HEALTH ASSESSMENT OF THE AQUATIC ECOSYSTEM IN AIYI RIVER

YIN, L.[1] – QIU, X.[2*] – ZHAO, R.[2]

[1]*School of Civil and Conservancy Engineering, Ningxia University, Yinchuan, Ningxia 750021, China*

[2]*College of Life Science, Ningxia University, Yinchuan, Ningxia 750021, China*

**Corresponding author*
e-mail: yinliang1001@163.com; phone: +86-187-2133-4685

(Received 9th Apr 2019; accepted 19th Jun 2019)

Abstract. Based on the investigation of the water environment factors and aquatic biodiversity of AiYi River from March to November 2018, 14 indicators were selected from water environment factors and aquatic biodiversity index using principal component analysis to construct the evaluation index system of aquatic ecosystem health of AiYi River. The gray correlative degree method was also used to evaluate the aquatic ecosystem's health condition of AiYi River from March to November 2018. The result showed that the aquatic ecosystem health condition of AiYi River was healthy in March and November, and that was sub-health in May, July, September. The aquatic ecosystem health of AiYi River was in the sub-health state due to the higher content of nitrogen, phosphorus and organic matter.
Keywords: *aquatic ecosystem, principal component analysis, gray correlative degree analysis*

Introduction

Ecosystem health refers to the structural integrity and functional stability of the ecosystem, and the ability of self-maintenance and self-repair. A healthy aquatic ecosystem plays an important role in protecting the water environment and maintaining its normal functions of the water environment. Accurate diagnosis and evaluation of the health status of the aquatic ecosystem has high theoretical and practical significance.

Aquatic ecosystem is a complex large-scale system. It is difficult to diagnose and evaluate the health status of aquatic ecosystem accurately by a single method. At present, the widely used method in the health evaluation of aquatic ecosystem is the index system method (Hossain et al., 2017; Milani et al., 2017; Janssens et al., 2017; Rongrong et al., 2018). A reasonable index system should reflect not only the overall health level of aquatic ecosystems, but also the changing trend of aquatic ecosystem health. The "Clean Water Act" issued by the United States in 1972 holds that maintaining the physical, chemical and biological integrity of the structure and function of river aquatic ecosystems is an important principle for river health assessment (Milani et al., 2017). Obolewski et al. (2019) proposed 16 indicators in 2019, including riparian zone integrity, river bed conditions, fish, aquatic plants, and classified the river health into five grades for evaluation. Some work has been done on the evaluation index system and methods of aquatic ecosystem health in China. Yu et al. (2017) put forward the contents of aquatic ecosystem health evaluation, such as the quality evaluation of biological habitat, hydrological evaluation and the evaluation of biological community. Maloney (2019) put forward the evaluation index system of water quantity, water quality, aquatic organism, physical structure and riparian zone,

http://www.aloki.hu ● ISSN 1589 1623 (Print) ● ISSN 1785 0037 (Online)
DOI: http://dx.doi.org/10.15666/aeer/1704_1001310025

as well as five evaluation criteria of "very healthy, healthy, sub-healthy, unhealthy and sick". Du et al. (2017) constructed the evaluation index system of aquatic ecosystem health, and used the analytic hierarchy process to evaluate the Luanhe River Basin comprehensively.

Although the index system method can well reflect the health status of aquatic ecosystems well, selecting reasonable indicators to construct the evaluation index system has not yet formed a recognized theoretical system and methods. In this study, the principal component analysis method was used to screen the candidate indicators for the health assessment of the Aquatic Ecosystem of Aiyi River, construct the evaluation index system, determine the weight of the corresponding indicators, and use the grey correlation method to evaluate the health status of the Aquatic Ecosystem of Aiyi River comprehensively, in order to provide some basis for the restoration of the Aquatic Ecosystem of Aiyi River and the comprehensive prevention and control of water pollution.

Materials and methods

Research area

Ningxia is short of water resources, arid and windy, and vegetation is scarce, which determines that its environmental capacity is small, the stability of ecosystem is poor, and the water environment is vulnerable to pollution and destruction. At present, the water environment situation in Ningxia is severe, and the regional water environmental pollution has become one of the biggest environmental problems. Aiyi River is the key project of river-lake system connection in Yinchuan City. It is the key water conservancy project of autonomous region integrating flood control, drainage, ecology and landscape. It is a National Water Conservancy Scenic spot. It has important social significance and far-reaching history for improving flood control and drainage conditions, Regulating Groundwater level, beautifying human settlement environment, upgrading urban grade, realizing human-water harmony and social harmony in Yinchuan City. Significance. The total length of Aiyi River is 158.5 km, the water surface is more than 50,000 mu, and the drainage area is controlled at 1.75 million mu. The main source of water is flood, Gully Water and channel discarded water. The amount of water that can be reused in the upper reaches of Aiyi River reaches 51 million m3 every year, of which farmland drainage accounts for 68.9%, rich in nitrogen and phosphorus nutrients. Agricultural and rural non-point source pollution in irrigation area is becoming the basic restrictive factor of the water quality of Aiyi River, and the backwater pollution in irrigation area with farmland as the core is becoming the main pollution source affecting the water quality of Aiyi River. Due to the large input of exogenous nutrients, the water exchange between rivers and lakes is weak, which makes the water body of Aiyi River tend to eutrophication gradually.

Screening of comprehensive assessment indicators of aquatic ecosystem health in Aiyi River

Composition of candidate index system

According to the results of factor analysis of water environment of Aiyi River, the main factors affecting water environment of Aiyi River are total phosphorus (TP), electrical conductivity (EC), ammonia nitrogen (NH3-N), total nitrogen (TN),

http://www.aloki.hu ● ISSN 1589 1623 (Print) ● ISSN 1785 0037 (Online)
DOI: http://dx.doi.org/10.15666/aeer/1704_1001310025

permanganate index (CODMn), five-day biochemical oxygen demand (BOD5), suspended solids (SS), transparency (SD), chlorophyll a (Chl.a), so this paper determines these nine physical and chemical indicators as love. Candidate indicators of comprehensive evaluation index system of aquatic ecosystem health of Yihe River. Biological indicators include phytoplankton biomass, phytoplankton Shannon-Wiener index (H'_a), zooplankton Shannon-Wiener index (H'_b), benthic animal Shannon-Wiener index (H'_c), aquatic plant Shannon-Wiener index (H'_d), and sediment heterotrophic bacteria. At the same time, the comprehensive trophic status index ($TLI_{(\Sigma)}$) which can reflect the eutrophication characteristics of water body is selected. The above indicators together constitute the candidate indicators of the Aiyi River aquatic ecosystem health evaluation index system.

Indicator screening method

Principal component analysis was carried out for each index value of Aiyi River in March, May, July, September and November 2018. The factor load matrix was rotated by maximum variance orthogonal rotation method. The principal component was extracted according to 85% cumulative variance contribution rate. Then, the index with load value greater than 0.6 after rotation was selected as the index for evaluating the health attributes of Aiyi River (Boltovskoy, 2017).

Determination of weight of evaluation index system

The above selected indicators constitute an index system for evaluating the health attributes of Aiyi River, and then the principal component analysis is carried out. The eigenvalues of principal components, the contribution rate of variance and the load value of factor after rotation are obtained. According to the 85% cumulative variance contribution rate, four principal components are extracted. According to the corresponding eigenvalues and contribution rate of variance of the four principal components, the weight of the index can be calculated (David et al., 2017; Łuczyńska et al., 2018). The calculation formula is as follows:

$$W_i = \sum_{j=1}^{k} \left| a_{ij} \right| \bullet E_j \qquad \text{(Eq.1)}$$

In the formula, a_{ij} is the factor score coefficient (eigenvalue) of factor i in the j principal component, that is the contribution of factor i to the j principal component; E_j is the contribution rate of the principal component to the variance; W_i is the weight value of factor i. Then the weights of each evaluation factor can be obtained by normalizing the W_i.

Determination of evaluation standard system

Referring to "Standard for Surface Water Environmental Quality" (GB 3838-2002) (Gdara et al., 2018) and Hyun et al. (2017), Boltovskoy (2017) and Xiao-Yun et al. (2018), the evaluation standard system of Aquatic Ecosystem Health of Aiyi River was established, which was divided into five evaluation levels: very healthy, sub-healthy, unhealthy and morbid (*Table 1*).

http://www.aloki.hu ● ISSN 1589 1623 (Print) ● ISSN 1785 0037 (Online)
DOI: http://dx.doi.org/10.15666/aeer/1704_1001310025

Table 1. *Classification of health assessment standard system*

Grade	Very healthy	Healthy	Sub-healthy	Unhealthy	Morbid
Meaning	The structure and function of aquatic ecosystem are complete and balanced, the flow of substance and energy is smooth, the vitality and resilience are very strong, and the health condition is very good	Aquatic ecosystems maintain a dynamic balance, strong vitality, reasonable structure, coordination, strong resilience and good health	The structure of aquatic ecosystem has changed, its function has declined, its ecological quality has declined, its vitality and resilience are general, and its health status is general	Aquatic ecosystems are deteriorating further, with weak vitality, inconsistent structure, poor resilience and poor health	Aquatic ecosystem deteriorates seriously, its vitality is very weak, its structure is completely unreasonable, its resilience is very poor, and its health is very poor

Health grade assessment of aquatic ecosystem in Aiyi River

The health grade of Aiyi River was evaluated by grey correlation method. Taking health standard grading as comparison series, the measured values of each index are reference series, and the correlation degree between monthly and annual average values and health levels is calculated. The health level of water body in each period is judged by the magnitude of correlation degree (Boltovskoy, 2017; Fleming et al., 2002).

The evaluation steps are as follows (Boltovskoy, 2017; Fleming et al., 2002):

(1) Normalize the evaluation month and the index values of the evaluation criteria;

(2) Calculate the absolute difference between the normalized index value and the corresponding evaluation criteria of five evaluation grades [$\Delta_{ik}(j)$].

(3) Find out the minimum absolute difference [$\Delta\min$] and the maximum absolute difference [$\Delta\max$] between all indexes and five evaluation grades.

(4) The correlation coefficients [$\varepsilon_{ik}(j)$] between the five-month and annual average values of each index and the corresponding evaluation criteria were calculated by taking the resolution coefficient p = 0.5.

$$\varepsilon_{ik}(j) = \frac{\Delta\min + \rho\Delta\max}{\Delta_{ik}(j) + \rho\Delta\max} \quad \text{(Eq.2)}$$

(5) According to the weight value of each index, the grey correlation degree (γ_{ij}) between the monthly and annual average and the five evaluation grades was calculated.

$$\gamma_{ij} = W_i \varepsilon_{ik}(j) \quad \text{(Eq.3)}$$

(6) According to the principle of maximum membership degree, the average health grade of 5 months and the whole year was evaluated.

http://www.aloki.hu ● ISSN 1589 1623 (Print) ● ISSN 1785 0037 (Online)
DOI: http://dx.doi.org/10.15666/aeer/1704_1001310025

Results

Selection of health assessment indicators for aquatic ecosystem of Aiyi River

Four principal components were extracted according to 85% cumulative variance contribution rate (*Table 2*). Fifteen factors were selected according to the principle that the factor load value was greater than 0.6. However, the number of heterotrophic bacteria in sediment has not been reported as an indicator of aquatic ecosystem health assessment. The evaluation criteria are uncertain, so 14 factors such as SS, EC, COD_{Mn}, BOD_5, TN, NH_3-N, TP, Chl.a, $TLI_{(\Sigma)}$, phytoplankton biomass (D), phytoplankton H'_a, zooplankton H'_b, benthic animal H'_c, and aquatic plant H'_d, are identified as the indicators for the health evaluation of the Aquatic Ecosystem of Aiyi River (see *Table 3*).

Composition and weight of health evaluation index system for aquatic ecosystem of Aiyi River

Fourteen health assessment factors of Aquatic Ecosystem of Aiyi River, including SS, EC, COD_{Mn}, BOD_5, TN, NH_3-N, TP, Chl.a, $TLI_{(\Sigma)}$, phytoplankton biomass (D), phytoplankton H'_a, zooplankton H'_b, benthic animal H'_c, and aquatic plant H'_d were screened and analyzed by principal component analysis. According to the analysis results (*Table 4*), the weights of each evaluation index were calculated, and the weights of 14 indicators were summed up. The normalized weights of each index can be obtained by dividing the weights of each index by the sum of weights (*Table 5*).

Table 2. *Characteristic number and principal constituent contribution rate and the cumulative contribution rate*

Composition	F1	F2	F3	F4
EC	0.3813	-0.0582	0.138	0.0336
SD	0.3115	0.0387	0.3545	0.0933
SS	-0.1348	0.4475	-0.1951	-0.1855
COD_{Mn}	-0.2872	-0.047	-0.0525	0.3513
BOD_5	-0.2852	-0.0468	-0.0297	0.3371
TN	0.2368	0.3261	0.0771	0.3273
NH_3-N	0.1831	0.3704	-0.0366	0.3359
TP	0.3009	0.0317	-0.2581	0.3026
Chl.a	-0.2917	0.1819	-0.0505	-0.3564
$TLI_{(\Sigma)}$	-0.2067	0.3387	-0.2682	0.1945
Phytoplankton biomass	-0.114	0.0237	0.4751	0.1424
Phytoplankton H'a	-0.263	0.2013	0.3765	0.0754
Zooplankton H'b	0.1178	0.1392	0.4363	-0.2858
Benthic animal H'c	-0.0916	0.4604	0.2166	0.0475
Aquatic plant H'd	0.1683	0.3406	-0.161	-0.3547
Number of heterotrophic bacteria	0.3673	0.0985	-0.1857	-0.0814
Characteristic value	6.1575	3.4362	2.9546	2.4977
Contribution rate%	38.48	21.48	18.47	15.61
Accumulated contribution rate%	38.48	59.96	78.43	94.04

http://www.aloki.hu ● ISSN 1589 1623 (Print) ● ISSN 1785 0037 (Online)
DOI: http://dx.doi.org/10.15666/aeer/1704_1001310025

Normalized weight values of SS, EC, COD_{Mn}, BOD_5, TN, NH_3-N, TP, Chl.a, $TLI_{(\Sigma)}$, phytoplankton biomass (D), phytoplankton H'_a, zooplankton H'_b, benthic animal H'_c, and aquatic plant H'_d are respectively set as 0.0636, 0.0724, 0.0723, 0.0711, 0.0787, 0.0764, 0.0716, 0.0756, 0.0771, 0.0790, 0.0571, 0.0599, 0.0717, 0.0736.

Table 3. *Rotated factor matrix*

	F1	F2	F3	F4
EC	**0.6343**	0.4997	-0.5434	-0.1365
SD	0.5750	0.5594	-0.5047	0.3120
SS	0.0311	0.0506	**0.9969**	0.0327
COD_{Mn}	**-0.8915**	-0.0718	0.0596	0.1687
BOD_5	**-0.8631**	-0.0835	0.0504	0.2010
TN	0.1681	**0.9749**	0.0504	0.1217
NH_3-N	0.0354	**0.9526**	0.2339	0.0163
TP	0.0703	**0.7545**	-0.2135	-0.6053
Chl.a	-0.0624	-0.5945	**0.7428**	0.2310
$TLI_{(\Sigma)}$	-0.5630	0.2432	**0.7657**	-0.0414
Phytoplankton biomass	-0.1349	0.0161	-0.2341	**0.8522**
Phytoplankton H'a	-0.2967	-0.0873	0.2603	**0.9138**
Zooplankton H'b	**0.7304**	-0.0023	-0.0459	0.6188
Benthic animal H'c	0.0278	0.3649	0.598	**0.6579**
Aquatic plant H'd	**0.6973**	0.1862	0.6199	-0.242
Number of heterotrophic bacteria	**0.6466**	0.5101	-0.0367	-0.5503

Table 4. *Characteristic number and principal constituent contribution rate and the cumulative contribution rate*

Composition	F1	F2	F3	F4
EC	-0.4211	0.0178	-0.1168	0.1645
SD	0.1993	0.4184	0.0275	-0.3055
SS	0.3177	-0.1062	0.3107	0.1964
COD_{Mn}	0.3178	-0.1066	0.2836	0.2038
BOD_5	-0.2185	0.3794	0.1362	0.3196
TN	-0.1622	0.416	0.2325	0.2324
NH_3-N	-0.3506	0.105	0.3736	0.0473
TP	0.3439	0.1183	-0.1813	-0.3296
Chl.a	0.2548	0.3043	0.3504	-0.0852
$TLI_{(\Sigma)}$	0.3423	0.141	-0.2143	0.3269
Phytoplankton biomass	0.1502	-0.0006	-0.2572	0.468
Phytoplankton H'a	-0.0796	0.1486	-0.5403	0.137
Zooplankton H'b	0.1819	0.4339	-0.1305	0.1926
Benthic animal H'c	-0.1474	0.3703	-0.1405	-0.3787
Aquatic plant H'd	4.7865	3.3635	2.5934	2.3328
Number of heterotrophic bacteria	34.19	24.03	18.52	16.66
Characteristic value	34.19	58.21	76.74	93.40

http://www.aloki.hu ● ISSN 1589 1623 (Print) ● ISSN 1785 0037 (Online)
DOI: http://dx.doi.org/10.15666/aeer/1704_1001310025

Table 5. *The weight and the normalized weight of evaluation indicators*

	Principal component eigenvalues of evaluation indicators				Variance contribution rate of each principal component				Weight	Normalized weight
	F1	F2	F3	F4	F1	F2	F3	F4		
SS	-0.4211	0.0178	-0.1168	0.1645	34.19	24.03	18.52	16.66	0.1973	0.0636
EC	0.1993	0.4184	0.0275	-0.3055	34.19	24.03	18.52	16.66	0.2247	0.0724
COD_{Mn}	0.3177	-0.1062	0.3107	0.1964	34.19	24.03	18.52	16.66	0.2244	0.0723
BOD_5	0.3178	-0.1066	0.2836	0.2038	34.19	24.03	18.52	16.66	0.2208	0.0711
TN	-0.2185	0.3794	0.1362	0.3196	34.19	24.03	18.52	16.66	0.2443	0.0787
NH_4-N	-0.1622	0.416	0.2325	0.2324	34.19	24.03	18.52	16.66	0.2372	0.0764
TP	-0.3506	0.105	0.3736	0.0473	34.19	24.03	18.52	16.66	0.2222	0.0716
Chl.a	0.3439	0.1183	-0.1813	-0.3296	34.19	24.03	18.52	16.66	0.2345	0.0756
$TLI_{(\Sigma)}$	0.2548	0.3043	0.3504	-0.0852	34.19	24.03	18.52	16.66	0.2393	0.0771
Phytoplankton biomass D	0.3423	0.141	-0.2143	0.3269	34.19	24.03	18.52	16.66	0.2451	0.079
Phytoplankton H'a	0.1502	-0.0006	-0.2572	0.468	34.19	24.03	18.52	16.66	0.1771	0.0571
Zooplankton H'b	-0.0796	0.1486	-0.5403	0.137	34.19	24.03	18.52	16.66	0.1858	0.0599
Benthic animal H'c	0.1819	0.4339	-0.1305	0.1926	34.19	24.03	18.52	16.66	0.2227	0.0717
Aquatic plant H'd	-0.1474	0.3703	-0.1405	-0.3787	34.19	24.03	18.52	16.66	0.2285	0.0736

Standard system for health assessment of aquatic ecosystem in Aiyi River

The classification standard of physical and chemical indexes of water body is based on "Surface Water Environmental Quality Standard" (GB 3838-2002). Five grades of very healthy, healthy, sub-healthy, unhealthy and sick correspond to I, II, III, IV and V water standards respectively. The classification standard of suspended solids (SS) and conductivity (EC) is determined by reference (Boltovskoy, 2017).

According to the relevant provisions of the "Evaluation Method of Eutrophication of Lakes (Reservoirs) and Technical Regulations for Classification" (Yang et al., 2019; Ochoa-Rivero et al., 2017; Sorokovikova et al., 2017), the comprehensive nutritional status index N = 50 is medium nutrition, which is regarded as sub-health level, N < 30 is poor nutrition, which is very healthy level, N > 70 is severe eutrophication, which is morbid level, 30-50 is health level, 60-70 is unhealthy level.

The Shannon-Wiener diversity index (H') of phytoplankton, zooplankton, benthic and aquatic plants reflects the diversity of community species. The value of H'(0-1) is eutrophic, 1-3 is mesotrophic and more than 3 is poor nutrition (Kozlov et al., 2017). Accordingly, 2-3 is considered as sub-health grade, 4 is considered as very health grade, H'(1) is considered as morbid grade, 3-4 is health grade, 1-2 is unhealthy grade.

According to the relevant evaluation criteria of lake eutrophication in China (Suzuki et al., 2018), phytoplankton biomass < 3 mg L^{-1} is a poor nutrition type, which is regarded as very healthy and healthy grade. 3-5 mg L^{-1} is a middle nutrition type, which is regarded as sub-health grade, 5-10 mg L^{-1} as eutrophic type, which is unhealthy grade, and > 10 mg L^{-1} as extremely eutrophic type, which is a morbid grade.

http://www.aloki.hu ● ISSN 1589 1623 (Print) ● ISSN 1785 0037 (Online)
DOI: http://dx.doi.org/10.15666/aeer/1704_1001310025

The health assessment standard system of the Aquatic Ecosystem of Aiyi River is shown in *Table 6*.

Table 6. *Health assessment standard system of Aiyi River aquatic ecosystem*

Index	Health grade				
	Very healthy	**Healthy**	**Sub-healthy**	**Unhealthy**	**Morbid**
EC(μS·cm^{-1})	≤ 200	(200, 300]	(300, 400]	(400, 500]	(500, 600]
SS (mg·L^{-1})	≤ 96	(96, 172]	(172, 364]	(364, 820]	(820, 1640]
COD_{Mn}(mg·L^{-1})	≤ 2	(2,4]	(4,6]	(6,10]	(10,15]
BOD_5(mg·L^{-1})	≤ 3.0	≤ 3.0	(3.0, 4.0]	(4.0, 6.0]	(6.0, 10.0]
TN (mg·L^{-1})	≤ 0.2	(0.2, 0.5]	(0.5, 1.0]	(1.0, 1.5]	(1.5, 2.0]
NH_3-N (mg·L^{-1})	≤ 0.15	(0.15, 0.50]	(0.50, 1.0]	(1.0, 1.5]	(1.5, 2.0]
TP (mg·L^{-1})	≤ 0.02	(0.02, 0.10]	(0.10, 0.20]	(0.20, 0.30]	(0.30, 0.40]
Chl.a(μg·L^{-1})	≤ 1.0	(1.0, 2.0]	(2.0, 4.0]	(4.0, 10.0]	(10.0,26.0]
$TLI_{(\Sigma)}$	≤ 30	(30,50]	(50,60]	(60,70]	> 70
Phytoplankton biomass D	≤ 3.0	≤ 3.0	[3.0, 5.0)	[5.0, 10.0)	≥ 10.0
Phytoplankton H'a	≥ 4.0	[3.0, 4.0)	[2.0, 3.0)	[1.0, 2.0)	≤ 1.0
Zooplankton H'b	≥ 3.0	[2.0, 3.0)	[1.0, 2.0)	[0.5, 1.0)	≤ 0.5
Benthic animal H'c	≥ 3.0	[2.0, 3.0)	[1.0, 2.0)	[0.5, 1.0)	≤ 0.5
Aquatic plant H'd	≥ 3.0	[2.0, 3.0)	[1.0, 2.0)	[0.5, 1.0)	≤ 0.5

Health grade assessment of aquatic ecosystem in Aiyi River

Taking the annual average index of Aiyi River as an example, the correlation degree between each evaluation index and evaluation standard grade was calculated (*Table 7*). The results of the difference calculation are shown in *Table 8*, and the correlation coefficient and correlation degree are shown in *Tables 9* and *10*.

Table 7. *The measured values of evaluation indicators in AiYi River*

	March	**May**	**July**	**September**	**November**	**Avg.**
EC(us·cm^{-1})	**1116.67**	**1056.67**	**991.67**	**928.33**	**981.67**	**1015.00**
SS(mg·L^{-1})	23.24	34.62	42.42	25.28	25.24	30.16
COD_{Mn}(mg·L^{-1})	6.03	6.13	9.98	8.93	5.75	7.36
BOD_5(mg·L^{-1})	2.98	3.17	5.18	5.78	3.01	4.02
TN(mg·L^{-1})	1.835	2.302	3.080	1.247	3.063	2.305
NH_3-N(mg·L^{-1})	0.634	0.745	0.989	0.866	0.440	0.735
TP(mg·L^{-1})	0.082	0.050	0.094	0.118	0.064	0.082
Chl.a(ug·L^{-1})	10.51	10.49	15.10	13.58	11.62	12.26
$TLI_{(\Sigma)}$	53.94	54.26	62.4	57.13	54.54	56.45
Phytoplankton biomass (mg·L^{-1})	4.52	6.58	6.02	5.17	3.43	5.15
Phytoplankton H'a	3.469	3.464	3.184	2.993	3.558	3.334
Zooplankton H'b	2.648	2.728	3.094	2.965	3.356	2.958
Benthic animal H'c	2.043	2.004	2.284	2.175	1.575	2.016
Aquatic plant H'd	2.441	2.002	2.118	2.294	2.410	2.424

http://www.aloki.hu ● ISSN 1589 1623 (Print) ● ISSN 1785 0037 (Online)
DOI: http://dx.doi.org/10.15666/aeer/1704_1001310025

Table 8. *D-value of average index and evaluation criterion*

	Difference value						
	Very healthy	**Healthy**	**Sub-healthy**	**Unhealthy**	**Morbid**	**Max**	**Min**
EC(μS·cm^{-1})	815	715	615	515	415	815	415
SS (mg·L^{-1})	65.84	141.84	333.84	789.84	1609.84	1609.84	65.84
COD_{Mn}(mg·L^{-1})	5.36	3.36	1.36	2.64	7.64	7.64	1.36
BOD_5(mg·L^{-1})	1.02	1.02	0.02	1.98	5.98	5.98	0.02
TN (mg·L^{-1})	2.105	1.805	1.305	0.805	0.305	2.105	0.305
NH_3-N (mg·L^{-1})	0.585	0.235	0.265	0.765	1.265	1.265	0.235
TP (mg·L^{-1})	0.062	0.018	0.118	0.218	0.318	0.318	0.018
Chl.a(μg·L^{-1})	11.26	10.26	8.26	2.26	7.74	11.26	2.26
$TLI_{(\Sigma)}$	26.45	6.45	3.55	13.55	43.55	43.55	3.55
Phytoplankton biomass (mg·L^{-1})	1.15	2.15	0.15	4.85	14.85	14.85	0.15
Phytoplankton H'a	0.666	0.334	1.334	2.334	3.334	3.334	0.334
Zooplankton H'b	1.042	0.042	0.958	1.958	2.958	2.958	0.042
Benthic animal H'c	1.984	0.984	0.016	1.016	2.016	2.016	0.016
Aquatic plant H'd	1.576	0.576	0.424	1.424	2.424	2.424	0.424

Table 9. *The grey relational coefficient of average index and evaluation criterion $\varepsilon_{ik}(j)$*

	Relational coefficient				
	Very healthy	**Healthy**	**Sub-healthy**	**Unhealthy**	**Morbid**
EC(μS·cm^{-1})	0.6728	0.7327	0.8044	0.8916	1.0000
SS (mg·L^{-1})	1.0000	0.9197	0.7647	0.546	0.3606
COD_{Mn}(mg·L^{-1})	0.5643	0.7214	1.0000	0.8019	0.452
BOD_5(mg·L^{-1})	0.7506	0.7506	1.0000	0.6056	0.3356
TN (mg·L^{-1})	0.4299	0.4751	0.5758	0.7308	1.0000
NH_3-N (mg·L^{-1})	0.7125	1.0000	0.9666	0.6208	0.4572
TP (mg·L^{-1})	0.8009	1.0000	0.639	0.4695	0.3711
Chl.a(μg·L^{-1})	0.4671	0.4965	0.568	1.0000	0.5901
$TLI_{(\Sigma)}$	0.5251	0.8973	1.0000	0.7169	0.3877
Phytoplankton biomass (mg·L^{-1})	0.8834	0.7911	1.0000	0.6171	0.3401
Phytoplankton H'a	0.8577	1.0000	0.6668	0.5001	0.4001
Zooplankton H'b	0.6033	1.0000	0.6241	0.4425	0.3428
Benthic animal H'c	0.3422	0.5141	1.0000	0.5059	0.3386
Aquatic plant H'd	0.5868	0.915	1.0000	0.6206	0.4499

The correlation between each month and the grade of evaluation criteria is calculated in *Table 11*. From *Table 11* we can see that the evaluation results of the Aiyi River in March and November are healthy, the evaluation results in May, July and September are sub-healthy, and the overall evaluation of the health status of the Aiyi River aquatic ecosystem is sub-healthy.

http://www.aloki.hu ● ISSN 1589 1623 (Print) ● ISSN 1785 0037 (Online)
DOI: http://dx.doi.org/10.15666/aeer/1704_1001310025

Table 10. *Grey relational degree of average index and evaluation criterion*

	Weight	Very healthy	Healthy	Sub-healthy	Unhealthy	Morbid
EC($\mu S \cdot cm^{-1}$)	0.0636	0.0428	0.0466	0.0512	0.0567	0.0636
SS ($mg \cdot L^{-1}$)	0.0724	0.0724	0.0666	0.0554	0.0395	0.0261
COD_{Mn}($mg \cdot L^{-1}$)	0.0723	0.0408	0.0522	0.0723	0.058	0.0327
BOD_5($mg \cdot L^{-1}$)	0.0711	0.0534	0.0534	0.0711	0.0431	0.0239
TN ($mg \cdot L^{-1}$)	0.0787	0.0338	0.0374	0.0453	0.0575	0.0787
NH_3-N ($mg \cdot L^{-1}$)	0.0764	0.0544	0.0764	0.0738	0.0474	0.0349
TP ($mg \cdot L^{-1}$)	0.0716	0.0573	0.0716	0.0458	0.0336	0.0266
Chl.a($\mu g \cdot L^{-1}$)	0.0756	0.0353	0.0375	0.0429	0.0756	0.0446
$TLI_{(\Sigma)}$	0.0771	0.0405	0.0692	0.0771	0.0553	0.0299
Phytoplankton biomass ($mg \cdot L^{-1}$)	0.079	0.0698	0.0625	0.079	0.0488	0.0269
Phytoplankton H'a	0.0571	0.049	0.0571	0.0381	0.0286	0.0228
Zooplankton H'b	0.0599	0.0361	0.0599	0.0374	0.0265	0.0205
Benthic animal H'c	0.0717	0.0245	0.0369	0.0717	0.0363	0.0243
Aquatic plant H'd	0.0736	0.0432	0.0673	0.0736	0.0457	0.0331
Correlation degree		0.6534	0.7945	0.8346	0.6525	0.4886

Table 11. *Calculation of grey relational degree*

Site	Very healthy	Healthy	Sub-healthy	Unhealthy	Morbid	Result
March	0.6743	0.8219	0.8093	0.64	0.4675	Healthy
May	0.6627	0.7751	0.8242	0.6461	0.4688	Sub-healthy
July	0.5995	0.7294	0.8078	0.7049	0.5171	Sub-healthy
September	0.5854	0.7521	0.8249	0.7102	0.4692	Sub-healthy
November	0.7428	0.8521	0.7944	0.6583	0.4939	Healthy
Comprehensive	0.6534	0.7945	0.8346	0.6525	0.4886	Sub-healthy

Conclusion

Health evaluation index of aquatic ecosystem in Aiyi River

The evaluation index of Aquatic Ecosystem Health of Aiyi River is mainly composed of four parts: The first part includes the factors of phytoplankton biomass (D), phytoplankton H'_a, zooplankton H'_b, benthic animal H'_c and aquatic plant H'_d which are the comprehensive reflection of the diversity and integrity of aquatic ecosystem structure, and the most important part of the evaluation index of aquatic ecosystem health. The second part includes SS, EC, Chl.a and $TLI_{(\Sigma)}$ which mainly describe the content of suspended solids and dissolved salts in water. The third part includes TN, NH_3-N and TP, which mainly describe the composition and content of nitrogen and phosphorus nutrients in water. The fourth part includes COD_{Mn} and BOD_5 which mainly describe the content of organic matter in water. The above indicators cover the main water quality factors such as suspended matter, dissolved salts, nutrients and organic matter, which can fully reflect the water environment quality of the Aiyi River. Biological indicators include phytoplankton biomass (D), phytoplankton H'_a, zooplankton H'_b, benthic animal H'_c, and aquatic plant H'_d which are comprehensive reflections of the structural diversity of aquatic ecosystems. In the process of research,

http://www.aloki.hu ● ISSN 1589 1623 (Print) ● ISSN 1785 0037 (Online)
DOI: http://dx.doi.org/10.15666/aeer/1704_1001310025

due to the lack of microbial research results, microbial indicators can not be included in the evaluation index system, and further in-depth and systematic research is needed to further improve the theory and methods of aquatic ecosystem health assessment.

Health status of aquatic ecosystem in Aiyi River

The contents of S S, CODMn, BOD5, NH3-N, TN and TP in Aiyi River in May, July and September were significantly higher than those in March and November, indicating that the contents of nutrients and organic matter in the water body of Aiyi River were higher in May, July and September, and the pollution degree of the water body was higher. The reason was that a large amount of organic matter and nutrients entered the water body due to the large amount of water recharge in the three periods. At the same time, under the high nutrient and high temperature environment, cyanobacteria multiply in large quantities, forming dominant species, inhibiting the growth of other phytoplankton species, decreasing phytoplankton diversity, increasing chlorophyll a content, phytoplankton density and biomass, resulting in serious impacts on the structure of the aquatic ecosystem and functional degradation of the Aiyi River, so the health status in May, July and September is worse than that in March and November. To be poor, in a sub-health state. $TLI_{(\Sigma)}$ indicates the degree of eutrophication of the water body. The $TLI_{(\Sigma)}$ in July and September of the Aiyi River is higher than that in March and November. It also shows that the water body of the Aiyi River has been moderately polluted, in a state of medium eutrophication, and its health has declined. In addition, the community structure of aquatic plants and benthic fauna in Aiyi River is not balanced and the diversity is low. The natural succession rate of aquatic plants and benthic fauna in Aiyi River can not adapt to the pressures of exogenous pollutants, and the inadequate ability to degrade nitrogen, phosphorus nutrients and organic matter is also an important reason for the sub-health of the aquatic ecosystem in Aiyi River.

The water source of Aiyi River is mainly farmland recession with high nutrient and organic matter content, which is the main cause of water pollution of Aiyi River. The aquatic ecosystem is greatly affected by external stress factors, resulting in sub-health of the overall health of the aquatic ecosystem of Aiyi River. The comprehensive evaluation results also reflect the water environment characteristics of the aquatic ecosystem of Aiyi River comprehensively. According to the results of health assessment of aquatic ecosystem, the prevention and control of water pollution in Aiyi River should mainly focus on reducing the content of exogenous nutrients and organic matter, rebuilding and restoring aquatic ecosystem, ensuring its structural integrity and functional stability.

The health status of river aquatic ecosystem varies greatly in different time and space scales. Based on the actual monitoring data in 2018, the health status of Aiyi River aquatic ecosystem is preliminarily evaluated. In the future, the characteristics of aquatic plant community, the characteristics of algae community and its diversity index, biological integrity index and comprehensive quality evaluation index of habitat need to be strengthened. In order to further improve the theory and method of river aquatic ecosystem health assessment, we should strengthen the observation of long time series aquatic ecosystem in different water periods.

Acknowledgements. This project is supported by “Major Innovation Projects for Building First-class Universities in China’s Western Region” (ZKZD2017002).

http://www.aloki.hu ● ISSN 1589 1623 (Print) ● ISSN 1785 0037 (Online)
DOI: http://dx.doi.org/10.15666/aeer/1704_1001310025

REFERENCES

[1] Boltovskoy, D. (2017): Traits and impacts of invasive species: myths and evidences from the perspective of introduced freshwater mussels. – Aquatic Ecosystem Health & Management. DOI: 10.1080/14634988.2017.1397483.

[2] David, B., Avinash, K., Warish, A., Stephen, C., Paul, M., Christopher, S. et al. (2017): A community multi-omics approach towards the assessment of surface water quality in an urban river system. – International Journal of Environmental Research and Public Health 14(3): 303-310.

[3] Du, Y., Ye, J., Wu, L., Yang, C., Wang, L., Hu, X. (2017): Physiological effects and toxin release in microcystis aeruginosa and microcystis viridis exposed to herbicide fenoxaprop-p-ethyl. – Environmental Science and Pollution Research 24(8): 7752-7763.

[4] Fleming, R. A., Barclay, H. J., Candau, J. N. (2002): Scaling-up an autoregressive time-series model (of spruce budworm population dynamics) changes its qualitative behaviour. – Ecological Modelling 149(1-2): 127-142.

[5] Gdara, I., Zrafi, I., Balducci, C., Cecinato, A., Ghrabi, A. (2018): Seasonal occurrence, source evaluation and ecological risk assessment of polycyclic aromatic hydrocarbons in industrial and agricultural effluents discharged in Wadi el Bey (Tunisia). – Environ Geochem Health 20: 1-19.

[6] Hossain, M., Stewart, T. J., Arhonditsis, G. B., Van Oevelen, D., Minns, C. K., Koops, M. A. (2017): Uncertainty assessment of trophic flows in hamilton harbour: a linear inverse modelling analysis. – Aquatic Ecosystem Health & Management 20(3): 265-277.

[7] Hyun, B., Baek, S. H., Shin, K., Choi, K. H. (2017): Assessment of phytoplankton invasion risks in the ballast water of international ships in different growth conditions. – Aquatic Ecosystem Health & Management. https://doi.org/10.1080/14634988. 2017.1406273.

[8] Islam, M. R., Das, N. G., Barua, P., Hossain, M. B., Venkatramanan, S., Chung, S. Y. (2017): Environmental assessment of water and soil contamination in rajakhali canal of karnaphuli river (bangladesh) impacted by anthropogenic influences: a preliminary case study. – Applied Water Science 7(2): 997-1010.

[9] Janssens, L., Lin, O. D. B., Stoks, R. (2017): Stoichiometric responses to an agricultural pesticide are modified by predator cues. – Environmental Science & Technology 51(1): 581-588.

[10] Kozlov, D. V., Nasonov, A. N., Tsvetkov, I. V., Zhogin, I. M. (2017): Multifractal principles of aquatic ecosystem development control by algacenosis correction. – Water Resources 44(2): 259-266.

[11] Łuczyńska, J., Paszczyk, B., Łuczyński, M. J. (2018): Fish as a bioindicator of heavy metals pollution in aquatic ecosystem of Pluszne Lake, Poland, and risk assessment for consumer's health. – Ecotoxicology & Environmental Safety 153: 60-67.

[12] Maloney, E. M. (2019): How do we take the pulse of an aquatic ecosystem? current and historical approaches to measuring ecosystem integrity. – Environmental Toxicology and Chemistry 38(2).

[13] Milani, D., Grapentine, L., Burniston, D. A., Graham, M., Marvin, C. (2017): Trends in sediment quality in hamilton harbour, lake ontario. – Aquatic Ecosystem Health & Management 20(3): 295-307.

[14] Obolewski, K., Glińska-Lewczuk, K., Bąkowska, M. (2018): From isolation to connectivity: the effect of floodplain lake restoration on sediments as habitats for macroinvertebrate communities. – Aquatic Sciences 80(1): 4.

[15] Ochoa-Rivero, J. M., Reyes-Fierro, A. V., Peralta-Pérez, M. D. R., Zavala-Díaz de la Serna, F. J. et al. (2017): Levels and distribution of pollutants in the waters of an aquatic ecosystem in northern Mexico. – International Journal of Environmental Research and Public Health 14(5): 456-465.

http://www.aloki.hu ● ISSN 1589 1623 (Print) ● ISSN 1785 0037 (Online)
DOI: http://dx.doi.org/10.15666/aeer/1704_1001310025

[16] Richman, L., Milani, D., Marvin, C. (2017): Trends in suspended sediment quality in the upper st. clair river: assessment of large-scale remediation of contaminated sediments in a dynamic riverine environment. – Aquatic Ecosystem Health & Management 21(1): 93-106.
[17] Rongrong, W., Guishan, Y., Xue, D., Yanhui, Z., Bing, L. I. (2018): Water security-based hydrological regime assessment method for lakes with extreme seasonal water level fluctuations: a case study of Poyang Lake, China. – Chinese Geographical Science 3: 1-14.
[18] Sorokovikova, L. M., Sinyukovich, V. N., Tomberg, I. V. (2017): The status of the aquatic ecosystem of the selenga river delta under long-duration low-water conditions. – Geography and Natural Resources 38(1): 60-67.
[19] Suzuki, K., Watanabe, S., Yuasa, Y., Yamashita, Y., Arai, H., Tanaka, H. et al. (2018): Adiocesium dynamics in the aquatic ecosystem of Lake Onuma on MT. AKAGI following the Fukushima Dai-Ichi nuclear power plant accident. – Science of the Total Environment 622-623: 1153-1164.
[20] Xiao-Yun, G. U., Zong-Xue, X. U., Lin-Fei, L., Xu-Wang, Y., Mi, W. (2018): Health assessment of the stream ecosystem in the North Canal River basin, Beijing, China. – Environmental Science 39(6): 2576.
[21] Yang, J., Wang, F., Lv, J., Liu, Q., Feng, J. (2019): Responses of freshwater algal cell density to hydrochemical variables in an urban aquatic ecosystem, northern China. – Environmental Monitoring and Assessment 191(1).
[22] Yu, C., Chen, S. S., Zhang, L., Gao, Q., Wang, Z., Shen, Q. (2017): Changes in water quality of the rivers discharging into Lake Tanganyika in Bujumbura, Burundi. – Aquatic Ecosystem Health & Management. https://doi.org/10.1080/14634988.2017.1394772.

http://www.aloki.hu ● ISSN 1589 1623 (Print) ● ISSN 1785 0037 (Online)
DOI: http://dx.doi.org/10.15666/aeer/1704_1001310025

SEDIMENTARY CHARACTERISTICS AND DEPOSITIONAL EVOLUTION OF LITTORAL-TIDAL FLAT SYSTEM OF SILURIAN ROCKS IN THE TABEI AREA, TARIM BASIN, NW CHINA

WANG, Y. N.[1] – XU, H. B.[2*] – ZHANG, S. F.[1] – XIA, Y. T.[3] – ZHANG, C.[1] – SHANG, J.[1] – BAO, C.[1]

[1]*College of Geosciences, Yangtze University, Wuhan, Hubei 430100, China*

[2]*Key Laboratory of Submarine Geoscience, Second Institute of Oceanography, SOA, Hangzhou, Zhejiang 310012, China*

[3]*Sinopec Northwest Company, Urumqi 830013, China*

**Corresponding author*
e-mail: wyn-ml@foxmail.com

(Received 9th Apr 2019; accepted 19th Jun 2019)

Abstract. The marine clastic rock of the Silurian in the Tabei Area is a favorable reservoir. Based on an analysis of geological data such as core, logging, and seismic information, this study investigated the characteristics and differences of the Silurian rocks in the Tabei area main sedimentary system types. Both tidal flat and littoral have been meticulously depicted. In addition, the paleogeographic environment and depositional evolution features of the Silurian rocks in this area have been remodeled. The obtained results show that: (1) according to the difference in sedimentary environment, tidal flat facies have been subdivided into shallow tidal flat and bay tidal flat. (2) During the Early Silurian stage, the center-western region of the study area developed an incised channel with curved characteristics, which was associated with the coastal plain. (3) The whole Silurian deposition was significantly controlled by tectonic movement. Consequently, under the background of Late Caledonian orogeny, the Tabei area was gradually uplifted, and its depocenter constantly migrated southward. This resulted in the vertical transformation of sedimentary types from an incised channel-coastal plain-shallow tidal flat system to a littoral-bay tidal flat system. Moreover, Backshore and supratidal zone were generally denuded due to uplifting at a later stage.
Keywords: *sedimentary facies, marine clastic rock, Kepingtage formation, stratigraphy, coastal plain*

Introduction

The Tabei Area is located in the northern parts of the Tarim Basin and includes the Halahatang Sag, the Akekule Uplift, the Caohu Sag, and the Shaya Uplift. Vertically, Silurian strata are divided into three formations, namely the Kalpintake formation (S_1k), the Tataiertage formation (S_1t), and the Yimugantawu (S_2y) formation from low to upper levels. In particular, the Yimugantawu formation was missing because it was denuded during the early Hercynian movement. Moreover, Kalpintake formation was subdivided into three parts, which are the lower part of the Kalpintake formation (S_1k^1), the middle part (S_1k^2), and the upper part (S_1k^3) (*Fig. 1a, b*).

During the Late Caledonian movement, sedimentary the facies of the Silurian in the Tabei area was controlled by factors such as constant uplifting and multiple cycles of increasing and descending sea level (*Fig. 1c, d*). With constant discoveries of oil and gas reservoirs, marine clastic rocks as favorable reservoirs developed in the Silurian formations, have attracted the attention of experts and scholars.

http://www.aloki.hu ● ISSN 1589 1623 (Print) ● ISSN 1785 0037 (Online)
DOI: http://dx.doi.org/10.15666/aeer/1704_1002710035

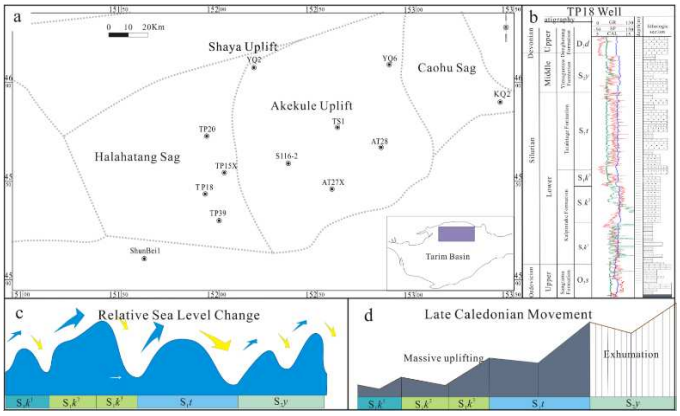

Figure 1. *Tectonic setting and stratigraphic characteristics in the Tabei area*

In recent years, the study of sedimentary facies of marine clastic rocks has achieved significant progress both in China and internationally. For example, Yamashita et al. (2009) analyzed the coefficient of variance (CV) of grain-size distribution and reported the three-dimensional distribution of the tidal flat sand body in the estuary of the Chlamara River. Tillmann and Wunderlich (2014) combined the ground penetrating radar (GPR) with sedimentology and defined different coastal environments of southern Sylt, an island in the North Sea. Zhao et al. (2015) proposed the use of grain-size-sensitive indicators to identify sedimentary facies in a study of modern tidal flat sediments. Gong et al. (2018) studied the relationship between the evolution of tidal channels and the changing sea level. In combination, these studies offer a new way of thinking for the study of marine clastic rocks. Furthermore, many studies have investigated the sedimentary characteristics and the depositional systems of the Silurian in the Tarim Basin. For example, Hu et al. (2007), Jiang et al. (2009), Liu et al. (2016), and Zeng et al. (2018) all suggested that the Tarim Basin developed a barrier-free clastic littoral, offshore shelf, tidal flat, and river delta during the Silurian. Niu et al. (2013) studied the sediment source. Liu et al. (2016) studied the palaeogeomorphology evolution during the Silurian in the Tarim Basin. On the one hand, it is important to clarify sedimentary characteristics, the underlying system, and its evolution, as these still remain poorly understood, which restricts the exploration and research of oil and gas resources resources. On the other hand, previous research typically focused on the description of sedimentary facies and their characteristics (El-Wahed, 2010; Guilbaud et al., 2012; Zhang et al., 2012; Zhang, 2014; Zhang, 2017). However, they ignored the relationship between the transformations of different sedimentary facies and the influence of tectonic movement. At present, the main questions are as follows: (1) What are the differences between the sedimentary characteristics of both shallow tidal flat and bay tidal flat under different depositional environments? (2) What are the sedimentary characteristics and distributions of the coastal plain and its incised channel? (3) How can different facies transform from one form to the other? The results of this study provide answers for these questions which offer a solid geological basis for further oil and gas exploration and their development.

Materials and methods

The utilized geological data contains 137 core sample photos of Silurian rocks, logging data, and seismic profiles, which were provided by the Sinopec Group Northwest Petroleum

http://www.aloki.hu ● ISSN 1589 1623 (Print) ● ISSN 1785 0037 (Online)
DOI: http://dx.doi.org/10.15666/aeer/1704_1002710035

Branch. The analysis is based on core observations, identification of sedimentary facies markers, analysis of single well, and interpretation of logging and seismic information. The aim was to define the different types of sedimentary facies and both its subfacies and microfacies. Through seismic profiles information, the sedimentary distribution was determined. Then, the distributions were combined with the tectonic evolution process to identify the depositional filling process and sedimentary systems in each period of the Silurian age.

Results

Sedimentary types and characteristics

In the study area, Silurian formations mainly deposited marine clastic rocks, developed tidal flat facies, littoral facies, coastal plain facies, and neritic shelf facies.

Tidal flat facies

Silurian formations in the Tabei area ware distributed as a clastic tidal flat. During the Early-middle Silurian period, the lower part of the Kalpintage (S_1k^1) extensively developed the shallow water tidal flat facies, while the upper part (S_1k^3) locally deposited the Bay tidal flat facies. Their subfacies are intertidal zone and subtidal zone. Furthermore, its microfacies include mud flat, mixed flat, sand flat, tidal channel, and tidal sand bar.

Shallow tidal flat facies

The shallow tidal flat facies is distributed throughout the lower part of the lower Silurian Kalpintage formation in the Tabei area. During the early Early Silurian period (S_1k^1 sedimentary period), a small-scale uplift of the terrain under the late Caledonian movement resulted in a stable subsidence. It is worth mentioning that the sedimentary environment at that time in the study was a wide epicontinental sea without barrier. The waves were weakened due to the particular environment with shallow water and gentle slope. As a result, the area widely developed shallow tidal flat facies, which directly contacted the neritic shelf, forming a widely distributed shallow sea shelf contact.

The log curve and seismic profile of the AT27X well provides the natural gamma (GR) curve of the shallow tidal flat in the lower part of the formation and shows the median value and the dentate type (*Fig. 2a*). The seismic reflection structure consists of two types: low continuity and middle amplitude as well as high continuity and middle-high amplitude. The shallow tidal flat facies above the Ordovician system shows the retrogradation progress and reflects the rise of the sea level (*Fig. 2b*).

Bay tidal flat

In contrast, bay tidal flat facies is locally distributed in the upper part of the Kalpintage formation (S_1k^3) and the Tataiertage formation (S_1t) of the lower-middle Silurian in the Tabei area. With the sustained enhancement of late Caledonian movement during the Early-Middle Silurian period, except the eastern and western region, the study area was subjected to rapid uplifting and formed a steep slope. At the same time, waves were significantly strengthened. However, the eastern and western

http://www.aloki.hu ● ISSN 1589 1623 (Print) ● ISSN 1785 0037 (Online)
DOI: http://dx.doi.org/10.15666/aeer/1704_1002710035

areas featured by no obvious barrier bay, which could have obstructed wave formation and thus boosted tidal shifts. The facies contacted the shelf or upper nearshore.

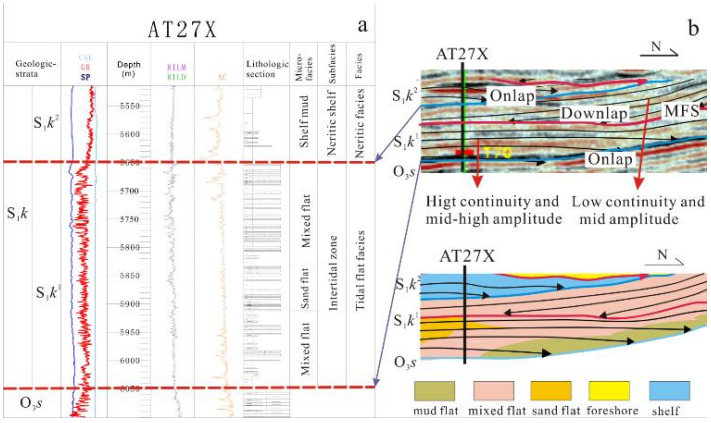

Figure 2. *Geophysical response characteristics of shallow tidal flat in the AT27X well*

Furthermore, the shallow tidal flat has a relatively high shale content. Its mud flat is well developed and other microfacies contain mixed flat, sand flat, and tidal bar. Especially the tidal channel is little developed. The mud flat consists of grey-green grey mudstone and silty mudstone (*Fig. 3a*). The mixed flat has an unequal thickness, is interbeded with fine sandstone and mudstone, and developed both tidal bedding and cross bedding (*Fig. 3b, c, d*). The lithology of the sand flat consist of gray-green gray fine litharenite with separation, cross bedding, and oblique bedding (*Fig. 3e*).

Because the strong uplift led to a rapid decrease of relative sea level, rocks of the bay tidal flat facies contain less muddy sediment but more sandy depositions, which differs from shallow tidal flat. It includes grey-green grey brown sandstone, reflecting the weak reduction/weak oxidation sedimentary environment. Its tidal channels are well developed and other microfacies include mixed flat, sand flat, and tidal sand bar, but no mud flat.

Then, the characteristics of the tidal channel lithology contains comparatively rough granularity with poor separation. Furthermore, the fine-coarse litharenite is visible. Sandy, argillaceous, and lime conglomerate developed at the bottom, with many erosion and truncated surfaces, and the fine gravelly deposit (*Fig. 3f, g, h*).

Littoral facies

Under the background of late Caledonian movement during the Early-Middle Silurian period, the central part of the Tabei area was greatly uplifted and became steep. Consequently, the hydrodynamic wave force was greatly strengthened. As a result, the upper part of the Kalpintage formation (S_1k^3) and the Tataaiertage formation (S_1t) developed littoral deposition.

In general, the facies have three main features in common: (1) as the near source deposits, the have a general composition and structural maturity; (2) the foreshore and nearshore developed, while backshore lacked. According to the lithologic difference of nearshore, the latter can be subdivided into an upper shoreface and a lower shoreface; (3) sand bodies were characteristic by acceleration progradation and reverse cycle due to the rapid descending of the relative sea level.

http://www.aloki.hu ● ISSN 1589 1623 (Print) ● ISSN 1785 0037 (Online)
DOI: http://dx.doi.org/10.15666/aeer/1704_1002710035

The lithology of foreshore contains gray and green-grayish medium-fine grained lithic quartz sandstone, with bidirectional cross bedding, oblique bedding, parallel bedding, and bottom scour upgrowing (*Fig. 3i, j, k*).

Due to the strong hydrodynamic force at the upper shore face, the lithology contains grey-grey green fine sandstone and gritstone. Parallel bedding and plate cross bedding developed (*Fig. 3l, m, n*). However, the lower part shore face, with its lower water hydrodynamic condition, is mainly composed of grey fine sandstone and siltstone with few gray-green gray silt and silty mudstone. The sandstone shows parallel bedding and striped argillaceous (*Fig. 3o, p*).

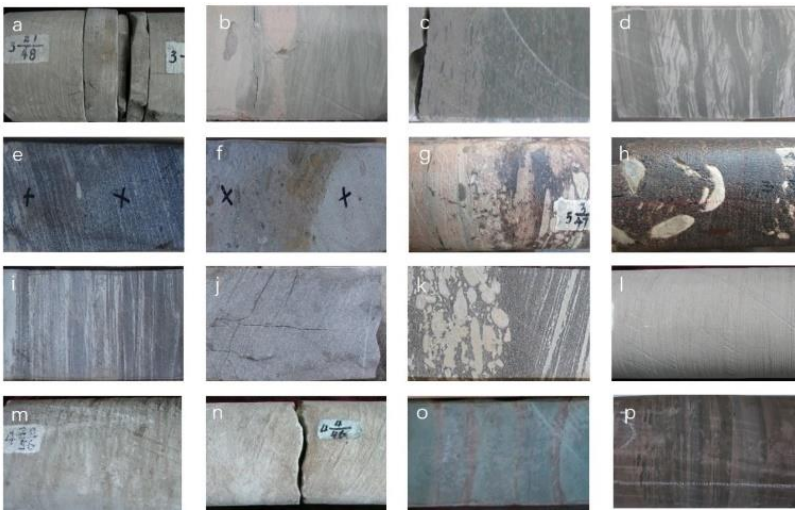

Figure 3. *Core of Littoral and tidal flat of the Silurian in the Tabei area. a. grey green horizontal bedding silty mudstone, S119 Well, 5331.5 m, S_1k; b. wavy bedding, mixed flat deposition, S116-2 Well, 5416.4 m, S_1k^1; c. light-grey green siltstone and grey green mudstone. S110 Well, 5495.06 m, S_1k^1; d. lenticular bedding, mixed flat deposition. S110 Well, 5487.74 m, S_1k^1; e. oblique bedding and sand flat deposition. TP5 Well, 5508.20-5508.77 m, S_1k^3; f. grey-green fine sandstone, tidal channel. TP3 Well, 5470.30 m, S_1k^3; g. grey brown fine conglomerate, lime and muddy gravel, tidal channel, TP3 Well, 5470.30 m, S_1k^3; h. parallel bedding. TP6 Well, 5711.32-5712.82 m, S_1k^3; i. oblique bedding. TP6 Well, 5711.32-5712.82 m, S_1k^3; j. bottom erosion. TP11 Well, 5855.35 m, S_1k^3; k. grey-green fine sandstone, small cross bedding. S112-2 Well, 5458.4 m, S_1k; l. top slaty bedding, S119 Well, 5346.7 m, S_1k; m. wave mark. TP2 Well, 5283.01 m, S_1t; n. light-grey green siltstone and fine sandstone with grey green thin-layer silty mudstone TP6 Well, 5708.03-5714.53 m, S_1k^3; o. striped argillaceous. TP22 Well, 6230.84-6231.44 m, S_1k; p. parallel bedding. TP3 Well, 5471.58-5472.20 m, S_1k^3*

Coastal plain

The coastal plain and its incised channels formed during the early Early Silurian period (S_1k^1 sedimentary period), and were distributed throughout the Tuopu district, central Tabei. Two main channels developed (*Fig. 4a*) whose lithology consisted of gray black fine grain lithic quartz sandstone and gray black mudstone with part of silty sand and a large number of brachiopoda. It showed characteristics of high value box type, bell type + funnel type, and bell type + box type of the GR curve (*Fig. 4b*). The seismic event of the channel through process of erosion and filling can be distinguished as incised valley and the seismic response is a strong amplitude and a medium continuous reflection *(Fig. 4c*).

http://www.aloki.hu ● ISSN 1589 1623 (Print) ● ISSN 1785 0037 (Online)
DOI: http://dx.doi.org/10.15666/aeer/1704_1002710035

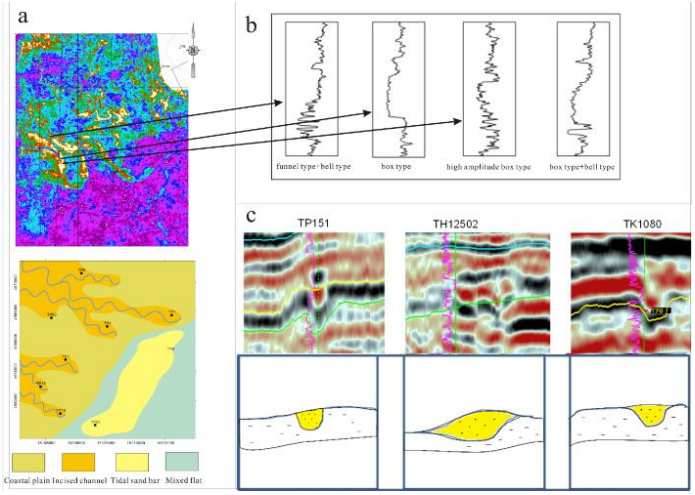

Figure 4. *Geophysical response and distribution of coastal plain and its incised channels of the early Silurian period*

Discussion

Depositional filling process

During the early Early Silurian period (S_1k^1 sedimentary period), the sedimentary center was located in the northeast of the study area. The uplift was not obvious, which led to a wide sedimentary range with great thickness. The shallow water tidal flat developed (*Fig. 5a*).

During the period of the middle part (S_1k^2 sedimentary period), the sea level rapidly rose, a large-scale transgression occurred, the sedimentary center moved southward, and the neristic shelf facies (*Fig. 5b*) developed. During the period of the upper part (S_1k^3 sedimentary period), the tidal flat and littoral developed, including sand flat, sandy foreshore, upper of shore, and the lower member (*Fig.5c*). The depositional period of the Tataaiertage formation (S_1t sedimentary period) is mainly dominated by both tidal flat and littoral deposits (*Fig. 5d*).

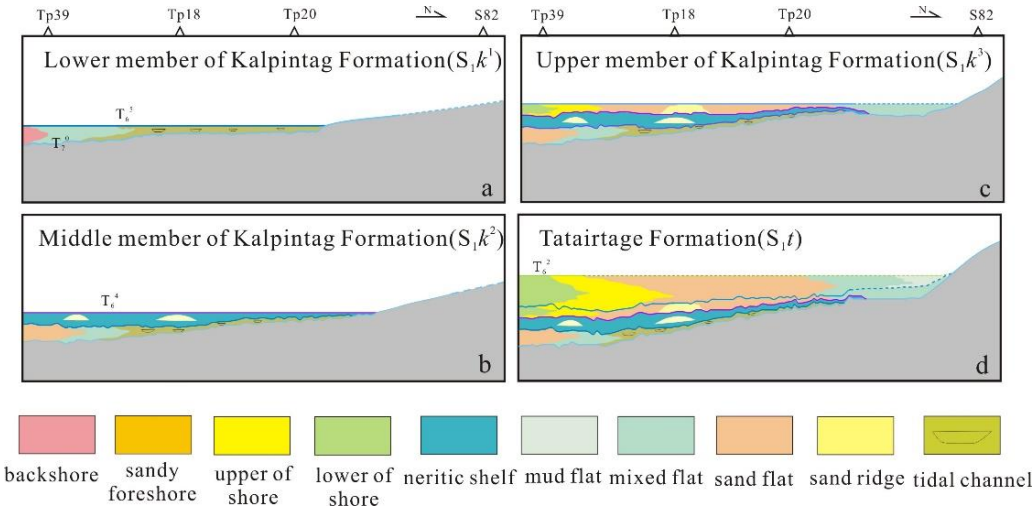

Figure 5. *Filling progress of Silurian sedimentary facies in the Tabei area*

http://www.aloki.hu ● ISSN 1589 1623 (Print) ● ISSN 1785 0037 (Online)
DOI: http://dx.doi.org/10.15666/aeer/1704_1002710035

Sedimentary system and depositional evolution

In the lower part of the Kalpintage formation of the Early Silurian age (S_1k^1 period), the uplift is not significant in the study area. This is a broad epicontinental sea sedimentary environment that features shallow water, gentle slopes, and wide intertidal zones, which results in weak wave action and the wide development of the shallow water clastic rock tidal flat. As a result, it is characterized by the shallow water tidal flat-coastal plain-incised channel depositional system. The tidal flat is stably distributed in east-west direction along the coast, developing sedimentary microfacies of mud flat, mixed flat, and sand flat, which reflects the gradual weakening of tidal hydrodynamic forces from sea and coast. In addition, the mud flat is thin due to erosion caused by the later-stage uplifting. The development of coastal plain deposits in the Tuopu area features two main channels and outwards into tidal flat facies (*Fig. 6a*).

During the middle part, the tectonic movement resulted in a slight uplift (S_1k^2 period). At the same time, the sea level rose rapidly, large-scale transgression occurred, and the sediment center migrated southward, which led to the development of the neritic shelf facies in most areas and sand ridges in part of the areas (*Fig. 6b*).

In the upper part (S_1k^3 period), the uplifting and topography variation of the Tabei area is more obvious. The center area is raised and the slope increased, which strengthened the wave action. The near source littoral facies developed. However, the relatively gentle slope and the shading of the bay weakened the action of the waves in the west and east area, which is dominated by bay tidal flat facies. Therefore, the Tabei area developed a bay tidal flat-littoral depositional system *(Fig. 6c*).

During the sedimentary period of the Tataaiertag formation of the Middle Silurian age (S_1t period), the area inherited the geomorphic features of the upper part and the sedimentary center continued to migrate southward. At the same time, the bay tidal flat-littoral depositional system developed (*Fig. 6d*).

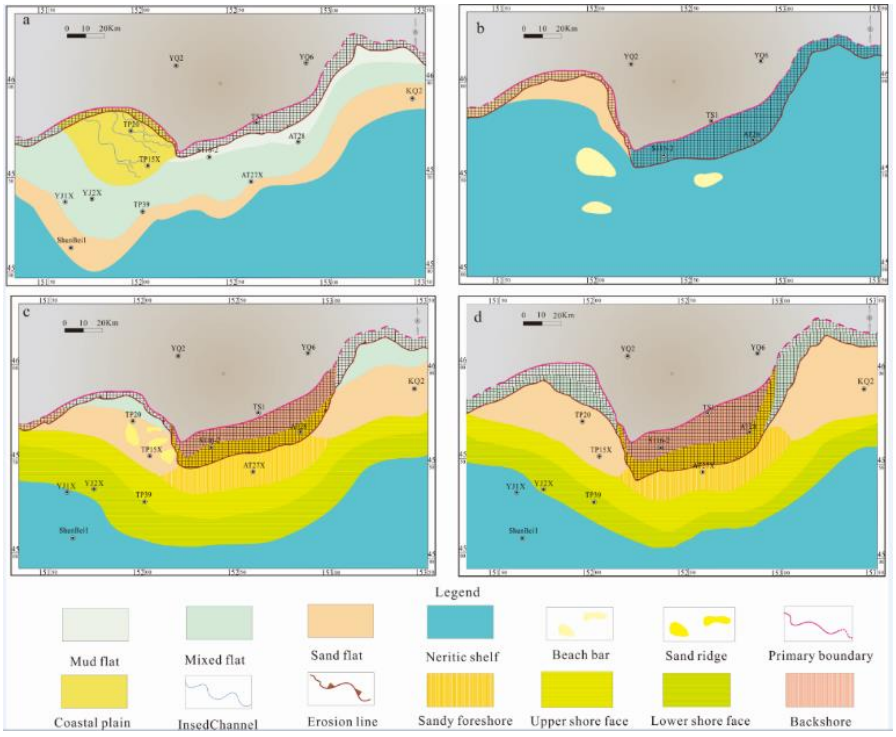

Figure 6. *Depositional system and its evolution during the Silurian in the Tabei area*

http://www.aloki.hu ● ISSN 1589 1623 (Print) ● ISSN 1785 0037 (Online)
DOI: http://dx.doi.org/10.15666/aeer/1704_1002710035

Conclusion

(1) The Silurian tidal flat in the study area can be divided into shallow tidal flat and bay tidal flat. The shallow tidal flat is located in the barrier-free and wide epicontinental sea during the stable subsidence period. This is characterized by extensive distribution and high mud content, among which, the mud flat developed very well, but the tidal channel did not develop; distribution in the bay area without obvious barrier during the period of rapidly declining sea level, thus limiting the bay tidal flat. The sand content of rocks is high and the tidal channel developed.

(2) During the Early Silurian period (the S_1k^1 period), the coastal plain and its incised channels in the central-western regions of the study area were characterized by the incised valley shape of the seismic profile, and the high amplitude and medium continuous reflection.

(3) The Silurian deposit is controlled by the late Caledonian movement. The Tabei area continues to rise and the sedimentary center moves southward. The depositional system is transformed from an incised channels-shallow tidal flat system to a littoral-bay tidal flat system. Among these, the backshore and the upper tidal zone are generally denuded by the late uplifting.

This research identified the Silurian strata sedimentary characteristics and how they evolved in the Tarim Basin, which provides a basis for further research. In addition, this paper discussed a previously ignored relationship between transformations of different sedimentary facies and the influence of the orogeny of the Late Caledonian. The next step will be to semi-quantitatively determine the relationship between tectonic movement, the changing sea level, and the depositional filling process to establish a relationship model between the depositional filling process and the changing sea level under this specific tectonic setting.

Acknowledgements. We are grateful to the support from Natural Science Foundation of China (project number: 41302095).

REFERENCES

[1] El-Wahed, M. A. A. (2010). The role of the Najd Fault System in the tectonic evolution of the Hammamat molasse sediments, Eastern Desert, Egypt. – Arabian Journal of Geosciences 3(1): 1-26.

[2] Gong, Z., Yan, J. W., Geng, L., Zhu, S. Y., Li, H., Zhang, C. K. (2018) Mechanisms underlying the dynamic evolution of an open-coast tidal flat-creek system: III: Impact of sea level rise. – Advances in Water Science 29(01): 109-117.

[3] Guilbaud, R., Bernet, M., Huyghe, P., Erens, V., Chirouze, F., Dupont-Nivet, G. (2012). On the influence of diagenesis on the original petrographic composition of Miocene–Pliocene fluvial sandstone in the Himalayan foreland basin of western-central Nepal. – Journal of Asian Earth Sciences 44(1): 107-116.

[4] Hu, S. H., Wang, Q. G., Li, X. Z. (2007). Sequence stratigraphic subdivision and sedimentary system characteristics of Silurian in Tarim Basin. – Journal of Daqing Petroleum Institute 31(2): 8-11 + 122-123.

[5] Jiang, Z., Wang, Y., Wei, C. (2009). Hemipelagic deposition of the Silurian Kepingtage formation in Tarim basin and its sedimentologic significance. – Journal of Earth Science 20(6): 921.

http://www.aloki.hu ● ISSN 1589 1623 (Print) ● ISSN 1785 0037 (Online)
DOI: http://dx.doi.org/10.15666/aeer/1704_1002710035

[6] Liu, H., Somerville, I. D., Lin, C., Zuo, S. (2016). Distribution of Palaeozoic tectonic superimposed unconformities in the Tarim Basin, NW China: significance for the evolution of palaeogeomorphology and sedimentary response. – Geological Journal 51(4): 627-651.

[7] Liu, R. H., Wang, M., Jiang, Z. X. (2016). Development of sedimentary facies type in Silurian lower Kepingtage formation, Tahe Area. – Acta Sedimentologica Sinica 34(2): 326-335.

[8] Niu, L., Yu, B. S., Zhang, W. B. (2013): Provenance analysis and dating of parent rocks of the sandstones from Kepingtage formation (Silurian) in the Northern Tarim Basin. – Acta Sedimentologica Sinica 31(03): 421-429.

[9] Tillmann, T., Wunderlich, J. (2014). Barrier spit accretion model of Southern Sylt, German North Sea: insights from ground-penetrating radar surveys and sedimentological data. – Zeitschrift für Geomorphologie (Supplementary Issues) 58(3): 137-161.

[10] Yamashita, S., Nakajo, T., Naruse, H., Sato, T. (2009). The three-dimensional distribution of sedimentary facies and characteristics of sediment grain-size distribution in a sandy tidal flat along the Kushida River estuary, Ise Bay, Central Japan. – Sedimentary Geology 215(1-4): 70-82.

[11] Zeng, Q., Zhang, X., Zhang, R., Zhao, J., Hou, G., Ji, Y. (2018). Characteristics of tidal action sedimentary system and distribution of favorable sand bodies of Silurian in Tazhong area, Tarim basin, NW China. – Quaternary International 468: 62-71.

[12] Zhang, J. L., Meng, Q., Qi, J. F. (2012) Characteristics of multi-stage structural deformation and oil and gas accumulation in fault depression basin: a case study of Nember Depression in Hailar-Tamtsag Basin. – Petroleum Geology & Experiment 34(4): 368-375.

[13] Zhang, T. (2017) Division of tectonic evolution stages in South Beier Sag. – West-China Exploration Engineering 29(50): 110-112 + 115.

[14] Zhang, Y. (2014) Study on characteristics of prototype basin of Nantun formation in Beier Sag of Hailar Basin. – Petroleum Geology and Engineering 28(6): 12-15.

[15] Zhao, Y. N., Wang, Z. H., Wu, X. X. (2015). Grain size distribution of modern tidal flat sediments at the Yangtze River mouth and its application to identification of sedimentary facies. – Journal of Palaeogeography 17(3): 405-416.

http://www.aloki.hu ● ISSN 1589 1623 (Print) ● ISSN 1785 0037 (Online)
DOI: http://dx.doi.org/10.15666/aeer/1704_1002710035

ASSESSMENT OF THE ACCURACY OF A SOIL SALINITY MODEL FOR SHALLOW GROUNDWATER AREAS IN XINJIANG BASED ON ELECTROMAGNETIC INDUCTION

SONG, J. H. – SHI, X. Y. – CUI, J. – ZHU, Y. Q. – WANG, H. J.*

Department of Resources and Environmental Science, Shihezi University
Shihezi, Xinjiang, PR China
(phone: +86-130-4054-6967)

**Corresponding author*
e-mail: wanghaijiang@shzu.edu.cn; phone: +86-189-6382-7056

(Received 9th Apr 2019; accepted 19th Jun 2019)

Abstract. Accurate and rapid assessment of soil salinity is a prerequisite for monitoring and management of soil salinization. Electromagnetic induction technology (EMI) has been broadly applied for scientific research and soil salinity monitoring. In this study, the path analysis method was used to analyze the influence of the soil properties of different soil layers and groundwater (GW) characteristics on apparent electrical conductivity (ECa) values measured at different heights of an EM38. The results showed that for all soil layers, the standard electrical conductivity of a saturated soil extract (ECe) was the most important factor affecting ECa measured at different heights. Both soil moisture content and GW characteristics (GW depth, GW conductivity) had an obvious effect on ECa, whereas the soil clay content had little effect. The reliability of ECe prediction models for different soil layers was improved to various degrees by the addition of soil water content and GW characteristics as auxiliary factors. The ECe prediction model was validated with the coefficient of determination (R^2) between the predicted and measured ECe values of each layer reaching more than 0.70. The ECe prediction model can be used to accurately estimate any unsampled points in a study area.
Keywords: *electromagnetic induction, soil profile, accurate interpretation, groundwater, soil properties*

Introduction

Soil salinization is a global problem, affecting more than 930 million hectares of land, and the extent of the problem continues to increase (Rengasamy, 2006). High evaporation rates in arid and semi-arid areas increase the problem of soil salinization (Butcher et al., 2016; Li et al., 2014). Soil salinization negatively affects soil quality and sustainable agricultural development (Cassel et al., 2015). Land areas that are potentially impacted by soil salinization remain important resources for agricultural development. The key strategy to ensure the development and utilization of such land resources lies in the development of accurate and rapid soil salinity assessment and measurement techniques (Kasim et al., 2018; Abdu et al., 2007; Yao et al., 2010; Singh, 2018). At present, electromagnetic induction (EMI) is the most important and broadly-applied scientific method for measuring and assessing soil salinity. EMI is used to measure soil apparent electrical conductivity (ECa) to predict the salt content of the soil profile (Heil and Schmidhalter, 2017). Based on the existing research results, soil salinity (Dakak et al., 2017; Scudiero et al., 2016; Aboelsoud and Abdel-Rahman, 2017), soil moisture (Hossain et al., 2010; Huang et al., 2018), soil clay content (Doolittle et al., 2002; Triantafilis and Lesch, 2005), cation exchange capacity (Triantafilis and Santos, 2010; Suddth, 2005), organic matter content (Martinez et al., 2016; Bekele et al., 2005), soil temperature (Brevik et al., 2004), soil compaction

http://www.aloki.hu ● ISSN 1589 1623 (Print) ● ISSN 1785 0037 (Online)
DOI: http://dx.doi.org/10.15666/aeer/1704_1003710057

(Krajco, 2007) and other major physical and chemical properties of the soil have an impact on its ECa. Therefore, the major factors affecting EMI of areas with different in soil properties differ considerably.

EM38 is a tool for rapid determination of ECa (McNeill, 1980). The assessment of soil salinity using ECa should be calibrated relative to the standard electrical conductivity of a saturated soil extract (ECe). Many scholars have used the EM38 to determine ECa to quantify and monitor soil salinity in arid and semi-arid irrigated agricultural areas (Jadoon et al., 2015; Ding and Yu, 2014; He et al., 2018). In the aforementioned research, almost all other soil physical and chemical properties were considered to be uniform; however, in the actual investigation process, the measurement accuracy of EM38 was often reduced due to uneven irrigation and differences in soil texture. A soil survey by Lesch and Corwin (2003) concluded that minimum water content should be at least 65% of the total capacity whenever possible. However, in arid and semi-arid regions, limited rainfall and irrigation water usually result inlarge differences in soil water (SW) content between plots. Therefore, the establishment of a calibration relationship between ECa and ECe depends on the soil type under specific field conditions and moisture status. In addition, the soil ECa increases with increasing clay content due to the fact that the clay content affects electromagnetic conductivity, whereas on the other hand soil clay content is closely related to cation exchange capacity (CEC) (Triantafilis and Lesch, 2005; Sudduth et al., 2005). In addition, partially exchangeable ions can produce ionic conductance, thus affecting ECa, and studies have shown that the variability of ECa conversion to ECe is greater in coarse-grained soils than in medium or fine-textured soils (McKenzie, 1993).

There have been many studies of the effects of SW content and soil salinity on ECa (Hanson and Kaita, 1997; Bennett et al., 2000; Wittler et al., 2006; Jiang et al., 2017). The results have shown that there is a linear relationship between SW content and ECa (Hanson and Kaita, 1997). ECa readings vary considerably with changes in SW content. Norman (1990) demonstrated that for clay soils, the water content of the soil profile should be greater than 20% to accurately obtain soil salinity values from the observed ECa data. Rahimian and Hasheminejhad (2011) found that the regression equation between ECah (horizontal mode) and ECav (vertical mode) and soil salinity obtained in the field with SW content of 35% was more reliable. Silberstein et al. (2007) found a significant correlation between ECa and groundwater (GW) level and GW conductivity ($R^2 = 0.75$, $P < 0.001$). Mankin and Karthikeyan (2002) conducted research in the central and mid-south regions of Kansas, USA to distinguish between the saline exudation zone and non-exudation zone and assessed the extent of saline exudation by means of ECa measured by EM38.

In summary, although the relationship between soil ECe and ECa is reliable, the factors affecting different regions and different soil layers (e.g., moisture, clay content, GW depth and GW conductivity) differ. To construct an accurate interpretation model of soil profile salt content, the present study aimed to characterize the soil characteristics of the Xinjiang arid area by: (1) analysis of soil properties at different depths and determining the influence of GW characteristics on EM38 readings; (2) determine the dominant factors impacting on ECa determination, and establishing an accurate soil ECe interpretation model; (3) validate the precision and stability of the soil ECe interpretation model.

http://www.aloki.hu ● ISSN 1589 1623 (Print) ● ISSN 1785 0037 (Online)
DOI: http://dx.doi.org/10.15666/aeer/1704_1003710057

Materials and methods

Overview of research region

The present study focused on the Karamay agricultural development area located within the lacustrine plain region on the southern side of the Dzungaria Basin in Xinjiang Province (84°50′–85°20′ E and 45°22′–45°40′ N). The region has a desert climate with an annual mean temperature of 8 °C and an annual rainfall of 105.3 mm. The average depth of GW in the area has risen by 6.90 m since 2000 due to improper irrigation methods, which has consequently resulted in soil salinization. To date, more than 66% of the area has been affected by soil salinization (Han et al., 2011).

The field within the Karamay agricultural development area of approximately 68 ha with the shallowest GW was chosen for the present study. Other factors considered were soil texture, salt status, vegetation types and irrigation methods. As shown in *Figure 1*, the GW depth (DGW) and quality were monitored from 11 positions. Sunflowers and matrimony vines planted in the field in 2016 were replaced with cotton in 2017. The crops were irrigated manually during their periods of growth using drip irrigation under mulch. Soil moisture content and GW characteristics were highly variable across the research region since the types of crops differ and the terrain is uneven, as shown in *Table 2*. Soil clay content at a depth of 1 m was spatially homogeneous, with an average value of approximately 56%. On the other hand, serious soil salinization has occurred with a minimum and maximum ECe of 1.69 mS cm^{-1} and 2.90 mS cm^{-1}, respectively. This relatively high salt content has restricted crop growth. *Table 1* lists the monthly mean variations of DGW in the research region from 2013 to 2017, which show that DGW has been significantly influenced by agricultural irrigation before 2016 with an annual mean depth ranging from 0.78 m to 1.12 m, and that DGW increased to a certain extent in 2016 and 2017 with a mean depth of 1.40 m.

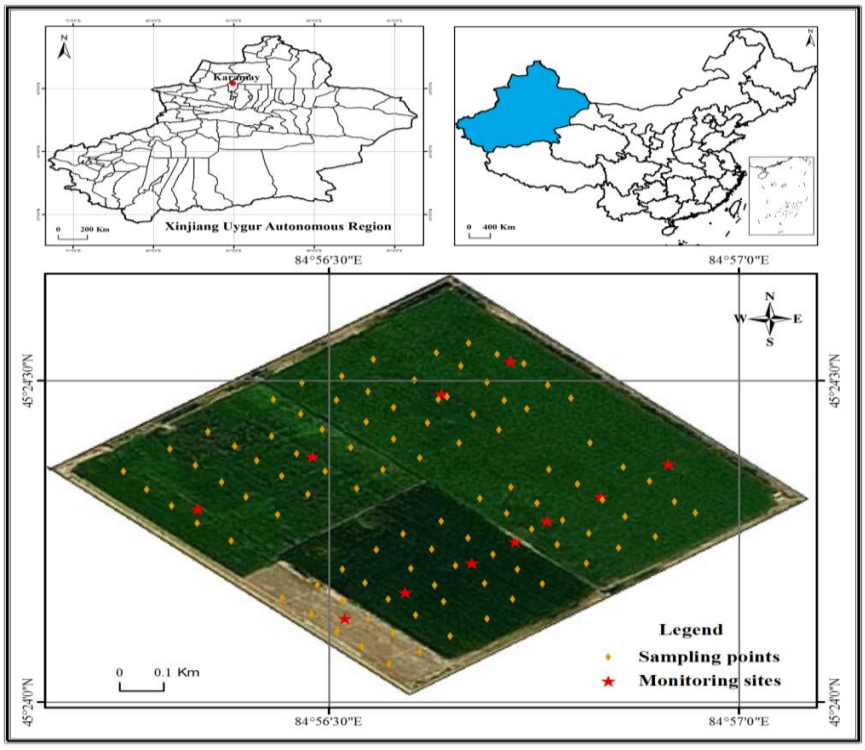

Figure 1. *Spatial location of the experimental sites*

http://www.aloki.hu ● ISSN 1589 1623 (Print) ● ISSN 1785 0037 (Online)
DOI: http://dx.doi.org/10.15666/aeer/1704_1003710057

Table 1. *Monthly mean change of groundwater level in the study area*

Years	June	July	August	September	October	November	Average	CV (%)
2013	0.69	0.69	0.41	1.28	0.82	0.78	0.78	0.36
2014	0.99	1.12	0.76	1.02	1.27	1.36	1.09	0.19
2015	0.91	0.99	1.25	1.38	1.28	0.89	1.12	0.19
2016	1.35	1.28	1.33	1.45	1.52	1.49	1.4	0.07
2017	1.36	1.44	1.4	1.28	1.4	1.52	1.4	0.06

Data collection

Electromagnetic interference (EMI) data collection

The EM38 had two receiver coils spaced at 0.5 m and 1 m from the transmitter coil. The transmitter coil was energised with an alternating current, generating a time-varying magnetic field in the earth. This magnetic field resulted in current flow in the soil, resulting in the generation of a secondary magnetic field. The strength of this secondary electromagnetic field was directly proportional to the ECa of the soil.

$$ECa = 4(Hs/Hp)/\omega\mu_0 S^2 \quad \text{(Eq.1)}$$

where ECa is the apparent electrical conductivity, Hs and Hp are the secondary magnetic field and the primary magnetic field, respectively, $\omega = 2\pi f$, where f is the transmission frequency (Hz), S is the distance between the transmitting end and the receiving end (m) and μ_0 is the spatial magnetic field conduction coefficient.

In the present study, the EM38-MK2 instrument (Geonics Limited, On-tario, Canada) with effective investigation depths in the vertical and horizontal modes of 1.5 m and 0.75 m (McNeill, 1980), respectively and transmitting coil and receiving coil separated by 1 m was used to measure EMI data throughout the research region. According to previous studies, ECa is influenced by both soil properties and soil depth, and soil layers at different depths contribute to ECa at different degrees. *Equations 2* and *3,* representing density functions of the contributions of a soil layer at a certain depth to ECa in the vertical and horizontal modes, respectively, show that 20% of ECa in the horizontal mode is contributed by soil layers at depths < 1.2 m and 27% of ECa in the vertical mode is contributed by soil layers at depths < 1.8 m. In the present study, the heights of EM38 during measurement were set at 1.30 m, 1.10 m, 0.90 m, 0.70 m and 0.50 m in sequence, corresponding to effective investigation depths of 0.20 m, 0.40 m, 0.60 m, 0.80 m and 1.00 m, respectively, in the vertical mode.

A total of 100 measurement positions were deployed using the systematic distribution method and the data were collected by EM38 in May, 2017. Before the measurement, EM38 was calibrated at a height of 1.5 m, following which the values of ECa were measured at the heights of 1.30 m, 1.10 m, 0.90 m, 0.70 m and 0.50 m in the horizontal and vertical modes. In addition, the positions of the measurement points were recorded via GPS (Trimble, USA).

$$\varphi^v(Z) = \frac{4Z}{(4Z^2+1)^{3/2}} \quad \text{(Eq.2)}$$

http://www.aloki.hu ● ISSN 1589 1623 (Print) ● ISSN 1785 0037 (Online)
DOI: http://dx.doi.org/10.15666/aeer/1704_1003710057

$$\varphi^h(z) = 2 - \frac{4z}{(4z^2+1)^{1/2}} \quad \text{(Eq.3)}$$

where z denotes the depth of EM38 in the vertical direction.

Collection and treatment of soil samples and GW

To obtain soil property information, manual sampling procedures were implemented at the measurement points. The soil was separated into five layers: 0 m to 0.20 m (L1),0.20 m to 0.40 m (L2), 0.40 m to 0.60 m (L3), 0.60 m to 0.80 m (L4) and 0.80 m to 1.00 m (L5). Effective soil profiles totaling 90 were chosen and 450 soil samples were collected in total. Soil profiles totaling 60 were used to derive the salt content prediction model whereas the remaining 30 were used to validate the model.

The collected soil samples were mixed and then transported to the laboratory for characterization. The soil moisture content per unit mass (θ) was determined using the oven drying method. EC of 5:1 water to soil extract (ECe) was determined using a conductivity meter. Soil clay content (γ) was determined using the hydrometer method.

The characteristic GW data were obtained from the 11 automated monitoring points. The monitored indices included GW depth (DGW), monitored by the DATA-5111 sensor (China), and GW EC (ECGW), monitored by the DATA-5102 water conductivity sensor (China). The sensors were set to collect data once every 2 h.

Data analysis method

Path analysis and its principles

A number of factors need to be considered when deriving an accurate model for interpreting soil salt information based on EMI. At the same time, path analysis is a useful numerical analysis method suitable for determining the effects of multiple factors. Path analysis divides correlation coefficients into those exerting direct and indirect effects, which indicates the relative importance of the factors. Therefore, when studying the linear relationships between multiple correlated variables, path analysis can reveal the direct and indirect contributions of each independent variable to the dependent variable. With that in mind, path analysis was used in the present study to establish the contribution of soil properties and GW characteristics to ECa.

Path coefficient

Path analysis is a statistical multiple linear regression analysis method applied to standardized variables and path coefficients are partial regression coefficients for standardized variables. The path coefficient of an independent variable reflects its relative magnitude and property in relation to the dependent variable.

Assuming the existence of a linear relationship between the dependent variable *y* and the independent variables x_i (i = 1,2,3,..., n), the regression equation can be written as:

$$y = b_0 + b_1x_1 + b_2x_2 + \cdots + b_nx_n \quad \text{(Eq.4)}$$

Then, based on the standardized multiple linear regression equation, the canonical equations can be derived as:

http://www.aloki.hu ● ISSN 1589 1623 (Print) ● ISSN 1785 0037 (Online)
DOI: http://dx.doi.org/10.15666/aeer/1704_1003710057

$$\begin{cases} P_{yx_1} + r_{x_1x_2}P_{yx_2} + \cdots + r_{x_1x_n}P_{yx_n} = r_{x_1y} \\ r_{x_1x_2}P_{yx_2} + P_{yx_2} + \cdots + r_{x_2x_n}P_{yx_n} = r_{x_2y} \\ \vdots \quad \vdots \quad \vdots \quad \vdots \quad \cdots \quad \vdots \quad \vdots \quad \vdots \\ r_{x_nx_1}P_{yx_1} + r_{x_nx_2}P_{yx_2} + \cdots + P_{yx_n} = r_{x_ny} \end{cases} \quad \text{(Eq.5)}$$

Equation 5 can be transformed into a normal matrix equation as:

$$\begin{bmatrix} 1 & r_{x_1x_2} & \cdots & r_{x_1x_n} \\ r_{x_2x_1} & 1 & \cdots & r_{x_2x_n} \\ \vdots & \vdots & \ddots & \vdots \\ r_{x_nx_1} & r_{x_nx_2} & \cdots & 1 \end{bmatrix} \begin{bmatrix} P_{yx_1} \\ P_{yx_2} \\ \vdots \\ P_{yx_n} \end{bmatrix} = \begin{bmatrix} r_{x_1y} \\ r_{x_2y} \\ \vdots \\ r_{x_ny} \end{bmatrix} \quad \text{(Eq.6)}$$

where $r_{x_ix_j}$ is the simple correlation coefficient of x_i and x_j, and r_{x_iy} is the simple correlation coefficient of x_i and y. The path coefficient P_{yx_i} can be obtained by solving *Equation 5*. $r_{x_ix_j}P_{yx_i}$ represents the indirect path coefficient of *xi* to *y* via x_j.

Contribution rates of variables

The influencing factors can be ordered according to their path coefficients. Furthermore, since the contributions of the variables are calculated from their direct path coefficients, the contribution rates of the influencing factors to ECa can also be calculated:

$$\eta = |a| / \left(|a| + |b| + |c| + |d| + \cdots \right) \quad \text{(Eq.7)}$$

where a, b, c, d… denote the direct path coefficients of the corresponding variables and η denotes the contribution rate of the first variable.

Derivation of the ECe prediction model

Path analysis was used to analyze how soil properties (including θ, γ and ECe) and GW characteristics are related to ECa as measured by EM38 at different heights. The non-salt factors with high contribution rates to ECa were then chosen as independent variables with soil conductivity as the dependent variable. The optimal soil salt interpretation model was then derived using multiple linear regression (MLR). The data analysis and model derivation were conducted using SPSS 20.0 (IBM, USA), and the figures and tables were compiled using Sigmaplot 12.0 (Systat Software, USA).

Model validation

The reserved 30 soil profiles were used to validate the reliability of the ECe prediction model using three indices: mean error (ME), root mean square error (RMSE) and coefficient of determination (R^2).

Among them:

Mean Error (ME):

http://www.aloki.hu ● ISSN 1589 1623 (Print) ● ISSN 1785 0037 (Online)
DOI: http://dx.doi.org/10.15666/aeer/1704_1003710057

$$ME = \frac{1}{N}\sum_{i=1}^{N}\left|x_i - y_i\right| \quad \text{(Eq.8)}$$

Root Mean Square Error (RMSE):

$$\mathrm{RMSE} = \sqrt{\frac{1}{\mathrm{N}}\sum_{i=1}^{N}(x_i - y_i)^2} \quad \text{(Eq.9)}$$

where *xi* is the interpreted value, y_i is the observed value and N is the number of data points.

When using the test model, root mean squared error (RMSE) was always used for statistical analysis of conformity between simulated values and measured values. The smaller the RMSE value, the better the consistency and the smaller the deviation between simulated values and measured values, and thus the more accurate and reliable the model.

Results and discussion

Data analysis

Table 2 lists the soil properties and GW characteristics (including ECGW and DGW) of different soil layers and readings of EM38 at different heights. The soil texture in the research region ranged from heavy loam to light clay, and the soil profile clay content was distributed relatively evenly. At L1–L5, γ ranged from 49% to 62%, with the maximum in L3. θ showed a trend of increasing from the top soil layer (8%) to the bottom soil layer (25%) and was not evenly distributed in the soil profiles. According Lesch and Corwin (2003), if θ is far less than field moisture capacity, the spatial variation in θ is likely to become the most important factor contributing to EM data, even if salt content shows significant spatial variation. Norman (1990) found that soil profile θ should be greater than 20% in clay soil to accurately estimate soil salt content according to measured EM data. Given the above information, the θ of the study area in the present study could preclude the development of an effective soil salt prediction model. At the same time, ECe showed a clear variation among different soil layers, with average ECe of each layer ranging from 1.69 mS cm^{-1} to 2.9 mS cm^{-1}. At L1–L4, the coefficient of variation of ECe decreased from 60.69% to 34.66% with increasing soil depth, whereas at L5, the coefficient of variation of ECe increased to 50.69%. This illustrated the complex spatial distribution of ECe. DGW was highly variable across the region with a minimum, maximum and average DGW of 1.12 m, 1.38 m and 1.34 m, respectively, and ECGW ranged from 35.8 mS cm^{-1} to 62.8 mS cm^{-1} with an average of 2.36 mS cm^{-1} due to high GW mineralization and poor water quality. Therefore, the moisture and salt contents of the soil profiles could be influenced by the shallow depths and high salt content of GW, thereby influencing EM38 measurements.

Corwin and Rhoades (1982) derived the EC of the soil profile in the vertical direction based on the linear hypothesis and using the values of ECa measured by EMI at different heights, a method which has been proven to effectively improve the accuracy of predicting soil salt using EM38 (Cook and Walker, 1992). In the present study, the EM38 readings decreased with increasing height. The signals received by

http://www.aloki.hu ● ISSN 1589 1623 (Print) ● ISSN 1785 0037 (Online)
DOI: http://dx.doi.org/10.15666/aeer/1704_1003710057

EM38 were generated mainly by the top soil layer and the contribution of the bottom soil layer to the EM38 readings decreased with increasing soil depth (McNeil, 1990). Soil at depths of 0 m–1.50 m accounted for 70% of the readings in the vertical mode, and with increasing EM38 height, the effective investigation depth decreased (Abdu et al., 2007). In addition, the aboveground atmosphere with an ECa of 0 made no contribution to EM38 readings (Misra and Padhi, 2014). The aforementioned facts explain the reason for a noticeable decrease in EM38 readings as height increased. Huang et al. (2015) found that ECa variations decreased significantly as height increased, which is consistent with the results of the present study.

Table 2. *Summary characteristics of soil properties at various soil depths, groundwater properties, and EM38 measurements collected invarious layers*

Soil layer		N	Max	Min	Average	Standard deviation	CV
0-0.20	EMh1.30	60	92	9	47.5	22.41	47.18%
	EMv1.30	60	170	21	94.88	43.86	46.23%
	ECe/mS cm^{-1}	60	6.89	0.5	2.9	1.76	60.69%
	θ/%	60	0.18	0.08	0.13	0.02	15.38%
	γ/%	60	0.82	0.16	0.49	0.16	32.65%
0.20-0.40	EMh1.10	60	131	15	66.93	34.25	51.17%
	EMv1.10	60	230	25	121.15	56.55	46.68%
	ECe/mS cm^{-1}	60	4	0.5	1.99	0.78	39.24%
	θ/%	60	0.22	0.09	0.16	0.03	21.16%
	γ/%	60	0.85	0.10	0.53	0.20	37.29%
0.40-0.60	EMh0.90	60	195.00	26.00	92.48	48.93	52.91%
	EMv0.90	60	268.00	37.00	152.88	65.56	42.88%
	ECe/mS cm^{-1}	60	3.52	0.85	2.05	0.73	35.63%
	θ/%	60	0.25	0.11	0.18	0.03	17.62%
	γ/%	60	0.84	0.27	0.62	0.18	29.14%
0.60-0.80	EMh0.70	60	360	35	137.75	77.60	56.33%
	EMv0.70	60	472	56	209.03	106.57	50.98%
	ECe/mS cm^{-1}	60	3.5	0.68	1.74	0.60	34.66%
	θ/%	60	0.24	0.1	0.18	0.04	20.12%
	γ/%	60	0.84	0.22	0.59	0.21	35.25%
0.80-1.00	EMh0.50	60	514	58	210.73	120.56	57.21%
	EMv0.50	60	636	84	282.50	140.52	49.74%
	ECe/mS cm^{-1}	60	4.26	0.42	1.69	0.85	50.69%
	θ/%	60	0.25	0.13	0.18	0.03	16.82%
	γ/%	60	0.88	0.13	0.59	0.22	37.28%
	ECGW/mS cm^{-1}	7	62.8	35.8	52.36	10.06	19.21%
	DGW/m	7	1.38	1.12	1.34	11.71	8.72%

Analysis of factors influencing ECa in different soil layers

Factors influencing ECa as measured by EM38 at a height of 1.30 m (EM1.30)

Path analysis in two modes was used to determine the factors influencing ECa (EMh1.30 and EMv1.30) and their degrees of influence. When conducting path analysisat L1, θ, γ, ECe, ECGW and DGW were regarded as independent variables and EMh1.30 and EMv1.30 were regarded as dependent variables. *Table 3* lists the results

http://www.aloki.hu ● ISSN 1589 1623 (Print) ● ISSN 1785 0037 (Online)
DOI: http://dx.doi.org/10.15666/aeer/1704_1003710057

of path analysis used to determine the factors influencing ECa (i.e., EMh1.30 and EMv1.30) measured at a height of 1.30 m. W) except for ECe, indicating that θ had a certain degree of influence on EMv1.30 at L1. ECe showed the best correlation with EMh1.30 and EMv1.30 at L1 measured at a height of 1.30 m, with the correlation being extremely significant at the P = 0.01 level with correlation coefficients of 0.86 and 0.83, respectively. On the other hand, no significant correlations were evident between ECa and θ, γ, ECGW or DGW, among which the correlation between ECa and θ was the lowest (R < 0.10). According to the results, the order of independent variables in regards to their influence on EMv1.30 at L1 was: ECe > θ > γ > ECGW > DGW. The order of independent variables in regards to their influence on EMh1.30 was ECe > DGW > γ > θ > ECGW. Therefore, since ECe had the largest effect on both EMh1.30 and EMv1.30 at L1, it can be concluded that ECe was the most important factor influencing ECa as measured by EM38 at a height of 1.30 m. Thus, ECe can be used to ECa. Among the other influencing factors, the influence of DGW on EMh1.30 was larger than that of θ, γ or ECGW. Generally speaking, with EM38 height set to 1.30 m, the effective investigation depth for EMh1.30 was not sufficiently deep to reach the soil surface. However, an extremely significant linear relationship (P < 0.001) existed between EMh1.30 and EMv1.30, and a significant correlation (R = −0.432, P < 0.01) existed between DGW and ECe at L1. Therefore, it is likely that the influence of DGW on ECe was responsible for the correlation between DGW and EMh1.30. On the other hand, the contribution of θ to EMv1.30 was 10.93%, larger than those of the other influencing factors (γ, ECGW and DG).

Table 3. *Path coefficients between influence factors to EM38 values at1.30 m above the ground of 0-0.20 m*

Dependent variable	Variable	ECe	θ	γ	ECGW	DGW	Contribution rate	Correlation coefficient with EM
EMv1.30	ECe	**0.7880**	-0.0013	0.0291	0.0233	0.0241	65.78%	0.86**
	θ	-0.0055	**0.1310**	-0.0302	-0.0089	0.0134	10.93%	0.10
	γ	-0.2017	0.0355	**-0.1120**	-0.0155	-0.0073	9.35%	-0.30
	ECGW	-0.1671	0.0102	-0.0157	**-0.1110**	-0.0246	9.27%	-0.31
	DGW	-0.3404	-0.0320	-0.0146	-0.0488	**-0.0560**	4.67%	-0.49
EMh1.30	ECe	**0.7530**	-0.0006	0.0218	0.0036	0.0538	72.68%	0.83**
	θ	-0.0053	**0.0570**	-0.0227	-0.0014	0.0300	5.50%	0.06
	γ	-0.1928	0.0154	**-0.0840**	-0.0024	-0.0163	8.11%	-0.28
	ECGW	-0.1596	0.0044	-0.0117	**-0.0170**	-0.0550	1.64%	-0.24
	DGW	-0.3253	-0.0139	-0.0113	-0.0075	**-0.1250**	12.07%	-0.48

EMh1.30—EM38 values of apparent electrical conductivity in horizontal operation mode; EMv1.30—EM38 values of apparent conductivity in vertical operation mode; ECe—soil electrical conductivity; θ—soil moisture; γ—soil clay content; ECGW—groundwater conductivity; DGW—groundwater level; ** indicates significant at 0.01 level, * indicates significant at 0.05 level. Bold font indicates direct path coefficient of corresponding factor

Factors influencing EC as measured by EM38 at a height of 1.10 m (EM1.10)

When conducting path analysis at L2, θ, γ, ECe, ECGW and DGW were regarded as independent variables whereas EMh1.10 and EMv1.10 were regarded as dependent

http://www.aloki.hu ● ISSN 1589 1623 (Print) ● ISSN 1785 0037 (Online)
DOI: http://dx.doi.org/10.15666/aeer/1704_1003710057

variables. *Table 4* lists the results of path analysis used to determine the factors influencing ECa (i.e., EMh1.10 and EMv1.10) measured at a height of 1.10 m. ECe also had a significant correlation with EMh1.10 and EMv1.10 measured at a height of 1.10 m in the two modes at L2, with correlation coefficients of 0.89 and 0.86 ($P < 0.01$), respectively. At L2, the correlations between θ and EMh1.10 and θ and EMv1.10 were 0.53 ($P < 0.05$) and 0.67 ($P < 0.01$), respectively, indicating that θ had an influence on ECa at L2. On the other hand, no significant correlations were evident between ECa measured at a height of 1.10 m and γ, ECGW or DGW. According to the results, the order of the independent variables according to their influence on EMv1.10 at L2 was: ECe > θ > DGW > ECGW > γ. The order of the independent variables according to their influence on EMh1.10 was: ECe > θ > DGW > ECGW > γ. Therefore, since ECe also had the largest influence on both EMh1.10 and EMv1.10 at L2, it can be concluded that ECe was the most important factor influencing ECa as measured by EM38 at a height of 1.30 m. Among the other factors, the contribution rates of θ to EMh1.10 and EMv1.10 (7.85% and 25.16%, respectively) were larger than those of DGW, γ, or ECGW, indicating that θ had a relatively significant influence on the data measured by EM38 at L2.

Table 4. *Path coefficients between influence factors to EM38 values at1.10 m above the ground of 0.20~0.40 m*

Dependent variable	Variable	ECe	θ	γ	ECGW	DGW	Contribution rate	Correlation coefficient with EM
EMv1.10	ECe	**0.8270**	0.0397	-0.0001	0.0043	0.0154	82.21%	0.89**
	θ	0.4160	**0.0790**	0.0007	0.0068	0.0246	7.85%	0.53*
	γ	-0.0298	0.0284	**0.0020**	-0.0017	-0.0002	0.20%	0.001
	ECGW	-0.0794	-0.0119	0.0001	**-0.0450**	-0.0231	4.47%	-0.16
	DGW	-0.2407	-0.0367	0.0000	-0.0196	**-0.0530**	5.27%	-0.35*
EMh1.10	ECe	**0.6880**	0.1393	-0.0002	0.0050	0.0230	62.49%	0.86**
	θ	0.3461	**0.2770**	0.0018	0.0078	0.0367	25.16%	0.67**
	γ	-0.0248	0.0997	**0.0050**	-0.0019	-0.0003	0.45%	0.08
	ECGW	-0.0660	-0.0416	0.0002	**-0.0520**	-0.0344	4.72%	-0.19
	DGW	-0.2002	-0.1285	0.0000	-0.0227	**-0.0790**	7.18%	-0.43**

EMh1.10—EM38 values of apparent electrical conductivity in horizontal operation mode; EMv1.10—EM38 values of apparent conductivity in vertical operation mode; ECe—soil electrical conductivity; θ—soil moisture; γ—soil clay content; ECGW—groundwater conductivity; DGW—groundwater level; ** indicates significant at 0.01 level, * indicates significant at 0.05 level. Bold font indicates direct path coefficient of corresponding factor

According to the density functions of EM38, i.e., *Equations 3* and *4,* at an EM38 height < 1.10 m, EMv1.10 was mainly influenced by soil properties at L1–L2. According to the present results, ECe at L2 had the largest influence on EMv1.10 and EMh1.10, with the second-most important factor being θ with a rate of contribution of 25.16%. Huang et al. (2015) found that at an EM38 height of 1.00 m, ECe showed the best correlations with EMh and EMv in the 0.15 m–0.30 m soil layer ($R = 0.750$ and $R = 0.773$, respectively), which supports the reliability of the results of the present

http://www.aloki.hu ● ISSN 1589 1623 (Print) ● ISSN 1785 0037 (Online)
DOI: http://dx.doi.org/10.15666/aeer/1704_1003710057

study. In addition, the correlations of ECe with EMh and EMv at L2 in the present study were even stronger (R = 0.86 and R = 0.89, respectively).

Factors influencing ECa as measured by EM38 at a height of 0.90 m (EM0.90)

When conducting path analysis at L3, θ, γ, ECe, ECGW and DGW were regarded as independent variables, whereas and EMh0.90 and EMv0.90 were regarded as dependent variables. *Table 5* lists the results of path analysis used to determine the factors influencing ECa (i.e., EMh0.90 and EMv0.90) measured at a height of 0.90 m. At L3, ECe showed significant correlations with both EMh0.90 and EMv0.90, with correlation coefficients of 0.86 for both ($P < 0.01$). θ and DGW also showed significant correlations with EM0.90 ($P < 0.05$) at L3, indicating that θ and DGW influenced ECa measured at a height of 0.90 m. According to the results, the rates of contribution of ECe to EMh0.90 and EMv0.90 at L3 were the highest among all the factors at 65.79% and 56.12%, respectively. The rates of contribution of ECGW and DGW to EMv0.90 were 12.75% and 10.64%, respectively, and they also had relatively significant influences on EMh0.90 with rates of contribution of 10.23% and 13.55%, respectively.

Table 5. *Path coefficients between influence factors to EM38 values at 0.90 m above the ground of 0.40~0.60 m*

Dependent variable	Variable	ECe	θ	γ	ECGW	DGW	Contribution rate	Correlation coefficient with EM
EMv0.90	**0.7480**	0.0686	0.0019	0.0049	0.0380	65.79%	0.86**	**0.7480**
	0.4937	**0.1040**	0.0066	-0.0038	0.0276	9.15%	0.63**	0.4937
	0.0741	0.0363	**0.0190**	-0.0067	-0.0096	1.67%	0.11	0.0741
	-0.0254	0.0027	0.0009	**-0.1450**	-0.0528	12.75%	-0.22	-0.0254
	-0.2349	-0.0237	0.0015	-0.0632	**-0.1210**	10.64%	-0.44**	-0.2349
EMh0.90	**0.6420**	0.1452	0.0010	0.0040	0.0487	56.12%	0.84**	**0.6420**
	0.4237	**0.2200**	0.0035	-0.0030	0.0353	19.23%	0.68**	0.4237
	0.0614	0.0768	**0.0100**	-0.0054	-0.0122	0.87%	0.13	0.0614
	-0.0218	0.0057	0.0005	**-0.1170**	-0.0676	10.23%	-0.20	-0.0218
	-0.2015	-0.0502	0.0008	-0.0510	**-0.1550**	13.55%	-0.46**	-0.2015

EMh0.90—EM38 values of apparent electrical conductivity in horizontal operation mode; EMv0.90—EM38 values of apparent conductivity in vertical operation mode; ECe—soil electrical conductivity; θ—soil moisture; γ—soil clay content; ECGW—groundwater conductivity; DGW –groundwater level; ** indicates significant at 0.01 level, * indicates significant at 0.05 level. Bold font indicates direct path coefficient of corresponding factor

Factors influencing ECa as measured by EM38 at a height of 0.70 m (EM0.70)

When conducting path analysis at L4, θ, γ, ECe, ECGW and DGW were regarded as independent variables and EMh0.70 and EMv0.70 were regarded as dependent variables. *Table 6* shows the results of path analysis to determine the factors influencing ECa (i.e., EMh0.70 and EMv0.70) measured at a height of 0.70 m. At L4, ECe showed significant correlations with both EMh0.70 and EMv0.70, with correlation coefficients of 0.81 and 0.80 ($P < 0.01$), respectively. θ and DGW also showed significant correlations with EM0.70 ($P < 0.05$) at L4, indicating that θ and DGW influenced ECa

http://www.aloki.hu ● ISSN 1589 1623 (Print) ● ISSN 1785 0037 (Online)
DOI: http://dx.doi.org/10.15666/aeer/1704_1003710057

measured at a height of 0.70 m. According to the results, the rates of contribution of ECe to EMh0.70 and EMv0.70 at L4 were 49.26% and 39.49%, respectively. On the other hand, θ and DGW had relatively significant influences on EMh0.70 and EMv0.70 with rates of contribution of 16.64% and 24.14% and 22.62% and 18.55%, respectively. Therefore, it can be inferred that as the height of EM38 decreased, the rates of contribution of ECe to EMh0.70 and EMv0.70 decreased with increasing soil depth, whereas the contribution rates of the other factors increased.

Table 6. *Path coefficients between influence factors to EM38 values at 0.70 m above the ground of 0.60~0.80 m*

Dependent variable	Variable	ECe	θ	γ	ECGW	DGW	Contribution rate	Correlation coefficient with EM
EMv0.70	**0.6010**	0.1153	0.0001	0.0082	0.0845	49.26%	0.81**	**0.6010**
	0.3414	**0.2030**	-0.0009	-0.0150	0.0560	16.64%	0.58**	0.3414
	-0.0126	0.0345	**-0.0050**	-0.0019	-0.0028	0.41%	0.01	-0.0126
	-0.0367	0.0225	-0.0001	**-0.1350**	-0.1203	11.07%	-0.27	-0.0367
	-0.1839	-0.0412	-0.0001	-0.0589	**-0.2760**	22.62%	-0.56**	-0.1839
EMh0.70	**0.5300**	0.1840	0.0024	0.0077	0.0762	39.49%	0.80**	**0.5300**
	0.3010	**0.3240**	-0.0192	-0.0140	0.0505	24.14%	0.64**	0.3010
	-0.0111	0.0551	**-0.1130**	-0.0018	-0.0025	8.42%	-0.07	-0.0111
	-0.0323	0.0360	-0.0016	**-0.1260**	-0.1086	9.39%	-0.23	-0.0323
	-0.1622	-0.0658	-0.0011	-0.0549	**-0.2490**	18.55%	-0.53**	-0.1622

EMh0.70—EM38 values of apparent electrical conductivity in horizontal operation mode; EMv0.70—EM38 values of apparent conductivity in vertical operation mode; ECe—soil electrical conductivity; θ—soil moisture; γ—soil clay content; ECGW—groundwater conductivity; DGW—groundwater level; ** indicates significant at 0.01 level, * indicates significant at 0.05 level. Bold font indicates direct path coefficient of corresponding factor

Factors influencing ECa as measured by EM38 at a height of 0.50 m (EM0.50)

When conducting the path analysis at L5, θ, γ, ECe, ECGW and DGW were regarded as the independent variables and EMh0.50 and EMv0.50 were regarded as dependent variables. *Table 7* lists the results of path analysis conducted to determine the factors influencing ECa (i.e., EMh0.50 and EMv0.50) measured at a height of 0.50 m. At L5, ECe showed significant correlations with both EMh0.50 and EMv0.50 with correlation coefficients of 0.80 and 0.78 ($P < 0.01$), respectively. θ and DGW also showed significant correlations with ECa ($P < 0.05$), possibly because ECa at L5 had shown a significant correlation with DGW (REC-Dgw = 0.34*, $P < 0.05$), which indirectly imposed an influence on EM0.50 through ECe. According to the results, the rates of contribution of ECe to EMh0.50 and EMv0.50 at L5 were 36.98% and 32.58%, respectively. On the other hand, θ had a greater influence on EMh0.50 than ECe, indicating that θ had a large influence at L5. GW characteristics also showed relatively significant influences on EMh0.50 and EMv0.50, with rates of contribution of 21.45% and 17.16%, respectively. DGW and ECGW showed negative correlations with ECa measured at a height of 0.50 m, although the correlation was only significant for DGW ($R = -0.58^{**}, -0.54^{**}$, $P < 0.01$), consistent with the study of Bouksila et al. (2012).

http://www.aloki.hu ● ISSN 1589 1623 (Print) ● ISSN 1785 0037 (Online)
DOI: http://dx.doi.org/10.15666/aeer/1704_1003710057

Table 7. *Path coefficients between influence factors to EM38 values at 0.50 m above the ground of 0.80~1.00 m*

Dependent variable	Variable	ECe	θ	γ	ECGW	DGW	Contribution rate	Correlation coefficient with EM
EMv0.50	**0.4500**	0.2682	-0.0123	0.0043	0.0906	36.98%	0.80**	**0.4500**
	0.2898	**0.4230**	-0.0254	0.0013	0.0890	34.76%	0.78**	0.2898
	0.0986	0.1916	**-0.0560**	-0.0087	0.0044	4.60%	0.23	0.0986
	-0.0711	-0.0207	-0.0181	**-0.0270**	-0.1138	2.22%	-0.25	-0.0711
	-0.1561	-0.1442	0.0010	-0.0118	**-0.2610**	21.45%	-0.57**	-0.1561
EMh0.50	**0.4291**	0.3132	-0.0339	-0.0021	0.0784	32.58%	0.78**	**0.4291**
	0.2721	**0.4940**	-0.0702	-0.0006	0.0771	37.51%	0.77**	0.2721
	0.0940	0.2238	**-0.1550**	0.0042	0.0038	11.77%	0.17	0.0940
	-0.0678	-0.0242	-0.0501	**0.0130**	-0.0985	0.99%	-0.23	-0.0678
	-0.1489	-0.1685	0.0026	0.0057	**-0.2260**	17.16%	-0.54**	-0.1489

EMh0.50—EM38 values of apparent electrical conductivity in horizontal operation mode; EMv0.50—EM38 values of apparent conductivity in vertical operation mode; ECe—soil electrical conductivity; θ—soil moisture; γ—soil clay content; ECGW—groundwater conductivity; DGW—groundwater level; *, ** significant at 0.05 and 0.01 level of probability, respectively. Bold font indicates direct path coefficient of corresponding factor

ECa measured by EM38 at a height of 0 m showed the best correlation with ECe at all soil layers (Huang et al., 2015; Yao and Yang, 2010). However, in the present study, the height of EM38 was set at 1.30 m, 1.10 m, 0.90 m, 0.70 m and 0.50 m in sequence, where the corresponding effective investigation depths were 0.20 m, 0.40 m, 0.60 m, 0.80 m and 1.00 m respectively. This approach was taken to more directly analyze influences of soil properties on ECa in the different layers. The results showed that ECe had the greatest influence on EMv regardless of EM38 height, with the influences of θ, DGW and ECGW increasing as EM38 height decreased, whereas the influence of clay content remained negligible. In general, soil ECa has been found to be mainly influenced by the factor showing the most spatial variability across the research region (Doolittle and Brevik, 2014). As a result, since γ showed less spatial variability than that of soil ECe and θ in the vertical direction, the fact that γ had a negligible effect on ECa was expected.

Prediction of ECe in different soil layers

Linear regression has been widely used to study the relationship between ECe and ECa of soil (Triantafilis et al., 2000; Bennett and George, 1995). In the present study, ECe of different soil layers was taken as the dependent variable and EMh and EMv were taken as the independent variables within simple linear regression analysis. ECe of different soil layers was then taken as the dependent variable and both EMh and EMv were taken as independent variables within binary linear regression analysis. Furthermore, the factors with large influences on ECa were gradually introduced as additional independent variables together with ECa to generate an MLR model for different soil layers. For all soil layers, θ, DGW and ECGW were chosen as the additional independent variables and were gradually introduced into the prediction

http://www.aloki.hu ● ISSN 1589 1623 (Print) ● ISSN 1785 0037 (Online)
DOI: http://dx.doi.org/10.15666/aeer/1704_1003710057

model. *Figure 2* shows the change in R^2 with the gradual addition of different variables into the prediction model. The optimal ECe interpretation models for different soil layers are shown in *Table 2*.

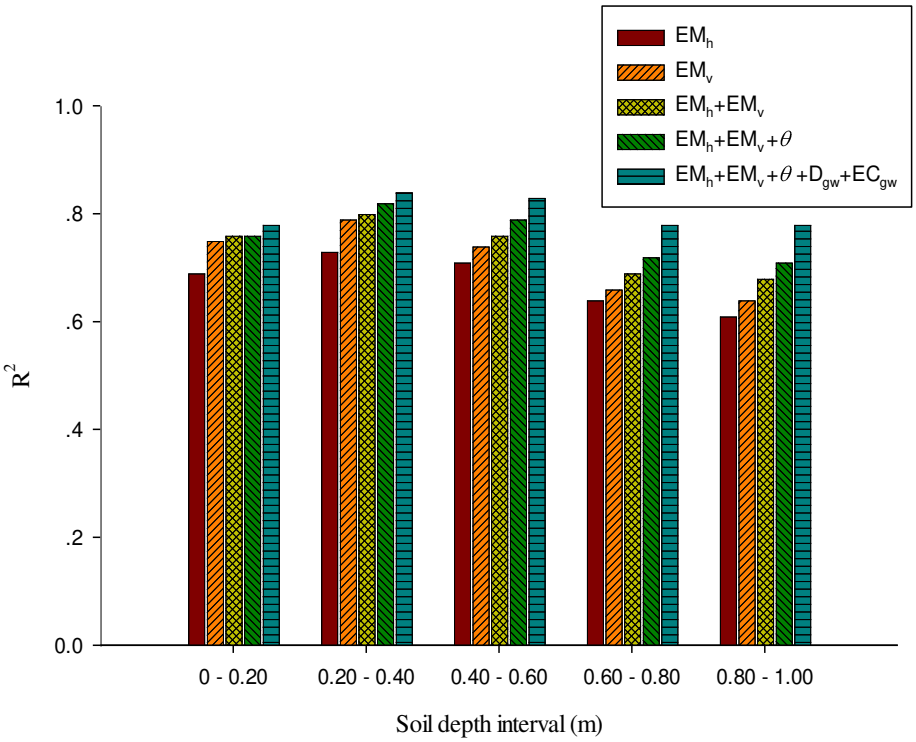

Figure 2. *The change in R^2 with the gradual addition of different variables into the prediction*

In general, at an EM38 height of 0 m and a separation of 1 m between the receiving coil and transmitting coil, the effective investigation depth was 0.75 m in the horizontal mode and 1.5 m in the vertical mode. Therefore, the correlation between ECe at the top soil layer and ECa measured in the horizontal mode was higher than that between ECe at the top soil layer and ECa measured in the vertical mode (Huang et al., 2015; Yao and Yang, 2010), whereas the correlation between ECe at the bottom soil layer and ECa measured in the vertical mode was higher than that between ECe at the bottom soil layer and ECa measured in the horizontal mode. In the present study, ECe values at different soil layers (L1–L5) were interpreted using ECa data measured at the corresponding heights (1.30 m, 1.10 m, 0.90 m, 0.70 m and 0.50 m, respectively). As shown in *Figure 2*, the effectiveness of EMv in providing an interpretation was better than that of EMh for all soil layers because at an EM38 height < 1.5 m, soil information could be effectively investigated in the vertical mode, whereas this was only true for the horizontal mode at EM38 height < 0.75 m. The prediction accuracy of ECe at L1 using EMv1.30 was low. On the other hand, the highest prediction accuracy of ECe using EMv1.10 was at L2. Below L2, the prediction accuracy of ECe decreased with increasing soil depth. A possible explanation is that since θ at L1 is low, some salt at L1 is likely to remain undissolved, thereby providing no contribution to the reading of EM38. In addition, with decreasing EM38 height, the thickness of the soil that can influence ECa increases; thus, the prediction accuracy of ECe using ECa within the deeper soil layer decreases.

http://www.aloki.hu ● ISSN 1589 1623 (Print) ● ISSN 1785 0037 (Online)
DOI: http://dx.doi.org/10.15666/aeer/1704_1003710057

Various studies have used EM38 data in both the horizontal and vertical modes to interpret soil salt content, and ECe prediction models have been developed with relatively high accuracies (Liu et al., 2016; Lesch et al., 2000). As shown in *Figure 1*, the accuracy of the model developed in the present study improved with the incorporation of both EMh and EMv. However, with the use of EMh1.30 and EMv1.30 to interpret ECe at L1 and EMh1.10 and EMv1.10 to interpret ECe at L2, the improvement in the accuracy of the interpretation model was not as high as those in the other three cases. This observation can be explained by the fact that the effective investigation depth in the horizontal mode was only 0.75 m. More specifically, at EM38 heights of 1.10 m or 1.30 m, despite EMh showing an extremely significant correlation with ECe, ECe was in fact mainly influenced by EMv because the linear relationship between EMv and EMh could be identified during EM38 calibration. This explains why introducing EMh into the model did not increase the accuracy of the model for predicting salt content at L1 and L2.

Among all the factors that can influence soil ECa in salinized regions, the concentration of soluble salt is the most prominent (Williams et al., 2006). However, due to upward leaching and evaporative processes, GW salt tends to accumulate in the soil (Richardson and Williams, 1994). Liu et al (2010) showed θ and ECGW to be the most important non-salt factors in regions of relatively shallow GW. Therefore, the accuracy of the soil salt prediction model can be improved by introducing θ and ECGW into the model as additional independent variables. Similar conclusions were made in the present study. At L1, DGW and ECGW showed significant correlations with ECe ($P < 0.05$), whereas θ did not. As a result, the introduction of θ into the model did not improve the model's accuracy, whereas the opposite was found with the introduction of GW characteristics (R^2 increased from 0.76 to 0.78). At L2, θ showed a significant correlation with γ and DGW ($P < 0.05$), indicating that θ at L2 is greatly affected by γ and GW characteristics. With an increase in θ, salt dissolved; thus, when θ, ECGW and DGW were introduced into the prediction model, R^2 increased from 0.80 to 0.84. This was also observed at L3–L5, where the ECe prediction accuracies increased to 0.83, 0.78 and 0.78 respectively. Hanson and Kaita (1997) found a positive relationship between θ and the sensitivity of EM38 to variation in soil salt content. Therefore, when using EM38 to measure soil salt content, the influence of θ on ECa should be taken into account (Brevik et al., 2002). In the present study, incorporating θ improved the accuracy of the ECe prediction model except at L1. In addition, incorporating GW characteristics improved the model accuracy for the deeper soil layers to a larger degree than that for the top soil layer, possible due to the relatively shallow DGW in the research region.

Validation of interpretation model for soil salt content

Table 8 shows the models used to predict salt content in the different soil layers. The reserved 30 soil profiles were used as test data to validate the reliability of the models. The independent variables can be used by the prediction models to estimate salt content in the test profiles for different soil layers. By comparing the model predictions of salt content with laboratory measurements, the accuracy and practicability of the interpretation model can be validated.

Figure 3 shows the R^2 values for the salt content predictions versus measurements in the test profiles of each layer. All values of R^2 were greater than 0.70, indicating highly significant correlations between the model predictions and the measurements. This

http://www.aloki.hu ● ISSN 1589 1623 (Print) ● ISSN 1785 0037 (Online)
DOI: http://dx.doi.org/10.15666/aeer/1704_1003710057

demonstrated that the model represented major processes affecting salt content in the different layers relatively well. On the other hand, the values of ME between the predictions and the ECe measurements for L1–L5 were 0.63, 0.46, 0.53, 0.25 and 0.24, respectively, whereas the values of RMSE were 0.77, 0.48, 0.21, 0.26 and 0.24, respectively.

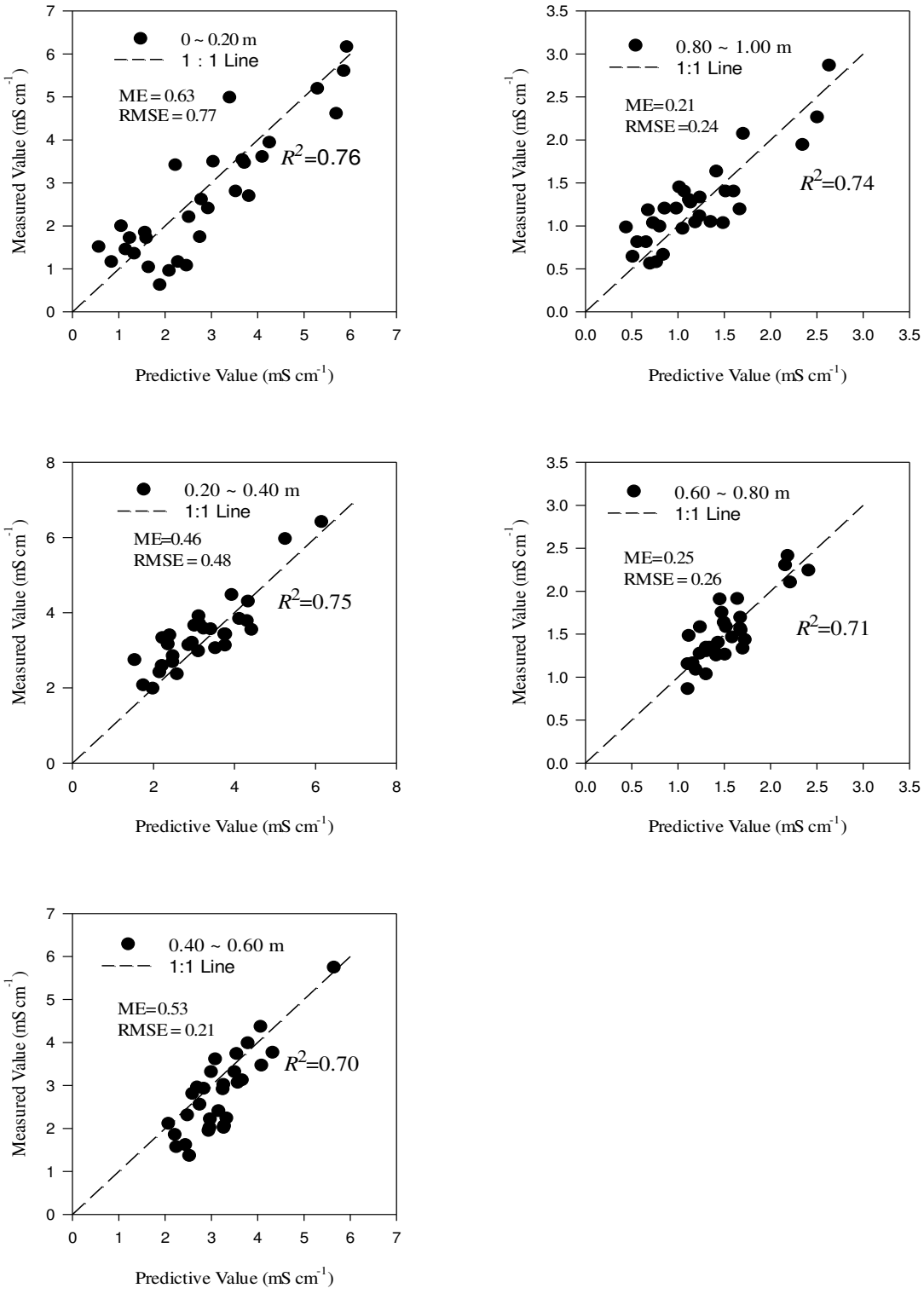

Figure 3. *Fitting of soil EC between predicted value and measured value in different soil layers*

http://www.aloki.hu ● ISSN 1589 1623 (Print) ● ISSN 1785 0037 (Online)
DOI: http://dx.doi.org/10.15666/aeer/1704_1003710057

Table 8. *The exact interpretation model of salt in different soil layers*

Soil layers	Model equation	R^2
0~20	$-0.317 + 0.035 \times EMv1.30 + 0.012 \times ECGW - 0.005 \times DGW$	0.78
20~40	$0.142 + 0.013 \times EMv1.10 - 2.56 \times \theta + 0.004 \times ECGW + 0.003 \times DGW$	0.84
40~60	$-0.51 + 0.004 \times EMh0.90 + 0.01 \times EMv0.90 + 2.385 \times \theta + 0.01 \times ECGW + 0.003 \times DGW$	0.83
60~80	$-0.85 + 0.005 \times EMh0.70 + 0.002 \times EMv0.70 + 0.634 \times \theta + 0.01 \times ECGW + 0.01 \times DGW$	0.78
80~100	$-1.48 + 0.006 \times EMh0.50 + 0.001 \times EMv0.50 - 4.68 \times \theta + 0.001 \times ECGW + 0.017 \times DGW$	0.78

Conclusions

Path analysis was used in the present study to analyze the influences of soil properties and GW characteristics in different soil layers on ECa as measured by EM38 at different heights. The results showed that ECe was the most important factor influencing ECa measured at different heights. The rates of contribution of ECe to EMv at L1–L5 were 65.78%, 82.21%, 65.79%, 49.26% and 36.98%, respectively. The results showed that the degree of influence of the bottom soil layer to ECa decreased whereas those of other soil properties increased with increasing soil depth. In addition, since θ at L1 was relatively low, the rate of contribution of ECe to ECa at L1 was also relatively small. The influence of θ on ECa was also noticeable, with rates of contribution to ECa at L1–L5 being 10.93%, 7.85%, 9.15%, 16.64% and 34.76%, respectively. The rates of contribution of DGW to ECa measured by EM38 at heights of 1.30 m, 1.10 m, 0.90 m, 0.70 m and 0.50 m were 4.67%, 5.27%, 10.64%, 22.62% and 21.45%, respectively, whereas those of ECGW were 9.27%, 4.47%, 12.75%, 11.07% and 2.22%, respectively. In arid and semi-arid areas, due to upward leaching and evaporative processes, GW salt tends to accumulate in the soil. In such areas, the soil salt content has significant correlations with unsuitable irrigation practices, evapotranspiration of farm land and DGW during crop growth. GW characteristics impose an influence on ECa by influencing ECe in each layer. In the research region, the influence of γ on the ECa was minor.

Linear regression was used to derive optimal ECe prediction models for different soil layers. Taking ECe of different soil layers as the dependent variable and EMh and EMv as the independent variables in sequence, simple linear regression analysis was conducted. Binary linear regression analysis was conducted by taking ECe of different soil layers as the dependent variable and both EMh and EMv as the independent variables. θ, DGW and ECGW were then gradually introduced into the prediction model as additional independent variables. The results showed EMv to provide a better interpretation than EMh in each soil layer. This was because at an EM38 height < 1.5 m, the soil information could be effectively investigated in the vertical mode, whereas this was only true for the horizontal mode at an EM38 height < 0.75 m. The ECe prediction accuracy at L1 using EMv1.30 was low due to low θ. On the other hand, the ECe prediction accuracy at L2 was the highest; however, as the depth of the soil layer increased below L2, the ECe prediction accuracy decreased. When EMh and EMv were both used to derive the interpretation model, the model accuracy improved.

θ and GW characteristics were important factors influencing ECa; therefore, their influences on ECa need to be considered when using EM38 to measure soil salt content. With the introduction of θ and GW characteristics to the prediction model as additional independent variables, the reliability of the ECe prediction model in each soil layer

http://www.aloki.hu ● ISSN 1589 1623 (Print) ● ISSN 1785 0037 (Online)
DOI: http://dx.doi.org/10.15666/aeer/1704_1003710057

improved. In addition, the addition of GW characteristics improved the prediction accuracy for the bottom soil layer more than that for the top soil layer.

The accuracies of the ECe prediction models for different soil layers were validated. R^2 values showing the correlations between model ECe predictions and measurements of each layer were > 0.70. ME and RMSE values at L1–L5 were 0.63, 0.46, 0.53, 0.25 and 0.24, respectively, and 0.77, 0.48, 0.21, 0.26 and 0.24, respectively. The results suggested that the models for L3–L5 were more accurate than those for L1–L2.

The EMI approach offers potential for improving the prediction accuracy of soil salinity information by the addition of influence factors into the multiple regression model. In the future research, it is necessary to study the denoising of data to help resolve some of the uncertainty issues associated with this non-contacting technology and further improve the accuracy of the interpretation model.

Acknowledgements. The authors are grateful for the financial support of the International Science & Technology Cooperation Program of China [grant number 2015DFA11660], Major Scientific Research Projects of Xinjiang Production and Construction Corps (2018AA004, 2018AA005). We would also like to thank the reviewers for their time spent in improving the paper.

REFERENCES

[1] Abdu, H., Robinson, D. A., Jones, S. B. (2007): Comparing bulk soil electrical conductivity determination using the DUALEM 1-S and EM-38DD EMI instruments. – Soil Science Society of America Journal 71(1): 189-196.

[2] Aboelsoud, H., Abdel-Rahman, M. (2017): Rapid field technique for soil salinity appraisal in north Nile delta using EM38 through some empirical relations. – International Journal of Plant & Soil Science 14: 1-9.

[3] Bekele, A., Hudnall, W. H., Daigle, J. J., Prudente, J. A., Wolcott, M. (2005): Scale dependent variability of soil electrical conductivity by indirect measures of soil properties. – Journal of Terramechanics 42(3-4): 339-351.

[4] Bennett, D. L., George, R. J. (1995): Using the em38 to measure the effect of soil salinity on Eucalyptus globulus, in South-Western Australia. – Agricultural Water Management 27(1): 69-85.

[5] Bennett, D. L., George, R. J., Whitfield, B. (2000): The use of ground EM systems to accurately assess salt store and help define land management options, for salinity management. – Exploration Geophysics 31(1/2): 249-254.

[6] Bouksila, F., Persson, M., Bahri, A., Berndtsson, R. (2012): Electromagnetic induction prediction of soil salinity and groundwater properties in a Tunisian Saharan oasis. – Hydrological Sciences Journal 57(7): 1473-1486.

[7] Brevik, E. C., Fenton, T. E. (2002): Influence of soil water content, clay, temperature, and carbonate minerals on electrical conductivity readings taken with an EM-38. – Soil Horizons 43(1): 9-13.

[8] Brevik, E. C., Fenton, T. E., Horton, R. (2004): Effect of daily soil temperature fluctuations on soil electrical conductivity as measured with the Geonics® EM-38. – Precision Agriculture 5(2): 145-152.

[9] Butcher, K., Wick, A. F., DeSutter, T., Chatterjee, A., Harmon, J. (2016): Soil salinity: a threat to global food security. – Agronomy Journal 108(6): 2189-2200.

[10] Cassel, F., Goorahoo, D., Sharmasarkar, S. (2015): Salinization and yield potential of a salt-laden Californian soil: an in situ geophysical analysis. – Water, Air, & Soil Pollution 226(12): 422.

http://www.aloki.hu ● ISSN 1589 1623 (Print) ● ISSN 1785 0037 (Online)
DOI: http://dx.doi.org/10.15666/aeer/1704_1003710057

[11] Cook, P. G., Walker, G. R. (1992): Depth profiles of electrical conductivity from linear combinations of electromagnetic induction measurements. – Soil Science Society of America Journal 56(4): 1015-1022.
[12] Corwin, D. L., Rhoades, J. D. (1982): An improved technique for determining soil electrical conductivity-depth relations from above-ground electromagnetic measurements 1. – Soil Science Society of America Journal 46(3): 517-520.
[13] Dakak, H., Huang, J., Zouahri, A., Douaik, A., Triantafilis, J. (2017): Mapping soil salinity in 3 - dimensions using an EM38 and EM4Soil inversion modelling at the reconnaissance scale in central Morocco. – Soil use and management 33(4): 553-567.
[14] Ding, J., Yu, D. (2014): Monitoring and evaluating spatial variability of soil salinity in dry and wet seasons in the Werigan–Kuqa Oasis, China, using remote sensing and electromagnetic induction instruments. – Geoderma 235: 316-322.
[15] Doolittle, J. A., Brevik, E. C. (2014): The use of electromagnetic induction techniques in soils studies. – Geoderma 223: 33-45.
[16] Doolittle, J. A., Indorante, S. J., Potter, D. K., Hefner, S. G., McCauley, W. M. (2002): Comparing three geophysical tools for locating sand blows in alluvial soils of southeast Missouri. – Journal of Soil and Water Conservation 57(3): 175-182.
[17] Liu, G., Yang, J., Yao, R. (2010): Electromagnetic induction based interpreting model of soil salinity in different soil layers. – Transactions of the Chinese Society of Agricultural Engineering 26(1): 61-66.
[18] Han, D., Song, X., Currell, M. J., Cao, G., Zhang, Y., Kang, Y. (2011): A survey of groundwater levels and hydrogeochemistry in irrigated fields in the Karamay Agricultural Development Area, Northwest China: implications for soil and groundwater salinity resulting from surface water transfer for irrigation. – Journal of Hydrology 405(3-4): 217-234.
[19] Hanson, B. R., Kaita, K. (1997): Response of electromagnetic conductivity meter to soil salinity and soil-water content. – Journal of irrigation and Drainage Engineering 123(2): 141-143.
[20] He, Y., Desutter, T., Norland, J., Chatterjee, A., Casey, F., Clay, D. (2018): The measurement, prediction, and development of soil management zones in low-relief sodic soils. – Precision Agriculture 1-18.
[21] Heil, K., Schmidhalter, U. (2017): The application of em38: determination of soil parameters, selection of soil sampling points and use in agriculture and archaeology. – Sensors 17(11): 2540.
[22] Hossain, M. B., Lamb, D. W., Lockwood, P. V., Frazier, P. (2010): Em38 for volumetric soil water content estimation in the root-zone of deep vertosol soils. – Computers & Electronics in Agriculture 74(1): 100-109.
[23] Huang, J., Purushothaman, R., McBratney, A., Bramley, H. (2018): Soil water extraction monitored per plot across a field experiment using repeated electromagnetic induction surveys. – Soil Systems 2(1): 11.
[24] Jadoon, K. Z., Moghadas, D., Jadoon, A., Missimer, T. M., Al-Mashharawi, S. K., McCabe, M. F. (2015): Estimation of soil salinity in a drip irrigation system by using joint inversion of multicoil electromagnetic induction measurements. – Water Resources Research 51(5): 3490-3504.
[25] Jiang, Z. Y., Li, X. Y., Wu, H. W., Zhang, S. Y., Zhao, G. Q., Wei, J. Q. (2017): Linking spatial distributions of the patchy grass Achnatherum splendens with dynamics of soil water and salt using electromagnetic induction. – Catena 149: 261-272.
[26] Kasim, N., Tiyip, T., Abliz, A., Nurmemet, I., Sawut, R., Maihemuti, B. (2018): Mapping and modeling of soil salinity using WorldView-2 data and EM38-KM2 in an arid region of the Keriya River, China. – Photogrammetric Engineering & Remote Sensing 84(1): 43-52.

http://www.aloki.hu ● ISSN 1589 1623 (Print) ● ISSN 1785 0037 (Online)
DOI: http://dx.doi.org/10.15666/aeer/1704_1003710057

[27] Krajco, B. J. (2007): Detection of soil compaction using soil electrical conductivity. – Journal of Physical Chemistry A 111(34): 8352-8356.
[28] Lesch, S. M., Corwin, D. L. (2003). Using the dual-pathway parallel conductance model to determine how different soil properties influence conductivity survey data. – Agronomy Journal 95(2): 365-379.
[29] Lesch, S. M., Rhoades, J. D., Corwin, D. L. (2000): ESAP-95 Version 2.01 R: User manual and tutorial guide. – Research Rpt. 146, USDA-ARS George E. Brown, Jr. Salinity Laboratory, Riverside, CA.
[30] Li, J. G., Pu, L. J., Han, M. F., Zhu, M., Zhang, R. S., Xiang, Y. Z. (2014): Soil salinization research in China: advances and prospects. – Journal of Geographical Sciences 24(5): 943-960.
[31] Liu, G. M., Li, J. B., Zhang, X. C., Wang, X. P., Lv, Z. Z., Yang, J. S., Shao, H. B., Yu, S. P. (2016): GIS-mapping spatial distribution of soil salinity for Eco-restoring the Yellow River Delta in combination with electromagnetic induction. – Ecological Engineering 94: 306-314.
[32] Mankin, K. R., Karthikeyan, R. (2002): Field assessment of saline seep remediation using electromagnetic induction. – Transactions of the ASAE 45(1): 99.
[33] Martinez, G., Vanderlinden, K., Ordóñez, R., Muriel, J. L. (2009). Can apparent electrical conductivity improve the spatial characterization of soil organic carbon?. – Vadose Zone Journal, 8(3), 586-593.
[34] McKenzie, R. C., Mathers, H. M., Robertson, J. M., Woods, S. A. (1993). Salinity and cold tolerance of ornamental trees and shrubs. – Alberta Special Crops and Horticultural Research Center.
[35] McNeill, J. D. (1980): Electromagnetic terrain conductivity measurement at low induction numbers. – Geonics Limited, Mississauga, ON, Canada.
[36] McNeill, J. D. (1990): Geonics EM38 ground conductivity meter: EM38 operating manual. – Geonics Ltd., Mississauga, ON, Canada.
[37] Misra, R. K., and Padhi, J. (2014): Assessing field-scale soil water distribution with electromagnetic induction method. – Journal of Hydrology 516: 200-209.
[38] Norman, C. P. (1990): Training manual on the use of the EM38 for soil salinity appraisal. – Victorian Department of Agriculture and Rural Affairs, Australia.
[39] Rahimian, M. H., Hasheminejhad, Y. (2011): Calibration of electromagnetic induction device (EM38) for soil salinity assessment. – Iranian Journal of Soil Research 24(3): 243-252.
[40] Rengasamy, P. (2006): World salinization with emphasis on Australia. – Journal of Experimental Botany 57(5): 1017-1023.
[41] Richardson, D. P., Williams, B. G. (1994): Assessing discharge characteristics of upland landscapes using electromagnetic induction techniques. – CSIRO, Canberra.
[42] Scudiero, E., Skaggs, T. H., Corwin, D. L. (2016). Comparative regional-scale soil salinity assessment with near-ground apparent electrical conductivity and remote sensing canopy reflectance. – Ecological indicators, 70, 276-284.
[43] Silberstein, R. et al. (2007): Does grazing perennial pastures on saline land affect farm salt and water balances? – SGSL Salt and Water Movement Theme Report. http://www.saltlandgenie.org.au/ literature_ 23944/RR — _SGSL_ Salt_and Water Movement and Site Characterisation Theme (Accessed 14 August 2012).
[44] Singh, A. (2018): Use of em-38 soil surveys in forage fields at a saline drainage water reuse site to calibrate a hydro-salinity model for decision support. – A thesis submitted in partial fulfillment of the requirements for the degree of Master of Science in Plant Science in the Jordon College of Agricultural Sciences and Technology California State University, Fresno.
[45] Sudduth, K. A., Kitchen, N. R., Wiebold, W. J., Batchelor, W. D., Bollero, G. A., Bullock, D. G. et al. (2005): Relating apparent electrical conductivity to soil properties

http://www.aloki.hu ● ISSN 1589 1623 (Print) ● ISSN 1785 0037 (Online)
DOI: http://dx.doi.org/10.15666/aeer/1704_1003710057

across the North-Central USA. – Computers and Electronics in Agriculture 46(1): 263-283.

[46] Triantafilis, J., Laslett, G. M., Mcbratney, A. B. (2000): Calibrating an electromagnetic induction instrument to measure salinity in soil under irrigated cotton. – Soil Science Society of America Journal 64(3): 1009-1017.

[47] Triantafilis, J., Lesch, S. M. (2005): Mapping clay content variation using electromagnetic induction techniques. – Computers and Electronics in Agriculture 46(1-3): 203-237.

[48] Triantafilis, J., Santos, F. M. (2010): Resolving the spatial distribution of the true electrical conductivity with depth using EM38 and EM31 signal data and a laterally constrained inversion model. – Soil Research 48(5): 434-446.

[49] Williams, B., Walker, J., Anderson, J. (2006): Spatial variability of regolith leaching and salinity in relation to whole farm planning. – Australian Journal of Experimental Agriculture 46(10): 1271-1277.

[50] Wittler, J. M., Cardon, G. E., Gates, T. K., Cooper, C. A., Sutherland, P. L. (2006): Calibration of electromagnetic induction for regional assessment of soil water salinity in an irrigated valley. – Journal of Irrigation and Drainage Engineering 132(5): 436-444.

[51] Yao, R., Yang, J. (2010): Quantitative evaluation of soil salinity and its spatial distribution using electromagnetic induction method. – Agricultural Water Management 97(12): 1961-1970.

http://www.aloki.hu ● ISSN 1589 1623 (Print) ● ISSN 1785 0037 (Online)
DOI: http://dx.doi.org/10.15666/aeer/1704_1003710057

ANALYSIS AND RESEARCH ON THE DIVERSITY OF MICROBIAL COMMUNITY STRUCTURE IN URBAN RIVER SEDIMENT

TU, B. H. – OU, Y.T. – ZHAO, Y.* – QIN, W. – XIAO, X. – ZHANG, S.* – LIU, Y.

School of Environmental and Safety Engineering, Changzhou University, Changzhou, Jiangsu 213164, China

Changzhou City New Materials Technology Co. LTD, Changzhou, Jiangsu 213000, China

**Corresponding authors*
e-mail/phone: zhaoyuan@cczu.edu.cn/+86-159-6123-8081 (ZHAO, Y.);
zhangsheng@cczu.edu.cn/+86-139-5122-6900 (ZHANG, S.)

(Received 9th Apr 2019; accepted 19th Jun 2019)

Abstract. In this study, sediment was sampled from the North River in Changzhou at five different loca-tions at the same time. Microbial DNA was extracted from the obtained samples, and the extracted DNA purity was compared by two different methods. After DNA amplification by 16S rRNA PCR, microspectrophotometry and agarose gel electrophoresis, the modified gradient gel electrophoresis (DGGE) was performed. The DGGE map was analyzed using Quantity one software of bio-rad to study the community diversity. The similarity matrix showed that the samples of different locations and time had high similarity, with the highest similarity reaching 82%. The proportion of similarity over 60% is extremely high, which indicates that the microbial population in North River is abundant, but the microbial community structure changes little in space.
Keywords: *sediment, spatial variation, PCR amplifiction, DGGE, microbial diversity*

Introduction

Urban rivers are part of natural river basins, playing an irreplaceable role in the process of urban ecological construction, namely, they have the functions of material circulation and ecological protection, weakening the urban heat island effect and regulating local climate (Yan and Wang, 1999). Due to the rapid development of human urbanization, the natural ecosystem of urban rivers is overused, damaged and difficult to recover. Resulting in the loss of self-purification capacity and the rapid deterioration of the environment, which seriously affects the urban ecological environment and the health of urban residents (Sun, 2015). With the continuous improvement of living standards, people are constantly strengthening their environmental awareness, and the quality of living environment is also constantly improving, which leads to the prominent problem of urban river pollution, and its governance is of great urgency. At present, physical, chemical and biological methods have been used to restore and manage damaged river ecosystems (Hu et al., 2005). Compared to physical and chemical methods, biological methods do not cause secondary pollution in the treatment, and the cost of investment and maintenance is low (Gu et al., 2013). In addition, the study on the microflora of urban river environments in China has been available in the 1980s. For example, since 1986, Zhao et al. used traditional culture methods to study the correlation between organic matter and water temperature in water and microbial quantity and population distribution (Zhao et al., 1986). Therefore, it is of great significance to study the community structure and functional diversity of microorganisms in known environments. Combined with the existing methods of

http://www.aloki.hu ● ISSN 1589 1623 (Print) ● ISSN 1785 0037 (Online)
DOI: http://dx.doi.org/10.15666/aeer/1704_1005910072

environmental microorganism community analysis, there are traditional culture and separation methods (Amann et al., 1995). Community level physiology fingerprint methods (CLPP) (Victorio et al., 1996; Ibekwe and Kennedy, 1998), biological marker methods (Bai, 1997) and modern molecular biology methods (Torsvik et al., 1990; Hill et al., 2002; Handelsman, 2004; Tunlid, 2007). Since 1985, Pace et al. (1997) used the accounting sequencing method to study microbial evolution, molecular biology technology has been gradually introduced into biodiversity research. In 1993, Muyzer et al. (1993) first introduced the denatured gradient gel electrophoresis DGGE technology into the study of microbial ecology (Zhang et al., 2009; Yu et al., 2010). Since then, DGGE technology has been applied and developed in environmental microorganism research. Therefore, in this study, taking the North River in Changzhou city as an example, the microbial community structure of the urban river is analyzed with the PCR-DGGE (Röttgers, 2007) technology. Through analyzing the target environment of microbial community structure and population diversity, we supplied a reference for optimizing the community structure, regulating functions of community, and discovering new important microbial groups.

Materials and methods

Experimental materials

River sediment

The river bottom sediment samples were collected in the North River, and the locations of the river bottom sediment samples were Jingu Manor, Boai Bridge, Chunting Bridge, Zhiyuan Bridge and Yuanfeng Bridge (as shown in *Fig. 1*). In order to facilitate the experimental record, the samples of the above five locations were recorded as no.1,2,3,4 and 5, respectively. As there are residential communities near the river section, part of the sewage will be directly discharged into the river section. But in recent years, beishi river has improved its water quality by adding aeration devices and installing biological floating islands. The samples of river surface sediment (0~20 cm) were collected from January to December 2017 and all of them were gathered using sterile bags. At 4 °C under the condition of back to the laboratory immediately, save under the condition of -80 °C, and completed within a week of sediment microbial total DNA extraction.

Preparation of buffer solution

(1) 50×TAE preparation: Tris 242 g, Na2EDTA·2H2O 37.2 g, and then 800 ml of deionized water was added, which was fully stirred to dissolve. Add 57.1 ml acetic acid and mix well. Finally, add the deionized water to 1 L for storage at room temperature. (50×TAE is the storage fluid. Dilute 50 times to get 1×TAE solution)

(2) 5×Loading buffer preparation: 10 mM tris-hcl, 5 mM EDTA, pH 7.6, 0.03% bromophenol blue, 0.03% xylene blue, 30% glycerin.

Experimental methods

Determination of physical and chemical properties of North River sediment

Dissolved oxygen and water temperature should be measured at the sampling site, and immediately measured by the Shanghai Jingke jpbj-608 portable dissolved oxygen meter. pH, ammonia nitrogen, total nitrogen, total phosphorus, chemical oxygen demand, nitrate nitrogen and chlorophyll a were measured in the laboratory. The determination of

http://www.aloki.hu ● ISSN 1589 1623 (Print) ● ISSN 1785 0037 (Online)
DOI: http://dx.doi.org/10.15666/aeer/1704_1005910072

chemical oxygen demand, ammonia nitrogen, total nitrogen and total phosphorus was carried out by the 6b-2000 multi-parameter water quality meter of Jiangsu Shengaohua Environmental Protection Technology Co. LTD. The determination of pH was carried out by using a multiple parameter analyzer. Chlorophyll a was determined by spectrophotometer (Röttgers, 2007). The determination of nitrate nitrogen was performed by UV spectrophotometry (Zhu et al., 2011), that is, the absorption area of nitrate ion at the wavelength of 220 nm was used for quantitative determination of nitrate nitrogen.

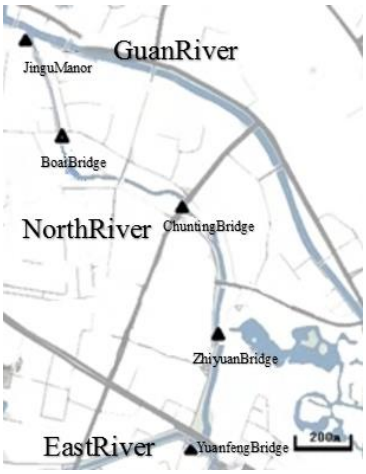

Figure 1. *North River sampling section distribution schematic diagram*

Total DNA extraction of river sediment microorganisms

The 1 g bottom sediment samples were respectively weighed and used in combination with humic acid by bioengineering (Shanghai) company, and 0.2-0.5 g bottom sediment samples were extracted from the bottom sediment samples by using Omega biotek soil DNA small-lift kit. The operation steps were performed according to the instructions, and the extraction effect was compared.

Inspection of DNA concentration and purity

This study used an ultra-micro spectrophotometer to determine the concentration of DNA. 2 μL of DEPC tretd water was taken as a blank sample and 2 μL of the total DNA solution of the sediment sample, and each was dropped in the measurement area of the micro spectrophotometer, and the relevant data was recorded by an analysis software. If the ratio of A260/A280 is around 1.8, it means that higher DNA concentration can be used for subsequent PCR and cloning experiments. If A260/A280 > 2.0, it means that the RNA interference is large and the DNA needs to be re-expressed (Hoefel et al., 2005).

PCR amplification

In the present study, the amplified DNA fragment was subjected to the V3 region of the bacterial 16S rRNA sequence, and the primers were 357f and 518r (Li et al., 2013), and the length was about 194 bp. Further, a "GC" splint having a base number of 40 bp was added to the 5' portion of the primer 357f. which is
"GC" splint: 5′-CGCCCGCCGCGCCCCGCGCCCGGCCCGCCGCCCCCGCCCC -3′

http://www.aloki.hu ● ISSN 1589 1623 (Print) ● ISSN 1785 0037 (Online)
DOI: http://dx.doi.org/10.15666/aeer/1704_1005910072

357f: 5′-CCTACGGGAGGCAGCAG-3′
518r: 5′-ATTACCGCGGCTGCTGG-3′

Reaction system: (1) PCR reaction system is 25 μL, the specific reagent amount: 2×Taq Master mix 12.5 μL; upstream primer 2 μL; downstream primer 2 μL; DNA template 1.25 μL; DDH_2O 7.25 μL; (2) PCR reaction system is 50 μL, the specific reagent amount: 2×Taq Master mix 25 μL; upstream primer 1 μL; downstream primer 1 μL. DNA template 2 μL; DDH_2O 21 μL.

Amplification procedure: pre-denaturation at 94 °C for 5 min, then 25 cycles, each cycle includes denaturation at 94 °C for 30 s, annealing at 61-56 °C for 30 s, extension at 72 °C for 1 min, and end of the cycle at 72 °C for a final extension of 7 min. Hold 4 °C.

DNA agarose gel electrophoresis experiment (qualitative analysis)

The extracted total DNA was qualitatively analyzed by agarose gel electrophoresis. 0.25 g of agarose was added to 1×TAE buffer, and a 1% agarose gel was subjected to electrophoresis, and the results were observed after photographing under an ultraviolet lamp.

DNA denaturing gradient gel electrophoresis (DGGE) experiment

Solidifying the gel in 1×TAE buffer, each sample well of a sample of about 15 μL, using horizontal electrophoresis, a gradient of denaturant is allowed to range from 40% to 55%, the voltage75 V, run time 14 h, electrophoresis was carried out at a temperature of 60 °C. After the electrophoresis of the DGGE gel was completed, it was stained with EB (ethidium bromide). After staining, images were taken using a gel imaging system and images were quantified using BIO-RAD's Quantity One software (Li et al., 2013). And by digitally converting DGGE maps, the species diversity was analyzed. In this study, Shannon-Wiener index (*H'*) (Xu et al., 2011), Simpson index (*D*) (Sun and Liu, 2004) and Pielou index (*J*) (Liu et al., 2013) were used to characterize the species diversity of their communities, which calculated as follows:

$$H' = -\sum_{i=1}^{n} p_i \ln p_i \quad \text{(Eq.1)}$$

$$D = \sum_{i=1}^{n} p_i^2 \quad \text{(Eq.2)}$$

$$J = -\sum_{i=1}^{n} (p_i \ln p_i) / \ln S = H' / \ln S \quad \text{(Eq.3)}$$

where *n* indicates the number of bands detected in each sample, and *S* indicates the sum of the different bands detected by DGGE, indicating the gray level of each band in the sample as a percentage of the total gray scale of the sample.

http://www.aloki.hu ● ISSN 1589 1623 (Print) ● ISSN 1785 0037 (Online)
DOI: http://dx.doi.org/10.15666/aeer/1704_1005910072

Results and discussion

Analysis of the pollution status of the sediments in The North River

Analysis of pollution status of nitrogen element in sediments of The North River

(1) Ammonia nitrogen

As shown in *Figure 2,* the ammonia nitrogen was varied in the range of 0.2 to 0.7 mg/g, and the average value was 0.45 mg/g. In terms of river flow, the content of ammonia nitrogen in each section is Boai Bridge > Chunting Bridge > Jingu Manor > Yuanfeng Bridge > Zhiyuan Bridge, that is, upstream ammonia nitrogen content > middlestream > inlet > export > downstream; in terms of time, ammonia nitrogen content The monthly value has changed slightly but the change has not changed much. It can be seen that the ammonia nitrogen value of river sediment is not affected by seasonal temperature changes (Qin et al., 2014).

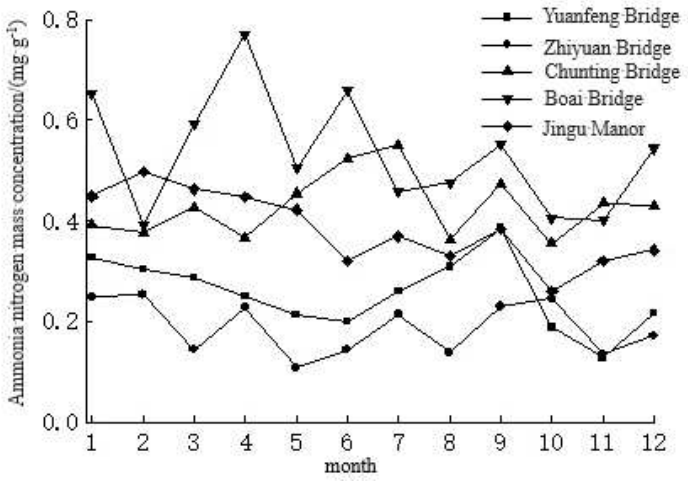

Figure 2. *The change trend of ammonia-nitrogen*

(2) Nitrate nitrogen

As shown in *Figure 3,* the nitrate nitrogen ranged from 0 to 0.06 mg/g with an average of 0.04 mg/g. In terms of river flow, the sediment content of each section is Jinyuan Manor > Boai Bridge > Chunting Bridge > Zheyuan Bridge > Yuanfeng Bridge, which is the inlet nitrate nitrogen content > upstream > middlestream > downstream > export; in terms of time, sediment The content of nitrate nitrogen did not change much, but the Boai Bridge increased slightly in the spring, and the Qiating Bridge increased in summer. The reason for this phenomenon is as follows: (1) The relative error of the measured value is too large due to the low nitrate content of the measured nitrate; (2) The resin adsorption treatment of the sediment sample is not carried out in this experiment, resulting in a high value measured at 220 nm, which causes it to be subjected to Interference with organic matter.

(3) Total nitrogen

As shown in *Figure 4,* the variation range of TN is between 1 and 3.5 mg/g, and the average value is 2.05 mg/g. In terms of river flow, the total nitrogen content of each

http://www.aloki.hu ● ISSN 1589 1623 (Print) ● ISSN 1785 0037 (Online)
DOI: http://dx.doi.org/10.15666/aeer/1704_1005910072

section of the sediment is Boai Bridge > Chunting Bridge > Jingu Manor > Yuanfeng Bridge > Zhiyuan Bridge, its variation law is consistent with the change of ammonia nitrogen content in all sections, that is, upstream ammonia nitrogen content > midstream > inlet > export > downstream; in terms of time, the total nitrogen content of sediment has little fluctuation in each month. It can be seen that the total nitrogen content of the sediment is not affected by seasonal temperature changes.

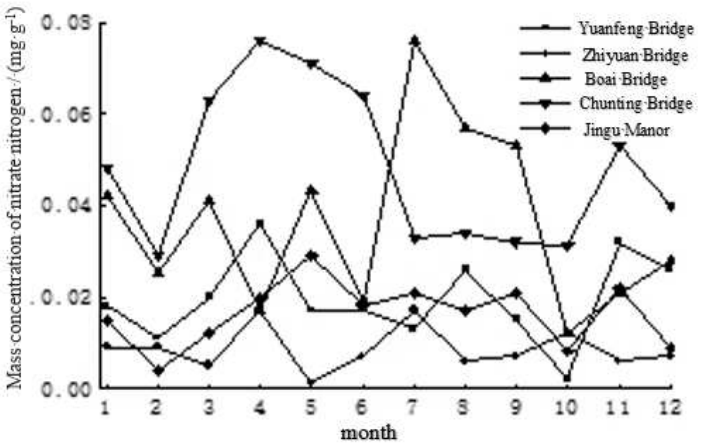

Figure 3. *The change trend of nitrate nitrogen*

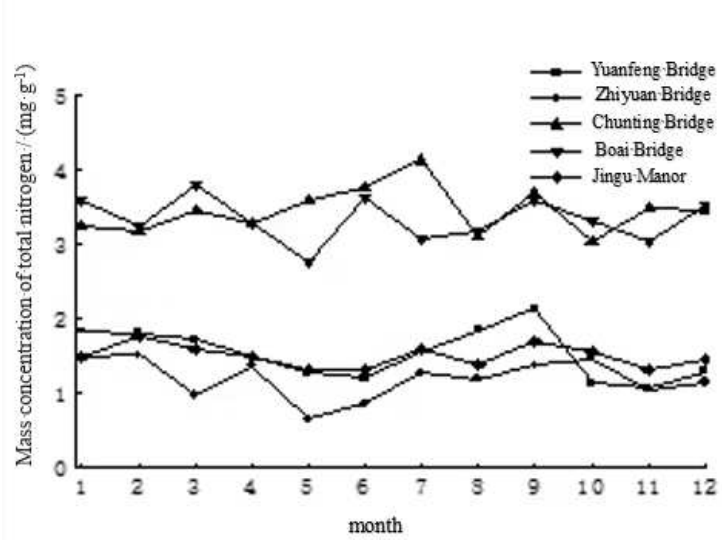

Figure 4. *The change trend of TN*

As Chunting Bridge and Boai Bridge are both in densely populated areas, the river is polluted more seriously, and the nutrient element nitrogen value is higher. In addition, Yuanfeng Bridge and Jinyin Manor are connected to Dongshi River and Guanhe River respectively, so the nutrient nitrogen element the content is affected by Donghe River and Guanhe River; and Zhiyuan Bridge is located in Hongmei Park of Changzhou City. The surrounding trees have a positive impact on the environment, which makes the nitrogen content of nutrient elements low. It can be seen that the nutrient nitrogen

http://www.aloki.hu ● ISSN 1589 1623 (Print) ● ISSN 1785 0037 (Online)
DOI: http://dx.doi.org/10.15666/aeer/1704_1005910072

content of the river bottom mud in Beishi is affected by human activities and the surrounding environment.

Analysis of pollution status of phosphorus in the sediment of The North River

As shown in *Figure 5,* the range of TP was 1 to 2 μg/g, and the average value was 1.35 μg/g. In terms of river flow, the content of TP in each section of the sediment is Boai Bridge > Chunting Bridge > Yuanfeng Bridge > Jingu Manor > Zhiyuan Bridge, which is the upstream TP content > middlestream > export > inlet > downstream; in terms of time, TP content in each month There has been a slight change, but the change is not large. It can be seen that the phosphorus content of the nutrient element in the sediment is not affected by seasonal temperature changes (Zeng et al., 2009).

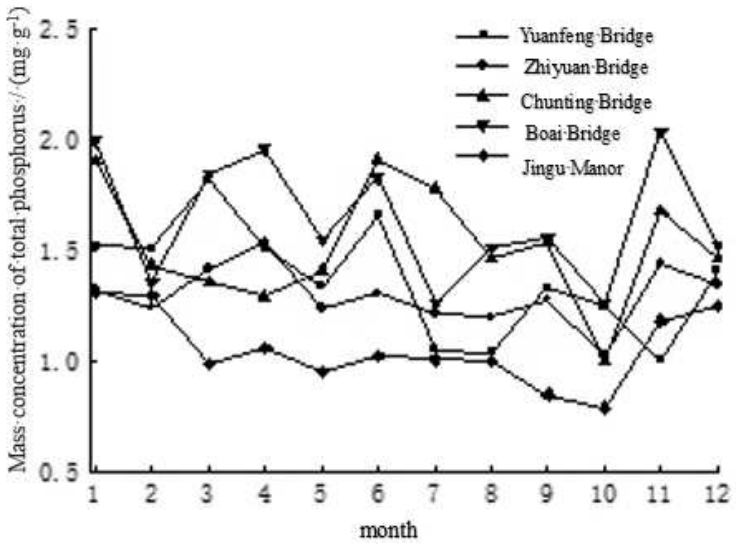

Figure 5. *The change trend of TP*

From the above analysis of pollution conditions, it can be seen that the changes in the contents of N and P in the river bottom mud of Changzhou City are consistent. In terms of time, the content of N and P did not change much in each month, and was basically not affected by seasonal temperature. In terms of river flow, the content of upstream N and P was greater than that of midstream and greater than downstream. The nitrogen and phosphorus in the sediment are mainly derived from the discharge of domestic sewage from nearby residents, landfill leachate, and discharge of restaurant wastewater from nearby restaurants.

The pH value of the sediment varies from 5 to 6.7, which is weakly acidic. The average value of TN is 2.05 mg/g, the average value of TP is 2.05 mg/g, the average value of ammonia nitrogen is 0.45 mg/g, and the average value of nitrate nitrogen is 0.04 mg/g. The river bottom mud has been polluted by N and P, N and P belong to medium pollution level, and the degree of TP pollution is slightly higher than TN. The benthic community has suffered some damage, but it is still within the acceptable range.

The N element in the sediment as a double indicator mainly reflects the pollution degree and nutritional status of the Beishi River, while the P element is one of the important indicators reflecting the pollution degree of the Beihe River. For microbial

http://www.aloki.hu ● ISSN 1589 1623 (Print) ● ISSN 1785 0037 (Online)
DOI: http://dx.doi.org/10.15666/aeer/1704_1005910072

community structure analysis, N and P have a certain correlation with microbial community diversity, but the effect of N element on microbial community is not significant, but P element has great influence on microbial community (Peng et al., 2009).

Extraction of microbial total DNA from sediment samples

The total DNA of the extracted sediment sample, if extracted by the soil DNA extraction kit, is invisible after drying, and the solution after dissolution with TE Buffer is light brown; if using the soil total DNA kit and humic acid It can be clearly seen after drying, and the white particles are clearly visible, and the brown matter is formed on the edge, and the solution dissolved by TE Buffer is colorless and transparent, or light brown.

The DNA extracted by the two methods was subjected to agarose gel electrophoresis. The map of the extract of the soil DNA extract kit was shown in *Figure 6*. The extract of the total DNA kit and the humic acid was as shown in *Figure 7*.

By observing the agarose gel electrophoresis patterns of the two methods, the soil extract kit has a small amount of DNA and more impurities. The total DNA kit combined with humic acid extracts more DNA and less impurities. In order to save costs and improve the accuracy of the experiment, only the extract obtained by the combination of the total DNA kit and the humic acid was used as the experimental material in the subsequent experiments.

Test of DNA concentration and purity

It can be seen from *Tables 1* and *2* that the OD260/OD280 values of the DNA extract of the soil extract kit are all greater than 2.0, indicating that the RNA and impurities contained therein are large, which does not meet the requirements of subsequent experiments. The total DNA purity of the sediment samples extracted from the total DNA kit combined with humic acid is higher and the content is higher. The OD260/OD280 values are less than 2.0 and greater than 1.6, which means that the extracted total DNA can be used as Subsequent PCR amplification experiments.

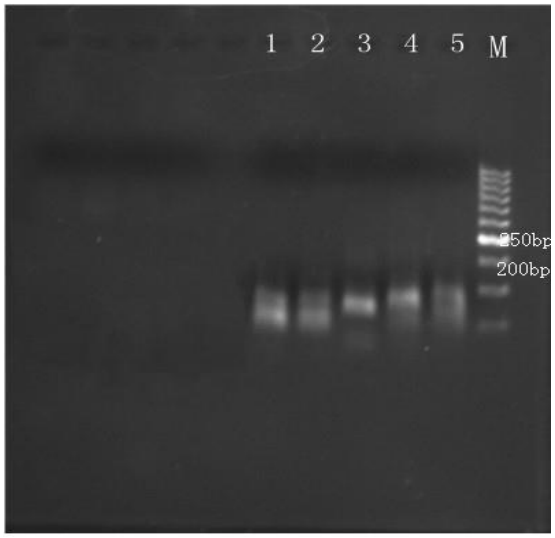

Figure 6. *Electrophoresis pattern of extracts of soil DNA kit by agarose gel*

http://www.aloki.hu ● ISSN 1589 1623 (Print) ● ISSN 1785 0037 (Online)
DOI: http://dx.doi.org/10.15666/aeer/1704_1005910072

Figure 7. *Electrophoresis pattern of extracts of soil total DNA kits and humus acids combined by agarose gel*

Table 1. *Extraction of DNA concentration and purity by soil DNA kit*

DNA sample	**1**	**2**	**3**	**4 5**
Sample size/(g)	0.3	0.3	0.3	0.3 0.3
OD260/OD280	1.64	1.72	1.57	1.62 1.60
OD260/OD230	1.12	1.10	1.13	1.12 1.11
DNA yield/(ng/μL)	57.92	62.97	57.32	58.73 60.02

Table 2. *Extraction of DNA concentration and purity by soil total DNA kits and humus acids combined*

DNA sample	1	2	3	4 5
Sample size/(g)	0.3	0.3	0.3	0.3 0.3
OD260/OD280	2.35	2.08	2.29	2.28 2.25
OD260/OD230	1.07	1.13	1.13	1.40 1.28
DNA yield/(ng/μL)	27.62	29.08	30.22	28.00 29.53

DNA samples 1, 2, 3, 4, and 5 in *Tables 1* and *2* are the DNA extracts of the Beihe River sediment samples from five different locations of Jingu Manor, Boyai Bridge, Qiting Bridge, Zhiyuan Bridge and Yuanfeng Bridge

Agarose gel electrophoresis test of PCR products (qualitative analysis)

After extracting the total DNA of the microbes in the sediment, the agarose gel electrophoresis experiment was carried out, and the DNA content was analyzed qualitatively. Its ultraviolet transmission spectrum is shown in *Figure 8*. This is a PCR amplified DNA agarose gel electrophoresis. Among them, M was the marker (normalruntm100bp-iv DNA Ladder), and 1 to 5 were the electrophoresis bands obtained after the amplification of microbial total DNA at five different sampling points, namely Jingu Manor, Boai Bridge, Chunting Bridge, Zhiyuan Bridge and

http://www.aloki.hu ● ISSN 1589 1623 (Print) ● ISSN 1785 0037 (Online)
DOI: http://dx.doi.org/10.15666/aeer/1704_1005910072

Yuanfeng Bridge. The figure shows that the amplified target band is bright and clear with good specificity, and the amplified product is about 200bp to 250bp.

Figure 8. *Electrophoresis pattern of PCR products by agarose gel*

Denaturing gradient gel electrophoresis (DGGE) experiment of DNA

The DGGE spectra of the sediment samples from five different sections of The North Riiver (Jingu Manor, Boai Bridge, Chunting Bridge, Zhiyuan Bridge and Yuanfeng Bridge) are shown in *Figure 9*. The DGGE map indicates that the strains in the sediments of The North River have a high degree of richness. In addition, the DGGE band spectrum has some differences in the number and position of the bands and the brightness of the bands, indicating that the microbial community composition of different samples is also different.

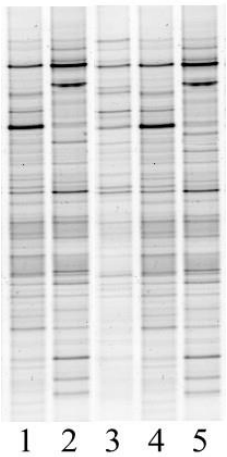

Figure 9. *DGGE map of five samples of North River mud*

BIO-RAD's Quantity One software analyzes DGGE maps, which allow manual and automated quantification of lanes and bands and then output results based on analysis needs. The chart below will be the lane/strip recognition map (*Fig. 10*) and the similarity matrix (*Fig. 11*) analyzed using Quantity One software.

http://www.aloki.hu ● ISSN 1589 1623 (Print) ● ISSN 1785 0037 (Online)
DOI: http://dx.doi.org/10.15666/aeer/1704_1005910072

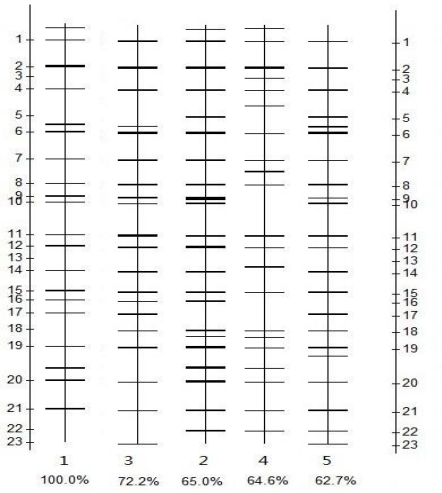

Figure 10. *Lane/strip identification maps of five samples of North River*

The sediment samples of the five different sections of the North River are shown in *Figure 10*. The standard for the lane identification map is C1. Identify the thickness of the lines in the figure, the thick strips indicate that the corresponding density on the DGGE glue is large, and the thin strips indicate that the density is relatively small; in the figure, 23 strips appearing more, 1 and 2 No. 4, No. 6, No. 6, No. 7, No. 8, No. 11, No. 15, No. 15, No. 20 and No. 21 appear in each sample; No. 9, No. 10, No. 14 And the frequency of the band 18 is also very high. The No. 2 strip is thicker in each lane, which means that the microbes represented by this strip are dominant microorganisms in the sediment of the North River.

Using the results of the strip comparison, a matrix of the similarity of each sample can be calculated from the Dyes coefficient Cs, as shown in *Figure 11*: the maximum similarity is 82% (No. 1 and No. 4), and the minimum similarity is 49.6% (4 and 5). By comparing the results of the pairwise comparison, there are 7 groups with similarity exceeding 60%, and the flora structure between them is similar.

Lane	1	2	3	4	5
1	00.0	64.0	66.7	82.0	50.8
2	64.0	100.0	65.0	72.2	64.6
3	66.7	65.0	100.0	65.5	53.2
4	82.0	72.2	65.5	100.0	49.6
5	50.8	64.6	53.2	49.6	100.0

Figure 11. *The similarity matrix of five samples of North River*

The variation of the DGGE band number, the Shannon-Wiener index, the Simpson index and the Pielou index of the five sediment samples of The North River is shown in *Figure 12*. With the increase of DGGE bands, the Shannon-Wiener index and the Pielou index also increased, while the Simpson index decreased accordingly. It can be seen that

http://www.aloki.hu ● ISSN 1589 1623 (Print) ● ISSN 1785 0037 (Online)
DOI: http://dx.doi.org/10.15666/aeer/1704_1005910072

with the increase of bacterial species, population diversity and uniformity increase, correspondingly The advantage is reduced. The maximum value of the Shannon-Wiener index appears in the Chunting Bridge in Section 3, and the minimum appears in the Zhiyuan Bridge in Section 4; the maximum value of the Simpson Index appears in the Chunting Bridge in Section 3, and the minimum appears in the Zhiyuan Bridge in Section 4; the Pielou Index The maximum value appears in the Zhiyuan Bridge in Section No.4, and the minimum value appears in the Chunting Bridge in Section No.3.

From the above analysis, the microbial diversity of the different locations of The North River is rich, with up to 23 bands appearing in a single lane. From the similarity matrix, the similarity of samples at different locations and times is high, the highest similarity is 82%, and the similarity is higher than 60%. Therefore, the North River has a rich microbial population, but its microbial community structure does not change much in space.

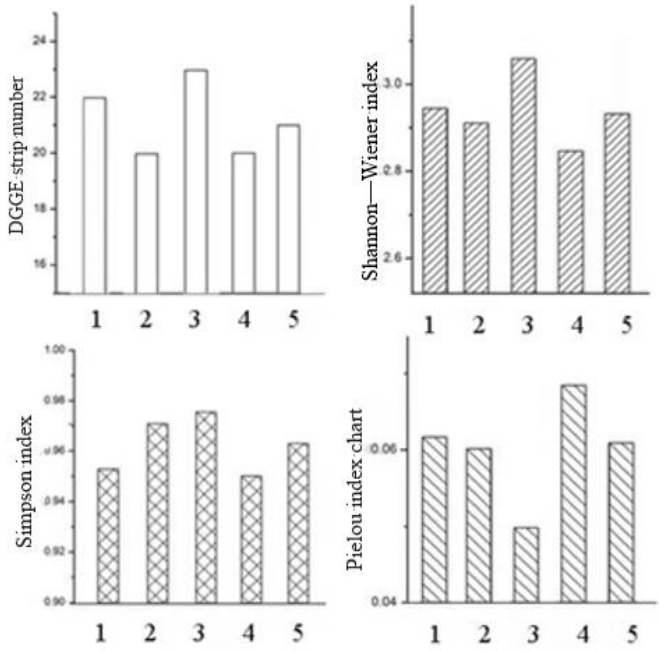

Figure 12. *DGGE number of bands, Shannon-Wiener exponents, Simpson exponents and Pielou exponents*

Conclusion

By comparing two methods of microbial DNA extraction from the sediments of the Beihe River (soil DNA mini-kit method and soil total DNA kit combined with humic acid), the latter can be compared with the former for the sediment samples of the Beihe River. The effect of DNA extraction is good. Although the total DNA purity and content of the sediment sample extracted by the total DNA kit and the humic acid method are high, the purity is still affected by protein, phenol and humus, so it is necessary to extract the total DNA of the environmental sample. Need to pay attention to reduce the pollution of proteins, humus, phenol and other substances.

(2) By analyzing the denaturing gradient gel electrophoresis pattern of the sample DNA, it can be seen that the microbial diversity of different locations in the Beishi River is rich, and at most, 23 bands appear in a single lane. From the similarity matrix,

http://www.aloki.hu ● ISSN 1589 1623 (Print) ● ISSN 1785 0037 (Online)
DOI: http://dx.doi.org/10.15666/aeer/1704_1005910072

the similarity of samples at different locations and times is high, the highest similarity is 82%, and the similarity is higher than 60%. Therefore, the micro-population of the Beishi River is abundant, but its microbial community structure does not change much in space.

(3) Based on the analysis and research on the microbial community structure diversity of Beizhou River in Changzhou, it will provide corresponding help for optimizing community structure, regulating community function and discovering new important microbial functional groups, and then cultivate specific dominant functional groups. Future studies concerning the treatment of polluted rivers by microorganisms and related research on water body repair in desperately needed.

Acknowledgements. This study was supported by National Science and Technology Support Program Project (No.2015BAC02B02-01), Changzhou Science and Technology Support Program (Social Development) (CE20175060).

REFERENCES

[1] Amann, R. I., Ludwig, W., Schleifer, K. H. (1995): Phylogenetic identification and in situ detection of individual microbial cells without cultivation. – Microbiological Reviews 59: 143-169.

[2] Bai, Q. (1997): Chemical valuation method of soil microbial community structure. – Agro-Environmental Protection 16(6): 252-256.

[3] Gu, Y., Li, M., Chen, S. (2013): Research progress on urban river eco-logical restoration technology. – Environmental Science and Management 38(4): 25-29.

[4] Handelsman, J. (2004): Metagenomics: application of genomics to uncultured microorganisms. – Microbiology and Molecular Biology Reviews (MMBR) 68(4): 669-685.

[5] Hill, J. E., Seipp, R. P., Betts, M., Hawkins, L., Kessel, A. G. V., Crosby, W. L. et al. (2002): Extensive profiling of a complex microbial community by high-throughput sequencing. – Applied and Environmental Microbiology 68(6): 3055-3066.

[6] Hoefel, D., Monis, P. T., Grooby, W. L., Andrews, S., Saint, C. P. (2005): Profiling bacterial survival through a water treatment process and subsequent distribution system. – Journal of Applied Microbiology 99(1): 175-186.

[7] Hu, H., He, M., Zhu, M. (2005): Water purification and ecological restoration technology for polluted rivers and its integration strategy. – Water Supply & Drainage 31: 1-9.

[8] Ibekwe, A. M., Kennedy, A. C. (1998): Phospholipid fatty acid profiles and carbon utilization patterns for analysis of microbial community structure under field and greenhouse conditions. – FEMS Microbiology Ecology 26(2): 151-163.

[9] Li, Y. H., Xu, Q. G., Zhao, Y., Li, Q., Wei, Z. M., Zhao, X. Y. (2013): Bacterial community structure in different spatial distribution of Songhua Lake. – Journal of Agro-Environment Science 32(4): 764-770.

[10] Liu, Y. J., Liang, Y. T., Qin, W., Xiao, X., Zhao, Y. (2013): An analysis of Beishi River's environmental status and dominant factors. – Journal of Changzhou University 25(2): 24-29.

[11] Muyzer, G., de Waal, E. C., Uitterlinden, A. G. (1993): Profiling of complex microbial populations by denaturing gradient gel electrophoresis analysis of polymerase chain reaction-amplified genes coding for 16S rRNA. – Applied and Environmental Microbiology 59(3): 695-700.

[12] Pace, N. R. (1997): A molecular view of microbial diversity and the biosphere. – Science 276: 734-740.

http://www.aloki.hu ● ISSN 1589 1623 (Print) ● ISSN 1785 0037 (Online)
DOI: http://dx.doi.org/10.15666/aeer/1704_1005910072

[13] Peng, D., Liu, L., Hu, J. (2009): Vertical distribution and bio-availability of various forms of phosphorus in the sediments of Xuanwu Lake. – Water Resources Protection 25(1): 31-35.
[14] Qin, W., Liu, Y., Zhao, Y. (2014): Evaluation of N and P in sediments of The North River and their effects on microbial population. – Journal of Changzhou University 26(1): 74-79.
[15] Röttgers, R. (2007): Comparison of different variable chlorophyll a fluorescence techniques to determine photosynthetic parameters of natural phytoplankton. – Deep-Sea Research Part I: Oceanographic Research Papers. DOI: 10.1016/j.dsr.2006.12.007.
[16] Sun, D. (2015): Advances in research on urban river ecological health assessment and environmental pollution remediation technology. – Environmental Protection and Circular Economy 1: 49-51.
[17] Sun, J., Liu, D. (2004): The application of diversity indices in marine phytoplankton studies. – Acta Oceanologica Sinica 26(1): 62-75.
[18] Torsvik, V., Goksoyr, J., Daae, F. L. (1990): High diversity in DNA of soil bacteria. – Applied and Environmental Microbiology 56: 782-787.
[19] Tunlid, A. (2007): Molecular biology: a linkage between microbial ecology, general ecology and organismal biology. – Oikos 1999(85): 177-189.
[20] Victorio, L., Gilbride, K. A., Allen, D. G., Liss, S. N. (1996): Phenotypic fingerprinting of microbial communities in wastewater treatment systems. – Water Research 30(5): 1077-1086.
[21] Xu, Q., Zhang, F., Xu, Z. (2011): Some characteristics of Simpson index and the Shannon-Wiener index and their dilution effect. – Pratacultural Science 28(4): 527-531.
[22] Yan, S., Wang, X. (1999): Preliminary study on the roles and applied ways of urban river in urban ecological construction. – Urban Environment & Urban Ecology 12(6): 36-38.
[23] Yu, J., Feng, X., Xie, Y. H., Liu, S. C. (2010): PCR-DGGE and its application in the research of environmental microbiology. – Journal of Northwest A & F University (Natural Science Edition) 38(6): 227-234.
[24] Zeng, J., Yang, L., Li, J., Liang, Y., Xiao, L., Jiang, L., Zhao, D. (2009): Vertical distribution of bacterial community structure in the sediments of two eutrophic lakes revealed by denaturing gradient gel electrophoresis (DGGE) and multivariate analysis techniques. – World Journal of Microbiology and Biotechnology 25(2): 225-233.
[25] Zhang, Z. N., Wu, X. F., Chen, Y. H. (2009): Application in research on microbial diversity of environment by DGGE technique. – Biotechnology Bulletin 12: 48-52.
[26] Zhao, Y. W., Cai, M. Y., Qian, B., Wang, D. S. (1986): A preliminary study on microbial ecology of the river in city. – Acta Microbiologica Sinica 26(3): 200-205.
[27] Zhu, L., Zhang, L., Wang, H. (2011): Comparative study of DNA extraction methods of microorganisms in river sediment. – Chinese Journal of Environmental Engineering 5(4): 935-938.

http://www.aloki.hu ● ISSN 1589 1623 (Print) ● ISSN 1785 0037 (Online)
DOI: http://dx.doi.org/10.15666/aeer/1704_1005910072

EFFECT OF IRRIGATION INTERVALS, BIOTIC AND ABIOTIC TREATMENTS ON WATER USE EFFICIENCY AND POTATOS YIELD IN SULAIMANI – IRAQI KURDISTAN REGION

KARIM, L. G.[1*] – MAHOOD, N. A.[2] – ALLAWI, M. M.[3]

[1]*Horticulture Department, College of Agricultural Sciences, University of Sulaimani Sulaimani-Kurdistan Region, Iraq*

[2]*Protected Agricultural Department, Bakrajo Technical Agriculture Institute, Sulaimani, Iraq*

[3]*Horticulture Department, College of Sciences Agricultural Engineering University of Baghdad, Iraq*

[*]*Corresponding author*
e-mail: luqman.karim@univsul.edu.iq; phone:+96-477-0143-4161

(Received 10th Apr 2019; accepted 19th Jun 2019)

Abstract. This study was carried out in two growing spring seasons 2017 and 2018 at Kanipanka Agricultural Research Station (Lat. 35°13'12", Long. 45°25'48", 550 MASL) in Shahrazoor valley 35 km east of Sulaimani – Iraqi Kurdistan Region to investigate the effect of two irrigation intervals (5 and 10 days) and thirteen different biotic and abiotic treatments on potatoes yield water use efficiency under the field condition. The results showed that the cumulative depth of irrigation in 2017 and 2018 for 5 and 10 days were 369, 228 and 363, 287 mm, respectively, while for both depth of irrigation and precipitation were 535, 394 and 513,437 mm, respectively. The effect of irrigation intervals on the WUE, IWUE and total yield (tons hectare^{-1}) was significant at 2017 and 2018 season and the average of both seasons, with exception of WUE in the first season. The 5 days irrigation intervals gave the highest values for the second season and the average of both seasons for the character WUE, while 10 days irrigation intervals gave the highest values in both seasons and their average. Regarding the first season and the average of both seasons, the mycorrhizal inoculation treatments gave the highest values of WUE, IWUE and total yield but at the second season, the KCl with *Glycyrrhiza glabra* (6 g L^{-1}) extract treatments gave the highest values for WUE, IWUE and total yield.
Keywords: *Solanum tuberosum, water management, mycorrhizae, KCl application, licorice extract*

Introduction

Potato (*Solanum tuberosum*), which belong Solanaceae family, is the fourth most agronomical important feed crops worldwide after winter wheat, maize, and rice. It is a global crop that is well-adapted wider range of altitude, latitude, and climatic conditions. Potato is a productive and exhaustive crop at the same time, requiring a variety of balanced plant nutrients for growth and development. The total world production of potatoes was 388 million tons in 2017 from this China have 25% of total production around the world with 99 million tons followed by India, Russia, Ukraine, and the United States with 48, 29, 22 and 20 million tons, respectively (FAOSTAT, 2019). Over two-thirds of the global potato production is consumed directly by humans, and the rest is used as animal feeds and starch production (FAOSTAT, 2019). The licorice roots (*Glycyrrhiza glabra*) extracted contain some compounds, which have similar effect to the growth promoters, and also have a wide range of minerals (phosphorus, potassium, zinc, magnesium, iron, calcium), amino acids (alanine, lysine, arginine), vitamins (B_1, B_2, B_6), with carbohydrate and nitrogen. In addition, it also

http://www.aloki.hu ● ISSN 1589 1623 (Print) ● ISSN 1785 0037 (Online)
DOI: http://dx.doi.org/10.15666/aeer/1704_1007310090

contains mevalonic acid that can be used in gibberellins synthesis (Sarby *et al.*, 2009). Potassium (K) foliar application is another factor that has been used for improved nutrient management and increasing potato growth and yield (Grewal *et al.*, 1992). Generally, Potassium is one of the vital elements that affect most of the biochemical and physiological processes. The physiological and molecular mechanisms of K function in plant stress resistance are studied by (Wang *et al.*, 2013). These researchers also demonstrated that adequate K nutritional status in the plants living under drought conditions has significant effect on root growth, leaf area, and increased cell membrane stability with total dry mass. In addition, role of potassium may facilitate osmotic adjustment, which is improved uptake of water via roots and minimize water loss during drought periods (regulates transpiratory water), consequently improving the ability of plants to tolerate drought stress (Egilla *et al.*, 2005). Furthermore, it has also a critical role for justifying ROS (reactive oxygen species) damage as induced by drought stress because ROS are significantly accumulated under a biotic stress conditions, which cause oxidative damage and eventually resulting in cell death (Wang *et al.*, 2013).

Microorganisms are vital component of the agricultural system. Arbuscular mycorrhizal (AM) fungi, a global soil microbe, can subordinate with the roots of most terrestrial crop species (Duc, 2017). Several benefits were observed when AM is colonized crops including; increased growth and yield, enhanced plant resistance to environmental adversities, improve plant tolerance to a biotic stress (Birhane *et al.*, 2012) Recently, researcher confirmed that improve stress tolerance of the host plants can be done by several AM-induced mechanisms of host tolerance to a biotic stresses, such as more effective anti-oxidative systems, defense enzymes; modifications in host physiology, e.g. osmotic adjustment, gas exchange, photosynthesis; remarkable alterations of sugars, proline, polyamines, stress phytohormones, expression patterns of stress-responsive genes (Latef and Miransari, 2014). AMF can produce glycoprotein glomalin, which is act similar a glue, binding carbon, nitrogen and other biological components of soil to the mineral components, clay and sand, that has an important role for increased soil organic matter, and consequently collected highly water stability (Duc, 2017). In addition, under drought condition, direct water uptake from soil into the host plant can improved by interlacing external hyphae of mycorrhizae, thus, it is believed that has resistance to drought condition by many mechanisms including; osmotic adjustment and altering display of stomatal conductance (Wu *et al.*, 2006).

Shock *et al.* (1992) studied that potato could be tolerating water deficit before tuber set without reduction in tuber quality under some water stress conditions. Potato may be quite sensitive to drought (Van Loon, 1981) as it needs frequently irrigations for suitable growth and optimum yield (Yuan *et al.*, 2003; Kiziloglu *et al.*, 2006). Hassan *et al.* (2002) found that the Stalinization and Tuberization stages were more sensitive than bulking and tuber enlargement stages. Thornton (2002) and Shock (2004) found that all growing stages of potato, especially tuber formation stage, are very sensitive to water deficit stress.

Irrigation scheduling is a means of supplying water according to crop needs. It is the process of determining when to irrigate and how much water to apply, as for factors which influencing irrigation scheduling which are soil characteristics, climatic factors, crop characters and management factors that are to be supposed in determining irrigation schedules (Reddy, 2007). Beder (2010) proposed that to appropriate irrigation scheduling can, it be conserved and maintained that avoid plant water stress.

http://www.aloki.hu ● ISSN 1589 1623 (Print) ● ISSN 1785 0037 (Online)
DOI: http://dx.doi.org/10.15666/aeer/1704_1007310090

To achieve this objective specific and fine data of soil, plant and climatic parameters could be gathered and analyzed at specific field conditions. Ati *et al.* (2010) found that the water consumption of potato were 441 mm, 429 mm for the agricultural season 2008 and 2009, respectively. Results showed by Ati and Nafaou (2012) indicated that highest potato production was achieved when the treatment depletion 50% of available water (30.26 ton ha^{-1}) compared to the treatment depletion 75% of available water (25.66 ton ha^{-1}). Ati *et al.* (2013) study the effect of different irrigation treatment (deficit irrigation) and potassium humate fertilizer on yield, the content of nitrogen, potassium, and phosphor in tuber of potato and water use efficiency in the Abu-Ghraib Region, Iraq. Potato was grown under drip irrigation with three treatments: irrigation applied when evaporation 75%, 100% and 125% from pan A, and three potassium humate fertilizers: 0, 1.2 and 2.4 kg ha^{-1} with three times additions. The seasonal potato evapotranspiration ranged from 267 mm to 372 mm. The drip irrigation treatments significantly affected tuber yield of potato and recorded 29.530, 27.630 and 24.880 kg ha^{-1} for 125%, 100% and 75% from pan A evapotranspiration, respectively. Humus fertilizers addition has the lowest value of ETa 309 mm and maximum value of yield 29300 kg ha^{-1}.

Water use efficiency (WUE) defined as the tuber yield obtained per unit of water consumed as ETa or water used in cubic meter by the potato (Doorenbos and Pruitt, 1977). Rashidi and Gholami (2008) illustrated that WUE of potato in Iran ranged from 1.92 to 5.25 kg m^{-3}. They added that few numbers of irrigation could reduce compactness of the soil. Nagaz *et al.* (2007) found that WUE varied around 8-14 kg m^{-3} for planted potato. Wright and Stark (1990) reported that the WUE for maximum yield range from approximately 0.05 to 0.1 kg ha m^{-3}. Kirda (2002) stated that the main objective of deficit irrigation is to increase the WUE of a crop by eliminating irrigation that have little impact on yield. The objective of this study was to determine the effects of irrigation intervals and different treatments biotechnologies on yield of potato (Actrice variety) and water use efficiency in Iraq -Kurdistan region.

Material and Method

This study carried out in two spring growing seasons in 2017 and 2018 at Kanipanka Agricultural Research Station (Lat. 35°13'12", Long. 45°25'48", 550 MASL) in Shahrazoor valley 35 km east of Sulaimani – Iraqi Kurdistan Region. GIS software was used to create the study sites shown in *Fig. 1*. Generally, elevation of this region ranges between 5-2368 m above sea levels. The climate of study area is generally characterised by worm, dry summer and cold winters (Najmaddin *et al.*, 2017).The meteorological data of Kanipanka during both growing seasons is shown in *Table 1* as well as some physical and chemical properties of Kanipanka soil shown in *Table 2*.

Bio Inoculation

The fungal inoculants *Glomus mosseae* was obtained from Al-Zaefaraniya Agricultural Research Station - Ministry of Science and Technology – Baghdad. The inoculants were consisting of mycorrhizal spore with 47 spore g^{-1} dry soil and the residual of the infected roots. Potato tubers were inoculated with the mycorrhizal spores by using 20 g from the mixture of the inoculums and the pet moss inside the pores which specified for inoculation treatment before planting the tubers where the pad method was used to ensure the infection by touching the inoculums during planting.

http://www.aloki.hu ● ISSN 1589 1623 (Print) ● ISSN 1785 0037 (Online)
DOI: http://dx.doi.org/10.15666/aeer/1704_1007310090

Preparation of Glycyrriza glabra Extraction

Three and Six gram of *Glycyrriza glabra* roots powder was soaked separately in one litter hot distilled water at 50°C for 24 hours in dark colure bottles with shaking continuously, then the solution filtered through several layers of Tapestry cloth, to obtained two concentrations of the extraction 3 and 6 g L^{-1} and several drop of Twin20 were added as a spread materials to reduce the surface tension. The plants were sprayed two times 45 and 60 days after planting date, after the sun seat in both years 2017 and 2018 (Lazim and Sulaiman, 2012).

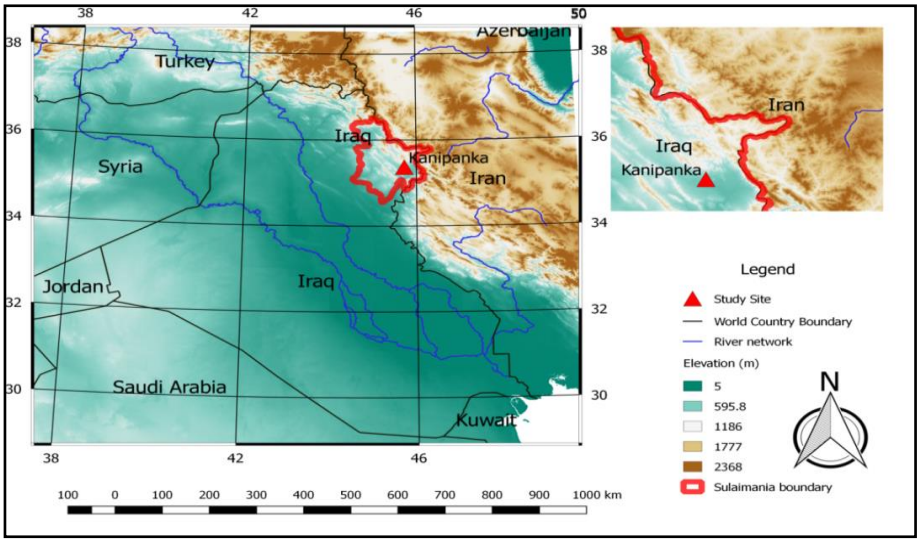

Figure 1. *Regional and local location of the study site*

Table 1. *Meteorological data of Kanipanka location during both growing seasons (2017 and 2018)*

Months	Air Temp. (°C)			Humidity (%)			Pre. (mm)	Pan Eva. (mm)	Soil Temp. (°C)
	Avg.	Max.	Min.	Avg.	Max.	Min.			
Season 2017									
March	12.2	23.0	4.0	49.7	84.0	22.0	107.1	70.2	12.0
April	17.4	31.1	7.0	42.0	79.0	17.0	39.6	119.9	17.6
May	24.6	39.3	12.2	30.3	75.0	16.0	19.3	164.4	23.9
June	30.4	45.7	15.2	21.4	32.0	14.0	0.0	216.0	29.4
Season 2018									
March	14.7	30.0	2.5	42.3	78.0	18.0	15.5	98.7	11.7
April	17.1	29.7	6.2	38.4	80.0	17.0	82.7	110.5	17.4
May	22.2	37.8	10.0	36.1	84.0	17.0	51.8	135.1	20.6
June	30.3	45.5	17.0	21.7	30.0	13.3	0.0	211.3	27.1

Preparation of Potassium Fertilizer (KCl)

Two half five gram of potassium chloride (KCl) was dissolved in one liter hot distilled water at 40°C with shaking the potassium completely dissolved and several drop of Twin20 were added as a spread material to reduce the surface tension. The plants were sprayed at the morning trice 40, 55 and 70 days after planting in both years 2017 and 2018.

http://www.aloki.hu ● ISSN 1589 1623 (Print) ● ISSN 1785 0037 (Online)
DOI: http://dx.doi.org/10.15666/aeer/1704_1007310090

Table 2. *Some physical and chemical properties of Kanipanka soil*

Soil components	Quantities	Unit
Sand	308.0	g kg^{-1}
Silt	340.0	g kg^{-1}
Clay	352.0	g kg^{-1}
Textured Class	Clay loam	
pH	7.10	
EC	0.38	dS m^{-1}
Field Capacity	290.0	g kg^{-1}
Wilting point	180.0	g kg^{-1}
Organic Matter	8.5	g kg^{-1}
Available Nitrogen	32.0	g kg^{-1}
Available Phosphate	8.0	g kg^{-1}
Available Potassium	73.11	g kg^{-1}
Carbonate Minerals	201.2	g kg^{-1}
Bulk density	1.32	g cm^{-3}
CEC	33.0	$cmol_c$ kg^{-1}
Calcium (Ca++)	2.29	meq L^{-1}
Magnesium (Mg++)	2.53	meq L^{-1}
Potassium (K+)	0.93	meq L^{-1}
Sodium (Na+)	2.10	meq L^{-1}
Carbonate (CO3=)	Nil	meq L^{-1}
Bicarbonate (HCO3-)	0.90	meq L^{-1}
Chloride (Cl-)	2.49	meq L^{-1}
Sulphate (SO4=)	2.16	meq L^{-1}

Table 3. *The experimental factors used in the study*

No.	Factors	Levels	Descriptions
First	Irrigation Intervals	I_5	5 days
		I_{10}	10 days
Second	Treatments	T_1	Control (Spray with distilled water).
		T_2	Di-Ammonium Phosphate (DAP).
		T_3	Mycorrhizal Inoculation.
		T_4	Spraying with (2.5g L^{-1}) KCl.
		T_5	Spraying with (3g L^{-1}) *Glycyrrhiza glabra* extract.
		T_6	Spraying with (6g L^{-1}) *Glycyrrhiza glabra* extract.
		T_7	Mycorrhizal Inoculation + Spraying with (2.5g L^{-1}) KCl.
		T_8	Mycorrhizal Inoculation + Spraying with (3g L^{-1}) *Glycyrrhiza glabra* extract.
		T_9	Mycorrhizal Inoculation + Spraying with (6g L^{-1}) *Glycyrrhiza glabra* extract.
		T_{10}	Spraying with (2.5g L^{-1}) KCl + Spraying with (3g L^{-1}) *Glycyrrhiza glabra* extract.
		T_{11}	Spraying with (2.5g L^{-1}) KCl + Spraying with (6g L^{-1}) *Glycyrrhiza glabra* extract.
		T_{12}	Mycorrhizal Inoculation + Spraying with (2.5g L^{-1}) KCl + Spraying with (3g L^{-1}) *Glycyrrhiza glabra* extract.
		T_{13}	Mycorrhizal Inoculation + Spraying with (2.5g L^{-1}) KCl + Spraying with (6g L^{-1}) *Glycyrrhiza glabra* extract.

http://www.aloki.hu ● ISSN 1589 1623 (Print) ● ISSN 1785 0037 (Online)
DOI: http://dx.doi.org/10.15666/aeer/1704_1007310090

Addition of Chemical Fertilizer

Six hundred kilograms per hectare of Di-Ammonium Phosphate (DAP) 18:18:0 fertilizer was added in two times, first during the cultivation of the tubers (spares on the furrows), the second addition was after one month from the first addition as recommended for the chemical fertilizer treatment only, (Esho *et al.*, 2009) while half of the recommended were added for the rest of the treatments.

Field Practices

Each experimental unit (furrow) was 3 m long and 0.8 m apart (2.4 m^2), each furrows consists of 12 plants in one side. Planting dates were 10 March 2017 and 5 March 2018 at the first and the second season respectively, while the harvesting were accomplished after 100 days on 20 June 2017 and 15 June 2018 at the first and the second season respectively. The furrows within the blocks were divided into 4 groups, each group consists of 4 furrows, the last one was one furrow, and each groups were conducted with a 10 cm diameter plastic pipes to feeding them with water from the main stream in order to calculate the timing for watering from the main stream to the furrows. The timing was calculate until the water reached the standardized line in each furrow in order to measure the quantity of water that entered the furrow through the plastic pipes in each irrigation intervals 5 and 10 days. The average volume of water and its operation time was calculated to estimate the discharge of sub main irrigation pipe:

$$Q\ t = A\ d \qquad \text{(Eq.1)}$$

where:

- Q: discharge of sub main (L/sec).
- t: operation time (sec).
- A: area of furrow (2.4 m^2).
- d: depth of irrigation water (mm).

Level furrows were created between rows to ensure uniform water distribution in plots irrigated by furrows. Furrows were closed at the end to prevent runoff and a square meter was used to measure the amounts of applied water. Since the Actual Evapotranspiration (ETa) was calculated using the soil water balance method:

$$ET_a = P + I - D \pm \Delta W \qquad \text{(Eq.2)}$$

where:

- ET_a: actual evapotranspiration (mm).
- P: is the rainfall (mm).
- I: is the irrigation applied to individual plots (mm).
- D: is the deep percolation.
- ΔW: is the change in water storage of the soil profile (mm).

Water use efficiency (WUE) and irrigation water use efficiency (IWUE) were calculated from the following equations (Kirda, 2002) and (Howell *et al.,* 1990):

$$WUE = \frac{Yield\ (kg)}{ETa\ (m^3)} \qquad \text{(Eq.3)}$$

http://www.aloki.hu ● ISSN 1589 1623 (Print) ● ISSN 1785 0037 (Online)
DOI: http://dx.doi.org/10.15666/aeer/1704_1007310090

$$IWUE = \frac{Yied\ (kg)}{Total\ water\ applied\ (m^3)} \quad \text{(Eq.4)}$$

Statistical Analysis

A factorial experiment was conducted in split-plot design with three replicates; the first factor (Irrigation intervals) were implemented in the main plots and conducted with Randomized Complete Block Design (RCBD), while the second factor (Treatments) were implemented in the sub plots. All possible comparisons among the means were carried out by using Least Significant Difference (L.S.D) test at a significant level of 5% after they show their significance in the general test (Al-Rawi and Khalafallah, 1980).

Results

Water is one of the most essential elements in growing plants, which constitutes more than 80% of the active cells. Thereby, the amount of applied water during crop irrigation, added time, irrigation methods, quality of added water, and prevailing micro-meteorological conditions have found to play limited roles in yield quality and quantity. In Asia, statistics showed that the yields for most crops have increased 100–400% after irrigation. Irrigation allows farmers to use water in the most efficient way and at the crucial times for the crop instead of being subject to the shortage of rainfall. Water becomes scarce, expensive, and necessitates to be utilized in a scientific manner.

In the first season of irrigation intervals 5 and 10 days were applied after 50 days from sowing and were ended at 96 days after sowing, since, the amount of irrigation water for 5 days interval was cover the most of depleted water at this time. The cumulative depth of irrigation for 5 and 10 days from 1 May 2017 to 15 June 2017 were practically measured and formed to be 369 and 228 mm, respectively. Since the numbers of irrigation were 10 and 6 times for 5 and 10 days of irrigation intervals respectively as shown in *Fig. 2*. While the amount of actual evapotranspiration for 2017 and 2018 were 529, 423, 515 and 440 mm, respectively (*Table 4* by applied *Equation 2*), while cumulate depth of irrigation and precipitation were 535 and 394 mm respectively as shown in *Fig. 3.*

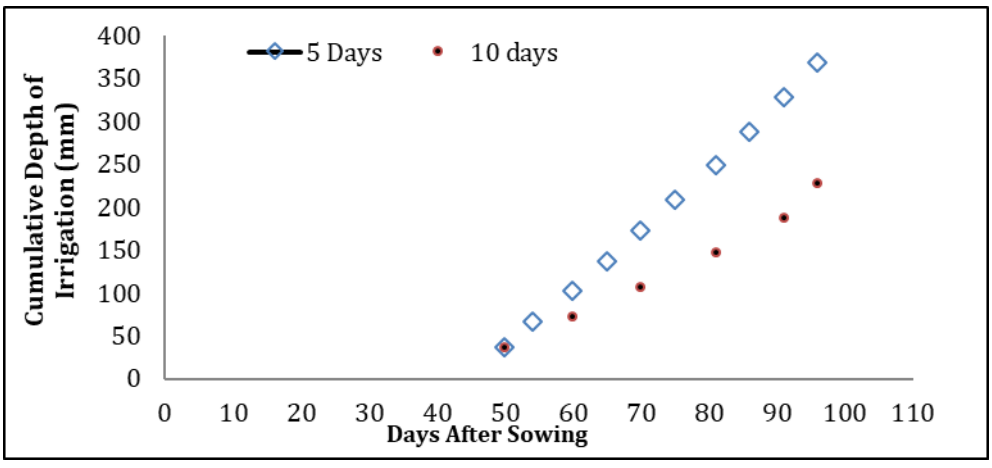

Figure 2. *Cumulative depth of irrigation (mm) for 5 and 10 days of irrigation intervals in 2017*

http://www.aloki.hu ● ISSN 1589 1623 (Print) ● ISSN 1785 0037 (Online)
DOI: http://dx.doi.org/10.15666/aeer/1704_1007310090

Table 4. *Actual evapotranspiration (ETa) for 5 and 10 days in 2017 and 2018*

Component	Season 2017		Season 2018	
	I_5	I_{10}	I_5	I_{10}
Rainfall (P) (mm)	166	166	150	150
Irrigation (I) (mm)	369	228	363	287
Deep percolation (D) (mm)	36	16	34	20
ΔW (mm)	30	45	36	23
Eta (mm)	529	423	515	440

$$\text{Eta } (m^3) \text{ for } (I_5 - 2017) = 1.104 + 0.384 = 1.488\ m^3$$
$$\text{Eta } (m^3) \text{ for } (I_{10} - 2017) = 0.680 + 0.468 = 1.148\ m^3$$
$$\text{Eta } (m^3) \text{ for } (I_5 - 2018) = 1.089 + 0.364 = 1.453\ m^3$$
$$\text{Eta } (m^3) \text{ for } (I_{10} - 2018) = 0.681 + 0.367 = 1.228\ m^3$$

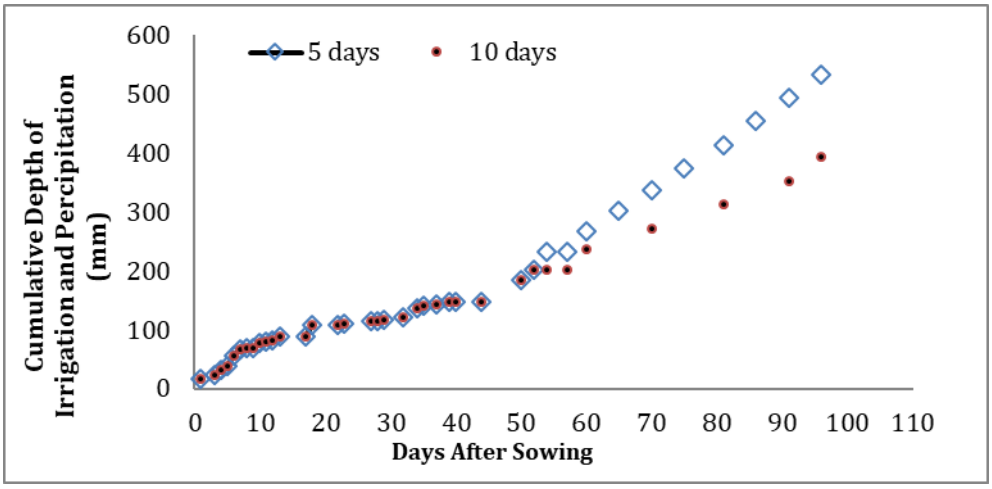

Figure 3. *Cumulative depth of irrigation and precipitation (mm) for 5 and 10 days of irrigation intervals in 2017*

In the season 2018 the irrigation intervals 5 and 10 days was applied from the sowing date and were ended at 95 days after sowing, the amount of irrigation water for 5 days interval which cover the most of depleted from 5 March 2018 to 10 June 2018 were practically measured 363 and 287 mm, respectively. Since the numbers of irrigation were 9 and 5 times for 5 and 10 days of irrigation intervals respectively as shown in *Fig. 4*. While accumulate depth irrigation and precipitation were 513 and 437 mm, respectively as shown in *Fig. 5.* These results are in agreement with the findings of several other researches (Ati *et al.*, 2012; Ati and Nafaou, 2012). Gander and Tanner (1976) showed that mild water stress of -3 to -5 bars greatly reduce leaf expansion in potatoes, and for best tuber yields, a 120-150 day potato crop requires 508-698.5 mm of the water.

The data in *Table 5* and *Appendix 1 and 2* show the effect of the irrigation intervals on the studied characters, significant differences were observed among all of the studied characters at the first, second and average of both seasons with exception of WUE in the first season this may be due to that rain fed in this season distributed throughout the growing season in the way that the deficit does not cause any reduction in the yield. The 5 days irrigation intervals achieved the highest values of WUE and in the second and average of both seasons with 7.085 and 6.802 kg m^{-3}, respectively, while the 10 days irrigation intervals achieved lowest

http://www.aloki.hu ● ISSN 1589 1623 (Print) ● ISSN 1785 0037 (Online)
DOI: http://dx.doi.org/10.15666/aeer/1704_1007310090

values with 6.144 and 6.439 kg m^{-3}, respectively. This agrees with the finding of Nagaz *et al.* (2007), which concluded that WUE varied around 8-9, 6-8 and 11-14 kg m^{-3} for autumn and spring planted potato, respectively in Southern Tunisia. Rashidi and Gholami (2008) reported that WUE of potato in Iran ranged from 1.92 to 5.25 kg m^{-3}. Erdem *et al.* (2006) reported that potatoes plant was grown under furrow and drip irrigation methods and three regimens irrigation applied when 30, 50, and 70% of the available water was consumed, water use efficiency values increased from 4.70 to 6.63 kg m^{-3} for furrow-irrigated treatments, and from 5.19 to 9.47 kg m^{-3} for drip-irrigated treatments.

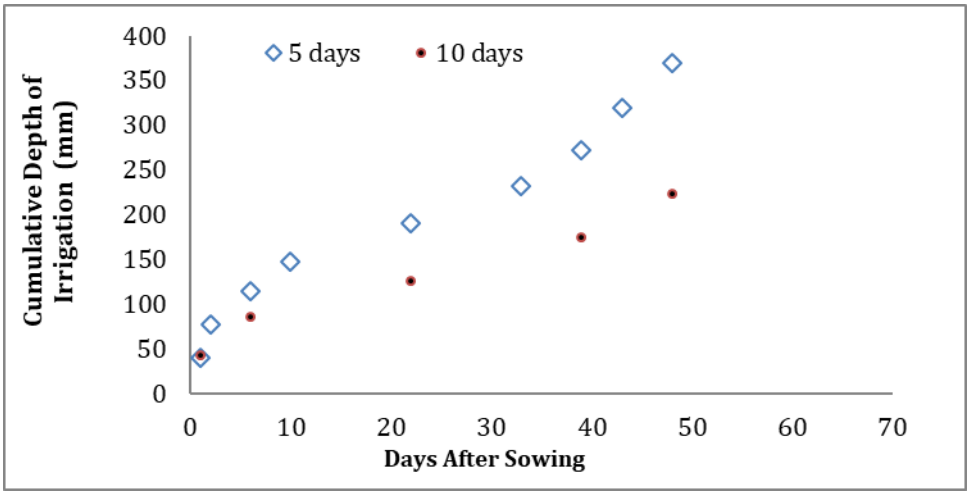

Figure 4. *Cumulative depth of irrigation (mm) for 5 and 10 days irrigation intervals in 2018*

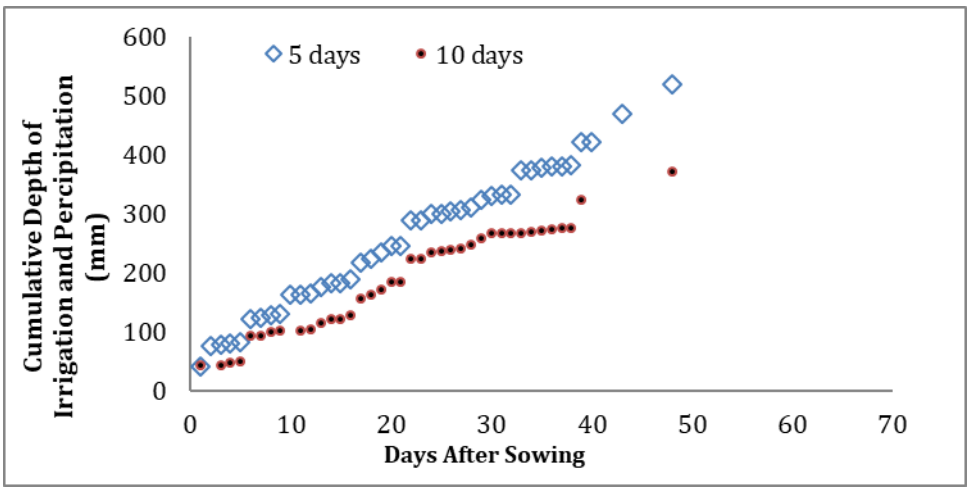

Figure 5. *Cumulative depth of irrigation and precipitation (mm) for 5 and 10 days irrigation intervals in 2018*

Concerning the IWUE in the first, second and average of both seasons the 10 days irrigation intervals gave the maximum values with 11.352, 11.281 and 11.316 kg m^{-3} respectively, while the 5 days irrigation intervals gave the lowest values with 8.788, 9.293 and 9.041kg m^{-3} respectively. Total yield gave the maximum values in the use of the 5 days

http://www.aloki.hu ● ISSN 1589 1623 (Print) ● ISSN 1785 0037 (Online)
DOI: http://dx.doi.org/10.15666/aeer/1704_1007310090

irrigation intervals at the first, second and the average of both seasons with 40.418, 42.886, and 41.652 tons hectare^{-1} respectively and overcome the yields of the 10 days intervals which gave 32.205, 31.431, and 31.818 tons hectare^{-1} at the first, second and the average of both seasons, respectively.

Table 5. *Effect of irrigation intervals on WUE, IWUE and total yield*

Irrigation Interval (A)	WUE (kg m^{-3})	IWUE (kg m^{-3})	Total yield (tons hectare^{-1})
First Season			
I_5	6.520 ^{a}	8.788 ^{b}	40.418 ^{a}
I_{10}	6.734 ^{a}	11.352 ^{a}	32.205 ^{b}
L.S.D $_{(p\leq0.05)}$	**n.s**	**1.193**	**2.012**
Second Season			
I_5	7.085 ^{a}	9.293 ^{b}	42.886 ^{a}
I_{10}	6.144 ^{b}	11.281^{a}	31.431 ^{b}
L.S.D $_{(p\leq0.05)}$	**0.761**	**1.280**	**4.117**
Average of Both Seasons			
I_5	6.802 ^{a}	9.041 ^{a}	41.652 ^{a}
I_{10}	6.439 ^{b}	11.316 ^{b}	31.818 ^{b}
L.S.D $_{(p\leq0.05)}$	**0.311**	**0.565**	**1.479**

Table 6A and *Appendix 1* illustrated the effect of the treatments on WUE, IWUE and yield plant^{-1} at the first season, the treatment had significant effect on all of the studied characters. The maximum values of WUE, IWUE and total yield achieved by T_3 with 8.141 kg m^{-3}, 12.297 kg m^{-3} and 44.912 tons hectare^{-1} respectively, while T_1 gave the minimum values with 4.753 kg m^{-3}, 7.236 kg m^{-3} and 25.984 tons hectare^{-1} respectively.

Table 6A. *Effect of the biotechnological treatments on WUE, IWUE and tota yield at the first season*

Treatments (B)	WUE (kg m^{-3})	IWUE (kg m^{-3})	Total yield (tons hectare^{-1})
First Season			
T_1	4.753 ^{d}	7.236 ^{d}	25.984 ^{d}
T_2	7.092 ^{ab}	10.746 ^{ab}	38.984 ^{b}
T_3	8.141 ^{a}	12.297 ^{a}	44.912 ^{a}
T_4	6.845 ^{bc}	10.371 ^{bc}	37.634 ^{b}
T_5	5.810 ^{cd}	8.872 ^{cd}	31.654 ^{cd}
T_6	6.872 ^{bc}	10.404 ^{bc}	37.812 ^{b}
T_7	7.178 ^{ab}	10.908 ^{ab}	39.331 ^{ab}
T_8	6.604 ^{bc}	10.072 ^{bc}	36.033 ^{bc}
T_9	6.203 ^{bc}	9.440 ^{bc}	33.924 ^{bc}
T_{10}	6.676 ^{bc}	10.201 ^{bc}	36.347 ^{bc}
T_{11}	6.629 ^{bc}	9.947 ^{bc}	36.856 ^{bc}
T_{12}	6.642 ^{bc}	10.115 ^{bc}	36.293 ^{bc}
T_{13}	6.705 ^{bc}	10.296 ^{bc}	36.284 ^{bc}
LSD $_{(p\leq0.05)}$	**1.079**	**1.654**	**5.940**

http://www.aloki.hu ● ISSN 1589 1623 (Print) ● ISSN 1785 0037 (Online)
DOI: http://dx.doi.org/10.15666/aeer/1704_1007310090

This may be due to the use of arbuscular mycorrhizal fungi (AMF) mitigates the effects of this stress in a sustainable way and given the increase in the tolerance to water deficit stress in plants inoculated with these fungi; however, the exact mechanism is unknown because the response depends on the water-deficit stress type and is specific to the AMF and the plant. These mechanisms may include modifications in the content of plant hormones, such as strigolactones, jasmonic acid (JA) and absicic acid (ABA). The JA appears to be involved in the stress signal in mycorrhizal plants through an increase of ABA concentrations and, at the same time, ABA has a regulating effect on strigolactones concentrations. Also, there is improvement of plant water status, stomatal conductance, nutritional status and plant responses to cope with a water deficit, such as osmotic adjustment, and antioxidant activity. These modifications cause an increase in CO_2 assimilation and photoassimilates production, improving plant growth as well as the yield during a drought.

The results in *Table 6B* and *Appendix 1* revealed that the treatments significantly influenced on WUE, IWUE and yield plant^{-1} during the second season 2018. The highest values were obtained by T_{11} with 7.495 kg m^{-3}, 11.655 kg m^{-3} and 42.106 tons hectare^{-1} respectively, while the lowest value was recorded by T_1 with 5.334 kg m^{-3}, 8.456 kg m^{-3}, and 29.678 tons hectare^{-1} for WUE, IWUE and total yield respectively. These results is agree with the study of Ati *et al.* (2013) which they stated that potassium humate had a great impact on tuber of potato and water use efficiency in the Abu-Graib Region, Iraq. In their study potato was grown under drip irrigation with three treatments: irrigation applied when evaporation 75%, 100% and 125% from pan A, and three potassium humate fertilizers: 0, 1.2 and 2.4 kg ha^{-1} with three times additions. The seasonal potato evapotranspiration ranged from 267 mm to 372 mm. The drip irrigation treatments had significant effecting tuber yield of potato recorder 29.530, 27.630 and 24.880 kg ha^{-1} for 125%, 100% and 75% from pan A evapotranspiration, respectively. Humus fertilizers addition has the lowest value of ETa 309 mm and maximum value of yield 29300 kg ha^{-1}.

Table 6B. *Effect of the biotechnological treatments on WUE, IWUE and total yield at the second season*

Treatments (B)	WUE (kg m^{-3})	IWUE (kg m^{-3})	Total yield (tons hectare^{-1})
Second Season			
T_1	5.334 ^{d}	8.456 ^{e}	29.678 ^{e}
T_2	7.155 ^{ab}	11.346 ^{ab}	39.809 ^{abc}
T_3	7.337 ^{ab}	11.280 ^{ab}	41.453 ^{ab}
T_4	5.957 ^{cd}	9.286 ^{cde}	33.424 ^{cde}
T_5	6.228 ^{bcd}	9.793 ^{bcde}	34.799 ^{abcde}
T_6	6.910 ^{abc}	10.688 ^{abcd}	38.924 ^{abcd}
T_7	7.301 ^{ab}	11.167 ^{ab}	41.351 ^{ab}
T_8	6.175 ^{bcd}	9.676 ^{bcde}	34.564 ^{bcde}
T_9	5.738 ^{cd}	8.977 ^{de}	32.142 ^{de}
T_{10}	7.085 ^{ab}	10.901 ^{abc}	40.014 ^{abc}
T_{11}	7.495 ^{a}	11.655 ^{a}	42.106 ^{a}
T_{12}	6.446 ^{abcd}	10.092 ^{abcde}	36.089 ^{abcde}
T_{13}	6.826 ^{abc}	10.416 ^{abcd}	38.709 ^{abcd}
LSD $_{(p\leq0.05)}$	**1.257**	**1.846**	**7.318**

http://www.aloki.hu ● ISSN 1589 1623 (Print) ● ISSN 1785 0037 (Online)
DOI: http://dx.doi.org/10.15666/aeer/1704_1007310090

Table 6C and *Appendix 2* showed the effect of the treatments on WUE, IWUE and total yield. The differences among treatments were significant at the average of both seasons. T_3 gave the maximum values for all of the characters with 7.739 kg m^{-3}, 11.789 kg m^{-3}, and 43.183 tons $hectar^{-1}$ respectively, however the minimum values recorded in T_1 with 5.034 kg m^{-3}, 7.846 kg m^{-3} and 27.831 tons $hectar^{-1}$ respectively. The results agreement with the finding of several other researches. Goussous and Mohammad (2009) reported that Arbuscular Mycorrhizal Fungi (AMF) and plant roots improve water and nutrient uptake such as phosphorus, nitrogen and micronutrients, thus enhance potato plants growth, and yield. AMF can produce glycoprotein glomalin, which is act similar a glue, binding carbon, nitrogen and other biological components of soil to the mineral components, clay and sand, that has an important role for increased soil organic matter, and consequently collected highly water stability (Duc, 2017). In addition, under drought condition, direct water uptake from soil into the host plant can improved by interlacing external hyphae of mycorrhizae, thus, it is believed that has resistance to drought condition by many mechanisms including; osmotic adjustment and altering display of stomatal conductance (Qiang-Sheng *et al.*, 2006).

Table 6C. *Effect of the treatments on WUE, IWUE and total yield at the average of both seasons*

Treatments (B)	WUE (kg m^{-3})	IWUE (kg m^{-3})	Total yield (tons $hectare^{-1}$)
Average of Both Seasons			
T_1	5.043 ^{d}	7.846 ^{e}	27.831 ^{e}
T_2	7.123 ^{abc}	11.046 ^{ab}	39.396 ^{abc}
T_3	7.739 ^{a}	11.789 ^{a}	43.183 ^{a}
T_4	6.401 ^{cd}	9.829 ^{bcd}	35.529 ^{cd}
T_5	6.019 ^{d}	9.332 ^{cd}	33.226 ^{d}
T_6	6.891 ^{bc}	10.546 ^{bc}	38.368 ^{bc}
T_7	7.240 ^{ab}	11.037 ^{ab}	40.341 ^{ab}
T_8	6.390 ^{cd}	9.874 ^{bcd}	35.298 ^{cd}
T_9	5.970 ^{d}	9.208 ^{d}	33.033 ^{d}
T_{10}	6.881 ^{bc}	10.551 ^{bc}	38.180 ^{bc}
T_{11}	7.062 ^{abc}	10.801 ^{ab}	39.481 ^{abc}
T_{12}	6.544 ^{bcd}	10.104 ^{bcd}	36.191 ^{bcd}
T_{13}	6.766 ^{bcd}	10.356 ^{bcd}	37.497 ^{bcd}
LSD $_{(p\leq0.05)}$	**0.818**	**1.223**	**4.653**

The data in *Table 7A, 7B and 7C* and *Appendix 1 and 2* reveal no significant differences for the interaction effects of irrigation intervals and the treatments on WUE, IWUE and total yield during the first season 2107, the second season 2018 and the average of both seasons.

Data in *Table 8* and *Appendix 2* show that seasons had no significant effect on WUE, IWUE and total yield.

http://www.aloki.hu ● ISSN 1589 1623 (Print) ● ISSN 1785 0037 (Online)
DOI: http://dx.doi.org/10.15666/aeer/1704_1007310090

Table 7A. *Interaction effects of irrigation intervals and treatments on WUE, IWUE and total yield at the first season*

Irrigation Interval × Treatments (A×B)	WUE (kg m^{-3})	IWUE (kg m^{-3})	Total yield (tons $hectare^{-1}$)
First Season			
$I_5 \times T_1$	4.593 [a]	6.191 [a]	28.472 [a]
$I_5 \times T_2$	7.155 [a]	9.643 [a]	44.353 [a]
$I_5 \times T_3$	8.441 [a]	11.377 [a]	52.324 [a]
$I_5 \times T_4$	6.914 [a]	9.319 [a]	42.859 [a]
$I_5 \times T_5$	5.459 [a]	7.358 [a]	33.840 [a]
$I_5 \times T_6$	6.986 [a]	9.416 [a]	43.307 [a]
$I_5 \times T_7$	7.060 [a]	9.515 [a]	43.763 [a]
$I_5 \times T_8$	6.280 [a]	8.465 [a]	38.931 [a]
$I_5 \times T_9$	6.015 [a]	8.107 [a]	37.284 [a]
$I_5 \times T_{10}$	6.236 [a]	8.405 [a]	38.657 [a]
$I_5 \times T_{11}$	7.272 [a]	9.801 [a]	45.077 [a]
$I_5 \times T_{12}$	6.395 [a]	8.619 [a]	39.642 [a]
$I_5 \times T_{13}$	5.956 [a]	8.028 [a]	36.923 [a]
$I_{10} \times T_1$	4.913 [a]	8.282 [a]	23.496 [a]
$I_{10} \times T_2$	7.029 [a]	11.848 [a]	33.615 [a]
$I_{10} \times T_3$	7.841 [a]	13.218 [a]	37.500 [a]
$I_{10} \times T_4$	6.777 [a]	11.424 [a]	32.410 [a]
$I_{10} \times T_5$	6.161 [a]	10.387 [a]	29.467 [a]
$I_{10} \times T_6$	6.757 [a]	11.391 [a]	32.318 [a]
$I_{10} \times T_7$	7.297 [a]	12.301 [a]	34.900 [a]
$I_{10} \times T_8$	6.928 [a]	11.679 [a]	33.134 [a]
$I_{10} \times T_9$	6.391 [a]	10.773 [a]	30.564 [a]
$I_{10} \times T_{10}$	7.117 [a]	11.997 [a]	34.037 [a]
$I_{10} \times T_{11}$	5.987 [a]	10.093 [a]	28.635 [a]
$I_{10} \times T_{12}$	6.888 [a]	11.612 [a]	32.943 [a]
$I_{10} \times T_{13}$	7.453 [a]	12.564 [a]	35.646 [a]
L.S.D $_{(p\leq0.05)}$	**n.s**	**n.s**	**n.s**

Table 7B. *Interaction effects of irrigation intervals and treatments on WUE, IWUE and total yield at the second season*

Irrigation Interval × Treatments (A×B)	WUE (kg m^{-3})	IWUE (kg m^{-3})	Total yield (tons $hectare^{-1}$)
Second Season			
$I_5 \times T_1$	5.102 [a]	6.693 [a]	30.886 [a]
$I_5 \times T_2$	6.836 [a]	8.966 [a]	41.377 [a]
$I_5 \times T_3$	8.359 [a]	10.964 [a]	50.598 [a]
$I_5 \times T_4$	6.296 [a]	8.258 [a]	38.109 [a]
$I_5 \times T_5$	6.266 [a]	8.219 [a]	37.928 [a]
$I_5 \times T_6$	7.625 [a]	10.002 [a]	46.156 [a]
$I_5 \times T_7$	8.537 [a]	11.198 [a]	51.678 [a]
$I_5 \times T_8$	6.341 [a]	8.318 [a]	38.385 [a]
$I_5 \times T_9$	5.947 [a]	7.800 [a]	35.996 [a]
$I_5 \times T_{10}$	8.040 [a]	10.546 [a]	48.668 [a]
$I_5 \times T_{11}$	8.032 [a]	10.536 [a]	48.619 [a]
$I_5 \times T_{12}$	6.645 [a]	8.716 [a]	40.223 [a]
$I_5 \times T_{13}$	8.078 [a]	10.596 [a]	48.900 [a]
$I_{10} \times T_1$	5.565 [a]	10.218 [a]	28.470 [a]
$I_{10} \times T_2$	7.475 [a]	13.725 [a]	38.241 [a]
$I_{10} \times T_3$	6.315 [a]	11.596 [a]	32.309 [a]
$I_{10} \times T_4$	5.618 [a]	10.315 [a]	28.739 [a]
$I_{10} \times T_5$	6.190 [a]	11.366 [a]	31.669 [a]
$I_{10} \times T_6$	6.195 [a]	11.375 [a]	31.692 [a]
$I_{10} \times T_7$	6.064 [a]	11.135 [a]	31.024 [a]
$I_{10} \times T_8$	6.009 [a]	11.034 [a]	30.742 [a]
$I_{10} \times T_9$	5.530 [a]	10.153 [a]	28.288 [a]
$I_{10} \times T_{10}$	6.130 [a]	11.256 [a]	31.360 [a]
$I_{10} \times T_{11}$	6.958 [a]	12.775 [a]	35.594 [a]
$I_{10} \times T_{12}$	6.246 [a]	11.469 [a]	31.955 [a]
$I_{10} \times T_{13}$	5.574 [a]	10.235 [a]	28.518 [a]
L.S.D $_{(p\leq0.05)}$	**n.s**	**n.s**	**n.s**

http://www.aloki.hu ● ISSN 1589 1623 (Print) ● ISSN 1785 0037 (Online)
DOI: http://dx.doi.org/10.15666/aeer/1704_1007310090

Table 7C. *Interaction effects of irrigation intervals and treatments on WUE, IWUE and total yield at the average of both seasons*

Irrigation Interval × Treatments (A×B)	WUE (kg m^{-3})	IWUE (kg m^{-3})	Total yield (tons $hectare^{-1}$)
Average of Both Seasons			
$I_5 \times T_1$	4.848 [a]	6.442 [a]	29.679 [a]
$I_5 \times T_2$	6.995 [a]	9.305 [a]	42.865 [a]
$I_5 \times T_3$	8.400 [a]	11.170 [a]	51.461 [a]
$I_5 \times T_4$	6.605 [a]	8.788 [a]	40.484 [a]
$I_5 \times T_5$	5.862 [a]	7.788 [a]	35.884 [a]
$I_5 \times T_6$	7.306 [a]	9.709 [a]	44.731 [a]
$I_5 \times T_7$	7.799 [a]	10.357 [a]	47.721 [a]
$I_5 \times T_8$	6.311 [a]	8.391 [a]	38.658 [a]
$I_5 \times T_9$	5.981 [a]	7.953 [a]	36.640 [a]
$I_5 \times T_{10}$	7.138 [a]	9.476 [a]	43.662 [a]
$I_5 \times T_{11}$	7.652 [a]	10.168 [a]	46.848 [a]
$I_5 \times T_{12}$	6.520 [a]	8.668 [a]	39.932 [a]
$I_5 \times T_{13}$	7.017 [a]	9.312 [a]	42.912 [a]
$I_{10} \times T_1$	5.239 [a]	9.250 [a]	25.983 [a]
$I_{10} \times T_2$	7.252 [a]	12.787 [a]	35.928 [a]
$I_{10} \times T_3$	7.078 [a]	12.407 [a]	34.904 [a]
$I_{10} \times T_4$	6.197 [a]	10.869 [a]	30.574 [a]
$I_{10} \times T_5$	6.176 [a]	10.877 [a]	30.568 [a]
$I_{10} \times T_6$	6.476 [a]	11.383 [a]	32.005 [a]
$I_{10} \times T_7$	6.681 [a]	11.718 [a]	32.962 [a]
$I_{10} \times T_8$	6.469 [a]	11.356 [a]	31.938 [a]
$I_{10} \times T_9$	5.960 [a]	10.463 [a]	29.426 [a]
$I_{10} \times T_{10}$	6.623 [a]	11.626 [a]	32.699 [a]
$I_{10} \times T_{11}$	6.472 [a]	11.434 [a]	32.114 [a]
$I_{10} \times T_{12}$	6.567 [a]	11.540 [a]	32.449 [a]
$I_{10} \times T_{13}$	6.514 [a]	11.400 [a]	32.082 [a]
L.S.D $_{(p\leq0.05)}$	**n.s**	**n.s**	**n.s**

Table 8. *The effect of seasons on WUE, IWUE and total yield*

Seasons	WUE (kg m^{-3})	IWUE (kg m^{-3})	Total yield (tons $hectare^{-1}$)
First Season 2017	6.627 [a]	10.070 [a]	36.311 [a]
Second Season 2018	6.614 [a]	10.287 [a]	37.159 [a]
L.S.D $_{(p\leq0.05)}$	**n.s**	**n.s**	**n.s**

Discussion

These result accused the role of the interaction of irrigation intervals and different treatments, increased wetted soil volume inside root zone, and this mean increasing in water volume which was stored in root zone. The differences on the total yield can be explained by the influence of the biotic and abiotic application on WUE and IWUE which in return maximize the total yield.

Results of WUE indicated the importance of the treatments to achieve good yield and better utilization of water, which can be attributed to the role of Mycorrhizal inoculation in improving crop resistance to water stress and other stresses. In the first season 2017, no significant difference was observed in term of WUE and this may be due to the distribution and the amount of rainfall in this season was enough to bear plants water requirement in the 10 days irrigation intervals.

Thus, increase of phosphorus uptake by mycorrhizae considering the role of phosphorus in molecular structures such as nucleic acids, stomatal conductance, and photosynthesis increases the tolerance of plants against water stress.

http://www.aloki.hu ● ISSN 1589 1623 (Print) ● ISSN 1785 0037 (Online)
DOI: http://dx.doi.org/10.15666/aeer/1704_1007310090

Biofertilization has emerged in order to minimize environmental impacts and take advantage of the resources available in the field.

Therefore, it can be concluded that the biotic application with good crop management can achieve good productivity and high WUE in Iraqi Kurdistan region conditions.

The treatment of mycorrhizae inoculation for the highest values in WUE and IWUE may be due to its high ability to produce the glomalin compound, which binds the soil minutes to each other and to the aggregation of aggregates, as well as the role played by the mycelium hypha in mass soil actions and increase its stability. Fokom *et al.* (2012) indicates that there are positive correlations of correlations between organic matter and chlorine associated with Glomalin Related Soil Protein (GRSP). Peng *et al.* (2013) noted that the soil fertilized with mycorrhizae increases the stability of its aggregates as a result of the action of the mycorrhizae hypha and the result of its production of glomalin, a watery and insoluble molybdenum protein compound that contributes to the formation and increase stability of the soil complexes where it is released to the and reduce their hydration because it is a glue-absorbing composite. Martin *et al.* (2012) and Wu *et al.* (2013) reported that organic matter also plays an important role in improving the properties of physical, chemical and biological soil. Microorganisms are fertilized with food and increase their activity, which positively affects the increase in the activity of the Mycorrhizae (Ochl *et al.*, 2003). All of these factors improve soil properties and increase their water retention.

The *Glycyrrhiza glabra* extract contains some acids, monosaccharide's, various vitamins (E, C and B), folic acid and various elements such as calcium, iron, silicon, aluminum, magnesium, sulfur, potassium, zinc and phosphorus, which play an important role in growth (Vispute and Khopade, 2011). *Glycyrrhiza glabra* extract also contains mevalonic acid, which enters the synthesis of gibberellins (Moses *et al.*, 2002).

Potassium is also associated with many other important phylogenetic functions, including activation of enzymes, regulation of opening and closing of stents, as well as its important role in the synthesis of ATP, where the electrostatic charge in the ATP production sites is closely related to the K^+ (Prajapati and Modi, 2012) and sugars (Van Brunt and Sultenfnss, 1998), water and nutrient transport (Thomas and Thomas, 2009) and protein synthesis and starch (Patil, 2011).

Conclusion

The irrigation intervals had great influence on WUE and the total yield of potato, the 5 days intervals overcome the 10 days intervals at 2017 and 2018 season's and the average of both seasons with exception of the character WUE of at the first season. Mycorrhizal inoculation maximize the WUE, IWUE and the total yield at the first season 2017 and the average of both seasons, this indicated that the Mycorrhizal inoculation will improve the WUE, IWUE and the total yield depending on the seasonal condition. At the second season the application of (2.5 g L^{-1}) KCl with (6 g L^{-1}) *Glycyrrhiza glabra* extract gave the highest value for the studied characters the rainfall quantity in this season was more in April and May 2018 comparing with the same months in 2017 which leads to increase the role of this combination.

http://www.aloki.hu ● ISSN 1589 1623 (Print) ● ISSN 1785 0037 (Online)
DOI: http://dx.doi.org/10.15666/aeer/1704_1007310090

REFERENCES

[1] Al-Rawi, K. M., Khalaf-Allah, A. M. (1980): Design and analysis of agricultural experiments. – El Mousel Univ. Iraq 19: 487.
[2] Ati, A. S., Shihab, R. M., Aziz, S. A., Ahmed, F. H. (2010): Production and water use of potato under regulated deficit irrigation treatments. – Annals of Agricultural Science (Cairo) 55(1): 123-128.
[3] Ati, A., Nafaou, S. M. (2012): Effect of potassium fertilization on growth, yield and water use efficiency of irrigated potato. – Misr Journal Agricultural Engineering 29(2): 735-744.
[4] Ati, A. S., Iyada, A. D., Najim, S. M. (2012): Water use efficiency of potato (*Solanum tuberosum* L.) under different irrigation methods and potassium fertilizer rates. – Annals of Agricultural Sciences 57(2): 99-103.
[5] Ati, A. S., Al-Sahaf, F., Wally, D. H., Thamer, T. E. (2013): Effects of Potassium Humate Fertilizers and Irrigation Rate on Potato Yield and Consumptive Use under Drip Irrigation Method. – Journal of Agricultural Science and Technology: 803-810.
[6] Beder, O. M. A. (2010): Recent Irrigation scheduling techniques for improving water use in landscaping. – Fourteenth International Water Technology Conference, IWTC 14 2010, Cairo, Egypt.
[7] Birhane, E., Sterck, F. J., Fetene, M., Bongers, F., Kuyper, T. W. (2012): Arbuscular mycorrhizal fungi enhance photosynthesis, water use efficiency, and growth of frankincense seedlings under pulsed water availability conditions. – Oecologia 169(4): 895-904.
[8] Doorenbos, J. (1977): Crop Water Requirements. – Irrigation and Drainage paper 24: 144.
[9] Duc, N. H., Mayer, Z., Pék, Z., Helyes, L., Posta, K. (2017): Combined inoculation of arbuscular mycorrhizal fungi, Pseudomonas fluorescens and Trichoderma spp. for enhancing defense enzymes and yield of three pepper cultivars. – Applied Ecology and Environmental Research 15(3): 1815-1829.
[10] Egilla, J. N., Davies, F. T., Boutton, T. W. (2005): Drought stress influences leaf water content, photosynthesis, and water-use efficiency of Hibiscus rosa-sinensis at three potassium concentrations. – Photosynthetica 43(1): 135-140.
[11] Erdem, T., Erdem, Y., Orta, H., Okursoy, H. (2006): Water-yield relationships of potato under different irrigation methods and regimens. – Scientia Agricola 63(3): 226-231.
[12] Esho, T., Enzlin, P., Van Wolputte, S., Temmerman, M. (2010): Female Genital Cutting and Sexual Functioning: in Search of an Alternate Theoretical Model. – African Identities 8(3): 221-234.
[13] FAOSTAT (2019): Food and Agricultural Organization of the United Nations, Statistics, Rome, Italy. – http://www.fao.org/faostat/en/#data/QC.
[14] Fokom, R., Adamou, S., Teugwa, M. C., Boyogueno, A. B., Nana, W. L., Ngonkeu, M. E. L., Zollo, P. A. (2012): Glomalin related soil protein, carbon, nitrogen and soil aggregate stability as affected by land use variation in the humid forest zone of south Cameroon. – Soil and Tillage Research 120: 69-75.
[15] Goussous, S. J., Mohammad, M. J. (2009): Comparative effect of two arbuscular mycorrhizae and N and P fertilizers on growth and nutrient uptake of onions. – International Journal of Agriculture and Biology 11(4): 463-467.
[16] Grewal, J. S., Sharma, R. C., Saini, S. S. (1992): Agrotechniques for intensive potato cultivation in India. – Indian Council of Agricultural Research; New Delhi.
[17] Hassan, A. A., Sarkar, A. A., Ali, M. H., Karim, N. N. (2002): Effect of deficit irrigation at different growth stages on the yield of potato. – Pakistan Journal of Biological Sciences 5(2): 128-134.

http://www.aloki.hu ● ISSN 1589 1623 (Print) ● ISSN 1785 0037 (Online)
DOI: http://dx.doi.org/10.15666/aeer/1704_1007310090

[18] Howell, T. A., Cuenca, R. H., Solomon, K. H. (1990): Crop yield response. – In: Hoffman, G. J., Howell, T. A., Solomon, K. H. (eds.) Management of Farm Irrigation Systems. Chapter 5, pp. 93-122. ASAE Monograph, ASAE, St. Joseph, Michigan.
[19] Kirda, C. (2002): Deficit irrigation scheduling based on plant growth stages showing water stress tolerance. – http://www.fao.org/library/library-home/en/.
[20] Kiziloglu, F. M., Sahin, U., Tune, T., Diler, S. (2006): The Effect of Deficit Irrigation on Potato Evapotranspiration and Tuber Yield under Cool Season and Semiarid Climatic Conditions. – Journal of Agronomy 5(2): 284-288.
[21] Latef, A. A. H. A., Miransari, M. (2014): The role of arbuscular mycorrhizal fungi in alleviation of salt stress. – Use of microbes for the alleviation of soil stresses, pp. 23-38, Springer, New York, NY.
[22] Lazim, Z. S., Sulaiman, S. M. (2012): Effect of gibberillic and liquorice extract on seed germination of black seed (*Nigella sativa* L.). – Iraq.J.Agric.Res. 17(1): 105-113.
[23] Martin, S. L., Mooney, S. J., Dickinson, M. J., West, H. M. (2012): Soil structural responses to alterations in soil micro biota induced by the dilution method and mycorrhizal fungal inoculation. – Pedobiologia 55(5): 271-281.
[24] Moses, T. N., AbdulJabbar, W. A., Elwy, A. N. (2002): Study of some local licorice root powder components (*Glycyrrihiza glabra* L.). – Iraq. J. of Agric. Sci. 33(4): 30-38.
[25] Nagaz, K., Masmoudi, M. M., Mechlia, N. B. (2007): Soil salinity and yield of drip-irrigated potato under different irrigation regimes with saline water in arid conditions of Southern Tunisia. – Journal of agronomy 6(2): 324.
[26] Najmaddin, P. M., Whelan, M. J., Balzter, H. (2017): Estimating daily reference evapotranspiration in a semi-arid region using remote sensing data. – Remote Sensing 9(8): 779.
[27] Oehl, F., Sieverding, E., Ineichen, K., Mäder, P., Boller, T., Wiemken, A. (2003): Impact of land use intensity on the species diversity of arbuscular mycorrhizal fungi in agro ecosystems of Central Europe. – Applied Environmental Microbiology 69(5): 2816-2824.
[28] Patil, R. B. (2011): Role of potassium humate on growth and yield of soybean and black gram. – International Journal of Pharma and Biosciences 2(1): 242-246.
[29] Peng, S., Guo, T., Liu, G. (2013): The effects of arbuscular mycorrhizal hyphal networks on soil aggregations of purple soil in southwest China. – Soil Biology and Biochemistry 57: 411-417.
[30] Prajapati, K., Modi, H. A. (2012): The importance of potassium in plant growth–a review. – Indian Journal of Plant Sciences 1(02-03): 177-186.
[31] Rashidi, M., Gholami, M. (2008): Review of crop water productivity values for tomato, potato, melon, watermelon and cantaloupe in Iran. – Int. J. Agric. Biol. 10: 432-436.
[32] Reddy, M. J., Nagesh Kumar, D. (2007): Multi-objective particle swarm optimization for generating optimal trade-offs in reservoir operation. – Hydrological Processes: An International Journal 21(21): 2897-2909.
[33] Sabry, G. H., Rizk-Alla, M. S., Abd El-Wahab, M. A. (2009): Influence of effective micro-organisms, seaweed extract and amino acids application on growth, yield and bunch quality of Red globe grapevines. – J. Agric. Sci. Mansoura Univ. 34(6): 5901-5921.
[34] Shock, C. C., Zalewski, J. C., Stieber, T. D., Burnett, D. S. (1992): Impact of early-season water deficits on Russet Burbank plant development, tuber yield and quality. – American Potato Journal 69(12): 793-803.
[35] Shock, C. C. (2004): Efficient irrigation scheduling. – Malheur Experiment Station, Oregon State University, Oregon, USA.
[36] Thomas, T. C., Thomas, A. C. (2009): Vital role of potassium in the osmotic mechanism of stomata aperture modulation and its link with potassium deficiency. – Plant Signal Behaviour 4(3): 240-243.
[37] Thornton, M. K. (2002): Effects of heat and water stress on the physiology of potatoes. – Idaho Potato Conference, Idaho.

http://www.aloki.hu ● ISSN 1589 1623 (Print) ● ISSN 1785 0037 (Online)
DOI: http://dx.doi.org/10.15666/aeer/1704_1007310090

[38] Van Brunt, J. M., Sultenfuss, J. H. (1998): Better crops with plant food. – Potassium: Functions of potassium 82(3): 4-5.
[39] Van Loon, C. D. (1981): The effect of water stress on potato growth, development, and yield. – American Potato Journal 58(1): 51-69.
[40] Vispute, S., Khopade, A. (2011): *Glycyrrhiza glabra* Linn.-"Klitaka": a review. – Int J Pharma Bio Sci. 2(3): 42-51.
[41] Wang, C., Deng, P., Chen, L., Wang, X., Ma, H., Hu, W., He, G. (2013): A wheat WRKY transcription factor TaWRKY10 confers tolerance to multiple abiotic stresses in transgenic tobacco. – PloS one 8(6): e65120.
[42] Wright, J. L., Stark, J. C. (1990): Potato. – In: Stewart, B. A., Nielson, D. R. (eds.) Irrigation of Agricultural Crops. American Society of Agronomy, Crop Science Society of America, Soil Science Society of America, Madison, USA. pp: 859-889.
[43] Wu, Q. S., Srivastava, A. K., Zou, Y. N. (2013): AMF-induced tolerance to drought stress in citrus: A review. – Scientia Horticulturae 164: 77-87.
[44] Yuan, B. Z., Nishiyama, S., Kang, Y. (2003): Effects of different irrigation regimes on the growth and yield of drip-irrigated potato. – Agricultural water management 63(3): 153-167.

APPENDICES

Appendix 1. *Mean squares of the analysis of variance for the characters WUE, IWUE and total yield*

S.O.V	d.f	WUE (kg m^{-3})	IWUE (kg m^{-3})	Total yield (tons $hectare^{-1}$)
First Season				
Blocks	2	3.244	8.034	89.522
Irrigation Interval (A)	1	0.891 $^{n.s}$	128.159*	1315.348*
Error (a)	**2**	**0.369**	**1.500**	**4.263**
Treatments (B)	12	3.644*	8.135*	114.325*
(A×B)	12	0.747 $^{n.s}$	1.553 $^{n.s}$	28.440 $^{n.s}$
Error (b)	**48**	**0.863**	**2.030**	**26.185**
Second Season				
Blocks	2	0.350	1.102	9.826
Irrigation Interval (A)	1	17.269*	77.034*	2558.859*
Error (a)	**2**	**0.609**	**1.726**	**17.857**
Treatments (B)	12	2.813*	6.018*	94.861*
A × B	12	1.678 $^{n.s}$	3.285 $^{n.s}$	59.723 $^{n.s}$
Error (b)	**48**	**1.173**	**2.528**	**39.745**

Appendix 2. *Combined analysis of variance for the characters WUE, IWUE and total yield for both seasons*

S.O.V	d.f	WUE (kg m^{-3})	IWUE (kg m^{-3})	Total yield (tons $hectare^{-1}$)
Seasons (S)	1	0.006 $^{n.s}$	1.842 $^{n.s}$	27.995 $^{n.s}$
Error (a)	**4**	**1.797**	**4.568**	**49.674**
Irrigation Interval (A)	1	5.157*	201.958*	3771.713*
A × S	1	13.002	3.235	102.494
Error (b)	**4**	**0.489**	**1.613**	**11.060**
Treatments (B)	12	5.623*	12.095*	183.647*
B × S	12	0.834	2.058	25.540
A × B	12	1.096 $^{n.s}$	1.668 $^{n.s}$	48.166 $^{n.s}$
A × B × S	12	1.329	3.170	39.998
Error (c)	**96**	**1.018**	**2.279**	**27.995**

http://www.aloki.hu ● ISSN 1589 1623 (Print) ● ISSN 1785 0037 (Online)
DOI: http://dx.doi.org/10.15666/aeer/1704_1007310090

CONSIDERING EFFECTS OF CLIMATE EXTREMES ON PLANT FUNCTIONAL TRAITS BENEFITS THE PREDICTION OF ECOSYSTEM FUNCTIONING

GUO, T.* – TANG, Y. H.

College of Urban and Environmental Sciences, Peking University, 100871 Beijing, China

**Corresponding author*
e-mail: tongg@pku.edu.cn

(Received 11th Apr 2019; accepted 13th Jun 2019)

Abstract. Climate extremes are recognized as main drivers of ecosystem functioning in terrestrial biomes. So far impacts and underlying mechanisms of which climate extremes shape ecosystem processes are poorly understood. This gap impedes an understanding of how climatic extremes modulate long-term and large landscape provisions of ecosystem functions. Trait-based studies render a feasible avenue that links climate extremes and ecosystem functioning. Plant functional traits are considered as a sensitive probe in terms of the response to changes in climatic conditions. Approaches that account for effects of climate extremes on plant functional traits may close this gap. We develop a stepwise framework that relates the response of functional traits to climate extremes and resolves relationships between patterns of functional traits and ecosystem functioning by a process-based dynamic vegetation model. We introduce an ongoing case study to demonstrate how this framework permits an accurate evaluation of ecosystem functioning under various scenarios of climate extremes. Our proposed framework may benefit functioning programs by providing key functional traits sensitive to climate extremes or determinants of ecosystem functions. The practice will in turn improve the parameterization and the validation of the vegetation model, especially in regions paucity of field data.
Keywords: *dynamic vegetation model, ecosystem process, patterns of functional traits, precipitation, temperature, alpine ecosystems*

Introduction

The intensity and the frequency of climatic extremes, namely abnormal climate variabilities, significantly shift the functioning of terrestrial ecosystems (Jentsch et al., 2011; Frank et al., 2015). There is an evidence that plant interactions (Filazzola et al., 2018), vegetation net primary productivity (Sun et al., 2016) and the resistant capacity of plant community (Dreesen et al., 2014) seemed to be more vulnerable to climate extremes than to average climatic conditions. Although effects of climate extremes on ecosystem processes and the resulting ecological consequences have been gradually tested (Wilcox et al., 2016), researches of climate extremes in terms of ecosystem functioning are far from perfection. An important reason is a hard quantification of drving impacts of climate extremes on the ecosystem dynamic. Moreover, mechanisms underlying responses of ecosystem processes to climate extremes, e.g. non-linear effects and threshold behaviors (Brotherton and Joyce, 2015), were not fully understood. Thus more concerns should be made on the ecological significance of climate extremes.

Until now, experimenters manipulated the magnitude of climatic factors like treatments of water reduction and open-top chamber warming, and assessed impacts of climate extremes on ecosystem functioning (Walter et al., 2011; Wang et al., 2012; Kreyling et al., 2017). However, they largely neglected potential interactions among climate extremes. Drought might offset effects of warming on aboveground biomass in a short time period. A combination of decreased rainfall and higher temperature was

http://www.aloki.hu ● ISSN 1589 1623 (Print) ● ISSN 1785 0037 (Online)
DOI: http://dx.doi.org/10.15666/aeer/1704_1009110104

likely to exacerbate deficits in water budgets through an increased evaporation in temperate grasslands (Brotherton and Joyce, 2015). The impact of various climate extremes to ecosystem functions should be disentangled since the complex nature of ecosystem response to climate extremes is non-linear and non-additive.

Understanding ecosystem response to climate extremes can be advanced by incorporating approaches emphasizing the role of plant functional traits. Plant traits are measurable properties of an individual plant such as plant height, leaf area and root depth. The functional characteristics of traits are showed by their depiction on the fitness of plant species (Violle et al., 2007). Distributions of functional traits could indicate selection effects of abnormal climatic variabilities on plant communities. Larger rainfalls together with less rainy days stimulated the growth of deep-rooted plants as individual rainstorm led to a greater infiltration into deeper soil layers (Knapp et al., 2008; Tietjen, 2016). Plants responded to drought stress by structural adjustments such as decreased leaf area and increased root–shoot ratio (Teuling et al., 2006; Greenwood et al., 2017). Drought events were found to enhance the dispersal capacity of plant seeds (Zavalloni et al., 2009). Communities composed of long-lived plants might be resistant to individual extremes but be vulnerable to abrupt changes in climate regimes owing to a low turnover rate (Beier et al., 2012), since long-lived plants were more likely to experience cumulative influences of multiple extremes in the course of their lifespan.

Distributions or compositions of plant functional traits have been broadly found to be related to ecosystem functioning (Orwin et al., 2010; Zirbel et al., 2017). Plant functional traits and their associated trade-offs determined vegetation competitive abilities for light, water resources and nutrients (Kunstler et al., 2016). Trait-based approaches have been proposed incorporating into dynamic vegetation models for predictions of vegetation distribution and ecosystem functions (Webb et al., 2010; Soussana et al., 2012; van Bodegom et al., 2014). Functional trait compositions can advance our understanding of how ecosystem functioning responds to climate change (Helge et al., 2018). Compositional changes in functional traits led to a shift in biomass productions of the grassland community under conditions of increased warming events (White et al., 2000). Biomass productions of the herbaceous community were more determined by reproductive traits than competitive traits under drought stress (Dreesen et al., 2014). However, trait-based studies of climate extremes are constrained by lack of systematically experimental trait data and the highly non-linear plant response to climate extremes. This makes a quantitative assessment of extreme impacts on ecosystem functions virtually difficult. Therefore, the strength and the direction of links between functional trait patterns and ecosystem functions need to be evaluated based on simulating multiple scenarios of climate extremes.

In summary, most studies did not consider the full path from climate extremes via plant functional traits to ecosystem functioning. What extent climate extremes shape variations of plant functional traits or trait combinations is not well understood. Empirical investigations are the fundamental step to deal with the problem. However, owing to their limited complexity of spatio-temporal scales, we might draw an incomplete conclusion of climate extreme effects on patterns of functional traits. To fill out the knowledge gap, a full factorial modelling design, in which properties and interactions of individual climate extremes as well as all combinations of plant functional traits, is simulated to predict long term changes in ecosystem functioning.

http://www.aloki.hu ● ISSN 1589 1623 (Print) ● ISSN 1785 0037 (Online)
DOI: http://dx.doi.org/10.15666/aeer/1704_1009110104

In the following, we present a stepwise research framework that includes a simulation of individual climate extremes and their interactions, modelling patterns of plant functional traits and their relationship with ecosystem functioning. Implementing this framework will pave the road towards benefiting practitioners in the aim of predicting ecosystem functioning. The methodology in the framework may play a greater role in regions susceptible to climate change, especially regions short of field data. Although we illustrate the research framework with reference to Qinghai-Tibetan alpine grassland ecosystems, we are confident that the framework is also feasible for studying effects of climate extremes on ecosystem functioning in a global scale.

Construction of the framework

Achieving an accurate prediction of ecosystem functioning toward future climate requires integrative knowledge from properties of climate extremes and trait-based studies as well as process-based dynamic vegetation models. Such approaches, however, have been so far missing. To achieve the above-mentioned goals, we put forward the following research questions to identify which plant functional traits are reliable indices for predictions of ecosystem functioning under conditions of climate extremes:

1) How should we simulate properties of climate extremes in the dynamic vegetation model?

2) What are patterns of functional traits under different scenarios of climate extremes?

3) How do functional trait patterns affect ecosystem functioning?

Here we briefly propose consecutive steps in a framework that describes how climate extremes and plant functional traits can be linked to achieve the ultimate goal. We thereafter elaborate these steps using an ongoing case study to illustrate the potential value of the approach.

How should we do at first: the simulation of individual climate extremes and their interactions

Assessing vegetation responses to precipitation and temperature should consider properties of climate extremes in reality. The consistent findings on precipitation patterns with increased extremity were not well covered by treatments applied in empirical experiments (Dwyer and O'Gorman, 2017). Similarly, current climate generators in ecosystem models did not fully capture abnormal variabilities of precipitation and temperature time-series recorded data (Reichstein et al., 2013). This may lead to an unrealistic simulation of driving effects on the vegetation dynamic. In addition, increased temperature resulting from long-term global warming was experimentally manipulated in short time periods. Rainfall extremes associated with increased temperature might be underestimated in terms of projections of future climate change (Allan and Soden, 2008). This urges us to simulate precipitation and temperature extremes in a more realistical way. It is necessary to at first identify types, the magnitude and the frequency of climate extremes based on studied regions. Designed scenarios of climate extreme should satisfy requirements that applied treatments are indeed ‘abnormal’ beyond current background variabilities of climate conditions over a time period. Otherwise we may run the risk of killing ‘real’ or maintain ‘no-existed’ plant types.

http://www.aloki.hu ● ISSN 1589 1623 (Print) ● ISSN 1785 0037 (Online)
DOI: http://dx.doi.org/10.15666/aeer/1704_1009110104

Link climate extremes with functional traits: Developing a process-based dynamic vegetation model

To assess effects of climate extremes on the vegetation dynamic, fundamental ecosystem processes should be included in the model like water cycle, carbon cycle and vegetation demographical processes (Frank et al., 2015). Simulations of ecosystem processes refer to descriptions in the literature and these need to be adjusted and adapted to the studied system. Dynamic vegetation models used plant functional types depicted by suits of functional traits rather than specific species. This allowed for direct assessments of functional traits responding to climate changes (Mouillot et al., 2013). It was necessary to explicitly incorporate representative functional traits that were closely linked to vegetation dynamics under multiple climatic conditions (Fernandez-Going et al., 2012). Sensitivity analysis is an effective way to find out key trait parameters that should be carefully assigned values. If a sensitive parameter is uncertain, this uncertainty should be conducted through model simulations to establish a full range of potential outcomes. Trait parameterization is a crucial step to gain full confidence of vegetation simulations which should be based on empirical data e.g. the corresponding relationship between simulated trait parameters and measured traits in reality.

Patterns of functional traits and their relationship with ecosystem functioning under different scenarios of climate extremes

A knowledge gap that cannot be filled by experimental data is that effects of climate extremes on ecosystem functioning are not additive. Modelling ecosystem behaviors after climate extremes requires in depth understanding of patterns at the level of plant functional traits. Patterns of functional traits may aid us to identify thresholds of community responses to individual climate extremes. In case pulses exerted by climate extremes went beyond thresholds of community resistance or tolerance, they would cause dramatic changes in ecosystem functioning (Diez et al., 2012). Plant communities adapted to dynamic environmental conditions and with a higher diversity of functional traits might have advantages in the recovery from climate extremes (Brotherton and Joyce, 2015). The relationship between patterns of functional traits and ecosystem functioning should be assessed in a full factorial design under multiple scenarios of climate extremes. We should be aware that specific trait combinations determine one function or single functional trait plays different roles for various function indices.

A case study in Qinghai-Tibetan alpine grasslands

We exemplify the framework using an ongoing case study with a focus on Qinghai-Tibetan alpine grasslands. Climate extremes largely drove ecosystem functioning in cold biomes with high altitudes (Marcolla et al., 2011; Wipf et al., 2013). The unique geographical and climatic conditions in Qinghai-Tibetan Plateau determine processes of water and carbon cycle in eastern Asia (Yao et al., 2012). In addition, most regions are characterized by arid or semi-arid biomes. Low temperature and water shortage were both limiting factors for resource acquisition of alpine plants. Demographical rates closely linked with traits of alpine plants (Blonder et al., 2018). Alpine plants were generally long-lived. Vegetation processes might work at a slower rate than warmer areas (Gottfried et al., 2012). Average plant height usually declined with an increased altitude (Butterfield and Suding, 2013). Alpine plants often developed opportunistic

http://www.aloki.hu ● ISSN 1589 1623 (Print) ● ISSN 1785 0037 (Online)
DOI: http://dx.doi.org/10.15666/aeer/1704_1009110104

traits in response to late snowmelt due to altitudinal constraints (Almeida et al., 2013). Functional trait diversity of alpine plants can regulate the response of vegetation productivity to regional climate change (Wu et al., 2016). Measured data of functional traits in most regions of Qinghai-Tibetan Plateau were much limited, characterized by a short time scale and lack of the comparability among regions. Thus, simulating effects of climate extremes on ecosystem functioning through plant functional traits may permit us to understand the underlying mechanisms of alpine ecosystem dynamic. We should have an awareness that part of areas in Qinghai-Tibetan Plateau already locate under so-called climate extreme conditions (e.g. very low temperature or covered by snow all year around), where plant functional traits are evolutionary outcomes of their environmental conditions. More extremes of climate conditions probably lead to weak or no changes in ecosystem functioning. To achieve the goal of accurately predicting ecosystem functioning, our approach integrates a database of plant functional traits and community properties in the Haibei station (one of typical experimental stations in Qinghai-Tibetan Plateau) with a process-based dynamic vegetation model. In the following we demonstrate the application of every consecutive step, that is, how we perform the framework in Haibei alpine grasslands to address our research questions (*Fig. 1*).

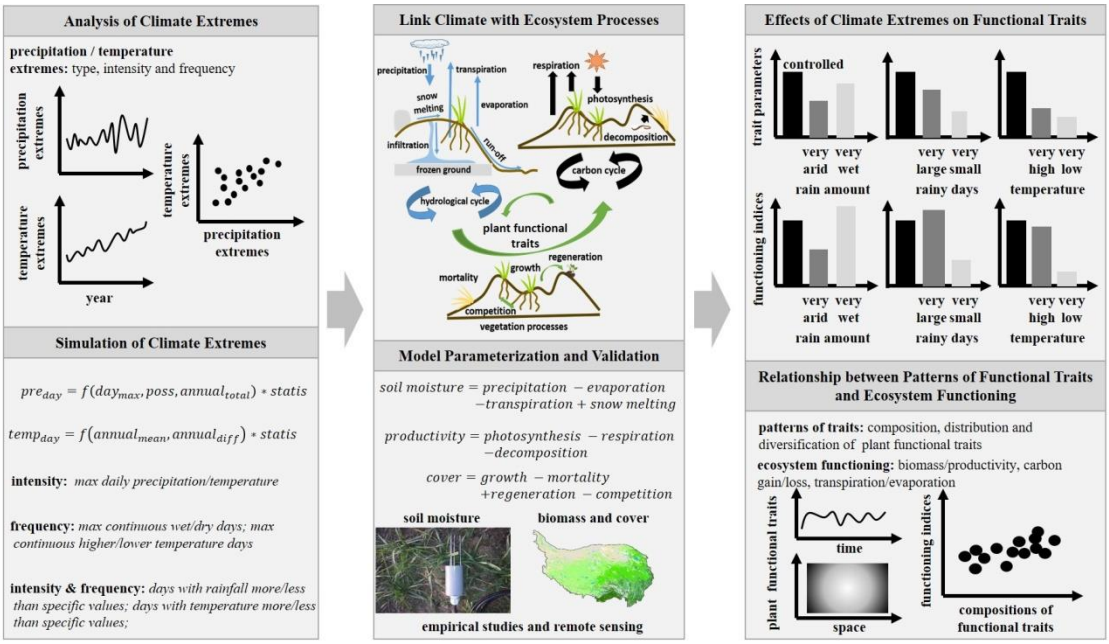

Figure 1. *Every steps performed in our case study for evaluating effects of climate extremes on functional traits patterns and their relationship with ecosystem functioning. The left panel: 1) we analyze temporal variations of precipitation and temperature extremes as well as interactions between individual extreme indices. 2) We incorporate properties of extreme indices into the climate generator to better simulate the vegetation dynamic in the model. The middle panel: 1) We simulate ecosystem processes related to carbon cycle, water cycle and vegetation demography. These processes interconnect and are adjusted by plant functional traits. 2) We calibrate and validate the model based on site-specific measured data at the Haibei station in Qinghai Province. The right panel: 1) We compare patterns of functional traits between the baseline scenario and various climate extreme scenarios; 2) W will evaluate the relationship between patterns of functional traits and ecosystem functioning under respective climatic scenarios*

http://www.aloki.hu ● ISSN 1589 1623 (Print) ● ISSN 1785 0037 (Online)
DOI: http://dx.doi.org/10.15666/aeer/1704_1009110104

Simulations of climate extremes

Properties of individual climate extremes should be depicted based on long term climate data. We obtained 56 years (1960 - 2015) climate data from two weather stations nearest to the Haibei station. Thereafter we analyzed the temporal variations of individual climate extreme indices recommended by Expert Team on Climate Change Detection, Monitoring and Indices (Alexander et al., 2006). We selected several representative extreme indices based on ecosystem characteristics of Qinghai-Tibetan Plateau. These extreme properties are incorporated into the climate generator (*Table 1*). To evaluate future threats of respective climate extremes, outcomes of the multiple extreme scenarios are compared with the cumulative outcomes of the single extreme scenario. Based on regional climatic characteristics and the temporal trend of historical data, we conduct an increased extremity for each scenario (a change of 10% and 20%) and covariations of individual climate extremes.

Table 1. *Simulating properties of climate extremes in the dynamic vegetation model*

Climate factors	Types	Dimensions
Precipitation	Max continuous dry/wet days in grow seasons	Frequency
	Increased precipitation intensity	Intensity/Frequency
	Increased inter-annual variability	Intensity/Frequency
	Rainy days larger than specific values in grow seasons	Intensity/Frequency
	Max snowy days and snowfall larger than 2 mm	Intensity/Frequency
Temperature	Increased annual temperature	Intensity
	Max/Min daily temperature deviations	Intensity
	Max continuous higher temperature days in grow seasons	Intensity/Frequency
	Days of temperature higher than specific values in and around grow seasons	Intensity/Frequency

Localizing a dynamic vegetation model in Qinghai-Tibetan alpine grasslands

There were so far few dynamic vegetation models applied in alpine grassland ecosystems. Most models used statistical or remote sensing ways since the parameterization of a dynamic vegetation model is a much difficult task owing to lack of systematically measured soil and plant data. The elements considered in the model include the vegetation dynamic, plant functional traits, soil properties, hydrological and carbon cycling processes. We simulate different scenarios of climate extremes and analyze the influences of extremes on ecosystem elements. In the model, we should be careful of the specificity of alpine ecosystem processes and their potential interactions. The alpine grasslands at high altitudes are characterized by a low temperature over a long time period, especially in winters the evaporation flux is quite low. Low temperature also leads to a slow decomposition rate of organic carbon. Thus the soil stock might be deemed as a carbon sink, which indirectly benefits vegetation growth. In addition, effects of snow cover on the vegetation dynamic were largely ignored in most vegetation models. We localize the dynamic vegetation model adapted to Qinghai-Tibetan alpine grasslands by calculating all relevant ecosystem processes with a reference to a process-based dynamic vegetation model (Tietjen et al., 2009, 2010; Guo et al., 2016, 2018). The model is characterized by explicit ecosystem processes and spatio-temporal scales.

http://www.aloki.hu ● ISSN 1589 1623 (Print) ● ISSN 1785 0037 (Online)
DOI: http://dx.doi.org/10.15666/aeer/1704_1009110104

Model overview

We simulate the landscape based on geographical characteristics, e.g. the elevation, the slope and soil conditions, of Haibei station. The simulated landscape is separated into grid cells (each cell: 20 by 20 m^2) and different layers per cell. We assume a homogeneity of soil properties within the size of grid cells. The depth of soil layers is determined by site-specific soil heterogeneity. The simulated soil depth is not more than 1 m as we do not consider the ecosystem dynamic in permafrost layers. Each layer is depicted by a combination of soil parameters (Guo et al., 2018). These parameters are calibrated by measured soil physic-chemical and hydraulic indices. Representative plant functional types (PFTs) are selected based on local dominant and constructive species. Proxies indicating ecosystem functioning include above- and belowground plant biomass, litter and dead biomass, carbon storage in plant and soil, plant transpiration and soil evaporation. In order to track the changes in these functions, water, carbon cycle and vegetation processes are calculated for each grid cell. We briefly describe these interrelated processes as follows.

Vegetation processes and the parameterization of plant functional traits

Vegetation processes capture the entire life cycle and describe demographical characteristics of herbaceous plants distributing over the landscape. Main processes include photosynthetic growth, seed dispersal/establishment, mortality and grazing by livestock. The competition among PFTs is explicitly simulated in terms of water, light and space. Vegetation processes dependent on specific plant functional traits (*Table 2*) are driven by available soil water and soil temperature.

Table 2. *Main vegetation processes and trait parameters in the model*

Vegetation processes	Influencing factors	Measured traits	Trait parameters
Growth	Precipitation Temperature	Biomass calculation in leaf, shoot and root	Growth rate
		Allocation of water in leaf, shoot and root	Water uptake and transmission rate
		Allocation of organic carbon in leaf, shoot and root	Carbon uptake and transmission rate
Mortality	Precipitation Temperature	Biomass reduction in leaf, shoot and root The decreased number of plant species or individuals	Mortality rate
Reproduction	Precipitation Temperature	The number and the size of seeds	Dispersal rate
		The distance between adult and child plants	Range of distance
		The number of child plants	Establishment rate
Competition	Precipitation Temperature	Vegetation cover or leaf area index	Competition for space
		Distribution of leaf and root	Competition for water and carbon

Equations of vegetation processes are mainly constructed through vegetation cover and biomass (Tietjen et al., 2010; Guo et al., 2016). Trait combinations of plant functional types are parameterized by local plant species based on their light and water capture strategy, growth form, leaf size, plant height, rooting depth. The trait parameterization mainly relies on the investigation of dominant and constructive species

http://www.aloki.hu ● ISSN 1589 1623 (Print) ● ISSN 1785 0037 (Online)
DOI: http://dx.doi.org/10.15666/aeer/1704_1009110104

in local areas. Moreover functional traits are assigned values partly based on reference data of Qinghai-Tibetan ecosystems (He et al., 2006; Qi et al., 2014; Wang et al., 2014). The sensitivity of trait variations has to be assessed through single trait change or joint trait changes. The simulated plant community is composed of different plant functional types depicted by sound trait combinations including covariations (e.g., growth rate & resistance to grazing; seed size & seed number; leaf area & plant height). There existed diverse trade-offs among traits in Qinghai alpine ecosystems (Du and Qi, 2010). The diversification of plant functional types in the model is constrained by proper values (maximum, minimum and average) of individual functional traits. We assume a completely balanced state of trade-offs within a newly constructed PFT. That is, the number of traits, whose values locate between average and maximum, equals the number of traits with values assigned between minimum and average. To test whether we define the 'right' functional types that match the real plant community, we should repeatedly and randomly conduct various trait combinations of plant functional types in long term simulations. Moreover, the local richness of plant species should be investigated to evaluate the simulated number of PFTs in grid cells.

Hydrological and carbon processes

Hydrological processes revolve round the calculation of soil moisture for different layers across all grid cells. Relevant processes include infiltration, runoff, evaporation and transpiration. These processes depend on site-specific soil texture, topography, weather and community properties. A challenge during this procedure is that water processes act on different temporal and spatial scales. This can be solved using a hierarchical setting, which calculated processes in separated sub-modules running on various spatio-temporal scales (Tietjen et al., 2009). Carbon storage and fluxes are assessed for each grid cell dependent on soil properties, soil moisture, vegetation cover and above- and belowground biomass. Main processes include photosynthesis, respiration, litter decomposition, biomass degradation. The parameterization and equations of water and carbon processes refer to previous empirical or modelling studies (Gu et al., 2008; Tan et al., 2010; Yan et al., 2015). Coupled interactions between water and carbon processes are very crucial for vegetation dynamic and ecosystem functioning. Carbon cycle was verified to be linked with nitrogen cycle in Qinghai-Tibetan Plateau (Lee et al., 2013). However, the model is currently not considering any nutrient cycling processes. To test the suitability of every ecosystem process in the selected areas, the model should be run under the very same climatic conditions. In addition, all indices that are employed to quantify ecosystem functions should be validated. Specifically, simulated soil moisture, community cover and biomass, plant and soil carbon content are compared to measured dynamics of the Haibei station.

Patterns of functional traits and their relationship with ecosystem functioning

In the following, we implement simulation experiments under various scenarios of climate extremes to assess how future climate extremes shape patterns of functional traits and the associated ecosystem functioning in alpine grasslands. Ecosystem functions like biomass, fluxes of resource cycling are evaluated via absolute as well as proxy measurements. We firstly assess the effects of climate extremes on ecosystem functioning with a limited number of plant functional types. To test the separated and interactive effects of individual climate extremes, all other extreme properties are kept

http://www.aloki.hu ● ISSN 1589 1623 (Print) ● ISSN 1785 0037 (Online)
DOI: http://dx.doi.org/10.15666/aeer/1704_1009110104

on a constant level. That is, all climate extremes should be run separately and in different combinations in a full factorial design. Then we diversify trait combinations and observe this effect. Combinations of functional traits are detected that are sensitive to specific climate extremes. More importantly we can know which plant functional traits are reliable indicators of ecosystem functions under different scenarios of climate extremes. The relationship between patterns of functional traits and ecosystem functioning should be assessed across all treatments of climate extremes. Our model approach clearly demonstrates site-specific characteristics of the Haibei station such as geographical and community properties. Through the application of a case study like this, we can propose specific plant functional traits or trait combinations that indicate abnormal variabilities in climatic conditions and thus strengthen assessments of ecosystem functioning. In a follow-up analysis, we can advance our knowledge on the Qinghai-Tibetan alpine ecosystems in general. E.g. in case we test whether the framework works in other Qinghai-Tibetan Plateau sites, we could modify soil, weather conditions and vegetation type if necessary while keeping ecosystem processes consistent. Model experiments can be performed for different Qinghai-Tibetan areas after the model has been calibrated and validated for respective sites. This can verify whether functional traits and trait combinations respond to climate extremes as well relate with ecosystem functioning is site specific. Future work could also consider other global change factors (grazing or nitrogen deposition) and trade-offs among ecosystem functions that deserve great attentions for the land restoration.

Conclusion

To our knowledge, there are few mechanistic approaches that can assess long-term vegetation dynamic and ecosystem functioning through patterns of functional traits under impacts of climate extremes. We believe that the proposed framework fill the gaps and therefore closely link abiotic climatic factors with biotic agents like alpine vegetation. We use the response of plant functional traits to climate extremes to predict ecosystem functioning since variations of ecosystem functions are sometimes difficultly captured by changes in climatic conditions. Through this endeavor, the relationship between patterns of functional traits and ecosystem functioning can be better understood under different scenarios of climate extremes. Achieving the goal of a precise prediction of ecosystem functioning under complex climatic conditions needs an integration of different research approaches. Our proposed framework provides a promising scheme for a scientific assessment of ecosystem functioning in Qinghai-Tibetan alpine ecosystems lack of long term measured data.

Acknowledgements. This work was supported by China Postdoctoral Science Foundation (2018M641072). We thank anonymous reviewers for very constructive suggestions on the original namuscript.

REFERENCES

[1] Alexander, L. V., Zhang, X., Peterson, T. C., Caesar, J., Gleason, B., Tank, A. M. G. K., Haylock, M., Collins, D., Trewin, B., Rahimzadeh, F., Tagipour, A., Kumar, K. R., Revadekar, J., Griffiths, G., Vincent, L., Stephenson, D. B., Burn, J., Aguilar, E., Brunet, M., Taylor, M., New, M., Zhai, P., Rusticucci, M., Vazquez-Aguirre, J. L. (2006): Global

http://www.aloki.hu ● ISSN 1589 1623 (Print) ● ISSN 1785 0037 (Online)
DOI: http://dx.doi.org/10.15666/aeer/1704_1009110104

observed changes in daily climate extremes of temperature and precipitation. – Journal of Geophysical Research-Atmospheres 111: 1-22. doi: 10.1029/2005jd006290.

[2] Allan, R. P., Soden, B. J. (2008): Atmospheric warming and the amplification of precipitation extremes. – Science 321: 1481-1484. doi:10.1126/science.1160787.

[3] Almeida, J. P., Montúfar, R., Anthelme, F. (2013): Patterns and origin of intraspecific functional variability in a tropical alpine species along an altitudinal gradient. – Plant Ecology & Diversity 6: 423-433. doi:10.1080/17550874.2012.702137.

[4] Beier, C., Beierkuhnlein, C., Wohlgemuth, T., Penuelas, J., Emmett, B., Korner, C., de Boeck, H. J., Christensen, J. H., Leuzinger, S., Janssens, I. A., Hansen, K. (2012): Precipitation manipulation experiments - challenges and recommendations for the future. – Ecology letters 15: 899-911. doi:10.1111/j.1461-0248.2012.01793.x.

[5] Blonder, B., Kapas Rozalia, E., Dalton Rebecca, M., Graae Bente, J., Heiling Jacob, M., Opedal Øystein, H. (2018): Microenvironment and functional-trait context dependence predict alpine plant community dynamics. – Journal of Ecology 106: 1323-1337. doi:10.1111/1365-2745.12973.

[6] Brotherton, S. J., Joyce, C. B. (2015): Extreme climate events and wet grasslands: plant traits for ecological resilience. – Hydrobiologia 750: 229-243. doi:10.1007/s10750-014-2129-5.

[7] Bruelheide, H., Dengler, J., Purschke, O., Lenoir, J., Jimenez-Alfaro, B., Hennekens, S. M., Botta-Dukat, Z., Chytry, M., Field, R., Jansen, F., Kattge, J., Pillar, V. D., Schrodt, F., Mahecha, M. D., Peet, R. K., Sandel, B., van Bodegom, P., Altman, J., Alvarez-Davila, E., Khan, M. A. S. A., Attorre, F., Aubin, I., Baraloto, C., Barroso, J. G., Bauters, M., Bergmeier, E., Biurrun, I., Bjorkman, A. D., Blonder, B., Carni, A., Cayuela, L., Cerny, T., Cornelissen, J. H. C., Craven, D., Dainese, M., Derroire, G., De Sanctis, M., Diaz, S., Dolezal, J., Farfan-Rios, W., Feldpausch, T. R., Fenton, N. J., Garnier, E., Guerin, G. R., Gutierrez, A. G., Haider, S., Hattab, T., Henry, G., Herault, B., Higuchi, P., Holzel, N., Homeier, J., Jentsch, A., Jurgens, N., Kacki, Z., Karger, D. N., Kessler, M., Kleyer, M., Knollova, I., Korolyuk, A. Y., Kuhn, I., Laughlin, D. C., Lens, F., Loos, J., Louault, F., Lyubenova, M. I., Malhi, Y., Marceno, C., Mencuccini, M., Muller, J. V., Munzinger, J., Myers-Smith, I. H., Neill, D. A., Niinemets, U., Orwin, K. H., Ozinga, W. A., Penuelas, J., Perez-Haase, A., Petrik, P., Phillips, O. L., Partel, M., Reich, P. B., Romermann, C., Rodrigues, A. V., Sabatini, F. M., Sardans, J., Schmidt, M., Seidler, G., Espejo, J. E. S., Silveira, M., Smyth, A., Sporbert, M., Svenning, J. C., Tang, Z. Y., Thomas, R., Tsiripidis, I., Vassilev, K., Violle, C., Virtanen, R., Weiher, E., Welk, E., Wesche, K., Winter, M., Wirth, C., Jandt, U. (2018): Global trait-environment relationships of plant communities. – Nature Ecology & Evolution 2: 1906-1917. doi:10.1038/s41559-018-0699-8.

[8] Butterfield, B. J., Suding, K. N. (2013): Single-trait functional indices outperform multi-trait indices in linking environmental gradients and ecosystem services in a complex landscape. – Journal of Ecology 101: 9-17. doi:10.1111/1365-2745.12013.

[9] Diez, J. M., D'Antonio, C. M., Dukes, J. S., Grosholz, E. D., Olden, J. D., Sorte, C. J. B., Blumenthal, D. M., Bradley, B. A., Early, R., Ibanez, I., Jones, S. J., Lawler, J. J., Miller, L. P. (2012): Will extreme climatic events facilitate biological invasions? – Frontiers in Ecology and the Environment 10: 249-257. doi:10.1890/110137.

[10] Dreesen, F. E., De Boeck, H. J., Janssens, I. A., Nijs, I. (2014): Do successive climate extremes weaken the resistance of plant communities? An experimental study using plant assemblages. – Biogeosciences 11: 109-121. doi:10.5194/bg-11-109-2014.

[11] Du, G. Z., Qi, W. (2010): Trade-offs between flowering time, plant height, and seed size within and across 11 communities of a QingHai-Tibetan flora. – Plant Ecology 209: 321-333. doi:10.1007/s11258-010-9763-4.

[12] Dwyer, J. G., O'Gorman, P. A. (2017): Changing duration and spatial extent of midlatitude precipitation extremes across different climates. – Geophysical Research Letters 44: 5863-5871. doi: 10.1002/2017gl072855.

http://www.aloki.hu ● ISSN 1589 1623 (Print) ● ISSN 1785 0037 (Online)
DOI: http://dx.doi.org/10.15666/aeer/1704_1009110104

[13] Fernandez-Going, B. M., Anacker, B. L., Harrison, S. P. (2012): Temporal variability in California grasslands: Soil type and species functional traits mediate response to precipitation. – Ecology 93: 2104-2114. doi:10.1890/11-2003.1.

[14] Filazzola, A., Liczner, A. R., Westphal, M., Lortie, C. J. (2018): The effect of consumer pressure and abiotic stress on positive plant interactions are mediated by extreme climatic events. – New Phytologist 217: 140-150. doi: 10.1111/nph.14778.

[15] Frank, D., Reichstein, M., Bahn, M., Thonicke, K., Frank, D., Mahecha, M. D., Smith, P., Van der Velde, M., Vicca, S., Babst, F., Beer, C., Buchmann, N., Canadell, J. G., Ciais, P., Cramer, W., Ibrom, A., Miglietta, F., Poulter, B., Rammig, A., Seneviratne, S. I., Walz, A., Wattenbach, M., Zavala, M. A., Zscheischler, J. (2015): Effects of climate extremes on the terrestrial carbon cycle: concepts, processes and potential future impacts. – Global Change Biology 21: 2861-2880. doi:10.1111/gcb.12916.

[16] Gottfried, M., Pauli, H., Futschik, A., Akhalkatsi, M., Barancok, P., Alonso, J. L. B., Coldea, G., Dick, J., Erschbamer, B., Calzado, M. R. F., Kazakis, G., Krajci, J., Larsson, P., Mallaun, M., Michelsen, O., Moiseev, D., Moiseev, P., Molau, U., Merzouki, A., Nagy, L., Nakhutsrishvili, G., Pedersen, B., Pelino, G., Puscas, M., Rossi, G., Stanisci, A., Theurillat, J. P., Tomaselli, M., Villar, L., Vittoz, P., Vogiatzakis, I., Grabherr, G. (2012): Continent-wide response of mountain vegetation to climate change. – Nature Climate Change 2: 111-115. doi:10.1038/Nclimate1329.

[17] Greenwood, S., Ruiz-Benito, P., Martínez-Vilalta, J., Lloret, F., Kitzberger, T., Allen, C. D., Fensham, R., Laughlin, D. C., Kattge, J., Bönisch, G., Kraft, N. J. B., Jump, A. S. (2017): Tree mortality across biomes is promoted by drought intensity, lower wood density and higher specific leaf area. – Ecology letters 20: 539-553. doi:10.1111/ele.12748.

[18] Gu, S., Tang, Y., Cui, X., Du, M., Zhao, L., Li, Y., Xu, S., Zhou, H., Kato, T., Qi, P., Zhao, X. (2008): Characterizing evapotranspiration over a meadow ecosystem on the Qinghai-Tibetan Plateau. – Journal of Geophysical Research 113. doi:10.1029/2007jd009173.

[19] Guo, T., Lohmann, D., Ratzmann, G., Tietjen, B. (2016): Response of semi-arid savanna vegetation composition towards grazing along a precipitation gradient—The effect of including plant heterogeneity into an ecohydrological savanna model. – Ecological Modelling 325: 47-56. doi:10.1016/j.ecolmodel.2016.01.004.

[20] Guo, T., Weise, H., Fiedler, S., Lohmann, D., Tietjen, B. (2018): The role of landscape heterogeneity in regulating plant functional diversity under different precipitation and grazing regimes in semi-arid savannas. – Ecological Modelling 379: 1-9. doi:10.1016/j.ecolmodel.2018.04.009.

[21] He, J. S., Wang, Z. H., Wang, X. P., Schmid, B., Zuo, W. Y., Zhou, M., Zheng, C. Y., Wang, M. F., Fang, J. Y. (2006): A test of the generality of leaf trait relationships on the Tibetan Plateau. – New Phytologist 170: 835-848. doi:10.1111/j.1469-8137.2006.01704.x.

[22] Jentsch, A., Kreyling, J., Elmer, M., Gellesch, E., Glaser, B., Grant, K., Hein, R., Lara, M., Mirzae, H., Nadler, S. E., Nagy, L., Otieno, D., Pritsch, K., Rascher, U., Schadler, M., Schloter, M., Singh, B. K., Stadler, J., Walter, J., Wellstein, C., Wollecke, J., Beierkuhnlein, C. (2011): Climate extremes initiate ecosystem-regulating functions while maintaining productivity. – Journal of Ecology 99: 689-702. doi:10.1111/j.1365-2745.2011.01817.x.

[23] Knapp, A. K., Beier, C., Briske, D. D., Classen, A. T., Luo, Y., Reichstein, M., Smith, M. D., Smith, S. D., Bell, J. E., Fay, P. A., Heisler, J. L., Leavitt, S. W., Sherry, R., Smith, B., Weng, E. (2008): Consequences of More Extreme Precipitation Regimes for Terrestrial Ecosystems. – Bioscience 58: 811-821. doi:10.1641/B580908.

[24] Kreyling, J., Dengler, J., Walter, J., Velev, N., Ugurlu, E., Sopotlieva, D., Ransijn, J., Picon-Cochard, C., Nijs, I., Hernandez, P., Guler, B., von Gillhaussen, P., De Boeck, H. J., Bloor, J. M. G., Berwaers, S., Beierkuhnlein, C., Arfin Khan, M. A. S., Apostolova, I.,

http://www.aloki.hu ● ISSN 1589 1623 (Print) ● ISSN 1785 0037 (Online)
DOI: http://dx.doi.org/10.15666/aeer/1704_1009110104

Altan, Y., Zeiter, M., Wellstein, C., Sternberg, M., Stampfli, A., Campetella, G., Bartha, S., Bahn, M., Jentsch, A. (2017): Species richness effects on grassland recovery from drought depend on community productivity in a multisite experiment. – Ecology Letters 20: 1405-1413. doi: 10.1111/ele.12848.

[25] Kunstler, G., Falster, D., Coomes, D. A., Hui, F., Kooyman, R. M., Laughlin, D. C., Poorter, L., Vanderwel, M., Vieilledent, G., Wright, S. J., Aiba, M., Baraloto, C., Caspersen, J., Cornelissen, J. H. C., Gourlet-Fleury, S., Hanewinkel, M., Herault, B., Kattge, J., Kurokawa, H., Onoda, Y., Penuelas, J., Poorter, H., Uriarte, M., Richardson, S., Ruiz-Benito, P., Sun, I. F., Stahl, G., Swenson, N. G., Thompson, J., Westerlund, B., Wirth, C., Zavala, M. A., Zeng, H. C., Zimmerman, J. K., Zimmermann, N. E., Westoby, M. (2016): Plant functional traits have globally consistent effects on competition. – Nature 529: 204-207. doi:10.1038/nature16476.

[26] Lee, Y. H., Lim, H. J., Ichii, K., Li, Y. N. (2013): Evaluation of the Community Land Model 3.5 with carbon and nitrogen cycles (CLM3.5CN) at a Tibetan grassland site. – Asia-Pacific Journal of Atmospheric Sciences 49: 561-570. doi:10.1007/s13143-013-0050-x.

[27] Marcolla, B., Cescatti, A., Manca, G., Zorer, R., Cavagna, M., Fiora, A., Gianelle, D., Rodeghiero, M., Sottocornola, M., Zampedri, R. (2011): Climatic controls and ecosystem responses drive the inter-annual variability of the net ecosystem exchange of an alpine meadow. – Agricultural and Forest Meteorology 151: 1233-1243. doi:10.1016/j.agrformet.2011.04.015.

[28] Mouillot, D., Graham, N. A. J., Villeger, S., Mason, N. W. H., Bellwood, D. R. (2013): A functional approach reveals community responses to disturbances. – Trends in Ecology & Evolution 28: 167-177. doi:10.1016/j.tree.2012.10.004.

[29] Orwin, K. H., Buckland, S. M., Johnson, D., Turner, B. L., Smart, S., Oakley, S., Bardgett, R. D. (2010): Linkages of plant traits to soil properties and the functioning of temperate grassland. – Journal of Ecology 98: 1074-1083. doi:10.1111/j.1365-2745.2010.01679.x.

[30] Qi, W., Bu, H. Y., Liu, K., Li, W. J., Knops, J. M. H., Wang, J. H., Li, W. L., Du, G. Z. (2014): Biological traits are correlated with elevational distribution range of eastern Tibetan herbaceous species. – Plant Ecology 215: 1187-1198. doi:10.1007/s11258-014-0377-0.

[31] Reichstein, M., Bahn, M., Ciais, P., Frank, D., Mahecha, M. D., Seneviratne, S. I., Zscheischler, J., Beer, C., Buchmann, N., Frank, D. C., Papale, D., Rammig, A., Smith, P., Thonicke, K., van der Velde, M., Vicca, S., Walz, A., Wattenbach, M. (2013): Climate extremes and the carbon cycle. – Nature 500: 287-295. doi:10.1038/nature12350.

[32] Soussana, J. F., Maire, V., Gross, N., Bachelet, B., Pages, L., Martin, R., Hill, D., Wirth, C. (2012): Gemini: A grassland model simulating the role of plant traits for community dynamics and ecosystem functioning. Parameterization and evaluation. – Ecological Modelling 231: 134-145. doi: 10.1016/j.ecolmodel.2012.02.002.

[33] Sun, G., Wang, Z. Y., Zhu-Barker, X., Zhang, N. N., Wu, N., Liu, L., Lei, Y. B. (2016): Biotic and abiotic controls in determining exceedingly variable responses of ecosystem functions to extreme seasonal precipitation in a mesophytic alpine grassland. – Agricultural Forest Meteorology 228: 180-190. doi: 10.1016/j.agrformet.2016.07.010.

[34] Tan, K., Ciais, P., Piao, S. L., Wu, X. P., Tang, Y. H., Vuichard, N., Liang, S., Fang, J. Y. (2010): Application of the ORCHIDEE global vegetation model to evaluate biomass and soil carbon stocks of Qinghai-Tibetan grasslands. – Global Biogeochemical Cycles 24. doi:10.1029/2009gb003530.

[35] Teuling, A. J., Uijlenhoet, R., Hupet, F., Troch, P. A. (2006): Impact of plant water uptake strategy on soil moisture and evapotranspiration dynamics during drydown. – Geophysical Research Letters 33. doi:10.1029/2005gl025019.

http://www.aloki.hu ● ISSN 1589 1623 (Print) ● ISSN 1785 0037 (Online)
DOI: http://dx.doi.org/10.15666/aeer/1704_1009110104

[36] Tietjen, B., Zehe, E., Jeltsch, F. (2009): Simulating plant water availability in dry lands under climate change: A generic model of two soil layers. – Water Resources Research 45: 1-14. doi:10.1029/2007wr006589.

[37] Tietjen, B., Jeltsch, F., Zehe, E., Classen, N., Groengroeft, A., Schiffers, K., Oldeland, J. (2010): Effects of climate change on the coupled dynamics of water and vegetation in drylands. – Ecohydrology 3: 226-237. doi:10.1002/eco.70.

[38] Tietjen, B. (2016): Same rainfall amount different vegetation—How environmental conditions and their interactions influence savanna dynamics. – Ecological Modelling 326: 13-22. doi: 10.1016/j.ecolmodel.2015.06.013.

[39] van Bodegom, P. M., Douma, J. C., Verheijen, L. M. (2014): A fully traits-based approach to modeling global vegetation distribution. – Proceedings of the National Academy of Sciences of the United States of America 111: 13733-13738. doi:10.1073/pnas.1304551110.

[40] Violle, C., Navas, M.-L., Vile, D., Kazakou, E., Fortunel, C., Hummel, I., Garnier, E. (2007): Let the concept of trait be functional! – Oikos 116: 882-892. doi:10.1111/j.0030-1299.2007.15559.x.

[41] Walter, J., Nagy, L., Hein, R., Rascher, U., Beierkuhnlein, C., Willner, E., Jentsch, A. (2011): Do plants remember drought? Hints towards a drought-memory in grasses. – Environmental and Experimental Botany 71: 34-40. doi:10.1016/j.envexpbot.2010.10.020.

[42] Wang, X., Nakatsubo, T., Nakane, K. (2012): Impacts of elevated CO_2 and temperature on soil respiration in warm temperate evergreen Quercus glauca stands: an open-top chamber experiment. – Ecological Research 27: 595-602. doi:10.1007/s11284-012-0932-x.

[43] Wang, Y. J., Wang, J. J., Lai, L. M., Jiang, L. H., Zhuang, P., Zhang, L. H., Zheng, Y. R., Baskin, J. M., Baskin, C. C. (2014): Geographic variation in seed traits within and among forty-two species of Rhododendron (Ericaceae) on the Tibetan plateau: relationships with altitude, habitat, plant height, and phylogeny. – Ecology and Evolution 4: 1913-1923. doi:10.1002/ece3.1067.

[44] Webb, C. T., Hoeting, J. A., Ames, G. M., Pyne, M. I., LeRoy Poff, N. (2010): A structured and dynamic framework to advance traits-based theory and prediction in ecology. – Ecology letters 13: 267-283. doi:10.1111/j.1461-0248.2010.01444.x.

[45] White, T. A., Campbell, B. D., Kemp, P. D., Hunt, C. L. (2000): Sensitivity of three grassland communities to simulated extreme temperature and rainfall events. – Global Change Biology 6: 671-684. doi:10.1046/j.1365-2486.2000.00344.x.

[46] Wilcox, K. R., Blair, J. M., Knapp, A. K. (2016): Stability of grassland soil C and N pools despite 25 years of an extreme climatic and disturbance regime. – Journal of Geophysical Research: Biogeosciences 121: 1934-1945. doi: 10.1002/2016JG003370.

[47] Wipf, S., Gottfried, M., Nagy, L. (2013): Climate change and extreme events - their impacts on alpine and arctic ecosystem structure and function. – Plant Ecology & Diversity 6: 303-306. doi:10.1080/17550874.2013.819533.

[48] Wu, J. S., Wurst, S., Zhang, X. Z. (2016): Plant functional trait diversity regulates the nonlinear response of productivity to regional climate change in Tibetan alpine grasslands. – Scientific Reports 6: 1-10. doi: 10.1038/srep35649.

[49] Yan, L., Zhou, G. S., Wang, Y. H., Hu, T. Y., Sui, X. H. (2015): The spatial and temporal dynamics of carbon budget in the alpine grasslands on the Qinghai-Tibetan Plateau using the Terrestrial Ecosystem Model. – Journal of Cleaner Production 107: 195-201. doi:10.1016/j.jclepro.2015.04.140.

[50] Yao, T. D., Thompson, L., Yang, W., Yu, W. S., Gao, Y., Guo, X. J., Yang, X. X., Duan, K. Q., Zhao, H. B., Xu, B. Q., Pu, J. C., Lu, A. X., Xiang, Y., Kattel, D. B., Joswiak, D. (2012): Different glacier status with atmospheric circulations in Tibetan Plateau and surroundings. – Nature Climate Change 2: 663-667. doi:10.1038/Nclimate1580.

http://www.aloki.hu ● ISSN 1589 1623 (Print) ● ISSN 1785 0037 (Online)
DOI: http://dx.doi.org/10.15666/aeer/1704_1009110104

[51] Zavalloni, C., Gielen, B., De Boeck, H. J., Lemmens, C. M. H. M., Ceulemans, R., Nijs, I. (2009): Greater impact of extreme drought on photosynthesis of grasslands exposed to a warmer climate in spite of acclimation. – Physiologia Plantarum 136: 57-72. doi:10.1111/j.1399-3054.2009.01214.x.

[52] Zirbel, C. R., Bassett, T., Grman, E., Brudvig, L. A. (2017): Plant functional traits and environmental conditions shape community assembly and ecosystem functioning during restoration. – Journal of Applied Ecology 54: 1070-1079. doi: 10.1111/1365-2664.12885.

http://www.aloki.hu ● ISSN 1589 1623 (Print) ● ISSN 1785 0037 (Online)
DOI: http://dx.doi.org/10.15666/aeer/1704_1009110104

THE IMPACT OF DIFFERENT SOWING-TIMES OF THE QUINOA (*CHENOPODIUM QUINOA* WILLD.) AND ITS VARIETIES ON THE YIELD AND YIELD COMPONENTS IN TURKEY-MARDIN ECOLOGY CONDITION

ALTUNER, F.[1*] – ORAL, E.[2] – KULAZ, H.[2]

[1]*Department of Plant and Animal Production, Gevaş Vocational School of Higher Education, Yüzüncü Yıl University, Gevaş, Van, Turkey*

[2]*Department of Field Crops, Faculty of Agriculture, Yüzüncü Yıl University, 65100, Van, Turkey*

**Corresponding author*
e-mail: faltuner@gmail.com

(Received 11th Apr 2019; accepted 19th Jun 2019)

Abstract. This research was planned to determine the correct sowing times of quinoa (*Chenopodium quinoa* Willd.) varieties under the ecological conditions of Turkey-Mardin. The study was conducted in three different sowing times (15 March, 30 March and 15 April) using 2 quinoa varieties in aqueous conditions in 2017 spring period with three repetitions. At the end of the research; according to the data obtained, the number of plants in the harvest (15.4- 29.2 plants/m^2), plant height (73.9-90.3 cm), the main panicle length (31.1-43.9 cm), the number of panicle branches (23.7-29.7 units plant), thousand weight (3.37-3.46 g), grain yield (125.6-1339 kg ha^{-1}), hectoliter weight (6220-6280 kg ha^{-1}) and crude protein ratio (14.8-15.7%) ranged. The highest grain yield was obtained from the application of Valiente and Titicaca (April 15) with 1345-1333 kg ha^{-1}, respectively. As a result of these properties, it was concluded that the most suitable planting time for quinoa (*Chenopodium quinoa* Willd.) cultivation in Mardin may be the second week of April.
Keywords: *quinoa, Mardin ecology, sowing date, grain yield, agronomy*

Introduction

Parallel to the increasing population of the world in our day, the dependency to the natural resources and consumption has increased. Additionally, the global warming, which has increased in the same period, caused important problems about sufficient and balanced nutrition (Kaya and Karaer, 2017). This case encouraged human beings to find and develop new resources. Particularly the usage of types and varieties of plants, which will increase the yield and quality in animal and plant production and which will be produced under all climates and natural conditions, has been obligatory (Kır, 2016). It is a known fact that grains such as wheat, barley, and rice, which constitute the most basic food source in human nutrition, cause celiac disease (Özkaya, 1999; Battais et al., 2005). Therefore, quinoa (*Chenopodium quinoa* Willd.) can play an important role as an alternative plant, which can be cultivated in a large geography and which has the potential to remove this negativity for the nutrition. To define botanically, quinoa (*Chenopodium quinoa* Willd.) is a dicotyledonous annual plant from the *Chenopodiaceae* family. It has been cultivated in many countries such as Bolivia, Peru, Ecuador, and Chile since the ancient times and its homeland is known to be the South America (Pearsall, 1992). In recent years, the trend in the US and European countries have started to plant quinoa while newly recognized in

http://www.aloki.hu ● ISSN 1589 1623 (Print) ● ISSN 1785 0037 (Online)
DOI: http://dx.doi.org/10.15666/aeer/1704_1010510117

Turkey. However, consumption in the world and Turkey is increasing rapidly. Quinoa is a region in the And mountain region on the west coast of South America, where its homeland is very cold and has high plateaus. It is mainly grown in Colombia, Argentina, Peru, Bolivia, Chile and Ecuador. According to data, 146.735 tons of yield is obtained from 173.242 hectares in the world (FAO, 2017). In our country there is no official data. The fact that this plant has a rich nutritional value caused a rapid increment in cultivation sites. Known little in our country, this plant attracted intensive attention particularly in America and Europe. In return to this attraction, the year 2013 was declared as the year of quinoa (*Chenopodium quinoa* Willd.) by the United Nations (Miranda et al., 2012).

Particularly today, when more than half of the world population is exposed to poor or irregular nutrition, there is a need for alternative products to solve this problem. Accepted as one of these plants, quinoa is named as "super food", "miracle grain", or "astronaut grain". The main reason to define it in these terms is the existence of protein and amino acid at high levels in the grains. Besides this content, the levels of A, B, C, D, E, and K vitamins are at high levels as well (FAO, 2017).

Quinoa cultivation should be generalized as an alternative product in our country and in regions with grain agriculture. It will make important contributions in adding a significant amount of marginal terrains, mined terrains being in the first place, to the production (Kır and Temel, 2017). For this purpose, successful results were obtained by the contracted farmers in the production of these seeds, which certain firms brought to Mardin province. Thus, an agricultural production with high added value will be introduced to the region. In this purpose, it is necessary to determine the most appropriate sowing time and accurate cultivation methods of the quinoa varieties and to encourage its cultivation.

In this study, it was aimed at determining the yield and yield components of quinoa (*Chenopodium quinoa* Willd.) varieties in different sowing times that are not being widely cultivated in our region but considered to increase in a short period.

Materials and methods

This study was conducted in a single year during the cropping season of the 2017 spring period in the ecological conditions of Mardin-Kızıltepe (37°11'12"N and 40°36'43"E) (*Fig. 1*). In the trial, South American-origin Valiente and Titicaca quinoa (*Chenopodium quinoa* Willd.) varieties were used, which were provided by certain companies.

The climate information concerning the research area is given in the *Table 1* and the properties of the soil are given in *Table 2*. As is seen in *Table 1*, it was observed that the temperature and precipitation were lower while the relative humidity was high during the research in the production season of 2017. According to these results, the distribution and amount of the precipitation over the year caused differences between the yield and yield components based on the cultivation times.

As the conclusion of the analysis of the soil samples taken from the research area, it was observed that there was no problem about the salinity and alkalinity. Moreover, it was determined that the soil samples were mid-calcareous and weak in terms of organic matters. The results concerning the pH, salt, lime, and organic matter analyses of the soil samples are given in *Table 2*.

http://www.aloki.hu ● ISSN 1589 1623 (Print) ● ISSN 1785 0037 (Online)
DOI: http://dx.doi.org/10.15666/aeer/1704_1010510117

Figure 1. *The research was conducted in Kiziltepe/Mardin of Turkey*

Table 1. *Climate data concerning the research period at Mardin Weather Regional Station, between February and July calculated from daily climate data, 2017 (Anonymous, 2017)*

Months	Rel. humidity (%)		Mean temp. (°C)		Precipitation (mm)	
	2017	ALY*	2017	ALY*	2017	ALY*
February	51.3	51.0	3.8	3.9	23.2	64.4
March	62.5	62.9	9.7	9.0	101.7	99.6
April	55.7	55.2	13.5	15.2	109.2	98.5
May	44.0	43.8	19.7	19.6	60.3	57.0
June	26.1	25.8	26.8	26.0	0.2	2.2
July	17.0	16.5	32.4	32.1	0.0	0.6
Total					294.6	322.3
Average	**42.8**	**42.5**	**17.6**	**17.7**		

ALY: average of the long years

Table 2. *Soil analysis results about the trial area*

Soil texture (%) Sand alluvium clay			pH	Organic matter (%)	P (phosphor) ppm	K (potassium) ppm	CaCO3 (lime) %
54.3	27.4	11.5	7.2	1.8	28	265	18.95

Mardin Artuklu University Central Laboratory

http://www.aloki.hu ● ISSN 1589 1623 (Print) ● ISSN 1785 0037 (Online)
DOI: http://dx.doi.org/10.15666/aeer/1704_1010510117

This study randomized blocks were developed as 3-repeat according to the experimental design. The quinoa varieties (Valiente and Titicaca), which were obtained by a special company and used in the research, were applied to main parcels, and the sowing times (15 March, 30 March, and 15 April) were applied to the sub-parcels (*Figs. 2* and *3*). In the trial, each parcel (6 m-long and 2 m-wide) was sewn at a 1.0-1.5 cm depth as 6 lines. The distances among the lines were 40 cm. The tillage process was elaborately conducted to prevent clods in the soil and for an orderly germination and first emergence. Since the quinoa seeds are not sewn too deep, and in order for the germination and the first emergence not to be interrupted as a conclusion of the shallow sowing and the crusting soil, springer irrigation was applied after each sowing time. In order to guarantee the number of plants in a unit area, the sowings were applied denser, and once the plants reached a height of 10-15 cm, the distances between the plants were kept at 8 cm through thinning. A distance of 2 m was left among the blocks and 0.5 m among the parcels. Before the sowing, 150 kg ha^{-1} DAP (Diammonium Phosphate) was applied as the bottom fertilizer. After the thinning (while the plants were about 10-15 cm) second nitrogenous manure (ammonium sulphate) was implemented with a calculation of 50 kg N ha^{-1}. One month after the sowing, hoeing was applied to clean the weeds. Hand and hoes were used mechanically in weeding. As the foils turned yellow, started to drop and as the flower clusters dried, the plants were harvested.

In each parcel, 10 plants were selected among the ones that became harvestable, and the following measurements were obtained respectively. Leaving the edge effect, the remaining parts of the parcels were sickled and they were blended after several days of drying. After the seeds matured in the plants were neglected as the edge effect of 50 cm from the parcel heads with 1 and 6 rows. The remaining $5 \times 1.2\ m^2 = 6\ m^2$ area was harvested and yield per decare was calculated. The observations in the research were determined as the number of plants in the harvest (plant number m^{-2}), plant height (cm), the main panicle length (cm), the number of panicle branches (plant $number^{-1}$), total yield (kg ha^{-1}), grain yield (kg ha^{-1}), harvest index (%), thousand weight (g), hectoliter weight (kg) and crude protein ratio (%) (Kır and Temel, 2017).

The data obtained from the research were analyzed through variance analysis by means of CoStat (version 6.303) program, and LSD (0.05, 0.01) multiple comparison test was implemented to determine the significance levels of the differences among the implementations.

Figure 2. *View of the area during the first sowing date*

http://www.aloki.hu ● ISSN 1589 1623 (Print) ● ISSN 1785 0037 (Online)
DOI: http://dx.doi.org/10.15666/aeer/1704_1010510117

Figure 3. *View of the area during the third sowing date*

Results

The mean squares, which were obtained through the variance analysis concerning the mean values of number of plants in the harvest (NPH), plant height (PH), the main panicle length (MPL), the number of panicle branches (NPB), grain yield (GY), thousand weight (TW), hectoliter weight (HW) and crude protein ratio (CPR) that were obtained from trials of 2 quinoa (*Chenopodium quinoa* Willd.) varieties in different times, are given in *Table 3* and the results of the comparisons of the mean values are given in *Table 4*.

Table 3. *Mean squares (MS) obtained from the variance analysis results*

V.K.	DF	NPH	PH	MPL	NPB	TW	GY	HW	CPR
V	1	52.70 *	875.10**	112.50*	4.50ns	0.03ns	144.5*	0.09ns	0.02ns
ST	2	6.92**	168.40ns	33.69ns	57.30**	0.02ns	316.12ns	0.05ns	1.14ns
V × ST	2	10.58ns	0.35 ns	46.33**	21.30ns	0.02ns	283.13**	1.72**	0.46ns
Error	12	366.14	787.12	224.05	383.33	0.05	203.54	3.38	5.25
C_{total}	17	436.6	1830.9	416.6	466.50	0.12	1671.1	5.24	6.87
LSD	-	6.30	9.24	4.83	6.45	0.15	10.05	0.61	0.75
CV (%)	-	13.7	8.3	5.2	8.3	8.9	10.5	4.1	3.7

LSD: least significant effect, CV: coefficient of variation, d.f.: degree of freedom, *value significant at 0.05 probability level, **value significant at 0.01, ns: not significant. V: variety, ST: sowing time, NPH: number of plants in the harvest, PH: plant height, MPL: main panicle length, NPB: number of panicle branches, GY: Grain YIELD, TW: thousand weight, HW: hectoliter weight, and CPR: crude protein ratio

Number of plants in the harvest (plants/m^2) and the plant height (cm)

According to the results of the research, the variety and the sowing time (ST) values of the quinoa were determined to be statistically significant (*Table 3*). The number of plants in the harvest was detected higher in the Titicaca (23.5 plants/m^2) variety

http://www.aloki.hu ● ISSN 1589 1623 (Print) ● ISSN 1785 0037 (Online)
DOI: http://dx.doi.org/10.15666/aeer/1704_1010510117

compared to the Valiente (20.1 plants/m^2) variety (*Table 4*). Based on the sowing times, it was determined that the highest NPH was 26.9 plants/m^2 during the 3rd sowing time (15 April), while the lowest NPH was 17.1 plants/m^2 in the 1st sowing time (1 March) (*Fig. 4*).

Table 4. *The impact of different sowing times on the number of plants in harvest and plant height of quinoa varieties*

Number of plants in the harvest (plants/m^2)					Plant height (cm)			
Sowing times					Sowing times			
Variety	**1**	**2**	**3**	**Mean**	**1**	**2**	**3**	**Mean**
Valiente	15.4	20.1	24.7	20.1 B	87.5	82.9	90.3	86.4 A
Titicaca	18.8	22.5	29.2	23.3 A	76.1	68.8	73.9	72.9 B
Mean	17.1 C	21.3 B	26.9 A		81.8	80.7	82.1	

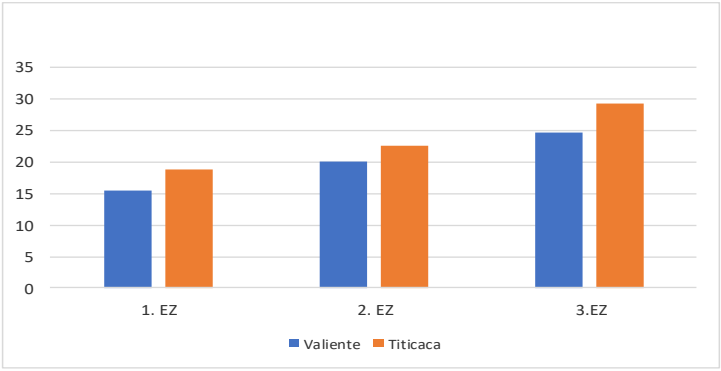

Figure 4. *The impact of sowing times on the number of plants in the harvest in Quinoa. (EZ: sowing time)*

The impact of different sowing times (ST) on the plant height in quinoa varieties was determined to be statistically significant ($p < 0.01$) (*Table 3*). According to the results, the plant height was detected as 86.9 cm in the Valiente variety, while it was 72.9 in Titicaca variety (*Table 4; Fig. 5*).

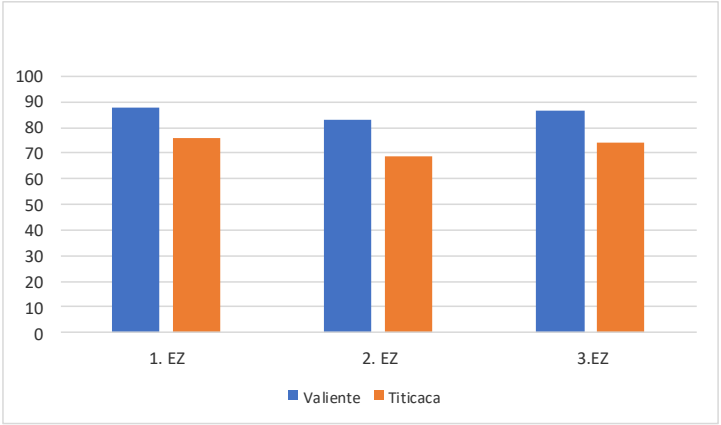

Figure 5. *The impact of sowing times on the plant heights in Quinoa. (EZ: sowing time)*

http://www.aloki.hu ● ISSN 1589 1623 (Print) ● ISSN 1785 0037 (Online)
DOI: http://dx.doi.org/10.15666/aeer/1704_10105010117

The main panicle length (cm) and the number of panicle branches (panicle branch^{-1})

As is seen in *Table 3*, according to the results, the variety and variety × sowing time (ST) interactions were determined to be statistically significant. According to the obtained results, the main panicle length in the Titicaca variety (38.1 cm) was lower compared to the Valiente variety (42.8 cm) (*Table 5*).

Table 5. *The impact of different sowing times on the main panicle length and number of panicle branches of quinoa varieties*

Number of plants in the harvest (plants/m^2)					Plant height (cm)			
Sowing times					Sowing times			
Variety	**1**	**2**	**3**	**Mean**	**1**	**2**	**3**	**Mean**
Valiente	43.1 e	41.4 e	43.9 cd	42.8 A	23.7	24.0	29.7	26.7
Titicaca	31.1 ef	43.1 cd	41.1 gh	38.4 B	27.7	27.6	24.7	25.7
Mean	37.1	42.2	42.5		25.7 B	25.8 B	27.2 A	

In this research, where the interaction of variety × sowing time was determined to be significant, the highest main panicle length was (42.8 cm) determined in the 3rd sowing time of the Valiente variety, while the lowest main panicle length was (31.1 cm) determined in the 1st sowing time of the Titicaca variety (*Fig. 6*).

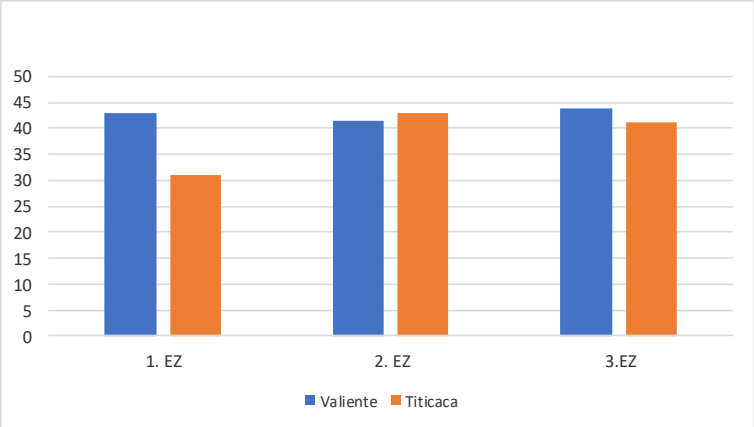

Figure 6. *The impact of sowing times on the main panicle length in Quinoa. (EZ: sowing time)*

In our study, it was determined that the impact of interactions of variety × sowing time (ST) on the number of panicle branches was insignificant, while the impact of the sowing time was determined to be statistically significant (*Table 3*). In this study, the highest number of panicle branches was 27.2 panicle branches^{-1} in the 3rd sowing time, while the lowest was 25.7 panicle branches^{-1} in the 1st sowing time (*Table 5; Fig. 7*).

Thousand weight (g) and grain yield (g)

In this study, the impact of sowing times (ST) on the thousand weight of the quinoa varieties was determined to be statistically insignificant (*Table 3*). According to these results, the thousand weights varied between 3.37-3.46 g (*Table 6; Fig. 8*).

http://www.aloki.hu ● ISSN 1589 1623 (Print) ● ISSN 1785 0037 (Online)
DOI: http://dx.doi.org/10.15666/aeer/1704_1010510117

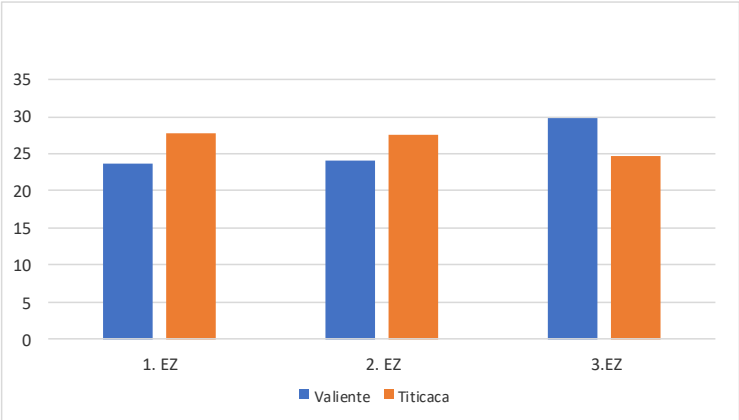

Figure 7. *The impact of sowing times on the number of panicle branches in Quinoa. (EZ: sowing time)*

Table 6. *The impact of different sowing times on the thousand weight and grain yield of quinoa varieties*

Number of plants in the harvest (plants/m^2)					Plant height (cm)			
Sowing times					Sowing times			
Variety	**1**	**2**	**3**	**Mean**	**1**	**2**	**3**	**Mean**
Valiente	43.1 c	41.4 e	43.9 cd	42.8 A	23.7	24.0	29.7	26.7
Titicaca	31.1 ef	43.1 cd	41.1 gh	38.4 B	27.7	27.6	24.7	25.7
Mean	37.1	42.2			25.7 B	25.8 B	27.2 A	

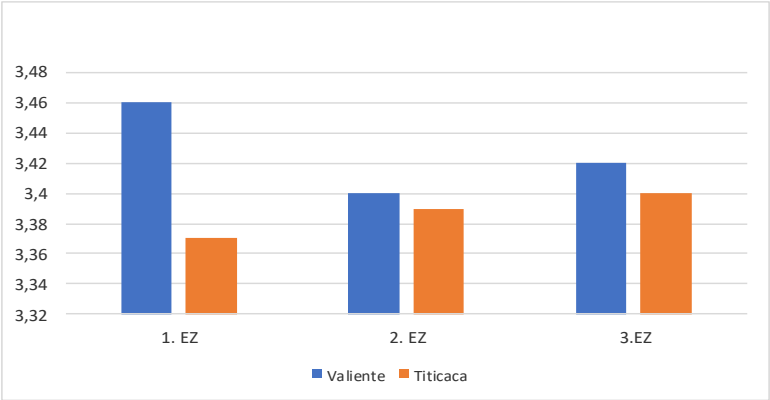

Figure 8. *The impact of sowing times on the thousand weight in Quinoa. (EZ: sowing time)*

As is seen in the *Table 3*, 131.9 g grain yield was obtained from the Valiente variety, which was found to be statistically significant for the variety and variety × sowing time interaction, and 128.7 g grain yield from the Titicaca variety (*Tables 3* and 6). The highest grain yield was 134.5 g in the 3rd sowing time of the Valiente variety, while the lowest grain yield was determined as 125.6 g in the 1st sowing time of the Titicaca variety (*Fig. 9*).

http://www.aloki.hu ● ISSN 1589 1623 (Print) ● ISSN 1785 0037 (Online)
DOI: http://dx.doi.org/10.15666/aeer/1704_1010510117

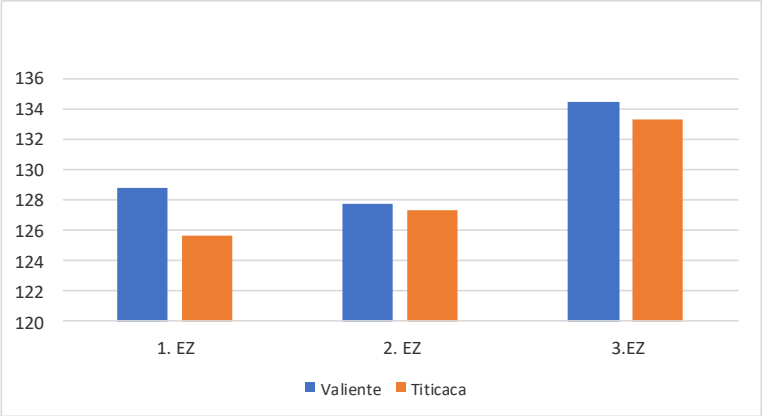

Figure 9. *The impact of sowing times on the grain yield in Quinoa. (EZ: sowing time)*

Hectoliter weight (kg) and crude protein ratio (%)

As is seen in the *Table 3*, while there was statistically no significant impact of the variety and sowing times (ST) on the hectoliter weight, the variety and sowing times interaction was determined to be statistically significant. According to the results of the study, the highest hectoliter weight was 62.8 kg in the 3rd sowing time of the Valiente variety, while the lowest was 62.2 kg in the 1st and 3rd sowing times of the Titicaca variety (*Table 7; Fig. 10*).

Table 7. *The impact of different sowing times on the hectoliter weight and crude protein ratio of quinoa varieties*

Hectoliter weight (kg)					Crude protein (cm)			
Sowing times					Sowing times			
Variety	**1**	**2**	**3**	**Mean**	**1**	**2**	**3**	**Mean**
Valiente	62.4 b	62.2 bc	62.8 a	62.5	15.7	15.2	15.1	15.3
Titicaca	62.2 bc	62.6 ab	62.2 ab	62.3	15.5	14.8	15.0	15.1
Mean	62.3	62.4	62.5		15.6	15.0	15.0	

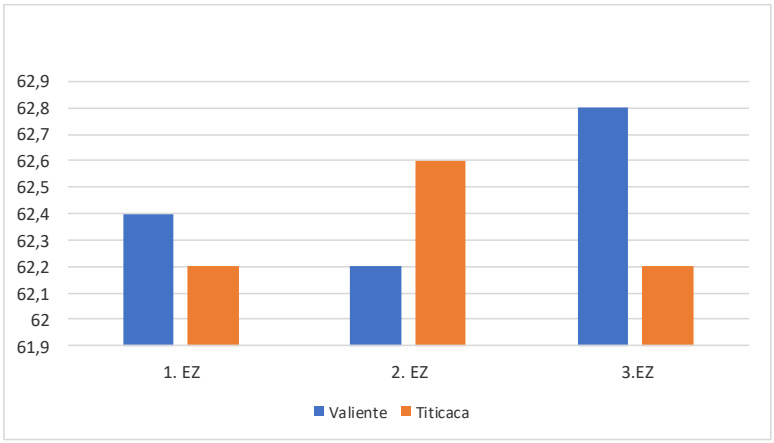

Figure 10. *The impact of sowing times on the hectoliter weight in Quinoa. (EZ: sowing time)*

http://www.aloki.hu ● ISSN 1589 1623 (Print) ● ISSN 1785 0037 (Online)
DOI: http://dx.doi.org/10.15666/aeer/1704_1010510117

It was determined that there was statistically no significant impact of the variety and sowing times (EZ) on the crude protein ratios (*Table 3*). However, the mean crude protein ratios obtained in different sowing times from the Valiente and Titicaca varieties were respectively, 15.3% and 15.1% (*Table 7; Fig. 11*).

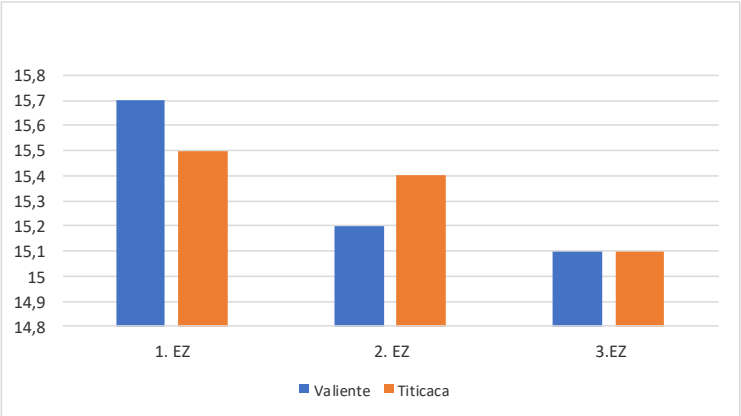

Figure 11. *The impact of sowing times on the crude protein ratios in Quinoa. (EZ: sowing time)*

Discussion

In similar studies, it was reported that the number of plants in the harvest is directly relevant to the grain yield (Bertero et al., 2004). The main reason of the lower NPH figure in the 1st sowing time was estimated to be emerging from that the precipitation and temperature levels of the March were lower compared to those of the April. Lower temperature and precipitation negatively influence the first emergence and development of quinoa, causing a decrease in the number of plants in the harvest (Geren et al., 2014).

In a study conducted by Geren et al. (2014), it was reported that the plant height varied between 63.8 cm and 111.7 cm. According to these results, it is estimated that the plant heights are influenced, to a large extent, from the agricultural implementations applied to the genotypes under different ecological conditions. In a study conducted on different ecology and genotypes, Pulvento et al. (2010) concluded that there were differences in the plant heights of the genotypes. According to the results of the study, the main reason behind the high results of the 3rd sowing time is the increasing temperature and the precipitation in our region. Therefore, we are of the opinion that the first week of the April month might be an appropriate time for a successful quinoa cultivation in our province. In similar studies, it was reported that main panicle length and number of panicle branches had a high and positive impact on the grain yield (Bertero et al., 2004; Bhargava et al., 2007). In a study conducted by Hirich et al. (2014) in the Southern Morocco, different sowing times were implemented ranging between 15 October and 15 March. In that study it was determined that the panicle weight per plant was firstly 24 g, subsequently increasing to 57 g and ultimately decreasing to 15 g.

Besides the fact that thousand weight is a genotypic characteristic, it is known that it is influenced from the environmental conditions. In a study conducted by Koziol (1993), it was reported that the thousand weight varied between 1.9 - 4.3 g based on the variety. In another study conducted by Kaya (2010) under Çukurove conditions, the thousand weight was determined between 2.1 g and 2.6 g (*Fig. 8*). It was considered that the most important motive behind the impact of the sowing times on the grain

http://www.aloki.hu ● ISSN 1589 1623 (Print) ● ISSN 1785 0037 (Online)
DOI: http://dx.doi.org/10.15666/aeer/1704_1010510117

yields of the varieties in the quinoa was that impact of changes in the temperature and precipitation on emergence and germination. This impact influences other herbal characteristics, particularly the number of plants in the unit area, and causes fluctuations in the grain yield (Geren et al., 2014). In similar studies, it was reported that not only the sowings in March, but also sowings in May negatively influence the blossoming and pollination, thus decrease the grain yield (Gonzales et al., 2012). Therefore, in order to determine the accurate sowing time, it was determined that over precipitation and humidity had negative impacts on pollen activity in addition to the negative impacts of dry and hot weather (Aguilar and Jacobsen, 2003). Hectoliter weight is an important criterion in particularly milling, and especially in grains. Moreover, it was reported that ecological factors and cultural implementations can significantly influence the storage and putting on market the seeds (Chauhan et al., 1992; Lindeboom, 2005; Peralta et al., 2006).

The protein ratio of the quinoa was reported to be higher compared to other grains, ranging between 8-22% (Jancurova et al., 2009). The growing season length has been affected by accumulated radiation. In addition to abiotic factors (temperature, radiation, rainfall) affecting quinoa growth, biotic factors such as downy mildew and weeds affected the yield (Hirich et al., 2014).

Conclusion

According to the results of this research study, it was considered that the most appropriate sowing time for the quinoa in Mardin province was the second week of April. The best values concerning the most important characters for the cultivation, the grain yield (133.9 g) and thousand weight (3.41 g) were obtained from the April 15 sowing time. In our region, where the first product wheat and second product corn agriculture is densely implemented, an alternative income can be created by cropping system among various products. Quinoa is quite appropriate for the mechanized agriculture, the sowing can be employed by the sowing machine, and the harvest can be conducted through harvester. The plant is resistant to drought, needing 250-380 mm water in the growing period. Particularly in our province, where the irrigation water is insufficient, if there is precipitation after the sowing in the first and second weeks of April, no need arises for irrigation until the mid-June. After this period, it is necessary to employ irrigation. Therefore, considering the high costs of the water obtained from wells based on intense drilling activities, it is necessary to encourage the cultivation of products with high added values and with an economical water use. Further studies can be conducted in this region as well, supporting this product to become widespread. After this study, similar multi-year researches will be conducted on quinoa. Fertilizer, frequency, irrigation time and other quality analyzes are planned for sowing.

REFERENCES

[1] Aguilar, P. C., Jacobsen, S. E. (2003): Cultivation of quinoa on the Peruvian Altiplano. – Food Reviews International 19: 31-41.

[2] Anonymous (2017): Mardin meteroloji bölge istasyonu verileri. – https://www.mgm.gov.tr/kurumsal/istasyonlarimiz.aspx (accessed: 20 Sept 2018).

http://www.aloki.hu ● ISSN 1589 1623 (Print) ● ISSN 1785 0037 (Online)
DOI: http://dx.doi.org/10.15666/aeer/1704_1010510117

[3] Battais, F., Courcoux, P., Popineau, Y., Kanny, G., Moneret-Vautrin, D. A., Denery-Paini, S. (2005): Food allergy to wheat: differences in immunoglobulin E-binding proteins as a function of age or symptoms. – Journal of Cereal Science 42: 109-117.
[4] Bertero H. D., de la Vega, A. J., Correa, G., Jacobsen, S. E., Mujica, A. (2004): Genotype and genotype-by-environment interaction effects for grain yield and grain size of quinoa (*Chenopodium quinoa* Willd.) as revealed by pattern analysis of international multienvironment trials. – Field Crops Research 89: 299-318.
[5] Bhargava, A., Shukla, S., Ohri, D. (2007): Genetic variability and interrelationship among various morphological and quality traits in quinoa (*Chenopodium quinoa* Willd.). – Field Crops Resarch 101(1): 104-116.
[6] Chauhan, G. S., Eskin, N. A. M., Tkachuk, R. (1992): Nutrients and antinutrients in quinoa seed. – Cereal Chemistry 69: 85-88.
[7] FAO (2017): Plataforma de información de la quinua. – http://www.fao.org/in-action/quinoa-platform/en/ (accessed: 10 Nov 2018).
[8] Geren, H., Kavut, Y. T., Topçu, G. D., Ekren, S., İştipliler, D. (2014): Akdeniz iklimi koşullarında yetiştirilen kinoa (*Chenopodium quinoa* Willd.)'da farklı ekim zamanlarının tane verimi ve bazı verim unsurlarına etkileri. – Ege Üniversitesi Ziraat Fakültesi Dergisi 51: 297-305.
[9] Gonzalez, J. A., Konishi, Y., Bruno, M., Valoya, M., Pradoc, F. E. (2012): Interrelationships among seed yield, total protein and amino acid composition of ten quinoa (*Chenopodium quinoa* Wild) cultivars from two different agroecological regions. – Journal Science Food Agriculture 92: 1222-1229.
[10] Hirich, A., Choukr-Allah, R., Jacobsen, S. E. (2014): Quinoa in Morocco - effect of sowing dates on development and yield. – Journal of Agronomy and Crop Science 1: 371-377.
[11] Jancurová, M., Minarovicová, L., Dandar, A. (2009): Quinoa - a review. – Czech Journal of Food Sciences 27: 71-79.
[12] Kaya, Ç. İ. (2010): Akdeniz bölgesinde damla sistemiyle tatlı ve tuzlu su kullanılarak uygulanan farklı sulama stratejilerinin kinoa bitkisinin verimiyle toprakta tuz birikimine etkileri ve saltmed modelinin test edilmesi. – Yüksek Lisans Tezi, Çukurova Üniversitesi Fen Bilimleri Enstitüsü, Adana.
[13] Kaya, E., Karaer, M. (2017): Kinoa yetiştiriciliği ve sağlık açısından önemi. – Türk Bilimsel Derlemeler Dergisi 10: 21-26.
[14] Kır, A. E., Temel, S. (2016): Iğdır ekolojik koşullarında farklı kinoa çeşit ve populasyonlarının tohum verimi ve bazı özelliklerinin belirlenmesi. – Yüksek Lisans Tezi, Iğdır Üniversitesi Fen Bilimleri Fakültesi Tarla Bitkileri Anabilim Dalı, Iğdır.
[15] Kır, A. E., Temel, S. (2017): Sulu Koşullarda Farklı Kinoa (Chenopodium quinoa Willd.) Genotiplerinin Tohum Verimi ile Bazı Tarımsal Özelliklerinin Belirlenmesi. – Iğdır Üni. Fen Bilimleri Enst. Der./Iğdır Univ. J. Inst. Sci. & Tech. 7(1): 353-361.
[16] Koziol, M. J. (1993): Quinoa: A Potential New Oil Crop. – In: Janick, J., Simon, J. E. (eds.) New Crops. Wiley, New York, pp. 328-336.
[17] Lindeboom, N. (2005): Studies on the characterization, biosynthesis and isolation of starch and protein from quinoa (*Chenopodium quinoa* Willd.). – Ph.D. Thesis, University of Saskatchewan, Department of Applied Microbiology and Food Science, Canada.
[18] Miranda, M., Vega-Galvez, A., Quispe-Fuentes, I., Rodriguez, M. J., Maureira, H., Martinez, E. A. (2012): Nutritional aspects of six quinoa (*Chenepodium quinoa* willd.) ecotypes from three geographical areas of Chile. – Chilean Journal of Agricultural Research 72: 175-181.
[19] Özkaya, B. (1999): Tahılların Neden Olduğu Alerjiler ve Önemi 2. – Food Hi-Tech 1: 82-88.
[20] Pearsall, D. M. (1992): The Origins of Plant Cultivation in South America. – In: Cowan, C. W., Watson, P. J. (eds.) The Origins of Agriculture. Smithsonian Institute Press Washington, DC, pp.173-205.

http://www.aloki.hu ● ISSN 1589 1623 (Print) ● ISSN 1785 0037 (Online)
DOI: http://dx.doi.org/10.15666/aeer/1704_1010510117

[21] Peralta, E., Mazón, N., Villacrés, E., Taipe, J., Olmos, W. (2006): Sustainable production systems for quaranteeing food security in poor communities of the province of Cotopaxi, Ecuador. – National Autonomous Institute for Agricultural Livestock Breeding Research, Year: 1 Progress Report.

[22] Pulvento, C., Riccardi, M., Lavini, A., d'Andria, R., Iafelice, G., Marconi, E. (2010): Field trial evaluation of two chenopodium quinoa genotypes grown under rain-fed conditions in a typical Mediterranean environment in South Italy. – Journal of Agronomy and Crop Science 196(6): 407-411.

http://www.aloki.hu ● ISSN 1589 1623 (Print) ● ISSN 1785 0037 (Online)
DOI: http://dx.doi.org/10.15666/aeer/1704_1010510117

SYNERGISTIC EFFECTS OF RHIZOBIAL INOCULUM WITH CHEMICAL FERTILIZER ON GROWTH AND YIELD OF WHEAT

SABER, T. D.* – KHURSHEED, M. Q.

Department of Biology, College of Education, University of Salahaddin-Erbil, Iraq

**Corresponding author*
e-mail: trifa.saber@su.edu.krd

(Received 12th Apr 2019; accepted 22nd May 2019)

Abstract. The present study was aimed at examining the combined effect of five species of rhizobial inoculation (Control, *Bradyrhizobium sp.* (Vigna), *Rhizobium leguminosarum bv. viciae*, *Bradyrhizobium* Mungbean, *Mesorhizobium ciceri*, and *Rhizobium leguminosarum bv phaseoli*) at three levels (120, 240, 360 kg.ha^{-1}) of NPK on the physiological characteristics, yield components, and leaf chemical content of two wheat species. The results indicated that all physiological characteristics and all nutrient contents of leaf under study, total dry weight of plant at harvest, spike weight, grain number, grain yield, biological yield, and harvest index increased significantly as a result of the interaction between the chemical fertilizer, the biofertilizer, and the wheat species. It was observed that the combination of rhizobial bacteria and wheat species had a positive effect on the physiological characteristics, leaf nutrient contents, and yield components, but not on spike length, spikelet number, and weight of 1000 grains. Our data suggested that a lower level of NPK fertilizer and rhizobial inoculation should be combined in order to achieve the greatest effect on yield components. Also, different types of rhizobial bacteria should be used as biofertilizer in order to improve wheat production.
Keywords: *physiological characteristics, bacteria, production, leaf, Triticum sp.*

Introduction

As one of the first cultivated plants, wheat is regarded as the most significant cereal because it is a major food supply for human. There are numerous species of wheat. For example, macaroni wheat (*Triticum durum*) is a tetraploid wheat species which are cultivated in order to fulfill the demands of the pasta market, whereas *Triticum aestivum* is a hexaploid species that is widely grown throughout the planet (Abou-Taleb and Gomaa, 2012). This species (i.e. *Triticum aestivum*) is one of the most important crops worldwide (Wang et al., 2018). Given the fact that there has been a huge global demand for food as a result of increased world population over the last few decades, a large number of research studies have been aimed at increasing food production so as to meet humanity needs around the world. These diverse researches have included environmental, physiological, agricultural, and genetic studies which all aimed to increased crops productivity (Elghair, 2012).

In order to increase the yields, there has been an increase in the use of mineral fertilizers which are very costly and cause pollution in many ways. Therefore, researchers have always attempted to control such threats by producing alternative substitutes which are more economical, environmentally friendly, and properly improved. In this regard, use of beneficial microbes or plant growth promoting rhizobacteria has been proposed as the best approach to improve crop yield (Adnan et al., 2014). Another widely utilized method to enhance soil fertility and crop productivity is the use of chemical fertilizers which have a negative effect on the complex system of biogeochemical cycles. One of their negative effects, for example,

http://www.aloki.hu ● ISSN 1589 1623 (Print) ● ISSN 1785 0037 (Online)
DOI: http://dx.doi.org/10.15666/aeer/1704_1011910138

is environmental degradation due to runoff and leaching of nutrients, particularly P and N (Yildirim et al., 2011). Another method to increase crop productivity is to use biofertilizers which are substances that contains living microorganisms and applied to plant surface, seeds, or soil. Biofertilizers add nutrients by stimulating plant growth through the synthesis of growth promoting substances and through the natural processes of nitrogen fixation, solubilizing phosphorus. By utilizing biofertilizers, it is expected that there will be a remarkable decrease in the use of chemical fertilizer and pesticides. It is stated that natural nutrient cycle of the soil can be restored and the soil organic matter can be built through the microorganisms in biofertilizers (Al-Shamma and Al-Shahwany, 2014). Moreover, soil contains a wide range of microbes that can act in symbiosis or non-symbiosis association with their host plant (Gray and Smith, 2005).

A range of bacterial genera like *Rhizobium*, *Bradyrhizobium, Sinorhizobium, Mesorhizobium, Allorhizobium,* and *Azorhizobium* exist in rhizobia through which a symbiosis can be established with leguminous plants. Special organs that are known as nodules are produced by these genera on the stems and roots of the hosts, leading to a decrease in atmospheric nitrogen that is delivered to the plant (Sessitsch et al., 2002). As plant growth promoting rhizobacteria (PGPR), rhizobia can also be used in non-legumes (Yanni et al., 1997). Moreover, by producing IAA, gibberellins, and cytokinins, it can enhance growth and yield of cereals (Zahir et al., 2010). Moreover, by producing organic acids, it increase the supply of insoluble nutrients such as phosphorus and iron (Fatima et al., 2006), making these nutrients easily available for plant uptake (Biswas et al., 2000). It is widely reported that the growth parameters, yield, components, and chemical constituents in treated plants can be improved through inoculation of such plants with *Azospirillum*, *Azotobacter*, *Rhizobium*, and *Pseudomonas* in dual or different combinations with organic and mineral fertilizers. According to previous experiments, the best results were obtained by mixing the various inoculations and applying on wheat plants, leading to reduced amount of mineral fertilizers (Mitkees et al., 1996).

The present study was carried out in order to assess the effectiveness of rhizobial bacteria in reducing the use of chemical fertilizer and improving wheat production.

Materials and methods

Pot experiment

The experiment was carried out in the Glasshouse of Biology Department, College of Science, University of Salahaddin-Erbil during winter 2016-2017. The experimental plants used in this experiment included wheat (*Triticum aestivum*) cultivar Hawler2 and (*Triticum durum*) cultivar Seminto that were obtained from the Agricultural Research Center in Erbil. The experiments were carried out using plastic pots with a depth of 25 cm and a diameter of 30 cm. Using a 4 mm pore size sieve, the soil was sieved and then sterilized using formalin 40% as described by Elia et al. (1987). Each pot was filled with 8 kg sandy clay loam soil. *Table 1* presents some of the chemical and physical properties of the soil before the treatments. A sufficient number of wheat seeds were separated and disinfected with 95% ethanol for 30 s and then washed with sterilized distilled water at least 8 times (Etesami et al., 2009). In each pot, 5 seeds were sown at a depth of 3-4 cm and later thinned to four plants.

http://www.aloki.hu ● ISSN 1589 1623 (Print) ● ISSN 1785 0037 (Online)
DOI: http://dx.doi.org/10.15666/aeer/1704_1011910138

Table 1. *Some physical and chemical properties of soil under investigation*

Properties		Value
Particle size distribution (%)	Sand	67.8
	Silt	10.9
	Clay	21.3
Soil texture		Sandy clay loam
pH		8.2
Electrical conductivity ($dS.m^{-1}$)		0.60
Total nitrogen%		0.56
Total phosphorous%		0.144
Total potassium%		0.056
Calcium%		0.253
Iron%		0.078

Isolation of Rhizobial sp

Five strains of rhizobia including *Bradyrhizobium sp*. (Vigna), *Rhizobium leguminosarum* bv. viciae, Bradyrhizobium Mungbean, *Mesorhizobium ciceri* and *Rhizobium leguminosarum* bv. phaseoli were isolated from *Vigna unguiculata*, *Vicia faba, Vigna radiata L., Cicer arietinum L.,* and *Phaseoulus vulgasrous* root nodules, respectively which were growing for 2-3 months under field conditions at a different area of Erbil city. Afterwards, the host plants which had some non-rhizopheric soil on them were uprooted, and they were placed in polythene bags and taken to the laboratory. By shaking the uprooted plants, their non-rhizospheric soil was removed. Moreover, by dipping and shaking them in water, their rhizospheric soil was removed. The nodules were separated from the roots with a sterilized razor blade, and each of them was placed in a separate Petri plates. The surface of the nodules was disinfected by dipping them in ethanol (95%) for 20 s and then in $HgCl_2$ (0.2%) solution for 3 min followed by washing them with sterilized distilled water 6 times. Using a sterilized glass rod, the surface-disinfected nodules of each host were crushed in a sterilized test tube containing sterilized distilled water. The obtained suspension was used to inoculate Petri plates that contained autoclaved and solidified yeast extract mannitol (YEM) media which was then incubated at 28 ± 1 °C for bacterial growth (Mehboob et al., 2011).

Preparation of inoculums

In order to complete the preparation of inoculum, the selected isolates of rhizobia were grown in 250 mL conical flask containing 100 mL YEM broth by incubating at 28 ± 1 °C in an orbital shaking incubator at 100 rpm for 3 days. In order to obtain uniform cell density (i.e. 10^8 to 10^9 CFU mL^{-1}), dilution method was employed in so as to record an optical density of 0.5 at a wavelength of 535 nm (Mehboob et al., 2011). Inoculation of 10 ml (10^8–10^9 $CFU.mL^{-1}$) per seedling was done at the base of the plant ten days after germination.

Experimental design and treatment

The current experiment included 6 treatments of rhizobial inoculums (i.e. Control, *Bradyrhizobium sp.* (Vigna), *Rhizobium leguminosarum bv. viciae*, *Bradyrhizobium*

http://www.aloki.hu ● ISSN 1589 1623 (Print) ● ISSN 1785 0037 (Online)
DOI: http://dx.doi.org/10.15666/aeer/1704_1011910138

Mungbean, *Mesorhizobium ciceri*, and *Rhizobium leguminosarum bv. phaseoli*) and 3 levels of NPK (20:20:20) fertilizers (120, 240 and 360 kg.ha^{-1}), making a total of 36 treatments per replication. The experiment was carried out using a factorial complete randomized design (Factorial C.R.D.) with 3 replications. The comparisons between means were made using Tukey test at significant level of 5% for field experiment parameters and 1% for laboratory parameters. SPSS version 16 was used for data analysis.

Experimental parameters

Physiological parameters

The spectrophotometric method as described by Lichtenthaler (1987) was employed to measure chlorophyll a, chlorophyll b, and carotenoid based on the flag leaf samples that were collected at flowering stage during the growing period.

$$Chlorophyll\ a = (13.36 \times A664.2) - (5.19 \times A648.6)$$

$$Chlorophyll\ b = (27.43 \times A648.6) - (8.12 \times A664.2)$$

$$Total\ Chlorophyll = Chlorophy\ a + Chlorophy\ b$$

$$Carotenoid = \{(1000 \times A470) - (2.13 \times Ch\ a) - (97.64 \times Ch\ b)\}/209$$

In order to determine the membrane stability index (MSI), the method proposed by Premachandra et al. (1991) was utilized.

$$MSI = [1 - (C1/C2)] \times 100$$

Biochemical contents

Dried leaves at flowering stage were ground by an electrical grinder. Afterwards, 0.3 g of the ground samples was digested by adding 10 ml H_2O_2 and 10 ml concentrated H_2SO_4, and they were heated. After that, Kjeldahl method was employed to determine the total nitrogen, spectrophotometer method was used to estimate the total phosphorus, atomic absorption method was utilized to estimate the total calcium and iron, and flame-photometer method as described by Ryan et al. (2001) was used to determine the total potassium determined. Moreover, by multiplying the value of total nitrogen by 5.75, the total protein was calculated (Dalaly and Al-Hakim, 1987). Also, the Anthron method (Sadasivam, 1996) was utilized to determine the total soluble carbohydrate.

Yield components

At harvest, main spike length (cm), number of grains.plant^{-1}, weight of spikes.plant^{-1}, grain yield (kg.ha^{-1}), biological yield (kg.ha^{-1}), number of spikelets.spike^{-1}, harvest index (%), weight of 1000 grains (g), and increase grain yield (%) were estimated. The following formula proposed by Ye et al. (2005) was employed to determine the increased grain yield.

http://www.aloki.hu ● ISSN 1589 1623 (Print) ● ISSN 1785 0037 (Online)
DOI: http://dx.doi.org/10.15666/aeer/1704_1011910138

$$Increase\ grain\ yield\% = \big((Grain\ yield\ of\ fertilized\ pot - Grain\ yield\ of\ control)/Grain\ yield\ of\ control\big) \times 100$$

Results

Physiological parameters

According to the data presented in *Table 2,* it was detected that soil application of B3 led to the highest levels of chlorophyll a, chlorophyll b, total chlorophyll, and carotenoid, while the highest value of cell membrane stability was obtained by utilizing B5.

Table 2. *Effects of different species of rhizobial bacteria on some physiological characteristics*

Bacterial species	Chlorophyll a ($mg.g^{-1}$)	Chlorophyll b ($mg.g^{-1}$)	Total chlorophyll ($mg.g^{-1}$)	Carotenoid ($mg.g^{-1}$)	Cell membrane stability %
Control	0.950	0.609	1.559	0.422	88.557
B1	1.326	1.061	2.387	0.666	93.079
B2	1.426	1.149	2.574	0.696	93.401
B3	1.438	1.199	2.638	0.725	93.105
B4	1.394	0.961	2.356	0.675	94.083
B5	1.343	1.130	2.473	0.671	94.248
Tukey 0.01	0.125	0.163	0.253	0.105	0.133

B1: *Bradyrhizobium sp.* (Vigna), B2: *Rhizobium leguminosarum bv. viciae*, B3: *Bradyrhizobium* Mungbean, B4: *Mesorhizobium ciceri,* B5: *Rhizobium leguminosarum bv phaseoli*

The results also indicated that the highest values of chlorophyll a and cell membrane stability were obtained by adding 360 $kg.ha^{-1}$ of NPK (see *Table 3*). On the other hand, using 240 $kg.ha^{-1}$ of NPK led to obtaining the maximum value of total chlorophyll and carotenoid.

Table 3. *Effects of different levels of chemical fertilizers on some physiological characteristic*

Chemical fertilizer ($kg.ha^{-1}$)	Chlorophyll a $(mg.g)^{-1}$	Chlorophyll b ($mg.g^{-1}$)	Total chlorophyll ($mg.g^{-1}$)	Carotenoid ($mg.g^{-1}$)	Cell membrane stability %
NPK1	1.216	0.9706	2.187	0.589	92.433
NPK2	1.353	1.052	2.405	0.671	92.700
NPK3	1.370	1.032	2.402	0.668	93.103
Tukey 0.01	0.075	n.s.	0.153	0.063	0.08

NPK1 = 120 $kg.ha^{-1}$, NPK2 = 240 $kg.ha^{-1}$, NPK3 = 360 $kg.ha^{-1}$

The results presented in *Table 4* revealed that *Triticum durum* significantly surpassed *Triticum aestivum* regarding the total chlorophyll and cell membrane stability, while wheat species had no effect on chlorophyll a, chlorophyll b, and carotenoid.

http://www.aloki.hu ● ISSN 1589 1623 (Print) ● ISSN 1785 0037 (Online)
DOI: http://dx.doi.org/10.15666/aeer/1704_1011910138

Table 4. *Effects of wheat species on some physiological characteristics*

Wheat species	Chlorophyll a $(mg.g)^{-1}$	Chlorophyll b $(mg.g^{-1})$	Total chlorophyll $(mg.g^{-1})$	Carotenoid $(mg.g^{-1})$	Cell membrane stability %
T. aestivum	1.289	0.990	2.279	0.637	91.879
T. durum	1.3370	1.0464	2.383	0.6480	93.612
Tukey 0.01	n.s.	n.s.	0.087	n.s.	0.057

As indicated in *Table 5*, Rhizobium inoculation resulted in significant increase in physiological parameters in both wheat species. The highest values of chlorophyll a and carotenoid were respectively 1.501 and 0.750 $mg.g^{-1}$ that were recorded in B2 of *Triticum durum*, while highest value of chlorophyll b was 1.258 $mg.g^{-1}$ and the total chlorophyll was 2.737 $mg.g^{-1}$, which were recorded in B3 of *Triticum durum.* The results presented in *Table 5* also revealed that the highest value of cell membrane stability was 94.417% that was recorded in B1 of *Triticum durum.*

Table 5. *Interaction effects of wheat species and rhizobial bacteria on some physiological characteristics*

Wheat species	Bacterial species	Chlorophyll a $(mg.g)^{-1}$	Chlorophyll b $(mg.g^{-1})$	Total chlorophyll $(mg.g^{-1})$	Carotenoid $(mg.g^{-1})$	Cell membrane stability %
T. aestivum	Control	0.928	0.596	1.523	0.452	86.529
	B1	1.204	0.980	2.184	0.631	91.740
	B2	1.350	1.091	2.441	0.643	92.735
	B3	1.397	1.142	2.539	0.717	92.075
	B4	1.445	0.965	2.410	0.709	93.916
	B5	1.408	1.169	2.577	0.672	94.281
T. durum	Control	0.972	0.624	1.595	0.391	90.586
	B1	1.448	1.142	2.590	0.702	94.417
	B2	1.501	1.207	2.708	0.750	94.067
	B3	1.480	1.258	2.737	0.734	94.136
	B4	1.344	0.958	2.302	0.642	94.250
	B5	1.278	1.091	2.368	0.670	94.215
Tukey 0.01		0.199	0.26	0.405	0.168	0.212

B1: *Bradyrhizobium sp.* (Vigna), B2: *Rhizobium leguminosarum bv. viciae*, B3: *Bradyrhizobium* Mungbean, B4: *Mesorhizobium ciceri,* B5: *Rhizobium leguminosarum bv phaseoli*

According to the results presented in *Table 6*, different levels of NPK fertilizer led to significant increase in photosynthetic pigments and cell membrane stability of the two wheat species. The highest value of all photosynthetic pigments was recorded at 240 $kg.ha^{-1}$ of *Triticum durum*, while using 360 $kg.ha^{-1}$ of *Triticum durum* resulted in the highest value of cell membrane stability.

The data presented in *Table 7* show how photosynthetic pigments and cell membrane stability were influenced by different combinations of different levels of NPK fertilizer and different species of rhizobial bacteria. As indicated, using 240 $kg.ha^{-1}$ with B4 led

http://www.aloki.hu ● ISSN 1589 1623 (Print) ● ISSN 1785 0037 (Online)
DOI: http://dx.doi.org/10.15666/aeer/1704_1011910138

to highly significant increases in chlorophyll a, total chlorophyll, and carotenoid. However, the highest value of chlorophyll b was obtained as result of using 240 kg.ha^{-1} with B5. Moreover, using 360 kg.ha^{-1} of NPK with B5 led to the highest cell membrane stability.

Table 6. *Interaction effect of wheat species and chemical fertilizers on some physiological characteristics*

Wheat species	Chemical fertilizer (kg.ha^{-1})	Chlorophyll a (mg.g)$^{-1}$	Chlorophyll b (mg.g^{-1})	Total chlorophyll (mg.g^{-1})	Carotenoid (mg.g^{-1})	Cell membrane stability %
T. aestivum	NPK1	1.227	0.996	2.224	0.605	91.483
	NPK2	1.242	0.918	2.160	0.624	91.988
	NPK3	1.396	1.056	2.453	0.683	92.167
T. durum	NPK1	1.205	0.945	2.150	0.573	93.384
	NPK2	1.463	1.187	2.650	0.718	93.412
	NPK3	1.343	1.008	2.350	0.652	94.039
Tukey 0.01		0.125	0.163	0.253	0.105	0.133

NPK1 = 120 kg.ha^{-1}, NPK2 = 240 kg.ha^{-1}, NPK3 = 360 kg.ha^{-1}

Table 7. *Interaction effect of chemical fertilizer and rhizobial bacteria on some physiological characteristics*

Chemical fertilizer (kg.ha^{-1})	Bacterial species	Chlorophyll a (mg.g)$^{-1}$	Chlorophyll b (mg.g^{-1})	Total chlorophyll (mg.g^{-1})	Carotenoid (mg.g^{-1})	Cell membrane stability %
NPK1	Control	0.931	0.627	1.558	0.430	87.755
	B1	1.252	0.978	2.230	0.607	93.996
	B2	1.344	1.204	2.547	0.669	92.720
	B3	1.318	1.106	2.423	0.658	91.919
	B4	1.184	0.863	2.046	0.553	94.155
	B5	1.269	1.047	2.316	0.616	94.056
NPK2	Control	0.898	0.495	1.393	0.395	87.843
	B1	1.290	0.977	2.267	0.677	92.460
	B2	1.427	1.094	2.520	0.696	93.486
	B3	1.475	1.252	2.727	0.773	94.135
	B4	1.580	1.206	2.786	0.778	94.005
	B5	1.445	1.291	2.736	0.709	94.273
NPK3	Control	1.019	0.706	1.726	0.439	90.075
	B1	1.436	1.229	2.665	0.715	92.780
	B2	1.506	1.148	2.655	0.724	93.998
	B3	1.522	1.242	2.764	0.745	93.262
	B4	1.419	0.816	2.235	0.695	94.089
	B5	1.315	1.051	2.366	0.687	94.415

B1: *Bradyrhizobium sp.* (Vigna), B2: *Rhizobium leguminosarum bv. viciae*, B3: *Bradyrhizobium* Mungbean, B4: *Mesorhizobium ciceri,* B5: *Rhizobium leguminosarum bv phaseoli.* NPK1 = 120 kg.ha^{-1}, NPK2 = 240 kg.ha^{-1}, NPK3 = 360 kg.ha^{-1}

http://www.aloki.hu ● ISSN 1589 1623 (Print) ● ISSN 1785 0037 (Online)
DOI: http://dx.doi.org/10.15666/aeer/1704_1011910138

Leaf photosynthetic pigments and cell membrane stability increased significantly in both wheat species as a result of *Rhizobium* inoculation and chemical fertilizer treatments (see *Table 8*). *Triticum durum* with 240 kg.ha^{-1} of NPK combined with B2 surpassed other interactions and resulted in the highest chlorophyll a and total chlorophyll. Furthermore, *Triticum durum* with 240 kg.ha^{-1} of NPK integrated with B5 and B4 led to the maximum chlorophyll b and carotenoid pigments, respectively, while adding 360 kg.ha^{-1} of NPK with B1 in *Triticum durum* brought about the highest value of cell membrane stability.

Table 8. *Interaction effect of wheat species, chemical fertilizer and rhizobial bacteria on some physiological characteristics*

Wheat species	Chemical fertilizer (kg.ha^{-1})	Bacterial species	Chlorophyll a (mg.g)$^{-1}$	Chlorophyll b (mg.g^{-1})	Total chlorophyll (mg.g^{-1})	Carotenoid (mg.g^{-1})	Cell membrane stability %
T. aestivum	NPK1	Control	0.814	0.615	1.430	0.357	86.978
		B1	1.206	1.009	2.214	0.637	93.604
		B2	1.442	1.286	2.729	0.712	90.955
		B3	1.255	0.991	2.246	0.633	89.425
		B4	1.258	0.935	2.193	0.630	93.875
		B5	1.388	1.141	2.530	0.659	94.058
	NPK2	Control	0.922	0.423	1.345	0.461	85.687
		B1	1.047	0.732	1.779	0.599	90.663
		B2	1.195	0.828	2.023	0.575	93.056
		B3	1.444	1.198	2.642	0.767	94.275
		B4	1.511	1.194	2.705	0.733	93.875
		B5	1.335	1.134	2.469	0.610	94.375
	NPK3	Control	1.047	0.748	1.795	0.538	86.923
		B1	1.359	1.201	2.560	0.658	90.955
		B2	1.413	1.157	2.570	0.642	94.195
		B3	1.492	1.236	2.729	0.749	92.524
		B4	1.566	0.766	2.331	0.764	93.998
		B5	1.501	1.231	2.732	0.749	94.410
T. durum	NPK1	Control	1.049	0.639	1.687	0.504	88.531
		B1	1.299	0.947	2.246	0.577	94.389
		B2	1.245	1.121	2.366	0.625	94.486
		B3	1.381	1.220	2.601	0.683	94.413
		B4	1.109	0.790	1.899	0.475	94.435
		B5	1.149	0.953	2.102	0.574	94.053
	NPK2	Control	0.874	0.568	1.442	0.329	89.999
		B1	1.534	1.221	2.755	0.755	94.258
		B2	1.658	1.359	3.017	0.817	93.915
		B3	1.507	1.305	2.812	0.778	93.996
		B4	1.649	1.219	2.868	0.823	94.135
		B5	1.555	1.448	3.003	0.809	94.170
	NPK3	Control	0.992	0.665	1.656	0.341	93.228
		B1	1.513	1.257	2.769	0.773	94.605
		B2	1.600	1.140	2.739	0.807	93.800
		B3	1.552	1.248	2.799	0.741	94.000
		B4	1.272	0.866	2.138	0.626	94.180
		B5	1.128	0.871	1.999	0.626	94.421
Tukey0.01			0.403	0.528	0.821	0.341	0.431

B1: *Bradyrhizobium sp.* (Vigna), B2: *Rhizobium leguminosarum bv. viciae*, B3: *Bradyrhizobium* Mungbean, B4: *Mesorhizobium ciceri,* B5: *Rhizobium leguminosarum bv phaseoli.* NPK1 = 120 kg.ha^{-1}, NPK2 = 240 kg.ha^{-1}, NPK3 = 360 kg.ha^{-1}

http://www.aloki.hu ● ISSN 1589 1623 (Print) ● ISSN 1785 0037 (Online)
DOI: http://dx.doi.org/10.15666/aeer/1704_1011910138

Biochemical contents

The results presented in *Table 9* demonstrate that the highest values of nitrogen, iron, and protein were recorded by adding B3. Also, phosphorus and carbohydrate reached their highest values as a result of adding B5. Moreover, the maximum values of potassium and calcium were recorded by adding B1 and B4, respectively.

In was also observed that the highest values of nitrogen, phosphorus, iron, and protein were obtained as a result of using 360 kg.ha^{-1} of NPK (see *Table 10*). Furthermore, adding 120 kg.ha^{-1} of NPK resulted in the greatest potassium content of leaves. Also, 240 kg.ha^{-1} of NPK brought about the highest values of calcium and carbohydrate.

According to the data presented in *Table 11, Triticum durum* surpassed *Triticum aestivum* significantly in all leaf nutrient contents under study except potassium and calcium which were better in *Triticum aestivum* than *Triticum durum*.

Table 9. *Effects of different species of rhizobial bacteria on some nutrient content of leaves*

Bacterial species	Protein mg.g^{-1}	Carbohydrate mg.g^{-1}	Nitrogen mg.kg^{-1}	Phosphorus mg.kg^{-1}	Potassium mg.kg^{-1}	Calcium mg.kg^{-1}	Iron mg.kg^{-1}
Control	182.44	250.47	34064.04	2254.53	8404.92	7443.14	121.62
B1	240.96	308.69	43479.46	2838.69	10481.95	8158.36	178.22
B2	250.70	300.24	44044.08	2569.27	10164.06	8175.40	191.88
B3	258.79	317.42	47026.08	3104.00	9836.24	8142.41	217.45
B4	232.19	324.36	40763.83	2724.08	10350.04	8287.79	183.37
B5	221.68	327.73	41212.83	3818.69	9890.59	8050.33	169.54
Tukey 0.01	2.24	0.58	389.437	9.981	125.046	103.398	3.338

B1: *Bradyrhizobium sp.* (Vigna), B2: *Rhizobium leguminosarum bv. viciae*, B3: *Bradyrhizobium* Mungbean, B4: *Mesorhizobium ciceri,* B5: *Rhizobium leguminosarum bv phaseoli*

Table 10. *Effects of different levels of chemical fertilizer on some nutrient content of leaves*

Chemical fertilizer (kg.ha^{-1})	Protein mg.g^{-1}	Carbohydrate mg.g^{-1}	Nitrogen mg.kg^{-1}	Phosphorus mg.kg^{-1}	Potassium mg.kg^{-1}	Calcium mg.kg^{-1}	Iron mg.kg^{-1}
NPK1	219.93	310.46	38248.73	2748.11	9968.80	7832.05	178.94
NPK2	236.26	312.80	41087.88	2791.14	9792.77	8208.84	165.82
NPK3	264.26	291.19	45958.54	3115.39	9802.33	8087.83	186.27
Tukey 0.01	1.35	0.35	234.783	6.017	75.388	62.336	2.012

NPK1 = 120 kg.ha^{-1}, NPK2 = 240 kg.ha^{-1}, NPK3 = 360 kg.ha^{-1}

Table 11. *Effect of wheat species on some nutrient content of leaves*

Wheat species	Protein mg.g^{-1}	Carbohydrate mg.g^{-1}	Nitrogen mg.kg^{-1}	Phosphorus mg.kg^{-1}	Potassium mg.kg^{-1}	Calcium mg.kg^{-1}	Iron mg.kg^{-1}
T. aestivum	230.17	293.05	40029.07	2750.18	10045.62	8248.84	168.64
T. durum	250.13	316.58	43501.04	3019.57	9663.65	7836.98	185.39
Tukey 0.01	0.96	0.25	167.715	4.299	53.852	44.529	1.437

http://www.aloki.hu ● ISSN 1589 1623 (Print) ● ISSN 1785 0037 (Online)
DOI: http://dx.doi.org/10.15666/aeer/1704_1011910138

It was also observed that the nutrient contents of the leaves in both wheat species increased significantly as a result of different species of Rhizobial inoculation compared with the control species (see *Table 12*). The highest values of N (50079.67 $mg.kg^{-1}$), Fe (263.34 $mg.kg^{-1}$), protein (287.96 $mg.g^{-1}$), and carbohydrate (356.79 $mg.g^{-1}$) were observed in B3 of *Triticum durum*, while the highest values of P (4350.08 $mg.kg^{-1}$), K (10555.82 $mg.kg^{-1}$), and Ca (8841.02 $mg.kg^{-1}$) were respectively recorded in B5 of *Triticum durum*, B1 of *Triticum aestivum*, B4 of *Triticum aestivum*.

Table 12. *Interaction effect of wheat species and rhizobial species on some nutrient content of leaves*

Wheat species	Bacterial species	Protein $mg.g^{-1}$	Carbohydrate $mg.g^{-1}$	Nitrogen $mg.kg^{-1}$	Phosphorus $mg.kg^{-1}$	Potassium $mg.kg^{-1}$	Calcium $mg.kg^{-1}$	Iron $mg.kg^{-1}$
T. aestivum	Control	184.24	230.56	32041.55	2336.67	9047.43	7618.78	129.89
	B1	241.62	314.89	42021.59	2750.52	10555.82	8085.04	177.47
	B2	254.52	291.72	44264.17	2598.20	10210.15	8737.96	210.69
	B3	252.84	278.05	43972.50	2866.62	10153.99	7968.21	171.57
	B4	235.59	299.09	40972.13	2661.77	10469.07	8841.02	171.90
	B5	212.19	344.01	36902.48	3287.30	9837.22	8242.00	150.31
T. durum	Control	207.50	270.37	36086.53	2172.39	7762.40	7267.50	113.36
	B1	258.39	302.49	44937.34	2926.86	10408.07	8231.68	178.97
	B2	251.99	308.76	43824.00	2540.35	10117.96	7612.83	173.07
	B3	287.96	356.79	50079.67	3341.37	9518.49	8316.61	263.34
	B3	233.19	349.63	40555.52	2786.40	10231.02	7734.57	194.83
	B5	261.76	311.45	45523.18	4350.08	9943.96	7858.67	188.77
Tukey 0.01		3.57	0.926	621.566	15.931	199.582	165.029	5.327

B1: *Bradyrhizobium sp.* (Vigna), B2: *Rhizobium leguminosarum bv. viciae*, B3: *Bradyrhizobium* Mungbean, B4: *Mesorhizobium ciceri,* B5: *Rhizobium leguminosarum bv phaseoli*

The results also revealed that NPK fertilizer had a significant effect on all nutrient contents of the leaves in both wheat species (see *Table 13*). In addition, using 360 $kg.ha^{-1}$ of NPK for *Triticum durum* led to the highest values of nitrogen, phosphorus, and protein. Moreover, 120 $kg.ha^{-1}$ NPK of *Triticum aestivum* and 240 $kg.ha^{-1}$ NPK of *Triticum aestivum* led to the maximum values of potassium and calcium, respectively. Furthermore, adding 120 $kg.ha^{-1}$ NPK of *Triticum durum* brought about the highest iron and carbohydrate content of the leaves.

Table 14 presents the data related to the effects of the chemical fertilizer combined with biofertilizer on the nutrient contents of the leaves. As observed, the highest values of nitrogen and protein contents of the leaves were obtained at 360 $kg.ha^{-1}$ of NPK with B3. On the other hand the maximum value of phosphorus contents of the leaves was obtained at 360 $kg.ha^{-1}$ of NPK with B5, while the greatest values of potassium and calcium were obtained in 240 $kg.ha^{-1}$ of NPK with B4. Moreover, adding 120 $kg.ha^{-1}$ with B3 led to the maximum values of iron and carbohydrate.

The interaction effects of different species of rhizobial bacteria and different levels of NPK on the two wheat species are presented in *Table 15*. Adding different types of rhizobial bacteria to the soil at different levels of NPK led to significant increase in Fe, P, N, Ca, K, protein, and the leaves' carbohydrate contents in both wheat species. Application of 360 $kg.ha^{-1}$ of NPK with B3 led to the highest nitrogen and protein

http://www.aloki.hu ● ISSN 1589 1623 (Print) ● ISSN 1785 0037 (Online)
DOI: http://dx.doi.org/10.15666/aeer/1704_1011910138

contents of the leaves in *Triticum durum*. The highest values of carbohydrate, phosphorus, and iron were recorded by utilizing 360 kg.ha^{-1} of NPK with B4 of *Triticum durum*, 120 kg.ha^{-1} of NPK with B5 of *Triticum durum*, and (120 kg.ha^{-1} of NPK with B3 of *Triticum durum*, respectively, while the highest values of potassium and calcium were obtained through 240 kg.ha^{-1} of NPK with B4 of *Triticum aestivum*.

Table 13. *Interaction effect of wheat species and chemical fertilizer on some nutrient content of leaves*

Wheat species	Chemical fertilizer (kg.ha^{-1})	Protein mg.g^{-1}	Carbohydrate mg.g^{-1}	Nitrogen mg.kg^{-1}	Phosphorus mg.kg^{-1}	Potassium mg.kg^{-1}	Calcium mg.kg^{-1}	Iron mg.kg^{-1}
T. aestivum	NPK1	217.05	295.59	37747.63	2355.21	10104.45	7965.86	148.11
	NPK2	222.61	317.32	38714.14	2858.63	10035.05	8495.70	161.28
	NPK3	250.85	266.25	43625.44	3036.70	9997.34	8284.95	196.53
T. durum	NPK1	222.81	325.33	38749.83	3141.00	9833.16	7698.24	209.77
	NPK2	249.90	308.28	43461.63	2723.64	9550.48	7921.99	170.37
	NPK3	277.68	316.14	48291.65	3194.08	9607.31	7890.70	176.02
Tukey 0.01		2.24	0.58	389.437	9.981	125.046	103.398	3.338

NPK1 = 120 kg.ha^{-1}, NPK2 = 240 kg.ha^{-1}, NPK3 = 360 kg.ha^{-1}

Table 14. *Interaction effect of chemical fertilizer and rhizobial bacteria on some nutrient content of leaves*

Chemical fertilizer (kg.ha^{-1})	Bacteria species	Protein mg.g^{-1}	Carbohydrate mg.g^{-1}	Nitrogen mg.kg^{-1}	Phosphorus mg.kg^{-1}	Potassium mg.kg^{-1}	Calcium mg.kg^{-1}	Iron mg.kg^{-1}
NPK1	Control	172.58	250.71	30014.22	1894.74	9064.47	7483.87	135.78
	B1	239.55	311.26	41661.58	2627.63	10505.41	7885.47	142.63
	B2	225.49	303.63	39215.14	2550.27	9899.13	7882.97	151.98
	B3	246.90	356.81	42938.43	2631.99	10036.23	7728.07	312.42
	B4	220.66	309.11	38375.89	2700.99	10668.13	8163.23	157.33
	B5	214.40	331.24	37287.13	4083.02	9639.46	7848.67	173.52
NPK2	Control	204.37	266.29	35542.27	2371.15	7993.57	7479.29	110.24
	B1	236.24	344.77	41084.41	2955.75	10268.68	8135.42	166.92
	B2	234.00	308.11	40694.83	2512.56	10079.10	7900.04	176.02
	B3	259.33	308.44	45101.62	2725.65	10024.42	8606.24	181.87
	B4	241.08	315.80	41927.17	2926.44	10685.93	8838.98	191.96
	B5	242.52	333.39	42177.01	3255.26	9704.90	8293.08	167.92
NPK3	Control	210.65	234.40	36635.62	2497.70	8156.72	7366.26	118.84
	B1	274.23	270.04	47692.40	2932.69	10671.75	8454.18	225.10
	B2	300.28	288.97	52222.28	2644.99	10513.95	8743.18	247.64
	B3	304.97	287.01	53038.20	3954.35	9448.07	8092.92	158.08
	B4	241.43	348.17	41988.42	2544.82	9696.07	7861.17	200.81
	B5	254.00	318.56	44174.36	4117.79	10327.41	8009.25	167.17
Tukey 0.01		4.65	1.205	808.749	20.728	259.685	214.728	6.932

B1: *Bradyrhizobium sp.* (Vigna), B2: *Rhizobium leguminosarum bv. viciae*, B3: *Bradyrhizobium* Mungbean, B4: *Mesorhizobium ciceri,* B5: *Rhizobium leguminosarum bv phaseoli.* NPK1 = 120 kg.ha^{-1}, NPK2 = 240 kg.ha^{-1}, NPK3 = 360 kg.ha^{-1}

http://www.aloki.hu ● ISSN 1589 1623 (Print) ● ISSN 1785 0037 (Online)
DOI: http://dx.doi.org/10.15666/aeer/1704_1011910138

Table 15. *Interaction effect of wheat species, chemical fertilizer and rhizobial species on some nutrient content of leaves*

Wheat species	Chemical fertilizer (kg.ha^{-1})	Bacteria species	Protein mg.g^{-1}	Carbohydrate mg.g^{-1}	Nitrogen mg.kg^{-1}	Phosphorus mg.kg^{-1}	Potassium mg.kg^{-1}	Calcium mg.kg^{-1}	Iron mg.kg^{-1}
T. aestivum	NPK1	Control	177.96	233.90	30950.32	2070.93	9501.22	7836.17	137.28
		B1	241.53	268.36	42005.92	*2231.45*	10734.78	7984.77	149.98
		B2	236.95	314.09	41208.25	2552.93	10088.08	8063.87	137.28
		B3	229.06	313.15	39837.23	2447.81	10054.35	7752.07	166.17
		B4	230.87	289.54	40150.90	*2073.90*	10588.20	8103.87	147.98
		B5	185.92	354.50	32333.16	2754.26	9660.07	8054.37	149.98
	NPK2	Control	167.25	242.17	29087.13	2438.10	8924.14	7399.21	117.59
		B1	229.05	406.81	39834.73	2669.14	9720.69	8215.98	166.17
		B2	226.49	296.13	39389.73	2475.00	9931.38	8150.51	200.56
		B3	241.49	293.03	41998.92	2645.24	10674.82	8093.69	182.37
		B4	234.41	320.56	40766.58	3438.10	11240.79	10583.01	166.67
		B5	236.94	345.23	41207.75	3486.21	9718.50	8531.78	134.28
	NPK3	Control	207.50	215.62	36087.20	2501.00	8716.94	7620.97	134.78
		B1	254.29	269.51	44224.11	3350.98	11212.00	8054.37	216.26
		B2	300.12	264.93	52194.53	2766.67	10611.00	9999.50	294.23
		B3	287.97	227.96	50081.34	3506.81	9732.80	8058.87	166.17
		B4	241.49	287.17	41998.92	2473.31	9578.22	7836.17	201.06
		B5	213.71	332.30	37166.54	3621.43	10133.08	8139.83	166.67
T. durum	NPK1	Control	167.20	267.51	29078.13	1718.55	8627.71	7131.56	134.28
		B1	237.57	354.16	41317.25	3023.81	10276.04	7786.17	135.28
		B2	214.03	293.17	37222.04	2547.62	9710.19	7702.07	166.67
		B3	264.73	400.46	46039.63	2816.17	10018.12	7704.07	458.67
		B4	210.45	328.69	36600.87	3328.07	10748.05	8222.58	166.67
		B5	242.89	307.99	42241.09	5411.79	9618.84	7642.97	197.06
	NPK2	Control	241.49	290.42	41997.42	2304.21	7063.00	7559.37	102.90
		B1	243.42	282.73	42334.09	3242.36	10816.67	8054.87	167.67
		B2	241.50	320.08	41999.92	2550.12	10226.81	7649.57	151.48
		B3	277.17	323.85	48204.32	2806.07	9374.03	9118.79	181.37
		B4	247.75	311.04	43087.77	2414.79	10131.08	7094.96	217.26
		B5	248.09	321.55	43146.27	3024.31	9691.30	8054.37	201.56
	NPK3	Control	213.81	253.19	37184.04	2494.40	7596.50	7111.56	102.90
		B1	294.17	270.58	51160.68	2514.40	10131.50	8853.98	233.95
		B2	300.44	313.02	52250.03	2523.31	10416.89	7486.87	201.06
		B3	321.97	346.06	55995.06	4401.88	9163.33	8126.98	149.98
		B4	241.37	409.16	41977.92	2616.33	9813.92	7886.17	200.56
		B5	294.30	304.81	51182.18	4614.14	10521.74	7878.67	167.67
Tukey 0.01			7.25	1.879	1260.856	32.316	404.854	334.765	10.807

B1: *Bradyrhizobium sp.* (Vigna), B2: *Rhizobium leguminosarum bv. viciae*, B3: *Bradyrhizobium* Mungbean, B4: *Mesorhizobium ciceri,* B5: *Rhizobium leguminosarum bv phaseoli.* NPK1 = 120 kg.ha^{-1}, NPK2 = 240 kg.ha^{-1}, NPK3 = 360kg.ha^{-1}

Yield components

The results presented in *Table 16* reveal that, compared with the control treatment, soil application of different rhizobial bacteria had a significant effect on some yield

http://www.aloki.hu ● ISSN 1589 1623 (Print) ● ISSN 1785 0037 (Online)
DOI: http://dx.doi.org/10.15666/aeer/1704_1011910138

components. In addition, using B4 led to the maximum values of total dry weight of 54.31 g.plant^{-1}, spike weight of 8.09 g, grain number of 106.22, and biological yield of 7895.18 kg.ha^{-1}, and utilizing B3 resulted in the highest grain yield of 2823.15 kg.ha^{-1} and harvest index of 38.43%.

Table 16. *Effects of different species of rhizobial bacteria on some yield components*

Bacterial species	Total dry weight g.pot^{-1}	Spike length plant^{-1}	Spike weight. plant^{-1}	Spikelet number plant^{-1}	Grain number plant^{-1}	Grain yield kg.ha^{-1}	Biological yield kg.ha^{-1}	Weight of 1000 grain (g)	Harvest index %
Control	38.80	8.07	5.54	17.33	68.75	1819.77	5492.33	47.99	33.68
B1	52.73	8.51	7.31	18.50	95.28	2550.29	7464.03	48.49	34.28
B2	54.05	8.33	7.59	18.83	97.08	2708.82	7650.86	50.40	36.22
B3	53.95	8.33	7.53	18.33	95.72	2823.15	7636.71	53.47	38.43
B4	54.31	8.60	8.09	18.83	106.22	2780.06	7686.72	47.64	37.04
B5	53.11	8.80	7.76	19.17	105.83	2661.63	7517.50	46.68	35.54
Tukey 0.05	3.31	n.s.	0.70	n.s.	6.578	271.42	468.25	n.s.	4.45

B1: *Bradyrhizobium sp.* (Vigna), B2: *Rhizobium leguminosarum bv. viciae*, B3: *Bradyrhizobium* Mungbean, B4: *Mesorhizobium ciceri,* B5: *Rhizobium leguminosarum bv phaseoli*

According to the results presented in *Table 17,* it can clearly be observed that adding 360 kg.ha^{-1} resulted in the maximum increment of total dry weight, spike weight, grain number, grain yield, and biological yield. Moreover, using 120 kg.ha^{-1} of NPK led to the highest value of harvest index.

According to *Table 18,* some yield components were affected by wheat species, such that *Triticum aestivum* surpassed *Triticum durum* regarding spike length, grain number, and harvest index, while *Triticum durum* surpassed *Triticum aestivum* significantly in terms of total dry weight, spike weight, grain yield, biological yield, and weight of 1000 grains.

Table 17. *Effects of different levels of chemical fertilizer on some yield components*

Chemical fertilizer (kg.ha^{-1})	Total dry weight g.pot^{-1}	Spike length plant^{-1}	Spike weight plant^{-1}	Spikelet number plant^{-1}	Grain number plant^{-1}	Grain yield kg.ha^{-1}	Biological yield kg.ha^{-1}	Weight of 1000 grain (g)	Harvest index %
NPK1	48.26	8.20	6.54	18.42	84.15	2452.47	6830.70	42.64	38.31
NPK2	49.44	8.33	7.16	18.42	93.76	2551.62	6998.19	42.41	37.12
NPK3	55.78	8.80	8.21	18.67	106.53	2632.70	7895.18	41.64	34.22
Tukey 0.05	1.91	n.s.	0.41	n.s.	3.80	156.86	270.6	n.s.	2.57

NPK1 = 120 kg.ha^{-1}, NPK2 = 240 kg.ha^{-1}, NPK3 = 360 kg.ha^{-1}

Table 18. *Effects of wheat species on some yield components*

Wheat species	Total dry weight g.pot^{-1}	Spike length plant^{-1}	Spike weight plant^{-1}	Spikelet number plant^{-1}	Grain number plant^{-1}	Grain yield kg/ha	Biological yield kg/ha	Weight of 1000 grain (g)	Harvest index %
T. aestivum	45.19	9.72	6.47	18.50	105.94	2465.78	6396.43	42.03	38.91
T. durum	57.13	7.16	8.13	18.50	83.69	2648.79	8086.29	56.19	32.82
Tukey 0.05	1.299	0.67	0.28	n.s.	2.58	106.60	183.91	2.4	1.75

http://www.aloki.hu ● ISSN 1589 1623 (Print) ● ISSN 1785 0037 (Online)
DOI: http://dx.doi.org/10.15666/aeer/1704_1011910138

The results presented in *Table 19* revealed that different species of rhizobial bacteria had a significant effect on some yield components of both wheat species. Applying B2 with *Triticum durum* resulted in the highest values of grain yield (2941.26 kg.ha^{-1}), total dry weight of plant (63.04 g.plant^{-1}), and biological yield (8922.86 kg.ha^{-1}). Also, B4 with *Triticum durum* led to the highest value of spike weight (9.21 g). Moreover, the highest value of grain number (127.50) was obtained by utilizing B5 with *Triticum aestivum*, and the maximum value of harvest index (45.76%) was obtained as a result of using B3 with *Triticum aestivum*.

Table 19. *Interaction effect of wheat species and rhizobial bacteria on some yield components*

Wheat species	Bacterial species	Total dry weight g.pot^{-1}	Spike length plant^{-1}	Spike weight plant^{-1}	Spikelet number plant^{-1}	Grain number plant^{-1}	Grain yield kg.ha^{-1}	Biological yield kg.ha^{-1}	Weight of 1000 grain (g)	Harvest index %
T. aestivum	Control	33.02	8.93	4.77	17.33	75.00	1631.83	4673.43	39.12	35.11
	B1	47.39	9.67	6.36	18.33	105.50	2342.69	6707.24	39.56	35.01
	B2	45.07	9.27	6.54	18.67	104.83	2476.37	6378.86	42.63	39.35
	B3	46.61	9.50	6.77	18.00	109.17	2939.37	6597.78	48.63	45.76
	B4	48.05	10.57	6.97	19.33	113.67	2663.52	6800.66	43.36	40.21
	B5	51.01	10.40	7.42	19.33	127.50	2740.90	7220.57	38.88	38.02
T. durum	Control	44.59	7.21	6.31	17.33	62.50	2007.71	6311.24	56.87	32.26
	B1	58.08	7.34	8.27	18.67	85.06	2757.88	8220.81	57.42	33.55
	B2	63.04	7.40	8.64	19.00	89.33	2941.26	8922.86	58.17	33.09
	B3	61.29	7.17	8.29	18.67	82.28	2706.93	8675.63	58.30	31.09
	B4	60.57	6.63	9.21	18.33	98.78	2896.60	8572.78	51.92	33.86
	B5	55.21	7.20	8.09	19.00	84.17	2582.37	7814.42	54.47	33.07
Tukey 0.05		5.409	n.s.	1.15	n.s.	10.76	443.82	765.67	n.s.	7.28

B1: *Bradyrhizobium sp.* (Vigna), B2: *Rhizobium leguminosarum bv. viciae*, B3: *Bradyrhizobium* Mungbean, B4: *Mesorhizobium ciceri,* B5: *Rhizobium leguminosarum bv phaseoli*

In addition, the two wheat species were significantly different in terms NPK levels (see *Table 20*). In general, the highest values of most yield components were observed at NPK3 for both species, while the highest values of weight of 1000 grains and harvest index were obtained by adding 240 kg.ha^{-1} of NPK of *Triticum durum* and 120 kg.ha^{-1} of NPK *Triticum aestivum*, respectively.

Table 20. *Interaction effect of wheat species and chemical fertilizer on some yield components*

Wheat species	Chemical fertilizer kg.ha^{-1}	Total dry weight g.pot^{-1}	Spike length plant^{-1}	Spike weight plant^{-1}	Spikelet number plant^{-1}	Grain number plant^{-1}	Grain yield kg.ha^{-1}	Biological yield kg.ha^{-1}	Weight of 1000 grain (g)	Harvest index %
T. aestivum	NPK1	39.38	9.35	5.57	17.50	90.25	2346.15	5573.48	45.50	41.83
	NPK2	44.39	9.63	6.18	18.67	104.25	2503.26	6283.56	42.97	40.08
	NPK3	51.80	10.18	7.67	19.33	123.33	2547.93	7332.23	37.62	34.82
T. durum	NPK1	57.14	7.04	7.50	19.33	78.06	2474.48	8087.91	56.28	30.89
	NPK2	54.49	7.02	8.14	18.17	83.28	2648.27	7712.83	56.47	34.21
	NPK3	59.76	7.42	8.76	18.00	89.72	2823.62	8458.13	45.65	33.62
Tukey 0.05		3.31	n.s	0.70	n.s	6.58	271.42	468.25	6.19	4.45

NPK1 = 120 kg.ha^{-1}, NPK2 = 240 kg.ha^{-1}, NPK3 = 360 kg.ha^{-1}

http://www.aloki.hu ● ISSN 1589 1623 (Print) ● ISSN 1785 0037 (Online)
DOI: http://dx.doi.org/10.15666/aeer/1704_1011910138

The results presented in *Table 21* indicate the interaction effects of chemical fertilizer and rhizobial bacteria on some yield components. As observed, the highest values of total dry weight, spike weight, grain number, and biological yield were gained by adding 360 kg.ha^{-1} of NPK with B4, and the highest values of grain yield and harvest index were obtained by adding 240 kg.ha^{-1} of NPK with B4.

Table 21. *Interaction effect of chemical fertilizer and rhizobial bacteria on some yield components*

Chemical fertilizer kg.ha^{-1}	Bacterial species	Total dry weight g.pot^{-1}	Spike length plant^{-1}	Spike weight plant^{-1}	Spikelet number plant^{-1}	Grain number plant^{-1}	Grain yield kg.ha^{-1}	Biological yield kg.ha^{-1}	Weight of 1000 grain (g)	Harvest index %
NPK1	Control	31.36	7.97	4.68	17.50	64.00	1622.55	4439.26	47.55	36.54
	B1	50.36	8.37	6.80	18.00	88.42	2379.34	7127.62	47.34	33.78
	B2	55.73	8.25	7.02	19.00	90.42	2836.99	7888.65	55.11	38.06
	B3	50.95	8.10	6.59	18.50	86.92	2751.12	7211.61	56.83	39.79
	B4	49.64	7.80	6.88	18.50	84.92	2384.05	7026.19	49.81	35.51
	B5	51.51	8.70	7.24	19.00	90.25	2487.85	7290.87	48.70	34.47
NPK2	Control	43.07	8.25	6.31	18.00	78.00	1943.38	6096.25	45.01	31.90
	B1	54.18	8.25	7.21	18.00	99.50	2533.62	7669.26	47.47	33.05
	B2	50.68	8.00	7.25	18.00	93.58	2564.76	7173.39	49.80	36.06
	B3	48.18	8.10	6.96	18.00	87.50	2751.59	6819.53	55.53	41.99
	B4	50.44	8.75	7.780	19.00	103.00	3000.24	7139.42	51.39	42.37
	B5	50.10	8.60	7.44	19.50	101.00	2661.01	7091.30	49.14	37.48
NPK3	Control	41.98	8.00	5.63	16.50	64.25	1893.37	5941.50	51.42	32.61
	B1	53.66	8.90	7.93	19.50	97.92	2737.91	7595.19	50.66	36.02
	B2	55.75	8.75	8.50	19.50	107.25	2724.70	7890.54	46.28	34.54
	B3	62.73	8.80	9.05	18.50	112.75	2966.74	8878.98	48.04	33.49
	B4	62.84	9.25	9.58	19.00	130.75	2955.89	8894.55	41.73	33.23
	B5	57.72	9.10	8.59	19.00	126.25	2836.05	8170.32	42.19	34.68
Tukey 0.05		7.11	n.s.	1.51	n.s.	14.13	583.11	1005.98	n.s.	9.56

B1: *Bradyrhizobium sp.* (Vigna), B2: *Rhizobium leguminosarum bv. viciae*, B3: *Bradyrhizobium* Mungbean, B4: *Mesorhizobium ciceri,* B5: *Rhizobium leguminosarum bv phaseoli.* NPK1 = 120 kg.ha^{-1}, NPK2 = 240 kg.ha^{-1}, NPK3 = 360 kg.ha^{-1}

The results presented in *Table 22* indicate that combining different species of rhizobium with different levels of NPK had significant effects on some yield components including total dry weight of plant, weight of spike, number of grains, grain yield, biological yield, and harvest index in both species. As observed, the highest grain number was obtained in *Triticum aestivum* with 360 kg.ha^{-1} of NPK with B5, while the maximum total dry weight and biological yield were observed in *Triticum durum* with 120 kg.ha^{-1} of NPK with B2. Moreover, the greatest grain yield was achieved in *Triticum aestivum* by adding 120 kg.ha^{-1} of NPK with B3, and the highest value of spike weight was recorded in *Triticum durum* by adding 240 kg.ha^{-1} of NPK with B4. Furthermore, the highest value of harvest index was obtained in *Triticum aestivum* by adding 120 kg.ha^{-1} of NPK with B3. *Figure 1* indicates that soil application of 120 kg.ha^{-1} of NPK with B2 increased the grain yield by 111.19% compared to the control. The results also showed that combining the lower level of NPK fertilizer with rhizobial inoculation had the greatest effect on the yield components.

http://www.aloki.hu ● ISSN 1589 1623 (Print) ● ISSN 1785 0037 (Online)
DOI: http://dx.doi.org/10.15666/aeer/1704_1011910138

Table 22. *Interaction effect of wheat species, chemical fertilizer and rhizobial bacteria on some yield components*

Wheat species	Chemical fertilizer (kg.ha^{-1})	Bacterial species	Total dry weight g.pot^{-1}	Spike length. plant^{-1}	Spike weight. plant^{-1}	Spikelet number plant^{-1}	Grain number plant^{-1}	Grain yield kg.ha^{-1}	Biological yield kg.ha^{-1}	Weight of 1000 grain (g)	Harvest index %
T. aestivum	NPK1	Control	31.60	8.80	5.12	16.00	81.00	1702.29	4472.75	37.12	38.06
		B1	40.22	9.00	5.13	*17.00*	85.00	2036.33	5692.85	42.31	35.77
		B2	38.16	9.50	5.27	19.00	84.00	2415.66	5401.27	50.79	44.72
		B3	44.68	9.00	6.43	17.00	111.00	3362.11	6324.13	53.50	53.16
		B4	38.80	9.60	5.72	*18.00*	90.00	2346.78	5491.86	46.06	42.73
		B5	42.80	10.20	5.75	18.00	90.50	2213.73	6058.03	43.20	36.54
	NPK2	Control	37.76	9.00	5.27	18.00	86.00	1715.50	5344.66	35.23	32.10
		B1	52.88	10.00	6.96	18.00	122.00	2516.63	7484.78	36.43	33.62
		B2	44.88	9.00	6.37	18.00	107.50	2460.01	6352.44	40.42	38.73
		B3	37.96	9.20	5.48	18.00	86.50	2673.27	5372.97	54.59	49.75
		B4	42.22	10.60	5.55	20.00	92.50	2659.12	5975.94	50.78	44.50
		B5	50.66	10.00	7.48	20.00	131.00	2995.05	7170.56	40.38	41.77
	NPK3	Control	29.69	9.00	3.93	18.00	58.00	1477.71	4202.88	45.00	35.16
		B1	49.06	10.00	6.98	20.00	109.50	2475.11	6944.09	39.92	35.64
		B2	52.16	9.30	7.99	19.00	123.00	2553.43	7382.87	36.67	34.59
		B3	57.20	10.30	8.41	19.00	130.00	2782.73	8096.25	37.81	34.37
		B4	63.12	11.50	9.65	20.00	158.50	2984.67	8934.18	33.26	33.41
		B5	59.58	11.00	9.05	20.00	161.00	3013.92	8433.12	33.06	35.74
T. durum	NPK1	Control	31.13	7.13	4.25	19.00	47.00	1542.82	4405.76	57.98	35.02
		B1	60.49	7.73	8.48	19.00	91.83	2722.34	8562.40	52.36	31.79
		B2	73.31	7.00	8.76	19.00	96.83	3258.32	10376.03	59.432	31.40
		B3	57.22	7.20	6.75	20.00	62.83	2140.13	8099.08	60.16	26.42
		B4	60.48	6.00	8.05	19.00	79.83	2421.33	8560.51	53.57	28.28
		B5	60.22	7.20	8.73	20.00	90.00	2761.97	8523.71	54.20	32.40
	NPK2	Control	48.38	7.50	7.36	18.00	70.00	2171.27	6847.84	54.79	31.71
		B1	55.49	6.50	7.45	18.00	77.00	2550.60	7853.74	58.51	32.48
		B2	56.48	7.00	8.14	18.00	79.67	2669.50	7994.34	59.18	33.40
		B3	58.40	7.00	8.45	18.00	88.50	2829.91	8266.10	56.48	34.24
		B4	58.66	6.90	10.05	18.00	113.50	3341.35	8302.90	52.00	40.24
		B5	49.54	7.20	7.40	19.00	71.00	2326.96	7012.03	57.89	33.19
	NPK3	Control	54.26	7.00	7.32	15.00	70.50	2309.04	7680.11	57.85	30.065
		B1	58.26	7.80	8.88	19.00	86.33	3000.71	8246.28	61.39	36.39
		B2	59.33	8.20	9.02	20.00	91.50	2895.97	8398.21	55.90	34.48
		B3	68.26	7.30	9.69	18.00	95.50	3150.74	9661.71	58.27	32.61
		B4	62.56	7.00	9.52	18.00	103.00	2927.11	8854.92	50.19	33.06
		B5	55.87	7.20	8.14	18.00	91.50	2658.17	7907.53	51.31	33.62
Tukey 0.05			11.12	n.s	2.37	n.s.	22.11	912.23	1573.76	n.s.	14.95

B1: *Bradyrhizobium sp.* (Vigna), B2: *Rhizobium leguminosarum bv. viciae*, B3: *Bradyrhizobium* Mungbean, B4: *Mesorhizobium ciceri,* B5: *Rhizobium leguminosarum bv phaseoli*. NPK1 = 120 kg.ha^{-1}, NPK2 = 240 kg.ha^{-1}, NPK3 = 360 kg.ha^{-1}

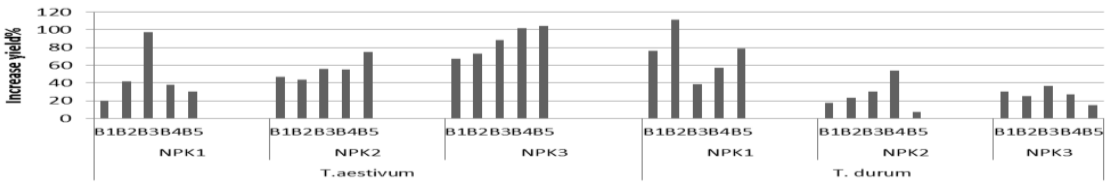

Figure 1. *Interaction effect of wheat species, chemical fertilizer, and rhizobial species on percentage increase of yield*

http://www.aloki.hu ● ISSN 1589 1623 (Print) ● ISSN 1785 0037 (Online)
DOI: http://dx.doi.org/10.15666/aeer/1704_1011910138

Discussion

A common anthropogenic alteration to terrestrial systems is application of fertilizers. An increase in nutrient input can have a direct impact on soil microbial diversity or function by altering soil environments, or an indirect effect through plant-microbe feedbacks with potentially important effects on ecologically-important plant-associated mutualists (Simonsen et al., 2015). Chemical fertilizers can be used in order to increase soil nutrients and crop yields (Jia et al., 2018). Nitrogen (N), phosphorus (P), and potassium (K) are the major nutrients required by the crop, and the reproductive capability, growth, and yield of the plant can negatively be affected by inadequate supply of any of these nutrients during crop growth (Okechukwu, 2011). However, excessive use of mineral fertilizers can generate several environmental problems such as potential pollution to soil, water, and air (Stajković-Srbinović et al., 2014). The present study was aimed at minimizing the use of chemical fertilizer and improving wheat production and environmental risks. The results showed that combining chemical fertilizer and biofertilizer can improve wheat growth and development. The positive effects of the biofertilizer on physiological parameters, biochemical contents of leaves, and yield components under study can be attributed to the fact that rhizobial bacteria are involved in the production of phytohormone, leading to changes in root morphology and physiology that resulted in an increase in nutrient and water uptake of the wheat species from the soil (Mia and Shamsuddin, 2010). Adesemoye and Kloepper (2009) pointed out that plant–PGPR interactions can lead to various benefits such as improvement in seed shoot weights, germination rate, yield, chlorophyll content, leaf area, hydraulic activity, and protein content. Given the production of siderophores and nutrient uptake due to better root system, rhizobial bacteria have mostly been used to promote photosynthetic pigments. Research has indicated that bacterial production of siderophores enhances chlorophyll content and growth of plants due to the selective iron uptake from the solutions of trace elements, and production of siderophores inhibits free radical formation, substantiates the oxidative stress, and prevents the uptake of heavy metals (Ullah et al., 2017). Moreover, the role of *Rhizobium sp.* in enhancement of stress tolerance leads to an increase in cell membrane stability (Mia and Shamsuddin, 2010) because cell membranes are one of the first targets of many plant stresses (Bajji et al., 2002). Due to urgent need for increased global wheat production, wheat tolerance to biotic and abiotic stresses should be should be improved more (ElBasyoni et al., 2017). As pointed out by Mehboob et al. (2011), growth and yield of wheat can be promoted by isolates of *Rhizobium spp*. Rhizobium inoculation can lead to yield enhancement in wheat parameters, which can be attributed to the fact that applying biofertilizers have been proved to lead to high quality yield and avoid environmental pollution (Das et al., 2008). The findings of the present study are in agreement with those of the studies carried out by Agamy et al. (2012) and Adnan et al. (2016). It should be noted that plant species and their genotypes are genetically different in terms of their ability to uptake and metabolize elements.

Conclusion

Based on the results of the present study, it was observed that the combination between lower levels of NPK fertilizer and rhizobial inoculation had the greatest effect on yield components; therefore, such combinations are recommended to be utilized. Recently, biofertilizers have become an important means in agriculture because they use

http://www.aloki.hu ● ISSN 1589 1623 (Print) ● ISSN 1785 0037 (Online)
DOI: http://dx.doi.org/10.15666/aeer/1704_1011910138

beneficial rhizobial bacteria to improve wheat production in a more economical and environmentally friendly way. Therefore, we suggested that the influence of combined effect of NPK fertilizer and rhizobial inoculation on growth and yield of wheat in soil needs further investigation to arrive at a conclusion where the effects are synergistic.

Acknowledgements. The authors of the present study would like to thank the staff of the greenhouse for their support and help with this research. Sincere thanks also go to the reviewers and editors for their exceptionally helpful comments on the manuscript.

REFERENCES

[1] Abou-Taleb, S. M., Gomaa, E. F. (2012): Morphological and anatomical study on some wheat cultivars and their response to seasonal variations. – Australian Journal of Basic and Applied Sciences 6: 13-22.
[2] Adesemoye, A. O., Kloepper, J. W. (2009): Plant–microbes interactions in enhanced fertilizer-use efficiency. – Applied Microbiology and Biotechnology 85: 1-12.
[3] Adnan, M., Shah, Z., Khan, A., Khan, G. A., Ali, A., Khan, N. A., Saleem, N., Nawaz, S., Akbar, S., Samreen, S. (2014): Integrated effects of Rhizobial inoculum and inorganic fertilizers on wheat yield and yield components. – American Journal of Plant Sciences 5: 2066.
[4] Agamy, R., Mohamed, G., Rady, M. (2012): Influence of the application of fertilizer type on growth, yield, anatomical structure and some chemical components of wheat (Triticum aestivum L.) grown in newly reclaimed soil. – Australian Journal of Basic and Applied Sciences 6: 561-570.
[5] Al-Shamma, U. H., Al-Shahwany, A. W. (2014): Effect of mineral and bio-fertilizer application on growth and yield of wheat Triticum aestivum L. – Iraqi Journal of Science 55: 1484-1495.
[6] Bajji, M., Kinet, J.-M., Lutts, S. (2002): The use of the electrolyte leakage method for assessing cell membrane stability as a water stress tolerance test in durum wheat. – Plant Growth Regulation 36: 61-70.
[7] Biswas, J., Ladha, J., Dazzo, F. (2000): Rhizobia inoculation improves nutrient uptake and growth of lowland rice. – Soil Science Society of America Journal. DOI: 10.2136/sssaj2000.6451644x.
[8] Dalaly, B., Al-Hakim, S. (1987): Food Analysis. – Mosel University, Iraq.
[9] Das, K., Dang, R., Shivananda, T. (2008): Influence of bio-fertilizers on the availability of nutrients (N, P and K) in soil in relation to growth and yield of Stevia rebaudiana grown in South India. – International Journal of Applied Research in Natural Products 1: 20-24.
[10] ElBasyoni, I., Saadalla, M., Baenziger, S., Bockelman, H., Morsy, S. (2017): Cell membrane stability and association mapping for drought and heat tolerance in a worldwide wheat collection. – Sustainability 9: 1606.
[11] Elghair, S. A. A. (2012): Effect of nitrogen on rhizobacteria associated with wheat shoot productivity. – Thesis Submitted to the Faculty of the Graduate College of the Oklahoma State University in partial fulfillment of the requirements for the Degree of Master of Science.
[12] Elia, Y., Al-Sahaf, N., Al-Khesraji, T. (1987): Preliminary studies on Orobanche aegyptiaca Pers. in tomato. – Iraqi J. Agric. Sci.'Zanco' 5: 233-244.
[13] Etesami, H., Alikhani, H. A., Jadidi, M., Aliakbari, A. (2009): Effect of superior IAA producing rhizobia on N, P, K uptake by wheat grown under greenhouse condition. – World Appl. Sci. J 6: 1629-1633.

http://www.aloki.hu ● ISSN 1589 1623 (Print) ● ISSN 1785 0037 (Online)
DOI: http://dx.doi.org/10.15666/aeer/1704_1011910138

[14] Fatima, Z., Zia, M., Chaudhary, M. F. (2006): Effect of Rhizobium strains and phosphorus on growth of soybean Glycine max and survival of Rhizobium and P solubilizing bacteria. – Pakistan Journal of Botany 38: 459.
[15] Gray, E., Smith, D. (2005): Intracellular and extracellular PGPR: commonalities and distinctions in the plant–bacterium signaling processes. – Soil Biology and Biochemistry 37: 395-412.
[16] Jia, Q., Kamran, M., Ali, S., Sun, L., Zhang, P., Ren, X., Jia, Z. (2018): Deficit irrigation and fertilization strategies to improve soil quality and alfalfa yield in arid and semi-arid areas of northern China. – Peer J 6: e4410.
[17] Lichtenthaler, H. K. (1987): Chlorophylls and carotenoids: pigments of photosynthetic biomembranes. – Methods in Enzymology 148: 350-382.
[18] Mehboob, I., Zahir, Z. A., Arshad, M., Tanveer, A., Azam, F. (2011): Growth promoting activities of different Rhizobium spp. in wheat. – Pak. J. Bot 43: 1643-1650.
[19] Mia, M. B., Shamsuddin, Z. (2010): Rhizobium as a crop enhancer and biofertilizer for increased cereal production. – African journal of Biotechnology 9: 6001-6009.
[20] Mitkees, R., Saad, H., Iman, M., Amer, H., Mahamoud, S. K. (1996): Importance of N2 fixing biofertilizer for decreasing the use of mineral nitrogen fertilizer for wheat plant. – Egypt J. Appl. Sci 11: 34-41.
[21] Okechukwu, V. (2011): Effects of NPK fertilizer on growth, drymatter production and yield of eggplant in southwestern Nigeria. – Agric. Biol. J. N. Am. 2(7): 1117-1125.
[22] Premachandra, G., Saneoka, H., Kanaya, M., Ogata, S. (1991): Cell membrane stability and leaf surface wax content as affected by increasing water deficits in maize. – Journal of Experimental Botany 42: 167-171.
[23] Ryan, J., Estefon, G., Rashid, A. (2001): Soil and Plant Analysis Laboratory Manual, 2nd edn. National Agriculture Research Center (NARC) Islamabad, Pakistan. – Bull. Fac. Sci 31: 395-303.
[24] Sadasivam, S. (1996): Biochemical Methods. – New Age International, Delhi.
[25] Sessitsch, A., Howieson, J., Perret, X., Antoun, H., Martinez-Romero, E. (2002): Advances in Rhizobium research. – Critical Reviews in Plant Sciences 21: 323-378.
[26] Simonsen, A. K., Han, S., Rekret, P., Rentschler, C. S., Heath, K. D., Stinchcombe, J. R. (2015): Short-term fertilizer application alters phenotypic traits of symbiotic nitrogen fixing bacteria. – Peer J 3: e1291.
[27] Stajković-Srbinović, O., Delić, D., Kuzmanović, D., Protić, N., Rasulić, N., Knežević-Vukčević, J. (2014): Growth and nutrient uptake in oat and barley plants as affected by rhizobacteria. – Rom. Biotechnol. Lett 19: 9429-9436.
[28] Ullah, S., Qureshi, M. A., Ali, M. A., Mujeeb, F., Yasin, S. (2017): Comparative potential of Rhizobium species for the growth promotion of sunflower (Helianthus annuus L.). – Eurasian Journal of Soil Science 6: 189-196.
[29] Wang, Y., Wei, S., Wang, J., Su, X., Suo, B., Qin, F., Zhao, H. (2018): Exogenous application of 5-aminolevulinic acid on wheat seedlings under drought stress enhances the transcription of psbA and psbD genes and improves photosynthesis. – Brazilian Journal of Botany 41: 275-285.
[30] Yanni, Y. G., Rizk, R., Corich, V., Squartini, A., Ninke, K., Philip-Hollingsworth, S., Orgambide, G., De Bruijn, F., Stoltzfus, J., Buckley, D. (1997): Natural Endophytic Association between Rhizobium Leguminosarum bv. trifolii and Rice Roots and Assessment of its Potential to Promote Rice Growth. – In: Ladha, J. K. et al. (eds.) Opportunities for Biological Nitrogen Fixation in Rice and Other Non-Legumes. Springer, Dordrecht, pp. 99-114.
[31] Ye, Q., Zhang, H., Wei, H., Zhang, Y., Wang, B.-F., Xia, K., Huo, Z.-Y., Dai, Q.-G., Xu, K. (2005): Effects of nitrogen fertilizer on nitrogen use efficiency and yield of rice under different soil conditions. – Acta Agronomica Sinica 31: 1422.

http://www.aloki.hu ● ISSN 1589 1623 (Print) ● ISSN 1785 0037 (Online)
DOI: http://dx.doi.org/10.15666/aeer/1704_1011910138

[32] Yildirim, E., Karlidag, H., Turan, M., Dursun, A., Goktepe, F. (2011): Growth, nutrient uptake, and yield promotion of broccoli by plant growth promoting rhizobacteria with manure. – HortScience 46: 932-936.
[33] Zahir, Z. A., Yasin, H., Naveed, M., Anjum, M., Khalid, M. (2010): L-tryptophan application enhances the effectiveness of rhizobium inoculation for improving growth and yield of mungbean (Vigna radiata (L.) Wilczek). – Pak J Bot 42: 1771-1780.

http://www.aloki.hu ● ISSN 1589 1623 (Print) ● ISSN 1785 0037 (Online)
DOI: http://dx.doi.org/10.15666/aeer/1704_1011910138

NITROGEN USE EFFICIENCY IN CEREALS UNDER HIGH PLANT DENSITY: MANUFACTURING, MANAGEMENT STRATEGIES AND FUTURE PROSPECTS

SHER, A.[1] – ZHANG, L. G.[2] – NOOR, M. A.[3] – NADEEM, M.[4] – ASHRAF, U.[5] – BALOCH, S. K.[6] – AMEEN, A.[7] – YUAN, X. Y.[1*] – GUO, P. Y.[1*]

[1]*Key Laboratory of Crop Chemical Regulation and Chemical Weed Control, College of Agronomy, Shanxi Agricultural University, Taigu, Shanxi, China*

[2]*Institute of Crop Sciences, Shanxi Academy of Agricultural Sciences, Taiyuan, China*

[3]*Institute of Crop Sciences, Chinese Academy of Agricultural Sciences, Key Laboratory of Crop Physiology and Ecology, Ministry of Agriculture, 100081 Beijing, China*

[4]*School of Agronomy, Anhui Agricultural University, Hefei, China*

[5]*Department of Botany, University of Education, Faisalabad-Campus, Faisalabad 38000, Punjab, Pakistan*

[6]*College of Agriculture, Shanxi Agricultural University, Taigu, Shanxi, China*

[7]*Department of Agronomy, Faculty of Agriculture, Gomal University, Dera Ismail Khan 29050, Pakistan*

**Corresponding authors*
e-mail: yuanxiangyang200@163.com; pyguo126@126.com

(Received 16th Oct 2018; accepted 28th Jan 2019)

Abstract. Increasing the crop yield is very important and depends relatively on high plant density. The high grain yield per unit area of cereals is due to the optimum plant density. In this review, recent improvements and future insights to obtain better information for the regulation of nitrogen use efficiency in cereals under high plant density are presented. An updated knowledge of the basic mechanisms controlling plant nitrogen interaction is very important in cereals, to increase nitrogen use efficiency and for decreasing high cost of fertilizers, to obtain high output. In view of this fact, we should emphasize to develop plant morpho-physiological, agronomic and molecular studies which focuses on phenomics, genomics, and metabolite profiling to understand comprehensive knowledge of the different steps of nitrogen uptake, assimilation, and recycling under high plant density in cereals. A very important piece of information is provided on understanding of the physiological assimilation of N under different environmental conditions in cereals under different plant densities that has been improved through the use of different strategies for future research. According to the global economic and environmental constraints for future, agronomic and physiological principles and application which were adapted to less fertilizer inputs are discussed under high plant density.
Keywords: *cereals, NUE, plant density, nitrogen management, physiological mechanism*

Introduction

Cereals are sine qua non for current and projected human food security being staple food nearly in every region and country. Across the globe, merely 5% of staple derives from root crops like cassava, yams and potato, while the rest is provided by cereals with a range of health benefits. To ensure and secure food security on sustainable basis, cereals have to produce grains with many-fold larger quantity. Further increase in yield

http://www.aloki.hu ● ISSN 1589 1623 (Print) ● ISSN 1785 0037 (Online)
DOI: http://dx.doi.org/10.15666/aeer/1704_1013910153

would largely come from optimal planting density in field (Tokatlidis et al., 2011; Sher et al., 2017, 2018). Increasing the planting density of cereals is an agronomical task/deed/process has evolved over the time and this management practice has changed from the past six decades (Tollenaar, 1992; Sher et al., 2016; Noor, 2017). For example in USA Corn Belt, maize planting density has evolved from 3 plants m^{-2} to 8 plants m^{-2} in 85 years from 1930 to 2015 (Li et al., 2015) which caused many fold increase in average yield.

In the USA hybrids of central Iowa have increased nearly 79 kg ha^{-1} annually (Duvick, 1996). These yield escalations have occurred however mean yield per plant has not been changed significantly, increased by just an average of 0.05 kg $plant^{-1}$ over the past 40 years (USDA, 2010) while average plant population has increased by an average 720 plants ha^{-1} per year over the past 44 years (USDA, 1965-2009). In European countries where climate is heterogeneous than USA row spacing for planting density of maize vary between 70-75 cm to facilitate intensive cultivation (Sharratt and McWilliams, 2005). Developing countries produced lower grains of maize from a unit of land than developed countries though environmental and irrigation are satisfactory for maize production. Therefore the main constrain is low plant density per unit of land than those of developed countries. Mean planting density of 58000 ha^{-1} in developed countries is about two times less intensive than current cultivation stand density in developed countries. Grain yield per unit land area is the product of grain yield $plant^{-1}$ and number of plants per unit area (Hashemi et al., 2005). Maximum yield per unit area may be obtained by growing cereals hybrids that can withstand high plant density, up to 100,000 plants ha^{-1} (Huseyin et al., 2003). Growing hybrid by maintaining high density may causes a radical decline in grain yield as these hybrids can be susceptible to high stand density. In such hybrids, one-eared bearing pattern, recumbent leaf, plant height and large-type plants are the reasons of non-significant tolerance against high plant population (Tang et al., 2018; Hou et al., 2019). On other hand, developed countries grow hybrids that are characterized by high yielding ability per unit land due to prolificacy, early silking and tasseling, short anthesis-silking interval (ASI), more grain filling period, rare barren stalks backed them to adopt high density field environments. Likewise genotypes with erect leaves intercept light more efficiently and are very desirable for increased population densities (Radenovic et al., 2007). Therefore, there is a great genetic difference in grains production by cereals owing to their response to altering planting density (Liu et al., 2004). Main purpose of higher plant densities is to increase grain yield or biomass over per unit of land which make the cropping system more efficient over a piece of land. In absence of environmental stresses, grain production is directly proportional to amount of solar radiation intercepted by plants. Thus, efficient light harvesting is of paramount importance for plants growing in competition in dense stands under natural conditions (Pearcy et al., 2004; Valladares and Niinemets, 2008). The plant density has been evolving for decades, but now more enhancements in density fails to upsurge grains production has been rising steadily. But advancement in hybrids to tolerate high canopy still can attain the goal. Researchers believes that high densities like 90,000 plants ha^{-1} are still below potential maximum yield densities, indicating even higher tolerance to stand density may be possible in advanced hybrids (Widdicombe and Thelen, 2002). Planting density is also critical for the wheat because it directly affects the morphological parameters like number of ears per unit area. Currently, the plant density for the wheat ranges from 250 to 400 viable

http://www.aloki.hu ● ISSN 1589 1623 (Print) ● ISSN 1785 0037 (Online)
DOI: http://dx.doi.org/10.15666/aeer/1704_1013910153

seeds. This is based on the hybrid cycle, as well as its dual ability as a forage and grain crop (Comissão et al., 2007).

In the rice production system higher densities are helpful in suppression of weeds (Ahmed et al., 2016). But extra cost on more seeds for high seedling density should be set off with more yield. Sorghum is most favorable for those areas where water availability is limited as it produced grains with less water compared to other cereals. Plant population of sorghum influence both tillering and panicle weight. The greater densities did support fewer tillers per plant. This response is due to the competitiveness of the stand and is normally associated with reduced weight of the inflorescence (Gardner et al., 2010). Yield response of barley also varies with changing planting densities (Soleymani et al., 2011). Therefore, optimal grains production come from optimal planting stand by taking into account the specific set of environmental conditions and available resources including the particular cultivar characteristic which are responsible for tolerance to dense canopy architecture. Several factors, such as hybrid maturity group, water availability, soil fertility and row spacing (Sangoi et al., 2002) are crucial in determining proper plant number per unit area. In this study the response of cereals to plant population and nutrient management are presented and future prospects and insights are discussed.

Importance of nitrogen use efficiency

For food security it is necessary to enhance NUE in cereal crops at low input of fertilizers (White and Brown, 2010). Cereal crops need large amount of nitrogen to produce optimum yield and for which NUE is calculated is below 50% (Wang et al., 2018; Zhu, 2000; Ruan and Johnson, 1999). Irrigation, fertilizer and soil management practices are very important to enhance the crop yield (Ruan and Johnson, 1999).

Nitrogen plays an important role in crop growth and yield (Noor, 2017). Among the major plants nutrient N is taken up by the plants in largest amount. N is an essential component of plant growth (protein, enzymes, DNA, RNA) and photosynthesis i.e. chlorophyll. Symbiosis process in leguminous crops provides more nitrogen to soil which ultimately increased crop yield. Plants use nitrogen in the form of ammonium and nitrate (*Fig. 1*). Excess of nitrogen adversely affect plant growth and environment and surface nitrogen often leads to its contamination, eutrophication which later produces a decline in oxygen content of water. To improve NUE in cereals, some strategies need to apply for example N management, plant breeding and genetics. NUE is economically and also environmentally beneficial to enhance irrigation use efficiency, diminish soil erosion, reduces the pest infestation, to maintain soil texture, increase soil organic matter and humidity, less reliance on agricultural chemicals and improve crop NUE (Noor, 2017; Halvorson et al., 2001; Riedell et al., 2009).

The plant life cycle in response to the nitrogen management is divided into two parts: the vegetative part and the reproductive part. During vegetative growth, smaller roots and leaves respond as sink organs before flowering and then reduced by the nitrate assimilatory pathway (Hirel and Lea, 2001). The amino acids are further used for the synthesis of enzymes and proteins which are involved in growing plant architecture and the different components of the photosynthetic pigments, in C3 species 50% of the total soluble leaf protein can be represent alone by Rubisco (ribulose 1,5- isphosphate carboxylase) (Mae, 1997) and 20% in C4 species.

http://www.aloki.hu ● ISSN 1589 1623 (Print) ● ISSN 1785 0037 (Online)
DOI: http://dx.doi.org/10.15666/aeer/1704_1013910153

Before anthesis in wheat, 60–95% N comes from the remobilization of N stored in young roots and shoots (Palta and Fillery, 1995). Post-flowering N uptake and N translocation to the grain is available in a very less quantity. Under N-deficient conditions the size and the N content of the grain significantly decreased (Dupont and Altenbach, 2003). Nitrogen (N) deficiency, is one of the major problem diminishing crop growth (Tanner et al., 1993; Teklu and Hailemariam, 2009). Three split applications at anthesis showed significant result for Higher NHI (Jan et al., 2010). It is not clear that storage protein synthesis and plant N availability or that decreases the determination of grain yield and protein synthesis N applications in wheat are generally calculated by the total N budget method. Until tillering, the soil supplies nitrogen to the plant. Three applications are generally recommended: one at tillering (50–80 kg ha^{-1}), one at the beginning of stem elongation (around 50 kg ha^{-1}), and one at the second node stage (40–50 kg h^{-1}). SPAD meter is a potential instrument used for predicting grain N requirements in cereals (Lopez-Bellido et al., 2004). In rice crop same pattern of N management exists but the plant mostly uses ammonium instead of nitrate. Vegetative organs uses the remobilized N 70–90% of the total panicle N (Mae, 1997; Tabuchi et al., 2005). Crop residues in rice belt farming patterns have small or no short-term benefits on rice yield (Thuy et al., 2008). In the field, at early growth phase and tillering 40 to 110 kg N ha^{-1} used in the form of ammonium or urea. At panicle primordial stage and the late stage of spikelet initiation, additional top-dressing N (15–45 kg ha^{-1}) is applied and is effective for spikelet production. Sink size of rice crop is little effected by N uptake. During the grain-filling stag, in a leaf blades N is accumulated and large part used by the grain and that contributes to grain N protein synthesis (Mae, 1997). Plant density and nitrogen use efficiency of cereals are represented in *Table 1*.

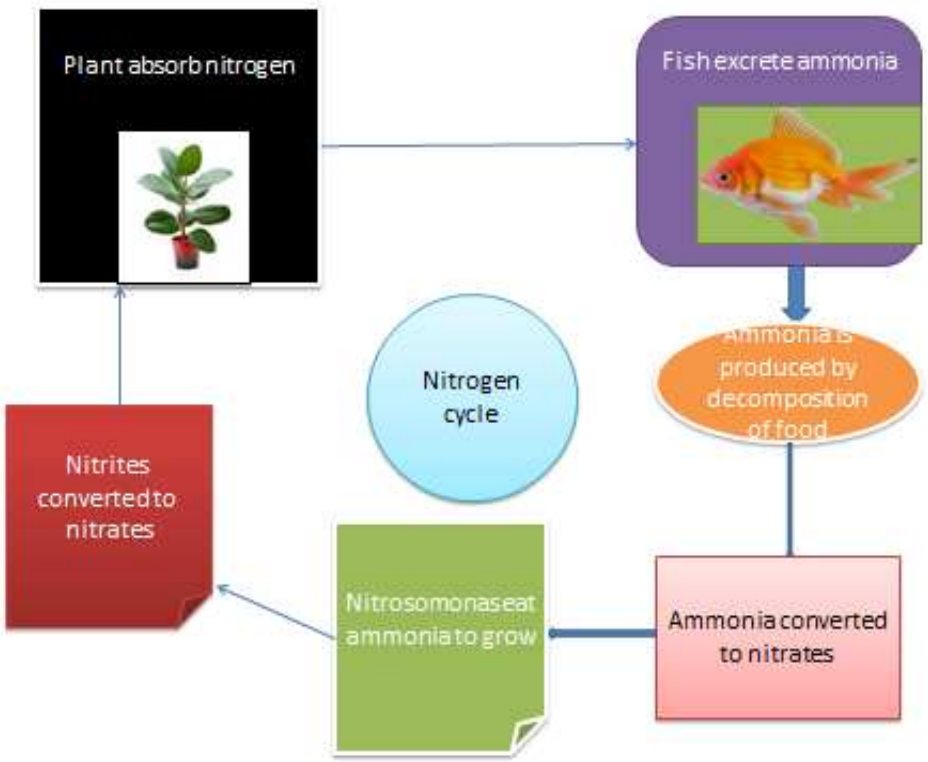

Figure 1. *Nitrogen cycle in agricultural systems.*

http://www.aloki.hu ● ISSN 1589 1623 (Print) ● ISSN 1785 0037 (Online)
DOI: http://dx.doi.org/10.15666/aeer/1704_1013910153

Physiological response of cereals to nitrogen use efficiency

Good et al. (2004) and Lea and Azevedo (2006), defined nitrogen use efficiency as nitrogen in grain per total N uptake. NUE is further divided into two parts i.e. uptake and utilization efficiency (Moose and Below, 2009). Winter wheat response to next crop and crop management the effect of next crop on the N uptake of the following crop has long been studied (Anderson, 2008).

Table 1. *Nitrogen use efficiency for different plant density and nitrogen regimes*

Planting density	Crop	Seed rate/PD*	Yield	NUE	Ref	Exp. duration
LD	Wheat	180 kg ha-1	2643 kg/ha	22.5	Gao et al., 2009	2003
HD	Wheat	225 kg ha-1	2657	25.9	Gao et al., 2009	2003
LD	Wheat	180 kg ha-1	3,477 kg/ha	45.3	Gao et al., 2009	2003-4
HD	Wheat	225 kg ha-1	3,745	54.6	Gao et al., 2009	2003-4
ND	Maize	27 cm	3.51 g/plant	46.51	Jiang et al., 2013	2007
HD	Maize	6cm	3.24	49.57	Jiang et al., 2013	2007
ND	Maize	27 cm	3.57	46.82	Jiang et al., 2013	2007-2008
HD	Maize	6 cm	3.40	50.87	Jiang et al., 2013	2007-2008
ND	Wheat	300 plants/m^2	676.40 g/m2	1.3 kg/ha	Jamaati-e-Somarin et al., 2010	2008
ND	Wheat	350	753.42	2.1 kg/ha	Jamaati-e-Somarin et al., 2010	2008
ND	Wheat	400	909.63	2.4 kg/ha	Jamaati-e-Somarin et al., 2010	2008
LD*^{LN}	Maize	54,000 p/hec	138.6 g/plant	8.68	Ciampitti & Vyn, 2011	2009
LD*^{HN}	Maize	54000 p/h	142.6 g/p	5.18	Ciampitti & Vyn, 2011	2009
MD*^{LN}	Maize	79,000 p/h	124.2 g/p	8.89	Ciampitti & Vyn, 2011	2009
MD*^{HN}	Maize	79,000 p/h	145.9 g/p	10.47	Ciampitti & Vyn, 2011	2009
HD*^{LN}	Maize	104,000 p/h	102.3 g/p	18.55	Ciampitti & Vyn, 2011	2009
HD*^{HN}	Maize	104,000 p/h	105.8 g/p	10.54	Ciampitti & Vyn, 2011	2009

LD = low density, HD = high density MD = medium density

NHI is defined as the ratio of grain protein content to the nutritional quality (Sinclair, 2004). Jan et al. (2010) reported that the higher NHI in the three split application at anthesis gave significant result. The genomics for grain composition indicates that grain yield and protein concentration in most grain crops has been reduced by an apparent inverse genetic relationship (Simmonds, 1995), including wheat (Canevara et al., 1994), oilseed rape (Brennan et al., 2000; Jackson, 2000) and maize (Feil et al., 1990). A negative regression is used to predict higher grain protein content among wheat line (Oury et al., 2003; Kade et al., 2005).

High yielding and high protein varieties are used to determine negative control present between yield and grain protein content. This is also helpful for understanding the comparison of N uptake and N use for protein deposition under less and high N condition (Uribalarrea et al., 2007). Modern varieties showed greater NUE than older ones (Sylvester-Bradley and Kindred, 2009), but this phenomena has not been identified. Crop management, fertilizer application methods to develop high yielding varieties through breeding are the two ways to enhance NUE for example root system can be modify in up taking the nitrate from the below soil that have negative effects on the uptake efficiency of phosphate, which is present in upper soil.

http://www.aloki.hu ● ISSN 1589 1623 (Print) ● ISSN 1785 0037 (Online)
DOI: http://dx.doi.org/10.15666/aeer/1704_1013910153

Impact of nitrogen use efficiency and plant density on photosynthesis

To increase light interception on plants to improve photosynthesis there is a tight relationship among radiation use efficiency (RUE), leaf N distribution, leaf photosynthetic pigments and N supply and plant population (Gastal and Lemaire, 2002) when C3 or C4 crop species are studied. It is very important to study the level of CO_2 saturation of Rubisco. As an example of a tillering Gramineae species, Bos and Vos (2000) analysed for wheat which morphological leaf components were influenced by plant population and which mechanisms were involved. They reported that the most significant effect of higher plant population on leaf area per plant was the absence of later formed tillers. When a species does not form tillers, plant density can only affect the growth of leaves on the main stem. A study into the effects of environmental factors on the morphological development of such a plant type could lead to a better understanding of mechanisms involved in the effects of plant density on leaf-area development. Moreover, at higher plant densities, leaf area per plant is decreased in later phases of growth (Hay and Walker, 1989).

In both Sorghum and maize N uptake capacity depends leaf senescence is the cause of increased photosynthetic activity (Borrel et al., 2001). For improving the characterization of plants that are stay-green, N uptake, N assimilation and N recycling of the fine regulatory mechanisms is very important (Rampino et al, 2006). To know more about the physiological and molecular basis of the stay-green phenotype, further research is needed. To characterize whether such a phenotype are used when N fertilization is decreased and when water resources are decreased in relation to nitrogen availability, root N uptake capacity and architecture (Borrell et al., 2000).

Plant N economy and their species specificities

Nitrogen (N) deficiency is big threat for limiting wheat production and yield (Tanner et al., 1993; Teklu and Hailemariam, 2009). In maize (*Zea mays* L.) before silking about 45–65% of the grain N already exists in stover and the remaining 35–55% of the grain N produces from post-silking N (Ta and Weiland, 1992; Rajcan and Tollenaar, 1999; Gallais and Coque, 2005). To obtain maximum yield, one application of N fertilizer is recommended at sowing, ranging from 100 to 240 kg N ha $^{-1}$. Chlorophyll meter is the best instrument to estimate leaf N in maize crop (Chapman and Baretto, 1997).

Barley (*Hordeum vulgare* L.) is the fourth major crop in cereals. Due to genetic, physiological and agronomic studies it is an established model plant (Raun and Jonhson, 1999). However, N uptake and assimilation through biochemical and molecular mechanisms and recycling is best in this crop. Future improvements require studying N fertilizer levels and timing of application to achieve best grain yield and good quality of protein content. However, symbiotic N crop species contributes half of the amount of N applied in inorganic N fertilizers (Smil, 2006).

Plant development stages related to nutrition and plant density

Cereal yield is linearly correlated to high plant density. Improved morphology was the key for promoting light use efficiency per plant (Yu et al., 1998; Li and Li, 2004) which influenced canopy architecture, light interception and yield (Maddoni et al., 2001; Stewart et al., 2003; Tollenaar et al., 2006; Li and Wang, 2010). Superoptimal

http://www.aloki.hu ● ISSN 1589 1623 (Print) ● ISSN 1785 0037 (Online)
DOI: http://dx.doi.org/10.15666/aeer/1704_1013910153

planting densities can affect canopy architecture particularly during the period bracketing silking and can lead to reduce the yield (Tollenar and Wu., 1999; Maddoni et al., 2001; Christopher et al., 2009). Increasing panting density accelerated leaf senescence (Tethio-Kagho and Gardner, 1988), increased the shading of leaves (Hashemi-Dezfouli and Herbert, 1992), and reduced the net assimilation of individual plants. An increase in plant population of 2–13 plants per m^2 reduced net assimilation per plant from 0.85 to 0.11 mg CO_2 m^{-2} s^{-1}, but increased grain yield per area (Dwyer et al., 1991). This enhancement in grain yield can be explained by the increase in LAI and net crop assimilation rate. Corn cultivars having erect leaves are very desirable for increased population densities, which increases light interception (Radenovic et al., 2007).

In plants N availability influences several developmental processes the number i.e. leaves and their rate of appearance (Snyder and Bunce, 1983; Mae, 1997), and the number of tillers (Vos and Biemond, 1992; Trapani and Hall, 1996) are reduced under N-limiting conditions both in spring wheat. The valuable contribution of Arabidopsis research community is to verifying the connection between N, N uptake and root development (Remans et al., 2006); However, recent studies have suggested that an increased acidification capacity of the rhizosphere could be targeted to increase nitrate uptake and improve NUE in addition, the NUE of agricultural system may be improved if plants could maintain internal nutrient concentrations and optimal growth with a lower outside concentration in the soil. Therefore understanding the response mechanisms of NAcE to nutrient deficiencies may improve the ability of crops to tolerate lower nutrient concentrations in the soil and thereby save fertilizer and reduce potential pollution. All abbreviations are added in *Table 2*.

Table 2. *Abbreviations*

LD	Low density
MD	Medium density
HD	High medium density
NUE	Nitrogen Use efficiency
NHI	Nitrogen harvest index
HHV	High heat value
AN	Ammonium nitrate
CN	calcium ammonium nitrate

Manufacturing and cost of production of nitrogenous fertilizers

The products of the fertilizer industry are unique and different, every product needs different production processes. Fertilizer industries use many input as raw materials for example (energy, electricity natural gas, and other hydrocarbons), mineral phosphate, potassium salts, sulphur ammonia and acids (phosphoric, sulphuric, nitric), blending mixtures. There are different small companies' uses basic fertilizer materials to process, blends and mix compounds, which may or may not be further processed into mixtures, blends or compound to make fertilizers. Due to this complex process, basic fertilizer material such as phosphate, potassium salts, sulphur and ammonia should be used to the soil directly, according to this scenario, one company raw material may be another company product.

http://www.aloki.hu ● ISSN 1589 1623 (Print) ● ISSN 1785 0037 (Online)
DOI: http://dx.doi.org/10.15666/aeer/1704_1013910153

Cost of production for nitric acid, ammonium nitrate (AN) and calcium ammonium (CN) nitrate production

Basic inputs per ton of AN in modern plants include 0.21 t NH3, 0.78 t 100% HNO_3 and 25-40 kWh of electricity. Steam and turbine power are according to the nitric acid concentration. Thus, the net steam requirement may vary from zero to 50 kg/t, and it depends if final product is only AN solution, steam may be exported (UNEP et al., 1998). Anhydrous ammonia production is represented in *Figure 2.*

The complete N budget is calculated as a function of N mineralization and the soil nitrate levels are used at the beginning of the season. Nitrogen mineralization are calculated as a function of soil texture and organic matter content. Most agricultural soils contain less naturally occurring plant available nitrogen to meet the needs of a crop throughout the growing season. Supplementary nitrogen applications are normally made each year to meet crop demand.

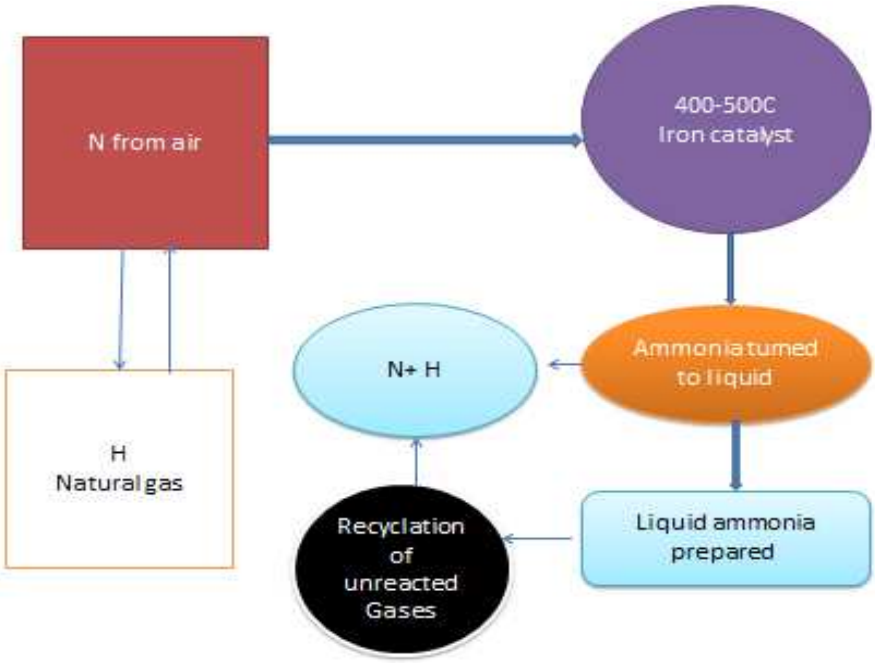

Figure 2. *Anhydrous ammonia production*

Strategies and practices to improve nitrogen use efficiency

Soil physical properties are very important to improve nitrogen use efficiency for example, soil texture, soil structure, organic matter.

Soil texture: Top soil texture is very important to determine lime requirement.

Soil structure: To obtain optimum economic yields, crops need sufficient nutrients and water from the soil through roots. To maintain good soil structure root growth is very important soil parameter, such as compaction.

Soil organic matter: Soil organic matter is a vital source of N used by crops. Organic matter consists of stable material called humus that has cumulated over a period of time.

There are different ways and procedure which are used to lower the price of fertilizers at farm-gate and to reduce the farmers' perception of the risk in the use of fertilizers by: (i) Hashemi-Dezfouli and Herbert (1992) sting in distribution

http://www.aloki.hu ● ISSN 1589 1623 (Print) ● ISSN 1785 0037 (Online)
DOI: http://dx.doi.org/10.15666/aeer/1704_1013910153

infrastructure; (ii) Researching innovative ideas to avoid losses and to provide finance; (iii) Encouraging sub regional measurement for country-level fertilizer manufacturing companies, facilities and/or procurement; and (iv) Encouraging dialogue between different agencies to arrive at a common approach to increase nitrogen use efficiency. Nitrogen management for intensification of cereals is widely researched topic across the globe.

Soil quality and NUE: Cycling of nutrients depends on the quality of agricultural soils, either directly through their capacity to receive nutrients and to convert them into or keep them in forms that are available to crops, or indirectly by governing the productivity and harvestability of crops and thereby the effective capture of nutrients from soils (Giller et al., 1997; Harris et al., 2011; Keesstra et al., 2016). Generally to improve nitrogen use efficiency following points should be considered (1) fertilizer use timing (2) Risk of N loss; (3) Placing N close to the period of maximum crop growth; (4) Even application of fertilizer and Fertilizer application rate; (5) Nitrogen fertilizer sources; (6) Application methods (7) Additives to reduce losses; (8) Managing nitrogen from manure; (9) Promoting efficient uptake and special consideration. Agronomic factors affecting plant population are (i) cultivar, (ii) length of the growing season, (iii) time of planting, (iv) water availability, (v) row spacing. Management and sources of nitrogen fertilizers are represented in *Figure 3.*

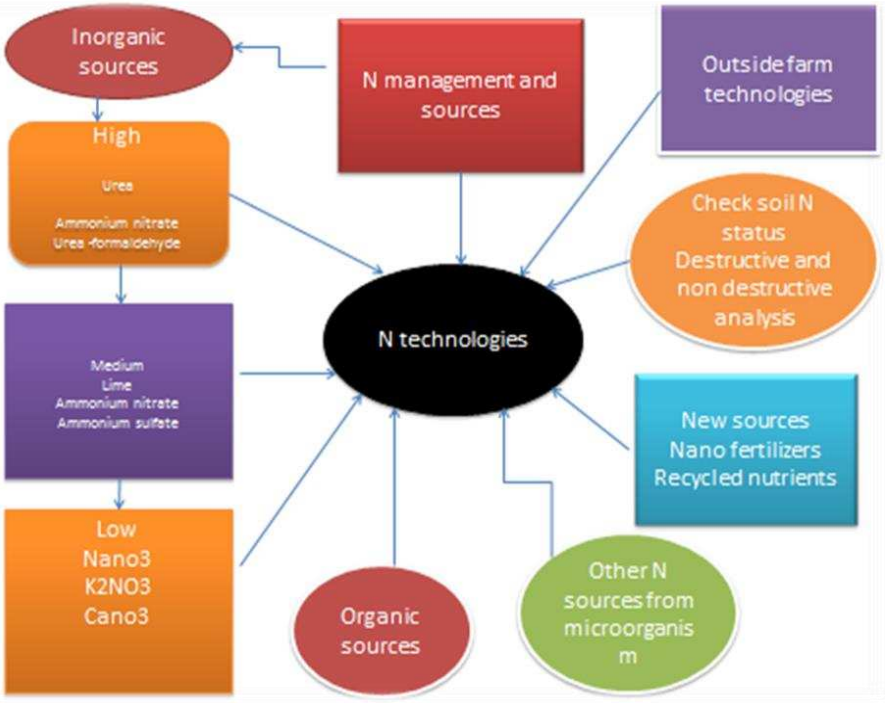

Figure 3. *Nitrogen production sources and management*

Concluding remarks

A genetic, physiological, and agronomic approach to N response and plant density will be useful for the use of NUE and is necessary to get key selection criteria for researchers and is important tool for farmers for fertilization protocol. This review will enhance the understanding to develop an integrated research work for discovering genes

http://www.aloki.hu ● ISSN 1589 1623 (Print) ● ISSN 1785 0037 (Online)
DOI: http://dx.doi.org/10.15666/aeer/1704_1013910153

by means of a complete phenotypic, agronomical, physiological, and biochemical under different plant population densities. High population density, important for high yields, causes greater competition for resources and morphological changes in the plant and may lead kernel abortion and lodging. Under different plant populations, due to leaching of NO_3-N and contamination of water the sufficient amount of N is not available to plant thus the NUE reduced. The future prospect is that how genetic, physiological, and agronomic approaches to high plant density and nitrogen to improve yield and quality of cereals. The breeders and agronomists should focus molecular and genetic aspects of cereals and should breed cultivars which are resistant to lodging and other problems under different plant densities.

Acknowledgements. We acknowledge the funding support from national modern agricultural industrial technology system project (CARS-06-13.5-A28), Youth fund of Crop Science, Shanxi Academy of Agricultural Sciences (ZQ1703), the Program for the Top Young Innovative Talents of Shanxi Agricultural University (TYIT201406).

REFERENCES

[1] Ahmed, S., Humphreys, E., Salim, M., Chauhan, B. S. (2016): Growth, yield and nitrogen use efficiency of dry-seeded rice as influenced by nitrogen and seed rates in Bangladesh. – Field Crops Research 186: 18-31.

[2] Anderson, R. L. (2008): Growth and yield of winter wheat as affected by preceding crop and crop management. – Agronomy Journal 100: 977-980.

[3] Borrell, A. K., Hammer, G. L., Van Oosterom, E. (2001): Stay-green: a consequence of the balance between supply and demand for nitrogen during grain filling. – Annals of Applied Biology 138: 91-95.

[4] Bos Bos, H. J. Vos, J., Struik, P. C. (2000): Morphological analysis of plant density effects on early leaf area growth in maize. – Netherlands Journal of Agricultural Science 48(2000): /99-212.

[5] Brennan, R. F., Mason, M. G., Walton, G. H. (2000): Effect of nitrogen fertilizer on the concentrations of oil and protein in canola (*Brassica napus*) seed. – Journal of Plant Nutrition 23: 339-348.

[6] Canevara, M. G., Romani, M., Corbellini, M., Perenzin, M., Borghi, B. (1994): Evolutionary trends in morphological, physiological, agronomical and qualitative traits of *Triticum aestivum* L. cultivars bred in Italy since 1990. – European Journal of Agronomy 3: 175-185.

[7] Chapman, S., Baretto, H. (1997): Using a chlorophyll meter to estimate specific leaf nitrogen of tropical maize during vegetative growth. – Agronomy Journal 89: 557-562.

[8] Christopher, R. B., Judith, B. S., Tollenaar, M., Tony, J. V. (2009): Maize morphophysiological responses to intense crowding and low nitrogen availability: an analysis and review. – Agronomy Journal 101: 1426-1452.

[9] Ciampitti, I. A., Vyn, T. J. (2011): A comprehensive study of plant density consequences on nitrogen uptake dynamics of maize plants from vegetative to reproductive stages. – Field Crops Research. 121(1):2-18.

[10] Comissão Brasileira de Pesquisa de Trigo (2007): Informaçõestécnicas da comissãobrasileira de Pesquisa de Trigo e Triticale para a Safra 2007 (Technical information from the Brazilian Wheat and Triticale Research Committee for the 2007 Season). – Embrapatrigo, Passo Fundo, RS, Brazil (in Portuguese).

[11] Dupont, F. M., Altenbach, S. B. (2003): Molecular and biochemical impacts of environmental factors on wheat grain development and during the life span of rice leaf (*Oryza sativa* L.). – Plant and Cell Physiology 24: 1079-1086.

http://www.aloki.hu ● ISSN 1589 1623 (Print) ● ISSN 1785 0037 (Online)
DOI: http://dx.doi.org/10.15666/aeer/1704_1013910153

[12] Duvick, D. N. (1996): What is Yield? – In: Edmeades, G. O., Banziger, M., Mickelson, H. R., Peña-Valdivia, C. B. Developing Drought and Low N-Tolerant Maize. El Batain, Mexico.
[13] Dwyer, T., Ponsonby, A. L., Newman, N. M., Gibbons, L. E. (1991): Prospective cohort study of prone sleeping position and sudden infant death syndrome. – Lancet 337(8752): 1244-7.
[14] Feil, B., Thiraporn, R., Geisler, G. (1990): Genotypic variation in grain nutrient concentration in tropical maize grown during a rainy and a dry season. – Agronomie 10: 717-725.
[15] Gallais, A., Coque, M. (2005): Genetic variation and selection for nitrogen use efficiency in maize: a synthesis. – Maydica 50: 531-537.
[16] Gao, Y., Li, Y., Zhang, J., Liu, W., Dang, Z., Cao, W., Qiang, Q. (2009): Effects of mulch, N fertilizer, and plant density on wheat yield, wheat nitrogen uptake, and residual soil nitrate in a dryland area of China. – Nutrient Cycling in Agroecosystems 85(2): 109-121.
[17] Gardner, J. C., Schnieter, A. A., Schatz, B. G. (2010): Effect of Plant Density on Grain Sorghum Production in North Dakota. – North Dakota Agricultural Experimental Station, Fargo, ND.
[18] Gastal, F., Lemaire, G. (2002): N uptake and distribution in crops: An agronomical and ecophysiological perspective. – Journal of Experimental Botany 53: 789-799. http://dx.doi.org/10.1093/jexbot/53.370.789.
[19] Giller, K. E., Beare, M. H., Lavelle, P., 'Izac, A.-M. N., Swift, M. J. (1997): Agricultural intensification, soil biodiversity and agroecosystem function. – Applied Soil Ecology 6: 3-16.
[20] Good, A. G., Shrawat, A. K., Muench, D. G. (2004): Can less yield more? Is reducing nutrient input into the environment compatible with maintaining crop production? – Trends in Plant Science 9: 597-605.
[21] Halvorson, A. D., Wienhold, B. J., Black, A. L. (2001): Tillage and nitrogen fertilization influence grain and soil nitrogen in an annual cropping system. – Agronomy Journal 93: 836-841.
[22] Harris, D. A., Kim, K., Nakahara, K., Vásquez-Doorman, C., Carthew, R. W. (2011): Cargo sorting to lysosome-related organelles regulates sirna-mediated gene silencing. – J. Cell Biol. 194(1): 77-87.
[23] Hashemi, A. M., Herbert, S. J., Putnam, D. H. (2005): Yield response of corn to crowding stress. – Agronomy Journal 97 839-846.
[24] Hashemi-Dezfouli, A., Herbert, S. J. (1992): Intensifying plant population response of corn with artificial shade. – Agronomy Journal 84: 547-551.
[25] Hay, R. K. M., Walker, A. J. (1989): Introduction to the Physiology of Crop Yield. – Longman Group UK Limited, Harlow.
[26] Hirel, B., Lea, P. (2001): Ammonia Assimilation. – In: Lea, P. J., Morot-Gaudry, J. F. (eds.) Plant Nitrogen. Springer-Verlag, Berlin, pp. 79-100. http://dx.doi.org/10.1007/978-3-662-04064-5_4.
[27] Hou H., Ma W., Noor, M.A., Tang L., Li C., Ding Z., Zhao M. (2019): Quantitative design of yield components to simulate yield formation for maize in China – Journal of Integrative Agriculture 18: 2–13. https://doi.org/ 10.1016/S2095-3119(19)62661-4
[28] Huseyin, G. K., Omer, M. K. (2003): Effect of hybrid and plant density on grain yield and yield components of maize (*Zea mays* L.). – Indian J. Agron. 48 203-205.
[29] Jackson, G. D. (2000): Effects of nitrogen and sulfur on canola yield and nutrient uptake. – Agronomy Journal 92: 44-49.
[30] Jamaati-e-Somarin, S., Zabihi-e-Mahmoodabad, R., Yari, A., Khayatnezhad, M., Gholamin, R. (2010): Study of Agronomical Nitrogen Use Efficiency of Durum Wheat, Affected by Nitrogen Fertilizer and Plant Density. – World Applied Sciences Journal 11(6): 674-681.

http://www.aloki.hu ● ISSN 1589 1623 (Print) ● ISSN 1785 0037 (Online)
DOI: http://dx.doi.org/10.15666/aeer/1704_1013910153

[31] Jan, M. T., Khan, J. M., Khan, A., Arif, M., Shafi, M., Nullah, N. (2010): Wheat nitrogen indices response to nitrogen source and application time. – Pakistan Journal of Botany 42(6): 4267-4279.
[32] Jiang, W., Wang, K., Wu, Q., Dong, S., Liu, P., Zhang, J. (2013): Effects of narrow plant spacing on root distribution and physiological nitrogen use efficiency in summer maize. – The Crop Journal 1(1): 77-83.
[33] Kade, M., Barneix, A. J., Olmos, S., Dubcovsky, J. (2005): Nitrogen uptake and remobilization in tetraploid 'Langdon' durum wheat and a recombinant substitution line with the high grain protein gene Gpc-B1. – Plant Breeding 124: 343-349.
[34] Keesstra, S. D. et al. (2016): Interactive comment on "FORUM" paper: The significance of soils and soil science towards realization of the UN sustainable development goals (SDGS). – Soil Discuss. DOI: 10.5194/soil-2015-88-AC1.
[35] Lea, P. J., Azevedo, R. A. (2006): Nitrogen use efficiency. 1. Uptake of nitrogen from the soil. – Annals of Applied Biology 149: 243-247.
[36] Li, J., Xie, R. Z., Wang, K. R., Ming, B., Guo, Y. Q., Zhang, G. Q., Li, S. K. (2015): Variations in maize dry matter, harvest index, and grain yield with plant density. – Agron. J. 107: 829. http://dx.doi.org/10.2134/agronj14.0522.
[37] Li, M., Li, W. (2004): Regulation of fertilizer and density on sink and source and yield of maize. – Sci. Agric. Sin. 37(8): 1130-1137 (in Chinese).
[38] Li, S. K., Wang, C. T. (2010): Potential and Ways to High Yield in Maize. – Science Press, Beijing, pp. 217-240 (in Chinese).
[39] Liu, W., Tollenaar, M., Stewart, G., Deen, W. (2004): Response of corn grain yield to spatial and temporal variability in emergence. – Crop Science 44: 847-854.
[40] Lopez-Bellido, R. J., Shepherd, C. E., Barraclough, P. B. (2004): Predicting post-anthesis N requirements of bread wheat with Minolta SPAD meter. – European Journal of Agronomy 20(3)313-320.
[41] Maddonni, G. A., Otegui, M. E., Cirilo, A. G. (2001): Plant population density, row spacing, and hybrid effects on maize canopy architecture and light attenuation. – Field Crops Research 71: 183-193.
[42] Mae, T. (1997): Physiological nitrogen efficiency in rice: nitrogen utilization, photosynthesis, and yield potential. – Plant and Soil 196(2): 201-211.
[43] Moose, S., Below, F. E. (2009): Biotechnology Approaches to Improving Maize Nitrogen Use Efficiency. – In: Kriz, A. L., Larkins, B. A. (eds.) Molecular Genetic Approaches to Maize Improvement, Biotechnology in Agriculture and Forestry. Springer-Verlag, Berlin, pp. 65-77.
[44] Noor, M. A. (2017): Nitrogen management and regulation for optimum NUE in maize - A mini review – Cogent Food & Agriculture, 3: 1348214.
[45] Oury, F. X., Be'rard, P., Brancourt-Hulmel, M., et al. (2003): Yield and grain protein concentration in bread wheat: a review and a study of multi-annual data from a French breeding program. – Journal of Genetics and Breeding 57: 59-68.
[46] Palta, J. A., Fillery, I. R. P. (1995): N application increases pre-anthesis contribution of dry matter to grain yield in wheat grown on duplex soil. – Australian Journal of Agricultural Research 46: 507-518.
[47] Pearcy, R. W., Valladares, F., Wright, S. J., Lasso de Paulis, E. (2004): A functional analysis of the crown architecture of tropical forest psychotria species: do species vary in light capture efficiency and consequently in carbon gain and growth? – Oecologia139: 163-177.
[48] Radenovic, C., Konstantinov, K., Delic, N., Stankovic, G. (2007): Photosynthetic and biolumine science properties of maize inbred lines with upright leaves. – Maydica 52: 347-356.
[49] Rajcan, I., Tollenaar, M. (1999). Source:sink ratio and leaf senescence in maize. II. Nitrogen metabolism during grain filling. – Field Crops Research 60: 255-265.

http://www.aloki.hu ● ISSN 1589 1623 (Print) ● ISSN 1785 0037 (Online)
DOI: http://dx.doi.org/10.15666/aeer/1704_1013910153

[50] Rampino, P., Pataleo, S. Gerardi, C., Carla Perrotta, G. (2006): Drought stress response in wheat: physiological and molecular analysis of resistant and sensitive genotypes. – Plant, Cell and Environment 29: 2143-2152.
[51] Raun, W. R., Johnson, G. V. (1999): Improving nitrogen use efficiency for cereal production. – Agronomy Journal 91: 357-363.
[52] Remans, T., Nacry, P., Pervent, M., Girin, T., Tillard, P., Lepetit, M., Gojon, A. (2006): A central role for the nitrate transporter NRT2.1 in the integrated morphological and physiological responses of the root system to nitrogen limitation in Arabidopsis. – Plant Physiol. 140(3): 909-21.
[53] Riedell, W. E., Pikul, J. L., Jaradat, A. A., Schumacher, T. E. (2009): Crop rotation and nitrogen input effects on soil fertility, maize mineral nutrition, yield and seed composition. – Agronomy Journal 101: 870-879.
[54] Sangoi, L., Gracietti, M. A., Rampazzo, C., Bianchetti, P. (2002): Response of Brazilian maize hybrids from different eras to changes in plant density. – Field Crops Research 79: 39-51.
[55] Sharratt, B. S., Mcwilliams, D., (2005): Microclimatic and rooting characteristics of narrow-row versus conventional-row corn. – Agronomy Journal 97: 1129-1135. http://dx.doi.org/10.2134/agronj2004.0292.
[56] Sher, A., He, L., Zhang, S., Li, J. C., Song, Y. (2016): Analysis and characterisation of interplant competition on maize canopy morphology for modelling. – In: Proceedings of the IEEE International Conference on Functional- Structural Plant Growth Modeling, Simulation, Visualization and Applications (FSPMA), Qingdao, pp. 189-193. DOI: 10.1109/FSPMA.2016.7818306.
[57] Sher, A., Khan, A., Li, J. C., Ahmad, M. I., Asharf, U., Jamoro, S. A. (2017): Response of maize grown under high plant density; performance, issues and management - a critical review. – Adv Crop Sci Tech. 5: 3.
[58] Sher, A., Khan, A., Liu, H. H., Ashraf, U., Li, J. C. (2018): Characterization of the effect of increased plant density on canopy morphology and stalk lodging risk. – Front. Plant Sci. 9: 1047.
[59] Simmonds, N. W. (1995): The relation between yield and protein in cereal grains. – Journal of the Science of Food and Agriculture 67: 309-315.
[60] Sinclair, T. R., Purcell, L. C., Sneller, C. H. (2004): Crop transformation and the challenge to increase yield potential. – Trends in Plant Science 9: 70-75.
[61] Smil, V. (2006): Transforming the 20th Century. – Oxford University Press, New York.
[62] Snyder, F. W., Bunce, J. A. (1983): Use of the plastochron index to evaluate effects of light, temperature and nitrogen on growth of soya bean (*Glycine max* L. Merr.). – Annals of Botany 52: 895-903.
[63] Soleymani, A., Shahrajabian, M. H., Naranjani, L. (2011): Determination of the suitable planting date and plant density for different cultivars of barley (*Hordeum vulgare* L.) – Fars. African Journal of Plant Science 5(4): 284-286.
[64] Stewart, D. W., Costa, C., Dwyer, L. M. Smith, D. L. Hamilton, R. I. Ma, B. L. (2003): Canopy structure, light interception, and photosynthesis in maize. – Agronomy Journal 95: 1465-11474.
[65] Sylvester-Bradley, R., Kindred, D. R. (2009): Analysing nitrogen responses of cereals to prioritize routes to the improvement of nitrogen use efficiency. – Journal of Experimental Botany 60: 1939-1951. http://dx.doi.org/10.1093/jxb/erp116.
[66] Ta, C. T., Weiland, R. T. (1992): Nitrogen partitioning in maize during ear development. – Crop Science 32: 443-451.
[67] Tabuchi, M., Sugiyama, T., Ishiyama, K., Inoue, E., Sato, T., Takahashi, H., Yamaya, T. (2005): Severe reduction in growth and grain filling of rice mutants lacking osgs1;1, a cytosolic glutamine synthetase 1;1. – The Plant Journal 42: 641-655.

http://www.aloki.hu ● ISSN 1589 1623 (Print) ● ISSN 1785 0037 (Online)
DOI: http://dx.doi.org/10.15666/aeer/1704_1013910153

[68] Tang, L., Ma, W., Noor, M.A., Li, L., Hou, H., Zhang, X., Zhao, M. (2018): Density resistance evaluation of maize varieties through new "*Density–Yield Model*" and quantification of varietal response to gradual planting density pressure – Scientific Reports, 8:17281. DOI:10.1038/s41598-018-35275-w

[69] Tanner, D., Amanuel, G., Asefa, T. (1993): Fertilizer effect on sustainability in the Wheat based small holder-farming systems of southeastern Ethiopia. – Field Crops Research 33: 235-248.

[70] Teklu, E., Hailemariam, T. (2009): Agronomic and economic efficiency of manure and urea fertilizers use on vertisols in Ethiopian highlands. – J. Agri. Sci. 8(3): 352-360.

[71] Tetio-Kagho, F., Gardner, F. (1988): Responses of maize to plant population density. I. Canopy development, light relationships, and vegetative growth. – Agronomy Journal 80: 930-935.

[72] Thuy, N. H., Shan Y., Singh B., Wang K., Cai Z., Singh Y., Buresh, R. J. (2008): Nitrogen supply in rice-based cropping systems as affected by crop residue management. – Soil Sci Soc Am J 72:.

[73] Tokatlidis, I. S., Has, V. Melidis, V. Has. I. Melonas, I., Evgenidis, G. Copandean, A., Ninou, E. Fasoula, V. A. (2011): Maize hybrids less dependent on high plant densities improve resource use efficiency in rainfed and irrigated conditions. – Field Crops Research 120. 345-351.

[74] Tollenaar, M., Wu, J. (1999): Yield improvement in temperate maize is attributable to greater stress tolerance. – Crop Science 39: 1597-1604.

[75] Tollenaar M., Dwyer, L. M., Stewart, D. W., (1992): Ear and kernel formation in maize hybrids representing three decades of grain yield improvement in Ontario. – Crop Science 32: 432-438.

[76] Tollenaar, M., Deen, W., Echarte, L., Liu, W. (2006): Effect of crowding stress on dry matter accumulation and harvest index in maize. – Agronomy Journal 98: 930-937. Doi: 10.2134/agronj2005.0336.

[77] Trapani N., Hall, A. J. (1996): Effects of leaf position and nitrogen supply on the extension of leaves of field-grown sunflower (*Helianthus annuus* L.). – Plant and Soil 184: 331-340.

[78] UNEP, UNIDO, IFA. (1998): Mineral Fertilizer Production and the Environment. Part 1. The fertilizer industry's Manufacturing Processes and Environmental Issues. Fertilizer Technical Report. – International Fertilizer Industry Association, United Nations Environment Programme, Paris, pp. 1-66.

[79] Uribelarrea M., Below, F. E., Moose, S. P. (2007): Divergent selection for grain protein affects nitrogen use in maize. – Field Crops Research 100: 82-90.

[80] USDA NASS (1965-2009): Compilation of Crop Production Reports. Agri-News. 09-18. – http://www.nass.usda.gov (verified 1 May 2001). USDA-NASS, Washington, DC.

[81] USDA-National Agricultural Statistics Service (2010): Published Estimates Data Base (PEDB). – http://www.nass.usda.gov (verified 1 May 2001). USDA-NASS, Washington, DC.

[82] Valladares, F., Niinemets, U. (2008): Shade tolerance, a key plant feature of complex nature and consequence. – Annual Review Ecology Systematics 257. https://doi.org/10.1146/annurev.ecolsys.39.110707.173506.

[83] Vos J., Biemond, H. (1992): Effects of nitrogen on the development and growth of the potato plant. 1. Leaf appearance, expansion growth, life span of leaves and stem branching. – Annals of Botany 70: 27-35.

[84] Wang, X., Yue, Y., Noor, M. A., Hou, H., Zhou, B., Ma, W., Zhao, M. (2018): Tillage time affects soil hydro-thermal properties, seedling growth and yield of maize (*Zea mays* L.). – Applied Ecology and Environmental Research 16(5): 6007-6023.

[85] White, P. J., Brown, P. H (2010): Plant nutrition for sustainable development and global health. – Annals of Botany 105(7): 1073-1080.

http://www.aloki.hu ● ISSN 1589 1623 (Print) ● ISSN 1785 0037 (Online)
DOI: http://dx.doi.org/10.15666/aeer/1704_1013910153

[86] Widdicombe, W. D., Thelen, K. D. (2002): Row width and plant density effects on corn grain production in the Northern Corn Belt. – Agronomy Journal 94: 1020-1023.
[87] Yu, Q., Wang, T., Liu, J., Sun, S (1998): Mathematical study on crop architecture and canopy photosynthesis. – J. Model. Acta. Agric. Sin. 24(1): 7-15 (in Chinese).
[88] Zhu, Z. (2000): Loss of fertilizer N from the plant–soil system and the strategies and techniques for its reduction in China. – Soil Environmental Science 9: 1-6.

http://www.aloki.hu ● ISSN 1589 1623 (Print) ● ISSN 1785 0037 (Online)
DOI: http://dx.doi.org/10.15666/aeer/1704_1013910153

THE USE OF PHYTOBENTHOS FOR THE ECOLOGICAL STATUS ASSESSMENT IN UPPER SAKARYA BASIN, TURKEY

ÇETIN, T.[1*] – DEMIR, N.[2]

[1]*General Directorate of Water Management, Ministry of Agriculture and Forestry, Republic of Turkey, 06560 Ankara, Turkey*

[2]*Department of Fisheries and Aquaculture Engineering, Faculty of Agriculture, Ankara University, 06110 Ankara, Turkey*
(phone: + 90-312-596-1643; fax: +90-312-318-5298)

**Corresponding author*
e-mail: tolga.cetin@tarimorman.gov.tr; phone: +90-312-207-5818; fax: +90-312-207-5573

(Received 13th Apr 2019; accepted 1st Jul 2019)

Abstract. In this study, it was aimed to use diatoms as representatives of phytobenthos for estimating the ecological status in Upper Sakarya Basin. Samples were taken seasonally from ten stations from April 2015 to December 2015. Stations 1, 2, 3, 4, 5, 6 and 7 were selected from rivers, stations 8 and 9 were selected from ponds which form Sakarya Springs. Station 10 was located at the outlet of Cifteler Aquaculture and Research Station. Diatoms were identified, counted and 19 diatom indices were calculated. Moreover, water temperature, dissolved oxygen, pH, electrical conductivity were measured *in situ*, and total nitrogen, orthophosphate and alkalinity were analysed. Finally, ecological status was estimated by evaluating biological, chemical and hydromorphological status according to Water Framework Directive. In total, 96 diatom species were identified from samples and *Achnanthidium minutissimum*, *Cymbella excisa*, *Craticula subminuscula* and *Fragilaria brevistriata* were the dominant species. Among diatom indices, IDP index which shows a high correlation with total nitrogen was used for the evaluation of the biological status. As a result, ecological status of the station 2 was estimated as high (class I), the status of stations 1, 4, 7, 8, 9 and 10 was estimated as good (class II), and the status of stations 3, 5, 6 was estimated as moderate (class III).
Keywords: *diatom, index, biological monitoring, reference site, water quality*

Introduction

Biological, chemical and hydromorphological monitoring has been carried out in Turkey since 2011 within the scope of alignment of Water Framework Directive (WFD). Rivers, lakes, coastal and transitional waters were monitored in 25 river basins. Water bodies were delineated, typology system was established, and sensitive areas were determined for that purpose. Preparation of river basin management plans and identification of reference sites are still ongoing.

The WFD requires to assess the status of rivers and lakes by using numerous parameters, one of which is phytobenthos. “Macrophytes and phytobenthos” are treated as two separate biological quality elements, and diatoms are frequently considered as representatives of phytobenthos (Kelly, 2013). Ecological status assessment is based on the status of biological, hydromorphological and physicochemical quality elements, by comparing data with the reference conditions (Muxika et al., 2007).

Phytobenthos is composed of many groups of living organisms such as macroalgae. However, reliable methods are developed mostly for diatoms. Some countries such as Czech Republic, Austria, Germany and Spain developed assessment methods for non-diatom communities. For instance, the activities regarding the identification of

http://www.aloki.hu ● ISSN 1589 1623 (Print) ● ISSN 1785 0037 (Online)
DOI: http://dx.doi.org/10.15666/aeer/1704_1015510172

macroalgae and development of indices are still ongoing. However, mostly diatoms are used for ecological status classification within the scope of the WFD.

Several studies were conducted on diatom indices for water quality assessment (Cemagref, 1982; Kelly and Whitton, 1995; Lenoir and Coste, 1996; Rott et al., 1999; Gomez and Licursi, 2001). Some studies were carried out in order to classify the water quality by using diatom indices in Turkey (Kalyoncu et al., 2009; Kıvrak et al., 2012; Morkoyunlu Yüce and Gönülol, 2016; Atıcı et al., 2018). In addition, other studies are also available which evaluate the phytobenthos for each river basin (Demir et al., 2017; Toudjani et al., 2017).

In diatom studies carried out in the Sakarya Basin, 117 epilithic diatoms were identified as a result of sampling from June 2006 to February 2007 from five stations in Felent Creek. Water quality was then assessed according to the Watanabe index (Watanabe et al., 1990) and the Sladecek index (Sladecek, 1986). In the light of results, organic pollution was recorded in summer, and species richness was higher mostly in winter than in summer (Solak et al., 2012). In total, 45 epipelic diatoms were identified in spring 2010 in Gürleyik stream, and the water quality was determined according to the Trophic Diatom Index (TDI) (Kelly and Whitton, 1995) and Biological Diatom Index (IBD) (Coste et al., 2009) as mesotrophic (Tokatlı, 2012).

The Upper Sakarya Basin which is covered by one of the largest river basins in Turkey (Sakarya Basin) was selected in this study. The aim of the study is to investigate the seasonal variation of diatom composition, and to estimate the ecological status with hydromorphological and physicochemical quality elements in the Upper Sakarya Basin.

Materials and methods

The Upper Sakarya Basin is located between 38°45'-39°45' latitudes and 30°15'-31°50' longitudes in the southeast of Eskişehir province in Turkey (DSİ, 1978). The most important stream in the basin is the Sakarya River which covers 5.816.000 ha, with 6.4×10^9 m^3 annual water potential and 824 km of length. In addition, Sakarbasi ponds consisting of East Pond (2.1 m^3 s^{-1}) and West Pond (0.41 m^3 s^{-1}) are among the most important sources of the river. The West Pond is the main water source of Cifteler Aquaculture and Research Station (CARS) which has a trout production capacity of 60 tons yr^{-1}. 10 stations were sampled (7 rivers, 2 ponds and the outlet of CARS) in April, July, September and December 2015 (*Fig. 1*). The coordinates of the sampling stations are given in *Table 1*.

Water temperature (°C), dissolved oxygen (DO), pH and electrical conductivity (EC) were measured *in situ* using WTW Multi 3430 Set G. Sampling bottles were submerged towards the main flow of the river in the homogeneous zone to collect a sample below the surface film. Water samples were taken below the surface (50 cm depth) from the ponds. At least 2 L of water was taken for each station per sampling season. They were then stored in iceboxes with ice packs and transferred immediately to the laboratory for later analyses. Total nitrogen (TN), orthophosphate (PO_4-P) and alkalinity were measured according to APHA (2012). The results of parameters were checked against the Surface Water Quality By-Law (YSKY, 2016).

Approximately 10 m river stretch or pond shore was selected for diatom sampling. In rivers, riffles were selected to better indicate the variety of natural hard surfaces. Single substrate was chosen for comparability of the samples. At least five cobbles were used for sampling. However, if cobbles were not present, five small boulders were sampled

http://www.aloki.hu ● ISSN 1589 1623 (Print) ● ISSN 1785 0037 (Online)
DOI: http://dx.doi.org/10.15666/aeer/1704_1015510172

instead. Epilithic diatoms were brushed from submerged substrates from removable cobbles and boulders approximately 10 cm^2. One epilithic diatom sample was taken for one station per sampling season. The samples were fixed with ethanol solution immediately after collection (European Committee for Standardization, 2014a). Hot hydrogen peroxide method was used to clean diatom frustules in the laboratory, and slides were prepared with Naphrax (European Committee for Standardization, 2014b). Diatoms were identified with a trinocular Leica microscope and a camera using the relevant taxonomic literature (Krammer and Lange-Bertalot, 1985, 1986, 1988, 1991a, b; Hofmann et al., 2013). At least three slides per sample and 400 specimen in each slide were counted. Diatom indices were calculated with OMNIDIA 6.0.2 (Lecointe et al., 1993) and brief information was given for diatom indices in *Table 2*.

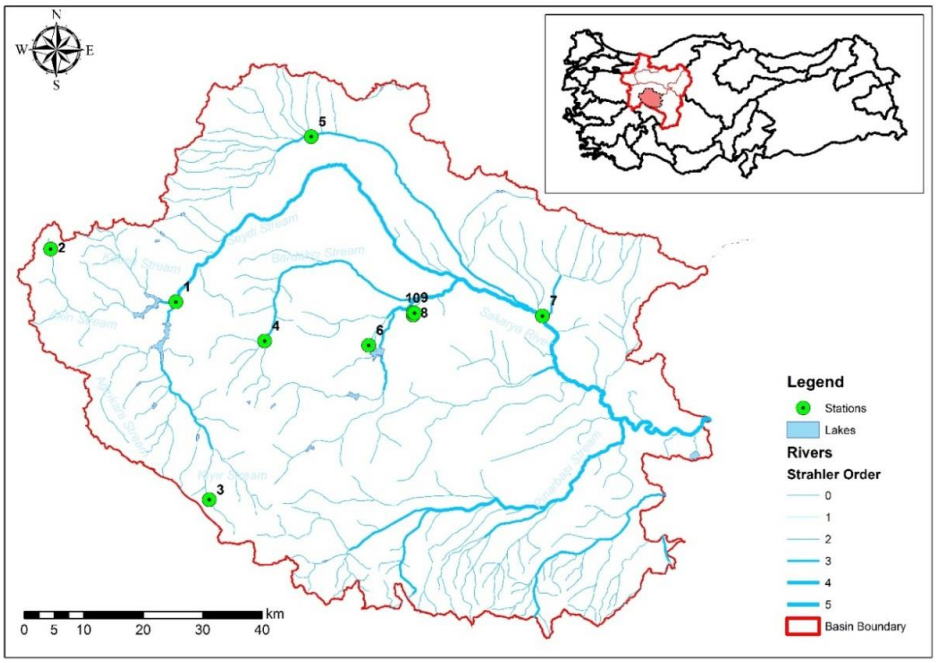

Figure 1. *The Upper Sakarya Basin and sampling stations. 1: Seydisuyu river; 2: Akin river; 3: Kıyır river; 4: Bardakçı river; 5: Sarısu river; 6: Ilıcabaşı river; 7: Sakarya river; 8: East pond (Sakarbasi); 9: West pond (Sakarbasi); 10: Outlet of CARS*

Table 1. *Coordinates of the sampling stations*

Stations	Water Body	Coordinates
1	Seydisuyu River	39º21.447' N - 30º35.627' E
2	Akin River	39º25.794' N - 30º20.741' E
3	Kıyır River	39º03.584' N - 30º40.435' E
4	Bardakçı River	39º18.209' N - 30º46.183' E
5	Sarısu River	39º36.959' N - 30º50.732' E
6	Ilıcabaşı River	39º18.155' N - 30º58.342' E
7	Sakarya River	39º21.359' N - 31º18.531' E
8	East Pond (Sakarbasi)	39º21.051' N - 31º03.412' E
9	West Pond (Sakarbasi)	39º21.282' N - 31º03.424' E
10	Outlet of CARS	39º21.233' N - 31º03.562' E

http://www.aloki.hu ● ISSN 1589 1623 (Print) ● ISSN 1785 0037 (Online)
DOI: http://dx.doi.org/10.15666/aeer/1704_1015510172

Table 2. *Information about the calculated diatom indices according to OMNIDA 6.0.2 (Lecointe et al., 1993)*

Index	Abbreviation	Reference	Scale	Water quality
Biological Diatom Index	IBD	Coste et al., 2009	20	20 (best)
Pollution Sensitivity Index	IPS	Cemagref, 1982	20	20 (best)
Generic Diatom Index	IDG	Cemagref, 1982; Rumeau and Coste, 1988	20	20 (best)
Descy Index	DESCY	Descy, 1979	5	5 (best)
Sladecek Index	SLA	Sladecek, 1986	4	4 (worst)
Leclercq and Maquet Index	IDSE	Leclercq and Maquet, 1987	5	5 (best)
Artois-Picardie Diatom Index	IDAP	Prygiel et al., 1996	20	20 (best)
Eutrophication Pollution Index-Diatoms	EPI-D	Dell'Uomo, 2004	4	4 (worst)
Lobo Index	LOBO	Lobo et al., 2004	4	4 (worst)
Swiss Diatom Index	DI-CH	Hürlimann and Niederhauser, 2002	8	8 (worst)
Rott Trophic Index	TID	Rott et al., 1999	4	4 (worst)
Rott Saprobic Index	SID	Rott et al., 1997	4	4 (worst)
Trophic Diatom Index for Lakes	TDIL	Stenger-Kovacs et al., 2007	5	5 (best)
Commission for Economical Community Index	CEE	Descy and Coste, 1991	20	20 (best)
Watanabe Index	WAT	Watanabe et al., 1990	100	100 (best)
Trophic Diatom Index	TDI	Kelly and Whitton, 1995	100	100 (worst)
Pollution Tolerant Taxa Index	% PT	Kelly and Whitton, 1995	%	100 (worst)
Pampean Diatom Index	IDP	Gomez and Licursi, 2001	4	4 (worst)
Steinberg and Schiefele Index	SHE	Steinberg and Schiefele, 1988	7	7 (best)

Detrended Correspondence Analysis (DCA) was performed to determine whether the ordination model was linear or unimodal before proceeding with the Canonical Correspondence Analysis (Leps and Smilauer, 2003). In order to link diatom species with water quality parameters, CCA was made with CANOCO 4.5 (ter Braak and Smilauer, 2002) and XLSTAT because the longest gradient length is above 4.0. Diatom species which were over 1% of general composition were taken into consideration. Physicochemical parameters were transformed $\ln(x + 1)$ except for pH in order to decrease skewness. CCA analysis was tested with 499 unrestricted permutations according to Monte Carlo simulation to clarify the significance of environmental variables on diatom species data. Significant variables ($P < 0.01$) were included in CCA analysis. The Pearson correlation between diatom indices and water quality parameters was calculated with XLSTAT software. In order to normalize the data, all index results were transformed to the scale 0-20 by the OMNIDIA 6.0.2. Since orthophosphate results were lower than the detection limits (< 0.01 mg L^{-1}) in some stations, they were excluded from CCA analysis. It was performed for 39 variables (22 diatom species and 6 physicochemical parameters) in 10 stations for 4 sampling periods due to the fact that station 2 was dry in September. The seasonal variations in physicochemical parameters and community structure were analysed by using one-way variance analysis (ANOVA). Diversity and evenness of diatoms calculated for community structure.

IHF index (Fluvial Habitat Index) (Pardo et al., 2002) and MPCA Stream Habitat Assessment (MSHA) (MPCA, 2014) were used in rivers, and the ECELS index (Boix et al., 2010) was used in ponds to estimate the hydromorphological status.

Ecological status was determined according to one-out-all-out principle in the WFD (Directive, 2000). According to this principle, the lowest score of all assessment results determined the overall ecological quality class in this study.

http://www.aloki.hu ● ISSN 1589 1623 (Print) ● ISSN 1785 0037 (Online)
DOI: http://dx.doi.org/10.15666/aeer/1704_1015510172

Results

Physical and chemical water quality parameters

In the research period, the lowest mean temperature (8.53 °C), alkalinity (11.55 mg L^{-1}), electrical conductivity (68.73 µS cm^{-1}), total nitrogen (0.50 mg L^{-1}) and the highest mean dissolved oxygen (9.99 mg L^{-1}) were measured in station 2 (*Table 3*). pH ranged between 7.05 and 8.0. The highest temperature (21.50 °C) and total nitrogen (4.06 mg L^{-1}) were found in station 6.

Table 3. *The variation of physicochemical parameters in sampling stations by season (n = 4) (mean ± standard deviation)*

Stations	Temperature (°C)	pH	EC (µS cm^{-1})	DO (mg L^{-1})	TN (mg L^{-1})	PO_4-P (mg L^{-1})	Alkalinity (mg $CaCO_3$ L^{-1})
1	11.53±6.35	7.68±0.28	359.00±27.31	9.43±1.49	1.25±0.36	0.03±0.04	118.11±24.89
2	8.53±4.65	7.52±0.46	68.73±10.18	9.99±0.83	0.50±0.65	0.01±0.01	11.55±4.16
3	15.95±4.97	7.58±0.15	491.00±54.94	8.62±1.07	1.82±0.76	0.03±0.05	164.05±42.28
4	16.28±7.82	8.07±0.26	549.25±46.18	9.00±2.11	2.81±0.66	0.02±0.01	200.66±57.42
5	13.15±6.34	7.56±0.17	986.50±53.10	4.82±2.54	3.66±1.43	0.01±0.01	189.88±42.77
6	21.50±3.59	7.05±0.08	715.00±12.68	5.39±0.27	4.06±1.01	0.01±0.01	203.21±51.63
7	15.25±5.88	7.72±0.36	897.25±164.29	7.90±1.45	1.68±0.19	0.03±0.02	198.87±29.90
8	19.28±3.93	7.15±0.07	870.00±19.78	7.14±0.58	1.90±0.64	0.01±0.02	224.18±49.62
9	18.88±3.14	7.17±0.10	857.75±14.17	7.03±0.67	1.84±0.45	0.01±0.00	224.96±49.39
10	19.15±3.02	7.45±0.18	856.25±16.32	7.06±0.63	1.77±0.41	0.01±0.01	223.34±48.20

Diatom composition

In total, 96 diatom species which belong to 43 genera were identified from the sampling stations of the Upper Sakarya Basin (*Table 4*). The dominant species were *Achnanthidium minutissimum, Cymbella excisa, Craticula subminuscula, Fragilaria brevistriata, Amphora pediculus, Diatoma moniliformis, Ulnaria ulna* and *Denticula kuetzingii*. On the other hand, *Cymatopleura elliptica, Caloneis bacillum, Nitzschia vitrea, Cocconeis disculus, Cymbella compacta, Cymbella parva, Gomphonema truncatum, Navicula oblonga* and *Pinnularia viridiformis* were found rarely.

Diatom indices

The seasonal average scores of diatom indices in the sampling stations were given in *Table 5*. Different diatom indices revealed different water quality classes in the stations.

Statistical analyses

The seasonal variations in physicochemical parameters were found to be significant ($P < 0.05$). The unimodal ordination model was found between physicochemical parameters and diatom taxa since the longest gradient length was above 4.0. CCA analysis was performed to explain the link between physicochemical parameters and diatom taxa. The eigenvalues of the first two CCA axes were 0.792 and 0.515. 18.8% of the cumulative variance (axis 1: 11.4%, axis 2: 7.4) in the diatom species was explained by the first two CCA axes with 92% of the diatom species-environment correlation (*Fig. 2*). The amount of species-environment variance explained was 63.4% (*Table 6*). The Monte Carlo test confirmed that temperature, dissolved oxygen, total nitrogen, alkalinity ($P = 0.002$) and pH ($P = 0.004$) were statistically significant ($P < 0.01$).

http://www.aloki.hu ● ISSN 1589 1623 (Print) ● ISSN 1785 0037 (Online)
DOI: http://dx.doi.org/10.15666/aeer/1704_1015510172

Table 4. *Diatom composition of the sampling stations (%)*

Species	Composition (%) of stations									
	1	**2**	**3**	**4**	**5**	**6**	**7**	**8**	**9**	**10**
Achnanthidium affine (Grunow) Czarnecki	0.52	-	-	0.06	0.23	-	-	-	-	0.06
Achnanthidium minutissimum (Kützing) Czarnecki	17.31	-	3.81	26.94	53.00	66.37	0.54	0.43	-	2.35
Achnanthidium pyrenaicum (Hustedt) H.Kobayasi	0.35	-	-	-	0.17	-	-	-	2.86	0.06
Amphipleura pellucida (Kützing) Kützing	0.06	6.07	-	-	0.06	-	0.18	0.12	-	-
Amphora copulata (Kützing) Schoeman & R.E.M.Archibald	-	-	-	0.12	0.11	0.30	-	-	-	-
Amphora ovalis (Kützing) Kützing	-	-	-	0.24	0.17	0.18	-	0.06	-	-
Amphora pediculus (Kützing) Grunow ex A.Schmidt	1.39	0.51	3.81	13.56	0.06	-	1.14	13.99	5.72	6.53
Aneumastus minor Lange-Bertalot	-	-	-	-	-	-	-	0.25	-	-
Aulacoseira granulata var. angustissima (Otto Müller) Simonsen	0.12	-	0.18	-	-	-	-	-	-	-
Bacillaria paxillifera (O.F.Müller) T.Marsson	-	-	-	-	-	-	3.06	-	0.06	-
Brebissonia lanceolata (C.Agardh) Mahoney & Reimer	-	-	0.18	-	-	-	0.66	-	-	-
Caloneis bacillum (Grunow) Cleve	-	-	-	-	-	0.12	-	-	-	-
Caloneis macedonica Hustedt	-	-	-	-	-	-	-	0.25	-	-
Cocconeis disculus (Schumann) Cleve	-	-	-	-	-	-	-	0.19	-	-
Cocconeis placentula Ehrenberg	-	1.03	1.97	0.12	1.43	0.06	2.94	0.37	0.73	-
Cocconeis placentula var. lineata (Ehrenberg) Van Heurck	0.29	2.31	1.97	0.54	2.34	0.06	4.92	0.06	3.71	0.41
Craticula accomoda (Hustedt) D.G.Mann	1.91	-	0.66	0.12	-	0.30	-	-	4.81	0.06
Craticula cuspidata (Kutzing) D.G.Mann	-	-	-	-	-	-	0.30	-	-	-
Craticula subminuscula (Manguin) C.E.Wetzel & L.Ector	16.62	6.92	40.33	2.29	0.40	-	2.22	-	0.06	0.24
Cyclostephanos dubius (Hustedt) Round	0.41	-	-	-	-	-	-	-	-	-
Cyclotella atomus Hustedt	0.29	-	-	-	-	-	0.06	-	0.06	-
Cyclotella distinguenda Hustedt	-	-	-	-	7.71	-	0.06	0.25	4.99	3.12
Cyclotella meneghiniana Kützing	0.29	0.77	-	-	0.29	0.06	1.86	0.25	-	0.29
Cymatopleura elliptica (Brébisson) W.Smith	-	-	-	0.06	-	-	-	-	-	-
Cymatopleura solea (Brébisson) W.Smith	-	-	0.06	-	-	-	0.30	-	-	-
Cymbella compacta Østrup	0.17	-	-	-	-	-	-	-	-	-

http://www.aloki.hu ● ISSN 1589 1623 (Print) ● ISSN 1785 0037 (Online)
DOI: http://dx.doi.org/10.15666/aeer/1704_1015510172

Cymbella cymbiformis C.Agardh	-	-	-	-	1.77	-	0.12	0.43	0.49	0.06
Cymbella excisa Kützing	2.26	3.25	1.61	13.44	6.45	5.88	4.20	19.18	30.44	17.12
Cymbella hustedtii Krasske	0.06	0.26	0.24	0.30	-	-	-	-	-	-
Cymbella lange-bertalotii Krammer	0.75	-	-	0.60	-	-	0.12	-	-	-
Cymbella neocistula Krammer	0.06	-	-	0.06	0.46	-	0.84	0.06	-	-
Cymbella parva (W.Smith) Kirchner	0.17	-	-	-	-	-	-	-	-	-
Cymbopleura amphicephala (Nägeli) Krammer	-	-	-	0.06	0.11	0.36	1.08	0.43	0.06	-
Denticula kuetzingii Grunow	0.17	-	-	0.66	12.79	11.99	0.24	0.37	2.50	0.53
Diatoma moniliformis (Kützing) D.M.Williams	1.16	-	-	15.67	-	0.06	14.27	-	-	4.41
Diatoma vulgaris Bory	0.41	-	-	0.30	-	-	0.66	0.99	-	7.00
Encyonema lacustre (C.Agardh) Pantocsek	0.12	-	-	-	-	-	-	0.12	-	0.06
Encyonema minutum (Hilse) D.G.Mann	0.35	-	-	-	-	-	-	-	-	-
Encyonema silesiacum (Bleisch) D.G.Mann	-	1.97	0.48	0.18	0.06	-	-	-	-	-
Encyonema ventricosum (C.Agardh) Grunow	2.61	2.14	1.67	0.54	0.11	-	0.12	-	-	-
Encyonopsis cesatii (Rabenhorst) Krammer	-	-	-	-	0.06	-	0.06	0.12	0.06	-
Encyonopsis minuta Krammer & E.Reichardt	0.69	-	1.19	7.23	1.83	0.59	3.36	0.99	1.89	1.29
Epithemia turgida (Ehrenberg) Kützing	-	-	-	-	-	-	-	-	-	0.65
Eunotia bilunaris (Ehrenberg) Schaarschmidt	-	11.62	-	-	-	-	-	-	-	-
Eunotia minor (Kützing) Grunow	-	-	-	-	-	-	-	0.25	-	-
Fragilaria brevistriata Grunow	0.06	1.20	-	0.06	1.43	1.07	5.40	51.77	0.97	1.59
Fragilaria construens (Ehrenberg) Grunow	-	-	-	-	-	0.06	0.18	0.93	0.30	-
Fragilaria recapitellata Lange-Bertalot & Metzeltin	-	3.76	-	-	-	-	-	-	-	-
Fragilaria vaucheriae (Kützing) J.B.Petersen	0.17	0.26	0.30	-	0.11	-	0.06	0.06	3.78	1.29
Gomphonema italicum Kützing	-	0.60	0.06	-	-	-	0.18	-	1.28	0.35
Gomphonema micropus Kützing	-	18.35	-	-	-	-	-	-	-	-
Gomphonema olivaceum (Hornemann) Brébisson	15.52	0.77	3.81	4.88	-	-	0.48	-	0.24	0.24
Gomphonema parvulum (Kützing) Kützing	4.86	0.77	9.71	0.48	1.66	2.08	0.24	0.06	4.87	0.18
Gomphonema subclavatum (Grunow) Grunow	-	2.22	-	-	-	-	-	-	-	-
Gomphonema truncatum Ehrenberg	-	-	-	-	-	-	-	-	0.18	-

http://www.aloki.hu ● ISSN 1589 1623 (Print) ● ISSN 1785 0037 (Online)
DOI: http://dx.doi.org/10.15666/aeer/1704_1015510172

Halamphora veneta (Kützing) Levkov	-	-	1.61	0.24	0.23	-	0.12	-	3.47	1.88
Hantzschia amphioxys (Ehrenberg) Grunow	0.06	0.85	-	0.24	0.57	0.06	-	-	-	0.12
Hippodonta capitata (Ehrenberg) Lange-Bertalot. Metzeltin & Witkowski	0.17	-	-	-	-	-	0.30	-	-	-
Karayevia clevei (Grunow) Round & Bukhtiyarova	-	0.51	0.06	-	-	-	0.24	2.41	-	-
Lindavia balatonis (Pantocsek) T.Nakov et al.	1.16	-	0.06	-	-	-	1.86	-	-	-
Lindavia ocellata (Pantocsek) T.Nakov et al.	4.00	0.43	0.18	0.12	-	-	3.18	-	0.06	0.18
Melosira varians C.Agardh	0.58	-	0.06	-	0.74	0.30	19.85	-	0.85	0.29
Meridion circulare (Greville) C.Agardh	-	17.52	-	0.18	-	-	-	-	-	-
Navicula antonii Lange-Bertalot	-	-	0.71	0.06	-	-	-	0.12	-	-
Navicula capitatoradiata H.Germain	0.29	-	0.71	0.24	-	-	0.18	-	-	-
Navicula cari Ehrenberg	-	-	-	-	-	-	-	1.61	-	0.06
Navicula cryptotenella Lange-Bertalot	0.17	0.43	0.30	1.27	0.17		3.66	0.62	0.97	0.12
Navicula kotschyi Grunow	-	-	-	-	0.17	3.74	-	0.37	0.06	-
Navicula oblonga (Kützing) Kützing	-	-	-	0.06	-	-	0.06	0.06	-	-
Navicula reichardtiana Lange-Bertalot	11.70	2.05	1.19	1.02	0.11	-	-	0.12	-	0.12
Navicula tripunctata (O.F.Müller) Bory	0.81	-	6.61	1.08	0.46	-	4.44	-	-	0.12
Nitzschia amphibia Grunow	1.33	-	1.61	-	-	0.12	1.32	-	0.12	14.47
Nitzschia capitellata Hustedt. nom. inval.	0.75	-	0.30	0.06	-	3.38	0.06	-	0.06	0.18
Nitzschia dissipata (Kützing) Rabenhorst	2.95	0.85	1.43	4.34	1.77	-	1.92	0.06	0.24	0.12
Nitzschia fonticola (Grunow) Grunow	2.37	0.26	2.92	-	0.29	-	-	-	0.49	18.45
Nitzschia frustulum (Kützing) Grunow	-	-	0.24	-	0.23	-	-	-	-	-
Nitzschia heufleriana Grunow	-	-	0.12	0.18	-	-	0.24	-	-	-
Nitzschia linearis W.Smith	-	1.37	2.44	0.36	0.34	0.06	1.68	-	0.24	-
Nitzschia recta Hantzsch ex Rabenhorst	-	-	-	-	0.11	-	0.96	-	-	-
Nitzschia vitrea G.Norman	-	-	-	-	-	-	0.12	-	-	-
Pinnularia viridiformis Krammer	-	-	-	-	-	-	0.18	-	-	-
Planothidium lanceolatum (Brébisson ex Kützing) Lange-Bertalot	-	5.64	0.66	-	0.06	1.07	-	-	-	-
Planothidium rostratum (Østrup) Lange-Bertalot	-	-	-	-	-	-	0.42	-	-	-
Reimeria sinuata (W.Gregory) Kociolek & Stoermer	0.64	0.26	0.60	0.24	0.06	-	0.06	-	0.12	-

http://www.aloki.hu ● ISSN 1589 1623 (Print) ● ISSN 1785 0037 (Online)
DOI: http://dx.doi.org/10.15666/aeer/1704_1015510172

Rhoicosphenia abbreviata (C.Agardh) Lange-Bertalot	0.41	0.51	0.24	-	-	-	1.26	-	-	0.06
Rhopalodia gibba (Ehrenberg) Otto Müller	-	0.60	-	-	-	-	-	-	0.18	-
Sellaphora pupula (Kützing) Mereschkovsky	-	0.43	0.60	-	-	0.12	0.12	0.12	-	-
Staurosira venter (Ehrenberg) Cleve & J.D.Möller	-	-	-	-	-	-	-	0.43	-	-
Stephanodiscus hantzschii Grunow	0.23	0.51	-	-	-	-	1.02	-	-	0.47
Surirella angusta Kützing	0.17	1.54	0.60	0.24	-	-	1.02	-	-	-
Surirella brebissoni Krammer & Lange-Bertalot	0.17	1.20	4.29	0.36	0.11	0.42	2.28	-	0.06	-
Tryblionella apiculata W.Gregory	0.23	-	0.36	0.12	0.11	-	1.20	-	-	-
Tryblionella hungarica (Grunow) Frenguelli	-	-	-	-	-	0.59	0.24	-	-	-
Ulnaria acus (Kützing) Aboal	0.23	-	-	0.60	0.06	-	0.30	0.68	0.06	0.24
Ulnaria biceps (Kützing) Compère	0.23	-	-	0.18	1.09	0.30	0.18	1.36	4.57	6.47
Ulnaria ulna (Nitzsch) Compère	2.20	0.26	0.06	0.30	0.51	0.30	1.68	0.06	18.39	8.76

Table 5. *Average scores of diatom indices in sampling stations (see abbreviations in Table 2)*

Stations	IBD	IPS	IDG	DESCY	SLA	IDSE	IDAP	EPI-D	LOBO	DI-CH	TID	SID	TDIL	CEE	WAT	TDI	PT	IDP	SHE
	20	20	20	5	4	5	20	4	4	8	4	4	5	20	100	100	%	4	7
1	13.7	12.7	12.2	3.50	2.03	3.11	11.6	1.75	2.11	4.15	2.81	2.39	2.96	11.4	58.30	77.23	26.3	1.80	4.35
2	15.9	14.3	14.9	4.29	1.27	3.75	11.0	1.26	2.00	3.97	2.85	1.97	2.76	15.2	61.93	52.46	29.5	1.13	5.09
3	10.1	10.0	9.6	3.73	2.20	2.81	8.7	2.41	2.02	5.97	3.34	2.64	1.83	10.0	39.69	84.74	57.3	2.20	3.33
4	19.1	16.0	14.8	4.50	1.41	4.09	16.1	1.20	3.33	3.33	2.23	2.03	3.53	15.4	72.77	51.03	3.6	1.49	5.47
5	18.8	16.8	16.1	3.97	1.22	4.14	17.6	0.76	3.64	2.90	1.64	1.46	3.53	16.0	79.02	42.09	3.4	1.29	5.86
6	18.2	15.6	16.0	3.85	1.23	4.21	18.8	0.86	3.98	3.33	1.81	1.58	3.84	15.4	83.24	38.15	6.3	1.21	5.72
7	15.6	13.3	12.6	3.94	1.67	3.45	13.0	1.84	3.08	4.23	2.77	2.06	2.93	11.5	54.64	71.34	6.3	1.98	4.96
8	15.9	13.1	13.9	4.80	1.48	3.87	15.2	1.44	2.79	3.33	2.79	1.50	2.98	14.7	58.73	73.22	2.5	1.73	5.45
9	14.7	12.0	14.5	3.02	1.82	3.16	7.7	1.72	2.65	4.88	3.07	2.08	2.57	11.9	54.25	63.62	9.3	1.95	5.21
10	15.0	12.2	10.4	3.53	1.64	3.35	9.2	1.75	2.65	4.91	3.24	2.22	3.34	11.7	64.34	72.57	20.2	1.86	5.37

http://www.aloki.hu ● ISSN 1589 1623 (Print) ● ISSN 1785 0037 (Online)
DOI: http://dx.doi.org/10.15666/aeer/1704_1015510172

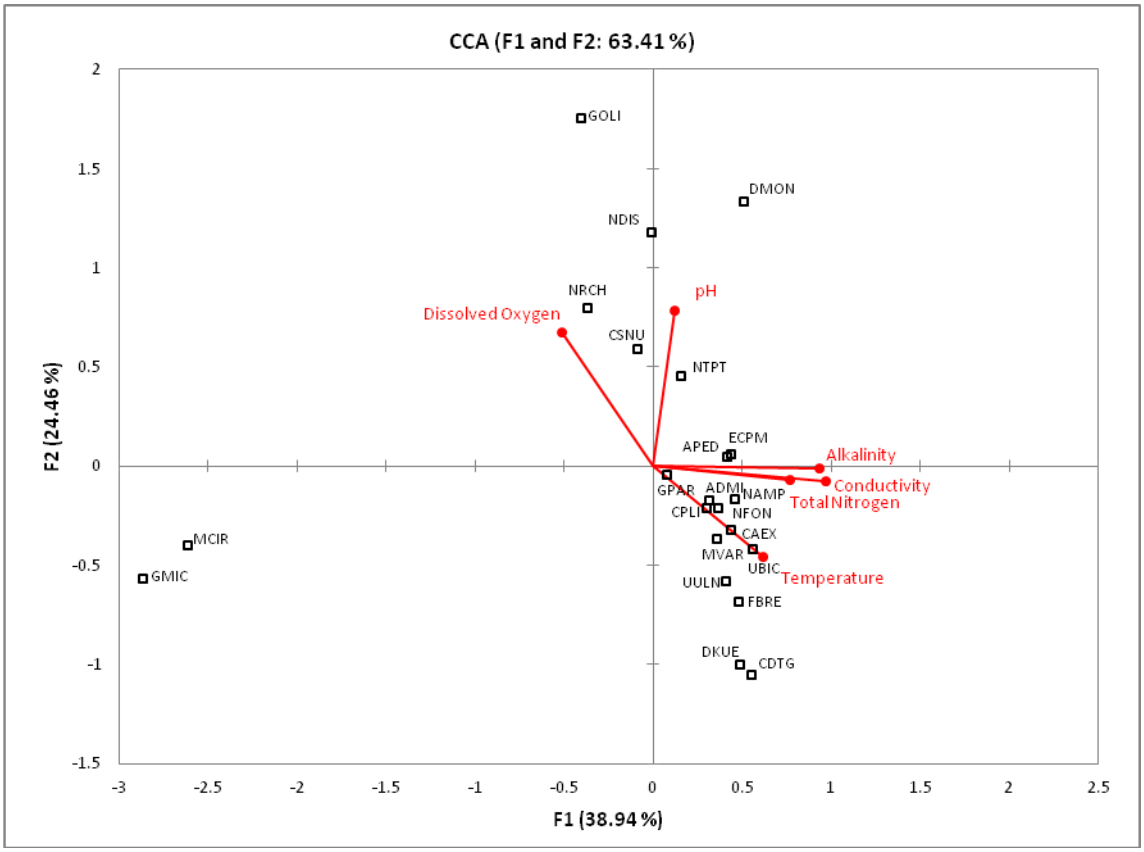

Figure 2. *CCA plot of species and physicochemical parameters in sampling stations. ADMI, Achnanthidium minutissimum; APED, Amphora pediculus; CPLI, Cocconeis placentula var. lineata; CSNU, Craticula subminuscula; CDTG, Cyclotella distinguenda; CAEX, Cymbella excisa; DKUE, Denticula kuetzingii; DMON, Diatoma moniliformis; ECPM, Encyonopsis minuta; FBRE, Fragilaria brevistriata; GMIC, Gomphonema micropus; GOLI, Gomphonema olivaceum; GPAR, Gomphonema parvulum; MVAR, Melosira varians; MCIR, Meridion circulare; NRCH, Navicula reichardtiana; NTPT, Navicula tripunctata; NAMP, Nitzschia amphibia; NDIS, Nitzschia dissipata; NFON, Nitzschia fonticola; UBIC, Ulnaria biceps; UULN, Ulnaria ulna*

Table 6. *Summary of canonical correspondence analysis for diatom species and physicochemical parameters*

Axes	1	2	3	4	Total inertia
Eigenvalues	0.792	0.515	0.384	0.199	6.961
Species-environment correlations	0.954	0.920	0.888	0.711	
Cumulative percentage varians of species data	11.4	18.8	24.3	27.1	
of species environment relation	38.9	63.4	81.2	90.8	
Sum of all eigenvalues					6.961
Sum of all canonical eigenvalues					2.080

Figure 2 shows the CCA biplot of physicochemical parameters and diatom species for the first two axes. As shown in *Figure 2*, there is a negative relation between

http://www.aloki.hu ● ISSN 1589 1623 (Print) ● ISSN 1785 0037 (Online)
DOI: http://dx.doi.org/10.15666/aeer/1704_1015510172

temperature and dissolved oxygen whereas a positive relation was found between alkalinity and conductivity. *Gomphonema micropus* and *Meridion circulare* were found to be in a separate quadrat from the other species and physicochemical parameters. Conductivity, alkalinity, total nitrogen and temperature were the parameters playing an important role in the distribution of species. When the clusters of species were examined, a large percentage of the species were clustered around temperature. In terms of nutrients, total nitrogen showed a close relation with temperature in the distribution of species. Pearson correlations between physicochemical parameters and diatom indices were shown in *Table 7*.

Table 7. *Pearson correlations between physicochemical parameters and diatom indices (n = 39) (see abbreviations in Table 2)*

	Temperature	**Dissolved oxygen**	**pH**	**Conductivity**	**Alkalinity**	**Total nitrogen**
IBD	-0.2319	-0.1942	-0.0253	0.1525	0.0380	0.1824
IPS	**-0.3759***	-0.1402	0.0327	0.0522	-0.0699	0.1537
IDG	-0.2359	-0.2117	-0.1855	0.0115	-0.0778	0.1581
DESCY	-0.2324	0.1304	0.0363	-0.0646	-0.0912	-0.0181
SLA	-0.3058	-0.1922	-0.2026	0.0194	-0.1307	0.0256
IDSE	-0.2704	-0.1818	-0.1078	0.0974	-0.0320	0.1812
IDAP	-0.1688	**-0.3192***	-0.0505	0.1989	0.1029	**0.4001***
EPI-D	**-0.3266***	-0.2527	-0.1503	0.0591	-0.0811	0.1614
LOBO	0.0603	**-0.3869***	-0.1503	**0.3671***	0.2625	**0.3811***
DI-CH	**-0.3680***	-0.0799	-0.0692	0.0647	-0.0363	0.0966
TID	-0.1553	**-0.3785***	-0.0525	0.1685	0.0917	**0.4513****
SID	-0.0618	**-0.4457****	**-0.3677***	0.2452	0.0950	0.2171
TDIL	-0.2510	-0.1764	-0.0224	0.2013	0.0946	0.2741
CEE	-0.3051	-0.1447	-0.1365	-0.0180	-0.1265	0.1088
WAT	-0.2061	-0.2569	-0.1052	0.1341	0.0211	0.2587
TDI	-0.1591	-0.2998	-0.0750	0.0050	-0.1057	0.3071
% PT	0.0783	0.2654	0.1024	**-0.3837***	-0.2226	-0.2390
IDP	**-0.4264****	-0.1075	0.0793	-0.2300	**-0.3224***	0.0087
SHE	-0.1191	-0.2922	-0.2020	0.2243	0.0750	0.1483

*$P < 0.05$, **$P < 0.01$

The IDP index which has the highest correlation with temperature and which plays an essential role in the distribution of species, was used to evaluate the diatom results. IPS, DI-CH and EPI-D indices were also correlated with temperature respectively after IDP index. The IDP index results regressed against total nitrogen which also affected the distribution of diatom species (*Fig. 2*). Station 2 is excluded from the regression since the species were found to be in completely different quadrats.

Hydromorphological results

The hydromorphological quality in the sampling stations varied between high and moderate (*Table 8*). Station 2 is in high hydromorphological status, whereas stations 5, 6 and 10 are in moderate hydromorphological status.

http://www.aloki.hu ● ISSN 1589 1623 (Print) ● ISSN 1785 0037 (Online)
DOI: http://dx.doi.org/10.15666/aeer/1704_1015510172

Table 8. *Hydromorphological status in sampling stations*

Stations	MSHA Score	IHF Score	ECELS Score	Status
1	62	65	-	Good
2	82	82	-	High
3	71	68	-	Good
4	61	66	-	Good
5	54	58	-	Moderate
6	49	56	-	Moderate
7	61	67	-	Good
8	-	-	71	Good
9	-	-	70	Good
10	45	52	-	Moderate

Ecological status

Ecological status was classified based on physicochemical parameters, biological results obtained by IDP index and hydromorphological findings (*Table 9*).

Table 9. *Ecological status in sampling stations*

Stations	Physicochemical status	Biological index results	Biological status	Hydromorphological status	Ecological status
1	I	1.80	II	II	II
2	I	1.13	I	I	I
3	II	2.20	III	II	III
4	II	1.49	I	II	II
5	III	1.29*	I*	III	III
6	III	1.21*	I*	III	III
7	II	1.98	II	II	II
8	II	1.73	II	II	II
9	II	1.95	II	II	II
10	II	1.86	II	III	II

*Given that *Achnanthidium minutissimum* which is found in stations 5 and 6 dominantly is excluded from the assessment, station 5 is found to be in class II (1.79) and station 6 is found to be in class III (2.04) according to IDP results

Discussion

Distribution of diatom species

In this study, *Achnanthidium minutissimum*, *Cymbella excisa*, *Craticula subminuscula* and *Fragilaria brevistriata* were determined as dominant species. The most dominant species, *Achnanthidium minutissimum*, is reported as a problematic both from taxonomic and ecological perspectives (Potapova, 2007). Kelly and Whitton (1995) stated that this species is dominant in high-altitude regions and in oligo-mesotrophic rivers. According to Steinberg and Schiefele (1988), it is a species that avoids conditions worse than β-mesosaprobic. In addition, according to Cox (1996), it is described as a species which commonly occurs in waters with a wide range of quality,

http://www.aloki.hu ● ISSN 1589 1623 (Print) ● ISSN 1785 0037 (Online)
DOI: http://dx.doi.org/10.15666/aeer/1704_1015510172

but which is sensitive to waste water and β-α-mesosaprobic conditions. In the present study, *Achnanthidium minutissimum* was found to be a dominant species in some stations with diverse water quality. This might result from the fact that this species occurs in wide quality range from clean to polluted waters.

Statistical analyses and diatom index

In this study, most of the species clustered around the temperature. Toman et al. (2014) reported that temperature is listed among critical parameters for diatom composition which covers *Achnanthidium minutissimum* as a dominant species. Similarly, Izagirre and Elosegi (2005) determined that temperature was a parameter which affected diatom composition.

CCA showed that station 2 revealed the greatest differences compared to the other stations. Station 2 could only be sampled three times since it was dry in September, and it was observed that the results of these three sampling campaigns were concentrated in a different quadrat from other stations. Türkmen Mountain, with an altitude of 1829 m, is the highest mountain in Eskişehir province (ÇSB, 2014). Solak ve Wojtal (2012) identified 304 species in a study conducted on that mountain, and described 59 species out of 304 as the most common ones for Turkey, on the other side which can occur in completely different water bodies. According to Levkov et al. (2013), new species such as *Luticola kemalii*, *Luticola angusta* and *Luticola rotunda* were identified in samples taken from Türkmen Mountain. The number of species in station 2 was found higher than the other stations.

When examining the correlations between the indices and temperature which affects the distribution of the large percentage of species, it was found out that the highest correlation is obtained with IDP ($r = -0.4264$, $P < 0.01$) index. The IDP index has also a correlation in the distribution of species with alkalinity which varies significantly ($r = -0.3224$, $P < 0.05$). A significant correlation was found between the index results of IDP, which is an eutrophication index, and log total nitrogen ($R^2 = 0.7091$). As a result, IDP index was used in the evaluation of diatoms in the Upper Sakarya Basin.

The IDP index was developed for rivers located in the Pampean Plain of Argentina. Sensitivity values of 210 diatom species against organic richness and eutrophication were determined taking into account BOD_5, $NH4^+$ and $PO4^{-3}$ (Gomez and Licursi, 2001). The IDP index was first used in Turkey by Kalyoncu et al. (2009) to determine the water quality of the Aksu River. In that study, the IDP index and $NH4^+$ ($r = 0.854$, $P < 0.01$) provided the highest correlation between diatom indices and physicochemical parameters.

Ecological status

Concerning chemical, biological and hydromorphological water quality, station 2 was estimated to be in class I according to Surface Water Quality By-law, IDP index and hydromorphological assessment respectively. According to one-out-all-out principle of WFD, the ecological status of station 2 is estimated as class I. Since the station 2 is located far away from pressures and species diversity of this station is different from the other stations, monitoring effort should be sustained in here. It is the only station in this study with a high hydromorphological status, which might be a reference site.

http://www.aloki.hu ● ISSN 1589 1623 (Print) ● ISSN 1785 0037 (Online)
DOI: http://dx.doi.org/10.15666/aeer/1704_1015510172

Stations 5 and 6 were estimated to be in class III chemical water quality according to the Surface Water Quality By-law, class I biological water quality according to the IDP index and class III according to hydromorphological assessments. This two-class difference between chemical and biological classification was only observed in these stations. According to one-out-all-out principle, the ecological status of both stations was estimated as class III. Both stations are fed by groundwater and there are agricultural areas in the vicinity. In addition, *Achnanthidium minutissimum* was the dominant species in each station. When these findings were tried to be confirmed by different indices, it was found out that stations 5 and 6 are categorized in class I water quality according to the IBD index but class V water quality according to the LOBO index. For this reason, station 5 is categorized in class II water quality (1.79) and station 6 is categorized in class III water quality (2.04) according to IDP index when *Achnanthidium minutissimum* is excluded from the assessment.

Station 10 is categorized in class II chemical and biological water quality according to the Surface Water Quality By-law and IDP index respectively, and in class III water quality according to hydromorphological assessment. According to one-out-all-out principle, the ecological status of station 10 was estimated as class II. Station 10 is located on a small creek where the effluents of CARS -which is fed by waters coming from station 9- confluence with the Sakarya River. However, chemical and biological classification results do not differ too much between stations 9 and 10. Only the diatom composition differs between the stations but this difference did not have any implications in the index results. Kırkağaç et al. (2009) stated that the invertebrate abundance in the inlet water was lower than the outlet water of CARS. However, the composition did not differ and only the Gastropoda species which are tolerant to pollution were found in the inlet and outlet water. As a result of this study, diatoms are concluded as important biological indicators for the monitoring the effluents of fish farms.

Generally, the results of chemical and biological assessment were similar for all stations. The results of five stations (2, 7, 8, 9, 10) were observed in the same quality class and there was one class difference among three stations (1, 3, 4). Two-class quality difference was only observed in stations 5 and 6, and the dominant species in those stations is *Achnanthidium minutissimum*, which is problematic in terms of taxonomy and ecology. According to the results of IDP index, which is calculated leaving aside this species, there is only one-class quality difference between chemical and biological status in station 5, while the same results were obtained in station 6.

According to a study conducted by Kalyoncu et al. (2004) in Ağlasun Stream, two different water quality classes were identified in terms of physicochemical parameters and epilithic algae. Water quality was then classified based on epilithic algae, which positively deviated half water quality class. In another study, Kalyoncu (2006) reported that water quality assessment was made according to epilithic diatoms, which positively deviated half water quality class from the assessment based on the results of physicochemical parameters. The differences between physicochemical and biological quality assessment observed in this study conducted in the Upper Sakarya Basin reveal similarities with the studies mentioned above.

http://www.aloki.hu ● ISSN 1589 1623 (Print) ● ISSN 1785 0037 (Online)
DOI: http://dx.doi.org/10.15666/aeer/1704_1015510172

Conclusions

As a summary, it is essential to develop biological indices for ecological status classification for water resources. Turkey is a very rich country in terms of biological diversity because of its geographical position. This diversity varies from region to region, and it affects the application of biological indices. For this reason, it might be recommended that eco-regions should be determined for monitoring of aquatic organisms, and the class boundaries of biological indices should be developed for these eco-regions.

Biological monitoring is carried out in river basins throughout Turkey. In this study, ecological status was estimated based on diatoms which are used as biological quality elements in rivers and ponds. The findings of this study may serve as an example both for water quality monitoring and management in Turkey. Sakarbasi Springs, which are the source of the Sakarya River, are used for several purposes, such as agriculture, recreation and aquaculture. It is therefore important to monitor these water bodies for controlling the pollution of the river.

In conclusion, it is necessary to take action for water bodies which are in moderate ecological status according to this study, and water bodies in good ecological status should be maintained. The Upper Sakarya Basin was monitored within the scope of the reference monitoring network since it forms the headwaters of the Sakarya Basin and has a high water potential. Station 2, Akin River which is in high ecological status might be proposed as a reference site for mountainous rivers with low alkalinity.

Acknowledgements. This study is a part of doctoral thesis "The Use of Phytobenthos for the Ecological Status Assessment in Upper Sakarya Basin" which was prepared in Turkey.

REFERENCES

[1] APHA (2012): Standard Methods for the Examination of Water and Wastewater. 22nd Ed. – American Public Health Association, Washington.

[2] Atıcı, T., Tokatlı, C., Çiçek, A. (2018): Diatoms of Seydisuyu stream basin (Turkey) and assessment of water quality by statistical and biological approaches. – Sigma Journal of Engineering and Natural Sciences 36(1): 271-288.

[3] Boix, D., Caiola, N., Canedo-Argüelles, M., Gascon, S., Ibanez, C., Nebra, A., Quintana, X. D., Rieradevall, M., Sala, J., Sanchez-Millaruelo, N., Sola, C., Munne, A. (2010): Avaluacio de l'estat ecologic de les zones humides i ajust dels indicadors de qualitat. – Generalitat de Catalunya: Agencia Catalana de l'Aigua, Departament de Medi Ambient i Habitatge, Barcelona.

[4] Cemagref (1982): Etude de Methodes Biologiques Quantitatives d'Appreciation de la Qualit des Eaux. – A.F.B. Rhône-Mediterrannee-Corse, Lyon.

[5] Coste, M., Boutry, S., Tison-Rosebery, J., Delmas, F. (2009): Improvements of the biological diatom index (BDI): Description and efficiency of the new version (BDI-2006). – Ecological Indicators 9: 621-650.

[6] Cox, E. J. (1996): Identification of Freshwater Diatoms from Live Material. – Chapman and Hall, London.

[7] ÇŞB (2014): Kütahya Province Environment Report. – ÇŞB, Kütahya (in Turkish).

[8] Dell'Uomo, A. (2004): L'indice diatomico di eutrofizzazione/polluzione (EPI-D) nel monitoraggio delle acque correnti. Lince guida. – APAT Agenzia per la protezione dell'ambiente e per I servizi tecnici, Roma.

http://www.aloki.hu ● ISSN 1589 1623 (Print) ● ISSN 1785 0037 (Online)
DOI: http://dx.doi.org/10.15666/aeer/1704_1015510172

[9] Demir, N., Çetin, T., Gök, C., Şanal, M. (2017): First biological monitoring in the Akarçay Basin according to the Water Framework Directive: phytoplankton and phytobenthos. – Turkish Journal of Water Science and Management 1: 90-107.
[10] Descy, J. P. (1979): A new approach to water quality estimation using diatoms. – Nowa Hedwigia 64: 305-323.
[11] Descy, J. P., Coste, M. (1991): A test of methods for assessing water quality based on diatoms. – Verhandlungen der Internationalen Vereinigung Für Theorestische und Angewandte Limnologie 24: 2112-2116.
[12] Directive (2000): Directive 2000/60/EC of the European parliament and of the council of 23 October 2000 establishing a framework for community action in the field of water policy. – O. J. E. C. 327: 1-72.
[13] DSİ (1978): Upper Sakarya Basin Hydrogeological Investigation Report. – DSİ Basım ve Foto-film İşletme Müdürlüğü Matbaası, Ankara (in Turkish).
[14] European Committee for Standardization (2014a): Water quality - guidance standard for the routine sampling and preparation of benthic diatoms from rivers and lakes. – European Standard EN 13946, Brussels.
[15] European Committee for Standardization (2014b): Water quality - guidance standard for the identification and enumeration of benthic diatoms from rivers and lakes. – European Standard EN 14407, Brussels.
[16] Gómez, N., Licursi, M. (2001): The Pampean Diatom Index (IDP) for assessment of rivers and streams in Argentina. – Aqua. Ecol. 35: 173-181.
[17] Hofmann, G., Werum, M., Lange-Bertalot, H. (2013): Diatomeen im Süßwasserbenthos von Mitteleuropa. – Koeltz Scientific Books, Königstein.
[18] Hürlimann, J. Niederhauser, P. (2002): Methode d'etude et d'appreciation de l'etat de santé des cours d'eau: Diatomees-niveau R (region). – OFEFP, Berne.
[19] Izagirre, O., Elosegi, A. (2005): Environmental control of seasonal and inter-annual variations of periphytic biomass in a North Iberian stream. – Ann. Limnol.-Int. J. Lim. 41(1): 35-46.
[20] Kalyoncu, H. (2006): Determination of water quality in Isparta stream according to physicochemical parameters and epilithic diatoms. – S. D. Ü. Fen Edebiyat Fakültesi, Fen Dergisi 1(1-2): 14-25 (in Turkish).
[21] Kalyoncu, H., Barlas, M., Ertan, Ö. O., Gülbay, H. (2004): Determination of water quality of Ağlasun stream according to physicochemical parameters and epilithic algae. – S. D. Ü. Eğirdir Su Ürünleri Dergisi 2(12): 7-14 (in Turkish).
[22] Kalyoncu, H., Barlas, M., Ertan, Ö. O. (2009): The study of the water quality of the Aksu stream according to the biotic index (diatoms and invertebrates) and physic-chemical parameters, the relations of the organisms with the water quality. – Türk Bilim Araştırma Vakfı 2: 45-57 (in Turkish).
[23] Kelly, M. (2013): Data rich, information poor? Phytobenthos assessment and the Water Framework Directive. – European Journal of Phycology 48: 437-450.
[24] Kelly, M. G., Whitton, B. A. (1995): The trophic diatom index: a new diatom index for monitoring eutrophication in rivers. – J. Appl. Phycol. 7: 433-444.
[25] Kırkağaç, M. Ü., Pulatsü, S., Topçu, A. (2009): Trout farm effluent effects on water sediment quality and benthos. – Clean 37(4-5): 386-391.
[26] Kıvrak, E., Uygun, A., Kalyoncu, H. (2012): Application of diatom indices to assess water quality of the Akarçay stream (Afyonkarahisar, Türkiye). – AKU J Sci 12: 27-38 (in Turkish).
[27] Krammer, K., Lange-Bertalot, H. (1985): Naviculaceae. Bibliotheca Diatomologia, Band 9. – J. Cramer, Berlin-Stuttgart.
[28] Krammer, K., Lange-Bertalot, H. (1986): Bacillariophyceae. 1. Teil: Naviculaceae. – In: Ettl, H., Gerloff, J., Heynig, H., Mollenhauer, D. (eds.) Süsswasser Flora von Mitteleuropa. Band 2/1. Gustav Fischer Verlag, Stuttgart.

http://www.aloki.hu ● ISSN 1589 1623 (Print) ● ISSN 1785 0037 (Online)
DOI: http://dx.doi.org/10.15666/aeer/1704_1015510172

[29] Krammer, K., Lange-Bertalot, H. (1988): Bacillariophyceae. 2. Teil: Bacillariaceae, Epithemiaceae, Surirellaceae. – In: Ettl, H., Gerloff, J., Heynig, H., Mollenhauer, D. (eds.) Süsswasserflora von Mitteleuropa, Band 2/2. VEB Gustav Fischer Verlag, Jena.
[30] Krammer, K., Lange-Bertalot, H. (1991a): Bacillariophyceae. 3. Teil: Centrales, Fragilariaceae, Eunotiaceae. – In: Ettl, H., Gerloff, J., Heynig, H., Mollenhauer, D. (eds.) Süsswasserflora von Mitteleuropa, Band 2/3. Gustav Fischer Verlag, Stuttgart, Jena.
[31] Krammer, K., Lange-Bertalot, H. (1991b): Bacillariophyceae. 4. Teil: Achnanthaceae, Kritische Ergänzungen zu Navicula (Lineolatae) und Gomphonema, Gesamtliteraturverzeichnis. Teil 1-4. – In: Ettl, H., Gärtner, G., Gerloff, J., Heynig, H., Mollenhauer, D. (eds.) Süsswasserflora von Mitteleuropa, Band 2/4. Gustav Fischer Verlag, Stuttgart, Jena.
[32] Leclercq, L., Maquet, B. (1987): Deux Nouveaux Indices Chimiques et Diatomiques de Qualite d'eau Courante. Application au Samson et Ses Affluents (Bassin de la Meuse Belge). Comparison Avec d'autres Indices Chimiques Biocenotiques et Diatomiques. – Institute Royal des Sciences Naturelles de Belgique, Document de Travail 38: 1-113.
[33] Lecointe, C., Coste, M., Prygiel, J. (1993): "Omnidia": software for taxonomy, calculation of diatom indices and inventories management. – Hydrobiologia 269/270: 509-513.
[34] Lenoir, A., Coste, M. (1996): Development of a Practical Diatom Index of Overall Water Quality Applicable to the French National Water Board Network. – In: Whitton, B. A., Rott, E. (eds.) Use of Algae for Monitoring Rivers II. Studia, Innsbruck, pp. 29-43.
[35] Leps, J., Smilauer, P. (2003): Multivariate Analysis of Ecological Data Using CANOCO. – Cambridge University Press, Cambridge.
[36] Levkov, Z., Metzeltin, D., Pavlov, A. (2013): *Luticola* and *Luticolopsis*. – In: Lange-Bertalot, H. (eds.) Diatoms of Europe, Diatoms of the European Inland Waters and Comparable Habitats. Vol. 7. Koeltz Scientific Books, Konigstein.
[37] Lobo, E. A., Bes, D., Tudesque, L. Ector, L. (2004): Water quality assessment of the Pardinho River, RS, Brazil, using epilithic diatom assemblages and faecal coliforms as biological indicators. – Vie et Milieu/Life and Environment 54: 115-125.
[38] Morkoyunlu Yüce, A., Gönülol, A. (2016): Evaluations of epilithic diatoms and biotic index in Sakarya River, Turkey. – Pak. J. Bot 48(5): 2153-2158.
[39] MPCA (2014): MPCA stream habitat assessment (MSHA) protocol for stream monitoring sites. – Minnesota Pollution Control Agency. Minnesota, USA.
[40] Muxika, I., Borja, A., Bald, J. (2007): Using historical data, expert judgement and multivariate analysis in assessing reference conditions and benthic ecological status, according to the European Water Framework Directive. – Marine Pollution Bulletin 55: 16-29.
[41] Pardo, I., Alvarez, M., Casas, J., Moreno, J. L., Vivas, S., Bonada, N., Alba-Tercedor, J., Jaimez-Cuellar, P., Moya, G., Prat, N., Robles, S., Suarez, M. L., Toro, M., Vidal-Abarca, M. R. (2002): El habitat de los rios mediterraneos. Diseno de un indice de diversidad de habitat. – Limnetica 21: 115-133.
[42] Potapova, M. (2007): Morphological and ecological variation within the *Achnanthidium minutissimum* (Bacillariophyceae) species complex. – J. Phycol. 43: 561-575.
[43] Prygiel, J., Leveque, L., Iserentant, R. (1996): L'IDP: Un nouvel indice diatomique pratique pour l'evaluation de la qualite des eaux en reseau de surveillance. – Revue des Sciences de I'eau 9: 97-113.
[44] Rott, E., Hofmann, G., Pall, K., Pfister, P. Pipp, E. (1997): Indikationslisten für Aufwuchsalgen in Österreichischen Fliessgewässern. Teil 1: Saprobielle Indikation. – Bundeministeriums für Land- und Forstwirtschaft, Wien.
[45] Rott, E., Pipp, E., Pfister, P., Van Dam, H., Ortler, K., Binder, N., Pall, K. (1999): Indikationslisten für Aufwuchsalgen in österreichischen Fliessgewässern. Teil 2: Trophieindikation (sowie geochemische Präferenzen, taxonomische und toxikologische

http://www.aloki.hu ● ISSN 1589 1623 (Print) ● ISSN 1785 0037 (Online)
DOI: http://dx.doi.org/10.15666/aeer/1704_1015510172

Anmerkungen). – Wasserwirtschaftskataster, Bundesministerium f. Land- u. Forstwirtschaft, Wien.
[46] Rumeau, A. Coste, M. (1988): Initiation à la systématique des diatomées d'eau douce. – Bull. Fr. Piscic. 309: 69.
[47] Sladecek, V. (1986): Diatoms as indicators of organic pollution. – Acta Hydroch Hydrobiol. 14: 555-566.
[48] Solak, C. N., Wojtal, A. Z. (2012): Diatoms in spring and streams of Türkmen Mt. (Sakarya River Basin) common in Turkish inland waters. – Polish Botanical Journal 57(2): 375-425.
[49] Solak, C. N., Barinova, S., Acs, E., Dayıoğlu, H. (2012): Diversity and ecology of diatoms from Felenk creek (Sakarya River basin) Turkey. – Turk J Bot. 36*:* 191-203.
[50] Steinberg, C., Schiefele, S. (1988): Biological indication of trophy and pollution of running waters. – Z. Wasser. Abwasser. Forsch. 21: 227-234.
[51] Stenger-Kovacs, C., Buczko, K., Hajnal, E. Padisak, J. (2007): Epiphytic, littoral diatoms as bioindicators of shallow lake trophic status: Trophic Diatom Index for Lakes (TDIL) developed in Hungary. – Hydrobiologia 589: 141-154.
[52] ter Braak, C. J. F., Milauer, P. (2002): CANOCO Reference Manual and CanoDraw for Windows User's Guide: Software for Canonical Community Ordination (Version 4.5). – Microcomputer Power Press, Ithaca.
[53] Tokatlı, C. (2012): Use of some diatom indices for evaluating water quality: Sample of Gürleyik stream (Eskişehir). – Dumlupınar Üniversitesi Fen Bilimleri Enstitüsü Dergisi 29: 21-28 (in Turkish).
[54] Toman, J. M., Groseli, A. M., Zelnik, I. (2014): The influence of selected factors on the distribution of epilithic diatoms in a torrential river the Kamniska Bistrica (Slovenia). – Acta Bot. Croat. 73(2): 447-463.
[55] Toudjani, A. A., Çelekli, A., Gümüş, E. Y., Kayhan, S., Lekesiz, H. Ö., Çetin, T. (2017): A new diatom index to assess ecological quality of running waters: a case study of water bodies in western Anatolia. – Int. J. Lim*,* 53: 333-343.
[56] Watanabe, T., Asai, K. Houki, A. (1990): Numerical Simulation of Organic Pollution in Flowing Waters. – In: Cheremisinoff, P. N. (ed.) Encyclopedia of Environmental Control Technology. Vol. 4. Hazardous Waste Containment and Treatment. Gulf Publishing Company, Houston, pp. 251-284.
[57] YSKY (2016): Surface Water Quality By-Law. – T. C. Orman ve Su İşleri Bakanlığı, Su Yönetimi Genel Müdürlüğü, Ankara (in Turkish).

http://www.aloki.hu ● ISSN 1589 1623 (Print) ● ISSN 1785 0037 (Online)
DOI: http://dx.doi.org/10.15666/aeer/1704_1015510172

DETERMINATION OF LICHEN DIVERSITY VARIATIONS IN HABITAT TYPE OF MEDITERRANEAN MAQUIS AND ARBORESCENT MATORRAL

TUFAN-ÇETIN, Ö.

Program of Environmental Protection and Control, Department of Environmental Protection Technology, Vocational School of Technical Sciences, University of Akdeniz, Antalya, Turkey (e-mail: ozgetufan@akdeniz.edu.tr; phone: +90-242-310-6758; fax: +90-242-227-4785)

**Corresponding author*
e-mail: ozgetufan@akdeniz.edu.tr

(Received 15th Apr 2019; accepted 13th Jun 2019)

Abstract. In this study, it was aimed to determine the epiphytic and non-epiphytic lichen diversity variations in Mediterranean maquis and arborescent matorral habitats. One of Turkey's national parks, Altınbeşik Cave National Park in Antalya, Turkey, was chosen as the research area as this habitat type is very common in the park. In this research, lichen diversity was calculated according to the data of species richness and species frequency. For identify possible variations of the lichen species composition in this habitat type, this research was planned on three major hills in the park. In addition, localities were selected from four different slope directions and tops of the hills. Statistical tests were used to analyze whether there was a difference or similarity on data. Moreover, the statistical relationships between the data of grouped localities with the data of diversity calculation classes were investigated. As a result of this study; lichen diversity of Mediterranean maquis and arborescent matorral habitats was put forth. Secondly, species richness and frequency of northern localities of Mediterranean maquis and arborescent matorral habitats were found to be significantly higher and community composition of northern localities was found to be much different than other localities.
Keywords: *Altınbeşik Cave National Park, biodiversity, community composition, Eastern Mediterranean, four cardinal directions, Turkey*

Introduction

Lichens are sensitive to even weak changes in their environments (Rose and Hawksworth, 1981; Ellis et al., 2007; Johansson, 2008; Nascimbene et al., 2012). Their sensitivity to environmental changes has been subject to numerous investigations (Gombert et al., 2004; Svoboda et al., 2010; De Guevara et al., 2014; Branquinho et al., 2015). When a change occurs in the environment of lichens, species richness and community composition changes to ones that are suitable for new conditions and replace previous lichen (Gadsdon et al., 2010; Johansson et al., 2012; Lang et al., 2012). This characteristic of the lichens is the reason why they are indicators of different ecosystem and habitat diversity (McCune, 2000; Rogers and Ryel, 2008; Nascimbene et al., 2012). In addition, by monitoring changes in lichen diversity, forest health can be determined (McCune, 2000; Thormann, 2006; Fenn et al., 1998; Geiser and Neitlich, 2007; McMurray et al., 2015). In order to determine the ecological condition of the areas according to the lichen diversity, it should be known which lichen composition is seen in which habitat.

Many researches have been done on lichen diversity variations of forests until now (Rogers and Ryel, 2008; McMullin et al., 2010; Koch et al., 2013; Bartels and Chen., 2015). There is also a large number of studies on the determination of the lichen richness in Mediterranean habitats (John, 1996; Litterski, 1997; Nimis and John, 1998;

http://www.aloki.hu ● ISSN 1589 1623 (Print) ● ISSN 1785 0037 (Online)
DOI: http://dx.doi.org/10.15666/aeer/1704_1017310193

Christensen and Svane, 2007; Ravera et al., 2011; Sipman and Raus, 2015). However, there are very few studies including variations of lichen diversity in the habitat composition of Mediterranean maquis and arborescent matorral (Aragón et al., 2006).

Mediterranean maquis and arborescent matorral habitat type is found across the entire Mediterranean biogeographical zone (Portugal, Spain, France, Italy, Sardinia, Sicily, Malta, Croatia, Macedonia, Montenegro, Serbia, Bulgaria, Greece, Crete, Aegean Islands, Cyprus, Turkey and Northern Africa) (EEA, 2016). According to the habitat types of EUNIS, this habitat has evergreen sclerophilous or lauriphyllous shrub vegetation which forms a dense enclosed canopy with or without emergent trees (EEA, 2017). In this habitat type there are matorrals that are covered top to bottom with leaves that hides the stem and some of these are arborescent that are sociologically isolated, with non-competitive root system (Tomaselli, 1977). *Quercus coccifera* L., *Pistacia palaestina* (Boiss) Engl., *Olea europaea* L. var. *sylvestris* (Mill.) Brot., *Phillyrea latifolia* L., *Juniperus excelsa* M. Bieb., *Pinus brutia* Ten are examples of Mediterranean arborescent matorrals. Although *J. excelsa* and *P. brutia* are originally forest trees but they are also found as arborescent matorrals within maquis in Mediterranean biogeography. This interesting habitat composition may suggest that its lichen diversity is unusual.

In this study, it was aimed to determine the epiphytic and non-epiphytic lichen diversity in Mediterranean maquis and arborescent matorral habitats. Therefore, one of Turkey's national parks, Altınbeşik Cave National Park, was chosen to determine lichen diversity of Mediterranean maquis and arborescent matorral habitats of park. Besides, there is a study showing that the vegetation type of park is suitable for this research (Çinbilgel and Gökçeoğlu, 2010a). Lichen diversity in this study was calculated according to the data of species richness and species frequency. The obtained data was used not only to examine the lichen diversity in Mediterranean maquis and arborescent matorral habitats but also to examine the existing differences or similarities of lichen diversity at different directions, altitudes, and substrates (epiphytic and non-epiphytic) in this habitat type. For identify possible variations of the lichen species composition, localities were selected on three major hills (Altınbeşik Hill, İnönü Hill, Kale Hill) and from four different slope directions, tops of the hills. Moreover, the statistical relationships between the data of grouped localities (according to directions, tops and hills) with the data of diversity classes (total richness, total frequency, epiphytic and non-epiphytic richness, epiphytic and non-epiphytic frequency) were investigated.

Materials and methods

Study area

Altınbeşik Cave and surrounding area were declared as national park in 1994; located between 37°01.19' to 37°04.37' N, and 31°35.49' to 31°38.52' E (*Fig. 1*). The park covers 1156 ha area, where the lowest altitude is 380 m, and the highest is 1165 m. The study was conducted on three major hills (Altınbeşik, İnönü and Kale) in the national park. The park is located in the rainy Mediterranean bioclimate zone according to the Emberger quotient (Çinbilgel and Gökçeoğlu, 2010b). The park generally covers with maqius and arborescent matorral habitats due to Mediterranean climate and karstic geomorphological structure of the area. *Quercus coccifera* L., *Pistacia palaestina* (Boiss) Engl., *Olea europea* L. var. *sylvestris* (Mill.) Brot., *Phillyrea latifolia* L., *Juniperus excelsa* M. Bieb., *Pinus brutia* Ten. are the most common members of the

http://www.aloki.hu ● ISSN 1589 1623 (Print) ● ISSN 1785 0037 (Online)
DOI: http://dx.doi.org/10.15666/aeer/1704_1017310193

park vegetation. In addition, although the surface geology of Altınbeşik Cave National Park is generally calcareous, there are also siliceous rocks on the area.

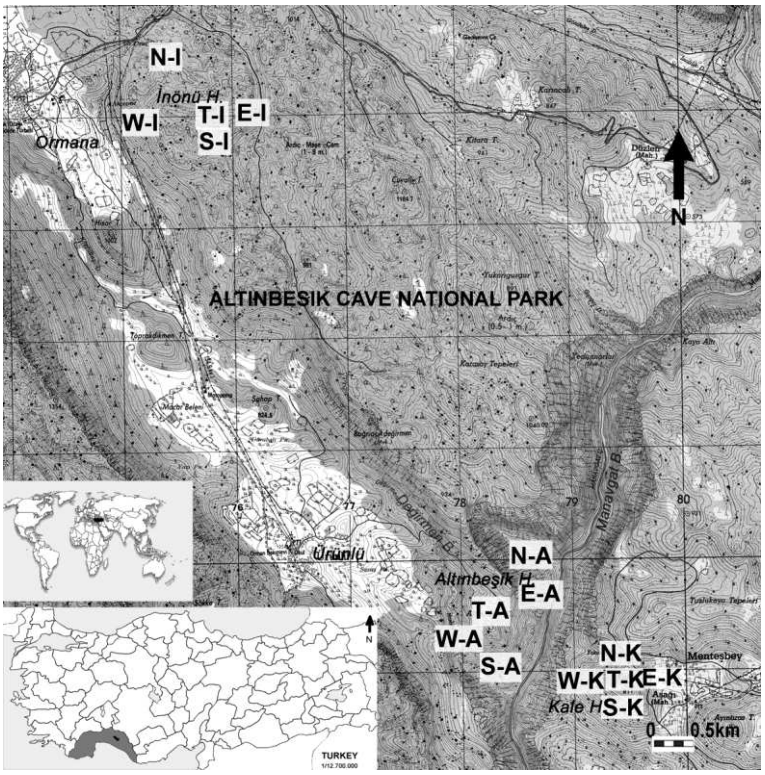

Figure 1. *Maps of Altınbeşik Cave National Park and studied localities (created with Adobe Photoshop 7.0). Abbreviations: -A: Altınbeşik Hill. E: East slopes.-I: İnönü Hill. -K: Kale Hill. N: North slopes. S: South slopes. W: West slopes T: Tops*

Sampling and data collection techniques

The lichen samples have been collected in April 2017, January 2019 and deposited in O. Tufan-Çetin's private fungarium in Akdeniz University. Field studies were carried out in 15 localities (sampling area approximately 1.5 ha) (*Table 1; Fig. 1*). The localities were selected from four different directions and tops of the 3 hills (Altınbeşik, İnönü and Kale; *Fig. 1*) and contain same habitat patterns (maquis and arborescent matorral habitat) and same superficial geological structure. The hills represent three different altitude groups: Altınbeşik (500-700 m), Kale (700-900 m), İnönü (900-1100 m). Detail information and the abbreviated names of all localities were listed in *Table 1*. Sampling for richness and frequency data of lichens were recorded in 5 × 25 cm quadrats with five units (5 × 5 cm) for both epiphytic and non-epiphytic lichens. Frequency data was determined that based on the ratio of occurrence of the species in quadrats (Asta et al., 2002a, b). Epiphytic lichens were obtained from the trunks or stems of *J. excelsa*, *P. latifolia, P. palaestina* and *Q. coccifera* that found on all localities. Six individuals of each four plant species were selected and quadrats were placed 1 m above the ground and on four sides of the trees in each locality (Asta et al., 2002a). Also; non-epiphytic lichens from ground and rocks (calcareous and siliceous) were sampled 96 times.

http://www.aloki.hu ● ISSN 1589 1623 (Print) ● ISSN 1785 0037 (Online)
DOI: http://dx.doi.org/10.15666/aeer/1704_1017310193

Table 1. *Information of studied localities in Altınbeşik Cave National Park (İbradı, Antalya, Turkey)*

Abbr.	Localities	Coordinates	Altitude (Approx.)
N-A	Manavgat Creek edges, North slopes of Altınbeşik Hill	37°02'18" N 31°37'55" E	585 m
E-A	Entrance of Altınbeşik Cave, East slopes of Altınbeşik Hill	37°02'15" N 31°37'56" E	537 m
S-A	South slopes of Altınbeşik Hill	37°01'49" N 31°37'53" E	598 m
W-A	West slopes of Altınbeşik Hill	37°01'53" N 31°37'44" E	560 m
T-A	Top of Altınbeşik Hill	37°02'05" N 31°37'56" E	653 m
N-I	North slopes of İnönü Hill	37°04'33" N 31°35'46" E	982 m
E-I	East slopes of İnönü Hill	37°04'22" N 31°36'26" E	996 m
S-I	South slopes of İnönü Hill	37°04'17" N 31°36'02" E	1066 m
W-I	West slopes of İnönü Hill	37°04'21" N 31°35'35" E	912 m
T-I	Top of the İnönü Hill	37°04'21" N 31°36'06" E	1089 m
N-K	North slopes of Kale Hill	37°01'40" N 31°38'40" E	747 m
E-K	East slopes of Kale Hill	37°01'35" N 31°38'46" E	745 m
S-K	South slopes of Kale Hill	37°01'33" N 31°38'40" E	757 m
W-K	West slopes of Kale Hill	37°01'32" N 31°38'32" E	703 m
T-K	Top of the Kale Hill	37°01'36" N 31°38'41" E	784 m

Abbr.: Abbreviation of localities; Approx.: Approximately

Identification of samples

Dried samples were examined by using a light microscope for microscopic characters; and a stereoscopic zoom microscope for macroscopic characters. For identification of the species, the following literature has been used: Moberg (1977), Goward et al. (1994), Fryday and Coppins (1997), Tucker and Thiers (1998), Giralt (2001), Wasser and Nevo (2005), Wetmore (2005), Smith et al. (2009), Wirth et al. (2013) and McCune (2016). When required spot tests, ultra violet light (UV) tests and thin layer chromatography (TLC) have also been carried out.

http://www.aloki.hu ● ISSN 1589 1623 (Print) ● ISSN 1785 0037 (Online)
DOI: http://dx.doi.org/10.15666/aeer/1704_1017310193

Data analysis

The relations in recorded richness and frequency data from Altınbeşik Cave National Park were analyzed by correlation tests. First, the normality of the data was examined by the Shapiro-Wilk test. Pearson correlation test was used for normal distribution data set where Spearman's rho was used in other cases. The significance of all rankings was calculated by linear regression analysis. As of species richness and frequency data were not normally distributed, the Kruskal Wallis test (Kruskal and Wallis, 1952) was used to determine whether there is a difference within the data obtained from the localities. Since the variances were found unequal, Tamhane's T2 post-hoc test was applied to determine which localities differ from the others. All these analyses were performed by SPSS 23.0.

In terms of the lichen richness data, similarity of localities was calculated by Sørensen (Bray-Curtis) similarity index with group average algorithm (UPGMA). On the other hand, differences of community composition on maquis and arborescent matorral habitats were analyzed with non-metric multidimensional scaling (NMS) (McCune et al., 2002) using "medium" autopilot mode with the Sørensen (Bray-Curtis) distance measurement. The relationship of diversity calculation classes (joint plots) with the community composition was also investigated. Joint plots (total richness, total frequency, epiphytic and non-epiphytic richness, epiphytic and non-epiphytic frequency) were included in NMS analysis. By multi-response permutation procedure (MRPP) analysis (McCune et al., 2002), community composition of four slope directions and tops of hills, also separately three hills were compared on PC-ORD 6.08.

Results

Total 123 lichen taxa were identified from 15 selected Mediterranean maquis and arborescent matorral habitat localities in Altınbeşik Cave National Park. They are listed in *Table 2* in alphabetic order. New lichen taxa for Antalya Province of Turkey are highlighted by an asterisk (*) in this list. Also, the list includes average frequencies of epiphytic and non-epiphytic taxa and their total average frequencies (total frequency) and total richness data. Total frequency and total richness data for each locality were examined and were not found normally distributed. Therefore, Spearman's rho test was used to determine whether there is any relationship between total frequency and total richness data. As a result; a strong linear relationship was found between total frequency and total richness of each localities in the positive direction ($p = 0.000$, $r = 0.991$).

Based on the data of total frequency and total richness of each locality, the graph in *Figure 2* was formed (The altitude of the localities are also shown in the graph). As shown in the graph, each localities were sorted from high to low total richness as follows N-A > N-K > S-A > T-A > T-K > N-I > E-I > W-K > S-I > S-K > T-I > W-A > E-A > W-I > E-K ($r = 0.868$) and according to total frequency; from high to low: N-A > N-K > W-K > S-A > T-K > S-I > T-I > T-A > S-K > N-I > E-A > W-I > E-I > W-A > E-K ($r = 0.852$). In terms of total richness and frequency, the highest results were obtained from northern slopes of Altınbeşik Hill (N-A), whereas lowest results were from eastern slopes of Kale Hill (E-K). In addition, while data of N-A constitutes 16.11% of the total frequency and 21.14 of the total richness, data of E-K constitutes 2.60% of the total frequency and 10.57% of the total richness. It can be seen from the *Figure 2* while the northern slopes show the highest variation in lichen diversity in maquis and arborescent matorral habitats, the eastern slopes show least. On the other hand, in terms of data of species richness and species frequency, at least one locality was found significantly different than the other localities,

http://www.aloki.hu ● ISSN 1589 1623 (Print) ● ISSN 1785 0037 (Online)
DOI: http://dx.doi.org/10.15666/aeer/1704_1017310193

statistically (Kruskal Wallis, p = 0.000). Since all variances are not homogeneous, non-parametric Tamhane's T2 post-hoc test was preferred to understand which localities are different. According to richness and frequency data, especially two north localities N-A and secondly N-K are different than other 13 localities. The post-hoc test results of both localities are given at *Table 3*. While the similarity of localities was examined, a Sørensen dendogram based on species richness was obtained (*Fig. 3*). According to dendrogram, lichen richness of same slope directions is similar and also tops localities show similarity. The northern localities are in a separate similarity group the rest being in another similarity group; top localities and western localities are also in separate similarity groups.

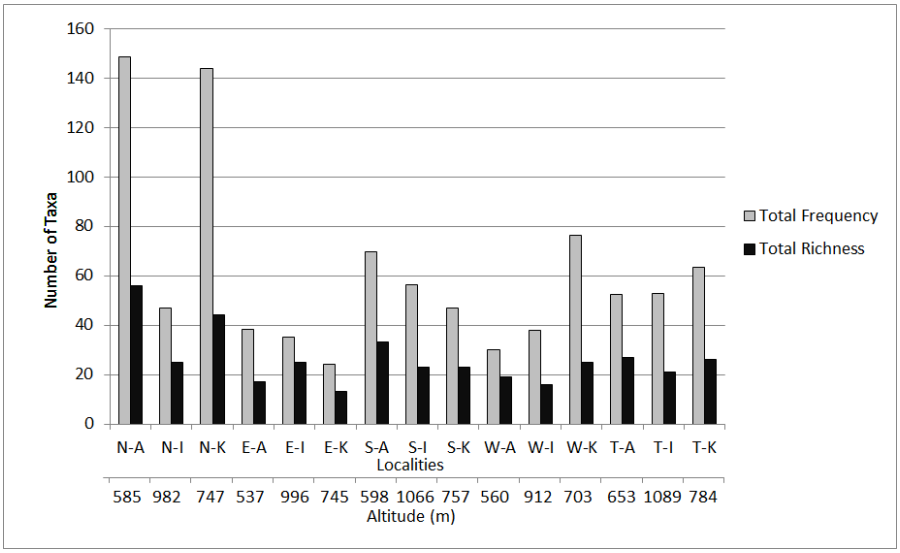

Figure 2. *Graphs about total frequency and total richness data based on all localities (created with Excel 2010). Abbreviations: -A: Altınbeşik Hill. E: East slopes. -I: İnönü Hill. -K: Kale Hill. N: North slopes. S: South slopes. W: West slopes T: Tops*

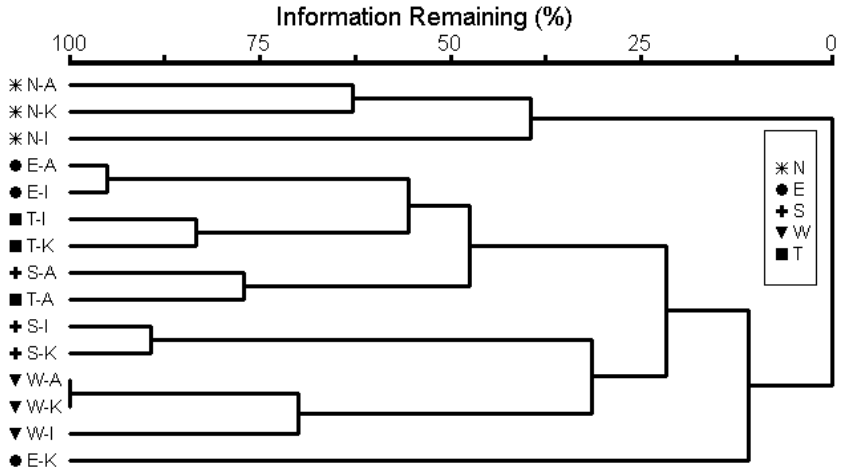

Figure 3. *Sørensen similarity dendrogram of all localities based on species richness in Altınbeşik Cave National Park (created with PC-ORD 6.08). Abbreviations: -A: Altınbeşik Hill. E: East slopes.-I: İnönü Hill. -K: Kale Hill. N: North slopes. S: South slopes. W: West slopes T: Tops*

http://www.aloki.hu ● ISSN 1589 1623 (Print) ● ISSN 1785 0037 (Online)
DOI: http://dx.doi.org/10.15666/aeer/1704_1017310193

Table 2. *List of determined epiphytic and non-epiphytic lichen taxa with distribution of the average of frequencies data according to localities (the total average of frequencies and the total richness were added to the bottom of each taxa group lists)*

Epiphytic Taxa on *P. palaestina*		**N-A**	**N-I**	**N-K**	**E-A**	**E-I**	**E-K**	**S-A**	**S-I**	**S-K**	**W-A**	**W-I**	**W-K**	**T-A**	**T-I**	**T-K**
Anaptychia ciliaris (L.) Körb. ex A.Massal.			4.00	5.67												
Athallia cerinella (Nyl.) Arup. Frödén & Søchting				3.67	0.33											
Caloplaca cerina (Ehrh. ex Hedw.) Th.Fr.				2.67											0.67	
Gyalolechia flavorubescens (Huds.) Søchting. Frödén & Arup				0.33					3.67							
Lecanora chlarotera Nyl.		1.00		1.00					1.00					1.00		
Lecidella elaeochroma (Ach.) M.Choisy				0.33												1.33
Melanohalea exasperatula (Nyl.) O. Blanco et al.												1.00				
Parmelina quercina (Willd.) Hale						0.33			3.00		0.33		4.00			
Phaeophyscia ciliata (Hoffm.) Moberg							1.33			3.33		2.00				
Physcia leptalea (Ach.) DC.									1.00							
Physconia distorta (With.) J.R.Laundon		2.00	3.00	1.33					3.00			3.67				
Rinodina exigua (Ach.) Gray								2.00		0.33						
Xanthoria parietina (L.) Th.Fr.			2.33	3.67					0.67				1.33			
Total Frequency of Taxa		3.00	9.33	18.67	0.33	0.33	1.33	2.00	12.34	3.66	0.33	6.67	5.33	1.00	0.67	1.33
Total Richness of Taxa		2	3	8	1	1	1	1	6	2	1	3	2	1	1	1
Epiphytic Taxa on *Q. coccifera*		**N-A**	**N-I**	**N-K**	**E-A**	**E-I**	**E-K**	**S-A**	**S-I**	**S-K**	**W-A**	**W-I**	**W-K**	**T-A**	**T-I**	**T-K**
Athallia holocarpa (Hoffm.) Arup. Frödén & Søchting								3.67								
Caloplaca cerina (Ehrh. ex Hedw.) Th.Fr.				3.33											2.33	
Candelariella xanthostigma (Pers.) Lettau															0.67	
Collema furfuraceum (Arnold) Du Rietz		5.67						1.33	3.00							
Evernia prunastri (L.) Ach.		4.00							3.00	2.33						
Lecanora carpinea (L.) Vain.														0.33	1.33	1.33
Lecidella elaeochroma (Ach.) M.Choisy		0.67			2.33											
Leptogium furfuraceum (Harm.) Sierk		1.33														
Melanohalea exasperatula (Nyl.) O. Blanco et al.									2.00							
Melanohalea laciniatula (Flagey ex H.Olivier) O.Blanco et al.	*	1.33														
Ochrolechia balcanica Vers.			0.33									1.33	2.00			
Physcia adscendens (Fr.) H.Olivier		5.67		4.33		0.67			2.00	2.33	1.33		5.33			
Physcia aipolia (Ehrh. ex Humb.) Hampe		3.00														
Physcia biziana (A.Massal.) Zahlbr.		1.33						2.00	2.00							

http://www.aloki.hu ● ISSN 1589 1623 (Print) ● ISSN 1785 0037 (Online)
DOI: http://dx.doi.org/10.15666/aeer/1704_1017310193

Physcia leptalea (Ach.) DC.		1.00				0.33			1.33							
Pleurosticta acetabulum (Neck.) Elix & Lumbsch									3.33							
Ramalina farinacea (L.) Ach.		3.33							3.00	1.33						
Rinodina capensis Hampe		1.33														
Xanthoria parietina (L.) Th.Fr.		6.57					0.67		0.67	4.33	1.33		2.00			
Total Frequency of Taxa		35.23	0.33	7.66	2.33	1.00	0.67	7.00	20.33	10.32	2.66	1.33	9.33	0.33	4.33	1.33
Total Richness of Taxa		12	1	2	1	2	1	3	9	4	2	1	3	1	3	1
Epiphytic Taxa on *J. excelsa*		**N-A**	**N-I**	**N-K**	**E-A**	**E-I**	**E-K**	**S-A**	**S-I**	**S-K**	**W-A**	**W-I**	**W-K**	**T-A**	**T-I**	**T-K**
Candelariella efflorescens R.C.Harris & W.R.Bucks.		0.67			1.00	0.67								1.33	4.00	
Candelariella xanthostigma (Pers.) Lettau					0.67		0.33						3.67	2.00		0.33
Hypogymnia tubulosa (Schaer.) Hav.			2.00	6.00												
Lecidella elaeochroma (Ach.) M.Choisy								0.67								
Parmelina tiliacea (Hoffm.) Hale		6.00		5.00	2.00	1.33			2.33							
Pertusaria albescens (Huds.) M.Choisy & Werner		3.67														
Polycaulina polycarpa (Hoffm.) Frödén. Arup & Søchting	*		1.33	2.00												
Total Frequency of Taxa		10.34	3.33	13.00	3.67	2.00	0.33	0.67	2.33	0	0	0	3.67	3.33	4.00	0.33
Total Richness of Taxa		3	2	3	3	2	1	1	1	0	0	0	1	2	1	1
Epiphytic Taxa on *P. latifolia*		**N-A**	**N-I**	**N-K**	**E-A**	**E-I**	**E-K**	**S-A**	**S-I**	**S-K**	**W-A**	**W-I**	**W-K**	**T-A**	**T-I**	**T-K**
Collema nigrescens (Huds.) DC.		4.67		2.00				2.33		0.67				0.33		
Collema subnigrescens Degel.		5.33			0.33									1.33		
Fuscopannaria olivacea (P.M.Jørg.) P.M.Jørg.		1.00		5.67										4.00		
Lecidella elaeochroma (Ach.) M.Choisy											0.33			2.33		
Leptogium brebissonii Mont.	*	1.33														
Leptogium cyanescens (Rabenh.) Körb.		0.67														
Melanelixia glabra (Schaer.) O. Blanco et al.				3.00												
Nephroma laevigatum Ach.		2.00														
Parmelina tiliacea (Hoffm.) Hale								2.00						4.67		
Pectenia plumbea (Lightf.) P.M.Jørg.. L.Lindblom. Wedin & S.Ekman		2.00												1.33		
Pertusaria albescens (Huds.) M.Choisy & Werner										0.33	1.00	2.33		1.33		
Phaeophyscia ciliata (Hoffm.) Moberg								3.00								
Phaeophyscia orbicularis (Neck.) Moberg								1.33		3.67			2.67	0.67	1.67	2.33
Phlyctis argena (Sprengel) Flot.		2.00		4.67												
Physcia aipolia (Ehrh. ex Humb.) Hampe				4.33				1.33						0.67		

http://www.aloki.hu ● ISSN 1589 1623 (Print) ● ISSN 1785 0037 (Online)
DOI: http://dx.doi.org/10.15666/aeer/1704_1017310193

Physcia biziana (A.Massal.) Zahlbr.													3.00		
Physcia leptalea (Ach.) DC.							1.33					4.00	0.67		
Physconia distorta (With.) J.R.Laundon		2.00		1.33			2.33				3.67				
Physconia venusta (Ach.) Poelt		5.33	3.33	5.67									3.67		
Pleurosticta acetabulum (Neck.) Elix & Lumbsch							2.00								
Ramalina fastigiata (Pers.) Ach.			1.33	2.33											
Total Frequency of Taxa		26.33	4.66	29.00	0.33	0	0	15.65	0	4.67	1.33	6.00	6.67	24.00	1.67	2.33
Total Richness of Taxa		10	2	8	1	0	0	8	0	3	2	2	2	12	1	1
Non-Epiphytic Taxa		**N-A**	**N-I**	**N-K**	**E-A**	**E-I**	**E-K**	**S-A**	**S-I**	**S-K**	**W-A**	**W-I**	**W-K**	**T-A**	**T-I**	**T-K**
Acarospora cervina (Ach.) A.Massal.																2.00
Aspicilia cheresina (Müll.Arg.) Hue															2.33	
Aspicilia farinosa (Flörke) Flagey					1.33	0.67		1.00		4.00	3.67	1.00		1.33	2.33	3.67
Bagliettoa calciseda (DC.) Gueidan & Cl.Roux						1.33		2.00		2.00	1.00	3.00				
Bagliettoa marmorea (Scop.) Gueidan & Cl.Roux		2.33	0.67		5.67	1.00		1.00					3.67		1.33	
Bagliettoa parmigera (J.Steiner) Vězda & Poelt				5.67										3.67	4.00	
Blennothallia crispa (Huds.) Otálora. P.M.Jørb. & Wedin				2.00												
Caloplaca adriatica (Zahlbr.) Servit								1.00	3.67						2.00	
Caloplaca atroflava (Turner) Mong														1.33		1.00
Caloplaca erythrocarpa (Pers.) Zwackh				3.00	2.00								3.00			
Caloplaca velana (A.Massal.) Du Rietz									4.00	3.67			2.00			2.00
Catapyrenium daedaleum (Kremp.) Stein		0.33	1.33	1.00					2.00	1.00	3.67		2.33			
Circinaria calcarea (L.) Mudd				5.67		0.67						0.33	5.67			
Circinaria contorta (L.) A. Nordin. Savić & Tibell subsp. *contorta*						0.67				2.33					1.33	1.00
Circinaria contorta subsp. *hoffmanniana* S.Ekman & Fröberg ex R.Sant.			2.00	6.00		1.33		1.00		1.00						5.33
Circinaria coronata (A.Massal.) B.de Lesd.				2.00												
Cladonia convoluta (Lam.) Anders				5.67				1.00			3.67	3.67				
Cladonia fimbriata (L.) Fr.		4.00	1.33				3.00									
Cladonia pocillum (Ach.) Grognot				3.00												
Cladonia pyxidata (L.) Hoffm.		1.00			1.00		1.33									
Cladonia rangiformis Hoffm.		5.67		4.67			1.00									
Clauzadea immersa (Hoffm.) Hafellner & Bellem.		6.00		4.00		2.00								3.67		
Dermatocarpon miniatum (L.) W.Mann		5.00	3.67												3.00	6.00

http://www.aloki.hu ● ISSN 1589 1623 (Print) ● ISSN 1785 0037 (Online)
DOI: http://dx.doi.org/10.15666/aeer/1704_1017310193

Diploschistes ocellatus (Vill.) Norman				5.33												
Diplotomma venustum (Körb. in Rabenh.) Körb.																1.00
Enchylium tenax (Sw.) Gray				1.00										1.00		4.00
Gyalolechia flavovirescens (Wulfen) Søchting. Frödén & Arup		2.00														
Gyalolechia fulgens (Sw.) Søchting. Frödén & Arup		4.00	1.33		1.00	1.33				2.67						
Gyalolechia subbracteata (Nyl.) Søchting. Frödén & Arup	*										1.00		1.33			
Lathagrium auriforme Otálora. P.M.Jørb. & Wedin		0.67										1.33	0.67			
Lathagrium cristatum Otálora. P.M.Jørb. & Wedin var. *cristatum*			5.00		5.67	2.33		5.67		0.33			3.00			2.00
Lathagrium cristatum var. *marginale* (Huds.) Degel.			0.33	0.67												
Lecanora bolcana (Pollini) Poelt					2.33	2.00					0.33	1.33	2.33	1.67	3.67	3.67
Lecanora campestris (Schaer.) Hue							0.67				1.33		3.00			
Lepraria incana (L.) Ach.						2.33		3.67								
Lepraria nivalis J.R.Laundon				4.00												
Leproplaca chrysodeta (Vain. ex Räsänen) J.R.Laundon						1.33		2.00		0.67						
Leproplaca xantholyta (Nyl.) Hue		4.00							3.67							
Lobothallia radiosa (Hoffm.) Hafellner				4.00		3.67	2.33	4.00		2.33	2.33	5.67	5.33		4.00	5.67
Neocatapyrenium rhizinosum (Müll.Arg.) Breuss				1.00												
Peltigera rufescens (Weiss) Humb.		1.33									0.33		1.00			
Petractis clausa (Hoffm.) Kremp.									0.33							
Placidium pilosellum (Breuss) Breuss				0.67								0.33				
Placidium squamulosum (Ach.) Breuss		0.33						0.33							0.33	1.33
Placopyrenium bucekii (Nádv. & Servít) Breuss		0.33														
Placynthium nigrum (Huds.) Gray					4.00	3.00	2.00									
Placynthium subradiatum (Nyl.) Arnold		1.33	3.33									0.67	0.67			
Protoparmeliopsis muralis (Schreb.) M.Choisy		5.33			2.33	2.33			1.33		1.67		0.33		2.33	1.33
Psora decipiens (Hedw.) Hoffm.		2.33		3.67		1.33		3.67						1.67		1.00
Psora vallesiaca (Schaer.) Timdal									1.33							3.67
Pyrenodesmia chalybaea (Fr.) A.Massal.					4.00	0.67										1.00
Pyrenodesmia variabilis (Pers.) A.Massal.			1.33	3.67	2.33	1.67	3.67									2.33
Rhizocarpon lecanorinum Anders											1.67		3.33			
Rinodina calcarea (Arnold) Arnold								2.33								6.33
Rinodina tunicata H.Mayrhofer & Poelt	*	1.00	0.67													
Sarcogyne regularis Körb.								1.00						1.33	0.67	

http://www.aloki.hu ● ISSN 1589 1623 (Print) ● ISSN 1785 0037 (Online)
DOI: http://dx.doi.org/10.15666/aeer/1704_1017310193

Scytinium gelatinosum (With.) Otálora. P.M.Jørg. & Wedin		1.00									2.33		3.67			
Scytinium palmatum (Huds.) Gray		0.33		0.33												
Scytinium schraderi (Bernh.) Otálora. P.M.Jørg. & Wedin			1.33	2.33												
Solenopsora cesatii (A.Massal.) Zahlbr.						0.67		2.33								
Solenopsora marina (Zahlbr.) Zahlbr.		0.67														
Solenopsora olivacea (Fr.) H.Kilias subsp. *olbiensis* (Nyl.) Clauzade & Cl.Roux		4.00														
Solenopsora olivacea (Fr.) H.Kilias subsp. *olivacea*		1.33														
Squamarina cartilaginea (With.) P.James		5.67	2.33	4.00			1.67	5.00						4.00	3.67	
Squamarina gypsacea (Sm.) Poelt									1.33	2.67				3.33		
Synalissa ramulosa (Hoffm. ex Bernh.) Fr.																1.33
Toninia candida (Weber) Th.Fr.		1.33	0.67													
Toninia diffracta (A.Massal.) Zahlbr.			1.00	2.00				1.33								
Toninia physaroides (Opiz) Zahlbr.																1.00
Toninia sedifolia (Scop.) Timdal											1.33		4.00			
Trapelia coarctata (Turner ex Sm.) M.Choisy		1.33														
Varicellaria lactea (L.) I.Schmitt & Lumbsch		4.33				1.33		2.00								
Variospora aurantia (Pers.) Arup. Frödén & Søchting							4.67	1.67	3.67	3.00	1.33	3.33	6.00	0.67	4.00	
Variospora flavescens (Huds.) Arup. Søchting & Frödén		2.33	1.67													
Verrucaria dolosa Hepp	*	2.00														
Verrucaria macrostoma Dufour ex DC.								2.33				3.33				
Verrucaria nigrescens Pers.							1.33			2.67					3.33	
Verruculopsis lecideoides (A.Massal.) Gueidan & Cl.Roux																1.33
Xanthocarpia ochracea (Schaer.) A.Massal. & De Not.		2.33	1.33												3.67	
Total Frequency of Non-Epiphytic Taxa		73.63	29.32	75.35	31.66	31.66	21.67	44.33	21.33	28.34	25.66	23.99	51.33	23.67	41.99	57.99
Total Richness of of Non-Epiphytic Taxa		30	17	24	11	20	10	20	9	13	14	11	18	11	16	22
Total Frequency of Epiphytic Taxa		74.9	17.65	68.33	6.66	3.33	2.33	25.32	35	18.65	4.32	14	25	28.66	10.67	5.32
Total Richness of Epiphytic Taxa		26	8	20	6	5	3	13	14	10	5	5	7	16	5	4
General Total Frequency of All Taxa		148.5	46.97	143.7	38.32	34.99	24.00	69.65	56.33	46.99	29.98	37.99	76.33	52.33	52.66	63.31
General Total Richness of All Taxa		56	25	44	17	25	13	33	23	23	19	16	25	27	21	26

*The mean lichen taxa are new for Antalya province of Turkey
Total frequency data were calculated by the ratio of the total frequency of taxa to the number of occurrence of the taxa. In the list, the average frequencies of epiphytic taxa were divided according to each tree species on which the taxa were placed
-A: Altınbeşik Hill, -I: İnönü Hill, -K: Kale Hill, E: East slopes, N: North slope, S: South slopes, W: West slopes, T: Tops

http://www.aloki.hu ● ISSN 1589 1623 (Print) ● ISSN 1785 0037 (Online)
DOI: http://dx.doi.org/10.15666/aeer/1704_1017310193

Table 3. *The most statistically different localities and multiple comparison results based on species richness and species frequency*

Localities		Taxa richness		Taxa frequency	
		Mean difference	**Sig.**	**Mean difference**	**Sig.**
N-A	N-I	.25203*	.002	.82569*	.002
	N-K	.09756	1.000	.03943	1.000
	E-A	.31707*	.000	.89602*	.000
	E-I	.25203*	.002	.92309*	.000
	E-K	.34959*	.000	1.01244*	.000
	S-A	.18699	.204	.64130	.119
	S-I	.26829*	.001	.74959*	.014
	S-K	.26829*	.001	.82553*	.002
	W-A	.30081*	.000	.96382*	.000
	W-I	.32520*	.000	.89870*	.000
	W-K	.25203*	.002	.58699	.446
	T-A	.23577*	.008	.78211*	.006
	T-I	.28455*	.000	.77943*	.008
	T-K	.24390*	.004	.69285	.076
N-K	N-I	-.09756	1.000	-.03943	1.000
	N-K	.15447	.516	.78626*	.007
	E-A	.21951*	.006	.85659*	.002
	E-I	.15447	.516	.88366*	.000
	E-K	.25203*	.000	.97301*	.000
	S-A	.08943	1.000	.60187	.278
	S-I	.17073	.234	.71016*	.043
	S-K	.17073	.234	.78610*	.007
	W-A	.20325*	.024	.92439*	.000
	W-I	.22764*	.003	.85927*	.002
	W-K	.15447	.516	.54756	.706
	T-A	.13821	.829	.74268*	.020
	T-I	.18699	.083	.74000*	.026
	T-K	.14634	.682	.65341	.183

*The mean difference is significant at the 0.05 level

After Kruskal Wallis analyses were used, at least one locality was found significantly different than the other localities. Since all variances are not homogeneous, non-parametric Tamhane's T2 post-hoc test was preferred

-A: Altınbeşik Hill, -I: İnönü Hill, -K: Kale Hill, E: East slopes, N: North slope, S: South slopes, W: West slopes, T: Tops

After these results were determined, total frequency and total richness data were grouped based on localities at different slope directions and tops of the hills (*Fig. 4*). Also; localities from three hills grouped separately and plotted accordingly (*Fig. 5*). As two comparison data showed normal distribution, Pearson test was used for correlation analysis of these. While there was a very strong linear relation in data of four slope directions and data of tops ($p = 0.008$, $r = 0.963$), no relation was found within the data of the three hills (and the three altitude groups). As seen from the graphs, the total

http://www.aloki.hu ● ISSN 1589 1623 (Print) ● ISSN 1785 0037 (Online)
DOI: http://dx.doi.org/10.15666/aeer/1704_1017310193

frequency of different slope directions and tops is sorted from high to low as follows: North > South > Top > West > East (r = 0.885); total richness data as North > South > Top > East > West (r = 0.911). Total northern data were found to be significantly higher than other directions and tops (*Fig. 4*).

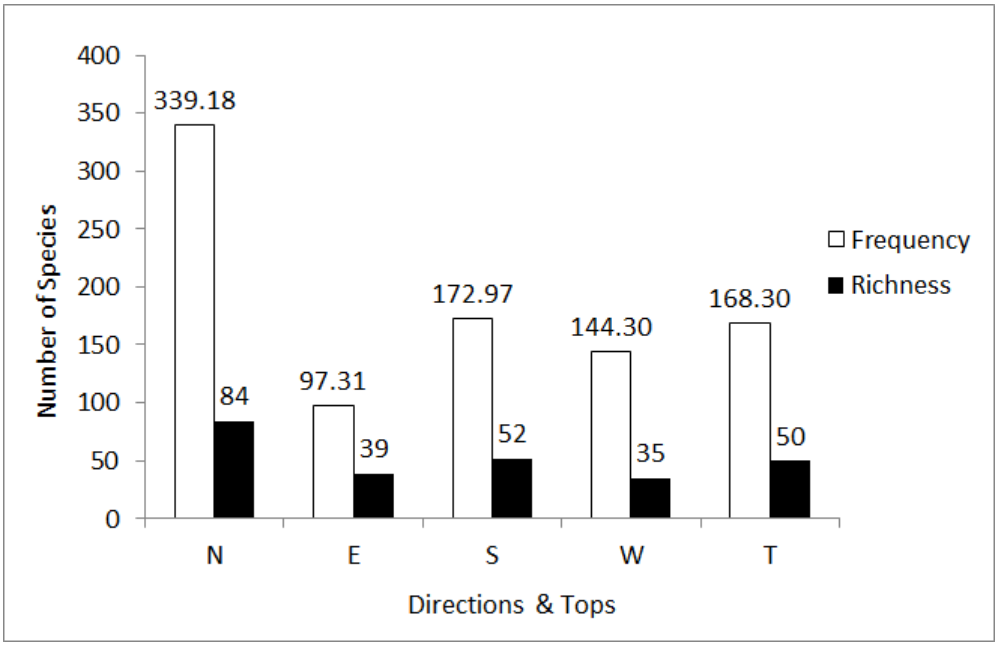

Figure 4. *Graphs about total frequency and total richness data based on localities of different slope directions and tops (created with Excel 2010). Abbreviations: E: East slopes, N: North slopes, S: South slopes, W: West slopes, T: Tops*

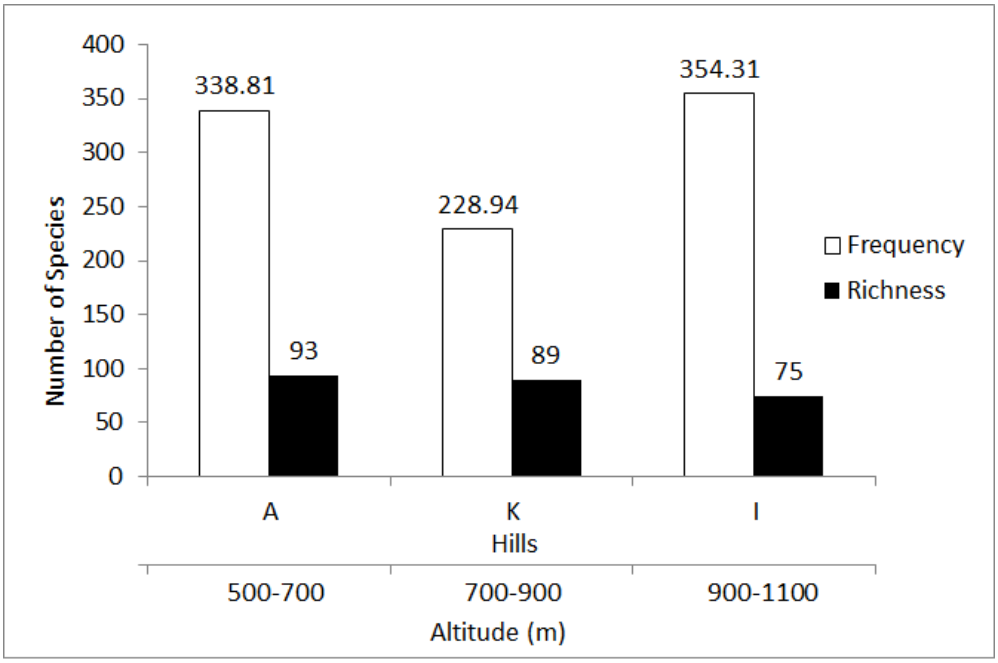

Figure 5. *Graphs about total frequency and total richness data based on localities of three hills (created with Excel 2010). Abbreviations: A: Altınbeşik Hill, I: İnönü Hill, K: Kale Hill*

http://www.aloki.hu ● ISSN 1589 1623 (Print) ● ISSN 1785 0037 (Online)
DOI: http://dx.doi.org/10.15666/aeer/1704_1017310193

Also; total frequency data results obtained from the three hills are as follows from high to low (These hills also represent different altitude groups): Altınbeşik (500-700 m) > Kale (700-900 m) > İnönü (900-1100 m) (r = 0.917); total richness data as: İnönü (900-1100 m) > Altınbeşik (500-700 m) > Kale (700-900 m) (r = 0.952) (*Fig. 5*). When Kruskal Wallis test was applied for data of species richness and species frequency of different slope directions and tops, at least one data group statistically differentiates from others (p = 0.000). In addition, according to Tamhane's T2 post-hoc test results; northern slopes data significantly differ from the data of other directions and tops (*Table 4*). When species richness and frequency data of the three hills were analyzed; difference is available for the frequency data (Kruskal Wallis, p = 0.033) and richness data (Kruskal Wallis, p = 0.011) of the three hill. Tamhane's T2 post-hoc test result showed; Inönü Hill (900-1100 m) is different from Altınbeşik Hill (500-700 m) based on species richness data and it is different from Altınbeşik and Kale (700-900 m) Hills based on frequency data (*Table 5*).

Table 4. *Multiple comparison results based on species richness and species frequency of data of slope directions and tops*

Directions & tops		Species richness		Species frequency	
		Mean difference	Sig.	Mean difference	Sig.
N	E	.36585*	.000	1.97724*	.000
	S	.26016*	.000	1.36211*	.001
	W	.39837*	.000	1.59520*	.000
	T	.27642*	.000	1.40008*	.001
E	N	-.36585*	.000	-1.97724*	.000
	S	-.10569	.596	-.61512	.111
	W	.03252	1.000	-.38203	.790
	T	-.08943	.793	-.57715	.219
S	N	-.26016*	.000	-1.36211*	.001
	E	.10569	.596	.61512	.111
	W	.13821	.211	.23309	.994
	T	.01626	1.000	.03797	1.000
W	N	-.39837*	.000	-1.59520*	.000
	E	-.03252	1.000	.38203	.790
	S	-.13821	.211	-.23309	.994
	T	-.12195	.366	-.19512	.999
T	N	-.27642*	.000	-1.40008*	.001
	E	.08943	.793	.57715	.219
	S	-.01626	1.000	-.03797	1.000
	W	.12195	.366	.19512	.999

*The mean difference is significant at the 0.05 level
After Kruskal Wallis analysis were used. At least one slope direction or top data was found significantly different than the other localities. Since all variances are not homogeneous. non-parametric Tamhane's T2 post-hoc test was preferred
E: East slopes. N: North slopes. S: South slopes. W: West slopes T: Tops

http://www.aloki.hu ● ISSN 1589 1623 (Print) ● ISSN 1785 0037 (Online)
DOI: http://dx.doi.org/10.15666/aeer/1704_1017310193

Table 5. *Multiple comparison results based on species richness and species frequency of data of three hills*

Hills		Species richness		Species frequency	
		Mean difference	Sig.	Mean difference	Sig.
A	I	.14634*	.040	.90407*	.030
	K	.03252	.916	-.11520	.989
I	A	-.14634*	.040	-.90407*	.030
	K	-.11382	.166	-1.01927*	.021
K	A	-.03252	.916	.11520	.989
	I	.11382	.166	1.01927*	.021

*The mean difference is significant at the 0.05 level
After Kruskal Wallis analysis were used. At least one hill data was found significantly different than the other localities. Since all variances are not homogeneous. non-parametric Tamhane's T2 post-hoc test was preferred
A: Altınbeşik Hill, I: İnönü Hill, K: Kale Hill

When species community composition was summarized according to frequency data by non-metric multidimensional scaling (NMS), it was seen that 3 axes explained total variation with 82.89% (axis 1 48.20%; axis 2 21.81%; axes 3 12.88%). For 3-dimensional solution, the final stress rate was 12.41% and instability was 0.00000. At *Figure 6*, an ordination graph was given based on these NMS results with joint plot vectors (total richness, total frequency, epiphytic and non-epiphytic richness, epiphytic and non-epiphytic frequency). Examining Pearson correlation of axes and vectors; it was found that total richness (r = 0.624), epiphytic richness (r = 0.610), non-epiphytic richness (r = 0.470), epiphytic frequency (r = 0.552), non-epiphytic frequency (r = 0.462) and total frequency (r = 0.556) showed high positive correlations with axis 1. At axis 2; whereas all diversity vectors had descending relation, epiphytic richness (r = 0.708) and epiphytic frequency (r = 0.715) were associated with ascending gradient. It can be understood from the results and graph; the epiphytic richness and frequency are more related to the data from southern slopes than data from the top and other slopes. Furthermore, while all other vector parameters were associated with the northern slopes, *Figure 6* shows non-epiphytic richness and frequency are also associated with the data of tops of hills.

Lichen community composition of tops and four slope directions of hills were compared as small-scale with MRPP. The results were presented in *Table 6.* In a MRPP analysis, in case chance-corrected within-group agreement (*A*) value is higher than 0.3, this *A* value is enough to say the compositions are different (McCune et al., 2002). When the results of analysis were evaluated according to this information, species composition of northern slopes versus southern, eastern, western slopes and tops were found distinctly different as well as western slopes versus tops (*Table 6*). On NMS graph, also MRPP results are reflected (*Fig. 6*). Also it was experimented comparison of lichen community composition as large-scale with the data of three hills. In *Table 6*, MRPP comparison of lichen community composition of three hills is given separately. According to this table, no significant difference is observed in any pairwise comparison.

http://www.aloki.hu ● ISSN 1589 1623 (Print) ● ISSN 1785 0037 (Online)
DOI: http://dx.doi.org/10.15666/aeer/1704_1017310193

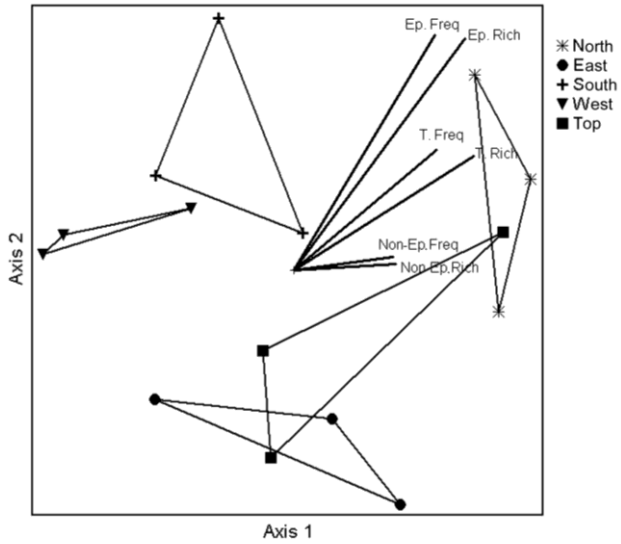

	Axis 1 r	Axis 2 r	Axis 3 r
Total Richness (T. Rich)	.624	.498	-.073
Total Frequency (T. Freq)	.556	.510	-.013
Non-Epiphytic Richness (Non-Ep. Rich)	.470	.128	-.033
Epiphytic Richness (Ep. Rich)	.610	.708	-.092
Non-Epiphytic Frequency (Non-Ep. Freq)	.462	.168	-.047
Epiphytic Frequency (Ep. Freq)	.552	.715	.016

Figure 6. *Ordination graph based on NMS results with diversity calculation classes (joint plot vectors) (created with PC-ORD 6.08)*

Table 6. *Pairwise comparison of lichen community composition of tops-four slope directions and separately hills with MRPP analysis*

	Directions & tops	
	***A* (MRPP)**	***p* (MRPP)**
N vs. E	0.41	0.02345
N vs. S	0.38	0.02852
N vs. W	0.43	0.02278
N vs. T	0.30	0.04784
E vs. S	0.24	0.05580
E vs. W	0.27	0.04174
E vs. T	0.11	0.16028
S vs. W	0.19	0.08800
S vs. T	0.25	0.03982
W vs. T	0.33	0.02374
	Hills	
	***A* (MRPP)**	***p* (MRPP)**
A vs. I	- 0.087	0.8898
A vs. K	0.014	0.3834
I vs. K	- 0.107	0.9607

A value is higher than 0.3, this A value is enough to say the compositions are different (McCune et al., 2002)

A: Altınbeşik Hill, A (MRPP): Chance-corrected within-group agreement, E: East slopes, I: İnönü Hill, K: Kale Hill, N: North slopes, p (MRPP): calculated probability, S: South slopes, vs.: versus, W: West slopes, T: Tops

http://www.aloki.hu ● ISSN 1589 1623 (Print) ● ISSN 1785 0037 (Online)
DOI: http://dx.doi.org/10.15666/aeer/1704_1017310193

Discussion

The study was carried out to determine the compositional diversity of lichen species in selected Mediterranean maquis and arborescent matorral habitats in Altınbeşik Cave National Park. Nascimbene et al. (2013) listed 35 articles examining lichen richness, diversity and composition of different habitats in different European countries. These articles were based on epiphytic lichens that live on forest trees. This study differentiates from those articles by examining epiphytic and non-epiphytic lichens on maquis and arborescent matorral habitats in the Mediterranean region. Therefore; it is the first research about lichen community composition subject on maquis habitats in Eastern Mediterranean Region.

Among the frequency and richness data of selected Mediterranean maquis and arborescent matorral habitats from tops and four slope directions of three hills in the northern data were found significantly higher and differ than others. According to results from Sorensen Similarity Index: slopes at same directions are similar, also top localities shows similarity within themselves. Among them northern localities shows the highest similarity. According to MRPP results; species composition of northern slopes is statistically different than southern, eastern, western slopes and top localities. In addition, it was found; all lichen diversity calculation classes (total richness, total frequency, epiphytic and non-epiphytic richness, epiphytic and non-epiphytic frequency) are related with the northern slopes according to NMS ordination test. Hence, it was concluded that all lichen diversity calculation classes are high in the northern localities. North slopes of hills are typically cool, shady and have high atmospheric humidity (Moser et al., 1979). As lichens are poikilohydric organisms, their water content changes according to the surrounding environmental conditions (Nash, 2008). After recurring hydration – drying cycles, they become metabolically active in humid air (Bidussi et al., 2013). In Mediterranean Region when temperature is sufficient for metabolic activity of lichens, humidity becomes more critical than light in terms of vitality (Aragón et al., 2010). Furthermore, dew is a very important water supply for lichens. Dew at Northern slopes has higher frequency and longer duration than the ones at the other directions (Kidron et al., 2002). All this information may be used to explain the reason for the higher similarities and diversities of the northern slopes in Mediterranean maquis and arborescent matorral habitats compared to the other localities observed in this study.

In a previous study, the response of lichen richness and abundance were examined according to land use intensity. According to this study; epilithic lichen diversity increases along the gradient of increase intensity of land use from forested to non-forested areas (Giordani et al., 2010). Similarly, according to NMS ordination test of current study; richness of non-epiphytic lichens, which lives on rocks and ground, was found to associate with the data of the tops of the hills which are the most non-vegetation areas of the Mediterranean maquis and arborescent matorral habitats. Besides, the epiphytic richness was determined to be more related to the southern slopes than other slopes. The most important environmental factor for epiphytic lichens is diffuse but fairly bright light (Rose, 1992; Renhorn et al., 1997; Sillett et al., 2000). This kind of light is mostly on the southern slopes. This may be one of the reasons to explain the relationship between southern slopes and epiphytic lichens in Mediterranean maquis and arborescent matorral habitats.

According to the results obtained from three hills in the Altınbeşik Cave National Park, least amount of lichen species richness but most frequency data were determined

http://www.aloki.hu ● ISSN 1589 1623 (Print) ● ISSN 1785 0037 (Online)
DOI: http://dx.doi.org/10.15666/aeer/1704_1017310193

from İnönü Hill. While species frequency of this hill was found statistically different than other hills, species richness is different than only Altınbeşik Hill. As İnönü hill represents altitudes of 900-1100 m, this finding suggests; it is possible to find interesting lichen composition in Mediterranean maquis and arborescent matorral habitats at these altitudes in comparison to other altitudes.

Also lichen community composition of 3 hills was found similar according to NMS results. In a similar research on macro lichen diversity; the species richness and species abundance of areas were compared (Wiersma and McMullin, 2018). According to this study, it is reported that there is no difference in species richness or abundance in large-scale areas. This case suggests that similarity and difference measurements of lichen community compositions may be misleading on large-scale research areas. Similarly in this study, it was found that the composition of lichen in Mediterranean maquis and arborescent matorral habitats can show great variation in small-scale areas.

Conclusion

Mediterranean maquis and arborescent matorral habitat type is found across the entire Mediterranean biogeographical zone. In this study, it was aimed to determine the epiphytic and non-epiphytic lichen diversity in Mediterranean maquis and arborescent matorral habitats. Lichen diversity in this study was calculated according to the data of species richness and species frequency. In addition, it was examined the existing differences or similarities of lichen diversity at different directions, altitudes, and substrates (epiphytic and non-epiphytic) in this habitat type. Among the frequency and richness data of selected Mediterranean maquis and arborescent matorral habitats from tops and four slope directions of three hills, the northern data were found significantly higher and differ than others. According to results from Sorensen Similarity Index: slopes at same directions are similar, also top localities shows similarity within themselves. Among them northern localities shows the highest similarity. According to MRPP results; species composition of northern slopes is statistically different than southern, eastern, western slopes and top localities. In addition, it was found; all lichen diversity calculation classes (total richness, total frequency, epiphytic and non-epiphytic richness, epiphytic and non-epiphytic frequency) are related with the northern slopes according to NMS ordination test. In addition, richness of non-epiphytic lichens, which lives on rocks and ground, was found to associate with the data of the tops of the hills which are the most non-vegetation areas of the Mediterranean maquis and arborescent matorral habitats. Besides, the epiphytic richness was determined to be more related to the southern slopes than other slopes. Though it was found that lichen community composition shows great variation in Mediterranean maquis and arborescent matorral habitat, community composition of 3 hills was found similar according to NMS results. This result suggests that choosing large-scale areas for determining differences on lichen communities may have misleading results.

REFERENCES

[1] Aragón, G., Rico, V. J., Belinchón, R. (2006): Lichen diversity from Cazorla, Segura and Las Villas Biosphere Reserve (SE Spain). – Nova Hedwigia 82(1-2): 31-50.

http://www.aloki.hu ● ISSN 1589 1623 (Print) ● ISSN 1785 0037 (Online)
DOI: http://dx.doi.org/10.15666/aeer/1704_1017310193

[2] Aragón, G., Martínez, I., Izquierdo, P., Belinchón, R., Escudero, A. (2010): Effects of forest management on epiphytic lichen diversity in Mediterranean forests. – Applied Vegetation Science 13: 183-194.
[3] Asta, J., Erhardt, W., Ferretti, M., Fornasier, F., Kirschbaum, U. Nimis, P. L., Purvis, O. W., Pirintsos, S., Scheidegger, C., Van Haluwyn, C., Wirth, V. (2002a): European Guideline for Mapping Lichen Diversity as an Indicator of Environmental Stress. The British Lichen Society. – Kluwer Academic Publishers, Dordrecht.
[4] Asta, J., Erhardt, W., Ferretti, M., Fornasier, F., Kirschbaum, U., Nimis, P. L., Purvis, O. W., Pirintsos, S., Scheidegger, C., Van Haluwyn, C., Wirth, V. (2002b): Mapping Lichen Diversity as an Indicator of Environmental Quality. – In: Nimis, P. L., Scheidegger, C., Wolseley, P. A. (eds.) Monitoring with Lichens. Kluwer Academic Publisher, Dordrecht, pp. 273-279.
[5] Bartels, S. F., Chen, H. Y. (2015): Epiphytic macrolichen cover, richness and composition in young successional boreal forest: a comparison of fire and logging disturbance. – Forest Ecology and Management 347: 149-155.
[6] Bidussi, M., Gauslaa, Y., Solhaug, K. A. (2013): Prolonging the hydration and active metabolism from light periods into nights substantially enhances lichen growth. – Planta 237: 1359-1366.
[7] Branquinho, C., Matos, P., Pinho, P. (2015): Lichens as Ecological Indicators to Track Atmospheric Changes: Future Challenges. – In: Lindenmayer, D. B., Pierson, J., Barton, P. (eds.) Surrogates and Indicators in Ecology, Conservation and Environmental Management. CSIRO Publishing and CRC Press, Melbourne and London.
[8] Christensen, S. N., Svane, S. (2007): Contribution to the knowledge of the lichen flora of Crete (Kriti), Greece. – Willdenowia 37(2): 587-593.
[9] Çinbilgel, I., Gökçeoğlu, M. (2010a): The vegetation of Altınbeşik Cavern National Park (İbradı-Akseki/Antalya-Turkey). A synecological study. – Spanish Journal of Rural Development (SJRD) 1(2): 1-18.
[10] Çinbilgel, I., Gökçeoğlu, M. (2010b): Flora of Altınbeşik Cavern National Park (İbradı-Akseki, Antalya/Turkey). – Biological Diversity and Conservation 3: 85-110.
[11] De Guevara, M. L., Lázaro, R., Quero, J. L., Ochoa, V., Gozalo, B. Berdugo, M., Uclés, O., Escolar, C., Maestre, F. T. (2014): Simulated climate change reduced the capacity of lichen-dominated biocrusts to act as carbon sinks in two semi-arid Mediterranean ecosystems. – Biological Conservation 23: 1787-1807.
[12] EEA (2016): European Red List of Habitats - Heathland Habitat Group, F5.1 Mediterranean Maquis and Arborescent Matorral. – EEA Eionet Report.
[13] EEA (2017): EUNIS habitat type hierarchical view revised. Visualization of revised groups of EUNIS habitat type classification – https://eunis.eea.europa.eu/habitats/6121. Accessed: 2019-01-22.
[14] Ellis, C. J., Coppins, B. J., Dawson, T. P., Seaward, M. R. (2007): Response of British lichens to climate change scenarios: Trends and uncertainties in the projected impact for contrasting biogeographic groups. – Biological Conservation 140: 217-235.
[15] Fenn, M. E., Poth, M. A., Aber, J. D., Baron, J. S., Bormann, B. T. Johnson, D. W., Lemly, A. D., McNulty, S. G., Ryan, D. E., Stottlemeyer, R. (1998): Nitrogen excess in North American ecosystems: predisposing factors, ecosystem responses, and management strategies. – Ecological Applications 8: 706-733.
[16] Fryday, A., Coppins, B. (1997): Keys to sterile, crustose saxicolous and terricolous lichens occurring in the British Isles. – Lichenologist 29: 301-332.
[17] Gadsdon, S. R., Dagley, J. R., Wolseley, P. A., Power, S. A. (2010): Relationships between lichen community composition and concentrations of NO_2 and NH_3. – Environmental Pollution 158(8): 2553-2560.
[18] Geiser, L., Neitlich, P. N. (2007): Air pollution and climate gradients in western. Oregon and Washington indicated by epiphytic macrolichens. – Environmental Pollution 145: 203-218.

http://www.aloki.hu ● ISSN 1589 1623 (Print) ● ISSN 1785 0037 (Online)
DOI: http://dx.doi.org/10.15666/aeer/1704_1017310193

[19] Giordani, P., Incert, G., Rizzi, G., Ginaldi, F., Viglione, S. Rellini, I., Modenesi, P. (2010): Land use intensity drives the local variation of lichen diversity in Mediterranean ecosystems sensitive to desertification. – Bibliotheca Lichenologica 105: 139-148.
[20] Giralt, M. (2001): The lichen genera *Rinodina* und *Rinodinella* (lichenized Ascomycetes, Physciaceae) in the Iberian Peninsula. – Bibliotheca Lichenologica 79: 1-160.
[21] Gombert, S., Asta, J., Seaward, M. R. D. (2004): Assessment of lichen diversity by index of atmospheric purity (IAP), index of human impact (IHI) and other environmental factors in an urban area (Grenoble, southeast France). – Science of the Total Environment 324: 183-199.
[22] Goward, T., McCune, B., Meidinger, D. (1994): The lichens of British Columbia, illustrated keys. Part 1: Foliose and squamulose species. – British Columbia Ministry of Forests, Special Report Series 8: 1-181.
[23] Johansson, O., Palmqvist, K., Olofsson, J. (2012): Nitrogen deposition drives lichen community changes through differential species responses. – Global Change Biology 18(8): 2626-2635.
[24] Johansson, P. (2008): Consequences of disturbance on epiphytic lichens in boreal and near boreal forests. – Biological Conservation 141: 1933-1944.
[25] John, V. (1996): Preliminary catalogue of lichenised and lichenicolous fungi of Mediterranean Turkey. – Bocconea 6: 173-216.
[26] Kidron, G. J., Herrnstadtw, I., Barzilay, E. (2002): The role of dew as a moisture source for sand microbiotic crusts in the Negev Desert, Israel. – Journal of Arid Environments 52: 517-533.
[27] Koch, N. M., de Azevedo Martins, S. M., Lucheta, F., Müller, S. C. (2013): Functional diversity and traits assembly patterns of lichens as indicators of successional stages in a tropical rainforest. – Ecological Indicators 34: 22-30.
[28] Kruskal, W. H., Wallis, W. A. (1952): Use of ranks in one-criterion variance analysis. – Journal of the American Statistical Association 47: 583-621.
[29] Lang, S. I., Cornelissen, J. H., Shaver, G. R., Ahrens, M., Callaghan, T. V., Molau, U., Ter Braak, C. J. F., Hölzer, A., Aerts, R. (2012): Arctic warming on two continents has consistent negative effects on lichen diversity and mixed effects on bryophyte diversity. – Global Change Biology 18(3): 1096-1107.
[30] Litterski, B. (1997): Lichen observations on the island of Cyprus. – Feddes Repertorium 108(5-6): 463-473.
[31] McCune, B. (2000): Lichen communities as indicators of forest health. – Bryologist 103: 353-356.
[32] McCune, B. (2016): Key to the lichen Genera of the Pacific Northwest. – Department of Botany and Plant Pathology, Oregon State University, Corvallis OR.
[33] McCune, B., Grace, J., Urban, D. L. (2002): Analysis of Ecological Communities. – Gleneden Beach, OR.
[34] McMullin, R. T., Duinker, P. N., Richardson, D. H., Cameron, R. P., Hamilton, D. C., Newmaster, S. G. (2010): Relationships between the structural complexity and lichen community in coniferous forests of southwestern Nova Scotia. – Forest Ecology and Management 260(5): 744-749.
[35] McMurray, J. A., Roberts, D. W., Geiser, L. H. (2015): Epiphytic lichen indication of nitrogen deposition and climate in the northern rocky mountains, USA. – Ecological Indicators 49: 154-161.
[36] Moberg, R. (1977): The lichen genus Physcia and allied genera in Fennoscandia. – Symbolae Botanicae Upsaliensis 22: 1-108.
[37] Moser, T. J., Nash, III T. H., Thomson, J. W. (1979): Lichens of Anaktuvuk Pass, Alaska, with emphasis on the impact of caribou grazing. – Bryologist 82: 393-408.
[38] Nascimbene, J., Thor, G., Nimis, P. L. (2012): Habitat types and lichen conservation in the Alps: Perspectives from a case study in the Stelvio National Park (Italy). – Plant Biosystems 146: 428-442.

http://www.aloki.hu ● ISSN 1589 1623 (Print) ● ISSN 1785 0037 (Online)
DOI: http://dx.doi.org/10.15666/aeer/1704_1017310193

[39] Nascimbene, J., Thor, G., Nimis, P. L. (2013): Effects of forest management on epiphytic lichens in temperate deciduous forests of Europe. A review. – Forest Ecology and Management 298: 27-38.
[40] Nash, III T. H. (2008): Lichen Sensitivity to Air Pollution. – In: Nash, III T. H. (ed.) Lichen Biology. Cambridge University Press, Cambridge, UK, pp. 299-314.
[41] Nimis, P. L., John, V. (1998): A contribution to the lichen flora of Mediterranean Turkey. – Cryptogamie. Bryologie, Lichénologie 19: 35-58.
[42] Ravera, S., Nimis, P. L., Brunialti, G., Frati, L., Isocrono, D., Martellos, S., Munzi, S., Nascimbene, J., Potenza, G., Tretiach, M. (2011): The role of lichens in selecting important plant areas in Italy. – Fitosociologia 48(2): 145-153.
[43] Renhorn, K. E., Esseen, P. A., Palmqvist, K., Sundberg, B. (1997): Growth and vitality of epiphytic lichens. I. Responses to microclimate along a forest edge–interior gradient. – Oecologia 109: 1-9.
[44] Rogers, P. C., Ryel, R. J. (2008): Lichen community change in response to succession in aspen forests of the Rocky Mountains, USA. – Forest Ecology and Management 256: 1760-1770.
[45] Rose, C. I., Hawksworth, D. L. (1981): Lichen recolonization in London's cleaner air. – Nature 289: 289-292.
[46] Rose, F. (1992): Temperate Forest Management: its Effects on Bryophyte and Lichen Floras and Habitats. – In: Bates, J. W., Farmer, A. M. (eds.) Bryophytes and Lichens in a Changing Environment. Clarendon, Oxford, UK, pp. 211-233.
[47] Sillett, S. C., McCune, B., Peck, J. E., Rambo, T. R., Ruchty, A. (2000): Dispersal limitations of epiphytic lichens result in species dependent on old-growth forests. – Ecological Applications 10: 789-799.
[48] Sipman, H. J. M., Raus, T. (2015): Lichens and lichenicolous fungi from the island of Chios (Aegean Sea, Greece). – Herzogia 28(2): 496-519.
[49] Smith, C. W., Aptroot, A., Coppins, B. J., Fletcher, A., Gilbert, O. L., James, P. W., Wolseley, P. A. (2009): The Lichens of Great Britain and Ireland. – British Lichen Society, London, UK.
[50] Svoboda, D., Peksa, O., Vesela, J. (2010): Epiphytic lichen diversity in central European oak forests: Assessment of the effects of natural environmental factors and human influences. – Environmental Pollution 158: 812-819.
[51] Thormann, M. N. (2006): Lichens as indicators of forest health in Canada. – The Forestry Chronicle 82: 335-343.
[52] Tomaselli, R. (1977): The degradation of the Mediterranean maquis. – Ambio 356-362.
[53] Tucker, S., Thiers, H. (1998): Key to crustose lichen genera of California. – Bulletin of the California Lichen Society 5: 1-18.
[54] Wasser, S. P., Nevo, E. (2005): Lichen-Forming, Lichenicolous and Allied Fungi of Israel. – Ganter, Ruggell.
[55] Wetmore, C. M. (2005): Keys to the Lichens of Minnesota. – Department of Plant Biology, University of Minnesota, St. Paul.
[56] Wiersma, Y. F., McMullin, R. T. (2018): Is it common to be rare on the landscape? A test using a novel model system. – Landscape Ecology 33: 183-195.
[57] Wirth, V., Hauck, M., Schultz, M. (2013): Die Flechten Deutschlands. – Ulmer, Stuttgart.

http://www.aloki.hu ● ISSN 1589 1623 (Print) ● ISSN 1785 0037 (Online)
DOI: http://dx.doi.org/10.15666/aeer/1704_1017310193

DETERMINATION OF EMITTER HYDRAULIC PROPERTIES OF DIFFERENT IN-LINE DRIPPER TYPES

AYDIN, Y.

Siirt University, Faculty of Agriculture, Department of Biosystem Engineering
Siirt 56100, Turkey
e-mail: yusufaydin@siirt.edu.tr; phone: +90-484-212-1111; fax: +90+484-223-1998

(Received 16th Apr 2019; accepted 13th Jun 2019)

Abstract. It is only possible by way of highly efficient system performance to provide uniform water distribution and sufficient soil moisture at the plant root zone in drip irrigation systems. Factors related with hydraulic and the emitter performance change should be known well for determining irrigation uniformity. In the study, 4 different emitter laterals were tested under 4 different pressure loads (5-10-15 and 20 m). The accordance of flow characteristics for the laterals, manufacturing variety coefficient (CV), emitter uniformity (EU) and irrigation water uniform distribution coefficient or Cristiansen Uniformity Coefficient (CU) and Statistical Uniformity (Us) values were evaluated in with regard to the American Society of Agricultural Engineers standards. It was determined based on the acquired results that there is an increase in the flow rates of emitters corresponding to the increasing pressure values and it was also determined that there were differences ranging between 0.75% to 25.5% with the flow values provided by manufacturing companies under 1 atm pressure. While the manufacturing variety coefficient class values were "weak", "moderate" and "good" for the A emitter, class values of "good" and "very good" were determined for irrigation uniformity (CU) and emitter uniformity (EU).
Keywords: *operating pressure, uniformity, drip irrigation, flow-rate, test-table*

Introduction

Recently, irrigation is also considered as, "maintaining the usable water at a suitable level at the root zone in addition to providing the water required for plant production". Irrigation applications are carried out using different methods due to changes in the topographic structure of the land, soil and plant type as well as changes in farmer preferences and cost factors. Among these methods, drip irrigation is preferred due to its superiorities over other methods with regard to yield, efficiency, irrigation water savings when compared with other irrigation methods, it is indicated that drip irrigation provides 44% water savings on apple trees in comparison with other surface irrigation methods (Mohammed, 2018), whereas drip irrigation consumes 60% less water in grapevine irrigation compared with furrow irrigation and 56% less water compared with micro sprink irrigation (Baştuğ et al., 1998). In general, about 30-60% water saving is possible with drip irrigation method in comparison to sprinkling and flood irrigation in agricultural irrigation (Anonymous, 2004). Drip irrigation is defined as, "slowly delivering filtered water to the plant roots in small amounts and at high intervals". Deep percolation, surface flow and evaporation losses can be minimized with this method (Wu et al., 1979; Korukçu, 1980; cited from Altın, 2009). Uniform distribution of water is a desired characteristic in drip irrigation. Failure of the system to distribute the water uniformly results in excessive or deficit irrigation of the plant roots. Both cases will inevitably yield to the emergence of conditions that are not suited for plant growth. Excessive irrigation leads to insufficient aeration of the roots due to bad drainage, washing of nutrients at the root and thereby reduced effectiveness of the fertilizer, while deficit irrigation results in higher energy consumption and low irrigation efficiency

http://www.aloki.hu ● ISSN 1589 1623 (Print) ● ISSN 1785 0037 (Online)
DOI: http://dx.doi.org/10.15666/aeer/1704_1019510205

(Çiçek, 2015). Hence, hydraulic change and emitter performance change should be taken into consideration as two important parameters causing changes in emitter flow rates when determining irrigation uniformity which is an important element when evaluating the drip irrigation system performances. Hydraulic change develops due to the pressure change resulting from the incline of side pipes and laterals on the land as well as pipe diameter and lateral length. Whereas emitter performance change can be considered as changes in emitters due to factors such as manufacturing varieties of emitters, level of clogging due to irrigation water, changes in irrigation water temperature and wear in emitters over time (Çamoğlu and Yavuz, 2004). Similarly, many factors such as operating pressure, water chemical and temperature, construction changes, effecting the uniformity of water distrubition. Therefore, the lack of such mentioned factors that caused to poor desing will bring changing in discharge and the distribution uniformity and low irrigation efficiency. The uniformity parameters are the main and basic criteria for designing an efficient of drip irrigation system (Elamin et al., 2017). Ideally, all emitters in a drip irrigation system should have equal flow rates (Özekici and Bozkurt, 1996). However, this is not possible in practice. Accurate emitter manufacturing is the main criteria and necessary in order to ensure a high effective system uniformity. Also the emission uniformity is essential to determining the total dept of water applied (Yeeshu et al., 2014). Manufacturing varieties that have a significant impact on system performance also cause variations in emitter flow rates. Emitters may differ with regard to characteristics such as volume, weight, surface shape and length due to factors such as raw materials used in manufacturing, manufacturing temperature, mold properties, manufacturing pressure and rate, cooling time etc. (Demir and Yürdem, 2000). There may be flow regime differences even in two emitters manufactured with the same technology using the same machine and the same manufacturing conditions (Solomon, 1979; Özekici and Sneed, 1995). Uniform distribution of irrigation water is one of the primary criteria taking into consideration when evaluating irrigation systems. However, irrigation systems differ with regard to uniform distribution due to many different reasons. Factors such as the uniform distribution of water at the application area, friction losses at the side pipe and laterals of the system, pressure changes due to the elevation differences between system elements, how well the system is maintained, level of clogs in the emitter due to contamination of irrigation water and the number of emitters per plant affect the uniform distribution of water (Ünal, 2011). It is also inevitable that there will be differences between local and foreign emitter laterals due to factors such as manufacturing conditions, raw material and manufacturing temperature even if they have been manufactured using similar technologies.

The purpose of this study was to put forth the impacts of manufacturing differences among emitters on their irrigation performances and to provide information to users on the different types of emitters in the market by carrying out analyses on their operating performances under different operating pressures as well as various hydraulic performance parameters. In the literature review, resently, there is no study in the GAP region which is compatible with the subject of this study or to determine the dripper hydraulic performances. There are large agricultural areas where pressurized irrigation systems are used in the region. Considering the excess amount of dripper lateral to be used in these areas, the use of drippers with good hydraulic performance is very important in terms of protection of water resources and providing the expected benefit from irrigation.

http://www.aloki.hu ● ISSN 1589 1623 (Print) ● ISSN 1785 0037 (Online)
DOI: http://dx.doi.org/10.15666/aeer/1704_1019510205

Materials and Methods

Test setup preparation

The present study was carried out at Siirt University which is located in the Southest Anatolia Region of Turkey Faculty of Agriculture Department of Biosystem Engineering irrigation laboratory. The test table in the laboratory (*Fig. 1*) was arranged such that the specially manufactured 4 lateral lines with an elevation of 1.2 m from ground level, lenght of 6 m and width of 1.8 m can be tested simultaneously.

Figure 1. *A view of test table used in this study*

The test setup was comprised of a main pipe, mounting system and lateral pipe lines. A 32 mm PPRC (Polypropylene Random Copolymer) pipe integrated to the municipal water outlet at the laboratory which is controlled by a ball valve was used as the main pipeline. The mounting system was affixed from its starting and ending points using a steel wire to make the incline at the laterals zero and the test laterals were fixed on these steel wires via clips. The test table for steel wires and laterals was mounted on a moving table at an elevation of 40 cm and a setup with 4 rows was prepared with lateral gaps of 35 cm. Plastic ball valves and manometers were used as return valve on the end of the main pipeline for pressure control at the lateral inlets and for ensuring lateral safety under high pressure conditions. The municipal water used in the test setup was directly connected since there was no contamination that may cause clogging. An additional electrical pump was not used in the system since the municipal operating pressure may reach up to 6 bars, however a 2 kW electrical pump was integrated to the system as a precaution against pressure drops. The municipal pressure was applied on the laterals after being reduced to the desired test pressure via ball valves. Temperature changes in the municipal water were monitored during the test at varying intervals using a portable thermometer and a difference of $\pm 0.5^{o}C$ was not included in the calculations since it is not effective on flow rate changes. Transparent plastic cups of 1.2 liters were used for collecting the water from the emitters.

Execution of the tests

Lateral flow rate tests were carried out at 4 different pressure intervals (5-10-15 and 20 m) on emitters the characteristics of which are given in *Table 1*.

A total of 28 emitters were selected on each lateral for determining the relationship between emitter pressure – flow rate and measurements were carried out with 3 repetitions. Water was given to the system which was subject to 10 minutes of natural dripping prior to starting the measurements and it was waited until the lateral input pressures became constant. Measurements were started and stopped simultaneously for all laterals. The emitter flow rates were determined in accordance with the volume

http://www.aloki.hu ● ISSN 1589 1623 (Print) ● ISSN 1785 0037 (Online)
DOI: http://dx.doi.org/10.15666/aeer/1704_1019510205

principle using the amount of water accumulated in drip pans placed under the laterals by way of 10 ml graded 1000 ml glass beakers (Tekin et al., 2016). The flow rate values determined for each emitter were evaluated in Excel software after which the flow regime, flow index subject to flow regime (x), flow coefficient (k), correlation coefficient (r), emitter uniformity (EU), Cristiansen Uniformity coefficient (CU), statistical uniformity coefficient (Us), manufacturing variety coefficient (CV) values were determined and the changes in these values subject to pressure were evaluated.

Table 1. *Characteristics of the emitters used in the test*

Emitter name	Flow rate(l h^{-1})	Emitter distance (m)	Type of lateral	Emitter Type
A (local)	4	0.33	Round	in-line-no diaphragm
B (local)	4	0.33	Round	in-line-no diaphragm
C (foreign)	4	0.33	Round	in-line-no diaphragm
D (foreign)	4	0.33	Round	in-line-no diaphragm

Determination of emitter flow characteristics

Emitter flow rate is a function of the pressure that characterizes flow. Hence, certain emitter characteristics such as manufacturing variety, emitter parameters can be easily determined via experimental studies (Karaca, 2008). The relationship between emitter inlet pressure and emitter flow rate is defined as a flow characteristic and is indicated with the $Q=kh^x$ equality given in *Table 2* and calculated using *Eq.1*. Here; Q: emitter flow rate, (l/h); k: coefficient expressing emitter dimensions, h: emitter inlet pressure (m) and x: emitter flow regime coefficient. The values of k and x indicate emitter characteristics and are two important parameters with an impact on uniform water distribution in drip irrigation as coefficients indicating emitter flow regime (Demir and Yürdem, 2000).

Table 2. *Hydraulic parameters and equations used in calculation*

Hydrolic parameters	Equations	
Flow Equation (Korukçu, 1980; Bralts, 1986)	$Q = kh^x$	(Eq.1)
Manufacturing Variety Coefficient (CV) (ASAE, 2002)	$Cv = \frac{S}{X_{ort}}$	(Eq.2)
Emitter uniformity (EU) (Keller and Karmeli, 1974)	$EU = 100 * \frac{q_x}{q_a}$	(Eq.3)
Irrigation water distrubition uniformity (CU) (Cristiansen, 1942)	$CU = 100(1 - \frac{\Delta q_o}{q_a})$	(Eq.4)
Statistical Uniformity (Us) (Bralts and Kesner, 1983)	$Us = 100(1 - \frac{S_q}{q_{ort}})$	(Eq.5)

In the above equations; q: emitter flowrate (l h^{-1}); k: flow coefficient; h: operating pressure, m; x: flow index subject to flow regime; q_x: average of ¼ of the emitters with the lowest flow rate (l h^{-1}); q_a: average of all emitter flow rates, (l h^{-1}); Δq_o: average of the absolute deviations from the average for each emitter or lateral flow rate, q_o: emitter or lateral input flow rate average, (l h^{-1}); S_q: standard deviation of emitter flow rates; q_{ort}: average emitter flow rate (l h^{-1}); X_{ort}: average emitter flow rate; (l h^{-1}); S: standard deviation of emitter flow rates

Flow index values suggested by different researchers that define emitter flow rate characteristics are given in *Table 3*. Results for the flow regime obtained in the study were evaluated according to *Table 3* and the flow regimes of the laterals used were determined.

http://www.aloki.hu ● ISSN 1589 1623 (Print) ● ISSN 1785 0037 (Online)
DOI: http://dx.doi.org/10.15666/aeer/1704_1019510205

Table 3. *Emitter flow regime coefficient values (Demir and Yürdem, 2000; Karaca, 2008)*

Flow Regime	**x value** (Bralts et al., 1987)
In pressure regülatör emitters	0-0.5
Partially turbulent flow and unstabil flow conditions	0.5-1.0
Full turbulance	0.5
Laminar flow	0.5-1.0
Partially regulated pressure	0-0.5
Regulated pressure fully	0

The evaluation principles provided in *Table 4* were used when determining emitter hydraulic parameters and the numerical values acquired as a result of the calculations were classified according to the provided criteria.

Table 4. *Recommended limits of coefficients (Tüzel, 1993; ASAE, 1994, 2002)*

Classification	**CV (%)**	**Us (%)**	**EU (%)**	**CU (%)**
Very good	<5	100-95	≥94	>90
Good	5-7	90-85	81-77	80-90
Moderate	7-11	80-75	68-75	70-80
Weak	11-15	70-65	56-62	60-70
Unacceptable	>15	<60	≤50	<60

Results and Discussion

Emitter flow characteristics

Table 5 summarizes the results related with flow characteristics for the emitters used in the study. Flow index values were determined between 0-0.5 for the B, C and D emitters used in the study and display a partially turbulent flow characteristic without pressure regulator. The flow index (x) value determined via graphic method for the emitter of A company was 0.5035 and it was evaluated to have a full turbulent flow regime.

Table 5. *Flow properties of emitters*

	Flow properties of emitters			
	A (local)	**B (local)**	**C (foreign)**	**D (foreign)**
Flow regime	Full Turbulence	Partial Turbulence	Full Turbulence	Full Turbulence
Flow equations	$q=1.6811*h^{0.5035}$	$q=1.3305*h^{0.4529}$	$q=1.3308*h^{0.4684}$	$q=1.386*h^{0.4706}$
k	1.6811	1.3305	1.3308	1.386
x	0.5035	0.4529	0.4686	0.4706
R^2	0.9795	0.9869	0.9881	0.9667

Pressure-Flow Rate relationship

The emitters used in the study were tested under 4 different operating pressures and the acquired results have been summarized in *Table 6* and *Figure 2*. It can be observed upon examining the pressure-flow rate change of emitters that different values have been obtained at different operating pressures. Whereas the lowest average flow rate value was 2.79 l h^{-1} for the B emitter at the lowest operating pressure (5 m), the highest

http://www.aloki.hu ● ISSN 1589 1623 (Print) ● ISSN 1785 0037 (Online)
DOI: http://dx.doi.org/10.15666/aeer/1704_1019510205

average flow rate value was obtained as 7.73 l h^{-1} for the A emitter at an operating pressure of 20 m.

As can be seen in *Table 6*, the flow rate values determined during the study carried out for determining the flow characteristics of the emitters displayed a tendency to increase with increasing operating pressure. Parallel to the developments in irrigation technologies, studies have been carried out by many researchers for determining the variation in emitter pipes as well as the flow characteristics of these emitters (Özekici and Sneed, 1995; Demir and Yürdem, 2000; Kırnak et al., 2004; Üğlü and Tanrıverdi, 2013; Tekin et al., 2016). It was put forth in studies carried out by researchers that flow rate changes especially in systems using emitters without pressure regulator tended to increase with increasing operating pressure. Results acquired in this study regarding the pressure-flow rate changes were in accordance with the findings of other researchers and an increase was observed in emitter flow rates corresponding to an increase in operating pressure.

Table 6. *Emitters' pressure-flow relationship*

Pressure (m)	Flow (l h^{-1})			
	A (local)	B (local)	C (foreign)	D (foreign)
5	3.89	2.79	2.87	3.02
10	5.02	3.75	3.86	4.03
15	6.70	4.36	4.57	4.65
20	7.73	5.35	5.61	6.02

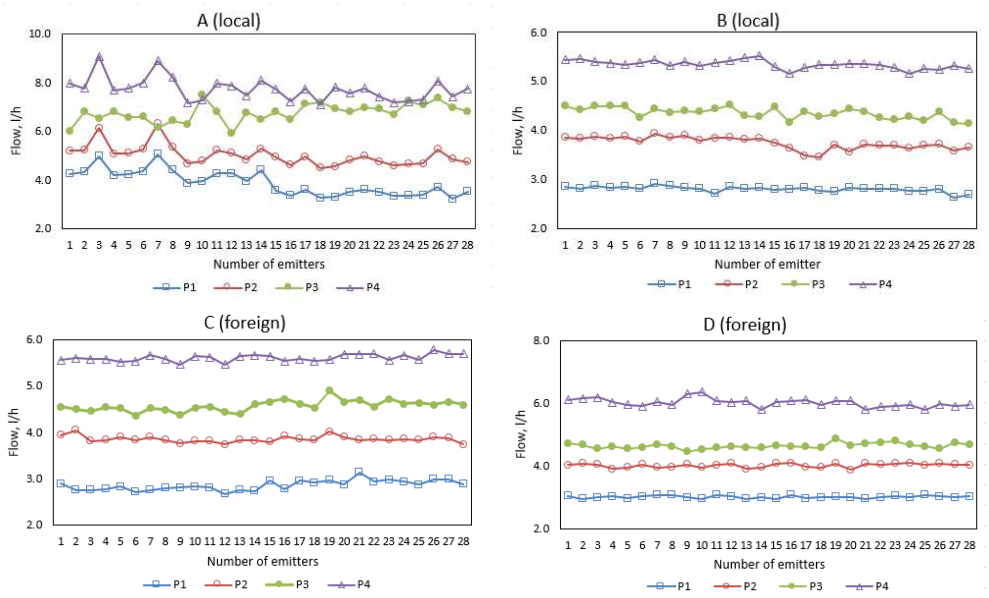

Figure 2. *Pressure-flow change in foreign dripper pipes*

Even though the flow rate for 1 atm pressure suggested by manufacturers of the emitters used in the study was 4 l h^{-1}, deviations from this value were observed. While the highest % change from the suggested flow rate was observed for the A emitter with 25.5%, the lowest change % was observed for the D emitter with 0.75%. The aforementioned values are similar with the findings of Tekin et al. (2016). Researchers

http://www.aloki.hu ● ISSN 1589 1623 (Print) ● ISSN 1785 0037 (Online)
DOI: http://dx.doi.org/10.15666/aeer/1704_1019510205

determined this change to vary between 1-15.5% subject to the companies of emitters used. The sudden decrease and increase in emitter B shown in *Figure 2* is thought to be due to the instantaneous pressure change in the emitter. The preference of emitters by system users with less flow rate change and which are classified as either "good" or "very good" should be taken into consideration with regard to both system performance and first facility cost.

Manufacturing variety coefficient

The manufacturing variety coefficients of the emitters used in the study were calculated using *Eq.2* and evaluated according to Wu and Gittling (1974) and ASAE (1994) and the manufacturing variety coefficients (CV) acquired along with classification have been given in *Table 7.* As can be seen when the table is examined that the CV coefficients have been subject to an evaluation based on different classification groups and received group values ranging between "very good" and "unacceptable". The emitters were classified into 4 groups as a result of this evaluation.

Table 7. *Manufacturing variety coefficient values*

Pressure (m)	CV_{cal} and Classification values							
	A (local)		B (local)		C (foreign)		D (foreign)	
5	13.27	*W*	5.68	G	3.74	VG	1.39	VG
10	8.46	*M*	3.33	VG	1.80	VG	1.57	VG
15	5.60	*G*	2.64	VG	2.50	VG	1.89	VG
20	6.16	*G*	1.62	VG	1.34	VG	2.25	VG

While the A emitter with an operating pressure of 5 m yielded a high (13.27) CV value, it was classified as "weak". Similarly, while the same emitter took on the value of "moderate with a load of 8.46 at a pressure load of 10 m, it was classified as "good" at pressure loads of 15 m and 20 m. The classification change interval ranged between "good" and "very good" for the B emitter as well even though the changes were not as dramatic as those of the emitter A. The change interval for the manufacturing variety coefficients under different pressure loads for exported emitters C and D was not very high with the lowest value of 1.34, highest value of 3.74 and a classification of "very good". Demir and Yürdem (2000) carried out a study in which a total of 32 emitters (22 without pressure regulator, 6 with pressure regulator and 4 with on-line emitters) were subject to tests under 5 different operating pressures and controlled laboratory conditions. It was observed as a result of the evaluation based on manufacturing variety coefficients that the emitters without pressure regulator were classified as "unacceptable" and "moderately perfect". The changes in CV values subject to pressure in the present study were in accordance with the findings of other researchers in literature. Even though the manufacturing variety coefficients of emitters vary between 2-15%, it is possible to obtain higher values (Çiçek, 2015). The CV values acquired in this study remained in the limits indicated by the researchers.

Emitter uniformity (EU)

The emitter uniformity coefficients for the emitters subject to the tests in the study were calculated using *Eq.3* and evaluated in accordance with ASAE (1994) and the acquired results together with the classification results are given in *Table 8*. As can be

http://www.aloki.hu ● ISSN 1589 1623 (Print) ● ISSN 1785 0037 (Online)
DOI: http://dx.doi.org/10.15666/aeer/1704_1019510205

seen upon examining the table that the emitter uniformity coefficients displayed increasing or decreasing changes. Whereas an increase was observed in emitters A, B and C subject to an increase in pressure, the converse was true for the emitter D. Tekin et al. (2016) carried out a study in which the emitter uniformity coefficient decreased at all pressures applied, only the results for emitter D were in accordance while the contrary was observed for all other emitters and the acquired results were not in accordance with the findings of other researchers. This is due to the fact that different brand laterals and emitters have been used.

Table 8. *Emitter Uniformity, EU*

Pressure (m)	EU_{cal} and classification values							
	A (local)		B (local)		C (foreign)		D (foreign)	
5	85.49	*G*	94.53	*VG*	95.64	*VG*	98.27	*VG*
10	91.86	*G*	95.46	*VG*	98.11	*VG*	97.82	*VG*
15	92.69	*G*	96.50	*VG*	96.93	*VG*	97.87	*VG*
20	93.23	*G*	97.93	*VG*	98.39	*VG*	97.37	*VG*

While emitter A was below the value of 94% for all applied pressures and took on the classification of "good", the other emitters were classified as "very good". The lowest emitter uniformity coefficient was determined as 85.49 for emitter A under a pressure load of 5 m, while the highest value was determined as 98.39 for emitter C under a pressure load of 20 m. Emitter uniformity coefficients were classified as "good" and "very good" for emitter A as was the case according to the findings of Özekici and Bozkurt (1996), the other emitters remained above 94% and were classified as "very good" in accordance with the results of studies by Çamoğlu and Yavuz (2004), Tekin et al. (2016). Uygan and Çetin (2015) carried out a study in which the emitter uniformity coefficient varied between 80-99% in plants using the emitter system in the Eskişehir-Sakarya region.

Irrigation water uniform distribution coefficient (CU)

The compliance of the irrigation water uniform distribution coefficients of emitters were calculated using *Eq.4* and evaluated according to ASAE (1994) and given in *Table 9.* While all coefficients obtained in the study were classified as "very good", only emitter A took on the "good" classification under a pressure load of 5 m. In general, Cu values increased with increasing pressure for emitters A, B and C, while all values were similar for emitter D under all pressure values. Çamoğlu and Yavuz (2004) determined the average CU value as 97.41, while Tekin et al. (2016) determined the average CU value as 97.20% and classified it as "very good". Based on these results, they concluded that the operating pressure value has an impact on the uniformity coefficient.

Statistical uniformity (Us)

The compliance of statistical uniformity coefficient values for the emitters was calculated using *Eq.5* and evaluated subject to ASAE (1994) and the acquired Us coefficients are given in *Table 10.* As can be seen when the table is examined that the lowest statistical uniformity coefficient was obtained as 5 m for emitter A under a pressure load of as 86.73, while the highest value was obtained as 98.66 for emitter C

http://www.aloki.hu ● ISSN 1589 1623 (Print) ● ISSN 1785 0037 (Online)
DOI: http://dx.doi.org/10.15666/aeer/1704_1019510205

under a pressure load of 20 m. In this case, the statistical uniformity classification values varied between "good" and "very good". In general, the Us values were determined to be under 94% only for emitter A under pressure loads of 5-10 and 20 m, while the average Us value was determined as above 94% and was classified as "very good". Çamoğlu and Yavuz (2004) carried out a study in which this value was determined as 97.11%, while Tekin et al. (2016) determined it as 96.49.

Table 9. *Irrigation Water Uniform Distribution Coefficients (CU)*

Pressure (m)	Coefficient of irrigation water distrubution uniformity (CU), %, and classification values							
	A (local)		B (local)		C (foreign)		D (foreign)	
5	89.41	*G*	95.47	*VG*	97.02	*VG*	98.89	*VG*
10	93.25	*VG*	97.34	*VG*	98.57	*VG*	98.75	*VG*
15	95.53	*VG*	97.90	*VG*	98.00	*VG*	98.49	*VG*
20	95.08	*VG*	98.71	*VG*	98.93	*VG*	98.21	*VG*

Table 10. *Coefficients of Statistical Uniformity (Us)*

Pressure (m)	Us (%) classification values							
	A (local)		B (local)		C (foreign)		D (foreign)	
5	86.73	*G*	94.32	*G*	96.26	*VG*	98.61	*VG*
10	91.54	*G*	96.67	*VG*	98.20	*VG*	98.43	*VG*
15	94.40	*G*	97.36	*VG*	97.50	*VG*	98.11	*VG*
20	93.84	*G*	98.38	*VG*	98.66	*VG*	97.75	*VG*

Selvaperumal et al. (2019) conducted a study in India on drip irrigation system in order to determine manufacturing variety coefficient (CV), uniformity coefficient (UC) and statistical uniformity (US) with the soil moisture distribution. Researchers declared that the coefficient of variation (CV) was obtained 0.0207 percent at a constant pressure of 50.66 kPa, statistical uniformity (US) as 97 percent and coefficient of uniformity (CU) as 0.9518. While US and CU values were consistent with our findings, CV values were found to be very low.

Conclusion

The fact that this study is conducted for the first time in the region is important in terms of guiding the future studies on this subject. The fact that this study is conducted for the first time in the region is important in terms of guiding the future studies on this subject. Beneficiaries who will benefit from the study outputs will be able to make more conscious choice in system planning, installation and dripper selection and thus contribute to the protection of water resources. It is expected from the drip irrigation system to provide the required performance, to be operated profitably and to provide the sufficient amount of water to the plant under optimum conditions with the best system hydraulic and flow parameters. Lowest values of the manufacturing variety coefficients which are among the most important factors that make up the system parameters lead to low flow rate variations between emitters and the ability to provide sufficient water to the plant root region. High values of Emitter Uniformity (EU), Cristiansen Uniformity Coefficient (CU) and statistical uniformity coefficients (Us) for all emitters increases the success of irrigation while also resulting in a uniform plant development and

http://www.aloki.hu ● ISSN 1589 1623 (Print) ● ISSN 1785 0037 (Online)
DOI: http://dx.doi.org/10.15666/aeer/1704_1019510205

optimum increase in yield. Due to the aforementioned reasons, all factors with adverse impacts on hydraulic performance should be eliminated when setting up the drip irrigation system and the system should be operated efficiently based on the principle of efficacy.

Acknowledgements. This study was carried out at the Siirt University, Biosystems Engineering Department Irrigation Laboratory in Siirt/TURKEY, using a test table manufactured under the scope of the 2017-SIUZIR-53 Research Project supported by Siirt University Scientific Research Project Office.

REFERENCES

[1] Altın, F. (2009): The Effect of Dripper Manufacturing Differences on System Design. – Ege Uni. Graduate School of Natural and Applied Science. Department of Agriculture Structure and Irrigation. M.Sc Thesis. p:84. (in Turkish).
[2] Anonymous (2004): Agricultural Irrigation Methods. – Ministry of Agriculture and Rural Affairs, Publication Department, Farmer Training Series 7. (in Turkish).
[3] ASAE (1994): Design and Installation of Microirrigation Systems. – ASAE EP405.1 Dec.93: 724-727.
[4] ASAE (2002): Design and Installation of Microirrigation Systems. – ASAE EP405.1 Dec.01: 903-907.
[5] Baştuğ, R., Uzun, İ., Hakgören, F. (1998): Effects of different irrigation methods on yield, quality and water usage in vines in Antalya conditions. – Akdeniz University, Journal of Agriculture Faculty 11(1): 81-89. (in Turkish).
[6] Bozkurt, S. (1996): The Effects of Manufacturing Differences on the Equal Distribution of in-line Drippers. – Çukurova Uni. Institute of Natural and Applied Science. Department of Agriculture Structure and Irrigation. M.Sc Thesis. p:116. (in Turkish).
[7] Bralts, V. F., Kesner, C. D. (1983): Drip Irrigation Field Uniformity Estimation. – Transactions of the ASAE.26(5): 1369-1374.
[8] Bralts, V. F. (1986): Operational Principles-Field Performance and Evaluation. – In: Nakayama, F. S., Bucks, D. A. (eds.) Trickle Irrigation for Crop Production. Elsevier Science Publisher, B. V. The Netherlands: 216-223.
[9] Bralts, V., Edwards, D. M., Wu, I. P. (1987): Drip Irrigation Design and Evaluation Based on the Statistical Uniformity Concept. – Advances in Irrigation 4: 72.
[10] Christiansen, J. E. (1942): Hydraulic of Springling Systems for Irrigation. – Trans. ASCE 107: 221-239.
[11] Çamoğlu, G., Yavuz, M. Y. (2004): Comparison of domestic and foreign production drippers in terms of irrigation performance. – Uludağ Uni. Journal of Agricultural Faculty 18(1):181-191. (in Turkish).
[12] Çiçek, Y. (2015): Investigation of Water Dispersion Smoothness in Drip Irrigation Systems Used in Olive Trees around İzmir. – Selçuk Uni. Graduate School of Natural Scıences, Department of Agriculture Structure and Irrigation. M.Sc Thesis. p:54. (in Turkish).
[13] Demir, V., Yürdem, H. (2000): Technical Characteristics and Manufacturing Differences of drippers with different production features produced and widely used in Turkey. – Ege Uni. Journal of Agriculture Faculty 37(2): 85-92. (in Turkish).
[14] Elamin, A. W. M., Abd Eldaiam, A. M., Abdalla, N. A., Hussain, M. E. (2017): Hydraulic performance of drip irrigation system under different emitter types, and operating pressures using treated wastewater at Khartoum state. – International Journal of Development and Sustainability 6(9): 1086-1095.
[15] Karaca, Y. (2008): Determination of Extension Distance of Circular Section Tubes of Drip Irrigation according to Different Dripper Range. – Namık Kemal Uni. Institute of

http://www.aloki.hu ● ISSN 1589 1623 (Print) ● ISSN 1785 0037 (Online)
DOI: http://dx.doi.org/10.15666/aeer/1704_1019510205

Natural and Applied Science. Department of Agricultural Structure and Irrigation. M.Sc Thesis, p: 64, Tekirdağ.

[16] Keller, J., Karmeli, D. (1974): Trickle Irrigation Design Parameters. – Trans of the ASAE 17(4): 678-684.

[17] Kırnak, H., Doğan, E., Demir, S., Yalçın, S. (2004): Determination of Hyraulic Performance of Trickle Irrigation Emitters Used in Irrigation Systems in the Harran Plain. – Tr. J. of Agr. and For. 28: 223-230.

[18] Korukçu, A. (1980): A Research on Determination of Side Pipe Lengths in Drip Irrigation. – Ankara Uni. Ankara Uni. Publications 742, p:75 Ankara. (in Turkish).

[19] Mohammed, M. M. Z. (2018): Evaluation of Drip Irrigation Method Used for Irrigation of Cherry Gardens in Konya-Akşehir District. – Selçuk Uni. Graduate School of Natural Scıences, Department of Agriculture Structure and Irrigation. M.Sc Thesis. p: 44. (in Turkish).

[20] Özekici, B., Sneed, R. E. (1995): Manufacturing Various Trickle Irrigation On-Line Emitters. – ASAE 0883-8542: 1102-0235.

[21] Özekici, B., Bozkurt, S. (1996): Determination of Hydraulic Performance of in-line Drippers. – Tr. J. of Agriculture and Forestry 23(1): 19-24.

[22] Selvaperumal, A., Sujitha, E., Muthuchami, I. (2019): Evaluation of uniformity Coefficient and Soil Moisture Distrubution under Drip Irrigation System. – Current Journal of Applied Science and Technology 34(5): 1-9. Article no.CJAST.48187, ISSN:2457-1024 (Past name: British Journal of Applied Science&Technology, Past ISSN:2231-0843, NLM ID:10166454).

[23] Solomon, K. (1979): Variability of Sprinkler Coefficient of Uniformity Test Results. – Transactions of the ASAE 22: 1078-1086.

[24] Tekin, S., Boyacı, S., Sezen, S. M., Gönen, E., Soylu, E., Soyugüzel, E., Özge, Z., Ketenci, A. M., Üstün, Y. (2016): Evaluation of Hydraulic Properties of Drip Irrigation Drippers which are Commonly Used in Kahramanmaraş Region. – KSU J. Nat. Sci. 19(4): 445-453. 2016, Research article. (in Turkish).

[25] Tüzel, H. (1990): A Study on Some Technical Properties and Project Criteria of Domestic Drip and Low Pressure Sprinkler Systems. – Ege Uni. Graduate School of Natural and Applied Science. Department of Agriculture Structure and Irrigation. Ph.D Thesis. p: 95. (in Turkish).

[26] Tüzel, H. (1993): Evaluation of Irrigation Uniformity in Drip Irrigation Systems. – Ege Univ. Journal of Agriculture Faculty 30: 119-126. (in Turkish).

[27] Uygan, D., Çetin, Ö. (2015): Evaluation of performance indicators in some drip irrigation systems installed in Eskişehir and Sakarya Provinces-Drip irrigation performance indicators. – Journal of Soil & Water 4(1): 27-35. (in Turkish).

[28] Üğlü, G., Tanrıverdi, Ç. (2013): Hydrolic Performance Analysis of in-line Drippers. – Agriculture for Life, Life for Agriculture, 5-8 June, 2013, Bucharest.

[29] Ünal, Y. (2011): Determination of Optimum Lateral Lengths of Some Drip Irrigation Pipes in Domestic Production. – Selçuk Uni. Graduate School of Natural Scıences, Department of Agriculture Structure and Irrigation. M.Sc Thesis. p: 55. (in Turkish).

[30] Wu, I. P., Gittlin, H. M. (1974): Drip Irrigation Design Based on Uniformity. – Transactions of the ASAE 17(3): 157-168.

[31] Wu, I. P., Howell, T. A., Hiler, E. A. (1979): Hydraulic Design of Drip Irrigation Systems. – Hawai Agricultural Experiment Station, University of Hawaii, Technical Bulletin No.105.

[32] Yeeshu, K. D., Verma, V. P., Sinha, J. (LM-10161), Verma, P. D. (2014): Hydraulic Performance of Drip Irrigation System under Different Operating Pressures. – Agricultural Engineering Today 38(3): 20-23. Print ISSN: 0970-2962. Online ISSN: 2230-7265.

http://www.aloki.hu ● ISSN 1589 1623 (Print) ● ISSN 1785 0037 (Online)
DOI: http://dx.doi.org/10.15666/aeer/1704_1019510205

EFFICACY OF DIFFERENT SAMPLING METHODS IN PEST MONITORING OF DIRECT SEEDED RICE AT DIFFERENT GROWTH STAGES

DUMAN, M.[1*] – MUTLU, Ç.[2]

[1]*Diyarbakır Plant Protection Research Institute, 21100 Sur, Diyarbakir, Turkey*

[2]*Department of Plant Protection, Faculty of Agriculture, Harran University, Sanliurfa, Turkey*

[*]*Corresponding author*
email: cetinmutlu21@hotmail.com; phone: +90-414-318-1248; fax: +90-414-318-3274

(Received 17th Apr 2019; accepted 13th Jun 2019)

Abstract. This two-year study was aimed at determining the efficacy of different sampling methods in pest monitoring of direct seeded rice in southeastern Anatolia, Turkey. Four direct seeded rice fields were selected in Sanliurfa and Diyarbakir provinces and insect species were monitored at four different BBCH rice growth stages (i.e., 21-39, 41-49, 51-69 and 71-89) with two different sampling methods (D-Vac and sweep net). The highest density of insects belonging to Tipulidae family was observed at Biologische Bundesanstalt, Bundessortenamt and Chemical industry (BBCH) 21-39 growth stage the both years of the study. Similarly, the highest density of Phloeothripidae species was noted during BBCH 71-89 growth stage during 1st year and BBCH 21-39 growth stage during 2nd year of the study. Likewise, the highest density for Tettigonidae insects was recorded at BBCH 51-69 growth stage during both years. The greatest density of Acrididae family was recorded at BBCH 41-649 growth stage during both years of study. Overall, D-Vac sampling method trapped higher number of insects belonging to Tipulidae and Acrididae families, whereas sweep net method trapped higher number of insects belonging to Tettigonidae and Phloeothripidae families. It is concluded that D-Vac sampling method can be used for sampling Tipulidae and Acrididae insect species infesting rice in the future studies.
Keywords: *Tipulidae, Phloeothripidae, Tettigonidae, D-Vac, Turkey*

Introduction

Rice provides dietary and caloric supplies for half of the population of the world (Muthayya et al., 2014). Globally rice is cultivated on 167 million hectares of land with an annual production of 769 million tons and an average yield of 4601 kg ha^{-1}. In Turkey, rice is grown on 109 thousand hectares with an annual production of 900 thousand tones with an average yield of 8218 kg ha^{-1} (FAOSTAT, 2019). In the Southeastern Anatolia Region of Turkey, rice occupies 1965 hectares, producing 9 thousand tones with an average yield of 4580 kg ha^{-1} (TURKSTAT, 2016). Turkey is among the top five countries in terms of average rice yield (FAOSTAT, 2019), yet there exists a yield gap compared to developed countries of the world, i.e., Australia and the United States. Rice cultivation faces various limitations ranging from climate, soil type and fertility, water supply, irrigation, pest and disease problems in Turkey.

Rice farming is gaining popularity among Turkish farmers due to higher demands and government support policies to increase production for gaining self-sufficiency in rice production (Duman and Mutlu, 2011; Duman et al., 2013, 2014; Mutlu et al., 2016). The increasing rice cultivation has given rise to several problems such as insect, disease and weed' infestation, which hamper the quantity and quality of rice. Several studies have determined the beneficial and harmful insect fauna in rice cultivation areas of

http://www.aloki.hu ● ISSN 1589 1623 (Print) ● ISSN 1785 0037 (Online)
DOI: http://dx.doi.org/10.15666/aeer/1704_1020710220

Aegean, Black Sea and Marmara regions in Turkey (Uzunali, 1976; Teoman and Kavut, 1979; Yürüten et al., 1982).

Transplanted rice fields are considered as the most diverse agricultural systems on the planet (Horgan, 2017). The rice productivity depends upon the flood cycles in transplanted rice where periodic shifts are recorded from flooded to dry period during the crop cycle. These changes in flood cycles promote a rich diversity of flora and fauna in transplanted rice (Catling, 1992; Way and Heong, 1994; Settle et al., 1996; Horgan et al., 2017). Over 800 insects have been recorded to feed on rice; however, ~20 of these species are considered as damaging pests of rice crop (Castro, 1970; Pathak and Dyck, 1973; Kiritani, 1979; Pathak and Khan, 1994). The most damaging pest species of rice include stem borers, gall midge, defoliators and vectors such as leaf and plant hoppers that cause direct damages and transmit various diseases. These pest species incur heavy losses to rice crop and various management strategies are opted or devised to keep their level below economic threshold. China, the largest rice producer has developed enough genomic strategies, which keep the harmful pests below their threshold level, whereas rice producers in the rest of the rice producing countries are still dependent on conventional pest management strategies.

Turkey is among the countries where farmers are still dependent on conventional pest management strategies for rice crop. The pest management studies in rice are mostly concentrated on the identification of beneficial and harmful pest species. Most of these studies have been conducted in transplanted rice, whereas direct seeded rice has been less studied (Duman and Mutlu, 2011; Duman et al., 2013, 2014; Mutlu et al., 2016). Rice is sown through direct seeding method in southeastern Anatolia region and scanty information is available on the pests of direct seeded rice crop in the region. Moreover, no information is available regarding the pest species' infestation at different growth stages of direct seeded rice in southeastern Anatolia region. Various studies in transplanted rice crop has revealed that relatively small number of arthropod herbivores damage rice plants; however, most arthropods species are beneficial. Herbivores invade the rice fields as crop grows and a small number of these can become pests if not effectively regulated. The pest attack at early crop growth stage relatively less damaging and negligible yield losses happen (Rubia et al., 1996; Horgan et al., 2016) or in some cases early stage pest attack results in more yield compared to pest attack-free crop (Nik Mohammad Noor et al., 1995; Islam and Karim, 1997). However, the pest attack at later growth stages can be more damaging and could result in heavy economic losses (Horgan, 2017). Therefore, monitoring pest density at different growth stages is necessary for effective pest management in rice crop (Reissig et al., 1986).

Different sampling methods are used to monitor pest densities in different crops. The sweep net and D-Vac sampling methods are most frequently used for pest monitoring (Turnipseed, 1974; Reissig et al., 1986; Schotzko and O'Keeffe, 1989; Buffington and Redak, 1998). These sampling methods have differential efficacy for trapping different insect species. The selection of accurate sampling method could help in effective monitoring of insect species (Schotzko and O'Keeffe, 1989; Binns and Nyrop, 1992; Buffington and Redak, 1998) However, limited information is available on the efficacy of insect monitoring in rice crop at different growth stages.

Therefore, the current study was designed with three major objectives, i.e., i) identify the harmful pest species infesting direct seeded rice crop in different districts of southeastern Anatolia region, ii) infer the density of different harmful pest species at different growth stages of rice and iii) determine the efficacy of different sampling

http://www.aloki.hu ● ISSN 1589 1623 (Print) ● ISSN 1785 0037 (Online)
DOI: http://dx.doi.org/10.15666/aeer/1704_1020710220

methods in monitoring insect species at different growth stages of rice crop. It was hypothesized that sampling districts and growth stages will significantly differ for the density of harmful pest species. It was further hypothesized that different sampling methods will differ in their efficacy for monitoring/trapping different insect species. To test these hypotheses, survey studies were conducted during two consecutive years in four districts of southeastern Anatolia region, Turkey. The results of the study will help to devise effective management strategies for the harmful pest species in direct seeded rice and help to improve sampling methods for pest monitoring of rice crop.

Material and Methods

Study area

This survey study was conducted in three districts of Diyarbakir province (Ergani, Cinar and Hazro) and one district of Sanliurfa (Siverek) province during rice growing seasons of 2010 and 2011. One rice field was selected from each district and surveys were accomplished in these selected fields during both years of the study. The geographic location of each surveyed field and prevailing long-term climatic conditions are provided in *Table 1*. Rice is cultivated by direct seeding method in the region. The farmers use different herbicide to manage weed infestation. Penoxulam, Bispyribac-Sodium and Bentazone+MCPA herbicides are used at the initial stage of rice crop for weed management. Insecticides are generally not used to control insect pests of rice crop in southeastern Anatolia region of Turkey.

Table 1. *Geographic location and long-term average (1979-2013) weather attributes of surveyed fields in southeastern Anatolia region, Turkey*

Surveyed Field	Latitude °N	Longitude °E	Area (ha)	Altitude	Rainfall (mm)	Max T °C	Min T °C	Avg T °C	Sunshine Hours	Aridity Index
Siverek	37.710583	39.246194	10.5	630	490.43	27.66	9.55	21.07	6.32	0.39
Ergani	37.881462	39.720773	11.0	1057	658.84	26.74	7.48	18.28	6.81	0.52
Hazro	38.168675	40.741611	14.0	821	617.05	26.22	8.27	19.61	6.72	0.52
Cinar	37.794088	40.156301	12.0	766	503.46	28.03	8.78	20.82	7.25	0.38

Max = Maximum, Min = Minimum, Avg = Average, Aridity index is opted from Çetin et al. (2007)

Survey timing and methods

Rice is typically cultivated during the month of May in southeastern Anatolia region of Turkey. The exploratory surveys to collect the insect species infesting rice crop were conducted at four different growth stages of rice. The growth stages according to BBCH scale were; 21-39 (tillering and stem elongation), 41-49 (booting), 51-69 (inflorescence emergence and anthesis) and 71-89 (fruit development and ripening) (Lancashire et al., 1991; Meier, 1997). The surveys were started from mid-June and continued until maturity with a fortnight interval. Two different sampling methods were used to test their efficacy in collecting the insect species. For sweep net method, insects were collected by sweeping the standard sweep net (Yiğit et al., 2003) at four different locations of each field. Twenty-five nets were swept at each location within a field making 100 sweeps per field. Similarly, in the D-Vac method (Mutlu et al., 2008; Yılmaz and Karsavuran, 2009), insects were sucked from four different locations within

http://www.aloki.hu ● ISSN 1589 1623 (Print) ● ISSN 1785 0037 (Online)
DOI: http://dx.doi.org/10.15666/aeer/1704_1020710220

each sampled field. The insects were sucked for one minute with vacuum sucking. For the sake of uniformity, twenty-five suctions were made at each location within each field. The collected insect species from both sampling methods were put in transparent polyethylene bags, labeled and brought to the laboratory. The collected species were identified according to the earlier specimens in the region, whereas the unidentified specimens were sent to taxonomists for accurate identification. The grasshopper specimens were identified by Prof. Dr. Ali SATAR (Faculty of Science and Literature, Dicle University, Diyarbakir, Turkey). Similarly, thrips specimens were identified by Prof. Dr. İrfan TUNÇ (Department of Plant Protection, Faculty of Agriculture, Akdeniz University, Antalya, Turkey). Crane fly (*Tipula orientalis*) was identified by Prof. Dr. Hasan KOÇ (Department of Biology, Faculty of Sciences, Muğla Sıtkı Koçman University, Muğla, Turkey).

The polyethene bags were kept in deep freezer to kill the insect species collected during the survey. The insect species were then placed over white papers and carefully counted. The counted species were separated into two groups (i.e., beneficial and harmful insects), and data relating to harmful insect species were used in this manuscript. The identified harmful insect species were then grouped into different families. The density of the insect species was then counted at family level and used for the interpretation of the results. A total 13 harmful insect species belonging to 4 families, i.e., Tipulidae (1 species), Acrididae (8 species), Tettigonidae (2 species) and Phloeothripidae (2 species) were identified during the survey.

Statistical analyses

The collected data regarding the density of insect species in different families were tested for normality, which indicated a normal distribution. Therefore, the statistical analyses were performed on non-transformed, original data. A paired t test was used to infer the differences among years, which indicated significant differences. Therefore, the data of both study years were analyzed and interpreted separately. Three-way Analysis of variance (ANOVA) technique was used to infer the effect of different growth stages, sampling methods and surveyed fields on the density of insect species belonging to different families (Steel et al., 1997). Least significant difference test at 99% probability level was used as post-hoc test to separate the means where ANOVA indicated significance. ANOVA indicated that all individual and interactive effects of growth stage, sampling method and surveyed field were significant for all insect families. Therefore, three-way interactions, i.e., growth stage × sampling method × surveyed fields were used for the interpretation of the results. All statistical analyses were performed using SPSS Version 20.0 (IBM, 2012).

Results

A total of 2472 insects belonging to 4 families were collected during 2010, whereas 3104 insects belonging to the same families were collected during 2011. The highest percentage (45.28%) of the insects belonged to Tettigonidae family, whereas the lowest percentage (8.09%) of the collected insect species belonged to Acrididae family (*Figure 1*).

The identified insect species with their corresponding families are summarized in *Table 2*. Some of the identified insect species are shown in *Figure 2*.

http://www.aloki.hu ● ISSN 1589 1623 (Print) ● ISSN 1785 0037 (Online)
DOI: http://dx.doi.org/10.15666/aeer/1704_1020710220

The individual and interactive effects of growth stage, sampling methods and surveyed fields significantly influenced the density of Tipulidae insect species during both years of the study, with an exception of non-significant effect of sampling methods × surveyed fields during 2011 (*Table 3*).

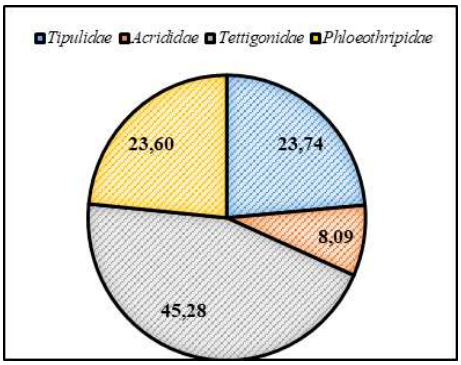

Figure 1. *The percentage of different harmful insect species belonging to various families collected from rice fields in southeastern Anatolia region, Turkey during 2010 and 2011*

Table 2. *Harmful insect species identified in different rice fields surveyed in southeastern Anatolia region, Turkey during 2010 and 2011*

Order	Family	Species
Diptera	Tipulidae	*Tipula orientalis* Lackschewitz
Orthoptera	Acrididae	*Aiolopus strepens* (Latr.)
Orthoptera	Acrididae	*Platycleis escalerai* Bolívar
Orthoptera	Acrididae	*Heteracris pterosticha* (Fischer von Waldheim)
Orthoptera	Acrididae	*Thisoicetrinus pterostichus* (Fischer de Waldheim)
Orthoptera	Acrididae	*Calliptamus barbarus* Fisher-Waldheim
Orthoptera	Acrididae	*Euprepocnemis plorans* Charp.
Orthoptera	Acrididae	*Oedipoda aurea Uvarov*
Orthoptera	Acrididae	*Aiolopus strepens* (Latreille)
Orthoptera	Tettigonidae	*Isophya sp.*
Orthoptera	Tettigonidae	*Conocephalus fuscus* (Fabricius)
Thysanoptera	Phloeothripidae	*Haplothrips aculeatus* (Fabr.)
Thysanoptera	Phloeothripidae	*Haplothrips reuteri* (Karny)

Figure 2. *Different hamrful insect species, (a) Conocephalus fuscus Fabricius (Tettigoniidae), (b) Thisoicetrinus pterostichus F.W. (Catantopidae) and (c) Tipula orientalis Lackschewitz identified from rice fields in southeastern Anatolia region, Turkey during 2010 and 2011*

The highest density of Tipulidae insect species during 2010 was recorded at BBCH 21-39 growth stage in Siverek field with D-Vac sampling method, whereas the lowest density was noted at BBCH 51-69 and BBCH 71-89 growth stages in Hazro and Cinar fields with D-Vac sampling method (*Table 4*). Similarly, D-Vac sampling method

http://www.aloki.hu ● ISSN 1589 1623 (Print) ● ISSN 1785 0037 (Online)
DOI: http://dx.doi.org/10.15666/aeer/1704_1020710220

collected the highest number of Tipulidae insect species at BBCH 21-39 growth stage from Cinar field during 2011, while the lowest number of insects were trapped by sweep net sampling method from Cinar field at BBCH 41-49 growth stage of rice (*Table 4*). Overall, D-Vac sampling method trapped higher number of Tipulidae insect species compared with sweep net sampling method during both years of the study. Siverek field had the higher density of Tipulidae insect species during both years of the study compared to the rest of the sampling fields (*Table 4*).

Table 3. *Three-way Analysis of variance of different growth stages, sampling methods, surveyed fields and their interaction for the number of individuals trapped belonging to different insect families*

2010									
Source of Variation		**Tipulidae**		**Phloeothripidae**		**Tettigonidae**		**Acrididae**	
	df	**F Value**	**P Value**	**F Value**	**P Value**	**F Value**	**P Value**	**F Value**	**P Value**
Growth Stage (G)	3	790.62	0.0001*	161.41	0.0001*	331.91	0.0001*	369.33	0.0001*
Sampling Method (M)	1	741.23	0.0001*	738.44	0.0001*	82.39	0.0001*	4.17	0.0452^{NS}
Surveyed Field (F)	3	1502.22	0.0001*	1636.76	0.0001*	721.70	0.0001*	251.75	0.0001*
G × M	3	254.46	0.0001*	434.20	0.0001*	36.80	0.0001*	58.15	0.0001*
G × F	9	277.14	0.0001*	184.07	0.0001*	59.52	0.0001*	117.51	0.0001*
M × F	3	55.14	0.0001*	78.26	0.0001*	7.17	0.0003*	39.51	0.0001*
G × M × F	9	121.17	0.0001*	166.06	0.0001*	52.76	0.0001*	53.30	0.0001*
2011									
Growth Stage (G)	3	9050.79	0.0001*	1179.58	0.0001*	8379.90	0.0001*	844.30	0.0001*
Sampling Method (M)	1	1635.57	0.0001*	2.50	0.12^{NS}	426.02	0.0001*	217.27	0.0001*
Surveyed Field (F)	3	39.21	0.0001*	12.78	0.0001*	13.49	0.0001*	2.36	0.08^{NS}
G × M	3	992.07	0.0001*	939.62	0.0001*	1243.95	0.0001*	740.73	0.0001*
G × F	9	22.00	0.0001*	8.22	0.0001*	21.36	0.0001*	2.57	0.01*
M × F	3	0.55	0.65^{NS}	8.05	0.0001*	5.90	0.0001*	5.31	0.0001*
G × M × F	9	23.33	0.0001*	5.70	0.0001*	10.47	0.0001*	4.89	0.0001*

df = degree of freedom, * = significant at P ≤ 0.01, NS = non-significant

Table 4. *Total number of individuals belonging to Tipulidae family trapped by two different sampling methods at different growth stages of rice from southeastern Anatolia region, Turkey during 2010 and 2011*

2010								
Growth stage	**D-Vac**				**Sweep net**			
	Siverek	**Ergani**	**Hazro**	**Çinar**	**Siverek**	**Ergani**	**Hazro**	**Çinar**
BBCH 21-39	76.33 a	16.00 ijk	15.00 jk	9.00 no	50.00 c	32.33 e	19.00 gh	12.00 lm
BBCH 41-49	8.00 no	30.00 e	5.00 pq	5.00 pq	41.33 d	60.33 b	21.00 g	9.00 no
BBCH 51-69	10.67 mn	12.00 lm	1.00 r	1.00 r	47.67 c	24.00 f	1.00 r	14.00 kl
BBCH 71-89	18.00 hi	7.00 op	1.00 r	1.00 r	17.00 hi	10.33 mn	1.00 r	2.33 qr
LSD 0.01	**2.68**							
2011								
BBCH 21-39	79.00 a	69.67 b	65.00 c	66.67 c	44.00 d	36.33 f	41.00 e	40.33 e
BBCH 41-49	10.00 lm	10.00 lm	9.00 m	10.00 lm	10.00 lm	9.00 m	9.00 m	6.00 n
BBCH 51-69	19.00 gh	15.00 i	19.00 gh	14.00 jk	14.00 jk	14.00 jk	11.00 l	13.00 k
BBCH 71-89	15.00 i	20.00 g	19.00 gh	19.00 gh	19.00 gh	18.00 h	16.00 i	16.00 i
LSD 0.01	**1.76**							

Means sharing the same letters within a column or a row are statistically similar (P > 0.01)

The density of insect species belonging to Phloeothripidae family was significantly altered by the individual and interactive effects of growth stage, sampling methods and surveyed fields, with only a non-significant effect of sampling methods 2011 (*Table 3*).

http://www.aloki.hu ● ISSN 1589 1623 (Print) ● ISSN 1785 0037 (Online)
DOI: http://dx.doi.org/10.15666/aeer/1704_1020710220

The highest and the lowest number of Phloeothripidae insect species were trapped by sweep net sampling method at BBCH 71-89 growth stage from Cinar and Siverek fields, respectively during 2010 (*Table 5*). However, the highest number of insect species belonging to Phloeothripidae family were trapped by D-Vac sampling method at BBCH 21-39 growth stage from Ergani field and by sweep net sampling method at BBCH 51-69 growth stage from Siverek field during 2011. The lowest number of Phloeothripidae insect species during 2011 were collected by sweep net sampling method at BBCH 71-89 growth stage from all the sampling fields included in the study (*Table 5*). The sweep net sampling method exhibited higher efficacy in trapping Phloeothripidae insect species during the first year, while both sampling method indicated similar performance during the second year of the study (*Table 5*).

Table 5. *Total number of individuals belonging to Phloeothripidae family trapped by two different sampling methods at different growth stages of rice from southeastern Anatolia region, Turkey during 2010 and 2011*

2010								
Growth stage	**D-Vac**				**Sweepnet**			
	Siverek	**Ergani**	**Hazro**	**Çinar**	**Siverek**	**Ergani**	**Hazro**	**Çinar**
BBCH 21-39	33.00 gh	17.67 mn	23.00 i	36.00 ef	15.00 op	21.00 jk	35.00 fg	24.00 i
BBCH 41-49	20.33 kl	14.00 p	16.33 no	25.00 i	19.00 klm	31.67 h	49.00 b	52.33 a
BBCH 51-69	10.00 q	7.00 rs	19.00 klm	38.00 de	35.00 fg	21.00 jk	34.00 fg	41.00 c
BBCH 71-89	5.00 st	3.00 tu	35.00 fg	39.67 cd	1.00 u	8.00 qr	18.33 lmn	52.67a
LSD 0.01	**2.13**							
2011								
BBCH 21-39	32.33 ab	34.00 a	32.00 ab	29.00 cd	12.67 i	14.00 hi	14.00 hi	13.00 hi
BBCH 41-49	22.00 e	21.00 ef	14.00 hi	14.00 hi	19.00 fg	15.00 h	18.00 g	15.00 h
BBCH 51-69	10.00 k	9.00 k	11.00 jk	10.00 k	34.00 a	28.00 d	30.33 bc	31.00 bc
BBCH 71-89	4.33 l	4.00 l	4.00 l	4.00 l	1.00 m	1.00 m	1.00 m	1.00 m
LSD 0.01	**2.10**							

Means sharing the same letters within a column or a row are statistically similar (P > 0.01)

All individual and interactive effects growth stage, sampling methods and surveyed fields significantly affected the density of insect species belonging to Tettigonidae family during both years of study (*Table 3*). The highest density of insect species belonging to Tettigonidae family was observed at BBCH 51-69 growth stage from Siverek field during both years of the study (*Table 6*). The sweep net sampling method collected the highest number of Tettigonidae insect species from Siverek field at BBCH 51-69 growth stage during both survey years. Similarly, the lowest number of insect species belonging to Tettigonidae family were trapped from Ergani field by both sampling methods at BBCH 71-89 growth stage during 2010. However, the lowest number of Tettigonidae insect species were trapped by D-Vac sampling method from Siverek field at BBCH 71-89 growth stage during 2011 (*Table 6*).

The density of Acrididae insect species belonging to family was significantly altered by all individual and interactive effects of growth stage, sampling methods and surveyed fields during both study years except non-significant effects of sampling methods during 2010 and surveyed fields during 2011 (*Table 3*). The highest number of Acrididae insect species were recorded at BBCH 41-49 growth stage of rice during both years of the study (*Table 7*). The D-Vac sampling method from Siverek field and sweep net sampling method from Cinar field collected the highest number of insects belonging to Acrididae family at BBCH 41-49 growth stage during first year of the study

http://www.aloki.hu ● ISSN 1589 1623 (Print) ● ISSN 1785 0037 (Online)
DOI: http://dx.doi.org/10.15666/aeer/1704_1020710220

(*Table 7*). The lowest number of Acrididae insect species were trapped by D-Vac sampling method from Siverek field at BBCH 21-39 growth stage during 2010 (*Table 7*). During the second year, D-Vac sampling method trapped the highest number of Acrididae insect species at BBCH 41-49 growth stage from Siverek and Cinar fields, whereas the lowest number of Acrididae species were collected by D-Vac sampling method at BBCH 71-89 growth stage from all sampling fields (*Table 7*).

Table 6. *Total number of individuals belonging to Tettigonidae family trapped by two different sampling methods at different growth stages of rice from southeastern Anatolia region, Turkey during 2010 and 2011*

2010								
Growth stage	**D-Vac**				**Sweepnet**			
	Siverek	**Ergani**	**Hazro**	**Çinar**	**Siverek**	**Ergani**	**Hazro**	**Çinar**
BBCH 21-39	60.33 c	14.00 jkl	20.00 h	10.00 l-o	39.67 ef	11.00 k-m	14.00 jkl	30.67 g
BBCH 41-49	59.67 c	21.00 hi	25.00 h	19.33 i	68.67 b	31.00 ge	44.00 de	48.33 d
BBCH 51-69	65.00 bc	6.67 no	12.33 klm	36.00 fg	99.67 a	8.00 mno	38.33 f	10.00 l-o
BBCH 71-89	11.67 k-m	0.83 p	12.00 ijk	16.00 g	30.67 g	1.00 p	5.00 op	10.33 l-o
LSD 0.01	**5.52**							
2011								
BBCH 21-39	56.00 h	52.33 i	56.33 h	60.33 g	38.33 k	29.00 m	33.00 l	31.00 lm
BBCH 41-49	60.33 g	60.33 g	55.67 h	50.00 j	68.00 e	65.00 f	60.33 g	65.00 f
BBCH 51-69	73.00 d	76.33 c	70.00 e	73.00 d	95.00 a	96.67 a	92.00 b	92.33 b
BBCH 71-89	9.00 o	12.67 n	13.00 n	12.00 n	29.00 m	31.00 lm	30.00 m	30.00 m
LSD 0.01	**2.30**							

Means sharing the same letters within a column or a row are statistically similar (P > 0.01)

Table 7. *Total number of individuals belonging to Acrididae family trapped by two different sampling methods at different growth stages of rice from southeastern Anatolia region, Turkey during 2010 and 2011*

2010								
Growth stage	**D-Vac**				**Sweepnet**			
	Siverek	**Ergani**	**Hazro**	**Çinar**	**Siverek**	**Ergani**	**Hazro**	**Çinar**
BBCH 21-39	1.00 n	1.67 mn	8.00 g	13.67 cd	4.00 jk	3.33 j-m	8.00 g	6.00 hi
BBCH 41-49	26.00 a	3.00 klm	15.33 c	23.67 b	7.00 gh	5.00 i	10.00 f	27.00 a
BBCH 51-69	10.00 f	2.00 lmn	2.00 lmn	11.00 ef	12.00 de	3.33 j-m	5.00 i	5.00 i
BBCH 71-89	2.00 lmn	5.00 i	3.00 klm	7.00 gh	3.67 jkl	14.00 c	2.67 k-m	11.00 ef
LSD 0.01	**1.79**							
2011								
BBCH 21-39	0.10 h	0.10 h	0.10 h	0.20 h	4.00 g	4.00 g	4.33 g	4.00 g
BBCH 41-49	24.00 a	21.00 b	21.00 b	23.33 a	4.00 g	5.00 g	3.67 g	5.00 g
BBCH 51-69	11.00 c	11.00 c	8.00 ef	9.00 de	10.33 cd	7.00 f	11.00 c	9.00 de
BBCH 71-89	1.00 h	1.00 h	1.00 h	1.00 h	4.00 g	4.00 g	5.00 g	4.00 g
LSD 0.01	**1.50**							

Means sharing the same letters within a column or a row are statistically similar (P> 0.01)

Discussion

The current study identified harmful insect species infesting direct seeded rice crop at different growth stages, which will provide valuable insights for the management of these species. A total of 13 species belonging to 4 families were identified, which are regarded as pests of different cultivated crops in earlier studies conducted by different researchers in Turkey. *Thisoicetrinus pteroschus* (Fischer de Waldheim) has been reported to cause significant damage to vegetables, tobacco and paddy fields in

http://www.aloki.hu ● ISSN 1589 1623 (Print) ● ISSN 1785 0037 (Online)
DOI: http://dx.doi.org/10.15666/aeer/1704_1020710220

Diyarbakir and its vicinity between 1960 and 1961 (Balamir, 1962). Similarly, *Euprepocnemis plorans* (Charpentier) is the most dangerous pest species of maize and cereals (Şimsek, 1988). *Platycleis escalerai* Bolívar, *Calliptamus barbarus* Fisher-Waldheim and *Aiolopus strepens* (Latr.) have been reported as harmful pests in numerous crops (Karabağ et al., 1971; Karabağ, 1975; Çıplak et al., 1991, 1996). Different studies have reported that different orthopteran species, i.e, *Gryllo gryllotalpa* (L.), *T. pterostichus*, *Locusta migratoria migratorioides* (R. & F.) and *Conocephalus discolor* (Thunberg) are noxious pests of rice crop (Alkan, 1948; Balamir, 1962; Uzunali, 1976; Serel, 1978). The identified insect species in the current study infest rice crop at different growth stages. Therefore, management strategies/efforts should be opted according to the infestation time of harmful insect species.

Different growth stages of rice crop, sampling methods and surveyed rice fields significantly differed for insect infestation. It is known that the life cycle of many insect pest species is closely linked with the development of the rice plant (Reissig et al., 1986) and the differences in the insect density at different growth stages of rice crop are owed to the feeding preference, life form and damaging habit of the insect species (Reissig et al., 1986; Pathak and Khan, 1994). Similarly, the differences among different surveyed fields are thought to be the result of micro environmental conditions (*Table 1*), weed infestation and site-specific management practices opted by the farmers (Reissig et al., 1986; Pathak and Khan, 1994). Likewise, the differences in the efficacy of different sampling methods for trapping insect species can be explained with the size, weight and life stage of the insect species (Reissig et al., 1986). The D-Vac sampling method usually sucks the insect which are smaller sized, lighter in weight and at the most mobile stage, whereas the sweep net method traps heavier insects, relatively less mobile and bigger in size (Turnipseed, 1974; Kogan and Herzog, 2012). Therefore, the selection of sampling methods should be based on the target insect species and growth stage of the crop.

Crane fly (Tipulidae) species infested the rice crop during early growth season, i.e., BBCH 21-39 growth stage during both years of the study. The highest density of crane fly species at early growth stage is directly linked to their damage caused to the rice crop. The larvae of crane fly species feed on pastures and spring cereals, roots and young seedlings of rice crop (Rao et al., 2006; Duman et al., 2014). The larval movement below soil uproots the emerging rice seedling leading to plant mortality (Duman et al., 2014). Therefore, the highest density of crane fly species at initial growth stage can be linked with the damaging habit, life cycle and growth stage of the species. The identified crane fly species (*Tipula orientalis*) is a widespread cosmopolitan species frequently found near streams and in cultivated wheat and rice fields (Duman et al., 2014). Rice is cultivated through direct seeding method in southeastern Anatolia region, and the irrigation applied to direct-seeded rice creates favorable environment for the development of *T. orientalis* larvae. Thus, sowing method of rice in the region is another reason of higher density of crane fly. The lowest density of crane fly species at later growth stages of rice crop can be explained with the life cycle of the pest. The pest completes its life cycle and switches to diapause at later growth stages of rice due to which the lowest number of insects were trapped at BBCH 71-89 growth stage of rice crop. Xingquan et al. (1993) stated that cold swamps and meadows are the primary habitats of *Tipula* sp and the larva of the species cause highest damage at the end of

http://www.aloki.hu ● ISSN 1589 1623 (Print) ● ISSN 1785 0037 (Online)
DOI: http://dx.doi.org/10.15666/aeer/1704_1020710220

May. The current results of the highest density of Tipulidae species at initial growth stage of rice crop are like the findings of Qian (1982) and Xingquan et al. (1993).

Thrips species had the highest infestation at different growth stages of rice crop in 1st and 2nd year of the study. The highest density was recorded at maturity (BBCH 71-89) during 1st year of the study, whereas the highest density was noted at BBCH 21-39 during 2nd year. The reasons for the differences in the density of thrips species at different growth stages in different years can be explained by the prevailing climatic conditions and weeds' infestation at different growth stages of rice crop. The farmers of southeastern Anatolia region stop irrigation at BBCH 71-89 growth stage of rice whereas temperature is high compared to the rest of the growth stages. The increased temperature coupled with no irrigation decreases relative humidity, thus, creating favorable conditions for the population development of thrips species. Thrips outbreaks are frequently reported during dry periods in rice crop (Hsu et al., 1978; Pathak and Khan, 1994). It is well known that thrips species mostly live in flowers, but many species complete their life cycle on leaves (Ananthakrishnan, 1993; Trdan et al. 2005; Van Haperen et al., 2019). A few of thrips species are predatory and probably about half of thrips species feed on fungi (Palmer et al., 1989). The damage caused to plants by thrips through feeding or egg laying is often ascribed to other pest species. Two thrips species were detected in the current study and discoloration on the leaves was noted during seedling stage. Besides feeding damage was also recorded during heading stage of rice (Hsu et al., 1978). *Stenchaetothrips biformis* (Bagnall) and *Haplothrips aculeatus* (Fabricius) have been recorded throughout rice growth season; however, these species are more abundant during the seedling and flowering stages of rice in some Asia countries (Madhusudhan and Gopalan, 1989; Pathak and Khan, 1994). The population declines in early September and disappears by mid-September (Pathak and Khan, 1994). Like the results of the first year of the current study, thrips infestation is generally recorded during the first week of August, with peak infestation during the second and third weeks in India. Hsu et al. (1978) reported that *Baliothrips biformis* (Bagn.) infests rice crop at 3-4-leaf seedling and tillering stages, whereas *Frankliniella tenuicornis* (Uzel) and *Haplothrips aculeatus* (F.) at late head-bearing and heading stages. These findings support the observation of current study.

Grasshopper species (Tettigonidae and Acrididae) had the highest density at BBCH 41-49 and BBCH 51-69 growth stages of rice crop. These findings are line with the results of Serel (1978) reported that grasshoppers appear in rice crop during first week of July. These results indicated that grasshopper species infest rice crop during mid to late growth season. Due to this reason, rice farmers use insecticides to control grasshopper species during July. However, the farmers in southeastern Anatolia region do not use any control measures against grasshoppers in rice crop. The insecticides are occasionally used to control grasshoppers in the region once the densities of grasshopper species are high. The higher density of grasshopper species observed in the current study is because the selected rice fields were closer to overwintering/migration areas of grasshoppers. The results obtained in the current study are similar to the results of several earlier studies reporting the identified insect species as harmful pests of rice crop (Balamir, 1962; Karabağ et al., 1971; Karabağ, 1975; Serel, 1978; Memişoğlu et al., 1986; Şimşek, 1988; Çıplak and Demirsoy, 1991; Çıplak et al., 1996; Satar and Özbay, 2003).

http://www.aloki.hu ● ISSN 1589 1623 (Print) ● ISSN 1785 0037 (Online)
DOI: http://dx.doi.org/10.15666/aeer/1704_1020710220

Conclusion

The current study concludes that different insect species infest direct seeded rice crop at different growth stages in southeastern Anatolia region of Turkey; however, actual losses caused by these species are still unknown. The studies relating to the losses caused by the identified insect species in the region are needed. It is also concluded that the differences in density of the insect species at different growth stages and in different fields necessitate site-specific and growth stage-specific management practices for the identified insect species in the region. Moreover, different sampling methods can be used for trapping harmful insect species (based on their size, weight and growth stage etc.) at different growth stages of rice.

Acknowledgements. The authors express their sincere gratitude to Commission of General Directorate of Agricultural Researches and Policies (TAGEM) for funding this study under project number TAGEM-B10/07-04(01-02)-08. We would like to thank several rice farmers who allowed the authors to conduct this research in their cultivated fields. Authors also express sincere thanks to Mahsum DEMİR and Deniz ÇAPLIK for their assistance in field selection and technical support.

REFERENCES

[1] Alkan, B. (1948): Cereal Pests in Central Anatolia. – Ankara University Publication, Ankara. 132 pp.
[2] Ananthakrishnan, T. N. (1993): Bionomics of thrips. – Annual Review of Entomology 38(1): 71-92.
[3] Balamir, S. (1962): Türkiye'de Son Yıllarda Zararı Görülen Bir Çekirge Türü *Thisocertrinus pterostichus* F.W. – Plant Protection Bulletin 2(2): 3-10.
[4] Binns, M. R., Nyrop, J. P. (1992): Sampling insect populations for the purpose of IPM decision making. – Annual Review of Entomology 37(1): 427-453.
[5] Buffington, M. L., Redak, R. A. (1998): A comparison of vacuum sampling versus sweep netting for arthropod biodiversity measurements in California coastal sage scrub. – Journal of Insect Conservation 2(2): 99-106.
[6] Castro, D. C. (1970): Rice Production Manual. – Los Banos: University of Philippines/IRRI, University of Philippines/IRRI.
[7] Catling, D. (1992): Rice in Deep Water. – London: MacMillan Press Ltd.; 1992.
[8] Çetin, S. C., Karaca, A., Haktanır, K., Yildiz, H. (2007): Global attention to Turkey due to desertification. – Environmental Monitoring and Assessment 128(1-3): 489-493.
[9] Çıplak, B., Demirsoy, A. (1991): Arguvan (Malatya) ve Çevresinde Orthoptera (Ins.) Faunasının İncelenmesi. – Turkish Journal of Zoology 15: 98-114.
[10] Çıplak, B., Demirsoy, A., Bozcuk, A. N. (1996): Malatya ve civarı Caelifera (Orthoptera-Insecta) Faunası. – Turkish Journal of Zoology 20: 17-31.
[11] Duman, M., Mutlu, Ç. (2011): Determination of Harmful and Beneficial Insect in the Karacadağ Rice Variety Cultivated Area. – Proceedings of the Fourth Turkish National Congress of Entomology, 28-30 June 2011, Kahramanmaras, Turkey. 287p.
[12] Duman, M., Mutlu, Ç., Büyük, M., Karaca, V. (2013): Beneficial insects, spider and polinater species determined in the Karacadağ paddy growing areas. – Turkish Journal of Biological Control 4(1): 53-64.
[13] Duman, M., Mutlu, Ç., Büyük, M. (2014): A new pest in rice growing fields in Southeastern Anatolia: *Tipula orientalis* Laskschewitz (Diptera: Tipulidae). – Turkish Bulettin of Entomology 4(2): 67-77.
[14] FAOSTAT. (2019): The Food and Agriculture Organization, FAO. – http://www.fao.org/faostat/en/#home (Date accessed: 28.03.2019).

http://www.aloki.hu ● ISSN 1589 1623 (Print) ● ISSN 1785 0037 (Online)
DOI: http://dx.doi.org/10.15666/aeer/1704_1020710220

[15] Horgan, F. G., Crisol Martinez, E., Almazan, M. L. P., Romena, A., Ramal, A. F., Ferrater, J. B. (2016): Susceptibility and tolerance in hybrid and pure-line rice varieties to herbivore attack: biomass partitioning and resources-based compensation in response to damage. – Annals of Applied Biology 169: 200-213.
[16] Horgan, F. G. (2017): Insect Herbivores of Rice: Their Natural Regulation and Ecologically Based Management. – In Rice Production Worldwide pp. 279-302, Springer, Cham.
[17] Horgan, F. G., Ramal, A. F., Villegas, J. M., Almazan, M. L. P., Bernal, C. C., Jamoralin, A., Arroyo, C. (2017): Ecological engineering with high diversity vegetation patches enhances bird activity and ecosystem services in Philippine rice fields. – Regional Environmental Change 17(5): 1355-1367.
[18] Hsu, Z. Y., Li, J. D., Chang, C. H., Hu, Z. C. (1978): Studies on the thrips infesting rice in Jin-ping, Kweichow Province. – Acta Entomologica Sinica 21(1): 13-26.
[19] IBM. (2012): SPSS Statistics for Windows v. 20. – 1-8. Armonk, NY: IBM Corporation.
[20] Islam, Z., Karim, A. N. M. R. (1997): Whiteheads associated with stem borer infestation in modern rice varieties: an attempt to resolve the dilemma of yield losses. – Crop Protection 16: 303-311.
[21] Karabağ, T., Gümüşsuyu, İ., Balamir, S., Tutkun, E. (1971): Orthoptera Fauna of Turkey (II). – Plant Protection Bulletin 2(2): 73-100.
[22] Karabağ, T. (1975): Studies in the Turkish Orthoptera (Ins.) I New Species and Less Known *Tettigoniidae*. – Journal of Natural History 9: 337-350.
[23] Kiritani, K. (1979): Pest management in rice. – Annual Review of Entomology 24: 279-312.
[24] Kogan, M., Herzog, D. C. (2012): Sampling methods in soybean entomology. – Springer Science & Business Media. 596 pp.
[25] Lancashire, P. D., Bleiholder, H., Boom, T. V. D., Langeluddeke, P., Stauss, R., Weber, E., Witzenberger, A. A. (1991): Uniform decimal code for growth stages of crops and weeds. – Annals of Applied Biology 119: 561-601.
[26] Madhusudhan, V. V., Gopalan, M. (1989): Studies on the biology of rice thrips, *Stenchaetothrips biformis* (Bagnall) in India. – Tropical Pest Management 35: 394-396.
[27] Meier, U. (1997): Growth stages of mono-and dicotyledonous plants. – Federal Biological Research Centre for Agriculture and Forestry.
[28] Memişoğlu, H., Özkan, M., Melan, K. (1986): Faunistic Survey Studies in the Rice Fields in Central Anatolia. – Plant Protection Bulletin 26(3-4): 97-111.
[29] Muthayya, S., Sugimoto, J. D., Montgomery, S., Maberly, G. F. (2014): An overview of global rice production, supply, trade, and consumption. – Annals of the New york Academy of Sciences 1324(1): 7-14.
[30] Mutlu, Ç., Sertkaya, E., Güçlü, Ş. (2008): Determination of Cicadellidae (Homoptera) species in second crop maize and their distribution in Diyarbakır province of Turkey. – Turkish Journal of Entomology 32(4): 281-301.
[31] Mutlu, Ç., Duman, M., Karaca, V., Bayram,Y., Süer, İ. E. (2016): he species of Cicadellidae, Cixiidae and Delphacidae (Hemiptera) on Karacadag rice and the effects of weeds on their populations. – Turkish Bulletin of Entomology 6(4): 279-289.
[32] Nik Mohammad Noor, N. S., Chang, P. M. (1995): Rice leaffolder in Malaysia and implications of not controlling them. – International Rice Research Institute. Proceedings of the workshop on reducing early season insecticide use for leaffolder control in rice: impact, economics and risks, Los Baños, pp. 1-15.
[33] Palmer, J. M., Mound, L. A., du Heaume, G. J. (1989): CIE guides to insects of importance to man 2. – Thysanoptera. CAB Int, Wallingford, pp 73.
[34] Pathak, M. D., Dyck, V. A. (1973): Developing an integrated method of rice insect pest control. – PANS Pest Articles & News Summaries 19(4): 534-544.
[35] Pathak, M. D., Khan, Z. R. (1994): Insect Pests of Rice. – International Rice Research Institute, Los Baños.

http://www.aloki.hu ● ISSN 1589 1623 (Print) ● ISSN 1785 0037 (Online)
DOI: http://dx.doi.org/10.15666/aeer/1704_1020710220

[36] Qian, K. C. (1982): A preliminary study on the biology of *Tipula aino* Alexander. – Insect Knowledge 19(5): 9-11.
[37] Rao, S., Liston, A., Crampton, L., Takeyasu, J. (2006): Identification of larvae of exotic *Tipula paludosa* (Diptera: Tipulidae) and *T. oleracea* in North America using mitochondrial cytB sequences. – Annals of the Entomological Society of America 99(1): 33-40.
[38] Reissig, W. H., Heinrichs, E. A., Litsinger, J. A., Moody, A., Fiedler, L., Mew, T. W, Barrion, A. T. (1986): Illustrated Guide to Integrated Pest Management in Rice in Tropical Asia. – International Rice Research Institute, Los Baños.
[39] Rubia, E. G., Heong, K. L., Zalucki, M., Gonzales, B., Norton, G. A. (1996): Mechanisms of compensation of rice plants to yellow stem borer *Scirpophaga incertulas* (Walker) injury. – Crop Protection 15: 335-340.
[40] Satar, A., Özbay, C. (2003): On the Orthoptera (insecta) Fauna of the Karacadağ Mountains and the Tigris Basin (Diyarbakir,Turkey). – Boletín SEA 32: 115-120.
[41] Schotzko, D. J., O'Keeffe, L. E. (1989): Comparison of Sweep Net., D-Vac., and Absolute Sampling., and Diel Variation of Sweep Net Sampling Estimates in Lentils for Pea Aphid (Homoptera: Aphididae)., Nabids (Hemiptera: Nabidae)., Lady Beetles (Coleoptera: Coccinellidae)., and Lacewings (Neuroptera: Chrysopidae). – Journal of Economic Entomology 82(2): 491-506.
[42] Serel, İ. (1978): Güneydoğu Anadolu Bölgesinde çeltik zararlılarının tanınmaları, yayılış alanları ve ekonomik önemleri üzerine araştırmalar. – (Ph.D Thesis) 92. Ege University. Agriculture Faculty, İzmir, Turkey. (In Turkish).
[43] Settle, W. H., Ariawan, H., Astuti, E. T., Cahyana, W., Hakim, A. L., Hindayana, D., Estari, A. S. (1996): Managing tropical rice pests through conservation of generalist natural enemies and alternative prey. – Ecology 77: 1975-1988.
[44] Steel, R. G. D., Torrie, J. H., Dickey, D. A. (1997): Principles and Procedures of Statistics: A Biological Approach. – New York: McGraw-Hill.
[45] Şimşek, Z. (1988): Studies on the Insect Species Harmful on Corn and Sorghum, Their Determination and Distribution in Eastern and Southeastern Anatolia Regions in Turkey. – Diyarbakir Plant Protection Research Institute, Series of Research Works No: 6, 87 p.
[46] Teoman, A., Kavut, H. (1979): Studying on insect fauna in the paddy fields of the Aegean Region. – Annals of Plant Protection Research 14: 10-12. İzmir, Turkey.
[47] Trdan, S., Andjus, L., Raspudić, E., Kač, M. (2005): Distribution of *Aeolothrips intermedius* Bagnall (Thysanoptera: Aeolothripidae) and its potential prey Thysanoptera species on different cultivated host plants. – Journal of pest science 78(4): 217-226.
[48] TURKSTAT. (2016): Turkish Statistical Institute. – www.tuik.gov.tr/Start.do. (Date accessed: December 2018).
[49] Turnipseed, S. G. (1974): Sampling soybean insects by various D-Vac, sweep, and ground cloth methods. – Florida entomologist 57(3): 217-223.
[50] Uzunali, S. (1976): Karadeniz Bölgesi Çeltiklerinde (*Oryza sativa* L.) zarar yapan önemli böcek türleri, tanınmaları, yayılış alanları ve zararları üzerinde araştırmalar. – (Ph.D thesis) 68 pp. Ege University Agriculture Faculty, İzmir, Turkey. (In Turkish).
[51] Van Haperen, P., Voorrips, R. E., Van Loon, J. J., Vosman, B. (2019): The effect of plant development on thrips resistance in Capsicum. – Arthropod-Plant Interactions 13(1): 11-18.
[52] Way, M. J., Heong, K. L. (1994): The role of biodiversity in the dynamics and management of insect pests of tropical irrigated rice – a review. – Bulletin Entomological Reserach 84: 567-587.
[53] Xingquan, Y., Jianhua, W., Taifang, W. (1993): Studies on the bionomics of *Tipula* sp. and its control. – Entomological Knowledge 30(1): 4-6.
[54] Yiğit, A., Doğanlar, M., Sertkaya, E., Evren, N. (2003): Comparison of two method used in sampling of sunn pest, *Eurygaster integriceps* Puton, (Het.; Scutelleridae) in Şanlıurfa, Turkey. – GAP III. Agriculture Congress, 02-03 November, Şanlıurfa, Turkey.

http://www.aloki.hu ● ISSN 1589 1623 (Print) ● ISSN 1785 0037 (Online)
DOI: http://dx.doi.org/10.15666/aeer/1704_1020710220

[55] Yılmaz, E., Karsavuran, Y. (2009): Fluctuations of *Zyginidia pullula* (Boheman, 1845) and *Asymmetrasca decedens* (Paoli) (Hom.: Cicadellidae) Populations in Maize Cultivation Areas of İzmir Province. – Proceedings of the Third Plant Protection Congress of Turkey, 15-18 July, Van, Turkey.
[56] Yürüten, O., Günaydın, T., Ersoy, G. (1982): Marmara Bölgesi çeltik tarlalarında zararlı ve faydalı fauna sürveyi. – Project Final Report (In Turkish). Plant Protection Research Institue, Istanbul, Turkey.

http://www.aloki.hu ● ISSN 1589 1623 (Print) ● ISSN 1785 0037 (Online)
DOI: http://dx.doi.org/10.15666/aeer/1704_1020710220

ASSESSMENT OF HEAVY METAL CONCENTRATION IN FEATHERS OF ARMENIAN GULL (*LARUS ARMENICUS* BUTURLIN, 1934) AND WATER SAMPLES OF HAZAR LAKE, TURKEY

NERGİZ, H.* – ŞAMAT, A. K.

Bitlis Eren University, Faculty of Scince and Art, Department of Biology, Bitlis 13000, Turkey

**Corresponding author*
e-mail: humeyranergiz@gmail.com; phone: +90-434-222-0020

(Received 23rd Apr 2019; accepted 4th Jul 2019)

Abstract. Accumulation levels of heavy metals in the feathers of birds reflect the abundance of these pollutants in the medium and birds can be useful indicators of this kind of pollution. The aim of the present study was to detected levels of some heavy metals of juvenile and adult Armenian Gull (*Larus armenicus*) and in the surface water of Hazar Lake, Turkey. The feather samples from different parts of the bodies of dead adult and juvenile Armenian Gulls were collected. Water samples were taken from different sampling stations distributed across the lake. Heavy metal concentrations were measured using a Thermo Scientific ICAP 600 Spectrometer. There was no significant statistical difference for bioaccumulation of heavy metals and trace elemets in adult and juvenile gull feathers ($p>0.05$). However, the highest metal concentrations were measured in juveniles. The highest average residue amounts in juvenile cover feathers were 0.02 mg/kg Cd, 0.46 mg/kg Pb, 0.72 mg/kg Cu, 58,31 mg/kg Fe, 0.04 mg/kg Ni, 8.38 mg/kg Zn, 0.07 mg/kg Se, 1.3 mg/kg Mn, 0.005 mg/kg Cr and 0. 01 mg/kg As. Mean values of all metals were within the acceptable limits of normal values for waterbirds, except Pb and Mn. When we evaluated the findings heavy metal concentration of the water were detected decrease in sequence of; Fe>As>Zn>Ni>Cd>Cu>Cr>Pb>Mn>Se. Compared with WHO (World Health Organization) and TSE-266 (Turkish Standarts Institution) standards; Cd, Cu, Zn and Cr concentrations in water were higher than the permissible levels for drinking water. It seems Armenian Gull feathers are useful monitoring tool for assessing heavy metal contamination.
Keywords: *bioindicator, biomonitoring, birds, toxic effect, wetland*

Introduction

Environmental degradation of wetland ecosystems by metals is a worldwide problem because of their toxic effects and long persistence (Mansouri et al., 2012; Klaassen, 2013; Zhang et al., 2018). As the trophic level rises in a food chain, the amount of toxic pollutant build up increases and therefore they involve great threat for all species and ecosystems (Ullah et al., 2014).

Indicator species are used to biomonitor environmental changes and to assess effects of pollution. Birds have been recognized as the useful bioindicators of environmental health (Erwin and Custer, 2000). They can be exposed to heavy metals through intake of food, drinking contaminated water and by physical contact (Becker, 2003; Burger and Gochfeld, 2004; Bostan et al., 2007).

One of the suitable methods of assessing level of the metal pollution in natural habitats is to determine the amount of it in bird feathers. Especially birds of prey species occupying higher trophic levels deemed indicative for bioaccumulation in the whole food chain (Boncompagni et al., 2003; Barbieri et al., 2010). Gulls are top predator species of their food web and they can give information about a large area around sampling site.

http://www.aloki.hu ● ISSN 1589 1623 (Print) ● ISSN 1785 0037 (Online)
DOI: http://dx.doi.org/10.15666/aeer/1704_1022110227

The Armenian Gull (*L. armenicus*) breeds in eastern Turkey, Armenia, southern Georgia and northwestern Iran. It is known that breeding population of species in Turkey has declined rapidly in recent years (Adızel et al., 2010; Nergiz and Durmuş, 2017; Durmuş et al., 2018). There is one known crowded native resident population of Armenian Gull in Hazar Lake in East Anatolia. But studies about Hazar Lake population of the species are scanty.

In this study, we measured levels of Cd, Pb, Cu, Fe, Ni, Zn, Se, Mn, Cr and As in feathers of *L. armenicus* and water samples of its foraging areas at Hazar Lake. The objectives of this study were was to assess relationships between the metal levels in the feather of adult and juvenile Armenian Gulls and to compare the concentration of these metals in feathers of the species and their habitat at Hazar Lake, Turkey. We hope that this study will be a useful reference for the determination of regional contamination and realization of a protection plan for this bioindicator species.

Materials and methods

Feather samples of Armenian Gull were collected during 2015-2016 breeding season from the dead individuals in Hazar Lake. Water samples (n=48) were taken once a month at sampling station distributed across the lake. The details of each sampling station are given in *Figure 1*. Collected specimens were labeled and transported to the laboratory under appropriate conditions.

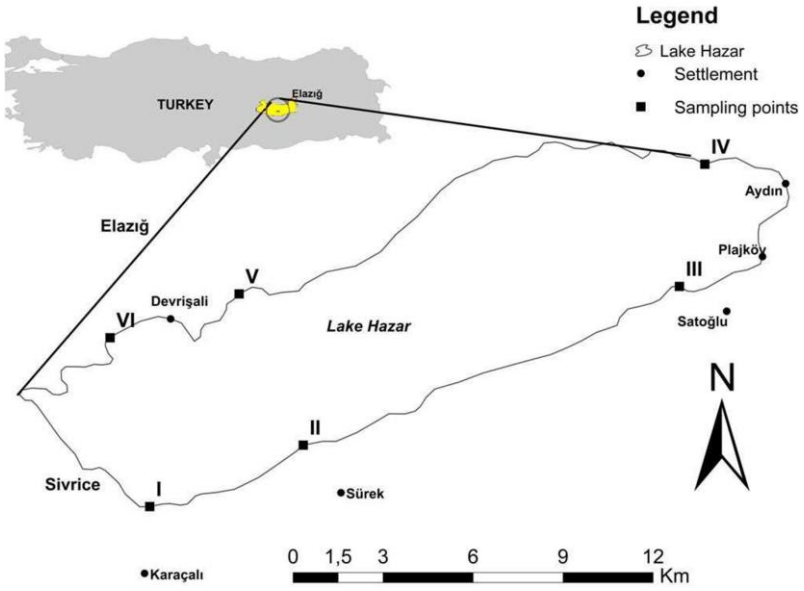

Figure 1. *Location of sampling stations in Lake Hazar*

Surface water samples were taken from 50 cm below the water surface using 100 ml sterile bottles, filtered and acidified with 1 ml of concentrated HNO_3 and then kept in a freezer at 4ºC until measured. Total 40 feather samples from different parts of the bodies of adult and juvenile Armenian Gulls were collected (APF: Adult Primary Wing Feather; ASF: Adult Secondary Wing Feather; ACF: Adult Cover Feather; JCF: Juvenile Cover Feather). Samples of feather transferred to the laboratory were washed with deionized water and rinsed with acetone to wash away the organic materials which

http://www.aloki.hu ● ISSN 1589 1623 (Print) ● ISSN 1785 0037 (Online)
DOI: http://dx.doi.org/10.15666/aeer/1704_1022110227

the water cannot dissolve. All samples were dried at 60ºC for 24 h to remove moisture. The dried feather samples were cut into small pieces with a steel scissors. 0.2 g (dry weight) from each sample were put into glass dissolution vessels and 5 ml HNO_3 (65%) added to each, and stored at room temperature for 24 h. The samples were heated to boiling on a hot plate until the color vapors of the samples vanished slowly and they were completely mineralized. After this, all samples were diluted to 10 ml with deionized water. Each sample was analysed at least three times for Cd, Pb, Cu, Fe, Ni, Zn, Se, Mn, Cr and As using ICP-AAS (Thermo Scientific ICAP 600 series).

Statistical analysis

All metal concentrations were detected as milligrams per liter for water samples and on a dry weight basis as milligrams per gram for feather samples. For this reason, average heavy metal levels were calculated as milligrams per kilogram. Statistical analysis was conducted in order to assess and compare the average values of metals in *L. armenicus*. Data were analyzed with SPSS software (Version 23). The average distribution of metals in *L. armenicus* (adults and juveniles) and water samples were assessed with independent t-test.

Results and discussion

The distribution of heavy metal and trace elements in feathers of *L. armenicus* for adults and juveniles respectively are given in *Table 1*. Results of our work confirm the findings by Burger (1993), Boncompagni et al. (2003) and Malik and Zeb (2009) that heavy metals pile up at different concentrations in feathers of adult and juvenile birds.

Table 1. *Concentrations of heavy metals and trace elements in feathers (mg/kg dry weight) of L. armenicus and in water samples of Hazar Lake (mg/l)*

Metal	Adults Mean ± SD	Juveniles Mean ± SD	Water samples Mean ± SD	p
Cd	0.0207± 0.0185	0.0265±0.0294	0.0091±0.0266	0.56
Pb	0.4491±0.4162	0.4689±0.2592	0.0046±0.01152	0.88
Cu	0.6302±0.1445	0.7295±0.1755	0.0081±0.0418	0.082
Fe	24.0938±19.3146	58.3160±15.0129	0.0697±0.1685	0.06
Ni	0.0063±0.0143	0.0490±0.1321	0.0101±0.03519	0.08
Zn	7.2498±1.7706	8.3848±1.9769	0.0146±0.0432	0.09
Se	0.0598±0.0289	0.0754±0.0238	*BDL	0.09
Mn	0.6212±0.4237	1.3006±0.3392	0.003±0.0055	0.07
Cr	0.0041±0.0125	0.0057±0.0134	0.0077±0.0418	0.18
As	0.0049±0.0037	0.0165±0.0311	0.0175±0.0032	0.25

*BDL: Below Detection Limit, statistically significance was accepted at $p<0.05$

Some studies have been conducted on heavy metals levels in feather of birds. Barbieri et al. (2010) showed that the levels of Cd, Co, Cr, Mn, Ni, Zn, and Pb increased with age. Furthermore, Burger (1996) indicated that the ratio of cadmium and lead in feathers of Franklin's gulls were lower in juveniles. Mansouri et al. (2012) pointed out that metal levels were always higher in adults, because of the age-related bioaccumulation. In the contrast, several studies have reported that there are significant differences in metal contamination in feathers with age related in which chicks had

http://www.aloki.hu ● ISSN 1589 1623 (Print) ● ISSN 1785 0037 (Online)
DOI: http://dx.doi.org/10.15666/aeer/1704_1022110227

significantly higher concentration of metal than adults (Stewart et al., 1997; Dauwe et al., 2000; Burger and Gochfeld, 2009; García-Tarrasón et al., 2013).

Present study provides additional supports for the suggestions by Burger et al. (2008) and Movalli (2000), that there was no significant statistical difference between feather samples taken from adults and juveniles for bioaccumulation of heavy metal and trace elements ($p>0.05$). The average levels of heavy metals detected in juvenile feathers in the present study were as; Cd 0.02 mg/kg, Pb 0.46 mg/kg, Cu 0.72 mg/kg, Fe 58.316 mg/kg, Ni 0.04 mg/kg, Zn 8.38 mg/kg, Se 0.07 mg/kg, Mn 1.3 mg/kg, Cr 0.005 mg/kg and As 0. 01 mg/kg. The chemical profiles of juveniles were as follows: Fe>Zn>Mn>Cu>Pb>Se>Cd>As>Ni>Cr. The highest trace metal concentrations were measured in juveniles. But the differences were smaller (*Figure 2*). This age related differences may be due to diet differences. Juveniles may have foraged in different habitats and fed more often than adults would have higher levels of metals in their feathers. The high levels of heavy metal accumulation in juveniles can be correlated with the egg and their food, which is derived locally.

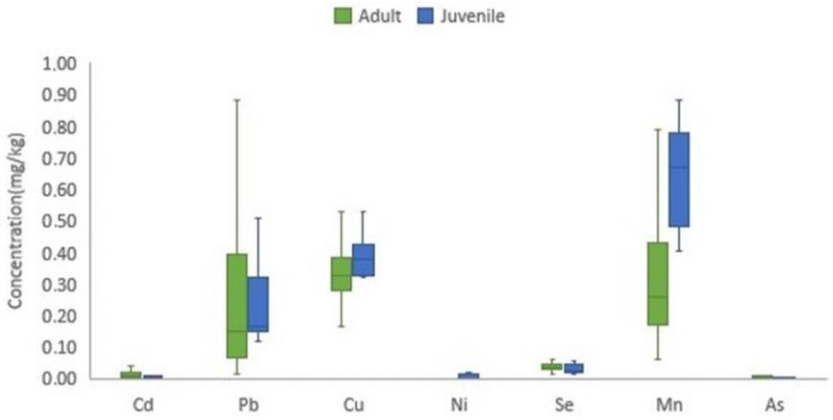

Figure 2. *Comparison of heavy metals in the feather samples taken from adult and juvenile Armenian Gulls*

Pb and Mn levels measured in present study were higher than those reported in previous researches. In the literature, an average of 0.51 ppm Mn and 0.19 ppm Cd was detected for marine birds (Burger, 2002). These values are much lower than that measured in our study. Greater than 2 mg/kg (dw) Cd, 4 mg/kg (dw) Pb, 1200 mg/kg (dw) Zn, 2.8 mg/kg (dw) Cr, 26 mg/kg (dw) Se, 0.96 mg/kg (dw) As concentrations in feathers were considered as abnormal poisoning and indicates increased environmental pollution (Burger, 1993; Heinz, 1996; Burger and Gochfeld, 2000; Taggart et al., 2006; Nighat, 2013). In the present study, mean heavy metal and trace element levels during 2015/2016 were in order of magnitude below known toxic effect levels.

Durmuş et al. (2018) studied metal deposition (Mg, Zn, Cu, Mn, Li, Sn, Co and Se) in feathers of the Armenian Gull from various regions of Van Lake Basin in Turkey. We found the mean concentration of Cr to be lower than their results but Zn, Mn and Se concentrations were slightly higher in our study which might be due to different nutrient density.

The heavy metal levels in water are given in *Table 1*. The mean values revealed that accumulation levels of heavy metals and trace elements in water varied from each other depending on the different sampling site. Pb, Fe, Zn and As were noted in all seasons.

http://www.aloki.hu ● ISSN 1589 1623 (Print) ● ISSN 1785 0037 (Online)
DOI: http://dx.doi.org/10.15666/aeer/1704_1022110227

Among the analyzed metals Fe was the highest and Se was the lowest metal which was below detection limit in all seasons while Cd and Cr were recorded only in autumn and winter, Mn in winter, Cu and Ni in summer, autumn and winter. There were no statistically significant differences in the concentration of metal among seasons ($p>0.05$). The highest levels of Cu, Cr, Fe, Mn, Ni, and Zn were noted during spring, Cd and Pb in summer and autumn (*Table 2*).

The heavy metal and trace elements accumulation in water decreased in the following order; Fe>As>Zn>Ni>Cd >Cu>Cr> Pb>Mn>Se. The highest Fe (1.29 mg/l), As (0.03 mg/l), Zn (0.28 mg/l), Ni (0.18 mg/l) levels were in sites 4 and 5. The highest heavy metal concentrations in the two sampling sites were associated with natural sources and human related activities.

Table 2. *The concentrations (mg/l) of some heavy metals in Hazar Lake*

Season	Cd	Pb	Cu	Fe	Ni	Zn	Se	Mn	Cr	As
Spring	0.01	0.001	0.03	0.11	0.04	0.03	*BDL	0.005	0.03	0.01
Summer	0.02	0.001	*BDL	0.06	*BDL	0.001	*BDL	0.004	0.0002	0.01
Autumn	*BDL	0.01	*BDL	0.1	*BDL	0.006	*BDL	0.002	*BDL	0.01
Winter	*BDL	0.005	*BDL	0.1	*BDL	0.01	*BDL	*BDL	*BDL	0.01

*BDL: Below Detection Limit

We compared the results of heavy metals in water of Hazar Lake with WHO and TSE-266 standards. According to these standards, Cu, Zn and Cr were higher than the permissible levels for drinking water in spring while Cd was in spring and summer.

Özmen et al. (2014) researched level of bioaccumulation of heavy metal and trace elements in water of Hazar Lake and recorded following highest concentrations (in mg/l) 0.43±0.11 Fe, 0.071±0.018 Zn, 0.012±0.002 Ni, 0.025–0.22 Cu. Their results indicated that a general absence of serious pollution caused by heavy metals such as Cd, Pb and As in the lake. Alp et al. (2011) reported that Cr, Pb and Cd levels were below detection limit in all seasons. According to our results the heavy metal concentrations of Hazar Lake' water increased which is presumed to be because of increased anthropological pressures.

Conclusions

Present study, we assessed the concentration of heavy metal and trace elements in feathers of Armenian gull, resident in the eastern Anatolia region of Turkey and breeding on Hazar Lake, for which scarce information existed. The results provide evidence that feathers are efficient metarial to understand heavy metals pollution levels and bioaccumulation along the wetland food chain with higher concentrations found in bird feathers than water. Metal concentrations detected during the study were within the acceptable range of normal concentrations for waterbirds except for Pb and Mn. Furthermore, the heavy metals (Cd, Cu, Zn, Cr) concentrations in water did exceeded WHO and TSE-266 guidelines in spring and summer. Although levels of heavy metals were not high, our results revealed that precautions need to be taken in order to prevent future heavy metal pollution in the lake basin. Consequently, we confirmed that feathers of Armenian Gull can reveal local contamination around the foraging and breeding sites and can be a very useful monitoring instrument for assessing heavy metal contamination.

http://www.aloki.hu ● ISSN 1589 1623 (Print) ● ISSN 1785 0037 (Online)
DOI: http://dx.doi.org/10.15666/aeer/1704_1022110227

Acknowledgements. This study was supported by Bitlis Eren University, BEBAP 2015.02 project. We wish to thank to The Scientific Research Project Unit of Bitlis Eren University for their financial support.

REFERENCES

[1] Adızel, Ö., Durmuş, A., Kiziroğlu, İ. (2010): Preliminary study on newly detected Yaylıyaka Marshes in the Lake Van Basin, Turkey. – The Journal of Animal and Plant sciences 20(4): 286-292.

[2] Alp, M. T., Şen, B., Özbay, Ö. (2011): Heavy metal levels in *Cladophora glomerata* which seasonally occurrence in the Lake of Hazar. – Ekoloji 8: 13-17.

[3] Barbieri, E., Passos, E. A., Filippini, A., Santos, I. S., Garcia, C. A. B. (2010): Assessment of trace metal concentration in feathers of seabird (Larus dominicanus) sampled in the Florianópolis, SC, Brazilian coast. – Environmental Monitoring and Assessment 169: 631-638.

[4] Becker, P. H. (2003): Trace metals and other contaminants in the environment. – Biomonitoring with birds 6(19): 677-736.

[5] Boncompagni, E., Muhammad, A., Jabeen, R., Orvini, E., Gandini, C., Sanpera, C., Ruiz, X., Fasola, M. (2003): Egrets as monitors of trace-metal contamination in wetlands of Pakistan. – Archives of Environmental Contamination and Toxicology 45: 399-406.

[6] Bostan, N., Ashrif, M., Mumtaz, A. S., Ahmad, I. (2007): Diagnosis of heavy metal contamination in agro-ecology of Gujranwala, Pakistan using cattle egret as bioindicator. – Ecotoxicology 6: 247-251.

[7] Burger, J. (1993): Metals in avian feathers: Bioindicators of environmental pollution. – Reviews in Environmental Contamination and Toxicology 5: 203-311.

[8] Burger, J. (1996): Heavy metal and selenium levels in feathers of Franklin's gulls in interior North America. – Auk 113: 399-407.

[9] Burger, J. (2002): Food chain differences affect heavy metals in bird eggs in Barnegat Bay, New Jersey. – Environmental Research 90: 33-39.

[10] Burger, J., Gochfeld, M. (2000): Metal levels in feathers of 12 species of seabirds from Midway Atoll in the northern Pacific Ocean. – Science of the Total Environment 257: 37-52.

[11] Burger, J., Gochfeld, M. (2004): Metal levels in eggs of common terns (Sterna hirundo) in New Jersey: temporal trends from 1971 to 2002. – Environmental Research 94: 336-343.

[12] Burger, J., Gochfeld, M. (2009): Comparison of arsenic, cadmium, chromium, lead, manganese, mercury and selenium in feathers in bald eagle (*Haliaeetus leucocephalus*), and comparison with common eider (*Somateria mollissima*), glaucous-winged gull (*Larus glaucescens*), pigeon guillemot (*Cepphus columba*), and tufted puffin (*Fratercula cirrhata*) from the Aleutian Chain of Alaska. – Environmental Monitoring and Assessment 152: 357-367.

[13] Burger, J., Gochfeld, M., Sullivan, K., Irons, D., McKnigh, A. (2008): Arsenic, cadmium, chromium, lead, manganese, mercury, and selenium in feathers of Black-legged Kittiwake (*Rissa tridactyla*) and Black Oystercatcher (*Haematopus bachmani*) from Prince William Sound, Alaska. – Science of the Total Environment 398: 20-25.

[14] Dauwe, T., Bervoets, L., Blust, R., Pinxten, R., Eens, M. (2000): Can Excrement and Feathers of Nestling Songbirds Be Used as Biomonitors for Heavy Metal Pollution? – Archives of Environmental Contamination and Toxicology 39: 541-546.

[15] Durmuş, A., Çelik, E., Cenger, C., Taşkın, N., Acar, Ş. (2018): Determination of metals and selenium concentrations in feather of Armenian gull (*Larus armenicus*) living in Van Lake Basin, Turkey. – Applied Ecology and Environmental Research 16: 3831-3837.

[16] Erwin, M., Custer, T. W. (2000): Herons as indicators. – In: Kushlan, J. A., Hanfer, H. (eds.) Heron Conservation. Academic Press, San Diego.

http://www.aloki.hu ● ISSN 1589 1623 (Print) ● ISSN 1785 0037 (Online)
DOI: http://dx.doi.org/10.15666/aeer/1704_1022110227

[17] García-Tarrasón, M., Pacho, S., Jover, L., Sanpera, C. (2013): Anthropogenic input of heavy metals in two Audouin's gull breeding colonies. – Marine Pollution Bulletin 74: 285-290.
[18] Heinz, G. H. (1996): Selenium in birds. – In: Beyer, W. M., Heinz, W. M. (eds.) Environmental Contaminants in Wildlife: Interpreting Tissue Concentrations. CRC Press: Boca Raton, FL, USA, pp. 447-458.
[19] Klaassen, C. (2013): Toxicology, The Basic Science of Poisons. – McGraw Hill Publishers, Newyork.
[20] Malik, R. N., Zeb, N. (2009): Assessment of environmental contamination using feathers of *Bubulcus ibis* L., as a biomonitor of heavy metal pollution, Pakistan. – Ecotoxicology 18: 522-536.
[21] Mansouri, B., Hoshyari, E., Pourkhabbaz, A., Babaei, H. (2012): Assessment of nickel levels in feathers of two bird species from southern Iran. – Podoces 7: 66-70.
[22] Movalli, P. A. (2000): Heavy metal and other residues in feathers of laggar falcon *Falco biarmicus jugger* from six districts of Pakistan. – Environmental Pollution 109: 267-275.
[23] Nergiz, H., Durmuş, A. (2017): Effects of habitat change on breeding water birds in Arin (Sodalı) Lake, Turkey. – Applied Ecology and Environmental Research 15: 1111-1118.
[24] Nighat, S., Iqbal, S., Nadeem, M. S., Mahmood, T., Shah, S. I. (2013): Estimation of heavy metal residues from the feathers of Falconidae, Accipitridae, and Strigidae in Punjab, Pakistan. – Turkish Journal of Zoology 37: 488-500.
[25] Özmen, H., Külahcı, F., Çukurovalı, A., Doğru, M. (2014): Concentrations of heavy metal and radioactivity in surface water and sediment of Hazar Lake (Elazığ, Turkey). – Chemosphere 55: 401-408.
[26] Stewart, F. M., Phillips, R. A., Catry, P., Furness, R. W. (1997): Influence of species, age and diet on mercury concentrations in Shetland seabirds. – Marine Ecology Progress Series 151: 237-244.
[27] Taggart, M. A., Figuerola, J., Green, A. J., Mateo, R., Deacon, C., Osborn, D., Meharg, A. A. (2006): After the Aznalcóllar mine spill: arsenic, zinc, selenium, lead and copper levels in the livers and bones of five waterfowl species. – Environmental Research 100: 349-361.
[28] Ullah, K., Hashmi, M. Z., Malik, R. N. (2014): Heavy-metal levels in feathers of cattle egret and their surrounding environment: a case of the Punjab province, Pakistan. – Archives of Environmental Contamination and Toxicology 66: 139-153.
[29] Zhang, J., Han, L., Ji, Y., Wei, J., Cai, G., Gao, G., Wu, J., Yao, Z. (2018): Heavy metal investigation and risk assessment along the Le'An River from non-ferrous metal mining and smelting activities in Poyang, China. – Journal of Environmental Biology 39: 536-545.

http://www.aloki.hu ● ISSN 1589 1623 (Print) ● ISSN 1785 0037 (Online)
DOI: http://dx.doi.org/10.15666/aeer/1704_1022110227

THE EFFECT OF *HMW-GS* ON *GLU-A1*, *GLU-B1*, *GLU-D1* IN SOME LOCAL BREAD (*Triticum aestivum* L.) WHEAT GENOTYPES

NANELI, İ.[1*] – TANRIKULU, A.[2] – BAŞDEMIR, F.[2] – SAKIN, M. A.[1]

[1]*Department of Field Crops, Faculty of Agriculture, Tokat Gaziosmanpaşa University, Taslıciftlik Campus, 60000 Tokat, Turkey*

[2]*Ceylanpınar Vocational High School, Harran University, 63570 Şanlıurfa, Turkey*

**Corresponding author*
e-mail: ismailnaneli@gmail.com; phone: +90-506-534-6031; fax: +90-252-1616-2184)

(Received 24th Apr 2019; accepted 24th Jun 2019)

Abstract. Wheat gluten proteins are extremely important proteins in terms of quality. Glutenin from the sub-units of gluten, because of the multi-polymer structure is effective in the rheological properties of the dough. In the study, samples taken from the endosperm section of local bread wheat (*Triticum aestivum* L.) genotypes; The *HMW-GS* band patterns in the *1A, 1B, 1D* genomes were determined, and the band patterns of the glutenin were determined using the vertical electrophoresis apparatus by *SDS-PAGE*. During the determination of *HMW-GSs*; *Cheyenne, Gabo, Chinese Spring, Janz, Insignia* genotypes were used as markers. According to the data obtained, some bread wheat genotypes carry high-quality glutenin bands found in the markers used in the study. As a result, in accordance with the data obtained from the study, the use of some bread wheat genotypes with high-quality scores in production will contribute to the development of high-quality products. However, a high-quality score with the improvement of genotypes used as parental lines, yield, and quality of high-new bread wheat cultivars will be developed.
Keywords: *band, genotype, HMW-GS, local bread wheat, mobility, molecular weight, quality, score*

Introduction

Wheat is a very important food material in terms of being the raw material of various nutrients. In order to meet the needs of the world population, the quality of flour should be increased due to wheat quality in order to meet the increasing demands along with the efficiency of the unit area. The quality of wheat produced in Turkey some years due to inadequate quality flour in some areas to meet the consumer demand is made by blending high-quality wheat. In addition, considering the self-sufficiency and the export of approximately 3.32 million tons of flour annually, it is essential to increase the flour quality of the bread wheat varieties (Anonymous, 2018). The most important parameter that determines the flour quality characteristics obtained from wheat is gluten proteins (Tatham and Shewry, 2000; Özberk, 2018). Gluten proteins are examined in two parts, gliadins and glutenins, and glutenin polymers form a multi-polymer structure by cross-linking of *HMW-GS* and *LMW-GSs* (Wrigley, 1996; D'Ovidio and Masci, 2004; Appelbee, 2006). Although *HMW-GSs* have a determinative role in dough basic properties, *LMW-GSs* also play an important factor (Cornish et al., 2001; D'Ovidio and Masci, 2004). Researchers also indicate that gluten proteins are highly effective in environmental factors as well as genetic factors (Payne et al., 1981; Troccoli et al., 2000). The use of sulfur fertilizers during wheat cultivation, in particular, increases the quality of gluten and thus increases the technological properties of flour (Zhao et al., 1999). *HMW-GS* is the bands that vary between *1-5* in bread and durum wheat (Waines and Payne,

http://www.aloki.hu ● ISSN 1589 1623 (Print) ● ISSN 1785 0037 (Online)
DOI: http://dx.doi.org/10.15666/aeer/1704_1022910238

1987), that number between *1-3* due to the absence in the durum wheat genome *1D*, the glutenin banding varies from *3-5* and in bread wheat. In the studies carried out by the researchers, the sulfur-deficient *omega-gliadin* and *HMW-GS* proteins increased in the wheat grown in the areas where sulfur deficiency was observed, on the other hand, they reported that sulfur-rich proteins such as *gamma* and *LMW-GS* were reduced (Wieser et al., 2004). *HMW-GS* in the long arms of *1A, 1B, 1D* genomes in bread wheat (*Triticum aestivum* L.) and gliadins found in short arms of *6A, 6B, 6D* genomes are extremely important for the quality of the flour (Garg et al., 2006). In particular, *HMW-GSs* are effective on the baking quality of the products obtained from bread wheat (Shewry et al., 1995). In terms of gluten quality, in the grain filling process, the *1D* genome *HMW-GSs* are more susceptible to the formation of poor gluten content with the high temperature occurring in the bread wheat (Deng et al., 2008) and this indicates the importance of environmental factors (Raza, et al., 2019). In this study, it was aimed to determine and score the *HMW-GS* protein bands in the *1A, 1B, 1D* genomes of local bread wheat genotypes which have a significant effect on the quality and to determine the bread wheat genotypes with superior quality bands.

Review of literature

HMW-GSs are important parameters to determine gluten quality characteristics. Numerous studies have been conducted to determine the formation and functional relationships of gluten in many researchers and research groups (Payne et al., 1987; Lawrence et al., 1988; Popineau et al., 1994; Gupta et al., 1995; Yu et al., 2019). However, the effect of the *Glu-1* locus allelic variations on dough formation and development was not fully characterized (Li et al., 2016a). Some researchers stated that hydrogen and disulfide bonds are important factors for gluten rheology during dough formation and development (Wang et al., 2013; Li et al., 2016b). According to Wang et al. (2003), the glutenin macropolymer structure and *HMW-GS* formations determine the rheological properties of dough and glutenin macropolymer structure with have found a close correlation between the end-use quality. Shewry and Halford (2003) stated that although *HMW-GSs* constitute approximately 20% of all glutenin proteins, they have a major effect on the viscoelastic properties of the dough. The number and distribution of cysteine residues in the *1A, 1B, 1D* genomes found in *HMW-GSs* is important for the formation of proteins due to the di-sulfide bonds they contain. These structures are important factors related to the technological properties of the dough. *HMW-GS* cysteine residues are important in determining the elastic and polymeric structure of the dough (Tatham et al., 1985; Buonocore et al., 1998; Wang et al., 2016). Payne (1987) and Roy et al. (2018) *Glu-1* locus allelic varieties have a significant effect on bread quality characteristics, especially in the end-use quality development has stated that a very high potential has been obtained. Zhang et al. (2018) *HMW-GSs* have been highly effective on dough elasticity and baking quality. *Glu-B1* and *Glu-D1* genomes were found in the study of different bread wheat genotypes, respectively; *17 + 18* and *5 + 10* bands have a high effect on the amount and quality of gluten (Gupta et al., 1994). The technological quality development of flour can be achieved by increasing the number of active *HMW-GS* in genomes or by regulation of allelic formation (Lafiandra et al., 1998).

http://www.aloki.hu ● ISSN 1589 1623 (Print) ● ISSN 1785 0037 (Online)
DOI: http://dx.doi.org/10.15666/aeer/1704_1022910238

Materials and methods

The research was conducted in Tokat Gaziosmanpaşa University Faculty of Agriculture, Grain Laboratory (*Fig. 1*). Gluten quality of bread wheat genotypes with *HMW-GS* bands (Gianibelli et al., 2002; Singh et al. 1991) were determined by using vertical electrophoresis device with a modified method of *Sodium Dodecyl Sulfate Polyacrylamide Gel Electrophoresis* (*SDS-PAGE*) (Koyuncu's, 2009) (*Fig. 2*). The used of 21 bread wheat genotypes in the study was obtained from Turkey Seed Gene Bank. Six bread wheat varieties used in the study were obtained from the International Maize and Wheat Improvement Center and used as a marker (*Table 1*). The scoring of the bands in *1A, 1B, 1D* genomes was determined by the method of scoring (*Figs. 3* and *4*) defined by Lasztity (2002), Lasztity and Abonyi (2009) and Payne (1987).

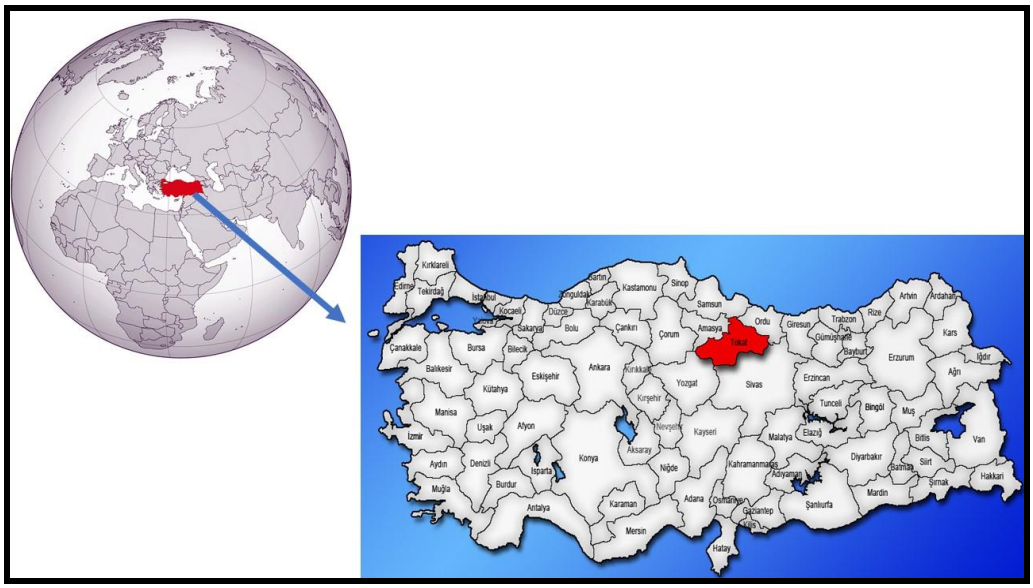

Figure 1. *The study was carried out in Tokat province*

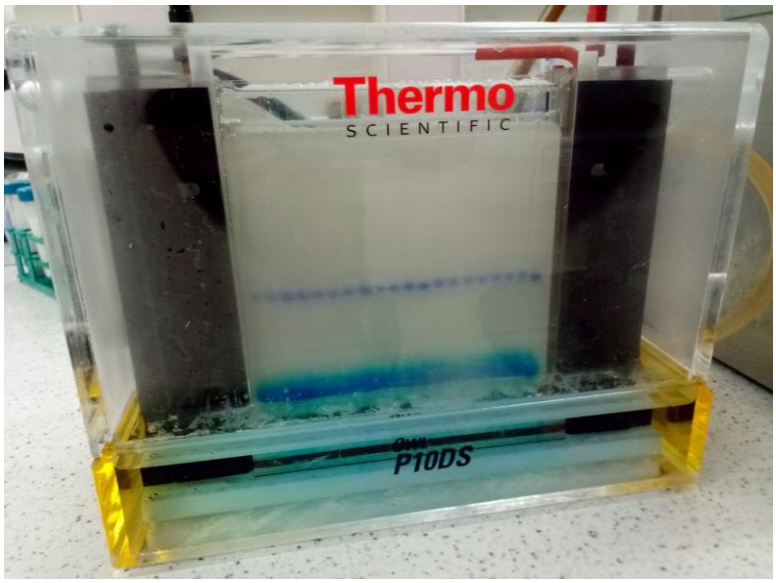

Figure 2. *Vertical electrophoresis device*

http://www.aloki.hu ● ISSN 1589 1623 (Print) ● ISSN 1785 0037 (Online)
DOI: http://dx.doi.org/10.15666/aeer/1704_1022910238

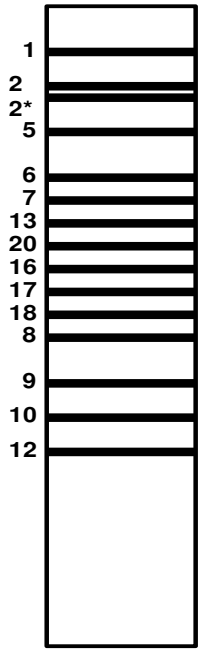

Figure 3. *1A, 1B, 1D genomes with the HMW-GS bands*

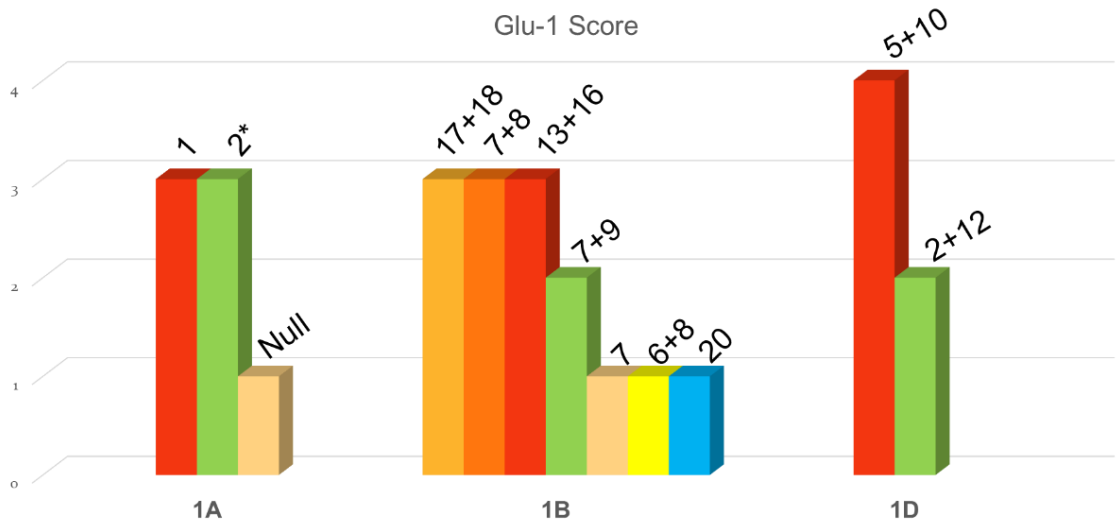

Figure 4. *1A, 1B, 1D found in the genome of protein bands and scores*

Table 1. *Bread wheat varieties that are used as markers*

Varieties	*1A genome bands*	*1B genome bands*	*1D genome bands*
Janz	*1*	*7 + 8*	*2 + 12*
Gabo	*2*/Null*	*17 + 18*	*2 + 12*
Chinese Spring	*Null*	*7 + 8*	*2 + 12*
Cheyenne	*2**	*7 + 9*	*5 + 10*
Baxter	*Null*	*13 + 16*	*Null*
Insignia	*1*	*20*	*5 + 10*

http://www.aloki.hu ● ISSN 1589 1623 (Print) ● ISSN 1785 0037 (Online)
DOI: http://dx.doi.org/10.15666/aeer/1704_1022910238

Results and discussion

Wheat breeders aim to ensure high gluten growth in genotypes where quality comes to the forefront with their yield characteristics (He et al., 2001). Studies conducted by researchers at *Glu-1* locus *1A, 1B, 1D* in wheat *HMW-GS* genome bands were detected in the relationship to between wheat quality (Payne et al., 1987; Vapa et al., 1996). Approximately 13-14%, 55-58% and 28-30% of *HMW-GSs* respectively; They were found in the *1A, 1B, 1D* genomes (Li et al., 2016a). Larroque et al. (2004) stated that in terms of the functional properties of bands contained *1A, 1B, 1D* genomes were found to be highly effective. In different studies examining the functional properties of *HMW-GSs*, they reported that it affects approximately 70% of the quality of bread, although it accounts for approximately 11% of the total protein content (Yu et al., 2019). In the study in which quality scoring was performed according to the protein bands found in the *HMW-GS; 1A, 1B, 1D* genomes, the genotypes examined were found to have *8, 7, 6, 5* (*Table 2*). *TR63581, TGB000534* genotypes *2** in the *1A* genome, *TGB000526* genotypes in the *1*, *1A* genome in the other genotypes have a null band (*Figs. 5* and *6*). The *1A* genome affects about 15% of the wheat quality changes according to the *1B* and *1D* genomes (Yu et al., 2019). One of the important quality parameters in terms of Farinograph values *1* and *2** bands in the genome *1A* has a higher value than the genotypes contain null bands (Bagulho et al., 2004), especially the *2** band has been determined to have a high *Farinograph-PSI* value. The *2** band carrying TR63581, *TGB000534* genotypes were determined to have a higher *Farinograph-PSI (Table 2). 1B* genome of *12* genotypes *7 + 8*, *7* genotypes *7 + 9*, *1* genotype *7*, *1* genotype determined to carry the *20* bands (*Fig. 3*), *7 + 8* band of the other band (*7 + 9, 7, 20*) having a higher quality score (*Fig. 4*). In the studies performed, the researchers found that *1A* genome *1, 2*, 1B* genome *14 + 15, 13 + 16, 7 + 8* and *7 + 9* bands were positive for the quality of gluten and thus the quality of the products (Kaan et al., 1995). Other researchers reported that *20* and *6 + 8* bands have negative effects (Oak et al., 2004; Naghavi et al., 2009). According to the obtained results, it was determined that the examined genotype of *TR44433* carrying *20* bands in the *1B* genome was determined that could show negative quality characteristics *(Table 2).* The *1B* genome of the *TGB000534* genotype only carries bands with high scores in the *1A* and *1D* genomes, despite the presence of only *7* bands *(Fig. 6).* Examined other genotypes had *7 + 8* or *7 + 9* bands that had positive gluten quality in *1B* genomes *(Table 2).* Branlard and Dardevet (1985) in the study; The dough elasticity of *17 + 18, 7 + 8* bands determined a positive effect on elasticity, Li et al. (2016b) reported that *17 + 18 > 14 + 15 > 7 + 8 > 7 + 9* sorting was performed between the bands in the 1B genome. In the *1D* genome, *8* genotypes with a high *HMW-GS* band score (*Fig. 4*) carry *5 + 10, 13* genotypes *2 + 12* bands (*Table 2*). The bands found in the genome *1D* affect the quality rather than the amount of protein. The *1A* genome was found to be more effective on the dough strength and gluten quality compared with the *1D* genome (Zhang et al., 2018). According to *1* and null bands, *2** in genome *1A* and, particularly, *5 + 10* bands in the *1D* genome had extra-strong flour and baking characteristics compared to the *2 + 12* band (Payne et al., 1981; Payne and Lawrence, 1983; Kolster et al., 1991; Lukow, 1991; Maruyama-Funatsuki et al., 2004). Altpeter et al. (1996) and Barro et al. (1997) examined the bands found in the *1D* genome and stated that the *10* band has an important relationship with the dough strength and bread-making quality (Wang et al., 2016).

http://www.aloki.hu ● ISSN 1589 1623 (Print) ● ISSN 1785 0037 (Online)
DOI: http://dx.doi.org/10.15666/aeer/1704_1022910238

Table 2. *Protein bands and quality scores of local bread wheat genomes*

No	*Genotypes*	*1A*	*1B*	*1D*	*Score*
1	*TGB003246*	*Null*	*7 + 9*	*2 + 12*	*5*
2	*TR63575*	*Null*	*7 + 8*	*2 + 12*	*6*
3	*TGB008249*	*Null*	*7 + 8*	*2 + 12*	*6*
4	*ZERUN*	*Null*	*7 + 8*	*2 + 12*	*6*
5	*TGB003247*	*Null*	*7 + 8*	*5 + 10*	*8*
6	*ÇALIBASAN*	*Null*	*7 + 9*	*5 + 10*	*7*
7	*TR63581*	*2**	*7 + 8*	*2 + 12*	*8*
8	*TGB000543*	*Null*	*7 + 8*	*5 + 10*	*8*
9	*TR63501*	*Null*	*7 + 8*	*2 + 12*	*6*
10	*TR48371*	*Null*	*7 + 8*	*2 + 12*	*6*
11	*ÖRMECE*	*Null*	*7 + 8*	*2 + 12*	*6*
12	*TGB003232*	*Null*	*7 + 9*	*5 + 10*	*7*
13	*AKSUNTERİ*	*Null*	*7 + 8*	*2 + 12*	*6*
14	*TR44433*	*Null*	*20*	*5 + 10*	*6*
15	*TGB000526*	*1*	*7 + 9*	*2 + 12*	*7*
16	*ÇAM BUĞDAYI*	*Null*	*7 + 9*	*2 + 12*	*5*
17	*TGB000534*	*2**	*7*	*5 + 10*	*8*
18	*DİMENİT*	*Null*	*7 + 8*	*5 + 10*	*8*
19	*TGB000521*	*Null*	*7 + 9*	*2 + 12*	*5*
20	*TR63497*	*Null*	*7 + 8*	*5 + 10*	*8*
21	*TR37373*	*Null*	*7 + 9*	*2 + 12*	*5*

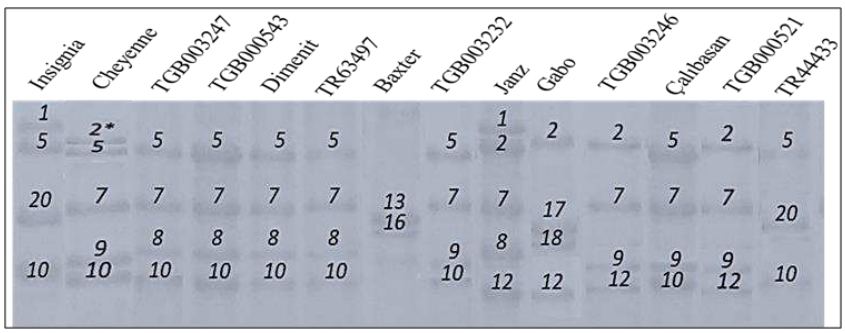

Figure 5. *HMW-GS band models of local bread wheat genotypes (a)*

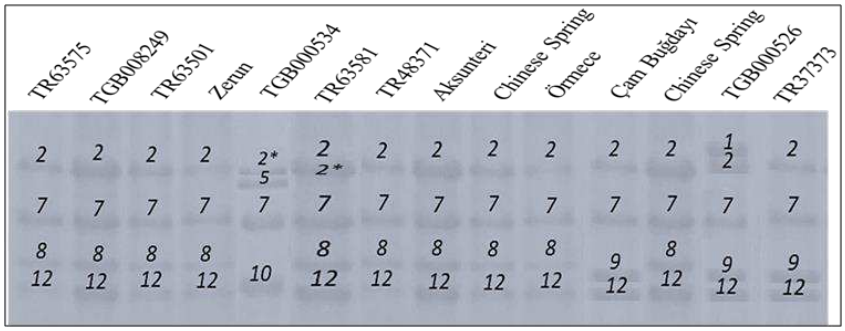

Figure 6. *HMW-GS band models of local bread wheat genotypes (b)*

http://www.aloki.hu ● ISSN 1589 1623 (Print) ● ISSN 1785 0037 (Online)
DOI: http://dx.doi.org/10.15666/aeer/1704_1022910238

Conclusion

HMW-GS is an important parameter in terms of quality in wheat. *TGB003247, TR63581, TGB000543, TGB000534, DİMENİT, TR63497* local bread wheat genotypes have high *HMW-GS* scores according to bands found in *1A, 1B, 1D* genomes. *TR63581, TGB000534, TGB000526* genotypes have come to the fore in some quality parameters with the bands they have in the genome *1A*. In this research, the *Glu-band* pattern of *1A, 1B, 1D* genomes of local bread wheat genotypes were determined and the effects of *HMW-GS* were explained in detail. Local bread wheat genotypes with high scores in terms of the parameters examined can be used as parental lines in breeding studies.

REFERENCES

[1] Altpeter, F., Vasil, V., Srivastava, V., Vasil, I. K. (1996): Integration and expression of the high-molecular-weight glutenin subunit 1Ax1 gene into wheat. – National Biotechnology 14: 1155-1159.
[2] Anonymous (2018): Turkey's Industrialists Federation. – http://www.tusaf.org/TR,2620/2018-yili-bugday-unu-ihracat-verileri.html
[3] Appelbee, M. J. (2006): Contribution of Glutenin Alleles to Dough Rheological Properties, Gluten Proteins. – AACC Int. Press, St. Paul, MN, pp. 238-243.
[4] Bagulho, A. S., Muacho, M. C., Carrillo, J. M., Brites, C. (2004): Influence of glutenin and puroindoline composition on the quality of bread wheat varieties grown in Portugal. – The Gluten Proteins 113-116.
[5] Barro, F., Rooke, L., Bekes, F., Gras, P., Tatham, A. S., Fido, R., Barcelo, P. (1997): Transformation of wheat with high molecular weight subunit genes results in improved functional properties. – National Biotechnology 15: 1295-1299.
[6] Branlard, G., Dardevet, M. (1985): Diversity of grain protein and bread wheat quality. 2. Correlation between high molecular weight subunits of glutenin and flour characteristic. – J. Cere. Sci 3: 345-354.
[7] Buonocore, F., Bertini, L., Ronchi, C., Bekes, F., Caporale, C., Lafiandra, D., Shewry, P. R. (1998): Expression and functional analysis of Mr 58000 peptides derived from the repetitive domain of high molecular weight glutenin subunit 1Dx5. – Journal of Cereal Science 27: 209-215.
[8] Cornish, G. B., Bekes, F., Allen, H. M., Martin, D. J. (2001): Flour proteins linked to quality traits in an australian doubled haploid wheat population. – Australian Journal of Agricultural Research 52: 1339-1348.
[9] Deng, Z., Tian, J., Zhao, L., Zhang, Y., Sun, C. (2008): High temperature-induced changes in high molecular weight glutenin subunits of Chinese winter wheat and its influences on the texture of Chinese noodles. – J. Agron. Crop Sci. 194: 262-269.
[10] D'Ovidio, R., Masci, S. (2004): The low-molecular-weight glutenin subunits of wheat gluten. – Journal of Cereal Science 39: 321-339.
[11] Garg, M., Tanaka, H., Tsujimoto, H. (2006): Chromosome location of genes controlling high molecular weight (*HMW*) glutenin locus in species related to wheat, gluten proteins. – AACC Int. Press, St. Paul, MN, pp. 17-22.
[12] Gianibelli, M. C., Lagudah, E. S., Wrigley, C. W., MacRitchie, F. (2002): Biochemical and genetic characterization of a monomeric storage protein (*T1*) with an unusually high molecular weight in *Triticum tauschii*. – Theoretical and Applied Genetics 104: 497-504.
[13] Gupta, R. B., MacRitchie, F. (1994): Allelic variation at gluten subunit and gliadin Loci, Glu-1, Glu-3 and Gli-1 of common wheats, II. biochemical basis of the allelic effects on dough properties. – Cereal Chemistry 19: 19-29.
[14] Gupta, R. B., Popineau, Y., Lefebvre, J., Cornec, M., Lawrence, G. J., MacRitchie, F. (1995): Biochemical basis of flour properties in bread wheats. II. Changes in polymeric

http://www.aloki.hu ● ISSN 1589 1623 (Print) ● ISSN 1785 0037 (Online)
DOI: http://dx.doi.org/10.15666/aeer/1704_1022910238

protein formation and dough/gluten properties associated with the loss of low Mr or high Mr glutenin subunits. – Journal of Cereal Science 21(2): 103-116.

[15] He, Z. H., Rajaram, S., Xin, Z. Y., Huang, G. Z. (2001): A History of Wheat Breeding in China. – CIMMYT, Mexico D. F.

[16] Kaan, F., Chihab, B., Borries, C., Monneveux, P., Branlard, G. (1995): Prebreeding and breeding durum wheat germplasm (*Triticum durum*) for quality products. – CIMMYT 22: 159-166.

[17] Kolster, P., van Eeuiwjk, F. A., van Gelder, W. M. J. (1991): Additive and epistatic effects of allelic variations at the high molecular weight glutenin subunit loci determining the bread-making quality of breeding lines of wheat. – Euphytica 55: 277-285.

[18] Koyuncu, M. (2009): Screening of durum wheat landraces for selected traits associated with pasta quality. – Master Thesis, Gaziosmanpaşa University, Graduate School of Natural and Applied Sciences.

[19] Lafiandra, D., Masci, S., Margiotta, B., De Ambrogio, E. (1998): Development of Durum and Bread Wheat with Increased Number of High Molecular Weight Glutenin Subunits. – In: Slinkard, A. E. (ed.) Proc. 9th International Wheat Genetics Symposium, Vol. 4. Grain Quality. University of Saskatchewan, Saskatoon, Canada, pp: 261-264.

[20] Larroque., O. R., Margiotta, B., Gianibelli, M. C., Bekes, F., Sharp, P., Lafiandra, D. (2004): Biochemical and Functional Studies of Wheat Isolines Containing Single Type High Molecular Weight Glutenin Subunits (*HMW-GS*). – In: Lafiandra, D. et al. (eds.) The Gluten Proteins, Royal Society of Chemistry, London, pp. 109-116.

[21] Lasztity, R. (2002): Prediction of wheat quality-success and doubts. – Periodica Polytechnica Ser. Chem. Eng. 46(1-2): 39-49.

[22] Lasztity, R., Abonyi, T. (2009): Prediction of wheat quality-past, present, future. A review. – Food Reviews International 25: 126-141.

[23] Lawrence, G. J., MacRitchie, F., Wrigley, C. W. (1988): Dough and baking quality of wheat lines deficient in glutenin subunits controlled by The *Glu-A1*, *Glu-B1* and *Glu-D1* loci. – Journal of Cereal Science 7(2): 109-112.

[24] Li, X., Liu, T., Gao, X., Li, L., Du, D., Cheng, X., Zhao, Y., Liu, Y. (2016a): Effects of *HMW-GS* at *Glu-B1* locus on the polymerization of glutenin during grain development and on the secondary and micro-structures of gluten in wheat (*Triticum aestivum* L.). – Journal of Cereal Science 72: 101-107.

[25] Li, X., Gao, X., Liu, T., Yu, J., Li, L., Feng, Yi. (2016b): Influence of high-molecular-weight glutenin subunit composition at *Glu-B1* locus on secondary and micro structures of gluten in wheat (*Triticum aestivum* L.). – Food Chemistry 197: 1184-1190.

[26] Lukow, O. M. (1991): Screening of bread wheats for milling and baking quality- a Canadian perspective. – Cereal Foods World 36(6): 497-501.

[27] Luo, C., Griffin, W. B., Branlard, G., McNeil, D. L. (2001): Comparison of low and high molecular weight wheat glutenin allele effects on flour quality. – Theor. Appl. Genet. 102(6-7): 1088-1098.

[28] Maruyama-Funatsuki, W., Takata, K., Nishio, Z., Tabiki, T., Yahata, E., Kato, A., Saito, K., Funatsuki, H., Saruyama, H., Yamauchi, H. (2004): Identification of low-molecular-weight glutenin subunits of wheat associated with bread-making quality. – Plant Breed 123: 355-360.

[29] Naghavi, M. R., Rashidi Monfared, S., Ahkami, A. H., Ombidbakhsh, M. A. (2009): Genetic variation of durum wheat landraces and cultivars using morphological and protein markers. – World Academy of Science, Engineering and Technology 49: 73-75.

[30] Oak, M. D., Tamhankar, S. A., Rao, V. S., Bhosale, S. S. B. (2004): Relationship of *HMW*, *LMW* glutenin subunit and gliadin with gluten strenght in Indian durum wheat. – J. Plant Biochemistry and Biotechnology 13: 51-55.

[31] Özberk, F. (2018): Impacts of khapra beetle (T. granarıum everts) onto marketing price and relevant traits in bread wheat (*T. aestıvum* L.). – Applied Ecology and Environmental Research 16(5): 6143-6153.

http://www.aloki.hu ● ISSN 1589 1623 (Print) ● ISSN 1785 0037 (Online)
DOI: http://dx.doi.org/10.15666/aeer/1704_1022910238

[32] Payne, P. I. (1987): The genetical basis of bread-making quality of wheat aspects. – Appl. Biol 15: 79-90.
[33] Payne, P. I., Lawrence, G. J. (1983): Detection by gel electrophoresis of oligomers formed by the association of high-molecular-weight glutenin protein subunits of wheat endosperm. – Journal of Experimental Botany 34(3): 254-267.
[34] Payne, P. I., Corfield, K. G., Holt, L. M., Blackman, J. A. (1981): Correlations between the inheritance of certain high-molecular weight subunits of glutenin and bread-making quality in progenies of six crosses of bread wheat. – J. Sci. Food Agric. 332: 51-60.
[35] Payne, P. I., Ninthingale, M. A., Krattiger, A. F., Holt, L. M. (1987): The relationship between HMW glutenin subunit composition and the bread-making quality of British grown wheat varieties. – J. Sci. Food Agric. 40: 51-65.
[36] Popineau, Y., Cornec, M., Lefebvre, J., Marchylo, B. (1994): Influence of high Mr glutenin subunits on glutenin polymers and rheological properties of glutens and gluten subfractions of near-isogenic lines of wheat sicco. – Journal of Cereal Sci. 19(3): 231-241.
[37] Raza, H., Khan, A. S., Ahmed, N. (2019): Genetic analysis for some phenological and morphological traits in wheat (*Triticum aestivum* L.) under two different sowing windows. – Applied Ecology and Environmental Research 17(2): 2059-2071.
[38] Roy, N., Islam, S., Ma, J., Lu, M., Torok, K., Tomoskozi, S., Bekes, F., Lafiandra, D., Appels, R., Ma, W. (2018): Expressed Ay HMW glutenin subunit in australian wheat cultivars indicates a positive effect on wheat quality. – Journal of Cereal Science 79: 494-500.
[39] Singh, N. K., Shepherd, K. W, Cornish, G. B. (1991): A simplified SDS-PAGE procedure for separating *LMW* subunits of glutenin. – Journal of Cereal Science 14: 203-208.
[40] Shewry, P. R., Halford, N. G. (2003): Genetics of Wheat Gluten Proteins. – In: Hall, J. C., Dunlap, J. C., Friedman, T. (eds.) Advances in Genetics. Elsevier Academic Press Inc, San Diego, pp. 111-184.
[41] Shewry, P. R., Tatham, A. S., Barro, P., Lazzeri, P. (1995): Biotechnology of breadmaking: unraveling and manipulating the multi-protein gluten complex. – Biotech. 13: 1185-1190.
[42] Tatham, A. S., Shewry, P. R. (2000): Elastomeric proteins: biological roles, structures and mechanisms. – Trends Biochemical Science 25(11): 567-571.
[43] Tatham, A. S., Miflin, B. J., Shewry, P. R. (1985): The Beta-turn conformation in wheat gluten proteins: relationship to gluten elasticity. – Cereal Chemistry 62: 405-412.
[44] Troccoli, A., Borrelli, G. M, DeVita, P., Fares, C., DiFonzo, N. (2000): Durum wheat quality: a multidisciplinary concept. – Journal of Cereal Science 32: 99-113.
[45] Vapa, Lj., Dencic, S., Soltes-Rak, E., Kevresan, S. (1996): Genetic variation in *Glu-1* loci breadmaking quality in wheat. – Cereal Research Communications 23: 361-364.
[46] Waines, J. G., Payne, P. I. (1987): Electrophoretic analysis of the high-molecular-weight glutenin subunits of *Triticum monococcum*, *T. Urartu*, and the a genome of bread wheat (*Triticum aestivum*). – Theor Appl Genet 6: 71-74.
[47] Wang, M., Oudgenoeg, G., Vliet, T. V., Hamer, R. J. (2003): Interaction of water unextractable solids with gluten protein: effect on dough properties and gluten quality. – Journal of Cereal Science 38: 95-104.
[48] Wang, Z., Dai, Z., Yin, Y., Li, Y., Cao, L. (2013): Variation of high-molecular-weight glutenin subunits and glutenin macropolymer particle distribution in wheat grains produced under different water regimes. – The Crop Journal 1: 84-89.
[49] Wang, Y., Zheng, Q. Y., Guo, Z. R., Qiao, Y. Y., Cao, Y. L., Liu, C. H., Xu, B. J., Wei, Z. Y., Zong, L. J., Chen, C., Han, Y. N., Chen, Q., Gong, X., Hua, S. Y., Zheng, Y. L., Qi, P. F., Wei, Y. M., Lan, X. J., Wang, J. R. (2016): A missense mutation affects the mobility of high molecular weight glutenin *Dy10* subunit in *SDS-PAGE.* – Agri Gene 2: 1-4.

http://www.aloki.hu ● ISSN 1589 1623 (Print) ● ISSN 1785 0037 (Online)
DOI: http://dx.doi.org/10.15666/aeer/1704_1022910238

[50] Wieser, H., Koehler, P., Tucher, S. V. (2006): Influence of Sulfur Fertilization on The Technological Properties of Wheat Flour, Gluten Proteins. – AACC Int. Press, St. Paul, MN, pp. 158-161.
[51] Wrigley, C. W. (1996): Giant proteins with flour power. – Nature 381: 738-739.
[52] Yu, Z., Ma, W., Peng, Y., Islam, M. d. S., She, M., Lu, M., Lafiandra, D., Roy, N., Juhasz, A., Yan, G. (2019): Molecular characterization and phylogenetic analysis of active y-type high molecular weight glutenin subunit genes at *Glu-A1* locus in wheat. – Journal of Cereal Science 86: 9-14.
[53] Zhang, X., Zhang, B., Wu., H., Lu, C., Lü, G., Liu, D., Li, M., Jiang, W., Song, G., Gao, D. (2018): Effect of high-molecular-weight glutenin subunit deletion on soft wheat quality properties and sugar-snap cookie quality estimated through near-isogenic lines. – Journal of Integrative Agriculture 17(5): 1066-1073.
[54] Zhao, F. J., Hawkesford, M. J., McGrath, S. P. (1999): Sulphur assimilation and effects on yield and quality of wheat. – J. Cereal Sci. 30: 1-17.

http://www.aloki.hu ● ISSN 1589 1623 (Print) ● ISSN 1785 0037 (Online)
DOI: http://dx.doi.org/10.15666/aeer/1704_1022910238

COMPARISON OF DIFFERENT DETERMINING METHODS OF REFERENCE ET_O BASED ON LIMITED WEATHER CONDITIONS IN GAP REGION

AYDIN, Y.

Department of Biosystem Engineering, Faculty of Agriculture, Siirt University, Siirt, Turkey
(e-mail: yusufaydin@siirt.edu.tr; phone: +90-484-212-1111; fax: +90-484-223-1998)

(Received 30th Apr 2019; accepted 13th Jun 2019)

Abstract. Reference crop evapotranspiration (ET_o) is among the most important components of the hydrologic cycle. Standard FAO-Penman-Monteith method is the most frequently used equation to estimate of ET_o. However, the usability of this method is limited due to its complexity Hargreaveas-Samani (HS) and Turc methods that can be operated with limited data such as temperature and solar radiation are used as an alternative to the standard method. In the present study, the reference ET_o values estimated with FAO-PM as the standard method, Hargreaveas-Samani and Turc methods were compared at semi-arid climate conditions. Based on the acquired results; highest R^2 value at the GAP region with semi-arid climate conditions was determined as 0.9872 from the monthly averages of $ET_{o\text{-}PM}$ and $ET_{o\text{-}HS}$ comparison, whereas the lowest RMSE value was also obtained from the same monthly comparison (0.08). $ET_{o\text{-}Turc}$ method yielded a monthly average comparison of 0.981 for the R^2 values comparison. While $ET_{o\text{-}CAP}$ put forth the lowest values for all three intervals. It is suggested that HS method can be used instead of Standart Penman-Monteith method (FAO-PM) under GAP region semi arid climate conditions for reference ET_o estimation if Penman-Monteith can not be calculated. The Turc method is also can be a good alternative to estimate potential evapotranspiration that can be measured by Class A pan. And that ET_o estimation should be made by determining the K_p value in case CAP based ET_o estimation is carried out.
Keywords: *reference ET_o, FAO-PM equation, Hargreaves-Samani equation, Turc equation, pistachio*

Introduction

Evapotranspiration is the most important component of the hydrologic cycle and occurs with the mutual impact of evaporation and transpiration from the soil and the leaf. In this regard, it is the most important parameter for water source planning, water budget methods and irrigation software used in crop water consumption calculations. Continuity and high yield in agricultural production is possible only by the accurate and timely completion of losses due to evaporation and transpiration. For this purpose, ET_o should be estimated accurately since it plays a critical role in the accurate estimation of water losses from the soil and the leaf, carrying out the plans accordingly as well as the planning of irrigation systems (Trajkovic, 2008; Çobaner et al., 2016). Evapotranspiration is generally estimated in two stages. It can be determined by estimating the evaporation gap of the air around the plant subject to certain climate parameters as well as by calculating the water consumption of the grass covering the soil surface completely which is used in estimating plant water consumption (ET_c) and multiplying it by a certain coefficient specific to the crop. It is known that there are over 50 methods or models for the estimation of potential evapotranspiration subject to the data sets used (temperature, radiation, Class A Pan, mass transfer etc.), ecological conditions (arid or humid) and assumptions (Lu et al., 2005). Many researchers have tested the compliance of these methods under certain ecological conditions while also carrying out studies for putting forth the performances of difference methods under different climate conditions (Castaneda and Rao, 2005; Tabari et al., 2013).

http://www.aloki.hu ● ISSN 1589 1623 (Print) ● ISSN 1785 0037 (Online)
DOI: http://dx.doi.org/10.15666/aeer/1704_1023910251

Empirical equations based on energy and mass transfer in compliance with different climate and environmental conditions have been developed for estimating ET_o. For this purpose, Allen et al. (1998) developed the FAO-56 Penman-Monteith method (PMF-56) which is the standard method that is widely used all over the world under different climate and agricultural conditions for ensuring that ET_o estimation is more understandable as well as for ensuring that the information provided is used commonly and frequently (Fisher and Pringle, 2013). This method is widely used for determining reference ET_o (Çobaner et al., 2016). However, there are difficulties related with the use of this model for estimating ETo due to its complexity. Daily data for many meteorological parameters such as temperature, relative humidity, solar radiation, evaporation, wind speed are required for using this model. It is not always possible to obtain this data set in full due to both technological and human based reasons and due to the fact that it is partially costly. On the other hand, calculation of water consumption on has become difficult in Turkey with a surface area of 783.562 km^2 since there are 275 meteorological stations with one station per each 275 km^2 (Çobaner et al., 2016). Therefore, researchers have developed easy to use reference ET_o methods which can be an alternative method for regions where it is not possible to provide the data set in full. Reference ET_o should be calculated using methods that require less climate data in cases when sufficient climate data are not available. For this purpose, Todoroviç et al. (2013) suggests the use of the best known Hargreveas-Samani equation and the "Penman Monteith Temperature Method" (PMT) in which the data required for calculation is calculated from the already existing climate data. Hargreavas and Samani (1985) developed an equation that can calculate the reference evapotranspiration value making use of only temperature and radiation data. Similarly, the Turc formula (1961) that uses only radiation, temperature and relative humidity values for determining reference ET_o was first developed for the regions of Southern France and Northern Africa (Diouf et al., 2016). The fact that the data used can be acquired easily is evaluated as the superiority of this formula for cases when the parameters required by other methods cannot be obtained. In addition, new methods developed which require a smaller data set have been used by many different researchers under different climate conditions for determining their performances in humid (Lu et al., 2005; Fisher and Pringle, 2013; Tabari et al., 2013) and arid regions (Todorovic et al., 2013) and for making a comparison with the FAO-56 PM method (Trajkovic, 2008; Gavilan et al., 2006; Castaneda and Rao, 2005; Shahidian et al., 2012). Since the Turc method is an empirical equation developed for estimating reference ET_o in humid regions, it uses only temperature and solar radiation as the data set. The radiation term used in this method is solved by the method provided in the Hargreaves-Samani equation. In addition to these methods, methods based on Class A Pan evaporation method as an alternative for many regions in the world where meteorological data cannot be obtained in full are used widely due to their ease of use, low cost and ease of application in irrigation software (Tabari et al., 2013). Different researchers (Kanber et al., 1992; Bilgel et al., 1999; Aydın, 2004) have carried out a limited number of studies on the determination of crop water consumption (ET_c) for pistachio. In these studies, ET_o-PM method has been used as the standard method for determining reference ET_o. The Food and Agriculture Organization (FAO) declared in 1990 together with the International Irrigation and Drainage Commission and World Meteorological Organization (WMO) that the FAO-PM (Allen et al., 1998) method can be taken as a reference since it yields more consistent and reliable results in comparison with other methods (Castaneda and

http://www.aloki.hu ● ISSN 1589 1623 (Print) ● ISSN 1785 0037 (Online)
DOI: http://dx.doi.org/10.15666/aeer/1704_1023910251

Rao, 2005; Çobaner et al., 2016). Hence, FAO-56-PM method was taken as the standard in this study with which the other methods were compared. Hargreaveas-Samani and Turc equations can be used frequently for crop water consumption calculations since they are easy to use, require less data and can be used only with temperature data. Therefore, some empirical methods used for determining reference crop water consumption and CAP evaporation method were evaluated comparatively in this study. The climate data used for this purpose in the study were acquired from the Provincial directorate of meteorology in Siirt. In this study, climate data and FAO-56 Penman Monteith values which are used as reference method were taken from the study carried out in Gaziantep in order to determine crop water consumption (ET_c) in pistachio by Aydın (2004). Gaziantep, one of the most important provinces for pistachio production was selected as the study area. Pistachio is produced in 56 provinces in Turkey (Anonymous, 2001) with the highest amount of production in Gaziantep and Şanlıurfa. Gaziantep is ranked first in Turkey with regard to its pistachio production area and product amount (Aslan, 2017) which is an important economical input for the economy of the province. In the aforementioned study, reference (ET_o) were determined according to FAO-56 Penman Monteith method and ET_c was calculated according to water budget technique. From this point of view, crop coefficients (K_c) were determined for the phenological stages of pistachio. The maximum and minimum values of K_c for the suggested treatment in July and November were calculated as 1.51 and 0.39, respectively. These values range from 0.49 to 1.1 for the Southeast 1st Region (Gaziantep, Şanlıurfa and Diyarbakır) (Anonymous, 2017). However, since it is not always possible to determine the ET_o by the Penman-Monteith method, it is possible to eliminate this deficiency with the Hargreaves-Samani model and to estimate ET_c using the determined K_c coefficients. On the other hand, no studies were conducted to determine pan coefficient (K_p) for Gaziantep and Southeastern Anatolia region. Similarly, Since a new issue in Southeastern Anatolia Region, there is no study about determination of K_p in pistachio. On the other hand, the K_p coefficients, which changed periodically for Pistachio in California conditions, were proposed as 0.96 in June and August (Anonymous, 2019). Therefore, K_p coefficient was accepted as 1 in this study.

The purpose of the present study was to carry out reference ET_o estimation in pistachio production regions, carry out reference ET_o estimations via FAO-PM, Hargreaves-Samani and Turc equations in addition to Class A Pan (CAP) method, evaluate the usability of these methods for alternative reference crop water consumption (ET_o) estimation in the GAP region and the put forth the relations between these methods. In addition, this study aims to contribute to the studies on determination of crop coefficient (K_c), evaporation pan coefficient (K_p) or crop-pan coefficient ($K_{cp\text{-}dual}$) in Southeast Anatolia region where pistachio is grown widely.

Materials and methods

Description of study area and weather data

The city of Gaziantep is located in the Southeast Anatolia Region (*Fig. 1*) between 36° 28’ and 38° 0’ eastern longitudes and 36° 38’ and 37° 32’ northern latitudes in WGS84 system and according to ED-50, 3° Central Meridian (CM): 36 coordinate system was shown in *Table 1*.

http://www.aloki.hu ● ISSN 1589 1623 (Print) ● ISSN 1785 0037 (Online)
DOI: http://dx.doi.org/10.15666/aeer/1704_1023910251

Figure1. *Locational view of the study area*

Table 1. *The place of Gaziantep in ED-50, 3° CM: 36 coordinate system*

Points	X	Y
1	541275.4225986	4155978.5921223
2	411633.5530552	4156345.4115202
3	410582.2394373	4056459.2749163
4	541765.9807594	4056095.7171703

Gaziantep has a climate structure with transition characteristics between the Mediterranean and the continental climate. Summers are quite hot and arid, while winters are cold and rainy. Mean annual temperature is + 14.9 °C, with the highest temperature of + 44 °C and lowest temperature of -17.5 °C. The hottest month is July with 27.7, while the coldest month is January with 3.4 and the annual rainfall for the province is 544.3 mm. Rains generally occur during the winter period with less rain during the summer months when evapotranspiration is high and the crops need plenty of water (Aydın, 2004). Thus, irrigation operation and management stands out for pistachio production.

ET_o estimation methods

FAO-56 PM method was used in this study for comparing the reference ET_o estimations obtained via Hargreaveas-Samani and Turc equations. For this purpose, the daily $ET_{o\text{-}PM}$ values were used which have been calculated in the study on pistachio by Aydın (2004) and Ünlü (2005). The climate data of Gaziantep, located in Southeastern Anatolia Region which is known as the most important pistachio producing region of Turkey were used in the aforementioned study. Climate data for the same province were used in Hargreaveas-Samani and Turc equations used for estimating reference ET_o.

FAO-56 Penman Monteith method

The FAO-56 Penman Monteith method used for determining reference crop water consumption requires only daily meteorological data. This equation can be written as indicated below (Allen et al., 1998).

http://www.aloki.hu ● ISSN 1589 1623 (Print) ● ISSN 1785 0037 (Online)
DOI: http://dx.doi.org/10.15666/aeer/1704_1023910251

$$ET_o = \frac{0.408*(R_n-G)+\gamma\frac{900}{T+273}\,u_2(e_s-e_a)}{\Delta+\gamma\ 1+0.34u_2} \quad \text{(Eq.1)}$$

where ET_o: reference evapotranspiration (mm day^{-1}); R_n: net radiation (MJ m^{-2}), G: soil heat flux ($MJ.m^{-2}$); T_{mean}: average air temperature (°C); U_2: wind speed at 2 m height ($m.sn^{-1}$), e_s: saturation vapor pressure (kPa), Δ: slope of vapor pressure curve ($kPa.°C^{-1}$), γ: psycrometric constant ($kPa.°C^{-1}$)

The ET_o software developed by FAO-56 was used for determining reference ET_o. All parameters used in this software are data measured daily and acquired from the meteorological station.

Hargreaves-Samani method

The Hargreaves-Samani equation used for determining reference crop water consumption which requires only the maximum and minimum (T_{max}-T_{min}) temperature values and extraterrestrial radiation (global radiation) (R_a) can be indicated as below (Hargreaves and Samani, 1985).

$$ET_{O-HS} = 0.0023\frac{R_a}{\lambda}\sqrt{(T_{max}-T_{min})}(T+17.8) \quad \text{(Eq.2)}$$

ET_o: Reference evapotranspiration (mm day^{-1}), 0.0023: an empirical coefficient, R_a: extraterrestrial radiation (mm day^{-1}), λ: the latent heat of vaporization (MJ kg^{-1}) for the mean air temperature (T_{mean} in °C) given as:

$$\lambda = 2.501 - 0.002361 * T_{mean} \quad \text{(Eq.3)}$$

λ is generally assumed 2.45 $MJ.kg^{-1}$

Since the temperature, humidity and radiation values used in the equation can be accessed easily, it has been used by many researchers for determining the reference crop water consumption (Todorovic et al., 2013; Fisher and Pringle., 2013; Djaman et al., 2015; Çobaner et al., 2016; Diouf et al., 2016; Yamaç, 2018). The R_a value used for calculating $ET_{o\text{-}HS}$ was calculated using the following equation suggested by Fisher and Pringle (2013) for the Turc method which is solved subject to temperature and by making use of the solar radiation data obtained from the meteorology.

$$R_s = 0.16(T_{max}-T_{min})^{0.5}\,R_a \quad \text{(Eq.4)}$$

R_s is the solar radiation (MJ m^{-2} day^{-1}).

Turc method

The Turc formula derived by Turc (1961) which is used for calculating the daily potential evapotranspiration can be written as below:

$$ET_{o-Turc} = a * C * (R_G + b)\frac{T}{r+15} \quad \text{(Eq.5)}$$

http://www.aloki.hu ● ISSN 1589 1623 (Print) ● ISSN 1785 0037 (Online)
DOI: http://dx.doi.org/10.15666/aeer/1704_1023910251

where ET_o: reference evapotranspiration (mm day^{-1}), T: mean daily temperature (°C), R_G: Global radiation (MJ m^{-2} day^{-1}), a and b: empirical constants and a = 0.31 (m^2 MJ^{-1} mm^{-1}) and b = 2.094 (MJ m^{-2} day^{-1}), C: defined by the relative humidity RH, (%) as:

$$C = 1 + \frac{50 - RH}{70} \quad if\ RH < 50\% \qquad \text{(Eq.6)}$$

$$C = 1 \quad if\ RH \geq 50\% \qquad \text{(Eq.7)}$$

Similarly, relative humidity and temperature values were obtained from meteorological records of Provincial Directorate of Meteorology in Siirt. The C value in the $ET_{o\text{-}Turc}$ equation used for calculating daily potential evapotranspiration was calculated using the aforementioned equations based on the average relative humidity ratio.

Pan evaporation method ($ET_{o\text{-}CAP}$)

The following equation suggested by Allen et al. (1998) was used for calculating reference crop water consumption (ET_o) according to the Class A Pan evaporation method.

$$ET_o = K_p * E_{pan} \qquad \text{(Eq.8)}$$

where ET_o: Reference evapotranspiration, mm day^{-1}; K_p: pan coefficient (assumed 1 as average value in this study). E_{pan}: pan evaporation, mm day^{-1}. However, the K_p value was not calculated separately in this comparison and was assumed theoretically as 1 and therefore the measured E_{pan} value was assumed to be equivalent to ET_o.

Statistical analysis

The ET_o values calculated daily according to the FAO-PM method were compared statistically with the daily ET_o values. Paired comparisons were made for determining the value of R^2 which were then subject to linear regression analysis and the R^2 equation was determined for the obtained curve. The equalities suggested by Djaman (2015) which are provided in *Table 2* were used for a more advanced evaluation of the compared equations.

Results and discussion

The climate data for 1999-2002 obtained from the meteorological records were used in the study. For this purpose, the maximum and minimum temperatures used in the Hargreaveas-Samani and Turc equations along with the relative humidity and radiation values used in the Turc equation were evaluated separately for each year and than converted to monthly average (*Fig. 2a*).

The solar radiation values measured in cal cm^{-2} day^{-1} at the meteorology stations were converted into the unit of MJ m^{-2} day^{-1} after which they were used for solving the equation. The radiation values for the study years are provided in *Figure 2b* as monthly average annually. As can be seen when the figures are examined, while solar radiation values were low in the beginning of the year (January-February) and in the last two months (November-December) of the year, the number of sunny days and sunshine

http://www.aloki.hu ● ISSN 1589 1623 (Print) ● ISSN 1785 0037 (Online)
DOI: http://dx.doi.org/10.15666/aeer/1704_1023910251

duration along with the amount of reflected radiation increased parallel to the increase in seasonal temperatures. Cloudy weather that sometimes occurred during measurement days appears as sudden decreases in radiation.

Table 2. *Statistical analysis equations*

Source	Equation	
Root mean squared error (RMSE	$RMSE = \sqrt{\sum_{k=0}^{n} \frac{(P_i - O_i)^2}{n}}$	(Eq.9)
Mean absolute error (MAE)	MAE = n-1$\sum_{1}^{n}(P_i - O_i)$	(Eq.10)
Percentage error (PE)	PE = $\left\lvert \frac{P_{ave} - O_{ave}}{O_{ave}} \right\rvert 100\%$	(Eq.11)
Mean ratio (MR)	MR = n-1$\sum_{1}^{n} \frac{P_i}{O_i}$	(Eq.12)
Determination coefficient (R2) (Todorovic et al., 2013)	$R^2 = \left\{ \frac{\sum_{i=1}^{n}(O_i - \bar{O}).(P_i - \bar{P})}{\sqrt{\sum_{i=1}^{n}(O_i - \bar{O})^2}.\sqrt{\sum_{i=1}^{n}(P_i - \bar{P})^2}} \right\}^2$	(Eq.13)

RMSE: root mean squared error; MAE: mean absolute error; MR: mean ratio; PE: percentage error of estimate; n: number of observations, P_i: estimated ET_o by other equations, O_i: PM-estimated ET_o (actual), P_{ave}: mean of the estimated ET_o, O_{ave}: mean of the O_i. In order to determine R^2, the pair wise comparisons were made by using linear regression

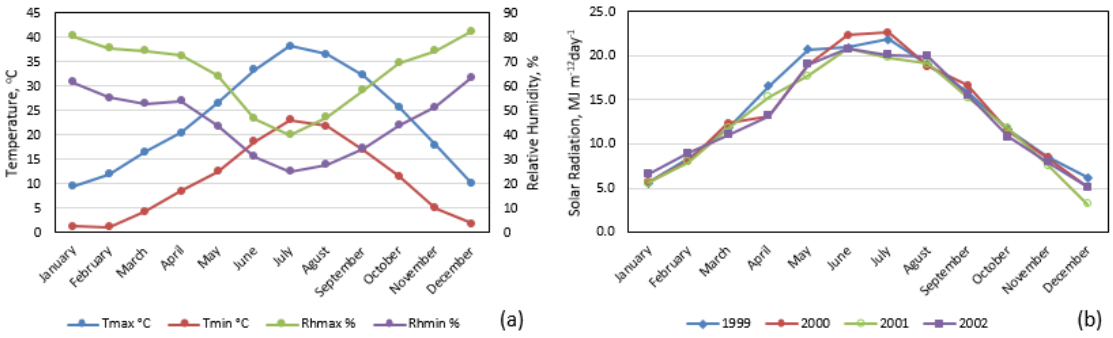

Figure 2. *Variation of long-term monthly average temperature and relative humidity (a) and solar radiation during study years (b)*

The 4 year mean values were calculated for the reference crop water consumption (ET_o) daily values obtained via the Hargreaveas-Samani ($ET_{o\text{-}HS}$), Turc ($ET_{o\text{-}TURC}$) and Pan evaporation methods ($ET_{o\text{-}CAP}$) compared in the study thereby obtaining long term average and annually total ET_o values which are presented in *Figure 3a* and *b*. As shown in *Figure 3a,* in the months which Class A Pan evaporation values measured were taken into consideration to compare the predicted plant water consumption values estimated by the models with the measured values. The period mentioned is the period in which pistachio is phenologically active and in this term, full bloom period is completed and begins the leafout period. The comparison of estimated and measured evaporation values was made until the end of October, which is the post-harvest period.

http://www.aloki.hu ● ISSN 1589 1623 (Print) ● ISSN 1785 0037 (Online)
DOI: http://dx.doi.org/10.15666/aeer/1704_1023910251

Likewise, as shown in *Figure 3b,* the monthly totals of the estimated and measured ET_o values were calculated for the mentioned period.

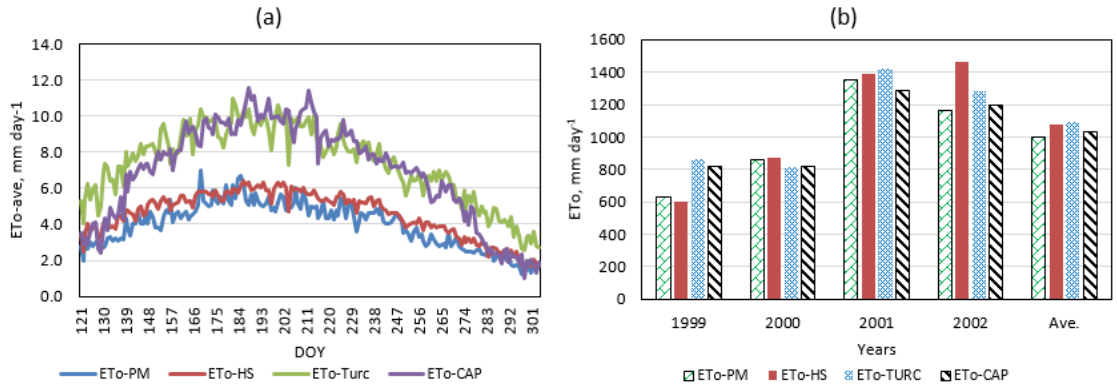

Figure 3. *Comparison of 4-year mean daily and total seasonally ET_o calculated from 4 methods during study years for evaporation season*

Average daily ET_o changing during study years. Similarly, The long term monthly mean values were calculated by taking the monthly mean ET_o values for the same years which are given in *Figure 4*. As can be seen in *Figure 4*, $ET_{o\text{-}PM}$ and $ET_{o\text{-}HS}$ values were determined to be close to each other, however the $ET_{o\text{-}Turc}$ and $ET_{o\text{-}Pan}$ values were observed to be greater than the $ET_{o\text{-}PM}$ and $ET_{o\text{-}HS}$ they were compared with. Long term mean monthly mean comparisons have yielded similar results as can be seen in *Figure 4.* Evaporation measurements are not carried out during the winter months (from November till April) in the study region, however other climate parameters are measured daily. Hence, it is not possible to calculate the $ET_{o\text{-}CAP}$ values for the aforementioned months. Çobaner et al. (2016) carried out a study for determining the best Hargreavas-Samani equation for the Mediterranean region as a result of which they put forth that the Hargreavas-Samani equation calibrated according to the temperature and humidity values put forth similar results with those calculated via Penman-Monteith. These findings of the researchers are in accordance with the results of the present study. Small differences in our results are due to the fact that the HS equation has not been calibrated for the GAP region and that it is used directly. Similarly, Trajkovic (2005) states that the Hargreaveas-Samani equation predicts ET_o higher than the actual value. The average values calculated via $ET_{o\text{-}CAP}$ and $ET_{o\text{-}Turc}$ methods showed a parallel change, similar to the change of radiation by temperature, as shown in *Figure 3a.* The $ET_{o\text{-}CAP}$ values increased rapidly during summer months when evaporation is measured.

Diouf et al. (2016) carried out a study for determining reference ET_o via Turc equation due to limited climate data under Senegal conditions as a result of which it was reported that the annual ET_o values were higher for the humid seasons according to the FAO-PM method. The researchers indicated that ET_o is mostly due to radiation and temperature under conditions of high humidity and that humidity does not have any impact on ET_o under any circumstance.

Fisher and Pringle (2013) carried out a study under humid regional conditions for comparing the Hargreavas–Samani and Turc methods with the FAO-56 model operated with reduced data as a result of which it was indicated that the FAO-56 reduced dataset

http://www.aloki.hu ● ISSN 1589 1623 (Print) ● ISSN 1785 0037 (Online)
DOI: http://dx.doi.org/10.15666/aeer/1704_1023910251

model yielded better results in comparison with the other two methods. The Turc equation developed for using the measured temperature and radiation value was tested with the equation using estimated radiation values and it was put forth that FAO-56 provides better estimations in comparison with the other methods.

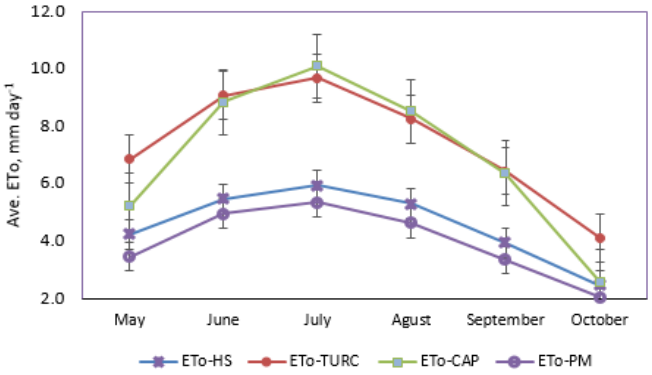

Figure. 4. *Comparison of 4-year mean monthly ET_o calculated from 4 methods during study years.*

Paired comparisons at the daily, 10 days and monthly average value levels were carried out for the reference crop water consumption values calculated in accordance with the methods used and the acquired results are presented graphically in *Figures 5–7*. As can be seen from *Figure 5,* the onset of the curve is at low levels during the first months when evaporation measured is not made in winter months while comparing $ET_{o\text{-}PM}$ and $ET_{o\text{-}CAP}$ values.

The methods used for reference ET_o were compared statistically and the acquired results have been summarized in *Table 3*.

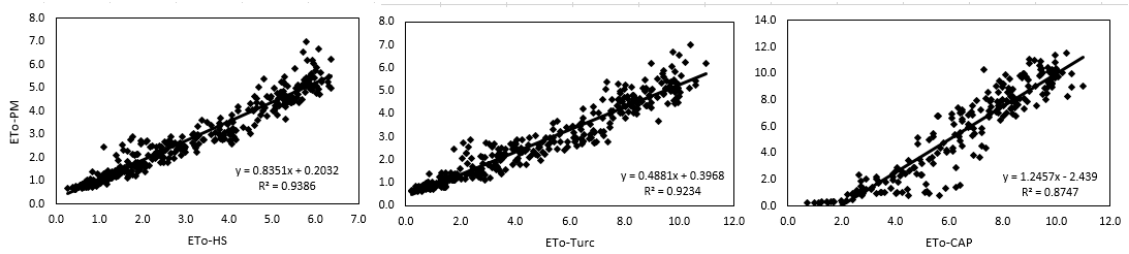

Figure 5. *Comparison of daily average ET_o for (1999-2002)*

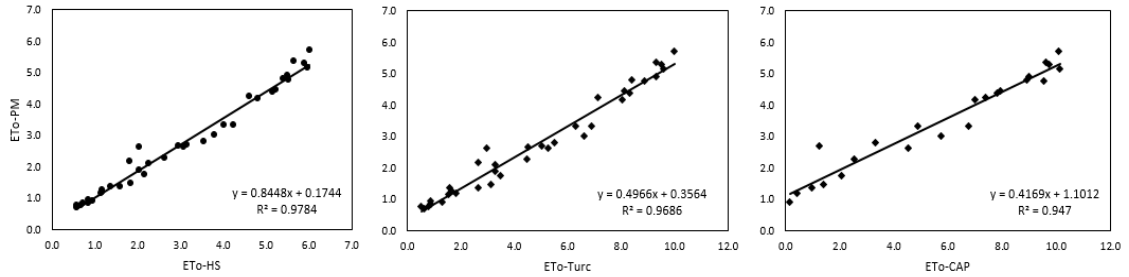

Figure 6. *Comparison of 10 days intervals average ET_o for (1999-2002)*

http://www.aloki.hu ● ISSN 1589 1623 (Print) ● ISSN 1785 0037 (Online)
DOI: http://dx.doi.org/10.15666/aeer/1704_1023910251

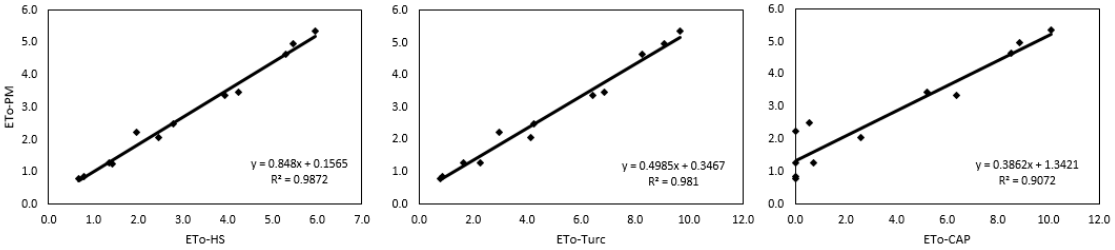

Figure 7. *Comparison of monthly average ET_o for (1999-2002)*

Table 3. *Error values of average daily ET_o estimates on daily basis as compared to FAO-PM method*

	Daily			10 days interval			Monthly		
	HS-PM	**Turc-PM**	**CAP-PM**	**HS-PM**	**Turc-PM**	**CAP-PM**	**HS-PM**	**Turc-PM**	**CAP-PM**
RMSE (mm/day)	0.58	2.65	2.62	0.15	0.82	0.81	0.08	0.47	0.46
MAE (mm)	0.45	2.11	2.14	0.04	0.21	0.21	0.01	0.07	0.07
MR	1.08	1.63	0.92	0.11	0.16	0.09	0.04	0.05	0.03
PE (%)	10.84	75.09	31.96	10.73	74.80	31.51	11.15	75.07	31.39
R^2	0.9386	0.9234	0.8747	0.9784	0.9686	0.947	0.9872	0.981	0.9072

Quantitative methods were applied for carrying out a statistical evaluation of the equations used in ET_o estimation. It is considered that the R^2 value approaching 1 and RMSE, MAE, MR and PE values approaching zero (0) from among the parameters given in *Table 3* which are used as criteria for comparing the methods indicate good performance and a high level of accordance between the compared values (Fisher and Pringle, 2013; Kaya et al., 2016).

The R^2 values of the studied methods were determined to be close but different in daily, weekly and monthly performance comparisons. It was determined as a result of the comparison made between reference crop water consumption methods for each of the three period intervals that the highest R^2 value was obtained as 0.9872 for $ET_{o\text{-}HS}$ and $ET_{o\text{-}PM}$ at the monthly level, while the lowest R^2 value was determined as 0.9386 for the comparison made at the daily level. The lowest R^2 value was also obtained as 0.8747 for the $ET_{o\text{-}PM}$-$ET_{o\text{-}CAP}$ method as a result of the comparison made for all three periods. Castaneda and Rao, (2005) compared Thornthwaite, Blaney Criddle, Turc and Makkink methods. It was indicated that the Turc method had the best performance among the compared methods since the values obtained were closest to the estimated values of the $ET_{o\text{-}PM}$ method prior to recalibration. They also put forth that other ET_o estimation methods also yield results within acceptable limits close to FAO-PM values in case regional parameters are used and the parameters are calibrated for the region. It will not be misleading to use the HS and Turc methods used in this study for making ET_o estimations in the region. When the compared methods are evaluated according to the RMSE values, lowest RMSE value should be obtained as is the case for other error parameters. As can be seen from the table, while the $ET_{o\text{-}HS}$-$ET_{o\text{-}PM}$ pair had the lowest RMSE value for monthly averages with 0.08, highest RMSE value was obtained as 2.65 from the $ET_{o\text{-}Turc}$ and $ET_{o\text{-}PM}$ paired comparison. Todorovic et al. (2013) carried out a comparison between HS and PMT models for reference ET_o estimation in the

http://www.aloki.hu ● ISSN 1589 1623 (Print) ● ISSN 1785 0037 (Online)
DOI: http://dx.doi.org/10.15666/aeer/1704_1023910251

Mediterranean climate region with limited data as a result of which similar HS and PMT values were obtained for the excessively arid and arid regions with those of MSE. While PMT yielded a lower RMSE value in semi-arid and humid regions as a result of which it was indicated to have a better performance in comparison with HS. It was observed as a result of the percentage error (PE) evaluations that the lowest percentage error was obtained as 10.73 for the 10 day interval comparison, while the highest percentage error was obtained as 75.09 for the $ET_{o\text{-}Turc}$ and $ET_{o\text{-}PM}$ comparison. Djaman et al. (2015) states that calibrated models display a better performance at cold and hot humid regions thereby leading to monthly values at an acceptable level, while the same performance has not been obtained for the semi-arid and tropical humid regions. Since the models are developed for use in the regional climate conditions for which they have been developed, they yield acceptable results only in similar climate conditions.

It was observed as a result of the statistical comparison between the studied methods that the highest R^2 value and the lowest percentage error value were obtained for the $ET_{o\text{-}HS}$-$ET_{o\text{-}PM}$ paired comparison in monthly average ET_o calculation. The results are observed to be in accordance with those of Çobaner et al. (2016) and Todorovic et al. (2013).

Conclusion

It was determined as a result of the study that the Hargreaveas-Samani model can be used for reference crop water consumption estimation in regions for Penman-Monteith model which full climate data cannot be obtained due to various reasons since these methods can be operated only with limited climate data and maximum temperature, minimum temperature, mean relative humidity and solar radiation inputs. Likewise the Turc model can also be a good alternative to estimate potential evapotranspiration which can be measured by Class A Pan. Moreover, the Penman-Monteith Temperature based (PMT) method used for ET_o estimation only with temperature data can also be used as an alternative for semi-arid climate conditions such as the GAP region.

REFERENCES

[1] Allen, R. G., Pereira, L. S., Raes, D., Smith, M. (1998): Crop Evapotranspiration (Guidelines for Computing Crop Water Requirements). – FAO-56 Irrigation and Drainage Paper No: 56. FAO, Rome.
[2] Anonymous (2001): Pistachio Breading. – Pistachio Research Institute Directorate. Publication Number: 13. Gaziantep-Turkey (in Turkish).
[3] Anonymous (2017): Water Consumption of Irrigated Crops in Turkey. – Ministry of Food Agriculture and Livestock, General Directorate of Agricultural Research and Policies, Ankara (in Turkish).
[4] Anonymous (2019): http://cekings.ucanr.edu/. – Date of access: 27th May 2019.
[5] Aslan, N. (2017): Pistachio production in the world and Turkey. – The Journal of Pistachio Research 6: 2-5 (in Turkish).
[6] Aydın, Y. (2004): The effect of different irrigation water and nitrogen levels on yield and alternate bearing in pistachio. – Ph.D Thesis. Çukurova Uni. Institute of Natural and Applied Science. Department of Agriculture Structure and Irrigation (in Turkish).
[7] Bilgel, L., Dağdeviren, İ., Nacar, A. S. (1999): Determination of water consumption and irrigation program of pistachio (Siirt cultivar) in Harran Plain conditions of the GAP

http://www.aloki.hu ● ISSN 1589 1623 (Print) ● ISSN 1785 0037 (Online)
DOI: http://dx.doi.org/10.15666/aeer/1704_1023910251

region. – III. Horticultural Plant Congress of Turkey, Sep, 14-17, Ankara, pp. 252-257 (in Turkish).

[8] Castaneda, L., Rao, P. (2005): Comparison of methods for estimating reference evapotranspiration in southern California. – Journal of Environmental Hydrology 13: 1-10.

[9] Çobaner, M., Çıtakoğlu, H., Haktanır, T., Yelkara, F. (2016): Determination of Hargreaves-Samani equation for the Mediterranean region. – Dicle Üniversity, Faculty of Engineering, Journal of Engineering 7(2): 181-190 (special issue, in Turkish).

[10] Diouf, O. C., Weihermüller, L., Ba, K., Faye, S. C., Faye, S., Vereecken, H. (2016): Estimation of Turc reference evapotranspiration with limited data against the Penman-Monteith formula in Senegal. – Journal of Agriculture and Environment for International Development - JAEID 110(1): 117-137 DOI: 10.12895/jaeid.20161.417.

[11] Djaman, K., Balde, A. B., Sow, A., Muller, B., Irmak, S., N'Diaye, M. K., Manneh, B., Moukoumbi, Y. D., Futakuchic, K., Kazuki Saito, S. (2015): Evaluation of sixteen reference evapotranspiration methods under sahelian conditions in the Senegal River Valley. – Journal of Hydrology: Regional Studies 3: 139-159. www.elsevier.com/locate/ejrh.

[12] Fisher, D. K., Pringle III, H. C. (2013): Evaluation of alternative methods for estimating reference evapotranspiration. – Agricultural Science 4(8A): 51-60. http://dx.doi.org/10.4236/as.2013.48A008.

[13] Gavilan, P., Lorite, I. J., Tornero, S., Berengena, J. (2006): Regional calibration of Hargreaves equation for estimating reference ET in a semiarid environment. – Agricultural Water Management 81: 257-281.

[14] Hargreaves, G. H., Samani, Z. A. (1985): Reference crop evapotranspiration from ambient air temperature. – American Society of Agricultural Engineers, Hyatt Regency, Chicago IL 1985 Winter Meeting, December 17-20, Paper No: 85-2517.

[15] Kanber, R., Önder, S., Köksal, H. (1992): Investigation of pistachio yield and water consumption in southeastern Anatolia conditions. – First International Symposium on Pistachio of Turkey, Gaziantep, pp. 145-160 (in Turkish).

[16] Kaya, S., Evren, S., Daşcı, E. (2016): Comparison of various equations for prediction of class A pan evaporation in semi-arid climatic conditions. – Uludağ Uni. Journal of Agriculture Faculty 30(2): 1-9 (in Turkish).

[17] Lu, J., Sun, G., McNulty, S. G., Amatya, D. M. (2005): A comparison of six potential evapotranspiration methods for regional use in the southeastern United States. – Journal of the American Water Resources Association 41: 621-633.

[18] Shahidian, S., Serralheiro, R., Serrano, J., Teixeira, J., Haie, N., Santos, F. (2012): Hargreaves and Other Reduced-Set Methods for Calculating Evapotranspiration. – In: Irmak, A. (ed.) Evapotranspiration—Remote Sensing and Modeling. InTech, Morn Hill, pp. 59-80. DOI: 10.5772/725.

[19] Tabari, H., Grismer, M. E., Trajkovic, S. (2013): Comparative analysis of 31 reference evapotranspiration methods under humid conditions. – Irrigation Science 31: 107-117.

[20] Todorovic, M., Karic, B., Pereira, L. S. (2013): Reference evapotranspiration estimate with limited weather data across a range of Mediterranean climates. – Journal of Hydrology 481: 166-176.

[21] Trajkovic, S. (2005): Temperature-based approaches for estimating reference evapotranspiration. – Journal of Irrigation Drainage Engineering 131(4): 316-323.

[22] Trajkovic, S., Stojnić, V. (2008): Simple daily ET_o estimation techniques. – Facta Universitatis Series: Architecture and Civil Engineering 6(2): 187-192. DOI: 10.2298/FUACE0802187T.

[23] Turc, L. (1961): Water requirements assessment of irrigation, potential evapotranspiration: simplified and updated climatic formula. – Annales Agronomiques 12: 13-49.

http://www.aloki.hu ● ISSN 1589 1623 (Print) ● ISSN 1785 0037 (Online)
DOI: http://dx.doi.org/10.15666/aeer/1704_1023910251

[24] Ünlü, M., Kanber, R., P. Steduto, P., Aydın, Y., Diker, K. (2005): Effects of different water and nitrogen levels on the yield and periodicity of pistachio (*Pistachia vera L*). – Turkish Journal of Agriculture and Forestry Sciences 29: 39-49.

[25] Yamaç, S. S. (2018): Estimation of long term reference evapotranspiration using limited weather data in sugar beet plantation area from Middle Anatolian, Turkey. – Süleyman Demirel Üniversity, Journal of Agriculture Faculty (1. International Congress on Agricultural Structure and Irrigation) Special Number: 160-1165.

http://www.aloki.hu ● ISSN 1589 1623 (Print) ● ISSN 1785 0037 (Online)
DOI: http://dx.doi.org/10.15666/aeer/1704_1023910251

CONSUMERS' ENVIRONMENTAL MANAGEMENT OF WASTE ANALYSIS OF THE FORMER YUGOSLAVIAN REPUBLICS

RALETIĆ JOTANOVIĆ, S.[1*] – SUDAREVIĆ, T.[2] – GRUBOR. A.[2] – KATIĆ, A.[3] – VUKSANOVIĆ, N.[1]

[1]*Professional College of Management and Business Communications*
Mitropolita Stratimirovića 110, Sremski Karlovci, Republic of Serbia

[2]*Faculty of Economics, University of Novi Sad*
Segedinski put 9-11, 24000 Subotica, Republic of Serbia

[3]*Faculty of Technical Sciences, University of Novi Sad*
Trg Dositeja Obradovića, 21000 Novi Sad, Republic of Serbia

**Corresponding author*
e-mail: raletic.sasa84@gmail.com

(Received 8th Dec 2018; accepted 10th Apr 2019)

Abstract. The aim of this study is to compare environmental management of waste between consumers of the former Yugoslavian republics. The starting points are H1: there are differences in environmental management of waste between consumers from the former Yugoslavian republics and H2: there are demographic differences in consumers' environmental management of waste between consumers from the former Yugoslavian republics. The survey was conducted on a sample of 1550 respondents from all the former Yugoslavian republics. The obtained results show that there are differences between consumers from Macedonia and all other former Yugoslavian republics as well as between Montenegro and Serbia, Croatia and Slovenia. Also, differences were noticed between consumers' environmental management of various types of waste. At the same time, results indicate that there are no differences in gender but differences in age, degree of education and monthly income by households exist related to environmental management of waste between consumers from former Yugoslavian republics. Through adequate implementation of obtained results, consumers' environmental management of waste may become a powerful tool of environmental protection, because it would contribute to the increase of environmentally responsible behavior of consumers in the region of former Yugoslavian republics as well as on a global basis.
Keywords: *consumers, waste disposal, ecological, former Yugoslavian republics, cross-cultural*

Introduction

Present level of consumer waste management is worrying level. This is indicated, among others, by facts related to plastic and electronic waste:

- 90% of waste floating in the oceans is plastic waste (http1://www.theworldcounts.com/stories/Plastic-Waste-Facts=).
- In the North Pacific Ocean there is 6 times more plastic waste than plankton, causing the death of the living world in the ocean (http1://www.theworldcounts.com/stories/Plastic-Waste-Facts=).
- Plastics are made from toxic materials such as benzene and vinyl hydrochloride, and these chemicals are known to cause cancer (http1://www.theworldcounts.com/stories/Plastic-Waste-Facts=).
- We generate about 40 million tons of electronic waste worldwide every year (http1://www.theworldcounts.com/stories/Plastic-Waste-Facts=).
- E-waste contains hundreds of substances, many of which are toxic. This includes mercury, lead, arsenic, cadmium, selenium, and chromium (http2://www.theworldcounts.com/stories/Electronic-Waste-Facts).

http://www.aloki.hu ● ISSN 1589 1623 (Print) ● ISSN 1785 0037 (Online)
DOI: http://dx.doi.org/10.15666/aeer/1704_72297248

- 70% of total toxic waste is e-waste (http2://www.theworldcounts.com/stories/Electronic-Waste-Facts).

This suggests that the adequate waste management by consumers, in a way that would not degrade the environment, is a necessity and a global problem today.

Disposal of waste in an ecological way implies the disposal of products that have expired or are defective and the disposal of product packaging after consuming the products at designated locations, in adequate containers and warehouses, and in an adequate manner.

Since consumers' environmental management of waste is a global problem, cross-cultural studies of consumers' habits regarding management of waste are excellent tools to provide information on the consumers' environmental management of waste and the way in which it may be improved at the regional level.

However, there are not enough cross-cultural studies on the topic of consumers' environmental management of waste, but only those comparing consumers from two countries: French – USA (United States of America) (Arbuthnot and Lingg, 1975), Belgium – Poland (Roozen and Pelsmacker, 2000), Switzerland – India (Sinha-Khetriwala et al., 2005), Norway – USA (Kipperberg, 2007) and USA – China (Xu et al., 2014).

Therefore the authors have concluded that there is no relevant cross-cultural research paper which analyses consumers' environmental management of waste between consumers from former Yugoslavian republics: the Republic of Serbia (Serbia), the Republic of Croatia (Croatia), the Republic of Slovenia (Slovenia), the Former Yugoslav Republic of Macedonia (FYR Macedonia), the Federation of Bosnia and Herzegovina (Bosnia and Herzegovina) and Republic of Montenegro (Montenegro).

There are two cross-cultural studies conducted on a sample of all six of the former Yugoslavian republics regarding environmentally responsible purchasing (Raletić Jotanović et al., 2016) and environmentally responsible consumption (Raletić Jotanović et al., 2017).

The aim of this study is to compare environmental management of waste between consumers from former Yugoslavian republics. The former Yugoslavian republics are selected for comparison because: a) they had 73 years of shared history which certainly influenced similarities in consumer behavior, and b) today all the former Yugoslavian republics are independent countries with different macro, structural, demographic, socio-economic, and other characteristics (State Statistical Office of Macedonia, 2018; Institute for Statistics of Serbia, 2018; Statistical Office of the Slovenia, 2018; Statistical Office of the Montenegro, 2018; Croatian Bureau of Statistics, 2018; Federal Office of Statistics of Bosnia and Herzegovina, 2018). According to the authors' knowledge this will be the first cross-cultural study of the former Yugoslavian republics regarding consumers' environmental management of waste.

Environmental management of waste between consumers from different countries

Consumers' environmental management of waste is different in different countries, according to the results of previous empirical comparative cross-cultural researches: (Arbuthnot and Lingg, 1975; Roozen and Pelsmacker, 2000; Sinha-Khetriwala et al., 2005; Kipperberg, 2007; Xu et al., 2014). Minimal differences were observed in consumers' environmental management of waste between in France and USA (Arbuthnot and Lingg, 1975). Belgian consumers manage their waste more environmentally than Polish ones (Roozen and Pelsmacker, 2000). The consumers from

http://www.aloki.hu ● ISSN 1589 1623 (Print) ● ISSN 1785 0037 (Online)
DOI: http://dx.doi.org/10.15666/aeer/1704_72297248

the Switzerland manage their e-waste (computers, television sets, microwave ovens, etc.) more environmentally than consumers from India (Sinha-Khetriwala et al., 2005). Environmental management of waste sometimes is better with consumers from Norway and sometimes with consumers from the USA, depending on the type of waste (Kipperberg, 2007). The consumers from the USA are more prone to dispose clothing and footwear at environmental way (using and buying second-hand clothing and footwear) than consumers from China (Xu et al., 2014). All these differences may be explained by differences in level of consciousness, knowledge and attitude towards environment in consumers from different countries (Arbuthnot and Lingg, 1975; Roozen and Pelsmacker, 2000; Sinha-Khetriwala et al., 2005; Kipperberg, 2007; Xu et al., 2014)

According to the results of previous studies, numerous macro factors have affected environmentally responsible consumer choice which also includes consumers' environmental management of waste (Dolan, 2002; Schaefer and Crane, 2005; Thøgersen, 2005; Assadourian, 2010; Marx et al., 2010). In other words, macro factors may be the basis for differences in environmental management of waste between consumers from various countries. Factors that could affect these differences between the former Yugoslavian countries are shown in *Table 1*.

Table 1. *Macro factors of former Yugoslavian countries. (Sources: WEF, 2018 pp. 499, 519, 363, 109, 403, 179; WEF, 2016 pp. 122, 156, 244, 266, 314, 322; WEF, 2014 p. 68)*

Factors \ Country	Serbia	Slovenia	Macedonia	Bosnia and Herzegovina	Montenegro	Croatia
GDP per capita (US$)	5,899.0[1]	20,732.5[2]	5,474.4[3]	5,149.0[4]	7,647.0[5]	13,138.3[6]
Environmental footprint	2.9[1]	4.7[2]	3.1[3]	3.3[4]	3.4[5]	3.6[6]
Quality of education	3.55[7]	4.6[8]	3.85[9]	3.15[10]	3.92[11]	3.7[12]
Sophistication of business	3.00[7]	4.03[8]	3.6[9]	3.23[10]	3.46[11]	3.53[12]
Environmental sustainability[13]	3.86 →	4.78 ↗	3.66 ↘		4.38 →	4.21 →

The World Economic Forum does not publish each year all the parameters for ranking countries listed *Table 1*, so, for example, environmental sustainability as a factor was last measured and published in the Global Competitive Report for 2014-2015.

Table 1 is obviously missing values for environmental sustainability for Bosnia and Herzegovina. Also, data in *Table 1* show that Slovenia had the highest values for all factors. Serbia had the lowest values for environmental footprint and sophisticated business, Bosnia and Herzegovina had the lowest values of GDP (gross domestic product) per capita and quality of education, while Macedonia had the lowest value of environmental sustainability.

Considering the results of earlier cross-cultural researches (Arbuthnot and Lingg, 1975; Roozen and Pelsmacker, 2000; Sinha-Khetriwala etal., 2005; Kipperberg, 2007;

http://www.aloki.hu ● ISSN 1589 1623 (Print) ● ISSN 1785 0037 (Online)
DOI: http://dx.doi.org/10.15666/aeer/1704_72297248

Xu et al., 2014) and macro and structural factors of former Yugoslavian republics shown in the *Table 1*, it can be assumed that:

H1: There are differences in consumers' environmental management of waste for different former Yugoslavian republics.

Relationships between consumers' environmental management of waste and demographic characteristics of consumers: gender, age, professional qualifications and monthly income by household, were analyzed in numerous studies conducted in different countries (Samdahland Robertson, 1989; Granzin and Olsen, 1991; Shamdasaniet al., 1993; Chan, 2001; Gilg et al., 2005; Jain and Kaur, 2006; Tilikidou and Delistavrou, 2008; Abeliotis et al., 2010; De Paço and Raposo, 2010; Pedrini and Ferri, 2014; Pinto et al., 2014; Pagiaslis and Krontalis, 2014; Aschemann-Witzel et al., 2017; Paço andLavrador, 2017; Pérez-Belis et al., 2017; Zhanget al., 2018; Scherer et al., 2018; Savchenkoet al., 2019; Talia et al., 2019). These relationships are shown in the *Table 2a-d*.

***Table 2a**. The relationships between consumers' environmental management of waste and the gender of consumers in different countries*

Country	Women and men are equal	Women are more active than men	Man are more active than women
USA		Granzin and Olsen, 1991	Savchenko et al., 2019
Singapore	Shamdasani et al., 1993		
UK	Gilg et al., 2005		
Greece	Tilikidou and Delistavrou, 2008; Abeliotis et al., 2010		
Portugal	De Paço and Raposo, 2010; Paço and Lavrador, 2017		
Italy	Pedrini and Ferri, 2014; Talia et al., 2019		
Spain		Pérez-Belis et al., 2017	
India		Jain and Kaur, 2006	
Germany	Scherer et al., 2018	Pinto et al., 2014	

***Table 2b.** The relationships between consumers' environmental management of waste and the age of consumers in different countries*

Country	Older consumers are more active	Younger consumers are more active	Age does not affect
USA	Savchenko et al., 2019	Granzin and Olsen, 1991	
Singapore			Shamdasani et al., 1993
UK	Samdahl and Robertson, 1989; Gilg et al., 2005		
China	Chan, 1999		
Portugal	De Paço and Raposo, 2010		
Italy		Talia et al., 2019	
Spanish	Pérez-Beliset al., 2017		
Denmark	Aschemann-Witzel et al., 2017		
Germany	Pagiaslis and Krontalis, 2014		Pinto et al., 2014; Scherer et al., 2018

http://www.aloki.hu ● ISSN 1589 1623 (Print) ● ISSN 1785 0037 (Online)
DOI: http://dx.doi.org/10.15666/aeer/1704_72297248

Table 2c. *The relationships between consumers' environmental management of waste and the professional qualifications of consumers in different countries*

Country	Educated consumers are more active	Less educated consumers are more active	Professional qualifications does not affect
USA	Granzin and Olsen, 1991	Arbuthnot and Lingg, 1975	
Singapore			Shamdasani et al., 1993
UK		Samdahl and Robertson, 1989	
China	Chan, 1999		
Greece	Tilikidou and Delistavrou, 2008; Abeliotis et al., 2010		
Portugal	De Paço and Raposo, 2010		
Italy	Pedrini and Ferri, 2014; Talia et al., 2019		
India	Jain and Kaur, 2006		
Denmark	Aschemann-Witzel et al., 2017		
Germany	Pagiaslis and Krontalis, 2014; Pinto et al., 2014		Scherer et al., 2018

Table 2d. *The relationships between consumers' environmental management of waste and the monthly income of consumers in different countries*

Country	Consumers who have higher incomes are more active	Consumers who have lower incomes are more active	Monthly earnings does not affect
USA	Granzin and Olsen, 1991		
Singapore			Shamdasani et al., 1993
UK		Samdahl and Robertson, 1989	
China	Chan, 1999	Zhang et al., 2018	
Portugal	De Paço and Raposo, 2010		
Italy	Pedrini and Ferri, 2014; Talia et al., 2019		
India	Jain and Kaur, 2006		
Greece	Tilikidou and Delistavrou, 2008; Abeliotis et al., 2010		
Germany	Pagiaslis and Krontalis, 2014; Pinto et al., 2014		Scherer et al., 2018
Denmark	Aschemann-Witzel et al., 2017		

Given the results of previously conducted research from *Table 2*, the basic assumption is that:

H2: There are differences in demographic characteristics of consumers related to consumers' environmental management of waste from different former Yugoslavian republics.

http://www.aloki.hu ● ISSN 1589 1623 (Print) ● ISSN 1785 0037 (Online)
DOI: http://dx.doi.org/10.15666/aeer/1704_72297248

Materials and methods

Sample

The study included 1,550 respondents from six former Yugoslavian republics: 17.81% (276) participants from Serbia, 16.13% (250) participants from Croatia, 17.10% (265) participants from Bosnia and Herzegovina, 16.13% (250) participants from Montenegro, 16.32% (253) participants from Macedonia and 16.51% (256) participants from Slovenia (*Table 3*).

Table 3. *Sample composition. (Source: authors' data)*

Demographic characteristics in %		Serbia	Slovenia	Macedonia	Bosnia and Herzegovina	Montenegro	Croatia	Total %
Gender	Male	41.30	27.34	36.76	41.89	43.6	31.2	**37.01**
	Female	58.70	72.66	63.24	58.11	56.4	68.8	**62.90**
Age	18-30	42.75	32.81	41.50	55.09	78.8	54.8	**50.76**
	31-40	31.16	34.77	26.88	24.91	13.6	19.2	**25.23**
	41-50	7.97	21.48	11.07	13.58	6.40	13.6	**12.52**
	51-60	11.59	8.60	9.49	6.04	0.8	9.6	**7.68**
	61-70	5.07	1.95	5.53	0.38	0.4	2.4	**2.65**
	71-80	0.72	0	3.16	0.00	0	0.4	**< 1**
Degree of education	Primary school	1.81	0.78	2.37	0.00	0	0.8	**< 1**
	High school	45.65	17.19	41.11	50.57	49.20	48.40	**39.81**
	College, university	33.70	59.77	27.27	31.32	35.6	38	**39.81**
	MSc/PhD	18.12	21.88	27.67	18.11	15.20	12.8	**19.61**
Monthly income by household	Below average	25.36	19.53	11.07	7.92	22.8	16.8	**33.68**
	Average	40.22	47.27	57.70	72.83	47.00	69.6	**48.90**
	Above average	34.06	32.81	31.23	19.25	30.2	13.6	**17.30**
Total		**276**	**256**	**253**	**265**	**250**	**250**	
%		**17.81**	**16.51**	**16.32**	**17.10**	**16.13**	**16.13**	**100**

When analyzing sample structure regarding the gender, that there is twice as much women than men (62.90% and 37.01%, respectively) (*Table 3*).

When considering the age structure of the sample, respondents between 18 and years of age make up the majority of the sample, i.e., 50.76% of the sample, while respondents between 71 and 80 are the least represented in the sample with <1% (*Table 3*). The second biggest category in the sample, according to age, is composed of respondents aged 31 to 40 with 25.23% of the sample, followed by respondents aged 41 to 50 years with 12.52% of the sample, then respondents between the age of 51 and 60 which make up 7.68% of the sample, while subjects between 61 and 70 years make up 2.65% of the sample. Seven of the respondents did not answer the question about their age (*Table 3*).

When considering the structure of the sample according to the professional qualification, the same number of respondents (39.81%) has graduated from a university and has completed high school. These categories make up the majority of respondents

http://www.aloki.hu ● ISSN 1589 1623 (Print) ● ISSN 1785 0037 (Online)
DOI: http://dx.doi.org/10.15666/aeer/1704_72297248

in the sample. Respondents with completed master studies, magisterium or doctorate make 19.16% of the sample. Less than 1% of the sample has completed elementary school only. Four respondents did not provide information on the qualifications (*Table 3*).

Finally, through the analysis of *Table 3*, it can be noted that most of the sample consists of respondents who live in the household with average monthly income, 48.90% of them. Respondents living in households below average monthly income make up 33.68% of the sample (*Table 3*). The lowest percentage of respondents, 17.30%, lives in households with monthly income above the average (*Table 3*). Two respondents did not answer the question about the monthly income of their households (*Table 3*).

The sampling method was the stratified sample. The total population from the territory of the former Yugoslavian republics is divided into strata, which are now independent countries: Serbia, Croatia, Bosnia and Herzegovina, Montenegro, Macedonia, and Slovenia. After that, simple random sample method was used for each stratum.

The total population from the territory of the former Yugoslavian republics is about 20 million people while the size of the sample analyzed is 1,550 respondents. The sample size is small but acceptable, having in mind that this sample mostly reflects demographic structure of the analyzed population (in all ex-Yugoslavian republics women are more numerous than men, most of population has graduated from a high school and then those with an university degree are following, most people live in household with average monthly income) (State Statistical Office of Macedonia, 2018; Institute for Statistics of Serbia, 2018; Statistical Office of the Slovenia, 2018; Statistical Office of the Montenegro, 2018; Croatian Bureau of Statistics, 2018; Federal Office of Statistics of Bosnia and Herzegovina, 2018). The sample size is small but acceptable regarding the nature of investigation, changes of population characteristics, changes of investigation object.

Instrument

For the purposes of this study, and following the example of previously conducted research (Roozen and Pelsmacker, 2000; Gilg et al., 2005; Sinha-Khetriwala etal., 2005; Kipperberg, 2007; Xu et al., 2014) an instrument – the questionnaire – was composed to test the difference between consumers' environmental management of waste in different former Yugoslavian republics. The items in the questionnaire were adapted to the national and the international environment of the countries in which the research was conducted.

The questionnaire is composed of three parts (see *Appendix*). The first part of the questionnaire is the respondents' consent for filling the questionnaire. Completing the questionnaire was anonymous. The second part of the questionnaire is based on the demographic characteristics of the respondents: state, gender, age, education and monthly household income. State, gender, education and household monthly income inquiries are of a closed type, while the question of the age of the respondents is of open type. In order to maximally adjust the questionnaire to cross-cultural research, it was necessary to standardize the data relating to monthly household income, given the fact that this data is differently shown in Statistical Yearbooks for the year 2018 of analyzed countries. Data on household income is reduced to a monthly level per household, because such type of data was found in most of the Statistical Yearbooks analyzed from former Yugoslavian republics. Questions related to monthly household income were set

http://www.aloki.hu ● ISSN 1589 1623 (Print) ● ISSN 1785 0037 (Online)
DOI: http://dx.doi.org/10.15666/aeer/1704_72297248

in the currency of the country in which the questionnaire was distributed, for easier understanding and answering questions. The third part of the questionnaire refers to consumers' environmental management of waste (*Table 4*). It has 7 items and every item connected to different group of waste (products): 1) food, 2) chemicals and pharmacy products, 3) clothing and footwear, 4) furniture, 5) electrical appliances, 6) means of transport, and 7) products of paper and cardboard (*Table 5*). Answers to the questionnaire were measured by Likert scale: 1-strongly disagree, 2-mostly disagree, 3-undefined, 4-mostly agree, and 5- completely agree.

Table 4. *Descriptive statistics of items in the total sample. (Source: authors' data)*

	Items	**M**	**SD**
Consumers' environmental management of waste	When possible, I put my leftover food in compost	3.23	1.39
	I do not throw expired medication in waste	3.04	1.50
	I do not throw away old clothes but rather donate it	4.42	.91
	I would leave an old sofa by the garbage container	3.01	1.60
	I put old electric appliances in the garbage container	2.33	1.41
	Parts of unusable bicycle, car and/or engine I would place next to the garbage container	2.59	1.50
	I put old paper into a paper container	3.64	1.45

Table 5. *Descriptive statistics of items regarding different groups of products and former Yugoslavian republics. (Source: authors' data)*

Country	**Serbia**		**Croatia**		**Bosnia and Herzegovina**		**Slovenia**		**Macedonia**		**Montenegro**	
Product	M	SD	M	SD	M	SD	M	SD	M	SD	M	SD
Food	3.0	1.36	3.3	1.42	3.0	1.40	4.3	.940	2.7	1.28	3.0	1.34
Medicaments	3.0	1.51	3.2	1.38	2.8	1.41	4.0	1.20	2.5	1.37	2.6	1.56
Clothing and footwear	4.4	.968	4.3	.939	4.4	.878	4.6	.772	4.4	.932	4.3	.981
Furniture	3.5	1.46	3.1	1.47	3.1	1.53	2.1	1.56	2.6	1.59	3.3	1.57
Technical devices (e-waste)	2.6	1.46	2.3	1.29	2.4	1.30	1.5	.975	2.2	1.44	2.7	1.54
Means of transport	3.0	1.54	2.6	1.42	2.8	1.54	1.7	1.14	2.4	1.44	2.8	1.52
Paper	3.4	1.43	4.1	1.17	3.4	1.42	4.8	.504	3.2	1.40	2.8	1.51

The questionnaires were translated into Slovenian, Macedonian, Croatian, and Serbian. Respondents from Serbia, Bosnia and Herzegovina, and Montenegro filled in questionnaires in Serbian considering that they can be classified in the same language area.

The questionnaire was distributed personally "paper and pencil" (PAPI – Paper and pencil interviewing) (Lavrakas, 2008) and through various Internet platforms (Google Drive, Facebook, email, etc.). It was given to the respondents by researchers, who had asked their colleagues, friends and family to fill the questionnaire and to send other

http://www.aloki.hu ● ISSN 1589 1623 (Print) ● ISSN 1785 0037 (Online)
DOI: http://dx.doi.org/10.15666/aeer/1704_72297248

copies to their friends and colleagues. Also, it was sent by the Internet to the e-mail addresses of various entities: private individuals, non-governmental organizations, higher education institutions, businesses, statistical bureaus of the countries, etc.

Variables

Independent variables in this study are: country, gender, age, professional qualification and monthly income by household, while the dependent variable is consumers' environmental management of waste.

Data analysis

For data processing, authors used the software package SPSS:16 (Norusis, 2008).

Preparing the data for the main analysis included the replacement of missing values by EM method and the treatment of extreme values that resulted in not showing even one outlier.

After preparing the data, exploratory factor analysis (EFA) was conducted. The results of EFA suggested that there is a relative satisfactory factor structure of the questionnaire. EFA was conducted for each country separately. Next, the obtained factor structure was confirmed by confirmatory factor analysis (CFA) in statistical packages "lavaan" and "semTools", written for the R environment.

One-way ANOVA with country as a factor (6 levels) and Tukey's HSD post hoc test were used as the methods for determining the differences in consumers' environmental management of waste between the former Yugoslavian republics. Also, two-way ANOVA and Tukey's HSD post hoc test were used to test the differences in demographic characteristics of respondents related to consumers' environmental management of waste between former Yugoslavian republics, with the following factors: country (6 levels) and gender (2 levels), country (6 levels) and age of respondents (6 levels), country (6 levels) and degree of education (4 levels), and country (6 levels) and monthly income by household (3 levels).

Results

Descriptive statistics

Descriptive statistics by arithmetic mean (M) and standard deviation (SD) of the questionnaire items regarding the consumers' environmental management of waste is shown in *Table 4*.

Table 5 shows descriptive statistics by arithmetic mean (M) and standard deviation (SD) of items regarding different groups of waste by products relative to former Yugoslavian republics.

Table 6 shows descriptive statistics for reliability of questionnaires by arithmetic mean (M) and standard deviation (SD). Results do not deviate significantly from the norm (the values of the skewness and kurtosis are within the allowed limits), despite the significant values of the K-S statistics (Kolmogorov-Smirnov test). Subscales reliability coefficients (α) for most of the individual countries are not proven to be quite adequate, since their values are lower than .70 (*Table 6*). The overall reliability coefficient for the sample is not entirely satisfactory since it is lower than the prescribed one. The reliability coefficient values could be explained by a small number of items for each subscale. The authors decided on a small number of items due to the nature of this cross-cultural study.

http://www.aloki.hu ● ISSN 1589 1623 (Print) ● ISSN 1785 0037 (Online)
DOI: http://dx.doi.org/10.15666/aeer/1704_72297248

Table 6. *Descriptive statistics and reliability coefficients of questionnaire. (Source: authors' data)*

Country	M	SD	Skewness	Kurtosis	K-S	α
Serbia	23.21	4.89	-.319	-.075	.070*	.490
Croatia	22.99	5.27	-.149	-.543	.064*	.660
Bosnia and Herzegovina	22.07	4.65	-.118	.001	.069*	.440
Montenegro	21.74	5.09	-.021	.164	.076*	.507
Macedonia	20.22	5.41	.531	.257	.089*	.647
Slovenia	23.22	3.28	.558	.725	.210*	.313
Total	22.26	4.92	-.061	-.037	.067*	.483

*p < .01

Differences in waste disposal among consumers from former Yugoslavian republics

The results of the one-factor variance analysis with country as an independent variable (6 levels) and the dependent variable of consumers' environmental management of waste show that there is a statistically significant difference between the respondents from different countries in terms of consumers' environmental management of waste, $F(5, 1544) = 14.91$, $p < .01$, $\eta^2_p = .05$. Post hoc tests (Tukey's HSD) showed that respondents from Macedonia (M = 20.22, SD = 5.42), dispose their waste in ecological way in the lowest degree in comparison to respondents from all other countries in the sample ($p < .01$). Also, it has been shown that respondents from Montenegro (M = 21.74, SD = 5.1) disposed less of the waste in an ecological manner compared to respondents from Serbia (M = 23.21, SD = 4.89, $p < .01$), Croatia (M = 23, SD = 5.27, $p < .01$), and Slovenia (M = 23.22, SD = 3.28, $p < .01$).

The results of the one-factor analysis of the variance with the country as a factor (6 levels) and the consumers' environmental management of food waste as a dependent variable indicate that there are significant differences between respondents from different countries, $F(5, 1544) = 48.02$, $p < .01$, $\eta^2_p = .14$. Post hoc tests show that respondents from Slovenia show a significantly higher level of ecological disposal of food waste, compared to respondents from all other countries ($p < .01$). Respondents from Macedonia are less prone to dispose of food waste in ecological manner in comparison to respondents from Bosnia and Herzegovina and Croatia ($p < .01$).

The results of the one-factor analysis of variance with the country as a factor (6 levels) and the consumers'' environmental management of medicament waste as a dependent variable indicate the existence of significant differences between respondents from different countries, $F (5, 1544) = 38.98$, $p < .01$, $\eta^2_p = .11$. Post hoc tests ($p < .01$ - .05) suggest that respondents from Slovenia apply more ecological disposal of medicament waste in comparison to respondents from all other countries, and that respondents from Macedonia and Montenegro are less prone to ecological disposal of medication waste in comparison to respondents from Serbia and Croatia ($p < .01$ - .05).

The results of the one-factor variance analysis with the country as a factor (6 levels) and the consumers' environmental disposal of clothing and footwear waste as a dependent variable show that there are significant differences between the respondents, $F (5, 1544) = 3.47$, $p < .01$, $\eta^2_p = .01$. Post hoc tests further show that respondents from Slovenia are ecologically disposing their clothing and footwear waste in a slightly higher degree, compared to respondents from Croatia and Montenegro ($p < .01$ - .05)

The results of the one-factor analysis of variance with the country as a factor (6 levels) and the consumers' environmental disposal of furniture waste as a dependent

http://www.aloki.hu ● ISSN 1589 1623 (Print) ● ISSN 1785 0037 (Online)
DOI: http://dx.doi.org/10.15666/aeer/1704_72297248

variable show significant differences between respondents, $F(5, 1544) = 29.47$, $p < .01$, $\eta^2_p = .09$. Post hoc tests ($p < .01$ - $.05$) further demonstrated that respondents from Slovenia and Macedonia dispose of waste from furniture in an environmentally friendly manner to the lowest degree when compared to respondents from all other countries. Also, it has been shown that respondents from Serbia are using this behavior to a greater extent in comparison to respondents from Croatia and Bosnia and Herzegovina.

The results of the one-factor analysis of variance with the country as a factor (6 levels) and the consumers' environmental management of electronic waste as a dependent variable show that there are significant differences between the respondents, $F (5, 1544) = 23.94$, $p < .01$, $\eta^2_p = .07$. Post hoc tests have shown ($p < .01$ - $.05$) that respondents from Slovenia are more prone to ecological disposing of electrical waste compared to respondents from all other countries.

The results of the one-factor analysis of variance with the country as a factor (6 levels) and the consumers' environmental management of waste from means of transport as a dependent variable indicate that there are significant differences between the respondents, $F (5, 1544) = 28.78$, $p < .01$, $\eta^2_p = .09$. Post hoc tests ($p < .01$ - $.05$) indicate that respondents from Slovenia, again, are most prone to ecologically dispose their means of transport waste, compared to respondents from all other countries. On the other hand, respondents from Serbia are more environmentally irresponsible when it comes to the disposal of waste from means of transport, in comparison to respondents from Croatia and Macedonia.

The results of the one-factor analysis of variance with the country as a factor (6 levels) and the consumers' environmental management of paper waste as a dependent variable indicate that there are statistically significant differences between respondents from different countries, $F (5, 1544) = 77.01$, $p < .01$, $\eta^2_p = .20$. Post hoc tests ($p < .01$) further demonstrated that respondents from Slovenia and Croatia to the greatest extent ecologically dispose their paper waste in comparison to respondents from all other countries. Also, it has been shown that the respondents from Montenegro are least prone to ecologically manage their paper waste in comparison to respondents from other countries ($p < .01$).

Differences in demographic characteristics in relation to waste disposal in an environmentally friendly manner

Gender – Disposal of waste in an environmentally friendly way: The results of a two-factor variance analysis with factors country (6 levels) and gender (2 levels) point to a statistically significant main effect of the sex, $F (1, 1537) = 5.44$, $p < .05$, $= .02$ $\eta p2 = .01$, and a statistically significant main effect of the country, $F (5, 1537) = 13.18$, $p < .01$, $\eta p2 = .04$. *Gender-to-country interaction is not statistically significant*, $F (5, 1537) = 1.97$, ns. The results of post hoc tests (Tukey's HSD) indicate that female respondents ($M = 22.53$, $SD = 4.85$) more dispose the waste in a way that does not degrade the environment, compared to male respondents ($M = 21.79$, $SD = 5.00$) in all countries.

Age – Disposal of waste in an environmentally friendly way: The results of a two-factor analysis of variance with factor country (6 levels) and age (5 levels) point to a statistically significant main effect of age, $F (2, 1537) = 19.27$, $p < . 01$, $.02 = \eta p2 = .02$, statistically significant main effect of the country, $F (4, 1510) = 11.84$, $p < .01$ $\eta p2 = .02$, and *statistically significant interaction between country and age*, $F (22, 1510) = 1.77$, $p < .05$, $\eta p2 = .02$. Post hock test (Tukey's HSD) indicates that the youngest respondents from Macedonia, aged 18-30 years ($M = 19.14$, $SD = 4.65$; $p < .01$), are less prone to disposing the waste in an ecological manner polluting the waste in an

http://www.aloki.hu ● ISSN 1589 1623 (Print) ● ISSN 1785 0037 (Online)
DOI: http://dx.doi.org/10.15666/aeer/1704_72297248

environmentally-friendly manner than respondents from Croatia, aged 31-40 (M = 25.22, SD = 4.86; p < .01).

Education – Disposal of waste in an environmentally friendly way: The results of a two-factor analysis of variance with factors country (6 levels) and education level (4 levels) point to the statistically significant main effect of the country, F (13, 1524) = 10.92, p < .01, ηp2 = .02, that the main effect of the education level is not statistically significant, F (2, 1524) = <1, ns, and that *the interaction between the country and the education level* is statistically significant, F (13, 1524) = 3.37, p < .01, ηp2 = .02. Post hoc test (Tukey's HSD) indicates that respondents from Macedonia with university degree (M = 19.43, SD = 5.26) are less involved in the disposal of waste in such a way as not to degrade the environment than respondents from: a) Serbia with completed high school (M = 23.37, SD = 4.99, p < .01), b) Croatia with university education (M = 23.61, SD = 5.01, p < .01), and c) Slovenia with a completed university education (M = 23.22, SD = 3.01; p < .01).

Monthly household income – Disposal of waste in an environmentally friendly way: The results of a two-factor variance analysis with factors country (6 levels) and monthly household income (3 levels) point to the statistically significant main effect of the country, F (5, 1530) = 8.99, p < .01, ηp2 = .02, that the main effect of monthly household income is not statistically significant, F (2, 1530) = 1.63, ns., and that the *interaction between the state and monthly household income*, F (10, 1530) = 2.02, p < .01, ηp2 = .01., is statistically significant. Post hoc test (Tukey's HSD) indicates that respondents from Macedonia with above-average household income (M = 19.53, SD = 5.49) are less involved in waste disposal in a way that does not degrade the environment than respondents from: a) Serbia with above-average monthly household income (M = 22.71, SD = 5.08, p < .01), with average monthly household income (M = 24, SD), and with below-average monthly household income (AS = 23.19, SD = 4.92, p < = 4.51, p < .01); b) Croatia with above-average monthly household income (AS = 24.92, SD = 5.04, p < .01) and average monthly household income (AS = 22.63, SD = 5.37, p < .01), c) Slovenia with above-average monthly household income (AS = 23.40, SD = 3.52, p < .01).

Discussion

The results show that there are differences in waste management in an environmentally friendly manner among consumers from different former Yugoslavian republics. The results obtained confirm the hypothesis H0 - there are differences in environmental management of waste between consumers from former Yugoslavian republics.

The results obtained confirm the differences between consumers' environmental management of waste in different countries, found in previously conducted cross-cultural studies (Arbuthnot and Lingg, 1975; Roozen and Pelsmacker, 2000; Sinha-Khetriwala et al., 2005; Kipperberg, 2007; Xu et al., 2014). The obtained results can be explained by the various macroeconomic factors mentioned in *Table 1*. Earlier studies confirm that different macroeconomic factors affect the diversity in the environmentally responsible behavior of consumers, which is the elimination of waste in an environmentally friendly manner (Dolan, 2002; Schaefer and Crane, 2005; Thøgersen, 2005; Assadourian, 2010; Marx et al., 2010). The results point that:

- Regarding the overall waste management in an environmentally friendly way (regardless of the type of waste), it can be concluded that the consumers from

http://www.aloki.hu ● ISSN 1589 1623 (Print) ● ISSN 1785 0037 (Online)
DOI: http://dx.doi.org/10.15666/aeer/1704_72297248

Macedonia have a lowest level of waste management in an environmentally friendly manner in comparison to all other countries in the sample. The above can be explained by the fact that Macedonia has the lowest value of the macroeconomic factor "Environmental sustainability" in comparison to all other former Yugoslavian republics (*Table 1*). Also, the "Environmental sustainability" factor has the decrease tendency for Macedonia only. Environmental sustainability is a factor that directly indicates the country's readiness to protect its environment, while managing waste in an ecologically friendly manner is the type of environmentally responsible consumer behavior that significantly depends on the government activity and the functionality of the waste management system at the state level.

- When consumers from Slovenia were analyzed, it was concluded that they are more ready than consumers from all other countries in the sample to environmentally manage different types of waste: food, medicaments, electrical appliances, means of transport and paper. This can be explained by the fact that Slovenia has the highest values for all of the macro factors analyzed in *Table 1*: GDP per capita, quality of education, sophisticated business and environmental sustainability, and each in its own way positively affects the environmental management of waste.
- Regarding the differences in the disposal of food waste in an environmentally friendly manner, the difference between the respondents from Macedonia and the respondents from Montenegro is evident, which can be explained by the fact that Montenegro has higher values for most of the factors analyzed in *Table 1*: GDP per capita, quality of education, and environmental sustainability.
- Respondents from Macedonia and Montenegro are less disposing of medical and chemical waste in an environmentally-friendly manner than respondents from Croatia, which can be explained by the fact that Macedonia and Montenegro in relation to Croatia have lower values for all mentioned macroeconomic factors from *Table 1*: GDP per capita, quality of education, sophisticated business and environmental sustainability.
- Respondents from Slovenia are more prone to disposing of clothing and footwear in an environmentally-friendly way than respondents from Croatia and Montenegro, which can also be explained by the fact that Slovenia in comparison to Croatia and Montenegro has higher values for all macroeconomic factors from *Table 1*: GDP per capita, quality of education, sophisticated business and environmental sustainability)
- If the disposal of furniture in an ecologically friendly way is analyzed, there are differences observed between Serbia on one side and Croatia and Bosnia and Herzegovina on the other side, where respondents from Serbia are more environmentally responsible when disposing of furniture waste than respondents from Croatia and Bosnia and Herzegovina, which can be explained by the fact that Serbia has the lowest value of the factor "Environmental footprint" (*Table 1*), which implies that Serbia is less prone to waste and degradation its natural resources for the better quality of life in relation to Croatia and Bosnia and Herzegovina. In other words, respondents from Serbia pollute less and less degrade the environment, among other things, with furniture waste.

http://www.aloki.hu ● ISSN 1589 1623 (Print) ● ISSN 1785 0037 (Online)
DOI: http://dx.doi.org/10.15666/aeer/1704_72297248

- Also, the observed differences in the disposal of furniture waste in an environmentally friendly manner are present between Slovenia and all other countries of the sample, in the sense that respondents from Slovenia are less likely to dispose of furniture waste in an environmentally friendly way than respondents from all other countries of the sample, which is explained by the fact that Slovenia has the highest value of the "Environmental footprint" factor (*Table 1*) than all other analyzed countries, which means that Slovenia mostly consumes and degrades its natural resources for a better standard of living, which includes furniture and waste disposal from it.
- Further, the observed differences between the disposal of waste in an environmentally friendly manner are such that respondents from Macedonia are less prone to dispose their furniture waste in an environmentally-friendly way than those from all other sample countries, which is explained by the lowest value of the macroeconomic factor "Environmental sustainability" in comparison with all other former Yugoslavian republics and the fact that this factor only in Macedonia has a decrease tendency in Macedonia only (*Table 1*).
- Respondents from Serbia are less able to dispose their transport vehicles and parts of transport vehicles in an environmentally-friendly manner than respondents from Croatia and Macedonia, which can be explained by the fact that Serbia has the lowest degree of macroeconomic factor "Sophistication of business", which also includes educational promotional campaigns on the importance of ecological manner of disposal of transportation means and their parts.

The obtained differences between countries that can not be explained by variations in macroeconomic factors (*Table 1*) can be explained by differences in the awareness, knowledge and attitude towards the environment in consumers from different analyzed countries (Arbuthnot and Lingg, 1975; Roozen and Pelsmacker, 2000; Sinha-Khetriwala et al., 2005; Kipperberg, 2007; Xu et al., 2014).

The obtained results indicate that there are no gender differences, while there are differences in age, education and monthly household income in relation to the disposal of waste in an environmentally friendly manner among consumers from the territory of the former Yugoslavia. The obtained results partially confirm the H2 hypothesis - there are demographic differences in the disposal of waste in a way that does not degrade the environment among consumers from the territory of the former Yugoslavia.

In all former Yugoslavian republics women environmentally dispose of waste more than men, which is also confirmed by previous research results conducted in: Singapore (Shamdasani et al., 1993), United Kingdom (Gilg et al., 2005), Greece (Tilikidou and Delistavrou, 2008; Abeliotis et al., 2010), Portugal (De Paço and Raposo, 2010; Paçoand Lavrador, 2017), Italy (Pedrini and Ferri, 2014; Talia et al., 2019), Germany (Scherer et al., 2018). Studies conducted in: United States of America (Granzin and Olsen, 1991; Savchenko et al., 2019), United Kingdom (Samdahl and Robertson, 1989; Gilg et al., 2005), China (Chan, 2001), Portugal (De Paço and Raposo, 2010), Italy (Talia et al., 2019), Germany (Pagiaslis and Krontalis, 2014), Spain (Pérez-Belis et al., 2017) and Denmark (Aschemann-Witzel et al., 2017) confirm that there are differences in consumers age related to their ecologically responsible waste disposal. Studies conducted in: United States of America (Arbuthnotand Lingg, 1975; Granzin and Olsen, 1991), United Kingdom (Samdahl and Robertson, 1989), China (Chan, 2001), India (Jain andKaur, 2006), Greece (Tilikidou and Delistavrou, 2008; Abeliotis et al., 2010), Portugal (De Paço and Raposo, 2010), Italy (Pedriniand Feri, 2014; Talia et al., 2019),

http://www.aloki.hu ● ISSN 1589 1623 (Print) ● ISSN 1785 0037 (Online)
DOI: http://dx.doi.org/10.15666/aeer/1704_72297248

Denmark (Aschemann-Witzel et al., 2017) and Germany (Pinto et al., 2014; Pagiaslis and Krontalis, 2014) confirm that there are differences in consumers' education level in comparison to environmentally responsible disposal of waste of consumers. That there are differences in certain countries regarding monthly household income in comparison to consumers' ecological waste disposal is confirmed by studies conducted in: United States of America (Granzin and Olsen, 1991), United Kingdom (Samdahl and Robertson, 1989), China (Chan, 2001; Zhang et al., 2018), India (Jain and Kaur, 2006), Greece (Tilikidou and Delistavrou, 2008; Abeliotis et al., 2010), Portugal (De Paço and Raposo, 2010), Italy (Pedrini and Feri, 2014; Talia et al., 2019) and Germany (Pinto et al., 2014; Pagiaslis and Krontalis, 2014) and Denmark (Aschemann-Witzel et al., 2017).

Limitations of research

Although this cross-cultural research was done with caution, it has certain limitations. The firstcan be that the questionnaire was designed for research purposes and it was not used elsewhere, and cannot be characterized as being of multiple uses. The second limitation can be the number of items in the questionnaire – seven. That is a small number of items, which is why maybe the structure of the questionnaire is not ideal. Consumers' environmental management of waste is a socially desirable behavior and it is assumed that respondents were subjective and that they were giving socially desirable answers, which is also considered a limitation of the study.

Conclusion

This is the first cross-cultural research of differences in environmental management of waste by consumers from the former Yugoslavian republics, and as such it provides valuable information.

The results indicate that there are differences in environmental management of waste between consumers from: Macedonia and all other former Yugoslavian republics, and from Montenegro in comparison to Serbia, Croatia and Slovenia. There are differences in consumers' environmental management of different types of waste: regarding food waste – between Slovenia and all other former Yugoslavian republics and Macedonia in comparison to Bosnia and Herzegovina and Croatia; regarding medicament waste – between Slovenia and all other former Yugoslavian republics and between Macedonia and Montenegro in comparison to Croatia and Serbia; regarding clothing and footwear waste – between Slovenia on one hand and Croatia and Montenegro on the other hand; regarding furniture waste –between Slovenia and Macedonia in comparison to all other former Yugoslavian republics; regarding e-waste – between Slovenia and all other former Yugoslavian republics; regarding waste from means of transport – between Slovenia and all other former Yugoslavian republics and Serbia in comparison to Croatia and Macedonia; regarding paper waste – between Slovenia and Croatia in comparison to all other former Yugoslavian republics and between Montenegro and all other former Yugoslavian republics.

Differences in environmental waste recycling between countries can largely be explained by the macroeconomic factors, while part of the results can be explained by differences in consumer awareness, attitude and knowledge regarding environment.

Results indicate that there are no differences in gender but that there are differences in age, degree of education and monthly income by households related to environmental management of waste between consumers from former Yugoslavian republics. As for the age, differences were noted between the youngest respondents from Macedonia,

http://www.aloki.hu ● ISSN 1589 1623 (Print) ● ISSN 1785 0037 (Online)
DOI: http://dx.doi.org/10.15666/aeer/1704_72297248

aged 18 to 30, and respondents from Croatia aged from 31 to 40 years, in sense that respondents from Macedonia are less likely to dispose of waste in an ecological way than respondents from Croatia. Regarding the level of education, respondents from Macedonia with higher education are less involved in the disposal of waste in such a way that the environment is not degraded than the respondents from: a) Serbia with a completed high school, b) Croatia with a university degree, and c) Slovenia with completed university degree. When it comes to monthly household income, the results show that respondents from Macedonia with above-average household income are less involved in waste disposal in a way that does not degrade the environment than respondents from: a) Serbia with above-average monthly household income, with average monthly household income, and below-average monthly income; b) Croatia with above-average monthly household income, and with average monthly household income, c) Slovenia with above-average monthly household income.

The practical application of the results is reflected in the possibility of more efficient management of consumer waste in an environmentally friendly manner on the territory of former Yugoslavian republics and also globally. Therefore, the consumer behavior can become a tool of environmental management and improve the quality of life in the region. The results indicate that in the territory of the former Yugoslavian republics there are different segments of consumers regarding behavioral variable of consumers' ecological waste management. However, it is necessary to adapt consumer waste management strategies in an environmentally friendly way to different segments i. e. countries. The most resources should be invested in order to bring the consumer waste management strategy in an environmentally friendly manner "most intensively" for consumers in Macedonia and the least resources for a consumer waste management strategy in an environmentally friendly way are needed for consumers from Slovenia. Also, the results indicate that there are market segments if we look at consumer management of different types of waste in an environmentally friendly manner, such as food, medicaments, clothing and footwear, furniture, e-waste, means of transport, or paper. For example, when analyzing waste from furniture, consumers from Slovenia only in this type of waste are less environmentally conscious than consumers from other countries in the sample, which indicates that the waste management strategy for ecologically oriented consumers in Slovenia should be created in such a way that it contributes most to the disposal of furniture waste in an environmentally friendly way in comparison to other types of waste. Or, if consumers from Montenegro are observed, it is concluded that of all the countries in the sample they are the least prone to ecological managing of paper waste. It further implies that the environmental management strategy for consumers in Montenegro should be focused on the environmentally friendly disposal of paper waste in comparison to other types of waste. If we look at the results obtained by analyzing the differences in demographic characteristics with respect to the environmentally responsible disposal of waste, it is concluded that in all the countries of the former Yugoslavia, male part of population should be encourage more to disposed of waste in ecological terms, since in all countries it has been observed that women are more represented in this type of behavior. Also, the same segment of results indicates that consumers from Macedonia aged 18-30 years should be encouraged, as well as consumers from Macedonia who have completed university education and those from Macedonia with above-average monthly income, since it was observed that these demographic groups were least involved in the disposal of waste in an environmentally friendly manner. The obtained data can serve as a starting point for entering into horizontal and vertical partnerships between different entities on national and

http://www.aloki.hu ● ISSN 1589 1623 (Print) ● ISSN 1785 0037 (Online)
DOI: http://dx.doi.org/10.15666/aeer/1704_72297248

international levels, with the aim of protecting the environment through increased consumers' environmental management of waste.

From a theoretical perspective, the data obtained is important because it provides an empirical basis for other studies by creating an environmental profile of responsible consumers. Also, the research was conducted with a newly created questionnaire that can be used for other research, and for creating other questionnaires on the same topic.

It is also proposed to carry out research in the territory of former Yugoslavia republics in order to determine the correlation between macroeconomic factors and different types of ecologically responsible behavior of consumers, including disposal of waste in an environmentally friendly way, which would show whether and which - if any - macroeconomic factors influence different ecological responsible consumers' behavior. Finally, the authors suggest that more studies should be carried out on the topic of consumers' environmental management of waste, as this is the only way to analyze the limits and motivators of the environmentally responsible behavior of consumers.

REFERENCES

[1] Abeliotis, K., Koniari, C., Sardianou, E. (2010): The profile of the green consumer in Greece. – International Journal of Consumer Studies 34(2): 153-160.

[2] Arbuthnot, J., Lingg, S. (1975): A comparison of French and American environmental behaviors, knowledge and attitude. – International Journal of Psychology 10(4): 275-281.

[3] Aschemann-Witzel, J., Jensen, J. H., Jensen, M. H., Kulikovskaja, V. (2017): Consumer behaviour towards price-reduced suboptimal foods in the supermarket and the relation to food waste in households. – Appetite 116: 246-258.

[4] Assadourian, E. (2010): Transforming cultures: from consumerism to sustainability. – Journal of Macromarketing 30(2): 186-191.

[5] Chan, R. Y. K. (2001): Environmental attitudes and behavior of consumers in China. – Journal of International Consumer Marketing 11(4): 25-52.

[6] Croatian Bureau of Statistics (2018): Statistical Yearbook. – Croatian Bureau of Statistics. https://www.dzs.hr/Hrv_Eng/ljetopis/2018/sljh2018.pdf. Accessed on 02 February 2019.

[7] De Paço, A. M. F., Raposo, M. L. B. (2010): Green consumer market segmentation: empirical findings from Portugal. – International Journal of Consumer Studies 34(4): 429-436.

[8] Dolan, P. (2002): The sustainability of "sustainable consumption". – Journal of Macromarketing 22(2): 170-181.

[9] Federal Office of Statistics of Bosnia and Herzegovina (2018): Statistical Yearbook. – Federal Office of Statistics of Bosnia and Herzegovina. https://docs.google.com/gview?url=http://fzs.ba/wp-content/uploads/2019/01/Godisnjak2018.pdf. Accessed on 02 February 2019.

[10] Gilg, A., Barr, S., Ford, N. (2005): Green consumption or sustainable lifestyles? Identifying the sustainable consumer. – Futures 37(6): 481-504.

[11] Granzin, K. L., Olsen, J. E. (1991): Characterizing participants in activities protecting the environment: A focus on donating, recycling and conservation behaviors. – Journal of Public Policy and Marketing 10(2): 1-27.

[12] Institute for Statistics of Republic Serbia (2018): Statistical Yearbook. – Institute for Statistics of Republic Serbia. http://publikacije.stat.gov.rs/G2018/Pdf/G20182051.pdf. Accessed on 02 February 2019.

[13] Jain, S., Kaur, G. (2006): Role of socio-demographics in segmenting and profiling green consumers: an exploratory study of consumers in India. – Journal of International Consumer Marketing 18(3): 107-117.

http://www.aloki.hu ● ISSN 1589 1623 (Print) ● ISSN 1785 0037 (Online)
DOI: http://dx.doi.org/10.15666/aeer/1704_72297248

[14] Kipperberg, G (2007): A Comparison of household recycling behaviors in Norway and the United States. – Environmental and Resource Economics 36(2): 215-235.
[15] Lavrakas, P. J. (2008): Encyclopedia of Survey Research Methods. – Sage, Thousand Oaks, CA.
[16] Marx, A. M., De Paula, I. C., Sum, F. (2010): Sustainable consumption in Brazil: identification of preliminary requirements to guide product development and the definition of public policies. – Natural Resources Forum 34(1): 51-62.
[17] Norusis, M. (2008): SPSS 16.0 Advanced Statistical Procedures Companion. – Prentice Hall, Upper Saddle River, NJ.
[18] Pagiaslis, A., Krontalis, A. K. (2014): Green consumption behavior antecedents: environmental concern, knowledge, and beliefs. – Psychology and Marketing 31(5): 335-348.
[19] Paço, A., Lavrador, T. (2017): Environmental knowledge and attitudes and behaviours towards energy consumption. – Journal of Environmental Management 197: 384-392.
[20] Pedrini, M., Ferri, L. M. (2014): Socio-demographic antecedents of responsible consumerism propensity. – International Journal of Consumer Studies 38(2): 127-138.
[21] Pérez-Belis, V., Braulio-Gonzalo, M., Juan, P., Bovea, D. M. (2017): Consumer attitude towards the repair and the second-hand purchase of small household electrical and electronic equipment. A Spanish case study. – Journal of Cleaner Production 158: 261-275.
[22] Pinto, C. D., Herter, M. M., Rossi, P., Borges, A. (2014): Going green for self or for others? Gender and identity salience effects on sustainable consumption. – International Journal of Consumer Studies 38(5): 540-549.
[23] Raletić Jotanović, S., Milijanka, R., Zakić, N. (2017): Pro-environmental activities of consumers. – Polish Journal of Management Studies 16(1): 55-66.
[24] Raletić Jotanović, S., Sudarević, T., Katić, A., Kalinić, M., Kalinić, Č. (2016): Environmentally responsible purchasing. Analysis of the ex-Yugoslavian republics. – Applied Ecology and Environmental Research 14(3): 559-572.
[25] Roozen, I. T. M., De Pelsmacker, P. (2000): Polish and Belgian consumers' perception of environmentally friendly behavior. – Journal of Consumer Studies and Home Economics 24(1): 9-21.
[26] Samdahl, D., Robertson, R. (1989): Social determinants of environmental concern: Specification and test of the model. – Environment and Behavior 21(1): 57-81.
[27] Savchenko, O., Kecinski, M., Li. T., Messer, K. (2019): Reclaimed water and food production: Cautionary tales from consumers research. – Environmental Research 120: 320-331.
[28] Schaefer, A., Crane, A. (2005): Addressing sustainability and consumption. – Journal of Macromarketing 25(1): 76-92.
[29] Scherer, C., Emberger-Klein, A., Menrad, K. (2018): Segmentation of interested and less interested consumers in sports equipment made of bio-based plastic. – Sustainable Production and Consumption 14: 53-65.
[30] Shamdasani, P., Chon-Lin, G. O., Richmond, D. (1993): Exploring green consumers in an oriental culture: role of personal and marketing mix factors. – Advances in Consumer Research 20(1): 488-493.
[31] Sinha-Khetriwala, D., Kraeuchi, P., Schwaninger, M. (2005): A comparison of electronic waste recycling in Switzerland and in India. – Environmental Impact Assessment Review 25(5): 492-504.
[32] State Statistical Office of the Macedonia (2018): Statistical Yearbook. – State Statistical Office of the Macedonia. http://www.stat.gov.mk/Publikacii/PDFSG2014/08-PrihodiPotrosCeni-IncomeExpPrices.pdf. Accessed on 02 February 2019.
[33] Statistical Office of the Montenegro (2018): Statistical Yearbook. – Statistical Office of the Montenegro. – http://monstat.org/eng/publikacije_page.php?id=1518. Accessed on 02 February 2019.

http://www.aloki.hu ● ISSN 1589 1623 (Print) ● ISSN 1785 0037 (Online)
DOI: http://dx.doi.org/10.15666/aeer/1704_72297248

[34] Statistical Office of Slovenia (2018): Statistical Yearbook. – Statistical Office of Slovenia. https://www.stat.si/StatWeb/File/DocSysFile/10179/STATOBOOK_2018.pdf. Accessed on 02 February 2019.
[35] Talia, D. E., Simeone, M., Scarpato, D. (2019): Consumer behaviour types in household food waste. – Journal of Cleaner Production 214: 166-172.
[36] Thøgersen, J. (2005): How many consumer policy empower consumers for sustainable lifestyles? – Journal of Consumer Policy 28(2): 143-78.
[37] Tilikidou, I., Delistavrou, A. (2008): Types and influential factors of consumers' non-purchasing ecological behaviors. – Business Strategy and the Environment 17(1): 61-76.
[38] WEF (2014): Global Competitiveness Report 2014-2015. – WEF, Geneva.
[39] WEF (2016-2017): Global Competitiveness Report 2016-2017. – WEF, Geneva.
[40] WEF (2018): Global Competitiveness Report 2018. – WEF, Geneva.
[41] Xu, Y., Chen, Y., Burman, R., Zhao, H. (2014): Second hand clothing consumption: a cross cultural comparison between American and Chinese young consumers. – International Journal of Consumer Studies 38(6): 670-677.
[42] Zhang, H., Duan, H., Andric, J. M., Song, M., Yang, B. (2018): Characterization of household food waste and strategies for its reduction: a Shenzhen City case study. – Waste Manag 78: 426-433.

APPENDIX

Questionnaire used in this study

Dear Sir/Madam,

Bearing in mind that this is one of rare cross cultural studies in our region, and that the results will provide valuable information on similarities and differences regarding our behavior as consumers, we kindly ask you to devote 10 minutes of your time, which will be enough to fill out this questionnaire.

This survey is entirely ANONYMOUS, which means that nobody will be able to associate you with your answers. Survey data will be processed in groups and will be used for scientific research purpose only.

We kindly ask you to answer ALL of the questions and check carefully whether you have completed the ENTIRE questionnaire.

You are free to send all of your questions and doubts relative to this research via e-mail: rsasaca@hotmail.com.

Filling out the questionnaire is voluntary and requires your consent. If you agree to participate in this survey, circle YES.

I AGREE TO PARTICIPATE IN THIS SURVEY:

YES NO

THANK YOU IN ADVANCE FOR YOUR COOPERATION!

Circle the number in front of the statement that applies to you.

Country:
1. Serbia 2. Croatia 3. Bosnia and Herzegovina 4. Slovenia 5. Macedonia 6. Monetenegro

http://www.aloki.hu ● ISSN 1589 1623 (Print) ● ISSN 1785 0037 (Online)
DOI: http://dx.doi.org/10.15666/aeer/1704_72297248

Gender:
1. male 2. female

Age (years) _____

Education:

1. elementary school 2. high school 3. University degree 4. MSc/Mr/Dr

The average monthly income per household in the Republic of Serbia, according to the Statistical Office, is 56,073.00 dinars for 2013. The total monthly income of your household is:
1. below average 2. average 3. above average

In the table below there are several statements describing different behaviors and attitudes which relate to ecological responsibility of consumers. Please, carefully read each of the statements and answer by circling the number and expressing to what degree you agree with each of the statements. Numbers have the following meaning:

1 - I strongly disagree, 2 - I disagree, 3 - Undecided, 4 - I agree, 5 - I strongly agree

	Items	
Environmental management of waste	When possible, I put my leftover food in compost	1 2 3 4 5
	I do not throw expired medication in waste	1 2 3 4 5
	I do not throw away old clothes but rather donate it	1 2 3 4 5
	I would leave an old sofa by the garbage container	1 2 3 4 5
	I put old electric appliances in the garbage container	1 2 3 4 5
	Parts of unusable bicycle, car and/or engine I would place next to the garbage container	1 2 3 4 5
	I put old paper into a paper container	1 2 3 4 5

http://www.aloki.hu ● ISSN 1589 1623 (Print) ● ISSN 1785 0037 (Online)
DOI: http://dx.doi.org/10.15666/aeer/1704_72297248

HIGH-SENSITIVITY AND SELECTIVITY DETECTION OF PERMANGANATE IONS BASED ON PIG LIVER-BASED CARBON QUANTUM DOTS

TU, Y. J.[1,2,3] –TIAN, Y. H.[4] –YANG, Y. L.[1*]

[1]*Faculty of Life Science and Technology, Kunming University of Science and Technology, Yunnan Province 650500, China*

[2]*Faculty of Environmental Science and Engineering, Kunming University of Science and Technology, Yunnan Province 650500, China*

[3]*Department of Chemical Science and Technology, Kunming University, Yunnan Province 650214, China*

[4]*School of Metallurgy and Energy Engineering, Kunming University of Science and Technology, Kunming 650500 Yunnan Province, China*

**Corresponding author*
e-mail: yilyil8@163.com

(Received 26th Dec 2018; accepted 3rd May 2019)

Abstract. In this paper, novel fluorescent carbon quantum dots (CQDs) were successfully prepared from pig liver by a simple one-step hydrothermal method. The prepared CQDs were characterized using TEM, XRD, XPS, FT-IR, UV-Vis, and fluorescence spectroscopy. It was found that the CQDs were uniformly distributed in size and exhibited good excitation dependence and excellent photostability. Fluorescent probe was used for detection of permanganate. This paper also studied the fluorescent staining performance of pig liver-based CQDs on four live/dead bacteria to evaluate the low toxicity and application prospects of the CQDs. Under the optimum experimental conditions, the probe showed a good linear range (R^2 = 0.9967) and a low detection limit (0.06 μM) in the concentration range of 0.1-50 μM. The pig liver based-CQDs were proved to be a low toxicity fluorescent dye. These attractive properties indicated that the new CQDs could adapt to various complex pH environments, and thus had extensive prospect and promising application for detection of permanganate in complex environmental samples.
Keywords: *carbon quantum dots, pig liver, bacterial staining, in vivo bio-imaging, MnO_4^-*

Introduction

Manganese is an essential trace element of human body. Too much or too little manganese in the body can cause adverse consequences (Teo and Chen, 2001). Manganese deficiency affects the body's reproductive function, lipid metabolism (da Silva et al., 2006), glucose metabolism (Doroschuk et al., 2004) and immune function (Rask et al., 2015), thus causing mental retardation, dysmotility and balance disorders (Gunter et al., 2010), and skeletal dysfunction (Liang et al., 2006). It can also deform the next generation. The excessive amount of manganese in the body can lead to mental symptoms (Zeng et al., 2017). Therefore, the analysis of manganese in food and environment samples is of important practical significance, and it is highly necessary to monitor the level of manganese in body fluids or environmental samples.

Permanganate is usually oxidable, hazardous explosion chemicals, precursor chemicals, and easy to decompose by heating because they all have the same anions-permanganate ions. Permanganate ion has strong oxidation in acidic solution (acidic

http://www.aloki.hu ● ISSN 1589 1623 (Print) ● ISSN 1785 0037 (Online)
DOI: http://dx.doi.org/10.15666/aeer/1704_72497263

$KMnO_4$ (potassium permanganate)). It also has certain oxidation in alkaline solution, which is purple red in solution. The oxidation of potassium permanganate can be found in both acidity and alkalinity, but it is more obvious in acidity. In recent years, many methods of manganese detection have been developed, including catalytic kinetic spectrophotometric for the determination of trace manganese, but there are few methods for the determination of permanganate ions. A new fluorescence method for the determination of trace manganese was established (Xu et al., 2004), where the concentration range of MnO_4^- is 1.0~2.4 mg/L, the maximum excitation wavelength is 278 nm, the maximum emission wavelength is 616 nm, and the fluorescence intensity and concentration show a good linear relationship by transforming the manganese into MnO_4^-. The results obtained in this method were satisfactory.

Carbon quantum dots (CQDs) are one of the most popular carbon nanomaterials after fullerene, carbon nanotubes and graphene. They were first discovered in 2004 (Wang and Hu, 2014) when electrophoresis was used to purify single-walled carbon nanotubes. They have attracted great attention due to their excellent optical properties, such as water solubility, chemical inertia, low toxicity, easy functionalization (Li et al., 2012) and high fluorescence intensity, photobleaching resistance and adjustable luminescence color. They have been widely used in detection of metal ions (Lu et al., 2012), anions (Zhao et al., 2011), small organic molecules (Li et al., 2013) and biological molecules (Deng et al., 2014). The method of detecting metal ions or other environmental pollutants using CQDs as a fluorescent probe has received extensive attention due to its excellent sensitivity and selectivity (Clarkson and Magos, 2006). Zhang and Chen (2014) used folic acid as carbon source and nitrogen source to trace mercury ions by nitrogen-doped carbon dots, and the detection limit was 0.23 mol/L.

In this study, fluorescent carbon quantum dots (CQDs) were successfully prepared by simple one-step hydrothermal method using pig liver as a carbon source. Since pig liver is a complex that contains a number of organics and biomolecules including fat, proteins, vitamin B, vitamin C, vitamin E, carbohydrates, cholesterol and minerals, it can be useful for doping of multiple hetero atoms in the CQDs without addition of any additives. In the experiment, we found that MnO_4^- could quench the fluorescence of CQDs, and the quenching degree was related to the concentration of MnO_4^-. To our knowledge, there is no report used CQDs fluorescent probe from pig liver for detection of MnO_4^- yet, which provides a new method for sensitive detection of MnO_4^-. In addition, this method has been successfully applied to detecting MnO_4^- in environmental water and soil samples.

Experiment

Instruments and reagents

Pig liver was purchased from a local supermarket in Kunming (Yunnan, China); all analytical reagents, including potassium permanganate ($KMnO_4$), citric acid, disodium hydrogen phosphate (Na_2HPO_4), $FeCl_3 \cdot 6H_2O$ and $FeCl_2 \cdot 4H_2O$, sodium nitrite, sodium nitrate, KI, NaCl, NaF, copper sulfate, aluminum sulfate, calcium chloride, $MnSO_4$, $BaCl_2$, $MgCl_2$ and sodium sulfide (NaS) were purchased from Shanghai Aladdin Biochemical Technology Co., Ltd. (Shanghai, China); and all solutions were prepared from Milli-Q system ultrapure water (18.2 MΩ.cm, 25 °C).

G9800A fluorospectrophotometer (Agilent Technologies, USA) was used to determine the fluorescence spectrum and its intensity; UV-2600 spectrophotometer

http://www.aloki.hu ● ISSN 1589 1623 (Print) ● ISSN 1785 0037 (Online)
DOI: http://dx.doi.org/10.15666/aeer/1704_72497263

(Shimadzu, Japan) was used to determine UV spectra; Tecnai G2 F30S-Twin high resolution field emission transmission electron microscope (FEI, Netherlands) was used to detect the particle size and morphology of fluorescent quantum dots; TENSOR 27 Fourier transform infrared spectrometer (Bruker, Germany) was used to determine the infrared spectrum and the structure of the material; D8-advance X-ray powder diffractometer (Bruker, Germany) was used to determine the crystal structure morphology; Thermo Scientific K-Alpha X-ray photoelectron spectrometer (Thermo Fisher Scientific Inc. U.S.A.) was used to analyze the elemental composition ratio and chemical oxidation state; XH-B vortex instrument (Shanghai Hanuo Instrument Co., Ltd., China) was used for vortex mixing; and 80-2 high speed centrifuge (Shanghai Surgical Instrument Factory, China) was used for centrifugal filtration.

Preparation of pig liver-based CQDs

The pig liver was dried naturally at room temperature and grinded into powders in a mortar. The CQDs of pig liver were prepared by simple hydrothermal method using pig liver powder as carbon source. Five grams of pig liver powder was dispersed in 150 mL deionized water. Then, the mixture was transferred into a high-pressure autoclave (200 mL) lined with polytetrafluoroethylene (PTFE), heated at 180 °C for 10 h, cooled naturally to room temperature, and centrifuged at 13,000 rpm for 20 min to obtain bright yellow solution, and filtered to remove insoluble substances. In order to obtain pure pig liver-based CQDs, the solution was filtered by 0.22 μm membrane. Finally, the obtained pig liver CQDs were stored at 4 °C for further use. Compared with other synthetic methods, the hydrothermal synthesis of pig liver CQDs is simpler and more feasible. In addition, pig liver as raw material for synthesis is cheap and easily available, and this method is greener and more environmentally friendly.

Fluorescence quenching test for permanganate

Typically, 50 μL of prepared pig liver-based CQDs solution and 1 mL of pH 7.0 citric acid-disodium hydrogen phosphate buffer solution mixed and diluted to 3.0 mL with deionized water were placed in a 10 mL glass centrifuge tube. Then, 2mL permanganate solution or sample with a different concentration was added to the centrifuge tube and the vortex was mixed with 30 s. After 3 min, the fluorescence intensity was measured at excitation wavelength 278 nm and emission wavelength 616 nm on the fluorescence spectrophotometer, and the fluorescence intensity was recorded. The slit width of excitation and emission was 5 nm. In order to evaluate the effect of coexisting interfering substances on the fluorescence intensity of pig liver-based CQDs and the selectivity of permanganate and other substances or ions (including $FeCl_3 \cdot 6H_2O$ and $FeCl_2 \cdot 4H_2O$, sodium nitrite, sodium nitrate, KI, NaCl, NaF, copper sulfate, aluminum sulfate, calcium chloride, $MnSO_4$, $BaCl_2$, $MgCl_2$ and sodium sulfide), the fluorescence quenching test was carried out under the same experimental conditions. The schematic diagram of detection of MnO_4^- with pig liver-based CQDs was shown in *Figure 1*.

http://www.aloki.hu ● ISSN 1589 1623 (Print) ● ISSN 1785 0037 (Online)
DOI: http://dx.doi.org/10.15666/aeer/1704_72497263

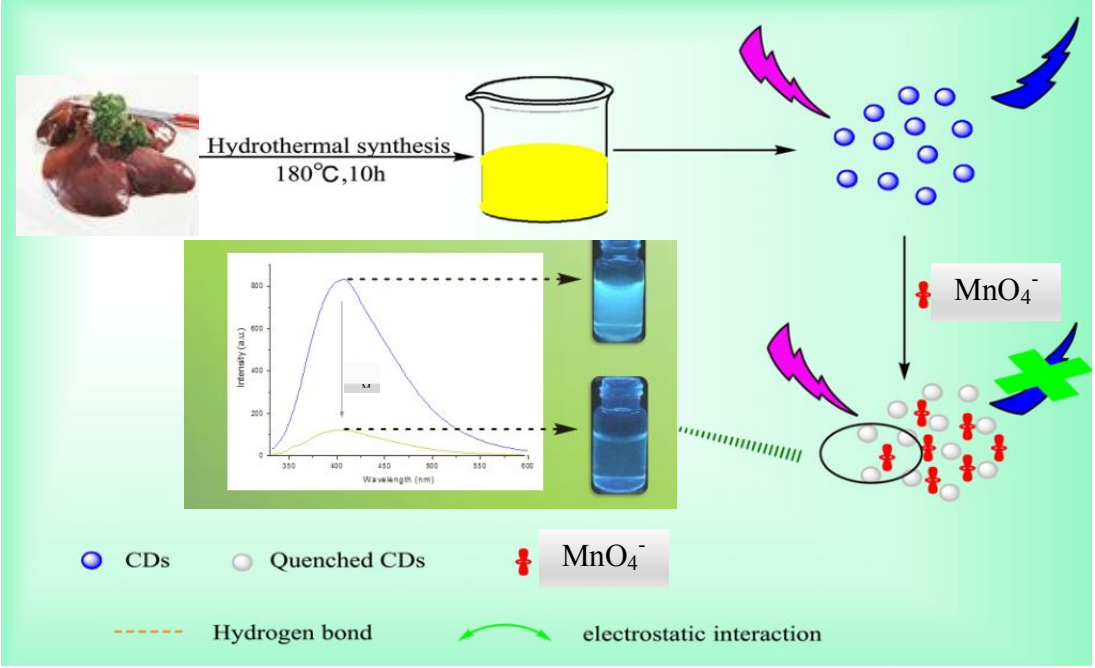

Figure 1. *Processing diagram for the synthesis and application of CQDs*

Collection and pretreatment of environmental samples

In this study, water samples were collected directly from our laboratory, Laoyuhe Lake and the domestic wastewater of the community next to a school. All water samples were filtered by simple centrifugal filtration to remove solid particles and suspended solids and then by 0.22 μm microporous membrane, and stored at 4 °C. The permanganate ion was added to the samples at a concentration of 0.01 mg/mL for spiked fluorescence analysis.

Soil samples were collected from the road outside the school after rain and dried under suitable environmental conditions (final moisture content 0.32%). One milliliter of methanol solution containing different concentrations of permanganate ions was added to 200 mg soil, mixed for 1 h on a 50 rpm shaker, and then allowed to stand overnight at room temperature (RT). On the second morning, the mixture was again vortexed and centrifuged for 2 min at 5,000 rpm and the supernatant was used for fluorescence detection.

Results and discussion

Characterization of the CQDs

The transmission electron microscopy (TEM) technique was used to explore the morphology and particle size distributions of CQDs. As shown in *Figure 2,* the CQDs present high dispersity, uniform spherical shapes, and a size distribution within the range of 3–10 nm and an average diameter of about 5.0 nm. The surface chemistry of CQDs was studied using Fourier transform infrared (FT-IR) spectroscopy. As shown in *Figure 3,* the strong absorption peak at 1469 cm^{-1} reveals the existence of -COOH stretching vibrations; the peak at 1652 cm^{-1} reveals the existence of O = C-NH stretching vibrations; and the absorption peak at 3190 cm^{-1} displays O-H stretching vibrations. As shown in *Figure 4,* the full scan XPS spectra present distinct peaks at

http://www.aloki.hu ● ISSN 1589 1623 (Print) ● ISSN 1785 0037 (Online)
DOI: http://dx.doi.org/10.15666/aeer/1704_72497263

287.3 and 532.7 eV, which are attributed to C1s and O1s, respectively. The result of XPS diagram was consistent with that of FT-IR analysis. Therefore, there should be hydrophilic groups on the surface of pig liver-based CQDs, such as -COOH, -OH, etc., which have good water solubility and broad application prospects.

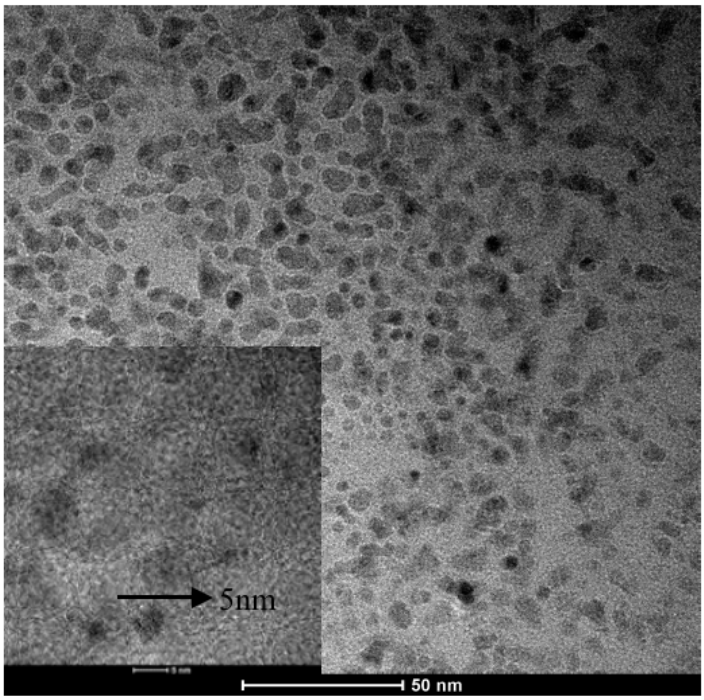

Figure 2. *TEM image (inset: HR-TEM image) of the synthesized CQDs*

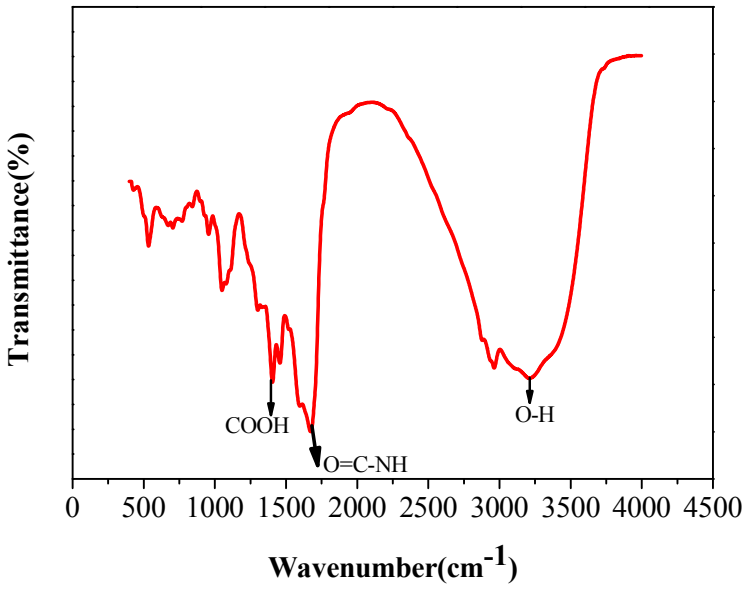

Figure 3. *FT-IR spectrum of pig liver-based CQDs*

http://www.aloki.hu ● ISSN 1589 1623 (Print) ● ISSN 1785 0037 (Online)
DOI: http://dx.doi.org/10.15666/aeer/1704_72497263

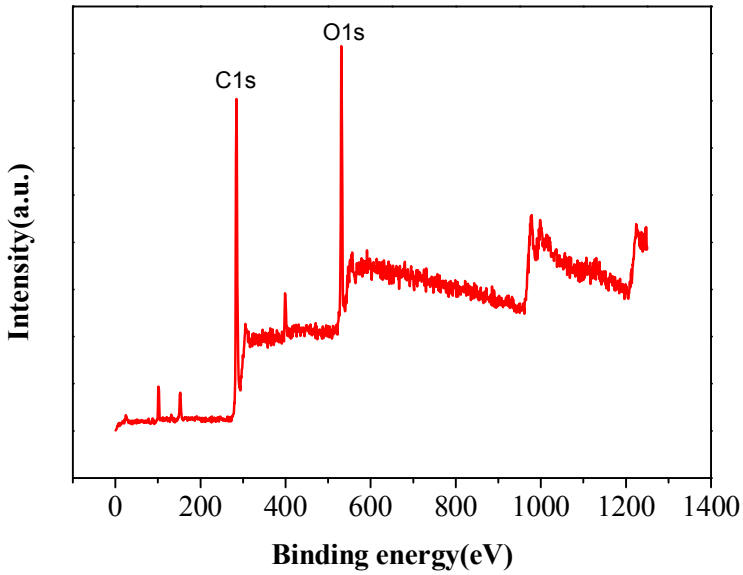

Figure 4. *XPS spectra of pig liver-based CQDs*

In order to study the optical properties of pig liver-based CQDS, the pig liver-based CQDs were characterized by UV-vis absorption spectrum and fluorescence emission spectrum. The UV-vis absorption spectrum (UV-vis) of pig liver-based CQDs is shown in *Figure 5*. The prepared pig liver-based CQDs had a weak absorption peak around 258 nm and an excitation wavelength of 278 nm at the maximum emission wavelength of 616 nm, as shown in *Figure 6,* a fluorescence spectrum (FS) and an excitation-dependent emission spectrum of pig liver-based CQDs. The results showed that when the excitation wavelength was changed from 300 to 360 nm in increments of 10 nm, the emission peak shifted toward the long wavelength direction.

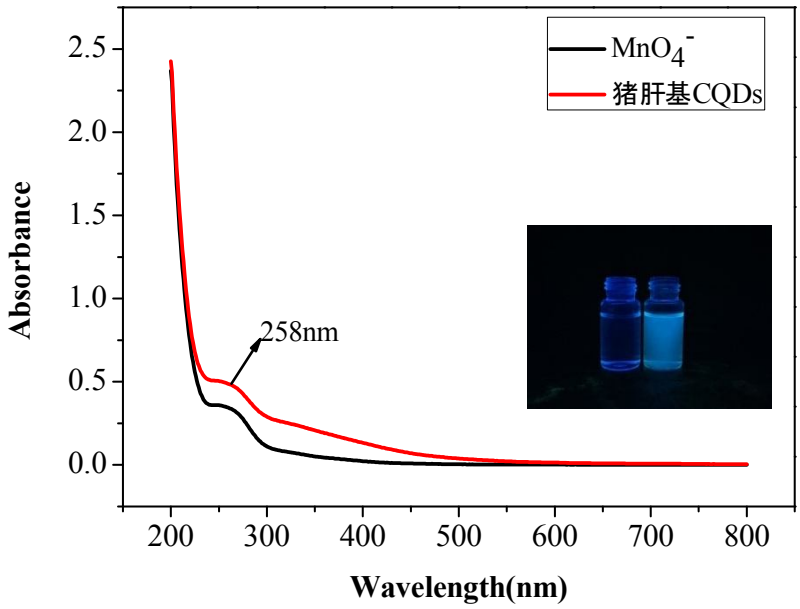

Figure 5. *UV-Vis absorption spectra of the synthesized pig liver-based CQDs. (Inset: photographs of pig liver-based CQDs under daylight (left) and UV (365 nm) irradiation (right))*

http://www.aloki.hu ● ISSN 1589 1623 (Print) ● ISSN 1785 0037 (Online)
DOI: http://dx.doi.org/10.15666/aeer/1704_72497263

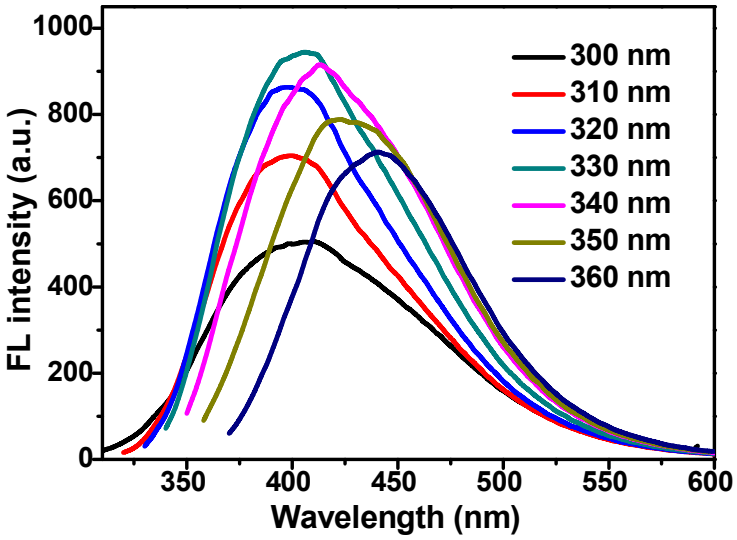

Figure 6. *Fluorescence emission spectra of pig liver-based CQDs at different excitation wavelengths*

Light stability test of pig liver-based CQDs

In order to study the stability of pig liver-based CQDs in detecting permanganate, the fluorescence intensity of pig liver-based CQDs at different storage time was studied. As shown in *Figure 7A,* the fluorescence intensity of the pig liver based-CQDs is substantially constant. In addition, the reaction time increased while the fluorescence intensity of the experimental system remained constant, indicating that the storage time had no effect on the fluorescence intensity of pig liver-based CQDs. The effects of ionic strength and pH on the fluorescence intensity of pig liver-based CQDs were also studied, as shown in *Figure 7B* and *C*. It is observed from the figures that with the gradual increase of the concentration of NaCl solution, the fluorescence intensity only slightly fluctuated without significant change; the pH of the citric acid-dibasic sodium phosphate buffer changed from 2.0 to 8.0; and the fluorescence intensity of pig liver-based CQDs remain unchanged, this demonstrates that pig liver-based CQDs can be used as fluorescent nanoprobe in any environmental conditions.

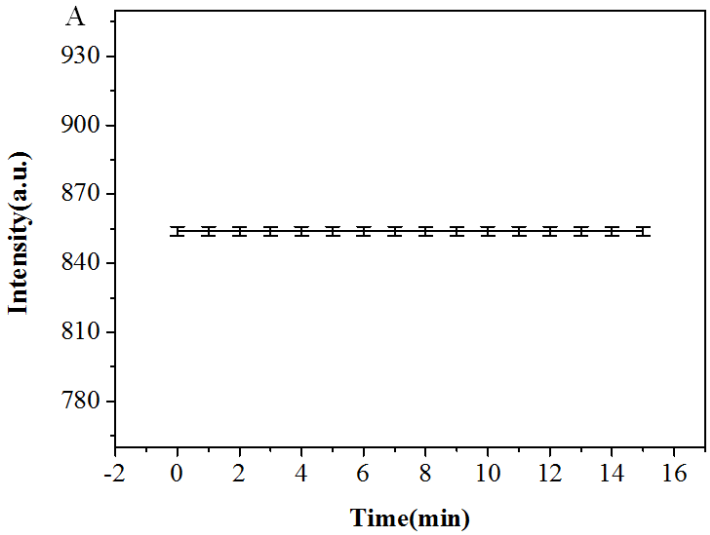

http://www.aloki.hu ● ISSN 1589 1623 (Print) ● ISSN 1785 0037 (Online)
DOI: http://dx.doi.org/10.15666/aeer/1704_72497263

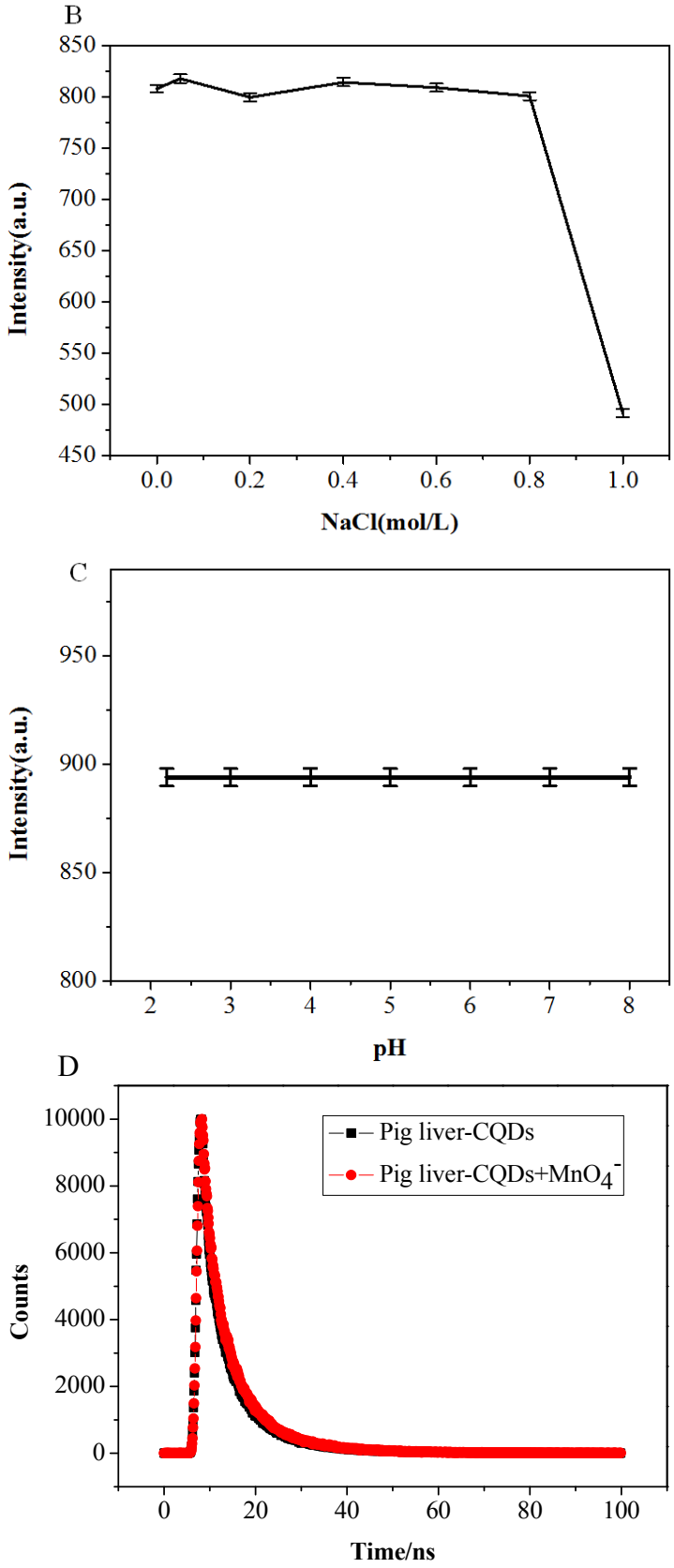

Figure 7. *Effects of various conditions on the fluorescence intensity of pig liver-based CQDs: (A) storage time; (B) NaCl concentration; (C) pH; (D) the Fluorescence lifetime decay curve*

http://www.aloki.hu ● ISSN 1589 1623 (Print) ● ISSN 1785 0037 (Online)
DOI: http://dx.doi.org/10.15666/aeer/1704_72497263

Selectivity

The selectivity of pig liver based-CQDs was investigated by monitoring the fluorescence intensity of different possible interfering substances such as MnO_4^-, Fe^{3+}, Fe^{2+}, NO_2, NO_3, I^-, Cl^-, F^-, Na^+, K^+, Cu^{2+}, Al^{3+}, Ca^{2+}, Mn^{2+}, Ba^{2+}, Mg^{2+} and S^{2-} in the presence of different concentrations or ions. As shown in *Figure 8,* only permanganate ion can effectively quench the fluorescence intensity of CQDs in pig liver, while the quenching effect of other possible interfering substances is negligible. The results show that there may be some quenching relationship between pig liver-based CQDs and permanganate ions, which is worthy of further study. Therefore, there is a high selectivity between permanganate ions and pig liver-based CQDs. This demonstrates that pig liver-based CQDs can be used to detect permanganate ions.

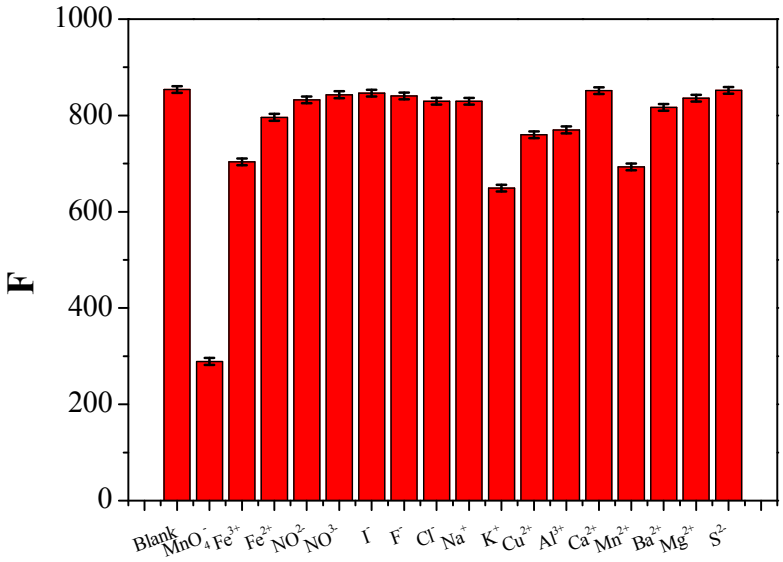

Figure 8. *Evaluation of method selectivity against possible interferents*

Optimization of experimental conditions

PH affects not only the fluorescence intensity of pig liver-based CQDs, but also the fluorescence quenching effect of permanganate ions on pig liver-based CQDs. Therefore, the effect of pH from 2.2 to 8.0 on the experimental system was investigated. As shown in *Figure 9A,* the fluorescence intensity of pig liver-based CQDs is related to pH. In the range of pH2.0-7.0, the fluorescence intensity increased gradually and the fluorescence quenching efficiency reached its maximum, but after pH 7.0, the fluorescence intensity decreased gradually. The results show that the fluorescence quenching response of the system is the largest at pH 7.0, according to which pH 70 is the optimum pH value of citric acid-disodium hydrogen phosphate buffer.

In order to study the stability of pig liver-based CQDs in detecting permanganate ions, the fluorescence intensity of pig liver-based CQDs in the presence of permanganate ions at the same concentration under different reaction time was studied. As shown in *Figure 9B,* the fluorescence intensity of pig liver based-CQDs decreased sharply within 0-1 min and gradually within 1-10 min, then tended to be stable, and reached the lowest fluorescence intensity in 2 min. Therefore, the reaction time of 2 min was chosen as the optimal fluorescence quenching response time.

http://www.aloki.hu ● ISSN 1589 1623 (Print) ● ISSN 1785 0037 (Online)
DOI: http://dx.doi.org/10.15666/aeer/1704_72497263

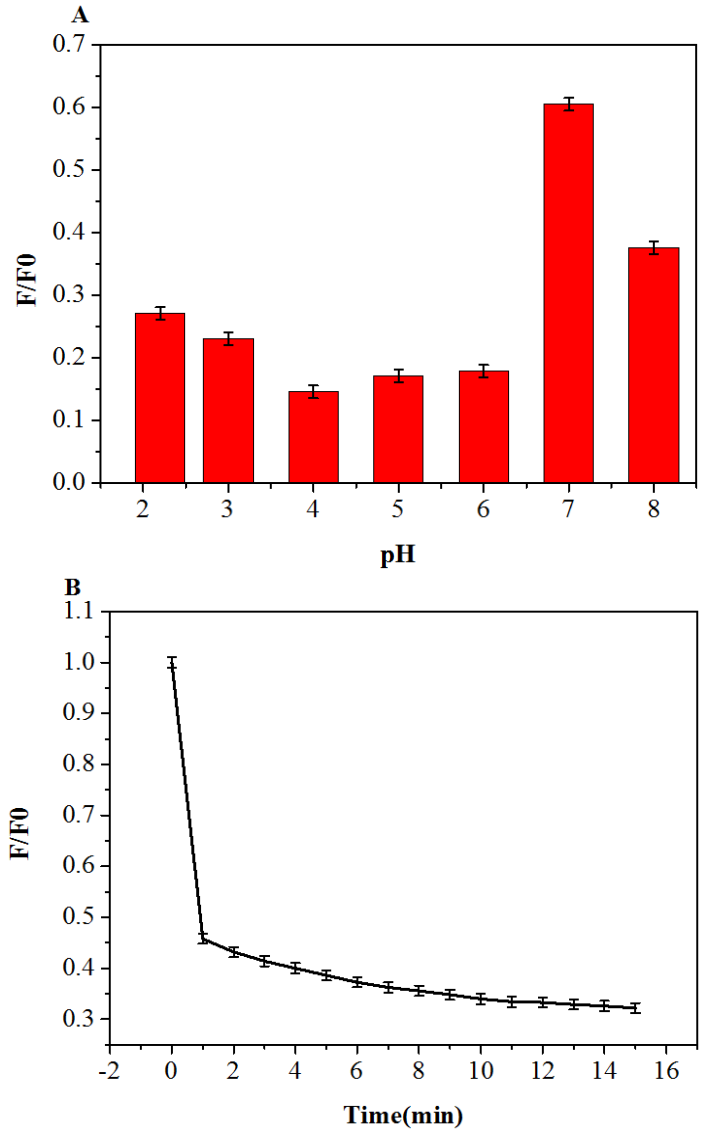

Figure 9. *Effect of pH (A) and (B) reaction time on the fluorescence intensity of the pig liver-based CQDs*

Method performance study

Under the optimal experimental conditions, the relationship between the fluorescence quenching intensity of pig liver-based CQDs and the concentration of MnO_4^- was studied, and the quantitative analysis method for fluorescence quenching of MnO_4^- was established. As shown in *Figure 10,* the fluorescence intensity of pig liver-based CQDs decreases gradually with the addition of MnO_4^- of different concentrations, and shows regular changes. As shown in *Figure 11,* the ratio of fluorescence intensity of the system was linear with the concentration of MnO_4^- in the range of 0-50 μM both before and after addition of pig liver-based CQDs. The regression equation is F/F0 = 0.0151C – 0.0112 (R^2 = 0.9967), where F and F0 are the fluorescence intensity of pig liver-based CQDs in the presence or absence of MnO_4^- respectively and C is the concentration of MnO_4^-. The detection limit of MnO_4^- was 0.06 μM and the signal-noise ratio was 3(S/N).

http://www.aloki.hu ● ISSN 1589 1623 (Print) ● ISSN 1785 0037 (Online)
DOI: http://dx.doi.org/10.15666/aeer/1704_72497263

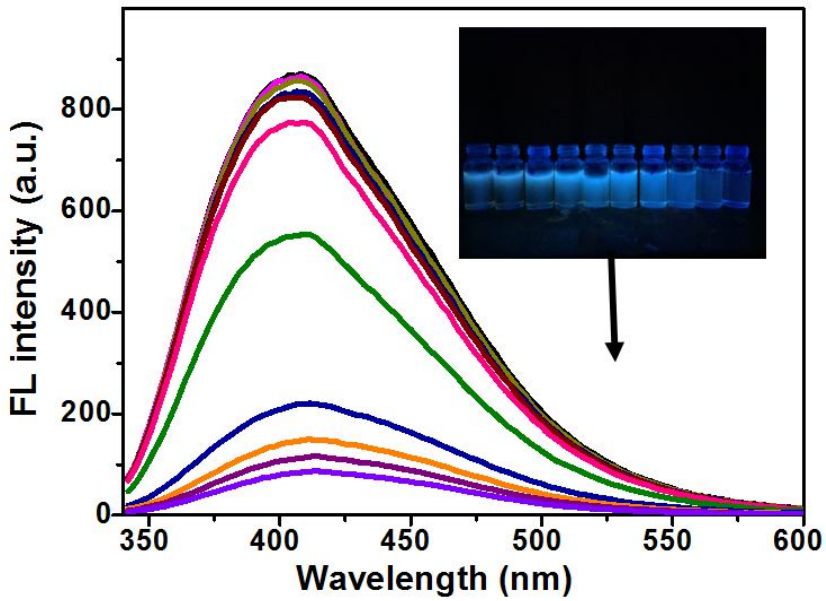

Figure 10. *Fluorescence response of pig liver-based CQDs upon addition of different concentrations of MnO_4^- (concentration gradient of pig liver based-CQDs under ultraviolet light)*

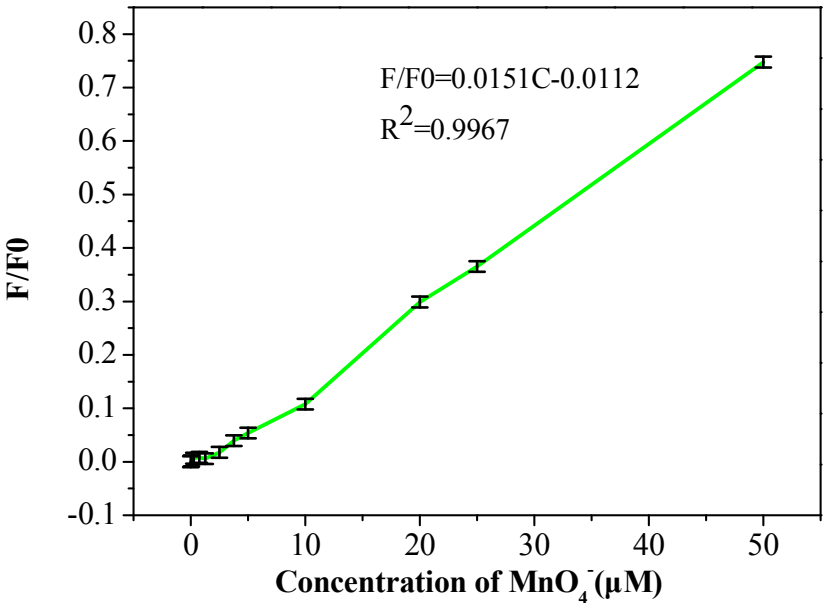

Figure 11. *Linear correlation of F0/F values versus the concentration of MnO_4^- over the range from 0.1 to 50 μM*

Possible fluorescence quenching mechanism

In recent years, many sensors have been established based on the fluorescence variation of carbon quantum dots. These sensors were primarily analytes that quenched or increased the fluorescence of the carbon dots (Mariappan et al., 2017). Theoretically, this fluorescence phenomenon is related to different mechanisms. For fluorescence

http://www.aloki.hu ● ISSN 1589 1623 (Print) ● ISSN 1785 0037 (Online)
DOI: http://dx.doi.org/10.15666/aeer/1704_72497263

quenching, the mechanism is usually divided into dynamic quenching and static quenching, caused by the collision between fluorescent materials and quencher and the formation of ground state complexes respectively (Kaviyarasu et al., 2017). In case of dynamic quenching, the Stern-Volmer equation can be used for analysis (Guo et al., 2015) with the following formula:

$$F0/F = 1 + K_{q\tau 0}[Q] = 1 + K_{SV}[Q]$$

where: F0 and F indicate the fluorescence intensity before and after the addition of MnO_4^- respectively, K_q is the bimolecular quenching constant, τ0 is the average lifetime of CQDs, generally 10^{-8} s, KSV is the Stern-Walmer quenching constant, and [Q] was the concentration of MnO_4^-. Therefore, the fluorescence quenching process may be caused by static quenching, i.e. the formation of ground state complexes in the reaction system (Lakowicz, 2006; Sun et al., 2015; Formica et al., 2012). The absorption strength of CQDs increased and the peak shifted to blue after addition of MnO_4^-, indicating that the interaction between MnO_4^- and CQDs produced the ground state complex. According to almost constant fluorescence lifetime, the fluorescence quenching caused by MnO_4^- may be static quenching due to the formation of stable non-fluorescent complexes (Zuo et al., 2016; Sun and Lei, 2017; Wu et al., 2011; Liu et al., 2017, 2014). FT-IR and XPS confirmed the presence of -COOH, -OH, etc. on the surface of CQDs, indicating good water solubility and good application prospect of the synthesized CQDs.

Analysis of MnO_4^- in real samples

The above mentioned environmental water and soil samples were pretreated, and then MnO_4^- in environmental water and soil samples was detected by prepared pig liver-based CQDs. The environmental water samples and soil samples were spiked and recovered using different concentrations of MnO_4^- and pretreated according to the same procedure. As shown in *Table 1,* the recovery of MnO_4^- in water samples is 94.2~102.5% and the relative standard deviations (RSD) of all samples are less than 5.8%. As shown in *Table 2,* the recovery of MnO_4^- in soil samples is 90.5 to 99.5% and the relative standard deviations (RSD) of all samples are below 4.7%. Therefore, this method has the potential for detecting MnO_4^- in environmental water samples and soil samples.

Table 1. *Analytical results of MnO_4^- in the water samples (n = 3)*

Samples	Spiked (μg/mL)	Found (μg/mL)	Recovery (%)	RSD (%, n = 3)
Tap water	0	ND	-	-
	5	4.71	94.2	4.3
	20	19.3	96.5	3.6
Lake water	0	ND	-	-
	5	4.92	98.4	5.8
	20	20.5	102.5	2.5
Waste water	0	ND	-	-
	5	5.10	102.0	5.3
	20	20.05	100.3	4.7

ND = not detected

http://www.aloki.hu ● ISSN 1589 1623 (Print) ● ISSN 1785 0037 (Online)
DOI: http://dx.doi.org/10.15666/aeer/1704_72497263

Table 2. *Analytical results of MnO_4^- in the soil samples (n = 3)*

Samples	Spiked (μg/mL)	Found (μg/mL)	Recovery (%)	RSD (%, n = 3)
Sample 1	0	ND	-	-
	5	4.97	99.5	4.5
	20	18.1	90.5	2.8
Sample 2	0	ND	-	-
	10	9.58	95.8	3.5
	20	18.34	91.7	3.1

ND = not detected

Conclusion

In summary, novel fluorescent CQDs were prepared from pig liver by hydrothermal synthesis method and the fluorescence intensity of CQDs could be quenched by MnO_4^-, so the CQDs were used as nanosensors for the sensitive and selective detection of MnO_4^- in environmental samples. For instance, morphology, particle size, crystal form, chemical element composition and optical properties of the prepared pig liver-based CQDs were characterized by TEM, FT-IR, XPS, UV-Vis and FS. The results showed that it had good stability and fluorescence characteristics. In addition, a good linear relationship was achieved between the fluorescence response of CQDs and the concentration of MnO_4^- in the range from 0.1 to 50 μM. The detection limit was 0.06 μM under optimized conditions. The developed method has been successfully applied to the determination of MnO_4^- in water samples and soils of environmental samples. This method is green, environmental friendly, simple and easy to operate, and shows great potential for application.

REFERENCES

[1] Bhunia, S. K., Saha, A., Maity, A. R., Ray, S. C., Jana, N. R. (2013): Carbon nanoparticle-based fluorescent bioimaging probes. – Sci. Rep. 3: 1473.

[2] Clarkson, T. W., Magos, L. (2006): The toxicology of mercury and its chemical compounds. – Crit. Rev. Toxicol. 36(8): 609-662.

[3] da Silva, E. G. P., do N. Santos, A. C., Costa, A. C. S., da N. Fortunato, D. M., José, N. M., Korn, M. G. A., dos Santos, W. N. L., Ferreira, S. L. C. (2006): Determination of manganese and zinc in powdered chocolate samples by slurry sampling using sequential multi-element flame atomic absorption spectrometry. – Microchemical Journal 82(2): 159-162.

[4] Deng, X. Y., Li, J. Y., Tan, K. J. (2014): Rapid screening and confirmation of pesticide residues in potato by high-resolution benchtop Q exactive LC-MS. – Chinese J. Anal. Chem. 42(4): 579-584.

[5] Doroschuk, V. O., Lelyushok, S. O., Ishchenko, V. B., Kulichenko, S. A. (2004): Flame atomic absorption determination of manganese (II) in natural water after cloud point extraction. – Talanta 64(4): 853-856.

[6] Formica, M., Fusi, V., Giorgi, L., Micheloni, M. (2012): New fluorescent chemosensors for metal ions in solution. – Coord. Chem. Rev. 256 170-192.

[7] Gunter, T. E., Miller, L. M., Gavin, C. E., Eliseev, R., Salter, J., Buntinas, L., Alexandrov, A., Hammond, S., Gunter, K. K. (2010): Determination of the oxidation states of manganese in brain, liver, and heart mitochondria. – Journal of Neurochemistry 88(2): 266-280.

http://www.aloki.hu ● ISSN 1589 1623 (Print) ● ISSN 1785 0037 (Online)
DOI: http://dx.doi.org/10.15666/aeer/1704_72497263

[8] Guo, Y., Zhang, L., Zhang, S., Yang, Y., Chen, X., Zhang, M. (2015): Fluorescent carbon nanoparticles for the fluorescent detection of metal ions. – Biosens. Bioelectron. 63 61-71.
[9] Hua, X.-W., Bao, Y.-W., Wang, H.-Y., Chen, Z., Wu, F.-G. (2017): Bacteria-derived fluorescent carbon dots for microbial live/dead differentiation. – Nanoscale 9: 2150-2161.
[10] Jones, K. H., Senft, J. A. (1985): An improved method to determine cell viability by simultaneous staining with fluorescein diacetate-propidium iodide. – J. Histochem. Cytochem. 33: 77-79.
[11] Kaviyarasu, K., Kanimozhi, K., Matinise, N., Maria, C. Magdalane, Mola, G. T., Kennedy, J., Maaza, M. (2017): Antiproliferative effects on human lung cell lines A549 activity of cadmium selenide nanoparticles extracted from cytotoxic effects: Investigation of bio-electronic application. – Mater. Sci. Eng. C. 76 1012-1025.
[12] Lakowicz, J. R. (2206): Principles of Fluorescence Spectroscopy. 3rd. Ed. – Springer, Singapore.
[13] Li, H., Kong, W. Q., Liu, J., Liu, N. Y., Huang, H., Liu, Y., Kang, Z. H. (2015): Fluorescent N-doped carbon dots for both cellular imaging and highly-sensitive catechol detection. – Carbon 91: 66-75.
[14] Li, H. T., Kang, Z. H, Liu, Y. et al. (2012): Carbon nanodots: synthesis, properties and applications. – J. Mater. Chem. 22(46): 24230-24253.
[15] Li, J. Z., Wang, N. Y., Tran, T. T. et al. (2013): Electrogenerated chemiluminescence detection of trace level pentachlorophenol using carbon quantum dots. – Analyst 138(7): 2038-2043.
[16] Li, Z., Yu, H. J., Bian, T., Zhao, Y. F., Zhou, C., Shang, L., Liu, Y. H., Wu, L. Z., Tung, C. H., Zhang, T. R. . (2015): Highly luminescent nitrogen-doped carbon quantum dots as effective fluorescent probes for mercuric and iodide ions. – Mater. Chem. C 3: 1922-1928.
[17] Liang, P., Sang, H., Sun, Z. (2006): Cloud point extraction and graphite furnace atomic absorption spectrometry determination of manganese (II) and iron(III) in water samples. – Journal of Colloid & Interface Science 304(2): 486-490.
[18] Lim, S. Y., Shen, W., Gao, Z. Q. (2015): – Chem. Soc. Rev. 44: 362.
[19] Liu, Y., Zhao, Y., Zhang, Y. (2014): One-step green synthesized fluorescent carbon nanodots from bamboo leaves for copper(II) ion detection. – Sens. Actuators B 196: 647-652.
[20] Liu, Y., Duan, W., Song, W., Liu, J., Ren, C., Wu, J., Liu, D., Chen, H. (2017): Red emission B, N, S-co-doped carbon dots for colorimetric and fluorescent dual mode detection of Fe3+ ions in complex biological fluids and living cells. – ACS Appl. Mat. Interfaces 9(14): 12663-12672.
[21] Lu, W., Qin, X., Liu, S. et al. (2012): Economical, green synthesis of fluorescent carbon nanoparticles and their use as probes for sensitive and selective detection of mercury(II) ions. – Analytical Chemistry 84(12): 5351-5357.
[22] Mariappan, A., Kaviyarasu, K., Neyvasagam, K., Ayeshamariam, A., Pandi, P., Palanichamy, R. R., Gopinathan, C., Mola, G. T., Maaza, M. (2017): – Surf. Interface. 6 247-255.
[23] Ming, H., Ma, Z., Liu, Y., Pan, K. M., Yu, H., Wang, F., Kang, Z. H. (2012): Large scale electrochemical synthesis of high quality carbon nanodots and their photocatalytic property. – Dalton Trans. 41: 9526-9531.
[24] Nocker, A., Cheung, C. Y., Camper, A. K. (2006): Comparison of propidium monoazide with ethidium monoazide for differentiation of live vs. dead bacteria by selective removal of DNA from dead cells. – J. Microbiol. Methods 67(2): 310-320.
[25] Rask, J. H., Miner, B. A. Buseck, P. R. (2015): Determination of manganese oxidation states in solids by electron energy-loss spectroscopy. – Ultramicroscopy 21(4): 321-326.
[26] Sun, J., Yang, S. W., Wang, Z. Y., Shen, H., Xu, T., Sun, L. T., Li, H., Chen, W. W., Jiang, X. Y., Ding, G. Q., Kang, Z. H., Xie, X. M., Jiang, M. H. (2015): Ultra-high

http://www.aloki.hu ● ISSN 1589 1623 (Print) ● ISSN 1785 0037 (Online)
DOI: http://dx.doi.org/10.15666/aeer/1704_72497263

quantum yield of graphene quantum dots: aromatic-nitrogen doping and photoluminescence mechanism. – Part. Part. Syst. Charact. 32: 434-440.

[27] Sun, X., Lei, Y. (2017): Fluorescent carbon dots and their sensing applications. – Trends in Analytical Chemistry 89 163-180.

[28] Sun, X., Wang, Y., Lei, Y. (2015): Fluorescence based explosive detection: from mechanisms to sensory materials. – Chem. Soc. Rev. 44 8019-8061.

[29] Teo, K. C., Chen, J. (2001): Determination of manganese in water samples by flame atomic absorption spectrometry after cloud point extraction. – Analyst 126(4): 534.

[30] Wang, Y. F., Hu, A. G. (2014): Carbon quantum dots: synthesis, properties and applications. – J. Mater. Chem. C 2(34): 6921-6939.

[31] Wu, J., Liu, W., Ge, J., Zhang, H., Wang, P. (2011): New sensing mechanisms for design of fluorescent chemosensors emerging in recent years. – Chem. Soc. Rev. 40: 3483-3495.

[32] Xu, X. Y., Robert, R., Gu, Y. L. et al. (2004): Electrophoretic analysis and purification of fluorescent single-walled carbon nanotube fragments. – J. am. Chem. Soc. 126(40): 12736-12737.

[33] Yu, H. J., Shi, R., Zhao, Y. F., Waterhouse, G. I. N., Wu, L. Z., Tung, C. H., Zhang, T. R. (2016): Nitrogen-doped porous carbon nanosheets templated from g-C3 N4 as metal-free electrocatalysts for efficient oxygen reduction reaction. – Adv. Mater. 28(25): 9454-9477.

[34] Zeng, C., Qin, P., Lan, L., Wei, H., Wu, W. (2017): Chemical vapor generation coupled with atomic fluorescence spectrometry for the determination of manganese in food samples. – Microchemical Journal 131: 31-35.

[35] Zhang, R., Chen, W. (2014): Nitrogen-doped carbon quantum dots: facile synthesis and application as a "turn-off" fluorescent probe for detection of Hg^{2+} ions. – Biosensors and Bioelectronics 55: 83-90.

[36] Zhao, H. X., Liu, L. Q., Liu, Z. D. et al. (2011): Highly selective detection of phosphate in very complicated matrixes with an off-on fluorescent probe of europium-adjusted carbon dots. – Chem. Commun. 47(9): 2604-2606.

[37] Zuo, P., Lu, X., Sun, Z., Guo, Y., He, H. (2016): A review on syntheses, properties, characterization and bioanalytical applications of fluorescent carbon dots. – Microchim. Acta 183 519-542.

http://www.aloki.hu ● ISSN 1589 1623 (Print) ● ISSN 1785 0037 (Online)
DOI: http://dx.doi.org/10.15666/aeer/1704_72497263

COMPOSITIONS OF PROKARYOTE COMMUNITES AND THEIR RELATIONSHIP TO PHYSIOCHEMICAL FACTORS IN DECEMBER IN CHAOHU LAKE AND THREE URBAN RIVERS IN CHINA

WU, L.[1*] – SHU, F.[2] – OU, Z.[1] – CHEN, Q.[1] – WANG, L.[1] – WANG, H.[1] – XU, Z.[1*]

[1]School of Life Science, Hefei Normal University, Hefei 230601, China (phone/fax: +86-551-6367-4150)

[2]Key Laboratory of Wetland Ecology and Environment Conservation of Lake Nansi, College of Life Sciences, Qufu Normal University, Qufu 273100, China (phone: +86-537-4456-415; fax: +86-537-4456-415)

**Corresponding authors*
e-mail: wuli090121@126.com (L. Wu), xuzhongdong@hftc.edu.cn (Z. Xu); phone/fax: +86-551-6367-4150

(Received 18th Jan 2019; accepted 28th Feb 2019)

Abstract. The aim of this study was to determine the impacts of anthropogenic disturbances on compositions of prokaryote communites (CPCs) in Chaohu Lake and its three urban tributaries, in China. Prokaryotic diversity in Chaohu Lake and its tributaries was high, and prokaryotic communities showed lower richness in Nanfei River than in Zhegao River and Hangbu River, with waterbody nutrient levels negatively corresponding to prokaryotic diversity. Except for a few rare prokaryotes, or where classification was unclear, the prokaryotes were distributed into 13 phyla and 924 genera. The dominant prokaryotic phyla were Proteobacteria (31.51%), Bacteroidetes (26.50%), Cyanobacteria (19.05%), and Actinobacteria (10.71%). Redundancy analysis (RDA) results showed CPCs, as well as abundances of Proteobacteria, Actinobacteria, and Firmicutes to be primarily affected by the concentration of total phosphorus (TP). Furthermore, Cyanobacteria showed a significant correlation with the concentrations of total nitrogen (TN), nitrate (NO_3) and ammonia nitrogen (NH_4). pH was correlated with Planctomycetes, while Thermotogae was generally associated with water temperature (WT). These results suggest that trophic status could play an important role in shaping CPCs in both freshwater lakes and rivers. Ultimately, urbanization was found to cause the deterioration of water quality within Chaohu Lake and its tributaries.

Keywords: *prokaryotic community structure, diversity, high-throughput sequencing, redundancy analysis, freshwater*

Introduction

With continued worldwide urban expansion and rapid economic and industrial development, discharge from anthropogenic activities (municipal, industrial, and agricultural) continues to expose freshwater systems to large quantities of anthropogenic pollutants. This pollution has resulted in a notable deterioration of freshwater quality (Martinuzzi et al., 2014; Jordaan and Bezuidenhout, 2016). In aquatic ecosystems, prokaryotes drive the transformation and cycling of most biologically active elements, so they play a critical role in the regeneration and mobilization of nutrients in freshwater food webs (Newton et al., 2011; Ren et al., 2013). Short generation times, high diversity, and quick reaction to (and recovery from) environmental change make prokaryotes ideal indicators of stress in freshwater systems. Anthropogenic disturbances on freshwater systems have major repercussion on the

http://www.aloki.hu ● ISSN 1589 1623 (Print) ● ISSN 1785 0037 (Online)
DOI: http://dx.doi.org/10.15666/aeer/1704_72657281

overall prokaryotic structure and function of these habitats (Jordaan and Bezuidenhout, 2016). To better manage and maintain the ecological environments of freshwater systems, we need to more fully understand how prokaryotic community diversity and distribution characteristics function in these environments. In recent years, culture-independent methods were used to characterize prokaryotic diversity. This approach avoids the cultivation bias and yields detailed insight into the prokaryotic diversity of diverse ecosystems (Ni et al., 2017; Wu et al., 2017; Xiang et al., 2018). The use of high-throughput sequencing has become an increasingly popular technique for the analysis of prokaryotic communities in a variety of freshwater ecosystems, and has led to the increased detection of rare prokaryotic species (Lin et al., 2012; Bashenkhaeva et al., 2015; Dai et al., 2016; Wu et al., 2017).

Chaohu Lake, one of the five largest freshwater lakes in China, is a shallow and subtropical freshwater system. Chaohu Lake has three urban-river tributaries–Nanfei, Zhegao, and Hangbu Rivers–which drain into the lake (Wang et al., 2011; *Fig. 1*). Chaohu Lake plays an important role in commercial fishing, water supply, irrigation, navigation, tourism, and recreational activity throughout the region. However, in recently years, due to the increase in anthropogenic activity within the lake's watershed, Chaohu Lake has suffered from severe pollution and eutrophication (Zan et al., 2011). This has resulted in large blooms of blue-green algae during the summer months, which have caused the production of highly toxic microcystins, and the subsequent fouling (and temporary interruption) of the local drinking water supply. The water quality of Chaohu Lake's three tributaries has also been adversely affected by human activity–including agricultural runoff, urban development, and the construction of informal settlements. The establishment of water management strategies requires previous knowledge of the ecological dynamics of target communities in the water body. To date, however, only two studies (Bao et al., 2008; Wei et al., 2008) have analyzed the phylogenetic composition of bacterioplankton communities in Chaohu Lake. This was accomplished by partially sequencing cloned 16S rRNA genes and PCR-DGGE (denaturing gradient gel electrophoresis) analysis. No further research has attempted to characterize the compositions of prokaryote communites (CPCs) in Chaohu Lake by way of high-throughput sequencing, and the information on the CPCs of the lake's three tributaries is virtually nonexistent. Ultimately, this has restricted the creation of an effective water management plan. Thus, it is important to collect data and conduct research on prokaryotic diversity within Chaohu Lake and its surrounding watershed. Moreover, much of our current understanding of local CPCs is primarily based on inter-lake or inter-river investigations, with less attention being given to the areas where rivers drain into the lake.

The objectives of this project were as follows: 1) characterize the CPCs in Chaohu Lake and its tributaries using high-throughput sequencing; 2) compare the CPCs among Chaohu Lake and its tributaries, and evaluate the importance of physicochemical parameters in the structuring of CPCs; 3) provide basic information for the restoration of Chaohu Lake and its tributaries.

Materials and methods

Study area

Chaohu Lake (E117°35'52.2", N31°40'26.5") has a surface area of 770 km^2, and is situated on the floodplain between the Yangtze River and the Huaihe River in the

http://www.aloki.hu ● ISSN 1589 1623 (Print) ● ISSN 1785 0037 (Online)
DOI: http://dx.doi.org/10.15666/aeer/1704_72657281

central Anhui Province of eastern China (Wang and Dou, 1998). The Nanfei River, Zhegao River, and Hangbu River, three tributaries of Chaohu Lake, flow through Hefei City, Zhegao Town, and Sanhe Town, respectively (*Fig. 1*). Farmland primarily surrounds the upper reaches of the three rivers, whereas cities and towns envelop the middle and lower reaches. Thus the middle and lower stretches are stressed from multiple anthropogenic sources, including untreated domestic and industrial wastewater discharge.

Sampling sites and sample collection

Samples were collected on 22 December 2017. We studied the Nanfei, Zhegao, and Hangbu Rivers, and established three sites along the upper reaches (U), middle reaches (M), and lower reaches (L) of all three rivers. Additionally, based on the shape and size of Chaohu Lake, three sites (I, II, III) were selected (*Fig. 1*). All stations were sampled within a 24-h period. The samples of three rivers were collected from the center of rivers. 500-ml water samples were collected at each sampling site for microbial DNA extraction. At each sampling site, 500-ml water samples were collected from surface waters (the top 50 cm) and filtered through 0.2-μm-pore-size Isopore filters (Millipore, Billerica, MA, USA). All samples were collected only once. DNA extraction was carried out within 24 h from the time of sample collection. Simultaneously, 1 L water samples were collected at each sampling site for physicochemical characterization (Huang, 2000).

Measurement of physical and chemical indices

Water temperature was measured using a multi-parameter water quality monitoring sonde (YSI 6600, USA). One liter of water was collected to measure pH, total phosphorus (TP), total nitrogen (TN), nitrate (NO_3) and ammonia nitrogen (NH_4). All of these physiochemical factors were measured according to standard methods (Huang, 2000).

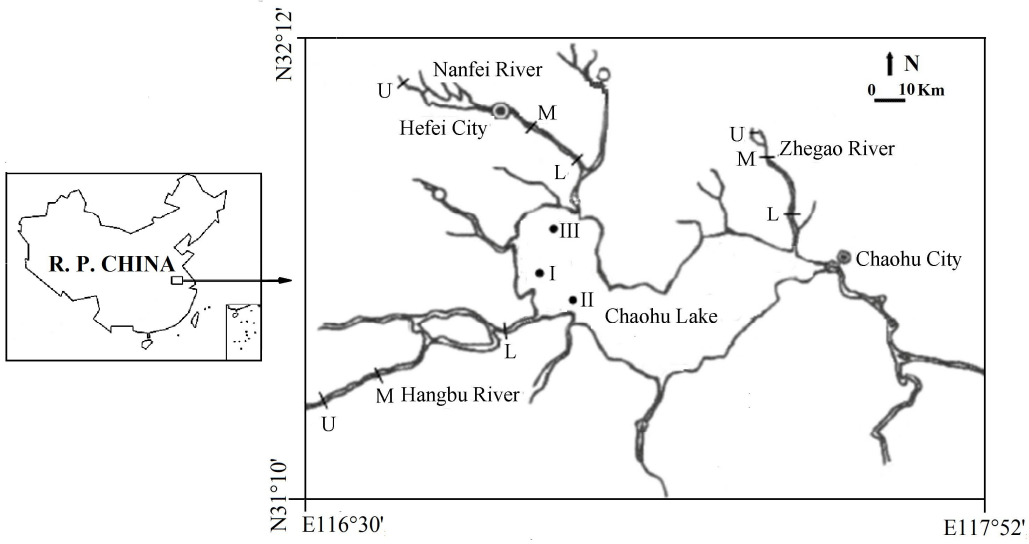

Figure 1. *Sampling sites of Chaohu Lake and three rivers. U, upper reaches; M, middle reaches; and L, lower reaches; I, site I of Chaohu Lake; II, site II of Chaohu Lake; III, site III of Chaohu Lake*

http://www.aloki.hu ● ISSN 1589 1623 (Print) ● ISSN 1785 0037 (Online)
DOI: http://dx.doi.org/10.15666/aeer/1704_72657281

DNA extraction and high-throughput sequencing of prokaryotic 16S rRNA gene

Genomic DNA of the water microbiota was extracted using the standard phenol-chloroform method (Wu et al., 2017). The extracted DNA was diluted to 10 ng/μL and stored at −40 °C for downstream use.

A prokaryotic universal primers 515F and 909R with a 12 nt unique barcode was used to amplify the V4-V5 hypervariable region of 16S rRNA gene for high-throughput sequencing according to a previous report (Ni et al., 2017). The PCR mixture (25 μl) contained 1× PCR buffer, 1.5 mM MgCl2, deoxynucleoside triphosphate at 0.4 μM, primer at 1.0 μM and 0.5 U of Ex Taq (TaKaRa, China), and 10 ng genomic DNA. The PCR amplification program included initial denaturation at 94 °C for 10 min, followed by 30 cycles of 94 °C for 40 s, 56 °C for 60 s, and 72 °C for 60 s, and a final extension at 72 °C for 10 min. Two PCR reactions were conducted for each sample and combined together after PCR amplification. PCR products were subjected to electrophoresis using 1% agarose gel. Each band showing the target size was excised and purified using a SanPrep DNA Gel Extraction Kit (Sangon Biotech, China) and quantified with Nanodrop. All samples were pooled together with equal molar amounts from each sample. The sequence samples were prepared using TruSeq DNA kit according to the manufacturer's instructions. The purified library was diluted, denatured, re-diluted, and mixed with PhiX (equal to 30% of the final DNA amount–as described in the Illumina library preparation protocols), and applied to an Illumina Miseq benchtop sequencer (Illumina, USA) at Guangdong Meilikang Bio-Science Ltd., China with the Reagent Kit (v2) 2 × 250 bp according to the manufacture manual.

Data analysis

The raw sequence data were merged using FLASH–1.2.8 software (Magoc and Salzberg, 2011). The merged sequences were trimmed and assigned to each sample based on their respective barcode sequences using QIIME Pipeline Version 1.7.0 (Caporaso et al., 2010). The sequences that are more than 300 bp of length, without ambiguous base 'N', and more than 30 of the average base quality score were used for downstream analysis (Xiang et al., 2018). Sequences were clustered into operational taxonomic units (OTUs) at a 97% identity threshold. The aligned gene sequences were used for chimera check using the Uchime algorithm (Edgar et al., 2011). Taxonomy was assigned using the Ribosomal Database Project classifier (Wang et al., 2007). Shannon index was calculated using QIIME 1.7.0 based on the composition of OTUs. Principal coordinate analysis (PCoA) based on a weighted UniFrac distance matrix was conducted using QIIME 1.7.0. Redundancy analysis (RDA) with a Monte Carlo permutation test was carried out using the 'vegan' package in R (Oksanen et al., 2015). P-values < 0.05 were considered statistically significant. We performed one-way analysis of variance (ANOVA) to test for significant differences in physicochemical characteristics. All statistical analyses were performed using SPSS 13.0.

Results

Physicochemical analysis

Concentrations of TP and NH_4 exhibited maxima in the Nanfei River, while concentrations of TN and NO_3 were greater in Chaohu Lake than in the three rivers (*Table 1*). According to the standard established by the Organisation for Economic and

http://www.aloki.hu ● ISSN 1589 1623 (Print) ● ISSN 1785 0037 (Online)
DOI: http://dx.doi.org/10.15666/aeer/1704_72657281

Co-operation and Development (OECD) (1982)–which is based on the concentration of total phosphorus (TP)–Chaohu Lake and its three associated rivers are eutrophic or hypereutrophic. The degree of eutrophication was as follows: Nanfei River > Chaohu Lake > Zhegao River > Hangbu River.

Table 1. *Physicochemical characteristics of Chaohu Lake and three rivers*

Physicochemical variables		WT (°C)	pH	TN (mg/L)	NH_4 (mg/L)	NO_3 (mg/L)	TP (mg/L)
Hangbu River	HBU	3.50	7.92	1.36	0.17	1.11	0.07
	HBM	4.50	7.54	0.82	0.04	0.31	0.10
	HBL	4.90	7.59	1.17	0.13	0.34	0.08
	Mean ± SD	4.30 ± 0.72	7.68 ± 0.21	1.12 ± 0.28	0.11 ± 0.06	0.59 ± 0.45	0.08 ± 0.02
Zhegao River	ZGU	5.00	8.10	1.91	0.24	1.24	0.15
	ZGM	4.80	8.01	0.86	0.06	0.61	0.06
	ZGL	4.70	7.98	1.67	0.07	0.92	0.05
	Mean ± SD	4.83 ± 0.15	8.03 ± 0.06	1.48 ± 0.55	0.12 ± 0.10	0.92 ± 0.32	0.09 ± 0.06
Nanfei River	NFU	2.50	7.53	10.79	3.58	4.64	0.35
	NFM	8.50	7.55	1.01	0.00	0.53	0.02
	NFL	8.70	7.78	18.88	7.18	6.53	1.39
	Mean ± SD	6.57 ± 3.52	7.62 ± 0.14	10.22 ± 8.95	3.59 ± 3.59	3.90 ± 3.06	0.59 ± 0.72
Chaohu Lake	CH I	4.00	7.96	7.96	0.40	4.17	0.19
	CH II	4.50	7.99	4.17	1.29	1.37	0.23
	CH III	4.40	7.75	28.44	8.80	8.58	0.23
	Mean ± SD	4.30 ± 0.26	7.90 ± 0.13	13.52 ± 13.06	3.49 ± 4.61	4.71 ± 3.63	0.21 ± 0.02
	P	N.S.	0.027	N.S.	N.S.	N.S.	N.S.

P: level of significance (ANOVA, $P < 0.05$); N.S.: not significant
NFU: upper reaches of Nanfei River; NFM: middle reaches of Nanfei River; NFL: lower reaches of Nanfei River; ZGU: upper reaches of Zhegao River; ZGM: middle reaches of Zhegao River; ZGL: lower reaches of Zhegao River; HBU: upper reaches of Hangbu River; HBM: middle reaches of Hangbu River; HBL: lower reaches of Hangbu River; CH I: site I of Chaohu Lake; CH II: site II of Chaohu Lake; CH III: site III of Chaohu Lake

Prokaryote community composition

In total, 296,004 effective sequences and 39,350 OTUs (not include the averages number of OTUs in Chaohu Lake and three rivers) were obtained from these samples (*Table 2*). Chaohu Lake had the highest number of OTUs (3,289) (*Table 2*). Additionally, prokaryote communities in Chaohu Lake showed higher richness than in the three rivers. The average Shannon diversity index for prokaryote communities in Chaohu Lake was 6.81. Among the three rivers, the highest observed prokaryotic diversity was in Zhegao River (7.60), followed by Hangbu River (6.99), and Nanfei River (6.21; *Table 2*). Thus, Chaohu Lake and its tributaries exhibited high prokaryotic diversity as well as an inverse relationship between water body trophic level and prokaryotic diversity.

Except for a small number of unclassified (0.03%) and rare (2.98%) prokaryotes, a total of 13 prokaryotic phyla were identified from Chaohu Lake and its tributaries. There were 13 dominant prokaryotic phyla, including Proteobacteria (31.51%), Bacteroidetes (26.50%), Cyanobacteria (19.05%), Actinobacteria (10.71%),

http://www.aloki.hu ● ISSN 1589 1623 (Print) ● ISSN 1785 0037 (Online)
DOI: http://dx.doi.org/10.15666/aeer/1704_72657281

Verrucomicrobia (2.73%), Firmicutes (2.29%), Planctomycetes (1.02%), Chloroflexi (0.82%), Acidobacteria (0.62%), Chlorobi (0.51%), Thermotogae (0.50%), Crenarchaeota (0.38%), and Euryarchaeota (0.35%; *Fig. 2A* and *Table 3*). The Proteobacteria were distributed (in descending order) as Betaproteobacteria (19.88%), Alphaproteobacteria (6.41%), Gammaproteobacteria (4.47%) and Deltaproteobacteria (0.57%). Within the Bacteroidetes phylum, Flavobacteriia (17.75%), Sphingobacteriia (7.11%) and Bacteroidia (1.16%) were the most frequently detected. Nostocophycideae (8.70%), Synechococcophycideae (1.55%), and Oscillatoriophycideae (1.24%) were the dominant classes of Cyanobacteria phylum; Actinobacteria (9.73%) and Verrucomicrobiae (1.57%) were the main classes of the Actinobacteria and Verrucomicrobia phyla; the Firmicutes phylum predominantly consisted of the Clostridia (1.20%) and Bacilli classes (1.00%; *Table 3*).

Table 2. *The richness and diversity of the prokaryotic community in Chaohu Lake and its tributaries*

	Site	Number of sequences	No. of OTU (97% identity)	Shannon index
Hangbu River	HBU	32615	2551	7.31
	HBM	16838	2010	6.9
	HBL	8918	1592	6.75
	Average	19457	2051	6.99
Zhegao River	ZGU	17535	2411	6.63
	ZGM	14868	2317	7.84
	ZGL	7465	1748	8.34
	Average	13289	2159	7.60
Nanfei River	NFU	24885	2685	6.75
	NFM	15424	2653	7.05
	NFL	7582	1678	4.82
	Average	15964	2339	6.21
Chaohu Lake	CH I	30711	3533	6.34
	CH II	28419	3720	7.77
	CH III	16743	2614	6.33
	Average	25291	3289	6.81
Total		296004	39350	

Abbreviations are the same as those in *Table 1*

There was a distinct difference in the distribution of the dominant prokaryotic phyla in Chaohu Lake and its tributaries. For example, Proteobacteria exhibited the highest abundance in all of the collection stations–especially in Nanfei River–while Bacteroidetes abundance was highest in Hangbu River. Furthermore, Chaohu Lake and Zhegao River had high abundances of Cyanobacteria, Nanfei River had a high abundance of Firmicutes, and the middle reaches of Zhegao River (ZGM) had a high abundance of Verrucomicrobia. The upper reaches of Hangbu River (HBU) and upper reaches of Nanfei River (NFU) exhibited lower nutrient levels than the other stations, and also had the lowest abundance of Acidobacteria (*Fig. 2A* and *Table 3*).

http://www.aloki.hu ● ISSN 1589 1623 (Print) ● ISSN 1785 0037 (Online)
DOI: http://dx.doi.org/10.15666/aeer/1704_72657281

Table 3. *Percentage of the most abundant phyla, classes, and genera in each sampling station (%)*

Taxon	HBU	HBM	HBL	ZGU	ZGM	ZGL	NFU	NFM	NFL	CH I	CH II	CH III	Percentage of the total prokaryotic abundant (%)
Proteobacteria	0.2304	0.3724	0.290	0.371	0.240	0.244	0.4905	0.5353	0.4877	0.154	0.1693	0.1959	31.5
Bacteroidetes	0.6896	0.4351	0.491	0.170	0.169	0.110	0.3589	0.245	0.1195	0.097	0.1483	0.1463	26.5
Cyanobacteria	0.0142	0.0625	0.020	0.222	0.197	0.309	0.052	0.0294	0.0667	0.525	0.4336	0.3536	19.1
Actinobacteria	0.0098	0.0602	0.083	0.094	0.118	0.169	0.013	0.0439	0.1947	0.124	0.1611	0.2142	10.7
Verrucomicrobia	0.0021	0.0066	0.035	0.028	0.137	0.038	0.0056	0.0052	0.0137	0.035	0.0161	0.0048	2.73
Firmicutes	0.0171	0.0189	0.019	0.018	0.025	0.026	0.0296	0.0473	0.0235	0.013	0.0177	0.0201	2.29
Planctomycetes	0.0010	0.0014	0.004	0.052	0.026	0.015	0.0014	0.0013	0.0083	0.006	0.0024	0.0041	1.02
Chloroflexi	0.0030	0.003	0.005	0.007	0.005	0.019	0.0041	0.0054	0.0231	0.007	0.0068	0.0105	0.82
Acidobacteria	0.0036	0.0042	0.007	0.005	0.007	0.008	0.0061	0.0106	0.0078	0.004	0.0048	0.0062	0.62
Chlorobi	0.0011	0.0015	0.004	0.0008	0.020	0.005	0.0016	0.0016	0.0102	0.004	0.0042	0.0066	0.51
Thermotogae	0.0048	0.0043	0.005	0.004	0.006	0.005	0.0047	0.0082	0.007	0.003	0.0043	0.0045	0.50
Crenarchaeota	0.0036	0.0038	0.005	0.002	0.004	0.006	0.0051	0.0034	0.0044	0.002	0.0029	0.0034	0.38
Euryarchaeota	0.0032	0.0031	0.004	0.001	0.004	0.003	0.0031	0.0056	0.0057	0.003	0.0027	0.0029	0.35
Taxon	**HBU**	**HBM**	**HBL**	**ZGU**	**ZGM**	**ZGL**	**NFU**	**NFM**	**NFL**	**CH I**	**CH II**	**CH III**	**Percentage of the total prokaryotic abundant (%)**
Proteobacteria;c__Betaproteobacteria	0.1726	0.3235	0.219	0.140	0.143	0.123	0.3052	0.3384	0.3578	0.053	0.0863	0.1237	19.9
Proteobacteria;c__Gammaproteobacteria	0.0453	0.0211	0.035	0.018	0.031	0.029	0.1422	0.1389	0.0305	0.011	0.0137	0.020	4.47
Proteobacteria;c__Alphaproteobacteria	0.0087	0.0233	0.029	0.204	0.055	0.082	0.0339	0.0447	0.0922	0.085	0.0649	0.0456	6.41
Proteobacteria;c__Deltaproteobacteria	0.0032	0.0036	0.006	0.007	0.007	0.008	0.0053	0.0104	0.0061	0.004	0.0038	0.0045	0.57
Bacteroidetes;c__Flavobacteriia	0.6459	0.278	0.413	0.08	0.074	0.03	0.2989	0.1701	0.0343	0.022	0.0554	0.0275	17.8

http://www.aloki.hu ● ISSN 1589 1623 (Print) ● ISSN 1785 0037 (Online)
DOI: http://dx.doi.org/10.15666/aeer/1704_72657281

Bacteroidetes;c__Sphingobacteriia	0.0258	0.1424	0.059	0.076	0.08	0.063	0.0423	0.0541	0.0677	0.063	0.0784	0.1009	7.11
Bacteroidetes;c__Bacteroidia	0.0137	0.011	0.015	0.008	0.01	0.011	0.014	0.0134	0.0115	0.007	0.0089	0.0143	1.16
Cyanobacteria;c__Nostocophycideae	0.0035	0.0024	0.003	0.006	0.003	0.133	0.0035	0.0029	0.0051	0.345	0.2285	0.3072	8.70
Cyanobacteria;c__Oscillatoriophycideae	0.0043	0.0029	0.003	0.010	0.009	0.006	0.0033	0.0033	0.0459	0.038	0.0185	0.0049	1.24
Cyanobacteria;c__Synechococcophycideae	0.0009	0.0007	0.001	0.121	0.002	0.014	0.0008	0.001	0.0024	0.022	0.0126	0.0077	1.55
Actinobacteria;c__Actinobacteria	0.0085	0.0538	0.068	0.078	0.104	0.147	0.0111	0.0412	0.1894	0.105	0.1566	0.2055	9.73
Firmicutes;c__Bacilli	0.0062	0.0082	0.006	0.008	0.011	0.011	0.0154	0.0274	0.0086	0.005	0.0072	0.0073	1.01
Firmicutes;c__Clostridia	0.0102	0.0104	0.013	0.009	0.013	0.014	0.0127	0.0191	0.0142	0.008	0.0091	0.012	1.2
Verrucomicrobia;c__Verrucomicrobiae	0.0004	0.0018	0.025	0.013	0.119	0.013	0.0026	0.0029	0.0004	0.009	0.0006	0.0004	1.57
Verrucomicrobia;c__Opitutae	0.0008	0.0035	0.007	0.009	0.010	0.015	0.0012	0.0006	0.012	0.015	0.0144	0.0026	0.76
Taxon	**HBU**	**HBM**	**HBL**	**ZGU**	**ZGM**	**ZGL**	**NFU**	**NFM**	**NFL**	**CH I**	**CH II**	**CH III**	**Percentage of the total prokaryotic abundant (%)**
Proteobacteria;g__Limnohabitans	0.1043	0.0558	0.096	0.055	0.053	0.046	0.0897	0.0651	0.0092	0.008	0.0284	0.0586	5.57
Proteobacteria;g__Hydrogenophaga	0.0066	0.2001	0.006	0.001	0.008	0.005	0.0929	0.0194	0.1916	0.0009	0.0019	0.0022	4.47
Proteobacteria;Other	0.0373	0.035	0.04	0.023	0.046	0.036	0.0334	0.0689	0.0877	0.013	0.0226	0.036	3.98
Proteobacteria;g__	0.0013	0.0011	0.006	0.166	0.003	0.066	0.0021	0.0032	0.0731	0.069	0.0527	0.0306	3.94
Proteobacteria;g__Pseudomonas	0.0204	0.0041	0.011	0.002	0.002	0.001	0.058	0.0171	0.0026	0.0006	0.001	0.0043	1.04
Bacteroidetes;g__Flavobacterium	0.640	0.2638	0.407	0.069	0.051	0.022	0.2933	0.1656	0.0108	0.012	0.0403	0.018	16.6
Bacteroidetes;g__	0.0058	0.016	0.016	0.047	0.046	0.020	0.0129	0.0121	0.0222	0.014	0.0277	0.0687	2.57
Cyanobacteria;g__Dolichospermum	0.0033	0.0024	0.003	0.006	0.003	0.132	0.0035	0.0029	0.0049	0.342	0.2258	0.3043	8.62
Cyanobacteria;g__	0.0032	0.0497	0.008	0.055	0.169	0.092	0.0393	0.003	0.0104	0.077	0.1224	0.0223	5.43
Cyanobacteria;g__Prochlorococcus	0.0009	0.0006	0.001	0.117	0.002	0.013	0.0008	0.0008	0.0022	0.021	0.012	0.0073	1.49
Cyanobacteria;g__	0.0009	0.0035	0.003	0.013	0.006	0.039	0.0026	0.0077	0.0017	0.024	0.0358	0.0042	1.17
Actinobacteria;g__	0.0055	0.0465	0.056	0.069	0.09	0.132	0.0078	0.0237	0.168	0.096	0.1416	0.1900	8.56

Abbreviations are the same as those in *Table 1*

http://www.aloki.hu ● ISSN 1589 1623 (Print) ● ISSN 1785 0037 (Online)
DOI: http://dx.doi.org/10.15666/aeer/1704_72657281

We identified 924 genera in 12 samples, with 12 dominant genera including *Flavobacterium* (16.60%), *Dolichospermum* (8.62%), *Limnohabitans* (5.57%), *Hydrogenophaga* (4.47%), *Prochlorococcus* (1.49%), *Pseudomonas* (1.04%), and 6 unidentified genera. These 6 identified genera included 3 dominant genera of Proteobacteria, 2 dominant genera of Cyanobacteria, 1 dominant genus of Bacteroidetes (*Table 3*). The changes in CPCs were mainly concentrated in Proteobacteria, Bacteroidetes, and Cyanobacteria.

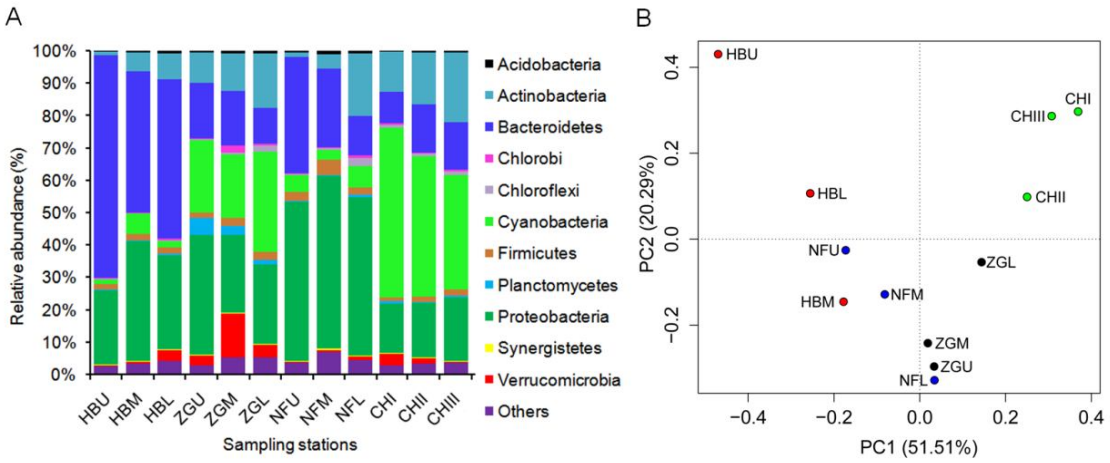

Figure 2. *Relative abundances of dominant phyla (A) and principal coordinate analysis (PCoA) profile (B) of samples. The PCoA profile was drawn based on a weighted UniFrac distance matrix. Abbreviations are the same as those in Table 1*

The results of PCoA showed a strong clustering of samples from Chaohu Lake, and a dispersed distribution among the rivers samples. This likely indicates a higher susceptibility among prokaryotic communities in Chaohu Lake than in the three rivers (*Fig. 2B*). Furthermore, the CPCs in Chaohu Lake were different from those in the three rivers and the spatial change patterns for prokaryotic communities were lake-specific and river-specific. This could imply that CPCs exhibit a high degree of spatial heterogeneity between the lake and the rivers.

Relationship between prokaryotic communities and environmental factors

According to the RDA analyses, 66% of the cumulative variance in the species-environment relationship was explained by the first two RDA axes. Furthermore, following forward selection and the Monte Carlo test, the prokaryotic community showed a significant correlation with the concentration of TP ($p < 0.01$; *Fig. 3* and *Table 4*). For example, among the 13 phyla, Proteobacteria, Actinobacteria, and Firmicutes were primarily affected by the concentration of total phosphorus (TP; $p < 0.05$, $p < 0.05$, $p < 0.05$, respectively). In contrast, Cyanobacteria showed a significant correlation with TN ($p < 0.01$), NH_4 ($p < 0.01$), and NO_3 ($p < 0.05$). Planctomycete showed a correlation with pH ($p < 0.05$), and Thermotogae was generally associated to WT ($p < 0.05$; *Fig. 3* and *Table 4*). Bacteroidetes, Acidobacteria, Chlorobi, Verrucomicrobia, Euryarchaeota, Chloroflexi, and Crenarchaeota exhibited no correlation with the examined physicochemical factors.

http://www.aloki.hu ● ISSN 1589 1623 (Print) ● ISSN 1785 0037 (Online)
DOI: http://dx.doi.org/10.15666/aeer/1704_72657281

Table 4. *Correlation matrix showing the relationship between prokaryotic community / 6 prokaryotic phyla and significantly associated environmental factors*

		Axis 1	Axis 2
Prokaryotic community	TP (mg/L)	-0.59	-0.80
Proteobacteria	TP (mg/L)	0.67	0.64
Cyanobacteria	TN (mg/L)	-0.54	0.53
	NH_4 (mg/L)	0.33	-0.59
	NO_3 (mg/L)	0.58	-0.50
Actinobacteria	TP (mg/L)	0.66	-0.65
Firmicutes	TP (mg/L)	-0.21	0.10
Planctomycetes	pH	0.86	0.39
Thermotogae	WT	0.72	0.40

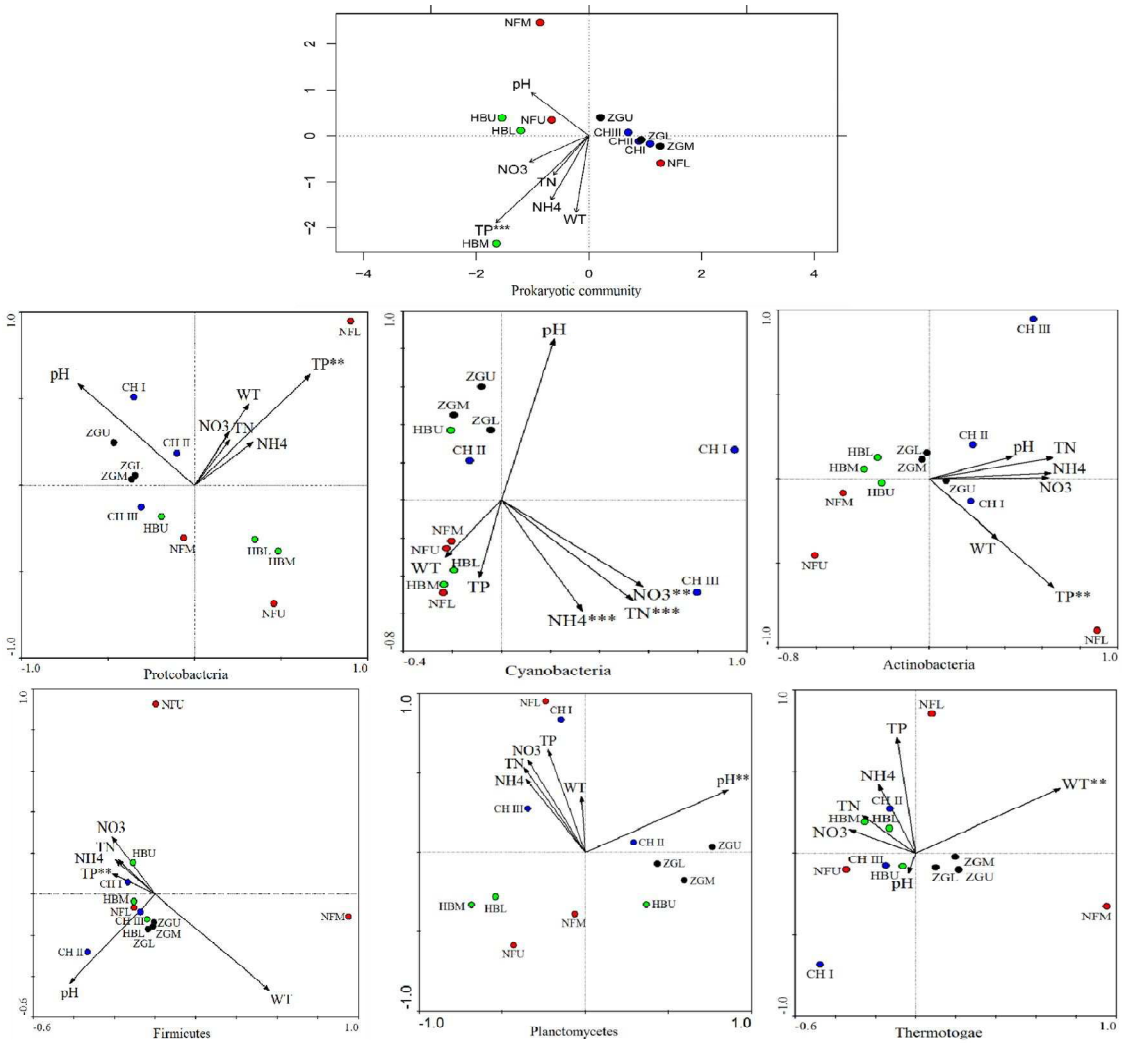

Figure 3. *Redundancy analysis (RDA) biplots of prokaryotic communities and 8 prokaryotic phyla in correlation with environmental variables. Abbreviations are the same as those in Table 1. ***Significant at p < 0.01; **Significant at p < 0.05*

http://www.aloki.hu ● ISSN 1589 1623 (Print) ● ISSN 1785 0037 (Online)
DOI: http://dx.doi.org/10.15666/aeer/1704_72657281

Discussion

Prokaryotic community structure characteristics

High-throughput sequencing has been widely used to study differences in prokaryotic communities (Dai et al., 2016; Jordaan and Bezuidenhout, 2016; Liu et al., 2015; Yang et al., 2016). Bao (2008) analyzed the CCBs of Chaohu Lake, using a combination of PCR amplification of 16S rRNA genes and DGGE, and reported that Chaohu Lake had 4 dominant phyla. In the present study, Chaohu Lake prokaryotes were distributed among 13 dominant phyla. Compared with the PCR-DGGE approach, high-throughput sequencing could identify more prokaryotic species, and is thus more suitable for describing prokaryotic community diversity in aquatic systems.

Proteobacteria, Cyanobacteria, Bacteroidetes, Actinobacteria, and Verrucomicrobia are the main prokaryotic phyla in freshwater ecosystems (Ren, 2013). Similarly, our results found Proteobacteria, Cyanobacteria, Bacteroidetes, and Actinobacteria to be the most common prokaryotic phyla of Chaohu Lake and its tributaries–results that are in agreement with those from previous studies (Wu et al., 2007; Dai et al., 2016; Jordaan and Bezuidenhout, 2016). Proteobacteria was the largest prokaryotic phylum of Chaohu Lake and its adjoining rivers, and exhibited high abundances in all samples, especially in Nanfei River, which showed the highest nutrient concentration. Proteobacteria abundance is known to be higher when environmental conditions are poor (Sun et al., 2016) and hence the present study suggests that the water quality of Chaohu Lake and its three tributaries is deteriorating.

Among the Proteoprokaryotic communities, Alphaproteobacteria, Betaproteobacteria, and Gammaproteobacteria dominated–with Betaproteobacteria exhibiting the highest abundance of the three. Betaproteobacteria represent one of the key components of freshwater bacterioplankton and play an important role in freshwater ecosystems (Crump and Hobbie, 2005; Newton et al., 2006; Salcher et al., 2013). *Limnohabitans* and *Hydrogenophaga* were the dominant genera of Betaproteobacteria. *Limnohabitans* belongs to BetI lineage of Betaproteobacteria, is the most abundant type of prokaryotes, and is widely distributed throughout of the world (Ren, 2013). Furthermore, *Limnohabitans* plays an important role in phosphorus cycling in eutrophic water and wastewater, and its distribution includes urban rivers (Jordaan and Bezuidenhout, 2016). The PhoD gene of the genus *Limnohabitans* codes the APase, which promotes the process of eutrophication by increasing the bioavailability of phosphorus (Zhao et al., 2015). Gammaproteobacteria and Alphaproteobacteria, the second and third classes of Proteobacteria, respectively, are found in a variety of aquatic habitats (Crump and Hobbie, 2005; Newton et al., 2011; Liu et al., 2012), but are generally more dominant in marine prokaryotic communities (Biers et al., 2009).

Hangbu River exhibited the highest abundance of Bacteroidetes, the second most abundant phylum. Within the Bacteroidetes, *Flavobacterium* was the most frequently detected genus–results that are consistent with bacterioplankton communities of Taihu Lake (Wu et al., 2007). Due to its algicidal activity and antagonism toward other bacteria, *Flavobacterium* has been associated with harmful algal blooms (Roth et al., 2008). Furthermore, it is often found in high abundance in eutrophic and hypertrophic urban rivers–usually correlating with high nutrient levels (Drury et al., 2013; Jordaan and Bezuidenhout, 2016).

Chaohu Lake and Zhegao River showed the highest abundances of Cyanobacteria, the third most dominant phylum. Cyanobacteria are the oldest known oxygen-producing

http://www.aloki.hu ● ISSN 1589 1623 (Print) ● ISSN 1785 0037 (Online)
DOI: http://dx.doi.org/10.15666/aeer/1704_72657281

organisms on Earth, and are widely distributed in freshwater ecosystems. Furthermore, these organisms are capable of adapting to environmental stresses, such as elevated nutrients (Paerl, 2008) and high temperatures (Briand et al., 2004). In shallow, non-stratified, lakes it has been suggested that the potential for cyanobacteria to dominate is greatest when the water temperature is high and the nutrient load is elevated (Elliot et al., 2006). In the present study, Cyanobacteria comprised four dominant genera: *Dolichospermum*, *Prochlorococcus*, and two unclassified genera. It should be noted that *Dolichospermum* is the most common genus in Cyanobacterial blooms (Liu et al., 2015).

Actinobacteria, the fourth dominant phylum in our study, are globally distributed and are often the most abundant phylum in a variety of freshwater ecosystems (Crump and Hobbie, 2005; Wilhelm et al., 2014). In Lake Taihu, a shallow hypertrophic freshwater lake in China, Actinobacteria are considered to be the most significant lineage (Wu et al., 2007).

Less abundant phylotypes were grouped with the Firmicutes, Verrucomicrobia, Chloroflexi, Planctomycetes, Acidobacteria, Chlorobi, Thermotogae, Crenarchaeota, Euryarchaeota, and unaffiliated. Firmicutes make up a small fraction of the prokaryotic community in some freshwater systems (Eiler and Bertilsson, 2004; Lymperopoulou et al., 2012), and predominantly consist of Gram-positive, rod-shaped, bacteria in the class Bacilli. Most of the species in this class exhibit strong environmental adaptability and can form stress resistant spores. Thus Bacilli play an important biological role in a variety of ecological systems, such as the treatment of industrial wastewater (Song et al., 2015). In this study, the highest abundance of Bacilli was found in the Nanfei River, in which the highest nutrient concentration was recorded. Verrucomicrobia exhibited a low abundance (1–4%) in all of our sample collections. This phylum is widely distributed in rivers and lakes, and its low abundance may be associated with surplus nutrients (Haukka et al., 2006).

There are contradictory reports of Bacteroidetes abundance in the literature. For example, Bacteroidetes have been detected in high frequencies in lakes associated with Cyanobacterial blooms (Eiler and Bertilsson, 2004; Newton et al., 2011). However, this phylum has characteristically been found in association with clear water or mesotrophic lakes (Van der Gucht et al., 2005; McLaughlin et al., 2015). We found that Bacteroidetes were more abundant at sample stations exhibiting relatively low nutrient concentrations. In contrast, Actinobacteria and Cyanobacteria were primarily distributed among stations with high nutrient levels.

The recorded dominance of phylotypes belonging to Bacteroidetes, Betaproteobacteria, Alphaproteobacteria, Cyanobacteria, and Actinobacteria may be the result of the strong eutrophication of Chaohu Lake and its three tributaries. For example, similar results have been recorded for other eutrophic water bodies, and this may indicate a decline in water quality in the near future (Eiler and Bertilsson, 2004; Van Der Gucht et al., 2005; de Figueiredo et al., 2007; Wiedner et al., 2007; Wu et al., 2007). Furthermore, the CPCs is altered with the production of some groups such as Cyanobacteria and Actinobacteria, whose abundances may threaten water quality (Van Der Gucht et al., 2005; de Figueiredo et al., 2007; Wiedner et al., 2007). In the present study, Actinobacteria, Bacteroidetes, Alphaproteobacteria, Cyanobacteria, and Betaproteobacteria were co-dominant in Chaohu Lake and its three tributaries–environments that were characterized as eutrophic or hypereutrophic.

http://www.aloki.hu ● ISSN 1589 1623 (Print) ● ISSN 1785 0037 (Online)
DOI: http://dx.doi.org/10.15666/aeer/1704_72657281

Environmental effects on prokaryotic community

The nutrient content of waterbodies has a significant impact on the diversity of prokaryotes (Lindström, 2000; Yan et al., 2017). Our RDA analysis showed that the prokaryotic communities and 3 prokaryotic phyla–including Proteobacteria, Actinobacteria, and Firmicutes–were significantly associated with TP. Furthermore, Cyanobacteria showed a significant correlation with TN, NH_4, and NO_3. These findings are consistent with those of previous studies (Liu et al., 2011; Zhang et al., 2012; Niu et al., 2015; Wang et al., 2015). Of the measured explanatory variables, phosphorus and nitrogen were shown to have the greatest effect on CPCs, and this result may hold the greatest significance for the management of nature reserves. Specifically, understanding how phosphorus and nitrogen affect CPCs could aid in the search for new strategies to combat the degradation of freshwater ecosystems due to anthropogenic pollution.

Previous research has shown prokaryotic diversity to increase with elevated nutrient levels (Feng et al., 2007; Pang et al., 2014). However, other studies have found prokaryotic community diversity to significant decrease with the increase of freshwater nutrients (Van der Gucht et al., 2005; McLaughlin et al., 2015). Compared with the Zhegao and Hangbu Rivers, Nanfei River and Chaohu Lake had higher nutrient levels, and lower prokaryotic diversity. Our results have shown a link between higher waterbody nutrients and lower prokaryotic diversity. Microorganisms that can use and/or survive in the presence of pollutants often dominate contaminated ecosystems. As the result, the diversity of microbial communities is less than that of non-contaminated systems (McLaughlin et al., 2015). Van der Gucht et al. (2005) indicated that, as a result of the disappearance of submerged macrophyte stands, this transition is associated with a loss of structural diversity and, consequently, a decrease in biodiversity at higher trophic levels.

Our RDA results indicate that pH is correlated with Planctomycetes, this result is consistent with those of Ren et al. (2015), who observed that pH was the strongest determinant of both overall bacterioplankton community composition and the composition of abundant bacterioplankton groups. Previous literature has shown that water temperature can affect freshwater bacterioplankton communities (Adams et al., 2010; de Figueiredo et al., 2010; Zhang et al., 2012; Jordaan and Bezuidenhout, 2016). We observed that water temperature (WT) is generally associated with Thermotogae. Hence, this study suggests that pH and water temperature may play crucial roles in shaping bacterioplankton community structure in freshwater lakes and rivers.

Conclusions

In this study, CPCs were characterized using high-throughput sequencing and the relationship between CPCs and environment factors was explored in Chaohu Lake and its three urban tributaries. Our results indicated that elevated nutrients, pH, and water temperature may be the primary environmental controllers of the variation in CPCs in Chaohu Lake and its three tributaries. Furthermore, we found that the variation of CPCs was influenced by anthropogenic perturbations–eutrophication processes that are continuing to increase within the Chaohu Lake watershed. Ultimately, these results add to our growing understanding of the ecology of CPCs in Chaohu Lake and its tributaries, and may offer crucial ecological background data for the development of management plans for this important urban freshwater system.

http://www.aloki.hu ● ISSN 1589 1623 (Print) ● ISSN 1785 0037 (Online)
DOI: http://dx.doi.org/10.15666/aeer/1704_72657281

Acknowledgements. This research was supported by the CRSRI Open Research Program (CKWV2015238/KY) and the Visiting Research Foundation at Home and Abroad for the Outstanding Young Backbone Talents of Colleges and Universities of Anhui Province (No. gxfx2017082).

REFERENCES

[1] Adams, H. E., Crump, B. C., Kling, G. W. (2010): Temperature controls on aquatic bacterial production and community dynamics in arctic lakes and streams. – Environmental Microbiology 12: 1319-1333.

[2] Bao, S. M. (2008): Horizontal and Seasonal Dynamics of the Bacterioplankton Community Composition in the Large Shallow Chaohu Lake, China. – Anhui Agricultural University, Hefei.

[3] Bashenkhaeva, M. V., Zakharova, Y. R., Petrova, D. P., Khanaev, I. V., Galachyants, Y. P., Likhoshway, Y. V. (2015): Sub-ice microalgal and bacterial communities in freshwater Lake Baikal Russia. – Microbial Ecology 70: 751-765.

[4] Biers, E. J., Sun, S. L., Howard, E. C. (2009): Prokaryotic genomes and diversity in surface ocean waters: interrogating the global ocean sampling metagenome. – Applied and Environmental Microbiology 75(7): 2221-2229.

[5] Briand, J. F., Leboulanger, C., Humbert, J. F. (2004): Cylindrospermopsis raciborskii (cyanobacteria) invasion at mid-latitudes: selection wide physiological tolerance or global warming. – Journal of Phycology 40: 231-238.

[6] Caporaso, J. G., Kuczynski, J., Stombaugh, J., Bittinger, K., Bushman, F. D., Costello, E. K., Fierer, N., Pena, A. G., Goodrich, J. K., Gordon, J. I., Huttley, G. A., Kelley, S. T., Knights, D., Koenig, J. E., Ley, R. E., Lozupone, C. A., McDonald, D., Muegge, B. D., Pirrung, M., Reeder, J., Sevinsky, J. R., Turnbaugh, P. J., Walters, W. A., Widmann, J., Yatsunenko, T., Zaneveld, J., Knight, R. (2010): QIIME allows analysis of high-throughput community sequencing data. – Nature Methods **7**(5): 335-336.

[7] Crump, B. C., Hobbie, J. E. (2005): Synchrony and seasonality in bacterioplankton communities of two temperate rivers. – Limnology and Oceanography 50(6): 1718-1729.

[8] Dai, Y., Yang, Y. Y., Wu, Z., Feng, Q. Y., Xie, S. G., Liu, Y. (2016): Spatiotemporal variation of planktonic and sediment bacterial assemblages in two plateau freshwater lakes at different trophic status. – Applied Microbiology and Biotechnology 100: 4161-4175.

[9] de Figueiredo, D. R., Pereira, M. J., Moura, A., Silva, L., Barrios, S., Fonseca, F., Henriques, I., Correia, A. (2007): Bacterial community composition over a dry winter in meso- and eutrophic Portuguese water bodies. – FEMS Microbiology Ecology 59: 638-650.

[10] de Figueiredo, D. R., Pereira, M. J., Correia, A. (2010): Seasonal modulation of bacterioplankton community at a temperate eutrophic shallow lake. – World Journal of Microbiology & Biotechnology 26: 1067-1077.

[11] Drury, B., Rosi-Marshall, E., Kelly, J. J. (2013): Wastewater treatment effluent reduces the abundance and diversity of benthic bacterial communities in urban and suburban rivers. – Applied and Environmental Microbiology 79(6): 1897-1905.

[12] Edgar, R. C., Haas, B. J., Clemente, J. C., Quince, C., Knight, R. (2011): UCHIME improves sensitivity and speed of chimera detection. – Bioinformatics 27: 2194-2200.

[13] Eiler, A., Bertilsson, S. (2004): Composition of freshwater bacterial communities associated with cyanobacterial blooms in four Swedish lakes. – Environmental Microbiology 6: 1228-1243.

[14] Elliot, J. A., Jones, I. D., Thackeray, S. J. (2006): Testing the sensitivity of phytoplankton communities to changes in water temperature on nutrient load in a temperate lake. – Hydrobiologia 559: 401-411.

http://www.aloki.hu ● ISSN 1589 1623 (Print) ● ISSN 1785 0037 (Online)
DOI: http://dx.doi.org/10.15666/aeer/1704_72657281

[15] Feng, S., Qin, B. Q., Gao, G. (2007): Response of bacterial communities to eutrophic water in Lake Taihu. – Acta Scientiae Circumstantiae 27(11): 1823-1829.
[16] Haukka, K., Kolmonen, E., Hyder, R., Hietala, J., Vakkilainen, K., Kairesalo, T., Haario, H., Sivonen, K. (2006): Effect of nutrient loading on bacterioplankton community composition in lake mesocosms. – Microbial Ecology 51(2): 137-146.
[17] Huang, X. F. (2000): Survey, Observation and Analysis of Lake Ecology. – Standard Press of China, Beijing.
[18] Jordaan, K., Bezuidenhout, C. C. (2016): Bacterial community composition of an urban river in the North West Province South Africa in relation to physico-chemical water quality. – Environmental Science and Pollution Research 23: 5868-5880.
[19] Lindström, E. S. (2000): Bacterioplankton community composition in five lakes differing in trophic status and humic content. – Microbial Ecology 40: 104-113.
[20] Liu, L. M., Yang, J., Zhang, Y. Y. (2011): Genetic diversity patterns of microbial communities in a subtropical riverine ecosystem (Jiulong River southeast China). – Hydrobiologia 678: 113-125.
[21] Liu, L. M., Yang, J., Yu, Z., Wilkinson, D. M.. (2015): The biogeography of abundant and rare bacterioplankton in the lakes and reservoirs of China. – ISME Journal 9: 2068-2077.
[22] Liu, Y., Gao, H. Y., Li, X. Y., Li, R. H. (2015): Identification and determination of mycosporine-like amino acids (MAAs) in dolichospermum flos-aquae. – Acta Hydrobiologica Sinica 39(3): 549-553.
[23] Liu, Z. H., Huang, S. B., Sun, G. P., Xu, Z. C., Xu, M. Y. (2012): Phylogenetic diversity composition and distribution of bacterioplankton community in the Dongjiang River China. – FEMS Microbiology Ecology 80(1): 30-44.
[24] Lin, X. J., McKinley, J., Resch, C. T., Kaluzny, R., Lauber, C. L., Fredrickson, J., Knight, R., Konopka, A. (2012): Spatial and temporal dynamics of the microbial community in the Hanford unconfined aquifer. – ISME Journal 6: 1665-1676.
[25] Lymperopoulou, D. S., Kormas, K. Ar., Karagouni, A. D. (2012): Variability of prokaryotic community structure in a drinking water Reservoir (Marathonas Greece). – Microbes and Environments 27(1): 1-8.
[26] Magoc, T., Salzberg, S. L. (2011): FLASH: Fast length adjustment of short reads to improve genome assemblies. – Bioinformatics 27: 2957-2963.
[27] Martinuzzi, S., Januchowski-Hartley, S. R., Pracheil, B. M., McIntyre, P. B., Plantinga, A. J., Lewis, D. J., Lewis, D. J., Radeloff, V. C. (2014): Threats and opportunities for freshwater conservation under future land use change scenarios in the United States. – Global Change Biology 20(1): 113-24.
[28] McLaughlin, R. W., Wang, S. B., Zhou, W., Cheng, G. J., Deng, K. J. (2015): A comparison of the bacterial diversity of two shallow freshwater lakes in China. – Proceedings of the National Academy of Sciences, India Section B: Biological Sciences 85(1): 137-146.
[29] Newton, R. J., Kent, A. D., Triplett, E. W., Mcmahon, K. D. (2006): Microbial community dynamics in a humic lake: differential persistence of common freshwater phylotypes. – Environmental Microbiology 8(6): 956-970.
[30] Newton, R. J., Jones, S. E., Eiler, A., Mcmahon, K. D., Bertilsson, S. (2011): A Guide to the natural history of freshwater lake bacteria. – Microbiology and Molecular Biology Reviews 75(1): 14-49.
[31] Ni, J. J., Li, X. J., He, Z. L., Xu, M. Y. (2017): A novel method to determine the minimum number of sequences required for reliable microbial community analysis. – Journal of Microbiological Methods 139: 196-201.
[32] Niu,Y., Yu, H., Jiang, X. (2015): Within-lake heterogeneity of environmental factors structuring bacterial community composition in Lake Dongting China. – World Journal of Microbiology & Biotechnology 31: 1683-168.

http://www.aloki.hu ● ISSN 1589 1623 (Print) ● ISSN 1785 0037 (Online)
DOI: http://dx.doi.org/10.15666/aeer/1704_72657281

[33] Oksanen, J., Blanchet, F. G., Kindt, R., Legendre, P., Minchin, P. R., OHara, R. B., Simpson, G. L., Solymos, P., Stevens, M. H. H., Wagner, H. (2015): Vegan: Community Ecology Package R Package Version 22-1. – http://CRANR-projectorg/package=vegan.
[34] Organisation for Economic and Co-operation and Development (OECD) (1982): Eutrophication of Waters: Monitoring Assessment and Control. – OECD, Paris.
[35] Paerl, H. W. (2008): Nutrient and other environmental controls of harmful cyanobacterial blooms along the freshwater-marine continuum. – Advances in Experimental Medicine and Biology 619: 216-241.
[36] Pang, X. H., Lü, L. Y., Niu, Y., Shen, H., Yuan, X. G., Chen, W. J., Chen, J., Xie, P. (2014): The spatial pattern of bacterioplankton communities composition in summer in Lake Taihu. – Acta Hydrobiologica Sinica 38(2): 335-341.
[37] Ren, L. J., He, D., Xing, P., Wang, Y. J., Wu, Q. L. (2013): Bacterial diversity and ecological function in lake water bodies. – Biodiversity Science 21(4): 421-432.
[38] Ren, L. J., Jeppesen, E., He, D., Wang, J. J., Liboriussen, L., Xing, P., Wu, Q. L. (2015): pH influences the importance of niche-related and neutral processes in lacustrine bacterioplankton assembly. – Applied and Environmental Microbiology 81(9): 3104-3114.
[39] Roth, P. A., Mikulski, C. M., Doucette, G. J. (2008): The influence of microbial interactions on the susceptibility of Karenia spp to algicidal bacteria. – Aquatic Microbial Ecology 50: 251-259.
[40] Salcher, M. M., Posch, T., Pernthaler, J. (2013): In situ substrate preferences of abundant bacterioplankton populations in a prealpine freshwater lake. – ISME Journal **7**(5): 896-907.
[41] Song, Z. Q., Wang, L., Liu, X. H., Liang, F. (2015): Diversities of Firmicutes in four hot springs in Yunnan and Tibet. – Biotechnology 25(5): 481-486.
[42] Sun, Y. J., Wang, T. Y., Peng, X. W., Wang, P., Lu, Y. L. (2016): Bacterial community compositions in sediment polluted by perfluoroalkyl acids (PFAAs) using Illumina high-throughput sequencing. – Environmental Science and Pollution Research 23: 10556-10565.
[43] Van der Gucht, K., Vandekerckhove, T., Vloemans, N., Cousin, S., Muylaert, K., Sabbe, K., Gillis, M., Declerk, S., De Meester, L., Vyverman, W. (2005): Characterization of bacterial communities in four freshwater lakes differing in nutrient load and food web structure. – FEMS Microbiology Ecology 53: 205-220.
[44] Wang, Q., Garrity, G. M., Tiedje, J. M., Cole, J. R. (2007): Naïve Bayesian classifier for rapid assignment of rRNA sequences into the new bacterial taxonomy. – Applied and Environmental Microbiology 73: 5261-5267.
[45] Wang, S., Jiang, X., Jin, X. (2011): Classification and pollution characteristic analysis for inflow rivers of lake Chaohu. – Environmental Science 32: 2834-2839.
[46] Wang, S. M., Dou, H. S. (1998): Biography of Lakes in China. – Science Press, Beijing.
[47] Wang, Y. M., Yang, J., Liu, L. M., Yu, Z. (2015): Quantifying the effects of geographical and environmental factors on distribution of stream bacterioplankton within nature reserves of Fujian China. – Environmental Science and Pollution Research 22: 11010-11021.
[48] Wei, C. L., Bao, S. M., Zhu, X. Y., Huang, X. M. (2008): Spatio-temporal variations of the bacterioplankton community composition in Chaohu Lake China. – Progress in Natural Science 18: 1115-1122.
[49] Wiedner, C., Rücker, J., Bruggemann, R., Nixdorf, B. (2007): Climate change affects timing and size of populations of an invasive cyanobacterium in temperate regions. – Oecologia 152: 473-484.
[50] Wilhelm, S. W., Le Cleir, G. R., Bullerjahn, G. S., McKay, R. M., Saxton, M. A., Twiss, M. R., Bourbonniere, R. A. (2014): Seasonal changes in microbial community structure and activity imply winter production is linked to summer hypoxia in a large lake. – FEMS Microbiology Ecology 87(2): 475-485.

http://www.aloki.hu ● ISSN 1589 1623 (Print) ● ISSN 1785 0037 (Online)
DOI: http://dx.doi.org/10.15666/aeer/1704_72657281

[51] Wu. L., Sun, Q. Y., Ni, J. J. (2017): Not all of the rare operational taxonomic units (OTUs) play the same role in maintaining community stability. – Applied Ecology and Environmental Research 15(1): 105-112.
[52] Wu, X., Xi, W., Ye, W., Yang, H. (2007): Bacterial community composition of a shallow hypertrophic freshwater lake in China revealed by 16S rRNA gene sequences. – FEMS Microbiology Ecology 61: 85-96.
[53] Xiang, J. G., He, T. Y., Wang, P. P., Xie, M., Xiang, J., Ni, J. J. (2018): Opprtunistic pathogens are abundant in the gut of cultured giant spiny frog (*Paa spinosa*). – Aquaculture Research 49: 2033-2041.
[54] Yan, Q. Y., Stegen, J. C., Yu, Y. H., Deng, Y., Li, X. H., Wu, S., Dai, L. L., Zhang, X., Li, J. J., Wang, C., Ni, J. J., Li, X. M., Hu, H. J., Xiao, F. S., Feng, W. S., Ning, D. L., He, Z. L., Van Nostrand, J. D., Wu, L. Y., Zhou, J. Z. (2017): Nearly a decade-long repeatable seasonal diversity patterns of bacterioplankton communities in the eutriphic Lake Donghu (Wuhan China). – Molecular Ecology 26: 3839-3850.
[55] Yang, J., Jiang, H. C., Wu, G., Liu, W., Zhang, G. J. (2016): Distinct factors shape aquatic and sedimentary microbial community structures in the lakes of western China. – Frontiers in Microbiology 08: 1-8.
[56] Zan, F. Y., Huo, S. L., Xi, B. D., Li, Q. Q., Liao, H. Q., Zhang, J. T. (2011): Phosphorus distribution in these dements of a shallow eutrophic lake, Lake Chaohu, China. – Environmental Earth Sciences 62: 1643-1653.
[57] Zhao, D. D., Luo, J. F., Huang, X. Y., Lin, W. T. (2015): Diversity of bacterial APase phoD gene in the Pearl River water. – Acta Scientiae Circumstantiae 35(3): 722-728.
[58] Zhang, M. L., Yu, N., Chen, L. Q., Jiang, C. H., Tao, Y. J., Zhang, T., Chen, J., Xue, D. (2012): Structure and seasonal dynamics of bacterial communities in three urban rivers in China. – Aquatic Sciences 74: 113-12.

http://www.aloki.hu ● ISSN 1589 1623 (Print) ● ISSN 1785 0037 (Online)
DOI: http://dx.doi.org/10.15666/aeer/1704_72657281

BALANCE BETWEEN CONSTRUCTION AND CONSERVATION: STRATEGY IN WATER SENSITIVE AREA PLANNING

YANG, J.-Y.[1*#] – ZHANG, B.[1#] – WU, Y.-F.[2] – FENG, Y.-R.[1] – ZHENG, Y.[1] – SHI, B.-X.[1]

[1]*Department of Architecture, Southeast University, 210096 Nanjing, China*

[2]*School of Energy and Environment, Southeast University, 210096 Nanjing, China*

[#]*These authors equally contributed to this paper.*

**Corresponding author*
e-mail: Yjy-2@163.com

(Received 2nd Feb 2019; accepted 1st May 2019)

Abstract. The paper comprehensively considers the interaction and balance between urban construction and protection of water ecology, breaks through the original concept of water protection, and formulates the planning concept of "balanced construction". In terms of planning strategy, a diversified strategy integrating empirical sampling, software simulation and an evaluation system is applied to realize the dynamic monitoring of urban construction and protection of water ecology. Firstly, the basis of water environment analysis is laid by collecting and analyzing current water samples. Secondly, the water quality and flow field are simulated and analyzed by DHI Mike 21 simulation software, which provides a basis for the planning of the surrounding water system. Thirdly, based on the calculation of water pollution capacity and future planning pollution load, the key factors affecting water quality are identified, and the urban land use planning model based on the concept of "balanced construction" is completed. Finally, the comprehensive evaluation index system of ecological water health is established to realize the objective evaluation of the balance between protection of water ecology and urban construction.
Keywords: *quantitative analysis of water, dynamic equilibrium, software simulation, indicator evaluation system, protection of water ecology, rapid urban development, DHI Mike 21*

Introduction

As a prerequisite to the development of civilization and the basis of human existence, water is of great importance to urban construction and development. There are numerous recordings of famous cities belonging to early human civilizations being built near water sources. Overall, the world is still in the process of rapid urbanization, especially in most developing countries. According to the forecast of the United Nations, by 2050, 6.7 billion people will live in cities, accounting for 68% of the total population, which is an increase of about 13% over the current proportion (United Nations, 2018). Significant changes have taken place during urbanization, including the fact that impervious materials such as asphalt and concrete have replaced soil; buildings have replaced forests; rainwater pipelines have replaced natural runoff. Urbanization has dramatically changed the original natural hydrological environment (Jacobson, 2011). While changing rainwater runoff, water pollution caused by urban development has become an important issue that cannot be ignored, especially in highly sensitive areas of water ecology.

In recent years, many cities have suffered from waterlogging disasters. Apart from the bad weather caused by climate and environmental changes, the built environment of the city itself is also one of the essential reasons. It is estimated that about 85% of precipitations becomes the runoff of completely hardened roads or roofs in urban areas,

http://www.aloki.hu ● ISSN 1589 1623 (Print) ● ISSN 1785 0037 (Online)
DOI: http://dx.doi.org/10.15666/aeer/1704_72837299

and another 15% is intercepted by streets, buildings, roofs or walls and other paved or gentle slope surfaces (Lull and Sopper, 1969; Hough, 2004). This not only leads to floods and erosion, but also reduces water quality. Meanwhile, rainwater resources are not effectively utilized, which is also one of the reasons of water shortage in some cities. Moreover, the impact of urbanization on water quality is shocking. The lack of supervision on pollutant discharge, the failure of discharge standards, the inadequate control of urban non-point source pollution, and the mixing of rainwater and sewage have caused severe pollution of urban surface water resources, including lakes and rivers. Facing such urban water environment problems, various countries have put forward diversified strategies, mainly including Low Impact Development (LID) in America (Pyke et al., 2011), Water Sensitive Urban Design (WSUD) in Australia (Morison and Brown, 2011), Sponge City in China (Chan et al., 2018), Sustainable Urban Drainage System (SuDs) (Griffiths, 2017; Mitchell, 2005) and Blue-Green Cities (BGCs) (Thorne et al., 2015) in England, Low Impact Urban Design and Development (LIDUD) in New Zealand (Voyde et al., 2010). The purpose of these strategies is to enhance the city's ability to deal with water environmental problems and enhance the overall utilization efficiency of water resources through planning strategies and engineering measures. According to the current similar development concepts, resilient cities (RC) mainly focus on the coping strategies and flexibility of cities when facing uncertainties, especially climate change (Meerow et al., 2016). In terms of overall development strategy, the International Symposium on Ecological Wisdom of Urban Sustainable Development held in Chongqing, China, in October 2014, focused on the ecological wisdom presented in urban development and construction (Xiang, 2014; Wang and Xiang, 2016), which provided a strategic reference for exploring the direction of urban construction in water-ecologically sensitive areas.

As an essential ecological and habitat bearing space of cities, highly sensitive areas of water ecology are also facing the intrusion of urban construction under the background of rapid urbanization. The solution to deal with the relationship between urban construction and ecological protection; positive measures to reduce the damage and interference of the urbanization process on the natural environment and a balance between urban construction and protection of water ecology are all important issues that cannot be avoided in the development of cities in highly sensitive areas of water ecology. Based on the summary of the current development model of water ecology in highly sensitive areas, it is found that there are two different tendencies in the current planning strategy. One is to emphasize the importance of water ecology protection while ignoring the actual needs of urban development. The other is to overemphasize the economic benefits of urban development while ignoring the protection of water ecology, thus causing severe damage to the natural ecological environment. Therefore, the two tendencies both have some defects in the actual development of cities. Therefore, it can be concluded that the current model is more from a single perspective to examine the future development scenarios of highly sensitive areas of water ecology, but lacks comprehensive, holistic, top-down planning and thinking.

On this basis, the authors put forward the idea of “balanced construction” in highly sensitive areas of water ecology, which takes into account the two-way value of environmental protection and urban development, to seek the balance between urban construction and ecological protection. Specifically, it can be divided into the following aspects:

http://www.aloki.hu ● ISSN 1589 1623 (Print) ● ISSN 1785 0037 (Online)
DOI: http://dx.doi.org/10.15666/aeer/1704_72837299

(1) The balance between dynamic development and static protection

The development of a city is a dynamic process, on which different times background, development direction and decision-making ideas will have a significant impact, while ecological protection is a relatively stable state. The balance between dynamic development and static protection through corresponding planning measures is the development basis of "balanced construction" in highly sensitive areas of water ecology.

(2) The balance between ecological benefit and economic benefit

The development of a city is a process of maximizing the comprehensive benefits of economy, society, culture and ecology. Ecological benefits are the basis and starting point of urban construction in highly sensitive areas of water ecology, but comprehensive benefits are the ultimate goal of urban construction. In urban construction, we should abandon the original idea of mechanical protection and pursue the maximization of comprehensive benefits. Urban construction and ecological protection are not entirely opposed to each other. By taking appropriate planning measures, urban construction can effectively promote ecological protection and achieve the balance between ecological benefits and economic benefits.

(3) The balance between natural environment and urban landscape

Urbanization has resulted in the fragmentation of natural ecological environment and landscape. As a heterogeneous factor, the method that helps urban landscape be more actively integrated into the natural environment is worth exploring. The continuity of natural ecological environment can be ensured by setting ecological patches, corridors and springboards. At the same time, the overall style, height and volume of the urban construction area are controlled and guided to maximize the balance between the natural environment and the urban landscape.

(4) The balance between ecological conservation and land use function

Based on ecology, a barrier has been established for urban construction. Negative list and other planning measures can be utilized to support urban development and construction in highly sensitive areas of water ecology. On the premise of ecological conservation, the central planning principles of urban industry selection, land use function layout and spatial structure form are defined to achieve the balance between ecological conservation and urban land use function.

(5) The balance between environmental capacity and the quantity of development and construction

The capacity of the natural environment is limited, and the restriction of environmental capacity is more stringent in highly sensitive areas of water ecology. Sustainable development cities are built on the basis of holding the restriction of limited capacity and seeking reasonable and moderate development and construction, and it needs rational planning for urban development mode and the total amount of development and construction, so as to achieve the balance between environmental capacity and development and construction quantity.

http://www.aloki.hu ● ISSN 1589 1623 (Print) ● ISSN 1785 0037 (Online)
DOI: http://dx.doi.org/10.15666/aeer/1704_72837299

While defining the planning concept, we should use corresponding planning strategies to achieve rational planning objectives. In order to realize the dynamic monitoring of urban construction and protection of water ecology, a diversified strategy of integrating empirical sampling, software simulation and evaluation system was constructed. On the basis of breaking through the original framework of mechanical protection of water ecological environment, this paper puts forward the planning concept of "balanced construction" between urban construction and water ecological health, which provides a new way of thinking for the development and construction of highly sensitive areas of water ecology. Therefore, this investigation aims to find out a method to monitor the dynamic mechanism of urban construction and water protection by utilizing the quantitative analysis of water ecology in the context of rapid urbanization. Moreover, based on this method, this investigation can achieve the dynamic balance between protection of water ecology and rapid urban development. It can also provide a reference for urbanization of water sensitive areas in other fast-growing regions of the world.

Materials and methods

Research framework

Under the guidance of the planning concept of "balanced construction", by taking the measures of mountain and water resources protection, water body ecological control, natural ecological environment conservation, ecological purification measures, ecological corridor control, urban construction guidance, urban landscape shaping, and evaluation index system construction, it is critical to adhere to the principle of protection of water ecology and build the ecological background of regional development. At the same time, it is necessary to actively guide urban development and construction, attach importance to and meet the actual needs of urban development on the basis of ecological protection, seek a sufficient balance between urban construction and protection of water ecology, and obtain the comprehensive optimal solution of economic, social, cultural and ecological benefits (Kiss and Kiss, 2018; Ahern, 2011).

In terms of research process, firstly, through collecting and analyzing the current water samples, the foundation of water environment analysis is laid, and the main focus of water ecological control is clarified. Secondly, DHI Mike 21 simulation software is used to simulate the water quality and flow field, which provides a basis for the planning of surrounding water system and guidance for the spatial layout of green and blue infrastructure. Thirdly, based on the calculation of water pollution capacity and future planning pollution load, the key factors affecting water quality are clarified, the urban land use planning model based on the concept of "balanced construction" is constructed, and the requirements of urban construction scale, spatial layout structure and urban dominant function are put forward. Finally, the comprehensive evaluation index system of water ecological health is established to realize the objective and dynamic evaluation of the balance between protection of water ecology and urban construction.

Step 1: Water environment and ecological investigation

The highly sensitive areas of water ecology have the superior ecological background and abundant habitat communities, and in the tide of urbanization, both water

http://www.aloki.hu ● ISSN 1589 1623 (Print) ● ISSN 1785 0037 (Online)
DOI: http://dx.doi.org/10.15666/aeer/1704_72837299

environment and natural ecology will be challenged severely. Seeking the path of balanced development of urban construction and protection of water ecology must be based on a thorough grasp of the current situation, including water environment, ecological resources, ecological community, water flow direction, water depth, control objectives and so on. Through collecting and analyzing the current water environment and ecological situation, the database of follow-up research and analysis is laid, and the criteria and key points of future water ecological control are defined in combination with the goal orientation, which provides the basis and support for the later urban spatial layout and the location of ecological facilities.

The investigation methods are mainly on-site survey and water sampling analysis, supplemented by literature review. Firstly, according to the judgment of the water shape and the relationship between the water body and the surrounding water body, the spot water quality sampling points are determined, and the water samples will be uniformly collected on the spot in good weather. The main purpose of field sampling is to acquire the current characteristics of a diversified water environment, to grasp the water environment and ecological situation in an all-around way. Therefore, the principle of sampling point setting is to select the heterogeneous water environment samples as many as possible and emphasize the uniqueness and representativeness of samples to ensure the comprehensiveness and integrity of water environment and ecological survey. The concentration of pollutants such as COD, TN, NH_3-N, TP and dissolved oxygen (DO) in water samples are measured. DO is measured on the spot by portable dissolved oxygen meter on the day of sampling, so as to grasp the pollutants in different locations and development environments of the current water body, and help to apply targeted planning strategies.

Step 2: Simulation analysis of water flow distribution and quality via MIKE 21 software

Based on the collection and analysis of water samples in the present, pollutant sources and types that need emphatically solving are determined during the city construction period and the computer simulation analysis of water flow distribution and quality is finished via DHI MIKE 21 software. The analysis and simulation not only help to confirm the potential blind spots and stagnant zones during the water circulation and water flow under the overall conditions such as the specific form of water and coastline layout, but also provide research support for the future urban space planning, coastline optimizing and water ecological facilities distributing.

The simulated results have important reference to water circulation optimization, water form, coastline setting and others since DHI Mike 21, the two-dimensional mathematical model developed by Denmark Hydra Institution, has been widely applied in water simulation and it has strong functions on the simulation of two-dimensional fluid data with a free-surface (Xu et al., 2012; Thompson et al., 2004; Devi et al., 2015).

Model equations of water flow distribution

The control equation of DHI MIKE 21 simulation software is the Navier-Stokes equation that is incompressible in three dimensions, enjoys uniformly distributed Reynolds values and complies with the Boussinesq assumption and hydrostatic pressure (Danish Hydraulic Institute (DHI), 2012). In the numerical calculation aspect, Finite Volume Method, which divides continuum into non-superposed units (the units uses the

http://www.aloki.hu ● ISSN 1589 1623 (Print) ● ISSN 1785 0037 (Online)
DOI: http://dx.doi.org/10.15666/aeer/1704_72837299

triangle mesh) is utilized to solve the spatial dispersion and model resolution of the computational area. In addition, the two-dimensional shallow water equation set can be expressed as follows (*Eqs. 1-3*):

$$\frac{\partial h}{\partial t}+\frac{\partial h\bar{u}}{\partial x}+\frac{\partial h\bar{v}}{\partial y}=hS \quad \text{(Eq.1)}$$

$$\frac{\partial h\bar{u}}{\partial t}+\frac{\partial h\bar{u}^2}{\partial x}+\frac{\partial h\bar{u}\bar{v}}{\partial y}=f\bar{v}h-gh\frac{\partial \eta}{\partial x}-\frac{h}{\rho_0}\frac{\partial p_a}{\partial x}-\frac{gh^2}{2\rho_0}\frac{\partial \rho}{\partial x}+\frac{\tau_{sx}}{\rho_0}-\frac{\tau_{bx}}{\rho_0}-\frac{1}{\rho_0}\left(\frac{\partial s_{xx}}{\partial x}+\frac{\partial s_{xy}}{\partial y}\right)+\frac{\partial}{\partial x}(hT_{xx})+\frac{\partial}{\partial y}(hT_{xy})+hu_sS \quad \text{(Eq.2)}$$

$$\frac{\partial h\bar{v}}{\partial t}+\frac{\partial h\bar{u}\bar{v}}{\partial x}+\frac{\partial h\bar{v}^2}{\partial y}=-f\bar{u}h-gh\frac{\partial \eta}{\partial y}-\frac{h}{\rho_0}\frac{\partial p_a}{\partial y}-\frac{gh^2}{2\rho_0}\frac{\partial \rho}{\partial y}+\frac{\tau_{sy}}{\rho_0}-\frac{\tau_{by}}{\rho_0}-\frac{1}{\rho_0}\left(\frac{\partial s_{yx}}{\partial x}+\frac{\partial s_{yy}}{\partial y}\right)+\frac{\partial}{\partial x}(hT_{xy})+\frac{\partial}{\partial y}(hT_{yy})+hv_sS \quad \text{(Eq.3)}$$

where t is the time. x,y is the coordinates of Cartesian coordinate system. η is the water level. d is the still depth of water. $h=\eta+d$ represents the total depth of water. u and v are the velocity components in x and y direction respectively. f is the coefficient of Coriolis force. In the $f=2\omega\sin\varphi$, ω represents rotational angular velocity of the earth and φ represents local latitude. g is the gravity acceleration. ρ is the density of water. s_{xx}, s_{xy} and s_{yy} are radiation stresses component. S is the source item. (u_s,v_s) represents water velocity of source item.

The letter with a line above represents average value. For instance, $\bar{u}$ and $\bar{v}$ is average water velocity along the water depth, which is defined as follows (*Eq. 4*):

$$h\bar{u}=\int_{-d}^{\eta}udz,\quad h\bar{v}=\int_{-d}^{\eta}vdz \quad \text{(Eq.4)}$$

T_{ij} is horizontal vibration stress term, including viscous force, turbulent stress and advection, and the calculation can be expressed as (*Eq. 5*):

$$T_{xx}=2A\frac{\partial\bar{u}}{\partial x},\quad T_{xy}=A(\frac{\partial\bar{u}}{\partial y}+\frac{\partial\bar{v}}{\partial x}),\quad T_{yy}=2A\frac{\partial\bar{v}}{\partial y} \quad \text{(Eq.5)}$$

Model equations of water quality

Based on the existing results, basic parameters of water quality collected from water simulation and surrounding out and in river are acquired by combining flow-field simulation and collected data of water samples as well as referring to recent water monitoring data. The simulation and analysis on the content of each pollutant that the future water could bear and special distribution of pollution are finished and the relative solutions are proposed based on the results.

2-d water quality simulation mainly uses ECO Lab software and HD Integrated Computing of MIKE 21. DO, which has significantly affected the water quality, TN, TP and other pollutants, should be focused continuously. Eutrophication Module (EU) mainly describes water oxygen dissolved state and nutrient recycling (*Eq. 6*).

$$\frac{\partial C}{\partial t}+u\frac{\partial C}{\partial x}+v\frac{\partial C}{\partial y}+w\frac{\partial C}{\partial z}=D_x\frac{\partial^2 C}{\partial x^2}+D_y\frac{\partial^2 C}{\partial y^2}+D_z\frac{\partial^2 C}{\partial z^2}+S_c+P_c \quad \text{(Eq.6)}$$

where C is the concentration of water quality index; u, v, w are the water velocity components in x, y and z direction respectively; S_c is the source sink term; P_c is the ecological process.

http://www.aloki.hu ● ISSN 1589 1623 (Print) ● ISSN 1785 0037 (Online)
DOI: http://dx.doi.org/10.15666/aeer/1704_72837299

Step 3: Calculation and analysis of assimilative capacity and pollution load

The hydrological conditions in the natural areas are changed due to the progress of urbanization and new pollutants are generated due to city development and construction as well as human activities. Overall, the polluted sources are the city-polluted water (point source pollution) that directly discharged to surrounding waters and the non-point source pollution brought by surrounding water in the city. However, with the improving facilities of city and upgrading planning and monitoring level, the negative influence of point source pollution has been controlled effectively. The non-point source has more noticeable effect on the local water environment, which continuously becomes the focus of water pollutant control in water sensitive area.

Calculation of assimilative capacity

Usually, lake and reservoir are regarded as completely homogeneous mixing water quality model to estimate the long-term dynamic change of water quality. When being steady, the environmental capacity model could be calculated via a water balance equation as shown in *Equation 7*.

$$V(t)\frac{dc}{dt} = Q_{in}(t) \times C_{in}(t) - Q_{out}(t) \times C_{out}(t) + S_c + kV(t)C \quad \text{(Eq.7)}$$

where V(t) is the water yield of time t (m^3). dc/dt is the change rate of the parameters such as COD and ammonia. Qin (t) is the input water yield (m^3/a) at time t. Qout (t) is the output water yield (m^3/a) at time t. Cin (t) is the input concentration (mg/L) at time t. Cout (t) is the output concentration (mg/L) at time t. C(t) is the lake concentration (mg/L) at time t. Sc is the external polluted content. k is the comprehensive degradation coefficient of COD and ammonia.

Without considering the mixing area, when the demand mass concentration is Cs in the water functional zone of lake and reservoir, the equation of their environmental capacity can be expressed as follows (*Eq. 8*):

$$W_{capacity} = 31.54 \times (QC_s + KC_sV \div 86400) \quad \text{(Eq.8)}$$

where $W_{capacity}$ is the environmental capacity (t/a); Cs is the target value of water quality (mg/L); Q is the input and output water yield at steady state; k is the comprehensive degradation coefficient of COD and ammonia; V is the water volume in lake and reservoir (m^3).

Step 3: Calculation and analysis of assimilative capacity and pollution load

The hydrological conditions in the natural areas are changed due to the progress of urbanization and new pollutants are generated due to city development and construction as well as human activities. Overall, the polluted sources are the city-polluted water (point source pollution) that directly discharged to surrounding waters and the non-point source pollution brought by surrounding water in the city. However, with the improving facilities of city and upgrading planning and monitoring level, the negative influence of point source pollution has been controlled effectively. The non-point source has more noticeable effect on the local water environment, which continuously becomes the focus of water pollutant control in water sensitive area.

http://www.aloki.hu ● ISSN 1589 1623 (Print) ● ISSN 1785 0037 (Online)
DOI: http://dx.doi.org/10.15666/aeer/1704_72837299

Calculation of assimilative capacity

Usually, lake and reservoir are regarded as completely homogeneous mixing water quality model to estimate the long-term dynamic change of water quality. When being steady, the environmental capacity model could be calculated via a water balance equation as shown in *Equation 7*.

$$V(t)\frac{dc}{dt} = Q_{in}(t) \times C_{in}(t) - Q_{out}(t) \times C_{out}(t) + S_c + kV(t)C \quad \text{(Eq.7)}$$

where V(t) is the water yield of time t (m^3). dc/dt is the change rate of the parameters such as COD and ammonia. Qin (t) is the input water yield (m^3/a) at time t. Qout (t) is the output water yield (m^3/a) at time t. Cin (t) is the input concentration (mg/L) at time t. Cout (t) is the output concentration (mg/L) at time t. C(t) is the lake concentration (mg/L) at time t. Sc is the external polluted content. k is the comprehensive degradation coefficient of COD and ammonia.

Without considering the mixing area, when the demand mass concentration is Cs in the water functional zone of lake and reservoir, the equation of their environmental capacity can be expressed as follows (*Eq. 8*):

$$W_{capacity} = 31.54 \times (QC_s + KC_sV \div 86400) \quad \text{(Eq.8)}$$

where $W_{capacity}$ is the environmental capacity (t/a); Cs is the target value of water quality (mg/L); Q is the input and output water yield at steady state; k is the comprehensive degradation coefficient of COD and ammonia; V is the water volume in lake and reservoir (m^3).

Calculation of pollution load

The water pollutant mainly comes from point source pollution and non-point source pollution. When calculating pollution load, one premise needs to be confirmed, that is, pollution load should focus more on the effect of non-point source pollution when the point source pollution of city is controlled effectively. The capacity of non-point source pollution in different land use is different. The dynamic relationship between pollution load produced in city construction and pollutant carrying capacity of water is explicated in different developing states and situations via analyzing and calculating the current and future urban land, thus adjusting, analyzing and checking the direction of city construction as well as constructing the foundation of balanced construction theory.

Firstly, the terrain features and the situation of city construction in water sensitive area are concluded. After confirming the water catchment regionalization via GIS and other analyzing tools, it is known that the regionalization includes direct water catchment area (overland runoff directly flows into main water body, getting through overland flow, concentration of channel flow and others) and indirect water catchment. Then, the construction situations of water catchment regionalization are classified by mathematical statistics method, thus calculating non-point source pollution load caused by different land types.

The land types for non-point source pollution load calculating in water catchment regionalization mainly includes residential, commercial, cultural, educational, industrial, scientific, road and entertainment, etc. The composite output coefficient of COD, TN and TP are 320 kg/(ha.a), 40 kg/(ha.a) and 7.0 kg/(ha.a) via weighted

http://www.aloki.hu ● ISSN 1589 1623 (Print) ● ISSN 1785 0037 (Online)
DOI: http://dx.doi.org/10.15666/aeer/1704_72837299

calculation after confirming the non-point source pollution load through relative experience numbers (Qi, 2005; Li, 2000).

In the water highly sensitive area, with the target of collecting and solving point source pollution, planning drainage pipe network of polluted water and constructing sewage treatment infrastructure could guarantee the effective solution of polluted water. At the same time, protective greenbelt, sponge facilities, constructed wetlands and others could assist intercepting and purifying non-point source pollutant generated by runoff water, thus making sure that the pollution load of the non-point source is smaller than the assimilative capacity of the main water body.

Step 4: Construction of a diagnostic indicator system for water ecosystem health

Diagnostic sand table for water ecosystem health

Based on "balanced construction" logos, the diagnostic indicator system for water ecosystem health is constructed, whose aim is to construct the evaluating trend and ideal sand table for water ecosystem. By dynamic monitor and adjustment based on water ecosystem and city construction, the objective evaluation concerning water ecosystem protection and balanced city construction is realized. This evaluating system is divided into rule hierarchy including water quality characteristic, hydrological characteristics, physical shape structure, ecosystem indicators, lake landscape, and marker bed which fractionalizes and dismantles the rule hierarchy, finally forming evaluating indicator system including two tiers, five types and seventeen subclasses (*Table 1*).

Table 1. *Diagnostic indicator system for water ecosystem health*

Rule hierarchy	Marker bed	Quantitative criteria
Water quality characteristic B1	Nemerow multi-factor index method (C11)	COD, NH_3-N, TN, TP
	Nutritional index (C12)	TLI
	Dissolve oxygen (C13)	DO
Hydrological characteristics B2	The lowest ecological water level satisfied state (C21)	The lowest ecological water level satisfied rate
	Water exchanging cycle period (C22)	Water exchanging cycle period
Physical shape structure B3	Lake basin stability (C31)	Stable degree of lake basin
	Lakeshore stability (C32)	Stable degree of lakeshore
	Vegetation integrity (C33)	Vegetation coverage
	Form of coastline and revetment (C34)	Hardening rate of slope
Ecosystem indicators B4	Green belt vegetation coverage (C41)	Coverage of shore side buffer, barrier and island
	Diversity of phytoplankton (C42)	Diversity of plankton
	Conservation rate of indigenous plant (C43)	Proportion of indigenous plant
	Proportion of natural surface (C44)	Proportion of natural surface
	Quality index of habitat (C45)	Diversity index of water habitats
Lake landscape B5	Aesthetic measure (C51)	Aesthetic measure
	Accessibility of landscape (C52)	Accessible degree of landscape
	Width of green belt in lakeside (C53)	Lake greening rate

The city construction in water highly sensitive should obey balance construction planning theory, seeking the balance between city construction and ecological protection. Moreover, the control of the ecological quality of water body has become

http://www.aloki.hu ● ISSN 1589 1623 (Print) ● ISSN 1785 0037 (Online)
DOI: http://dx.doi.org/10.15666/aeer/1704_72837299

the ecological basis of city development, especially the development of water sensitive area. By diversified city construction management and purification treatment measures, the focus of water ecosystem control is put into water quality conservation. It guarantees the quality of water body and fully plays the role of the water body, thus producing comprehensive profits in ecology, landscape, society, economy. Therefore, when constructing evaluating indicator system which synthetically and roundly reflects multiple values of water ecosystem sensitive area, it is necessary to fully consider the influence of city construction, ecology conservation, function constitute and other factors, take ecological protection as background and regards city construction as extension.

Weight of evaluation indicator for water ecological health

For water quality characteristic, hydrological characteristics, physical shape, biological state and landscape aesthetics, judgment matrix as shown in *Table 2* is established based on a 1-9 scale norm.

Table 2. *Judgment matrix of marker bed*

	Water quality characteristic	**Hydrological characteristics**	**Physical shape structure**	**Biological state**	**Landscape aesthetics**
Water quality characteristic	1	3	5	2	5
Hydrological characteristics	0.33	1	3	0.5	2
Physical shape structure	0.2	0.33	1	0.33	1
Biological state	0.5	2	3	1	4
Landscape aesthetics	0.2	0.5	1	0.25	1

By calculating and judging the max eigenvalue and relevant feature vector of the matrix, the obtained weight of rule hierarchy relative to the overall goal $w = [0.43\ 0.16\ 0.07\ 0.26\ 0.08]$, CI = 0.013, RI = 1.12, CR = 0.0117 < 0.1 obtains consistency checks. For rule hierarchy of water quality characteristic, the judgment matrix is established as shown in *Table 3*.

Table 3. *Judgment matrix of water quality indicator*

Indicator	**Nemerow multi-factor index**	**Trophic status index**	**Dissolve oxygen**
Nemerow multi-factor index	1	3	5
Trophic status index	0.33	1	3
Dissolve oxygen	0.2	0.33	1

Compared with the rule hierarchy of water quality characteristic, the weights of Nemerow multi-factor index, trophic status index, and dissolved oxygen are $w_1 = [0.64\ 0.26\ 0.1]$, respectively. Similarly, the weights of the rest marker beds are $w_2 = [0.75\ 0.25]$, $w_3 = [0.25\ 0.25\ 0.25\ 0.25]$, $w_4 = [0.09\ 0.06\ 0.07\ 0.39\ 0.39]$, $w_5 = [0.33\ 0.33\ 0.33]$. According to the index system of Lake Ecosystem health risk

http://www.aloki.hu ● ISSN 1589 1623 (Print) ● ISSN 1785 0037 (Online)
DOI: http://dx.doi.org/10.15666/aeer/1704_72837299

assessment integrated from top to bottom and combined with the weight of each index, the comprehensive index of Lake Ecosystem health risk assessment is as follows (*Eq. 9*):

$$EHRI = \sum_{i=1}^{n} w_i I_i \quad \text{(Eq.9)}$$

In the equation, EHRI is the comprehensive index of lake healthy risk assessment. w_i is the weight of the evaluation index and I_i is the result of the evaluation index. Referring to the relevant standards of lake health research at home and abroad, we can divide the lake healthy risk assessment level into five levels: excellent, good, medium, poor and very poor, as shown in *Table 4*.

Table 4. *Level division of lake ecological health risk evaluation*

Level	*EHRI*	Health risk status
I	4	Excellent
II	3	Good
III	2	Medium
IV	1	Poor
V	0	Very poor

Results: case study of Xianghu Lake

We applied this method to the actual urban planning practice to test the operability of the method. We apply it in the urban planning of the Xianghu area in Hangzhou. The site of planning practice is located on the eastern coast of China, Hangzhou, Zhejiang Province. The geographical coordinates of Hangzhou are 118°21′-120°30′ east longitude and 29°11′-30°33′ north latitude. It is one of the critical central cities in the Yangtze River Delta region of eastern China. In 2018, the urban population was about 9.8 million. The rapid development of the urban economy and the concentration of the urban population have also caused a dramatic expansion of urban space.

The Xianghu area is located in the northeast of Hangzhou, which is adjacent to the Qiantang River (*Fig. 1*). As a backup water source for urban development, its water body has higher ecological sensitivity and protection requirements. In addition, the landscape resources in the area are one of the critical parts of the urban habitat core. In recent years, with the rapid development of urbanization taking tourism industry as an engine, Xianghu region is gradually being incorporated into a series of built-up areas. Therefore, Xianghu Lake is facing tremendous pressure of urban development and construction. How to protect the natural ecological background and landscape characteristics of Xianghu Lake under the premise of ensuring the city's rapid development and its gradually improving function? How to seek the balance between urban development and ecological environment protection? How to place the fast-growing city in the superior natural ecological environment? These problems deserve our attention.

(1) Results of current water quality sampling analysis

At present, the catchment area of Xianghu Lake is about 10.6 km^2, the water area is 3.2 km^2, and the total water storage capacity is 13.5 million m^3. With the expansion of

http://www.aloki.hu ● ISSN 1589 1623 (Print) ● ISSN 1785 0037 (Online)
DOI: http://dx.doi.org/10.15666/aeer/1704_72837299

the lake in the future, the water of Qiantang River will be introduced into the lake. The total water area of Xianghu Lake can exceed 6 km^2. The water storage capacity can reach 23 million cubic meters. According to the relationship between the shape of Xianghu Lake and the surrounding water bodies, a total of 16 water sampling points were set up for sampling and analysis, including 12 points in the water of Xianghu Lake (*Fig. 2*), 3 points in surrounding rivers, and one sampling point in Qiantang River. On December 16, 2017, the water samples were collected on site and brought back to the Southeast University Environmental Laboratory for testing and analysis. The DO was tested by a portable dissolved oxygen meter. The temperature on the day of sampling was 4~15 °C, and the weather was fine.

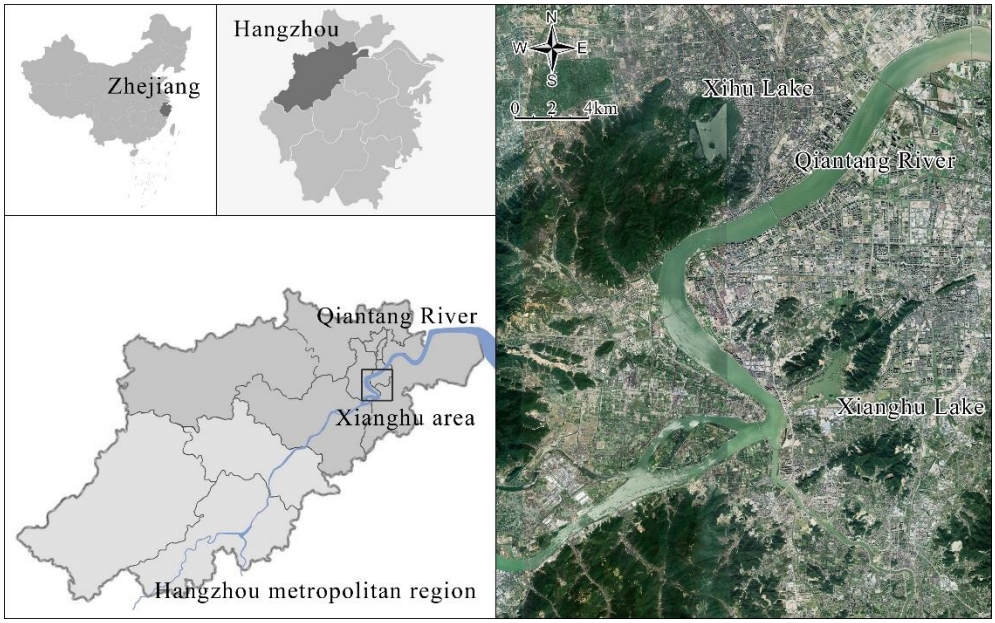

Figure 1. *Location of Xianghu Lake*

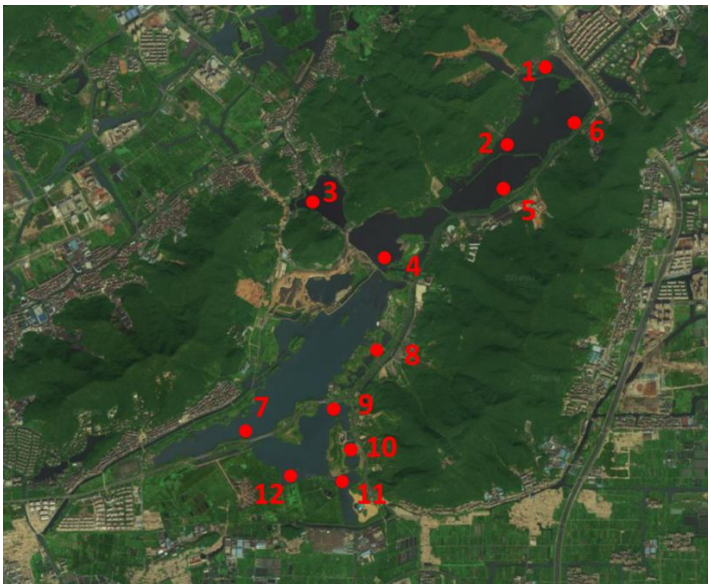

Figure 2. *Water quality sampling point of Xianghu Lake*

http://www.aloki.hu ● ISSN 1589 1623 (Print) ● ISSN 1785 0037 (Online)
DOI: http://dx.doi.org/10.15666/aeer/1704_72837299

Through experimental analysis of sample water collected on field, the water quality of Xianghu Lake is IV or V (GB3838-2002) according to the single factor evaluation method. Compared with the set water quality target of Class III, the main factor that exceeds the standard is TN. Therefore, controlling TN concentration is the primary way to improve the water quality of Xianghu Lake. The water quality of nearby rivers is IV or V. The main pollutant factors are COD_{Mn} and ammonia nitrogen. The water quality of rural rivers is better than that of urban rivers, and urban built-up areas have a significant impact on the water quality of rivers. Ensuring sufficient width of ecological corridor is also one of the measures to reduce the impact of water quality.

(2) Results of Mike 21 flow field and water quality simulation

The water flow field plays an active role in improving water purification capacity and environmental capacity. Through the simulation with DHI Mike 21, the critical areas of Xianghu Lake featured with slow flow, vulnerable to pollution and eutrophication are identified. The external running water from the Qiantang River is introduced to enhance the water cycle of Xianghu Lake (*Fig. 3*). Measures are taken including setting up ecological wetlands, increasing the width of ecological corridors, planting purified aquatic plants, and controlling the inflow of pollution sources to enhance the self-purification capacity of the water body in the region, which can greatly meet the needs of urbanization development and construction, enhance nearby construction capacity and raise the threshold of "balanced construction" under the premise of ensuring ecological priority.

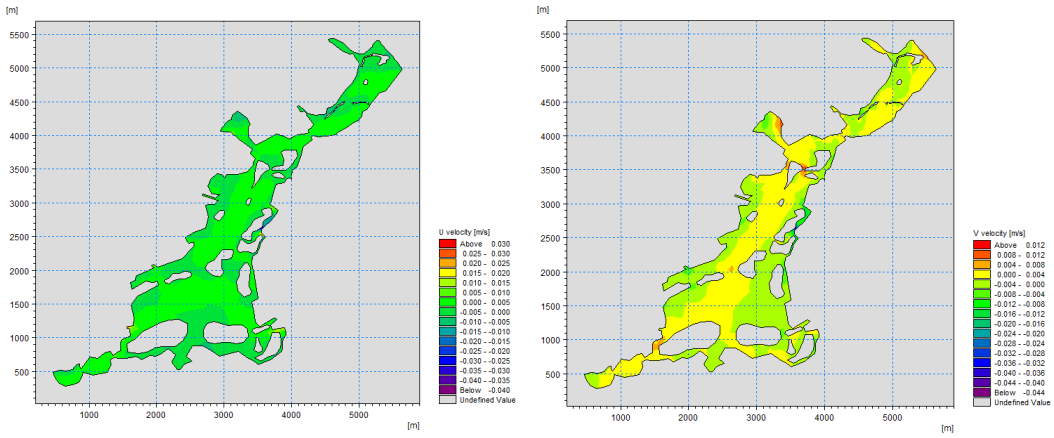

Figure 3. *Simulated distribution of X (left) and Y (right) directional velocity of Xianghu Lake with introduce of running water of Qiangtang River*

(3) Comparisons between pollution capacity and pollution load

The capacity of Xianghu water body to absorb pollutants directly affects the scale of urban development and construction. After clarifying the significant influence of non-point source pollution on the water quality conservation of Xianghu Lake, the authors optimized the proportion of land use and the division of spatial groups in the planning scheme by calculating the non-point source pollution load od the planning land use scheme and comparing with the capacity of Xianghu water body to absorb pollutants

http://www.aloki.hu ● ISSN 1589 1623 (Print) ● ISSN 1785 0037 (Online)
DOI: http://dx.doi.org/10.15666/aeer/1704_72837299

horizontally. Through many times of adjustments, analyses and checks, the interaction and balance between the layout of planned land and water ecology have been achieved.

(4) Calculation of ecological health evaluation index of Xianghu Lake

Through calculation of current ecological health evaluation index of Xianghu Lake, the health status of it can be reflected as feedback to urban development and construction in order to seek a dynamic balance between protection and construction. The weight of the health evaluation index reflects the importance of each index in the health system of Xianghu Lake. The weight of water quality index and ecosystem index is larger, 0.43 and 0.26, respectively, followed by hydrological characteristics, which is consistent with the status of Xianghu Lake as an important backup water source and habitat core of the city. The specific calculation process is shown in *Table 5*. The final calculation result is 2.95, indicating the current health evaluation level of Xianghu Lake is good.

Table 5. *The weight and assignment of health evaluation index of Xianghu Lake in 2018*

Rule hierarchy	Weight	Marker bed	Weight	Assignment
Water quality characteristic B1	0.43	Nemerow multi-factor index (C11)	0.64	3
		Nutrition index (C12)	0.26	2
		Dissolved oxygen (C13)	0.10	1.55
Hydrologcial characteristics B2	0.16	The lowest ecological water level satisfied state (C21)	0.75	4
		Water exchanging cycle period (C22)	0.25	3
Physical shape B3	0.07	Lake basin stability (C31)	0.25	3
		Lakeshore stability (C32)	0.25	3
		Vegetation integrity (C33)	0.25	3
		Form of coastline and revetment (C34)	0.25	4
Ecosystem indicators B4	0.26	Green belt vegetation coverage (C41)	0.09	4
		Diversity of phytoplankton (C42)	0.06	3
		Conservation rate of indigenous plant (C43)	0.07	4
		Proportion of natural surface (C44)	0.39	2
		Quality index of habitat (C45)	0.39	3
Lakeside landscape B5	0.08	Aesthetic measure (C51)	0.33	4
		Accessibility of landscape (C52)	0.33	3
		Green belt vegetation coverage (C53)	0.34	4

According to the orientation of the ecological function of Xianghu Lake, the health evaluation factors constructed include 17 evaluation indexes, such as hydrology and water resources, water system structure, ecological function, ecosystem health, and tourism landscape value. The calculation results can show the health status of Xianghu Lake with the level from good to excellent. Based on guaranteeing excellent ecological background, the healthy evaluation index system provides not only a dynamic grasp for monitoring the water ecological quality of Xianghu Lake, but also regular feedback for urban construction. The urban development and construction is a dynamic and long-term process. The results of water health assessment of Xianghu Lake can provide a basis of optimization for the development and construction of Xianghu Lake region, to achieve the dynamic balance between protection of water ecology and urban

http://www.aloki.hu ● ISSN 1589 1623 (Print) ● ISSN 1785 0037 (Online)
DOI: http://dx.doi.org/10.15666/aeer/1704_72837299

construction. Moreover, the results of health assessment can reflect the direction of improving the water health of Xianghu Lake in the future. For Xianghu Lake, if the water quality pollution index, natural water area and habitat index can be taken up to one higher level respectively, the health index of Xianghu Lake can reach 3.53, namely, the excellent level of health.

Discussion and conclusion

In the process of "balanced construction" in highly sensitive areas of water ecology, we utilized calculation of water ecology and software simulation to lay the ecological foundation of subsequent urban planning and design and seek for interaction between water ecology and subsequent urban planning and design. According to the results of simulation analysis, measures to help seek urban design strategies are included as follows:

(1) Flow field simulation of water body. We collect and investigate the current water body. Then, we simulate and analyze the water body by using Mike simulation software. In this way, we find out the current problems and areas with poor fluidity (water quality is vulnerable to deterioration) so that we can take appropriate measures to deal with in the planning process.

(2) Water purification methods. After clarifying the types of main pollution sources in the future development process, we should strictly control the point source pollution and minimize its adverse impact on the environment. Besides, we should pay full attention to the calculation and treatment of non-point source pollution. We can take diversified ecological purification measures such as eco-embankment, constructed wetlands, aquatic animal and plant communities to improve the capacity of water to absorb and treat pollutants. At the same time, through the ecological treatment of peripheral rivers and construction of sponge facilities, the water quality of the catchment can be purified to ensure the water quality health and finally achieve the stated planning goals of water ecological conservation.

(3) Dynamic balanced monitoring methods. Supported by the established water healthy evaluation index system, periodic and dynamic inspection of water health status is carried out to reflect the impacts of urban construction on highly sensitive areas of water ecology. Based on the evaluation results, feedback and guidance are provided for urban development and construction in terms of construction and development capacity, spatial distribution, selection of leading functions, blue-green infrastructure construction and urban landscape construction, to achieve the dynamic balance between protection of water ecology and urban construction.

In this paper, there are also several aspects that need to be discussed:

(1) In this paper, the evaluation of water quality and related application standards are all based on the national standards of China. If the methods are applied in other areas, the corresponding standards need to be re-checked to meet the actual local requirements.

(2) In this paper, the research object is the lake. If the lake is transformed into other kinds of water form, the corresponding Mike 21 simulation analysis equation may need to be adjusted accordingly.

(3) The paper focuses on the current development of Chinese cities, especially the big cities. The control standard of point source pollution in cities is relatively higher, which can achieve municipal collection and treatment. Therefore, the impact of point

http://www.aloki.hu ● ISSN 1589 1623 (Print) ● ISSN 1785 0037 (Online)
DOI: http://dx.doi.org/10.15666/aeer/1704_72837299

source pollution on water quality has not been fully considered in the calculation of pollution load. If point source pollution cannot be effectively controlled, the development of water ecologically sensitive area could be catastrophic. Under such prerequisite, it is necessary to take a relatively conservative attitude towards urban construction in water ecologically sensitive areas. When the cities fail to deal with the discharge of point source pollutants, urban development and construction in highly sensitive areas of water ecology need to be controlled.

Overall, the urbanization process of the world is still in a stage of rapid development. In the process of rapid urbanization, urban and natural, construction and protection are two factors that cannot be avoided. Based on the experience in China's urbanization practice, the paper summarizes the planning evaluation methods that seek the dynamic equilibrium of construction and protection. It can also provide a reference for subsequent research. Ecological protection is the foundation of urban development. The development should be high quality and sustainable, which is under the premise of protection. It is recommended that in the future research and practice process, the importance of ecological protection should be fully emphasized. By the application of scientific quantitative research methods, we can seek the maximum comprehensive benefits of urban development on the basis of meeting ecological capacity.

Acknowledgements. This work was supported by the major program of National Natural Science Foundation of China under Grant 51838002; general program of National Natural Science Foundation of China under Grant 51578128; and major program of science and technology of Ministry of Housing and Urban-Rural Development of the People's Republic of China.

REFERENCES

[1] Ahern, J. (2011): From fail-safe to safe-to-fail: sustainability and resilience in the new urban world. – Landscape and Urban Planning 100: 341-343.
[2] Chan, F. K. S., Griffiths, J. A., Higgitt, D., Xu, S.-Y., Zhu, F.-F., Tang, Y.-T. et al. (2018): "Sponge City" in China—A breakthrough of planning and flood risk management in the urban context. – Land Use Policy 76: 772-778.
[3] Danish Hydraulic Institute (DHI) (2012): MIKE 21 Flow Model: Hydrodynamic Module User Guide (Chinese Edition). – DHI Water and Environment, Horsholm, Denmark.
[4] Devi, G. K., Ganasri, B. P., Dwarakish, G. S. (2015): A review on hydrological models. – Aquatic Procedia 4: 1001-1007.
[5] Griffiths, J. A. (2017): Sustainable urban drainage. – Encyclopedia of Sustainable Technologies: 403-413.
[6] Hough, M. (2004): Cities and Natural Process: A Basis for Sustainability. 2nd Ed. – Routledge, New York.
[7] Jacobson, C. R. (2011): Identification and quantification of the hydrological impacts of imperviousness in urban catchments: A review. – Journal of Environmental Management 92: 1438-1448.
[8] Kiss, T., Kiss, V. M. (2018): Ecology-related resilience in urban planning. A complex approach for Pécs (Hungary). – Ecological Economics 144: 160-170.
[9] Li, H.-E. (2000): Average concentration method for non-point source pollution load and its application. – Acta Scientiae Circumstantiae 20(4): 397-400.
[10] Lull, H. W., Sopper, W. E. (1969): Hydrological Effects from Urbanization of Forested Watersheds in the NE. – USDA Forest Service Research Paper NE 146. US Department of Agriculture, Washington, DC.

http://www.aloki.hu ● ISSN 1589 1623 (Print) ● ISSN 1785 0037 (Online)
DOI: http://dx.doi.org/10.15666/aeer/1704_72837299

[11] Meerow, S., Newell, J. P., Stults, M. (2016): Defining urban resilience: a review. – Landscape and Urban Planning 147: 38-49.
[12] Mitchell, G. (2005): Mapping hazard from urban non-point pollution: a screening model to support sustainable urban drainage planning. – Journal of Environmental Management. https://doi.org/10.1016/j.jenvman.2004.08.002.
[13] Morison, P. J., Brown, R. R. (2011): Understanding the nature of publics and local policy commitment to Water Sensitive Urban Design. – Landscape and Urban Planning 99: 82.
[14] Pyke, C., Warren, M. P., Johnson, T., Lagro Jr., J., Scharfenberg, J., Groth, P. et al. (2011): Assessment of low impact development for managing stormwater with changing precipitation due to climate change. – Landscape and Urban Planning 103: 166-173.
[15] Qi, J.-Y. (2005): Study on Urban Non-Point Source Pollution Load Quantification. – Master's Thesis of Hehai University, Nanjing, China.
[16] Thompson, J. R., Sørenson, H. R., Gavin, H., Refsgaard, A. (2004): Application of the coupled MIKE SHE/MIKE 11 modelling system to a lowland wet grassland in southeast England. – Journal of Hydrology 293: 151-179.
[17] Thorne, C. R., Lawson, E. C., Ozawa, C., Hamlin, S. L., Smith, L. A. (2015): Overcoming uncertainty and barriers to adoption of Blue-Green Infrastructure for urban flood risk management. – Journal of Flood Risk Management 11(S2): S960-S972.
[18] United Nations (2018): The 2018 Revision of the World Urbanization Prospects. – The Population Division of the United Nations Department of Economic and Social Affairs (UN DESA), NewYork.
[19] Voyde, E., Fassman, E., Simcock, R. (2010): Hydrology of an extensive living roof under sub-tropical climate conditions in Auckland, New Zealand. – Journal of Hydrology 394: 3895.
[20] Wang, X.-H., Xiang, W.-N. (2016): Ecological wisdom for urban sustainability: doing real and permanent good in ecological practice. – Landscape and Urban Planning 155: 1-2.
[21] Xiang, W.-N. (2014): Doing real and permanent good in landscape and urban planning: Ecological wisdom for urban sustainability. – Landscape and Urban Planning 121: 65-69.
[22] Xu, M. J., Yu, L., Zhao, Y. W., Li, M. (2012): The simulation of shallow reservoir eutrophication based on MIKE21: a case study of Douhe Reservoir in North China. – Procedia Environmental Sciences 13: 1975-1988.

http://www.aloki.hu ● ISSN 1589 1623 (Print) ● ISSN 1785 0037 (Online)
DOI: http://dx.doi.org/10.15666/aeer/1704_72837299

INVESTIGATION OF HEAVY METAL ADSORPTION ON MICROPLASTICS

OZ, N.* – KADİZADE, G. – YURTSEVER, M.

Sakarya University, Engineering Faculty, Sakarya, Turkey
(e-mail: goksin.kadizade1@ogr.sakarya.edu.tr; mevci@sakarya.edu.tr
phone: +90-264-295-5639; fax: +90-264-295-5601)

**Corresponding author*
e-mail: nuroz@sakarya.edu.tr

(Received 5th Feb 2019; accepted 8th Apr 2019)

Abstract. Microplastics and heavy metals represent two pollutant classes which have adverse impacts on aquatic ecosystems. This study has investigated the adsorption of two heavy metals [Lead (Pb)II and Aluminum (Al)III] on three different types of microplastics [polyethylene terephthalate (PET), polyamide (PA), ethylene vinyl acetate (EVA)]. The Scanning Electron Microscope (SEM) analysis has shown that microplastics have different surface characteristics. The effects of parameters such as the pH of solution, duration of contact, initial concentration and temperature on adsorption capacity have been examined. Experimental results have been applied to the adsorption isotherm models of Langmuir and Freundlich and it has been seen that the Freundlich model has been seen as more suitable than the Langmuir model. Moreover, the pseudo-second kinetic has been found to be more appropriate than the pseudo-first kinetic model. Adsorption percentages have changed according to the type of microplastic and working conditions. Finally, the study has investigated the potential of microplastics to act as an instrument of transport for heavy metals to the food chain and for their bioaccumulation.
Keywords: *polyethylene terephthalate, polyamide, ethylene vinyl acetate, bioaccumulation*

Introduction

The term microplastic was first used in 2004 to define microscopic plastic particles with a diameter of approximately 20 microns (Thompson et al., 2004). In time, this definition widened to include plastic parts with diameters smaller than 5 mm (Arthur et al., 2008). Today, it is estimated that there are at least 5.25 trillion microplastics in the seas with a weight of 268,940 tons. Microplastics are generally transported to the seas and oceans by river flows (Okubo et al., 2018). It is thought that 10% of plastics in the oceans stem from ships and fishing activities. Furthermore, detergents, cleaning agents and cosmetic products contain microplastics as well (Aytan et al., 2016).

It is known that plastic parts in the seas and freshwater ecosystems are divided into tiny particles by small sea creatures. Microplastics can spread widely in water environment through currents and hydrodynamic processes due to their persistent characteristics (Ng and Obbard, 2006). Particles with a high density deposit and accumulate, while low-density particles float on water (Cauwenberghe and Janssen, 2014). Moreover, it is more likely for buoyant particles into be swallowed and transferred to the food chain (Boerger et al., 2010). Micrometer-sized plastic particles are swallowed by sea creatures like fish, worms, sea birds, crustaceans and clams (Hu et al., 2017). This type of feeding might obstruct the gastrointestinal tract, leading to limited nutrition. These particles might even be transferred into the circulation system through intestinal wall. Swallowing microplastics may cause serious harm to vital functions of living creatures (Cauwenberghe and Janssen, 2014).

http://www.aloki.hu ● ISSN 1589 1623 (Print) ● ISSN 1785 0037 (Online)
DOI: http://dx.doi.org/10.15666/aeer/1704_73017310

Microplastics are potential carriers that can adsorb heavy metals in aquatic environments due to their specific surface areas. It is even possible for heavy metals adsorbed onto microplastics to be transferred to a great variety of aquatic organisms in both seas and freshwaters (Digka et al., 2018). Thus, microplastics have bioaccumulation potential throughout the food chain (Galloway, 2015).

Metal pollution is rather high in seas and freshwaters due to industrial wastes, paints containing metals and fuel combustion (Fu and Wang, 2011; Brennecke et al., 2016; Yousefzadeh et al., 2018). In the same manner, microplastics are known to abound in seas and freshwaters because of human activities (Brennecke et al., 2016). Until recently, interactions between plastics and metals have not been considered important. It is probably thought that polymers are ineffective against metals. However, microplastics are an important intermediary for the transportation of metals in aquatic environments and they display a higher inclination for adsorption of heavy metals in freshwaters (Holmes et al., 2012).

The adsorption of heavy metals by microplastics may differ according to the physical properties of microplastics, the size of pores, surface area and the type of microplastics. Therefore, the type of microplastics is influential on adsorption efficiency. Three different types of microplastics were used in this experimental study, which are polyethylene terephthalate (PET), polyamide (PA) and ethylene vinyl acetate (EVA) found in the sea ecosystem. The aim of this study is to investigate the adsorption of heavy metals onto microplastics.

Material and Methods

Stock Solutions of Lead and Aluminum Ions

As the lead stock solution, 1000 mg/L of $Pb(NO_3)_2$ (Merck) was used and as the aluminum stock solution, 1000 mg/L of $Al(NO_3)_3$ (Merck) was used. Solutions with varying concentrations were prepared with these stock solutions and 1 gr of microplastics was added.

Microplastic Pellets

PET, PA and EVA were purchased as granules. These granules had sizes of 0.5-1 mm. The morphological features of plastics were examined in the Scanning Electron Microscope (SEM). *Figure 1* displays the SEM micrographs of PET, PA and EVA, respectively. As can be seen in *Figure 1*, the surfaces of microplastics vary according to their type.

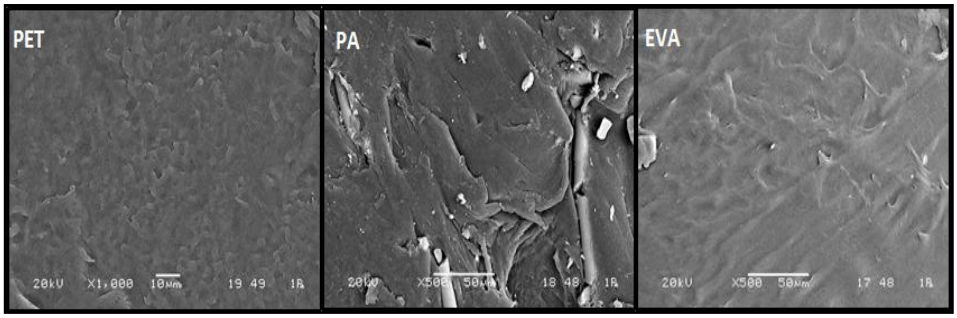

Figure 1. *SEM images of PET, PA, and EVA raw pellets*

http://www.aloki.hu ● ISSN 1589 1623 (Print) ● ISSN 1785 0037 (Online)
DOI: http://dx.doi.org/10.15666/aeer/1704_73017310

Experimental Study Methods

This study investigated how the adsorption capacity is affected by pH (2, 3, 4, 5, 6, 7, 8, 9, 10) duration of contact (5, 15, 30, 60, 90 min), initial concentration (0.5, 1, 2, 3, 4, 5, 6, 7 ppm) and temperature (25, 35, 45, 55°C), which are significant parameters in adsorption processes and which affect the solution, and the features of the adsorbent and it was tried to find optimum conditions. A solution volume of 1000 mL was used in all the adsorption experiments. The pH adjustment was carried out with 0.1 M HCl or NaOH solutions. Solutions with different concentrations were prepared by diluting the standard stock solution of Pb or A1. The solutions were added with 1 gr of PET, PA and EVA, respectively, and stirred on a magnetic stirrer with a fixed stirring speed of 180 rpm. The filtrate water was put into falcon tubes of 50 mL. Three replicates were carried out for each experiment. The concentration of metal in the filtrate was examined with ICP-OES and adsorption removal efficiencies were determined based on the results. The adsorption percentage was calculated based on the *Equation 1*.

$$\%Ads = 100 - \frac{[A]_t}{[A]_0} \times 100 \quad \text{(Eq.1)}$$

where, %ads is the adsorption percentage; $[A]_t$ is the concentration of heavy metal remaining in the solution after time t; and $[A]_0$ is the concentration of heavy metal at time 0.

Adsorption models

The adsorption isotherm models of Langmuir and Freundlich were used in this study. Linear forms of the Langmuir isotherm are shown in *Equations 2, 3 and 4*:

$$q_e = \frac{Q_{max}\, a_L\, C_e}{1 + a_L\, C_e} \quad \text{(Eq.2)}$$

$$q_e = \frac{K_L\, C_e}{1 + a_L\, C_e} \quad \text{(Eq.3)}$$

To show this in a linear way;

$$\frac{1}{q_e} = \left(\frac{1}{K_L}\right).\frac{1}{C_e} + \frac{a_L}{K_L} \quad \text{(Eq.4)}$$

where, q_{max} is the single layer capacity of heavy metal (mg/g); C_e is the concentration of heavy metal molecules remaining in solution at equilibrium (mg/L); K is the Langmuir constant related to the adsorption balance and energy (L/mg); a_L is the constant based on adsorption energy (L/mg); and q_e is the amount of material adsorbed on unit adsorbent (mg/g).

When the graph of C_e/q_e was drawn against C_e, the curve of the linear graph gives a_L/K_L and the point where it cuts the y-axis gives $1/K_L$. The R^2 constant was calculated to find the suitability of adsorption and this constant requires the suitability condition to have values between 0 and 1 (Hamdaoui and Naffrechoux, 2007).

The linear forms of the Freundlich isotherm are shown in the *Equations 5 and 6*.

$$qe = K_f\, Ce^{1/n} \quad \text{(Eq.5)}$$

http://www.aloki.hu ● ISSN 1589 1623 (Print) ● ISSN 1785 0037 (Online)
DOI: http://dx.doi.org/10.15666/aeer/1704_73017310

where; C_e is the concentration of the material remaining after adsorption (mg/L); q_e is the amount of adsorbed material on unit adsorbent (mg/g); K_f is calculated experimentally. Adsorption capacity (L/g); n is the heterogeneity factor (without unit).

In the Freundlich isotherm, the logarithm of both sides of the *Equation 5* is taken and linearized.

$$q_e = \log K_f + \frac{1}{n} \log C_e \quad \text{(Eq.6)}$$

The K_f and n constants are determined by drawing the change of log q_e according to log C_e. The cut off point of the y-axis of the line obtained from the graph gives log K_f and its curve 1/n (Aksu and Yener, 2001).

Adsorption Kinetics

In order to explain the adsorption of heavy metals on any adsorbent, usually the pseudo-first order and pseudo-second order models are used. In the pseudo-first order model of Lagergren, it is seen that a proportional change occurs in time when solid surface is saturated in different concentrations.

The pseudo-first order equation is given with (*Eq. 7*);

$$\ln(qe - qt) = \ln qe - k1t \quad \text{(Eq.7)}$$

where; q_t is the amount of adsorbate on adsorbent at any time (mg/g); k_1 is the first order kinetic rate constant (min^{-1}).

If a graph is drawn between ln(q_e-q_t) and t, a straight line is obtained. The curve of this line gives the k_1 constant and the point where it cuts the y-axis gives the lnqe value (Lagergren, 1898).

The pseudo-second order equation is given with (*Eq. 8*);

$$\frac{t}{q_t} = \left[\frac{1}{k_2 . q_e 2}\right] + \frac{1}{q_e} . t \quad \text{(Eq.8)}$$

where; k_2 is the second order kinetic rate constant is (gr/mg.min).

When a graph is drawn between t/q_t and t, a straight line is obtained. The curve of this line gives the 1/q_e value and the point where it cuts the y-axis gives the 1/k_2.qe_2 value (Ho and Mckay, 1999).

Results and Discussion

Adsorption Experiments

The most significant factor in heavy metal adsorption is pH. During the experiments, initially concentration, the duration of contact and temperature were kept constant and pH values ranging between 2–10 were used. When heavy metals had a tendency to precipitate at pH 6 or higher, the pH was determined to be 5.5.

The optimum pH was set as 5.5 against the precipitation tendency of heavy metals (Li et al., 2008). Pb(II) or Al(III) solutions were studied for 5–90 min in pH 5.5 with a concentration of 1 ppm and it was established that the optimum duration of contact was 60 min. Furthermore, solutions were prepared with a pH value of 5.5 between the

http://www.aloki.hu ● ISSN 1589 1623 (Print) ● ISSN 1785 0037 (Online)
DOI: http://dx.doi.org/10.15666/aeer/1704_73017310

ranges of 0.5–7 ppm and stirred at 25°C for 60 min in order to examine the concentration changes of Pb(II) and Al(III) ions. At the end of the experiment, it was seen that the optimum concentration was 4 ppm for Pb(II) and 3 ppm for Al(III).

The experiment results in *Figure 2* and *Figure 3* were obtained by working at optimum pH, contact time and initial concentration to investigate the temperature effect of Pb (II) and Al (III) ions on adsorption. The highest adsorption capacities were obtained in experiments conducted in optimum conditions with a pH value of 5.5, an initial concentration of 4 ppm, a temperature of 55°C and with a 60-min stirring time.

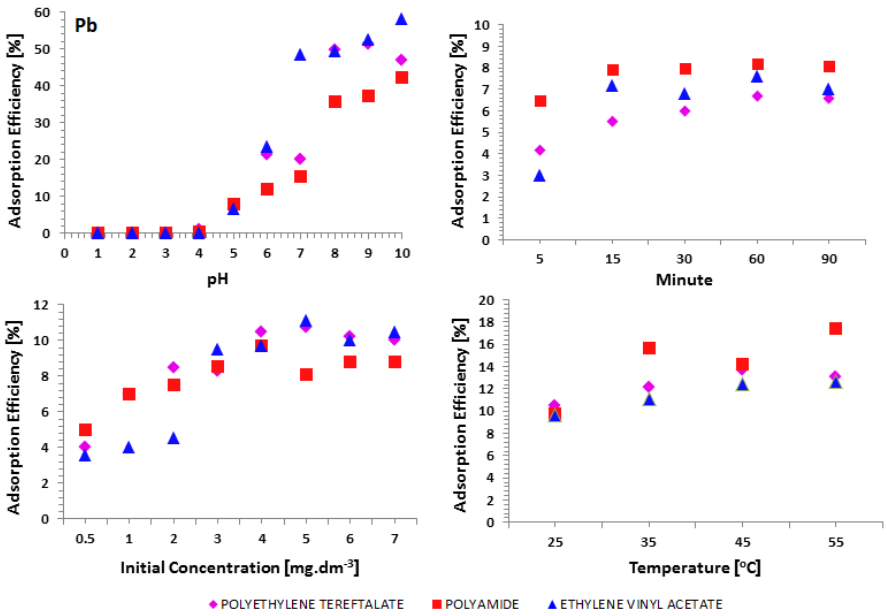

Figure 2. *Pb(II) adsorption temperature (pH: 5.5, time: 60 min, initial concentration: 4 ppm)*

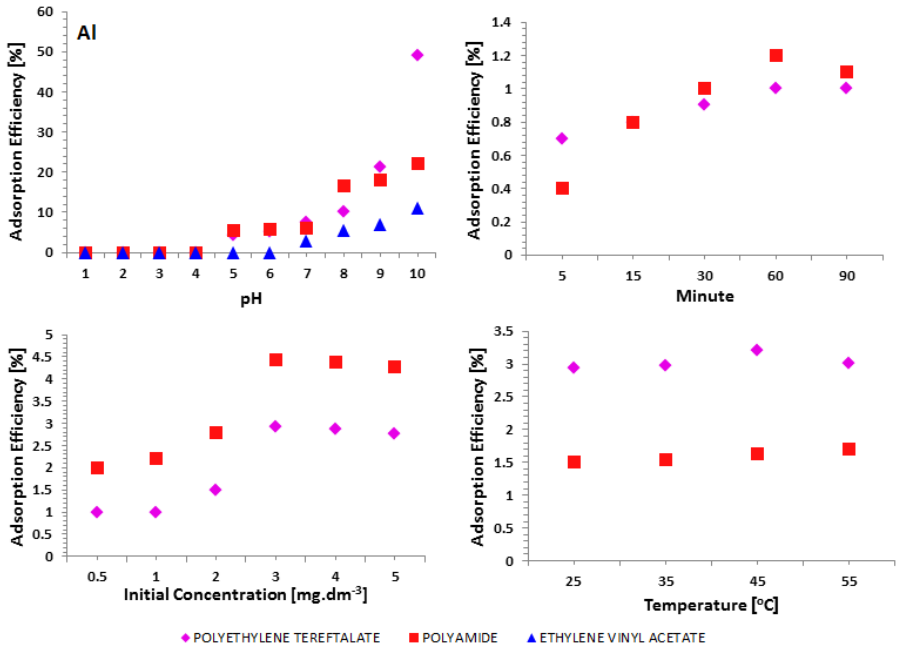

Figure 3. *Al (III) adsorption temperature (pH: 5.5, time: 60 min, initial concentration: 3 ppm)*

http://www.aloki.hu ● ISSN 1589 1623 (Print) ● ISSN 1785 0037 (Online)
DOI: http://dx.doi.org/10.15666/aeer/1704_73017310

It is seen in the graph given in *Figure 2* that the adsorption capacity increased for PET, PA and EVA with increasing temperatures but it was not affected much. The adsorption capacity also changed based on the type of microplastic. The adsorption capacities were detected as PA, PET, and EVA in the descending order. The high adsorption capacity of PA supports the results of other studies in literature (Wang et al., 2015; Li et al., 2018).

Experiments were repeated for the adsorption of PET, PA and EVA on Al(III) and the adsorption of EVA on Al(III) did not occur in any circumstances. It is seen in the graph given in *Figure 3* that the adsorption capacity of PET and PA increased with increasing temperatures but it was not affected much. The adsorption capacity also changed based on the type of microplastic. The adsorption capacity of PET was higher than that of PA in adsorption experiments carried out under the same conditions. The studies suggest that the polarity of MPs can affect the adsorption levels of polar chemicals. Physicochemical properties of MPs may affect the adsorption capacity (Teuten et al., 2009; Wang et al., 2015; Li et al., 2018).

Adsorption isotherm of heavy metals in microplastics

Experiments for adsorption isotherms were carried out in concentrations of 0.5-1-2-3-4-5-6-7 mg/L. When the R^2 values of the Langmuir and Freundlich isotherms were studied in experimental results obtained in adsorption equilibrium state for all three microplastics, it was determined that the regression coefficients of the Freundlich isotherm were higher than the Langmuir isotherm and they were more suitable for the Freundlich isotherm (*Figure 4*). Several studies have reported that the sorption of pollutants on microplastics fit well with Freundlich model (Razanajatovo et al., 2018; Zhang et al., 2018; Llorca et al., 2018; Wu et al., 2019). This indicates that the relationship between microplastics and heavy metals is multi-layer adsorption on heterogeneous surfaces (Andersson et al., 2011).

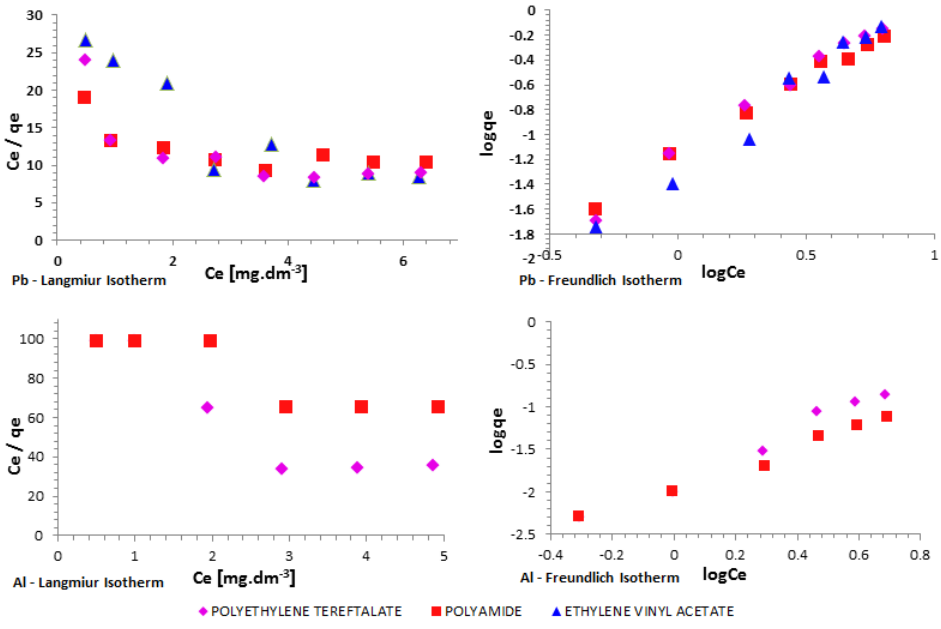

Figure 4. *Adsorption isotherms of Pb(II) and Al(III) onto PET, PA, EVA*

http://www.aloki.hu ● ISSN 1589 1623 (Print) ● ISSN 1785 0037 (Online)
DOI: http://dx.doi.org/10.15666/aeer/1704_73017310

The balance data obtained were applied to the Freundlich and Langmuir models, which are widely used to explain the adsorption process, and the constants of both isotherms were calculated. The predicted Langmuir and Freundlich constants are summarized in *Table 1* and *Table 2*.

Table 1. *Parameters of Langmuir and Freundlich isotherms for Pb(II) adsorption*

Pb	Langmuir Isotherm Constants			Freundlich Isotherm Constants		
	q_{max} (mg / gr)	K_L (L / mg)	R^2	K_f (mg / gr)	n	R^2
PET	-0.551	-0.103	0.526	0.065	0.733	0.988
PA	-0.978	-0.065	0.513	0.069	0.822	0.991
EVA	-0.303	-0.128	0.791	0.047	0.661	0.978

Table 2. *Parameters of Langmuir and Freundlich isotherms for Al(III) adsorption*

Al	Langmuir Isotherm Constants			Freundlich Isotherm Constants		
	q_{max} (mg / gr)	K_L (L / mg)	R^2	K_f (mg / gr)	n	R^2
PET	-0.058	-0.165	0.831	0.012	0.64	0.98
PA	-0.105	-0.089	0.79	0.01	0.821	0.987

Adsorption Kinetic of Microplastics and Heavy Metals

Adsorption kinetics is important when assessing adsorption efficiency. The kinetic study was conducted in order to understand the time-dependent behavior of heavy metal adsorption on microplastics. Adsorption capacities (q_e) and adsorption rate constants (k_1 and k_2) were calculated using the curve values of the lines in the graphs which were drawn by calculating the values corresponding to different adsorption durations (t) and given in *Figure 5*. For Pb(II) and Al(III), the adsorption efficiency in the first 60 min after adsorption experiments began and later it reached adsorption equilibrium and slowed down. Based on these results, a contact duration of 60 min was selected.

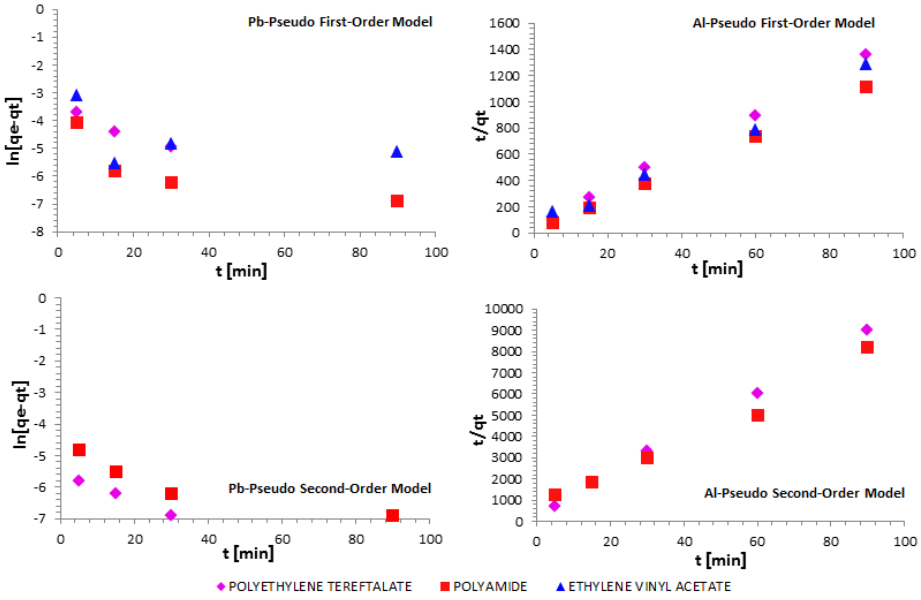

Figure 5. *Pseudo-first order and pseudo-second order kinetic models for Pb(II) and Al(III)*

http://www.aloki.hu ● ISSN 1589 1623 (Print) ● ISSN 1785 0037 (Online)
DOI: http://dx.doi.org/10.15666/aeer/1704_73017310

The pseudo-first and pseudo-second order models determine the adsorption rate. While the adsorption rate is a physical process for the pseudo-first order model, it is a chemical process for the pseudo-second order model involving the adsorbent force (Mohan et al., 2006). Therefore, the data in the kinetic study in *Figure 5* were applied to the pseudo-first and pseudo-second order models to investigate rate limiting mechanisms. The results of the pseudo-first and pseudo-second order models are summarized in *Table 3* and *Table 4* including parameters like k_1 and k_2 and experimental ($q_{e,exp}$). For both metals ($q_{e,cal}$), the values of the balance adsorption amount and the correlation coefficient (R^2) are suitable with the pseudo-second order model, which is higher than the pseudo-first order model.

Table 3. *Parameters of pseudo-first order and pseudo-second order kinetic models for Pb(II)*

Pb			**pseudo first-order (PFO)**			**pseudo second-order (PSO)**		
	Co (mg/L)	$q_{e,exp}$ (mg/gr)	k_1 (1/min)	$q_{e,cal}$ (mg/gr)	R^2	k_2 (gr/mg.min)	$q_{e,cal}$ (mg/gr)	R^2
PET	1	0.067	0.035	0.023	0.982	4.03	0.069	0.999
PA	1	0.082	0.0254	0.007	0.642	14.49	0.082	0.999
EVA	1	0.076	0.0125	0.015	0.196	3.937	0.075	0.989

Table 4. *Parameters of pseudo-first-order and pseudo-second-order kinetic models for Al(III)*

Pb			**pseudo first-order (PFO)**			**pseudo second-order (PSO)**		
	Co (mg/L)	$q_{e,exp}$ (mg/gr)	k_1 (1/min)	$q_{e,cal}$ (mg/gr)	R^2	k_2 (gr/mg.min)	$q_{e,cal}$ (mg/gr)	R^2
PET	1	0.01	0.044	0.003	0.998	26.385	0.01	0.999
PA	1	0.012	0.021	0.006	0.837	9.765	0.012	0.988

Conclusion

Microplastics and heavy metals are sources of pollution in sea and freshwater ecosystems. The interaction between these two pollutants may create a serious problem to aquatic ecosystems. This study investigated the role of PA, PET and EVA in the transport of the heavy metals of Pb and Al to the food chain and in their bioaccumulation.

The adsorption behaviors of 2 heavy metals on 3 types of microplastic pellets were carefully evaluated. Our results showed that adsorption capacities varied among heavy metals, plastic types, and environmental conditions (e.g., pH). Overall, the adsorption percentage in the study was low. In addition, literature studies, laboratory tests and environmental monitoring using plastic pellets have shown that plastics can accumulate metals (Wang et al., 2017). Heavy metals and persistent organic pollutants enter into the food chain and bioaccumulation may occur in living things that swallow these microplastics (Wang et al., 2016). Because of the abundance of plastics in aquatic ecosystem their role in respect of bioaccumulation of a broader range of contaminants merits further study.

http://www.aloki.hu ● ISSN 1589 1623 (Print) ● ISSN 1785 0037 (Online)
DOI: http://dx.doi.org/10.15666/aeer/1704_73017310

Acknowledgements. This research work was supported and granted by the Graduate School of Scientific Research, Project Commission (Proje no: 2017-50-01-069) of Sakarya University.

REFERENCES

[1] Aksu, Z., Yener, J. (2001): A comperative adsorption/biosorption study of mono-chlorinated phenols onto various sorbents. – Waste Management 21: 695-702.
[2] Andersson, K. I., Eriksson, M., Norgren, M. (2011): Removal of lignin from wastewater generated by mechanical pulping using activated carbon and fly ash: adsorption isotherms and thermodynamics. – Ind. Eng. Chem. Res 50: 7722-7732.
[3] Arthur, C., Baker, J., Bamford, H. (eds.) (2008): Proceedings of the International Research Workshop on the Occurrence, Effects and Fate of Micro-plastic Marine Debris. – NOAA Technical Memorandum NOS-OR&R-30, USA.
[4] Aytan, U., Valente, A., Senturk, Y., Usta, R., Sahin, F. B. E., Mazlum, R. E., Agirbas, E. (2016): First evaluation of neustonic microplastics in Black Sea waters. – Marine Environmental Research 119: 22-30.
[5] Boerger, C. M., Lattin, G. L., Moore, S. L., Moore, C. J. (2010): Plastic ingestion by planktivorous fishes in the North Pacific Central Gyre. – Marine Pollution Bulletin 60: 2275-2278.
[6] Brennecke, D., Duarte, B., Paiva, F., Caçador, I., Clode, J. (2016): Microplastics as vector for heavy metal contamination from the marine environment. – Estuarine, Coastal and Shelf Science 178: 189-195.
[7] Cauwenberghe, L. V., Janssen, C. R. (2014): Microplastics in bivalves cultured for human consumption. – Environmental Pollution 193: 65-70.
[8] Digka, N., Tsangaris, C., Torre, M., Anastasopoulou, A., Zeri, C. (2018): Microplastics in mussels and fish from the Northern Ionian Sea. – Marine Pollution Bulletin135: 30-40.
[9] Fu, F., Wang, Q. (2011): Removal of heavy metal ions from wastewaters: A review. – Journal of Environmental Management 92: 407-418.
[10] Galloway, T. S. (2015): Micro- and nano-plastics and human health. – In: Bergmann, M., Gutow, L., Klages, M. (eds.) Marine Anthropogenic Litter. Springer International Publishing: 343-366.
[11] Hamdaoui, O., Naffrechoux, E. (2007): Modeling of adsorption isotherms of phenol and chlorophenols onto granular activated carbon: Part I. Two-parameter models and equations allowing determination of thermodynamic parameters. – Journal of Hazardous Materials 147: 381-394.
[12] Ho, Y. S., Mckay, G. (1999): Pseudo-second order model for sorption processes. – Process Biochemistry 34: 451-465.
[13] Holmes, L. A., Turner, A., Thompson, R. C. (2012): Adsorption of trace metals to plastic resin pellets in the marine environment. – Environmental Pollution 160: 42-48.
[14] Hu, J. Q., Yang, S. Z., Guo, L., Xu, X., Yao, T., Xie, F. (2017): Microscopic investigation on the adsorption of lubrication oil on microplastics. – Journal of Molecular Liquids 227: 351-355
[15] Lagergren, S. (1898): Zur theorie der sogenannten adsorption gelöster stoffe, Kungliga Svenska Vetenskapsakademiens. – Handlingar 24: 1-39.
[16] Li, W., Zhang, L., Peng, J., Li, N., Zhang, S., Guo, S. (2008): Tobacco stems as a low cost adsorbent for the removal of Pb(II) from wastewater: Equilibrium and kinetic studies. – Industrial Crops and Products 28: 294-302.
[17] Li, J., Zhang, K., Zhang, H. (2018): Adsorption of antibiotics on microplastics. – Environmental Pollution 237: 460-467.
[18] Llorca, M., Schirinzi, G., Martínez, M., Barcelo, D., Farre, M. (2018): Adsorption of perfluoroalkyl substances on microplastics under environmental conditions. – Environmental Pollution 235: 680-691.

http://www.aloki.hu ● ISSN 1589 1623 (Print) ● ISSN 1785 0037 (Online)
DOI: http://dx.doi.org/10.15666/aeer/1704_73017310

[19] Mohan, D., Singh, K. P., Singh, V. K. (2006): Trivalent chromium removal from wastewater using low cost activated carbon derived from agricultural waste material and activated carbon fabric cloth. – Journal of Hazardous Materials 135: 280-295.
[20] Ng, K. L., Obbard, J. P. (2006): Prevalence of microplastics in Singapore's coastal marine environment. – Marine Pollution Bulletin 52: 761-767.
[21] Okubo, N., Takahashi, S., Nakano, Y. (2018): Microplastics disturb the anthozoan-algae symbiotic relationship. – Marine Pollution Bulletin 135: 83-89.
[22] Razanajatovoa, R. M., Dinga, J., Zhanga, S., Jianga, H., Zoua, H. (2018): Sorption and desorption of selected pharmaceuticals by polyethylene microplastics. – Marine Pollution Bulletin 136: 516-523.
[23] Teuten, E. L., Saquing, J. M., Knappe, D. R. U., Barlaz, M. A., Jonsson, S., Bjorn, A., Rowland, S. J., Thompson, R. C., Galloway, T. S., Yamashita, R., Ochi, D., Watanuki, Y., Moore, C., Hung, P. V., Tana, T. S., Prudente, M., Boonyatumanond, R., Zakaria, M. P., Akkhavong, K., Ogata, Y., Hirai, H., Iwasa, S., Mizukawa, K., Hagino, Y., Imamura, A., Saha, M., Takada, H. (2009): Transport and release of chemicals from plastics to the environment and to wildlife. – Philos. Trans. R. Soc. B 364: 2027-2045.
[24] Thompson, R. C., Olsen, Y., Mitchell, R. P., Davis, A., Rowland, S. J., John, W. G., McGonicle, D., Russell, A. E. (2004): Lost at sea: where is all the plastic? – Science 304: 838.
[25] Wang, F., Shih, K. M., Li, X. Y. (2015): The partition behavior of perfluorooctanesulfonate (PFOS) and perfluorooctanesulfonamide (FOSA) on microplastics. – Chemosphere 119: 841-847.
[26] Wang, J., Tan, Z., Peng, J., Qiu, Q., Li, M. (2016): The behaviors of microplastics in the marine environment. – Mar. Environ. Res 113: 7-17.
[27] Wang, J., Peng, J., Tan, Z., Gao, Y., Zhan, Z., Chen, Q., Cai, L. (2017): Microplastics in the surface sediments from the Beijiang River littoral zone: Composition, abundance, surface textures and interaction with heavy metals. – Chemosphere 171: 248-258.
[28] Wu, P., Cai, Z., Jin, H., Tang, Y. (2019): Adsorption mechanisms of five bisphenol analogues on PVC microplastics. – Science of the Total Environment 650: 671-678.
[29] Yousefzadeh, H., Salarian, A. A., Kalal, H. S. (2018): Study of Pb (II) adsorption from aqueous solutions by TiO2 functionalized with hydroxide ethyl aniline (PHEA/n-TiO2). – Journal of Molecular Liquids 263: 294-302.
[30] Zhang, H., Wang, J., Zhou, B., Zhou, Y., Dai, Z., Zhou, Q., Chriestie, P., Luo Y. (2018): Enhanced adsorption of oxytetracycline to weathered microplastic polystyrene: Kinetics, isotherms and influencing factors. – Environmental Pollution 243: 1550-1557.

http://www.aloki.hu ● ISSN 1589 1623 (Print) ● ISSN 1785 0037 (Online)
DOI: http://dx.doi.org/10.15666/aeer/1704_73017310

GENETIC POTENTIAL AND ASSOCIATION AMONG MORPHO-PHYSIOLOGICAL TRAITS OF *PETUNIA* INBRED LINES

MAHMOOD, A.[1] – ALI, Q.[2,6*] – AHMAD, S.[1] – BAKHSH, A.[3] – MAHPARA, S.[3] – KAMARAN, S.[3] – MAMOON-UR-RASHID, M.[4] – SALMAN, S.[5] – WASEEM, M.[6] – HAIDER, M. S.[1] – NASIR, I. A.[7]

[1]*Institute of Agricultural Sciences, University of the Punjab Lahore, Lahore, Pakistan*

[2]*Institute of Molecular Biology and Biotechnology, University of Lahore, Lahore, Pakistan*

[3]*Department of Plant Breeding and Genetics, Ghazi University, Dera Ghazi Khan, Pakistan*

[4]*Department of Entomology, Faculty of Agriculture, Gomal University, Dera Ismail Khan, Pakistan*

[5]*Department of Plant Breeding and Genetics, Gomal University, Dera Ismail Khan, Pakistan*

[6]*Department of Agronomy, Faculty Agriculture, Lasbela University of Agriculture, Water and Marine Science, Uthal, Lasbela, Pakistan*

[7]*Centre of Excellence in Molecular Biology, University of the Punjab Lahore, Lahore, Pakistan*

**Corresponding author*
e-mail: saim1692@gmail.com

(Received 7th Feb 2019; accepted 8th Apr 2019)

Abstract. *Petunia hybrida* is considered as an important and beautiful ornamental flowering plant, grown throughout the world for its beauty and attractiveness. Various petunia hybrids have been produced by different countries. The present study was carried out to investigate the higher seed yield petunia line developed through selfing to produce F_1 hybrids during the experimental seasons of the 2011-2014 period. The lines IAGS-P8, IAGS-P9 and IAGS-P11 performed well, both in the cluster analysis and minimum spanning tree, the inbred lines IAGS-P8 and IAGS-P9 showed to a higher similarity percentage. From statistical and regression analysis showed that stomata conductance, chlorophyll 'a' contents, chlorophyll 'b' contents, flowers per plant, flower fresh weight, seed area, seed weight and abscisic acid contributed higher to seed yield per plant in petunia. The higher abscisic acid concentration suggested that the petunia genotypes may be used to develop better seed yields and higher number of flowers per plant in petunia under environmental stress. This method proved to be more efficient as it reduced the cost, time and efficacy for better selection in petunia improvement program. Still, further studies are required which should cover different years and locations.
Keywords: *Petunia hybrida, abscisic acid, multivariate analysis, heritability, genetic advance*

Introduction

Petunia hybrida is an important and the mostly used ornamental plant throughout the world from several years as commercially grown ornamental plant. *Petunia hybrida* is an important and mostly used genera to develop *Petunia* new varieties and hybrids. Griesbach (2007) has reported that *Petunia* has an old history in sense of development as an ornamental plant as compared with new emerging ornamental crops plant species. Ganga et al. (2011) suggested that the production of hybrid seed has been adapted by various ornamental crop plants breeding program to develop new colour and varieties of ornamental plants. It has been found that there are 20 South American origin species of

http://www.aloki.hu ● ISSN 1589 1623 (Print) ● ISSN 1785 0037 (Online)
DOI: http://dx.doi.org/10.15666/aeer/1704_73117332

Petunia (Selaru, 2008), 14 herbaceous species (Toma, 2009). Selaru (2008) reported that the specie *Petunia hybrida* Hort. (*P. axillaris Lam.* × *P. violacea* Lindl.) has been presented with higher decorative value. It has been confirmed from findings of various researchers that the 14 familiar species are consisted of genus *Petunia* (Stehmann et al., 2009). The *Petunia hybrida* Hort. as an ornamental plant species, used as ornamental plant in loans, fields and gardens for its abundant flowering ability (Toma et al., 2011). Dole and Wilkins (1999) reported that most of the *Petunia* species have been developed in Brazil, Uruguay or Argentina. In modern era a large number of cultivars have been developed in the form of varieties, hybrids and cultivars with variety of colors and patterns. Depending on flower size, color and habit, four groups of *Petunias* have been defined as, multiflora, milliflora, grandiflora, ground cover or spreading. Even every year new varieties of *Petunia* have been developed by ornamental breeders (Toma, 2009).

Bender (2006) found that the new and modern species of petunias are hybrids in nature like garden petunia (*Petunia axillaris*) or ambrosial white and violet *petunia* (*P. integrifolia*, and *P. violacea*). The old or wild type *petunia* species, varieties or hybrids use has been less down now a day. *Petunia* is grown throughout the world for its beauty, higher growth rate, different color ranges and continued flowering up to about 6 months of plant life cycle. It blossoms most abundantly under hot summers conditions (Bala, 2012; Selaru, 2008). Erwin (2006) found that the higher blooming ability, *petunia* is even grown in baskets, landscaping by the forms, in alloyed trays on roads and even in room open spaces (Erwin, 2006). The present study was conducted to develop inbred lines of petunia through selfing at growing seasons. The data of various morphological, physiological and seed yield traits was recorded to access the performance of inbred lines under development. The identification of promising inbred lines was also done.

Material and methods

The prescribed study was carried out in the research area of Institute of Agricultural Sciences, University of the Punjab Lahore, Pakistan located at 31.4779° N, 74.2623° E with average higher temperature of about 37 °C with highest up to 45 °C during summer season, 11 °C with lowest 3 °C during winter season. Twelve petunia lines, IAGS-P1, IAGS-P2, IAGS-P3, IAGS-P4, IAGS-P5, IAGS-P6, IAGS-P7, IAGS-P8, IAGS-P9, IAGS-P10, IAGS-P11 and IAGS-P12 were selected and grown in the field during 2014, selfing of all the lines was carried out for three successive growing seasons (2011-13) to develop inbred lines, the selfed seed were collected to develop next generation (*Figs. 1* and *2*). The selfed seed was grown in three replication under completely randomized block design during growing season of 2014, and data for various traits of 10 selected plants from each of three replications was recorded during all three growing seasons and average of data was used for results and interpretation, the traits were included photosynthetic rate (A), leaf temperature (LT), transpiration rate (E), stomata conductance (gs) and Sub-stomata CO_2 Concentration (Ci) through the use of IRGA (Infrared Gas Analyzer, Model: LI-6400XT), chlorophyll 'a' content (Chl. a), chlorophyll 'b' content (Chl. b) in fresh matter was measured using the dimethyl sulfoxide extraction method (Hiscox and Israelstam, 1978), leaves per plant (LPP), plant height (PH), stem diameter (SD), flowers per plant (FPP), leaf length (LL), leaf width (LW), leaf area (LA), fresh leaf weight (FLW), fresh stem weight (FSW), flower

http://www.aloki.hu ● ISSN 1589 1623 (Print) ● ISSN 1785 0037 (Online)
DOI: http://dx.doi.org/10.15666/aeer/1704_73117332

weight (FW), seeds per fruit (SPF), 100-seed weight (HSW), seed area (SA), capsule weight (CW), abscisic acid (ABA) by using HPLC method (Seo and Koshiba, 2002), and seed yield per plant (SYP) were collected. Water use efficiency (WUE) was recorded through using given formula:

$$\text{Water use efficiency } (\%) = \frac{\text{Transpiration rate}}{\text{Photosynthetic rate}} \times 100$$

The collected data was statistically analyzed by using analysis of variance technique, principal component analysis, correlation analysis, regression analysis, factor analysis, spinning tree and cluster analysis (Steel et al., 1997) through using GenStat 18 (SP1) version.

Figure 1. *Twelve lines petunia hybrida grown in filed*

Heritability estimate

Broad sense heritability was calculated by using genotypic, phenotypic and environmental variances according to Burton (1951):

$$\text{Broad sense heritability} = \frac{\left(\partial^2_g + \partial^2_e\right) - \partial^2_e}{\partial^2_g + \partial^2_e} \times 100$$

http://www.aloki.hu ● ISSN 1589 1623 (Print) ● ISSN 1785 0037 (Online)
DOI: http://dx.doi.org/10.15666/aeer/1704_73117332

∂^2_g = genotypic variance, ∂^2_e = environmental variance, $\partial^2_g + \partial^2_e$ = phenotypic variance, $(\partial^2_g + \partial^2_e) - \partial^2_e$ = genotypic variance.

Genetic advance (GA) was calculated by the following formula (Falconer, 1989):

$$GA = \sigma_p x\, h^2 x\, i$$

where: σ_p = the phenotypic standard deviation; h^2 = estimate of broad sense heritability; i = constant value (1.755) that reflects selection intensity (10%).

Figure 2. *Close view of different petunia hybrid in field and pot (for transplanting in field)*

Results and discussions

It was persuaded from the results (*Table 1*) that significant differences were found for all studied traits. Broad sense heritability was found higher for photosynthetic rate (90.825%), stomata conductance (80.268%), sub-stomata CO_2 concentration (96.035%), water use efficiency (89.847%), leaves per plant (98.750%), plant height (92.613%), leaf length (83.584%), flowers per plant (92.911%), leaf area (84.460%), fresh stem weight (85.266%), seeds per fruit (96.379%) and abscisic acid (85.205%) while lower for chlorophyll b (23.527%), leaf width (37.084%), fresh leaf weight (24.074%), flower weight (26.145%), seed area (26.781%) and seed yield per plant (4.359%). Genetic advance was found higher for all of the studied traits seeds per fruit. Higher heritability suggested that the selection of petunia lines on the basis of these traits for the development of hybrids may be fruitful. Various researchers while working on different crop plants have described about higher heritability for these traits as reported in our study (Ali et al., 2013, 2014; Fawad et al., 2017). Higher genetic advance suggested that the selection of lines may also be helpful to develop synthetic varieties. The similar findings for different crops have been reported by various researchers (Ali et al., 2013, 2016). It was found from results (see *Appendix*) that the line IAGS-P8, IAGS-P9 and IAGS-P11 performed better than all other lines. Correlation analysis provides an opportunity to the research to select genotypes of crop plant to improve crop plant growth and production. In our study, significant correlation (*Table 2*) was found for

http://www.aloki.hu ● ISSN 1589 1623 (Print) ● ISSN 1785 0037 (Online)
DOI: http://dx.doi.org/10.15666/aeer/1704_73117332

photosynthetic rate with chlorophyll 'a' contents, sub-stomata CO_2 concentration, water use efficiency, plant height, flowers per plant, leaf width and abscisic acid. Abscisic acid was found to be significantly correlated with most of the studied traits including seed yield per plant. Stomata conductance showed also significant correlation with transpiration rate, water use efficiency, flowers per plant, leaf area, fresh shoot weight, seeds per fruit, abscisic acid and leaf width. Seed yield per plant was significantly correlated with photosynthetic rate, leaf temperature, leaves per plant, stem diameter, seed weight and abscisic acid. The positive and significant correlation suggested that the selection of lines to develop hybrids and synthetic varieties may be helpful to improve the growth and development of petunia, the significant correlation of abscisic acid with morphological, seed yield and physiological traits indicated that the selection of petunia lines on the basis of good abscisic acid production may be fruitful to improve drought tolerance in petunia (Mahmood et al., 2017; Sah et al., 2016; Skubacz et al., 2016; Zao et al., 2016; Saradadevi et al., 2017). Kaczperski et al. (1991) estimated growth of the petunia and development in combined effects of light and temperatures. The adverse effect of an optimum temperature environment for minimum time to *petunia hybrida* was begin to be 25 °C, and a minimum circadian light intensity for adequate growth was begin to be 13 $molm^{-2}$ d^{-1}. The adeptness for petunia to growth and development with increase in light and temperature has afresh been appeared, so there is befalling to optimize development, crop plant growth, crop scheduling and higher with ecology changes in light and increase in temperature. However, the accessible delay of growth and development with top abundance and the access of CO_2 in an optimized environment showed not extensively have adverse effects (Ahmad and Tahir, 2017; Blanchard and Runkle, 2009; Mustafa et al., 2017).

The stepwise regression (*Table 3*) was performed to find out the traits that were highly contributing to the seed yield per plant of petunia, from results it was predicted that stomata conductance (120.311), chlorophyll 'a' contents (2.775), chlorophyll 'b' contents (2.1040, flowers per plant (2.484), flower fresh weight (11.364), seed area (7.062), seed weight (31.497) and abscisic acid (15.356) contributed higher to seed yield per plant in petunia but it could be biased as previous literature also reported the error effect of stepwise regression (El-Badaway and Mehasen, 2011; Ahmad et al.; 2012, 2016) while handling a large number of independent variables. The Intercept = 128.387, $R^2 = 0.832$, Adjust $R^2 = 0.276$ and Standard Error = 0.728 was found with expected regression equation as follows:

$$\begin{aligned} Y = {} & 128.387 + (0.224X_1) + (-0.235\,X_2) + (2.775\,X_3) + (2.2.104X_4) + (120.311X_5) \\ & + (-4.418X_6) + (-0.007X_7) + (-0.070X_8) + (-0.252X_9) + (0.116X_{10}) + (0.004X_{11}) \\ & + (2.484X_{12}) + (-0.115X_{13}) + (-17.234X_{14}) + (-80.073X_{15}) + (11.364X_{16}) + (-10.121X_{17}) \\ & + (0.068X_{18}) + (-12.101X_{19}) + (-0.033X_{20}) + (7.062X_{21}) + (31.497X_{22}) + (15.356X_{23}) \end{aligned}$$

Various researchers have used PCA (Principal Component Analysis) to evaluate the effects of independent traits (*Table 4*) in large number for selecting the fruitful variability percentage from a large population (Fawad et al., 2017; Ali et al., 2014). It has been reported from study conducted by Greenacre (2010) that the eigenvalues (used in PCA) shows the primary importance of numerical diagnostics for assessing the variation which a number of large traits/variables contributed for the dependent structure also to display the data matrix in a graphical form.

http://www.aloki.hu ● ISSN 1589 1623 (Print) ● ISSN 1785 0037 (Online)
DOI: http://dx.doi.org/10.15666/aeer/1704_73117332

Table 1. *Genetic components for various morpho-physiology and yield traits of petunia*

Traits	M.S	G.M ± SE	GV	GCV %	PV	PCV %	EV	ECV %	h^2bs%	GA%
Photosynthetic rate ($\mu gCO_2\ s^{-1}$)	124.356*	15.114 ± 0.0094	40.102	168.621	44.153	176.933	4.051	53.593	90.825	75.097
Leaf temperature (°C)	139.563*	22.184 ± 0.0613	38.703	135.136	62.157	171.255	23.454	105.198	62.267	40.651
Chlorphyll a (mg g^{-1} fr. wt.)	13.467*	3.219 ± 0.0579	4.074	112.848	5.319	128.943	1.245	62.383	76.593	96.905
Chlorphyll b (mg g^{-1} fr. wt.)	17.972*	1.268 ± 0.0386	2.875	135.008	12.221	278.339	9.346	243.404	23.527	91.503
Stomata conductance (mmol $m^{-2}\ s^{-1}$)	1.294*	0.042 ± 0.0068	0.399	361.210	0.497	403.169	0.098	179.089	80.268	324.911
Transpiration rate (mm day^{-1})	1.029*	0.914 ± 0.0176	0.272	55.482	0.485	74.087	0.213	49.097	56.082	77.574
Sub-stomata CO_2 concentration (µmol mol^{-1} CO_2)	238.323*	149.119 ± 0.8165	78.363	72.548	81.598	74.030	3.235	14.740	96.035	10.226
Water use efficiency (%)	37.356*	7.781 ± 0.1471	12.000	132.920	13.356	140.229	1.356	44.682	89.847	84.844
Leaves per plant	234.974*	87.742 ± 0.4714	77.996	94.820	78.983	95.418	0.987	10.669	98.750	17.755
Plant height (cm)	209.803*	53.719 ± 0.0910	68.123	110.474	73.557	114.795	5.434	31.201	92.613	24.974
Stem diameter (cm)	1.073*	0.532 ± 0.0012	0.311	78.057	0.450	93.879	0.139	52.157	69.134	159.345
Flowers per plant	398.244*	147.16 ± 0.4714	129.456	95.819	139.333	99.407	9.877	26.467	92.911	13.651
Leaf length (cm)	36.357*	7.121 ± 0.0216	11.374	134.112	13.608	146.692	2.234	59.435	83.584	85.567
Leaf width (cm)	5.459*	1.618 ± 0.0294	1.162	92.533	3.134	151.951	1.972	120.527	37.084	84.878
Leaf Area (cm^2)	39.023*	6.124 ± 0.1392	12.256	138.894	14.511	151.133	2.255	59.578	84.460	88.879
Fresh leaf weight (g)	3.214*	0.661 ± 0.0249	0.522	89.340	2.169	182.086	1.647	158.662	24.074	95.103
Fresh stem weight (g)	204.224*	46.321 ± 0.0535	64.367	114.352	75.490	123.838	11.123	47.536	85.266	26.413
Flower weight (g)	2.029*	0.636 ± 0.0205	0.348	76.110	1.332	144.736	0.984	124.385	26.145	98.045
Seeds per fruit	998.267*	869.169 ± 0.4714	328.640	61.597	340.986	62.743	12.346	11.939	96.379	3.606
100-seed weight (mg)	65.324*	13.131 ± 0.0082	17.363	120.043	30.597	159.354	13.234	104.801	56.748	45.721
Seed area (mm)	2.091*	0.418 ± 0.0052	0.365	101.044	1.362	195.254	0.997	167.075	26.781	153.556
Seed yield per plant	1.129*	52.213 ± 0.0294	0.099	4.354	1.092	14.462	0.993	13.791	9.066	5.769
Capsule weight (mg)	98.672*	115.121 ± 0.0618	25.447	47.015	47.779	64.423	22.332	44.044	53.259	62.284
Abscisic acid (mg/100 g fresh leaf weigh)	572.897*	127.126 ± 0.0163	180.517	125.221	211.862	135.658	31.345	52.180	85.205	18.906

*Significant at 5% probability level. Mean Sum of Squares (M.S), Grand mean (G.M), Genotypic variance (GV), Genotypic coefficient of variance (GCV %), Phenotypic variance (PV), Phenotypic coefficient of variance (PCV %), Environmental Variance (EV), Environmental coefficient of variance (ECV %), Broad sense heritability (h2bs %), Genetic advance (GA)

http://www.aloki.hu ● ISSN 1589 1623 (Print) ● ISSN 1785 0037 (Online)
DOI: http://dx.doi.org/10.15666/aeer/1704_73117332

Table 2. *Correlation among various morpho-physiology and yield traits of petunia*

Traits	A	LT	Chl. a	Chl. b	gs	E	Ci	WUE	LPP	PH	SD	FPP	LL	LW	LA	FLW	FSW	FW	SPF	HSW	SA	SW	ABA
LT	-0.1013																						
Chl. a	0.8128*	-0.0851																					
Chl. b	-0.0597	-0.2476	-0.0181																				
gs	-0.2867	0.1704	-0.1030	0.4668*																			
E	-0.0079	0.4530*	-0.0727	0.8146*	0.4579*																		
Ci	0.3950*	-0.2423	0.3196*	0.0541	0.3187	0.0697																	
WUE	0.5112*	-0.2758	0.3659*	0.7206*	0.4996*	0.8432*	0.2287																
LPP	0.2184	0.1949	-0.1063	-0.2864	-0.1038	-0.6049*	-0.2114	-0.6657*															
PH	0.4889*	0.0884	0.5840*	-0.3759*	-0.2407	-0.3948*	0.5473*	-0.0364	-0.2126														
SD	-0.0771	0.2057	0.2103	-0.1540	-0.1632	-0.4087*	0.1115	-0.2716	0.0482	0.5810*													
FPP	0.5809*	-0.3171	0.4399*	-0.3461*	0.6668*	-0.2286	-0.1656	-0.4426*	-0.1203	0.1310	0.1846												
LL	0.0572	0.5487*	-0.0572	0.3546*	0.3167	0.5373*	-0.0113	0.3584*	0.1298	0.6172*	0.7836*	-0.3034											
LW	0.4323*	-0.1097	0.2583	0.1649	0.4055*	0.2566	0.5872*	0.3416*	-0.3639*	0.4110*	0.1859	-0.3387	-0.0998										
LA	-0.0988	0.5709*	0.0384	0.4181*	0.4586*	0.6219*	0.2168	0.4765*	-0.0118	0.4380*	0.6828*	-0.4192*	0.9250*	0.2848									
FLW	-0.1776	0.0755	0.2038	0.4141*	0.1044	0.0602	0.1902	0.1690	0.3791	-0.0838	-0.2435	-0.3787*	0.2378	-0.1561	0.1826								
FSW	0.2286	0.0874	-0.0975	0.8117*	0.7284*	0.7186*	-0.1976	0.6657*	0.1219	0.4128*	0.3056	0.7602*	0.5195*	0.3838*	0.6544*	-0.3962*							
FW	-0.3168	0.3892	0.2256	0.5522*	-0.2800	0.5444*	-0.3062	-0.3209	0.1814	0.3695*	0.2475	-0.0049	-0.4342*	0.2129	-0.3496*	-0.2250	0.4368*						
SPF	0.3357*	-0.2624	-0.2190	0.0261	0.6072*	0.2327	-0.3290	0.0701	-0.5112*	-0.0825	-0.2852	0.6372*	-0.0504	-0.2489	-0.1388	-0.2299	0.3457*	-0.0509					
HSW	-0.2110	-0.0802	0.0189	0.2805	0.2698	0.2135	-0.2069	0.1428	0.1302	0.4799*	-0.2091	-0.4771*	0.3224	0.3372	0.4300*	-0.0049	-0.5089*	0.2117	-0.1950				
SA	-0.2123	-0.0176	0.4387*	-0.3649*	-0.3544*	-0.3596*	-0.2203	-0.1311	0.0090	0.4723*	0.5642*	0.2387	-0.3503*	-0.1822	-0.4146*	-0.4584*	0.5161*	0.3473*	-0.0084	-0.3245			
SW	-0.1780	0.5446*	0.1105	0.1083	0.2293*	-0.0731	-0.0224	0.1543	-0.1874	0.1312	0.3928*	-0.1639	-0.4553*	-0.3195	-0.5608*	0.0272	-0.0047	-0.2391	-0.2006	-0.3778*	0.2548		
ABA	0.4873*	0.5678*	0.4295*	0.6059*	0.6105*	0.5155*	0.1939	0.6303*	0.6055*	0.0500	-0.1248	-0.1071	0.2178	0.4029*	0.3521*	-0.1509	0.3672*	-0.0245	0.4402*	0.4521*	-0.0221	0.5046*	
SYP	0.4686*	0.3733*	-0.2753	-0.2215	0.3062	-0.3579*	-0.1311	-0.3978*	0.3493*	-0.0664	0.3580*	-0.0343	-0.1842	-0.1173	-0.2242	-0.4212*	0.1257	0.0152	-0.4284*	-0.0631	0.3865*	0.3295*	0.5632*

*Significant at 5% probability level. A = Photosynthetic rate, LT = Leaf temperature, Chl. a = Chlorophyll 'a' content, Chl. b = Chlorophyll 'b' content, E = transpiration rate, gs = stomata conductance, Ci = Sub-stomata CO_2 Concentration, WUE = water use efficiency, LPP = leaves per plant, PH = Plant height, SD = Stem diameter, FPP = Flowers per plant, LL = Leaf length, LW = Leaf width, LA = Leaf area, FLW = Fresh leaf weight, FSW = Fresh stem weight, FW = Flower weight, SPF = Seeds per fruit, HSW = 100-seed weight, SA = Seed area, CW = Capsule weight, ABA = Abscisic acid, SYP = Seed yield per plant

http://www.aloki.hu ● ISSN 1589 1623 (Print) ● ISSN 1785 0037 (Online)
DOI: http://dx.doi.org/10.15666/aeer/1704_73117332

Table 3. *Stepwise regression analysis for various traits of petunia for seed yield*

	Traits	*Coefficients B*	*Standard error*	*t Stat*	*Cumulative R^2*	*Partial R^2 %*
X_1	Photosynthetic rate	0.224	0.213	1.053	0.403	40.30
X_2	Leaf temperature	-0.235	0.176	-1.330	0.315	31.50
X_3	Chlorphyll a	2.775	2.329	1.192	0.356	35.60
X_4	Chlorphyll b	2.104	1.920	1.096	0.387	38.70
X_5	Stomata conductance	120.311	47.385	2.539	-0.126	12.60
X_6	Transpiration rate	-4.418	3.471	-1.273	0.331	33.10
X_7	Sub-stomata CO_2 concentration	-0.007	0.004	-1.689	-0.233	23.30
X_8	Water use efficiency	-0.070	0.364	-0.191	0.866	86.60
X_9	Leaves per plant	-0.252	0.157	-1.607	0.249	24.90
X_{10}	Plant height	0.116	0.088	1.325	0.277	27.70
X_{11}	Stem diameter	0.004	0.0627	0.068	0.950	95.00
X_{12}	Flowers per plant	2.484	8.886	0.279	0.798	79.80
X_{13}	Leaf length	-0.115	0.096	-1.203	-0.315	31.50
X_{14}	Leaf width	-17.234	17.825	-0.967	0.405	40.50
X_{15}	Leaf area	-80.073	80.280	-0.997	-0.392	39.20
X_{16}	Fresh leaf weight	11.364	11.769	0.966	0.406	40.60
X_{17}	Fresh stem weight	-10.121	5.151	-1.965	-0.144	14.40
X_{18}	Flower weight	0.068	0.1356	0.501	0.643	64.30
X_{19}	Seeds per fruit	-12.101	10.544	-1.148	-0.315	31.50
X_{20}	100-seed weight	-0.033	0.0589	-0.563	0.604	60.40
X_{21}	Seed area	7.062	4.326	1.632	-0.178	17.80
X_{22}	Capsule weight	31.497	18.527	1.701	0.164	16.40
X_{23}	Abscisic acid	15.356	30.458	0.504	0.641	64.10

Intercept = 128.387, R^2 = 0.832, Adjust R^2 = 0.276, Standard Error = 0.728

We performed principle component analysis to investigate the traits contributing higher towards seed yield per plant in petunia, four PCA (*Table 4*) were estimated which diverse variation among the studied traits. The PC1, PC2, PC3 and PC4 contributed variations of 29.60%, 16.60%, 13.90% and 10.5% while their cumulative proportion was 29.6%, 46.20%, 60.10% and 70.60% respectively. PC1 and PC2 contributed higher variation for respective studied traits (*Fig. 3a*) the eigenvalues of PCs was higher than 1 (*Fig. 3b*). Through the use of principle component analysis, principle factor analysis was performed to check the traits that were directly and highly associated with the seed yield per plant in petunia. The highly contributing factor traits from factor 1 which contributes 36.20% in total variation were chlorophyll a, chlorophyll b, stomata conductance, transpiration rate, water use efficiency, leaves per plant, stem diameter, leaf length, leaf area, seed yield per plant and abscisic acid (*Table 5*). Fawad et al. (2017) and Ali et al. (2014) suggested that the selection of genotypes on the basis of factor analysis (traits from factor 1) may be helpful to develop higher yield synthetic varieties and hybrids. The traits in factor 2 (from factor loading *Table 5*) showed that the selection on the basis of these traits will not be useful as segregation takes place in the next generation. The higher performance of petunia genotypes for chlorophyll a, chlorophyll b, stomata conductance, transpiration rate, water use efficiency, leaves per plant, stem diameter, leaf length, leaf area, seed yield per plant and abscisic acid indicated that the accumulation of organic compounds will be higher in the plant body. The accumulation of biomass in plant body is essential for

http://www.aloki.hu ● ISSN 1589 1623 (Print) ● ISSN 1785 0037 (Online)
DOI: http://dx.doi.org/10.15666/aeer/1704_73117332

the proper and enhanced growth and development of petunia (Huang, 2007; Huang and Yeh, 2009; Ali et al., 2011; Munir et al., 2016), the accumulation is generally in the leaf, stem and flowering parts of the plant body. Our findings are well supported by Filipovic et al. (2014) who demonstrated the role of factor analysis for effective selection criteria in maize breeding program. For understanding of the association among the petunia lines, we performed cluster analysis (Mahmood et al., 2016; Khorasani et al., 2011; Mostafavi et al., 2011; Ali et al. 2015, 2016). The results from clustering showed that the petunia lines IAGS-P8 and IAGS-P9 were highly associated with each other as compared with all other petunia lines (*Fig. 4a*) the association was verified through the development of minimum spanning tree (*Fig. 4b*) that showed very less distance between petunia lines IAGS-P8 and IAGS-P9 through the use of eigen values. The results showed that the petunia lines IAGS-P8 and IAGS-P9 may be used as two separate male or female lines to develop petunia hybrids. The petunia line IAGS-P11 performed better for almost all studied traits, it may be used as male to develop good quality petunia hybrids. It also indicated that in future breeding program of IAGS-P8, IAGS-P9 and IAGS-P11, these traits are important for primary selection to increase seed yield per plant of petunia under various environmental regimes. Moreover, this method proved to be more efficient as it reduced the cost, money, time and efficacy for better selection in petunia improvement program because the hybridization procedure of petunia is very difficult. When researcher take important traits like seed yield and flower size in account then there may be a chance to improve yield and quality of petunia. However, further studies are required which should cover different years and locations.

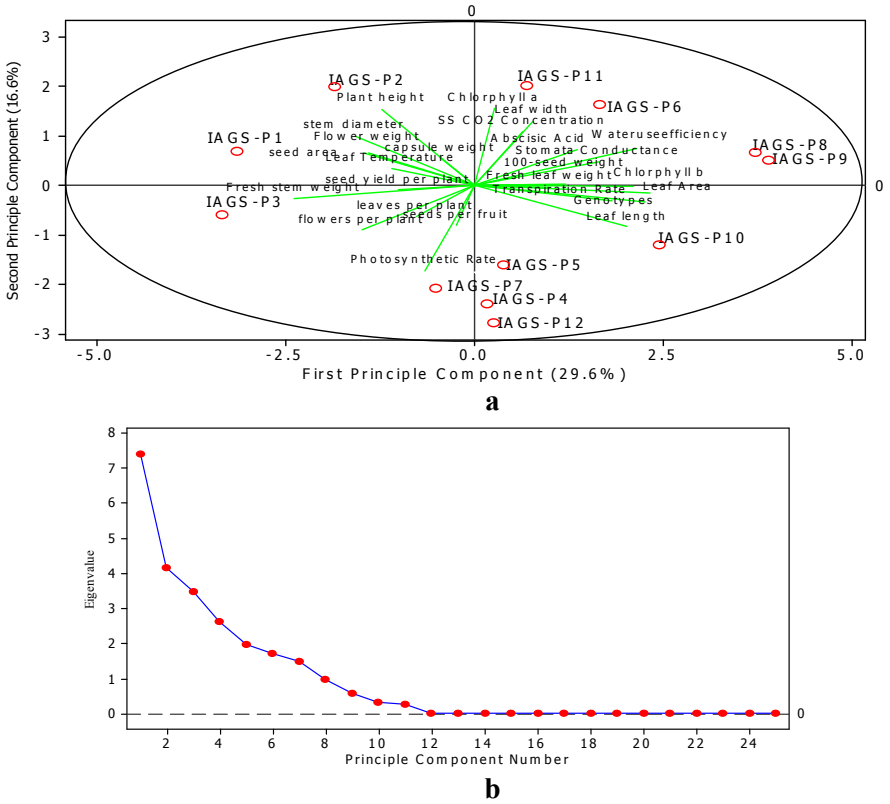

Figure 3. a *Principle component analysis of yield and its attributing traits.* ***b*** *Scree plot and respective eigen values*

http://www.aloki.hu ● ISSN 1589 1623 (Print) ● ISSN 1785 0037 (Online)
DOI: http://dx.doi.org/10.15666/aeer/1704_73117332

Table 4. *Principal component analysis*

Eigen value	7.3977	4.1516	3.4767	2.6343
Proportion	0.296	0.166	0.139	0.105
Cumulative	0.296	0.462	0.601	0.706
Traits	**PC1**	**PC2**	**PC3**	**PC4**
Photosynthetic rate	0.689	0.415	0.016	0.055
Leaf temperature	-0.15	0.083	-0.336	-0.093
Chlorphyll a	0.035	0.376	0.07	0.036
Chlorphyll b	0.286	-0.005	-0.025	-0.217
Stomata conductance	0.221	0.118	-0.297	-0.047
Transpiration rate	0.313	-0.037	0.151	-0.162
Sub-stomata CO2 concentration	0.087	0.263	0.029	0.002
Water use efficiency	0.29	0.183	0.123	-0.202
Leaves per plant	-0.104	-0.15	-0.34	0.257
Plant height	-0.166	0.371	0.137	-0.033
Stem diameter	-0.213	0.243	-0.044	-0.124
Flowers per plant	-0.203	-0.216	0.315	-0.108
Leaf length	0.274	-0.201	-0.01	0.158
Leaf width	0.104	0.313	0.076	0.248
Leaf area	0.305	-0.077	0.018	0.241
Fresh leaf weight	0.136	-0.007	-0.185	-0.041
Fresh stem weight	-0.324	-0.064	0.176	0.002
Flower weight	-0.191	0.16	0.018	0.337
Seeds per fruit	-0.032	-0.196	0.414	-0.134
100-seed weight	0.161	0.009	-0.074	0.371
Seed area	-0.199	0.162	0.082	-0.106
Seed yield per plant	-0.136	-0.021	-0.316	-0.056
Capsule weight	-0.062	0.135	-0.205	-0.499
Abscisic acid	0.184	0.178	0.336	0.075

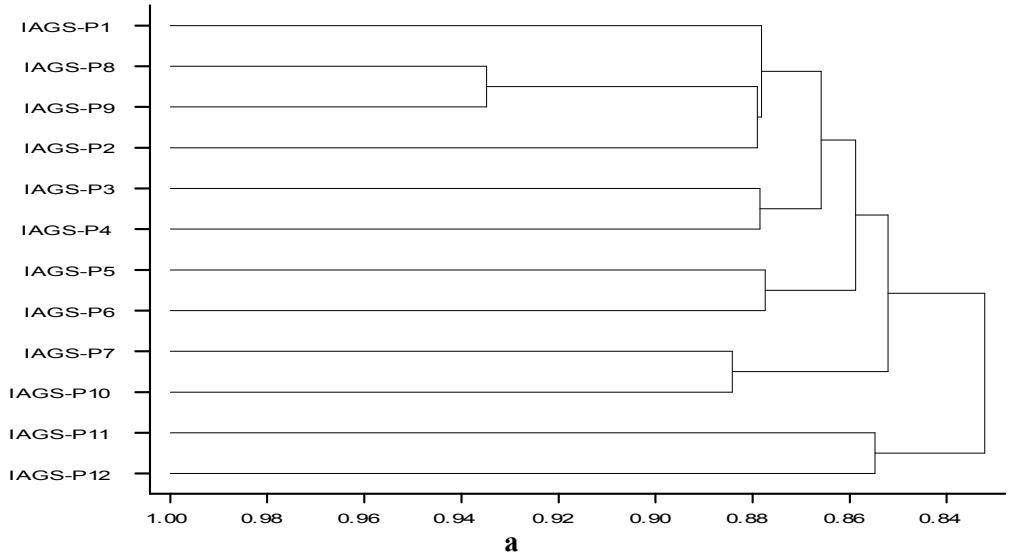

a

http://www.aloki.hu ● ISSN 1589 1623 (Print) ● ISSN 1785 0037 (Online)
DOI: http://dx.doi.org/10.15666/aeer/1704_73117332

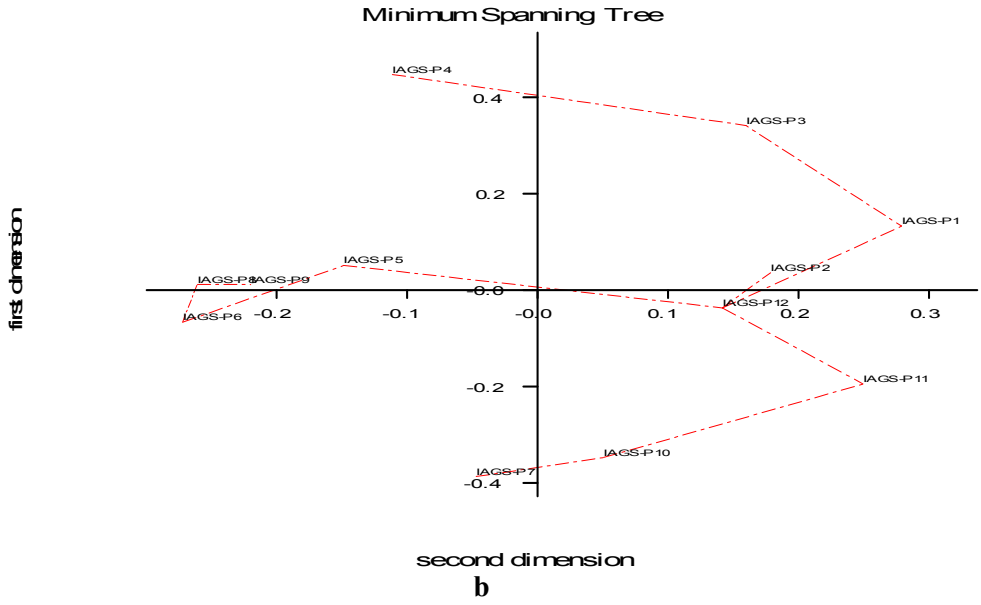

b

Figure 4. a *Dendrogram analysis based on hierarchal clustering. Association of petunia lines on genetic basis of all studied traits.* ***b*** *Minimum spanning tree using egine values for petunia lines on the basis of all studied traits*

Table 5. *Factor loadings for various traits of petunia*

Factor1	Factor loadings	% Communality
Chlorophyll a	0.603	
Chlorophyll b	0.766	
Stomata conductance	0.564	
Transpiration rate	0.873	
Water use efficiency	0.970	
leaves per plant	0.659	
stem diameter	0.929	
Leaf length	0.887	
Leaf area	0.850	
Seed yield per plant	0.867	
Abscisic acid	0.836	
Number of flowers per plant	0.756	36.2
Factor2		
Sub-stomata CO2 concentration	-0.545	
Plant height	-0.894	
Fresh shoot weight	-0.628	27.1
Factor3		
Seed size	0.309	
Leaf length	0.333	
Leaf area	0.307	
Fresh leaf weight	0.369	
Seed per fruit	0.354	13.1
Factor4		
Photosynthetic rate	0.211	
Capsule weight	0.116	
Leaf width	0.129	
stem diameter	0.279	
Leaf temperature	0.217	
Flower weight	0.163	
100-seed weight	0.296	9.40
Cumulative variance		85.80

http://www.aloki.hu ● ISSN 1589 1623 (Print) ● ISSN 1785 0037 (Online)
DOI: http://dx.doi.org/10.15666/aeer/1704_73117332

Conclusion

The present study was carried out to investigate the higher seed yield petunia line during the experimental seasons of 2011-2014. The data for various morphological, physiological and seed yield traits were recorded, analyzed and interpreted for final inferences. It was found that the lines IAGS-P8, IAGS-P9 and IAGS-P11 performed well. From correlation analysis, heritability, genetic advance, principle component analysis, factor analysis and regression analysis that stomata conductance, chlorophyll 'a' contents, chlorophyll 'b' contents, flowers per plant, flower fresh weight, seed area, seed weight and abscisic acid contributed higher to seed yield per plant in petunia. The higher abscisic acid contribution suggested that the petunia genotypes may be used to develop good seed yield per plant and large number of flowers per plant in petunia. The more research and experimentation should be carried out to improve yield and quality of petunia flower.

Conflict of interests. The authors declare the absence of potential conflict of interests.

REFERENCES

[1] Ahmad, A., Tahir, M. (2017): Role of Zinc Sulphate for Maize (Zea mays L.) and Mungbean (Vigna radiata L. Wilczek) yield improvement: a review. – Bulletin of Biological and Allied Sciences Research 2: 1-17.

[2] Ahmad, H. M., Ahsan, M., Ali, Q., Javed, I. (2012): Genetic variability, heritability and correlation studies of various quantitative traits of mungbean (Vigna radiate L.) at different radiation levels. – International Research Journal of Microbiology 3(11): 352-362.

[3] Ali, F., Kanwal, N., Ahsan, M., Ali, Q., Bibi, I., Niazi, N. K. (2015): Multivariate analysis of grain yield and its attributing traits in different maize hybrids grown under heat and drought stress. – Scientifica. http://dx.doi.org/10.1155/2015/563869.

[4] Ali, Q., Ahsan, M., Hussain, B., Elahi, M., Khan, N. H., Ali, F., Elahi, F., Shahbaz, M., Ejaz, M., Naees, M. (2011): Genetic evaluation of maize (Zea mays L.) accessions under drought stress. – International Research Journal of Microbiology 11: 437-441.

[5] Ali, Q., Ahsan, M., Ali, F., Aslam, M., Khan, N. H., Munzoor, M., Mustafa, H. S. B., Muhammad, S. (2013): Heritability, heterosis and heterobeltiosis studies for morphological traits of maize (Zea mays L.) seedlings. – Advancements in Life Sciences 1(1): 52-63.

[6] Ali, Q., Ali, A., Ahsan, M., Ali, S., Khan, N. H., Muhammad, S., Abbas, H. G., Nasir, I. A., Husnain, T. (2014): Line × Tester analysis for morpho-physiological traits of *Zea mays* L. seedlings. – Advancements in Life Sciences 1(4): 242-253.

[7] Ali, Q., Ahsan, M., Malook, S., Kanwal, N., Ali, F., Ali, A., Ahmed, W., Ishfaq, M., Saleem, M. (2016): Screening for drought tolerance: comparison of maize hybrids under water deficit condition. – Advancements in Life Sciences 3(2): 51-58.

[8] Bala, M. (2012): Floriculture General and Special. – Partos Timisoara.

[9] Bender, S. (2006): New Types of Perfect Petunias. – Issue of Southern Living. www.southernliving.com/.../new-typesperfect.

[10] Blanchard, M., Runkle, E. (2009): Energy efficient annuals part 6: Petunias. – Greenhouse Grower 27(9): 36-41.

[11] Burton, G. W. (1951): Quantitative Inheritance in pearl millet (*Pennisetum glaucum* L) 1. – Agronomy Journal 43(9): 409-417.

http://www.aloki.hu ● ISSN 1589 1623 (Print) ● ISSN 1785 0037 (Online)
DOI: http://dx.doi.org/10.15666/aeer/1704_73117332

[12] Dole, J., Wilkins, H. (1999): Floriculture Principles and Species. – Prentice Hall, Upper Saddle River, NJ.
[13] EL-Badawy, M. E. M., Mehasen, S. A. S. (2011): Multivariate analysis for yield and its components in maize under zinc and nitrogen fertilization levels. – Australian Journal of Basic and Applied Sciences 5: 3008-3015.
[14] Erwin, J. (2006): Flower Breeding and Genetics. Factor Affecting Flowering in Ornamental Plants. – In: Anderson, N. O. (ed.) Flower Breeding and Genetics: Issues, Challenges and Opportunities for the 21st Century. Springer Netherlands.
[15] Falconer, D. S. (1989): Introduction to Quantitative Genetics. 3rd Ed. – Longman Scientific & Technical, Harlow.
[16] Fawad, A., Ahsan, M., Ali, Q., Kanwal, N. (2017): Phenotypic stability of Zea mays grain yield and its attributing traits under drought stress. – Frontiers in Plant Science 8: 1397.
[17] Filipovic, M., Babic, M., Delic, N., Bekavac, G., Babic, V. (2014): Determination of relevant breeding criteria by the path and factor analysis in maize. – Genetika 46: 41-49.
[18] Ganga, M., Jayalakshmi, S., Jegadeeswari, K., Padmadevi, K., Jawaharlal, M. (2011): Petunia. – In: Kole, C. (ed). Wild Crop Relatives: Genomic and Breeding Resources Plantation and Ornamental Crop. Springer, Berlin.
[19] Greenacre, M. (2010): Niplots in Practice. – BBVA Foundation, Madrid. www.multivariatestatistics.org.
[20] Griesbach, J. R. (2007): Petunia. – In: Anderson, N. O. (ed.) Flower Breeding and Genetics. – Springer, Netherlands, pp: 301-336.
[21] Hiscox, J. D., Israelstam, G. F. (1978): A method for the extraction of chlorophyll from leaf tissue without maceration. – Canadian Journal of Botany 57: 1332-1334.
[22] Huang, L. C. (2007): Behavioral differences in pre-purchase processes between purchasers of flowers for self use and for gift use. – Horticultural Technology 17: 183-190.
[23] Huang, L. C., Yeh, T. F. (2009): Floral consumption values for consumer groups with different purchase choices for flowers. – Horticulture Technology 19: 563-571.
[24] Kaczperski, M. P., Carlson, W. H., Karlsson, M. G. (1991): Growth and development of Petunia. hybrids as a function of temperature and irradiance. – Journal of American Society of Horticultural Sciences 116: 232-237.
[25] Khorasani, S. K., Mostafavi, K., Zandipour, E., Heidarian, K. (2011): Multivariate analysis of agronomic traits of new corn hybrids (*Zea mays* L.). – International Journal of Agricultural Sciences 1: 314-322.
[26] Mahmood, A., Haider, M. S., Ali, Q., Nasir, I. A. (2017): Multivariate analysis to assess abscisic acid content association with different physiological and plant growth related traits of Petunia. – Acta Agriculturae Slovenica 109(2): 175-186.
[27] Mahmood, Z., Afzal, M., Ahmad, M., Munir, M. A., Ali, M. I., Sharif, M. N., Maqbool, R. (2016): Genetic analysis for morphological traits of *Euphorbia helioscopia*. – Bulletin of Biological and Allied Sciences Research 1: 5.
[28] Mostafavi, K., Shoahosseini, M., Geive, H. S. (2011): Multivariate analysis of variation among traits of corn hybrids traits under drought stress. – International Journal of Agricultural Sciences 1: 416-422.
[29] Munir, M. A., Ahmad, M., Ali, M. I., Mahmood, Z., Afzal, M., Sharif, M. N., Aslam, M. (2016): Correlation and regression analysis of morphological traits in *Rumex dentatus*. – Bulletin of Biological and Allied Sciences Research 1: 2.
[30] Mustafa, H. S. B., Tariq, M., Ahsan, U., Amjad, S., Abdul, N. B., Muhammad, N., Rahat, A. (2017): Role of seed priming to enhance growth and development of crop plants against biotic and abiotic stresses. – Bulletin of Biological and Allied Sciences Research 2: 1-11.
[31] Sah, S. K., Reddy, K. R., Li, J. (2016): Abscisic acid and abiotic stress tolerance in crop plants. – Frontiers in Plant Science 7: 571.

http://www.aloki.hu ● ISSN 1589 1623 (Print) ● ISSN 1785 0037 (Online)
DOI: http://dx.doi.org/10.15666/aeer/1704_73117332

[32] Saradadevi, R., Palta, J. A., Siddique, K. H. (2017): ABA-mediated stomatal response in regulating water use during the development of terminal drought in wheat. – Frontiers in Plant Science 8: 1251.
[33] Selaru, E. (2008): Culture Flowers for Garden. – Ceres, Bucharest.
[34] Seo M and Koshiba T (2002): Complex regulation of ABA biosynthesis in plants. – Trends in Plant Science 7(1): 41-8.
[35] Skubacz, A., Daszkowska-Golec, A., Szarejko, I. (2016): The role and regulation of ABI5 (ABA-Insensitive 5) in plant development, abiotic stress responses and phytohormone crosstalk. – Frontiers in Plant Science 7: 1884.
[36] Steel, R. G. D., Torrie, J. H., Dicky, D. A. (1997): Principles and Procedures of Statistics. A Biometrical Approach. 3rd Ed. – McGraw Hill, New York, pp: 400-428.
[37] Stehmann, J. R., Forzza, R. C., Salino, A., Sobral, M., da Costa, D. P., Kamino, L. H. (eds.) Plantas, da floresta Atlântica. – Jardim Botânico do Rio de Janeiro, Rio de Janeiro.
[38] Stuurman, J., Hoballah, M. E., Broger, L., Moore, J., Basten, C., Kuhlemeier, C. (2004): Dissection of floral pollination syndromes in Petunia. – Genetics 168: 1585-1599.
[39] Toma, F. (2009): Floriculture and Floral Art. – INVEL Multimedia, Bucharest.
[40] Toma, F., Vasilescu, T., Petra, S., Zamfir-Vasca, D. (2011): Research concerning the propagation by cutting of some new cultivars of petunia. – USAMV Bucharest Seria B 55: 253-256.
[41] Zhao, Y., Wang, Y., Yang, H., Wang, W., Wu, J., Hu, X. (2016): Quantitative proteomic analyses identify ABA-related proteins and signal pathways in maize leaves under drought conditions. – Frontiers in Plant Science 7: 1827.

APPENDIX

1. Photosynthetic rate

Genotypes mean homogeneous groups

IAGS-P11 19.578 A
IAGS-P8 19.267 B
IAGS-P9 18.245 C
IAGS-P7 16.888 D
IAGS-P4 16.102 E
IAGS-P5 15.334 F
IAGS-P3 13.572 G
IAGS-P10 11.245 H
IAGS-P1 11.112 I
IAGS-P6 9.9033 J
IAGS-P2 9.1093 K
IAGS-P12 8.8883 L
Alpha 0.05 Standard Error for Comparison 9.393E-03

2. Leaf temperature

Genotypes mean homogeneous groups

IAGS-P11 24.620 A
IAGS-P8 24.175 B
IAGS-P9 23.835 C
IAGS-P3 23.730 C
IAGS-P1 22.176 D
IAGS-P2 21.428 E

http://www.aloki.hu ● ISSN 1589 1623 (Print) ● ISSN 1785 0037 (Online)
DOI: http://dx.doi.org/10.15666/aeer/1704_73117332

IAGS-P4 21.166 F
IAGS-P10 19.288 G
IAGS-P5 18.951 H
IAGS-P12 18.930 H
IAGS-P7 18.288 I
IAGS-P6 17.732 J
Alpha 0.05 Standard Error for Comparison 0.0613

3. Chlorphyll a

Genotypes mean homogeneous groups

IAGS-P11 3.5467 A
IAGS-P12 3.5267 AB
IAGS-P9 3.5167 AB
IAGS-P8 3.4267 B
IAGS-P7 3.1867 C
IAGS-P2 3.1667 CD
IAGS-P3 3.0867 CDE
IAGS-P1 3.0867 CDE
IAGS-P4 3.0567 DE
IAGS-P5 3.0367 E
IAGS-P10 3.0067 E
IAGS-P6 2.7467 F
Alpha 0.05 Standard Error for Comparison 0.0579

4. Chlorphyll b

Genotypes mean homogeneous groups

IAGS-P11 1.9267 A
IAGS-P9 1.9067 A
IAGS-P8 1.9067 A
IAGS-P6 1.8167 B
IAGS-P10 1.7567 B
IAGS-P12 1.5967 C
IAGS-P2 1.4167 D
IAGS-P4 1.4067 D
IAGS-P1 1.3667 DE
IAGS-P5 1.3067 EF
IAGS-P7 1.2667 F
IAGS-P3 1.2567 F
Alpha 0.05 Standard Error for Comparison 0.0386

5. Stomata conductance

Genotypes mean homogeneous groups

IAGS-P11 0.0567 A
IAGS-P7 0.0433 AB
IAGS-P9 0.0400 BC
IAGS-P8 0.0367 BCD
IAGS-P10 0.0367 BCD
IAGS-P1 0.0267 CDE
IAGS-P12 0.0267 CDE
IAGS-P6 0.0267 CDE

http://www.aloki.hu ● ISSN 1589 1623 (Print) ● ISSN 1785 0037 (Online)
DOI: http://dx.doi.org/10.15666/aeer/1704_73117332

IAGS-P3 0.0233 DE
IAGS-P2 0.0200 E
IAGS-P4 0.0167 E
IAGS-P5 0.0133 E
Alpha 0.05 Standard Error for Comparison 6.804E-03

6. Transpiration rate

Genotypes mean homogeneous groups

IAGS-P10 1.4567 A
IAGS-P11 1.4500 A
IAGS-P8 1.3933 B
IAGS-P9 1.2500 C
IAGS-P5 0.8633 D
IAGS-P1 0.8267 E
IAGS-P12 0.7733 F
IAGS-P7 0.7700 F
IAGS-P6 0.6833 G
IAGS-P2 0.5233 H
IAGS-P4 0.5167 H
IAGS-P3 0.0967 I
Alpha 0.05 Standard Error for Comparison 0.0176

7. Sub-stomata CO_2 concentration

Genotypes mean homogeneous groups

IAGS-P11 255.00 A
IAGS-P8 247.33 B
IAGS-P12 237.00 C
IAGS-P9 205.33 D
IAGS-P10 181.00 E
IAGS-P3 174.00 F
IAGS-P1 148.00 G
IAGS-P2 143.33 H
IAGS-P4 68.667 I
IAGS-P6 66.000 J
IAGS-P5 33.333 K
IAGS-P7 27.667 L
Alpha 0.05 Standard Error for Comparison 0.8165

8. Water use efficiency

Genotypes mean homogeneous groups

IAGS-P11 14.641 A
IAGS-P8 12.953 B
IAGS-P9 8.7000 C
IAGS-P7 8.2507 D
IAGS-P1 7.4390 E
IAGS-P6 6.3847 F
IAGS-P2 5.7450 G
IAGS-P10 5.0213 H
IAGS-P5 4.7317 H
IAGS-P12 4.2437 I

http://www.aloki.hu ● ISSN 1589 1623 (Print) ● ISSN 1785 0037 (Online)
DOI: http://dx.doi.org/10.15666/aeer/1704_73117332

IAGS-P4 2.6817 J
IAGS-P3 0.7123 K
Alpha 0.05 Standard Error for Comparison 0.1471

9. Leaves per plant

Genotypes mean homogeneous groups

IAGS-P9 91.333 A
IAGS-P11 91.333 A
IAGS-P8 90.333 B
IAGS-P2 89.333 C
IAGS-P7 88.333 D
IAGS-P4 87.333 E
IAGS-P12 86.333 F
IAGS-P6 85.333 G
IAGS-P5 84.333 H
IAGS-P3 83.333 I
IAGS-P10 82.333 J
IAGS-P1 81.333 K
Alpha 0.05 Standard Error for Comparison 0.4714

10. Plant height

Genotypes mean homogeneous groups

IAGS-P11 62.357 A
IAGS-P9 62.247 A
IAGS-P8 61.127 B
IAGS-P3 60.247 C
IAGS-P4 59.997 D
IAGS-P12 59.347 E
IAGS-P5 56.797 F
IAGS-P7 52.367 G
IAGS-P10 51.947 H
IAGS-P6 49.017 I
IAGS-P1 47.357 J
IAGS-P2 47.017 K
Alpha 0.05 Standard Error for Comparison 0.0910

11. Stem diameter

Genotypes mean homogeneous groups

IAGS-P11 0.5967 A
IAGS-P9 0.5733 B
IAGS-P8 0.5507 C
IAGS-P3 0.5480 D
IAGS-P6 0.5210 E
IAGS-P4 0.5120 F
IAGS-P2 0.5047 G
IAGS-P7 0.4930 H
IAGS-P12 0.4920 H
IAGS-P5 0.4550 I
IAGS-P10 0.4433 J
IAGS-P1 0.4420 J

http://www.aloki.hu ● ISSN 1589 1623 (Print) ● ISSN 1785 0037 (Online)
DOI: http://dx.doi.org/10.15666/aeer/1704_73117332

Alpha 0.05 Standard Error for Comparison 1.217E-03

12. Flowers per plant

Genotypes mean homogeneous groups

IAGS-P11 147.33 A
IAGS-P9 146.33 B
IAGS-P8 145.33 C
IAGS-P12 141.33 D
IAGS-P3 141.33 D
IAGS-P1 140.33 E
IAGS-P6 139.33 F
IAGS-P2 139.33 F
IAGS-P4 139.33 F
IAGS-P5 138.33 G
IAGS-P7 137.33 H
IAGS-P10 136.33 I
Alpha 0.05 Standard Error for Comparison 0.4714

13. Leaf length

Genotypes mean homogeneous groups

IAGS-P8 7.000 A
IAGS-P11 6.9100 B
IAGS-P12 6.3400 C
IAGS-P9 6.1500 D
IAGS-P5 6.1000 E
IAGS-P6 6.0900 E
IAGS-P7 6.0400 F
IAGS-P2 5.8900 G
IAGS-P10 5.8900 G
IAGS-P4 5.2100 H
IAGS-P1 5.1600 I
IAGS-P3 5.1300 I
Alpha 0.05 Standard Error for Comparison 0.0216

14. Leaf width

Genotypes mean homogeneous groups

IAGS-P11 1.1033 A
IAGS-P8 1.1033 A
IAGS-P9 1.1033 A
IAGS-P10 1.0833 AB
IAGS-P3 1.0633 ABC
IAGS-P1 1.0433 BCD
IAGS-P6 1.0333 BCD
IAGS-P5 1.0133 CDE
IAGS-P12 1.0033 DEF
IAGS-P4 0.9733 EF
IAGS-P2 0.9733 EF
IAGS-P7 0.9533 F
Alpha 0.05 Standard Error for Comparison 0.0249

http://www.aloki.hu ● ISSN 1589 1623 (Print) ● ISSN 1785 0037 (Online)
DOI: http://dx.doi.org/10.15666/aeer/1704_73117332

15. Leaf area

Genotypes mean homogeneous groups

IAGS-P11 7.423 A
IAGS-P8 6.603 B
IAGS-P9 6.107 C
IAGS-P12 5.847 CD
IAGS-P2 5.837 CDE
IAGS-P6 5.677 DE
IAGS-P7 5.667 DE
IAGS-P5 5.557 E
IAGS-P10 4.850 F
IAGS-P1 4.703 F
IAGS-P3 4.413 G
IAGS-P4 3.990 H
Alpha 0.05 Standard Error for Comparison 0.1392

16. Fresh leaf weight

Genotypes mean homogeneous groups

IAGS-P9 0.7660 A
IAGS-P11 0.7120 AB
IAGS-P8 0.7100 AB
IAGS-P10 0.6920 B
IAGS-P7 0.6880 B
IAGS-P12 0.6840 B
IAGS-P5 0.6680 BC
IAGS-P3 0.6600 BC
IAGS-P4 0.6220 CD
IAGS-P2 0.5880 D
IAGS-P6 0.5760 D
IAGS-P1 0.4860 E
Alpha 0.05 Standard Error for Comparison 0.0294

17. Fresh stem weight

Genotypes mean homogeneous groups

IAGS-P8 52.610 A
IAGS-P11 51.960 B
IAGS-P9 51.190 C
IAGS-P1 50.070 D
IAGS-P2 49.960 DE
IAGS-P12 49.940 E
IAGS-P6 49.940 E
IAGS-P4 49.940 E
IAGS-P3 47.740 F
IAGS-P5 47.440 G
IAGS-P10 45.410 H
IAGS-P7 44.490 I
Alpha 0.05 Standard Error for Comparison 0.0535

18. Flower weight

http://www.aloki.hu ● ISSN 1589 1623 (Print) ● ISSN 1785 0037 (Online)
DOI: http://dx.doi.org/10.15666/aeer/1704_73117332

Genotypes mean homogeneous groups

IAGS-P9 0.6633 A
IAGS-P11 0.6233 AB
IAGS-P3 0.6143 BC
IAGS-P8 0.6143 BC
IAGS-P4 0.6053 BC
IAGS-P6 0.5963 BCD
IAGS-P2 0.5943 BCD
IAGS-P10 0.5923 BCD
IAGS-P1 0.5903 BCD
IAGS-P5 0.5863 BCD
IAGS-P12 0.5763 CD
IAGS-P7 0.5593 D
Alpha 0.05 Standard Error for Comparison 0.0205

19. Seeds per fruit

Genotypes mean homogeneous groups

IAGS-P11 872.33 A
IAGS-P9 871.33 B
IAGS-P8 870.33 C
IAGS-P1 867.33 D
IAGS-P12 867.33 D
IAGS-P10 866.33 E
IAGS-P2 866.33 E
IAGS-P5 865.33 F
IAGS-P5 864.33 G
IAGS-P4 863.33 H
IAGS-P7 862.33 I
IAGS-P3 857.33 J
Alpha 0.05 Standard Error for Comparison 0.4714

20. 100-seed weight

Genotypes mean homogeneous groups

IAGS-P11 12.130 A
IAGS-P8 12.120 AB
IAGS-P9 12.110 BC
IAGS-P1 12.100 CD
IAGS-P7 12.090 DE
IAGS-P10 12.080 E
IAGS-P2 12.080 E
IAGS-P12 12.020 F
IAGS-P3 12.010 F
IAGS-P6 11.990 G
IAGS-P5 11.970 H
IAGS-P4 11.890 I
Alpha 0.05 Standard Error for Comparison 8.165E-03

21. Seed area

Genotypes mean homogeneous groups

http://www.aloki.hu ● ISSN 1589 1623 (Print) ● ISSN 1785 0037 (Online)
DOI: http://dx.doi.org/10.15666/aeer/1704_73117332

IAGS-P11 0.3753 A
IAGS-P9 0.3723 A
IAGS-P8 0.3693 AB
IAGS-P12 0.3683 ABC
IAGS-P1 0.3653 ABCD
IAGS-P2 0.3593 BCD
IAGS-P3 0.3583 CD
IAGS-P6 0.3563 DE
IAGS-P4 0.3463 EF
IAGS-P7 0.3433 F
IAGS-P5 0.3393 FG
IAGS-P10 0.3323 G
Alpha 0.05 Standard Error for Comparison 5.249E-03

22. Seed weight

Genotypes mean homogeneous groups

IAGS-P11 116.20 A
IAGS-P4 115.98 B
IAGS-P8 115.85 C
IAGS-P9 115.40 D
IAGS-P12 115.32 D
IAGS-P7 115.32 D
IAGS-P6 115.31 D
IAGS-P10 115.06 E
IAGS-P1 114.87 F
IAGS-P2 114.32 G
IAGS-P3 114.26 G
IAGS-P5 113.63 H
Alpha 0.05 Standard Error for Comparison 0.0618

23. Abscisic acid

Genotypes mean homogeneous groups

IAGS-P11 0.1250 A
IAGS-P8 0.1240 AB
IAGS-P9 0.1240 AB
IAGS-P10 0.1230 AB
IAGS-P3 0.1230 AB
IAGS-P1 0.1220 AB
IAGS-P12 0.1210 B
IAGS-P4 0.1140 C
IAGS-P5 0.1110 CD
IAGS-P6 0.1100 D
IAGS-P7 0.1090 D
IAGS-P2 0.1030 E
Alpha 0.05 Standard Error for Comparison 1.633E-03

24. Seed yield per plant

Genotypes mean homogeneous groups

IAGS-P11 54.153 A
IAGS-P9 53.353 B

http://www.aloki.hu ● ISSN 1589 1623 (Print) ● ISSN 1785 0037 (Online)
DOI: http://dx.doi.org/10.15666/aeer/1704_73117332

IAGS-P8 52.263 C
IAGS-P6 52.143 D
IAGS-P2 51.263 E
IAGS-P5 51.263 E
IAGS-P10 50.153 F
IAGS-P7 49.593 G
IAGS-P1 48.923 H
IAGS-P12 48.703 I
IAGS-P3 46.263 J
IAGS-P4 43.603 K
Alpha 0.05 Standard Error for Comparison 0.0249

http://www.aloki.hu ● ISSN 1589 1623 (Print) ● ISSN 1785 0037 (Online)
DOI: http://dx.doi.org/10.15666/aeer/1704_73117332

FINE SCREENING FOR RESISTANCE TO COLD-INDUCED SWEETENING IN A WILD POTATO POPULATION

ALI, A.[1,2,4] – ALI, Q.[3,4*] – IQBAL, M. S.[3] – NASIR, I. A.[3] – WANG, X.[1*]

[1]*Department of Plant Pathology, China Agricultural University, No. 2 West Yuanmingyuan Road Haidian District, 100093 Beijing, China*

[2]*1-FB Genetics, Four Brothers Group, Lahore, Pakistan*

[3]*Centre of Excellence in Molecular Biology, University of the Punjab Lahore, Punjab, Pakistan*

[4]*Institute of Molecular Biology and Biotechnology, University of Lahore, Lahore, Punjab, Pakistan*

**Corresponding authors*
e-mail: wxd_210@126.com, saim1692@gmail.com

(Received 12th Feb 2019; accepted 8th Apr 2019)

Abstract. Potato is the most important indispensable part of human food. Cold induced sweetening is a phenomenon in which reducing sugars react with free available amino acid and give brown to black color when fried at high temperature which is not acceptable at end consumers. Moreover, acrylamide a potent carcinogenic is also produced during this process. So many wild and cultivated species have been utilized for screening the best potato germplasm against many potato diseases and quality but only a small sample of the available biodiversity has been exploited. An effort was made in this study to sort out the best potato germplasm from five different wild families on the basis of fine Molecular screening at different research station against cold induced sweetening. Crosses were made between potato families and then stored at 4 °C. Total RNA was isolated for Quantification of mRNA. Protein was isolated and invertase activity was measured through Plate reader at 5.9 λ. Sucrose and reducing sugars were measured through High Performance Liquid Chromatography. After 4 months of 4 °C storage incubation families were screened on the basis of chips color, invertase enzyme activity, Sucrose, reducing sugars contents and mRNA expression level. Resistance against cold induced sweetening was genotype and trial dependent especially for chip color. Invertase activity was corresponding with genotypes and trails. Locations with good chip color were having low invertase action and reducing sugars along with low mRNA expression of invertase enzyme while at other locations vice versa. Same genotype showed variable resistance at different trial satiations and conclusively invertase activity was genotypes and trials dependent. Significant trial effects were detected; all subsequent analyses were carried by trial.
Keywords: *fine screening, mRNA, invertase, germplasm, cold induced sweetening*

Introduction

In most potato producing regions worldwide, the crop is typically harvested during a narrow window of time, but it is consumed throughout the year. Consequently, most of the potato crop is stored before it is shipped to packing facilities and processing plants. Metabolic stability of potato tubers during this storage period is one of the prime trait targets for breeding programs worldwide (Bradshaw and Ramsay, 2005; Dale and Bradshaw, 2003; Hirsch et al., 2013). Potatoes need to be cool-stored throughout the year to maintain a continuous supply to the industry, and storage at low temperature (<8 °C) is beneficial because it reduces bacterial soft rots, decreases water and dry matter loss, and prevents sprouting without the need to add sprout inhibitors (Sowokinos, 2001a). However, storage at low temperature leads to an accumulation of

http://www.aloki.hu ● ISSN 1589 1623 (Print) ● ISSN 1785 0037 (Online)
DOI: http://dx.doi.org/10.15666/aeer/1704_73337344

the reducing sugars glucose and fructose, in a process known as cold-induced sweetening (CIS) (Herrman et al., 1996). Sugars that accumulate in non-photosynthetic tissues are recruited from the starch degradation pathway (Malone et al., 2006; Sowokinos et al., 2004). Tuber sugar content is affected by amount and activity of carbohydrate metabolizing enzymes in source (leaf) and sink (tuber) tissues and by the flux of sucrose from source (Menéndez et al., 2002). When potatoes that have undergone CIS are processed into crisps or chips, high fry temperature causes reducing sugars to react with free amino acids via the Millard reaction, resulting in an unacceptable blackening of the product (Benzing-Purdie et al., 1985). The Millard reaction also leads to the formation of the probable carcinogen acrylamide (Mottram et al., 2002).

Studies on carbohydrate metabolism in potato have shown that several enzymes contribute to low temperature sweetening. During low temperature storage, starch breakdown into sucrose is usually driven by UDP-glucose pyrophosphorylase and sucrose-6-phosphate synthase (Sowokinos, 2001b; McKenzie et al., 2005). Acid invertase converts sucrose into the reducing sugars glucose and fructose. A relationship between light chip color and low levels UDP-glucose pyrophosphorylase activity has been demonstrated (Menéndez et al., 2002; Sowokinos, 2001a). Similarly, low acid invertase activity is associated with light chip color (Bhaskar et al., 2010; Li et al., 2005; Liu et al., 2011; Wu et al., 2011). However, QTL studies have found associations between a number of additional carbohydrate metabolism genes and cold-induced sweetening (Draffehn et al., 2010). More recently, association genetics demonstrated that DNA polymorphisms in genes encoding invertase and starch phosphorylases were associated with potato chip color; starch content and starch yield. Association analysis found that SNP2746 in the StLapN gene was strongly associated with chip quality (Urbany et al., 2011). These genetic studies support the working model that natural variation in tuber starch and sugar content is controlled by allelic variants of enzymes that function in starch and sugar metabolism (Fischer et al., 2013; Theocharis et al., 2012).

Microarray hybridization experiments using a tomato gene chip hybridized with potato mRNA allowed the identification of known and novel genes that were differentially expressed during tuber cold storage in a potato clone. Transcript levels of known candidate genes, such as invertase, were correlated with sugar accumulation (Bagnaresi et al., 2008). Comparative proteome analysis has previously proven successful in identifying new candidate genes controlling tuber quality traits (Yang et al., 2011; Hoehenwarter et al., 2008). One approach to breeding for resistance to CIS is to reduce acid invertase activity. Silencing of the acid invertase gene has effectively reduced CIS, resulting in acceptable fry products (Bhaskar et al., 2010). Alternatively, resistance to CIS is found in wild relatives of potato. The wild diploid species *Solanum raphanifolium* is sexually compatible with diploid forms of cultivated potato. Its hybrid offspring have been shown to exhibit resistance to CIS (Hamernik et al., 2009). In fact, acid invertase activity in germplasm carrying CIS resistance genes from *S. raphanifolium* is as low as that in clones in which the gene has been silenced (Bhaskar et al., 2010). Wild potato species are useful sources of genes for potato improvement (Bradshaw and Ramsay, 2005; Herrman et al., 1996; Jansky et al., 2009; Bethke and Jansky, 2008). However, most wild germplasm is self-incompatible and maintained by intercrossing within populations. Consequently, genetic variation within and among accessions is common (Jansky et al., 2009; Cai et al., 2011; Chung et al., 2011; Jansky,

http://www.aloki.hu ● ISSN 1589 1623 (Print) ● ISSN 1785 0037 (Online)
DOI: http://dx.doi.org/10.15666/aeer/1704_73337344

2000; Jansky et al., 2006). It is important, therefore, to identify individuals within a population carrying genes of interest. We followed for two purposes in the present study: First, we were interested in fine screening a population of *S. raphanifolium* for resistance to CIS at different stations within country. Second, we determined the relationship between chip color and potential sources of chip color variation. Since we know that low levels of acid invertase are associated with resistance to CIS in this germplasm, we focused on expression of the acid invertase gene, acid invertase enzyme activity, and levels of the sugars sucrose, glucose, and fructose.

Materials and methods

Potato plant crosses

Crosses were made between clone hap-chc as a female and five plants of *S. raphanifolium* PI 310998 as a male. Hap-chc is a hybrid between a *S. tuberosum* dihaploid (US-W730) and *S. chacoense* PI 310998 from Horticulture Lab, University of Wisconsin Madison USA. In previous work, this cross has produced clones with moderate resistance to cold-induced sweetening (Bhaskar et al., 2010; Hamernik et al., 2009). Seeds were sown on August 14, 2009, transplanted to 48-well flats three weeks later (*Fig. 1a*) and then 16-21 plants per family were transplanted into 10 cm square pots on October 5 (*Fig. 1b*). They were grown in a greenhouse at Muree, Pakistan, until maturity. Plants were harvested on January 27-29, 2010 and placed in 4 °C storage on February 2. Two tubers of each plant in each family were chipped during the first week of June and two were retained for clonal maintenance. This trial is designated M1. Thirty-five clones produced at least eight tubers each, so four tubers were planted in the field at Sahiwal, Pakistan, on May 6, 2010. Two replications of two plants each were included in a randomized complete block design. On September 10, each plant was harvested by hand and tubers were collected. The tubers were stored at 4.4 °C until the first week of June, 2011, when two tubers per plot were chipped and were named trial S1. On September 30, 2010, one tuber per clone from the M1 trial was planted again at Sahiwal, Pakistan. Tubers were harvested from mature plants on January 28, 2011. They were stored at 4 °C until June 6, when they were chipped. This was trial S2. Tubers from the S2 trial were planted on September 15, 2011 at a greenhouse in CEMB, Pakistan. Mature plants were harvested on March 8, 2012 and stored at 6 °C. On April 9, samples were collected for sugar, RNA, and invertase assays as described below. In addition, two tubers per clone were chipped. This was trial L1. Each clone was again planted in the Multan greenhouse on April 16, harvested on July 27, and tubers were stored at 6 °C for one month. Two tubers per clone were then chipped. This was trial M2.

Chipping analysis

Chip color was evaluated by taking a 1-2 mm slice from the center of a transverse tuber cut, rinsing it in tap water and frying it in 190 °C corn oil until bubbling ceased. Each chip was visually scored for color using a scale of 1 (light) to 10 (dark), at 0.5 intervals, based on the International Chip Color Institute (Cleveland, OH) color chart). In the M1 trial, each of two tubers per clone was cut into half longitudinally and one half was again cut in half longitudinally. After cutting, the samples were immediately frozen in liquid nitrogen and stored at -70 °C for gene expression analysis. The tuber

http://www.aloki.hu ● ISSN 1589 1623 (Print) ● ISSN 1785 0037 (Online)
DOI: http://dx.doi.org/10.15666/aeer/1704_73337344

halves were used for sugar analyses. One of the quarter tuber pieces was used for the invertase enzyme activity assay and the other quarter was used for mRNA isolation. Tuber samples were passed through a Wiley freeze mill with a 40 mesh screen and stored in a -80 °C freezer.

a b

Figure 1. a *Potatoes varieties grown under control conditions on MS media.* ***b*** *Potatoes varieties grown in the pots under greenhouse conditions*

Invertase assay

For the invertase enzyme assay, 100 g protein was extracted by using PD Midi Trap G25 column. The extraction buffer consisted of 0.50 mM HEPES-KOH pH 7.5, 5 mM $MgCl_2.6H_20$, 1 mM EDTA, 1 mM EGTA, 0.1% w/v Triton X-100, and 10% w/v glycerol. Phenyl methyl sulfonyl fluoride (PMSF) was added to extraction buffer to a final concentration of 5 mM immediately before use. Before using the Midi Trap column, the cap was removed and the storage solution was poured off. The bottom cap was also removed and the column was put into 50 ml Falcon tube on ice. Then, 5 ml extraction buffer was put into column to wash it; this step was repeated thrice to a total volume ~15 ml extraction buffer and flow through was discarded. Then, 1 g tuber sample was put into a 15 ml tube along with 2 ml extraction buffer and 2-3 small glass beads. After incubating on ice for 10 min, samples were spun in a micro centrifuge for 10 min at 4 °C at maximum speed to pellet debris, and 1 ml supernatant was added to the equilibrated Midi Trap column and allowed to pack the bed completely. Flow through was discarded and the column was placed into a new Falcon tube. Then, 1.5 ml extraction buffer, along with dichlorodiphenyltrichloroethane DDT and PMSF, was added and this time the flow through was collected as it contained the protein sample. A 450 µl sample of protein was collected, frozen in liquid nitrogen, and stored at 0 °C.

Protein concentration measurements

Protein concentration was measured using the Bio-Rad assay. 10 µl sample of Bovine Serum Albumin (BSA) were used as standard. 2 ul of extracted protein along with dye was loaded into a 96 well plate. After incubating for 30 min at room temperature, absorbance at 595 nm was taken using a plate reader. Vacuolar Acid Invertase activity was measured before and after destroying invertase inhibitor proteins. The crude extract of potato tubers contains proteins which may inhibit soluble invertase activity (Pressey, 1971; Ewing and McAdoo, 1971; Barichello et al., 1990; Steel and

http://www.aloki.hu ● ISSN 1589 1623 (Print) ● ISSN 1785 0037 (Online)
DOI: http://dx.doi.org/10.15666/aeer/1704_73337344

Whitehead, 1994). However, Ross and Davis have pointed out that technique to destroy inhibitors, such as rapid vortexing of the extract, may result in a loss of invertase (Ross and Davies, 1992). So, the protein aliquot was divided in half and one half was vortexed at low speed for 30 min in cold room (10 °C) while the remaining half was also put in cold room for 30 min, but was not vortexed. The reaction buffer was prepared for measuring enzyme activity by using 133 mM sucrose, 26.7 mM sodium acetate (NaOAc) pH 4.7, 0.1 M sodium phosphate (Napi) pH 7.4 and 50 mM NaPi pH 7.4 were prepared separately, 100 U/ml glucose oxidase (GO), 100 U/ml Horseradish Peroxide (HRP), 10 mM Amplex red (AR) and dimethyl Sulfoxide (DMSO) for preparing Amplex red was also used. 10 mM NaOAc pH 5 was also used for making up volume. For each sample two tubes of 0.2 ml were used. Each containing 20 µg total protein and 10 mM sodium acetate pH 5 was used to bring volume upto 20 µl. One set of tube was put on ice to serve as zero min control, while in other 60 µl reaction buffer was used and incubated at 30 °C for 60 min. After incubating at 30 °C the reaction buffer was added to zero min control, and 8 µl 1 M NaPi pH 7.4 to each of the zero and 60-min tubes to stop the reaction. After mixing well, the reaction was incubated at 97 °C for 3 min to deactivate the enzyme.72 µl 50 mM NaPi was added and centrifuged to pellet the precipitated protein. Then, the enzyme assay mix was prepared using 5.3 ml 50 mM NaPi pH 7.4, 100 µl GO, 100 µl HRP and 100 µl AR. 50 µl enzyme assay mix was added into 96 well plates along with 50 µl reaction mixture. 200 µM glucose was used as standard. After incubating the plates for 30 min in dark reading of absorbance were taken at 560 nm. Activity of VInv was calculated as nmol glucose formed per minute per mg of protein.

Reducing sugars analysis

For sugar analyses (Spiro, 1966), freeze dried 5 mg samples were put into 1.5 ml tubes along with 4-5 beads and shaken in pulverize shaker for ~1 min to pulverize the sample. Samples were suspended in 4 ml 80% ethanol and then vortexes and placed in a 60 °C shaking water bath overnight. The next day, tubes were spin for 10 min at 20 °C at 4000 rpm and the supernatant was transferred into new tubes. The pellets were re-suspended in 4 ml 80% ethanol and placed in a 60 °C shaking water bath set overnight. The next day, samples were spin for 10 min at 20 °C at 4000 rpm and the supernatant was transferred added to the tubes from the first extraction. At this point, the supernatant was nearly 8 ml and the volume was brought to 10 ml with 80% ethanol. The sample was mixed by inversion and a 1.5 ml sample was pipetted into a 2 ml tube. The tube was placed in a vacuumfuge overnight to dry it without heat. For HPLC, 1 ml of distilled water was added to the dried sample and incubated at room temperature for 30 min and vortexes at high speed for 10 min to dissolve the pellet completely. Then samples were placed in centrifuge at 13,000 rpm for 10 min. The supernatant was filtered using a tuberculin syringe, carrying 0.2 um regenerated cellulose filter with care. Then HPLC was done, glucose, fructose, and sucrose were calculated in mg/ml.

mRNA extraction and analysis

RNA was extracted using Agilent Plant RNA isolation Mini Kit (catalog no. 5155-2780). DNA was degraded using with Ambion DNase treatment Kit (Catalogue no. AM1906). Single-stranded cDNA was synthesized using the Invitrogen Super-Script III kit (Catalogue no.18080-051). Then, this cDNA was used as a template for quantitative

http://www.aloki.hu ● ISSN 1589 1623 (Print) ● ISSN 1785 0037 (Online)
DOI: http://dx.doi.org/10.15666/aeer/1704_73337344

PCR using a Bio Rad PCR system. The PCR reaction mix consisted of 2 µl of cDNA (200 ng), short length primers 10 pico mole (Forward-AAACGGGTTGGACACATCAT, Reverse -AACCCAATTCCACAATCCAA) for Vacuolar Acid Invertase gene and Fermentas Maxima SYBP Green /fluorescein qPCR Master mix (catalog no. K0241). Actin was used as the control (forward primer 5'ATGTTCCCGGGTATTGCTGACAGA-3'; reverse 5'-CTGCCTTTGCAATCCACATCTGCT-3'). Reaction containing primers of actin and invertase samples were run in on 96-well plates, PCR cycles were run at 95 °C for 10 min, 95 °C for 15 s, 55 °C for 30 s,72 °C for 30 s at melt curve 55- 95 °C. One sample each positive control (genomic DNA) of actin and invertase was also run on each plate. Fluorescence data during the extension phase and melt curve temperatures were recorded. Real time PCR Data were analyzed using the general linear model in SAS. Means comparison was carried out using a least significant difference test at $p = 0.05$. Pearson correlation coefficients were used to evaluate relationships among chips scores and biochemical parameters. The data on all studied traits was recorded from all of the performed experiments, the average data from all experiments was calculated for statistical analysis by using analysis of variance technique and significance of mean differences (Steel et al., 1997) through using SPSS 23 version.

Results

The significant differences were found among all of the families under study as shown by *Table 1*. Family 15 consistently produced light chips, while Family 14 produced darker chips (*Table 2*). All five families were generated by crossing the same female clone (HC) to plants from one wild species accession. The *S. raphanifolium* clone that was crossed to hap-chc to produce Family 15 is more desirable than the others tested in PI 310998. The lightest chips were produced from Murree (M1) greenhouse tubers stored for 4 months at 4 °C, followed by Sahiwal-1 greenhouse tubers stored for 1 month at 6 °C (*Table 2*). The darkest chips were produced from tubers grown at Sahiwal-2 and stored for 9 months at 4 °C. Significant differences ($P = 0.05$) were detected among families in this trial for PCR cycle time, enzyme activity, sucrose, glucose, and fructose. There was a significant effect of clone on PCR cycle time ($P = 0.0009$), enzyme activity ($P < 0.0001$), sucrose ($P < 0.0001$), glucose ($P < 0.0001$), and fructose ($P < 0.0001$) (*Table 3*). However, there was a significant correlation between sucrose and glucose ($P = 0.0002$), sucrose and fructose ($P = 0.0213$) and glucose and fructose ($P < 0.0001$). There was no correlation between clone chip score in the M1 trial and any of the biochemical traits. Based on clone means, correlations between pairs of biochemical traits were calculated (*Table 4*). There was found a significant but negative correlation between enzymes with Multan location, sucrose with mRNA expression. Positive and significant correlation of mRNA expression with glucose and fructose was recorded.

Table 1a. *ANOVA for chip color and biochemical traits*

Traits/locations	CEMB (L1)	Sahiwal (S1)	Multan (M2)	Murree (M1)
Replication	1.082ns	2.123ns	0.531ns	3.7823ns
Family	7.6916*	11.8038*	1.5918*	31.4569*

ns = non-significant, * = significant at 5% probability level

http://www.aloki.hu ● ISSN 1589 1623 (Print) ● ISSN 1785 0037 (Online)
DOI: http://dx.doi.org/10.15666/aeer/1704_73337344

Table 1b. *ANOVA for chip color and biochemical traits*

Traits/Locations	Sahiwal (S2)	RNA	Fructose	Glucose	Sucrose
Replication	5.608ns	0.042ns	1.028ns	1.001ns	5.123ns
Family	44.927*	0.48585*	6.82822*	7.1807*	30.7049*

ns = non-significant, * = significant at 5% probability level

Table 2. *Mean chip score of five families in five cold storage trials. Chip score ratings were based on a scale of 1 (light) to 10 (dark). Chip color scores of 4 or less are commercially acceptable*

Traits Family	CEMB Mean±SE	Sahiwal Mean±SE	Multan Mean±SE	Murree Mean±SE	Sahiwal 2 Mean±SE
11	4.4750±0.2311	4.1750±0.2495	4.8125±0.1932	3.4750±0.1915	6.4000±0.2350
13	4.1250±0.2311	3.9750±0.2495	4.2875±0.1932	4.1475±0.1915	4.3500±0.2350
14	4.7750±0.2311	5.0000±0.2495	4.4250±0.1932	5.8550±0.1915	4.5000±0.2350
15	3.9600±0.2311	3.9500±0.2495	4.0125±0.1932	3.1025±0.1915	4.0500±0.2350
18	4.1667±0.2255	4.2381±0.2435	4.4762±0.1886	4.9905±0.1869	4.1714±0.2293

Table 3. *RNA extraction amount and biochemical analysis for different families*

Traits Family	RNA Mean±SE	Fructose Mean±SE	Glucose Mean±SE	Sucrose Mean±SE
11	0.1398±0.0355	1.4443±0.2058	1.5095±0.2801	10.609±0.8381
13	1.2483±0.0355	2.6723±0.2058	2.2382±0.2801	8.433±0.8381
14	0.3337±0.0355	1.6860±0.2058	1.9653±0.2801	6.542±0.8381
15	0.0675±0.0355	0.6482±0.2058	0.4572±0.2801	9.243±0.8381
18	0.2305±0.0347	1.6902±0.2008	1.9419±0.2733	6.000±0.8179

Table 4. *Correlation among various traits of potato*

Traits	CEMB	Sahiwal	Multan	Murree	Sahiwal 2	RNA	Invertase enzyme	Fructose	Glucose
Sahiwal	0.0138								
Multan	-0.0546	0.0205							
Murree	0.0193	0.0631	0.0761						
Sahiwal 2	-0.0163	-0.013	-0.0279	0.0383					
RNA	-0.1026	-0.1226	0.1004	0.0075	-0.0735				
Invertase enzyme	0.0941	0.6511*	-0.1326*	0.0354	0.2175*	-0.0899			
Fructose	0.0602	0.2164	-0.0152	0.1028	0.0991	0.1409*	0.2887*		
Glucose	0.2356	0.2372	-0.0594	-0.0664	-0.0153	0.1202*	0.3352*	0.8197*	
Sucrose	0.1539	0.1284	-0.0143	0.3109	-0.0713	-0.0747*	0.1545*	0.2741*	0.2583*

* = significant at 5% probability level

http://www.aloki.hu ● ISSN 1589 1623 (Print) ● ISSN 1785 0037 (Online)
DOI: http://dx.doi.org/10.15666/aeer/1704_73337344

Discussion

HC is a heterozygous interspecific hybrid, so it may segregate for CIS alleles. However, the set of alleles it contributes to offspring is expected to be the same among the five families. Consequently, differences among families are likely due mainly to differences genetic variability among male parents from the same *S. raphanifolium* accession within each trial. All five families were generated by crossing the same female clone (HC) to plants from one wild species accession. ANOVA revealed a significant effect of family ($P < 0.05$), but not replication, on chip score at all locations except S2 (*Table 1*). Family 15 consistently produced light chips, while Family 14 produced darker chips (*Table 2*). Individuals from a population of an outcrossing species are likely to be heterozygous and heterogeneous. While PI 310998 is a good source of CIS resistance genes, fine screening of the population for individuals that produce a high proportion of resistant offspring is likely to be productive. Fine screening of accessions for individuals carrying traits of interest has been reported in potato (Bamberg et al., 1996; Bamberg et al., 1998; Douches et al., 2001). The *S. raphanifolium* clone that was crossed to hap-chc to produce Family 15 is more desirable than the others tested in PI 310998.

The lightest chips were produced from Murree (M1) greenhouse tubers stored for 4 months at 4 °C, followed by Sahiwal-1 greenhouse tubers stored for 1 month at 6 °C (*Table 2*). The darkest chips were produced from tubers grown at Sahiwal-2 and stored for 9 months at 4 °C. We did not expect lighter chip color from tubers stored at 6 °C than at 4 °C. However, the combined effect of environmental and cultural practices can affect tuber quality, which we visualized in the finished processed products. Suboptimal environments result in an increase in internal tuber disorders (Zhou et al., 1994). Long-term storage of potato tubers (six month or more) has significant, variety-dependent effects on sugar and amino acid concentrations (Muttucumaru et al., 2014). Consequently, darker chip color in the long storage trials (M2 and L1) was expected. Tubers from trial Murree were chosen for analyses of acid invertase RNA levels (as measured by the number of PCR cycles to reach the threshold), acid invertase activity, and levels of the sugars sucrose, glucose, and fructose. Significant differences ($P = 0.05$) were detected among families in this trial for PCR cycle time, enzyme activity, sucrose, glucose, and fructose. However, since there was no difference in chip color among families in trial Murree, additional analyses were based on clones without regard to family. There was a significant effect of clone on PCR cycle time ($P = 0.0009$), enzyme activity ($P < 0.0001$), sucrose ($P < 0.0001$), glucose ($P < 0.0001$), and fructose ($P < 0.0001$) (*Table 3*).

Based on clone means, correlations between pairs of biochemical traits were calculated. There was no significant correlation between acid invertase RNA or activity and any of the three sugars. However, there was a significant correlation between sucrose and glucose ($P = 0.0002$), sucrose and fructose ($P = 0.0213$) and glucose and fructose ($P < 0.0001$). There was no correlation between clone chip score in the M1 trial and any of the biochemical traits. Based on clone means, correlations between pairs of biochemical traits were calculated (*Table 4*). There was found a significant but negative correlation between enzymes with Multan location, sucrose with mRNA expression. Positive and significant correlation of mRNA expression with glucose and fructose was recorded. It was suggested from positive correlation may be used to improve in the quality traits while improving the related traits and improvement may be fixed in next generations. The negative correlations suggested that the decrease in the trait may be

http://www.aloki.hu ● ISSN 1589 1623 (Print) ● ISSN 1785 0037 (Online)
DOI: http://dx.doi.org/10.15666/aeer/1704_73337344

fixed in next generations. For the improvement of qualitative and quantitative traits positive correlations are used for selection (Ali and Jansky, 2015; Ali et al., 2014, 2016, 2013). The ratio of sucrose to glucose is a reflection of acid invertase enzyme activity. Again however, there was no significant difference in the sucrose: glucose ratio between the clones with high enzyme activity and those with low activity. It is interesting that acid invertase enzyme activity and mRNA production is negatively correlated with chip color in this study. In a previous study using the same accession of *S. raphanifolium*, silencing the potato vacuolar acid invertase gene resulted in light colored chips (Bhaskar et al., 2010). In that study, relatively high levels of invertase transcript were detected in hap-chc, but transcript levels were low in some hap-chc x *S. raphanifolium* 310998 hybrids. Several studies have demonstrated high sequence variability and genotype specific variants among potato protease inhibitors. These inhibitors significantly affect the Vacuolar Acid invertase activity (Bauw et al., 2006; Jørgensen et al., 2005). Effects of patatins and phospholipas in altering membrane lipid composition could explain differences between genotypes with strong (CIS-s) and weak (CIS-t) cold acclimation responses (Theocharis et al., 2012). More recently, association genetics demonstrated that DNA polymorphisms in genes encoding invertases and starch phosphorylases were associated with potato chip color, starch content and starch yield (Fischer et al., 2013).

Conclusions

Same genotype can show variable resistance in different trial satiations and in conclusive invertase activity is genotypes and trials dependent. Significant trial effects can be detected; if all subsequent analyses are carried by trial. Invertase enzyme is responsible for cold induced sweetening but not exclusively. Its activity is trail, genotype and environmental conditions dependent. Along with fine screening it is the need of time to sort out best potato germplasm based on the action of other genes involved in glycolysis pathway.

Acknowledgements. The authors highly acknowledge their research wok to Higher Education Commission of Pakistan for providing scholarship and National Natural Science Foundation of China (31601600).

Conflict of interests. The authors declare that the research was conducted in the absence of any commercial or financial relationships that could be construed as a potential conflict of interests.

REFERENCES

[1] Ali, A., Jansky, S. (2015): Fine screening for resistance to cold-induced sweetening in potato hybrids containing Solanum raphanifolium germplasm. – Advances in Agriculture. http://dx.doi.org/10.1155/2015/327969.

[2] Ali, Q., Ahsan, M., Ali, F., Aslam, M., Khan, N. H., Munzoor, M., Mustafa, H. S. B., Muhammad, S. (2013): Heritability, heterosis and heterobeltiosis studies for morphological traits of maize (Zea mays L.) seedlings. – Advancements in Life Sciences 1(1) 52-63.

[3] Ali, Q., Ali, A., Waseem, M., Muzaffar, A., Ahmad, S., Ali, S., Awan, M., Samiullah, T., Nasir, I., Tayyab H. (2014): Correlation analysis for morpho-physiological traits of maize (Zea mays L.). – Life Science Journal 11: 9-13.

http://www.aloki.hu ● ISSN 1589 1623 (Print) ● ISSN 1785 0037 (Online)
DOI: http://dx.doi.org/10.15666/aeer/1704_73337344

[4] Ali, Q., Ahsan, M., Malook, S., Kanwal, N., Ali, F., Ali, A., Ahmed, W., Ishfaq, M., Saleem, M. (2016): Screening for drought tolerance: comparison of maize hybrids under water deficit condition. – Advancements in Life Sciences 3(2): 51-58.
[5] Bagnaresi, P., Moschella, A., Beretta, O., Vitulli, F., Ranalli, P., Perata, P. (2008): Heterologous microarray experiments allow the identification of the early events associated with potato tuber cold sweetening. – BMC Genomics 9: 176. DOI: 10.1186/1471-2164-9-176.
[6] Bamberg, J., Longtine, C., Radcliffe, E. (1996): Fine screening Solanum (potato) germplasm accessions for resistance to Colorado potato beetle. – American Journal of Potato Research 73: 211-223.
[7] Bamberg, J., Palta, J., Peterson, L., Martin, M., Krueger, A. (1998): Fine screening potato (Solanum) species germplasm for tuber calcium. – American Journal of Potato Research 75: 181-186.
[8] Barichello, V., Yada, R. Y., Coffin, R. H., Stanley, D. W. (1990): Respiratory enzyme activity in low temperature sweetening of susceptible and resistant potatoes. – Journal of Food Science 55: 1060-1063.
[9] Bauw, G., Nielsen, H. V., Emmersen, J., Nielsen, K. L., Jørgensen, M., Welinder, K. G. (2006): Patatins, Kunitz protease inhibitors and other major proteins in tuber of potato cv. Kuras. – The FEBS Journal 273: 3569-3584.
[10] Benzing-Purdie, L. M., Ripmeester, J. A., Ratcliffe, C. I. (1985): Effects of temperature on Maillard reaction products. – Journal of Agricultural and Food Chemistry 33: 31-33.
[11] Bethke, P., Jansky, S. (2008): The effects of boiling and leaching on the content of potassium and other minerals in potatoes. – Journal of Food Science 73: H80-H85.
[12] Bhaskar, P. B., Wu, L., Busse, J. S., Whitty, B. R., Hamernik, A. J., Jansky, S. H., Buell, C. R., Bethke, P. C., Jiang, J. (2010): Suppression of the vacuolar invertase gene prevents cold-induced sweetening in potato. – Plant Physiology 154: 939-948.
[13] Bradshaw, J. E., Ramsay, G. (2005): Utilisation of the Commonwealth Potato Collection in potato breeding. – Euphytica 146: 9-19.
[14] Cai, X., Spooner, D., Jansky, S. (2011): A test of taxonomic and biogeographic predictivity: resistance to potato virus Y in wild relatives of the cultivated potato. – Phytopathology 101: 1074-1080.
[15] Chung, Y. S., Holmquist, K., Spooner, D. M., Jansky, S. H. (2011): A test of taxonomic and biogeographic predictivity: resistance to soft rot in wild relatives of cultivated potato. – Phytopathology 101: 205-212.
[16] Dale, M. F. B., Bradshaw, J. E. (2003): Progress in improving processing attributes in potato. – Trends in Plant Science 8: 310-312.
[17] Douches, D., Bamberg, J., Kirk, W., Jastrzebski, K., Niemira, B., Coombs, J., Bisognin, D., Felcher, K. (2001): Evaluation of wildSolanum species for resistance to the US-8 genotype ofPhytophthora infestans utilizing a fine-screening technique. – American Journal of Potato Research 78: 159-165.
[18] Draffehn, A. M., Meller, S., Li, L., Gebhardt, C. (2010): Natural diversity of potato (Solanum tuberosum) invertases. – BMC Plant Biology 10: 271.
[19] Ewing, E., McAdoo, M. H. (1971): An examination of methods used to assay potato tuber invertase and its naturally occurring inhibitor. – Plant Physiology 48: 366-370.
[20] Fischer, M., Schreiber, L., Colby, T., Kuckenberg, M., Tacke, E., Hofferbert, H. R., Schmidt, J., Gebhardt, C. (2013): Novel candidate genes influencing natural variation in potato tuber cold sweetening identified by comparative proteomics and association mapping. – BMC Plant Biology 13: 113.
[21] Hamernik, A., Hanneman, R., Jansky, S. (2009): Introgression of wild species germplasm with extreme resistance to cold sweetening into the cultivated potato. – Crop Science 49: 529-542.

http://www.aloki.hu ● ISSN 1589 1623 (Print) ● ISSN 1785 0037 (Online)
DOI: http://dx.doi.org/10.15666/aeer/1704_73337344

[22] Herrman, T. J., Love, S. L., Shafii, B., Dwelle, R. B. (1996): Chipping performance of three processing potato cultivars during long-term storage at two temperature regimes. – American potato journal 73: 411-425.
[23] Hirsch, C. N., Hirsch, C. D., Felcher, K., Coombs, J., Zarka, D., Van Deynze, A., De Jong, W., Veilleux, R. E., Jansky, S., Bethke, P. (2013): Retrospective view of North American potato (Solanum tuberosum L.) breeding in the 20th and 21st centuries. – G3: Genes| Genomes| Genetics 3: 1003-1013.
[24] Hoehenwarter, W., van Dongen, J. T., Wienkoop, S., Steinfath, M., Hummel, J., Erban, A., Sulpice, R., Regierer, B., Kopka, J., Geigenberger, P. (2008): A rapid approach for phenotype-screening and database independent detection of cSNP/protein polymorphism using mass accuracy precursor alignment. – Proteomics 8: 4214-4225.
[25] Jansky, S. (2000): Breeding for disease resistance in potato. – Plant Breeding Reviews 19: 69-155.
[26] Jansky, S., Simon, R., Spooner, D. (2009): A test of taxonomic predictivity: resistance to the Colorado potato beetle in wild relatives of cultivated potato. – Journal of Economic Entomology 102: 422-431.
[27] Jansky, S. H., Simon, R., Spooner, D. M. (2006): A test of taxonomic predictivity. – Crop Science 46: 2561-2570.
[28] Jørgensen, H. J., Mathisen, T., Løvseth, A., Omoe, K., Qvale, K. S., Loncarevic, S. (2005): An outbreak of staphylococcal food poisoning caused by enterotoxin H in mashed potato made with raw milk. – FEMS Microbiology Letters 252: 267-272.
[29] Li, L., Strahwald, J., Hofferbert, H.-R., Lübeck, J., Tacke, E., Junghans, H., Wunder, J., Gebhardt, C. (2005): DNA variation at the invertase locus invGE/GF is associated with tuber quality traits in populations of potato breeding clones. – Genetics 170: 813-821.
[30] Liu, X., Zhang, C., Ou, Y., Lin, Y., Song, B., Xie, C., Liu, J., Li, X. Q. (2011): Systematic analysis of potato acid invertase genes reveals that a cold-responsive member, StvacINV1: regulates cold-induced sweetening of tubers. – Molecular Genetics and Genomics 286: 109-118.
[31] Malone, J. G., Mittova, V., Ratcliffe, R. G., Kruger, N. J. (2006): The response of carbohydrate metabolism in potato tubers to low temperature. – Plant and Cell Physiology 47: 1309-1322.
[32] McKenzie, M. J., Sowokinos, J. R., Shea, I. M., Gupta, S. K., Lindlauf, R. R., Anderson, J. A. (2005): Investigations on the role of acid invertase and UDP-glucose pyrophosphorylase in potato clones with varying resistance to cold-induced sweetening. – American Journal of Potato Research 82: 231-239.
[33] Menéndez, C. M., Ritter, E., Schäfer-Pregl, R., Walkemeier, B., Kalde, A., Salamini, F., Gebhardt, C. (2002): Cold sweetening in diploid potato: mapping quantitative trait loci and candidate genes. – Genetics 162: 1423-1434.
[34] Mottram, D. S., Wedzicha, B. L., Dodson, A. T. (2002): Food chemistry: acrylamide is formed in the Maillard reaction. – Nature 419: 448-449.
[35] Muttucumaru, N., Powers, S., Elmore, J., Briddon, A., Mottram, D., Halford, N. (2014): Evidence for the complex relationship between free amino acid and sugar concentrations and acrylamide-forming potential in potato. – Annals of Applied Biology 164: 286-300.
[36] Pressey, A. (1971): An extension of assimilation theory to illusions of size, area, and direction. – Attention, Perception, and Psychophysics 9: 172-176.
[37] Ross, H., Davies, H. (1992): Sucrose metabolism in tubers of potato (Solanum tuberosum L.) Effects of sink removal and sucrose flux on sucrose-degrading enzymes. – Plant Physiology 98: 287-293.
[38] Sowokinos, J. R. (2001a): Allele and isozyme patterns of UDP-glucose pyrophosphorylase as a marker for cold-sweetening resistance in potatoes. – American Journal of Potato Research 78: 57-64.
[39] Sowokinos, J. R. (2001b): Biochemical and molecular control of cold-induced sweetening in potatoes. – American Journal of Potato Research 78: 221-236.

http://www.aloki.hu ● ISSN 1589 1623 (Print) ● ISSN 1785 0037 (Online)
DOI: http://dx.doi.org/10.15666/aeer/1704_73337344

[40] Sowokinos, J. R., Vigdorovich, V., Abrahamsen, M. (2004): Molecular cloning and sequence variation of UDP-glucose pyrophosphorylase cDNAs from potatoes sensitive and resistant to cold sweetening. – Journal of Plant Physiology 161: 947-955.
[41] Spiro, R. G. (1966): Analysis of Sugars Found in Glycoproteins. – In: Neufild, E. F., Ginsburg, V. (eds.) Complex Carbohydrates. (Series: Methods in Enzymology Vol. 8). Academic Press, Cambridge, MA, pp. 3-26.
[42] Steel, D. M., Whitehead, A. S. (1994): The major acute phase reactants: C-reactive protein, serum amyloid P component and serum amyloid A protein. – Immunology Today 15: 81-88.
[43] Steel, R. J. D., Torrie, J. H. Dicky, D. A. (1997): Principles and Procedures of Statistics: A Biometrical Approach (Vol. 633). – McGraw-Hill, New York.
[44] Theocharis, A., Clément, C., Barka, E. A. (2012): Physiological and molecular changes in plants grown at low temperatures. – Planta 235: 1091-1105.
[45] Urbany, C., Colby, T., Stich, B., Schmidt, L., Schmidt, J. r., Gebhardt, C. (2011): Analysis of natural variation of the potato tuber proteome reveals novel candidate genes for tuber bruising. – Journal of Proteome Research 11: 703-716.
[46] Wu, L., Bhaskar, P. B., Busse, J. S., Zhang, R., Bethke, P. C., Jiang, J. (2011): Developing cold-chipping potato varieties by silencing the vacuolar invertase gene. – Crop Science 51: 981-990.
[47] Yang, Y., Qiang, X., Owsiany, K., Zhang, S., Thannhauser, T. W., Li, L. (2011): Evaluation of different multidimensional LC–MS/MS pipelines for isobaric tags for relative and absolute quantitation (iTRAQ)-based proteomic analysis of potato tubers in response to cold storage. – Journal of Proteome Research 10: 4647-4660.
[48] Zhou, D., Mattoo, A., Li, N., Imaseki, H., Solomos, T. (1994): Complete nucleotide sequence of potato tuber acid invertase cDNA. – Plant Physiology 106: 397.

http://www.aloki.hu ● ISSN 1589 1623 (Print) ● ISSN 1785 0037 (Online)
DOI: http://dx.doi.org/10.15666/aeer/1704_73337344

PERCEPTIONS OF SMALL-SCALE MAIZE FARMERS ON CLIMATE CHANGE IMPACTS IN HHOHHO, MANZINI AND SHISELWENI REGIONS OF THE KINGDOM OF ESWATINI

KUNENE, M. N. – MTHOMBENI, D. L.* – ANTWI, M. A.

Department of Agriculture and Animal Health, College of Agriculture and Environmental Sciences, University of South Africa, 1710 Florida, South Africa

**Corresponding author*
e-mail: mthomdl@unisa.ac.za

(Received 15th Feb 2019; accepted 10th Apr 2019)

Abstract. The study examined the perceptions of small-scale maize farmers in the Kingdom of eSwatini regarding the impacts of climate change. These perceptions were assessed by means of a five-point Likert scale; 59% of the respondents strongly agreed and 41% agreed that climate change has a significant influence on maize production and low yield. Multi-stage sampling involving purposive and random sampling was used in the study. The study was based on data from 188 small-scale maize farmers supplying the National Maize Corporation (NMC) depots in eSwatini. Principal component analysis (PCA) was used to analyse the data, and four factors that farmers perceived as influencing climate change were identified. The conclusion reached was that any adaptation strategies developed by smallholder maize farmers to combat climate change were largely influenced by the farmers' perceptions of climate change.
Keywords: *principal component analysis, maize, National Maize Corporation, climate change, eSwatini*

Introduction

Maize is a staple food in the Kingdom of eSwatini, and most small-scale farmers cultivate this crop, which is their most important source of income. Maize is highly susceptible to climate change (Sutcliffe et al., 2016); the small-scale farmers who participated in the study mentioned heat waves, drought, floods, water scarcity and plant diseases as the main factors affecting their maize production and associated these phenomena with climate change. The perceptions of small-scale maize farmers with regard to external influences are an important element determining their decisions and course of action. However, limited research has been conducted into the perceptions of maize farmers in the Kingdom of eSwatini relating to climate change. According to Debela et al. (2015), many of the studies on perceptions regarding climate change are aimed at better understanding the extent of farmers' perceptions but fail to identify the factors that influence the level at which small-scale farmers perceive climate change and its impact. Small-scale farmers and the general population find it necessary to make decisions every day concerning how to cope with and adapt to the impacts of climate change in both agricultural production and their daily lives. In eSwatini, smallholder maize farmers are already experiencing the unfavourable effects of climate change, and the impact of this phenomenon is already being felt across the socio-economic and agricultural sectors. The degree of vulnerability of communities to the effects of climate change has increased sharply, and this has negatively affected various sectors of the economy such as agriculture, water, energy, health and forestry. Establishing the perceptions of small-scale maize farmers is necessary for informed policy decisions and mitigation strategies among farmers, hence the study objective of investigating the

http://www.aloki.hu ● ISSN 1589 1623 (Print) ● ISSN 1785 0037 (Online)
DOI: http://dx.doi.org/10.15666/aeer/1704_73457356

perceptions of small-scale maize farmers in the Hhohho, Manzini and Shiselweni regions of eSwatini as these related to the impact of climate change.

Literature review

Sub-Saharan Africa is expected to have rainfall above the global average, yet rainfall is declining. There is growing evidence that extreme events, such as drought and floods, have been common occurrences, and these affect small-scale farmers in developing countries, who depend heavily on rainfed agriculture for their livelihoods (Belay et al., 2017). As stated above, smallholder farmers and the general population find it necessary to make decisions every day concerning how to cope with and adapt to the impacts of climate change both in agricultural production and in their daily lives. A study by Jacobi et al. (2015) indicated that small-scale farmers are affected by the negative impacts of global climate change and that livelihood based on small-scale agriculture tends to be highly vulnerable to climate change, since these farmers have limited coping options. A better understanding of farmers' concerns and the way they perceive climate change is crucial and will assist in equipping farmers to take the correct adaptive measures (Abid et al., 2017; Ayanlade et al., 2016). Perception significantly affects the way in which farmers deal with climate-induced risks and opportunities (Debela et al., 2015).

The rapid pace of climate change has been seen to have marked effects on food availability in Swaziland, as it affects crop production (Mamba et al., 2015). Adebayo et al. (2012) have reported that smallholder maize farmers with poor resources demonstrate low levels of awareness concerning climate change, and that this in turn affects their food production. Therefore, the need to identify farmers' perceptions regarding climate change is a vital step in dealing with the impacts of this phenomenon (Abid et al., 2015).

Materials and methods

Sampling and data collection

The study reported on in this article was carried out in the Kingdom of eSwatini, previously known as the Kingdom of Swaziland. The Kingdom of eSwatini (*Fig. 1*) is a small, landlocked, mountainous country in southern Africa, covering an area of 17 364 km^2 (Mamba et al., 2015). The sample frame error was controlled by obtaining a list of the 539 maize farmers who supplied maize to National Maize Corporation (NMC) depots from 2010 to 2014. This list was obtained from the NMC in 2017, and data was collected during the period 2017 to 2018. The multi-stage sampling technique was used in the study; to involve maize farmers who produced for both consumption and for sale, purposive selection criteria were used. These criteria were very useful for identifying those farmers who supplied maize to NMC depots during the period 2012 to 2014; random sampling was then used to give each small-scale farmer a chance to be selected for questionnaire administration. According to Krejcie and Morgan, as discussed by Rahi (2017), the sample size for a population of 539 should be 217; in this study, 219 questionnaires were administered to small-scale maize farmers in the three maize-producing regions of eSwatini, namely, Hhohho, Manzini and Shiselweni. During data capture and analysis, 31 questionnaires were found to be incomplete and invalid, and the sample size was therefore reduced to 188 respondents.

http://www.aloki.hu ● ISSN 1589 1623 (Print) ● ISSN 1785 0037 (Online)
DOI: http://dx.doi.org/10.15666/aeer/1704_73457356

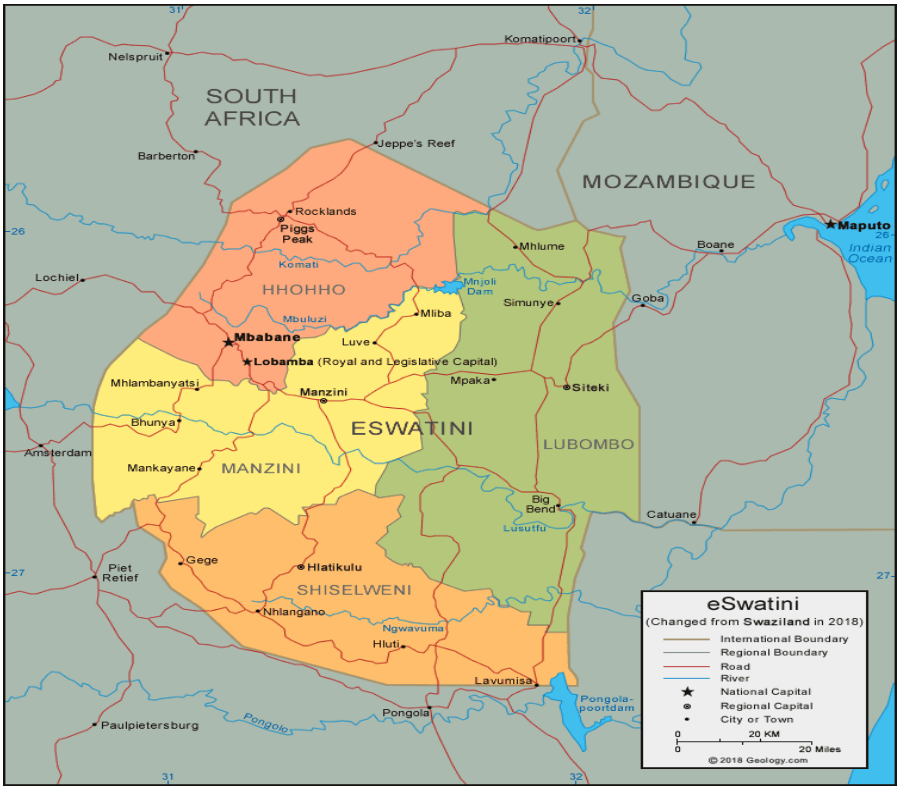

Figure 1. *Map of eSwatini. (Source: https://geology.com/world/swaziland-satellite-image.shtml – accessed: 10 March 2019)*

Analysis of variance results

The Kaiser-Meyer-Olkin (KMO) measure of sampling adequacy and Bartlett's test of sphericity were used to assess the appropriateness of the data for factor analysis. The Chi-square was 480.330 with 36 degrees of freedom, which was significant at ($p < 0.05$), as shown in *Table 1*. At 0.471, the KMO measure of sampling adequacy was less than 0.50, and so factor analysis was considered an appropriate technique for further analysis of the data.

Table 1. *Analysis of variance results and KMO Bartlett's test of sphericity. (Source: own calculations based on the survey (2017–2018); Kaiser-Meyer-Olkin measure of sampling adequacy = 0.471)*

Chi-square	df	Significance
480.330	36	0.000

Data analysis

In terms of gender distribution, 47.9% of the respondents were male and 52.1% female. The respondents' perceptions were measured using a five-point Likert scale, which was applied to rank responses according to how respondents perceived climate change impact in the three maize producing regions; responses ranged as follows: 1. Strongly agree, 2. Agree, 3. Don't know 4. Disagree, and 5. Strongly disagree. A mean

http://www.aloki.hu ● ISSN 1589 1623 (Print) ● ISSN 1785 0037 (Online)
DOI: http://dx.doi.org/10.15666/aeer/1704_73457356

score for each variable was calculated based on questions measuring perceptions. Questions relating to how the small-scale maize farmers perceived climate change covered the following domains: incidences of floods, shifts in rainfall seasonality, persistent droughts, increasing food crop costs, destruction of buildings, infrastructure and soil erosion. A "strongly agree" score on the scale indicated a positive perception of climate change and a "strongly disagree" indicated a negative perception of climate change.

Principal component analysis (PCA) was used to rank a small number of variables that could account for the variability found in a relatively large number of variables, not including all the original variables in the analysis. This method allowed the researcher to find new variables representing the underlying or latent variables of the dataset of the statement, considered to be the factors that best described the ideas that conveyed farmers' perceptions of the impacts of climate change. Criteria such as eigenvalues greater than one and cumulative variance were explained by increasing the number of factors that were included in the factor model, and the interpretability of extracted factors was used to guide the choice of the appropriate number of factors to be included in the model of choice, or best fit model.

Results and discussion

Demographic of respondents

According to Debela et al. (2015), perceptions regarding climate change among small-scale farmers and rural communities is driven by multiple forces, such as household demographics and farm factors. The demographics of the respondents are presented in *Table 2*.

Table 2. *Summary of demographics. (Source: own calculations based on the survey (2017–2018), N = 188)*

Variables	Percentages
Age of the respondents	
Below the age of 25 years	7.5%
25–30 years old	3.9%
31–40 years old	30.3%
41–50 years old	25%
Over the age of 51 years	
Educational level	33.3%
No formal education	15.4%
Primary education	39.9%
Secondary education	27.1%
Tertiary education	17.6%
Household size	
Fewer than 2 members	11.7%
3–6 members	40.4%
7–10 members	36.2%
More than 10 members	11.7 %

http://www.aloki.hu ● ISSN 1589 1623 (Print) ● ISSN 1785 0037 (Online)
DOI: http://dx.doi.org/10.15666/aeer/1704_73457356

Age of the respondents

Table 2 presents the age distribution of respondents. The age of the respondents was analysed as a reflection of their agricultural production experience. Debela et al. (2015) identified a close relationship between the age of a farmer and farming experience and his or her accumulated knowledge of the environment, including changes in climate conditions. 33.3% of the respondents were over the age of 50, 30.3% of the respondents were between the ages of 31 and 40, and 25% of the respondents were between the ages of 41 and 50. The remaining 3.9% of the respondents were between the ages of 25 and 30. This suggests that maize farming in the Kingdom is dominated by older smallholder farmers. The results also revealed that 30.3% of the heads of households were in the productive age group of 31 to 40 and more than 51 and would therefore be in a position to take action with regard to climate change.

Education level

The distribution of respondents by education level is shown in *Table 2*. The highest number of respondents (39.9%) had higher primary education, followed by secondary education (27.1%), tertiary education (17.6%) and non-formal education (15.4%). Farmers with a higher level of education had slightly more knowledge and information about good agricultural principles, and those with university education were able to analyse and interpret information much better than farmers with no formal education. The results also showed that farmers with education and agricultural skills made a significant contribution in the context of maize production activities. The level of formal education attained by farmers influences their ability to perceive climate change and its impact (Debela et al., 2015).

Household size

In the maize production areas in the three regions, 11.7% of households consisted of fewer than 2 members, and a further 11.7% of households consisted of more than 10 members. 40.4% of households consisted of 3 to 6 members, and 36.2% of households comprised 7 to 10 members (*Table 2*). The fact that there were so many large households would be expected to have a positive impact on maize production when all household members were fully engaged in agricultural activities. The results also showed that as the number of household members increased, so did the chances that the household was engaged in agricultural production, since it would be possible to take advantage of a readily available labour force, and the chances of adapting to climate change impact would therefore be high. According to Debela et al. (2015), households consisting of many members are more likely to engage in non-farm income generating activities, because non-farm income buffers financial losses from farming; in consequence, householders are less likely to perceive climate change.

Percentage ratings of the perceptions regarding climate change impact

Table 3 presents the descriptive statistics of the variables that indicated perceptions of climate change. About 59% of the respondents perceived climate change to have a very significant influence on maize production, while 44.7% of the farmers strongly agreed that shifts in rainfall patterns have caused crop failures and low yield.

http://www.aloki.hu ● ISSN 1589 1623 (Print) ● ISSN 1785 0037 (Online)
DOI: http://dx.doi.org/10.15666/aeer/1704_73457356

Table 3. *Percentage ratings of respondents' perceptions regarding climate change impact. (Source: own calculations based on the survey (2017–2018), N = 188)*

Perceptions regarding climate change impact	Strongly agree	Agree	I do not know	Disagree	Strongly disagree
Climate change has a very big impact on maize production	59%	41%	00%	00%	00%
Variations in climate have caused an increase in incidences of floods	7.4%	12.2%	29.3%	16.5%	34.6%
Shifts in rainfall seasonality have caused crop failures and low yield	44.7%	34.0%	12.2%	4.8%	4.3%
Crop varieties have no longer been productive due to persistent droughts	25.5%	20.7%	29.3%	14.9%	9.6%
Climate change has led to crop infestation and diseases due to droughts	7.4%	31.9%	37.8%	22.9%	00%
Climate change has led to rural–urban migration	00%	15.4%	46.3%	24.5%	13.8%
Excessive rainfall contributes to destruction of buildings and infrastructure	67.0%	17.6%	11.7%	3.7%	00%
Flood does not contribute to soil erosion	20.2%	5.9%	28.7%	24.5%	20.7%
Water becomes scarce due to droughts and low rainfall	72.3%	20.2%	00%	3.2%	4.3%
Dry spell of crops is the result of drought	30.9%	45.7%	12.2%	3.7%	7.4%
Climate variability has an impact on rain-fed production	42.0%	10.1%	31.9%	7.4%	8.5%
Decrease in rainfall reduces water stored in bands	27.7%	27.7%	3.1.9%	4.3%	8.5%
Climate change has led to deforestation	20.7%	31.4%	42.0%	3.7%	2.1%
The cost of food crops is increasing because of climate change	24.5%	36.2%	25.0%	4.3%	10.1%

67% of the small-scale maize farmers strongly agreed that excessive rainfall contributes to destruction of buildings and infrastructure, 72.3% strongly agreed that water becomes scarce due to droughts and low rainfall. The results further reveal that 42% of smallholder maize farmers perceived climate variability to have a significant impact on rainfed maize production. Mamba et al. (2015) reported different perceptions of climate change among farmers, further showing that these farmers tended to overestimate the negative impact of climate change, and that this misperception affected crop production.

Scree plot

In the scree plot in *Figure 2,* eigenvalues were plotted against principal component (PC) numbers. The PC numbers were plotted on the X-axis, while the eigenvalues were plotted on the Y-axis. The PCs that were kept were those on the slope of the graph before the decrease in eigenvalues levels off to the right of the plot. Using this criterion,

http://www.aloki.hu ● ISSN 1589 1623 (Print) ● ISSN 1785 0037 (Online)
DOI: http://dx.doi.org/10.15666/aeer/1704_73457356

4 PCs, namely: impact on maize production, climate change, flood incidences, shifts in rainfall and droughts were retained in the analysis of this study.

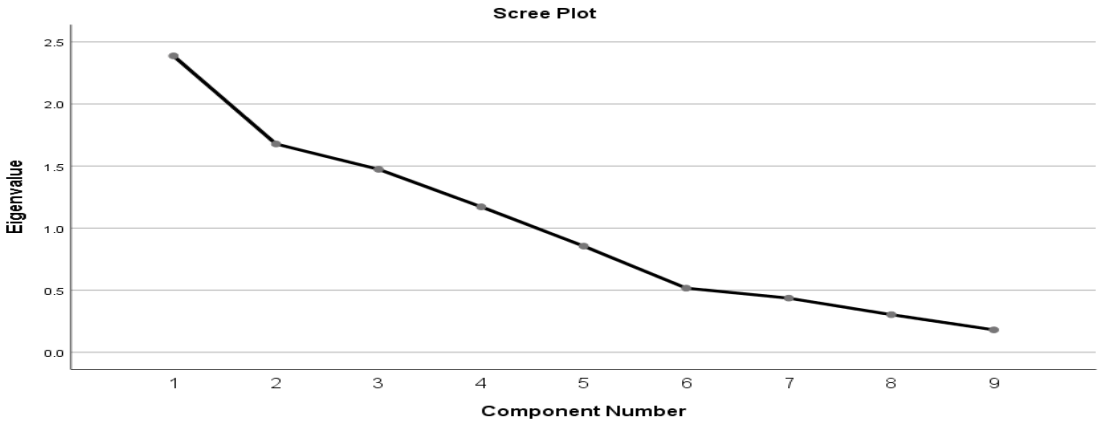

Figure 2. *Scree plot*

In *Figure 2,* the different variables represented different patterns of perceptions of small-scale maize farmers regarding climate change. The grouping of the original variables was done by observing the magnitude of the factor loadings. Each PC was considered a weighted linear combination of the variables and was written with the heavy loadings and given the most descriptive name.

Cumulative column

The eigenvalue table was divided into three sub-sections, namely Initial eigenvalues, Extracted sums of squared loadings and Rotation of sums of squared loadings. For analysis and interpretation purposes we were concerned only with the extracted sums of squared loadings. Note that the first factor accounts for 26.525% of the variance, the second 18.640%, the third 16.373% and the fourth 13.017%. All the remaining factors were not significant. *Table 4* presents the number of principals, from which 4 were selected. The cumulative column indicates that extracting the 4 factors made it possible to explain roughly 75% of the variation in the data.

Principal component factor analysis (Rotated factor pattern)

Principal component 1 (PC1) contributed 26.525% of the variations, with an eigenvalue of 29.419, and represented small-scale farmers who were aware of the impact of climate change, such as floods, soil erosion and water scarcity between 2010 and 2014 (see the Component 1 column in *Table 5*). Of the four coefficients, three were positive, indicating a positive correlation among the significant variables, for instance, an increase in flood incidences will result in an increase in soil erosion; on the other hand, an increase in flood incidences decreases water scarcity. The PC1 equation is presented below:

$$PC1 = 0.465X_1 + 0.754X_2 + 0.400X_8 - 0.907X_9 \quad \text{(Eq.1)}$$

http://www.aloki.hu ● ISSN 1589 1623 (Print) ● ISSN 1785 0037 (Online)
DOI: http://dx.doi.org/10.15666/aeer/1704_73457356

Table 4. *Cumulative percentages of variance. (Source: own calculations based on the survey (2017–2018), N = 188)*

	Initial eigenvalues			Extraction sums of squared loading			Rotation sums of squared loadings		
Variables	**Total**	**% of variance**	**Cumulative %**	**Total**	**% of variance**	**Cumulative %**	**Total**	**% of variance**	**Cumulative %**
Impact on maize production	2.39	26.53	29.419	2.39	26.53	26.53	1.86	20.66	20.66
Flood incidences	1.678	18.640	45.165	1.678	18.640	45.165	1.762	19.577	40.240
Shifts in rainfall	1.474	16.373	61.537	1.47	16.373	61.537	1.671	18.562	58.802
Droughts	1.171	13.017	74.554	1.171	13.017	74.554	1.418	15.752	74.554
Crop disease	0.855	9.499	84.053						
Rural–urban migration	0.516	5.737	89.790						
Structural destruction	0.436	4.840	94.630						
Soil erosion	0.303	3.367	97.996						
Water scarcity	0.180	2.004	100.000						

Table 5. *Rotated factor pattern. (Source: own calculations based on the survey (2017–2018))*

Variables	Component 1	Component 2	Component 3	Component 4
Impact on maize production (X_1)	**0.465**	**-0.349**	0.429	**0.477**
Flood incidences (X_2)	**0.754**	-0.051	0.184	-0.097
Shifts in rainfall (X_3)	-0.057	**0.298**	**- 0.646**	**0.404**
Droughts (X_4)	0.006	0.080	**0.860**	0.191
Crop disease (X_5)	0.159	**0.897**	0.016	-0.070
Rural–urban migration (X_6)	0.082	0.082	**0.519**	-0.366
Structural destruction (X_7)	-0.238	0.069	-0.029	**0.859**
Soil erosion (X_8)	**0.400**	**-0.729**	0.072	-0.286
Water scarcity (X_9)	**-0.907**	-0.076	0.143	0.146

http://www.aloki.hu ● ISSN 1589 1623 (Print) ● ISSN 1785 0037 (Online)
DOI: http://dx.doi.org/10.15666/aeer/1704_73457356

Principal component 2 (PC2) contributed 18.640% of the variations, with an eigenvalue of 45.165. The variables included small-scale maize farmers who were aware of the impacts of climate change on maize production, and experienced shifts in rainfall, crop diseases and soil erosion between 2010 and 2014. The results in the Component 2 column in *Table 5* imply that shifts in rainfall to higher levels decreases the impact on maize production. However, an increase in shifts in rainfall increases crop diseases. The PC2 equation is presented below:

$$PC2 = -0.349X_1 + 0.298X_3 + 0.897X_5 - 0.729X_8 \quad \text{(Eq.2)}$$

Principal component 3 (PC3) contributed 16.373% of the variations, with an eigenvalue of 61.537. The variables included small-scale maize farmers who held perceptions on climate change and who had experienced a significant shift in rainfall, droughts patterns and rural–urban migration. The results in the Component 3 column in *Table 5* indicate that a decrease in rainfall increases drought patterns and rural urban migration. The PC equation between 2010 and 2014 is presented below:

$$PC3 = -0.646X_3 + 0.860X_4 + 0.519X_6 \quad \text{(Eq.3)}$$

Principal component 4 (PC4) contributed to 13.017% of the variations, with an eigenvalue of 70.506. The variables included small-scale maize farmers who held perceptions on climate change and who had experienced impact on maize production, shifts in rainfall and structural destruction between 2010 and 2014. The results in the Component 4 column in *Table 5* show a positive correlation among the variables. The PC equation between 2010 and 2014 is presented below:

$$PC4 = 0.477X_1 + 0.404X_3 + 0.859X_7 \quad \text{(Eq.4)}$$

Correlation between the explanatory variables in the analysis of variance

To determine the degree and nature of the relationship and the direction of association among the independent and dependent variables, a correlation analysis was worked out and presented in the form of a correlation matrix. *Table 6* shows a correlation or relationship between the perceptions of small-scale maize farmers regarding impacts of climate change and the independent variables: the impact on maize production, floods, shifts in rainfall, droughts, crop diseases, rural–urban migration, structural destruction, soil erosion and water scarcity. A positive relationship between perception and the independent variables was established. Of the nine independent variables, five, namely crop diseases, rural–urban migration, structural destruction, soil erosion and water scarcity, were positively and significantly correlated ($p < 0.05$) with the perceptions of farmers regarding climate change.

Table 6 shows that crop diseases were positively and significantly correlated ($p < 0.373$) with floods and droughts (0.375). This meant that farmers who perceived that crop diseases were associated with climate change had high perceptions of floods and droughts as the effects of climate change. A study conducted in Swaziland by Mamba et al. (2015) showed that the majority of farmers (88.1%) indicated that they had noted changes in the frequency, intensity and duration of drought over the preceding years.

http://www.aloki.hu ● ISSN 1589 1623 (Print) ● ISSN 1785 0037 (Online)
DOI: http://dx.doi.org/10.15666/aeer/1704_73457356

Table 6. *Correlation between the explanatory variable in the analysis of variance. (Source: own calculations based on the survey (2017–2018))*

Variables	1	2	3	4	5	6	7	8	9
1. Impact on maize production	1.000								
2. Flood incidences	0.002	1.000							
3. Shifts in rainfall	0.016	0.000	1.000						
4. Droughts	0.000	0.003	0.000	1.000					
5. Crop disease	0.008	**0.373**	0.033	**0.375**	1.000				
6. Rural–urban migration	**0.305**	**0.307**	0.005	0.000	0.000	1.000			
7. Structural destruction	0.010	0.000	0.000	**0.250**	**0.274**	0.001	1.000		
8. Soil erosion	0.000	0.002	0.000	0.129	0.000	0.001	0.000	1.000	
9. Water scarcity	0.001	0.000	**0.255**	0.069	0.003	0.118	0.000	0.000	1.000

$P < 0.05$, $P < 0.01$, $N = 188$

Rural–urban migration was positively correlated (sig. 0.305) with impact on maize production and floods (0.307), and it affected the perceptions of farmers regarding climate change. The more aware the farmers were of rural–urban migration, the more they perceived maize production and floods to be effects of climate change.

The results in *Table 6* showed that structural destruction was positively associated with drought at (sig. 0.250) and crop diseases at (sig. 0.274). From the results, it could be inferred that farmers who perceived structural destruction to be caused by climate change also perceived that droughts and crop diseases were caused by climate change. Water scarcity was also positively correlated with shifts in rainfall. The likelihood of water scarcity as a result of shifts in rainfall was statistically significant (sig. 0.255).

Interpretation of the independent variables

The results of descriptive statistics for all the variables under investigation is presented in *Table 7*. The means and the standard deviation of respondents are given. The means showed rural–urban migration, floods, soil erosion, crop diseases and droughts to be the most important variables influencing small-scale maize farmers' perceptions of climate change. These variables had the highest means, namely 3.4734, 3.4043. 3.2340, 2.9894 and 2.6755, respectively.

Table 7. *Descriptive statistics of the variables. (Source: own calculations based on the survey (2017–2018), N = 188)*

Variables	Mean	Std. deviation
Impact on maize production	1.4096	0.49307
Flood incidences	3.4043	1.12644
Shifts in rainfall	1.9043	1.08040
Droughts	2.6755	1.35079
Crop disease	2.9894	1.24096
Rural–urban migration	3.4734	1.02604
Structural destruction	1.5585	0.96560
Soil erosion	3.2340	1.41743
Water scarcity	1.41743	0.94405

http://www.aloki.hu ● ISSN 1589 1623 (Print) ● ISSN 1785 0037 (Online)
DOI: http://dx.doi.org/10.15666/aeer/1704_73457356

Box plots

Box plots were used to show patterns of responses for each group, as shown in *Figure 3.* They provided a useful way of visualising the range and other characteristics of responses for large groups. As an indicator of centrality, the box plot was of a sample of 5 points from a population centred on 3. As an indicator of symmetry, the box plot was a sample of 5 points from a symmetrical population.

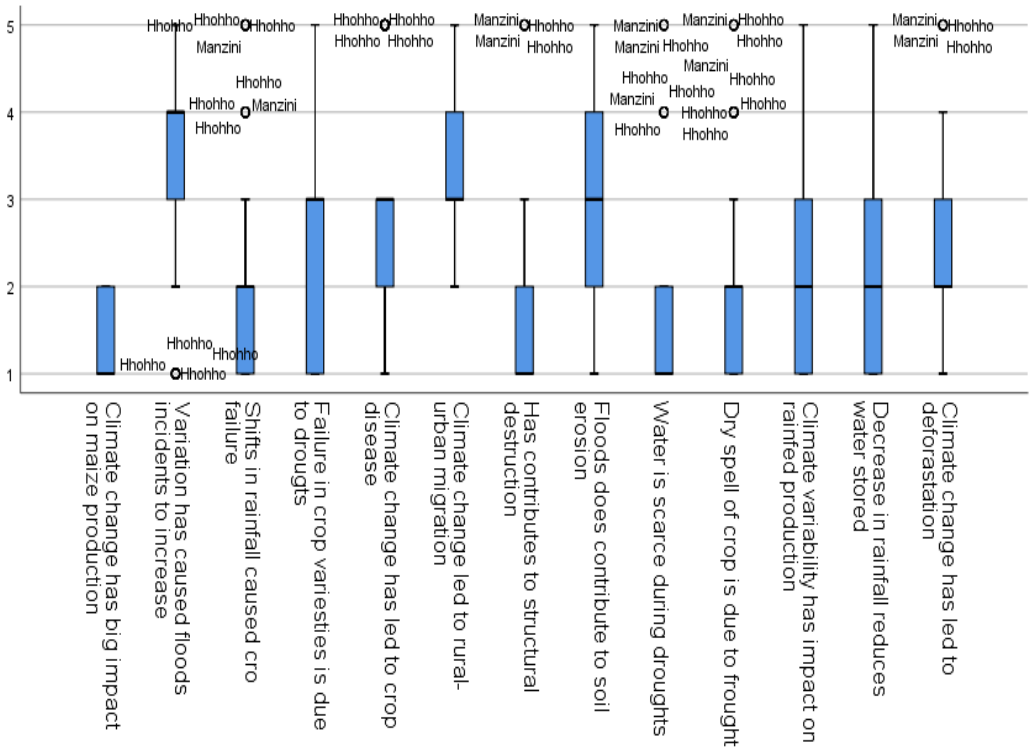

Figure 3. *Box plots showing overall patterns of response for groups*

The data sets for variables 1 and 9, namely impacts on maize production and water scarcity during drought, were skewed to the left with a median of 1. Variables 2 and 6, namely caused floods to increase and rural–urban migration, were skewed to the right and to the left, respectively. The data sets for variables 3 and 10, shift in rainfall caused crop failure and dry spells of crops due to drought, were skewed to the right. According to Debela et al. (2015), farmers perceived the onset of rainfall to be much later over the past ten years than 20 years ago, and they also perceived rainfall to cease halfway through the growing season. Variable 8, floods which contributed to soil erosion, was symmetrical. This showed that small-scale maize farmers perceived soil erosion to be a significant result of climate change.

The line for 1 variable (Floods contributes to soil erosion) is in the centre of the box, and the whisker lengths are the same. In the case of 6 variables (shift in rainfall, structural destruction, dry spells, climate variability and reduced rainfall), the top whisker is much longer than the bottom whisker, and the line gravitates towards the bottom of the box. In the case of 1 variable (climate change has led to crop failure), the bottom whisker is much longer than the top whisker, and the line rises to the top of the box.

http://www.aloki.hu ● ISSN 1589 1623 (Print) ● ISSN 1785 0037 (Online)
DOI: http://dx.doi.org/10.15666/aeer/1704_73457356

Conclusion

The perceptions of small-scale maize farmers regarding climate change was analysed using information from maize farmers relating to the farming seasons during the period 2010 to 2014. Results showed that farmers had different levels of perception regarding climate change. They also showed that maize production declined in the 2012 to 2014 cropping seasons. Principal component analysis revealed that it was possible to place different perception factors affecting climate change in different groups. In conclusion, smallholder maize farmers in the three regions held a range of perceptions regarding climate change. The results indicated that any adaptation strategies developed by smallholder maize farmers to combat climate change were largely influenced by their perceptions regarding climate changes. Farmers' perceptions, if well articulated, have a significant influence on how the government responds or intervenes in such situations.

REFERENCES

[1] Abid, M. E. A., Scheffran, J., Schneider, U. A., Ashfaq, M. (2015): Farmers' perceptions of and adaptation strategies to climate change and their determinants: the case of Punjab province, Pakistan. – Earth System Dynamics 6(1): 225–243.

[2] Adebayo, A. A., Onu, J. I., Adebayo, E. F., Anyanwu, S. O. (2012): Farmers' awareness, vulnerability and adaptation to climate change in Adamawa State, Nigeria. – British Journal of Arts and Social Sciences 9(2): 104–115.

[3] Ayanlade, A., Radeny, M., Morton, J. F. (2017): Comparing smallholder farmers' perception of climate change with meteorological data: a case study from southwestern Nigeria. – Weather and Climate Extremes 15: 24–33.

[4] Belay, A., Recha, J. W., Woldeamanuel, T., Morton, J. F. (2017): Smallholder farmers' adaptation to climate change and determinants of their adaptation decisions in the Central Rift Valley of Ethiopia. – Agriculture & Food Security 6(1): 24.

[5] Debela, N., Mohammed, C., Bridle, K., Corkrey, R., McNeil, D. (2015): Perception of climate change and its impact by smallholders in pastoral/agropastoral systems of Borana, South Ethiopia. – SpringerPlus 4(1): 236.

[6] Jacobi, J., Schneider, M., Bottazzi, P., Pillco, M., Calizaya, P., Rist, S. (2015): Agroecosystem resilience and farmers' perceptions of climate change impacts on cocoa farms in Alto Beni, Bolivia. – Renewable Agriculture and Food Systems 30(2): 170–183.

[7] Mamba, S. F., Salam, A., Peter, G. (2015): Farmers' perception of climate change: a case study in Swaziland. – Journal of Food Security 3(2): 47–61.

[8] Rahi, S. (2017): Research design and methods: A systematic review of research paradigms, sampling issues and instruments development. – International Journal of Economics & Management Sciences 6(2): 1–5.

[9] Sutcliffe, C., Dougill, A. J., Quinn, C. H. (2016): Evidence and perceptions of rainfall change in Malawi: do maize cultivar choices enhance climate change adaptation in sub-Saharan Africa? – Regional Environmental Change 16(4): 1215–1224.

http://www.aloki.hu ● ISSN 1589 1623 (Print) ● ISSN 1785 0037 (Online)
DOI: http://dx.doi.org/10.15666/aeer/1704_73457356

EVALUATION OF HEAT TOLERANCE INDEX, SUSCEPTIBILITY INDEX OF CANOPY TEMPERATURE AND LEAF CHLOROPHYLL CONTENT OF WHEAT (*TRITICUM AESTIVUM* L.)

LI, Q.[1,2,3] – MENG, X. H.[1,2,3] – LI, D.[1,2,3] – ZHAO, M. H.[1,2,3] – SUN, S. L.[1,2,3] – LI, H. M[1,2,3] – LI, W.[1,2,3] – QIAO, W. C[1,2,3*]

[1]*Dryland Farming Institute, Hebei Academy of Agricultural and Forestry Sciences, Hengshui, China*

[2]*Key Lab of Crop Drought Tolerance Research of Hebei Province, Hengshui, China*

[3]*Hengshui Branch, National Wheat Improvement Center, Hengshui, China*

**Corresponding author*
e-mail: qwc7228@126.com; phone: +86-031-8792-0618; fax: +86-031-8792-0312

(Received 18th Feb 2019; accepted 8th Apr 2019)

Abstract. Heat negatively affects wheat production in the world. At present, heat tolerance remains one least understood field in wheat genetics and breeding, because there are not enough effective methods for identification of heat stress and tolerance. This study used sixteen cultivars of winter wheat to evaluate a new method with stress intensity (δ) and heat tolerance index (HTI), and assess the susceptibility index of canopy temperature (SCT) and leaf chlorophyll content (SLCC) at different days after the anthesis to identify heat tolerance. The result showed HTI had significant positive correlations with yield under heat stress, and significant negative correlations with yield reduction rate, indicating that HTI is a good indicator of both yield potential and stability under heat stress which can be used to identify heat tolerance in later generations. SCT at 28 DAA had significant positive correlation with yield and significant negative correlation with yield reduction rate under heat stress. SLCC at 29 DAA had positive correlation with yield and significant negative correlation with yield reduction rate, and especially kernel weight reduction under heat stress. The two indicators may be used to screen for heat tolerant germplasm in early generations, or to identify a large number of wheat cultivars concurrently.
Keywords: *wheat, heat stress, stress intensity, yield, yield reduction*

Introduction

Wheat (*Triticum aestivum* L.) is one of the most important foods in the world, and it has become a basic food staple in Asia, Europe, and North Africa. Therefore, global wheat yield needs to be increased to meet the rising demand for this grain, and high grain value must be maintained under climate change to ensure ongoing human nutrition, end-use functional properties, as well as commodity value (Nuttall et al., 2017). As climates warm, heat stress during the post-anthesis period (terminal heat) negatively affects wheat production. This increased temperature not only hastens the phenological stages of wheat development but also reduces the duration of the grain filling stages, thereby lowering grain yield and quality (Faroop et al., 2011; Figueiredo et al., 2015; Gooding et al., 2003; Hoffmann et al., 2006). Increases in mean daily air temperatures of 1 °C during wheat development are projected to shorten the grain filling period by 3.1 d and decrease the weight per grain by as much as 2.8 mg (Wiegand and Cuellar, 1981). These wheat yield losses severely threaten global food security.

Most heat stress studies were aimed at predicting and maximizing yield (Amani et al., 1996; Blum et al., 2001; Rane and Nagarajan, 2004; Reynolds et al., 1998; Tewolde

http://www.aloki.hu ● ISSN 1589 1623 (Print) ● ISSN 1785 0037 (Online)
DOI: http://dx.doi.org/10.15666/aeer/1704_73577369

et al., 2006; Xu et al., 2000). Some other studies focused on stability under heat stress. For example, some wheat genotypes were demonstrated to be tolerant to the effects of heat stress on grain quality at 29 days after anthesis (days after anthesis, DAA) (Blumenthal et al., 1995). In a recent paper, 54 genotypes were classified in two overall groups: stable and unstable, based on their rank shifts in different environments (Hernández-Espinosa et al., 2018). However, these numerical values cannot completely reflect the heat resistance of different wheat cultivars. The ultimate indicator of cultivar-specific heat resistance is manifested in the absolute and relative yield, that is, both yield potential and stability. Ideal heat resistance would be displayed as a durable, consistent yield with minimal yield reduction under heat stress conditions.

Some characteristics like leaf chlorophyll content and canopy temperature depression may be correlated with field performance, especially under heat stress (Jin et al., 2012; Wu et al., 2015). Ayeneh et al. (2002) compared the leaf, spike, peduncle, and canopy temperature depression in wheat under heat stress. Bahar et al. (2008) studied the effect of canopy temperature depression on grain yield and yield components in bread and durum wheat. Webber et al. (2015) used a multi-model approach including canopy temperature to simulate heat stress in irrigated wheat in a semi-arid environment. Gautam et al. (2015) found canopy temperature may be used as a selection parameter for grain yield and its components in Durum Wheat under terminal heat stress in late sown conditions. The term of susceptibility index ($1\text{-}Y/Y_p$) was used to reflect response of plant yield to heat stress, where Y is yield under stress, Yp is yield without stress, which was commonly used for estimating stress resistance (Li et al., 2018; Mason et al., 2010).

The purpose of this study was to evaluate a new method for identifying the heat tolerance of wheat cultivars based on yield and yield reduction under heat stress, and the related physiological indicators of canopy temperature and leaf chlorophyll content at different times after heat stress treatment. We designed a movable greenhouse for temperature control and created a heat tolerance index (heat tolerance index, HTI) for testing different wheat cultivars. This identifying method combining yield potential and stability could be a useful selection method for characterizing cultivar performance under heat stress. The susceptibility index of canopy temperature (susceptibility index of canopy temperature, S_{CT}) and leaf chlorophyll content (susceptibility index of leaf chlorophyll content, S_{LCC}) at different days after the anthesis have potential application for breeding in indirect selection to identify physiologically superior genotypes under heat stressed environment.

Materials and methods

Cultivars

The 16 winter wheat (*Triticum aestivum* L.) cultivars most commonly grown in the North China Plain (*Table 1*) were evaluated for heat tolerance. Cultivars were mechanically sown by Wintersteiger plotseed TC at the research station in Hebei Hengshui (37°44′N, 115°42′E; elev. 20 m). Meteorological data for this area is shown in *Figure 1*.

The experiment was conducted on sandy loam soil in field conditions. A split block design with 3 × 2 treatments and three replicates was employed during the 2016-2017 and 2017-2018 crop seasons. Each cultivar was grown in an 11.16-m^2 plot (nine rows of 8 m length with 15.5 cm space between rows). After adjusting for seed size, the seed

http://www.aloki.hu ● ISSN 1589 1623 (Print) ● ISSN 1785 0037 (Online)
DOI: http://dx.doi.org/10.15666/aeer/1704_73577369

density was maintained at a uniform population of 300 plants per m^2 (3 million plants per hectare), according to the 1000 grain weight and germination percentage. Standard agronomic practices recommended for normal fertility (340 kg/ha N: 172.5 kg/ha P_2O_5: 40 kg/ha K_2O) were followed. All K_2O and P_2O_5 were applied at the time of sowing. Nitrogen was supplied in split applications: 170 kg/ha N at sowing and 170 kg/ha N at the first irrigation. Care was taken to avoid moisture and biotic stress by ensuring timely irrigation and pesticide control. Cultivars were harvested by Wintersteiger and weighted by electronic scale.

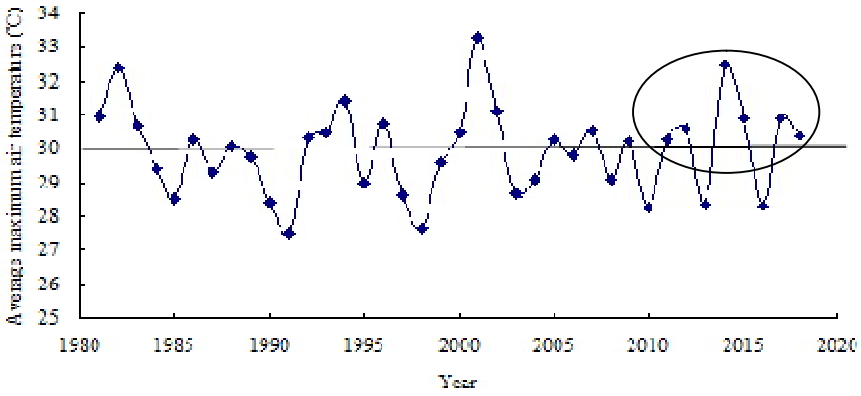

Figure 1. *Average daily maximum air temperature (14 May - 14 June) per year from 1981 to 2018 in the wheat growing region from this study. Temperature varied from 27.5 °C in 1991 to 33.3 °C in 2001. The increased frequency with higher daily maximum temperature than average value in a 10-year cycle indicates an increased risk in environmental heat pressure during the wheat grain filling stage in this region*

Table 1. *The 16 winter wheat cultivars evaluated in this study*

No.	Cultivar	No.	Cultivar
1	Heng11-6021	9	HengH14-4019
2	Heng9966	10	HengH14-5051
3	HengH14Guan14	11	HengH15-4489
4	HengH13Guan26	12	HengH13-5062
5	Heng5835	13	Heng12-6098
6	HengS13-5022	14	Heng14-K2-3
7	Heng5109	15	Jimai22
8	HengH15-4585	16	Heng4399

Heat treatments

On 14 May 2016, the mobile temperature-controlled greenhouse was used to cover the 16 cultivars at 14 DAA (for 80% of individuals). Heat treatments continued for 32 d, increasing the daily maximum temperature from 28.1 °C to 48.0 °C during 2016-2017 and from 22.3 °C to 48.6 °C during 2017-2018 (*Fig. 2*). Temperature was maintained 5 °C (± 1 °C) higher than ambient conditions.

http://www.aloki.hu ● ISSN 1589 1623 (Print) ● ISSN 1785 0037 (Online)
DOI: http://dx.doi.org/10.15666/aeer/1704_73577369

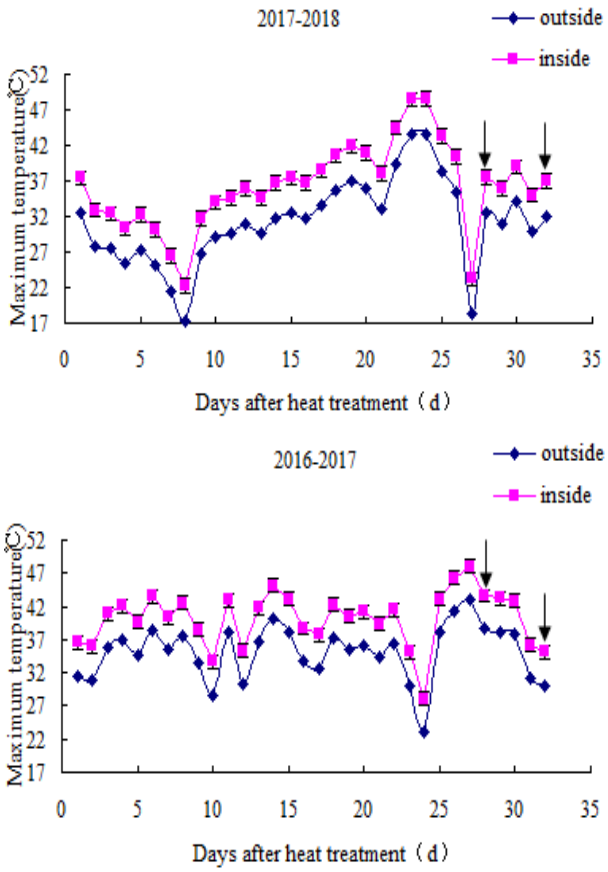

Figure 2. *Daily maximum temperature inside and outside of the greenhouse in the 2016-2017 and 2017-2018 seasons. An approximate 5 °C difference between the inside and outside temperatures was maintained for 32 d. Bars mean SE. Arrows indicate the time of canopy temperature measurements. The air temperature had been measured parallel with the canopy temperature*

X and Xp indicate yield averaged over all cultivars under stress and control treatments, respectively. 1-X/Xp represents 'stress intensity' (δ). These criteria can be used to estimate resistance to stress (Li et al., 2018; Mason et al., 2010).

The heat tolerance index (HTI) includes both yield potential and stability after heat stress. To include the value of yield potential after heat stress, we substituted absolute yield under heat stress (yield, Y) into the formula, resulting in:

$$HTI = \frac{Y_S^{\,2}}{Y_{S.P}} \times \frac{Y_{CK.P}}{Y_{CK}^{\,2}} \qquad \text{(Eq.1)}$$

where Y_S: yield of identified cultivars under heat stress; $Y_{S.P}$: yield of identified cultivars under normal treatment; $Y_{CK.P}$: yield of CK cultivar under normal treatment; Y_{CK}: yield of CK cultivar under heat stress. We calculated relative yield (Y/Y_P) to account for variation in yield under the control conditions. Relative yield is commonly used in studies of stress resistance (Blum, 1973; Fischer and Maurer, 1978). We also included control data to account for variability in other environmental factors.

http://www.aloki.hu ● ISSN 1589 1623 (Print) ● ISSN 1785 0037 (Online)
DOI: http://dx.doi.org/10.15666/aeer/1704_73577369

HTI was used to classify each cultivar (*Table 2*) as tolerant (≥ 1.20), moderately tolerant (1.00 to ≤ 1.19), moderately susceptible (0.80 to ≤ 0.99), or susceptible (≤ 0.79).

Table 2. *HTI scale for tolerance of or susceptibility to heat stress for different wheat cultivars*

Scale	HRI	Opinion
1	≥ 1.20	Tolerant
2	1.00-1.19	Moderately tolerant
3	0.80-0.99	Moderately susceptible
4	≤ 0.79	Susceptible

Canopy temperature measurements

Canopy temperature was measured using a hand-held infrared thermometer (IRT) (Model AG-42, Telatemp Crop, Fullerton, CA) at 15 and 20 d after heat treatment (28 May and 2 June). Three measurements were taken per plot with the instrument held at an angle of 30° to the horizontal plane, 1 m away from the edge of the plot and approximately 50 cm above the plants, giving a canopy view of 10 cm × 25 cm. Measurements were taken 0.5 h before and 2 h after solar noon, in full sunshine, 3 or 4 d after irrigation had been applied, as recommended by Amani et al. (1996). The equation of S_{CT} is as follows:

$$S_{CT} = \frac{CT}{CT_P} - 1 \qquad \text{(Eq.2)}$$

where CT (canopy temperature, CT) is canopy temperature under stress, CT_p is canopy temperature without stress.

Leaf chlorophyll content measurements

Chlorophyll content was measured in 10 randomly selected flag leaves in each plot by using a portable chlorophyll content meter (CCM-200, Opti-Sciences Inc., NH, USA). Ten measurements were taken for each plot. The measurements were taken at 29DAA and 33DAA. The equation of S_{LCC} is as follows:

$$SLCC = 1 - \frac{LCC}{LCC_P} \qquad \text{(Eq.3)}$$

where LCC (leaf chlorophyll content, LCC) is leaf chlorophyll content under stress, LCCp is leaf chlorophyll content without stress.

Statistical analysis

Statistical analysis was done using SAS software (SAS Institute 2003). Statistical analysis using HTI values, SCT, SLCC, yield and yield reduction were performed for sixteen genotypes. The linear correlation coefficient was calculated to determine the

http://www.aloki.hu ● ISSN 1589 1623 (Print) ● ISSN 1785 0037 (Online)
DOI: http://dx.doi.org/10.15666/aeer/1704_73577369

association among of HTI values, SCT and SLCC with yield and yield reduction under heat stress. Differences were considered significant at the $P < 0.01$ level.

Results

Meteorological data

The average maximum temperature (14^{th} May - 14^{th} June) in Hengshui from 1981 to 2018 was 30 °C. The highest average temperature recorded was 27.5 °C in 1991, and the highest temperature during the grain filling stage was 33.3 °C in 2001. These maximum temperatures have a difference of 5.8 °C. We used this temperature difference in the controlled greenhouse experiments by exposing the treatment plants to a heat stress treatment 5 °C higher than the control treatment. In the first decade (1981-1990), the average maximum temperature was 30 °C, and five of these years were greater than the average value; in the second decade (1991-2000), the average maximum temperature was 29.6 °C, and five years were greater than the average value; in the third decade (2001-2010), the average maximum temperature was 30 °C, with another five years greater than the average value; in 2011-2018, the average maximum temperature was 30.3 °C, which has been higher than the long-term average during six years. The increased frequency with higher daily maximum temperature than average value in a 10-year cycle indicates an increased risk in environmental heat pressure during the wheat grain filling stage in this region.

We obtained the values for 'stress intensity' of $\delta_{2017} = 0.33$ and $\delta_{2018} = 0.11$ in 2016-2017 and 2017-2018 respectively, in accordance with the trend of average maximum air temperature change from 2017 to 2018.

The maximum daily temperature inside and outside of the greenhouse during the 2016-2017 and 2017-2018 crop growing seasons are presented in *Figure 2*. The ranges of the daily maximum temperature inside the greenhouse were from 28.1 °C to 48.0 °C and from 22.3 °C to 48.6 °C during 2016-2017 and 2017-2018, respectively.

Evaluation and application of heat tolerance index (HTI)

Heat stress affected values for mean yield, which dropped from 8864.9 to 5978 kg/ha in 2017 and from 7425.8 to 6588.3 kg/ha in 2018, when comparing the control to the heat stress treatments (*Table 3*). Stress intensity (δ) was 0.33 in 2017 and 0.11 in 2018 (*Fig. 3*). Average yield of the 16 wheat cultivars decreased by 18 kg/ha (2017) and 5.2 kg/ha (2018) under heat stress during the grain filling stages.

HTI calculated by *Equation 1* with maximum value in cultivars exhibited lower YR and higher yield under heat stress. HTI reached a maximum of 1.42 for the HengH15-4489 cultivar in 2017 and of 1.16 for the Heng14-K2-3 cultivar in 2018. HTI attained a minimum of 0.74 for the Heng9966 cultivar in 2017 and 0.84 for the HengH14-5051 cultivar in 2018. There was no detectable difference in HTI between the two experimental years. Cultivars, yield, reduction under heat stress, and HTI showed significant correlations (*Table 4*). Positive correlations ($R = 0.9775$ and $R = 0.9415$ in 2017 and 2018, respectively) were found between HTI and mean yield under heat stress (*Fig. 3*). Significant negative correlations ($R = -0.9419$ and $R = -0.7458$ in 2017 and 2018, respectively) existed between HTI and YR rate (*Fig. 3*).

http://www.aloki.hu ● ISSN 1589 1623 (Print) ● ISSN 1785 0037 (Online)
DOI: http://dx.doi.org/10.15666/aeer/1704_73577369

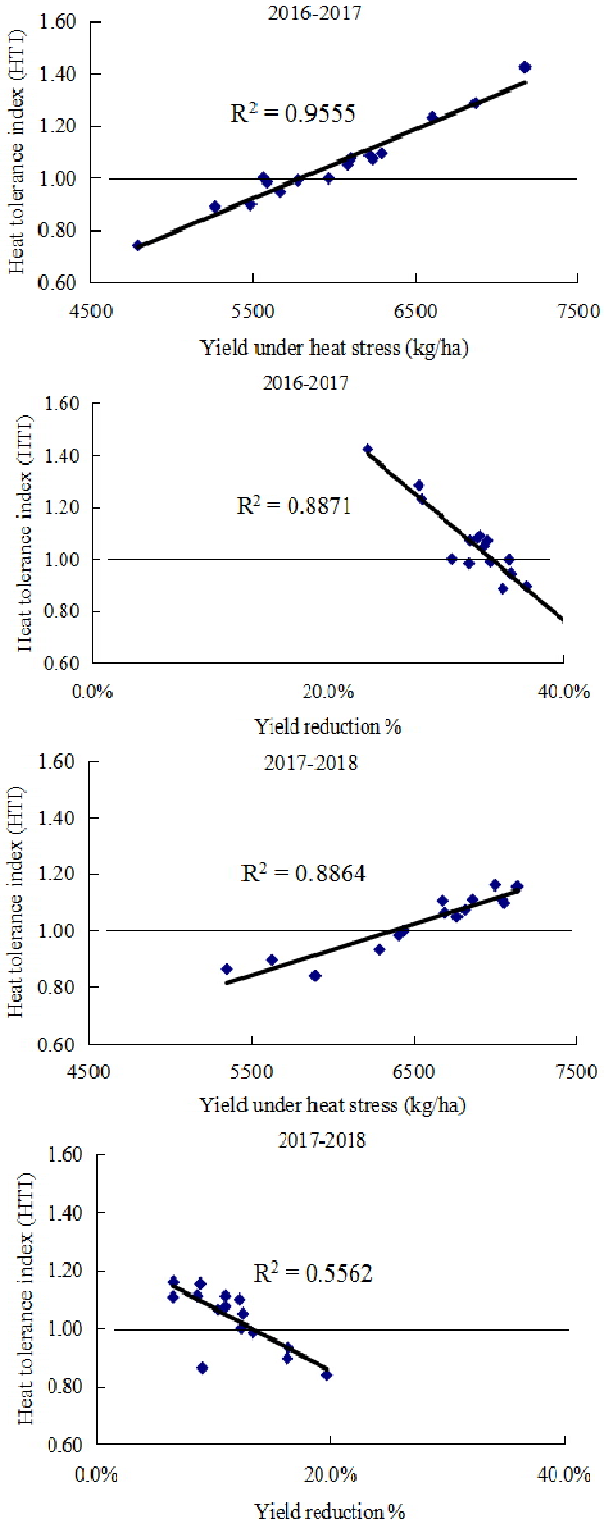

Figure 3. *Correlations based on averaged values for the 16 wheat studied cultivars for yield under heat stress (kg/ha) and yield reduction (YR) with heat tolerance index (HTI) in the 2016-2017 and 2017-2018 growth seasons. Positive correlations (R = 0.9775 in 2016-2017; R = 0.9415 in 2017-2018, P < 0.001) existed between HTI and yield under heat stress. Negative correlations (R = -0.9419 in 2016-2017; R = -0.7458 in 2017-2018, P < 0.001) were observed between HTI and YR. The line at 1 on the y-axis indicates standard heat tolerance. Dots indicate average values for each cultivar*

http://www.aloki.hu ● ISSN 1589 1623 (Print) ● ISSN 1785 0037 (Online)
DOI: http://dx.doi.org/10.15666/aeer/1704_73577369

Across the two years, 5 cultivars consistently showed HTI < 1 (Heng9966, Heng12-6098, Hengs13-5022, Heng5835, and Hengh14-5051) with low yield and high yield reduction under heat stress (*Table 3*). There were 8 cultivars, HTI > 1 (Heng5109, Jimai22, Heng11-6021, Heng14-K2-3, HengH15-4585, HengH13Guan26, HengH14-4019, and HengH15-4489), indicating high yield and low yield reduction under heat stress.

Table 3. *The evaluation on the yield, yield reduction, HTI, S_{CT} at 28DAA and S_{LCC} at 29DAA of 16 wheat cultivars. Y: yield, YR: yield reduction, HTI: heat tolerance index, S_{CT}: susceptibility index of canopy temperature, S_{LCC}: susceptibility index of leaf chlorophyll content*

Cultivar	2016-2017					2017-2018				
	Y	YR	HTI	S_{CT}	S_{LCC}	Y	YR	HTI	S_{CT}	S_{LCC}
HengH15-4489	7172.73	23.37%	1.42	0.50	0.69	6859.94	8.7%	1.11	0.22	0.22
HengH14-4019	6867.01	27.72%	1.28	0.37	0.19	7143.68	8.9%	1.15	0.25	0.25
HengH13Guan26	6600.57	27.95%	1.23	0.26	0.37	7057.68	12.3%	1.10	0.17	0.19
HengH15-4585	6289.61	32.90%	1.09	0.21	0.19	6813.76	11.1%	1.07	0.21	0.18
Jimai22	6215.86	32.66%	1.08	0.24	0.19	7045.74	11.1%	1.11	0.20	0.20
Heng14-K2-3	6102.14	32.06%	1.07	0.32	0.10	7001.97	6.6%	1.16	0.22	0.26
Heng11-6021	6233.34	33.53%	1.07	0.26	0.13	6693.87	10.4%	1.06	0.19	0.16
Heng5109	6082.20	33.26%	1.05	0.23	0.09	7136.10	8.9%	1.15	0.23	0.21
Heng4399	5559.11	30.51%	1.00	0.30	0.25	6439.05	12.4%	1.00	0.14	0.12
Heng5835	5962.75	35.37%	1.00	0.21	0.11	5352.49	9.1%	0.86	0.18	0.18
Heng12-6098	5777.02	33.78%	0.99	0.25	0.19	6292.44	16.4%	0.93	0.19	0.14
HengH14Guan14	5582.43	31.98%	0.98	0.21	0.01	6766.73	12.5%	1.05	0.20	0.09
HengH13-5062	5664.56	35.52%	0.95	0.29	0.12	6680.69	6.6%	1.11	0.28	0.11
HengH14-5051	5484.24	36.84%	0.90	0.19	0.23	5894.21	19.7%	0.84	0.10	0.14
HengS13-5022	5262.46	34.83%	0.89	0.08	0.11	5627.07	16.3%	0.90	0.06	0.07
Heng9966	4792.11	40.40%	0.74	0.19	0.16	6406.01	13.4%	0.98	0.17	0.12

Evaluation of susceptibility index of canopy temperature (S_{CT}) and leaf chlorophyll content (S_{LCC})

In order to evaluate the susceptibility index related physiological indicators, we detected canopy temperature and chlorophyll content. S_{CT} and S_{LCC} were calculated by *Equations 2* and *3* respectively. S_{CT} reached a maximum of average value 0.36 for the HengH15-4489 in 2017 and 2018. Meanwhile S_{CT} attained a minimum of average value 0.07 for the HengS13-5022 in 2017 and 2018. S_{LCC} reached a maximum of average value 0.46 for the HengH15-4489 in 2017 and 2018. Meanwhile S_{LCC} attained a minimum of average value 0.05 for the HengH14Guan14 in 2017 and 2018. The result (*Table 4*) showed that there were significant positive correlations (R = 0.7356 and R = 0.6579 in 2017 and 2018, respectively; $P < 0.01$) between S_{CT} at 28DAA and yield under heat stress, and significant negative correlations (R = -0.7645 and R = -0.8164 in 2017 and 2018, respectively; $P < 0.001$) between S_{CT} and yield reduction under heat treatment. Meanwhile there were significant negative correlations (R = -0.6762 and R = -0.5548 in 2017 and 2018, $P < 0.01$ and $P < 0.05$, respectively) between S_{LCC} at 29 DAA and yield reduction under heat stress, and significant negative correlations (R = -

http://www.aloki.hu ● ISSN 1589 1623 (Print) ● ISSN 1785 0037 (Online)
DOI: http://dx.doi.org/10.15666/aeer/1704_73577369

0.7497 and R = -0.8556 in 2017 and 2018, respectively; $P < 0.001$) between S_{LCC} and kernel weight reduction under heat treatment.

Table 4. *Correlations among yield under heat stress (Y), yield reduction under heat stress (YR%) and kernel weight reduction (KWR%) as canopy temperature (CT), leaf chlorophyll content (LCC), susceptibility index of canopy temperature (S_{CT}), and susceptibility index of leaf chlorophyll content (S_{LCC}) in 2016-2017 and 2017-2018*

Time	Content	2016-2017			Daily maximum temperature	2017-2018			Daily maximum temperature
		Y	YR	KWR		Y	YR	KWR	
28 DAA	CT	-0.6984**	0.6336**	0.3517	38.1 ℃	-0.6763**	0.5888*	0.5872*	32.4 ℃
	S_{CT}	0.7356**	-0.7645***	-0.5975*		0.6579**	-0.8164***	-0.4093	
29 DAA	LCC	-0.1605	0.3492	0.6289**	33.7 ℃	0.0123	-0.2359	0.2013	31.8 ℃
	S_{LCC}	0.5870*	-0.6762**	-0.7497***		0.5614*	-0.5548*	-0.8556***	
32 DAA	CT	0.0611	0.0062	-0.3757	35.5 ℃	0.3611	-0.0752	-0.2019	36.9 ℃
	S_{CT}	-0.1131	-0.2099	0.1720		0.0006	0.3464	-0.3252	
33 DAA	LCC	-0.0316	0.1222	0.1788	36.2 ℃	-0.3246	-0.0845	0.1610	35.9 ℃
	S_{LCC}	-0.4802	0.4129	0.6002*		0.2476	0.0317	0.1477	

*, **, *** significant at $P < 0.05$, $P < 0.01$, and $P < 0.001$, respectively

Discussion

Meteorological change

According to the meteorological data in 38 years, the frequency of the average maximum temperatures appeared in the winter wheat grain filling stage (14 May-14 June) in Hengshui are increasing, which is similar with findings of the Intergovernmental Panel on Climatic Change (IPCC, 2013). Heat tolerance identification and breeding should be preferred to be researched, even with extremely high temperature.

Evaluation and application of heat tolerance index (HTI)

HTI showed significant correlations with yield and yield reduction under heat stress in 2 crop seasons, which supports the conclusion that HTI can be used to identify heat tolerance by indicating the yield potential and yield stability of wheat cultivars under heat stress.

HTI has several advantages over other methods for identifying heat tolerance. It is easier to quantify using the 'stress intensity' (δ) and HTI. Correlations between HTI, yield, and yield reduction were significant across the two experimental years, indicating reliability across variable growth conditions. HTI can also measure heat tolerance by incorporating both the values of yield stability and potential, linking yield reduction under heat stress to maximum possible yield.

There were 8 wheat cultivars whose HTI reached or exceeded level 2 ('moderately tolerant') across both years indicating adequate heat tolerance. These cultivars should be considered for wheat breeding with high heat tolerance. There were 5 wheat cultivars that reached level 3-4, indicating adequate heat susceptibility, and may be used for genetic analysis. In further study, we can use HengH15-4489 with the highest HTI and Heng9966 with the lowest HTI according to the two-year average, as parents to construct genetic population to analysis heat tolerant mechanism, heat tolerant genes mapping and tagging.

http://www.aloki.hu ● ISSN 1589 1623 (Print) ● ISSN 1785 0037 (Online)
DOI: http://dx.doi.org/10.15666/aeer/1704_73577369

HTI can give a fuller picture of heat tolerance than yield reduction alone. In one cultivar, Heng5835, HTI in 2017-2018 was low as 0.86, but the yield reduction reached only 9.1%. This may be due to its early and low yield in the control treatment. Therefore, the use of only yield reduction may give incorrect information about heat tolerance.

HTI may be more able to identify heat tolerance when stress intensity is higher. In 2017-2018, stress intensity reached $\delta_{2018} = 0.11$ due to the severe heat waves that occurred in late stage of filling, and the yield under the control treatment reduced. Results would otherwise be clustered due to this strong effect, but HTI was reliable.

Evaluation of susceptibility index of canopy temperature (S_{CT}) and leaf chlorophyll content (S_{LCC})

Measuring Canopy temperature and leaf chlorophyll content was inexpensive, fast, easy, and suitable for breeding applications (Brennan et al., 2007; Reynolds et al., 2007). In this study we used susceptibility index of canopy temperature (S_{CT}) and leaf chlorophyll content (S_{LCC}) at different days after the anthesis to identify heat tolerance. The wheat cultivar with the highest S_{CT} and S_{LCC} during 2017-2018 was HengH15-4489, which was in agreement with the result of HTI. This cultivar performed heat tolerance well during 2017-2018. In further research, we can study on heat tolerant mechanism by using this cultivar.

The result showed that S_{CT} at 28 DAA had significant positive correlation with yield and significant negative correlation with yield reduction rate under heat stress, indicating that the wheat lines with higher S_{CT} may have high yield potential and yield stability in early generation under heat stress. It was reported that the canopy temperature and transpiration rate had a very significant negative correlation (Wall et al., 2006). Here, the canopy temperature of the cultivars with good heat tolerance increases greatly. It may be related to the regulation of reducing the transpiration rate with water loss getting slower and plant function keeping longer. The result need to be further verified.

S_{LCC} at 29 DAA had positive correlation with yield and significant negative correlation with yield reduction rate, and especially kernel weight reduction under heat stress, indicating that wheat lines with higher S_{LCC} may have lower yield and kernel weight reduction for stability under heat stress**.** The results agree with previous studies, showing that plant adapt to stress environment by reducing chlorophyll content in plant leaves to alleviate photo-inhibition and improve photosynthesis (Melis, 2009; Ort et al., 2011, 2015; Polle et al., 2003).

The result also indirectly proved the mechanism of heat tolerance: under heat stress, stomatal closure reduces transpiration, and then canopy temperature rise; meanwhile chlorophyll content in plant leaves reduce to alleviate photo-inhibition then improve photosynthesis, and to reduce light absorption then reduce canopy temperature.

The new methodology better estimated heat tolerance compared to other methods for four reasons. First, the heat treatment was easier to quantify because of using ‘stress intensity’ (δi). Second, HTI, SCT and SLCC had greater repeatability over different years and different stress intensities. Third, the correlations among HTI, SCT, SLCC, yield and yield reduction under heat stress was always significant in different years. Finally, HTI, SCT and SLCC linked the yield under heat stress to the yield reduction and reflected a heat tolerance with yield potential and stability in heat stress of different wheat cultivars simultaneously.

http://www.aloki.hu ● ISSN 1589 1623 (Print) ● ISSN 1785 0037 (Online)
DOI: http://dx.doi.org/10.15666/aeer/1704_73577369

The different cultivar responses to heat stress indicated that the heat resistance ability of wheat cultivars varied. HTI and SCT was able to represent these varied responses and significantly correlate with the yield and yield reduction of wheat under heat stress. Accordingly, this new methodology can be used to reflect the yield potential and the stability to heat stress of different wheat varieties simultaneously. Cultivars with a high HTI (> 1) or higher SCT can be considered to be heat tolerance, as they exhibited higher yield and smaller yield reductions under heat stress compared with the other cultivars. The new methodology was a reliable evaluation for heat-tolerance of wheat cultivars. HTI is a good indicator of both yield potential and stability under heat stress which can be used to identify heat tolerance in advanced generations. The other two indicators SCT and SLCC may be used to screen for heat tolerance germplasm in early generations, or to identify a large number of wheat cultivars concurrently. HTI combined with SCT and SLCC maybe a good breeding strategy for heat tolerance improving.

Conclusions

In this study of heat tolerance across 16 wheat cultivars, HTI, S_{CT} and S_{LCC} showed significant correlations with yield and yield reduction under heat stress, and may be efficient indicators reflecting heat tolerance, including both yield potential and stability simultaneously. HTI can be used to identify heat tolerance of wheat cultivars in advanced generations, and S_{CT} at 28 DAA and S_{LCC} at 29 DAA may be used to screen for heat tolerant germplasm in early generations, or to identify a large number of wheat cultivars concurrently.

Acknowledgements. This research was financially supported by the National Key Technology R&D Program of China under Grant [2016YFD0100502]; National Key Technology R&D Program of China under Grant [2016YFD0300407]; National Wheat Cultivation Industry System under Grant [CARS-3-1-1]; and the HAAFS Technological Innovation Program [4-01-03].

REFERENCES

[1] Amani, I., Fischer, R. A., Reynolds, M. P. (1996): Canopy temperature depression associated with yield of irrigated spring wheat cultivars in a hot climate. – Journal of Agronomy and Crop Science 176: 119-129.

[2] Ayeneh, A., Mvan, G., Reynolds, M. P., Ammar, K. (2002): Comparison of leaf, spike, peduncle and canopy temperature depression in wheat under heat stress. – Field Crops Research 79(2): 173-184.

[3] Bahar, B., Yıldırım, M., Barutcular, C., Genc, I. (2008): Effect of canopy temperature depression on grain yield and yield components in bread and durum wheat. – Notulae Botanicae Horti Agrobotanici Cluj-Napoca 36(1): 34-37.

[4] Blum, A. (1973): Components analysis of yield responses to drought of sorghum hybrids. – Experimental Agriculture 9: 159-167.

[5] Blum, A., Klueva, N., Nguyen, H. T. (2001): Wheat cellular thermotolerance is related to yield under heat stress. – Euphytica 117: 117-123.

[6] Blumenthal, C., Bekes, F., Gras, P. W., Barlow, E. W. R., Wrigley, C. W. (1995): Identification of wheat genotypes tolerant to the effects of heat stress on grain quality. – Cereal Chemistry 72(6): 539-544.

http://www.aloki.hu ● ISSN 1589 1623 (Print) ● ISSN 1785 0037 (Online)
DOI: http://dx.doi.org/10.15666/aeer/1704_73577369

[7] Brennan, J. P., Condon, A. G., Van, G. M., Reynolds, M. P. (2007): An economic assessment of the use of physiological selection for stomatal aperture-related traits in the CIMMYT wheat breeding programme. – Journal of Agricultural Science 145(1): 187-194.
[8] Farooq, M., Bramley, H., Palta, J. A., Siddique, K. H. M. (2011): Heat stress in wheat during reproductive and grain filling phases. – Critical Reviews in Plant Sciences 30: 491-507.
[9] Figueiredo, I. C. R. D., Pinto, C. A. B. P., Ribeiro, G. H. M. R. (2015): Efficiency of selection in early generations of potato families with a view toward heat tolerance. – Crop Breeding and Applied Biotechnology 15(4): 210-217.
[10] Fischer, R. A., Maurer, R. (1978): Drought resistance in spring wheat cultivars. I: Grain yield response. – Australian Journal of Agricultural Research 29: 897-912.
[11] Gautam, A., Prasad, S. V. S., Jajoo, A., Ambati, D. (2015): Canopy temperature as a selection parameter for grain yield and its components in durum wheat under terminal heat stress in late sown conditions. – Agricultural Research 4(3): 238-244.
[12] Gooding, M. J., Ellis, R. H., Shewry, P. R., Schofield, J. D. (2003): Effects of restricted water availability and increased temperature on the grain filling, drying and quality of winter wheat. – Journal of Cereal Science 37: 295-309.
[13] Hernández-Espinosa, N., Mondal, S., Autrique, E., Gonzalez-Santoyo, H., Crossa, J., Huerta-Espino, J., Singh, R. P., Guzmán, C. (2018): Milling, processing and end-use quality traits of CIMMYT spring bread wheat germplasm under drought and heat stress. – Field Crops Research 215: 104-112.
[14] Hoffmann, S., Debreczeni, K., Hoffmann, B. Nagy, E. (2006): Grain yield and baking quality of wheat as affected by crop year and plant nutrition. – Cereal Research Communications 34(1): 473-476.
[15] Intergovernmental Panel on Climatic Change (2014): Climate change 2013: the physical science basis. – Contribution of Working Group I to the Fifth Assessment Report of IPCC the Intergovernmental Panel on Climate Change 18(2): 95-123.
[16] Jin, X. L., Wang, K. R., Xiao, C. H., Diao, W. Y., Wang, F. Y., Chen, B., Li, S. K. (2012): Comparison of two methods for estimation of leaf total chlorophyll content using remote sensing in wheat. – Field Crops Research 135(3): 24-29.
[17] Li, Q., Wang, Z. R., Li, D., Wei, J. W., Qiao, W. C., Meng, X. H., Sun, S. L., ... Zhao, F. W. (2018): Evaluation of a new method for quantification of heat tolerance in different wheat cultivars. – Journal of Integrative Agriculture 17(4): 786-795.
[18] Mason, R. E., Mondal, S., Beecher, F. W. (2010): QTL associated with heat susceptibility index in wheat (*Triticum aestivum* L.) under short-term reproductive stage heat stress. – Euphytica 174: 423-436.
[19] Melis, A. (2009): Solar energy conversion efficiencies in photosynthesis: Minimizing the chlorophyll antennae to maximize efficiency. – Plant Science 177: 272-280.
[20] Nuttall, J. G., O'Leary, G. J., Panozzo, J. F., Walker, C. K., Barlow, K. M., Fitzgerald, G. J. (2017): Models of grain quality in wheat-A review. – Field Crops Research 202: 136-145.
[21] Ort, D. R., Zhu, X. G., Melis, A. (2011): Optimizing antenna size to maximize photosynthetic efficiency. – Plant Physiology 155: 79-85.
[22] Ort, D. R., Merchant, S. S., Alric, J. et al. (2015): Redesigning photosynthesis to sustainably meet global food and bioenergy demand. – Proceedings of the National Academy of Science of the USA 112: 8529-8536.
[23] Polle, J. E., Kanakagiri, S. D., Melis, A. (2003): tla1, a DNA insertional transformant of the green alga Chlamydomonas reinhardtii with a truncated light-harvesting chlorophyll antenna size. – Planta 217: 49-59.
[24] Rane, J., Nagarajan, S. (2004); High temperature index-for field evaluation of heat tolerance in wheat varieties. – Agricultural Systems 79: 243-255.

http://www.aloki.hu ● ISSN 1589 1623 (Print) ● ISSN 1785 0037 (Online)
DOI: http://dx.doi.org/10.15666/aeer/1704_73577369

[25] Reynolds, M. P., Singh, R. P., Ibrahim, A., Ageeb, O. A. A., Larque-Saavedra, A., Quick, J. S. (1998): Evaluating physiological traits to complement empirical selection for wheat in warm environments. – Euphytica 100: 85-94.
[26] Reynolds, M. P., Pierre, C. S., Saad, A. S. I., Vargas, M., Condon, A. G. (2007): Evaluating potential genetic gains in wheat associated with stress-adaptive trait expression in elite genetic resources under drought and heat stress. – Crop Science 47: 172-189.
[27] Tewolde, H., Fernandez, C. J., Erickson, C. A. (2006): Wheat cultivars adapted to post-heading high temperature stress. – Journal of Agronomy and Crop Science 192: 111-120.
[28] Wall, G., Garcia, R., Kimball, B. et al. (2006): Interactive effects of elevated carbon dioxide and drought on wheat. – Agronomy Journal 98: 354-381.
[29] Webber, H., Martre, P., Asseng, S. et al. (2015): Canopy temperature for simulation of heat stress in irrigated wheat in a semi-arid environment: a multi-model comparison. – Field Crops Research 202: 21-35.
[30] Wiegand, C. L., Cuellar, J. A. (1981): Duration of grain filling and kernel weight of wheat as effected by temperature. – Crop Science 21: 95-101.
[31] Wu, X. L., Tang, Y. L., Li, C. S., Wu, C., Huang, G.(2015): Chlorophyll fluorescence and yield responses of winter wheat to waterlogging at different growth stages. – Plant Production Science 18(3): 284-294.
[32] Xu, W., Rosenow, D. T., Nguyen, H. T. (2000): Stay-green trait in grain sorghum: Relationship between visual rating and leaf chlorophyll concentration. – Plant Breeding 119: 365-367.

http://www.aloki.hu ● ISSN 1589 1623 (Print) ● ISSN 1785 0037 (Online)
DOI: http://dx.doi.org/10.15666/aeer/1704_73577369

ENERGY EFFICIENCY AND ECONOMIC ANALYSIS IN TOMATO PRODUCTION: A CASE STUDY OF MERSIN PROVINCE IN THE MEDITERRANEAN REGION

YELMEN, B.[1*] – ŞAHIN, H. H.[2] – ÇAKIR, M. T.[3]

[1]*Wastewater Treatment Department, Adana Metropolitan Municipality, 01120 Adana, Turkey*

[2]*Adana Metropolitan Municipality, 01120 Adana, Turkey*

[3]*Health Institutes of Turkey (TUSEB), 06590 Ankara, Turkey*

**Corresponding author*
e-mail: bekiryelmen@gmail.com

(Received 22nd Feb 2019; accepted 3rd May 2019)

Abstract. This study was carried out to find the energy equivalents of inputs and outputs in tomato cultivation in the Mediterranean region of Mersin province. For this aim, the energy balance between values of the input and output energies per unit field for tomato cultivation in open-field and greenhouses was investigated. Energy efficiency, energy density, energy efficiency were compared in terms of cost-benefit ratio. Data were collected and analyzed in open-field (112) and in greenhouses (14) from producers of tomato cultivation. The results showed that the total energy requirement in open fields and greenhouses was 56127.77 and 245246.78 MJ ha^{-1}, respectively. Energy use efficiency in the open-fields and in greenhouses was realized as 1.12 and 0.75 respectively. The cost-benefit-ratios were 2.32 in open-fields and 3.06 in greenhouses. According to the current results, the open-fields tomato production system has a higher energy efficiency than the greenhouse tomato production system, while the greenhouse system has a higher economic benefit.
Keywords: *tomato production, greenhouse, energy, energy consumption, cost benefit ratio*

Introduction

Tomato (*Lycopersicon esculentum* Mill.) is a perennial plant in tropical regions which is Solanales of the family of Solanaceae Lycopersicon family, depending on the single-year in temperate climates (Kinet and Peet, 1997). In total vegetable production, which is 1.1 billion tons in the world, tomatoes have 15% ratio with 162 million tons. In Turkey, the share of total vegetable production with production reaching 12.6 million tons exceeded 40%. In the current figures of tomato production; Turkey ranks 4th in the world (FAO, 2013). High adaptability, open the predisposition to greenhouse cultivation next to agriculture, as well as one of the various forms of reasons such as the availability of the processing industry, where most heavily cultivated and most widely consumed and the Mediterranean Basin which Turkey involved in. The amount of tomato consumption per capita in Turkey is 115 kg/year around (Yanmaz et al., 2015). Regional distribution in the largest ratio, is Mediterranean region with the 31% of the total (Abak, 2018). Mersin province is one of Turkey's largest tomato growing fields (ha) (Anonymous, 2017). From 2000 to 2015; Turkey's greenhouse fields increased with the ratio of 58.41%, from 47355.5 ha to 75015.5 (Turemiş, 2015). Today agricultural production is dependent on the consumption of fossil fuels (Taskın and Vardar, 2016). The use of energy in agriculture has increased due to the increasing human population, the limited supply of arable land and the will to improve the standard of living (Banaeian et al., 2010). Agriculture is an energy user and energy supplier (Alam et al., 2005). From the sowing-

http://www.aloki.hu ● ISSN 1589 1623 (Print) ● ISSN 1785 0037 (Online)
DOI: http://dx.doi.org/10.15666/aeer/1704_73717379

planting processes to the harvest-blending operations, direct energy is needed (Singh, 2007). Indirect energy is needed in the process from sowing to harvesting and transportation of products (Ozkan et al., 2004a). Yield, annual production, energy consumption, investments and costs are very high in greenhouses (Heidari and Omid, 2011). Inputs such as electricity, machinery, seeds, chemical fertilizers constitute a significant part of the inputs in the tomato production system (Hatirli et al., 2006). On the other hand, efficient use of energy contributes to increased production, profitability and competitiveness (Singh et al., 2002). Thus, sustainability in agriculture can be achieved in rural life (Park and Seaton, 1996). By using energy efficient in agriculture and by saving fossil fuels, air pollution can be reduced (Pervanchon et al., 2002). More efficient use of energy can be achieved so that the same level of development can be achieved with less energy use and less emissions (Ozturk et al., 2018). Using energy efficiently is very important for the terms of sustainability and the reduction of emissions of greenhouse gases (Alluvione et al., 2011). Energy used in agriculture is 17% of the world's energy (Mohammadi and Omid, 2010). The financial and technical analysis of the tomato production system is called the energy budget (Canakci and Akıncı, 2006). In terms of energy input-output relations, seed bed preparation, fertilizer quantity, soil cultivation processes and productivity etc. subjects are looked at (Mandal et al., 2002). In terms of production efficiency, input-output energy analysis is used (Alluvione et al., 2011). Production efficiency can be increased by reducing energy inputs. In the energy consumption in agriculture, mechanization is important (Ozkan et al., 2004b). The efficient use of energy provides sustainability (Dalgaard et al., 2001). In the world; there are important researches had done about field crops, fruits and the use of energy for vegetables. Energy inputs and outputs of apricot cultivation were examined (Gezer et al., 2003). Many researchers; soybean, corn and wheat in Italy (Sartori et al., 2005), tomatoes and tomato paste in Turkey (Esengün et al., 2007), lettuce in Colombia, radishes and spinach (Bojaca and Schrevens, 2010), rice in Malaysia (Bockari et al., 2005), kiwi in Iran production (Mohammadi et al., 2010), apple (Rafiee et al., 2010), onion and coriander Pennsylvania in the USA (Moore, 2010), the productivity of crops such as sugar cane production in Morocco (Mrini et al., 2001) has made energy issues and economic analysis. Work efficiency and alternative energy consumption in tomato production were analyzed (Onal and Tozan, 1986). Detailed energy usability surveys were conducted (Yılmaz et al., 2005). Greenhouse energy and cost analysis were carried out in the Serik district of Antalya for the production of grapes in open-field and greenhouses (Ozkan et al., 2007). Some studies have been carried out on the use of energy in peach production in Tokat province (Goktolga et al., 2006). Economic analysis of the input energy requirements and costs are made in tomato production in Turkey (Cetin and Vardar, 2008).

The objectives of this study are; determine the effectiveness of tomato production systems, energy utilization rates, energy output-input ratio, cost/benefit ratio, energy inputs optimization of energy use efficiency and to determine the economic analysis. Thus in Mersin, greenhouse tomatoes and open-field tomato production systems will be compared.

Materials and methods

In this study, data were collected from 126 producers in open-fields and greenhouses in Mersin. In the Mediterranean city of Mersin, located south of Turkey. 36° 48' north

http://www.aloki.hu ● ISSN 1589 1623 (Print) ● ISSN 1785 0037 (Online)
DOI: http://dx.doi.org/10.15666/aeer/1704_73717379

latitude and 34° 38' east longitude. The average annual temperature is approximately 19.2 °C and the total annual rainfall is 592.1 mm. Approximately 94% rainfall falls from October to May (TSMS, 2017). The total number of registered farmers in Mersin, in 2016 is 35039 (MAF, 2016). Data on the production of tomatoes collected by face-to-face survey from growers are belong to 2016 production period. in the province of Mersin, 941.232 tons of tomatoes were obtained from 91.211 decares of field. Sample farms were randomly selected from the study area by using a random sampling technique. However, it should be taken into account the factor in which variability can be observed in basic datasets. The sample size was calculated using the Neyman method (*Eq. 1*) (Yamane, 1967).

$$n = \frac{N \times S^2}{(N-1)S^2_x + S^2} \quad \text{(Eq.1)}$$

For this equation; n is the required sample size, N population volume, S standard deviation, Sx standard deviation of the sample average (Sx = d/z), z reliability coefficient, d is based on the allowable error equation of the sample size. For open-field and greenhouse tomato cultivation, the number of samples examined was 112 and 14 (126) respectively. The permissible error (d) was defined as 5%, and for the 95% reliability (z), 126 sampling sizes were calculated. Firstly, the most common production systems for each product were identified, and then all inputs and outputs from the systems were identified and digitized, and then converted to energy units. By adding partial energies to total energies (ha) per production unit; energy inputs include human labor, diesel fuel, machinery, farm manure, irrigation, nitrogenous, phosphorus and potassium chemical fertilizers. In order to estimate the energy in MJ/ha and to find the amount of inputs in terms of efficiency values by the energy analysis of the tomato, the equivalents in *Table 1* are used.

Table 1. *Energy equivalents for different inputs and outputs in agricultural production*

Particulars	Unit	Energy equivalent (MJ unit^{-1})	Reference
A. Inputs			
1. Human labor	h	1.96	Mohammadi et al., 2008
2. Machinery	h	64.80	Singh et al., 2002
3. Diesel fuel	l	47.80	Canakcı and Akıncı, 2006
4. Chemical fertilizers			
(a) Nitrogen	kg	66.14	Mohammadi et al., 2008
(b) Phosphate	kg	11.10	Mani et al., 2007
(c) Potassium	kg	11.15	Kousar et al., 2006; Sartori et al., 2005
(d) Sulfur	kg	1.12	Mohammadi et al., 2008
(e) Zinc	kg	8.40	Mohammadi et al., 2008
(f) Mixed micronutrients	kg or l	120.00	Alam et al., 2005
5. Chemicals	kg or l		
(a) Herbicides		238.30	Esengun et al.,2007 Erdal et al., 2007
(c) Pesticides		101.20	Esengun et al., 2007
(d) Fungicides		216.00	Esengun et al., 2007
6. Cattle manure	kg	0.30	Mohammadi et al., 2008
7. Electricity	kWh	11.93	Mani et al., 2007
8. Water for irrigation	m3	1.02	Rafiee et al., 2010
9. Seeds	kg	1.00	Esengun et al., 2007
B. Outputs			
1. Fruit yield	kg	0.80	Taki et al., 2012

http://www.aloki.hu ● ISSN 1589 1623 (Print) ● ISSN 1785 0037 (Online)
DOI: http://dx.doi.org/10.15666/aeer/1704_73717379

Energy use efficiency (*Eq. 2*), energy productivity (*Eq. 3*), specific energy (*Eq. 4*), energy intensiveness (*Eq. 5*) and net energy (*Eq. 6*) were calculated (Banaeian et al., 2010; Ghorbani et al., 2011).

$$\text{Energy use efficiency} = \frac{\text{Energy output}(MJha^{-1})}{\text{Energy input}(MJha^{-1})} \quad \text{(Eq.2)}$$

$$\text{Energy produvtivity} = \frac{\text{Crops output}(Kgha^{-1})}{\text{Energy input}(MJha^{-1})} \quad \text{(Eq.3)}$$

$$\text{Specific energy} = \frac{\text{Energy inpute}(MJha^{-1})}{\text{Crops output}(t.ha^{-1})} \quad \text{(Eq.4)}$$

$$\text{Energy intensiveness} = \frac{\text{Energy inpute}(MJha^{-1})}{\text{Cost of cultivation}(\$\,ha^{-1})} \quad \text{(Eq.5)}$$

$$\text{Net energy} = \left[\text{Energy output}(MJha^{-1}) - \text{Energy input}(MJha^{-1})\right] \quad \text{(Eq.6)}$$

The energy equivalents of the inputs are mega joule (MJ) per unit. In particularly this calculated ratio was used to express energy deficiency with input fossil fuel energy and output food ratio. The increase in the rate of crop production indicates improvement. It is possible to determine the energy efficiency trends of agricultural production by evaluating energy efficiency rates. Total value of production (*Eq. 7*), Gross return (*Eq. 8*), Net return (*Eq. 9*), Total cost of production (*Eq. 10*), Benefit to cost ratio (*Eq. 11*) and Productivity (*Eq. 12*) (Economic analysis of tomato cultivation) were investigated (Zangeneh et al., 2010):

$$\text{Total value of production} = \text{tomato yield (kg ha}^{-1}) \times \text{tomato price (\$ kg}^{-1}) \quad \text{(Eq.7)}$$

$$\text{Gross return} = \text{total value of production (\$ ha}^{-1}) - \text{variable cost of production (\$ ha}^{-1}) \quad \text{(Eq.8)}$$

$$\text{Net return} = \text{total value of production (\$ ha}^{-1}) - \text{total cost of production (\$ ha}^{-1}) \quad \text{(Eq.9)}$$

$$\text{Total cost of production} = \text{variable cost of production (\$ ha}^{-1}) + \text{fixed cost of production (\$ ha}^{-1}) \quad \text{(Eq.10)}$$

$$\text{Benefit to cost ratio} = \text{total value of production (\$ ha}^{-1}) / \text{total cost of production (\$ ha}^{-1}) \quad \text{(Eq.11)}$$

$$\text{Productivity} = \text{tomato yield (kg ha}^{-1}) / \text{total cost of production (\$ ha}^{-1}) \quad \text{(Eq.12)}$$

Results

Energy input-output relationship in open-field and greenhouse tomato production system

In tomato production systems, per hectare in open-fields and greenhouses, 1088.25 and 2347.82 h of human labor respectively and showed that 32.44 and 98.65 h machine power

http://www.aloki.hu ● ISSN 1589 1623 (Print) ● ISSN 1785 0037 (Online)
DOI: http://dx.doi.org/10.15666/aeer/1704_73717379

is required. The total energy used in production in open fields and green houses is 62862.93 and 183866.38 MJ ha^{-1} (*Table 2*). It is the electricity sector which has the highest energy consumption in tomato production system in open-fields (32.89%), followed by nitrogen (22.08%), irrigation (13.55%) and diesel fuel (12.66%) (*Table 2*) If the highest energy consumption in the tomato production system in greenhouses is diesel fuel (60.90% of total energy input), followed by electricity (14.68%) and micro nutrients (fertilizer, 11.34%) (*Table 2*). For tomato production systems, the average fruit yield in open fields and greenhouses were 147854 kg ha^{-1} with 52429.8 respectively, while the straw yield were 2789.21 and 8744.37 kg ha^{-1}. While total energy output per hectare was 62862.93 MJ in open fields and 183866.38 MJ in greenhouses. The input-output energy ratio in open fields and greenhouse systems is 1.12 and 0.75, respectively. The energy use efficiency in the open-field was nearly 1.49 times more than the greenhouse system due to the use of more input energy than the greenhouse system.

Table 2. *Energy input-output relationship in openfield and greenhouse tomato production system*

Energy inputs	Quantity per unit area (ha)		Energy equivalent (MJ $unit^{-1}$)		Total energy equivalent (MJ)		Percentage of total energy input (%)	
	Open field	Green house	Open field	Green house	Open field	Green house	Open field	Green house
Human labor (h)	1088.25	2347.82	1.96	1.96	2132.97	4601.73	3.80	1.88
Machinery (h)	32.44	98.65	64.80	64.80	2102.11	6392.52	3.75	2.61
Diesel fuel (l)	148.64	3124.57	47.80	47.80	7104.99	149354.45	12.66	60.90
Nitrogen (kg)	187.39	121.84	66.14	66.14	12393.97	8058.50	22.08	3.29
Phosphate (kg)	96.27	73.15	11.10	11.10	1068.60	811.97	1.90	0.33
Potassium (kg)	34.86		11.15		388.69	0.00	0.69	0.00
Sulphur (kg)		317.52		1.12	0.00	355.62	0.00	0.15
Cattle manure (kg)	11207.23	10621.46	0.30	0.30	3362.17	3186.44	5.99	1.30
Micro nutrients (kg or l)	3.89	231.71	120.00	120.00	466.80	27805.20	0.83	11.34
Herbicides (kg or l)	1.91	0	238.30	238.30	455.15	0.00	0.81	0.00
Pesticides (l)	1.63	4.43	101.20	101.20	164.96	448.32	0.29	0.18
Fungicide (kg or l)	1.94	16.25	216.00	216.00	419.04	3510.00	0.75	1.43
Electricity (kWh)	1547.36	3018	11.93	11.93	18460.00	36004.74	32.89	14.68
Water for irrigation (m^3)	7458.28	4624.54	1.02	1.02	7607.45	4717.03	13.55	1.92
Seeds (kg)	0.87	0.28	1.00	1.00	0.87	0.28	0.00	0.00
Total energy input (MJ)					56127.77	245246.78	100.00	100.00
Outputs								
Fruit yield (kg)	52429.8	147854.5	0.80	0.80	41943.86	118283.61	66.72	68.09
Straw yield (kg)	2789.21	8744.37	7.50	7.50	20919.08	65582.78	31.91	31.91
Total energy output (MJ)					62862.93	183866.38		
Energy efficiency					1.12	0.75		

Efficiency and specific energy in open-field and greenhouse systems

Energy use efficiency is 1.12 in open-field and 0.75 in greenhouse tomato production systems. The energy intensiveness was calculated as 14.61 in open-field and 3.79 MJ$\$^{-1}$ in greenhouse systems. The average energy productivity of the open-field and greenhouse is 0.93 and 0.60 kg MJ^{-1}, respectively. Specific energy is 1.07 and 1.66 MJ

http://www.aloki.hu ● ISSN 1589 1623 (Print) ● ISSN 1785 0037 (Online)
DOI: http://dx.doi.org/10.15666/aeer/1704_73717379

kg^{-1} in the open-field and in the greenhouse, respectively. Net energy is 6735.16 and -61380.40 MJ ha^{-1} in open-field and greenhouse respectively (*Table 3*).

Table 3. *Tomato production energy indices in open field and greenhouse systems*

Items	Unit	Open field	Greenhouse
Energy input	MJ ha^{-1}	56127.77	245246.78
Energy output	MJ ha^{-1}	62862.93	183866.38
Energy use efficiency	-	1.12	0.75
Energy intensiveness	MJ $\$^{-1}$	14.61	3.79
Specific energy	MJ kg^{-1}	1.07	1.66
Energy productivity	kg MJ^{-1}	0.93	0.60
Net energy	MJ ha^{-1}	6735.16	-61380.40

Relationship between economic indices and analysis in tomato production system in open-field and greenhouse

The production cost of our two works and our gross product can be seen at *Table 4*. In open-field and greenhouse tomato production systems, the gross production value is 14680.35 and 93148.34 \$ ha^{-1}. The tomato production and stability in the open-field was 3925.23 and 2390.94 \$ ha^{-1}, greenhouse facilities 15977.42 and 14486.52 \$ ha^{-1}. The production amount per hectare (6316.16 \$ ha^{-1}) in the open-field is lower than the greenhouse system (30463.94 \$ ha^{-1}). Total production amount in the greenhouse system is 79.27% higher than the open-field system. The gross return and net return (10755.12 and 8364.19 \$ ha^{-1}) available in open-field production is very low from the greenhouse production system (77170.92 and 62684.40 \$ ha^{-1}). The gross and net return in the open field system is 7.2 and 7.5 times lower. In greenhouses (3.06), the benefit cost ratio is higher than the open-field system (2.32). Productivity is expressed in 1 US\$, this means how much product we can produce with 1 US dollar. This study efficiency is 8.30 and 4.85 kg^{-1} for open-field and greenhouse systems.

Table 4. *Economic indices of tomato production in open space and greenhouse systems and relationship between analysis*

Cost and return components	Open field (value)	Greenhouse (value)
Fruit yield (kg ha^{-1})	52429.82	147854.51
Sale price (\$ kg^{-1})	0.28	0.63
Gross value of production (\$ ha^{-1})	14680.35	93148.34
Variable cost of production (\$ ha^{-1})	3925.23	15977.42
Fixed cost of production (\$ ha^{-1})	2390.94	14486.52
Total cost of production (\$ ha^{-1})	6316.16	30463.94
Total cost of production (\$ kg^{-1})	0.12	0.21
Total cost production (\$ MJ^{-1})	0.06	0.09
Gross return (\$ ha^{-1})	10755.12	77170.92
Gross return (\$ kg^{-1})	0.21	0.52
Gross return (\$ MJ^{-1})	0.10	0.22
Net return (\$ ha^{-1})	8364.19	62684.40
Net return (\$ kg^{-1})	0.16	0.42
Net return (\$ MJ^{-1})	0.08	0.18
Benefit to cost ratio	2.32	3.06
Productivity (kg $\$^{-1}$)	8.30	4.85

http://www.aloki.hu ● ISSN 1589 1623 (Print) ● ISSN 1785 0037 (Online)
DOI: http://dx.doi.org/10.15666/aeer/1704_73717379

Discussion

In tomato production systems, the total energy input (56127.77 MJ ha^{-1}) used in the open-field has shown that it is approximately 4.37 times lower than the greenhouse production system (245246.78 MJ ha^{-1}). Diesel fuel consumption in the production of tomatoes in greenhouses is very high. In addition, energy consumption in greenhouse production systems is higher than the open-field production system. But, the energy use rate is lower (Cetin and Vardar, 2008). In addition, tomato yield in the open field (52429.82 kg ha^{-1}) is 2.82 times lower than the greenhouse system (147854.51 kg ha^{-1}) (Özkan et al., 2004b). Energy output-input ratio is higher in open-field (1.12) than in greenhouse systems (0.75).

Conclusions

Reducing the share of fertilizers and diesel fuel may increase energy efficiency. Net energy is -61380.40 and 6735.16 MJ ha^{-1} in greenhouse systems and outdoor field. A negative value of the energy gain in the greenhouse is due to the heating technology used for heating diesel engines at high temperatures, such as low heating technology (Banaeian et al., 2010). In the open field, respectively, 10755.12 $, 8364.19 $ and 2.32; The gross, net return and benefit cost ratio is lower than the greenhouse tomato production system. Total production cost of greenhouse is higher than open-field due to heavy fuel usage. The high price of greenhouse tomatoes is owing to the lack of tomatoes in autumn and winter. Effective use of inputs contributes to economic profitability and competitiveness, while increasing productivity (Singh et al., 2002). The results show that water for diesel fuel, irrigation, fertilization, machinery and electrical energies is the major part of the energy inputs used in tomato production systems. In terms of energy efficiency, the tomato production system in the open-field is 1.49 times higher than the greenhouse system. This leads to an increase towards higher sustainability. In addition, the most effective factors affecting the efficiency of energy use in greenhouse and open-field systems are diesel fuel and nitrogen fertilizer inputs. Therefore, reducing the consumption of these inputs may increase the efficiency of energy use in tomato production systems in Mersin province.

REFERENCES

[1] Abak, K. (2018): Tomatoes yesterday in Turkey, today and tomorrow. – Lefke European University Faculty of Agricultural Sciences, Gemikonağı - Lefke, Mersin, TTOB Journal 17: 8-9. www.turktob.org.tr/dergi/makaleler/dergi17/TTOB_Dergi17WEB-8_13.pdf.

[2] Alam, M. S., Alam, M. R., Islam, K. K. (2005): Energy flow in agriculture: Bangladesh. – American Journal of Environmental Sciences 1(3): 213-220.

[3] Alluvione, F., Moretti, B., Sacco, D., Grignani, C. (2011): EUE (energy use efficiency) of cropping systems for a sustainable agriculture. – Energy 36: 4468-4481.

[4] Anonymous (2017): https://www.mersinportal.com/mersin/mersinde-940-bin-ton-domates-uretiliyor-h39341.html.

[5] Banaeian, N., Omid, M., Ahmadi, H. (2010): Energy and economic analysis of greenhouse strawberry production in Tehran province of Iran. – Energy Conversion and Management 52(2): 1020-1025

http://www.aloki.hu ● ISSN 1589 1623 (Print) ● ISSN 1785 0037 (Online)
DOI: http://dx.doi.org/10.15666/aeer/1704_73717379

[6] Bockari Gevao, S. M., Wan Ishak, W. I., Azmi, Y., Chan, C. W. (2005): Analysis of energy consumption in lowland rice-based cropping system of Malaysia. – Sci Technol 27(4): 819-826.
[7] Bojaca, C. R., Schrevens, E. (2010): Energy assessment of peri-urban horticulture and its uncertainty: case study for Bogota, Colombia. – Energy 35: 2109-2118.
[8] Canakci, M., Akinci, I. (2006): Energy use pattern analyses of greenhouse vegetable production. – Energy 31: 1243-1256. 31(8-9): 1243-56.
[9] Cetin, B., Vardar, A. (2008): An economic analysis of energy requirements and input costs for tomato production in Turkey. – Renewable Energy 33: 428-433.
[10] Dalgaard, T., Halberg, N., Porter, J. R. (2001): A model for fossil energy use in Danish agriculture used to compare organic and conventional farming. – Agric. Ecosyst. Environ. 87: 51-65.
[11] Erdal, G., Esengun, K., Guduz, O. (2007): Energy use and economic analysis of sugar beet production in Tokat province of Turkey. – Energy 32: 34-41.
[12] Esengun, K., Gunduz, O., Erdal, G. (2007): Input–output energy analysis in dry apricot production of Turkey. – Energy Conversion and Management 48(2): 592-598.
[13] FAO (2013): Faostat Agricultural Database. – www.faostat.org. Accessed: 17.02.2015.
[14] Gezer, I., Acaroglu, M., Hacseferogullari, H. (2003): Use of energy and labour in apricot agriculture in Turkey. – Biomass Bioenerg 24: 215-9.
[15] Ghorbani, R., Mondani, F., Amirmoradi, S., Feizi, H., Khorramdel, S., Teimouri, M., Sanjani, S., Anvarkhah, S., Aghel, H. (2011): A case study of energy use and economical analysis of irrigated and dryland wheat production systems. – Appl Energy 88: 283-288.
[16] Goktolga, Z. G., Gozener, B., Karkacier, O. (2006): Energy use in peach production: Case of Tokat province. – GOU. J. Agric. Faculty 23(2): 39-44.
[17] Hatirli, S. A., Ozkan, B., Fert, C. (2006): Energy inputs and crop yield relationship in greenhouse tomato production. – Renewable Energy 31: 427-438.
[18] Heidari, M. D., Omid, M. (2011): Energy use patterns and econometric models of major greenhouse vegetable productions in Iran. – Energy 36(1): 220-225.
[19] Kinet, J.M., Peet , M.M. (1997): Tomato : In Wien , H.C.(Ed), The Physiology of Vegetable Crops. CAB, International. New York, pp.207-258.
[20] Kousar, R., Makhdum, S. A., Yagoob, S., Saghir, A. (2006): Economics of energy use in cotton production on small farms in district Sahiwal, Punjab, Pakistan. – J Agric Social Sci 2(4): 219-221.
[21] MAF (2016): Republic of Turkey Ministry of Agriculture and Forestry. https://www.tarimorman.gov.tr/SGB/TARYAT/Belgeler/il_yatirim_rehberleri/mersin.pdf
[22] Mandal, K. G., Saha, K. P., Gosh, P. L., Hati, K. M., Bandyopadhyay, K. K. (2002): Bioenergy and economic analyses of soybean based crop production systems in central India. – Biomass Bioenerg 23: 337-45.
[23] Mani, I., Kumar, P., Panwar, J. S., Kant, K. (2007): Variation in energy consumption in production of wheat-maize with varying altitudes in hilly regions of Himachal Pradesh, India. – Energy 32: 2336-2339.
[24] Mohammadi, A., Omid, M. (2010): Economical analysis and relation between energy inputs and yield of greenhouse cucumber production in Iran. – Appl Energy 87: 191-196.
[25] Mohammadi, A., Tabatabaeefar, A., Shahin, S., Rafiee, S., Keyhani, A. (2008): Energy use and economical analysis of potato production in Iran, a case study: Ardabil province. – Energy Conver Manage 49: 3566-3570.
[26] Mohammadi, A., Rafiee, S., Mohtasebi, S., Rafiee, H. (2010): Energy inputs-yield relationship and cost analysis of kiwifruit production in Iran. – Renew Energy 35: 1071-1075.
[27] Moore, S. R. (2010): Energy efficiency in small-scale biointensive organic onion production in Pennsylvania, USA. – Renewable Agriculture and Food Systems 25: 181-188.

http://www.aloki.hu ● ISSN 1589 1623 (Print) ● ISSN 1785 0037 (Online)
DOI: http://dx.doi.org/10.15666/aeer/1704_73717379

[28] Mrini, M., Senhaji, F., Pimentel, D. (2001): Energy analysis of sugarcane production in Morocco. – Environ Dev Sustain 3: 109-126.
[29] Onal, I., Tozan, M. (1986): Energy budget and work requirements of the alternative production systems in the processing tomato production. – In: 10th National Agricultural Mechanization Congress, Adana, Turkey, May 5-7, pp. 216-28 [in Turkish].
[30] Ozkan, B., Kurklu, A., Akcaoz, H. (2004a): An input-output energy analysis in greenhouse vegetable production: a case study for Antalya region of Turkey. – Biomass Bioenergy 26(1): 189-195.
[31] Ozkan, B., Akcaoz, H., Fert, C. (2004b): Energy input-output analysis in Turkish agriculture. – Renew Energy 29: 39-51.
[32] Ozkan B., Fert C., Karadeniz, C. F. (2007): Energy and cost analysis for greenhouse and open field grape production. – Energy 32: 1500-04.
[33] Ozturk, H. H., Kücukerdem, K., Mutlu, N., Gozubuyuk, Z., Atay, U. (2018): Sustainability indicators for energy use and environmental impacts in agricultural production. – Journal of Agricultural Machinery Science 14(3): 199-204.
[34] Park, J., Seaton, R. A. F. (1996): Integrative research and sustainable agriculture. – Agricultural Systems 50(1): 81-100.
[35] Pervanchon, F., Bocstaller, C., Girardin, P. (2002): Assessment of energy use in arable farming systems by means of an agro-ecological indicator: the energy indicator. – Agric. Syst. 72: 149-172.
[36] Rafiee, S., Mousavi, S. H., Mohammadi, A. (2010): Modeling and sensitivity analysis of energy inputs for apple production in Iran. – Energy 35: 3301-3306.
[37] Sartori, L., Basso, B., Bertocco, M., Oliviero, G. (2005): Energy use and economic evaluation of a three year crop rotation for conservation and organic farming in NE Italy. – Biosyst. Eng. 91(2): 245-256.
[38] Singh, H., Mishra, D., Nahar, N. M. (2002): Energy use pattern in production agriculture of a typical village in arid zone India - Part I. – Energy Convers Manage 43(16): 2275-2286.
[39] Singh, H., Singh, A. K., Kushwaha, H. L., Singh, A. (2007): Energy consumption pattern of wheat production in India. – Energy 32: 1848-1854.
[40] Taki, M., Ajabshirchi, Y., Mobtaker, H. G., Abdi, R. (2012): Energy consumption, input-output relationship and cost analysis for greenhouse productions in Esfahan Province of Iran. – American Journal of Experimental Agriculture 2(3): 485-501.
[41] Taskın, O., Vardar, A. (2016): Use of some renewable energy resources in agricultural production. – Journal of Agricultural Faculty of Uludag University 30(1): 179-184.
[42] TSMS (2017): Turkish State Meteorological Service. – https://www.mgm.gov.tr/?il=Mersin.
[43] Turemiş, N. (2015): Greenhouse Growing in Turkey. – http://bahcebitkileri.cu.edu.tr/upload/nturemis/turkiyeortualti.pdf.
[44] Yamane, T. (1967): Elementary Sampling Theory. – Prentice Hall, Englewood Cliffs, NJ.
[45] Yanmaz, R., Duman, İ., Yaralı, F., Demir, K., Sarıkamış, G., Sarı, N., Balkaya, A., Kaymak, H. Ç., Akan, S., Özalp, R. (2015): Changes in vegetable production and new explorations. – Chamber of Agricultural Engineers of TMMOB VIII. Technical Congress Proceedings, pp. 579-605.
[46] Yilmaz, I., Akcaoz, H., Ozkan, B. (2005): An analysis of energy uses and input–output costs for cotton production in Turkey. – Renewable Energy 30(1): 145-55.
[47] Zangeneh, M., Omid, M., Akram, A. (2010): Comparative study on energy use and cost analysis of potato production under different farming technologies in Hamadan province of Iran. – Energy 35: 2927-2933.

http://www.aloki.hu ● ISSN 1589 1623 (Print) ● ISSN 1785 0037 (Online)
DOI: http://dx.doi.org/10.15666/aeer/1704_73717379

ASSESSMENT AND MONITORING OF REHABILITATION STUDIES ON COAL MINE DUMP SITE WITH UAV'S

KUN, M.

Department of Mining Engineering, Faculty of Engineering, Dokuz Eylul University
Izmir, Turkey
(e-mail: mete.kun@deu.edu.tr; phone: +90-232-301-7540; fax: +90-232-453-0868)

(Received 25th Feb 2019; accepted 1st May 2019)

Abstract. Today, the rapidly increasing environmental awareness and the need for available space posed environmentally sensitive change of mining activities and created the target of producing alternative economic values in the fields it is used. For this reason, especially for the last two decades, in the context of the rehabilitation and reactivation in the nature of open-cast mines whose production is either finisher or ongoing, nature restoration work after mining activities have gained momentum. In terms of country and regional planning studies, in the mining activities especially carried out in large areas, the rehabilitation of the sites in terms of the preservation and sustainability of the natural balance within the area is of great importance. With advanced technological equipment, remote sensing systems, unmanned aerial vehicles and increasing data processing techniques, it is possible to follow up the mining initiatives and rehabilitation works carried out especially in large areas. In this way, transaction tracking and success percentages of transactions can be revealed. In the study prepared for this purpose, a sample coal operation was taken into consideration and the rehabilitation works carried out especially at the dump sites were examined. As a result of the study, the adaptation of the species planted to the nature and the survival percent obtained were revealed. In addition to this, the rehabilitation processes on the dump sites were monitored with the help of plant index maps obtained by using unmanned aerial vehicle (UAV) and photogrammetric software and the success of applied methods was evaluated.
Keywords: *mining, reclamation, plant index map, UAV, TGI, VARI*

Introduction

Mines and mining are of great importance in continuation of today's modern lifestyle and achieving the goals set. Today, as in the past, mining is one of the largest industries. Some adverse effects on the environment are inevitable according to the methods followed during the running of a mine. When compared to underground mining, open pit mining has a more negative effect on the natural environment and the negative visual impact it creates is known to be greater than the underground mining.

The negative impacts of mining activities on the environment can be local and regional, as well as globally. These effects may vary slightly depending on the characteristics of the natural environment, the structure of the mine, the mining technique applied and the nature of the enterprise. Additionally, the realization, estimation, prevention or reduction of these environmental impacts caused by mining activities in real terms is possible with the measures to be taken during the planning of the activity.

Since mining is an activity that changes terrain surfaces, active mining activities in a given time period significantly change the landscape and tend to destroy all traces of land use in the past. The negative effects such as degradation of the visual environment, damage to the landscape, damage to agricultural and forest areas, erosion, land subsidence, etc. are focused on (Sengupta, 1993). However, the dump sites, which are formed in the immediate vicinity of the mine areas, are often larger than the active mining sites. The rehabilitation of these dump sites is a necessary and compulsory

http://www.aloki.hu ● ISSN 1589 1623 (Print) ● ISSN 1785 0037 (Online)
DOI: http://dx.doi.org/10.15666/aeer/1704_73817393

action (Mallı. et al., 2018). For this reason, field rehabilitation practices were included in the operation procedure and costs, before starting the production, taking into account in the feasibility stages of their enterprises. Thus, when the mining works in the sites are completed, a large part of the sites become rehabilitated (*Fig. 1*).

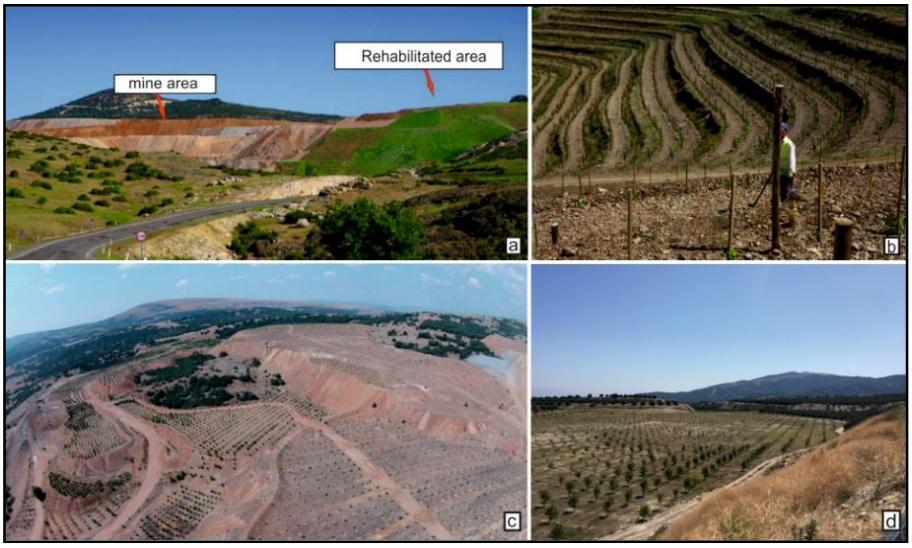

Figure 1. *Rehabilitated mining sites [(a),(b) – Kısladag gold mine in Uşak /Turkey; (c)- Tutluca magnesite quary in Eskisehir/Turkey; (d)-coal mine rehabilitated area in Aydın/Turkey)]*

Rehabilitation studies are generally divided into four stages by different researchers. These stages are classified as the site usage plan, reorganizing, improvement, monitoring and maintenance works (Topay and Kaya, 2007; Düzgün, 2009; Mallı et al., 2018). All of these steps were completed in the prepared study and especially as a result of the completed studies, the use of UAVs in the monitoring and research of tree planting sections were put forward.

Firstly planted areas were followed in five to seven year period and the results of planting studies in different fields were evaluated for this purpose. Secondly, the fields were visualized with UAV progress and the results were evaluated by using TGI and VARI values. As a result of the study, especially the planting of large areas, using UAVs and related visual processing software, according to the indexes given above as a result of the evaluation of plant life and long-term follow-up of the results obtained by classical means overlapped. This situation shows that the results of UAVs, 3D mining software, TGI and VARI values together can be performed accurately, reliably and fast, especially in the pursuit of the rehabilitation of large mining sites.

Review of Literature

Claim is the preparation of the mining operation area for post-mining use, and also the consolidation of the post-operational land by adapting to the environment (Ramani, 1990). In other words, it is defined as returning the area to its natural state or to a more suitable use, as bringing out the efficient, useful, clean and aesthetically beautiful appearance of the destroyed area (Michaud, 1981). The re-efficiency of a destroyed area and regaining its ecological, economic and aesthetic values is possible by the nature repair works.

http://www.aloki.hu ● ISSN 1589 1623 (Print) ● ISSN 1785 0037 (Online)
DOI: http://dx.doi.org/10.15666/aeer/1704_73817393

Site usage plan is defined as the formation of the conditions for the land and the determination of ecological targets for re-planting before mining. Reorganizing involves activities such as excavation, soil laying, planting, drainage works etc. The improvement phase is the studies of recovery of biological efficiency in the destroyed area and evaluation and improvement of the soil and the re-planting. The monitoring phase, which is the last stage, can be defined as the phase during which plant development is monitored and evaluated in line with the determined targets after the stages of organizing and improvement. In the study, these processes were done both by classical means and with the help of UAVs and the results were compared.

There are many studies that show the use of UAVs and their successful use in the fields of mining and the environmental relation. For example, Ozcan and Sari (2019) and Gül (2019), in their studies on the environmental effects and monitoring of quarries, respectively, have demonstrated the success of UAVs in open mines planning. Again, Lee and Choi (2016) focused on the safe use of UAVs for different purposes (planning and monitoring) in mining operations in a study called reviews of unmanned aerial vehicle (drone) technology trends and its applications in the mining industry. Shahbazi et al. (2014) the management, monitoring and management of natural resources unmanned aerial imagery has clearly demonstrated the latest developments and achievements. Özcan (2017) and Öztürk et al. (2017), the effects of the images taken with different elevation and camera angles, respectively, were investigated and the differences between the steep and sloping image acquisition from mining sites were determined.

There can be found several other examples in the literature that have assessed suitability of mined lands for post-mining land-uses, and mentioned the effective criteria in the evaluations. For expample, Maiti and Ghose (2005); Tafi (2006) and Carrick and Kruger (2007) have evaluated the factors limiting plant growth on mined soils and mentioned the most serious soil limitations. Some other researchers e.g. Gizikoff (2004) and Zavadskas and Antucheviciene (2006) have investigated on so many other factors such as topography, climate, environment, society, economy, etc. which arise in land-use evaluations of mined or other disturbed lands. Paschke et al. (2003); Meech et al. (2006); Li (2006) and Cao (2007) have focused on special post-mining land-uses thatwere exercised in some mine sites.

Moreover, extensive studies are carried out in different parts of the world. For example, the value of claim costs in the US West Kentucky basin was estimated to be around 8% of the total operating cost. In another study, it was determined that the cover/coal ratio was 8:1 and for each 100 tons production, 0.2 hectares of land was damaged; the cost of claim in an open pit mine was determined to be $ 0.32 / ton or 7.6% of the total cost. In the literature, this value varies between $ 1000 and $ 20000 per hectare. In addition, with the project of East Germany rehabilitation of lignite mines, more than 100 thousand hectares of land became usable and was regained to the environment by spending 7.5 billion euros (Kuyumcu, 2005).

As seen in the above-mentioned similar studies, the necessity of rehabilitation of the sites as well as the need to regain economic values from the mining areas, encourages enterprises in this direction. Therefore, in the following parts of the study, the rehabilitation studies carried out in the new and old dump sites of the coal mine discussed and follow-up and monitoring of these studies with today's technologies were mentioned.

http://www.aloki.hu ● ISSN 1589 1623 (Print) ● ISSN 1785 0037 (Online)
DOI: http://dx.doi.org/10.15666/aeer/1704_73817393

Materials and Methods

Description of the study area

Lignite production site discussed in the study is located in western Turkey, on the Aegean Coast, in the province of Aydin. Until the year 1984 the production was only underground and since 84 to the present day it has functioned as both underground and open-pit production. Until today, about 7 million tons of coal were produced from underground mine and 10 million tons of coal were produced from the open pit mine. In the production process, approximately 160 million m^3 of excavation was carried out on the open pit mine. *Fig. 2* shows the site location map, the study area and the rehabilitation areas belonging to the lignite pit.

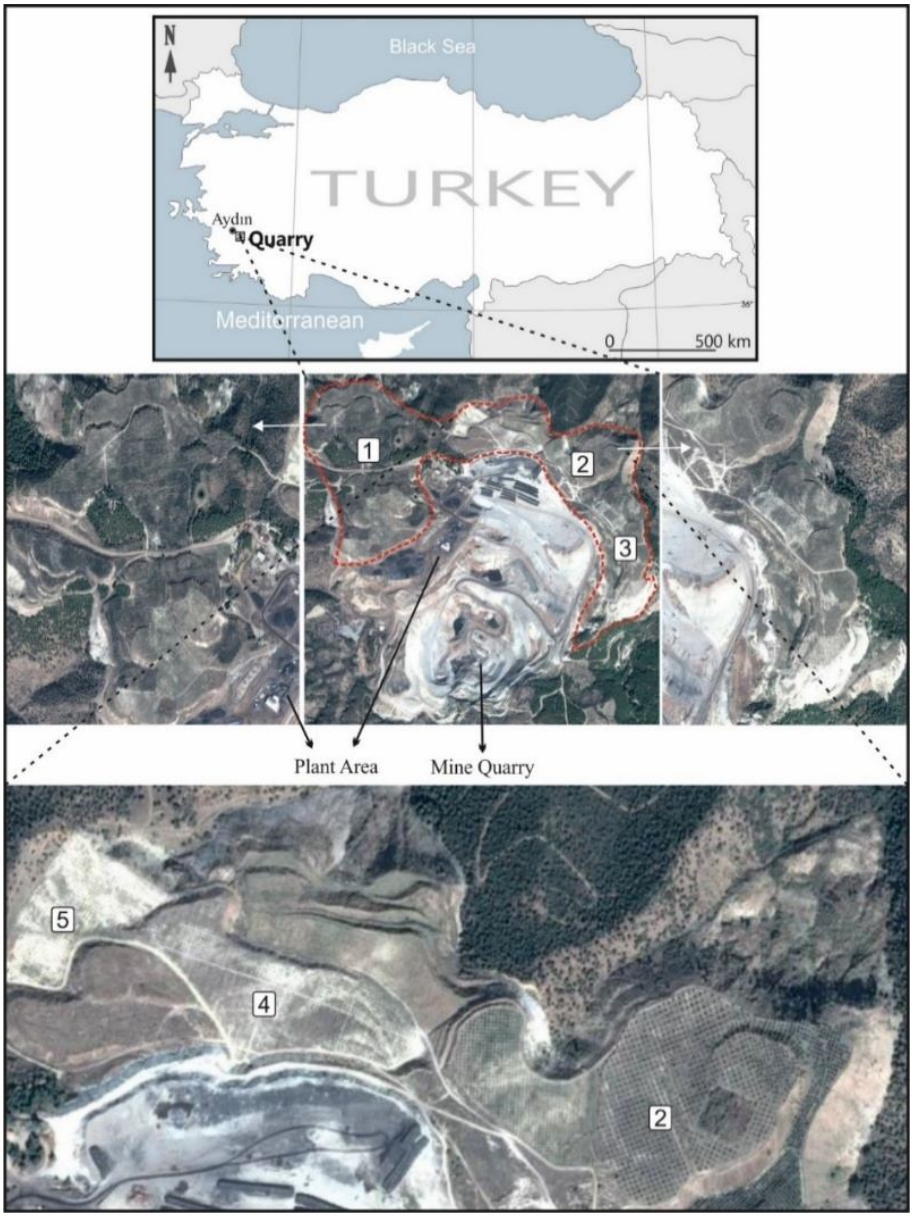

Figure 2. *Open pit mine quaryy and dump sites (number 1-5 and area coordinates: between longitudes 27° 56' 12.80" E to 27° 55' 44.25" E and latitudes 37° 46' 47.86" N to 37° 46' 32.87" N).*

http://www.aloki.hu ● ISSN 1589 1623 (Print) ● ISSN 1785 0037 (Online)
DOI: http://dx.doi.org/10.15666/aeer/1704_73817393

Data collection

Planting studies and applications in the field

Field studies are listed as the determination of the species that are available before the mining operation, establishment of research zones on the damaged areas and the casting areas, conducting the soil analysis of the areas, sapling planting in the areas formed and maintenance and monitoring of the planted areas.

According to this, the active species in the vicinity of the mine and in the region were determined. Most active tree species in the region are; *Pinus Brutia Ten*, *Rolium Olivaru*m, *Robinia Pseudoacacia* and *Amygdolus Communi*s. These identified species were planted in the experimental areas determined on the casting areas whose analysis are given in *Table 1*. Soil analyzes in the determined planting areas were made every 6 months starting 1 year before planting, and every 50 x 100 meters. The average values of these soil analyzes in *Table 1* are given. In addition, the planting process has been completed with a 5 x 5 meter square and a 20-25 square meter seedling has been completed.

Table 1. *The characteristics of soil used in plantation*

Parameters	Unit	
Sand	%	54.5 ± 2.5
Dust	%	38.56 ± 2.11
Clay	%	6.88 ± 1.2
$CaCO_3$	%	9.98 ± 2
pH	-	6.92 ± 1.2
Organic Subs.	%	2.55 ± 0.7
N	%	0.008 ± 0.001
P	mg kg^{-1}	3.0 ± 0.5
K	mg kg^{-1}	156 ± 12
Ca	mg kg^{-1}	2700 ± 22
Na	mg kg^{-1}	75 ± 8
B	mg kg^{-1}	3.22 ± 1.03

*The samples were taken from 30/50 centimeter depth

The evaluation of the seven years data for *Rolium Olivaru*m and also two years data for *Amygdolus Communi*s obtained from this phase were made by evaluating min 1000 saplings and the data were interpreted statistically. As a result of the evaluations, there were differences in terms of survival percent among the species mentioned above. According to this; about 99% of *Rolium Olivarum*, about 94% of *Robinia Pseudoacacia*, 82% of *Amygdolus Communi*s and about % 77 of *Pinus Brutia Ten* survived in the dump sites (*Table 2*). These values were obtained for *Rolium Olivarum* eight years later and for *Amygdalus Communis* two years after planting.

Table 2. *Survival statistics of several tree species on dump sites (%)*

Tree Specie	Chance of Survival (%)
Rolium Olivarum	99
Robinia Pseudoacacia	94
Amygdolus Communis	80
Pinus Brutia Ten	77

http://www.aloki.hu ● ISSN 1589 1623 (Print) ● ISSN 1785 0037 (Online)
DOI: http://dx.doi.org/10.15666/aeer/1704_73817393

Considering the high survival percent of *Rolium Olivarum*; both because it would increase the success in the rehabilitation process and in order to commercially evaluate the crop obtained from *Rolium Olivarum* planting, areas numbered 1,2,3 in the casting areas shown in *Fig. 2* were totally planted Olivarum trees. The casting sites where *Rolium Olivarum* are planted in a geometry of 5 m x 5 m and crop today (20 kg oil/tree) are given in *Fig. 3*.

Figure 3. *Planting dump sites (Rolium Olivarum)*

Because of the factors such as the spreading of open pit casting sites to a very large area, the presence of *Amygdolus Communis* with *Rolium Olivarum* among the primary tree species in the region, ensuring diversity in the areas to be planted, and economic yield obtained from the crop of *Amygdolus Communis* trees, areas numbered 4 and 5 shown in *Fig. 2* were planned to plant *Amygdolus Communis*. For this reason, samples were taken from 30/50 cm from the casting sites corresponding to the regions numbered 4 and 5 in the site and the soil properties given in *Table 3* were obtained. Soil samples were taken for each 50 x 100 meter square area. The planting of 1750 *Amygdolus Communis* trees in the area of approximately 70 hectares numbered 5 and 6 in *Fig. 2* and their current situation are shown in *Fig. 4*. About 2 years old trees were planted in 5 x 5 geometry. Watering the trees is done by drip irrigation as in olive.

In addition to this, the fertilization process done when necessary (rarely applied) also yielded positive results. As a result of research, the main element of the success in the afforestation was determined as the suitability of the characteristics of the soil (casting material) to be planted to the rapid root development. The plants tested in the field can be evaluated in the selection of species in the afforestation of different fields unless there is another restriction giving positive results in the expected direction. However, when afforestation is done with mixed tree species, planting in groups should be preferred by taking different biology of species into consideration (fast growing tree species are light trees). It is also advised to fertilize with organic fertilizers where possible and to irrigate especially in the first two years. Due to the facts that it has the highest survival percent in the area of re-cultivation and will provide economic contribution in terms of mine's economy in the future, approximately 50,000 olive saplings were planted. As a result of the investigations carried out in this area, it was determined that about 20 kg of crop per tree is obtained from these saplings and approximately 1000 tons of olives are produced annually.

http://www.aloki.hu ● ISSN 1589 1623 (Print) ● ISSN 1785 0037 (Online)
DOI: http://dx.doi.org/10.15666/aeer/1704_73817393

Table 3. *The characteristics of soil used in Amygdolus Communis*

Parameters	Unit	
Salt	(µS/cm)	418
$CaCO_3$	%	7.83
pH	-	7.8
Organic Subs.	%	1.08
N	%	-
P	ppm	0.50
K	ppm	110
Ca	ppm	5134
Mg	ppm	226
Cu	ppm	0.36
Fe	ppm	4.27
Mn	ppm	3.24
Zn	ppm	0.68
B	ppm	0.32

Figure 4. *Planting dump sites (Amygdolus Communis)*

UAV data's and technical parameters

UAV used in the acquisition of images has 1 inch 20 MP CMOS sensor and 35 mm focal length, with a single piece lens also the device can take 5472 × 3648 pixel resolution in JPG and RAW format image. In addition, it has GLONASS and GPS satellite support positioning module, 10 m / s wind resistance, 7 km horizontal, 500 m vertical control control distance, 0 - 40°C temperature range, between 2.4 and 5.8 Ghz frequency channels in case of need can make the transition.

In addition to the UAV used in the study, the Ashtech Promark 800 GNSS device was used as the positioning system. Real time positioning most accurate tolerance are 10 mm ± 1.0 ppm in horizontally and 20 mm ± 1.0 ppm in vertically. The system is able to deliver real-time raw data and location output up to 20 Hz. Also, unmanned aerial system flight parameters are clearly shown in *Table 4*.

http://www.aloki.hu ● ISSN 1589 1623 (Print) ● ISSN 1785 0037 (Online)
DOI: http://dx.doi.org/10.15666/aeer/1704_73817393

Table 4. *Unmanned Aerial Vehicle Flight Parameters*

Flight parameters	Values
Flight altitude	70 meters
Flight velocity	32 kilometers per hour
Flight overlap (Side – Front)	%70 - %70
Area covered	0.401 square kilometers
Image amount	303 images
Average ground sampling distance	2.84 centimeters

Research methodology

Unmanned aerial vehicles and photogrammetric software, which are used in many different branches of industry, are used effectively in mining industry especially in planning and rehabilitation studies. The facts that the rehabilitation areas are quite large and difficult to access from time to time, and that the measurements and determinations are made in a short time and they are repeatable allowed the UAVs to be included in these areas. With the UAV, "plant index maps" of the fields can be obtained and the health status of the areas that are brought back to the nature can be determined and controlled.

In the field of especially newly planted *Amygdolus Communis (Fig. 2*, field numbered 4) and olive fields in close vicinity (*Fig. 2*, field numbered 2) shown in *Fig. 4*, flights were made on the dump sites to reveal the rehabilitation model of the site. The flight plans for the flights are given in *Fig. 5a*. In total 313 visual reception fields, four aboveground control points were used for the purpose of controlling the system. In the study which especially focused on the new planting areas where *Amygdolus Communis* trees are located and the vicinity, an area of approximately five hectares was investigated in the first place. The position of the UAV on the site numbered 4 (*Amygdolus Communis* tree planting area) is shown in *Fig. 5b* as an example.

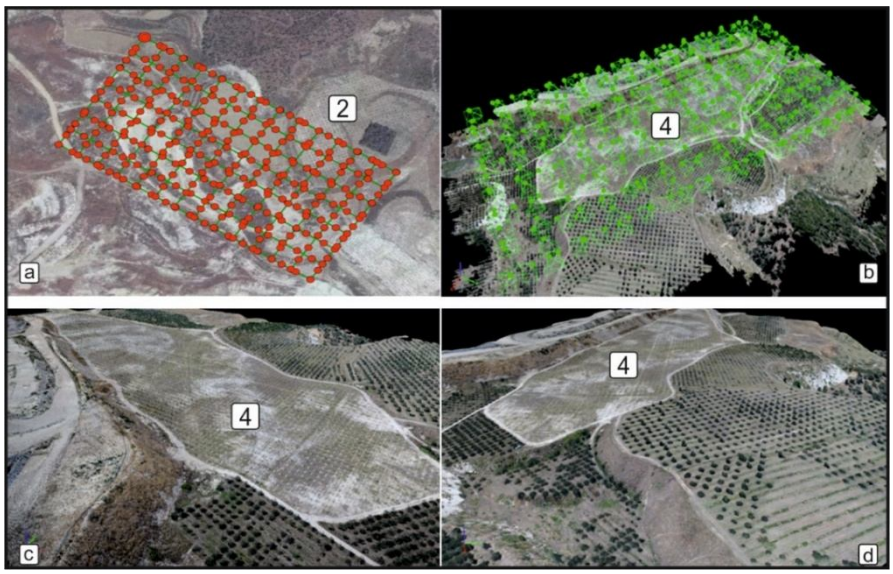

Figure 5. *UAV datas on dump sites [(a) UAV fligth plan; (b) UAV position on Amygdolus Communis plant area; (c) and (d) solid models]*

http://www.aloki.hu ● ISSN 1589 1623 (Print) ● ISSN 1785 0037 (Online)
DOI: http://dx.doi.org/10.15666/aeer/1704_73817393

High-resolution images of the planted area were processed using pix4D software, and a cloud of approximately 10 million 735 thousand points was obtained from the entire area with a mean error margin of less than 4 cm in the measurement. *Fig. 5d* shows the solid model of the sites produced from the point cloud.

"Vegetation index maps" were obtained by processing of received images. The purpose here is to determine the health status of the plants in the field studied and to follow the development process. Since the study was done with a UAV with integrated RGB camera, TGI (Triangular Greenness Index) and VARI (Visible Atmospheric Resistant Index) indices were used together as vegetation index. The TGI and VARI indices were preferred because of the facts that they stand out among other visual indexes and especially that the VARI index can be used in all stages of plant life (Hunt et al., 2011).

TGI index, the reflected spectrum value from the plant; is the junction area of the triangle that ground on blue (480 nm), green (550 nm) and red (670 nm) spectral values as the corner point (*Fig. 6*). The TGI index value (green reflection value) is has a positive value if it is above the line combining 480nm and 670 nm values; and if not it has a negative value. While the positive value (green color) indicates healthy vegetation, the negative value (red color) indicates soil cover (Hunt et al., 2011).

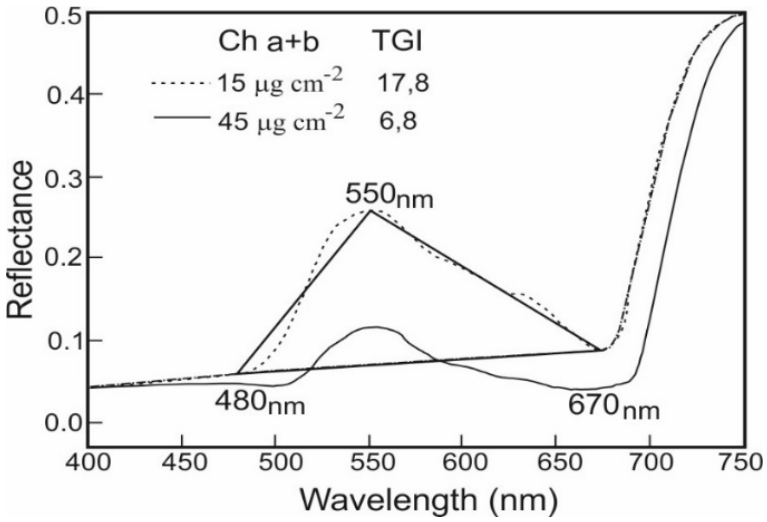

Figure 6. *TGI indeks (Reflected spectrum value from the plant)*

Red, green and blue colors contain information throughout the growing season. The VARI index is determined by the transitions of the green's reflection value with the red edges. VARI is designed to provide an atmospheric correction and is a good and valid index to predict the vegetation fraction from the visible range of the spectrum. This index can be used to analyze plants in all growth stages (Gitelson et al., 2002).

The VARI and TGI index maps and index value distributions divided into four parts of the rehabilitation area studied are visualized as histograms in *Fig. 7* and *Fig. 8*.

Because newly planted almond seedlings are considered first, TGI index was used as subsidiary index by basing on the VARI index applicable to all stages of plant life. The range of values for the VARI index: Value ranges changing between "-1"and "1" that are frequently used in field work are used. In *Table 5*, VARI index values and their meanings are given.

http://www.aloki.hu ● ISSN 1589 1623 (Print) ● ISSN 1785 0037 (Online)
DOI: http://dx.doi.org/10.15666/aeer/1704_73817393

Results

Within the scope of the study, the close geography of the site was examined and the experimental plantings for olive and almond trees, which were determined as a priority, were observed and examined between two and seven years. When the experimental plantings in the casting areas yielded positive results by 99% in *Rolium Olivaru*m and by 80-82% in *Amygdolus Communis*, the sites were mainly afforested with these two species. 50.000 olive saplings were planted in a large part of the dump sites, which has the highest percentage of survival, and which will provide economic contribution in terms of business economy. Today, an average of 20 kg crop per tree is obtained from these planted sites and approximately 1000 tons of olives are produced annually. In other dump sites, to increase plant diversity and produce economic return, *Amygdolus Communis* were planted in almost 70 hectares and they were monitored.

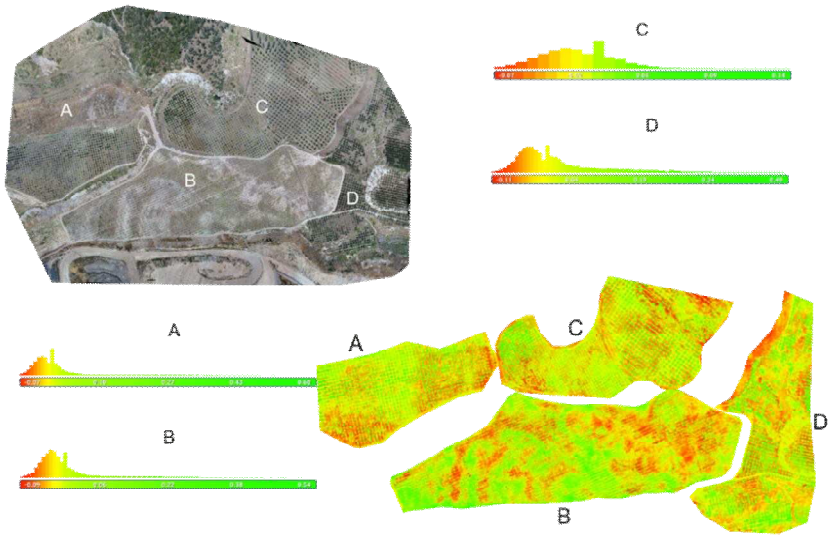

Figure 7. *Visible atmospherically resistant indeks (VARI) of planting dump sites*

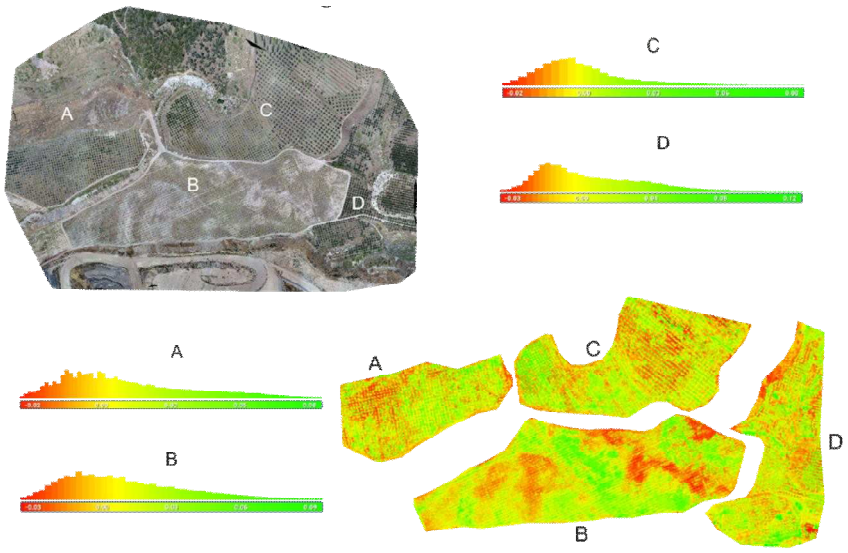

Figure 8. *Triangular greenness indeks (TGI) of dump sites planting dump sites*

http://www.aloki.hu ● ISSN 1589 1623 (Print) ● ISSN 1785 0037 (Online)
DOI: http://dx.doi.org/10.15666/aeer/1704_73817393

Table 5. *VARI Index value range and meanings*

VARI index value	Meanings
< 0	Lifeless or dead plant
0 – 0.33	Immature plant
0.33 – 0.66	Healty plant
> 0.66	Very healthy plant

"Plant index maps" were prepared in the site in order to follow and evaluate the plantation and afforestation processes, which is another stage of the study, with UAVs (*Fig. 7* and *Fig. 8*). According to the obtained plant index maps, when the VARI index values are examined in parallel with the high survival percent of *Rolium Olivarum* both in the experimental areas and in the site, it was determined that it the ones in the range of 0.33 and 0.66 are in the class of "Healthy Plant". This value indicates the class of "immature plant". Additionally, with the UAVs, the visualization of the sites and the processing of the obtained point clouds and the success of the planting process in the site were followed by color scales. Similarly, the intense green color (90-92%) observed in the olive tree region demonstrates the success of the application and monitoring technique. This ratio was obtained between 75-80% in *Amygdolus Communis* planting area.

Discussions

In the present study, a sample study was conducted in order to rehabilitate the heaps of dump sites formed by pickling materials in open coal pits and to monitor the rehabilitated sites. The purpose of the rehabilitation site while mining activities continue was determined as to ensure nature restoration after mining activities by re-creating natural vegetation of the site before mining activities and to generate economic income by planting in these fields.

In this context, the field studies conducted with the help of long-term field studies and the UAVs can be used actively in monitoring the plants and determining the faces of life. Furthermore, with the help of the UAVs, the removal of plant index maps in the course of the restoration of large mining sites has been shown to be a fast, reliable and modern method to control the success of the rehabilitation processes at the sites.

Acknowledgements. The author would like to thank Dokuz Eylul University Department of Scientific Research Projects for the support of 2017.KBFEN.021. Also, the author would like to thank Mining Engineer Ahmet Ozer of Aydın Lignite Enterprises and Yücel Açıkgöz and Ali Ince from the Agriculture Department of the same corporation.

REFERENCES

[1] Cao, X. (2007): Regulating mine land reclamation in developing countries: the case of China. – Land Use Policy 24: 472-483.

[2] Carrick, P. J., Kruger, R. (2007): Restoring degraded landscapes in lowland Namaqualand: Lessons from the mining experience and from regional ecological dynamics. – Journal of Arid Environments 32: 52-67.

http://www.aloki.hu ● ISSN 1589 1623 (Print) ● ISSN 1785 0037 (Online)
DOI: http://dx.doi.org/10.15666/aeer/1704_73817393

[3] Düzgün, Ş. (2009): The basic principles of restoration and mine closure. – In: Chamber of Mining Engineers of Turkey: 3th International Symposium on Mining And Environment, Ankara, June 11-12, 2009: 1-4.
[4] Gitelson, A., Kaufman, Y., Stark, R., Rundquist, D. (2002): Novel algorithms for remote estimation of vegetation fraction. – Remote Sensing of Environment 80: 76-87.
[5] Gizikoff, K. G. (2004): Re-Establishing livestock use on mined landscapes in the southern interior of BC. – In: UBC: Proceedings In: Annual British Columbia Mine Reclamation in Campbell River, BC, June 20-31, 2009: 1-11.
[6] Gül, Y. (2019): Applications of Unmanned Aerial vehicle (UAV) in open-pit mines. – Geological Bulletin of Turkey 62: 99-112.
[7] Hunt, J. E., Daughtry, C., Eitel, J. U., Long, D. (2011): Remote sensing leaf chlorophyll content using a visible band index. – Agronomy Journal 103: 1090-1099.
[8] Kuyumcu, M. (2005): The rehabilitation and integration of lignite mines in Western Germany. – In: Chamber of Mining Engineers of Turkey: International Symposium on Mining and Environment, Ankara, June 11-12, 2005: 165-172.
[9] Lee, S., Choi, Y. (2016): Reviews of unmanned aerial vehicle (drone) technology trends and its applications in the mining industry. – Geosystem Engineering 9(4): 197-204.
[10] Li, M. S. (2006): Ecological restoration of mineland with particular reference to the metalliferous mine wasteland in China: a review of research and practice. – Science of the Total Environment 357: 38-53.
[11] Maiti, S. K., Ghose, M. K. (2005): Ecological restoration of acidic coalmine overburden dumps - an Indian case study. – Journal of Land Contamination and Reclamation 13: 361-370.
[12] Mallı, T., Kun, M., Tufan, B. (2018): The technical and economic evaluation of reclamation studies in open pit mining. – Environmental Engineering and Management Journal 17: 11-18.
[13] Meech, J. A., McPhie, M., Clausen, K., Simpson, Y., Lang, B., Campbell, E., Johnstone, S., Condon, P. (2006): Transformation of a derelict mine site into a sustainable community: the Britannia project. – Journal of Cleaner Production 14: 349-365.
[14] Michaud, L. H. (1981): A manual of reclamation practice. – International Academic Services Ltd.
[15] Ozcan, O., Sari, H. (2019): Determining the spatial effects of quarries using a drone: the case of the Suleymanpasa-Tekirdag quarries. – Fresenius Envitonmental Bulletin 28(1): 53-61.
[16] Özcan, O. (2017): Accuracy assessment of the digital surface models (DSMs) generated from different altitudes using unmanned aerial vehicle. – Journal of Engineering and Earth Science 1: 1-7.
[17] Öztürk, O., Bilgilioğlu, B. B., Çelik, F., Bilbilioğlu, S. S., Uluğ, R. (2017): The investigation of the height and the camera angle in the production of orthoimage with Images of unmanned aerial vehicle (UAV). – Journal of Geomatics 2(3): 135-141.
[18] Paschke, M. W., Redente, E. F., Brown, S. L. (2003): Biology and establishment of mountain shrubs on mining disturbances in the rocky mountains. – Land Degradation and Development 14: 459-480.
[19] Ramani, R. V., Sweigard, R. J., Clar, M. L. (1990): Reclamation Planning-surface Mining Handbook. – SME: 750-769.
[20] Sengupta, M. (1993): Environmental Impacts of Mining: Monitoring Restoration, and Control. – Lewis Publisher.
[21] Shahbazi, M., Théau, J., Ménard, P. (2014): Recent applications of unmanned aerial imagery in natural resource management. – GIScience & Remote Sensing 51: 339-365.
[22] Tafi, T. C. (2006): Reclamation effectiveness at three reclaimed abandoned mine sites in Jefferson County, Montana. – MsC Thesis, Montana State University, Bozeman, Montana.

http://www.aloki.hu ● ISSN 1589 1623 (Print) ● ISSN 1785 0037 (Online)
DOI: http://dx.doi.org/10.15666/aeer/1704_73817393

[23] Topay, M., Kaya, L. G. (2007): The education of landscaping in Turkey. – 3rd Landscape Architecture Congress, Antalya, Turkey, 554-557.
[24] Zavadskas, K. E., Antucheviciene, J. (2006): Development of an indicator model and ranking of sustainable revitalization alternatives of derelict property: a Lithuanian case study. – Sustainable Development 14: 287-299.

http://www.aloki.hu ● ISSN 1589 1623 (Print) ● ISSN 1785 0037 (Online)
DOI: http://dx.doi.org/10.15666/aeer/1704_73817393

THE TAXONOMICAL CHARACTERIZATION OF SOME *HELVELLA* AND ITS RELATIVES BY MORPHOLOGICAL AND MOLECULAR DATA FROM TURKEY

AKTAŞ, S.* – KARASELEK, M. A.

Department of Biology, Faculty of Science, Selçuk University, Konya, Turkey

**Corresponding author*
e-mail: sinaktas@yahoo.com; phone: +90-332-223-1867; fax: +90-332-241-2499

(Received 28th Feb 2019; accepted 3rd May 2019)

Abstract. Herein, 15 fungi species belonging to different genera of Pezizales were studied morphologically and molecularly. During the morphological analyses performed by means of Primer 7 software, 28 characters were used, mainly including the stalk, cap, asci, and spores, to assess the taxonomical relationships of the fungi species. The data matrix and nMDS plot approaches based on the morphological data were highly functional in the determination of the taxonomical relationship of very closely related fungi taxa, particularly at the genus level. Moreover, the data from the ISSR locus analyses significantly supported the current morphological relationships on a wide scale. Contrary to the morphological data expressing taxonomical relationships related to morels or early morels, a minor exceptional condition was determined inferring to the relatively higher genetic similarity among Verpa and Gyromitra in the dendrogram connected with the ISSR analyses.
Keywords: *fungi, DNA, genetic relationships, ISSR, numerical analyses*

Introduction

Helvella L. is a widespread and interesting genus of large apothecial ascomycet (Pezizomycete: *Pezizales* J. Schröt.) that are found in terrestrial biomes of the Northern and Southern Hemispheres. The genus contains many of the larger and charismatic species of the order *Pezizales* and comprises a range of elaborate apothecia, from cupulate to saddle-shaped, and convex to campanulate, including species with folded and lobed caps seated on a simple, ribbed, or furrowed stipe (Skrede et al., 2017). Compared to other close relatives, *Helvella* is a relatively more crowded group in terms of the number of taxa and it is represented by 21 species in Turkey (Sesli and Denchev, 2014).

Morchella Dill. ex Pers. taxa are known as Morels, which occur in different types of forests with different mycelial dynamics, alternating between saprotrophic and symbiotic behaviors (Stefani et al., 2010). The changes in the developmental process may induce a high degree of variability in the ascocarps (Yoon et al., 1990).

Verpa Sw. is a genus of ascomycete fungi related to the morels, resembling the latter genus; hence, they are called false or early morels. There are 5 species in the widespread genus (Kirk et al., 2008). *Verpa* comes from the Latin for erection or little rod. Thus, the 3 genera are now included in the family *Morchellaceae* Rchb. (O'Donnell et al., 1997).

Gyromitra esculenta (Pers.) Fr. is a beautiful spring time mushroom that is often encountered by morel hunters in northern and montane areas of the continent. It can be distinguished from other species of *Gyromitra* Fr. by its convoluted and brain-like, reddish-brown cap, and by the fact that its stem is not massive in proportion to its cap

http://www.aloki.hu ● ISSN 1589 1623 (Print) ● ISSN 1785 0037 (Online)
DOI: http://dx.doi.org/10.15666/aeer/1704_73957405

(Kuo, 2014). Additionally, the species display high similarity with morel taxa in terms of their ascocarp features.

Sarcoscypha coccinea (Jacq.) Sacc., commonly known as the scarlet elf cup, or the scarlet cup, is a species of fungus in the family *Sarcoscyphaceae* Le Gal ex Eckblad of the order Pezizales. The fungus, widely distributed in the Northern Hemisphere, has been found in Africa, Asia, Europe, North and South America, and Australia. The type species of the genus *Sarcoscypha* Roum., *S. coccinea*, has been known by many names since its first appearance in the scientific literature in 1772. The species was originally named *Helvella coccinea* by the Italian naturalist Giovanni Antonio Scopoli in 1772 (Scopoli, 1772). Other early names include *Peziza coccinea* (Jacquin, 1774) and *Peziza dichroa* (Holmskjold, 1799). Although some authors in older literature have applied the generic name *Plectania* to the taxon, following Fuckel's 1870 name change (e.g., Seaver, 1928; Kanouse, 1948; Nannfeldt, 1949; Le Gal, 1953), that name is now used for a fungus with brownish-black fruit bodies (Korf and Harrington, 1990). *S. coccinea* was given its current name by Lambotte in 1889.

In recent years, developments in molecular biology and genetic have made inevitable the emergence of new techniques in the systematic field, and these developments have also been effective in fungal systematics. Previous classifications of the fungi could be checked via molecular studies to determine whether it is natural or not. The marker system, called inter-simple sequence repeats (ISSRs), is also a polymerase chain reaction (PCR)-based technique (Wolfe, 1998) that has been successfully applied for the genetic analyses of plants (Fang et al., 1997; Prevost et al., 1999; Song et al., 2006; Uysal et al., 2012 a, b; Bozkurt et al., 2013) and fungal classification (Tang et al., 2005). In particular, ISSR markers can be highly variable within a species and have an advantage over others in utilizing longer primers that allow more stringent annealing temperatures (Camacho and Liston., 2001; Tsumura et al., 1996; Nazrul and Bian, 2010). Recently, the development of molecular systematics, thanks to ISSR and similar molecular markers, has made it possible to identify specimens of closely related species and, to some extent, it has been applied to taxonomic studies of *Helvella* (Landvik et al., 1999; Nguyen et al., 2013; Landeros et al., 2015; Ariyawansa et al., 2015; Zhao et al., 2017). In previous studies were also reported that some cryptic fungi species would be recognized by means of applying molecular markers (Nguyen et al., 2013; Balasundaram et al., 2015). Hence, ISSR has been chosen for the taxonomical characterization of some *Helvella* taxa from Turkey herein. Our aim was to first reveal the natural taxonomical positions of some *Helvella* species with their taxonomical characters and then solve the natural relationships between *Helvella* and its relatives.

Materials and methods

In this study, 15 *Ascomycota* taxa were collected from different localities in Turkey (*Table 1* and *Fig. 1)*.

Morphology

The morphological analyses of the studied fungi taxa were conducted on 15 samples from each taxa in the field from 2011–2016. A total of 28 qualitative (15) and quantitative (13) morphological characters were used (*Table 2*). The diagnostic traits at the species or genera level were measured, including the stalk, ascocarp, cap, spores, and asci. The qualitative and quantitative characters determined were measured and

http://www.aloki.hu ● ISSN 1589 1623 (Print) ● ISSN 1785 0037 (Online)
DOI: http://dx.doi.org/10.15666/aeer/1704_73957405

scored over the samples and finally turned into a data matrix. Morphometric data (*Table 2*) were analyzed using multivariate techniques with the PRIMER7 software package (Plymouth Marine Laboratory, Plymouth, UK; Clarke and Warwick, 1994). The Bray-Curtis similarity matrix was used to generate a 2-dimensional ordination plot applying non-metric multidimensional scaling in the PRIMER7 software (nMDS; Clarke, 1993).

Table 1. *Ascomycota taxa used for ISSR and morphological analyses*

Sample number	Taxa	Locality, Collector(s) and collector's number
HM1	*Helvella ephippium* Lév.	Adana, pine forest, 30.10.2011, Aktaş 1112; Isparta, pine forest, 17.12.2011, Aktaş 1128; Amasya, pine forest, 20.04.2012, Aktaş 1130; Amasya, pine forest, 22.04.2012, Aktaş 1145; Amasya, pine forest, 23.04.2012, Aktaş 1152; Amasya, pine forest, 11.06.2012, Aktaş 1154; Amasya, pine forest, 12.06.2012, Aktaş 1158
HM2	*H. lacunosa* Afzel.	Antalya, fir forest, 26.11.2011, Aktaş 1122; Amasya, fir-pine forest, 21.04.2012, Aktaş 1142; Amasya, fir-pine forest, 22.04.2012, Aktaş 1146
HM3	*H. leucomelaena* (Pers.) Nannf.	Adana, pine forest, 28.10.2011, Aktaş 1111; Antalya, pine forest, 25.11.2011, Aktaş 1119; Antalya, pine forest, 26.11.2011 Aktaş 1121; Isparta, pine forest, 16.12.2011, Aktaş 1125; Amasya, pine forest, 20.04.2012, Aktaş 1131; Amasya, pine forest, 21.04.2012, Aktaş 1141; Amasya, pine forest, 22.04.2012, Aktaş 1147; Amasya, pine forest, 10.06.2012, Aktaş 1153; Amasya, pine forest, 11.06.2012, Aktaş 1155
HM4	*H. queletii* Bres.	Antalya, fir forest, 27.11.2011, Aktaş 1123; Amasya, fir-pine forest, 20.04.2012, Aktaş 1132; Amasya, fir-pine forest, 12.06.2012, Aktaş 1157
HM5	*H. acetabulum* (L.) Quél.	Amasya, pine forest, 21.04.2012, Aktaş 1140; Amasya, pine forest, 22.04.2012, Aktaş 1148
HM6	*H. spadicea* Schaeff.	Isparta, among poplar woods, 16.12.2011, Aktaş 1124; Amasya, among poplar woods, 20.04.2012, Aktaş 1133; Amasya, among poplar woods, 21.04.2012, Aktaş 1139
HM13	*H. crispa* Sowerby	Antalya; Akseki, fir-pine forest, 26.11.2011, Aktaş 1121
HM14	*H. solitaria* P. Karst.	Samsun; Ladik, beech forest, 22.10.2016, Aktaş 2033
HM15	*H. leucopus* Pers.	Konya; Akşehir, near stream, 15.10.2016, Aktaş 2027
HM7	*Peziza michelii* (Boud.) Dennis	Amasya, pine forest, 23.04.2012, Aktaş 1153
HM8	*P. varia* (Hedw.) Alb. & Schwein.	Amasya, pine forest, 22.04.2012, Aktaş 1149
HM9	*Gyromitra esculenta* (Pers.) Fr.	Antalya, pine forest, 25.11.2011, Aktaş 1120; Amasya, fir-pine forest, 21.04.2012, Aktaş 1138; Amasya, pine forest, 20.04.2012, Aktaş 1134; Amasya, pine forest, 21.04.2012, Aktaş 1143; Amasya, pine forest, 12.06.2012, Aktaş 1156
HM10	*Verpa conica* (O.F. Müll.) Sw.	Amasya, among poplar woods, 21.04.2012, Aktaş 1136
HM11	*Sarcoscypha coccinea* (Gray) Boud.	Isparta, pine forest, 16.12.2011, Aktaş 1126; Isparta, pine forest, 17.12.2011, Aktaş 1127; Isparta, pine forest, 18.12.2011, Aktaş 1129; Amasya, pine forest, 23.04.2012, Aktaş 1150
HM12	*Morchella esculenta* (L.) Pers.	Amasya, pine forest, 20.04.2012, Aktaş 1135; Amasya, pine forest, 21.04.2012, Aktaş 1137; Amasya, pine forest, 22.04.2012, Aktaş 1144

http://www.aloki.hu ● ISSN 1589 1623 (Print) ● ISSN 1785 0037 (Online)
DOI: http://dx.doi.org/10.15666/aeer/1704_73957405

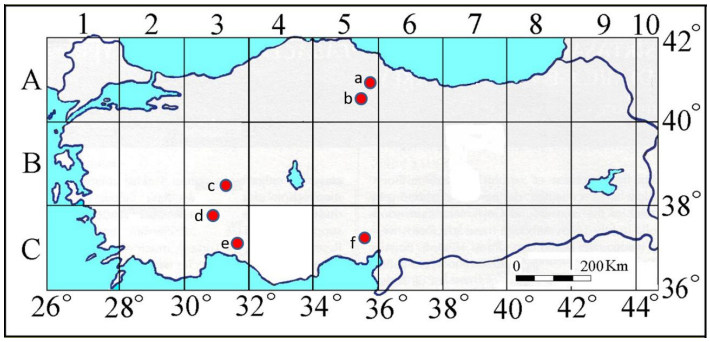

Figure 1. *The location of collected samples on map (a: Samsun; b: Amasya; c: Konya; d: Isparta; e: Antalya; f: Adana)*

Table 2. *Characters used in numerical analysis*

Diagnostic characters of the Ascomycota species		
Stalk	Absent (0), present (1)	HS1
Stalk	Whitish (0), yellowish (1), brownish (2), blackish (3), absent (4)	HS2
Stalk	Smooth (0), ribbed or veined (1), absent (2)	HS3
Stalk	Narrowed at the base (0), enlarged at the base (1), same anywhere (2), absent (3)	HS4
Stalk	Up to 20 mm (0), between 21–50 mm (1), 51–80 mm (2), more than 81 mm (3)	HS5
Stalk	Up to 15 mm (0), between 16–30 mm (1), more than 31 mm (2)	HS6
Rate of stalk length/diameter	Unit	HS7
The type of ascocarp	Apothecium (0), other (1)	HS8
Ascocarp	Saddle-shaped (0), cup-shaped (1), Globose (2), conical (3)	HS9
Ascocarp	Smooth (0), lobed (1), curved-brain (2), alveolate (3)	HS10
Ascocarp (outer surface)	Cream (0), reddish-brown (1), yellowish (2), greyish (3)	HS11
Ascocarp (inner surface; Hymenium)	Greyish brown (0) brownish-black (1) yellowish (2), reddish-brown (3), red (4), light brown (5)	HS12
Ascocarp (inner surface; Hymenium)	Glabrous (0), hairy (1)	HS13
Cap	Up to 25 mm (0), 26–60 mm (1), more than 61 mm (2)	HS14
Cap	Up to 25 mm (0), 26–60 mm (1), more than 61 mm (2)	HS15
Rate of cap length/diameter	Unit	HS16
Cap	Convex (0), concave (1), semi-convex (2)	HS17
Spores	Ellipsoidal (0), elliptic (1), weakly-elliptic (2)	HS18
Spores (oil drop number)	Only one (0), two (1), more (2)	HS19
Spores (oil drop position)	Inside of spores (0), outside of spores (1)	HS20
Spores	Between 16 and 21 µm (0), 22–27 µm (1), more than 27 µm (2)	HS21
Spores	Between 8 and 10 µm (0), 11–13 µm (1), 14-16 µm (2)	HS22
Rate of spore length/diameter	Unit	HS23
Spores (surfacial)	Smooth (0), verrucose (1)	HS24
Asci	Between 225 and 300 µm (0), 301–375 µm (1), more than 376 µm (2)	HS25
Asci	Between 14 and 18 µm (0), more than 18 µm (1)	HS26
Rate of asci length/width	Unit	HS27
Asci (number of spores)	Number	HS28

http://www.aloki.hu ● ISSN 1589 1623 (Print) ● ISSN 1785 0037 (Online)
DOI: http://dx.doi.org/10.15666/aeer/1704_73957405

DNA extraction

Total genomic DNA was extracted following the 2xCTAB method of Doyle and Doyle (1987) as was modified by Soltis et al. (1991) and Cullings (1992) from silica gel-dried leaves collected in the field.

ISSR-PCR

Our modified ISSR-PCR analyses were basically performed according to the method of Zietkiewicz et al. (1994). During the PCR-optimization reactions, some modifications were quantitatively carried out, particularly for the Mg and primer amounts, as well as the Tm selection. The designed ISSR primers by British Colombia University were chosen for the PCR-amplifications. Amplification products were separated by electrophoresis in 1.2% agarose gel run in a TAE buffer at 100 V. The fragment size was estimated using a 20,000–75 bp molecular size DNA ladder (Thermoscientific, SM1331).

Data analysis

The ISSR profiles were scored as present (1) or absent (0). Only reproducible bands were scored as monomorphic or polymorphic. The dendrogram was created using NTSYS-pc version 2.1 (Rohlf, 1998).

Results

Molecular results

A total of 15 taxa were tested with 20 ISSR primers and only 10 of them provided reproducible and analyzable amplification products for all taxa and a total of 477 bands ranging from 80–2500 bp were obtained to put the relativeness of the fungi species (*Fig. 2*). All of the ISSR primers showed 100% polymorphism for Ascomycota taxa (*Table 3*).

Table 3. *Number and percentage of polymorphic ISSR markers*

Primers	Primer sequences (5'-3')	Fragment size (bp)	Total number of bands	Total number of polymorphic bands
UBC827	ACA CAC ACA CAC ACA CG	1500-100	47	47
UBC812	GAG AGA GAG AGA GAG AA	1400-80	47	47
UBC810	GAG AGA GAG AGA GAG AT	1250-80	51	51
UBC847	CAC ACA CAC ACA CAC ARC	1100-80	35	35
UBC857	ACA CAC ACA CAC ACA CYG	2000-80	46	46
UBC808	AGA GAG AGA GAG AGA GC	1250-80	46	46
UBC855	ACA CAC ACA CAC ACA CYT	2000-250	45	45
UBC834	AGA GAG AGA GAG AGA GYT	2500-80	79	79
UBC840	GAG AGA GAG AGA GAG AYT	1750-80	45	45
UBC856	ACA CAC ACA CAC ACA CYA	1250-80	36	36

When we look at the dendrogram that was created using the locus analysis based on the ISSR primers, all of the *Helvella* taxa were positioned together as only one group (*Fig. 3*). However, the relationships and positions of the *Helvella* species among

http://www.aloki.hu ● ISSN 1589 1623 (Print) ● ISSN 1785 0037 (Online)
DOI: http://dx.doi.org/10.15666/aeer/1704_73957405

themselves did not fit exactly with the performed previously classification on a morphology basis. In the dendrogram, the *Helvella* species displayed very close genetic relationships with at least 80% similarity and they were placed in the core of dendrogram. As the furthest taxa, *Morchella esculenta* was placed in the outermost area with 75% similarity to others. Compared to the first taxa, *Sarcoscypha coccinea* showed a closer similarity with the remaining taxa and its genetic relationship was more than 76%. Another relatively smaller group (subclade B) consisted of 3 taxa representing 3 different genera and they showed at least 81% genetic similarity. Even if classified morphologically in different families, *Gyromitra esculenta* is genetically closer to *Verpa conica* when compared to *Peziza* and others analyzed herein. Naturally, *Peziza michelii* and *P. varia* are very similar genetically and the distance between them is less than 15%.

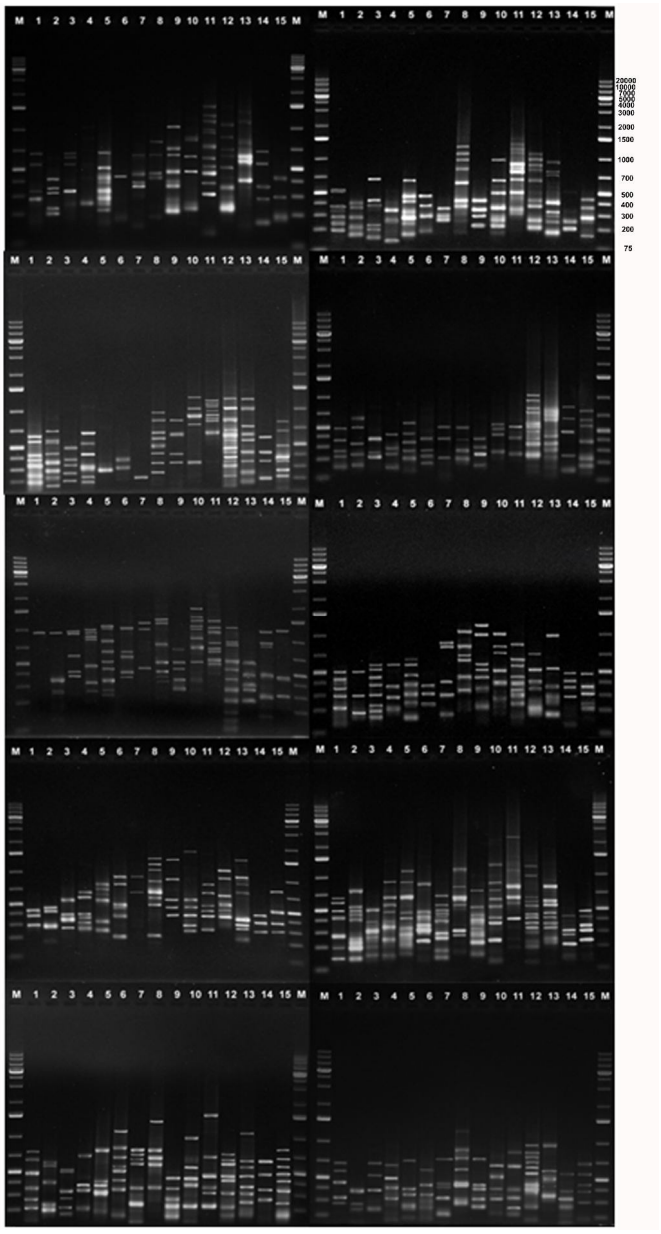

Figure 2. *Electrophoresis Patterns of ISSR products amplified with primers UBC827, 812, 810, 847, 857, 808, 855, 834, 840 and 856 for Ascomycota taxa*

http://www.aloki.hu ● ISSN 1589 1623 (Print) ● ISSN 1785 0037 (Online)
DOI: http://dx.doi.org/10.15666/aeer/1704_73957405

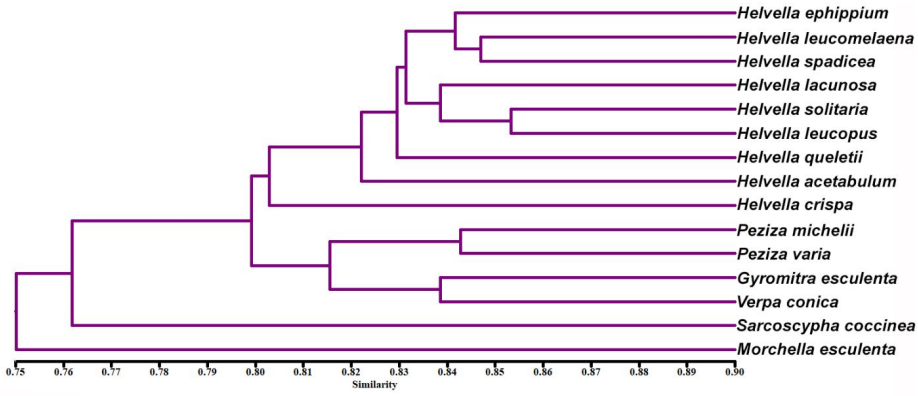

Figure 3. *The dendrogram showing the genetic relationships among Ascomycota taxa based on ISSR data*

Morphological results

The nMDS plots revealed the morphological differences among the studied taxa and helped to make prominent separations among them (*Fig. 4*). The phenogram pointed out very important characters which were very functional in classifying the fungi at different taxonomical levels (for instance, levels of species, genera, or higher). According to the phenogram (*Fig. 5*), it could be said that the characters belonging to the cap and the stalk are important at the primary level; hence, the taxa were divided in the main 2 groups according to these characters. Second, it was seen that the fungal species were divided into 2 subgroups according to whether the cap surface was smooth or not, and that this separation was largely compatible with previous classifications based on morphology. Finally, it was determined that the structural ornamentations made by the cap inside or outside were important in the classification of the fungi, especially to determine the 2 different groups of taxa located in the *Helvella* genus as saddle or cup (*Fig. 5*).

Discussion and conclusion

True morels (*Morchella* spp.) are highly popular for their edibility and appearance, and they have been examined in many broad-scale studies at different times (Kirk et al., 2011); however, other relatives have not be researched as deeply until now. We can emphasize clearly from our results that ISSR markers and morphometric analyses are very effective tools to assess close relative fungi, particularly at the genera level.

Traditionally, *Verpa* and *Gyromitra* were found to be very close to the genus *Morchella* and so, they were named false morels (Kirk et al., 2008). Our examinations indicated that these taxonomical groups are very close in terms of genetic and morphological features, and clear differences can be displayed among them. According to our findings, *Morchella esculenta* is the farthest taxa genetically and the alveolate ascocarp was not seen in any other relatives. From these, we can say that the alveolate cap is an important character for true morels to separate it from its close relative genera. Analysis of the ribosomal DNA of many of the *Pezizales* showed the genus *Verpa* to be closely related to the genus *Morchella* (Bunyard et al., 1995; O'Donnell et al., 1997). The results from the ISSR analyses did not exactly reflect this information, such that *S. coccinea* was positioned exceptionally among them.

http://www.aloki.hu ● ISSN 1589 1623 (Print) ● ISSN 1785 0037 (Online)
DOI: http://dx.doi.org/10.15666/aeer/1704_73957405

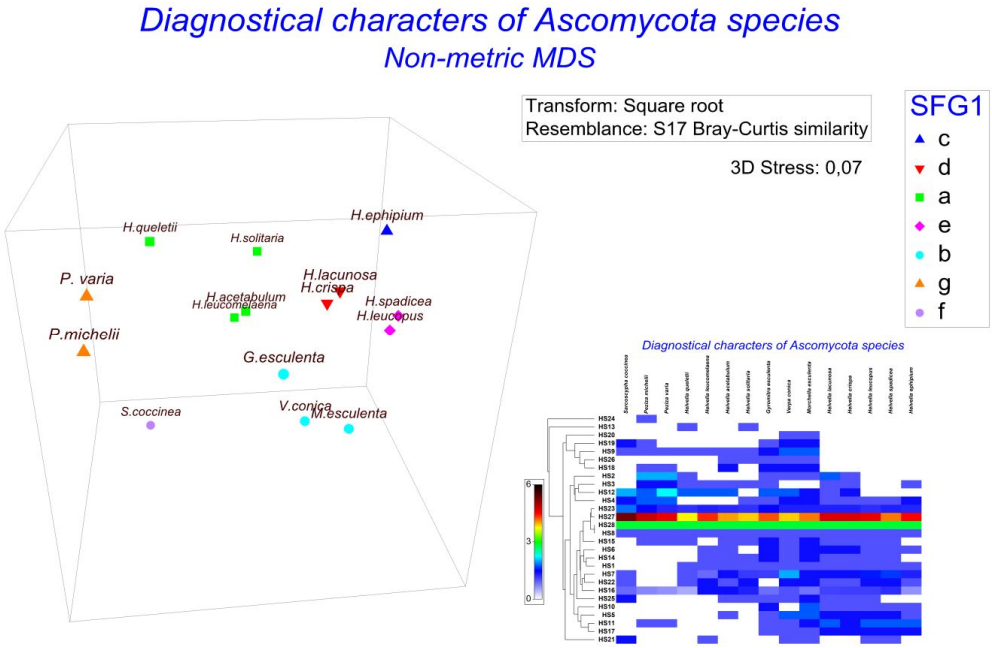

Figure 4. *Two-dimensional nMDS ordination belonging to morphological characters*

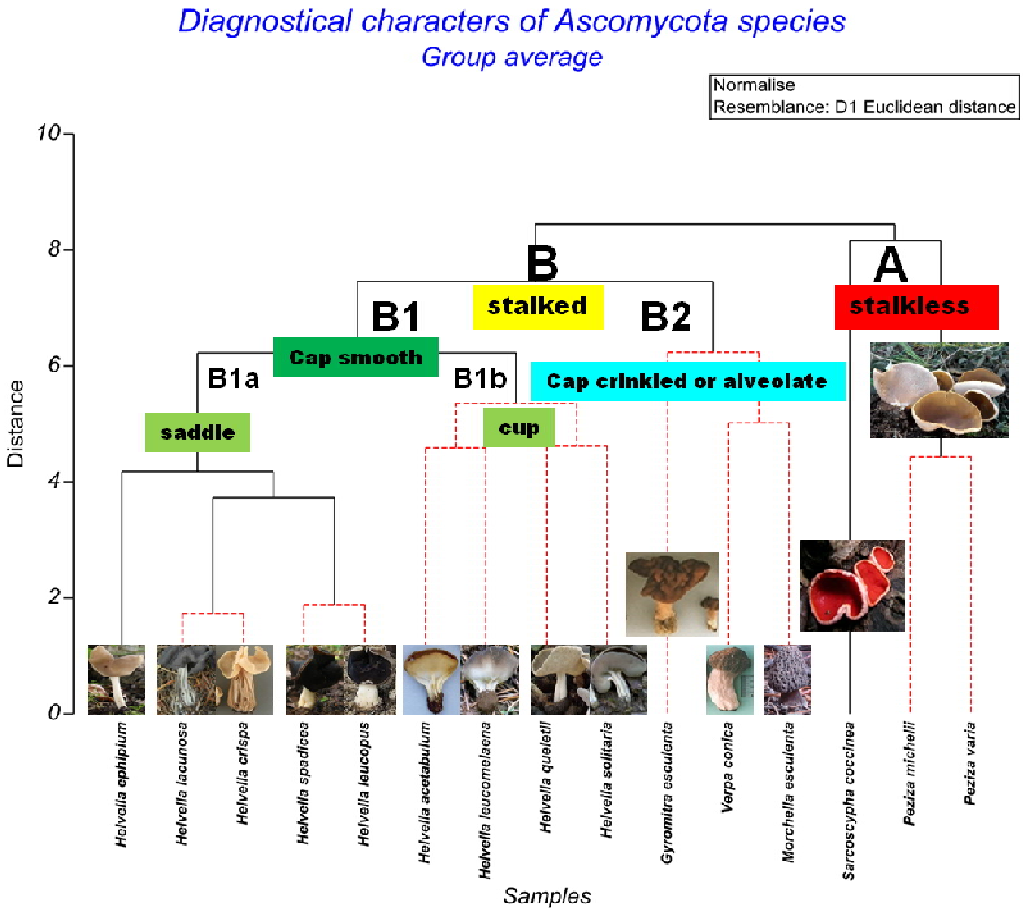

Figure 5. *The phenogram showing relationships among Ascomycota taxa according to morphological characters*

http://www.aloki.hu ● ISSN 1589 1623 (Print) ● ISSN 1785 0037 (Online)
DOI: http://dx.doi.org/10.15666/aeer/1704_73957405

The morphological data has been found largely correlated with the genetic information based on the ISSR locus analyses in except of a limited homoplasy and pseudocriptic variation. It is an interesting finding that species such as *H. lacunosa* and *H. crispa*, which are very close taxa morphologically within the genus *Helvella*, constituted the main body of this study, and are taken place genetically relatively remote (*Fig. 3*). This observed homoplasic similarity on their morphologies might be sourced from similar environmental conditions and habitats rather than genealogy. As together with this, Skrede et al. (2017) reported a pseudocryptic variation, in which 2 taxa could be recognized morphologically, only after molecular systematic data unveiled their existence. The authors suggested that the morphologically similar species pairs of *H. corium/H. macrosperma, H. lactea/H. pallescens,* and *H. elastica/H. panormitana*, which were initially indiscernible due to the lack of discriminating morphological characters, could be resolved as genealogically exclusive using the sequence data. This was true with our 4 fungi, such as with *H. lacunosa* and *H. crispa* or *H. spadicea* and *H. leucopus*. The results indicated that these species pairs are genetically divergent and located in relatively distant related *Helvella* lineages according to the ISSR data. The use of molecular characters is important in cases whether the morphological characters of the taxa are identical to each other or not, or may have been reduced or absent from the taxa (Blackwell et al., 2007). The genus *Helvella*, which constitutes the main body of this work, is relatively taxonomically problematic and shows a series of relationships with the other genera mentioned in this paper. Although easily separated from other macrofungi by conspicuous polymorphic apothecia, it is surprisingly difficult to distinguish between *Helvella* species. Historically, the shape, color, and outer surface characters have been emphasized in species discrimination, while the microanatomy of the sterile and fertile structures added few characters of value in species recognition. In a previous study performed on *Helvella* (Weber, 1972), it was concluded that most morphological and anatomical characters exhibited a nearly continuous variation in the genus as a whole. Unlike the expressed critics, we think that the trustable and functional characters could be revealed for the genus *Helvella* in light of the molecular or morphological data, as illustrated via the nMDS plot of Primer7, and they could be used to explain taxonomical relationships. In conclusion, it was decided that both the stalk and cap features were quite efficient when the characters were handled comprehensively.

Acknowledgements. The authors would like to thank TÜBİTAK (Project No, 111T633) and Selçuk University Scientific Research Projects (BAP, Project No. 11201012) for their financial support of this project.

REFERENCES

[1] Ariyawansa, H. A., Hyde, K. H., Jayasiri, S. C., Buyck, B., Chethana, K. W. T., Dai, D. Q., Dai, Y. C. et al. (2015): Fungal diversity notes 111-252 - taxonomic and phylogenetic contributions to fungal taxa. – Fungal Diversity 75: 27-274.

[2] Balasundaram, S. V., Engh, I. B., Skrede, I., Kauserud, H. (2015): How many DNA markers are needed to reveal cryptic fungal species. – Fungal Biology 119: 940-945.

[3] Bozkurt, M., Ertuğrul, K., Uysal, T. (2013): The determination of genetic relationships among some Vicia L. (Vetch) taxa by using ISSR markers. – Biological Diversity and Conservation 6(3): 135-139.

http://www.aloki.hu ● ISSN 1589 1623 (Print) ● ISSN 1785 0037 (Online)
DOI: http://dx.doi.org/10.15666/aeer/1704_73957405

[4] Bunyard, B. A., Nicholson, M. S., Royse, D. J. (1995): Phylogenetic resolution of Morchella, Verpa and Disciotis [Pezizales: Morchellaceae] based on restriction enzyme analysis of the 28S ribosomal gene. – Exp Mycol 19: 223-233.
[5] Camacho, F. J., Liston, A. (2001): Population structure and genetic diversity of Botrychium pumicola (Ophioglossaceae) based on inter-simple sequence repeats (ISSR). – Am. J. Bot. 88: 1065-1070.
[6] Clarke, K. R. (1993): Non-parametric multivariate analyses of changes in community structure. – Aust J Ecol 18: 117-143.
[7] Clarke, K. R., Warwick, R. M. (1994): Change in Marine Communities: An Approach to Statistical Analysis and Interpretation. – Natural Environment Research Council, Swindon.
[8] Cullings, K. W. (1992): Design and testing of a plant-specific PCR primer for ecological and evolutionary studies. – Molecular Ecology 1: 233-240.
[9] Fang, D. Q., Roose, M. L. (1997): Identification of closely related citrus cultivars with inter-simple sequence repeats markers. – Theor. Appl. Genet. 95: 408-417.
[10] Fuckel, L. (1870): Symbolae mycologicae. Beiträge zur Kenntnis der rheinischen Pilze [Contributions to the knowledge of mushrooms of the Rhein]. – Jahrbücher des Nassauischen Vereins für Naturkunde 23-24: 324 (in German).
[11] Holmskjold T (1799): Beata Ruris Otia Fungis Danicis. – Sumtibus Universitatis Bibliopolae Friderico Brummer, Havniae (in Latin)
[12] Jacquin, N. J. (1774): Flora Austriaca. – Vienna, Austria.
[13] Kanouse, B. C. (1948): The genus Plectania and its segregates in North America. – Mycologia 40(4): 482-97. DOI: 10.2307/3755155. JSTOR 3755155.
[14] Korf, R. P., Harrington, F. A. (1990): Proposal to conserve a type for Sarcoscypha (Fries) Boudier, S. coccinea (Jacq.) Lambotte (Fungi). – Taxon. 39(2): 342-3. DOI: 10.2307/1223069. JSTOR 1223069.
[15] Kuo, M. (2014): Contributors. – http://www.mushroomexpert.com/contributors.html.
[16] Kirk, P. M., Cannon, P. F., Minter, D. W., Stalpers, J. A. (2008): Dictionary of the Fungi (10th Ed.). – CABI, Wallingford, UK.
[17] Lambotte, J. B. E. (1889): *Sarcoscypha coccinea* (Scop.). – MycoBank, International Mycological Association (retrieved 2010-08-21).
[18] Landeros, F., Iturriaga, T., Rodriguez, A., Vargas-Amadoc, G., Guzmán-Dávalos, L. (2015): Advances in the phylogeny of Helvella (Fungi: Ascomycota), inferred from nuclear ribosomal LSU sequences and morphological data. – Revista Mexicana de Boversidad 86: 856-871.
[19] Landvik, S., Kristiansen, R., Schumacher, T. (1999): Pindara: a miniature Helvella. – Mycologia 91: 278-285.
[20] Le Gal, M. (1953): Les Discomycètes de Madagascar [The Discomycetes of Madagascar]. Prodrome à Flore Mycologique de Madagascar et Dépendanes. – Muséum National d'Histoire Naturelle, Paris 4: 1-465 (in French).
[21] Nannfeldt, J. A. (1949): Contributions to the microflora of Sweden. 7. A new winter Discomycete, Urnula hiemalis Nannf. n. sp., and a short account of the Swedish species of *Sarcoscyphaceae*. – Svensk Botanisk Tidskrift. 43: 468-84.
[22] Nazrul, M. I., Bian, Y. B. (2010): Efficiency of RAPD and ISSR markers in differentiation of homo- and heterokaryotic protoclones of Agaricus bisporus. – J. Microbiol. Biotechnol. 20(4): 683-692.
[23] Nguyen, N. H., Landeros, F., Garibay-Orijel, R., Hansen, K., Vellinga, E. C. (2013): The *Helvella lacunosa* species complex in western North America: cryptic species, misapplied names and parasites. – Mycologia 105(5): 1275-1286.
[24] O'Donnell, K., Cigelnik, E., Weber, N. S., Trappe, J. M. (1997): Phylogenetic relationships among ascomycetous truffles and the true and false morels inferred from 18S and 28S ribosomal DNA sequence analysis. – Mycologia 89(1): 48-65. DOI: 10.2307/3761172. JSTOR 3761172.

http://www.aloki.hu ● ISSN 1589 1623 (Print) ● ISSN 1785 0037 (Online)
DOI: http://dx.doi.org/10.15666/aeer/1704_73957405

[25] Prevost, A., Wilkinson, M. J. (1999): A new system of comparing PCR primers applied to ISSR fingerprinting of potato cultivars. – Theor. Appl. Genet. 98: 107-112.
[26] Rohlf, F. J. (1998): NTSYSpc Numerical Taxonomy and Multivariate Analysis System User Guide. – Exeter Software, New York, 0-925031-28-3.
[27] Scopoli, G. A. (1772): Flora Carniolica. 2nd Ed.. – Sumptibus J. T. Trattner, Vienna (in Latin).
[28] Seaver, F. J. (1928): The North American Cup-Fungi (Operculates). – Self Published, New York, pp. 191-2.
[29] Sesli, E., Denchev, C. M. (2014): Checklists of the Myxomycetes, Larger Ascomycetes, and Larger Basidiomycetes in Turkey. 6th Ed. – Mycotaxon Checklists Online. http://www.mycotaxon.com/resources/checklists/sesli-v106-checklist.pdf.
[30] Skrede, I., Carlsen, T., Schumacher, T. (2017): A synopsis of the saddle fungi (Helvella: Ascomycota) in Europe-species delimitation, taxonomy and typification. – Persoonia 39: 201-253.
[31] Soltis, D. E., Collõer, T. G., Edgerton, M. L. (1991): The Heuchera group (Saxifragaceae): Evidence for chloroplast transfer and paraphyly. – Amer. J. Bot.78: 1091-1112.
[32] Song, Z. P., Guan, Y., Rong, J., Xu, X., Lu, B. R. (2006): Inter-simple sequence repeat (ISSR) variation in populations of the cutgrass Leersia hexandra. – Aquat. Bot. 84: 359-362.
[33] Stefani, O. P. F., Sokolski, S., Wurtz, T., Piche, Y., Hamelin, R., Fortin, A., Berube, J. A. (2010): *Morchella tomentosa*: a unique belowground structure and a new clade of morels. – Mycologia 102: 1082-1088.
[34] Tang, L. H., Xiao, Y., Bian, Y. B. (2005): The orthogonal optimization of ISSR-PCR amplification system in *Auricularia auricula*. – J. Fungal Res. 3: 15-18.
[35] Tsumura, Y., Ohba, K., Strauss, S. H. (1996): Diversity and inheritance of inter-simple sequence repeat polymorphisms in Douglas-fir (Pseudotsuga menziesii) and sugi (Cryptomeria japonica). – Theor. Appl. Genet. 92: 40-45.
[36] Uysal, T., Özel, E., Bozkurt, M., Ertuğrul, K. (2012a): Genetic diversity in threatened populations of the endemic species Centaurea lycaonica Boiss. & Heldr. (Asteraceae). – Research Journal of Biology 2(3): 110-116.
[37] Uysal, T., Özel, E., Ertuğrul, K., Bozkurt, M. (2012b): Determination of genetic relationship among *Cheirolepis* (*Centaurea*/Asteraceae) section and its relatives in Turkey. – Research Journal of Biology 2(3): 104-109.
[38] Weber, N. S. (1972): The genus Helvella in Michigan. – The Michigan Botanist 11: 147-201.
[39] Wolfe, A. D., Liston, A. (1998): Contributions of PCR-Based Methods to Plant Systematics and Evolutionary Biology. – In: Soltis, D. E., Soltis, P. S., Doyle, J. J. (eds.) Molecular Systematics of Plants II: DNA Sequencing. Kluwer, New York, pp. 43-86.
[40] Yoon, C. S., Gessner, R. V., Romano, M. A. (1990): Population genetics and systematics of the *Morchella esculenta* complex. – Mycologia 82: 227-235.
[41] Zhao, Q., Zhang, X., Li, S., Chai, H., Bahkali, A. H., Hyde, K. D. (2017): New species and records of saddle fungi (Helvella, Helvellaceae) from Jiuzhaigou Natural Reserve, China. – Mycoscience 57: 422-430.
[42] Zietkiewicz, E., Rafalski. A., Labuda, D. (1994): Genome fingerprinting by simple sequence repeat (SSR)-anchored polymerase chain reaction amplification. – Genomics 20: 176-183.

http://www.aloki.hu ● ISSN 1589 1623 (Print) ● ISSN 1785 0037 (Online)
DOI: http://dx.doi.org/10.15666/aeer/1704_73957405

DETERMINATION OF THE CYTOTOXIC EFFECT ON HUMAN COLON CANCER AND PHENOLIC SUBSTANCE CONTENT OF THE ENDEMIC SPECIES *SIDERITIS OZTURKII* AYTAÇ & AKSOY

DEMIRELMA, H.* – GELINCI, E.

Department of Biology, Faculty of Science, Selçuk University, Konya 42031, Turkey

**Corresponding author*
e-mail: demirelma@gmail.com; phone: +90-532-635-0305

(Received 28th Feb 2019; accepted 3rd May 2019)

Abstract. *Sideritis* L. species that we based on in this study are annual or perennial flowering plants which are widely used as herbal medicine, and also called mountain tea or shepherd's tea. They are common in the Mediterranean Region, the Balkans, Iberian Peninsula, Greece, Central Asia and Anatolia. They are xerophytic shrub or herbs between 8 and 90 cm. They usually grow on arid cliffs, calcareous slopes, high-altitude mountainous regions (650-1400 m). Full bloom usually occurs in July. It is commonly used in Albania, Greece, Kosova, Bulgaria, Macedonia, Asia, Central Europe and Anatolia as herbal tea and for therapeutic purposes. It is usually used to aid digestion, strengthen the immune system, suppress common cold, allergy, sinusitis and influenza and as therapeutic for pain and mild anxiety. The methanol extracts obtained from the flower and leaf parts of the species *Sideritis ozturkii* Aytaç & Aksoy, which is endemic in Turkey, were applied at different concentrations and for different times on DLD-1 human colorectal cancer cells cultured in RPMI-1640 medium. The cytotoxicity measurements were made through the use of MTT and the cytotoxicity indices were calculated using an Elisa Reader. As a result of the study, it was determined that the flower and leaf extracts obtained from the species *Sideritis ozturkii* exhibit cytotoxic activity on DLD-1 cells in a dose- and time-dependent manner. It is believed that the extracts obtained from the species *Sideritis ozturkii* could be beneficial as a natural anti-proliferative agent.
Keywords: *Sideritis, cytotoxicity, cancer, phenolic, DLD-1, MTT*

Introduction

Cancer is characterized by abnormal growth of cells that have the potential to spread to other parts of the body, and the body's normal control mechanism is a disease that develops when it stops working and causes death. Today more than 100 types of cancer affect people. Cancer is a global health problem; it is known that 9% of deaths in developed countries and 21% of deaths in developing countries are caused by cancer. The World Health Organization estimates that in the year 2050, about 27 million new cases of cancer will occur annually and 17.5 million people will die from these cases (Hussain et al., 2016).

The word cancer means the growth of malignant tumors resulting from the irregular division and proliferation of the cells in an organ or tissue. In the general sense, the cancer refers to a group of more than 100 diseases caused by the uncontrolled proliferation of the cells in various regions of our body. Although there are a great variety of cancer types, all begin with an uncontrolled proliferation of the abnormal cells. These may cause serious disorders, even death, in case left untreated (Horner et al., 2009).

Colon cancer is the third most common type of cancer in the world, and colorectal cancer is the second most common cause of death. Although colon cancer is a disease that can be seen at any age, its incidence is generally higher in people aged 40 years and older. Among all cancers, the incidence is in the third place in females and the second in males (Giardiello, 2014). According to the Ministry of Health data, it is among the five most

http://www.aloki.hu ● ISSN 1589 1623 (Print) ● ISSN 1785 0037 (Online)
DOI: http://dx.doi.org/10.15666/aeer/1704_74077419

common types of cancer in Turkey. Globally, more than a million people per year are caught in colorectal cancer. In 1990, 490,000 people per year of death of the colon cancer, which led to the death of 715,000 people annually was announced to cause death. Colorectal cancer is the second largest cause of male and female deaths in the United States. In 2011, there were 141,210 cases per year in the United States and 41,000 cases in the United Kingdom. Environmental factors are the major factors in the incidence of colon cancer in the community. Especially in developed countries, unhealthy eating habits of people with unbalanced life and high fat increase the incidence of colon cancer. In addition, the genetic predispositions and characteristics of people as well as environmental factors increase the incidence of colon cancer.

Increase in the incidence of cancer cases, chemotherapy and radiotherapy used in the treatment of many cancer patients to damage the normal cells and reducing the percentage of success of these treatments in targeted cancer cells has encouraged scientists to develop new anticancer drugs from plants (Shah et al., 2013).

It is seen that in many archaeological findings, people have been using plants for treatment and nutrition purposes for thousands of years (Koçyiğit, 2005). The belief in the power of plants to treat diseases is almost as old as the history of humanity. Throughout the history of humanity, plants with many different forms have been used in the treatment of diseases. There is much historical evidence that plants are used for treatment in all continents of the world. The first written information about the ethnobotanical field, which refers to the use of plants for medical purposes, dates back to 3000 BC, namely the periods of Egypt, Hittite, Greek and Roman periods (Dağcı et al., 2002).

At the end of the 5th century BC, the book de De Mataria Medica rod by Diockrodidas in the 1st century AD is shown as the basis of modern pharmacology. Plants still present in these works and new species of these plants continue to be used in traditional treatment (Cowan, 1999).

In recent years, especially after the 1980s, the chemical industry began to take the place of herbal medicines as a result of the rapid progress of the synthetic (chemical) drugs. However, because of the occurrence of many side effects of these synthetic drugs and the high prices of many of them, people have turned to prefer treatment with herbal remedies (Yücel, 2010).

As in all countries of the world, plants are seen important from a medical point of centuries people in Turkey, tea, ointments, spices and so on. used in the treatment of diseases in the shapes. Nowadays, interest in natural herbal medicines has increased again because microorganisms have more resistance to synthetic drugs (Nakipoğlu and Otan, 1992).

The genus *Sideritis* L. constituting the basis for our present study are the annual or perennial flowering plants, which are also called the mountain tea or the shepherd's tea and are commonly used as herbal medicine (Barber et al., 2015). They are abundant in Mediterranean region, the Balkans, the Iberian Peninsula, Greece, Central Asia and Anatolia. These are xerophilous shrubs or herbs with a height in the range of 8-90 cm. They usually grow on the arid rocks, on calcareous slopes and in mountainous regions with high altitude (650-1400 m). The inflorescence is generally verticillate. The blooming is usually observed in July (Aytaç and Aksoy, 2000). It is commonly used as herbal tea for therapeutic purposes in Albania, Greece, Kosovo, Bulgaria, Macedonia, Asia, Central Europe and Anatolia. It is generally used to aid digestion, strengthen the immune system, suppress common cold, allergies, sinusitis and flu and treat pain and mild anxiety (Todorova and Trendafilova, 2014).

http://www.aloki.hu ● ISSN 1589 1623 (Print) ● ISSN 1785 0037 (Online)
DOI: http://dx.doi.org/10.15666/aeer/1704_74077419

Studies have been made regarding the plant's antimicrobial, antibacterial, anti-inflammatory, antioxidant and cytotoxic effects on the diseases. Diterpenes and flavonoids were identified as the predominant active ingredients as the result of the extraction process (Petreska et al., 2011).

The cytotoxicity is the quality of being toxic to cells (Tokur and Aksoy, 2017). Cytotoxicity determines the effect of the active ingredients, particularly flavonoids, glucosides, alkaloids, terpenoids, which are obtained as a result of the extraction of the medicinal plants, on the cancer cells (Kuntz et al., 1999). The most important stage in the research related to the anticancer drugs is the determination of the in-vitro cytotoxicity B. The cultures of the human or animal cancer cells are performed in-vitro in the culture plates where the reproducing cells are grown. Then, the effective dose is determined as a result of a study that is based on the steps of collecting the plants, subjecting the same to mechanical fractionation followed by extraction, introducing to the cancer cells the active ingredients resulting from the extraction and identifying the dose of these active ingredients that kills 50 percent of the cancer cells (Riss et al., 2014).

In the light of this information, this study is to determine the cytotoxic effect of the extracts obtained from the leaves and flower parts of the Sideritis ozturkii species (*Fig. 1*) which are endemic to the province of Konya endemic to the province of Konya on the DLD-1 cell line and to have fewer side effects in the treatment of the cancer of our time. In order to support the production of an economical drug, which is more effective, it has been researched. The cytotoxic effects of *Sideritis* species on the cancer cells began in 1981 and have continued until the present (Jeremic et al., 2013). The literature research on the *Sideritis* species reveals that the studies are generally focused on the species *Sideritis scardia* Griseb. In the present study, the cytotoxic effects of the species *Sideritis ozturkii* of the plant *Sideritis*, an endemic species of Konya Province that has not yet been studied, were investigated on the cancer cells (particularly on the colon cancer cells).

Sideritis ozturkii is an endemic plant in the province of Konya and this is the first study on colon cancer cell line with *Sideritis ozturkii*. Therefore, we believe that this study will contribute to the literature. With the present study, it was aimed to provide support for the manufacture of an economical drug with fewer side effects and with the possibility of being more effective in treating the cancer, the disease of our age. The distribution map of the species *Sideritis ozturkii* is given in *Figure 2*.

Figure 1. *Sideritis ozturkii Aytaç & Aksoy*

http://www.aloki.hu ● ISSN 1589 1623 (Print) ● ISSN 1785 0037 (Online)
DOI: http://dx.doi.org/10.15666/aeer/1704_74077419

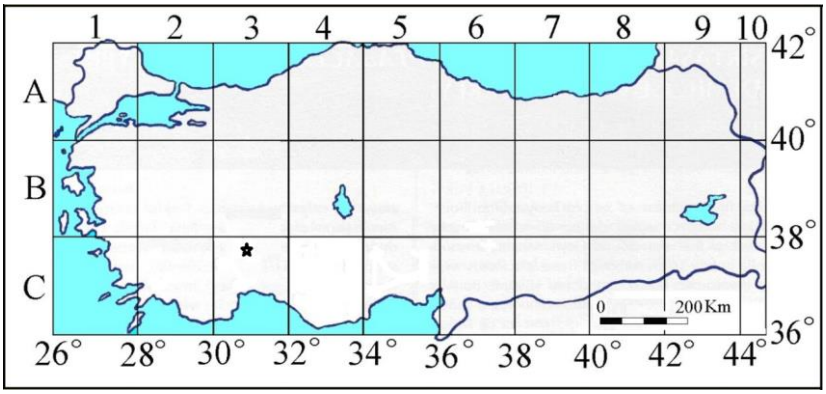

Figure 2. *Distribution map of Sideritis ozturkii (*) Aytaç & Aksoy*

Materials and methods

Collection material

Sideritis ozturkii type used in this study is located 3 km north of Konya Derebucak district Çamlık village; Kızıldağ's 1450-1700 m high mountainous area collected approximately 1 kg in flowering period in July 2016.

Drying of the plant

The plant was allowed to dry in a room away from the direct sunlight. When the plant was completely dried after two months, the flower and leaf parts were separated. Next, the leaf and flower parts were separately triturated with a plant grinder, subjected to sieving and then moved on to the extraction process. The reason for collecting the plant during flowering period. The extract of the flower part was also intended to be obtained.

Extraction

Of the triturated plants, first a quantity of 15 g was weighed from the leaf part by means of precision scales, placed into the soxhlet apparatus and subjected to the extraction process with 200 mL of methanol for 6-8 h. We have used methanol in our study because methanol is often preferred in studies with *Sideritis*. The extracts recovered from the extraction process were kept overnight in a refrigerator at + 4 °C. On the following day, the extracts were evaporated in a rotary evaporator at 40 °C in order to remove the solvents thereof. The recovered raw extracts were kept at -20 °C until their use in order to prevent any loss of activity. The extraction process with the Soxhlet device is shown in *Figure 3*.

Preparation of cell culture

In order to ensure that DLD-1 cells proliferate in vitro such as in vivo, the appropriate medium was prepared. For this purpose; 10% fetal bovine serum (FBS) and 1% penicillin-streptomycin RPMI-1640 (Sigma) cell medium were used. A few minutes were kept at 37 °C for fast dissolution of DLD-1 cells from the liquid nitrogen tank. The dissolved cells were added to a falcon tube and FBS was added to remove DMSO and pipetted several times. It was then centrifuged for 5 min. After centrifugation, the

http://www.aloki.hu ● ISSN 1589 1623 (Print) ● ISSN 1785 0037 (Online)
DOI: http://dx.doi.org/10.15666/aeer/1704_74077419

supernatant was discarded and the remaining cell pellet was plated on the prepared medium and sown to 25 cm² flask. Cells were cultured in 25 cm² flasks with 95% humidity and 5% CO2 gas and 37 °C CO2 incubator. The density of DLD-1 cells in the flask maintained in the CO 2 incubator was increased over time by invert microscopy, and the cells from the flask were observed to be propagated by passaging.

Figure 3. *Soxhlet device extraction process*

Determination of cytotoxic effect

The cytotoxic effect of the obtained extracts was tested on the DLD-1 cell line comprising the colorectal cancer cells where in said cell line was cultured in RPMI-1640 medium. The obtained extract was subjected to characterization via HPLC in order to reveal the phenolic substance composition. The extract was first dissolved in a solvent, was then passed through the respective chromatography column under high pressure and the phenolic substance content was checked.

High performance liquid chromatography (HPLC)

HPLC is the most widely used device for the purpose of analytical separation techniques. The reasons for widespread use are that it is easily adaptable to quantitative determinations, suitable for the separation of compounds that are not volatile or easily decomposed by temperature. Most importantly, it is the wide applicability of many disciplines of science to the subjects of primary interest of the society. Examples of such compounds include amino acids, proteins, nucleic acids, carbohydrates, drugs and pesticides. HPLC unit: Degasser, pump, autosampler, column and detector consist of four parts. The Degasser; It provides removal of dissolved gases present in mobile phases.

http://www.aloki.hu ● ISSN 1589 1623 (Print) ● ISSN 1785 0037 (Online)
DOI: http://dx.doi.org/10.15666/aeer/1704_74077419

HPLC (High Performance Liquid Chromatography) High Performance Liquid Chromatography is briefly referred to as HPLC.

High performance; expresses high resolution. It is also called High-pressure Liquid Chromatography since the mobile phase is progressed with high pressure (Lindsay, 1987).

Calculation of cytotoxicity indexes

The prepared extract was dissolved using DMSO at a nontoxic level and it was used on the cell line at different concentrations and for different time intervals. After different concentrations of the extract were added on the cell line, the measurement of cytotoxicity was performed through the use of MTT. Four hours after the addition of MTT on the cells, DMSO or isopropanol was added and the cells were incubated for four hours in an ambience not exposed to light. After the exposure of the cells to the extract for 24 and 48 h, the cytotoxicity indices based on absorbance were calculated by using an Elisa Reader. The cells allowed to proliferate under appropriate conditions were removed from the flask base by treatment with trypsin-EDTA when they covered 70% of the flask surface. The cells stained with Trypan blue dye were counted 3 times with the help of thoma slide and suspended in the number of cells required for MTT testing. 100 µl of cell suspension was then transferred to a 96-well cell culture plate. 24 h incubation at 37 °C was achieved to allow the cells to adhere and adapt to the new environment. After 24 h, fresh media containing (100 µg/ml, 250 µg/ml, 500 µg/ml, 750 µg/ml and 1000 µg/ml) the desired final concentrations of extracts were added to the cells to determine the cytotoxic effects of the extracts and incubated for 24 and 48 h at 37 °C in a CO2 incubator.

Results

The % viability graphs obtained in line with the MTT test data, which were measured at time points of 24 and 48 h after the application, on DLD-1 cell line, of the methanolic extracts obtained from the leaf and flower parts of the plant *Sideritis ozturkii* and of the extract obtained by way of brewing from the leaf thereof are in *Figures 4, 5* and *6*.

When the mitochondrial activity after 24 h of application was evaluated as the % viability in the plates that were started with equal numbers of cells, the extract obtained from the leaf led to the cell death rates of 1% at the dose of 100 µg/mL, 26% at the dose of 250 µg/mL, 54% at the dose of 500 µg/mL, 67% at the dose of 750 µg/mL and 74% at the dose of 1000 µg/mL, while the extract obtained from the flower part, though causing an increase in the number of cells at the dose of 100 µg/mL, resulted in the death of the cells at increasing doses; namely the cell death rates of 12% at the dose of 250 µg/mL, 32% at the dose of 500 µg/mL, 45% at the dose of 750 µg/mL and 80% at the dose of 1000 µg/mL. On the other hand, the extract obtained by the brewing method from the leaf resulted in cell death rates of 57% at the dilution of 1/10, 70% at the dilution of 1/5 and 79% at the dilution of 1/2. Taking the % viability values into consideration, it was observed that the extracts obtained from the leaf were more effective in causing the death of the DLD-1 cells as compared to the extract obtained from the flower. The extracts obtained from the flower were also effective in providing the cell death, but they exhibited lower effect than the leaf extracts.

http://www.aloki.hu ● ISSN 1589 1623 (Print) ● ISSN 1785 0037 (Online)
DOI: http://dx.doi.org/10.15666/aeer/1704_74077419

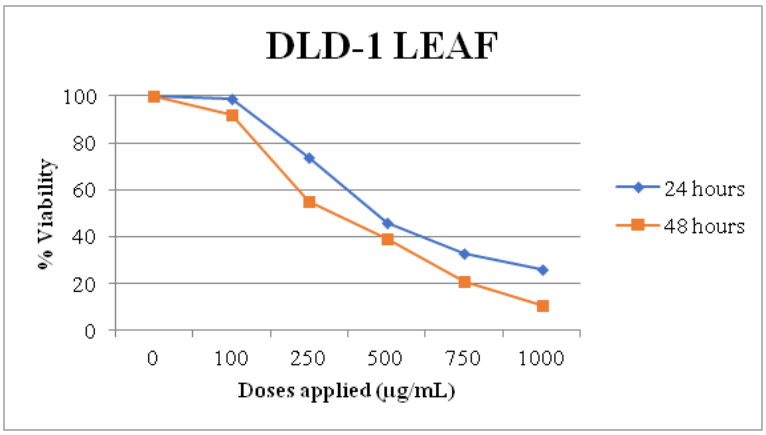

Figure 4. *24- and 48-h effects of the extract obtained from the leaf on DLD-1 cell line*

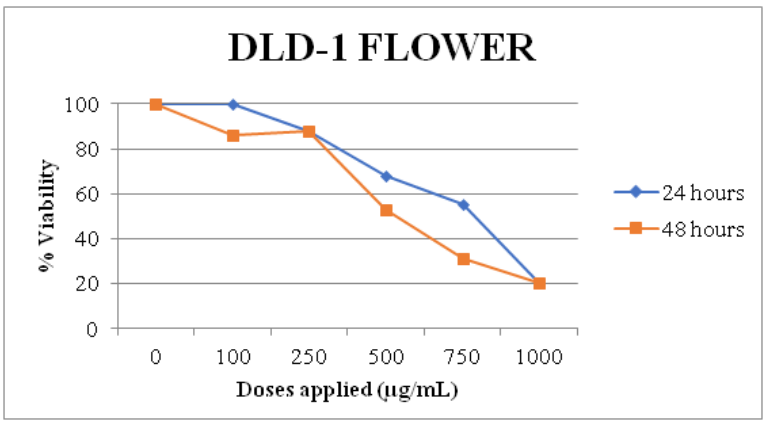

Figure 5. *24- and 48-h effects of the extract obtained from the flower on DLD-1 cell line*

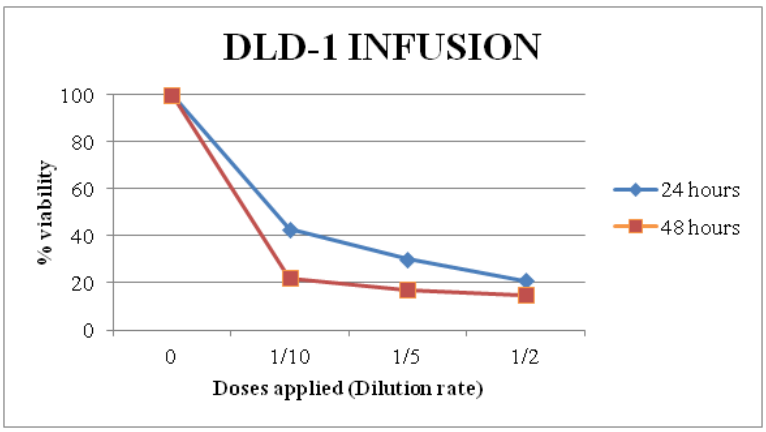

Figure 6. *24- and 48-h effects of the extract obtained by way of brewing from the leaf on DLD-1 cell line*

When the results for 48 h of extract application were compared to those for the 24-h application, some increase was observed in the cell death in a time-dependent manner. The extract obtained from the leaf led to the cell death rates of8% at the dose of

http://www.aloki.hu ● ISSN 1589 1623 (Print) ● ISSN 1785 0037 (Online)
DOI: http://dx.doi.org/10.15666/aeer/1704_74077419

100 µg/mL, 45% at the dose of 250 µg/mL, 61% at the dose of 500 µg/mL, 79% at the dose of 750 µg/mL and 89% at the dose of 1000 µg/mL; the extract obtained from the flower part led to the cell death rates of 24% at the dose of 100 µg/mL, 22% at the dose of 250 µg/mL, 47% at the dose of 500 µg/mL, 69% at the dose of 750 µg/mL and 80% at the dose of 1000 µg/mL; and the extract obtained by the brewing method from the leaf led to the cell death rates of 78% at the dilution of 1/10, 83% at the dilution of 1/5 and 85% at the dilution of 1/2.

The IC_{50} dose for the extract obtained from the leaf was calculated as 0.46 mg/mL for 24 h and 0.33 mg/mL for 48 h. On the other hand, a higher IC_{50} dose was found for the extract obtained from the flower, as compared to the extract obtained from the leaf. For the extract obtained from the flower, the values of 0.7 mg/mL and 0.53 mg/mL were calculated for 24 h and 48 h, respectively (*Fig. 7*).

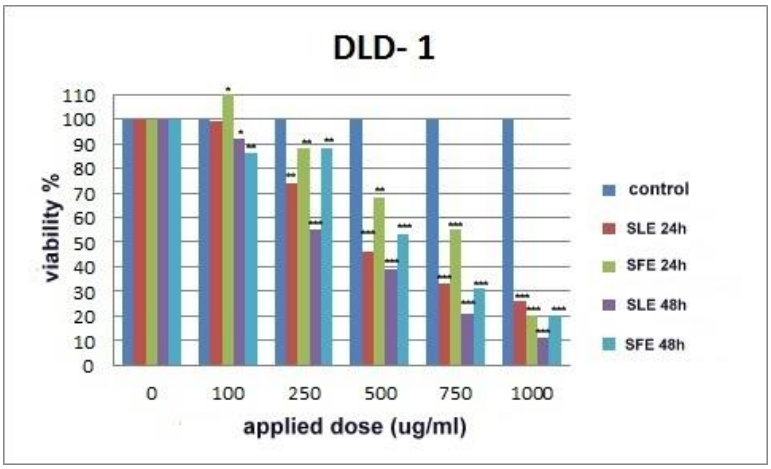

Figure 7. *24- and 48-h effects of the obtained extracts on DLD-1 cell line*

The graphs for the results of HPLC (high pressure liquid chromatography) we performed on two methanolic extracts obtained from the plant *Sideritis ozturkii* are in *Figures 8* and *9*.

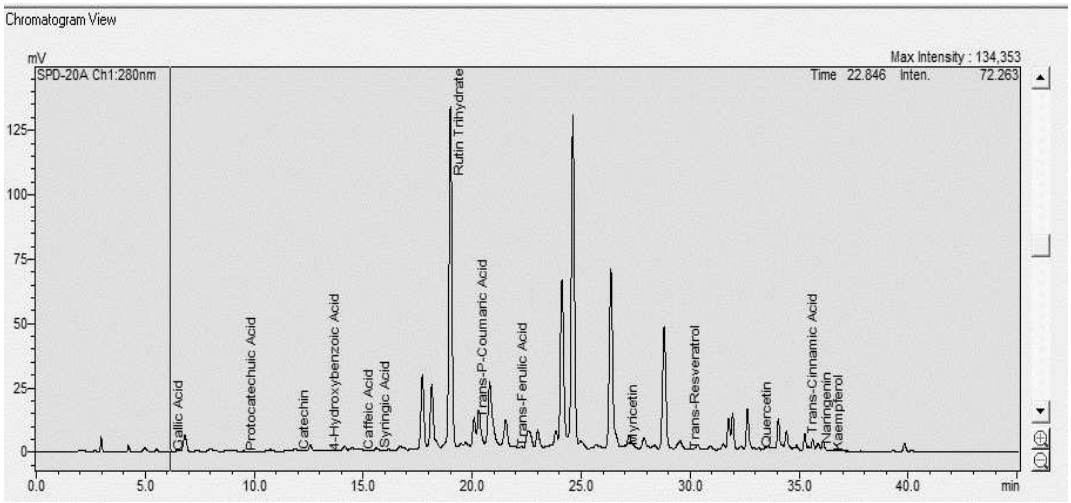

Figure 8. *View of the HPLC chromatogram for the methanolic extract obtained from the leaf of Sideritis ozturkii*

http://www.aloki.hu ● ISSN 1589 1623 (Print) ● ISSN 1785 0037 (Online)
DOI: http://dx.doi.org/10.15666/aeer/1704_74077419

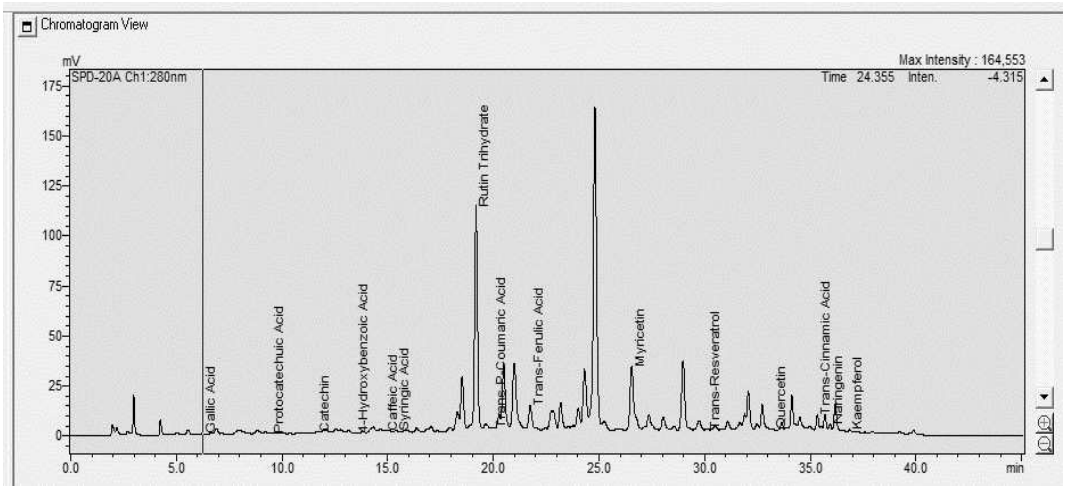

Figure 9. *View of the HPLC chromatogram for the methanolic extract obtained from the flower of Sideritis ozturkii*

The screening was performed on both extracts for 15 phenolic substances. The phenolic substances used as the standard were as follows: Gallic Acid, Protocatechuic Acid, Catechin, 4-Hydroxybenzoic Acid, Caffeic Acid, Syringic Acid, Rutin Trihydrate, Trans-P-Coumaric Acid, Trans-Ferulic Acid, Myricetin, Trans-Resveratrol, Quercetin, Trans-Cinnamic Acid, Naringenin and Kaempferol. The standards were prepared by way of dissolving the same in methanol. The phenolic substances found in each extract and their respective quantities are given in (*Table 1*).

When the extracts were compared in terms of the phenolic substance content, the extract obtained from the leaf was found to contain the highest quantities of rutin trihydrate and Trans-P-Coumaric Acid.

Table 1. *Phenolic substances present in the extracts obtained from Sideritis ozturkii and their respective quantities*

Phenolic substance	***Sideritis ozturkii* leaf (mg/100 g)**	***Sideritis ozturkii* flower (mg/100 g)**
Gallic Acid	7.278	11.067
Protocatechuic Acid	10.244	4.972
Catechin	70.056	64.100
4-Hydroxybenzoic Acid	11.178	15.922
Caffeic Acid	8.844	8.467
Syringic Acid	12.722	13.472
Rutin Trihydrate	1805.756	823.367
Trans-P-Coumaric Acid	49.811	9.556
Trans-Ferulic Acid	24.289	98.372
Myricetin	37.811	424.517
Trans-Resveratrol	6.089	29.856
Quercetin	19.811	22.433
Trans-Cinnamic Acid	4.900	4.506
Naringenin	14.367	12.328
Kaempferol	7.900	72.367

http://www.aloki.hu ● ISSN 1589 1623 (Print) ● ISSN 1785 0037 (Online)
DOI: http://dx.doi.org/10.15666/aeer/1704_74077419

Discussion

Cancer is one of the most important reasons of disease-caused deaths in the world. World Health Organization reports that approximately 84 million people lost their lives due to cancer between 2005 and 2012 (Behzad et al., 2014). Despite the frequent use of chemotherapy in the treatment of cancer, the toxic effects that occur over time limit the use of these drugs. Both the high mortality rate of cancer cases and the emergence of serious side effects of chemotherapy and radiotherapy lead cancer patients to alternative and/or complementary therapies (Shah et al., 2013). At this point, natural products are viewed as potential raw materials for new drug discoveries, and phenolic compounds found in natural products come to the forefront with their structures and activities. For this reason, the search for the anticancer effects of natural products, either as whole extracts or compounds isolated from them, has become one of the most popular study areas. In preliminary studies to determine the availability of natural products for humans, the use of in vitro methods is recommended. Clinical trials are recommended only if positive results are obtained from in vitro and in vivo studies (Demir et al., 2016, 2017). Some criteria have been established to demonstrate if a natural compound is effective and acceptable in terms of chemopreventive or chemotherapeutic efficacy. The most important of these criteria is that the natural product (that is cytotoxic to cancerous cells) used should not exhibit the cytotoxic effect in normal cells, and should be effective against multiple cancer cell lines (Demir et al., 2017).

In line with this information, in order to support the production of a herbal preparation that has less side effects in treating cancer -the disease of the century- or at least has the potential to reduce the side effects of chemotherapy; *Sideritis ozturkii* (which is endemic to Konya province and has not been studied before) extracts of leaf and flower parts (extracted with methanol) were isolated and their cytotoxic effects on colon cancer were examined through MTT method.

Tadić et al. (2012) evaluated the cytotoxic effects of plant extracts in PBMC, B16 and HL-60 cells. Cytotoxic effects were analyzed by dual staining of apoptosis cell death and neurotic cell death with annexin V and PI-coupled fluorescein isothiocyanate (FITC). All plant extracts were also analyzed phytochemically. Analysis by HPLC revealed that ferulic acid was the predominant active ingredient of the phenolic compounds. It has been determined that this phenolic compound has a higher cytotoxic effect in PBMC, B16 and HL-60 cells than that of the other active substances. In this study, the cytotoxic effects of the extracts of the flower and leaves of the *Sideritis ozturkii* plant on the DLD-1 cell line were investigated. Cytotoxicity was analyzed by MTT test. All phytochemical analysis of the plant was carried out by HPLC method. As a result of this analysis, it was determined that the dominant active substances of the plant were routine trihydrate, myricetin and catechin. It has been found that routine trihydrate, the predominant active ingredient in the leaf, has a higher cytotoxic effect on colon cancer cells than other active agents.

Jeremic et al. (2015) have examined the mechanisms of cytotoxic action of flavonoids (from the active ingredients of *Sideritis scardia* L. extracts) on rat C6 glioma cells. As a result of their study, flavonoids (detected as the predominant active ingredient in *Sideritis scardia* L. extracts) were found to have elevated rates of apoptosis, necrosis and autophagic cancer cell death in C6 glioma cells, and thus have a high cytotoxic effect. In this study, cytotoxic effects of *Sideritis ozturkii* extracts on colon cancer cells were investigated. In the results, it was found that mathanol extracts had a significant cytotoxic effect on the detected tumor line. As a result of the HPLC

http://www.aloki.hu ● ISSN 1589 1623 (Print) ● ISSN 1785 0037 (Online)
DOI: http://dx.doi.org/10.15666/aeer/1704_74077419

analysis, it is thought that *Sideritis ozturkii* has an anti-tumor characteristic due to its rich flavonoid content and therefore it can be proposed as an anti-tumor agent with cancer prevention and an alternative cancer prevention food.

Radovaroic (2015) in this study, chemical components of plants with cytotoxic activity and plant extracts selected for producing chemotherapeutic drugs were evaluated. Various plant extracts (*Sideritis scardia* L. *S. linearifolia*) were studied and polyphenolic, diterpenoids, flavanoids, betulinic acid, triterpenoids, anthraquinone and berberine were determined as predominant active agents and their effect rates on cytotoxicity were compared. These active ingredients were measured on the effects of apoptosis to stop the cycle of cancer cells on viability. As a result of these studies, it has been determined that plant extracts have potential cytotoxic effects on cancer cells and especially flavonoids are effective anti-chemotherapeutic agents.

Zegerac (2015) investigated the cytotoxic, antioxidant and antimicrobial effects of the active substances in extracts extracted from *Sideritis lamiaceae* in in vitro studies on cancer cells in mice. However, *Sideritis lamiaceae* L. extracts were not as effective as *Sideritis scardia* L. in cancer cells. However, flavonoids, the dominant active ingredient in antioxidant properties, were found to be positive according to ORAC 5.0 assay. The in-vitro studies of the active ingredients in extracts from the leaves and flower parts of the endemic Sideritis ozturkii investigated the cytotoxic effects on the DLD-1 cell line (colon cancer cells). Sideritis ozturkii extracts have been found to have a higher cytotoxic effect than Sideritis congesta species in which Zegerac works in cancer cells. This has also shown us that Sideritis ozturkii's cancer prevention may also be an alternative anti-cancer agent.

To our knowledge, no cytotoxic effect studies on *Sideritis ozturkii* have been reported so far. However, studies on similar species of *Sideritis* have shown cytotoxic effects on cancer cells.

In this study, cytotoxic effects of methanol extracts, obtained from endemic *Sideritis ozturkii* leaves and flowers, on DLD-1 cell line were investigated by MTT method and Elisa reading. As a result of this study, leaf and flower extracts obtained from *Sideritis ozturkii* displayed cytotoxic effects on DLD-1 cells, depending on the dose and time. The extracts obtained from the leaves were found to be more effective than the ones obtained from the flowers. The IC_{50} doses for leaves and flowers were estimated to be approximately 0.3 μg/ml and 0.5 μg/ml, respectively. When extracts were compared to phenolic substance content, it was found that the extract obtained from leaf yielded the highest amount of routine trihydrate and Trans-P-Coumaric Acid. We think that this phenolic substance content of the leaves causes these results.

Conclusions

According to the results obtained from the MTT test, the extracts obtained from the leaf and flower parts of the species *Sideritis ozturkii* showed cytotoxic effects on DLD-1 cells in a dose- and time-dependent manner. The leaf extract was determined to be more effective than the flower extract. The IC_{50} dose was calculated to be approximately 0.3 μg/mL for the leaf extract and 0.5 μg/mL for the flower extract. The data suggest that the extracts obtained from the species *Sideritis ozturkii* could be beneficial as a natural anti-proliferative agent.

http://www.aloki.hu ● ISSN 1589 1623 (Print) ● ISSN 1785 0037 (Online)
DOI: http://dx.doi.org/10.15666/aeer/1704_74077419

Acknowledgements. We would like to thank Selçuk University BAP (Coordination Office for Scientific Research Projects) for supporting this study with the project no. 16201095.

REFERENCES

[1] Aytaç, Z., Aksoy, A. (2000): A new Sideritis species (Labiatae) from Turkey. – Flora Medit 10: 181-184.
[2] Barber, J. C., Ortega, J. F., Santos Guerra, A., Marrero, A., Jansen, R. K. (2000): Evolution of endemic Sideritis (Lamiaceae) in Macaronesia: insights from a chloroplast DNA restriction site analysis. – Systematic Botany 25: 633-647.
[3] Behzad, S., Pirani, A., Mosaddegh, M. (2014): Cytotoxic activity of some medicinal plants from Hamedan district of Iran. – Iranian Journal of Pharmaceutical Research: IJPR 13(Supplement): 199-205.
[4] Cowan, M. (1999): Plant products as antimicrobial agents. – Clinical Microbiology Reviews 12(4): 564-582.
[5] Dağcı, E., İzmirli, M., Dığrak, M. (2002): Kahramanmaraş ilinde yetişen bazı ağaç türlerinin antimikrobiyal aktivitelerinin araştırılması. – KSU Fen ve Mühendislik Dergisi, 5(1): 38-46.
[6] Demir, S., Aliyazicioglu, Y., Turan, I., Misir, S., Mentese, A., Yaman, S. O., Deger, O. (2016): Antiproliferative and proapoptotic activity of Turkish propolis on human lung cancer cell line. – Nutrition and Cancer 68(1): 165-172.
[7] Demir, S., Turan, İ., Aliyazıcıoğlu, R., Aliyazıcıoğlu, Y. (2017): Primula vulgaris Yaprak Ekstraktının Antioksidan ve Sitotoksik Özelliklerinin Değerlendirilmesi. – KSU Doğa Bil. Derg 20(4): 361-367.
[8] Giardiello, F. M., Allen, J. I., Axilbund, J. E., Boland, C. R., Burke, C. A., Burt, R. W. et al. (2014): Guidelines on genetic evaluation and management of Lynch syndrome: a consensus statement by the US Multi-Society Task Force on Colorectal Cancer. – Gastroenterology 147(2): 502-526.
[9] Horner M, Ries L, Krapcho M, Neyman N, Aminou R, Howlader, N., Altekruse, S. F., Feuer, E. J., Huang, L., Mariotto, A., Miller, B. A. (2009): SEER Cancer Statistics Review, 1975-2006. – National Cancer Institute, Bethesda, MD.
[10] Hussain, A., Chauhan, J., Singh, A. K., Yousuf, S. (2016): A study on adoption behaviour of farmers in Kashmir valley. – Indian Research Journal of Extension Education 9(2): 46-49.
[11] Jeremic, I., Tadic, V., Isakovic, A, Trajkovic V, Markovic I, Redzic, Z., Isakovic, A. (2013): The mechanisms of in vitro cytotoxicity of mountain tea, Sideritis scardica, against the C6 glioma cell line. – Planta Medica 79: 1516-1524.
[12] Jeremic, I., Petrovic, D., Zivkovic, M., Petricevic, S., Tadic, V., Petronijevic, M., Isakovic, A. (2015): Sideritis scardica extract prevents bone loss in ovariectomized rats. – Annals of the Rheumatic 74: 921.
[13] Koçyiğit, M. (2005): Yalova ilinde etnobotanik bir araştırma. – Yüksek Lisans Tezi, İstanbul Üniversitesi Sağlık Bilimleri Enstitüsü, İstanbul.
[14] Kuntz, S., Wenzel, U., Daniel, H. (1999): Comparative analysis of the effects of flavonoids on proliferation, cytotoxicity, and apoptosis in human colon cancer cell lines. – European Journal of Nutrition 38: 133-142.
[15] Lindsay, S., Kealey, D. (1987): Chromatography, High Performance Liquid. – Wiley & Sons, London.
[16] Nakipoğlu, M., Otan, H. (1992): Tıbbi bitkilerin flavonitleri. – Journal of AARI 4(1): 70-93.
[17] Petreska, J., Stefkov, G., Kulevanova, S., Alipieva, K., Bankova, V., Stefova, M. (2011): Phenolic compounds of mountain tea from the Balkans: LC/DAD/ESI/MSn profile and content. – Natural Product Communications 6: 21-30.

http://www.aloki.hu ● ISSN 1589 1623 (Print) ● ISSN 1785 0037 (Online)
DOI: http://dx.doi.org/10.15666/aeer/1704_74077419

[18] Radovaroic, A. (2015): Evaluation of potential cytotoxic effects of herbal extracts. – Serbian Journal of Experimental and Clinical Research 16(4): 333-342.
[19] Riss, T. L., Niles, A., Moravec, R. A. (2014): Kits for luminogenic and nonluminogenic multiplex assays. – Google Patents.
[20] Shah, U., Shah R., Acharya S., Acharya N. (2013): Novel anticancer agents from plant sources. – Chinese Journal of Natural Medicines 11: 16-23.
[21] Tadić, V. M., Jeremic, I., Dobric, S., Isakovic, A., Markovic, I., Trajkovic, V., Arsic, I. (2012): Anti-inflammatory, gastroprotective, and cytotoxic effects of Sideritis scardica extracts. – Planta Medica 78(05): 415-427.
[22] Todorova, M., Trendafilova, A. (2014): Sideritis scardica Griseb., an endemic species of Balkan peninsula: Traditional uses, cultivation, chemical composition, biological activity. – J Ethnopharmacol 152: 256-265.
[23] Tokur, O., Aksoy, A. (2017): In Vitro Sitotoksisite Testleri (Turkish). – Harran Üniversitesi Veterinerlik Fakültesi Dergisi 6: 112-118.
[24] Yücel, E. (2010): Tıbbi ve Aromatik Bitkilerin Yetiştiriciliği. – Anadolu Üniversitesi Yayını, 2101.
[25] Zegerac, J. P. (2015): Greek Mountain Tea (Sideritis L.): Functional Components and Biological Activity. Ingredient Corner Greek Mountain Tea. – Brunswick Laboratories, Southborough. – http://www.brunswicklabs.com/ingredient-corner/greek-mountain-tea. Accessed on 2 Jan 2016

http://www.aloki.hu ● ISSN 1589 1623 (Print) ● ISSN 1785 0037 (Online)
DOI: http://dx.doi.org/10.15666/aeer/1704_74077419

EFFECT OF MINERAL FERTILIZERS ON FUNGI COMMUNITIES IN A MOLLISOL OF NORTHEAST CHINA

YAN, L.[1] – WANG, C.[1] – FENG, G.[1] – GAO, Q.[1*] – ZHANG, J.[1*] – WEI, D.[2*]

[1]*Key Laboratory of Sustainable Utilization of Soil Resources in the Commodity Grain Bases of Jilin Province, College of Resource and Environmental Science, Jilin Agricultural University, 130118 Changchun, China*
(phone: +86-155-2686-6351)

[2]*Chinese Academy for Environmental Planning, 100000 Beijing, China*

**Corresponding authors*
e-mail/phone: gaoqinglunwen@163.com/+86-131-3445-7702 (Q. Gao); zhangjinjing@126.com/+86-132-5260-6675 (J. Zhang); lunwen20189@163.com/+86-173-9099-8916 (D. Wei)

(Received 1st Mar 2019; accepted 3rd May 2019)

Abstract. The purpose of this research has been to identify the fungi communities abundance and structure of different fertilization management and their relationship with soil environment with 32-year fertilization experiment which included no fertilization (CK), phosphorus plus potassium fertilization (PK) and nitrogen, phosphorus and potassium fertilization (NPK) on Mollisol in Northeast China by pyrosequencing analysis. It was found that mineral fertilizer application caused shifts in the structure of fungi communities. Soil physical and chemical properties and fungi diversity and abundance were significantly affected by long-term mineral fertilization, especially in fungi diversity reduction and soil acidification.
Keywords: *long-term experiment, diversity, enzyme activity, phylogenetic analysis, CCA analysis*

Introduction

Fertilization has been widely used as a common agricultural practice to maintain soil fertility and increase crop production (Robertson and Vitousek, 2009; Shen et al., 2010). Microbial community composition is sensitive to nitrogen (N), phosphorus (P), and potassium (K) fertilization (Allison and Martiny, 2008), especially in the long-term fertilizer experiments (Shen et al., 2010). N fertilizer is the limiting nutrient for primary production in many countries. N input to unmanaged agricultural ecosystem often resulted in microorganism composition and diversity change, which finally impacted microbial and fungi communities (Cleland and Harpole, 2010; Clark et al., 2007). Many researches found that inorganic fertilizer applications change the soil physical and chemical characteristics, such as pH (Tripathi et al., 2012), electrolytic conductivity (EC) (Rezapouret al., 2013) and organic materials concentration (Chávez-Romero et al., 2016; Sul et al., 2013). Furthermore, previous studies have shown that the application of N fertilizer suppressed microbial activity in soil (Lu et al., 2011; Liu and Greaver, 2010). China began to large-scale application of mineral fertilizer since 1980s, to better understand how Phosphorus plus Potassium (PK) and nitrogen addition (NPK) impact the soil environment in black soil, we have set up a series of long-term fertilizer experiments in order to explore the effect of mineral fertilizer on soil environment and soil quality since 1984.

Previous studies were mainly focused on the impact of long-term fertilization on crop production and microbial communities. However, little information is obtainable about

http://www.aloki.hu ● ISSN 1589 1623 (Print) ● ISSN 1785 0037 (Online)
DOI: http://dx.doi.org/10.15666/aeer/1704_74217429

the fungi construction and the relationship between fungi community and soil environment under long-term fertilization. In this study, we collected soil samples of three kinds of fertilization management from a 32-year fertilization experiment which included no fertilization (CK), phosphorus and potassium fertilization (PK) and nitrogen, phosphorus and potassium fertilization (NPK) to investigate the effect of different fertilization management on soil fungi communities. The objective of this study was therefore to know the fungi communities abundance and structure of different fertilization management and their relationship with soil environment by pyrosequencing analysis.

Materials and methods

Sampling site

Soil samples were collected from long-term fertilizer experiment station in Jilin Agricultural University, Changchun city, Jilin Province, Northeast China (43°26'N, 125°45'E). The station was established in 1984 with continuous maize cropping system in a Mollisol. The region was characterized by a temperate continental monsoon climate, with an average annual precipitation of 570 mm and an average temperature of 4.8 °C. Three fertilization treatments with three replicates for each treatment were selected for the present study, i.e., CK (no fertilizer), PK (phosphorus and potassium fertilization at a rate of 75 kg P/ha and 75 kg K/ha), and NPK (nitrogen, phosphorus and potassium fertilization at a rate of 150 kg N/ha, 75 kg P/ha and 75 kg K/ha). In September 2015, four soil cores from each plot were collected from the top 30 cm soil layer with auger (10 cm diameter) and then mixed into a composite sample. The soil samples were sieved through a 2 mm sieve, and preserved at -80 °C for DNA extraction.

Soil characteristics

pH was determined using a glass combination electrode with soil: water of 1:1. Soil organic matter and total N were determined by the ultraviolet spectrophotometric method, the total phosphorus (TP) were determined using the acidic molybdate-ascorbic acid spectrophotometric method. The initial physical and chemical characteristics of soil in 1983 were shown in *Table 1*. Catalase and sucrase activity was determined according to Claiborne (1985) and Tabatabai (1977). Phosphatases were analyzed by soil zymography according to Spohn et al. (2013).

Table 1. *The basic physical and chemical characteristics of background soil which was tested in 1983 (Lu et al., 2006)*

pH	OM (g/kg)	T N (g/kg)	T P (g/kg)	Available N (mg/kg)	Available P (mg/kg)	Available K (mg/kg)	Organic C (g/kg)
7.4	22.8	1.39	0.53	125.0	13.6	218	17.90

OM: organic matter; TN: total nitrogen; TP: total phosphorus. Available N: available nitrogen; Available P: available phosphorus; Available K: available potassium; Organic C: organic carbon

Soil DNA extraction

The DNA was extracted from 0.25 g soil using the Power soil DNA Isolation Kit (MOBIO Laboratories Inc., Carlsbad, CA, USA) according to the manufacturer's instructions. The DNA samples were purified with Axyprep^{TM} DNA Gel Extraction Kit.

http://www.aloki.hu ● ISSN 1589 1623 (Print) ● ISSN 1785 0037 (Online)
DOI: http://dx.doi.org/10.15666/aeer/1704_74217429

ITS gene amplification and sequencing

To amplify the fungal specific fragments for Miseq, primers ITS1F (5'-CTTGGTCATTTAGAGGAAGTAA-3') and ITS2R (5'-TCCTCCGCTTATTGATATGC-3') which target for fungal ITS genes were selected. Both forward and reverse primers were tagged with adapter, pad and linker sequences. Each barcode sequence (12 mer) was added to the reverse primer for pooling multiple samples in one run of Miseq sequencing. The PCR conditions were 94 °C for 2 min, 32 cycles of 94 °C for 1 min, 59 °C for 45 s and 72 °C for 1 min of extension, followed by 72 °C for 7 min. PCR products were purified and combined in equimolar rations with the quantitative DNA binding method in order to create a DNA pool that was further used for sequencing from the adaptor. The ITS genes were sequenced using the Illumina Miseq platform. The resultant high-quality sequences were then clustered into operational taxonomic units (OTUs) at 97% similarity using UPARSE (Edgar, 2013). The RDP fungal ITS database was used as a reference for classification.

Phylogenetic analysis

After sequencing, the raw fastq files were demultiplexed and quality-filtered using QIIME (version 1.17). As the number of spurious phylotypes increases with sequencing effort, equal number of sequence reads should be used to compare microbial community among samples to minimize the sequencing artifact (Schloss et al., 2011). In this work, about 74503 reads from every sample were randomly picked and grouped into operational units (OTUs) with 97% similarity cutoff using UPARSE (version 7.1 http://drive5.com/uparse/). Chimeric sequences were identified and removed using UCHIME. Community diversity index (Chao, Simpson, Coverage, Shannon diversity index) and rarefaction curves were generated using the MOTHUR program. The taxonomic assignment of OTUs was performed by RDP Classifier (http://rdp.cme.msu.edu/) against the Warcup fungal ITS database.

Statistical analysis

Canonical correspondence analyses (CCA) were carried out by Canoco 4.5 to compare the effects of soil characteristics on fungi community structure. Statistical significant analyses were performed by SPSS ($p < 0.05$).

Results and discussion

Soil characteristics

After 32 years with different fertilizer application, the physical and chemical properties of soil significantly changed (*Table 2*). Comparing with the initial soil, the pH value in the CK treatment only slightly decreased, which was probably attributed to the continuous crop system with no nutrient input. Among the three fertilizer treatments, the pH value in the NPK treatment was the lowest, indicating that soil acidification occurred. N additions have resulted in a significant decrease in soil pH (Guo et al., 2010; Zhou et al., 2016). Stamatiadis (1999) reported that an intensive soil nitrification process resulted in soil acidification which is the main predictor of bacterial diversity in soils (Zhalnina et al., 2015), when amounts of ammonium fertilizer input, especially as N fertilizer was applied. The content of soil organic matter decreased

http://www.aloki.hu ● ISSN 1589 1623 (Print) ● ISSN 1785 0037 (Online)
DOI: http://dx.doi.org/10.15666/aeer/1704_74217429

significantly from 22.8 g kg^{-1} to lowest 17.4 g kg^{-1}, which resulted from long-term chemical fertilization or no nutrient management without organic materials input. Soil organic carbon also exhibited the same trend. Achiba et al. (2010) showed that manure application could increase soil organic carbon content. Tian (2015) reported the crop straw residue could improve microbial population and increased soil organic carbon content. Comparing with the initial soil, the contents of available N and K reduced slightly, while the content of available P increased remarkably. This indicated that the application of nitrogen and potassium fertilizer was little deficiency and the application of phosphorus fertilizer was in excessive.

Table 2. *The physical and chemical characteristics of soil samples in 2015*

Treatment	pH	OM (g/kg)	Available N (mg/kg)	Available P (mg/kg)	Available K (mg/kg)	Organic C (g/kg)
S_0CK	7.31 b	19.18 a	92.47 b	8.42 c	162.55 b	11.13 a
S_0PK	7.59 a	17.43 b	88.14 c	60.57 a	190.78 a	10.11 a
S_0NPK	7.10 c	20.13 a	115.67 a	41.43 b	185.13 a	11.68 a

Microbial community diversity

Illumina Miseq sequencing analysis was performed to investigate the microbial community structure in the three fertilizer treatments. There were 98793, 74503 and 120939 effective sequence tags were observed in the CK, PK and NPK treatment, respectively, with an average red length of 320 bp. A total of 74503 reads from each sample were picked randomly for further analysis. The OTUs, richness, diversity, and rerefaction curves of microbial communities were shown in *Table 1*. A total of 670, 618 and 664 OTUs were obtained in CK, PK and NPK treatments, respectively, with clustering at a 97% similarity level. There are significant differences in the OTUs and Shannon index for different fertilization. PK treatment has less OTUs than the other treatments. The higher the Shannon index, the more the microbial community diversity. Among the three treatments, the Shannon index in the NPK treatment was lower than that in the CK and PK treatments, suggesting that N addition has significant effect on fungus diversity. Geisseler (2014) reported that increasing N inputs could suppress soil microbial activity according to the meta-analysis of predominantly unmanaged ecosystems (Paungfoo-Lonhienne et al., 2015; Lu et al., 2011; Liu and Greaver, 2010; Theseder, 2008). As one of the most important microbial parameters in soils (Zhang and Cai, 2007; Tian et al., 2015), microbial diversity was affected remarkably by fertilization (Zhang et al., 2012; Esperschuetz et al., 2007).

ITS pyrosequencing method can reveal the differences of soil fungi communities under long-term fertilization. The mean effective reads obtained from the CK, PK and NPK treatments were 98 793, 74 503 and 120 939, respectively. The coverage showed that the three fertilization samples were greater than 0.99, indicating that the sequencing capability was large enough to capture the complete diversity of each sample. Three fertilization treatments had no significant effect on fungi richness, however, balanced fertilization management (NPK) treatment had significantly influenced on fungi diversity according to Shannon indices; and PK treatment remarkably reduced the OTUs number. Fungi diversity is one of the most important fungi parameters in soil (Zhong and Cai, 2007).

http://www.aloki.hu ● ISSN 1589 1623 (Print) ● ISSN 1785 0037 (Online)
DOI: http://dx.doi.org/10.15666/aeer/1704_74217429

Changes of microbial composition at different levels

The classifiable sequences in the CK treatment were affiliated with 5 phyla, 19 classes and 125 genera; the classifiable sequence in the PK treatment were affiliated with 6 phyla, 19 classes and 118 genera; and the classifiable sequences in the NPK treatment were affiliated with 5 phyla, 19 classes and 123 genera. The phylogenetic classification of sequences at phylum, class and genus levels from the three treatments was summarized in *Figure 1*. Ascomycota was the first dominant phyla in all the three treatments, representing 89.13%, 86.72% and 87.70%, respectively. And other main dominant phyla included Basidiomycota, Chytridiomycota, Glomeromycota, and Zygomycota. The rate of Basidiomycota Phylum in the PK and NPK treatments was higher compared with that in the CK treatment, which was favorable to the cultivation of crops and afforestation. Furthermore, the rate of Zygomycota and Chytridiomycota Phylum in the NPK treatment increased two times and five times than that in the others fertilizer treatments.

At class level by the phylogenetic classification, *Dothideomycetes* and *Sordariomycetes* are the main compositions in the three fertilizer treatments, followed by *Eurotiomycetes*, *Leotiomycetes* and *Agaricomycetes*. Thus, the long-term application of mineral fertilizers has no significant impacts on fungi community composition, which was consistent with findings from previous studies (Esperschuetz et al., 2007; Ogilvie et al., 2008; Boerjesson et al., 2012). Dothideomycetes Class as the second most abundant Class is very important for ecosystem environment and global carbon cycle by speeding up cell wall decay (Freedman et al., 2015), the results in our research showed that long-term only P plus K addition would reduce the composition rate in soil. The application of NPK fertilizer significantly increased *Alternaria* and *Pseudogymnoascus* at genus level, compared with the CK and PK treatments. Many pesudogymnoascus species are cellulolytic, function as saprothrophs and are either psychrophilic or psychrotolerant. *Alternaria* is a genus of *ascomycete* fungi. *Alternaria* species are known as major plant pathogens. They are also common allergens in humans, growing indoors and causing hay fever or hypersensitivity reactions that sometimes lead to asthma. At least 20% of agricultural spoilage is caused by Alternaria species; most severe losses may reach up to 80% of yield (Nowicki, et al., 2012). The above results indicated that N fertilizer application could improve the resistance, but also bring about the risk of plant diseases. However, the rate of *Fusarium* at genus level in the NPK treatment reduced less 70% than that of the others treatments. Some species in *Fusarium* genus produce mycotoxins in cereal crops that can affect human and animal health if they enter the food chain. The rate of genus of Penicillium in Eurotiomycetes Class in the NPK treatment obviously increased; on the contrary, the rate of genus of and Ceratobasidium in Agaricomycetes class decreased significantly, comparing with the CK and PK treatments. *Penicillium* bacteria can decompose many agricultural products, and Gratobasidium cornigerum (Bourd.) Rogers in Ceratobasidium could result in crop banded sclerotial blight. Therefore, suitable N addition could improve soil ability of degraded cellulose, as well as reduce the chance of plant banded sclerotial blight.

Relationships between fungi community and environmental variables

According to CCA analysis, catalase had large variance inflation factor (VIF), which implied that its variables are redundant with other variables in the environmental factors

http://www.aloki.hu ● ISSN 1589 1623 (Print) ● ISSN 1785 0037 (Online)
DOI: http://dx.doi.org/10.15666/aeer/1704_74217429

(*Fig. 2*). All the environmental variables together explained 99.3% of the variation in fungi communities among fertilizer treatments. A total of 32.2% of the total variance were explained by the first two constrained axes of CCA analysis, in which the first axis explaining 23.0% and second explaining 8.9% of the total variance. The CCA clearly demonstrates that *Pseudogymnoascus*, *Alternaria*, *Penicillium* and *Chaetomium* are sensitive to N fertilizer application.

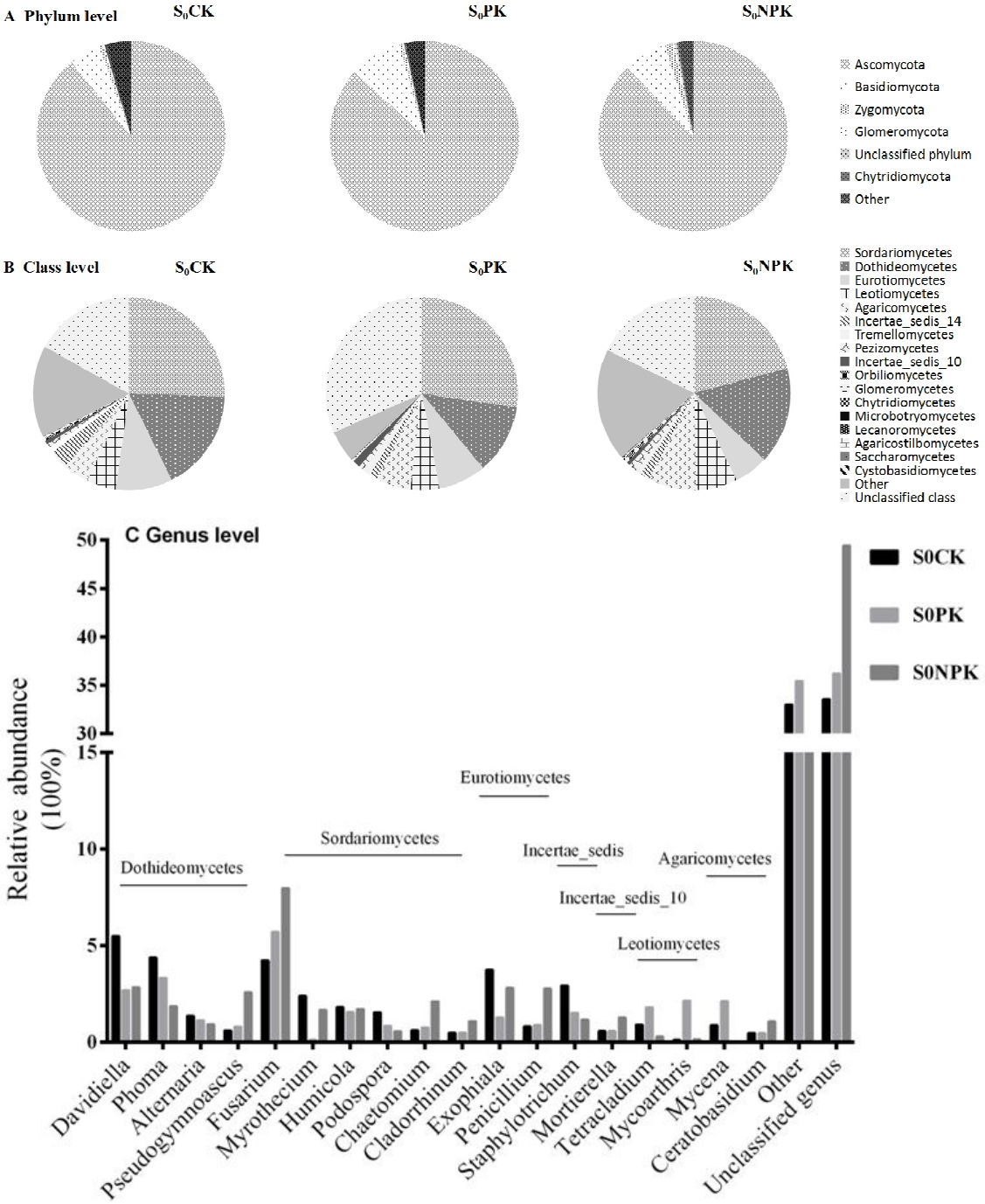

Figure 1. *Fungal community structures at (A) Phylum level, (B) Class and (C) genus level of the SoCK, SoPK and SoNPK. The relative abundance was defined as the percentage of the in total effective fungal sequences in sample. Genera making up less than 1% of total composition was classified as 'other'*

http://www.aloki.hu ● ISSN 1589 1623 (Print) ● ISSN 1785 0037 (Online)
DOI: http://dx.doi.org/10.15666/aeer/1704_74217429

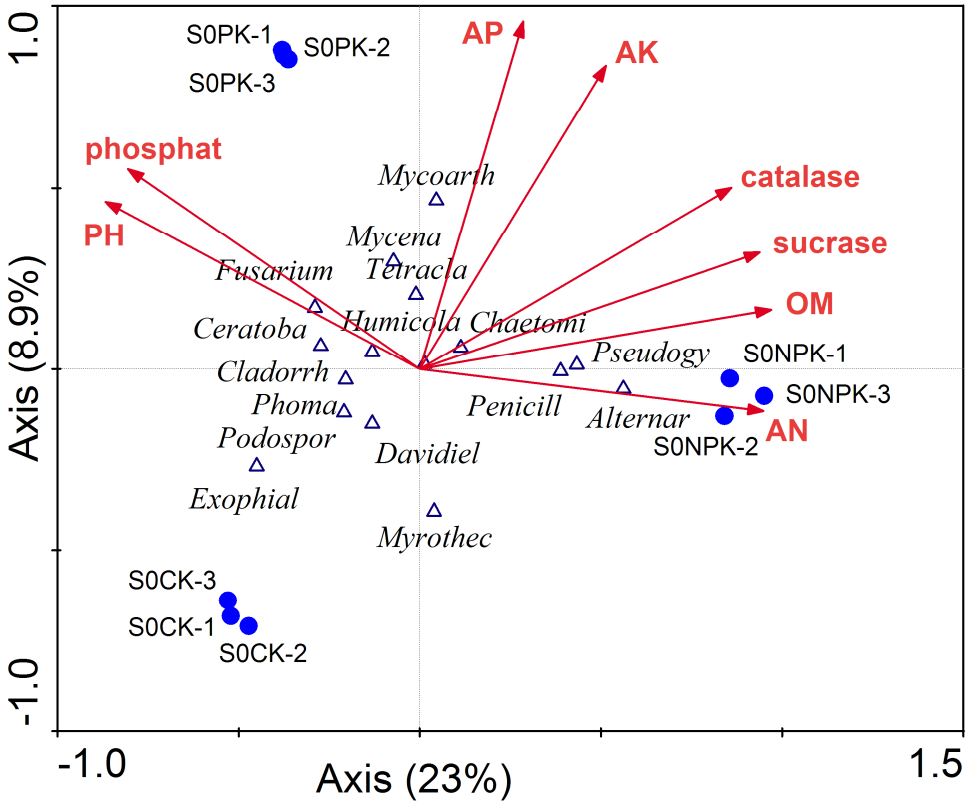

Figure 2. *CCA analysis of different fertilization treatments with soil environmental characteristics as arrows. Triangle symbols represent different genus fungal community structures. OM: organic matter; AN: available nitrogen; AP: available phosphorus; AK: available potassium*

Conclusion

The results presented in this paper unequivocally demonstrate that mineral fertilizer application caused shifts in the structure of fungi communities in Mollisol soil. Soil physical and chemical properties and fungi diversity and abundance were significantly affected by long-term mineral fertilization, especially in fungi diversity reduction and soil acidification.

Acknowledgements. The authors would like to acknowledge the Technology Key Project of Jilin Province (20170101004JC), National Key Research and Development Program of China (2017YFD0201804), and Project supported by the National Natural Science Foundation of China (Grant No.31301850) for their financial support.

REFERENCES

[1] Achiba, W. B., Lakhdar, A., Gabteni, N., Laing, G. D., Verloo, M., Boeckx, P., Cleemput, O. V., Jedidi, N., Gallali, T. (2010): Accumulation and fractionation of trace metals in a Tunisian calcareous soil amended with farmyard manure and municipal solid waste compost. – Journal of Hazardous Materials 176: 99-108.

http://www.aloki.hu ● ISSN 1589 1623 (Print) ● ISSN 1785 0037 (Online)
DOI: http://dx.doi.org/10.15666/aeer/1704_74217429

[2] Allison, S. D., Martiny, J. B. H. (2008): Resistance, resilience, and redundancy in microbial communities. – Proceedings of the National Academy of Sciences of the USA 105: 11512-11519.
[3] Boerjesson, G., Menichetti, L., Kirchmann, H., Kaetterer, T. (2012): Soil microbial community structure affected by 53 years of nitrogen fertilization and different organic amendments. – Biology & Fertility of Soil 48: 245-257.
[4] Chávez-Romeroa, Y., Navarro-Noyab, Y. E., Reynoso-Martíneza, S. C., Sarria-Guzmána, Y., Govaertsc, B., Verhulstc, N., Dendoovena, L., Luna-Guido, M. (2016): 16s metagenomics reveals changes in the soil bacterial community driven by soil organic c, n-fertilizer and tillage-crop residue management. – Soil and Tillage Research 159: 1-8.
[5] Claiborne, A. (1985): Catalase Activity – In: Greenwald, R. A. (ed.) CRC Handbook of Methods for Oxygen Radical Research. CRC Press, Boca Raton, FL.
[6] Clark, C. M., Cleland, E. E., Collins, S. L., Fargione, J. E., Gough, L., Gross, K. L., Pennings, S. C., Suding, K. N., Grace, J. B. (2007): Environmental and plant community determinants of species loss following nitrogen enrichment. – Ecology Letters 10: 596-607.
[7] Cleland, E. E., Harpole, W. S. (2010): Nitrogen enrichment and plant communities. – Annals of the New York Academy of Sciences 1195: 46-61.
[8] Edgar, R. C. (2013): UPARSE: highly accurate OTU sequences from microbial amplicon reads. – Nat Methods 10: 996-998.
[9] Esperschuetz, J., Gattinger, A., Maeder, P., Schloter, M., Fliessbach, A. (2007): Response of soil microbial biomass and community structures to conventional and organic farming systems under identical crop rotation. – FEMS Microbiology Ecology 61: 26-37.
[10] Freedman, Z. B., Romanowicz, K. J., Upchurch, R. A., Zak, D. R. (2015): Differential responses of total and active soil microbial communities to long-term experimental N deposition. – Soil Biology and Biochemistry 90: 275-282.
[11] Geisseler, D., Scow, K. M. (2014): Long-term effects of mineral fertilizers on soil microorganisms -A review. – Soil Biology and Biochemistry 75: 54-63.
[12] Guo, J. H., Liu, X. J., Zhang, Y., Shen, J. L., Han, W. X., Zhang, W. F., Christie, P., Goulding, K. W. T., Vitousek, P. M. Zhang, F. S. (2010): Significant acidification in major Chinese croplands. – Science 327: 1008-1010.
[13] Liu, L., Greaver, T. L. (2010): A global perspective on belowground carbon dynamics under nitrogen enrichment. – Ecology Letters 13: 819-828.
[14] Lu, H. Y., Li, N. (2006): effect of long-term fixed position fertilization on nutrition in topsoil of black earth. – Journal of Jilin Agricultural Sciences 31: 33-36 (in Chinese with English abstract).
[15] Lu, M., Yang, Y., Luo, Y., Fang, C., Zhou, X., Chen, J., Yang, X., Li, B. (2011): Responses of ecosystem nitrogen cycle to nitrogen addition: a meta-analysis. – New Phytologist 189: 1040-1050.
[16] Nowichi, M., Nowakowska, M., Niezgoda, A., Kozik, E. U. (2012): Alternaria black spot of crucifers: symptoms, importance of disease, and perspectives of resistance breeding. – Vegetable Crops Research Bulletin 76: 5-19.
[17] Ogilvie, L. A., Hirsch, P. R., Johnston, A. W. B. (2008): Bacterial diversity of broadbalk 'Classical' winter wheat experiment in relation to long-term fertilizer inputs. – Microbial Ecology 56: 525-537.
[18] Paungfoo-Lonhienne, C., Yeoh, Y. K., Kasinadhuni, N. R., Lonhienne, T. G., Robinson, N., Hugenholtz, P., Ragan, M. A., Schmidt, S. (2015): Nitrogen fertilizer dose alters fungal ommunities in sugarcane soil and rhizosphere. – Scientific Report 58678: 1-6.
[19] Rezapour, S., Taghipour, A., Samadi, A. (2013): Modifications in selected soil attributes as inflfluenced by long-term continuous cropping in a calcareous semiarid environment. – Nat. Hazards 69: 1951-1966.
[20] Robertson, G. P., Vitousek, P. M. (2009): Nitrogen in agriculture: balancing the cost of an essential resource. – Annual Review of Environment and Resources 34: 97-125.

http://www.aloki.hu ● ISSN 1589 1623 (Print) ● ISSN 1785 0037 (Online)
DOI: http://dx.doi.org/10.15666/aeer/1704_74217429

[21] Shen, J. P., Zhang, L. M., Guo, J. F., Ray, J. L., He, J. Z. (2010): Impact of long-term fertilization practices on the abundance and composition of soil bacterial communities in Northeast China. – Applied Soil Ecology 46: 119-124.
[22] Spohn, M., Kuzyakov, Y. (2013): Distribution of microbial and root-derived phosphates activities in the rhizosphere depending on P availability and C allocation - coupling soil zymography with ^{14}C imaging. – Soil Biology and Biochemistry 67: 106-113.
[23] Stamatiadis, S., Werner, M., Buchanan, M. (1999): Field assessment of soil quality as affected by compost and fertilizer application in a broccoli field (San Benito County, California). – Applied Soil Ecology 12: 217-225.
[24] Sul, W. J., Asuming-Brempong, S., Wang, Q., Tourlousse, D. M., Penton, C. R., Deng, Y., Rodrigues, J. L. M., Adiku, S. G. K., Jones, J. W., Zhou, J., Cole, J. R., Tiedje, J. M. (2013): Tropical agricultural land management influences on soil microbial communities through its effect on soil organic carbon. – Soil Biol. Biochem. 65: 33-38.
[25] Tabatabai, M. A. (1977): Effects of trace elements on urease activity in soils. – Soil Biology & Biochemistry 9: 9-13.
[26] Tian, W., Wang, L., Li, Y., Zhuang, K. M., Li, G., Zhang, J. B., Xiao, X. J., Xi, Y. G. (2015): Responses of microbial activity, abundance, and community in wheat soil after three years of heavy fertilization with manure-based compost and inorganic nitrogen. – Agriculture Ecosystems and Environment 213: 219-227.
[27] Treseder, K. K. (2008): Nitrogen additions and microbial biomass: a meta-analysis of ecosystem studies. – Ecology Letters 11: 1111-1120.
[28] Tripathi, B. M., Kim, M., Singh, D., Lee-Cruz, L., Lai-Hoe, A., Ainuddin, A. N., Go, R., Rahim, R. A., Husni, M. H. A., Chun, J., Adams, J. M. (2012): Tropical soil bacterial communities in Malaysia: pH dominates in the Equatorial Tropics too. – Microb Ecol 64: 474-484.
[29] Zhalnina, K., Dias, R., de Quadros, P. D., Davis-Richardson, A., Camargo, F. A., Clark, I. M., McGrath, S. P., Hirsch, P. R., Triplett, E. W. (2015): Soil pH determines microbial diversity and composition in the park grass experiment. – Microbial Ecology 69: 395-406.
[30] Zhang, Q. C., Ahamsi, I. H., Xu, D. T., Wang, G. H., Lin, X. Y., Jilani, G., Hussain, N., Nawaz, A. (2012): Chemical fertilizer and organic manure inputs in soil exhibit a vice versa pattern of microbial community structure. – Applied Soil Ecology 57: 1-8.
[31] Zhong, W. H., Cai, Z. C. (2007): Long-term effects of inorganic fertilizers on microbial biomass and community functional diversity in a paddy soil derived from quaternary red clay. – Applied Soil Ecology 36: 84-91.
[32] Zhou, J., Jiang, X., Zhou, B., Zhao, B., Ma, M., Guan, D., Qin, J., Chen, S., Cao, F., Shen, D., Li, J. (2016): Thirty four years of nitrogen fertilization decreases fungal diversity and alters fungal community composition in black soil in northeast China. – Soil Biology and Biochemistry 95: 135-143.

http://www.aloki.hu ● ISSN 1589 1623 (Print) ● ISSN 1785 0037 (Online)
DOI: http://dx.doi.org/10.15666/aeer/1704_74217429

IDENTIFICATION OF AN ALKALINE PROTEASE PRODUCING BACTERIUM ISOLATED FROM PANJIN RED BEACH, CHINA

YUAN, Y.[1] – GAO, J. Y.[2] – DU, L. Q.[2] – LI, X. M.[1] – LI, Y. Y.[1] – WANG, L. L.[1] – BU, N.[1*] – MA, L. J.[1*]

[1]*College of Life Science, Shenyang Normal University*
No. 253 Huanghe North Street, Shenyang, Liaoning 110034, China

[2]*College of Life Science, Wuhan University, Wuhan 430072, China*

[*]*Corresponding authors*
e-mail: malianju@163.com, buning60@sohu.com

(Received 1st Mar 2019; accepted 1st May 2019)

Abstract. Extremophilic bacteria surviving in extreme environmental conditions possess the special abilities to adapt adverse environment. There are very high salinization and alkalinization contents in Panjin Red Beach's soil. A productive alkline protease strain HHT597 was isolated from the soil samples and identified as *Bacillus altitudinis* based on the 16s rDNA sequence. The HHT597 strain was characterized as a gram positive, rod-shaped bacterial strain with flagellum. The optimum temperature for protease activity by the strain HHT597 was 60°C. There was a broad pH active range of protease from 7.0–11.0 with having optima pH 9.0. The media containing 2.0% glucose and 1% yeast extract as carbon and nitrogen sources could improve protease activity. The strain HHT597 could degrade casein, hemoglobin (HGB) and albumin (ALB) protein. The results indicated that the strain HHT597 might be potential for biotechnological applications.
Keywords: *extreme environment, isolation, 16S rRNA gene, identification, Bacillus*

Introduction

Proteases, which catalyze proteolysis by performing cleavage of peptide bonds, are widely used industrial enzymes, accounting for more than 65% of the total worldwide sale of the enzymes (Rao et al., 1998; Shankar et al., 2011; Annamalai et al., 2014). Proteases include alkaline, acid, thiol and metallo proteases. Among these categories of proteases, alkaline proteases are a class of extracellular enzyme that performs proteolysis and have wide applications as industrial catalysts in various of industries and research laboratories, which could be used in enzymatic peptide synthesis, biotransformation reactions, detergent, surfactants, food processing, diagnostic reagents, preparation of organic fertilizers, silver recovery from used X-ray film and wastes treatment (Kalisz, 1988; Anwar and Saleemuddin, 1998; Shah et al., 2010; Rathod and Pathak, 2016; Hakim et al., 2018). A wide range of sources was found to produce alkaline protease such as bacteria, molds, yeasts, certain insects or mammalian tissues (Mabrouk et al., 1999; Kumar et al., 2014). Bacteria producing

http://www.aloki.hu ● ISSN 1589 1623 (Print) ● ISSN 1785 0037 (Online)
DOI: http://dx.doi.org/10.15666/aeer/1704_74317438

alkaline protease are the most important approach relative to plants, animal, and fungus because of their extracellular nature, high yield of production, limited space, convenient cultivation and feasibility to genetic manipulation (Breithaupt, 2001; Selvamohan and Sherin, 2010).

With previous studies gaining a better understanding of the physical, chemical and biological properties of alkaline proteases, researchers nowadays focus more on searching for alkaline proteases with specificities such as high temperature and pH tolerance. Active ranges of temperatures of alkaline (serine) proteases were 35°C–80°C and pH was 7–12 (Rao et al., 1998). Morozkina et al. (2010) reported that the extremophiles could produce extremozymes. Through the long term of natural selection, extremophilic bacteria possess the special abilities associated tightly with their structures, physiological mechanisms, genetic characteristics and biochemical pathways. For example, they can produce extracellular proteases. At high pH and temperatures, there were remarkable activity and stability in alkaline protease produced by marine bacteria (Arastoo and Zahra, 2013). Therefore, extreme environments, in particular, marine environments are a valuable approach for bacteria producing microbial enzymes (Mirete et al., 2016).

Panjin Red Beach which locates in Liaoning, China, is a famous wetland landscape covering an area of 133.33 km^2 on a flat and broad terrain (Wang et al., 2011). Years of marine corrosion leads to the soil a sandy, humid and heavy texture with a high level of salinization and alkalinization. The inartificial edatope creates a unique ecosystem that provides native habitats for variety of halophilic and basophilic microorganisms. Therefore, it is likely to find functional strains that are adaptation to saline-alkali environment. Our research focused on isolating and identification bacteria producing alkaline protease with protease activity in the natural saline-alkaline soil of the Red Beach.

Materials and Methods

Isolation of Bacterial Strain Producing Alkaline Protease

Five representative plots were selected during September 2017 in Panjin Red Beach. Soil samples, five soil cores (5 cm diameter) were collected in triplicate from the topsoil (0-15 cm) in each sampling site and mixed evenly, then placed in aseptic polyvinyl chloride soil bag.

Soil samples (10 g) collected were suspended in 90 mL of sterile distilled water. After a serial dilution (10^{-3} to 10^{-5}) of the soil suspension with sterile distilled water, 0.1 mL soil suspension was spread on selective agar plates and incubated at 37℃ for 2 d. The selective agent in the agar plates contained beef extract 0.3% (w/v), casein 1% (w/v), NaCl 1.5% (w/v), agar 2% (w/v). Ten plates were screened in soil samples and about 150 plates altogether were screened. The strain having the largest clear zone was selected by secondary screening for this study.

http://www.aloki.hu ● ISSN 1589 1623 (Print) ● ISSN 1785 0037 (Online)
DOI: http://dx.doi.org/10.15666/aeer/1704_74317438

Identification of Bacteria Strain

Bacteria strain was performed by Gram staining and biochemical tests such as methyl red test, V-P test, carbohydrate fermentation test and hydrogen sulfide production test following commonly used microbial identification manuals like Bergey's manual (Holt, 1994). Each treatment was conducted with three replicates.

The total genomic DNA of the bacteria strain was extracted and purified using Bacterial DNA Isolation Kit (Sangon Biotech Co., Ltd, China) according to maufacturer's instructions. The 16S rDNA of the isolate was amplified through PCR reaction using the universal primers 27f (5'-AGAGTTTGATCATCCTGGCTCAG-3') and 1492r (5'-TACGGTTACCTTGTTACGACTT-3') synthesized by Sangon Biotech Co., Ltd (Shanghai, China). The PCR reaction process was as follows: 95°C for 5 min, 35 cycles of 95°C for 1 min, 55°C for 1 min, 72°C for 2 min, and a final extension at 72°C for 10 min. PCR product was sent to Sangon BiotechCo., Ltd (Shanghai, China) for sequencing. The similarities of the sequence were identified using online EzBioCloud database (https://www.ezbiocloud.net/). Construction of phylogenetic tree was carried out using MEGA 7 (Kumar et al., 2016).

Enzyme Assay Estimation

Alkaline protease activity was determined by using casein as a substrate by method of Yang and Wang (1999). One unit of protease activity was defined as the amount of the enzyme that produces 1μg/mL/min of tyrosine equivalent under the assay conditions.

Optimum Conditions for Protease Activity

Optimum Temperature and pH: Preheat 2.0% casein solution for 5 min by water bath at temperature ranging from 10°C to 80°C. Mix 1 mL of each casein solution with 1mL preheated crude protease solution and water bath at 40℃ for 10 min, then end the reaction with 5 mL TCA solution. The basal media was adjusted to seven different pH ranging 6.0-12.0. The seed culture (1.0% V/V) was inoculated to each 150 mL liquid medium and was carried out at 37°C, 160 rpm for 2 d. Enzyme assay determination was as stated above.

Carbon and Nitrogen Sources: 2.0% each of glucose, maltose, sucrose and lactose was added in the basal media to investigate the effects of different carbon sources. To observe the effects of various nitrogen sources on protease activity, 1.0% each of beef extract, peptone, yeast extract, sodium nitrate, ammonium nitrate and ammonium chloride was added to the basal media. Fermentation was carried out under optimum temperature and pH at 130 rpm for optimum period. Enzyme assay determination was as stated according to the method described above.

Substrate Specificity Assay: Prepare 2% (w/v) of each casein, gelatin, hemoglobin (HGB), albumin (ALB) solution as substrate. Mix 1 mL substrate solution with 1 mL preheated the crude protease solution and water bath at 40°C for 10 min, then end the reaction with 5 mL TCA solution. Enzyme assay determination was as already mentioned.

http://www.aloki.hu ● ISSN 1589 1623 (Print) ● ISSN 1785 0037 (Online)
DOI: http://dx.doi.org/10.15666/aeer/1704_74317438

Statistical analysis

All data were analyzed according to Duncan's multiple range tests using the SPSS 11.0 software package.

Results and Discussion

Isolation, Screening and Identification of Strain HHT597

Eight isolates from soil samples showed clear zone around bacterial colonies on the selective medium, indicating that these strains can produce extracellular alkaline protease. These eight strains were named for from HHT591 to 598. Finally, bacterium strain HHT597 was chosen for further study based on the intensity of clear zone.

The strain HHT597 was characterized as a gram positive, rod-shaped bacterial strain with flagellum (*Figure 1A*). Colony morphology was faint yellow, round, marginal tidy, dry surface (*Figure 1B, C*).

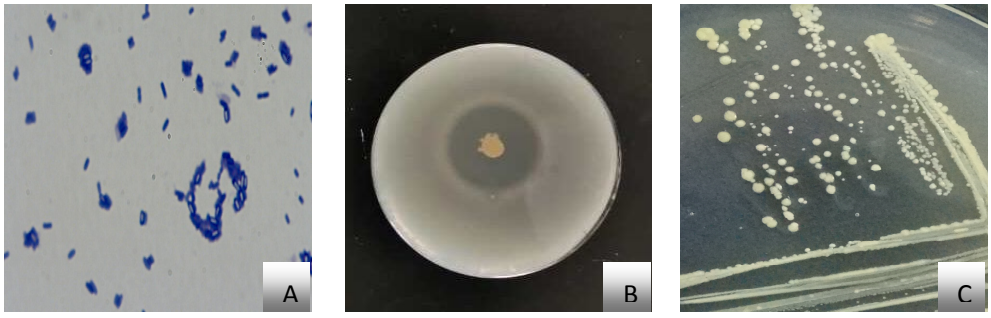

Figure 1. *The colony morphology (A, B) and Gram stain (C) of bacteria strain HHT597*

Biochemical characteristics were listed in *Table 1*. Based on the morphological and biochemical characteristics, isolate HHT597 was identified as *Bacillus* sp. Among all the alkaolphilic microorganisms, *Bacillus* spp. is the most predominant and a prolific source of alkaline proteases (Kumar and Takagi, 1999).

Table 1. *Biochemical characteristics of strain HHT597*

Glucose	Lactose	Acid production	Gas production	Voges Proskauer	Methyl red	H_2S production
+	-	-	+	+	+	+

To carry out the 16S rDNA gene sequencing analysis, the genome of strain HHT597 was used for PCR amplification of 16S rDNA. The molecular weight of PCR product of strain HHT597 was corresponding to 1500 bp of the DNA marker and the amplification was successful. The DNA sequence of 1456 bp product was uploaded to EzBioCloud database for phylogenetic identification and comparison. Phylogenetic tree was

http://www.aloki.hu ● ISSN 1589 1623 (Print) ● ISSN 1785 0037 (Online)
DOI: http://dx.doi.org/10.15666/aeer/1704_74317438

constructed based on neighbour-joining statistical algorithms. According to phylogenetic tree (*Figure 2*), the strain HHT597 were clustered with *Bacillus* altitudinis strain G65 with high (99%) 16S rDNA sequence similarity. The strain HHT597 was affiliated to the genus *Bacillus*.

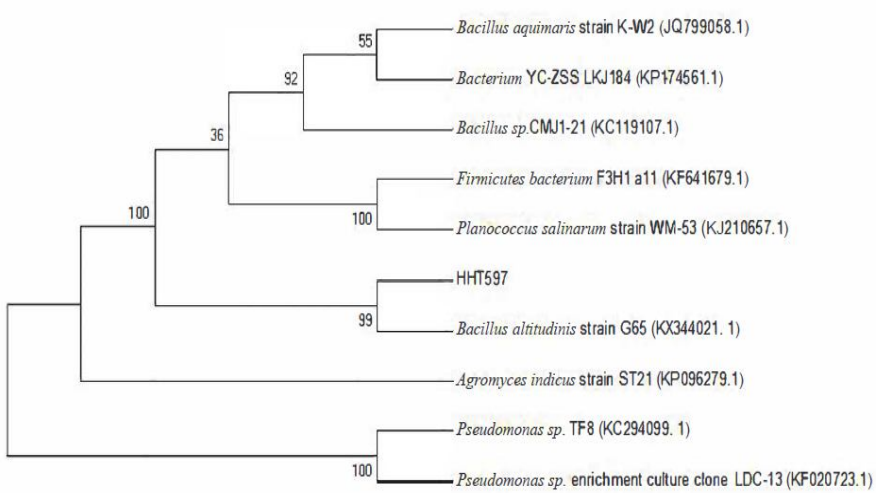

Figure 2. *Phylogenetic tree of HHT597 and B. altitudinis strain G65 with other B. species*

Effects of Temperature and pH on Protease Activity

Generally, the protease activity is easily decreased by high temperature. The temperature optima of protease depended on the bacterial species (Iqbal et al., 2018). In the present study, the alkaline protease activity first gradually increased then gradually decreased with increasing temperature (*Figure 3a*).

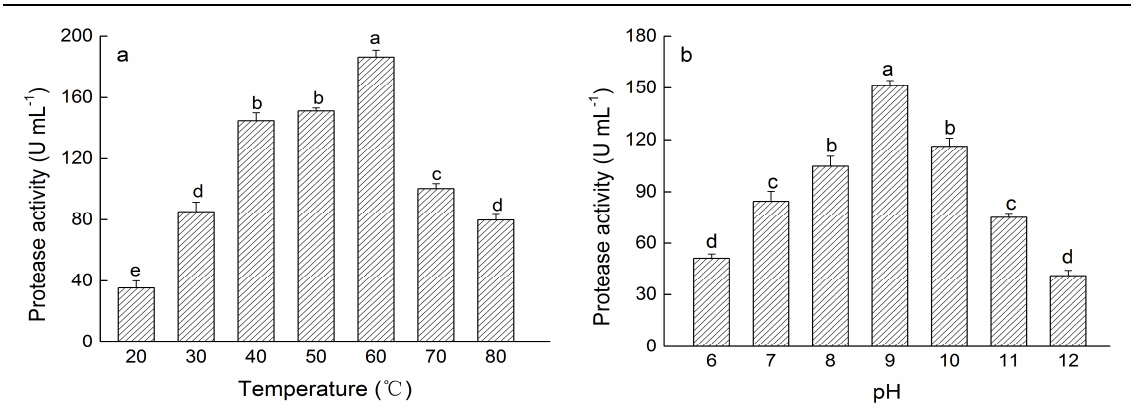

Figure 3. *Effects of temperature (a) and pH (b) sources on alkaline protease activity*

The optimum temperature of protease activity produced by strain HHT597 was 60°C and protease activity reached 186.35 U/mL. When temperature was up to 70°C, the protease activity began gradually to decrease. The results indicated that the protease

http://www.aloki.hu ● ISSN 1589 1623 (Print) ● ISSN 1785 0037 (Online)
DOI: http://dx.doi.org/10.15666/aeer/1704_74317438

produced by the strain HHT597 could work at high temperatures. Nevertheless, almost similar protease activity was found at 40–50°C (Hakim et al., 2018).

Many enzymatic processes are strongly influenced by the pH (Ellaiah et al., 2002; Hakim et al., 2018). In the present study, the pH active range of protease was from 7.0 to 11.0. The optimum pH for alkline protease activity was 9.0, and the protease activity was 151.21 U/mL (*Figure 3b*). Rao et al (1998) reported that pH optima of alkaline protease in commerce were from 8.0 to 12.0.

Effects of Carbon and Nitrogen Sources on Protease Activity

The carbon and nitrogen sources used in the media highly influenced production of alkaline protease (Hakim et al., 2018). The media containing glucose at 2% was the most favorable source supported the highest alkaline protease production compared to other carbon sources (*Table 2*). The results were similar with other reports (Ellaiah et al., 2002; Hakim et al., 2018). Among the different nitrogen sources studies, 1% yeast extract was the most benefit for alkaline protease production (*Table 2*), which is consistent with previous results of *B*. subtilis AKAL7 (Hakim et al., 2018) and *B*. sp MA6 (Azad and Hoq, 2000). However, the strain HHT597 could not use inorganic nitrogen compounds as nitrogen sources.

Table 2. *Effects of carbon source, nitrogen source and substrate on alkaline protease activity*

Treatment		Protease activity（U/mL）
Carbon source	Glucose	89.26±1.73a
	Maltose	79.37±2.38b
	Sucrose	35.43±1.2c
	Lactose	78.34±1.34b
Nitrogen source	Beef extract	117.26±4.16b
	Yeast extract	186.24±8.56a
	Peptone	109.32±6.52b
	Ammonium nitrate	—
	Sodium nitrate	—
	Ammonium chloride	—
Substrate	Casein	136.63±7.65a
	Gelatin	—
	Hemoglobin	112.06±4.31b
	Albumin	108.63±2.62b

The different letters indicate significant differences at $P < 0.05$

Optimum Substrate on Protease Activity

Casein, HGB, AHL and gelatin was used as substrate to detect the protease degradation ability, respectively. Among four substrates, casein was the most appropriate substrate and the maximum protease activity was 136.63 U/mL (*Table 2*). HGB and AHL could also be the substrate of alkline protease extracted from HHT597. However, gelatin was not used as the protease substrate.

http://www.aloki.hu ● ISSN 1589 1623 (Print) ● ISSN 1785 0037 (Online)
DOI: http://dx.doi.org/10.15666/aeer/1704_74317438

Conclusion

A productive alkline protease, gram positive bacterial strain of the genus *Bacillus* was isolated from the soil samples of Panjin Red in China and identified as *B. altitudinis* strain HHT597. The optimum temperature for maximum protease activity produced by the strain HHT597 was 60°C. There was a broad pH active range of protease from 7.0-11.0. The optimum carbon and nitrogen sources for protease activity produced by the strain HHT597 was 2% glucose and 1% yeast extract, respectively. The strain HHT597 could degrade casein, HGB and AHL protein. The research results showed that the strain HHT597 might be potential for industrial applications.

Acknowledgements. This work was supported by Shenyang city Science and Technology plan (F16-205-1-50), Major incubating project of Shenyang Normal University (ZD201705) and Liaoning Province Science and Technology Plan Progect (No.2017208001).

REFERENCES

[1] Annamalai, N., Rajeswari, M. V., Balasubramanian, T. (2014): Extraction, purification and application of thermostable and halostable alkaline protease from Bacillus alveayuensis CAS5 using marine wastes. – Food Bioprod Process 92(4): 335-342.

[2] Anwar, A., Saleemuddin, M. (1998): Alkaline proteases: a review. – Bioresour Technol 64: 175-183.

[3] Arastoo, B. D., Zahra, K. (2013): Screening and isolation of an organic solvent tolerant-protease from Bacillus sp. JER02: Activity optimization by response surface methodology. – J Mol Cataly B: Enzymatic 89: 15-23.

[4] Azad, A. K., Hoq, M. M. (2000): Production of alkaline serine protease by Bacillus sp. MA6. – Bangladesh J Microbiol 11(2): 143-149.

[5] Breithaupt, H. (2001): The hunt for living gold. – EMBO Rep 2(11): 968-971.

[6] Ellaiah, P., Srinivasulu, B., Adinarayana, K. (2002): A review on microbial alkaline proteases. – J Sci Ind Res 61: 690-704.

[7] Hakim, A., Bhuiyan, F. R., Qbal, A., Emon, T. H., Ahmed, J., Azad, A. K. (2018): Production and partial haracterization of dehairing alkaline protease from Bacillus subtilis AKAL7 and Exiguobacterium indicum AKAL11 by using organic municipal solid wastes. – Heliyon 4: e00646.

[8] Holt, J. G. (1994): Bergey's manual of determinative bacteriology. – 9th Edition, Lippincott Williams and Wilkins, Baltimore.

[9] Iqbal, A., Hakim, A., Hossain, M. S., Rahman, M. R., Islam, K., Azim, M. F., Ahmed, J., Assaduzzaman, M., Hoq, M. M., Azad, A. K. (2018): Partial purification and characterization of serine protease produced through fermentation of organic municipal solid wastes by Serratia marcescens A3 and Pseudomonas putida A2. – J Genet Eng Biotechnol 16: 29-37.

[10] Kalisz, H. M. (1988): Microbial proteinases. – Adv Biochem Eng Biotechnol 36: 1-65.

http://www.aloki.hu ● ISSN 1589 1623 (Print) ● ISSN 1785 0037 (Online)
DOI: http://dx.doi.org/10.15666/aeer/1704_74317438

[11] Kuma, C. G., Takagi, H. (1999): Microbial alkaline proteases: From a bioindustrial viewpoint. – Biotechnol Adv 17: 561-594.
[12] Kumar, R. S., Ananthan, G., Prabhu, A. S. (2014): Optimization of medium composition for alkaline protease production by Marinobacter sp. GA CAS9 using response surface methodology-A statistical approach. – Biocataly Agric Biotechnol 3: 191-197.
[13] Kumar, S., Stecher, G., Tamura, K. (2016): MEGA 7: Molecular evolutionary genetics analysis version 7.0 for bigger datasets. – Mol Biol Evol 33: 870-874.
[14] Mabrouk, S. S., Hashem, A. M., El-Shayeb, N. M. A., Ismail, A. M. S., Abdel-Fattah, A. F. (1999): Optimization of alkaline protease productivity by Bacillus licheniformis ATCC 21415. – Bioresour Technol 69(2): 155-159.
[15] Mirete, S., Morgante, V., González-Pastor, J. E. (2016): Functional metagenomics of extreme environments. – Curr Opin Biotech 38: 143-149.
[16] Morozkina, E. V., Slutskaya, E. S., Fedorova, T. V., Tugay, T. I., Golubeva, L. I., Koroleva, O. V. (2010): Extremophilic microorganisms: Biochemical adaptation and biotechnological application (review). – Appl Biochem Microbiol 46: 1-14.
[17] Rao, M. B., Tanksale, A. M., Ghatge, M. S., Deshpande, V. V. (1998): Molecular and biotechnological aspects of microbial protease. – Microbiol Mol Biol Rev 62(3): 597-635.
[18] Rathod, M. G., Pathak, A. P. (2016): Optimized production, characterization and application of alkaline proteases from taxonomically assessed microbial isolates from Lonar soda lake, India. – Biocatal Agric Biotechnol 7: 164-173.
[19] Selvamohan, T., Sherin, S. (2010): Optimization of protease production from Bacillus cereus using different substrates. – Plant Arch 10(2): 651-656.
[20] Shah, K., Mody, K., Keshri, J., Jha, B. (2010): Purification and characterization of a solvent, detergent and oxidizing agent tolerant protease from Bacillus cereus isolated from the Gulf of Khambhat. – J Mol Catal B-Enzym 67: 85-91.
[21] Shankar, S., Rao, M., Laxman, R. S. (2011): Purification and characterization of an alkaline protease by a new strain of Beauveria sp. – Process Biochem 46(2): 579-585.
[22] Wang, J. L., Huang, X. J., Zhong, T. Y., Chen, Z. G. (2011): Review on sustainable utilization of salt-affected land. – Acta Geogr Sin. 66: 673-684.
[23] Yang, S. S., Wang, J. Y. (1999): Protease and amylase production of Streptomyces rimosus in submerged and solid state cultivations. – Bot Bull Acad Sin. 40: 259-265.

http://www.aloki.hu ● ISSN 1589 1623 (Print) ● ISSN 1785 0037 (Online)
DOI: http://dx.doi.org/10.15666/aeer/1704_74317438

MORPHOLOGICAL AND MOLECULAR IDENTIFICATION OF *CAPOETA TRUTTA* (CYPRINIDAE) AND *PLANILIZA ABU* (MUGILIDAE) FRESHWATER FISH IN SULAIMANI GOVERNORATE, IRAQ

ALI, M. K.[1*] – ABDULLAH, S. M. A.[2]

[1]*Department of Animal Science, College of Agricultural Science, University of Sulaimani, Sulaimani, Iraq*

[2]*Department of Fish and Aquatic Resource, College of Agriculture, University of Salahaddin, Erbil, Iraq*
(phone: +964-770-365-5545)

**Corresponding author*
e-mail: muqdad.ali@univsul.edu.iq

(Received 3rd Mar 2019; accepted 1st May 2019)

Abstract. The morphological similarities of species of *Capoeta* and *Planiliza* genera make the identification difficult in some cases. Thus, this classification should be confirmed by molecular examination. In this study, 150 specimens of *Capoeta trutta* (Cyprinidae) were collected from Dukan Lake and 120 specimens of *Planiliza abu* (Mugilidae) from Sirwan River in northwestern and southeastern Sulaimani Governorate, respectively. The two fish species recorded were native species. The DNA sequences of both species of fish (*C. trutta* and *P. abu*) were mitochondrial DNA cytochrome c oxidase subunit I (mtDNA COI) locus 617 bp with 61 cytochrome b (cytb) gene, partial cds; mitochondrial, 446 bp respectively. Following analysis the sequences were compared with sequences of other genera and fish species stored in GenBank. DNA sequencing results showed that studied species belong to *Capoeta trutta* and *Planiliza abu*. We conclude, in the view of the results of the present study, that DNA sequence analysis revealed and confirmed the validity of these two species.
Keywords: *fishes, morphometric measure and meristic, molecular examination, DNA sequencing, Iraq*

Introduction

Among the several families of freshwater fishes in the world the most diverse one is Cyprinidae having 220 genera including 2420 species, which belong to Cypriniformes order (Nelson, 2006). Most of Iraqi fish belong to Cyprinidae family, which involving 16 genera with 32 cyprinid species (Coad, 1998; Coad and Hussein, 2007). The distribution area of cyprinid genus *Capoeta* includes Western to Central Asia, such as Armenia, Azerbaijan, Afghanistan, Israel, Anatolia, Iraq, Uzbekistan, Georgia, and Iran (Banarescu, 1991). Genus *Capoeta* includes almost 10 species, 4 out of these occur in Iraq (Coad, 2010). The species commonly appear in streams and lakes, thus in both fast and slow flowing waters (Geldiay and Balik, 1996). *Capoeta trutta* (Heckel, 1843) is a fish species having economic importance with wide distribution in Turkey, Iran, Iraq and Syria (Gunduz et al., 2014), which is dominantly thriving in both the Euphrates and Tigris river systems (Geldiay and Balik, 2007).

The grey mullets or mullets were discovered world-wide in temperate to tropical coastal waters directly entering in estuaries and they are also resident in freshwaters. There are around 75 species and 20 genera in world (Nelson et al., 2016). In Iraq only four species are exist (Coad, 2010). *Planiliza abu* is a mugilid species discovered in

http://www.aloki.hu ● ISSN 1589 1623 (Print) ● ISSN 1785 0037 (Online)
DOI: http://dx.doi.org/10.15666/aeer/1704_74397451

channels, drains, lakes, reservoirs ponds, canals, rivers, and streams on fish farms with entering estuaries. Ozdilek (2003) and Kuru (1979) state that in Syria, Iraq, Pakistan, Turkey and Iran, mullet often occurs in inhabited places or schools. *Liza abu*, mugilid fish (Heckel, 1843), locally known as khisni, is distributed in all part of mid and south inland waters of Iraq (Al-Daham, 1984).

Fishes in the genera *Chelon*, *Ellochelon* and *Planiliza* were previously in the genus *Liza* (Jordan and Swain, 1884). Molecular data has caused a re-assessment that can be found in the literature (Durand et al., 2012*;* Nematzadeh et al., 2013; Xia et al., 2016). Various authors have or have not accepted, these generic replacements but the review of these opinions is beyond the scope of this paper. Most of the literature cited below refers to the species discussed under the genus *Liza* (except for *Mugil cephalus*) but the genus name has been changed in this text for consistency.

Nowadays via using characteristics other than morphological traits mullet species phylogenic relationships were determined based on molecular genetics and advanced techniques have been developed for studying DNAs in diverse populations and also for identifying fish species via using nuclear (nDNA) and mitochondrial (mtDNA) genomes (Semina et al., 2007; Avis, 1991; Papasotiropoulos et al., 2007). For the study of phylogenetic relationships and molecular systematic in population genetics the mtDNA is an efficient genetic marker due to maternal inheritance, and lesser mean rate of recombination, of replacement and exchange in mtDNA nucleotides than those in nDNA (Ghorashi et al., 2008; Asensio, 2007).

The morphological similarities of species of *Capoeta* and *Planiliza* genera make the identification difficult in some cases. Thus, the aim of this study is to confirm this classification by molecular examination.

Materials and methods

Description of study area

Dukan Lake is situated in north western Sulaimani City, Kurdistan Region, in the north of Iraq. It is approximately 76 km far from the city center (Shaban, 1980). According to Toma (2000) the lake has unregulated spillway at 515 m above sea level and full-pool operating altitude of 511 m, its boundaries extend between 34°17'N – 36°33'N latitude with 43°17'E – 46°24'E longitude (*Fig. 1*).

Sirwan River is situated in south eastern Sulaimani City. It is called Diyala in Arabic and Sirwan in Kurdish. It flows in western Iran from its headwaters in Zagros Mountains to south of Baghdad to its ultimate confluence with the Tigris River. The latitude of Sirwan River is 33° 13' 14.88" N and its longitude is 44° 30' 23.04" E (*Fig. 1*).

Sample collection

A total of 150 *Capoeta trutta* specimens have been collected from Dukan Lake in north western Sulaimani governorate and 120 individual of *Planiliza abu* were collected from Sirwan River in the Sulaimani governorate by fishermen using gill nets, during the period from November, 2017 until May 2018. Fish were transported with local river water in a cool box to laboratory.

http://www.aloki.hu ● ISSN 1589 1623 (Print) ● ISSN 1785 0037 (Online)
DOI: http://dx.doi.org/10.15666/aeer/1704_74397451

Figure 1. *Map of Iraq showing Dukan Lake and Sirwan River*

Morphometric measure and meristic study

The specimens were brought out of the cool box and the body length was measured using a one-meter measuring board graduated in millimetres (mm). The morphometric parameters were measured from left side of each specimen. According to Beckman (1962) and Coad (2010, 2017), morphometric characters and meristic were studied as shown in *Table 1*.

Extraction of DNA

Samples were taken from the liver of two fish species their identification by morphological characters only. Samples (20 mg) collected from the liver tissue samples were digested and homogenized, and stored in liquid nitrogen. According the protocol of AccuPrep® Genomic DNA extraction Kit (Bioneer Corporation Cat. No.: K-3032 Korea), genomic DNA was extracted.

Agarose gel (1%) electrophoresis used to assess and identify the quality of the extracted DNA.

PCR amplification

In *Capoeta trutta* to amplify mtDNA COI locus by Darabi (2014) viz., the following primer was used COI-625F: 5'-TCAACCAACCACAAAGACATTGGCAC-3' and COI-625 R: 5'-GACTTCTGGGTGGCCAAA-GAATCA-3' have been used in this study. Amplifications of DNA were performed using a thermal cycler (MultiGene OptiMax Thermal Cycler TC9610 /TC9610-230, Applied Bio systems, USA) with the

http://www.aloki.hu ● ISSN 1589 1623 (Print) ● ISSN 1785 0037 (Online)
DOI: http://dx.doi.org/10.15666/aeer/1704_74397451

final reaction volume of 25 µl. Each reaction contained prime *taq* premix (2X) Genet Bio PCR master mix (*Taq* DNA Polymerase 1 unit/10 µl, 20 mM Tris-HCl, 80 mM KCl, 4 mM MgCl2, enzyme stabilizer, sediment, loading dye, pH 9.0, 0.5 mM of each dATP, dCTP, dGTP, dTTP), primers (10 pmoles/µl), DNA template (40 ng) and water free DNase. Initial denaturation was carried out for 3 min at 95 °C, followed by 35 cycles of denaturation at 95 °C for 30 s; annealing at 62 °C for 30 s and extension at 72 °C for 45 s followed by a final extension at 72 °C for 10 min (Parmaksiz and Eksi, 2017).

Table 1. *Morphological characters and meristic abbreviations and description*

Abbreviations	Description
TL	Total length
SL	Standard length
HL	Head length
BD	Body depth
ED	Eye diameter
SnL	Snout length
Pre-O	Pre orbital distance
PrD	Pre dorsal fin distance
LD	Length of the dorsal-fin ray
Pre-Pectoral	Pre pectoral fin distance
Pre-Pelv	Pre pelvic fin distance
Pre-ans	Pre – anal distance
LA	Length of the anal-fin ray
ALL	Above lateral line scales
BLL	Below lateral line scales
PrD1	First pre dorsal fin distance
PrD2	Second pre dorsal fin distance

Primers have been used to amplify 61 cytochrome b (cytb) gene, partial cds; mitochondrial, primers designed from cytochrome b (cytb) gene GenBank: (JQ060190.1), F: CTGCATTCGTAGGCTATGTC and R: GTGCTAGAACCCCTCCTAGC for *Planiliza abu* fish. PCR was performed with a profile of initial denaturation at 95 °C for 5 min, followed by 40 cycles of denaturation at 95 °C for 30 s, annealing at 61 °C for 30 s, extension at 72 °C for 30 s and final extension at 72 °C for10 min.

Agarose gel electrophoresis separation

A volume of 10 µl PCR product on 2% agarose gel was electrophoresed. Ethidium bromide was used to stain bands, which were visualized on a gel documentation (ENDURO™ GDS Touch Gel Documentation System) by using 100 bp DNA ladder (gene direx). The ladder was supplied in a ready for using format having fluorescent tracking dyes and DNA stain. The expected size of the PCR amplicon was 625 bp for *Capoeta trutta* and 521 bp for *Planiliza abu*.

http://www.aloki.hu ● ISSN 1589 1623 (Print) ● ISSN 1785 0037 (Online)
DOI: http://dx.doi.org/10.15666/aeer/1704_74397451

DNA sequencing

A mitochondrial DNA cytochrome c oxidase subunit I (mtDNA *COI*) locus and cytochrome b (cytb) gene were amplified by PCR. In the present study, Genetic analyzer 3500, Applied Bio systems (USA) was used to find the nucleotides order of mtDNA *COI* and cytb for *C. trutta* and *P. abu* fish samples, respectively. The PCR product of the fish samples were used for sequence specific PCR amplification and sent to the Macrogen Company in South Korea for nucleotide sequence analyses.

Results

A total of 150 *Capoeta trutta* specimens were collected from Dukan Lake in north western Sulaimani governorate and 120 specimens of the *Planiliza abu* were collected from Sirwan River in south eastern Sulaimani governorate.

Morphology

The morphological characters and meristic of *Capoeta trutta* and *Planiliza abu* are indicated in *Table 2*. *Figures 2* and *3* show the general morphology of *Capoeta trutta* and *Planiliza abu*, respectively.

Table 2. *The results of morphological characters and meristic for Capoeta trutta (Heckel, 1843) and Planiliza abu (Heckel, 1843)*

Abbreviations	Range *Capoeta trutta*	Range *Planiliza abu*
TL	18-32 (25) cm.	14 - 21 (17.5) cm.
SL	15 -27.5 (21.25) cm.	12 -18 (15) cm.
HL	4-5 (4.5) cm	3 – 3.5 (3.25) cm
BD	4.5-7 (5.75) cm	4–5.5 (4.75) cm
ED	0.7 – 1.3(1) cm	0.8 – 0.9 (0.85) cm
SnL	0.9 – 1.5 (1.2) cm	1 cm
Pre-O	1.5-2 (1.75) cm	1 – 1.5 (1.25) cm
PrD	8 – 12.5 (10.25)	-
LD	3.2 – 5.5 (4.35) cm	2.5–3.5 (3) cm
Pre-Pectoral	4 – 5.5 (4.75) cm	4 – 4.5 (4.25) cm
Pre-Pelv	9.5 – 13 (11.25) cm	6 – 7 (6.5) cm
Pre-ans	14 – 20 (17) cm	11.5 – 13 (12.25) cm
LA	3-5 (4) cm	2 – 3 (2.5) cm
ALL	14-17	7
BLL	11-14	6
Number of barbels	One pair barbels on the upper jaw	No barbels
The pectoral fin ray length	3 – 3.8 (3.4) cm	2 – 2.8 (2.4) cm
PrD1	-	7 – 8 (7.5) cm
PrD2	-	11.5 – 13 (12.25)

http://www.aloki.hu ● ISSN 1589 1623 (Print) ● ISSN 1785 0037 (Online)
DOI: http://dx.doi.org/10.15666/aeer/1704_74397451

Figure 2. *Capoeta trutta*

Figure 3. *Planiliza abu*

DNA sequence

DNA extraction performed on 150 and 120 specimens for *Capoeta trutta* and *Planiliza abu,* respectively were successfully generated product containing DNA.

The result of the present study of sequencing DNA of two species of fish, were mtDNA *COI* locus in *Capoeta trutta* about 617 bp and cytochrome b (cytb) gene, partial cds; mitochondrial in *Planiliza abu* about 446 bp put to BLAST then compared with sequences of other genera and fish species stored in GenBank. The molecular study showed the presence of two species belonging to *Capoeta trutta* and *Planiliza abu*. BLAST results are indicated in *Table 3*.

Table 3. *The BLAST results of fish species*

No. Samples	Genus and species	Molecular based homology (%)
1	*Capoeta trutta*	100% identified homology
2	*Planiliza abu*	100% identified homology

Partial cds, Cytochrome oxidase subunit I (*COI*) gene mitochondrial and partial cds 61 cytochrome b (cytb) gene mitochondrial are compatible with the same sequence fragment marker, which is available at the GeneBank in the National Center for Biotechnology Information (NCBI). *Figures 4a, b* and *5a, b* showed pair wise analysis and partial sequence of the two fish specimens.

http://www.aloki.hu ● ISSN 1589 1623 (Print) ● ISSN 1785 0037 (Online)
DOI: http://dx.doi.org/10.15666/aeer/1704_74397451

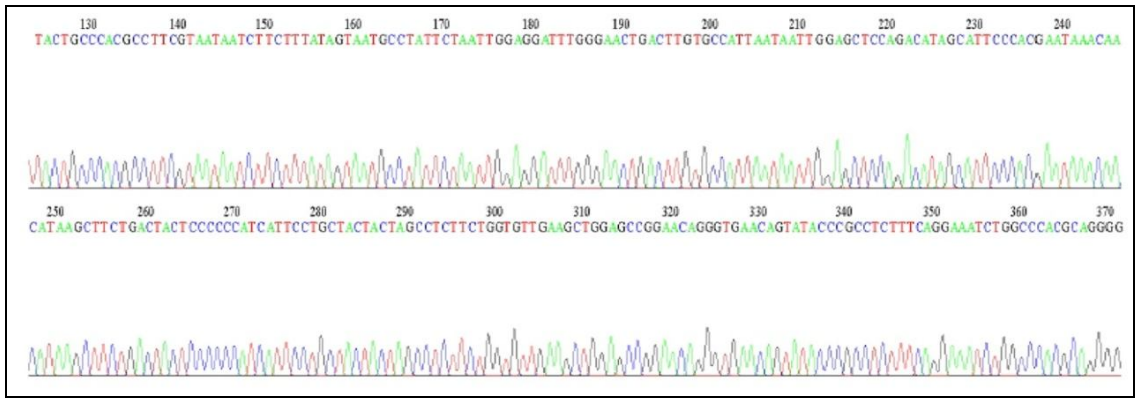

Figure 4a. *The partial sequencing result of partial cds, Cytochrome oxidase subunit I (COI) gene; of Capoeta trutta*

```
Query  37   TGGGCACTGCTTTAAGCCTTCTCATTCGAGCCGAATTAAGCCAACCCGGATCACTTCTAG  96
            ||||||||||||||||||||||||||||||||||||||||||||||||||||||||||||
Sbjct  29   TGGGCACTGCTTTAAGCCTTCTCATTCGAGCCGAATTAAGCCAACCCGGATCACTTCTAG  88
Query  97   GCGATGACCAAATTTATAATGTTATCGTTACTGCCCACGCCTTCGTAATAATCTTCTTTA  156
            ||||||||||||||||||||||||||||||||||||||||||||||||||||||||||||
Sbjct  89   GCGATGACCAAATTTATAATGTTATCGTTACTGCCCACGCCTTCGTAATAATCTTCTTTA  148
Query  157  TAGTAATGCCTATTCTAATTGGAGGATTTGGGAACTGACTTGTGCCATTAATAATTGGAG  216
            ||||||||||||||||||||||||||||||||||||||||||||||||||||||||||||
Sbjct  149  TAGTAATGCCTATTCTAATTGGAGGATTTGGGAACTGACTTGTGCCATTAATAATTGGAG  208
Query  217  CTCCAGACATAGCATTCCCACGAATAAACAACATAAGCTTCTGACTACTCCCCCCATCAT  276
            ||||||||||||||||||||||||||||||||||||||||||||||||||||||||||||
Sbjct  209  CTCCAGACATAGCATTCCCACGAATAAACAACATAAGCTTCTGACTACTCCCCCCATCAT  268
Query  277  TCCTGCTACTACTAGCCTCTTCTGGTGTTGAAGCTGGAGCCGGAACAGGGTGAACAGTAT  336
            ||||||||||||||||||||||||||||||||||||||||||||||||||||||||||||
Sbjct  269  TCCTGCTACTACTAGCCTCTTCTGGTGTTGAAGCTGGAGCCGGAACAGGGTGAACAGTAT  328
Query  337  ACCCGCCTCTTTCAGGAAATCTGGCCCACGCAGGGGCATCAGTAGACCTAACAATCTTCT  396
            ||||||||||||||||||||||||||||||||||||||||||||||||||||||||||||
Sbjct  329  ACCCGCCTCTTTCAGGAAATCTGGCCCACGCAGGGGCATCAGTAGACCTAACAATCTTCT  388
Query  397  CACTCCATCTGGCAGGTGTTTCATCAATCCTGGGAGCAATCAATTTCATTACTACAACTA  456
            ||||||||||||||||||||||||||||||||||||||||||||||||||||||||||||
Sbjct  389  CACTCCATCTGGCAGGTGTTTCATCAATCCTGGGAGCAATCAATTTCATTACTACAACTA  448
Query  457  TTAACATAAAACCCCCAGCCATTTCCCAATATCAAACACCCCTATTCGTCTGATCCGTGC  516
            ||||||||||||||||||||||||||||||||||||||||||||||||||||||||||||
Sbjct  449  TTAACATAAAACCCCCAGCCATTTCCCAATATCAAACACCCCTATTCGTCTGATCCGTGC  508
Query  517  TCGTAACCGCCGTGTTACTTCTTCTGTCACTACCCGTTCTAGCCGCTGGGATTACAATAC  576
            ||||||||||||||||||||||||||||||||||||||||||||||||||||||||||||
Sbjct  509  TCGTAACCGCCGTGTTACTTCTTCTGTCACTACCCGTTCTAGCCGCTGGGATTACAATAC  568
Query  577  TCCTAACAGACCGAAACCTCAACACCACATTCTTTGACCCCGCCGGAGGAGGAGACCCAA  636
            ||||||||||||||||||||||||||||||||||||||||||||||||||||||||||||
Sbjct  569  TCCTAACAGACCGAAACCTCAACACCACATTCTTTGACCCCGCCGGAGGAGGAGACCCAA  628
Query  637  TCCTCTACCAACACCTA  653
            |||||||||||||||||
Sbjct  629  TCCTCTACCAACACCTA  645
```

Figure 4b. *Pair wise alignment partial cds, Cytochrome oxidase subunit I (COI) gene of Capoeta trutta. Query is the study or sample sequence and Subject is the GenBank sequence*

http://www.aloki.hu ● ISSN 1589 1623 (Print) ● ISSN 1785 0037 (Online)
DOI: http://dx.doi.org/10.15666/aeer/1704_74397451

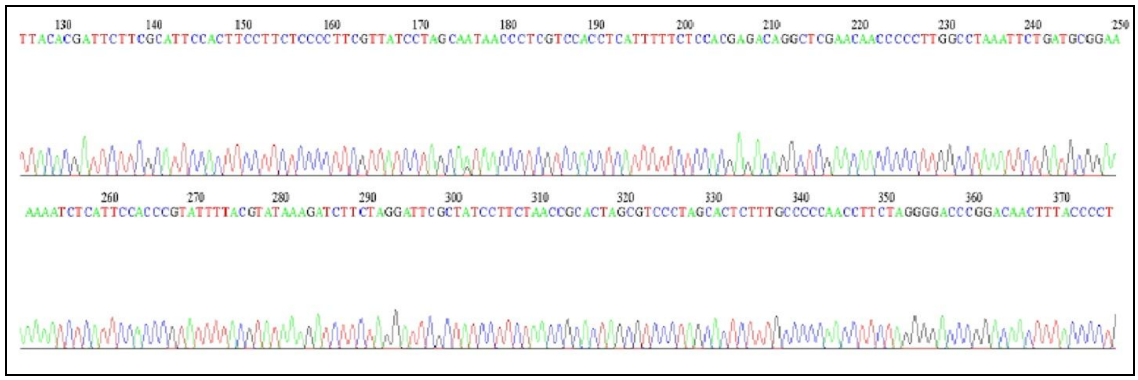

Figure 5a. *The partial sequencing result of Cytochrome oxidase subunit I (COI) gene, of Planiliza abu*

```
Query  27   GCGCCACCGTCATTACAAACCTCCTCTCTGCTGTTCCTTATATTGGAGACGCCCTTGTCC  86
            ||||||||||||||||||||||||||||||||||||||||||||||||||||||||||||
Sbjct  329  GCGCCACCGTCATTACAAACCTCCTCTCTGCTGTTCCTTATATTGGAGACGCCCTTGTCC  388
Query  87   AATGAATTTGAGGCGGCTTCTCAGTAGATAATGCTACCCTTACACGATTCTTCGCATTCC  146
            ||||||||||||||||||||||||||||||||||||||||||||||||||||||||||||
Sbjct  389  AATGAATTTGAGGCGGCTTCTCAGTAGATAATGCTACCCTTACACGATTCTTCGCATTCC  448
Query  147  ACTTCCTTCTCCCCTTCGTTATCCTAGCAATAACCCTCGTCCACCTCATTTTTCTCCACG  206
            ||||||||||||||||||||||||||||||||||||||||||||||||||||||||||||
Sbjct  449  ACTTCCTTCTCCCCTTCGTTATCCTAGCAATAACCCTCGTCCACCTCATTTTTCTCCACG  508
Query  207  AGACAGGCTCGAACAACCCCCTTGGCCTAAATTCTGATGCGGAAAAAATCTCATTCCACC  266
            ||||||||||||||||||||||||||||||||||||||||||||||||||||||||||||
Sbjct  509  AGACAGGCTCGAACAACCCCCTTGGCCTAAATTCTGATGCGGAAAAAATCTCATTCCACC  568
Query  267  CGTATTTTACGTATAAAGATCTTCTAGGATTCGCTATCCTTCTAACCGCACTAGCGTCCC  326
            ||||||||||||||||||||||||||||||||||||||||||||||||||||||||||||
Sbjct  569  CGTATTTTACGTATAAAGATCTTCTAGGATTCGCTATCCTTCTAACCGCACTAGCGTCCC  628
Query  327  TAGCACTCTTTGCCCCCAACCTTCTAGGGGACCCGGACAACTTTACCCCTGCAAACCCCC  386
            ||||||||||||||||||||||||||||||||||||||||||||||||||||||||||||
Sbjct  629  TAGCACTCTTTGCCCCCAACCTTCTAGGGGACCCGGACAACTTTACCCCTGCAAACCCCC  688
Query  387  TAGTCACCCCACCCCACATCAAGCCCGAATGATATTTCCTCTTTGCATACGCTATTCTCC  446
            ||||||||||||||||||||||||||||||||||||||||||||||||||||||||||||
Sbjct  689  TAGTCACCCCACCCCACATCAAGCCCGAATGATATTTCCTCTTTGCATACGCTATTCTCC  748
Query  447  GCTCCATCCCCAACAAGCTAGGAGGG  472
            |||||||||||||||||||||||||
Sbjct  749  GCTCCATCCCCAACAAGCTAGGAGGG  774
```

Figure 5b. *Pair wise alignment of partial cds, Cytochrome oxidase subunit I (COI) gene of Planiliza abu. Query is the study or sample sequence and subject is the GenBank sequence*

http://www.aloki.hu ● ISSN 1589 1623 (Print) ● ISSN 1785 0037 (Online)
DOI: http://dx.doi.org/10.15666/aeer/1704_74397451

Discussion

Traditionally, in the freshwaters of Iraq, four species (*Capoeta aculeata*, *Capoeta barroisi*, *Capoeta damascina* and *Capoeta trutta*) represent the genus *Capoeta* and four species (*Liza abu*, *Liza klunzingeri*, *Liza oligolepis* and *Liza subviridis*) represent the genus *Liza* (Coad, 2010).

The presences of two species of fish in this study are showed belonging to the family of Cyprinidae and Mugilidae. The description and measurement of present samples of two fish species in this study are similar to those received from Beckman (1962) and Coad (2010).

As a comparison between some characteristics of *Capoeta trutta* in this study such as standard length, total length, body depth, head length, eye diameter, length of the dorsal-fin ray, snout length, length of the anal-fin ray, above lateral line scales and below lateral line scales are 25, 21.25, 4.5, 5.75, 1, 1.2, 4.35, 4, (14-17) and (11-14), respectively are in agreement with the results of Agha (2017), which are 28.18, 23.74, 4.86, 5.7, 0.76, 1.5, 4.98, 3.6, (15-16) and (10-11).

Standard length, total length, body depth, head length, eye diameter, length of the dorsal-fin ray, snout length, length of the anal-fin ray, above lateral line scales and below lateral line scales of *Planiliza abu* in this study are 17.5, 15, 3.25, 4.75, 0.85, 1, 7 and 6, respectively are in agreement with the results of Agha (2017), which are 18.38, 16, 3.53, 4.45, 0.75, 1, 7, 6.

The morphological results of *Planiliza abu* in this study are similar to the results of Khayyami et al. (2014) on morphological variability of *Liza abu* and Mohamed et al. (2016) on comparative taxonomical for (*Planiliza subviridis*, *P. klunzingeri*, *P. carinata* and *Osteomugil speigleri*). Standard length of *Planiliza abu* in this study is in agreement with the results of Mohamed et al. (2018)**.**

In Iraq, there has not been any molecular research on *Capoeta trutta* and *Planiliza abu*, but Cyprinidae and Mugilidae families have been examined. The results of *Capoeta trutta* in family Cyprinidae in this study are in agreement with the results of Faddagh et al. (2012a) who identified eight cyprinid fish species, and discovered high similarity between *Barbus* species, from 84.4% between *B. Kersin* and *B. xanthopterus* to 52% between *B. sharpeyi* and *B. barbulus* to 86.9% between *A. vorax* and *B. grypus.* Faddagh et al. (2012b) also used the mitochondrial 16S rRNA gene fragment as a molecular marker to study taxonomical status of seven cyprinin fish species in Iraqi inland waters: *Barbus kersin*, *B. xanthopterus*, *B. barbulus*, *B. sharpeyi*, *B. grypus*, *Cyprinus carpio* and *C. luteus,* the results assured that the six *Barbus* species genetically belong to sub-family Cyprininae which belong to family Cyprinidae. Aziz (2015) examined nine species of Cyprinidae family, the result of DNA sequencing showed that all species belong to family Cyprinidae the phylogenetic relationship degree with this family for *C. luteus* was a BP of 87%, for *C. regium*, *C. carpio* and *C. Carassius* was a BP of 75%, for *C. macrostomum*, *L. esocinus*, *C. trutta* and *L. xanthopterus*a was a BP of 90% and for *Barbus grypus* was a BP of 76%.

In this study the results are in agreement with Parmaksiz and Eksi (2017) who used mtDNA *COI* 625 locus to study the genetic diversity of populations from 47 samples of *Capoeta trutta.* The result of sequence analysis showed six polymorphic sites and seven haplotypes on that locus, which is also in agreement with Turan (2008) determination of subspecies of *Capoeta* corresponding to taxonomic entities and defined species using traditional gene sequencing of mitochondrial 16S rDNA. The database included 124 variable sites, parsimony informative was 103 sites. The results in this study are similar

http://www.aloki.hu ● ISSN 1589 1623 (Print) ● ISSN 1785 0037 (Online)
DOI: http://dx.doi.org/10.15666/aeer/1704_74397451

to the results of Zareian et al. (2016) who used mitochondrial cytochrome *b* gene sequences for phylogenetic relationship of *Capoeta* species, and it was found that three major groups were detected: Clade I: *Capoeta trutta* group which is the Mesopotamian *Capoeta* group having very close related taxa (*barroisi*, *trutta and turani)*. Clade II: *Capoeta damascina* complex group (*capoeta* group small scale) including the Anatolian-Iranian groups such us (*buhsei*, *saadii*, *banarescui* and *damascina*) and widespread highly diversified groups. Clade III comprises closely related taxa; *Capoeta capoeta* complex group (the Aralo-Caspian group, large scale *capoeta* group).

The results in this study are in agreement with Nematzadeh et al. (2013) using PCR-sequencing method to establish phylogenetic relationships among six mugilidae species (*M. capito*, *Valamugil buchanani*, *Mugil cephalus*, *Liza subviridis*, *L. saliens* and *L. aurata)* and genetic differences were determined. The results demonstrate that in the mitochondrial 16s rRNA genome number of bases was approximated 600 base pairs. Also (Lai et al., 2011) (80) random primers for random amplified polymorphic DNA (RAPD) were used for the examination of 15 fish families. Results clarify that in the Mugilidae family a novel specific PCR product was found, OPAV04 primer was employed also in the *Liza* genus, by using OPAV10 primer other novel specific PCR product was found.

The results of the present study are not in agreement with Faddagh et al. (2012b the *Liza abu* and *Liza klunzingeri* did not respond to the modified primer in mitochondrial 16S rRNA gene but in this study *Planiliza abu* responded to the cytochrome b (cytb) gene, partial cds; mitochondrial.

This taxonomic position has changed and most researchers in the field now agree that DNA coding is a useful tool in the process of identifying and indexing species. There are still researchers who doubt that one can distinguish the gene of all species and refers to the fact that taxonomists who evaluate their findings on morphological basis have a range of many different characters, not one, to help them identify, for this the present study used a molecular tool for identification. Molecular techniques such as PCR and DNA sequencing were proven to be very specific and highly sensitive to detect species of fish. However, using them in diagnostic laboratories are very rare.. Moreover, DNA amplification is not cheap and it is tedious, also samples can face cross contamination which is dangerous, fortunately nowadays by developed methods these issues are decreased (Agha, 2017).

In the present study, 617 and 446 bp were aligned for *Capoeta trutta* and *Planiliza abu* respectively; the two specimens were morphologically identified by using Coad keys. The sequences compared with sequences of other genera and fish species stored in Gen Bank. The results showed that the morphometric data and molecular methods were successful in identifying of *C. trutta* and *P. abu*.

Samples of *Capoeta trutta* and *Planiliza abu* have been morphologically identified. DNA sequencing results showed that the studied two fish species belong to *Capoeta trutta* and *Planiliza abu.* Gen Bank analysis indicated that the two sequenced species were correctly identified.

Conclusions

In the view of the results of the present study, *Capoeta trutta* and *Planiliza abu* were morphologically identified. The results of DNA sequencing revealed and confirmed the

http://www.aloki.hu ● ISSN 1589 1623 (Print) ● ISSN 1785 0037 (Online)
DOI: http://dx.doi.org/10.15666/aeer/1704_74397451

validity of the two fish species and indicated that the two sequenced species were correctly identified by using *COI* and cytochrom b gene.

Acknowledgements. A special thanks to Asst. Prof. Dr. Bahzad Hama Salih Mustafa the Head of Animal Science Department for his continuous help during the study.

REFERENCES

[1] Agha, G. F. (2017): Morphological and molecular identification of some inhabitant fishes in greater Zab River/Aski-Kalak in Kurdistan Region, Iraq. – M.Sc. Thesis, College of Agriculture, University of Salahaddin, Arbil, Iraq.
[2] AL-Daham, N. K. (1984): Fishes of Iraq and the Arab Gulf, Vol. 3, Perciformes (Mugiloidei) to Tetraodontiformes. – Basrah University Press, Basrah (in Arabic).
[3] Asensio, L. G. (2007): PCR-based methods for fish and fishery products authentication. – Food Science &Technology Journal 18: 558-568.
[4] Avis, J. C. (1991): Molecular Markers, Natural History and Evolution. – Chapman and Hall, New York.
[5] Aziz, D. M. A. (2015): Comparative hemato-biochemical profiles and phylogenetic study of some Cyprinids in Dukan Lake, Kurdistan. – Master of Science Thesis, College of Science, University of Salahaddin, Arbil.
[6] Banarescu, P. (1991): Zoogeography of Fresh Waters. Distribution and Dispersal of Freshwater Animals in North America and Eurasia. Vol. 2. – Aula-Verlag, Wiesbaden.
[7] Beckman, W. C. (1962): The Freshwater Fishes of Syria and Their General Biology and Management. – Fisheries Biology Branch Technical Paper. FAO, Rome.
[8] Coad, B. W. (1998): Systematic biodiversity in the freshwater fishes of Iran. – Ital. J. Zool. 65: 101-108.
[9] Coad, B. W., Hussain, N. A. (2007): First record of the exotic species Hemiculter leucisculus (Actinopterygii: Cy-prinidae) in Iraq. – Zoology in the Middle East 40: 107-109.
[10] Coad, B. W. (2010): Freshwater Fishes of Iraq. – Pensoft Series Faunistica, 93. Pensoft, Moscow.
[11] Coad, B. W. (2017): Freshwater Fishes of Iran. – www.braincoad.com.
[12] Darabi, A. R., Kashan, N., Fayazi, J., Aminafshar, M., Chamani, M. (2014): Investigation of phylogenetic relationship among two *Barbus* species (*Cyprinidae*) populations with mitochondrial DNA using PCR sequencing. – IJBPAS 4(2): 302-311. DOI: 10.12692/ijb/5.2. 41-46.
[13] Durand, J –D., Shen, K-N., Chen, W.-J., Jamandre, B. W., Biel, H., Diop, K., Nirchio, M., Garciade león, F. J., Whitfield, A. K., Chang, C.-W., Borsa, P. (2012): Systematics of the grey mullets (Teleostei: Mugiliformes: Mugilidae): Molecular phylogenetic evidence challenges two centuries of morphology based taxonomy. – Molecular Phylogenetics and Evolution 64(1): 63-92.
[14] Faddagh, M. S., Hussain, N. A., AL-Badran, A. I. (2012a): DNA fingerprinting of eight cyprinid fish species of Iraqi inland waters using RAPD-PCR technique. – Advances in Life Sciences 2(2): 9-16.
[15] Faddagh, M. S., Hussain, N. A., AL-Badran, A. I. (2012b): Usage mitochondrial 16S rRNA gene as molecular marker in taxonomy of Cyprinin fish species (Cyprinidae: Teleostei). – JKAU: Mar. Sci. 23(1): 39-49.
[16] Geldiay, R., Balik, S. (1996): Turkiye Tatlısu Balıkları. – Ege Unv. Fen Fak. Kitaplar Serisi No: 46, Ege Universitesi Basımevi, İzmir, 532.
[17] Geldiay, R., Balik, S. (2007): Turkiye Tatlisu Balıkları. – Ders Kitabı, Ege Universitesi BasımEvi. 97: 250.

http://www.aloki.hu ● ISSN 1589 1623 (Print) ● ISSN 1785 0037 (Online)
DOI: http://dx.doi.org/10.15666/aeer/1704_74397451

[18] Ghorashi, S. A., Fatemi, S. M., Amini, F., Houshmand, M., Salehitabar, R, Hazaie, K. (2008): Phylogenetic analysis of anemone fishes of the Persian Gulf using mtDNA sequences. – African Journal of Biotechnology 7(12): 2074-2080.
[19] Gunduz, F., Coban, M. Z., Yuksel, F., Demirol, F., Kurtoglu, M., Yildiz, N. (2014): Uzuncayır Baraj Golu'ndeki (Tunceli) *Capoeta trutta* (Heckel, 1843) 'nınBazı Populasyon Parametreleri. – Yunus Araştırma Bülteni 2: 3-14. DOI: 10.1 7693/yunusae.vi.235393.
[20] Heckel, J. J. (1843): Abbildungen und Beschreibungen der Fische Syriens nebst einer neuen Classification und Characteristiks sämmtlicher Gattungen der Cyprinen Süsswasser-Fische Syriens. – Schweizerbart, Stuttgart.
[21] Jordan, D. S., Swain, J. (1884): A review of the American species of marine Mugilidae. – Proceedings of the United States National Museum 7(434): 261-275.
[22] Khayyami, H., Movahedinia, A., Zolgharnein, H., Salamat, N. (2014): Morphological variability of *Liza abu* (Heckel, 1843) from Northwestern part of the Persian Gulf. – World Journal of Fish and Marine Sciences 6(5): 386-394.
[23] Kuru, M. (1979): The Freshwater fish of South-Eastern Turkey-2 (Euphrates-Tigris System). – Hacettepe Bulletin of Natural Sciences and Engineering 7: 105-114.
[24] Lai, S., Wang, Y., Yang, K., Chen, C., Huang, M. (2011): Novel family- an genus specific DNA markers in Mugilidae. – African Journal of Biotechnology 10(59): 12722-12728.
[25] Mohamed, A. M., Abood, A. N., Hussein, S. A. (2016): Comparative taxonomical study of four mullet species (Mugiliformes: Mugilidae) from Iraqi marine waters, Arabian Gulf. – Basrah J. Agric. Sci. 29 (2): 11-20.
[26] Mohamed, A. M., Abood, A. N., Hussein, S. A. (2018): Taxonomical study of *Planiliza abu* in Qarmat Ali River, Iraq. – Scientific Journal of King Faisal University, Basic and Applied Sciences 19(1).
[27] Nelson, J. S. (2006): Fishes of the World. – John Wiley & Sons, Inc, Hoboken. http://en.wikipedia.org/wiki /Cyprinid.
[28] Nelson, J. S., Grande, T. C., Wilson, M. V. H. (2016): Fishes of the World. Fifth Ed. – John Wiley & Sons, Hoboken.
[29] Nematzadeh, M., Rezvani, S., Khalesi, M. K., Laloei, F., Fahim, A. A. (2013): Phylogeny analysis on six mullet species (Teleosti: Mugillidae) using PCR-sequencing method. – Iranian Journal of Fisheries Sciences 12(3): 669-679.
[30] Özdilek, Ş. Y. (2003): Occurrence of the Abu mullet, Liza abu (Heckel, 1843) (Pisces, Mugilidae), in the Orontes River. – Zoology in the Middle East 30: 111-113.
[31] Papasotiropoulos, V., Klossa-Kilia, E., Alahiotis, S., Kilias, G. (2007): Molecular phylogeny o Grey Mullets (Teleostei: Mugilidae) in Greece: evidence from sequence analysis of mtDNA segments. – Biochem. Genet. 45: 623-636.
[32] Parmaksiz, A., Eksi, E. (2017): Genetic diversity of the cyprinid fish *Capoeta trutta* (Heckel, 1843) populations from Euphrates and Tigris rivers in Turkey based on mtDNA *COI* sequences. – Indian J. Fish 64(1): 18-22.
[33] Semina, A. V., Polyakova, N. E., Barykov, V. A. (2007): Analysis of mitochondrial DNA: taxonomic and phylogenic relationships in two fish taxa (pisces: Mugilidae and Cyprinidae). – www.ncbi.nlm.nih.gov/pubmed/18205618.
[34] Shaban, A. A. G. (1980): An ecological study on phytoplankton in Dokan Lake. – M.Sc. Thesis. University of Salahaddin, Arbil, Iraq.
[35] Toma, J. J. (2000): Limnological study of Dokan Lake, Kurdistan region of Iraq. – M.Sc. Thesis. University of Salahaddin, Arbil, Iraq.
[36] Turan, C. (2008): Molecular systematic of the *Capoeta* (Cypriniformes: Cyprinidae) species complex inferred from mitochondrial 16S rDNA sequence data. – Acta Zoologica Acracoviensia 51A (1-2): 1 14.

http://www.aloki.hu ● ISSN 1589 1623 (Print) ● ISSN 1785 0037 (Online)
DOI: http://dx.doi.org/10.15666/aeer/1704_74397451

[37] Xia, R., Durand, J-D., Fu, C. (2016): Multi locus resolution of Mugilidae phylogeny (Teleostei: Mugiliformes): implications for the family's taxonomy. – Molecular Phylogenetics and Evolution 96: 161 177.
[38] Zareian, H., Esmaeili, H., Heidari, A., Khoshkholgh, M., Mousavi-Sabet, H. (2016): Contribution to the molecular systematic of the genus Capoeta from the south Caspian Sea basin using mitochondrial cytochrome b sequences (Teleosstei: Cyprinidae). – Molecular Biology Research Communications 5(2): 65-75.

http://www.aloki.hu ● ISSN 1589 1623 (Print) ● ISSN 1785 0037 (Online)
DOI: http://dx.doi.org/10.15666/aeer/1704_74397451

COMPARISON OF COLOR AND ATTRACTANT TRAPS EFFECT USED FOR SAMPLING APPLE BLOSSOM BEETLE (*TROPINOTA HIRTA* (PODA, 1761) (COLEOPTERA, SCARABAEIDAE, CETONIINAE))

AYDIN, G.[1*] – YAŞAR, B.[2]

[1]*Atabey Vocational School, Isparta University of Applied Science, 32670 Atabey, Isparta, Turkey*

[2]*Plant Protection Dept, Agricultural Faculty, Isparta University of Applied Science, Isparta, Turkey*

**Corresponding author*
e-mail: gokhanaydin@isparta.edu.tr; phone: +90-507-672-5309

(Received 4th Mar 2019; accepted 1st May 2019)

Abstract. This study was carried out to determine the most appropriate trap design for monitoring *Tropinota hirta* (Poda, 1761) (Coleoptera: Cetoniidae) among the commonly used traps in the world during the 2018. For this purpose, cherry gardens with three different loc. Atabey district, İslamköy and Pembeli villages of Isparta province were selected and the adult catch rates of the known binary attractant mixture (cinnamyl alcohol (3-phenyl-2-propen-1-ol) and transanethole [(1-methoxy-4-(1-propenyl) benzene)]) and white, light and dark blue color traps were compared with each other during the blooming period. As a result of the present study, the amount of adult catch of light blue color traps in the cherry blooming period was found to be significantly higher than the attractant and dark blue color traps which are regularly used in the world hence the use of this mentioned trap was found as the most effective biotechnical method for the controlling of *T. hirta* among the frequently used traps.
Keywords: *apple blossom beetle, attractant traps, cherry, color traps, Isparta*

Introduction

Apple blossom beetle has been expressed in the INPN which is the reference information system for data related to Nature (INPN) (https://inpn.mnhn.fr/accueil/a-propos-inpn) as *Tropinota hirta* (Poda, 1761) (Coleoptera: Cetoniidae) however the species every so often expressed as *Epicometris (Tropinota) hirta* (Poda, 1761) (57 scientific articles), *Tropinota* (*Epicometris*) *hirta* (33 scientific articles), *E. hirta* (11) and or *T. hirta* (12) and sometimes even expressed as under the family of Scarabaeidae instead of Cetoniidae.

Adults of *T. hirta* is polifagous and causing serious damage through feeding on pistils and stamens of the flowers of numerous plants such as apple, barley, blackberry, blackcurrant, broomrape, canola, cherry, lupine, narcissus, pear quince, plum, raspberry, rye, tulip, wheat, and other plants of agricultural importance even ornamental plants (Milenkovic and Stanisavljevic, 2003; Çetin et al., 2006; Ertop and Özpınar, 2011; Perez and Traveset, 2011). *T. hirta* may damage 70% of the blossoms on some plants of agricultural importance (Kutinkova and Andreev, 2004; Ražov et al., 2009). Control of *T. hirta* is difficult since most of the pesticide cannot applied during blooming period without affecting beneficial organisms that provide pollination, specially honey bees (Vuts et al., 2011a, b). Besides, long-acting pesticides also have an adverse effect on exports. Therefore, the application of biotechnical methods to control of the mentioned

http://www.aloki.hu ● ISSN 1589 1623 (Print) ● ISSN 1785 0037 (Online)
DOI: http://dx.doi.org/10.15666/aeer/1704_74537462

pest will be extremely beneficial both in terms of environment and human-animal health. Recent studies show that the most recommended biotechnical methods are color traps and color with attractant against *T. hirta* which is widespread in parts of Eurasia, from the Mediterranean to the Middle East and Central Asia. Baits have been used as biotechnical method to control and monitoring of *T. hirta* and it has been mostly prepared with *cinnamyl alcohol* (3-*phenyl*-2-*propen*-1-*ol*) and *transanethole* [(1-*methoxy*-4-(1-*propenyl*) *benzene*)] which compounds are common flower scent constituents by a 1:1 mixture (Knudsen et al., 1993).

Lot of valuable research have been conducted on controlling of *T. hirta* however it has been found that the results of scientific studies on the best biotechnical methods to be used for *T. hirta* have not corresponded with each other. Therefore the present study was conducted in order to find out the most suitable biotechnical methods for *T. hirta*.

Materials and methods

The study was carried out in cherry blooming period between April 30 and May 14 to compare efficiency of attractant (cinnamyl alcohol and transanethole) and color traps (dark blue, light blue and white) for sampling adults of apple blossom beetle adults during 2018.

Localities

Three different locations; (Atabey district (a: loc.1), (37°56'48.58"N/30°39'5.16"E) Pembeli (p: loc.2) (37°56'20.07"N/30°41'12.60"E) and İslamköy (i: loc.3) (37°54'51.77"N/30°39'14.76"E) villages in Isparta province, Turkey) were selected for the study. While color traps were placed in each locations with 10 pieces (3 colors × 10 pieces × 4 locations = 120 units), attractant traps were set up in Atabey district with 10 pieces.

Traps

Ten attractive traps (A) were placed on the cherry branches which are approximately 2 m high from the ground for the purpose of sampling of the adults of *T. hirta* in the cherry orchard in Atabey district, Isparta province, Turkey. Three different colors (hex code are inside brackets), light blue (LB) (#87CEFA), dark blue (DB) (#1E90FF), and white (W) (#FFFAF0), and 10 pieces for each one, were set up for three cherry orchards in Atabey, Pembeli and İslamköy (Isparta province). The ratios of *T. hirta* adults sampled from attractants and color traps were compared during the blooming period.

Baits were prepared with *cinnamyl alcohol* (3-*phenyl*-2-*propen*-1-*ol*) and *transanethole* [(1-*methoxy*-4-(1-*propenyl*) *benzene*)] by a 1:1 mixture according to the suggestions of Tóth et al. (2004) and Schmera et al. (2004) suggestions to catch *T. hirta*. A total of 10 units of cottons prepared in equal length were impregnated with attractive (1:1 mixture-20 µl) and placed inside the perforated (20 pieces with a diameter of 0.3 mm) falcon tubes (50 ml). Falcon tubes (3 × 13 cm length) with lures fixed with upside part of the light blue funnels (22 cm diameters and 25 cm length). Five liters (approx. 1.32 gallon) of plastic water containers which placed at the bottom of the funnels were used as traps to collect adults of apple blossom beetles. Totally 10 attractant traps prepared as mentioned above were hung tree branches nearly 2 meters

http://www.aloki.hu ● ISSN 1589 1623 (Print) ● ISSN 1785 0037 (Online)
DOI: http://dx.doi.org/10.15666/aeer/1704_74537462

above from the ground where the traps were a location representing the cherry garden. These attractive traps were placed only in Atabey district.

Color traps were designed as 25 cm in diameter and 10 cm in depth plastic basins. The order of colored traps were changed incidentally and set up 10 pieces for each locations. The distance between color traps were about one meter within a block and each block were set up 50 m distant from the next. 1/3 water was filled into the color traps to prevent adult of *T. hirta* from escaping. Blocks containing 3 traps with the above colors, were replicated 10 times, in the cherry orchard at each of the 3 locations. Each block the colors were distributed randomly hence the total number of traps was 90. Traps were set up on the soil surface in sunny places within the cherry orchards.

Both attractant and color traps were checked daily and the captured adults were counted and recorded.

Data analysis

All data from both adult numbers for each traps and groups of traps were analysed using ANOVA (one-way analysis of variance) and separated by Tukey's HSD (honestly significant difference) test at $P < 0.05$ to examine the differences between capture capability of attractant and color traps in SPSS.

Cluster analysis was performed using percent similarity and dendrogram based on the data was constructed with the help of MVSP software using the unweighted pair group method of arithmetic mean (UPGMA).

Results

It was found out that the number of individuals caught with color traps was found higher than individuals caught with attractant traps and differences was found out statistically significant. It was also compared the effects of the color traps with each other during the sampling adults of *T. hirta*. Light blue color traps were sampled more adults than the dark blue color traps.

Totally 776 individuals of *T. hirta* adults were sampled by attractant and color traps during the present study. The most of the proportion of *T. hirta* adults were caught by LB traps at Atabey, Pembeli, and Islamköy with 152, 136, and 126 individuals respectively. This means; nearly half of the specimens were sampled with LB traps at three loc. (Average: 138; individuals; proportion: 43.58%). The lowest of individuals were sampled by W traps at loc.1, loc.2, and loc.3 8, 12, and 11 respectively (Average: 10.33 individuals; proportion: 3.26%). Average of sampled adults of *T. hirta* were found similar with attractant and DB traps, with 87.0 and 81.3, respectively (Proportion: 27.47% and 25.68% respectively).

Capture rates of *T. hirta* adults with W set up at loc.1; loc.2, and loc.3 were found statistically different from the captures of other traps (*Table 1*).

It was determined that the least attractive trap for the adults of apple blossom beetle was W while the most attractive one was LB. Although no statistical differences were found between LBi with A, the adult capture averages of LBa and LBp were found statistically different from all other traps (*Table 1*). A was found not statistically significant with all DB traps at loc.1, loc.2, and loc.3 (*Table 1*).

Traps with the same color were grouped in terms of ease of understanding capture rates differences between color and attractant traps. Result of the capture means of all traps were given in *Table 2*.

http://www.aloki.hu ● ISSN 1589 1623 (Print) ● ISSN 1785 0037 (Online)
DOI: http://dx.doi.org/10.15666/aeer/1704_74537462

Table 1. *Comparison of capture rates of T. hirta adults sampled by attractant and color traps at loc.1., loc. 2, and loc. 3 in Isparta province*

Traps*	N	Mean ± Std. error	Std. deviation
Aa	10	8.7 ± 0.84 bc**	2.6687
LBa	10	15.2 ± 1.85 d	5.8652
DBa	10	8.6 ± 0.65 bc	2.0656
Wa	10	0.8 ± 0.25 a	0.7888
LBp	10	13.6 ± 1.34 d	4.2216
DBp	10	8.8 ± 0.74 bc	2.3476
Wp	10	1.2 ± 0.42 a	1.3166
LBi	10	12.6 ± 0.73 cd	2.3190
DBi	10	7.0 ± 0.67 b	2.1082
Wi	10	1.1 ± 0.31 a	0.9944

*A: Attractant; LB: Light Blue; DB: Dark Blue; W: White; a: loc. 1 (Atabey); p: loc. 2 (Pembeli); i: loc. 3 (Islamköy)
**According to a Tukey HSD test; means with the same letter in their superscript are not significantly different ($P < 0.05$)

Table 2. *Comparison of capture rates of T. hirta adults sampled by attractant and grouped color traps (values obtained from the same color were combined)*

Traps*	N	Mean ± Std. error	Std. deviation
Aa	10	8.7 ± 0.84 b	2.669
LB	30	13.8 ± 0.80 c	4.366
DB	30	8.13 ± 0.41 b	2.255
W	30	1.03 ± 0.19 a	1.033

*A: Attractant; LB: Light Blue; DB: Dark Blue; W: White; a: loc. 1 (Atabey); p: loc. 2 (Pembeli); i: loc. 3 (İslamköy)
**According to a Tukey HSD test; means with the same letter in their superscript are not significantly different ($P < 0.05$)

ANOVA test of data showed that no difference was found between the capture rates of A and DB traps ($P = 0.949$) however capture rates differences between them and the other traps (DB and W) were considered statistically significant (*Table 2*). The differences of catch proportions between DB-W and DB-LB traps were also found statistically significant ($P \leq 0.000$) (*Table 2*).

The dendrogram composed from the insect numbers sampled in all the set traps distinctly showed that all the same colors come together as a group while attractant trap was included with the DB color group (*Fig. 1*). Besides similarity values of A and DBa was found 90.17% as the most similar traps. It was seen that three main groups, W, LB, and DB with A were formed on the dendrogram. The similarity values of Wa and Wi traps captured by the least number of adults were seen as 63.15% (*Fig. 1*). Similarity values of Wp and the group formed by Wa and Wi was found 36.74% as the most dissimilar. The group formed by W traps at three localities showed 13.7% similarity with the group designed by all other traps, LB, DB, and A.

The following dendrogram is better at explaining dissimilarities and also shows statistically significant grades between groups. It was seen that A and DB traps were

http://www.aloki.hu ● ISSN 1589 1623 (Print) ● ISSN 1785 0037 (Online)
DOI: http://dx.doi.org/10.15666/aeer/1704_74537462

similar to each other by 84% while LB trap was found similar with this mentioned group by 74.9% (*Fig. 2*). W was equivalent to only with 19.2% of all other groups.

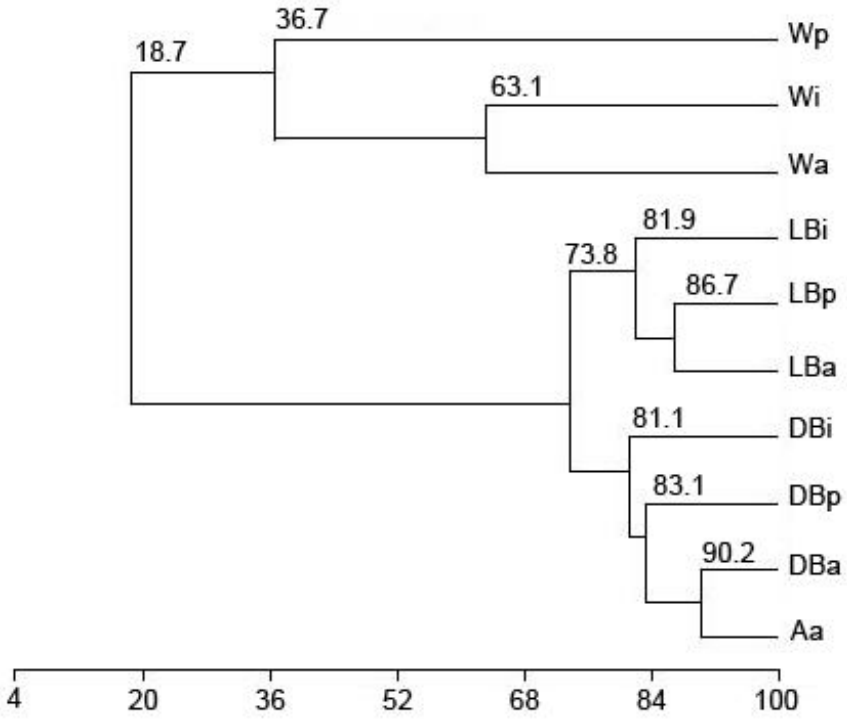

Figure 1. *Dendrogram of sampled T. hirta adults from the 9 colors and one attractant traps (A: Attractant; LB: Light Blue; DB: Dark Blue; W: White) in study locations (a: Atabey (loc. 1); p: Pembeli (loc. 2); i: İslamköy (loc. 3)). The cluster analysis was performed using Percent similarity*

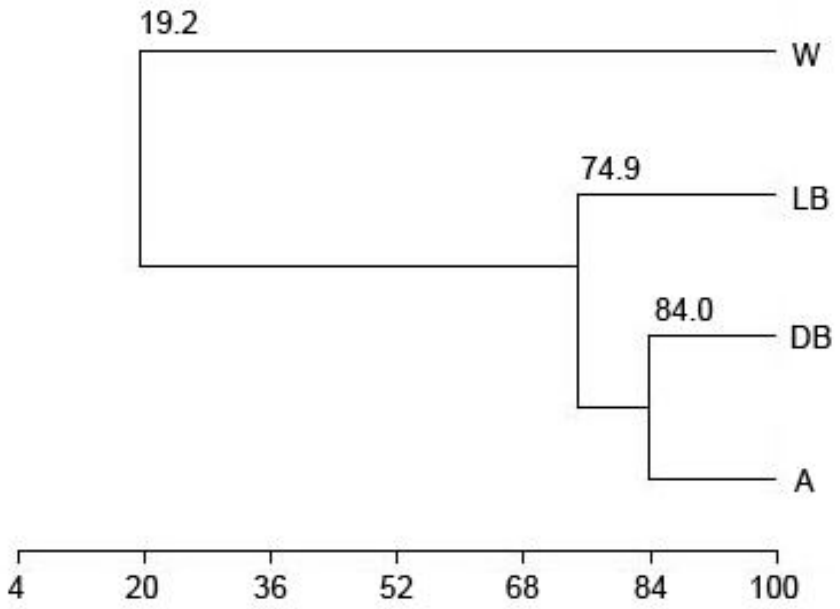

Figure 2. *Dendrogram of sampled T. hirta adults from the color traps (traps with the same color were grouped) and an attractant trap (A: Attractant; LB: Light Blue; DB: Dark Blue; W: White) in study area. The cluster analysis was performed using Percent similarity*

http://www.aloki.hu ● ISSN 1589 1623 (Print) ● ISSN 1785 0037 (Online)
DOI: http://dx.doi.org/10.15666/aeer/1704_74537462

Discussion

Many colors, yellow, fluorescent yellow, white, brown, transparent, chartreuse, coral, dodger blue, golden rod, hot pink, light sea green, light sky blue, medium orchid, etc have been evaluated to find out the most attractant colors for *T. hirta* in numerous scientific studies (Schmera et al., 2004; Kozár, 1972; Tóth et al., 2005, 2009; Aydın, 2011; Subchev et al., 2011; Vuts et al., 2012; Trotus et al., 2015). Some researchers declared that adults of *T. hirta* were strongly attracted to objects of light blue color (Kozár, 1972; Aydın, 2011) while some of them affirmed that the blue color has been the most attractive color for *T. hirta* (Tóth et al., 2005). Likewise some of the scientific study results showed that *T. hirta* had been attracted to yellow, light blue or white color in a field test, but they found no significant differences between colors (Schmera et al., 2004). On the contrary of the mentioned results, Aydin (2011) declared that the susceptibility of *T. hirta* to white and light blue colors was found statistically significant. We have tried three different colors of traps; white, light blue and dark blue during the blooming period of cherry orchard. Result of our study has showed that light blue color trap is the best attractant compared the other used traps for adults of apple blossom beetle and can be used for controlling of *T. hirta*

For the last decades researchers have tried different colors with different lures (Tóth et al., 2004, 2009, 1998, 2003; Schmera et al., 2004; Vuts et al., 2012; Trotus et al., 2015; Subchev et al., 2012) experiments were also carried out in different places at the same time (Vuts et al., 2010a). Cinnamyl alcohol, transanethol and cinnamyl acetate were found as compounds attracting *T. hirta* by Tóth et al. (2003). Thereupon Schmera et al. (2004) declared that combination of light blue color and a bait of 1:1 mixture of *cinnamyl alcohol* and *transanethol* used in dry funnel traps were very effective tool for catching of *T. hirta.* As for chemical attractive stimuli for *T. hirta*, a binary floral attractant consisting of (E)-cinnamyl alcohol and (E)-anethol has been optimised (Tóth et al., 2004, 2009, 1998, 2003). Finally a new coattractant, 4-methoxyphenethyl alcohol, developed for increasing the attractiveness of known binary attractant mixture, cinnamyl alcohol/trans-anethol (Vuts et al., 2010b). Vuts et al. (2010b) found that traps baited with the mixtures of known binary attractant with 4-methoxyphenethyl in 1:1:1 or 1:1:0.3 ratios sampled significantly more *T. hirta* than known binary attractant alone. However, Güvenç and Yaşar (2014) declared that there were no statistical differences between known binary attractant mixtures and known binary attractant with 4-methoxyphenethyl for catching of *T. hirta.* We have tried known binary attractant in our study. When we compare the effective of colors with mentioned attractant, almost similar number of individuals of *T. hirta* were caught with both attractant and dark blue color (87 individuals with attractant; 86, 88, and 70 with dark blue color in loc.1, loc.2, and loc.3, respectively) while the light blue color has been found the most effective tool for catching of adults of *T. hirta* (152, 136 and 126 individuals in loc.1, loc.2, and loc.3, respectively).

Some of the traps were used in the study of Yasar and Sagdas (2014) at apple orchards. Authors declared that the highest number of adults were obtained through the blue funnel trap in loc.1 however the most of the adults were caught by blue funnel + attractant traps when they compare with all four locations of the study. The results of our study coincide with study of Yasar and Sagdas (2014) however light blue traps were not include the mentioned previous study to compare efficiency of traps. Attractant and dark blue traps have been used detection and monitoring of apple

http://www.aloki.hu ● ISSN 1589 1623 (Print) ● ISSN 1785 0037 (Online)
DOI: http://dx.doi.org/10.15666/aeer/1704_74537462

blossom beetle on the other hand using light blue trap is highly recommended to control of *T. hirta* in cherry orchards according to our study results.

The study of Yasar and Uysal (2013) was conducted to evaluate the most effective traps for capturing *T. hirta* on plum and pear orchards. The most of the adults were sampled by blue funnel plus water traps with attractant (containing cinnamyl alcohol, trans-anethol, dipropylene glycol and 2 - propanol, 1, 1 - oxybis). They declared that use of an attractant with a blue funnel trap is an effective biotechnical method for controlling *T. hirta* when insecticides cannot be applied during the blooming period. Our study results showed that the attractant and dark blue color have not been found statistically different for catching adults of *T. hirta*. However the light blue traps caught the most individuals while the white color caught the least individuals when they compare to each other.

Gezer and Ozpinar (2015) were tested the different traps to determine the adult density of apple blossom beetle, in different orchards; peach, cherry, apricot and apple in Canakkale. They declared that the highest number of adults had been captured by the blue bowl plus water traps with attractant in all orchards. However there were no statistical differences between blue color bowl traps and blue color bowl traps with attractant containing trans-anethole + cinamyl alcohol, (1:1). It is an interesting result of the mentioned study that just blue bowl plus water trap was found the most effective than the all other traps with attractant. The authors explained this situation as the wind effect (Gezer and Ozpinar, 2015). Although we have got similar result with the mentioned study showed that blue color trap was the most effective traps, we believe that color is very effective tool for adult of *T. hirta* instead of wind condition instead of attractant.

The several scientific studies have been carried out on the subject and mentioned attractant mixtures have been used for controlling and/or seasonal monitoring of T. *hirta* in most of Central and Eastern Europe (Bulgaria, Hungary, Croatia and Italy) (Vuts et al., 2010a; Tóth et al., 2005, 2009; Subchev et al., 2011; Mircheva et al., 2004; Sivcev et al., 2006). We agree with these results that blue funnel with attractant trap can be suggested as an effective biotechnical method for controlling *T. hirta* however we believe that it is possible to control *T. hirta* without applying insecticide and population density of the mentioned species can be kept below the "economic damage threshold" by using the correct traps at the right time.

Some studies show that white color is the most attractive trap in terms of individual catching of *T. hirta* adults compared with light and dark blue color traps (Aydın, 2011). But some authors do not agree with this result and they declared that light or dark blue color has been found more attractive for the species than white color trap. On the other hand, the results of the studies carried out under different geographical conditions that do not coincide with each other as in the case of the study carried out in Central and Eastern Europe. The result of the study has been showed that CA-baited trap caught the most individual in Bulgaria, Hungary, and Croatia however scientists could not found the same result in Italy.

In fact, many studies have shown that the apple blossom beetle responds to different colors at different times. Scarcely, no studies reveal this result openly or expressed. It can be revealed that the color sensitivity of the beetle is in fact related to the plant phenology when all the results of the works are taken together instead of evaluating all the works separately.

http://www.aloki.hu ● ISSN 1589 1623 (Print) ● ISSN 1785 0037 (Online)
DOI: http://dx.doi.org/10.15666/aeer/1704_74537462

Result of our study showed that there is no statistically significant difference between the attractant and dark blue color whereas highest number of individuals caught with light blue color trap has been found statistically significant compared the other used traps. However, we are not sure that the same result can be obtained in studies to be done pre and post bloom period because we think that the color preference of the *T. hirta* changed depending on blooming periods. If behaviour pattern of apple blossom beetle is linked to plant phenology the color of traps should be changed considering the bloom period. Aydin (2011) has found same result with our study during blooming period of cherry however he has suggested using white color traps instead of traps with dark and light blue colors to catch more individuals of adult of *T. hirta* during pre and post blooming periods.

Results of many scientific studies and present study results showed that known binary attractant or known binary attractant with 4-methoxyphenethyl used with the light blue or dark blue colors cannot catch the similar number of individuals as the light blue traps which are set up at the ground surface. We think that the traps placed in the ground level can be more easily and earlier recognized than attractants hanged on branches of trees by *T. hirta*. Moreover it should be investigated that the rate of pest's flower damage on branches with an attractant hanging might be higher than the branches with not attractant hanging (Aydin and Yaşar, 2019). If pest is attracted to the trees with attractants damage rate can be increased. It may be more appropriate to set up the traps at a distance from the trees where adults of *T. hirta* can recognize easily rather than hang the traps on the branches.

Conclusion

There have been many scientific studies to understand which color or the attractant or even color and attractant use in conjunction is the best attraction method for sampling of *T. hirta*. When the studies conducted so far have been evaluated, we see that different sampling tools are suggested. Despite these confusing conclusions we wonder whether or not it is possible that the *T. hirta* color sensitivity changes at different times.

The second contradiction is that the necessity of using the attractors with color has not been explained in scientific studies. If the species is attracted to known binary attractant mixtures (or even known binary attractant with 4-methoxyphenethyl) why is the attractant has been recommended usage with color? It is understood from the related studies that only attractors do not affect the adults of apple blossom beetle. If the attractant used alone does not affect the insect and it is necessary to use it with color, so it can be said that the color is important. Some studies have emphasized that the use of color with known binary attractant and the use of only color (shades of blue) have not been found that has a statistically significant difference between their roles in attracting the insect. Our study results show that there is no difference between the number of individuals caught with the attractant and dark blue color trap. However, it is revealed that the number of individuals caught with light blue color is considerably higher than the others while the number of individuals caught with white color is very low. Both results have been found statistically significant.

The results of our study and the other related studies so far have been examined can be summarized as follows:

1. Plant phenology related shifts in color preferences of *T. hirta* adults.

1.1. Light blue color traps can be used during blooming periods of cherry orchards

http://www.aloki.hu ● ISSN 1589 1623 (Print) ● ISSN 1785 0037 (Online)
DOI: http://dx.doi.org/10.15666/aeer/1704_74537462

1.2. White color traps can be used during the pre and post blooming periods. The white color traps set up during pre-bloom can reduce the damage of *T. hirta* adults at present season while white color traps set up during post-bloom can reduce the population of the next year. Thus application order of this methods can be suggested both "as an effective biotechnical method for controlling *T. hirta*" and "population density of the pest can be kept below the "economic damage threshold".

1.3. Pesticide application against mentioned pest may not be needed with choosing right traps on time for monitoring of *T. hirta.* Thus non-target organisms such as honey bees, predator ladybirds, etc would not be negatively affected by applying insecticides.

2. Traps even including attractants should be installed in a visible place where the pest can easily recognize instead of hanging them on tree branches. Thus the rate of flower damage caused by the pest can be decreased and more numbers of adults can be caught

Acknowledgements. Part of the work has been orally presented in the International Symposium on EuroAsian Biodiversity (SEAB 2018), 03-06 July 2018 Kiev-Ukraine

REFERENCES

[1] Aydın, G. (2011): Plant phenology-related shift in color preference of *Epicometis* (*Tropinota*) *hirta* (Coleoptera: Scarabaeidae: Cetoniinae) adults - key to effective population monitoring and suppression. – Fla Entomol 94(4): 832-838.

[2] Çetin, G., Hantaş, C., Erenoğlu, B. (2006): Determination on fauna of pest insect and mites in *Rubus fruticocus* orchards in Bursa and Yalova. – Bahce 35(1-2): 61-74.

[3] Ertop, S., Özpınar, A. (2011): Population dynamics of phytophagous species and predators in cherry orchards in Çanakkale. – Turk J Entomol 1(2): 109-118.

[4] Gezer, B., Özpinar, A. (2015): Evaluation of different traps to determine of adults of *Tropinota hirta* (Poda) (Coleoptera: Cetoniidae) density in peach, apple, cherry and apricot. – COMU J Agric Fac 3(2): 27-34.

[5] Güvenç, C., Yaşar, B. (2014): The effect of different chemical attractants on the capture of *Tropinota hirta* (poda) (coleoptera: scarabaeidae) feeding on cherry flowers. – SDU J Nat Appl Sci 18(3): 97-104.

[6] Knudsen, J. T., Tollesten, L., Bergström, L. G. (1993): Floral scents - a checklist of volatile compounds isolated by head-space techniques. – Phytochemistry 33: 253-280.

[7] Kozár, F. (1972): A new method of studying the swarming of *Epicometis hirta* Poda. – Acta Agron Acad Sci Hung 21: 373-376.

[8] Kutinkova, H., Andreev, R. (2004): Integrated pest management in sweet cherry (*Prunus avium* L.) orchards in Bulgaria. – J Fruit Omam Plant Res 12: 41-47.

[9] Milenkovic, S., Stanisavljevic, M. (2003): Raspberry pests in Serbia. Integrated plant protection in orchards - Soft Fruits. – IOBC/WPRS Bulletin 26(2): 23-27.

[10] Mircheva, A., Subchev, M., Sredkov, I., Tóth, M. (2004): Seasonal flight of *Epicometis hirta* Poda (Coleoptera, Scarabaeiddae) established by attractant traps. – Annuaire de l'Université de Sofia St. Kliment Ohridski 96: 201-204.

[11] Perez, R. J., Traveset, A. (2011): Influence of reproductive traits on pollination success in two daphne species (Thymelaeaceae). – J Plant Res 124: 277-287.

[12] Ražov, J., Barić, B., Dutto, M. (2009): Fauna of the Cetoniid beetles (Coleoptera: Cetoniidae) and the ir damages on peach fruits in orchards of Northern Dalmatia, Croatia. – Entomol Croat 13(2): 7-20.

[13] Schmera, D., Tóth, M., Subchev, M., Sredkov, I., Szarukan, I., Jermy, T., Szentesi, A. (2004): Importance of visual and chemical cues in the development of an attractant trap

http://www.aloki.hu ● ISSN 1589 1623 (Print) ● ISSN 1785 0037 (Online)
DOI: http://dx.doi.org/10.15666/aeer/1704_74537462

for *Epicometis* (*Tropinota*) *hirta* Poda (Coleoptera: Scarabaeidae): – Crop Prot 23(10): 939-944.

[14] Sivcev, I., Tóth, M., Tomasev, I. (2006): Application of attractants in control of the sugar-beet weevil and the blossom feeder scarab (*Bothynoderes punctiventris*, *Epicometis hirta*). – Poljoprivredni Kalendar 138-140.

[15] Subchev, M., Toshova, T. B., Andreev, R. A., Petrova, V. D., Maneva, V. D., Spasova, T. S., Marinova, N. T., Minkov, P. M., Velchev, D. I. (2011): Employing floral baited traps for detection and seasonal monitorin g of *Tropinota* (*Epicometis*) *hirta* (Poda) (Coleoptera: Cetoniidae) in Bulgaria. – Acta Zool Bulg 63(3): 269-276.

[16] Subchev, M., Toshova, T., Andreev, R., Petrova, V., Maneva, V., Spasova, T., Marinova, N., Minkov, P., Velchev, D. (2012): Using floral baited colour traps for detection and seasonal monitoring of *Oxythyrea funesta* (Poda) (Coleoptera: Cetoniidae) in Bulgaria. – Acta Zool Bulg 64: 439-443.

[17] Tóth, M., Szarukán, I., Klein, M. (1998): Trapping scarab beetles (Coleoptera, Scarabaeidae, Melolonthinae): tests on orchard pests in Hungary. – Abstract of IOBC-wprs Meeting "Scents in Orchards", Dachau, September 21-24.

[18] Tóth, M., Klein, M. G., Imrei, Z. (2003): Field screening for attractants of scarab pests in Hungary (Coleoptera: Scarabaeidae). – Acta Phytopathol Entomol Hung 38: 323-331.

[19] Tóth, M., Schmera, D., Imrei, Z. (2004): Optimization of a chemical attractant for *Epicometis* (*Tropinota*) *hirta* Poda. – Z Naturforsch 59c: 288-292.

[20] Tóth, M., Imrei, Z., Szarukán, I., Voigt, E., Schmera, D., Vuts, J., Harmincz, K., Subchev, M. (2005): Chemical communication of fruit- and flower-damaging scarabs: results of one decade's research efforts. – Növényvédelem 41: 581-588.

[21] Tóth, M., Vuts, J., Difranco, F., Tabilio, R., Baric, B., Razov, J., Toshova, T., Subchev, M., Sredkov, I. (2009): Detection and monitoring of *Epicometis hirta* Poda and *Tropinota squalida* Scop. with the same trap. – Acta Phytopathol Entomol Hung 44(2): 337-344.

[22] Trotus, E., Pochiscanu, S. F., Naie, M. (2015): Flowers hairy beetle (*Epicometes hirta* Poda): dangerous pest of rapeseed crops. An. – INCDA Fundulea 83: 179-187.

[23] Vuts, J., Baric, B., Razov, J., Toshova, T. B., Subchev, M., Sredkov, I., Tabilio, R., DiFranco, F., Tóth, M. (2010a): Performance and selectivity of floral attractant-baited traps targeted for cetoniin scarabs (Coleoptera: Scarabaeidae) in Central and Southern Europe. – Crop Prot 29: 1177-1183.

[24] Vuts, J., Szarukan, I., Subchev, M., Toshova, T., Tóth, M. (2010b): Improving the floral attractant to lure *Epicometis hirta* Poda (Coleoptera: Scarabaeidae, Cetoniinae). – J Pest Sci 83(1): 15-20.

[25] Vuts, J., Kaydan, M. B., Yarimbatman, A., Tóth, N. (2012): Field catches of *Oxythyrea cinctella* using visual and olfactory cues. – Physiol Entomol 37: 92-96.

[26] Yaşar, B., Sağdaş, A. (2014): The Capturing of the apple blossom beetle, *Tropinota hirta* (Poda) (Coleoptera: Scarabaeidae): by different traps in Afyonkarahisar. – Turk J Agric For 1: 29-34.

[27] Yaşar, B., Uysal, O. (2013): Evaluation of the efficacy of different traps in capturing apple blossom beetle (*Tropinota hirta* (Poda, 1761)) (Coleoptera: Scarabaeidae). – Turk Entomol Derg-TU 37(2): 169-177.

http://www.aloki.hu ● ISSN 1589 1623 (Print) ● ISSN 1785 0037 (Online)
DOI: http://dx.doi.org/10.15666/aeer/1704_74537462

EFFECT OF LOW-TEMPERATURE THERMAL-ALKALINE PRETREATMENT WITH ALKYL POLYGLUCOSIDES (APGS) FOR LOW-ORGANIC-CONTENT SLUDGE ON ANAEROBIC DIGESTION

LIU, X.[1,2] – ZHANG, C.[1,2*] – YU, Z.[1,2]

[1]*College of Environmental Science and Engineering, Hunan University, Changsha 410082, China*

[2]*Key Laboratory of Environmental Biology and Pollution Control (Hunan University), Ministry of Education, Changsha 410082, China*

**Corresponding author*
e-mail: zhangchang@hnu.edu.cn; phone/fax: +86-731-8882-2312

(Received 6th Mar 2019; accepted 3rd May 2019)

Abstract. Low-temperature thermo-alkaline pretreatment with alkyl polyglucosides (APGs) was employed for improving the utilization of low-organic-content sludge in anaerobic digestion (AD). An orthogonal experiment (L_9 (3^4)) was designed to estimate the influence of four factors on pretreatment, and the order determined by significance level was: pH > temperature > APG dosage > time. Under the conditions of pH 11, 60 °C, and 60 min, the content of organic matter dissolved from sludge increased as the APG dosage increased to 18 g/L. When fermenting at a dosage above its critical micelle concentration (CMC), however, APG inhibited aerogenesis due to the adverse impact on methanogen activity. Thus, the optimal APG dosage was fixed at 3.0 g/L. After 35 days of mesophilic AD, the biogas volume, the methane volume fraction, and the organics utilization rate reached their respective peaks. The methane volume fraction (45.8%) was lower than normal biogas (at least 53%), so further evaluation is needed.
Keywords: *surfactant, CMC, mesophilic, methanogenesis, orthogonal experiment*

Introduction

The large amount of sludge generated by wastewater treatment plants (WWTPs) has been a great challenge and has raised significant concerns in China (Yang et al., 2015). Disposal methods, including sanitary landfill, land application, and incineration, are the main final destinations of sludge after treatment (Murakami et al., 2009; Song and Lee, 2010; Hale et al., 2012). Processes such as thickening, conditioning, dewatering, stabilization, and drying are commonly employed as sludge treatment methods (Yang et al., 2015). Stabilization, a well-developed approach, is an important way to reduce the environmental risks of sewage sludge. In particular, anaerobic and aerobic digestion are the most common stabilization methods, and they are usually applied in cases of small WWTPs, although the majority of produced sludge is treated anaerobically (Kelessidis and Stasinakis, 2012).

Anaerobic digestion (AD) is a complex process which is generally considered to have a rate limited by the hydrolysis of sludge (Appels et al., 2008). Therefore, pretreatments facilitating sludge hydrolysis enhance the efficiency of AD. Generally speaking, pretreatment methods include biological, thermal, mechanical (ultrasonic treatment, lysis-centrifugation, liquid shear, and grinding), and chemical (oxidation and alkalization) (Carrere et al., 2010) treatments, among which thermal treatment has been paid much attention. Thermal pretreatment can be mainly classified into two categories

http://www.aloki.hu ● ISSN 1589 1623 (Print) ● ISSN 1785 0037 (Online)
DOI: http://dx.doi.org/10.15666/aeer/1704_74637476

based on the temperature applied, i.e., pretreatment higher than 100 °C (need a high-pressure installation) (Bougrier et al., 2008; Ennouri et al., 2016; Jae et al., 2018) and pretreatment lower than 100 °C (under atmospheric pressure) (Appels et al., 2010; Fernández-Marchante, 2018). However, treatment in a mild temperature is often combined with a chemical method (Mendez et al., 2013), most commonly with an alkali. Some researchers (Kim et al., 2015; Zhang et al., 2015; Li et al., 2016; Du et al., 2019) have concluded that a low-temperature thermo-alkali pretreatment significantly enhances the efficiency of AD.

From studies on sludge dewatering, it was found that surfactants were highly effective in releasing extracellular polymeric substances (EPSs) from sludge (Wang et al., 2014; Liu et al., 2019). EPSs consist of high-molecular-weight secretions from microorganisms, and products of cellular lysis and macromolecule hydrolysis. A higher EPS content in sludge results in greater sludge stability (Sheng et al., 2010), so the release of EPSs from cells can facilitate the dissolution of organics, thus making a positive contribution to the hydrolysis of sludge. In short, surfactants can be chosen for sludge pretreatment (Guan et al., 2017), but their environmental friendliness must be taken into consideration.

Alkyl polyglucoside (APG) is a nonionic surfactant synthesized from renewable raw materials, and it has excellent ecotoxicological profiles, so it is readily biodegradable (Geetha and Tyagi, 2012). Luo et al. (2015) reported that adding APG to an anaerobic treatment system of waste activated sludge (WAS) improved the production of short-chain fatty acids remarkably. However, so far, no one has tried to pretreat sludge with APG before AD.

WAS with comparatively low organic content has not been qualified for AD. This study, therefore, explored the effect of low-temperature thermo-alkaline pretreatment, optimized by APG dosing of low-organic-content sludge, on AD. An orthogonal experiment was firstly designed to estimate the effects of pH, temperature, APG dosage, and time on the pretreatment, and single factor experiments were also conducted to meet the shortcomings of the orthogonal experiment. More importantly, the role of APG dosage in AD was investigated by a series of fermentation experiments.

Materials and methods

Test materials

Waste activated sludge

The sludge used in this study was collected from Kaifu Wastewater Treatment Plant (Changsha, China) through a Modified Sequencing Batch Reactor (MSBR). It was dewatered by belt filter press in the plant, and it was then stored in a plastic hermetic bag at 4 °C in the laboratory. The moisture content of the sludge was 81.3 ± 0.05%.

Before each experiment, the dewatered sludge was diluted with deionized water into approximate 15 g/L (total solids), and the ratio of volatile solids (VS) to total solids (TS) was 51.32 ± 0.10%, which is comparatively low (VS/TS of WAS for AD in the literature was generally above 70%). The main characteristics of the sludge solution were total chemical oxygen demand (TCOD) = 6976.8 ± 77.5 mg/L, soluble chemical oxygen demand (SCOD) = 85.3 ± 7.7 mg/L, soluble total organic carbon (STOC) = 60.45 ± 5.38 mg/L, soluble total phosphorus (soluble TP) = 10.18 ± 0.20 mg/L, pH = 6.96 ± 0.01.

http://www.aloki.hu ● ISSN 1589 1623 (Print) ● ISSN 1785 0037 (Online)
DOI: http://dx.doi.org/10.15666/aeer/1704_74637476

Inocula

For the anaerobic digestion tests, the sludge solution was anaerobically cultivated at 37 °C for 3 days in a constant-temperature incubator in order to activate the anaerobe, and to prepare for the inocula (it is feasible to use raw WAS as inocula, as shown in the literature; Nguyen et al., 2014). Its main characteristics were TCOD = 6821.8 ± 155.0 mg/L, SCOD = 100.8 ± 23.3 mg/L, STOC = 66.45 ± 3.62 mg/L, soluble TP = 14.30 ± 0.11 mg/L, pH = 6.91 ± 0.01.

Alkyl polyglucoside

The surfactant alkyl polyglucoside (APG0810), which was a faint yellow thick fluid (solid content≥50%), was purchased from Shanghai Fine Chemical CO., LTD and was used with no further purification. Thus, APG concentration in this paper refers to the concentration of the fluid. Its carbon content was 34.9 ± 0.3%.

Critical micelle concentration (CMC) is an important characteristic of a surfactant, and it is defined as the concentration of surfactants above which micelles form, and all additional surfactants added to the system form micelles (IUPAC, 1997). Before reaching the CMC, the surface tension changes strongly with the concentration of the surfactant. After reaching the CMC, the surface tension remains relatively constant, or it changes at a slower rate.

The surface tensions of the surfactant aqueous solution and sludge solution were measured and are shown in *Figure 1*. The CMC of the APG aqueous solution was about 1.5 g/L, which corresponds with the data provided by the manufacturer, while the CMC of the APG sludge solution was approximately 3.0 g/L. *Figure 1* also indicates that NaOH treatment nearly had no effect on the surface tension of the sludge solution.

Methods

Low-temperature thermo-alkaline pretreatment with APG

The pretreatment tests were conducted in 150 mL conical flasks with covers (to avoid water loss by evaporation) fed with 100 mL of sludge solution. Different volumes of 1 mol/L NaOH and 100 g/L APG solution were added to adjust the pH and APG concentration, respectively. The volume of NaOH added for reaching a set pH was determined by a preliminary experiment, whose results are shown in *Table 1*.

Table 1. *The relationship between pH and volumes of NaOH*

Volume of NaOH (mL/100 mL)	0.0	0.6	1.4	2.0
pH	7	10	11	12

All flasks were maintained in a digital thermostat water bath oscillator, and the solution temperatures were detected by a thermometer. The timer was started as soon as the temperature reached the desired value. Each test was repeated twice.

After completion, samples were centrifuged at 8000 rpm (3785×*g*) for 15 min, the supernatant was filtered by a 0.45 μm microporous membrane, and the soluble total organic carbon and soluble total phosphorus were analyzed. In the present study, mixed-STOC = the data from the experimental analysis which included organic carbon both from sludge and APG, and STOC = mixed-STOC –APG × 349 (1 g APG = 349 mg TOC, which can be deduced from section 2.1.3), which included the TOC dissolved just from sludge.

http://www.aloki.hu ● ISSN 1589 1623 (Print) ● ISSN 1785 0037 (Online)
DOI: http://dx.doi.org/10.15666/aeer/1704_74637476

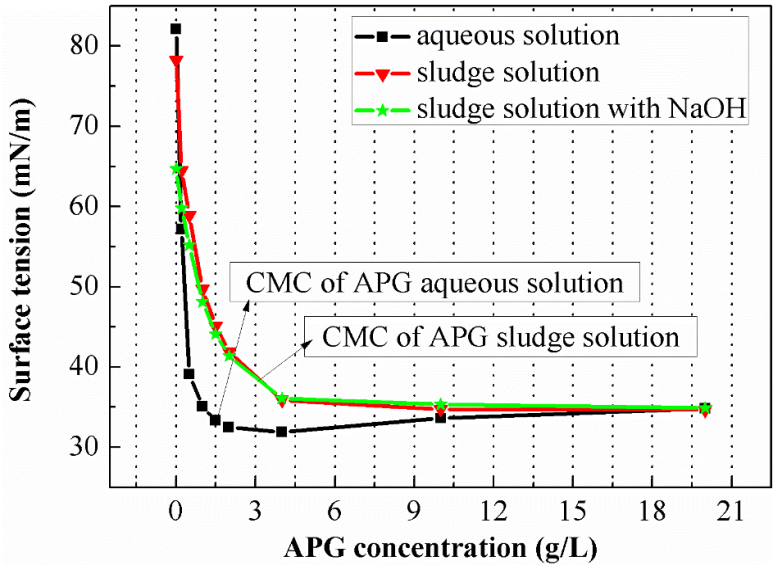

Figure 1. *Surface tension of different APG concentrations*

STOC represents the effect of the pretreatment. Soluble TP indicates the disintegration of the microbial cells due to those in the WWTPs, polyphosphate accumulation organisms (PAOs) are able to store phosphate as intracellular polyphosphate, leading to P removal via PAO cells in WAS (Oehmen et al., 2007). As a result, soluble TP comes almost entirely from the cellular interior, having dissolved when cells were destroyed.

Orthogonal experiment design

For the pretreatment tests, sludge was mainly affected by temperature, time, pH, and APG concentration. It was assumed that the four factors had significant influences on pretreatment. The results described herein are from an orthogonal experiment, which was designed for evaluating such experimental factors. Each factor includes three levels, as follows. Temperature: 40, 60, and 80 °C; time: 30, 60, and 90 min; pH: 7, 10, and 12 (neutral, alkaline, and strongly alkaline); and APG: 1.5, 3, and 4.5 g/L (below CMC, CMC, and above CMC). Since there were four experimental factors and three levels for each factor, the orthogonal matrix denoted as $L_9(3^4)$ was chosen as the experimental scheme to arrange the tests. Each test was repeated two times, and SPSS software was used for the experiment design and statistical analysis.

Anaerobic digestion tests

The experiments were conducted using conical flasks in duplicate with a working volume of 500 mL. The bottles contained a magnet rotor (for stirring automatically once a day) and were filled with 200 mL inocula and 300 mL pretreated sludge. All pretreatments were under the conditions of pH = 11, temperature = 60 °C, time = 60 min, APG = 0, 1.5, 3.0, and 5.0 g/L (preliminary experiments had proved that when pretreating at APG > 5 g/L, there is no gas produced in the AD system). The bottles of APG were named T0, T1.5, T3.0, and T5.0, respectively. For comparison, a blank test was run in a flask filled with 200 mL inocula and 300 mL raw sludge solution.

http://www.aloki.hu ● ISSN 1589 1623 (Print) ● ISSN 1785 0037 (Online)
DOI: http://dx.doi.org/10.15666/aeer/1704_74637476

All flasks were incubated at 35 °C in an electrically heated thermostatic water bath for 35 days until gas was no longer produced. The gas was collected by aluminum foil gas-collecting bags, and gas volume was measured using a syringe. Moreover, the biogas composition was analyzed using gas chromatography (GC). Each test was repeated twice.

Analysis methods

The analyses of sludge moisture content, TS, VS, COD, TP, and pH were conducted according to standard methods (APHA, 2005). The surface tension was determined by pulling escape using a JZ-200A automatic interface tensiometer. By using a Shimadzu TOC-Vcph/cpn instrument, TOC was detected by catalytic oxidation nondispersive infrared analysis. The methane was analyzed by a gas chromatograph (Agilent, 6890N) equipped with a flame ionization detector (FID) and a 30 m × 0.32 mm capillary column (HP-5). The temperature of the injector, detector, and column were kept at 100 °C, 180 °C, and 80 °C, respectively. Helium was used as the carrier gas at a flow rate of 30 mL/min. Three parallel samples were used for each analysis.

Data calculation formula

The energy efficiency from the single factor experiments was calculated as in *Equation 1*.

$$\text{energy efficiency} = \frac{c \times v}{m \times (T - 20) \times C} \quad \text{(Eq.1)}$$

where c is the average concentration value when time ≥ 30 min, v is the volume, m is the mass, T is the desired temperature, 20 is the room temperature, and C is the specific heat capacity of water (4.2 kJ/°C·kg). The unit for energy efficiency is mg/kJ, which refers to the dissolved quantity of sludge per kJ energy consumed. The heat loss that occurs during the constant temperature process was ignored because of its small value and the difficulties in its calculation.

Results and discussion

Orthogonal experiment

The results of the orthogonal experiment for estimating the effects of temperature, time, pH, and APG concentration on the pretreatment of sludge are summarized in *Table 2*. The F-value shown in *Table 2* indicates that the order of the effects of factors on STOC is pH > temperature > APG concentration > time. For soluble TP, the order of pH and temperature was the same, but the order of the other two factors (APG concentration and time) was opposite. This distinction indicates that the dissolution of organics was not caused solely by cell disintegration, but was also related to the dissolution of EPSs.

However, dissolution of EPSs contributes to the destruction of cells, and, as a result, the effects of the factors on STOC and soluble TP have a lot in common. As shown in *Figure 2,* pH (the most important factor) and temperature (the second most important factor) have similar effects, agreeing with the previous literature (Kim et al., 2015) that an increase of pH and temperature both enhance the dissolution of organics and

http://www.aloki.hu ● ISSN 1589 1623 (Print) ● ISSN 1785 0037 (Online)
DOI: http://dx.doi.org/10.15666/aeer/1704_74637476

phosphorus from sludge. Taking into consideration the effects of pH and temperature on anaerobic digestion (Zhao et al., 2015a) and the energy consumption of the pretreatment, the final pH of the pretreatment was adjusted to 11 for both pretreatment efficiency and the reducing effect of alkalinity on AD, but the temperature needed some additional experiments.

Table 2. *Tests of between-subject effects*

Source	Dependent variable: STOC R Squared = .996 (Adjusted R Squared = .992)		Dependent variable: soluble TP R Squared = .999 (Adjusted R Squared = .997)	
	F	Sig.	F	Sig.
Corrected Model	260.748	.000	785.335	.000
Intercept	11235.690	.000	17368.888	.000
Temp	**186.670**	**.000**	**199.503**	**.000**
Time	**3.603**	**.071**	**25.473**	**.000**
APG	**25.808**	**.000**	**7.907**	**.010**
pH	**826.909**	**.000**	**2908.456**	**.000**

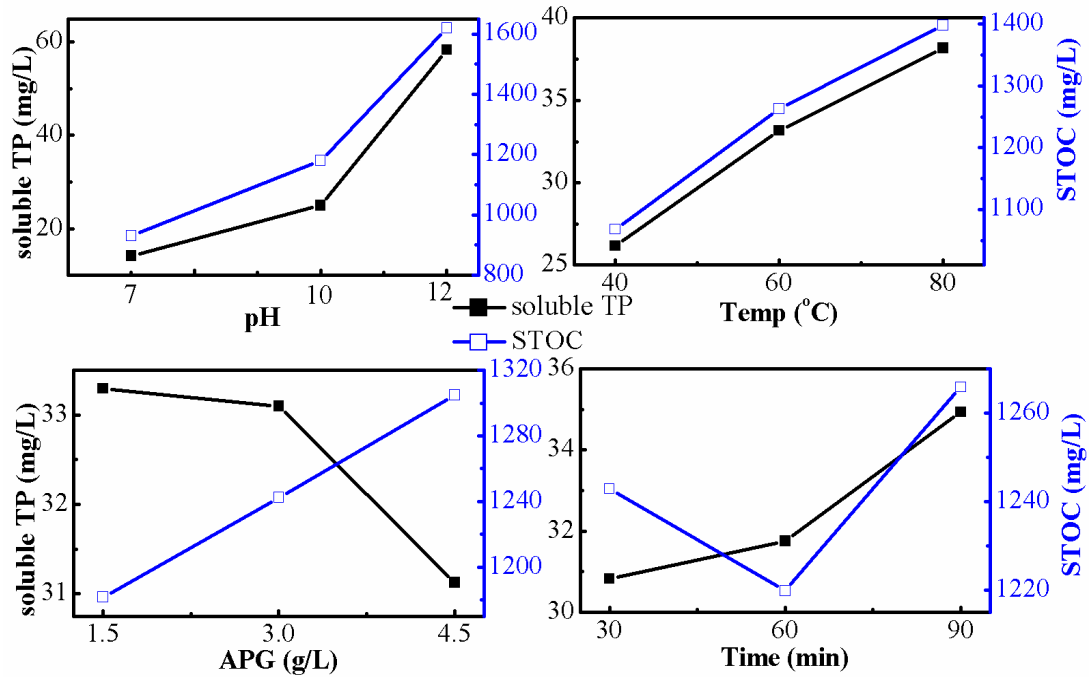

Figure 2. *Level effects of each factor on STOC and soluble TP*

Figure 2 also shows that for STOC and soluble TP, the least significant factors (time of STOC, APG concentration of soluble TP) have abnormal data, which could be explained by that time and APG concentration were easily affected by the other factors. The orthogonal design has two fundamental limitations: one is that it considers only first-order effects, and the other is that it does not account for the interaction among factors (Zeng et al., 2004). As a result, single factor experiments were required for demonstrating the effects of those two factors.

http://www.aloki.hu ● ISSN 1589 1623 (Print) ● ISSN 1785 0037 (Online)
DOI: http://dx.doi.org/10.15666/aeer/1704_74637476

Single factor experiments

Effect of time and determination of appropriate temperature

The effect of time at various temperatures is shown in *Figure 3a* for the conditions: pH = 11; APG = 5 g/L; and temperature = 40 °C, 60 °C, and 80 °C. Once alkali and APG were added to the sludge solution, organic matter and phosphorus dissolved in the water rapidly until 30 min had elapsed, then the dissolving speed slowed down considerably. Referring to the literature (Kim et al., 2013; Ruffino et al., 2016), 60 min was chosen as a pretreatment time to ensure that the pretreatment was comparatively complete.

It is shown in *Figure 3a* that temperature enhanced the dissolution of organics and phosphorus in the sludge, which is consistent with the result of the orthogonal experiment. However, in *Figure 3b,* the energy efficiency decreased as the temperature increased, which negates the notion that the hotter the better. Although the dissolved quantity of sludge at 80 °C was higher than that at 60 °C, the amount of energy consumed at 80 °C was higher, or the energy efficiency was lower at 80 °C. Besides, it shows that the energy efficiency at 40 °C was the highest, but the dissolved quantity was compromised (the lowest). Thus, to obtain both the optimal dissolved quantity and energy efficiency, 60 °C was selected as the optimal temperature.

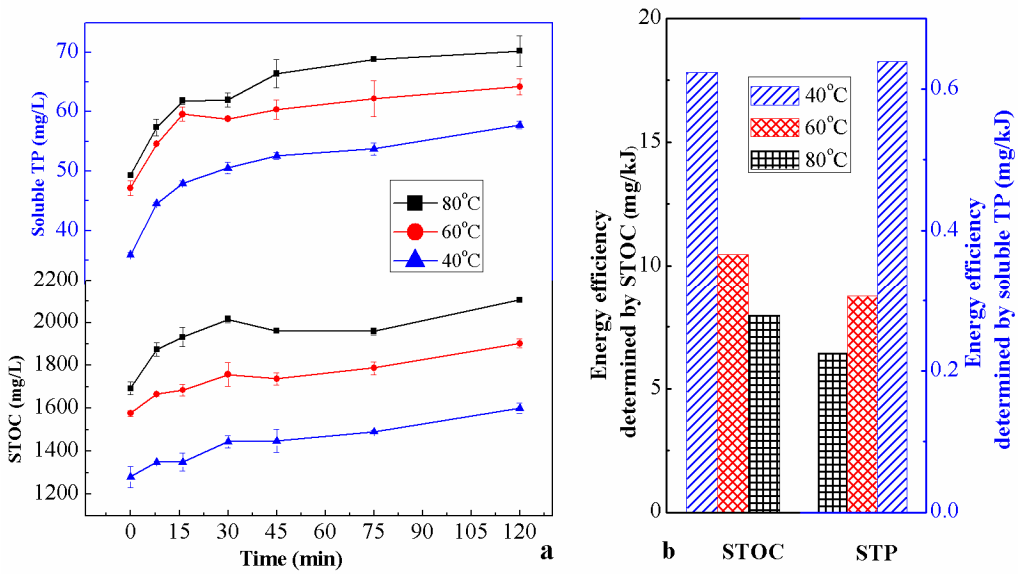

Figure 3. *Effects of time on pretreatment*

Effect of APG concentration

The effect of APG is shown in *Figure 4* for the conditions of pH = 11, temperature = 60 °C, and time = 60 min. The mixed-TOC (TOC from both sludge and APG) had a good linear relationship with APG (*Table 3*), but there is a discontinuity when APG = 18 g/L (*Fig. 4a*). The trend of STOC is from rising to declining, which could be explained as follows: Setting APG as x and mixed-STOC as y, then $y = k x + b$, and setting STOC as y', then $y' = (k - 349) x + b$. It is easy to conclude from the equation that the slope coefficient of y' (k – 349) changed due to the change of the coefficient of y (k, from 446.1 to 275.4) at the point where APG = 18 g/L. Also, it is

http://www.aloki.hu ● ISSN 1589 1623 (Print) ● ISSN 1785 0037 (Online)
DOI: http://dx.doi.org/10.15666/aeer/1704_74637476

clear from the figure that at the point where APG = 18 g/L, the efficiency of APG decreased slowly and then rapidly.

Table 3. *Linear fitting equation of APG (x) and mixed-STOC (y)*

APG concentration (mg/L)	Linear equation	R^2
[0,18]	y = 446.1x + 970.7	0.999
[18,30]	y = 275.4x + 4017	0.998

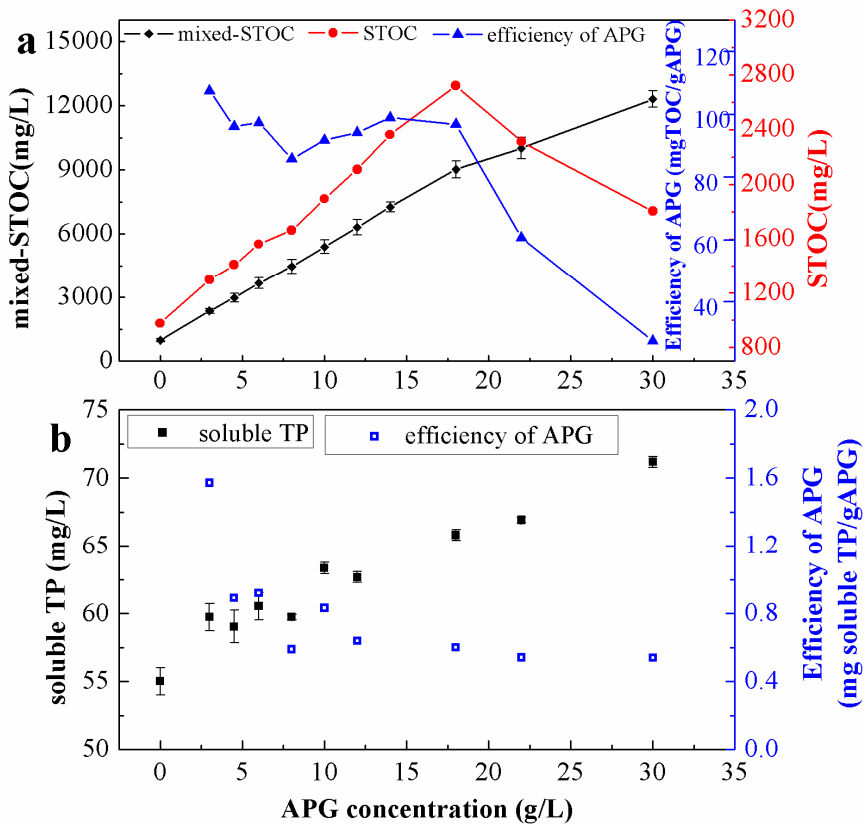

Figure 4. *Effects of APG concentration on STOC (a) and soluble TP (b). In (a), the efficiency of APG = (STOC – $STOC_0$)/APG, where the $STOC_0$ is STOC with APG = 0 mg/L. In (b), the efficiency of APG = (soluble TP – soluble TP_0)/APG, where the soluble TP_0 is soluble TP with APG = 0 g/L*

In *Figure 4a,* when APG < 18 g/L, the higher the APG concentration, the more organics dissolved from the sludge. However, when APG concentration is over 18 g/L, STOC inversely decreases as APG increases. This could be explained as follows: When the concentration of a surfactant is above its CMC, micelles transform from spherical to rod-like. The rod-like micelles would even become associated if continuously adding the surfactant (Rakshit, 2008). In other words, a concentration above the CMC induces the formation of bigger micelles. When the micelles are large enough to be blocked by a microporous membrane, the organics in these micelles may not appear in the dissolved form. In this solution system, 18 g/L was the critical concentration, at which there were micelles blocked by a 0.45 μm microporous membrane.

http://www.aloki.hu ● ISSN 1589 1623 (Print) ● ISSN 1785 0037 (Online)
DOI: http://dx.doi.org/10.15666/aeer/1704_74637476

In *Figure 4b,* soluble TP increases with increasing APG dosage, which indicates that more APG led to more cell disintegration. Phosphorus was not contained in micelles, so big micelles blocked by the microporous membrane did not affect it; therefore, there was no discontinuity insoluble TP.

Similar to other surfactants, some APG molecules formed micelles when the concentration was above its CMC. Thus, the quantity of effective APG molecules did not have a linear increase with its concentration, resulting in the decreasing efficiency of APG in both *Figure 4a* and *b*.

Anaerobic digestion

Gas production

The biogas production from AD is shown in *Figure 5* as a function of fermentation time (on the x-axis) and cumulative gas volume (on they-axis). Comparing the blank with T0 shows that after the low-temperature thermo-alkaline pretreatment without APG, there was higher biogas production efficiency of T0, which is consistent with the literature (Li et al., 2016). However, pretreatment with different dosages of APG had a significant effect on the gas production.

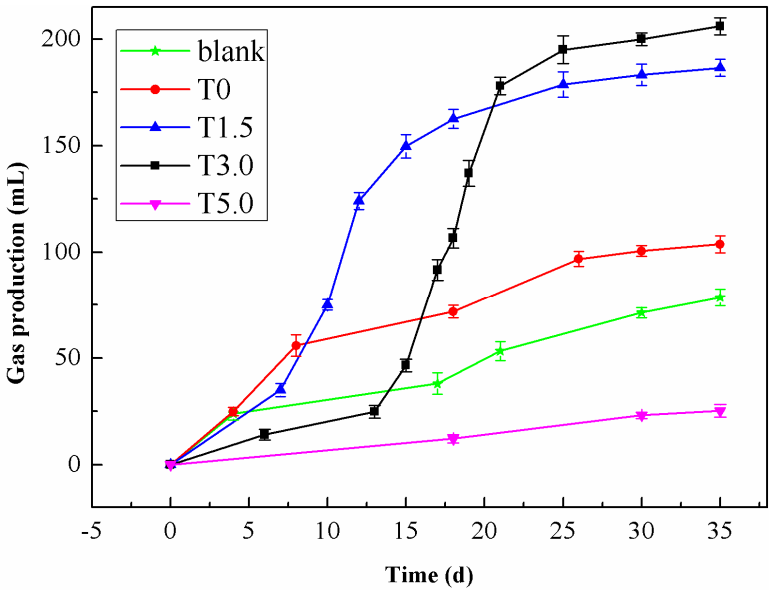

Figure 5. *Total volume of biogas in AD*

Comparing T0 with T1.5, it was found that adding APG to the pretreatment had a greater impact on AD than adding solely alkali. Moreover, the gas production of T1.5 increased rapidly about 7 days later, which means that the microorganisms in T1.5 had an adaptive phase of 7 days.

In comparison with T1.5, it was observed that the gas production rate of T3.0 started rising rapidly on the 13th day. The longer adaptive phase defines the inhibiting effect of APG on the microorganisms in the anaerobic system. When the APG concentration is less than the CMC, the adaptive phase increases with increasing APG dosage.

Assuming that there was no wastage of APG during the process of pretreatment, APG concentration in the fermentation broth was 0.9 g/L for T1.5, 1.8 g/L for T3.0, and

http://www.aloki.hu ● ISSN 1589 1623 (Print) ● ISSN 1785 0037 (Online)
DOI: http://dx.doi.org/10.15666/aeer/1704_74637476

3.0 g/L for T5.0 (APG was diluted 5/3 times by inocula). It is shown in *Figure 5* that T5.0 produced a small amount of biogas, which suggests that the aerogen can hardly adapt to the APG concentration at CMC (the CMC of the APG sludge solution was approximately 3.0 g/L, section 2.1.3). Considering the result of preliminary experiments indicating that there were no bubbles in the fermentation liquor when pretreating at APG > 5.0 g/L, it is the APG micelles that have a negative impact of activity on the aerogen. However, in the study by Xia and Onyukse (2000), they found that it was the surfactant monomer, not the micelle, that went through the cell membrane to damage the cell. Therefore, as they stated, "micelles may act as a depot to continuously replace aqueous surfactant monomers taken up by the membrane."

Property analysis of fermentation liquor and biogas

The compositions of the liquor and biogas during fermentation are shown in *Figure 6*. The sludge solutions of T0, T1.5, T3.0, and T5.0 pretreated by the low-temperature thermo-alkaline method (initial pH = 11) were mixed with inocula. All pH was between 8.8 and 8.9, as shown in *Figure 6a,* and all pH values were significantly reduced after 35 days. The AD of the organic material basically follows hydrolysis, acidogenesis, acetogenesis, and methanogenesis (Appels et al., 2008). It could be deduced that the main cause of the pH reduction was acidogenesis and acetogenesis.

It is known that methanogens are extremely sensitive to pH, with an optimum between 6.5 and 7.2 (Appels et al., 2008), and the optimal pH of hydrolysis and acidogenesis is between 5.5 and 6.5 (Ward et al., 2008). As shown in *Figure 6a,* the pH values of the blank, T0, T1.5, and T3.0 after AD were between 6.5 and 7.2, which may indicate that the maximal activity strain in the fermentation reactor was a methanogen. However, *Figure 6b* also shows that it is only in T1.5 and T3.0 that there was a relatively large CH_4 volume fraction. Only 1.66 vol% methane in the blank was produced, which is because the poor efficiency of hydrolysis made acidogenesis difficult (the pH changed just from 6.97 to 6.80), so of course acetogenesis and methanogenesis were limited. In T0, the pretreatment facilitated hydrolysis, so acidogenesis and acetogenesis made the pH drop sharply from 8.80 to 7.13. The low methane yield may be caused by the limitation of low organic substrate concentration, since the ratio of VS to TS of sludge used in this study was just 51.32 ± 0.10% (shown in section2.1.1). Adding APG to the pretreatments more effectively promoted the dissolution of organics in the sludge, and APG could even act as an organic substrate, thus leading to the relatively large amount of CH_4 in T1.5 and T3.0, compared to that in T0.

Meanwhile, the pH of T5.0 was at the optimum for hydrolysis and acidogenesis (5.5–6.5, *Fig. 6a*), and there was no methane detected (*Fig. 6b*), both of which suggest that the activity of the methanogens in the T5.0 anaerobic system was extremely low. This conclusion could be also deduced by its STOC reduction rate (*Fig. 6c*).

The STOC reduction rate is unequal to the carbon utilization rate of methanogens, because hydrolysis, acidogenesis, acetogenesis, and methanogenesis simultaneously occur in a mixed anaerobic system. That is to say, when soluble carbon was being converted into CH_4, and CO_2 volatilizing from the liquor, the carbon in the suspended solids was being dissolved into the water by hydrolysis and acidogenesis. However, it is only soluble carbon that methanogens can utilize, so the STOC reduction rate is, to some extent, equal to the activity of methanogens. *Figure 6c* shows that T5.0 had a STOC reduction rate far below that of the other tests, showing its low methanogen

http://www.aloki.hu ● ISSN 1589 1623 (Print) ● ISSN 1785 0037 (Online)
DOI: http://dx.doi.org/10.15666/aeer/1704_74637476

activity. Taking the conclusion of section 3.3.1 into consideration, APGs have more of a negative impact of activity on methanogens than on other strains in the AD system. The literature (Luo et al., 2015) reports that there was far more Firmicutes in WAS anaerobic reactors with APG than without APG (42.6% vs. 9.8%), from which it could be deduced that a firm cell wall can help to protect the bacteria from the toxic effect of APG. Methanogens belong to Archaea, whose cell wall is comparatively weak, so APG monomers easily go through cell membranes and cause them damage.

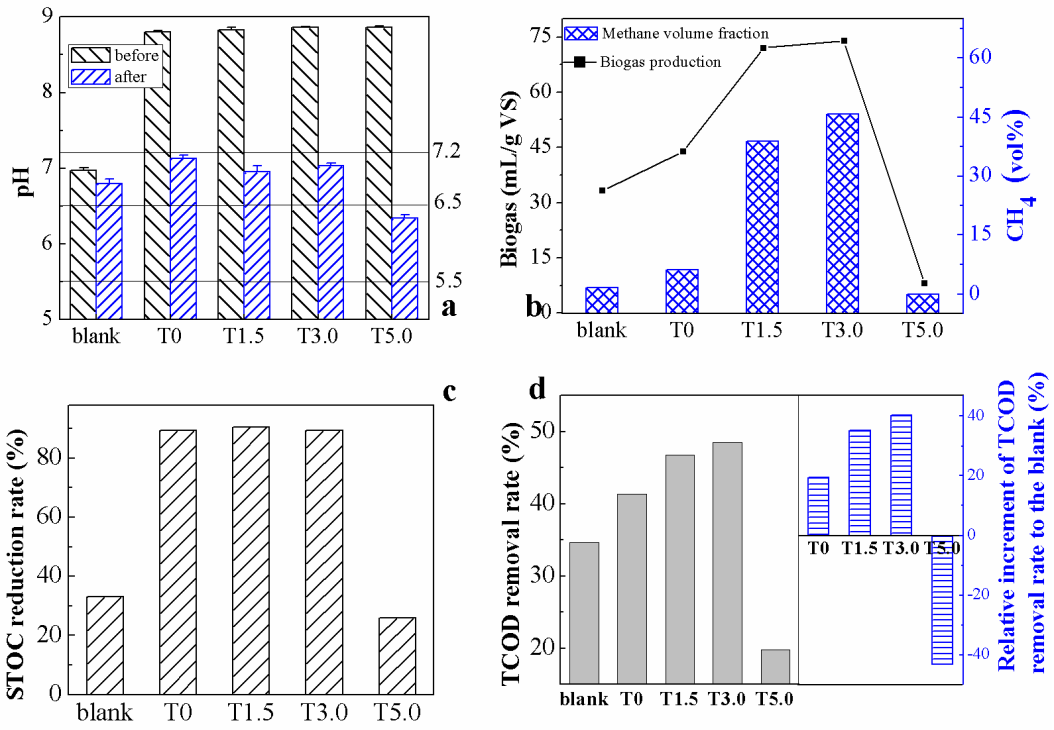

Figure 6. *Property analysis of fermentation liquor and biogas. (a) The change of pH before and after AD. (b) Biogas yield and volume fraction of CH_4. In (c), STOC reduction rate = ($STOC_b$– $STOC_a$)/$STOC_b$, where $STOC_b$ is soluble total organic carbon in the fermentation broth before fermenting, and $STOC_a$ is after fermenting. In (d), TCOD removal rate = ($TCOD_b$ – $TCOD_a$)/$TCOD_b$, where $TCOD_b$ is total chemical oxygen demand in the fermentation broth before fermenting, and $TCOD_a$ is after fermenting. The relative increase of the TCOD removal rate, compared to the blank = TCOD removal rate of (Tα– blank)/blank × 100%, which quantifies the comparison between TCOD removed by AD with pretreatment (T0, T1.5, T3.0, T5.0) and without pretreatment (blank)*

The rate of TCOD removal can be considered to represent the organics utilization rate in the AD system. It is observed from *Figure 6d* that the APG dosage increased the organics utilization rate when the APG concentration was under the CMC. However, when the APG was plentiful enough to generate abundant micelles (APG concentration ≥ CMC), the micelles sharply lowered the activity of the methanogens to inhibit methanogenesis, so the organics utilization rate of T5.0 decreased obviously. This is why Zhao et al. (2015b) and Luo et al. (2015) added APG to anaerobic fermentation systems to inhibit methanogenesis in order to accumulate short-chain fatty acids (SCFAs).

http://www.aloki.hu ● ISSN 1589 1623 (Print) ● ISSN 1785 0037 (Online)
DOI: http://dx.doi.org/10.15666/aeer/1704_74637476

The relative increase of the TCOD removal rate compared to the blank (*Fig. 6d*) suggests that pretreatment does improve the efficiency of AD. The relative increase of T0 was 19.37%, and that of T3.0 was 40.30%. It was easy to calculate that 40.30 is108.07% greater than 19.37, significantly demonstrating that 3.0 g/L is a reasonable selection for the optimal APG dosage. This is due to the fact that, during pretreatment, APG at the CMC promotes dissolution of EPSs, which accelerates hydrolysis. Further, when fermenting, APG is diluted to below CMC, so its toxicity to methanogens is reduced.

In addition, the methane volume fraction of T3.0 was 45.84% (*Fig. 6b*), which is lower than normal biogas (CH_4 volume fraction of digestion biogas was 53–70%; Appels et al., 2008). In comparison with the blank (1.66%) and T0 (6.17%), T3.0 nearly realized sludge recycling.

Although there was an adaption phase in the AD system because of APG, this disadvantage could be overcome by additional high-efficiency gas production studies in a continuous fermentation system (not in a sequencing batch reactor, as in the present experiment). Further, although the methane content was low because of the lack of organic substrate, other degradable organic waste, such as food waste, could be used to increase the organic substrate concentration. However, these suppositions need to be confirmed by more experiments.

Conclusion

A low-temperature thermo-alkaline pretreatment with APG for WAS with low organic content could greatly improve the sludge utilization in AD systems. More APG led to more dissolution of organic matter during the pretreatment, but in fermentation, APG above the CMC severely inhibited methanogenesis. As a result, 3.0 g/L was chosen as the optimal APG dosage. Under optimum conditions, pretreated sludge was fermented anaerobically at mesophilic temperatures to obtain the best biogas production, CH_4 volume fraction, and organics utilization rate. Although there was an adaptive phase of 13 days and the methane content was low, additional experiments could be conducted to find solutions that overcome these disadvantages.

Acknowledgements. This research was financially supported by the project of National Natural Science Foundation of China (NSFC) (Nos.51179068, 51521006).

REFERENCES

[1] APHA (2005): Standard Methods for the Examination of Water and Wastewater. 21st Ed. – Public Health Association, Washington, DC.

[2] Appels, L., Baeyens, J. et al. (2008): Principles and potential of the anaerobic digestion of waste-activated sludge. – Progress in Energy and Combustion Science 34(6): 755-781.

[3] Appels, L., Degrève, J. et al. (2010): Influence of low temperature thermal pre-treatment on sludge solubilisation, heavy metal release and anaerobic digestion. – Bioresource Technology 101(15): 5743-5748.

[4] Bougrier, C., Delgenès, J. P. et al. (2008): Effects of thermal treatments on five different waste activated sludge samples solubilisation, physical properties and anaerobic digestion. – Chemical Engineering Journal 139(2): 236-244.

http://www.aloki.hu ● ISSN 1589 1623 (Print) ● ISSN 1785 0037 (Online)
DOI: http://dx.doi.org/10.15666/aeer/1704_74637476

[5] Carrere, H., Dumas, C. et al. (2010): Pretreatment methods to improve sludge anaerobic degradability: a review. – J Hazard Mater 183(1-3): 1-15.
[6] Du, J., Qian, Y. et al. (2019): Hydrothermal and alkaline thermal pretreatment at mild temperature in solid state for physicochemical properties and biogas production from anaerobic digestion of rice straw. – Renewable Energy 139: 261-267.
[7] Ennouri, H., Miladi, B. et al. (2016): Effect of thermal pretreatment on the biogas production and microbial communities balance during anaerobic digestion of urban and industrial waste activated sludge. – Bioresour Technol 214: 184-191.
[8] Fernández-Marchante, C. M., Asensio, Y., León, L. F. ... Lobato, J., Rodrigo, M. A. (2018): Thermally-treated algal suspensions as fuel for microbial fuel cells. – Journal of Electroanalytical Chemistry 814: 77-82.
[9] Geetha, D., Tyagi, R. (2012): Alkyl Poly Glucosides (APGs) Surfactants and their properties: a review. – Tenside Surfactants Detergents 49(5): 417-427.
[10] Guan, R., Yuan, X. et al. (2017): Functionality of surfactants in waste-activated sludge treatment: a review. – Sci Total Environ 609: 1433-1442.
[11] Hale, R. C., La Guardia, M. J. et al. (2012): Polybrominated diphenyl ethers in U.S. sewage sludges and biosolids: temporal and geographical trends and uptake by corn following land application. – Environ Sci Technol 46(4): 2055-2063.
[12] IUPAC (1997): Compendium of Chemical Terminology (Compiled by A. D. McNaught and A. Wilkinson). – Blackwell Scientific Publications, Oxford.
[13] Jae, M., Sun, K. et al. (2018): Enhancement of methane production in anaerobic digestion of sewage sludge by thermal hydrolysis pretreatment. – Bioresource Technology 259: 207-213.
[14] Kelessidis, A., Stasinakis, A. S. (2012): Comparative study of the methods used for treatment and final disposal of sewage sludge in European countries. – Waste Manag 32(6): 1186-1195.
[15] Kim, J., Yu, Y. et al. (2013): Thermo-alkaline pretreatment of waste activated sludge at low-temperatures: effects on sludge disintegration, methane production, and methanogen community structure. – Bioresour Technol 144: 194-201.
[16] Kim, M., Han, D. W. et al. (2015): Selective release of phosphorus and nitrogen from waste activated sludge with combined thermal and alkali treatment. – Bioresour Technol 190: 522-528.
[17] Li, C., Zhang, G. et al. (2016): Alkaline thermal pretreatment at mild temperatures for biogas production from anaerobic digestion of antibiotic mycelial residue. – Bioresour Technol 208: 49-57.
[18] Liu, R., Yu, X. et al. (2019): New insights into the effect of thermal treatment on sludge dewaterability. – Science of the Total Environment 656: 1082-1090.
[19] Luo, J., Feng, L. et al. (2015): Alkyl polyglucose enhancing propionic acid enriched short-chain fatty acids production during anaerobic treatment of waste activated sludge and mechanisms. – Water Res 73: 332-341.
[20] Mendez, L., Mahdy, A. et al. (2013): Enhancing methane production of Chlorella vulgaris via thermochemical pretreatments. – Bioresour Technol 149: 136-141.
[21] Murakami, T., Suzuki, Y. et al. (2009): Combustion characteristics of sewage sludge in an incineration plant for energy recovery. – Fuel Processing Technology 90(6): 778-783.
[22] Nguyen, M. T., Mohd Yasin, N. H. et al. (2014): Enhancement of sludge reduction and methane production by removing extracellular polymeric substances from waste activated sludge. – Chemosphere 117: 552-558.
[23] Oehmen, A., Lemos, P. C. et al. (2007): Advances in enhanced biological phosphorus removal: from micro to macro scale. – Water Res 41(11): 2271-2300.
[24] Rakshit, A. K. (2008): Micelles: a short review. – Journal of the Indian Chemical Society 85(12): 1289-1300.

http://www.aloki.hu ● ISSN 1589 1623 (Print) ● ISSN 1785 0037 (Online)
DOI: http://dx.doi.org/10.15666/aeer/1704_74637476

[25] Ruffino, B., Campo, G. et al. (2016): Preliminary technical and economic analysis of alkali and low temperature thermo-alkali pretreatments for the anaerobic digestion of waste activated sludge. – Waste and Biomass Valorization 7(4): 667-675.
[26] Sheng, G. P., Yu, H. Q. et al. (2010): Extracellular polymeric substances (EPS) of microbial aggregates in biological wastewater treatment systems: a review. – Biotechnol Adv 28(6): 882-894.
[27] Song, U., Lee, E. J. (2010): Environmental and economical assessment of sewage sludge compost application on soil and plants in a landfill. – Resources, Conservation and Recycling 54(12): 1109-1116.
[28] Wang, L.-F., He, D.-Q. et al. (2014): Characterization of dewatering process of activated sludge assisted by cationic surfactants. – Biochemical Engineering Journal 91: 174-178.
[29] Ward, A. J., Hobbs, P. J. et al. (2008): Optimisation of the anaerobic digestion of agricultural resources. – Bioresour Technol 99(17): 7928-7940.
[30] Xia, W. J., Onyuksel, H. (2000): Mechanistic studies on surfactant-induced membrane permeability enhancement. – Pharmaceutical Research 17(5): 612-618.
[31] Yang, G., Zhang, G. et al. (2015): Current state of sludge production, management, treatment and disposal in China. – Water Res 78: 60-73.
[32] Zeng, S. Y., Kang, L. S. et al. (2004): An orthogonal multi-objective evolutionary algorithm for multi-objective optimization problems with constraints. – Evol Comput 12: 77-98.
[33] Zhang, Y., Feng, Y. et al. (2015): Zero-valent iron enhanced methanogenic activity in anaerobic digestion of waste activated sludge after heat and alkali pretreatment. – Waste Management 38: 297-302.
[34] Zhao, J., Yang, Q. et al. (2015a): Effect of initial pH on short chain fatty acid production during the anaerobic fermentation of membrane bioreactor sludge enhanced by alkyl polyglcoside. – International Biodeterioration & Biodegradation 104: 283-289.
[35] Zhao, J., Yang, Q. et al. (2015b): Enhanced production of short-chain fatty acid from food waste stimulated by alkyl polyglycosides and its mechanism. – Waste Manag 46: 133-139.

http://www.aloki.hu ● ISSN 1589 1623 (Print) ● ISSN 1785 0037 (Online)
DOI: http://dx.doi.org/10.15666/aeer/1704_74637476

STUDY ON CARBON FOOTPRINT AND SPATIAL DISTRIBUTION CHARACTERISTICS OF HUMAN ACTIVITIES IN JIUZHAI VALLEY SCENIC AREA

SUN, R. H.[1] – YE, X. L.[1*] – GAO, J.[2] – ZHU, Z. F.[3] – DU, J.[3]

[1]*Department of Business Administration, School of Management, Shanghai University of Engineering Science, 333 Longteng Road, Songjiang District, Shanghai, China*
(e-mail: sunruihong@sues.edu.cn; phone/fax: +86-21-6787-4142)

[2]*School of Tourism, Shanghai Normal University,*
100 Guilin Road, Xuhui District, Shanghai, China
(e-mail: gaojun@shnu.edu.cn; phone/fax: +86-21-6432-2447)

[3]*Jiuzhai Valley Scenic Area Administration, Zhangzha Town, Jiuzhaigou County, Aba Tibetan and Qiang Autonomous Prefecture, Sichuan Province, China*
(e-mail: 183796414@qq.com; phone/fax: +86-83-7773-9753)

**Corresponding author*
e-mail: yexinliang@sues.edu.cn

(Received 27th Feb 2019; accepted 3rd May 2019)

Abstract. As a nature reserve with extremely vulnerable ecological system, Jiuzhai Valley must strike a balance between climate change, tourism growth and environmental protection in the future development. Carbon footprint is a key tool to measure the environmental impact of human activities. The key factors of carbon emission reduction in Jiuzhai Valley Nature Reserve can be found through carbon footprint evaluation and targeted carbon emission reduction measures can be put forward. In this paper, the carbon emission inventory based on mixed life cycle is introduced to calculate the carbon emissions within the boundary of Jiuzhai Valley Nature Reserve, evaluate its carbon footprint and find out its spatial distribution pattern in order to find out the key factors and links in the improvement of the low-carbon management in Jiuzhai Valley. The study found that the commercial activities of operating companies providing services to tourists (such as transportation and catering) are a major part of carbon emissions, followed by tourist tours and the management and maintenance activities of the Authority, the residential carbon emissions which come from the village daily life and private car driving. The low carbon emission reduction in Jiuzhai Valley should focus on the optimization of land use, the control of the number of residents and tourists, and the sharing of responsibility for emission reduction.
Keywords: *carbon emission, carbon footprint, spatial distribution, human activities, Jiuzhai Valley scenic area*

Introduction

Jiuzhai Valley Nature Reserve was established in 1978, and was approved to establish national scenic area in 1984. In 1992, UNESCO designated Jiuzhai Valley as "World Natural Heritage", and then Jiuzhai Valley joined the World Network of Man and Biosphere Reserves. Jiuzhai Valley Nature Reserve is located on the eastern edge of the Qinghai-Tibet Plateau. In general, it belongs to the alpine and gorge region landform。 The unique geological, geomorphological and natural geography conditions have created the alpine karst landscape and lake canyon scenery with large scale and unique shape. The ecological environment of Jiuzhai Valley is very fragile and sensitive, belonging to the "environmentally and cultural vulnerable areas" (Zhang and Zhu, 2007). In theory, Jiuzhai Valley should rely on ecotourism to protect the World Natural Heritage through

http://www.aloki.hu ● ISSN 1589 1623 (Print) ● ISSN 1785 0037 (Online)
DOI: http://dx.doi.org/10.15666/aeer/1704_74777493

small scale tourism that strictly limits the number of tourists according to the environmental capacity. However, this concept is challenged by mass tourism, aboriginal people getting rich from poverty and local economic growth in practice. Therefore, Jiuzhai Valley's scenic area management needs to consider a variety of demands to promote operational strategies.

This paper selects Jiuzhai Valley to carry out carbon footprint research based on the following considerations: first of all, tourism has become the economic artery of Jiuzhai Valley, and Jiuzhai Valley scenic area has become the local pillar industry and economic artery. Since its development in 1980, Jiuzhai Valley has experienced an average annual increase of 27%. In 2012, the number of tourists has reached 3,638,618, and tourism income has accounted for more than 90% of the local economic income. Tourism has effectively promoted local economic development and the employment of residents out of poverty. Secondly, tourism growth poses a severe challenge to the ecological carrying capacity of scenic spot, which are often overloaded. According to Zhang Xiaoping, former director general of Jiuzhai Valley Administration, and related scholars, the daily tourist psychological capacity of Jiuzhai Valley scenic area is 12000 people (with different values in different seasons), the best (most appropriate) daily capacity is 18000 people, and the comprehensive environmental capacity is 22000 people, the maximum daily capacity can reach 28000 people, and the annual capacity is 2.6 million to 4.38 million people (Zhang and Zhu, 2007). According to the tourism scale of Jiuzhai Valley in 2016, the number of tourists was already at the carrying capacity boundary and breaking the limiting value. Thirdly, Jiuzhai Valley Administration ecological protection work has been carried out in an orderly manner and the data has been sorted out and improved. The Academic Research Office and Protection Department of Jiuzhai Valley Administration has carried out a general survey and quantitative statistics on the species of animals and plants inside the reserve area, and has more detailed records and observation data on the land use change of Jiuzhai Valley. The Protection Department is responsible for the disposal of waste and feces and sewage in the scenic area of Jiuzhai Valley, which can obtain basic information through interviews. The Jiuzhai Valley Administration has a Resident Management Office, which is responsible for the management of residents in the scenic area, has relatively complete information on residents' living conditions, income changes, vehicle ownership situation and so on.

This paper applies the theory of carbon footprint to Jiuzhai Valley Nature Reserve and discusses how to reduce carbon footprint and implement carbon management to balance ecological vulnerability protection and tourism economic growth. This paper combines the international common carbon footprint inventory to construct the evaluation model of tourism carbon footprint suitable for minority areas, and verifies it through the field interview data of Jiuzhai Valley, introduces stakeholders to distinguish the responsibilities of Jiuzhai Valley tourism industry in reducing emissions according to the results of carbon footprint evaluation, and provides theoretical and empirical support for putting forward and perfecting low-carbon construction and sustainable development of Jiuzhai Valley tourism industry.

Research object and scheme design

The basic situation of Jiuzhai Valley scenic area

Tourism activities are mainly carried out in the experimental area of Jiuzhai Valley scenic area, accounting for 8.53% of the total area of nature reserve. The changes in

http://www.aloki.hu ● ISSN 1589 1623 (Print) ● ISSN 1785 0037 (Online)
DOI: http://dx.doi.org/10.15666/aeer/1704_74777493

population and land use in Jiuzhai Valley are closely related to its history of development. *Figure 1* shows the changes of tourists and population in Jiuzhai Valley from 1978 to 2012. The number of tourists fluctuated greatly during that period. The two biggest fluctuations occurred in the early stages of tourism development in Jiuzhai Valley in 1980 with a sharp increase of tourists and the rapid development of tourism after 1989, followed by three small fluctuations, which are respectively after the 1997 financial crisis, after SARS in 2003 and after Sichuan earthquake in 2008. In contrast, the number of residents has maintained a steady and slow growth, its population growth rate showed a downward trend.

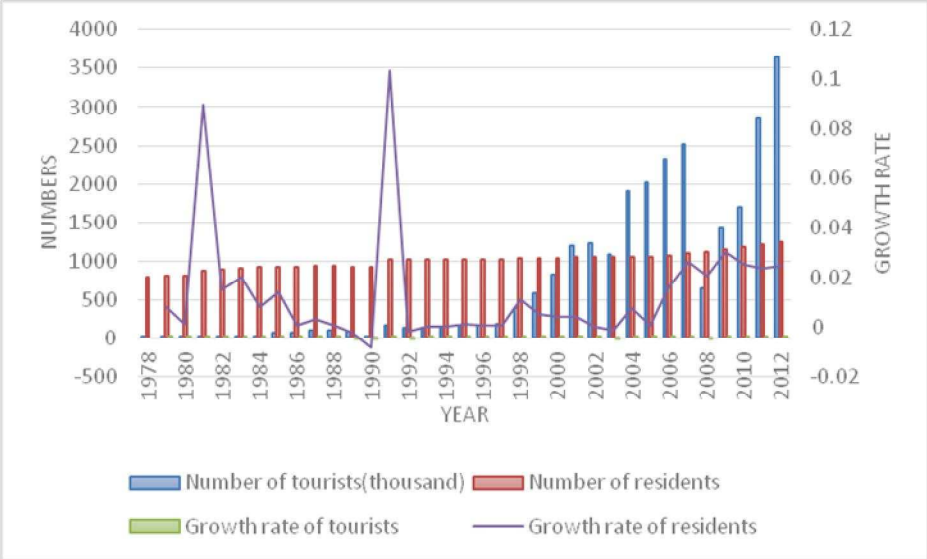

Figure 1. *Changes in the number of tourists and residents in Jiuzhai Valley*

Human activities in different periods have a great influence on the landscape pattern and land use of Jiuzhai Valley Nature Reserve. *Figure 2* reflects the land use changes in Jiuzhai Valley Nature Reserve in four periods from 1975 to 2012. The reasons of the land use change of each period can be found in the development decision and course of the specific period at that time.

Before 1978, Jiuzhai Valley production method and life style were mainly agricultural grazing and forestry felling. The local people made a living by logging, farming, grazing, hunting and digging medicine and lived a life of half farming and half grazing. In 1966, the original Bailong River Forestry Bureau began opening work circle to felling timber in Jiuzhai Valley. Jiuzhai Valley Nature Reserve was established in 1978, but forest logging was not completely banned because of sectoral economic interest until 1992 when it was listed as the World Natural Heritage. In 1984, the national scenic spot was established, and Jiuzhai Valley officially opened to the outside world. Tourism started and the construction of tourist facilities was started. Since 1987, especially in 1990, Jiuzhai Valley tourism has entered a period of rapid growth-the number of tourists had increased exponentially and the tourism economy had grown rapidly. However, due to extensive management, the phenomenon of urbanization and over-commercialization gradually appeared in the reserve, which caused certain damage to the ecological environment (Zhou, 1998). Since 1999, Jiuzhai Valley has taken strict and scientific measures to protect the environment. On the one hand, the traditional

http://www.aloki.hu ● ISSN 1589 1623 (Print) ● ISSN 1785 0037 (Online)
DOI: http://dx.doi.org/10.15666/aeer/1704_74777493

living habits of residents have been changed, and natural gas cooking has been realized. In 2000, the hotels in the reserve was dismantled comprehensively, and implement the policy of returning the grain plots to forestry. From 2008 till now, Jiuzhai Valley has been hit hard by the earthquake and the tourists have plummeted, and the water area and mountain body within the territory have been significantly destroyed by earthquake and debris flow. Post-disaster reconstruction of the scenic area and tourism industry recovery has become the main theme. From the perspective of land use changes in Jiuzhai Valley, such events as stopping forest harvesting, developing tourism, returning the grain plots to forestry, demolishing hotels and other operational sites in scenic spots, and rebuilding after the earthquake have played a very important role in restoring and increasing the forest land of Jiuzhai Valley, changing the way of residents life by returning grain plots to forestry to engage in tourism, reducing a large amount of constructive land and standardizing the land management of Jiuzhai Valley.

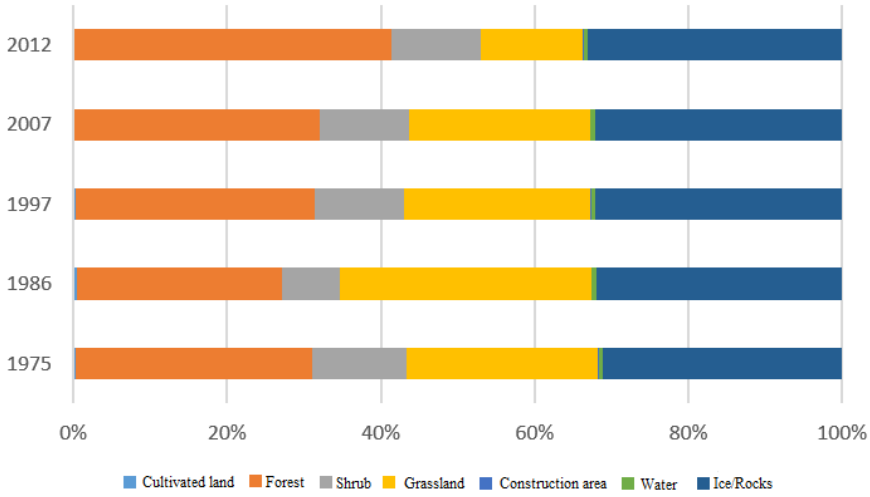

Figure 2. *Percentage change of different land use types in Jiuzhai Valley*

Review of carbon footprint research

From the perspective of source and nature, carbon footprint is a spatial concept, which is measured in the unit of area. Kitzes and other scholars (Kitzes et al., 2009, 2007) regard carbon footprint as part of the ecological footprint, known as the "fossil energy footprint" or "carbon dioxide land", which is measured in gha (gha, the abbreviation of global hectare, one unit global hectare refers to a productivity space of 1 ha with an average global yield, the unit is hm^2). There are also many scholars who tend to express carbon footprint in terms of carbon dioxide emissions or carbon dioxide equivalents, typical of which is that Wiedmann and Minx (2007) and Hertwich and Peters (2009) define carbon footprint as the total amount of carbon dioxide and other greenhouse gases emitted by a product's supply chain or life-cycle. Although the carbon footprint originated from the ecological footprint, it has formed its unique meaning on the basis of its "ecological footprint of carbon emissions" in practice, which becomes a token of greenhouse gas emissions taking into account global warming potential (GWP). Whether the area or the quality of measurement units are inadequate. Converting greenhouse gas emissions into land area requires a series of assumptions that increase the error and uncertainty of carbon footprint accounting (Lenzen, 2006).

http://www.aloki.hu ● ISSN 1589 1623 (Print) ● ISSN 1785 0037 (Online)
DOI: http://dx.doi.org/10.15666/aeer/1704_74777493

On the other hand, it is not accurate to express the carbon footprint by the quality of greenhouse gas, because carbon footprint is a spatial concept, and it is easy to lead misunderstanding if taking mass as the unit (Hertwich and Peters, 2009).

In order to distinguish the concept of carbon footprint and carbon emission, this paper adopts the definition of "productive land area needed to absorb carbon dioxide emissions from human activities". Carbon emissions are defined as "the direct or indirect carbon dioxide emissions in the entire life cycle or within a certain geographical range of an activity, a product (or service)".

Carbon footprint inventory of carbon emission sources is the first step in carbon footprint evaluation. Although greenhouse gas accounting standard is commonly used in footprint calculations, there is no mandatory carbon footprint verification (Pandey et al., 2011). The domestic and international studies on carbon emissions in specific regions based on greenhouse gas emission inventories mainly focus on the research of regional carbon emissions on the large and mesoscale scale, with the largest number of studies on the assessment of carbon footprint between countries and continents on a large scale. In view of the pressure of greenhouse gas emission reduction on countries brought by global climate change, different scholars put forward some practical amendments to the IPCC and other emission inventories and carry out the design and statistics of carbon emission inventory according to the characteristics of their respective countries and regions characteristics. Some scholars also put forward their views on the design and method of greenhouse gas emission inventory (Ravindranath and Ostwald, 2008). Ramaswami et al. (2008) developed a demand-oriented hybrid life-cycle approach that focuses on demand-oriented mixed greenhouse gas inventory method including urban direct greenhouse gas emissions related to final energy use, and indirect greenhouse gas emissions related to the main substances supporting the city. After that, some scholars have improved and applied the city inventory method based on the mixed life cycle inventory method (Kennedy et al., 2010, 2011).

Evaluation and design of carbon footprint in Jiuzhai Valley

Tourism is the only economic industry in Jiuzhai Valley. The type of economic activity in Jiuzhai Valley is tourism industry. All the main bodies in Jiuzhai Valley can be divided into tourists and organizations and individuals who provide services for tourists. Tourist activities in the scenic area impact on the environment is waste and sewage, feces. Organizations and individuals providing services to tourists include: residents, the commercial sector of the scenic area and the administration in Jiuzhai Valley. Jiuzhai Valley residents basically turn to tourism employment, their working carbon emissions can basically be included in the tourism industry carbon emissions, so the resident carbon emissions in Jiuzhai Valley come from the daily life and transportation of residents. The scenic area commerce provides the service of catering, shopping, transportation and sightseeing for tourists. Its environmental impact includes: fuel and electricity consumption, waste gas and waste water produced by business activities and so on. Administration carbon emissions are reflected in the daily office energy use, construction waste and vehicle use for construction and maintenance of scenic area, and the use of working vehicles for safety management and protection in scenic area.

According to the types of human activities in Jiuzhai Valley scenic area, there are mainly four kinds of activities: the first is the daily life of the residents in the reserve and the activities of participating in tourism management. The second is the tourism

http://www.aloki.hu ● ISSN 1589 1623 (Print) ● ISSN 1785 0037 (Online)
DOI: http://dx.doi.org/10.15666/aeer/1704_74777493

activities of tourists. The third is the commercial operation activities in the scenic area, involving the business activities of the three companies under the jurisdiction of the Jiuzhai Valley Administration, such as the joint venture company (operating the Nourilang Center), the tourist products company (operating the Shopping Center, VIP building and Heye Guesthouse), and sightseeing company (operating tourist vehicles). The fourth kind is the management and maintenance activities of the scenic area, including the construction and repair of the scenic area, the daily office work of the Administration Bureau, the safety protection and management of the scenic spot of the Administration, etc. *Figure 3* lists the various departments involved in the statistics of the carbon emission inventory, among which, the Administration Bureau belongs to scenic area management department, the tourism company, the product company, and the jointly venture company are the scenic area commercial operation company.

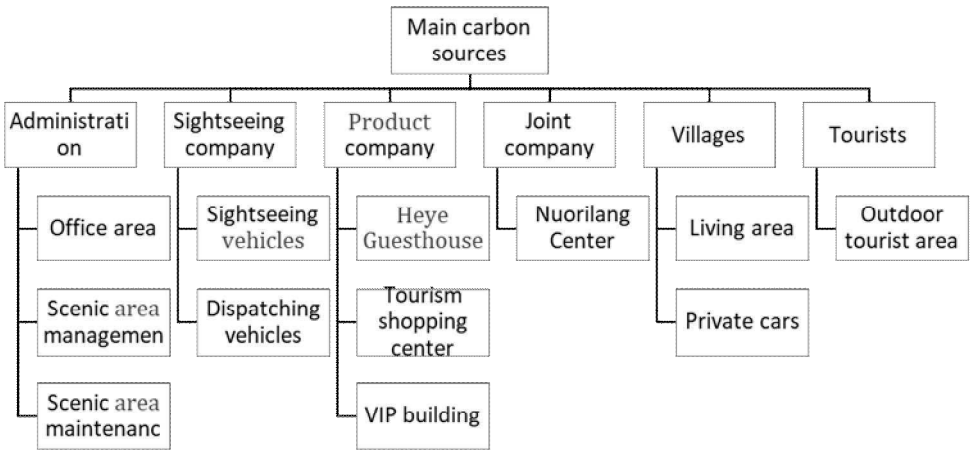

Figure 3. *The main bodies involved in the Jiuzhai Valley carbon inventory*

The inventory of carbon emissions based on mixed life cycle includes not only direct carbon emissions from energy activities but also indirect carbon emissions from power consumption and indirect carbon emissions from waste disposal. Direct carbon emissions of Jiuzhai Valley mainly come from energy activities, such as fuel consumption of traffic vehicles, use of natural gas, energy consumption of Nourilang diesel stove and charcoal heating in winter of residents in the scenic area. Electricity belongs to indirect carbon emissions. The feces, garbage, sewage are also considered as indirect carbon emission because all of them are transported out of Jiuzhai Valley for treatment and its carbon emissions occur outside the scenic area. The projects in Jiuzhai Valley that can be included in carbon inventory statistics are as follows, as shown in *Figure 4*.

Greenhouse gas emissions need to focus not only on direct emissions inside the nature reserve, but also on indirect emissions from energy consumption and waste disposal. Compared with the IPCC inventory classification statistics, Jiuzhai Valley's greenhouse gas accounting is clear and simple, because Jiuzhai Valley's economic activity type is only tourism industry. All the main bodies in Jiuzhai Valley can be divided into tourists and organizations and individuals that provide services for tourists. Tourist activities in the scenic area impact on the environment is waste and sewage, feces. Organizations and individuals providing services to tourists include: residents, the commercial sector of the scenic area and the administration in Jiuzhai Valley. Jiuzhai

http://www.aloki.hu ● ISSN 1589 1623 (Print) ● ISSN 1785 0037 (Online)
DOI: http://dx.doi.org/10.15666/aeer/1704_74777493

Valley residents basically turn to tourism employment, their working carbon emissions can basically be included in the tourism industry carbon emissions, so the resident carbon emissions in Jiuzhai Valley come from the daily life and transportation of residents. The scenic area commerce provides the service of catering, shopping, transportation and sightseeing for tourists. Its environmental impact includes: fuel and electricity consumption, waste gas and waste water produced by business activities and so on. Administration carbon emissions are reflected in the daily office energy use, construction waste and vehicle use for construction and maintenance of scenic area, and the use of working vehicles for safety management and protection in scenic area.

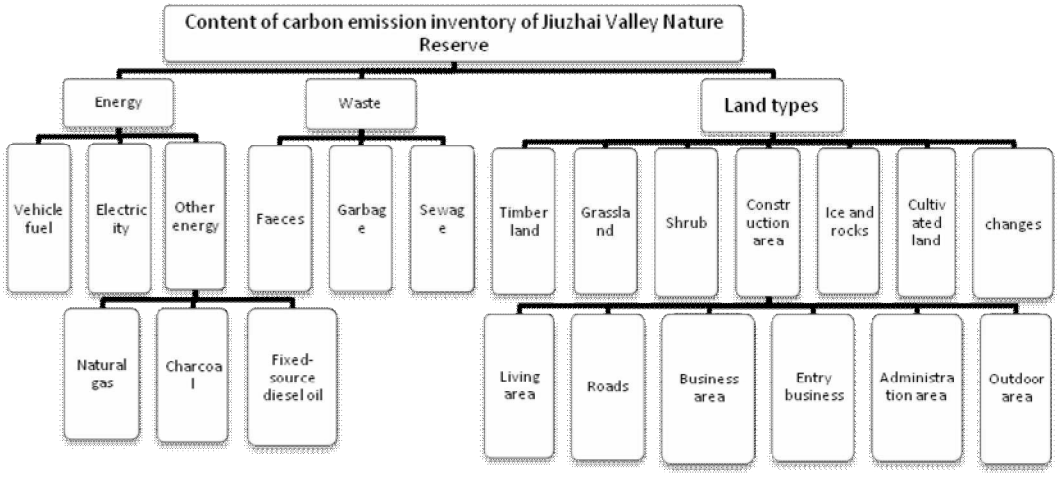

Figure 4. *Statistics on carbon emission inventory in Jiuzhai Valley*

There are three sources of carbon emissions in Jiuzhai Valley: energy, waste, and land use. Among them, construction land and cultivated land in land use are sources of carbon emissions. But since 2003-2004, the cultivated land in Jiuzhai Valley has been converted into forestry, and the carbon source of cultivated land has not existed. Carbon emissions from construction land are energy consumption and waste emissions from that region, so there is no need for double counting. The other land types of Jiuzhai Valley play a role of carbon sink and have the function of carbon storage and carbon absorption except for construction land. According to the carbon emission inventory, the activities data level of the carbon source in Jiuzhai Valley is counted, and the emission coefficient method is used to calculate the carbon emissions of each carbon source in Jiuzhai Valley. NPP carbon sink method can be adopted in the evaluation of carbon footprint and carbon balance. *Figure 5* shows the process of carbon footprint evaluation in Jiuzhai Valley Nature Reserve.

Evaluation methods and data acquisition

Evaluation methods

The evaluation of carbon emission and the selection of emission coefficient

The calculation of carbon emissions from energy and waste refers to the calculation method recommended by *IPCC2006 Greenhouse Gas Emission Inventory Guidelines*, which is also adopted and used for reference by international general inventory

http://www.aloki.hu ● ISSN 1589 1623 (Print) ● ISSN 1785 0037 (Online)
DOI: http://dx.doi.org/10.15666/aeer/1704_74777493

guidelines such as PAS2050, ISO14064. Energy carbon emission calculation is relatively simple, the key of which is to determine the corresponding energy carbon emission coefficient. As for the units of measurement, carbon emissions, carbon storage, and carbon absorption all use kilograms or tons (kg or t), the unit of land area and carbon footprint is hectares (hm^2), and the units of other indexes in this paper all refer to the national standard *GB 3101-1993 General Principles of Quantities, Units and Symbols*.

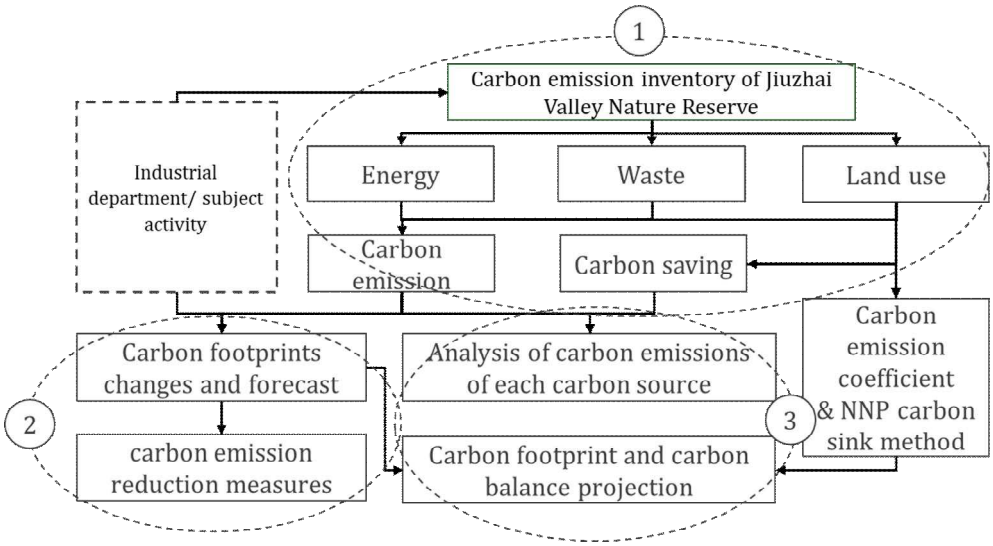

Figure 5. *Evaluation design of carbon footprint in Jiuzhai Valley*

Carbon footprint calculation

This paper adopts the net primary productivity (NPP) index to reflect the carbon absorption of different vegetation, and calculate the area of productive land needed to absorb carbon emissions, that is, carbon footprint. The NPP of forests, grasslands, thinly forested shrubs and water bodies refer to the studies of different domestic scholars (Du et al., 2010; Gu et al., 2007; Liu et al., 2010), while the NPP of bare rock refers to Lu et al. (2005) study on Sichuan in the western region, which makes a detailed analysis of the calculation in the paper.

Calculation of carbon balance in Jiuzhai Valley

This paper analyzes the carbon balance of Jiuzhai Valley reserve ecosystem from two aspects. One is the comparison between carbon emission from human activities and carbon storage and carbon absorption in Jiuzhai Valley. The other is the comparison between the human activities carbon footprint and Jiuzhai Valley productive land area. The former analysis is based on the carbon emission inventory. According to the national carbon emission inventory, the types and quantities of carbon emission sources and absorption sinks in Jiuzhai Valley Nature Reserve are listed in the form of incoming and outgoings, which is convenient to observe the situation of carbon balance. The latter one refers to the analysis based on ecological carbon balance index. If the ecological carbon balance index is greater than 1, it means that there is ecological deficit. If the ecological carbon balance index is equal to 1, it shows that ecology is in the critical

http://www.aloki.hu ● ISSN 1589 1623 (Print) ● ISSN 1785 0037 (Online)
DOI: http://dx.doi.org/10.15666/aeer/1704_74777493

state of carbon balance. If the ecological carbon balance index is less than 1, it indicates that there is ecological surplus. The smaller the ecological carbon balance index, the more intact the ecosystem is and is less disturbed by human activities.

Data acquisition

The interview with various department in Jiuzhai Valley

In December 2012, the author conducted a half-month departmental interview in Jiuzhai Valley Nature Reserve, covering 16 departments, the departments and interview content are as shown in *Table 1*.

Table 1. *Interview department and content of Jiuzhai Valley administration*

Interview department	Interview content
HR Office	For the division and arrangement of responsibilities of the Jiuzhai Valley Administration, final report of the Administration over the years
Marketing Department	Get the number of tourists, the origin and composition of tourists, the consumption of tourists and sample survey conditions
Information Center	For its management of tourist ticketing and the tracing of tourists
Office of Academic Research	Protection of vegetation, types and changes of land use, boundary of reserve
Resident Management Office	The number of residents, the number of households in village, the building area of village, the conversion of farmland to forests, etc.
Security Department	Reserve waste disposal, fecal disposal, sewage treatment, resident charcoal procurement
Legal Department	Number and type of private cars owned by the residents
Supervision Department	Monitoring the energy consumption of each department
Construction Department	Construction of scenic area, construction waste and use of vehicles
Administration Office and Drivers Office	Number of vehicles, types of vehicles, usage condition in the Valley, mileage and fuel consumption owned by the Administration
Sightseeing Company	Vehicle types and quantity changes, fuel consumption and usage, vehicle scheduling management
Product Company	Energy consumption of the commerce in the Valley such as catering, accommodation, shopping, number of visitors and consumption
Joint Venture Company	Telephone interviews to learn about vehicles, energy use
Tourist Center	Jiuzhai Valley scientific research achievements presentation, tourist survey
Finance Department	Involving confidential not being interviewed
Stockaded Village	Go to the village committee and residents' home of Heye Village, Zharu Village, and Shuzheng Village to interview and observe
Postdoctoral Research Station	Understanding the construction of low carbon scenic area

Public data acquisition

Statistical yearbook

China Energy Statistics Yearbook 2011, Sichuan Energy Statistics Yearbook, National Statistical Yearbook, Tourism Statistics Yearbook.

Google data base

The data of total carbon emissions, per capita carbon emission, electricity production, power carbon emission both at home and abroad, population size and population growth rate of China are selected from World Bank to analyze in this paper.

http://www.aloki.hu ● ISSN 1589 1623 (Print) ● ISSN 1785 0037 (Online)
DOI: http://dx.doi.org/10.15666/aeer/1704_74777493

Authoritative report

IPCC 2006 Inventory Guideline, 2011 Datum Line Emission Factor of China Regional Power Grid released by the Climate Department of the State Development and Reform Commission.

Other data acquisition

Survey data on vegetation and water bodies in Jiuzhai Valley

Referring to Liu and Zhang (2007) Biodiversity of Jiuzhai Valley Nature Reserve.

Data on land use types and changes in Jiuzhai Valley from 1975 to 2007

Referring to Deng (2011) Landscape Change and Protection in Jiuzhai Valley Nature Reserve, The Influence of Tourism Development on Landscape Pattern Change of Jiuzhai Valley Nature Reserve, and the doctoral thesis of Research on the Causes and Protection of Tourism Landscape of Jiuzhai Valley World Heritage Site.

The data of land use changes in 1997, 2007, 2012

Remote sensing images from the Chinese resource satellite remote sensing processor.

Research results and analysis

According to the carbon emission sources of Jiuzhai Valley scenic area, the carbon emissions from energy, waste and different land use are calculated respectively. The results show that the total carbon emissions of human activities in Jiuzhai Valley in 2012 was 21118.41 tons. From the emission source of the carbon footprint of human activities, the carbon footprint generated by energy consumption accounted for 81.86% of the total carbon footprint, while the carbon footprint of waste accounted for 18.14%. In the energy carbon footprint, the carbon footprint of traffic vehicles using moving source fuel accounted for 54.84%, in which, the size of the carbon footprint was followed by tourists sightseeing transportation, private cars of residents and working vehicles. The carbon footprint of electric power accounted for 35.62%, the other energy consumption produces the smallest carbon footprint, and the size of carbon footprint of which was followed by gas, charcoal and fixed-source diesel.

According to the conversion formula of carbon emission and ecological footprint, the carbon footprint of human activities in Jiuzhai Valley can be calculated to be 3872.9 hm^2 in 2012, accounting for 5.94% of the biological productivity area (excluding construction land) in Jiuzhai Valley Nature Reserve. In terms of ecological footprint, carbon emissions from human activities in Jiuzhai Valley have very little impact on the environment of the reserve, far from reaching the upper limit of ecological carrying capacity in Jiuzhai Valley Nature Reserve. Jiuzhai Valley Nature Reserve still has 94.06% of the land to provide China with carbon sinks while supporting the development of tourism and the life of the residents at the same time.

Carbon footprint analysis of different subjects

From the subjects of human activity carbon footprint, the operating company that provides tourists with transportation, catering, accommodation (guesthouse), shopping company has the largest carbon footprint, accounting for 56.78% of the total. Tourists' carbon footprint due to toilet use, water use, abandonment of waste and other behavior

http://www.aloki.hu ● ISSN 1589 1623 (Print) ● ISSN 1785 0037 (Online)
DOI: http://dx.doi.org/10.15666/aeer/1704_74777493

in the process of sightseeing ranks second, accounting for 22.38% of the total. The carbon footprint of the residents in the reserve caused by family life, the family car, the family commerce and so on ranks the third, accounting for 11.12% of the total. The carbon footprint of Administration caused by the daily work, the construction and maintenance of protected area facilities and the management of protected areas accounts for 9.72% of the total.

From the point of view of the final allocation of carbon footprint, the management and maintenance of reserve by commerce and Administration are all carried out to meet the material and spiritual needs of the tourist during their tourism process, and their carbon footprint will eventually be transferred to the tourists. From this point of view, tourists eventually bear 88.88% of the carbon footprint and the rest are born by the residents. In 2012, the total number of tourists in Jiuzhai Valley was 3,638,618, and the total number of residents in Jiuzhai Valley was 1,241. The average carbon footprint per tourist was 0.00095 hm^2, while the carbon footprint per inhabitant was 0.347 hm^2.

Per capita carbon footprint of tourists and residents

As *Table 2* shows, the carbon footprint per resident is 366.81 times the carbon footprint per tourist. In other words, the carbon footprint of 367 tourists is the same as that of one resident. Or one tourists come to Jiuzhai Valley Reserve 367 times can produce a carbon footprint equal to the carbon footprint of one resident. It is true that residents live in the Valley 365 days a year, and each tourist stays for only one day. However, if you compare the carbon footprint of 0.000951 per person per day to that of a tourist, the carbon footprint of the resident is still greater. It shows that the impact of individual resident on the ecological environment of Jiuzhai Valley is greater than that of individual tourist.

Table 2. *Carbon footprint of tourists versus residents in 2012*

Carbon footprint allocation objects	Carbon emissions t	Carbon footprint hm^2	Percentage	Number of people in 2012	Per capita carbon emissions t	Per capita carbon footprint hm^2
Reserve residents	2348.26	430.65	11.78%	1241	1.89	0.35
Tourists	18770.15	3442.26	88.22%	3638618	0.01	0.00095
Total	21118.41	3872.90	100.00%	3639859		

The carbon footprint of one resident is the same as that of 367 tourists in the Reserve. In 2012, for example, 1241 residents in the Reserve produced the same carbon footprint as 455212 tourists. If the number of tourists is less than 455212, the activity of residents is the main cause of the negative impact of human activities on the environment of the Reserve, and tourist activity is the secondary motivation. This also explains why we have observed that residents have much greater impact on the environmental problems of many tourist destinations than tourists. Especially for the tourist destination which is in the early stage of tourism development or has few tourists due to the lack of fame, the carbon footprint of resident activities is the largest among all human activities. The reasons are as follows: firstly, it is due to the lack of effective management of resident activities. Secondly, the tourist facilities and services are not perfect, so that the tourist stay time and consumption are less. Thirdly, the management and operation of tourist

http://www.aloki.hu ● ISSN 1589 1623 (Print) ● ISSN 1785 0037 (Online)
DOI: http://dx.doi.org/10.15666/aeer/1704_74777493

destination is not mature, which makes the Reserve lack of attraction and appeal, and lack of lasting competitiveness. As a result, the number of tourists is small, the number of returned customers is also small, and the public praise is not high.

Spatial distribution of carbon footprint in Jiuzhai Valley in 2012

Analysis of carbon footprint distribution and carbon emission sources

In view of that there is NPP coefficient transformation relationship between carbon footprint and carbon emissions, and the carbon footprint can also be explained from the perspective of carbon emissions, this part uses Jiuzhai Valley carbon emissions to analyze.

The location of the carbon footprint is shown in *Figure 6*. The highway in the Reserve is the largest carbon footprint producing area, accounting for 44.89% of the total carbon footprint, which is mainly caused by the traffic carbon emissions of sightseeing vehicles, working vehicles and private cars. Jiuzhai Valley outdoor tourism area (excluding highway) is the second largest area of carbon footprint, accounting for 22.43% of all carbon footprint, which is mainly caused by waste and power consumption in the Reserve. The carbon footprint in the entrance of Jiuzhai Valley accounted for 20.62%, which mainly comes from the work of the commerce and Administration in the entrance of Jiuzhai Valley. Village carbon footprint should not be ignored, accounting for 10.40%, mainly from the lives of residents and a small number of family business activities. The carbon footprint of Nuorilang is the smallest, mainly because there are only 10% tourists eating here, and the office and shopping space is small, so the carbon emission is low, which is 1.67%. If the entrance of Jiuzhai Valley Nature Reserve is taken as the boundary, the carbon footprint inside the gate of Jiuzhai Valley Nature Reserve is only 3073.924 hm^2, accounting for 79.38% of the total carbon footprint and 4.71% of the biological productivity area of Jiuzhai Valley Nature Reserve.

Combined with the area of the site generating carbon footprint, it can be found that there are differences in carbon emission intensity of different plots in Jiuzhai Valley construction land. The road is the highest, which is followed by the village, the entrance of the Valley, Nuorilang, and the tourist area.

Analysis of carbon emission intensity in different regions

From the analysis of *Figure 7*, Jiuzhai Valley entrance Administration office has the highest carbon emission intensity, followed by the business in the entrance, the scenic tourist areas, scenic roads, Shuzheng Village, Zharu Village, Heye Village and so on. The reason for the high carbon emissions in the office building in the entrance lies in the fact that the office building has concentrated most of the staff of the Jiuzhai Valley Administration, and as a scenic spot, the staff are all on duty without holidays in the peak season. The calculation of carbon intensity adopts the land area rather than building area, so the carbon emission intensity is high, but the total amount is not big. The commerce in the entrance is the second largest area of carbon emission intensity, because the tourist's limited tourist demand in Jiuzhai Valley is released outside the Valley, and the commercial location in the entrance is good so that the consumption of dining, shopping and accommodation is increasing, so the intensity of carbon emission is relatively high. Scenic tourist area is the third largest area of carbon emission, because the tourist solid waste, feces, sewage produced the most in this area. Scenic

http://www.aloki.hu ● ISSN 1589 1623 (Print) ● ISSN 1785 0037 (Online)
DOI: http://dx.doi.org/10.15666/aeer/1704_74777493

road carbon intensity is also large, mainly because the total amount of vehicle carbon emissions is large. In summary, it can be seen that the office of the Administration should design corresponding energy saving and emission reduction daily norms, promote the staff to participate in the construction of low-carbon scenic area. The green consumption standards can be implemented for the commerce in the entrance, and carbon reduction targets should be put forward to commercial organizations. For waste management, it should focus on the management of tourists' abandonment of garbage and the cultivation of water-saving awareness. The management of road carbon emissions can be achieved by improving vehicle emission standards and operational efficiency.

Environmental externality analysis of carbon footprint

From the regional transfer of final carbon emissions, 47.3% of the carbon emissions generated by human activities in Jiuzhai Valley Nature Reserve are transferred outside the Reserve, while 52.7% of which are still in the Reserve. The total carbon footprint generated by 52.7% carbon emissions is 2041.05 hm^2, which accounts for only 3.13% of the biological productivity areas in Jiuzhai Valley, as shown in *Table 3*.

Table 3. *Environmental externalities analysis of carbon footprint in Jiuzhai Valley*

Externality	Carbon emission t	NPP/hm^2a	Carbon footprint (hm^2)	Percentage
Carbon emissions still in the reserve	11129.56	5.45	2041.05	52.70%
Carbon emissions moved out of reserve	9988.85	5.45	1831.85	47.30%

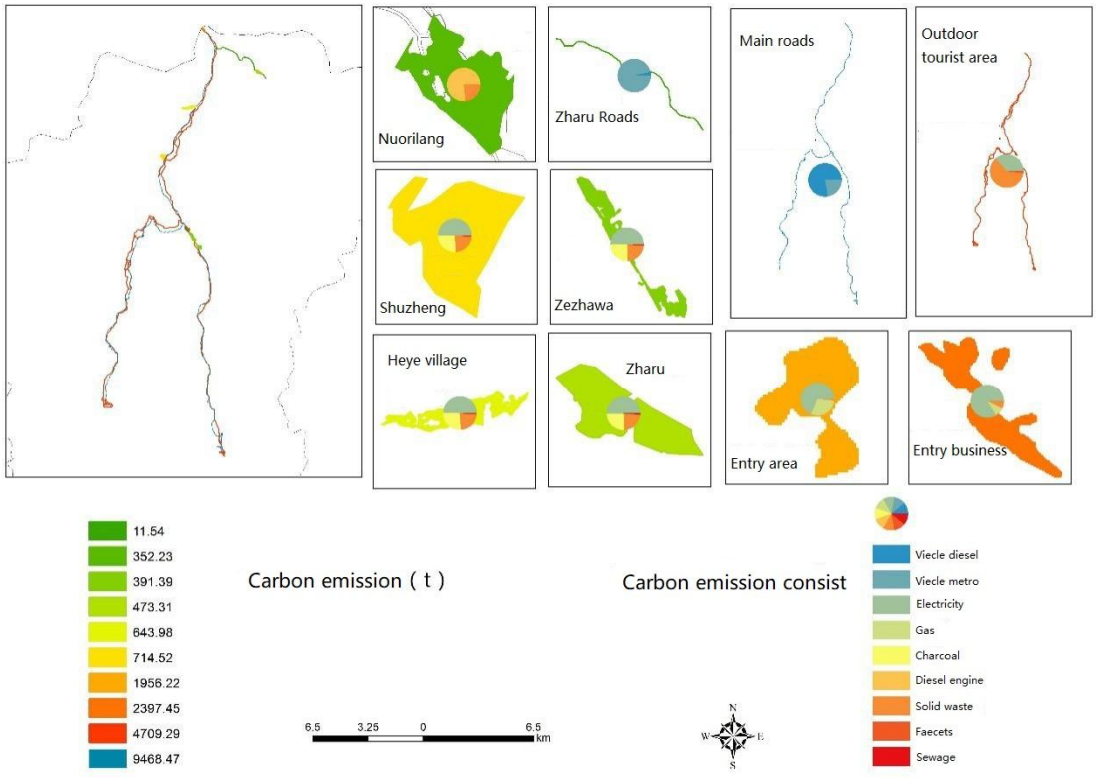

Figure 6. *Regional analysis of carbon emissions in Jiuzhai Valley*

http://www.aloki.hu ● ISSN 1589 1623 (Print) ● ISSN 1785 0037 (Online)
DOI: http://dx.doi.org/10.15666/aeer/1704_74777493

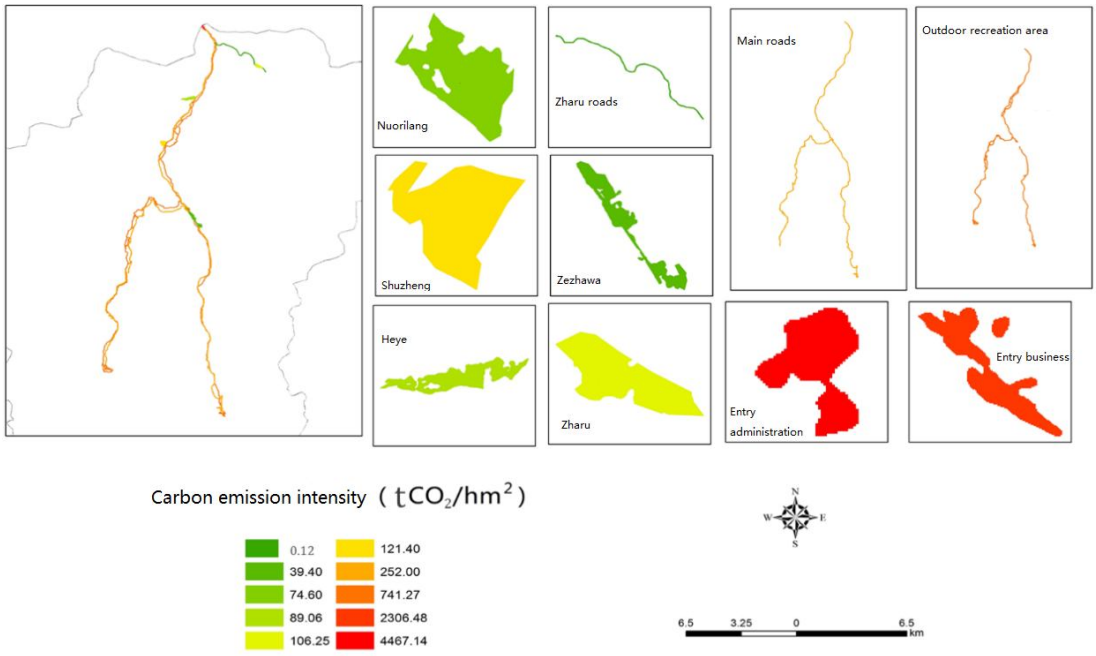

Figure 7. *Carbon intensity analysis of different regions of Jiuzhai Valley construction land*

The main reasons are as follows. First of all, the electric energy that used a lot in Jiuzhai Valley is the indirect carbon emission in the Reserve, and its actual carbon emissions occur in power plants and power stations. The carbon footprint generated by electricity use accounts for 29.16% of the total carbon footprint. Secondly, Jiuzhai Valley transfers all the waste treatment to the treatment plant outside the Valley. For example, the excrement is sent to Jiuzhai Valley fecal plant for decomposition, and sewage and refuse are transported to sewage treatment plant and refuse treatment plant, thus avoiding environmental pollution in the Reserve. The waste carbon footprint accounts for 18.14% of the total carbon footprint of Jiuzhai Valley.

The external transfer of carbon footprint in Jiuzhai Valley Nature Reserve reflects the transfer or shift of environmental costs, or environmental externalities, or the Not In My Back Yard (NIMBY) of the nature reserves. The fact that Jiuzhai Valley Nature Reserve transfers its carbon emissions to the external environment can contribute to the protection of its fragile ecosystem and diverse biological environment and to the increase of carbon storage and carbon absorption capacity of the vegetation in the protected areas, and the prevention of the conversion of soil to carbon emission. It is also beneficial to realize scale effect, save energy cost and improve energy utilization efficiency by unified treatment of waste outside the Valley.

Conclusion and discussion

In 2012, the carbon footprint of human activities in Jiuzhai Valley was 3872.9 hm^2, accounting for only 5.94% of the biological productivity area in Jiuzhai Valley Nature Reserve, and the average carbon emission per capita in Jiuzhai Valley was much lower than that in China and the world. This indicates that there is a huge ecological surplus

http://www.aloki.hu ● ISSN 1589 1623 (Print) ● ISSN 1785 0037 (Online)
DOI: http://dx.doi.org/10.15666/aeer/1704_74777493

between the total supply of productive land provided by the ecosystem of Jiuzhai Valley Nature Reserve and the carbon footprint generated by absorbing human activities, which can not only support the sustainable development of tourism in Jiuzhai Valley in the future, but also make a great contribution to our ecological environment, providing a large number of carbon sinks.

From the perspective of the main body of the carbon footprint, the final carbon footprint that tourists need to bear is 88.88% of the total carbon footprint, in which the direct carbon footprint generated by tourists' own activities accounts for only a third of the total carbon footprint, while the other two thirds of the total carbon footprint are transferred by the commerce and Reserve management. The operating company that provide tourists with transportation, catering, accommodation (guesthouse in the entrance), the shopping companies causes the largest carbon footprint, accounting for 44.78% of the total carbon footprint in Jiuzhai Valley.

Comparing the carbon footprint of tourists with that of residents, the carbon footprint produced by one resident in the Reserve is equivalent to that of 367 tourists. In 2012, for example, 1241 residents in the Reserve produced the same carbon footprint as 455212 tourists. If the number of tourists is less than 455212, the activity of residents is the main cause of the negative impact of human activities on the environment of the Reserve, and tourist activity is the secondary motivation.

From the perspective of the location of the carbon footprint, the Reserve road is the largest carbon footprint producing area, accounting for 44.89% of the total carbon footprint, which is caused by the traffic carbon emissions from tourist vehicles, working vehicles and private cars. Jiuzhai Valley outdoor tourism area (excluding highway) is the second largest area of carbon footprint, accounting for 22.43% of all carbon footprint, which is mainly caused by waste and power consumption in the Reserve. The carbon footprint in the entrance of Jiuzhai Valley accounted for 20.62%, which mainly comes from the work of the commerce and Administration in the entrance of Jiuzhai Valley. Village carbon footprint should not be ignored, accounting for 10.40%, mainly from the lives of residents and a small number of family business activities. The carbon footprint of Nuorilang is the smallest, accounting for 1.67%.

From the regional transfer of final carbon emissions, 47.3% of the carbon emissions generated by human activities in Jiuzhai Valley Nature Reserve are transferred outside the Reserve, while 52.7% of which are still in the Reserve. The total carbon footprint generated by 52.7% carbon emissions is 2041.05 hm^2, which accounts for only 3.13% of the biological productivity areas in Jiuzhai Valley. The external transfer of carbon footprint in Jiuzhai Valley Nature Reserve reflects the transfer or shift of environmental costs, or environmental externalities, or the Not In My Back Yard (NIMBY) of the nature reserves.

From the perspective of the role of tourism development in carbon reduction, tourism development cannot reduce the carbon footprint of human activities in tourist areas, and tourism development is only conducive to the industrial transformation of tourist destinations, which may helps to avoid extensive industrial development producing a larger carbon footprint. Tourism development limits the unlimited growth of residents' carbon footprint, but increases the carbon footprint generated by tourists' tourism activities. Tourism activities become the main driving factor of the carbon footprint of nature reserves. If the environmental impact of nature reserve residents is greater than that of tourists, the reason is that the tourist destination is still in its early stage of

http://www.aloki.hu ● ISSN 1589 1623 (Print) ● ISSN 1785 0037 (Online)
DOI: http://dx.doi.org/10.15666/aeer/1704_74777493

development, or the tourism industry is not attractive enough to allow residents to move to tourism employment, and of course, the lack of supervision should be also to blame.

Acknowledgements. We are very grateful to Shangguan Xiaoyan in Jiuzhai Valley Administration Bureau, for helping data collection, thereby making our investigation proceeding smoothly; to Ye Bin for his unpublished energy consumption data; to director Deng Guiping for help at diverse aspects; to Zhan Qilin for technical help at various phases of the project. At last, but in the first place of course, we would like to express our special thanks to the grant of the National Social Science Foundation to the project study "Research on the development of domestic cruise tourism in China under the adjustment of supply structure" (No. 16BGL110), and the Ministry of Education to the youth planning project study "Research on the Environmental Externality and Green Governance Path of China's Cruise Industry from the Perspective of Ecological Economy" (No. 19YJC790117), and the National Science Foundation of China Funded Project: Investigation on the Pro-poor Tourism Effects and It's Influencing Mechanism on Settlement Space Evolution in Southwest Minority Villages (No.41661031).

REFERENCES

[1] Becken, S., Patterson, M. (2006): Measuring national carbon dioxide emissions from tourism as a key step towards achieving sustainable tourism. – Journal of Sustainable Tourism 14(4): 323-338.
[2] Chavez, A., Ramaswami, A. (2011): Progress toward low carbon cities: approaches for transboundary GHG emissions' footprinting. – Carbon 2(4): 471-482.
[3] Dong, Y., Yang, X. (2012): Review of low-carbon tourism research at home and abroad. – Journal of Southwest Agricultural University (Social Science Edition) 9(12): 5-11.
[4] Du, J., Shu, J., Zhang, L. (2010): The ecological footprint model based on net primary productivity and the comparative analysis with traditional model. – Ecology and Environmental Sciences 19(1): 191-196.
[5] Du, Q., Chen, Q., Lu, N. (2012): Forecast of China's carbon emissions based on modified IPAT model. – Journal of Environmental Science 32(9).
[6] Dubois, G., Ceron, J. P. (2006): Tourism/leisure greenhouse gas emissions forecasts for 2050: Factors for change in France. – Journal of Sustainable Tourism 14(2): 172-191.
[7] Fang, K., Dong, D., Lin, Z., Shen, W. (2012): Calculation method of energy ecological footprint based on global net primary productivity. – Acta Ecologica Sinica 32(9): 2900-2909.
[8] Geng, Y., Dong, H., Xi, F., Liu, Z. (2010): A review of the research on carbon footprint responding to climate change. – China Population Resources and Environment 20(010): 6-12.
[9] Gu, X., Huang, M., Ji, J., Wu, Z. (2007): The influence of climate change on vegetation net primary productivity in southwestern China during recent 20 years period. – Journal of Natural Resources 22(2).
[10] Han, L., Wu, J., Ren, R., Wang, Y. (2013): Researches on the structure trend of inbound tourism origin countries of China from 1995 to 2010. – Areal Research and Development 32(1).
[11] Hao, Y., Jiang, H., Wang, J., Jin, J., Ma, Y. (2009): Study on vegetation landscape change and habitat fragmentation in Jiuzhai Valley reserve. – Scientia Geographica Sinica 29(6): 886-892.
[12] Hertwich, E., Peters, G., Glen, P. (2009): Carbon footprint of nations: a global, trade-linked analysis. – Environmental science & technology 43(16): 6414-6420.
[13] Kitzes, J., Peller, A., Goldfinger, S., Wackernagel, M. (2007): Current methods for calculating national ecological footprint accounts. – Science for Environment & Sustainable Society 4(1): 1-9.

http://www.aloki.hu ● ISSN 1589 1623 (Print) ● ISSN 1785 0037 (Online)
DOI: http://dx.doi.org/10.15666/aeer/1704_74777493

[14] Kitzes, J., Galli, A., Bagliani, M., Barrett, J., Dige, G. et al. (2009): A research agenda for improving national Ecological Footprint accounts. – Ecological Economics 68(7): 1991-2007.
[15] Lenzen, M. (2006): Uncertainty in impact and externality assessments-implications for decision-making. – The International Journal of Life Cycle Assessment 11(3): 189-199.
[16] Lin, Z., Yin, P. (1994): Studies on the soil genetic characteristics and geographical distribution in Jiuzhai Valley region. – Journal of Southwest China Normal University (Natural Science) 19(001): 90-99.
[17] Liu, M., Li, W., Xie, G. (2010): Estimation of China ecological footprint production coefficient based on net primary productivity. – Chinese Journal of Ecology 29(3): 592-597.
[18] Liu, S., Zhang, X. (2007): Biodiversity of Jiuzhai Valley Nature Reserve. – Sichuan Science and Technology Press, Chengdu.
[19] Lu, L., Li, X., Veroustraete, F. (2005): Terrestrial net primary productivity and its spatial-temporal variability in western China. – Acta Ecologica Sinica 25(5): 1026-1032.
[20] Pandey, D., Agrawal, M., Pandey, J. S. (2011): Carbon footprint: current methods of estimation. – Environmental Monitoring and Assessment 178(1-4): 135-160.
[21] Pandey, D. N. (2002): Global climate change and carbon management in multifunctional forests. – Current Science 83(5): 593-602.
[22] Pang, X., Bao, W. Jiang, Y., Wang, C. (2009): Comparison of soil physical properties under primary and secondary forests in Jiuzhai Valley and Huanglong Nature Reserves, Sichuan, China. – Chinese Journal of Applied & Environmental Biology 6: 768-773.
[23] Ramaswami, A., Hillman, T., Janson, B., Reiner, M., Thomas, G. (2008): A demand-centered, hybrid life-cycle methodology for city-scale greenhouse gas inventories. – Environmental Science & Technology 42(17): 6455-6461.
[24] Ravindranath, N., Ostwald, M. (2008): Carbon Inventory Methods: Handbook for Greenhouse Gas Inventory, Carbon Mitigation and Roundwood Production Projects. – Springer, Netherlands.
[25] Shi, P., Wu, P., Feng, L., Zheng, B. (2010): Study on the design of emission reduction policy framework in China's tourism industry and strategic measures. – Tourism Tribune 25(6): 13-18.
[26] Wang, Q., Yang, X. (2012): Overseas study review of carbon emissions for tourism industry. – Tourism Tribune 1: 73-82.
[27] Wiedmann, T. (2009): A review of recent multi-region input–output models used for consumption-based emission and resource accounting. – Ecological Economics 69(2): 211-222.
[28] Zhang, J., Zhang, J. (2006): Research progress and model modification of ecological footprint. – Resource Science 28(6): 196-203.
[29] Zhang, J., Zhang, J., Liang, Y., Li, N., Liu, Z. (2005): An analysis of touristic ecological footprint and eco compensation of Jiuzhai Valley in 2002. – Journal of Natural Resource 20(5).
[30] Zhang, X., Zhu, Z. (2007): An analysis of tourism environment capacity in Jiuzhai Valley scenic area. – Tourism Tribune 22(9): 50-57.
[31] Zhang, X., Ren, P., Deng, G. (2009): A Study on the strategic management of the sustainable development of Jiuzhai Valley. – Journal of Southwest University for Nationalities (Humanities and Social Sciences Edition) 6: 213-216.
[32] Zhou, X. (1998): Influence of geological environmental deterioration on Jiuzhai Valley ravine landscape. – Carsologica Sinica 17(3): 301-310.

http://www.aloki.hu ● ISSN 1589 1623 (Print) ● ISSN 1785 0037 (Online)
DOI: http://dx.doi.org/10.15666/aeer/1704_74777493

CLONING AND CHARACTERIZATION OF A WHEAT RING FINGER GENE *TaRHA2b* WHOSE EXPRESSION IS UP-REGULATED BY ABA TREATMENT

LI, D. B. – LYU, G. Z. – LYU, J. P. – NIU, H. B. – WANG, X. – YIN, J.*

National Engineering Research Center for Wheat, State Key Laboratory of Wheat and Maize Crop Science, Collaborative Innovation Center of Henan Grain Crop Henan Agricultural University, Zhengzhou 450002, China

**Corresponding author*
e-mail: xmzxyj@126.com; phone: +86-03-716-355-8203

(Received 27th Feb 2019; accepted 3rd May 2019)

Abstract. Preharvest sprouting in wheat (*Triticum aestivum L.*) is the germination of grains in the ears when long range rainfall or damp conditions prior to harvest occur. E3 ubiquitination (type RING-H2) RING finger protein plays a key role in dealing with abiotic stresses in plants, which could be used to improve the PHS resistance of wheat. The full-length cDNA of a wheat RING finger gene named *TaRHA2b* was firstly cloned from wheat. Bioinformatic analysis and expression profile analysis of the *TaRHA2b* gene were carried out. The results indicated that the full-length cDNA of *TaRHA2b* was 845bp containing 465bp open reading frame which encoded 154 amino acid residues. The genomic *TaRHA2b* gene had no introns. The protein encoded by *TaRHA2b* gene was consisted of Zinc finger RING-type profile. Blast and phylogenetic analysis showed that the protein encoded by *TaRHA2b* shared the identity with *RHA2b* from the *Arabidopsis*. The result of semi RT-PCR showed that expression of *TaRHA2b* gene was significantly tissue-specific. The result of qRT-PCR showed that the expression of *TaRHA2b* in the seeds was significantly higher than the expression of gene expression after soaking germination. The sensitivity of this gene to abscisic acid was significantly increased. *TaRHA2b* gene may play an important role in seed dormancy during germination, which could be used to improve the PHS resistance of wheat.
Keywords: *wheat, bioinformatics analysis, expression profile, seed dormancy, preharvest sprouting*

Abbreviations: ABA, abscisic acid; PHS, preharvest sprouting; RING, Really Interesting New Gene; E1, ubiquitin-activating enzymes; E2, ubiquitin-conjugating enzymes; E3, ubiquitin protein ligase; ORF, open reading frame; Rel.Exp, relative expression of gene

Introduction

Pre-harvest sprouting (PHS) is one of the major adverse effects of high yield and stable yield of wheat (Xiao et al., 2002a; Li et al., 2004). In China, the phenomenon of wheat spike germination is particularly serious. Spike germination occurred frequently and seriously in the world's major wheat producers, including Canada, the United States, Britain, Australia, Brazil, Germany, Sweden and so on. Direct annual losses caused by PHS approach $1 billion dollars worldwide (Liu et al., 2013). The yield reduction caused by the problem of wheat spike germination accounts for nearly 83% of the total wheat planting area. Seed viability and hydrolysis of starch and protein in the endosperm are always reduced after PHS (Xiao et al., 2002b). At present, most of the wheat varieties used in the production have certain ear sprouting characteristics. The way to solve the PHS was as follows: firstly, the application of chemical control technology; secondly, breeding varieties with resistance to PHS. Breeding resistant cultivars is the best way to solve the problem of sprouting, but the selection and application was restricted by limited resistance source. It is very important to excavate

http://www.aloki.hu ● ISSN 1589 1623 (Print) ● ISSN 1785 0037 (Online)
DOI: http://dx.doi.org/10.15666/aeer/1704_74957510

good genes of PHS resistance, which is an ideal way to solve the PHS problem. In order to make full use of the RING finger gene to improve the resistance to PHS in wheat, a RING finger transcription factor gene *TaRHA2b* was cloned from wheat by RT-PCR and RACE amplification. Bioinformatic analysis and expression profile analysis of the *TaRHA2b* gene with the treatment of different abscisic acid (ABA) concentration were carried out. The research could provide some reference for studying the mechanism of *TaRHA2b* gene in wheat dormancy, which may be used as an excellent gene resource to improve PHS resistance.

Review of literature

The ubiquitination process is accomplished by the continuous action of ubiquitin-activating enzymes (E1), ubiquitin-conjugating enzymes (E2) and ubiquitin protein ligases (E3), and the specificity of the ubiquitin-conjugating enzyme E3 binding substrate to a great extent (Smalle and Vierstra, 2004). In the *Arabidopsis* genome, more than 1300 genes are predicted to encode different types of E3 ligases, which means that ubiquitination is involved in a wide range of cellular metabolic processes and fine adjustment of life activities (Li et al., 2017). It was found that ubiquitination linked many components of plant biology through molecular genetic analysis, including cell cycle, embryonic development, light morphogenesis, regulation of day and night patterns, hormone signaling, homologous transformation, resistance to disease and aging (Liu et al., 2017).

Ubiquitin E3 ligases are mainly classified into three groups: RING (Really Interesting New Gene) finger protein family, HECT protein family and U-box family. At present, Ring finger protein family was found to be the largest among them. There were 469, 488, 399, 725, 330 and 688 possible RING finger E3 ligase family members in *Arabidopsis thaliana*, rice, poplar, soybean, grape and apple, respectively (Kraft et al., 2005; Du et al., 2009; Lim et al., 2010; Li et al., 2011).

RING finger protein consists of a large family of proteins, which is ubiquitous in eukaryotic organisms. The RING finger domain is a typical structural feature, and it has been shown that RING finger domain plays an important role in abiotic stress of plants (Zeba et al., 2009). The RING finger domain contains a conserved amino acid sequence: Cys-X2-Cys-Xn (9-39)-Cys-X (1-3) -His-X (2-3) –Cys/His-X2-Cys-X (4-48) -Cys-X2-Cys (Cys is a cysteine residue, His is a histidine residue, X is an arbitrary amino acid residue) (Kraft et al., 2005). According to the number and location of Zn^{2+} binding residues Cys and His, the RING finger family can be divided into nine subgroups: RING-HC, RING-H2, RING-v, RING-C2, RING-D, RING-S/T, RING-G, RING-mH2 and RING-mHC (Li et al., 2011). At present, many RING finger proteins have been isolated from many plants.

In the previous study, RHA2b played an important positive role in ABA-mediated seed maturity and early germination in *Arabidopsis* (Li et al., 2011). In order to solve the problem of wheat PHS, scholars at home and abroad have conducted a series of studies on the mechanism of wheat ear germination and made many remarkable achievements. The apparent physical and physiological characteristics of wheat seeds, including ear morphology (Zanetti et al., 2000), the color of the seed coat (Torada and Amano, 2002; Bassoi and Flintham, 2005), seed structure and water absorption (King and von Wettstein-Knowles, 2000), seed dormancy (Andreoli et al., 2006; Hughes et al., 2010), ABA content (Gerjets et al., 2010) and α-amylase activity (Major et al., 2001), was studied. The characteristics of genes related to PHS or seed dormancy and the

http://www.aloki.hu ● ISSN 1589 1623 (Print) ● ISSN 1785 0037 (Online)
DOI: http://dx.doi.org/10.15666/aeer/1704_74957510

positional cloning of QTLs (Zanetti et al., 2000; Major et al., 2001; Bassoi and Flintham, 2005; Somers et al., 2007; Chen et al., 2008) was studied. PHS resistance in wheat is a quantitative trait, and relevant quantitative trait locuses linked to PHS have been reported on almost all chromosomes (Ogbonnaya et al., 2008; Munkvold et al., 2009). From the existing research results, most researchers agree that the germination of wheat spike is the result of the interaction between genotype and environment. The dormancy characteristics of plants are closely related to their spike germination characteristics. PHS-resistant wheat germplasm resources are scarce. The *VP1* and *Trx* genes have been used to increase the PHS resistance of wheat (Li et al., 2009; Huang et al., 2012). Although these attempts have yielded some progress in controlling seed dormancy and PHS, more work is required.

Materials and methods

The wheat variety "Zhengmai 9023" was tested. Zheng mai 9023 is an excellent wheat variety, but it is prone to sprouting. Further research will be carried out based on the transgenic operation of this variety to improve the resistance of PHS. Plant expression vector PGM-T, Escherichia coli DH5a and Taq DNA polymerase were purchased from Tiangen (Tiangen Biotech (Beijing) Co., Ltd., Beijing, China). MiniBEST Plant Genomic DNA Extraction Kit, Plant total RNA extraction reagent Trizol, PrimeScript^{TM} RT reagent Kit (Perfect Real Time) kit, T4 DNA ligase, TranZol^{TM} Plant kit and SYBR Premix Ex Taq^{TM} II (Tli RNaseH plus) were purchased from TaKaRa (TaKaRa Biotechnology (Dalian) Co., Ltd., Dalian, Japan).

Extraction of total DNA and RNA and synthesis of cDNA first strand

DNA was extracted from wheat germ with MiniBEST Plant Genomic DNA Extraction Kit. Trizol reagent was used to extract the total RNA from wheat germ. The extracted RNA was tested for quality and purity and then stored in a refrigerator at -80°C for reserve. PrimeScript^{TM} RT reagent Kit (Perfect Real Time) was used to synthesize cDNA from total RNA. All operations are performed according to the instructions of the kits. The cDNA was stored at -80°C for later use.

Cloning of TaRHA2b gene

According to the amino acid sequence of RING finger gene *AtRHA2b* of *Arabidopsis thaliana*, GenBank EST data was searched and many expression sequences of its highly homologous origin were obtained. By software splicing, analysis and in vitro splicing, a complete cDNA sequence with RING finger structure domain was obtained from wheat database (National Center for Biotechnology information). According to splicing products, specific Primer5.0 software was used to design the primers for the experiment (*Table 1*), and target gene prediction and in vitro splicing were conducted.

The wheat cDNA was used as template for PCR amplification. PCR reaction system 20 μL: 10x PCR Buffer 2.0 μL, 2.5 mM dNTPs 1.6 μL, 10 mM upstream and downstream primers each 0.8 μL, Taq enzyme 0.3 μL, cDNA template 1.0 μL, ddH_2O complement 20 μL. Response procedures: 94°C pre degeneration 3 min; 94°C modified 30 s, 50°C annealing 40 s, 72°C for 1 min, 30 cycle; 72°C extension time for 10 min.

The primer pairs P1-F and P1-R were designed according to the sequence. By using bioinformatics mosaic and RACE amplification, the unknown segment of the gene was

http://www.aloki.hu ● ISSN 1589 1623 (Print) ● ISSN 1785 0037 (Online)
DOI: http://dx.doi.org/10.15666/aeer/1704_74957510

cloned. The full-length cDNA sequence of wheat *TaRHA2b* gene was obtained by RT-PCR amplification with specific primers P2-F and P2-R designed according to the above product sequences. The PCR products were recovered and connected with the pGEMT vector, and the recombinant plasmid transformed into E. coli DH5α competent cells, and the positive clones were screened and sent to BGI (HuaDa Biotechnology co., ltd., China) for sequencing.

Table 1. *Primers sequences of the experiment*

Primers name	Primer sequence (from 5'sequence-3'sequence)
P1	F: TGCCCGAGGAGGTCAAGGAG
	R: CGTGATTGGATGGCTACTATACAAAGTG
P2-1	F: CAGGTGGTCCGGCCGAGGTCGAT
	R: CCAGGCACACGATGCACGTCGCCG
P2-2	F: GCGGTGGCGGCCGACACAGAGA
	R: CAAAATTGGGATTTTATTTAGCTTATTATTAG
P2	F: CGCAAACGATAGACAGGCCTG
	R: GCTCGACAACTGTAAAGTCTAGGT
P2-3	F: GTCTCCGGCCATGGGGTTCCC
	R: CGAGCTGTTGACATTTCAGATCCACTAGC
P3	F: GTTCCAATCTATGAGGGATACACGC
	R: GAACCTCCACTGAGAACAACATTACC
P4	F: GGTGGATCGACCTCGGC
	R: GCTGGGAAAACGAAAGACG

Bioinformatics analysis of TaRHA2b gene

Based on cDNA sequence, using NCBI site ORF Finder (https://www.ncbi.nlm.nih.gov/orffinder/) speculation TaRHA2b open reading frame, SingaIP TaRHA2b protein 4.1 (http://www.cbs.dtu.dk/services/SignalP/) analysis of signal peptide, TMHMM Server2.0 (http://www.cbs.dtu.dk/services/TMHMM/) to predict transmembrane regions (Krogh et al., 2001). Using SMART online server (http://smart.embl-heidelberg.de/) domain analysis of protein structure. The consistency of *TaRHA2b* homologous genes with other species was analyzed using DNAMAN, and the evolution tree was constructed with the software MEGA 7.0. The RHA2b interacting proteins network can be predicted by string software.

Tissue specific expression analysis of TaRHA2b gene

The Root, stem, leaf, cob, lemma and endosperm from 25d flowering wheat plants were taken. RNA was extracted, and reverse transcription was conducted to synthesize the first strand of cDNA.

And PCR amplification was conducted with the first strand of cDNA as template. The reaction system was the same as above. Reaction conditions: 94°C for 3 min, 94°C for 30 s, 54°C for 30 s, 72°C for 40 s, a total of 28 cycle, 72°C extension time for 10 min, electrophoresis detection of PCR products.

The *Actin* gene products amplified by wheat *Actin* gene specific primers were taken as internal reference. The primers of *Actin* gene used in PCR reaction were P3-F and P3-R (*Table 1*). And the primers of *TaRHA2b* gene were P4-F and P4-R (*Table 1*). According to the PCR reaction mixture system, PCR amplification conditions as follows: 94°C 3 min, 94°C for 30 s, 54°C for 30 s, 72°C for 35 s, a total of 28 cycle. 72°C

http://www.aloki.hu ● ISSN 1589 1623 (Print) ● ISSN 1785 0037 (Online)
DOI: http://dx.doi.org/10.15666/aeer/1704_74957510

for 10 min, RT-PCR product after 1.0% agarose electrophoresis detecting camera, preservation. The experiment was repeated for three times.

Analysis of TaRHA2b gene expression under ABA treatment

To further study the ABA response of *TaRHA2b* gene during seed germination, qRT-PCR was used to analyze the expression of *TaRHA2b* gene by ABA treatment at different concentrations and at different times at the same concentration. ABA solutions of different concentrations (*Table 2*) were used to treat wheat seeds with full and equal grain size three days after germination after disinfection. RNA was extracted with TranZol^{TM} Plant kit after 12 hours of sampling. PrimeScript^{TM} RT reagent Kit (Perfect Real Time) was used to synthesize cDNA from total RNA. All operations are performed according to the instructions of the kits. The cDNA was stored at -80°C for later use.

Table 2. *Different content of the ABA in the present study*

Group number	ABA content (μM)
1	0
2	0.25
3	0.5
4	1.0
5	2.0
6	3.0
7	4.0
8	5.0

Wheat seeds with full and equal size after disinfection were soaked with ABA solution of 0.5 μM, treatment without ABA was set for control, and samples were taken at different time (*Table 3*). RNA of dry seeds without soaking was extracted at the same time. PrimeScript^{TM} RT reagent Kit (Perfect Real Time) was used to synthesize cDNA from total RNA. The cDNA was numbered and stored at -80°C for later use.

Table 3. *Sampling time of the experiments with the treatment of 0.5 μM ABA*

Group number	Sampling time (h)
1	0
2	12
3	24
4	36
5	48

Fluorescence quantitative PCR was used to analyze the *TaRHA2b* gene expression under ABA treatment with the primers P4-F and P4-R and internal reference *Actin* gene primers P3-F and P3-R (*Table 1*). According to the relative quantitative method to calculate: The relative expression of gene (Rel.Exp) = $2^{-\Delta\Delta Ct}$, among them $-\Delta\Delta Ct$ = Calibrator ΔCt - ΔCt (the unknown sample), ΔCt (unknown sample) = (Ct) internal gene - (Ct) target gene, Calibrator ΔCt = (Ct) reference sample internal gene - (Ct) reference sample target gene. The reaction system of fluorescence quantitative PCR was 20 μL: SYBR Premix Ex Taq^{TM} II, 10 μL, PCR Forward Premer (10 μM) 0.8 μL, PCR Reverse Premer (10 μM) 0.8 μL, ROX Reference Dye II (50x), cDNA template 2 μL, ddH_2O up to 20 μL.

http://www.aloki.hu ● ISSN 1589 1623 (Print) ● ISSN 1785 0037 (Online)
DOI: http://dx.doi.org/10.15666/aeer/1704_74957510

Statistical analysis

The software package SPSS 13.0 was used for statistical analysis. For comparing results of different treatments, the Tukey ANOVA test was performed. Differences were considered significant for $P<0.05$.

Results

Analysis of TaRHA2b gene sequence and its coding protein structure

cDNA cloning of wheat *TaRHA2b* gene was synthesized using bioinformatics splicing combined with RACE amplification. First, the amino acid sequence of RING finger gene *AtRHA2b* was used to search for GenBank EST data, and the wheat EST (CA741783) with high homology was obtained (*Fig. 1A*). Secondly, specific primers P2-1-F and P2-1-R, P2-2-F and P2-2-R were designed according to the wheat EST sequence, and 5 'RACE (*Fig. 1B*) and 3' RACE (*Fig. 1C*) were respectively used to clone the unknown regions of the TaRHA2b gene. Finally, according to the above product sequence design, the specific primers P2-F and P2-R were used to amplify the full-length *TaRHA2b* fragment by RT-PCR (*Fig. 1D*), and the target sequence was obtained. The sequencing results confirmed that the length of *TaRHA2b* gene was 845 bp, including the 5 '-end non-coding sequence of 79 bp, the 3' -end non-coding sequence of 301 bp and the open reading frame (ORF) of 465 bp, encoding 155 amino acids (*Fig. 2*), the molecular weight was about 16.94 kD, and the isoelectric point was 7.77, belonging to weakly alkaline protein. This gene was named *TaRHA2b*. The GenBank accession number of the *TaRHA2b* gene is JN661690.1.

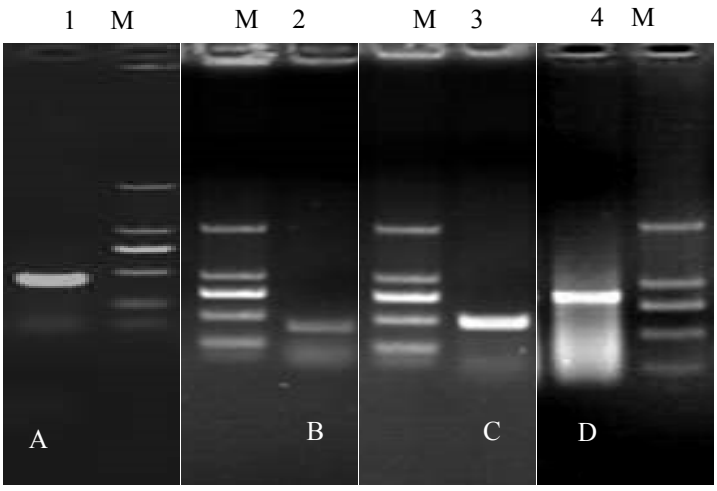

Figure 1. *Amplification of cDNA fragments of TaRHA2b gene in wheat immature endosperm. A, EST of TaRHA2b fragment; B, 3' RACE of TaRHA2b fragment; C, 5' RACE of TaRHA2b fragment; D, full-length TaRHA2b fragment; M, marker*

To further obtain the detailed information of the *TaRHA2b* gene, PCR amplification was performed using primers P2-3-F and P2-3-R (*Table 1*) with wheat genomic DNA as the template. The amplification products were sequenced. The analysis of sequencing showed that *TaRHA2b* gene had no introns.

http://www.aloki.hu ● ISSN 1589 1623 (Print) ● ISSN 1785 0037 (Online)
DOI: http://dx.doi.org/10.15666/aeer/1704_74957510

The results of SingaIP 4.1 analysis of the signal peptide software showed that TaRHA2b contains a signal peptide sequence with a length of 32 (S^1-F^{32}) and 39 (M^1-M^{40}) amino acid residues, indicating that this kind of protein needs transmembrane transfer (localization) during the synthesis process, and then the signal peptide can be removed under the specific protease to form the mature protein sequence. Further structural analysis revealed that all RHA transcription factors, including TaRHA2b, contained motif with a length of 49 amino acid residues (RING-H2 motif), $CX_2CX_{14-15}CXHX_2HX_2CX_3WX_{6-8}CPXC$.

```
1         CGCAAACGATAGACAGGCCTGGCCGGCGCAGCCTGTGACGTTCGAGCTCCCGCCGGGCGT
61        CCACGCGTCGTCTCCGGCCATGGGGTTCCCCCTGGTGTGCTACTGCGTCGCCATCCCCAA
1                           M  G  F  P  L  V  C  Y  C  V  A  I  P  K

121       GCCGGTCATCGCCTTCTGCAAGCTCGTCGCCGCCGTCAGGGACGCCCTCCTCCTGCTGCT
15          P  V  I  A  F  C  K  L  V  A  A  V  R  D  A  L  L  L  L  L

181       CTCCCTCGTCGGCCTCTGCCGCTCCCCGCGCCGCTCTGTGGACGACGCCCCGCTGCCCGA
35          S  L  V  G  L  C  R  S  P  R  R  S  V  D  D  A  P  L  P  E

241       GGAGGTCAAGGAGCGCCTCCCGGCCGTCGAGTTCGGCTGCCTGGCGCGTCCGGCGCAGCA
55          E  V  K  E  R  L  P  A  V  E  F  G  C  L  A  R  P  A  Q  Q

301       GCAGCAGCACGACGGGGACGACGACGAGGTCGCCGCCGCGGCGACGTGCATCGTGTGCCT
75          Q  Q  H  D  G  D  D  D  E  V  A  A  A  A  T  C  I  V  C  L

361       GGAGAGGCTGCGGGCGACGGACGAGGTGCGGCGGCTGGGCAACTGCGCGCACGCCTTCCA
95          E  R  L  R  A  T  D  E  V  R  R  L  G  N  C  A  H  A  F  H

421       CCGGGGCTGCATCGACGGGTGGATCGACCTCGGCCGGACCACCTGCCCGCTGTGTCGCTC
115         R  G  C  I  D  G  W  I  D  L  G  R  T  T  C  P  L  C  R  S

481       CCACCTACTGCCTCGCGCGCGGAGGGACGGCCCGCTCGCCAGCCTCCTCACGCGCGTTTG
135         H  L  L  P  R  A  R  R  D  G  P  L  A  S  L  L  T  R  V  W

541       GTGACGACCAACCGCGCCAGGTTAGCTCGAAGGCCACGTCTTTCGTTTTCCCAGCGCGGT
155         *

601       GGCGGCCGACACAGAGATTCGCGATCTCGACCGGCTGCATGTGTATTTAATGTGGGTTTA
661       CATCATCTCAAAATTGGGATTTTATTTAGCTTATTATTAGGGCGCCACTTTGTATAGTAG
721       CCATCCAATCACGAGGTCACCAATAGGTGCATACGCATAGTTTTTTCCCCCCGTAGAGAA
781       GGATTCTTTGGTCGAACATATGTGTACTAGCGTTTGGCTAGTGGATCTGAAATGTCAACA
841       GCTCG
```

Figure 2. *Nucleotide and deduced amino acid sequences of the TaRHA2b gene*

TaRHA2b encoding amino acid sequence alignment and phylogenetic tree

The bioinformatics software DNAMAN was used to sequence and predict the amino acid sequence of *TaRHA2b* gene (*Fig. 2*). The protein encoded by *TaRHA2b* gene was consisted of Zinc finger RING-type profile (*Fig. 3*).

```
MGFPLVCYCVAIPKPVIAFCKLVAAVRDALLLLLSLVGLCRSPRRSVDDAPLPEEVKERLPAVEFG
CLARPAQQQQHDGDDDEVAAAATCIVCLERLRATDEVRRLGNCAHAFHRGCIDGWIDLGRTTCPLC
RSHLLPRARRDGPLASLLTRVW
```

Figure 3. *Domain analysis of TaRHA2b protein. The yellow part of the amino acid corresponds to the blue part of the functional domain*

http://www.aloki.hu ● ISSN 1589 1623 (Print) ● ISSN 1785 0037 (Online)
DOI: http://dx.doi.org/10.15666/aeer/1704_74957510

The sequence combination and similarity analysis of RING-H2 motif with 4 types of RING finger proteins (BOXSHADE 1.80) were performed (*Fig. 4*). The results showed that the amino acid sequence from wheat was similar with RHA2a and RHA2b from the *Arabidopsis*, indicating that this RING finger transcription factor and AtRHA2b belonged to the same family.

Figure 4. *Comparison of the RING finger motif sequences of four type RHA proteins. The missed base is marked with "-"; conserver residues are marked with "*"; TaRHA2b (AEQ67396), AtRHA1a (NP_192876), AtRHA1b (NP_192875), AtRHA2a (NP_172962), AtRHA2b (OAP11108), AtRHA3a (NP_179337), AtRHA3b (NP_195273) and NaRHA4a (XP_019266728) are the RING finger motif sequences of four type RHA proteins from Triticum aestivum, Arabidopsis thaliana and Nicotiana attenuate*

http://www.aloki.hu ● ISSN 1589 1623 (Print) ● ISSN 1785 0037 (Online)
DOI: http://dx.doi.org/10.15666/aeer/1704_74957510

By applying MAGE software, the protein sequence of RING finger transcription factor was compared multiple times to map the phylogenetic tree (*Fig. 5*). The results showed that *TaRHA2b* gene was very similar to *AtRHA2b* gene.

The interacting protein network of RHA2b includes KIN1(AT5G15960.1), ATDI8(AT5G66400.1), AT5G12110(AT5G12110.1), KUOX1(AT5G07480.1), KUF1(AT1G31350.1), AIRP1(AT4G23450.2), SDIR1(AT3G55530.1), KEG(AT5G13530.1), AT5G58410(AT5G58410.1) and NAC019(AT1G52890.1) (*Fig. 6*). RHA2b is involved in the ubiquitination of proteins, cell protein metabolism, and response to acidic compounds. The function of proteins interacting with RHA2b is listed in *Table 4*. The results showed that *RHA2b* gene is essential for plant growth and development and stress response.

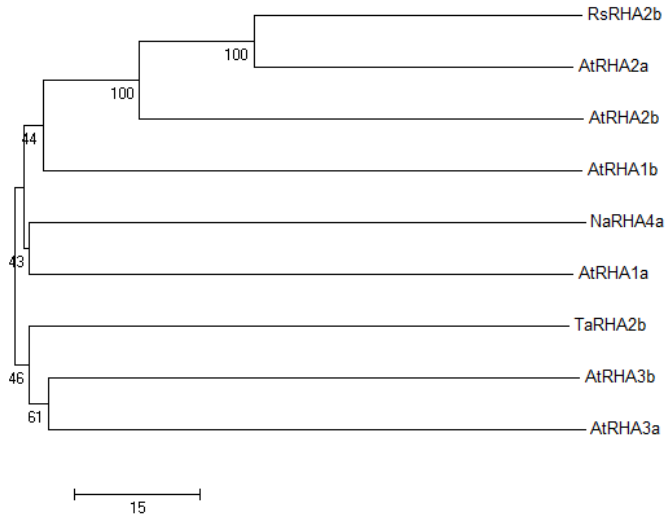

Figure 5. *A phylogenetic tree of the RING finger motifs (with the software MEGA 7.0)*

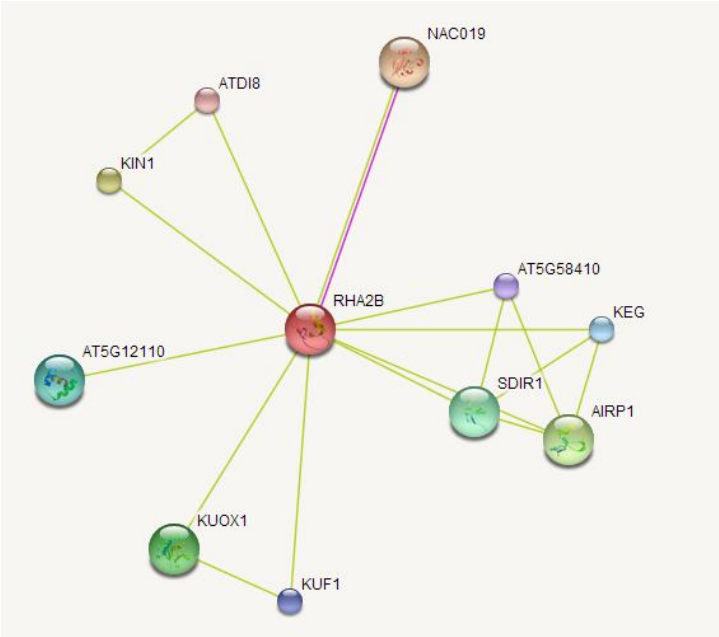

Figure 6. *Interaction network of RHA2b protein (prediction by string software)*

http://www.aloki.hu ● ISSN 1589 1623 (Print) ● ISSN 1785 0037 (Online)
DOI: http://dx.doi.org/10.15666/aeer/1704_74957510

Table 4. *The function of proteins interacting with RHA2b (prediction by string software)*

Proteins	Function
KIN1, ATDI8, SDIR1 and KEG	ABA stress response
KIN1, ATDI8, SDIR1 and NAC019	water loss stress response
RHA2b, SDIR1, KEG, AT5G58410 and AIRP1	the process of protein ubiquitination
KIN1, ATDI8, SDIR1, NAC019, RHA2b and KUF1	non-biological stress response
KIN1, ATDI8, SDIR1, NAC019 and KEG	acidic and oxygen-containing stress response
KIN1 and ATDI8	low temperature stress response
SDIR1, KEG, RHA2b, AT5G58410, AT5G12110 and KUF1	the process of cell protein metabolism

Tissue specific expression analysis of TaRHA2b gene

The root, stem, leaf, cob, lemma and endosperm of wheat were used to detect expression arrays of *TaRHA2b* gene (*Fig. 7*). There was strong expression of *TaRHA2b* gene in the cob, lemma and endosperm tissue, while weak expression of *TaRHA2b* gene in root, stem and leaf tissue. The result showed that the expression of *TaRHA2b* gene in wheat is tissue-specific.

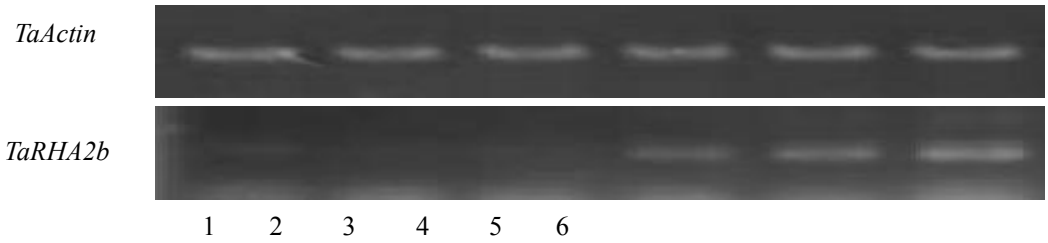

Figure 7. *Expression analysis of TaRHA2b gene in different organs of wheat. Expression was analyzed by semi-quantitative RT-PCR.1, roots; 2, stems; 3, leaves; 4, cob; 5, lemma; 6, endosperm*

Expression profile of TaRHA2b gene under ABA treatment

The results of tissue specific expression analysis of *TaRHA2b* gene showed that *TaRHA2b* gene was highly expressed in endosperm, and it can be inferred that *TaRHA2b* gene may be involved in seed germination. ABA is an important plant hormone that regulates seed maturation, development and germination. Therefore, in order to study whether *TaRHA2b* gene is involved in ABA signaling pathway, we analyzed the response of *TaRHA2b* gene to exogenous ABA during wheat seed germination.

The results showed that the transcription expression of *TaRHA2b* gene was induced by ABA (*Fig. 8*). The different ABA concentration (0 μM, 0.25 μM, 0.5 μM, 1.0 μM, 2.0 μM, 3.0 μM, 4 μM and 5 μM) was used to explore whether the *TaRHA2b* gene was sensitive to ABA or not. With the increase of ABA concentration, the gene expression level gradually increased. The gene expression level was at the expression peak at 0.5 μM, which was extremely significant compared with the control ($p < 0.01$). After that, the *TaRHA2b* gene expression level gradually decreased. And The expression level of the *TaRHA2b* gene was similar between the experimental group and the control group. So the 0.5 μM ABA concentration was used for follow-up research.

http://www.aloki.hu ● ISSN 1589 1623 (Print) ● ISSN 1785 0037 (Online)
DOI: http://dx.doi.org/10.15666/aeer/1704_74957510

ABA response analysis of TaRHA2b gene in early stage after germination

It showed that *TaRHA2b* gene expression is highest in dry seeds (*Fig. 9*). During seed germination, *TaRHA2b* gene expression decreased as a whole compared with dry seeds. It decreased most significantly at the stage of 12 h with 0.5 μM ABA treatment and increased at the stage of 24 h with 0.5 μM ABA treatment. The expression of *TaRHA2b* gene in the samples with the treatment of 0.5 μM ABA was higher than the samples without the treatment of ABA, and the second half of the S curve of *TaRHA2b* gene expression in the treatment group showed a tendency to be straightened.

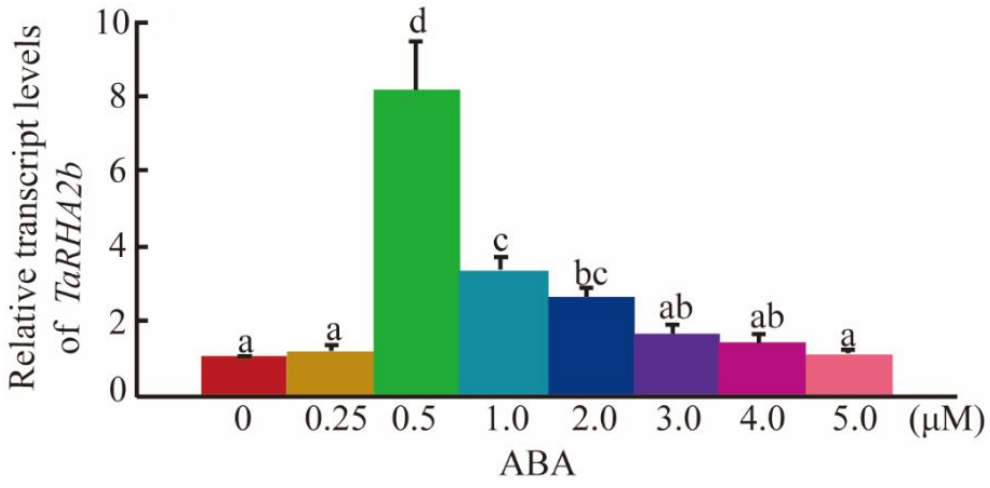

Figure 8. *TaRHA2b expression in 3-d-old seedlings with the treatment of different ABA content for 12h. The letters 'a' to 'd' indicate statistically significant differences by Turkey's least significantly difference test ($p<0.05$)*

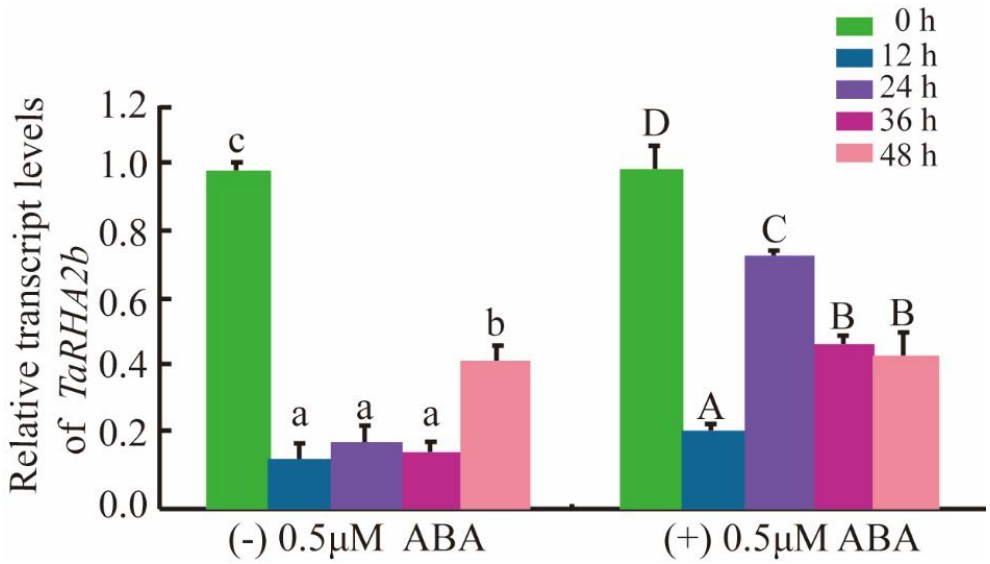

Figure 9. *TaRHA2b expression in seeds during germination with the treatment of 0.5μM ABA. (-) 0.5μM ABA, the letters 'a' to 'd' indicate statistically significant differences by Turkey's least significantly difference test ($p<0.05$); (+) 0.5μM ABA, the letters 'A' to 'D' indicate statistically significant differences by Turkey's least significantly difference test ($p<0.05$)*

http://www.aloki.hu ● ISSN 1589 1623 (Print) ● ISSN 1785 0037 (Online)
DOI: http://dx.doi.org/10.15666/aeer/1704_74957510

Discussion

Many studies have shown that over-expression of RING-H2 protein in model plant can affect abiotic stress (Lyzenga and Stone, 2012; Stone, 2014). Some RING finger type E3 ubiquitin ligase is involved in some specific plant signaling pathways, mainly ABA signaling pathways (Devoto and Turner, 2003; Moon et al., 2004; Schwechheimer and Schwager, 2004; Hoecker, 2005; Dreher and Callis, 2007). Several RING finger genes have been reported. AIP2 and KEG, two proteins with RING finger structure in ABA signaling pathway, are two important positive regulators of ABI3 and ABI5, respectively, which are negative regulators of ABA signaling pathway (Stone et al., 2006). It was found that CIPK26 interacted with KEG through yeast two-hybridization, and proved that CIPK26 participated in ABI5-mediated and KEG-mediated ABA stress response (Lyzenga et al., 2013).Whether there is an interaction among the three protein (CIPK26, ABI5 and KEG) is unclear. SDIRIP1, the substrate of SDIR1, was degraded by ubiquitin-proteasome pathway. SDIR1 controlled ABA related germination and stress response. SDIRIP1 participates in ABA and salt stress pathways by negatively regulating ABI5 expression (Zhang et al., 2015). Overexpression of *AtXerico* in *Arabidopsis thaliana* and rice significantly increased plant sensitivity to ABA and salt, and significantly increased plant drought resistance (Ko et al., 2006; Zeng et al., 2015). Overexpression of *AtXerico* homologous gene *OsRHP1* in rice showed increased drought and salt tolerance, ABA content, and the expression of ABA biosynthetic genes and related genes (Zeng et al., 2014). The overexpression of *ZmXerico* in maize can improve drought resistance and ABA content. It is also proved that *ZmXerico1* plays a role in ABA dynamic equilibrium by regulating the stability of ABA 8 '-hydroxylase protein and is a new control point in the ABA regulation pathway (Brugiere et al., 2017).

A RING finger transcription factor gene *TaRHA2b* was cloned by RT-PCR and RACE in this study. It was found that the gene belonged to the typical RING-H2 finger family. The bioinformatics analysis results showed that *TaRHA2b* gene was very similar to *AtRHA2b*. Therefore, it is speculated that *TaRHA2b* is similar in function to *AtRHA2b*.

It can be seen that spike germination caused certain physiological damage to wheat (*Fig. 10*). The dormancy and germination of seeds are regulated by hormones and metabolic pathways inside the seeds. PHS resistance is closely related to seed dormancy. Varieties with strong dormancy have strong PHS resistance, while those with weak dormancy are easy to germinate. The external environment can influence the PHS resistance of wheat to some extent, but the most critical determinant is seed dormancy, especially the endogenous ABA content and the sensitivity of seeds to ABA. Genetic studies of several species have also confirmed that ABA can effectively induce seed dormancy.

Overexpression of *RHA2a* in transgenic *Arabidopsis* increased the sensitivity to ABA, increased seed dormancy and decreased seed germination rate (Bu et al., 2009). The *rha2b-1* mutant with high homology between AtRHA2b and AtRHA2a also showed ABA insensitive phenotype and drought sensitivity (Li et al., 2011). The interaction between ATAF2 and RHA2a in yeast were found. RHA2a could negatively regulate Flg22-induced root growth inhibition and seedling growth inhibition in *Arabidopsis thaliana* and promote the growth of Pst DC3000. RHA2a can activate positive regulators by mono-ubiquitinating and stabilizing certain key regulators of the ABA signaling pathway. ANAC019 and ANAC055, two closely related NAC family proteins, were identified as RHA2a-interacting proteins (Bu et al., 2008; Jiang et al.,

http://www.aloki.hu ● ISSN 1589 1623 (Print) ● ISSN 1785 0037 (Online)
DOI: http://dx.doi.org/10.15666/aeer/1704_74957510

2009). RHA2b targets MYB30 degradation to regulate ABA signal transduction (Zheng et al., 2018).

The analysis of the expression of wheat *TaRHA2b* gene showed its tissue specificity. There was higher expression of *TaRHA2b* gene in the cob, lemma and endosperm tissues than other tissues. It showed that *TaRHA2b* gene was involved in the regulation of seed formation and dormancy.

The germination rate of *Arabidopsis thaliana* seeds over-expression *AtRHA2a* and *AtRHA2b* significantly decreased and the sensitivity to exogenous ABA of them were enhanced. It suggested that *TaRHA2b* may play an equally important role in the dormancy-germination process and could be used as an excellent genetic resource to improve the germination characteristics of spike.

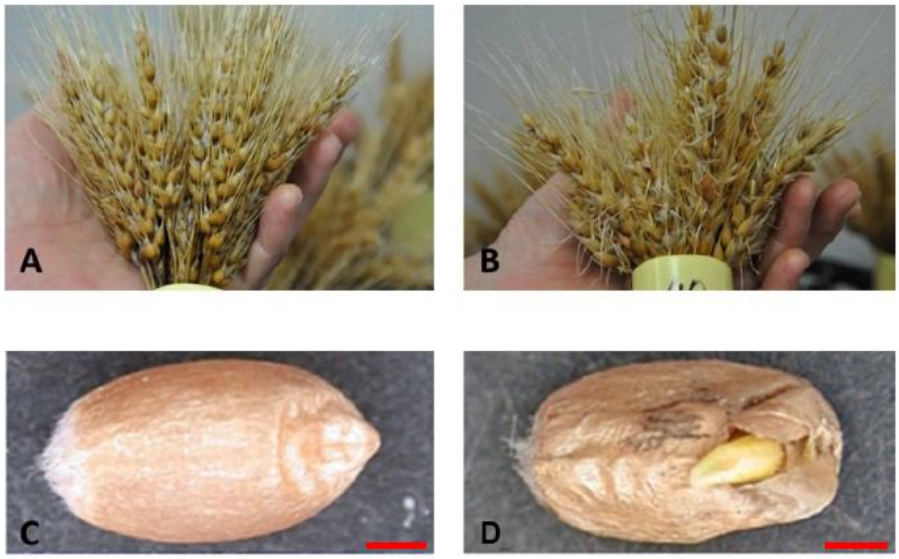

Figure 10. *Physical damage of wheat caused by PHS. A: Spike of PHS-resistant germplasm; B: Spike of PHS-susceptible germplasm; C: Grain of PHS-resistant germplasm; D: Grain of PHS-susceptible germplasm. The bar value is 1 mm*

The expression profile of *TaRHA2b* gene with the treatment of different ABA concentration showed that *TaRHA2b* gene was highly expressed in dry seeds. And its expression decreased rapidly after soaking germination, which was similar to the expression pattern of similar *AtRHA2b* gene in *Arabidopsis thaliana*. The results indicated that the function of *RHA2b* gene in plants is relatively similar, especially in ABA signal transduction pathway. The results showed that *TaRHA2b* gene may be an excellent genetic resource to improve PHS resistance. More work is needed for using *TaRHA2b* gene to improve dormancy and PHS tolerance in wheat.

Conclusion

The full-length cDNA of the RING finger gene *TaRHA2b* was cloned from wheat. The full-length cDNA of *TaRHA2b* encoded 154 amino acid residues, which was consisted of Zinc finger RING-type profile. The genomic *TaRHA2b* gene had no introns. TaRHA2b shared the identity with RHA2b from the *Arabidopsis*. The main result are as

http://www.aloki.hu ● ISSN 1589 1623 (Print) ● ISSN 1785 0037 (Online)
DOI: http://dx.doi.org/10.15666/aeer/1704_74957510

follows: (1) the expression of *TaRHA2b* gene was significantly tissue-specific; (1) the expression of *TaRHA2b* in the seeds was significantly higher than the expression of gene expression after soaking germination; (3) the sensitivity of the *TaRHA2b* gene to ABA was significantly increased. Some questions are as follows: (1) the distribution of *TaRHA2b* gene coding region in donor ancestors and different varieties could be studied to explore the mechanism mediated with *TaRHA2b* gene in PHS resistance;(2) the proteins interacted with TaRHA2b could be screened by yeast two hybrid system, which may be the new genes of PHS resistance genes; (3) how does the *TaRHA2b* gene regulate in ABA signal transduction. Further researches on the mechanism of wheat mediated with *TaRHA2b* gene in PHS resistance should be futher expanded in the future.

Acknowledgements. This work was supported by the "Twelfth Five-Year" National Science and Technology Projects in Rural Areas (2013BADD04B01-02) and Henan Science and Technology Project (162102110007). Hongbin Niu designed the research; Dongbing Li and Junpeng Lyu performed the experiment; Dongbing Li drafted the manuscript; Guizhen Lyu provided ideas; Xiang Wang and Jun Yin edited the manuscript; Dongbing Li and Guizhen Lyu read and approved the final manuscript. Authors state no conflict of interest.

REFERENCES

[1] Andreoli, C., Bassoi, M. C., Brunetta, D. (2006): Genetic control of seed dormancy and pre-harvest sprouting in wheat. – Scientia Agricola 63: 564-566.
[2] Bassoi, M. C., Flintham, J. (2005): Relationship between grain colour and preharvest sprouting-resistance in wheat. – Pesquisa Agropecuária Brasileira 40: 981-988.
[3] Brugiere, N., Zhang, W., Xu, Q., Scolaro, E. J., Lu, C., Kahsay, R. Y., Kise, R., Trecker, L., Williams, R. W., Hakimi, S., Niu, X., Lafitte, R., Habben, J. E. (2017): Overexpression of ring domain E3 ligase ZmXerico1 confers drought tolerance through regulation of ABA homeostasis. – Plant Physiol 175: 1350-1369.
[4] Bu, Q., Jiang, H., Li, C.-B., Zhai, Q., Zhang, J., Wu, X., Sun, J., Xie, Q., Li, C. (2008): Role of the Arabidopsis thaliana NAC transcription factors ANAC019 and ANAC055 in regulating jasmonic acid-signaled defense responses. – Cell Research 18: 756-767.
[5] Bu, Q. Y., Li, H. M., Zhao, Q. Z., Jiang, H. L., Zhai, Q. Z., Zhang, J., Wu, X. Y., Sun, J. Q., Xie, Q., Wang, D. W., Li, C. Y. (2009): The Arabidopsis ring finger E3 ligase RHA2a Is a novel positive regulator of abscisic acid signaling during seed germination and early seedling development. – Plant Physiology 150: 463-481.
[6] Chen, C. X., Cai, S. B., Bai, G. H. (2008): A major QTL controlling seed dormancy and pre-harvest sprouting resistance on chromosome 4A in a Chinese wheat landrace. – Molecular Breeding 21: 351-358.
[7] Devoto, A., Turner, J. G. (2003): Regulation of jasmonate-mediated plant responses in Arabidopsis. – Annals of Botany 92: 329-337.
[8] Dreher, K., Callis, J. (2007): Ubiquitin, hormones and biotic stress in plants. – Annals of Botany 99: 787-822.
[9] Du, Z., Zhou, X., Li, L., Su, Z. (2009): plantsUPS: a database of plants' Ubiquitin Proteasome System. – BMC Genomics 10: 227.
[10] Gerjets, T., Scholefield, D., Foulkes, M. J., Lenton, J. R., Holdsworth, M. J. (2010): An analysis of dormancy, ABA responsiveness, after-ripening and pre-harvest sprouting in hexaploid wheat (Triticum aestivum L.) caryopses. – Journal of Experimental Botany 61: 597-607.
[11] Hoecker, U. (2005): Regulated proteolysis in light signaling. – Current Opinion in Plant Biology 8: 469-476.

http://www.aloki.hu ● ISSN 1589 1623 (Print) ● ISSN 1785 0037 (Online)
DOI: http://dx.doi.org/10.15666/aeer/1704_74957510

[12] Huang, T., Qu, B., Li, H. P., Zuo, D. Y., Zhao, Z. X., Liao, Y. C. (2012): A maize viviparous 1 gene increases seed dormancy and preharvest sprouting tolerance in transgenic wheat. – Journal of Cereal Science 55: 166-173.
[13] Hughes, K., Griffey, C., Parrish, D., Barbeau, W., Souza, E., Thomason, W. (2010): Preharvest Sprouting Tolerance in Current Soft Red Winter Wheat Cultivars. – Crop science 50: 1449-1457.
[14] Jiang, H., Li, H., Bu, Q., Li, C. (2009): The RHA2a-interacting proteins ANAC019 and ANAC055 may play a dual role in regulating ABA response and jasmonate response. – Plant signaling & behavior 4: 464-466.
[15] King, R., von Wettstein-Knowles, P. (2000): Epicuticular waxes and regulation of ear wetting and pre-harvest sprouting in barley and wheat. – Euphytica 112: 157-166.
[16] Ko, J. H., Yang, S. H., Han, K. H. (2006): Upregulation of an Arabidopsis RING-H2 gene, XERICO, confers drought tolerance through increased abscisic acid biosynthesis. – Plant Journal 47: 343-355.
[17] Kraft, E., Stone, S. L., Ma, L., Su, N., Gao, Y., Lau, O. S., Deng, X. W., Callis, J. (2005): Genome analysis and functional characterization of the E2 and ring-type E3 ligase ubiquitination enzymes of Arabidopsis. – Plant Physiology 139: 1597-1611.
[18] Krogh, A., Larsson, B., Von, H. G., Sonnhammer, E. L. (2001): Predicting transmembrane protein topology with a hidden Markov model: application to complete genomes. – Journal of Molecular Biology 305: 567-580.
[19] Li, C., Ni, P., Francki, M., Hunter, A., Zhang, Y., Schibeci, D., Li, H., Tarr, A., Wang, J., Cakir, M. (2004): Genes controlling seed dormancy and pre-harvest sprouting in a rice-wheat-barley comparison. – Functional & integrative genomics 4: 84-93.
[20] Li, Y. C., Ren, J. P., Cho, M. J., Zhou, S. M., Kim, Y. B., Guo, H. X., Wong, J. H., Niu, H. B., Kim, H. K., Morigasaki, S. (2009): The level of expression of thioredoxin is linked to fundamental properties and applications of wheat seeds. – Molecular plant 2: 430-441.
[21] Li, H., Jiang, H., Bu, Q., Zhao, Q., Sun, J., Xie, Q., Li, C. (2011): The Arabidopsis RING finger E3 ligase RHA2b acts additively with RHA2a in regulating abscisic acid signaling and drought response. – Plant Physiol 156: 550-63.
[22] Li, X., Hasegawa, Y., Lu, Y., Sato, T. (2017): Ubiquitin related enzymes and plant-specific ubiquitin ligase ATL family in tomato plants. – Plant Biotechnology 34: 71-78.
[23] Lim, S. D., Yim, W. C., Moon, J. C., Dong, S. K., Lee, B. M., Jang, C. S. (2010): A gene family encoding RING finger proteins in rice: their expansion, expression diversity, and co-expressed genes. – Plant Molecular Biology 72: 369.
[24] Liu, S., Sehgal, S. K., Li, J., Lin, M., Trick, H. N., Yu, J., Gill, B. S., Bai, G. (2013): Cloning and characterization of a critical regulator for preharvest sprouting in wheat. – Genetics 195: 263-273.
[25] Liu, H., Ravichandran, S., Teh, O. K., Mcvey, S., Lilley, C., Teresinski, H. J., Gonzalez-Ferrer, C., Mullen, R. T., Hofius, D., Prithiviraj, B., Stone, S. L. (2017): The ring-type E3 ligase XBAT35.2 is involved in cell death induction and pathogen response. – Plant Physiol 175: 1469-1483.
[26] Lyzenga, W. J., Stone, S. L. (2012): Abiotic stress tolerance mediated by protein ubiquitination. – Journal of Experimental Botany 63: 599-616.
[27] Lyzenga, W. J., Liu, H., Schofield, A., Muisehennessey, A., Stone, S. L. (2013): Arabidopsis CIPK26 interacts with KEG, components of the ABA signalling network and is degraded by the ubiquitin–proteasome system. – Journal of Experimental Botany 64: 2779-2791.
[28] Major, B., Kettlewell, P., Scott, R. (2001): Mechanisms leading to excess alpha-amylase activity in wheat (Triticum aestivum, L) grain in the UK. – Journal of Cereal Science 33: 313-329.
[29] Moon, R. T., Kohn, A. D., De Ferrari, G. V., Kaykas, A. (2004): WNT and beta-catenin signalling: diseases and therapies. – Nature Reviews Genetics 5: 691-701.

http://www.aloki.hu ● ISSN 1589 1623 (Print) ● ISSN 1785 0037 (Online)
DOI: http://dx.doi.org/10.15666/aeer/1704_74957510

[30] Munkvold, J. D., Tanaka, J., Benscher, D., Sorrells, M. E. (2009): Mapping quantitative trait loci for preharvest sprouting resistance in white wheat. – Theoretical and applied genetics 119: 1223-1235.
[31] Ogbonnaya, F. C., Imtiaz, M., Ye, G., Hearnden, P. R., Hernandez, E., Eastwood, R. F., van Ginkel, M., Shorter, S., Winchester, J. (2008): Genetic and QTL analyses of seed dormancy and preharvest sprouting resistance in the wheat germplasm CN10955. – Theoretical and Applied Genetics 116: 891-902.
[32] Schwechheimer, C., Schwager, K. (2004): Regulated proteolysis and plant development. – Plant Cell Reports 23: 353-364.
[33] Smalle, J., Vierstra, R. D. (2004): Ubiquitin 26S proteasome proteolytic pathway. – Annual Review of Plant Biology 55: 555-590.
[34] Somers, D., Ogbonnaya, F. C., Imtiaz, M., Depauw, R. M. (2007): Haplotype diversity of preharvest sprouting QTLs in wheat. – Genome 50: 107-118.
[35] Stone, S. L., Williams, L. A., Farmer, L. M., Vierstra, R. D., Callis, J. (2006): KEEP ON GOING, a RING E3 ligase essential for Arabidopsis growth and development, is involved in abscisic acid signaling. – Plant Cell 18: 3415-28.
[36] Stone, S. L. (2014): The role of ubiquitin and the 26S proteasome in plant abiotic stress signaling. – Frontiers in Plant Science 5: 135.
[37] Torada, A., Amano, Y. (2002): Effect of seed coat color on seed dormancy in different environments. – Euphytica 126: 99-105.
[38] Xiao, S.-H., Zhang, X.-Y., Yan, C.-S., Lin, H. (2002a): Germplasm improvement for preharvest sprouting resistance in Chinese white-grained wheat: an overview of the current strategy. – Euphytica 126: 35-38.
[39] Xiao, S., Zhang, X., Yan, C., Lin, H. (2002b): Germplasm improvement for preharvest sprouting resistance in Chinese white-grained wheat: An overview of the current strategy. – Euphytica 126: 35-38.
[40] Zanetti, S., Winzeler, M., Keller, M., Keller, B., Messmer, M. (2000): Genetic analysis of pre-harvest sprouting resistance in a wheat× spelt cross. – Crop science 40: 1406-1417.
[41] Zeba, N., Isbat, M., Kwon, N. J., Lee, M. O., Kim, S. R., Hong, C. B. (2009): Heat-inducible C3HC4 type RING zinc finger protein gene from Capsicum annuum enhances growth of transgenic tobacco. – Planta 229: 861-71.
[42] Zeng, D. E., Hou, P., Xiao, F., Liu, Y. (2014): Overexpressing a novel RING-H2 finger protein gene, OsRHP1 , enhances drought and salt tolerance in rice (Oryza sativa L.). – Journal of Plant Biology 57: 357-365.
[43] Zeng, D. E., Hou, P., XIAO, F. & LIU, Y. (2015): Overexpression of Arabidopsis XERICO gene confers enhanced drought and salt stress tolerance in rice (Oryza Sativa L.). - Journal of Plant Biochemistry & Biotechnology 24: 56-64.
[44] Zhang, H., Cui, F., Liu, L., Tian, M., Ning, Y., Lou, L., Shu, K., Wu, Y., Tang, S., Xie, Q. (2015): The ring finger ubiquitin E3 ligase SDIR1 targets SDIR1-INTERACTING PROTEIN1 for degradation to modulate the salt stress response and ABA signaling in Arabidopsis. – Plant Cell 27: 214-227.
[45] Zheng, Y., Chen, Z., Ma, L., Liao, C. (2018): The ubiquitin E3 ligase RHA2b promotes degradation of MYB30 in abscisic acid signaling. – Plant Physiology 178: 428-440.

http://www.aloki.hu ● ISSN 1589 1623 (Print) ● ISSN 1785 0037 (Online)
DOI: http://dx.doi.org/10.15666/aeer/1704_74957510

THE INFLUENCE OF LAND USE AND MANAGEMENT MEASURES ON THE QUALITY OF GRASSLAND SOIL

WANG, K.[1] – JIAO, Z.[2] – TIAN, X.[1,3*] – FAN, H.[1] – ZHANG, F.[1] – LI, Y.[1]

[1]*The Agriculture of Shihezi University, 832000 Xinjiang, Shihezi, China*

[2]*College of Biology and Geography, Yili Normal University, 835000 Xinjiang, China*

[3]*College of Agriculture and Forestry, Hebei North University, 075000 Zhangjiakou, Hebei, China*

**Corresponding author*
e-mail: wky20@163.com

(Received 27th Feb 2019; accepted 3rd May 2019)

Abstract. Improper conversion of grassland utilization patterns leads to soil quality degradation and increased soil erosion. Analysis of the differences and sensitivities of soil physical, chemical and biological quality indicators under different agricultural management practices, research with the development of Xinjiang YiLi Nalati representing the natural grassland grazing grassland, conventional farming and organic farming fields as the research object. The results showed that the degeneration of soil chemical mass will be much more to see for grazing mode. The most sensitive chemical quality index is soil total nitrogen and organic carbon, especially 0.25-2 mm and 2-8 mm soil organic carbon content. The farmland cultivation mode stimulates the soil microorganism's ability of absorbing carbon and nitrogen, which goes against the soil carbon and nitrogen's conservation especially for a long-term fertilizer application in the regular farming mode.
Keywords: *conventional farming, organic farming, land use, lawn, soil quality*

Introduction

Many ecological processes by nature and humans such as vegetation succession, the changes of land use pattern, have influences on the changes of the soil quality. The most profound and directive factors are utilization pattern of soil and the level of management. On the one hand, these factors can lead to soil degradation, soil erosion. On the other hand, they can improve the soil quality and ecological environment. Nowadays, the main reason of the soil degradation is that unreasonable way of land utilization used by humans. There is not a single or multiple index could reflect the combined action between the soil organisms, physics and chemistry. So, there is not established a uniform soil measurement. After many small watershed are developed, the land utilization begins to be diversity. The changes of the soil environment lead to that the function and structure of the ecosystem begin to change. The situation of the soil quality not only reflect the influences of the soil utilization on the soil physics, chemistry and soil quality, but also clear and definite the influences that decision of the soil utilization has on the nutrient cycling, leaching, soil structure, carbon accumulation and other related process.

The change of land to make it arable, which makes the soil organic matter lower. The transformation of arable land from woodland or grassland makes the soil property depredated (Meriles et al., 2008; Chen et al., 2008). For the ecologically fragile area, the soil parent material (parent material), altitude (altitude) and the use of a greater impact on soil properties, which affect the most is how to use the land (Fermont et al., 2008). In recent years, because of the overdevelopment of some where's water and land resource in Ili Valley, the valley terrace pastures which mainly used for animal husbandry degenerate

http://www.aloki.hu ● ISSN 1589 1623 (Print) ● ISSN 1785 0037 (Online)
DOI: http://dx.doi.org/10.15666/aeer/1704_75117522

seriously and is becoming the soil and water loss of the basin becoming more and more serious. Yang and Zhang (Yang and Zhang, 2009) analysis the use of change in cross-strait land of the Ili Valley, compared with the year of 1985, the arable land increases of 4.99×10^4 hm^2 entirely. Grassland is the only type of land which is reducing, whose reduced area contains 7.02×10^4 hm^2. The conversion from grassland to cropland accounted for 90.4%. Because of the land development utilization improperly, the net increase of the useless land is 1.07×10^4 hm^2, the net increase of the saline land is 13.04×10^4 hm^2, which all of them cause a series of environmental problems of soil erosion and desertification and salinization. As is regarded to be the research object from the soil in Ili Nalati prairie and developed different kinds of land utilization on soil, the research on grassland development made it a theory evidence to Grazed Grassland, conventional field and organic field on the impact on soil quality and the rational exploitation of regional grassland resources definitely. The research also helps growers make the appropriate land management measures to adjust with.

Materials and methods

Basic situation of region

The study area located at long-term observation sites of grassland management central station of Yili State (North latitude 43°18′-43°22′, East longitude 84°05′-84°09′). The grassland was located in Piedmont plains of altitude 1480 m, perennial resistance to low temperature and drought resistance of Gramineae and soil type was mainly meadow chernozem. The Kunes River was a temperate continental climate type, which belongs to the seasonal snow melt water and rainwater recharge rivers, intra annual variation of small diameter. the length of 258 km, the catchment area of 3532 km^2, The annual average temperature of 8 degrees, the annual rainfall of about 800 mm, The high temperature period is 7-8 months, and the precipitation concentration in 4-6 months, in May the most.

Test design and sample collection

The test set Native Grassland (NG), Grazed Grassland (GG), Six years conventional field (6-yr CF), More than twenty years conventional field (20-yr CF), Six years organic field (6-yr OF) and Thirteen years organic field (13-yr OF) Six treatments. Artificial disturbance of natural grassland is very small, most of the natural grassland has been cultivated for grazing grassland or over 20 years, Grazing period was mainly from September to June. The application of chemical fertilizer (pure nitrogen amount of about 170 kg/hm^2) in Conventional tillage models and The application of organic fertilizer (pure nitrogen amount of about 170 kg/hm^2) in organic cultivation. Soil samples in late September 2010 before the winter collection. Frist dig a pit (30 cm wide and 45 cm deep), and then in the 0-20 cm soil layer collection size consistent with the undisturbed soil sample (length * width * high = 20 cm * 10 cm * 10 cm) and the sampling point as close as possible in the whole soil and bulk density of the samples nearby, to as much as possible to reduce the spatial variability of soil samples, In order to obtain the aggregate distribution of undisturbed soil sample determination. Each treatment takes three undisturbed soil samples, into the square plastic box and carefully transported to the laboratory. Then immediately soil samples screened out by 8 mm soil sieve and the large clods gently crushing along natural fractures, finally analysis of soil aggregates and stability in dried soil samples within the laboratory.

http://www.aloki.hu ● ISSN 1589 1623 (Print) ● ISSN 1785 0037 (Online)
DOI: http://dx.doi.org/10.15666/aeer/1704_75117522

Research methods and measurement items

The study accessed to the soil quality index dividing into soil physical, chemical and biological quality indexes of three types. The first was principal component analysis (PCA), and then was correlation analysis and t-test, which orders to determine the significant factors affecting soil quality changes. Soil aggregate separations use the wet sieving method. According to the above 8 particle size mm soil sieve samples were divided into the following categories: large aggregates (2-8 mm), smaller aggregates (0.250-2 mm), micro-aggregate (0.053-0.25 mm) and silt plus clay group (< 0.053 mm). The soil samples were separated and arranged to determine the particle composition, soil organic carbon, total nitrogen and so on. The soil aggregate : 0.053 mm, 0.053-0.25 mm, 0.250-2 mm < 2-8 mm in turn representing as SAP1, SAP2, SAP3 and SAP4, and the particle size of the soil organic carbon content are expressed as SOC1, SOC2, SOC3 and SOC4, the content of soil organic carbon of 0-20 cm representing SOCT. The main indexes measuring methods are shown in *Table 1*. The AWCD and diversity index calculation methods are as follows:

(1) The average absorbance of AWCD can be used to estimate the total capacity of microbial community in the use of carbon sources. (Ai is the relative absorbance of i, and A A1 is the relative absorbance of A1.)

$$AWCD = \sum(Ai - AA1) / 31 \quad \text{(Eq.1)}$$

(2) Shannon-Wiener richness index H was used to evaluate the species richness.

$$H = -\sum Pi \bullet \ln(Pi) \quad \text{(Eq.2)}$$

(3) Shannon-Wiener richness index E was used to evaluate the species richness. (S is the number of the carbon source.)

$$E = H / \ln S \quad \text{(Eq.3)}$$

(4) Shannon-Wiener advantage of D number is used to evaluate some of the most common species of a moderate.

$$D = 1 - \sum(Pi)^2 \quad \text{(Eq.4)}$$

Statistical analysis

Through the SPSS Base Ver17.0 statistical software (SPSS, Chicago, IL, USA) analysis correlation of the data. The multivariate methods such as principal component analysis (PCA) was employed to determine how the samples were different as a whole.

Results and analyses

The influence of grassland development to soil physical quality index

On soil physical quality index for PCA analysis (*Fig. 1*). The projection information indicates that the land use patterns are divided into three categories. The first category is organic farming for 6 years and 13 years. The second category is conventional farming for 6 years and 20 years. Others are processed as the third category. Using correlation analysis,

http://www.aloki.hu ● ISSN 1589 1623 (Print) ● ISSN 1785 0037 (Online)
DOI: http://dx.doi.org/10.15666/aeer/1704_75117522

of which the results reached a very significant level, for further description of influencing factors of the soil physical quality indicators are shown in *Table 2*. Soil physical indicator of 0.053-0.25 mm aggregates percentage and first principal component PC1 (principal component 1) is a significant positive correlation, 2-8 mm aggregates percentage and first principal component PC1 is a significant negative correlation. That means the positive direction of PC1 and PC2 spindle are organic farming mode. 0.25-2 mm aggregates percentage and second principal component PC2 is a significant positive correlation. That means the negative direction of PC2 spindle and the positive direction of PC1 spindle are conventional farming mode. The negative direction of PC1 and PC2 spindle are the third type of grass mode. Aggregates of particles percentage change indicate the effect of management measures under different land use patterns on soil aggregate. The positive direction of the first principal component is the percentage increase of 0.053-0.25 mm aggregates. The negative direction of it is the percentage increase of 2-8 mm aggregates. All this shows that the farmland management (organic and conventional) mode causes the macro-aggregates crushing and 0.053-0.25 mm micro-aggregates increasing and the grassland management mode is conducive to maintaining 2-8 mm macro-aggregates. The positive direction of the second principal component is the percentage increase of 0.25-2 mm aggregates. This shows that the organic management mode is conducive to the formation of 0.25-2 mm aggregates, but the effect of its formation rate is less than the breakage rate of 0.053-0.25 mm aggregates. This indicates that after the grassland convert to cropland; farmland mode makes soil crush from macro-aggregates into 0.053-0.25 mm micro-aggregates and the overall degradation of soil physical quality. But organic farming management mode can alleviate soil particles' broken, which can make 0.25-2 mm macro-aggregates increase.

Table 1. *Main index measuring method*

Item	Measuring method
Soil bulk (SB)	Cutting-ring method
Soil pH value (pH)	2.5:1 water-soil ratio electrode
Soil organic carbon (SOC) and total nitrogen (TN)	Analysis of carbon and nitrogen analyzer
Soil available phosphorus (AP) and total phosphorus (TP)	MO Ti Sc colorimetry
Soil available potassium (AK) and total potassium (TK)	Flame photometric determination
Soil alkaline hydrolysis nitrogen (AN)	Alkali solution diffusion method
Soil ammonium nitrogen (NH_4^+-N) and nitrate nitrogen (NO_3^--N)	Flow analyzer determination
Soil microbial carbon (SMC) and soil microbial nitrogen (SMN)	Chloroform fumigation extraction method
Oxidized organic carbon (OOC)	Potassium permanganate oxidation colorimetry
Hot water soluble organic carbon (HWSOC)	Distilled water extraction and Potassium dichromate titration
Acid hydrolysis carbon (AOC)	6 M concentrated hydrochloric acid extraction, Potassium dichromate titration
Average color change rate of soil (AWCD)	Biolog analyzer determination
Soil fungi (SFUNG), Bacteria (SBACT) and Actinomycetes Strain (SACTI)	Plate counting method

http://www.aloki.hu ● ISSN 1589 1623 (Print) ● ISSN 1785 0037 (Online)
DOI: http://dx.doi.org/10.15666/aeer/1704_75117522

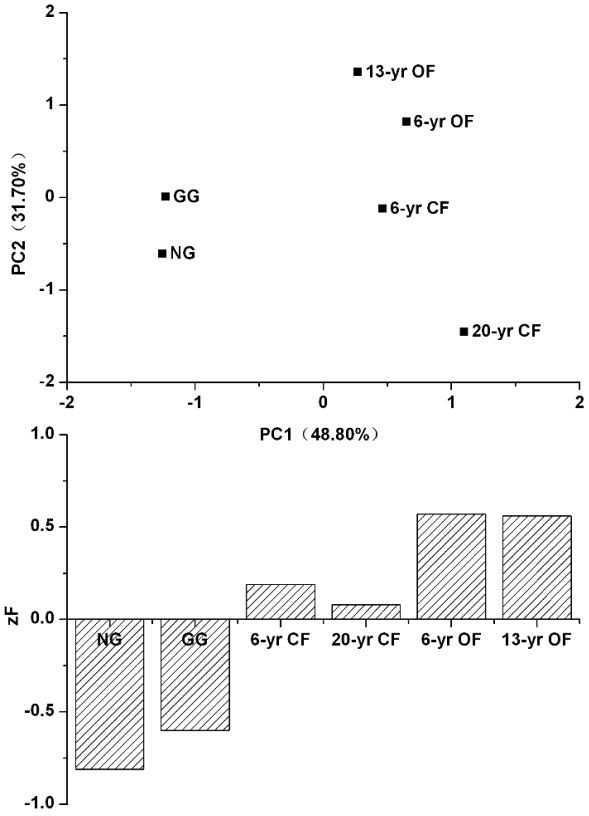

Figure 1. *PCA of physics index and composite scores of soil quality. (zF indicates PCA of composite scores. The same below)*

Table 2. *Correlativity between physics index of soil quality*

Factor	PC1	PC2
SB	0.45	0.44
SAP1	0.68	-0.69
SAP2	0.88**	-0.11
SAP3	0.24	0.94**
SAP4	-0.98**	-0.15
Eigenvalue	2.442	1.584
Contribution rate (%)	48.801	31.704
Cumulative contribution rate (%)	48.801	80.505

*Indicates significant difference ($p < 0.05$), **indicates extremely significant difference ($p < 0.01$). The same below

The influence of grassland development to soil chemical mass index

The PCA analysis (*Fig. 2*) on soil chemical mass, the projection information indicates that the land use patterns are divided into four categories, the first category includes six years of organic farming, 13 years of organic farming and six years of conventional farming, the second category is grazing meadow, the third category is natural grassland, and the fourth category is 20-year conventional tillage. Use correlation analysis can further indicates that soil chemical quality indicators

http://www.aloki.hu ● ISSN 1589 1623 (Print) ● ISSN 1785 0037 (Online)
DOI: http://dx.doi.org/10.15666/aeer/1704_75117522

influencing factors shown in *Table 3,* the correlation analysis results reach a significant level. First principal component PC1 and soil total nitrogen content of the soil chemistry indicators, 0.25-2 mm soil organic carbon content, 2-8 mm soil organic carbon content and soil organic carbon content are a significant positive correlation with soil potassium content, soil phosphorus content, < 0.053 mm soil organic of carbon content, 0.053-0.25 mm soil organic carbon content, namely that the positive direction of PC1 spindle are natural grass, 13 years of organic farming, 6 years of organic farming and 6 years of conventional farming; the second principal component PC2 and available potassium content was extremely significant with positive correlation with ammonium nitrogen content, and an acid solution of carbon content was significantly significant negative correlation, i.e. PC2 spindle positive direction represents natural grassland, 6 years of grazing grassland and six years of conventional tillage, the negative direction means 6 years of organic farming, 13 years of conventional tillage or 20 years beyond. The third principal component the PC3, active carbon dioxide content and hot water-soluble carbon content was significantly positively related. The positive direction of the PC3 spindle represents 6 years of conventional tillage, 6 years of grazing grassland and organic farming; therefore, the land use pattern can be divided into four main categories. Soil organic carbon and its components play an important role in many of the features in the soil, as it is considered to be an important indicator of soil quality. The positive direction of the first principal component represents the increase of soil total nitrogen content of the soil chemistry indicators, 0.25-2 mm soil organic carbon content, 2-8 mm soil organic carbon content, soil organic carbon content of soil potassium content, soil total phosphorus, < 0.053 mm soil increased organic carbon content, 0.053-0.25 mm soil organic carbon content. And it shows that soil organic carbon and soil total nutrient have the essential influence on soil chemical quality, especially soil organic carbon and total nitrogen reached a significant positive correlation, which decides the reaction of soil chemical quality to management measures in the land-use mode. The second principal component in the positive direction for the content of soil soluble potassium and ammonium nitrogen increases, the negative direction for the content of acid solution of carbon increases. It shows that the condition that at a certain level of total nutrient, soil available potassium, ammonium nitrogen and hydrolysable carbon content is most sensitive in the secondary impact factor. The field husbandry (organic and conventional) management model destroys soil aggregates, which made the physical protection of the nutrients reduced. Farmland management model led a significant reduction to the soil available potassium and ammonium nitrogen contents, but the content of acid hydrolysis organic carbon increased significantly. The third main component of the positive direction is the content of active carbon dioxide and hot-water-soluble carbon increases, indicating that under the six years of grazing and short-term farming mode (conventional farming and organic farming) the activity of carbon dioxide and hot water soluble carbon can get easily use. With the growth of the cultivation age, organic carbon which is easy to use gradually reduced. This indicates that after the grassland conversed to cropland, the total nutrient in the soil, organic carbon, active carbon dioxide and hot water-soluble carbon first increased under the short-term tillage. With the growth of cultivation age, the content of soil available potassium and ammonium nitrogen decrease significantly at first, and finally the quality of soil chemistry in the farmland all get decreased gradually. Because grazing pattern does not use any exogenous substances, the degradation of soil chemical quality is the most obvious.

http://www.aloki.hu ● ISSN 1589 1623 (Print) ● ISSN 1785 0037 (Online)
DOI: http://dx.doi.org/10.15666/aeer/1704_75117522

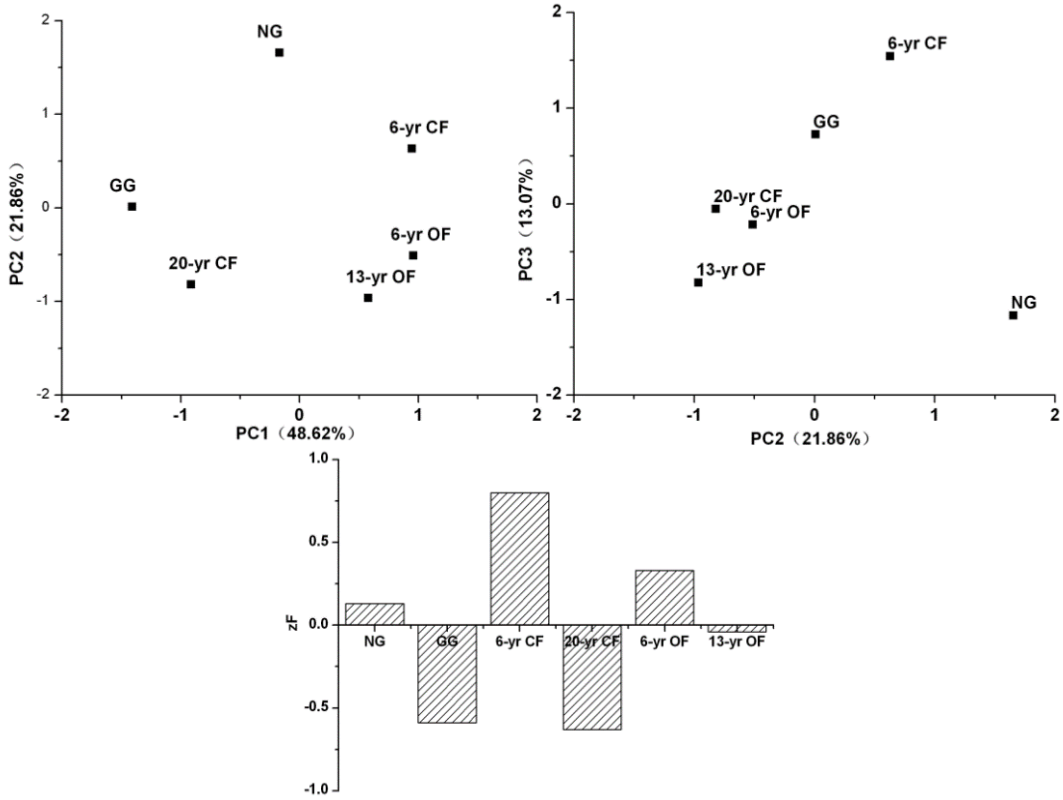

Figure 2. *PCA of chemistry index of soil quality*

Table 3. *Correlativity between chemistry index of soil quality*

Factor	PC1	PC2	PC3
pH	0.11	-0.58	-0.07
NH_4^+-N	-0.17	0.80*	0.08
NO_3^--N	0.60	0.17	0.10
AN	-0.61	0.14	0.60
AP	0.42	-0.71	-0.42
AK	0.13	0.90**	-0.26
TN	0.94**	0.30	-0.07
TK	0.76*	-0.51	0.04
TP	0.76*	0.04	0.07
SOC1	0.77*	-0.14	-0.56
SOC2	0.80*	0.52	0.16
SOC3	0.99**	0.03	0.12
SOC4	0.96**	0.03	0.26
SOCT	0.96**	0.16	-0.18
OOC	0.29	0.03	0.82*
HWSOC	0.48	-0.28	0.80*
AOC	-0.06	-0.82*	0.22
Eigenvalue	8.269	3.716	2.221
Contribution rate (%)	48.642	21.859	13.065
Cumulative contribution rate (%)	48.642	70.501	83.567

http://www.aloki.hu ● ISSN 1589 1623 (Print) ● ISSN 1785 0037 (Online)
DOI: http://dx.doi.org/10.15666/aeer/1704_75117522

The influence of grassland development to soil bio-quality index

On soil biological quality index for PCA analysis (*Fig. 3*), the projection information indicates that the mode of land use is mainly divided into two categories, the first category for tillage (organic and conventional) mode, second kinds of grass mode, using correlation analysis further illustrate the soil biological quality index impact factors in *Table 4,* the results of correlation analysis at significant level. The first principal component PC1 and soil biological indicators of AWCD, microbial nitrogen content was significant positive correlation, namely PC1 spindle orientation for tillage (organic and conventional) mode, the negative direction for second kinds of grassland pattern; as a result of the second main components of PC2 and biological indicators of the quality of impact factors are not significant correlation exists, so on the mode of land utilization soil biological quality impact is very small. The first principal component is the direction for tillage (organic and conventional) model, AWCD and microbial nitrogen content increased, description of farming (organic and conventional) mode of microbial communities using carbon and microbial nitrogen capability is strong, namely farmland management pattern is enhanced by microorganisms on soil carbon and nitrogen utilization ability, relatively speaking, grassland management model for carbon and nitrogen resources conservation. Suggesting that the conversion of grassland to farmland, farmland tillage mode to promote soil microorganisms on carbon and nitrogen resource utilization ability, is not conducive to the soil carbon and nitrogen retention.

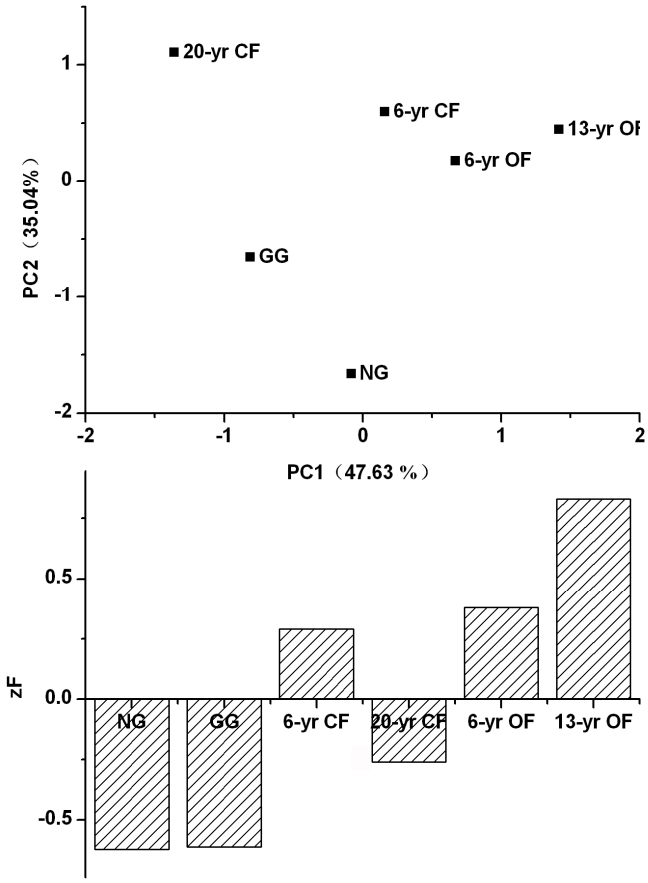

Figure 3. *PCA of biology index of soil quality*

http://www.aloki.hu ● ISSN 1589 1623 (Print) ● ISSN 1785 0037 (Online)
DOI: http://dx.doi.org/10.15666/aeer/1704_75117522

Table 4. *Correlativity between biology index of soil quality*

Factor	PC1	PC2
SFUNG	0.73	-0.6
SBACT	0.65	-0.58
SACTI	0.58	-0.69
AWCD	0.97**	0.14
H	0.53	0.74
E	-0.57	0.35
D	0.51	0.75
SMC	0.63	0.33
SMN	0.92**	0.32
Eigenvalue	4.286	3.154
Contribution rate (%)	47.626	35.041
Cumulative contribution rate (%)	47.626	82.667

Discussion

Soil physical quality index

The analysis and ordination diagram of the principal component of the soil physical quality indicators can reflect the reaction of the soil physical quality due to the change of the land management practices. As the lawn developed to different form with different pattern of land usage, the 0.053-0.25 mm, 0.25-2 mm, 2-8 mm soil aggregates experience significant influence. With the pattern of grassland turns to be conventional or organic farmland, 2-8 mm soil macro aggregate has broken into the smaller micro aggregate, which is consistent with the former research that the water stable aggregate in natural grassland, forest land and grazing grassland are much higher than the farmlands' (Kremer and Kussman, 2011; Kremer and Li, 2003; Guo et al., 2010).

The increase of 0.25-2 mm soil aggregate is the important reflecting for a stability tend of the basic substance in soil and its function unit (Jastrow, 1996; Puget et al., 2000; Six and Elliott, 1998). The results show that the 0.25-2 mm soil aggregate increases gradually in organic farming at the year of 6 and 13, and the 0.25-2 mm soil aggregate decreases gradually in conventional tillage beyond the year of 6 and 20, it may be directly related to the fresh organic material who return back to the soil (Chen et al., 2016; Cole et al., 1993). This shows that organic farming mode is favorable to optimize the soil aggregate's structure. Therefore, land use patterns are determined to be the major factor of soil physical quality under the premise of same climate, same terrain and same soil property. Soil management behavior can future reflects the good or bad of soil physical property.

Soil chemical quality index

Land use and management measures changed the natural grassland soil chemical characteristics, organic farming mode soil chemistry quality is best, conventional tillage 20 years of soil chemistry quality relative worst, the most sensitive chemical quality index is soil total nitrogen and organic carbon ($P < 0.01$), especially 0.25-2 mm and 2-8 mm soil organic carbon content ($P < 0.01$). Conventional farming mode weakened the soil structure, and lead to soil organic carbon and total nitrogen significantly reduced

http://www.aloki.hu ● ISSN 1589 1623 (Print) ● ISSN 1785 0037 (Online)
DOI: http://dx.doi.org/10.15666/aeer/1704_75117522

(Jacobs et al., 2009; Koch and Stockfisch, 2006), this may be as cultivation increased soil organic matter mineralization rate relevant (Blair et al., 2006), but organic farming mode organic material not only directly for aggregate function to provide cementing material, compensation soil mineralization, carbon and nitrogen loss, and for soil biological activity provide energy, promoting the soil large aggregate and micro aggregate composition and the stability of the organic matter (Alagoz and Yilmaz, 2009).

At the same time, land use and management measures first cause, total content of soil nutrients and soil organic carbon content changes ($P < 0.01$), the second is ammonium nitrogen ($P < 0.05$) and phosphorus and potassium content ($P < 0.01$), and the last is easy oxidation of organic carbon and thermal hydrolysis organic carbon content ($P < 0.05$). There have been many literature compared the land use and management measures on soil chemical quality index influence, considered that soil organic carbon, total nitrogen, available phosphorus, pH and vulnerable to agronomic measures influence (Voundi and Tonye, 2003; Nosrati et al., 2011), but not for land use and management measures to the chemical quality index of influence sorting, this may and soil chemical properties vulnerable to soil environmental change and crop management measures about influence (Paudel et al., 2012).

Soil bio-quality index

The principal component analysis and correlation analysis interpret the influence of land use and regulative measure to soil bio-quality index, which changes the value of soil microorganism's ability of utilization from carbon source AWCD ($p < 0.01$) and the content of nitrogen in microbial biomass ($p < 0.01$), and both the influence from the two numerical value of tillage pattern (organic and conventional) are larger than the figure from grass pattern. Via an analysis of utilization ability on soil microbial biomass carbon source by Juliet (Juliet et al., 2002) and Cooksona (Cooksona et al., 2008), they also told planting pattern has a big effect on soil microorganism. Applying organic materials can stimulate microbial activity (Tian et al., 2016), applying chemical fertilizer has a little effect on soil microbial activity and microbial biomass (Lovella et al., 1995); however, the long-term applying chemical fertilizer may decrease soil microbial activity (Li et al., 2017). Thus, soil microbial activity can be enhanced when the grassland exploited to the farmland. But the soil microbial activity whose usage is beyond 20 years by conventional tillage decrease, the farmland need fertilization reasonable in order to optimize the environment of soil microorganism and maintain soil microbial activity.

Conclusion

The effect of land use patterns on soil physical quality is more influential than the land management measures, the farmland cultivation mode break the soil macroaggregate to 0.053-0.25 mm smaller microaggregate, but the organic farming management mode can alleviate soil particle crushing and increase the number of 0.25-2 mm macroaggregate.

After the grassland being conversed to the farmland, total soil nutrient, organic carbon, activated carbon oxide and hot water soluble carbon will get much increase in a short-term cultivation mode. But the content of soil available potassium and ammonium nitrogen will get reduced significantly along with the increasing cultivation time, and

http://www.aloki.hu ● ISSN 1589 1623 (Print) ● ISSN 1785 0037 (Online)
DOI: http://dx.doi.org/10.15666/aeer/1704_75117522

finally the soil chemistry quality index of farmland are all decreasing generally. For grazing mode, as it does not use any foreign matter, the degeneration of soil chemical mass will be much more to see.

After the grassland being conversed to the farmland, the farmland cultivation mode stimulate the soil microorganism's ability of absorbing carbon and nitrogen, which goes against the soil carbon and nitrogen's conservation especially for a long-term fertilizer application in the regular farming mode.

Acknowledgements. Science and Technology Support Program of Xinjiang Production and Construction Corps (2018AA005), the National key research and development program of China (2016YFC0501406), This research was supported by the National Natural Science Foundation of China (31560169), the International Science & Technology Cooperation Program of China (2015DFA11660), and Shihezi University level project (GJHZ201706, GJHZ201802).

REFERENCES

[1] Alagoz, Z., Yilmaz, E. (2009): Effects of different sources of organic matter on soil aggregate formation and stability: a laboratory study on a Lithic Rhodoxeralf from Turkey. – Soil Tillage Research 103: 419-424.

[2] Blair, N., Faulkner, R. D., Till, A. R., Korschens, M., Schulz, E. (2006): Long-term management impacts on soil C, N and physical fertility: Part II: Bad Lauchstadt static and extreme FYM experiments. – Soil Tillage Res 91: 39-47.

[3] Chen, G. Q., Jiang, M. M., Yang, Z. F., Chen, B., Zhou, J. B. (2008): Exergetic assessment for ecological economic system: Chinese agriculture. – Ecological Modeling 220(3): 397-410.

[4] Chen, Z., Guo, Y. B., Du, Z. L., Wu, W. L., Meng, F. Q. (2016): Change in the abundance and community composition of ammonia-oxidizing bacteria and archaea at soil aggregate level as native pasture converted to cropland in a semiarid alpine steppe of central Asia. – Journal of Soils and Sediments 16(1): 243-254.

[5] Cole, C. V., Flach, K., Lee, J., Sauerbeck, D., Stewart, B. (1993): Agricultural sources and sinks of carbon. – Water Air Soil Pollut 70: 111-122.

[6] Cooksona, W. R., Daniel, V. M., Margaret, M. R. (2008): Characterizing the relationships between soil organic matter components and microbial function and composition along a tillage disturbance gradient. – Soil Biology and Biochemistry 40(3): 763-777.

[7] Fermont, A. M., van Asten, P. J. A., Giller, K. E. (2008): Increasing land pressure in East Africa: the changing role of cassava and consequences for sustainability of farming systems. – Agriculture, Ecosystems and Environment 128: 239-250.

[8] Guo, Z. B., Yan, G. J., Zhang, R. H., Li, F. M. (2010): Improvement of soil physical properties and aggregate-associated C, N, and P after cropland was converted to grassland in semiarid Loess Plateau. – Soil Sci 175: 99-104.

[9] Jacobs, A., Rauber, R., Ludwig, B. (2009): Impact of reduced tillage on carbon and nitrogen storage of two Haplic Luvisols after 40 years. – Soil Tillage Res 102: 158-164.

[10] Jastrow, J. D. (1996): Soil aggregate formation and the accrual of particulate and mineral-associated organic matter. – Soil Biol. Biochem 28: 656-676.

[11] Juliet, P. M, Lynne, B., Randerson, P. F. (2002): Analysis of microbial community functional diversity using sole-carbon-source utilisation profiles-acritique. – FEMS Microbiology Ecology 42(1): 1-14.

[12] Koch, H. J., Stockfisch, N. (2006): Loss of soil organic matter upon ploughing under a loess soil after several years of conservation tillage. – Soil Tillage Res 86: 73-83.

[13] Kremer, R. J., Kussman, R. D. (2011): Soil quality in a pecan–Kura clover alley cropping system in the Midwestern USA. – Agroforestry Systems 83: 213-223.

http://www.aloki.hu ● ISSN 1589 1623 (Print) ● ISSN 1785 0037 (Online)
DOI: http://dx.doi.org/10.15666/aeer/1704_75117522

[14] Kremer, R. J., Li, J. (2003): Developing weed-suppressive soils through improved soil quality management. – Soil Till Res 72: 193-202.
[15] Li, R., Tao, R., Ling, N., Chu, G. X. (2017): Chemical, organic and bio-fertilizer management practices effect on soil physicochemical property and antagonistic bacteria abundance of a cotton field: Implications for soil biological quality. – Soil & Tillage Research 167: 30-38.
[16] Lovella, R. D., Jarvisa, S. C., Bardgettb, R. D. (1995): Soil microbial biomass and activity in long-term grassland: effects of management changes. – Soil Biology and Biochemistry 27(7): 969-975.
[17] Meriles, J. M., Vargas Gil, S., Conforto, C., Figoni, G., Lovera, E., March, G. J., Guzmán, C. A. (2008): Soil microbial communities under different soybean cropping systems: Characterization of microbial population dynamics, soil microbial activity, microbial biomass, and fatty acid profiles. – Soil Tillage Research 103(2): 271-281.
[18] Nosrati, K., Feiznia, S., Van Den Eeckhaut, M., Duiker, S. W. (2011): Assessment of soil erodibility in Taleghan Drainage Basin, Iran, using multi variate statistics. – Physical Geography 32(1): 78-96.
[19] Paudel, B. R., Udawatta, R. P., Kremer, R. J., Anderson, S. H. (2012): Soil quality indicator responses to row crop, grazed pasture, and agroforestry buffer management. – Agroforestry Systems 84(2): 311-323.
[20] Puget, P., Chenu, C., Balesdent, J. (2000): Dynamics of soil organic matter associated with particle-size fractions of water-stable aggregates. – Eur. J. Soil Sci 51: 595-605.
[21] Six, J., Elliott, E. T. (1998): Aggregation and soil organic matter accumulation in cultivated and native grassland soils. – Soil Science Society of America 62: 1367-1377.
[22] Tian, X, M., Zhang, F. H., Li, J. H., Fan, H., Cheng, Z. B., Wang, K. Y. (2016): Effects of bio-organic fertilizer on soil microbiome against Verticillium dahlia. – Int. J. Agric. Biol. 18(5): 923-931.
[23] Voundi, N. J. C., Tonye, J. (2003): Assessment of certain soil properties related to different land-use systems in the Kaya watershed of the humid forest zone of Cameroon. – Land Degradation and Development 14: 57-67.
[24] Yang, Y., Zhang, H. Q. (2009): Analysis of land use and land cover change in the Yili Newly reclaimed area in recent 20 years (in Chinese). – Resources Science 31(12): 2029-2034.

http://www.aloki.hu ● ISSN 1589 1623 (Print) ● ISSN 1785 0037 (Online)
DOI: http://dx.doi.org/10.15666/aeer/1704_75117522

ANALYSIS ON EVOLUTION AND CHARACTERISTICS OF CARBON EMISSIONS OF SHANXI PROVINCE, CHINA

XU, L. N.[1,2,3,4,5] – SHI, X. J.[5] – FAN, C. Y.[1,2*] – CHEN, S. Z.[2] – YANG, X. F.[1,2] – LIU, H.[4,6]

[1]*Energy Economics and Environmental Policy Research Centre, Datong University Datong, Shanxi 037009, China (e-mail: xulina1999@163.com)*

[2]*Business School, Datong University, Datong, Shanxi 037009, China*

[3]*Datong Macroeconomic Research Center, Datong, Shanxi 037009, China*

[4]*School of Environment, Tsinghua University, Beijing 100084, China*

[5]*National Energy Conservation Centre, Beijing 100045, China*

[6]*Regional Economic Teaching and Research Department Sichuan Administration College Chengdu, Sichuan 610071, China*

[*]*Corresponding author*
e-mail: dtfcy@sohu.com

(Received 27th Feb 2019; accepted 3rd May 2019)

Abstract. The paper calculates carbon emissions, and analyses relationship among economic growth, industrial structure, energy structure and carbon emissions using environmental quality equation based on the terminal energy consumption data in 1990-2017 based on Shanxi province in China. The results show that economic development is the main positive driving factor of carbon emissions, industrial structure has an inverted u-shaped curve related with the carbon emissions and there is not a high linear correlation between energy structure and carbon emissions. Finally, some suggestions are proposed to reduce carbon emissions. The energy-intensive provinces should adjust industrial structure and pay more attention to the improvement of technologies, at the same time, should keep the population rate not increasing rapidly and energy structure not degenerating.
Keywords: *carbon emissions; economic growth; industrial structure; energy structure; diversity factors; environmental quality equation*

Introduction

As the biggest carbon emission increment country in the world, China is facing more and more international pressure on carbon emission reduction. As a responsible big country, the Chinese government, in accordance with China's national conditions, stage of development, sustainable development strategy and international responsibilities, has set the goal of self-action to reach the peak of carbon emissions by 2030 and reach the peak as soon as possible. In China, the implementation of energy-saving target responsibility system and the provincial-level decomposition of energy-saving targets require provinces to find out the evolution law of carbon emissions in accordance with their own natural and geographical conditions, resource endowment constraints, economic development models and economic development stages, based on which, to formulate reasonable emission reduction policies, and to achieve the decomposition goals. Rational emission reduction policies promote the smooth completion of the overall emission reduction targets. On the one hand, Energy-intensive provinces need to provide energy for China's development. On the other hand, they have great pressure on

http://www.aloki.hu ● ISSN 1589 1623 (Print) ● ISSN 1785 0037 (Online)
DOI: http://dx.doi.org/10.15666/aeer/1704_75237534

emissions, which has become a bottleneck for China to achieve the overall emission reduction goals. Therefore, it is of great practical significance to study the evolution of carbon emissions in energy-intensive provinces, find out the inherent mechanism of carbon emissions growth, and formulate reasonable emission reduction paths for specific provinces, so as to achieve the overall emission reduction goals in China.

Review of literature

In recent years, the growth of carbon emissions has been a hot topic both at home and abroad, and has made great progress. The existing research is mainly as follows, one aspect is the relationship between carbon emissions and the level of economic development and energy consumption. For example, Qi et al. (2015) selected six provinces in central China as the research object and used a variety of econometric analysis methods to study the relationship between economic growth and carbon emissions. Gao et al. (2017) discussed the possibility of the existence of environmental Kuznets curve and the existence of inflection point between carbon emission and economic growth in urban agricultural sector. Gao (2017) empirically analyzed the relationship between the relationship between energy consumption, carbon emissions and economic growth in Beijing Tianjin and Hebei region. Another aspect is to explore the driving forces of carbon emissions, and analyze the influencing factors of carbon emissions. Such as Chen et al. (2012), he analyzed the driving forces of carbon emissions from the theoretical and empirical level. Zhao and Yang (2012) used the factor analyzing method to study the driving force of China's carbon emissions. Xu et al. (2013) explored the driving force of carbon emissions in resource-based provinces combining with the PATH-STIRPA model. Song and Xu (2011), Wu et al. (2014), Li et al. (2015), Wang and Xie (2015), Ma et al. (2017), Zhou and Mao (2017), Yuan et al. (2017) analyzed the influencing factors of carbon emissions in China's cities and towns, China's provinces, China's power sector, China's industrial sector, China's export implied carbon emissions, China's provincial transport sector and China's provincial agricultural sector. Another aspect is the analysis of carbon emission forecasts. Such as Chi (2007), Huang et al. (2010), Liu (2011), Mirzaei and Bekri (2017), Wang et al. (2017) they used linear regression methods, ARIMA models, Logistic curves, and system dynamics methods to investigate and study issues related to predict carbon emissions in different regions combined with regression analysis methods.

At present, there are not many researches on the evolution of carbon emissions in China. Liu et al. (2013) used the dynamic distribution analysis method (MEDD) to empirically analyze the dynamic distribution and evolution of China's carbon emission intensity. Hu et al. (2016) selected panel data from 30 provinces and municipalities in China from 1997 to 2012 to analyze the evolution trend of carbon emission intensity in China and the regional differences. Tian et al. (2014) and Gao et al. (2017) analyzed the evolution trend of carbon emissions in China's agricultural sector and regional agricultural sector respectively. Sun et al. (2011) and Liang and Li (2014) explored the evolution characteristics of carbon emissions in the Bohai rim and Shandong province. Most of the existing research only selecting a certain industry in China as a whole sample, there are less research on the evolution of carbon emissions. Therefore, the author chose energy-intensive provinces as the research object, constructed the coefficient of diversification of industrial structure, the coefficient of diversification of energy consumption results, studied the evolution law of carbon emissions with the aid of environmental-quality equation and environmental Kuznets curve, and put forward

http://www.aloki.hu ● ISSN 1589 1623 (Print) ● ISSN 1785 0037 (Online)
DOI: http://dx.doi.org/10.15666/aeer/1704_75237534

practical policy suggestions for carbon emission reduction to provides policy reference and decision-making basis for the realization of carbon emission reduction goal in energy-intensive provinces.

Estimation of total carbon emission

Calculation method of carbon emission

According to the fourth assessment from IPCC (Intergovernmental Panel on Climate Change) (Lin and Liu, 2010; Lin and Huang, 2011; China National Development and Reform Commission, 2012), the carbon emissions calculated in this section are mainly carbon emissions caused by fossil energy consumption. Shanxi Province in China, a large coal resource province, is chosen as the representative of energy intensive provinces. Carbon emissions are estimated by the method from Lin and Liu (2010).

$$C = \sum_i C_i = \sum_i E_i \times \alpha_i \times f_i \quad \text{(Eq.1)}$$

Among the *equation (1)*, C is total carbon emission, C_i is carbon emissions from category i energy, E_i is the category i energy consumption, α_i is the conversion coefficient of standard coal of the category i energy consumption, f_i is the carbon emission coefficient of the category i energy.

Data sources

The study period was selected from 1990 to 2017, and all the energy data came from the Shanxi statistical yearbook (1991-2018). The final energy consumption is calculated based on the total conversion of physical consumption. In this paper, all the value calculation, was calculated setting 1952 as a benchmark year for the reduction, because the year of 1952 was setting as a base period which value was 100 in the statistical yearbook. In addition, this author estimated the end of fossil energy consumption according to the standard amount of carbon emissions, not calculating the carbon emissions from the energy losses generated during the process of conversion, transportation and distribution. The energy conversion coefficient was calculated by Appendix 4 of China Energy Statistics Yearbook (2018). The emission coefficients of coal, coke and natural gas was calculated by the carbon emission inventory published by IPCC. The numbers are 0.7559, 0.8550, 0.4483 in turn. The oil carbon emission coefficient (Song, 2012) comes from the data published by the Energy Research Institute of the National Development and Reform Commission, the number is 0.5825.

Characteristics of carbon emissions

According to Eq.1, the carbon emission of Shanxi province is shown in *Figure 1*. As can be seen from *Figure 1*, Shanxi's carbon emissions in 1990 were 26.57 million tons, increasing to 73.27 million tons in 2017, an increase of almost two times. The carbon emissions are in the trend of increasing year by year. The growth rate of carbon emissions in the study cycle can be divided into three stages: from 1991 to 1996, the overall carbon emissions in Shanxi Province showed an upward trend, but the growth was slow; from 1997 to 2005, there was a short-term fluctuation in carbon emissions,

http://www.aloki.hu ● ISSN 1589 1623 (Print) ● ISSN 1785 0037 (Online)
DOI: http://dx.doi.org/10.15666/aeer/1704_75237534

but the overall trend was upward; after 2005, the total carbon emissions entered a linear upward state, in the following year, carbon emissions entered a fluctuation period again.

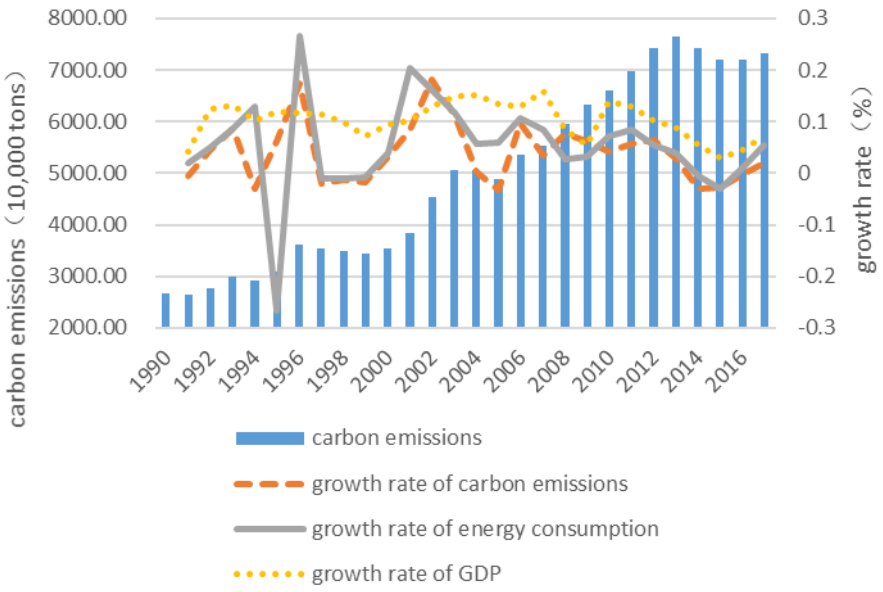

Figure 1. *The carbon emission, energy consumption and GDP output in Shanxi province in 1990-2017*

From 1990 to 2017, the carbon emissions of Shanxi Province basically kept pace with the growth of energy consumption. There was a sudden change in energy consumption in 1995 because an adjustment was made in statistical caliber in this year. From 2000 to 2003, the growth rate of carbon emissions was slightly faster than the growth rate of gross domestic product. After that, with the evolution of energy consumption structure and industrial structure in Shanxi province, the total carbon emissions are increasing, but the growth rate is slowing down. The growth rate of GDP has begun to be slightly faster than the growth rate of carbon emissions (as in *Fig 1*).

Analysis of evolution characteristics of carbon emissions

Existing research on the growth factors of carbon emissions mainly focuses on population, economic growth, industrial structure, energy structure. In this paper, the author does not focus on the analysis of factors affecting the growth of carbon emissions, so she quoted the existing research conclusions (He, 2012; Tong et al., 2015; Ren, 2015; Chen et al., 2016). The academic community has reached a consensus on the role of population in promoting carbon emissions, so the author will not repeat it.

Analysis on the relationship between economic growth and carbon emissions evolution

In order to investigate the quantitative relationship between economic growth and carbon emissions, we use the commonly used environmental Kuznets curve to analyze.

$$c = \beta_0 + \beta_1 y + \beta_2 y^2 + \beta_3 y^3 + u_i \quad \text{(Eq.2)}$$

http://www.aloki.hu ● ISSN 1589 1623 (Print) ● ISSN 1785 0037 (Online)
DOI: http://dx.doi.org/10.15666/aeer/1704_75237534

In the *equation (2)*, c is the carbon emissions over years, y is GDP per capita over years (The data are derived from the statistical yearbook of Shanxi province. The year 1952 is used as the benchmark year to calculate the reduction). Regression results are obtained by using Eviews8, as shown in *Table 1*.

Table 1. *The regression results of carbon emissions and economic growth in Shanxi province*

Parameters	**Model 1** $c = \beta_0 + \beta_1 y + \mu$	**Model 2** $c = \beta_0 + \beta_1 y + \beta_2 y^2 + \mu$	**Model 3** $c = \beta_0 + \beta_1 y + \beta_2 y^2 + \beta_3 y^3 + u_i$
β_0	2276.179 (22.98478)	1847.739 (-12.46559)	1534.06 (-5.535005)
β_1	0.902713 (-28.01651)	1.297577 (-11.05064)	1.738635 (-4.952082)
β_2		-6.14E-05 (-3.450783)	-0.000217 (-1.835032)
β_3			1.53E-08 (-1.330053)
adjusted R^2	0.971497	0.980945	0.981618
F-statistics	784.9247	593.0045	410.4036

Note: The test value of t statistics for each parameter are in brackets

Regression results show that the three models can effectively fit the relationship between carbon emissions and economic growth, but the parameters are significantly different. The fitting effect of model three is the best, below 5% level. The constant term and the linear term of per capita GDP are checked by significance test and it shows that between 1990 and 2013, there is a monotonic trend between carbon emissions and economic growth in Shanxi Province, the corresponding increase of carbon emissions is 1.74% for every 1% economic growth.

Analysis on the relationship between industrial structure evolution and carbon emissions

Method of calculating the diversity coefficient of industrial structure

The evolution of carbon emissions is not only related to economic growth, but also to industrial structure. In the existing studies, most of the measurement of the impact of industrial structure on carbon emissions is based on the industrial structure diversification coefficient proposed by Zhang et al. (2010) and Huang (2014). This coefficient is representative and reasonable to a certain extent, and can effectively show the proportion of the secondary and tertiary industries in the economic structure, but also has certain limitations. Because this coefficient is based on the primary industry as a benchmark, if the proportion of the primary industry in the economic structure is reduced, the coefficient will increase with the proportion of the primary industry decreasing, while the adjustment coefficient between the secondary industry and the tertiary industry can not be reflected. Therefore, the author used industrial structure correction coefficient from Huang (2014) to analyze the relationship between industrial structure and carbon emissions.

In order to quantitatively measure the impact of industrial structure on the evolution of carbon emissions, the author constructed an environmental-quality regression equation between carbon emissions and industrial structure diversification coefficient by using the industrial structure diversification coefficient.

http://www.aloki.hu ● ISSN 1589 1623 (Print) ● ISSN 1785 0037 (Online)
DOI: http://dx.doi.org/10.15666/aeer/1704_75237534

The construction method of industrial structure coefficient is to use A (agriculture), I (industry), S (service) to represent the output value of the first, second and third industry respectively, and D to represent the diversification coefficient of industrial structure. Then:

$$ISF = \sum \left(\frac{A}{A}, \frac{I}{A}, \frac{S}{A}\right) \quad \text{(Eq.3)}$$

According to the relevant data of Shanxi Statistical Yearbook, the industrial structure diversification coefficient of Shanxi Province from 1990 to 2017 was calculated by *equation (3)*. The output value is calculated on the basis of the year of 1952 as the following *Figure 2*.

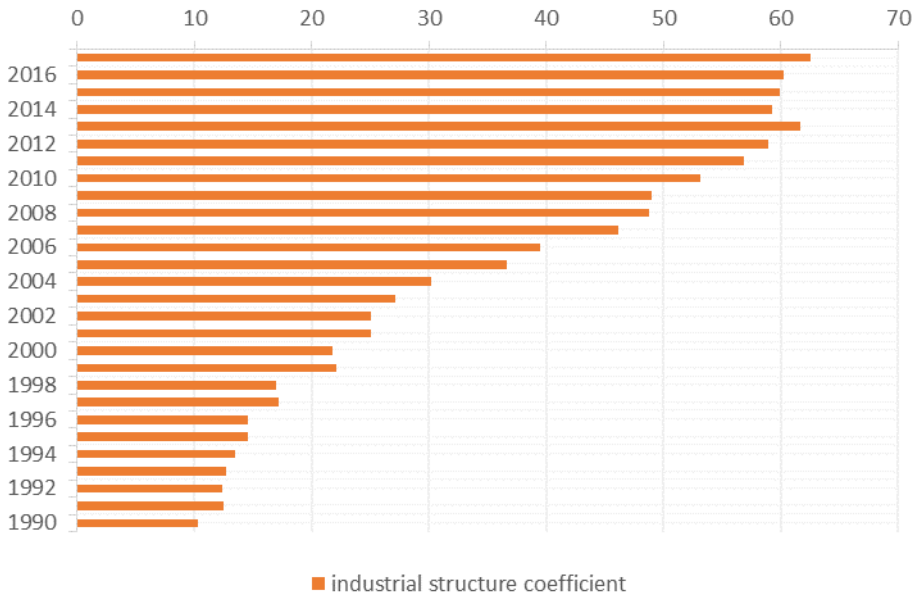

Figure 2. *Industrial structure diversification coefficient of Shanxi province 1990-2017*

From *Figure 2* we can find that, the diversification coefficient of Shanxi province industrial structure basically showed a linear upward trend in the research stage.

Regression result of industrial structure diversification coefficient and carbon emissions

In order to investigate the role of industrial structure change in the evolution process of carbon emissions in Shanxi Province, the regression equation of industrial structure evolution coefficient and carbon emissions was established by using the Environment-Quality equation:

$$c = \beta_0 + \beta_1 y + \beta_2 y^2 + \beta_3 y^3 + u_i \quad \text{(Eq.4)}$$

The parameters were estimated by stepwise changing the curve form by Eq. 4, and the regression results are shown in *Table 2*.

From the regression results of *Table 2*, we can see that the fitting result of Model 3 is the best, which reflects the characteristics between the evolution of industrial structure

http://www.aloki.hu ● ISSN 1589 1623 (Print) ● ISSN 1785 0037 (Online)
DOI: http://dx.doi.org/10.15666/aeer/1704_75237534

and carbon emissions. From 1990 to 2017, there is an inverted U-shaped curve between carbon emissions and the coefficient of industrial structure diversification in Shanxi Province. When the coefficient of industrial structure diversification is 25.08, the turning point of the curve corresponding to the time axis between 2002 and 2003 appears. That is, when the diversity coefficient of industrial structure is less than 25.8, the evolution of industrial structure brings about an increase in carbon emissions.

Table 2. *The regression results of carbon emissions and industrial structure diversity coefficient in Shanxi province*

Parameters	**Model 1** $c = \beta_0 + \beta_1 y + \mu$	**Model 2** $c = \beta_0 + \beta_1 y + \beta_2 y^2 + \mu$	**Model 3** $c = \beta_0 + \beta_1 y + \beta_2 y^2 + \beta_3 y^3 + u_i$
β_0	1819.606 (13.6308)	1807.974 (5.638141)	554.082 (0.823589)
β_1	91.27689 (23.67227)	92.17266 (4.062833)	238.2008 (3.247835)
β_2		-0.012914 (-0.040096)	-4.749545 (-2.066715)
β_3			0.044947 (2.078798)
adjusted R^2	0.960507	0.958629	0.964279
F-statistics	560.3766	267.4737	207.9591

Note: The test value of t statistics for each parameter are in brackets

When the coefficient of industrial structure diversification is greater than 25.8, the evolution of industrial structure can promote the reduction of carbon emissions. This coincides with the results of carbon emission growth rate and industrial output value growth rate in *Figure 2*, indicating that the industrial restructuring policy of Shanxi Province has achieved initial effect.

Analysis of the relationship between energy consumption structure and carbon emissions evolution

The energy structure of a country or region will change with the development of economy, from unification to diversification. In order to measure this change, this author constructed a pluralistic model of energy structure. F (first) denotes the dominant energy consumption in the economic development of a country or region, S (second), T (third) … denotes the subsequent energy consumption, and ESF denotes the coefficient of energy structure diversification in Eq. 5.

$$ESF = \sum \left(\frac{F}{F}, \frac{S}{F}, \frac{T}{F} \right) \quad \text{(Eq.5)}$$

From 1990 to 2017, coal has been the dominant energy consumption type in Shanxi Province. Therefore, coal was selected as unitary element in the evolution of energy structure, and other energy types as pluralistic elements of energy consumption structure. So the diversification coefficient of consumption structure in Shanxi province is as follow:

$$ESF = \sum \left(\frac{c}{c}, \frac{o}{c}, \frac{e}{c}, \frac{g}{c} \right) \quad \text{(Eq.6)}$$

http://www.aloki.hu ● ISSN 1589 1623 (Print) ● ISSN 1785 0037 (Online)
DOI: http://dx.doi.org/10.15666/aeer/1704_75237534

In the *equation (6) c,o,e,g* represents energy consumption of coal, oil, electricity, natural gas and other gases, respectively.

According to *equation (6)* and the data of Shanxi Statistical Yearbook, we calculated the coefficient of energy structure diversification, such as *Table 3*.

Table 3. *The consumption structure diversification coefficient of Shanxi province in 1990-2017*

Year	Coefficient	Year	Coefficient
1990	1.632569	2004	1.727133
1991	1.69738	2005	2.059616
1992	1.709464	2006	2.105542
1993	1.732847	2007	2.204329
1994	1.280864	2008	2.122848
1995	1.287026	2009	2.08718
1996	1.596045	2010	2.143757
1997	1.63661	2011	2.194854
1998	1.642659	2012	2.149954
1999	1.67804	2013	2.181708
2000	1.688116	2014	2.469229
2001	1.604971	2015	2.498509
2002	1.567656	2016	2.506846
2003	1.569563	2017	2.664153

From *Table 3*, we can see that Shanxi Province's energy consumption structure diversification coefficient rose slowly, from 1990 to 2017, it increased by about 1.0, the entire evolution process shows certain phased features. (1) The rising stage from 1990 to 1995. At this stage, the structure of energy consumption is basically on the rise stage, and in very few years, the energy structure has regressed. It shows that the energy consumption structure in this stage has been improved to a certain extent, and the energy structure adjustment policies in Shanxi Province have achieved certain results. The proportion of electricity in the structure of energy consumption is gradually increasing. (2) From 1996 to 2004, the stage of rebound decline. Affected by the Asian financial crisis, in order to stimulate economic development, some of the small coal kilns shut down have been rekindled, and some of the high energy consumption projects have been restarted, resulting in a re-increase in coal consumption, a decline in energy structure coefficient, and a return to the development model relying on coal consumption. (3) The slow recovery stage from 2005 to 2017. At this stage, Shanxi's industrialization was developing rapidly, urbanization was steadily advancing, and energy consumption had undergone some new changes. At the same time, the government of Shanxi Province decided to change the economic structure of "the coal dominant" and put forward the "coal-based, multi-development" strategy. The consumption of electricity and natural gas increased steadily, and the diversification coefficient of energy structure increased steadily (Xu, 2014).

In order to investigate the role of energy structure change in the evolution process of carbon emissions in Shanxi Province, this section still adopts the regression analysis of environmental quality curve. The regression equation is the same as *equation 4*, but the Y in the equation is expressed as the coefficient of energy structure diversification in this section. Model regression estimates are shown in *Table 4*.

http://www.aloki.hu ● ISSN 1589 1623 (Print) ● ISSN 1785 0037 (Online)
DOI: http://dx.doi.org/10.15666/aeer/1704_75237534

Table 4. *the regression results of carbon emissions and energy structure diversity coefficient in Shanxi province*

Parameters	Model 1 $c = \beta_0 + \beta_1 y + \mu$	Model 2 $c = \beta_0 + \beta_1 y + \beta_2 y^2 + \mu$	Model 3 $c = \beta_0 + \beta_1 y + \beta_2 y^2 + \beta_3 y^3 + u_i$
β_0	-3639.798 (-2.952779)	14304.97 (0.0677)	-63060.86 (-1.00861)
β_1	4557.069 (6.7509)	-15796.35 (0.0724)	125231.2 (1.10351)
β_2		5630.887 (2.444072)	-78363.93 (-1.16181)
β_3			16342.16 (1.2460)
adjusted R^2	0.659636	0.722393	0.72951
F-statistics	45.57465	30.92554	21.67697

Note: The test value of t statistics for each parameter are in brackets

The regression results showed that the adjusted R^2 of the third model is the maximum among the three models. However, at the 5% significance level, the parameters of the model are not significant, only the parameters of model 1 are significant at the 5% level and its adjusted number is only 0.66, indicating that between 1990 and 2017, there was no simple linear relationship between the diversity coefficient of energy consumption structure and carbon emissions in Shanxi Province. There was a more complex relationship between energy consumption structure evolution and carbon emissions growth, which needs further discussion. This is similar to the result of the relationship between the diversification coefficient of China's energy consumption structure and carbon emissions calculated by Zhang (2003) and Li and Cui (2011).

Conclusion

Based on the time series data from 1990 to 2017, the author selected Shanxi Province as the representative of energy-intensive provinces, empirically analyzed the changing characteristics of carbon emissions and carbon emissions intensity in energy-intensive provinces. Using environmental Kuznets curve, environmental-quality equation, and with the help of the constructed industrial structure diversification coefficient, energy structure diversification coefficient, the author examined the role of economic growth, industrial restructuring, energy consumption structure changes in the evolution of carbon emissions. The conclusions are as follows:

1) From 1990 to 2017, the carbon emissions of Shanxi Province in general were in the state of growth, but the increase rate was different.
2) Economic growth has a direct pull on the growth of carbon emissions, and every 1% increase in economic growth, carbon emissions will increase accordingly.
3) Industrial evolution is a bi-directional pulling factor of carbon emissions growth: When the industrial structure transits from the primary industry to the secondary industry, the industrial structure evolution has a pulling effect on carbon emissions growth. When the industrial structure transits from the secondary industry to the tertiary industry, the industrial structure reduces the growth of carbon emissions, showing the characteristics of inverted U-shaped curve. Before

http://www.aloki.hu ● ISSN 1589 1623 (Print) ● ISSN 1785 0037 (Online)
DOI: http://dx.doi.org/10.15666/aeer/1704_75237534

2003, there was an inflection point between the relationship of industrial structure diversification coefficient and carbon emissions.

4) The linear relationship between the evolution of energy structure and carbon emissions is not obvious. There is no inverted U-shaped curve between energy consumption and carbon emissions in Shanxi Province. This shows that the rebound effect of energy consumption may occur in the evolution process of energy structure in Shanxi Province, which needs further discussion.

At present, most studies believe that to control the growth of carbon emissions is to control the population, adjust the industrial structure, adjust the energy structure, and increase the proportion of non-mineral resource in energy consumption. Among the measures, which measures are more effective for carbon emission reduction in energy intensive provinces? The liberalization of the single second child policy in 2013 did not cause a small peak in fertility, and the implementation of the national family planning policy over the past few decades has changed people's conception of fertility. This shows that the policy effect of controlling population growth to reduce carbon emissions will not be significant for some time to come. From the perspective of energy consumption structure, Shanxi Province is a big province of coal production and consumption, although the energy structure reform has been carried out, but the coal-based energy consumption structure cannot be rapidly changed in a short time. At the same time, with the industrialization and urbanization process of Shanxi Province, the demand for primary energy will increase. The regression results also show that the linear relationship between the evolution of energy consumption structure and carbon emissions is not very obvious, and the potential to reduce carbon emissions through the evolution of energy structure is very small. The most effective policy to reduce carbon emissions in Shanxi is industrial restructuring. In the future, we need to continue to promote industrial restructuring, from the secondary industry to the tertiary industry. At the same time, in order to promote the transformation of high energy-consuming sectors in the secondary industry to low energy-consuming sectors, the support of technological progress is also needed in the process of transformation. To sum up, the main potential of carbon emission reduction in energy-intensive provinces lies in the rational evolution of industrial structure and technological progress, at the same time, ensuring that the population does not soar, the energy structure retrogression or reasonable evolution.

Acknowledgements. The authors gratefully acknowledge the financial support from Shanxi Datong University PhD Start-up Foundation (2014-b-16), Datong Soft Science Foundation (2017151), Shanxi Province Philosophy and Social Science Planning Foundation, Shanxi Province Soft Science Foundation (2018041067-4), Shanxi Province Soft Science Foundation (2018041060-7) and West Program of the National Social Science Fund of China (No. 15XGL018).

REFERENCES

[1] Chen, S. F., Liu, Y., Zou, X. P. (2012): A Theoretical and empirical study on Driving Forces of Carbon Dioxide Emissions Evolution. – Scientific Management Research 1: 43-48.

[2] Chen, J. L., Li, P. X., Gao, J. L. (2016): Spatiotemporal patterns and influencing factors of carbon emissions in the Pan-Yangtze River Delta region, 1990-2014. – Progress in Geography 12: 1472-1482.

[3] Chi, Q.-S. (2007): Forecasting the Increase of Petroleum Consumption in China based on the ARIMA Model. – Resources Science 5: 69-73.

http://www.aloki.hu ● ISSN 1589 1623 (Print) ● ISSN 1785 0037 (Online)
DOI: http://dx.doi.org/10.15666/aeer/1704_75237534

[4] China National Development and Reform Commission (2012): The Second National Information Circular on Climate Change of the People's Republic of China.
[5] Gao, B. (2017): The Empirical Study on the Relationship Between Energy Consumption, Carbon Emissions and Economic Growth in Beijing ─ Tianjin ─ Hebei. – Journal of Industrial Technological & Economics: 82-92.
[6] Gao, B., Fang, J., Lu, X. (2017): Evolution relationship between agricultural carbon emissions and economic growth and its reduction potential. – Journal of Arid Land Resources and Environment: 13-18.
[7] He, H. B. (2012): Factors Analysis of Influencing China's Carbon Emissions. – Huazhong University of Science and Technology.
[8] Hu, Y., Liu, J.-F., Hu, W. (2016): Regional Variance, Trend Evolution and Factors of China's Carbon Emission Intensity Based on 30 Provinces (Cities and Districts)' 1997—2012 panel data. – Resources & Industries: 7-13.
[9] Huang, R., Zhe, Y., Wang, Z. (2010): Prediction on Shanghai's Energy Consumption Trend and Carbon Emission Pink. – Shanghai Journal of Economics 4: 81-90.
[10] Huang, H. (2014): Research on the Pertinence Between Shanghai's Economic Polynary Structure and Carbon Emission. – China Population, Resources and Environment: 32-35.
[11] Li, Z. H., Cui, Y. A. (2011): An Empirical Study on the Evolution Characteristics of China's Carbon Emissions. – Statistics & Decision: 122-126.
[12] Li, J.-B. Huang, X.-J., Wu, C.-Y. (2015): Analysis of Spatial Heterogeneity Impact Factors on Carbon Emissions in China. – Economic Geography 11: 21-28.
[13] Liang, H.-M., Li, H.-L. (2014): Evolution Characteristics of Carbon Emissions and Its Influencing Factors in Circum-Bohai Sea Region. – Journal of Beihua University (Natural Science): 274-280.
[14] Lin, B., Liu, X. (2010): China's Carbon Dioxide Emissions under the Urbanization Process: Influence Factors and Abatement Policies. – Economic Research Journal 8: 20-30.
[15] Lin. B., Huang, X. G. (2011): The Evolution Trend of China's Regional Carbon Emissions under Gradient Development Mode——Based on the Perspective of Spatial Analysis. – Journal of Financial Research 12: 35-46.
[16] Liu, J. C. (2011): Energy Saving Potential and Carbon Emissions Prediction for the Transportation Sector in China. – Resources Science 4: 640-646.
[17] Liu, H., Bao, Z., Yang, Q. (2013): Distributional Dynamic and Evolution of China's CO2 Emissions. – Resources Science 4: 1925-1932.
[18] Ma, D., Wu, W., Dong, Z. (2017): Industrial Carbon Emission Performance and Its Influencing Factors in China: Based on an Empirical Study of Spatial Panel Data Model. – China Economic Studies 1: 121-135.
[19] Mirzaei, M., Bekri, M. (2017): Energy Consumption and CO2 Emissions in Iran, 2025. – Environmental Research: 345-351.
[20] Qi, S. Z., Lin, S., Wang, B.-B. (2015): Impact of Economic Growth Pattern of the Six Provinces of Central China on Regional Carbon Emission:Based on the Tapio Model and Lag Instrumental Variable Analysis of Panel Data. – China Population Resources and Environment 5: 59-66.
[21] Ren, J. (2015): Reviews on Carbon Emission Factors. – Resources & Industries: 79-83.
[22] Song, D., Xu, A. (2011): Regional Difference and Influencing factors of China's Urban Carbon Emissions. – China Population, Resources and Environment 11: 8-14.
[23] Song, J. (2012): Factor Decomposition of Carbon Emissions from Energy Consumption of Shandong Province Based on LMDI. – Resources Science: 35-41.
[24] Sun, X. M., Zhou, M., Qi, Z.-F. (2011): Empirical Study on Evolution Characteristics and Factors of Carbon Emissions in Shandong Province. – East China Economic Management 7: 11-15.

http://www.aloki.hu ● ISSN 1589 1623 (Print) ● ISSN 1785 0037 (Online)
DOI: http://dx.doi.org/10.15666/aeer/1704_75237534

[25] Tian, Y., Zhang, J.-B., Yin, C.-J., (2014): Distributional Dynamics and Trend Evolution of China's Agricultural Carbon Emissions—An Analysis on Panel Data of 31 Provinces from 2002 to 2011. – Population, Resources and Environment 7: 91-98.
[26] Tong, X., Chen, K., Li, G. (2015): An Empirical Study of Chinese Carbon Emissions and Influencing Factors—Grey Correlation Analysis of China and 30 Provincial between 2000 and 2011. – Journal of Industrial Technological Economics: 66-78.
[27] Wang, C.-K., Xie, H. Z. (2015): Study on Dynamic Characteristics and Influencing Factors of China's Power Carbon Emissions. – China Population, Resources and Environment 4: 21-27.
[28] Wang, R., Jiang, Z. (2017): Energy Consumption in China's Rural Areas: A Study Based On the Village Energy Survey. – Journal of Cleaner Production: 452-461.
[29] Wu, X. R., Zhang, J. (2014): Provincial Agricultural Carbon Emissions in China: Calculation, Performance Change and Influencing Factors. – Resources Science 4: 129-138.
[30] Xu, L., Zhao, T., Yang, X. F. (2013): Study on Driving Forces of Resource Provinces' Carbon Emissions—Based On the PATH-STIR PAT Model. – Forum on Science and Technology in China 12: 52-58.
[31] Xu, L. (2014): Analysis of Influence Factors and Prediction of Carbon Emissions during the Process of Urbanization in Shanxi Province. – Tianjin University.
[32] Yuan, C. W., Zhang, S., Jiao, P. (2017): Temporal and spatial variation and influencing factors research on total factor efficiency for transportation carbon emissions in China. – Resources Science 4: 687-697.
[33] Zhang, L. (2003): Economic Development and Its Bearing on CO2 Emission. – Acta Geographica Sinica: 629-637.
[34] Zhang, L., Huang, Y., Li, Y. (2010): An Investigation on Spatial Changing Pattern of CO2 Emissions in China. – Resources Science: 211-217.
[35] Zhao, Z. Y., Yang, C.-F. (2012): Decomposition analysis of China's carbon emission driving factors. – China Soft Science 6: 175-183.
[36] Zhou, K., Mao, Y.-Y. (2017): Research on the factors of implied carbon export in China: based on the analysis of counter factual method. – China Population, Resources and Environment 6: 16-26.

http://www.aloki.hu ● ISSN 1589 1623 (Print) ● ISSN 1785 0037 (Online)
DOI: http://dx.doi.org/10.15666/aeer/1704_75237534

STUDY ON THE SPATIAL RELATIONSHIP BETWEEN LANDSCAPE RECREATION SERVICE DEMAND AND URBANIZATION – A CASE STUDY IN SHANGHAI

BING, Z.* – QIU, Y. – ZHONG, W. – JIANG, H.

College of Hospitality Management, Shanghai Business School
123 Fengpu Avenue, Fengxian District, Shanghai, China
(e-mail: xiaobing0707@126.com, caddy513416@126.com, jianghong007@126.com; phone: +86-136-6186-0799)

**Corresponding author*
e-mail: xiaobing0707@126.com

(Received 27th Feb 2019; accepted 3rd May 2019)

Abstract. In the traditional ecosystem service evaluation, non-material services such as culture and recreation services are difficult to accurately quantify due to the lack of a powerful evaluation model. Compared with ecosystem services, landscape services emphasize all the tangible and intangible services that landscape ecosystems provide to humans in the spatial pattern. Social media photos can be used for perceived services demand evaluation on the landscape scale. The study of spatial relationship between recreation service demand (RSD) and urbanization complements the integrity of the landscape service supply and demand relationship framework. Firstly, this paper analyzes the spatial autocorrelation and seasonal differences of landscape recreation service demand through Global Moran's I. The analysis shows that there is a highly significant spatial agglomeration and certain seasonal differences in landscape recreation service demand. Secondly, the bivariate Global Moran's I is used to analyze spatial correlation between landscape recreation service demand and urbanization, The result shows that there is a positive spatial correlation between urbanization indicators and landscape recreation service demand in different seasons. Thirdly, the bivariate LISA method is used to show the spatial agglomeration relationship between landscape recreation service demand and urbanization indicators in different seasons. Finally, it is verified that the spatial lag model and the spatial error model are more suitable for measuring the dependence than the linear regression least squares (OLS). At the same time, population density (PD) has a positive impact on landscape recreation service demand in different seasons, while landscape recreation service demand in autumn is also positively affected by non-urbanization factors and negative impact of GDP, which also proves space spillover effect between landscape recreation service demand and urbanization. The above conclusions can be used as important information for urban landscape planning and decision-making.

Keywords: *recreation services demand, landscape services, spatial dependence, spatial correlation, Moran's I, urbanization*

Introduction

Today, human beings are considered an indispensable part of the landscape. At the same time, human beings also benefit from the functions provided by the landscape and the natural environment. Therefore, the research on ecosystem service demand is gradually starting (Burkhard et al., 2014; Schroter et al., 2015; Villamagna et al., 2013), the difficulty of data collection and the measurement limitations of time scales have relatively limited the progress of demand research. At the same time, the spatial alienation of ecosystem service demand, supply and consumption have limited the study of ecosystem service supply and demand trade-offs and spatial heterogeneity (Syrbe and Walz, 2012).

http://www.aloki.hu ● ISSN 1589 1623 (Print) ● ISSN 1785 0037 (Online)
DOI: http://dx.doi.org/10.15666/aeer/1704_75357548

The International Classification of Ecosystem Services (Hainesyoung et al., 2009; Hainesyoung and Potschin, 2013) identifies Cultural Ecosystem Services (CES) as a very important component. In recent years, cultural service value assessment research has developed rapidly (Bieling et al., 2014; Hermes et al., 2018; Van Berkel and Verburg, 2014). Recreational services are defined as the "recreational pleasure people derive from natural or cultivated ecosystems" (MEA, 2005; TEEB, 2010), which have a positive impact on social well-being (Hermes et al., 2018). However, non-material services such as cultural services and recreation are difficult to accurately quantify due to the lack of a powerful model for evaluation (Shaw et al., 2016; Tenerelli et al., 2016), the spatial and temporal ectopicity of service supply and demand is more pronounced (Milcu et al., 2013).

The basic spatial unit of the ecosystem service flow includes the supply unit, the connection unit and the use unit. The recreation service can be used by the beneficiary without passing through the carrier, the first assessment perspective should come from the beneficiary itself (Lie et al., 2017). Ecosystem services perceived by consumers and generating benefits can constitute effective demand (Yan et al., 2017), people's aesthetic preferences can be used as a means of recreational services demand assessment (Peña et al., 2015). The social media photos provide an opportunity to "excavate the perception, cognition or activity of many people" and reflect the relationship between landscape attributes and landscape preferences (Tieskens et al., 2018), which can be used for perceived recreation service demand evaluation on a landscape scale (Michael et al., 2018), is becoming an increasingly attractive source of cultural service assessment (Oteros-Rozas et al., 2017). The data and content analysis reflects recreation services supply on the landscape scale, while demonstrating the effective demand of people, and promotes the improvement of existing assessment methods on time scales and spatial scales (Michael et al., 2018).

Population and economic factors often affect ecosystem service demand, while land cover and land use are directly related to ecosystem service supply capacity (Oteros-Rozas et al., 2017). Among them, there is a certain spatial correlation between the supply of ecosystem services and landscape features and urbanization (Oteros-Rozas et al., 2017; Syrbe et al., 2012; Zhang et al., 2018). In recent years, ecosystem services research has emphasized the relationship between ecosystems and human social systems at the landscape scale (Wu et al., 2013), focusing on ecosystem service needs assessments. At present, the spatial correlation between recreational service demand and landscape features has also been verified (Oteros-Rozas et al., 2017). So, is there a spatial correlation between recreational service demand and urbanization? This answer will complement the integrity of the LRS supply-demand relationship study at the landscape scale (*Fig. 1*).

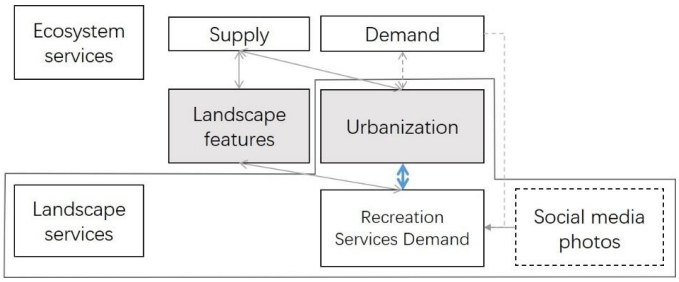

Figure 1. *Conceptual framework linking ecosystem services supply and demand. The contents of block diagram are the research topics of this paper*

http://www.aloki.hu ● ISSN 1589 1623 (Print) ● ISSN 1785 0037 (Online)
DOI: http://dx.doi.org/10.15666/aeer/1704_75357548

Is there a spatial autocorrelation of landscape recreation service demand in cities with developed tourism (Goal 1)? Is there any seasonal difference in this spatial autocorrelation (Goal 2)? Is there a spatial correlation between landscape recreation service demand and urbanization (Goal 3)? Does the demand for landscape recreation services have a spatial dependence on the level of urbanization (Goal 4)? The above questions are the research objectives of this paper. This paper aims to discuss the spatial distribution of landscape recreation service demand from the perspective of people's needs. This method can explain whether landscape recreation service supply and demand are affected by landscape features and urbanization at the same time, provide important information for landscape planning and decision making (Maes et al., 2012; Syrbe and Walz, 2012).

Methodology

Study area

The city is a region where human society and ecosystems interact closely. Landscape recreation services are an important contribution of landscape to human well-being. As a famous international tourist city, Shanghai's tourism demand has certain seasonal differences, and the off-season and peak seasons are more obvious (*Table 1*).

Table 1. *The number and ratio tourist receptions and social media photos in different seasons*

	Spring	Summer	Autumn	Winter	Whole year
Inbound tourists (thousand)	2273.5	2011.75	2266.5	1745	8297.75
Ratio (%)	27.40%	24.25%	27.32%	21.03%	100%
Social media photos	855	741	838	522	2956
Ratio (%)	28.92%	25.07%	28.35%	17.66%	100%

The number of inbound tourists is calculated by the average of the data from 2014 to 2017. The data comes from the website of the Shanghai Municipal Culture and Tourism Bureau (http://lyw.sh.gov.cn/)

Therefore, this paper selects Shanghai urban area as the research scope. Shanghai's urban ecosystem is highly complex, human activities are intensive, and tourism is developed. It can be used as a typical area for studying landscape recreation service demand (*Fig. 2*).

Data

Social media photos

The data of social media photos used in this study belongs the Yahoo Lab Research Project (Thomee et al., 2015), which includes 100 million global photo information published on the Flickr platform from 2004 to 2014, in addition to photo elements. It includes 23 types of information such as photo number, shooting time, title, description, deep learning label, latitude and longitude. In this database, all photos of Shanghai geographic coordinates are extracted, and several types of information indicators such as photo number, shooting time, deep learning label, and latitude and longitude are selected for this study.

http://www.aloki.hu ● ISSN 1589 1623 (Print) ● ISSN 1785 0037 (Online)
DOI: http://dx.doi.org/10.15666/aeer/1704_75357548

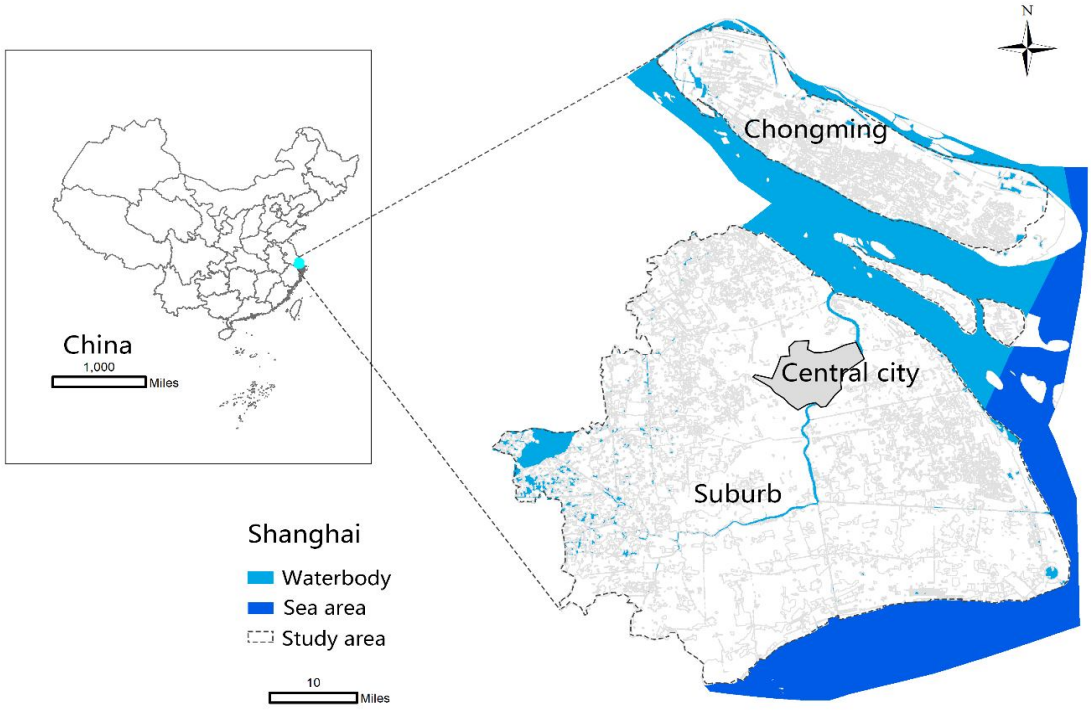

Figure 2. *The dotted line in the figure is the study area*

There are a total of 125,327 photos in Shanghai. First, in order not to repeatedly calculate the same tourist's perception of the same landscape, the duplicate data released at the same time is excluded. Secondly, in order to analyze the tourist's perception of the natural landscape, we remove the deep learning label as "empty". "Indoor", "outdoor", "People", "architecture", etc., which do not reflect the relationship between human activities and natural landscapes; finally, a total of 2,956 data records (*Table 1*) that meet the criteria are selected, according to spring (March to May), summer (June to August), autumn (September to November), winter (December to February), and the whole year. The proportion of photo data in different quarters is similar to that of inbound tourism. The proportion in spring is the highest, which is 11.26% higher than that in winter. It can be seen that the social meida photos data can be used to analyze the seasonal differences in landscape recreation demand. In this paper, the filtered data table is imported into Arcgis10.1 software and converted into projection data. The projection uses the WGS_1984_UTM_Zone_51N coordinate system.

Urbanization

Spatial distribution data of population density and GDP density in 1 × 1 km resolution raster, obtained from the Resource and Environment Data Cloud Platform (http://www.data.ac.cn). The two datasets were spatialized by Interpolating statistical data to spatial grids with consideration of local land use, the nighttime light index, and other remote sensing information. The data format is gird. The author imported the data into ArcGIS10.1 software, intercepted the data according to the boundary of the study

http://www.aloki.hu ● ISSN 1589 1623 (Print) ● ISSN 1785 0037 (Online)
DOI: http://dx.doi.org/10.15666/aeer/1704_75357548

area, converted it into vector data, and adjusted the projected coordinate system to be consistent with the photo data.

Spatial correlation analysis

Spatial autocorrelation of landscape recreation services demand

Spatial autocorrelation is an important indicator to test whether the attribute value of an element is significantly associated with the attribute value of its adjacent space point. Global Moran's I is used to assess whether landscape recreation service demand belong to cluster distribution, discrete distribution or random distribution, p value indicates the probability of occurrence of this trend, and z score is a multiple of standard deviation. Moran's $I > 0$ represents spatial positive correlation, the larger the value, the more obvious the spatial correlation; Moran's $I < 0$ represents the spatial negative correlation, the smaller the value, the larger the spatial difference; Moran's $I = 0$, indicating a random distribution.

At the same time, Anselin Local Moran's I is used to identify spatial clusters with high or low value elements, ie, statistically significant hotspots, cold spots, and spatial outliers. This tool can effectively obtain hotspots and cold spots for landscape recreation service demand (Figueroa-Alfaro and Tang, 2016).

In this paper, Arcgis10.1 software is used for data processing to generate a square grid map of 1 km × 1 km in Shanghai urban area. The square grid is superimposed with geotag photo data for spatial feature analysis of landscape recreation services demand. The Spatial Autocorrelation (Global Moran's I) tool and the clustering and outlier analysis (Anselin Local Moran's I) tool were analyzed using GeoDa1.10 software. The spatial clustering analysis in the paper defines the spatial weight based on the polygon Queen contiguity, and uses the average of all adjacent positions to evaluate the degree of correlation between the X variable value of a position and the value of the Y variable.

Spatial correlation between landscape recreation service demand and urbanization

The Bivariate Moran's I tool is used to explore the spatial clustering (positive spatial correlation) and spatial discrete (negative spatial correlation) relationships between landscape recreation service demand and urbanization. The global bivariate Moran's I is used for spatial correlation analysis between landscape recreation service demand and urbanization, and the local bivariate Moran's I can be used for visual spatial correlation analysis (Anselin and Rey, 2014). For the pseudo value obtained, the spatial correlation between RSD and urbanization is set to b0.01. Four types of local spatial autocorrelation are generated by bivariate LISA: quadrant I (HH) represents a high RED value surrounded by high urbanization values; quadrant II (HL) represents a high RSD value surrounded by low urbanization values; quadrant III (LH) represents a low RSD value surrounded by a high urbanization value and a quadrant IV (LL) representing a low RSD value surrounded by a low urbanization value.

Spatial regression analysis

In spatial cluster analysis, if there is no spatial autocorrelation in the variable, the OLS regression model can be used for analysis. If the observed value of the variable has spatial autocorrelation, it means that the residual value is not random. This situation needs to use spatial regression analysis. However, the spatial lag model and the spatial

http://www.aloki.hu ● ISSN 1589 1623 (Print) ● ISSN 1785 0037 (Online)
DOI: http://dx.doi.org/10.15666/aeer/1704_75357548

error model are more suitable for regression analysis (Wang, 2009). Therefore, based on the spatial autocorrelation analysis, this paper compares the significance of OLS, SLM and SEM regression analysis results and selects the best analytical model.

Results

Spatial autocorrelation of landscape recreation service demand

The results of Global Moran's I analysis show that (*Table 2*), the annual RSD spatial pattern shows a highly significant spatial agglomeration, with Moran's I index of 0.5094 and Z score of 80.3762, which can reject null hypothesis and random distribution. Compared with different seasons, RSD has the highest concentration in spring, Moran's I index is 0.5256, Z score is 84.0242; LRS demand is the lowest in autumn, Moran's I index is 0.412, Z score is 55.2689. In general, the spatial agglomeration patterns of RSD in different seasons have certain differences, but the differences are not significant.

Table 2. *Spatial autocorrelation analysis of RSD in spring, summer, autumn, winter, and whole year. Statistically significant at 1% level*

RSD	Moran's I index	Expected index	Variance	Z score
Whole year	0.5094	-0.0002	0.0063	80.3762
Winter	0.4748	-0.0002	0.0055	86.5094
Autumn	0.412	-0.0002	0.0074	55.2689
Summer	0.4397	-0.0002	0.0059	74.7128
Spring	0.5256	-0.0002	0.0063	84.0242

The results of Local Moran's I show different types of RSD spatial aggregating patterns. It can be seen from the annual RSD spatial agglomeration feature that the HH area is mainly concentrated in the central area of Shanghai, and this feature has similar performance in different seasons. The HL area distribution is relatively discrete. The LH area is distributed in the southwest and south of the study area, and the spatial aggregation of RSD is most similar in autumn and whole year. The LL area is mainly distributed in Chongming Island and suburban areas in the north; the number of RSD cold spots in spring and summer is large, distributed in the marginal areas of Chongming Island and suburban areas, while the number of cold spots in autumn and winter is small. It can be seen that the regional spatial agglomeration of high RSD is strong, and the seasonal difference is relatively low; the area of low RSD has spatial agglomeration and seasonal differences (*Fig. 3*).

Correlation analysis between landscape recreation service demand and urbanization

This paper uses Bivariate Moran's I to test the spatial correlation between RSD and urbanization. The level of urbanization is represented by two indicators: population density (PD) and GDP. *Figure 4* shows a significant positive correlation between RSD and PD. There is also a positive correlation between RSD and GDP, but the correlation is weak, and the correlation is between 0.084 and 0.118. It can be seen that the

http://www.aloki.hu ● ISSN 1589 1623 (Print) ● ISSN 1785 0037 (Online)
DOI: http://dx.doi.org/10.15666/aeer/1704_75357548

correlation between urbanization and RSD is relatively stable, and the seasonal difference is not large (*Fig. 4*).

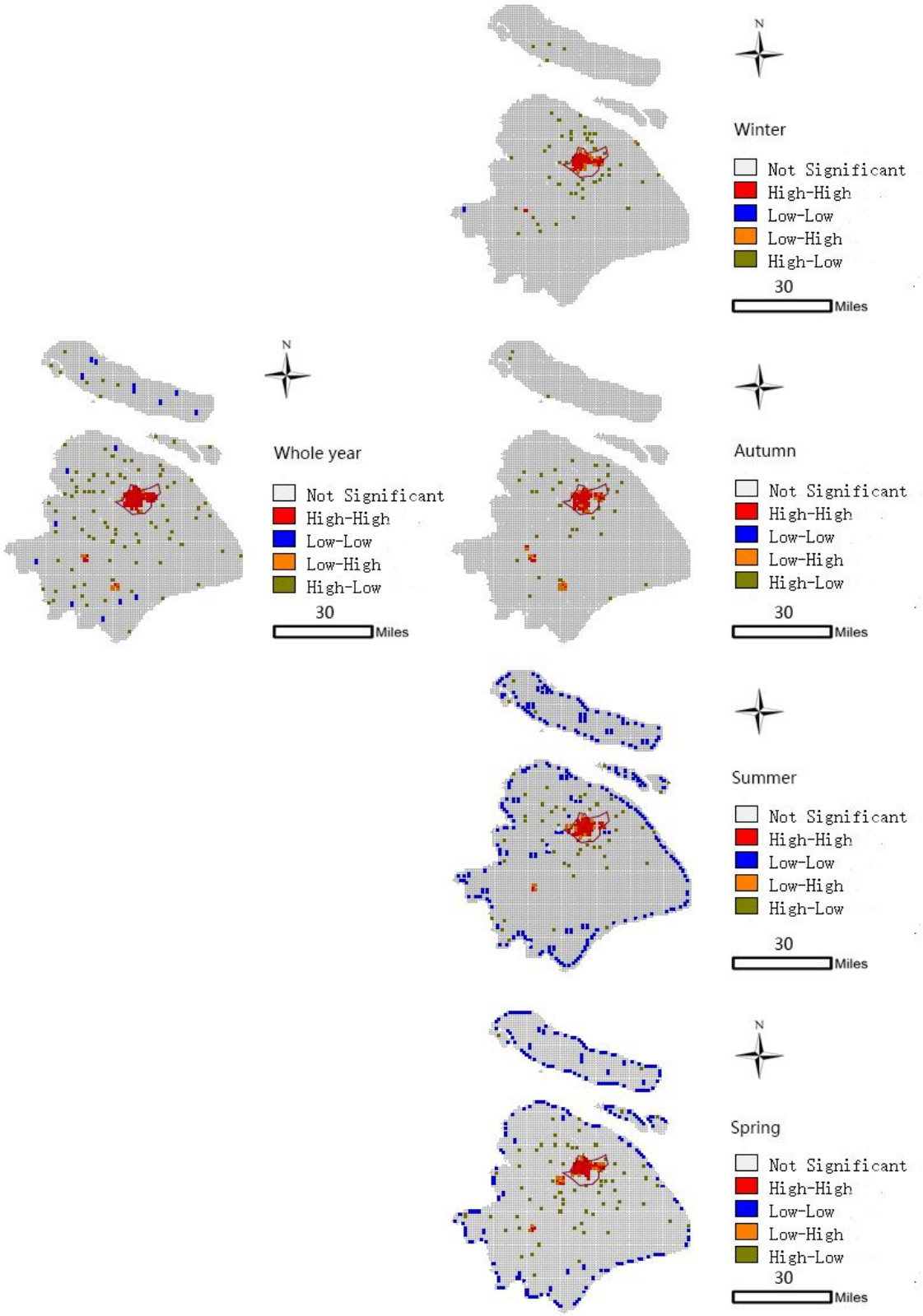

Figure 3. *LISA cluster map of local Moran's I. Statistically significant at 1% level*

http://www.aloki.hu ● ISSN 1589 1623 (Print) ● ISSN 1785 0037 (Online)
DOI: http://dx.doi.org/10.15666/aeer/1704_75357548

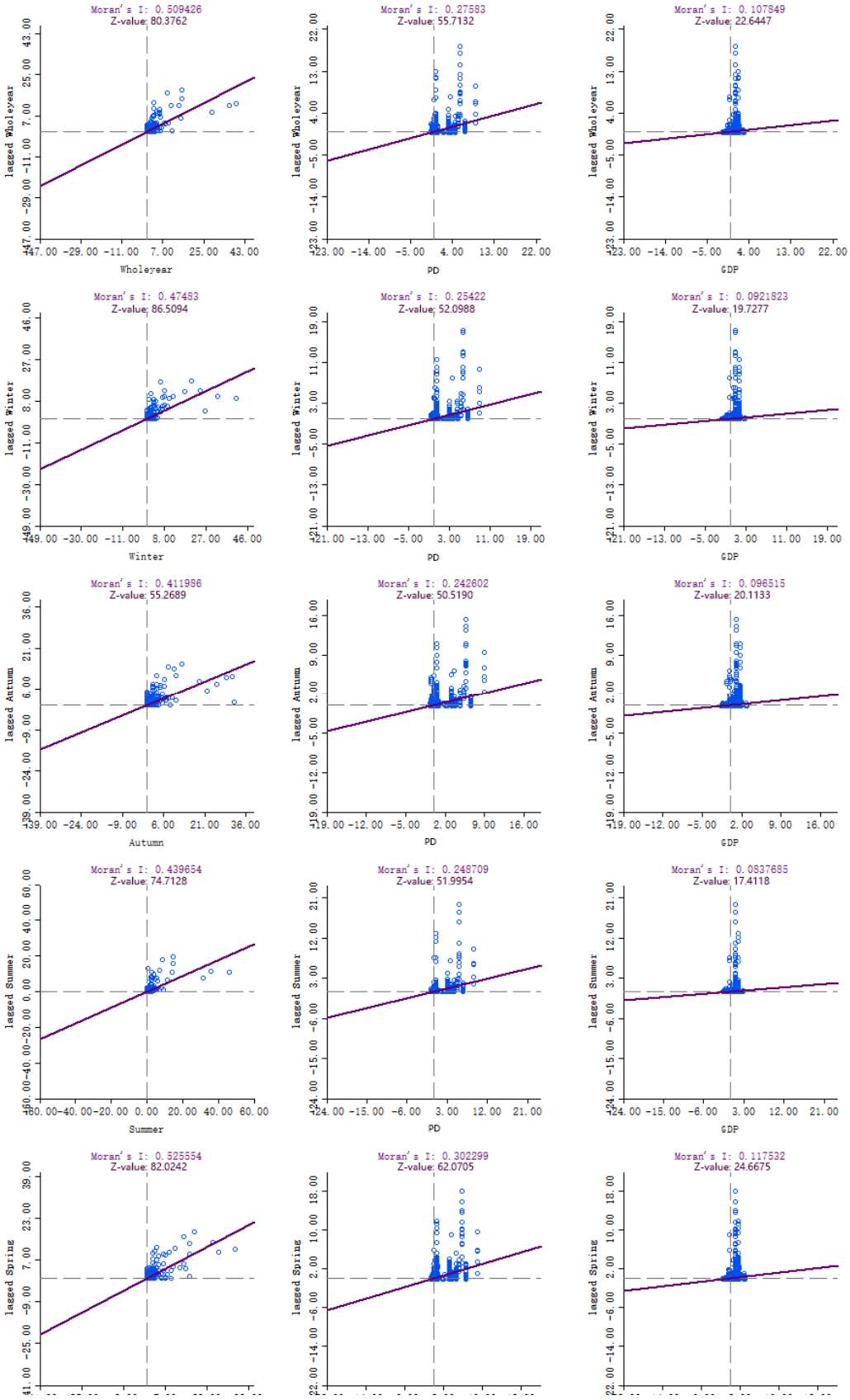

Figure 4. *Bivariate Moran's I between RSD and urbanization (PD & GDP). Statistically significant at 1% level*

http://www.aloki.hu ● ISSN 1589 1623 (Print) ● ISSN 1785 0037 (Online)
DOI: http://dx.doi.org/10.15666/aeer/1704_75357548

The BiLISA Cluster map (*Fig. 5*) shows the spatial agglomeration of RSD and urbanization in different seasons. The HH area of urbanization and RSD is still mainly concentrated in the central city, with a high degree of concentration. The seasonal distribution of GDP and RSD is not much different; the high values of PD and RSD are the largest in spring. HL has the widest distribution range, PD has a high value distribution in the middle and northeast of the study area, and RSD has a low value distribution, GDP has a high value distribution in the middle and northwest of the study area, while RSD has a low value distribution. The LH region is dispersedly distributed in the southwestern part of the study area. The spatial agglomeration of urbanization and RSD is more obvious in autumn and the whole year. The LL value distribution area presents a certain space and seasonal agglomeration, mainly concentrated in the urban fringe area of spring and summer and the edge area of Chongming Island. We can get several conclusions: First, compared with the spatial distribution of urbanization, the RSD high-value space is more concentrated, mainly concentrated in the central city; second, in the low-value area of urbanization indicators, RSD appears a large range of high values in autumn. At the same time, in the low-value areas of urbanization, the low RSD is mainly in the urban fringe of spring and summer.

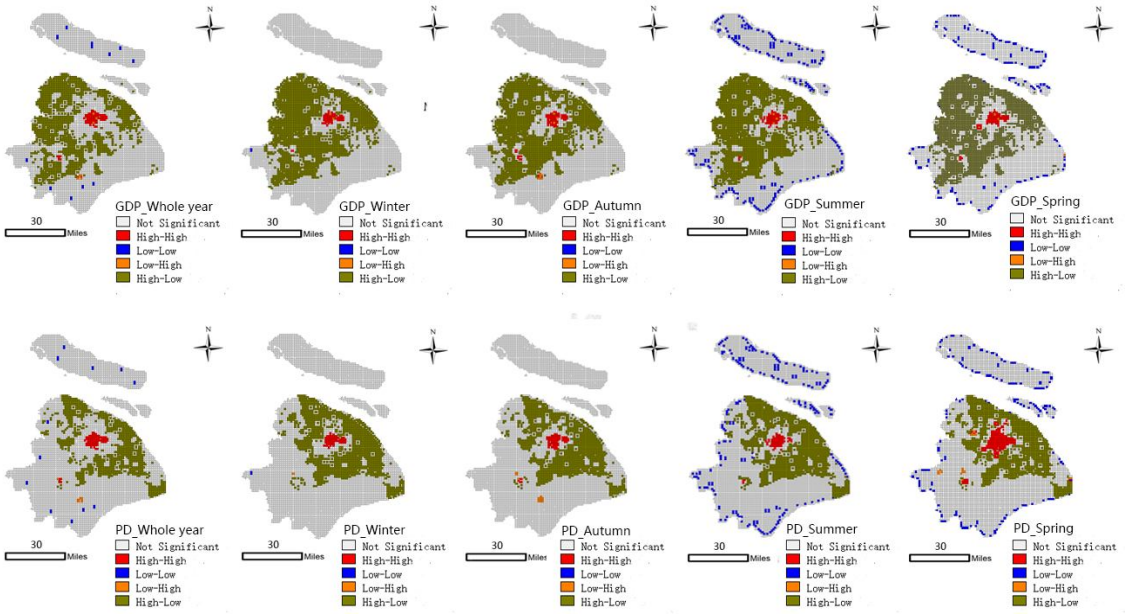

Figure 5. *BiLISA Cluster map between RSD and urbanization (PD & GDP). Statistically significant at 1% level*

Spatial dependence analysis of landscape recreation service demand on urbanization

The previous analysis has obtained that the observation value of RSD is related to the geographical location, then the residuals are no longer independent of each other, and there is a certain spatial positive correlation between RSD and urbanization. Therefore, when further analyzing the causal relationship between urbanization indicators and RSD, the OLS model is no longer applicable. In this paper, the urbanized PD and GDP indicators are used as independent variables, and the RSD of different seasons is used as the dependent variable. The maximum likelihood estimation method (SLM & SEM) is

http://www.aloki.hu ● ISSN 1589 1623 (Print) ● ISSN 1785 0037 (Online)
DOI: http://dx.doi.org/10.15666/aeer/1704_75357548

used for spatial regression analysis, and the OLS model results are used for comparison test (*Table 3*).

The OLS results show that the simulation fit is not ideal and the adjusted R^2 value is relatively low. Among them, the regression fit of PD with RSD in different seasons is highly significant, while the GDP index only fits significantly with the regression of RSD in autumn and whole year. At the same time, LM tests show that LM (Lag) and LM (Error) are significant for regression analysis of RSD in different seasons, and this indicates that SLM and SEM are more suitable than OLS.

Spatial regression analysis shows that SRM is superior to OLS because Log Likelihood values increase and AIC and SC values decrease (*Tables 3* and *4*). SLM has the best results in RSD regression analysis in spring, summer, winter and whole year. The lag coefficient (W_LRS) in SLM is positive under pb0.001 significant condition, indicating that the RSD of four time dimensions is adjacent. The SEM has the best positive results in autumn, and the error coefficient (LAMBDA) is also positive under the pb 0.001 significance condition in the SEM, indicating that the RSD is also positively affected by non-urbanization factors in autumn.

Table 3. *The results of OLS model between RSD and urbanization*

Variables	Whole year	Spring	Summer	Autumn	Winter
Constant	-0.164	-0.009**	-0.003	-0.008**	-0.005*
GDP	-13.67**	9.015	0.446	-3.126**	5.452
PD	0.0002***	16.482***	10.98***	9.36***	5.42***
Adjusted R^2	0.08	0.09	0.061	0.058	0.048
Log likelihood	-17043.4	3362.47	3841.11	3836.18	5341.67
Akaike info criterion	34092.8	-6718.93	-7676.23	-7666.37	-10677.3
Schwarz criterion	34112.9	-6698.76	-7656.06	-7646.2	-10657.2
Lagrange multiplier (lag)	4844.73***	151.16***	403.02***	463.44***	128.92***
Robust LM (lag)	45.25***	24.65***	4.01*	125.86***	27.28***
Lagrange multiplier (error)	4824.96***	134.98***	399.65***	408.90***	116.58***
Robust LM (error)	25.49***	8.46**	0.64*	71.32***	14.94***

*Statistically significant at 5% level. **Statistically significant at 1% level. ***Statistically significant at 0.1% level

All PD coefficients are significant positive values, indicating that PD growth drives RSD growth. In the order of decreasing absolute values of PD coefficients, as the PD increases, the RSD in spring increases the most, while the demand for RSD in winter increases the least.

GDP coefficients are only significant negative values in the autumn, indicating that the RSD in the autumn has a degrading effect with the increase of GDP. At the same time, compared with the OLS model analysis, the absolute value of GDP coefficients in the SEM regression analysis of RSD in autumn is higher, indicating that the effect of spatial autocorrelation is that the negative impact of GDP increase on RSD in autumn is reduced.

http://www.aloki.hu ● ISSN 1589 1623 (Print) ● ISSN 1785 0037 (Online)
DOI: http://dx.doi.org/10.15666/aeer/1704_75357548

Table 4. *Results of spatial regression between RSD and urbanization, only the most suitable models are shown*

	Whole year[a]	Spring[a]	Summer[a]	Autumn[b]	Winter[a]
W_LRS	0.792***	0.245***	0.34***		0.22***
LAMBDA		-	-	0.378***	
Constant	-0.044	-0.007*	-0.002	-0.006	-0.004
GDP	-27.74	4.48	-4.00	-2.09**	2.51
PD	10.42***	11.24***	5.79***	4.94***	2.99***
Log likelihood	-15505.1	3426.36	3988.16	3999.89	5394.12
Akaike info criterion	31018.2	-6844.71	-7968.31	-7993.78	-10780.2
Schwarz criterion	31045.1	-6817.82	-7941.42	-7973.61	-10753.3

[a]Spatial lag model
[b]Spatial error model
W_LRS denotes spatial lag term of individual ecosystem service equation. This parameter only makes sense in spatial lag models, namely in LRS in whole year regressions. LAMBDA denotes spatial error term of individual ecosystem service equation. This parameter only makes sense in spatial lag models, namely in regressions
*Statistically significant at 5% level. **Statistically significant at 1% level. ***Statistically significant at 0.1% level

Discussion

Spatial autocorrelation and seasonal differences in landscape recreation service demand

There are certain seasonal differences in the number of tourists in the city, and this conclusion has been verified in related research on tourism activities. This paper explores the RSD spatial agglomeration model and seasonal differences through Global Moran's I and local Moran's I. The results show that the RSD in different seasons shows a highly significant spatial autocorrelation. Among them, the HH region is concentrated in the central city, and the seasonal difference is low; the LH region shows a certain concentration outside the central city, and the RSD in autumn is the most concentrated obviously. As an international tourist city, the hotspots of RSD in Shanghai are concentrated and stable, and are almost unaffected by the seasons. In September, "Shanghai Tourism Festival" and other events have an impact on RSD and form some new hotspots in the spatial distribution. Although it has not formed a role in other seasons, it has a significant impact on the spatial distribution of RSD throughout the year.

Study on the relationship between supply and demand of recreation services

As mentioned above, the alienation of the demand, supply and consumption of ecosystem services has limited research on supply and demand. This problem is more prominent in non-material services such as recreational services.

On the basis of the verification of the spatial supply of ecosystem services and the spatial characteristics of landscape and urbanization, the spatial correlation between RSD and landscape features is also explained by relevant research results from the perspective of consumer demand. In this paper, there is a significant positive correlation

http://www.aloki.hu ● ISSN 1589 1623 (Print) ● ISSN 1785 0037 (Online)
DOI: http://dx.doi.org/10.15666/aeer/1704_75357548

between RSD and urbanization, and it is not affected by seasonal differences, indicating that the spatial relationship is relatively stable. This stable spatial correlation conclusion will complement the research framework for the relationship between supply and demand of recreational services (*Fig. 1*). We can understand that the supply and demand capacity of recreation services is spatially related to landscape characteristics and urbanization, and can be used for supply and demand relationship models. At the same time, photo data based on geographic coordinates provides a data source for the research of recreational service demand in landscape scale and time dimension (Michael et al., 2018). The deep learning of photo content can help to analyze the specific demand of people and promote spatial heterogeneity research.

Enlightenment of spatial dependence analysis on urban landscape planning

The SLM model performed optimally in RSD regression analysis in spring, summer, winter, and year-round, and was positively affected by adjacent values (*Table 4*), indicating that RSD was affected by both PD and adjacent values. Therefore, it is necessary to pay attention to the protection and planning of natural landscapes in densely populated areas. Natural landscape is an important part of maintaining the sustainable development of urban ecosystems. It not only protects the natural landscape of RSD hotspots, but also drives demand growth around hotspots.

As the tourist season in Shanghai in the autumn, the distribution of high-value points of RSD also shows a certain concentration. At the same time, the SEM model is optimal for RSD regression analysis in autumn. The RSD in autumn is affected by the positive influence of PD and the negative impact of GDP, and the RSD in autumn is also positively affected by non-urbanization factors (*Table 4*). The research and management of RSD supply and demand in autumn needs to be comprehensively considered and evaluated, and as far as possible to plan the development of areas with high population density, while avoiding the economic business center area. It is particularly important to note that the RSD cold spots area (urban fringe area and Chongming Island fringe area) in spring and summer can be the focus of landscape planning to promote the balanced development of supply and demand.

Conclusion

This paper improves the supply and demand research framework of landscape recreation services through the study of spatial relationship between RSD and urbanization.

The spatial autocorrelation of RSD is the first research goal of this paper. Global Moran's I analysis shows that RSD has a highly spatial agglomeration. The hotspots are highly concentrated in the central area of the city, and the cold spots are relatively discrete. There are some differences in the RSD spatial agglomeration patterns in different seasons, and the distribution of cold spots in spring and summer is discrete.

The spatial correlation between RSD and urbanization is the second research goal. Bivariate Global Moran's I verifies that there is a positive spatial correlation between urbanization and RSD in different seasons.

The spatial dependence of RSD on urbanization is also a research goal. In order to avoid the influence of spatial autocorrelation, this paper uses the maximum likelihood estimation method (SLM & SEM) for spatial regression analysis, and compares the OLS model results. The LM test showed that LM (Lag) and LM (Error) were significant

http://www.aloki.hu ● ISSN 1589 1623 (Print) ● ISSN 1785 0037 (Online)
DOI: http://dx.doi.org/10.15666/aeer/1704_75357548

for RSD regression analysis in different seasons, and this indicates that SLM and SEM are more suitable than OLS. The results show that the regression fit of PD with RSD in different seasons is highly significant, while GDP only fits significantly to the regression between RSD in autumn. SLM has the best results in RSD regression analysis in spring, summer, winter and whole year, indicating that RSD is positively affected by PD and adjacent values; SEM is optimal in RSD regression analysis in autumn, and RSD in autumn is positively affected by PD and non-urbanization factors, while being negatively affected by GDP, also proves the spatial spillover effect between RSD and urbanization.

Acknowledgements. The completion of this paper is funded by the project of China National Natural Science Foundation "Landscape Services spatial heterogeneity assessment and supply forecasting simulation—A Case Study of Chongming Dongtan Wetland Bird Nature Reserve in Shanghai" (41701633).

REFERENCES

[1] Anselin, L., Rey, S. J. (2014): Modern Spatial Econometrics in Practice: A Guide to GeoDa. – GeoDa Press LLC, GeoDaSpace and PySAL, Chicago, IL.
[2] Bieling, C., Plieninger, T., Pirker, H., Vogl, C. R. (2014): Linkages between landscapes and human well-being: an empirical exploration with short interviews. – Ecological Economics 105(5): 19-30.
[3] Burkhard, B., Kroll, F., Nedkov, S., Müller, F. (2012): Mapping ecosystem service supply, demand and budgets. – Ecological Indicators 21: 17-29.
[4] Figueroa-Alfaro, R. W., Tang, Z. (2016): Evaluating the aesthetic value of cultural ecosystem services by mapping geo-tagged photographs from social media data on Panoramio and Flickr. – Journal of Environmental Planning and Management. https://doi.org/10.1080/09640568.2016.1151772.
[5] Hainesyoung, R. et al. (2009): Towards a common international classification of ecosystem services (CICES)) for integrated environmental common international classification of ecosystem services (CICES)) for integrated environmental and economic accounting. – Interspeech, Conference of the International Speech Communication Association, Makuhari, Chiba, Japan, September.
[6] Hainesyoung, R., Potschin, M. (2013): Common International Classification of Ecosystem services (CICES). – Report to the European Environment Agency. www.cices.eu.
[7] Hermes, J., Berkel, D. V., Burkhard, B., Plieninger, T., Fagerholm, N., Haaren, C. V. et al. (2018): Assessment and valuation of recreational ecosystem services of landscapes. – Ecosystem Services 31: 289-295.
[8] Liu, H. M., Liu, L. Y., Ding, S. Y. (2017): The impact of human activities on ecosystem services flow. – Acta Ecologica Sinica 37(10): 3232-3242 (in Chinese).
[9] Maes, J., Paracchini, M. L., Zulian, G., Dunbar, M. B., Alkemade, R. (2012): Synergies and trade-offs between ecosystem service supply, biodiversity, and habitat conservation status in Europe. – Biological Conservation 155(4): 1-12.
[10] MEA (2005): Ecosystems and Human Well-Being: Synthesis of the Millennium Ecosystem Assessment. – Island Press, Washington DC.
[11] Michael, S., Andrea, G., Sheela, A. M. (2018): A crowdsourced valuation of recreational ecosystem services using social media data: an application to a tropical wetland in India. – Science of the Total Environment 642: 356-365.

http://www.aloki.hu ● ISSN 1589 1623 (Print) ● ISSN 1785 0037 (Online)
DOI: http://dx.doi.org/10.15666/aeer/1704_75357548

[12] Milcu, A. J., Hanspach, J., Abson, D., Fischer, J. (2013): Cultural ecosystem services: a literature review and prospects for future research. – Ecology and Society 18(3): 261-272.
[13] Oteros-Rozas, E., Martín-López, Berta, Fagerholm, N., Bieling, C., Plieninger, T. (2017): Using social media photos to explore the relation between cultural ecosystem services and landscape features across five european sites. – Ecological Indicators 94(2): 74-86.
[14] Peña, L., Casado-Arzuaga, I., Onaindia, M. (2015): Mapping recreation supply and demand using an ecological and a social evaluation approach. – Ecosystem Services 13: 108-118.
[15] Schroter, M., Barton, D. N., Remme, R. P., Hein, L. G. (2014): Accounting for capacity and flow of ecosystem services: a conceptual model and a case study for Telemark, Norway. – Ecological Indicators 36(1): 539-551.
[16] Shaw, E., Kumar, V., Lange, E., Lerner, D. N. (2016): Exploring the utility of Bayesian networks for modelling cultural ecosystem services: a canoeing case study. – Science of the Total Environment 540: 71-78.
[17] Syrbe, R. U., Walz, U. (2012): Spatial indicators for the assessment of ecosystem services: providing, benefiting and connecting areas and landscape metrics. – Ecological Indicators 21: 0-88.
[18] TEEB (2010): The Economics of Ecosystems and Biodiversity: Ecological and Economic Foundations. Edited by Pushpam Kumar. – Earthscan, London and Washington.
[19] Tenerelli, P., Demšar, U., Luque, S. (2016): Crowdsourcing indicators for cultural ecosystem services: a geographically weighted approach for mountain landscapes. – Ecological Indicators 64: 237-248.
[20] Thomee, B., Shamma, D. A., Friedland, G., Elizalde, B., Ni, K., Poland, D. et al. (2015): Yfcc100m: the new data in multimedia research. – Communications of the ACM 59(2): 64-73.
[21] Tieskens, K. F., Zanten, B. T. V., Schulp, C. J. E., Verburg, P. H. (2018): Aesthetic appreciation of the cultural landscape through social media: an analysis of revealed preference in the dutch river landscape – Landscape & Urban Planning177: 128-137.
[22] Van Berkel, D. B., Verburg, P. H. (2014): Spatial quantification and valuation of cultural ecosystem services in an agricultural landscape. – Ecological Indicators37: 163-174.
[23] Villamagna, A. M. et al. (2013): Capacity, pressure, demand, and flow: A conceptual framework for analyzing ecosystem service provision and delivery. – Ecological Complexity 15(5): 114-121.
[24] Wang, F. H. (2009): Quantitative Method and Application Based on GIS. – Commercial Press, Beijing.
[25] Wu, J., Feng, Z., Gao, Y., Peng, J. (2013): Hotspot and relationship identification in multiple landscape services: a case study on an area with intensive human activities. – Ecological Indicators 29: 529-537.
[26] Yan, Y., Zhu, J. Y., Wu, G., Zhan, Y. J. (2017): Review and prospective applications of demand supply and consumption of ecosystem services. – Acta Ecologica Sinica 37(8): 2489-2496 (in Chinese).
[27] Yao, J., He, X. Y., Chen, W. (2018): The latest process in ecosystem service flow research methods. – Chinese Journal of Applied Ecology 29(1): 335-342 (in Chinese).
[28] Zhang, Y., et al. (2018): On the spatial relationship between ecosystem services and urbanization: a case study in Wuhan, China. – Science of the Total Environment 637-638: 780-790.

http://www.aloki.hu ● ISSN 1589 1623 (Print) ● ISSN 1785 0037 (Online)
DOI: http://dx.doi.org/10.15666/aeer/1704_75357548

EFFECT OF CONTROL SYSTEMS ON BACTERIA COMMUNITY STRUCTURE IN SEQUENCING BATCH BIOFILM REACTORS TO TREAT WASTEWATER

JIN, Y.[1*] – WU, C.[2]

[1]*Department of Civil Engineering, Luoyang Institute of Science and Technology, Luoyang 471023, China*

[2]*Department of Environmental Engineering and Chemistry, Luoyang Institute of Science and Technology, Luoyang 471023, China*
(e-mail: ch_wu70l@163.com; phone: +86-188-3883-2915)

**Corresponding author*
e-mail: jyx9988@126.com; phone: +86-135-2595-4418

(Received 27th Feb 2019; accepted 3rd May 2019)

Abstract. This study aimed to evaluate the effect of control systems, including an intelligent control system (ICS) and a conventional timer control system (TCS), on bacteria community structure. Clone library methods for 16S rDNA were used in sequencing batch biofilm reactors (SBBRs) to treat wastewater. A total of 108 clones were randomly selected and individually sequenced from 16S rDNA libraries. Results indicated that the community structure was different in each SBBR under different controlled systems. The dominant bacterial communities and their contents showed significant differences. The dominant bacterial community Bacteroidetes has a proportion of 45%, whereas β-proteobacteria has 37%. The significant difference in the performance of nitrogen and phosphorus removal in ICS from TCS was the dominant bacterial community.
Keywords: *intelligent control system (ICS), sequencing batch biofilm reactor (SBBR), 16S rDNA library, bacterial community, denitrification*

Introduction

The most fundamental method for controlling water eutrophication and preventing water pollution is to treat pollution sources and control pollutant emissions. This approach will enable the nitrogen and phosphorus obtained from the wastewater treatment plants to meet emission standards (Zou et al., 2006). The wastewater discharge standard at present is increasingly becoming strict in all countries around the world. Many new and original wastewater treatment plants are facing the pressure of standard nitrogen and phosphorus emissions (Mielcarek et al., 2015; Ge, 2010; Wen et al., 2015).

Sequencing batch biofilm reactor (SBBR) is novel of composite biofilm reactor and a new technology for nitrogen and phosphorus removal that is being studied by scholars at home and abroad. SBBR utilizes time sequence. Construction cost is low because biological reaction proceeds in a single tank without physical partition (Yang et al., 2014). Given a large amount of biomass, the reactor can resist shock load (Goh et al., 2009; Fu et al., 2018). Sludge bulking is not a problem because of low sludge

Production (Amulya et al., 2015; Zhao et al., 2017) SBBR has been used in the research of nitrogen and phosphorus removal from urban wastewater (Choi et al., 2008; Zhang et al., 2009; Fu et al., 2010; Hosseini et al., 2012). Microorganisms in SBBR are attached to the carrier to form a biofilm with long sludge age and food chain. The

http://www.aloki.hu ● ISSN 1589 1623 (Print) ● ISSN 1785 0037 (Online)
DOI: http://dx.doi.org/10.15666/aeer/1704_75497559

biofilm has certain thickness. Under aerobic conditions, the biofilm creates a hypoxic microenvironment where nitrification and denitrification can occur simultaneously; this condition leads to high nitrogen removal efficiency (Isanta et al., 2015). Changing the operating conditions of the reactor will change the environment where microorganisms depend on for survival, as well as the bacterial community structure of microorganisms, thus leading to the change of nitrogen and phosphorus removal efficiency (Aydin et al., 2015). Therefore, the present study on the effect of control systems on the bacterial community structure in SBBR system is important to optimize the bacterial community structure and improve the efficiency of nitrogen and phosphorus removal.

The 16S rDNA clone library method is used to amplify and analyze the full-length sequence of 16S rDNA to analyze the bacterial community structure in the environmental samples (Cantafio et al., 1996; Sanapareddy et al., 2009; Yu et al., 2010). Given its high speed, accuracy, good repeatability, and abundant information, this method has become the main approach used in the research of bacterial community structure and diversity in wastewater treatment systems. In the present paper, two SBBRs under different control systems were adopted to treat urban wastewater. SBBR under an intelligent control system (ICS) controls the process of wastewater treatment based on DO and temperature. By contrast, SBBR under a timer control system (TCS) changes the operation conditions based on time setting. The 16S rDNA clone library method was adopted to study the similarities and differences of the bacterial community structures of these two reaction systems and to determine the dominant bacterial communities. This approach identifies the effect of control systems on the bacterial community structure of the system.

Materials and methods

SBBRs configurations and operational conditions

Experiments were conducted in two SBBRs controlled by an ICS and a TCS. *Figure 1* shows that the acrylic reactors were composed of polymethyl methacryate with a capacity of 30 L and a working volume of 20 L. Two SBBRs and operations conditions were described in an earlier publication (Jin et al., 2012).

ICS

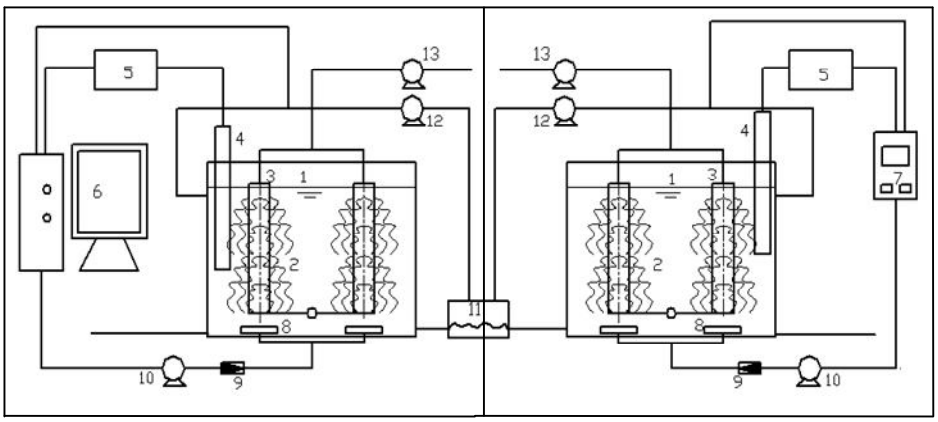

TCS

Figure 1. *Schematic of two SBBRs. 1. Bioreactor. 2. Fiber threads carrier. 3. Cylinder. 4. DO sensor. 5. DO detector. 6. Computer. 7. Timer. 8. Porous stones. 9. Rotameter. 10. Air compressor. 11. Thermostatic bash. 12. Circulation pump. 13. Drawn pump*

http://www.aloki.hu ● ISSN 1589 1623 (Print) ● ISSN 1785 0037 (Online)
DOI: http://dx.doi.org/10.15666/aeer/1704_75497559

Synthetic wastewater

Synthetic wastewater was used as feed to evaluate SBBR performance. Wastewater was prepared based on the characteristics of Chinese municipal wastewater with the following composition (concentrations in mg/L): glucose ($C_6H_{12}O_6$) (332); NH_4Cl (213 at C/N ratio of around 5.0) l; KH_2PO_4 (21.95); $ZnCl_2$ (50), $MgSO_4$ (50); and a 1 ml trace element mixture consisting of $CaCl_2$, $CuCl_2$, $NiCl_2$, $FeSO_4$ and H_3BO_3. $NaHCO_3$ measuring 100 mg/L was used to maintain the pH of the wastewater at 6.8 to 7.2. Synthetic wastewater is characterized in *Table 1*. All chemicals and reagents were of analytical grade.

Table 1. *Characteristics of synthetic wastewater during stable operation*

Parameter	COD (mg/L)	NH_4^+-N (mg/L)	TN (mg/L)	TP (mg/L)	pH
Values	326 ± 30	61 ± 10	65 + 10	5 ± 1	7 ± 0.2

Experimental methods

Sample collection and DNA extraction

After about five weeks of domestication, the biofilm was successfully cultured in two reactors before being entered into the operating period. Through 30 days of sample analysis, the results showed that the reaction period was 6 h for ICS and 9 h for TCS. The operation results of a cycle were extracted as the example. The concentrations of COD, TN, NH_4^+-N, and TP in inflow water were 309.5, 63.61, 60.28, and 5.16 mg/L, respectively. The removal rates of COD, TN, NH_4^+-N, and TP were 93.4%, 85.6%, 100%, and 100% in ICS and 91.1%, 70.9%, 100%, and 100% in TCS, respectively. Thus, TN removal rate in ICS was 14.7% higher than that in TCS.

Bacteria Sampling of the two reactors obtained according to the method of Hao et al. (2009). During the stable operation of two SBBRs, the biofilm samples were taken with sterile scissors and sterile brush from the fillers at different vertical depths and horizontal positions in the SBBRs under ICS and TCS. The samples were dissolved in 500 mL distilled water and fully shaken. The supernatants were removed after precipitation for 30 min. Then, 40 mL of the solutions was taken from the precipitation layers and placed in 50 mL centrifuge tubes. After 3 min of centrifugal separation (5147R centrifuge, Germany, Eppdorf) at the rate of 1000 r/min, 30 mL of sterile TE buffers (10 mmol/L, Tris-HCl, 1 mmol EDTA, adjusted to pH = 8, 121 °C and sterilized for 20 min) was added in the solutions. The supernatants were removed after re-centrifugation. Then, 15 mL of distilled water was added and fully shaken. Afterward, 5 mL of solution was taken for DNA extraction in the biofilms. The pretreated water samples were filtered (0.22 μm bacterial filter film). The filter films were soaked in 10 mL of sterilized saline water after filtration and then placed in an ultrasonic cleaning instrument (KH2200DB, Kunshan Hechuang in China) and shaken for 10 min. The solutions were then repeatedly beaten by the liquid drawing gun to enable the cells on the membrane to enter completely into the solutions. The solutions were placed in centrifuge tubes (1.5 mL) and underwent centrifugation for 3 min at the rate of 10000 r/min to facilitate bacteria collection. The metagenomics DNA extraction kits produced by Shanghai Sangon were adopted to extract ICS samples and TCS samples.

http://www.aloki.hu ● ISSN 1589 1623 (Print) ● ISSN 1785 0037 (Online)
DOI: http://dx.doi.org/10.15666/aeer/1704_75497559

16S rDNA gene full-length amplification and carrier connection transformation

Bacteria 16S rDNA universal primer 27F (5'-AGAGTTTGATCCTGGCTCAG-3', M = CorA) and 1492R (5'-CTACGGCTACCTTGTTACGA-3', T = 3', Y = CorT) were adopted to amplify the target genes of two groups of samples (Masoud et al., 2011). The PCR reaction procedure (Hao et al., 2009) was predegenerated at 95 °C for 5 min, degenerated at 94 °C for 30 s; annealed at 52 °C for 30 s, and extended to 72 °C for 2 min for a total of 35 circulations. The procedure also involved extension at 72 °C for 10 min before preservation at 4 °C. PCR amplification products were detected by 1.2% agarose gel electrophoresis. The products were connected to PGEM-T clone by PGEM-T cloning (Promage Company) kits and heat-shock transformed into escherichia coli DH5α competent cells. The products were then coated with Amp/IPTG-Gal that contains LB culture mediums. After 16 h of culture at 37 °C, the samples were subjected to 4 °C color development process for 1 h. White-blue plaque selection and white plaque validation were conducted. The positive clones in each sample were randomly selected for sequencing by Shanghai Sangon Co., Ltd.

System development analysis

Chimera detection was conducted on the sequences using a Chimera detection program on the Ribosomal database project (RDP) website. The obtained sequences were then classified by Dutor software, and similar sequences were excluded. The remaining sequences were entered into the BLAST facility of the National Center for Biotechnology Information (http://www.ncbi.nlm.nih.gov). Comparative analysis was conducted on the remaining sequences and those existing in GenBank + EMBL + DDBJ + PDB. Sequences with the highest similarity and those with species that have high similarity were downloaded as reference. All sequences were compared by ClustalW program in BioEdit. The system development tree diagram was generated using MEGA 4.0.

Results and discussion

Bacterial diversity analysis of samples in ICS and TCS

The sequences were analyzed with Dutor software. After eliminating similar sequences, ICS obtained 30 genotypes and 32 for TCS. The sequence of each genotype in ICS and TCS was entered into the RDP website. The sample system group was determined by a classifier program. After analysis, 16S rDNA sequences of 108 positive clones of bacteria were identified in the ICS sample library, which belonged to 7 bacterial communities (as shown in *Figs. 2* and *3*). These sequences are *Bacteroidetes* (45%), *β-proteobacteria* (27%), *γ-proteobacteria* (16%), *α-proteobacteria* (3%), *Verrucomicrobia (*3%), *Chloroflexi* (3%), and unclassified_Proteobacteria (3%). The dominant bacterial communities were *Bacteroidetes* (45%), *β-proteobacteria (*27%), and *γ-proteobacteria* (16%). The 16S rDNA sequences of 108 positive clones of bacteria in TCS sample library belonged to 9 bacterial communities (as shown in *Figs. 4* and *5*), namely, *β-proteobacteria* (37%), *γ-proteobacteria* (25%), *Bacteroidetes* (24%), *δ-proteobacteria* (3%), *Firmicutes* (3%), *Nitrospira* (3%), *Actinobacteria (*3%), *Acidobacteria (*3%), and unclassified_Proteobacteria (5%). The dominant bacterial communities in ICS were *Bacteroidetes*, *β-proteobacteria*, *andγ-proteobacteria*, which account for 45%, 27%, and 16%, respectively. The dominant bacterial communities in

http://www.aloki.hu ● ISSN 1589 1623 (Print) ● ISSN 1785 0037 (Online)
DOI: http://dx.doi.org/10.15666/aeer/1704_75497559

TCS were*β-proteobacteria*, *γ-proteobacteria*, and *Bacteroidetes*, accounting 37%, 25%, and 24%, respectively. Different operation modes and different growth environments for microorganism between ICS and TCS led to different dominant bacterial communities and different community structures. In ICS, the growth environment for biofilm microorganisms was (aerobic/hypoxic)^n. *Bacteroidetes* was the dominant bacterial community, which has a proportion of 45%. In TCS, the growth environment for biofilm microorganisms was anaerobic/aerobic, in which *β-proteobacteria* was the dominant bacterial community with a proportion of 37%. The community structure of ICS was more stable than that of TCS, and the communities in ICS were less than those in TCS.

System development analysis of bacteria in samples in ICS and TCS

To further understand the system development of bacteria in biofilm samples in ICS and TCS, the genotypes that represent different sequences were ordered in accordance with the principle of maximum homology. This approach was adopted to construct the system development tree diagrams of Proteobacteria and other communities in ICS and TCS gene libraries, as shown in *Figures 4, 5, 6,* and *7*. *Figures 4* and *5* show the system development trees of Proteobacteria and other communities based on 16S rDNA sequence in ICS system. *Figures 6* and *7* show the system development trees of Proteobacteria and other communities based on 16S rDNA sequence in ICS system.

System development analysis of bacterial in ICS

In ICS, *Bacteroidetes* was the dominant community with a proportion of 45%. This finding means that nearly half of bacteria in the biofilm samples in ICS were *Bacteroidetes*. The most similar structure of this sequence is from eutrophic lakes (Cantafio et al., 1996), which include 12 genotypes of uncultured bacteria. The bacteria in *Bacteroidetes* community were bacillus of different sizes. These bacteria were reported only in the phosphorus removal system, but were barely investigated in the activated sludge and nitrogen removal system (Amann et al., 1995). ICS did not adopt anaerobic phosphorus release, but it showed significant phosphorus removal effect. Moreover, the performance of ICS in TN removal was obviously better than that of TCS. Thus, we can conclude the presence of microorganisms with functions of anoxic phosphorus uptake and denitrifying phosphorus removal, which exist in the form of polyphosphate under the aerobic condition in *Bacteroidetes* (Liu et al., 1996). Therefore, new bacteria exist that are related to nitrogen and phosphorus removal in *Bacteroidetes*. These bacteria accounted for 27% of bacteria in the library, including 9 genotypes. The homology between Z-28 and *Thauera sp.* (CP001281) was as high as 99%. *Thauera sp.* was the denitrification bacterium that could remove NO_3^--N and PO_4^{3-}-P from wastewater through denitrification (Manz et al., 1994; Amann et al., 1995). This bacterium played a very important role in denitrification and in the degradation process of organic matters (Ayara et al., 2011). In the anoxic or aerobic period, the exterior of the biofilm was the aerobic layer and the interior was the special structure for the anaerobic/anoxic layer. This structure provided favorable conditions for the existence of denitrifying bacteria and benefited nitrogen removal or denitrifying phosphorus removal in ICS. The other clones were uncultured bacteria. The *γ-proteobacteria* was the third largest bacterial community with the proportion of 16% in the library. This bacterium included three genotypes, among which the homology

http://www.aloki.hu ● ISSN 1589 1623 (Print) ● ISSN 1785 0037 (Online)
DOI: http://dx.doi.org/10.15666/aeer/1704_75497559

between Z-15 and *Xanthomonas sp.* (AJ786786) was 98%. *Xanthomonas sp.* had strong degradation ability for organic carbon. Thus, it was beneficial for COD removal.

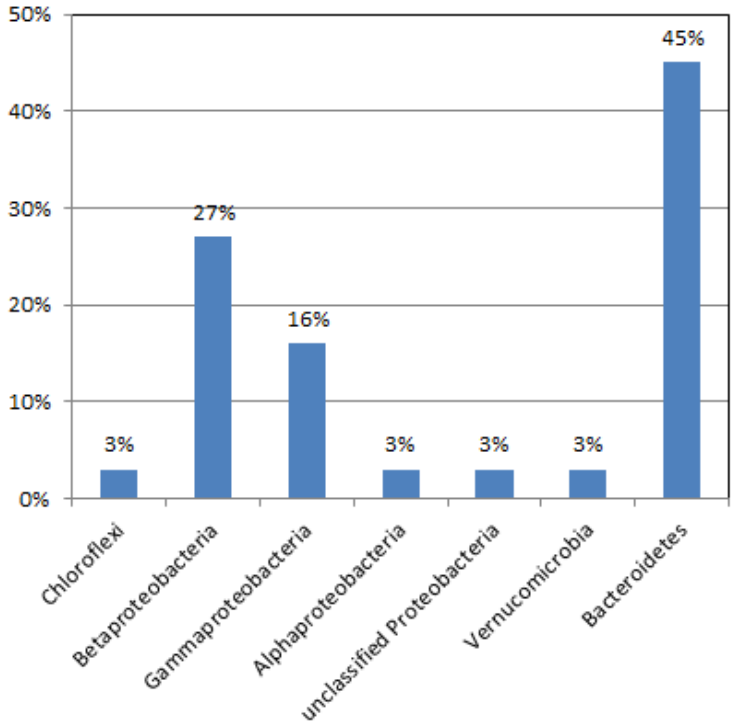

Figure 2. *Proportion of phyla in the clone library from ICS*

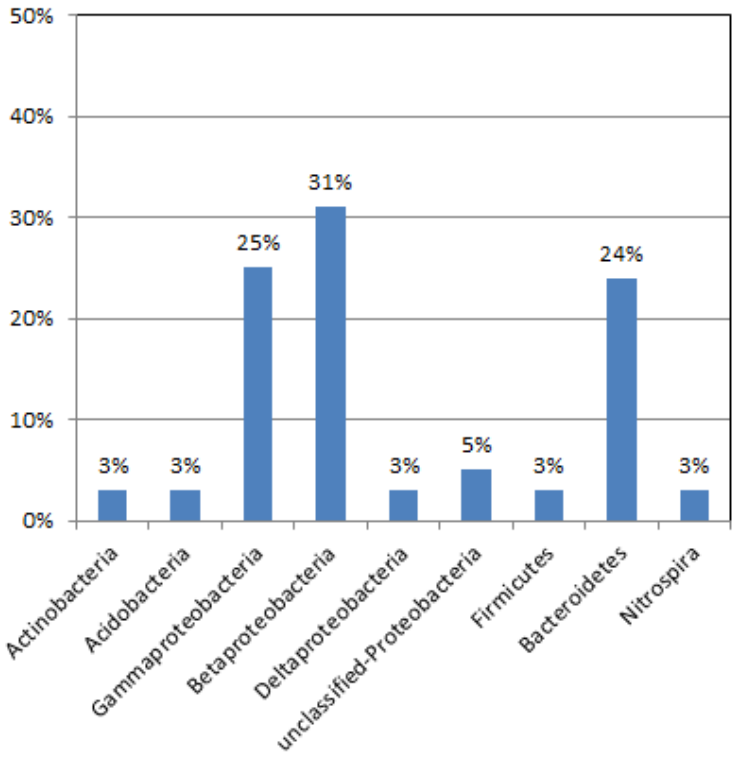

Figure 3. *Proportion of phyla in the clone library from TCS*

http://www.aloki.hu ● ISSN 1589 1623 (Print) ● ISSN 1785 0037 (Online)
DOI: http://dx.doi.org/10.15666/aeer/1704_75497559

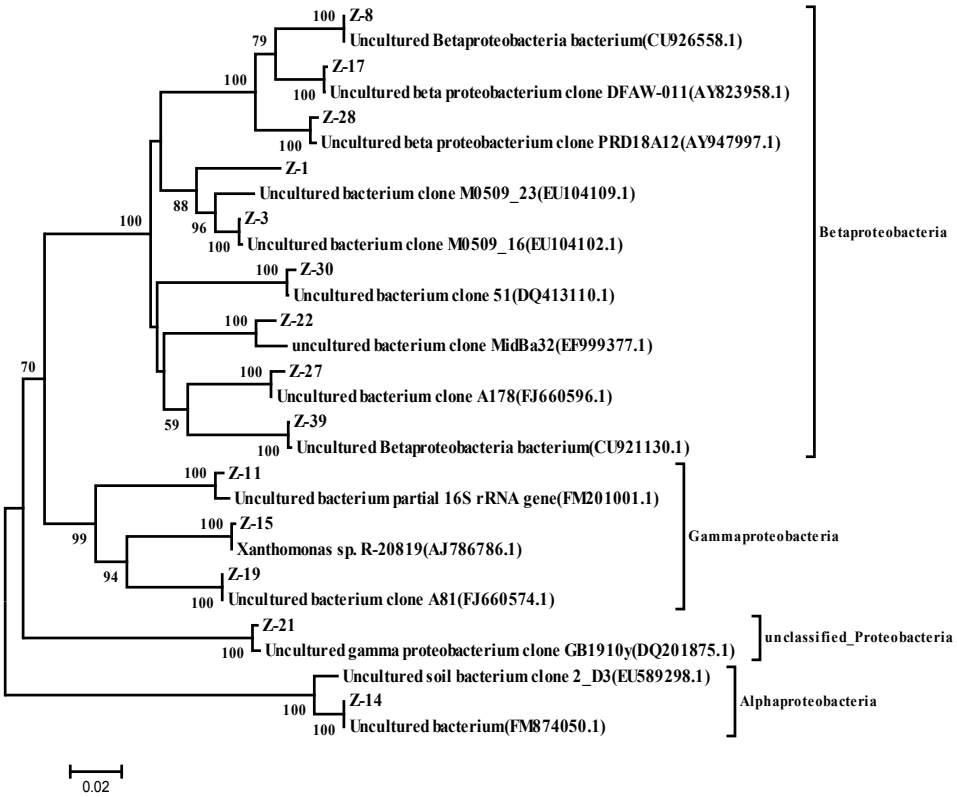

Figure 4. *Phylogenetic tree of proteobacteria isolated from ICS column based on 16S rDNA sequences*

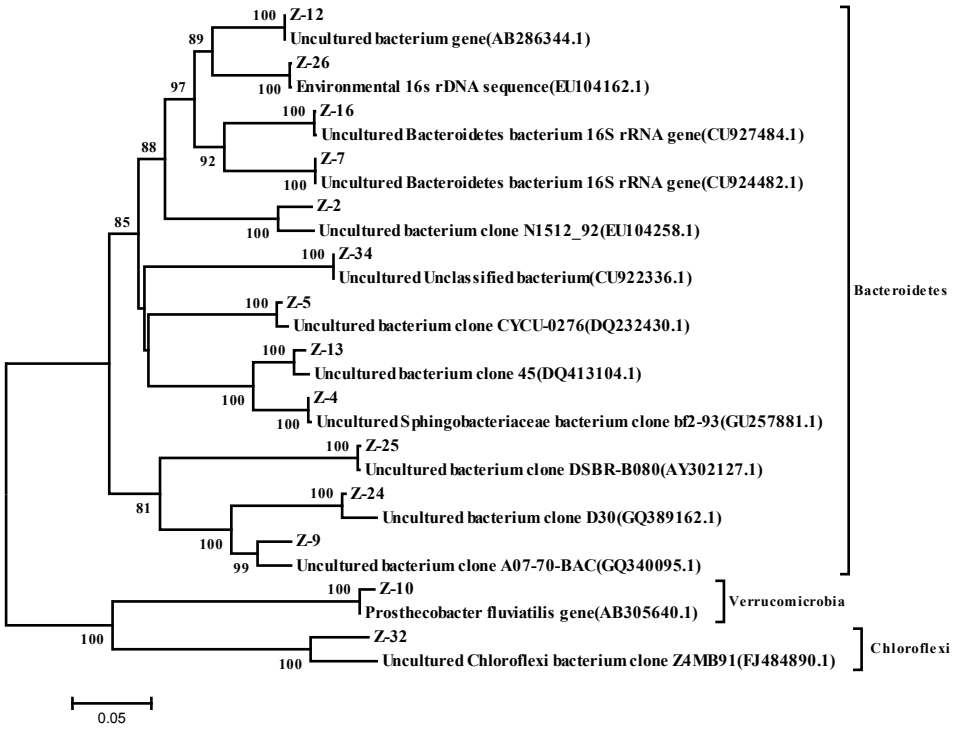

Figure 5. *Phylogenetic tree of other bacteriophyta isolated from ICS column based on 16S rDNA sequences*

http://www.aloki.hu ● ISSN 1589 1623 (Print) ● ISSN 1785 0037 (Online)
DOI: http://dx.doi.org/10.15666/aeer/1704_75497559

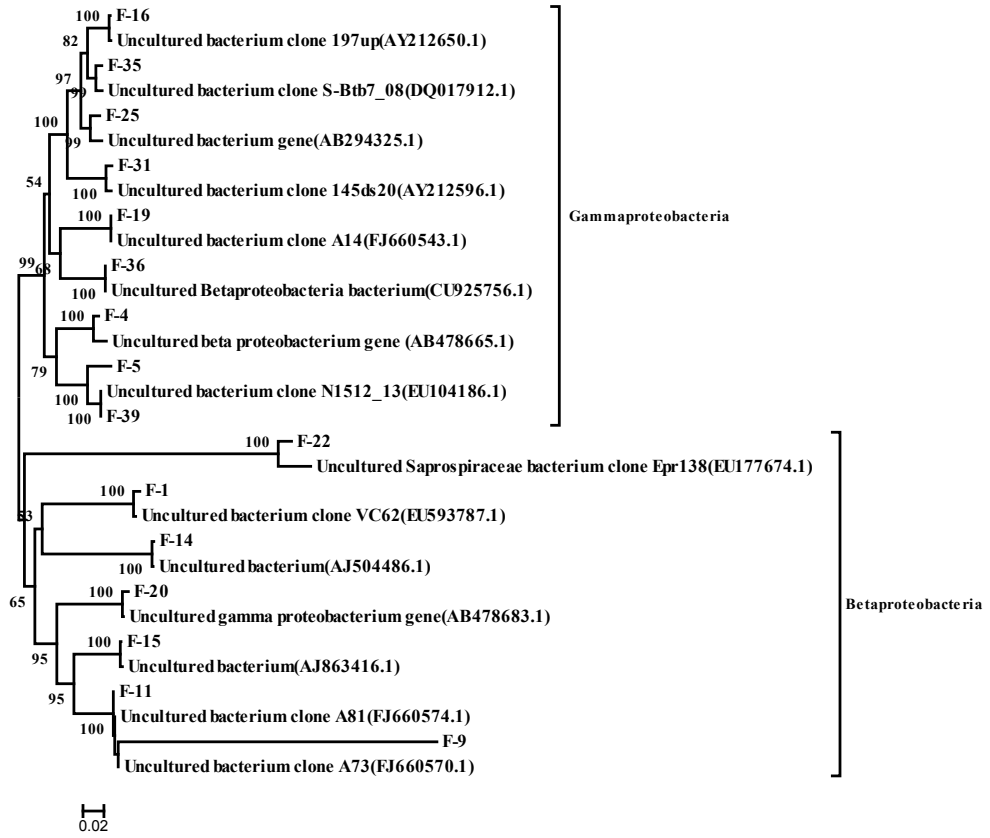

Figure 6. *Phylogenetic tree of proteobacteria isolated from TCS column based on 16S rDNA sequences*

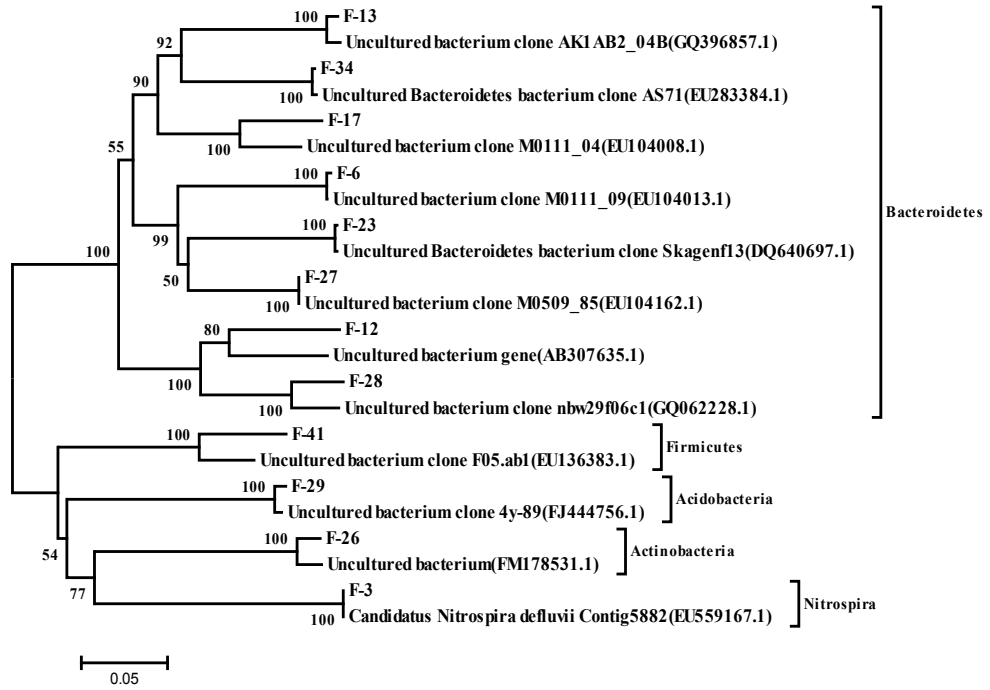

Figure 7. *Phylogenetic tree of other bacteriophyta isolated from ICS column based on 16S rDNA sequences*

http://www.aloki.hu ● ISSN 1589 1623 (Print) ● ISSN 1785 0037 (Online)
DOI: http://dx.doi.org/10.15666/aeer/1704_75497559

System development analysis of bacterial in TCS

In TCS, *β-proteobacteria* was the dominant bacterial community with proportion of 37%. However, it was the second largest bacterium in ICS with proportion of 27%. This bacterium included 12 genotypes, in which the homology between F-2 and *Bacterium AEOC009* (AB208727) was 99% and that between F-42 and *Arabidopsis lyrata* was 99%. Other clones were uncultured bacteria. According to Amann et al.'s study of the bacterial community structure in the biological reactor, *β-proteobacteria* and *Bacteroidetes* were the most dominant communities in the wastewater treatment system. The former played an important role in organic matter degradation, nitrogen and phosphorus removal, and flocculation structure formation (Burrell et al., 1999). Second, *γ-proteobacteria, δ-proteobacteria, and* unclassified *Proteobacteria* accounted for 25%, 3%, and 5.5% of bacteria in the library, respectively. They were all *Proteobacteri*a, which could efficiently remove organic matters, nitrogen, and phosphorus. *Bacteroidetes* was the third largest community in the library with proportion of 24%, but it was the dominant community in ICS. The bacteria in this community were related to nitrogen and phosphorus removal. Thus, ICS had better performance than TCS in nitrogen and phosphorus removal. *Nitrospira* (nitrification spirillum) accounted for 3% of bacteria in the library. The homology among F-3 and other two unnamed *Nitrospira* (EU55916 and DQ059545) was 99%. *Nitrospira* was an important NO_2^--N oxidation bacterium. The research of Burrell et al. (1999), Lee et al. (2002) and Benítez-Páez et al. (2016) showed that the bacteria in *Nitrospira* species could have played the role of NO_2^--N oxidation during nitrification rather than *nitrobacter*.

Conclusions

(1) The concentrations of COD, TN, NH4 + -N, and TP in inflow water were 309.5, 63.61, 60.28, and 5.16 mg/L, respectively. The removal rates of COD, TN, NH4 + -N, and TP were 93.4%, 85.6%, 100%, and 100% in ICS and 91.1%, 70.9%, 100%, and 100% in TCS, respectively. Thus, TN removal rate in ICS was 14.7% higher than that in TCS.

(2) Different control systems of SBBR will cause differences in bacterial community structures and their relative proportions. In the ICS sample library, 16S rDNA sequences by bacterial clones belonged to 7 bacterial communities, namely, *Bacteroidetes*, *β-proteobacteria*, *γ-proteobacteria*, *α-proteobacteria, Verrucomicrobia*, *Chloroflexi,* and unclassified_Proteobacteria. In the TCS sample library, 16S rDNA sequences by bacterial clones belonged to 9 bacterial communities, namely, *β-proteobacteria*, *γ-proteobacteria, Bacteroidetes*, *δ-proteobacteria*, *Firmicutes*, *Nitrospira, Actinobacteria, Acidobacteria,* and unclassified_Proteobacteria.

(3) The growth environment of the biofilm microorganisms in ICS was aerobic/hypoxic, in which *Bacteroidetes* was the dominant community with the proportion of 45%. The growth environment of the biofilm microorganisms in TCS was anaerobic/aerobic, in which *Betaproteobacteria* was the dominant community with the proportion of 37%.

Acknowledgements. This study was supported by the key scientific and technological project of Henan Province (172102310730 and 172102310736), and Henan Province Key research projects of higher education institutions (17A610011).

http://www.aloki.hu ● ISSN 1589 1623 (Print) ● ISSN 1785 0037 (Online)
DOI: http://dx.doi.org/10.15666/aeer/1704_75497559

REFERENCES

[1] Amann, R. I., Ludwig, W., Schleifer, K. H. (1995): Phylogenetic identification and in situ detection of individual microbial cells without cultivation. – Fems Microbiology Reviews 59(1): 143-69.

[2] Amulya, K., Jukuri, S., Mohan, S. V. (2015): Sustainable multistage process for enhanced productivity of bioplastics from waste remediation through aerobic dynamic feeding strategy: Process integration for up-scaling. – Bioresource Technology 188: 231-240.

[3] Ayara, J. M., Erijman, L. (2011): Balance of neutral and deterministic components in the dynamics of activated sludge floc assembly. – Microbial Ecology 61: 486-492.

[4] Aydin, S., Ince, B., Ince, O. (2015): Development of antibiotic resistance genes in microbial communities during long-term operation of anaerobic reactors in the treatment of pharmaceutical wastewater. – Water Research 83: 337-345.

[5] Benítez-Páez A., Portune K. J., Sanz Y. (2016): Species-level resolution of 16S rRNA gene amplicons sequenced through the MinION™ portable nanopore sequencer. – GigaScience 5: 4-11.

[6] Burrell, H. P., Keller, J., Blackall, L. (1999): Characterisation of the bacterial consortium involved in nitrite oxidation in activated sludge. – Water Sci. Technol. 39: 45-53.

[7] Cantafio, A. W., Hagen, K. D., Lewis, G. E. (1996): Pilot-scalese-lenium bioremediation of San Joaquin drainage water with Thauera selenatis. – Applied and Environmental Microbiology 62(9): 3298-303.

[8] Choi, H. J., Lee, S. M., Choi, C. H., Kwon, M. C., Lee, H. Y. (2008): Influence of the wastewater composition on denitrification and biological p-removal in the SDN-P-process (b) Effect of acetate. – Journal of Hazardous Materials 158: 151-160.

[9] Fu, B., Liao, X. Y., Ding, L. L., Ren, H. Q. (2010): Characterization of microbial community in an aerobic moving bed biofilm reactor applied for simultaneous nitrification and denitrification. – World J. Microbiol. Biotechnol. 26: 1981-1990.

[10] Fu, K., Fu, Ch., Wang, H., Su, X., Li, Hui 1, Qiu, F., Cao, X. Q. (2018): Effects of nitrite on nitrogen removal performance and N_2O emission in a biofilm CANON process. – Chinese Journal of Environmental Engineering 12: 2776-2782.

[11] Ge, S. J., Peng, Y. Z., Wang, S. Y., Guo, J. H., Ma, B., Zhang, L. A., Cao, X. (2010): Enhanced nutrient removal in a modified step feed process treating municipal wastewater with different inflow distribution ratios and nutrient ratios. – Bioresour Technol. 101: 9012-9019.

[12] Goh, C. P., Seng, C. E., Sujari, A., Lim, P. E. (2009): Performance of sequencing batch biofilm and sequencing batch reactors in simultaneous p-nitrophenol and nitrogen removal. – Environmental Technology 30: 725-733.

[13] Hao, C. B., Wang, G. C., Dong, J. N., Zhang, Q., Cai, W. T. (2009): Bacterial Biodiversity in the Groundwater Contaminated by Oil. – Environmental Science 8: 2464-2472.

[14] Hosseini, K. E., Alavi, M. R., Hashemi, S. H. (2012): Investigation of decolorization kinetics and biodegradation of azo dye Acid Red 18 using sequential process of anaerobic sequencing batch reactor/moving bed sequencing batch biofilm reactor. – International Biodeterioration & Biodegradation. 71: 43-51.

[15] Isanta, E., Reino, C., Caarera, J. (2015): Stable partial nitritation for low-strength wastewater at low temperature in an aerobic granular reactor. – Water Research 80: 149-158.

[16] Jin, Y. X., Ding, D. H., Feng, C. P., Tong, S., Suemura, T., Zhang, F. (2012): Performance of sequencing batch biofilm reactors with different control systems in treating synthetic municipal wastewater. – Bioresource Technology 104: 12-19.

[17] Kim, T. S., Jeong, J. Y., Wells, G. F., Park, H. D. (2013): General and rare bacterial taxa demonstrating different temporal dynamic patterns in an activated sludge bioreactor. – Applied and Environmental Microbiology 97: 1755-1763.

http://www.aloki.hu ● ISSN 1589 1623 (Print) ● ISSN 1785 0037 (Online)
DOI: http://dx.doi.org/10.15666/aeer/1704_75497559

[18] Lee, S., Lee, J., Lee, J. (2002): Molecular characterization of microbial community in nitrate-removing activated sludge. – Fems Microbiology Reviews 41: 85-93.
[19] Liu, B. B., Zhang, F., Feng, X. X. (2006): Thauera and Azoarcus as functionally important genera in a denitrifying quinoline-removal bioreactor as revealed by microbial community structure comparison. – FEMS Microbiology Ecology 55(2): 274-86.
[20] Manz, W., Wagner, M., Amann, R. (1994): Characterization of the microbial consortia active in two wastewater treatment plants. – Water Research 28: 1715-1723.
[21] Masoud, W., Takamiya, M., Vogensen, F. K., Lillevang, S. (2011): Characterization of bacterial populations in Danish raw milk cheeses made with different starter cultures by denaturating gradient gel electrophoresis and pyrosequencing. – International Dairy Journal 21: 142-148.
[22] Mielcarek, A., Rodziewicz, J., Janczukowicz, W., Thornton, A. J., Jóźwiak, T., Szymczyk, P. (2015): Effect of the C:N:P ratio on the denitrifying dephosphatation in a sequencing batch biofilm reactor (SBBR). – Journal of Environmental Sciences 4: 1-7.
[23] Sanapareddy, N., Hamp, T. J., Gonzalez, L. C., Hilger, H. A., Fodora. A., Clinton, S. M. (2009): Molecular Diversity of a North Carolina Wastewater Treatment Plant as by Pyrosequencing. – Applied and Environmental Microbiology 75: 1688-690.
[24] Wen, Y., Jin, Y. X., Wang, J. Y., Cai, L. P. (2015): MiSeq sequencing analysis of bacterial community structures in wastewater treatment plants. – Polish Journal of Environmental Studies 24: 1809-1815.
[25] Yang, K., Ji, B., Wang, H., Zhang, H., Zhang, Q. (2014): Bio-augmentation as a tool for improving the modified sequencing batch biofilm reactor. – Journal of Bioscience and Bioengineering 117: 763-771.
[26] Yu, F. B., Li, S. W., Guan, L. B., Li, S. P., Zhou, S. (2010): Bioaugmentation of a sequencing batch reactor with Pseudomonas putida ONBA-17, and its impact on reactor bacterial communities. – Journal of Hazardous Materials 176: 20-31.
[27] Zhang, L. Q., Wei, C. H., Zhang, K. F., Zhang, C. S., Fang, Q., Li, S. G. (2009): Effects of temperature on simultaneous nitrification and denitrification via nitrite in a sequencing batch biofilm reactor. – Bioprocess Biosystems Engineering 32: 175-182.
[28] Zhao, X. Y., Bian, W., Hou, A. Y. (2017): Characteristics of microbial community structure in the stable operation of the partial cut nitrification system with seasonal temperature. – China Environmental Science 4: 1366-1374.
[29] Zou, H., Du, G., Ruan, W., Chen, J. (2006): Role of nitrate in biological phosphorus removal in a sequencing batch reactor. – World J. Microbiol. Biotechnol. 22: 701-710.

http://www.aloki.hu ● ISSN 1589 1623 (Print) ● ISSN 1785 0037 (Online)
DOI: http://dx.doi.org/10.15666/aeer/1704_75497559

SOIL PROPERTIES IN DIFFERENT YEARS OF CULTIVATION ABANDONMENT IN THE MIDSTREAM AND DOWNSTREAM OF SHIYANG RIVER AREA

WANG, L. D.[1,2,3*] – GUO, C. X.[1,2,3] – XU, B. Y.[1,2,3] – WU, H.[1,2,3] – WANG, F. L.[1,2,3] – LI, X. J.[1,2,3]

[1]*Gansu Desert Control Research Institute, Lanzhou 730070, China*

[2]*Gansu Hexi Corridor Forest Ecosystem National Research Station, Wuwei 733000, China*

[3]*State Key Laboratory Breeding Base of Desertification and Aeolian Sand Disaster Combating, Wuwei 733000, China*
(e-mail: wld69@tom.com, guochunxiu0414@163.com, 68428666@qq.com, wuhao4832@163.com, 466961776@qq.com, 124213741@qq.com)

[*]*Corresponding author*
e-mail: wld69@tom.com

(Received 27th Feb 2019; accepted 3rd May 2019)

Abstract. To understand changes of soil properties in different years of cultivation abandonment in the midstream and downstream of Shiyang River area, soil physicochemical characteristics, microbial population, soil microbial biomass, relationships between them and comprehensive evaluation of soil fertility quality were analyzed. The results showed that soil pH increased slightly, soil water content, sand content, the number of bacteria ,the number of actinomycetes and SMBN (soil microbial biomass nitrogen) decreased then increased, soil organic carbon, total potassium, Quick-available K, Quick-available P, SMBC (soil microbial biomass carbon), SMBP (soil microbial biomass phosphorus) and SMBC/SMBN increased then decreased, total nitrogen increased then decreased and tended to be stable, total phosphorus and the number of fungi decreased then increased and decreased finally, and different abandoned years had different significant difference. From the correlation analysis and principal component analysis (PCA), there were close correlations among the soil physical characteristics, soil chemical characteristics and the number of soil microbes, soil microbial biomass. The key factors determining the soil quality were the soil pH, sand content, soil water content, soil water content, total nitrogen, Quick-available K, the number of fungi, SMBC and SMBN. The results that the effects of 4a on the soil during restoration were better for soil improvement than the other abandoned years, making the abandoned years of 4a more critical for use in the ecological restoration and control of the midstream and downstream of Shiyang River area.
Keywords: *soil microbial characteristics, soil physicochemical characteristics, soil fertility, midstream and downstream of Shiyang river, years of abandoned cultivated lands*

Introduction

Shiyang River is a typical inland river in the arid regions of northwestern China. Its downstream Minqin area was once a natural oasis with plenty water and rush grass (Feng, 1963). However, in recent decades, with the continuous expansion of the population and economic scale of midstream area of Shiyang River, especially the expansion of artificial oases, the downstream surface water resources are decreasing day by day, the groundwater is seriously over-exploited, the degree of mineralization is rising, natural vegetation is subject to serious disturbance and damage, a series of ecological problems such as desertification and salinization have been intensified (Zhang et al., 2016; Chang et al., 2016), causing large-scale land to be abandoned and uncultivated which deteriorates into secondary grassland. If these secondary grasslands

http://www.aloki.hu ● ISSN 1589 1623 (Print) ● ISSN 1785 0037 (Online)
DOI: http://dx.doi.org/10.15666/aeer/1704_75617572

are not properly protected, degradation will speed up, wind erosion and desertification will occur with emergence of new source of sand and dust, forming a vicious circle and seriously damaging soil ecosystem of the secondary grassland in the middle and lower reaches of Shiyang River (Chai et al., 2015). Therefore, how to properly protect and restore secondary grassland in abandoned oasis area in the middle and lower reaches of Shiyang River is an ecological problem that needs to be settled urgently.

Soil serves as the carrier of many ecological processes in ecosystems and the substrate for plant growth (Hu and Guo, 2012). Its physicochemical properties and biological properties are key indicators reflecting restoration degree of soil ecosystems (Yuan et al., 2012). Studies have shown that soil microbes in soil ecosystems mainly participate in material circulation and energy flow by decomposing animal and plant residues, which serve as supply source and reservoir pool of soil nutrients, affecting vegetation succession and soil quality (Kardol et al., 2007). The amount of soil microbes is used to study and evaluate soil microbial regulation functions, which can reflect the effects of various soil factors on soil microbes and its effects on plant growth and soil fertility, and exert certain regulation on the whole ecosystem (Harris, 2003). Soil microbial biomass constitutes living soil organic matter, which is a sign of soil activity and one of the early warning indicators of soil ecosystem changes (Singh et al., 2014). At present, research on the evolution of soil properties mainly focuses on physicochemical properties of soil (Zhao et al., 2012), while there are few reports on the evolution of soil properties in the Shiyang River Basin. In view of this, this paper studies change characteristics of physical properties, chemical properties and microbial properties of secondary grassland with different abandoned years in different middle and lower reaches of Shiyang River, discusses the relationship between them and makes comprehensive evaluation of soil quality in this area, with a view to making in-depth exploration into evolution process of soil properties in Shiyang River Basin, and providing a theoretical basis for ecological restoration and management in the area.

Materials and methods

Overview of the study area

The test site was selected in Huanghui Village and Ziyun Village, Xiqu Town, north of Minqin County, Gansu Province. The geographical coordinates are located at east longitude 103°07′50″~103°37′56″ and north latitude 39°01′30″-39°03′28″. The altitude is 1297~1306 m, the annual average temperature is 7.4°C, the average annual precipitation is 110 mm which is mainly concentrated in July~ September, the annual average evaporation is 2644 mm, the annual sunshine hours are 2832.1 h, and the annual average wind speed is 2.3 m/s. The soil type is gray brown desert soil. The main shrub plants in the plot include Nitraria schoberi, Kalidium foliatum, Lycium chinense, Nitraria sibirica, Reaumuria songarica, etc. The herbaceous plants include Convolvulus arvensis, Chenopodium album, Halogeton arachnoideus, Suaeda glauca, Peganum harmala, Salsola ikonnikovii, etc. (Chai et al., 2015).

Sample site setting and soil sample collection

In September 2012, interview and investigation was conducted in the forestry department and local residents of Minqin County to accurately grasp abandoned time in the middle and lower reaches of Shiyang River. By using method of space replacement

http://www.aloki.hu ● ISSN 1589 1623 (Print) ● ISSN 1785 0037 (Online)
DOI: http://dx.doi.org/10.15666/aeer/1704_75617572

time, sections with uniform plant growth, small changes in microtopography, and without topography change owing to natural factors or soil material redistribution caused by human factors were selected as test area. While ensuring that soil parent materials of the sample site was consistent, 9 wastelands where crops have been planted 1, 2, 3, 4, 5, 8, and 15. 24 and 31a with an area of 1 hm2 was selected as sample site (see *Table 1*).

Table 1. *Basic condition of sample sites*

Abandoned years(a)	Altitude (m)	Longitude/ Latitude	Dominant plants species	Accompanying species	(Plant type before abandonment)
1a	1304	E103°36′03 N39°03′28″	Chenopodium album, Convolvulus arvensis, *Echinopilon divaricatum,* Peganum harmala	*P. nigellastrum, Chloris virgata, Corispermum hyssopifolium, Polygonumaviculare* et al	The autumn crops
2a	1303	E103°36′09″ N39°03′25″	*Sonchus oleraceus, P. nigellastrum,* Halogeton arachnoideus, *Lepidium lotifolium*	*Atriplex sibirica,* Chenopodium album, *Chloris virgata, Euphorbia pekinensis* et al.	The autumn crops
3a	1297	E103°36′09″ N39°02′36″	*P. nigellastrum,* Halogeton arachnoideus, *Lepidium lotifolium, Acroptilon repens*	*Limoniumau-reum, Phragmites australis,* Peganum harmala, *Eragrostis pilosa* et al.	The autumn crops
4a	1305	E103°36′13″ N39°02′34″	Peganum harmala, *Acroptilon repens, P. nigellastrum,* Suaeda glauca	*Phragmites australis, Chloris virgata,* Halogeton arachnoideus et al.	The autumn crops
5	1304	E103°35′58″ N39°02′9″	*Lycium ruthenicum,* Halogeton arachnoideus, *Lepidium lotifolium,* Peganum harmala	*Cardaria draba, Clematis florida, P. nigellastrum, Chloris virgata* et al.	The autumn crops
8a	1304	E103°07′54″ N39°02′54″	*Lycium ruthenicum,* Halogeton arachnoideus, Peganum harmala, *P. nigellastrum*	*Phragmites australis, Acroptilon repens, Limoniumau-reum, Achnatherum splendens* et al.	The autumn crops
15a	1304	E103°37′02″ N39°01′45″	*Lycium ruthenicum,* Halogeton arachnoideus, *P. nigellastrum, Limoniumau-reum*	*Atriplex sibirica,* Salsola ikonnikovii, *Lepidium lotifolium, Echinopilon divaricatum* et al.	The autumn crops
24a	1306	E103°36′24″ N39°02′34″	*Lycium ruthenicum,* Kalidium foliatum, Reaumuria songarica, *Phragmites australis*	Halogeton arachnoideus, Nitraria schoberi, *P. nigellastrum, Eragrostis pilosa* et al.	The autumn crops
31a	1306	E103°36′13″ N39°02′34″	*Lycium ruthenicum,* Kalidium foliatum, Reaumuria songarica, *P. nigellastrum*	Nitraria schoberi, *Scorzonera hispanica,* Halogeton arachnoideus, Peganum harmala et al.	The autumn crops

Five soil sample collection points were selected in each site using “S” method, and each collection point was repeated three times. 0～10 cm soil samples were taken with soil drill (soil drills type: SoilMoisture0200.0206L06.0215F1L05). After the same soil samples were uniformly mixed, the soil samples were separated into two parts by quartering and enclosed to be brought back to the laboratory. One part is used for the determination of soil physicochemical properties, and the other part is used for the determination of soil biological properties (at 4°C for less than 24 h).

Determination method

Determination of soil physicochemical properties

Soil pH was determined by pH instrument (PHS-3S), soil moisture content was measured by oven drying method in incubator (Shanghai yiheng DHG-9030A electric thermostat), and the sand content (the sum of coarse sand and fine sand) was measured by Malvern Mastersizer 2000. The organic carbon was determined by potassium dichromate-sulfuric acid external heating method, total nitrogen was determined by Kjeldahl distillation method, total phosphorus, available phosphorus were determined by NaHCO3 extraction- Mo-Sb-Vc colorimetric method, total potassium, available

http://www.aloki.hu ● ISSN 1589 1623 (Print) ● ISSN 1785 0037 (Online)
DOI: http://dx.doi.org/10.15666/aeer/1704_75617572

potassium were determined by atomic absorption spectrophotometry. Refer to "Soil Agricultural Chemistry Analysis" for the specific methods (Bao, 2005).

Determination of soil microbial properties

(1) The amount of soil bacteria, fungi and actinomycetes was determined by flat surface smearing (Xu and Zheng, 1986), in which beef extract peptone medium was used for bacteria, Martin-Bengal red medium was used for fungus, and modified Gaoshi No.1 medium was used for actinomycete.

(2) Determination of soil microbial biomass

Soil microbial biomass was determined by chloroform fumigation incubation method (Sparling et al., 1997; Yao and Huang, 2006).

1) Soil microbial biomass carbon (SMBC): was determined by K2Cr2O7-H2SO4 external heating method. The calculation formula is:

$$SMBC\ (mg/kg) = (Ec- Ec0) / kEc \quad (Eq.1)$$

2) Soil microbial biomass nitrogen (SMBN): was determined by Kjeldahl determination method. The calculation formula is:

$$SMBN\ (mg/kg) = (En- En0) / kEn \quad (Eq.2)$$

3) Soil microbial biomass phosphorus (SMBP): was determined by molybdenum blue colorimetric method. The calculation formula is:

$$SMBP\ (mg/kg) = (Ep- Ep0) / kEp \quad (Eq.3)$$

In the formula: Ec, En and Ep are the contents of organic carbon, total nitrogen and phosphorus in the fumigated soil extract, Ec0, En0 and Ep0 are the contents of organic carbon, total nitrogen and phosphorus in the unfumigation soil extract, and kEc, kEn and kEp are correction coefficients which are 0.38, 0.54 and 0.40, respectively.

Data Analysis and Processing

The test data was the average of 3 replications, and analysis of variance, correlation analysis, and principal components analysis (PCA) were performed using SPSS 19.0 software and tabulated with Excel 2010.

Results and analysis

Characteristics of physic-chemical properties of soil

The soil physicochemical properties of secondary grassland with different abandoned years are shown in *Table 2*. With the extension of abandoned years, soil pH generally shows an upward trend with a range of 8.0-8.5; the soil water content decreases first in 1-4a, 8- 24a and then increases in 4-8a, 24-31a, with significant difference between different years ($P<0.05$), of which the maximum is reached at 8a (7.26%); the sand content in the soil decreases first in 1-4a, 5- 8a, 15-24a and then increases in 4-5a, 8-15a, 24-31a, with significant difference between different years ($P<0.05$).

With the extension of abandoned years, soil organic carbon increases first in 1-2a, 3-4a, 5-15a, 24-31a and then decreases in 2-3a, 4-5a, 15-24a, with maximum of 1.76%

http://www.aloki.hu ● ISSN 1589 1623 (Print) ● ISSN 1785 0037 (Online)
DOI: http://dx.doi.org/10.15666/aeer/1704_75617572

achieved at 4a; the total nitrogen increases first in 1-2a and 3-4a, then decreases (2-3a) and finally stabilizes (4-31a), with the maximum of 0.07 achieved at 1a, 4a; the total phosphorus decreases first in 1-3a, 4-5a, 8-15a, 24-31a and then increases in 3-4a, 5-8a, 15-24a, with significant difference between different abandoned years($P<0.05$), and the maximum of 0.66 g/kg is achieved at 1a, followed by 4a (0.58 g/kg); the total potassium increases first in 1-2a, 4-5a, 15-24a and then decreases in 2-4a, 5-15a, 24-31a, with the maximum of 38.17g/kg achieved at 5a. The available potassium increases first in 1-3a, 4a-15a, 24-31a and then decreases in 3-4a, 15-24a, with the maximum of 636.09 mg/kg achieved at 15a, showing significant difference between different years ($P<0.05$); the available phosphorus decreases first in 1-2a, 3-5a, 15-24a and then increases in 2- 3a, 5-15a, 24-31a, with the maximum of 0.178 mg/kg achieved at 3a, showing no significant difference between different abandoned years ($P>0.05$).

Soil microbial properties

As can be seen from *Table 3*, the number of soil bacteria decreases sharply (1-2a) with the extension of abandoned years, increasing first after 2a (2-4a, 8-24a) and then decreasing (4-8a, 24- 31a); the number of fungi decreases first (1-2a, 4-5a, 8-31a) and then increases (2-4a, 5-8a); the number of actinomycetes decreases first (1-3a, 4-5a, 8-15a, 24-31a) and then increases (3-4a, 5-8a, 15-24a), reaching the maximum of 8.37×105cfu/g at 8a and showing significant difference between different abandoned years ($P <0.05$); soil microbes have different compositions, and with the extension of abandoned years, the proportion of bacteria, fungi and actinomycetes decreases to a different extent, of which bacteria accounts for the largest proportion, with the maximum of 95.65% achieved at 1a, while the proportion of fungi is less than 1%.

With the extension of abandoned years, SMBC fluctuates, increasing first (1-2a, 3-8a, 15-24a) and then decreasing (2-3a, 8-15a, 24-31a), showing significant difference between different abandoned years ($P< 0.05$), with the maximum of 979.13 mg/kg achieved at 8a; SMBN decreases first (1-2a, 4-8a, 15-24a) and then increases (2-4a, 8-15a, 24-31a); SMBP increases first (1-2a, 3-4a) and then decreases (2-3a, 4-31a), reaching the maximum of 168.35 mg/kg at 4a; SMBC/SMBN increases first (1-2a, 3-8a, 15-24a) and then decreases (2-3a, 8-15a, 24-31a), reaching the maximum of 9.2 at 8a.

Correlation between soil microbial properties and soil physic-chemical properties

From *Table 4*, it can be known that the number of soil bacteria is significantly positively correlated with total phosphorus ($P<0.01$), and significantly negatively correlated with pH, total potassium and available potassium ($P<0.01$). The number of fungi is significantly positively correlated with organic carbon and total nitrogen ($P<0.01$), significantly negatively correlated with available potassium ($P<0.01$), and negatively correlated with water content ($P<0.05$). The number of actinomycetes is significantly negatively correlated with sand ($P<0.01$), and positively correlated with organic carbon ($P<0.05$); SMBC is significantly positively correlated with pH ($P<0.01$), positively correlated with available potassium ($P<0.05$), and negatively correlated with sand and available phosphorus ($P<0.05$). SMBN is significantly positively correlated with organic carbon ($P<0.01$), significantly negatively correlated with water content and available potassium ($P<0.01$), and positively correlated with total nitrogen ($P<0.05$). SMBP is significantly positively correlated with organic carbon ($P<0.01$), and positively correlated with total nitrogen ($P<0.05$). The correlation between the remaining is not obvious.

http://www.aloki.hu ● ISSN 1589 1623 (Print) ● ISSN 1785 0037 (Online)
DOI: http://dx.doi.org/10.15666/aeer/1704_75617572

Table 2. *Soil physic-chemical properties under different abandoned years*

Index	Abandoned years (a)								
	1	2	3	4	5	8	15	24	31
pH	8±0.06f	8.09±0.04ef	8.18±0.05de	8.24±0.04cd	8.27±0.02bcd	8.32±0.01bc	8.38±0.04ab	8.45±0.04a	8.5±0.02a
Water content	5.85±0.121b	5.66±0.123b	2.89±0.156d	1.32±0.038e	2.92±0.048ad	7.26±0.047a	3.90±0.286c	1.63±0.020e	3.27±0.239d
Sand content/%	60.15±0.19c	55.51±0.13de	54.87±0.08ef	54.54±0.12ef	65.63±0.15a	54.11±0.55f	62.45±0.02b	53.67±0.92f	56.38±0.07d
Organic carbon/%	1.02±0.009c	1.1±0.012b	0.95±0.46c	1.76±0.046a	0.73±0.011e	0.99±0.008c	1.12±0.013b	0.75±0.013e	0.87±0.015d
Total nitrogen/%	0.05±0.008b	0.07±0.004a	0.03±0.003c	0.07±0.006a	0.03±0.002c	0.03±0.002c	0.03±0.002c	0.03±0.003c	0.03±0.002c
Total phosphorus(g/kg)	0.66±0.002a	0.57±0.004b	0.54±0.008d	0.58±0.006b	0.45±0.003f	0.57±0.006b	0.38±0.005g	0.55±0.001c	0.51±0.005e
Total potassium(g/kg)	34.57±0.05e	37.18±0.40b	36.54±0.25bc	35.60±0.19cd	38.17±0.19a	36.23±0.24bc	34.99±0.48de	37.02±0.49b	36.60±0.28bc
Quick-available K(mg/kg)	266.26±17.07d	357.54±5.75c	383.56±2.94c	277.86±9.29d	380.22±54.61c	479.97±6.46b	636.09±11.43a	520.63±13.83b	529.94±1.33b
Quick-available P (mg/kg)	0.177±0.053a	0.159±0.035ab	0.178±0.12a	0.115±0.064cd	0.106±0.30d	0.132±0.05bcd	0.150±0.001abc	0.106±0.18d	0.134±0.092bcd

The different lowercase letters in the same line indicate different years abandoned cultivated lands have significant different at 0.05 level, the same below

Table 3. *The number of soil microbe under different abandoned years*

Index	Abandoned years (a)								
	1	2	3	4	5	8	15	24	31
Bacteria/（$\times10^5$cfu/g）	23.06±0.299a	2.22±0.173c	2.68±0.067c	7.30±0.232b	1.11±0.067de	0.45±0.063e	1.37±0.113d	7.71±0.616b	0.45±0.063e
Fungi/（$\times10^3$cfu/g）	0.72±0.063de	0.52±0.067ef	2.16±0.113b	4.65±0.110a	0.72±0.067de	1.10±0.067c	0.91±0.067cd	0.45±0.063f	0.45±0.063f
Actinomycetes/（$\times10^5$cfu/g）	1.04±0.063de	0.46±0.067f	0.46±0.067f	7.69±0.282b	0.59±0.000ef	8.37±0.299a	1.43±0.063d	3.63±0.234c	0.97±0.110def
Percentage of bacteria/%	95.65±0.002a	82.9±0.01b	84.92±0.02b	48.56±0.004d	65±0.01c	5.13±0.006f	48.57±0.03d	67.89±0.01c	31.84±0.04e
Percentage of fungi/%	0.03±0.0002e	0.19±0.0002d	0.69±0.0005a	0.31±0.0001c	0.42±0.0002b	0.12±0.00003d	0.32±0.0002c	0.04±0.00003e	0.32±0.0004c
Percentage of actinomycetes/%	4.32±0.002f	16.9±0.01e	14.39±0.02e	51.13±0.003c	34.58±0.01d	94.75±0.006a	51.1±0.03c	32.07±0.01d	67.84±0.04b
SMBC（mg/kg）	437.40±8.245de	523.13±13.08c	257.91±13.542f	417.86±5.158e	469.75±5.065d	979.13±13.536a	433.27±8.842e	959.48±13.154a	773.17±13.105b
SMBN（mg/kg）	154.45±1.352c	108.98±0.954e	169.59±1.484b	215.50±1.885a	153.84±1.346c	106.42±0.930e	122.65±1.073d	121.64±1.063d	124.32±1.089d
SMBP（mg/kg）	105.89±0.813f	125.88±0.813d	122.64±0.813e	168.35±0.814a	148.14±0.814b	133.65±0.815c	126.73±0.814d	102.81±0.814g	92.92±0.813h
SMBC/SMBN	2.83±0.08f	4.8±0.12d	1.52±0.08h	1.94±0.02g	3.05±0.03f	9.2±0.16a	3.53±0.08e	7.89±0.13b	6.22±0.12c

http://www.aloki.hu ● ISSN 1589 1623 (Print) ● ISSN 1785 0037 (Online)
DOI: http://dx.doi.org/10.15666/aeer/1704_75617572

Table 4. *Correlation analysis between soil microbial properties and Soil physic-chemical properties*

Index	Bacteria	Fungi	Actinomycetes	SMBC	SMBN	SMBP
pH	-0.536**	-0.145	0.188	0.541**	-0.274	-0.204
Water content	0.104	-0.435*	0.045	0.2	-0.572**	-0.182
Sand content	0.048	-0.031	-0.491**	-0.407*	0.021	0.139
Organic carbon	0.124	0.816**	0.475*	-0.372	0.573**	0.620**
Total nitrogen	0.345	0.531**	0.256	-0.320	0.430*	0.438*
Total phosphorus	0.666**	0.181	0.288	0.133	0.190	-0.125
Total potassium	-0.535**	-0.241	-0.185	0.198	-0.189	0.076
Quick-available K	-0.538**	-0.443**	-0.057	0.442*	-0.609**	-0.372
Available P	0.275	-0.097	-0.380	-0.435*	-0.056	-0.283

**: indicate very significant correlation (P<0.01); *: indicate significant correlation (P<0.05)

Comprehensive evaluation of soil fertility quality

Soil quality assessment can provide a theoretical basis for the restoration and management of degraded land (Kirkegaard et al., 2000). In this study, principal component analysis was used to comprehensively evaluate soil quality (*Table 5*). The cumulative contribution rate of the first 5 principal components is 87.61%, which is in line with the requirements of principal component analysis. Therefore, the 5 principal component analysis can represent the variation information of soil quality of secondary lands with different abandoned years in the lower reaches of Shiyang River.

Table 5. *The loading factor, eigenvalue and contribution ratio of 5 PCAs*

Index	The first principal component	The second principal component	The third principal component	The forth principal component	The fifth principal component
pH	-0.634	0.614	0.179	0.184	-0.270
Water content	-0.100	-0.630	0.329	0.168	0.621
Sand content	-0.199	-0.117	-0.770	0.011	0.150
Organic carbon	0.812	0.291	0.098	0.340	0.152
Total nitrogen	0.824	-0.079	0.171	-0.138	0.224
Total phosphorus	0.558	-0.458	0.586	-0.293	-0.171
Total potassium	-0.381	0.293	-0.139	-0.757	0.241
Quick-available K	-0.810	0.252	0.052	0.469	-0.014
Available P	0.164	-0.692	-0.166	0.375	0.091
Bacteria	0.480	-0.596	0.091	-0.031	-0.473
Fungi	0.802	0.530	-0.005	0.155	-0.076
Actinomycetes	0.332	0.506	0.682	0.147	0.147
Soil microbial C	-0.537	0.145	0.785	-0.139	-0.022
Soil microbial N	0.783	0.325	-0.330	-0.055	-0.340
Soil microbial P	0.582	0.574	-0.212	-0.041	0.458
Eigenvalue	5.154	3.065	2.408	1.287	1.227
Rate of variance %	34.361	20.433	16.051	8.578	8.179
Cumulative rate %	34.361	54.794	70.845	79.423	87.603

The first principal component mainly reflects pH, organic matter, total nitrogen, available potassium, fungi and soil microbial biomass nitrogen index (absolute value of load value > 0.6), indicating that it is the most important impact factor in soil quality assessment. The second principal component mainly reflects pH, water content and

http://www.aloki.hu ● ISSN 1589 1623 (Print) ● ISSN 1785 0037 (Online)
DOI: http://dx.doi.org/10.15666/aeer/1704_75617572

bacteria. The third principal component mainly reflects sand content, actinomycetes and soil microbial biomass carbon. The fourth principal component mainly reflects total potassium, and the fifth principal component mainly reflects water content.

From weighting of the eigenvectors and the normalized data, the scores of the 5 common factors in different abandoned years are obtained, and then comprehensive scores of soil fertility quality under different abandoned years are obtained by weighting of scores of the factors and the variance contribution rate (soil quality comprehensive evaluation index). See *Table 6* for the result, which is sorted as abandoned year 4a (1.087) > abandoned year 8a (0.333) > abandoned year 2a (0.007) > abandoned year 3a (-0.087) > abandoned year 15a (-0.157) > abandoned year 1a (-0.183) > abandoned year 24a (- 0.253) > abandoned year 31a(-0.363) > abandoned year 5a(-0.383), indicating that abandoned year 4a is a key period of restoration. After abandoned year 5a, soil quality decreased to varying degrees. It can be seen that the sorting results of soil quality comprehensive evaluation index are consistent with the previous demonstration results, so the results of principal component analysis can better reflect the actual conditions of the soil.

Table 6. *General sores and ranking under different managements*

Abandoned years(a)	Factor score					General sores	Ranking
	Factor1	Factor2	Factor3	Factor4	Factor5		
1	0.917	-2.150	-0.009	0.100	-0.806	-0.183	6
2	0.244	-0.811	0.166	-0.694	1.488	0.007	3
3	0.347	-0.227	-0.801	0.041	-0.417	-0.087	4
4	2.136	1.584	0.243	0.211	-0.310	1.087	1
5	-0.494	0.591	-1.594	-1.489	0.604	-0.383	9
8	-0.389	0.171	1.771	0.351	1.424	0.333	2
15	-0.748	0.289	-1.041	2.118	0.313	-0.157	5
24	-0.916	0.425	1.009	-0.782	-1.471	-0.253	7
31	-1.097	0.128	0.257	0.144	-0.825	-0.363	8

Discussion

The experimental study found that with the extension of abandoned years, soil pH of the secondary grassland with different abandoned years in the lower reaches of Shiyang River gradually increased but did not show significant difference, which was generally alkaline. Soil available potassium content increased in fluctuations, which may be because soil leaching effect increased the available potassium content in the soil surface (Wang, 2016); the soil water content was generally "V"-shaped, and the maximum value appeared at abandoned year 8a, which may be due to the decline of vegetation coverage and surface exposure with the return of farmland to forest (Wang, 2016). In addition, because of the combined effect of precipitation and natural sedimentation, the soil structure is continuously restored, and the soil capillary water is effectively stored (Wang, 2016). Moreover, as abandoned year 8a vegetation is mainly perennial shrubs, such plants can obtain water in deeper soil layers, while surface soil water content contributes little to it (Walter, 1979); soil sand content decreased gradually during abandoned years 1-4a, fluctuated after 5a, and gradually increased after abandoned year 24a. Soil organic carbon, total nitrogen, total phosphorus, total potassium and available phosphorus decreased with the extension of abandoned years. The reason for this change may be that the vegetation richness index and diversity index decreased in

http://www.aloki.hu ● ISSN 1589 1623 (Print) ● ISSN 1785 0037 (Online)
DOI: http://dx.doi.org/10.15666/aeer/1704_75617572

varying degrees with the extension of abandoned years, and then the bare soil area increased gradually. In addition, the lower reaches of Shiyang River has strong wind (Chang et al., 2007), desertification and wind erosion of the sample site thus deteriorate, while soil sand is not easily eroded by wind, causing a large loss of nutrients. Due to the limitation of water and heat, the slow decomposition rate of organic matter reduces the ability of nutrient return (Liu et al., 2016). At the same time, with the extension of abandoned years, vegetation coverage and biomass decrease, which reduces the supplement of soil nutrients by plant residue (Li et al., 2010).

Bacteria in the soil constitute the main microbial group, its maximum number is up to 23.06×105 cfu/g, accounting for 95.65% followed by actinomycetes and fungi was the least. This may be because the soil in this study area is slightly alkaline, which is beneficial to the growth of bacteria and actinomycetes, while fungus grows poorly in a slightly alkaline environment. This is consistent with the results of Tan Qiujin (Tan et al., 2014). The number of soil bacteria, fungi and actinomycetes in different abandoned years reaches the highest at abandoned year 1a, abandoned year 4a and abandoned year 8a. During abandoned years 1-8a, field husbandry, fertilization and other agricultural management measures just stopped or stopped for a short time, so the good soil moisture conditions and ventilation, coupled with higher soil nutrient content enabled strong microbial activity. In addition, an increase in the number of soil microbes leads to a corresponding increase in the proportion. With the extension of abandoned years, the trend of soil microbial biomass changed slightly. SMBC content was the highest at abandoned year 8a, SMBN and SMBP contents were the highest at abandoned year 4a, which was significantly higher than that at other abandoned years ($P<0.05$).This may be because vegetation grew fast at abandoned years 4a and 8a, root biomass and root exudates then increased, so that soil nutrients accumulated continuously. It was also related to the fact that the collected sample was surface soil (0~10 cm). The surface layer accumulated a large number of plant residues which enriched soil organic matter, and also the layer had good hydrothermal and ventilation condition (Wen et al., 2010), providing a suitable environment for microbial growth and reproduction, and promoting biological activity of microbes. The soil microbial biomass carbon and nitrogen ratio are important indicators to characterize whether soil microbial growth is restricted by carbon or nitrogen, which affect the community structure of soil microbes (Yang et al., 2014). Soil SMBC/SMBN≥30 and SMBC/SMBN≤20 indicate that soil microbial growth is respectively limited by nitrogen source and carbon source. When SMBC/SMBN=25, it is most beneficial to soil microbial growth, which is conducive to the normal function of soil microbes in ecosystem (Zhang et al., 2012). SMBC/SMBN ranged from 1.5~9.2 in the secondary grassland with different abandoned years in the lower reaches of Shiyang River, indicating that supply quantity of carbon source is the main limiting factor for soil microbial growth. The correlation results also show that soil microbial biomass is related to soil nutrients in different degrees (Niu et al., 2011), which is significantly correlated with soil organic matter, so this conclusion is further confirmed. However, soil represents a relatively complex ecosystem, and soil microbial biomass is also affected by factors such as temperature, air temperature, soil bulk density, etc. which demands comprehensive considerations.

Soil microbes are reservoirs of soil nutrients and play an important role in soil organic matter and nutrient conversion and cycling (Singh et al., 2014). Wang et al. (2010) and Yang et al. (2014) have found that there is a certain correlation between soil microbes and soil physicochemical properties. This study also shows that soil microbial

http://www.aloki.hu ● ISSN 1589 1623 (Print) ● ISSN 1785 0037 (Online)
DOI: http://dx.doi.org/10.15666/aeer/1704_75617572

quantity, soil microbial biomass under different abandoned years are closely related to soil physicochemical properties, good physical environment (moisture, pH and gas permeability) will promote the growth of soil bacteria, fungi and actinomycetes, thereby increasing the number of microbes, and the change in soil microbial quantity will accelerate the soil nutrient cycle, leading to an increase in soil nutrients (Taylor et al., 2002). The principal component analysis showed that indicators such as soil pH, sand, water content, organic matter, total nitrogen, available potassium, fungi, soil microbial biomass carbon, soil microbial biomass nitrogen have a large contribution rate in each principal component, which can be used to evaluate important factors in soil fertility quality of the area. The results of comprehensive evaluation of soil fertility indicated that abandoned year 4a> abandoned year 8a> abandoned year 2a> abandoned year 3a> abandoned year 15a> abandoned year 1a> abandoned year 24a> abandoned year 31a> abandoned year 5a, of which abandoned year 4a is a key period of recovery. This conclusion is consistent with the conclusions obtained from single factor analysis to a certain extent and the two are mutually confirmed.

Conclusion

With the extension of abandoned years, soil pH gradually increased, soil water content, sand content, bacteria number, actinomycetes number, SMBN decreased first and then increased; soil organic carbon, total potassium, available potassium, available phosphorus, SMBC, SMBP, The SMBC/SMBN increased first and then decreased; the total nitrogen first increased, then decreased, then increased and finally stabilized; the total phosphorus and fungi decreased first, then increased and finally decreased. There is a close correlation between soil physicochemical properties and soil microbial quantity and soil microbial biomass. Indicators such as soil pH, sand, water content, organic matter, total nitrogen, available potassium, fungi, soil microbial biomass carbon and soil microbial biomass nitrogen are important factors for evaluating soil fertility quality in this area. It can be inferred from the comprehensive evaluation of soil fertility quality that the abandoned year 4a is the key stage of restoration and control process in Shiyang River Basin management.

Acknowledgements. This paper belongs to the project of the China National Natural Science Foundation (31760709), Gansu provincial youth science and technology fund project (18JR3RA019) and Gansu provincial forestry science and technology project (2017kj025).

REFERENCES

[1] Bao, S. D. (2005): Agrochemistry soil analysis Handbook. – Beijing: China Agricultural Press: 23-107.
[2] Chai, X. H., Wang, L. D., Yao, T. (2015): Effects of different years of cultivation abandonment on soil physical, chemical and microbial characteristics in the midstream and downstream of Shiyang river area. – Acta Prataculturae Sinica 24(8): 24-34.
[3] Chang, Z. F., Zhao, M., Liu, H. J. (2007): Study on dynamic degenerate ecological characteristic of desertification in Minqin. – Chinese Agricultural Science Bulletin 23(11): 333-338.

http://www.aloki.hu ● ISSN 1589 1623 (Print) ● ISSN 1785 0037 (Online)
DOI: http://dx.doi.org/10.15666/aeer/1704_75617572

[4] Chang, G. Y., Wang, L., Zhang, W. X. (2016): Perceptions of peasants in Minqin County for the water conservation polices of Shiyang river basin and their effects. – Journal of Arid Land Resources and Environment 30(2): 13-19.
[5] Feng, S. W. (1963): The evolution of drainage system of the Minqin oasis. – Journal of Geographical Science 29(3): 241-249.
[6] Harris, J. A. (2003): Measurements of the soil microbial community for estimating the success of restoration. – European Journal of Soil Science 54(4): 801-808.
[7] Hu, C. J., Guo, L. (2012): Advances in research of ecological effects of vegetation restoration. – Ecology and Environmental Sciences 21(9): 1640-1646.
[8] Kardol, P., Cornips, N. J., Van Kempen, M. M. L., Bakx-Schotman, J. M. T., van der Putten, W. H. (2007): Microbe-mediated plant-soil feedback causes historical contingency effects in plant community assembly. – Ecological Monographs 77(2): 147-162.
[9] Kirkegaard, J. A., Sarwar, M., Wong, P. T. W., Mead, A., Howe, G. N., Newell, M. (2000): Field studies on the biofumigation of take-all by Brassica break crops. – Crop and Pasture Science 51(4): 445-456.
[10] Li, Z. Y., Li, C. L., Wang, D. Z. (2010): Characteristics of vegetation succession on salinized abandoned fields in lower reaches in Shiyang river. – Acta Botanica Boreali-Occidentalia Sinica 30(10): 2087-2092.
[11] Liu, X. T., Wei, Y. C., Yang, X. L., Hao, M. D., Wei, X. R. (2016): Effects of different re-vegetation patterns on soil organic carbon and total nitrogen in the wind-water erosion crisscross region. – Chinese Journal of Applied Ecology 27(1): 91-98.
[12] Niu, S. Q., Yang, T. T., Li, J. F., Da, W. Y., Yang, J. W. (2011): Seasonal trends of microbial functional groups in Saline-alkali soil and their relationship with soil physicochemical factors in the east Hexi corridor. – Arid Zone Research 28(2): 328-334.
[13] Singh, A. K., Bordoloi, L. J., Kumar, M., Hazarika, S., Parmar, B. (2014): Land use impact on soil quality in eastern Himalayan region of India. – Environmental Monitoring and Assessment 186(4): 2013-2024.
[14] Sparling, G. P., Pankhurst, C., Doube, B. M. (1997): Soil microbial biomass, activity and nutrient cycling as indicators of soil health. – Biological Indicators of Soil Health: 97-119.
[15] Tan, Q. J., Song, T. Q., Peng, W. X., Zeng, F., Du, H. M., Zhang, H., Fan, F. (2014): Characteristics of soil microbial populations and biomass under different ecosystems in a canyon karst region. – Acta Ecologica Sinica 34(12): 3302-3310.
[16] Taylor, J. P., Wilson, B., Mills, M. S., Burns, R. G. (2002): Comparison of numbers and enzymatic activities in surface soils and subsoils using various techniques. – Soil Biology and Biochemistry 34: 387-401.
[17] Walter, H. (1979): Vegetation of the earth: second edition Handbook. – NewYork: Springer-Verlag.
[18] Wang, C. T., Long, R. J., Wang, G. X. (2010): Relationship between plant communities, characters, soil physical and chemical properties, and soil microbiology in alpine meadows. – Acta Prataculturae Sinica 19(6): 25-34.
[19] Wang, L. D. (2016): Evolution of vegetation and soil system on secondary grassland of abandoned land area in Minqin. – Lanzhou: Gansu agricultural university.
[20] Wen, D. R. Y., Li, G., Zhang, J. N. (2010): The study of soil microbial biomass and soil enzyme activity on different grassland in Hulunbeier, Inner Mongolia. – Acta Pratacultural Sinica 19(5): 94-102.
[21] Xu, G. H., Zheng, H. Y. (1986): Soil Microbial Analysis Method of Manual Handbook. – Beijing: Agricultural Press: 102-109.
[22] Yang, N., Zou, D. S., Yang, M. Y., Lin, Z. G., Song, G. T., Chen, Z. Y., Zhao, L. F. (2014): Changes of soil properties in re-vegetation stages on sloping-land with purple soils in hengyang of Hunan Province, South-central China. – Acta Ecologica Sinica 34(10): 2693-2701.
[23] Yao, H. Y., Huang, C. Y. (2006): Soil Microbial Ecology and Experimental TechniquesHandbook. – Beijing: Science Press.

http://www.aloki.hu ● ISSN 1589 1623 (Print) ● ISSN 1785 0037 (Online)
DOI: http://dx.doi.org/10.15666/aeer/1704_75617572

[24] Yuan, J. Y., Ouyang, Z. Y., Zheng, H., Xu, W. H. (2012): Effects of different grassland restoration approaches on soil properties in the southeastern Horqin sandy land, northern China. – Applied Soil Ecology (61): 34-39.
[25] Zhang, L. Q., Peng, W. X., Song, T. Q., Zou, D. S., Zeng, F. P., Song, M., Yu, Z., Liu, Y. (2012): Spatial heterogeneity of soil microbial biomass carbon, nitrogen and phosphorus in sloping farmland in a karst region on the Yunnan-Guizhou Plateau. – Acta Ecologica Sinica 32(7): 2056-2065.
[26] Zhang, Y. H., Liu, S. Z., Ji, Y. F. (2016): Spatial distribution pattern and spatial association of phragmites australis in the middle reaches of Shiyang river. – Journal of Desert Research 36(2): 342-348.
[27] Zhao, H. L., Zhou, R. L., Zhao, X. Y. (2012): Desertification mechanisms and process of soil chemical and physical properties in Hulunbeir sandy grassland, Inner Mongolia. – Acta Prataculturae Sinica 21(2): 1-7.

http://www.aloki.hu ● ISSN 1589 1623 (Print) ● ISSN 1785 0037 (Online)
DOI: http://dx.doi.org/10.15666/aeer/1704_75617572

ANALYSIS OF THE CORRELATION BETWEEN FRACTAL DIMENSION OF GRAVELLY SOIL AND DEBRIS-FLOW INITIATION THROUGH IN-SITU EXPERIMENTS

ZHONG, W.[1,2] – HE, N.[3*] – COSGROVE, T.[4] – ZHU, Y. J.[3] – FU, L.[3]

[1]*Institute of Mountain Hazards and Environment, Chinese Academy of Sciences, Chengdu 610041, China*

[2]*Key Laboratory of Mountain Hazards and Surface Processes, Chinese Academy of Sciences, Chengdu 610041, China*

[3]*School of Civil Engineering, Henan Polytechnic University, Jiaozuo, Henan 454003, China*

[4]*Department of Civil Engineering & Materials Science, University of Limerick, Limerick, Ireland*

**Corresponding author*
e-mail: hn61886@163.com; phone: +86-133-2382-2010

(Received 27th Feb 2019; accepted 3rd May 2019)

Abstract. Particle size distribution of the gravelly soil in debris flow source area has a great impact on the formation mechanism of debris-flow. In order to explore the relationship between particle composition and debris flow initiation, we collected 182 soil samples from debris flow source areas. Sieving tests have been conducted in the laboratory to acquire the fundamental particle size distribution data. Subsequently, the fractal theory was employed to compute the fractal dimension of each soil sample, analyzing the results of calculation we found that the gravelly soil in debris flow source area is mainly concentrated in one fractal dimension, the value of which ranges from about 2.250 to 2.798. Comparing the results of calculation and sieving experimentation, the underlying relationship between particle composition and fractal dimension can be revealed: the particle compositions of the gravelly soil tend to remain uniform as the fractal dimension increases. On the basis of the calculation results, the in-situ artificial rainfall experiments can be designed and performed. Analyzing the phenomenon during the processes of the experiments, the initiation mechanism with different fractal dimensions can be preliminarily identified: The gravelly soil which can mobilise into debris flows exhibits significant criticality feature, and the gravelly soil with fractal dimension ranges from 2.4 to 2.6 are more susceptible to mobilise into debris flow, and the scale of the debris flow is relatively larger. For slopes with fractal dimension < 2.4, the possibility of mobilisation into debris flow is extremely low. When fractal dimension ranges from about 2.6 to 2.7, the density of the formed debris flow is relatively lower, under which the formation of debris flows exhibits significant intermittent characteristics.
Keywords: *debris flow, fractal theory, particle size distribution, initiation mechanism, in-situ experiments, disaster mitigation*

Introduction

Debris flows form a class of slope failures (Varnes, 1978) encompassing a wide range of characteristics and varying widely in magnitude (Jakob, 2005), composition (Coussot and Meunier, 1996), and mechanism of initiation (Coe et al., 2008a). Debris flows are recognized as a significant hazard in mountainous areas, and have been shown to be an important process controlling the transport of sediment and woody debris from hill slopes to channels in mountainous areas, with implications for channel form and riparian habitat (Brayshaw, 2009; Hogan and Schwab, 1991; Smadja, 1992). Because of

http://www.aloki.hu ● ISSN 1589 1623 (Print) ● ISSN 1785 0037 (Online)
DOI: http://dx.doi.org/10.15666/aeer/1704_75737589

their high mobility, velocity and density, debris flows can be very destructive and damaging when they encounter infrastructure such as buildings, roads, bridges, pipelines and hydropower facilities, and may lead to loss of human life (Park et al., 2016; Chen and Lee, 2000; Gregoretti et al., 2016; Wang et al., 2017).

To mitigate and prevent hazards induced by debris flows and related risks, one must understand the formation of these in order to make reliable forecasts (Yu et al., 2014). Many factors are related to the occurrence of debris flows such as the basin gradient, the percentage of basin area with slopes greater than or equal to 30%, basin ruggedness, slope aspect, rainfall intensity, and soil properties, including the clay percentage, the percentage of organic matter, the soil composition, and the soil liquid limit (Cannon et al., 2010; Liu et al., 2009). Many researchers have focused on the prediction of their occurrence (Bathurst et al., 1997; Giannecchini et al., 2007; Ho et al., 2000) and estimation of their magnitude and runout distance (Hungr et al., 2008; Johnson et al., 2000; Miller and Burnett, 2008) in order to reduce associated risk. In addition, established prediction models include the Water-Soil coupling forecast model, the I-D (rainfall intensity-duration) prediction model and other statistical prediction models (Yang et al., 2016, 2002; Saito et al., 2010; Zhang et al., 2014a, b). Moreover, other parameter combination modes for defining a threshold for debris flow activity in terms of mean intensity, duration and mean annual precipitation were also presented for the debris flow prediction of dolomites in northeastern Italy (Bacchini and Zannoni, 2003; Giannecchini et al., 2016; Maggioni et al., 2016; Papa et al., 2013). Some researchers carried out experiments on slope stability considering mechanical property variations of the soil mass and established the model of debris flow initiation (Berti and Simoni, 2005; Iverson and LaHusen, 1989; Iverson et al., 1997). Other scientists used different approaches and discussed the relationship between particle composition and properties of debris flows (Li et al., 2007; Yong et al., 2013, 2005), and some models have been established (He et al., 2014; Ningsheng et al., 2004; Zhou et al., 2012), which greatly facilitate debris flows prediction and mitigation. However, due to the complexity of debris flow formation and subsequent dynamic process, the accuracy of the prediction often cannot meet adequately the requirements of disaster mitigation (Turkington et al., 2016). Prediction models based on the formation mechanism of debris flows promises an effective way to ameliorate the impact of such disasters.

Basically, three necessary conditions are required to fulfill debris flow initiation: energy conditions (slope gradient), meteorological conditions (rainfall condition) and material condition (particle size distribution and density). In the short term, the energy conditions can be taken as a constant, and the precipitation can be measured at nearby meteorological stations. The mechanical property of the loose solid material plays an extremely important role in debris flow initiation. From soil mechanics we know that the soil mechanical property with the major influence on debris flow initiation is soil composition. Therefore, identifying the particle size distribution of the loose solid material is the precondition for an accurate analysis of debris flow initiation. But the particle size distribution of the gravelly soil in the debris-flow source area is so wide that the critical particle grading features are not yet well understood. The composition and gradation of the particles in debris flow source areas have significant influence on debris flow formation, subsequent movement and resulting dynamic forces (Chen et al., 2010; He et al., 2016). Previous studies explored the characteristics of the gravelly soil (Li et al., 2007; MacDonald et al., 2012), and some models were established to reveal the relationship between mechanical properties of the gravelly soil and its particle size

http://www.aloki.hu ● ISSN 1589 1623 (Print) ● ISSN 1785 0037 (Online)
DOI: http://dx.doi.org/10.15666/aeer/1704_75737589

distribution (Chen, 2004; Hwang and Powers, 2003; Shimizu et al., 2011; Wang and Sassa, 2003; Zhou et al., 2012), but the influential of particle composition on debris flow initiation is still unclear. In addition, the complexity of the particle size distribution results in a non-deterministic and anisotropic gravelly soil structure, which poses great difficulties when attempting to use traditional methods based on linear analysis to quantitatively describe it (https://www.benthamopen.com/contents/pdf/TOCIEJ/TOCIEJ-10-877.pdf).

Based on the aforementioned discussion, to better understand the characteristics of the gravelly soil and reveal the relationship between mechanical properties and debris flow initiation, the main objective of this paper is to explore the characteristics of particle size distribution taken from areas prone to debris flows, and using fractal theory to calculate the fractal dimension of each sample. After the particle size distribution is established, the fractal dimension can be calculated, and the fractal characteristics can be fully understood. Taking into account of this data, the in-situ artificial rainfall experiments can then be conducted. By analyzing rainfall data, water content, and pore water pressure, the initiation mechanism of debris flow can be revealed, and the influence of particle composition on debris flow initiation can be identified, which in turn can greatly facilitate future debris flow prediction and mitigation.

Methodology

In this research, 182 soil samples were taken from 116 gullies before September 2013 that were identified highly prone to debris flows (all of the gullies are situated on Longmenshan fault zone; *Fig. 1*). The soil samples were sorted and dried in the laboratory to facilitate the sieve tests. Using sieve tests, the particle size distribution curves were established, and plotted in both plane-coordinate and double logarithmic coordinates.

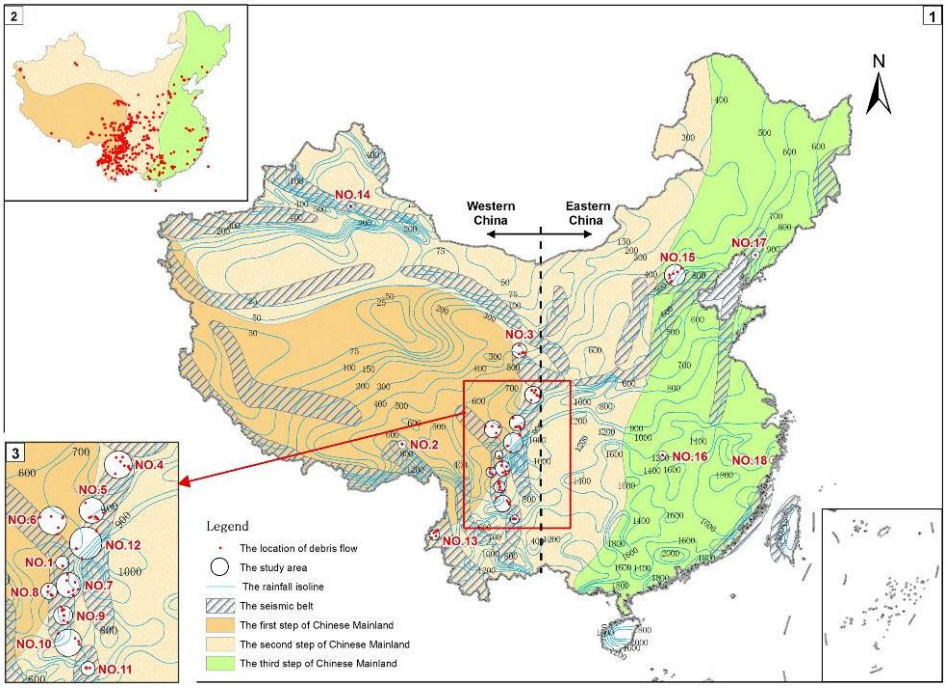

Figure 1. *Sampling sites (Lu, 2013)*

http://www.aloki.hu ● ISSN 1589 1623 (Print) ● ISSN 1785 0037 (Online)
DOI: http://dx.doi.org/10.15666/aeer/1704_75737589

Fractal theory

The gravelly soil in the debris-flow source areas shares some characteristics with the fragmented rocks. Therefore, the particle fractal dimension can be calculated using a rock-crushing model, which is derived from fractal theory (Carpinteri et al., 2004; Chen Yong, 1998). It is presumed that the diameter of a gravelly soil particle is R, while $N(R)$ denotes the number of particles whose diameter is larger than R, and these two parameters satisfy the general fractal equation:

$$N(R) = R^{-D} \quad \text{(Eq.1)}$$

where D is the fractal dimension. After differentiating we obtain *Equation 2:*

$$dN(R) \sim R^{-D-1} dR \quad \text{(Eq.2)}$$

The particle size distribution and frequency of gravelly soil fits the Weibull distribution well:

$$\frac{M(<R)}{M_0} = 1 - \exp[-(\frac{R}{R_0})^k] \quad \text{(Eq.3)}$$

where $M(<R)$ denotes the total mass of the particles whose diameter is smaller than R, M_0 is the total mass of the gravelly soil, R_0 is the average diameter of the gravelly soil, and k is a constant. For $R << R_0$, *Equation 3* was further manipulated, ignoring the quadratic term, and the following equation is obtained:

$$\frac{M(<R)}{M_0} = (\frac{R}{R_0})^k \quad \text{(Eq.4)}$$

From which we obtain *Equation 5:*

$$dM(<R) \sim \mathrm{R}^{\mathrm{k-1}} dR \quad \text{(Eq.5)}$$

The particle number of the gravelly soil and the mass of the gravelly soil satisfies the following equation:

$$dM(<R) \sim \mathrm{R}^3 dN(R) \quad \text{(Eq.6)}$$

Combining *Equations 2, 5* and *6,* the following equation can be derived:

$$\mathrm{D} = 3 - \mathrm{k} \quad \text{(Eq.7)}$$

Equation 7 is the function employed in this paper to calculate the fractal dimension, where D is the fractal dimension, while k is the slope of the line we are fitting in the

http://www.aloki.hu ● ISSN 1589 1623 (Print) ● ISSN 1785 0037 (Online)
DOI: http://dx.doi.org/10.15666/aeer/1704_75737589

double logarithmic coordinates, where the X-axis is $\lg R$ and the Y-axis is $\lg[M(<R)/M_0]$.

A fractal phenomenon approximates self-similarity or statistical self-similarity. This similarity exists only within a certain range of scales. Therefore the similarity will not exist outside certain ranges. Outside of these ranges the objects do not possess fractal feature, which indicates the fractal scale-free interval is limited. On the basis of the complexity and particular nature of the gravelly soil, this paper chooses the coefficient of determination (R^2) of the fitted line as the index to determine if the soil samples possesses fractal features or not. If the coefficient of determination (R^2) of the fitted line is greater than 0.9, it means that the soil samples present good similarity and the fractal dimension can be calculated through $D = 3 - k$. On the other hand, if the coefficient of determination (R^2) of the fitted line is less than 0.9, the soil samples do not have fractal features, and *Equation 7* cannot be employed to calculate the fractal dimension.

Fractal features of the gravelly soil in debris flow source area

In total, 182 samples were sorted and prepared first (*Fig. 2*). Using sieve tests, the particle size distribution data were acquired and the particle size distribution curves were plotted using plane-coordinates and a double logarithmic scale (*Figs. 3* and *4*). By means of linear fitting we obtained the slope of the straight line, and then *Equation 7* was employed to calculate the fractal dimensions of all 182 soil samples. On analyzing the results, we found that the soil samples were mainly concentrated in one fractal dimension. About 161 soil samples satisfied the requirements of fractal theory well, and one fractal dimension accounted for 88.46% of the total samples. Therefore, we concluded that the gravelly soil is mainly concentrated in one fractal dimension. The dimension value ranges from about 2.25 to 2.98. The sample with the largest dimension was taken from Jiangjia gully, while the smallest was taken from Ganxi gully, and their double logarithm curves are depicted in *Figure 4a* and *b,* respectively. The distribution interval of one fractal dimension is illustrated in *Figure 5*. Through *Figure 5,* we found that the fractal dimensions of the 130 soil samples are within the range of 2.4–2.7, with one fractal dimension accounting for 80.75% of the total samples. This raises an obvious question: is it the case that gravelly soil with fractal dimension ranging from 2.4 to 2.7 is more susceptible to debris flow? This question merits further study in the future.

Figure 2. *Sorting and drying the soil in the laboratory*

http://www.aloki.hu ● ISSN 1589 1623 (Print) ● ISSN 1785 0037 (Online)
DOI: http://dx.doi.org/10.15666/aeer/1704_75737589

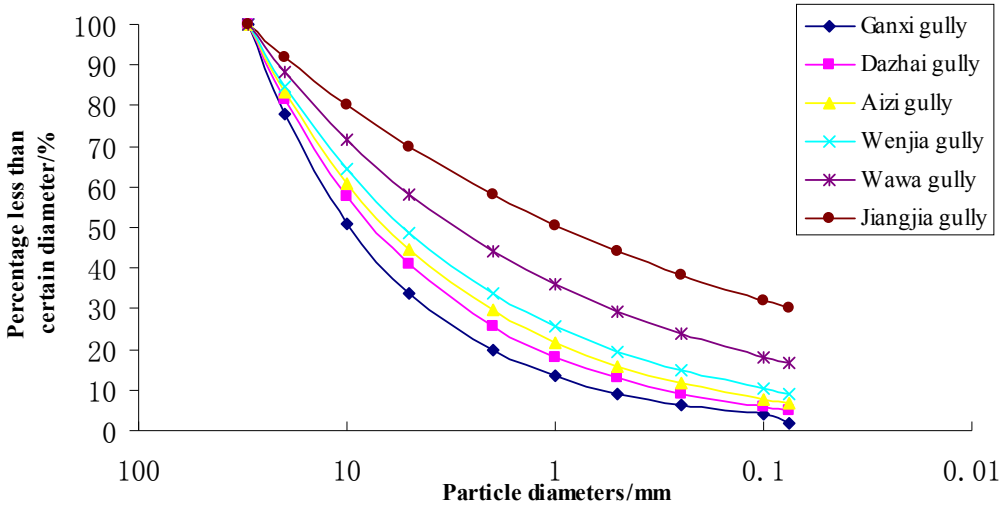

Figure 3. *Particle size distribution curves*

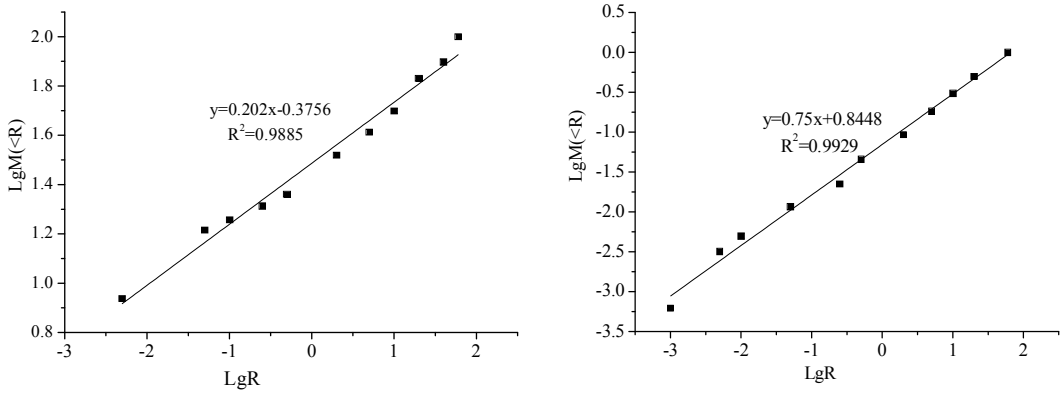

a. Sample from Jiangjia gully **b. Sample from Ganxi gully**

Figure 4. *Double logarithm curves of Jiangjia gully and Ganxi gully (where R denotes the diameter of the particles, while M (< R) is the percentage whose diameters are less than R)*

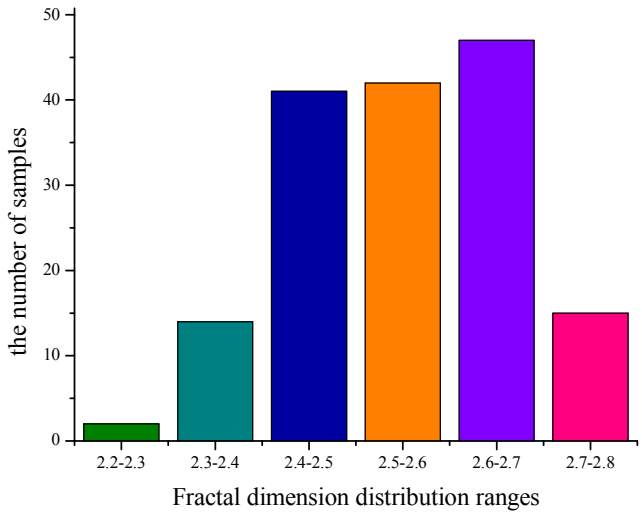

Figure 5. *Distribution interval of one fractal dimension*

http://www.aloki.hu ● ISSN 1589 1623 (Print) ● ISSN 1785 0037 (Online)
DOI: http://dx.doi.org/10.15666/aeer/1704_75737589

By comparing *Figures 3* and *4,* we found that the particle size distribution tends to remain uniform as the fractal dimension increases. In addition, as the coarse particle content increases, the fractal dimension decreases. The particle composition determines the kind of skeleton or mechanical properties of the gravelly soil, which in turn determines the strength and hydraulic conductivity.

Figures 3 and *4* illustrate that the fractal dimension varied with the particle size distribution. The more uniform the particle size distribution, the larger the fractal dimension becomes. The larger particles formed the skeleton of the gravelly soil, while the relatively smaller particles filled the pores. For soil samples with larger fractal dimension, the pores formed by larger particles are well filled with small particles. Under such circumstances, the hydraulic conductivity can be greatly reduced. Moreover, the strength of a gravelly soil with a larger fractal dimension is mainly provided by cohesion and sliding friction between particles. As the fractal dimension decreases, the porosity formed by larger particles could not be fully filled by the smaller particles. Therefore, the hydraulic conductivity becomes larger. For soil samples with a smaller fractal dimension, the strength of the soil is mainly determined by cohesion and occlusal friction.

In addition, soil strength plays a crucial role in slope stability analysis. Debris-flow initiation can generally be subdivided into two mechanisms: 1) failure of shallow landslides, which transform into debris flows, and 2) concentrated run-off (flash flood) erosion in channels filled with sediments, which may be augmented by landslides from the slope. To better understand the debris-flow initiation mechanism, the relationship between fractal dimension of gravelly soil and debris-flow initiation was investigated by conducting in situ artificial rainfall experiments in areas prone to debris flow.

In-situ debris flow initiation experiment

Based on the aforementioned dataset, a debris flow initiation experiment can be designed and conducted. A schematic diagram of the experiment is shown in *Figure 6*. The artificial rainfall experiment involved mainly the following equipments: an artificial rainfall system (water pump, water tank, bracket and spay nozzle), rainfall gauge, pore-water pressure sensors, water content sensors, video camera, and data collection system. As noted in section 2.2 we found that the soil fractal dimension ranges from about 2.25 to 2.98. Therefore we selected 2.3, 2.35, 2.4, 2.45, 2.5, 2.55, 2.6 and 2.7 as the experimental fractal dimension value to back-calculate the corresponding particle compositions. Through field investigation the dry density of the gravelly soil can be determined. The dry density ranges from 1.55 to 2.2 g/cm^3. In this research the dry density of the soil sample was assumed as 1.7, 1.8 and 1.9 g/cm^3, respectively. Previous research revealed that slope angle ranging from 25 to 45° gives favourable conditions for debris flow initiation. Due to the complexity and difficulties in the process of performing in-situ experiments, the slope angle is assumed as 35°. The slope size is 1.5 m × 2.3 m, the position and depth of the sensors are shown in *Figure 6*. A total of 12 sensors were used in the experiment. The sensors are buried in six locations, 0.7 and 0.17 m in depth, and 0.7 and 1.5 m away from the upper edge of the experimental slope. Rainfall intensity is 75.2 mm/h during the experiments, and the duration time are mainly dependent on the initiation of debris flows, after debris flow initiated, the rainfall processes will last 30-40 minutes in order to identify the scale of the debris flows.

http://www.aloki.hu ● ISSN 1589 1623 (Print) ● ISSN 1785 0037 (Online)
DOI: http://dx.doi.org/10.15666/aeer/1704_75737589

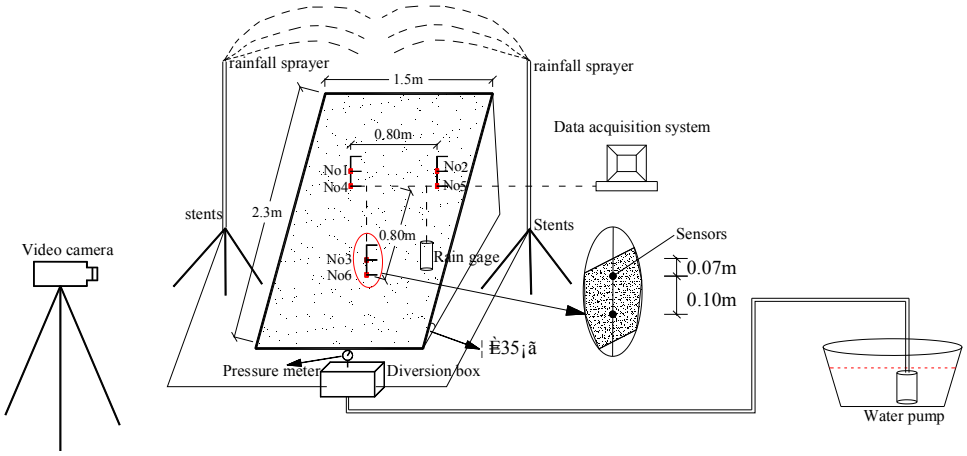

Figure 6. *Experimental scheme figure*

Test preparations

Based on the selected fractal dimension value, the particle size distribution for different particle diameters and different dry densities can be back-calculated, and the soil sample can be prepared. Subsequently the prepared soil can be placed on the slope at the chosen slope angle and the sensors positioned as shown in *Figure 7*. Based on the typical debris flow records in the past, most rainfall intensities that induced debris flows are over 30 mm/h, and in some areas they can exceed 100 mm/h. In this study, the rainfall intensities are controlled by a water pump. The sprinkler nozzle is 11 mm in diameter, and the rainfall intensity is set at 75 mm/h. The actual rainfall intensity of the experiment is found to be 75.2 mm/h during calibration. Then the rainfall gauge, pore water sensors and water content sensors are connected to the data collection system. The video camera, water pump and data collection system are turned on simultaneously to start the experiment (*Fig. 8*).

Experiment procedure

The particle composition under different fractal dimension and dry density can be back-calculated. According to the required slope angle (35°) and the slope size (1.5 m × 2.3 m), the slope can be modified. To facilitate and ensure the homogeneity of the samples, the initial water content is set as 10%, and the required water can be added and mixed uniformly with the gravelly soil. The soil can then be placed step by step on the modified slope. The thickness of the gravely soil is 35 cm, and the soil samples were placed in three layers, with the thickness of the upper, middle and lower layer of 10, 10 and 15 cm, respectively. After the lower layer is fully placed on the slope, the surface is scratched to avoid sliding slip plane between the lower and the mid-layer. Then the pore-water pressure sensors and water content sensors are placed in the correct locations. The sampling process is then repeated until the slope meets the requirements of the experiment. The rainfall gauge was placed on the edge of slope (as shown in *Figs. 6* and *8a*) with the aim of collecting real time precipitation data during the experiment. In order to analyze the formation mechanism, and to better illustrate the underlying reasons for each phenomenon in the experimental process, the video camera was placed in front of the slope. When the experiment was started, the artificial rainfall system, data collection system and video camera were turned on simultaneously.

http://www.aloki.hu ● ISSN 1589 1623 (Print) ● ISSN 1785 0037 (Online)
DOI: http://dx.doi.org/10.15666/aeer/1704_75737589

a. Buried sensors **b. Control slope angle**

c. Measure the size of the slope **d. Bury sensors**

Figure 7. *Experiment preparation*

a. Rainfall process **b. Data collection system**

Figure 8. *In-situ experiment progress*

Results

Following careful analysis of the results of the in-situ artificial rainfall experiments, we found that for gravelly soil, certain conditions are critical for debris flow initiation, and the gravelly soil that mobilized into debris flows manifests obvious criticality: The results indicate that while the fractal dimension of the slope is less than 2.4, regardless of the density or cumulative rainfall amount, no debris flows occurred during the whole

http://www.aloki.hu ● ISSN 1589 1623 (Print) ● ISSN 1785 0037 (Online)
DOI: http://dx.doi.org/10.15666/aeer/1704_75737589

rainfall process. Moreover, as the fractal dimension of the soil increased, the probability of debris flow initiating on the slope becomes higher, the unit weight of the formed debris flow becomes larger, varying from dilute debris flow (unit weight less than 1.8 g/cm^3) to viscous debris flow (unit weight greater than 1.8 g/cm^3).

By comparing the data from all the experiments the following results can be established: under identical dry density, slope angle and rainfall condition, the gravelly soil with lower fractal dimension (less than 2.4) experienced short term creep deformation during the rainfall process, which thereafter tends to stabilize, and the slope maintains its stability during the subsequent rainfall process. Under such circumstances, no overland runoff was witnessed on the slope and the infiltrated water flowed out at the base of the slope mainly through internal flow. In addition, the internal flow entrained the vast majority of the fine particles. Therefore the soil structure can be changed dramatically, and obvious sinking can be witnessed on the slope (*Fig. 9*). Due to the washing away of fine particles, the pore water sensors and water content sensors were finally exposed (*Fig. 9d*). But no debris flow was witnessed from beginning to the end of the experiments.

a. At the beginning of the experiment

b. During the process of the experiment

c. During the process of the experiment

d. At the end of the experiment (the sensors were exposed due to the continuous rainfall)

Figure 9. *Phenomenon of the experiment (here the fractal dimension of the soil sample is 2.35)*

After the fractal dimension exceeds 2.4, the creep deformation lasted longer and the distance of the creep deformation is larger during the rainfall process. By analyzing the recorded videos, two types of runoff were identified: internal runoff and overland

http://www.aloki.hu ● ISSN 1589 1623 (Print) ● ISSN 1785 0037 (Online)
DOI: http://dx.doi.org/10.15666/aeer/1704_75737589

runoff. Comparing the internal runoff we found that for larger fractal dimension (larger than 2.4) very little of the fine particle fraction were washed out by the internal runoff. As the rainfall process continued, many erosion gullies were induced by overland flow, which subsequently caused an accumulation of material collapsed from banks. This subsequently failed as shallow slides when saturated, transforming the process into debris in a second stage. After this initial phase, the debris flow volume increased rapidly by a chain of subsequent cascading processes starting with collapses of the sidewalls, damming and breaching, leading to a rapid widening of the erosion channel. In terms of erosion amount, the subsequent mechanisms were much more important than the initial one. The damming and breaching were found to be the main reasons for the huge magnitude of the debris flows, and this agrees well with previous research (Hu et al., 2016).

The samples from the formed debris flows were collected and analyzed. Comparing them, we found that the unit weight of the debris flow increases as the fractal dimension increase. For slopes with fractal dimension 2.4, the unit weight of the formed debris flow is around 1.63 g/cm^3, but the unit weight of samples taken from slope with fractal dimension 2.7 is more than 1.82 g/cm^3. These results indicate that as the fractal dimension of the soil increases, the formed debris flow is likely to change from dilute to viscous debris flow. These results demonstrate that the unit weight of the formed debris flow is closely linked to particle size distribution. This can provide useful information for future debris flow prevention. For slope with identical fractal dimension, as the dry density increases, debris flow initiation process takes a longer time, but for slopes with fractal dimension smaller than 2.4, no debris flows were witnessed.

Analyzing the pore-water pressure and water content pressure we found that regardless of whether a debris flow was formed or not, the pore water pressure and water content curves exhibit similar characteristics. At the beginning of the rainfall process, the pore water pressure gradually increased to its peak value and then decreased to a given value, as shown in *Figure 10*. But the water content first increased and then maintains a peak value for the duration of the rainfall. For soil with different fractal dimension and dry density, the peak value and fixed value may show some variations, but the trends are identical. Here we take the pore water pressure and water content from the slope with fractal dimension 2.35 as an example to illustrate this phenomenon (*Fig. 10*).

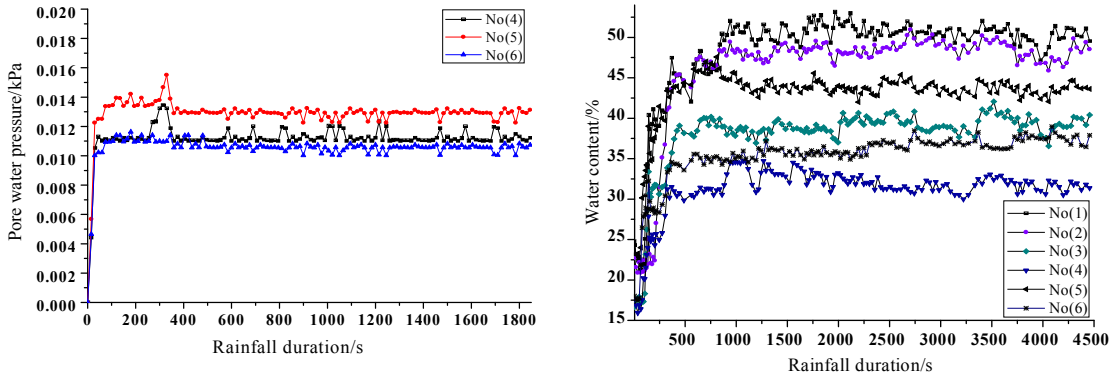

a. pore-water pressure curves **b. water content curves**

Figure 10. *Pore-water pressure curves and water content curves of gravelly soil with fractal dimension 2.3*

http://www.aloki.hu ● ISSN 1589 1623 (Print) ● ISSN 1785 0037 (Online)
DOI: http://dx.doi.org/10.15666/aeer/1704_75737589

Analyzing the pore water pressure curves and debris flow initiation process, it was also found that debris flow initiation always happens before the occurrence of peak pore water pressure. For slopes with different fractal dimensions, the time from initiation to the peak value of pore water pressure varied greatly.

Discussion

Based on the analysis in section 2.2, we concluded that the fine particle portion increases with the increasing of fractal dimension. Previous research (He et al., 2014) revealed that permeability coefficient and fractal dimension displays an exponential relationship, and the function is presented in *Equation 8,* where k denotes coefficient of permeability, D is fractal dimension of the gravelly soil, and ρ_d is dry density. Through *Equation 8* we found that for a given dry density, the permeability coefficient decreased dramatically as fractal dimension increased. The in-situ artificial rainfall experiment agrees well with previous research: for slope with lower fractal dimension (less than 2.4), no overland flow was identified during the entire experiment, and no obvious peak pore-water pressure was witnessed, and the fluctuation of the pore water pressure is relatively small, as shown in *Figure 11*. This is mainly due to the high permeability, so water can freely infiltrate and flow out of the slope in a short time without causing a sharp increase in pore water pressure. Surface sinking of the slope was induced mainly due to the losses of fine particles and structural reorganization. Moreover, the strength of the slope decreased slightly due to a small pore-water pressure increase. Therefore, the strength is sufficient to resist the sliding forces, and the slope can maintain its stability.

$$k = f(\rho_d, D) = 6.051 \times 10^4 \times \rho_d^{-7.297} \times D^{-9.196} \quad \text{(Eq.8)}$$

As the fractal dimension increases, the fine particle fraction increases gradually, and the permeability of the soil decreases rapidly. During the rainfall process, the infiltrated water cannot release timely. This will cause a sharp increase in pore water pressure. Effective stress and pore water pressure is negatively correlated, a sharp increase in pore water pressure directly causing a dramatic decrease in effective stress. Under the combined effect of pore-water pressure increasing, along with an increased entrained and scour capacity of the overland flow, the large-scale debris flow was finally formed. For slopes with fractal dimension more than 2.4, during the rainfall process debris flow was identified. But comparing the videos and pore water pressure curves, we found that even though all such slopes formed debris flows, the mechanism of debris flow formation were radically different.

For slopes with fractal dimension ranging from 2.4 to 2.6, the formation mechanism can be understood using Soil Mechanics: the coefficient of permeability of the slope is larger than slopes with fractal dimension more than 2.6 (He et al., 2014). Therefore, under same rainfall conditions, more water infiltrated into the slope, which resulted in a raised pore-water pressure. Due to the continuous rainfall, the pore-water pressure increased a lot, and finally reached its peak value. The soil strength decreased to its minimal value, and the debris flow formed thereby. Theoretically, debris flow should be formed simultaneously with pore-water pressure reaching its peak value. Owing to the sensitivity of the sensors, it takes a period of time for the sensors to record the data, so

http://www.aloki.hu ● ISSN 1589 1623 (Print) ● ISSN 1785 0037 (Online)
DOI: http://dx.doi.org/10.15666/aeer/1704_75737589

the collected data lags behind the real situation. This is the reason why initiation of debris flow appeared to be ahead of the occurrence of peak pore water pressure. For slopes with fractal dimension more than 2.6, the infiltration capacity is relatively lower, little rainfall can infiltrate into the slope. Debris flow formed under such condition can be shown to be due to a run-off generated mechanism (Hu et al., 2016, 2014; Kean et al., 2013b; Yu et al., 2014). Superficial run-off erosion first generated a small erosion gully in the upper part of the slope and the eroded material was deposited in the lower part. The debris flow process initiated through saturation and breaching of this deposited material, which blocked the run-off water. Bed erosion and lateral erosion then continued to enlarge the erosion gully providing future material to the debris flow at lower concentrations. The subsequent erosion peaks with high debris-flow solid concentrations, were related to the cyclic damming by side-wall failures and dam breaching which enlarged the erosion gully, the size and the unit weight of the debris flow (Coe et al., 2008b; Kean et al., 2013a).

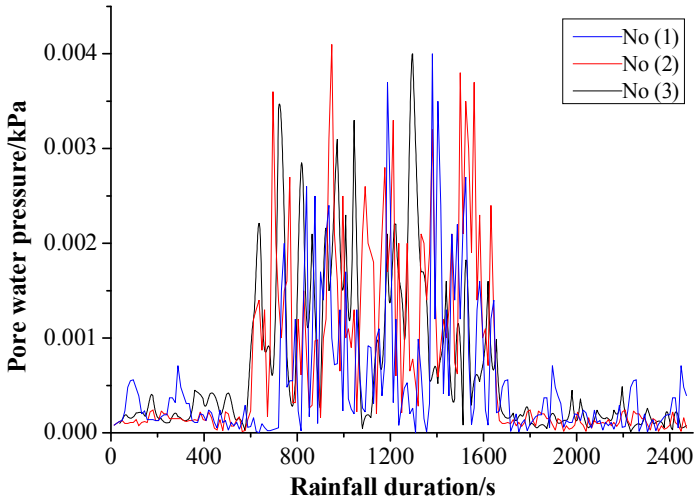

Figure 11. *Pore water pressure curves (slope with fractal dimension 2.35)*

The criticality is mainly due to the internal structure of the gravelly soil, which significantly influenced its coefficient of permeability and strength. When the fractal dimension is less than 2.4, the soil is constituted of coarse particles, and the strength is mainly determined by occlusal forces. Therefore, the permeability is larger and the strength is relatively higher, so the infiltrated water can be released freely without causing a pore-water pressure increase, and the slope can maintain its stability very well under continuous rainfall conditions. When the fractal dimension ranges from 2.4 to 2.6, cohesion forces and the internal friction angle both determined the soil strength, and the permeability coefficient allows water infiltrate into the slope and causes a pore-water pressure increase. The permeability coefficient is smaller than the rainfall intensity, so the rainfall will generate two types of water flow: internal flow and overland flow. The internal flow results in decreasing of soil strength, and the overland flow provides impact force to trigger debris flow. That is why slopes with fractal dimension ranges from 2.4 to 2.6 are more susceptible to debris flow. As the fractal dimension increases to more than 2.6, the soil structure properties are mainly governed by the fine particles. The soil strength is determined by the internal friction angle. Previous research found

http://www.aloki.hu ● ISSN 1589 1623 (Print) ● ISSN 1785 0037 (Online)
DOI: http://dx.doi.org/10.15666/aeer/1704_75737589

that water content has a slight influence on internal friction angle. Hence, soil strength decreased slightly during the whole rainfall duration. For soils with fractal dimension larger than 2.6, the coefficient of permeability is extremely small, and the precipitation mainly resulted in overland water flow. Under these circumstances, debris flow initiation is triggered by overland flow, and the mechanism can be understood using hydraulic theory.

Conclusions

From sampling and sieve testing the particle size distributions of the gravelly soil in debris flow source area can be established. With the aid of fractal theory, the fractal dimension of the samples can be computed and the fractal characteristics can be determined. Using the fractal characteristics of the gravelly soil, an in-situ artificial rainfall experiments were conducted, and some important findings were made. Following an analysis of the aforementioned experimental results, the following conclusions can be drawn:

(a) Gravelly soil in debris flow source area is mainly concentrated in one fractal dimension. The dimension value ranges from about 2.25 to 2.98. A close link between fractal dimension and particle size distribution was revealed: as fractal dimension increased, the particle composition tends to be more evenly.

(b) Our previous research established that the strength and permeability coefficient of gravelly soil is governed by fractal dimension (particle size composition or distribution). As fractal dimension increased, the permeability coefficient decreased (He et al., 2014).

(c) Gravelly soil manifests criticality, which means that slopes with fractal dimension less than 2.4 cannot (or can only with extremely low probability) mobilise into debris flow, regardless of rainfall intensity, duration or cumulative rainfall. Moreover, as the fractal dimension of the soil increases, the probability of the slope mobilising into debris flow becomes higher, and the unit weight of the formed debris flow becomes larger, ranging from dilute debris flow (unit weight less than 1.8 g/cm^3) to viscous debris flow (unit weight greater than 1.8 g/cm^3).

(d) As the fractal dimension falls into different intervals, the appropriate debris flow formation or initiation mechanism can be understood using different theories: For slopes with fractal dimension ranges from 2.4 to 2.6 and more than 2.6, the formation mechanism can be understood using soil mechanics and hydraulics theories, respectively.

(e) Debris flow initiation and peak pore-water pressure did not occur simultaneously. The initiation time always happened before the occurrence of peak pore-water pressure.

The results presents in this article provide a useful tool for debris flow forecast and prevention in the future. With the aim of improving the accuracy of debris flow prediction, the soil composition characteristics can be analyzed, and the fractal dimension of the soils can be computed. Comparing the fractal dimension with the results in this paper, a preliminary evaluation of the probability of debris flow initiation can be made. Furthermore, a comprehensive analysis of the slope angles, meteorological conditions and watershed features in the study area should be completed, then the scale, property and probable dynamic processes and dynamic characteristics of the potential debris flow can then be assessed. This can greatly

http://www.aloki.hu ● ISSN 1589 1623 (Print) ● ISSN 1785 0037 (Online)
DOI: http://dx.doi.org/10.15666/aeer/1704_75737589

improve the accuracy of prediction, and provide important information for disaster mitigation.

Acknowledgements. This work was financially supported by National Key R&D Program of China (No. 2018YFC1505205), the National Natural Science Foundation of China (41302284 &41661144028), and the doctoral fund of Henan Polytechnic University (Grant No B2015-58), and Henan Postdoctoral Foundation (Grant No.19030069).

REFERENCES

[1] Bacchini, M., Zannoni, A. (2003): Relations between rainfall and triggering of debris-flow: case study of Cancia (Dolomites, Northeastern Italy). – Natural Hazards and Earth System Science 3(1-2): 71-79.
[2] Bathurst, J. C., Burton, A., Ward, T. J. (1997): Debris flow run-out and landslide sediment delivery model tests. – Journal of Hydraulic Engineering 123(5): 410-419.
[3] Berti, M., Simoni, A. (2005): Experimental evidences and numerical modelling of debris flow initiated by channel runoff. – Landslides 2(3): 171-182.
[4] Brayshaw, D. H. M. A. (2009): Debris flow initiation and sediment recharge in gullies. – Geomorphology 109(3-4): 122-131.
[5] Cannon, S. H., Gartner, J. E., Rupert, M. G., Michael, J. A., Rea, A. H., Parrett, C. (2010): Predicting the probability and volume of postwildfire debris flows in the intermountain western United States. – Geological Society of America Bulletin 122(1-2): 127-144.
[6] Carpinteri, A., Lacidogna, G., Pugno, N. (2004): Scaling of energy dissipation in crushing and fragmentation: a fractal and statistical analysis based on particle size distribution. – International Journal of Fracture 129(2): 131-139.
[7] Chen, H., Lee, C. F. (2000): Numerical simulation of debris flows. – Canadian Geotechnical Journal 37(1): 146-160.
[8] Chen N. C., Wang, X., Di, B. (2004): Testing study on strength reduction of gravelly soil in triggering areaof debris flow under earthquake. – Chinese Journal of Rock Mechanics and Engineering 23(16): 2743-2747 (in Chinese).
[9] Chen, N. S., Zhou, W., Yang, C. L., Hu, G. S., Gao, Y. C., Han, D. (2010): The processes and mechanism of failure and debris flow initiation for gravel soil with different clay content. – Geomorphology 121(3-4): 222-230.
[10] Chen, Y. (1998): Fractal Geometry. – Earthquake Press, Beijing.
[11] Coe, J. A., Cannon, S. H., Santi, P. M. (2008a): Introduction to the special issue on debris flows initiated by runoff, erosion, and sediment entrainment in western North America. – Geomorphology 96(3): 247-249.
[12] Coe, J. A., Kinner, D. A., Godt, J. W. (2008b): Initiation conditions for debris flows generated by runoff at Chalk Cliffs, central Colorado. – Geomorphology 96(3): 270-297.
[13] Coussot, P., Meunier, M. (1996): Recognition, classification and mechanical description of debris flows. – Earth-Science Reviews 40(3): 209-227.
[14] Giannecchini, R., Naldini, D., Avanzi, G. D. A., Puccinelli, A. (2007): Modelling of the initiation of rainfall-induced debris flows in the Cardoso basin (Apuan Alps, Italy). – Quaternary International 171: 108-117.
[15] Giannecchini, R., Galanti, Y., D'Amato Avanzi, G., Barsanti, M. (2016): Probabilistic rainfall thresholds for triggering debris flows in a human-modified landscape. – Geomorphology 257: 94-107.
[16] Gregoretti, C., Degetto, M., Boreggio, M. (2016): GIS-based cell model for simulating debris flow runout on a fan. – Journal of Hydrology 534: 326-340.

http://www.aloki.hu ● ISSN 1589 1623 (Print) ● ISSN 1785 0037 (Online)
DOI: http://dx.doi.org/10.15666/aeer/1704_75737589

[17] He, N., Chen, N. S., Zhu, Y. H., Yang, J. Y., Yang, C. L. (2014): Experiment study of fractal feature and relationship between fractal dimension and permeability coefficient of gravelly soil in debris flow source area. – Yantu Lixue/Rock and Soil Mechanics 35(9): 2543-2548.
[18] He, S., Liu, W., Li, X. (2016): Prediction of impact force of debris flows based on distribution and size of particles. – Environmental Earth Sciences 75(4): 1-8.
[19] Ho, K., Leroi, E., Roberds, B. (2000): Quantitative Risk Assessment: Application, Myths and Future Direction. – International Society for Rock Mechanics, Lisbon.
[20] Hogan, D. L., Schwab, J. W. (1991): Stream channel response to landslides in the Queen Charlotte Islands, BC: changes affecting pink and chum salmon habitat. – Proceedings of the 15th Northeast Pacific Pink and Chum Salmon Workshop, Parksville, BC, pp. 222-236.
[21] Hu, W., Xu, Q., Rui, C., Huang, R. Q., Asch, T. W. J., Zhu, X., Xu, Q. Q. (2014): An instrumented flume to investigate the initiation mechanism of the post-earthquake huge debris flow in the southwest of China. – Bulletin of Engineering Geology and the Environment 74(2): 393-404.
[22] Hu, W., Dong, X. J., Xu, Q., Wang, G. H., van Asch, T. W. J., Hicher, P. Y. (2016): Initiation processes for run-off generated debris flows in the Wenchuan earthquake area of China. – Geomorphology 253: 468-477.
[23] Hungr, O., McDougall, S., Wise, M., Cullen, M. (2008): Magnitude–frequency relationships of debris flows and debris avalanches in relation to slope relief. – Geomorphology 96(3): 355-365.
[24] Hwang, S. I., Powers, S. E. (2003): Using particle-size distribution models to estimate soil hydraulic properties. – Soil Science Society of America Journal 67(4): 1103-1112.
[25] Iverson, R. M., LaHusen, R. G. (1989): Dynamic pore-pressure fluctuations in rapidly shearing granular materials. – Science 246(4931): 796-799.
[26] Iverson, R. M., Reid, M. E., LaHusen, R. G. (1997): DEBRIS-FLOW MOBILIZATION FROM LANDSLIDES 1. – Annual Review of Earth and Planetary Sciences 25(1): 85-138.
[27] Jakob, M. (2005): A size classification for debris flows. – Engineering Geology 79(3): 151-161.
[28] Johnson, A. C., Swanston, D. N., McGee, K. E. (2000): Landslide initiation, runout, and deposition within clearcuts and old-growth forests of Alaska. – JAWRA Journal of the American Water Resources Association 36(1): 17-30.
[29] Kean, J. W., McCoy, S. W., Tucker, G. E., Staley, D. M., Coe, J. A. (2013): Runoff-generated debris flows: Observations and modeling of surge initiation, magnitude, and frequency. – Journal of Geophysical Research: Earth Surface 118(4): 2190-2207.
[30] Li, Y., Liu, J., Chen, X., Wei, F. (2007): Grain composition and erosive equilibrium of debris flows. – Journal of Mountain Science 4(1): 71-76.
[31] Liu, C.-N., Dong, J.-J., Peng, Y.-F., Huang, H.-F. (2009): Effects of strong ground motion on the susceptibility of gully type debris flows. – Engineering Geology 104(3): 241-253.
[32] Lu, Y. (2013): Study for the effect mode and mechanism of Earthquakes & droughts on debris flows. – Doctorate. University of Chinese Academy of Sciences, Huairou, China.
[33] MacDonald, A., Maurice, L., Dobbs, M., Reeves, H., Auton, C. (2012): Relating in situ hydraulic conductivity, particle size and relative density of superficial deposits in a heterogeneous catchment. – Journal of Hydrology 434: 130-141.
[34] Maggioni, V., Nikolopoulos, E. I., Marra, F., Destro, E., Borga, M. (2016): Satellite-rainfall estimation for identification of rainfall thresholds used for landslide/debris flow prediction. – Proceedings EGU General Assembly Conference Abstracts 18: 15006.
[35] Miller, D. J., Burnett, K. M. (2008): A probabilistic model of debris-flow delivery to stream channels, demonstrated for the coast range of Oregon, USA. – Geomorphology 94(1): 184-205.

http://www.aloki.hu ● ISSN 1589 1623 (Print) ● ISSN 1785 0037 (Online)
DOI: http://dx.doi.org/10.15666/aeer/1704_75737589

[36] Ningsheng, C., Peng, C., Xiaoying, W., Baofeng, D. (2004): Testing study on strength reduction of gravelly soil in triggering area of debris flow under earthquake. – Chinese Journal of Rock Mechanics and Engineering, 23(16): 2743-2747 (Chinese paper).
[37] Papa, M., Medina, V., Ciervo, F., Bateman, A. (2013): Derivation of critical rainfall thresholds for shallow landslides as a tool for debris flow early warning systems. – Hydrology and Earth System Sciences 17(10): 4095-4107.
[38] Park, D. W., Lee, S. R., Vasu, N. N., Kang, S. H., Park, J. Y. (2016): Coupled model for simulation of landslides and debris flows at local scale. – Natural Hazards 1-30.
[39] Saito, H., Nakayama, D., Matsuyama, H. (2010): Relationship between the initiation of a shallow landslide and rainfall intensity—duration thresholds in Japan. – Geomorphology 118(1): 167-175.
[40] Shimizu, H., Murata, S., Ishida, T. (2011): The distinct element analysis for hydraulic fracturing in hard rock considering fluid viscosity and particle size distribution. – International Journal of Rock Mechanics and Mining Sciences 48(5): 712-727.
[41] Smadja, J. (1992): Studies of climatic and human impacts and their relationship on a mountain slope above Salme in the Himalayan Middle Mountains, Nepal. – Mountain Research and Development 12(1): 1-28.
[42] Turkington, T., Remaître, A., Ettema, J., Hussin, H., Westen, C. (2016): Assessing debris flow activity in a changing climate. – Climatic Change 137(1): 1-13.
[43] Varnes, D. J. (1978): Slope Movement Types and Processes. – Transportation Research Board Special Report, Washington, DC.
[44] Wang, G., Sassa, K. (2003): Pore-pressure generation and movement of rainfall-induced landslides: effects of grain size and fine-particle content. – Engineering Geology 69(1): 109-125.
[45] Wang, Y., Zhao, B., Li, J. (2017): Mechanism of the catastrophic June 2017 landslide at Xinmo Village, Songping River, Sichuan Province, China. – Landslides 4: 1-13.
[46] Yang, D., Herath, S., Musiake, K. (2002): A hillslope-based hydrological model using catchment area and width functions. – Hydrological Sciences Journal 47(1): 49-65.
[47] Yang, Z.-Y., Pourghasemi, H. R., Lee, Y.-H. (2016): Fractal analysis of rainfall-induced landslide and debris flow spread distribution in the Chenyulan Creek Basin, Taiwan. – Journal of Earth Science 27(1): 151-159.
[48] Yong, L., Xiaoqing, C., Kaiheng, H., Shufen, H. (2005): Fractality of grain composition of debris flows. – Journal of Geographical Sciences 15(3): 353-359.
[49] Yong, L., Xiaojun, Z., Pengcheng, S., Yingde, K., Jingjing, L. (2013): A scaling distribution for grain composition of debris flow. – Geomorphology 192: 30-42.
[50] Yu, B., Zhu, Y., Wang, T., Chen, Y., Zhu, Y., Tie, Y., Lu, K. (2014): A prediction model for debris flows triggered by a runoff-induced mechanism. – Natural Hazards 74(2): 1141-1161.
[51] Zhang, S. J., Wei, F. Q., Liu, D., Yang, H. J., Jiang, Y. H. (2014a): A regional-scale method of forecasting debris flow events based on water-soil coupling mechanism. – Journal of Mountain Science 11(6): 1531-1542.
[52] Zhang, S., Yang, H., Wei, F., Jiang, Y., Liu, D. (2014b): A model of debris flow forecast based on the water-soil coupling mechanism. – Journal of Earth Science 25(4): 757-763.
[53] Zhou, X., Cui, P., Li, Z. (2012): Development and application of integrated test equipment for permeability and settlement of gravelly soil in triggering area of debris flow. – Chinese Journal of Rock Mechanics and Engineering 31(6): 1281-1289.

http://www.aloki.hu ● ISSN 1589 1623 (Print) ● ISSN 1785 0037 (Online)
DOI: http://dx.doi.org/10.15666/aeer/1704_75737589

THE EFFECTS OF NITROGEN AND ZINC APPLICATIONS ON THE YIELD, YIELD COMPONENTS AND OIL RATIO OF SAFFLOWER (*Carthamus tinctorius* L.) UNDER SEMI-ARID CONDITIONS

HALILOGLU, H.[1*] – BEYYAVAS, V.[2]

[1]*Department of Field Crops, Faculty of Agriculture, Harran University, Sanliurfa, Turkey*

[2]*Suruc Vocational College, Harran University, Sanliurfa, Turkey*

**Corresponding author*
e-mail: haliloglu@harran.edu.tr; phone: +90-530-205-0794

(Received 6th Mar 2019; accepted 3rd May 2019)

Abstract. This study was conducted in order to determine the effect of Nitrogen (N) and Zinc (Zn) on the yield, yield components and oil ratio of safflower under semi-arid conditions in 2011-2012 and 2012-2013 growing seasons. Field trials was established in the randomized complete blocks design split plots with three replications in the experimental area Department of Field Crops of Agricultural Faculty, Harran University in Turkey. In the study, N applications (N_0 = no fertilization, N_5 = 50 kg ha^{-1}, N_{10} = 100 kg ha^{-1} and N_{15} = 150 kg ha^{-1}) were placed in the main plots, Zn applications (Zn_0 = no fertilization, Zn_1 = 10 kg ha^{-1}, Zn_2 = 20 kg ha^{-1} and Zn_3 = 30 kg ha^{-1}) were in the sub-plots. Seed yield (kg ha^{-1}), seed yield per plant (g plant^{-1}), plant height (cm), number of heads per plant (pieces plant^{-1}), number of seeds per head (pieces head^{-1}), 1000 seeds weight (g), dry petal yield (g plant^{-1}), oil ratio (%) and biomass yield (kg ha^{-1}) were examined in the study. The results indicated that; the highest seed yields were obtained from the N_{15} (1171 and 1651 kg ha^{-1}) and Zn_3 (1233 and 1675 kg ha^{-1}) applications in both years. N applications comparing control plots affected the yield per plant, plant height, number of heads per plant, number of seeds per head, 1000 seed weight and biomass yield, had negative effect on the dry petal yield and oil ratio. Zn applications according to control plots whereas had positive effects on the seed yield per plant and number of heads per plant but had no significant effect on the dry petal yield and oil ratio. NxZn interactions affected the seed yield, number of heads per plant, number of seeds per head and biomass yield. 150 kg N ha^{-1} and 30 kg Zn ha^{-1} should be given to safflower under semi-arid conditions.

Keywords: *Carthamus, nutrients, dry petal, oil ratio, interaction*

Introduction and literature review

Sanliurfa is the hottest province of Southeastern Anatolia Region in Turkey. Harran Plain is located in the Sanliurfa city where continental climate, summers are very hot and dry and the winter are relatively temperate (Kose et al., 2018). Average annual rainfall is around 350-400 mm. Most of the rainfall falls in the winter season. Therefore, it is great important to cultivate drought-resistant plants in areas where irrigation is not possible. Safflower plant can be grown in this region under drought.

Safflower plant (*Carthamus tinctorius* L.) has quite various usage by stem, leaves, seeds and flowers. It is a very important industrial plant neglected and could not reach the place deserved. It is an historical species and it was cultivated in the Middle East 3000 years ago (Knowles, 1982). All parts of the plant are used in the treatment of various illnesses in India and Pakistan (Nimbkar, 2002). The flowers are used in the food, cosmetic, dye and pharmaceutical industries (Dajue and Mundel, 1996; Abd El-Mohsen and Mahmoud, 2013). Safflower was reported to be one of the alternative

http://www.aloki.hu ● ISSN 1589 1623 (Print) ● ISSN 1785 0037 (Online)
DOI: http://dx.doi.org/10.15666/aeer/1704_75917604

plants that can be considered in irrigated areas with its tolerance to salinity and weeds, and especially due to its high tolerance to cold and heat climatic conditions in arid regions (Emongor et al., 2015).

Safflower (*Carthamus tinctorius* L.) is one of the most important annual oil plants to be grown in winter season (Eslam, 2010; Gursoy et al., 2018). It is more resistant to drought and lower temperatures than other non-selective oil crops in terms of growth requirements safflower can also be grown in fallow areas especially in arid regions (Johnson et al., 1993). Due to these properties, safflower can be an alternative crop in crop rotation vs. wheat, barley, lentil and tobacco. It can help to alleviate the shortage of vegetable oil demand of Turkey (Eryigit et al., 2015; Kose, 2017). Safflower has yellow, red, orange and cream-colored flowers with thorny and thorn less forms, and it has been used for he production of edible oil and biofuels having 30-45% fat on average in its seeds (Demir and Kara, 2018).

Safflower seeds contain 13-46% oil, about 90% of this oil consisted of unsaturated fatty acids (oleic and linoleic acid) (Johnson et al., 1993; Belgin et al., 2007). Safflower oil containing an average of 75% linoleic acid (Weiss, 2000), and there are also its antioxidant effects and tocopherols with high vitamin E values. Therefore, safflower oil is used in diets applied by cardiovascular patients and has a great importance because of its anti-cholesterol effects (Pongracz et al., 1995).

Safflower petals are very important as a source of medicinal preparations, natural food colour and dyes for colouring fabrics. In addition to the colouring properties, safflower petals are used for curing several chronic diseases such as hypertension, coronary heart ailments, rheumatism and male and female fertility problems (Rajvanshi, 2005).

Since the safflower oil is suitable for biodiesel production, intensive researches on biodiesel production from safflower oil are carried out (Ogut and Oguz, 2006; Nosheen et al., 2011). The cartharmia substance obtained from the safflower is great important as a natural dye raw material (Nagaraj et al., 2001; Emongor, 2010). Especially the petals are used as food dyes and spices have potential to increase income from the unit area in the arid regions (Esendal, 2001).

In addition, some plant nutrients were found to be effective together with irrigation in direct to yield and yield components. Two of these important nutrients are nitrogen and zinc.

Nitrogen fertilizers are one of the important inputs in dry rainfed agricultural systems. In order to obtain optimum yield and quality product in these regions, sufficient amount of nitrogen in suitable time and form should be given to the plant. Excessive or insufficient N fertilizer applications result in some economic losses, excessive nitrogen application causes environmental problems over time (Grant, 2006). It was reported by many researches that the nitrogen fertilizer affected on the safflower growth, yield and quality properties significantly (Ahmed et al., 1985; El-Nakhlawy, 1991; Ibrahim, 1994). N fertilization increased seed yield (Strasil and Vorlicek, 2002); 300, 600 and 900 kg ha^{-1} N applications according to the control plots increased the biomass of safflower by 13.4%, 15.3% and 22.9% respectively (Haghighati, 2010). Nitrogen was effective on the vegetative and reproductive stages of safflower (Bitarafan et al., 2011); nitrogen applications increased seed yield 44.6-60.5% on average compared to the control plots (Singh and Singh, 2013); seed yield, 1000 seed weight, number of heads per plant and plant height were affected positively (Eryigit et al., 2015), and plant height and seed yield were increased (Revant Nathan et al., 2018) by

http://www.aloki.hu ● ISSN 1589 1623 (Print) ● ISSN 1785 0037 (Online)
DOI: http://dx.doi.org/10.15666/aeer/1704_75917604

the nitrogen fertilization. The effect of nitrogen may vary according to the amount, time and form of the application.

Zinc applications exhibited positive effect on the oil yield and seed quality, and besides, do the plant more resistant to drought conditions were reported by many researchers (Mengel, 2001; Khoshgoftarmanesh, 2010; Taha et al., 2013). Zinc has an important effect on the oil yield and quality, seed yield and biomass production (Lewis and McFarlane, 1986); Zinc sulphate application under water stress conditions increased seed yield, biomass and biological yield than control plots (Lakzayi, 2015); zinc application comparing central increased seed yield and number of heads per plant (Gulmezoglu and Aytac, 2016).

In this study, it is important to determine the effect of N and Zinc separately and in combination on the safflower crop under semi-arid climate conditions in the Harran Plain conditions. There have not been done such a study before under Harran plain conditions, because of that this study is important. As it is known, the genotypic structure of each plant is affected more or less from the environmental factors. The dose of the plant nutrient that is applied in a region has a good result, may not work well under any other environmental conditions. Therefore, it is great important to conduct these studies and determine the most appropriate doses in every ecological condition.

This study was carried out to asses the appropriate doses of the nitrogen and zinc on to seed yield and seed quality as well as disseminate the cultivation of safflower under semi-arid climatic conditions.

Materials and methods

Remzibey-05 safflower cultivar with yellow flowers, spiny leaves and head was used as plant material. The experimental area has a flat topography. It is well-drained deep, stone-free, with high clay content (54-56%). Soil pH is between 7.3-7.2, the salt content is 0.088-0.092%, and low in organic material 1.25-1.19%. In addition, the amount of pure N 25-19 kg ha^{-1}, P_2O_5 amount of pure 27-30 kg ha^{-1} and K_2O 1086-1129 kg ha^{-1} was determined (*Table 1*).

Table 1. *Some soil properties of experimental area (Anonymous, 2012)*

Years	Total Salt (%)	Lime (%)	Sand (%)	Clay (%)	Silt (%)	Organic Matter (%)	pH	N (kg ha^{-1})	P_2O_5 (kg ha^{-1})	K_2O (kg ha^{-1})
2011	0.088	5.1	25.12	54	20.20	1.25	7.3	25	27	1086
2012	0.092	5.4	26.03	56	20.32	1.19	7.2	19	30	1129

Field trials were setup employing according to the randomized complete block design split plots with three replications in the experimental area Department of Field Crops of Agricultural Faculty, Harran University Eyyubiye Campus (37°06'59.1" N 38°49'15.8" E) (altitude = 510 m from sea level) (*Fig. 1*).

Each plot consisted of 5 m long with 5 rows. Inter-row and intra-row spaces were 35 and 15 cm respectively (*Fig. 2*). After experimental area had been ploughed, herbicide (*Trifluarin* active ingredient) was applied by a sprayer before planting. Then, Disk-harrowing was practiced for trial seedbed preparation tillage.

The sowing was practiced on 5th November, 2011 and 3th November, 2012 by the experimental drill. 2 m alley was left between each plot. After the emergence, thinning

http://www.aloki.hu ● ISSN 1589 1623 (Print) ● ISSN 1785 0037 (Online)
DOI: http://dx.doi.org/10.15666/aeer/1704_75917604

was practised in the stages of 3 or 4 leaves. The cultural practices (hoeing, weeding and pest management) were performed when needed in accordance with the conventional methods.

Figure 1. *The map of the experimental area*

Figure 2. *Experimental area*

In both growing seasons, total precipitation occurred close to each other. The average temperature (13.76 °C) for the 2011-2012 growing season was very close to the average for long years (13.68 °C), but the average temperature for the 2012-2013 growing period (15.31 °C) was higher than the average of the first year and long years of the experiment (*Table 2*). The higher average temperature in the second year of the

http://www.aloki.hu ● ISSN 1589 1623 (Print) ● ISSN 1785 0037 (Online)
DOI: http://dx.doi.org/10.15666/aeer/1704_75917604

experiment and the higher monthly precipitation, especially in May, may have caused the better development of the plant.

Table 2. *Some of meteorological characteristics for long term (1929-2013) and 20011-2013 period in Sanliurfa, Turkey (Anonymous, 2013)*

	2011-2012			2012-2013			1929-2013
Months	**Average monthly temp. (°C)**	**Precipitation (kg m^{-2})**	**Average relative humidity (%)**	**Average monthly temp. (°C)**	**Precipitation (kg m^{-2})**	**Average relative humidity (%)**	**Average of long-term (°C)**
November	9.4	62.1	53.7	14.9	68.4	65.6	12.9
December	7.4	47.1	57.4	8.3	142.8	73.0	7.5
January	5.5	170.9	81.0	6.8	86.8	69.5	5.4
February	5.8	95.8	57.0	9.3	107.2	73.6	6.8
March	9.7	35.8	47.3	12.9	12.1	-	10.7
April	19.3	23.3	42.4	18.4	18.0	44.9	16.0
May	22.4	42.3	40.8	22.9	56.2	43.4	22.1
June	30.6	5.8	21.2	29.0	-	24.0	28.0
Average	13.76		50.1	15.31		49.25	13.68
Total		483.1			491.5		

In the study, N applications (N_0 = no fertilization, N_5 = 50 kg ha^{-1}, N_{10} = 100 kg ha^{-1} and N_{15} = 150 kg ha^{-1}) were placed in the main plots, Zn applications were assigned in the sub-plots (Zn_0 = no fertilization, Zn_1 = 10 kg ha^{-1}, Zn_2 = 20 kg ha^{-1} and Zn_3 = 30 kg ha^{-1}). Half of the nitrogen was applied in the form of Ammonium Sulphate (21%) with the sowing, the remaining half in the form of ammonium nitrate (33%) at the branching stage. All the zinc in the form of ZnSO4 7H_2O (23%) was applied with the sowing in 5-6 cm next to the plant rows and 5-6 cm deep by hand. Superphosphate (pure phosphorus 80 kg ha^{-1}) was applied as basal fertilizer at sowing.

Harvest was performed by hand for the seed and biomass yield from the remaining area (4 m × 1.05 m = 4.2 m^2) by thrown away the side effects of 0.5 m at the beginning and end of 3 rows in the middle of each plots on 5th June, 2013 and 6th June, 2013. Seed yield per plant (g plant^{-1}), plant height (cm), number of heads per plant (pieces plant^{-1}), number of seeds per head (pieces head^{-1}), 1000 seed weight (g) and dry petal yield (g plant^{-1}) were determined on randomly selected 10 plants (Esendal et al., 1992). A sufficient amount of seed (10 g) was grinded for each application and dried in the oven at 70 °C for 72 hours. 5 g of each sample boiled for 6 hours by using hexane in soxhlet extraction device and so on oil ratios (%) were scored.

The data was subjected to analysis of variance utilizing the JMP 11 (SAS Institute 2013, USA) statistical program in the randomized complete blocks design split plots and averages were grouped by the Tukey HSD test ($p \leq 0.05$).

Results and discussion

In the analysis of variance (ANOVA) according to the combined years of the properties examined in the trial, statistical differences were found between years. Due to that the results of each year were analyzed separately.

http://www.aloki.hu ● ISSN 1589 1623 (Print) ● ISSN 1785 0037 (Online)
DOI: http://dx.doi.org/10.15666/aeer/1704_75917604

Seed yield (kg ha^{-1})

N_{15} application gave the highest seed yield (1171 and 1651 kg ha^{-1}) in both years of the experiment. Strasil and Vorlicek (2002), Singh and Singh (2013), Eryigit et al. (2015) and Revant Nathan et al. (2018) reported that the nitrogen fertilization increased yield is consistent with the research results. The highest seed yield in Zn application was obtained from the Zn_3 application (1233 and 1675 kg ha^{-1}) in both years. Taha et al. (2013), Lakzayi (2015) and Gulmezoglu and Aytac (2016) observed that the zinc applications increased seed yield comparing to the control. In the first year of the experiment N_{15} x Zn_3 interaction (1463 kg ha^{-1}), in the second year N_0 x Zn_3 (1887 kg ha^{-1}), N_{10} x Zn_2 (1865 kg ha^{-1}) and N_{15} x Zn_3 (1900 kg ha^{-1}) interactions gave the highest seed yield (*Table 3*). N_{15} x Zn_3 interaction gave the highest seed yield (1463 and 1900 kg ha^{-1}) in both years shows that the application in these doses increase the seed yield. High yield in second year comparing that of first year can be attributed to fluctuating climate and environmental factors.

Seed yield per plant (g plant^{-1})

Statistically significant differences were found between N and Zn applications in both years. N_{15} (8.44 and 11.98 g) and Zn_3 (8.68 and 11.25 g) applications gave the highest seed yield per plant in both years. In general, obtained the better yields in the second year than the first year can be attributed to environmental and climatic conditions. N_{15} x Zn_3 interaction gave the highest seed yield (10.83 and 13.57 g) in both years indicates that the application at these doses increases seed yield per plant (*Table 3*).

Seed yield per plant is a factor that directly affects seed yield per hectare. As a matter of fact, the highest values obtained from the N_{15} and Zn_3 applications for seed yield per hectare confirmed the research results. Eryigit et al. (2015) and Revant Nathan et al. (2018) reported that the nitrogen fertilization increased seed yield per plant, and Taha et al. (2013); Gulmezoglu and Aytac (2016) zinc fertilization as well.

Plant height (cm)

N_5 application (142.0 cm) in the first year, N_{15} application (141.6 cm) in the second year gave the highest plant height values (*Table 1*). Khalil et al. (2013) and Eryigit et al. (2015) report that the nitrogen fertilization increases plant height which was consistent with the research results. Similar results were also reported by Katar et al. (2012) and Bitarafan et al. (2011).

As the zinc applications had not any effects on the plant height in the first year, Zn_2 application gave the highest plant height (140.3 cm) in the second year. N_5 x Zn_2 interaction (144.8 cm) in the first year, N_0 x Zn_3 (143.3 cm) and N_5 x Zn_2 (143.0 cm) interactions in the second year gave the highest plant height scores (*Table 3*).

Plant height is significantly affected by environmental factors. The highest plant height scores from the different applications in both years can be due to the fact that the plants grow in all kinds of natural areas that are open to various impacts and they are very much under different environmental conditions during the growth and development periods (Arslan and Bayraktar, 2015). However, the highest plant height from the N_5 x Zn_2 (144.8 and 143.0 cm) interaction in both years showed that the application at these doses increases the plant height.

http://www.aloki.hu ● ISSN 1589 1623 (Print) ● ISSN 1785 0037 (Online)
DOI: http://dx.doi.org/10.15666/aeer/1704_75917604

Table 3. *Averages and groups of main (N), sub variables (Zn) and interactions (NxZn) for seed yield (kg ha^{-1}), seed yield per plant (g plant^{-1}) and plant height (cm)*

Treatments		Seed yield (kg ha^{-1})		Seed yield per plant (g plant^{-1})		Plant height (cm)	
N		**2011-12**	**2012-13**	**2011-12**	**2012-13**	**2011-12**	**2012-13**
N_0		1045 b*	1612 b*	8.07 a*	9.85 c*	139.7 b*	140.1 b*
N_5		985 c	1565 c	6.55 b	11.10 ab	142.0 a	139.1 b
N_{10}		1147 a	1594 b	8.43 a	10.14 bc	139.6 b	135.3 c
N_{15}		1171 a	1651 a	8.44 a	11.98 a	138.2 b	141.6 a
Zn		**2011-12**	**2012-13**	**2011-12**	**2012-13**	**2011-12**	**2012-13**
Zn_0		1110 b*	1473 c*	8.03 b*	10.65 b*	140.4 ns	138.4 bc*
Zn_1		1020 c	1674 a	7.83 b	11.35 a	140.2	137.6 c
Zn_2		985 c	1602 b	6.94 c	9.81 c	139.4	140.3 a
Zn_3		1233 a	1675 a	8.68 a	11.25 a	139.5	139.7 ab
Interactions		**2011-12**	**2012-13**	**2011-12**	**2012-13**	**2011-12**	**2012-13**
N_o	Zn_0	1207 bcd*	1461 gh*	8.54 b*	10.57cd*	140.6 abc*	138.2 b-f*
	Zn_1	1158 b-e	1698 c	7.69 bd	11.31 bc	138.5 bc	136.7 c-g
	Zn_2	984 gh	1560 de	7.57 bcd	10.30 cd	139.4bc	142.3 ab
	Zn_3	1243 b	1887 a	8.49 bce	12.65 ab	140.2 abc	143.3 a
N_5	Zn_0	1015 fg	1414 h	6.58 cde	10.35 cd	139.2 bc	139.9 a-e
	Zn_1	894 h	1599 d	6.56 de	9.25 d	141.6 ab	136.2 efg
	Zn_2	921 gh	1564 de	6.14 e	9.90 cd	144.8 a	143.0 a
	Zn_3	1111 de	1683 c	6.92 cde	13.67 a	142.5 ab	137.4 c-g
N_{10}	Zn_0	1209 bc	1494 fg	8.79 b	10.52 cd	142.6 ab	133.3 g
	Zn_1	923 gh	1790 b	8.99 b	10.31 cd	142.6 ab	136.6 d-g
	Zn_2	932 gh	1865 a	7.94 bcd	9.56 d	135.5 c	135.3 fg
	Zn_3	1115 cde	1228 ı	8.00 bcd	10.14 cd	137.6 bc	135.8 efg
N_{15}	Zn_0	1012 fg	1523 ef	8.72 b	10.44 cd	139.1 bc	142.3 ab
	Zn_1	1106 ef	1607 d	8.08 bc	10.22 cd	138.1 bc	141.0 abc
	Zn_2	1105 ef	1419 h	6.13 e	9.48 d	137.9 bc	140.8 a-d
	Zn_3	1463 a	1900 a	10.83 a	13.57 a	137.6 bc	142.5 ab
CV %		13.74	11.61	16.22	10.12	10.96	12.40
				F value			
	N	85.97 **	42.61 **	37.40 **	51.03 **	9.38 **	44.19 **
	Zn	141.55 **	295.95 **	24.63 **	27.01 **	0.97 ns	8.90 **
	NxZn	34.05 **	379.11 **	9.28 **	15.70 **	5.73 **	7.88 **

*Means followed by different letters within columns are significantly different ($p \leq 0.05$)
*$p \leq 0.05$, **$p \leq 0.01$, ns: non-significant

Number of heads per plant (pieces plant^{-1})

N_{10} application gave the highest number of heads per plant (17.7 pcs plant^{-1}) in the first year, N_{15} application gave the highest number of heads per plant (21.2 pcs plant^{-1}) in the second year. Bitarafan et al. (2011) and Eryigit et al. (2015) reported that nitrogen fertilization increases the number of heads per plant. In the first year of the experiment Zn_3 (18.7 pcs plant^{-1}), in the second year Zn_1 and Zn_3 applications (20.3 pcs plant^{-1})

http://www.aloki.hu ● ISSN 1589 1623 (Print) ● ISSN 1785 0037 (Online)
DOI: http://dx.doi.org/10.15666/aeer/1704_75917604

gave the highest number of heads per plant. Gulmezoglu and Aytac (2016) declared that Zinc application increased the number of heads per plant compared to the control plots in a research which was consistent with the research results. $N_{10}xZn_1$ (19.7 pcs plant^{-1}) and $N_{10}xZn_3$ (19.6 pcs plant^{-1}) interactions in the first year of the experiment, N_5xZn_3 (22.8 pcs plant^{-1}) in the second year gave the highest number of heads per plant (*Table 4*).

Table 4. *Averages and groups of main (N), sub variables (Zn) and interactions (NxZn) for number of heads per plant (pieces plant^{-1}), number of seeds per head (pieces head^{-1}) and 1000 seed weight (g)*

Treatments		**Number of heads per plant (pieces plant^{-1})**		**Number of seeds per head (pieces head^{-1})**		**1000 seed weight (g)**	
N		**2011-12**	**2012-13**	**2011-12**	**2012-13**	**2011-12**	**2012-13**
N_0		17.5 ab*	19.2 b*	14.3 ab*	11.7 b*	29.11 ab*	28.77 b*
N_5		16.9 b	19.2 b	12.5 b	11.6 b	27.86 b	29.45 ab
N_{10}		17.7 a	18.7 b	14.5 a	12.6 a	29.76 ab	29.85 a
N_{15}		17.2 b	21.2 a	15.5 a	12.9 a	30.01 a	29.88 a
Zn		**2011-12**	**2012-13**	**2011-12**	**2012-13**	**2011-12**	**2012-13**
Zn_0		17.3 b*	19.6 b*	14.8 ab*	12.4^{ns}	29.68^{ns}	29.94 a*
Zn_1		17.2 b	20.3 a	13.2 b	12.2	29.80	29.25 ab
Zn_2		16.1 c	18.2 c	13.2 b	12.3	28.58	28.62 b
Zn_3		18.7 a	20.3 a	15.6 a	11.9	28.69	30.15 a
Interaction		**2011-12**	**2012-13**	**2011-12**	**2012-13**	**2011-12**	**2012-13**
N_o	Zn_0	17.2 cde*	22.1 ab*	15.5 abc*	12.0 d-g*	30.73^{ns}	30.97 ab*
	Zn_1	18.8 ab	20.2 b-e	13.2 bc	12.1 c-f	29.33	28.98 ab
	Zn_2	16.2 efg	19.6 efg	13.1 bc	11.1 efg	28.07	28.94 ab
	Zn_3	17.7 bcd	22.1 abc	15.9 abc	11.1 efg	28.32	29.88 ab
N_5	Zn_0	18.5 abc	17.9 gh	11.3 c	11.7 d-g	27.97	29.05 ab
	Zn_1	15.5 fg	21.7 a-d	13.0 bc	10.6 fg	27.98	28.90 ab
	Zn_2	16.4 d-g	15.4 ı	12.9 bc	13.8 abc	27.70	28.88 ab
	Zn_3	17.3 cde	22.8 a	12.9 bc	10.4 g	27.81	31.72 a
N_{10}	Zn_0	19.0 ab	18.0 fgh	14.1 abc	12.7 b-e	29.37	29.66 ab
	Zn_1	19.7 a	19.3 e-h	14.2 abc	14.0 ab	31.20	30.59 ab
	Zn_2	15.3 g	20.0 def	14.5 abc	12.5 b-e	29.12	28.53 b
	Zn_3	19.6 a	17.6 h	15.4 abc	11.1 efg	29.33	30.64 ab
N_{15}	Zn_0	16.8 def	20.3 b-e	18.1 ab	13.2 a-d	30.67	29.33 ab
	Zn_1	15.4 g	20.1 cde	12.4 c	12.0 d-g	30.67	28.52 b
	Zn_2	16.3 d-g	17.8 gh	12.3 c	11.7 d-g	29.42	28.10 b
	Zn_3	17.3 cde	18.7 e-h	19.0 a	14.7 a	29.30	29.12 ab
CV %		8.56	10.38	17.26	10.60	5.93	4.20
				F value			
	N	5.98 *	33.28 **	5.21 *	16.84 **	4.40 *	3.53 *
	Zn	62.12 **	28.05 **	5.54 *	1.81 ns	2.09 ns	6.37 *
	NxZn	24.18 **	26.38 **	3.32 *	19.65 **	0.46 ns	2.24 ns

*Means followed by different letters within columns are significantly different ($p \leq 0.05$)
*$p \leq 0.05$, **$p \leq 0.01$, ns: non-significant

http://www.aloki.hu ● ISSN 1589 1623 (Print) ● ISSN 1785 0037 (Online)
DOI: http://dx.doi.org/10.15666/aeer/1704_75917604

The most important selection criteria for seed yield was the number of heads per plant. The number of heads is a property that is affected by the plant genetic structure, sowing density, fertilization and other environmental factors. Implemented that the difference between the results and applications of other researchers in terms of number of heads per plant could be caused by the variations in climate and soil structure of the location where the research was carried out and cultivar, and the differences between different cultural techniques, sowing and harvest dates.

Number of seeds per head (pieces head^{-1})

N_{10} and N_{15} applications gave the highest number of seeds per head in both years. The highest number of seeds per head by the nitrogen fertilization increased seed yield per plant, and therefore contributed positively to the seed yield per hectare in the trial. Strasil and Vorlicek (2002); Singh and Singh (2013) and Eryigit et al. (2015) reported that the nitrogen fertilization increased yield was consistent with our research results. As the Zn_3 application gave the highest number of seeds per head (15.6 pcs head^{-1}) in the first year, there were no statistically significant differences between the applications in the second year. N_{15}xZn_3 interaction gave the highest number of seeds per head (19.0 and 14.7 pcs head^{-1}) in two years (*Table 4*).

When examined the interactions, N_{15} x Zn_3 interactions was promising. Bitarafan et al. (2011) indicated that nitrogen was effective in vegetative and reproductive development; Soleymani and Shahrajabian (2011), nitrogen increased the number of seeds per head, and Lewis and McFarlane (1986), Zn had an important role on the oil yield and quality, seed yield and biomass production are compatible with the research results. The number of seeds per head as well as the number of heads per plant were the important criterion for yield. The number of seeds per head was directly related to the head size and that can be affected fairly by genetic and environmental factors. Although an average of 100 flowers were formed in each safflower head, 20% of these flowers formed seed (Baydar, 2000).

1000 seed weight (g)

N_{15} application (30.01 g) in the first year of the experiment, N_{10} and N_{15} applications (29.85 and 29.88 g) in the second year gave the highest 1000 seed weight. Nitrogen fertilization gave the more 1000 seed weight values than control plots in both years. Bitarafan et al. (2011); Khalil et al. (2013) and Eryigit et al. (2015) reported that nitrogen doses increased 1000 seed weight comparing the control. Although Zn applications were insignificant in the first year, Zn_0 and Zn_3 applications (29.94 and 30.15 g) gave the maximum 1000 seed weight values in the second year. At the same time, N x Zn interactions were in non-significant in the first year, N_5 x Zn_3 interaction gave the highest 1000 seed weight (31.72 g) in the second year (*Table 4*). These differences between years might be due to different soil and climate factors.

Dry petal yield (g plant^{-1})

The highest petal yields (1.12 and 1.19 g) were obtained from control N_0 subject according to the N application, from the Zn_0 (1.17 and 1.27 g) subject according to the Zn application in both years. N_0 x Zn_1 and N_{10} x Zn_0 interactions gave the highest petal yield in the first (1.47 and 1.45 g) and second year (1.70 and 1.65 g) (*Table 5*). Control

http://www.aloki.hu ● ISSN 1589 1623 (Print) ● ISSN 1785 0037 (Online)
DOI: http://dx.doi.org/10.15666/aeer/1704_75917604

plots created more petal yields. This indicated that N and Zn applications had negative effects on the petal yields.

Table 5. *Averages and groups of main (N), sub variables (Zn) and interactions (NxZn) for dry petal yield (g plant^{-1}), oil ratio (%) and biomass yield (tons ha^{-1})*

Treatments		Dry petal yield (g plant^{-1})		Oil ratio (%)		Biomass yield (tons ha^{-1})	
N		**2011-12**	**2012-13**	**2011-12**	**2012-13**	**2011-12**	**2012-13**
N_0		1.12 a*	1.19 a*	30.0 a*	31.3 a*	5.808 c*	9.238 ab*
N_5		1.02 bc	1.04 c	30.1 a	31.4 a	6.617 a	8.612 b
N_{10}		0.98 c	1.00 d	29.5 b	29.8 b	6.058 b	9.467 a
N_{15}		1.04 b	1.12 b	30.1 a	30.6 ab	6.217 b	9.648 a
Zn		**2011-12**	**2012-13**	**2011-12**	**2012-13**	**2011-12**	**2012-13**
Zn_0		1.17 a*	1.27 a*	29.9^{ns}	30.4^{ns}	6.571 a*	9.111 b*
Zn_1		1.08 b	1.13 b	30.0	30.9	5.742 c	9.600 a
Zn_2		1.05 c	1.11 b	29.1	30.7	6.137 b	9.215 b
Zn_3		0.86 d	0.84 c	29.7	31.0	6.250 b	9.040 b
Interaction		**2011-12**	**2012-13**	**2011-12**	**2012-13**	**2011-12**	**2012-13**
N_o	Zn_0	1.13 cd*	1.27 c*	29.9^{ns}	30.3 c-f*	6.550 abc*	9.420 bcd*
	Zn_1	1.47 a	1.70 a	30.0	30.5 b-f	4.700 g	9.000 cd
	Zn_2	0.77 fg	0.71 fg	30.0	33.1 a	5.617 ef	8.640 de
	Zn_3	1.09 d	1.08 d	30.2	31.2 b-e	6.367 a-d	9.893 bc
N_5	Zn_0	1.20 c	1.24 c	30.3	30.7 b-f	6.700 ab	7.667 f
	Zn_1	0.84 ef	0.84 e	29.7	31.0 b-f	6.533 abc	9.827 bc
	Zn_2	1.17 c	1.20 c	30.3	31.8 a-d	6.833 a	7.413 f
	Zn_3	0.84 ef	0.89 e	30.0	32.1 abc	6.400 a-d	9.543 bcd
N_{10}	Zn_0	1.45 a	1.65 a	29.2	30.0 efg	6.933 a	9.260 bcd
	Zn_1	0.66 h	0.63g	30.3	30.0 efg	5.967 c-f	9.800 bc
	Zn_2	1.09 d	1.05 d	29.2	28.6 g	6.000 c-f	10.900 a
	Zn_3	0.75 g	0.67 fg	29.3	30.6 b-f	5.333 fg	7.907 ef
N_{15}	Zn_0	0.91 e	0.91 e	30.1	30.6 b-f	6.100 b-e	10.097 ab
	Zn_1	1.35 b	1.37 b	30.1	32.2 ab	5.767 def	9.773 bc
	Zn_2	1.17 cd	1.45 b	30.4	29.4 fg	6.100 b-e	9.907 bc
	Zn_3	0.75 g	0.74 f	29.4	30.2 d-g	6.900 a	8.817 de
CV %		14.46	11.82	5.93	4.20	10.10	10.57
F Value							
	N	54.90 **	95.21 **	4.80 *	20.35 **	24.03 **	26.97 **
	Zn	312.99 **	425.03 **	1.25 ns	2.91 ns	28.82 **	8.24 **
	NxZn	364.42 **	479.56 **	3.15 *	12.06 **	17.78 **	38.28 **

*Means followed by different letters within columns are significantly different ($p \leq 0.05$)
*$p \leq 0.05$, **$p \leq 0.01$, ns: non-significant

Oil ratio (%)

N_0 (30.0%), N_5 (30.1%) and N_{15} (30.1%) subjects gave the highest oil ratio in the first year, N_0 and N_5 (31.3 and 31.4%) treatments in the second year and these formed in

http://www.aloki.hu ● ISSN 1589 1623 (Print) ● ISSN 1785 0037 (Online)
DOI: http://dx.doi.org/10.15666/aeer/1704_75917604

the same group. The formation of similar groups in two years reveals that the application of N did not have a positive effect on oil ratios. Kolsarici et al. (2005) and Elfadl et al. (2009) reported the similar results in their studies. Zn applications had not statistically significant in both years. Although N x Zn interaction was insignificant in the first year, N_0 x Zn_2 interaction gave the highest oil ratio (33.1%) in the second year (*Table 5*). These differences between the experimental years might be due to the various effects of environmental factors.

Biomass yield (tons ha^{-1})

N_5 application gave the highest biomass yield (6.617 tons ha^{-1}) in the first year, N_{10} and N_{15} applications (9.467 and 9.648 tons ha^{-1}) in the second year. When scores of characteristics for two years were evaluated, N applications generated the more biomass yield than the control plots. Several researchers reported that N applications increased biomass yield comparing to the control (Haghighati, 2010; Singh and Singh, 2013 and Revant Nathan et al., 2018). The highest biomass yield (6.571 tons ha^{-1}) in Zn applications was obtained from the Zn_0 application in the first year, from the Zn_1 application (9.600 tons ha^{-1}) in the second year. N_0 x Zn_2 (6.933 tons ha^{-1}) and N_{15} x Zn_3 (6.900 tons ha^{-1}) interactions in the first year, N_{10} x Zn_2 (10.900 tons ha^{-1}) interaction in the second year gave the highest biomass values (*Table 5*).

Biomass yields are affected by environmental factors. Especially, N applications with high precipitation enhance the vegetative development of the plant. Nitrogen with water, is the most vital nutrient. Therefore, it appears to be a nutrient that controls plant growth (Fageria, 2009). Zinc affects the nitrogen metabolism, starch formation and seed maturation in plants. Zinc a plant nutrient element necessary for the production of growth hormones (auxin hormone), and especially for the prolongation of the internode (Gardiner and Miller, 2008; McCauley et al., 2009). For these reasons, N and Zn applications are important in safflower production. The differences between N x Zn interactions in the research may have been caused by the diversities of climate and soil factors.

Conclusions

It was concluded that; the highest seed yield and seed yield per plant were obtained from the both N_{15} x Zn_3 interaction and N_{15} and Zn_3 applications. Although N applications had the positive effects comparing to the control plots on the seed yield per plant, plant height, number of heads per plant, number of seeds per head, 1000 seed weight and biomass yield and had no any positive effects on the dry petal yield and oil ratio. Zn applications had showed positive effects comparing to the control plots on the seed yield per plant and number of heads per plant and had negative effects on the oil ratio and dry petal yield. As a result of the research; the highest seed yield and seed yield per plant from the N_{15} and Zn_3 applications were lower than those of the N_{15} x Zn_3 interaction, and the doses of 150 kg N ha^{-1} and 30 kg Zn ha^{-1} should be given together in N and Zn applications under semi-arid conditions. However, as each region has its own climate and soil conditions, it is useful to perform these studies where safflower cultivation is done.

http://www.aloki.hu ● ISSN 1589 1623 (Print) ● ISSN 1785 0037 (Online)
DOI: http://dx.doi.org/10.15666/aeer/1704_75917604

Acknowledgements. This study was financially supported by the Harran University Scientific Research Board (HÜBAK Project No: 0985).

REFERENCES

[1] Abd El-Mohsen, A. A., Mahmoud, G. O. (2013): Modeling the influence of nitrogen rate and plant density on seed yield, yield components and seed quality of safflower. – American Journal of Experimental Agriculture 3(2): 336-360.
[2] Ahmed, Z., Medekkar, S., Mohammad, S. (1985): Response of safflower to nitrogen and phosphorus. – Indian Journal of Agronomy 39(1): 128-130.
[3] Anonymous (2012): GAP Agricultural Research Institute. – Sanliurfa, Turkey.
[4] Anonymous (2013): Meteorological data obtained from Sanliurfa Meteorological Station.
[5] Arslan, Y., Bayraktar, N. (2015): Effect of different levels Nitrogen and Phosphorus on the some yield components of Safflower (*Carthamus tinctorius* L.) in dry conditions. – International Journal of agricultural and Wildlife Science (IJAWS) 1(2): 91-103.
[6] Baydar, H. (2000): Effects of gibberellic acid on male sterility, seed yield and oil and fatty acid syntheses of safflower (*Carthamus tinctorius* L.). – Tr. J. Biology 24(2000): 159-168.
[7] Belgin, C., Bilal, G., Mustafa, K. (2007): Oil content and fatty acid composition of some safflower (*Carthamus tinctorius* L.) varieties sown in spring and winter. – International Journal of Natural and Engineering Sciences 1(3): 11-15.
[8] Bitarafan, Z., Shirani-Rad, A. H., Delkhosh, B. (2011): Nitrogen rates and sowing date effect on yield and oil content of spring safflower. – International Journal of Science and Advanced Technology 1(6): 25-30.
[9] Dajue, L., Mundel, H. H. (1996): Safflower. Promoting the Conservation and Use of Underutilized and Neglected Crops. – 7. Institute of Plant Genetics and Crop Plant Reasarch, Gatersleben/International Plant Genetic Resources Institute, Rome.
[10] Demir, I., Kara, K. (2018): The effect of different environmental conditions on yield and oil rates of safflower (*Carthamus tinctorius* L.). – Fresenius Environmental Bulletin 27(2): 989-995.
[11] Esendal, E. (2001): Safflower production and research in Turkey. – Vth International Safflower Conference, Williston, North Dakota, Sidney, Montana, USA, July 23-27, pp. 203-206.
[12] Esendal, E., Kevseroglu, K., Uslu, N., Aytac, S. (1992): The effect of spring and winter planting on yield and important characters of safflower. – University of Ondokuz Mayıs, Faculty of Agriculture, Years of Research, Project No: Z-044, pp. 119-121.
[13] Eslam, B. P., Monirifar, H., Ghassemi, M. T. (2010): Evaluation of late season drought effects on seed and oil yields in spring safflower genotypes. – Turk J. Agric. For. 34(2010): 373-380.
[14] El-Nakhlawy, F. S. (1991): Response of safflower to different levels of nitrogen, phosphorus and potassium. – Acta Agronomica Hungarica 40(1-2): 37-92.
[15] Elfadl, E., Reinbrecht, C., Frick, C., Claupein, W. (2009): Optimization of nitrogen rate and seed density for safflower (*Carthamus tinctorius* L.) production under low input farming conditions in temperate climate. – Field Crops Research 114(1): 2-13.
[16] Emongor, V. E. (2010): Safflower (*Carthamus tinctorius L.*) the underutilized and neglected crop: A review. – Asian Journal of Plant Sciences 9(6): 299-306.
[17] Emongor, V. E., Oagile, O., Kedikanetswe, B. (2015): Effects of plant population and season on growth and development of safflower (*Carthamus tinctorius L.*) as an ornamental plant. – Acta Horticulturae 1077(1077): 35-45.
[18] Eryigit, T., Yildirim, B., A. M., Kumlay, A. M., Sancaktaroglu, S. (2015): The Effects of different row distances and nitrogen fertilizer rates on yield and yield components of safflower (*Carthamus tinctorious*) under micro-climate conditions of Iğdır plain, Turkey.

http://www.aloki.hu ● ISSN 1589 1623 (Print) ● ISSN 1785 0037 (Online)
DOI: http://dx.doi.org/10.15666/aeer/1704_75917604

– 3rd International Conference on Biological, Chemical & Environmental Sciences (BCES-2015) Sept. 21-22, 2015 Kuala Lumpur (Malaysia).

[19] Fageria, N. K. (2009): The Use of Nutrients in Crop Plants. – CRC Press, Boca Raton, FL.

[20] Gardiner, D. T., Miller, R. W. (2008): Soils in Our Environment. 11th Ed. – Pearson/Prentice Hall, Upper Saddle Hill, NJ.

[21] Grant, C. (2006): Enhancing nitrogen use efficiency in dryland cropping systems on the Northern Great Plains. – 18th World Congress of Soil Science, Philadelphia, PA.

[22] Gulmezoglu, N., Aytac, Z. (2016): The influences of various zinc applications on seed yield and zinc uptake of safflower. – Soil Water Journal 5(2): 11-17.

[23] Gursoy, M., Basalma, D., Farzad Nofouzi, F. (2018): Effects of safflower cultivars (*Carthamus tinctorius* L.) on yield and yield components of different row and row spaces. – Selcuk Journal of Agriculture and Food Sciences 32(1): 20-28.

[24] Haghighati, A. (2010): Study on the effects of nitrogen and phosphorus fertilizers on the yield and oil content of safflower lines in drylands. – Research Journal of Agronomy 4(3): 57-62.

[25] Ibrahim, Y. M. (1994): Response of safflower to different nitrogen levels in United Arab Emirates. – Annals of Arid Zone 33(1): 77-78.

[26] Johnson, R. C., Stout, D. M., Bradley. V. L. (1993): A rich source of safflower germplasm. The U.S. Collection. – Proceeding Third International Safflower Conference, Beijing Botanical Garden Institute of Botany Chinese Academy of Sciences, 14-18 June, Beijing, China, pp. 202-208.

[27] Katar, D., Arslan, Y., Subasi, I. (2012): Effect of different doses of nitrogen on the yield and yield components of safflower (*Carthamus tinctorius* L.) under Ankara ecological conditions. – Suleyman Demirel University Journal of the Faculty of Agriculture 7(2): 56-64.

[28] Khalil, N. A. A., Dagash, Y. M., Yagoub, S. O. (2013): Effect of sowing date, irrigation intervals and fertilizers on safflower (*Carthamus tinctorius* L.) yield. – Discourse Journal of Agriculture and Food Sciences 1(5): 97-102.

[29] Khoshgoftarmanesh, A. H., Schulin, S., Chaney, R. L., Daneshbakhsh, B., Afyuni, M. (2010): Micronutrient-efficient genotypes for crop yield and nutritional quality in sustainable agriculture. A review. – Agron. Sustain. 30: 83-107.

[30] Knowles, P. F. (1982): Safflower: Genetics and Breeding. – In: Improvement of Oil-Seed and Industrial Crops by Induced Mutations. International Atomic Energy Agency, Vienna, pp. 89-101.

[31] Kolsarici, O., Allusoglu, S., Kaya, M. D. (2005): The effects of tillage and nitrogen doses on water use efficiency, soil moisture and seed characters of safflower (*Carthamus tinctorius* L.) in wheat-safflower rotation system. – VIth International Safflower Conference, Istanbul, 6-10 June 2005, pp. 126-131.

[32] Kose, A. (2017): Agricultural performances of some safflower (*Carthamus tinctorius* L.) varieties under Eskisehir conditions. – Selcuk Journal of Agriculture and Food Science 31(2): 1-7.

[33] Kose, A., Hatipoglu, H., Arslan, H. (2018): Genotype reaction and effect of the sowing time under arid ecological conditions in Safflower (*Carthamus tinctorius* L.). – Fresenius Environmental Bulletin 27(5A): 3577-3586.

[34] Lakzayi, M. (2015): Influence of foliar application on safflower yield. – International Journal of Multidisciplinary Research and Development Online 2(12): 336-339.

[35] Lewis, D. C., McFarlane, J. D. (1986): Effect of foliar applied manganese on the growth of safflower (*Carthamus tinctorius* L.) and the diagnosis of manganese deficiency by plant tissue and seed analysis. – Australian Journal of Agricultural Research 37(6): 567-572.

http://www.aloki.hu ● ISSN 1589 1623 (Print) ● ISSN 1785 0037 (Online)
DOI: http://dx.doi.org/10.15666/aeer/1704_75917604

[36] McCauley, A., Jones, C., Jacobsen, J. (2009): Nutrient Management. – Nutrient Management Module 9. Montana State University Extension Service Publication 4449(9): 1-16.
[37] Mengel, K., Kirkby, E. A. (2001): Principles of Plant Nutrition. 5th Ed. – Kluwer Academic Publishers, Dordrecht.
[38] Nagaraj, G., Devi, G. N., Surivas, C. V. S. (2001): Safflower petals and their chemical composition. – Proc. V. International Safflower Conference, July 23-27, USA.
[39] Nimbkar, N. (2002): Safflower rediscovered. – Times Agricultural Journal 2(1): 32-36.
[40] Nosheen, A., Bano, A., Ullah, F., Farooq, U., Yasmin, H., Hussain, I. (2011): Effect of plant growth promoting rhizobacteria on root morphology of Safflower (*Carthamus tinctorius* L.). – African Journal of Biotechnology 10(59): 12639-12649.
[41] Ogut, H., Oguz, H. (2006): Biodiesel: Third Millennium Fuel. – Nobel Publication, Ankara, pp. 55-60.
[42] Pongracz, G., Weiser, H., Matzinger, D. (1995): Tocopherol, Antioxidation. – Journal of Natural Fatty Acid Science and Technology 97: 90-104.
[43] Rajvanshi, A. K. (2005): – In: Esendal, E. (ed.) VIth International Safflower Conference, Istanbul, Turkey, 6-10 June 2005, pp. 80-85.
[44] Revanth Nathan, J. K., Madhavi Lata, A., Joseph, B., Madhavi, A. (2018): Influence of nitrogen and sulphur on growth yield and economics of spineless safflower under irrigated conditions. – Int. J. Pure App. Biosci. 6(3): 77-81.
[45] Singh, R. K., Singh, A. K. (2013): Effect of nitrogen, phosphorus and sulphur fertilization on productivity, nutrient-use efficiency and economics of safflower (*Carthamus tinctorius* L.) under late-sown condition. – Indian Journal of Agronomy 58(4): 583-586.
[46] Soleymani, A., Shahrajabian, M. H. (2011): Effect of planting dates and different levels of nitrogen on seed yield and yield components of safflower grown after harvesting of corn in Isfahan, Iran. – Research on Crops 12(3): 739-743.
[47] Strasil, Z., Vorlicek, Z. (2002): The effect of nitrogen fertilization, sowing rates and site on yields and yield components of selected varieties of safflower (*Carthamus tinctorius* L.). – Rostlinna Vyroba. 48(7): 307-311.
[48] Taha, M. H., Shalaby, E. A., Nermeen, T. S. (2013): Improving safflower (*Carthamus tinctorius* L.) growth and biological activities under saline water irrigation by using iron and zinc foliar applications. – J. Plant Production, Mansoura Univ. 4(8): 1219-1234.
[49] Weiss, E. A. (2000): Castor, Sesame, and Safflower. – Barnes and Noble, Inc., New York, pp. 529-44.

http://www.aloki.hu ● ISSN 1589 1623 (Print) ● ISSN 1785 0037 (Online)
DOI: http://dx.doi.org/10.15666/aeer/1704_75917604

THE SENSITIVITY OF DIFFERENT GROWTH STAGES OF SUNFLOWER (*HELIANTHUS ANNUUS* L.) UNDER DEFICIT IRRIGATION

MAHMOOD, H. N.[1*] – TOWFIQ, S. I.[1] – RASHID, K. A.[2]

[1]*Crop Science Department, College of Agricultural Sciences, University of Sulaimani, Sulaimani-Kurdistan Region, Iraq*

[2]*Soil and Water Science Department, College of Agricultural Sciences, University of Sulaimani, Sulaimani-Kurdistan Region, Iraq*

**Corresponding author*
e-mail: hekmat.mahmood@univsul.edu.iq; phone: +964-750-126-9838

(Received 8th Mar 2019; accepted 3rd May 2019)

Abstract. Sunflower-like all other plants have several growth stages such as vegetative, flowering, and achene formation. Water stress mainly results in a reduction in seed yield during the flowering more than the achene formation stage. A randomized complete block design was applied with irrigation as main plots (skipping irrigation at stages of vegetation, flowering, achene formation, and full irrigation), and sunflower genotypes (Barolo RO, Velko, and Local) as sub-plots. Each treatment replicated three times. This study was conducted at two different locations (Kanipanka and Qlyasan) under the semiarid region of Sulaimani province, Iraq. Velko genotype had the highest seed yield of 4,993.705, and 6,247.265 kg ha^{-1} respectively at both locations, under full irrigation. Under skipping irrigation, at both stages of flowering and achene formation, irrigation water use efficiency value was lower than the value of water use efficiency. Crop response factor was less than one for all genotypes. At the flowering stage and under skipping irrigation, the crop response factor was higher at both locations. The result of this study concluded that Barolo RO genotype has the highest performance under deficit irrigation. Also, under skipped irrigation, the flowering stage was more effective in seed yield increase than stages of vegetation and achene formation in sunflower. The objective of this study was to determine the sensitivity of sunflower growth stages under deficit irrigation.
Keywords: *irrigation requirement, saving water, seed yield, water use efficiency, yield response factor*

Introduction

Sunflower (*Helianthus annuus* L.) is considered one of the top four edible vegetable oils in the world. Globally, it is counted for about 12% of the edible vegetable oil production following palm, soybean, and canola oil (Demir et al., 2006; Rauf et al., 2017). It is the most effective unconventional oilseed crops in the world due to its high oil quality, and it is advantages in crop rotation systems, such as high adoption capability, suitability to mechanization and low labor needs (Reddy et al., 2003; Kazemeini et al., 2009).

Agriculture uses the highest amount of freshwater which accounts for 70%, that driven from rivers, lakes, and aquifers up to more than 90% in some developing countries (WWP, 2017). The IPCC AR5 (2013) stressed low confidence in a global-scale observed trend in drought, owing to lack of direct observations, dependencies of inferred trends on the index choice, as well as difficulties in distinguishing long-term climate change from decadal-scale drought variability.

Ghani et al. (2000) found that irrigation is a substantial factor which directly influences the yield of sunflower. Wise application in time for irrigation in critical

http://www.aloki.hu ● ISSN 1589 1623 (Print) ● ISSN 1785 0037 (Online)
DOI: http://dx.doi.org/10.15666/aeer/1704_76057623

stages of growth from increased sunflower seeds produces dramatically. Sunflower plants can achieve maximum water productivity under water deficit environment (Ali, 2009). Indeed, flowering and seed filling stages have been reported as the most critical for water stress in sunflower (Iqbal et al., 2005). Shafi et al. (2013) indicated that water stress during the flowering stage causes a considerable reduction in seed yield of sunflower.

The identification of the relationship between water use efficiency and seed yield under deficit irrigation has been a high concern for agricultural research in semi-arid areas (Fan et al., 2005; Sun et al., 2006; Sinaki et al., 2007; Faraji et al., 2009). However, one of the biggest challenges facing agriculture is the development of technological options or to improve the efficiency of agricultural water use (Turner, 2004).

Drought is one of the tops stress abiotic factor which causes low yield especially in arid and semi-arid regions of the world (Tian et al., 2016; Viscardi et al., 2016). Martinek (2008) stated that drought tolerance differs strongly between the growth stages of many crops. Deficit irrigation is known as the application of water at levels below full crop water requirements, and it is one of the new strategies designed to improve water savings in agriculture (Bashir and Mohamed, 2014). The purpose of deficit irrigation is to raise the water use efficiency (WUE) and to obtain the highest yield per unit water (Kirda et al., 2006), further De Pascale et al. (2011) describe the ration of crop yield per unit as water use efficiency in agriculture.

By knowing the value of crop response factor, farmers can get optimum yield without withdrawing irrigation water at that stage if water scarcity persists. Doorenbos and Kassam (1979) found the crop response factor (*ky*) for some crops. Crop response factor values of more than one indicate more stress, and from this value, the critical stage can be obtained. As reported by Ali (2009), the response factor various by locations, which influence by soil types, weather conditions, seasons and varieties. Therefore, a location-specific response factor should be considered for the efficient management of water. Here sunflower crop was used to estimate crop response factor as it can tolerate low to medium water and salinity stress (Tolga and Lokman, 2003).

The genotype differences may be due to the differences in genetic structure between the sunflower genotype, to the differences in growth characters and the differences in photosynthetic partitioning (Ahmed and Hassanein, 2000; Abou El-Seoud and Wafaa, 2010). Hybrid seed yield is a condition by its capacity to use the environmental variables efficiently in different phenophases (Gonzáles et al., 2013). Thus, the genetic potential of the hybrid sunflower is reduced by the action of the growth factors, either environmental or technological. In addition to high yield sunflower varieties, agronomic practices are essential for maximum seed yield (Beg et al., 2007). Ibrahim (2012) reported that the plant population and varieties could determine seed yield per unit area.

The objective of this study was to highlight the sensitivity of different growth stages of three genotypes of sunflower to different irrigation levels.

Materials and methods

Study area

This study was carryout during the summer of 2016 at two locations: first the Agricultural Research Station at Kanipanka, Sulaimani with (Longitude of 045° 43’ 22” E, altitude of 548 masL, and latitude of 35° 22’ 22” N). The second location was

http://www.aloki.hu ● ISSN 1589 1623 (Print) ● ISSN 1785 0037 (Online)
DOI: http://dx.doi.org/10.15666/aeer/1704_76057623

Qlyasan, the experimental station of the College of Agricultural Sciences, the University of Sulaimani, (latitude: 35° 34' 17" N, Longitude: 045° 22' 00" E, altitude: 757 masL) "Garmin, GPSmap60 Cx" (*Fig. 1*).

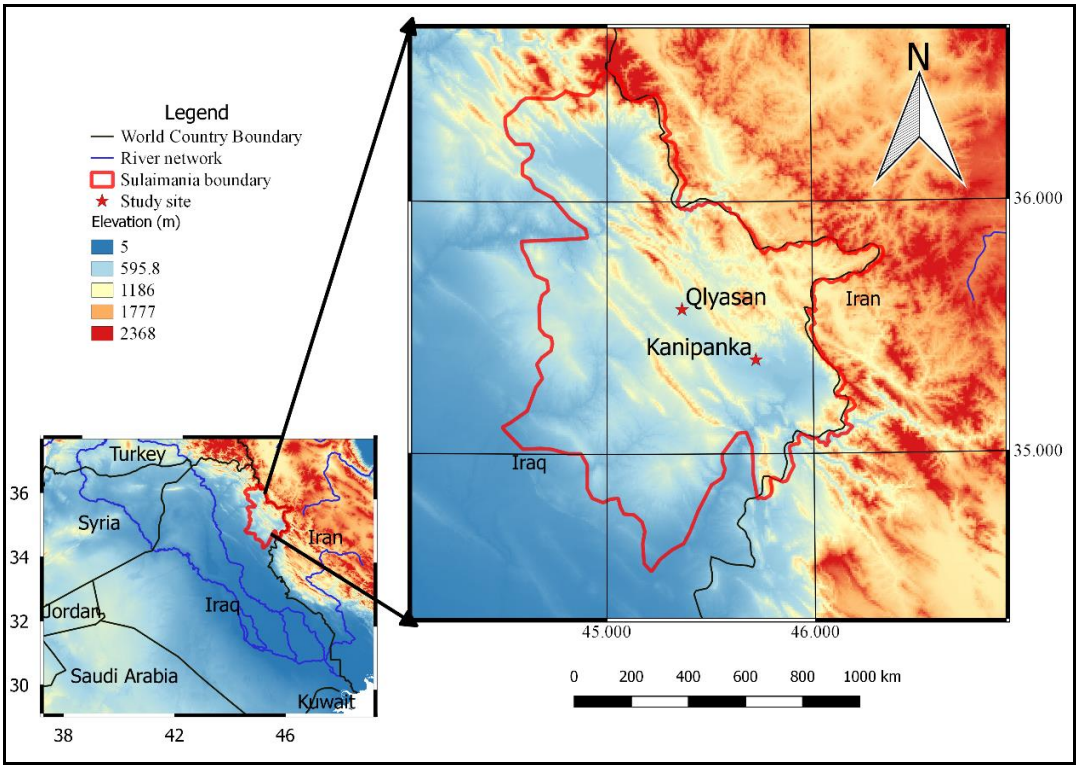

Figure 1. *Map of the study site in Sulaimani-Kurdistan region, Iraq*

At each location, a composite soil sample of about 5 kg was obtained by mixing subsamples from 6 sites using a shovel. Each soil sample was freed from plant roots and other debris. All samples were dried at room temperature for seven days. Each sample was cleaned using 2 mm stainless-steel sieve.

A split-plot factorial with full and deficit irrigation as the main plot was replicated three times, a in randomized complete block design. The water deficit of various degrees was imposed at different growth stages with the irrigation treatments. There were three sunflower growth stages which are vegetative (S_1), flowering (S_2), and achene formation (S_3) stages. The four levels of irrigation treatments were: skipping irrigation at vegetative stage (I_1), skipping irrigation at flowering stage (I_2), skipping irrigation at the achene formation stage (I_3), and full irrigation (I_4). *Table 1* exhibits the details of the irrigation treatments. *Table 2* shows the sum of water applied at different treatments for both locations.

Table 1. *Details of the irrigation treatments*

Irrigation treatments symbol	Description
I_1	Skipping irrigation at vegetative stage
I_2	Skipping irrigation at flowering stage
I_3	Skipping irrigation at the achene formation stage
I_4	Full irrigation (non-skipping irrigation)

http://www.aloki.hu ● ISSN 1589 1623 (Print) ● ISSN 1785 0037 (Online)
DOI: http://dx.doi.org/10.15666/aeer/1704_76057623

Table 2. *Total number of irrigations along with the gross depth of applied water as influenced by different irrigation treatments during the sunflower growing season at the study locations*

Irrigation treatments	Number of irrigations	Total applied water			
		Liters (L)	(mm)	(m ha^{-1})	ET_a (m^3 ha^{-1})
Kanipanka Location					
I_1	11	3416	632.59	6325.93	4428.148
I_2	11	3511	650.19	6501.85	4551.296
I_3	10	2872	531.85	5318.52	3722.963
I_4	18	4111	761.3	7612.96	5329.074
Qlyasan Location					
I_1	10	3500	648.15	6481.48	4212.963
I_2	11	3642	674.44	6744.44	4383.889
I_3	10	2669	494.26	4942.59	3212.685
I_4	18	4073	754.26	7542.59	4902.685

The sub-plot factors encompassed of the genotypes which were a single cross hybrid Barolo RO, single cross hybrid Velko and Local variety.

The size of each sub-plots was 3 m by 1.8 m, and consisted of three rows, with 0.60 m apart. The spaces between plants were 0.30 m. The least significant difference at confidence levels of 0.05 and 0.01 were used for treatments comparison.

Cultural practices

Before planting and delineating the plots, an area with a gentle slope was selected an irrigated. The field was then plowed with moldboard plow at the optimum water content for tillage. At both locations, three sunflower seeds at a depth of 2-4 cm were placed in each hole on July 11 and 15, 2016. After two weeks, the seedling was thine out to one per hole. The nitrogen fertilizer in the form of Urea applied one before the second irrigation and the other before flowering at a rate of 43 kg ha^{-1} as recommended. Hand weeding practiced as needed. There was not treated with any pesticide. At the flowering stage, plants were protected from bird attack by installing a screen over the heads.

Sulaimani governorate climate

The climate of Sulaimani governorate is considered as a semi-arid environment: cold and wet in winter, hot and dry in summer. The average temperature from July to August is between 39-43 °C and often reaching nearly 50 °C. October means high temperatures are 24-29 °C and slightly cooling down in November. The rainfall is limited to winter and spring months Kurdistan Regional Government, 2018; see *Table 3*).

Watering schedules

As recommended by Allen et al. (1988), irrigation scheduling was based on an allowable root zone water depletion of 45% (p = 0.45) during the whole growing cycle. SOTERA digital meter was used to measure the water flow (*Fig. 2*).

http://www.aloki.hu ● ISSN 1589 1623 (Print) ● ISSN 1785 0037 (Online)
DOI: http://dx.doi.org/10.15666/aeer/1704_76057623

Table 3. *Agrometeorological parameters at Kanipanka and Qlyasan locations 2015-2016*

Locations	Month	Air temperature °C		Average humidity (%)	Average wind speed (ms^{-1})	Precipitation (mm)
		Minimum	Maximum			
Kanipanka	October	10.2	38.00	40.50	1.63	186.1
	November	4.5	21.80	51.90	1.81	143.6
	December	-2.0	15.90	54.40	2.23	86.1
	January	-3.0	16.50	56.80	2.86	51.7
	February	0.5	22.40	49.50	2.26	87.1
	March	3.2	23.00	45.90	2.33	113.5
	April	5.2	32.70	41.30	2.37	74.0
	May	12.0	40.00	31.40	2.60	10.0
	June	18.7	44.80	21.70	2.68	0
	July	27.05	44.33	20.30	1.65	0
	August	29.34	45.88	19.56	1.50	0
	September	21.42	39.55	22.68	1.61	0
	October	15.66	34.69	28.56	1.38	
Qlyasan	October	22.7	25.3	42.0	1.41	96.7
	November	12.0	17.6	50.6	1.54	152
	December	7.4	12.45	40.5	1.63	52.7
	January	5.7	10.6	40.3	1.61	72.5
	February	9.8	15.7	50.0	1.67	64.8
	March	12.4	18.4	51.8	2.35	122.6
	April	17.1	23.9	43.1	1.36	55.2
	May	22.4	29.8	30.2	1.40	6.0
	June	30.6	37.6	14.1	1.94	0
	July	25.84	43.46	22.9	1.77	0
	August	27.49	45.36	20.35	1.60	0
	September	19.95	38.26	26.17	1.65	0
	October	14.95	32.01	29.42	1.44	0

Figure 2. *SOTERA digital display meter*

A small auger 5 cm in diameter (Lorenz and Maynard, 1980) was used to observe soil water content. The average water requirement (consumptive crop use) was calculated from soil moisture. The soil moisture was brought to field capacity when the

http://www.aloki.hu ● ISSN 1589 1623 (Print) ● ISSN 1785 0037 (Online)
DOI: http://dx.doi.org/10.15666/aeer/1704_76057623

available soil moisture was depleted by 45%. The net depth of applied water was calculated from (Michael, 1978):

$$d_n = \frac{(\omega_{FC} - \omega_{WP})}{100} \frac{\rho_b}{\rho_w} P\ D \quad \text{(Eq.1)}$$

where:
d_n = net depth of applied water (mm)
ω_{FC} = Soil water retention at -33 kPa
ω_{PW} = Soil water retention at -1500 kPa
ρ_b = Average soil bulk density of the root zone (gcm^{-3})
ρ_w = Water density (gcm^{-3})
P = Depletion fraction = 0.45
D = Root zone depth (mm)

The gross depth of applied water (dg) was obtained from the following relationship:

$$dg = \frac{d_n}{Ea} \quad \text{(Eq.2)}$$

where Ea = Irrigation application efficiency.
The values of this parameters were 0.70 and 0.65 for Kanipanka and Qlyasan locations, respectively (*Table 4*).

Table 4. *Irrigation application efficiencies for the locations under study based on average land slope and basic infiltration rate*

Locations	Average land slope (%)	Basic infiltration rate, ib (mm hr^{-1})	Irrigation application efficiency, e_a
Kanipanka	Nearly level	44	0.70
Qlyasan	1.16	80	0.65

The consumptive crop use mean during the growing season was comparable with that computed by the Penman-Monteith equation. In each plot, middle row plants were harvested at maturity for seed yield determination at 10% seed moisture content. On October 19 and 24, 2016 mature plants were harvested from a deficit and full irrigation plots, respectively, at Kanipanka location, while the harvesting dates at Qlyasan location, was on October 25 for all the irrigation treatments.

The following equation was used to estimate water use efficiency (WUE), and irrigation water use efficiency (IWUE), as the ratio of crop yield per unit of water applied (Kang et al., 2000):

$$WUE = \frac{Y}{ET_c} \quad \text{(Eq.3)}$$

$$IWUE = \frac{Y}{I} \quad \text{(Eq.4)}$$

http://www.aloki.hu ● ISSN 1589 1623 (Print) ● ISSN 1785 0037 (Online)
DOI: http://dx.doi.org/10.15666/aeer/1704_76057623

where:
Y = The total sunflower seed yield (kg ha^{-1})
ET_c = The seasonal evapotranspiration (m^3 ha^{-1})
I = The total volume of applied irrigation water (m^3 ha^{-1})

While the irrigation application efficiencies for the locations under study based on average land slop and basic infiltration rate was calculated according to Karim and Karim (2001), and the results are revealed in *Table 4*.

The crop response factor *ky* was based on the formula recommended by (Doorenbos and Kassam, 1979).

$$\left(1 - \frac{Y_a}{Y_m}\right) = ky\left(1 - \frac{ET_a}{ET_{max}}\right) \quad \text{(Eq.5)}$$

where:
Y_a = Actual crop yield (kg ha^{-1})
Y_m = Maximum crop yield (kg ha^{-1})
ET_a = Actual evapotranspiration (mm)
ET_{max} = Maximum evapotranspiration (mm)
ky = Yield response factor (dimensionless)

The crop response factor for different stages of growth can be described by:

$$\frac{Y}{Y_m} = \Pi^n{}_{i=1}\left[1 - K_{yi}\left(1 - \frac{ET}{ET_m}\right)_i\right] \quad \text{(Eq.6)}$$

By expanding *Equation 4,* we find:

$$\frac{Y}{Y_m} = \left[1 - k_{y1}\left(1 - \frac{ET_a}{ET_m}\right)_1\right]\left[1 - k_{y2}\left(1 - \frac{ET_a}{ET_m}\right)_2\right]\left[1 - k_{y3}\left(1 - \frac{ET_a}{ET_m}\right)_3\right] \quad \text{(Eq.7)}$$

where the subscripts 1, 2, and 3 represent the first, second and third stages of growth and the other symbols retain the same meanings.

By putting $\frac{ET_a}{ET_{max}} = 1.0$ for the stages under full irrigation, and replacing $\frac{ET_a}{ET_{max}}$ by stress coefficient (ky) for the stage at which deficit irrigation was applied, we obtain:

$$k_{yi} = \left(1 - \frac{Y_{ai}}{Y_{max}}\right)(1 - k_{si}) \quad \text{(Eq.8)}$$

where the subscript i denotes the stage at which deficit irrigation was implemented.

Table 5 shows the calculation of k_s for different growth stages of sunflower at both locations. The obtained values of k_s from *Table 3* were used for calculating k_y for different growth stages of sunflower genotypes. The study was focused on the stages of sunflower irrespective of genotype due to the soil moisture status under different genotypes.

The uniformity coefficient (UC) for some selected parameters was determined according to (Devitt et al., 1992):

http://www.aloki.hu ● ISSN 1589 1623 (Print) ● ISSN 1785 0037 (Online)
DOI: http://dx.doi.org/10.15666/aeer/1704_76057623

$$UC = 1 - (\text{Standard deviation/mean}) \quad \text{(Eq.9)}$$

Laboratory analysis

Table 6 shows the results of the investigated soil parameters. Particle size distribution for textural class assessing was carried out by international pipette method as described by Black et al. (1965). Hydrogen ion concentration (pH) and electrical conductivity (EC) in a suspension ratio of 1:10, soil to H_2O were determined by Thomas (1996), using pH model of WTW 330i, whereas for EC the model WTW 330i EC-meter was used. Organic carbon percentage (O.M%) in soil were determined by wet oxidation method according to the Walkley-Black method (Black et al.,1965). Then after the percent of organic matter was calculated through % Organic matter = % Organic carbon × 1.724 (factor). Calcium carbonate CaCO3% (g kg^{-1}) was determined according to a 23c method of U.S. Salinity Laboratory Staff, 1954 as mentioned in (Black et al., 1965).

Table 5. *Calculation of stress coefficient during the stages when irrigation water skipped*

Locations	Stage	θ_{FC}	θ_{PWP}	TAW	θ	(1-P)TAW	Depletion (D)	TAW-D	Ks=(TAW-D)/(1-P)TAW
Kanipanka	S_1	0.303	0.196	0.107	0.221	0.05885	0.082	0.025	0.42
	S_2	0.303	0.196	0.107	0.216	0.05885	0.087	0.02	0.34
	S_3	0.303	0.196	0.107	0.207	0.05885	0.096	0.011	0.19
Qlyasan	S_1	0.302	0.195	0.107	0.219	0.05885	0.083	0.024	0.41
	S_2	0.302	0.195	0.107	0.220	0.05885	0.082	0.025	0.42
	S_3	0.302	0.195	0.107	0.211	0.05885	0.091	0.016	0.27

θ_{FC} = Water retention at -33 kPa on mass basis (kg ha^{-1}), θ_{PWP} = Water retention at -1500 kPa on mass basis (kg ha^{-1}), θ = Average water content of the root zone on a mass basis during the stage when irrigation was skipping (kg ha^{-1}), *TAW* = Total available water (kg ha^{-1}), *P* = Fraction of TAW that a crop can extract from the root zone without suffering water stress = 0.45, *D* = Root zone depletion, *Ks* = Stress coefficient

Table 6. *Physicochemical properties of the soil samples for locations of the experiment*

Physicochemical properties		Locations	
		Kanipanka	Qlyasan
Particles size distribution kg^{-1}	Sand	36	87
	Silt	529	435
	Clay	435	458
	Texture	SiC	SiC
PH		7.70	7.59
ECe (micro siemens cm^{-1}) or (µS cm^{-1})		218	490
O.M. (g kg^{-1})		14.8	22.4
CaCO3 (g kg^{-1})		208.3	304.3

http://www.aloki.hu ● ISSN 1589 1623 (Print) ● ISSN 1785 0037 (Online)
DOI: http://dx.doi.org/10.15666/aeer/1704_76057623

Statistical analysis

All collected data were statistically analyzed using XLSTAT (2017). A direct comparison of treatments, the least significant difference test (LSD) at levels of 0.05 and 0.01 levels was used. The analysis of variance (ANOVA) was used for testing the main effects of deficit irrigation on sunflower genotypes.

Results

Table 7 shows that the response of the parameters, seed yield, irrigation water use efficiency, and water use efficiency was highly significant to the effect of skipping irrigation treatments (*Appendix*). As seen in this table the most sensitive stage of irrigation skipping at flowering stage (I_2) at both Kanipanka and Qlyasan locations in which produced the lowest value of these parameters which were 3258.652 kg ha^{-1}, 5.012, and 7.160 kg ha^{-1} mm^{-1} respectively at Kanipanka location, while it reached 3853.858 kg ha^{-1}, 5.714, and 8.791 kg ha^{-1} mm^{-1} respectively at the Qlyasan location. Based on the average values of seed yields at both locations, during skipping irrigation the results showed that the $I_4 > I_1 > I_3 > I_2$. The result indicates that the lowest value for irrigation water use efficiency and water use efficiency were obtained at the flowering stage (I_2) at both locations. The order of different growth stages of irrigation skipping for IWUE, and WUE was as follows: achene formation stage > vegetative stage > flowering stage. The results confirm that the I_2 and I_3 offered the lowest and the highest effect in these two parameters respectively.

Table 7. *Effect of skipping irrigation treatments on seed yield, irrigation water use efficiency, and water use efficiency at Kanipanka and Qlyasan locations*

Irrigation treatments	Total applied water (mm)	Seed yield (kg ha^{-1})	Irrigation water use efficiency IWUE (kg ha^{-1} mm^{-1})	Water use efficiency WUE (kg ha^{-1} mm^{-1})
Kanipanka Location				
I_1	632.59	3842.512 b	6.074 b	8.677 b
I_2	650.19	3258.652 d	5.012 d	7.160 d
I_3	531.85	3544.538 c	6.664 a	9.521 a
I_4	761.3	4159.478 a	5.463 c	7.805 c
LSD 0.05		175.104**	0.265**	0.379**
Qlyasan Location				
I_1	648.15	4264.867 b	6.580 b	10.123 b
I_2	674.44	3853.858 d	5.714 c	8.791 c
I_3	494.26	4031.335 c	8.156 a	12.548 a
I_4	754.26	4734.582 a	6.277bc	9.657bc
LSD 0.05		385.936**	0.684**	1.053**

As shown in *Table 8,* a highly significant difference among the sunflower genotypes for seed yield, as related to IWUE, and WUE at both locations (*Appendix*). In relation to irrigation water use efficiency and water use efficiency, Velko genotype seed yields were higher values at Kanipanka location were 4405.035 kg ha^{-1}, 6.911, and 9.873 kg

http://www.aloki.hu ● ISSN 1589 1623 (Print) ● ISSN 1785 0037 (Online)
DOI: http://dx.doi.org/10.15666/aeer/1704_76057623

ha^{-1} mm^{-1} respectively than at the Qlyasan location 5356.999 kg ha^{-1}, 8.47, and 13.03 kg ha^{-1} mm^{-1} respectively. Based on the average values of these parameters for both locations, regarding the genotype performance; the order of performance; Velko > Barolo RO > Local. The results indicated that the Velko and Local genotypes had the highest and lowest performance respectively.

Table 8. *Averages of seed yield, irrigation water use efficiency, and water use efficiency of sunflower genotypes at Kanipanka and Qlyasan locations*

Sunflower genotypes	**Seed yield (kg ha^{-1})**	**Irrigation water use efficiency IWUE (kg ha^{-1} mm^{-1})**	**Water use efficiency WUE (kg ha^{-1} mm^{-1})**
Kanipanka Location			
Barolo RO	3431.935 b	5.384 b	7.692 b
Velko	4405.035 a	6.911 a	9.873 a
Local	3266.915 c	5.115 c	7.308 c
LSD 0.05	118.837 **	0.180 **	0.257 **
Qlyasan Location			
Barolo RO	3809.474 b	6.075 b	9.347 b
Velko	5356.999 a	8.470 a	13.03 a
Local	3497.009 c	5.501 c	8.463 c
LSD 0.05	250.958 **	0.385 **	0.592 **

There were statistically significant differences in seed yield among the sunflower genotypes under different irrigation treatments (*Table 9* and *Appendix*). The flowering and achene formation stage respectively were the most sensitive stage to water deficit, which had a considerable yield decreases at both locations. It is evident from this table that at Kanipanka location Barolo RO genotype had the lowest yield of 2952.785 kg ha^{-1} under I_2 treatment, while at the Qlyasan location the local genotype showed the lowest seed yield of 3117.805 kg ha^{-1} under I_3 treatment. Seed yield increased with increasing amount of applied irrigation water quantities, for instance, Velko genotype gave the highest seed yield under full irrigation treatment (I_4) at both locations 4993.705 and 6247.265 kg ha^{-1} respectively.

As seen in this table the irrigation water use efficiency and water use efficiency restricted from as low as 4.541 and 6.488 kg ha^{-1} mm^{-1} respectively at first location for the Barolo RO genotype under I_2 treatment, while as high as 10.347 and 15.918 kg ha^{-1} mm^{-1} respectively for the Velko genotype under I_3 irrigation treatment at the second location. The results above stated that both IWUE and WUE values decreased with increasing irrigation water quantities except full irrigation (I_4).

Table 10 represents a yield response (*ky*) factor for three individual sunflower growth stages. The crop response factor value varies depending on season, location and intensity of water deficit. Among three sunflower genotypes and water deficit at different growth stages at both study locations, the highest crop response factor (*ky*) value was found at flowering stage (S_2), followed by achene formation (S_3) and vegetative (S_1) stages at Kanipanka and Qlyasan locations respectively.

The yield response factor *ky* of 0.366, 0.350, and 0.253 was found at S_2 for Velko, Barolo RO, and Local genotypes respectively at Kanipanka location. The water stress at

http://www.aloki.hu ● ISSN 1589 1623 (Print) ● ISSN 1785 0037 (Online)
DOI: http://dx.doi.org/10.15666/aeer/1704_76057623

S_1 and S_3 exerted (56.83 and 53.28%; 73.43 and 50.86%; and 44.66 and 18.18%) respectively, less stress than most stressed treatment S_2.

At Qlyasan location, the yield response factor *ky* of 0.426, 0.338 and 0.144 was found at S_2 for Velko, Local, and Barolo RO genotype. The water stress at S_1 and S_3 exerted (43.19 and 41.55%; 39.35 and 6.51%; and 93.75 and 89.58%) respectively, less than the most stressed treatment S_2.

Therefore, the order of sensitive stages to water deficit arrangement for individual growth stages can be written at both locations as follows: $S_2 > S_3 > S_1$ for all of the genotypes.

Table 9. *Seed yield, irrigation water use efficiency, and water use efficiency of three sunflower genotypes as influenced by different irrigation treatments at both locations*

Sunflower genotypes and irrigation treatments		Total applied water (mm)	Total applied water (m^3 ha^{-1})	ET_a (m^3 ha^{-1})	Seed yield (kg ha^{-1})	Irrigation water use efficiency (IWUE) (kg ha^{-1} mm^{-1})	Water use efficiency (WUE) (kg ha^{-1} mm^{-1})
Kanipanka Location							
Barolo RO	I_1	632.59	6325.93	4428.148	3633.770 d	5.744 d	8.206 d
	I_2	650.19	6501.85	4551.296	2952.785 f	4.541 g	6.488 g
	I_3	531.85	5318.52	3722.963	3302.435 e	6.209 c	8.87 c
	I_4	761.3	7612.96	5329.074	3838.750 d	5.042 ef	7.203 ef
Velko	I_1	632.59	6325.93	4428.148	4541.010 b	7.178 b	10.255 b
	I_2	650.19	6501.85	4551.296	3786.950 d	5.824 d	8.321 d
	I_3	531.85	5318.52	3722.963	4298.475 c	8.082 a	11.546 a
	I_4	761.3	7612.96	5329.074	4993.705 a	6.559 c	9.371 c
Local	I_1	632.59	6325.93	4428.148	3352.755 e	5.3 e	7.571 e
	I_2	650.19	6501.85	4551.296	3036.220 f	4.67 g	6.671 g
	I_3	531.85	5318.52	3722.963	3032.705 f	5.702 d	8.146 d
	I_4	761.3	7612.96	5329.074	3645.980 d	4.789 fg	6.842 fg
LSD 0.05					237.673*	0.359**	0.513*
Qlyasan Location							
Barolo RO	I_1	648.15	6481.48	4212.963	3885.74 d	5.995 de	9.223 de
	I_2	674.44	6744.44	4383.889	3583.635 de	5.313 ef	8.175 ef
	I_3	494.26	4942.59	3212.685	3862.245 d	7.814 b	12.022 b
	I_4	754.26	7542.59	4902.685	3906.275 d	5.179 f	7.968 f
Velko	I_1	648.15	6481.48	4212.963	5351.125 b	8.256 b	12.702 b
	I_2	674.44	6744.44	4383.889	4715.65 c	6.992 c	10.757 c
	I_3	494.26	4942.59	3212.685	5113.955 bc	10.347 a	15.918 a
	I_4	754.26	7542.59	4902.685	6247.265 a	8.283 b	12.743 b
Local	I_1	648.15	6481.48	4212.963	3557.735 de	5.489 ef	8.445 ef
	I_2	674.44	6744.44	4383.889	3262.29 e	4.837 f	7.442 f
	I_3	494.26	4942.59	3212.685	3117.805 e	6.308 cd	9.705 cd
	I_4	754.26	7542.59	4902.685	4050.205 d	5.37 ef	8.261 ef
LSD 0.05					501.915*	0.770*	1.184*

http://www.aloki.hu ● ISSN 1589 1623 (Print) ● ISSN 1785 0037 (Online)
DOI: http://dx.doi.org/10.15666/aeer/1704_76057623

Table 10. *Crop response factor (ky) for individual Sunflower growth stages at which irrigation was skipped at both locations*

Locations	Sunflower genotype	Sunflower growth stage	Y	Y_{max}	Y/Y_m	$1-Y/Y_m$	K_s	1-Ks	$K_Y = (1-Y/Y_m)/(1-K_s)$
Kanipanka	Barolo RO	S_1	3633.77	3838.75	0.947	0.053	0.425	0.575	0.093
		S_2	2952.79	3838.75	0.769	0.231	0.340	0.660	0.350
		S_3	3302.44	3838.75	0.860	0.140	0.187	0.813	0.172
	Velko	S_1	4541.01	4993.71	0.909	0.091	0.425	0.575	0.158
		S_2	3786.95	4993.71	0.758	0.242	0.340	0.660	0.366
		S_3	4298.48	4993.71	0.861	0.139	0.187	0.813	0.171
	Local	S_1	3352.76	3645.98	0.920	0.080	0.425	0.575	0.140
		S_2	3036.22	3645.98	0.833	0.167	0.340	0.660	0.253
		S_3	3032.71	3645.98	0.832	0.168	0.187	0.813	0.207
									SE = 0.031
Qlyasan	Barolo RO	S_1	3885.74	3906.28	0.995	0.005	0.408	0.592	0.009
		S_2	3583.64	3906.28	0.917	0.083	0.425	0.575	0.144
		S_3	3862.25	3906.28	0.989	0.011	0.272	0.728	0.015
	Velko	S_1	5351.13	6247.27	0.857	0.143	0.408	0.592	0.242
		S_2	4715.65	6247.27	0.755	0.245	0.425	0.575	0.426
		S_3	5113.96	6247.27	0.819	0.181	0.272	0.728	0.249
	Local	S_1	3557.74	4050.21	0.878	0.122	0.408	0.592	0.205
		S_2	3262.29	4050.21	0.805	0.195	0.425	0.575	0.338
		S_3	3117.81	4050.21	0.770	0.230	0.272	0.728	0.316
									SE = 0.047

The highest value of *ky* were 0.366, 0.350 and 0.253 at the first location, while it was 0.426, 0.144 and 0.338 at the second locations, for Velko, Barolo RO and Local genotype by imposing water deficit at critical growth stages (flowering stage).

Data represented in *Table 11* illustrate the crop yield response factor (*ky*) for sunflower genotypes at both locations, which estimated according to Doorenbos and Kassam (1979), the results were tabulated in this table. The crop response factor values ranged from the minimum of 0.089 for the Barolo RO genotype at the Qlyasan location to a maximum of 0.781 for the Local genotype at the same location. Also, among the genotypes, Barolo RO exhibited the least value of (*ky*) at both locations. All genotypes yield response factor were of less than 1.0.

Table 11. *Crop response factor for different sunflower genotypes to limited irrigation at both locations*

Locations	Sunflower genotypes	Seed yield (kg ha^{-1})	ET_a (m^3 ha^{-1})	*ky*
Kanipanka	Barolo RO	3431.935 b	4507.87	0.603
	Velko	4405.035 a	4507.87	0.658
	Local	3266.915 b	4507.87	0.630
		LSD .05 175.104		*SE* = 0.016
Qlyasan	Barolo RO	3809.474 b	4178.056	0.089
	Velko	5356.999 a	4178.056	0.725
	Local	3497.009 b	4178.056	0.781
		LSD .05 385.936		*SE* = 0.222

http://www.aloki.hu ● ISSN 1589 1623 (Print) ● ISSN 1785 0037 (Online)
DOI: http://dx.doi.org/10.15666/aeer/1704_76057623

Table 12 illustrate the yield reduction and water saving for sunflower genotypes under different irrigation treatments. It was shown that the percent yield reduction decreased with an increase in the amount of applied water at various growth stages. The maximum percentage of yield reduction was 24.17 and 24.52% for Velko genotype under skipping irrigation at flowering stage (I_2) at both locations, respectively. Deficit irrigations applied in vegetative stages have fewer effects on seed yield losses, while the effects were higher at flowering and achene formation stages. Also, seed yields were affected by water stress at later growth stages, which could result in about 40% water saving as compared with full irrigation.

Table 12. *Percent of yield reduction and water saving under limited irrigation of both locations*

Genotypes and irrigation treatments		Total applied water (mm)	Seed yield (kg ha^{-1})	Yield reduction %	Water saving %
Kanipanka Location					
Barolo RO	I_1	632.59	3633.770 d	5.34	16.91
	I_2	650.19	2952.785 f	23.08	14.59
	I_3	531.85	3302.435 e	13.97	30.14
	I_4	761.3	3838.750 d	0.00	0.00
Velko	I_1	632.59	4541.010 b	9.07	16.91
	I_2	650.19	3786.950 d	24.17	14.59
	I_3	531.85	4298.475 c	13.92	30.14
	I_4	761.3	4993.705 a	0.00	0.00
Local	I_1	632.59	3352.755 e	8.04	16.91
	I_2	650.19	3036.220 f	16.72	14.59
	I_3	531.85	3032.705 f	16.82	30.14
	I_4	761.3	3645.980 d	0.00	0.00
			$LSD_{0.05}$ 237.673*	*SE* = 2.478	
Qlyasan Location					
Barolo RO	I_1	648.15	3885.74 d	0.53	14.07
	I_2	674.44	3583.635 de	8.26	10.58
	I_3	494.26	3862.245 d	1.13	34.47
	I_4	754.26	3906.275 d	0.00	0.00
Velko	I_1	648.15	5351.125 b	14.34	14.07
	I_2	674.44	4715.65 c	24.52	10.58
	I_3	494.26	5113.955bc	18.14	34.47
	I_4	754.26	6247.265 a	0.00	0.00
Local	I_1	648.15	3557.735 de	12.16	14.07
	I_2	674.44	3262.29 e	19.45	10.58
	I_3	494.26	3117.805 e	23.02	34.47
	I_4	754.26	4050.205 d	0.00	0.00
			$LSD_{0.05}$ 501.915*	*SE* = 2.794	

As listed in *Table 13,* the uniformity coefficient values were 0.93 for Velko genotype, and it was below this value for the Barolo RO and Local genotype. Also, there was a statistical difference between genotypes and locations data.

http://www.aloki.hu ● ISSN 1589 1623 (Print) ● ISSN 1785 0037 (Online)
DOI: http://dx.doi.org/10.15666/aeer/1704_76057623

Table 13. *Yield response factor (Ky) of sunflower genotypes under different irrigation treatments*

Sunflower genotypes	ET_a ($m^3\ ha^{-1}$)		Ky value			Standard deviation (SD)	Uniformity coefficient (UC)	Coefficient of variance (CV) %
	Kanipanka location	Qlyasan location	Kanipanka location	Qlyasan location	Ky mean			
Barolo RO	4507.87	4178.056	0.6028	0.0892	0.346	0.36317	-0.04962	104.96
Velko	4507.87	4178.056	0.6577	0.7253	0.6915	0.0478	0.930874	6.913
Local	4507.87	4178.056	0.6303	0.7813	0.7058	0.106773	0.84872	15.128

Discussion

The lowest and highest seed yields under irrigation water use efficiency (IWUE) and water use efficiency (WUE) at both I_2 and I_3 stages were due to a deficit in irrigation. This may be due the effect of deficit irrigation. Therefore, such effect could be less significant if water stress were applied to the crop during specific growth stages that were less sensitive to moisture deficiency. Kazemeini et al. (2009) also reached the same conclusions. Also, Iqbal et al. (2005) reported that flowering and seed filling stages had been the most critical for water stress in sunflower. Therefore, Anastasi et al. (2010) signified that sunflower provides the highest seed yield under full irrigation.

Genotypes and irrigation stages were the main factors in higher seed yields of Velko genotype. Our results collaborate (Mahender et al., 2000; Kakar and Soomro, 2001) results in which genotypes and irrigation intervals are two main factors in seed yield increases in oilseed sunflower. Various genotypes of sunflower have different responses to water stress. Our results were similar to (Angadi and Entz, 2002; Bakht et al., 2010) who observed the genotypic differences in sunflower for drought tolerance.

Velko genotype produced the highest seed yields under full irrigation (I_4), and drought stress statically decreased seed yield compared to no-stress. This indicates that skipping of irrigation at these stages can minimize seed yield to a great extent. Irrigation skipping at the achene formation stage (I_3) should be preferred due to higher IWUE and WUE if water resources are limited. Our finding collaborates (Cicek et al., 2015; Baba et al., 2016). The results stated that there is a steady decrease in both irrigation water use efficiency and water use efficiency with an increase in the amount of water quantities with the exception of control treatment (I_4). Our study showed that IWUE and WUE values were higher than those in literature in the neighboring countries under limited irrigation. Kassab et al. (2012) found that the WUE under drought condition higher than it is under plain irrigation. Regarding the genotypes, the second and third stage, i.e., skipped irrigation at flowering and achene formation stages are the critical stages for deficit irrigation. Therefore, skipping of irrigation at these stages can minimize crop yield to a great extent. Irrigation skipping at the achene formation stage should be preferred due to higher IWUE and WUE when water resources are limited, and the cost of irrigation water is high.

The crop response (*ky*) factor value for individual growth stages varies depending on season, location and intensity of water deficit. Among three sunflower genotypes and water deficit at different growth stages, the highest crop response factor value was found at flowering (S_2), followed by achene formation (S_3) and vegetative (S_1) stages. This may explain that the flowering stage is critical in sunflower seed production.

http://www.aloki.hu ● ISSN 1589 1623 (Print) ● ISSN 1785 0037 (Online)
DOI: http://dx.doi.org/10.15666/aeer/1704_76057623

Therefore, the water deficit at flowering stage must be avoided if possible. Martyniak (2008) stated that drought tolerance differs strongly among the growth stages of many crops. Thus, water stress at flowering stage (S_2) will not be allowed because of yield reduction was found higher than other stages (*Table 12*). The flowering stage was the most critical stage to deficit irrigation for sunflower cultivation. The flowering stage is the most sensitive to water deficits which cause considerable seed yield decreases since fewer flower come to full development (Beyazgul et al., 2000; Ali and Shui, 2009). Water deficit at the flowering stage should be avoided. It is clear that the value of response factor varies from location to location (depending on weather and soil), variety to variety, crop to crop, season to season and also for individual growth stages to entire growing season what Ali (2009) discussed in determining response factor of winter wheat in Bangladesh.

The crop response factor (*ky*) value for the entire cropping season was determined by Doorenbos and Kassam (1979). Several research reports exist on yield response of sunflower to water, while other reported that the (*ky*) values were between 0.80 – 0.95 for sunflower (Demir et al., 2006; Moutonnet, 2002). But, Mila and Ali (2016) found that the (*ky*) values were in the range of 0.25 to 0.64 for the whole growing season of sunflower. Similarly, (Sullu and Dagdelen, 2015) reported that the crop response factor as 0.74 for the entire growth season. However, our *ky* values for all genotypes were between 0.09 – 0.78. This confirmed that the genotypes under our study are more tolerant to water deficit, and partly recovering from stress, exhibiting less than relative reductions in yield with reduced water use. Regarding the previous studies, there are agreements ($ky < 1$) (Silva et al., 2014; Steduto et al., 2012) and divergences ($ky > 1$) (Sezen et al., 2011), with respect to tolerance sunflower. However, slight differences in yield response factors were mainly because of differences in climate parameters, plant water consumptions, cultivars, soil conditions, irrigation programs and other cultural practices (Çiçek et al., 2015).

The maximum percentage of seed yield reduction was recorded by Velko genotype under skipping irrigation at flowering stage (I_2) treatment at both locations. This confirmed that the most sensitive stage to water deficit is a flowering stage, which similar to the result reported by Shafi et al. (2013) who indicated a considerable reduction in seed yield of sunflower due to water stress at the flowering stage. Therefore, plant growth stages should be taken into consideration, and irrigation scheduling should accordingly be created to have optimum water use efficiency in semi-arid climates.

It was noticed that the highest uniformity coefficient value recorded by Velko genotype, compared to the values of Barolo RO and Local genotypes, could be due to various factors such as growing season, region and intensity of water deficit (Mila and Ali, 2016).

The study showed that the most active growth stage of irrigation was skipping irrigation at flowering stage, compared with other stages; therefore irrigation during this period would ensure the least yield reduction of sunflower. This implies that irrigation treatment at the middle stage was more efficient to increase the seed yield of sunflower genotypes rather than the early and last irrigation. The tolerance of the full-grown plant to drought may be due to sufficient root penetration without water deficit in the early stages of growth. Also, the increase in the production of antioxidant enzymes when plants are subjected to stress may also provide plant resistance to drought (Langeroodi et al., 2014).

http://www.aloki.hu ● ISSN 1589 1623 (Print) ● ISSN 1785 0037 (Online)
DOI: http://dx.doi.org/10.15666/aeer/1704_76057623

Conclusion

The results indicated that skipping irrigation at the flowering stage was more effective to decrease the seed yield of sunflower genotypes than the achene formation and vegetative stages; it is the most sensitive stage to water deficit which causes considerable yield reduction. It was observed that the water deficit should be avoided at the flowering stage. Thus, water must be ensured at this stage to prevent severe yield loss. Greater water stress may be contributed to higher crop response factor, which indicated that sufficient water supply during flowering and achene formation stage is important. The results showed that water deficit at the flowering stage should be eliminated. However, this will change with location, the intensity of water deficit, and stages of growth. Water stress can influence seed yield in sunflower during the stages of flowering and seed formation due to its effect on reproductive organs and the increase in the number of empty seeds; this may be due to abortion of ovaries, embryo, and sterility of pollen grains.

In view of the existing values of water efficiency, it is recommended to give high priority to Velko genotype coupled with none skipping irrigation at the flowering stage.

REFERENCES

[1] Abou El-Seoud, I. I. A., Wafaa, H. M. (2010): Phosphorus efficiency of different maize (Zea mays, L.) genotypes grown on calcareous soil. – Alex. Sci. Exch. J. 31(1): 1-9.
[2] Ahmed, M. A., Hassanein, M. E. S. (2000): Partition of photosynthates in yellow maize hybrids. – Egyptian Journal of Agronomy 22: 39-63.
[3] Allen, R. G., Pereira, L. S., Raes, D., Smith, M. (1998): Crop evapotranspiration-Guidelines for computing crop water requirements. – FAO Irrigation and Drainage Paper 56. Fao, Rome 300(9): D05109.
[4] Ali, M. H. (2009): Irrigation-yield response factor of winter wheat for different growth phases. – Journal of Agrometeorology 11(1): 9-14.
[5] Ali, M. H., Shui, L. T. (2009): Potential evapotranspiration model for Muda irrigation project, Malaysia. – Water Resources Management 23(1): 57.
[6] Anastasi, U., Santonoceto, C., Giuffrè, A. M., Sortino, O., Gresta, F., Abbate, V. (2010): Yield performance and grain lipid composition of standard and oleic sunflower as affected by water supply. – Field Crops Research 119(1): 145-153.
[7] Angadi, S. V., Entz, M. H. (2002): Water relations of standard height and dwarf sunflower cultivars. – Crop Science 42(1): 152-159.
[8] Baba, H., Zumre, M., Ozyigit, I. I. (2016): A comparative biogeographical study of myxomycetes in four different habitats of eastern Mediterranean part of Turkey. – Fresenius Environmental Bulletin 25(5): 1449-1460.
[9] Bakht, J., Shafi, M., Yousaf, M., Raziuddin, K. M., Khan, M. A. (2010): Effect of irrigation on physiology and yield of sunflower hybrids. – Pak. J. Bot 42(2): 1317-1326.
[10] Bashir, M. A., Mohamed, Y. M. (2014): Evaluation of full and deficit irrigation on two sunflower hybrids under semi-arid environment of Gezira, Sudan. – Journal of Agri-Food and Applied Sciences 2(3): 53-59.
[11] Beg, A., Pourdad, S. S., Alipour, S. (2007): Row and plant spacing effects on agronomic performance of sunflower in warm and semi-cold areas of Iran. – Helia 30(47): 99-104.
[12] Beyazgül, M., Kayam, Y., Engelsman, F. (2000): Estimation methods for crop water requirements in the Gediz Basin of western Turkey. – Journal of Hydrology 229(1-2): 19-26.
[13] Black, C. A., Evans, D. D., Dinauer, R. C. (1965): Methods of Soil Analysis. Vol. 9. – American Society of Agronomy, Madison, WI, pp. 653-708.

http://www.aloki.hu ● ISSN 1589 1623 (Print) ● ISSN 1785 0037 (Online)
DOI: http://dx.doi.org/10.15666/aeer/1704_76057623

[14] Çiçek, N., Arslan, Ö., Çulha-Erdal, Ş., Eyidoğan, F., Ekmekçi, Y. (2015): Are the photosynthetic performance indexes and the drought factor index satisfactory selection criterion for stress. – Fresen. Environ. Bull 24(11c): 4190-4198.
[15] De Pascale, S., Dalla Costa, L., Vallone, S., Barbieri, G., Maggio, A. (2011): Increasing water use efficiency in vegetable crop production: from plant to irrigation systems efficiency. – Hort Technology 21(3): 301-308.
[16] Demir, A. O., Göksoy, A. T., Büyükcangaz, H., Turan, Z. M., Köksal, E. S. (2006): Deficit irrigation of sunflower (Helianthus annuus L.) in a sub-humid climate. – Irrigation Science 24(4): 279-289.
[17] Devitt, D. A., Morris, R. L., Bowman, D. C. (1992): Evapotranspiration, crop coefficients, and leaching fractions of irrigated desert turfgrass systems. – Agronomy Journal 84(4): 717-723.
[18] Doorenbos, J., Kassam, A. H. (1979): Yield response to water. – Irrigation and Drainage Paper 33: 257.
[19] Fan, T., Stewart, B. A., Payne, W. A., Wang, Y., Song, S., Luo, J., Robinson, C. A. (2005): Supplemental irrigation and water–yield relationships for plasticulture crops in the Loess Plateau of China. – Agronomy Journal 97(1): 177-188.
[20] Faraji, A., Latifi, N., Soltani, A., Rad, A. H. S. (2009): Seed yield and water use efficiency of canola (Brassica napus L.) as affected by high-temperature stress and supplemental irrigation. – Agricultural Water Management 96(1): 132-140.
[21] Ghani, A., Hussain, M., Qureshi, M. S. (2000): Effect of different irrigation regimens on the growth and yield of sunflower. – International Journal of Agriculture and Biology 2(4): 334-335.
[22] González, J., Mancuso, N., Ludueña, P. (2013): Sunflower yield and climatic variables. – Helia 36(58): 69-76.
[23] Ibrahim, H. M.(2012): Response of some sunflower hybrids to different levels of plant density. – APCBEE Procedia 4: 175-182.
[24] IPCC (Intergovernmental Panel on Climate Change) (2013): Drought in a Changing Climate: AR5 and Recent Scientific Advances. – IPCC, Geneva.
[25] Iqbal, N., Ashraf, M. Y., Ashraf, M. (2005): Influence of water stress and exogenous glycinebetaine on sunflower achene weight and oil percentage. – International Journal of Environmental Science & Technology 2(2): 155-160.
[26] Kakar, A. A., Soomro, A. G. (2001): Effect of water stress on the growth, yield and oil content of sunflower. – Pak. J. Agri. Sei. 38: 1-2.
[27] Kang, S., Shi, W., Zhang, J. (2000): An improved water-use efficiency for maize grown under regulated deficit irrigation. – Field Crops Research 67(3): 207-214.
[28] Karim, T. H., Karim, K. (2001): Water demand of crops at Smaquly Watershed/ Koya. – FAO Representation in Iraq. FAO Coordination Office for Northern Iraq, Erbil, Iraq.
[29] Kassab, O. M., Abo Ellil, A. A., Abo El-Kheir, M. S. (2012): Water use efficiency and productivity of two sunflower cultivars as influenced by three rates of drip irrigation water. – Journal of Applied Sciences Research 8(7): 3524-3529.
[30] Kazemeini, S. A., Edalat, M., Shekoofa, A. (2009): Interaction effects of deficit irrigation and row spacing on sunflower (Helianthus annuus L.) growth, seed yield, and oil yield. – African Journal of Agricultural Research 4(11): 1165-1170.
[31] Kirda, C., Topcu, S., Çetın, M., Kaman, H., Topaloğlu, F., Derıcı, M. R., Daşgan, Y. (2006): Partial Root Drying and Conventional Deficit Irrigation for Increasing Irrigation-Water Use Efficiency of Major Crops in the Mediterranean Region. – 18th International Soil Meeting (ISM) on "Soils Sustaining Life on Earth, Managing Soil and Technology" Proceedings 1: 272-278.
[32] Kurdistan Regional Government (2018): Kurdistan's geography and climate. – http://cabinet.gov.krd/a/d.aspx?s=010000&l=12&a=18656.
[33] Langeroodi, A. R. S., Kamkar, B., da Silva, J. A. T., Ataei, M. (2014): Response of sunflower cultivars to deficit irrigation. – Helia 37(60): 37-58.

http://www.aloki.hu ● ISSN 1589 1623 (Print) ● ISSN 1785 0037 (Online)
DOI: http://dx.doi.org/10.15666/aeer/1704_76057623

[34] Lorenz, O. A., Maynard, D. N. (1980): Knott's Handbook for Vegetable Growers. – John Wiley & Sons, New York.
[35] Mahender, S., Harbir, S., Tej, S., Jhorar, R. K., Singh, B. P. (2000): Seed yield, water use and water-use efficiency of sunflower (Helianthus annuus) genotypes under irrigation and nitrogen variables. – Indian Journal of Agronomy 45(1): 188-192.
[36] Martyniak, L. (2008): Response of spring cereals to a deficit of atmospheric precipitation in the particular stages of plant growth and development. – Agricultural Water Management 95(3): 171-178.
[37] Michael, A. (1978): Irrigation and Theory Practice. – Vikas Pub. House PVT LTD, New Delhi.
[38] Mila, A. J., Ali, M. H. (2016): Irrigation yield response factor of mustard at different growth phases. – International Journal of Experimental Agriculture 6(1): 15-21.
[39] Moutonnet, P. (2002): Yield response factors of field crops to deficit irrigation. – Deficit Irrigation Practices. Water Reports 22, FAO, Rome, pp. 11-15.
[40] Rauf, S., Jamil, N., Tariq, S. A., Khan, M., Kausar, M., Kaya, Y. (2017): Progress in modification of sunflower oil to expand its industrial value. – Journal of the Science of Food and Agriculture 97(7): 1997-2006.
[41] Reddy, G. K. M., Dangi, K. S., Kumar, S. S., Reddy, A. V. (2003): Effect of moisture stress on seed yield and quality in sunflower. – Journal of Oilseeds Research 20: 282-283.
[42] Sezen, S. M., Yazar, A., Kapur, B., Tekin, S. (2011): Comparison of drip and sprinkler irrigation strategies on sunflower seed and oil yield and quality under Mediterranean climatic conditions. – Agricultural Water Management 98(7): 1153-1161.
[43] Shafi, M., Bakht, J., Mohammad, Y., Aman, K. (2013): Effects of irrigation regime on growth and seed yield of sunflower (Helianthus annuus L.). – Pak. J. Bot. 45(6): 1995-2000.
[44] Silva, A. R. A., Bezerra, F. M. L., de Freitas, C. A. S., Amorim, A. V., de Carvalho, L. C. C., Pereira Filho, J. V. (2014): Coeficientes de sensibilidade ao déficit hídrico para a cultura do girassol nas condições do semiárido cearense. – Revista Brasileira De Agricultura Irrigada-RBAI 8(1): 38-51.
[45] Sinaki, J. M., Heravan, E. M., Rad, A. H. S., Noor Mohammadi Gand, G., Zarei, G. (2007): The effects of water deficit during growth stages of oilseed rape (Brassica napus L). – American-Eurasian Journal of Agricultural and Environmental Sciences 2: 417-422.
[46] Steduto, P., Hsiao, T. C., Fereres, E., Raes, D. (2012): Crop Yield Response to Water. Vol. 1028. – FAO, Rome.
[47] Sullu, A., Dagdelen, N. (2015): The evaluation of drip irrigation on second crop sunflower yield and quality in Soke region. – Journal of Adnan Menderes University Agricultural Faculty 12(1): 45-54.
[48] Sun, H. Y., Liu, C. M., Zhang, X. Y., Shen, Y. J., Zhang, Y. Q. (2006): Effects of irrigation on water balance, yield and WUE of winter wheat in the North China Plain. – Agricultural Water Management 85(1-2): 211-218.
[49] Thomas, G. W. (1996): Soil pH and Soil Acidity. Methods of Soil Analysis. Part 3. Chemical Methods. – ASA, Madison, WI, pp. 475-490.
[50] Tian, F. P., Zhang, Z. N., Chang, X. F., Sun, L., Wie, X. H., Wu, G. L. (2016): Effects of biotic and abiotic factors on soil organic carbon in a semi-arid grassland. – Journal of Soil Science and Plant Nutrition 16(4): 1087-1096.
[51] Tolga, E., Lokman, D. (2003): Yield response of sunflower to water stress under Tekirdag conditions. – Helia 26(38): 149-158.
[52] Turner, N. C. (2004): Agronomic options for improving rainfall-use efficiency of crops in dryland farming systems. – Journal of Experimental Botany 55(407): 2413-2425.
[53] Viscardi, S., Ventorino, V., Duran, P., Maggio, A., De Pascale, S., Mora, M. L., Pepe, O. (2016): Assessment of plant growth promoting activities and abiotic stress tolerance of Azotobacter chroococcum strains for potential use in sustainable agriculture. – Journal of Soil Science and Plant Nutrition 16(3): 848-863.

http://www.aloki.hu ● ISSN 1589 1623 (Print) ● ISSN 1785 0037 (Online)
DOI: http://dx.doi.org/10.15666/aeer/1704_76057623

[54] WWP (2017): The United Nations World Water Development Report 2017. Wastewater: The Untapped Resource. – WWP, Jacksonville, FL.
[55] XLSTAT (2017): Data Analysis and Statistical Solution for Microsoft Excel. – Addinsoft, Paris, France.

APPENDIX

Mean squares of variance analysis for seed yield, IWUE, and WUE at both locations

S.O.V	d.f	Seed yield kg ha^{-1}	Irrigation water use efficiency (kg ha^{-1} mm^{-1})	Water use efficiency (kg ha^{-1} mm^{-1})
Kanipanka Location				
Block	2	19239.73	0.036	0.073
Irrigation	3	1351140**	4.671**	9.531**
E (a)	6	23042.79	0.053	0.108
Genotype	2	4538945**	11.257**	22.973**
Irrigation $_X$ Genotype	6	59495.04**	0.199**	0.406**
E (b)	16	18852.97	0.043	0.088
Qlyasan Location				
Block	2	36831.84	0.134	0.318
Irrigation	3	1309368**	9.854**	23.323**
E (a)	6	111937.5	0.352	0.833
Genotype	2	11904062**	29.743**	70.399**
Irrigation $_X$ Genotype	6	265607.9**	0.729**	1.724*
E (b)	16	84077.5	0.198	0.468

*Significant at 0.05, **significant at 0.01

http://www.aloki.hu ● ISSN 1589 1623 (Print) ● ISSN 1785 0037 (Online)
DOI: http://dx.doi.org/10.15666/aeer/1704_76057623

OCCUPATIONAL HEALTH PROBLEMS OF SAWMILL WORKERS PROCESSING RED PINE IN TURKEY

SÜTÇÜ, A.* – SEMERCI, N. T.

Isparta University of Applied Science, Faculty of Forestry, Department of Forest Products Engineering, 32260 Isparta, Turkey
(phone: +90-246-2113966; fax: +90-246-2371810)

**Corresponding author*
e-mail: abdullahsutcu@isparta.edu.tr; phone: +90-246-211-3966; fax: +90-246-237-1810

(Received ; accepted)

Abstract. Red pine (*Pinus brutia* Ten.) is one of the most common and most processed softwood species in the forest products sector in Turkey. It is essential to learn as much information as possible about potential employee health problems that may occur during processing of this wood. For this reason, sawmill workers that produce lumber from the red pine species were investigated in terms of employee health problems. A face-to-face survey method of employees was used to conduct this study. The questionnaire contained three sub-sections: demographic, physical, and environmental and ergonomic factors that affect employee health. The collected data were statistically evaluated and compared with findings from the literature. Certain important findings are presented as crosstabs and graphs for comparison. Based on the study results, employee complaints about the red pine sawing process during working hours are as follows: allergic reactions due to wood dust: 23.2%; burning eyes and redness: 27.4%; dyspnea: 30.5%; prolonged standing and discomfort: 64.9%; noise-induced hearing loss: 38.5%. It is also realized, however, that occupational diseases such as vascular disorders depend not only on the working environment and conditions but also on the age of employees.
Keywords: *work healthy, woodwork, work-related symptoms, Pinus brutia, occupational hazards*

Introduction

According to a recent press release from the International Council of Forest and Paper Associations (ICFPA), 90% of wood and paper production comes from 43 countries and the forest products industry has a volume of more than $470 billion with more than 14-million people employed worldwide. Approximately 300,000 people provide employment opportunities in Turkey's wood and forestry products industry, with an annual worth of $19-billion (OAIB, 2017).

However, timber manufacturing in Turkey is a sub-sector of the overall manufacturing sector and consists mainly of private sector enterprises of which the majority are small enterprises that grow slowly. Although there is a total of 10.000 sawmills (small or medium to large) with an annual timber capacity of 10 million m^3, at present the current production capacity is reported to be approximately 6-million $m^3$of sawn timber (Sakarya and Canlı, 2011; Görgün and Unsal, 2015).

However, it has been reported that most wood processing plants are exposed to gas, steam, and wood dust that is harmful to workers, but occupational health has not been given enough importance in these enterprises (Barlı, 1996). In recent years, increased sensitivity to occupational health and diseases has led to a comprehensive review of the lumber and forest products sectors. As a result, international authorities have established some legal arrangements with certain risk groups.

One of the first studies on the subject of health problems in the wood-working industry was conducted in England in 1965. This study established that a critical

http://www.aloki.hu ● ISSN 1589 1623 (Print) ● ISSN 1785 0037 (Online)
DOI: http://dx.doi.org/10.15666/aeer/1704_76257639

number of workers exposed to furniture and wood dust developed sino-nasal adenocarcinoma. Since then, many scientific studies of employees working in various wood-related industries have been conducted that reported that these types of workers are at risk. It has been reported that beech and oak species are two of the most common species that cause workers to develop some type of disorder, although many other species cause health problems in workers (Demers et al., 1997). It was also reported that quercetin and Δ3-carene isolated from wood is mutagenic (Jensen et al., 2001).

It was reported that wood dust generated different types of processing could cause work-related respiratory and skin problems or disorders, such as eczema, shortness of breath, nasal cancer, headache, and cramps (Bozkurt and Bozkurt, 1979). It was also reported that workers exposed to high levels of hardwood or softwood dust after smoking and consuming alcohol are at risk for laryngeal cancer (Ramroth et al., 2008). In another study conducted on pine wood sawmills, asthma and cough symptoms were observed for employees that were associated with increased levels of eye and nose irritation resulting from dust exposure (Douwers et al., 2001). It was also proposed that cutting of green wood releases essential oils and monoterpenes into the environment along with wood dust that could cause eye irritation, mucous membrane defects, and skin irritation (Rosenberg et al., 2002). It is clear that dust exposure may result in declining lung function, bronchial hyper-responsiveness, and various other problems such as allergic alveolitis, toxic dust syndrome, chronic bronchitis, rhinitis, mucous irritation, and asthma.

The International Agency for Research on Cancer (IARC) has already classified wood dust as a Group 1 agent that is carcinogenic to humans, based on evidence of the effects of exposure to hardwood dust on the nasal cavities and paranasal sinuses of exposed woodworkers (IARC, 1995). In 2009, the IARC concluded that wood dust should be avoided by workers and could cause cancer of the nasal cavities, paranasal sinuses, and nasopharynx (Siew et al., 2012).

In view of the physical and psychological effects of working conditions in the workplace, it was suggested that musculoskeletal injuries of the upper limbs were the most common type of injury in the timber industry (Jones and Kumar, 2004). Similarly, it was found that the highest rate of injury was associated with the transport of logs to timber processing sites (Bello ve Mijinyawa, 2010). Work-related symptoms in sawmill workers typically are chest tightness, cough, dyspnoea, hoarseness, headache, weakness, sweating, eye and body itching, and skin rash (Dutkiewitcz, 2001).

Based on the results of this comprehensive literature survey, a detailed study focused on the occupational health problems of employees working in red pine processing sawmills was not found. However, the red pine species is spread widely throughout not only Turkey but also throughout the forests of Mediterranean countries. The aim of this research was to evaluate the working conditions of red pine processing sawmills in order to identify general health problems for employees and to develop solutions to problems that may arise in terms of occupational health in depends on the perception of employees. Results of this study will provide simple but high-impact information concerning the quality of life of employees.

Materials and methods

In this study, health problems that may occur in employees were directly evaluated with a standard questionnaire that was distributed to employees. This survey was given

http://www.aloki.hu ● ISSN 1589 1623 (Print) ● ISSN 1785 0037 (Online)
DOI: http://dx.doi.org/10.15666/aeer/1704_76257639

to 413 employees across 17 enterprises in Turkey. The study was conducted among sawmill workers processing red pine wood in west mediterrian region between July 2013 and February 2014. The open-ended questions included in the questionnaire form were distributed to employees about 10-15 min. Participants were asked to respond and their opinions about the general problems and their solutions were recorded.

According to a forest activity report from the Union of Chambers and Commodity Exchanges of Turkey (TOBB), 13285 people are employed in the sawmill and parquet sector and 67.3% of them are workers (8945) (TOBB, 2012). No official information was available that reported the species of wood processed by the sawmills. However, a previous study conducted on the Isparta region found that 90% of the primary forest production enterprises used red pine (Sütçü et al., 2008).

In order to determine the minimum sample size to be surveyed and to provide statistical reliability, the number of samples needed for a 95% confidence level was determined to be a minimum of 368 people according to the following equation (*Eq. 1*) (Krejcie and Morgan, 1970).

$$s = \frac{X^2 NP(1-P)}{d^2(N-1)+X^2P(1-P)} \quad \text{(Eq.1)}$$

where; s: *required sample size*; χ^2: *the table value of chi-square for one degree of freedom at the desired confidence level (1.96^2)*; N: *the population size (8945)*; P: *the population proportion (assumed to be 0.5 since this would provide the maximum sample size)*; d: *the degree of accuracy expressed as a proportion (0.05), s=368*.

In this study, a total of 413 randomly selected people were given the questionnaire in order to produce more accurate results. The study's data information and survey specifications are shown in *Table 1*.

Table 1. *The survey and questionnaire specifications*

Country	Population*		Samples			
	Number of work places (Nw)	Number of employees (Ne)	Number of work places (nw)	Number of employees (ne)	Workplace rate (nw/Nw)	Employees rate (ne/Ne)
Isparta	402	1.070	12	315	2.99%	29.44%
Burdur	235	780	1	15	0.43%	1.92%
Antalya	1.027	2.496	1	40	0.10%	1.60%
Adana	755	1.699	3	43	0.40%	2.53%
Total	2419	6045	17	413	0.7%	6.83%

* According to TUIK (2007)

The questionnaire forms, which were prepared with the literature reports, contained 23 topics under three headings (demographic, current, physical and environmental factors).

For statistical evaluation of survey data, the necessary analyses were conducted using statistical software SPSS 13.0 and the results of these analyses were interpreted by graphs and tables. Due to the discontinuous data of the study, the results were graded with 0-1 variables that are expressed as discrete variables (yes-no, good-bad, existent-non-existent). Therefore, it was decided to simultaneously use Chi-square for trend test and Student's t-test, assuming $p < 0.05$ as the significance level. However, a Chi-square for trend test was performed whether there was a linear trend for an outcome to increase

http://www.aloki.hu ● ISSN 1589 1623 (Print) ● ISSN 1785 0037 (Online)
DOI: http://dx.doi.org/10.15666/aeer/1704_76257639

or decrease over the range of an ordered categorical exposure variable (Peat et al., 2009).

Results and discussion

Evaluation of demographic factors for sawmill employees processing red pine

Demographic data of the employees in the pine wood processing sawmills are presented in *Table 2*. According to the survey results, the majority of the employees in the sector are predominately male with an age distribution greater than middle-age. However, according to the Turkish 2002 general manufacturing industry workplace report, the rate of women working in the sub-sector of sawnwood and cork production (excluding furniture) is 6.84% (TUIK, 2007). In this study, the rate of female employees was found to be only 3.6%. Moreover, more than half of the employees in this sector are in the age group of 30 to 40 years of age. This clearly shows that young people (18-30 years) are not interested in the sawmill industry. It is also important to note that approximately 70% of employees have primary education while the undergraduate level is not even 1%. Similar results were found in Turkish studies of the sawmill sector (Osman and Pala, 2009).

Table 2. *Demographic characteristics of participants*

Gender	**Female**			**Male**	
	%3,6			%96,4	
Age (Year)	**<20**	**20-30**	**31-40**	**41-50**	**50<**
	%1	%19	%50	%23	%7
Education level	**Primary Education**	**High School**	**Vocational High School**		**Higher Education**
	66.8%	14.5%	17.9%		0.7%
Length of employment (in industry)	**<1**	**2-5 year**	**6-10 year**	**10<**	
	%13	%27	%23	%37	

It was also found that approximately 40% of the workers have worked in the same sawmill for 10 years or longer. The work time of employees in the forest products industry also supports the results of our current work (Osman and Pala, 2009). Of the employees in this sector, 45% had previously worked with furniture or as carpenters and 3% worked in other manufacturing sectors such as marble-mining, which is different from woodworking sector.

Working units in sawmills are broadly divided into two parts: the sawmill workshop-manufacturing area and sawmill yards. Sawmill workshops refer to the units where activities such as processing, sawing, planning, and sanding are performed and 67% of employees working in Sawmill workshops. In sawmill yards, activities such as stacking logs, and drying the sawn timber in the open air are performed and 33% of the employees work in sawmill yards.

Evaluation of physical working comfort for red pine sawmill employees

Physical working comfort is dependent on the physical working circumstances and the ergonomic characteristics of the manufacturing environment. Conditions such as a poor working environment, noise, inadequate lighting, ventilation, excessive and

http://www.aloki.hu ● ISSN 1589 1623 (Print) ● ISSN 1785 0037 (Online)
DOI: http://dx.doi.org/10.15666/aeer/1704_76257639

prolonged work hours, absolute temperature and failure to comply with ergonomic standards adversely affects the productivity of employees. However, the most important work environment factors that affect occupational health in the woodworking industry are noise and wood dust (Barlı, 1996). In this study, noise was found to be the most important factor (*Figure 1*). The main sources of noise in sawmills are band saws, planers, gang saw, and compressors, and the noise level usually exceeds 85 dB (Reinhold et al., 2006; Gomez et al., 2010). Although this situation may cause temporary deafness and hearing loss, it is reported that this noise is effective even on retention of coronary heart failure and this risk continues even after retirement (Virkkunen et al., 2005). De Souza et al. (2015) claims that noise exposure is independently associated to hypertension. In our study, we considered only for auditory effects. As a result 62% of the employees stated that they had experienced hearing loss as a result of excessive noise.

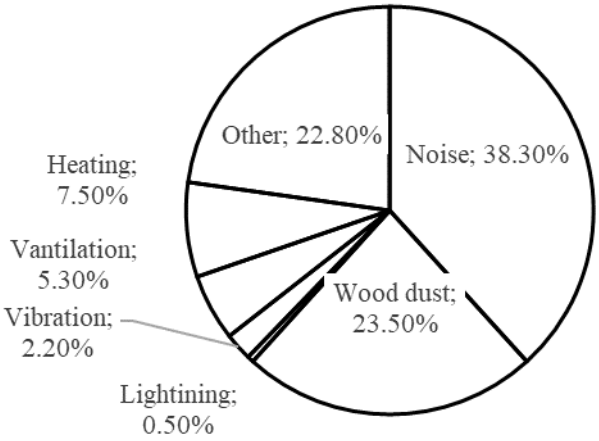

Figure 1. *Response of sawmill workers about working conditions*

It was reported that the woodwork industry usually utilizes low technology and the average age of many machine-plants is over ten years (Sütçü et.al., 2008; Sakarya and Canlı, 2011). The use of old machinery and facilities deprives the sector of new technologies that have taken the necessary measures in terms of the health and safety of employees. As a result of the observations made within the scope of the evaluated enterprises, significant differences in noise and vibration between the use of old and new technology, especially with compressor, multi-slitting, and profile machines, were observed. Ülker (2018) reported that, in furniture manufacturing, most of the machines exceed the threshold of 85 dB, even when operating in the idle position. Vibration, as a noise factor, causes pain in various limbs (e.g., wrist, arm, elbow, leg) of the workers. Pain was reported in the body as a result of exposure to vibration in 60.3 percent of employees.

Another important factor is 'wood dust' (with a rate of about 24%), as shown in *Figure 1*. Wood dust is known to cause respiratory symptoms related to asthma, dermatitis, eye irritation, and upper respiratory tract. However, wood dust is also classified as a human carcinogen by IARC (IARC, 1995). And it has only been conclusively linked to sinonasal cancers, despite individual studies suggesting an association with a range of respiratory tract cancers. Hancock et al. (2014) has

http://www.aloki.hu ● ISSN 1589 1623 (Print) ● ISSN 1785 0037 (Online)
DOI: http://dx.doi.org/10.15666/aeer/1704_76257639

demonstrated significant associations between lung cancer and wood dust exposure or employment in wood dust-related occupations. Moreover, respiratory protective equipment and local exhaust ventilation reduce the risk of occupational sinonasal cancer (Emanuelli et al., 2016).

Lighting and ventilation are important working condition factors. Adequate levels of lighting reduces the risk of accidents that may occur when using machinery and equipment. According to this study, the lighting situation is considered to be sufficient by a high percentage of employees (91.5%). However, ventilation conditions were not quite as high by those employees who considered the lighting conditions to be adequate (84.3%).

Temperature and humidity conditions are other important factors that affect the subjective feeling of human comfort. Too low or too high ambient temperature and high humidity negatively affect the productivity of employees. Based on the results of our study, although the majority of the employees thought that thermal comfort was adequate in the winter and summer months, approximately 40% of them reported that they felt very hot or very cold in terms of thermal comfort. This indicates that enterprises do not take adequate measures for heating in cold areas and cooling in hot areas. In regions with cold winter conditions, such as Isparta, experienced warming problems due to the lack of adequate heating systems in the facility; warm regions, such as Adana, due to the heat and humidity in summer conditions, climatic disturbance is felt. Despite this, the ratio of those who feel that thermal comfort is sufficient (62%) should not be underestimated.

Evaluation of general health problems in sawmill activities

In the forest product industry, it is inevitable for employees to avoid joint disturbances as a result of long-term outpatient work, loading and unloading of loggers, transporting large and heavy materials between machines, and loading the machine. But this factor can cause work related musculoskeletal syndrome disorders (MSD's) or different kinds of problems in organisms (Gedik and Akyüz, 2004). However, it was proposed that low back pain, tendonitis, and tenosynovitis are the most common MSD's that accounted for 25% of occupational injuries in the United States in 1997 (Wu et al., 2009). Bello and Mijinyawa (2010) reported that 57.81% of those working in the sawmill industry in Nigeria had pain in the back and in the lower back. According to our findings as summarized in *Table 3*, the number and incidence of joint pain (back, waist, foot) caused by prolonged standing during work has been quite high (64.9%). Also, the situation of vascular diseases that has emerged as an occupational discomfort due to prolonged standing during work conducted by sawmill workers.

Table 3. *Symptoms to body area for sawmill tasks*

Symptoms (n=413)	**Frequency**	**Percentage (%)**
Work Related Musculoskeletal Syndrome Disorders (MSD's)	268	64.9
Joint pain due to vibratory	164	39.7
Hearing Impairment	159	38.5
Respiratory dysfunction (dyspnea)	126	30.5
Eye irritation due to wood dust	113	27.4
Varicose veins	106	25.7
Work related allergic reactions	96	23.2

http://www.aloki.hu ● ISSN 1589 1623 (Print) ● ISSN 1785 0037 (Online)
DOI: http://dx.doi.org/10.15666/aeer/1704_76257639

The distribution of vascular disease in the participants according to demographic characteristics is shown in *Table 4*. The incidence of vascular disease was not significantly different according to gender and work unit ($p > 0.005$). Although there was a decrease in the trend of educational status (26.8%; 23.9%; 0.0%), the incidence of vascular disease was not significantly different based on the education level of the employees (χ^2 for trend = 0.820, $p = 0.365$, *Table 4*). According to the data evaluated and the statements of the employees participating in the survey, a significant difference was found between vocational education and vascular disease (χ^2 for trend=24.294, p=0.0001). Although the frequency of vascular disturbance based on length of employment showed a significant difference, the results of the analysis (χ^2 for trend=10.304, p=0.005) show that, when the direction of the trend is taken into consideration and employees with 6-10 years of experience are excluded from the evaluation, the significant difference in the analysis is lost (χ^2 for trend= 4.42, p=0.110). This situation applies to employees who work in the red pine processing sawmills and shows that the length of employment has no effect on the risk of vascular disease.

Based on the t-test, the relative age of patients that developed vascular disease was older than no patients, but the difference was not significant (37.3, SD:7.58; 36.6, SD:4.7; $p = 0.428$).

The incidence of MSD's was not significantly different based on gender, educational status, and occupational education ($p > 0.05$, *Table 4*). However, the relationship of MSD's with the working area showed a significant difference ($\chi^2 = 3.426$, $p < 0.05$). This indicates that workers (71.1%) in the yards face more risk of joint pain than those working in the workshop (61.9%).

According to the length of employment, the incidence of MSD's showed a significant difference (χ^2 for trend = 11.374, $p< 0.05$, *Table 4*). However, when employees with a work duration less than one year were excluded from the evaluation, the significant difference in the analysis was lost (χ^2 for trend = 4.66, $p = 0.097$). According to the results of the analysis, workers with a work duration of less than one year had many complaints about MSD's (80.8%). Although there is a gradual increase in length of employment of more than one year, no significant difference was observed based on the results of the analysis, but this situation can be explained by the "training and practice" effect (Yıldırım, 1989).

Workers in woodwork industries are exposed to hand–arm vibrations, awkward posture, repetitive tasks, and high grip force. Also, vibration has been reported to introduce fatigue in muscles, further augmenting postural stress (Bhardwaj and Khan, 2018). In this study, the change in the occurrence of MSD's (especially joint pain) caused by demographic-based vibration exposure is shown in *Table 4*.

Joint pain caused by vibration and its correlation to gender, working unit, and work time does not show a significant difference. However, there is a significant difference based on the education level of the employees (χ^2 for trend = 5.683, $p < 0.05$, *Table 4*). Based on the occupational education of employees, the presence of joint pain caused by exposure to vibration showed a significant difference ($\chi^2 = 8.077$, $p < 0.05$). However, the mean age (35.7; SD:8.0) of participants with complaints about joint pain resulting from exposure to vibration was lower than the mean age of those without joint pain (37.5; SD:7.6, $p < 0.05$). As a result of these observations made in sawmills, the employment of highly qualified personnel with a higher education level in more qualified jobs, low level of education, new entry into the business and unqualified personnel can be related to the work in units of older model machines, which work more noisily and vibrate.

http://www.aloki.hu ● ISSN 1589 1623 (Print) ● ISSN 1785 0037 (Online)
DOI: http://dx.doi.org/10.15666/aeer/1704_76257639

Table 4. *The Crosstab about relationship with Symptoms for sawmill employees processing red pine according to demographic characteristics*

Symptoms	Demog-raphic Characters		**Gender**		**Education level**			**Voc. Education**		**Production area**		**Length of Employment**			
			Female	Male	Pri. Edu	H. Sch.	H. Edu.	Yes	No	Work-shop	Yards	<1	2-5 year	6-10 year	10<
		Count	15	398	276	134	3	105	308	278	135	52	111	97	153
Varicose veins	Yes	Count	1	105	74	32	0	46	60	75	31	12	26	16	52
		%	6.7	26.4	26.8	23.9	0	43.8	19.5	27	23	23.1	23.4	16.5	34
	No	Count	14	293	202	102	3	59	248	203	104	40	85	81	101
		%	93.3	73.6	73.2	76.1	100	56.2	80.5	73	77	76.9	76.6	83.5	66
		χ^2	2.945		0.82			24.294		0.768		0.768			
		p	0.069		0.365			0.0001		0.226		0.226			
Arthrosis Pain	Yes	Count	8	260	174	93	1	64	204	172	96	42	61	61	104
		%	53.3	65.3	63	69.4	33.3	61	66.2	61.9	71.1	80.8	55	62.9	68
	No	Count	7	138	102	41	2	41	104	106	39	10	50	36	49
		%	46.7	34.7	37	30.6	66.7	39	33.8	38.1	28.9	19.2	45	37.1	32
		χ^2	0.811		16.679			2.144		2.41		2.669			
		p	0.278		0.0001			0.091		0.076		0.445			
Respiratory dysfunction	Yes	Count	3	123	102	23	1	38	88	38	88	15	40	30	41
		%	20	30.9	37	17.2	33.3	36.2	28.6	36.2	28.6	28.8	36	30.9	26.8
	No	Count	12	275	174	111	2	67	220	67	220	37	71	67	112
		%	80	69.1	63	82.8	66.7	63.8	71.4	63.8	71.4	71.2	64	69.1	73.2
		χ^2	0.811		16.679			2.144		2.41		2.669			
		p	0.278		0.0001			0.091		0.076		0.445			
Work related allergic reactions	Yes	Count	4	92	66	30	0	28	68	63	33	21	20	20	35
		%	26.7	23.1	23.9	22.4	0	26.7	22.1	22.7	24.4	40.4	18	20.6	22.9
	No	Count	11	306	210	104	3	77	240	215	102	31	91	77	118
		%	73.3	76.9	76.1	77.6	100	73.3	77.9	77.3	75.6	59.6	82	79.4	77.1
		χ^2	0.102		0.367			0.924		0.162		10.649			
		p	0.475		0.545			0.203		0.388		0.014			

http://www.aloki.hu ● ISSN 1589 1623 (Print) ● ISSN 1785 0037 (Online)
DOI: http://dx.doi.org/10.15666/aeer/1704_76257639

Symptoms	Demog-raphic Characters		Gender		Education level			Voc. Education		Production area		Length of Employment			
			Female	Male	Pri. Edu	H. Sch.	H. Edu.	Yes	No	Work-shop	Yards	<1	2-5 year	6-10 year	10<
		Count	15	398	276	134	3	105	308	278	135	52	111	97	153
Eye irritation due to wood dust	Yes	Count	5	108	85	28	0	26	87	70	43	18	33	33	29
		%	33.3	27.1	30.8	20.9	0	24.8	28.2	25.2	32.9	34.6	29.7	34	19
	No	Count	10	290	191	106	3	79	221	208	92	34	78	64	124
		%	66.7	72.9	69.2	79.1	100	75.2	71.8	74.8	68.1	65.4	70.3	66	81
		χ^2	0.279		5.409			0.478		2.035		9.295			
		p	0.393		0.02			0.288		0.096		0.026			
Hearing Impairments	Yes	Count	2	157	109	50	0	39	120	100	59	26	44	38	51
		%	13.3	39.4	39.5	37.3	0	37.1	39	36	43.7	50	39.6	39.2	33.3
	No	Count	13	241	167	84	3	66	188	178	76	26	67	59	102
		%	86.7	60.6	60.5	62.7	100	62.9	61	64	56.3	50	60.4	60.8	66.7
		χ^2	4.163		0.65			0.109		2.295		4.709			
		p	0.033		0.42			0.417		0.08		0.194			
Joint pain caused by vibration	Yes	Count	3	161	120	44	0	54	110	111	53	27	42	30	65
		%	20	40.5	43.5	32.8	0	51.4	35.7	39.9	39.3	51.9	37.8	30.9	42.5
	No	Count	12	237	156	90	3	51	198	167	82	25	69	67	88
		%	80	59.5	56.5	67.2	100	48.6	64.3	60.1	60.7	48.1	62.2	69.1	57.5
		χ^2	2.526		5.683			8.077		0.017		7.019			
		p	0.09		0.017			0.003		0.492		0.071			

Abbreviations: Voc. Education :Vocational Education; Pri. Edu.: Primary Education (basic education for eight years); H. Sch.: High School (4 years of High School); H.Edu.: Higher Education (4 years of University and upper)

http://www.aloki.hu ● ISSN 1589 1623 (Print) ● ISSN 1785 0037 (Online)
DOI: http://dx.doi.org/10.15666/aeer/1704_76257639

Wood dust is one of the most important health risks in forest product workplaces, as described in the literature. Required limit values have been established by international organizations (Siew et al., 2012; IARC, 2012). However, the mechanism of pathogenesis involving the lungs in woodworkers could be due to exposure to airborne dust of different particle sizes, concentrations and compositions.

Moreover, these structural components are also responsible for most toxic, irritant, and sensitizing effects which become a cause of impairment and worsening of lung function. In addition, it is well known that wood contains many microorganisms (including fungi) and toxins, agents such as; terpenes, abietic acid, and plicatic acid in different types are, potentially, implicated in the occurrence of asthma by inducing increased bronchial responsiveness or by damaging the bronchial epithelial cells (Kherde et al., 2017). According to the results of the survey, 30% of the workers experienced dyspnea that was caused by exposure to wood dust. *Table 4* illustrates the change in dyspnea frequency caused by participants' exposure to wood dust based on demographic characteristics. The frequency of dyspnea was not significantly different according to gender, occupational education, work unit, and work time. But it was significantly different based on education level of employees (χ^2 for trend=1.679, p=0.0001). This situation can be explained by qualified personnel that graduated from high school working in more qualified work units (technical units-departments which are less exposed to wood dust). When the ratio of university graduates contrasts with the above explanation, only three university graduates participated in the survey, which makes it difficult to propose a valid interpretation.

There was no statistically significant difference ($p > 0,05$) in the mean age between employees who have shortness of breath (37.1; SD:7.3) and those that do not (36.6; SD:8.0).

The frequency of allergic reactions did not show a significant difference based on gender, education, occupational education status, and working area (*Table 4*). The frequency of allergic reactions based on length of employment showed a significant difference (χ^2 for trend = 10.649, $p < 0,05$). This difference is due to the frequency of high allergic reactions in less than one year (40.4%). When employees less than one year are excluded from the evaluation, the significant difference is lost (χ^2 for trend = 0.92, $p> 0,05$).

The mean age (35.4, SD:7.5) of participants having allergic reactions was lower than the mean age of participants without allergic reactions (37.2, SD:7.8; p= 0.051). As a result of exposure to dust in the workplace, 27.4% of the workers had itching, redness, and burning in the eyes caused by wood dust but 72.6% of the participants did not have such complaints (*Table 4*). In the literature, allergic reactions to sawdust from softwood are more common among sawmill workers than allergic reactions to sawdust from hardwood (Dutkiewicz, 2001). Rosenberg et al. (2002) reported for pine processing industries the focused on monoterpene exposure which causes work-related subjective symptoms.

There was no significant difference in the occurrence of redness and burning in the eyes based on gender, the level of vocational education, and the work area (*Table 4*). A significant difference was observed based the education level of the employees (χ^2 for trend = 5.490, $p<0.05$). Similarly, a significant difference was observed based on length of employment (χ^2 for trend = 9.295, $p < 0.05$). This difference was due to redness and burning complaints ranging from 6 to 10 years (34%). When these employees are excluded from the evaluation, the significant difference is lost (χ^2 for trend = 0.59,

http://www.aloki.hu ● ISSN 1589 1623 (Print) ● ISSN 1785 0037 (Online)
DOI: http://dx.doi.org/10.15666/aeer/1704_76257639

p> 0.05). The mean age (35.3, SD:6.4) of the participants that have redness and burning in the eyes was lower than the mean age of the participants without these complaints (37.3, SD:8.8; p = 0.051).

The percentage of participants who stated that they experienced hearing loss as a result of exposure to noise in the red pine processing sawmill was high (38.5%, *Table 3*). The frequency of hearing loss based on gender showed a significant difference ($\chi 2$=4.163, p=0.033). Male employees (39.4%) expressed that they experienced hearing loss due to more noise so than women. Male employees are exposed to greater levels of noise depend on working in noise-intensive environments and may experience more health problems related to hearing loss. Female are generally employed in classification-standardization and packaging units. In addition, no significant difference was found in terms of hearing loss status based on education level, vocational education, working area, and length of employment. Similarly, there was no significant difference in the 95% confidence level between the average age of the participants with hearing loss and the mean age of those who did not experience hearing loss (p = 0.167). According to *Table 4*, the rate of hearing loss was found to be as high as 50% in employees with less than one year of work experience. However, it is known that at least two years of working in a noisy environment are required for the formation of hearing loss as a result of continuous noise exposure. According to these data, it is estimated that the employees experience temporary hearing loss.

General complaints about ergonomic conditions in red pine processing sawmills

Figure 2 shows a summary for the question of 'What do you think is the most important factor that negatively affects the health of employees in the environment where you work?' The most important complaints expressed by workers were "ignore use of personal protective equipment (PPE)" and "overtime work".

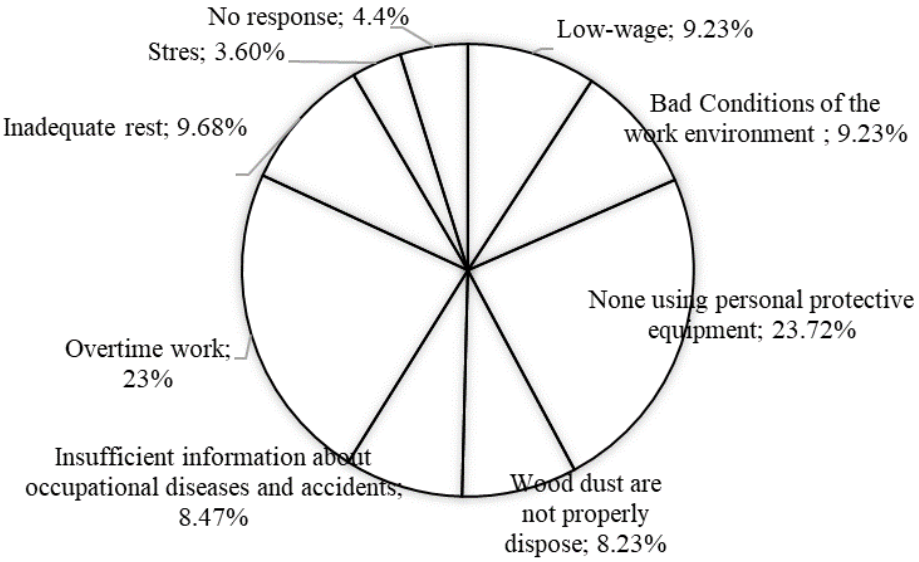

Figure 2. *Complaints in red pine processing sawmills expressed by workers*

It is understood that the use of PPE, such as earmuffs or plugs, hand gloves, or masks, has been poor and inappropriate in the wood processing industries and they are

http://www.aloki.hu ● ISSN 1589 1623 (Print) ● ISSN 1785 0037 (Online)
DOI: http://dx.doi.org/10.15666/aeer/1704_76257639

often considered to be irrelevant and disturbing. According to the results of the survey; approximately 25% of employees complain of non-use of PPE in the work environment. One of the most common reason for not using it, was mentioned that PPE causes discomfort while working (Top et al., 2016). Effendi and Pratama (2017) found a significant relationship between knowledge with the use of personal protective equipment. Similar findings were made by other groups (Bello and Mijinyawa, 2010; Jerie, 2012). These groups also reported that some workers (23%) complained about overtime. However, the majority of these employees are ungrudging in to work under the overtime work to meet their economic requirements due to their unqualified employee status and minimum wage. In Turkey, according to the Regulation on Working Hours of Labor Law, uninterrupted work time cannot exceed 11 hours per day (RG, 25425). Overtime work causes problems such as fatigue, weariness, and carelessness in employees and also decreases job dissatisfaction and work performance. This is why the risk of accidents can be reduced while increasing employee motivation and work efficiency with organizational configuration measures such as more efficient organization of break times, job expansion, and job enrichment. In addition, 9% of employees reported that they do not have any information or knowledge about occupational health and safety. This shows that the risks to employees in the work environment, the hazards that may arise from these risks, and the rights of employees against these risks are not known. In this scenario, employers have a significant role. Employers should organize information seminars for their employees through their occupational health and safety experts. The studies done by various authors have also recommended implementation of an occupational health service and development of a means for collective and individual prevention to reduce the risk maximally. It has already proposed that the health risk should be minimized by the mutual collaboration between health officials, woodworkers and their management (Kherde et al., 2016).

Conclusions

The employees studied in this work are exposed to wood dust generated during the processing of red pine wood, to chemicals formed by the extracts and essential oils in the wood, and to hazardous preservatives that are used to prevent biological and physical degradation of these raw materials. In addition, it is inevitable that occupational health problems will be experienced by the employees due to the fact that working conditions are not sufficiently ergonomic, heavy material is manipulated manually, and physical factors such as overtime work.

However, inevitable muscular and skeletal syndrome disorders develop as a result of prolonged standing during work, loading and unloading of loggers, transportation of large and heavy planks between the machines. However, workers in the yards encounter more risk of joint pain than those working in the workshop. In addition, use of PPE, improvements to the working environment, and organization of information seminars about occupational health and safety have been suggested by workers.

The length of the work day causes problems such as fatigue, weariness, absence, turnover, carelessness, poor performance, and decreased job satisfaction. For these reasons, the risk of accidents can be reduced while implementing work structuring principles such as more effective organization of break times, job enrichment, job enlargement, and job rotation to increase motivation and work efficiency.

http://www.aloki.hu ● ISSN 1589 1623 (Print) ● ISSN 1785 0037 (Online)
DOI: http://dx.doi.org/10.15666/aeer/1704_76257639

Acknowledgements. This study is derived from Nazik Tugba Semerci's MSc Thesis. The authors wish to thank the Suleyman Demirel University, Scientific Research Projects Coordination Unit (SDU-BAP) Project number: 3559-YL1-13 for the financial support received for this research.

REFERENCES

[1] Barlı, Ö. (1996): Physical Environment Factors That Influence Human Health in Forest Product Industry. – Tr. J. of Agriculture and Forestry 22: 521-524. (in Turkish).
[2] Bello, R. S., Mijinyawa, Y. (2010): Assessment Of Injuries in Small Scale Sawmill Industry of South Western Nigeria. – Agric Eng Int: CIGR Journal 12(1): 151-157.
[3] Bhardwaj, S., Khan, A. A. (2018): Ergonomics investigation for orientation of the handles of wood routers. – International Journal of Occupational Safety and Ergonomics (JOSE) 24(4): 592-604.
[4] Bozkurt, A. Y., Bozkurt, T. (1979): Healthy problems in woodworking industries. – Journal of the Faculty of Forestry Istanbul University, Series B 29(2): 60-67. (in Turkish).
[5] Demers, P., Teschke, K., Kennedy, S. (1997): What to Do About Softwood? A Review of Respiratory Effects and Recommendations Regarding Exposure Limits. – American Journal of Industrial Medicine 31: 385-398.
[6] De Souza, T. C. F., Périssé, A. R. S., Moura, M. (2015): Noise exposure and hypertension: Investigation of a silent relationship Environmental and occupational health. – BMC Public Health 15(1): 328.
[7] Douwes, J., McLean, D., Slater, T., Pearce, N. (2001): Asthma and Other Respiratory Symptoms in New Zealand Pine Processing Sawmill Workers. – American Journal Of Industrial Medicine 39(6): 608-615.
[8] Dutkiewicz, J., Skorska, C., Krysinska-Traczyk, E., Dutkiewicz, E., Matuszyk, A., Sitkowska, J. (2001): Response of Sawmill Workers to Work-Related Airborne Allergens. – Ann Agric Environ Med 8(1): 81-90.
[9] Effendi, L., Pratama, A. P. (2017): Factors Related For Use Of Personal Protective Equipment on Worker Carpenter in Ciputat District South Tangerang City Bante. – International Conference of Occupational Health and Safety (ICOHS) 2017, Proceeding Book, 1–2 Nov. 2017, Bali, Indonesia, FKM UI, Depok, pp.113-123.
[10] Emanuelli, E., Alexandre, E., Cazzador, D., Comiati, V., Volo, T., Zanon, A., Scapellato, M. L., Carrieri, M., Martini, A., Mastrangelo, G. (2016): A case-case study on sinonasal cancer prevention: effect from dust reduction in woodworking and risk of mastic/solvents in shoemaking. – Journal of Occupational Medicine & Toxicology 11(1): 1-7.
[11] Gedik, T., Akyüz, İ. (2004): Investigation of working conditions based on sectors. – Kafkas Üniversitesi Artvin Orman Fakültesi Dergisi 5(2): 182-192. (in Turkish).
[12] Gomez, M. E., Sanchez, J. F., Cardona, M. A., Pioquinto, J. F., Torres, P., Sanchez, D., Camargo, L. M., Castaneda, R. A., Villamizar, R. H., Cremades, V. L. (2010): Health and Working Conditions in Carpenter's Workshop in Armenia (Colombia). – Industrial Health 48(2): 222-230.
[13] Görgün, H. V., Ünsal, Ö. (2015): Past, present and future of the lumber industry in Turkey. – 2023'e Doğru 3. Doğa ve Ormancılık Sempozyumu, Antalya, Türkiye. pp.1-1. (in Turkish).
[14] Hancock, D. G., Langley, M. E., Chia, K. L., Woodman, R. J., Shanahan, E. M. (2015): Wood dust exposure and lung cancer risk:a meta-analysis. – Occup Environ Med 72: 889-898.
[15] IARC. (1995): IARC Monographs on the Evaluation of Carcinogenic Risks to Humans: Wood Dust and Formaldehyde. – Vol. 62. Lyon, France: IARC, World Health Organization.
[16] IARC. (2012): IARC Monographs on the Evaluation of Carcinogenic Risks to Humans: Wood Dust. – Vol. 100C [Online], https://monographs.iarc.fr [accessed 02 Dec., 2018].

http://www.aloki.hu ● ISSN 1589 1623 (Print) ● ISSN 1785 0037 (Online)
DOI: http://dx.doi.org/10.15666/aeer/1704_76257639

[17] Jensen, L. K., Larsen, A., M∅lhave, L., Hansen, M. G., Knudsen, B. (2001): Health Evaluation of Volatile Organic Compound (VOC) Emissions from Wood and Wood-Based Materials. – Archives of Environmental Health: An International Journal 56(5): 419-432.
[18] Jerie, S. (2012): Occupational health and safety problems among workers in the wood processing industries in Mutare, Zimbabwe. – Journal of Emerging Trends in Economics and Management Sciences (JETEMS) 3(3): 278-285.
[19] Jones, T., Kumar, S. (2004): Occupational Injuries and Illnesses in The Sawmill Industry of Alberta. – International Journal of Industrial Ergonomics 33: 415-427.
[20] Kherde, P. M., Mishra, N. V., Chitta, S. S., Gahukar, S. D. (2017): Influence of sawdust on peak expiratory flow rate in sawmill workers of central India working in unprotected environment and its correlation with duration of exposure. – National Journal of Physiology, Pharmacy and Pharmacology 7(1): 68-73.
[21] Krejcie, R. V., Morgan, D. W. (1970): Determining Sample Size for Research Activities. – Educational and Psychological Measurement 30: 607-610.
[22] OAIB. (2017): Development of Foreign Trade in Turkey, Wood, Paper and Forest Products Sector Report. – www.turkishwood.org [accessed 24 Dec., 2018] (in Turkish).
[23] Osman, E., Pala, K. (2009): Occupational Exposure to Wood Dust and Health Effects on the Respiratory System in a Minor Industrial Estate in Bursa/Turkey. – International Journal of Occupational Medicine and Environmental Health 22(1): 43-50.
[24] Peat, J., Barton, B., Elliott, E. (2009): Statistics Workbook for Evidence-based Health Care. – Chichester: Wiley-Blackwell.
[25] Ramroth, H., Dietz, A., Ahrens, W., Bechen, H. (2008): Occupational Wood Dust Exposure and the Risk of Laryngeal Cancer: A Population Based Case-Control Study in Germany. – American Journal of Industrial Medicine 51(9): 648-655.
[26] Reinhold, K., Tint, P., Kiivet, G. (2006): Risk Assessment In Textile And Wood Processing Industry. – International Journal of Reliability, Quality and Safety Engineering 13(2): 115-125.
[27] RG 25425. (2004): Regulation on working time related to labor law. – Resmi Gazete, (2004, 6 April) (in Turkish).
[28] Rosenberg, C., Liukkonen, T., Kallas-Tarpila, T., Ruonakangas, A., Ranta, R., Nurminen, M., Welling, I., JaÈppinen, P. (2002): Monoterpene and Wood Dust Exposures: Work-Related Symptoms Among Finnish Sawmill Workers. – American Journal of Industrial Medicine 41(1): 38-53.
[29] Sakarya, S., Canlı, Ş. (2011): Lumber Report [Online]. – Central Anatolian Furniture, Paper and Forestry Products Exporters' Union, www.turkishwood.org [accessed 05 May, 2013] (in Turkish).
[30] Semerci, N. T. (2014): Occupational health problems in red pine (*pinus brutia*) processing sawmills. – MSc Thesis, Suleyman Demirel University, Isparta, Turkey (in Turkish).
[31] Siew, S. S., Kauppinen, T., Kyyrönen, P., Heikkilä, P., Pukkala, E. (2012): Occupational exposure to wood dust and formaldehyde and risk of nasal, nasopharyngeal, and lung cancer among Finnish men. – Cancer Manag Res. 4: 223-232.
[32] Sütçü, A., Keskin, H., Demirgil, H., Sezgin, A., Dulupçu, M. A., Karakuş, B., Demirel, O., Şentürk, C., Çakmakçı, H. A. (2008): Investigation on Forest Products Industry in Isparta. – Isparta Governorship Provincial Directorate of Industry and Trade, Isparta, Turkey (in Turkish).
[33] TOBB. (2012): Sectoral Report of Turkish Forestry Products Council 2011. – The Union of Chambers and Commodity Exchanges of Turkey (TOBB) [Online], www.tobb.org.tr [accessed 04 Jan., 2013] (in Turkish).
[34] Top, Y., Adanur, H., Öz, M. (2016): Comparison of practices related to occupational health and safety in microscale wood-product enterprises. – Safety Science 82: 374-381.

http://www.aloki.hu ● ISSN 1589 1623 (Print) ● ISSN 1785 0037 (Online)
DOI: http://dx.doi.org/10.15666/aeer/1704_76257639

[35] TUIK. (2007): General Census of Industry and Business Local Units Provinces 2002. – Turkish Statistical Institute, Printing Division, Ankara,Turkey.
[36] Ülker, O. (2018): Investigation of Noise Exposure at Furniture Production and Analyzing Noise Levels. – International Journal of Engineering Research and Development 10(2): 225-244. (in Turkish).
[37] Virkkunen, H., Kauppinen, T., Tenkanen, L. (2005): Long-term effect of occupational noise on the risk of coronary heart disease. – Scandinavian Journal of Work Environment and Health 31(4): 291-199.
[38] Wu, H. C., Chen, H. C., Chen, T. (2009): Effects of ergonomics-based wafer-handling training on reduction in musculoskeletal disorders among wafer handlers. – International Journal of Industrial Ergonomics 39(1): 127-132.
[39] Yıldırım, M. (1989): Work Study and Planning. – Publication of the Faculty of Forestry Istanbul University, Pub. No:3556, Taş Matbaası, İstanbul, Turkey (in Turkish).

http://www.aloki.hu ● ISSN 1589 1623 (Print) ● ISSN 1785 0037 (Online)
DOI: http://dx.doi.org/10.15666/aeer/1704_76257639

THE EFFECT OF PLOUGH TILLAGE ON PRODUCTIVITY OF RATOONING RICE SYSTEM AND SOIL ORGANIC MATTER

DU, P.[1,2#] – LUO, H. W.[3#] – HE, L. X.[3#] – MAO, T.[1,2] – LAI, R. F.[3] – TANG, X. R.[3] – TANG, Q. Y.[4] – HU, L.[1,2*]

[1]*College of Engineering, South China Agricultural University, Guangzhou 510642, PR China*

[2]*Key Laboratory of Key Technology for South Agricultural Machine and Equipment Ministry of Education, Guangzhou 510642, PR China*

[3]*Department of Crop Science and Technology, College of Agriculture, South China Agricultural University, Guangzhou 510642, PR China*

[4]*College of Agriculture, Hunan Agricultural University, Changsha 410128, PR China*

[#]*These authors have contributed equally to this work.*

**Corresponding author*
e-mail: lianhu@scau.edu.cn

(Received 9th Mar 2019; accepted 1st May 2019)

Abstract. Plough tillage had existed in Chinese agricultural history for a very long time. However, more and more farmers prefer to use the rotary machine to do the land preparation due to its ability to provide better soil fragmentation in recent years. The present study was conducted in order to study the effect of plough tillage on grain yield, quality and soil organic matter in ratooning rice systems, in Hunan Province, China, using a rice cultivar, *Huanghuazhan* as material and two tillage treatments were applied in present study. Conventional rotary tillage was named as CK and plough tillage was named as PT. The result showed that compared to CK, PT treatment not only could improve the grain yield of both main-crop rice and ratooning rice, but also increased the grinding quality and nutrition quality of grains in main-crop rice. Furthermore, higher soil organic matter was recorded under PT.
Keywords: *ratooning rice, grain quality, yield, paddy soil, land preparation methods*

Introduction

Ratooning rice is a special cultivation method in rice production. It has a long history in China which can be traced back to 1700 years ago (Min et al., 2017). It is characterized by cutting only about two-thirds of the upper part of the rice plant, collecting rice panicles, leaving behind one-third of the plant and root system, fertilization and cultivation, so that it can grow another season of rice. Normally, there will be some axillary buds when rice matures in the first season and after harvesting in the first season, they will be retained. On the basis of the original root system, these axillary buds will grow and heading again. After about 2 months, they will mature again and can be harvested (Rogé et al., 2016). Generally, the grain size of rice in the second season is smaller than that in the first season, but the number of panicles in the second season is higher than that in the first season (where the original panicle is cut, more than two panicles will grow), so the yield is not small.

The areas suitable for planting ratooning rice are mainly those where sunshine and heat are not enough to grow two-crop rice, but there are many areas where one-crop rice is planted. Because it grows again on the original roots, it saves the period from the first crop to the middle of the second crop (so it is called Ratooning rice, not Two-crop rice) in the second crop rice growing area. In this way, ratooning rice can be planted in areas with more than one

http://www.aloki.hu ● ISSN 1589 1623 (Print) ● ISSN 1785 0037 (Online)
DOI: http://dx.doi.org/10.15666/aeer/1704_76417647

season, thus increasing yield (Kupkanchanakul et al., 1990). At present, many areas in China, such as Sichuan and Fujian provinces, are experimenting to popularize this cultivation (Luzhou and Hz, 2000). Thus, developing ratooning rice is an important task to ensure China's future food security.

As an important part in rice production, tillage is required to reduce the loss of water and fertilizers through excessive percolation and it also could decrease weeds and enhance nutrient availability (Alam et al., 2018). In Chinese agricultural history, there were two tillage methods including plough tillage and rotary tillage. Recently, because of the better soil fragmentation, most of framers are likely to use rotary machine to do the land preparation. However, excessive soil fragmentation under rotary tillage could induce the reduction in soil's ability to regulate water, air and heat (Abu-Hamdeh, 2000). The study of SUN (2017) revealed that compared to rotary tillage, plough tillage not only could improve the soil environment, but also could promote the root activity and the production of tobacco leaf.

In order to study the effect of plough tillage on ratooning rice system productivity and soil organic matter, present study was conducted in Hunan Province (major rice producing province in Central China) with the hypothesis that plough tillage could improve rice yield and grain quality in ratooning rice system.

Materials and methods

Plant material and growing conditions

A rice cultivar, *Huanghuazhan*, which having a growth period of 129-131 days and widely grown in Central China, was used in present experiment and planted at Hongshuo Farm, Datong Lake District, Yiyang, Hunan Province (29 08' N, 112 26' E) in 2017. Before sowing, the seeds were soaked in water for 24 h, germinated in manual climatic boxes for another 12 h and shade-dried. Then, the germinated seeds were sown in polyvinyl chloride trays for nursery raising. The experimental site enjoyed a subtropical monsoon climate and the air temperature during the experiment was shown in *Figure 1*. The soil type of paddy field is fluvo-aquic soil and mechanical composition is as follows: sand (0.05~2 mm) accounts for 34%, silt (0.002~0.05 mm) for 56.7%, clay (0~0.002) for 9.3%. It contained organic matter 29.30 g kg^{-1}, total N 1.94 g kg^{-1}, total P 1.31 g kg^{-1}, and total K 26.70 g kg^{-1}.

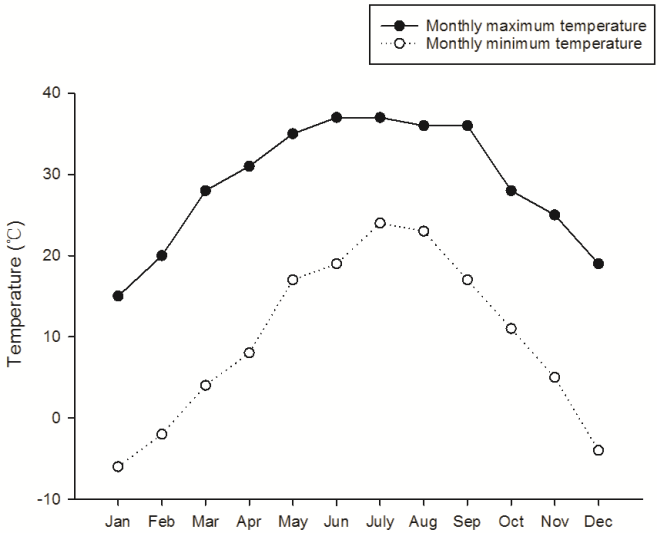

Figure 1. *The temperature during the field experiment*

http://www.aloki.hu ● ISSN 1589 1623 (Print) ● ISSN 1785 0037 (Online)
DOI: http://dx.doi.org/10.15666/aeer/1704_76417647

Treatment description and sampling

Two land preparations, plough tillage and rotary tillage were adopted in present study. We set rotary tillage as control (CK) and name plough tillage as PT.

CK: Before transplanting, the paddy field was puddle twice with rotary cultivator.

PT: Before transplanting, the paddy field was puddle twice with plough cultivator.

The treatments were arranged in randomized complete block design (RCBD) in triplicate with net plot size of 665 m^2. After the harvest of main-crop rice and ratooning rice, five soil cores (0–20 cm depth, 2 cm in diameter) were collected in each plot for the determination of soil organic matter.

Estimation of soil organic matter

The light fraction (LF) and heavy fraction (HF) of soil organic matter were separated using the method described by Camberdella and Elliott (1993). Briefly, 10 g of air-dried soil was homogenized with 30 ml NaI solution (gravity 1.8 g cm^{-3}) in a 100 ml centrifuge tube by shaking on a reciprocating shaker for 60 min at 200 rpm, after which it was centrifuged at 1000 × g for 15 min. The LF, all floating material after centrifugation, was poured into a vacuum filter unit with a 0.45-μm nylon film, and the material retained by the film was washed with 0.01 M CaCl2 and distilled water. This process was repeated three times. The HF remaining in the centrifuge tube was washed three times with ethanol to remove excess NaI, after which it was washed twice with distilled water. Next, the LF and HF were dried at 60 °C for 48 h, and then weighed and ground to pass through a 0.15-mm sieve for organic determinations. The organic matter in LF and HF were determined by the wet oxidation method with K2Cr2O7 at 170–180 °C (Zhao et al., 2016).

Yield and yield related traits

At maturity stage, the rice grains were harvested from ten-unit sampling area (1 m^2) in each plot and then threshed by machine. The harvested grains were sun-dried and weighted in order to determinate the grain yield. Twenty hills of rice from different locations in each plot were sampled for estimate the average effective panicles number per hill. Then, eight hills representative plants were taken for estimation of the yield related traits.

Grain quality

After sun drying, grains were stored at room temperature for at least a month to determine grain quality components. About 1.0 kg rice grains from each treatment was taken from storage and brown rice rate was estimated using a rice huller (Jiangsu, China) while milled rice and head rice recovery rates were calculated by using a Jingmi testing rice grader (Zhejiang, China). Grains with chalkiness and chalkiness degree were estimated by using an SDE-A light box (Guangzhou, China) while an Infratec-1241 grain analyzer (FOSS-TECATOR) was used to determine the grain amylose and protein contents.

Statistical analysis

Data were analyzed on Statistix 8.1 (Analytical Software, Tallahassee, FL, USA) while differences among means were separated by using least significant difference

http://www.aloki.hu ● ISSN 1589 1623 (Print) ● ISSN 1785 0037 (Online)
DOI: http://dx.doi.org/10.15666/aeer/1704_76417647

(LSD) test at 5% probability level. Graphical representation was conducted via Sigma Plot 14.0 (Systat Software Inc., California, USA).

Results

Soil organic matter

As shown in *Figure 2,* plough tillage significantly influenced the soil organic matter compared to CK. After the harvest of main-crop rice, 28.11% higher soil organic matter was recorded in PT than CK. After the harvest of ratooning rice, compared to CK, PT treatment increased soil organic matter by 19.56%.

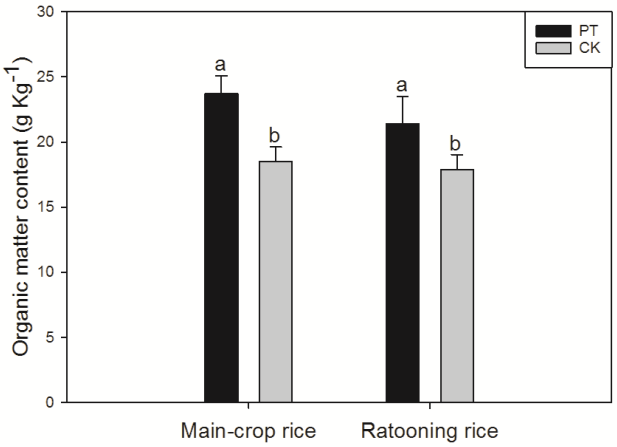

Figure 2. *The effect of plough tillage on soil organic matter in ratooning rice system (Means sharing a common letter do not differ significantly at (P ≤ 0.05) according to least significant difference (LSD) test)*

Yield and yield related trails

As shown in *Table 1*, plough tillage affected rice yield and related trails in ratooning rice system significantly. For main-crop rice, PT treatment increased panicle number, grains number and yield by 12.03, 7.02 and 10.99%, respectively whilst there was no significant difference between PT and CK in both seed-setting rate and 1000-grain weight. For ratooning rice, compared to CK, 4.51, 7.47, 4.42 and 4.72% higher panicle number, grains number, 1000-grain weight and yield were recorded in PT.

Table 1. *The effect of plough tillage on rice yield and related trails in ratooning rice system*

	Treatment	Panicle number per hill	Grains number per panicle	Seed-setting rate (%)	1000-grain weight (g)	Yield (t ha^{-2})
Main-crop rice	PT	326.97±16.78a	128.56±3.76a	86.60±3.71a	22.82±0.65a	7.50±0.39a
	CK	291.87±15.99b	120.12±2.64b	85.61±2.29a	22.42±1.03a	6.76±0.41b
Ratooning rice	PT	355.94±8.65a	56.36±1.48a	78.51±1.90a	22.69±0.43a	3.46±0.06a
	CK	340.70b±6.40b	52.44±0.71b	77.64±2.00a	21.73±0.55b	3.30±0.07b

Values sharing a common letter within a column do not differ significantly at (P ≤ 0.05) according to least significant difference (LSD) test for both the years. The same as below

http://www.aloki.hu ● ISSN 1589 1623 (Print) ● ISSN 1785 0037 (Online)
DOI: http://dx.doi.org/10.15666/aeer/1704_76417647

Grain quality

As shown in *Table 2*, plough tillage affected grain quality in ratooning rice system significantly. For main-crop rice, compared to CK, PT treatment significantly increased brown rice rate, milled rice rate, head rice rate, crude protein content, amylose content and Akali value by 6.27, 1.51, 10.76, 1.40, 8.82 and 2.92%, respectively. Moreover, 25.64% lower chalky rice rate was recorded in PT treatment than CK. For ratooning rice, PT treatment increased both brown rice rate and Akali values significantly compared to CK. However, there was remarkable difference between CK and PT in milled rice rate, head rice rate, crude protein content, amylose content, chalky rice rate and chalkiness.

Table 2. *The effect of plough tillage on grain quality in ratooning rice system*

	Treatment	Brown rice rate (%)	Milled rice rate (%)	Head rice rate (%)	Crude protein content (%)	Amylose content (%)	Akali	Chalky rice rate (%)	Chalkiness (%)
Main-crop rice	PT	73.13±0.34a	64.60±0.33a	42.52±0.05a	7.26±0.03a	18.50±0.04a	5.86±0.07a	19.33±0.88b	14.96±0.90a
	CK	68.82±0.30b	63.64±0.16b	38.39±0.05b	7.16±0.03b	17.00±0.40b	5.70±0.05b	26.00±0.78a	14.10±2.84a
Ratooning rice	PT	73.13±0.32a	65.26±0.94a	46.73±1.97a	10.76±0.09a	17.90±0.10a	7.03±0.07a	5.06±0.58a	14.83±1.36a
	CK	71.10±0.31b	65.78±0.89a	47.99±1.63a	11.00±0.05a	17.77±0.07a	6.90±0.03b	4.33±0.67a	13.16±1.98a

Correlation analysis

As shown in *Figure 3,* there exited a significant positive correlation between rice yield and grain number. However, panicle number, seed-setting rate and grain weight all did not have significant correlation with the grain yield. Furthermore, there also existed a significant positive correlation between yield and soil organic matter (*Fig. 4*).

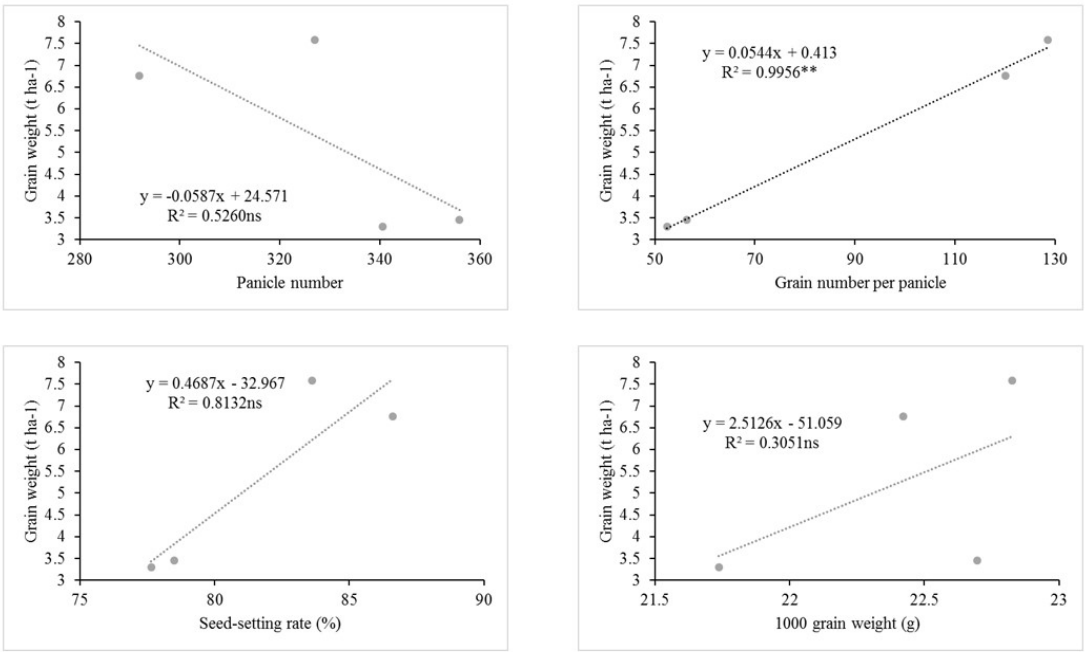

Figure 3. *The correlation between yield related trails and yield in ratooning rice system*

http://www.aloki.hu ● ISSN 1589 1623 (Print) ● ISSN 1785 0037 (Online)
DOI: http://dx.doi.org/10.15666/aeer/1704_76417647

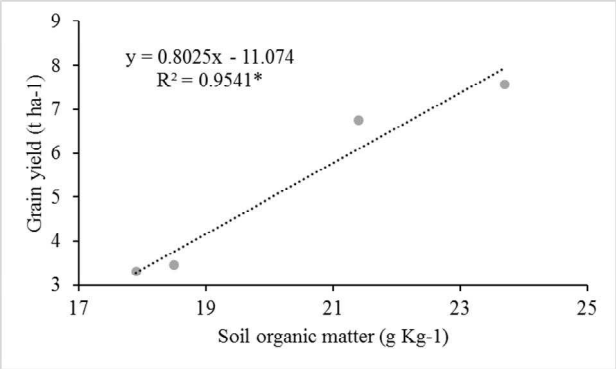

Figure 4. *The correlation between yield and soil organic matter*

Discussion

The development of ratooning rice is a vital way to achieve a full utilization of the solar-thermal resources in autumn and promote the profit of rice field. Previous study (Fu-Xian et al., 2015) already showed some key regulation technologies in ratooning rice cultivation such as varieties selection and fertilizer application. Present study revealed the effect of different tillage on yield, grain quality and soil organic matter in ratooning rice. Compared with conventional rotary tillage, plough tillage significantly increased the yields of both main-crop rice and ratooning rice. The increment in main crop rice yield could be explained by the improvement in panicle number and grain number. The increment in ratooning rice yield not only because of the enhancement of panicle number and grain number, but also due to the higher grain weight under plough tillage. Furthermore, we also observed a significant positive correlation between yield and soil organic matter which indicated that the improvement in soil organic matter due to plough tillage might be the direct reason of the yield increment. This result agreed with the study of Wei et al. (2016) who demonstrated that soil organic matter was an important factor which affected rice productivity significantly. Normally, the degree of soil fragmentation under rotary tillage is higher than plough tillage. But it also means the rotary tillage had rotary tillage destroys the soil more severely and excessive soil fragmentation can induce the decrement of biodiversity in farmland soil (Biswas et al., 2017). Our study showed that plough tillage was more suitable for ratooning rice cultivation because it not only improved the rice yield, but also had less soil fragmentation and improved the soil organic matter.

Moreover, in our study, we observed that plough tillage improved some grain quality attributes. Normally, rice price in market mostly depend on grain quality (Luo et al., 2018). For main-crop rice, plough tillage not only improved rice grinding quality such as brown rice rate, milled rice and head rice rate, but also increased the grain nutrition quality such as protein and amylose content. The increments in grain quality might because the plough tillage improved rice growth and development.

Conclusion

In ratooning rice system, compared to rotary tillage, plough tillage not only could improve the grain yield of both main-crop rice and ratooning rice, but also increased the grinding quality and nutrition quality of grains in main-crop rice. Moreover, higher soil

http://www.aloki.hu ● ISSN 1589 1623 (Print) ● ISSN 1785 0037 (Online)
DOI: http://dx.doi.org/10.15666/aeer/1704_76417647

organic matter was recorded in plough tillage than rotary tillage. In order to explore the mechanism of how tillage affects ratooning rice performance, further investigation should be at the field trials.

Acknowledgements. This study was supported by the National Key Research and Development Program of China (2016YFD0700301) and National Natural Science Foundation of China (31601225).

REFERENCES

[1] Abu-Hamdeh, N. H. (2000): Effect of tillage treatments on soil thermal conductivity for some Jordanian clay loam and loam soils. – Soil & Tillage Research 56: 145-151.
[2] Alam, M. J., Humphreys, E., Sarkar, M. A. R., Yadav, S. (2018): Comparison of dry seeded and puddled transplanted rainy season rice on the High Ganges River Floodplain of Bangladesh. – European Journal of Agronomy 96: 120-130.
[3] Biswas, S., Hazra, G. C., Purakayastha, T. J., Saha, N., Mitran, T., Roy, S. S., Basak, N., Mandal, B. (2017): Establishment of critical limits of indicators and indices of soil quality in rice-rice cropping systems under different soil orders. – Geoderma 292: 34-48.
[4] Cambardella, C. A., Elliott, E. T. (1993): Methods for physical separation and characterization of soil organic matter fractions. – Geoderma 56: 449-457.
[5] Fu-Xian, X. U., Xiong, H., Zhang, L., Zhu, Y. C., Jiang, P., Guo, X. Y., Liu, M. (2015): Progress in research of yield formation of ratooning rice and its high-yielding key regulation technologies. – Scientia Agricultura Sinica 9: 1702-1717.
[6] Kupkanchanakul, T., Vergara, B. S., Kupkanchanakul, K. (1990): Ratooning ability and potential herbage production from ratoon crops of rice cultivars. – International Rice Research Newsletter 15(5): 10.
[7] Luo, H. W., Wang, Z. M., Chen, Y. Y., Zheng, A. X., Chen, Y. L., Du, P., Mao, T., Meng, S. B., Tang, X. R. (2018): The effects of different temperatures on the biosynthesis of grain protein in rice at filling stage. – Applied Ecology and Environmental Research 16: 8017-8027.
[8] Luzhou, K. M. Hz, W. (2000): Achievements and developments of ratooning rice in South of China. – Acta Agronomica Sinica 26(3): 1-5.
[9] Min, X. I., Wenge, W. U., Wang, J., Wang, H., Chen, G., Youzun, X. U. (2017): Study on formation of grain yield differences in ratooning rice cultivation. – Acta Agriculturae Boreali-Sinica 32(1): 104-110.
[10] Rogé, P., Snapp, S., Kakwera, M. N., Mungai, L., Jambo, I., Peter, B. (2016): Ratooning and perennial staple crops in Malawi. A review. – Agronomy for Sustainable Development 36: 50.
[11] Sun Jingguo, W. C. C. Z. (2017): The influence of different tillage on soil and flue-cured tobacco. – Journal of Hubei University (Natural Science) 39: 299-304.
[12] Wei, W., Yun, Y., Jian, C., Christie, P., Zhang, F., Fan, M. (2016): Effects of combined application of organic amendments and fertilizers on crop yield and soil organic matter: An integrated analysis of long-term experiments. – Agriculture Ecosystems & Environment 225: 86-92.
[13] Zhao, S., Li, K., Wei, Z., Qiu, S., Huang, S., Ping, H. (2016): Changes in soil microbial community, enzyme activities and organic matter fractions under long-term straw return in north-central China. – Agriculture Ecosystems & Environment 216: 82-88.

http://www.aloki.hu ● ISSN 1589 1623 (Print) ● ISSN 1785 0037 (Online)
DOI: http://dx.doi.org/10.15666/aeer/1704_76417647

DYNAMICS OF LIVESTOCK PRODUCTION DEVELOPEMENT IN THE SLOVAK REPUBLIC BETWEEN THE YEARS 2004 AND 2017 AND POTENTIAL IMPACT OF THE CHANGES ON THE AGRICULTURAL SECTOR AND LANDSCAPE

NÉMETHOVÁ, J.[1*] – HUDÁKOVÁ, M.[2]

[1]*Department of Geography and Regional Development, Faculty of Natural Sciences*
Constantine the Philosopher University in Nitra
Trieda A. Hlinku 1, 949 74 Nitra, Slovak Republic

[2]*Department of Management, Faculty of Economics and Management*
Slovak University of Agriculture in Nitra, Trieda A. Hlinku 2, 949 01 Nitra, Slovak Republic

[*]*Corresponding author*
e-mail: jnemethova@ukf.sk; phone: +42-1-905-274-138

(Received 11th Mar 2019; accepted 1st May 2019)

Abstract. The paper deals with the dynamics of changes in livestock production in Slovakia in the period between 2004 and 2017 from the viewpoint of productive and non-productive factors with a special focus on environmental factors in the breeding of four groups of farm animals. The development was evaluated on the basis of the indicator of stock intensity. The data was analysed at the levels of NUTS 3 (regions) and LAU 1 (districts) for Slovakia. The study showed that the changes in the agricultural sector after the year 2004 due to Slovakia´s entering the European Union have manifested themselves in an overall decrease of livestock production as well as in further aggravation of regional disparities. The aforementioned changes not only pose a direct risk to the agrarian sector but they also affect the environment in a broader context. The positive ecological impacts associated with the attenuation of primary livestock production spotted at first glance can negatively affect the environment, biological diversity and quality of life. The current status quo requires a consequent application of the principles of organic farming and its support in form of government subsidies and legislation.
Keywords: *animal production intensity, ecological agriculture, regional disparities, environmental impact, Slovakia*

Introduction

Before the transformation process in the agrarian sector livestock production in Slovakia was to one of those fields, which had been financed by state subsidies. After the transition to the new model of economic relations the government incentives were minimized and abolished respectively. This resulted in a significant decrease of livestock population, particularly in the traditional (majority) groups such as beef cattle and pigs. It became problematic to cover the costs of breeding and producing livestock. The reduction in the number of the individual types of livestock had already started in the 1990´s and it has been continuing ever since. In this period not only the regional disparities in primary livestock production in Slovakia became apparent (Némethová et al., 2017b) but the development insinuated that the stability of the agricultural commodity markets was at stake. This developement persists and livestock production in Slovakia has been on the decline for a long time (Chrastinová et al., 2014). This fact is also connected with the economic conditions such as higher costs of breeding farm animals (Buday et al., 2012). The decline in livestock production is related to the decrease in the numbers of the individual types of farm animals but also to the import of

http://www.aloki.hu ● ISSN 1589 1623 (Print) ● ISSN 1785 0037 (Online)
DOI: http://dx.doi.org/10.15666/aeer/1704_76497666

finished products of animal origin to the Slovak market. The structural changes in Slovak agriculture after Slovakia´s accession to the European Union (EU) in the year 2004 and the Common Agricultural Policy (CAP) aggravated the regional disparities in livestock production (Némethová et al., 2004). As a result in Slovakia not only livestock population drastically dropped but in some regions the breeding was completely abandoned. The positive aspect in the process is the growing efficiency of farm animals, which is however conditioned by other than economic factors. The EU´s Common Agricultural Policy motivated the farmers with its instruments to reduce livestock production and to favour vegetable production focussing on large-scale crop production and primarily crops in the area of renewable energy sources, which ultimately brought about other specific implications and consequences.

The changes in Slovak agriculture associated with the consequences of a state´s entering the European Union and adopting the EU´s CAP are theoretically reflected in the works of experts from various aspects (Spišiak et al., 2005; Falťanová, 2008; Spišiak and Némethová, 2008; Buday et al., 2012; Némethová and Civáň, 2017; Némethová et al., 2014, 2017a). The problems do not concern only Slovakia. After the dissolution of Czechoslovakia Czech farmers also had to come to terms with the new situation. The impact of the CAP on agriculture and rural areas in the Czech Republic and the issue of regional disparities have been analysed by several authors (Kabrda and Jančák, 2006; Svobodová and Věžník, 2011; Věžník and Konečný, 2011; Král et al., 2012; Doucha et al., 2012 and others). Over the past 30 years the Czech Republic has seen a rapid decline in some types of farm animals as well as a change in their internal structure and method of breeding (Věžník et al., 2013, 2017). The impacts of the EU´s CAP on the development of agriculture, the analyses and evaluation of the impacts are written down in the works of many foreign experts (Kulikowski, 2005; Kołodziejczak, 2006; Buchenrieder and Möllers, 2009; Kołodziejczak and Kossowski, 2011). The approach of the individual farmers in Portugal as far as the impact of the EU´s CAP is concerned is presented by Dos Santos et al. (2010). Rudnicki (2013) assessed the situation in Poland from the viewpoint of a recipient of European subsidies. The approach and opinions of selected farmers in the new EU member states regarding the changes in the CAP after the year 2003 were dealt with by Gorton et al. (2008). Ilbery and Maye (2005) analysed selected changes in the trend of cattle breeding and its importance for the food market in Great Britain.

Ecologization of agriculture and protection of the environment are important on a global scale. The European Union supports this aera of agro-environmental production. Apart from producing healthy food organic farming strives to eliminate damaging and devastating of the environment by preventive measures and special farming and breeding practices (Petrovič et al., 2017). Unlike convenational agriculture it prefers the quality of production, versatile production and a varied cropping pattern. It excludes chemistry and machinery from its production. The system of organic farming is the research topic of several experts in Slovakia, e.g. Schlosserová and Juršík (2009), Némethová and Mesárošová (2013), Kozáková et al. (2015), Némethová et al. (2017b) in the Czech Republic, e.g. Hrabalová and Zander (2006), Brožová (2011), Doležalová et al. (2014). The analysis of the transition from the conventional farming system to organic farming is dealt with by e.g. Lockie and Halpin (2005), Stolze and Lampkin (2009), Moschitz and Stolze (2009), Mzoughi (2011). The measures applied by the government and the market economy aim at supporting organic farming and

http://www.aloki.hu ● ISSN 1589 1623 (Print) ● ISSN 1785 0037 (Online)
DOI: http://dx.doi.org/10.15666/aeer/1704_76497666

consumption of organic products (Milestad and Darnhofer, 2003; Häring et al., 2004; Nieberg and Kuhnert, 2007).

The aim of the paper was to analyse the developmental trends and the level of animal production in Slovakia in the period 2004 to 2017 and to point out regional disparities – at the level of regions and districts of Slovakia – in the context of environmental effects. Main attention was focused on the dynamics of livestock production developement and potential impact of the changes on the agricultural sector and landscape.

Material and methods

Dataset characteristics

The main statistical set comprised the official data of the Statistical office of the Slovak Republic referring to the basic indicators of livestock production in the period between 2004 and 2017 (MS Excel). The data was analysed at the level of NUTS 3 (regions) and LAU 1 (districts) of Slovakia.

The principal livestock production indicator used in this study was the stock density on the declared area: heads on 100 hectares of agricultural area (cattle and sheep) or arable land (pigs and poultry) and its alternation during the reference period. The impact of the changes in primary livestock production on the subsequent production on the market is illustrated by the data regarding sales from livestock farming during the evalutation period from 2004 to 2017.

Dataset processing

In order to statistically process and cartographically visualize stock density in the initial situation in the year 2004 and the situation in the year 2017 as well as sales development we applied descriptive statitics and the ArcView programme for visualizing spatial information. For the needs of illustrating the modelling of potential development of stock density in the coming period (identification of expected trends) we applied a procedure based on the evaluation of the dynamics of timelines aided by the ARIMA model in the R software.

Results and discussion

Dataset general characteristics

For the needs of the study the basic statistical set was analysed at the level of the regional statististical territorial units NUTS 3 (regions) and LAU 1 (districts). Slovakia is administratively divided into eight self-governing regions: the Bratislava Region, the Trnava Region, the Trenčín Region, the Nitra Region, the Žilina Region, the Bánska Bystrica Region, the Prešov Region and the Košice Region. The regions are further subdivided into 79 districts.

Stock density of selected livestock groups

The dynamics of the changes in livestock farming between the years 2004 and 2017 is processed in form of analyses; the cartographic visualization consists of maps documenting the initial state (the year 2004) and the state in the year 2017.

http://www.aloki.hu ● ISSN 1589 1623 (Print) ● ISSN 1785 0037 (Online)
DOI: http://dx.doi.org/10.15666/aeer/1704_76497666

Stock density of cattle – Situation in the year 2004 and 2017

In the year 1993 more than 900 000 heads of cattle were bred in Slovakia, in the year 2004 it was only 540 146 heads and at present in the year 2017 the figure amounts to 439 826 heads (when comparing the years 2004 and 2017 the decrease equals to 100 320 heads), which is a decline of 18.6%. A decline over 30% was seen in the Nitra and Trnava Regions. All the regions reported a reduction in livestock population except for the Prešov Region, which recorded a moderate increase of 3.5%. The milk producers keep on producing milk with a loss. The level of the purchase prices of milk does not cover the production costs, which are high. For instance in the year 2000 in Slovakia 246 000 milking cows were bred and in the year 2017 it was roughly only 125 000. The drop in the numbers of cattle is also shown in stock density on the declared area, i.e. heads on 100 hectares of agricultural area. This indicator in the year 2004 amounted to 28 heads of cattle per 100 hectares of agricultural area and in the year 2017 it was only 23, which results in a decrease of 17.7%. The decrease of beef cattle numbers expressed by stock density was seen in all Slovak regions except for the Prešov Region (*Fig. 1* and *Fig. 2*).

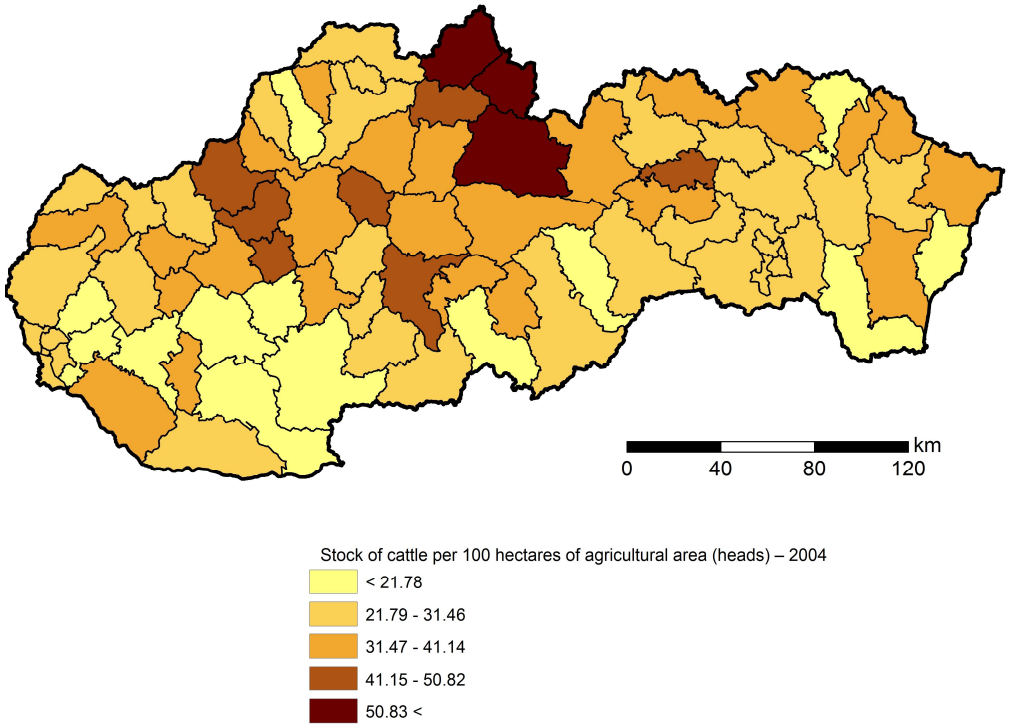

Figure 1. *Stock of cattle per 100 hectares of agricultural area (heads) – 2004*

The falling numbers of cattle influenced the structure of vegetable production particularly the production volume of grain feed and bulk feed. After the entry of Slovakia into the EU the subsidy policy had a positive impact on the breeding of suckler cows. This type of breeding is of relevance especially for landscape maintenance in the agriculturally disadvantaged regions. In the long run an increase of cattle numbers would bring positive results such as for instance the increase of the production of stable manure, which is increasingly lacking on Slovak soils.

http://www.aloki.hu ● ISSN 1589 1623 (Print) ● ISSN 1785 0037 (Online)
DOI: http://dx.doi.org/10.15666/aeer/1704_76497666

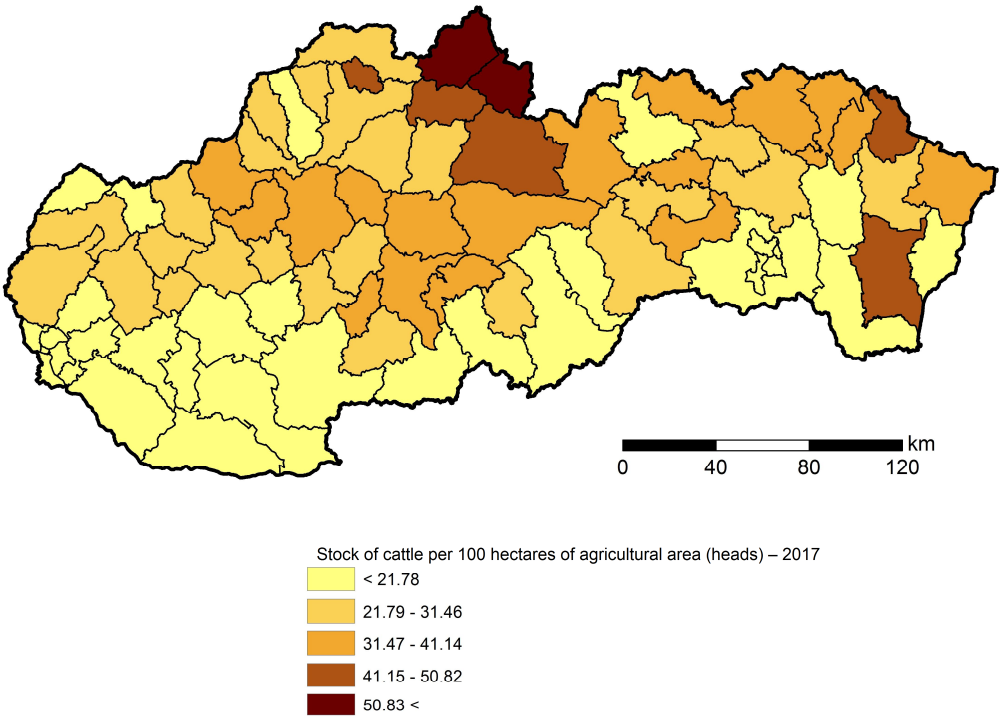

Figure 2. *Stock of cattle per 100 hectares of agricultural area (heads) – 2017*

Stock density of pigs – Situation in the year 2004 and 2017

In the year 1993 in Slovakia 1.8 million heads of pigs were bred. At the time when Slovakia was entering the EU it was 1,1 million heads and in the year 2017 it was only 614 384 heads (a decrease of 534 898 heads). This was the biggest decrease reported among all farm animals (-46.5%). The numbers of pigs fell primarily due to the impossibility to receive subsidies in the field of pig farming as a consequence of the overall surplus production of pigs in the EU states. The next factor influencing the falling numbers of pigs was the increase of the prices of feed, lower purchase prices of pork and cheaper import of meat from abroad. The decrease of the numbers of pigs was seen in all the Slovak regions. In the Košice and Žilina Regions the decline exceeded 70%. A decrease over 50% was reported in the Banská Bystrica, Nitra and Trenčín Regions. Pork is being imported to Slovakia from almost all of Europe, however in particular from the neighbouring countries such as Poland, the Czech Republic and Hungary. More than 50% of the slaughter pigs are being exported due to the closing of a number of important slaugher houses. At the present day in Slovakia there are only smaller slaughter houses in operation such as for example in Myjava, Tešedíkov and Komárno. Most Slovakian slaughter houses process meat from foreign production, which is cheaper and thus more profitable. Slovakia attempts to revitalize the sector of pig farming, which was permanently ignored, with the help of subsidies coming either from the EU or the state itsself. Nowadays Slovakia is beginning to put more emphasis on the freshness and quality of meat, which cannot be guaranteed to the consumer in case of imported meat but only with meat produced by Slovak farmers. From the point of view of future development the growth potential in the area of pig breeding in Slovakia is obvious and it can be expected that the country will become fully

http://www.aloki.hu ● ISSN 1589 1623 (Print) ● ISSN 1785 0037 (Online)
DOI: http://dx.doi.org/10.15666/aeer/1704_76497666

sustainable in pork production. Also the stock density of pigs expressed in the numbers of pigs per 100 hectares of arable land points to a decrease of pig population during the reference period from 2004 to 2017. In Slovakia the stock of pigs in 2004 totalled to 84.5 heads, which in 2017 fell to 45.8 heads, which presents a decrese of 45.9%. A significant decline of more than 70% was reported in the Košice and Žilina Regions (*Fig. 3* and *Fig. 4*). The decrease in the numbers of pigs expressed by stock density of pigs was seen in all the regions of Slovakia.

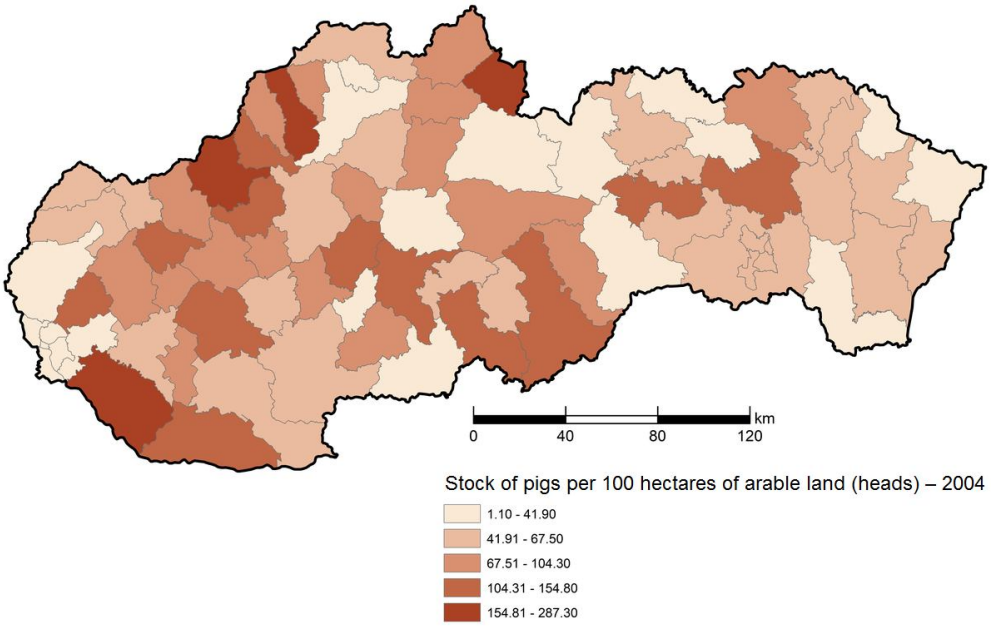

Figure 3. *Stock of pigs per 100 hectares of arable land (heads) – 2004*

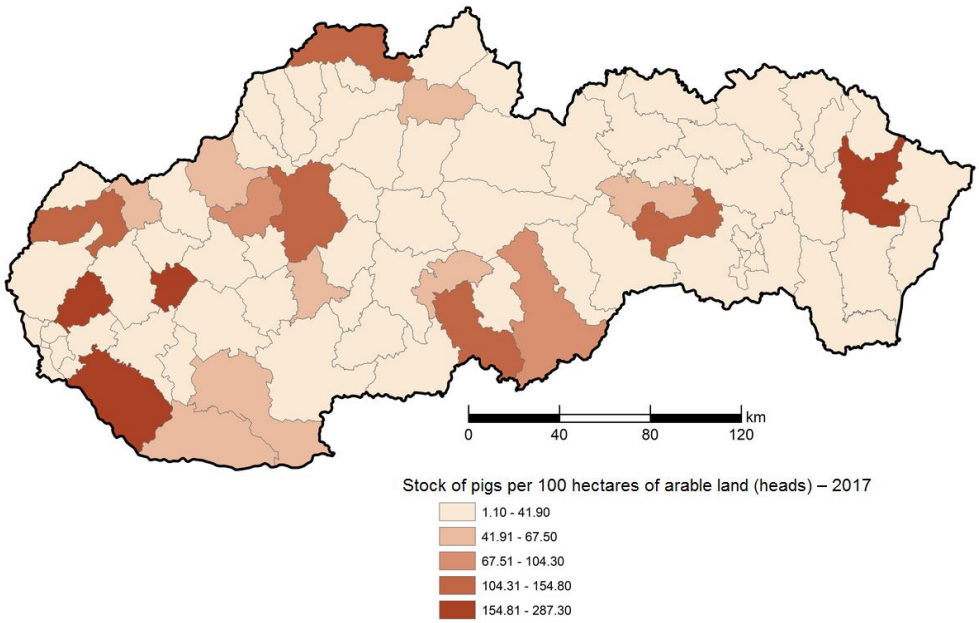

Figure 4. *Stock of pigs per 100 hectares of arable land (heads) - 2017*

http://www.aloki.hu ● ISSN 1589 1623 (Print) ● ISSN 1785 0037 (Online)
DOI: http://dx.doi.org/10.15666/aeer/1704_76497666

Stock density of poultry – Situation in the year 2004 and 2017

In case of poultry Slovakia did not record such a significant decline as with pigs and beef cattle. In the year 2004 in Slovakia 13.7 million heads of poultry were bred, before the year 2017 the numbers fell to 13.4 million heads (-2.6%, a decrease of 359 402 heads). A bigger decline was seen in the Trnava Region (-32.2%) and Prešov Region (-53.9%). This decline can be attributed to the common European market connected with the import of cheaper poultry meat from abrod especially from Poland and Hungary. In consequence of the pressure by the supermarket chains regarding the reduction of poultry meat purchase prices, the price fell over several years and does not longer cover the production costs of the breeders. Prior to the year 2000 Slovakia was self-sustainable in the production of poultry meat. As of today the production of poultry meat covers approximately 50% of the consumption of the Slovak population. An increase of the numbers of poultry in the reference period from 2004 to 2017 was seen only in the Bratislava Region and Košice Region. In all the other Slovak regions we state a moderate decline. The decline in poultry numbers can be illustrated with a next indicator, stock density expressed by the number of heads per 100 hectares of arable land. In the year 2004 in Slovakia this value amounted to 1009.8 heads of poultry per 100 hectares of arable land, by 2017 the value went down to 994.4 heads, which presents a 1.5% decrease. The increase in poultry population in the Bratislava and Košice Regions is also reflected in the stock density of poultry (*Fig. 5* and *Fig. 6*). According to this indicator the remaining regions report a decline.

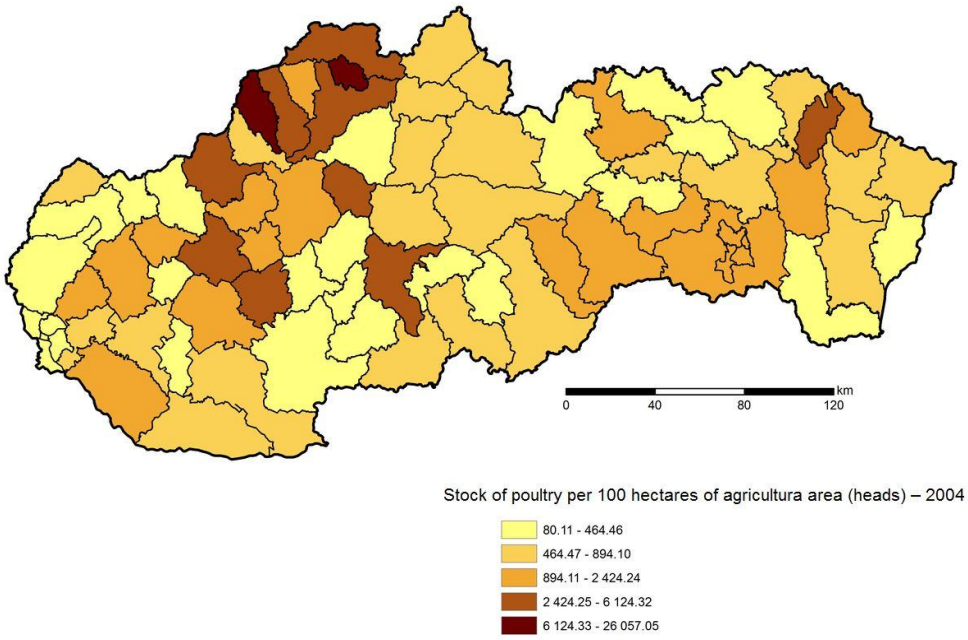

Figure 5. *Stock of poultry per 100 hectares of agricultura area (heads) – 2004*

Stock density of sheep – Situation in the year 2004 and 2017

In case of sheep Slovakia has seen a moderate increase of 13.7%. In the year 2004 the numbers of sheep amounted to 321 227 heads and in the year 2017 it was 365 344 (an increase by 44 117 heads). In all the regions of Slovakia the numbers of sheep

http://www.aloki.hu ● ISSN 1589 1623 (Print) ● ISSN 1785 0037 (Online)
DOI: http://dx.doi.org/10.15666/aeer/1704_76497666

increased in the reference period from 2004 to 2017. There was a decrease only in the Nitra Region (-15.1%). The biggest increase was seen in the Bratislava Region (93.3%) and the Trenčín Region (51.6%). In the year 2004 there were 16.6 sheep on 100 hectares of agricultural area and by 2017 the value of the indicator went up to 19.1 heads (an increase by 15%) (*Fig. 7* and *Fig. 8*).

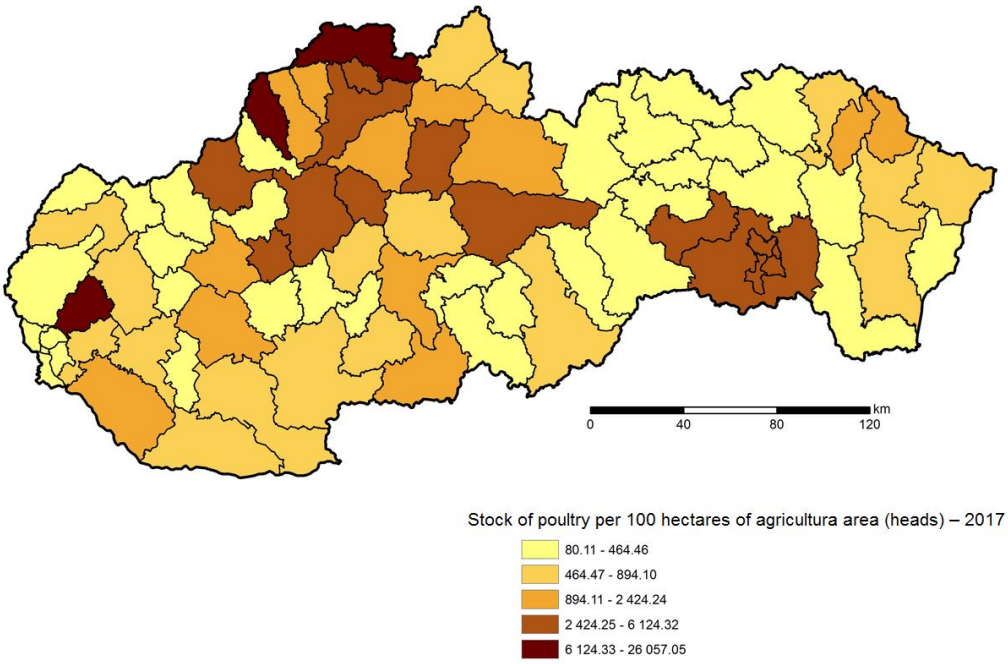

Figure 6. *Stock of poultry per 100 hectares of agicultura area (heads) – 2017*

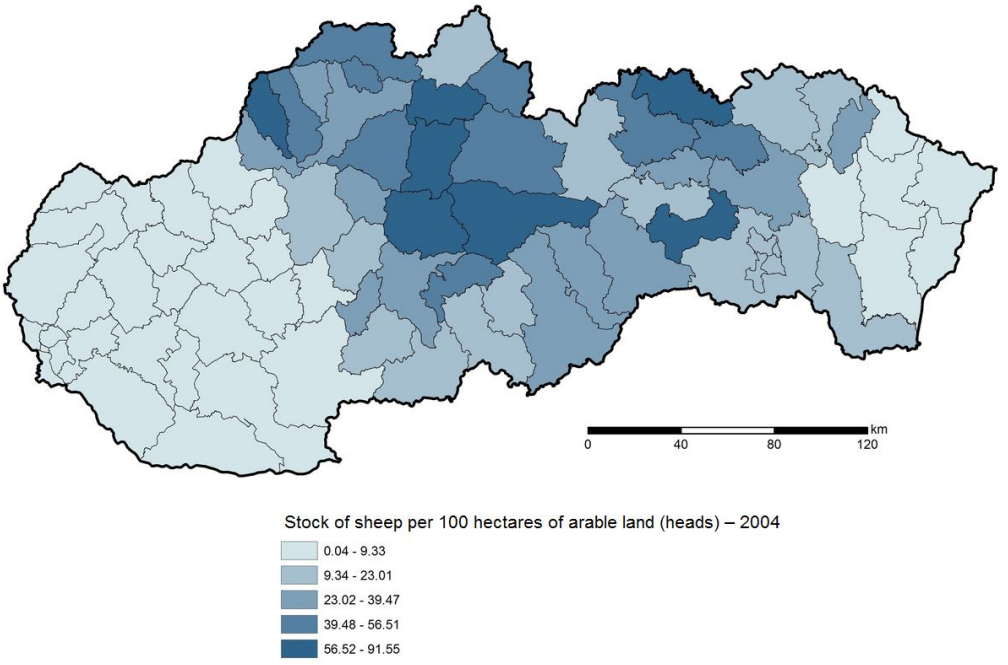

Figure 7. *Stock of sheep per 100 hectares of arable land (heads) – 2004*

http://www.aloki.hu ● ISSN 1589 1623 (Print) ● ISSN 1785 0037 (Online)
DOI: http://dx.doi.org/10.15666/aeer/1704_76497666

This was primarily due to the EU´s supporting the breeding of farm animals on permanent grassland. The increase in numbers was seen in all the regions of Slovakia except the Nitra Region, in which the stock density of sheep fell by 16%. The domestic consumer market is little interested in sheep meat and thus most of the production is being exported to the markets of developed EU countries. The subsidies and payments in relation to the area of permanent grassland in Slovakia will contribute to further expanding the sector of sheep breeding. Potential development model of stock density in the coming period (identification of expected trends) is presented bellow (*Fig. 9*).

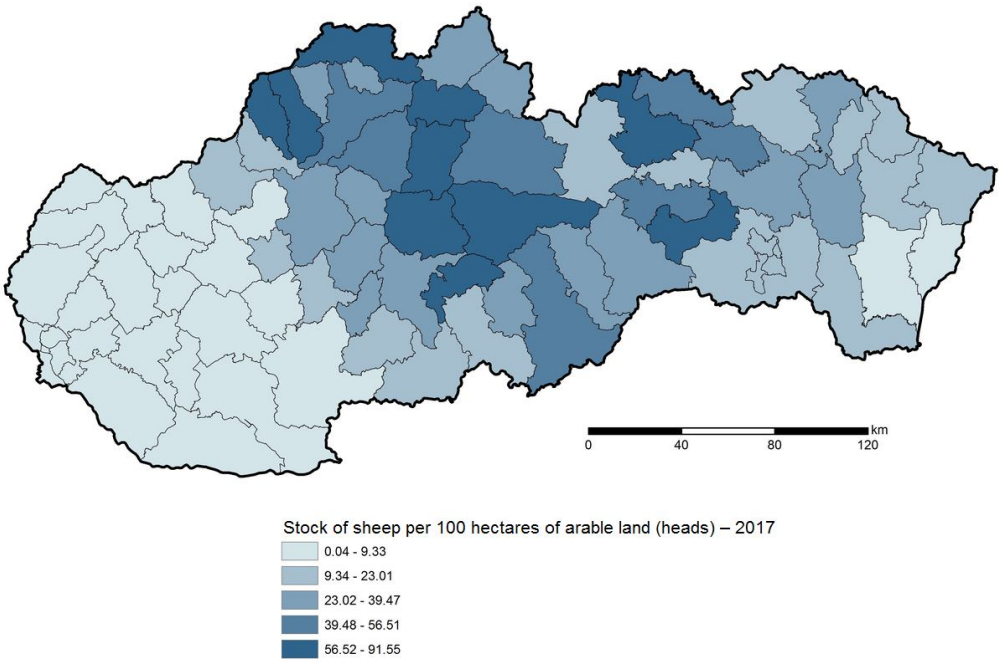

Figure 8. *Stock of sheep per 100 hectares of arable land (heads) – 2017*

Dynamics of sales from livestock production over the period from 2004 to 2017 – share of livestock production sales in total sales from agriculture

Over the past 30 years the breeding of farm animals in Slovakia has significantly decreased especially the breeding of pigs (by more than 66%) and breeding of beef cattle (by more than 50%). This negative phenomenon has translated into the falling employment rates in agriculture. After the accession to the EU Slovak agriculture has not sufficiently used its potential arising from the implementation of the CAP, the common European market and the two rural development programmes. The sector has been financially undernourished for a long period. Unequal conditions among EU countries have contributed to a further decrease of the numbers of farm animals, which led to Slovakia´s not longer being self-sustainable in the field of meat production and meat processing. Also the fact can be seen as negative that the export of living farm animals abroad has increased due to the fact that Slovakia lacks meat-processing enterprises. A next reason is the lower redemption price of meat as compared with abroad. Slovakia is able to cover domestic meat consumption, however over the past years the import of farm animals and mainly the import of meat from abroad have been on the increase. The incorrectly set system of subsidies for livestock production as well

http://www.aloki.hu ● ISSN 1589 1623 (Print) ● ISSN 1785 0037 (Online)
DOI: http://dx.doi.org/10.15666/aeer/1704_76497666

as the milk crisis in 2015 made the population of farm animals gradually drop. The unequal level of support among the individual EU member states weakens the competitiveness of Slovak agriculture. A lower level of support on the part of the state does not create favourable conditions for running a farm business either. Slovak agriculture must have adequate conditions for enterprenial activities as it is the case with the other EU states. Livestock production in Slovakia has been on the decline and vegetable production is starting to gain the upperhand. In the year 2004 the share of livestock production sales in the total sales amounted to 58% and in the year 2017 it only made for 44%. The lower share of livestock production in the total sales has been seen since the year 2009, when the livestock production sales amounted to 47.03% and the sales from vegetable production to 52.97%. The share of livestock production sales in the total sales generated in the Slovak Republic reveals a decline in livestock production, as demonstrated of maps from the years 2004 and 2017 (*Fig. 10* and *Fig. 11*). When comparing the years 2004 and 2017 the sales from livestock production in Slovakia fell by 7.6%. The biggiest decrease was seen in the Trenčín Region (-20.7%), the Banská Bystrica Region (-20.2%) and the Nitra Region (-14.7%).

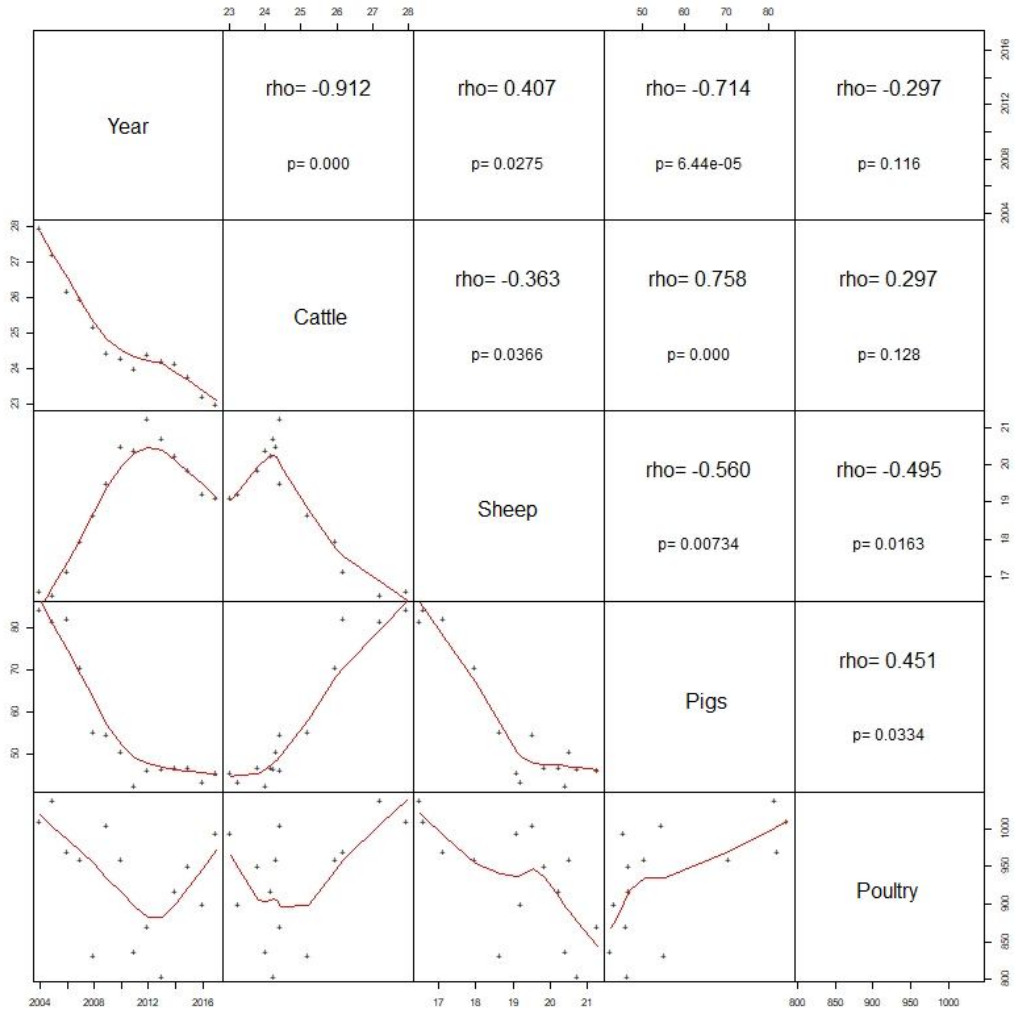

Figure 9. *Animal production trends model in the Slovak Republic (model based on time series analysis)*

http://www.aloki.hu ● ISSN 1589 1623 (Print) ● ISSN 1785 0037 (Online)
DOI: http://dx.doi.org/10.15666/aeer/1704_76497666

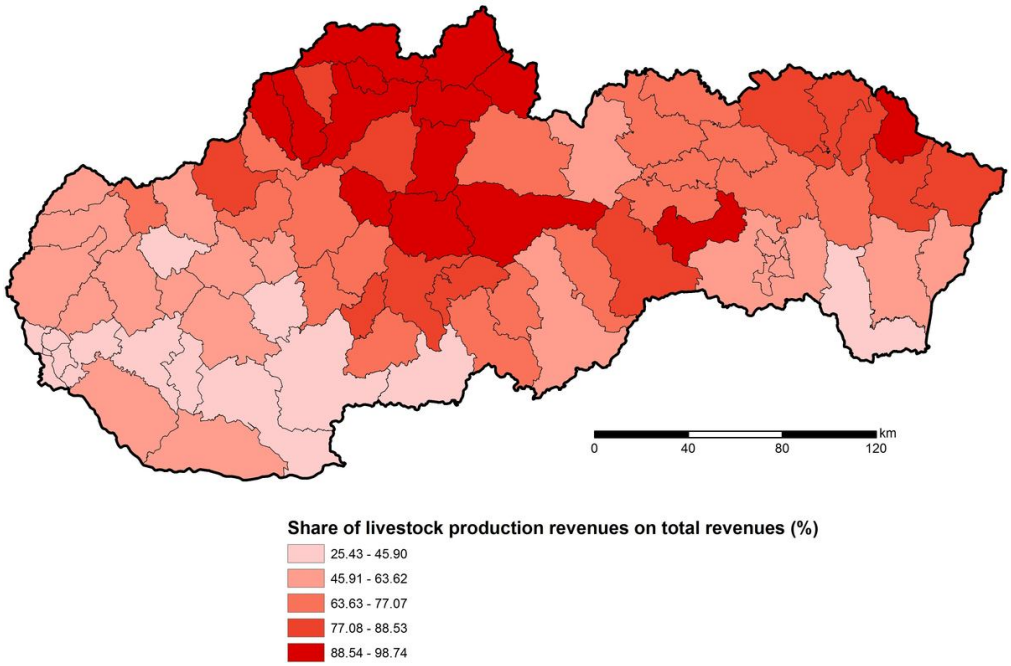

Figure 10. *Share of livestock production revenues on total revenues (%) – 2004*

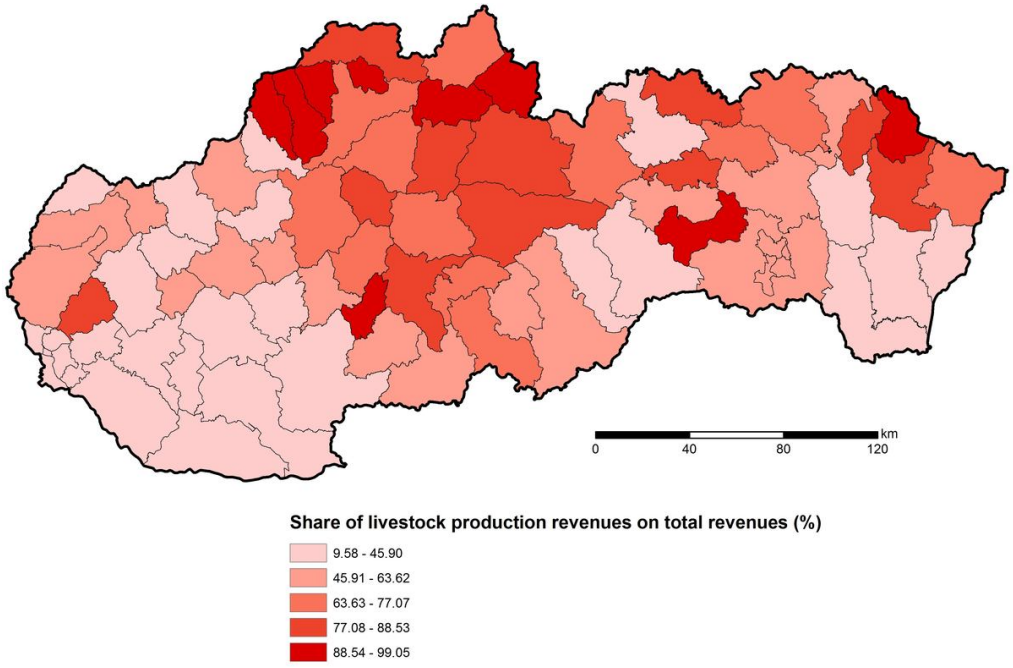

Figure 11. *Share of livestock production revenues on total revenues (%) – 2017*

Vegetable production compared to livestock production is being more supported in Slovakia. According to the Ministry of Agriculture and Rural Development of the Slovak Republic, 2006 the direct payments into agriculture in Slovakia in the year 2005 amounted to 203 MioEUR, while less than 8 MioEUR went to livestock production. It is regarded as positive that the direct payments were gradually increasing and in the

http://www.aloki.hu ● ISSN 1589 1623 (Print) ● ISSN 1785 0037 (Online)
DOI: http://dx.doi.org/10.15666/aeer/1704_76497666

year 2016 they totalled to 408 MioEUR, from which the breeders of farm animals only received 54 MioEUR (Ministry of Agriculture and Rural Development of the Slovak Republic, 2017). The above-mentioned disproportion in funding the livestock production sector in form of a lower number of types of direct support from the EU could be alleviated by funding from the state budget; however this support can not be compared with the level of funding provided in the remaining EU states.

Changes in livestock production and their potential impact on quality of environment

The changes in livestock production in Slovakia between the years 2004 and 2017 may at first sight suggest a favourable development in reducing damage connected with the direct impact of the agrarian sector on the environment. In case of farm animal breeding it is the potential impact on air quality as well as the quality of soil and water sources. In this respect environmental pollution was particulary seen in relation to large-capacity agricultural farmyards but also with other activities carried out outside the premises of agricultural businesses. The decline in the population of farm animals might in this context appear as a naturally positive factor. However, in a broader context it is necessary to point out the importance of non-productive factors related to a targeted breeding of farm animals. These non-productive factors have a wider impact on the whole society but there is also their biological impact including the preservation of the cultural character of landscape and protection of the environment.

- Reduction of the population of farm animals decreased the production of biomass as renewable energy source and this not only in the form of excrements but also in form of reducing areas under crops for selected commodities, which belonged to the fodder base of livestock production as well as selected types of fermented feed (e.g. silage).
- Reduction of the population of farm animals made natural fertilizers such as the production of stable manure less accessible.
- Livestock production and farm animal breeding generate a quantity of greenhouse gases emissions such as carbon dioxide CO_2 and nitrogen oxide. Most greenhouse gases are released into the air from stable manure. The decrease of the population of farm animals has a positive impact on the reduction of emissions responsible for the greenhouse effect.
- The falling population of farm animals reduces the levels of methane, which has a harmful impact on the climate.
- The drop in the population of farm animals also leads to lowering the level of ammonia (NH_3) emissions. Ammonia contributes to the creation of acid rains.
- Livestock production also causes damage and pollutes soil by excessive overgrazing of pastures by the farm animals and can thus provoke erosive soils. The reduction of the population of livestock therefore has a positive impact on soil.
- Livestock production further contributes to polluting waters. Ground water is mainly polluted by animal droppings, chemicals, synthetic fertilizers, pesticides, hormones and antibiotics that are being served to the animals with fodder. In this respect the decline in the population of farm animals has a positive impact on the environment.
- As it is stated in many documents of the European Union selected groups of farm animals (particularly sheep and beef cattle) play an irreplaceable role in

http://www.aloki.hu ● ISSN 1589 1623 (Print) ● ISSN 1785 0037 (Online)
DOI: http://dx.doi.org/10.15666/aeer/1704_76497666

form of ecological benefits because they help preserve biodiversity and landscape in areas that are naturally disadvantaged or less fertile. The preserveration of biodiversity affects both the flora and fauna and the whole ecosystems respectively. In many countries, Slovakia included, we find national as well as local breeds, which presents a unique gene pool from the point of view of reproduction and sustainability of the gene pool and animal genetic sources, which foregrounds also the impact on the protection and preservation of agrobiodiversity.

- Farm animals play an equally important role in fighting such phenomena as soil erosion particularly as a result of deforestation but also the changing structure of vegetation, avalanches, fires, inundations and torrential rainfalls.
- The grazing of natural pastures often prevents progradation of various air-raid/ invasive types of plantes (either herbs or woody plants), maintaining i.a. healthy vegetation from the point of view of assimilation of nutrients. Bad accessibility is also a relevant factor.

Possibilities for development of organic farming with focus on livestock production

A sustainable agroecosystem prioritizes organic farming practices, functions and objectives in farming on soil and breeding of animal farms. In comparison with the conventional methods of farming organic farming has more positive effects on the protection of natural elements and landscape. An indispensable factor is the biodiversity of the flora and fauna in areas with arable land, permanent grassland and in the surrounding biotopes as well as the preservation and protection of agrobiodiversity. Since Slovakia entered the EU organic farming has been booming as never before. The positive trend of the development of organic farming in Slovakia has been reflected in an increased number of producers of bioproducts, the area of organic soil has risen and the number of enterprises processing bioproducts has seen a moderate increase too. In the year 2017 there are more than 400 farms operating in the field of organic farming registered in Slovakia. The share in organically farmed land has increased up to 9%. Also the demand of the consumers for organic products significantly contributes to the development of organic farming. In spite of the fact that the prices of organic products are not exactly low the present-day consumers are committed to eating healthy food and protecting their environment at the same time. An essential advantage of organic products is the fact that their production does not pollute the environment. On organic farms, where permanent grassland prevails, the breeding of beef cattle, sheep and goats is strongly represented. As to the orientation of livestock production in the regions of Slovakia it is particularly cattle breeding in combination with other types of farm animals such as sheep, goats and horses. When it comes to cattle breeding two central Slovakian regions stand out: the Žilina and Banská Bystrica Regions and also the Prešov and Košice Regions in eastern Slovakia. The breeding of sheep in combination with other farm animals is less represented (goats, horses and pigs). The farmers deal the least with the breeding of pigs and poultry. It is in this very type of breeding that Slovakia can develop a lot in future. In the Western Slovak Regions and in the Danubian Lowland organic breeding of farm animals is almost not being carried out. In Western Slovakia it is vegetable production of the conventional type but also alternative vegetable production that is more developed. As negative the fact can be regarded that there is an absence of the processors of organic products, their quantity is still not sufficient though the number is rising. As of 2017 Slovakia reports more than 80

http://www.aloki.hu ● ISSN 1589 1623 (Print) ● ISSN 1785 0037 (Online)
DOI: http://dx.doi.org/10.15666/aeer/1704_76497666

processors in the field of organic farming, while a majoritiy of the enterprises processing the products of organic farming are located in the regions of Western Slovakia, Eastern Slovakia and in the northern part of the country. These entities mainly concentrate on processing and producing dairy products (17 processors).

In the programming period from 2014 to 2020 the territory of Slovakia falls under the Rural Development Programme 2014 – 2020, which supports organic farming within Priority 4 "Restoring, preserving and enhancing ecosystems related to agriculture and forestry", measures 11 "Organic farming, sub-measures Payments for conversion to organic farming practices and methods" and "Payments for the preservation of organic farming practices and methods". In Slovakia organic farming can become an important element not only when it comes to increasing employment in rural areas, development of agrotourism and production of traditional organic food but in landscape maintenance in particular.

Conclusions

The entry of Slovakia into the European Union introduced new possibilities of receiving subsidies and non-refundable financial resources, which nonetheless did not slow down the falling trend in the population of farm animals particulary of cattle and pigs. Slovak agriculture would not only be helped by a higher level of support from the state budget but also if the direct EU funding were aligned, which would contribute to increasing the employment rates in rural areas and put an end to Slovakia´s lagging behind the other EU countries. Slovakia´s competitiveness on the common European market would increase, while the importation of food from abroad would decrease. The CAP for the period 2014 – 2020 meant a revaluation of direct payments to farmers and of the rural development policy, a greener more ecologically oriented policy of the state, support of smaller farms and small farmers, the support of suckler cows breeding and last but not least the abolishing of the system of milk quotas, which is however related to an overproduction of milk and milk products on the European market. The new reform should enable gradual improvement of efficiency in agriculture and at the same time decrease the share of agrarian policy in the total EU budget (Common Agricultural Policy Reform 2014 – 2020, 2015).

In the new programming period 2014 – 2020 the Ministry of Agriculture of the Slovak Republic has decided to increase the financial support for the breeding of certain farm animals, e.g. milk cows, brood sows, pigs for fattening, broiler chicken and sheep. The amount of the subsidy is derived from the number of the specific animals and the costs necessary for their life (Rural Development Programme of the Slovak Republic 2014 – 2020, 2015). The main objective of this kind of support is to increase the numbers of farm animals in the individual types of breeding.

The funding from the European Union in the new programming period 2014 – 2020 mainly targets revitalization of the dropping livestock production. Although at present Slovakia is not self-sustainable in the production of any kind of meat the country is capable of changing this situation. As far as the breeding of beef cattle is concerned the population of suckle cows is expected to grow. These changes are supported by the transfer of a part of arable land into permanent grassland. Slovakia has a considerable growth potential in the pig farming and there is the assumption to attain full self-sustainability in the production of pork and even to export it. The presently increasing interest of the consumers for poultry meat will contribute to increasing the domestic

http://www.aloki.hu ● ISSN 1589 1623 (Print) ● ISSN 1785 0037 (Online)
DOI: http://dx.doi.org/10.15666/aeer/1704_76497666

production of slaughtered poultry. Slovak consumers are minimally interested in purchasing sheep meat and most of the production is being exported to developed EU countries. It can be presumed that the breeding of sheep in Slovakia will increase due to support and payments according to the area of permanent grassland. Along with cattle farming sheep breeding is of considerable importance for a sustainable development of rural landscape in mountain and submontane regions. The Slovak consumer is increasingly more interested in not only the quality but also the origin of meat. The freshness of meat is a sign of quality and this cannot be guaranteed by any kind of imported meat. This is the reason why Slovakia endeavours to support young beginning farmers. Young farmers are expected to particularly develop the sensible sectors such as livestock production but also truck farming and fruit growing. It is these very products that are absent on the regional markets (Common Agricultural Policy Partnership between Europe and farmers, 2012). Hole et al. (2004) assess the impact of organic farming on landscape biodiversity compared to conventional farming. Intensification and expansion of modern agriculture rank among the biggest current threats to global biodiversity. Organic farming is a potential solution for increasing biodiversity. This system focusses on food production while minimally damaging the ecosystems. Slovakia meets the preconditions for further development of organic farming.

The dynamics of animal production from 2004 to 2017 in Slovakia, changes of its intensity and structure reflect wider changes in the context of the accession to the European Union and the application of common rules in the form of the CAP. As our study has shown, these changes has been significantly negative impact. The results, among other, are a livestock stocks decrease, a change in the share of livestock production revenues on total revenues, and a deepening of regional disparities. A systematic monitoring of the further development of livestock numbers/stocks (decline, stabilization, increase) and structure of animals / herds appears to be of importance. Furthermore, it will be important to monitor the impact of animal production development on total agricultural production and the agro-food complex, on the agricultural landscape, effect on the environment quality in the context of organic land management and sustainable land development.

Acknowledgements. This paper was elaborated within the project VEGA 1/0934/17 Land-use changes of Slovak cultural landscape over the past 250 years and prediction of its further development and project APVV-18-0185 Land-use changes of Slovak cultural landscape and prediction of its further development.

REFERENCES

[1] Brožová, I. (2011): The economic performance analysis of organic farms in the Czech Republic. – Agricultural Economics 57: 240-246.

[2] Buchenrieder, G., Möllers, J. (eds.). (2009): Structural change in Europe's rural regions, Farm livelihoods between subsistence orientation, modernisation and non-farm diversification. – Studies on the Agricultural and Food Sector in central and Eastern Europe, 49. – http://ageconsearch.umn.edu/bitstream/53334/2/IAMO%20studies%20series_vol49.pdf.

[3] Buday, Š., Chrastinová, Z., Krížová, S., Gálik, J. (2012): Porovnanie dopadov SPP na vývoj poľnohospodárskej výroby a objem zahraničného obchodu. – Výskumný ústav ekonomiky poľnohospodárstva a potravinárstva, Bratislava, 19p.

http://www.aloki.hu ● ISSN 1589 1623 (Print) ● ISSN 1785 0037 (Online)
DOI: http://dx.doi.org/10.15666/aeer/1704_76497666

[4] Chrastinová, Z., Trubačová, A., Ďuričová, I., Krížová, S. (2014): Ekonomická efektívnosť chovu hovädzieho dobytka a oviec. – Ekonomika poľnohospodárstva XIV: 33-56.
[5] Common Agricultural Policy Partnership between Europe and farmers. (2012): Availabe at: https://ec.europa.eu/info/food-farming-fisheries/key-policies/common-agricultural-plicy/cap-glance.
[6] Common Agricultural Policy Reform 2014 – 2020 (2015): Available at: http://www.euractiv.sk/podnikanie-v-eu/zoznam_liniek/reforma-spolocnej-polnohospodarskej-politiky-2014--2020-000303.
[7] Doležalová, H., Pícha, K., Navrátil, J., Bezemková, A. (2014): Changes in the structure of the regional agricultural production (South Bohemian region). – Journal of Central European Agriculture 15: 335-353.
[8] Dos Santos, M. J. P. L., Henriques, P. D., Fragoso, R. M., Carvalho, M. L. P. V. (2010): Attitudes of the Portuguese farmers to the EU Common Agricultural Policy. – Agricultural Economics 56: 460-469.
[9] Falťanová, N. (2008): Očakávané vplyvy agrárnej politiky EÚ na vývoj poľnohospodárskej výroby SR. – Prognostický ústav SAV, Bratislava.
[10] Gorton, S., Douarin, E., Davidova, S., Latruffe, L. (2008): Attitudes to agricultural policy and farming futures in the context of the 2003 CAP reform: A comparison of farmers in selected established and new member states. – Journal of Rural Studies 24: 322-336.
[11] Häring, A. M., Dabbert, S., Aurbacher, J., Bichler, B., Eichert, C. H., Gambelli, D., Lampkin, N., Offermann, F., Olmos, S., Tuson, J., Zanoli, R. (2004): Organic farming and measures of European agricultural policy. – Organic Farming in Europe: Economics and Policy, volume 11. University of Hohenheim, Stuttgart, 243p.
[12] Hole, D. G., Perkins, A. J., Wilson, J. D., Alexander, I. H., Grice, P. V., Evans, A. D. (2004): Does organic farming benefit biodiversity? – Biological Conservation 122: 113-130.
[13] Hrabalová, A., Zander, K. (2006): Organic beef farming in the Czech Republic: structure, development and economic performance. – Agricultural Economics 52: 89-100.
[14] Ilbery, B., Maye, D. (2005): Alternative (shorter) food supply chains and specialist livestock products in the Scottish-English borders. – Environment and Planning A 37: 823-844.
[15] Kabrda, J., Jančák, V. (2006): České zemědělství a krajina po vstupu Česka do EU: nový institucionální rámec. – XXI. sjezd České geografické společnosti. České Budějovice.
[16] Kołodziejczak, A. (2006): Agriculture and the countryside in Poland: alternative scenarios of change. – Quaestiones Geographicae 25: 47-52.
[17] Kołodziejczak, A., Kossowski, T. (2011): Diversification of farming systems in Poland in the years 2006–2009. – Quaestiones Geographicae 30: 49-52.
[18] Kozáková, J., Lančarič, D., Tóth, M., Savov, R. (2015). Ekonomické zhodnotenie vybraných rozdielov ekologického a konvenčného hospodárenia na Slovensku. – Ekonomika poľnohospodárstva XV.
[19] Král, M., Palasová, P., Svobodová, H., Věžník, A. (2012): Dopady SZP EU na rozvoj zemědělství v centrální části Drahanské vrchoviny. – Geographia Cassoviensis VI: 78-90.
[20] Kulikowski, R. (2005): Agricultural problems areas, in Poland, 2002. – Moravian Geographical Reports 19: 50-60.
[21] Lockie, S., Halpin, D. (2005): The 'Conventionalisation' Thesis Reconsidered: Structural and Ideological Transformation of Australian Organic Agriculture. – Sociologia Ruralis 45: 284-307. DOI:10.1111/j.1467-9523.2005.00306.x.
[22] Milestad, R., Darnhofer, I. (2003): Building farm resilience: The prospects and challenges of organic farming. – Journal of sustainable agriculture 22: 81-97. DOI:101300/J064v22n03_09.

http://www.aloki.hu ● ISSN 1589 1623 (Print) ● ISSN 1785 0037 (Online)
DOI: http://dx.doi.org/10.15666/aeer/1704_76497666

[23] Ministry of Agriculture and Rural Development of the Slovak Republic (2006): Správa o poľnohospodárstve a potravinárstve v Slovenskej republike za rok 2005 (Zelená správa). – NPPC-VÚEPP, Bratislava, 257p.
[24] Ministry of Agriculture and Rural Development of the Slovak Republic (2017): Správa o poľnohospodárstve a potravinárstve v Slovenskej republike za rok 2016 (Zelená správa). – NPPC-VÚEPP, Bratislava, 44p.
[25] Moschitz, H., Stolze, M. (2009): Organic farming policy networks in Europe: Context, actors and variation. – Food Policy 34: 258-264. DOI: 10.1016/j.foodpol.2009.03.007.
[26] Mzoughi, N. (2011): Farmers adoption of integrated crop protection and organic farming: Do moral and social concerns matter? – Ecological Economics 78: 1536-1545. DOI:http://dx.doi.org/10.1016/j.ecolecon.2011.03.016.
[27] Némethová, J., Mesárošová, J. (2013): The Development and Current Situation of Organic Farming in the Trnava Region, 2013. – Geographical Information 17: 4-25.
[28] Némethová, J., Dubcová, A., Kramáreková, H. (2014): The Impacts of the European Union's common agricultural policy in Slovakia. – Moravian Geographical Reports 22: 51-64. DOI: 10.1515/mgr-2014-0023.
[29] Némethová, J., Civáň, M. (2017): Regional differences in agriculture in Slovakia after its accession to the European union, 2017. – Quaestiones Geographicae 36: 9-21. DOI:10.1515/quageo– 2017–0011.
[30] Némethová, J., Dubcová, A., Kramáreková, H. (2017a): Slovak agriculture in 2002 – 2014 and its regional differentiations. – Geographical Journal 69: 281-298.
[31] Némethová, J., Dubcová, A., Nagyová, Ľ., Kramáreková, H. (2017b): Ecological Farming in Slovakia and its Regional Disparities. – European Countryside 9: 746-768. DOI: 10.1515/euco-2017-0042.
[32] Nieberg, H., Kuhnert, H. (2007): Support Policy for Organic Farming in Germany. – Landbauforschung Völkenrode 57: 95-106.
[33] Petrovič, F., Stránovský, P., Muchová, Z., Falťan, V., Skokanová, H., Havlíček, M., Gábor, M., Špulerová, J. (2017): Landscape-ecological optimization of hydric potential in foothills region with dispersed settlements – a case study of Nová Bošáca, Slovakia. – Applied Ecology and Environmental Research 15: 379-400.
[34] Rudnicki, R. (2013): Spatial differences in the number of applications for payments under the EU common agrocultural policy submitted by agricultural holdings in Poland over the yers 2002-2010. – Quaestiones Geographicae 32: 15-31.
[35] Rural Development Programme of the Slovak Republic 2014 – 2020 (2015): Available at: http://www.pomocvidieku.sk/sites/default/files/program_rozvoja_vidieka_sr_2014_-_2020_-_neprojektove_opatrenia.pdf.
[36] Schlosserová, J., Juršík, J. (2009): Ekologické poľnohospodárstvo. – Inštitút vzdelávania veterinárnych lekárov, Košice, 88p.
[37] Spišiak, P., Kusendová, D., Pavličková, K., Halás, M., Kolény, M., Zubriczký, G., Švoňavec, M., Hurbánek, P., Paľúch, T., Labuda, M. (2005): Agrorurálne štruktúry Slovenska po roku 1989. – Bratislava, Geo-grafika.
[38] Spišiak, P., Némethová, J. (2008): Agrosubjekty regiónu Nitra vo vzťahu k odberateľom poľnohospodárskych surovín = Agricultural entities of the Nitra region in relation to the purchasers of agricultural raw materials, 2008. – Geographical Journal 60: 63-87.
[39] Stolze, M., Lampkin, N. (2009): Policy for organic farming: Rationale and concepts. – Food Policy 34: 237-244.
[40] Svobodová, H., Věžník, A. (2011): Impacts of the commom agricultural policy of the European union in the Vysočina region (Czech republic) by the view of the farmers. – Journal of Central European Agriculture 12: 733-743.
[41] Věžník, A., Konečný, O. (2011): Agriculture of the Czech republic after accession to the EU: regional differentiation. – Moravian Geographical Reports 19: 50-60.
[42] Věžník, A., Král, M., Svobodová, H. (2013): Agriculture of the Czech republic in the 21st century: From productivism to post-productivism. – Quaestiones Geographicae 32: 7-14.

http://www.aloki.hu ● ISSN 1589 1623 (Print) ● ISSN 1785 0037 (Online)
DOI: http://dx.doi.org/10.15666/aeer/1704_76497666

[43] Věžník, A., Svobodová, H., Némethová, J., Hradický, J. (2017): Livestock production in Czechia and Slovakia, ten years beyond EU accession, 2017. – Human Geographies: Journal of Studies and Research in Human Geography 11: 77-94. DOI: 10.5719/hgeo.2017.111.5.

http://www.aloki.hu ● ISSN 1589 1623 (Print) ● ISSN 1785 0037 (Online)
DOI: http://dx.doi.org/10.15666/aeer/1704_76497666

EFFECTS OF RAINFALL SHORTAGE AND CLIMATIC WATER BALANCE CHANGE ON AGRICULTURE

RADZKA, E.* – JANKOWSKI, K. – JANKOWSKA, J.

Faculty of Natural Sciences, Siedlce University of Natural Sciences and Humanities
ul. Prusa14, 08-110 Siedlce, Poland

**Corresponding author*
e-mail: elzbieta.radzka@uph.edu.pl; phone:+48-25-643-1351

(Received 11th Mar 2019; accepted 3rd May 2019)

Abstract. This paper assesses of climatic water balance (CWB) in the 2000-2018 vegetation seasons and the rainfall requirements of selected crops. Extreme values and the range of variation for that time period are given emphasis to, paired with statistical significance of the slope of linear trends. The study found that the biggest difference in climatic water balance between 2018 and the 2000-2017 period was recorded in June (29 mm). Water shortages for cereals occurred in all months of the growing seasons both form 2000 to 2017 and in 2018, but in May 2018 water deficit was much larger than in the multiannual period. In the case of maize the last months of the 2018 growing season exhibited high deficiency of rainfall. For early potato varieties water shortages were not higher in 2018 than the average of the multiannual period. However, significant rainfall shortages for sugar beet were recorded in May and August 2018. In the 2000-2017 period the highest average monthly rainfall deficiencies for meadows and pastures were in July. In the same month there was also a statistically significant increase in the CWB value, on average, by about 6.4 mm per 10 years.
Keywords: *precipitation, air temperature, drought, crops, Poland*

Introduction

The ongoing climate change has a direct impact on agriculture. With the change of weather conditions, some factors determining plant yields such as requirements for agro technical practices and for fertilizer also change, together with incidence and severity of diseases and pests. The decisive factor shaping production systems in agriculture in the next few years, alongside climate change, may be the rising demand for food and competition for water. Climate change significantly increases the threat of drought (Sulewski and Czekaj, 2015), but for agriculture global warming may be sometimes beneficial as it opens the possibility of growing new varieties, not used earlier in some parts of the world (Gendron St-Marseille et al., 2019). Scientists predict that the trend in drought incidence in southern Europe and the North-Eastern part of South America will last up to 2050 (Ruane et al., 2018). The increasing frequency of droughts observed in recent years is a result of rising air temperature, lower than average rainfall, or even a complete lack of precipitation for a longer time (Górski, 2006; Kundzewicz et al., 2006; Łabędzki, 2006; Kozyra et al., 2009). Droughts cause significant yield losses (Łabędzki, 2006; Doroszewski et al., 2008). In the drought monitoring system (SMSR) in Poland, weather conditions causing water shortages in agriculture are measured by using climatic water balance (CWB) (Rojek, 1987; Kołodziej et al., 2003; Legates and Mccabe, 2005; Łabędzki, 2006; Kanecka-Geszke and Smarzyńska, 2007; Doroszewski et al., 2008). This period is referred to as agricultural drought (Niedźwiedź, 2003). The agricultural drought monitoring system has been developed on the basis of agro-meteorological studies

http://www.aloki.hu ● ISSN 1589 1623 (Print) ● ISSN 1785 0037 (Online)
DOI: http://dx.doi.org/10.15666/aeer/1704_76677678

(Doroszewski and Górski, 1995; Demidowicz et al., 1996, 1997; Doroszewski et al., 1997).

The aim of the research was to characterise climatic water balance and rainfall deficiency for selected crops in eastern Poland in 2018 compared to the 2000-2017 period. Attention was drawn to extreme values and variation range in that time series. Additionally, statistical significance of linear trend slopes was determined.

Material and methods

The analysis is based on the data recorded between 2000 and 2018 which was provided by the meteorological station in Siedlce (φ°=52°10′03″N ; λ°=22°17′24″E; 150 m above sea level).

The following meteorological elements were analysed:

- daily mean air temperature.
- daily total precipitation.
- daily mean relative humidity.

The basic characteristics of the distribution of the tested parameters were determined: their arithmetic means, and minimum, and maximum values. To present the dynamics of monthly arithmetic means the coefficient of variation was calculated (*Eq.1*).

$$V = \frac{S}{X} * 100\% \quad \text{(Eq.1)}$$

where:

CV – coefficient of variation,

SD – standard deviation,

X – arithmetic mean.

Then evaporation was calculated using Ivanov's equation (Przedpełska, 1971) (*Eq.2*).

$$E = 0.0018(25 + t)^2(100 - f) \quad \text{(Eq.2)}$$

where:

t – mean monthly air temperature, °C,

f – mean monthly relative humidity,%.

Monthly values of climatic water balance were designated using the following formula (*Eq.3*):

$$CWB = P - E \quad \text{(Eq.3)}$$

where:

P – monthly sum of precipitation (mm),

E – monthly evaporation (mm).

Water needs of selected crops were estimated based on optimal precipitation according to the method specified by Klatt (after Nyc, 2006) (*Eq.4*).

$$Popt = Pk + 5 * tk \quad \text{(Eq.4)}$$

where:

http://www.aloki.hu ● ISSN 1589 1623 (Print) ● ISSN 1785 0037 (Online)
DOI: http://dx.doi.org/10.15666/aeer/1704_76677678

Popt – optimal precipitation (mm),

Pk – optimal monthly precipitation according to the Klatt table (mm),

tk – mean monthly air temperature (°C) for which Klatt determined the optimal precipitation (Pk),

Shortages of rainfall were calculated according to the formula (*Eq.5*):

$$N = Prz - Popt \quad \text{(Eq.5)}$$

where:

N – precipitation deficit (mm),

Prz – recorded precipitation (mm),

Popt – optimal precipitation according to Klatt (mm).

Water shortages were calculated for the following crops: spring wheat, oats, corn, early potato, sugar beet, meadows and pastures.

The values of the analyzed meteorological parameters, climatic water balance, and precipitation deficit in 2018 were compared to the values for the 2000-2017 period. The direction and significance of the trend of climatic water balance changes were established on the basis of the linear trend equation. The significance of the slope of the trend was assessed with Student's t-test with a significance level of $\alpha = 0.05$.

Result analysis and discussion

The greatest average monthly precipitation during the 2000-20017 period was in July (72 mm), and the smallest in October and April with 37 mm and 38 mm, respectively (*Table 1*). The minimum value of this parameter was noted in October (only 2 mm), and the maximum in August (257 mm). Precipitation in October had the largest variation with the CV of 93%. The first half of the growing season (April, May, June and July) exhibited around a 50% monthly variability of rainfall.

Table 1. *Average mean, maximum, and minimum values of some meteorological parameters, with the coefficient of variation in Siedlce during the 2000-2017 period*

Parameter/Month		April	May	June	July	August	September	October
Precipitation (mm)	Mean	38	60	64	72	66	53	37
	Max	82	138	166	180	257	165	130
	Min	6	22	18	9	12	14	2
	CV	53	52	56	53	81	78	93
Air temperature (°C)	Mean	8.6	13.9	16.6	19.2	18.5	13.5	8.2
	Max	12.1	16.7	18.3	21.8	20.8	15.7	10.8
	Min	6.2	11.3	14.2	16.4	16.8	11.3	5.1
	CV	16.0	9.9	7.1	7.2	5.5	9.2	21.1
Relative humidity (%)	Mean	69.5	71.2	72.6	73.9	74.2	80.2	83.5
	Max	80.0	84.9	83.2	85.5	83.1	88.7	93.8
	Min	61.5	62.0	63.2	57.6	59.1	68.7	76.2
	CV	7.7	7.7	8.0	8.2	7.4	6.6	5.5
CWB (mm)	Mean	-64	-79	-86	-91	-89	-54	-32
	Max	-40	-38	-44	-44	-54	-23	-9
	Min	-85	-109	-124	-168	-156	-92	-53
	CV	20	23	25	28	25	33	34

http://www.aloki.hu ● ISSN 1589 1623 (Print) ● ISSN 1785 0037 (Online)
DOI: http://dx.doi.org/10.15666/aeer/1704_76677678

The warmest month in the 2000-2017 period was August with the average air temperature of 18,5°C, while October with 8.2°C was the coldest. In the same month the minimum value of this parameter was recorded (5.1°C), while the largest (21.8°C) was in July. The largest variation of the monthly average temperature was in October (CV = 21.1%) and the lowest in August (CV=5,4%).

The observed trend of rising temperature and changing evaporation conditions increased the area of the moderately dry region in Poland from 13% in the 1931-1960 period to 20% in the 1971-2000 period, and the area of land with high soil moisture decreased from 32% to 10% (Ziernicka-Wojtaszek, 2009).

Average relative air humidity in the growing season varied from 69.5% in April to 83.5% in October. The maximum value for this parameter was noted in October (93.8%), and the minimum in July (57.6%). The variability of humidity ranged from 5.5% in October to 8.2% in July. The average monthly values of the climatic water balance in the 2000-2017 growing seasons were negative. The maximum value of this parameter was noted in October (-9 mm) and minimum in July (-168 mm), while CWB variation remained at around 27%.

Multiannual average rainfall (2000-2017) in the growing season was 390 mm, and in 2018 it was 347 mm, which was only about 43 mm less (*Fig. 1*). However, monthly sums of precipitation were slightly larger than the multiannual average only in April, June, and July 2018 (*Fig. 1*). Compared to the average in May 2018 rainfall was lower by 34 mm, in August by about 37 mm, in September by 11 mm, and in October by 3 mm.

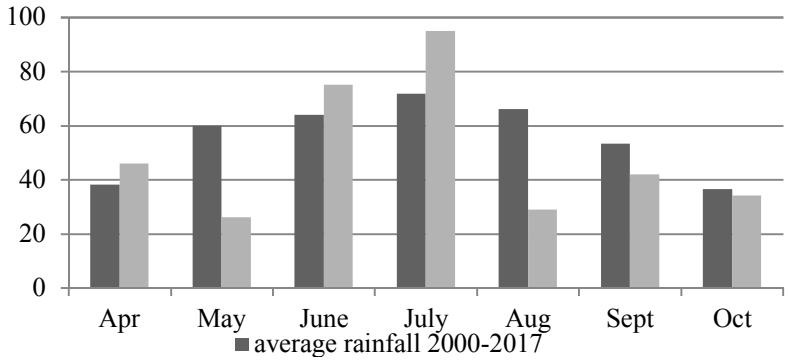

Figure 1. *Average monthly rainfall (mm) of the 2000-2017 period and in 2018 in Siedlce*

It was found that in all months of the 2018 growing season the average monthly air temperature was higher than the average multiannual (*Fig. 2*). In April 2018 it was higher than the average multinational by 4ºC. The smallest difference in thermal conditions between 2018 and the multiannual period was in July, with the temperature in 2018 higher by only 0.3°C.

Changes in relative air humidity in 2018 were inverse to changes in air temperature (*Fig. 3*). In all the months of the 2018 growing season, with the exception of July, the value of this parameter was a few percent less than the multiannual average.

Similarly, the values of climatic water balance in July 2018 were 7 mm higher than the multiannual average (*Figs. 4 and 5*). In the remaining months of the 2018 growing season precipitation shortage was bigger than the perennial values, and the biggest difference was recorded in June (29 mm).

http://www.aloki.hu ● ISSN 1589 1623 (Print) ● ISSN 1785 0037 (Online)
DOI: http://dx.doi.org/10.15666/aeer/1704_76677678

Using the Penman-Monteith equation Łabędzki et al. (2012) found that the average evapotranspiration in Poznań, Olsztyn, and Cracow ranged from 50-60 mm in April and September to 100-120 mm in the remaining months of the growing season. The largest value of evapotranspiration in those areas was in July.

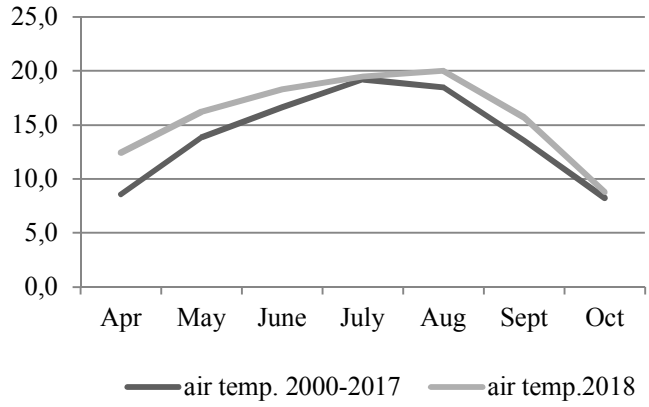

Figure 2. *Average monthly air temperature (°C) in the 2000-2017 period and in 2018 in Siedlce*

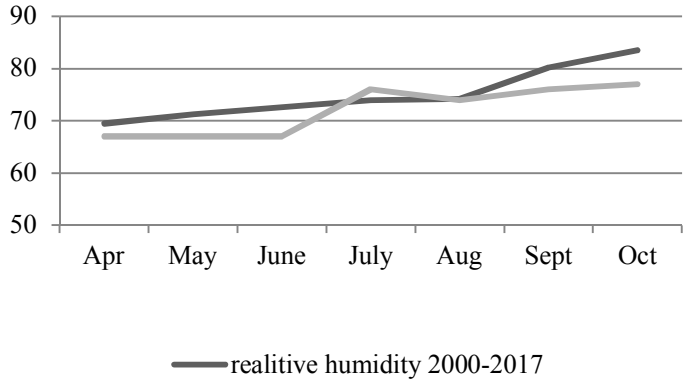

Figure 3. *Average monthly relative humidity (%) in 2000-2017 and in 2018 in Siedlce*

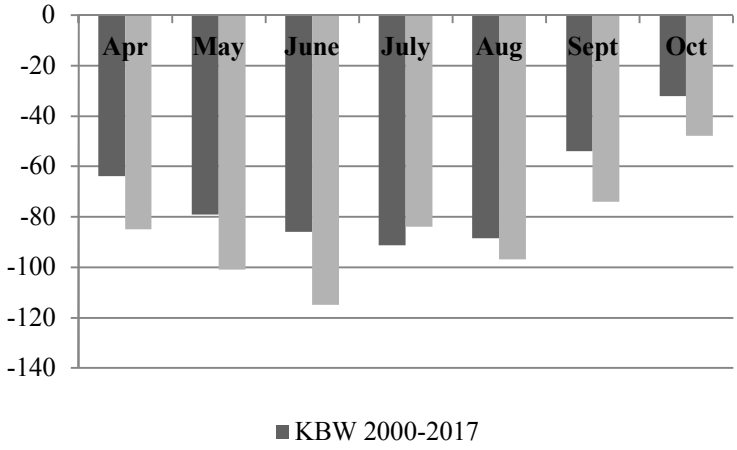

Figure 4. *Average monthly climatic water balance (mm) in the 2000-2017 period and in 2018 in Siedlce*

http://www.aloki.hu ● ISSN 1589 1623 (Print) ● ISSN 1785 0037 (Online)
DOI: http://dx.doi.org/10.15666/aeer/1704_76677678

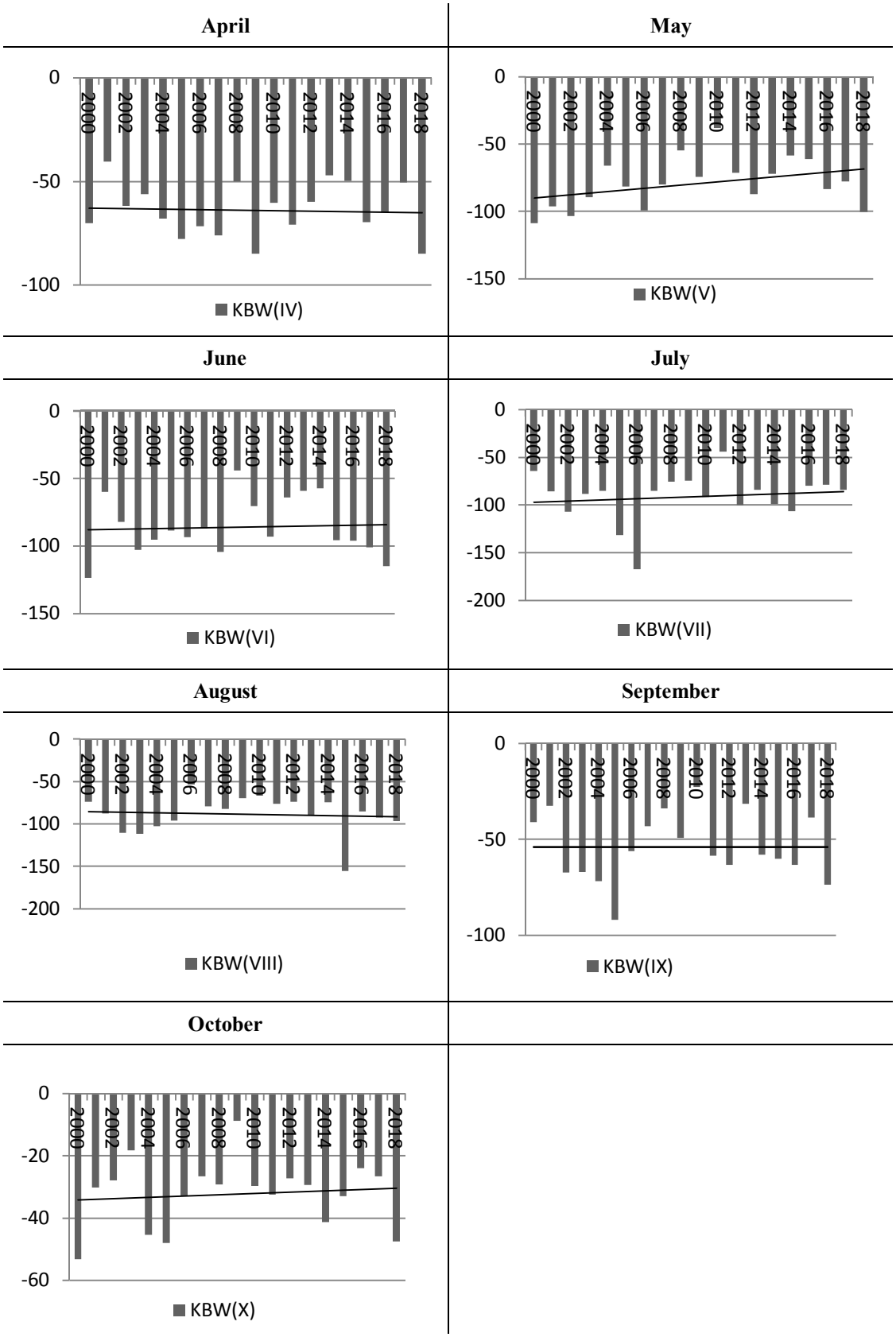

Figure 5. *Climatic water balance (mm) and linear trend in the 2000- 2018 vegetation seasons in Siedlce*

http://www.aloki.hu ● ISSN 1589 1623 (Print) ● ISSN 1785 0037 (Online)
DOI: http://dx.doi.org/10.15666/aeer/1704_76677678

Projected climate change (Watson et al., 1997; Stuczyński et al., 2000) justifies the need for the current monitoring of the incidence and extent of drought. A prolonged lack of precipitation and resulting evapotranspiration processes reduce agricultural productivity. Agricultural drought seriously reduces plant growth, which leads to a significant drop in crop yields. A longer period of reduced precipitation leads to soil drought (Łabędzki, 2007; Vicente-Serrano et al., 2010). Changes in both precipitation and air temperature affect climatic water balance. In 2018 agricultural drought occurred in Poland for all monitored plants in all provinces with 1923 communes affected, which constituted 49% of agricultural land. Analysis of the linear trend of climate change impact on water balance showed that slope values were positive only in May, June, and July (*Table 2*). Furthermore, it was found that in July there was a statistically significant increase in the CBW value, on average, by about 6.4 mm in 10 years. However, in the rest of the growing season there was a declining tendency, but it was not statistically significant. Changes in the structure of water balance led to water deficit which significantly affected the level of plant production and changes in the structure of crop production.

Table 2. *Linear regression of climatic water balance changes in 2000-2018 in Siedlce*

Month	Linear regression
April	y= - 0.136x + 210.95
May	y= 1.214x - 2518.42
June	y= 0.202x - 491.27
July	y= 0.637*x - 1370.89
August	y= - 0.372x + 658.52
September	y= - 0.005x - 43.32
October	y= - 0.005x - 43.32

By analyzing the 1970-2010 period Łabędzki et al. (2012) found that in Poland there had been a significant statistically significant increase of total evapotranspiration in the growing seasons (April-September). There was a change in the temporal distribution of rainfall, with an increase in the amount of precipitation during the winter and early spring, and a decrease in spring and summer. This reduced climatic water balance, with an increase in rainfall shortage in relation to potential evaporation. Especially in recent years, spring and early summer climatic water balance values have been getting smaller, which means that periods of drought are becoming more and more severe. This coincides with the period of greatest water requirements of crops, especially of cereals. The manifestation of water scarcity trends was the extreme drought of 2018, resulting in the average yield of certain crops decreasing by up to 30% in Poland.

In all months of the 2018 growing season there were water shortages for the analyzed cereals (*Fig. 5*). When compared to the average multinational values it was found that they were the biggest in May. For wheat and oats the shortage of rainfall in the same month was 55 mm, and it was larger than the multiannual value by 28 mm. For maize it was 40 mm and surpassed the perennial average by 17 mm.

Demand for water is related to the species and its stage of growth and development. It increases as the weight of the fresh matter and transpiration increase. The greatest demand for water is usually during the critical period in plant development. This corresponds to the end of vegetative development and the beginning of the formation of generative organs. The critical period for cereals is during the following stages: stem formation,

http://www.aloki.hu ● ISSN 1589 1623 (Print) ● ISSN 1785 0037 (Online)
DOI: http://dx.doi.org/10.15666/aeer/1704_76677678

heading, and grain development and filling (Chmura et al., 2009). Spring wheat reacts to shortage and excess of water particularly adversely during tillering and stem formation. Rain excess causes extension of the growing season, delays maturity, increases the incidence of disease, and it can cause sprouting during the harvest. Dmowski et al. (2008) found that sufficient rainfall in April and May is conducive to germination and tillering, and in June to the formation of the main shoot, side shoots, and grain development. Moderate rainfall in July is conducive to further grain filling and grain maturing on the main and side shoots. Research of Zagdańska and Wiśniewski (2001) has shown that the ability of spring wheat to increase its resilience (acclimatization) under the influence of the previously occurring drought is a varietal characteristic. Among cereals, oat is distinguished by its low resistance to drought due to a high transpiration rate and lower water use efficiency (Anderson and Mc Lean, 1989; Wojcieska, 1993). Considering the frequent occurrence of the shortage of rainfall in the most recent period in Poland, it can be assumed that drought negatively affects not only the yield of oats but also grain quality.

In the case of maize the last months of the 2018 growing season (August and September) also exhibited high water deficiency. In August that year the shortage was 58 mm, and in September it reached as much as 73 mm. Deficiencies in these months exceeded multiannual values by 22 mm and 48 mm. A lack of water during the growing season for maize causes uneven growth and development of plants, and withering in extreme cases (Dudek et al., 2009). According to Stuczyński et al. (2000) despite the prevailing water scarcity the importance of maize in Poland will increase, and it will become the primary spring cereal.

In the case of early potato varieties water shortages in 2018 were not higher than the average multiannual. The critical period of potato plants is during the following stages: flower bud formation, flowering, tuber formation, and leaf yellowing. In the period from planting to shoot formation, the potato plant uses water supplies stored in the parent tuber. During the time from shooting to flower bud formation water needs are also small. From flower bud formation onwards water needs regularly increase (Chmura et al., 2009). Varieties of early potatoes respond to water shortages especially negatively (Rykaczewska, 2007) because of an intense increase in the mass of above-ground parts and fast growth of tubers (Wheeler et al., 2003; Smith, 2006).

For sugar beet significant rainfall shortages were in May and August 2018, with 40 mm in the former and 73 mm in the latter. In the remaining months of the growing season that year they were not higher than average values for the 2000-2017 period. Sugar beet has the greatest sensitivity to a lack of soil moisture in the initial period, and later, especially after the end of August, dry and warm weather is more favourable, increasing its quality (Svachula and Pulkrabek, 2000). The critical stage of sugar beet lasts about 60 days when the leaf canopy covers the ground and during the intense thickening of the root (Chmura et al., 2009).

For meadows and pastures the highest average monthly rainfall deficiency with -43 mm and -53 mm, respectively, occurred in July of the 2000-2017 period (*Fig. 6*). On the other hand, in July 2018 shortages were the smallest (-5 mm for meadows and -15 mm for pastures). It was found that the greatest shortage of rainfall in 2018 was in May (-55 mm for meadows, and -60 mm for pasture) and in August (-68 mm for meadows and pastures). In the remaining months of the 2018 growing season water deficit was smaller than the average multiannual. Meadow water needs are different for each of the growth cycles.

http://www.aloki.hu ● ISSN 1589 1623 (Print) ● ISSN 1785 0037 (Online)
DOI: http://dx.doi.org/10.15666/aeer/1704_76677678

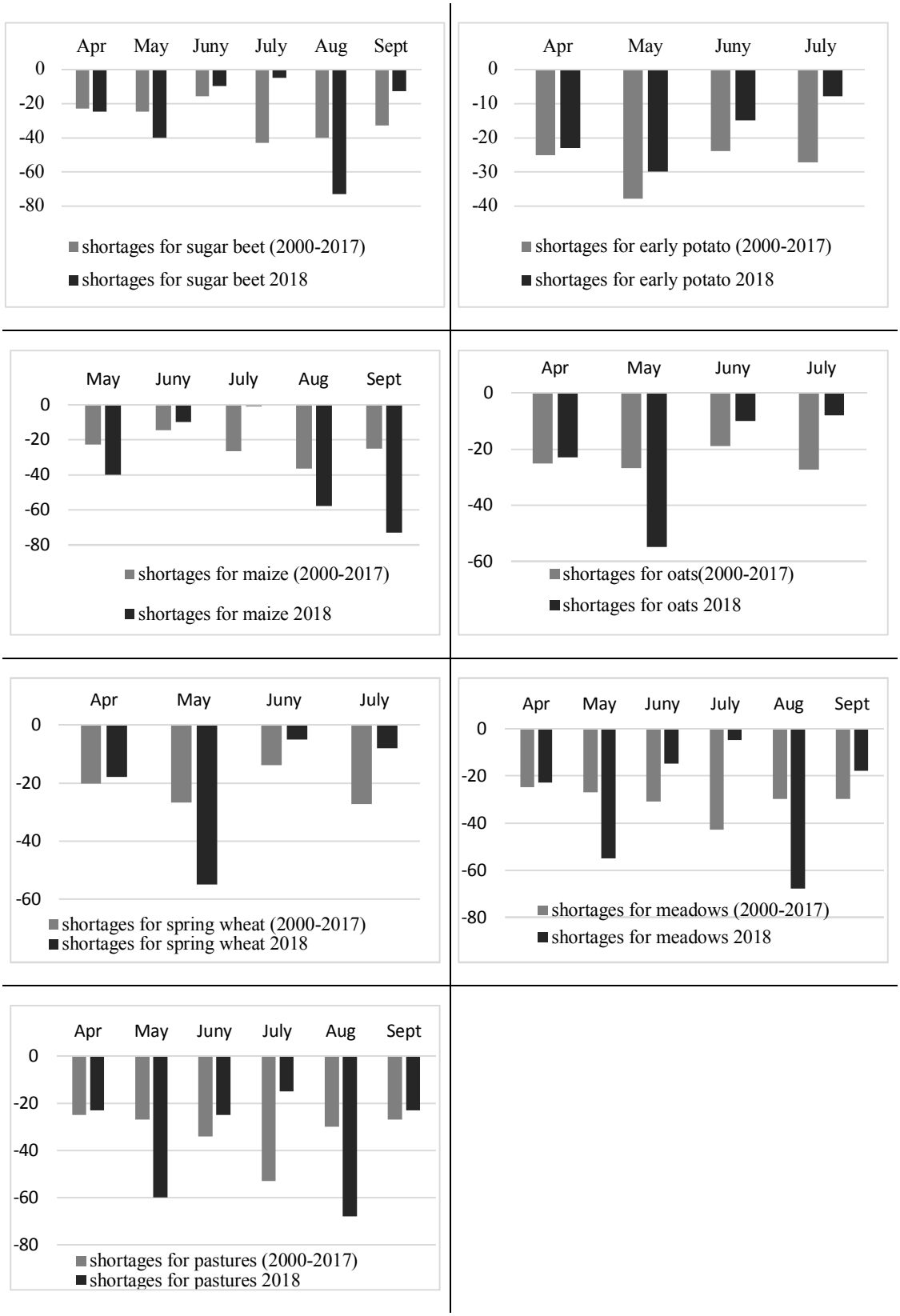

Figure 6. *Average monthly rainfall shortages (mm) for selected crops during the 2000-2018 period and in 2018 in Siedlce*

http://www.aloki.hu ● ISSN 1589 1623 (Print) ● ISSN 1785 0037 (Online)
DOI: http://dx.doi.org/10.15666/aeer/1704_76677678

The greatest demand for water is during the second one, i.e. in June and July. Grabarczyk (1989) found that, depending on the region, water needs in the first growth cycle are 125-158 mm, 186-240 mm in the second, and 160-190 mm in the third. On pastures when vegetation becomes yellowish and there is no biomass increase, grazing should stop until grass regenerates after rainfall. Such regeneration should last at least 3 weeks. Kasperska-Wołowicz (2007) points out that the most common instances of insufficient moisture in meadows and pastures can be expected in August. Leśny and Juszczak (2005) report that both in dry and wet growing seasons in grassland areas most winter precipitation surplus evaporates in May. Insufficient rainfall and increasing grassland dryness often lead to very large and adverse changes in both soil and plants. Stuczyński et al. (2000) argue that the period of animals grazing will significantly increase, although in summer it can be inefficient due to periodic droughts.

Conclusions

Values of climatic water balance in July 2018 were 7 mm higher than the multiannual average. In the remaining months of the 2018 growing season precipitation shortage was bigger than the average values of the 2000-2017 period. The biggest difference in climatic water balance between 2018 and the multinational was recorded in June (29 mm). It was found that in July there was a statistically significant increase in the value of CWB, on average, of about 6.4 mm per 10 years. For analysed cereals water shortages occurred in all months of the growing season both in 2000-2017 and in 2018. In May 2018 deficits were much larger than the average perennial value. In the case of maize the last months of the 2018 growing season (August and September) also exhibited high deficiency of rainfall. An important solution will be suitable agricultural practices that can mitigate the effects of drought. Earlier varieties of plants with the period of greatest demand for water before strong droughts will be introduced. For early potato varieties water shortages in 2018 were not higher than the average multinational. However, significant rainfall shortages for sugar beet were in May and August 2018. Those deficiencies were well above the critical values and could have resulted in a decline in the level of crop yield and deterioration of the quality of raw material. For meadows and pastures the highest average monthly rainfall deficiencies in the 2000-2017 period occurred in July (-43 mm for meadows and -53 pastures). In 2018 the greatest shortage of rainfall was recorded in May (-55 mm for the meadows and -60 mm for pastures) and in August (-68 mm both for meadows and pastures).

Drought causes withering and significant loss of some fodder species; forage on meadows should be harvested earlier because in drought conditions its quality worsens every day. Changes of water balance basic components occurring in temperate latitudes are a result of an increase in air temperature and evaporation. An increase in the air temperature with unchanging annual total precipitation can cause water shortages lowering crop yields, especially on sandy soils with poor retention. It can be inferred from the present analysis that the composition of crop species should be adapted to changing climatic conditions. The studies indicate that a drought should be monitored to assess its impact on crops. Persistent unfavourable weather conditions lasting for a longer time may determine the choice of plant species to be grown in the region. Additionally, by designating areas that are particularly vulnerable to the effects of droughts it is possible to carry out a more complete assessment of the impact of climate change on agriculture in Europe.

http://www.aloki.hu ● ISSN 1589 1623 (Print) ● ISSN 1785 0037 (Online)
DOI: http://dx.doi.org/10.15666/aeer/1704_76677678

REFERENCES

[1] Anderson, W. K., Mc Lean, R. (1989): Increased responsiveness of short oat cultivars to early sowing, nitrogen fertilization and seeding rate. – Aust. J. Agric. Res. 40: 729-744.
[2] Chmura, K., Chylińska, E., Dmowski, Z., Nowak, L. (2009): Role of the water factor in yield formation of chosen field crops. – Infrastructure and Ecology of Fural Areas 9: 33-44.
[3] Demidowicz, G., Doroszewski, A., Górski, T. (1996): The impact of rainfall shortages on potato and sugar beet production losses. – Zeszyty Problemowe Postępów Nauk Rolniczych. Iss. 438: 43-52. (in Polish).
[4] Demidowicz, G., Doroszewski, A., Górski, T. (1997): Methodology of the estimation of agricultural production losses caused by rainfall deficit. – Roczniki AR w Poznaniu. T. 291. Melioracje i Inżynieria Środowiska. Iss. 17: 233-243. (in Polish).
[5] Dmowski, Z., Dzieżyc, H., Nowak, L. (2008): The assessment of the impact of selected parameters - precipitation and soil – on the spring wheat yield in South-Western Poland. – Acta Agrophysica 11(3): 613-622. (in Polish).
[6] Doroszewski, A., Górski, T. (1995): A simple coefficient of potential evapotranspiration. – Roczniki AR w Poznaniu. Vol. 271. Melioracje i Inżynieria Środowiska. Iss. 16: 3-8. (in Polish).
[7] Doroszewski, A., Kozyra, J., Pudełko, R., Stuczyński, T., Jadczyszyn, J., Koza, P., Łopatka, A. (2008): Monitoring of agricultural drought in Poland. – Wiadomości Melioracyjne i Łąkarskie. Iss. 1: 35-38. (in Polish).
[8] Dudek, S., Żarski, J., Kuśmierek-Tomaszewska, R. (2009): Results of a multiannual field experiment on maize response to irrigation. – Infrastruktura i Ekologia Terenów Wiejskich, Iss. 3: 167-174. (in Polish).
[9] Górski, T. (2006): The variation of agroclimatic conditions and the length of the growing period in the last century. – In: Gutry-Korycka, M., Kędziora, A., Starkel, L., Ryszkowski, L. (eds.) Long-term transformation of Polish landscape as a result of changes in climate and land use. Poznań. Joint publication. IGBP Komitet Narodowy: 65-77. (in Polish).
[10] Grabarczyk, S. (1989): Water needs of grassland and grass. – Zesz. Probl. Postępów Nauk Rol. Z 343: 43-55. (in Polish).
[11] Kanecka-Geszke, E., Smarzyńska, K. (2007): Evaluation of meteorological drought with a variety of indexes in selected agroclimatic regions of Poland. – Acta Scientiarum Polonorum. Formatio Circumiectus. Iss. 6. Z. 2: 41-50. (in Polish).
[12] Kasperska-Wołowicz, W. (2007): Water shortages of meadows on peat-muck soil in different agroclimatic regions of Poland. – Acta Agrophysica 9(3): 645-655. (in Polish).
[13] Kołodziej, J., Liniewicz, K., Bednarek, H. (2003): Precipitation in the Lublin area and water requirements of crops. – Annales UMCS. Sect. E. Vol. 58: 101-110. (in Polish).
[14] Kozyra, J., Doroszewski, A., Nieróbca, A. (2009): Climate change and its expected impact on agriculture in Poland. – Studia i Raporty IUNG-PIB. Puławy. Iss. 14: 243-257. (in Polish).
[15] Kundzewicz, Z., Szwed, M., Radziejewski, M. (2006): Climate change and extreme hydrological phenomena: floods and droughts. – In: Gutry-Korycka, M., Kędziora, A., Starkel, L., Ryszkowski, L. (eds.) Long-term transformation of Polish landscape as a result of climate and land use change. Joint publication. Komitet Narodowy IGBP: 169-180. (in Polish).
[16] Łabędzki, L. (2006): Agricultural drought - an outline of the problem. Methods of monitoring and classification. – Woda Środowisko Obszary Wiejskie. Rozprawy Naukowe Monografie. Iss. 17: 107. (in Polish).
[17] Łabędzki, L. (2007): Estimation of local drought frequency in central Poland using the standardized precipitation index SPI. – Irrigation and Drainage 56(1): 67-77.
[18] Łabędzki, L., Bąk, B., Kanecka-Geszke, E. (2012): The size and variability of transpiration coefficient according to Penman-Monteith in the 1970-2004 growing periods in selected

http://www.aloki.hu ● ISSN 1589 1623 (Print) ● ISSN 1785 0037 (Online)
DOI: http://dx.doi.org/10.15666/aeer/1704_76677678

regions of Poland. – Woda-Środowisko-Obszary Wiejskie. Vol. 12. Iss. 2(38): 159-170. (in Polish).
[19] Legates, D. R., Mccabe, G. J. (2005): A re-evaluation of the average annual global water balance. – Physical Geography 26: 467-479.
[20] Leśny, J., Juszczak, R. (2005): Atmospheric water balance in agricultural and woodland areas. – Woda, Środ. Obsz. Wiej. 5, 2(15): 53-65. (in Polish).
[21] Niedźwiedź, T. (2003): A dictionary of weather. – Seria Atlasy i Monografie IMGW. Warszawa. PTGeof. ISBN 83-88897-25-X pp. 496. (in Polish).
[22] Nowak, L. (2006): Irrigation of root crops. – In: Karczmarczyk, S., Nowak, L. (eds.) Irrigation of crops. Joint publications. Poznań. PWRiL: 368-372. (in Polish).
[23] Nyc, K. (2006): The introduction of irrigation systems. – In: Karczmarczyk, S., Nowak, L. (eds.) Irrigation of crops. PWRiL, Poznań, chapter 7: 157-174. (in Polish).
[24] Przedpełska, W. (1971): The issue of atmospheric drought in Poland and methods of its determination. – Prace PIHM. Iss.103: 3-27. (in Polish).
[25] Rojek, M. (1987): Temporal and spatial distribution of climatic and agroclimatic water balance in Poland. – Zeszyty Naukowe AR we Wrocławiu. Z. 62 pp. 68. (in Polish).
[26] Rykaczewska, K. (2007): Comparison of the productivity of several early potato varieties, domestic and foreign. – Zeszyty Problemowe Postępów Nauk Rolniczych. Iss. 517: 629-638. (in Polish).
[27] St-Marseille, A. F. G., Bourgeois, G., Brodeur, J., Mimee B. (2019): Simulating the impacts of climate change on soybean cyst nematode and the distribution of soybean. – Agricultural and Forest Meteorology 264: 178-187.
[28] Stuczyński, T., Demidowicz, G., Deputat, T., Górski, T., Krasowicz, S., Kuś, J. (2000): Adaptation scenarios of future climate change. – Environmental Monitoring and Assessment 61: 133-144.
[29] Sulewski, P., Czekaj, S. (2015): Climate and institutional change and projected economic performance of Polish farms. – Szkoła Główna Gospodarstwa Wiejskiego Warszawa. DOI: 10.5604/00441600.1146932. (in Polish).
[30] Svachula, V., Pulkrabek, J. (2000): Dependence of betaine content in sugar beet on the rainfall and air temperature during the vegetation. – Rostl. Vyroba no 46(2): 77-80.
[31] Vicente-Serrano, S., Begueri´a, S., Lo´pez-Moreno, J. (2010): A Multiscalar Drought Index Sensitive to Global Warming: The Standardized Precipitation Evapotranspiration Index. – Journal of Climate 23: 1696-1718.
[32] Watson, R. T, Zinyowera, M. C., Moss, R. H., Dokken, D. J. (1997): IPCC The regional impact of climate change: IPCC special report on the regional impacts of climate change. – An assessment of vulnerability [online].
[33] Wiśniewski, K., Zagdańska, B. (2001): Genotype-dependent proteolytic response of spring wheat to water deficiency. – J. Exp. Bot.: 1455-1463.
[34] Wojcieska, U. (1993): Oat physiology. – In: Puławy, I. (ed.) Oat biology and agriculture. R(304): 53-94. (in Polish).

http://www.aloki.hu ● ISSN 1589 1623 (Print) ● ISSN 1785 0037 (Online)
DOI: http://dx.doi.org/10.15666/aeer/1704_76677678

OCCURRENCE OF *ARTICHOKE LATENT POTYVIRUS* (ARLV) AND *TOMATO SPOTTED WILT VIRUS* (TSWV) AS MIXED INFECTION IN ARTICHOKE PRODUCTION AREAS

FIDAN, H.[1*] – KOÇ, G.[2]

[1]*Plant Protection Department, Faculty of Agriculture, Akdeniz University, Antalya, Turkey*

[2]*Subtropical Fruits Research and Experimental Center, Çukurova University, Adana, Turkey*

**Corresponding author*
e-mail: hakanfidantr@hotmail.com.tr

(Received 11th Mar 2019; accepted 1st May 2019)

Abstract. Artichoke (*Cynara scolymus*), is one of the most important agricultural products of North Cyprus (NC) due to its importance in export. During field surveys in artichokes production fields between 2013 and 2016, little and indistinguishable leaves, light shaded regions taking after mosaic with yellowish wilting of the leaves and little head development plants were gathered and broken down by DAS-ELISA for the examination of infections (most of them mentioned by Gallitelli et al. (2004)) which could be harmful to artichokes (belonging to groups of *Nepovirus*, *Cheravirus*, *Fabavirus, Ilarvirus*, *Cucumovirus*, *Tombusvirus, Tobamovirus, Tobravirus, Potyvirus*, *Carlavirus*, *Potexvirus*, *Crinivirus, Tospovirus*, *Anulavirus*, in the families of *Rhabdoviridae and Bromoviridae* respectively*)*. Thirty-three samples were detected positive for mix infection of *Artichoke Latent Potyvirus* (ArLV) and *Tomato spotted wilt virus* (TSWV) in Laboratory assays (ELISA and RT-PCR). The results were also confirmed by RT-PCR using total RNA which was extracted from the leaves. RT-PCR assay was conducted by newly designed Sense and antisense primer pairs specific to ArLV; L1TSWVR and L2TSWVF primer pairs specific to TSWV. As results of RT-PCR, the region of 485 bp special to coat protein of ArLV and 276 bp of TSWV were obtained in 2% agarose gel. While occurrence of remaining viruses was not detected in the tested samples, it was observed that disease incidence increased due to non-sterile equipment and devices during the harvest. Additionally, infected product materials, transmission with aphid and thrips vectors also increased disease incidence. In NC, the occurrence of ArLV was assigned as a new virus disease in Artichoke and also mixed infection with TSWV.
Keywords: *Northern Cyprus, artichoke, RT-PCR, DAS-ELISA, ArLV, TSWV*

Introduction

Artichoke (*Cynara scolymus Linneus*, 1753) is a financially essential vegetable. It is developed for its huge meaty juvenile inflorescences (capitula) that are broadly expended in both new and saved frame. Production is not confined to the Mediterranean region, yet additional export is needed in the Central East, North Africa, South America United States, and China (FAO, 2015). There are numerous components diminishing the amount and nature of artichoke production in different harvests. Plant viral diseases are amongst the most critical prohibitive components incorporating plant malady and irritations. Among the critical agronomic qualities, as a few maladies caused by infections have significant reproducing targets and have extraordinary monetary effect on artichoke generation around the world. *Cucumber mosaic virus*, *Artichoke mottled crinkle virus*, *Tomato black ring virus*, *Artichoke Italian latent virus*, *Artichoke Aegean ringspot virus*, *Artichoke vein banding virus*, *Broad bean wilt virus, Tobacco streak virus*, *Artichoke yellow ringspot virus*, *Tobacco mosaic virus, Pelargonium zonate spot virus*; *Tobacco rattle virus*; *Artichoke latent virus, Bean yellow mosaic virus*, Artichoke

http://www.aloki.hu ● ISSN 1589 1623 (Print) ● ISSN 1785 0037 (Online)
DOI: http://dx.doi.org/10.15666/aeer/1704_76797691

latent virus S, *Turnip mosaic virus*, Artichoke latent virus M, an anonymous infection remotely related serologically to *Poplar mosaic virus*, Artichoke curly dwarf virus, Artichoke degeneration virus, *Potato virus X*, *Tomato infectious chlorosis virus*, *Tomato spotted wilt virus* have caused infections. Morphology, scientific categorization, symptomatology, cytopathology, the study of disease transmission, determination and sanitation of these Cynara tainting species (since 1950s) have been investigated by Gallitelli et al. (2004). Furthermore, Arabis Mosaic Virus, Alfalfa Mosaic Virus, Tomato Bushy Stunt Virus, Potygroup specific antisera and *Potato Virus Y* were also reviewed in Gallitelli et al. (2004).

Another Artichoke disease caused by Artichoke Yellow Ringspot Virus was first reported in Globe Artichoke in Turkey by Paylan et al. (2013). Same researchers also reported CMV in globe artichoke.

The ArLV is a potyvirus, which is able to transmit experimentally in non-persistent manner to artichoke seedlings by afid species (*Aphis fabae, Myzus persicae and Brachycaudus cardui* by Rana et al., 1982). Its first detection from symptomless globe artichoke plants was found in Tunisia by Marrou and Mehani (1964). Transmission efficiency was higher by the quick re-infection rate (over 75% in two years) registered in a field trial in Sardinia, Italy (Foddai et al., 1985). The *C.* syriaca and C. *cardunculus* species are not resistant to ArLV (Manzanares et al. (1995). The ArLV is responsible for reductions in plant thrive and blossom what is more, instigates misfortunes in the number and the heaviness of gathered plates running from 3 to 47% (Pecaut et al., 1983; Foddai and Man-as, 1984; Migliori et al., 1987). Moreover, ArLV infection causes subjective and quantitative changes in 'Brindisino' artichoke, for example, leaf and bracts staining, opening of head peak, postponement of first reap, shortening of head stalk, decrease of head distance across and diminishing of yield (Rana et al., 1992).

This paper aims to decide the possibility and predictability of regular artichoke infections, incorporating ArLV in North Cyprus (NC) where presence of artichoke infections has not been investigated yet.

Materials and methods

The exploration was led in NC in 2013-2016 (*Fig. 1*). An aggregate of 97 tests were gathered from suspected plants in artichoke fields at various areas in the Island. Amid the overviews, little and indistinguishable leaves, light shaded zones looking like mosaic with yellowish shrinking of the leaves and little head development were seen on artichoke plants. Studies were directed amid the developing season and just symptomatic examples were gathered haphazardly all through the zone in the district.

Serological tests

The samples, were named and put in isolated plastic packs, conveyed to the Virology Lab by putting in ice pail and kept at 4 °C. All examples were handled inside 24 h.

Double antibody sandwich enzyme linked immunosorbent assay (DAS-ELISA)

For distinguishing proof infections contaminating artichoke, leaf tests were tried by DAS-ELISA utilizing polyclonal antiserum explicit to infections which has a place with gatherings of *Nepovirus*, *Cheravirus*, *Fabavirus, Ilarvirus*, *Cucumovirus*, *Tombusvirus, Tobamovirus, Tobravirus, Potyvirus*, *Carlavirus*, *Potexvirus*, *Crinivirus, Tospovirus*, in

http://www.aloki.hu ● ISSN 1589 1623 (Print) ● ISSN 1785 0037 (Online)
DOI: http://dx.doi.org/10.15666/aeer/1704_76797691

the families of *Rhabdoviridae and Bromoviridae,* which are given in *Table 1,* Each explicit antisera separately obtained from Agdia USA, Bioreba AG, Switzerland and Loewe® Biochemica GmbH, Germany.

Figure 1. *The map of Cyprus Island with positive locations (http://www.cyprus-properties.comcyprusgeography.htm; http://www.emapsworld.comcyprus-location-map.html, in small)*

Tests included location of infections in tainted fresh leaves and conveyed by Clark and Adams (1977). Polystyrene microtiter plates were covered with 1:200 weakening of gamma globulin. The leaves of contaminated fresh explants were grounded in the extraction cradle (phosphate cushioned saline, PBS, pH 7.0). Plant tests were connected at a weakening of l/5 (Wff) in PBS (pH7.0), containing 0.05 volumes Tween-20, 0.2% polyvinyl pyrolidone (PVP-40) and 2% bovine serum albumin (BSA). IgG-conjugate was applied at the concentration of 1 ul/200 ul (Agdia and Loewe) and 1 ul/1000 ul (Bioreba). Alkaline phosphatase conjugate was utilized at a 1/1000 dilution.

Results were obtained spectrophotometrically at 405 nm wave length at Medispec ESR 200 ELISA microplate peruser. Additionally, negative controls (healthy samples), double the mean estimation of healthy sample were considered as positive. Positive controls of all infections were provided in lyophilized frame with the units and were resuspended in the examined support as prescribed by the manufacturer (Agdia, Inc.).

Molecular analysis (phylogeny, total RNA isolation and reverse-transcription polymerase chain reaction (RT-PCR)

Add up to RNA separates (Dellaporta et al., 1983) of ArLV and TSWV contaminated artichoke plants were utilized in a Reverse-Transcription Polymerase Chain Response (RT-PCR) with new sense (Forward primer) 5'-ATCTCGTGACGAAGCAACAA-3' and antisense (Reverse primer) 5'-CGAGACCATCGTGAATCTCC-5' primers, designed based on nucleotide sequences alignment of CP genes of diverse isolates Artichoke latent virus isolates, complete genome GenBank: KF155694.1 7163..7642 /product="CP protein"485 bp from NCBI via Primer-BLAST program and L1TSWVR

http://www.aloki.hu ● ISSN 1589 1623 (Print) ● ISSN 1785 0037 (Online)
DOI: http://dx.doi.org/10.15666/aeer/1704_76797691

and L2TSWVF specific to TSWV (Adkins et al., 2005). First and second strand cDNAs were blended from ArLV and TSWV RNAs utilizing Thermo Scientific Verso 1-Step RT-PCR Hot-Start Kit pack according to producer's convention. Enhancement for ArLV continued through a cycle of denaturation at 95 ^{0}C (45 s), toughening at 55 °C (45 s.) and expansion at 72 °C (45 s) for a sum of 35 cycles in Techne Genius thermal cycler. Steps mentioned above were utilized for TSWV likewise.

Table 1. *Serologic and molecular studies and results of Cynara scolymus (artichoke) plant samples*

Virus Species	Plant species	Assays	*Result
TBRSV (*Tomato Black RingVirus*)	*Cynara scolymus*	DAS-ELISA	-
TSV (*Tomato Streak Virus*)	″	DAS-ELISA	-
TEV (*Tobacco Etch Potyvirus*)	″	DAS-ELISA	-
TuMV (*Turnip Mosaic Potyvirus*)	″	DAS-ELISA	-
WMV-2 (*Watermelon Mosaic 2 Potyvirus*)	″	DAS-ELISA	-
TBSV (*Tomato Bushy Stunt Tombusvirus*)	″	DAS-ELISA	-
ArMV (*Arabis Mosaic Virus*)	″	DAS-ELISA	-
CMV (Cucumber Mosaic Virus)	″	DAS-ELISA	-
PepMoV (*Pepper Mottle Potyvirus*)	″	DAS-ELISA	-
TMV (*Tobacco Mosaic Virus*)	″	DAS-ELISA	-
TRV (*Tobacco Rattle Tobravirus*)	″	DAS-ELISA	-
ToMV (*Tomato Mosaic Virus*)	″	DAS-ELISA	-
Tospo (Tospovirus)	″	DAS-ELISA	+
PVX (*Potato Virus* X)	″	DAS-ELISA	-
BCMV (*Bean common mosaic potyvirus*)	″	DAS-ELISA	-
Poty (Group Poty Virus)	″	DAS-ELISA	+
PVY (*Potato Virus Y*)	″	DAS-ELISA	-
AMV (*Alfalfa Mosaic Virus*)	″	DAS-ELISA	-
ZYMV (*Zucchini Yellow Mosaic Virus*)	″	DAS-ELISA	-
LMV (*Lettuce mosaic potyvirus*)	″	DAS-ELISA	-
LYSV (*Leek yellow stripe potyvirus*)	″	DAS-ELISA	-
OYDV (*Onion yellow dwarf potyvirus*)	″	DAS-ELISA	-
TSWV (*Tomato Spotted Wilt Virus*)	*Cynara scolymus* *Lycopersicon esculantum* (***mi****)* *Capsicum annum* (***mi****)*	DAS-ELISA RT-PCR	+ + +
ArLV (*Artichoke Latent Potyvirus*)	*Cynara scolymus* *Nicotiana clevelandii* (***mi****)* *Chenopodium amaranticolor* (***mi****)*	RT-PCR	+ + +

*(-) Negative (not infected); (+) Positive (infected); mi (mechanically inoculated)

Analysis of RT-PCR products

Ten microliters of the PCR reaction blend was joined with gel loading buffer and dissected on a 2% agarose gel containing 0.5 mg/ml of ethidium bromide and shot (Sambrook et al., 1989). 100 bp DNA stepping ladder (thermo) or Bio Marker TM Low (Bio Ventures, Inc.) were utilized on each gel to decide the length of the amplified item.

http://www.aloki.hu ● ISSN 1589 1623 (Print) ● ISSN 1785 0037 (Online)
DOI: http://dx.doi.org/10.15666/aeer/1704_76797691

Phylogenetic analysis

The RT PCR products were sequenced and dnasp5 program conducted for haplodisation analysis. Phylogeny performed by MEGA 7 software program and neighbor joining process, according to convention analysis.

Mechanical inoculation

Inoculation were processed when the first real leaves of seedlings appeared and approximately 15 cm in length. 1 g inoculum (Positive Samples via DAS-ELISA&RT-PCR) was added into 2 ml 0.01% M phosphate buffer solution with carborandum and silicon oxide. The mixture was prepared for mechanical inoculation, and was applied on the first real leaves of plants by hand etching. The temperature was kept at 22-24 °C and proportional humidity at 60-70% in test greenhouses (Garland et al., 2005).

Results

Detection and occurrence of viruses by serology (ELISA)

Positive results were obtained from Tospovirus groups, TSWV and Potyvirus. *Tomato spotted wilt tospovirus (TSWV)* is one of the unique member of *Tospovirus. Orthotospoviruses* or *Tospoviruses* are genera of negative RNA virus found within the *Tospoviridae* family of the *Bunyavirales* order (Lima et al. (2017)).

Assay results were given as positive reactions from samples against both TSWV and Tospovirus group specific antiserum.

Serological analyses were repeated at least two times to approve, 27 out of 33 positive samples also produced positive reaction with the potyvirus group specific antiserum. Samples of artichoke, were 33 positive, collected from six provinces, *6/Girne (Krynea), 8/Güzelyurt (Omorpho), 4/Lefke, 2/ Iskele (Trikomo), 4/Lefkoşa (Nicosea) and 9/ Gazimağusa (Famagusta)* (*Fig. 1*). However, none of the PVY, BCMV, LMV, LYSV, OYDV, PepMoV, TEV, TuMV, WMV, ZYMV viruses has had positive reaction. ArLV member of the Potyvirus genus in the Potyviridae family have been previously reported in Artichoke worldwide (Gallitelli et al., 2004; Martelli and Gallitelli, 2008; Pasquini and Barba, 2003; Erkan et al., 2014; Fidan et al., 2015; Rana et al., 1982). Due to having positive result to Potyvirus group and non-absence of ArLV commercial antiserum, the test by RT-PCR is performed on the artichoke plants.

Type of symptoms

Virus tainted leaves with yellowish wilting in the fields have diminished in size and weight (*Figs. 2* and *3*). There is likewise, leaf twisting or distortion (*Fig. 4*), little head development and general staining were seen on the artichoke plants (*Fig. 5*). Amid head reaping, the plant heads were sliced from start of line to end of line. Rural workers have not changed or surface cleaned all types of cutting gear. Consequently, all collected artichokes have indicated extreme maladies (*Fig. 3*). This unmistakably shows that mechanical reaping will spread the infections. The symptoms from collected samples were similar with Spanò et al. (2018).

http://www.aloki.hu ● ISSN 1589 1623 (Print) ● ISSN 1785 0037 (Online)
DOI: http://dx.doi.org/10.15666/aeer/1704_76797691

Figure 2. *Chlorotic spots and mosaic on artichoke leaf induced by infected by ArLV + TSWV*

Figure 3. *Yellowish withering of the leaves on infected plants*

Figure 4. *Leaf distortion, mosaic, necrosis spots on Artichoke induced by ArLV*

http://www.aloki.hu ● ISSN 1589 1623 (Print) ● ISSN 1785 0037 (Online)
DOI: http://dx.doi.org/10.15666/aeer/1704_76797691

Figure 5. *Small-head formation and general discoloration on artichoke plants*

Mechanical inoculation studies

About 20 days after the date of mechanical inoculation, observations and investigations about the symptoms of diseases in tomato, pepper, tobacco and *Chenopodium spp.* plants have been conducted. At the end of the test, characteristic dark brown lesion, yellow concentric ring and necrotic spot, systemic mosaic and Necrotic local lesion symptoms via TSWV and ArLV were recorded between the leaf veins of sensitive plants (*Figs. 6* and *7*). Symptoms on assayed indicators were tested to confirm the infections in these plants by serologic and molecular based diagnosis.

Figure 6. *Dark brown lesions on Lycopersicon esculantum (A1-A2). Yellow concentric rings and necrotic spots on Capsicum annum (A3). (Mechanically inoculated by TSWV Artichoke Cyprus isolate)*

http://www.aloki.hu ● ISSN 1589 1623 (Print) ● ISSN 1785 0037 (Online)
DOI: http://dx.doi.org/10.15666/aeer/1704_76797691

Figure 7. *Severe systemic mosaics on Nicotiana clevelandii (B1). Necrotic local lesions on Chenopodium amaranticolor (B2). (Mechanically inoculated by ArLV Artichoke Cyprus isolate)*

The RT-PCR

With the end goal to confirm the disease, RT-PCR examinations have intensified ArLV RNA, yielding an expected result of 485 bp (*Fig. 8*) on agarose gel (2%) in all samples of artichoke. Subsequently, RT-PCR results affirmed that the diseases of ArLV in DAS-ELISA were positive for the plants. Furthermore, 276 bp cDNA bands of TSWV were observed correspondingly (*Fig. 9*) in all examples. During the test, healthy plant material was used as negative control in order to eliminate plant misleading factors.

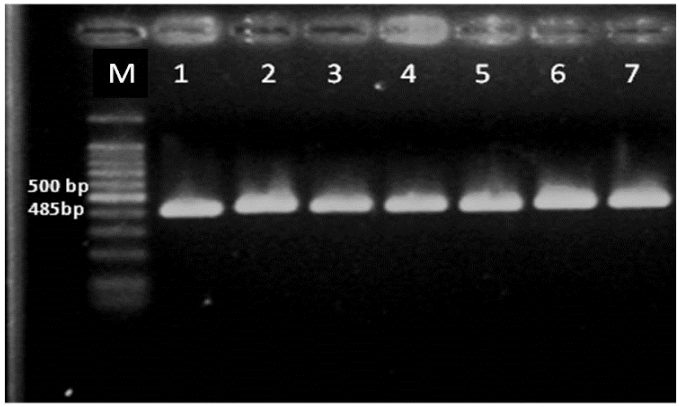

Figure 8. *RT-PCR product of 485 bp of ArLV CP on agarose gel (2%); DNA ladder (first lane M), Lane 1-3 samples positive of Artichoke in NC; Lane 4 positive control; Lane 5-7 samples positive of Artichoke in NC*

Phylogenetic analysis

Phylogeny performed by MEGA 7 software program and neighbor joining process, according to conventional analysis for all ArLV isolates (*Fig. 8*). Two different haplotypes were determined from 7 isolates by RT-PCR and sequences. These two distinctive isolates were compared with each other and other known world's isolates.

http://www.aloki.hu ● ISSN 1589 1623 (Print) ● ISSN 1785 0037 (Online)
DOI: http://dx.doi.org/10.15666/aeer/1704_76797691

Their outcomes were submitted to NCBI framework as new records. The outcomes were cleared up that these two isolates have comparative homology with KF 155694.1 (99%-Italy) and KP405233.1 (96%-France) separately (*Fig. 10*).

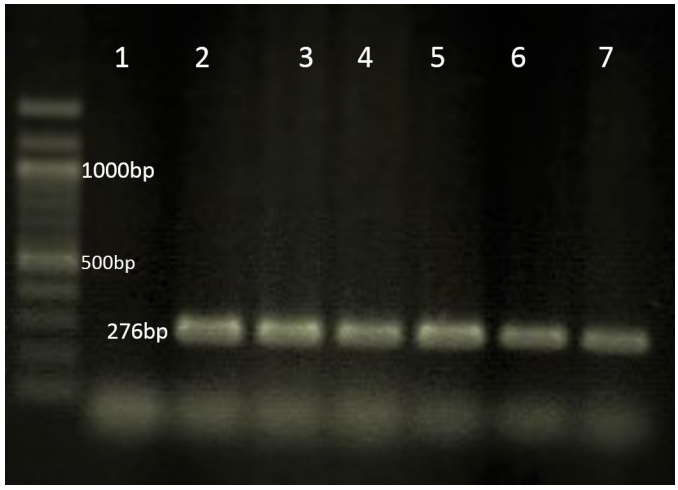

Figure 9. *RT-PCR product of 276 bp of TSWV CP on agarose gel (2%); DNA ladder (First lane M), Lane 1 negative control; Lane 2 positive control (TSWV infected pepper); Lane 3-7 positive samples of Artichoke in NC*

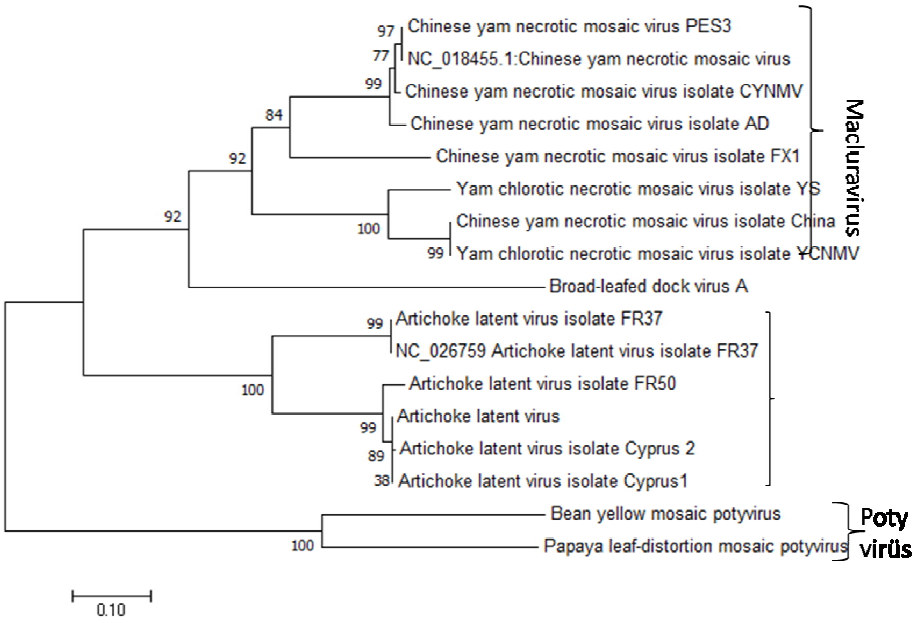

Figure 10. *Phylogenetic tree of two different North Cyprus ARLV haplotypes which belong to Potyviridae and group of Macluravirus, had branched with same branch. While Macluraviruses clustered within intersection, Potyviruses have various subsets*

Discussion

This investigation uncovered the characteristic conveyance and event of artichoke infections in territories situated in NC. Our outcomes called attention to the clean conditions for basic plant infections in growing fields in NC. ArLV and TSWV have the

http://www.aloki.hu ● ISSN 1589 1623 (Print) ● ISSN 1785 0037 (Online)
DOI: http://dx.doi.org/10.15666/aeer/1704_76797691

most across the board infections contaminating artichoke edits in NC. Genera Potyvirus and Tospovirus are transmitted by aphids and thrips separately. The board of these vectors are troublesome. The indications on gathered plants have seriously appointed to ArLV and TSWV by mixed contamination. These outcomes were fitted Testa et al. (2008) results where their Sardinian examples demonstrated a serious mosaic for the most part, and had ArLV mixed infection with Tomato spotted wilt virus (TSWV). The study was focused on ArLV due to first occurrence on artichoke. Although ArLV has a less host range than TSWV, the ArLV may survive in different weed species that are not having a place with the Asteraceae family filling in as a supply. These outcomes permit ArLV to be spread all the more continuously and to happen with high frequency, after essential contamination by infected seedling or inoculums sources. These results have confirmed Costa et al. (1959) results where it was reported that ArLV had isolated from symptomless artichoke plants in California. Severe systemic mosaics on *Nicotiana clevelandii,* necrotic local lesions on *Chenopodium amaranticolor* mechanically inoculated by ArLV Artichoke isolates gave identical symptoms which were confirmed by RT-PCR, previously recorded by Ciffou et al. (2011).

Previous studies have revealed artichoke latent virus found in Northern Cyprus and the Aegean region in Turkey (Fidan et al, 2015; Erkan et al., 2014). The current results have verified the previous results that artichoke plants infection with ArLV is limiting artichoke production in the Mediterranean basin as reported by other articles as well (Rana and Russo, 1980; Ortega et al., 2000). Also Minutillo et al. (2015) impressed that Ranunculus latent virus should be demonstrated as unique strain of ArLV. They also underlined that it is not a distinct species.

This is the first report of TSWV and ArLV + TSWV mix infection for artichoke in NC. This paper also indicates that uncontrolled distribution of infected artichoke plants in countries will create the viral problems. Molecular analyses have distinguished that there are two different ArLV haplotypes present in NC according to their sequence alignments in NCBI system. Although the Mediterranean Sea as a limiting factor separate the island from the mainland the same viral diseases occur on both places. In any case, sequence grouping arrangements have demonstrated NC's ArLV haplotypes are like Italian (KF155694.1 99)% and French (KP405233.1 98%) haplotypes showing all fare and import plant material can be disseminated without any quarantine direction. The NC is an important harbour in the Mediterranean Sea and all sort of business ships have been visiting for exchange (Lumia et al., 2003; Saitou and Nei, 1987; Tamura et al., 2007).

Conclusion

Further investigations ought to be gotten ready for recognizing individual vectors and obscure epidemiological highlights and qualities of the infections for instance potyviruses like ArLV which transmitted by aphids (Adams et al. , 2012). There are new virus infections sustaining in weeds and neighboring yield species in the Island. ArLV is the most severe of the 25 viruses recorded in *Cynara scolymus* L. and *Cynara cardunculus* L. from Europe and the Mediterranean. These viruses were having decreasing effectivity for the aspect of the productivity and the quality artichoke crop head (Gallitelli et al., 2012). The ArLV + TSWV mix infection in artichoke have synergistic effectivity and severity (Acquadro et al., 2010). Elbeaino et al. (2017) reported some artichoke viruses specially Artichoke Italian latent virus via Next

http://www.aloki.hu ● ISSN 1589 1623 (Print) ● ISSN 1785 0037 (Online)
DOI: http://dx.doi.org/10.15666/aeer/1704_76797691

Generation Sequencing technique and molecular analysis, focused on RNA1 and RNA2 sequences. Novel administration techniques for ailments will be formulated upon these examinations to ensure sanitized plants. Accordingly, the disease pathway and transmissibility of major infections could be counteracted.

Salleh et al. (2017) commented that Artichoke viruses could infect broad range of crop species and weeds as reservoir plants due to having potential for spreading by vectors. Also they mentioned the same viral factors could play important role in the ecology and viral epidemiology. Additionally, all verification, the use of inappropriate cuttings practices by farmers have critical point in same objections.

A certification programme for artichoke has become necessary. It is also indispensable for the globe artichoke biodiversity conservation. And breeding of virus free genetic resources is essential (Spanò et al., 2018). In order to block invasion of critical viruses which are potentially destructive for artichoke quarantine applications should be effectively applied in the island.

Acknowledgments. This work was supported by Virology Labs of Akdeniz University, Faculty of Agriculture, Plant Protection Department and Pozantı Vocational School of Çukurova University.

Conflict of interests. The authors declare that they have no conflict of interests.

Ethical approval. This article does not contain any studies with human participants or animals performed by any of the authors.

REFERENCES

[1] Acquadro, A., Papanice, M. A., Lanteri, S., Bottalico, G., Portis, E., Campanale, A., Finetti-Sialer, M. M., Mascia, T., Sumerano, P., Gallitelli, D. (2010): Production and fingerprinting of virus-free clones in a reflowering globe artichoke. – Plant Cell Tiss Organ Cult 100: 329-337.

[2] Adams, M. J., Zerbini, F. M., French, R., Rabenstein, F., Stenger, D. C., Valkonen, J. P. T. (2012): Family Potyviridae. – In: King, A. M. Q., Adams, M. J., Carstens, E. B., Lefkowitz, E. J. (eds.) Virus Taxonomy. Elsevier, San Diego, pp. 1069-1090.

[3] Adkins, S., Zitter, T., Momol, T. (2005): Tospoviruses (Family Bunyaviridae, Genus Tospovirus). – Institute of Food and Agricultural Sciences, University of Florida, Gainesville.

[4] Ciuffo, M., Testa, M., Lenzi, R., Turina, M. (2011): Ranunculus latent virus: a strain of artichoke latent virus or a new macluravirus infecting artichoke? – Arch Virol 156: 1053-1057.

[5] Clark, M. F., Adams, A. N. (1977): Characteristic of microplate method of enzyme-linked immunosorbent assay for detection of plant viruses. – J. Gen. Virol. 34: 475-483.

[6] Costa, A. S., Duffus, J. E., Morton, D., Yarwood, C. E., Bardin, R. (1959): A latent virus of California artichokes. – Phytopathology 49: 49-53.

[7] Dellaporta, S. L., Wood, J., Hicks, J. B. (1983): A plant DNA mini-preparation: version 2. – Plant Mol Biol Rep. 1(4): 19-21. DOI: 10.1007/BF02712670.

[8] Erkan, S., Gümüş, M., Duman, İ., Paylan, İ. C., Ergün, M. (2014): The new report of artichoke latent virus (ArLV) from globe artichoke in Turkey. – Ege Üniv. Ziraat Fak. Derg. 51(3): 265-269.

[9] Elbeaino, T., Belghacem, I., Mascia, T., Gallitelli, D., Digiaro, M. (2017): Next generation sequencing and molecular analysis of artichoke Italian latent virus. – Arch Virol 162: 1805-1809. DOI: 10.1007/s00705-017-3290-8.

http://www.aloki.hu ● ISSN 1589 1623 (Print) ● ISSN 1785 0037 (Online)
DOI: http://dx.doi.org/10.15666/aeer/1704_76797691

[10] FAO (2015): Food and Agriculture Organization of the United Nations. The Statistics Division of FAO. – http://faostat.fao.org/.
[11] Fidan, H., Karanfiloğlu, H., Karamanlı, A., Kocadal, E., Baydar, K. (2015): A new virus disease, *Artichoke Latent Virus Potyvirus* (Arlv). – Artichoke Production Areas of NC. V. Plant Protection Congress, Antalya, Türkiye, 3-5 February 2015.
[12] Foddai, A., Marras, F. (1984): Influenza di ALV (Artichoke Latent Virus) sulla produttività del carciofo Spinoso Sardo. Considerazioni conclusive dopo un biennio di indagini. – Atti Giorn. Fitopat III: 353-358.
[13] Foddai, A., Manas, E., Idini, G. (1985): Indagine sulla reinfezione naturale del carciofo Spinoso Sardo risanato da ALV. – Informatore Fitopatologico 35: 57-58.
[14] Gallitelli, D., Rana, G. L., Vovlas, C., Martelli, G. P. (2004): Viruses of globe artichoke: an overview. – J. Plant Pathol. 86: 267-281.
[15] Gallitelli, D., Mascia, T., Martelli, G. P. (2012): Viruses in artichoke. – Advances in Virus Research 84: 289-324.
[16] Garland, S., Sharman, M., Persley, D., McGrath, D. (2005): The development of an improved PCR-based marker system for Sw-5, an important TSWV resistance gene of tomato. – Australian J. Agric. Research 56: 285-289.
[17] Lima, M. F., Carvalho, S. I. C., Ragassi, C. F., Bianchetti, L. B., Faleiro, F. G. Reifschneider, F. J. B. (2017): Characterization of a pepper collection (*Capsicum frutescens* L.) from Brazil Genet. – Mol. Res. 16(3): gmr16039704.
[18] Lumia, V., Pasquini, G., Barba, M. (2003): Sensitive detection of artichoke latent virus in globe artichoke field samples by onestep RT-PCR or tissue imprint hybridization. – Journal of Phytopathology 151: 477-479.
[19] Manzanares, M. J. et al. (1995): Evaluation of globe artichoke and related germplasm for resistance to artichoke latent virus. – Euphytica 84: 219-228.
[20] Marrou, J., Mehani, S. (1964): Etude d'un virus parasite de l'artichaut. – Comptes Rendues de l'Académie d' Agriculture de France 50: 1051-1064.
[21] Martelli, G. P., Gallitelli, D. (2008): Viruses of Cynara. Characterization, Diagnosis and Management of Plant Viruses. Vol. 1. Industrial Crops. – Studium Press, Texas.
[22] Migliori, A., Homo, E., Corre, J., Marzin, H., Legal, V., Curvale, J. P. (1987): Repartition, fréquence et nuisibilité des virus chez l'artichaut en Bretagne. – PHM.-Revue Horticole 274: 29-36.
[23] Minutillo, S. A., Marais, A., Mascia, T., Faure, C., Svanella-Dumas, L., Theil, S. et al. (2015): Complete nucleotide sequence of artichoke latent virus shows it to be a member of the genus Macluravirus in the family Potyviridae. – Phytopathology 105: 1155-1160. DOI: 10.1094/PHYTO-01-15-0010-R.
[24] Ortega, A. M., Juarez, M., Armengol, J., Jorda, M. C. (2000): Viral diseases in artichoke crops in Spain. – Acta Hort. 681: 611-616.
[25] Pasquini, G., Barba, M. (2003): Evidence of viral infections in late artichoke cv. Romanesco. – Acta Hort. 681: 597-602.
[26] Paylan, I. C., Ergun, M., Erkan, S. (2013): First report of artichoke yellow ringspot virus in globe artichoke in Turkey. – Plant Disease 97(10): 1388-1388.
[27] Pecaut, P. (1994): Globe Artichoke. – In: Kalloo, G., Bergh, B. O. (eds.) Genetic Improvement of Vegetable Crops. Pergamon Press, Oxford, pp. 737-746.
[28] Pecaut, P., Dumas de Vaulx, R., Lof, H. (1983): Virus-free clones of globe artichoke (*Cynara scolymus*) obtained after in vitro propagation. – Acta Hortic 131: 303-309.
[29] Rana, G. L., Russo, M. (1980): Le virosi del carciofo in Italia: possibilita` di prevenzione e lotta. – Atti Giorn. Fitopatol. 2: 85- 93.
[30] Rana, G. L., Russo, M., Gallitelli, D., Martelli, G. P. (1982): Artichoke latent virus: characterization, ultrastructure, and geographical distribution. – Ann. App. Biol. 101: 279-289.

http://www.aloki.hu ● ISSN 1589 1623 (Print) ● ISSN 1785 0037 (Online)
DOI: http://dx.doi.org/10.15666/aeer/1704_76797691

[31] Rana, G. L., Elia, A., Nuzzaci, M., Lafortezza, R. (1992): Effects of artichoke latent virus infection on the production of artichoke heads. – Journal of Phytopathology 135: 153-159. DOI: 10.1111/j.1439-0434.1992.tb01261.x.
[32] Saitou, N., Nei, M. (1987): The neighbor-joining method—a new method for reconstructing phylogenetic trees. – Mol Biol Evol 4: 406-425.
[33] Salleh, W., Minutillo, S. A., Spanò, R., Zammouri, S., Gallitelli, D., Mnari-Hattab, M. (2017): Occurrence of artichoke-infecting viruses in Tunisia. – EPPO Bull 47: 48-56. DOI: 10.1111/epp.12360.
[34] Sambrook, J., Fritschi, E. F., Maniatis, T. (1989): Molecular Cloning: A Laboratory Manual. – Cold Spring Harbor Laboratory Press, New York.
[35] Spanò, R., Bottalico, G., Corrado, A., Campanale, A., Di Franco, A., Mascia, T. (2018): A protocol for producing virus-free artichoke genetic resources for conservation, breeding, and production. – Agriculture 8: 36.
[36] Tamura, K., Peterson, D., Peterson, N., Stecher, G., Nei, M., Kumar, S. (2011): MEGA5: Molecular evolutionary genetics analysis using maximum likelihood, evolutionary distance and maximum parsimony methods. – Mol. Biol. Evol. 28: 2731-2739.
[37] Testa, M., Marras, P. M., Turina, M., Ciuffo, M. (2008): Resenza del virus dell'avvizzimento maculato del pomodoro (TSWV) su carciofo in Sardegna. – Protezione Delle Colture 2: 34-36.

http://www.aloki.hu ● ISSN 1589 1623 (Print) ● ISSN 1785 0037 (Online)
DOI: http://dx.doi.org/10.15666/aeer/1704_76797691

CLIMATE CHANGE AND ITS EFFECT ON LAND USE CHANGE IN THE CENTRAL RIFT VALLEY OF ETHIOPIA

BEKELE, B.[1, 2] – WU, W.[1, 3*] – YIRSAW, E.[4] – NEGUSSIE, W.[1, 2] – ALEMAYEHU, A.[1, 2]

[1]*College of Land Management, Nanjing Agricultural University, Nanjing 210095, China (e-mail: belewbekele@yahoo.com (B.B.); wube14@yahoo.com (N.W.); asferaalem2011@yahoo.com (A.A))*

[2]*Department of Natural Resources Management, Assosa ATVET College, Assosa 242, Ethiopia*

[3]*National and Joint Local Engineering, Research Center for Rural Land Resources Use and Consolidation, Nanjing 210095, China*

[4]*Department of Natural Resources Management, Dilla University, Dilla 419, Ethiopia (e-mail: eshetu.yirsaw@yahoo.com)*

[*]*Corresponding author*
e-mail: ww@njau.edu.cn; phone: +86-137-7065-1675

(Received 11th Mar 2019; accepted 1st May 2019)

Abstract. Climate change and variability have been one of the challenges to socioeconomic and environmental sustainability in the twenty-first century. Meteorological analyses of historical drought occurrences are common in East Africa, but studies devoted to its effect on land use change are yet limited. This paper aimed to assess the long-term rainfall and temperature variability and its effects on farmers' land use change in the Central Rift Valley of Ethiopia over the past 30-36 years using a combination of meteorological and socioeconomic data. Results show that the overall coefficient of variation for rainfall was more than 35% for rainy seasons. Out of the 36 years, total rainfall of the rainy season showed negative anomalies for about half of these years. Summer season rainfall started after the average time of onset for about 42% of the database years, and it ceased ahead of the average time of the stop for about 56% of these years. As a result of such rainfall shortage and variability, about 82% of the drought-vulnerable farmers had already changed their land use from pastoralist/agropastoralist to mixed farming while 10% have a wish to shift to other land use options in the future. Hence, future policies need to consider strategies that strengthen the adaptation capacity of farmers to climate change in East Africa.
Keywords: *'Belg', coefficient of variation, drought, 'Kirmet', rainfall, temperature*

Introduction

Climate change and variability have been one of the challenges to socioeconomic and environmental sustainability in the twenty-first century (UNFCCC, 2018). The change in climate is accelerating faster than the global effort to address it. Studies show that the atmospheric concentration of greenhouse gases (GHG) has increased more in recent decades than at any time in the past of human history (IPCC, 2007, 2014). This increase in GHGs, in turn, lead to global warming with its related catastrophes to life on Earth like extreme storms, droughts, fires, floods, ice melting, and rising in sea levels (IPCC, 2007, 2014; Eckstein et al., 2017). According to Maharjan and Joshi (2013), global average surface temperature and atmospheric concentration of CO_2 have been rising at an increasing rate, especially since the 1900s. With current mitigation efforts, future projections also indicate a continual increase for GHGs and temperature trends (Ravindranath and Sathaye, 2002; IPCC, 2014). Such threats, in general, made the

http://www.aloki.hu ● ISSN 1589 1623 (Print) ● ISSN 1785 0037 (Online)
DOI: http://dx.doi.org/10.15666/aeer/1704_76937713

climate change issue, one of the top agendas of discussion among the global research community and political leaders in recent decades.

Climate change could affect the ecosystem and human well-being in several ways. For instance, climate change could affect regional agricultural production yield, food price and food security (Sivakumar, 1992; Ravindranath and Sathaye, 2002; Barron et al., 2003), and it could affect human, plant, and animal health through its direct and indirect impact on physiology (Maharjan and Joshi, 2013; Pedrono et al., 2016). Climate change also affects ecosystem services and functioning by deteriorating biological, hydrological and atmospheric systems (Ravindranath and Sathaye, 2002; Pedrono et al., 2016). Additionally, climate change can force vulnerable communities to wholly or partially change their land use systems and livelihoods (Biazin and Sterk, 2013), and hence affect household income and social security. Furthermore, climate change can increase the costs incurred by mitigation and adaptation to overcome its impacts (Maharjan and Joshi, 2013).

The impact of climate change is more severe in developing nations where the income of the majority of the population directly depends on climate-sensitive economic sectors (e.g., agriculture) (UNFCCC, 2007; Torquebiau et al., 2016), as agriculture is not only contributing to climate change through GHG emissions, but is also most affected by it. According to Ravindranath and Sathaye (2002) and UNFCCC (2007), the region of Sub-Saharan Africa, south and east Asia, and the tropics of Latin America are particularly vulnerable to climate change. Studies show that the Sahel region in West Africa is well known for its severe environmental problems of drought and desertification over a long period of its history (Sivakumar, 1992; Agnew and Chappell, 1999). Similarly, the East African region is known for its recurrent severe drought in the last several decades (Barron et al., 2003). Beside such a high degree of vulnerability in developing countries, the adaptive capacity to overcome climate change impact is low due to financial, institutional, technological, and political constraints. For instance, Collier et al. (2008) and Gemeda and Sima (2015), pointed out that the impact of climate change on Africa is probably severe because of high agricultural dependency and limited capacity to adapt.

Besides primary socioeconomic drivers, climate change vulnerability is another crucial factor affecting agricultural land use (Dale, 1997; Reid et al., 2000; Biazin and Sterk, 2013; Ahmed et al., 2016). For example, Ahmed et al. (2016), found that the expansion in agricultural land use was mainly due to climate change in West Africa. These authors pointed out that unless agriculture is intensified, the climate-induced decline in crop yield coupled with a future increase in food demand will continue to increase agricultural area at the expense of forest and grassland loss in West Africa. The other study elsewhere showed that in addition to climatological deviations, drought vulnerability is also affected by the type of land use and social traditions of life. For instance, according to Biazin and Sterk (2013), the pastoral way of life was found to be more vulnerable to severe drought than mixed farming land use system. Similarly, a rain-fed cultivation is likely to be more susceptible to climate change than irrigated cropping, and a mono-cropping system is expected to be more vulnerable than a mixed cropping system, for example, agroforestry. Hence, according to Dale (1997) as a means of adaptation to climate change, vulnerable farmers usually try to modify/shift from a land use system that is more vulnerable to a land use system that is less vulnerable.

http://www.aloki.hu ● ISSN 1589 1623 (Print) ● ISSN 1785 0037 (Online)
DOI: http://dx.doi.org/10.15666/aeer/1704_76937713

Climate change and variability can be evaluated using different climatic indices and datasets. Studies show that temperature and precipitation are the two most frequently used climatic variables for evaluating climate variability and its impacts (Maharjan and Joshi, 2013). This is because there is an advantage of data availability in using, for example, rainfall, to investigate drought occurrence instead of using other variables, for example, river flow, which is increasingly managed by human action (Agnew and Chappell, 1999). Mean, median, a coefficient of variation, standard deviation, and the probability of dry spells are commonly used statistical parameters to describe both rainfall and temperature variability (Stern et al., 2006). In addition, the Standardized Precipitation Index is usually employed to evaluate long-term rainfall deviation from the usual norm (Agnew and Chappell, 1999; Agnew, 2000; Bewket and Conway, 2007; WMO, 2012; Viste et al., 2013). Irrespective of the type of indices used for climate change analysis, most climatologists advise using precipitation and temperature data of the long-term period and data from the wider gaging stations for better accuracy of results (Ali and Lebel, 2009).

Ethiopia is one of the countries in the Horn of East Africa hit by frequent drought over the last century. This was confirmed by various local and national level studies conducted in the country (Bewket and Conway, 2007; Cheung et al., 2008; Viste et al., 2013). For instance, Seleshi and Zanke (2004) found a significant decline in the annual and summer season total rainfalls since 1982 for the eastern, southern, and southwestern parts of the country. Cheung et al. (2008) in their long-term (1960-2002) rainfall data series analysis, found a significant decline in summer rainfall in southwestern and central parts of Ethiopia and pointed rainfall trends as one of the most important factors determining different socioeconomic constraints such as food insecurity in the country. The study by Rosell (2011) for three decades (1987-2007), indicated a decline in rainfall and an increase in temperature for the spring season in the central highlands of Ethiopia. Besides, Viste et al. (2013) found that the years 1972-1975, 1980-1982, 1984, 1987, 1990-1992, 1999-2000, 2002-2003, and 2008-2011 were the periods of severe drought episodes in Ethiopia. Furthermore, the recent 3-5 decades temperature and rainfall data analysis by Fazzini et al. (2015) reported a markedly increasing and decreasing trend for minimum temperature and annual spring season rainfall respectively in the country. However, there are studies reported the absence of significant variation, particularly in terms of total annual rainfall, as opposed to the farmers' usual perception of total rainfall shortage in most parts of Ethiopia (Conway, 2000; Conway et al., 2004; Seleshi and Zanke, 2004; Kassie et al., 2013; Adimassu et al., 2014). The main reason for these divergent results in the trend analysis of the annual rainfall of the country is the difference in base periods used for analysis (Agnew and Chappell, 1999; Bewket and Conway, 2007). In general, Ethiopia as a country whose economy is mainly dependent on rain-fed agriculture, the trend of seasonal rainfall is an important factor determining the socioeconomic functioning, particularly food production potential of the country (Bewket and Conway, 2007; Mideksa, 2010; Fazzini et al., 2015; Fekadu, 2015).

The Central Rift Valley (CRV) of Ethiopia is a semi-arid region known for its persisted shortage of agricultural rainfall in the country. Previous studies indicated the presence of drought vulnerability due to seasonal rainfall variability in the area (Biazin and Sterk, 2013; Kassie et al., 2013; Gizachew and Shimelis, 2014; Getachew and Tesfaye, 2015). However, works of literature devoted to climate variability and its impacts on farmers' land use change are currently limited in Ethiopia. Additionally, in a

http://www.aloki.hu ● ISSN 1589 1623 (Print) ● ISSN 1785 0037 (Online)
DOI: http://dx.doi.org/10.15666/aeer/1704_76937713

diversified agroclimatic condition, like in Ethiopia, a local level analysis is quite important as meteorological results usually vary for regional, local and even individual gaging stations. Furthermore, for climate change-prone and rain-fed dependent agricultural area, like in CRV, up-to-date climatic trend information is quite crucial to practice climate-responsive agriculture and to minimize climate-related production risks. Hence, this study is intended to 1) assess long-term rainfall and temperature change and variability over the last 30-36 years and 2) assess the possible effects of this climatic variability on land use/livelihood change by vulnerable farmers. It is believed that the output of such analysis partly helps the stakeholders to have an informed decision for future policy direction and better management strategies.

Materials and Methods

The study area

The CRV is located about 160 km south of the capital city Addis Ababa, Ethiopia. Geographically, the study site is situated within 7º10'- 8º30' north latitude and 38º15'-39º25' east longitude (*Figure*). It is part of the Main Ethiopian Rift system which is characterized by an area of depression zone with steep marginal faults along its eastern and western edges. It is found within the current administrative boundary of Oromia and Southern Nations, Nationalities and Peoples (SNNP) Regional States.

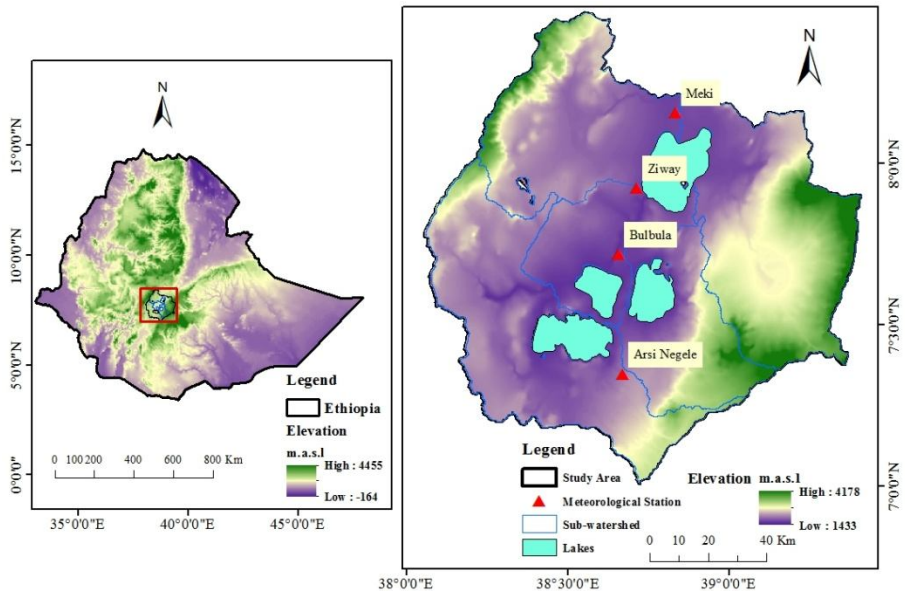

Figure 1. *The study site location map with agroclimatic zones*

Due to the unique topographical and geological feature of the region, the climate of CRV is known to vary markedly with altitude and season (Jansen et al., 2007). It is semi-arid in the areas along rift floor, and humid to sub-humid in the highland zone. As shown in *Figure*, the study area receives a bimodal annual rainfall distribution pattern in which the small light rain occurs during *Belg* (spring) season (February to May), and this is followed by the main rain that occurs during *Kirmet* (summer) season (June to September). The peak rainy months are July and August. The dry season (*Bega*)

http://www.aloki.hu ● ISSN 1589 1623 (Print) ● ISSN 1785 0037 (Online)
DOI: http://dx.doi.org/10.15666/aeer/1704_76937713

(winter), on the other hand, extends from October to January. According to data from the National Meteorological Agency (NMA), the mean annual rainfall is about 740 mm, and the mean minimum and maximum annual temperatures are 13ºC and 27ºC, respectively. In general, studies show that rain-fed agriculture in CRV is constrained by the highly erratic nature of rainfall in the region in recent decades (Jansen et al., 2007).

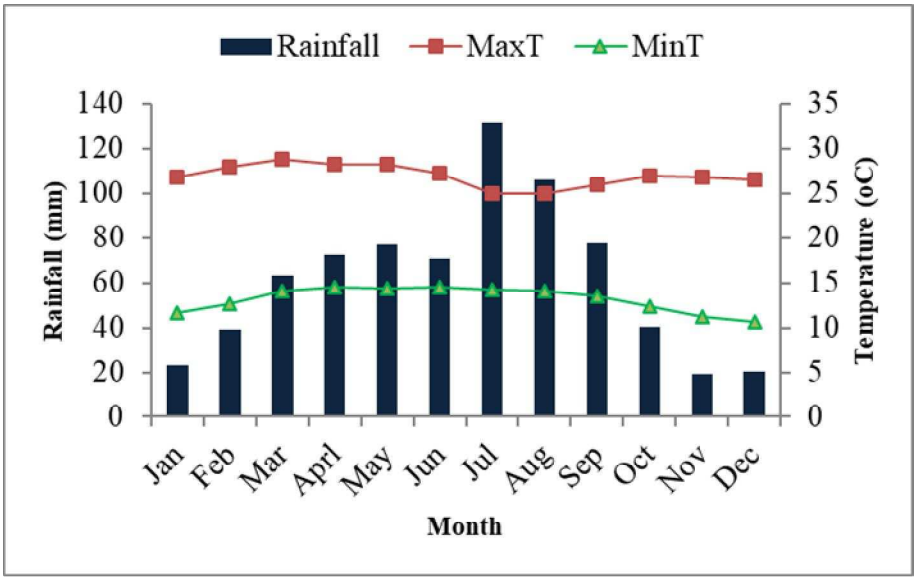

Figure 2. *Average monthly rainfall and temperature at CRV: MaxT = maximum temperature, MinT = minimum temperature: Data from NMA*

The common land use/cover types of the study area include agricultural land, scattered acacia woodland, water body, shrub/bushland, grass/grazing land, marshy/swampy land, and bare land as described in Bekele et al. (2018a). The dominant and peculiar vegetation type in the region is acacia woodland. As a result of continual deforestation for agricultural land expansion, charcoal making, and fuelwood extraction, the acacia woodland of the region has been highly decreased from time to time over the last half century (Garedew et al., 2009; Biazin and Sterk, 2013; Temesgen et al., 2013; Ariti et al., 2015). Four of the principal Ethiopian lakes namely: Abijata, Shalla, Ziway, and Langano are found within the catchment of CRV basin. The first two lakes are known for their soda ash (salt) content and home for a variety of migratory bird species while the latter two are intensively used for a fishery, irrigation, and domestic water consumption currently (Hengsdijk and Jansen, 2006). As a result of such high anthropogenic-induced pressures on land resources and poor management, the study area is presently highly threatened by extensive land degradation, lake water retreat and pollution, and drought and food insecurity (Meshesha et al., 2012; Bekele et al., 2018b).

The population of the study area has increased with an annual average growth rate of about 3% over the last three decades (Bekele et al., 2018b). The average number of a family is about seven in a rural area. According to data from CSA (CSA, 1994, 2007), the total population of three districts in CRV namely: Arsi Negele, Adami-Tulu-Jido Kombolcha, and Dugda had increased by about 86% in 2016 from its figure in 1994. About 85% of the population is still known to live in a rural area (CSA, 2007).

http://www.aloki.hu ● ISSN 1589 1623 (Print) ● ISSN 1785 0037 (Online)
DOI: http://dx.doi.org/10.15666/aeer/1704_76937713

For the vast majority (85%) of the population in the region, smallholder mixed rain-fed agricultural production is the main economic activity (Melka et al., 2015). There are also a few portions of the rural community who are still engaged in the agropastoral livelihood system. Despite significant attempts made to promote irrigated agriculture over the last two decades in the area, agricultural productivity is still subsistent due to erratic rainfall, recurrent drought, and limited technological applications. Due to this, the majority of the rural population is food insecure and still dependent on external relief aid programs (Bekele et al., 2018b).

Data used and sources

Long-term meteorological data (30-36 years) and socioeconomic data are the two main data sources used in this study. According to Maharjan and Joshi (2013), temperature and precipitation are widely used to assess climate change and its subsequent impacts. Hence, for climate variability and change analysis, long-term historical temperature and rainfall data were mainly used in this study. Data was specifically obtained from four selected Gaging Stations in CRV namely Meki, Ziway, Bulbula, and Arsi Negele (*Table*) which are monitored by Ethiopian National Meteorological Agency (NMA). All the stations are found along the rift-floor of the CRV and selected based on proximity to study Districts which were vulnerable to climate change and land use change in recent decades. The 1981-2017 database period was selected to make it match with the period for which land use/cover change was analyzed in previous work by the authors (Bekele et al., 2018a). Data for rural farmers' perception towards climate variability and its effect on their historical land use change was generated through formal households' interview and discussion with focus group and key informants — detail as explained in Bekele et al. (2018b). Accordingly, about 297 survey households were randomly selected and interviewed from two study districts namely Arsi Negele and Adami Tulu-Jido Kombolcha.

Table 1. *Data sources and period for rainfall and temperature*

Station	Latitude	Longitude	Elevation (m.a.s.l.)	Database period	
				Rainfall	Temperature
Arsi Negele	7°21'	38°39'	1800	1981-2016	1988-2017
Bulbula	7°43'	38°43'	1700	1981-2016	NA
Meki	8°09'	38°49'	1400	1981-2016	NA
Ziway	7°56'	38°43'	1640	1981-2016	1981-2017

m.a.s.l. = meter above sea level, NA = data not available (Source: NMA)

Data processing and analysis

Analysis of mean, standard deviation, coefficient of variation, precipitation concentration index, and standardized precipitation index

The daily time series rainfall and temperature data from each station and for the respective year were checked for homogeneity, outliers, discontinuities, and errors during analysis. Suspected outlier data were cross-checked with data from neighboring stations for typographical errors and corrected when found. Missing data value was filled by using data from a neighboring station. The inter-seasonal/annual trend of

http://www.aloki.hu ● ISSN 1589 1623 (Print) ● ISSN 1785 0037 (Online)
DOI: http://dx.doi.org/10.15666/aeer/1704_76937713

rainfall and temperature was examined for the study period and each station by processing data using the climatic analysis software, INSTAT version 3.36 following the guideline given by Stern et al. (2006). Mean values, standard deviation (SD), a coefficient of variance (CV), Precipitation Concentration Index (PCI), and standardized precipitation index (SPI) were employed for the analysis. The formula in *Equation 1* was used to calculate the SD for rainfall and temperature variability. Rainfall variability is also statistically described by using CV and PCI (Bewket and Conway, 2007). The CV is calculated as the ratio of the SD to the mean in a given period (*Eq. 2*), and the PCI values were calculated using *Equation 3* as given by Oliver (1980). SPI, also known as Standardized Rainfall Anomaly (SRA), *is simply the difference of precipitation from the mean for a specified period divided by SD, where the mean and SD are determined from recorded data* (McKee et al., 1993). The SPI values of the rainy season were calculated using the formula given in *Equation 4* as in Agnew and Chappell (1999) and Bewket and Conway (2007).

$$SD = \sqrt{\left[\sum_{i=1}^{n} \frac{(x_i - X)^2}{n}\right]} \quad \text{(Eq.1)}$$

$$CV = \frac{SD}{X} * 100 \quad \text{(Eq.2)}$$

$$PCI = \left[\frac{\sum P_i^2}{(\sum P_i)^2}\right] * 100 \quad \text{(Eq.3)}$$

$$SPI = \frac{P_t - P_m}{SD} \quad \text{(Eq.4)}$$

where, SD = standard deviation, CV = coefficient of variation, x_i = individual temperature/rainfall observation, X = mean rainfall/temperature, n = number of years considered, PCI = Precipitation Concentration Index, P_i = the rainfall amount of the i^{th} month, SPI = standardized precipitation index, P_t = annual rainfall in year t, P_m = long term mean annual rainfall over a period of observation.

Analysis of onset and cessation of rain, probability of dry spells, and length of growing season

Previous studies in dryland areas of Africa, including Ethiopia, defined the 'onset of rain' (a successful planting date) as *the first occasion after March 1st when the rainfall accumulates for three consecutive days and rainfall is at least 20 mm and no dry spell of more than ten days in the next 30 days* (Sivakumar, 1988; Simane and Struik, 1993; Tesfaye and Walker, 2004). Studies elsewhere described a 'rainy day' as a day receiving rainfall amount of >= 0.85 mm (Barron et al., 2003; Stern et al., 2006), whereas in this study the value given by Ethiopian National Meteorological Agency (NMA, 2001) (i.e., >=1 mm) was used as a reference for rainfall start which was also used by Seleshi and Zanke (2004). A first-order Markov Chain Model was applied by using INSTAT version 3.36 to analyze the onset of wet and dry spells as described by Stern et al. (2006). This model assumes that the probability of rainfall on a given day depends on whether rainfall did or did not occur on the previous day (Biazin and Sterk, 2013). To get an overview of drought at the study area for the whole year, probabilities of the maximum dry spell lengths over the next 30 days from planting was calculated

http://www.aloki.hu ● ISSN 1589 1623 (Print) ● ISSN 1785 0037 (Online)
DOI: http://dx.doi.org/10.15666/aeer/1704_76937713

(Tesfaye and Walker, 2004). For this study, a 'dry day' is a day receiving less than 1 mm of rain and a 'dry spell' is any consecutive number of days defined as 'dry'. The end of the rainy season or cessation was determined by using the water balance dialogue in the INSTAT climatic guide (Stern et al., 2006) and defined as a day after 'first September' when the soil water drops to 10 mm m^{-2}. Consequently, the length of the growing season is simply the difference between the rainfall onset date and cessation date (Sivakumar, 1988; Tesfaye and Walker, 2004; Stern et al., 2006). Frequency (F) of dry spells was computed using *Equation 5* below as in Sivakumar (1992).

$$F(D < x) = \frac{N(D_i)}{M} X\ 100 \quad \text{(Eq.5)}$$

where, $N(D_i)$ is the number of years a dry spell of length < x started in a prescribed 10-day period i, and M is the total data period (year).

Analysis of effect of climate change vulnerability on land use change

Studies show that drought vulnerability is much affected not only by climatological events but also by land use type and social contexts. For instance, Biazin and Sterk (2013) analyzed drought vulnerability based on locally perceived criteria of drought and found that the pastoral way of life was more vulnerable to severe drought than the mixed farming (livestock and crop combined) system. Based on these previous vulnerability findings, past historical land use type and future preferences of farmers who are currently engaged in two different land use system (agropastoralist versus mixed farming) were assessed by using a semi-structured questionnaire. The detail about household socioeconomic survey is explained in Bekele et al. (2018b). Accordingly, the study analyzed the change in land use of farmers during the study period, the main reason for changing, and their future preferences (either to continue as agropastoralist, mixed-farmer or other). Additional evidence for land use history was also collected from key informants and experts who were working in the study area for a long period. Finally, simple descriptive statistics were used to evaluate such climate change-induced farmers' historical land use change.

Results

Rainfall variability and change

Seasonal and annual rainfall characteristics

Rainfall of the study area showed both temporal and spatial variability over the study period. *Table* and *Table* summarizes the long-term statistics of spatial and seasonal rainfall for four selected sites in CRV while *Figure* illustrates a time series of bar graph that shows inter-seasonal and inter-annual total rainfall variability. The average precipitation of the driest month (19.2 mm) and wettest month (106.1 mm) was observed for November and August respectively. Mean annual total rainfall was below average for about 44% of the study years. The mean annual total rainfall is lowest (708 mm) at Bulbula and highest (769 mm) at Arsi Negele. The CV for rainfall is higher at Arsi Negele (43%) and lower at Ziway (20%). On the other hand, monthly rainfall distribution is less concentrated (PCI = 9) at Bulbula and more concentrated (PCI = 14) at Meki.

http://www.aloki.hu ● ISSN 1589 1623 (Print) ● ISSN 1785 0037 (Online)
DOI: http://dx.doi.org/10.15666/aeer/1704_76937713

Table 2. *Spatial rainfall characteristics at four stations in CRV*

Station	Mean	SD	CV (%)	PCI
Arsi Negele	769.52	328.12	42.64	10.58
Bulbula	708.33	254.76	35.97	8.66
Meki	744.19	164.16	22.06	13.59
Ziway	737.94	144.98	19.65	12.72
Study site	739.99	140.01	18.92	11.39

SD = standard deviation, CV = coefficient of variation, PCI = Precipitation Concentration Index

Table 3. *Seasonal rainfall statistics at four sites in CRV*

Station name	Season	Minimum	%tile			Maximum	Mean	SD	CV (%)
			25	50	75				
Arsi Negele	FMAM	26.90	142.70	274.20	359.40	594.40	272.04	149.07	54.80
	JJAS	70.40	235.60	354.50	487.85	1001.00	392.04	207.83	53.01
	ONDJ	0.00	43.10	97.50	160.10	287.25	105.44	75.32	71.43
Bulbula	FMAM	64.20	173.10	248.60	321.90	635.45	264.19	119.15	45.10
	JJAS	99.40	156.95	234.60	290.80	664.25	253.49	120.03	47.35
	ONDJ	0.00	102.75	181.00	240.80	604.65	190.65	116.59	61.15
Meki	FMAM	71.20	152.70	207.50	295.40	517.50	234.12	106.30	45.41
	JJAS	110.95	383.00	446.70	527.20	855.10	460.68	127.87	27.76
	ONDJ	0.00	11.30	43.20	85.30	164.30	49.39	45.19	91.48
Ziway	FMAM	75.10	142.20	247.30	302.80	413.50	236.42	101.72	43.02
	JJAS	182.50	391.40	441.60	489.10	660.70	437.36	89.80	20.53
	ONDJ	0.00	8.50	34.80	102.00	289.80	64.16	70.74	110.25
Study site	FMAM	59.35	152.68	244.40	319.88	540.21	251.69	117.72	46.77
	JJAS	115.81	291.74	369.35	448.74	795.26	385.89	133.69	34.65
	ONDJ	0.00	41.41	89.13	147.05	336.50	102.41	75.90	74.12

FMAM = February-May, JJAS = June-September, ONDJ = October-January, SD = standard deviation, CV = coefficient of variation

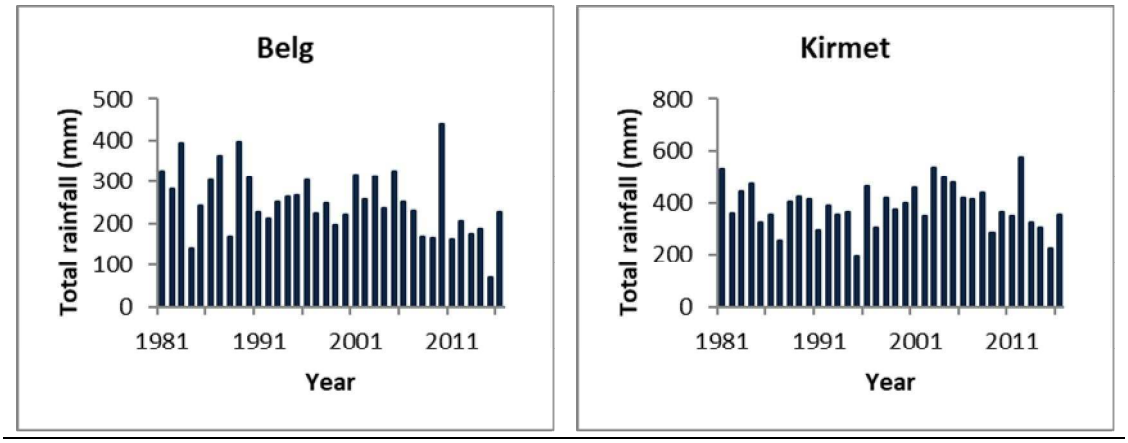

Figure 3. *Long-term seasonal total rainfall at CRV*

http://www.aloki.hu ● ISSN 1589 1623 (Print) ● ISSN 1785 0037 (Online)
DOI: http://dx.doi.org/10.15666/aeer/1704_76937713

Rainfall variability along the sites is also observed for both rainy seasons (*Table*). The overall mean seasonal rainfall ranged from 252 mm in *Belg* season (FMAM) to 386 mm in *Kirmet* season (JJAS). The coefficient of rainfall variation is higher for *Belg* season (47%) than for *Kirmet* season (35%). The long-term *Belg* season minimum rainfall ranged from 27 mm at Arsi Negele to 75 mm at Ziway, while the long-term maximum rainfall of the same season ranged from 413 mm at Ziway to 635 mm at Bulbula. Mean rainfall of the *Belg* season was lowest (234 mm) at Meki and highest (272 mm) at Arsi Negele. During this season, rainfall is more variable (CV=55%) at Arsi Negele and less variable (CV=43%) at Ziway. On the other hand, the minimum rainfall of the *Kirmet* season ranged from 70 mm at Arsi Negele to 182 mm at Ziway, while the maximum rainfall of the same season ranged from its 661 mm at Ziway to 1001 mm at Arsi Negele. The lowest (253 mm) and highest (461 mm) mean *Kirmet* rainfall was recorded for Bulbula and Meki sites respectively. *Kirmet* season rainfall is more variable (CV=53%) at Arsi Negele and less variable (CV=20%) at Ziway.

Standardized Precipitation Index (SPI)

The Standardized Precipitation Index (SPI) (*Figure*) shows an overall picture of average (normal), above average (wet) and below average (dry) years, while *Table* gives the classification of SPI based on McKee et al. (1993). SPI values ranged from (-)2.34 to (+)2.42 for *Belg* season and (-)2.23 to (+)2.21 for *Kirmet* season. As can be seen from *Figure*, both seasons experienced dry and wet years over the last 36 years.

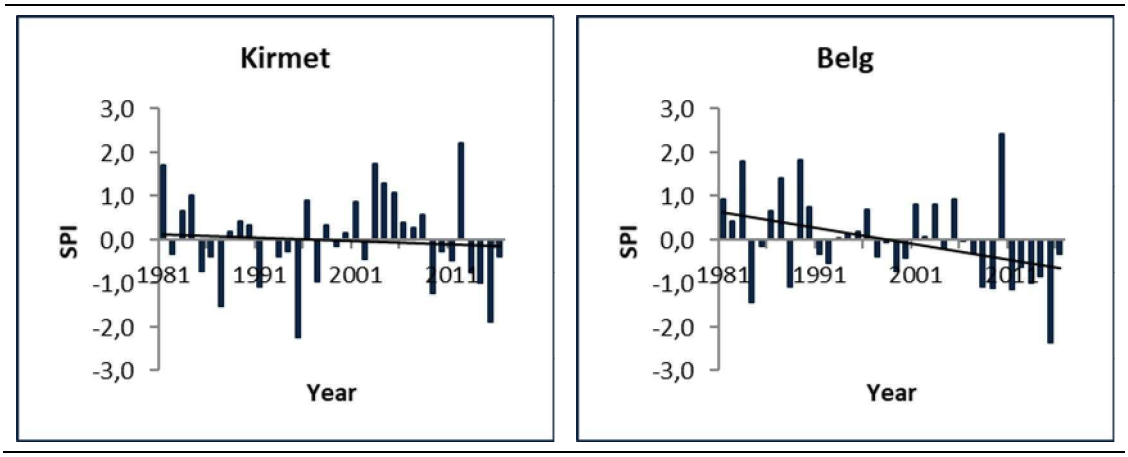

Figure 4. *Standardized Precipitation Index (SPI) of the growing season in CRV*

For instance, out of the 36 database years considered, rainfall was below average (dry years) during 20 years (56%) of *Belg* season and 18 years (50%) of *Kirmet* season. On the other hand, the linear trend line in *Figure* indicates that the total annual rainfall showed a general decreasing trend since 1981 during both seasons. According to the SPI classification given by McKee et al. (1993), rainfall of about 44% and 50% of the study years fall in the category of *no drought/normal* for *Belg* and *Kirmet* seasons respectively (*Table*). For the *Belg* season, the 'extreme drought' year was 2015, whereas for *Kirmet* season the 'severe drought' and 'extreme drought' years were 1987 and 2015, and 1995, respectively.

http://www.aloki.hu ● ISSN 1589 1623 (Print) ● ISSN 1785 0037 (Online)
DOI: http://dx.doi.org/10.15666/aeer/1704_76937713

Table 4. *Drought evaluation in CRV based on McKee et al. (1993)*

Season	Drought class	Drought/normal years	Frequency	Percentage of frequency
Belg	Extreme drought	2015	1	2.8
	Severe drought	-	0	0
	Moderate drought	1984, 1988, 2008-2009, 2011	5	13.9
	Mild drought	1985, 1991-1992, 1997-2000, 2004, 2006-2007, 2012-2014, 2016	14	38.9
	No drought	1981-1983, 1986-1987, 1989-1990, 1993-1996, 2001-2003, 2005, 2010	16	44.4
	Total		36	100
Kirmet	Extreme drought	1995	1	2.8
	Severe drought	1987, 2015	2	5.6
	Moderate drought	1991, 2009	2	5.6
	Mild drought	1982, 1985-1986, 1993-1994, 1997, 1999, 2002, 2010-2011, 2013-2014, 2016	13	36.0
	No drought	1981, 1983-1984, 1988-1990, 1992, 1996, 1998, 2000-2001, 2003-2008, 2012	18	50.0
	Total		36	100

Rainfall onset, cessation, and length of growing season

The onset (start) and cessation (end) date of rainfall for the main rainy season, averaged for the study site is shown in *Figure*. The average rainfall onset date of the study area is 25 June. Out of the 36 database years considered, for 15 years (42%), rainfall started later than the average onset date (June 25). On the other hand, the average rainfall cessation date in CRV is 17 September. For 20 years (56%), out of the 36 years, rainfall stopped earlier than the average cessation date (September 17). The average length of the crop growing season (i.e., the difference between cessation date and onset date) is as shown in *Figure*. The average growing season in the study area is about three months (84 days), and the median value is 85 days. 1985, 1987, and 1995 were years with a growing season of less than 60 days, whereas 1982, 1988, 1996, 1998, 1999, 2000, and 2012 were years with more than 100 days of growing season.

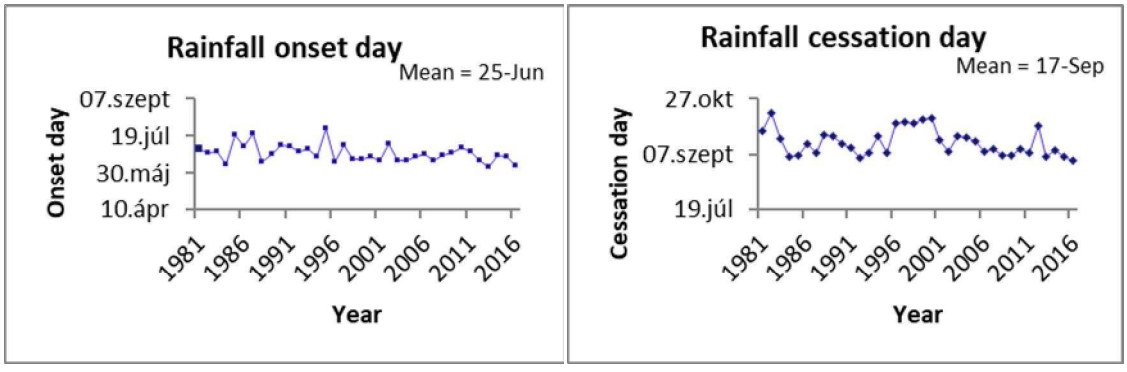

Figure 5. *Rainfall onset and cessation day variability in CRV*

http://www.aloki.hu ● ISSN 1589 1623 (Print) ● ISSN 1785 0037 (Online)
DOI: http://dx.doi.org/10.15666/aeer/1704_76937713

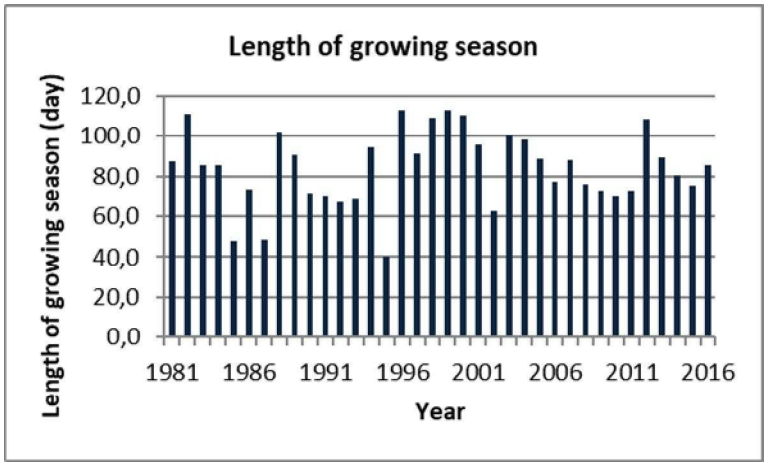

Figure 6. *Length of the growing season in CRV*

Number of rainy days and probability of dry spells

Figure depicts the trend of rainy days (days with rainfall >=1 mm) and dry spells (days with rainfall < 1 mm) for *Belg* and *Kirmet* seasons and respective study years. The average number of rainy days in the study area is 23 and 38, while the average number of dry spells is 97 and 84 for *Belg* and *Kirmet* seasons respectively. As presented in *Figure*, the number of rainy days showed a general decreasing trend, whereas the number of dry spells showed a generally increasing trend since 1981 for both *Belg* and *Kirmet* seasons.

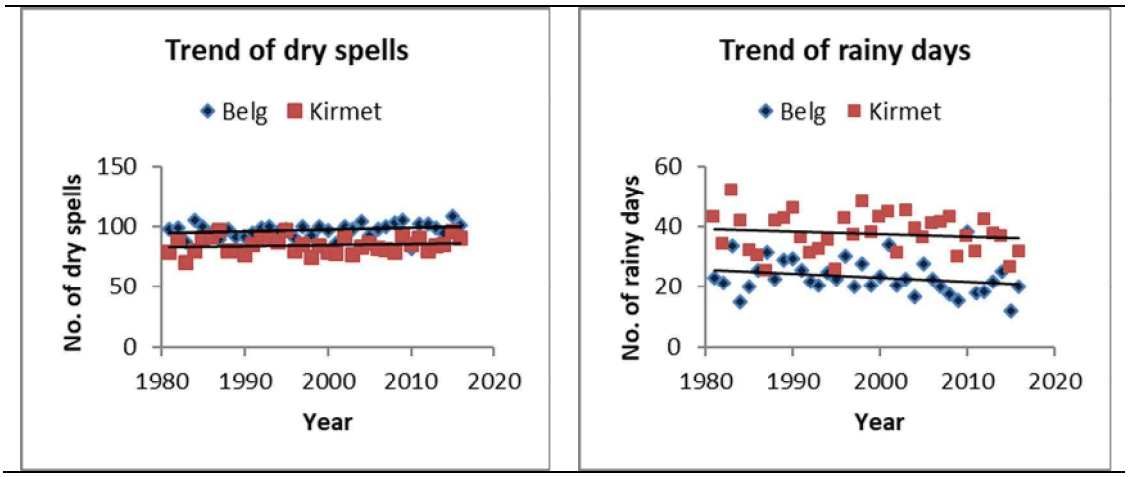

Figure 7. *Trend of number of rainy days and dry spells in CRV*

For example, for *Belg* season, the average number of rainy days was declined from 25 during 1981-1990 to 20 during 2007-2016 (18% decline), whereas for the same period, average number of dry spells was increased from 95 to 99. Similarly, for *Kirmet* season, during the same period, the average number of rainy days was declined from 39 to 36 (8% decline), whereas the average number of dry spells was increased from 83 to 86. On the other hand, the probability of dry spells was found to be higher during *Belg* season than during *Kirmet* season of the study years (*Figure*).

http://www.aloki.hu ● ISSN 1589 1623 (Print) ● ISSN 1785 0037 (Online)
DOI: http://dx.doi.org/10.15666/aeer/1704_76937713

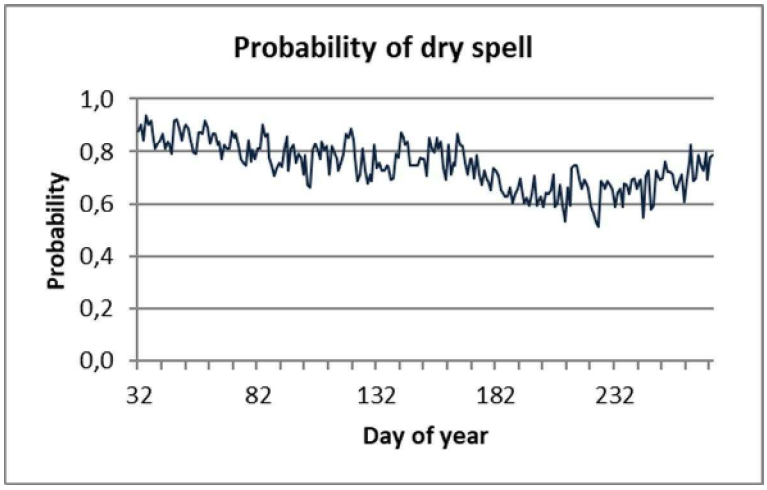

Figure 8. *Trend of the probability of dry spells in CRV*

Temperature variability and change

Results indicated that the temperature of the study area has shown minor inter-annual and inter-station variability over the study periods (*Table* and *Figure*). The average minimum temperature of the coldest month (10.7°C) and the average maximum temperature of the hottest month (28.8°C) was observed for December and March respectively.

Table 5. *Temperature characteristics at four stations in CRV*

Station	Minimum temperature			Maximum temperature		
	Mean	SD	CV	Mean	SD	CV
Arsi Negele	12.20	2.22	18.19	26.57	0.88	3.32
Bulbula	ND	ND	ND	ND	ND	ND
Meki	ND	ND	ND	ND	ND	ND
Ziway	14.14	0.89	6.28	27.36	0.97	3.55
Study site	13.24	1.26	9.51	27.12	0.55	2.03

SD = standard deviation, CV = coefficient of variation, ND = no data available

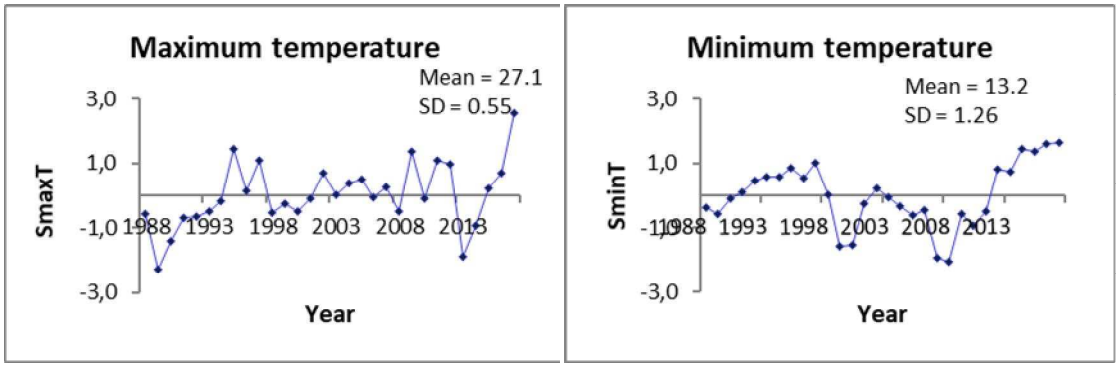

Figure 9. *Variability in minimum and maximum temperature in CRV: SminT = standardized minimum temperature, SmaxT = standardized maximum temperature*

http://www.aloki.hu ● ISSN 1589 1623 (Print) ● ISSN 1785 0037 (Online)
DOI: http://dx.doi.org/10.15666/aeer/1704_76937713

Both minimum and maximum temperature values are higher at Ziway than at Arsi Negele. The minimum temperature ranged from its lowest value (10.6ºC) in 2008 to its highest value (15.3ºC) in 2017, while the maximum temperature ranged from its lowest value (25.9ºC) in 1989 to its highest value (28.5ºC) in 2017. The minimum temperature had risen above the average value for 15 years (50%) out of the 30 years considered. Similarly, the maximum temperature was above average value for 16 years (53%) of the data years. On the other hand, both minimum and maximum temperatures showed a relatively continuous increment after 2013.

Effect of climate variability on farmers' land use change

Table indicates how farmers of the study area have shifted/wish to change their land use system through time in order to adapt to the impacts of climatic and environmental changes over time. About 15 and 35% of respondents in CRV claimed that they had been pastoralists and agropastoralists respectively before the government change in 1991. However, currently, only 9% of respondents claimed as being agropastoralists and none of them claimed as fully pastoralist. This indicates about 82% of farmers who were pastoralists and agropastoralists before three decades had changed their land use to mixed farming and other livelihood activities. On the other hand, as indicated in *Table*, though the majorities (about 90%) of the farmers wish to continue as a mixed farmer, none of them wish to continue either as pastoralist or agropastoralist in the future. The rest 10% of respondents have a wish to shift their livelihood to other activities like off-farm jobs, mini trading, and cattle fattening.

Table 6. *Farmers land use change through time (N=297)*

Type of land use	30 years before (%)	Current (%)	Future wish (Yes, %)
Pastoralist	15.00	0.00	0.00
Agropatoralist	35.50	9.10	0.00
Mixed farming	48.50	89.00	90.10
Other activity	1.00	1.90	9.90

The major factors that forced farmers to change their land use system through time are as listed in *Table*. This change in land use is more observed in communities whose livelihood is more vulnerable to climate change for example, in pastoralists and agropastoralists than in mixed farming communities who are less vulnerable. According to 40% of respondents, climate variability is the main factor forcing farmers to change their land use system which was followed by the shortage of land due to population growth (30%), as a second driver of change.

Table 7. *Forcing factors of farmers' land use change (N=297)*

Factors	Number of respondents (%)
Climate change	40
Population growth and shortage of land	30
Access to market and infrastructure	15
Institutional and policy changes	10
Others	5

http://www.aloki.hu ● ISSN 1589 1623 (Print) ● ISSN 1785 0037 (Online)
DOI: http://dx.doi.org/10.15666/aeer/1704_76937713

Improvements in access to infrastructure and market from time to time and institutional changes following the subsequent government changes in 1974 and 1991 in Ethiopia were also mentioned as substantial factors that contributed for such land use changes in the study area.

Discussion

Results indicated that rainfall in the study area experienced a high inter-seasonal, inter-annual, and inter-station variability over the last 36 years. For instance, mean annual total rainfall was below average for about 44% of study years, and the CV of rainfall is about 20% and above for all seasons and sites. This long-term rainfall variability was also confirmed by the perceived results of the discussion with farmers and experts of the study area (Bekele et al., 2018b). As per the classification given by Hare (1983), total rainfall of CV < 20% is classified as less variable; CV of 20-30% as moderately variable, and CV of > 30% as highly variable and vulnerable to drought. According to this classification, the overall rainfall in CRV can be categorized in the threshold of 'moderately variable', even though inter-seasonal/station variations are 'highly variable'. On the other hand, the overall PCI value for the study site is about 11, which indicates that the monthly rainfall distribution of the study area is highly concentrated. According to Oliver (1980), PCI values of less than 10, 11-20, and above 21 are indicators of 'uniform', 'high concentration' and 'very high concentration' monthly distribution of rainfall respectively.

This result is in line with results of previous studies on climate variability in the region (Biazin and Sterk, 2013; Getachew and Tesfaye, 2015; Muluneh et al., 2017) and studies in other parts of Ethiopia (Seleshi and Zanke, 2004; Bewket and Conway, 2007; Cheung et al., 2008; Viste et al., 2013) who reported the prevalence of seasonal rainfall variability and drought in the country over the last decades. Besides climatic fluctuations, there are studies reported the non-stationarity in hydrological variables particularly stream flow and lake level in the Rift Valley Lakes Basin of Ethiopia (Wagesho et al., 2012; Getnet et al., 2014). This affects the available water which, in turn, affects land use. However, other studies reported the absence of significant variation particularly in terms of total annual rainfall as opposed to farmers' usual perception of the presence of total rainfall shortage in the country in recent decades (Rosell, 2011; Kassie et al., 2013; Adimassu et al., 2014). In addition to seasonal variation, Ethiopian precipitation exhibits great spatial variation due to high altitudinal variation over the country (Viste et al., 2013). Coupled with the semi-arid climate and hence moisture-deficient soil of the CRV, variability in rainfall is one of the challenges to the sustainable production of the rain-fed agriculture in the region (Kassie et al., 2013; Gizachew and Shimelis, 2014; Getachew and Tesfaye, 2015), in Ethiopia (Mideksa, 2010), and other semi-arid and dry sub-humid areas in Sub-Saharan Africa (Barron et al., 2003; Viste et al., 2013; Fekadu, 2015; Serdeczny et al., 2017).

In the study area, out of the 36 study years considered, total rainfall was below average (i.e., negative anomalies) for about half of these years. According to the threshold suggested by McKee et al. (1993), SPI values of less than zero are indicators of the presence of drought. SPI and probabilities of drought occurrence are commonly used in evaluating trends of rainfall over a long period (McKee et al., 1993; Agnew and Chappell, 1999; Agnew, 2000; Bewket and Conway, 2007; WMO, 2012; Viste et al., 2013). This is because using SPI has advantages in that other input parameter is not

http://www.aloki.hu ● ISSN 1589 1623 (Print) ● ISSN 1785 0037 (Online)
DOI: http://dx.doi.org/10.15666/aeer/1704_76937713

needed except precipitation, it can be compared for varied climatic zones and timescales, it gives drought early warning and helps to evaluate the severity of the drought, and it is less complex than the other indices (Agnew, 2000; WMO, 2012). In addition, in areas where data accessibility is limited, Viste et al. (2013) recommend using precipitation-based drought measurements. On the other hand, SPI has weaknesses in that it requires the data to be normally distributed and also its output is affected by the time of the base data period used (Agnew and Chappell, 1999; Agnew, 2000; Ali and Lebel, 2009; WMO, 2012). In addition, there exists a confusion on the definition of the term 'drought' as its impacts can be evaluated in terms of meteorological, climatological, hydrological, agricultural, ecological, and economic aspects (McKee et al., 1993; Agnew, 2000; Viste et al., 2013). However, meteorological drought is the main form of drought, and there is a consensus that drought occurs when rainfall is 'below average' (Agnew and Chappell, 1999).

For a moisture-deficient, semi-arid climate, and a rain-fed dependent agriculture like the one in CRV of Ethiopia, the time of the start of rainfall (onset), the time at which rainfall stop (cessation), and the length of the growing season are very important climatic phenomenon that affects not only the crop cultivation calendar, but also the final yield of production (Seleshi and Zanke, 2004; Segele and Lamb, 2005). Hence, such rainfall analysis has important applications in initiating weather-responsive farming for drought-prone areas like the Sahel and East Africa (Sivakumar, 1988, 1992). As seen from the result, out of the 36 years considered, *Kirmet* season rainfall in the study area started after the average time of onset for about 42% of the years, and it ceased ahead of the average time of a stop for about 56% of the years. This shortens the length of the growing season which directly affects crop productivity due to moisture deficiency in the soil before crop grain filling time. Studies show that there exists a significant relationship between the length of the growing season and the date of onset of rain (Sivakumar, 1988). Early onset of rain is usually followed by a prolonged growing season and vice versa. As pointed in Bekele et al. (2018b), during the discussion, farmers also blamed that late onsets and early cessations of rainfall are the main reasons for the reduction of their crop yield in recent decades.

The average ratio of rainy days to dry spells for the rainy season in the study area is about 1:3. This indicates that the number of dry spells is three times that of rainy days. The number of dry spells showed a generally increasing trend while the number of rainy days has experienced a generally decreasing trend since 1981 for both *Belg* and *Kirmet* seasons. On the other hand, the probability of dry spell occurrence was found to be less during *Kirmet* season than during *Belg* season. Previous studies also reported the presence of frequent drought in Ethiopia. For example, the years 1972-1975, 1980-1982, 1984, 1987, 1990-1992, 1999-2000, 2002-2003, and 2008-2011 were the periods of severe drought episodes while the years 1973/74, 1984/85, and 2009 were the nationally widespread and worst drought years in Ethiopia (Jury, 2010; Gebrehiwot et al., 2011; Viste et al., 2013). It is important to match the crop phenology with the dry-spell lengths to meet the crop water requirements in the semi-arid and arid regions where moisture is available for a relatively short period during the year (Sivakumar, 1992). Hence, for the choice of a particular crop or variety, such information on the length of dry spells for a given region could be used as a guide.

Similar to rainfall, the temperature (particularly of minimum temperature) has shown an inter-annual variability and a generally increasing trend in recent years. It is evident that an evapotranspiration rate will increase with an increase in temperature which, in

http://www.aloki.hu ● ISSN 1589 1623 (Print) ● ISSN 1785 0037 (Online)
DOI: http://dx.doi.org/10.15666/aeer/1704_76937713

turn, will contribute to crop productivity decline due to a shortage of available soil moisture in drought-prone areas. Studies in different parts of the country also reported a slight increase in temperature over recent decades (Rosell, 2011; Fazzini et al., 2015; Getachew and Tesfaye, 2015). Local communities and experts relate such an increase in diurnal temperature to massive losses in vegetation coverage of the region due to deforestation over the last decades (Bekele et al., 2018b). An increase in temperature could also be ascribed to global warming effect due to an accumulation of greenhouse gases from intensive agricultural production (Maharjan and Joshi, 2013).

This study finally considered how climate change vulnerability shapes farmers' historical land use. Climate change perception survey results indicated that the variability in climate, particularly the occurrence of recurrent drought, is one of the factors that force drought vulnerable farmers to modify/change their land use system through time. Previous studies also indicate that land use change in CRV is driven by the interaction of frequent drought, socioeconomic and institutional dynamics, and access to market and infrastructures (Biazin and Sterk, 2013; Bekele et al., 2018b). Such climate change-induced change in land use is taken as a means of adaptation strategy to overcome climate change and its impacts (Dale, 1997; Reid et al., 2000; Ahmed et al., 2016). Besides such permanent changes in land use, farmers also use other short-term climate change adaptation mechanisms like changing cropping time, changing crop variety, using off-farm income sources, and selling cattle to overcome critical drought years. Studies show that coupled with climatological changes, the degree of drought vulnerability is also affected by the type of land-uses and social contexts (Biazin and Sterk, 2013). For instance, Biazin and Sterk (2013) in their study found that the pastoral way of life was more vulnerable to severe drought than the mixed farming (livestock and crop combined) system. This indicates that due to drought vulnerability farmers try to shift from a land use system that is more vulnerable to drought (e.g., pastoralist) to a land use system that is less vulnerable (e.g., mixed farming) through time. Another study by Ahmed et al. (2016) in western Africa also confirmed that the increase in agricultural land use in the region was primarily climate-driven.

Conclusions

Rainfall and temperature data analysis are in common practice to describe climate change and variability. Such analysis not only helps to evaluate the variation exists along spatial and temporal scales but also to see its impacts on the agrarian community. In this study, descriptive statistical tools were used to show long-term inter-seasonal, inter-annual, and inter-site rainfall and temperature variations, and its impacts on land use change in a drought-prone CRV region of Ethiopia. Results indicated that there existed a high inter-seasonal and inter-annual rainfall and temperature variability over the last three decades. For example, total annual rainfall was below average for about 44% of the 36 years data period. Late-onset and early cessation of rainfall were observed for the majority of the database period. The number of rainy days generally showed a decreasing trend while the number of dry spells showed a generally increasing trend since 1981. Standardized Precipitation Index of the crop growing season also showed negative anomalies (i.e., less than average) for the majority of the study years considered. Extreme and severe drought years were also noted for both rainy seasons (*Belg* and *Kirmet*).

http://www.aloki.hu ● ISSN 1589 1623 (Print) ● ISSN 1785 0037 (Online)
DOI: http://dx.doi.org/10.15666/aeer/1704_76937713

In line with meteorological evidence for drought, vulnerable farmers in the study area well perceived such recurrent drought occurrence over the last three decades and they blamed the change in climate as one of the important forcing factors to change their land use system through time. Majority of the farmers who had been pastoralists/agropastoralists before three decades are currently already changed their land use system to mixed farming, and the rest also have a wish to change in the future. In general, it is evident that climate change plays a significant role in driving historical land use change in drought-prone areas like East Africa. Hence, future policies need to consider strategies that strengthen the adaptation capacity of farmers to overcome drought impact while combating anthropogenic activities that aggravate climate change, for instance, land degradation, in Sub-Saharan countries.

It is believed that for a climate change-prone and rain-fed dependent agriculture, like in East Africa, up-to-date local climatic trend information is quite crucial to practice climate-responsive agricultural management activities like cultivation, water management, health management, and to reduce drought-induced catastrophes. However, this study might have limitations in that we used data from limited meteorological stations and hence future studies better incorporate data from the wider stations in CRV lakes basin. In addition, missing data observed in each station might affect the accuracy of the results to some extent and hence a cross-comparison of the results with reference data elsewhere, for example, World Climate Research Program Global Precipitation Climatology Center (GPCC) might be important. The role of climate change vulnerability in governing land use change also need further detail study. Future studies also need to address the adaptation strategies of farmers to overcome climate change, and the barriers hinder the success of such efforts.

Acknowledgements. The authors are indebted to thank the National Natural Sciences Foundation of China [Grant No. 41571176] and Sino-Africa Cooperation and Exchange Special Program [Fund No. 2018-AF-22) for financial support in conducting this study. We are grateful to thank the Chinese Government Scholarship Council (CSC) for giving the first author a chance to pursue his Ph.D. study in China. Special thanks also go to the Ethiopian National Meteorological Agency (NMA) for providing rainfall and temperature data and all the rural farmers of the three Districts: Dugda, Adami Tulu-Jido Kombolcha, and Arsi Negele, who took part during the field survey. The anonymous referees and editor are thankful for their valuable comments on the initial version of this manuscript.

REFERENCES

[1] Adimassu, Z., Kessler, A., Stroosnijder, L. (2014): Farmers′ strategies to perceived trends of rainfall and crop productivity in the Central Rift Valley of Ethiopia. – Environmental Development 11: 123-140.
[2] Agnew, C. (2000): Using the SPI to identify drought. – Drought Network News (1994-2001). Paper 1.
[3] Agnew, C., Chappell, A. (1999): Drought in the Sahel. – GeoJournal 48(4): 299-311.
[4] Ahmed, K. F., Wang, G., You, L., Yu, M. (2016): Potential impact of climate and socioeconomic changes on future agricultural land use in West Africa. – Earth System Dynamics 7(1): 151-165.
[5] Ali, A., Lebel, T. (2009): The Sahelian standardized rainfall index revisited. – International Journal of Climatology 29(12): 1705-1714.

http://www.aloki.hu ● ISSN 1589 1623 (Print) ● ISSN 1785 0037 (Online)
DOI: http://dx.doi.org/10.15666/aeer/1704_76937713

[6] Ariti, A. T., van Vliet, J., Verburg, P. H. (2015): Land-use and land-cover changes in the Central Rift Valley of Ethiopia: Assessment of perception and adaptation of stakeholders. – Applied Geography 65: 28-37.
[7] Barron, J., Rockström, J., Gichuki, F., Hatibu, N. (2003): Dry spell analysis and maize yields for two semi-arid locations in east Africa. – Agricultural and Forest Meteorology 117(1-2): 23-37.
[8] Bekele, B., Wu, W., Legesse, A., Temesgen, H., Yirsaw, E. (2018a): Random and Systematic Land Use/Land Cover Transitions in Semi-arid Landscapes of Ethiopian Central Rift Valley Lakes Region (East Africa). – Applied Ecology and Environmental Research 16(4): 3993-4014.
[9] Bekele, B., Wu, W., Legesse, A., Temesgen, H., Yirsaw, E. (2018b): Socio-environmental impacts of land use/cover change in Ethiopian Central Rift Valley lakes region, East Africa. – Applied Ecology and Environmental Research 16(5): 6607-6632.
[10] Bewket, W., Conway, D. (2007): A note on the temporal and spatial variability of rainfall in the drought-prone Amhara region of Ethiopia. – International Journal of Climatology 27(11): 1467-1477.
[11] Biazin, B., Sterk, G. (2013): Drought vulnerability drives land-use and land cover changes in the Rift Valley dry lands of Ethiopia. – Agr Ecosyst Environ 164: 100-113.
[12] Cheung, W. H., Senay, G. B., Singh, A. (2008): Trends and spatial distribution of annual and seasonal rainfall in Ethiopia. – International Journal of Climatology 28(13): 1723-1734.
[13] Collier, P., Conway, G., Venables, T. (2008): Climate change and Africa. – Oxford Review of Economic Policy 24(2): 337-353.
[14] Conway, D. (2000): Some aspects of climate variability in the north east Ethiopian Highlands-Wollo and Tigray. – Sinet: Ethiopian Journal of Science 23(2): 139-161.
[15] Conway, D., Mould, C., Bewket, W. (2004): Over one century of rainfall and temperature observations in Addis Ababa, Ethiopia. – International Journal of Climatology: A Journal of the Royal Meteorological Society 24(1): 77-91.
[16] CSA (1994): The 1994 population and housing census results for Oromiya Region. – Central Statistical Agency, Addis Ababa, Ethiopia.
[17] CSA (2007): The 2007 population and housing census results for Oromiya Region. – Central Statistical Agency, Addis Ababa, Ethiopia.
[18] Dale, V. H. (1997): The relationship between land-use change and climate change. – Ecol App 7(3): 753-769.
[19] Eckstein, D., Künzel, V., Schäfer, L. (2017): Global climate risk index 2018. – Germanwatch eV: Bonn, Germany.
[20] Fazzini, M., Bisci, C., Billi, P. (2015): The climate of Ethiopia. – In: Billi, P. (ed.) Landscapes and Landforms of Ethiopia. Springer, Dordrecht, pp 65-87.
[21] Fekadu, K. (2015): Ethiopian seasonal rainfall variability and prediction using canonical correlation analysis (CCA). – Earth Sciences 4(3): 112.
[22] Garedew, E., Sandewall, M., Soderberg, U., Campbell, B. M. (2009): Land-use and land-cover dynamics in the central rift valley of Ethiopia. – Environ Manage 44(4): 683-694.
[23] Gebrehiwot, T., van der Veen, A., Maathuis, B. (2011): Spatial and temporal assessment of drought in the Northern highlands of Ethiopia. – Theoretical and Applied Climatology 13(3): 309-321.
[24] Gemeda, D. O., Sima, A. D. (2015): The impacts of climate change on African continent and the way forward. – Journal of Ecology and the Natural environment 7(10): 256-262.
[25] Getachew, H., Tesfaye, K. (2015): Analysis of risks in crop production due to climate change in the Central Rift Valley of Ethiopia. – African Journal of Agricultural Research 10(16): 1913-1922.
[26] Getnet, M., Hengsdijk, H., van Ittersum, M. (2014): Disentangling the impacts of climate change, land use change and irrigation on the Central Rift Valley water system of Ethiopia. – Agricultural Water Management 137: 104-115.

http://www.aloki.hu ● ISSN 1589 1623 (Print) ● ISSN 1785 0037 (Online)
DOI: http://dx.doi.org/10.15666/aeer/1704_76937713

[27] Gizachew, L., Shimelis, A. (2014): Analysis and mapping of climate change risk and vulnerability in Central Rift Valley of Ethiopia. – African Crop Science Journal 22: 807-818.
[28] Hare, F. (1983): Climate and Desertification: a revised analysis. – World Climate Program, report, Geneva, Switzerland.
[29] Hengsdijk, H., Jansen, H. (2006): Agricultural development in the Central Ethiopian Rift valley: A desk-study on water-related issues and knowledge to support a policy dialogue. – Note 375. Plant Research International BV., Wageningen.
[30] IPCC (2007): Climate change 2007: impacts, adaptation, and vulnerability. – Contribution of working group II to the fourth assessment report of the intergovernmental panel on climate change. Cambridge University Press, Cambridge.
[31] IPCC (2014): Climate Change 2014 Synthesis Report Summary for Policymakers. – Contribution of working group to the fifth assessment report of the intergovernmental panel on climate change. Cambridge University Press, Cambridge.
[32] Jansen, H., Hengsdijk, H., Legesse, D., Ayenew, T., Hellegers, P., Spliethoff, P. (2007): Land and water resources assessment in the Ethiopian Central Rift Valley. – Project: Ecosystems for water, food and economic development in the Ethiopian Central Rift Valley, Alterra-rapport 1587. Wageningen, Alterra.
[33] Jury, M. R. (2010): Ethiopian decadal climate variability. – Theoretical and Applied Climatology 101(1-2): 29-40.
[34] Kassie, B. T., Hengsdijk, H., Rotter, R., Kahiluoto, H., Asseng, S., Van Ittersum, M. (2013): Adapting to climate variability and change: experiences from cereal-based farming in the central rift and Kobo Valleys, Ethiopia. – Environ Manage 52(5): 1115-1131.
[35] Maharjan, K. L., Joshi, N. P. (2013): Climate change, agriculture and rural livelihoods in developing countries. – Springer, Japan.
[36] McKee, T. B., Doesken, N. J., Kleist, J. (1993): The relationship of drought frequency and duration to time scales. – In: Proceedings of the 8th Conference on Applied Climatology, vol 22. American Meteorological Society Boston, MA, pp 179-183.
[37] Melka, Y., Kassa, H., Ketema, M., Abebaw, D., Schmiedel, U. (2015): The effect of drought risk perception on local people coping decisions in the Central Rift Valley of Ethiopia. – J Dev Agric Econ 7(9): 292-302.
[38] Meshesha, D. T., Tsunekawa, A., Tsubo, M. (2012): Continuing land degradation: cause–effect in Ethiopia's Central Rift Valley. – Land Degrad Dev 23(2): 130-143.
[39] Mideksa, T. K. (2010): Economic and distributional impacts of climate change: The case of Ethiopia. – Global Environmental Change 20: 278-286.
[40] Muluneh, A., Bewket, W., Keesstra, S., Stroosnijder, L. (2017): Searching for evidence of changes in extreme rainfall indices in the Central Rift Valley of Ethiopia. – Theoretical and Applied Climatology 128(3-4): 795-809.
[41] NMA (2001): Report submitted to initial national communication of Ethiopia to the United Nations Framework Convention on Climate Change. – National Meteorological Services Agency, Addis Ababa, Ethiopia.
[42] Oliver, J. E. (1980): Monthly precipitation distribution: a comparative index. – The Professional Geographer 32(3): 300-309.
[43] Pedrono, M., Locatelli, B., Ezzine-de-Blas, D., Pesche, D., Morand, S., Binot, A. (2016): Impact of climate change on ecosystem services. – In: Torquebiau, E. (ed.) Climate Change and Agriculture Worldwide. Springer, London pp 251-261.
[44] Ravindranath, N. H., Sathaye, J. A. (2002): Climate Change and Developing Countries. – Kluwer Academic Publishers, Dordrecht, The Nitherlands.
[45] Reid, R. S., Kruska, R. L., Muthui, N., Taye, A., Wotton, S., Wilson, C. J., Mulatu, W. (2000): Land-use and land-cover dynamics in response to changes in climatic, biological and socio-political forces: the case of southwestern Ethiopia. – Landscape Ecol 15(4): 339-355.

http://www.aloki.hu ● ISSN 1589 1623 (Print) ● ISSN 1785 0037 (Online)
DOI: http://dx.doi.org/10.15666/aeer/1704_76937713

[46] Rosell, S. (2011): Regional perspective on rainfall change and variability in the central highlands of Ethiopia, 1978–2007. – Applied Geography 31(1): 329-338.
[47] Segele, Z. T., Lamb, P. J. (2005): Characterization and variability of Kiremt rainy season over Ethiopia. – Meteorology and Atmospheric Physics 89(1-4): 153-180.
[48] Seleshi, Y., Zanke, U. (2004): Recent changes in rainfall and rainy days in Ethiopia. – International journal of climatology 24(8): 973-983.
[49] Serdeczny, O., Adams, S., Baarsch, F., Coumou, D., Robinson, A., Hare, W., Schaeffer, M., Perrette, M., Reinhardt, J. (2017): Climate change impacts in Sub-Saharan Africa: from physical changes to their social repercussions. – Regional Environmental Change 17(6): 1585-1600.
[50] Simane, B., Struik, P. (1993): Agroclimatic analysis: a tool for planning sustainable durum wheat (Triticum turgidum var. durum) production in Ethiopia. – Agriculture, Ecosystems & Environment 47(1): 31-46.
[51] Sivakumar, M. (1988): Predicting rainy season potential from the onset of rains in Southern Sahelian and Sudanian climatic zones of West Africa. – Agricultural and Forest Meteorology 42(4): 295-305.
[52] Sivakumar, M. (1992): Empirical analysis of dry spells for agricultural applications in West Africa. – Journal of Climate 5(5): 532-539.
[53] Stern, R., Rijks, D., Dale, I., Knock, J. (2006): INSTAT climatic guide. – University of Reading.
[54] Temesgen, H., Nyssen, J., Zenebe, A., Haregeweyn, N., Kindu, M., Lemenih, M., Haile, M. (2013): Ecological succession and land use changes in a lake retreat area (Main Ethiopian Rift Valley). – J Arid Environ 91: 53-60.
[55] Tesfaye, K., Walker, S. (2004): Matching of crop and environment for optimal water use: the case of Ethiopia. – Physics and Chemistry of the Earth, Parts A/B/C 29(15-18): 1061-1067.
[56] Torquebiau, E., Tissier, J., Grosclaude, J.-Y. (2016): How climate change reshuffles the cards for agriculture. – In: Torquebiau, E. (ed.) Climate Change and Agriculture Worldwide. Springer, pp 1-16.
[57] UNFCCC (2007): Climate change: Impacts, vulnerabilities and adaptation in developing countries. – United Nations Framework Convention on Climate Change.
[58] UNFCCC (2018): UN Climate Change Annual Report 2017. – United Nations Framework Convention on Climate Change. Bonn.
[59] Viste, E., Korecha, D., Sorteberg, A. (2013): Recent drought and precipitation tendencies in Ethiopia. – Theoretical and Applied Climatology 112(3-4): 535-551.
[60] Wagesho, N., Goel, N., Jain, M. (2012): Investigation of non-stationarity in hydro-climatic variables at Rift Valley lakes basin of Ethiopia. – Journal of Hydrology 444: 113-133.
[61] WMO (2012): Standardized precipitation index user guide. – United Nations Geneva, Switzerland.

http://www.aloki.hu ● ISSN 1589 1623 (Print) ● ISSN 1785 0037 (Online)
DOI: http://dx.doi.org/10.15666/aeer/1704_76937713

FEEDING EVALUATION OF MICROCRUSTACEA (CLADOCERA): RESPONSES TO VARIATIONS IN CELL VOLUME OF GREEN AND BLUE-GREEN ALGAE

ISMAIL, A. H.[1*] – MILLS, S.[2] – RECKNAGEL, F.[2]

[1]*School of Biological Sciences, Universiti Sains Malaysia, Penang, Malaysia*

[2]*School of Biological Sciences, University of Adelaide, Adelaide, Australia*

[*]*Corresponding author*
e-mail: azmahanim@usm.my; phone: +604-653 6170; fax: +604-656 5125

(Received 12th Mar 2019; accepted 1st May 2019)

Abstract. The grazing rate of three zooplankton species; *Daphnia carinata*, *D. lumholtzi* and *Ceriodaphnia* cf. *quadrangula* on six algal species at three concentrations are described in this paper. The effect of food density on ingestion rate was assessed by adding a suspension of algae to the tumblers and following the changes in concentration in the tumbler as the cladocerans consumed the suspension. Samples were taken and algal densities were measured every 15 minutes with a spectrophotometer. This study aimed to examine the role of cladoceran as grazers of algae under laboratory conditions. *D. carinata* removed algal cells at higher rates than the other two species when feeding in unialgal suspension. Quantitative differences in rate of food intake were found in suspensions of *Ankistrodesmus falcatus*, *Scenedesmus obliquus*, *Chlorella vulgaris*, *Chlamydomonas reinhardtii*, *Anabaena circinalis* and *Microcystis flos-aquae*. The small cells contributed by far the greatest fragment of green algae ingested by grazers. Filamentous *A. circinalis* and colonial *M. flos-aquae* can also be utilized by the grazers though the species was previously reported to have lethal toxic effects on cladocerans. Therefore, a management strategy using cladocerans for controlling undesirable cyanobacteria in aquatic ecosystem is contemplated to be necessary in the future.
Keywords: *grazing, zooplankton, Daphnia, Ceriodaphnia, ingestion rate*

Introduction

Zooplankton grazing is currently facing a crucial phase as the changes in the grazer population translate into changes in ecosystem properties, particularly in the phytoplankton biomass (Horn, 1981; Elser, 1992). Thus, it has attracted a lot of attention among scientists and has inspired them to conduct more research and experimental investigations into the plankton ecology. Measuring feeding rates of herbivorous zooplankton is important in order to understand the interaction between phytoplankton and zooplankton. Even though zooplankton grazing has been studied in laboratories worldwide, in Australia, little information is available on the subject. Zooplankton grazing directly affects the phytoplankton structure and changes the algal growth rates (Lampert et al., 1986). Algal losses in the aquatic ecosystems are caused by many factors such as grazing, sinking, parasitism, and nutrient levels (Tilman et al., 1982; Finkel et al., 2010). However, this paper focuses on zooplankton grazing through measurements in the laboratory as this approach has been known to be the best to estimate the increase and decrease of the algal population. The most important advantage of the laboratory method is the food type, food concentration quality and densities of grazers can all be defined by the researcher. Comprehensive laboratory determination of cladocerans feeding rates is essential to define the role of these important grazers in the freshwater ecosystems.

http://www.aloki.hu ● ISSN 1589 1623 (Print) ● ISSN 1785 0037 (Online)
DOI: http://dx.doi.org/10.15666/aeer/1704_77157725

Food uptake of suspension feeders can usually be described by the ingestion rate (IR). Ingestion rate or feeding rate is expressed as the amount, number or biomass of food cells consumed by an animal in a time interval (Wirtz, 2013). Zooplankton ingestion rate increases with food concentration. It increases up to about 100,000 cells mL^{-1} after which, a plateau will be reached; body length will increase and the body temperature will rise up to 20°C (Burns and Rigler, 1967).

In terms of food, zooplankton require high quality food with appropriate size range, to allow them to grow healthily in their ecosystem. Therefore, food size is an important factor related to cladoceran feeding. Nonetheless, not all phytoplankton cells are suitable for ingestion. Often, they refuse to feed on algae that are inedible, toxic and are in the form colonies or filaments. Furthermore, the biochemical composition, the cell wall thickness and the digestibility of algae may affect the growth and the species composition of cladoceran. Several studies have shown that different species of cladoceran have different preferences in terms of food (Bogdan and Gilbert, 1984; Knisely and Geller, 1986). Consequently, food size preferences affect their body size (Urabe et al., 1996).

In general, this study aimed to examine the role of cladoceran as grazers of algae under laboratory conditions. More specifically, it was the aim of the study:

- To determine the grazing rates of three different species of cladoceran and density of unialgal populations;
- To determine if cladocerans' algal grazing is size selective;
- To compare the feeding preferences of cladocerans between green and blue green algae.

Materials and Methods

Two medium cultures have been used in this study; AlgaBoost f/2 from AusAqua Pty. Ltd. as green algae medium culture and BG - 11 based on Rippka et al. (1979) for blue-green algae culture. Algae collection was obtained from cultures maintained by the SAW and Commonwealth Scientific & Industrial Research Organisation (CSIRO). Six species of algae were used in the grazing experiments, namely *Ankistrodesmus falcatus*, *Chlamydomonas reinhardtii*, *Scenedesmus obliquus*, *Chlorella vulgaris*, *Anabaena circinalis* and *Microcystis flos-aquae*. Algae were cultured by the method described by Hoff and Snell (1987) and Kilham et al. (1998).

Cell biovolume is the most common approach used to estimate biomass of phytoplankton. The calculation of biovolume was based on geometric approximation, calculated from microscopically measured linear dimensions (Hillebrand and Sommer, 1996). Altogether, 360 cells from each species were measured and the cell sizes were grouped into various size classes. Then, the median of measured linear dimensions of the biovolume were calculated as proposed by Hillebrand et al. (1999), not as a median or mean value of a set of individually calculated biovolumes. In this experiment, the value was expressed in cell volume, rather than cell concentration as the unit will standardize the different sizes of algae.

Wild *Daphnia carinata*, *D. lumholtzi* and *Ceriodaphnia* cf. *quadrangula* were collected from Myponga and South Para Reservoirs and reared or cloned over at least 30 generations in the laboratory. Cladocerans collected from the wild were placed in Petri dishes under a dissecting microscope for sorting. Each organism was separated using T-pipette and transferred into six well plates containing filtered lake water. The

http://www.aloki.hu ● ISSN 1589 1623 (Print) ● ISSN 1785 0037 (Online)
DOI: http://dx.doi.org/10.15666/aeer/1704_77157725

entire set up was placed in a lighted cabinet at 20°C and light regime for 10:14 hr light and dark. To maintain the uniformity of algal cells, the plates were gently agitated by hand twice a day. The plates were incubated in a lighted cabinet at approximately 1000 – 1500 lux and checked daily for clonal neonates. At least five individuals were present in the cell, the population was then transferred into a 50 mL falcon tube filled with filtered water and algae culture using a 10 µL pipette. Cultures in falcon tubes were incubated at the same temperature and light regime as indicated above. Cultures were then replenished once a week by removing 25 mL of media and adding 25 mL of 1:1 filtered lake water and algae. Once the culture was established, it was transferred to approximately 6 L aquarium containing lake water (*Fig.1*). The zooplankton were fed with a mixed culture of algae (*Ankistrodesmus falcatus*, *Scenedesmus obliquus* and *Chlorella vulgaris*) every two days (*Fig. 2*).

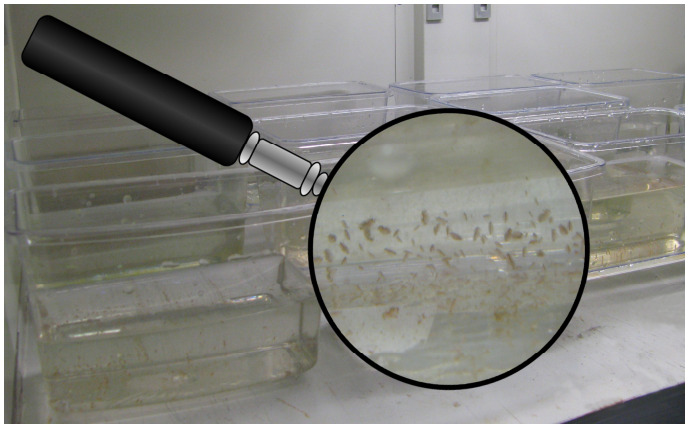

Figure 1. *Zooplankton culture*

Figure 2. *Algae culture*

In the grazing experiments, individuals with the largest adult length (*Daphnia carinata*, 3.4 – 3.8 mm; *D. lumholtzi*, 1.2 – 1.3 mm; and *Ceriodaphnia* cf. *quadrangula*, 0.65 – 0.75 mm) were used. The animals were acclimatized to the experimental temperature of 20°C for 24 hours before experiments in 50 mL of filtered lake water. Then, five adults were transferred to the 50 mL tumbler filled with filtered

http://www.aloki.hu ● ISSN 1589 1623 (Print) ● ISSN 1785 0037 (Online)
DOI: http://dx.doi.org/10.15666/aeer/1704_77157725

lake water (*Fig. 3*), enriched with an appropriate suspension of algae (Ismail et al., 2015). Five tumblers without animals served as the control sample. The experiments were run for two hours in a temperature-controlled cabinet at 20°C in the laboratory at 980 – 1045 lux.

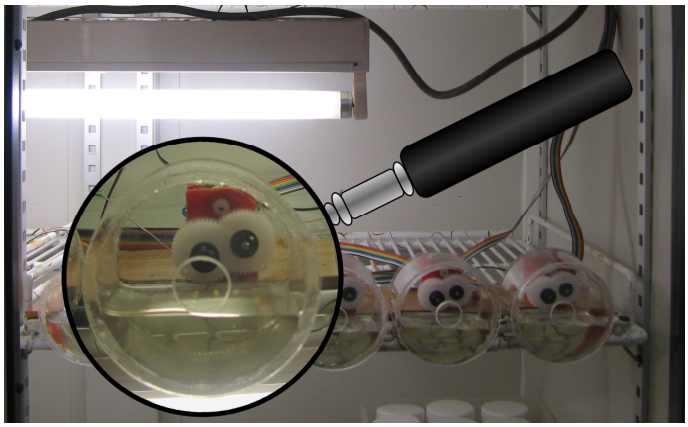

Figure 3. *Rotating tumblers filled with filtered lake water, enriched with an appropriate suspension of algae*

The effect of food density on ingestion rate was assessed by adding a suspension of algae to the tumblers following the changes in concentration in the tumbler as the cladocerans grazed the suspension down. Ingestion rate of cladocerans were measured every 15 min. All counts were made in five replicates using a spectrophotometer (Model 340). The instrument was adjusted to the desired wavelength such as 470 nm for green algae and 645 nm for cyanobacteria. Ingestion rate was calculated according to the formula in Frost (1972). There were three different cell concentrations at which ingestion rate was measured. Each concentration was replicated five times. The initial concentration of algae was the same for all species used which were 1.5 x 10^6 μm^3/mL, 3.0 x 10^6 μm^3/mL and 4.5 x 10^6 μm^3/mL. The tumblers were rotated at 1.5 rpm throughout the 2-hr experiment to minimize the sedimentation of algae. The ingestion rate was analysed using 3-way ANOVA to test the effects of the three cladocerans species, three food types and three concentrations for the eight time intervals. Significant differences among groups were tested using Tukey HSD test.

Results

The results of the grazing experiments on unialgal suspension were graphically presented in *Figures 4 and 5*, which show experiments from three different cell volumes on six algal species. All three species of Cladocera had a significant effect on the ingestion rate ($p < 0.05$), while all food concentrations showed a significant difference ($p < 0.05$), except at food volume of 3.0 x 10^6 μm^3/mL and 4.5 x 10^6 μm^3/mL ($p > 0.05$). The results displayed large fluctuating patterns for *A. falcatus* (*Fig. 1*), *C. vulgaris* (*Fig. 4*) and *M. flos-aquae* (*Fig. 5*), while small fluctuating trends occurred on *S. obliquus* (*Fig. 4*) and *C. reinhardtii* (*Fig. 5*). On the contrary, Cladocera grazing on *A. circinalis* showed low and almost constant trend throughout the experiment, which means that the rate was small compared with those of the other species of algae

http://www.aloki.hu ● ISSN 1589 1623 (Print) ● ISSN 1785 0037 (Online)
DOI: http://dx.doi.org/10.15666/aeer/1704_77157725

(*Fig. 5*). The results of the 3-way ANOVA did not show any significant difference in the Cladocera, algae and concentration ($p > 0.05$) (*Table 1*). Based on the fact that at $p < 0.05$, the ingestion rate of algal species varied significantly between the algal concentrations for the eight time intervals.

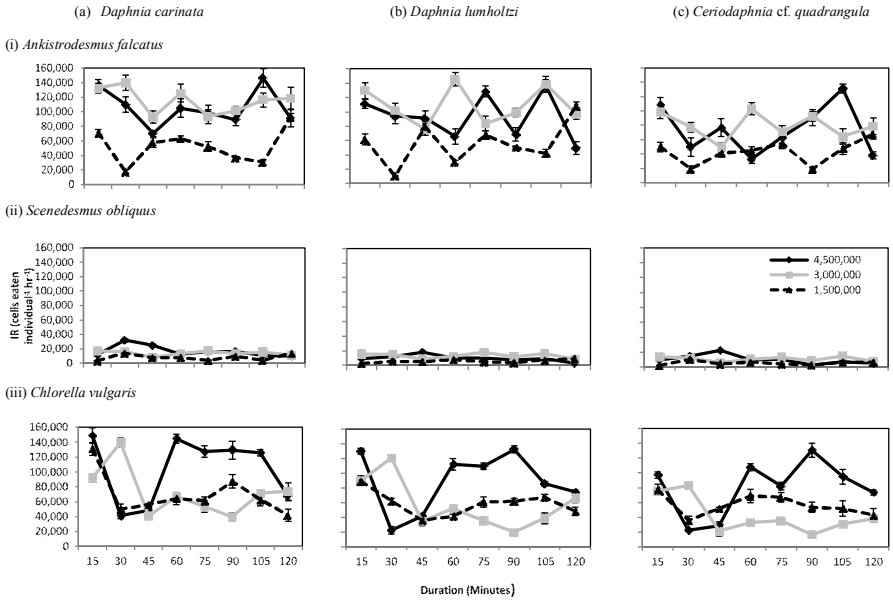

Figure 4. *Ingestion rates of (a) Daphnia carinata, (b) D. lumholtzi and (c) Ceriodaphnia cf. quadrangula in the presence of (i) Ankistrodesmus falcatus, (ii) Scenedesmus obliquus and (iii) Chlorella vulgaris at three volume concentration, calculated for the duration of 15 minutes intervals (0 - 2 hours). Error bars represent the standard error for five experimental replicates*

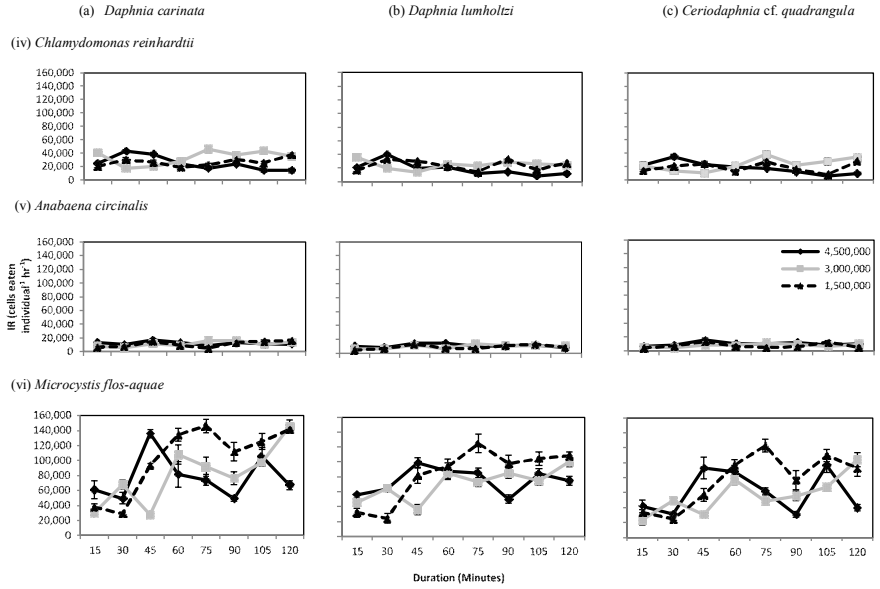

Figure 5. *Ingestion rates of (a) Daphnia carinata, (b) D. lumholtzi and (c) Ceriodaphnia cf. quadrangula in the presence of (iv) Chlamydomonas reinhardtii, (v) Anabaena circinalis and (vi) Microcystis flos-aquae at three volume concentration, calculated for the duration of 15 minutes intervals (0 - 2 hours). Error bars represent the standard error for five experimental replicat*

http://www.aloki.hu ● ISSN 1589 1623 (Print) ● ISSN 1785 0037 (Online)
DOI: http://dx.doi.org/10.15666/aeer/1704_77157725

Table 1. *Results of an ANOVA performed on ingestion rates by time interval*

Source of variation	SS	d.f	MS	F	P
Zooplankton	8.404	2	4.202	68.282	0.000*
Algae	323.257	5	64.651	1050.545	0.000*
Concentration	5.770	2	2.885	46.882	0.000*
Duration	1.395	7	0.199	3.239	0.002*
Zooplankton x Algae	0.699	10	0.070	1.136	0.331
Zooplankton x Concentration	0.053	4	0.013	0.214	0.931
Zooplankton x Duration	0.863	14	0.062	1.002	0.448
Algae x Concentration	15.551	10	1.555	25.269	0.000*
Algae x Duration	20.874	35	0.596	9.691	0.000*
Concentration x Duration	9.694	14	0.692	11.251	0.000*
Zooplankton x Algae x Concentration	1.554	20	0.078	1.262	0.194
Zooplankton x Algae x Duration	4.714	70	0.067	1.094	0.280
Zooplankton x Concentration x Duration	1.372	28	0.049	0.796	0.767
Algae x Concentration x Duration	30.152	70	0.431	6.999	0.000*

* $P<0.05$

Discussion

This paper focused on the outcomes of grazing rates of three cladocerans species in six single species of algae. The selection of zooplankton and algal species was based on the most common species found in Myponga and South Para Reservoirs. The mean body size of adult animals cultured in the laboratory was larger than those of the ones collected from the reservoirs, probably due to biotic factors such as predation, competition, and disease. To gain the maximum grazing rate, adult size was chosen for the experiments as representatives of all the body sizes present in the culture tanks.

In terms of quality, the six species of algae used were divided into two categories. The first one consisted of *A. falcatus*, *S. obliquus*, *C. vulgaris* and *C. reinhardtii*; all of them are edible algae. The other category included *M. flos-aquae* and *A. circinalis*, which are potentially toxic blue-green algae that require the cells to break away from the colony and filament before ingestion. In fact, cultured *M. flos-aquae* grew in smaller colonies than in their natural habitat. This observation corroborates that of Benndorf and Egerer (1981), which say that *Microcystis* change cell size and/or colony size in the culture. However, results obtained from the experiments may not be representative of their grazing behaviour in their natural environment.

In this experiment, 2-hr incubation periods for all zooplankton species were chosen. This was based on the pilot study, which showed that the zooplankton started to produce offsprings after two hours of incubation. Thus, it would not be relevant to measure feeding rates over longer periods because they might result in measurement bias. Moreover, within a 2-hr period, the animals' guts were believed to be full, thus they would produce faecal while they are simultaneously feeding. Further work on *D. magna* by Lotocka (2001) revealed that the intestines of adult individuals fed with mixture of *S. microspina* and *C. kessleri* were completely filled with food within 45 min while 50% of their guts would be full when exposed to *Aphanizomenon flos-aquae* after 30 min. Although the duration of this experiment was considered shorter than the findings in past literatures, the results are believed to be sufficiently accurate to determine the feeding rate of zooplankton on the selected foods. Even though in

http://www.aloki.hu ● ISSN 1589 1623 (Print) ● ISSN 1785 0037 (Online)
DOI: http://dx.doi.org/10.15666/aeer/1704_77157725

previous literatures various grazing methods have been applied, this study chose to measure them via spectrophotometer, as this is the common method to measure cell density. Moreover, the method is simple, quick and yields reliable results. However, the accuracy of the results can be improved by using more replicates of samples, cautiously.

In this study, zooplankton ingested at large amount of food at the beginning of the experiment. Indeed, a higher ingestion rate was expected at the first part of the time interval due to the 24-hr starvation period before the incubation. Acclimatization time was set for 24 hr prior to carrying out the grazing experiment, as some cladocerans would die when starved for more than 24 hr. Subsequently, all the starved animals were exposed to a single alga species in different concentrations. Apparently, the animals tested fed at reduced rate at low concentrations, but fed at their maximum rates when exposed to the high concentrations of algae. Ingestion rate was dependent on the density of food until a certain critical concentration, after which the ingestion rate became constant. Previous literatures supported this general pattern (Rothhaupt, 1990; Navarro, 1999). The results of ingestion rate for six species of algae at three cell concentrations affirmed the model by McMahon and Rigler (1965) and agreed with the ILL value obtained by Kersting and Leeuw (1976). Although the observations of algal concentrations may not be sufficient to establish this result absolutely, the result was reliable and able to show how the feeding behaviours changed in different cell concentrations.

D. carinata ingestion rate was higher than that of *D. lumholtzi* and *C.* cf. *quadrangula* for both blue-green algae *M. flos-aquae* and *A. circinalis*. However, the ingestion rates were significantly lower in *A. circinalis* filamants, compared with *M. flos-aquae*. This may be due to the ability of the grazers to break the small colonies of *M. flos-aquae*, making them easier to graze compared with 50 – 100 μm of *A. circinalis* filaments during ingestion. Some scientists (Geller and Muller, 1981; Gliwicz and Lampert, 1990) pointed out that it could possibly be due to the size restrictions and rejection, while Infante and Litt (1985) and Hartmann and Kunkel (1991) concluded that the reasons were excessive handling time and poor interception of filaments when compared with non-filamentous algae. Further evidence from observations by Kirk and Gilbert (1992) showed that the presence of *Anabaena* filaments causes an increase in post-abdominal rejections in the large *Daphnia pulex*. Therefore, the findings of the present study are in accord with those of previous studies that reported lower grazing rates of *A. circinalis*.

On the other hand, in this study, *C.* cf. *quadrangula* ingested at the lowest rate when exposed to the single *A. circinalis* suspension, and followed by *D. lumholtzi*. Thus, clearly the ingestion rate decreased with increasing body size. This has been confirmed by investigations that indicated that small cladocerans are more able to avoid *Anabaena* cells than larger cladocerans, probably due to their smaller size, which forbids them to ingest the large *Anabaena* filaments (Kirk and Gilbert, 1992).

Even though the algae were potentially toxic species, the observation on ingestion rate in unialgal suspension of *M. flos-aquae* showed that the three species of Cladocera ingested the potentially toxic form of algal colony (Ismail et al., 2015). Many studies (Fulton, 1988; DeBernardi and Giussani, 1990; Kirk and Gilbert, 1992; Repka, 1996; Kurmayer and Juttner, 1999) have shown subtle toxic effect on fecundity and survival rate of zooplankton fed on cyanobacteria. However, the consequences were not considered in the short-term experiments. Some authors demonstrated that food size affects the differences in the ability of zooplankton to graze on algal species (Persson,

http://www.aloki.hu ● ISSN 1589 1623 (Print) ● ISSN 1785 0037 (Online)
DOI: http://dx.doi.org/10.15666/aeer/1704_77157725

1985; Borsheim and Andersen, 1987; Urabe et al., 1996). Ingestion rates of *A. falcatus* (2.3 µm), *C. vulgaris* (3.3 µm) and *M. flos-aquae* (1.9 µm) by the three species of Cladocera were confirmed to be faster than those of *S. obliquus* (4.2 µm), *C. reinhardtii* (4.4 µm) and *A. circinalis* (5.8 µm). Undoubtedly, the three species of Cladocera preferred to graze on smaller sized cells. The cell size of *S. obliquus*, *C. reinhardtii* and *A. circinalis* might be too large for ingestion or to pass through their mouth gapes. According to Gliwicz (1980), the uptake of large particles by zooplankton is limited by the opening width of carapace gap.

Under laboratory conditions, *M. flos-aquae* grow in smaller colonies than in their natural ecosystems. Moreover, the suspension has been dispersed with strong shaking before the experiments to obtain the maximum ingestion rate. Apparently, the grazers can handle small colonies of *M. flos-aquae* efficiently compared with the filamentous form of *A. circinalis*. Possibly the cells of *M. flos-aquae* are more easily separated and ingested than the filamentous form of *A. circinalis*.

Despite the factor of particle size, differences in the grazability of algal species might be due to several other factors which can be considered, such as cell wall characteristic (Horn, 1981), flagella (DeMott, 1982), spines (Schnack, 1979), gelatinous sheath (McNaught et al., 1980), taste (Poulett and Marsot, 1978) and digestion (Porter, 1976). Knisely and Geller (1986) pointed out that smooth-walled species such as *Chlorella* would be possibly swept away after they are first captured. On the other hand, *A. circinalis* is a poor food for zooplankton due to the toxic strain that might affect the growth and the reproduction of Cladocera.

Furthermore, the results of this present study showed that ingestion rate varies with body size. The result is in agreement with those of other studies, which supported the size-efficiency hypothesis described by Brooks and Dodson (1965) which says that larger zooplankton body sizes provide a greater filtering capacity. The largest animal tested, *D. carinata* ingested at the highest rate among all algal species compared with the intermediate-sized *D. lumholtzi* and the small-sized species of *C.* cf. *quadrangula*. This outcome agrees with the results obtained by Geller and Muller (1981) who indicated that smaller sized grazers may have smaller carapace gaps and mesh sizes.

As observed in the experimental results, feeding behaviour of zooplankton depends on several factors when they are offered as food, algae as a single diet in terms of size, structure, quality and concentration as food. Besides, differences in body size certainly influence grazing efficiency between zooplankton species. Therefore, a combination of these factors may increase or decrease grazability despite the abiotic factors during the experiment.

Conclusion

The ingestion rate varies depending on the cladocerans' body size and species. In terms of feeding efficiency, larger cladocerans can ingest larger food items than smaller species. Algal size and concentration are major factors affecting the ingestion rate of cladocerans. Different sized algae were grazed at different efficiencies. Feeding on small and large particles appears to be qualitatively different. *D. carinata* ingested the largest food items most efficiently followed by *D. lumholtzi* and *C.* cf. *quadrangula*. The success of *D. carinata* may be explained partly by its ability to feed effectively on a variety of food organisms with a wide spectrum of cell sizes.

http://www.aloki.hu ● ISSN 1589 1623 (Print) ● ISSN 1785 0037 (Online)
DOI: http://dx.doi.org/10.15666/aeer/1704_77157725

A. circinalis has the lowest rate of ingestion among all grazers. However, all the Cladocera tested do feed on colonies of *M. flos-aquae* at a comparable rate. In the present study, zooplankton feed on both green algae as well as potentially toxic algae, hence, may control the algal biomass in the water column.

In conclusion, the study has determined the feeding rate of zooplankton under laboratory culture conditions, which has been assumed to be close to the natural environment, even though the food concentrations and temperatures varied in both situations. The information on the ingestion of cladocerans can provide useful knowledge for practising efficient management and ideally, for the sustainability of the ecosystem. Undeniably, the results presented here are still limited and considered as preliminary to yielding a better understanding of the grazing and selectivity behaviours of zooplankton in drinking water reservoirs. Thus, it is hoped that future studies will uncover additional information and render some improvements such as using more species of zooplankton and algae at more varied cell concentrations.

Acknowledgements. Appreciation and thanks are due to Peter Baker, Peter Hobson, Steve Amos and Hossain Siddiqui for generously provided cultures of the algae and for advice on maintaining laboratory cultures.

REFERENCES

[1] Benndorf, J., Egerer, G. (1981): A note on the variability of the diatom *Cyclotella meneghiniana* (Kiitz) after isolation from the natural environment. – Int. Revue. ges. Hydrobiol. 66: 771-774.

[2] Bogdan, K. G., Gilbert, J. J. (1984): Body size and food size in freshwater zooplankton. – Ecology 81: 6427-6431.

[3] Borsheim, K. Y., Andersen, S. (1987): Grazing and food size selection by crustacean zooplankton compared to production of bacteria and phytoplankton in a shallow Norwegian mountain lake. – J. Plankton Res. 9: 367-379.

[4] Brooks, J. L., Dodson, S. I. (1965): Predation, body size and composition of plankton. – Science 150: 28-35.

[5] Burns, C. W., Rigler, F. H. (1967): Comparison of filtering rates of *Daphnia rosea* in lake water and in suspensions of yeast. – Limnol. Oceanogr. 12: 492-502.

[6] Debernardi, R., Giussani, G. (1990): Are blue-green algae a suitable food for zooplankton? An overview. – Hydrobiologia 200/201: 29-41.

[7] Demott, W. R. (1982): Feeding selectivity and relative ingestion rates of *Daphnia* and *Bosmina*. – Limnol. Oceanogr. 27: 518-527.

[8] Elser, J. J. (1992): Phytoplankton Dynamics and the Role of Grazers in Castle Lake, California. – Ecology 73: 887-902.

[9] Finkel, Z. V., Beardall, J., Flynn, K. J., Quigg, A., Rees, T. A. V., Raven, J. A. (2010): Phytoplankton in a changing world: cell size and elemental stoichiometry. – J. Plankton Res. 32: 119-137.

[10] Frost, B. W. (1972): Effects of size and concentration of food particles on the feeding behavior of the marine planktonic copepod *Calanus pacificus*. – Limnol. Oceanogr. 17: 805-815.

[11] Fulton, R. S. I. (1988): Resistance to blue-green algal toxins by *Bosmina longirostris*. – J. Plankton Res. 10: 771-778.

[12] Geller, W., Muller, H. (1981): The filtration apparatus of Cladocera: Filter mesh-sizes and their implications on food selectivity. – Oceanologia 49: 316-321.

http://www.aloki.hu ● ISSN 1589 1623 (Print) ● ISSN 1785 0037 (Online)
DOI: http://dx.doi.org/10.15666/aeer/1704_77157725

[13] Gliwicz, Z. M. (1980): Filtering rates, food size selection and feeding rates in cladocerans - Another aspect of interspecific competition in filter feeding zooplankton. – In: Kerfoot, W. C. (ed.) Evolution and ecology of zooplankton communities. New England Press, Hanover.
[14] Gliwicz, Z. M., Lampert, W. (1990): Food thresholds in *Daphnia* species in the absence and presence of blue-green filaments. – Ecology 71: 691-702.
[15] Hartmann, H. J., Kunkel, D. D. (1991): Mechanisms of food selection in *Daphnia*. – Hydrobiologia 225: 129-154.
[16] Hillebrand, H., Sommer, U. (1996): Nitrogenous nutrition of the potential toxic diatom *Pseudonitzschia pungens f. multiseries* Hasle. – J. Plankton. Res. 18: 295-301.
[17] Hillebrand, H., Durselen, C.-D., Kirschtel, D., Pollingher, U., Zohary, T. (1999): Biovolume calculation for pelagic and benthic microalgae. – J. Phycol. 35: 403-424.
[18] Hoff, F. H., Snell, T. W. (1987): Plankton Culture Manual. – Florida Aqua Farms Inc.
[19] Horn, W. (1981): Phytoplankton losses due to zooplankton grazing in a drinking water reservoir. – Internat. Revue. ges. Hydrobiol. 66: 787-810.
[20] Infante, A., Litt, A. H. (1985): Differences between two species of *Dapnhia* in the use of 10 species of algae in Lake Washington. – Limnol. Oceanogr. 30: 1053-1059.
[21] Ismail, A. H., Mills, S., Recknagel, F. (2015): A new rotating tumbler apparatus for zooplankton grazing in laboratory. – Ekoloji 24(97): 54-59.
[22] Kersting, K., Leeuw, W. V. D. (1976): The use of the coulter counter for measuring the feeding rates of *Daphnia magna*. – Hydrobiologia 49: 233-237.
[23] Kilham, S. S., Kreeger, D. A., Lynn, S. G., Goulden, C. E., Herrera, L. (1998): COMBO: A defined freshwater culture medium for algae and zooplankton. – Hydrobiologia 377: 147-159.
[24] Kirk, K. L., Gilbert, J. J. (1992): Variation in herbivore response to chemical defenses: Zooplankton foraging on toxic cyanobacteria. – Ecology 73: 2208-2217.
[25] Knisely, K., Geller, W. (1986): Selective feeding of four zooplankton species on natural lake phytoplankton. – Oecologia 69: 86-94.
[26] Kurmayer, R., Juttner, F. (1999): Strategies for the co-existence of zooplankton with the toxic cyanobacterium *Planktothrix rubescens* in Lake Zurich. – J. Plankton Res. 21: 659-683.
[27] Lampert, W., Fleckner, W., Rai, H., Taylor, B. E. (1986): Phytoplankton control by grazing zooplankton: A study on the spring clear-water phase. – Limnol. Oceanogr. 31: 478-490.
[28] Lotocka, M. (2001): Toxic effect of cyanobacterial blooms on the grazing activity of *Daphnia magna* Straus. – Oceanologia 43: 441-453.
[29] McMahon, J. W., Rigler, F. H. (1965): Feeding rate of *Daphnia magna* Straus in different foods labeled with radioactive phosphorus. – Limnol. Oceanogr. 10: 105-113.
[30] McNaught, D. C., Griesmer, D., Kennedy, M. (1980): Resource characteristics modifying selective grazing in copepods. – In: Kerfoot, W. C. (ed.) Evolution and ecology of zooplankton communities. University Press, New England.
[31] Navarro, N. (1999): Feeding behaviour of the rotifers *Brachionus plicatilis* and *Brachionus rotundiformis* with two types of food: Live and freeze-dried microalgae. – J. Exp. Mar. Biol. Ecol. 237: 75-87.
[32] Persson, G. (1985): Clearance rates of crustacean microfiltrators: The nature of in-situ rate depressions in a fertilized oligotrophic lake in the Kuokkel area, Northern Sweden. – Internat. Revue ges. Hydrobiol. 70: 335-358.
[33] Porter, K. G. (1976): Enhancement of algal growth and productivity by grazing zooplankton. – Science 192: 1332-1334.
[34] Poulet, S. A., Marsot, P. (1978): Chemosensory grazing by marine calanoid copepods (Arthropoda: Crustacea). – Science 200(4348): 1403-1405.

http://www.aloki.hu ● ISSN 1589 1623 (Print) ● ISSN 1785 0037 (Online)
DOI: http://dx.doi.org/10.15666/aeer/1704_77157725

[35] Repka, S. (1996): Inter- and intra specific differences in *Daphnia* life histories in response to two food sources: The green alga *Scenedesmus* and the filamentous cyanobacterium *Oscillatoria*. – J. Plankton Res. 18: 1213-1223.
[36] Rippka, R., Deruelles, J., Waterbury, J. B., Herdman, M., Stanier, R. Y. (1979): Generic assignments, strain histories and properties of pure cultures of cyanobacteria. – J. Gen. Microbiol. 111: 1-61.
[37] Rothhaupt, K. O. (1990): Changes of the functional responses of the rotifers *Brachionus rubens* and *Brachionus calyciflorus* with particle sizes. – Limnol. Oceanogr. 35: 24-32.
[38] Schnack, S. B. (1979): Feeding of *Calanus helgolandieus* on phytoplankton mixtures. – Mar. Ecol. Prog. Ser. 1: 41-47.
[39] Tilman, D., Kilham, S., Kilham, P. (1982): Phytoplankton community ecology: The role of limiting nutrients. – Annu. Rev. Ecol. Syst. 13: 349-372.
[40] Urabe, J., Kawabata, K., Nakanishi, M., Shimizu, K. (1996): Grazing and food size selection of zooplankton community in Lake Biwa during BITEX' 93. – Jpn. J. Limnol. 57: 27-37.
[41] Wirtz, K. W. (2013): How fast can plankton feed? Maximum ingestion rate scales with digestive surface area. – J. Plankton. Res. 35(1): 33-48.

http://www.aloki.hu ● ISSN 1589 1623 (Print) ● ISSN 1785 0037 (Online)
DOI: http://dx.doi.org/10.15666/aeer/1704_77157725

SEASONAL VARIATIONS OF ZOOPLANKTON FUNCTIONAL GROUPS AND RELATIONSHIP WITH ENVIRONMENTAL FACTORS IN A EUTROPHIC RESERVOIR FROM COLD REGION

SUN, X.[1] – CHAI, F. Y.[2] – MWAGONA, P. C.[1] – SHABANI, I. E.[1] – HOU, W. J.[1] – LI, X. Y.[1] – MA, C. X.[1] – PAN, H. F.[1] – LI, S.[1] – YU, H. X.[1*]

[1]*Department of Wetland Science, College of Wildlife Resources, Northeast Forestry University, Harbin 150040, China*

[2]*Water Saving Technology Center of Heilongjiang Province, Harbin 150001, China*

**Corresponding author*
e-mail: china.yhx@163.com

(Received 12th Mar 2019; accepted 3rd May 2019)

Abstract. In this study, the concept of functional feeding groups was used to classify zooplankton community into functional groups among three seasons (spring, summer and autumn). A total of 30 zooplankton species were sampled in the Tuanjie Reservoir and identified into seven functional groups. Environmental factors and zooplankton functional group biomass were both varied in spatially and seasonally. Water transparency (SD), dissolved oxygen (DO), pH, N:P and dissolved iron (Fe^{3+}) were higher in autumn while total phosphorus (TP), chemical oxygen demand (COD_{Mn}) and dissolved copper (Cu^{2+}) were higher in spring, and temperature (T) and ammonium nitrogen (NH_4^+-N) were higher in summer. Zooplankton functional groups biomass was higher in summer, followed by spring and autumn. In spring, zooplankton functional group only dominated by group PF, while in summer and autumn dominated by group PF and RF. Spearman and RDA results showed that SD, conductivity (COND), DO, NH_4^+-N, nitrate nitrogen (NO_3^--N) and COD_{Mn} were the major factors influencing zooplankton functional groups in Tuanjie Reservoir.
Keywords: *seasonal dynamics, zooplankton functional groups, abundance and biomass, northeast of China*

Introduction

Zooplankton is found in almost all kinds of waterbodies. Compared with other aquatic animals, they are small in size, numerous in numbers and have strong metabolic activities. They feed on phytoplankton, bacteria, fragments and other organisms. Zooplankton also participates in the decomposition and circulation of organic matter in the water ecosystem through excretion and secretion, energy transfer from the primary producers to higher consumers (Wetzel, 2001). Variation of zooplankton can influence the structure of other nutrient levels in water ecosystems (Beaugrand et al., 2000; David et al., 2005; Lobry et al., 2008; Steinberg and Condon, 2009). The zooplankton community structure, their abundance and biomass is influenced by top-down and bottom-up control (Jeppesen et al., 2003), and is one of determinants for water quality (Jeppesen et al., 2011). This is due to the interaction between biological organisms and environmental factors (Ejsmont-Karabin and Karabin, 2013).

Traditional methods of zooplankton classification are usually based on the taxonomy system. However, it is difficult to reflect the aquatic ecological function. Therefore, ecologists have put forward the concept of functional groups, species characteristics of the functional group more closely in touch with environment, through the study of functional groups, can more directly reflect the ecological process of ecological

http://www.aloki.hu ● ISSN 1589 1623 (Print) ● ISSN 1785 0037 (Online)
DOI: http://dx.doi.org/10.15666/aeer/1704_77277740

environmental impact of aquatic biological communities (Hood et al., 2006). In recent years, the use plankton functional groups have been applied in several studies of biogeochemical models (Anderson, 2005). Zooplankton is divided into three functional groups: mico-, meso- and macrozooplankton (Quéré et al., 2010). By using the concept of functional groups, zooplankton community composition can be used to model the ecosystem process of the aquatic ecosystem and it is also conducive to analyzing the seasonal variation of zooplankton community (Sun et al., 2010).

Tuanjie Reservoir was built in 1981 with the aim of supplying drinking water to the local village people. The main sources water of the reservoir is Muling River, which is the largest tributary of the Ussuri River on the left bank of the border between China and Russia. In this study the concept of functional feeding groups was used to reveal the seasonal variation of zooplankton functional groups in relation to environmental factors in Tuanjie Reservoir. Understanding the variation of zooplankton functional groups biomass in relation to environmental factors is very important to better understand the environmental factors that significantly structure the zooplankton community in the reservoir. This study aims at: (1) identifying and classifying zooplankton species of Tuanjie Reservoir into functional group, and (2) to determine the seasonal and spatial dynamics of the biomass of zooplankton functional groups and their relationship to environmental factors. We hypothesized that seasonal and spatial change in biomass of zooplankton functional groups will be strongly influenced by environmental factors.

Materials and methods

Study area

Tuanjie Reservoir (130°8'-130°11'E, 44°01'-44°04'N) is located in the southeast of Heilongjiang Province Northeastern China (*Fig. 1*). The reservoir was built in 1981 in order to control floods, provide water for irrigation, fish farming, power generation and for aesthetic value. Tuanjie Reservoir has a surface area of 445 km^2, a capacity of 8.63×10^7 m^3 and it shaped like big "Y". The region where located the reservoir is influenced by temperate continental monsoon. The average annual evaporation and precipitation of the reservoir are 950 mm and 534 mm, respectively. The annual mean temperature is 1 °C, which ranged between -44.1 °C to 37.6 °C. In winter, the surface water of the reservoir is covered by ice.

Field sampling and laboratory analysis

Based on the reservoir shape, 5 sampling sites (*Table 1*) were selected for sampling on spring (May), summer (July) and autumn (September). Samples were collected from top (0.5 m from the surface water), middle and bottom (0.5 m from the waterbed) of water column according to the different water depth among sites inside the Tuanjie Reservoir (*Fig. 1*). At every sampling site, water temperature (T), pH, conductivity (COND), dissolved oxygen (DO) was measured in the field using a portable multi-probe (YSI 6600, YSI Inc.). Water transparency (SD) and depth (D) were measured using Secchi disk and longline method. Triplicate water samples for chemical analyses were collected at each sampling sites and put on acid-washed plastic bottles, placed in ice box and transported to laboratory for analysis. The concentration of total nitrogen (TN), total phosphorus (TP), N:P ratio (N:P), ammonium nitrogen (NH_4^+-N), nitrate nitrogen (NO_3^--N), chemical oxygen demand (COD_{Mn}) and dissolved iron (Fe^{3+}) and dissolved

http://www.aloki.hu ● ISSN 1589 1623 (Print) ● ISSN 1785 0037 (Online)
DOI: http://dx.doi.org/10.15666/aeer/1704_77277740

copper (Cu^{2+}) were measured according to the standard methods for China (MEP, 2002).

Table 1. *Five sampling sites coordinates in Tuanjie Reservoir*

Sampling sites	Latitude	Longitude
S1	N44°01'48"	E130°11'24"
S2	N44°03'36"	E130°10'48"
S3	N44°03'00"	E130°09'36"
S4	N44°04'12"	E130°10'36"
S5	N44°04'48"	E130°10'48"

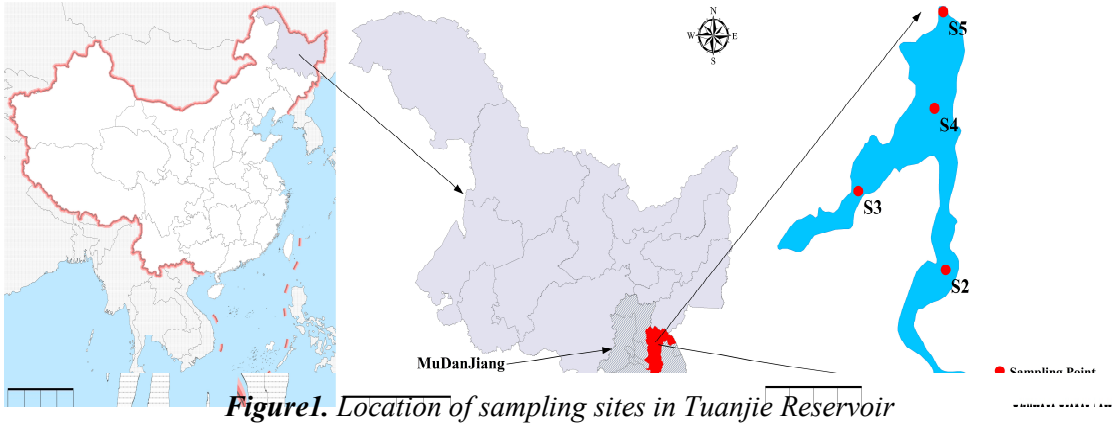

Figure1. *Location of sampling sites in Tuanjie Reservoir*

Zooplankton samples (20 L water filtered through 64 mm mesh size) were fixed with formaldehyde solution (4% concentration). Protozoa and rotifera samples were obtained by taking 1 L subsamples to form the 20 L pooled sample. The samples were preserved with Lugol's iodine and formaldehyde and allowed to sediment in 1 L jar for at least 48 h. The supernatant water was carefully removed and the residue was then collected and made to a known volume of 30 mL (Thompson et al., 2013). Identification and counting of the zooplankton specimen were using an inverted microscope at 400× magnification following the species keys (Chen, 1974; Chiang and Du, 1979; Yeatman, 1959). We calculated zooplankton functional group biomass by using dry weight (mg) obtained from length-weight relationship of the filtered water volume (L) (Zuo et al., 2003).

Zooplankton functional groups classification

Zooplankton species in Tuanjie Reservoir were classified into seven functional groups mainly according to body size/length and feeding mode (Benedetti et al., 2018; Ma et al., 2019; Mwagona et al., 2018). The seven functional groups are: group PF (protozoa filter feeders), group RF (rotifera filter feeders), group SCF (small copepods and cladoceran filter feeders, body size < 0.7 mm), group MCC (middle copepods and cladoceran carnivore, body size 0.7~1.5 mm), group MCF (middle copepods and cladoceran filter feeders, body size 0.7~1.5 mm), group LCC (large copepods and cladoceran carnivore, body size > 1.5 mm) and group LCF (large copepod filter feeders, body size > 1.5 mm).

http://www.aloki.hu ● ISSN 1589 1623 (Print) ● ISSN 1785 0037 (Online)
DOI: http://dx.doi.org/10.15666/aeer/1704_77277740

Data analysis

Statistical analyses were carried out using the SPSS 19.0 software. Variation and correlation of environmental factors and biomass of zooplankton functional groups in different seasons were analyzed by using One-way ANOVA and Tukey's honesty significant difference (HSD) tests, and Spearman analysis, respectively. Relationship between zooplankton functional group biomass and environmental factors was done using CANOCO 4.5 software (Microcomputer Power, New York, USA). Before analysis, the biological and abiotic data were transformed by $\log_{10}(x + 1)$ to satisfy the normal distribution. We found that the detrended corresponding analysis (DCA) of the largest gradient length of the four axes was 1.889 (< 3). Therefore, linear ordination method of the redundancy analysis (RDA) was used to reveal the relationship. Monte Carlo simulations with 499 permutations were used to test the significance of the environmental factors in explaining the biomass of zooplankton functional groups data in the RDA.

Results

Seasonal variation of environmental factors

The mean values of environmental factors presented among seasons are shown in *Table 2*. Most of the factors varied significantly (One-way ANOVA and Tukey HSD test). The mean values of D, COND, TN and NO_3^--N were not statistically significant difference among the seasons ($P > 0.05$). While the mean values of DO, pH, NH_4^+-N, COD_{Mn}, Fe^{3+}, Cu^{2+}, T, TP, N:P and SD varied significantly with seasons ($P < 0.05$). The minimum mean values of DO, pH, N:P and Fe^{3+}were observed in summer, while their maximum values were observed in autumn except for COD_{Mn}. On the contrary, the maximum mean values of T and NH_4^+-N were observed in summer and minimum presented in autumn.

Table 2. *The seasonal variations (mean ± SE, n = 32) of environmental factors: water transparency (SD), depth (D), conductivity (COND), dissolved oxygen (DO), pH, water temperature (T), total nitrogen (TN), total phosphorus (TP), N:P ratio (N:P), ammonium nitrogen (NH_4^+-N), nitrate nitrogen (NO_3^--N), chemical oxygen demand (COD_{Mn}) and dissolved iron (Fe^{3+}) and dissolved copper (Cu^{2+}), P-value from One-way ANOVA and a, b, c mean differences between the seasons were tested by post-hoc test using Tukey HSD ANOVA*

	Spring	Summer	Autumn	*P*-value
SD (m)	0.76 ± 0.12^a	1.01 ± 0.16^b	1.11 ± 0.12^b	0.037
D (m)	8.48 ± 3.26^a	10.93 ± 3.99^a	10.57 ± 3.70^a	0.716
COND (ms/cm)	0.11 ± 0.04^a	0.15 ± 0.05^a	0.12 ± 0.03^a	0.603
DO (mg/L)	7.66 ± 0.24^a	7.39 ± 0.43^a	8.91 ± 0.20^b	0.000
pH	7.44 ± 0.10^a	7.17 ± 0.15^a	7.80 ± 0.10^b	0.000
T (°C)	17.3 ± 0.90^a	22.94 ± 0.45^b	10.23 ± 0.74^c	0.002
TN (mg/L)	0.99 ± 0.20^a	0.87 ± 0.08^a	0.91 ± 0.09^a	0.277
TP (mg/L)	0.74 ± 0.16^a	0.52 ± 0.05^{ab}	0.36 ± 0.06^b	0.002
N:P	1.97 ± 0.67^a	1.67 ± 0.04^a	2.92 ± 0.56^b	0.005
NH_4^+-N (mg/L)	0.13 ± 0.01^a	0.23 ± 0.04^b	0.12 ± 0.02^a	0.000
NO_3^--N (mg/L)	0.36 ± 0.06^a	0.28 ± 0.07^a	0.20 ± 0.05^a	0.069
COD_{Mn} (mg/L)	4.44 ± 0.07^a	3.78 ± 0.12^b	4.24 ± 0.04^a	0.000
Fe^{3+}(mg/L)	0.32 ± 0.04^a	0.21 ± 0.07^b	0.42 ± 0.01^a	0.000
Cu^{2+}(mg/L)	0.21 ± 0.04^a	0.16 ± 0.03^a	0.03 ± 0.01^b	0.000

http://www.aloki.hu ● ISSN 1589 1623 (Print) ● ISSN 1785 0037 (Online)
DOI: http://dx.doi.org/10.15666/aeer/1704_77277740

Variation of zooplankton functional groups in Tuanjie Reservoir

A total of 30 zooplankton species belonging to 25 genera and four taxonomic groups including protozoa (33.33%), rotifera (36.67%), cladoceran (16.67%) and copepods (13.33%) were identified in the Tuanjie Reservoir (*Table 3*). The biomass of zooplankton functional groups showed seasonal and spatial variation (*Figs. 2* and *3*). Summer recorded the highest number of zooplankton species (20) followed by spring (19) and autumn (17). In summer, the dominant zooplankton functional group was PF mainly comprised by *Paramecium* (43.81%) and *Didinium nasutum* (37.55%), and RF which was presented by *Keratella cochlearis* (3.27%) and *Polyarthra trigla* (2.03%). While in spring, the dominant zooplankton functional group PF was presented only by *Paramecium* (74%). In autumn, the dominant zooplankton functional group PF was contributed by *Paramecium* (44.82%) and that of group RF was *Keratella cochlearis* (26.89%).

Table 3. *Zooplankton functional groups and biomass (%) in Tuanjie Reservoir, PF (protozoa filter feeders), RF (rotifera filter feeders), SCF (small copepods and cladoceran filter feeders), MCC (middle copepods and cladoceran carnivore), MCF (middle copepods and cladoceran filter feeders), LCC (large copepods and cladoceran carnivore), LCF (large copepod filter feeders)*

Taxonomic group	Species	Functional groups	Spring	Summer	Autumn
Protozoa	*Lagynophrya conifera*	PF	2.43	-	-
	Strombidium viride	PF	2.97	-	2.79
	Strobilidium velox	PF	1.35	1.88	2.69
	Strobilidium gyrans	PF	0.72	-	-
	Tetrahymena priformis	PF	3.67	0.69	1.61
	Vorticella campanula	PF	0.46	0.88	1.26
	Paramecium sp.	PF	74.00	43.81	44.82
	Didinium balbianii nanum	PF	4.49	-	-
	Didinium nasutum	PF	-	37.55	-
	Difflugia avellana	PF	0.60	-	-
Rotifera	*Polyarthra trigla*	RF	2.47	2.03	4.55
	Filinia longiseta	RF	0.50	-	-
	Keratella cochlearis	RF	-	3.27	26.89
	Keratella quadrata	RF	2.34	-	-
	Trichocerca Lamarck	RF	1.05	1.20	2.90
	Trichocerca porcellus	RF	-	0.21	-
	Lecane luna	RF	1.78	-	-
	Lecane tenuiseta Harring	RF	-	1.77	-
	Pompholyx sulcata Hudson	RF	-	0.55	-
	Colurella uncinata	RF	-	0.08	-
	Brachionus diversicornis	RF	-	0.96	-
Cladoceran	*Bosmina longirostris*	SCF	0.43	-	0.05
	Diaphanosoma leuchtenbergianum	MCF	-	-	1.21
	Leptodora kindti	LCC	-	0.05	0.44
	Daphnia cristata Sars	SCF	-	0.13	1.09
	Daphnia magna	MCF	-	4.09	7.24
Copepoda	*Cyclops strenuns*	MCC	0.26	0.35	0.60
	Calanioda.sp	LCF	0.12	0.16	0.45
	Thermocyclops dybowskii	MCC	0.19	0.25	1.00
	Microcyclops javanus	SCF	0.18	0.09	0.41

http://www.aloki.hu ● ISSN 1589 1623 (Print) ● ISSN 1785 0037 (Online)
DOI: http://dx.doi.org/10.15666/aeer/1704_77277740

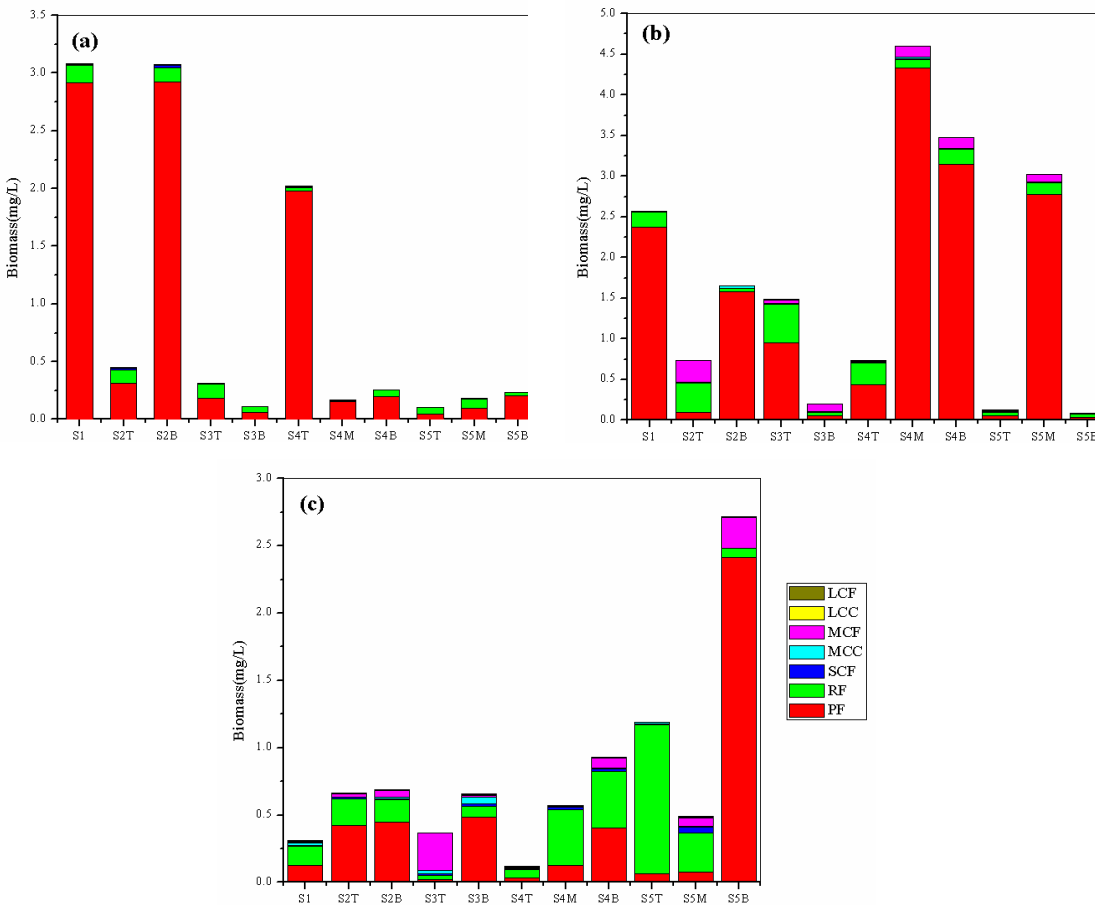

Figure 2. *Zooplankton functional group biomass of spring (a), summer (b) and autumn (c), S2T (Sampling site 2 top water layer), S4M (Sampling site 4 middle water layer), S2B (Sampling site 2 bottom water layer), PF (protozoa filter feeders), RF (rotifera filter feeders), SCF (small copepods and cladoceran filter feeders), MCC (middle copepods and cladoceran carnivore), MCF (middle copepods and cladoceran filter feeders), LCC (large copepods and cladoceran carnivore), LCF (large copepod filter feeders)*

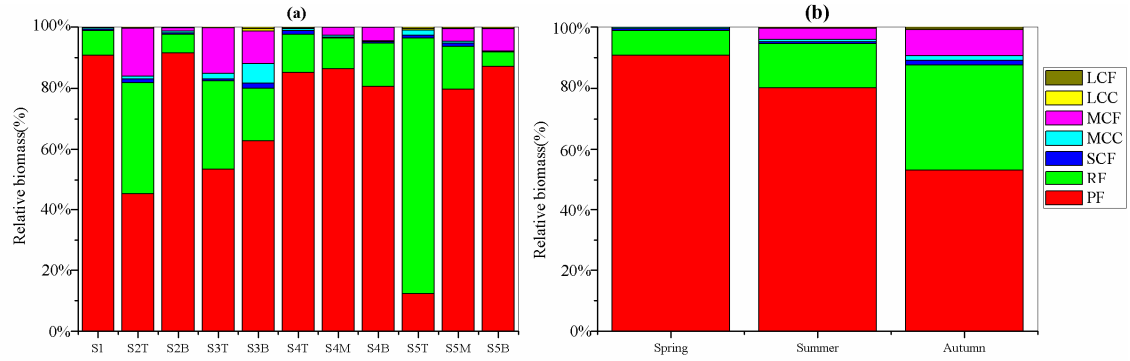

Figure 3. *Relative biomass of zooplankton functional groups among sampling sites (a) and seasons (b), S2T (Sampling site 2 top water layer), S4M (Sampling site 4 middle water layer), S2B (Sampling site 2 bottom water layer), PF (protozoa filter feeders), RF (rotifera filter feeders), SCF (small copepods and cladoceran filter feeders), MCC (middle copepods and cladoceran carnivore), MCF (middle copepods and cladoceran filter feeders), LCC (large copepods and cladoceran carnivore), LCF (large copepod filter feeders)*

http://www.aloki.hu ● ISSN 1589 1623 (Print) ● ISSN 1785 0037 (Online)
DOI: http://dx.doi.org/10.15666/aeer/1704_77277740

Correlation of zooplankton functional groups and environmental factors

The Spearman correlation analysis of zooplankton functional group biomass and environmental factors were listed in *Tables 4* and *5,* respectively. Group PF influenced RF, and group LCC influenced SCF and LCF. The feeding relationship of zooplankton functional groups has been proved by the results. Meanwhile, most environmental factors were correlated with zooplankton functional groups. Like group LCC, was significantly influenced by SD ($r = 0.374$), T ($r = 0.347$), NH_4^+-N ($r = 0.494$) and COD_{Mn} ($r = -0.541$). Groups MCF was negatively correlated with NO_3^--N ($r = -0.419$) and COD_{Mn} ($r = -0.541$). Other side, COND was positively correlated with group PF ($r = 0.407$), RF ($r = 0.392$) and SCF ($r = 0.477$). However, the DO and NH_4^+-N was only significant positively correlated with group MCC ($r = 0.386$) and LCF ($r = 0.410$) respectively.

Table 4. *Spearman correlation of zooplankton functional group biomass. PF (protozoa filter feeders), RF (rotifera filter feeders), SCF (small copepods and cladoceran filter feeders), MCC (middle copepods and cladoceran carnivore), MCF (middle copepods and cladoceran filter feeders), LCC (large copepods and cladoceran carnivore), LCF (large copepod filter feeders)*

	PF	RF	SCF	MCC	MCF	LCC	LCF
PF	1	.253	.112	.010	.080	-.044	.071
RF	.253	1	.313	.197	.344*	.296	.035
SCF	.112	.313	1	.178	.065	.421*	.225
MCC	.010	.197	.178	1	.273	.261	-.100
MCF	.080	.344*	.065	.273	1	.340	.011
LCC	-.044	.296	.421*	.261	.340	1	.356*
LCF	.071	.035	.225	-.100	.011	.356*	1

$^{**}p < 0.01$, $^{*}p < 0.05$

Table 5. *Spearman correlation between zooplankton functional group biomass and environmental factors, water transparency (SD), depth (D), conductivity (COND), dissolved oxygen (DO), pH, water temperature (T), total nitrogen (TN), total phosphorus (TP), N:P ratio (N:P), ammonium nitrogen (NH_4^+-N), nitrate nitrogen (NO_3^--N), chemical oxygen demand (COD_{Mn}) and dissolved iron (Fe^{3+}) and dissolved copper (Cu^{2+}). PF (protozoa filter feeders), RF (rotifera filter feeders), SCF (small copepods and cladoceran filter feeders), MCC (middle copepods and cladoceran carnivore), MCF (middle copepods and cladoceran filter feeders), LCC (large copepods and cladoceran carnivore), LCF (large copepod filter feeders)*

	SD	**D**	**COND**	**DO**	**pH**	**T**	**TN**	**TP**	**N:P**	**NH_4^+-N**	**NO_3^--N**	**COD_{Mn}**	**Fe^{3+}**	**Cu^{2+}**
PF	-.075	.121	.407*	.152	.302	-.178	.040	-.074	.041	-.272	-.157	.220	.164	-.050
RF	.099	-.154	.392*	-.126	.095	.102	.100	-.109	-.050	.196	-.119	-.306	-.021	-.137
SCF	-.004	-.179	.477**	-.247	-.201	.262	-.061	-.068	-.086	.149	.034	-.147	-.286	.140
MCC	-.011	-.332	.007	.386*	.189	-.092	.083	-.017	.038	-.125	-.149	-.294	.257	-.291
MCF	.339	.174	.182	-.015	.049	.107	-.144	.032	-.203	.067	-.419*	-.541**	-.133	-.262
LCC	.374*	.160	.148	-.312	-.193	.347*	-.171	.031	-.187	.494**	-.160	-.541**	-.324	-.013
LCF	.209	-.071	-.033	-.128	-.118	-.052	-.054	-.153	.154	.410*	.179	.089	.122	-.048

$^{**}p < 0.01$, $^{*}p < 0.05$

http://www.aloki.hu ● ISSN 1589 1623 (Print) ● ISSN 1785 0037 (Online)
DOI: http://dx.doi.org/10.15666/aeer/1704_77277740

RDA analysis between zooplankton functional groups and environmental factors

The results of Monte Carlo test showed that the first canonical axis and all canonical axes were significant ($F = 13.521$, $p = 0.002$; $F = 1.130$, $p = 0.002$; 499 random permutations). The eigenvalues of the four axes were 0.429, 0.033, 0.015, 0.004, respectively (*Table 6*). The functional groups-environment correlations for Axis 1 and Axis 2 were 0.686 and 0.691, respectively. The first two axes account for 46.2% of functional groups-environment variables relation (axis 1: 42.9%, axis 2: 3.3%) and 98.8% of the functional groups variables (axis 1: 91.7%, axis 2: 7.1%). Axis 1 was mainly positive correlated with pH ($r = 0.728$) and DO ($r = 0.683$) and negatively correlated with T ($r = -0.672$). Axis 2 was positively correlated with NH_4^+-N ($r = 0.602$), SD ($r = 0.481$) and negatively correlated with COD_{Mn} ($r = -0.658$), Fe^{3+}($r = -0.501$). Groups PF was positively related with pH, COND and COD_{Mn}, and negatively related with T, NH_4^+-N, NO_3^--N and Cu^{2+}. Group RF, SCF, MCF, LCF and LCC were positively related with NH_4^+-N and SD, and negatively related with COD_{Mn}, Fe^{3+}, DO, $Cu^{2+}$and NO_3^--N. Nevertheless, the group MCC was not related with most of environmental factors (*Fig. 4*).

Table 6. *RDA results of zooplankton functional group biomass*

Axes	Eigenvalues	Species-environment correlations	Cumulative percentage variance of species data	Cumulative percentage variance of species-environment relation
1	0.429	0.686	42.9	91.7
2	0.033	0.691	46.2	98.8
3	0.015	0.563	46.8	100
4	0.004	0.468	46.8	100

Discussion

Zooplankton, as an important part of the food chain in the aquatic ecosystem, is mainly composed of free-living protozoa, rotifera, cladocera and copepod. Zooplankton is very sensitive to environmental changes and hence considered as good indicator. Many previous studies focused on zooplankton community structure in relation to environmental factors (Bachiller et al., 2018; Coz et al., 2018; Jeppesen et al., 2011; Li et al., 2014; Matsuzaki et al., 2018; Neumann-Leitão et al., 2018). Recently, using functional groups to reveal the reaction of environmental factors are considered as a new method (Ma et al., 2019; Mwagona et al., 2018; Shi et al., 2015; Sun et al., 2010). Functional groups are species with similar morphological and physiological traits (Reynolds et al., 2002). In marine ecosystems, six functional groups have been classified according to zooplankton species individual size and feeding habits from the yellow sea (Sun et al., 2010). In Western English channel, the researchers analyzed the food web using three zooplankton functional groups (Araújo et al., 2006). On the other hand, in freshwater ecosystems, six and eight zooplankton functional groups have been confirmed in Small Xingkai Wetland Lake and Xiquanyan Reservoir in Heilongjiang Province, Northeast of China, respectively (Ma et al., 2019; Mwagona et al., 2018). In our study, we identified 30 species belonging to seven zooplankton functional groups in Tuanjie Reservoir, including group PF, RF, SCF, MCC, MCF, LCC and LCF.

http://www.aloki.hu ● ISSN 1589 1623 (Print) ● ISSN 1785 0037 (Online)
DOI: http://dx.doi.org/10.15666/aeer/1704_77277740

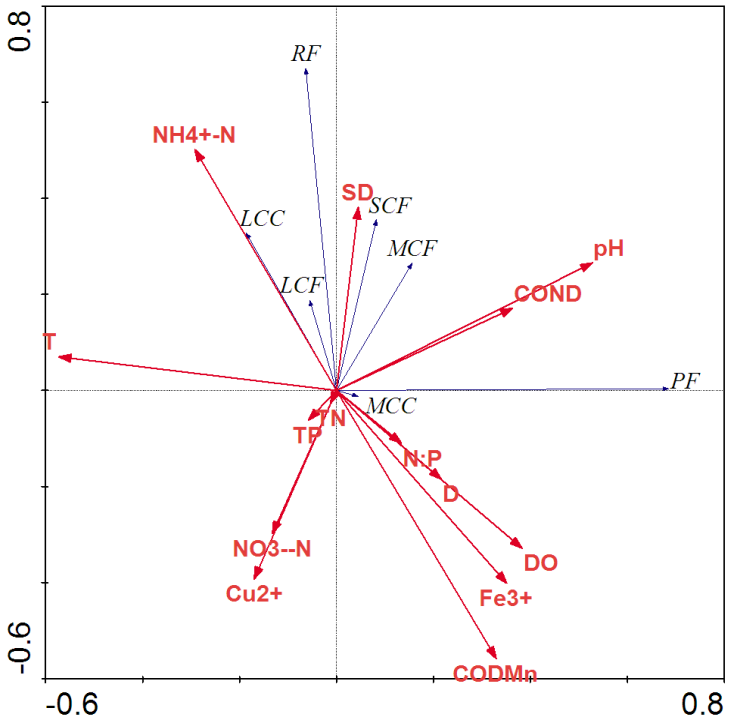

Figure 4. *RDA bioplot of zooplankton functional groups and environmental factors, water transparency (SD), depth (D), conductivity (COND), dissolved oxygen (DO), pH, water temperature (T), total nitrogen (TN), total phosphorus (TP), N:P ratio (N:P), ammonium nitrogen (NH_4^+-N), nitrate nitrogen (NO_3^--N), chemical oxygen demand (COD_{Mn}) and dissolved iron (Fe^{3+}) and dissolved copper (Cu^{2+}). PF (protozoa filter feeders), RF (rotifera filter feeders), SCF (small copepods and cladoceran filter feeders), MCC (middle copepods and cladoceran carnivore), MCF (middle copepods and cladoceran filter feeders), LCC (large copepods and cladoceran carnivore), LCF (large copepod filter feeders)*

Composition and variations of zooplankton functional groups in Tuanjie Reservoir

Seasonal and spatial variations of zooplankton biomass were demonstrated in aquatic ecosystems by Dube et al. (2017). In this study, the biomass of zooplankton functional groups varied significantly differences among seasons and sites. The mean values of biomass reported in spring (0.91 mg/L), summer (1.70 mg/L) and autumn (0.79 mg/L) were higher than those recorded by Mwagona et al. (2018) in the oligotrophic Xiquanyan Reservoir during spring (54.25 µg/L), summer (245.81 µg/L) and autumn (196.54 µg/L) and also higher than those found by Ma et al. (2019) in Small Xingkai Lake during spring (0.28 mg/L) and autumn (0.72 mg/L) in the same province. Mwagona et al. (2018) found that low nutrients level, which unable to meet the demand of the growth of zooplankton. While, Ma et al. (2019) noted that nutrient-rich level could promote the zooplankton breeding, and high turbid with low transparency also may contribute to zooplankton avoid predators.

As shown in *Figure 2,* during spring and summer seasons, zooplankton biomass was both dominated by protozoa filter feeders (group PF) accounting for 90.68% and 84.8% of total biomass, respectively. In spring, group PF mainly composed of *Paramecium sp.* (74%), while in summer mainly composed of *Paramecium sp.* (43.81%) and *Didinium nasutum* (37.55%). Group PF (protozoa filter feeders) are filter feeding on bacteria, algae and organic detritus and found in all sampling sites and water layer. We found

http://www.aloki.hu ● ISSN 1589 1623 (Print) ● ISSN 1785 0037 (Online)
DOI: http://dx.doi.org/10.15666/aeer/1704_77277740

that the biomass of group PF in summer was significantly higher than that in spring probably due to higher temperature and nutrients contributed to algae growth of their food resources (Duggan et al., 2001; Špoljar et al., 2010), and higher water transparency help them locate prey more clearly and predation activities more easily (Ma et al., 2019). Besides, *Didinium nasutum* could use their flagella enhance swimming ability in favor of avoiding predators and harvesting suitable light and food for growth, therefore became an dominant species (Bovo-Scomparin and Train, 2008). In autumn, zooplankton biomass was dominated by protozoa filter feeders (group PF) and rotifera filter feeders (group RF) accounted for 53.17% and 34.34% of total biomass, respectively. Group PF mainly composed of *Paramecium sp.* (44.82%) and group RF mainly composed of *Keratella cochlearis* (26.89%). This could be due to higher temperature in summer was suitable for rotifera breeding in large numbers (Galkovskaja, 1987), so they formed a dominant species in autumn. Another reason could be some environmental factors such as nutrients and turbidity can influence rotifera community structure in autumn (Armengol et al., 1998; Ma et al., 2019), and finally, it leads to the change of the structure and composition of zooplankton community. Moreover, other zooplankton functional groups preyed by their predators such as *Hypophthalmichthys molitrix* and *Aristichthys nobilis*, and some competitive interactions between those functional groups lead to relative low biomass among sampling sites and seasons in the reservoir during study (*Fig. 3a* and *b*).

Driving factors of zooplankton functional groups in Tuanjie Reservoir

There are so many driving factors influence the zooplankton community structure in aquatic ecosystems (Li et al., 2014; Ma et al., 2019; Mwagona et al., 2018; Shi et al., 2015; Sun et al., 2010). Among zooplankton functional groups, group MCF was positively correlated with group RF, and group LCC were both positively correlated with group SCF and LCF, which could due to intraspecific competition (*Table 4*). However, between environment and zooplankton, water depth did not affect the distribution of zooplankton functional groups (*Table 5*). Similarly, there was seemingly no significant variation in the abundance patterns of the dominant zooplankton taxa in response to changing pH value (Morgan, 1985a). The Spearman correlation results showed that pH was not related with the biomass of zooplankton functional groups in Tuanjie Reservoir (*Table 5*). The fluctuation of pH value in the freshwater ecosystem was primarily the result of enhanced primary productivity (Morgan, 1985b). Further studies also proved that the density of zooplankton individuals is influenced by the primary producers phytoplankton biomass (Trevisan and Forsberg, 2007).

On the other hand, this present study showing that nitrogen and phosphorus can usually be considered the main limiting nutrient (Fasham et al., 1990; Shumka et al., 2018). While in our study, both Spearman correlation and RDA results showing that the zooplankton functional groups were not affected by TN, TP and N:P ratio in Tuanjie Reservoir (*Table 5; Fig. 4*). That could be due to trophic level weakened their effect on plankton community in the reservoir, because an increase in trophic state can caused an increase in the total numbers of crustaceans (Ejsmont-Karabin and Karabin, 2013). The Spearman correlation and RDA results both showed that NH_4^+-N was positively influence group LCC and LCF, and NO_3^--N was negatively influence group MCF (*Table 5; Fig. 4*).

Metallic element concentrations were strongly correlated with plankton structure and biomass composition (Long et al., 2018). Such as iron (Fe) considered as important

http://www.aloki.hu ● ISSN 1589 1623 (Print) ● ISSN 1785 0037 (Online)
DOI: http://dx.doi.org/10.15666/aeer/1704_77277740

nutrient affecting the growth of phytoplankton (Alderkamp et al., 2015). Some phytoplankton species can take up Fe through their specialized transport mechanisms (Morel et al., 2008). Some researchers also found that zooplankton could directly obtain enough Fe to maintain growth (Baines et al., 2016). Similarly, copper (Cu) plays an important role in the physiology of natural plankton communities (Semeniuk et al., 2009). In Tuanjie Reservoir, there was no relationship among metal ion (Fe^{3+}, Cu^{2+}) with the biomass of zooplankton functional groups, which results consistent with RDA (*Table 5, Fig. 4*). We suspect that could be the zooplankton functional groups affected by the top-down and bottom-up control in the food webs (Carvalho, 1994; Prowe et al., 2012; Sinistro, 2010; Stephen, 2010; Sun et al., 2013). This proof confirmed a complex interaction between Fe and Cu physiology in plankton communities (Semeniuk et al., 2016). Besides, the primary correlated factors included chlorophyll a levels, cyanobacterial toxin levels, and temperature, suggesting that both phytoplankton biomass and composition play important roles in zooplankton dynamics (Srifa, 2010).

In addition, turbulence and turbidity of water column intensified the competition among zooplankton species (Zhou et al., 2018). These environmental factors should be considered as the new influencing variables in Tuanjie Reservoir for further studies in the future.

Conclusion

In this study, a total of 30 zooplankton species belonging to protozoa, rotifera, cladoceran and copepod were identified and classified into seven functional groups including PF, RF, SCF, MCC, MCF, LCC and LCF. Both environmental factors and zooplankton functional groups biomass in Tuanjie Reservoir varied seasonally and spatially. SD, DO, pH, N:P and Fe^{3+}were significant higher in autumn, while TP and T was higher in spring and summer. Zooplankton functional group biomass was higher in summer (0.62 mg/L), followed by spring (0.33 mg/L) and autumn (0.29 mg/L). In spring group PF was the dominant functional group, while in summer and autumn group PF and RF were both the dominant functional group. SD, COND, DO, NH_4^+-N, NO_3^--N and COD_{Mn} considered as the major factors influence zooplankton functional groups in Tuanjie Reservoir. Group PF was positively correlated with pH and COND while negatively correlated with T. Groups RF, SCF and LCC were positively influenced by NH_4^+-N and SD, while negatively influenced by COD_{Mn}, Fe^{3+}, DO, $Cu^{2+}$and NO_3^--N.

Acknowledgements. We thank to the leaders and workers from Muling city Fendou Reservoir construction headquarters for their assistance and support during field sampling work. The study was supported by programs of the National Key Research and Development Program of China (Grant No. 2016YFC0500406).

REFERENCES

[1] Alderkamp, A. C., Dijken, G. L. V., Lowry, K. E., Connelly, T. L., Lagerström, M., Sherrell, R. M., Haskins, C., Rogalsky, E., Schofield, O., Stammerjohn, S. E., Yager, P. L., Arrigo, K. R. (2015): Fe availability drives phytoplankton photosynthesis rates during spring bloom in the Amundsen Sea Polynya, Antarctica. – Elementa: Science of the Anthropocene 3: 1-26.

http://www.aloki.hu ● ISSN 1589 1623 (Print) ● ISSN 1785 0037 (Online)
DOI: http://dx.doi.org/10.15666/aeer/1704_77277740

[2] Anderson, T. (2005): Plankton functional type modelling: running before we can walk? – Journal of Plankton Research 27: 1073-1081.
[3] Araújo, J. N., Mackinson, S., Stanford, R. J., Sims, D. W., Southward, A. J., Hawkins, S. J., Ellis, J. R., Hart, P. J. B. (2006): Modelling food web interactions, variation in plankton production, and fisheries in the western English Channel ecosystem. – Marine Ecology Progress Series 309: 175-187.
[4] Armengol, X., Esparcia, A., Miracle, M. R. (1998): Rotifera vertical distribution in a strongly stratified lake: a multivariate analysis. – Hydrobiologia 387-388: 161-170.
[5] Bachiller, E., Utne, K. R., Jansen, T., Huse, G. (2018): Bioenergetics modeling of the annual consumption of zooplankton by pelagic fish feeding in the Northeast Atlantic. – Plos One 13: e0190345-.
[6] Baines, S. B., Chen, X., Twining, B. S., Fisher, N. S., Landry, M. R. (2016): Factors affecting Fe and Zn contents of mesozooplankton from the Costa Rica Dome. – Journal of Plankton Research 38: 331-347.
[7] Beaugrand, G., Ibañez, F., Reid, P. C. (2000): Spatial, seasonal and long-term fluctuations of plankton in relation to hydroclimatic features in the English Channel, Celtic Sea and Bay of Biscay. – Marine Ecology Progress Series 200: 93-102.
[8] Benedetti, F., Vogt, M., Righetti, D., Guilhaumon, F., Ayata, S. D. (2018): Do functional groups of planktonic copepods differ in their ecological niches? – Journal of Biogeography. https://doi.org/10.1111/jbi.13166.
[9] Bovo-Scomparin, V. M., Train, S. (2008): Long-term variability of the phytoplankton community in an isolated floodplain lake of the Ivinhema River State Park, Brazil. – Hydrobiologia 610(1): 331-344.
[10] Carvalho, L. (1994): Top-down control of phytoplankton in a shallow hypertrophic lake: Little Mere (England). – Hydrobiologia 275-276: 53-63.
[11] Chen, Q. C. (1974): On planktonic copepods of the Yellow Sea and the East China Sea, II. Cyclopoida and Harpacticoida. – Studia Marina Sinica 9: 1-24.
[12] Chiang, S. C., Du, N. S. (1979): Fauna Sinica, Crustacea, Freshwater Cladocera. – Science Press, Beijing.
[13] Coz, M. L., Chambord, S., Souissi, S., Meire, P., Ovaert, J., Buffan-Dubau, E., Prygiel, J., Azémar, F., Sossou, A. C., Lamothe, S. (2018): Are zooplankton communities structured by taxa ecological niches or by hydrological features? – Ecohydrology: e1956.
[14] David, V., Sautour, B., Chardy, P., Leconte, M. (2005): Long-term changes of the zooplankton variability in a turbid environment: the Gironde estuary (France). – Estuarine, Coastal and Shelf Science 64: 171-184.
[15] Dube, T., Denecker, L., Vuren, J. H. J. V., Wepener, V., Smit, N. J., Brendonck, L. (2017): Spatial and temporal variation of invertebrate community structure in flood-controlled tropical floodplain wetlands. – Journal of Freshwater Ecology 32: 1-15.
[16] Duggan, I. C., Green, J. D., Shiel, R. J. (2001): Distribution of rotiferas in north island, new zealand, and their potential use as bioindicators of lake trophic state. – Hydrobiologia 446/447: 155-164.
[17] Ejsmont-Karabin, J., Karabin, A. (2013): The suitability of zooplankton as lake ecosystemindicators: crustacean trophic state index. – Polish Journal of Ecology 61: 561-573.
[18] Fasham, M. J. R., Ducklow, H. W., Mckelvie, S. M. (1990): A nitrogen-based model of plankton dynamics in the oceanic mixed layer. – Journal of Marine Research 48: 591-639.
[19] Galkovskaja, G. A. (1987): Planktonic rotiferas and temperature. – Hydrobiologia 147: 307-317.
[20] Hood, R. R., Laws, E. A., Armstrong, R. A., Bates, N. R., Brown, C. W., Carlson, C. A., Chai, F., Doney, S. C., Falkowski, P. G., Feely, R. A. (2006): Pelagic functional group modeling: progress, challenges and prospects. – Deep-Sea Research Part II 53: 459-512.

http://www.aloki.hu ● ISSN 1589 1623 (Print) ● ISSN 1785 0037 (Online)
DOI: http://dx.doi.org/10.15666/aeer/1704_77277740

[21] Jeppesen, E., Jensen, J. P., Jensen, C., Faafeng, B., Hessen, D. O., Søndergaard, M., Lauridsen, T., Brettum, P., Christoffersen, K. (2003): The impact of nutrient state and lake depth on top-down control in the pelagic zone of lakes: a study of 466 lakes from the temperate zone to the Arctic. – Ecosystems 6: 313-325.
[22] Jeppesen, E., Nõges, P., Davidson, T. A., Haberman, J., Nõges, T., Blank, K., Amsinck, S. L. (2011): Zooplankton as indicators in lakes: a scientific-based plea for including zooplankton in the ecological quality assessment of lakes according to the European Water Framework Directive (WFD). – Hydrobiologia 676: 279-297.
[23] Li, X. Y., Yu, H. X., Ma, C. X. (2014): Zooplankton community structure in relation to environmental factors and ecological assessment of water quality in the Harbin Section of the Songhua River. – Chinese Journal of Oceanology & Limnology 32: 1344-1351.
[24] Lobry, J., David, V., Pasquaud, S., Lepage, M., Sautour, B., Rochard, E. (2008): Diversity and stability of an estuarine trophic network. – Marine Ecology Progress Series 358: 13-25.
[25] Long, S. X., Hamilton, P. B., Yang, Y., Wang, S., Huang, W. D., Chen, C., Ran, T. (2018): Differential bioaccumulation of mercury by zooplankton taxa in a mercury-contaminated reservoir Guizhou China. – Environmental Pollution 239: 147-160.
[26] Ma, C. X., Mwagona, P. C., Yu, H. X., Sun, X. W., Liang, L. Q. (2019): Seasonal dynamics of zooplankton functional group and its relationship with physicochemical variables in high turbid nutrient-rich Small Xingkai Wetland Lake, Northeast China. – Journal of Freshwater Ecology 34: 65-79.
[27] Matsuzaki, S. S., Suzuki, K., Kadoya, T., Nakagawa, M., Takamura, N. (2018): Bottom-up linkages between primary production, zooplankton, and fish in a shallow, hypereutrophic lake. – Ecology.
[28] MEP (2002): China national environmental quality standards for surface water. – GB3838-2002 (in Chinese).
[29] Morel, F. M. M., Kustka, A. B., Shaked, Y. (2008): The role of unchelated Fe in the iron nutrition of phytoplankton. – Limnology and Oceanography 53: 400-404.
[30] Morgan, M. D. (1985a): The effect of altered pH on zooplankton community structure in a disturbed New Jersey pine barrens pond. – Journal of Freshwater Ecology 3: 467-476.
[31] Morgan, M. D. (1985b): Photosynthetically elevated pH in acid waters with high nutrient content and its significance for the zooplankton community. – Hydrobiologia 128: 239-247.
[32] Mwagona, P. C., Ma, C. X., Yu, H. X. (2018): Seasonal dynamics of Zooplankton functional groups in relation to environmental variables in Xiquanyan Reservoir, Northeast China. – Annales de Limnologie-International Journal of Limnology 54: 33.
[33] Neumann-Leitão, S., Melo, P. A. M. C., Schwamborn, R., Diaz, X. F. G., Figueiredo, L. G. P., Silva, A. P., Campelo, R. P. S., Júnior, M. D. M., Melo, N. F. A. C., Costa, A. E. S. F. (2018): Zooplankton from a reef system under the influence of the Amazon River plume. – Frontiers in Microbiology 9: 1-15.
[34] Prowe, A. E. F., Pahlow, M., Dutkiewicz, S., Follows, M., Oschlies, A. (2012): Top-down control of marine phytoplankton diversity in a global ecosystem model. – Progress in Oceanography 101: 1-13.
[35] Quéré, C. L., Harrison, S. P., Prentice, I. C., Buitenhuis, E. T., Aumont, O., Bopp, L., Claustre, H., Cunha, L. C. D., Geider, R., Giraud, X. (2010): Ecosystem dynamics based on plankton functional types for global ocean biogeochemistry models. – Global Change Biology 11: 2016-2040.
[36] Reynolds, C. S., Huszar, V., Kruk, C., NaselliFlores, L., Melo, S. (2002): Towards a functional classification of the freshwater phytoplankton. – Journal of Plankton Research 24: 417-428.
[37] Semeniuk, D. M., Cullen, J. T., Johnson, W. K., Gagnon, K., Ruth, T. J., Maldonado, M. T. (2009): Plankton copper requirements and uptake in the subarctic Northeast Pacific Ocean. – Deep Sea Research Part I Oceanographic Research Papers 56: 1130-1142.

http://www.aloki.hu ● ISSN 1589 1623 (Print) ● ISSN 1785 0037 (Online)
DOI: http://dx.doi.org/10.15666/aeer/1704_77277740

[38] Semeniuk, D. M., Taylor, R. L., Bundy, R. M., Johnson, W. K., Cullen, J. T., Robert, M., Barbeau, K. A., Maldonado, M. T. (2016): Iron–copper interactions in iron-limited phytoplankton in the northeast subarctic Pacific Ocean. – Limnology & Oceanography 61: 279-297.
[39] Shi, Y. Q., Sun, S., Zhang, G. T., Wang, S. W., Li, C. L. (2015): Distribution pattern of zooplankton functional groups in the Yellow Sea in June: a possible cause for geographical separation of giant jellyfish species. – Hydrobiologia 754: 43-58.
[40] Shumka, S., Špoljar, Tasevska, M. O. (2018): The Zooplankton of Lake Skadar/Shkodra: Species Diversity and Abundance. – Pešić, V., Kostianoy, A. G., Karaman, G. S. (eds.) The Skadar/Shkodra Lake Environment. Springer, Berlin.
[41] Sinistro, R. (2010): Top-down and bottom-up regulation of planktonic communities in a warm temperate wetland. – Journal of Plankton Research 32: 209-220.
[42] Špoljar, M., Habdija, I., Primc, H. B., Sipos, L. (2010): Impact of environmental variables and food availability on rotifera assemblage in the karstic barrage lake Visovac (Krka River, Croatia). – International Review of Hydrobiology 90: 555-579.
[43] Srifa, A. (2010): Factors Controlling Zooplankton Dynamics in a Subtropical Lake During Cyanobacterial Bloom Events. – University of Florida, Gainesville, FL.
[44] Steinberg, D. K., Condon, R. H. (2009): Zooplankton of the York River. – Journal of Coastal Research 10057: 66-79.
[45] Stephen, D. (2010): The relative importance of top-down and bottom-up control of phytoplankton in a shallow macrophyte-dominated lake. – Freshwater Biology 39: 699-713.
[46] Sun, J., Feng, Y., Wang, D., Song, S., Jiang, Y., Ding, C., Wu, Y. (2013): Bottom-up control of phytoplankton growth in spring blooms in Central Yellow Sea, China. – Deep Sea Research Part II Topical Studies in Oceanography 97: 61-71.
[47] Sun, S., Huo, Y., Yang, B. (2010): Zooplankton functional groups on the continental shelf of the yellow sea. – Deep-Sea Research Part II 57: 1006-1016.
[48] Thompson, G. A., Dinofrio, E. O., Alder, V. A. (2013): Structure, abundance and biomass size spectra of copepods and other zooplankton communities in upper waters of the Southwestern Atlantic Ocean during summer. – Journal of Plankton Research 35: 610-629.
[49] Trevisan, G. V., Forsberg, B. R. (2007): Relationships among nitrogen and total phosphorus, algal biomass and zooplankton density in the central Amazonia lakes. – Hydrobiologia 586: 357-365.
[50] Wetzel, R. G. (2001): Limnology. – Academic Press, San Diego, CA.
[51] Yeatman, H. C. (1959): Cyclopoida. Freshwater Biology. 2nd Ed. – Wiley, New York.
[52] Zhou, J., Qin, B., Han, X. (2018): The synergetic effects of turbulence and turbidity on the zooplankton community structure in large, shallow Lake Taihu. – Environmental Science & Pollution Research 25: 1168-1175.
[53] Zuo, T., Wang, K. (2003): Length-dry weight relationship of Calanus sinicus in the southern part of the Yellow Sea. – Journal of Fisheries of China 27(Suppl.): 103-107.

http://www.aloki.hu ● ISSN 1589 1623 (Print) ● ISSN 1785 0037 (Online)
DOI: http://dx.doi.org/10.15666/aeer/1704_77277740

ESTIMATION OF SOIL EROSION AND RIVER SEDIMENT YIELD IN A RURAL BASIN OF NORTH ANATOLIA, TURKEY

OĞUZ, I.[1*] – SUSAM, T.[2] – KOCYIGIT, R.[1] – BICAK, H.[1] – DEMIRKIRAN, O.[3] – DEMIR, S.[1]

[1]*Department of Soil Science and Plant Nutrition, Gaziosmanpaşa University, Tokat, Turkey*

[2]*Department of Geomatics, Gaziosmanpaşa University, Tokat, Turkey*

[3]*Soil, Fertilizer and Water Resources Central Research Institute, Ankara, Turkey*

**Corresponding author*
e-mail: irfan.oguz@gop.edu.tr

(Received 14th Mar 2019; accepted 3rd May 2019)

Abstract. The aim of the study was to evaluate the sediment prediction performance of Revised Universal Equation (RUSLE) and Musgrave Equation at the Ekinli pond catchment, North central part of Turkey. Ekinli pond was built in 1977 for irrigation purposes. The accumulation of sediment in the ponds negatively affects their functions. There are many dams located within the study area whose operations have been adversely affected by excessive reservoir sedimentation. Accurate estimation of sediment deposition is important in the design of a pond. The calculated amount of sediment volume deposited in the Ekinli reservoir was 21600.75 m^3 and the average sediment yield was 514.3 m^3 y^{-1} between 1977 and 2018. In the Ekinli basin, the availability of bathymetry measurements between 1981 and 2006, provided the appropriate conditions to validate the results of the predicted sediment yield since the deposited sediment volume could be quantified as 552.3 m^3 y^{-1}. The measured and estimated sediment amounts for the Ekinli reservoir have shown an excellent accordance. In the 42-year time period, 6.74% of the water storage capacity of the pond has been lost. From 1977 to 2000, the entire basin was grassland and 38% of the basin area has been afforested. The landuse change reduced a little the amount of sediment in the reservoir. The Mann–Kendal and Theil–Sen Slope estimator statistics indicated a decreasing trend of sediment amount.
Keywords: *RUSLE, Musgrave Equation, sedimentation, pond, modified Fournier Index, trend analysis, Turkey*

Introduction

Generally, arid and semi-arid ecosystems, where limited rainfalls, floods, droughts and high population restrict rainfed crop production. For the solution of the problem, ponds present a significant contribution as a water conservation structure. The benefit of ponds is to keep water during periods of peak flows, thus preventing flood disasters, and then permit gradual release of water during periods of lower flows.

Pond construction involves high costs and environmental risks. In spite of this, they are built by taking into consideration of the benefits. All ponds negatively affect surface and subsurface hydrology, the aquatic environments of rivers, natural life. But those effects are often negated by the stated purpose of pond as being flood control, irrigation, drinking water supply and other functions. The expected life of a pond is essential for the evaluation of its function, viability, and the economic feasibility. The most important threat on the life of a pond is sedimentation. Deposition of sediment reduces reservoir's active water storage volume and hereby shortens its useful life. It has been reported that the reservoir capacity of world are decreasing each year about 0.5–1.0% (World Bank, 1998; World Commission on Dams Report, 2000). Soil erosion stands as the major factor controlling sedimentation of reservoirs in semi-arid regions (Wang et

http://www.aloki.hu ● ISSN 1589 1623 (Print) ● ISSN 1785 0037 (Online)
DOI: http://dx.doi.org/10.15666/aeer/1704_77417763

al., 2016); soils are usually shallower with sparse vegetation, low soil structural stability, non-negligible slopes and intense rainstorms (Cheviron et al., 2011; Gourfi et al., 2018). The useful life of reservoirs is limited by the excess sediment accumulation within the pond (Alighalehbabakhani et al., 2017). Several important factors such as climate change, glacial processes, and human induced activities (urbanization, deforestation, and changes in farm practices) in the watersheds can cause in accelerated soil erosion rates (Jordan et al., 2014; Toy et al., 2002).

There are several erosion models to estimate soil erosion in a field or a basin. One of them is USLE/RUSLE model (Wischmeier and Smith, 1978; Renard et al., 1997). The RUSLE, an empiric model, is a revised form of USLE model. The USLE/RUSLE is one of the most widely used soil erosion model worldwide, as well as in Turkey. Since this model is an erosion model, it needs sediment delivery ratio (SDR) to use in sediment calculations (Jobin et al., 2018). The RUSLE/SDR model has been widely used to evaluate soil erosion and sediment yield in numerous locations due to high efficiency and ease of implementation (e.g., Poirier et al., 2016; Gelagay, 2016; Yan et al., 2018; Ebrahimzadeh et al., 2018; Das et al., 2018; Wijesundara et al., 2018).

The RUSLE model is used with a calibrated SDR to obtain a simulated suspended sediment yield, which was compared with the observed values in 42 catchments of Morocco. The long-term observed values of sedimentation in all selected reservoirs in Morocco showed an annual mean sediment yield of 1.51 million m^3. A very strong positive relationship was determined between sedimentation in reservoirs and the corresponding drainage areas. The combination of RUSLE and SDR gave a very strong correlation with the observed suspended sediment yield (Gourfi et al., 2018).

The bathymetric measurement technique can be used to measure sediment yield in a reservoir by subtraction of the pre topographic elevations from current topographic elevations of a reservoir. This technique gives a possibility to compare between simulated sediment estimation to real sediment data in a reservoir.

In the Great Lakes watershed, the sediment accumulation rates of twelve reservoirs were evaluated using the Soil and Water Assessment Tool (SWAT). The estimated sediment accumulation rates by SWAT were compared on radionuclide dating of sediment cores and bathymetric survey methods. Based on the sediment accumulation rate, the remaining reservoir capacity for each study site was estimated. Evaluations of the anthropogenic impacts including land use change and pond construction on the sediment yield were assessed in this research. The regression analysis indicated a strong correlation between sediment yield and drainage area (Alighalehbabakhani et al., 2017).

In the present work, potential soil erosion of Ekinli basin and the sediment accumulation rate within the Ekinli reservoir was assessed by Revised Universal Equation (RUSLE) and Musgrave Equation, using the Geographic Information System (GIS)-based approach for reservoir sediment storage and post and pre-construction pond capacity. The objectives of this study are:

- The validation of applied sediment estimation method by comparing the sediment yields measured with the bathymetric surveys and calculated by some equations.
- To estimate the yearly sediment accumulation rate in the reservoir and predict the remaining capacity of the pond.
- To determine the effect of the partly afforestation on sediment yield in Ekinli basin.

http://www.aloki.hu ● ISSN 1589 1623 (Print) ● ISSN 1785 0037 (Online)
DOI: http://dx.doi.org/10.15666/aeer/1704_77417763

- To investigate the trends of rainfall and sedimentation and estimate the steepness of the slope used the Mann-Kendall for testing trend and Sen's slope estimator to determine trends of variables in Ekinli basin from 1977 to 2018.

Materials and methods

Study area

The study is carried out in the Ekinli basin in the North central part of Turkey, The reservoir was built in 1977 and its basin area is 591 ha. The Ekinli basin is located 49 km away from Tokat city (*Fig. 1*).

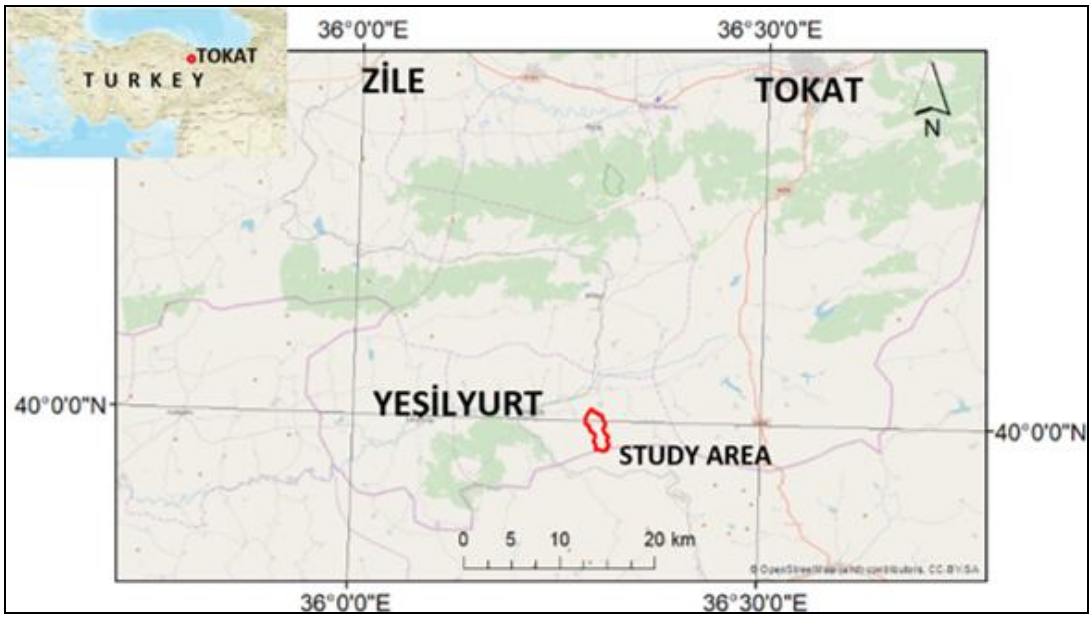

Figure 1. *The location of the study area*

The Ekinli reservoir at the Cayderesi outlet is a sub-unit of the Yesilirmak basin. Ekinli reservoir basin is located between 36°17'30"-36°18'00" latitudes and 40°00'30"-40°01'00" longitudes. The minimum and maximum elevation is 1118 m and 1440 m respectively and the average elevation is 1271 m. The digital elevation model (DEM) of Ekinli Basin is given in *Figure 2*.

The climate is semi-arid, and the annual precipitation is 419.6 mm. Approximately 49% of the annual precipitation falls between March and June. The mean annual temperature is 8.1 °C, the highest monthly temperature is in August (19.1°°C) and the lowest is in January (-2.1°°C). The mean annual evaporation is 1108 mm. The average snowy days are 22.6 in the basin.

The soils in the basin are calcareous brown forest soils with A and C profiles. Soils are generally vulnerable to degradation with steep slopes and lower vegetation density. The slope varies between 0 and 45% with an average of 26.15%.

The basin area was completely grassland up to 2000 year. In 2000, 38% of the basin area is converted to forestland. Currently, 38% of the basin area is forestland and 62% is grassland (*Fig. 3*). Some properties of Ekinli basin and reservoir are presented in *Table 1*.

http://www.aloki.hu ● ISSN 1589 1623 (Print) ● ISSN 1785 0037 (Online)
DOI: http://dx.doi.org/10.15666/aeer/1704_77417763

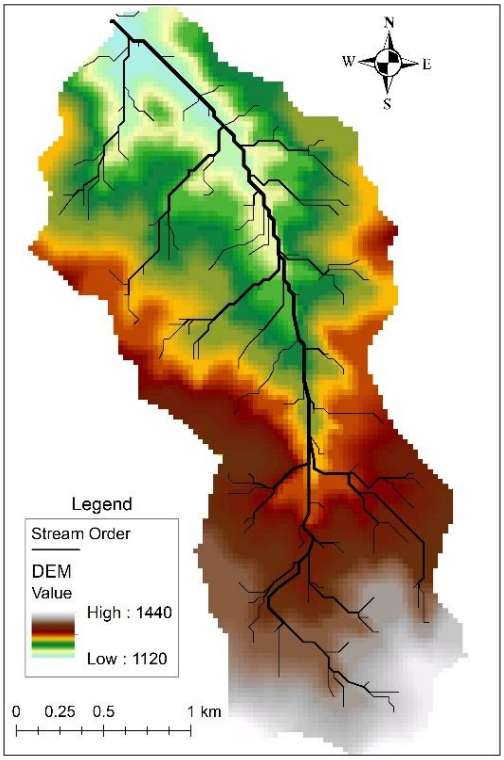

Figure 2. *Stream order and digital elevation model of Ekinli Basin*

Table 1. *Some properties of Ekinli basin and reservoir*

Attribute	Symbol	Ekinli pond basin
Water district	WD	Northern Turkey
Area	Ar (km^2)	5.91
Basin length	BL (km)	4.475
Basin width	BW (km)	1.29
Basin relief	r (m)	312
Minimum elevation	Hmin (m)	1118
Mean elevation	Hmean (m)	1271.03
Median elevation	Hm (m)	1220
Maximum elevation	Hmax (m)	1440
Mean slope	J (%)	26.15
Circulatory Ratio	Rc	0.51
Main stream length	L (km)	4.5
Main stream mean slope	Js (%)	6.4
Stream length	Lu (km)	6.4
Water storage volume	W (m^3)	320370
Active storage volume	As (m^3)	305635
Dead storage volume	Ds (m^3)	14735
Planned Sediment accumulation	Ps (m^3 25 y^{-1})	589.4
Crest height	Cr (m)	19.5
Crest width	Cw (m)	6
Irrigation area	(ha)	66

http://www.aloki.hu ● ISSN 1589 1623 (Print) ● ISSN 1785 0037 (Online)
DOI: http://dx.doi.org/10.15666/aeer/1704_77417763

Soil and sediment sampling and analyses

The coordinated soil samples from 150 locations were taken in June 2015 at the basin (*Fig. 3*). Sediment sampling was done in October when the pond was rather empty. Total 36 sediment samples were taken from crest to river discharge point through a line. Approximately 1000 cm^3 of disturbed soil was collected from 0.2 m depth, then sieved from 2 mm. The disturbed soil samples were used to determine soil organic matter and particle distribution. The undisturbed soil samples were obtained from 0 to 0.20 m by using a steel ring (0.05 × 0.05 m) to determinate saturated hydraulic conductivity and soil bulk density.

Soil organic matter was determined by Walkley-Black methods (Nelson and Sommers, 1982). Soil texture was analyzed using the hydrometer method (Gee and Bauder, 1986). Very fine sand content was measured by sieving (Soil Survey Staff, 1999). Saturated hydraulic conductivity was measured in the undisturbed cores (Black, 1965). Bulk density was determined by the core method (Blake and Hartge, 1986).

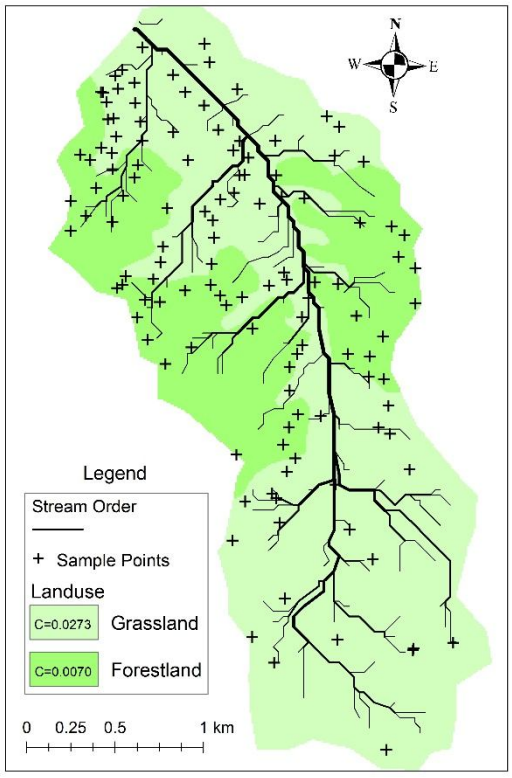

Figure 3. *Sample points, landuse and cover management factors map*

Bathymetric measurements

Bathymetric measurements of Ekinli reservoir were done three times in 1981, 1987 and 2006. The depth measurements of Ekinli reservoir were performed at 292 fix gridded points (10 × 20 m) in1981 and 1987 years. At these periods, the study was carried out at a limited number of fixed measurement points due to technical difficulties. For this purpose, iron bars were placed along both sides of the pond in order to precisely determine the fixed points. Iron bars were connected to each other by ropes during the measurement times. These ropes enabled the measurements on the same line

http://www.aloki.hu ● ISSN 1589 1623 (Print) ● ISSN 1785 0037 (Online)
DOI: http://dx.doi.org/10.15666/aeer/1704_77417763

in both measurement periods. The depth measurements were performed with the 10 m interval for each line. The first two periods of measurement were done by previous researchers using a boat and a plumb. The last measurement was carried out at 11366 points with LAZ 4100 echocaunder in 2006 by our research team. The points were measured by a freely movement of a zodiac boat in the pond.

The water storage volume of the pond was calculated for each measurement period by Surfer Software (Surfer, 1997). According to each bathymetric measurement periods, the reservoir water storage capacities were calculated.

Soil erosion and sediment yield calculation

The RUSLE erosion model and Musgrave Equation were employed for the calculation of soil loss and sediment yield for the study of basin. Required all calculation were done in geographic information system (GIS) environment within ArcGIS Version 10.1 (ESRI, 2011).

The factors used in the Revised Universal Soil Loss Equation (RUSLE) were used to estimate the average annual soil loss (Renard et al., 1997). According to RUSLE, soil erosion is directly affected by a region's rainfall erosivity, soil erodibility, slope length, slope steepness, land use type and supporting practices. Hereby, mean annual soil loss in per unit of area is estimated from six erosion factors according to *Equation 1*.

The RUSLE is as follows:

$$A = R \times K \times L \times S \times C \times P \quad \text{(Eq.1)}$$

where A is computed soil loss (ton ha^{-1} y^{-1}); R is the rainfall-runoff erosivity factor (MJ mm ha^{-1} h^{-1} y^{-1}); K is a soil erodibility factor (t h ha MJ^{-1} mm^{-1}); L is the slope length factor (dimensionless); S is the slope steepness factor (dimensionless); C is a cover management factor (dimensionless); and P is a supporting practices factor (dimensionless).

The rainfall erosivity is determined by the various characteristics of a rainfall event, such as rainfall intensity and duration, the kinetic energy of raindrops, their size (diameter), and velocity (Petan et al., 2010). The unit rainfall energy, as proposed by the RUSLE methodology, is defined by the following equation (*Eq. 2*) and is calculated for each time interval as follows (Brown and Foster, 1987).

$$e_m = 0{,}29\,[1 - 0{,}72\exp(-0{,}05\,i)] \quad \text{(Eq.2)}$$

where e_m is unit rainfall energy (MJ ha^{-1} mm^{-1}); i is rainfall intensity during the time interval (mm h^{-1}).

The calculation of RUSLE R factor required pluviograph records. In Ekinli basin, only daily pluviometer rainfall depth data was available. The Modified Fournier Index (MFI) of Arnoldus (1980) is widely used worldwide to calculate rainfall erosivity which is not available pluviograph data. The MFI is a parameter of rainfall erosivity and makes use of mean monthly and annual rainfall depth data (*Eq. 3*). The equation is expressed as:

$$MFI = \sum_{i=1}^{12} \frac{p_i^2}{P} \quad \text{(Eq.3)}$$

http://www.aloki.hu ● ISSN 1589 1623 (Print) ● ISSN 1785 0037 (Online)
DOI: http://dx.doi.org/10.15666/aeer/1704_77417763

where pi is monthly rainfall depth (mm); p is annual rainfall depth (mm).

Soil erodibility (K) is the sensitivity of a soil to erosion by runoff and raindrop impact. The higher K value is the greater the susceptibility of the soil to rill and sheet erosion. Soil erodibility factor was estimated using *Equation 4* given by Foster et al. (1991).

$$100K = 2.1M^{1.14}10^{-4}(12-a) + 3.25(b-2) + 2.5(c-3) \quad \text{(Eq.4)}$$

where K is soil erodibility (t h ha MJ^{-1} mm^{-1} ha^{-1}); M is the particle-size parameter; a is percent organic matter, b is soil structure code (very fine granular: 1, fine granular: 2, medium or coarse granular: 3, and blockish, platy, or massive: 4), which was determined in the field; c is soil profile permeability class (rapid: 1, moderate-to-rapid: 2, moderate: 3, slow-to-moderate: 4, slow: 5, and very slow: 6).

Slope length is defined as the distance from the point of origin of runoff to the point where deposition occurs. The slope length factor (L) was calculated with the help of *Equation 5* (Mc Cool et al., 1987).

$$L = (\lambda/22.1)^m \quad \text{(Eq.5)}$$

where L is slope length factor (dimensionless), which is field slope length (m); m is a coefficient that depends on slope steepness, being 0.5 for slopes exceeding 5%, 0.4 for 4% slopes and 0.3 for slopes less than 3%.

The slope steepness is a site slope, usually expressed as a percentage. The percent slope was determined from DEM with the help of *Equation 6*.

$$S = 10.8sin\theta + 0.03 \quad s < 9\% \qquad S = 16.8sin\theta - 0.05 \quad s \geq 9\% \quad \text{(Eq.6)}$$

where S is slope steepness factor (dimensionless) and ɵ is slope angle in degree.

In the RUSLE, the subfactor C were calculated by *Equation 7*. In this method, a factor called soil loss ratio (SLR) for given conditions is calculated by using 5 different subfactors.

$$SLR = PLU * CC * SC * SR * SM \quad \text{(Eq.7)}$$

where PLU is the prior land use subfactor, CC is the canopy subfactor, SC is the surface cover subfactor, SR is the surface roughness subfactor, and SM is the soil moisture subfactor.

Once the SLR's have been calculated for each time interval, they are multiplied by their corresponding percentage of annual EI (Wischmeier and Smith 1978). These values are then summed and divided by the total percentage of annual EI value for the entire time period (*Eq. 8*) (Renard et al., 1997).

$$C = (SLR_1 * EI_1 + SLR_2 * EI_2 + \cdots\cdots + SLR_n * EI_n / EI_t) \quad \text{(Eq.8)}$$

where C is average annual or crop value; SLR_i is the value for time period i; EI_i is percentage of the annual or crop EI occurring during that time period; n is number of periods used in the summation; and EI_t is sum of the EI percentages for the entire time

http://www.aloki.hu ● ISSN 1589 1623 (Print) ● ISSN 1785 0037 (Online)
DOI: http://dx.doi.org/10.15666/aeer/1704_77417763

period. The cover management factor (C factor) represents a combined effect of interrelated cover and management variables.

Erosion control practices factor (P) is determined to be the ratio between the soil losses expected for a certain soil conservation practice and that of up-and-down slope ploughing (Liu et al., 2001). The support practice factor (P factor) represents a combined effect of support practices and management variables. They are also known as structural methods for controlling erosion. In an area, if conservation practices are not followed P value should assign as 1.

RUSLE is a soil erosion model and is not capable to estimate sediment amount directly. The calculated soil loss amount, according to RUSLE model was multiplied by sediment delivery ratio (SDR) of the basin. Thus, calculated soil loss of the basin area has been converted to sediment amount. Therefore, the SDR of the basin is calculated by Renfro Method (*Eq. 9*).

Renfro (1975) developed an equation relating SDR with the drainage area. It is based on Maner's (1962) equation and the sediment yields observed in 14 watersheds in the Blackland Prairie Area in Texas. The model shows a good relationship between SDR and the drainage area ($R^2 = 0.92$). The equation is expressed as:

$$\log(SDR) = 1.7935 - 0.14191 * \log(A) \quad \text{(Eq.9)}$$

where A is drainage area (km^2).

The RUSLE equation is only capable of calculating sheet and rill erosions, and cannot calculate bed load. Therefore, for a more realistic calculation, it is necessary to add stream bed load to the calculations made with these equations. To obtain a more realistic sediment estimation, the amount of sediment calculated by the Musgrave Equation (Sevinç, 1993) was added to the amount of sediment calculated by the RUSLE equation. The Musgrave equation (*Eq. 10*) is given by:

$$E = U * D * A * Y \quad \text{(Eq.10)}$$

where E is stream bed load ($m^3\ y^{-1}$); U is length of waterway (m); D is eroded coastal height (m); A is active erosion rate of riverbank (%) and Y is horizontal advance distance (m).

In the meteorological variables, parametric and non-parametric approaches have been used over the years. The most frequently used tests for identifying the variations in meteorological variables have been nonparametric. The most popularized approach among them is Mann–Kendal test (Kendall, 1975; Mann, 1945). The Mann-Kendall nonparametric test was used to test for trend (*Eq. 11*). This test is calculated as (Mohtar et al., 2015; Yurekli, 2015):

$$S = \sum_{i=1}^{n-1} \sum_{j=i+1}^{n} \mathrm{sgn}\left(x_j - x_i\right) \quad \text{(Eq.11)}$$

where n is the number of event, Xj and Xi are the observed events, and sgn is the sign function.

The variance is given by *Equation 12*:

http://www.aloki.hu ● ISSN 1589 1623 (Print) ● ISSN 1785 0037 (Online)
DOI: http://dx.doi.org/10.15666/aeer/1704_77417763

$$\sigma_S^2 = 18^{-1}\left[n(n-1)(2n+5) - \sum_{i=1}^{m} t_i (t_i - 1)(2t_i + 5) \right] \quad \text{(Eq.12)}$$

where n is the number of events, m is the number of tied events, t_i is the number of events that are tied. For sample size greater than 10 the test can be given in *Equation 13*:

$$Z_{MK} = \begin{cases} \dfrac{S-1}{\sqrt{\sigma_S^2}} & \text{if} \quad S > 0 \\ 0 & \text{if} \quad S = 0 \\ \dfrac{S+1}{\sqrt{\sigma_S^2}} & \text{if} \quad S < 0 \end{cases} \quad \text{(Eq.13)}$$

For increasing rainfall trends, the values of Z_{MK} is positive while for decreasing trends the value of Z_{MK} is negative.

Sen's estimator for slope is a nonparametric test for the steepness of the trend. For N pairs of data is given in *Equation 14:*

$$Q_k = \frac{x_j - x_i}{j - i} \text{ for } k = 1,..., N \quad \text{(Eq.14)}$$

where Xj and Xk are the values at times j and k (j > k) respectively. The N values of Qk are ranked from smallest to largest. According to condition that N is odd or even, the median concerning with total N values of is calculated by *Equation 15:*

$$Q_{med} = \begin{cases} Q_{\left[(N+1)/2\right]} & \text{if N is odd} \\ 2^{-1}\left\{ Q_{\left[(N)/2\right]} + Q_{\left[(N+2)/2\right]} \right\} & \text{if N is even} \end{cases} \quad \text{(Eq.15)}$$

The confidence interval for Q_{med} was obtained to determine the significance of the slope.

Results and discussion

Bathymetric measurements

In the Ekinli reservoir, three bathymetric measurements were conducted in 1981, 1987 and 2006. The three-dimensional map of the pond according to last bathimetric measurement in 11366 measurement points is given in *Figure 4*. We considered 1120 m sea level for volume computations in all bathimetric measurements. The amount of the sediment volumes stored in the pond was calculated on the basis of x, y and z coordinates. The sediment amounts accumulated in the pond during the bathymetric measurement periods are given in *Table 2*.

http://www.aloki.hu ● ISSN 1589 1623 (Print) ● ISSN 1785 0037 (Online)
DOI: http://dx.doi.org/10.15666/aeer/1704_77417763

Table 2. *The change in the water storage volume of the Ekinli pond and the amount of sediment accumulation*

Years	Water storage capacity, m^3	The amount of sediment accumulated in the pond, m^3	Annual average sediment amount		Water storage capacity, %
			m^3 $year^{-1}$	mm $year^{-1}$	
1981	54873.6	0.0	-	-	100.00
1987	50626.2	4247.7	707.95	0.12	92.26
2006	45246.5	9627.1	534.84	0.09	82.46

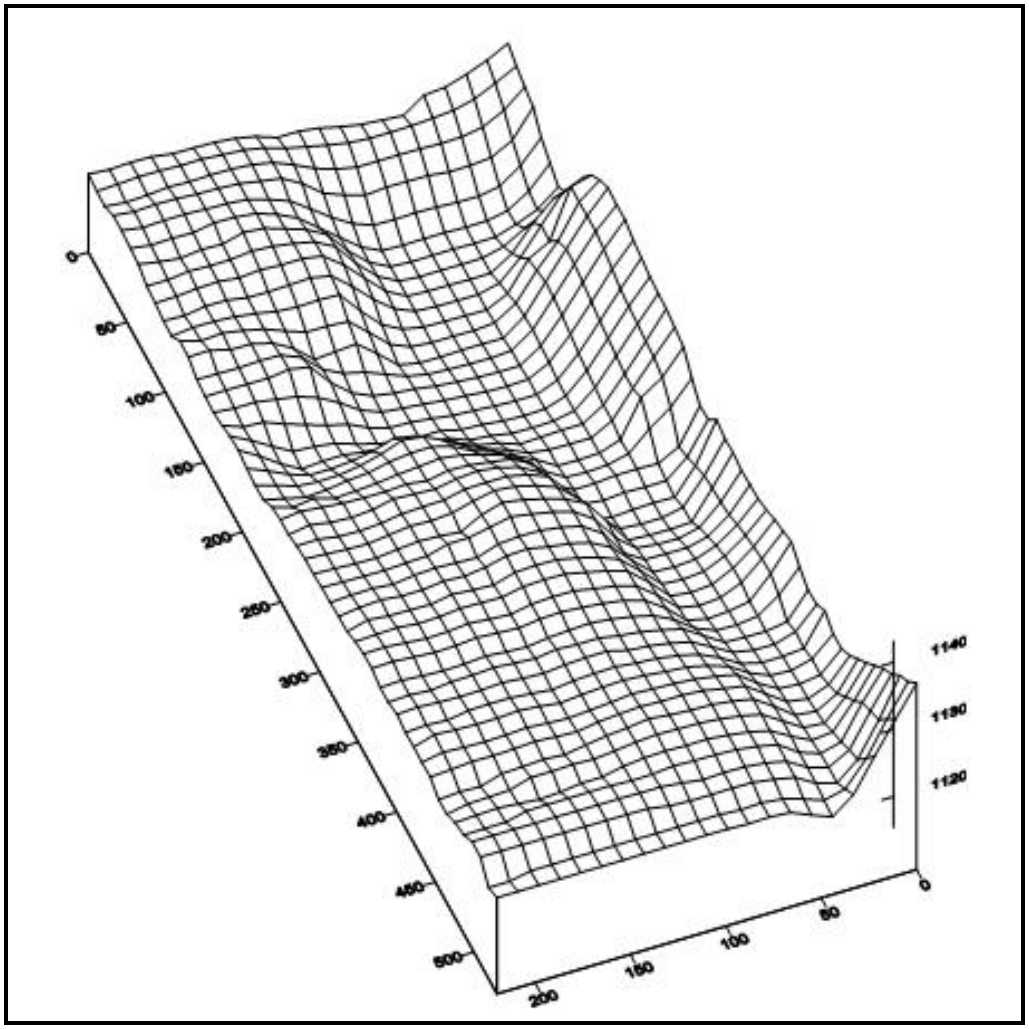

Figure 4. *Three-dimensional view of the pond (m)*

In 1981, the water storage capacity of the pond was calculated as 54873.6 m^3 according to 1120 m sea level by Surfer software. The water storage capacity of the pond decreased gradually due to accumulation of sediment amount during the experimental period. The water storage capacity of the pond decreased by 92.26% between the years 1981 and 2006. Considering the decrease in water storage capacity, a total of 4247.7 m^3 and 9627.1 m^3 sediment accumulated in the pond in 1981-1987 and 1987-2006 years respectively. The average sediment accumulation was 707.9 m^3 $year^{-1}$

http://www.aloki.hu ● ISSN 1589 1623 (Print) ● ISSN 1785 0037 (Online)
DOI: http://dx.doi.org/10.15666/aeer/1704_77417763

in 1981-1987 and 534.8 m^3 $year^{-1}$ in 1987-2006 periods, respectively. The decrease in the annual average sediment amount accumulated in the pond between 1987 and 2006 can be attributed to the afforestation of the Ekinli basin. The annual sediment volume to reach the reservoir is estimated as 589.4 m^3 y^{-1} when the pond was planned. The estimation of sediment for pond planning is quite accurate according to the results of the bathymetric measurements.

Sediment properties

A total 36 surface sediment samples of reservoir base were taken from crest to river discharge point to determine average sediment bulk density and sediment size distribution. The mean bulk density of sediment was measured as 1.48 g cm^{-3}. The highest clay and silt contents in the sediments were observed near the crest. The sand content was lower than 30% at this location. The clay content of sediments was measured over 25% up to 160 m from the crest. After this distance the clay content was below 5%. The silt content of the sediments was greater than 40%, from 0 to 150 m. Maximum sand content was observed at a distance of between 200 and 400 m from the crest (*Fig. 5*). Through the reservoir larger suspended particles generally sedimented earlier when reach to the pond compared to the fine particles which usually measured around the crest.

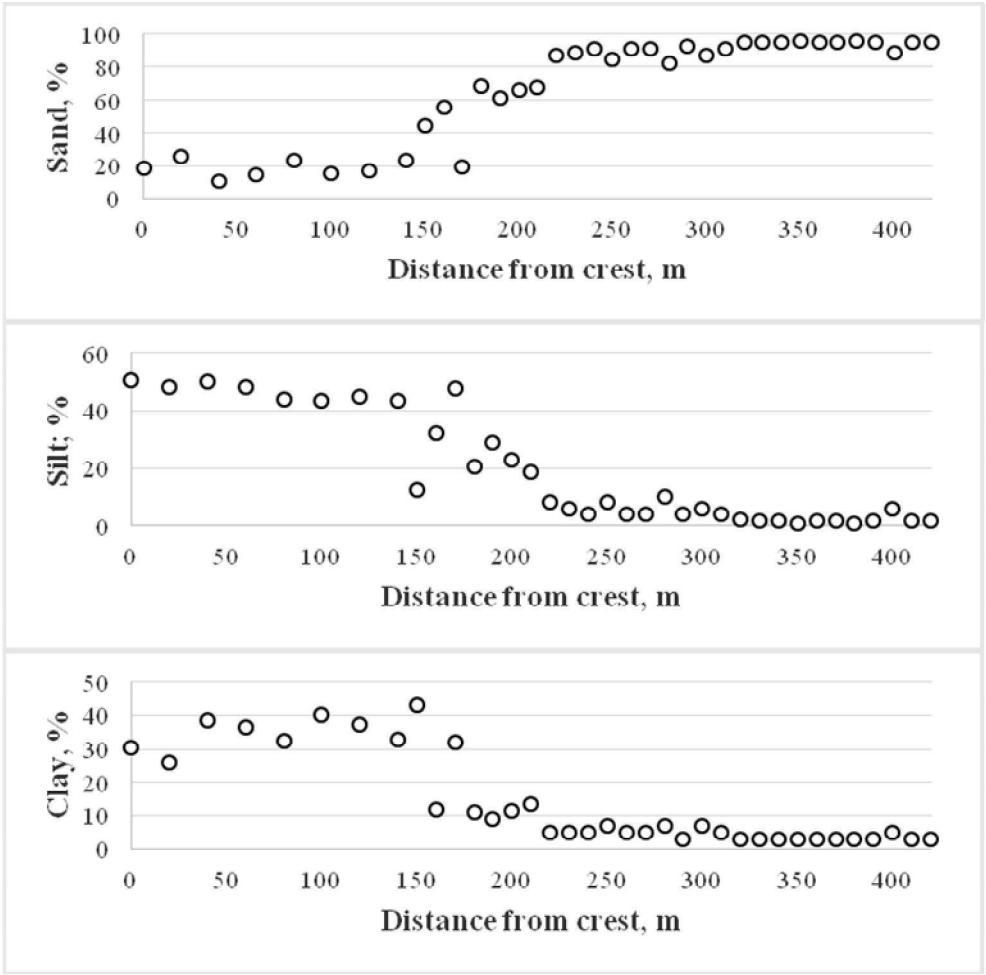

Figure 5. *Sediment size distribution according to distance from crest*

http://www.aloki.hu ● ISSN 1589 1623 (Print) ● ISSN 1785 0037 (Online)
DOI: http://dx.doi.org/10.15666/aeer/1704_77417763

Estimation of gross erosion of Ekinli Basin

Gross erosion includes sheet, rill, gully and channel erosions. The RUSLE estimates sheet and rill erosion only. For this reason, gully and channel erosions were modelled by Musgrave equation in the study (*Eq. 9*). The amount of sediment deposited in the pond was estimated by combining RUSLE and the Musgrave methods.

RUSLE erosion model calculations

As the required input parameters of RUSLE were obtained and prepared in ArcMap for soil loss calculation.

The rainfall erosivity (R) factor

Several studies showed that rainfall erosivity is one of the most sensitive factor for soil erosion (Ganasri and Ramesh, 2016). In Ekinli basin there were not pluviograph records hence, Modified Fournier Index (MFI) was used for the calculation of R factor. Using the MFI data, Tokat city pluviograph records were used to obtain a more realistic R-factor calculation. Tokat is 49 km away from the research site and pluviograph records for 18 years are available. The linear regression relationship equation was obtained between R factor and MFI values of Tokat province by 18 years data (*Fig. 6*). The regression analysis indicated a good correlation between R factor and MFI values. The R^2 which represents how close the data are to the regression line is 0.61. For the erosion studies with high level of uncertainty in the linear model, the R^2 of observation and parameter data were found as 0.61 which is adequate for the study.

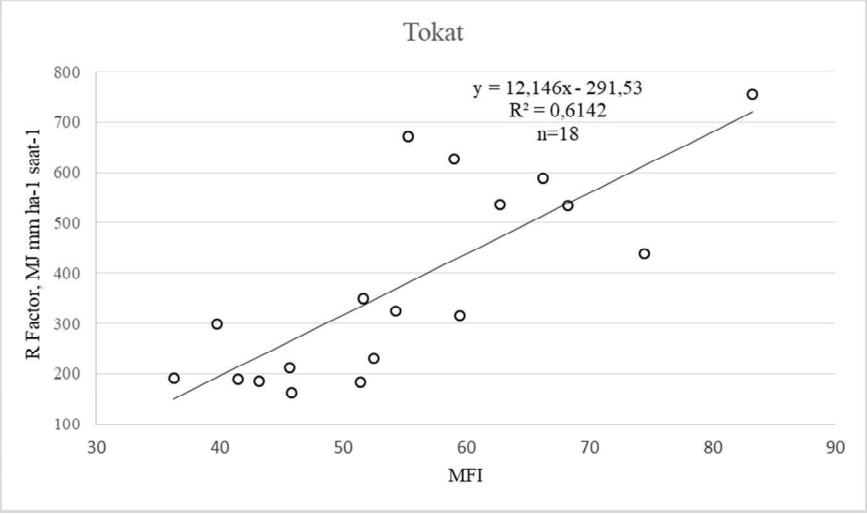

Figure 6. *Relationship between R factor and MFI values of Tokat*

The linear regression relationship equation between R factor and MFI of Tokat province were applied to Ekinli basin MFI values, which has been calculated from monthly rainfall data. Such regressions using local research areas have been used in literature where no rainfall intensity data are available (Gelagay and Minale, 2016; Zeng et al., 2017). Thus, the annual R-factor values of Ekinli basin were obtained (*Table 3*). The mean, lowest and highest R Factors values were 415.32, 98.12 and 800.09 MJ mm ha^{-1} h^{-1} y^{-1} respectively.

http://www.aloki.hu ● ISSN 1589 1623 (Print) ● ISSN 1785 0037 (Online)
DOI: http://dx.doi.org/10.15666/aeer/1704_77417763

Table 3. *The rainfall erosivity factor values of Ekinli basin (1977-2018)*

Year	R Factor MJmmha^{-1}h^{-1}yr^{-1}	Year	R Factor MJmmha^{-1}h^{-1}yr^{-1}	Year	R Factor MJmmha^{-1}h^{-1}yr^{-1}	Year	R Factor MJmmha^{-1}h^{-1}yr^{-1}
1977	468.05	1988	567.51	1999	328.78	2010	644.57
1978	241.90	1989	475.11	2000	358.03	2011	331.32
1979	429.57	1990	502.49	2001	271.33	2012	338.25
1980	609.37	1991	507.60	2002	317.81	2013	207.40
1981	392.84	1992	185.78	2003	142.07	2014	416.30
1982	335.12	1993	563.20	2004	323.05	2015	542.25
1983	633.47	1994	130.47	2005	224.15	2016	632.86
1984	932.23	1995	429.72	2006	518.08	2017	235.59
1985	800.09	1996	501.42	2007	256.17	2018	498.29
1986	357.28	1997	344.84	2008	98.12		
1987	390.44	1998	558.38	2009	402.06	Average	415.32

The K factor

To estimate the soil erodibility (K factor) values indirectly, soil physical features (texture, very fine sand, organic matter, saturated hydraulic conductivity and structural properties) were obtained in topsoil of 150 sampling points in the basin (Wischmeier and Smith, 1978). The soil erodibility characteristics of the Ekinli basin were determined with the help of *Equation 4*. Coordinated K factor point values of study area have been converted to K factor surface map by ArcMap software (*Fig. 7*).

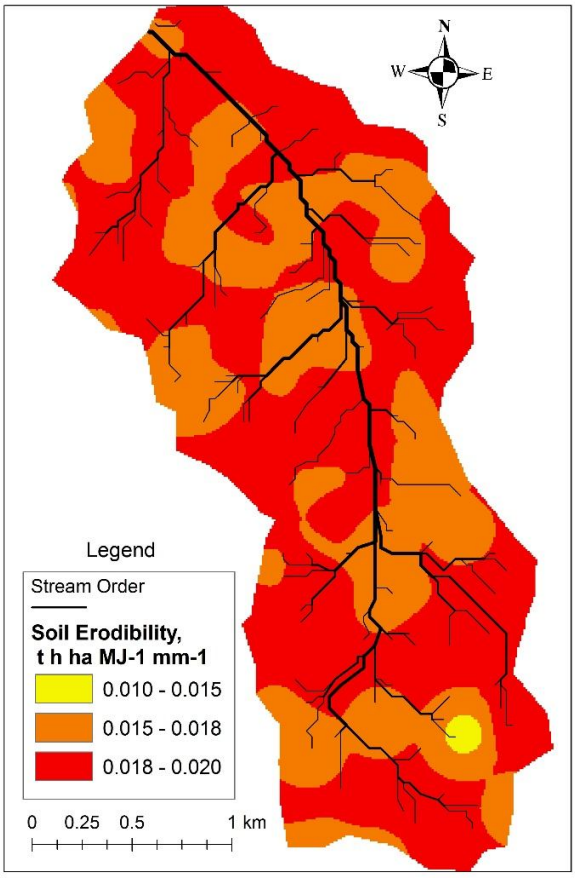

Figure 7. *The soil erodibility map*

http://www.aloki.hu ● ISSN 1589 1623 (Print) ● ISSN 1785 0037 (Online)
DOI: http://dx.doi.org/10.15666/aeer/1704_77417763

The spatial distribution of soil erodibility factor map ranged from 0.010 to 0.020 t ha h ha^{-1} MJ^{-1} mm^{-1}.

The LS factor

The slope length factor (L) and the slope steepness factor (S) illustrate the contribution of topography on soil loss. The L factor equals to 1 for 22.1 m slope length, and the S factor equals to 1 for 9% slope. L and S factor layers were directly calculated from DEM of the study area by the help of *Equations 5* and *6* in ArcMap (*Fig. 8*). The values of slope length and slope steepness factor (LS) varied from 0 to 22.04 with a mean value of 2.26; the highest values were recorded in areas with high altitudes and slopes, while flat lands had the lowest values.

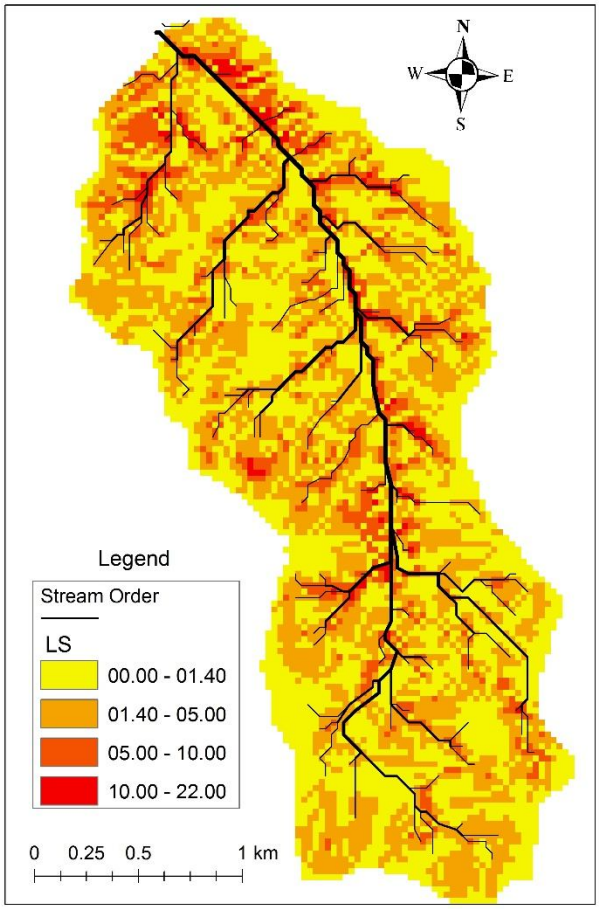

Figure 8. *The topographic factor of RUSLE map*

The C factor

In RUSLE, C factor represents the effects of plants, soil cover, soil biomass, and soil disturbing activities on erosion. The C factor values were determined by C factor calculation procedure (Renard et al., 1997) based on the field works. Field measurements were done in grassland and forestland separately. Various measurements and vegetation samplings were carried out at both locations in 15 days periods, excluding snow-covered days. A total of 18 field studies were carried out to obtain the

http://www.aloki.hu ● ISSN 1589 1623 (Print) ● ISSN 1785 0037 (Online)
DOI: http://dx.doi.org/10.15666/aeer/1704_77417763

C factor values. Some of the data were mass densities of live and dead roots, mass density of incorporated surface residue in the upper depth of soil, fraction of land surface covered by canopy, crop height, surface roughness, percent residue covers and dryweight of crop residue. As a result, SLR value was calculated for different time periods for forest and grassland by the help of *Equation 7* (*Table 4*). Weighted average values was also calculated and annual average C factor was determined according to *Equation 8* for the time frame corresponding to the annual erosion index (EI) value percentage. The annual C values were calculated as 0.007 and 0.0273 for forestland and grassland of the basin respectively (*Fig. 3*).

Table 4. *Calculated SLR values for forestland and grassland in Ekinli basin*

Months	**January**		**February**		**March**		**April**		**May**		**June**	
Forestland	0.034	0.035	0.034	0.032	0.034	0.026	0.026	0.026	0.001	0.001	0.000	0.000
Grassland	0.081	0.082	0.103	0.133	0.124	0.125	0.125	0.125	0.001	0.001	0.000	0.000
EI. %	1.17	1.16	0.74	1.61	0.59	0.32	9.69	5.41	14.78	13.56	25.06	5.76
Months	**July**		**August**		**September**		**October**		**November**		**December**	
Forestland	0.000	0.000	0.000	0.000	0.000	0.000	0.000	0.000	0.013	0.014	0.030	0.026
Grassland	0.000	0.000	0.000	0.000	0.000	0.000	0.000	0.000	0.024	0.026	0.062	0.065
EI. %	1.98	1.23	0.00	0.13	4.00	0.65	4.25	2.27	2.52	1.20	1.05	0.86

The P factor

The P factor is computed for individual support practices that are used in combination to reduce erosion. Such practices include terracing, contour tillage, and strip farming. In the case of rare conservation structures in a region, usually P Factor value of 1 is assigned (Tamene et al., 2015). There were no significant conservation measures so we used 1 value for soil loss calculation.

Soil erosion map of basin

Layers were created in GIS environment for each RUSLE equation factor. Thus, the annual potential sheet and rill erosion were calculated for the basin from 1977 to 2018. The average soil loss map is presented in *Figure 9*. The values of soil loss varied from 0 to 4.22 ton ha^{-1} y^{-1} with a mean value of 0.36; the highest values recorded in areas with high altitudes and slopes, while flat lands had the lowest values.

Sediment delivery ratio of Ekinli basin

The sediment delivery ratio (SDR) is commonly used in erosion and transport studies to describe the extent of sediment storage within the basin. Ekinli basin with small drainage area and the short distance of fields to the streams created a high SDR potential. Thus, the soil particles of reaching the water channel system are high. In order to calculate the SDR of the basin Renfro Equation (*Eq. 9*) was used and provided 48.31% value.

Stream bed load calculation by Musgrave equation

The waterway length of Ekinli basin is 4500 m. Since there has been active erosion on both sides of the waterway, total coastal length was considered as 9000 m. Eroded

http://www.aloki.hu ● ISSN 1589 1623 (Print) ● ISSN 1785 0037 (Online)
DOI: http://dx.doi.org/10.15666/aeer/1704_77417763

coastal height is 1.5 m and active erosion rate is 48.31% while horizontal advance distance is 0.051 m. According to *Equation 10,* stream bed load of Ekinli basin was calculated as 332 m^3 y^{-1}. This calculated value was added to the amount of sediment computation by RUSLE and the annual total amount of sediment reaching to the pond was determined (*Table 5*).

The sediment accumulation of reservoir was calculated as 21600.75 m^3 for 42 years study period. The minimum (370.03 m^3) and the maximum (775.69 m^3) sediment amounts were calculated in 2008 and 1984 respectively.

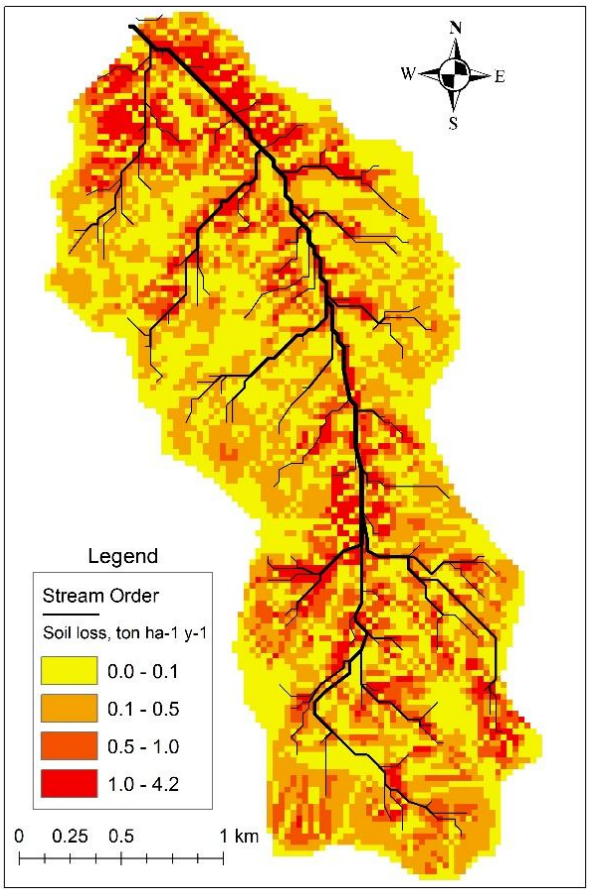

Figure 9. *Potential soil loss map of basin according to RUSLE method*

Comparison of sediment yield of Ekinli basin measured by bathymetry and computed by RUSLE and Musgrave method

In our study, the calculated sediment yield was compared with the results of bathymetric measurements. Thus, the accuracy of the calculations was tested. Because the last bathymetric measurement was carried out in 2006, the measurement values performed on this date do not provide sufficient information about the current water storage capacity of the pond. However, it gives valuable information about the validity of the calculations.

The effect of sedimentation on pond is only possible when the basin sediment yield is accurately modeled. Measured and calculated basin sediment yields are compared in *Table 6* by comparing two different bathymetric measurement periods.

http://www.aloki.hu ● ISSN 1589 1623 (Print) ● ISSN 1785 0037 (Online)
DOI: http://dx.doi.org/10.15666/aeer/1704_77417763

Table 5. *Total sediment accumulation to the pond*

Year	Average soil loss (RUSLE) ton ha^{-1} y^{-1}	Sediment (RUSLE) m^3*	Stream bed load (Musgrave) m^3	Total sediment accumulation m^3**
1977	0.53	223.96	332	555.96
1978	0.27	114.09	332	446.09
1979	0.48	202.83	332	534.83
1980	0.69	291.56	332	623.56
1981	0.44	185.93	332	517.93
1982	0.38	160.57	332	492.57
1983	0.87	367.63	332	699.63
1984	1.05	443.69	332	775.69
1985	0.90	380.30	332	712.30
1986	0.40	169.02	332	501.02
1987	0.44	185.93	332	517.93
1988	0.64	270.44	332	602.44
1989	0.54	228.18	332	560.18
1990	0.57	240.86	332	572.86
1991	0.57	240.86	332	572.86
1992	0.21	88.74	332	420.74
1993	0.64	270.44	332	602.44
1994	0.15	63.38	332	395.38
1995	0.49	207.05	332	539.05
1996	0.57	240.86	332	572.86
1997	0.39	164.80	332	496.80
1998	0.63	266.21	332	598.21
1999	0.37	156.35	332	488.35
2000	0.31	130.99	332	462.99
2001	0.24	101.41	332	433.41
2002	0.28	118.32	332	450.32
2003	0.12	50.71	332	382.71
2004	0.28	118.32	332	450.32
2005	0.20	84.51	332	416.51
2006	0.45	190.15	332	522.15
2007	0.22	92.96	332	424.96
2008	0.09	38.03	332	370.03
2009	0.35	147.90	332	479.90
2010	0.56	236.63	332	568.63
2011	0.29	122.54	332	454.54
2012	0.30	126.77	332	458.77
2013	0.18	76.06	332	408.06
2014	0.36	152.12	332	484.12
2015	0.47	198.60	332	530.60
2016	0.55	232.41	332	564.41
2017	0.21	88.74	332	420.74
2018	0.44	185.93	332	517.93
Total				**21600.75**

*This value was calculated as: calculated mean soil loss by RUSLE (ton ha^{-1} y^{-1}) × basin area (591 ha) × bulk density of sediment (1.48 g cm^{-3}) × sediment delivery ratio (% 48.31)

** This value was calculated as: calculated total sediment amount by RUSLE (m^3) + calculated stream bed load by Musgrave equation (m^3)

http://www.aloki.hu ● ISSN 1589 1623 (Print) ● ISSN 1785 0037 (Online)
DOI: http://dx.doi.org/10.15666/aeer/1704_77417763

Table 6. *Comparison of measured and calculated sediment yields in Ekinli basin*

Period	Measured		Calculated		Variation
	Total, m^3	Average, $m^3\ y^{-1}$	Total, m^3	Average, $m^3\ y^{-1}$	m^3
1981-1987	4200	600.00	4217.06	602.44	+17.06
1988-2006	9600	505.26	9540.57	502.14	-59.43

According to the bathymetric measurements, the amounts of sediment deposited in the basin for the periods between 1981-1987 and 1988-2006 were 4200 m^3 and 9600 m^3, respectively. At the same period, the calculated sediment yield of the Ekinli basin was 4217.06 m^3 and 9540.57 m^3 respectively.

The first bathymetric measurement period was identified 7 years of sediment accumulation. The average sediment yield was 600 $m^3\ y^{-1}$ in this period. Calculated sediment yield was very close to the measured sediment yield during the same period. The predicted sediment yield was only 17.06 m^3 higher than the actual measurement results.

The second bathymetric measurement period was identified 19 years of sediment accumulation. The average sediment yield was 505.26 $m^3\ y^{-1}$ during this period. At the same period, the calculated sediment yield was also very close to the measured sediment yield. The predicted sediment yield was only 59.43 m^3, lower than the actual measurement results.

The measured and estimated sediment amounts for the Ekinli reservoir represented an excellent adaptation. According to this result, it is possible that the estimation of adaptation is also being quite accurate for non-measured years.

The effects of sediment accumulation on the water storage capacity of the pond

The sluice way height of the pond was planned according to 14735 m^3 volume for the 25-year duration, considering the amount of sediment accumulation in the reservoir. For the planning calculations, the dead volume of the pond is expected to be filled in 2001. According to our sediment calculation results, the dead volume of the pond was filled in 2004. The results of the bathymetric measurements confirmed that the dead volume has been filled in the planned period. The bed of reservoir elevated with sediment accumulation over time and the sluice way remained below the current pond floor. However, the special design of the sluice way intake and the whirlpool effect by water movement have ensured seamless water flow from reservoir for irrigation up to date.

In 2017 the open channel irrigation system was canceled and the pipe system was switched to irrigation. Thus, the irrigation area of the pond was expanded.

The cumulative sediment accumulation in the reservoir from 1977 to 2018 is presented in *Figure 10*. According to our calculations, a total of 21600.75 m^3 sediments were deposited in the reservoir for 42 years. According to pond planning calculation, our computation and bathimetric measurements, the mean sediment accumulation were 589.4 m^3, 514.3 m^3 and 552.3 m^3 respectively. According to these comparisons, all three computations showed a perfect fit.

Considering the amount of sediment calculated with the help of RUSLE and Musgrave equation, 6.74% of the total volume of the pond has been filled with sediment. 623 years are required for the pond to be filled completely with sediment.

http://www.aloki.hu ● ISSN 1589 1623 (Print) ● ISSN 1785 0037 (Online)
DOI: http://dx.doi.org/10.15666/aeer/1704_77417763

RUSLE has been used and accepted by many researchers for erosion prediction because of its high reliability in erosion prediction studies (Ullah et al., 2018). The calculated and measured sediment yields in the basin were very low. The methods used in the study were successful on the prediction of even low sediment yield. Presence of forest and lower mean annual rainfall in the upstream may contribute to comparatively lower erosion rates (Fayas, 2019). In the study area, grassland and forestland had low rainfall erosivity. Therefore, the sediment accumulation calculated in the pond was low.

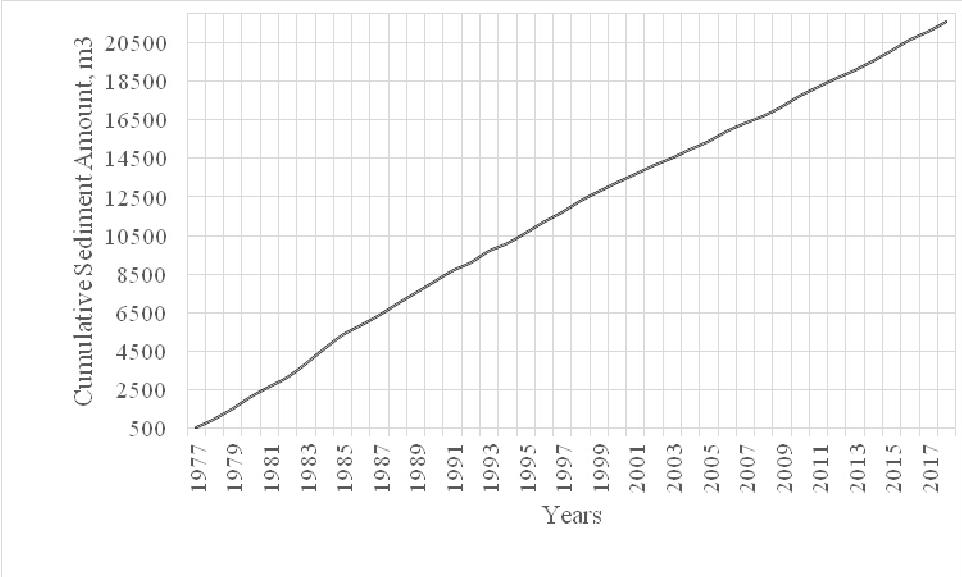

Figure 10. *Cumulative sediment accumulation (1977-2018)*

The effect of landuse chance on sediment yield

At the pond planning, the entire Ekinli basin was grassland. So the effects of forestation on sediment yield were not considered when the pond planned. As a result of the afforestation activities carried out in 2010 in the basin, 38% of the basin area was converted into forestland from grassland. The effect of this landuse change on sedimentation with the help of RUSLE equation was investigated. For this purpose, sediment accumulation was calculated by using RUSLE equation and Musgrave Equation for both situations (whole basin is grassland or 38% forestland and 62% grassland) for the years 2000-2018 (*Fig. 11*).

C factors values for grassland and forestland were calculated by the help of *Equations 7, 8* and the C value was used to detect of landuse change effect on sediment yield. According to these calculations, forestland was more effective in reducing erosion than grassland. The partial afforestation of the basin caused the sediment yield to drop from 9519 m^3 to 8801 m^3 between 2000 and 2018. The difference affected only 1.08% of sediment deposition over a 19-year period. The low difference could be the result of forestland and grassland which have a very close effect on reducing soil losses. Many studies have shown that the changes in land-use or vegetation have a large impact on soil erosion and sedimentation (Diyabalanage et al., 2017; Ganasri and Ramesh, 2016; Zhang et al., 2017; Chen et al., 2019). Conversion of a land from farmland to grassland or forestland is expected to contribute lower sedimentation. In a small basin in Poland, the increase in grassland and forestland at the catchment about 90% and 10%

http://www.aloki.hu ● ISSN 1589 1623 (Print) ● ISSN 1785 0037 (Online)
DOI: http://dx.doi.org/10.15666/aeer/1704_77417763

respectively and a decrease in cultivated land as 82% reduced soil erosion by 74% as being calculated using the Revised Universal Soil Loss Equation (Strugała, 2019). The aforestration of Ekinli basin extended the life span from 603 to 623 years.

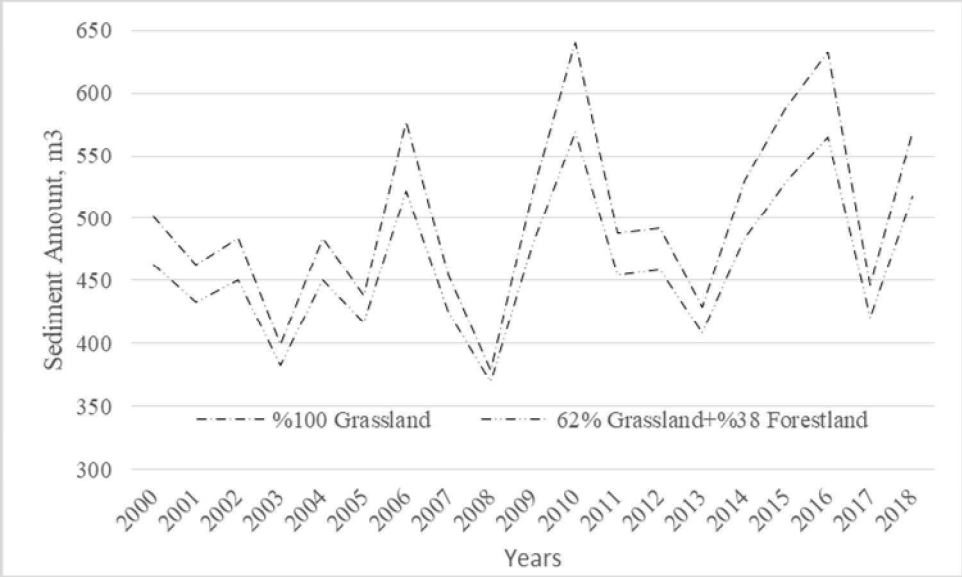

Figure 11. *The effect of this landuse change on sedimentation*

Trend and slope analyses

The Mann-Kendall test and Sen's slope estimator were used for rainfall, R factor and sediment amount of Ekinli basin. The Mann-Kendall statistics for trend and Sen's slope estimator result is given in *Table 7*. The Mann-Kendall statistics showed significant trend for sediment. The Sen's slope estimator had negative slope. The H_o hypothesis related to no monotonic trend was rejected for sediment data sets.

There were not a trend for rainfall and R factor in the basin. The calculated p value for sediment is smaller than the critical p value from the table of the standard normal distribution.

Although there was no trend for rainfall and rainfall erosivity, the trend for sedimentation was attributed to landuse change after 2000 in the basin.

Table 7. *Trend and slope results for Ekinli basin (1977-2018)*

Parameters	z	p-value	Sen	CI for Sen
Rainfall, mm	-1.41	0.08	-1.562	(-3.848, -0.657)
R Factor, MJ mm ha^{-1} h^{-1} yr^{-1}	-1.52	0.06	-3.511	(-8.193, -1.163)
Sediment, m^3	-2.77	0.00	-3.002	(-5.282, -0.919)

Conclusion

The silt accumulation of dams is complex event that affects negatively water storage capacity of pond. The economic life of the ponds are necessary for their sustainability since the most important event effecting the life of the ponds is sedimentation. The agricultural importance of the region has led to the construction of many small ponds.

http://www.aloki.hu ● ISSN 1589 1623 (Print) ● ISSN 1785 0037 (Online)
DOI: http://dx.doi.org/10.15666/aeer/1704_77417763

The calculations of reasonable sediment amount by the help of RUSLE/SDR and Musgrave equation can be helpful for the new planning of small ponds. This study showed that the GIS systems combined with RUSLE and Musgrave equation is a practical, reliable, inexpensive and relevant method for assessing sediment amount in a basin. The results of the study revealed that the sediment estimation was considerably valid for the basin.

The dead volume of the pond is filled in 2004. Hence, the aquatic life of pond could be under the risk especially in the irrigation seasons. The water storage capacity of the pond decreased by 6.7% due to sedimentation thus the irrigation potential in the area also decreased. In case the sediment accumulated in the pond would have been spread all over the basin, it would correspond to a soil layer of 3.65 mm thickness.

The RUSLE equation can be used successfully in sediment calculations. The biggest limitation of this equation is the accurate calculation of the sediment delivery ratio. In addition, calculation of gully and stream erosion by using different methods that the RUSLE equation cannot calculate will provide a more accurate sediment estimation. Even in the lower sedimentation such as grassland and forestland uses the estimation of model was very accurate compared to the results of bathymetric measurements.

According to the results, land use changes from pasture to forest have a poor effect on sediment yield. In order to provide a control on the intensive sedimentation, conversion from cropland to grassland or forestland will be more effective on sedimentation.

REFERENCES

[1] Alighalehbabakhani, F., Miller, C. J., Baskaran, M., Selegean, J. P., Barkach, J. H., Dahl, T., Abkenar, S. M. S. (2017): Forecasting the remaining reservoir capacity in the Laurentian Great Lakes watershed. – Journal of Hydrology 555: 926-937.

[2] Arnoldus, H. M. J. (1980): An Approximation of Rainfall Factor in the Universal Soil Loss Equation – In: Boodt, M. Gabriels, D. (eds.) Assessment of Erosion. Wiley, Chichester, pp. 127-132.

[3] Black, C. A. (1965): Methods of Soil Analysis Part 2. Chemical and Microbiological Properties. – American Society of Agronom, Inc., Madison, WI, pp. 771-1572.

[4] Blake, G. R., Hartge, K. H. (1986): Bulk Density. – In: Klute, A. (ed.) Methods of Soil Analysis, Part I. Physical and Mineralogical Methods. Agronomy Monograph No. 9. 2nd Ed. ASA, Madison, WI, pp. 363-375.

[5] Brown, L. C., Foster, G. R. (1987): Storm erosivity using idealized intensity distribution. – Transactions of the ASAE 30: 379-386.

[6] Chen, Z., Wang, L., Wei, A., Gao, J., Lu, Y., Zhou, J. (2019): Land-use change from arable lands to orchards reduced soil erosion and increased nutrient loss in a small catchment. – Science of the Total Environment 648: 1097-1104.

[7] Cheviron, B., Delmas, M., Cerdan, O., Mouchel, J. M. (2011): Parameter uncertainty and sensitivity analysis in sediment flux calculation. – Hydrology and Earth System Science 8: 1469-1506.

[8] Das, B., Paul, A., Bordoloi, R., Tripathi, O. P., Pandey, P. K. (2018): Soil erosion risk assessment of hilly terrain through integrated approach of RUSLE and geospatial technology: a case study of Tirap District, Arunachal Pradesh. – Modeling Earth Systems and Environment 4: 373-381.

[9] Diyabalanage, S., Samarakoon, K. K., Adikari, S. B., Hewawasam, T. (2017): Impact of soil and water conservation measures on soil erosion rate and sediment yields in a tropical watershed in the Central Highlands of Sri Lanka. – Applied Geography 79: 103-114.

http://www.aloki.hu ● ISSN 1589 1623 (Print) ● ISSN 1785 0037 (Online)
DOI: http://dx.doi.org/10.15666/aeer/1704_77417763

[10] Ebrahimzadeh, S., Motagh, M., Mahboub, V., Harijani, F. M. (2018): An improved RUSLE/SDR model for the evaluation of soil erosion. – Environmental Earth Sciences 77: 454.
[11] ESRI (2011): Environmental Systems Research Institute, ArcGIS for Desktop, Version 10.1. – Redlands CD ROM.
[12] Fayas, C. M., Abeysingha, N. S., Nirmanee, K. G. S., Samaratunga, D., Mallawatantri, A. (2019): Soil loss estimation using rusle model to prioritize erosion control in Kelani riverbasin in Sri Lanka. – International Soil and Water Conservation Research 7(2): 130-137.
[13] Foster, G. R., Mc Cool, D. K., Renard, K. G., Moldenhauer, W. C. (1991): Conversion of the universal soil loss equation to SI metric units. – Journal of Soil and Water Conservation 36: 355-359.
[14] Ganasri, B. P., Ramesh, H. (2016): Assessment of soil erosion by RUSLE model using remote sensing and GIS-A case study of Nethravathi Basin. – Geoscience Frontiers 7: 953-961.
[15] Gee, G. W., Bauder, J. W. (1986): Particle Size Analysis. – In: Klute, A. (ed.) Methods of Soil Analysis. Part 1. 2nd Ed. Agron. Mongr. 9. ASA, Madison, WI, pp. 383-411.
[16] Gelagay, H. S. (2016): RUSLE and SDR model based sediment yield assessment in a GIS and remote sensing environment: a case study of Koga watershed, upper Blue Nile basin, Ethiopia. – Hydrol Current Res 7(239): 2.
[17] Gelagay, H. S., Minale, A. S. (2016): Soil loss estimation using GIS and Remote sensing techniques: case of Koga watershed, Northwestern Ethiopia. – International Soil and Water Conservation Research 4(2): 126-136.
[18] Gourfi, A., Daoudi, L., Shi, Z. (2018): The assessment of soil erosion risk, sediment yield and their controlling factors on a large scale: Example of Morocco. – Journal of African Earth Sciences 147: 281-299.
[19] Jobin, T., Sabu, J., Thrivikramji, K. P. (2018): Assessment of soil erosion in a monsoon-dominated mountain river basin in India using RUSLE-SDR and AHP. – Hydrological Sciences Journal 63(4): 542-560.
[20] Jordan, Y. C., Ghulam, A., Hartling, S. (2014): Traits of surface water pollution under climate and land use changes: a remote sensing and hydrological modeling approach. – Earth-Science Reviews 128: 181-195.
[21] Kendall, M. G. (1975): Rank Correlation Methods. Fourth Ed. – Charles Griffin, London.
[22] Liu, C., Qi, S., Shi, M. (2001): Process of study on relationship between land use change and soil erosion. – Journal of Soil and Water Conservation 15: 510-513.
[23] Maner, S. B. (1962): Factors influencing sediment delivery ratios in the Blackland Prairie land resource area. – US Dept. of Agriculture, Soil Conservation Service, Fort Worth, TX.
[24] Mann, H. B. (1945): Non-parametric test against trend. – Econometrica 13: 245-259.
[25] Mc Cool, D. K., Foster, G. R., Mutchler, C. K., Meyer, L. D. (1987): Revised slope steepness factor for the universal soil loss equation. – Transactions of the AAE 30(5): 1387-1396.
[26] Mohtar, Z. A., Yahaya, A. S, Ahmad, F. (2015): Rainfall erosivity estimation for Northern and Southern peninsular Malaysia using Fourneir indexes. – Procedia Engineering 125: 179-184.
[27] Nelson, D. W., Sommers, L. E. (1982): Total Carbon, Organic Carbon, and Organic Matter. – In: Page, A. L. (ed.) Methods of Soil Analysis. Part 2. 2nd Ed. Agron. Monogr. 9. ASA and SSSA, Madison, WI, pp. 539-579.
[28] Petan, S., Rusjan, S., Vidmar, A., Mikos, M. (2010): The rainfall kinetic-energy intensity relationship for rainfall erosivity estimation in the Mediterranean part of Slovenia. – Journal of Hydrology 391: 314-321.

http://www.aloki.hu ● ISSN 1589 1623 (Print) ● ISSN 1785 0037 (Online)
DOI: http://dx.doi.org/10.15666/aeer/1704_77417763

[29] Poirier, C., Poitevin, C., Chaumillon, E. (2016): Comparison of estuarine sediment record with modelled rates of sediment supply from a western European catchment since 1500. – CR Geosci 348(7): 479-488.
[30] Renard, K. G., Foster, G. A., Weesies, G. A., McCool, D. K. (1997): Predicting soil erosion by water: a guide to conservation planning with RUSLE. – USDA, Agriculture Handbook No. 703, Washington, DC.
[31] Renfro, W. G. (1975): Use of Erosion Equation and Sediment Delivery Ratios for Predicting Sediment Yield. – In: Present and Prospective Technology for Predicting Sediment Yields and Sources. ARS-S-40, US Dept. Agric, Publ., Washington, DC, pp. 33-45.
[32] Sevinc, A. N. (1993): Havza sediment verimi. – KHGM, Ankara Araştirma Enstitusu (in Turkish).
[33] Soil Survey Staff. (1999): Soil Taxonomy: A Basic System of Soil Classification for Making and Interpreting Soil Surveys, – USDA Handbook No. 436. US Government Printing Office, Washington, DC.
[34] Strugała, M. K. (2019): Sediment variability in a small catchment of the Polish Western Carpathians during transition from centrally planned to freemarket economics. – Geomorphology 325: 119-129.
[35] Surfer (1997): Surfer for Windows User's Guide. Version 6. – Golden Software Inc., USA.
[36] Tamene, L., Le, Q. (2015): Estimating soil erosion in sub-Saharan Africa based on landscape similarity mapping and using the revised universal soil loss equation (RUSLE). – Nutrient Cycling in Agroecosystems 101: 1-15.
[37] Toy, T. J., Foster, G. R., Renard, K. G. (2002): Soil Erosion: Processes, Prediction, Measurement, and Control. – John Wiley & Sons, pp. 338.
[38] Ullah, S., Ali, A., Iqbal, M., Javid, M., Imran, M. (2018): Geospatial assessment of soil erosion intensity and sediment yield: a case study of Potohar Region, Pakistan. – Environmental Earth Sciences 77: 705.
[39] Wang, X., Zhao, X., Zhang, Z., Yi, L., Zuo, L., Wen, Q., Liu, F., Xu, J., Hu, S., Liu, B. (2016): Assessment of soil erosion change and its relationships with land use/cover change in China from the end of the 1980s to 2010. – Catena 137: 256-268.
[40] Wijesundara, N. C., Abeysingha, N. S., Dissanayake, D. M. S. L. B. (2018): GIS-based soil loss estimation using RUSLE model: a case of Kirindi Oya river basin, Sri Lanka. – Modeling Earth Systems and Environment 4(1): 251-262.
[41] Wischmeier, W. H., Smith, D. D. (1978): Predicting rainfall erosion losses. A guide to conservation planning. – USDA Agric. HB No 537, Washington, DC.
[42] World Bank (1998): Sustainability of Dams–Reservoir Sedimentation Management and Safety Implications. – World Bank, Washington, DC.
[43] World Commission on Dams Report (2000): Dams and Development. A New Framework for Decision-Making. – Earthscan Publications Ltd, London, pp. 356.
[44] Yan, R., Zhang, X., Yan, S., Chen, H. (2018): Estimating soil erosion response to land use/cover change in a catchment of the Loess Plateau, China. – International Soil and Water Conservation Research 6: 13-22.
[45] Yurekli, K. (2015): Impact of climate variability on precipitation in the Upper Euphrates–Tigris Rivers Basin of Southeast Turkey. – Atmospheric Research 154: 25-38.
[46] Zeng, C., Wang, S., Bai, X., Li, Y., Tian, Y., Li, Y., Luo, G. (2017): Soil erosion evolution and spatial correlation analysis in a typical karst geomorphology using RUSLE with GIS. – Solid Earth 8: 721-736.
[47] Zhang, S. H., Fan, W. W., Li, Y. Q., Yi, Y. J. (2017): Influence of changes in land use and landscape patterns on soil erosion in a watershed. – Science of the Total Environment 574: 34-45.

http://www.aloki.hu ● ISSN 1589 1623 (Print) ● ISSN 1785 0037 (Online)
DOI: http://dx.doi.org/10.15666/aeer/1704_77417763

WATER-YIELD RELATIONSHIPS OF DEFICIT IRRIGATED TOMATO (*LYCOPERSICON LYCOPERSICUM* L. VAR. HAZAR F1)

AYAS, S.

Yenisehir İbrahim Orhan Vocational School, Uludag University
Iznik Way 2. km Yenisehir, Bursa, Turkey
(e-mail: serayas@uludag.edu.tr; phone: +90-224-773-6069; fax: +90-224-773-6041)

(Received 13th Mar 2019; accepted 3rd May 2019)

Abstract. This trial was realized in the greenhouses of Uludag University Yenisehir Vocational School in Bursa province of Turkey between 2009 and 2010 to investigate effects of water deficit on yield and quality parameters of tomato during four crop growth stages. In this trial, fourteen irrigation treatments in four growth periods (vegetative, flowering, yield formation and ripening) of tomato (*Lycopersicon lycopersicum* L. var. Hazar F1) were constituted and the yield and quality parameters found from these treatments were evaluated. The layout of the experiment was a completely randomized block design with three replications for each of the fourteen irrigation treatments tested. According to the content of the treatments, the irrigation amount water applied to the plants varied between 0 and 554 mm in the first year, and between 0 and 556 mm in the second year. Water consumption of tomato in the first year ranged between 300 and 725 mm and in the second year ranged between 340 and 746 mm. Yield, fruit weight, diameter, height and dry matter ratio were determined statistically significant. In 2009 and 2010 years, the maximum yield were found as 92.2 t ha^{-1} and 93.4 t ha^{-1} in $V_{100}F_{100}Y_{100}R_{100}$ treatments, while the minimum yield were found as 2.0 t ha^{-1} and 4.0 ha^{-1} in the $V_0F_0Y_0R_0$ treatments, respectively. Water- yield relationship factors (k_y) in 2009 and 2010 years were found as 1.05 and 1.06, respectively. The maximum WUE and IWUE values were obtained from vegetative and ripening periods. Vegetative and ripening periods may be suggested as the maximum efficient irrigation periods for the tomato applied with drip irrigation under unheated greenhouse conditions.
Keywords: *tomato, deficit irrigation, WUE and IWUE values, yield and quality parameters of tomato, irrigation planning*

Introduction

Decreases in water resources together with increasing impacts of global warming and climate changes and increasing demands of increasing population make effective utilization of water resources a must. Increasing demands of sectors also deplete the ground water resources, pollute water ecosystems and developing new water resources is getting more and more expensive each day. Since about 75% of water resources of Turkey is allocated for agricultural purposes, effective water utilization and water saving in irrigation are the most critical issues to be considered. Pressurized piped systems and especially drip irrigation should be widespread for effective water utilization in agriculture (Cakmak and Gokalp, 2011).

Van Straten et al. (2010) stated that the greenhousing is worldwide the fastest growing sector of all agricultural production activities. There are two essential causes for this. First, the plant grows in greenhouse differently from the external environment, in this way supplying in a sort of way of abri from the flat-out effect of the exterior air conditions. This allows the production of crops at that specific place. Second, the greenhouse allows to be produced of many crops. Thus, grower allows the farming to come true as desired. It also offers advantages such as higher crop yield, longer production period, better quality and less use of chemicals. The output unit of area in greenhouses is much higher than that in field agriculture. This situation permits the

http://www.aloki.hu ● ISSN 1589 1623 (Print) ● ISSN 1785 0037 (Online)
DOI: http://dx.doi.org/10.15666/aeer/1704_77657781

grower to direct the farming in a desirable aspect. It causes to higher crop yield, extended production period, better quality and less use of chemicals. The value added per unit surface area in greenhouse crops is much higher than that in field agriculture.

China, India are United States are the world's three biggest tomato producers with 57, 19, 15 million tons, respectively. United States is the largest tomato exporting country. Turkey is one of the significant tomato producer with Turkey 12 750 000 tons (fourthly in the world) in the world (FAOSTAT, 2017).

Papadopoulos (1992) pointed out the tomato is a major vegetable that has reached immense demand over the last hundred years. Tomato contains vitamins of A and C and is very useful for human heath. Tomato fruit is the best source of lycopene and lycopene is a cancer hampering antioxidant. Hence, tomato is very important in developed countries and its production is production is being tried to increase. Greenhouse cultivation is the optimum option for tomato producer because of higher quality of tomato. In addition, the crop is protected from insect, disease and pest. Moreover, the size of all fruit stays uniform because of optimum environment. Water is vital input for tomato to remain alive in greenhouse. Water is saved by the drip irrigation and plant gives better yield and quality.

Sezen (2005) found that surface irrigation is not suggested due to low irrigation efficiency originated from salinity and drainage problems in irrigated areas. From a different viewpoint, traditional irrigation systems where excess water inputs and poor drainage occur, cause environmental problems such as salinity and water logging. In irrigation methods where irrigation water is used efficiently do not have the problems of conventional irrigation methods (Buyukcangaz et al., 2007). Thus, the use of less water consuming irrigation methods is of great importance with regard to irrigation planning (Anonymous, 2005). The objective of irrigation planning is to prevent the soil moisture level falling below the critical line for a specific soil and crop condition. This may enable to avoid the harmful effect of water stress by means of estimating the earliest date (Ritchie and Johnson, 1990).

Irrigation planning with drip irrigation relies on approaches connected with evapotranspiration estimations (Bar-Yosef and Sagiv, 1982; McNeeish et al., 1985; Clough et al., 1990; Hartz, 1993) and permissible soil-water depletion (Bogle et al., 1989). *Ky* represents the declines in the yield as a result of each deficit level in water consumption. *Ky* values usually difficult to create accurately. *Ky* values are affected by regional conditions, soil properties, crop physiology and cultural practices. A suggested *Ky* value for irrigation planning must be high enough to avoid the water stress caused by the needs and specific local situations. It remains low enough for effective water management (Yuan et al., 2003). Some studies have been realized to investigate the effect of deficient irrigation on tomato. The purposes of this experiment were to obtain a prospectus for tomato growers and to determine drip irrigated tomato response to deficit irrigation regimes in Bursa conditions.

Materials and methods

The study was realized in Yenisehir Vocational School, Bursa of Turkey in 2009 and 2010 years. For practical purposes, plastic greenhouse (8 m x 40 m) was used. In the study place, wintertimes are cold and summertimes are hot. The average annual rainfall and temperature values for the region where the greenhouse experiments were made in 2009 and 2010 were 531.3-804.4 mm and 13.3-14.6 °C, respectively. While the average

http://www.aloki.hu ● ISSN 1589 1623 (Print) ● ISSN 1785 0037 (Online)
DOI: http://dx.doi.org/10.15666/aeer/1704_77657781

minimum temperature for 2009 and 2010 were -3.6 - (5.9) °C between January and December, the average maximum temperature in August was measured as 30.6 and 34.6 °C (Anonymous, 2011a). Maximum and minimum temperature values in greenhouse during the plant growing period (92 days) were 38-38 °C and 0.9-1.3 °C, respectively in 2009-2010 years (*Figs. 1* and *2*). The highest and lowest relative humidity values in greenhouse in 2009 and 2010 years were found as 88-87% and 39-39%, respectively (*Fig. 3*). In addition, the highest and lowest radiation values in greenhouse in 2009-2010 years were measured as 1974-1542 W/m^2 and 335-139 W/m^2, respectively (*Fig. 4*) (Anonymous, 2011b).

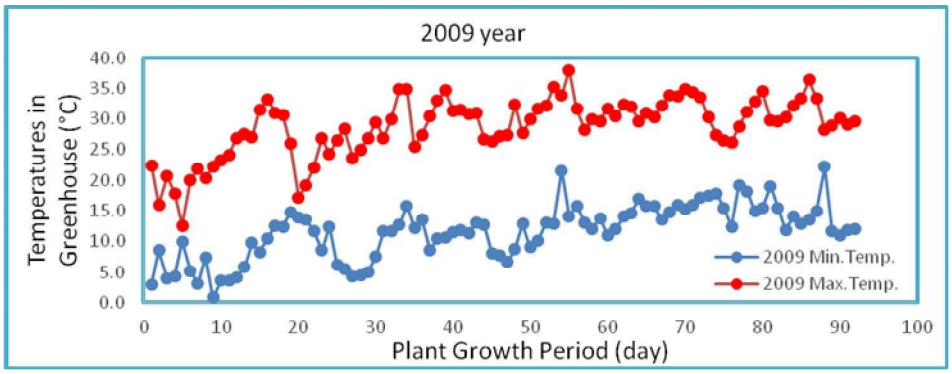

Figure 1. *Temperatures in greenhouse during the plant growth period in 2009 year*

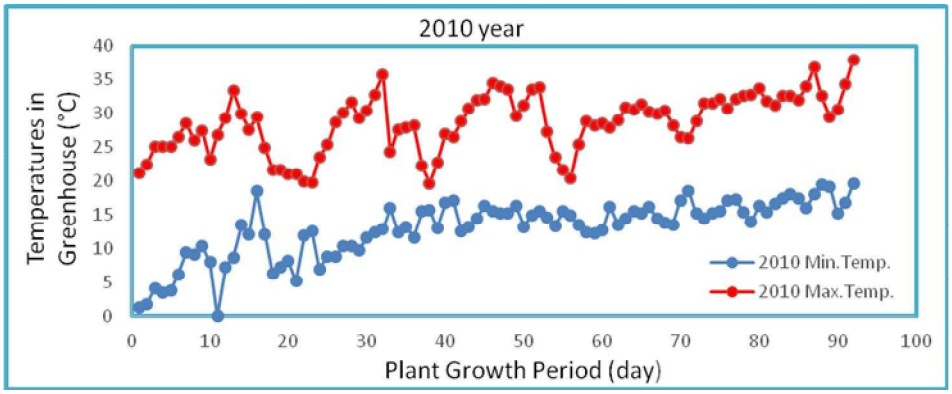

Figure 2. *Temperatures in greenhouse during the plant growth period in 2010 year*

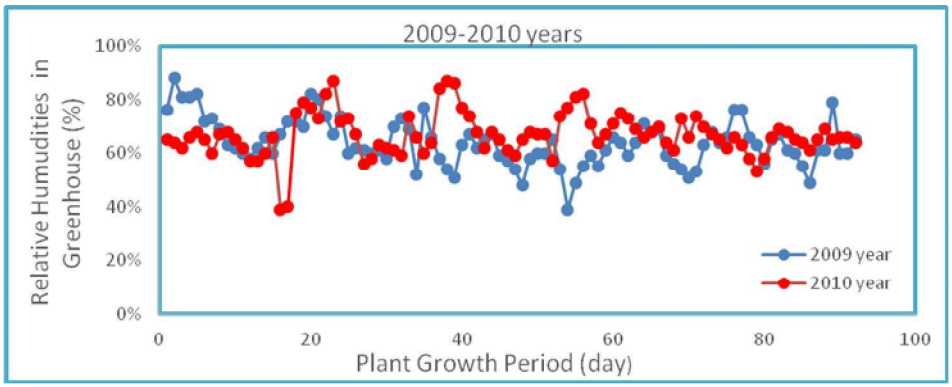

Figure 3. *Relative humidities in greenhouse during the plant growth period in 2009-2010 years*

http://www.aloki.hu ● ISSN 1589 1623 (Print) ● ISSN 1785 0037 (Online)
DOI: http://dx.doi.org/10.15666/aeer/1704_77657781

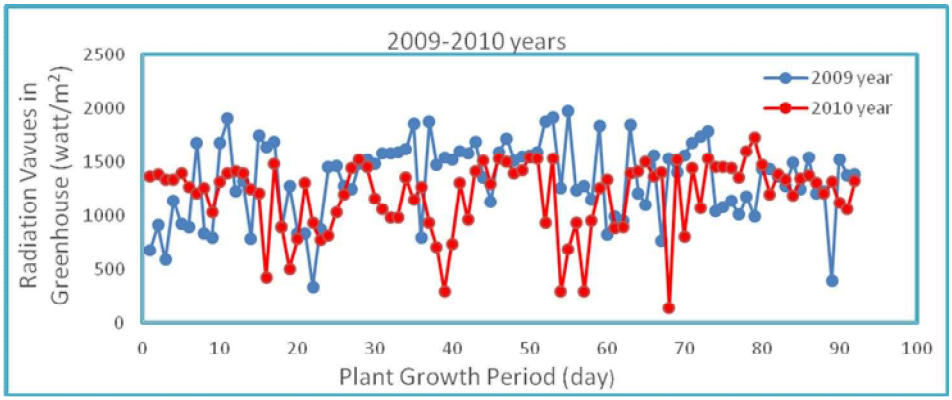

Figure 4. *Radiation values in greenhouse during the plant growth period in 2009-2010 years*

The soil of study place was sandy clay and pH value of soil ranged between 7.86 and 8.05. The specific features of the soil are given in *Table 1*.

Table 1. *Some specific properties of the experimental soil*

Soil depth (cm)	Soil type	Unit weight (g/cm^3)	Field capacity (%)	Wilting point (%)	pH	Total salt (%)	$CaCO_3$ (%)	Organic matter (%)
0-30	SL	1.34	29.73	21.74	7.99	0.037	16.5	2.92
30-60	SL	1.37	27.26	19.37	8.04	0.031	29.5	1.39
60-90	SL	1.58	33.92	23.72	7.86	0.034	31.5	1.08
90-120	SL	1.50	36.30	27.73	8.05	0.032	33.0	0.94

SL: sandy loam

Hazar F1 variety was used in the study. Hazar F1 is a mid-early type and its fruits are around 15-25 g. Hazar F1 has a strong plant structure. The fruits of Hazar F1 are oval, bright, charming and are resistant to waiting and transporting. This variety has a wide adaptability and high efficiency. In addition, this variety is tolerant to early leaf blight. In the experimental area, an irrigation well was utilized as the source and the water was of the class C_1S_1 after the analysis done. NPK 15-15-15 fertilizer was sprinkled on the soil by hand before planting the seedlings as bottom fertilizer. The application depth of the fertilizer ranged from 15 to 20 cm depending on the soil structure and the root depth of the plant grown. NPK 15-15-15 fertilizer was utilized to trial plots while the tomatoes were being planted, and 750 kg of NPK 15-15-15 fertilizer per hectares were utilized. The urea form of the nitrogen was applied to the plots together with the irrigation water. The first manure was applied as 250 kg/ha (% 46 N) in the flowering stage and the second fertilizer was utilized as 250 kg/ha in yield formation stage together with the irrigation water. Furthermore, in 2009 and 2010 years, 250 kg of magnesium nitrate manure per hectares (11 – 0 – 0 + 16 MgO - Nitrogen % 11 and MgO % 16) were used in the flowering and early yield formation stages to support the generative development.

The experimental blocks were formed with three replications and 14 trial treatments were randomly scattered. The size of the experimental plots was 4 m^2 (2.0 m × 2.0 m). The distances between the plots were 0.80 m and blocks were placed with 1.5 m distances. The tomato seeds were sown in viyols on 01 April 2009 and on 04 April 2010 in the experimental years. The tomato seedlings were transplanted to the plots on 02

http://www.aloki.hu ● ISSN 1589 1623 (Print) ● ISSN 1785 0037 (Online)
DOI: http://dx.doi.org/10.15666/aeer/1704_77657781

May 2009 and on 05 May 2010. The seedlings were grown with 50 cm intervals on the same row and with 50 cm intervals between the plant lines. Into each plot, 25 plants were planted.

Some quality parameters of tomato are yield, fruit weight, diameter, height and dry matter ratio. The fruit weight was determined by weighting 15 plants in the harvest part and fruit diameter and height were calculated by gauging the weighted fruit with a ruler and by taking the average of these values. The dry matter ratio was obtained after they were dried at 65 °C in a drying oven for 48 h and fruit dry matter ratio was calculated. The detail of the experimental plot is shown in *Figure 5*.

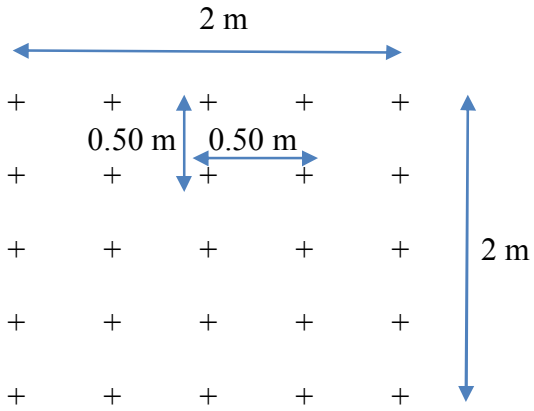

Figure 5. *The detail of a plot*

In different growth periods of tomato (vegetative, flowering, yield formation and ripening) fourteen deficit irrigation treatments were formed depending on full or deficit irrigation treatments. 75-50-25% of the deficit irrigations were applied in different growth stages of the plant, while 100% of irrigation water was used in full irrigation treatment. In line with this planning, irrigation treatments were planned like this: $V_{100}F_{100}Y_{100}R_{100}$, $V_{75}FYR$, $V_{50}FYR$, $V_{25}FYR$, $VF_{75}YR$, $VF_{50}YR$, $VF_{25}YR$, $VFY_{75}R$, $VFY_{50}R$, $VFY_{25}R$, $VFYR_{75}$, $VFYR_{50}$, $VFYR_{25}$, $V_0F_0Y_0R_0$ (*Table 2.*).

Table 2. *The experimental treatments*

Irrigation treatments	Growth Stages			
	Vegetative	Flowering	Yield Formation	Ripening
$V_{100}F_{100}Y_{100}R_{100}$	+	+	+	+
$V_{75}FYR$	+ %25 deficit irrigation	+	+	+
$V_{50}FYR$	+ %50 deficit irrigation	+	+	+
$V_{25}FYR$	+ %75 deficit irrigation	+	+	+
$VF_{75}YR$	+	+ %25 deficit irrigation	+	+
$VF_{50}YR$	+	+ %50 deficit irrigation	+	+
$VF_{25}YR$	+	+ %75 deficit irrigation	+	+
$VFY_{75}R$	+	+	+ %25 deficit irrigation	+
$VFY_{50}R$	+	+	+ %50 deficit irrigation	+
$VFY_{25}R$	+	+	+ %75 deficit irrigation	+
$VFYR_{75}$	+	+	+	+ %25 deficit irrigation
$VFYR_{50}$	+	+	+	+ %50 deficit irrigation
VFYR25	+	+	+	+ %75 deficit irrigation
$V_0F_0Y_0R_0$	-	-	-	-

+: Water application in the specified period, -: without irrigation

http://www.aloki.hu ● ISSN 1589 1623 (Print) ● ISSN 1785 0037 (Online)
DOI: http://dx.doi.org/10.15666/aeer/1704_77657781

The irrigation equipment in greenhouse used in the study was given in *Figure 6*.

a b

***Figure 6. a** Drip irrigation system. **b** Main and lateral pipes*

In the trial, the plants were irrigated by drip irrigation method and water was used an irrigation well. Some features of the irrigation water were given in *Table 3*. The irrigation water has low-sodium risk and medium EC and its class is C_2S_1 class. C2S1 irrigation water quality class has low sodium and medium electrical conductivity (salinity). Water in the C2S1 quality class can be used for be irrigated medium and highly resistant plants to salinity. In addition, C1S1 quality class water can be used in all plants and soil without creating harmful alkalinity. A study has been conducted on irrigating tomato by using C2S1 quality class water (Ashraf and Ewees, 2008).

***Table 3.** Specific properties of irrigation water*

Water source	$EC_{25}x$ (10^6)	Na^+	K^+	Ca^{2+}	Mg^{2+}	PH	Class	SAR
		(me L^{-1})						
Deep well	715	2.3	2.56	9.25	5.7	7.12	C_2S_1	0.85

In four growth stages the soil moisture contains of the soil was followed before and after irrigation with a gravimetric method in every 30 cm up to 120 cm depth.

The water balance equation was used to calculate evapotranspiration (ET) (*Eq. 1*).

$$ET = I + P - R_f - D_p \pm \Delta S \quad \text{(Eq.1)}$$

where ET represents the evapotranspiration, I shows the irrigation water amount during the period (mm), P is the total precipitation, R_f is the amount of the surface flow (mm), D_p indicates the deep drainage (mm) and ΔS is the soil water content at the beginning and end of the period (mm/120 cm). Before planting seedlings, water was given to the crop by the drip irrigation method. Total precipitation (P) and surface flow (R_f) were omitted due to the plant production in the greenhouse. The soil water in the deeper than 120 cm was taken as the deep drainage (D_p) and the deep drainage (Dp) was neglected.

The intervals of lateral were equal to the plant row intervals in the trial. Therefore the percentage of wetted area was calculated by the equation as follows (*Eq. 2*).

http://www.aloki.hu ● ISSN 1589 1623 (Print) ● ISSN 1785 0037 (Online)
DOI: http://dx.doi.org/10.15666/aeer/1704_77657781

$$P = \frac{Sd}{Sl} 100 \quad \text{(Eq.2)}$$

where P is the percentage of wetted area, Sd and Sl are the interval of dripper and the intervals of lateral, respectively. The amount of irrigation water to be applied in each irrigation (*Eq. 3*) was found by the equation given below.

$$dn = \frac{(FC - WP) Ry}{100} \gamma t \, D \frac{P}{100} \quad \text{(Eq.3)}$$

where dn is the amount of irrigation water to be applied in each irrigation, FC and WP are the field capacity and wilting point, respectively. γt is the soil bulk density, D is wetted soil depth, P is the percentage of wetted area.

In this trial, the relationships between yield and ET was described by Steward Model (*Eq. 4*) (Stewart et al., 1975; Doorenbos and Kassam, 1979). The equation can be given as:

$$\left(1 - \frac{Ya}{Ym}\right) = ky\left(1 - \frac{ETa}{ETm}\right) \quad \text{(Eq.4)}$$

where Y_m (t/ha) and Y_a (t/ha) are maximal and actual yield, respectively, ET_m (mm) and ET_a (mm) are maximal and actual evapotranspiration, respectively. The yield response factor is shown as k_y. WUE values were determined to assess irrigation efficiency in treatments. WUE and IWUE terms refer to contribution of irrigation water to effective use of plant production stages (Bos, 1980). WUE was calculated by dividing the fruit yield by seasonal evapotranspiration (ET). IWUE was predicted as (Zhang et al., 1999):

$$IWUE = \frac{(Y1 - YNI)}{I} \quad \text{(Eq.5)}$$

where Y_1 is fruit yield of irrigated treatments (t ha $^{-1}$) and Y_{NI} is the fruit yield of non-irrigated treatment (t ha $^{-1}$) and I is the amount of irrigation water (mm). The water content of the soil up to 120 cm depth was calculated before the seedlings were planted into the soil. Before starting irrigations, moisture level of the soil was completed to the level of field capacity in all treatments. Irrigation was begun on May 02 in 2009 and May 05 in 2010 and it was repeated every 7 days. The irrigation water amounts for the four growth stages were given in *Table 4*. Crop evapotranspiration for growth periods of tomato are given in *Table 5*.

Yield and quality parameters were evaluated. Variance analysis of yield and quality parameters were evaluated according to LSD multiple comparison test ($p < 0.05$). Variance analysis was done with the values of yield productivity and quality parameters by using MSTAT-C and MINITAB software (Steel and Torrie, 1980).

Results

In 2009 and 2010 years, the highest irrigation water was found in $V_{100}F_{100}Y_{100}R_{100}$ treatment as 554-556 mm and minimal irrigation water was found in $V_0F_0Y_0R_0$

http://www.aloki.hu ● ISSN 1589 1623 (Print) ● ISSN 1785 0037 (Online)
DOI: http://dx.doi.org/10.15666/aeer/1704_77657781

treatment as 0-0 mm respectively. Crop water use of tomato (ET_c) increased with the increment in the water amount. ET was found as 300-735 mm in 2009 and as 340-746 mm in 2010 in $V_{100}F_{100}Y_{100}R_{100}$ and $V_0F_0Y_0R_0$ treatments, respectively. The irrigation water and yields are presented in *Table 6*.

Crop water production functions (ky and R^2 values) obtained for each growth stage (vegetative, flowering, yield formation, ripening) and total growing season in 2009 and 2010 were given in *Table 7*.

Linear relationships between ET_c with Y_a, and IW with Y_a were observed for 2009 year. The relationship equation is as follows; $Y_a = 0.2185ET_c - 58.437$ with $R^2 = 0.9402$ and $Y_a = 0.1576IW + 2.2813$ with $R^2 = 0.99$ (*Figs. 2* and *3*). Linear relationships between ET_c with (Y_a), and IW with Y_a were observed for 2010 year. The relationship equation is as follows: $Y_a = 0.228ET_c - 67.477$ with $R^2 = 0.9115$ and $Y_a = 0.1569IW + 3.4724$ with $R^2 = 0.99$ (*Fig. 7*).

When the results were taken into consideration, yield was substantially affected by irrigation applications (*Figs. 2* and *3*) the maximum values of yield were found as 92.2 t ha^{-1} and 93.4 t ha^{-1} in $V_{100}F_{100}Y_{100}R_{100}$ treatment for 2009 and 2010 years, respectively (*Tables 8* and *9*).

Table 4. *The irrigation water applied for the four growth stages*

Irrigation Water (mm)										
Treatments	Vegetative		Flowering		Yield Formation		Ripening		Total	
	2009	2010	2009	2010	2009	2010	2009	2010	2009	2010
$V_{100}F_{100}Y_{100}R_{100}$	60	50	240	230	200	198	54	78	554,0	556,0
$V_{75}FYR$	45	38	240	230	200	198	54	78	532,0	544,0
$V_{50}FYR$	30	25	240	230	200	198	54	78	524,0	531,0
$V_{25}FYR$	15	12	240	230	200	198	54	78	509,0	518,0
$VF_{75}YR$	80	70	180	172,5	200	198	54	78	550,0	518,0
$VF_{50}YR$	80	70	120	115	200	198	54	78	535,0	481,0
$VF_{25}YR$	80	70	60	57,5	200	198	54	78	534,0	454,0
$VFY_{75}R$	80	70	240	230	150	148,5	54	78	524,0	526,0
$VFY_{50}R$	80	70	240	230	100	99	54	78	514,0	507,0
$VFY_{25}R$	80	70	240	230	50	49,5	54	78	504,0	495,0
$VFYR_{75}$	80	70	240	230	200	198	40,5	58,5	525,0	556,0
$VFYR_{50}$	80	70	240	230	200	198	27	39	517,0	537,0
VFYR25	80	70	240	230	200	198	13,5	19,5	514,0	518,0
$V_0F_0Y_0R_0$	0	0	0	0	0	0	0	0	0,0	0,0

Table 5. *Crop evapotranspiration for growth periods of tomato*

Crop Evapotranspiration (mm)										
Treatments	Vegetative		Flowering		Yield Formation		Ripening		Total	
	2009	2010	2009	2010	2009	2010	2009	2010	2009	2010
$V_{100}F_{100}Y_{100}R_{100}$	140	145	240	240	210	226	135	135	725	746
$V_{75}FYR$	130	132	226	225	192	220	117	107	665	684
$V_{50}FYR$	126	132	214	225	184	196	116	107	640	660
$V_{25}FYR$	126	130	212	222	178	190	116	104	632	646
$VF_{75}YR$	137	138	224	230	206	202	123	118	690	688
$VF_{50}YR$	138	138	230	228	208	183	104	112	680	661
$VF_{25}YR$	136	135	227	225	206	174	101	110	670	644
$VFY_{75}R$	129	137	206	232	200	206	120	117	655	692
$VFY_{50}R$	129	132	215	226	190	188	112	92	646	638
$VFY_{25}R$	130	125	216	210	185	164	103	105	634	604
$VFYR_{75}$	131	137	220	211	180	220	109	113	640	681
$VFYR_{50}$	122	138	219	214	190	202	104	116	635	670
VFYR25	134	140	222	220	142	172	112	109	610	641
$V_0F_0Y_0R_0$	70	80	90	100	80	90	60	70	300	340

http://www.aloki.hu ● ISSN 1589 1623 (Print) ● ISSN 1785 0037 (Online)
DOI: http://dx.doi.org/10.15666/aeer/1704_77657781

Table 6. *Relationship between yield and yield response factor (ky) with the decrease in water use, for tomato in 2009 and 2010 years*

Irrigation Treatment	Yield (t ha^{-1})	Applied Water (mm)	ETa (mm)	ETa/ETm	Ya/Ym	1-(ETa/Etm)	1-(Ya/Ym)	ky	ky
$V_{100}F_{100}Y_{100}R_{100}$	92,2	554,0	725	1,000	1,000	0,000	0,000	0,000	0,000
$V_{75}FYR$	88,6	532,0	665	0,917	0,961	0,083	0,039	0,472	
$V_{50}FYR$	86,4	524,0	640	0,883	0,937	0,117	0,063	0,537	0,595
$V_{25}FYR$	83,0	509,0	632	0,872	0,900	0,128	0,100	0,778	
$VF_{75}YR$	83,8	550,0	690	0,952	0,909	0,048	0,091	1,887	
$VF_{50}YR$	83,6	535,0	680	0,938	0,907	0,062	0,093	1,503	1,592
$VF_{25}YR$	82,5	534,0	670	0,924	0,895	0,076	0,105	1,387	
$VFY_{75}R$	85,8	524,0	655	0,903	0,931	0,097	0,069	0,719	
$VFY_{50}R$	84,6	514,0	646	0,891	0,918	0,109	0,082	0,756	0,763
$VFY_{25}R$	82,8	504,0	634	0,874	0,898	0,126	0,102	0,812	
$VFYR_{75}$	86,7	525,0	640	0,883	0,940	0,117	0,060	0,509	
$VFYR_{50}$	84,4	517,0	635	0,876	0,915	0,124	0,085	0,681	0,613
VFYR25	82,7	514,0	610	0,841	0,897	0,159	0,103	0,650	
$V_0F_0Y_0R_0$	2,00	0,0	300	0,414	0,022	0,586	0,978	1,669	1,669
									1,05
Irrigation Treatment	Yield (t ha^{-1})	Applied Water (mm)	ETa (mm)	ETa/ETm	Ya/Ym	1-(ETa/Etm)	1-(Ya/Ym)	ky	ky
$V_{100}F_{100}Y_{100}R_{100}$	93,4	556	746	1,000	1,000	0,000	0,000	0,000	0,000
$V_{75}FYR$	90,1	544	684	0,917	0,965	0,083	0,035	0,425	
$V_{50}FYR$	87,9	531	660	0,885	0,941	0,115	0,059	0,511	
$V_{25}FYR$	85,3	518	646	0,866	0,913	0,134	0,087	0,647	0,528
$VF_{75}YR$	80,5	518	688	0,922	0,862	0,078	0,138	1,776	
$VF_{50}YR$	78,6	481	661	0,886	0,842	0,114	0,158	1,391	
$VF_{25}YR$	73,2	454	644	0,863	0,784	0,137	0,216	1,582	1,583
$VFY_{75}R$	83,8	526	692	0,928	0,897	0,072	0,103	1,420	
$VFY_{50}R$	82,8	507	638	0,855	0,887	0,145	0,113	0,784	
$VFY_{25}R$	80,9	495	604	0,810	0,866	0,190	0,134	0,703	0,969
$VFYR_{75}$	90,6	556	681	0,913	0,970	0,087	0,030	0,344	
$VFYR_{50}$	89,2	537	670	0,913	0,955	0,087	0,045	0,516	
VFYR25	85,8	518	641	0,859	0,919	0,141	0,081	0,578	0,479
$V_0F_0Y_0R_0$	4,0	0	340	0,456	0,043	0,544	0,957	1,759	1,759
									1,06

Table 7. *Crop water production functions obtained for each growth stage and total growing season in 2009 and 2010 years*

Year	Period	Production Functions
2009	V	ky= 0.60, R^2= 0.8395
	F	ky=1.59, R^2= 0.8622
	Y	ky=0.76, R^2= 0.9989
	R	ky=0.61, R^2= 0.8078
	Seasonal	ky=1.05, R^2= 0.9402
2010	V	ky= 0.52, R2= 0.9610
	F	ky=1.58, R2= 0.8480
	Y	ky=0.97, R2= 0.9082
	R	ky=0.48, R2= 0.9997
	Seasonal	ky=1.06, R2= 0.9115

http://www.aloki.hu ● ISSN 1589 1623 (Print) ● ISSN 1785 0037 (Online)
DOI: http://dx.doi.org/10.15666/aeer/1704_77657781

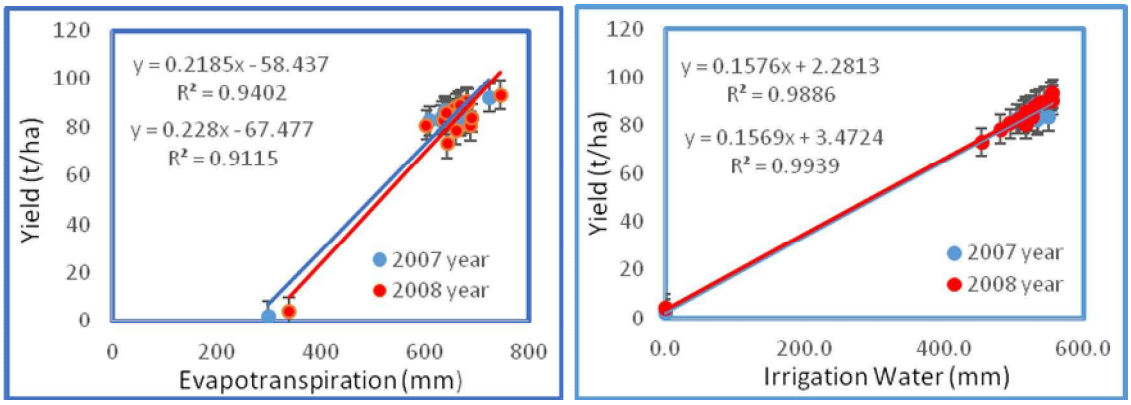

a **b**

Figure 7. a *The relationship between crop water consumption and yield.* ***b*** *The relationship between irrigation water and yield*

Table 8. *Effects of irrigation treatments on yield and quality parameters of tomato in 2009 year*

Irrigation treatment	Yield (t ha $^{-1}$)	Fruit weight (g)	Fruit diameter (cm)	Fruit height (cm)	Dry matter ratio (%)
V100F100Y100R100	92.2 a	220.0 a	8.2 a	7.5 a	6.0 h
V75FYR	88.6 b	217.0 ab	8.0 ab	7.4ab	7.4 g
V50FYR	86.4 c	214.0 bc	7.7 bc	7.2 abc	7.6 fg
V25FYR	83.0 fg	213.0 bc	7.5 cd	7.1 abcd	7.9 adefg
VF75YR	83.8 efg	190.0 hı	6.8 ef	6.8 cdef	7.7 efg
VF50YR	83.6 efg	187.0 ıj	6.5 fg	6.6 efg	7.9 defg
VF25YR	82.5 g	182.0 j	6.2 g	6.3 g	7.9 defg
VFY75R	85.8 cd	198.0 fg	7.3 cd	7.0 bcde	8.0 def
VFY50R	84.6 de	195.0 gh	7.1 de	6.7 defg	8.2 cde
VFY25R	82.8 g	191.0 hı	7.1 de	6.5 fg	8.3 cd
VFYR75	86.7 c	210.0 cd	7.4 cd	7.3 ab	8.4 bcd
VFYR50	84.4 def	206.0 de	7.3 cd	7.1 abcd	8.6 bc
VFYR25	82.7 g	202.0 ef	7.2 de	6.8 cdef	8.9 b
V0F0Y0R0	2.0 h	62.0 k	2.0 h	2.7 h	13,5 a
Treatments	*	*	*	*	*
Blocks	is	is	is	is	is

**Correlation is significant at the 0.05 level. ns: non-significant correlation

When $V_{100}F_{100}Y_{100}R_{100}$ treatment was made comparison with the other irrigation treatments, yield losses were determined as 4.1%, 6.7%, 11.1%, 10.0%, 10.3%, 11.8%, 7.5%, 9.0%, 11.4%, 6.3%, 9.2%, 11.5%, and 4510.0% in 2009 and 3.7%, 6.3%, 9.5%, 16.0%, 18.8%, 27.6%, 11.5%, 12.8%, 15.5%, 3.1%, 4.7%, 8.9% and 2235.0% in 2010. In the trial, it was observed that at $P < 0.05$ level has a significant effect on the yield and quality parameters of deficit irrigation.

http://www.aloki.hu ● ISSN 1589 1623 (Print) ● ISSN 1785 0037 (Online)
DOI: http://dx.doi.org/10.15666/aeer/1704_77657781

Table 9. *Effects of irrigation treatments on yield and quality parameters of tomato in 2010 year*

Irrigation treatment	Yield (t ha^{-1})	Fruit weight (kg)	Fruit diameter (cm)	Fruit height (cm)	Dry matter ratio (%)
V100F100Y100R100	93.4 a	220 a	8.6 a	7.5 a	6.5 e
V75FYR	90.1 bc	210 ab	8.2 a	7.2 ab	8.0 d
V50FYR	89.9 d	207 b	7.9 ab	6.9 ab	8.3 cd
V25FYR	89.7 e	203 b	7.7 bc	6.7 bc	8.6 bc
VF75YR	82.5 g	115 f	5.0 efg	5.2 cd	8.4bcd
VF50YR	79.6 h	109 fg	4.7 gh	4.8 de	8.7 bc
VF25YR	74.5 ı	102 g	4.5 h	4.5 e	8.9 b
VFY75R	85.4 f	131 cd	5.8 def	5.8 bc	8.4 bcd
VFY50R	83.0 f	125 de	5.4 fgh	5.5 cde	8.6 bc
VFY25R	82.8 g	117 e	5.1 gh	5.1 de	8.9 b
VFYR75	90.6 b	210 c	8.3 cd	7.3 cd	8.3 cd
VFYR50	90.2 cd	207 cd	8.0 cde	7.0 bc	8.7 bc
VFYR25	89.8 e	203 de	7.7 efg	6.8 ab	8.9 b
V0F0Y0R0	4.0 j	58 h	3.5 ı	3.7 f	13.7 a
Treatments	*	*	*	*	*
Blocks	is	is	is	is	is

**Correlation is significant at the 0.05 level. ns: non-significant correlation

While a positive straight line relationship was obtained between the water amount and the yield, fruit weight, diameter, height; a negative straight line relationship was obtained between the irrigation amount and dry matter ratio. As for that the relationship, these results were determined: fruit weight (2009) = 0.2637W + 63.179, R^2 = 0.90 and fruit weight (2010) = 0.288IW + 56.976, R^2 = 0.98 (*Fig. 8a*); fruit diameter (2009) = 0.0099IW + 2.0412, R^2 = 0.87 and fruit diameter (2010) = 0.0096 + 2.3538, R^2 = 0.92 (*Fig. 8b*); fruit height (2009) = 0.0081IW + 2.7108, R^2 = 0.91 and fruit height (2010) = 0.0089IW + 2.4269, R^2 = 0.98 (*Fig. 8c*); dry matter ratio (2009) = -0.0109IW + 13.619, R^2 = 0.88 and dry matter ratio (2010) = -0.0104 + 13.763, R^2 = 0.90 (*Fig. 8d*).

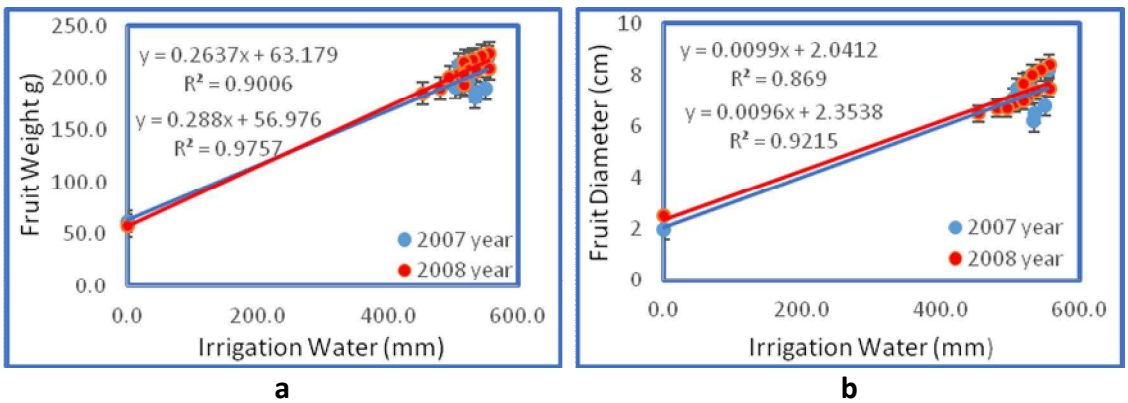

a **b**

http://www.aloki.hu ● ISSN 1589 1623 (Print) ● ISSN 1785 0037 (Online)
DOI: http://dx.doi.org/10.15666/aeer/1704_77657781

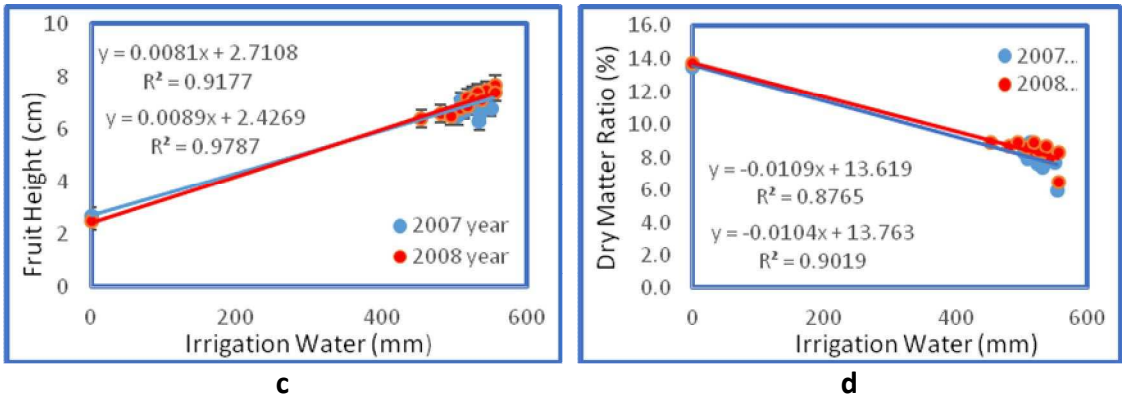

Figure 8. *Relationship between irrigation water and fruit weight, diameter, height and dry matter ratio*

Crop yield response factor (k_y)

The linear relationship between relative crop evapotranspiration and relative yield decrease is given the ky value. It is regarded as the yield response to the relative crop evapotranspiration. In another saying, it represents the declines in the yield as a result of each deficient level in water depletion. Seasonal ky values were determined as 1.05 (2009 year) and 1.06 (2010 year) (*Fig. 9*). Ky value increased with the increase in the water deficit. This result was relatively small with regard to seasonal crop yield response factors in four different crop growth stages of the tomatoes, while it was consistent with the crop yield response factors in each growth factors given in literature. The difference between these two results may refer to the differences between the empirical, climatic and seedling quality.

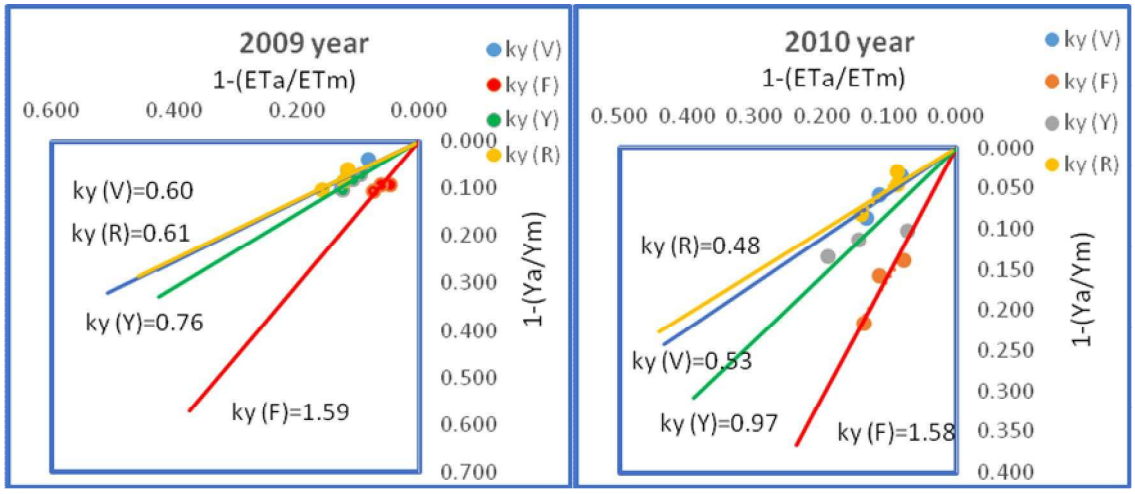

Figure 9. *The relationship between relative yield decrease and relative evapotranspiration deficit for the experimental years*

Water use efficiencies

WUE and IWUE values of the 2009 and 2010 years appeared differently in different treatments (*Table 10*). The maximum WUE values for 2009 year were found as 0.13,

http://www.aloki.hu ● ISSN 1589 1623 (Print) ● ISSN 1785 0037 (Online)
DOI: http://dx.doi.org/10.15666/aeer/1704_77657781

0.14, 0.13 – 0.14, 0.13, 0.14 kg mm^{-1} and were found 0.13, 0.13, 013 - 0.13, 0.13, 0.13 kg mm^{-1} from V75FYR, V50FYR, V25FYR and $VFYR_{75}$, $VFYR_{50}$, $VFYR_{25}$ treatments for 2010 year, respectively. IWUE values for 2009 year were found as 0.17, 0.16, 0.16 – 0.17, 0.16, 0.16 kg.mm^{-1} and were found 0.17, 0.17, 0.16 – 0.16, 0.17, 0.17 kg mm^{-1} from V75FYR, V50FYR, V25FYR and $VFYR_{75}$, $VFYR_{50}$, $VFYR_{25}$ treatments for 2010 year, respectively. When WUE and IWUE values were taken into consideration, the maximum WUE and IWUE values were obtained in vegetative and ripening periods and the lowest value was obtained from flowering and yield formation periods. In other words, the maximum yields were obtained from vegetative and ripening periods and the most water saving was supplied with deficit irrigation only in the vegetative and ripening periods of the tomato.

Table 10. *WUE and IWUE values for the tomato at fourteen irrigation treatments*

2009 year				2010 year			
Irrigation Treatment	Yield (t ha^{-1})	WUE (kg/m^3)	IWUE (kg/m^3)	Irrigation Treatment	Yield (t ha^{-1})	WUE (kg/m^3)	IWUE (kg/m^3)
$V_{100}F_{100}Y_{100}R_{100}$	92,2	0,13	0,17	$V_{100}F_{100}Y_{100}R_{100}$	93,4	0,13	0,17
V_{75}FYR	88,6	0,13	0,17	V_{75}FYR	90,1	0,13	0,17
V_{50}FYR	86,4	0,14	0,16	V_{50}FYR	87,9	0,13	0,17
V_{25}FYR	83	0,13	0,16	V_{25}FYR	85,3	0,13	0,16
VF_{75}YR	83,8	0,12	0,15	VF_{75}YR	80,5	0,12	0,16
VF_{50}YR	83,6	0,12	0,16	VF_{50}YR	78,6	0,12	0,16
VF_{25}YR	82,5	0,12	0,15	VF_{25}YR	73,2	0,11	0,16
VFY_{75}R	85,8	0,13	0,16	VFY_{75}R	83,8	0,12	0,16
VFY_{50}R	84,6	0,13	0,16	VFY_{50}R	82,8	0,13	0,16
VFY_{25}R	82,8	0,13	0,16	VFY_{25}R	80,9	0,13	0,16
$VFYR_{75}$	86,7	0,14	0,17	$VFYR_{75}$	90,6	0,13	0,16
$VFYR_{50}$	84,4	0,13	0,16	$VFYR_{50}$	89,2	0,13	0,17
VFYR25	82,7	0,14	0,16	VFYR25	85,8	0,13	0,17
$V_0F_0Y_0R_0$	2,00	0,01	0,00	$V_0F_0Y_0R_0$	4,0	0,01	0,00

Discussion

In this experiment, irrigation treatments considerably influenced yield, fruit weight, diameter, height and dry matter. In both experimental years, the maximum amounts of water applied to the crop were 554-556 mm for from $V_{100}F_{100}Y_{100}R_{100}$ while the seasonal evapotranspiration (ETa) values were changed between 725-300 and 746-340 mm for $V_0F_0Y_0R_0$ treatment. Total water amounts varied from 400 to 600 mm depending upon climate and length of growing season (Doorenbos and Kassam, 1979). Water applied for tomato ranged from 415 to 800 mm under different controlling sistems (Mahajan and Singh, 2006). Ayas (2015) stated that irrigation water amount applied for tomato varied from 65 to 564 mm in different treatments in the province of Bursa of Turkey. Kirda et al. (2004) reported that total seasonal evapotranspiration by tomato for spring and fall planted varied from 274 to 447 mm and irrigation water applied varied from 173 to 456 mm. Hanson and May (2011) determined that applied water ranged from 582 to 1018 mm. Berihun (2011) also reported that two days irrigation interval was used and a factorial combination of three levels of water (namely 315, 440 and 565 mm) combined with three mulch treatments. Wan et al. (2007) specified that for three years, evapotranspiration of tomato was 607 mm/season for drip irrigation with saline water. Seasonal evapotranspiration varied from 405 to 946 mm and irrigation amount applied from 271 to 832 mm in the province of Eskişehir in

http://www.aloki.hu ● ISSN 1589 1623 (Print) ● ISSN 1785 0037 (Online)
DOI: http://dx.doi.org/10.15666/aeer/1704_77657781

Turkey between 1998 and 2000 years (Cetin et al., 2002). These results are notably in accordance with the irrigation water amounts and crop water consumption values obtained from previous studies (Kuscu et al., 2014; Ayas, 2015; Gatta et al., 2015; Biswas et al., 2015; Linker et al., 2016).

The tomato yield ranged between 92.2-2.0 and 93.4-4.0 t ha^{-1} for 2009 and 2010 years, respectively. Yield was decreased as the irrigation water amount reduced. As a result, the effect of deficit irrigation was found significant on total yield. This result was compatible with those of (Liu et al., 2013; Kuscu et al., 2014; Saadi et al., 2015; Ayas, 2015; Gatta et al., 2015; Biswas et al., 2015; Nangare et al., 2016). As in yield, some quality parameters of tomato (fruit weight, diameter, height and dry matter) showed a similar response to deficit irrigation.

As for fruit weight, there was influence of deficiency irrigation on single fruit weight with respect to quality parameters. As observed in yield, the fruit diameter and weight gave similar response to deficit irrigation. The highest quality parameters were obtained from $E_{100}V_{100}Y_{100}R_{100}$ treatments every two experiment years. The non-irrigated ($V_0F_0Y_0R_0$) treatment had lower values than all irrigation treatments. The result of study were in conformance with (Akhtar et al., 2014; Kuscu et al., 2014; Ayas, 2015; Biswas et al., 2015; Nangare et al., 2016). Since $V_{100}F_{100}Y_{100}R_{100}$ treatments had higher fruit weight than the other treatments, the lowest dry matters have been found at $V_{100}F_{100}Y_{100}R_{100}$ treatments when the highest dry matter values were observed at $E_0V_0Y_0R_0$ treatments in both years of the experiment. As a result, we may say that as the amount of irrigation water decrease, the number of dry matter increases. These values are similar to those of previous studies (Birhanu and Tilahun, 2010; Ayas, 2015; Gatta et al., 2015; Candido et al., 2015).

The maximum WUE and IWUE values were found as 0.14-0.19 and 0.14-0.19 for 2009 and 2010 years, respectively. The maximal WUE and IWUE values were obtained in vegetative and ripening periods and the lowest value was obtained from flowering and yield formation periods. When the results concerning WUE values were in comparison to the findings of different researchers, they were in agreement with those of the other studies (Alomran et al., 2012; Mukherjee et al., 2012; Kuscu et al., 2014; Ayas, 2015; Cantore et al., 2016).

The variety of tomato, climate of the region, soil properties and effective use of water also influence yield and quality parameters of tomato. As explained by Davis et al. (2008), it may be attributed to the variety and applied cultural practices handling under different climate and geographical conditions. Crop yield response factor (k_y) for 2009 and 2010 year were calculated as 1.05 and 1.06 for tomato, respectively. The specified values of k_y (1.05-1.06) which is bigger than 1.00 shows that tomato is responsive to the water. The factor of k_y also matches up with the values obtained by researchers who studied on similar issues (Doorenbos and Kassam, 1979; Kuscu et al., 2014; Ayas, 2015; Cantore et al., 2016).

Conclusion

According to the results of the study, irrigation water were applied 554 and 556 mm in $V_{100}F_{100}Y_{100}R_{100}$ treatment applied of full irrigation in 2009 and 2010 years. The plant water consumption of tomato was determined as 300-725 mm and 340-746 mm for $V_0F_0Y_0R_0$ treatment 2009 and 2010 years. The factors of k_y for the different irrigation levels ($V_{100}F_{100}Y_{100}R_{100}$, $V_{75}FYR$, $V_{50}FYR$, $V_{25}FYR$, $VF_{75}YR$, $VF_{50}YR$, $VF_{25}YR$, $VFY_{75}R$,

http://www.aloki.hu ● ISSN 1589 1623 (Print) ● ISSN 1785 0037 (Online)
DOI: http://dx.doi.org/10.15666/aeer/1704_77657781

$VFY_{50}R$, $VFY_{25}R$, $VFYR_{75}$, $VFYR_{50}$, $VFYR_{25}$, $V_0F_0Y_0R_0$ treatments) in 2009 and 2010 years were calculated as 1.05 and 1.06 for tomato, respectively. The factors of k_y (1.05 and 1.06) values are bigger than 1.00 showed that the tomato was susceptible to water. The crop yield response factors (k_y) were close to each other in both years of the study. The highest yield decreases in all treatments were in *$V_0F_0Y_0R_0$* treatments, while the lowest yield decreases were in *$V_{100}F_{100}Y_{100}R_{100}$* treatments. In our trial, it was studied out that irrigation treatments considerable influences yield, fruit diameter, weight, height and dry matter ratio.

In this study, it was studied out that irrigation applications considerably influences yield, fruit weight, diameter, height and dry matter. In both years of the study, the highest yield was 92.2 t h^{-1} and 93.4 t h^{-1} and it was observed in $V_{100}F_{100}Y_{100}R_{100}$ treatment. The lowest yield was observed as 2.0 t h^{-1} and 4.0 t h^{-1} in $V_0F_0Y_0R_0$ treatment. Yield decreased considerably as a result of the diminishment in the water amount. Relative yield decreases in the irrigation treatments in 2009 and 2010 were 4.1%, 6.7%, 11.1%, 10.0%, 10.3%, 11.8%, 7.5%, 9.0%, 11.4%, 6.3%, 9.2%, 11.5%, 4510.0% and 3.7%, 6.3%, 9.5%, 16.0%, 18.8%, 27.6%, 11.5%, 12.8%, 15.5%, 3.1%, 4.7%, 8.9%, 2235.0%, respectively. WUE and IWUE values of vegetative and ripening periods were the maximum of all the treatments.

As a result of a possible deficit irrigation in a semi-humid climate condition, it is necessary to plan carefully and it is possible to say that the levels and times of the deficit irrigation were significantly effective on tomato yield. If deficit irrigation treatment is obligatory, water deficiency should be planned only for vegetative and ripening periods of tomato. The water deficiency should not be applied in flowering and yield formation periods and irrigations in these periods should be exactly applied. In addition, in the irrigation planning to be applied in similar climatic conditions may be benefited from crop yield response factor (ky) values. The results used to determine the amount of reduction in yield in response to the water deficiency applied to the plant may be used in studies related to tomato. It can be recommended that vegetative and ripening periods is most suitable periods for the deficit irrigation practices for tomato irrigation by drip irrigation.

REFERENCES

[1] Akhtar, S. S., Li, G., Andersen, M. N., Liu, F. (2014): Biochar enhances yield and quality of tomato under reduced irrigation. – Agric. Water Management 138: 37-44.

[2] Alomran, A. M., Al-Harbi, A. A. R., Wahb-Allah, M. A., Alwabel, M. A., Nadeem, M. E. A., Al-Eter, A. (2012): Management of irrigation water salinity in greenhouse tomato production under calcareous sandy soil and drip irrigation. – J. Agr. Sci. Tech. 14: 939-950.

[3] Anonymous (2005): The Annual Report of Meteorological Station, Bursa, Turkey. www.mgm.gov.tr/verideğerlendirme/il-ve-ilceler-istatistic.aspx?k

[4] Anonymous (2011a): The Annual Report of Meteorological Station, Bursa, Turkey. www.mgm.gov.tr/verideğerlendirme/il-ve-ilceler-istatistic.aspx?k

[5] Anonymous (2011b): The Meteorological Station of Greenhouse Application Area, Yenişehir-Bursa, Turkey. www.mgm.gov.tr/verideğerlendirme/il-ve-ilceler-istatistic.aspx?k

[6] Ashraf, S. O. and Ewees, M. S. A. (2008): The possible use of humic acid incorporated with drip irrigation system to alleviate the harmful effects of saline water on tomato plants. – Fayoum J. Agric. Res. & Dev. 22(1).

http://www.aloki.hu ● ISSN 1589 1623 (Print) ● ISSN 1785 0037 (Online)
DOI: http://dx.doi.org/10.15666/aeer/1704_77657781

[7] Ayas, S. (2015): The effects of different regimes on tomato (Lycopersicon lycopersicum L. Var. Hazal) yield and quality characteristics under unheated greenhouse conditions. – Bulgarian Journal of Agricultural Science 21(6): 1235-1241.
[8] Bar-Yosef, B., Sagiv, B. (1982): Response of tomatoes to N and water applied via a trickle irrigation system. – II Water. Argon. J. 74: 637-639.
[9] Berihun, B. (2011): Effect of mulching and amount of water on the yield of tomato under drip irrigation. Journal of Horticulture and Forestry 3(7): 200-206.
[10] Birhanu, K., Tilahun, K. (2010): Fruit yield and quality of dripirrigated tomato under deficit irrigation. – African Journal of Food, Agriculture, Nutrition and Development 10(2): 1684-5358.
[11] Bogle, C. R., Hartz, T. K., Nuntoez, C. (1989): Comparison of subsurface trickle and furrow irrigation on plastic mulched and bare soil for tomato production. – J. Am. Soc. Hortic. Sci. 114: 40-43.
[12] Bos, M. G. (1980): Irrigation efficiencies at crop production level. – ICID Bull.29: 18-25.
[13] Büyükcangaz, H., Demirtas C, Yazgan S, Korukcu, A. 2007. Efficient water use in agriculture in Turkey: The need for pressurized irrigation systems. – Water International 32(suppl 1): 776-785.
[14] Cakmak, B., Gokalp, Z. (2011): Climate change and effective water utilization. – Journal of Agricultural Sciences Research 4(1): 87-95.
[15] Candido, V., Campanelli, G., D'Addabbo, T., Castronuova, D., Perniola, M., Camele, I. (2015): Growth and yield promoting effect of artificial mycorrhization on field tomato at different irrigation regimes. – Scientia Horticulturae 187: 35-43.
[16] Cantore, V., Lechkar, O., Karabulut, E., Sellami, M. H., Albrizio, R., Boari, F., Stellaci, A. M., Todorovic, M. (2016): Combined effect of deficit irrigation and strobilurin application on yield, fruit quality and water use efficiency of "cherry" tomato (Solanum lycopersicum L.). – Agric. Water Management 167: 53-61.
[17] Cetin, Ö., Yıldırım, O., Uygan, D., Boyacı, H. (2002): Irrigation scheduling of drip-irrigated tomatoes using class a pan evaporation. – Turkish Journal of Agriculture and Forestry 26: 171-178.
[18] Clough, G. H., Locasio, S. J., Olsen, S. M. (1990): The yield of successively cropped polyethylene mulched vegetables as affected by irrigation method and fertilization management. – J. Am. Soc. Hortic. Sci. 115: 884-887.
[19] Davis, A. R., Webber, C. L., Perkins-Veazie, P., Ruso, V., Lopez Galarza, S., Sakata, Y. (2008): A Review of Production Systems on Watermelon Quality. – In: Pitrat, M. (ed.) Proceedings of the IXth EUCARPIA Meeting on 98 Genetics and Breeding of Cucurbitaceae, INRA, Avignon, France, pp. 515-520.
[20] Doorenbos, J., Kassam, A. H. (1979): Yield Response to Water. – FAO Irrigation and Drainage Paper No. 33, Rome.
[21] FAOSTAT (2017): Food and Agriculture Organization Corporate Statistical Database. – http://www.fao.org/faostat/en/#data/QC.
[22] Gatta, G., Libutti, A., Gagliardi, A., Beneduce, L., Brusetti, L., Borruso, L., Disciglio, G., Tarantino, E. (2015): Treated agro-industrial wastewater irrigation of tomato crop: Effects on qualitative/quantitative characteristics of production and microbiological properties of the soil. – Agric. Water Management 149: 33-43.
[23] Hanson, B., May, D. (2011): Crop evapotranspiration of processing tomato in the San Joaquin Valley of California, USA. – Irrigation Science 24: 211.
[24] Hartz, T. K. (1993): Drip irrigation scheduling for fresh market tomato production. – Hort. Science 28: 35-37.
[25] Kirda, C., Çetin, M., Dasgan, Y., Topçu, S., Kaman, H., Ekici, B., Derici, M. R., Özgüven, A. İ. (2004): Yield response of greenhouse grown tomato to partial root drying and conventional deficit irrigation. – Agric. Water Management 69: 191-201.

http://www.aloki.hu ● ISSN 1589 1623 (Print) ● ISSN 1785 0037 (Online)
DOI: http://dx.doi.org/10.15666/aeer/1704_77657781

[26] Kuscu, H., Turhan, A., Demir, A. O. (2014): The response of processing tomato to deficit irrigation at various phenological stages in a sub-humid environment. – Agric. Water Management 133: 92-103.
[27] Linker, R., Loslovich, I., Sylaios, G., Plauborg, F., Battilani, A. (2016): Optimal model-based deficit irrigation scheduling using Aqua Crop: a simulation study with cotton, potato and tomato. – Agric. Water Management 163: 236-243.
[28] Liu, H., Duan, A. W., Li, F. S., Sun, J. S., Wang, Y. C., Sun, C. T. (2013): Drip irrigation scheduling for tomato grown in solar greenhouse based on pan evaporation in North China Plain. – Journal of Integrative Agriculture 12(3): 520-531.
[29] Mahajan, G., Singh, K. G. (2006): Response of greenhouse tomato to irrigation and fertigation. – Agric. Water Management 84: 202-206.
[30] McNeish, C. M., Welch, N. C., Nelson, R. D. (1985): Trickle irrigation requirements for stawberries in coastal California. – J. Am. Soc. Hortic. Sci. 110: 714-718.
[31] Mukherjee, A., Sarkar, S., Chakraborty, P. K. (2012): Marginal analysis of water productivity function of tomato crop grown under different irrigation regimes and mulch managements. – Agric. Water Management 104: 121-127.
[32] Nangare, D. D., Singh, Y., Kumar, P. S., Minhas, P. S. (2016): Growth, fruit yield and quality of tomato (Lycopersicon esculentum Mill.) as affected by deficit irrigation regulated on phenological basis. – Agric. Water Management 171: 73-79.
[33] Papadopoulos, L. (1992): Fertigation of vegetables in plastic house: present situation and future aspects. – Acta Horticulturae 323: 151-174.
[34] Ritchie, J. T., Johnson, B. S. (1990): Irrigation of agricultural crops. – Agronomy Monograph 30: 363-390.
[35] Saadi, S., Todorovic, M., Tanasijevic, L., Pereira, L. S., Pizzigalli, C., Lionello, P. (2015): Climate change and Mediterranean agriculture: Impacts on winter wheat and tomato crop evapotranspiration, irrigation requirements and yield. – Agricultural Water Management 147: 103-115.
[36] Sezen, S. M. (2005): Effects of drip irrigation management on yield and quality of field grown green beans. – Agricultural Water Management 71: 243-255.
[37] Steel, R. G. D., Torrie, J. H. (1980): Principles and Procedures of Statistics. A Biometrical Approach. – McGraw-Hill, NewYork, pp.186-187.
[38] Stewart, J. I., Misra, R. D., Pruitt, W. O., Hagan, R. M. (1975): Irrigating corn and sorghum with a deficient water supply. – Trans. ASAE 18: 270-280.
[39] Van Straten, G., Van Willingenburg, G., Van Henten, E., Van Ooteghem, R. (2010): Optimum Control of Greenhouse Cultivation. – CRC Press, USA.
[40] Wan, S., Kang, Y., Wang, D., Liu, S. P., Feng, L. P. (2007): Effect of drip irrigation with saline water on tomato yield and water use in semi-humid area. – Agric. Water Management 90: 63-74.
[41] Yuan, B. Z., Sun, J., Nishiyama, S. (2003): Effect of drip irrigation on strawberry growth inside a plastic greenhouse. – Biosystems Engineering 87(2): 237-245.
[42] Zhang, H., Wang, X., You, M., Liu, C. (1999): Water-yield relations and water-use efficiency of winter wheat in the North China Plain. – Irrigation Science 19: 37-45.

http://www.aloki.hu ● ISSN 1589 1623 (Print) ● ISSN 1785 0037 (Online)
DOI: http://dx.doi.org/10.15666/aeer/1704_77657781

ORGANIC VS CONVENTIONAL ALMOND: MARKET QUALITY, FATTY ACID COMPOSITION AND VOLATILE AROMA COMPOUNDS

KARAAT, F. E.

Adıyaman University, Faculty of Agricultural Sciences and Technologies
Department of Plant Protection, 02040 Adıyaman, Turkey
e-mail: fkaraat@adiyaman.edu.tr

(Received 17th Mar 2019; accepted 3rd May 2019)

Abstract. Organic agriculture is an integrated form of agriculture combines techniques of ancient knowledge with current science and targets to exclude inorganic fertilizers, growth regulators and pesticides. Generally organic products are accepted as healthier and better tasting. This opinion is more common for fruits and vegetables. Series of studies on comparison of organic and conventional fruits and vegetables have been performed but comparison of analytical quality parameters lacks in previous studies especially fatty acids and volatile aroma compounds. This study compares pomological parameters, some selected chemical properties, fatty acid composition and volatile aroma compounds of organic and conventionally grown Ferragnes and Ferraduel almond cultivars. Results indicated significant differences between cultivars and growing systems suggesting a better overall market quality for organic kernel samples. Total oil and linoleic acid was lower in organic samples, whereas oleic was higher (82.4% in both cultivars) when compared with conventional samples (78.9% for Ferragnes and 75.8% for Ferraduel). Most of the aroma compounds detected in this present study are new record for almond aroma-active compounds. In an overall view, organic samples resulted with higher contents of aroma compounds.
Keywords: *composition, kernel, quality, Prunus amygdalus, taste*

Introduction

The most widely cultivated nut crop of Mediterranean area is the almond. World almond production was more than two tons, and The United States was the leading producing country (1.029.655 tons) followed by Spain (255.503 tons) and Turkey was the fifth country with the production of 90 thousand tons (FAO, 2019). Almond growing areas have significantly increased in last decades, and this increase is due to increasing demand for almond thanks to its natural and healthy food ingredients. Many reports have been published on nuts as a beneficial food source for human consumption, and considered as an essential balancing component in diets especially because of rich nutritional value. Even though almond contents high amount of fat, it has high amounts of unsaturated fatty acids (both mono and poly) and fiber (Sánchez-Bel et al., 2008).

Main quality aspects of almonds are their chemical composition, fatty acids composition, aroma compounds, protein and ash content, etc. Varying mainly depending on genetic background and ecological factors, but also cultural practices, general chemical composition of an almond is fat, proteins and carbohydrates in the percentages of 50-60, 20-25 and 20, respectively (Sánchez-Bel et al., 2008).

Today, agricultural practices are designed by knowledge of intense research, and especially studies on organic agriculture including organic fertilization have strong effects on the capacity of food production. Therefore, many studies have been performed to observe the increase in yield and quality of the almond in ecological agriculture and organic fertilization (Heeb et al., 2006; Lester et al., 2007; Sánchez-Bel

http://www.aloki.hu ● ISSN 1589 1623 (Print) ● ISSN 1785 0037 (Online)
DOI: http://dx.doi.org/10.15666/aeer/1704_77837793

et al., 2008). Organic farming benefits biodiversity (Bengtsson et al., 2005; Hole et al., 2005), and have the potential of increasing yield in some cases, especially with better water use efficiency and less carbon sequestration and pesticide use (Pretty et al., 2006; Wood et al., 2006). On the other hand, organic growing has the disadvantages of higher input and lower yield for the farmers (Guichard et al., 2001). In terms of consumer acceptance, organic foods are better welcomed, since consumers assume organic crops as higher quality (better tasting and more nutritious) rather than those conventionally grown crops (Ekelund and Tjarnemo, 2004; Gąstoł et al., 2011). Indeed, there are various reports on health benefits of organic crops (Lester et al., 2007). For that reason, organic crops growers ask higher prices for their crops to balance the relevant disadvantages. However, this demand of the growers is generally met by displeasure of traders and consumers.

Previously, some comparison studies about organic and conventional almond were published. Venkatasubramanian (2011) conducted a retail level study and compared some nutritional quality aspects of organic and conventional market foods including almond snacks. Sánchez-Bel et al. (2008) compared organic and inorganic fertilizers on potted almond trees, cv. Guara. A profitability comparison study was performed for organic and conventional almond orchards (Anonymous, 2011). On the other hand, a number of studies compared organic and conventional fruits based on sensory tests (Bourn and Prescott, 2002). But, previous studies about comparison of organic and conventional grown almond fruit quality are limited, especially for fatty acid composition and volatile aroma compounds.

In the previous studies, generally two methods of investigating differences between organic and conventional products have been applied which are cultivation and retail market studies. Both of them are focused on advantages and disadvantages. The approach used in this study is the compositional analysis of crops obtained from farm and cultivation rather than purchasing products from market. Farm and cultivation studies differ from retail market studies with the information available on cultivar, environmental conditions, harvest and post-harvest influences etc. Therefore, retail studies are reported as representative of the growing system in broad sense (Magkos et al., 2006).

For all of those reasons, in order to evaluate flavor related aroma compounds and various quality aspects of organic and conventional growing in almond this study was conducted to compare final quality of almonds grown organic and conventionally.

Materials and Methods

The study was conducted in Konuklu Village located in Besni County of Adıyaman Province, Turkey (37°36'11.13"N and 37°56'00.15"E) in 2018 which was a normal year in terms of climatic conditions for the area (*Table 1*). Plant materials of the study consisted of 8 years old organic and conventionally grown trees of Ferragnes and Ferraduel cultivars grafted on wild almond (*Prunus amygdalus* var. amara). Organic and conventional trees were grown in two nearby orchards that eliminate climatic influences. Pest management, weed control and soil cultivation were done as required. Drip irrigation and fertigation were utilized, and no nutrient deficiencies and water stress were observed during the season.

The study was conducted according to randomized block design including the plantation and fruit sampling, and from each genotype representing fruit samples were

http://www.aloki.hu ● ISSN 1589 1623 (Print) ● ISSN 1785 0037 (Online)
DOI: http://dx.doi.org/10.15666/aeer/1704_77837793

collected as required at harvest maturity stage (Anonymous, 2014). Fruit samples were subjected to hull separation and obtained nuts were sun dried for 4 days until 7% moisture level. Totally 10 kg of nuts (kernel with shell) samples were collected from each cultivar in each orchard. After two months of preservation of dried nuts at room temperature, pomological properties, chemical composition, fatty acid composition, and volatile aroma compounds of collected fruit samples were examined.

Table 1. *Meteorological records of experimental area (MGM, 2019)*

	May		June		July		August		September	
	2018	**MYA**	**2018**	**MYA**	**2018**	**MYA**	**2018**	**MYA**	**2018**	**MYA**
MT	19.8	20.6	24.2	26.8	28.3	31.1	28.8	30.6	25.4	25.8
MMT	27.1	26.6	32.0	33.2	36.4	37.6	36.6	37.5	32.8	33.0
MNT	12.5	14.3	16.3	19.7	20.4	23.7	21.4	23.4	17.9	19.0
MP	45.2	43.3	52	8.2	0.0	1.0	0.0	0.7	1.2	6.0

MT: Mean Temperature, MMT: Maximum Temperature, MNT: Minimum Temperature, MP: Monthly Precipitation, MYA: Multi-Year-Average

Pomological Evaluations and Sensory Analysis

With this regard, nut weight (NWE), nut length (NLE), nut width (NWI), nut thickness (NTH), kernel weight (KWE), kernel length (KLE), kernel width (KWI), kernel thickness (KTH), kernel/nut ratio (K/N), and Unit Kernel Number, number of kernels in 28.35 g (UKN), were measured. Nut and kernel width (mm), height (mm), and thickness (mm) were measured using digital calipers. Nut and kernel weight (g) were measured by precision scales (0.1 g), and kernel/nut ratio was calculated by division of these values. As part of market quality evaluation of the samples, consumer acceptability was also assessed by sensory analysis. For this aim, five judges (one a regular almond consumer, two almond growers, and two agriculture professionals) compared organic and conventional kernel samples in terms of their size & shape, color, and flavor.

Chemical composition

Total oil, total protein, total ash, and moisture were detected in terms of chemical composition. Total oil content was analyzed by extraction of oil with n-hexane (60 C) for 6 h using Soxhlet extractor (Anonymous, 2000). Total protein content was calculated by multiplication of total N content which was detected according to Kjeldahl method with 6.25 (James, 1995). Total ash were determined by burning almond kernels for 24 hours at 200°C and 6 hours at 600°C, respectively (Baymış, 2008). Kernel moisture content was measured according to the weight difference after heating the samples in an oven at 105°C for 24 hours (USDA, 1970).

Fatty acid composition

Fatty acid composition was evaluated by determination of palmitic acid, palmitoleic acid, stearic acid, oleic acid, linoleic acid contents. The fatty acid methyl esters were detected in a gas chromatograph (Shimatzu, QP2010 ULTRA) with a flame ionization

http://www.aloki.hu ● ISSN 1589 1623 (Print) ● ISSN 1785 0037 (Online)
DOI: http://dx.doi.org/10.15666/aeer/1704_77837793

detector and Rtx-5 MS capillary column according to Anonymous (1993). Obtained results were expressed as percentages of each fatty acid with regard to total oil content.

Volatile aroma compounds

Volatile aroma compounds were detected semi-quantitatively. Semi-quantitation (peak measurement) was done using another gas chromatograph (Agilent GC7890A) with a flame ionization detector and DB-5 ms capillary column (60 m×0.320 mm i.d. and 1 μm, film thickness) and 2-methyl-3-heptanone (internal standard) was used as internal standard. Peaks were identified by comparing retention times and mass spectra of eluted compounds with those of the Wiley library (Wiley7, Nist 05, J. Wiley & Sons Ltd., West Sussex, England).

Statistical calculations

Pomological parameters were measured in four replicates and obtained results were analyzed according to Duncan's test ($P \leq 0.05$) using SPSS 23.0 for Windows software. Data of compositional analyzes represents the average of multiple parallel measurements. Semi-quantitation was performed by comparing relative peak areas observed using FID detection, divided by the concentration in solution and compared again to that of 2-methyl-3-heptanone using headspace analysis.

Results

Fruit samples of almond trees grown organic and conventionally were evaluated in terms of pomological traits, sensorial quality, chemical, fatty acids and volatile aroma compounds composition. Pomological and sensorial evaluations were presented in *Table 2* and, results of the chemical, fatty acids and volatile aroma compounds compositions were shown in *Table 3, Table 4* and *Table 5*, respectively.

Pomological Evaluations and Sensory Analysis

Significant differences for all evaluated pomological parameters, except NLE which was not significantly differed between cultivars and growing systems. Although differences between nut and kernel sizes were significant between cultivars, they were not found significant between organic and conventional samples. NWE and KWE were significantly changed between organic and conventionally grown Ferraduel cultivar. NWE and KWE of organic Ferraduel samples were higher than conventional samples (4.9 and 4.6 g, 1.3 and 1.2 g, respectively). Both kernel and nut weight parameters were significantly changed between cultivars. Similarly, differences of K/N results were significant between cultivars but not between growing systems. On the other hand, UKN was significantly varied both between cultivars and between organic and conventionally grown Ferraduel cultivar. UKN of conventionally grown Ferraduel cultivar was higher than organic samples (23.8 and 21.4, respectively). Results indicated heavier nuts and kernels for organic samples of Ferraduel cultivar comparing to those conventional samples. Sensorial evaluations approved no difference between organic and conventional kernels in terms of size & shape, but indicated that organic kernels were slightly darker and richer in flavor. Results of the pomological evaluations are presented in *Table 2*.

http://www.aloki.hu ● ISSN 1589 1623 (Print) ● ISSN 1785 0037 (Online)
DOI: http://dx.doi.org/10.15666/aeer/1704_77837793

Chemical Composition

Highest total oil content was found in conventional Ferragnes samples (46.7%), whereas organic Ferraduel samples presented the lowest total oil content (41.1%). Highest total protein and moisture were found in organic Ferraduel samples. The lowest values for these contents were found in conventional Ferragnes (20.7% for total protein, and 4.5% for moisture). While ash content was not significantly varied between organic and conventional samples, in both cultivars organic kernels presented lower total oil, but higher total protein content and moisture when compared to conventional samples. Ferragnes was higher in total oil content, whereas Ferraduel was higher in total protein and moisture. Proximate chemical compositions results are presented in *Table 3*.

Table 2. *Pomological properties of almonds at organic and conventional orchards*

		Ferragnes		Ferraduel	
		Organic	**Conventional**	**Organic**	**Conventional**
NWE	(g)	4.2 ± 0.1 c	4.0 ± 0.1 c	4.9 ± 0.3 a	4.6 ± 0.2 b
NLE	(mm)	34.5 ± 0.6 ns	33.7 ± 0.7 ns	34.1 ± 0.9 ns	34.4 ± 1.0 ns
NWI	(mm)	21.1 ± 0.4 b	21.6 ± 0.4 b	24.5 ± 0.6 a	23.8 ± 0.9 a
NTH	(mm)	16.0 ± 0.2 bc	15.6 ± 0.2 c	16.5 ± 0.4 a	16.2 ± 0.4 ab
KWE	(g)	1.5 ± 0.0 a	1.4 ± 0.0 a	1.3 ± 0.1 b	1.2 ± 0.1 c
KLE	(mm)	26.8 ± 0.2 a	26.7 ± 0.1 a	25.1 ± 0.9 b	24.7 ± 0.7 b
KWI	(mm)	13.9 ± 0.2 b	14.1 ± 0.4 b	15.2 ± 0.2 a	14.8 ± 0.5 a
KTH	(mm)	8.5 ± 0.1 a	8.3 ± 0.2 ab	8.1 ± 0.3 bc	7.9 ± 0.2 c
K/N	(%)	35.9 ± 1.3 a	35.4 ± 1.1 a	26.9 ± 0.9 b	26.0 ± 1.5 b
UKN	Nr	19.0 ± 0.2 c	20.1 ± 0.4 bc	21.4 ± 1.1 b	23.8 ± 1.6 a

Differences between values signed with different letters within the rows are significant at $P \leq 0.05$.
NWE: Nut Weight, NLE: Nut Length, NWI: Nut Width, NTH: Nut Thickness, KWE: Kernel Weight, KLE: Kernel Length, KWI: Kernel Width, KTH: Kernel Thickness, K/N: Kernel /Nut Ratio, UKN: Unit Kernel Number

Table 3. *Proximate chemical composition of almonds at organic and conventional orchards*

%	Ferragnes		Ferraduel	
	Organic	**Conventional**	**Organic**	**Conventional**
Total oil	44.5	46.7	41.1	45.6
Total protein	20.9	20.7	21.3	20.8
Total ash	3.3	3.2	3.2	3.2
Moisture	4.7	4.5	4.8	4.7

Fatty Acid Composition

As part of fatty acid composition, the most significant differences were found in oleic and linoleic acid contents. Oleic acid contents were higher in organic samples, whereas linoleic acid contents were lower in both cultivars. Highest oleic acid content was found in organic samples which were the same in average for both cultivars (82.4%). Conventional Ferraduel samples were found with highest linoleic acid content

http://www.aloki.hu ● ISSN 1589 1623 (Print) ● ISSN 1785 0037 (Online)
DOI: http://dx.doi.org/10.15666/aeer/1704_77837793

(15.3%) followed by conventional Ferragnes samples (12.7%). Palmitic, palmitoleic and stearic acid contents were also higher in organic samples of both cultivars, and among the cultivars these values were higher in organic Ferraduel samples (7.9, 0.8, 2.7%). Fatty acid compositions of the samples included in the study are presented in *Table 4*.

Table 4. *Fatty acid compositions (percent) of almonds at organic and conventional orchards*

%	Ferragnes		Ferraduel	
	Organic	Conventional	Organic	Conventional
Palmitic Acid (C16:0)	6.4	5.9	7.9	6.0
Palmitoleic Acid (C16:1)	0.7	0.6	0.8	0.7
Stearic Acid (C18:0)	2.1	1.9	2.7	2.2
Oleic Acid (C18:1)	82.4	78.9	82.4	75.8
Linoleic Acid (C18:2)	8.4	12.7	6.2	15.3

Volatile Aroma Compounds

A total of 39 volatile aroma compounds were identified in almond kernel samples included in the study. The volatile aroma compounds consisted of ketones (17), terpenes (6), alcohols (5), esters (5), alkanes (4), and aldehydes (2). When all of the volatile compounds were classified according to absence in organic or conventional samples, most of the compounds were found higher in organic samples. Indeed, overall volatile compound contents were calculated as 1519 and 1193 µg/kg for organic and conventional samples of Ferragnes cultivar, 1417.4 and 1325.2 µg/kg for organic and conventional samples of Ferraduel cultivar.

Among the detected volatile compounds Butanal, Butyl acetate, Ethylbenzene, p-Chlorotoluene, 4-Octanone were found in higher concentrations in organic samples when compared with conventional samples in both cultivars. Pentadecane, 2-methyl-2-phenyl- was only detected in organic samples of both cultivars. On the other hand, some of the volatile compounds were detected in organic samples of one of the cultivar, while not found in other cultivar. 6-Hepten-3-one, 4-methyl-, 2.3-Dimethyl-1-butene, 3-Heptanone-5-methyl-, 2.6-Decadiene-4.5-diol-6-ethyl-, Decyl decanoate, Gamma-decalactone were detected in organic samples of Ferragnes, but not found in conventional Ferragnes samples and both of the Ferraduel samples. Similarly, Ethanone-1-(1-methylcyclopentyl)-and m-Cymene were detected in organic samples of Ferraduel, but not found in the rest of the samples. Butyl valerate and 3-Chloropentane-2.4-dione were not detected in conventional samples of Ferragnes cultivar but found in the rest of the samples.

The volatile compounds that found higher in conventional samples were butanol, 2-Methyl-3-heptanol, 2.5-Dimethyl-3-hexanone, isobutyric acid. On the other hand, 2.4-Dimethylpentane and 2-Hepten-4-one-2-methyl- were only found in conventional samples of Ferragnes, and similarly Octane-2.4.6-trimethyl-, diethyl phthalate, and gamma-undecalactone were only found in conventional samples of Ferraduel. While 3-Methyl-2-pentanone was not detected in both of the Ferragnes samples, it was detected in both organic and conventional samples of Ferraduel, and was found higher in concentration in organic samples when compared with conventional ones. Results of the volatile aroma compounds are presented in *Table 5*.

http://www.aloki.hu ● ISSN 1589 1623 (Print) ● ISSN 1785 0037 (Online)
DOI: http://dx.doi.org/10.15666/aeer/1704_77837793

Table 5. *Volatile aroma compounds of almonds at organic and conventional orchards*

t_r (min)	Volatile aroma compounds (µg/kg)	Ferragnes		Ferraduel	
		Organic	Conventional	Organic	Conventional
1.43	Acetone	56.0	23.7	20.3	23.0
1.82	Butanal	8.8	2.8	2.2	1.2
1.85	2.4-Dimethylpentane	-	0.3	-	-
1.85	3-Methyl-2-pentanone	-	-	0.2	0.4
2.42	Butanol	11.3	14.3	14.8	16.1
5.39	Butyl acetate	31.5	25.0	24.7	20.1
6.36	2-Phenyl-2-propanol	16.2	5.6	5.5	6.2
6.93	Ethylbenzene	23.8	19.6	21.6	18.1
7.69	6-Hepten-3-one-4-methyl-	5.9	-	-	-
7.79	3-Heptanone	7.2	8.2	9.0	8.7
9.94	o-Chlorotoluene	198.6	159.1	202.4	211.9
10.11	p-Chlorotoluene	91.8	81.2	171.1	103.0
10.15	2.3-Dimethyl-1-butene	6.3	-	-	-
10.34	2-Methyl-3-heptanol	8.4	17.1	7.9	13.8
10.68	4-Octanone	364.5	333.3	388.0	331.4
10.93	Octane-2.4.6-trimethyl-	-	-	-	2.4
10.93	2-Hepten-4-one-2-methyl-	-	1.2	-	-
10.94	Ethanone-1-(1-methylcyclopentyl)-	-	-	1.3	-
11.12	3-Octanone	-	1.9	3.1	2.1
11.14	3-Heptanone-5-methyl-	3.0	-	-	-
11.75	2-Methylpentanal	299.6	296.5	312.8	315.3
11.97	Pinacol	192.5	91.1	97.5	108.5
12.40	m-Cymene	-	-	6.0	-
12.43	Butyroin	7.1	-	-	4.6
12.53	2.5-Dimethyl-3-hexanone	25.2	29.3	30.2	32.9
12.87	Isobutyroin	6.7	5.5	5.9	7.3
13.04	Isobutyric acid	36.2	39.4	40.7	44.0
13.63	Diethylbenzol	9.3	9.1	8.6	11.0
14.65	Nonanone	11.4	12.4	15.5	15.1
14.71	Butyl valerate	1.3	-	0.7	0.6
16.88	Pentadecane-2-methyl-2-phenyl-	11.1	-	10.4	-
18.23	2-Methyl-1.3-dithiane	7.0	6.3	7.2	7.8
18.29	3-Chloropentane-2.4-dione	1.8	-	2.0	1.9
20.61	4-hydroxyheptanoic acid	44.2	10.1	7.8	9.5
28.88	Diethyl phthalate	-	-	-	4.4
29.08	2.6-Decadiene-4.5-diol-6-ethyl-	4.1	-	-	-
29.90	Decyl decanoate	10.2	-	-	-
31.39	Gamma-decalactone	18.0	-	-	-
31.40	Gamma-undecalactone	-	-	-	3.9
	Total	1519.0	1193.0	1417.4	1325.2

t_r: Retention time

Discussion

Almond cultivars included in this study were investigated in terms of pomological parameters under conventional growing conditions. Gülsoy and Balta (2014) reported an almond selection study included Ferragnes cultivar grown at Aydın city of Turkey. They reported NWE, NLE, KWE, KLE, and K/N as 3.4 g, 33.4 mm, 1.1 g, 25.5 mm, and 32.6, respectively. Parlakçı (2007) performed an adaptation study in Şanlıurfa city of Turkey and included Ferragnes and Ferraduel cultivars. They reported NWE, NLE,

http://www.aloki.hu ● ISSN 1589 1623 (Print) ● ISSN 1785 0037 (Online)
DOI: http://dx.doi.org/10.15666/aeer/1704_77837793

KWE, KLE, and K/N as 3.3 g, 32.6 mm, 1.2 g, 25.1 mm, and 31.1 for Ferragnes, and 3.7 g, 33.4 mm, 1.2 g, 25.7 mm, and 31.0 for Ferraduel, respectively. Results of these studies were similar each other but slightly lower than this study that probably caused by climatic differences caused by the year and environment.

Only a few previous studies have performed on comparison of chemical differences between organic and conventional almond. Venkatasubramanian (2011) compared commercial food samples of nuts from organic and conventional growing in terms of some sensory characteristics and chemical properties. Even though organic samples were found slightly darker and richer in flavor based on the sensory evaluations of this study, Venkatasubramanian (2011) reported a lighter color for organic almond, and no difference in terms of flavor. The difference of the flavor differences may be caused by fatty acid and volatile aroma compounds compositions. On the other hand, Venkatasubramanian (2011) reported higher protein, but lower fat and moisture content for organic samples when compared with conventional ones. These results are in accordance with total oil results of this current study but in opposite way for protein and moisture content. Relevant differences could be caused by multiple factors including cultivar, environmental differences, post-harvest processing, packaging, storage conditions etc. (Valdés et al., 2015). Yildirim et al. (2016) investigated total oil content of some almond cultivars and reported total oil contents as 61.3% for Ferragnes and 58.2% for Ferraduel. Houmy et al. (2016) measured total oil content of Ferragnes and Ferraduel kernel mixture and reported the value as 59.0% in average.

Sánchez-Bel et al. (2008) compared fatty acid composition of almond kernels sampled from trees fertilized with organic and inorganic fertilizers, and found no difference between the treatments in terms of fatty acid composition. However, current study resulted with significant differences especially in oleic and linoleic acid contents. Yildirim et al. (2016) investigated fatty acid compositions of conventionally grown Ferragnes and Ferraduel cultivars and indicated results in accordance with the results of conventional samples included in this present study. The differences between results of the studies would mainly are caused by growing conditions, and also cultivar difference. Samman et al. (2008) reported an inconsistently varied trend in the fatty acid compositions of edible oil samples of different crops grown organic and conventional including olive, coconut, canola, sesame, and sunflower.

Almonds are one of the most preferred nuts which are a regular part of the human diet since thanks to high nutritional value, and also sensory properties (Sathe et al., 2008; Gonçalves et al., 2018). Consumer preferences are related to nut quality which is associated with attractiveness such as color, size and shape (Kader, 2008), but aroma also play key role in market acceptability (Aceña et al., 2009; Shakerardekani et al., 2013). For this reason, evaluation of aroma compounds is important for determination of final quality of the products. Xiao et al. (2014) analyzed aroma compounds in raw almond samples and detected totally 41 volatile compounds from the groups of alcohols, aldehydes, ketones, and pyrazines. Erten et al. (2017) investigated aroma-active compounds in raw, dry roasted and oil roasted almonds and detected totally 59 aroma compounds including aldehydes, ketones, Nitrogen-containing compounds, Sulfur-containing compounds, acids, furanones, and other unknown compounds. Previously reported studies on volatile compounds in almonds showed that there are a large variety of compounds active in aroma specification of almonds that varies in absence and concentration in depending on various factors (Valdés et al., 2015; Erten, 2016). Erten et al. (2017) also suggested further studies for the identification of

http://www.aloki.hu ● ISSN 1589 1623 (Print) ● ISSN 1785 0037 (Online)
DOI: http://dx.doi.org/10.15666/aeer/1704_77837793

potentially important unknown aroma compounds in almonds. In furtherance of this suggestion of the authors, most of the aroma-active compounds detected in this present study (all compounds except acetone, butanal, 2-Phenyl-2-propanol, ethylbenzene, and 3-Heptanone) were not reported by previous studies in almonds (Erten, 2016; Kesen et al., 2018).

Conclusions

This study was conducted to compare organic and conventional almond samples of two different cultivars. Overall physical quality evaluations indicated not a worse even better market quality potential for organic samples of both almond cultivars. Consistent differences were found between fatty acid compositions of organic and conventional samples both of the cultivars. In conclusion, together with various aroma-active compounds detected, organic samples were found richer in total amount and the range of compound diversity.

REFERENCES

[1] Aceña, L., Vera, L., Guasch, J., Busto, O., Mestres, M. (2010): Comparative study of two extraction techniques to obtain representative aroma extracts for being analysed by gas chromatographyolfactometry: Application to roasted pistachio aroma. – Journal of Chromatography A 1217: 7781-7787.

[2] Anonymous (1993): Me´todos oficiales de ana´lisis; preparacio´n de los e´steres meti´licos (Official methods of analysis; preparation of metallic esters). – Ministerio de Agricultura Pesca y Alimentacio´n; Direccio´n General de Poli´tica Alimentaria (Ministry of Agriculture, Fisheries and Food; General Directorate of Food Policy); Madrid/Spain, 41(2): 135.

[3] Anonymous (2000): Sherlock microbial identification system. – Version 4 MIS operating manual, Newark DE, USA.

[4] Anonymous (2011): Profitability Comparison study of an organic almond orchard versus a conventionally farmed almond orchard in stanislaus county. – California Polytechnic State University, Digital Commons, https://digitalcommons.calpoly.edu/agbsp/61/ (Available Date: 17.03.2019).

[5] Anonymous (2014): Ilıman iklim meyve türlerinde hasat kriterleri (Harvest criteria in temperate fruits). – Gıda, Tarım ve Hayvancılık Bakanlığı, Meyvecilik Araştırma Enstitüsü (Minisry of Food, Agriculture and Livestock, Fruit Research Institute) http://arastirma.tarim.gov.tr/marem/Belgeler/Yeti%C5%9Ftiricilik%20Bilgileri/Il%C4%B1man%20%C4%B0klim%20Meyvelerinde%20Hasat%20Kriterleri.pdf (Available Date: 17.03.2019).

[6] Baymış, M. (2008): Yerli ve Yabancı Bazı Ceviz (*Juglans regia* L.) Tip ve Çeşitlerinin Kahramanmaraş Ekolojik Şartlarında Performanslarının Belirlenmesi (Assessing of Some Local and Foreign Walnut Type and Varieties (*Juglans regia* L.) Performances in the Kahramanmaraş Ecological Conditions). – MSc Thesis, Kahramanmaraş Sütçü İmam University, Kahramanmaraş/Turkey.

[7] Bengtsson, J., Ahnstrom, J., Weibull, A. C. (2005): The effects of organic agriculture on biodiversity and abundance: a meta-analysis. – Journal of Applied Ecology 42: 261-269.

[8] Bourn, D., Prescott, J. (2002): A comparison of the nutritional value, sensory qualities, and food safety of organically and conventionally produced foods. – Critical Reviews in Food Science and Nutrition 42(1): 1-34.

http://www.aloki.hu ● ISSN 1589 1623 (Print) ● ISSN 1785 0037 (Online)
DOI: http://dx.doi.org/10.15666/aeer/1704_77837793

[9] Ekelund, L., Tjarnemo, H. (2004): Consumer preferences for organic vegetables - the case of Sweden. – Acta Horticulturae 655: 121-128.
[10] Erten, E. S. (2016): Characterization of aroma components of raw and roasted almonds and the effect of the oxidative state of the nut on roasted flavor formation. – Phd Dissertation Thesis, University of Illinois at Urbana-Champaign, Illionis/USA.
[11] Erten, E. S., Cadwallader, K. R. (2017): Identification of predominant aroma components of raw, dry roasted and oil roasted almonds. – Food Chemistry 217: 244-253.
[12] FAO (2019): Food and Agriculture Organization, Crop Statistics. – http://www.fao.org/faostat/en/#data/QC (Available Date: 14.04.2019).
[13] Gąstoł, M., Domagała-Świątkiewicz, I., Krośniak, M. (2011): Organic versus conventional–a comparative study on quality and nutritional value of fruit and vegetable juices. – Biological Agriculture & Horticulture 27(3-4): 310-319.
[14] Gonçalves, B., Oliveira, I., Bacelar, E., Morais, M. C., Aires, A., Cosme, F., Ventura-Cardoso, J., Anjos, R., Pinto, T. (2018): Aromas and Flavours of Fruits. – In: Generation of Aromas and Flavours DOI: 10.5772/intechopen.72489.
[15] Guichard, S., Bertin, N., Leonardi, C., Gary, C. (2001): Tomato fruit quality in relation to water and carbon fluxes. – Agronomie 21: 385-392.
[16] Gülsoy, E., Balta, F. (2014): Aydın ili Yenipazar, Bozdoğan ve Karacasu ilçeleri badem (*Prunus amygdalus* Batch) seleksiyonu: pomolojik özellikler (Selection almond (*Prunus amygdalus* Batch) in Yenipazar, Bozdogan and Karacasu (Aydın): Pomological characteristics). – Akademik Ziraat Dergisi 3(2): 61-68.
[17] Heeb, A., Lundegardh, B., Savage, G., Ericsson, T. (2006): Impact of organic and inorganic fertilizers on yield, taste, and nutritional quality of tomatoes. – Journal of Plant Nutrition and Soil Science 169: 535-541.
[18] Hole, D. G., Perkins, A. J., Wilson, J. D., Alexander, I. H., Grice, P. V., Evans, A. D. (2005): Does organic farming benefit biodiversity. – Biological Conservation 122: 113-130.
[19] Houmy, N., Mansouri, F., Benmoumen, A., Elmouden, S., Boujnah, M., Sindic, M., Fauconnier, M. L., Serghini-Caid, H., Elamrani, A. (2016): Characterization of almond kernel oils of five almonds varieties cultivated in Eastern Morocco. – Cahiers Options Méditerranéennes: 1-5.
[20] James, G. S. (1995): Analytical Chemistry of Foods. – Blackie Academic and Professional, London: 117-120.
[21] Kader, A. A. (2008): Impact of nut postharvest handling, de-shelling, drying and storage on quality. – In: Harris, L. J. (ed.) Improving the Safety and Quality of Nuts. Woodhead Publishing, Cambridge/UK.
[22] Kesen, S., Amanpour, A., Selli, S. (2018): Comparative evaluation of the fatty acids and aroma compounds in selected Iranian nut oils. – European Journal of Lipid Science and Technology 120(10): 1800152.
[23] Lester, G. E., Manthey, J. A., Busling, B. S. (2007): Organic vs conventionally grown Rio Red whole grapefruit and juice: comparison of production inputs, market quality, consumer acceptance, and human health-bioactive compounds. – Journal of Agricultural and Food Chemistry 55: 4474-4480.
[24] Magkos, F., Arvaniti, F., Zampelas, A. (2006): Organic food: buying more safety or just peace of mind? a critical review of the literature. – Critical Reviews in Food Science and Nutrition 46: 23-56.
[25] MGM (2019): Resmi İstatistikler, T.C. Tarım ve Orman Bakanlığı, Meteoroloji Genel Müdürlüğü (Cities & Holiday Resorts, Turkish State Meteorological Service).
[26] Parlakçı, H. (2007): Yabancı Kökenli Değişik Badem Çeşitlerinin Bazı Pomolojik ve Kimyasal Özellikleri ile Bitki Besin Maddesi Kapsamlarının Belirlenmesi (Determination of Some Pomological and Chemical Traits with Nutrient Elements Contents for Some Foreign Originated Different Almond Cultivars). – MSc Thesis, Harran Üniversitesi, Şanlıurfa/Turkey.

http://www.aloki.hu ● ISSN 1589 1623 (Print) ● ISSN 1785 0037 (Online)
DOI: http://dx.doi.org/10.15666/aeer/1704_77837793

[27] Pretty, J. N., Noble, A. D., Bossio, D., Dixon, J., Hine, R. E., Penning de Vries, F. W. T., Morison, J. I. L. (2006): Resource-conserving agriculture increases yields in developing countries. – Environmental Science and Technology 40: 1114-1119.
[28] Samman, S., Chow, J. W., Foster, M. J., Ahmad, Z. I., Phuyal, J. L., Petocz, P. (2008): Fatty acid composition of edible oils derived from certified organic and conventional agricultural methods. – Food Chemistry 109(3): 670-674.
[29] Sánchez-Bel, P., Egea, I., Martínez-Madrid, M. C., Flores, B., Romojaro, F. (2008): Influence of irrigation and organic/inorganic fertilization on chemical quality of almond (*Prunus amygdalus* cv. Guara). – Journal of Agricultural and Food Chemistry 56(21): 10056-10062.
[30] Sathe, S., Monaghan, E., Kshiesagar, H., Venkatachalam, M. (2008): Chemical composition of edible nut seeds and its implications in human health. – In: Alsalvar, C., Shahidi, F. (ed.) Tree Nuts Composition, Phytochemicals and Health Effects. Taylor & Francis Group, Florida/USA.
[31] Shakerardekani, A., Karim, R., Ghazali, H., Chin, N. (2013): Textural, rheological and sensory properties and oxidative stability of nut spreads-a review. – International Journal of Molecular Sciences 14: 4223-4241.
[32] USDA (1970): Official grain standards of the United States. – US Department of Agricultural Consumer and Marketing Service, Grain Division, Revised.
[33] Valdés, A., Beltrán, A., Karabagias, I., Badeka, A., Kontominas, M. G., Garrigós, M. C. (2015): Monitoring the oxidative stability and volatiles in blanched, roasted andfried almonds under normal and accelerated storage conditions by DSC, thermogravimetric analysis and ATR-FTIR. – European Journal of Lipid Science and Technology 117: 1199-1213.
[34] Venkatasubramanian, C. (2011): Nutritional quality and acceptability of organic and conventional foods. – Indian Journal of Science and Technology 4(3): 361-365.
[35] Wood, R., Lenzen, M., Dey, C., Lundie, S. (2006): A comparative study of some environmental impacts of conventional and organic farming in Australia. – Agricultural Systems 89: 324-348.
[36] Xiao, L., Lee, J., Zhang, G., Ebeler, S., Niramani, W., Seiber, J., Mitchell, A. (2014): HS-SPME GC/MS characterization of volatiles in raw and dry-roasted almonds (*Prunus dulcis*). – Food Chemistry 151: 31-39.
[37] Yildirim, A. N., Akinci-Yildirim, F., Şan, B., Sesli, Y. (2016): Total oil content and fatty acid profile of some almond (*Amygdalus communis* L.) cultivars. – Polish Journal of Food and Nutrition Sciences 66(3): 173-178.

http://www.aloki.hu ● ISSN 1589 1623 (Print) ● ISSN 1785 0037 (Online)
DOI: http://dx.doi.org/10.15666/aeer/1704_77837793

THE RELATIONSHIP BETWEEN LAND USE, LAND COVER CHANGE, AND THE HEAT ISLAND EFFECT IN XI'AN CITY, CHINA

WANG, Z. F.[1,2*] – GONG, C. C.[1,2*] – BIAN, Z. H.[1]

[1]*Key Laboratory of Subsurface Hydrology and Ecological Effect in Arid Region of Ministry of Education, School of environmental science and engineering, Chang'an University Xi'an, Shaanxi, China*

[2]*Engineering Research Center of Groundwater and Eco-Environment of Shaanxi Province, Chang'an University, Xi'an, Shaanxi, China*
(e-mail: wangzf@chd.edu.cn, 895470127@qq.com, 2437035537@qq.com)

[*]*Corresponding author*
e-mail: wangzf@chd.edu.cn, 895470127@qq.com

(Received 23rd Feb 2019; accepted 3rd May 2019)

Abstract. With the acceleration of urbanization and the change of land use, the urban heat island effect has been significantly enhanced, leading to the rise of urban temperature, changing local air circulation, and influencing local microclimate. For investigating the temporal and spatial rules of the urban heat island effect in Xi'an City, China, this study combined Landsat TM, ETM remote sensing image, and surface meteorological station observation data to probe the trend of the urban heat island intensity in Xi'an City from 1993-2013 and to analyze its influencing factors. The results show that, from 1993 to 2009, the heat island intensity presented an increasing trend, with a temperature rise rate of 0.38°C/10y, while the heat island intensity showed a decreasing trend from 2009 to 2013. There was a positive correlation between heat island intensity and the urban area in Xi'an city. By a comprehensive analysis, the expansion of the urban land area, the heat island intensity followed a constantly increasing radius of influence are the main reasons.
Keywords: *urbanization, heat island intensity, urban land, forest land, farmland*

Introduction

Urban heat island refers to a phenomenon of increasing urban surface and atmospheric temperature in comparison to peripheral non-urban environments as a result of urbanization (Peng et al., 2013; Soltanifard et al., 2019). Urban heat island intensity typically measured by the mean difference between urban temperature and suburban temperature. According to existing publications, due to the urban heat island effect, the urban temperature of a city is typically 2-5°C higher than its peripheral suburban temperature (Ackerman, 2010). In recent years, with the acceleration of urbanization, the original use patterns of natural land have changed considerably, and the construction of buildings, roads, and other impermeable surfaces (Estoque et al., 2017) have further fragmented the urban landscape, increased the urban area and population, and enhanced the urban heat island effect (Alberti et al., 2004; Ciren et al., 2012; Zhou et al., 2017). Before 1980, the urban-suburban difference in annual mean minimum temperature of Shijiazhuang City had been rising by 0.26°C/10y; after 1980, it has been rising by about 1.7°C/10y (Yang et al., 2013a). On the temporal and spatial change characteristics of the heat island effect of Nanjing City, since 1985, the heat island intensity and scope have both increased, and the area affected by the grade-4 heat island effect in the built-up areas has increased by 107.88 km^2 (Yang et al., 2007). Beijing City, the capital of the People's Republic of China, reported that the area

http://www.aloki.hu ● ISSN 1589 1623 (Print) ● ISSN 1785 0037 (Online)
DOI: http://dx.doi.org/10.15666/aeer/1704_77957806

affected by urban heat island effect has constantly increased (Wang et al., 2006). In the Athens region, during the research period, the difference between its urban temperature and its suburban temperature was very significant, with a rising rate of 0.2°C/10y (Founda et al., 2015). The enhanced urban heat island effect has severely influenced both biodiversity and human life (Wu et al., 2014). Thus, in the context of changing patterns of urban land use, exploring the change rules and trend of the urban heat island effect has become one of the hotspot issues related to urban development under global climate change (Dong et al., 2011; Zhang, 2013a; Zhang et al., 2013b).

Studies on the urban heat island effect mainly conducted according to three methods: the ground meteorological data observation method, the remote sensing monitoring method, and the numerical simulation of the boundary layer (Yang, 2013b). Early studies mainly completed through an atmospheric temperature comparison between the urban and suburban areas of a city in the same period or of its different development stages (Song et al., 2009). With the development of remote sensing science and technology, the remote sensing monitoring method has become the primary method for investigating the heat island effect. In particular, aerospace sensors used to observe urban underlying surface temperature and other factors, while thermal infrared remote sensors are used to measure urban land cover temperature, thus obtaining heat distribution maps of different land covers via calculation and analysis (Yang, 2013b). For instance, remote sensing image for the inversion of land surface temperature and reported that changes in land use and land cover constitute the major drive behind the change in land surface temperatureb (Jiang et al., 2010). Other scholars (Chen et al., 2006; Qian et al., 2006; Xiao et al., 2007; Buyadi et al., 2013) reported that the increase of urban land area has led to a rise of land surface temperature, enhancing the urban heat island effect. The land surface temperature obtained through inversion via thermal infrared remote sensing can cover the land surface by a large scale, thus ensuring the relatively high spatial continuity and spatial resolution of the results (Voogt et al., 2003; Arnfield, 2003; Chen et al., 2012). However, given that the thermal infrared remote sensing phenomenon of the land surface is more significant during the daytime than during the nighttime, the results obtained with this method differ from the results calculated by atmospheric temperature data (Chen et al., 2012). It is thus clear that the data integration of aerial remote sensing and ground monitoring provides an effective method of researching the urban heat island effect.

With the acceleration of urbanization in China and the consequent increase of urban heat island intensity and expansion of heat island effect scope, accurately assessing and monitoring the development of the urban heat island effect has become particularly important at this point (Weilin et al., 2017). For explore the relationship between the urban heat island effect in Xi'an City and land use, land cover change (LUCC), this study integrated the remote sensing imaging technique and ground-measured atmospheric temperature data, probed into their relationships from both temporal and spatial scales, and analyzed the main controlling factors of the urban heat island effect through statistical comparison.

Research Contents and Methods

Research area

The study area, the Xi'an city, the People's Republic of China, located in the middle of the Guanzhong Basin, consisting of nine districts and four counties (geographical

http://www.aloki.hu ● ISSN 1589 1623 (Print) ● ISSN 1785 0037 (Online)
DOI: http://dx.doi.org/10.15666/aeer/1704_77957806

coordinates: 33°49′N-34°45′N, 107°40′E-109° 49′E). Xi'an city, situated between the Weihe River on the north and the Qinling Mountains on the south and adjoining, with the Taibai Mountain on the west and the Weinan City on the east. It is a temperate continental climate, with an annual mean temperature of 13.00°C and annual mean precipitation of 604.2 mm. It's maximum north-south width, and east-west lengths are about 116 km and 204 km, respectively. The total area of the city is 10,108 km^2.

Data sources

The temperature observation data came from the surface meteorological stations distributed in the urban districts and in Chang'an District, Lantian County, Gaoling County, Lintong County, Huxian County, and Zhouzhi County (*Fig. 1*). In particular, the annual mean temperature data of 1993, 1995, 2000, 2006, 2009, and 2013 were used to investigate the changing trend of heat island intensity; monthly mean temperature data were used to explore the spatial rules of heat island intensity change.

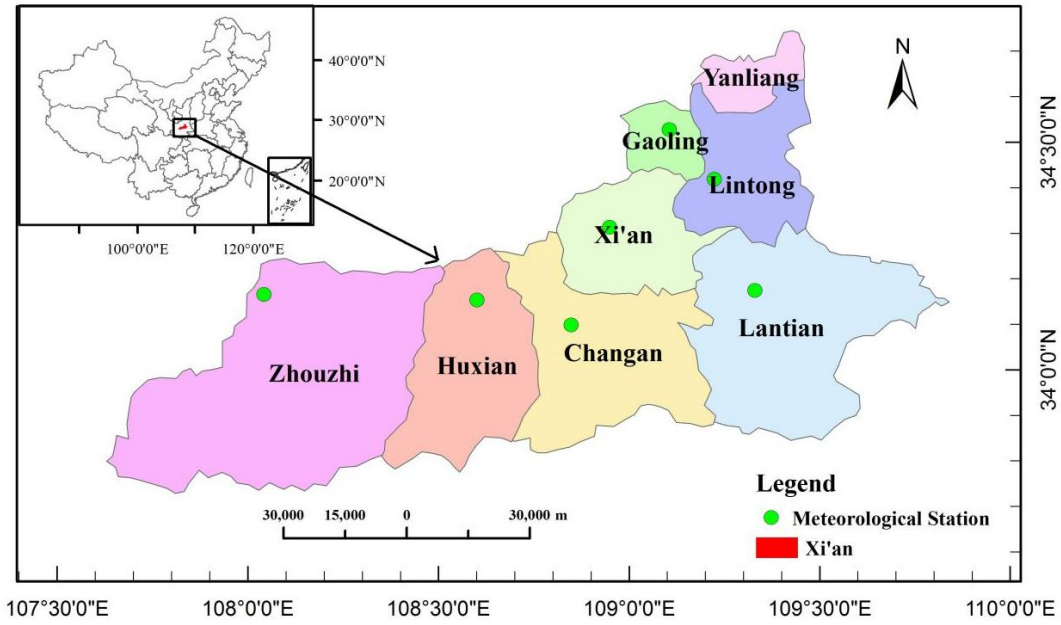

Figure 1. *Xi'an Administrative Region*

The remote sensing images were derived from the Geospatial Data Cloud of the Chinese Academy of Sciences (CAS), and Landsat TM and ETM remote sensing image data were selected from six years, i.e., 1993-6-18, 1995-6-8, 2000-5-20, 2006-7-24, 2009-6-30, and 2013-6-29.

Data processing

(1) The ENVI5.1 software used for the interpretation of remote sensing images and the supervised classification method was used to classify these images. According to national standards (Classification of land use status, GB/T 21010-2017), there are a total of six land use types, i.e., urban land, forest land, grassland, farmland, water area, and unused land. Based on the areas of various land use types obtained through statistical methods, a comparison conducted between acquired data and data from the statistical

http://www.aloki.hu ● ISSN 1589 1623 (Print) ● ISSN 1785 0037 (Online)
DOI: http://dx.doi.org/10.15666/aeer/1704_77957806

yearbooks, with the purpose of ensuring that the acquired data all fall within the allowable error range.

(2) Calculation of urban heat island intensity was done with the following formula:

$$\Delta T_{u-r} = T_u - \frac{1}{n}\sum_{i=1}^{n} T_r \quad \text{(Eq.1)}$$

where, ΔT_{u-r} is the urban heat island intensity; T_u is the annual mean temperature of downtown districts; T_r represents the annual mean temperature of suburban areas, covering six districts (counties), i.e., Chang'an District, Lantian County, Gaoling County, Lintong County, Huxian County, and Zhouzhi County; and n represents the number of suburban meteorological stations (n = 6).

Statistical analysis

The correlation between heat island intensity and various land cover types was analyzed according to the multivariate stepwise regression analysis and using SPSS software.

Results

Spatial change of the heat island effect in Xi'an City

Fig. 2 shows the temporal and spatial change rules of the temperature of Xi'an City. As can be seen from the interpretation of the remote sensing images during 1993-2009, the area of urban land showed a significantly increasing trend, and the area of downtown Xi'an City significantly increased as well. In the mountainous terrain of the Qinling Mountains to the south, and affected by human activities, the farmland and urban land of the intermontane valley region all increased, further fragmenting the forest there. The water area in this region accounted for a small proportion and did not present any significant change trend. Correspondingly, as indicated by the isothermal diagram of Xi'an City, with the expansion of urban land area, the isothermal diagram became more concentrated, pointing toward an increase of temperature gradients.

For comparatively analyze the changes in the urban heat island effect, this study calculated the change values of urban heat island intensity with time (*Eq. 1*). Affected by urban expansion and human activities, the mean temperature of Xi'an City increased significantly (*Fig. 3*). From 1993-2009, its urban heat island intensity presented a significantly increasing trend and increased from 0.42 in 1993 to 1.0 in 2009, and the five-year mean temperature rising rate of the city was 0.19°C/5y. Thus it is clear that after 2009, the urban heat island intensity index presented a decreasing trend. To discuss the cause of such a decrease, we evaluated the data of the statistical yearbooks of Xi'an City. According to statistical data from 2009 to 2013, the population of the city increased from 8.4346 million to 8.5881 million, and its urban land area was also constantly increased. However, it's forest land area remained unchanged. The improved urban landscape construction and increased green area weakened its heat island intensity to some extent (Huang et al., 2012). Furthermore, the climatic environment and local weather conditions also influenced the urban heat island effect, including inversion intensity, cloud cover, wind speed, wind direction, relative humidity, precipitation, and sunshine duration(Wang et al., 2006; Liu et al., 2008; Huang, 2011).

http://www.aloki.hu ● ISSN 1589 1623 (Print) ● ISSN 1785 0037 (Online)
DOI: http://dx.doi.org/10.15666/aeer/1704_77957806

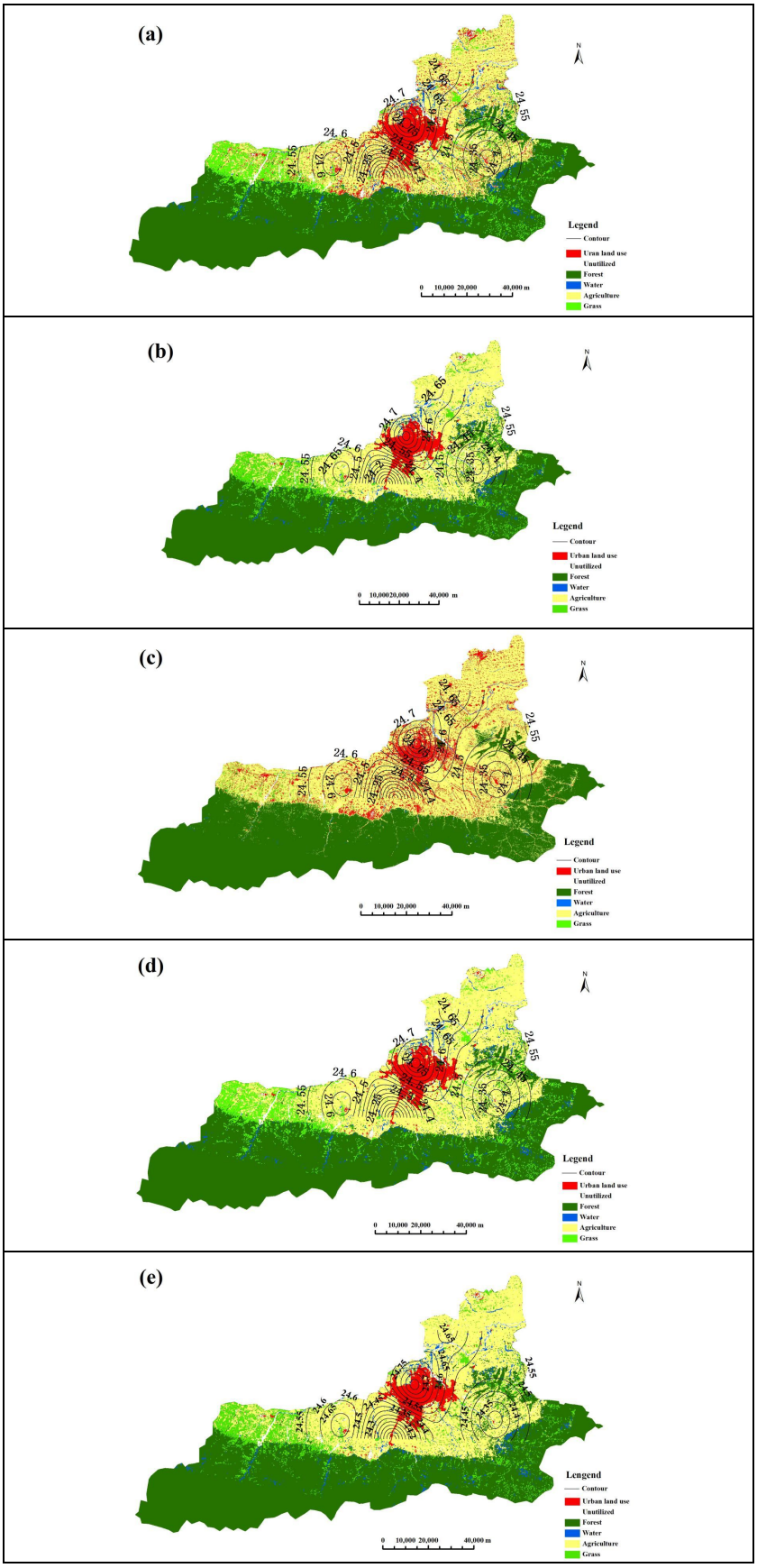

Figure 2. *Temporal and spatial changes in the temperature of Xi'an City*

http://www.aloki.hu ● ISSN 1589 1623 (Print) ● ISSN 1785 0037 (Online)
DOI: http://dx.doi.org/10.15666/aeer/1704_77957806

The relationship between heat island intensity and land use change of Xi'an City

To further analyze the relationship between heat island effect and land use in Xi'an City, remote sensing images were used to extract the urban land area, farmland area, forest land area and water area in the period of 1993-2009 to comparatively analyze their changing trends with time. *Fig. 4* depicts the change trends of the proportions of the urban land area, farmland area, forest land area, and water area in the total land area of Xi'an City with time. In summary, the urban land area of Xi'an City presented an increasing trend from 0.086 in 1993 to 0.100 in 2013. Xi'an's farmland area decreased from 0.316 in 1993 to 0.242 in 2013, while it's forest land area presented an increasing trend from 0.344 in 1993 to 0.503 in 2006. However, from 2006-2009, the water area showed a decreasing trend before 2000, an increasing trend observed after 2006.

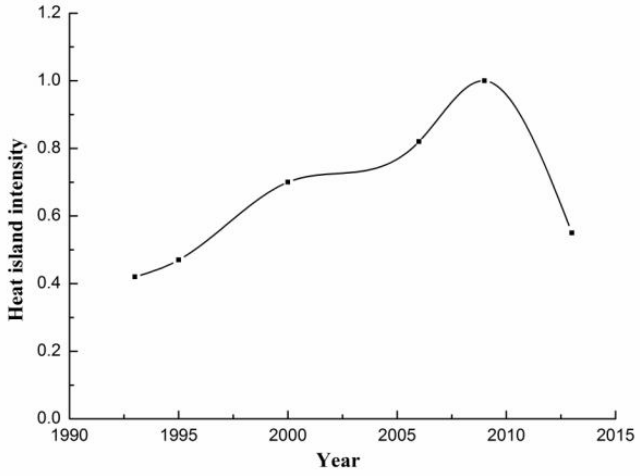

Figure 3. *Change trend of the urban heat island intensity of Xi'an City*

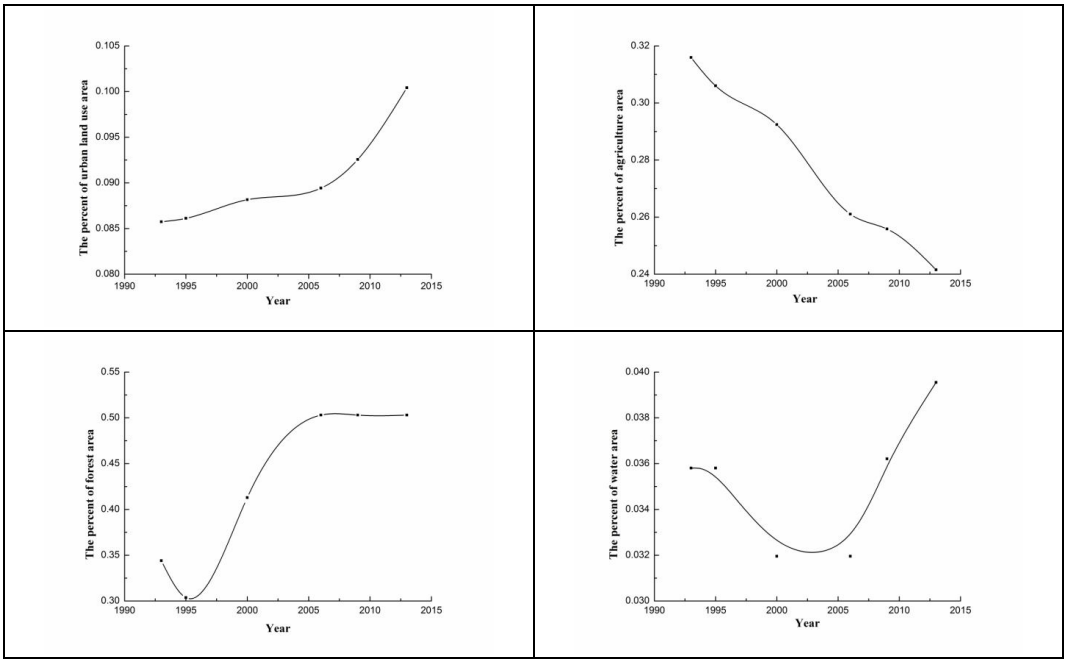

Figure 4. *Trend chart of main land use patterns of Xi'an City*

http://www.aloki.hu ● ISSN 1589 1623 (Print) ● ISSN 1785 0037 (Online)
DOI: http://dx.doi.org/10.15666/aeer/1704_77957806

Correlation between land use area change and heat island intensity of Xi'an City

Multivariate stepwise regression analysis was employed to analyze the correlation between the change of land use and heat island intensity, as well as to quantitatively investigate the correlation between heat island intensity and the areas of various land use types. The analysis results presented in *Table 1*.

Table 1. *Relationship between land use change and heat island intensity of Xi'an City*

Land use types	Urban land	Farmland	Forest land	Water area
Coefficient of correlation	0.985	-0.965	0.938	-0.223

The analysis results show a positive correlation between heat island intensity and urban land area (coefficient of correlation = 0.985), suggesting that the increase of urban land area exerted a very significant influence on the heat island intensity. A positive correlation was observed between heat island intensity and farmland area, as the decrease of farmland area would enhance the heat island effect. A positive correlation also observed between heat island intensity and forest land area, which is inconsistent with the results reported in other studies (Zhang et al., 1988; Liu, 2007; Liu et al., 2011). It's might because Xi'an City leans on the Qinling Mountains on the south and its forest land mainly distributed in the mountainous terrain of the Qinling Mountains. However, the airflow motion of Xi'an City mainly influenced by the northwest monsoon climate. In other words, the forest land of the mountainous terrain of the Qinling Mountains exerted no significant influence on the heat island effect of Xi'an City (Miao, 1998; Wang et al., 2008; Miao, 2014). A negative correlation found between heat island intensity and water area. However, the correlation was not strong, mainly because the water area in this region only accounted for a small proportion. After 2006, the water area showed an increasing trend, but small-area urban water bodies still exerted no significant regulatory effect on urban temperature (Liu et al., 2011).

To this regard, this study introduced multivariate stepwise regression analysis to investigate the relationship between the proportions of the urban land area, farmland area, forest land area, and water area in the total land area of Xi'an City and its heat island intensity. The results of stepwise regression shown in *Table 2*, and the regression model acquired:

$$Y = 85.912X_1 - 6.913 \quad \text{(Eq.2)}$$

where Y represents heat island intensity, and X_1 represents the proportion of urban land area in the total land area.

Table 2. *Stepwise regression analysis results*

Model	Unstandardized coefficient		Standardized	t	Sig.
	B	Standardized coefficient	Trial version		
Constant	-6.913	0.769	0.985	-8.992	0.003
Urban land	85.912	8.693		9.883	0.002

All correlations were statistically significant ($p<0.01$)

http://www.aloki.hu ● ISSN 1589 1623 (Print) ● ISSN 1785 0037 (Online)
DOI: http://dx.doi.org/10.15666/aeer/1704_77957806

Discussion

During recent years and with the acceleration of urbanization, China's large and medium-sized cities have witnessed an enhanced urban heat island effect (Weilin et al., 2017). Zigong City, in Sichuan Province, P. R. China, experienced relatively fast urbanization from 2000 to 2009, and the significant increase of urban land area changed the nature of the urban surface, thus enhancing the heat island effect (Deng et al., 2015). Guo et al. (2015) explored the thermal environmental characteristics and heat island intensity of urban villages in Shenzhen City and discovered a significant heat island effect in these villages. Using remote sensing images, Yao et al. (2013) analyzed the temporal and spatial change characteristics and causes for the heat island effect in Hefei, and the results show that the spatial distribution and extension of heat islands matched the layout of the city's built-up areas in the period of 1995-2010. Furthermore, the scope of heat islands continuously expanded with the development of Hefei city. In Shenyang City, P. R. China, compared to 2001, the year 2010 saw a significantly expanded urban heat island area (Wang et al., 2015). Heat island intensity, being closely related to LUCC, population, greening, and urban landscape environment, which is also influenced by the sum of climatic environmental and local weather conditions. In particular, local weather and meteorological conditions constitute the external cause, while land use change incurred by population growth, urbanization, and industrialization constitute the internal cause (Peng et al., 2013). Focused on the influence of the urbanization development of City on the heat island effect, Wang et al. (2010) found that the urban heat island effect of Shanghai City has gradually enhanced during recent years, mainly due to the increase of population density and the increase of built-up areas to a very large extent. Feng (2011) investigated the heat island effect in the metropolitan circle of Xi'an City and found the heat island effect in all the typical towns in its metropolitan circle to varying extents. In Liaoning Province, among the six cities, five suffered from an enhanced heat island effect (Li et al., 2012). Also, many other domestic cities experienced a heat island effect to varying degrees, and with the warming of the global climate and the acceleration of urbanization, the heat island effect gradually enhanced in China (Ran, 2010; Li, 2012). From the above results, we can say that the heat island effect poses a significant threat to human life and health. Therefore, it is of vital importance to decrease heat island intensity. Judging from the research results of this study, the urban heat island effect of Xi'an City presents an enhancing trend, mainly as a result of the increased urban area.

According to existing research, a negative correlation exists between the urban heat island effect and forest land area (Yang et al., 2007, 2014; Dai et al., 2009; Liu et al., 2011; Chen et al., 2012). However, according to our research, there is a positive correlation between urban heat island intensity and forest land area of Xi'an City. We think mainly due to two reasons. Firstly, Xi'an City leans to the Qinling Mountains on the south and its forest land mainly distributed in the mountainous terrain of the Qinling Mountain. However, the forest land area accounted for an extremely small proportion of the total land area of Xi'an City and did not change significantly. Therefore, the forest land in the mountainous terrain of the Qinling Mountains exerts no significant influence on its heat island intensity. Secondly, the prevailing wind in the Xi'an region is an easterly-westerly wind, and the Qinling Mountains on the south only block the entry of southerly airflow but exert no significant influence on the climate or general circulation of Xi'an City. The relatively weak correlation between heat island intensity and water area is due to the area of urban water bodies in Xi'an being relatively small and

http://www.aloki.hu ● ISSN 1589 1623 (Print) ● ISSN 1785 0037 (Online)
DOI: http://dx.doi.org/10.15666/aeer/1704_77957806

absorbing only a small proportion of surface heat. Consequently, water area exerts no significant influence on urban temperature.

Urbanization represents an inevitable trend of development all over the world, signifying the progress of human civilization (Li, 2006). The increasingly rapid urbanization has increased land surface temperature will no doubt intensely influence the mass and energy flows of the urban ecosystem, change its structure and functions, produce a series of eco-environmental effects, and impact urban climate, urban hydrology, urban soil physicochemical properties, urban atmospheric environment, urban biological habits, urban material cycle, urban energy metabolism, and urban residential health (Bo et al., 2005). The heat island effect is one of the extremely severe problems caused by urbanization. An extreme weather environment, particularly an extreme thermal environment, exerts a considerable influence on both mortality and morbidity. As an extra factor in the thermal environment, the heat island effect not only threatens human health but also increases mortality; furthermore, intensifies air pollution and increases energy consumption (Ketterer et al., 2014). Thus, to weaken the heat island effect, in the development process of its urbanization, Xi'an City should strengthen urban landscape construction, increase the extent of green and water area, control the increase of urban land area, and seek more rational patterns, scale, and spatial distribution of land use.

Conclusions

This study integrated the remote sensing imaging technique with ground-measured atmospheric temperature data, probed into the relationship between the urban heat island effect and LUCC from both temporal and spatial scales, and analyzed the main controlling factors of the urban heat island effect via statistical comparison. The mainly results as follows:

(1) From 1993 to 2009, the heat island intensity of Xi'an City presented an increasing trend, with a rate of temperature rise of 0.193°C/5y. However, from 2009 to 2013, its heat island intensity showed a decreasing trend, which might be related to both landscape construction and greening and the entire climatic environment.

(2) The heat island intensity of Xi'an City mainly influenced by urban land area, farmland area, increasing urban land area and decreasing farmland area. The city's heat island intensity increased. The stepwise regression analysis model for the correlation between heat island intensity and the urban land area in Xi'an City is $Y=85.912X_1-6.913$.

Acknowledgements. This work was supported by the National Science Foundation of China (NSFC, Grant No. 41202164), and the Open Research Fund of State Key Laboratory of Loess and Quaternary Geology, Institute of Earth Environment, CAS (Grant No. SKLLQG1623).

REFERENCES

[1] Ackerman, B. (2010): Temporal march of the Chicago heat island. – Journal of Applied Meteorology 24(6): 547-554.

[2] Alberti, M., Marzluff, J. M. (2004): Ecological resilience in urban ecosystems: linking urban patterns to human and ecological functions. – Urban Ecosystems 7(3): 241-265.

http://www.aloki.hu ● ISSN 1589 1623 (Print) ● ISSN 1785 0037 (Online)
DOI: http://dx.doi.org/10.15666/aeer/1704_77957806

[3] Arnfield, A. J. (2003): Two decades of urban climate research: a review of turbulence, exchanges of energy and water, and the urban heat island. – International Journal of Climatology 23(1): 1-26.
[4] Buyadi, S. N. A., Wan, M. N. W. M., Misni, A. (2013): Impact of land use changes on the surface temperature distribution of the area surrounding the national botanic garden, Shahalam. – Procedia Social and Behavioral Sciences 101: 516-525.
[5] Chen, X. L., Zhao, H. M., Li, P. X., Yin, Z. Y. (2006): Remote sensing image-based analysis of the relationship between urban heat island and land use/cover changes. – Remote Sensing of Environment 104(2): 133-146.
[6] Chen, A. L., Sun, R. H., Chen, L. X. (2012): Studies on urban heat island from a landscape pattern view: a review. – Acta Ecologica Sinica 14: 4553-4565. (in Chinese with English abstract).
[7] Ciren, L., Zhuo, G., Luo, B., Ciren, P. (2012): Temporal and spatial distribution of urban heat islands around Lhasa city. – Resources Science 34(12): 2364-2373.
[8] Dai, X. Y., Zhang, L. Q., Guo, Z. Y., Wu, J. P., Li, X. D., Zhu, Y. L. (2009): Mechanism of formation of urban heat island effect and its spatial pattern in Shanghai. – Acta Ecologica Sinica 07: 3995-4004.
[9] Deng, C., Yang, W. (2015): Spatial and temporal study on urban heat island in Zigong city, China based on TM data. – Earth and Environment 01: 86-91.
[10] Dong, H. Y., Hou, J. W., Liu, X. Z. (2011): Study on urban heat island effect in the Qingdao area. – The annual meeting of the twenty-eighth China Meteorological Society-S7 city weather forecast and service. Shamen (in Chinese).
[11] Estoque, R. C., Murayama, Y. Myint, S. W. (2017): Effects of landscape composition and pattern on land surface temperature: an urban heat island study in the megacities of southeast asia. – Science of the Total Environment DOI: 10.1016/j.scitotenv.2016.10.195.
[12] Feng, X. G. (2011): Study on the evolution of urban heat island effect and the cause of formation of Urban Heat Island [D]. – Shanxi Normal University (in Chinese).
[13] Founda, D., Pierros, F., Petrakis, M., Zerefos, C. (2015): Interdecadal variations and trends of the urban heat island in Athens (Greece) and its response to heat waves. – Atmospheric Research 161-162: 1-13.
[14] Guo, Q., Zou, Z., Hongyong, L. I., Qiu, G. (2015): Analysis of the thermal environment of an urban village in Shenzhen. – Ecology & Environmental Sciences 03: 427-435.
[15] Huang, L. P. (2011): Study on urban heat island effect in the Tianjin area. – Nanjing University of Information Science & Techonlogy (in Chinese).
[16] Huang, J. C., Zhao, X. F., Tang, L. N., (2012): Analysis of spatiotemporal changes of urban thermal landscape pattern in the context of urbanization: a case study of Xiamen City. – Acta Ecologica Sinica 02: 622-631. (in Chinese with English abstract).
[17] Jiang, J., Tian, G. (2010): Analysis of the impact of land use/land cover change on land surface temperature with remote sensing. – Procedia Environmental Sciences 2(1): 571-575.
[18] Ketterer, C., Matzarakis, A. (2014): Human-biometeorological assessment of the urban heat island in a city with complex topography - the case of Stuttgart, Germany. – Urban Climate 10(10): 573-584.
[19] Li, B. C. (2006): Problems of municipal ecological environment and the sustainable development in China. – Journal of Arid Land Resources & Environment 20(2): 1-6. (in Chinese with English abstract).
[20] Li, J. Q. (2012): Dynamic change analysis for heat island effects of Hefei based on remote sensing data and landscape ecology theory. – Anhui Agricultural University.
[21] Li, L. G., Wang, H. B., Jia, Q. Y., Lü, G. H., Wang, X. Y., Zhang, Y. S., Ai, J. F. (2012): Urban heat island intensity and its grading in Liaoning province of northeast China. – Chinese Journal of Applied Ecology 23(5): 1345-1350. (in Chinese with English abstract).

http://www.aloki.hu ● ISSN 1589 1623 (Print) ● ISSN 1785 0037 (Online)
DOI: http://dx.doi.org/10.15666/aeer/1704_77957806

[22] Liu, Y. (2007): Advance in the study on urban landscape pattern and heat island effect. – Journal of Meteorology & Environment 06: 46-50. (in Chinese with English abstract).
[23] Liu, Z. N., Yin, X. J. (2008): Urban heat island effect and meteorologic factors in Xi'an. – Journal of Arid Land Resources and Environment 22(2): 87-90. (in Chinese with English abstract).
[24] Liu, K., Xingfa, G. U., Tao, Y. U., Gao, Z., Gao, W. (2011): Relationships between urban heat island effect and land use and land cover change around urban weather stations. – Climatic & Environmental Research 16(6): 707-716. (in Chinese with English abstract).
[25] Miao, M. Q. (1998): The interaction between sea and land breeze and heat island circulation during the summer over the delta region of the Yangtze river and urbanization effect on climate. – Plateau Meteorology 03: 59-68. (in Chinese with English abstract).
[26] Miao, J. F. (2014): An overview of numerical studies of the interaction of urban heat island and sea breeze circulations. – Transactions of Atmospheric Sciences 04: 521-528. (in Chinese with English abstract).
[27] Peng, B., Shi, Y., Wang, H., Wang, Y. (2013): The impacting mechanism and laws of the function of urban heat islands effect: a case study of Shanghai. – Acta Geographica Sinica 68(11): 1461-1471. (in Chinese with English abstract).
[28] Qian, L. X., Cui, H. S., Chang, J. (2006): Impacts of land use and cover change on land surface temperature in the Zhujiang delta 1. – Pedosphere 16(6): 681-689. (in Chinese with English abstract).
[29] Ran, G. (2010): Analysis of urban heat island effect in Ji'nan. – Meteorological Science & Technology S1: 97-101. (in Chinese with English abstract).
[30] Soltanifard, H., Aliabadi, K. (2019): Impact of urban spatial configuration on land surface temperature and urban heat islands: a case study of mashhad, iran. – Theoretical and Applied Climatology. https://doi.org/10.1007/s00704-018-2738-4.
[31] Song, X., Duan, J., Du, L. (2009): Research overview of the urban heat island effect. – Meteorological & Environmental Sciences 32(3): 68-72. (in Chinese with English abstract).
[32] Voogt, J. A., Oke, T. R. (2003): Thermal remote sensing of urban climates. – Remote Sensing of Environment 86(3): 370-384.
[33] Wang, W. J., Shen, W. M., Liu, X. M., Zhang, F., Pan, Y. Z., Luo, H. J. (2006): Research on the relation of the urbanization and urban heat island effect changes in Beijing based on remote sensing. – Research of Environmental Sciences 19(2): 44-48. (in Chinese with English abstract).
[34] Wang, X. Q., Wang, Z. F. (2006): The study of the urban heat island in Beijing city. – Climatic & Environmental Research 11(5): 627-636. (in Chinese with English abstract).
[35] Wang, X. Q., Wang, Z. F., Gong, Y. B. (2008): Modulation of urban heat island circulation on the mountain-plain wind in the Beijing area. – Climatic & Environmental Research 13(5): 639-644.
[36] Wang, G. X., Shen, X. L. (2010): On the relationship between urbanization and heat island effect in Shanghai. – Journal of Subtropical Resources & Environment 02: 1-11. (in Chinese with English abstract).
[37] Wang, H. B., Li, L. G., Zhao, Z. Q., Cai, F., Wu, J. W., Xu, S. L., Jiang, P. (2015): Urban heat island variation of each district in Shenyang based on TM/ETM+ data. – Chinese Journal of Ecology 34(1): 219-226. (in Chinese with English abstract).
[38] Weilin, L., Xiaoping, L., Dagang, W., Yanling, S. (2017): The impact of energy consumption on the surface urban heat island in china's 32 major cities. – Remote Sensing doi:10.3390/rs9030250.
[39] Wu, H., Ye, L. P., Shi, W. Z., Clarke, K. C. (2014): Assessing the effects of land use spatial structure on urban heat islands using hj-1b remote sensing imagery in Wuhan, China. – International Journal of Applied Earth Observation & Geoinformation 32(1): 67-78. (in Chinese with English abstract).

http://www.aloki.hu ● ISSN 1589 1623 (Print) ● ISSN 1785 0037 (Online)
DOI: http://dx.doi.org/10.15666/aeer/1704_77957806

[40] Xiao, R. B., Ouyang, Z. Y., Li, W. F., Zhang, Z. M., Jr Tarver, G., Wang, X. K., Miao, H. Z. (2005): A review of the eco-environmental consequences of urban heat islands. – Acta Ecologica Sinica 25(8): 2055-2060. (in Chinese with English abstract).
[41] Xiao, H., Weng, Q. (2007): The impact of land use and land cover changes on the land surface temperature in a karst area of China. – Journal of Environmental Management 85(1): 245-257. (in Chinese with English abstract).
[42] Yang, Y. B., Wei-Zhong, S. U., Jiang, N., Zhen, F. (2007): Temporal and spatial characteristics of urban heat island effect change of Nanjing city and its relation with land use change. – Geographical Research 26(5): 877-876. (in Chinese with English abstract).
[43] Yang, B. (2013): The progress of urban heat island effect. – Journal of Meteorology & Environment 29(2): 101-106. (in Chinese with English abstract).
[44] Yang, P., Chen, J., Hou, X. W., Gao, Q., Zhao, Q. (2013): Study of Urban heat island based on multi-source data by the example of the Shijiazhuang Area. – Meteorological Monthly 10: 1304-1313. (in Chinese with English abstract).
[45] Yang, P., Chen, J., Gao, Q. (2014): Effect of different land cover types on urban heat island. – The annual meeting of the thirty-first China Meteorological Society S11-The third city meteorological Forum - city and environment. Beijing:14 (in Chinese).
[46] Yao, Y., Liu, P., Chen, L. (2013): Spatiotemporal variation characteristics and causes of urban heat islands in Hefei city, Anhui province of China based on remote sensing. – Chinese Journal of Ecology 12: 3351-3359. (in Chinese with English abstract).
[47] Zhang, J., Liu, Q. (1988): Temporal variations 1n the relationship between urban temperature and the structure of the urban surface in Beijing. – Acta Geographica Sinica 2: 159-168. (in Chinese with English abstract).
[48] Zhang, Z. (2013): Analysis on Heat Island Effect in Coastal Urbanization Area Using Remote Sensing Data: A Case Study in the Qingdao Area. – Ocean University of China (in Chinese).
[49] Zhang, H., Qi, Z. F., Ye, X. Y., Cai, Y. B., Ma, W. C., Chen, M. N. (2013): Analysis of land use/land cover change, population shift, and their effects on spatiotemporal patterns of urban heat islands in metropolitan Shanghai, China. – Applied Geography 44(4): 121-133. (in Chinese with English abstract).
[50] Zhou, B., Rybski, D., Kropp, J. P. (2017): The role of city size and urban form in the surface urban heat island. – Scientific Reports DOI:10.1038/s41598-017-04242-2.

http://www.aloki.hu ● ISSN 1589 1623 (Print) ● ISSN 1785 0037 (Online)
DOI: http://dx.doi.org/10.15666/aeer/1704_77957806

STABILITY ANALYSIS OF UNFAVOURABLE GEOLOGICAL BODIES IN A POST-EARTHQUAKE AREA: A CASE STUDY IN GENGDA TOWNSHIP CHINA

ZHONG, W.[1,2] – HE, N.[3,4*] – MEI, Z.[5] – KHAN, M. A.[6]

[1]*Key Laboratory of Mountain Hazards and Surface Processes, Chinese Academy of Sciences, Chengdu 610041, China*

[2]*Institute of Mountain Hazards and Environment, Chinese Academy of Sciences, Chengdu 610041, China*

[3]*School of Civil Engineering, Henan Polytechnic University, Jiaozuo, Henan 454000, China*

[4]*International Joint Research Laboratory of Henan Province for Underground Space Development and Disaster Prevention, Jiaozuo, Henan 454000, China*

[5]*Henan College of Industry and Information Technology, Jiaozuo, Henan 454003, China*

[6]*Karakoram International University, Gilgit-Baltistan, Pakistan*

**Corresponding author*
e-mail: hn61886@163.com

(Received 23rd Feb 2019; accepted 3rd May 2019)

Abstract. On 12 May 2008, a devastating mega-earthquake of magnitude 8.0 struck the Wenchuan area, northwestern Sichuan Province, China. Following this earthquake event, many areas in the affected areas were susceptible to geological disasters, such as debris flows, landslides and other secondary disasters. To better understand the mechanism of the formation processes of geological disasters, and to reduce the economic loss caused by the disasters, a comprehensive analysis is required. With the aim of obtaining the characteristics of unfavourable geological bodies, and analysing their stability, we choose the Gengda Township as an example (there are many unfavourable geological bodies distributed in this area, including landslides and deformation bodies). Field investigations and computational models are employed to analyse the stability of the unfavourable geological bodies. Through preliminary analysis and model calculation, the following conclusions can be drawn: under natural conditions, the stability factor of the landslide ranges from about 1.02–1.03, which means that the landslide is in a basically stable or less stable condition. Under the effect of continuous heavy rainfall, the stability factor of the landslide will be significantly reduced, and the corresponding value ranges from 0.9–0.96, which signifies that the landslide is in an unstable condition. For No 1 and No 2 deformation bodies (named by local inhabitants), the stability varied from less stable to unstable, and basically stable to unstable, respectively. On the basis of the results of the calculation, some countermeasures are proposed to mitigate the effects of these disasters probably caused by geological bodies.
Keywords: *case study, stability, model calculation, safety factor, transfer coefficient method*

Introduction

The 2008 Wenchuan Earthquake in Sichuan Province, China generated many unfavourable geological bodies, which can provide a huge amount of loose deposits, which have caused a dramatic increase in debris-flow occurrence in subsequent years (Hu et al., 2016; Tang et al., 2009; Zhuang et al., 2013). The epicenter Wenchuan Earthquake was in Wenchuan County, Sichuan (31°1'15.60"N, 103°22'1.20"E). As a consequence of the severe shocks, most valleys and slopes were destabilized and

http://www.aloki.hu ● ISSN 1589 1623 (Print) ● ISSN 1785 0037 (Online)
DOI: http://dx.doi.org/10.15666/aeer/1704_78077819

numerous geo-hazards, such as landslides, collapses, and unstable slopes, were triggered in the earthquake-affected area, which covered 50 badly affected counties and ten worst-affected counties in Sichuan province, SW China (Chen et al., 2009; Lee et al., 2017; Wang et al., 2017). The earthquake-stricken area is also the key area for torrent and debris flow mitigation in Sichuan. It was observed that the availability of masses of loose materials was the most important contributing factor for debris flows. Therefore, rock avalanches and landslides induced by the earthquake would supply abundant solid materials to form subsequent debris flows (Chen et al., 1989; Jiayuan, 1995; Postance et al., 2017; Sun et al., 2016). Gengda township is located in the worst-stricken area, Wenchuan earthquake not only caused a lot of casualties and economic losses, but also induced numerous secondary geological disasters, which including collapses, landslides and debris flows (Ni et al., 2012). As triggered by the Wenchuan earthquake, abundant rock falls and landslides were deposited in the gully drainages, which could provide a large amount of loose solid materials that might be directly turned into debris flows or easily entrained by debris flows. The abundant loose solid materials produced by an earthquake is usually recognized as the most important factor contributing to the occurrence of debris flow. Furthermore, the threshold of trigger factors, such as rainfall, significantly decreases after earthquake events. Thus, areas affected by the Wenchuan earthquake were prone to geological disasters (Ni et al., 2011; Zhuang et al., 2010; Kang and Kim, 2016; Shima et al., 2016).

Through field investigations, the lithology, seismic activity, and tectonic movements of the study area can be determined and consist of the following: exposed strata mainly concentrated in the Quaternary alluvial layer (Q_4^{al+pl}), the eluvial layer (Q_4^{el+dl}), colluvium (Q_4^{col}), and the landslide deposition layer (Q_4^{del}). Moreover, the bedrock in the study area is fragmentized due to the effect of tectonic movement and weathering, which can greatly facilitate landslide movement in subsequent rainfall conditions.

The study area is located in Huaxia tectonic belt, which belongs to Longmenshan tectonic system, and the tectonic movement is extremely complex. Due to the effect of strong tectonic movements, the bedrock becomes loose and can thus provide favourable conditions for the development of collapse, landslides, and other geological disasters.

On 12 May 2008, a devastating mega-earthquake of magnitude 8.0 struck the Wenchuan area of northwestern Sichuan Province, China. The focal mechanism of the earthquake was successive massive rock fracturing at 15 km depth at Yingxiu. Seismic analysis confirmed that the major shock occurred on the Beichuan–Yingxiu Fault and that aftershocks rapidly extended in a straight northeast–southeast direction along the Longmenshan Fault zone. The total number of fatalities approached 15000, with a significant number resulting from seismically triggered geohazards (Cui et al., 2011). The study area is located in Longmenshan seismic zone. Several earthquakes hit this area before the 12 May 2008 Wenchuan earthquake, including the 1933 Diexi earthquake (with a magnitude of 7.5), the 1657 Wenchuan earthquake (with a magnitude of 6.5), and the 1976 Pingwu earthquake (with a magnitude of 7.2). The study area influenced by these earthquakes reached degree V.

In order to mitigate the disasters that were caused by unfavourable geological bodies after the Wenchuan earthquake, field investigations and calculation models are employed in this paper to analyse the stability of the unfavourable bodies. After analysis, the stability of the unfavourable bodies can be identified, and the corresponding engineering countermeasures can be proposed. Thus, the magnitude of

http://www.aloki.hu ● ISSN 1589 1623 (Print) ● ISSN 1785 0037 (Online)
DOI: http://dx.doi.org/10.15666/aeer/1704_78077819

the disasters caused by the unfavourable bodies can be significantly reduced, and the security of the inhabitants living adjacent to the unfavourable bodies can be guaranteed.

Materials and methods

Study area

Wenchuan earthquake of 12 May 2008 which caused numerous coseismic landslides. After earthquakes of this magnitude, most valleys and slopes are destabilized and conditions for debris flows and landslides are amplified. These hazards are typically very active during the following 10-20 years. As a consequence of the severe shocks, most valleys and slopes were destabilized and numerous geo-hazards, such as landslides (*Fig. 1*), collapses (*Fig. 2a*), and unstable slopes (*Fig. 2b*), were triggered in the earthquake-affected area, which covered 50 badly affected counties and ten worst-affected counties in Sichuan province, SW China (Chen et al., 2009). The Gengda township is located in an earthquake-stricken area; due to the effect of seismic activity, many slopes located in the Gengda township are seriously affected. Thus, in the subsequent rainy seasons, these unfavourable bodies can be transferred into secondary disasters in response to heavy rainfall. The main objective of this paper is twofold. First, through field investigation, the fundamental data of the study area and the distribution of the unfavourable bodies can be identified; then, computational models are employed to compute the safety factor of each slope, which could allow us to analyse the stability of the slopes distributed within the study area. On the basis of the model calculations, the risk of each slope can be mapped, and preventative engineering can be designed. Thus, the threat caused by the unfavourable bodies can be greatly reduced.

Characteristics of the unfavourable geological bodies

The unfavourable geological bodies in the Gengda township mainly fall into the following four types: landslides, slippery bodies, deformation bodies, and perilous rock. These unfavourable geological bodies cause a great risk to the security of the nearby inhabitants. Moreover, many facilities are also under their threat (*Table 1*). In order to compute the safety factors of the unfavourable geological bodies, field investigations were conducted meticulously. Through these investigations, the fundamental data of the study area could be obtained, including meteorological data, geological conditions, topography, rainfall data, tectonic and earthquake history, hydrological conditions, and human activity. With the help of the data obtained through field investigations, the stability of the bodies can be analysed preliminarily. Then, calculation models are employed to compute the corresponding safety factors of he bodies. By comparing the calculation results to preliminary analysis results, the stability of the unfavourable geological bodies can be reasonably analysed.

Methods

In this paper, two basic approaches (field investigations and model calculations) are employed to explore the stability of the unfavourable bodies. The field investigations can help us acquire data that are closely related with the unstable bodies, which will be useful and can greatly facilitate the subsequent model calculation processes. Based on the fundamental data of the study area and the results of model calculations, a comprehensive stability analysis of each body can be performed.

http://www.aloki.hu ● ISSN 1589 1623 (Print) ● ISSN 1785 0037 (Online)
DOI: http://dx.doi.org/10.15666/aeer/1704_78077819

Field investigations

The field investigations were conducted from the period between June 2009 and July 2009, and these work lasted for around one month. Our investigations are primarily concentrate in Gengda township, Wenchuan prefecture, Sichuan Province. During the processes of investigations, we mainly collected the data with regard to rainfall conditions, geological conditions, topography, etc. The main purpose of the field investigations concerned the following main issues: an initial consideration of the distribution, scale, geological conditions, and triggering factors of each unstable body, followed by a preliminary analysis of the formation mechanism of each unstable body alongside an evaluation of its stability. These results can be compared with subsequent model computations, which can help us to draw reasonable and accurate conclusions. These conclusions can provide a reliable geological basis for designing preventative engineering measures for each unstable body. With the help of Wolong Reserve Management Bureau, Wolong Land Resources Bureau, and Wolong township government, field investigations were conducted and lasted for around one month. The scope of the investigations not only concentrated on the unstable body itself but also included the adjacent zone (within a 20 metre radius) and the area susceptible to these unstable bodies. Through the field investigations, it was possible to acquire the fundamental data of the study area, which are described in the following sections.

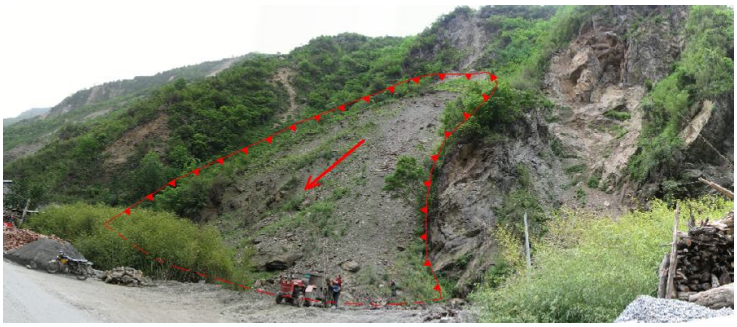

a

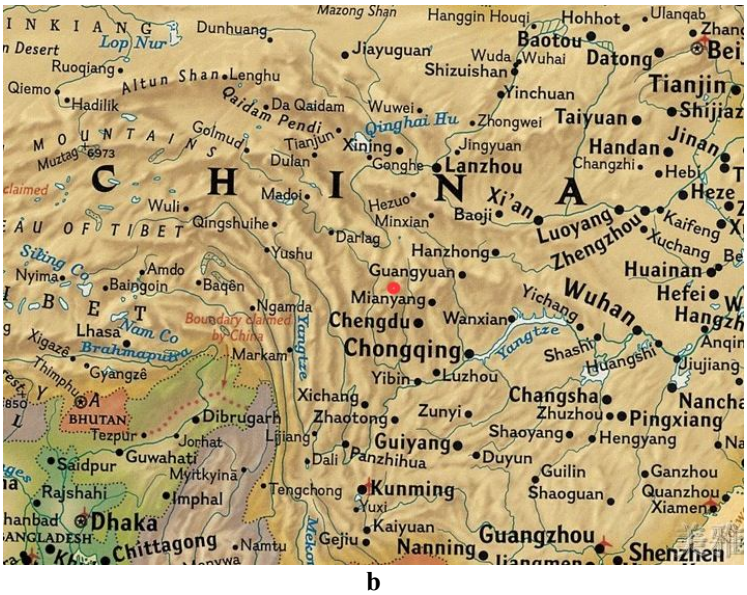

b

Figure 1. *Full view of Nitianguo landslide (red point is the study area).* ***a*** *Landslide range,* ***b*** *location of the study area*

http://www.aloki.hu ● ISSN 1589 1623 (Print) ● ISSN 1785 0037 (Online)
DOI: http://dx.doi.org/10.15666/aeer/1704_78077819

a **b**

Figure 2. *Other types of unstable geological bodies.* ***a*** *Collapses ,* ***b*** *unstable slopes*

Table 1. *Number of buildings and inhabitants under the threat of unfavourable geological bodies in Gengda township*

Object under threat of unfavourable geological bodies	Name of household	Inhabitants	Area of building (m^2)	Potential economic loss (10^4)	Notes
Gengda township	Shunfang Liu	5	230	10	
	Qing Jian	4	300	20	Original building was damaged
	Xing Jian	4	140	8	
	Lin Jian	5	380	30	
	Fugui Yu	4	400	12	
	Tianguo Ni	5	500	180	
	Shaoxiu Zhou	10	600	20	
	Tianyuan Ni	5	400	15	
	Tianhua Ni	5	150	12	
	Wenxiang Tang	6	150	4	
	Bing Jian	5	120	10	Under construction
	Huachuan Gong Highway Construction Group Co., Ltd. 303 Project Department	50	Rented building	200	
	Workers of Huachuan Gong Highway Construction Group Co., Ltd	50	Rented building	5	
Transmission facilities	Transmission tower			60	
Disaster prevention facilities	Retaining wall (2×8×85 m)		85		Under construction
Highway	Highway 303		500	150	
Number	11 households, 58 people, floating population 100, 2 transmission towers and 500 m highway			736	

http://www.aloki.hu ● ISSN 1589 1623 (Print) ● ISSN 1785 0037 (Online)
DOI: http://dx.doi.org/10.15666/aeer/1704_78077819

Model calculations

Since most slopes and other deformable bodies distributed within the study area mainly consist of soil, the deformation of the slope is mainly governed by the weak interface with maximum shear stress. Therefore, we can use the Transfer Coefficient Method (GB 50330-2013) to compute the safety factors of the slopes. Following this method, and to facilitate the subsequent deducing processes, the soil is initially divided vertically into several strips (*Fig. 3*) and each strip is taken as a rigid body while taking the interaction forces between the strips into consideration at the same time. The deducing results can be employed to calculate the safety factor of each strip from the slope, and the safety factor of the whole slope can be determined. On the basis of the above description, we assumed that the residual sliding force was parallel to the sliding surface, and then the driving moment and the resisting moment exerted on individual strips can be calculated, as shown by the stress analysis diagram in *Figure 3*.

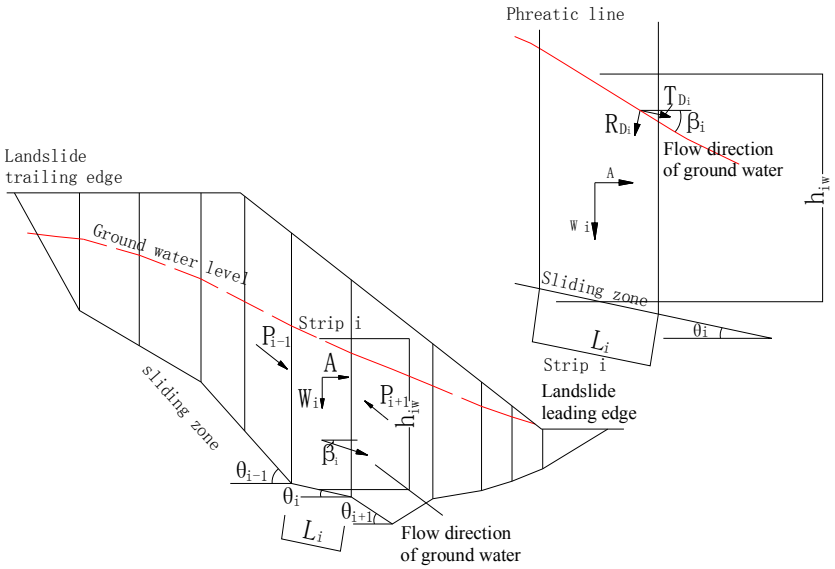

Figure 3. *Calculation model of transfer coefficient method*

(1) The computational formula for computing the safety factor is expressed as follows:

$$K_f = \frac{\sum_{i=1}^{n-1}((W_i(1-r_u)\cos\theta_i)tg\phi_i + C_iL_i\prod_{j=i}^{n-1}\psi_j) + R_n}{\sum_{i=1}^{n-1}(W_i(\sin\theta_i + A\cos\theta_i)\prod_{j=i}^{n-1}\psi_j) + T_n} \quad \text{(Eq.1)}$$

$$R_i = (W_i((1-r_U)\cos\theta_i - A\sin\theta_i) - R_{Di})tg\phi_i + C_iL_i \quad \text{(Eq.2)}$$

$$T_i = W_i(\sin\theta_i + A\cos\theta_i) + T_{Di} \quad \text{(Eq.3)}$$

$$\prod_{j=i}^{n-1}\psi_j = \psi_i\psi_{i+1}\cdots\cdots\psi_{n-1} \quad \text{(Eq.4)}$$

http://www.aloki.hu ● ISSN 1589 1623 (Print) ● ISSN 1785 0037 (Online)
DOI: http://dx.doi.org/10.15666/aeer/1704_78077819

Ψ_i is the residual sliding force transferred from strip i to strip i + 1 ($j = i$); that is:

$$\Psi_i = \cos(\theta_i - \theta_{i+1}) - \sin(\theta_i - \theta_{i+1}) \tan\phi_{i+1} \quad \text{(Eq.5)}$$

where W_i is the weight of the i-th strip; T_i is the sliding force of the i-th strip; R_i is the resistance force of the i-th strip; θ_i is the inclination of the sliding surface of the i-th strip; β_i is the angle between the sliding surface and the ground water (here, ground water denotes the water level below the i-th strip); ψ_i is the cohesion forces of the i-th strip; ϕ_i is the internal friction angle of the i-th strip; L_i is the length of the sliding surface of i-th strip; A is the coefficient of earthquake acceleration in the area where the seismic fortification grade is level 6, A is equal to 0.05; R_{D_i} is the component of seepage force perpendicular to the sliding surface, and R_{Di} is equal to $N_{Wi} \tan\beta_i \sin(\alpha_i - \beta_i)$; T_{Di} is the component of seepage force parallel to the sliding surface, and T_{Di} is equal to $N_{Wi} \tan\beta_i \cos(\alpha_i - \beta_i)$; N_{Wi} is pore water pressure, and N_{Wi} is equal to $\gamma_W h_{iW} L_i$; r_U is the ratio of pore pressure, and $r_U = \frac{v_w \times \gamma_w}{v_s \times \gamma_s} \approx \frac{s_u}{s_t \times 2}$, where v_w is the volume of the strip below water level, v_s is the total volume of the strip, s_u is the area of the strip below the water level, s_t is the total area of the strip, and γ_w and γ_s represent the unit weight of the water and strip (sliding body), respectively.

(2) The computational formula for computing the residual sliding force is expressed as follows:

$$P_i = P_{i-1}\Psi_{i-1} + K_s \times T_i - R_i \quad \text{(Eq.6)}$$

where P_i is the sliding thrust of the i-th strip (kN/m); P_{i-1} is the residual sliding force of i-th strip (kN/m); and K_s is the designed safety factor, with a value of 1.15 here.

Climatic and geological settings

Climatically, the study area falls into the subtropical humid climate zone; during winter the area is significantly affected by the Qinghai-Tibet Plateau climate, while in summer it is mainly dominated by the southwest and southeast monsoon climate. The mean annual precipitation is 930.2 mm, and the rainfall is mainly concentrated during the period from May to September, which contributes more than 78% of the total precipitation throughout the year. According to the rainfall contour diagram of Sichuan province illustrated in the manual of flood calculations for small and medium-sized basins, the rainfall data for 10 min and 1, 6, and 24 h can be acquired and the corresponding amounts are 10, 20, 65, and 120 mm, respectively. Some slopes in the study area have been loosened by the effect of seismic activity, which will result in instability under subsequent heavy rainfall conditions (Tang et al., 2011). The rainfall data from 2000 to 2009 were gathered, as shown in *Table 2*, and the historical rainfall histogram is shown in *Figure 4*.

http://www.aloki.hu ● ISSN 1589 1623 (Print) ● ISSN 1785 0037 (Online)
DOI: http://dx.doi.org/10.15666/aeer/1704_78077819

Table 2. *Rainfall data from 2000 to 2009 (the dataset are collected from county annals)*

Year	Rainfall (mm)												Annual rainfall (mm)
	Jan	Feb	Mar	Apr	May	June	July	Aug	Sep	Oct	Nov	Dec	
2000	8.0	13.0	30.0	122.0	144.0	122.0	/	/	29.0	78.0	46.0	1.0	
2001	8.0	11.0	26.0	89.0	94.0	154.0	161.0	165.0	149.0	111.0	16.0	9.0	993
2002	4.0	24.0	46.0	68.0	155.0	244.0	303.0	115.0	114.0	92.0	12.0	0	1177
2003	7.0	11.0	32.0	82.0	96.0	159.0	207.0	139.0	123.0	91.0	15.0	2.0	964
2004	6.0	11.0	24.0	117.0	97.0	189.0	152.0	106.0	168.0	73.0	28.0	6.0	977
2005	/	/	/	24.0	133.0	160.0	235.0	184.0	99.0	34.0	/	/	
2006	/	/	/	11.0	113.0	95.0	152.0	118.0	43.0	36.0	9.0	2.0	
2007	4.0	33.0	36.0	83.0	338.0	146.0	132.0	9.0	/	/	/	/	
2008	7.0	23.0	32.0	81.0	113.0	103.0	218.0	186.0	98.0	118.0	35.0	5.0	1019
2009	4.0	14.0	16.0	132.0	141.0	140.0	195.0	177.0	132.0	32.0	41.0	20.0	1044

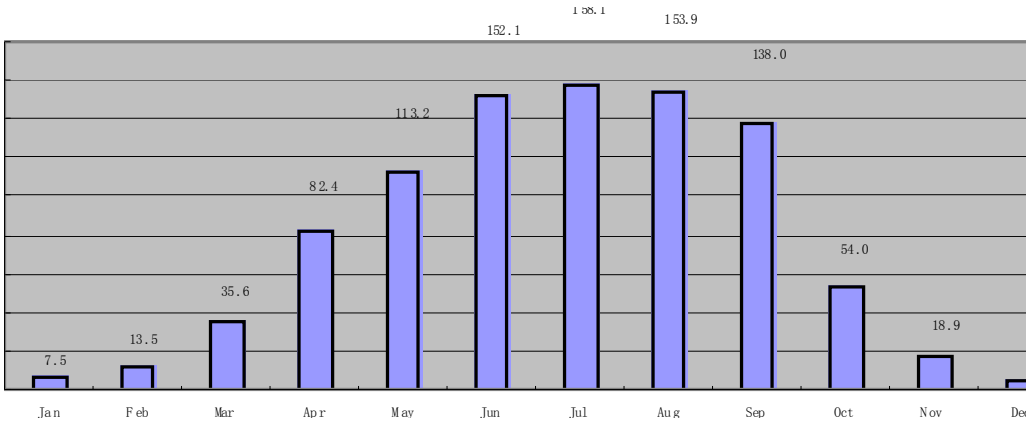

Figure 4. *Histogram of historical average rainfall (mm)*

Determination of the load condition parameters for model calculations

Through field investigations, the influential factors of the unstable bodies in the study area were studied meticulously. By analysis we found that the slopes in this area are mainly affected by the own weight of the slope, rainfall, and seismic activity. Based on these influential factors, we determined the load conditions and computed the safety factors under different load conditions. The load conditions were mainly grouped into three types: condition 1 represents the effect of the own weight of the slope, condition 2 represents the combined effect of the own weight of the slope and rainfall conditions (34 mm/h), and condition 3 represents the effect under the own weight of the slope, rainfall conditions (34 mm/h), and seismic activity.

During field investigations, we conducted some in-situ bulk density tests (we dug a hole in the field, measured the size of the hole in order to calculate the volume of the soil, and weighing the weight of the soil that was dug out, thus the unit weight can be figured out. Use similar method, we can also determine the saturated unit weight of the soil), and obtained the corresponding data, then combined with local rock-mass unit weight the unit weight of the slope body can be determined, the value of unit weight and saturated unit weight of the slope body is 17.1 and 25 kN/m^3, respectively. Soil strength

http://www.aloki.hu ● ISSN 1589 1623 (Print) ● ISSN 1785 0037 (Online)
DOI: http://dx.doi.org/10.15666/aeer/1704_78077819

parameters can be obtained by laboratory experiments (direct shear tests in the laboratory were conducted to identify strength of the soil collected from study area), by experiments the shear strength under fast shear and under fully saturated shear can be acquired simultaneously, their corresponding value shown in *Table 3*.

Table 3. *Shear strength of sliding body under different conditions*

Parameters / Landslide	Shear strength under natural conditions		Shear strength under fully saturated conditions	
	C (kPa)	Φ (°)	C (kPa)	Φ (°)
Sliding body and No 1 deformation body	8.5	29	7.5	28
No 2 deformation body	3.5	23.5	2.5	22

Results and discussion

According to the principle of the Transfer Coefficient Method, the unfavourable bodies in the study area can be vertically divided into several strips. Through preliminary analysis, we found that strips 6 and 7 are the most dangerous sliding bodies in the whole landslide, strips 1 and 2 are the most dangerous sliding bodies in No 1 deformation body, and strip 5 is the most dangerous body in No 2 deformation body. The stability calculation diagrams are shown in *Figure 5a-c*.

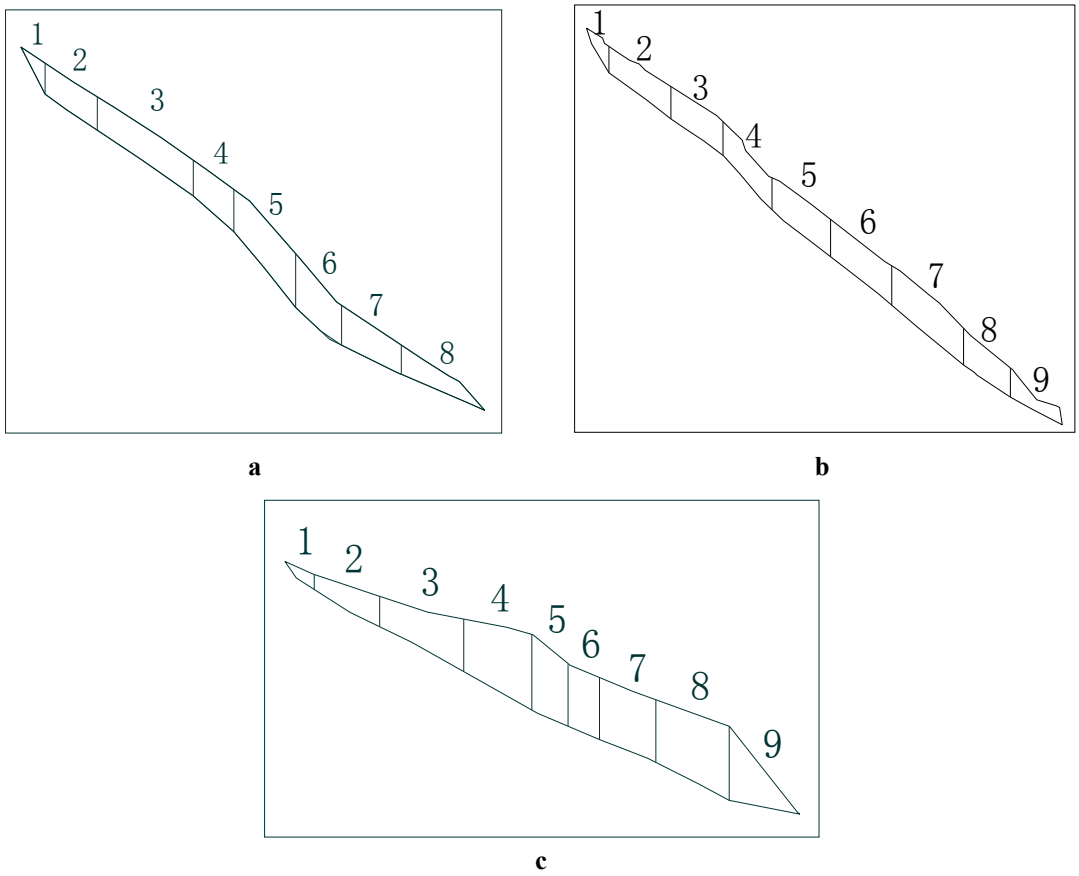

Figure 5. *Stability calculation diagram of* ***a*** *strip 1 of No 1 deformation body (profile);* ***b*** *strip 2 of No 1 deformation body (profile) and* ***c*** *strip 5 of No 2 deformation body (profile)*

http://www.aloki.hu ● ISSN 1589 1623 (Print) ● ISSN 1785 0037 (Online)
DOI: http://dx.doi.org/10.15666/aeer/1704_78077819

On the basis of Section 4, the calculation can be conducted and the calculation results can be obtained. Then the safety factors of strips 6 and 7 of the landslide, strips 1 and 2 of No 1 deformation body and strip 5 of No 2 deformation body can be obtained under different load conditions, as shown in *Table 4*. For No 1 deformation body, under the influence of the own weight of sliding body, the safety factor is 1.04, and under the effects of the own weight of sliding body and rainfall (34 mm/h), the safety factor is 1.03, results of the analysis can also be applied to landslide and No 2 deformation body.

Table 4. *Model calculation results. Conditions 1, 2 and 3 represent the effects under the own weight of landslide, the effects under the own weight of landslide and rainfall (34 mm/h), the effects under the own weight of landslide, rainfall (34 mm/h), and seismic activity*

Load conditions unstable bodies and strips		**1**	**2**	**3**
		Safety factor	**Safety factor**	**Safety factor**
Landslide	6	1.02	0.9	0.61
	7	1.13	0.96	0.66
No 1 deformation body	1	1.04	0.89	0.62
	2	1.03	0.89	0.63
No 2 deformation body	5	1.1	0.92	0.60

According to "Landslide Prevention Engineering Design and Construction of Calculation Specification", on the basis of the classification of landslide stability, the stability state under different stability factors can be determined, as shown in *Table 5*. With the help of *Table 5*, the safety factors under three different load conditions can be set as 1.30, 1.10, and 1.05, respectively. Then the residual sliding thrust can be calculated, and the calculation results are shown in *Table 6*.

Table 5. *Classification of landslide stability (Kst is the designed safety factor) Conditions 1, 2 and 3 represent the effects under the own weight of landslide, the effects under the own weight of landslide and rainfall (34 mm/h), the effects under the own weight of landslide, rainfall (34 mm/h), and seismic activity*

Stability factor of the slope	$K_s < 1.00$	$1.00 < K_s \leq 1.05$	$1.05 < K_s \leq K_{st}$	$K_s \geq K_{st}$
Stability status	Unstable	Less stable	Basically stable	Stable

According to landslide engineering investigation specifications, the stability of landslides can be subdivided into four classes. If the stability factor of a landslide under certain load conditions is larger than the safety factor, we can state that the stability of the landslide matches the stability criteria well. Based on this principle, the following conclusions can be drawn:

Under natural conditions, the stability factor of strip 6 is 1.02; thus referring to *Table 5*, the landslide is in the less stable state. Through field investigations, we found that many cracks developed at the location of strip 6. Moreover, under continuous rainfall, the stability factor decreased to 0.9, which means that the landslide is unstable under such conditions, which is in good agreement with the preliminary analysis. Under natural conditions, the stability factor of strip 6 is 1.13; referring to *Table 5*, the

http://www.aloki.hu ● ISSN 1589 1623 (Print) ● ISSN 1785 0037 (Online)
DOI: http://dx.doi.org/10.15666/aeer/1704_78077819

landslide is in the basically stable state. Similarly, under continuous rainfall, the stability factor decreased to 0.96, i.e. the landslide is unstable under such conditions, which is in good agreement with the real situation.

Table 6. *Calculation results of the residual sliding thrust*

Unfavourable bodies and strips		Load conditions	Safety factor F_s	Stability factor F_{st}	Residual sliding thrust E（kN/m）
Landslide	No.6	Condition 1	1.02	1.2	479.22
		Condition 2	0.9	1.10	800.28
		Condition 3	0.61	1.05	2230.20
	No.7	Condition 1	1.13	1.2	87.77
		Condition 2	0.96	1.10	274.38
		Condition 3	0.66	1.05	945.36
No 1 deformation body	1-1′	Condition 1	1.04	1.2	222.72
		Condition 2	0.89	1.10	433.78
		Condition 3	0.62	1.05	1139.49
	2-2′	Condition 1	1.03	1.2	348.58
		Condition 2	0.89	1.10	634.06
		Condition 3	0.63	1.05	1580.44
No 2 deformation body	5-5′	Condition 1	1.10	1.2	55.34
		Condition 2	0.92	1.10	147.33
		Condition 3	0.60	1.05	511.87

Under natural conditions, the safety factors of strips 1 and 2 of No 1 deformation body are 1.04 and 1.03, respectively. Referring to *Table 5*, the No 1 deformation body is in the less stable state. These findings agreed well with preliminary analysis. Under continuous rainfall, the stability factors of strips 1 and 2 both decreased to 0.89, meaning that the No 1 deformation body is unstable under such conditions, which is in good agreement with the real situation.

Under natural conditions, the safety factor of strip 5 of No 2 deformation body is 1.10. Referring to *Table 5*, the No 2 deformation body is in the basically stable state. This agreed well with the preliminary analysis. Under continuous rainfall, the stability factor of strip 5 decreased to 0.92, meaning that the No 2 deformation body is unstable under such conditions, which is in good agreement with the real situation.

Based on this analysis, the following conclusions can be drawn. The stability of the landslide and deformation bodies varied as the load conditions changed. From condition 1 (i.e. under the effect of the own weight of the slope) to condition 3 (i.e. under the effect of the own weight of the slope, rainfall, and seismic activity), the stability of the landslide varied from basically stable to less stable and finally to unstable; the stability of the No 1 deformation body varied from less stable to unstable; and the stability of the No 2 deformation body varied from basically stable to unstable. Due to the discrepancy of the slope in the study area, the deformation and stability variations have some differences; under some circumstances, partial failure may occur in the stable state.

http://www.aloki.hu ● ISSN 1589 1623 (Print) ● ISSN 1785 0037 (Online)
DOI: http://dx.doi.org/10.15666/aeer/1704_78077819

Conclusions

By means of field investigation ands model calculations, the following conclusions can be drawn. The stability of the unfavourable bodies was mainly affected by the 12 May 2008 Wenchuan Earthquake and subsequent rainfall infiltration. Continuous heavy rainfall plays a crucial role in slope stability analysis. In addition, human activity and weathering have also influenced the stability of unfavourable geological bodies in the study area.

Under natural conditions, the stability factor of the landslide ranges from about 1.02–1.03, which means that this landslide is in the basically stable or less stable condition. Under the effect of continuous heavy rainfall, the stability factor of the landslide will be significantly reduced, and the corresponding value ranges from 0.9–0.96, which means that the landslide is in the unstable condition. For No 1 and No 2 deformation bodies, the stability varied from less stable to unstable, and basically stable to unstable, respectively.

At present, some of the unfavourable bodies are in the less stable state, under the effect of continuous heavy rainfall, seismic activity, or other influential factors; some geological bodies will probably change to the unstable state. Considering the property of the landslide itself, a cut slope is recommended as a preventative and mitigation measure. For the No 1 deformation body, anti-slide piles are recommended as prevention and mitigation measures. Due to the small volume and simplicity of the No 2 deformation body, it is recommended to clear it directly.

Acknowledgements. This work is financially supported by the National Natural Science Foundation of China (41302284 &41661144028), the national Key R&D Program of China (No. 2018YFC1505205), and the doctoral fund of Henan Polytechnic University (Grant No B2015-58).

REFERENCES

[1] Chen, B., Wei, L., Wu, C. (1989): Analysis on the method of pattern recognition on the development, distribution and the restrictive elements of debris flows in southwestern China. – Bulletin of Soil and Water Conservation 9(2): 54-56.

[2] Chen, N., Yang, C., Zhou, W., Hu, G., Li, H., Hand, D. (2009): The critical rainfall characteristics for torrents and debris flows in the Wenchuan earthquake stricken area. – Journal of Mountain Science 6(4): 362-372.

[3] Chuan, T., Jing, Z., Xin, Q., Jun, D. (2011): Landslides induced by the Wenchuan earthquake and the subsequent strong rainfall event. A case study in the Beichuan area of China. – Engineering Geology 122: 22-33.

[4] Cui, P., Chen, X.-Q., Zhu, Y.-Y., Su, F.-H., Wei, F.-Q., Han, Y.-S., Liu, H.-J., Zhuang, J.-Q. (2011): The Wenchuan earthquake (May 12, 2008), Sichuan province, China, and resulting geohazards. – Natural Hazards 56(1): 19-36.

[5] GB 50330-2013 (2013): Technical Code for Building Slope Engineering. – National Standard of People's Republic of China.

[6] Hu, W., Dong, X. J., Xu, Q., Wang, G. H., van Asch, T. W. J., Hicher, P. Y. (2016): Initiation processes for run-off generated debris flows in the Wenchuan earthquake area of China. – Geomorphology 253: 468-477.

[7] Jiayuan, T. A. O. (1995): The distribution of disastrous debris flow in China. – Journal of Higher Correspondence Education (Natural Science) 4: 6-7.

[8] Kang, H.-S., Kim, Y.-T. (2016): The physical vulnerability of different types of building structure to debris flow events. – Natural Hazards 80(3): 1475-1493.

http://www.aloki.hu ● ISSN 1589 1623 (Print) ● ISSN 1785 0037 (Online)
DOI: http://dx.doi.org/10.15666/aeer/1704_78077819

[9] Lee, C. F., Huang, W. K., Chang, Y. L., Chi, S. Y., Liao, W. C. (2017): Regional landslide susceptibility assessment using multi-stage remote sensing data along the coastal range highway in northeastern Taiwan. – Geomorphology 300: 113-127.
[10] Ni, H. Y., Zheng, W. M., Tie, Y. B., Su, P. C., Tang, Y. Q., Xu, R. G., Wang, D. W., Chen, X. Y. (2011): Formation and characteristics of post-earthquake debris flow: a case study from Wenjia gully in Mianzhu, Sichuan, SW China. – Natural Hazards 61(2): 317-335.
[11] Ni, H., Zheng, W., Tie, Y., Su, P., Tang, Y., Xu, R., Wang, D., Chen, X. (2012): Formation and characteristics of post-earthquake debris flow: a case study from Wenjia gully in Mianzhu, Sichuan, SW China. – Natural Hazards 61(2): 317-335.
[12] Postance, B., Hillier, J., Dijkstra, T., Dixon, N. (2017): Comparing threshold definition techniques for rainfall-induced landslides: a national assessment using radar rainfall. – Earth Surface Processes & Landforms. DOI: 10.1002/esp.4202.
[13] Shima, J., Moriyama, H., Kokuryo, H., Ishikawa, N., Mizuyama, T. (2016): Prevention and mitigation of debris flow hazards by using steel open-type Sabo dams. – International Journal of Erosion Control Engineering 9(3): 135-144.
[14] Sun, G., Huang, Y., Li, C., Zheng, H. (2016): Formation mechanism, deformation characteristics and stability analysis of Wujiang landslide near Centianhe reservoir dam. – Engineering Geology 211: 27-38.
[15] Tang, C., Zhu, J., Li, W., Liang, J. (2009): Rainfall-triggered debris flows following the Wenchuan earthquake. – Bulletin of Engineering Geology and the Environment 68(2): 187-194.
[16] Wang, J., Yang, S., Ou, G., Gong, Q., Yuan, S. (2017): Debris flow hazard assessment by combining numerical simulation and land utilization. – Bulletin of Engineering Geology and the Environment77(1): 13-27.
[17] Wang, Y., Zhao, B., Li, J. (2017): Mechanism of the catastrophic June 2017 landslide at Xinmo Village, Songping River, Sichuan Province, China. – Landslides 4: 1-13.
[18] Zhuang, J., Cui, P., Hu, K., Chen, X., Ge, Y. (2010): Characteristics of earthquake-triggered landslides and post-earthquake debris flows in Beichuan County. – Journal of Mountain Science 7(3): 246-254.
[19] Zhuang, J.-Q., Cui, P., Peng, J.-B., Hu, K.-H., Iqbal, J. (2013): Initiation process of debris flows on different slopes due to surface flow and trigger-specific strategies for mitigating post-earthquake in old Beichuan County, China. – Environmental Earth Sciences 68(5): 1391-1403.

http://www.aloki.hu ● ISSN 1589 1623 (Print) ● ISSN 1785 0037 (Online)
DOI: http://dx.doi.org/10.15666/aeer/1704_78077819

QUANTIFYING ALUMINUM SCRAP GENERATION FROM SEVEN END-USE SECTORS TO SUPPORT SUSTAINABLE DEVELOPMENT IN CHINA

LIU, S.[1*] – LIANG, Y.[2]

[1]*Zhengzhou University of Aeronautics*
No.15, West Wenyuan Road, Zhengdong New District, Zhengzhou, China
(phone: +86-134-6022-5539)

[2]*College of Management Science, Chengdu University of Technology*
No. 1, Dongsan road, Erxian Bridge, Chenghua District, Chengdu, China
(phone: +86-156-7035-9739)

[*]*Corresponding author*
e-mail: liusl0223@sina.com

(Received 23rd Feb 2019; accepted 3rd May 2019)

Abstract. Nowadays, the domestic mineral resources are short, and the ecological environment is becoming worse and worse. Besides, the trade protectionism is on the rise, and the international trade environment is uncertain and unsafe. This paper simulates the potential old scrap generated from actual aluminum products consumption of seven end-use sectors during 1996-2017 on the basis of Weibull distribution. The object is to facilitate the exploitation and cyclic utilization of old scrap and "urban mines". During this period, the building and construction (B&C) and transportation (T) sectors are still the most and second consumers, accounting for 30% and 17% of the total consumption. Most aluminum products haven't entered into the scrapping stage yet, and only one fifth of consumed aluminum (about 52 Mt) became old scrap. In the in-use reservoir, B&C and T sectors take up about 60% due to their longer lifetime intervals. If the potential old scrap will be recycled efficiently, then the secondary aluminum produced by the scrap can meet around nine years' consumption demands at current consumption level. Therefore, the cyclic utilization of old scrap prompts resources saving, energy conservation, emission reduction and may remove the impacts of international trade instability.
Keywords: *aluminum resource, scrap generation, in-use stock, recycling and cyclic utilization*

Introduction

Aluminum, a popular metal, and its alloys are applied widely all over the world. They are raw material sources of tens of thousands of products, and the production amount of aluminum nowadays is more than the sum of other nonferrous metals (Halvor, 2014). However, it has been produced in commercial quantities for just over 100 years (USGS, 2016) since the first electrolytic aluminium plant established by Pittsburgh, USA. So to speak, aluminum is a comparatively new industrial metal (USGS, 2016). In 1956, the world's aluminum production yield exceeded copper, ranking first among non-ferrous metals because of its wonderful characteristics (Chen et al., 2009a; Luca et al., 2013; USGS, 2016): light weight; excellent corrosion resistance and durability; no low-temperature brittleness and magnetism; good electrical conductivity and reflectivity; high thermal conductivity, and the like. Aluminum metal, its alloys and by-products are usually used in building & construction (B&C), transportation (T), consumer durables

http://www.aloki.hu ● ISSN 1589 1623 (Print) ● ISSN 1785 0037 (Online)
DOI: http://dx.doi.org/10.15666/aeer/1704_78217835

(CD), containers & packaging (C&P), machinery & equipment (M&E), electrical engineering (EE), and other products. With the popularization of material lightweight requirement, aluminum metal and its alloys are more widely utilized, especially in national defense science field and some sophisticated industries such as aerospace engineering, medical apparatus and instruments, rail traffic and so on.

China, a populous and rapidly developing country, has the potential to influence the global material use (Wang et al., 2008). There is a significance increase in aluminum production and consumption amount after the reform and opening-up policy. During the period of 1991 to 2007, China's average growth rate of aluminum production and consumption was four times higher than the global average (Yue et al., 2014), especially after 2000, with the alumina and primary aluminum shares of global production rising from 9% and 13.2% in 2000, to 37.7% and 51.1% in 2008 (Chen et al., 2010, 2012). China has long been the world's largest producer and consumer of aluminium (Yue et al., 2015). Nevertheless, China's bauxite reserves are only about 3 percent of the world's, and its per capita reserves are also small, one-tenth of the global average (Chen et al., 2008). They are mostly unserviceable diaspore, which are characterized by high aluminum, high silicon and low aluminum-silicon ratio. These characteristics increase the difficulty to mine and smelt bauxite ores, and lead to weak productivity growth (Chen et al., 2009b; Liu et al., 2011, Liu and Müller, 2012). As a result, China relies heavily on importing bauxite. In the previous study, its external dependence increased continuously, from 1.9% in 1996 to 40% in 2016, among them 52.4% in 2007 and 54.3% in 2013 (Liu, 2017). The trade protectionism is on the rise, and the international trade environment is uncertain and unsafe. This situation is an obstacle to the realization of sustainable supply and sustainable economic and social development.

The supply structure of China’s aluminum metal in recent years is about: 80% for primary aluminum, 20% for recycled aluminum (Liu et al., 2016). And the average annual increase rate of secondary aluminum is above 25% after 1996 (Liu et al., 2016). Besides, the contribution degree of recycled aluminum supply is rising gradually (Liu, 2018). The energy required and pollution emission for producing secondary aluminum might be only 5-10% of that needed for smelting and producing primary aluminum (Melo, 1999). Remelting recycled aluminum can not only make up for the shortage of domestic bauxite ores, but also promote energy conservation and emissions reduction.

Review of literature

MFA is a systematic resource management means for stocks and flows of entire life cycle of materials within predefined anthropogenic temporal and spatial boundary (Brunner and Rechberger, 2004; Pauliuk and Müller, 2014; Nakamura and Halada, 2015; Maung et al., 2017; Wang et al., 2017). In recent years, it was extensively used in the research of noxious or specific chemical elements and in the fields of resources appropriate use and waste management. It usually divides the entire life cycle of elements into four main stages: Production (P); Fabrication & Manufacture (F&M); Use (U); and Waste Management & Recycling (WM&R) (*Fig. 1*).

Many experts and scholars use this approach to analyze non-ferrous metallic element such as iron (Wang et al., 2007), copper (Graedel et al., 2002; Spatari et al., 2002; Bertram et al., 2002; Rechberger and Graedel, 2002; Reck et al., 2006; Daigo et al., 2009), aluminum (Melo, 1999; Boin and Bertram, 2005; Hatayama et al., 2007; Dhalström and Ekins, 2007; Chen et al., 2009a,b, 2010; Chen and Shi, 2012; Chen and

http://www.aloki.hu ● ISSN 1589 1623 (Print) ● ISSN 1785 0037 (Online)
DOI: http://dx.doi.org/10.15666/aeer/1704_78217835

Graedel, 2012; Buchner et al., 2014), zinc (Graedel et al., 2005; Reck et al., 2006; Guo et al., 2010), lead (Mao et al., 2008a,b), phosphorus (Liu and Chen, 2006a,b) and the like. For the last few years, on the one hand, the studies on a more micro level (small scale of area, some kind or some certain kind of product) are more and more extensive. On the other hand, the WM&R stage such as recovery amount, recovery rate, and recovery potential are hot topics (Hoyle, 1995; Gesing and Wolanski, 2001; Müller, 2006; Modaresi and Müller, 2012; Gu et al., 2016a,b).

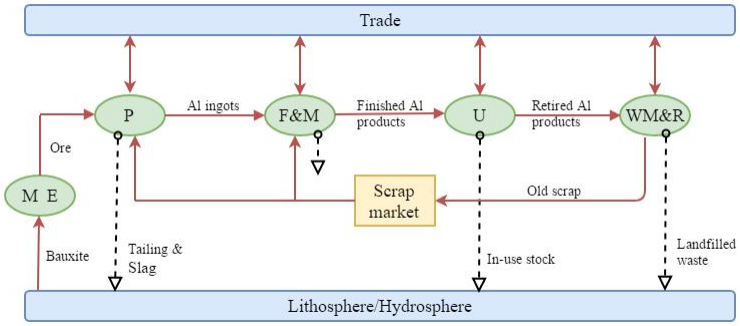

Figure 1. *Simplified aluminum life cycle diagram (M E: Mine Extraction, P: Production; F&M: Fabrication & Manufacture; U: Use; WM&R: Waste Management & Recycling)*

Among them, scrap generated from end-use sectors and in-use stocks of still existing in society are so complicated that researchers applied various methods to investigate them. McMillan et al. (2010) quantified aluminum in-use stocks and old scrap recycling and recovery in the United States for the period of 1900 to 2007 by a dynamic material flow analysis model and top-down approach. The in-use stock of aluminium in the State of Connecticut has been established by an extensive bottom-up study by Recalde et al. (2008), and the percentages of end-use sectors accounting for total stock have also been measured. Zhang et al. (2012, 2015a,b) mainly research on the flows and stocks of China's copper resource, and its spatial and temporal patterns by SFA, top-down, and bottom-up estimation. Yue et al. (2016) analyzed the iron in-use stocks in China by top-down and bottom-up methods, and related economic methods. Of course, estimation a sort of metal scrap and in-use stock of an industry is popular in researchers nowadays. The building stocks from urban to transnational scales was analyzed by Mastrucci et al. (2017) through bottom-up life cycle assessment, and Warrings and Fellner (2018) conducted a detailed material flow analysis for aluminum used in packaging & household non-packaging in 2013 in Austria. A MS (material stocks) accounting for 10 materials in 6 major infrastructures in Beijing, Tianjin and Shanghai were conducted by Huang et al. (2017).

Materials and methods

The aluminum products transform into retired products and generate old scrap after serving for society for a while. Nevertheless, their lifetimes are diverse for end-use products of different categories, and this study adopts the following lifetime intervals in *Table 1* on the basis of previous studies (Melo, 1999; Chen and Shi, 2012; Luca et al., 2013; Zhang et al., 2015a). Lifetime intervals of aluminum products are crucial for

http://www.aloki.hu ● ISSN 1589 1623 (Print) ● ISSN 1785 0037 (Online)
DOI: http://dx.doi.org/10.15666/aeer/1704_78217835

quantifying potential aluminum scrap, and Weibull distribution is proved to be a good way to simulate the life span of products. This paper applies the classical Weibull distribution to simulate the lifetimes of aluminum products from cradle to grave, and this is the foundation of aluminum scrap generation model.

Table1. *Lifetimes of seven categories Al products assumed for this study*

	B&C	T	CD	C&P	M&E	EE	Others
Lifetimes							
Low (a)	23	10	5	1	10	10	5
High (b)	40	16	15	1	30	25	15

The probability density function (pdf) of the Weibull distribution function in this study can be expressed in *equation (1)*, and the scale and shape parameters are taken from some researchers as a reference (Melo, 1999; Chen and Shi, 2012; Luca et al., 2013; Zhang et al., 2015a; Wang et al., 2017). Thus it can be seen that the random variable T is described by three parameters: a location parameter a, a scale parameter α, and a shape parameter β; and the mathematical constraint conditions of this function are $a \geq 0, \alpha > 0, \beta > 0$.

$$f(t;a,\alpha,\beta) = \begin{cases} \alpha\beta^{-\alpha}(t-a)^{\alpha-1}\exp\left\{-\left(\frac{t-a}{\beta}\right)^{\alpha}\right\}, & if\ t > a \\ 0, & otherwise \end{cases} \quad \text{(Eq.1)}$$

If a product ends its service life in society and become to useless waste after t years, then the probability of it is given by *equation (2)*.

$$p_t = \exp\left\{-\left(\frac{t-a}{\beta}\right)^{\alpha}\right\} - \exp\left\{-\left(\frac{t+1-a}{\beta}\right)^{\alpha}\right\}, \quad a \leq t < b \quad \text{(Eq.2)}$$

The value range [a,b] of the distribution function is given by lifetime intervals in *Table 1*. In other words, 100% of the total area under the curve of the density function must be located within the ranges a and b. But the realistic situation is so complicated that not all of aluminum products will retire within b years. So, this study stipulates that the cumulative distribution probability is set as 99.7%, that is, 99.7% of the total area is under the density function curve within the lifetime interval [a,b]. The corresponding cumulative probability function IP and the distribution function $F_{(t)}$ is measured by *equations (3) and (4)*, and γ =99.7%.

$$IP(a \leq T \leq b) = 1 - \exp\left\{-\left(\frac{b-a}{\beta}\right)^{\alpha}\right\} = \gamma \quad \text{(Eq.3)}$$

$$F_{(t)} = 1 - \exp\left\{-\left(\frac{t}{\beta}\right)^{\alpha}\right\} \quad \text{(Eq.4)}$$

http://www.aloki.hu ● ISSN 1589 1623 (Print) ● ISSN 1785 0037 (Online)
DOI: http://dx.doi.org/10.15666/aeer/1704_78217835

Quantifying the scrap generation of end-of-life aluminum products is based on the Weibull distribution described above, and this paper adopts top-down method (McMillan et al., 2010; Park J-a et al., 2011; Yan et al., 2013; Müller et al., 2014; Chen and Graedel, 2015). The mechanism of scrap generation of end-of-life aluminum products is a very complex process, and this study simplifies it as: the finished aluminum products flow into society for multiple use, and they get retired after different given life spans. Therefore, the theoretical scrap generation of year n can be measured by *equation (5)*:

$$F'_{(n)} = \exp\left\{-\left(\frac{n-1}{\beta}\right)^{\alpha}\right\} - \exp\left\{-\left(\frac{n}{\beta}\right)^{\alpha}\right\} \quad \text{(Eq.5)}$$

Within this paper, the rate of theoretical old scrap generation in year n is assumed as $f_{(n)}$, the cumulative rate of which is $F_{(n)}$. Then $F'_{(n)}$ refers to the probability of old scrap generation of aluminum end-of-life products (Park J-a et al., 2011; Yan et al., 2013). Besides, α and β still represent scale parameter and shape parameter. There is a hypothesis that $T_{(t)}$ denotes the mount of realistic consumption of various aluminum-containing products in year t, and $P_{(n)}$ is defined as the corresponding old scrap generation amount in year n. So $P_{(n)}$ can be expressed as *equation (6)*:

$$P_{(n)} = \sum_{t=0}^{n-1} T_{(t)} F'_{(n-t)} \quad \text{(Eq.6)}$$

The temporal boundary of this paper is the period of 1996-2017, the spatial boundary is mainland China, of course, and the major research objects are simulated aluminum old scrap generation for sum and end-of-life sectors. Most of various data used in calculation stems from official statistics, for example, the Yearbook of Nonferrous Metals Industry of China and World Bureau of Metal Statistics. Some missing data, especially aluminum products consumption amounts of seven end-use sectors, are borrowed from some reports and articles (Chen et al., 2009a, 2010; Chen and Shi, 2012; Yue et al., 2014).

In order to strengthen the scientific preciseness and conciseness of research, there are some assumptions and explanations: (1) This study just considers actual consumption statistics and focuses on old scrap generation of studied period of 1996-2017. That is, this study ignores the generated scrap from the years before 1996 and after 2017. (2) The length of service life of aluminum products follows the Weibull distribution. (3) The losses to the environment during the transformation from this flow into other flows are excluded from consideration.

Results

Nowadays, China is the country that produces and consumes the most aluminum metal, and the average growth rates of them are well above the world average (Yue et

http://www.aloki.hu ● ISSN 1589 1623 (Print) ● ISSN 1785 0037 (Online)
DOI: http://dx.doi.org/10.15666/aeer/1704_78217835

al., 2014). *Fig. 2* clearly describes this phenomenon and the variation trend of consumption amounts of seven end-use sectors.

The total consumption amounts of aluminum metal in China have maintained a trend of continuous increase since 1996, even during in global financial crisis, and the average growth rate reaches up to 14.58%. In China, the large-scale production and consumption of aluminum metal is relatively late, so the production and consumption of aluminum metal is very few before 1996. Besides, few consumption only generates fewer old scrap, and that is why the temporal boundary of this study begins in 1996.

Although the consumption amounts of seven end-use sectors all have been rising for decades, the consumption structure has also changed dramatically because of needs for economic and social development. From 1998 to 2000 was the period that has the most rapid changes in the consumption structure. Before 1998, the amounts of aluminum products in CD and EE fields were the most and second relatively, while the amount of aluminum products in B&C field was far more than any other sector in 2000, accounting for a third of total consumption. After 2000, the consumption structure of seven fields also changed, but not too much.

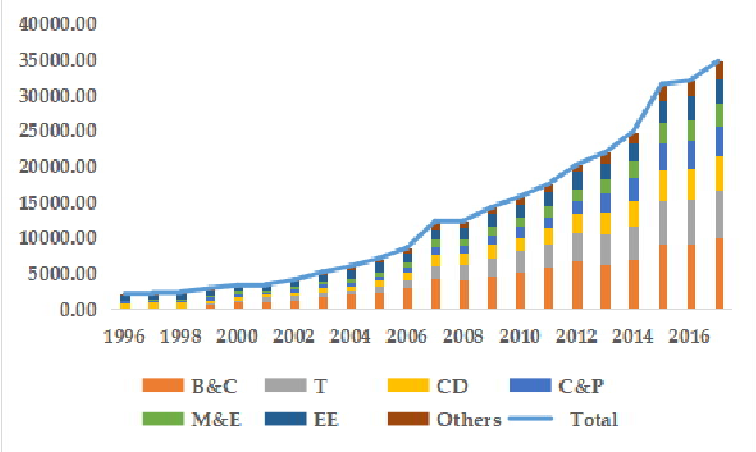

Figure 2. *Consumption amounts of total and end-use sectors (Unit: kt)*

The percentage of aluminum products in T sector was from less than 10% in 2000 up to 20% in 2017, nevertheless the percentage in EE sector was from about 20% in 2000 down to 10% in 2017. In the period of 1996-2017, the cumulative consumption amounts of seven end-use sectors are around 87.7 Mt, 49.2 Mt, 39.1 Mt, 30 Mt, 25.5 Mt, 34.2 Mt, 20 Mt, respectively, and account for 30%, 17%, 14%, 10%, 9%, 12% and 7% of total consumption. At present, the B&C and T sectors are the two sectors that consume most aluminum metal, and they account for a half of total consumption. This situation is closely related to the general background of China's economic development: higher urbanization rates and convenient, comfortable, plentiful life for more people.

Old scrap generation

Scrap generation of seven end-use sectors

As we all know, the lifetime of aluminum-containing products in B&C sector is relatively long due to its durability, so theoretically, the consumption in the period of

http://www.aloki.hu ● ISSN 1589 1623 (Print) ● ISSN 1785 0037 (Online)
DOI: http://dx.doi.org/10.15666/aeer/1704_78217835

1996-2017 has not produced old scrap yet. The starting year and ending year of old scrap generation in B&C sector are 2019 and 2056, respectively (*Fig. 3*).

The total amounts of annual potential scrap from B&C sector rise smoothly and then fall gradually, the peak of which is at around 2043. Accordingly, the change trend of cumulative scrap amount is: increases slowly, increases rapidly and then remains at high position. The variation trends of potential scrap generation amounts annually and cumulatively from M&E and EE sectors are the same with B&C sector, but the lifetime intervals are completely different. The starting year and ending year of old scrap generation in M&E sector are 2006 and 2046, and they are 2006 and 2041 in EE sector. Besides, the peak of annual scrap generation amount in M&E and EE sectors are all in about 2028 (*Fig. 3*).

The consumption quantity of aluminum products in T sector increases more and more rapidly because of the macro social background and lightweight requirement. The period of old scrap generation in T sector is from 2006 to 2032, and the annual scrap amount increases gradually, then increases quickly and drops more quickly after reaching the peak around 2027. The change trends of potential old scrap in CD and Others sectors are similar to the situation in T sector. Moreover, the periods of old scrap generation in these two sectors are all from 2001 to 2031, and the peaks are at around 2022. The tendency of the cumulative curve in these three fields is similar to other three fields described above, but the CD and Others fields increase smoothly, not increase slowly and then increase rapidly before reaching the high position. There is a striking common point in in these three fields: the growth change of annual scrap generation amount is not so regular. This is because their actual consumption amounts don't increase all the time before the peak, and they change unsteadily, sometimes more and sometimes less. However, the annual scrap generation in B&C, M&E and EE fields increase little by little before reaching the peak.

Aluminum packaging materials can be said to be the most common aluminum products in life, but the mean lifetime of it is so short that the starting year and ending year of its old scrap generation are 1997 and 2018. This paper defined its lifetime interval as 1 year, therefore the annual scrap generation amount is closely related to the actual consumption of previous year. It's precisely because of its defined lifetime interval as well, the annual scrap generation amount augments all the time accompanying its consumption in the period of 1997-2018. Furthermore, the cumulative curve of C&P sector is very different from other six sectors, and it is always on the rise. This situation also has to do with its lifetime interval.

Annual and cumulative scrap generation

From the bars of various colors in *Fig. 4*, the scrapping time nodes and scrap generation amounts of aluminum products of each sector can be obtained. In the beginning, only the aluminum products in C&P sector enters the scrapping period, and the amount is nothing much.

Follow that, the aluminum products in CD, Others, T, M&E and EE sectors enter the scrapping periods successively, so there is a large growth in the annual scrap amounts. The latest aluminum products to enter the scrapping stage come from the B&C sector, and it's in 2019. However, the potential scrap decreases a lot in this year.

The fundamental cause of this phenomenon is that C&P sector is completely out of scrapping stage. Due to the plentiful aluminum scrap generated from B&C field, the total scrap has a big increase in amount.

http://www.aloki.hu ● ISSN 1589 1623 (Print) ● ISSN 1785 0037 (Online)
DOI: http://dx.doi.org/10.15666/aeer/1704_78217835

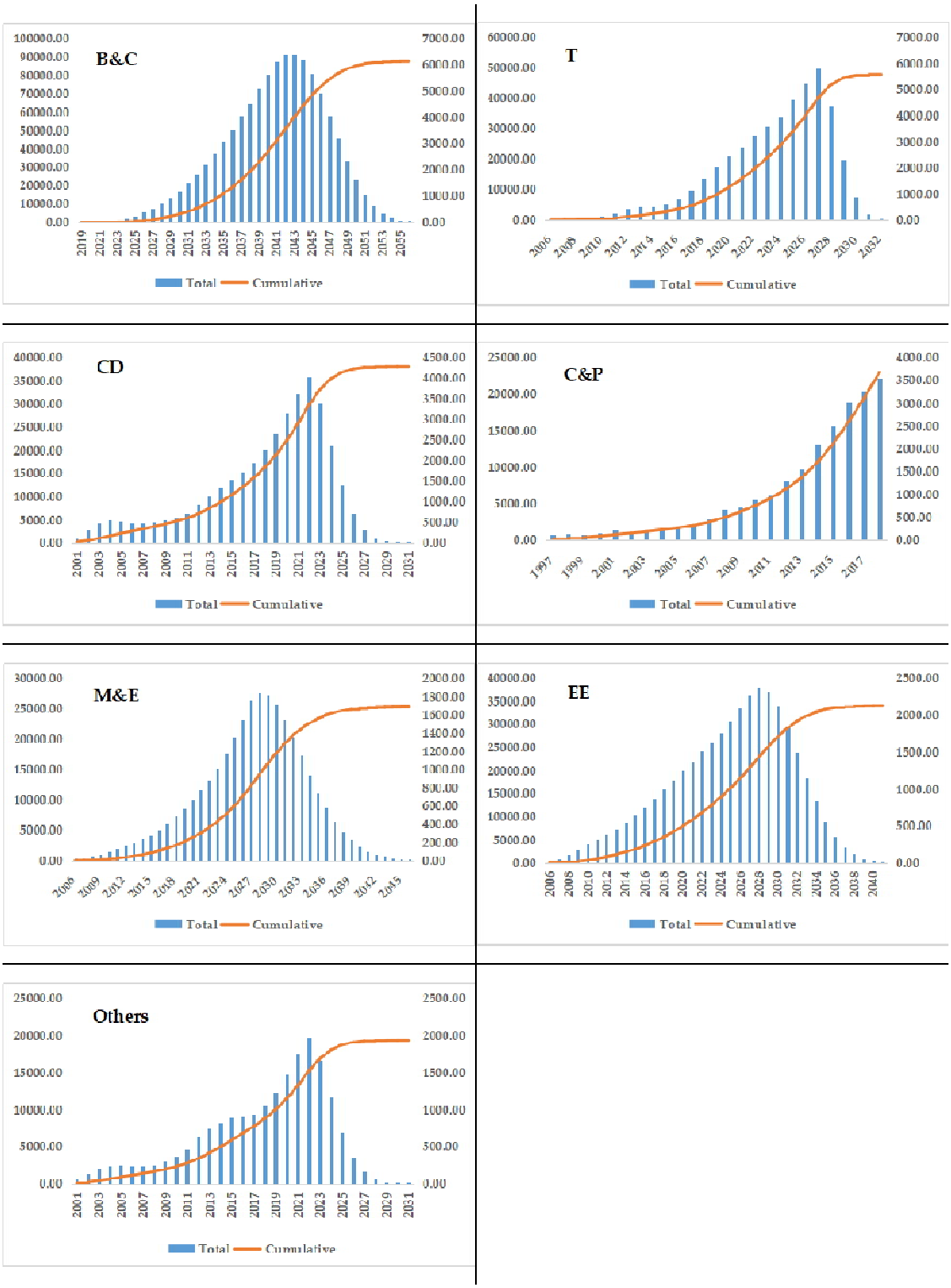

Figure 3. *Theoretical old scrap generation of seven end-use sectors (In all charts, the starting year is the first time that the various consumed aluminum products entered the scrap stage, and the ending year is the last time. "Total" denotes the total scrap amounts annually, and "Cumulative" denotes the cumulative scrap amounts within the lifetime intervals. The larger scale values on the left describe "Cumulative", and the smaller scale values on the right describe "Total". Unit: kt)*

http://www.aloki.hu ● ISSN 1589 1623 (Print) ● ISSN 1785 0037 (Online)
DOI: http://dx.doi.org/10.15666/aeer/1704_78217835

Then, the CD, T and Others fields also gradually exit the scrapping stage, so the potential scrap from these three fields is on the decrease until around 2030. For a while after that, the theoretical scrap generated from B&C, M&E and EE sectors is near the maximum or at the maximum, so the annual scrap generation amount continues to increase until the M&E and EE sectors exiting the scrapping period. In the end, there is B&C sector left, and the annual scrap generation amount is on the decrease step by step until it exiting the scrapping stage in about 2056. The complex old scrap generation amounts are attributed to the out-of-step of entering and exiting the scrapping stage of seven end-use sectors of aluminum products. There is no doubt that the cumulative amount increases continuously. The cumulative curve of the total potential old scrap in *Fig. 4* is analogous to the cumulative curves of those six end-use sectors in *Fig. 3*: rises slowly, then rises rapidly, and remains at the high position.

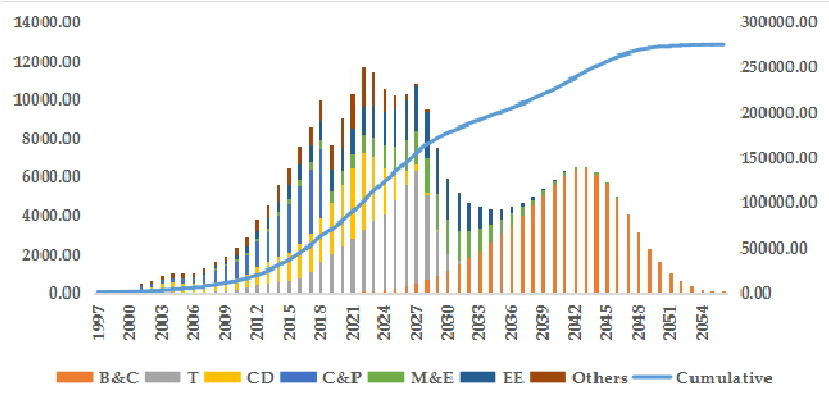

Figure 4. *Annual and cumulative scrap generated from seven categories aluminum products consumption. (The larger scale values on the right describe "Cumulative", and the smaller scale values on the left describe "Annual". Unit: kt)*

The total consumption of aluminum-containing products supports the twenty years' aluminum metal demands of the national economics. If most of the potential old scrap can be recycled, the secondary aluminum produced by it will meet nine years' consumption demands at current consumption level. It has a far-reaching significance for the country's sustainable development, and improves the ecological environment, reduces energy consumption and greenhouse gas emissions.

In-use reservoir

Theoretically, the cumulative old scrap generated from actual consumption in the period of 1996-2017 is 275 million tons, and the scrap generation amount before 2018 is about 52 million tons, accounting for one fifth or so. That is, there are four fifths of the theoretical old scrap still in the in-use reservoir, more than 220 million tons. The in-use stock is still under the ground to be mined, and will become the resource bank to support future consumption for economic development.

In in-use reservoir, there is no doubt that the largest proportion is in B&C field (*Fig. 5*), and 100% of them are still in anthropogenic cycle (*Fig. 6*) because they haven't entered into scrapping stage in the given period. It accounts for about 40% in the total in-use stock, and T sector followed by it. But the amount and percentage is only half of

http://www.aloki.hu ● ISSN 1589 1623 (Print) ● ISSN 1785 0037 (Online)
DOI: http://dx.doi.org/10.15666/aeer/1704_78217835

it, far less than B&C field. Because it hasn't entered into a large-scale scrapping stage, most (90%) of aluminum-containing products in T sector is still in use stage. This situation is closely similar to M&E sector, however, it only accounts for about 10% in the total in-use stock. Besides, the slightly greater proportions in the in-use stock are EE and CD sectors, and the proportions are 13% and 11%, respectively. But 86.5% of electrical engineering products and 63.3% of consumer durables are in the use stage. The aluminum products amount consumed by others sector is less than other fields, nevertheless the in-use stock quantity is not the least due to its longer lifetime interval. In addition, 60.2% of aluminum metal in others sector is still serving the society in different positions. The least in-use stock magnitude occurs in C&P field, and its recycling period is very short. Although the year 2018 is its last recovery period, there are still 15.4% in the use stage. So the consumption quantity of aluminum packaging materials is large in last several years.

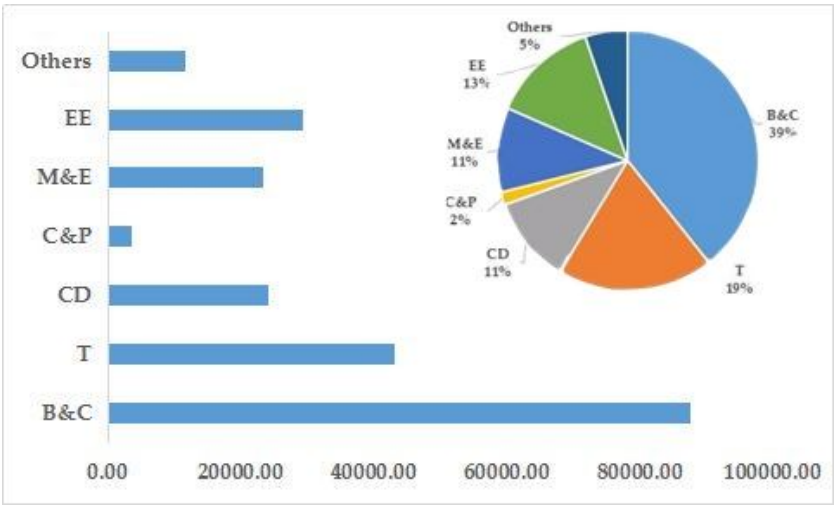

Figure 5. *The amounts and percentages of in-use stock in seven end-use sectors. (Unit: kt)*

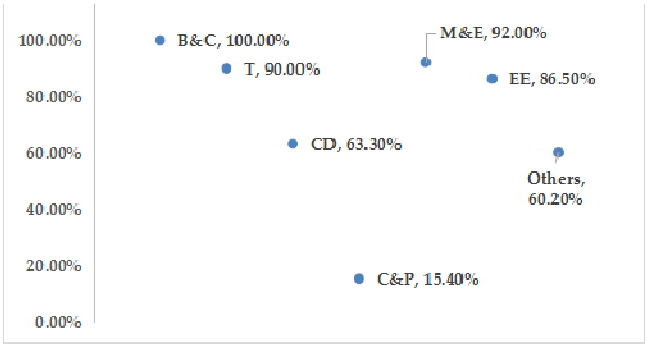

Figure 6. *The percentages of in-use stock in their theoretical scrap generation*

In general, the longer the lifetime interval, the more complex the scrapping process and the more uncertain the scrap generation. Therefore, the aluminum product consumed by B&C sector is more difficult to simulate its old scrap. On the contrary, the recovery rate of aluminum packaging materials is relatively high and is easy to calculate and utilize its old scrap. The research hot topics of old scrap and in-use stock

http://www.aloki.hu ● ISSN 1589 1623 (Print) ● ISSN 1785 0037 (Online)
DOI: http://dx.doi.org/10.15666/aeer/1704_78217835

management of aluminum products focus on the B&C, T and CD fields, and other fields are studied much less than them due to the lack of detailed statistics, a variety of products, complicated models to be established difficultly and so on. If the recycling system is relatively sound and perfect, like some developed countries, these in-use stock will be cyclic utilized in all walks of life in the future and achieve the proposed closed-loop for resource use. The closed-loop aluminum resource utilization, on the one hand, saves substantial primary ore consumption; and on the other hand, also saves energy consumption, reduces greenhouse gas emission and the influence of international trade environment.

Discussion

In real production process, there are so many kinds of aluminum-containing finished products and intermediate products to meet the actual demands, and the lifetime intervals of them are very different from each other even though the same kind of products. So the lifetime intervals are far more complicated than the simplified scrapping time assumed in this paper. For example, a car should become the retired product in its eighth year, then to be recycled, dismantled and other treatments. However, it may be scrapped in its fifth or tenth year due to the various reasons, or some components and parts are directly applied in other products, not recycled. In a word, the anthropogenic cycle course for serving the society of aluminum metal is not easy to investigate clearly, and in general varieties of scholars apply lots of methods and models to simulate it.

The research temporal boundary of this paper is the period of 1996-2017, and the scrapping interval of those aluminum products is relatively longer. But the aluminum products in other years also generate old scrap in this scrapping stage, nevertheless this study only pays attention to the old scrap generated from the period of 1996-2017. Hence the actual annual and cumulative scrap amounts are entirely different from the results in Section 3, and in the meantime, this is also not a dynamic study to some extent. Furthermore, the calculations of potential scrap in this study are only based on the actual consumption of sum and seven end-use sectors, but the scrap generation amount is restricted and affected by many factors. This is also what needs to be improved in later research course.

Besides, the aluminum metal in-use stock is not 100% recycled after the service lifetime, some of which will become post-consumer waste or waste left in the remelting course, and they will be delivered to the landfills, metallurgical waste residue storage sites or the ecological environment. In addition, the loss of resources in the recycling process is also large such as transport, classify, dismantle, remelt and other treatments. Therefore, the cyclic utilization of resource is easier said than done, and the joint efforts of responsible departments and the public are required to bear the responsibility for reducing the resource waste, energy consumption and greenhouse gas emission.

Conclusions

In addition to the various costs of importing raw materials, the trade wars are also getting more and more intense, and the international trade environment becomes very uncertain. These factors will drive the increasingly chaotic international trade order, and

http://www.aloki.hu ● ISSN 1589 1623 (Print) ● ISSN 1785 0037 (Online)
DOI: http://dx.doi.org/10.15666/aeer/1704_78217835

importing raw materials will be more and more difficult. Therefore, the focus of acquiring resources ought to turn to the homeland, and exploit and utilize the domestic resource (old scrap and "urban mines").

This paper simulates the potential old scrap generated from actual aluminum products consumption of seven end-use sectors during the period of 1996-2017 on the basis of Weibull distribution. The main results and conclusions are as follows. (1) The B&C and T sectors are still the most and second consumers. The cumulative consumption amounts of seven end-use sectors (B&C, T, CD, C&P, M&E, EE, and Others) are around 87.7 Mt, 49.2 Mt, 39.1 Mt, 30 Mt, 25.5 Mt, 34.2 Mt, 20 Mt, respectively, and account for 30%, 17%, 14%, 10%, 9%, 12% and 7% of total consumption. (2) Most aluminum products haven't entered into the scrapping stage yet. Only one fifth of consumed aluminum (about 52 Mt) became old scrap, and the rest are serving the society in the form of in-use stock. In the in-use reservoir, B&C and T sectors account for about 60% due to their longer lifetime intervals. (3) The percentages of in-use stock existing in those end-use sectors consumed in the period of 1996-2017 are 100%, 90%, 63.3%, 15.4%, 92%, 86.5% and 60.2%. The majority of aluminum-containing products delay for supporting the country's economic development, industrialization and urbanization. (4) If the recycling system and related supporting policies are improved and completed, the potential old scrap will be recycled efficiently. Then the secondary aluminum produced by the scrap can meet around nine years' consumption demands at current consumption level.

In recent years, the government established a number of renewable resource industrial parks or ecological industrial parks along with the increasingly serious resource situation and promised energy conservation and emission reduction requirements. This is the successful experience of developed countries, and makes the waste recycling and reuse form a complete industrialization development model. The government needs to formulate various policies for key support, mainly from tax policy, technology research and development support policy, land use policy and other related supporting measurements, to overall coordinate the development of the industry. This industry will recycle generated old scrap and in-use reservoir to support domestic production and consumption, and drive the aluminum industry away from importing bauxite and scrap gradually to reduce the influence of international trade environment. However, the realities of aluminum products consumption, usage, retire, recovery, treatment and the like are so tanglesome that this study simplified the calculation model, and still has many shortcomings. In later course of research, these shortcomings will be made up step by step.

REFERENCES

[1] Bertram, M., Graedel, T. E., Rechberger, H., Spatari, S. (2002): The contemporary European copper cycle: waste management subsystem. – Ecol Econ 42: 43-57.

[2] Boin, U. M. J., Bertram, M. (2005): Melting standardized aluminum scrap: A mass balance model for Europe. – J Metals 57: 26-33.

[3] Brunner, P. H., Rechberger, H. (2004): Practical handbook of material flow analysis. – Lewis Publishers: Boca Raton, FL, USA.

[4] Buchner, H., Laner, D., Rechberger, H. (2014): In-depth analysis of aluminum flows in Austria as a basis to increase resource efficiency. – Resour Conserv Recy 93: 112-123.

http://www.aloki.hu ● ISSN 1589 1623 (Print) ● ISSN 1785 0037 (Online)
DOI: http://dx.doi.org/10.15666/aeer/1704_78217835

[5] Chen, W. Q., Shi, L., Qian, Y. (2008): Description of anthropogenic aluminum cycles. – Resources Science 30: 1004-1012. (in Chinese).
[6] Chen, W. Q., Shi, L., Chang, X. Y., Qian, Y. (2009a): Substance flow analysis of aluminum in China for 1991-2007 (I): Trade of aluminum from a perspective of life cycle and its policy implications. – Resource Science 31: 1887-1897. (in Chinese).
[7] Chen, W. Q., Wan, H. Y., Wu, J. N., Shi, L. (2009b): Life cycle assessment of aluminum and the environmental impacts of aluminum industry. – Light Metal 5: 3-10. (in Chinese).
[8] Chen, W. Q., Shi, L., Qian, Y. (2010): Substance flow analysis of aluminum in mainland China for 2001, 2004, and 2007: Exploring its initial sources, eventual sinks and the pathways linking them. – Resour Conserv Recy 54: 557-570.
[9] Chen, W. Q., Graedel, T. E. (2012): Dynamic analysis of aluminum stocks and flows in the United States: 1900-2009. – Ecol Econ 81: 92-102.
[10] Chen, W. Q., Shi, L. (2012): Analysis of aluminum stocks and flows in mainland China from 1950 to 2009: Exploring the dynamics driving the rapid increase in China's aluminum production. – Resour Conserv Recy 65: 18-28.
[11] Chen, W. Q., Graedel, T. (2015): Improved alternatives for estimating in-use material stocks. – Environ Sci Technol 49(5): 3048-3055.
[12] Daigo, I., Hashimoto, S., Matsuno, Y., Adachi, Y. (2009): Material stocks and flows accounting for copper and copper-based alloys in Japan. – Resour Conserv Recy 53: 208-217.
[13] Dhalström, K., Ekins, P. (2007): Combining economic and environmental dimensions: Value chain analysis of UK aluminum flows. – Resour Conserv Recy 51: 541-560.
[14] Gesing, A., Wolanski, R. (2001): Recycling light metals from end-of-life vehicle. – JOM 53: 21-23.
[15] Graedel, T. E., Bertram, M., Fuse, K., Gordon, R. B., Lifset, R., Rechberger, H., Spatari, S. (2002): The contemporary European copper cycle: The characterization of technological copper cycles. – Ecol Econ 42: 9-26.
[16] Graedel, T. E., van Beers, D., Bertram, M., Fuse, K., Gordon, R. B. (2005): The multilevel cycle of anthropogenic zinc. – J Ind Ecol 9: 67-90.
[17] Gu, Y. F., Wu, Y. F., Xu, M., Mu, X. Z., Zuo, T. Y. (2016a): Waste electrical and electronic equipment (WEEE) recycling for a sustainable resource supply in the electronics industry in China. – J Clean Prod 127: 331-338.
[18] Gu, Y. F., Wu, Y. F., Xu, M. (2016b): The stability and profitability of the informal WEEE collector in developing countries: A case study of China. – Resour Conserv Recy 107: 18-26.
[19] Guo, X. Y., Zhong, J. Y., Song, Y., Tian, Q. H. (2010): Substance flow analysis of zinc in China. – Resour Conserv Recy 54: 171-177.
[20] Halvor, K. (2014): The aluminum smelting process. – J Occup Environ Med 56: S2-S4.
[21] Hatayama, H., Yamada, H., Daigo, I., Matsuno, Y., Adachi, Y. (2007): Dynamic substance flow analysis of aluminum and its alloying elements. – Mater Trans 48: 2518-2524.
[22] Hoyle, G. (1995): Recycling opportunities in the UK for aluminum-bodied motor cars. – Resour Conserv Recy 15: 181-191.
[23] Huang, C., Han, J., Chen, W. Q. (2017): Changing patterns and determinants of infrastructures' material stocks in Chinese cities. – Resour Conserv Recy 123: 47-53.
[24] Liu, Y., Chen, J. N. (2006a): Substance flow analysis of phosphorus cycle system in China. – China Environmental Science 26: 238-242. (in Chinese).
[25] Liu, Y., Chen, J. N. (2006b): Substance flow analysis on phosphorus cycle in Dianchi basin, China. – Environment Science 27: 1549-1553. (in Chinese).
[26] Liu, G., Bangs, C. E., Müller, D. B. (2011): Unearthing potentials for decarbonizing the US aluminum cycle. – Environ Sci Technol 45: 9515-9522.

http://www.aloki.hu ● ISSN 1589 1623 (Print) ● ISSN 1785 0037 (Online)
DOI: http://dx.doi.org/10.15666/aeer/1704_78217835

[27] Liu, G., Müller, D. B. (2012): Addressing sustainability in the aluminum industry: a critical review of life cycle assessments. – J Clean Prod 35: 108-117.
[28] Liu, S. L., Li, X., Wang, M. X. (2016): Analysis of aluminum resource supply structure and guarantee degree in China based on sustainable perspective. – Sustainability 8(12): 1335-1351.
[29] Liu, S. L. (2017): Dynamic analysis of aluminum flows in production stage in mainland China: 1996-2014. – Bulg Chem Commun 49 (Special Issue K1): 224-227.
[30] Liu, S. L. (2018): Contribution analysis of recycled aluminum supply in China based on sustainable supply. – IOP Conference Series: Materials Science and Engineering 397: 012107.
[31] Luca, C., Chen, W. Q., Fabrizio, P. (2013): Historical evolution of anthropogenic aluminum stocks and flows in Italy. – Resour Conserv Recy 72: 1-8.
[32] Mao, J. S., Dong, J., Graedel, T. E. (2008a): The multilevel cycle of anthropogenic lead Ⅰ.Methodology. – Resour Conserv Recy 52: 1058-1064.
[33] Mao, J. S., Dong, J., Graedel, T. E. (2008b): The multilevel cycle of anthropogenic lead Ⅱ. Recults and Discussion. – Resour Conserv Recy 52: 1050-1057.
[34] Mastrucci, A., Marvuglia, A., Leopold, U. (2017): Life cycle assessment of building stocks from urban to transnational scales: A review. – Renew Sust Energ Rev 74: 316-332.
[35] Maung, K. N., Yoshida, T., Liu, G., Lwin, C. M., Muller, D. B., Hashimoto, S. (2017): Assessment of secondary aluminum reserves of nations. – Resour Conserv Recy 126: 34-41.
[36] McMillan, C. A., Moore, M. R., Keoleian, G. A. (2010): Quantifying U.S. aluminum in-use stocks and their relationship with economic output. – Ecol Econ 69: 2606-2613.
[37] Melo, M. T. (1999): Statistical analyses of metal scrap generation: the case of aluminum in Germany. – Resour Conserv Recy 26: 91-113.
[38] Modaresi, R., Müller, D. B. (2012): The role of automobiles for the future of aluminum recycling. – Environ Sci Technol 46: 8587-8594.
[39] Müller, D. B. (2006): Stock dynamics for forecasting material flows-case study for housing in the Netherland. – Ecol Econ 59: 142-156.
[40] Müller, E., Hilty, L. M., Widmer, R. (2014) Modeling metal stocks and flows: a review of dynamic material flow analysis methods. – Environ Sci Technol 48(4): 2102-2113.
[41] Nakamura, T., Halada, K. (2015): Urban Mining Systems. – In: SpringerBriefs in Applied Sciences and Technology. Springer, Germany, Japan, pp 7-29.
[42] Park, J-a., Hong, S-j., Kim, I., Lee, J-y., Hur, T. (2011): Dynamic material flow analysis of steel resources in Korea. – Resour Conserv Recy 55(4): 456-462.
[43] Pauliuk, S., Müller, D. B. (2014): The role of in-use stocks in the social metabolism and in climate change mitigation. – Global Environ Chang 24: 132-142.
[44] Recalde, K., Wang, J. L. Graedel, T. E. (2008): Aluminium in-use stocks in the state of Connecticut. – Resour Conserv Recy 52: 1271-1282.
[45] Rechberger, H., Graedel, T. E. (2002): The contemporary European copper cycle: statistical entropy analysis. – Ecol Econ 42: 59-72.
[46] Reck, B. R., Bertram, M., Müller, D. B., Graedel, T. E. (2006): Multilevel anthropogenic cycles of copper and zinc: A comparative statistical analysis. – J Ind Ecol 10: 89-110.
[47] Spatari, S., Bertram, M., Fuse, K., Graedel, T. E., Rechberger, H. (2002): The contemporary European copper cycle:1 year stocks and flows. – Ecol Econ 42: 27-42.
[48] U.S. Geological Survey (2016): Aluminum Statistics and Information. – http://minerals.usgs.gov/minerals/pubs/commodity/aluminum/.
[49] Wang, T., Müller, D. B., Graedel, T. E. (2007): Forging the anthropogenic iron cycle. – Environ Sci Technol 41: 5120-5129.

http://www.aloki.hu ● ISSN 1589 1623 (Print) ● ISSN 1785 0037 (Online)
DOI: http://dx.doi.org/10.15666/aeer/1704_78217835

[50] Wang, T., Mao, J. S., Johnson, J., Reck, B. K., Graedel, T. E. (2008): Anthropogenic metal cycles in China. – J Mater Cycles Waste 10(2): 188-197.
[51] Wang, M. X., Chen, W., Zhou, Y., Li, X. (2017): Assessment of potential copper scrap in China and policy recommendation. – Resour Policy 52: 235-244.
[52] Warrings, R., Fellner, J. (2018): Current status of circularity for aluminum from household waste in Austria. – Waste Manage 76: 217-224.
[53] Yan, L. Y., Wang, A. J., Chen, Q. S., Li, J. W. (2013): Dynamic material flow analysis of zinc resources in China. – Resour Conserv Recy 75: 23-31.
[54] Yue, Q., Wang, H. M., Lu, Z. W., Zhi, S. K. (2014): Analysis of anthropogenic aluminum cycle in China. – T Nonferr Metal Soc 24(4): 1134-1144.
[55] Yue, Q., Du, Y., Wang, H. M. (2015): Analysis of Al-contents in social stock and the regeneration index of depreciated aluminum products. – J Northeast Univ (Nat Sci Ed) 36(9): 1297-1301. (in Chinese).
[56] Yue, Q., Wang, H. M., Gao, C. K. (2016): Analysis of iron in-use stocks in China. – Resour Policy 49: 315-322.
[57] Zhang, L., Yuan, Z. W., Bi, J. (2012): Estimation of copper in-use stocks in Nanjing, China. – J Ind Ecol 16(2): 191-202.
[58] Zhang, L., Yang, J. M., Cai, Z. J., Yuan, Z. W. (2015a): Understanding the spatial and temporal patterns of copper in-use stocks in China. – Environ Sci Technol 49(11): 6430-6437.
[59] Zhang, L., Cai, Z. J., Yang, J. M., Yuan, Z. W. (2015b): The future of copper in China—A perspective based on analysis of copper flows and stocks. – Sci Total Environ 536: 142-149.

http://www.aloki.hu ● ISSN 1589 1623 (Print) ● ISSN 1785 0037 (Online)
DOI: http://dx.doi.org/10.15666/aeer/1704_78217835

EXPERIMENTAL STUDY ON THE MECHANISM FOR WATER INFILTRATING INTO AN AIR BLOCK AREA

MENG, L.[1,2] – ZHAO, G.[3] – ZHANG, C.[3*] – WANG, L.[3] – XU, Y.[3]

[1]*School of Water Resources and Environment, China University of Geosciences, Beijing 100083, China*

[2]*Institute of Hydrogeology and Environmental Geology, Chinese Academy of Geological Sciences, Shijiazhuang 050061, China*

[3]*College of Geosciences and Engineering, North China University of Water Resources and Electric Power, Zhengzhou 450046, China*

**Corresponding author*
e-mail: hydrozcy@163.com; phone: +86-186-3900-6624

(Received 23rd Feb 2019; accepted 3rd May 2019)

Abstract. Gas is usually ignored in traditional studies of water movement processes in the vadose zone. However, a large number of simulation experiments show that gas is an important factor effecting water movement. In this paper, a two-dimensional sand tank model is built to observe the changes of gas pressure and negative pressure during rainfall events with different intensities and boundaries and investigate the interaction between gas and water to reveal the block effect of gas on water movement. The results show three main effects of gas affecting water infiltration. Firstly, the water infiltration causes the gas pressure increased, which results in the decrease of unsaturated hydraulic conductivity. Secondly, the gas will escape to surroundings even break through the overlying saturated layer if the infiltration causes the gas pressure to increase to a critical value. The movement of gas in the vadose zone is mainly in vertical under the condition of gas insulation boundary, while in both vertical and horizontal under the condition of gas exhaust boundary. Finally, according to the variations of gas pressure with depths in the central profile, the vadose zone is divided into three zones: gas escaping zone, gas pressure fluctuating zone and gas pressure fast-decreasing zone.
Keywords: *sand tank, rainfall intensity, gas pressure, infiltration, physical experiments, moisture content*

Introduction

Gas flow is usually ignored in research into water movement processes in the vadose zone, and it is generally assumed that gas can freely discharge or invasive, so the gas pressure and atmospheric pressure are balanced (Peng, 2002). In fact, water movement in the vadose zone is the result of the mutual displacement of gas and water in the vadose zone pores, especially during events of heavy rainfall infiltration and pressured water infiltration. Water infiltration causes the gas to be constantly compressed under the weight of water and the gas cannot dissipate within a short time period, resulting in an increase in gas pressure and a reduction in the infiltration rate (Jarrelt, 1978; Lei, 1988; Lu, 1994).

It was found that the water infiltration rate was smaller under gas insulation conditions than under free exhaust conditions, and that gas will break through the overlying layer to escape when the pressure reaches a breakthrough value in the one-dimensional soil column infiltration experiment (Wang, 1997). Others had also come to this conclusion (Peck, 1965; Toma, 1986; Grismerand, 1994. Weir and Kissling divided the soil column into three regions to describe the water phase and gas phase: an upper

http://www.aloki.hu ● ISSN 1589 1623 (Print) ● ISSN 1785 0037 (Online)
DOI: http://dx.doi.org/10.15666/aeer/1704_78377853

layer, a transition layer and a lower layer. Water-gas phase interactions mainly occur in the transition layer, where the existence of gas will affect the water penetration coefficient. Peng et al. (2002) found that the water infiltration rate obviously declined when the air flow rate at the bottom of the soil column was controlled instead of exhausting freely in a one-dimensional two-phase flow experiment. The flow movement to ambient infiltration zone and surface is due to gas pressure persistent arise and gas displacement by water is the main characteristic in infiltration process (Lei, 2009). Ghosh et al. (2012) made an experimental investigation on vertical gas–liquid counter-current two-phase flow and obtained nonlinear relationships between the developed flow regimes and input parameters. Jie et al. (2013) illustrated the essential of consideration of gas resistance. It was found that the calculated infiltration time considering gas resistance term in the stratified hypothesis model agrees with the measured value with low deviation degree and a very small fluctuation. Herrada et al. (2014) proposed a model to simulate infiltration into heterogeneous soils, with arbitrary initial water content distributions, subject to unsteady rainfall, and under the free draining condition. Li et al. (2015) obtained the results that the channel differential pressure on both sides brings obvious fluctuations when the liquid is infiltrated. It is the gas flow rate not the amount of liquid infiltration affects the fluctuation significantly in the amplitude of the pressure differential. Du et al. (2017) analyze the mechanisms of soil water and vapour transport in the desert vadose zone using the Hydrus-1D model. Xiao et al. (2018) created an artificial-intelligence system that identifies nanofluid gas-liquid two-phase flow states in a vertical mini-channel. Min et al. (2018) investigated the groundwater recharge and seepage velocity in the deep vadose zone under typical irrigated agricultural land-use types.

Most researchers focus on one-dimensional soil column infiltration experiments, studying the effect of the presence of gas in the vadose zone by controlling the air flow rate at the bottom of the column, with little consideration given to the existence of the overlying aquifer. Although pressure changes under infiltration conditions are analysed, the relationship between air pressure and moisture content are not presented. Research of two-dimensional problems of rainfall infiltration is relatively barely (Zhao, 2011). In this paper, based on a two-dimensional physical model, experiments are designed to investigate rainfall infiltration processes under conditions of four different rainfall intensities and two different boundaries. That the changes of gas pressure and the hydrodynamic filed under different rainfall intensities and boundaries are investigated. The gas pressure on the profile along the central line and at three typical points is chosen to make data analysis. The relationship between negative gas pressure and moisture content is also analysed.

Methods

Experimental equipment

The experimental equipment comprises a sand tank, a rainfall simulator and a rainfall collector, shown in *Figure 1*. The size of the sand tank is 130 cm × 120 cm × 30 cm. The rainfall simulator is a plate with circular holes (diameter is 0.2 mm). The size of the rainfall simulator is 50 cm × 30 cm × 20 cm.

The sand tank is the main body of the test device. It is made of a high-quality, water-resistant wood-based material, with a metal box at the bottom forming the saturated zone. The tank is fitted with intake pipes, drainage pipes and piezometric tubes.

http://www.aloki.hu ● ISSN 1589 1623 (Print) ● ISSN 1785 0037 (Online)
DOI: http://dx.doi.org/10.15666/aeer/1704_78377853

Because the tank is symmetrical, so 19 gas pressure sensors (measuring range: -1000~1000 Pa; resolution: ±0.25% FS; manufacturer: Chang'an University and Huarui Transducer Technology Company) are installed in the front side of the sand tank, and 17 negative pressure sensors (measuring range: 0~-50 kPa; resolution; ±0.25%FS; manufacturer: Chang'an University and Huarui Transducer Technology Company) are installed in the back side of the sand tank. The effective rainfall simulation zone is 50 cm × 30 cm on the top of the setup. The experimental medium filled in the tank is silty sand. The joint parts of the device are well sealed to prevent water from flowing out of the device. Several air outlets with a diameter of 1 cm are installed at not only the left side but also the right side of the device for free exhaust. The origin of the coordinate system is at the left-bottom corner of the sand tank. The X axis increases positively to the right, and the Z axis increases positively upwards, so the coordinate of each pressure observation point is obtained. A markovian bottle is used to keep the phreatic level at 25 cm considering the base level at X axis.

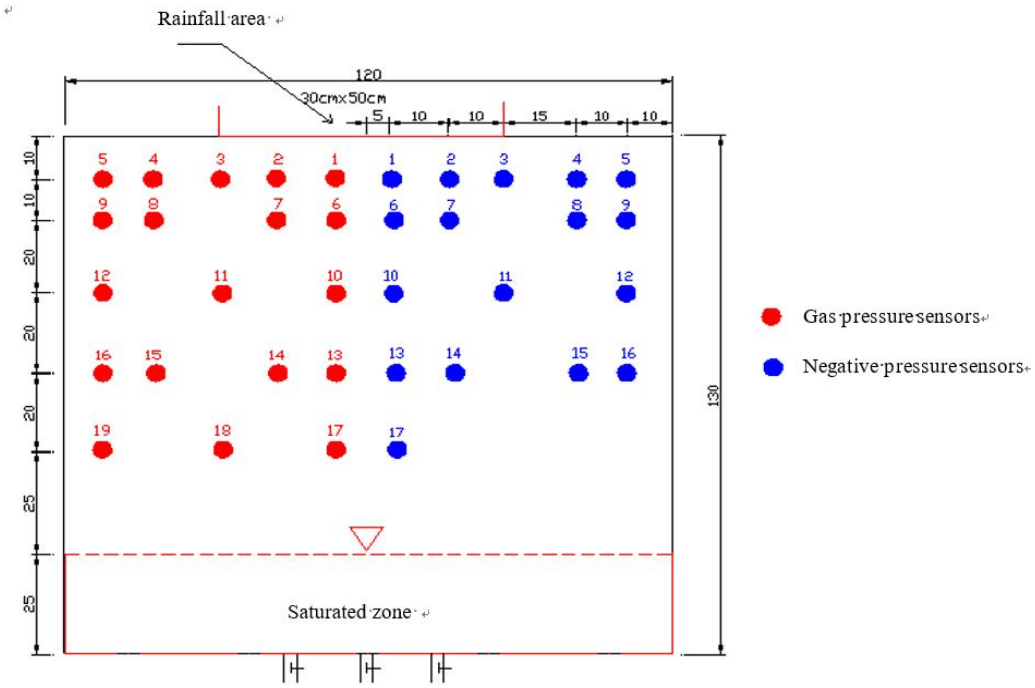

Figure 1. *Schematic diagram of experimental setup*

Experimental design

In order to analyze the affecting factors on water–gas phase flow migration law in the vadose zone, several different rainfall intensities and two different boundaries are set in the experiments. Two different boundaries are gas insulation condition and free exhaust condition. Gas insulation condition is that both the left and right boundaries of the sand tank model are closed and gas cannot be discharged (zero flux boundary). Free exhaust condition is that both the left and right sides of the sand tank model are partly open (flux boundary). The detailed experimental design is shown in *Table 1*. The rainfall duration is 30 min in each experiment. The groundwater level of saturated zone is kept at 25 cm. In each experiment, the negative gas pressure (matric potential) and the gas pressure and moisture content are measured and recorded continually.

http://www.aloki.hu ● ISSN 1589 1623 (Print) ● ISSN 1785 0037 (Online)
DOI: http://dx.doi.org/10.15666/aeer/1704_78377853

Table 1. *The experimental design*

Research content	Boundary	Rainfall intensity (cm/h)/ amount of rainfall (cm)
Changes of the aerodynamic field	Gas insulation condition	58/29
	Free exhaust condition	53/26.5
Changes of the gas pressure with the depth	Free exhaust condition	65/32.5
	Gas insulation condition	58/29; 40/20; 20/10
Changes of gas pressure at typical points	Gas insulation condition	78/39; 20/10
Changes of the hydrodynamic field	Gas insulation condition	58/29; 20/10
Distributions of moisture content in the central profile	Gas insulation condition	78/39; 20/10
Relationship between the gas phase and the water phase	Gas insulation condition	58/29; 20/10

Experimental results

Changes of the aerodynamic field under different boundaries

Distributions of the gas pressure field with a rainfall intensity of 58 cm/h (gas insulation boundary, presented in grey solid lines) and 53 cm/h (free exhaust boundary, presented in grey dotted lines) at different rainfall durations are shown in *Figures 2* and *3* respectively. The time varying maximum gas pressure of the central profile at X = 60 cm under different boundary conditions are presented in *Figure 4*.

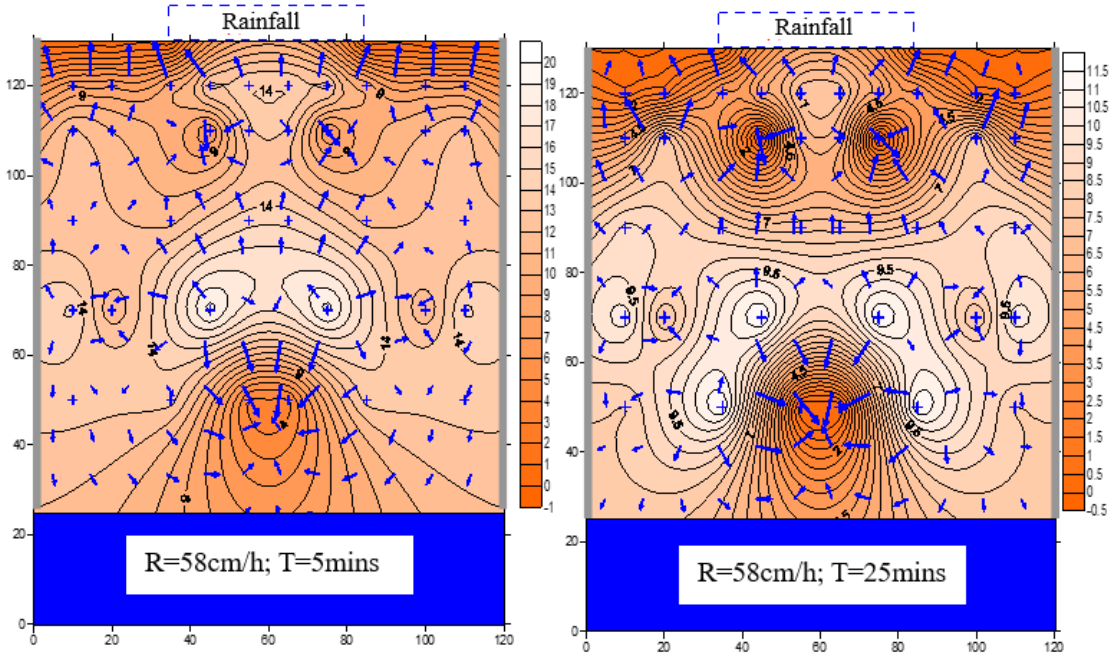

Figure 2. *Gas pressure distributions for a rainfall intensity of 58 cm/h (left: the rainfall duration is 5 min; right: the rainfall duration is 25 min; unit of gas pressure: Pa)*

http://www.aloki.hu ● ISSN 1589 1623 (Print) ● ISSN 1785 0037 (Online)
DOI: http://dx.doi.org/10.15666/aeer/1704_78377853

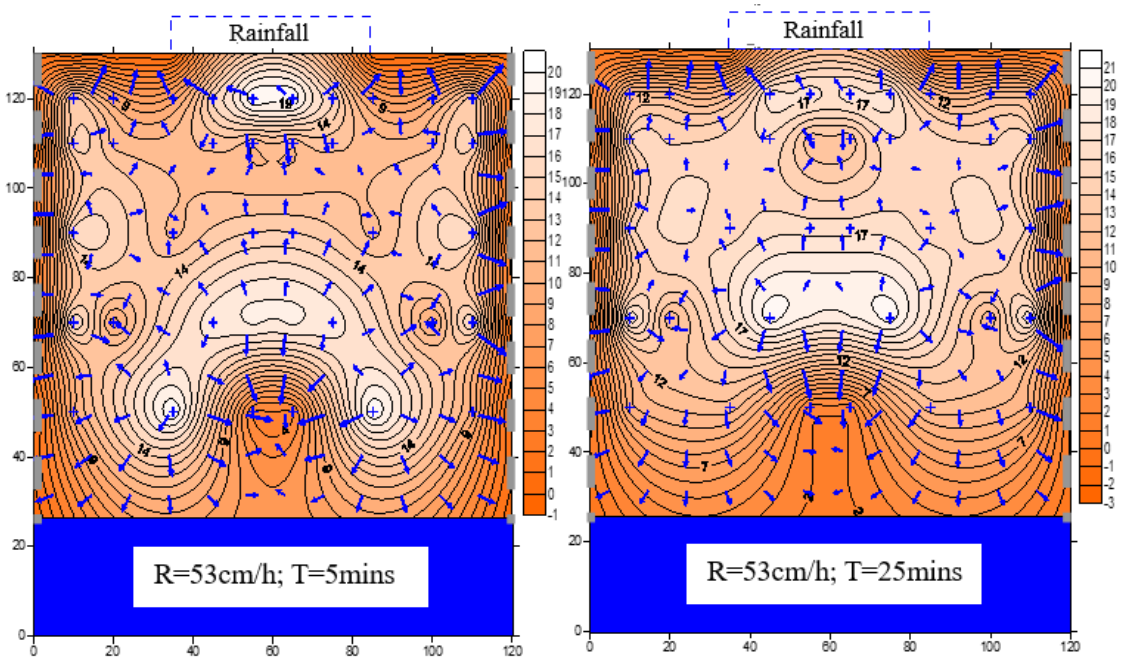

Figure 3. *Gas pressure distributions for a rainfall intensity of 53 cm/h (left: the rainfall duration is 5 min; right: the rainfall duration is 25 min; unit of gas pressure: Pa)*

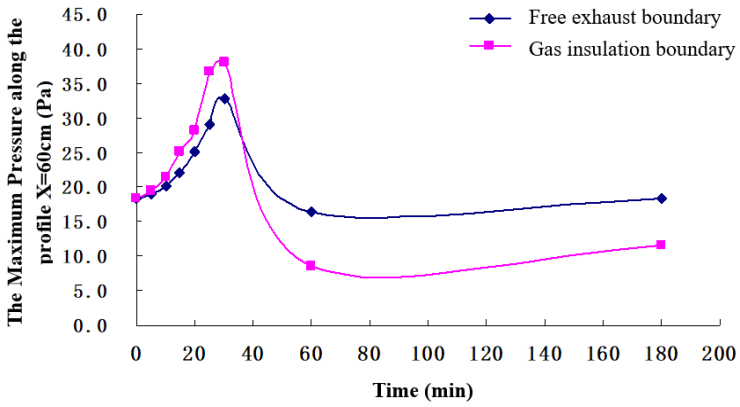

Figure 4. *The time varying of the maximum gas pressure of the central profile at X = 60 cm under different boundary conditions*

Changes of the gas pressure with the depth

Take the gas pressure at the central profile along X = 60 cm for example, the time-varying relationships between the gas pressure and depth in the vadose zone under different rainfall intensities and rainfall durations are shown in *Figure 5*. The rainfall duration is 0, 11, 20, 26 min respectively for each line in each figure.

Changes of gas pressure at typical points

Three gas pressure observation points at different locations in the vadose zone are selected. The first point (1#) locates at the rainfall area. The second point (3#) locates at

http://www.aloki.hu ● ISSN 1589 1623 (Print) ● ISSN 1785 0037 (Online)
DOI: http://dx.doi.org/10.15666/aeer/1704_78377853

the front of rainfall area and non-rainfall area. The third point (5#) locates at non-rainfall area. The changes of gas pressure values of the above three points are plotted in *Figure 6*.

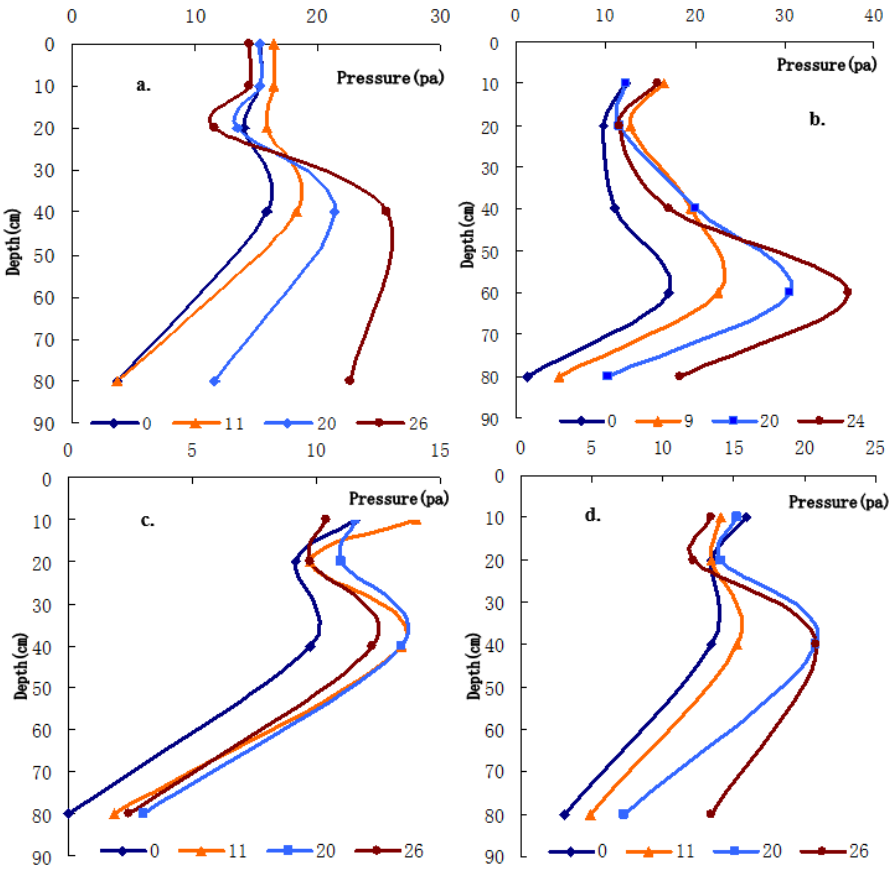

Figure 5. *Relationship between gas pressure and depth in the vadose zone for different rainfall intensities and different rainfall durations (a: rainfall intensity is 65 cm/h; b: rainfall intensity is 58 cm/h; c: rainfall intensity is 40 cm/h; d: rainfall intensity is 20 cm/h)*

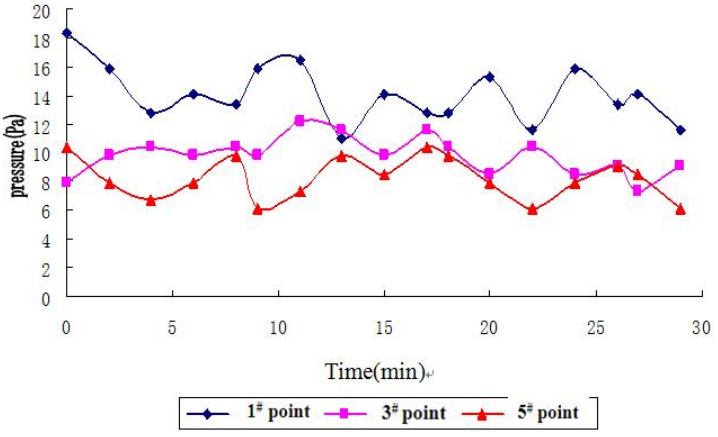

Figure 6. *Gas pressure variations with time at different observation points (1# point is located at the rainfall area; 3# point is located at the front of rainfall area and non-rainfall area; 5# point is located at the non-rainfall area)*

http://www.aloki.hu ● ISSN 1589 1623 (Print) ● ISSN 1785 0037 (Online)
DOI: http://dx.doi.org/10.15666/aeer/1704_78377853

The changes of gas pressure with time under different rainfall intensities are shown in *Figure 7*. It shows that the pressure fluctuates constantly around a mean value during a rainfall event. The mean value is 12.65 Pa when the rainfall intensity is 20 cm/h, while the mean value is 16.24 Pa when the rainfall intensity is 78 cm/h. The mean value of the pressure is greater when the rainfall rate is 78 cm/h than that when the rainfall rate is 20 cm/h. This proves that rainfall intensity has an important effect on the changes in gas pressure in the vadose zone.

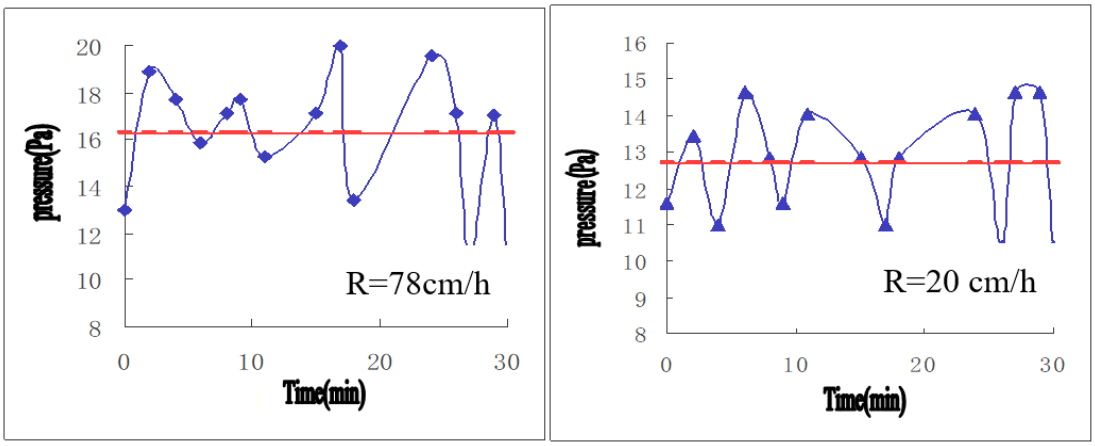

Figure 7. *Gas pressure variations with time in the vadose zone under different rainfall intensities*

Fluctuations in gas pressure are mainly related to unevenly distributed rainfall, surface disturbance, and the density of the experimental medium. These factors led to a change in the hydrodynamic field in the vadose zone, and to gas pressure fluctuations. It can be concluded that the water and gas phases are closely linked in the vadose zone and the mutual displacement processes should not be ignored.

Changes of the hydrodynamic field

The distributions of hydrodynamic fields under different rainfall intensities and different rainfall durations in the vadose zone are shown in *Figure 8*.

Figure 8 shows the downward migration of moisture in the vadose zone for different rainfall intensities. The hydraulic heads become increasingly concentrated in the vertical direction below the rainfall area as the rainfall time increases. The water flow usually moves vertically between the rainfall area and the groundwater table, and water infiltration in the vertical is much quicker than the percolation in the horizontal.

Contour plots of moisture content show the water infiltration process and the moving of wetting front. The figures showing the moving of the wetting front are presented in *Figure 9* for rainfall durations of 5, 20, 30 min and 15 min after the rainfall event respectively. The figure shows the distribution of moisture content within the vadose zone during a rainfall event. The red solid line represents the position of wetting front, at which the moisture content is approximately 20%. In addition, the movement of the wetting front shows a semi-oval shaped outward expansion. It can be obtained that for a rainfall duration of 29 min, the penetration distance of the water flow in vertical is about 50 cm, while the penetration distance in horizontal is only about 12 cm. This means the

http://www.aloki.hu ● ISSN 1589 1623 (Print) ● ISSN 1785 0037 (Online)
DOI: http://dx.doi.org/10.15666/aeer/1704_78377853

vertical penetration of water flow is much larger than the horizontal penetration, which causes the differences of gas expansion and compression in the vertical and horizontal directions. The unevenly moving of wetting front in directions is one of the causes of complicated gas migration and gas pressure changes.

Water flow infiltration rate ($q_i = dL_i/dt$, i = x, z) in the vertical and horizontal directions can be derived from the distance moved by a moisture peak at different times, shown in *Figure 10* (line a and b). In addition, the surface infiltration flux is 78 cm/h. From Darcy's law, the rate of water flow infiltration can be calculated. At the sand surface:

$$R = -K_{w0}\left(\frac{h_1 - h_0}{\Delta z} - 1\right) \quad \text{(Eq.1)}$$

where h_0 and K_{w0} are the hydraulic head and infiltration rate of the surface node respectively. The calculation results from Darcy's law are shown in *Figure 10* (line c).

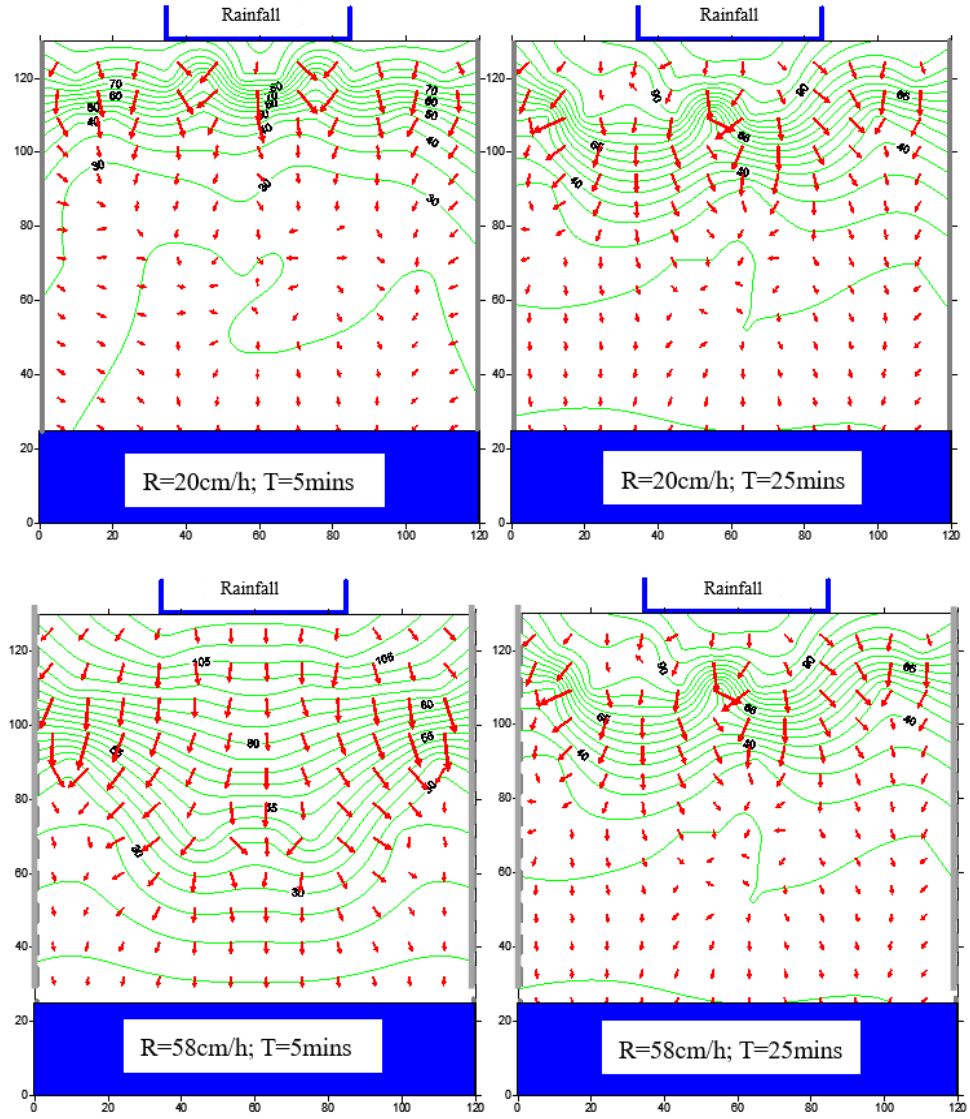

Figure 8. *Distributions of hydrodynamic field for different rainfall intensities and different rainfall durations (unit of hydrodynamic field: cm)*

http://www.aloki.hu ● ISSN 1589 1623 (Print) ● ISSN 1785 0037 (Online)
DOI: http://dx.doi.org/10.15666/aeer/1704_78377853

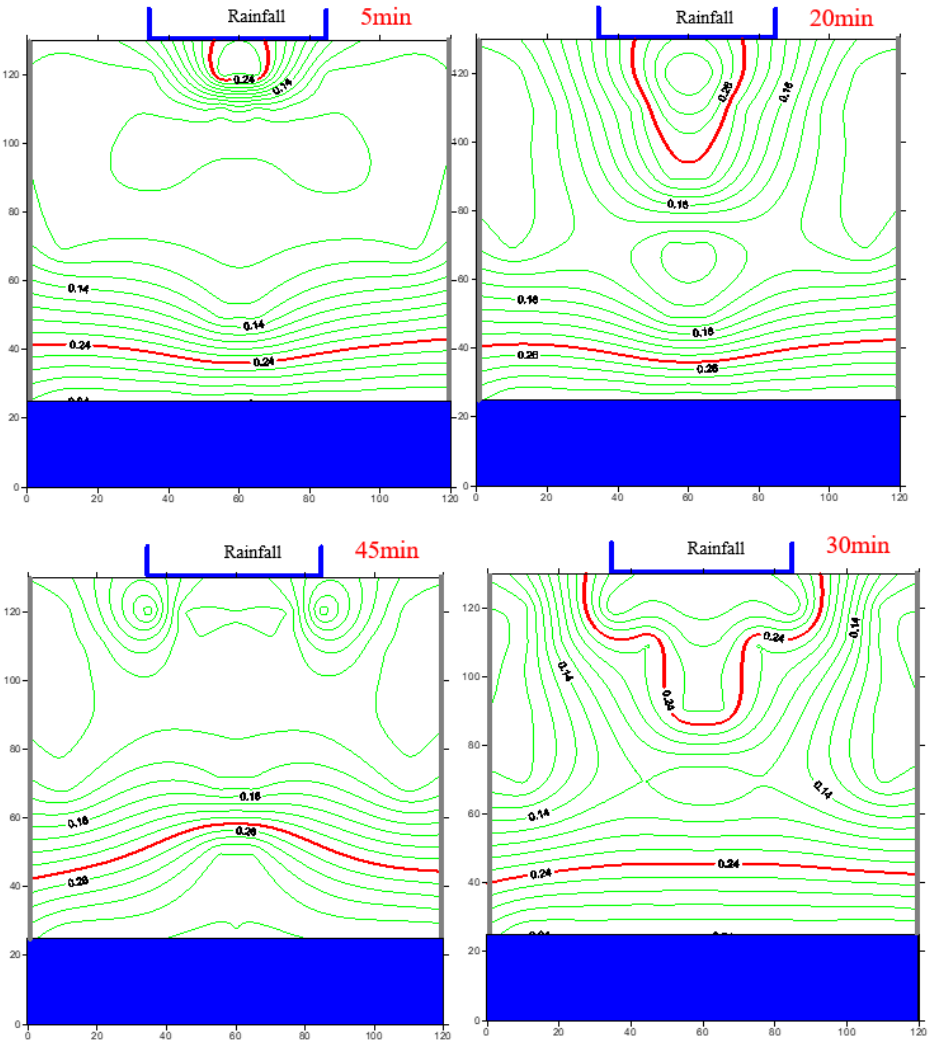

Figure 9. *Distributions of moisture content within the vadose zone at different times after the onset of rainfall (the rainfall duration is 30 min)*

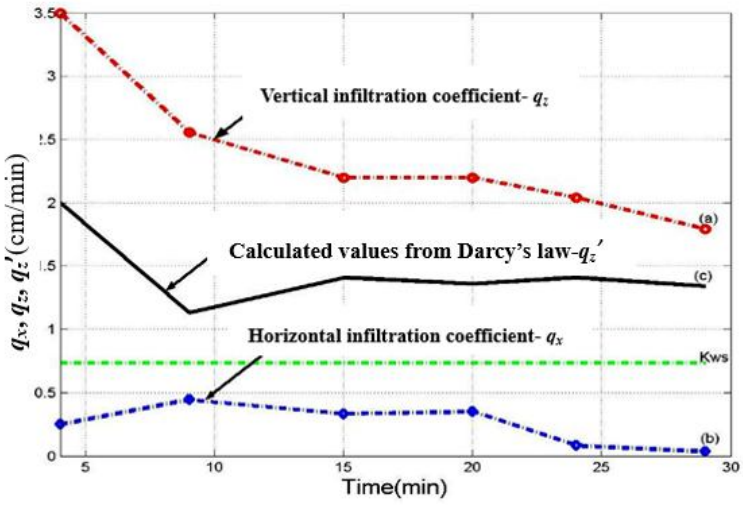

Figure 10. *Time series for the rainfall infiltration rates*

http://www.aloki.hu ● ISSN 1589 1623 (Print) ● ISSN 1785 0037 (Online)
DOI: http://dx.doi.org/10.15666/aeer/1704_78377853

From *Figure 10,* we can see that water infiltration rate in the vertical (q_z) is significantly greater than that in the horizontal (q_x), that is $q_z >> q_x$. The calculated vertical infiltration rate from Darcy's law (*Fig. 10,* line c) is in accordance with the changing vertical infiltration rate derived from the movement of wetting front (*Fig. 10,* line a), but much larger. Early in the rainfall event, the flow infiltration rate is significantly greater than the saturated hydraulic conductivity K_{ws}. As the vadose zone soil porosity gradually become saturated, the vertical infiltration rate decreases, ultimately tending to the saturated hydraulic conductivity K_{ws}. The horizontal infiltration rate is much smaller throughout the rainfall event, and eventually tends to zero (*Fig. 10,* line b).

Distributions of moisture content in the central profile at X = 60cm

Negative pressure (matric potential) varies with moisture content. So the changes of negative pressure are a useful mean of indirect measurement of moisture content in the vadose zone. Water column height (in cm) is used to represent the values of the negative pressure. The changes of negative pressure with depths under conditions of different rainfall intensities and rainfall durations are shown in *Figures 11* and *12*.

The relationship between the gas phase and the water phase

Soil pores in the vadose zone are filled with either water or gas, so moisture migration resulting from rainfall infiltration is actually a mutual displacement process between the water and gas phases. The changes in moisture content cause the changes in gas pressure, while the negative pressure (matric potential) varies with moisture content, so there is a close relationship between air pressure, moisture content and negative pressure. The research of the relationship is important to understand the mechanisms of water and air migration in the vadose zone.

The time series of air pressure and negative pressure under conditions of different rainfall intensities are shown in *Figure 13*.

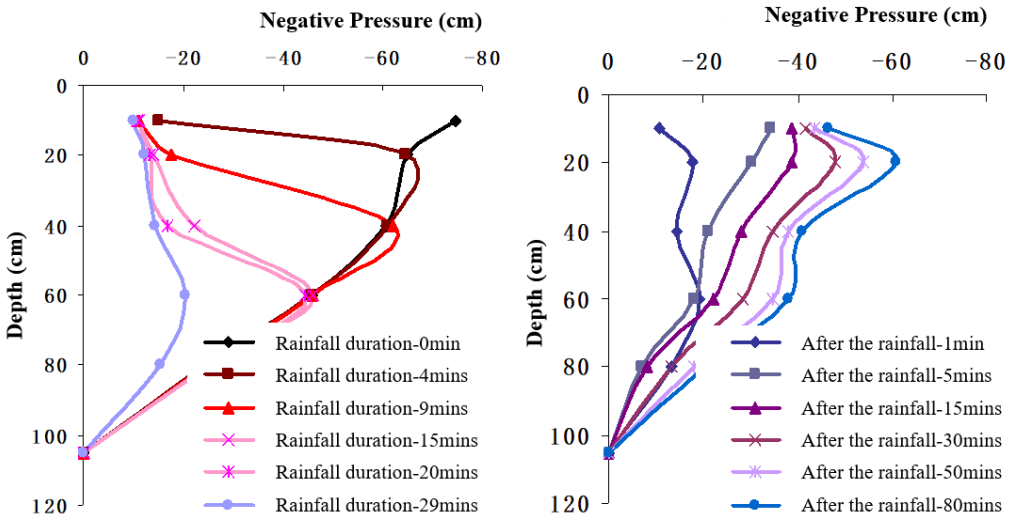

Figure 11. *Changes of negative pressure with depths in the vadose zone for a rainfall intensity of 20 cm/h*

http://www.aloki.hu ● ISSN 1589 1623 (Print) ● ISSN 1785 0037 (Online)
DOI: http://dx.doi.org/10.15666/aeer/1704_78377853

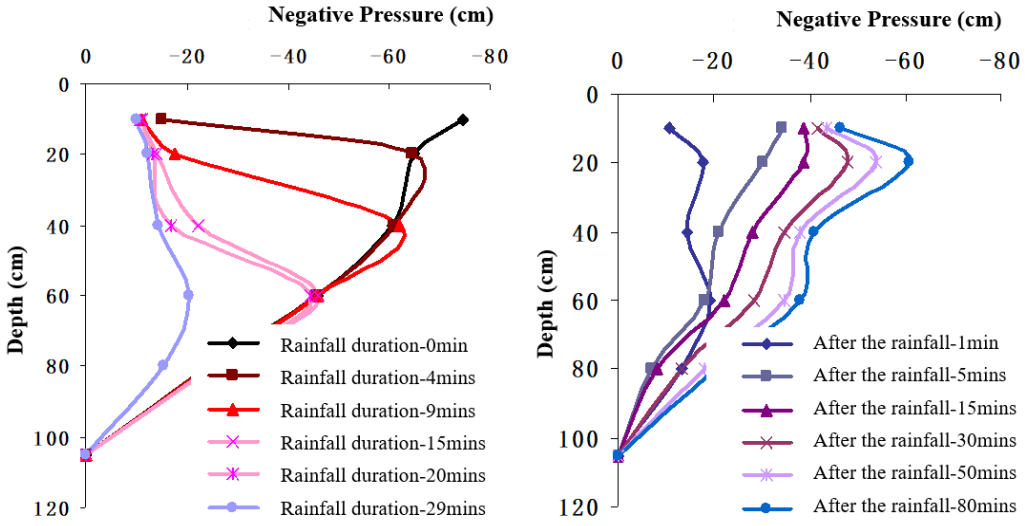

Figure 12. *Changes of negative pressure with depths in the vadose zone for a rainfall intensity of 78 cm/h*

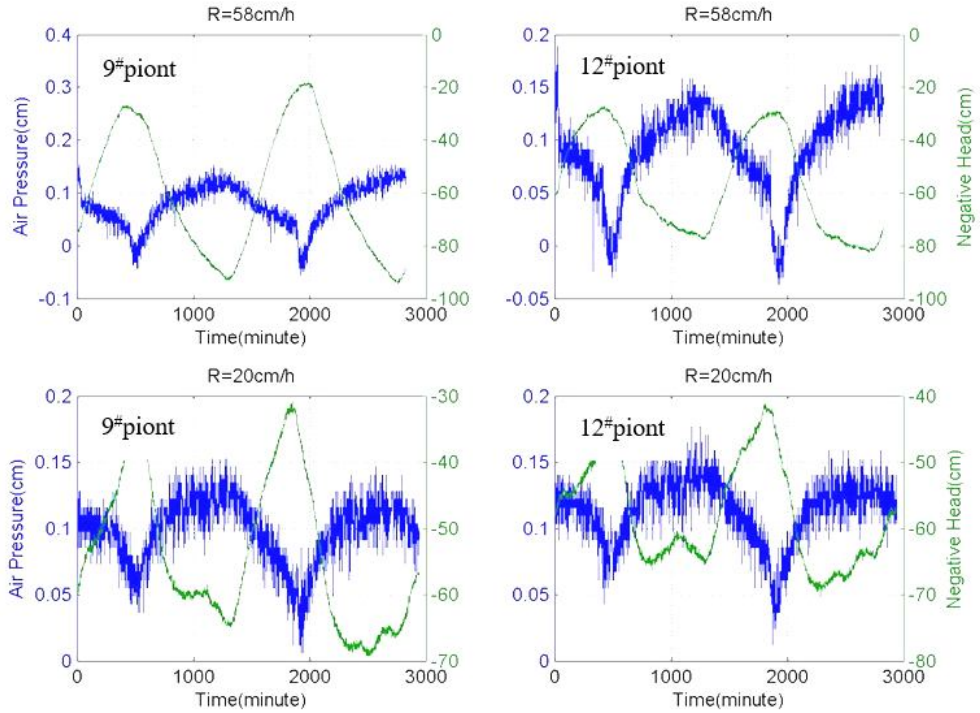

Figure 13. *Time series of gas pressure and negative gas pressure for different pressure measuring points under different rainfall intensities*

How the gas phase blocks water infiltration

The impact of the gas on the moisture migration. The mutual displacement relationship between the water phase and gas phase in the vadose zone is an important

http://www.aloki.hu ● ISSN 1589 1623 (Print) ● ISSN 1785 0037 (Online)
DOI: http://dx.doi.org/10.15666/aeer/1704_78377853

aspect of rainfall infiltration processes, and the blocking effect of the gas phase on water infiltration is particularly important. Using the groundwater recharge rate obtained from the rainfall infiltration experiments, Darcy's law can be expressed as the following equation:

$$q = -K_i\left(\frac{h_i - h_{i-1}}{\Delta z} - 1\right) \quad \text{(Eq.2)}$$

where h_i and h_{i-1} are the hydraulic head values for adjacent nodes near the groundwater table.

The unsaturated permeability coefficient *K(h)* can be obtained from *Equation 2*. The changes of *K(h)* with the pressure at node i are shown in *Figure 14*.

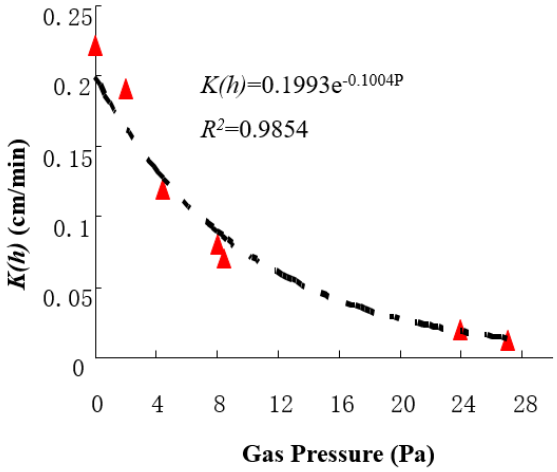

Figure 14. *The relationship between the unsaturated permeability coefficient K(h) and gas pressure*

The response time of rainfall recharge. Define the response time of rainfall recharge as the period between the time at which the rainfall infiltrates into the vadose zone to the time at which the infiltrated water begins to recharge groundwater. This response time is closely related to rainfall duration, vadose zone lithology and structure, surface vegetation cover and groundwater depth. The changes of the response time under different rainfall intensities conditions are depicted in *Figure 15*.

Discussion

Changes of the aerodynamic field under different boundaries

From *Figures 2* and *3,* it is found that the high pressure center, where the gas pressure increases quickly and the gas compression degree is the highest, is located just below the rainfall area, but not close to the groundwater table whether under the gas insulation boundary or free exhaust boundary. When the gas pressure increases to a critical level, the gas begin to escape to surroundings or even break through the overlying water layer to escape out of the sand surface as a result of the pressure gradient. Under gas insulation conditions, the gas cannot escape from the sides, and so

http://www.aloki.hu ● ISSN 1589 1623 (Print) ● ISSN 1785 0037 (Online)
DOI: http://dx.doi.org/10.15666/aeer/1704_78377853

is eventually released from the sand surface. And the maximum pressure of the compressed gas is about 38 Pa after 29 min rainfall (*Fig. 4*). The gas movement is mainly in vertical. Under the free exhaust condition, the gas escapes from both sides of the tank and exchanges with the air outside exhibiting significant horizontal movement besides vertical movement. The maximum gas pressure is about 32 Pa after 29 min rainfall (*Fig. 4*).

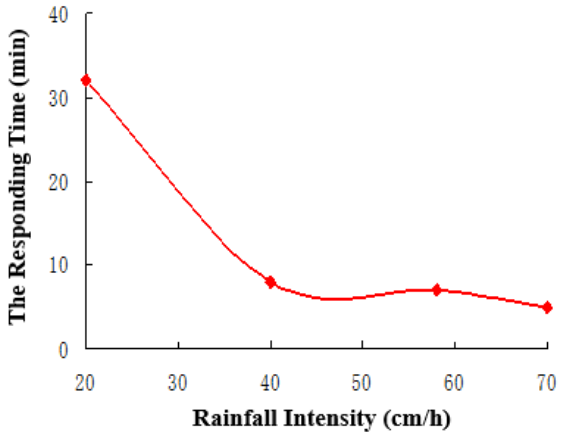

Figure 15. *The changes of the response time under different rainfall intensities conditions*

From *Figure 4,* it can be seen that the maximum pressure is larger under the gas insulation condition than that under the free exhaust condition during rainfall infiltrating. Almost at the end time of the rainfall, the gas pressure reaches a critical value, after which the gas breaks through the overlying water layer and escapes, causing the pressure to reduce rapidly. After rainfall (from 40 to 180 min), the maximum profile pressure decreases much more rapidly under gas insulation condition than that under free exhaust boundary condition. In addition, the pressure values under gas insulation condition keep lower than that under free exhaust boundary condition after rainfall. The above results demonstrate that the degree of gas compression under the gas insulation condition is much greater than that under the free exhaust condition. The boundary has a significant influence on the gas migration in the vadose zone.

Changes of the gas pressure with the depth

The gas pressure fluctuates strongly but approximately follows an "S" type with the depth from the surface to the bottom of the vadose zone either under a gas exhaust boundary or a gas insulation boundary. The difference is the location of the lower turning point. The location is at 60 cm under a gas exhaust boundary while it is at 20 cm under a 20 cm. The "S" type relationship between the gas pressure and depth divides the vadose zone into three zones. Zone I (at about 0–20 cm) is the gas escaping zone, where is close to the sand surface. The gas pressure in this zone decreases with the depth very slowly and reaches a minimum value at the depth of 20 cm. This is because this area reaches near-saturated in a comparatively short time during a rainfall event and the gas is quickly displaced by water. Zone II (at about 20-40 cm for gas insulation boundary; at about 20-60 cm for gas exhaust boundary) is the gas fluctuating zone. In this zone, the gas pressure increases quickly with the depth and reaches a maximum value at the

http://www.aloki.hu ● ISSN 1589 1623 (Print) ● ISSN 1785 0037 (Online)
DOI: http://dx.doi.org/10.15666/aeer/1704_78377853

depth of 40 cm (gas insulation boundary) or 60 cm (gas exhaust boundary). The maximum value decreases with the rainfall intensity. The reason is that the infiltrating flow advances rapidly in this zone, resulting in great changes in moisture content. The sustained infiltrating flow causes the gas resistance. And the downward movement of wetting front causes the gas compressed, so the gas cannot dissipate in time. Zone III (40–80 cm for gas insulation boundary; 60-80 cm for gas exhaust boundary) is the gas pressure fast-decreasing zone. In this zone, the gas pressure decreases with the depth. The flow tends to be steady due to the large infiltration distance and the reduced infiltration rate. Gas here slowly dissipates and escapes in the effect of the wetting front. Only a small amount of gas is transported to the groundwater table. The turning point illustrates that the gas movement does not only occur in the vertical direction but also in the horizontal direction. The turning point is where the gas is compressed and dissipated. The increase of gas pressure prevents the water from infiltrating and causes a lower hydraulic conductivity.

Changes of gas pressure at typical points

Figure 6 shows that the gas pressure fluctuates with time continuously around a mean value, exhibiting peaks and troughs. This is because the water infiltration causes gas to be constantly compressed during rainfall events. The increase in pressure causes the gas to break through the overlying water layer, which forms a pore channel. Then the pressure begins to decay rapidly and the pore channel is quickly re-occupied by water. This process repeats in the whole infiltration process, so the gas pressure in the vadose zone is not increasing or decreasing continuously, but in a state of fluctuation. The shape of the gas pressure time series curve shows that the changes of gas pressure in the vadose zone is similar with the fluctuations of the atmospheric pressure (Li, 2010). Pore channels form in the vadose zone and connect with the outside atmosphere, so the gas pressure changes are primarily related to the ambient atmospheric fluctuations. This result is consistent with the phenomenon described by Buckingham (1904), who considered that fluctuations in gas pressure in the vadose zone were related to changes in the near-surface atmospheric pressure. Massmann (1992) explained the near-surface atmospheric pressure fluctuations in detail. Massmann believed that the main causes of it were firstly the effect of heat conduction and gravity, and secondly the regional scaled weather conditions.

Distributions of moisture content in the central profile at X = 60 cm

The results (*Figs. 11* and *12*) show that saturation state can be reached near the surface in a short period of time. At the onset of a rainfall, the moisture content is approximately the saturated moisture content and the negative pressure head is small. As the rainfall continues, the water-gas front moves downwards and the moisture content increases and the negative pressure head decreases. After the rainfall event, groundwater in the vadose zone is transported downwards under the influence of gravity. The negative pressure shows the trend of larger values at the lower depth and smaller values at the deeper depth.

Analysis of the relationship between the gas phase and the water phase

The results (*Fig. 13*) show that the air pressure and negative pressure fluctuates with time: the negative pressure increases (negatively) with the air pressure increases, and

http://www.aloki.hu ● ISSN 1589 1623 (Print) ● ISSN 1785 0037 (Online)
DOI: http://dx.doi.org/10.15666/aeer/1704_78377853

vice versa. The increase in gas pressure at a point in the unsaturated zone indicates the entry of gas into pores near that point and the discharge of water from the pores. This corresponds to a decrease in the moisture content at that point, and a consequent increase in negative pressure. Similarly, a decrease in pressure indicates the entry of water into a pore near that point, following the discharge of gas from the pore, which corresponds to a decrease in negative pressure because of the increase in moisture content.

Analysis of how the gas phase blocks water infiltration

The curve in *Figure 14* shows that the unsaturated permeability coefficient varies with gas pressure following the empirical relationship ($K(h) = 0.1993e^{-0.1004P}$). It is clear that the increase of the gas pressure results in the reducing of the unsaturated permeability coefficient during a rainfall event. It illustrates that increasing pressure will strongly attenuate the flow infiltration rate. For example, when the gas pressure reaches 270 Pa, the unsaturated permeability coefficient of water decreases from 0.22 cm/min to 0.03 cm/min. The effect of the gas phase on the unsaturated permeability coefficient gradually becomes weakened with the gas pressure increases, and the curve becomes flattened. Although this relationship does not provide a clear quantification of the relationship between gas pressure and the unsaturated permeability coefficient, it does clearly demonstrate how the increasing pressure has a blocking effect on the water flow, resulting in the water infiltration rate reduction.

Figure 15 shows that the response time decreases as rainfall intensity increases. The greater the rainfall intensity, the faster the flow infiltration rate, and the shorter time taken for the flow to reach the groundwater table. Although rainfall infiltration leads to gas compression and creates a partial block to the flow, this does not completely prevent the flow, and the response time is mainly determined by the magnitude of the rainfall intensity.

Conclusions

In order to obtain the mechanism of water infiltrating into an air block area in the vadose zone under conditions of different rainfall intensities and boundaries, a two-dimensional sand tank is made and lots of experiments are conducted. From the data analysis, the following conclusions can be drawn:

(1) The boundary has a significant influence on the gas pressure. The gas moves primarily in the vertical direction under a gas insulation boundary. However, the gas exhibits significant lateral diffusion besides vertical movement under a gas exhaust boundary. When the gas pressure reaches to a sufficiently high value, the gas escapes to the surroundings even break through the overlying water layer.

(2) The gas pressure fluctuates strongly but approximately follows an “S” type with the depths. So the vadose zone can be divided into three zones: Zone I is the gas escaping zone; Zone II is the gas pressure fluctuating zone; Zone III is the gas pressure fast-decreasing zone.

(3) The unsaturated permeability coefficient varies with gas pressure following an empirical relationship. The block effect of the gas phase on the unsaturated permeability coefficient gradually becomes weakened with the gas pressure increases.

http://www.aloki.hu ● ISSN 1589 1623 (Print) ● ISSN 1785 0037 (Online)
DOI: http://dx.doi.org/10.15666/aeer/1704_78377853

Acknowledgements. This research was funded by The National Natural Science Foundation of China (41702285, 41372260) and the Scientific Starting Project of High-Level Talents of North China University of Water Resources and Electric Power (201702002) and the Geological Survey Projects Foundation of Institute of Hydrogeology and Environmental Geology (SK201505).

REFERENCES

[1] Buckingham, E. (1904): Contributions to our knowledge of the aeration of soils. – Science 25: 5-52.
[2] Du, C., Yu, J., Wang, P. et al. (2017): Analysing the mechanisms of soil water and vapour transport in the desert vadose zone of the extremely arid region of northern China. – Journal of Hydrology S0022169417306583.
[3] Ghosh, S., Pratihar D. K., Maiti, B. et al. (2012): Identification of flow regimes using conductivity probe signals and neural networks for counter-current gas–liquid two-phase flow. – Chemical Engineering Science 84: 417-436.
[4] Grismer, M. E., Orang, M. N., Clausitzer, V., Kinney, K. (1994): Effects of air compression and counter flow on infiltration into soils. – Journal of Irrigation & Drainage Engineering 120: 775-795.
[5] Herrada, M. A., Gutiérrez-Martin, A., Montanero, J. M. (2014): Modeling infiltration rates in a saturated/unsaturated soil under the free draining condition. – Journal of Hydrology 515: 10-15.
[6] Jarrett, A. R., Friton, D. D. (1978): Effect of entrapped soil air on infiltration. – Transactions of the ASAE 21(5): 901-906.
[7] Jie, Z., Tong-Chun, H., Hong-Qiang, D. et al. (2013): Analysis model for rainwater infiltration considering gas resistance under stratified assumption. – Yantu Gongcheng Xuebao/Chinese Journal of Geotechnical Engineering 35(12): 2219-2225.
[8] Lei, L., Bing, L., Qiang, X. (2009): Prediction analysis of water infiltration effect on landfill gas transport. – Physical and Numerical Simulation of Geotechnical Engineering 15: 43-45.
[9] Lei, Z. D., Yang, S. H., Xie, C. S. (1988): Soil Water Dynamics. – Tsinghua University Press, Beijing, pp. 21-22.
[10] Lu, T. X., Biggar, J. E., Nielsen, D. R. (1994): Water movement in glass bead porous media: 2. Experiments of infiltration and finger flow. – Water Resources Research 30: 3283-3290.
[11] Li, J., Zhao, J., Wang, S. (2015): Gas–liquid two-phase flow in a mini-channel with water infiltration continuously along the flow direction. – International Journal of Green Energy 12(3): 8.
[12] Li, Y. L. (2010): Simulation Study of Two-Phases (Water and Air) Flow in Unsaturated Zone under Infiltration Condition. – Chang'an University, Xi'an, China.
[13] Massmann, J., Farrier, D. (1992): Effects of atmospheric pressure on gas transport in the vadose zone. – Water Resources Research 28(3): 777-791.
[14] Min, L., Shen, Y., Pei, H. et al. (2018): Water movement and solute transport in deep vadose zone under four irrigated agricultural land-use types in the North China Plain. – Journal of Hydrology S0022169418301136.
[15] Peck, A. J. (1965a): Moisture profile development and air compression during water uptake by bounded porous bodies: 2. Horizontal columns. – Soil Science 100: 333-340.
[16] Peck, A. J. (1965b): Moisture profile development and air compression during water uptake by bounded porous bodies: 3. Vertical columns. – Soil Science 100: 44-51.
[17] Peng, S., Chen, J. J., Wang, J. S. (2002): Two-phase flow in soil vadose zone. – Acta Pedologica Sinica 39(4): 505-511.
[18] Touma, J., Vauclin, M. (1986): Experimental and numerical analysis of two-phase infiltration in a partially saturated soil. – Transport in Porous Media 1: 27-55.

http://www.aloki.hu ● ISSN 1589 1623 (Print) ● ISSN 1785 0037 (Online)
DOI: http://dx.doi.org/10.15666/aeer/1704_78377853

[19] Wang, Z., Feyen, J., Nielsen, D. R., Genuchten, M. T. V. (1997): Two-phase flow infiltration equations accounting for air entrapment effects. – Water Resources Research 33: 2759-2767.
[20] Xiao, J., Luo, X., Feng, Z. et al. (2018): Using artificial intelligence to improve identification of nanofluid gas–liquid two-phase flow pattern in mini-channel. – AIP Advances 8(1): 015123.
[21] Zhao, G. Z. (2011): Study on Transformation Mechanism of Vadose Zone Water-Groundwater in the Wind-blown Sand Area of the Ordos Basin. – Chang'an University, Xi'an, China.

http://www.aloki.hu ● ISSN 1589 1623 (Print) ● ISSN 1785 0037 (Online)
DOI: http://dx.doi.org/10.15666/aeer/1704_78377853

RESPONSE OF RUNOFF IN NINGXIA SECTION OF YELLOW RIVER BASIN OF CHINA TO CLIMATE CHANGES

WANG, Z. P.[1,2,4*] – TIAN, J. C.[1,3,4] – FENG, K. P.[1,3,4]

[1]*College of Civil and Hydraulic Engineering, Ningxia University, Yinchuan 750021, China*

[2]*School of Mathematics and Statistics, Ningxia University, Yinchuan 750021, China*

[3]*Ningxia Research Center of Technology on Water-Saving Irrigation and Water Resources Regulation, Yinchuan 750021, China*

[4]*Engineering Research Center for the Efficient Utilization of Water Resources in Modern Agricultural in Arid Regions, Yinchuan 750021, China*
(phone: +86-13895005003)

[*]*Corresponding author*
e-mail: wzp_0416@163.com

(Received 23rd Feb 2019; accepted 3rd May 2019)

Abstract. As one of the major water sources in Ningxia of China, it is of great importance to maintain healthy ecological environment of the Yellow River. In this essay, basin hydrological model is adopted to simulate the influences of prediction of climate changes on runoff in river basin, which is of great theoretical and realistic significance to flood and draught control plans as well as long-term exploitation and utilization of water resources in Ningxia Section of Yellow River Basin of China. Based on analysis of the changing characteristics of major climates and hydrological features in Ningxia Section of Yellow River Basin of China , distributed hydrological model SWAT (Soil and Water Assessment Tool) coupled with GIS is used in this study to simulate the yearly and monthly runoff volumes under 15 different climate changes, with the aim to explore the influences of climate changes to runoff. The results show that the runoff volume in the basin has negative correlation with the temperature but in positive correlation with the rainfall, and that the influence of the changes of rainfall in the basin on the runoff is greater than that of the temperature, which could provide basis for decision making of water resource management in Ningxia Section of the Yellow River Basin of China.
Keywords: *SWAT model, climate scenes, simulation, temperature, rainfall*

Introduction

As the environment in which human beings live, climate could affect human activities, which has been know by all. The influences of climate changes are comprehensive, multi-dimensional and multi-layered, with positive and negative influences co-existing. Generally, people concern more the negative influences. Global warming caused by carbon dioxide affects directly water supply and distribution in the world and has influenced the natural ecosystem in many areas of the world. Due to limited adaptability, natural ecosystem is easily to be destroyed severely and even irreversibly. Rainfall changes caused by climate warming is an essential factor to study the influences of potential climate on water supply, for rainfall is the fundamental source of fresh water on the earth. Water resources planning depends on mainly space-time distribution of rainfall and soil water. In the future, rainfall distribution would change obviously on the warmed earth and rainfall in many areas located in semi-arid subtropical zone would increase. Because global warming could cause profound changes of the global climate system, the coadaptation established between mankind

http://www.aloki.hu ● ISSN 1589 1623 (Print) ● ISSN 1785 0037 (Online)
DOI: http://dx.doi.org/10.15666/aeer/1704_78557863

and the ecological environmental system would be affected and disturbed significantly; therefore, global changes, especially climate changes, have attracted great concerns from governments of the world and the public.

Certain irrational activities of human beings have caused global warming in the world, which results in finally frequent draughts, floods and other natural disasters. In the past several decades, the global climate has had inconvenient changes, among which global warming has become an undisputed fact. Since IPCC (Intergovernmental Panel on Climate Change) was found in 1988, it has completed five evaluation reports on global climate changes (IPCC, 2013), among which it was pointed out in the fifth evaluation report: the average global surface temperature in the world between 1880-2012 rose 0.85ºC. Comparing the middle and late 21st century and the period from 1986-2005, the average global temperature will keep rising 1.0～ 2.0 and 1.0 ～ 3.7ºC. According to the observation results in the past hundred years in China, the average surface temperature in China in the 20th century had rose 0.5～ 0.8ºC, which showed similar trend of global warming. Climate changes could affect various fields and could change the conditions of global water circulation, which could result in spatial and temporal redistribution of water resource. In recent years, due to climate changes and the increase of human activities, about 31% annual runoff of 145 major rivers in the world shows rising tendency (9%) or descending tendency (22%) (Walling and Fang, 2003). Runoff of many major rivers in China declines, especially that in Haihe Basion and the Yellow River Basin (Wang et al., 2010; Bao et al., 2012; Feng et al., 2016). In recent years, many areas had floods or draughts often (Kunkelet al., 1999; Lindner et al., 2010; Zhang et al., 2015). For example, draught occurred in downstream of the Yellow River Basin, floods occurred in the Yangtze River Basin and Songhua River area respectively in 1997 and 1998, which had caused immense damages(Xu et al., 2010). Therefore, it is of great significance for understanding hydrological changing mechanisms and relieving future draughts and floods to know the reasons of the runoff changes in the changing environment.

Climate changes and human activities are two essential factors that could affect runoff changes. Climate changes affect runoff mainly through rainfall and potential evaporation (Chien et al., 2013; Zhao et al., 2015). A great number of studies have shown that global warming will aggravate global hydrological circulation (Huntington, 2006; Milliman et al., 2008). It has been predicated by the observation data and climate model studies that climate warming could result in significant increase of rainstorms (Wu and Lau, 2016). Many studies have used GCM and hydrologic model to evaluate the influences of climate changes on runoff (Eisner et al., 2017; Teklesadik et al., 2017). However, climate simulation factors could also affect runoff changes. The experiment adopted various factors (such as GCM model, project stage, emission scenes, downscaling method and deviation correction) to show the predicted flow is an factor for the modeling and that it is unnecessary to take all factors into consideration but to keep the overall design balance (Ringius et al., 1996; Aamery et al., 2016). Li et al. (2013) used two rainfall–runoff models to simulate the yearly and monthly runoff of southeastern Tibetan Plateau under the historical and future conditions of climate changes. Coles et al. (2017) studied the influences of climate changes on the hillslope runoff in the north of the Great Plains. Besides, with the increase of the population and the urbanization (Kuang et al., 2016), human activities, such as land use/cover changes (Rahman et al., 2015; Zhang et al., 2017; Yhang et al., 2019), operation of dam and reservoir, water and soil conservation projects as well as direct taking of surface water

http://www.aloki.hu ● ISSN 1589 1623 (Print) ● ISSN 1785 0037 (Online)
DOI: http://dx.doi.org/10.15666/aeer/1704_78557863

and groundwater, all could cause great influences on water resources. Zhai et al. (2017) investigated the climates and runoff tendencies of seven typical basins in China from 1961 to 2014 and attributed the runoff change within three periods to climate changes and human activities of each basin. The problem of water resources has aroused concerns of various scholars; moreover, it has become the bottle-neck of economic development of many countries and areas. In recent years, many professional scholars have begun to study the influences of climate changes on water resources, which could provide scientific theoretical basis for rational development and utilization of water resources, disaster prevention and reduction, water loss and soil erosion as well as comprehensive planning of the basin and could offer relevant policy reference to the decision-makers.

In this paper, distributed hydrological model SWAT coupled with GIS is used in this study to simulate the yearly and monthly runoff volumes under 15 different climate changes, with the aim to explore the influences of climate changes to runoff, and it can provide decision-making basis for water resource management in the Ningxia Section of the Yellow River Basin of China.

Material and methods

Overview of the research area

The Yellow River enters the downstream of Zhongwei City, Ningxia province, running through the Yellow River irrigation area of Zhongning County, Qingtongxia City, Litong District, Lingwu City, Yongning County, Yinchuan City, Helan County, Pinluo County, Dawukou District and Huinong District and flowing in Inner Mongolia at Shizuishan. There are three hydrological stations along the mainstream of the Yellow River, i.e., Xiaheyan, Qingtongxia and Shizuishan hydrological stations. The Yellow River Basin within Ningxia is located in north latitude $36^{\circ}0'\sim39^{\circ}23'$, east longitude $104^{\circ}17'\sim107^{\circ}39'$, with the drainage area of 51400 km^2. The geomorphic type is alluvial plain of Yellow River, where the terrain is flat with various ditches. The altitude is 1100~2500. It is arid region of temperate zone with abundant sunshine. The average annual sunshine hours are within 2750～2950 h, the average annual wind speed is within 1.7～2.5 m/s. The temperature varies greatly, with abundant heat and longer frost-free period. The drainage basin belongs to continental climate, drought with less rainfall, with the average rainfall of 180～220 mm. The inter-annual rainfall changes decrease from north to south gradually; the difference of average monthly rainfall in the Yellow River irrigation area is relatively obvious but the annual distribution is non-uniform; the changes of inter-annual rainfall in the central arid area and the south mountainous area are relatively mild, showing seasonal variation. The inter-annual rainfall in the basin is distributed unevenly; the dry and humid seasons are obvious; rainfall of July to September covers 60%～70% of the annual total amount; the evaporation is high, with the annual amount of evaporation of 1100～1600 mm. The types of land use are mainly lawn and farmland, covering respectively 33.74% and 48.76% of the basin area, the woodland covering 3.60%, the water area covering 1.43%, the urban and rural industrial and mining land and the residential land covering 1.46%, and the unused land covering 11.01%.

http://www.aloki.hu ● ISSN 1589 1623 (Print) ● ISSN 1785 0037 (Online)
DOI: http://dx.doi.org/10.15666/aeer/1704_78557863

Model calibration

SWAT (Soil and Water Assessment Tool) model was adopted as hydrological forecast model to simulate the hydrological circulation process in Ningxia section of the Yellow River Basin. This model could be used for short-term, middle-term and long-term hydrological forecast as well as for the evaluation of water resource regime in future climate scenarios. In the modeling process, the testing data of the meteorological and hydrological stations were taken as the input source to calibrate and test the model parameters. The simulation was based on the meteorological and hydrological data of Ningxia section from 1990 to 2012. With relative error R_e, correlation coefficient R^2 and Nash-Suttcliffe coefficient Ens as the standards, the sensitive parameters of the model were calibrated with the actually measured monthly runoff volumes within 2000-2006 and the model was validated with the actually measured monthly runoff volume within 2007-2012. The relative error R_e between the calibration period and the verification period was close to 10%, the correlation coefficient R^2 and Nash-Suttcliffe coefficientEns were larger than 0.86 and 0.85 during the calibration period, with good simulationresults. This suggests that this model is applicable to hydrological simulation of Ningxia section of the Yellow River Basin and could be used for quantitative and qualitative study of the basin under future climate changes. The DEM map of study area see *Fig. 1*.

Figure 1. *DEM Map of Ningxia Section of the Yellow River Basin*

Scene design of the climate changes

There are various reasons for climate changes, of which natural climate change caused by human activities affecting directly or indirectly global atmosphere is the key one. Climate change is naturally to cause the change of water circulation, redistribution of water resources in time and space as well as the change of quantity of water resource, which could in turn affect the development of ecological environment and the social economy. Global climate warming could cause rise of the seal level, gradual drop of groundwater level, melting of glacier and frequent occurrence of extreme climates. In

http://www.aloki.hu ● ISSN 1589 1623 (Print) ● ISSN 1785 0037 (Online)
DOI: http://dx.doi.org/10.15666/aeer/1704_78557863

terms of hydrological circulation, climate change could change redistribution of water resources in time and space and could cause the changes of rainfall and evaporation, which could in turn affect the water balance of the overall basin. Rise of the temperature could accelerate the melting of glacier snow. Certainly, it could also affect other hydrological factors and then affect the runoff volumes of rivers as well as the hydrological process of the overall basin. Rainfall is the major influencing factor of water resource in the basin as well as the major water resource of the basin, that is, rainfall is the basis of the formation of runoff. Changes of rainfall plays significant roles in water resources quantity. It could influence directly water resources quantity of the basin and then the hydrological process of the basin.

Generally, there are two design methods of climate scenes: (1) Arbitrary scene setting: Based on the actual conditions of the study area, taking advantage of the interlocking combination of the supposed rainfall changes and the temperature rising scene, study the influences of climate changes on water resources with appropriate hydrological model. (2) Atmospheric circulation pattern (GCMs) method: This model forecasts the climate changes in the future based on the influences of different CO_2 emissions on climate changes (Feng et al., 2016), and analyzes influences of climate changes on water resources by coupling with hydrological model. However, because the grid interval of the GCMs model data is larger, the spatial resolution is low and the confidence degree is not high when it is used to analyze the influences of climate changes on water resources. So, this essay adopts arbitrary scene setting to establish the scene of climate change in the study area.

Entering the 1980s, the major problems concerned by the human society in the world is no other than global climate changes. There are sufficient evidences to show that with the increase of CO_2 and other greenhouse gases, the global climate is having sharp changes that have never had in history. It was pointed out in the fourth evaluation report of the first working group of Intergovernmental Panel on Climate Change (IPCC) that in the past 100 years from 1906 to 2005, the global climate became warm obviously and it was shown by the statistic results the surface temperature on the earth rose 0.74ºC. Especially, in the recent 50 years, the rising rate of the temperature was higher than the former 50 years, during which the temperature rose 0.65ºC; while 11 of the latest 12 years ranked in the 12 warmest years since 1850 (IPCC, 2013). In the past 100 years, the temperature in China rose 0.4～0.5ºC, slightly lower than the average of the world but in line with the general trend of climate changes. In the latest 50 years, the average temperature in summer in China has no obvious changes, but that in winter increased obviously, increasing 0.42ºC every 10 years. Since 1985, China has had continuously 16 nationwide warm winter, among which the winter in 1998 was the warmest, 1.4ºC warmer. Scientists have made prediction of the global climate in the future 100 years based on population growth, the environmental condition, globalization, economic development and technological progress, the result of which suggested that by the end of the 21st century, the average global temperature would increase 1.1～6.4ºC, the rainfall would transmit seasonally from south to north, among which the arid and semiarid areas would become drier with varying changing tendencies in different areas. Chinese scientist used different global climate patterns and regional climate patterns in China to study the climate changing scenes of China after CO_2 is increased. Supposing atmospheric CO_2 keeping increasing, it is expected the temperature would rise1.68ºC by 2020～2030; 2.22ºC by 2050; it is predicted the temperature could reach 2.94ºC in case the concentration of CO_2 doubles and the warming amplitude in the north is higher than

http://www.aloki.hu ● ISSN 1589 1623 (Print) ● ISSN 1785 0037 (Online)
DOI: http://dx.doi.org/10.15666/aeer/1704_78557863

the south. Temperature in Northwest China could rise, 1.9～2.3ºC, rise 1.6～2.0ºC in southwest and in Tibetan Plateau rise 2.2～2.6ºC. Rainfall shows rising tendency in many areas, with the south-eastern coast the largest, where the annual rainfall could increase 6.4%～11% (Jiang et al., 2008).

Based on the above predictions of the global and Chinese climate changes, 15 different climate scenes are set in this essay to reflect the influences of climate changes on runoff. The established climate changes in the future are: Change of the temperature on the original bases are 0ºC, +1ºC and +2ºC, while the changes of the rainfall are respectively -20%, -10%, 0%, 10% and 20% of the original. Specific combinations see *Table 1*.

Table 1. *15 different climate scene settings*

		Rainfall changes				
		P×(1-20%)	P×(1-10%)	P	P×(1+10%)	P×(1+20%)
Temperature changes	T	A11	A12	A13	A14	A15
	T+1℃	A21	A22	A23	A24	A25
	T+2℃	A31	A32	A33	A34	A35

Results and discussion

The actually measured temperatures and rainfall amounts are increased and decreased accordingly based on the above 15 scenes to generate the meteorological data corresponding to 15 climate scenes. Based on SWAT model established in Model calibration Section, the changed meteorological data are input in SWAT model to simulate the average monthly runoff volumes of tributary station and the simulation results of different scenes are as shown in *Table 2*.

Table 2. *Runoff simulation of 15 different climate scenes*

			Rainfall changes				
			P×(1-20%)	P×(1-10%)	P	P×(1+10%)	P×(1+20%)
Temperature changes	Average yearly runoff （ten thousand m^3）	T	7568.3	8567.1	9683.2	10987.5	12334.9
		T+1℃	7002.4	8011.7	9234.9	10468.8	11975.3
		T+2℃	6253.6	7498.8	8806.7	10023.4	11334.4
	Variation amount （ten thousand m^3）	T	-2114.7	-1115.9	0.2	1304.5	2651.9
		T+1℃	-2680.6	-1671.3	-448.1	785.8	2292.3
		T+2℃	-3429.4	-2184.2	-876.3	340.4	1651.4
	Changing rate （%）	T	-21.8%	-11.5%	0.0%	13.5%	27.4%
		T+1℃	-27.7%	-17.3%	-4.6%	8.1%	23.7%
		T+2℃	-35.4%	-22.6%	-9.0%	3.5%	17.1%

It could be seen from *Table 2* that the runoff in Ningxia section of Yellow River Basin changes with the temperature and the rainfall in the following rules:

(1) The runoff volume in the basin is in negative correlation with the temperature and in positive correlation with the rainfall. With the temperature unchanged and the rainfall increasing 10%, the runoff increases 1304.5 ten thousand m^3, increasing 13.5%; with the temperature unchanged and the rainfall increasing 20%, the runoff increases 2651.9 ten thousand m^3, increasing 27.4%, with the rainfall unchanged but the temperature increasing 1ºC, the runoff decreases 448.1 ten thousand m^3, decreasing 4.6%; with the

http://www.aloki.hu ● ISSN 1589 1623 (Print) ● ISSN 1785 0037 (Online)
DOI: http://dx.doi.org/10.15666/aeer/1704_78557863

rainfall unchanged by the temperature increasing 2ºC, the runoff decreasing 876.3 ten thousand m^3, decreasing 9.0%. It could be seen thus rise of temperature could cause decrease of the runoff, the reason for which is rise of temperature could make the amount of evaporation greater; while increase of rainfall could make the runoff increase and the reason is that increase of rainfall could make the surface runoff yield increase.

(2) Rainfall changes in the basin have greater influences on the runoff than temperature. With the rainfall unchanged but the temperature increasing 2ºC, the runoff decreases 876.3 ten thousand m^3, decreasing 9.0%, which is in small scale; with the temperature unchanged by the rainfall increasing 20%, the runoff increases 2651.9 ten thousand m^3, increasing 27.4%, which is in large scale.

Runoff simulation under the condition with the rainfall unchanged but the temperature changed is as shown in *Fig. 2* and the runoff simulation under the condition with the temperature unchanged but the rainfall changed is as shown in *Fig. 3*.

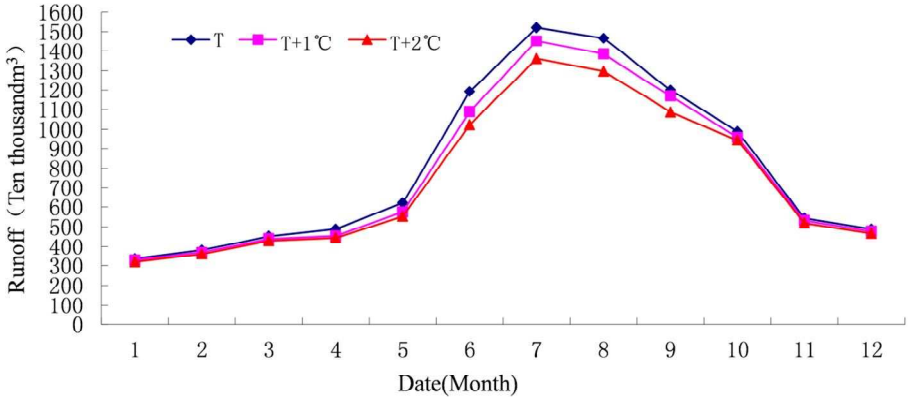

Figure 2. *Comparison between runoff volumes in climate scenes with the rainfall unchanged but the temperature changed*

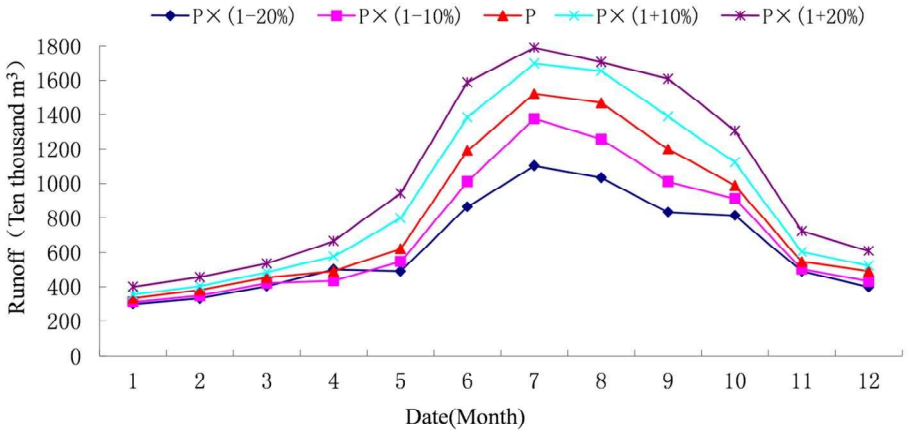

Figure 3. *Comparison between runoff volumes in climate scenes with the temperature*

It could be seen from *Fig. 2* with the rainfall unchanged, the runoff volumes show decreasing tendency. When the temperature rises, the evaporation amount would also increase so that the runoff decreases. It could be seen from *Fig. 3* with the temperature unchanged, the monthly runoff volumes and the rainfall changes have the same

http://www.aloki.hu ● ISSN 1589 1623 (Print) ● ISSN 1785 0037 (Online)
DOI: http://dx.doi.org/10.15666/aeer/1704_78557863

tendency, which begins to increase in spring and increases the most in summer; however, it decreases gradually in autumn but with the smallest increase in winter.

Conclusion

Distributed hydrological model SWAT coupled with GIS is used in this study to simulate the yearly and monthly runoff volumes under 15 different climate changes, with the aim to explore the influences of climate changes to runoff. The results show that the runoff volume in the basin has negative correlation with the temperature but in positive correlation with the rainfall, and that the changes of temperature has greater influences on the changes of rainfall but has little influences on the runoff. Its prediction of climate warming in the future has high credibility but the prediction of rainfall increase in the future is of certain degree of uncertainty; however, the influence of rainfall on runoff volume is more significant than that of temperature. Generally, it could provide some scientific basis for management and utilization of river basin water resources.

Acknowledgements. The study was completed with the support of the First-class Major Foundation of Ningxia Institutions of High Education in China. (NXYLXK2017A03).

REFERENCES

[1] Aamery, N. A., Fox, J. F., Snyder, M. (2016): Evaluation of climate modeling factors impacting the variance of streamflow. – J. Hydrol. 542: 125-142.
[2] Bao, Z. X., Zhang, J. Y., Wang, G. Q., Fu, G. B., He, R. M., Yan, X. L., Jin, J. L., Liu, Y. L., Zhang, A. J. (2012): Attribution for decreasing stream flow of the Haihe River basin, northern China: climate variability or human activities? – J. Hydrol. 460-461: 117-129.
[3] Chien, H. C., Yeh, P. J. F., Knouft, J. H. (2013): Modeling the potential impacts of climate change on streamflow in agricultural watersheds of the Midwestern United States. – J. Hydrol. 491: 73-88.
[4] Coles, A. E., Conkey, B. G. M., McDonnell, J. J. (2017): Climate change impacts on hillslope runoff on the northern Great Plains,1962-2013. – Journal of Hydrology 550: 538-548.
[5] Eisner, S., Flörke, M., Chamorro, A., Daggupati, P., Donnelly, C., Huang, J., Hundecha, Y., Koch, H., Kalugin, A., Krylenko, I., Mishra, V. (2017): An ensemble analysis of climate change impacts on stream flow seasonality across 11 large river basins. – Clim. Change 141(3): 1-17.
[6] Feng, X. M., Cheng, W., Fu, B. J., Lu, Y. H. (2016): The role of climatic and anthropogenic stresses on long-term runoff reduction from the Loess Plateau, China. – Sci. Total Environ. 571: 688-698.
[7] Huntington, T. G. (2006): Evidence for intensification of the global water cycle: review and synthesis. – J. Hydrol. 319(1-4): 83-95.
[8] IPCC. (2013): Working group i contribution to the IPCC fifth assessment report, climate change: the physical science basis: summary forpolicymakers[R/OL]. – http://www. climatechange2013. org /images /uploads /WGIAR5SPM_Approved27Sep2013. Pdf, 2013-10-28.
[9] IPCC: IPCC Fourth Assessment Report (AR4). – http: //ipcc-wg1. ucar. edu/wg1 /wg1-report. Htm, l 200.

http://www.aloki.hu ● ISSN 1589 1623 (Print) ● ISSN 1785 0037 (Online)
DOI: http://dx.doi.org/10.15666/aeer/1704_78557863

[10] Jiang, Z. H., Zhang, X., Wang, J. (2008): IPCC-AR4 Estimation of China's 21st Century Climate Change by IPCC-AR4 Model. – Geographic research 27(4): 787-799.
[11] Kuang, W., Liu, J., Dong, J., Chi, W., Zhang, C. (2016): The rapid and massive urban and industrial land expansions in China between 1990 and 2010: a CLUD-based analysis of their trajectories, patterns, and drivers. Landsc. – Urban Plan. 145: 21-33.
[12] Li, F., Zhang, Y., Xu, Z., Teng, J., Liu, C., Liu, W., Mpelasoka, F. (2013): The impact of climate change on runoff in the southeastern Tibetan Plateau. – Journal of Hydrology 505: 188-201.
[13] Lindner, M., Maroschek, M., Netherer, S., Kremer, A., Barbati, A., Garcia-Gonzalo, J., Seidl, R., Delzon, S., Corona, P., Kolstrom, M., Lexer, M. J., Marchetti, M. (2010): Climate change impacts, adaptive capacity, and vulnerability of European forest ecosystems. – For. Ecol. Manag. 259(4): 698-709.
[14] Milliman, J. D., Farnsworth, K. L., Jones, P. D., Xu, K. H., Smith, L. C. (2008): Climatic and anthropogenic factors affecting river discharge to the global ocean, 1951–2000. – Glob. Planet. Chang. 62(3-4): 187-194.
[15] Rahman, K., da Silva, A. G., Tejeda, E. M., Gobiet, A., Beniston, M., Lehmann, A. (2015): An independent and combined effect analysis of land use and climate change in the upper Rhone River watershed, Switzerland. – Applied Geography 63: 264-272.
[16] Ringius, L., Downing, T. E., Hulme, M. (1996): Climate change in Africa: Issue and challenges in Agriculture and water for Sustainable envelopment. – CICERO Report[R]. University of Oslo, Norway, 151.
[17] Teklesadik, A. D., Alemayehu, T., van Griensven, A., Kumar, R., Liersch, S., Eisner, S., Tecklenburg, J., Ewunte, S., Wang, X. (2017): Inter-model comparison of hydrological impacts of climate change on the Upper Blue Nile basin using ensemble of hydrological models and global climate models. – Clim. Change 1-16.
[18] Walling, D. E., Fang, D. (2003): Recent trends in the suspended sediment loads of the world's rivers. – Glob. Planet. Chang. 39(1-2): 111-126.
[19] Wang, J. H., Hong, Y., Gourley, J., Adhikari, P., Li, L., Su, F. G. (2010): Quantitative assessment of climate change and human impacts on long-term hydrologic response: a case study in a sub-basin of the Yellow River, China. – Int. J. Climatol. 30(14): 2130-2137.
[20] Wu, H.-T. J., Lau, W. K. M. (2016): Detecting climate signals in precipitation extremes from TRMM (1998-2013)-increasing contrast between wet and dry extremes during the "global warming hiatus". – Geophys. Res. Lett. 43(3): 1340-1348.
[21] Xu, K. H., Milliman, J. D., Xu, H. (2010): Temporal trend of precipitation and runoff in major Chinese Rivers since 1951. – Glob. Planet. Chang. 73(3-4): 219-232.
[22] Yang, W., Long, D., Bai, P. (2019): Impacts of future land cover and climate changes on runoff in the mostly afforested river basin in North China. – Journal of Hydrology 570: 201-219.
[23] Zhai, R., Tao, F. (2017): Contributions of climate change and human activities to runoff change in seven typical catchments across China. – Science of the Total Environment (605-606): 219-229.
[24] Zhang, Y. Q., You, Q. L., Lin, H. B., Chen, C. C. (2015): Analysis of dry/wet conditions in the Gan River Basin, China, and their association with large-scale atmospheric circulation. – Glob. Planet. Chang. 133: 309-317.
[25] Zhang, L., Karthikeyan, R., Bai, Z. K., Srinivasan, R. (2017): Analysis of stream flow responses to climate variability and land use change in the Loess Plateau region of China. – CATENA 154: 1-11.
[26] Zhao, Y., Zou, X., Gao, J., Xu, X., Wang, C., Tang, D., Wang, T., Wu, X. (2015): Quantifying the anthropogenic and climatic contributions to changes in water discharge and sediment load into the sea: a case study of the Yangtze River, China. – Sci. Total Environ. 536: 803-812.

http://www.aloki.hu ● ISSN 1589 1623 (Print) ● ISSN 1785 0037 (Online)
DOI: http://dx.doi.org/10.15666/aeer/1704_78557863

AMELIORATION OF ALKALIZED SOLONCHAK SOILS BY SUBSURFACE GRAVEL BLIND DITCHES AND DESULFURIZED GYPSUM

WANG, X.[1,2] – SUN, Z. J.[2,3,4,5*] – LIU, X. J.[1] – BAO, Z. Y.[1] – JIAO, B. Z.[2] – LI, X. Q.[2] – ZENG, Y. X.[2] – SAMEH, E.[6]

[1]*The Scientific Research Institute of the Water Conservancy of Ningxia, Yinchuan 750021, Ningxia, China*

[2]*School of Civil Engineering and Hydraulic Engineering, Ningxia University, Yinchuan 750021, Ningxia, China*

[3]*School of Resources and Environmental Science, Ningxia University, Yinchuan 750021, Ningxia, China*

[4]*Ningxia Key Laboratory of Resources Assessment and Environmental Regulation in Arid Regions, Yinchuan 750021, Ningxia, China*

[5]*China-Arab Joint International Research Laboratory for Featured Resources and Environmental Governance in Arid Region, Yinchuan 750021, Ningxia, China*

[6]*Vegetable Research Department, Agricultural and Biological Division, National Research Centre, Dokki, Giza 12311, Egypt*

**Corresponding author*
e-mail: sunzhaojunyx@126.com

(Received 23rd Feb 2019; accepted 3rd May 2019)

Abstract. This study aims to investigate the subsurface gravel ditches and desulfurization gypsum (DG) as amelioration methods for alkalized solonchak soils in Gansu Jingyuan of China (37°02' N, 104°96' E). Three blind ditch spacing (6, 9 and 12 m) and three application rates of desulfurization gypsum (20, 22 and 24 t/hm^2) were used to alkalized solonchak soil and increasing the yield of Chinese wolfberry (*Lycium bararum* L.*)*, as compared with the control treatments without blind ditch and DG. The findings show that a larger blind ditch density and appropriate DG application rate contributes to discharge salts easily by reducing the migration distance for soil solutes moving. Under the treatment with blind ditches with 6-metre spacing and a 22 t/hm^2 DG application rate, the values of pH, exchangeable sodium percentage (ESP) and electrical conductivity (EC) of the soil layer up to 40 cm from the surface were decreased by 11.0%, 38.1% and 34.5%, respectively, than those of the control which had no blind ditch and DG treatment in the first year. The yield of Chinese wolfberry was increased by 228.8% than that of the control in the second year.
Keywords: *alkalinity, irrigation, leaching, soil salinity, alkalized solonchak*

Introduction

Saline-sodic soils cover an extensive land surface around the world (Qadir and Oster, 2004). One particular form of these soils is alkalized solonchak which is characterized by an excessively high concentration of sodium with high pH on the surface (Feng et al., 2017). According to a study (Kameli, 2017), the alkalized solonchak mainly distributes in Liaoning, Gansu and Xinjiang province of China.

Solonetz is also found in other regions such as central Asia and central Australia as well as patches in other continents (Driessen et al., 2000). The area of alkalized solonchak in

http://www.aloki.hu ● ISSN 1589 1623 (Print) ● ISSN 1785 0037 (Online)
DOI: http://dx.doi.org/10.15666/aeer/1704_78657879

Gansu is approximately 21.18×10^4 hm^2 (Lin et al., 2016). The amelioration of saline-sodic requires a complex and long-term practice (Zhang et al., 2012a). The particles of this type of soils are dispersed and swelled after irrigation, causing the pores to close (Chi and Wang, 2014), which makes it difficult to be rapidly leached. Soluble salts accumulated in the soil surface cause changes in soil physical and chemical properties (Vance, 2008), which directly affect its ability for providing water, air and nutrients to plants (Heng et al., 2018) which is one of the main factors restricting the local agricultural production and ecological improvement.

The key to the amelioration of alkali soils is improving soil physical and chemical properties, providing a suitable soil environment for crops (De et al., 2014; Sakai et al., 2011). Presently, there are published reports on the amelioration of alkali soils with measures including planting saline-alkali tolerant crops (Mohsenian and Roosta, 2015), soil improvement by applying desulfurization gypsum (DG) (Mao et al., 2016), drip irrigation (Chen et al., 2015) and straw mulching etc (Xue et al., 2014). However due to a lower permeability of the alkalized solonchak soil, the leached salts from the upper layer may accumulate in the deeper layer resulting in secondary salinization occasionally, and in some cases the long improvement time and high cost make any single amelioration technique impractical and difficult to be extended.

The key ingredient in DG is $CaSO_4$ (Sakai et al., 2004), which increases Ca^{2+} concentration in the soil once it is applied. As the Ca^{2+} capacity of adsorption to soil colloids is stronger than that of Na^+ and the adsorbed Na^+ on soil colloids can exchange with Ca^{2+} in the soil solution, the increase in the Na^+ concentration in the soil solution results in an increase in alkalinity which damages soil aggregates. For this reason any improvement in soil aggregates and texture can effectively improve soil physical and chemical properties (Yu et al., 2015; Rhoton and McChesney, 2011).

Other experiments for the amelioration of saline-sodic show that the application of DG can decrease the soil pH and exchangeable sodium percentage (ESP) remarkably, but there is a problem associated with salt deposition within 60 cm of the soil layer (Lin et al., 2016). Due to the lower permeability of alkalized solonchak, the salts leached from the surface do not effectively discharge out of the soil, and instead they move to the land surface during evaporation. To facilitate salt leaching, mechanical means are effective which include the underground drainage facility to accelerate soil water movement and promote leaching of salts (Min, 2014; Christen and Skehan, 2001). The blind ditch is one form of underground drainage facilities which has advantages with a long lifespan and the benefit to farming operations without blocking the land surface (Pan and Zhao, 1998).

The blind ditches, backfilled with materials including straw and gravels etc., can accelerate infiltration of water and discharge saline water (Tao et al., 2016). It also allows soil water to dissolve salts sufficiently and drain it out of the soil through the blind ditches to reduce soil salinity/alkalinity which is an advantage over the traditional treatments that cannot discharge salts from the soil (Yu et al., 2012). The published research findings (Yang et al., 2015b) suggest that the blind ditch treatment on low-lying saline land with a clay layer can improve the soil permeability, increase the internal drainage ability and accelerate the salt mobility in the soil, resulting in a better leaching of ions such as Na^+, SO_4^{2-}, and Cl^- in the soil. Chinese wolfberry (*Lycium barbarum*) belongs to deciduous shrub with a high degree of economic value and medicinal value. It is mainly distributed in arid and semi-arid regions of northwest China. It has the characteristics of salt and drought tolerance and is very suitable to plant in saline-alkali soils (Liu et al., 2015).

http://www.aloki.hu ● ISSN 1589 1623 (Print) ● ISSN 1785 0037 (Online)
DOI: http://dx.doi.org/10.15666/aeer/1704_78657879

At present, the blind ditch is used in Ningxia (Pan and Zhao, 1998) and on coastal saline soils in Jiangsu in China (Yang et al., 2015b). There are extensive reports on the amelioration of alkali soils through the application of DG (Sakai et al., 2011; Yu et al., 2015), but there are few published reports about the effects of blind ditches combined with DG on the physical and chemical properties of alkalized solonchak and ions. Research on the amelioration effects of alkalized solonchak on the spacing of blind ditches and the application rate of DG is still needed to apply this method more efficiently and cost effectively. The present study examines the application of DG and blind ditches on a farmland using gravels and straw as backfilling materials to investigate the effects on subsurface physical and chemical properties of alkalized solonchak in Gansu, China. The concentrations of salt ions and the yield of Chinese wolfberry under different treatments are examined. The outcomes of this study can provide a theoretical and technical guidance for the amelioration and utilization of alkalized solonchak in China.

Materials and methods

Site characterization

The experimental site is located in Dongsheng, Jingyuan county, Gansu Province (37°03'N, 104°96'E), China. The climate is typically arid continental with mean annual precipitations of 240 mm, which is mainly concentrated between July and September, and mean annual evaporation of 1,634 mm, up to 6-7 times the annual average precipitations. Annual average temperature is 9 °C. Seasonal drought is frequent in spring, the soluble salts accumulate in the upper soil profile during spring. The groundwater level changes from 1.3 to 1.8 m. The soil organic matter ranges from 5.12 to 8.97 g/kg, available nitrogen from 17.52 to 29.25 mg/kg, available P from 0.7 to 5.98 mg/kg, available K from 179.64 to 244.58 mg/kg. Other physical and chemical properties of the soil are listed in *Table 1*. Data in *Table 1* show that EC in the surface soil gradually decreases with the soil depth. ESP is over 21% and pH is above 8.5. The primary cation in the top 100 cm of the soil is Na^+ ion, whereas the primary anion is Cl^- ion.

Table 1. *Main physical and chemical properties of tested soils*

Depth cm	Ion ingredients cmol/kg								pH	EC dS/m	ESP %	Bulk density g·cm^{-3}
	Na^+	Ca^{2+}	K^+	Mg^{2+}	CO_3^{2-}	HCO_3^-	Cl^-	SO_4^{2-}				
0-20	4.21	0.27	0.08	0.23	1.19	1.01	1.42	1.25	9.1	2.89	28.5	1.52
20-40	3.44	0.33	0.09	0.20	1.02	0.84	1.19	1.02	8.8	2.72	24.8	1.57
40-60	2.78	0.31	0.07	0.31	0.88	0.72	0.65	0.84	8.6	1.83	22.5	1.62
60-80	2.22	0.28	0.08	0.25	0.67	0.54	0.54	0.72	8.5	1.32	21.1	1.68
80-100	1.15	0.24	0.06	0.22	0.52	0.32	0.31	0.68	8.5	1.02	21.9	1.67

Soil pH was measured using a Mettler Toledo S220-K pH meter. Soil EC value was measured using a Mettler Toledo S230. Exchangeable Na^+ was measured using an ammonium acetate-ammonium hydroxide-flam photometric method, and ESP was calculated as the percentage of exchangeable Na^+ and cation exchange capacity (CEC). The concentrations of K^+ and Na^+ were measured with a subtraction method. Ca^{2+} and Mg^{2+} were measured using the Ethylene Diamine Tetraacetic Acid (EDTA) titration

http://www.aloki.hu ● ISSN 1589 1623 (Print) ● ISSN 1785 0037 (Online)
DOI: http://dx.doi.org/10.15666/aeer/1704_78657879

method. Cl^- was measured using $AgNO_3$ titration. SO_4^{2-} was measured using the EDTA back-dropping method, and CO_2^{-3} and HCO^{-3} were measured using double indicator titration (Bigham, 1965). The application process is shown in *Figure 1*.

Figure 1. *Blind ditch and laying cushion*

Experimental design

The research was carried out between 2016 and 2017 with a unified leaching quota of 4.5×10^3 m^3/hm^2 (Yang et al., 2015a). According to previous reports (Yang et al., 2015b) and known characteristics of alkalized solonchak, three blind ditches were set up at spacing of 6 m, 9 m and 12 m, respectively. In this study, the spacing is the horizontal distance between two blind ditches. Three application rates were used at 20 t/hm^2, 22 t/hm^2 and 24 t/hm^2. A site without the blind ditch and DG was as the control site (CK), each treatment was repeated 3 times. The experimental design is shown in *Table 2*.

Table 2. *Experimental design*

Treatments	Blind ditch spacing m	Desulfurized gypsum application rate t/hm^2
CK	Non	Non
T1	6	20
T2	6	22
T3	6	24
T4	9	20
T5	9	22
T6	9	24
T7	12	20
T8	12	22
T9	12	24

CK means the control treatment

Ditches were dug with a ditching machine (Chain, CASE860) with a width of 30 cm and depth of 90 to 120 cm which have a slope gradient of 1% from the field to the drain. Gravels were laid at the bottom of each ditch with 20 cm, and then covered with 40 cm of straw as a filter, and finally backfilled with soils. The blind ditches were dug perpendicular to the drain

http://www.aloki.hu ● ISSN 1589 1623 (Print) ● ISSN 1785 0037 (Online)
DOI: http://dx.doi.org/10.15666/aeer/1704_78657879

which was deeper than the ditch. Sheep manure was applied at a rate of 45 t/hm^2 uniformly at each site. According to the experimental design DG was applied between different treatments. Deep tillage was then performed to guarantee sufficient mixing. According to the previous studies (Yang et al., 2015a), the salts in the soil should to leach in total 3 times, the volume of leached water after the first operation was 1/2 of the leaching quota (ca. 2,250 m^3/hm^2) and the leached water was immersion for 24 h and then drained off the land surface. The volume of leached water after the second operation was 1/3 of the leaching quota (ca. 1,500 × 10^3 m^3/hm^2) and the leached water was immersion for 48 h and then drained off the land surface. Finally, the volume of leached water after the third operation was 1/6 of the leaching quota (750 m^3/hm^2). Chinese wolfberry seedlings were planted on 26 April 2016 with row spacing of 2.0 m and plant spacing of 1.5 m. The planted sites were irrigated once, respectively, during the May to November with 1.2 × 10^3 m^3/hm^2 (irrigation quota) water at every month.

Experimental methods

In order to analyze the amelioration effects, the soil samples were collected before the ditches were dug on 5 April 2016 and on 25 April 2016 in the first year, and on 25 April 2017 in the second year. Based on the principle of randomness and multipoint mixture, soil samples were collected using an auger by a random method in layers with spacing of 20 cm from the land surface. Samples were collected at 0 to 20 cm, 20 to 40 cm, 40 to 60 cm, 60 to 80 cm, and 80 to 100 cm in each treatment in triplicates. After the removing of gravel and crop residues, all soil samples were air-dried and passed through a 1 mm sieve.

The soil permeability was measured using a permeability cylinder, and the measured permeability is its value at a temperature 10 °C, expressed as K_{10} (mm/min) (Tian et al., 2013):

$$K_{10} = K_t / (0.7 + 0.03t) \quad \text{(Eq.1)}$$

where K_{10} (mm/min) is the permeability at 10 °C, K_t (mm/min) is the permeability at t, and t (°C) is the temperature of infiltrating water at the time of measurement.

On 30 May 2016, the survival rate of Chinese wolfberry seedlings was calculated, while the preservation rate was calculated on 2 May 2017. When the fruits of Chinese wolfberry were mature, the fruits were picked once every seven days. The fruits were collected in each plot and dried in a 45 °C oven, and the yield of Chinese wolfberry in every plot can be measured. The survival rate and preservation rate were calculated as follows:

$$\text{Survival rate} = \frac{\text{Actual alive number in the first year}}{\text{Seedling number}} 100\% \quad \text{(Eq.2)}$$

$$\text{Preservation rate} = \frac{\text{Actual alive number in the second year}}{\text{Seedling number}} 100\% \quad \text{(Eq.3)}$$

Data processing

Using an analytical approach of membership functions in fuzzy mathematics (Zhang, 2014), the membership values of various physical and chemical indexes were accumulated for different treatments and the average value was calculated. The values

http://www.aloki.hu ● ISSN 1589 1623 (Print) ● ISSN 1785 0037 (Online)
DOI: http://dx.doi.org/10.15666/aeer/1704_78657879

were then compared between different treatments to evaluate the improvement effects on alkalized solonchak.

The membership function X(u) of each index is determined using the following formula:

$$X(u)=\begin{cases}\dfrac{X-X_{\min}}{X_{\max}-X_{\min}} & \text{Positive correlation between index and improvement effect}\\ 1-\dfrac{X-X_{\min}}{X_{\max}-X_{\min}} & \text{Negative correlation between index and improvement effect}\end{cases} \quad \text{(Eq.4)}$$

where X(u) is the value of the membership function of an index for different treatments, X is the measured value of an index for different treatments, X_{max} is the maximum measured value of an index between all treatments, and X_{min} is the minimum measured value of an index between all treatments.

All the statistical tests were performed using SPSS software (version 19.0, USA).

Results

Soil permeability

The effect of different treatments on the permeability of soil from 0 to 40 cm is shown in *Figure 2*. It can be seen from *Figure 2* that the control site had a lower permeability compared to the other experimental sites, where its K_{10} was only 0.25 ± 0.02 mm/min in the first year. Each treatment significantly increased the soil permeability measured in terms of K_{10} values compared to the control site. The increase in treatment T2 by 308.0% (K_{10} = 1.02 ± 0.01 mm/min) is the largest while T7 increased the least (K_{10} = 0.55 ± 0.02 mm/min) in the first year. The permeability of the soil following the treatments in the second year was better in all treatments than the first year.

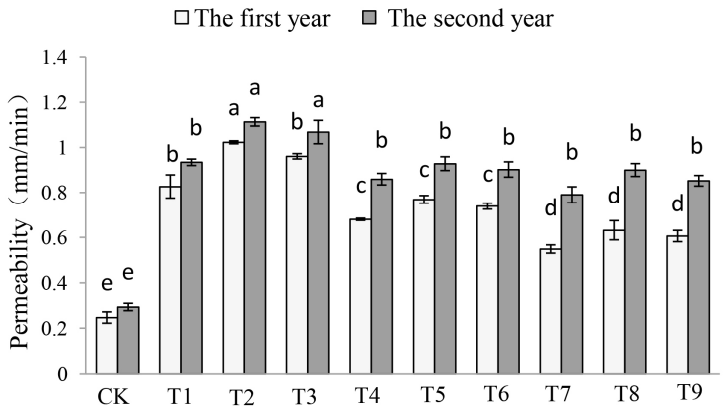

Figure 2. *Effect of different treatments on permeability of the soil from 0–40 cm, in which different letters indicate significant differences among treatments (P ≤ 0.05) and values = mean ± standard error, n = 3*

Regarding the blind ditch spacing, it is clearly to notice in *Figure 2* that, a 6-m blind ditch spacing treatments (T1, T2 and T3) have the highest values of soil permeability

http://www.aloki.hu ● ISSN 1589 1623 (Print) ● ISSN 1785 0037 (Online)
DOI: http://dx.doi.org/10.15666/aeer/1704_78657879

and followed by a 9-m spacing treatments (T4, T5 and T6), which have also superiority on a 12-m spacing treatments (T7, T8 and T9).

Respecting to the DG application rate, *Figure 2* shows that the DG application with a 22 t/hm^2 (T2, T5 and T8) gives rise to the highest soil permeability as compared with the other treatments (20 t/hm^2 and 24 t/hm^2 DG application rate). In addition, T2 in the second year shows the highest improvement in soil permeability (K_{10} = 1.11 ± 0.02 mm/min).

Soil pH

The effect of each treatment on pH of the soil from 0 to 40 cm is shown in *Figure 3*.

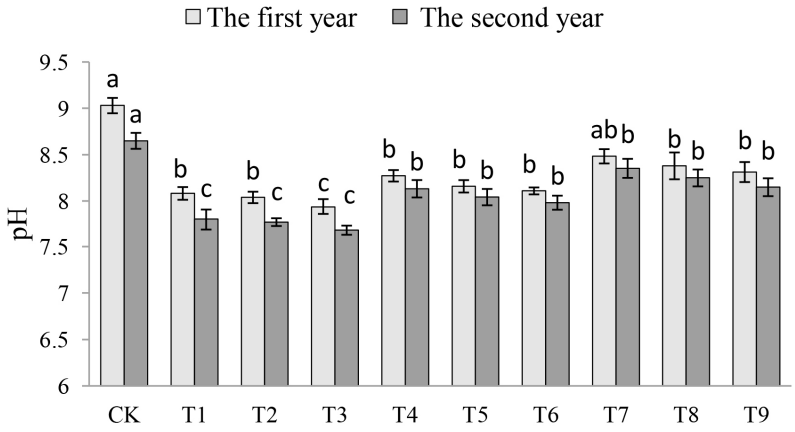

Figure 3. *Effects of different treatments on the pH of soil from 0–40 cm, in which different letters indicate significant differences among treatments (P ≤ 0.05) and values = mean ± standard error, n = 3*

Figure 3 illustrates that pH values of other treatment are lower than that of the control site except T7, and pH of T3 decreased by 12.1% compared to the control site in the first year. T3 in the second year has the minimum pH (7.7 ± 0.05). The pH of treatments with blind ditch spacing of 6-m, 9-m and 12-m in the first year on average decreased by 9.9%, 8.1% and 5.7%, respectively, compared to those before the treatments. In the second year, the pH of treatments with blind ditch spacing of 6-m, 9-m and 12-m on average decreased by 13.0%, 9.5% and 7.3%, respectively, compared to those before the treatments. It clear that the blind ditch with smaller spacing is more effective to reduce the soil pH compared to the other treatments.

Respecting to the DG application rate, *Figure 3* show that the DG application with a 24 t/hm^2 (T3, T6 and T9) produced the lowest pH compared to other treatments (20 t/hm^2 and 22 t/hm^2 DG application rate).

Exchangeable sodium percentage (ESP)

The effect of each treatment on the ESP of the soil from 0 to 40 cm is illustrated in *Figure 4*. It is seen from *Figure 4* that the ESP of each treatment is lower than that of the control site, and the ESP of T3 has the largest decrease of 51.0% than that before the treatment in the first year.

http://www.aloki.hu ● ISSN 1589 1623 (Print) ● ISSN 1785 0037 (Online)
DOI: http://dx.doi.org/10.15666/aeer/1704_78657879

The ESP of treatments with blind ditch spacing of 6-m, 9-m and 12-m in the first year on average decreased by 47.5%, 40.5% and 37.4%, respectively, compared to those before the treatments. In the second year, the ESP of treatments with blind ditch spacing of 6-m, 9-m and 12-m on average decreased by 52.8%, 45.5% and 41.6%, respectively, compared to those before the treatments. Regarding the blind ditch spacing, it is clearly to notice in *Figure 4* that, a 6-m blind ditch spacing treatments have the lowest values of ESP, compared to 9-m and 12-m spacing treatments.

According to the DG application rate, *Figure 4* shows that the DG application with a 24 t/hm^2 (T3, T6 and T9) produced the lowest ESP compared to other treatments (20 t/hm^2 and 22 t/hm^2 DG application rate). In addition, T3 in the second year had the lowest ESP (11.8 ± 0.09%).

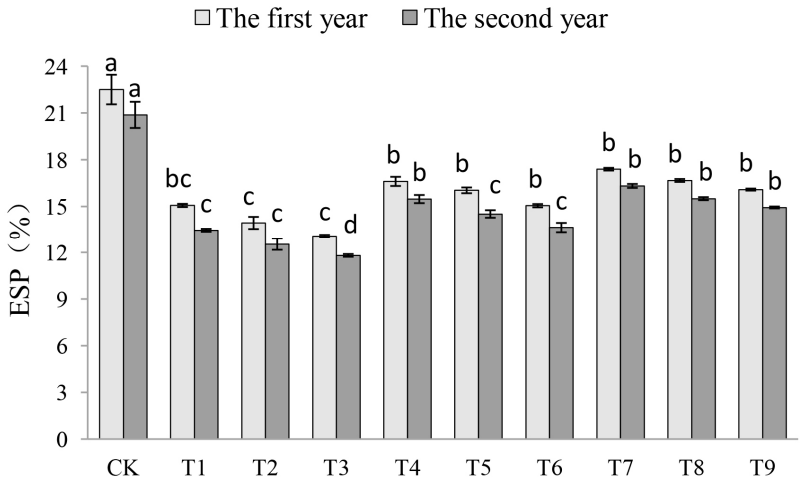

Figure 4. *Effects of different treatments on ESP of soil from 0–40 cm, in which different letters indicate significant differences among treatments (P ≤ 0.05) and values = mean ± standard error, n = 3*

Electrical conductivity (EC)

Before the soil improvement, the EC values of soil layers at 0 to 20 cm, 20 to 40 cm and 40 to 60 cm were 2.89 dS/m, 2.72 dS/m and 1.83 dS/m, respectively. The effect of each treatment on EC values in the soil layer from 0 to 60 cm is illustrated in *Figure 5*. As shown in *Figure 5a,* in the first year salts in the layers at 0 to 60 cm of each treatment were leached and the desalination effect on the land surface was significant. The EC values of the control site at 0 to 60 cm depth gradually increased with the soil depth in the first year. Salt accumulation indicated by an EC reading higher than its original value appeared at the depth of 40 to 60 cm. As to the data in *Figure 5b* for the second year, the EC value was highest at 0 to 20 cm of the control site. Treatments T1 to T9 did not appear to generate any secondary salinization. This is approved that, subsurface gravel blind ditches technique clearly leached the salts from soil layers and desalination effect on the land surface was significant.

In the first year, the EC of T2 at the 0 to 20 cm soil depth declined the most (75.1%) following the improvement. There were no significant differences for T1, T2, T3, T4, T5 and T6 at 0 to 20 cm, 20 to 40 cm and 40 to 60 cm soil depths in the first and second years. In the first year, the EC values of T1, T2, T3, T4, T5, T6, T7, T8 and T9

http://www.aloki.hu ● ISSN 1589 1623 (Print) ● ISSN 1785 0037 (Online)
DOI: http://dx.doi.org/10.15666/aeer/1704_78657879

decreased by 40.1%, 45.4%, 42.3%, 33.7%, 37.4%, 35.4%, 19.5%, 23.9% and 22.0% at 0 to 60 cm, respectively, compared to the control site. In the second year, the EC values of T1, T2, T3, T4, T5, T6, T7, T8 and T9 decreased by 49.4%, 55.2%, 52.2%, 42.5%, 47.7%, 45.1%, 32.5%, 37.2% and 34.9% at 0 to 60 cm, respectively, compared to the control site.

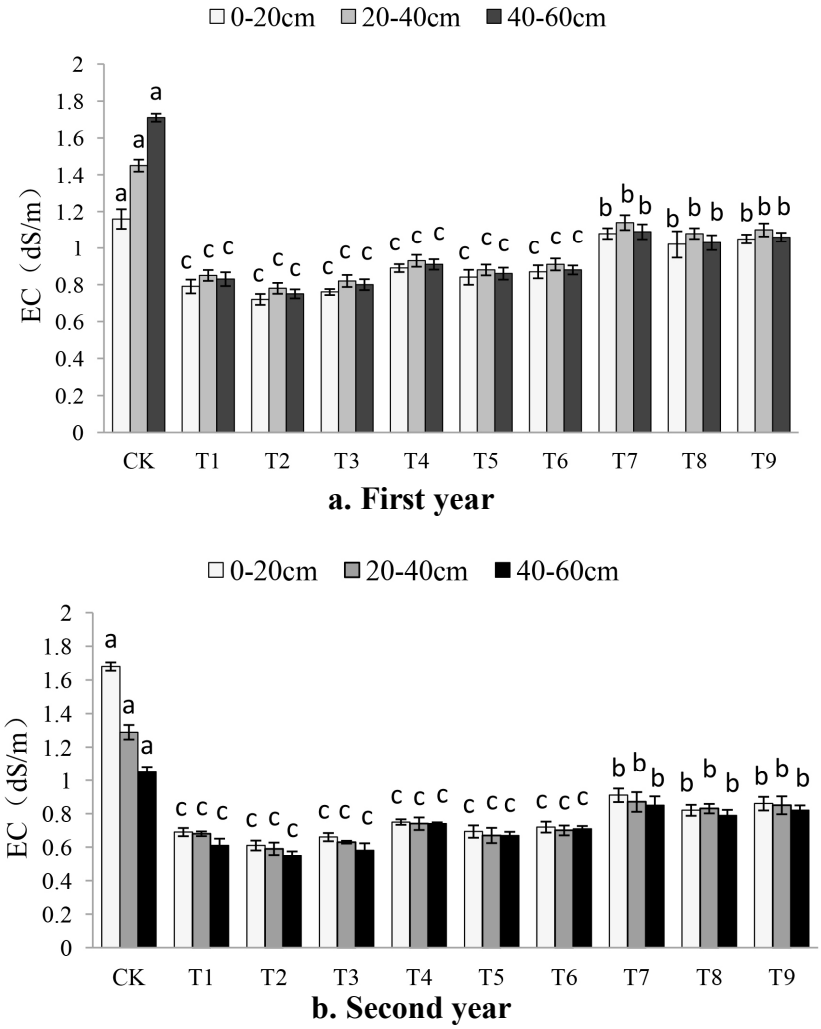

Figure 5. *Effects of different treatments on EC value of soil from 0–60 cm, in which different letters indicate significant differences among treatments ($P \leq 0.05$) and values = mean ± standard error, n = 3*

Soil salt ions

The effect of each treatment on ions is illustrated in *Table 3*. The concentrations of Na^+, Cl^-, CO_3^{2-}, HCO_3^- of the soil significantly declined following the treatment, and Mg^{2+}, K^+ did not change after the treatment while the concentration of SO_4^{2-} increased. The concentration of Ca^{2+} in each treatment was higher than that on the control site. The concentration of Na^+ declined over 60% in the first year following the treatment, and declined over 75% in the second year following the treatment compared to those before the treatments. The concentration of Na^+ in T3 had the largest decrease. CO_3^{2-} and HCO^{-3} of T3 decreased the most in the first year by 49.1% and 51.8%, respectively, compared

http://www.aloki.hu ● ISSN 1589 1623 (Print) ● ISSN 1785 0037 (Online)
DOI: http://dx.doi.org/10.15666/aeer/1704_78657879

to those before the treatments. In the second year, the concentrations of CO_3^{2-} and HCO_3^- of T3 were 0.01 cmol/kg and 0.04 cmol/kg, respectively, and continued decreasing compared with the first year.

In the first year, the concentrations of Cl^- in nine treatments were lower than 0.09 cmol/kg, Cl^- of T3 decreased the most by 95.4% compared to that before the improving treatments. In the second year, the concentrations of Cl^- in nine treatments were lower than 0.07 cmol/kg, and continued the decrease compared with the first year.

In the first year, DG was applied to increase the concentrations of Ca^{2+} and SO_4^{2-}, which had the greatest increase in T9, by 133.3% and 47.4%, respectively, comparing with before improvement. The data illustrated that the concentrations of Ca^{2+} in each treatment was higher than that on the control site, and the concentrations of Ca^{2+} and SO_4^{2-} of T1 were 0.25 cmol/kg and 0.72 cmol/kg, respectively, which were the lowest in the nine treatments in the second year. Compared to the control site, the difference in Mg^{2+} and K^+ concentrations of each treatment were insignificant in both first and second years.

Table 3. *Effect of different treatments on the distribution of salt ions in 0-40 cm soil layer (cmol/kg)*

Year	Treatment	Na^+	Ca^{2+}	Mg^{2+}	K^+	CO_3^{2-}	HCO_3^-	Cl^-	SO_4^{2-}
2016	CK	3.49±0.16^{a}	0.33±0.04^{c}	0.24±0.04^{a}	0.07±0.02^{a}	0.94±0.07^{a}	0.87±0.09^{a}	0.15±0.04^{a}	1.12±0.09^{d}
	T1	1.36±0.12^{b}	0.52±0.05^{b}	0.23±0.04^{a}	0.08±0.01^{a}	0.67±0.04^{b}	0.55±0.06^{b}	0.08±0.01^{b}	1.45±0.08^{c}
	T2	1.19±0.06^{c}	0.59±0.08^{ab}	0.19±0.03^{a}	0.07±0.01^{a}	0.64±0.07^{b}	0.55±0.07^{b}	0.07±0.01^{b}	1.51±0.05^{b}
	T3	1.01±0.12^{e}	0.64±0.07^{a}	0.18±0.02^{a}	0.08±0.00^{a}	0.56±0.04^{b}	0.53±0.07^{b}	0.06±0.01^{b}	1.57±0.07^{ab}
	T4	1.38±0.07^{b}	0.54±0.03^{b}	0.21±0.03^{a}	0.09±0.01^{a}	0.68±0.06^{b}	0.56±0.06^{b}	0.08±0.02^{b}	1.46±0.06^{c}
	T5	1.21±0.11^{bc}	0.63±0.04^{a}	0.19±0.02^{a}	0.08±0.01^{a}	0.65±0.06^{b}	0.56±0.05^{b}	0.08±0.02^{b}	1.54±0.05^{b}
	T6	1.07±0.05^{e}	0.68±0.04^{a}	0.19±0.03^{a}	0.08±0.00^{a}	0.62±0.06^{b}	0.53±0.05^{b}	0.09±0.02^{b}	1.60±0.03^{a}
	T7	1.36±0.04^{b}	0.57±0.09^{b}	0.21±0.03^{a}	0.08±0.01^{a}	0.69±0.07^{b}	0.58±0.09^{b}	0.09±0.02^{b}	1.51±0.06^{b}
	T8	1.15±0.06^{d}	0.65±0.02^{a}	0.23±0.04^{a}	0.09±0.01^{a}	0.68±0.06^{b}	0.57±0.09^{b}	0.08±0.03^{b}	1.63±0.12^{a}
	T9	1.12±0.07^{c}	0.70±0.02^{a}	0.22±0.05^{a}	0.08±0.02^{a}	0.66±0.07^{b}	0.54±0.06^{b}	0.08±0.02^{b}	1.68±0.05^{a}
2017	CK	3.36±0.09^{a}	0.32±0.05^{a}	0.23±0.05^{a}	0.08±0.01^{a}	0.85±0.11^{a}	0.12±0.04^{a}	0.11±0.05^{a}	1.06±0.03^{a}
	T1	0.81±0.05^{b}	0.35±0.05^{a}	0.24±0.06^{a}	0.06±0.01^{a}	0.03±0.01^{b}	0.09±0.03^{ab}	0.05±0.02^{b}	0.72±0.09^{c}
	T2	0.76±0.05^{c}	0.30±0.05^{a}	0.20±0.05^{a}	0.07±0.01^{a}	0.03±0.01^{b}	0.05±0.02^{b}	0.04±0.01^{b}	0.78±0.07^{c}
	T3	0.71±0.04^{c}	0.33±0.04^{a}	0.19±0.06^{a}	0.07±0.01^{a}	0.01±0.00^{b}	0.04±0.01^{b}	0.03±0.01^{b}	0.82±0.04^{b}
	T4	0.84±0.12^{b}	0.30±0.02^{a}	0.22±0.05^{a}	0.08±0.01^{a}	0.03±0.01^{b}	0.09±0.02^{ab}	0.05±0.01^{b}	0.79±0.02^{c}
	T5	0.79±0.10^{bc}	0.32±0.02^{a}	0.20±0.06^{a}	0.07±0.01^{a}	0.04±0.00^{b}	0.08±0.02^{b}	0.06±0.01^{b}	0.83±0.09^{b}
	T6	0.72±0.08^{bc}	0.35±0.03^{a}	0.21±0.04^{a}	0.09±0.01^{a}	0.03±0.01^{b}	0.07±0.01^{b}	0.06±0.01^{b}	0.89±0.07^{b}
	T7	0.85±0.10^{b}	0.34±0.03^{a}	0.19±0.02^{a}	0.07±0.02^{a}	0.06±0.01^{b}	0.10±0.01^{a}	0.07±0.01^{b}	0.86±0.05^{b}
	T8	0.83±0.10^{b}	0.38±0.02^{a}	0.21±0.03^{a}	0.08±0.02^{a}	0.06±0.01^{b}	0.09±0.01^{ab}	0.06±0.01^{b}	0.91±0.03^{b}
	T9	0.83±0.08^{b}	0.42±0.02^{a}	0.22±0.05^{a}	0.07±0.02^{a}	0.05±0.02^{b}	0.09±0.00^{ab}	0.06±0.01^{b}	1.02±0.05^{a}

Different letters indicate significant difference among treatments at 0.05 level
Values = mean ± standard error, n = 3

Analysis of treatments on improvement effects of alkalized solonchak

Different expressions for evaluating the membership function values are used following a comprehensive analysis of the data from different treatments. The results are shown in *Table 4*. As shown in *Table 4*, T2 had the greatest improvement effect on alkalized solonchak among the nine treatments. The soil treatment effect had the following order of improvement: T2 > T3 > T1 > T6 > T5 > T4 > T8 > T9 > T7. The

http://www.aloki.hu ● ISSN 1589 1623 (Print) ● ISSN 1785 0037 (Online)
DOI: http://dx.doi.org/10.15666/aeer/1704_78657879

results of T1, T2 and T3 show that under the condition with 6-m blind ditch spacing, an appropriate DG application rate will have better improvement effects. The results of T3, T6 and T9 show that with 24 t/hm^2 of DG application rate, the smaller spacing of blind ditches the better improvement effect.

Table 4. *Comprehensive appraisal index of soil improvement effects of different treatments*

Index	T1	T2	T3	T4	T5	T6	T7	T8	T9
Permeability	0.784	1	0.902	0.692	0.777	0.745	0.607	0.743	0.724
pH	0.876	0.943	1	0.536	0.629	0.598	0.206	0.412	0.340
EC	0.878	1	0.912	0.797	0.892	0.851	0.608	0.689	0.649
ESP	0.764	0.895	1	0.480	0.616	0.740	0.362	0.477	0.556
Comprehensive evaluation	0.826	0.960	0.954	0.627	0.728	0.734	0.446	0.580	0.567
Sorting	3	1	2	6	5	4	9	7	8

Survival rate, height and yield of Chinese wolfberry

The crop yield is an important index for measuring the productivity of land, and *Table 5* lists the effects of different treatments on survival rate, height and yield of Chinese wolfberry. It can be seen from *Table 5* that the survival rate and preservation rate on the control site are lowest than other treatments. The seedling survival rate, preservation rate and the yield of Chinese wolfberry increased significantly in nine treatments compared to the control site in the first year. The yields of T1, T2 and T3 increased than those of T4, T5, T6, T7, T8 and T9. The yields of T1, T2 and T3 did not have significant differences. In the first year, the yield of Chinese wolfberry of the treatments with a 6-m blind ditch spacing was higher than those with 9-m and 12-m spacing. The treatment of T2 had the highest yield is 1.08 t/hm^2 in the first year, and increased by 78.7% in the second year than that for the first year.

Table 5. *Effects of different treatments on survival rate, height and yield of Chinese wolfberry*

Year	Treatment	Survival rate (%)	Preservation rate (%)	Height (cm)	Yield (t/hm^2)
The first year	CK	43.3 ± 2.36^b	-	68.3 ± 0.78^c	0.49 ± 0.01^c
	T1	88.3 ± 4.71^a	-	87.4 ± 1.07^b	1.03 ± 0.01^b
	T2	93.3 ± 2.36^a	-	91.2 ± 0.78^b	1.08 ± 0.01^b
	T3	86.7 ± 4.71^a	-	90.9 ± 0.34^b	1.04 ± 0.01^b
	T4	86.7 ± 2.36^a	-	86.1 ± 2.64^b	0.94 ± 0.02^b
	T5	90.0 ± 4.08^a	-	87.5 ± 0.78^b	0.99 ± 0.02^b
	T6	85.0 ± 4.08^a	-	86.4 ± 1.02^b	0.96 ± 0.01^b
	T7	83.3 ± 2.36^a	-	83.5 ± 0.79^b	0.91 ± 0.01^b
	T8	86.7 ± 2.36^a	-	84.5 ± 0.75^b	0.95 ± 0.01^b
	T9	80.0 ± 4.08^a	-	83.7 ± 0.39^b	0.92 ± 0.01^b
The second year	CK	-	40.0 ± 4.08^b	86.6 ± 0.76^c	0.59 ± 0.01^c
	T1	-	81.7 ± 6.24^a	113.8 ± 1.17^a	1.91 ± 0.04^a
	T2	-	90.0 ± 4.08^a	119.8 ± 1.15^a	1.93 ± 0.02^a
	T3	-	83.3 ± 4.71^a	115.6 ± 0.71^a	1.94 ± 0.01^a

http://www.aloki.hu ● ISSN 1589 1623 (Print) ● ISSN 1785 0037 (Online)
DOI: http://dx.doi.org/10.15666/aeer/1704_78657879

	T4	-	85.0 ± 4.08[a]	111.2 ± 1.64[a]	1.89 ± 0.04[a]
	T5	-	88.3 ± 4.71[a]	115.4 ± 0.88[a]	1.91 ± 0.03[a]
	T6	-	85.0 ± 4.08[a]	113.5 ± 0.66[a]	1.90 ± 0.04[a]
	T7	-	81.7 ± 6.24[a]	108.9 ± 1.24[a]	1.86 ± 0.03[a]
	T8	-	83.3 ± 2.36[a]	113.7 ± 0.74[a]	1.90 ± 0.04[a]
	T9	-	78.3 ± 2.36[a]	110.8 ± 1.20[a]	1.88 ± 0.02[a]

The yield of Chinese wolfberry is the yield of dried fruits. Values = mean ± standard error, n = 3. Different letters indicate significant difference among treatments ($P \leq 0.05$)

Discussion

Alkalized solonchak has a high ESP, and under high alkaline conditions, the ion exchange with Na^+ during soil cementation results in the increased hydration of the cementing substance causing the soil to peptize and disperse easily in the presence of water (Ahmad et al., 2016). The macropores in the alkaline soils, once wetted, collapse to form fine pores leading to the impedance of soil water movement. The amelioration of saline-alkaline soils reduced both soil pH and ESP rapidly and effectively (Nan et al., 2016). As Ca^{2+} can flocculate soil colloids to form water stable aggregates which promote soil water movement (Morillo et al., 2002; Mahdy, 2011), the application of DG increases the concentration of Ca^{2+} in the soil which increases the capacity of adsorption to soil colloids more than that Na^+, thereby playing a role in improving the soil texture. The adsorbed Na^+ on soil colloids can exchange with Ca^{2+} in the soil solution, which decreases the exchangeable Na^+, thus decreasing soil ESP. Meanwhile, SO_4^{2-} is an acid radical with certain neutralization effects. The concentrations of CO_3^{2-} and HCO_3^- in the soil are important factors for determining the pH value of saline-alkaline soils (Chen et al., 2014). Consequently, a decrease in CO_3^{2-} and HCO_3^- in the soils content results in a decline in soil pH. However, DG is also a moderately soluble salt, which can increase the amount of salt in the soil if DG application rate is too much (Sakai et al., 2011). Therefore, in this experiment, the optimal application rate is 22 t/hm^2.

In order to enhance the treatment effects, the clay layer in the deeper soil must be disturbed to increase leaching. A clay layer between 60 cm and 80 cm at our experimental site was impervious to water, and collected the leached salts from the soil surface. In this arid region with little rainfall and strong evaporation, salts migrate through soil capillary forces to the surface of the soil leading to a higher EC value on the soil surface. The depth of our blind ditches is up to 120 cm, which broke the clay layer and promoted the migration of soil salts downward. The bottoms of the blind ditches are laid with gravels and straws to change the uniformity of soil texture, and to improve the soil water potential and permeability (Qu and Wang, 1997). Subsurface pipes can capture and drain infiltrating water to enhance desalinization and reduce the EC of the soil (Qu and Wang, 1997; Zhang et al., 2012b). Pores in gravels and straws are larger than those in the soil, and facilitate soil water movement. Our results are consistent with findings from other experiments on the improvement of soil structure with straws (Qu and Wang, 1997) and gravels (Zhang et al., 2012a).

The results presented here also show that soil water concentrates in straws forming a desalting zone after irrigation and expediting the desalting process (Zhen and Hao, 2010). We found that the application of gravels and straws not only accelerates the leaching of soil salts, but also prevents secondary salinization in the second year. Burying gravel and straw in a homogeneous soil can also improve soil aeration and crop

http://www.aloki.hu ● ISSN 1589 1623 (Print) ● ISSN 1785 0037 (Online)
DOI: http://dx.doi.org/10.15666/aeer/1704_78657879

growth and reduce the upward water movement. In addition, the organic acid released during the decomposition of straws can promote the dissolution of Ca^{2+} (Lu et al., 2017).

Cl^- has stable chemical properties with slow chemical reactions such as adsorption (Yang et al., 2015a). Yang et al. (2015a) found through an amelioration experiment of alkaline soil that with leaching, Cl^- easily accumulates in the soil deeper than 60 cm from the surface and is difficult to discharge through the soil layers again (Yang et al., 2015a). However, in our research, the concentrations of Cl^- for all treatments were significantly reduced, proving that the blind ditches help discharge Cl^-. The application of DG will increase the concentration of SO_4^{2-}, SO_4^{2-} and Na^+ producing Na_2SO_4 (Buckley and Wolkowski, 2014), which is leached to blind ditches by irrigation water and discharged from the soil.

Conclusion

With desulfurized gypsum which can effectively improve physical and chemical properties of alkalized solonchak, subsurface gravel blind ditches can further accelerate the leaching of salts from the soil and ameliorate the soil by improving its chemical and mechanical properties. Subsurface gravel blind ditches promoted the DG amelioration effect, which effectively improves the soil permeability and promotes salt leaching. The ESP, EC and the concentrations of Na^+, Cl^-, CO_3^{2-} and HCO_3^- in the soils are significantly reduced by the blind ditches and DG. Chinese wolfberry yield was significantly increased by the treatments. The best design scenario is one which has 6-m blind ditch spacing combined with a 22 t/hm^2 desulfurization gypsum application rate.

Acknowledgements. This work was supported by the "Major Innovation Projects for Building First-class Universities in China's Western Region" (No. ZKZD2017004). In addition, we would like to thank Dr. Ninghu Su from the James Cook University for his constructive suggestions on the present work.

REFERENCES

[1] Ahmad, S., Ghafoor, A., Akhtar, M. E. (2016): Implication of gypsum rates to optimize hydraulic conductivity for variable-texture saline-sodic soils reclamation. – Land Degradation & Development 3: 550-560.
[2] Bigham, J. M. (1965): Methods of soil analysis. – American Potato Journal 11: 345-346.
[3] Buckley, M., Wolkowski, R. (2014): In-season effect of flue gas desulfurization gypsum on soil physical properties. – Journal of Environmental Quality 1: 322-327.
[4] Christen, E., Skehan, D. (2001): Design and management of subsurface pipe drainage to reduce salt loads. – Journal of Irrigation & Drainage Engineering 3: 148-155.
[5] Chi, C. M., Wang, Z. C. (2014): Saturated hydraulic conductivity and its influence factors of saline-alkali soils. – Chinese Journal of Soil Science 3: 601-607 (in Chinese).
[6] Chen, J. R., Chen, X. H., Liu, Z. H. (2014): The experimental study on the process and effect to the FGD-gypsum as an improvement in coastal saline-alkali soil. – China Environmental Science 6: 1505-1513 (in Chinese).
[7] Chen, X., Kang, Y. H., Wan, S. Q. (2015): Influence of mulches on urban vegetation construction in coastal saline land under drip irrigation in North China. – Agricultural Water Management 158: 145-155.
[8] Cucci, G., Lacolla, G., Mastro, M. A. (2016): Leaching effect of rainfall on soil under four-year saline water irrigation. – Soil & Water Research 11: 181-189.

http://www.aloki.hu ● ISSN 1589 1623 (Print) ● ISSN 1785 0037 (Online)
DOI: http://dx.doi.org/10.15666/aeer/1704_78657879

[9] Driessen, P., Deckers, J., Spaargaren, O. (2000): Lecture notes on the major soils of the world. – Food and Agriculture Organization (FAO).
[10] De Sutter, T., Cihacek, L., Rahman, S. (2014): Application of flue gas desulfurization gypsum and its impact on wheat grain and soil chemistry. – Journal of Environmental Quality 1: 303-311.
[11] Feng, D., Wan, S. Q., Kang, Y. H. (2017): Drip irrigation scheduling for annual crops in an impermeable saline-sodic soil with an improved method. – Journal of Soil and Water Conservation 4: 351-360.
[12] Heng, T., Liao, R. K., Wang, Z. H. et al. (2018): Effects of combined drip irrigation and sub-surface pipe drainage on water and salt transport of saline-alkali soil in Xinjiang, China. – Journal of Arid Land 6: 932-945.
[13] Kameli, M. A., Chorom, M., Jaafarzadeh, N. et al. (2017): Application of wastewater with high organic load for saline-sodic soil reclamation focusing on soil purification ability. – Global Journal of Environmental Science & Management 3: 197-206.
[14] Lin, Y. L., Li, Y. J., Chen, Y. H. (2016): Effects adding sand on soil physical and chemical property and corn yield in alkalized solonchak soil. – Soil and Fertilizer Sciences 1: 119-123 (in Chinese).
[15] Liu, J. H., Ali, A., Yu, M. F. et al. (2015): Risk evaluation of main pests and integrated management in Chinese wolfberry, *Lycium barbarum L*. – Pakistan Journal of Zoology 47: 21-29.
[16] Lu, P. R., Zhang, Z. Y., Feng, G. X. (2017): Effect of straw draining piece depth in soil on soil water-salt distribution in saline soil and its drainage-salt inhibiting performance. – Transactions of the Chinese Society of Agricultural Engineering 5: 115-121 (in Chinese).
[17] Mahdy, A. M. (2011): Comparative effects of different soil amendments on amelioration of saline-sodic soils. – Soil and Water Research - UZEI (Czech Republic) 4: 205-216.
[18] Mao, Y. M., Li, X. P., Warren, A. D. (2016): Remediation of saline-sodic soil with flue gas desulfurization gypsum in a reclaimed tidal flat of southeast China. – Journal of Environmental Sciences 45: 224-232.
[19] Morillo, E., Maqueda, C., Reinoso, R. (2002): Effect of two organic amendments on norflurazon retention and release by soils of different characteristics. – Environmental Science & Technology 20: 4319-4325.
[20] Min, W., Hou ZA, Ma, L. J. et al. (2014): Effects of water salinity and N application rate on water- and N-use efficiency of cotton under drip irrigation. – Journal of Arid Land 4: 454-467.
[21] Mohsenian, Y., Roosta, H. (2015): Effects of grafting on alkali stress in tomato plants: datura rootstock improve alkalinity tolerance of tomato plants. – Journal of Plant Nutrition 1: 51-72.
[22] Nan, J., Chen, X., Chen, C. (2016): Impact of flue gas desulfurization gypsum and lignite humic acid application on soil organic matter and physical properties of a saline-sodic farmland soil in Eastern China. – Journal of Soils & Sediments 9: 1-11.
[23] Pan, P., Zhao, T. (1998): The study of simple blind ditch improvement of saline soil. – Ningxia Agriculture and Forestry Technology 3: 28-30 (in Chinese).
[24] Qu, C. X., Wang, W. (1997): Mechanisms of water reserved by sand interlayer in soil profile. – Journal of Huazhong Agricultural University 5: 43-50 (in Chinese).
[25] Qadir, M., Oster, J. D. (2004): Crop and irrigation management strategies for saline-sodic soils and waters aimed at environmentally sustainable agriculture. – Science of the Total Environment 1: 1-19.
[26] Rhoton, F., McChesney, D. (2011): Effect of FGD gypsum on the properties of a highly erodible soil under conservation Tillage. – Communications in Soil Science & Plant Analysis 16: 2012-2023.
[27] Sakai, Y., Matsumoto, S., Sadakata, M. (2004): Alkali soil reclamation with flue gas desulfurization gypsum in China and assessment of metal content in corn grains. – Soil and Sediment Contamination 1: 65-80.

http://www.aloki.hu ● ISSN 1589 1623 (Print) ● ISSN 1785 0037 (Online)
DOI: http://dx.doi.org/10.15666/aeer/1704_78657879

[28] Sakai, Y., Ren, S. H., Wang, C. (2011): Salt-affected soil amelioration with flue gas desulfurization by-products and waste gypsum board in Tianjin, China. – Journal of Chemical Engineering of Japan 10: 750-756.
[29] Tian, Y. F., Dou, S., Zhang, Y. G. (2013): Improvement effects of subsurface pipe with different spacing on sodic-alkali soil. – Transactions of the Chinese Society of Agricultural Engineering 12: 145-153 (in Chinese).
[30] Tao, Y., Wang, S. L., Xu, D. (2016): Experimental study of clogging defense measures for improved subsurface drainage. – Transactions of the Chinese Society for Agricultural Machinery 6: 187-192 (in Chinese).
[31] Vance, G., King, L., Ganjegunte, G. (2008): Soil and plant responses from land application of saline-sodic waters: implications of management. – Journal of Environmental Quality 1: 139-148.
[32] Xue, Z., Wan, S. Q., Kang, Y. H. (2014): Effect of sand-filled depth and straw mulching on crops growth in takyric solonetz. – Journal of Irrigation & Drainage 1: 38-41.
[33] Yang, J., Sun, Z. J., Luo, C. K. (2015a): Effect of salt-water regulation on improving takyric solonetz land and yield of oil sunflower. – Transactions of the Chinese Society of Agricultural Engineering 18: 121-128 (in Chinese).
[34] Yang, Y. C., Pan, D. F., Zou, Z. G. (2015a): Experiment of blind ditch of rice straw in Jiangsu coastal saline soil. – Jiangsu Agricultural Science 3: 373-375 (in Chinese).
[35] Yu, H. L., Gu, W., Tao, J. (2015): Impact of addition of FGDB as a soil amendment on physical and chemical properties of an alkali soil and crop yield of maize in Northern China Coastal Plain. – Journal of Chemistry 8: 1-11.
[36] Yu, S. H., Liu, J. T., Li, Z. X. (2012): Mechanism of saline-alkali lands improvement of subsurface pipe drainage systems and agro-ecosystem response. – Chinese Journal of Eco-Agriculture 12: 1664-1672.
[37] Zhen, W., Hao, F. (2010): Effect of straw-incorporation on soil infiltration characteristics and soil water holding capacity. – Transactions of the Chinese Society of Agricultural Engineering 4: 75-80.
[38] Zhang, J., Chang, T. T., Shao, X. H. (2012a): Improvement effect of subsurface drainage on secondary salinization of greenhouses oil and tomato yield. – Transactions of the Chinese Society of Agricultural Engineering 3: 81-86 (in Chinese).
[39] Zhang, T. B., Kang, Y. H., Hu, W. (2012b): Study on salinity characteristics of takyric solonetz in Ningxia Yinbei region. – Soils 6: 1001-1008 (in Chinese).
[40] Zhang, P. (2014): Effect of Different Afforestation Tree Species on Soil Physical and Chemical Properties of Saline-Alkali Soil. – Shandong Agricultural University, Shandong (in Chinese).

http://www.aloki.hu ● ISSN 1589 1623 (Print) ● ISSN 1785 0037 (Online)
DOI: http://dx.doi.org/10.15666/aeer/1704_78657879

THE EFFECT OF DRY-WET CYCLE ON CRACK PROPAGATION AND SHEAR STRENGTH INDEX OF YUNNAN LATERITE IN CHINA

ZHU, W.-W.

School of Urban and Rural Construction & Engineering Management, Kunming University
No. 2 Puxin Road, Kunming Economic Development Zone, Yunnan Province, China
(e-mail: zwwswfc@126.com; phone: +86-158-1202-5370; fax: +86-871-6509-8321)

(Received 23rd Feb 2019; accepted 3rd May 2019)

Abstract. To understand the changing pattern of crack propagation and shear strength index of Yunnan laterite in China after dry-wet cycle, prepared the Yunnan laterite with certain moisture content and made the soil cake samples after compaction which underwent indoor spraying and air dry to simulate the dry-wet cycle caused by multiple precipitation and evaporation in the project, and the determination of crack width and direct shear test were carried out for samples with various numbers of cycles. The results indicated that the crack process of Yunnan laterite could be classified into three stages upon dry-wet cycle: crack developmental stage, crack progression stage and crack stable stage. The cohesion and internal friction angle of the samples were reduced as the crack propagation of continued, with the reduction amplitude of cohesion greater than that of the internal friction angle, and the reduction law of both in line with the logistic curve pattern.
Keywords: *Yunnan laterite, dry-wet cycle, shrinkage, crack width, shear strength*

Introduction

Yunnan is one of the most developed areas of laterite in China. Laterite is a red color-based soil formed by weathering, micro-agglomeration and soil-forming processes of iron-rich mother rocks in hot and humid climates (Huang et al., 1998). Yunnan laterite is a special kind of clay, showing the characteristics of high clay content, high liquid limit, large natural porosity ratio, low permeability coefficient, high dispersivity, weak expansibility and strong shrinkage (Liu et al., 2005). Due to the little knowledge of the basic properties of Yunnan laterite, quite a few engineering disasters related to laterite have occurred in Yunnan Province. For example, the development of shrinkage cracks in lateritic foundation led to the settlement of buildings caused by strength reduction, and mining groundwater resulted in the shrinkage and cracking of red soil slope, strength reduction, and landslides after rainfall.

Yunnan, a region with slow economic development in China, is faced with quite a lot of laterite problems with the commencement of a large number of railway and highway projects. At present, the study on Yunnan laterite is mainly focused on the basic physical and mechanical properties index (Huang et al., 1998; Liu et al., 2005; Yuan, 2002; He et al., 2008), chemical composition (Huang, 2002), and the effect of rainfall scouring laterite slope on its physical and chemical properties (Zhang et al., 2016). The study on the cracking mechanism of soils under dry-wet cycles is mainly concentrated in common clay (Sun et al., 2015; He et al., 2012; Rayhani et al., 2007, 2008) and expansive soils (Tang et al., 2011, 2012, 2013), and the engineering properties of Yunnan laterite are different from those of the two types of soil. The objective of this study is to understand the changing pattern of crack propagation and shear strength index of Yunnan laterite. The present study directly reflected the occurrence and expansion of cracks in Yunnan laterite during the dry-wet cycle by indoor simulating

http://www.aloki.hu ● ISSN 1589 1623 (Print) ● ISSN 1785 0037 (Online)
DOI: http://dx.doi.org/10.15666/aeer/1704_78817889

the reciprocating process of natural rainfall and evaporation and revealed that the decrease of laterite strength was caused by the occurrence and expansion of cracks. In this paper, an empirical formula reflecting the decrease in the shear strength index of Yunnan laterite with the increase in the number of dry-wet cycles, and the mechanism of the occurrence and propagation of cracks in Yunnan laterite after dry-wet cycles was also discussed.

Experiment schemes

The soil material was excavated from Luoyang Section of East Ring Expressway in Kunming on September 2. The excavation amount was about 80 kg. Yunnan laterite soil with the certain moisture content was prepared and compacted according to the heavy-duty II-1 standard (Ministry of Communications of the People's Republic of China, 2007), which was used to make soil cake samples. To stimulate the state of laterite after experiencing rainfall and evaporation cycles in nature, multiple dry-wet cycles were performed indoors to create cracks and expansion. The change pattern of cracks during dry-wet cycles was observed morphologically, and the maximum crack width and saturated shear strength index were determined after experiencing various numbers of dry-wet cycles. Shear strength index was measured by direct fast shear test.

The selected laterite was brown in dry and red brown after immersion with the clay particles of 41.25%, the granule particles of 47.93% and the sand particles of 10.82%, whose basic physical and mechanical properties were shown in *Table 1*. Using standard compaction test, the maximum dry density (ρ_{dmax}) and the optimal water content (ω_{op}) were determined as 1.62 g/cm^3 and 17.8%, respectively.

Table 1. *Basic physical and mechanical properties of lateritic soil*

Natural wet density ρ(g/cm^3)	**Specific density of solid particles** G_s	**Natural moisture content** ω(%)	**Liquid limit** ω_L(%)	**Plastic limit** ω_P(%)	**Plasticity index** I_P
1.76	2.64	29.2	52.0	28.0	25.0

In this experiment, the soil was prepared according to moisture content ω = 21%, and the prepared soil was sealed in plastic bags for 24 hours to ensure the uniform moisture content. The samples were then placed in the compaction cylinders (inner diameter of 100 mm and height of 127 mm) to compact, and the soil moisture content ω, dry density ρ_d and the compaction coefficient were 20.8%, 1.53 g/cm^3 and 94.4%, respectively. The soil in the compaction cylinder was slowly lifted by a jack, and the soil cake with the thickness of 20 mm was obtained by carefully cutting with a wire saw, using which a total of 72 samples were prepared. The 72 samples were divided into 9 groups with 8 in each group, and the dry-wet cycles of 0, 1, 2, 3, 4, 5, 6, 7 and 8 were carried out. A small portion of the soil cake was collected via using small ring knife (inner diameter of 61.8 cm and height of 20 mm) to determine the shear strength index.

The dry and wet in the cycles of the present study were not absolute dry and wet, but the stimulation of the humidification and dehumidification process of Yunnan laterite in nature. The control standard of "dry" was air dry of the soil cake in the lab for 48 h. The standard of "wet" was: (1) spraying the surface of samples by using a syringe with needle (with the distance from needle tip to sample surface of 1 cm and the spraying

http://www.aloki.hu ● ISSN 1589 1623 (Print) ● ISSN 1785 0037 (Online)
DOI: http://dx.doi.org/10.15666/aeer/1704_78817889

rate of 0.5 ml/s) until the surface was covered in water. Spray was continued after water was absorbed by samples until the water stayed at the same level after 5 min; or (2) spray was conducted until free water seeped from the bottom of the sample if the water sprayed to the sample surface was always absorbed completely within 5 min.

The experiment was performed in October in Kunming in which the minimum night temperature, the maximum day temperature and relative humidity were 12 °C, 26 °C and 43-58%, respectively.

Results and analysis

The surface cracks of Yunnan laterite samples were clearly visible after various cycles of dry-wet cycles. The expansion status of the cracks after 1, 2, 3, 4, 5 and 6 dry-wet cycles were as shown in *Figure 1*. Almost all the samples showed the development of annular microfracture after the first dry-wet cycle, and some samples showed a relatively wide crack during the first air dry process, which might be due to the weak structural plane resulted from the unequal stress during the sample preparation, so the cracks were formed during the first air dry process because of the uneven contraction distortion after dehydration. After multiple dry-wet cycles, the crack width was gradually increased and secondary cracks were formed. The initial annular crack gradually radiated to the periphery, and the maximum crack width reached the scale of millimeter after the fourth dry-wet cycle. The cracks expansion tended to be stable and the width was no longer increased after the sixth cycle. With the 100x visualizer of crack width (1 DIV/0.02 mm, Shangyu Jingnuo Instrument Factory, Zhejiang Province, China; *Fig. 2*), the maximum crack width after various numbers was determined which was shown in *Figure 3*.

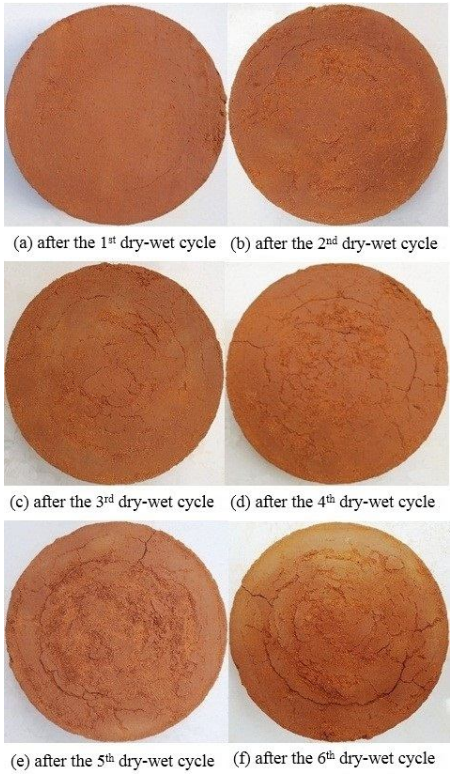

Figure 1. *The crack expansion in soil samples after dry-wet cycle*

http://www.aloki.hu ● ISSN 1589 1623 (Print) ● ISSN 1785 0037 (Online)
DOI: http://dx.doi.org/10.15666/aeer/1704_78817889

Figure 2. *The visualizer of crack width (100x)*

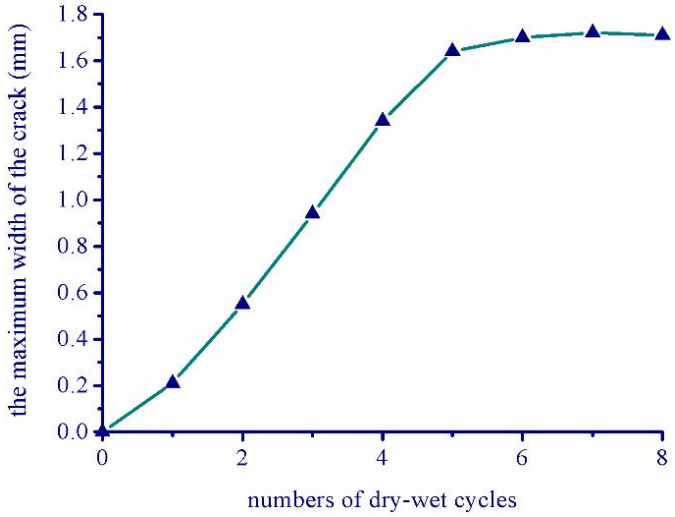

Figure 3. *The maximum crack width after dry-wet cycles*

Although the propagation of cracks is one of the contents of this study, for road engineering, more attention is paid to the shear strength attenuation of soil caused by cracks. The variation of soil moisture content during rainfall or evaporation in nature is not as dramatic as that of water saturation or oven drying. Therefore, the shear test was performed after each dry-wet cycle, and such shear strength index could reflect the effect of the crack development process on the strength of Yunnan laterite after the expansion-contraction cycle due to the dry-wet cycles caused by the external climate. The relationship of cohesive strength (c) and internal friction angle (φ) to the numbers of dry-wet cycles was as shown in *Figure 4*. Cohesion and internal friction angle are two indexes of shear strength of soil. Cohesion is the mutual attraction between the adjacent parts of the soil. This mutual attraction is the expression of the molecular force between the molecules of the same substance. cohesion is also the shear strength of the

http://www.aloki.hu ● ISSN 1589 1623 (Print) ● ISSN 1785 0037 (Online)
DOI: http://dx.doi.org/10.15666/aeer/1704_78817889

failure surface without any positive stress. The internal friction angle reflects the friction characteristics of soil, including the sliding friction caused by the rough surface of particles and the occlusal friction caused by the embedding, interlocking and disengaging of particles.

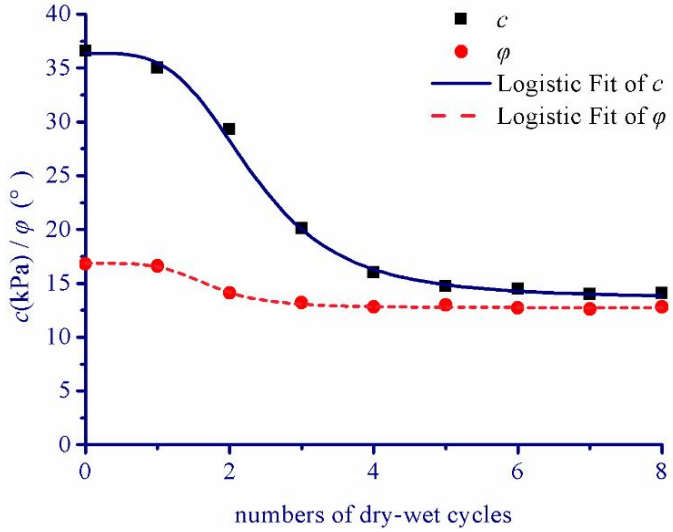

Figure 4. *The relationship of cohesive strength (c) and internal friction angle (φ) to the numbers of dry-wet cycles*

The results indicated that as the cycle increased, the cracks were formed from scratch and became larger, leading to the damage in the integrity of the soil and the gradual strength reduction of Yunnan laterite, which is consistent with the general knowledge of the variation pattern of shear strength in clay soil. Among these, the change in cohesive strength was most significant, which only retained 40% of its initial value after 5 cycles. Cohesion took on the trend of constant reduction due to successive crack development. Although some small cracks might close or partially close during humidification, the scars still existed, and the gradual increase in such damage of soil integrity resulted in looser soil and lowered strength. However, crack propagation followed the basic rule of being fast then slow, thus, the change to the number of dry-wet cycles of cohesion showed a form of being steep and then gentle as a whole. The internal friction angle of Yunnan laterite also decreased, but the altitude was much smaller than that of cohesive strength, showing 77% of the initial value after five dry-wet cycles. On one hand, the existence of cracks in the soil allowed Yunnan laterite to become fragmented. Furthermore, the expansion and shrinkage deformation led to loosen soil and reduced compactness, which tended to be stable after five cycles. Therefore, the decrease of internal friction angle at the beginning of dry-wet cycles might be related to the decrease of soil density caused by expansion and contraction.

Cracks lead to the decrease or lose of the cementation force between soil particles. Therefore, cohesion is significantly reduced, the further impact of crack propagation on it is not significant, and the main factor affecting the internal friction angle is the property of soil particles. Compared with cohesive strength, the reduction of internal friction angle entered stable stage with minimal variation.

Experiments revealed the expansion of cracks with increasing the numbers of dry-wet cycles, and the process of crack expansion was generally consistent with the

http://www.aloki.hu ● ISSN 1589 1623 (Print) ● ISSN 1785 0037 (Online)
DOI: http://dx.doi.org/10.15666/aeer/1704_78817889

reduction in the strength of Yunnan laterite, and it was shown that the strength reduction was resulted from the crack propagation.

The relationship of cohesive strength c and internal friction angle φ to dry-wet cycle number exhibited inversed S-shape curve (*Fig. 4*), and it could be fitted via using the mathematical expression of logistic curve, which were:

$$c = \frac{A_1 - A_2}{1+\left(n/n_1\right)^p} + A_2 \quad \text{(Eq.1)}$$

$$\varphi = \frac{A_3 - A_4}{1+\left(n/n_2\right)^q} + A_4 \quad \text{(Eq.2)}$$

In *Equations 1* and *2, n* is the number of dry-wet cycles; A_1, A_2, A_3, A_4, n_1 and n_2 indicate the fitting parameters.

The above formula, as an empirical formula reflecting the rule that the shear strength index of Yunnan laterite is reduced with the increase in the number of dry-wet cycles, can be used to estimate the final value of shear strength index of laterite under the long-term action of sunshine and rain. The fitting results of the present study were as follows:

$$c = \frac{36.878 - 13.635}{1+\left(n/2.337\right)^{3.782}} + 13.635 \quad \text{(Eq.3)}$$

$$\varphi = \frac{16.854 - 12.745}{1+\left(n/1.733\right)^{4.487}} + 12.745 \quad \text{(Eq.4)}$$

Calculated by *Equations 3* and *4,* the ultimate reduction value of the shear strength of the laterite as the cycle numbers increased were c = 13.635 kPa and φ = 12.745°. The cohesive strength and internal friction angle were reduced to 37% and 76% of the initial value, respectively.

The simplified Bishop method is a quantitative analysis method for the stability of subgrade slope. The basic principle is: assuming that the slope has an arc sliding surface, the slope stability factor can be calculated by comparing the sliding moment produced by the sliding surface with the sliding moment produced by the sliding body. When calculating, the stability coefficient K is assumed first, and then the calculated value F_S of the stability coefficient is inversely calculated. Then the assumed value K is adjusted according to the calculated value F_S of the stability coefficient, and the relative error between K and F_S is repeated until the relative error between K and F_S is within the prescribed range. To intuitively demonstrate the effect of the decrease in the shear strength of Yunnan laterite caused by dry and wet cycles on the slope stability, the stability coefficient F_S was calculated (simplified Bishop method) for the homogeneous embankment (soil bulk density of 18.5 kN/m^3) with the height of 10 m, the width of 20 m and the slope ratio of 1:1 using the strength index obtained in the test, which was shown in *Figure 5*.

Discussion

According to the data, the developmental process of cracks in the Yunnan laterite samples upon dry-wet cycles can be classified into 3 stages: crack developmental stage, crack progression stage and crack stable stage.

http://www.aloki.hu ● ISSN 1589 1623 (Print) ● ISSN 1785 0037 (Online)
DOI: http://dx.doi.org/10.15666/aeer/1704_78817889

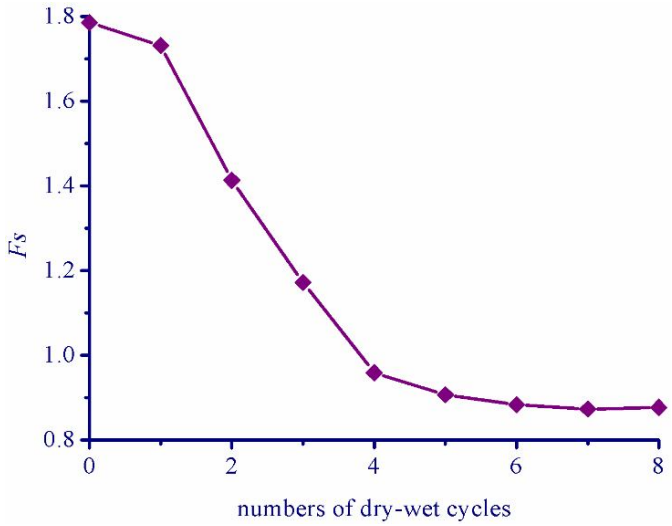

Figure 5. *The relationship of safety factor (F_S) and numbers of dry-wet cycles*

(1) Crack developmental stage. The first dry-wet cycle is the crack developmental stage. During this process, humidification of laterite samples occurs only in the original pores, the effect of humidification only lies in enabling the laterite to absorb water, and the effect of dehumidification only lies in emigration of partial moisture in the pores. However, such dry-wet cycle results in moisture gradient in laterite samples, and a large amount of moisture in the samples softens the connection between laterite particles, leading to the formation of micro-cracks in the samples, which creates favorable conditions for further expansion cracking and shrinkage cracking during later dehumidification. In the present study, the dry density of laterite sample was relatively high, so the swelling force caused in the process of humidification was also large, and the micro-cracks were produced after the first dry-wet cycle. It has been demonstrated that cracks were hard to form in the samples with relatively low dry density (Zhao et al., 2017).

(2) Crack progression stage. The 2^{nd}-5^{th} cycle is the crack progression stage. After the 1^{st} dry-wet cycle, the main effect of water absorption and humidification of laterite sample is to increase the thickness of water film between laterite particles, resulting in the swelling and cracking of laterite sample. The main effect of dehumidification is to reduce the thickness of water film between laterite particles, resulting in shrinkage and cracking of laterite samples, so the micro-cracks gradually develop into macro-cracks. With increasing the cycles, the thickness of water film among soil particles further increases, and the swelling and cracking laterite become more significant. During this development stage, the originally formed cracks have been further deepened and widened, and crack propagation has been achieved. In this process, crack propagation comes with the decrease in the shear strength index.

(3) Crack stable stage. Cycle beyond the 6^{th} is crack stable stage. During such a process, the main effect of water absorption and humidification of laterite sample is not to increase the thickness of water film between laterite particles and cause expansion cracking, but to fill the existing cracks, and the main function of dehumidification is to reduce moisture between laterite particles in existing fractures. Due to the large crack width and high moisture content, there is no water loss, shrinkage and crack deepening in a short time, which is not enough to form new cracks, so the expansion of cracks

http://www.aloki.hu ● ISSN 1589 1623 (Print) ● ISSN 1785 0037 (Online)
DOI: http://dx.doi.org/10.15666/aeer/1704_78817889

enters into a stable stage. In the repeated dry-wet cycles, the cracks are opened, closed and propagated under the combined effect of expansion and shrinkage, and they gradually reach a stable state after certain cycles. During this process, the attenuation of shear strength index in the soil samples also entered a stable period.

Although there are still some unreasonable factors in the method employed here, such as the artificial disturbance in sample preparation, the small size of sample, and the discrepancy between the simulated humidification and dehumidification and natural process, such a method is still preferable considering the difficulties in the present study on the cracking and strength of Yunnan laterite. Such a method makes it possible to study the crack initiation and propagation in Yunnan laterite caused by dry-wet cycles and the effect pattern of crack propagation on its strength by conventional geotechnical instruments, which provides a reasonable and effective basis for the analysis of laterite engineering problems in Yunnan. In the present study, the dry density of laterite sample was relatively high, and its compaction coefficient was similar to that of embankment. Therefore, the process of cracking during dry-wet cycles and the attenuation process of shear strength index are representative.

Conclusion and suggestion

(1) With a reasonable and simple experimental procedure, determined the crack width of Yunnan laterite and the variation pattern of shear strength index as the cracks expanded during dry-wet cycles. The data showed the phenomenon of the occurrence and expansion of cracks in Yunnan laterite upon dry-wet cycles, and revealed that the reduction in the strength of laterite was resulted from the occurrence and expansion of such cracks.

(2) The results indicated that either cohesive strength or internal friction angle exhibited certain decrease with the propagation of cracks which had a stronger effect on cohesive strength. An empirical formula was also presented showing the decrease of shear strength index of Yunnan laterite with the increase of dry-wet cycles as well as the development of cracks. Such a formula can be used to estimate the ultimate strength index of dense Yunnan laterite under long-term sunshine and rain.

(3) The mechanism of occurrence and expansion of Yunnan laterite after dry-wet cycles was discussed. During the crack developmental stage, the wetting process softens the connection between laterite particles, leading to the formation of microfractures after drying. During the crack expansion stage, the wetting process increases the thickness of water film between laterite particles to cause crack expansion of samples, whereas the drying process reduces the water film thickness between particles resulting in the shrinkage and cracking, and the micro-cracks gradually develop into macro-cracks. During the crack stable stage, because of the large width of cracks, the wetting process is to fill the cracks. The moisture content is relatively high during this stage, shrinkage and deepened cracks due to dehydration will not occur in a short time, and water loss is not enough to rip soil and form new cracks.

(4) In the future, investigations are needed to understand the pattern of crack propagation and strength attenuation of Yunnan laterite under various regulated conditions of dry-wet cycle and large-sized samples. For the foundation, embankment or slope of Yunnan laterite, more attention should be paid to the crack formation and strength degradation caused by rainfall and drought, especially with the large gradient of moisture content and uneven expansion. Because the effect of crack on the cohesive

http://www.aloki.hu ● ISSN 1589 1623 (Print) ● ISSN 1785 0037 (Online)
DOI: http://dx.doi.org/10.15666/aeer/1704_78817889

strength is more significant, the value of clay cohesive strength should be cautiously identified in engineering design, and the uniform moisture content is desired in the actual projects with Yunnan laterite.

Acknowledgements. This research was funded by Yunnan Applied Basic Research Projects (2016FD108).

REFERENCES

[1] He, J., Wan, J., Wang, Y. (2012): Desiccation cracks and hydraulic performance of compacted clay liner via laboratory wet-dry cycling tests. – Journal of Engineering Geology 20(3): 397-402.
[2] He, X. M., Su, H., Yan, H. H. et al. (2008): Study on engineering properties of red clay at Kunming New International Airport. – Yangtze River 39(24): 49-52.
[3] Huang, Y., Fu, B. C. (1998): Research on laterization and specific property of laterite in engineering geology. – Chinese Journal of Geotechnical Engineering 20(3): 40-44.
[4] Huang, Y., Fu, B. C. (2002): The change properties of the chemical compositions for laterite. – Journal of Kunming University of Science and Technology 27(4): 63-70.
[5] Liu, Z. B. (2005): Engineering characteristics and geotechnical engineering problems of Yunnan red clay. – Yunnan Electric Power 33(4): 44-47.
[6] Ministry of Communications of the People's Republic of China. (2007): Test Methods of Soils for Highway Engineering. – JTG E40-2007.
[7] Rayhani, M. H., Yanful, E. K., Fakher, A. (2007): Desiccation-induced cracking and its effect on the hydraulic conductivity of clayey soils from Iran. – Canadian Geotechnical Journal 44(3): 276-283.
[8] Rayhani, M. H. T., Yanful, E. K., Fakher, A. (2008): Physical modeling of desiccation cracking in plastic soils. – Engineering Geology 97(1): 25-31.
[9] Sun, D. A., Huang, D. J. (2015): Soil-water and deformation characteristics of Nanyang expansive soil after wetting-drying cycles. – Rock and Soil Mechanics 36(S1): 115-119.
[10] Tang, C. S., Shi, B., Liu, C., Suo, W. B., Gao, L. (2011): Experimental characterization of shrinkage and desiccation cracking in thin clay layer. – Applied Clay Science 52(1): 69-77.
[11] Tang, C. S., Cui, Y. J., Tang, A. M., Shi, B. (2012): Shrinkage and desiccation cracking process of expansive soil and its temperature-dependent behaviour. – Chinese Journal of Geotechnical Engineering 4(12): 2181-2187.
[12] Tang, C. S., Wang, D. Y., Shi, B., Liu, C. (2013): Quantitative analysis of soil desiccation crack network. – Chinese Journal of Geotechnical Engineering 35(12): 2298-2305.
[13] Yuan, X. (2002): Engineering property and its application of red clay in Yunnan. – Journal of Nanchang College of Water Conservancy and Hydroelectric Power 21(1): 59-62.
[14] Zhang, Z. L., Hong, B., Huang, Y. et al. (2016): Impact of physical chemical properties and the erosion on the slope of the Yunnan laterite under rainfall conditions. – Journal of Water and Soil Conservation 30(3): 6-18.
[15] Zhao, G. G., Huang, Y., Zhang, J. F. et al. (2017): Investigation on the development of cracks of laterite of Yunnan under wetting-drying cycles. – Journal of Soil and Water Conservation 31(2): 157-165.

http://www.aloki.hu ● ISSN 1589 1623 (Print) ● ISSN 1785 0037 (Online)
DOI: http://dx.doi.org/10.15666/aeer/1704_78817889

SEASONAL INFLUENCE OF REED (*PHRAGMITES AUSTRALIS*) AND LOTUS (*NELUMBO NUCIFERA*) ON URBAN WETLAND OF YI RIVER

XU, S. Z.[1] – WANG, Y. X.[2] – WANG, Y. D.[2] – ZHAO, Y. J.[3] – GAO, Y.[4,5*]

[1]*Linyi No. 7 Middle School of Shandong Province, Linyi 276000, China*
(e-mail: 1306934800@qq.com)

[2]*Linyi No. 4 Middle School of Shandong Province, Linyi 276000, China*
(e-mail: 327887987@qq.com; ykyyjyk@163.com)

[3]*College of Agriculture and Forestry, Linyi University, Linyi 276005, China*
(e-mail: zhaoyanjie1882@126.com)

[4]*Shandong Provincial Key Laboratory of Water and Soil Conservation and Environmental Protection, College of Resources and Environment, Linyi University, Linyi 276005, China*

[5]*Linyi Scientific Exploration Laboratory, Linyi 276037, China*

**Corresponding author*
e-mail: gaoyuan1182@tom.com, gaoy@lyu.edu.cn

(Received 23rd Feb 2019; accepted 3rd May 2019)

Abstract. Our research objective was to compare the eutrophication inhibition of reeds and lotuses on water body of wetland system of Yi River, evaluate ecological benefits of the two wetland systems, and reveal the response mechanism of water environmental factors, which not only has ecological theoretical significance, but also has extensive practical application value in the management and evaluation of wetland water ecosystem of Yi River. Three research sample plots were set up in Yimeng Lake of Yi River: reed water area, lotus water area and natural water area. In August (summer), October (autumn), December (winter) of 2018 and February 2019 (spring), subsurface water samples were collected and analyzed by laboratory detection for pH, chromaticity, total hardness, dissolved oxygen, BOD, COD, ammonia nitrogen, total nitrogen, total phosphorus, nitrate and chlorophyll a. Research results were as follows: 1) pH appeared as that of lotus water area > natural water area > reed water area, chromaticity appeared as that of natural water area > reed water area > lotus water area. Total hardness appeared as that of natural water area > lotus water area > reed water area, dissolved oxygen appeared as reed water area > lotus water area > natural water area. BOD appeared as that of lotus water area > natural water area > reed water area, COD appeared as that of lotus water area > natural water area > reed water area. Ammonia nitrogen appeared as that of reed water area > lotus water area > natural water area, total nitrogen appeared as that of natural water area > lotus water area > reed water area, total phosphorus appeared as that of reed water area > natural water area > lotus water area, nitrate appeared as that of natural water area > lotus water area > reed water area, and chlorophyll a appeared as that of lotus water area > natural water area > reed water area. 2) pH appeared as that of winter > spring > summer > autumn, chromaticity appeared as that of summer > autumn > winter > spring. Total hardness appeared as that of winter > autumn > spring > summer, dissolved oxygen appeared as that of spring > summer > winter > autumn. BOD appeared as that of spring > winter > autumn > summer, COD appeared as that of autumn > summer > winter > spring. Ammonia nitrogen appeared as that of winter > spring > autumn > summer, total nitrogen appeared as that of spring > summer > autumn > winter, total phosphorus appeared as that of winter > spring > autumn > summer, nitrate appeared as that of spring > summer > autumn > winter, and chlorophyll a appeared as that of autumn > summer > spring > winter. Our research conclusion is that reed can effectively increase dissolved oxygen and greatly reduce BOD, COD, total nitrogen, nitrate and chlorophyll a. Lotus can effectively increase pH, BOD, COD, chlorophyll a, and greatly reduce total phosphorus. It is recommended to increase reed community area and try to expand lotus community in the water areas with severe phosphorus load.

Keywords: *urban wetland, water quality, emergent plant, eutrophication, rubber dam, lacustrine river*

http://www.aloki.hu ● ISSN 1589 1623 (Print) ● ISSN 1785 0037 (Online)
DOI: http://dx.doi.org/10.15666/aeer/1704_78917900

Introduction

Water eutrophication is an environmental problem that has aroused worldwide attention. A large amount of nutrients such as nitrogen and phosphorus of point source and non-point source pollutants enter the water body, which is an important cause of eutrophication (Schaffner et al., 2009; Zhang and Huang, 2011). The sensitivity of various water bodies such as rivers, lakes and reservoirs to eutrophication is closely related to hydrodynamic conditions and climatic conditions of the area where they are located. It is subjected to influence of hydrological, hydrodynamic, physical and chemical environmental factors and food web structures. Therefore, significant differences may exist between different water bodies and geographic locations (Li et al., 2012). Studies have shown that lakes and waters in the Asia-Pacific region are prone to eutrophication in various degrees, with 54% of water bodies exceeding the standard (Wang et al., 2012). Eutrophication degree of lakes in China is obviously higher than the average level in the Asia-Pacific region, and the water body over-standard-rate is up to 66% (Jin and Hu, 2010). At present, wetland water bodies like rivers and lakes have also entered the ranking of eutrophication, and the situation is increasingly serious (Ge et al., 2017).

Yi River, a large river in the Huaihe River Basin, is located in Southern Shandong and Northern Jiangsu, China, with geographical coordinates of 34°23′-36°20′N, 117°25′-118°42′E. About 574 kilometers long, it originates from Yiyuan County, Shandong Province, China, turns into Xinyi River (Yi River Diversion Canal) from Wulou Village, Peixian County, Jiangsu Province, China, and then flows into the Yellow Sea from Yanwei Harbor (Gao et al., 2008, 2009, 2010). Yi River is included in the "10th Five-Year Plan" on water pollution prevention and control in Huaihe River Basin for important control and monitoring. In the plan, the Chinese government points out that the plan is an important basis for the prevention and control of water pollution in the Huaihe River Basin of China, and that the economic construction activities in the Huaihe River Basin must meet the requirements of the plan. In 1997, the longest rubber dam in Asia was built in Xiaobudong, Linyi City section of Yi River, with a total length of 1,135 m. After the successive completion of the stepped rubber dam, water volume in Linyi City section of Yi River increased significantly, and the original shallow wetland conditions changed as demonstrated by cyanobacteria blooms of Yi River urban section in 2009, 2011 and 2015.

A large number of studies have shown that aquatic plants, especially wetland plants, have positive significance in reducing water eutrophication (Huang, 2015). Reed (*Phragmites australis*) wetland is the world's main type of wetland, with a wide distribution and large coverage (Wang et al., 2018). It can treat wastewater through physical, chemical and biological functions (Zeng et al., 2012). Landscape plants or tool species introduced into European urban wetlands are mainly reeds (Korboulewsky et al., 2012), while reeds and lotus (*Nelumbo nucifera*) are widely present in urban wetlands in China (Ge et al., 2017). Lotus and reed have different ecological effects on wetland restoration. Comparing eutrophication inhibition of the two on water body of wetland system of Yi River, evaluating ecological benefits of the two wetland systems, and revealing the response mechanism of water environmental factors not only has ecological theoretical significance, but also has extensive practical application value in the management and evaluation of wetland water ecosystem of Yi River.

http://www.aloki.hu ● ISSN 1589 1623 (Print) ● ISSN 1785 0037 (Online)
DOI: http://dx.doi.org/10.15666/aeer/1704_78917900

Materials and methods

Research basin overview

The average annual precipitation of Yi River Basin is about 850 mm, and the average annual evaporation from water surface is about 1100 mm. There exists an urban wetland of about 3.6 square meters in Xiaobudong Rubber Dam and Jiaoyi Rubber Dam in Yihe City section, Taoyuan Rubber Dam and Liujiadaokou Hub - Yimeng Lake (Gao et al., 2008, 2009, 2010; Li and Gao, 2018).

Water sample collection and detection

In this field survey, three research sample plots were set up in Yimeng Lake of Yi River urban wetland: reed water area (35°107′N, 118°324′E), lotus water area (35°101′N, 118°351′E) and natural water area (35°081′N, 118°356′E). Three sets of duplicate plots were set for each plot, and three sets of duplicate water sample collection points were set for each plot, with one near shore, one in the center and one in the far shore. The sampling time was August 15 (summer), October 20 (autumn), December 16 (winter) of 2018 and February 14 2019 (spring). Sub-surface water samples (about 50 cm underwater) are collected for analysis and detection using 2.5 L clean water buckets.

In laboratory tests, pH, chromaticity, total hardness, dissolved oxygen, BOD, COD, ammonia nitrogen, total nitrogen, total phosphorus, nitrate and chlorophyll a were analyzed. pH was measured by a portable waterproof pH meter (08533797) using glass-electrode method (GB-6920-1986). Chromaticity was determined by dilution factor method according to GB/T 11903-1989. Total hardness was determined according to GB/T 5750.4-2006 by EDTA titration. Dissolved oxygen (DO) was determined by electrochemical probe method according to HJ 506-2009. BOD (5-day biochemical oxygen demand) was determined by 25 mL acid burette (B193) using dilution and inoculation (HJ 505-2009) method. COD (chemical oxygen demand) was determined by 50 mL acid burette (B192) using dichromate method (HJ 828-2017). Ammonia nitrogen (NH_3-N) and total phosphorus (TP) were determined by DR2008 visible spectrophotometer (1429121) using Nessler's reagent spectrophotometry (HJ 535-2009) and ammonium molybdate spectrophotometry (GB-11839-1989). Total nitrogen (TN) was determined by UV-1750ultraviolet-uisible spectrophotometer (A11605031003CS) using UV spectrophotometry (HJ 636-2012). Nitrate was determined by phenol disulfonic acid spectrophotometer according to GB/T 7480-1987. Chlorophyll a (Chla) was detected by acetone spectrophotometry according to HJ 897-2017.

Results and analysis

Water quality evaluation

According to the surface water environmental quality standard (GB 3838-2002), DO, BOD, COD, NH_3-N, TN and TP single indicators were used to evaluate the water quality of reed water area, lotus water area and natural water area of Yimeng Lake in different seasons. In China's surface water environmental quality standards, water quality grades are used to evaluate water quality. If the water level is high, that is the water quality is worse. I-II water is clean, IV water is contaminated, and super IV water is heavily polluted.

http://www.aloki.hu ● ISSN 1589 1623 (Print) ● ISSN 1785 0037 (Online)
DOI: http://dx.doi.org/10.15666/aeer/1704_78917900

In terms of DO, the reed water area has type III water in summer, autumn, winter and spring; the lotus water area has type III water in summer, type IV water in autumn, and type III-IV water in winter and spring; the natural water area has type III-IV water in summer and spring, type IV water in autumn and type III water in winter.

In terms of BOD, the reed water area has type IV-V water in summer and spring, and type V water in autumn and winter; the lotus water area has type V-inferior V water in summer, type V water in autumn and winter, and type IV waster in spring; the natural water area has type V water in summer, autumn and winter, and type IV water in spring.

In terms of COD, the reed water area has type III water in summer, type III-IV water in autumn, and type IV water in winter and spring; the lotus water area has type IV water in summer and autumn, and type III-IV water in winter and spring; the natural water area has type IV water in summer and autumn, and type III water in winter and spring.

In terms of NH_3-N, the reed water area has type II water in summer and spring, type I-II water in autumn, and type III water in winter; the lotus water area has type I-II water in summer, and type II in autumn, winter and spring.

In terms of TN, all of the reed water area, lotus water area and natural water area have inferior type V water in summer, autumn, winter and spring seasons.

In terms of TP, all of reed water area, lotus water area and natural water area have type I water in summer, autumn and spring, and type II water in winter.

Seasonal dynamics of water environment factors

Statistical analysis was performed on all data using SPSS 17.0 Chinese version.

pH characteristics of reed water area, lotus water area and natural water area (*Fig. 1A*). show: that of lotus water area > natural water area > reed water area ($p < 0.01$) in summer; that of lotus water area > natural water area > reed water area ($p > 0.05$) in autumn, with that of reed water area significantly lower than that of lotus water area and natural water area ($p < 0.01$); that of natural water area > natural water area > reed water area ($p > 0.05$) in winter; that of lotus water area > natural water area > reeds water area ($p > 0.05$) in spring.

Chromaticity characteristics of reed water area, lotus water area and natural water area (*Fig. 1B*) show: that of reed water area = natural water area > lotus water area ($p > 0.05$) in summer, with that of lotus water area significantly lower than that of natural water area and reed water area ($p < 0.01$); that of natural water area > reed water area > lotus water area in autumn, with that of lotus water area significantly lower than that of natural water area and reed water area ($p < 0.01$); that of natural water area > reed water area > lotus water area in winter, with that of lotus water area significantly lower than that of natural water area and reed water area ($p < 0.01$); that of reed water area = lotus water area = natural water in spring.

Total hardness characteristics of reed water area, lotus water area and natural water area (*Fig. 1C*) show: that of lotus water area > reed water area > natural water area in summer ($p < 0.01$); that of natural water area > lotus water area > reed water area in autumn ($p < 0.01$), that of reed water area > natural water area > lotus water area in winter ($p < 0.01$); that of natural water area > lotus water area > reed water area ($p > 0.05$) in spring.

Dissolved oxygen characteristics of reed water area, lotus water area and natural water area (*Fig. 1D*) show: that of lotus water area > reed water area > natural water area ($p > 0.05$) in summer, with that of lotus water area significantly higher than that of natural water area ($p < 0.01$); that of reed water area > natural water area > lotus water area in

http://www.aloki.hu ● ISSN 1589 1623 (Print) ● ISSN 1785 0037 (Online)
DOI: http://dx.doi.org/10.15666/aeer/1704_78917900

autumn ($p < 0.01$); that of reed water area > natural water area > lotus water area ($p > 0.05$) in winter, with that of lotus water area significantly lower than that of reed water area and natural water area ($p < 0.01$); that of reed water area > lotus water area > natural water area in spring, with that of reed water area significantly higher than that of lotus water area and natural water area ($p < 0.01$).

BOD characteristics of reed water area, lotus water area and natural water area (*Fig. 1E*) show: that of lotus water area > natural water area > reed water area ($p < 0.01$) in summer; that of natural water area > lotus water area > reed water area ($p < 0.01$) in autumn, with that of reed water area significantly lower than that of natural water area and lotus water area ($p < 0.01$); that of natural water area > lotus water area > reed water area ($p < 0.01$) in winter; that of reed water area > lotus water area > natural water area ($p < 0.01$) in spring.

COD characteristics of reed water area, lotus water area and natural water area (*Fig. 1F*) show: that of lotus water area > natural water area > reed water area in summer ($p < 0.01$); that of natural water area > lotus water area > reed water area in autumn ($p < 0.01$), with that of reed water area significantly lower than that of natural water area and lotus water area ($p < 0.01$); that of reed water area > lotus water area > natural water area in winter ($p < 0.01$)); that of reed water area > lotus water area > natural water area in spring ($p < 0.01$).

The characteristics of ammonia nitrogen in reed water area, lotus water area and natural water area (*Fig. 1G*) show: that of reed water area > lotus water area > natural water area ($p > 0.05$) in summer, with that of reed water area significantly higher than that of lotus water area and natural water area ($p < 0.01$); that of lotus water area > reed water area > natural water area in autumn ($p < 0.01$); that of reed water area > lotus water area > natural water area in winter ($p < 0.01$); that of reed water area > natural water area > lotus water area ($p > 0.05$) in winter.

The characteristics of total nitrogen in reed water area, lotus water area and natural water area (*Fig. 1H*) show: that of lotus water area > natural water area > reed water area in summer ($p < 0.01$); that of natural water area > lotus water area > reed water area in autumn ($p < 0.01$); that of natural water area > reed water area > lotus water area in both winter and spring ($p < 0.01$).

The characteristics of total phosphorus in reed water area, lotus water area and natural water area (*Fig. 1I*) show: that of reed water area > lotus water area > natural water area in summer, with that of reed water area significantly higher than that of natural water area ($p < 0.01$); that of reed water area = natural water area > lotus water area in autumn; that of natural water area > reed water area > lotus water area in winter, with that of natural water area significantly higher than that of lotus water area ($p < 0.01$); that of lotus water area > natural water area > reeds water area ($p > 0.05$) in spring.

Nitrate characteristics of reed water area, lotus water area and natural water area show (*Fig. 1J*) show: that of lotus water area > natural water area > reed water area ($p < 0.01$) in summer; that of natural water area > lotus water area > reed water area in autumn ($p < 0.01$); that of natural water area > reed water area > lotus water area in winter ($p < 0.01$); that of lotus water area > natural water area > reeds water area ($p > 0.05$) in spring.

Nitrate characteristics of reed water area, lotus water area and natural water area show (*Fig. 1K*) show: that of lotus water area > natural water area > reed water area in summer, with that of reed water area significantly lower than that of lotus water area and natural water area ($p < 0.01$); that of lotus water area > reed water area > natural water area in

http://www.aloki.hu ● ISSN 1589 1623 (Print) ● ISSN 1785 0037 (Online)
DOI: http://dx.doi.org/10.15666/aeer/1704_78917900

autumn, with that of natural water area significantly lower than that of lotus water area and reed water area ($p < 0.01$); that of reed water area > lotus water area > natural water area in winter; that of lotus water area > natural water area > reeds water area ($p > 0.05$) in spring.

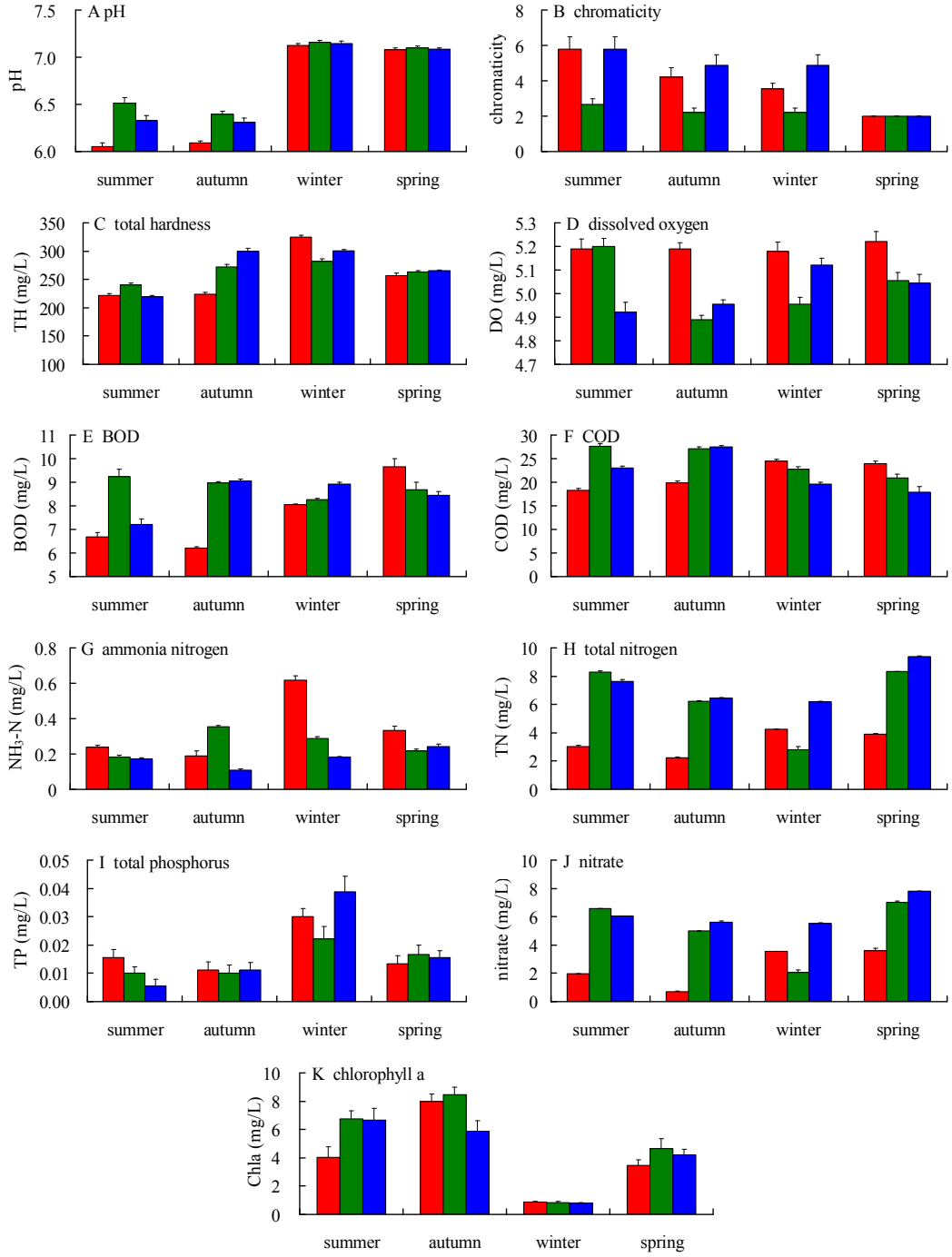

Figure 1. *Differences pH (A), chromaticity (B), total hardness (C), dissolved oxygen (D), BOD (E), COD (F), ammonia nitrogen (G), total nitrogen (H), total phosphorus (I), nitrate (J) and chlorophyll a (K) between water environment factors of reed water area, lotus water area and natural water area in Linyi urban wetland in different seasons.* ■ *reed water area;* ■ *lotus water area;* ■ *natural water area*

http://www.aloki.hu ● ISSN 1589 1623 (Print) ● ISSN 1785 0037 (Online)
DOI: http://dx.doi.org/10.15666/aeer/1704_78917900

Water environmental factor correlation

The correlation between water environmental factors of reed water area (see *Table 1*) shows: pH, total hardness, BOD, COD, ammonia nitrogen, total nitrogen, total phosphorus and nitrate are significantly positively correlated with each other ($p < 0.01$), and significantly negatively correlated with chlorophyll a ($p < 0.01$); chromaticity is significantly negatively correlated with total hardness and COD ($p < 0.01$).

Table 1. *Relevance of water environmental factors of reed water area in Linyi urban wetland in different seasons, China*

	pH	CH	TH	DO	BOD	COD	AN	TN	TP	NI
CH	-0.31									
TH	0.98**	-0.34*								
DO	-0.00	0.04	-0.07							
BOD	0.90**	-0.22	0.86**	0.02						
COD	0.87**	-0.51**	0.88**	-0.06	0.81**					
AN	0.92**	-0.32	0.90**	0.04	0.87**	0.81**				
TN	0.90**	-0.14	0.90**	-0.05	0.93**	0.72**	0.88**			
TP	0.59**	-0.27	0.59**	-0.10	0.67**	0.61**	0.70**	0.61**		
NI	0.87**	-0.16	0.87**	-0.06	0.89**	0.69**	0.89**	0.98**	0.61**	
Chla	-0.68**	0.25	-0.72**	0.18	-0.73**	-0.55**	-0.75**	-0.83**	-0.56**	-0.88**

CH: chromaticity; TH: total hardness; DO: dissolved oxygen; AN: ammonia nitrogen; NI: nitrate
*$p < 0.05$; **$p < 0.01$

The correlation between environmental factors water of lotus water area shows (see *Table 2*): pH is significantly positively correlated with total hardness and total nitrogen ($p < 0.01$), and significantly negatively correlated with BOD, COD, total phosphorus, nitrate and chlorophyll a ($p < 0.01$); total hardness is significantly positively correlated with ammonia nitrogen and total phosphorus ($p < 0.01$), and significantly negatively correlated with dissolved oxygen, BOD, COD, total nitrogen, nitrate and chlorophyll a ($p < 0.01$); dissolved oxygen is significantly positively correlated with total nitrogen and nitrate ($p < 0.01$), and significantly negatively correlated with ammonia nitrogen ($p < 0.01$); BOD, COD, total nitrogen, nitrate and chlorophyll a are significantly positively correlated with each other ($p < 0.01$).

The correlation between water environment factors of natural water area shows (see *Table 3*): pH is significantly positively correlated with total hardness, BOD, dissolved oxygen, ammonia nitrogen and total phosphorus ($p < 0.01$), and significantly negatively correlated with COD, total nitrogen, nitrate and chlorophyll a ($p < 0.01$); total hardness is significantly positively correlated with BOD, dissolved oxygen and total phosphorus ($p < 0.01$), and significantly negatively correlated with total nitrogen, nitrate and chlorophyll a ($p < 0.01$); dissolved oxygen is significantly positively correlated with BOD and total phosphorus ($p < 0.01$), and significantly negatively correlated with COD, total nitrogen, nitrate and chlorophyll a ($p < 0.01$). BOD is significantly positively correlated with total phosphorus ($p < 0.01$), and significantly negatively correlated with ammonia nitrogen, total nitrogen, nitrate and chlorophyll a ($p < 0.01$); COD is significantly positively correlated with chlorophyll a ($p < 0.01$), and significantly negatively correlated with ammonia nitrogen and total phosphorus ($p < 0.01$). Ammonia

http://www.aloki.hu ● ISSN 1589 1623 (Print) ● ISSN 1785 0037 (Online)
DOI: http://dx.doi.org/10.15666/aeer/1704_78917900

nitrogen is significantly positively correlated with total phosphorus ($p < 0.01$), and significantly negatively correlated with chlorophyll a ($p < 0.01$). Total nitrogen is positively correlated with nitrate and chlorophyll a ($p < 0.01$), and significantly negatively correlated with total phosphorus ($p < 0.01$).

Table 2. *Relevance of water environmental factors of lotus water area in Linyi urban wetland in different seasons, China*

	pH	CH	TH	DO	BOD	COD	AN	TN	TP	NI
CH	-0.23									
TH	0.45**	-0.19								
DO	-0.24	0.20	-0.62**							
BOD	-0.39*	-0.19	-0.56**	0.16						
COD	-0.72**	-0.01	-0.57**	0.31	0.727**					
AN	-0.02	-0.31	0.59**	-0.73**	-0.16	-0.17				
TN	-0.82**	0.27	-0.75**	0.55**	0.58**	0.78**	-0.46**			
TP	0.47**	-0.09	0.35*	-0.01	-0.25	-0.35	0.17	-0.50**		
NI	-0.83**	0.23	-0.73**	0.52**	0.59**	0.79**	-0.42*	1.00**	-0.50**	
Chla	-0.83**	0.04	-0.47**	0.01	0.67**	0.81**	0.10	0.75**	-0.48**	0.77**

CH: chromaticity; TH: total hardness; DO: dissolved oxygen; AN: ammonia nitrogen; NI: nitrate
*$p < 0.05$; **$p < 0.01$

Table 3. *Relevance of water environmental factors of natural water area in Linyi urban wetland in different seasons, China*

	pH	CH	TH	DO	BOD	COD	AN	TN	TP	NI
CH	-0.20									
TH	0.47**	-0.18								
DO	0.58**	-0.13	0.413*							
BOD	0.39*	-0.32	0.84**	0.43*						
COD	-0.75**	-0.12	0.06	-0.51**	0.17					
AN	0.52**	0.14	-0.27	0.30	-0.37*	-0.79**				
TN	-0.55**	0.26	-0.91**	-0.57**	-0.85**	0.05	0.24			
TP	0.75**	-0.04	0.52**	0.61**	0.36*	-0.56**	0.39*	-0.56**		
NI	-0.43*	0.10	-0.81**	-0.43*	-0.77**	0.04	0.21	0.83**	-0.52**	
Chla	-0.82**	0.07	-0.53**	-0.65**	-0.43*	0.57**	-0.40*	0.61**	-0.67**	0.40*

CH: chromaticity; TH: total hardness; DO: dissolved oxygen; AN: ammonia nitrogen; NI: nitrate
*$p < 0.05$; **$p < 0.01$

Discussion

Studies in Wuliangsuhai Lake and Baiyangdian Lake show that lotus planting can significantly improve water quality and significantly inhibit the growth of algae in water bodies (He et al., 2013; Li et al., 2018), but attention should be paid to planting density as lotus has a hormesis effect on water algae (Li and Hou, 2007). For reeds with good water purification effect, Dawen River wetland N shows net release when the reeds die and rot in winter, while P shows a net accumulation (Liu and Liu, 2012), which is contrary to our research result. In eutrophic ponds, the increase of total phosphorus

http://www.aloki.hu ● ISSN 1589 1623 (Print) ● ISSN 1785 0037 (Online)
DOI: http://dx.doi.org/10.15666/aeer/1704_78917900

decreases the relative abundance of annual plants without memory officer and increases the relative abundance of annual plants with memory officer (Arthaud et al., 2012). Eutrophication accelerates the decomposition of organic matter in plant litter (Deegan et al., 2012). Jinhewan Urban Wetland is the Driving Type of Total Nitrogen (Fan et al., 2012). Yihe urban wetlands with similar water environment background are also driven by total nitrogen.

Conclusion

Reed can effectively increase dissolved oxygen and greatly reduce BOD, COD, total nitrogen, nitrate and chlorophyll a. Lotus can effectively increase pH, BOD, COD, chlorophyll a, and greatly reduce total phosphorus. In view of the fact that the current urban wetlands in Yihe River are mainly driven by total nitrogen nutrients. We think that the main controlled nutrient parameters of urban wetlands in Yihe River should be total nitrogen. It is recommended to increase natural and artificial reed community area and try to expand lotus community in the water areas with severe phosphorus load.

Acknowledgements. Funded by the Fund of Shandong Provincial Key Laboratory of Water and Soil Conservation and Environmental Protection, Linyi University, NO. STKF201906.

REFERENCES

[1] Arthaud, F., Vallod, D., Robin, J., Bornette, G. (2012): Eutrophication and drought disturbance shape functional diversity and life-history traits of aquatic plants in shallow lakes. – Aquatic Sciences 74: 471-481.

[2] Deegan, L. A., Johnson, D. S., Warren, R. S., Peterson, B. J., Wollheim, W. M. (2012): Coastal eutrophication as a driver of salt marsh loss. – Nature 490(7420): 388-392.

[3] Fan, X. C., Dai, C. F., Lu, X. X., Fan, Y. W. (2018): Studyonphytoplankton functional groups uccession and ddrivingparameters in the Jinhewan UrbanWe Tland. – Acta Ecologica Sinica 38: 5726-5738 (in Chinese).

[4] Gao, Y., Su, Y. X., Qi, S. C. (2008): Phytoplankton and evaluation of water quality in Yi River watershed. – Journal of Lake Sciences 20: 544-548 (in Chinese).

[5] Gao, Y., Ci, H. X., Qi, S. C., Su, Y. X. (2009): Seasonal changes of phytoplankton diversity and assessment of water quality in four tributaries of Yi River. – Research of Environmental Sciences 22: 176-180 (in Chinese).

[6] Gao, Y., Qi, S. C., Su, Y. X., Ci, H. X. (2010): Seasonal changes of phytoplankton diversity and water quality in Yi River and Beng River. – Transactions of Oceanology and Limnology 32(2): 109-113 (in Chinese).

[7] Ge, Z. W., Fang, S. Y., Li, C., Li, Q., Bu, Q. Q., Xue, J. H. (2017): Analysis of the plant N and P sequestration from common reed and common reed + cattail communities in wetland soil in Qinhu Lake of northern Jiangsu, China. – Journal of Lake Sciences 29: 585-593 (in Chinese).

[8] He, L. S., Meng, F. L., Meng, R., Huang, C. H., Li, Y. W., Xi, B. D., Shu, J. M. (2013): In Situ Enclosure Experiment on Nelumbo nucifera for Eutrophication Control in Baiyangdian Lake. – Wetland Science 11: 282-285 (in Chinese).

[9] Huang, X. Y. (2015): Biological cycling of nutrient elements of two plantations in southeast coastal area, China. – Journal of Northwest Forestry University 30(2): 84-89 (in Chinese).

http://www.aloki.hu ● ISSN 1589 1623 (Print) ● ISSN 1785 0037 (Online)
DOI: http://dx.doi.org/10.15666/aeer/1704_78917900

[10] Jin, X. C., Hu, X. Z. (2010): Concept and tactic of clean water runoff generation mechanism restoration in lake watershed. – China Environmental Science 30: 374-379 (in Chinese).
[11] Korboulewsky, N., Wang, R., Baldy, V. (2012): Purification processes involved in sludge treatment by a vertical flow wetland system: Focus on the role of the substrate and plants on N and P removal. – Bioresour Technol 105: 9-14.
[12] Li, D. L., Zhang, T., Xiao, T. Y., Yu, J. B., Wang, H. Q., Chen, K. J., Liu, A. M., Li, Z. J. (2012): Phytoplankton's community structure and its relationships with environmental factors in an aquaculture lake, Datong Lake of China. – Chinese Journal of Applied Ecology 23: 2107-2113 (in Chinese).
[13] Li, L., Hou, W. H. (2007): Inhibitory Effects of Liquor Cultured with Nelumbo nucifera and Nymphaea tetragona on the Growth of Microcystis aeruginosa. – Environmental Science 28: 2180-2186 (in Chinese).
[14] Li, X., Gao, Y. (2018): Influence of the island with grass and the island with trees to water quality in Yihe River, China. – Desalination and Water Treatment 121: 186-190.
[15] Li, X., Xu, X. Q., Gou, M. M. (2018): Study on the influence of lotus planting in Wuliangsu of Inner Mongolia on water environment. – Journal of Environment and Health 35: 457-459 (in Chinese).
[16] Liu, X. W., Liu, J. (2012): N and P dynamic of Phragmites australis and Typha angustata litter in Dawen River wetland during the decomposition. – Journal of Qingdao Agricultural University (Natural Science) 29(4): 289-293 (in Chinese).
[17] Schaffner, M., Bader, H. P., Scheidegger, R. (2009): Modeling the contribution of point sources and nonpoint sources to Thachin River water pollution. – Science of the Total Environment 407: 4902-4915.
[18] Wang, J. L., Li, Y. H., Li, F. D. (2018): Emission fluxes of CO_2, CH_4, and N_2O from artificial and natural reed wetlands in Bosten Lake, China. – Acta Ecologica Sinica 38: 668-677 (in Chinese).
[19] Wang, Z., Zhang, Z. Y., Zhang, J. Q., Zhang, Y. Y., Yan, S. H. (2012): The fauna structure of benthic macro-invertebrates for environmental restoration in a eutrophic lake using water hyacinths. – China Environmental Science 32: 142-149 (in Chinese).
[20] Zeng, W. J., Liu, X., Liu, C. H., Chen, G. C., Liao, B. W. (2012): Comparison on purification effects of *Sonneratia apetala* and *Phragmites communis* wetland systems on nitrogen and phosphorus. – Ecological Science 31: 26-30 (in Chinese).
[21] Zhang, H., Huang, G. H. (2011): Assessment of non-point source pollution using a spatial multicriteria analysis approach. – Ecological Modeling 222: 313-321.

http://www.aloki.hu ● ISSN 1589 1623 (Print) ● ISSN 1785 0037 (Online)
DOI: http://dx.doi.org/10.15666/aeer/1704_78917900

THE INFLUENCE MECHANISM OF A NONLINEAR SYSTEM ON PRECIPITATION INFILTRATION

HE, Y. – WANG, G.*

Institute of Hydrogeology and Environmental Geology, CAGS, 050061 Shijiazhuang, China (phone: +86-186-3308-5615; fax: +86-311-6759-8531)

**Corresponding author*
e-mail: ihegwh@163.com; phone: +86-157-3696-0130; fax: +86-311-6759-8537

(Received 23rd Feb 2019; accepted 3rd May 2019)

Abstract. In order to uncover the heavy precipitation percolation feature and formation mechanism intensity in the deep vadose zone called black box, the nonlinear dynamical system theory was introduced in this paper. By in-situ monitoring the water dynamics in Taihang piedmont deep aeration zone, the heavy precipitation infiltration-evaporation process, wetting front advancing process, water storage changing process were analyzed. The result showed that: (1) the deep vadose zone was a "balance-unbalance-balance" nonlinear dynamical system. And the water infiltration was a typical nonlinear process; (2) the forming mechanism comprised of the internal control parameter vector C determined by vadose zone lithology, and the external forcing terms G(t) determined by rainfall, evaporation and human activities ect.; (3) when the time, space scale is large enough, the non-autonomous system could be transformed into a free system and linear system.
Keywords: *deep vadose zone, soil water distribution, heavy precipitation, nonlinear infiltration, TDR100 system*

Introduction

A nonlinear system cannot be described by a linear mathematical model. In the system at least one part or all parts have nonlinear characteristics and have nonlinear interaction among them. The basic characteristics of nonlinear system lead to the diversity and multiple scales of dynamic process in the system, so the nonlinear system's study is more complicated than the linear system's study. The nonlinear system cannot satisfy superposition principle and its mass action is greater than the sum of partial actions. The interaction of many small nonlinear factors in the nonlinear system may generate unpredictable results. The continual dynamic system could be expressed by the following equations (Li, 2006).

$$\begin{cases} \dot{x}_1 = f_1[(x_1 \mathrm{K}\ x_n)(c_1 \mathrm{K}\ c_m)] \\ \dot{x}_2 = f_2[(x_1 \mathrm{K}\ x_n)(c_1 \mathrm{K}\ c_m)] \\ \qquad \mathrm{M} \\ \dot{x}_n = f_n[(x_1 \mathrm{K}\ x_n)(c_1 \mathrm{K}\ c_m)] \\ \qquad \mathrm{M} \end{cases} \qquad \text{(Eq.1)}$$

At least one of f1, …, fn is nonlinear function, C = (C1, C2, …, Cm) represents control parameter vector and F = (f1, f2, …, fn). So *Equation 1* can be considered a vector.

http://www.aloki.hu ● ISSN 1589 1623 (Print) ● ISSN 1785 0037 (Online)
DOI: http://dx.doi.org/10.15666/aeer/1704_79017907

$$Z = F(X, C) \quad \text{(Eq.2)}$$

The system described by *Equation 2* has no external forcing and is a free system. If external forcing G (t) is introduced the system will be a forcing system which can be expressed by *Equation 3*.

$$Z = F(X, C) + G(t) \quad \text{(Eq.3)}$$

Equation 2 contains the time t so the system is known as non-autonomous system which can be expressed by *Equation 4*.

$$Z = F(X, C, t) \quad \text{(Eq.4)}$$

In *Equations 3* and *4,* G(t) and t are considered as a new state variable and the system can be conformed to free system.

The continual decline in groundwater level in Taihang Piedmont led to the depth of zone of aeration becoming greater (Baram et al., 2016). This is the typical nonlinear system under the interaction of precipitation, evaporation and human activity.

Every layer in the zone of aeration can be marked as Z1, Z2, …, Zn, f1, f2,…,fn are the nonlinear function of soil water potential or water content. The parameters of soil hydraulic properties can be expressed by C1, C2, …, Cm. The external forcing G(t) contains precipitation, evaporation, temperature and mankind's activity. The infiltration process of heavy precipitation takes place on the zone of aeration and be controlled by this nonlinear dynamic system, such as spatial variability (Dahan et al., 2017) inner the system. Meanwhile, the infiltration of heavy precipitation has an adverse effect on this nonlinear system, such as a new external forcing was added to the system over a period of time and cause the infiltration process analysis and simulation of nonlinear dynamic system more complicated (Gupta et al., 2018). Most of the traditional seepage researches in the zone of aeration separate the soil from the infiltration-evaporation process and less likely to carry the above two into a system (Turkeltaub et al., 2016) to explore the inner migration process and mechanism of black box.

In order to subtly study the soil hydraulic characteristics in the zone of aeration under various factors, this paper introduced the nonlinear dynamic systemic mathematic principle and take the heavy precipitation infiltrated into the zone of aeration and the soil as an entity (Min et al., 2017). And this paper analyzes the infiltration-evaporation process, moisture storage variation process, etc and tried to apply the nonlinear dynamic system to interpret the mechanism of the process.

Materials and methods

The study area

From 2012-2013, the study carried out in key field experimental base of the Ministry of Land and Resources in Zhengding, China. The study area has a temperate and semi-humid continental monsoon climate with clearly cut seasons. The annual average temperature is 12.9 °C, the average temperature in July is 26.5 °C and is the highest in a year and in January is the lowest with the temperature is -2.9 °C. The precipitation is focus on June-September and the annual average precipitation is 569.8 mm. The annual average evaporation is 1092.3 mm. The study time period was from April 15th to June

http://www.aloki.hu ● ISSN 1589 1623 (Print) ● ISSN 1785 0037 (Online)
DOI: http://dx.doi.org/10.15666/aeer/1704_79017907

5th. *Figure 1* showed that the heavy precipitation with 70 mm at April 18th, 16 mm at April 21th and 26 mm at April 24th and long-time evaporation process from April 24th to May 16th.

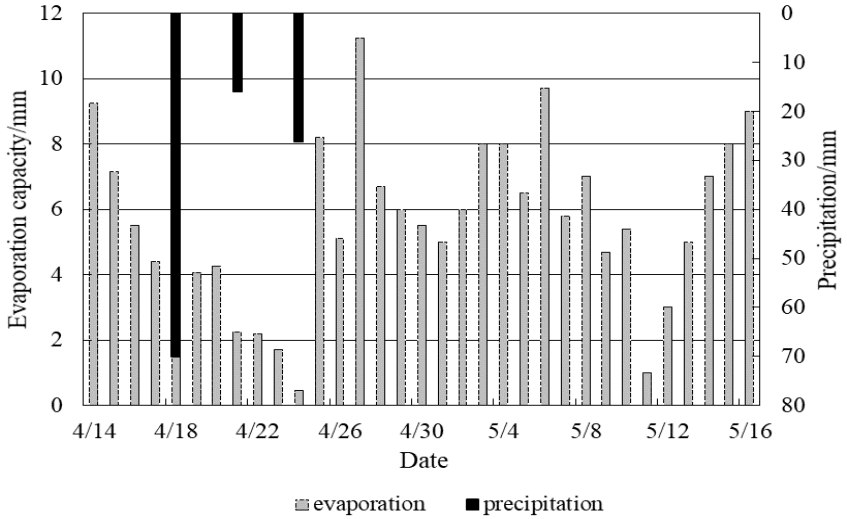

Figure 1. *Rainfall and evaporation (2012)*

Zhengding is located in the Piedmont Clinoplain in the midst of Taihang Mountain with the depth of shallow groundwater depth 36.1-49.1 m. The soil is composed mainly of silt clay and sandy clay, and specific gravity of soil is 2.2-2.74 g/cm^3 (Min et al., 2018).

Monitoring system layout

The study uncovered a typical multi-phase monitoring profile with 33 m depth, 2.5 m inner radius and 3.5 m outer diameter. The Time-Domain Reflectometry system developed by CAMPBELL Company in USA was applied to monitor the soil moisture. The detectors were installed on the inside of the typical profile. 36 CS630 were installed to measure the soil volumetric water content, 36 WATERMARK200-253/257 to measure the soil matric potential and 36 MODEL109 to measure the soil temperature. The buried depth of three kinds of detectors was the same. From the depth of 0.1 m, a detector was installed every 20 cm within 2 m and every 30~70 cm below 2 m. All the detectors were calibrated by the neutron probe and soil sampling.

The monitoring period was from August in 2011 and the monitoring interval was 0.5 h. The TDR systemic time was set up according to the Beijing time. At the same time the meteorological observation was carried out and its observation interval was 0.5 h. It includes 19 general meteorological data, such as precipitation, evaporation, the solar radiation, etc.

Results and discussion

The effect of lithology on infiltration

The control parameter vector $C = (C_1, C_2, \ldots, C_m)$ was internal effect factor of the nonlinear dynamic system. For the nonlinear dynamic system in the zone of aeration the

http://www.aloki.hu ● ISSN 1589 1623 (Print) ● ISSN 1785 0037 (Online)
DOI: http://dx.doi.org/10.15666/aeer/1704_79017907

control parameters are determined by the lithology of every layer. Suppose that C1 was soil particle size, C2 was soil specific retention and C3 was hydraulic conductivity of soil, and among them C1 and C2 was a constant at a particular depth and C3 was a variable changing with the soil moisture content. The above three parameters had an effect on the nonlinear function and there had correlation among them. And the above three parameters were determined by the soil lithology characteristics.

The TDR system was applied to measure and analyze the soil matric potential during the three precipitation-infiltration process and evaporation process. Because the evaporation intensity was great during the April to June so the measurement value was the value at 20:00 of the day for the evaporation process was essentially completed. *Figure 2* shows that 12 detectors measure the soil matric potential daily at different depth of the profile.

According to the measured value at different times, the initial matric potential was significantly lower than the adjacent layers. The initial matric potential was measured under the longstanding stable weak-evaporation condition, and so the main influencing factor of the difference of the soil matric potential at different layer was the lithology. Besides, at April 22th, three days behind the precipitation, the matric potential drop rapidly by 20 cm and the falling speed was greater than other layers. This phenomenon illustrated that water retention capability of soil at 30 cm depth was poor and the soil permeability was high so this layer was the best water passage in relation to the other layers. At the 180 m depth there has the similar simulation.

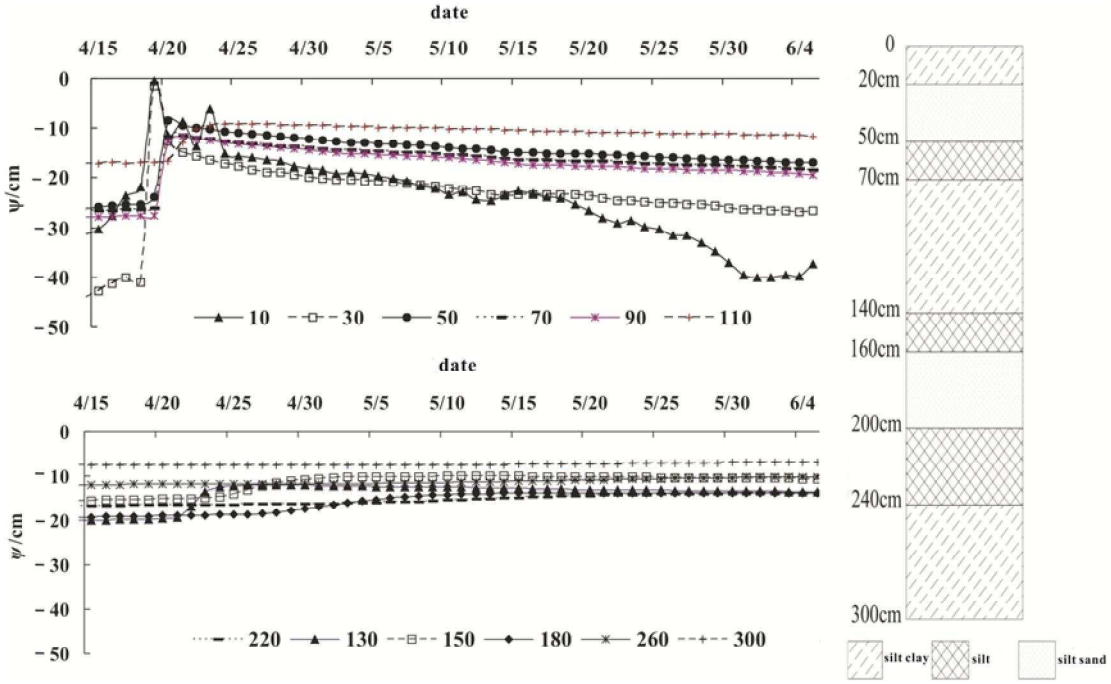

Figure 2. *Soil matrix potential variations of different depth*

The effect of lithology on soil water storage

The lithology has a significant effect on the soil water storage. The precipitation and evaporation changes the soil water storage and this process is a dynamic changing process. For the water storage compute of zone of aeration under one-dimensional

http://www.aloki.hu ● ISSN 1589 1623 (Print) ● ISSN 1785 0037 (Online)
DOI: http://dx.doi.org/10.15666/aeer/1704_79017907

condition, the soil volumetric water content at different depth can be measured, then accumulated the difference value of the soil water content at different time period and finally get the dynamic soil water storage. The CS630 detectors were applied to monitor the soil water content at different depth before heavy precipitation, 4 h and 720 h after precipitation. *Table 1* showed the soil moisture content dynamics at different time period by calculating changes in moisture content at each layer and then cumulated to get the total storage variation.

Table 1. *Soil moisture content dynamics and storage variations at different depth*

Moisture / Depth/cm	θ_1(0h)	θ_2(4h)	(θ_2-θ_1)	ΔW_1/mm	θ_3(720h)	(θ_2-θ_3)	ΔW_2/mm	(θ_3-θ_1)	ΔW_3/mm
10	0.177	0.369	0.192	19.2	0.16	0.209	20.9	-0.017	-1.7
30	0.106	0.26	0.154	30.8	0.164	0.096	19.2	0.058	11.6
50	0.103	0.23	0.127	25.4	0.18	0.05	10	0.077	15.4
70	0.105	0.117	0.012	2.4	0.15	-0.033	-6.6	0.045	9
90	0.123	0.124	0.001	0.2	0.14	-0.016	-3.2	0.017	3.4
110	0.105	0.104	-0.001	-0.2	0.13	-0.026	-5.2	0.025	5
130	0.124	0.124	0	0	0.14	-0.016	-3.2	0.016	3.2
150	0.133	0.134	0.001	0.2	0.16	-0.026	-5.2	0.027	5.4
180	0.12	0.12	0	0	0.15	-0.03	-9	0.03	9
220	0.146	0.145	-0.001	-0.4	0.16	-0.015	-6	0.014	5.6
260	0.25	0.25	0	0	0.265	-0.015	-6	0.015	6
300	0.045	0.045	0	0	0.045	0	0	0	0
Sum				77.6			5.7		71.9

The precipitation was 70 mm and lasted 4 h. θ_1, θ_2, $\theta_3$represented the soil volumetric water content 0 h, 4 h and 720 h after precipitation respectively, ΔW_1 represented the storage variation 4 h after precipitation at different depth, ΔW2 represented the storage variation between 4 and 720 h after precipitation at different depth, ΔW_3 represented the storage variation between 0 and 720 h after precipitation at different depth

In *Table 1,* the storage variation was up to 30.8 mm between 0 and 4 h after precipitation at 30 cm depth and was the maximum at the depth of 0-300 cm. that is because there were coarse soil particles and great porosity. The soil water storage can be increased rapidly during heavy precipitation and dropped quickly from 26% to 18% after 24 h. The high infiltration capacity of this layer was proved again. The storage variation simulation at 180 cm depth was similar to the above situation.

The above phenomenon was determined by the difference of the soil lithologic characters. For the high-content of sands at depth of 30 cm and 180 cm so the soil was named as silty sand according to the international standard. If the natural soil was not disturbed, it is difficult to monitor the mid-deep part of the vadose zone directly and accurately, so the hydrological cycle problem was settled from the point of lithology may be a new idea.

The effect of two and evaporation on infiltration and soil water storage

The nonlinear dynamic system was affected by the external forcing G (t) and was transformed to non-autonomous system. Its character was varying with the time significantly. Two precipitations, relative to the first heavy precipitation, and

http://www.aloki.hu ● ISSN 1589 1623 (Print) ● ISSN 1785 0037 (Online)
DOI: http://dx.doi.org/10.15666/aeer/1704_79017907

evaporation were consistent with this character. The shallow vadose zone approached saturation after heavy precipitation, the soil water content of deep- layers was increased and the permeability of unsaturated soil enhanced. So the two precipitations were easily to form the infiltration and increased the soil water storage. For the deep vadose zone two precipitations were hardly leaked to the groundwater level during the short time period. The process of evaporation varying with time was more significantly, especially at different layers. G (t) in the shallow non-autonomous system was nonlinear and below a certain depth was linear. In this paper the certain depth was 220 cm. When evaporation tends to be constant, G (t) was a constant and the system reached a new balance, the non-autonomous system was transformed to free system. The water storage of vadose zone reverted to the state before heavy precipitation and the storage was again determined by the lithology characteristics.

Conclusions

According to the analysis of the process of infiltration-evaporation, wetting front progradation, storage variation and dynamic variation of total water potential, the infiltration process occurring in the nonlinear dynamic system was typical nonlinear process. The formation mechanism of nonlinear infiltration process includes the inner control parameter vector C and the outer external forcing G(t). When the system suffering the heavy precipitation and evaporation becomes a non-autonomous system and the infiltration process will be determined by G(t) varying with time. When the system tends to be constant, the system becomes a free system and the infiltration process will be determined by the inner parameter vector C, such as the lithology of each layer in vadose zone. And further study is required to establish the specific range of soil particle sizes which can determine the lithology characteristics.

Acknowledgements. This study was funded by the National Natural Science Foundation of China (41877201) and (41672249). We thank the Key Laboratory of China geological survey geothermal resources research center for technical support and all of the partners in this project for their fruitful discussions.

REFERENCES

[1] Baram, S., Couvreur, V., Harter, T., Read, M., Brown, P. H., Kandelous, M., Hopmans, J. W. (2016): Estimating nitrate leaching to groundwater from orchards: Comparing crop nitrogen excess, deep vadose zone data-driven estimates, and HYDRUS modeling. – Vadose Zone Journal 15(11): 1-13.

[2] Dahan, O., Katz, I., Avishai, L., Ronen, Z. (2017): Transport and degradation of perchlorate in deep vadose zone: implications from direct observations during bioremediation treatment. – Hydrology and Earth System Sciences 21(8): 4011.

[3] Gupta, P. K., Yadav, B. K. (2018): Spatial and Temporal Nitrate Transport in Deep Heterogeneous Vadose Zone of India's Alluvial Plain. – In: Thangarajan, M. (ed.) Groundwater. Springer, Singapore, pp. 171-178.

[4] He, Y., Lin, W., Wang, G. (2015): The effect of winter flood irrigation with saline water on groundwater in a typical irrigation area. – Water Science and Technology: Water Supply 15(2): 356-361.

[5] Li, S. Y. (2006): Nonlinear Science and Complexity Science. – Harbin Institute of Technology Press, China.

http://www.aloki.hu ● ISSN 1589 1623 (Print) ● ISSN 1785 0037 (Online)
DOI: http://dx.doi.org/10.15666/aeer/1704_79017907

[6] Min, L., Shen, Y., Pei, H., Jing, B. (2017): Characterising deep vadose zone water movement and solute transport under typical irrigated cropland in the North China Plain. – Hydrological Processes 31(7): 1498-1509.
[7] Min, L., Shen, Y., Pei, H., Wang, P. (2018): Water movement and solute transport in deep vadose zone under four irrigated agricultural land-use types in the North China Plain. – Journal of Hydrology 559: 510-522.
[8] Turkeltaub, T., Kurtzman, D., Dahan, O. (2016): Real-time monitoring of nitrate transport in the deep vadose zone under a crop field – implications for groundwater protection. – Hydrology and Earth System Sciences Discussions 20: 3099-3108.

http://www.aloki.hu ● ISSN 1589 1623 (Print) ● ISSN 1785 0037 (Online)
DOI: http://dx.doi.org/10.15666/aeer/1704_79017907

INDOOR THERMAL ENVIRONMENT OF URBAN RESIDENTIAL BUILDINGS IN LHASA, CHINA

WANG, Q. – ZHAO, J. Y.*

School of Architecture, Chang'an University
No. 75 Chang'an Middle Road, 710061 Xi'an, China
(phone: +86-29-8233-7241; fax: +86-29-8220-2729)

**Corresponding author*
e-mail: zjyqtt@163.com; phone: +86-186-9182-0234; fax: +86-29-8220-2729

(Received 23rd Feb 2019; accepted 3rd May 2019)

Abstract. In Lhasa area, the solar radiation intensity is relatively high, so in order to satisfy the indoor natural lighting quality, it is easy to cause overheating in the south-facing room and non-uniform heat in the north-facing room with lower room temperature. In this paper, Dest-h software is used to simulate and study the base temperature and average energy consumption of non-heating residential buildings under different window-wall ratio and partition wall conditions, trying to find out the structural measures and design methods to improve the indoor thermal uniformity.
Keywords: *solar radiation intensity, non-uniformity, Dest-h, base temperature, building energy consumption*

Introduction

As a cold area, Lhasa needs heating in winter according to the Code of Thermal Design of Civil Buildings in China. But heating is expensive because fuel and coal are imported from other areas. However, thanks to the strong solar radiation, the annual sunshine time of more than 3,000 h, and the annual total solar radiation of 7,000 MJ/m^2 (Xiao, 2010), Lhasa region has unique solar energy resources. Through literature review (Zhang and Liu, 2008; Li and Liu, 2017; Liu, 2017; Kang, 2012; Li, 2017) and field review in 2016-2017, it was found that the flat roof buildings sitting north and south are adopted most commonly in this area, maximizing the use of opening area of south-facing glass window or passive energy-saving technology with additional sunshine, so as to obtain more solar radiation heat, thereby increasing the indoor temperature of the room, and ultimately reducing the heating load demand of the building. Nonetheless, the contradiction between excessive heating area and strong solar radiation resources makes indoor thermal non-uniformity the most significant thermal comfort problem of residential buildings in this area. For example, in winter, the south-facing room is overheated during the day, residents need to open windows, and the north-facing room has a lower temperature all day, residents are unwilling to stay in it.

Based on the field test and simulation analysis of residential buildings in cities and towns in Tibet Plateau, Liu et al. (2011) put forward the basic theory and calculation method of low-energy building design suitable for the natural and climatic conditions of Tibet Plateau. In view of the abundant solar energy resources in this area, Yang et al. (2010) put forward a heating mode that is mainly passive solar heating, supplemented by active heating and other heating modes, and combined it with passive and active heating, in order to improve the indoor thermal environment quality and reduce building energy consumption. Liu et al. (2008) tested the indoor and outdoor temperature of traditional houses in Lhasa area, and concluded that increasing the area of south-to-

http://www.aloki.hu ● ISSN 1589 1623 (Print) ● ISSN 1785 0037 (Online)
DOI: http://dx.doi.org/10.15666/aeer/1704_79097916

outdoor windows does not reduce the indoor minimum temperature, but can also improve the indoor average temperature and maximum temperature. Wang et al. (2012) tested and compared the indoor thermal environment of two residential buildings in Tibet using traditional building materials and modern building materials. It was concluded that the thermal insulation performance of traditional building materials in eastern Tibet was better than that of modern building materials. Wang (2018) divided the typical rural buildings in Tibet into space zoning modes, determined the structural parameters and thermal performance of the local typical building envelopes, and simulated and analysed the zoning modes. Domestic papers building thermal environment research in Tibet focuses, mainly on rural building envelope materials or indoor thermal environment energy-saving design, but there are few studies on indoor thermal heterogeneity, especially in urban residential buildings.

Aiming at the problem of indoor thermal non-uniformity in Lhasa area, the dynamic simulation of energy consumption of typical buildings in south and north rooms was carried out in this paper, according to the requirement of 65% energy saving in Lhasa area by means of Dest-h software simulation analysis, and the structural measures and design methods to improve the indoor thermal non-uniformity were explored in order to further improve the indoor thermal environment quality of buildings there.

Methodology

Climate parameters

In order to avoid the influence of weather instability on the accuracy of the calculation results, the typical meteorological year data (TMY) was used as the input condition, which is the hourly meteorological data of DeST software, and the number of air exchange is 0.5 times/h (Tianjin Eco-city Green Building Research Institute, Tsinghua University Building Energy Research Center, 2009). Room heat disturbance is determined by its use function. Indoor per capita calorific value was set at 53 W; lighting load was set at 60 W according to gross index input; the equipment load was set at 12.7 W/m^2 according to the average index input.

The slab buildings with two families sharing one staircase are the most representative residential building model in Lhasa. Usually, the buildings in this area are oriented to the south, with 6 stories and 3 m high. The plan is shown in *Figure 1*.

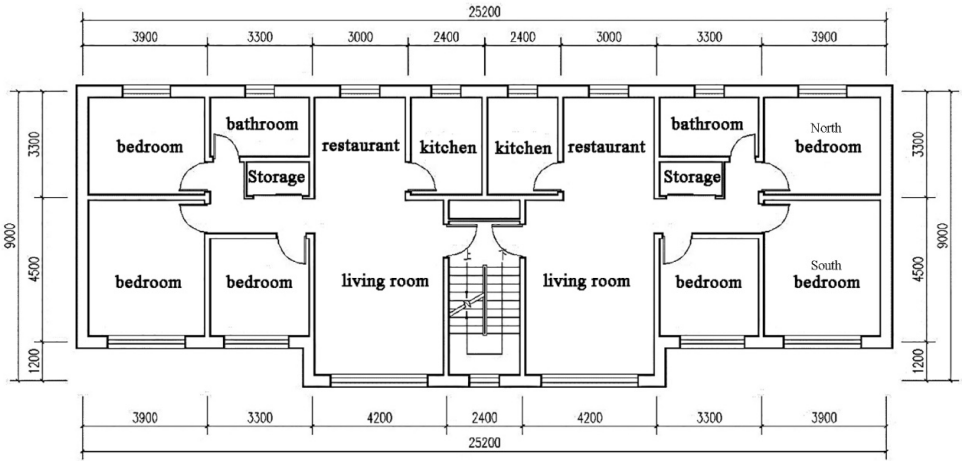

Figure 1. *Simulated model plan*

http://www.aloki.hu ● ISSN 1589 1623 (Print) ● ISSN 1785 0037 (Online)
DOI: http://dx.doi.org/10.15666/aeer/1704_79097916

Building envelope parameters

The parameters of roof, exterior wall, interior wall, ground, floor, exterior window and exterior door are set at the limit value prescribed by the code (DBJ540001-2016, 2016). The thermal parameters of materials and components are selected from the *Code for Thermal Design of Civil Buildings*, as shown in *Table 1*.

Table 1. *Thermal parameters of building envelope*

Name of envelops	Materials of envelops	Heat transfer coefficient K W/(m^2·K)
Roof	20 thick lime mortar + 50 thick polyurethane insulation layer + 20 thick cement mortar + 100 thick reinforced concrete slab + 20 thick cement mortar	0.42
Exterior wall	20 thick lime mortar + 40 thick extruded polystyrene board + 370 thick lime sand brick wall + 20 thick cement mortar	0.53
Interior wall	20 thick cement mortar + 240 thick cement-sand brick wall + 20 thick cement mortar	2.0
Ground	Concrete floor	2.9
Floor	20 thick cement mortar + 60 thick lightweight aggregate concrete + 100 thick reinforced concrete slab + 20 thick cement Mortar	4.8
Exterior window	6 + 12 + 6 double glazed window	2.8
Exterior door	Solid wood door	2.0

Results

Window-wall ratio

The window-wall ratio is a key index affecting indoor thermal environment. It is stipulated in the *Design Standard for Energy Efficiency of Residential Buildings in Severe Cold and Cold Zones* that the window-wall ratio of residential buildings in Cold Area A is not more than 0.5 (JGJ 26-2010, 2010). However, there is no limit value of window-wall ratio in the *Standard for Energy-saving Design of Civil Buildings in Tibet Autonomous Region*. But Lhasa is a cold area with strong solar radiation. The larger the size of the window opening, the greater the heat loss in the room. For the north room, the window size only needs to meet the functional lighting requirements of the room. Therefore, the northward window-wall ratio is set to 0.12. For the south room, it is necessary to maximize the solar radiation heat, but also to prevent indoor overheating. As a result, the south-facing window-wall ratio range is 0.3-0.8.

With the same thickness of partition wall and different window-wall ratios, the dynamic simulation of energy consumption of typical buildings in south and north rooms was carried out by using Dest-h software. Results are shown in *Figure 2,* when the window-wall ratio in residential buildings is too large, that is, above 0.6, the average building energy consumption value has dropped to 0 w/m^2, the base temperature of the south room has reached 26.37 °C, and that of the north room is 19.96 °C, and the temperature difference between the two rooms is 6.41 °C. As shown in *Figure 3,* the base temperatures of the south room and north room increases with the increase of the south window-wall ratio. With the increase of the south window-wall ratio, the

http://www.aloki.hu ● ISSN 1589 1623 (Print) ● ISSN 1785 0037 (Online)
DOI: http://dx.doi.org/10.15666/aeer/1704_79097916

temperature fluctuation of the south room increases from 1.52 to 3.45 °C, and the temperature fluctuation of the north room increases from 0.8 to 1 °C. The temperature difference between the south room and north room increases from 4.31 to 7.28 °C, and the fluctuation also increases significantly. If only the south window is used to obtain the solar radiation, when the window-wall ratio is 0.4 and above, the average temperature of the room is above 16 °C, which basically meets the requirements of indoor thermal environment.

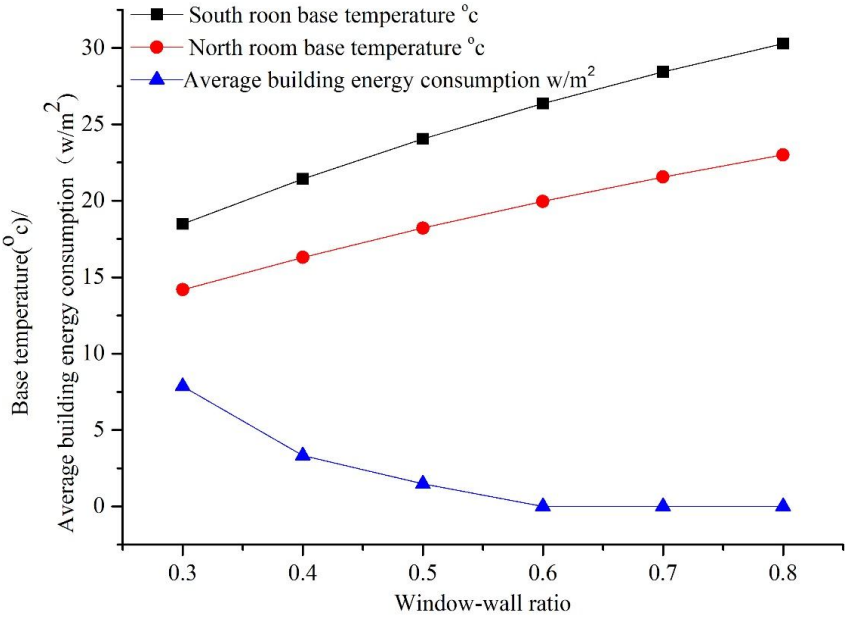

Figure 2. *The base temperature and average building energy consumption of south room and north room on the coldest day in Lhasa area with different window-wall ratios*

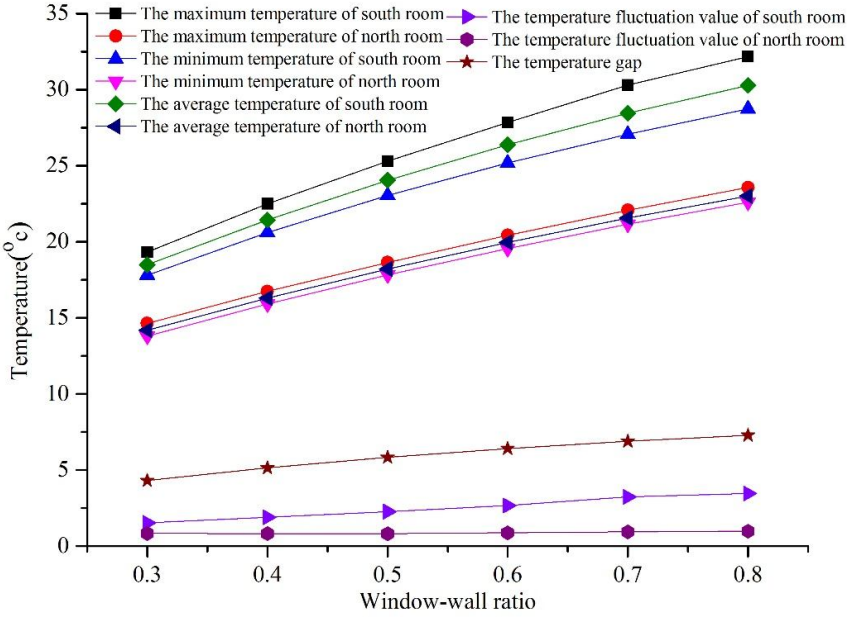

Figure 3. *The maximum, minimum, average temperature and temperature difference of south room and north room on the coldest day without heating (°C)*

http://www.aloki.hu ● ISSN 1589 1623 (Print) ● ISSN 1785 0037 (Online)
DOI: http://dx.doi.org/10.15666/aeer/1704_79097916

Partition wall

Under different heat transfer coefficients, the base temperature of rooms facing south and north of residential buildings in Lhasa area was simulated and analyzed. The values of different heat transfer coefficients K and the corresponding partition construction methods are shown in *Table 2*.

Table 2. *Values of different heat transfer coefficients K and their corresponding partition construction practices*

Conditions	Heat transfer coefficient K[W/(m^2·K)]	Recommended practices of partition wall construction
Case1	0.7	200 thick aerated concrete block wall (0.723)
Case2	1.2	100 thick aerated concrete block wall (1.207)
Case3		370 thick porous brick wall (1.248)
Case4	1.6	240 thick porous brick wall (1.624)
Case5		370 thick lime sand brick wall (1.641)
Case6	2.0	240 thick lime sand brick wall (2.036)
Case7	2.3	120 thick porous brick wall (2.251)
Case8	2.6	120 thick lime sand brick wall (2.618)
Case9	3.2	50 thick plasterboard partition (3.23)
Case10	6.3	12 thick glass partition wall (6.3)

Under the same window-wall area ratio, different thickness of partitions and construction methods, the hourly room temperature comparison curves of south and north-facing rooms in winter solstice are shown in *Figures 4* and *5*. Even in the case of glass partitioning, although the thermal non-uniformity of rooms in the south and north directions decreases, there is still a temperature difference of 5.01 °C. The results show that after the passive energy-saving technology is maximized, the large temperature difference between the south and north-facing rooms still exists. Therefore, the main method to solve the problem of indoor thermal non-uniformity is how to make rational use of the south-facing heat collection area to store or transfer heat to the north-facing room.

Discussion

If only the south window is used to obtain the solar radiant, when the east and the west window-wall ratios are 0, the north window-wall ratios is 0.12, the south window-wall ratio is greater than or equal to 0.4. On the coldest day, the average temperature of the south and the north rooms is above 16 °C, which basically meets the requirements of indoor thermal environment. If the south window-wall ratio is greater than 0.4, the fluctuation value of base temperature in south room is greater than that in north room, and the fluctuation value of base temperature in north room is basically unchanged, which indicates that the heat from the south room is difficult to transfer to the north room. Therefore, it is considered to adopt a solar building form to solve indoor thermal non-uniformity when the south in south direction is greater than 0.4.

http://www.aloki.hu ● ISSN 1589 1623 (Print) ● ISSN 1785 0037 (Online)
DOI: http://dx.doi.org/10.15666/aeer/1704_79097916

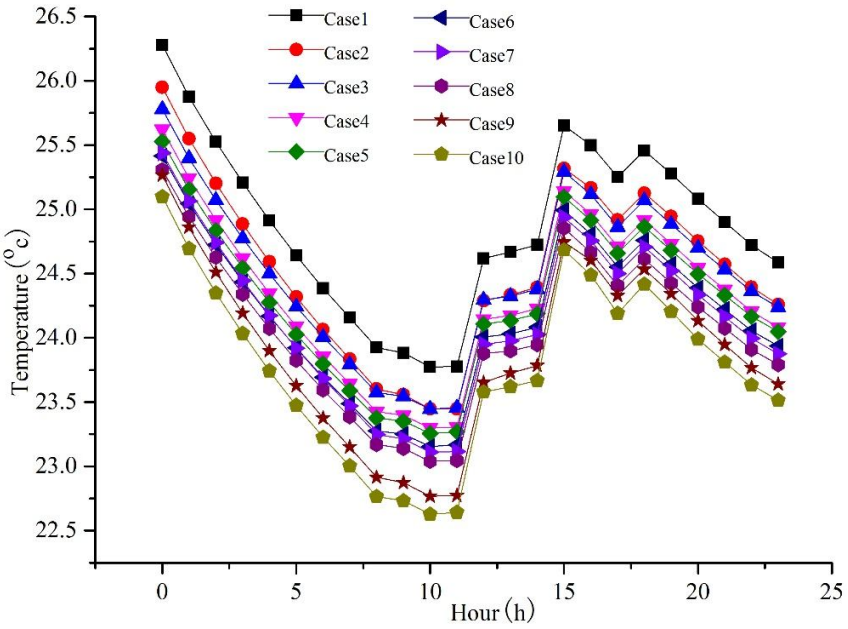

Figure 4. *Comparison of room temperature in south room under different partition conditions on winter solstice*

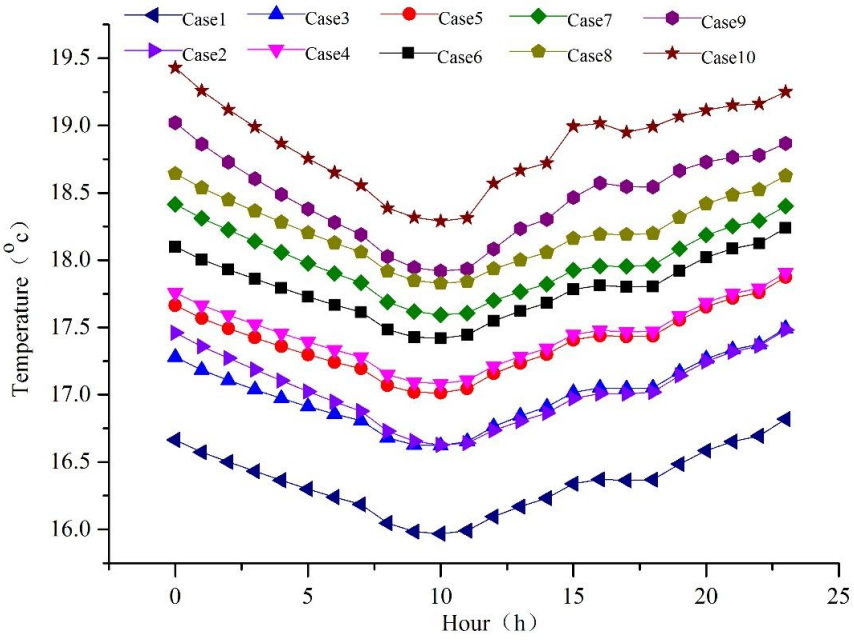

Figure 5. *Comparison of room temperature in north room under different partition conditions on winter solstice*

At present, the research focus of solar energy utilization in Lhasa area is on improving the efficiency of heat collection, which should be transferred to utilizing heat transfer to solve the non-uniformity of indoor temperature field. However, in the organic integration and utilization of building materials, building structures, building

http://www.aloki.hu ● ISSN 1589 1623 (Print) ● ISSN 1785 0037 (Online)
DOI: http://dx.doi.org/10.15666/aeer/1704_79097916

equipment and intelligent control methods, it still has the characteristics of simplification and one-sidedness. How to utilize the seasonality, randomness, periodicity and controllability of solar energy in different seasons, different periods and different heating areas to obtain the reasonable heat control, storage and use management of solar energy in time-sharing, zoning and seasons is an effective means to reduce energy consumption, improve indoor thermal comfort and solve the problem of non-uniformity of indoor temperature field.

In terms of installation mode, flat-plate solar collectors are mostly installed in fixed way in solar energy building, and wall-mounted type is adopted in order to ensure solar energy collection area in installation position. However, the former cannot adjust the angle of solar panels according to the change of all-day solar elevation angle, which leads to low efficiency of solar energy acquisition; the latter affects the facade design of buildings on the one hand. The latter on the one hand affects the design of building exterior facade, on the other hand has some potential safety hazards because it hangs directly on the wall surface. Therefore, the integrated design method of solar building with window solar energy system as heat storage component can be considered. At the same time, glass partition or light partition wall with large heat transfer coefficient should be adopted as indoor partition wall as far as possible.

Conclusions

In this paper, the indoor thermal environment and energy consumption of residential buildings in Lhasa under different window-to-wall ratios and partition conditions were simulated and analyzed. The results show that the indoor thermal environment of residential buildings in Lhasa still exhibits thermal non-uniformity under the condition of maximizing the use of passive energy-saving technology. When the east and the west window-wall ratios are 0, the north window-wall ratios is 0.12, the south window-wall ratio is greater than or equal to 0.4, glass partition or light partition wall with large heat transfer coefficient should be adopted as indoor partition wall as far as possible. On this basis, it is necessary to build window solar energy storage and energy-using equipment in combination with local climate, so that thermal energy can be transferred from south to north-facing rooms, reduce or avoid indoor discomfort, and reduce energy consumption.

Acknowledgements. This work was financially supported by National Key Research Project of China (Project No.: 2016YFC0700400); Fundamental Research Funds for the Central Universities of China (Project No.: 310841172101).

REFERENCES

[1] DBJ540001-2016 (2016): Tibet Autonomous Region Energy Efficiency Design Standard for Civil Buildings. – Tibet People's Publishing House, Tibet.
[2] JGJ 26-2010 (2010): Energy-saving design standards for residential buildings in severe cold and cold regions. – China Building Industry Press, Beijing.
[3] Kang, H. T. (2012): Study on design of low energy consumption residential buildings in Plateau alpine region. – Xi'an University of Architecture and Technology, Xi'an.

http://www.aloki.hu ● ISSN 1589 1623 (Print) ● ISSN 1785 0037 (Online)
DOI: http://dx.doi.org/10.15666/aeer/1704_79097916

[4] Li, E. (2017): Analyses of influence of residential building space organization on heating energy consumption in Lhasa. – Journal of Southeast University (English Edition) 33(4): 457-465.
[5] Li, E., Liu, J. P. (2017): Influence of the buffer-space design on winter heating energy consumption in Lhasa. – Journal of Civil, Architectural & Environmental Engineering 39(04): 40-47.
[6] Liu, J. P., Yang, L., Liu, Y. F., Tian, G. M. (2011): Key technological research and application of low energy consumption building design in Tibet. – China Engineering Science 13(10): 40-46.
[7] Liu, L. (2017): Study on Energy-saving Reconstruction Scheme of Residential Building Envelope in Lhasa Area. – Xi Hua University, Chengdu.
[8] Liu, Y. F., Liu, J. P., Yang, L., Li. J. (2008): Measuring study of passive solar house for traditional dwelling building in LhaSa area. – Solar Energy 4: 391-394.
[9] Tianjin Eco-City Green Building Research Institute, Tsinghua University Building Energy Research Center (2009): Building Energy Simulation and Operating Tutorial of eQUEST & DeST. – China Building Industry Press, Beijing.
[10] Wang, P. Q., Leng, Y. H., Xu, G. T. (2012): Analysis on thermal environment current situation of residential buildings in the south-eastern of Tibet. – Architecture Science 28(03): 65-68.
[11] Wang, W. K. (2018): Study on Thermal Design and Energy Saving Structure of Indoor Partition Solar Heating Building. – Xi'an University of Technology, Xi'an.
[12] Xiao, W. (2010): Study on the Direct-Gain Solar Heating in Remote Southwest Tibet. – Tsinghua University, Beijing.
[13] Yang, L., Zhu, X. R., Liu, Y. F., Liu, J. P. (2010): Review of design standard for energy efficiency of residential buildings in Tibet Autonomous Region. – HVAC 40(09): 51-54.
[14] Zhang, Y. Z., Liu, J. P. (2008): Current state and the trend of development of residential building in Lhasa. – Journal of Architecture 11: 33-35.

http://www.aloki.hu ● ISSN 1589 1623 (Print) ● ISSN 1785 0037 (Online)
DOI: http://dx.doi.org/10.15666/aeer/1704_79097916

GRANULAR FERTILIZER MASS PREDICTION FOR ELECTRIC FERTILIZER DISTRIBUTION DEVICE BASED ON RANSAC

HAN, J.[1] – WANG, X. T.[1] – ZHOU, Z.[1] – WANG, X.[2*]

[1]*Electrical and Information College, Heilongjiang Bayi Agricultural University Daqing 163319, PR China*

[2]*Engineering College, Heilongjiang Bayi Agricultural University, Daqing 163319, PR China*

[*]*Corresponding author*
e-mail: byndwangx@163.com

(Received 23rd Feb 2019; accepted 3rd May 2019)

Abstract. To improve the precision of granular fertilizer mass measured via microwave Doppler technology, this study proposed a method based on RANSAC to predict granular fertilizer mass for fertilizer apparatus. The maximum value, the minimum value, and a random value in the sample data were selected to obtain the best-fitting line that contained most interior points using iterative method. The fitting result of LS method was also presented to compare with the proposed scheme. Simulation results and experimental results illustrate that RANSAC method has a higher prediction precision than traditional LS method and a better ability to reduce the effect of measurement error.
Keywords: *microwave Doppler, sensor, solid flow and mass, electric fertilizer distribution, opening degree*

Introduction

In recent years, grain system applied in agricultural production has been modernized and normalized in China. Solid flow meter is widely used in the field of variable rate fertilization, grain storage, and flour milling measurement. Online continuous measurement and the follow-up control of solid mass plays an important role in different agricultural industries, and creates a massive demand for solid flow and mass monitoring system. The precision of solid flow and mass measurement has a significant meaning on precision fertilization and energy saving. A large variety of methods used to measure solid flow and mass have been proposed in the past twenty years.

Invasive method and non-invasive method are the two common ways to measure solid flow and mass in delivery pipe (Yan and Stewart, 2000). Invasive method using apparatus with direct connection to the measuring object. Invasive instrument is regularly utilized to measure the flow of stive and corrosion without direct contact, which has a better stability, a higher precision and a longer service life. Hence the invasive method has been studied in the previous research of solid flow and mass measurement field (Zheng, 2010). Using Doppler frequency shift in the wave propagation, Doppler measurement is an invasive method, which includes laser Doppler measurement, ultrasound Doppler measurement, and photon Doppler measurement (Dimaczek et al., 1994).

Crame indicated the advantages of Doppler method applying ultrasound Doppler to different kinds of liquid metal flow measurement (Cramer et al., 2013). Shames et al. (2013) studied target location and signal of Doppler frequency shift (Shames et al., 2013; Karaboga and Latifoglu, 2013). Isa and Wu (2004) designed a solid flow

http://www.aloki.hu ● ISSN 1589 1623 (Print) ● ISSN 1785 0037 (Online)
DOI: http://dx.doi.org/10.15666/aeer/1704_79177925

monitoring system based on microwave Doppler radar sensor, and pointed out that the echo energy, which was transformed from solid flow signal using FFT (Fast Fourier Transform), and solid mass had a linear relation (Isa and Wu, 2004, 2006). Pang et al. (2018) investigated the relation between grain size and dielectric constant and proposed a real time invasive measurement for solid granule.

Random Sample Consensus (RANSAC) method builds a mathematics model to estimate parameters even if there is abnormal data in the data set (Hossein-Nejad and Nasri, 2016; Niedfeldt et al., 2017). Wang et al. (2016) presented a RANSAC method based on screening and matching, which has a high robustness in the environment of contamination and low computation complexity. Based on RLS model, granular mass was obtained via power spectral density in the previous studies, resulting in low sampling precision. As an iterative algorithm, RANSAC method is used to estimate the parameter of mathematics model in an outlier observation data. RANSAC method is usually applied in the field of spectral analysis and image processing. To the authors' best knowledge, RANSAC has been rarely used in the granule fertilizer mass measurement. To improve the accuracy of the granule fertilizer mass, RANSAC method is used to obtain the optimal linear function of the sample in this study.

The study focused on fertilizing mass measurement of granular fertilizer. Data set collected by Doppler sensor is the voltage of echo signal, and output of the mathematics model is the mass of granule fertilizer. A granular fertilizer applicator was developed in Heilongjiang Bayi Agricultural University to collect echo signal voltage by microwave Doppler radar sensor. The relationship of fertilizer apparatus open degree and granular fertilizer mass was investigated using Random Sample Consensus (RANSAC) algorithm. The fertilizer mass prediction model provides reference for the optimization of solid flow and mass measurement. Simulation and experimental results show that the RANSAC method used to predict the mass of granular fertilizer online has a high precision and stability. The presented method provides a scientific fundament for mass measurement of granular material, which has a great meaning of improving the grain quality and yield.

Materials and methods

Materials

In this research, this fertilizer is granular compound fertilizer diammonium phosphate, and the total nutrient of granule fertilizer: (N+P2O5)≥64.0%.This granular fertilizer is irregular granular and its surface is smooth, which is suitable for signal acquisition by microwave Doppler sensor.

Methods of the RANSAC Algorithm for granular fertilizer mass prediction

Structure of granular fertilizer applicator

Figure 1 shows the structure of the granular fertilizer applicator. The appliance is consisted of fertilizer box, electric fertilizer apparatus, microwave Doppler radar sensor, data collector, and a computer. Capacity of the fertilizer box is 20 L. Power of the fertilizer apparatus is 12V / 50W. Diameter of the fertilizer pipeline is 4 cm. Microwave Doppler radar sensor is installed outside of the pipeline 30 cm away from the release location of the granular fertilizer.

http://www.aloki.hu ● ISSN 1589 1623 (Print) ● ISSN 1785 0037 (Online)
DOI: http://dx.doi.org/10.15666/aeer/1704_79177925

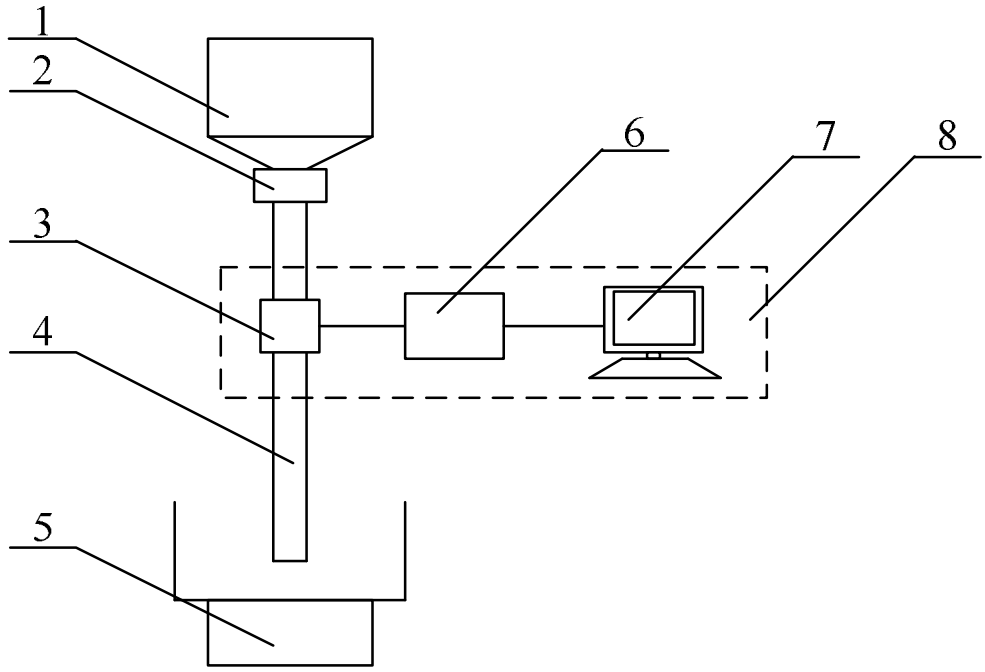

Figure 1. *Structure of granular fertilizer flow measurement appliance. 1-Storage Silo, 2-Electric Fertilizer Distribution Device, 3-Microwave Doppler Sensor, 4-Distributing Pipe, 5-Weighing Machine, 6-Data Acquisition Unit, 7-Computer, 8-Micorwave Doppler Solid Mass Flow Measurement System*

Algorithm description

For the granular fertilizer mass prediction model, voltage value of echo signal is taken as data set, unknown parameter of the sample model is granular fertilizer mass. The Voltage measured by Doppler sensor is linearly related to the opening degree of fertilizer apparatus. To improve the accuracy of the fitting line obtained by RANSAC method, the minimum value (X1, Y1), the maximum value (X2, Y2), and a random value (X3, Y3) are chosen in the establishment process of the initialized model. The three values are reserved in subset $\mathbf{M_i}$. The optimal linear model determined by the three feature points is given as *Eq.1*.

$$\mathbf{Ax + By + C = 0} \tag{Eq.1}$$

The distance from other point (Xi, Yi) to the optimal line is given as *Eq.2*.

$$d_i = \frac{|Ax_i + By_i + C|}{\sqrt{A^2 + B^2}} \tag{Eq.2}$$

If di<dh, (Xi, Yi) is inside the sample set $\mathbf{M_i}$, otherwise is outside the sample set. The inside point set is used to estimate a new line via least square (LS) method.

t is the probability of the inside point appearing in the sample set, which is expressed as *Eq.3*.

$$\mathbf{t} = \frac{n_{inliers}}{n_{inliers} + n_{outliners}} \tag{Eq.3}$$

http://www.aloki.hu ● ISSN 1589 1623 (Print) ● ISSN 1785 0037 (Online)
DOI: http://dx.doi.org/10.15666/aeer/1704_79177925

The probability of at least one of the three points exiting outside the sample set is defined as *Eq.4*.

$$1 - t^3 \quad \text{(Eq.4)}$$

If none of the three points is inside point in k times random sampling, there is $(1 - t^3)^k$. The wrong solution is obtained as *Eq.5*.

$$P = 1 - (1 - t^3)^k \quad \text{(Eq.5)}$$

where, *k* is iteration step, which is the minimum number of random sampling. *P* is the probability of obtaining the right solution.

The probability of inside point *t* is a priori value, which has a crucial influence on the judgement of inside point and outside point. To ensure the probability *P* of the right solution, iteration step *k* must increase even if *t* is large. From *Eq.6*, *k* can be calculated if *P* is known.

$$k = \frac{\lg(1-p)}{\lg(1-t^3)} \quad \text{(Eq.6)}$$

Simulation results

Data acquisition

Data acquisition instrument developed at Heilongjiang Bayi Agriculture University was employed to measure the flow of large granular urea in the field experiment. Diameter of the urea granular fertilizer used in experiment was 2.00 mm-4.75 mm. The acquisition frequency was 500 Hz. Echo signal voltage of the granular fertilizer flow waveform was obtained. The waveform of 10%, 50% and 100% opening degree is shown in *Figure 2*.

The voltage of each 10 percent of the fertilizer apparatus opening degree was measured for six times. Mass of each 10 percent opening degree was also measured using electronic scale for six times. The acquisition time was 10 seconds, which was counted by a time relay to improve the timing precision. *Table 1* is the average mass. To indicate accuracy of the measurement, maximum error between acquisition value and average value is also presented in *Table 1*.

Granular fertilizer mass prediction based on LS

Table 2 is granular fertilizer mass in one-unit interval and quadratic sum of voltage amplitude at each 10% opening degree. $\frac{1}{n}\sum_{i=1}^{n} V^2$ is the average value of the echo signal voltage amplitude. *Figure 3* is the fitting line of voltage amplitude average value and mass of different opening degree in one-unit interval based on LS.

The predicting equation based on LS method shown in *Figure 3* is expressed as *Eq.7*.

$$y = 0.0885x - 0.0992 \quad \text{(Eq.7)}$$

http://www.aloki.hu ● ISSN 1589 1623 (Print) ● ISSN 1785 0037 (Online)
DOI: http://dx.doi.org/10.15666/aeer/1704_79177925

where, y is average value of the voltage amplitude, x is granular fertilizer mass in one unit interval. *Table 3* is the absolute error between actual value and LS prediction value.

The nonlinear error is given by Eq.8.

$$\epsilon_{LS} = \frac{|(\Delta y_L)_{max}|}{y_{FS}} \times 100\% \quad \text{(Eq.8)}$$

where, y_{FS} is full range output, $\Delta(y_L)_{max}$ is the maximum deviation in the measurement points.

The maximum deviation occurred when the fertilizer apparatus opening degree was 60%. According to *Eq.8*, the linearity degree ϵ_{LS} is 11.7%.

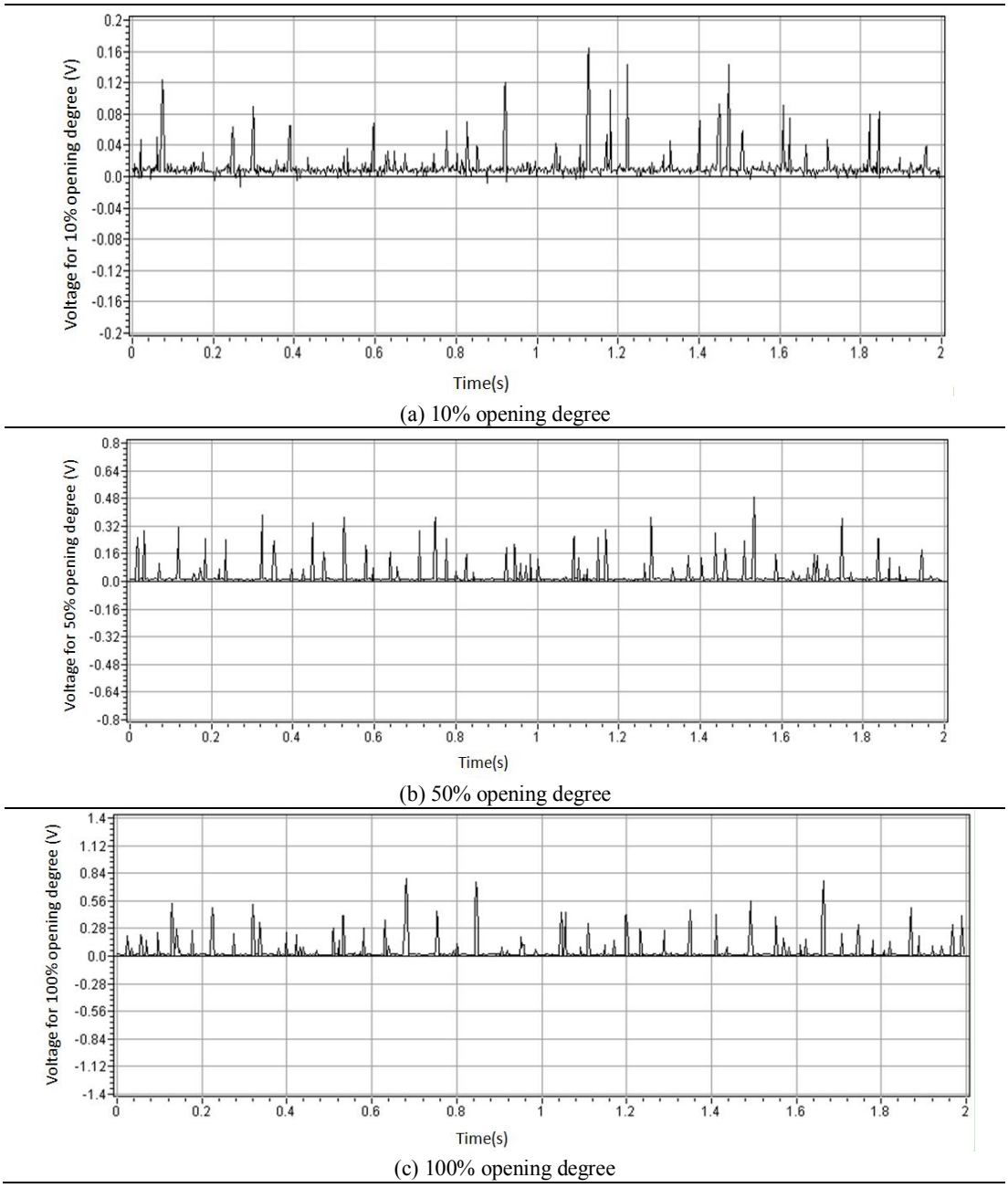

Figure 2. *Waveform of granular fertilizer flow voltage*

http://www.aloki.hu ● ISSN 1589 1623 (Print) ● ISSN 1785 0037 (Online)
DOI: http://dx.doi.org/10.15666/aeer/1704_79177925

Table 1. *Manual measurement statistics of granular fertilizer*

Opening degree	10%	20%	30%	40%	50%	60%	70%	80%	90%	100%
Average Mass (g)	28.55	135	215.35	262.37	327.64	400.8	467.17	550.83	601.6	675.32
Maximum error (%)	7.88%	2.96%	2.40%	1.46%	1.17%	0.85%	1.42%	0.48%	0.37%	0.91%

Table 2. *Granular fertilizer mass and quadratic sum of the voltage amplitude*

Opening degree (%)	Unit time mass (g/s)	$\frac{1}{n}\sum_{i=1}^{n}V^2$	Opening degree (%)	Mass (g)	$\frac{1}{n}\sum_{i=1}^{n}V^2$
10%	2.855	0.226014	60%	40.08	3.85177
20%	13.5	0.981529	70%	46.71667	3.944421
30%	21.535	1.678178	80%	55.08333	5.102993
40%	26.21667	2.191701	90%	60.16	5.090327
50%	32.764	2.703428	100%	67.532	5.679472

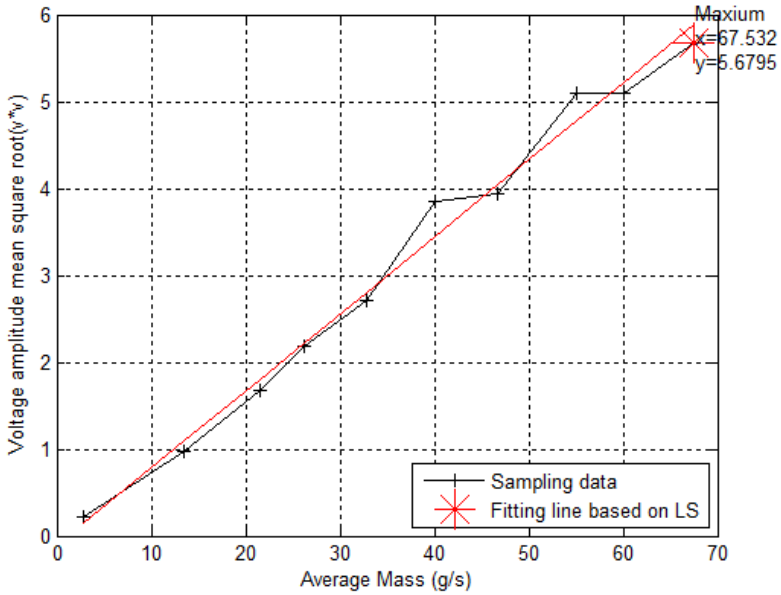

Figure 3. *Fitting line based on LS*

Table 3. *Absolute error between actual value and LS prediction value*

Fertilizer apparatus opening degree	Granular fertilizer mass (g)	$\frac{1}{n}\sum_{i=1}^{n}V^2$	Sampling point of LS linear equation	Error
10%	2.855	0.2260138	0.1535	0.072514
20%	13.5	0.978848294	1.0959	-0.11705
30%	21.535	1.678178	1.8072	-0.12902
40%	26.21667	2.191701	2.2216	-0.0299
50%	32.764	2.703428	2.8012	-0.09777
60%	40.08	3.85177	3.4489	0.40287
70%	46.7166	3.944421	4.0364	-0.09198
80%	55.08333	5.102993	4.7770	0.325993
90%	60.16	5.090327	5.2265	-0.13617
100%	67.532	5.679472	5.8791	-0.19963

http://www.aloki.hu ● ISSN 1589 1623 (Print) ● ISSN 1785 0037 (Online)
DOI: http://dx.doi.org/10.15666/aeer/1704_79177925

Granular fertilizer mass prediction based on RANSAC

Figure 4 is the fitting line of voltage amplitude average value and mass of different opening degree in one-unit interval based on RANSAC. *Table 4* is the absolute error between actual value and RANSAC prediction value.

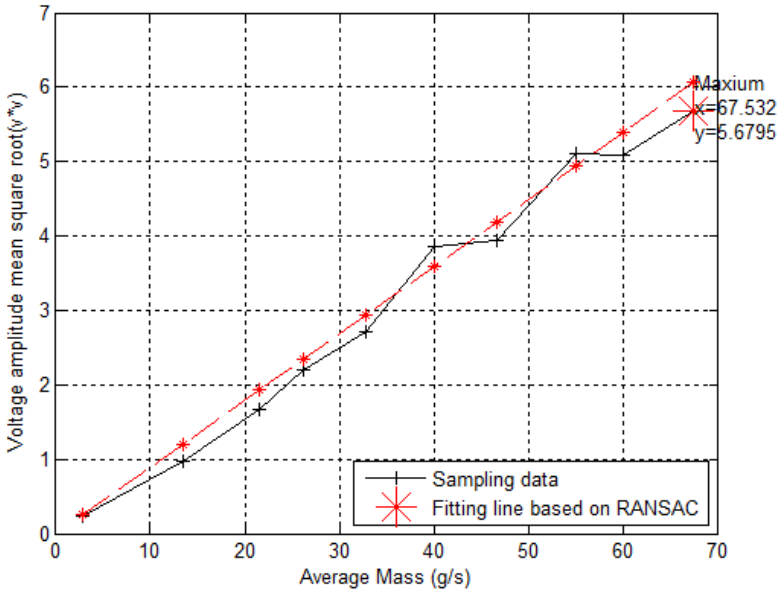

Figure 4. *Fitting line based on RANSAC*

Table 4. *Absolute error between actual value and RANSAC prediction value*

Fertilizer apparatus opening degree	Granular fertilizer mass (g)	$\frac{1}{n}\sum_{i=1}^{n} V^2$	Sampling point of RANSAC linear equation	Error
10%	2.855	0.2260138	0.2464	-0.02039
20%	13.5	0.978848294	1.2038	-0.22495
30%	21.535	1.678178	1.9265	-0.24832
40%	26.21667	2.191701	2.3476	-0.1559
50%	32.764	2.703428	2.9365	-0.23307
60%	40.08	3.85177	3.5946	0.25717
70%	46.7166	3.944421	4.1915	-0.24708
80%	55.08333	5.102993	4.9441	0.158893
90%	60.16	5.090327	5.4007	-0.31037
100%	67.532	5.679472	6.0637	-0.38423

The predicting equation based on RANSAC method shown in *Figure 5* is defined as *Eq.9*.

$$y = 0.089945x\text{-}0.010418 \quad \text{(Eq.9)}$$

The maximum deviation occurred when the fertilizer apparatus opening degree was 100%. According to *Eq.9*, the nonlinear error ϵ_{LS} is 6.34%.

The nonlinear error of the RANSAC line, which is less than the nonlinear error of LS. To obtained a minimum sum of squared error, if there is large deviation point, the error

http://www.aloki.hu ● ISSN 1589 1623 (Print) ● ISSN 1785 0037 (Online)
DOI: http://dx.doi.org/10.15666/aeer/1704_79177925

of fitting method based on LS is large. As regards to RANSAC method, the points near the fitting line are selected by eliminating the large deviation point. Hence, the prediction accuracy with RANSAC is higher than LS.

Result

Figure 5 is the comparison of the actual value and prediction value. The well-fitted line demonstrates the effectiveness of the proposed RANSAC method. which is better fitting than the LS line. *Table 5* is the result of MSE and nonlinear error with RANSAC and LS method.

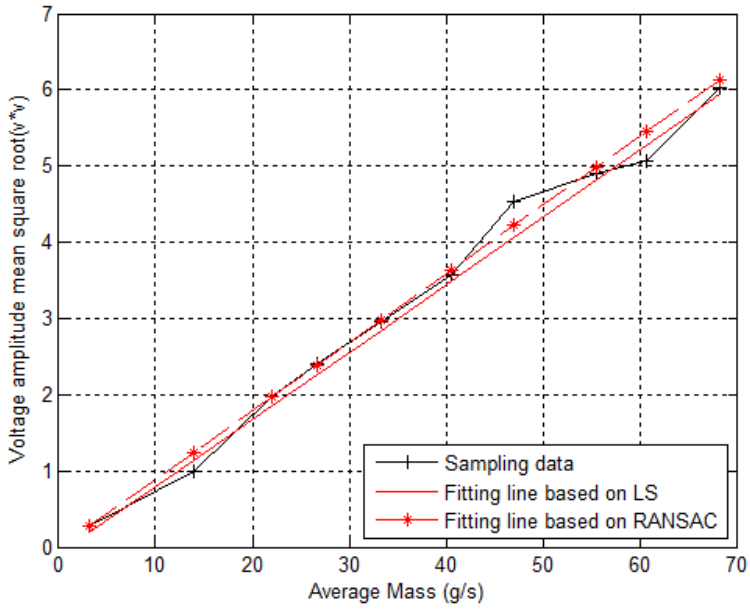

Figure 5. *Fitting lines based on RANSAC and LS*

Table 5. *Results of MSE and nonlinear error*

Fitting method	MSE	Nonlinear error
LS	0.45702	11.2%
RANSAC	0.37787	5.43%

Conclusion and discussion

The echo signal voltage of urea granular fertilizer was measured by Doppler sensor. The prediction model of granular fertilizer mass based on RANSAC was built. The proposed method was compared with LS algorithm. Simulation results demonstrate that the prediction accuracy with RANSAC is higher than LS.

The LS method considers the minimum square error of all location points in linear fitting. When there are several points with larger deviation, the fitting error is larger. Using RANSAC to estimate the Doppler signal, we can select consistent sets that conform to the straight line when fitting straight lines, automatically eliminate the larger error points, and improve the fitting accuracy. Subsequent research will further improve signal sampling accuracy, reduce computation time and improve operational efficiency.

http://www.aloki.hu ● ISSN 1589 1623 (Print) ● ISSN 1785 0037 (Online)
DOI: http://dx.doi.org/10.15666/aeer/1704_79177925

Acknowledgements. This work was supported by 13th Five-year Plan of National Key Research and Development Project (NO. 2016YFD020060802).

REFERENCES

[1] Cramer, A., Eckert, S., Gerbeth, G. (2013): Flow measurements in liquid metals by means of ultrasonic Doppler method and local potential probes. – European Physical Journal Special Topics 220: 25-41.
[2] Dimaczek, G., Fassbinder, H.-G., Emmel, A., Kupfer, R. (1994): High-precision Coriolis mass flowmeter for bulk material two-phase flows. – Flow Measurement & Instrumentation 5: 295-302.
[3] Hossein-Nejad, Z., Nasri, M. (2016): Image registration based on SIFT features and adaptive RANSAC transform. – International Conference on Communication and Signal Processing. IEEE.
[4] Hossein-Nejad, Z., Nasri, M. (2018): A-RANSAC: Adaptive random sample consensus method in multimodal retinal image registration. – Biomedical Signal Processing and Control 45: 325-338.
[5] Isa, M. M., Wu, Z. Q. (2004): Microwave radar sensor as solid flow counter. – High Frequency Postgraduate Student Colloquium. IEEE: 37-40.
[6] Isa, M. M., Wu, Z. Q. (2006): Microwave Doppler Radar Sensor for Solid Flow Measurements. – Eruopean microwave Conference. IEEE: 1508-1510.
[7] Karaboga, N., Latifoglu, F. (2013): Elimination of noise on transcranial Doppler signal using IIR filters designed with bee colony-ABC -algorithm. – Digital Signal Processing: 1051-1058.
[8] Le, V.-H., Vu, H., Nguyen, T. T., Le, T.-L., Tran, T.-H. (2018): Acquiring qualified samples for RNSAC using geometrical constraints. – Pattern Recognition Letters 102: 58-66.
[9] Niedfeldt, P. C., Ingersoll, K., Beard, R. W. (2017): Comparison and analysis of recursive-RANSAC for multiple target tracking. – IEEE Transactions on Aerospace & Electronic Systems PP (99): 1-1.
[10] Pang, L., Shao, Y., Geng, C., Zhong, W., Liu, G., Liu, L., Tian, W. (2018): Measurement of solid mass flow rate by a non-intrusive microwave method. – Powder Technology 323: 525-532.
[11] Shames, I., Bishop, A. N., Smith, M., Anderson, B. D. O. (2013): Doppler shift target localization. – IEEE Transactions on Aerospace and Electronic Systems 49: 266-276.
[12] Wu, Z., Wang, H. G., Isa, M., Liu, C. G. (2014): Laboratory evaluation of microwave Doppler velocimeter for solid flow measurements. – American Institute of Physics Conference Series. American Institute of Physics: 57-62.
[13] Xu, J. J., Huang, L., Yin, S., Gao, B., Chen, P. (2018): All-fiber self-mixing interferometer for displacement measurement based on the quadrature demodulation technique. – Opt Rev. 25(1): 40-45.
[14] Yan, Y., Stewart, D. (2000): Flow measurement of particulate solids in pipelines. – Flow Measurement & Instrumentation 11: 151-151.
[15] Zhang, N.-B., Xu, J.-J., Xue, C.-G. (2011): Core-shell structured mesoporous silica nanoparticles equipped with pyrene-based chemosensor: Synthesis, characterization, and sensing activity towards Hg(II). – Journal of Luminescence 131: 2021-2025.
[16] Zhu, L., Xu, J., Yan, L. (2017): Research on congestion elimination method of circuit overload and transmission congestion in the internet of things. – Multimedia Tools and Applications 76: 18047-18066.

http://www.aloki.hu ● ISSN 1589 1623 (Print) ● ISSN 1785 0037 (Online)
DOI: http://dx.doi.org/10.15666/aeer/1704_79177925

FREQUENCY SPECTRUM AND VARIABILITY ANALYSIS FOR BIG DATA IN GEOLOGICAL SPACE –TAKING DRILLING BIG SAMPLE DATA IN ORDOS BASIN AS A CASE STUDY

CAO, M. X.[1*] – LU, L. J.[2] – XIN, S.[2]

[1]*College of GeoExploration Science and Technology, Jilin University, Changchun 130021, China*

[2]*College of Earth Sciences, Jilin University, Changchun 130061, China*

**Corresponding author*
e-mail: caomx_lovely@163.com

(Received 23rd Feb 2019; accepted 3rd May 2019)

Abstract. The scientific problem of fusion analysis for geospatial big data is to obtain the structure, composition, spatial distribution and variation law of geological bodies from interdisciplinary data. The key technology is to carry out a geospatial three-dimensional reconstruction and visualization, and perform spatial analysis, prediction and decision. Spatial distribution and variability analysis of Ordos sandstone uranium mining is an important concern for uranium formation research. This study is based on big sample data of typical drilling and constructs a digital frequency spectrum model reflecting uranium oxidation-reduction space and lithofacies combination relationship, to describe uranium change of Zhiluo formation strata combination and spatial coupling relationship with the surrounding rock. Modeling process involves a series of key assessments which are structure analysis for big sample data of typical drilling, scale calculation, digital frequency spectrum and variation function principle, geological interpretation. Using stratum as minimum geological unit by spatial frequency spectrum calculation, this study can directly make frequency spectrum synthesis calculation with different levels such as stratum combination, sedimentary facies combination and basin, so as to build geological spatial digital feature model, which can be used as a basis for quantitative analogy and extrapolation prediction in the northern sandstone uranium basin.
Keywords: *Geospatial big data, fusion analysis, big sample space scale, digital frequency spectrum, variation function*

Introduction

The geological space is the complex material accumulation body with mixed characteristics produced in the upper crust. The geoscience big data based on geological space has four characteristics: complexity, heterogeneity, periodicity and extensiveness. Processing analysis of geoscience big data belongs to complexly giant system. The scientific essence of geoscience big data research is to realize geological space abstraction through geological spatial distribution and variability exploration; to establish geoscience space model, and carry out geological process simulation, then implement geological space prediction and decision-making, which serves the two major geosciences needs of mineral resource prediction and geological hazard warning. Due to the particularity of the geological space, it brings more uncertainty and cannot fully (or very well) express geological entity information for space modeling of geological big data. The major theoretical and technical issues for complex analysis of geospatial big data include: discussion of multi-heterogeneity and synergy of geological big data, discussion of randomness and chaotic nature of geological space, science division of geological space, cross-fusion of geological big data, complex modeling,

http://www.aloki.hu ● ISSN 1589 1623 (Print) ● ISSN 1785 0037 (Online)
DOI: http://dx.doi.org/10.15666/aeer/1704_79277941

spatial computing visualization, spatial prediction and spatial decision-making, etc. (Zhang and Zhou, 2017; Zhou et al., 2018, 2017).

Ordos continental uranium-bearing basin is giant accumulation area of uranium mining in north China, and Zhiluo formation in continental sedimentary construction is stratum combination with uranium-bearing specificity (Liu et al., 2013; Min et al., 2005; Jiao et al., 2016; Yang et al., 2015). Distribution variation of uranium mining space has a close relationship with sedimentary construction evolution, and borehole logging data is the important data set to reflect vertical lithology combination of the basin and the change of its physical properties; the logging data is divided into two types of direct uranium anomaly data and indirect associated data (Feng et al., 2016; Hao et al., 2015; Jiang et al., 2016; Liu et al., 2016; Yi et al., 2015). Application of logging data to depict digital features of uranium-bearing construction, which is not only very important for identifying change rule of uranium-bearing rock series of sedimentary facies and other sedimentary stratum combination, but also is important for identifying uranium-bearing characteristics of basin space (Ahmed and Arnous, 2015; Cai et al., 2015; Li et al., 2015; Luo et al., 2015). Therefore, the quantitative analysis of basin sedimentary facies, sedimentary construction, and uranium-bearing series is a hot and difficult problem for sandstone type uranium deposits assessment.

From the angle of geological analysis, basin sedimentary construction represents oxidation-reduction environment space of sedimentary environment and uranium element, and the smallest unit of sedimentary construction is stratum, different forms of stratum combination reflect overall characteristics of sedimentary facies and sedimentary construction, in general, geological information contained in these variation characteristics are drowned out by logging data (Guo and Xue, 2014; Wu, 2005; Zhao et al., 2015). Sometimes, it is impossible to directly extract uranium variation information from logging data, which objectively requires make systematic, comprehensive analysis about data structure and digital feature for logging data, and this is the objective of this study.

Uranium-bearing construction or lithofacies combination is constituted of different stratums. According to a certain space order relation, geologic body is constituted, and each stratum lithology has dependent and inheritance with overlying stratum, underlying stratum lithology in space, which in overall presents correlation and additivity (Li, 2012; Wang et al., 2014; Zhu, 2013). Therefore, digital feature model of basin sedimentary space should have structure and extensionality, and these are general principles which basin digital feature analysis should follow, which shows that analysis calculation of basin digital features depends on space order and logic recursive relationships of the construction, sedimentary facies, and uranium-bearing rock series.

Materials and methods

Every stratum geologic body in basin construction is deemed as independent monomer, and its thickness is L, logging data samples according to equal interval, so each stratum with different depth gets different number of samples, in special cases encryption interpolation processing for sample number of some stratum are made. Thereby a digital frequency spectrum model is established, the detailed process is as follows.

http://www.aloki.hu ● ISSN 1589 1623 (Print) ● ISSN 1785 0037 (Online)
DOI: http://dx.doi.org/10.15666/aeer/1704_79277941

Sample capacity determination

The average depth of all boreholes in the Ordos basin is in the range of 500-700 m, the sampling interval in the logging is generally 5 cm, and interpolation processing can reach 1 cm. The number of logging samples for each borehole can reach at least 10000; logging parameters of each sample point respectively contain four items, which are natural gamma, caliper, density, and resistivity. These parameters also contain 25 lithology parameters, which are all nominal type geological data. According to sample matching scale analysis, four logging curves data have a unique representation under the target association significance of the uranium bearing could be informed. Therefore, four logging curves as main variable parameters were made, and radioactive r spectrum parameter was used as target variable, other three curve parameters as independent variables. First, causal relationship model between target variable and independent variables was established, and calculated independent weights of each variable under the condition with best curve fitting, and calculated correlation weight of target variable to satisfy the criterion of maximum correlation between independent variables combination and target variable. Next combination calculation for independent weights and correlation weight of each sample were made, and then obtained spatial scale value of the sample, thus formed the sample sequence.

The specific process was as follows:

Obtained borehole logging data matrix, and made the following translation transforms:

$$x_{ij} = \frac{x_{ij}^* - \boldsymbol{min}(x_{lj}^*)}{\sigma_j} \qquad 1 \le l \le n, \quad i = 1,2,\cdots,n, \quad j = 1,2,\cdots m \tag{Eq.1}$$

Here, x_{ij}^* was the original logging data, n was the sample size and constituted a computing matrix $X = (x_{ij})_{n\times m} = (X_1, X_2, \cdots, X_m)$, among $X_1, X_2, \cdots, X_m$ was the independent variables. In this study, $m = 3$; and target variable $Y = (Y_1, Y_2, \cdots, Y_n)'$.

The problem of this study was to compute independent weights of independent variable and correlation weight of target variable, so the following causal relationship model were established, as follows:

$$\begin{cases} y = b_0 + \sum_{j=1}^{m} b_j X_j \\ y = b_0 \, \boldsymbol{exp}[\sum_{j=1}^{m} b_j X_j] \\ y = b_0 \, \boldsymbol{exp}[\sum_{j=1}^{m} b_j X_j]^2 \end{cases} \tag{Eq.2}$$

In all above equations, least-squares solution or optimal simulation solution was strived, and chose most remarkable equation as regression equation, then calculated partial regression square sum of each independent variable: $V_j = \frac{b_j^2}{c_{jj}} \quad j = 1,2,\cdots,m$,

http://www.aloki.hu ● ISSN 1589 1623 (Print) ● ISSN 1785 0037 (Online)
DOI: http://dx.doi.org/10.15666/aeer/1704_79277941

here, b_j was regression coefficients of remarkable regression equation, c_{jj} was main diagonal elements of inverse matrix of regression equation coefficient matrix, V_j would be defined as independent weights of corresponding variables X_j.

Considered the contribution of independent variables combination for target variable, correlation weight of target variable was calculated according to the following transformation: supposed constant α, β, and satisfied $\alpha + \beta = 1$, made:

$$q = \sum_{i=1}^{n} (\alpha y_i - \beta \sum_{j=1}^{m} V_j X_j)^2 \rightarrow \boldsymbol{min} \quad \text{(Eq.3)}$$

This meant that it had least fitting relationship between target variable and square for weighted residuals of independent variable combination, there had to be: $\frac{dq}{d\alpha} = 0$, and got:

$$\alpha = \frac{\sum_{j=1}^{m} V_j \overline{X_j}}{\overline{y} + \sum_{j=1}^{m} V_j \overline{X_j}} \quad \text{(Eq.4)}$$

Then defined sample space scale value of four logging curves were: $d_i = \alpha y_i + \beta \sum_{j=1}^{m} V_j \overline{X_j}$, $i = 1,2,\cdots n$ and gained spatial scaling sequence set: $D = (d_1, d_2, \cdots d_n)'$.

Samples spatial spectrum density calculation

For sample *D* sequence, according to the following process to calculate spatial spectral density of samples (Cui and Singh, 2016; Khalid et al., 2013; Lu and Liu, 2015; Ma et al., 2012; Mariotti et al., 2014; Silbert and Thomas, 2013), here had two cases:

Big sample scale sequence of individual geology body

Calculation procedure was as follows:

Supposed *D* sequence of a stratum sample scale as stable process, which had: $\{D(i), i \in R\}$.

Defined Fourier transform of $D(i)$ as spectral function, as follows:

$$F_D(\omega, I) = \int_{-I}^{I} D(i) e^{-j\omega i} di \quad \text{(Eq.5)}$$

Defined $S_D(\omega) = \boldsymbol{lim}_{I \to \infty} \frac{1}{2I} E\left\{ \left| F_D(\omega, I) \right|^2 \right\} < \infty$ as spatial spectral density of $D(i)$, this was distribution relationship of $D(i)$ about frequency ω ($\omega = 2\pi f$ is angular frequency).

http://www.aloki.hu ● ISSN 1589 1623 (Print) ● ISSN 1785 0037 (Online)
DOI: http://dx.doi.org/10.15666/aeer/1704_79277941

Further defined autocorrelation function of $D(i)$ (Chen, 2009), there was:

$$\begin{aligned} R_D(i_1,i_2) &= E\left[D(i_1)D(i_2)\right] \\ &= \int_{-\infty}^{\infty}\int_{-\infty}^{\infty} D_1 D_2 f(D_1,D_2;i_1,i_2)dD_1 dD_2 \end{aligned} \quad \text{(Eq.6)}$$

This was autocorrelation function of $D(i)$, such as $D(i)$ is stable process, so $R_D(i_1,i_2)$ in unrelated to choice of location i_1 and i_2, only related to the size of $(i_2 - i_1)$. Supposed $i_2 - i_1 = \tau$, then autocorrelation function was represented as $R_D(\tau)$, therefore, which was also called as spatial variation function.

The relationship expression between spatial spectral density function $S_D(\omega)$ and spatial variation function $R_D(\tau)$:

$$\begin{cases} S_D(\omega) = \int_{-\infty}^{\infty} R_D(\tau)^{-j\omega\tau} d\tau \\ R_D(\tau) = \dfrac{1}{2\pi}\int_{-\infty}^{\infty} S_D(\omega)^{j\omega\tau} d\omega \end{cases} \quad \text{(Eq.7)}$$

Here, it meant that $S_D(\omega)$ and $R_D(\tau)$ were mutually Fourier inverse transform pair. $S_D(\omega)$ represented concentration degree index of space attribute set in the same geology body, which was domain function about frequency, this set was also called spectrum, and represented unique digital features of this geology body.

Big sample scale sequence of two geology bodies

Calculation procedure was as follows:

Above $D(i)$ sequence represented geology monomer, for scale sequence $D(i)$ and $H(i)$ of two geology bodies, cross-spectral density and cross-correlation function was calculated (Hotelling, 2012; Lei et al., 2011; Liang et al., 2011; Lv et al., 2011; Xie et al., 2011), this was:

$$S_{DH}(\omega) = \lim_{I\to\infty} \frac{1}{2I} E\left\{F_D(\omega,I)F_H(\omega,I)\right\} \quad \text{(Eq.8)}$$

Further there was:

$$S_{DH}(\omega) = \int_{-\infty}^{\infty} R_{DH}(\tau) e^{-j\omega\tau} d\tau \quad \text{(Eq.9)}$$

$$R_{DH}(\tau) = \frac{1}{2\pi}\int_{-\infty}^{\infty} S_{DH}(\omega) e^{j\omega\tau} d\omega \quad \text{(Eq.10)}$$

http://www.aloki.hu ● ISSN 1589 1623 (Print) ● ISSN 1785 0037 (Online)
DOI: http://dx.doi.org/10.15666/aeer/1704_79277941

It could be seen that these two were Fourier inverse transform pair. It should be pointed out that establishing of cross-spectral density and cross-correlation function should be carried out under the premise that two geology bodies should have spatial correlation.

Additive operation of big sample space spectrum density

When two or more than geology bodies need to make cumulative calculation of spectral density, the formula could be $Z = \bigcup_{i=1}^{p} D_i$, which expressed that P geology bodies superimposed. Therefore, combined spectral density after superimposing was $S_Z(\omega) = \sum_{i=1}^{p} S_{D_i}(\omega)$, and average variation function of the geology body after superimposing was $R_Z(\tau) = \int_{-\infty}^{\infty} S_z(\omega) e^{-j\omega\tau} d\tau$.

Synthesis calculation for stratum combination

It is well known, all substance has vibration frequency, but vibration frequency of irregular geology body such as geological space is unable to estimate, this study can only start from multiple observation data to estimate. In this sense, spatial frequency spectrum function is expressed as frequency domain function, which completely can satisfy superposition operation conditions, and it also has the function of transforming into spatial domain, so as to make variability analysis.

Stratum combination (construction, sedimentary facies and rock facies) analysis is an indispensable part for basin analysis. Spatial frequency spectrum of geology body belongs to non-dimensional measurement, which can be made additive operation in the mathematical sense. Spatial frequency spectrum of different geology bodies exists the difference in the magnitude and structure. Oxidation, oxidation and reduction, boundary classification of reduction space for basin uranium involves synthesis calculations problem of spatial frequency spectrum, therefore according to the different levels of stratum combination to make synthesis calculations of spatial frequency spectrum, and constitute the whole content for digital features analysis of stratum, sedimentary facies, sedimentary formation and even the whole basin.

About superposition conditions of stratum, apart from according to geological methods such as sedimentary facies analysis, etc., also judge from the cross-correlation function and cross-spectral density function defined by this study. Generally, higher cross-correlation function in two stratums can be considered to make spectrum synthetically calculation. Cross-correlation function can also be used as the basis for three-division space.

Results

Background

Logging data of ZKA-7 borehole in the A exploration line of Daying uranium area in Ordos basin is used in this study, the distribution of boreholes in the A exploration line is shown in *Figure 1*. Then trial calculation based on above models was make, the result is as follows.

http://www.aloki.hu ● ISSN 1589 1623 (Print) ● ISSN 1785 0037 (Online)
DOI: http://dx.doi.org/10.15666/aeer/1704_79277941

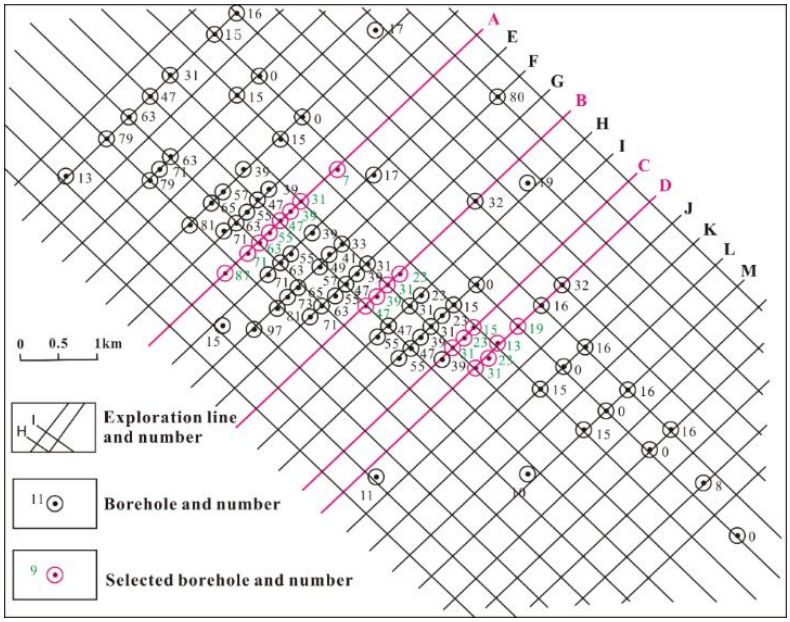

Figure 1. *Boreholes distribution in the A exploration line*

Spectrum density curves and spatial variation curves of each section interval for ZKA-7 borehole in the A exploration line are shown in *Figures 2* and *3*; 20-716 m variation comprehensive curve is shown in *Figure 4*. It should be noted that the depth markings on the figure do not correspond to the exact location, and it represents only the general characteristics of some section interval.

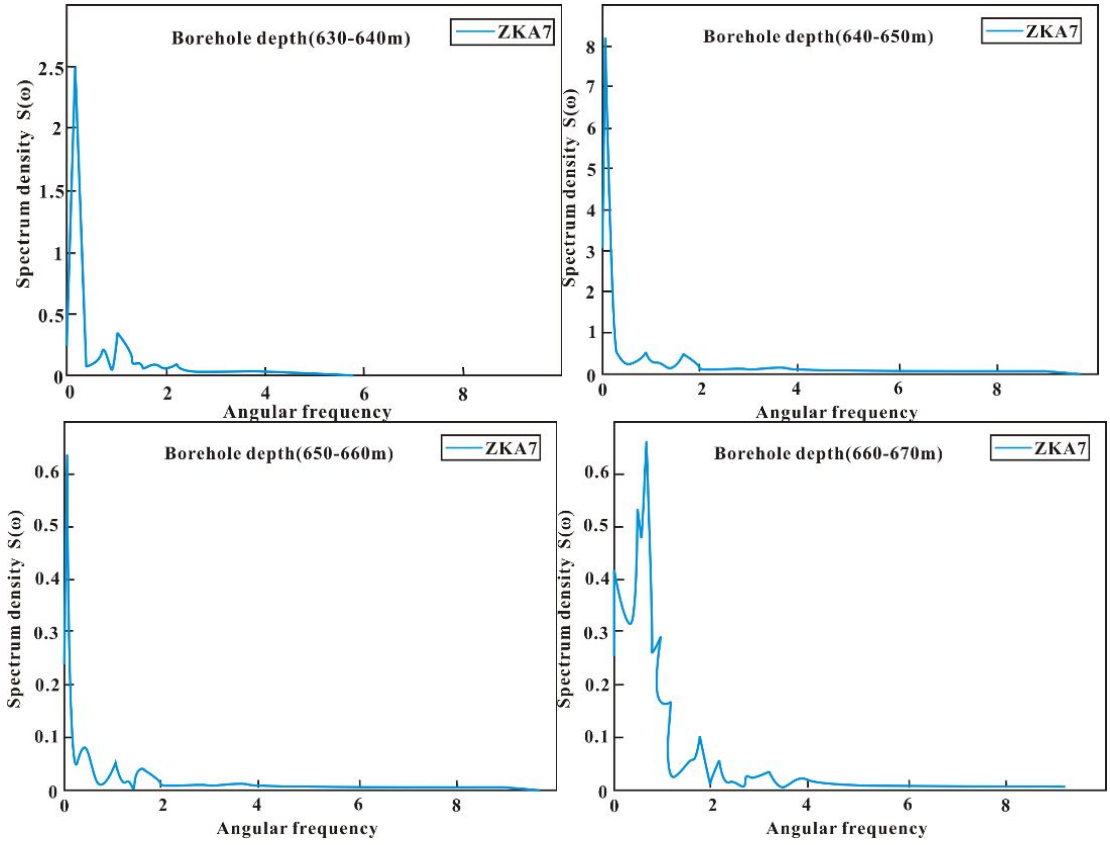

http://www.aloki.hu ● ISSN 1589 1623 (Print) ● ISSN 1785 0037 (Online)
DOI: http://dx.doi.org/10.15666/aeer/1704_79277941

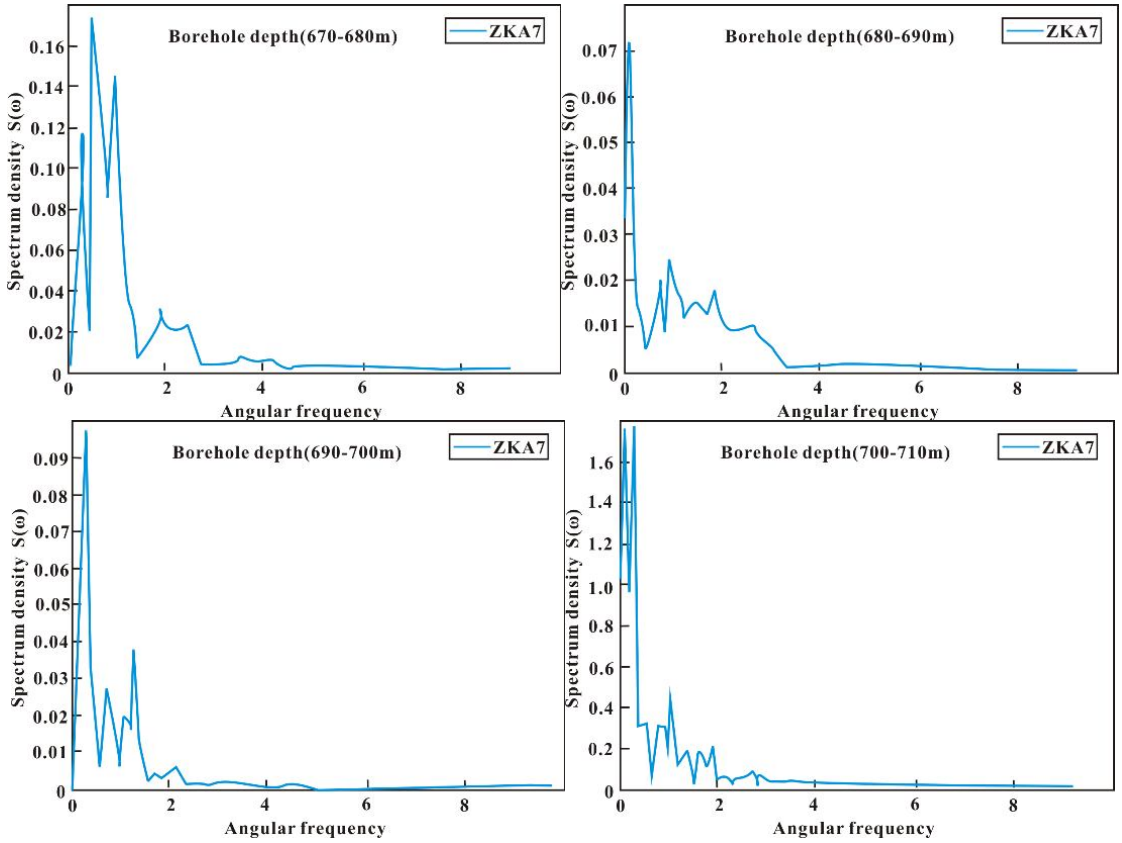

Figure 2. *Spectrum density curves of A drill for 630-710 m*

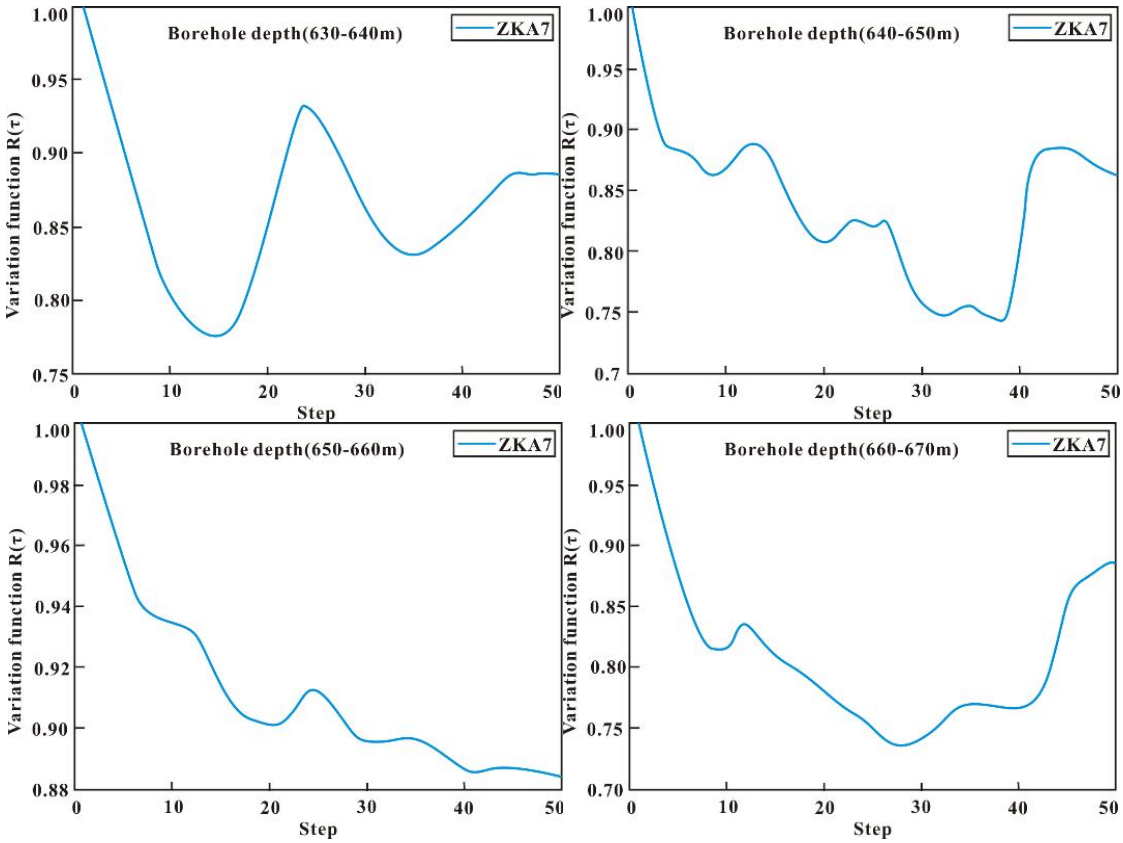

http://www.aloki.hu ● ISSN 1589 1623 (Print) ● ISSN 1785 0037 (Online)
DOI: http://dx.doi.org/10.15666/aeer/1704_79277941

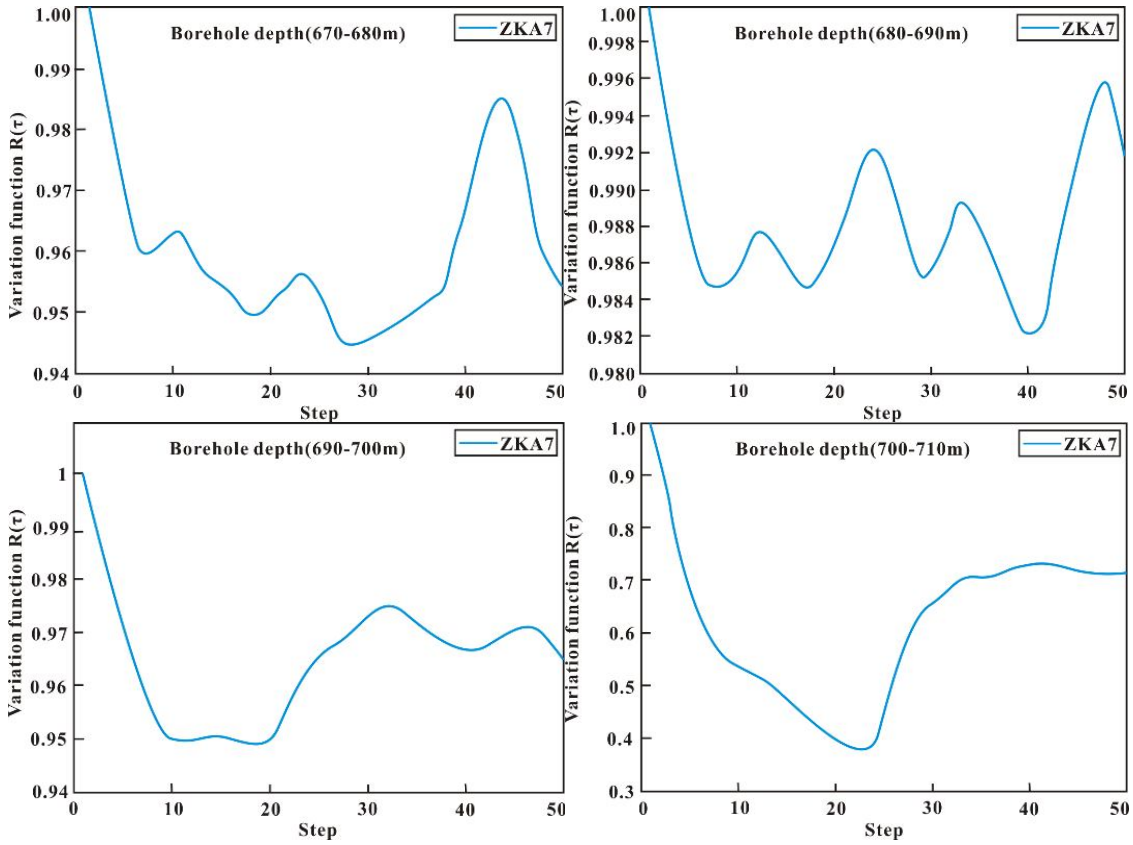

Figure 3. *Variation curves of A drill for 630-710 m*

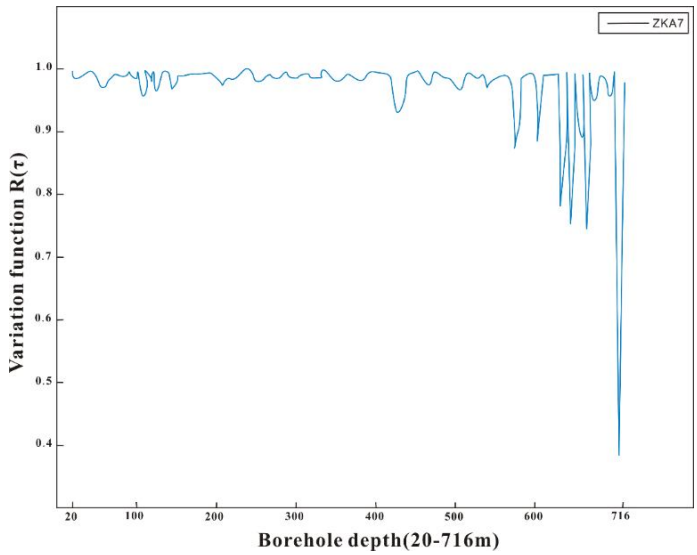

Figure 4. *Comprehensive variation curve for ZKA-7 borehole (20-716 m)*

In order to express the distribution of variation function $R_x(\tau_n)$ of all boreholes in A exploration line, specifically it will synthesize all variation curves of all boreholes in A exploration line, and finally generate variation comprehensive curve of the whole borehole, as shown in *Figure 5*.

http://www.aloki.hu ● ISSN 1589 1623 (Print) ● ISSN 1785 0037 (Online)
DOI: http://dx.doi.org/10.15666/aeer/1704_79277941

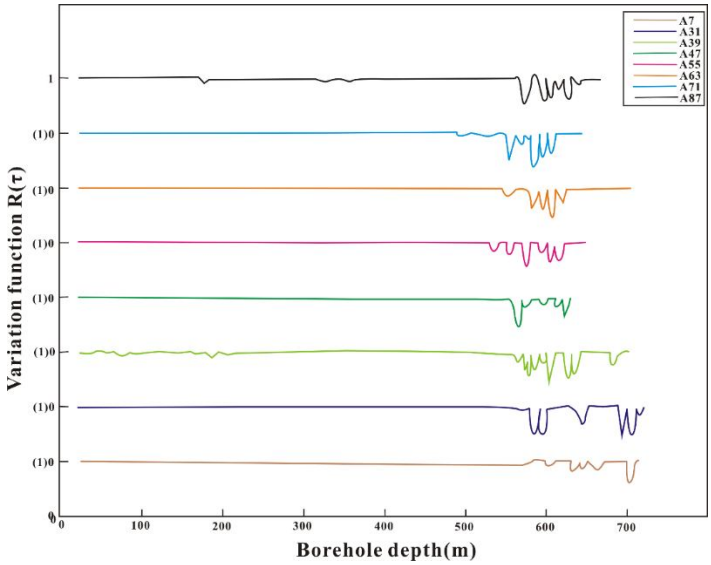

Figure 5. *Comprehensive variation curves for 8 boreholes in A exploration line*

In order to express the variation characteristics of lithologic assemblages of different strata at different depths, according to the statistical calculation of A borehole, 50 m is used as the interval standard, and the spatial spectrum density value of each section and the corresponding spatial variation value are calculated respectively. This part focuses on the section of 630-710 m with gamma anomaly characteristic.

Discussion

The spatial spectrum density curves represent the aggregate degree of the uranium mineralization factor (attribute set) combined by four parameters in the unit space measure (depth distance), which reflects the comprehensive intensity index of regional uranium mineralization, and call as generalized spatial attribute density (hereinafter referred to as density). This kind of parameters combination indicates a measure of the comprehensive information, which is more comprehensive than traditionally measured by single natural gamma or quantitative gamma, and the identified information is more reliable.

Due to the imbalance of geological actions in the region, resulting in the imbalance of comprehensive strength index or density distribution for the uranium mineralization, so the spatial distribution sometimes shows singularity characteristics, which is so-called anomaly phenomenon. The singularity characteristics or anomaly phenomenon is an important research content for spatial data distribution, and its scientific nature reflects the intensity change of geology action caused by regional environment, such as: magma intrusion with heat source intrude into the region is selective, so mineralization enrichment of the polymetallic elements formed during the process of magma emplacement is imbalanced.

From *Figure 2* it can be seen that distribution state of uranium mineralization factor density. Spectrum density curves of uranium mineralization factor for logging data about the entire borehole shows that the oscillation form, but oscillation frequency and density amplitude (ie, amplitude value, which is the corresponding function value) are different as different depth. Each spectrum density curve shows the frequency closer to

http://www.aloki.hu ● ISSN 1589 1623 (Print) ● ISSN 1785 0037 (Online)
DOI: http://dx.doi.org/10.15666/aeer/1704_79277941

0 points, the greater the marginal density, where the marginal density can also be identified as the maximum density distribution of this section, and with the frequency increases, the density gradually decay, which is the unique characteristics of the model algorithm.

From the view of section, the amplitude of the spectrum curves for the 65 sections (20-630 m, 670-700 m and 710-716 m) in the calculation is smaller, usually fluctuates between 0.01 ~0.35, and the features of density variation is not obvious, and the scale average in these sections is also lower, as shown in *Table 1* and *Figure 4*. But the amplitude for the five sections (630-670 m, 700-710 m) is larger, fluctuates between 0.7 and 9, as the frequency changes with same interval, the change of the density is also larger, and original scale average for these sections is also higher (*Table 1*). The comparison shows: the amplitude of the spectrum curves, original scale average for these five sections are significantly higher than other 66 sections of the ZKA-7 borehole. This can be understood as that in areas where the density is high, the density changes significantly and original scale average is also high, the comprehensive intensity of uranium mineralization is stronger. It is shown that these uranium combinations under the conditions of the redox environment achieve the best state, very conducive to precipitation mineralization for uranium element.

Table 1. *Original scale average in different depth interval*

Depth interval	Original scale average	Depth interval	Original scale average	Depth interval	Original scale average	Depth interval	Original scale average	Depth interval	Original scale average
20-30m	1.12	30-40m	1.18	40-50m	1.16	50-60m	1.18	60-70m	1.11
70-80m	1.17	80-90m	1.21	90-100m	1.32	100-110m	1.04	110-120m	1.17
120-130m	1.26	130-140m	1.25	140-150m	1.22	150-160m	1.13	160-170m	0.99
170-180m	1.20	180-190m	1.19	190-200m	1.32	200-210m	1.15	210-220m	1.04
220-230m	1.25	230-240m	1.44	240-250m	1.25	250-260m	1.17	260-270m	1.41
270-280m	1.46	280-290m	1.50	290-300m	1.27	300-310m	1.20	310-320m	1.17
320-330m	1.28	330-340m	1.33	340-350m	0.97	350-360m	0.93	360-370m	1.06
370-380m	1.22	380-390m	1.20	390-400m	1.11	400-410m	1.05	410-420m	1.16
420-430m	0.89	430-440m	0.68	440-450m	1.07	450-460m	1.11	460-470m	1.13
470-480m	1.01	480-490m	1.03	490-500m	0.91	500-510m	1.07	510-520m	1.20
520-530m	1.13	530-540m	1.22	540-550m	1.08	550-560m	1.13	560-570m	1.12
570-580m	1.24	580-590m	1.10	590-600m	1.21	600-610m	1.38	610-620m	1.17
620-630m	1.20	630-640m	2.89	640-650m	4.47	650-660m	1.45	660-670m	2.49
670-680m	1.75	680-690m	1.42	690-700m	1.31	700-710m	2.43	710-716m	1.49

On the other hand, it can be seen from the variation curves of different sections for ZKA-7 borehole, these curves can be divided into four categories: (1) the spatial variance with less fluctuates and high original scale; (2) the spatial variance with less fluctuates and low original scale; (3) the spatial variance with greatly fluctuates and high original scale; (4) the spatial variance with greatly fluctuates and low original scale.

The curves of these 66 sections (20-630 m, 650-660 m, 670-700 m, 710-716 m) in the ZKA-7 borehole belong to (2) and (4) categories, the internal variation has no big difference. Variability is more balanced with 10% fluctuations, which indicates that the

http://www.aloki.hu ● ISSN 1589 1623 (Print) ● ISSN 1785 0037 (Online)
DOI: http://dx.doi.org/10.15666/aeer/1704_79277941

distribution for the uranium mineralization scale is more uniform, and the original scale average of these sections are relatively low.

The curves of these 4 sections (630-650 m, 660-670 m, 700 m) belong to (1) and (3) categories, the internal variation has big difference. Variability has abrupt changes with 60% fluctuations, which indicates that the distribution of uranium mineralization scale is not balanced, and original scale average of these sections is relatively high, which means that there are anomalies in the sections with such features.

The anomaly sections of the spectrum density curves and the variation curves corresponds to the location of the mineralization body of known geological exploration profile. It can be found that the mineralization anomalies also present in these anomaly sections, and there are distribution signs of metallogenic belt.

It can be seen from *Figure 5,* abrupt variability usually occurs in the lower section of Zhiluo Formation. According to the size of the original scale value, it can be judged that abrupt sections present strong uranium mineralization information, which indicates that these sections may be gathering zone of uranium mineralization. In order to better verify this explanation, according to the comprehensive distribution characteristics of the spatial variation curves of all boreholes, the anomaly area of A exploration profile was determined, that is, mineralized anomaly area. The determination area is aligned with the mineralized body location map of the known geological profile, as shown in *Figure 6*. It can be found that the mineralization anomaly region determined by the spatial variation characteristics has relatively better coincidence with the known mineralization zone. So, this determining method can be used as an attempt to determine mineralization anomaly.

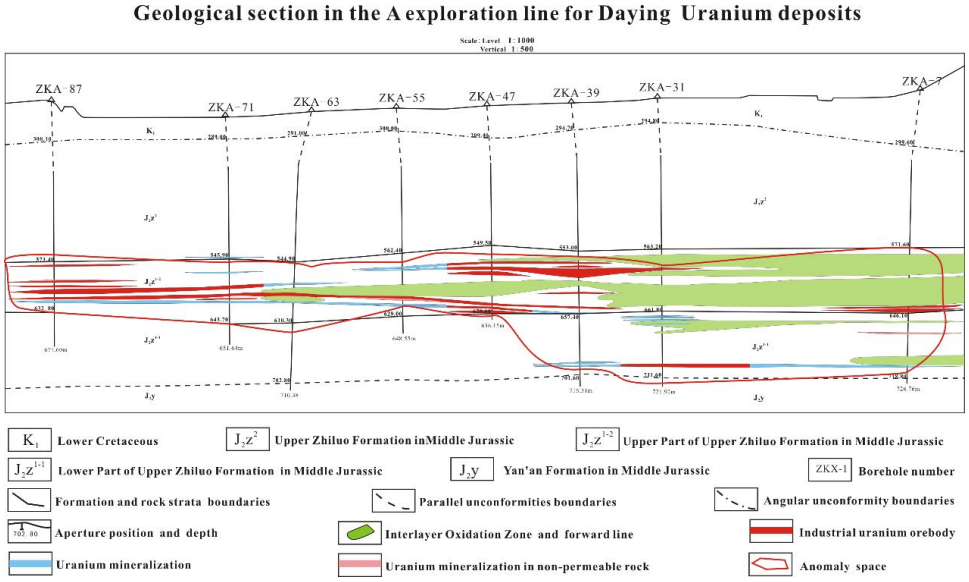

Figure 6. *Mineralization anomaly region delineated by the spatial variation characteristics*

Conclusion

The digital spectrum analysis of borehole logging data in Ordos Basin is essentially the fusion analysis of multivariate logging big data. The spatial spectrum density reflects the generalized density of geological elements set, which represents spatial concentration energy intensity of the geological properties. The spatial variation

http://www.aloki.hu ● ISSN 1589 1623 (Print) ● ISSN 1785 0037 (Online)
DOI: http://dx.doi.org/10.15666/aeer/1704_79277941

function reflects the spatial variation trend of geological element set or uranium mineralization factor. From the digital point of view, these two indicators (spatial spectrum density and spatial variation function) describe the spatial distribution and variation characteristics of the uranium mineralization combination and even mineralization anomalies, which provides a quantitative basis for determining the mineralization anomalies by using the digital features of the geology body

Through the case analysis, it is known that the size of density amplitude and the intensity of density change for the spectrum curves reflect the impact intensity of comprehensive indicators of the geology action. In the case of a larger original scale average, it presents that density amplitude is larger, simultaneously, the zone with greater fluctuations indicates that the comprehensive intensity of uranium mineralization is stronger, and such sections are easy to gather uranium element to achieve the best condition, which is favorable for uranium precipitation mineralization.

The features of spatial variation curves reflect spatial variation degree of the mineralization combined information. The larger original scale average, the greater fluctuations degree and the sections with abrupt change mean that there is a stronger uranium mineralization anomaly information, which indicates that these sections are favorable for forming the uranium mineralization zone, then to determine the spatial range of ore-bearing for A exploration profile. In the four categories of variance curves recognition, (1) and (3) categories indicate the mineralization section, where (3) categories indicates greater significance.

The better coincidence between the mineralization body location map and the mineralization anomaly area determined by the features of spatial spectrum density and variation curves shows that the digital spectrum calculation based on fusion analysis of multiple logging curves can be used as the effective and tentative method for identifying determination anomaly information.

Because data science system is uncertain and the constituent components are unknown, this study only uses known data to describe the unknown information, and uses the correlation between the data to construct the information identification method. This is also the limitation of this study. In order to better improve the limitations, this study can replace the most basic transform method with others, and make the tests. Then it also encrypts the multi-dimensional data density to improve the accuracy and make the result information more refined. The construction of this study belongs to the accurate prediction of the behavior or state of the natural science system. Now, it has been applied in the accurate prediction of geological mineralization, and will develop in the direction of precision medical evaluation and ecological critical identification in the future, this is also the future direction for this study.

Acknowledgements. This research was supported by the National Key Basic Research Program of China (No. 2015CB453005), the National Natural Science Foundation of China (No. 41802245).

REFERENCES

[1] Ahmed, E.-R., Arnous, M. O. (2015): A novel approach in hydrogeochemical exploration for uranium mineralization: an example from West Central Sinai, Egypt. – Acta Geologica Sinica 6: 1895-1913.

http://www.aloki.hu ● ISSN 1589 1623 (Print) ● ISSN 1785 0037 (Online)
DOI: http://dx.doi.org/10.15666/aeer/1704_79277941

[2] Cai, Y. Q., Zhang, J. D., Li, Z. Y., Guo, Q. Y., Somg, J. Y., Fan, H. H., Liu, W. S., Qi, F. C., Zhang, M. L. (2015): outline of uranium resources characteristics and metallogenetic regularity in China. – Acta Geologica Sinica 3: 918-937.
[3] Chen, Y. G. (2009): Reconstructing the mathematical process of spatial autocorrelation based on Moran' s statistics. – Geographical Research 28(6): 1449-1463.
[4] Cui, H. J., Singh, V. P. (2016): Maximum entropy spectral analysis for streamflow forecasting. – Physica-Statistical Mechanics and Its Applications 442(4): 91-99.
[5] Feng, Z. Q., Liu, D., Huang, S. P., Gong, D. Y., Peng, W. L. (2016): Geochemical characteristics and genesis of natural gas in the Yan'an gas field, Ordos Basin, China. – Organic Geochemistry 102: 67-76.
[6] Guo, X., Xue, C. J. (2014): Hydrodynamic regime as a major control on localization of uranium mineralization in sedimentary basins. – Science China 12: 2928-2933.
[7] Hao, G. Q., Yin, Y. P., Wei, A. J. (2015): Characteristics of sand body and mineralization condition of uranium in Zhiluo Formation of Shanghaimiao area of Ordos Basin. – Science and Technology of West China 14(8): 27-30.
[8] Hotelling, H. (2012): Analysis of a complex of statistical variables into principal components. – Journal of Educational Psychology 24(6): 417-441.
[9] Jiang, L., Qiu, Z., Wang, Q. C., Guo, Y. S., Wu, C. F., Wu, Z. J., Xue, Z. H. (2016): Joint development and tectonic stress field evolution in the southeastern Mesozoic Ordos Basin, west part of North China. – Journal of Asian Earth Sciences. DOI: 10.1016/j.jseaes.2016.06.017.
[10] Jiao, Y. Q., Wu, L. Q., Rong, H., Peng, Y. B., Maio, A. S., Wang, X. M. (2016): The Relationship between Jurassic coal measures and sandstone-type uranium deposits in the northeastern Ordos Basin, China. – Acta Geologica Sinica 6: 2117-2132.
[11] Khalid, T., White, P., De, L., C. B., Persad, R., Ewen, R., Johnson, E. (2013): A Pilot study combining a GC-sensor device with a statistical model for the identification of bladder cancer from urine headspace. – Plos One 8(7): UNSP e69602.
[12] Lei, J. Y., Yao, Q. F., Lei, Y., Liu, C. (2011): Structural damage detection method based on correlation function analysis of vibration measurement data. – Journal of Vibration and Shock 30(8): 221-224.
[13] Li, B. L. (2012): The Methods Research of Lithology Identification Based on Logging Data. – Xi'an University of Science and Technology, Xi'an.
[14] Li, Z. Y., Huang, Z. Z., Li, X. Z., Guo, J., Fan, C. (2015): The discovery of natural native uranium and its significance. – Acta Geologica Sinica 5: 1561-1567.
[15] Liang, Y., Ma, L., Na, X., Chen, C. (2011): Research of time delay estimation based on GCC algorithm. – Computer Science 38(B10): 454-456.
[16] Liu, D., Zhang, W. Z., Kong, Q. F., Feng, Z. Q., Fang, C. C., Peng, W. L. (2016): Lower PALEOZOIC source rocks and natural gas origins in Ordos Basin, NW China. – Petroleum Exploration and Development Online 43(4).
[17] Liu, G. D., Sun, M. L., Zhao, Z. Y., Wang, X. B., Wu, S. H. (2013): Characteristics and accumulation mechanism of tight sandstone gas reservoirs in the Upper Paleozoic, northern Ordos Basin, China. – Petroleum Science 4: 442-449.
[18] Lu, L. J., Liu. W. B. (2015): Digital spectral analysis method of geological space. – ICIC Express Letters 9(6): 1699-1706.
[19] Luo, J. C., Hu, R. Z., Shi, S. H. (2015): Timing of uranium mineralization and geological implications of Shazijiang granite-hosted uranium deposit in Guangxi, South China: new constraint from chemical U-Pb age. – Journal of Earth Science 6: 911-919.
[20] Lv, P., Ding, Z. F., Zhu, L. P. (2011): Application of double-difference relocation technique to aftershocks of 2008 Wenchuan earthquake using waveform cross-correlation. – Acta Seismologica Sinica 33(4): 407-419.
[21] Ma, K., Vitek, O., Nesvizhskii, A. I. (2012): A statistical model-building perspective to identification of MS/MS spectra with PeptideProphet. – BMC Bioinformatics 13(Suppl 16): 96-103.

http://www.aloki.hu ● ISSN 1589 1623 (Print) ● ISSN 1785 0037 (Online)
DOI: http://dx.doi.org/10.15666/aeer/1704_79277941

[22] Mariotti, E., Veronese, M., Dunn, J. T., Southworth, R., Eykyn, T. R. (2014): Kinetic analysis of hyperpolarized data with minimum a priori knowledge: Hybrid maximum entropy and nonlinear least squares method (MEM/NLS). – Magnetic Resonance in Medicine 73(6): 2332-2342.
[23] Min, M. Z., Xu, H. F., Chen, J., Fayek. M. (2005): Evidence of uranium biomineralization in sand stone-hosted roll-front uranium deposits, northwestern China. – Ore Geology Reviews 26: 198-206.
[24] Silbert, N. H., Thomas, R. D. (2013): Decisional separability, model identification, and statistical inference in the general recognition theory framework. – Psychonomic Bulletin & Review 20(1): 1-20.
[25] Wang, Y., Yang, W. L., Deng, J., Wu, B. L., Li, Z. Y., Wang, M. Z. (2014): Accumulation system of cohabitating Multi-Energy minerals and their comprehensive exploration in sedimentary basin–A case of Ordos Basin, NW China. – Acta Geologica Sinica 88(5): 815-824.
[26] Wu, B. L. (2005): Geological and Mineralization of Sandstone Type Uranium Deposits in the Mesozoic and Cenozoic Basins in Northwest China. – Northwest University, Xi'an.
[27] Xie, W. D., Zhou, Y. H., Kou, R. L. (2011): An improved fast normalized cross correlation algorithm. – Journal of Tongji University (Natural Science) 39(8): 1233-1237.
[28] Yang, M. H., Li, L., Zhou, J., Jia, H. C., Sun, X., Gong, T., Ding, C. (2015): Structural evolution and hydrocarbon potential of the upper Paleozoic Northern Ordos Basin, North China. – Acta Geologica Sinica 5: 1636-1648.
[29] Yi, C., Gao, H. W., Li, X. D., Zhang, K., Chen, X. L., Li, J. X. (2015): Study on indicative significance of major elements for sandstone-type uranium deposit in Zhiluo Formation in northeastern Ordos Basin. – Mineral Deposits 34(4): 801-813.
[30] Zhang, Q., Zhou, Y. Z. (2017): Big data will lead to a profound revolution in the field of geological science. – Chinese Journal of Geology 52(3): 637-648.
[31] Zhao, Z. Y., Guo, Y. R., Wang, Y., Lin, D. J. (2012): Research progress of tectonic evolution and ancient geographical features of Ordos Basin. – Special Oil and Gas Reservoirs 19(5): 15-20.
[32] Zhou, Y. Z., Li, P. X., Wang, S. G., Xiao, F., Li, J. Z., Gao, L. (2017): Research progress on big data and intelligent modelling of mineral deposits. – Bulletin of Mineralogy, Petrology and Geochemistry 36(2): 334-339.
[33] Zhou, Y. Z., Chen, S., Zhang, Q., Xiao, F., Wang, S. G., Liu, Y. P., Jiao, S. T. (2018): Advances and prospects of big data and mathematical geoscience. – Acta Petrologica Sinica 34(2): 256-263.
[34] Zhu, L. (2013): Research of visualization and analysis methods of logging data. – Wuhan Institute of Technology, Wuhan.

http://www.aloki.hu ● ISSN 1589 1623 (Print) ● ISSN 1785 0037 (Online)
DOI: http://dx.doi.org/10.15666/aeer/1704_79277941

STUDY ON THE ANALYTICAL METHOD OF INORGANIC ARSENIC SPECIES IN ENVIRONMENTAL SAMPLES

WU, J.[1] – ZHANG, S. D.[2] – ZHU, X. S.[1,3*]

[1]*School of Chemistry & Chemical Engineering, Yangzhou University, Yangzhou, China*

[2]*Bureau of Ecology and Environment of Yangzhou, Jiangsu, China*

[3]*Guangling College of Yangzhou University, Yangzhou, China*

**Corresponding author*
e-mail: xszhu@yzu.edu.cn, zhuxiashi@sina.com; phone: +86-514-8797-5244

(Received 23rd Feb 2019; accepted 3rd May 2019)

Abstract. A simple and rapid method based on ionic liquid liquid-liquid microextraction with room temperature ionic liquid 1-butyl-3-methylimidazolium hexafluorophosphate ([BMIM][PF_6]) coupled to electrothermal atomic absorption spectrometry (ETAAS) was developed for the speciation of arsenite (As(V))/ arsenate (As(III)) in environmental samples. In this method, As(V) can be extracted by [BMIM][PF_6] at pH 6.5 due to the formation of a hydrophobic complex, whereas As(III) remains in the aqueous solution. The As(V) and As(III) concentration were analyzed by ETAAS respectively. Various factors including pH, volume of [BMIM][PF_6], equilibrium temperature and time, effect of salt by single factor experiment design and orthogonal experimental design. Under the optimized conditions, the limits of detection (3σ) were 0.04 ng/mL and 0.35 ng/mL for As(V) and As(III), and its relative standard deviations was 3.5% and 2.9% respectively (n = 9, c = 20.00 ng/mL). The proposed procedure was applied without any chelating agent or dispersive agent. The method was validated against the certified reference materials (GBW08666), and successfully applied to determine As(V) and As(III) in real environmental samples.

Keywords: *As(V), As(III), ionic liquid, liquid-liquid microextraction, 1-butyl-3-methylimidazolium hexafluorophosphate, atomic absorption spectrometry, orthogonal experiment design, single factor optimization method*

Introduction

Arsenic is an abundant and high toxic element in the natural. The sources of arsenic can be divided into natural and man-made sources. The former is mainly arsenic in geological rocks, which is determined by the arsenic content in the soil, and the latter comes mainly from pesticides, fertilizers and mining smelters, such as lead arsenate and calcium arsenate, which are used to control insect pests of fruit trees or cottons; zinc methylarsonate used to control rice sheath blight, arsenic in medicament present in dentistry, used to kill nerve. Arsenic containing waste water, waste gas and waste residue were carried into the environment and raised environmental pollution, this pollution must be controlled by human beings. An important step in controlling this pollution is the determination of arsenic, and this involves the determination of arsenic speciation. Arsenic is divided into inorganic arsenic and organic arsenic, and their toxicity is very different. Inorganic arsenic and organic arsenic species have different toxicological behavior and biochemical activity. The As(III) is 10 times greater toxicity than As(V), and also seven times than methyl arsenate (MMA) and dimethyl arsenate (DMA) (Squibb et al., 1983). Many countries and regions have therefore established the maximum allowable limits of arsenic and its compounds in drinking water (United States Environmental Protection Agency, 2002; Ministry of Public Health of the People's Republic

http://www.aloki.hu ● ISSN 1589 1623 (Print) ● ISSN 1785 0037 (Online)
DOI: http://dx.doi.org/10.15666/aeer/1704_79437955

of China, 2007). Arsenic speciation is of more significant than total arsenic determination for evaluating their toxicity on human beings, as well as monitoring environmental pollution.

The direct determination of arsenic species at very low concentrations is always an impossible task due to the insufficient sensitivity of method, as well as the complicated matrix interferences occurring in samples. Generally, a preliminary separation and preconcentration step is often required for this reason. Numerous separation/analysis methods with primary separation steps for the speciation of As(V) and As(III) have been proposed, such as high-performance liquid chromatography and inductively coupled plasma mass spectrometry (Li et al., 2017), flow injection analysis and chemiluminescence detection (FIA-CD) (Nellaiappan et al., 2018), solid phase extraction electrothermal atomic absorption spectrometry/atomic fluorescence spectrometry (SPE-ETAAS) (Tunçeli et al., 2015; Abdolmohammad-Zadeh et al., 2013; Pourghazi et al., 2015), liquid–liquid microextraction-electrothermal atomic absorption spectrometry (LLME-ETAAS) (Wang et al., 2018). LLME is one of the efficient techniques to separate and concentrate metal ions, our research team has developed this method for the determination of many metals (Wen et al., 2013, 2014; Wen and Zhu, 2014). There are many advantages for LLME, such as easy operation, fewer solvents and rapidness. However, the method involves the use of organic solvents which generally are toxic and hazardous to organisms and environment.

Ionic liquids (ILs) were deemed as new green solvents (Wen et al., 2014), they seem very promising replacements for the traditional volatile organic solvents in the sample preparation. The ionic liquid liquid-liquid microextraction (IL-LLME) has received considerable attention for its convenience and simplicity compared with traditional liquid-liquid extraction, including lower cost, higher enrichment factor, and lower consumption of toxic organic solvent (Stanisz et al., 2014). 1-butyl-3-methylimidazolium hexafluorophosphate ([BMIM][PF_6])-based microextration procedures were proved to be environmentally friendly and efficient for the preconcentration of heavy metal ions in biological and environmental samples (Arain et al., 2016; Sha et al., 2014). However, the application of [BMIM]PF_6] for the speciation of As(V) and As(III) based on IL-LLME has not been explored so far.

In this work, [BMIM][PF_6] was synthesized, and used to extract/separate inorganic arsenic. As(V) was extracted by ionic liquid directly, while As(III) remains in aqueous phase at pH 6.5, then, a new method for the determination of arsenic by LLME-ETAAS was established. The new method is simple to operate. The proposed procedure does not need any chelating agent, and it also does not require any dispersants, reduce the harm to environment in preliminary separation/preconcentration step obviously. All parameters are optimized by single factor experiment design; furthermore, the orthogonal experiment design is used to optimize the conditions based on the above results. Under the optimized experimental conditions, the developed method was applied for the determination of As(V)/As(III) of different samples with satisfactory results.

Experimental

Instrumentation and reagents

Instrumentation

A ZEEnit 700 electrothermal atomic absorption spectrometer (Analytik Jena Instrument Co., Ltd., Germany) equipped with a arsenic hollow cathode lamp, and a Zeeman-based background corrector were used for arsenic determination. The instrumental settings are listed as follows, wavelength: 193.7 nm, spectrum bandwidth:

http://www.aloki.hu ● ISSN 1589 1623 (Print) ● ISSN 1785 0037 (Online)
DOI: http://dx.doi.org/10.15666/aeer/1704_79437955

0.8 nm, lamp current: 6.0 mA, matrix modifier: 0.1% $Pd(NO_3)_2$. All the absorbance measurements were performed by integrating peak areas. Operating parameters and electrothermal temperature program for arsenic determination were given in *Table 1*. Fourier transform infrared (FTIR) spectra were recorded by a TENSOR-27 Fourier transform infrared spectrophotometer (Bruker Corporation, Germany). A mode TDL80-2B centrifuge (Shanghai Anting Science Instrument Factory, Shanghai, China) was used to blend the mixture. pH measurements were made with a PHS-25B pH meter (Shanghai Precision & Scientific Instrument Co., Ltd., Shanghai, China) using a combined glass electrode. A digital constant temperature water-bath (Guohua Co., Ltd., China) was used to heat the mixture. Vacuum was achieved by a 2K-82B vacuum drying oven (Yichuan, Co., Ltd., China).

Table 1. *Instrumental conditions for arsenic species determination*

Step	Temperature (°C)	Heating rate (°C/S)	Hold time (S)	Argon flow rate (mL/min)
Drying 1	90	5	20	250
Drying2	110	2	20	250
Pyrolysis	300	250	10	250
Atomization	2100	3000	4	-
Cleaning	2200	500	4	250

Reagents

1-Bromohexane, N-methylimidazole, As(III) stock standard solution (1.00 g/L) was prepared by dissolving 0.1320 g dried As_2O_3 in 2.0 mL of 1.0 mmol/mL NaOH solution and adjusting the pH to 7.0 with 0.5 mol/L HCl. As(V) stock standard solution (1.00 mg/mL) was prepared by sodium arsenate. Working standard solutions were prepared by stepwise diluting the stock solutions just before use. N-Butylimidazole (98%, Shanghai Darui Fine Chemical Reagent Co., Ltd., Shanghai, China), KPF_6 (Aladdin Chemical Reagent Co., Ltd., Los Angeles, USA) and 1-bromobutane were used. Buffer solutions of acetic acid sodium-acetate (0.2 mol/L), polyethylene oxide pyridine, glycerol. A certified reference material for arsenic (V) GBW08666 was supplied by Research Center for Eco-Environmental Science, Chinese Academy of Sciences (Beijing, China). All chemicals and reagents used were of analytical reagent grade or higher purity and purchased from Sinopharm Chemical Reagent Co., Ltd. (Shanghai, China) unless otherwise specified. Deionized water used throughout entire work.

River water sample: The river water sample near Yangzhou Thermal Power Plant was collected to study the circulation of inorganic arsenic, the river water sample was filtrated and diluted 10 times prior to detect.

Air sample: For the same reason as above, air sample was collected near Yangzhou Thermal Power Plant. 10 g polyethylene oxide pyridine was added into 10 mL glycerol, then mixed with 100 mL water, neutral filter paper was immersed in the mixture solution for 6 h, then the filter paper was dried under infrared light and packed into a sampler to collect 15.0 m^3 gas with the flow rate of 60 L/min. After the sampling, the filter paper was shredded and put into a 100 mL beaker. Instead of adding such as nitric acid to digest sample for the determination of total arsenic, only 20 mL water was added

http://www.aloki.hu ● ISSN 1589 1623 (Print) ● ISSN 1785 0037 (Online)
DOI: http://dx.doi.org/10.15666/aeer/1704_79437955

to the beaker in this word in order to prevent V(III) from being oxidized to As(V), then stirring violently for 10 min. The sample solution was filtered with quantitative filter paper, the filtrate was fixed to 100 mL. Finally, 1.0 mL solution was put it in a 100 ml volume bottle, then set the volume to scale, which was used for the determination of water-soluble inorganic arsenic. It must be pointed out that in the actual sample determination in this experiment the result of air sample determination refers to the concentration of arsenic in the 100 mL volumetric flask, not the concentration of arsenic in the air.

Soil sample: Soil sample collected was near Yangzhou Thermal Power Plant too. 20 mL water was added to 0.5 g soil sample, then the mixture was stirred violently for 10 min. After filter, the filtrate was moved into 100 mL volumetric flask, the solution was diluted 1000 times prior to detect. Similarly, in the actual sample determination in this experiment, the result of soil sample is that the data was diluted 1000 times, not the concentration of arsenic in the soil sample.

Procedure

Synthesis of IL (Huddleston et al., 2001)

1-Butyl-3-methylimidazolium chloride was prepared by reaction of equal molar amounts of 1-methylimidazole and chlorobutane in a round-bottomed flask fitted with a reflux condenser by heating and stirring at 70 °C for 48–72 h. The resulting viscous liquid was allowed to cool to room temperature and then was washed three times with 200 mL portions of ethyl acetate. The remaining ethyl acetate was removed by heating to 70 °C under vacuum. To prepare the ionic liquid, hexa-fluorophosphoric acid (1.3 mol) was added (slowly to prevent the temperature from rising significantly) to a mixture of 1-butyl-3-methylimi-dazolium chloride (1.0 mol) in 500 mL of water. After stirring for 12 h, the upper acidic aqueous layer was decanted, the lower ionic liquid portion was washed with water until the washings were no longer acidic. The ionic liquid was then heated under vacuum at 70 °C to remove excess water. The product was verified by IR spectrum, the results are in agreement with references.

Extraction procedure

A 0.30 mL [BMIM][PF_6] with 1.0 mL arsenic sample solution was added into a 5 mL glass marked centrifuge tube, and added 1.0 mL acetate/acetic acid buffer, and then diluted to 5 mL with deionized water. For optimization procedures, 20 ug/mL As(V) was used instead of water sample. The tube was first shaken violently, and then the mixture was heated in a water bath for obtaining a dispersion of the ionic liquid into the aqueous media. Finally, the tube was centrifuged at 4000 r/min, then the formation of two well-defined phases was achieved. The aqueous phase were manually removed to analysis the concentration As(III) by ETAAS, and the viscous ionic liquid phase was dissolved in 0.40 mL of methanol prior to ETAAS measurement.

Results and discussion

In the research, the optimization method of single factor experiment design is first used to optimize the experimental conditions, and on the basis of the optimization conditions of the single factor experiment method, the cross-effect of each factor is

http://www.aloki.hu ● ISSN 1589 1623 (Print) ● ISSN 1785 0037 (Online)
DOI: http://dx.doi.org/10.15666/aeer/1704_79437955

considered comprehensively. Then, the experimental conditions was optimized by orthogonal experiment design.

Optimization of experimental parameters by single factor optimization method

Effect of pH

The effect of pH on the extraction efficiency of As(V) and As(III) was investigated separately over the pH range of 4.0–11.0. The results presented in *Figure 1* indicate that the quantitative recovery (>92.0%) of As(V) was achieved at a pH range of 4.0 to 7.0, while the extraction rate of As(III) was less than 7.0%. The reason for the selective extraction of As(V) maybe explained that As(V) was associated with positive ion of [BMIM][PF_6] by electrostatic interaction to form a hydrophobic complex compound, leading to the quantitative recovery of As(V).

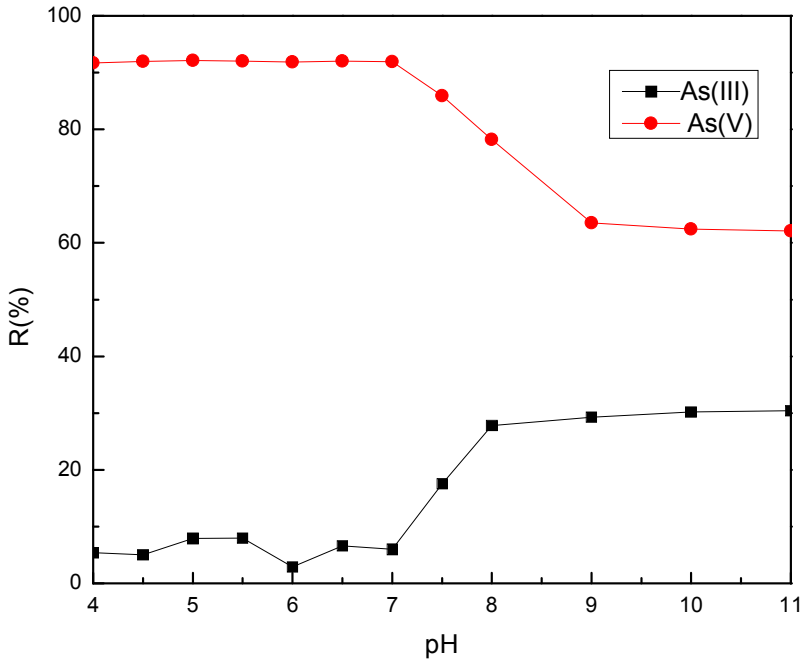

Figure 1. *Effect of pH*

As(V) and As(III) exist in both molecular and ionic forms depending on the pH value of the solution. The stability and speciation of inorganic arsenic compounds depend on pH of solution, as presented in *Figure 2* (Sullivan et al., 2010). In the range of pH 4.0-7.0, As(V) mainly exists as $H_2AsO_4^-$, which can be easily reacted with positive ion of [BMIM][PF_6] to form a stable compound:

$$C_6H_{11}N_2^+.PF_6^- + H_2AsO_4^- \rightarrow C_6H_{11}N_2^+.H_2AsO_4^- + PF_6^-$$

Therefore, the higher recovery rate of As(V) was obtained when pH ≤ 7.0.

However, As(III) tends to be as a neutral molecule(H_3AsO_3) when pH ≤ 7.0, it can not combine with the cation of [BMIM][PF_6], decreasing the recovery of As(III).

In order to selectively determine As(V) and avoid the interference of As(III), the pH 6.0 was chosen in the rest of the work.

http://www.aloki.hu ● ISSN 1589 1623 (Print) ● ISSN 1785 0037 (Online)
DOI: http://dx.doi.org/10.15666/aeer/1704_79437955

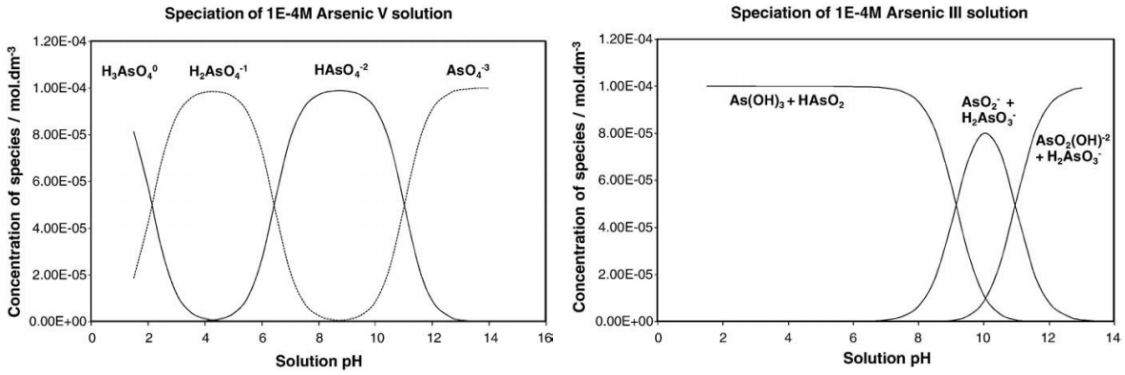

Figure 2. *Stability and speciation of arsenic compounds*

Effect of volume of [BMIM]PF$_6$]

Different volumes of [BMIM]PF$_6$] were investigated, and the results were shown in *Figure 3*. For As(V), the recovery rate increased with the increase of [BMIM]PF$_6$] amount from 0.1 mL to 0.3 mL, and the maximum recovery was obtained when the volume of [BMIM]PF$_6$] was 0.3 mL, whereas the recovery of As(III) was less than 7%. A 0.3 mL of [BMIM]PF$_6$] was selected.

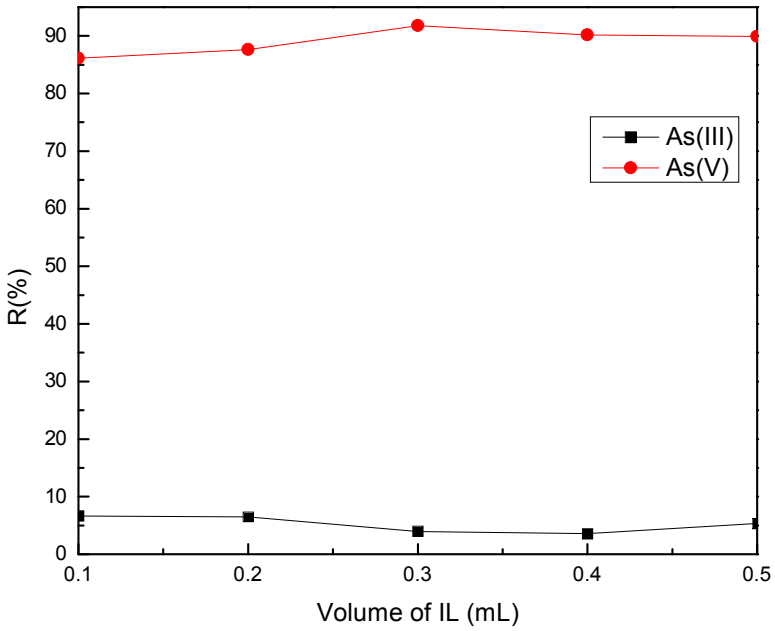

Figure 3. *Effect of the volume of [BMIM]PF$_6$]*

Effect of salt

The effect of salt was investigated with NaCl concentration ranging from 0 to 15% (W/V). As shown in *Figure 4,* the recovery ratio of As(V) decreased tardily with the addition of salts concentration, for the solubility of As(V) was increased with salts addition, as a result, the extraction ration decreased lightly when salts was added. Thus, salt addition was not adopted for further experiments.

http://www.aloki.hu ● ISSN 1589 1623 (Print) ● ISSN 1785 0037 (Online)
DOI: http://dx.doi.org/10.15666/aeer/1704_79437955

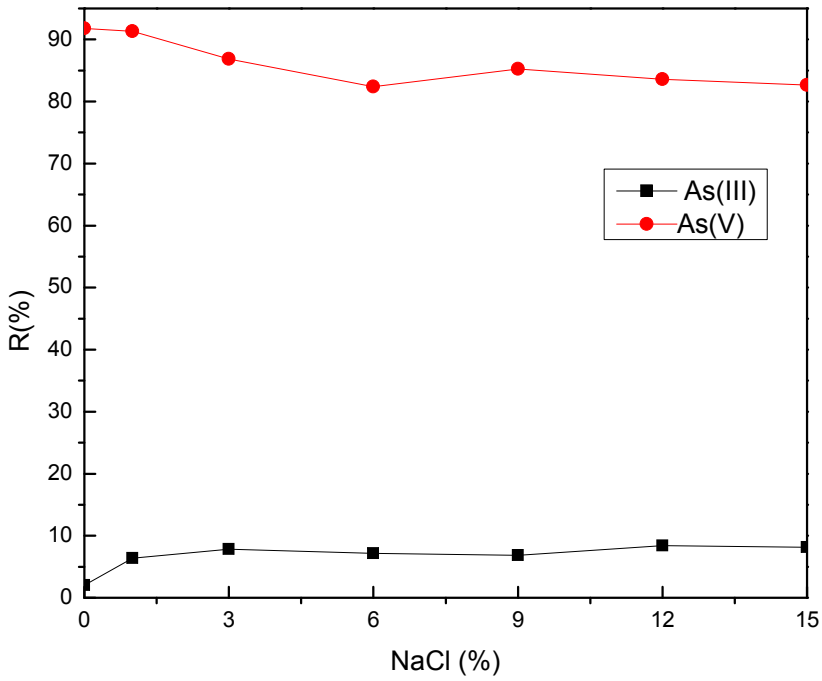

Figure 4. *Effect of salt*

Effect of extraction temperature

The effect of extraction temperature was examined in the range of 15-65 °C, as shown in *Figure 5*. Recovery ratio of As(V) was maximum at 45 °C; so 45 °C was selected.

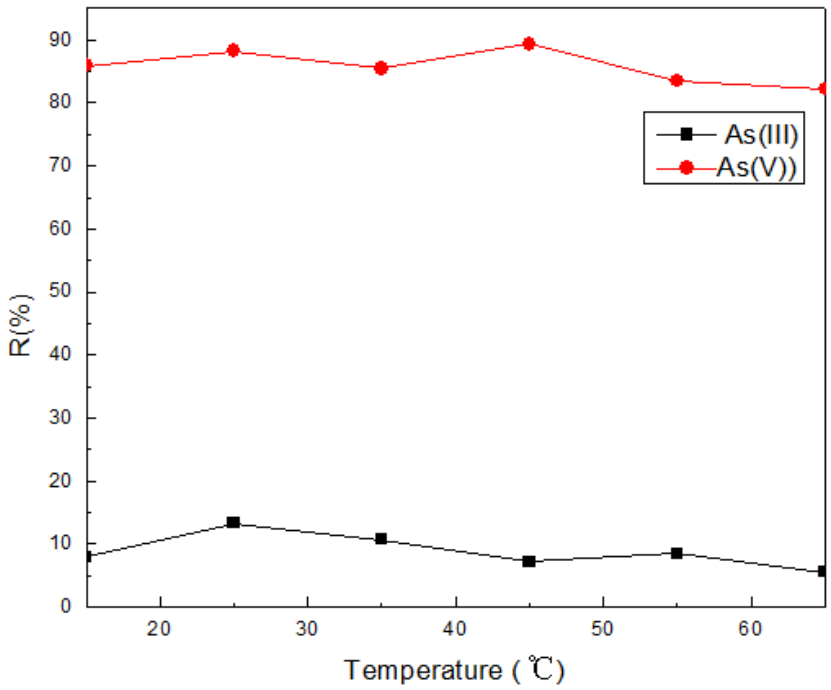

Figure 5. *Effect of temperature*

http://www.aloki.hu ● ISSN 1589 1623 (Print) ● ISSN 1785 0037 (Online)
DOI: http://dx.doi.org/10.15666/aeer/1704_79437955

Effect of extraction time

The influence of extraction time was investigated in the range from 5 to 30 min. *Figure 6* shows that 20 min was sufficient for the quantitative extraction (90%) of As(V), while the extraction efficiency of As(III) was very low (below 10%) in the tested time range. Thus, the extraction time of 20 min was used.

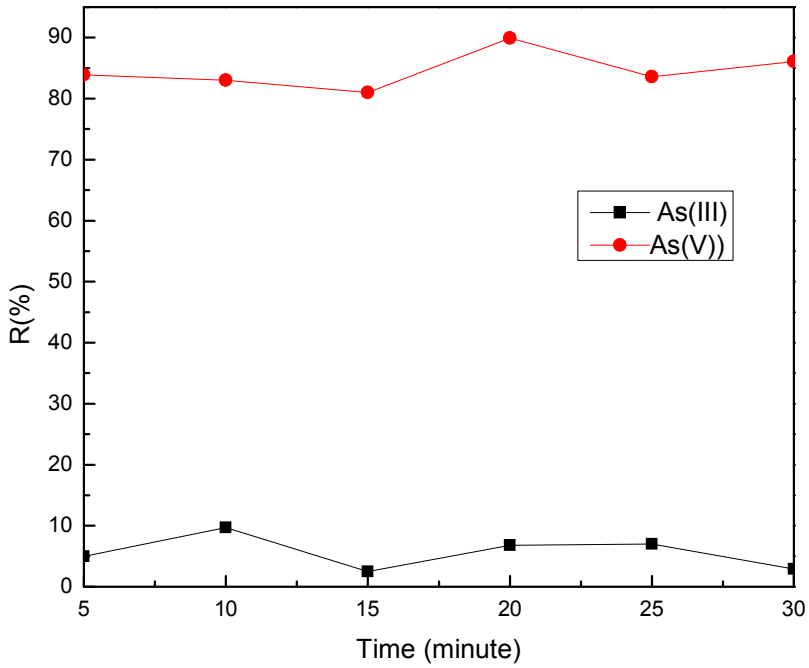

Figure 6. *Effect of the time of extraction*

Optimization of adsorption parameters by orthogonal experiment design

It is simple to use the single factor experiment method when optimizing the experimental conditions, but it must be assumed that the method can only be used when there is no interference between factors. If there is a cross-effect between factors, the use of this method may lead to a wrong result. In fact, factors are less independent of each other. Therefore, on the basis of single factor experiment, the orthogonal design is used to optimize the extraction conditions in this study. For there is little effect of salt on the extraction process, the effect of salt is not taken into account in orthogonal design. Above and below the optimum experimental conditions obtained by single factor experiment method, the orthogonal experiment design is used to optimize the experimental parameters, details are shown in the *Table 2.*

As can be seen from *Table 2*, the importance of the factors that affect the extraction rate of As(V) is significantly different, the order of factors is (from large to small): pH > volume of [BMIM]PF_6 > extraction temperature > extraction time. For As(III), there is little difference in the range of factors affecting the extraction. In pursuit of an increase in the extraction rate of As(V), the selected experimental conditions are as follows, pH:6.5, volume of [BMIM]PF_6: 0.5 mL, extraction temperature is 35 °C, and extraction time is 20 min, under this condition, the extraction rate of As(V) is more than 92% with the extraction rate of As(III) is less than 7%.

http://www.aloki.hu ● ISSN 1589 1623 (Print) ● ISSN 1785 0037 (Online)
DOI: http://dx.doi.org/10.15666/aeer/1704_79437955

Table 2. *Optimization of parameters by orthogonal experiment design*

Level		pH	V (mL)	Et (°C)	T (min)	Er (%)	
						As(III)	As(V)
1		6.0	0.2	35	10	2.0	81.4
2		6.0	0.3	45	15	4.5	88.5
3		6.0	0.4	55	20	8.2	85.7
4		6.0	0.5	65	25	8.8	83.2
5		6.5	0.2	45	20	7.7	86.9
6		6.5	0.3	35	25	7.1	87.8
7		6.5	0.4	65	10	8.1	84.1
8		6.5	0.5	55	15	8.5	84.9
9		7.0	0.2	55	25	8.9	83.2
10		7.0	0.3	65	20	6.7	87.4
11		7.0	0.4	35	15	12.2	88.3
12		7.0	0.5	45	10	6.9	85.1
13		7.5	0.2	65	15	7.2	68.7
14		7.5	0.3	55	10	9.2	70.4
15		7.5	0.4	45	25	7.0	72.5
16		7.5	0.5	35	20	6.7	76.8
As (V)	K1	85.575	77.275	84.1	80.85		
	K2	85.95	83.4	83.4	82.15		
	K3	85.725	84.375	81.3	83.425		
	K4	72.4	84.6	80.85	83.225		
	Range	13.55	7.325	3.25	2.575		
As (III)	K1	5.875	6.45	7	6.55		
	K2	7.85	6.875	6.525	8.1		
	K3	8.675	8.875	8.7	7.325		
	K4	7.525	7.725	7.7	7.95		
	Range	2.8	2.425	2.175	1.55		

V: volume of [BMIM]PF_6, Et: extraction temperature, T: extraction time, Er: extraction rate

Interference

Interference of As(III)

The interference between As(III) and As(V) was evaluated. The results showed that no remarkable influences were observed on the determination of As(V)/As(III) at the concentration ratio of As(III) to As(V) within 20-fold, the good recoveries have been obtained and the two species can be separated.

Interference of other metal ions

To evaluate the potential interference of other metal ions, different foreign metal ions were added individually to a series of standard working solution containing 20.00 ng/mLAs(V)/As(III). A variation on the recovery higher than ±5% was considered as interference. The tolerance limits (metal ion/As, w/w) of foreign ions on the determination of As(III)/As(V) were summarized as in *Table 3*.

http://www.aloki.hu ● ISSN 1589 1623 (Print) ● ISSN 1785 0037 (Online)
DOI: http://dx.doi.org/10.15666/aeer/1704_79437955

Table 3. *Effect of interfering ions of As*

Interferences ions	Tolerance ratio (w/w)
Pb^{2+}, Sn(IV) ,Zn^{2+},Cd^{2+}	10
Fe^{3+}, Mg^{2+}, Ca^{2+}, Cr(VI), Cl^-, F^-, HCO_3^-	100
K^+, Na^+, Cu^{2+}, Ni^{2+}, SO_4^{2-}, NH_4^+	200

Performance of the method

The proposed method was evaluated under the optimum conditions described above. According to the International Union of Pure and Applied Chemistry definition, the detection limits (3σ) of this method was 0.04 ng/mL for As(V) and 0.53 ng/mL for As(III).The relative standard deviations for six replicates extractions at 20.00 ng/mL level of As(V) was 3.5%, and As(III) was 2.9%. The preconcentration factor was 12.5-fold for As(V), which was calculated as the volume ratio of the sample solution (5.00 mL) to the [BMIM][PF_6] phase after the dilution with methanol (0.40 mL).

Comparison of the present method with others

Comparing the analytical features of the method with other studies (*Table 4*), the results demonstrates that this method is superior in terms of LOD of As(V). It should be noted in particular that no chelating reagent has been added to this method and no organic reagent has been used in the whole extraction process. Compared with other methods, this is less harmful to the environment, greener, more economical, and more environmentally friendly.

Table 4. *Comparison of analytical features of proposed method with other methods*

Method	LOD (ug.L^{-1})		Calibration range(ug.L-1)		Reference
	As(V)	As(III)	As(V)	As(III)	
ASCP	0.55	0.42	0.5-200	0.5-200	Jedryczko et al.(2016)
HPLC-HG-ICP-MS	0.3	0.1	1-750	1-300	Gomez-Ariza et al. (2000)
LC-HG-AFS	1.5	0.5	>800	>800	Vilanó et al. (2000)
FI-HG-AFS	0.05	-	0.1-3.0	-	Leal et al. (2006)
PCL	0.44	0.27	0-50	0-50	Sengupta et al. (2010)
SPE-ETAAS	20	28	-	-	Arain et al. (2016)
IL-LLME-ETAAS	0.04	0.35	0.47-72.0	1.02-75.3	This paper

LOD: limits of detection

Method application

To validate the accuracy and precision of the proposed method, arsenic species were analyzed in a certified reference material for GBW08666. The results in *Table 3* shows that almost no As(III) was detected in the reference GBW08666, and the content of As(V) was in good agreement with the certified value of 14.39 ng/mL. Furthermore, the recovery results for As(V)/As(III) in the reference were in the range of 93.4–104.4%. That could be concluded that the method was feasible and accurate for the determination of As(V)/As(III) species.

http://www.aloki.hu ● ISSN 1589 1623 (Print) ● ISSN 1785 0037 (Online)
DOI: http://dx.doi.org/10.15666/aeer/1704_79437955

The method was also applied to the determination of As(V)/As(III) in three kinds of samples. The results and the recovery for the spiked samples are given in *Table 5*. The As(V) extraction rate of standard addition is between 96.5% and 106.4% in the detection of various practical sample, while As(III) is between 97.2% and 106.8%.

Table 5. *Determination of As(III) and As(V) in real samples and certified reference material*

Sample	Added (ng/mL)		Found (ng/mL)			Recovery (%)		
	As(III)	As(V)	As(III)	As(V)	Total As	As(III)	As(V)	Total As
GBW08666*	0	0	ND	14.84	14.84	-	103.1	103.1
	14.76	12.87	13.78	27.52	41.30	93.4	102.0	98.3
	29.52	25.74	27.83	41.27	69.10	94.3	104.4	99.2
Air sample	0	0	0.75	1.22	1.97	-	-	-
	5.0	5.0	5.61	6.42	12.03	97.2	104.0	100.6
	10.0	10.0	10.59	10.87	21.46	98.4	96.5	97.5
River water	0	0	1.23	2.15	3.38	-	-	-
	5.0	5.0	6.07	7.23	13.32	96.8	101.3	99.4
	10.0	10.0	11.33	12.49	23.82	101.0	106.4	102.2
Soil sample	0	0	4.34	10.42	14.76	-	-	-
	5.0	5.0	9.68	15.25	24.93	106.8	96.6	101.7
	10.0	10.0	14.57	20.83	35.40	102.3	104.1	103.2

*Standard samples ($C_{As(V)}$ = 14.39 ng/mL) was diluted appropriately before determination
ND: not founded

Conclusion

In this paper, hydrophobic ionic liquid 1-butyl-3-methylimidazolium hexafluorophosphate was synthesized to extract and separate iAs species, The experimental conditions were optimized by single factor experiment and orthogonal design method. The whole process was carried out without any chelating/dispersive agent. The method sees to be simple, sensitive, and efficient. With the proposed procedures, satisfactory results of iAs species in different samples were obtained. The proposed method is recommended for iAs determinations in environmental samples.

Acknowledgements. The authors acknowledge the financial support from the National Natural Science Foundation of China (21375117), a project funded by the Priority Academic Program Development of Jiangsu Higher Education Institutions, and a funded by Yangzhou environmental protection bureau.

REFERENCES

[1] Abdolmohammad-Zadeh, H., Jouyban, A., Amini, R. (2013): Ultratrace determination of arsenic in water samples by electrothermal atomic absorption spectrometry after pre-concentration with Mg-Al-Fe ternary layered double hydroxide nano-sorbent. – Talanta 116(22): 604-610.

[2] Arain, S. A., Kazi, T. G., Afridi, H. I., Arain, M. S., Panhwar, A. H., Khan. N., Baig, J. A., Shah, F. (2016): A new dispersive liquid-liquid microextraction using ionic liquid based microemulsion coupled with cloud point extraction for determination of copper in serum and water samples. – Ecotoxicology Environmental Safety 126: 186-192.

http://www.aloki.hu ● ISSN 1589 1623 (Print) ● ISSN 1785 0037 (Online)
DOI: http://dx.doi.org/10.15666/aeer/1704_79437955

[3] Gomez-Ariza, J. L., Sanchez-Rodas, D., Giraldez, I., Morales, E. (2000): A comparison between ICP-MS and AFS detection for arsenic speciation in environmental samples – Talanta 51(2): 257-268.
[4] Huddleston, J. G., Visser, A. E., Reichert, W. M., Willauer, H. D., Broker, G. A., Rogers, R. D. (2001): Characterization and comparison of hydrophilic and hydrophobic room temperature ionic liquids incorporating the imidazoliumcation cation. – Green Chemistry 3(4): 156-164.
[5] Jedryczko, D., Pohl, P., Welna, M. (2016): Inorganic arsenic speciation in natural mineral drinking waters by flow-through anodic stripping chronopotentiometry. – Talanta 150: 265-271.
[6] Leal, L. O., Forteza, R., Cerdà, V. (2006): Speciation analysis of inorganic arsenic by a multisyringe flow injection system with hydride generation–atomic fluorescence spectrometric detection. – Talanta 69(2): 500-508.
[7] Li, J., Sun, C., Zheng, L., Jiang, F., Wang, S., Zhuang, Z., Wang, X. (2017): Determination of trace metals and analysis of arsenic species in tropical marine fishes from Spratly islands. – Marine Pollution Bulletin 122(1-2): 464-469.
[8] Ministry of Public Health of the People's Republic of China (2007): Occupational exposure limits for hazardous agents in the workplace. – Dissertation.
[9] Nellaiappan, S., Pillai, K. C., Kumar, A. S. (2018): Flow-injection analysis coupled electrochemical detection of poisonous inorganic arsenic(III) species using a gold nanoparticle/carbon nanofiber/chitosan chemically modified carbon screen printed electrode in neutral pH solution. – Analytical Methods 10(7)799-808.
[10] Pourghazi, K., Amoli-Diva, M., Beiraghi, A. (2015): Speciation of ultra-trace amounts of inorganic arsenic in water and rice samples by electrothermal atomic absorption spectrometry after solid-phase extraction with modified Fe3O4 nanoparticles. – International Journal of Environmental Analytical Chemistry 95(4): 15.
[11] Sha, O., Zhu, X. S. (2014): Determination of gold(III) by simplified room-temperature ionic liquid extraction with flame atomic absorption spectrometry. – Analytical Letters 47(6): 1052-1062.
[12] Sengupta, M. K., Hossain, Z. A., Ohira, S. I., Dasgupta, P. K. (2010): A simple inexpensive gas phase chemiluminescence analyzer for measuring trace levels of arsenic in drinking water. – Environmental Pollution 158(1): 252-257.
[13] Squibb, K. S., Fowler, B. A. (1983): The Toxicity of Arsenic and Its Compounds. – Elsevier Science, New York.
[14] Stanisz, E., Werner, J., Zgoła-Grześkowiak, A. (2014): Liquid-phase microextraction techniques based on ionic liquids for preconcentration and determination of metals. – TrAC Trends in Analytical Chemistry 61: 54-66.
[15] Sullivan, C., Tyrer, M., Cheeseman, C. R., Graham, N. J. D. (2010) Disposal of water treatment wastes containing arsenic—a review. – Science of the Total Environment 408: 1770-1778.
[16] Tunçeli, A., Ocak, G., Acar, O., Türker, A. R. (2015): Development of a method for speciation of inorganic arsenic in waters using solid phase extraction and electrothermal atomic absorption spectrometry. – International Journal of Environmental Analytical Chemistry 95(14): 1-17.
[17] United States Environmental Protection Agency (2002): Implementation Guidance for the Arsenic Rule. Drinking Water Regulations for Arsenic and Clarifications to Compliance and New Source Contaminants Monitoring Guidance. – EPA, Washington, DC.
[18] Vilanó, M., Padró, A., Rubio, R. (2000): Coupled techniques based on liquid chromatography and atomic fluorescence detection for arsenic speciation. – Analytical Chimica Acta 411(1-2): 71-79.
[19] Wang, X, Xu, G., Chen, P., Sun, Y. S., Yao, X.T., Lv, Y., Guo, W. W., Wang, G. Z. (2018): Fully-automated magnetic stirring-assisted lab-in-syringe dispersive liquid–liquid

http://www.aloki.hu ● ISSN 1589 1623 (Print) ● ISSN 1785 0037 (Online)
DOI: http://dx.doi.org/10.15666/aeer/1704_79437955

microextraction for the determination of arsenic species in rice samples. – RSC Advances 8(30): 16858-16865.

[20] Wen, S. P., Zhu, X. S. (2014) Speciation analysis of Mn(II)/Mn(VII) in tea samples using flame atomic absorption spectrometry after room temperature ionic liquid-based dispersive liquid–liquid microextraction. – Food Analytical Methods 7(2): 291-297.

[21] Wen, S. P., Wu, J., Zhu, X. S. (2013): Room temperature ionic liquid-based dispersive liquid–liquid microextraction combined with flame atomic absorption spectrometry for the speciation of chromium(III) and chromium(VI). – Journal of Molecular Liquids 180(4): 59-64.

[22] Wen, S. P., Zhu, X. S., Wu, X. Y., Qin, X. X. (2014): Directly suspended droplet microextractioncoupled with electrothermal atomic absorption spectrometry for the speciation of chromium(III)/chromium(VI). – Analytical Methods 6(24): 9777-9782.

http://www.aloki.hu ● ISSN 1589 1623 (Print) ● ISSN 1785 0037 (Online)
DOI: http://dx.doi.org/10.15666/aeer/1704_79437955

MONITORING OF PHYTOREMEDIATING WETLAND MACROPHYTES USING REMOTE SENSING: THE CASE OF COMMON REED (*PHRAGMITES AUSTRALIS* (CAV.) TRIN. EX STEUD.) AND THE GIANT REED (*ARUNDO DONAX* L.). A REVIEW

MABHUNGU, L.[1*] – ADAM, E.[1] – NEWETE, S. W.[2,3]

[1]*School of Geography, Archaeology and Environmental Studies*
University of the Witwatersrand, Private Bag X3, 2050 Johannesburg, South Africa

[2]*Agricultural Research Council-Institute for Soil, Climate and Water (ARC-ISCW)*
Geo-Information Science Programme, Arcadia, Private Bag X79, 0001 Pretoria, South Africa

[3]*School of Animal, Plant and Environmental Sciences, University of the Witwatersrand*
Private Bag X3, 2050 Johannesburg, South Africa

[*]*Corresponding author*
e-mail: loveness.mabhungu@gmail.com

(Received 7th Nov 2018; accepted 25th Jan 2019)

Abstract. Contaminants from various anthropogenic activities such as agriculture, mining, and recreation negatively affect wetland water quality and vegetation health and composition. Phytoremediation is an effective, sustainable and eco-friendly pollution abatement method using green plants. *Arundo donax* L. and *Phragmites australis* (Cav.) Trin. ex Steud. are two morphologically similar reeds commonly used for phytoremediation in wetlands of South Africa. *Arundo donax* is however, a declared category '1b' weed under the National Environmental Management: Biodiversity Act (NEM:BA, Act No. 10 of 2004), requiring its immediate removal. Thus, determining the phytoremediation efficiency of the two reeds could help making the right choice between them for potential use in wetlands. Furthermore, the effeciency of wetlands depends on a robust monitoring system for phytoremediating plants to determine the appropriate time for biomass harvest before they die and release contaminants taken up in plant tissues back into the source through decomposition. Remote sensing can be used for mapping and monitoring of such aquatic macrophytes at species level effectively. Satellites imageries with high spatial and spectral resolutions not only are capable of detecting heavy metal-induced plant stresses, but also can effectively discriminate between morphologically similar species like *A. donax* and *P. Australis* and facilitate wetland managment.
Keywords: *Acid Mine Drainage; Heavy metal uptake, Maping; hyperspectral; Rhizofiltration*

Introduction

Phytoremediation is a relatively low-cost and environmentally friendly method of reducing environmental pollutants to harmless levels using green plants (Emmanuel et al., 2014; Kaewtubtim et al., 2016; Newete and Byrne, 2016). Based on the plant tissues involved in removal of pollutants and their specific sites of accumulation in the plants, phytoremediation is sub-categorized as phytoextraction, rhizofiltration, phytovolotalization, phytostabilization, phytodegradation, and rhizodegradation (Pilon-Smits, 2005; Newete and Byrne, 2016). Phytostabilisation refers to the process of plants stabilising pollutants in the soil to harmless levels; phytoextraction is when pollutants are transported and concentrated in the above ground plant tissues and involves subsequent harvest of aerial plant biomass; rhizofiltration is when plants, or

http://www.aloki.hu ● ISSN 1589 1623 (Print) ● ISSN 1785 0037 (Online)
DOI: http://dx.doi.org/10.15666/aeer/1704_79577972

microorganisms associated with the rhizosphere, remove contaminants from water; phytodegradation occurs when plant enzymes break down pollutants inside their tissues and convert them into harmless compounds; phytovolatilisation involves extraction of volatile compounds by plants which are released as volatile compounds through the leaves (Raskin, 1997; Wong, 2003). Phytoremediation can occur in both dry and wet environments. Phytoextraction is commonly used for cleaning contaminants from soil, rhizofiltration to clean contaminants from water medium, while phytostabilization, phytovolatilization and phytodegradation can be used to clean either from soil or water mediums (Frick et al., 1999; Wong, 2003; Yang et al., 2005). The degree of pollutant accumulation by plants tends to increase with the wetness of the environment (Aryal et al., 2016). Compared to conventional or engineering methods of cleaning polluted environments, phytoremediation is potentially cheaper, environmentally friendly, sustainable, and has the possibility of bio-recovering heavy metals (Yang et al., 2005).

According to Ramsar Convention Secretariat (2016) wetlands are "areas of marsh, fen, peatland or water, whether natural or artificial, permanent or temporary, with water that is static or flowing, fresh, brackish or salt, including areas of marine water the depth of which at low tide does not exceed six metres". Wetlands are essential to both humans and the ecological environment, and once their health and functions are disturbed, the effects are detrimental on all life forms supported by wetlands. Their functions include nutrient removal from water, trapping of sediments, pollutant trapping, control of erosion, stream flow augmentation, provision of habitat for wildlife, and recreational benefits (Bruneau, 2017; Luo et al., 2017). According to Zedler and Kercher (2004), wetlands account for approximately 6% of the world's land surface. Depending on their positioning, wetlands are subjected to impacts from human activities such as agriculture, mining and urban development. Impacts of mining on wetlands include water pollution from Acid Mine Drainage (AMD) and heavy metals, land degradation, vegetation biodiversity degradation, and destruction of a wide range of habitat for wetland wildlife (Gupta and Nikhil, 2016). From these, the major effect of mining activities on wetlands is AMD pollution, which emanates from seepage of both active and abandoned mining areas near wetlands (Newete and Byrne, 2016). Acid mine drainage is the outflow of acidic water from mining sites, and this is mainly due to the oxidation of iron pyrites (FeS_2) (Akcil and Koldas, 2006; Ochieng et al., 2010). Due to its low pH of usually 2 - 3, AMD dissolves mining ores, and thus contains, high concentrations of metals which include manganese, aluminum, iron, nickel, zinc, cobalt, copper, and cadmium (Bell et al., 2001; Coetzee et al., 2006). AMD pollution from wetlands can also end up in streams, rivers and dams, which supply potable water for humans (McCarthy and Humphries, 2013). This makes the water quality unsuitable for human consumption and adds a toll to the costs of water purification. Research has shown that low pH and high concentrations of heavy metals negatively affect wetland species composition (Ochieng et al., 2010). Destruction of wetland vegetation or alteration of vegetation composition will also affect wild animals which use the plants as habitats. However, some aquatic plant species have adapted mechanisms to survive in such conditions (Deng et al., 2004; Papazoglou et al., 2005; Vymazal and Březinová, 2015), thus, they can be used as bio-indicators to evaluate the presence and amount of heavy metal contaminants in wetlands. These plants have an extensive root system and root surface area that enhances contaminant uptake by adsorption of metal cations onto the negatively charged root surfaces (Newete et al., 2016; Newete and Byrne, 2016). The subsequent harvest of the phytoremediating plants with a cocktail of organic and

http://www.aloki.hu ● ISSN 1589 1623 (Print) ● ISSN 1785 0037 (Online)
DOI: http://dx.doi.org/10.15666/aeer/1704_79577972

inorganic contaminants from polluted wetlands means an improvement of the existing water quality. Thus, many artificial wetlands are constructed for treatment of wastewater using green plants (Liu et al., 2007; Vymazal and Březinová, 2015). Among the common emergent macropytes used in wetlands are *Phragmites australis* (Cav.) Trin. ex Steud. (Vymazal and Brezinova, 2016), *Arundo donax* L. (Elhawat et al., 2014), *Phalaris arundinacea Scirpus* spp. and *Typha* spp. (Papazoglou et al., 2005; Newete and Byrne, 2016). From these, *P. australis* is the most commonly used and studied plant species (Vymazal and Brezinova, 2016). This could be because it is a cosmopolitan plant species which is widely distributed across the world (Adams and Bate, 1999). *Arundo donax* L., which is morphologically similar to *P. australis*, is another such species with wide geographical distribution in many polluted wetland systems of South Africa outside its natural habitat (Rouget et al., 2004). *Phragmites australis* also known as common reed, is native to South Africa (Adams and Bate, 1999), while *A. donax*, known as the Spanish or the giant reed, is a declared Category 1b weed in South Africa (Henderson, 2001; Department of Environmental Affairs, 2016). Although the two reeds have proved to be effective as tools of phytoremediation in wetlands, their capacities to uptake heavy metals have not been compared under similar and controlled conditions.

Although the efficiency of metal uptake by phytoremediating plants depends on plant species, size of plant biomass particularly large root surface area in aquatic macrophytes, type and amount of elements targeted for removal (Newete and Byrne, 2016), it is equally important to monitor the level of such pollutants' removal from the polluted environment and accumulation in the plant tissues. This is because it allows subsequent management of the phytoremediating plants by determining the appropriate time for harvest of plant biomass and safe disposal (Carson et al., 2018). The conventional method of determining metal accumulation in plant tissue in the laboratory is often expensive, destructive and labour intensive (Van Deventer and Cho, 2014). Thus, there is a need for effective and non-destructive method to monitor heavy metal uptake by various wetland plants. Remote sensing has the potential to be that method. This is because the spectral reflectance by green vegetation depends, *inter alia*, on the amount of specific biochemical in plant leaves (Gates et al., 1965; Zwiggelaar, 1998). Remote sensing has extensively been used to monitor the effect of individual metal pollutants on plants using their effects on chlorophyll and net photosynthesis (Sridhar et al., 2007).

There is a large number of literature reviews on phytoremediation (Raskin et al., 1997; Pilon-Smits, 2005; Laghlimi et al., 2015; Rizwan et al., 2017) and for wetlands (Matagi et al., 1998; Usharani and Vasudevan, 2016; Newete and Byrne, 2016; Leguizamo et al., 2017). However, only few of them focused on wetland phytoremediating plants. This study will therefore, review the efficiency of phytoremediation by emergent aquatic macrophytes in wetlands with specific reference to two morphologically similar reeds, *P. australis* and *A. donax*, in South Africa. It will also investigate the potential of remote sensing technique in monitoring heavy metal accumulation by the plants effectively.

http://www.aloki.hu ● ISSN 1589 1623 (Print) ● ISSN 1785 0037 (Online)
DOI: http://dx.doi.org/10.15666/aeer/1704_79577972

Reeds in South Africa

Reed is the general botanical term used for tall, grass-like plants that grow in wet places. They occur in reed beds. They are all members of the order Poales, but under different families. *Table 1* gives a list of some of the commonly known reeds.

Table 1. *Some of commonly known reeds in the world*

Family	Reed's common name and species name
Poaceae grass	Common reed *(Phragmites australis (Cav.) Trin. ex Steud.*)
	Giant reed (*Arundo donax L.*)
	Burma reed (*Neyraudia reynaudiana*)
	Reed canary-grass (*Phalaris arundinacea*)
	Reed sweet-grass (*Glyceria maxima*)
	Small-reed (*Calamagrostis species*)
Cyperaceae (sedge)	Paper reed or papyrus (*Cyperus papyrus*)
Sparganiaceae	Bur-reed (*Sparganium species*)
Typhaceae	Reed-mace (*Typha species*)
Restionaceae	Cape thatching reed (*Elegia tectorum*)
	Thatching reed (*Thamnochortus insignis*)

From the list in *Table 1*, *Cyperus papyrus*, *A. donax*, *Calamagrostis* species, *P. australis* and *Typha* species were identified in wetlands of South Africa (De Villiers et al., 2011). *Cyperus papyrus* is a tall perennial grass-like emergent plant. It is naturally found in KwaZulu-Natal, Mpumalanga and Limpopo provinces. It grows along the edges of rivers, seasonal or permanent pools, or swamps. The reed is unpalatable and has low forage quality, and thus does not support many plantivores (De Villiers et al., 2011). *Calamagrostis* is a perennial grass which inhabits vleis and marshes. It is sparsely distributed in Eastern Cape, Mpumalanga, Gauteng, North West and Northern Cape provinces of South Africa (De Villiers et al., 2011). *Typha* species is widely distributed in South Africa and it grows in wetlands and all aquatic habitats (Masoko et al., 2008; Ilfergane, 2016). The species forms large dense and dominant stands. *Arundo donax* and *P. australis* are tall, robust and perennial grass-like plants with hollow stems, and are widely distributed in Western Cape, Eastern Cape, KwaZulu-Natal, Mpumalanga and Gauteng provinces of South Africa (De Villiers et al., 2011). Morphologically the two reeds resemble each other. They are both aggressive invaders outside their native ranges (Lambert et al., 2010). The slight differences between them are shown in *Table 2*, extracted from Lusweti (2011). Images for *A. donax* (*Fig. 1*) and *P. australis* (*Fig. 2*) in Johannesburg, South Africa, extracted from google earth, are also shown below.

Table 2. *Morphological differences between Phragmites australis (Cav.) Trin. ex Steud. and Arundo donax L.*

Arundo donax L.	***Phragmites australis (Cav.) Trin. ex Steud.***
Very tall grass, 2 – 7 m tall	relatively tall grass, 1.5 – 3m tall
Relatively broad leaves, 10 – 80 mm wide	relatively narrow leaves 10 – 35 mm wide

Arundo donax L. is native to the Mediterranean Basin and the middle east in Asia, and some parts of Africa and southern Arabian Peninsula, while *P. australis* is a cosmopolitan species with wide distribution spanning the five continents (excluding the polar continents) of the world, and it is also known as native to South Africa

http://www.aloki.hu ● ISSN 1589 1623 (Print) ● ISSN 1785 0037 (Online)
DOI: http://dx.doi.org/10.15666/aeer/1704_79577972

(Henderson and Cillier, 2004). *Arundo donax* L. is a naturalised alien species in South Africa (Milton, 2004), and was introduced in the late 1700s for soil erosion control. It invades riparian areas across South Africa and its spread is facilitated by human activities such as building of dams and soil stabilisation (Canavan et al., 2017). Alien invasive plant species have negative impacts on indigenous plant ecosystems. They form dense stands which reduce biodiversity of indigenous communities, affect food-webs, and hence change ecosystem processes (Milton, 2004). *Arundo donax* L. is highly flammable and can alter fire regimes in invaded areas, thus changing the communities of native plants into a dense mono stand of *A. donax* (Lusweti, 2011). To address the invasive potential and negative impacts of *A. donax* in South Africa, biological control methods are being considered (Canavan et al., 2017).

Figure 1. *Image of the giant reed (Arundo donax). Source: US Department of State Geographer, Google earth, 2018.*

Figure 2. *Image of the common reed (Phragmites australis). Source: US Department of State Geographer, Google earth, 2018.*

Both *A. donax* and *P. australis* can adapt well in both dry and damp or wet areas, as well as in heavily polluted areas. As such, they are common in most wetlands. Their dense stands often crowds or shade other wetland vegetation. Their ability to uptake and accumulate nutrients and other pollutants makes them the most suitable macrophytes for phytoremediation in polluted wetlands (Bonanno, 2012; Aminsharei et al., 2017; Bello et al., 2018). As such the two plants have been used for phytoremediation in constructed and natural wetlands.

http://www.aloki.hu ● ISSN 1589 1623 (Print) ● ISSN 1785 0037 (Online)
DOI: http://dx.doi.org/10.15666/aeer/1704_79577972

Phytoremediation by aquatic plants

Wetland vegetation is an important part of the wetland ecosystem, as it plays a major role in environmental sustainability (Adam et al., 2010). Naturally wetlands are sinks for many contaminants, and as such they accumulate materials resulting from both terrestrial and wetland disturbances like sediments, nutrients, salts, heavy metals and other contaminants (Kaplan et al., 2017). According to De Villier et al. (2011), 50% of wetlands in South Africa have already been destroyed due to anthropogenic activities such as agriculture, mining, and urban development. Disturbances from these activities negatively affect the native wetland ecosystems. As a result of this, wetlands are vulnerable to invasion, and presence of particular invasive macrophytes in a wetland may be an indicator of the status of the wetland medium and system (Zedler and Kercher, 2004). Most invasive macrophytes are hyper-accumulators and have the ability to absorb harmful substances and pollutants from the wetland medium into their plant tissues (Zedler and Kercher, 2004). High concentration of pollutants in plant tissues is an important indicator of water quality status in wetlands and other water systems (Deng et al., 2004; Allende et al., 2011). All forms of aquatic plants (emergent, submerged and floating aquatic species) are used for phytoremediation of polluted wetlands (Newete and Byrne, 2016). Nevertheless, emergent aquatic macrophytes like *P. australis* (and *A. donax* are more prevalent in most wetland systems and have proven to be more resilient and effective in removal of heavy metals (Sheoran and Sheoran, 2006; Yang et al., 2006). The degree to which plants accumulate heavy metals is determined by the individual plant uptake capacity and intracellular transportation within the plant (Yang et al., 2005). For example *P. australis* has the potential to accumulate Cd, Cu, Cr, Ni and Pb up to 0.1% of plant dry mass and Fe and Zn up to 1% plant dry mass (Kalra, 1998; Sasmaz et al., 2008). Research conducted by Yang et al. (2006) in Guangdon province, China, showed that *Typha latifolia*, *P. australis* and *Cyperus malaccensis* significantly removed 94% of Cd, 99.04% of lead (Pb), and 97.30% of zinc (Zn) from a constructed wetland. Vymazal and Březinová (2016) revealed that *P. australis* planted in constructed wetlands removed 59% Zn, 55% Cd and 38% Cr, from the inflow annual load of the metals into wetlands. Vymazal and Březinová (2016) also concluded that the plant shoots in constructed wetlands can sequester up to 55% Cr, 49% Zn and 71% Cd, of the total heavy metals removed by the *P. australis*. In another study 19 plant species, among which were *P. australis* and *Cyperus* species, were planted in a constructed wetland in China and irrigated with waste water containing concentrations of Zn, Cd and Pb at 5.0, 0.5 and 2.0 mg/L, respectively. The results showed that the plants had more than 90% removal efficiency for the heavy metals (Liu et al., 2007). Bello et al. (2018), in Saudi Arabia, investigated the capacity of *P. australis* in removing Cd, Pb and Ni in hydroponic experiments with 5 mg/L concentration for each heavy metal. The results showed that the capacity of heavy metal removal by *P. australis* was 93%, 95% and 84% for Cd, Pb and Ni, respectively. In another research conducted in Catania, Italy, the roots, stems, and leaves of *A. donax* were tested as potential bio-monitors of trace elements such as Al, As, Cd, Cr, Cu, Hg, Mn, Ni, Pb, and Zn. The results showed that *A. donax* had the capacity to significantly bioaccumulate the trace elements, with root/sediment Bioaccumulation factors of: Cr (0.08), Cu (0.05), Mn (0.02), Ni (0.1), and Pb (0.03) (Bonanno, 2012). Mojiri et al. (2015) investigated the effectiveness of *P. australis* for heavy metal uptake from municipal waste leachate. At the end of their experiment, the amount of Fe, Mn, Cu and Ni removed by *P. australis* were 25.049, 9.623, 6.112, and 0.900 mg/kg, respectively. The translocation factors were 0.34, 0.89,

http://www.aloki.hu ● ISSN 1589 1623 (Print) ● ISSN 1785 0037 (Online)
DOI: http://dx.doi.org/10.15666/aeer/1704_79577972

1.30 and 1.01, respectively. Translocation Factor (TF) is the ratio of metal concentration in shoots to the metal concentration in roots, and measures the ability of a plant to translocate metals from roots to shoots (Mojiri et al., 2015). A plant has potential to be used for phytoextraction when its TF for a particular metal is above 1. Thus, according to Mojiri et al. (2015), it is apparent that *P. australis* has the potential for the phytoextraction of Cu and Ni, from wetlands, but not for Fe and Mn.

Aquatic plants are very useful in natural and constructed wetlands in the abatement of water contaminants and improving the water quality for domestic and agricultural purposes. *Table 3* is a summary of some literature showing the removal of heavy metals from contaminated wetlands by aquatic macrophytes.

Table 3. *Removal of heavy metal contaminants from wetlands by aquatic macrophytes*

Species	Metals purified	Place	Reference
Typha capensis and *Arundo donax L.*	Zn, Mn, Ni and Fe	Johannesburg, South Africa; Natural wetland	Van der Merwe et al., 1990
Cyperus vaginatus	Cr, Mn, Fe, Co, Ni, Cu, Zn, Cd, and Pb	South Australia; Constructed wetland	Aryal et al., 2016
Typha domingensis, *Phragmites australis (Cav.) Trin. ex Steud.* and *Arundo donax L.*	Al, As, Cd, Cr, Cu, Hg, Mn, Ni, Pb, Zn.	Italy; Natural wetland	Bonanno, 2013
Phragmites australis (Cav.) Trin. ex Steud. and *Bolboschoenus maritimus*	Cr, Ni, Cu and Zn	Northeast Italy; Constructed wetland	Bragato et al., 2006
Bolboschoenus Maritimus	Al, Fe, Cu, Zn	Western Cape, South Africa; Natural wetland	Shuping et al., 2011

The efficiencies of *P. australis* and *A. donax* in heavy metal uptake have been studied by a number of researchers worldwide (Papazoglou et al., 2005; Bonanno, 2012; Kumari and Tripathi, 2015), including in South Africa (Van der Merwe et al., 1990; Zingelwa and Wooldridge, 2016). Kumari and Tripathi (2015) demonstrated the removal of Cu, Cd, Cr, Ni, Fe, Pb and Zn from urban sewage mixed with industrial effluents using *P. australis* and *T. latifolia*, as a cost effective and promising technology in India. Their resuts showed that *P. australis* perfomed better than *T. latifolia* for all the metals, and mixing the two plants increased the removal efficiency of the metals from the effluent. Papazoglou et al. (2005) investigated *A. donax* irrigated with tap water containing increased concentrations of Cd and Ni in Greece. At the end of the experiment the parameters measured, namely, stem height and diameter, number of nodes, fresh and dry weight of leaves, and net photosynthesis, were found not affected, indicating that *A. donax* tolerates high concentrations of Cd and Ni, and thus can be used for phytoremediation. Van der Merwe et al. (1990) measured the accumulation of Zn, Mn, Ni and Fe by *A. donax* and *T. capensis* under acidic and alkaline conditions in the Burgspruit catchment area near Germiston, Ekurhuleni, South Africa and concluded that the metal accumulation capacity of *A. donax* was higher than that of *T. capensis*. Zingelwa and Wooldridge (2016) studied the mineral element uptake and accumulation by *T. latifolia* and *P. australis* from waste water in constructed wetlands in South Africa. They found that *T. latifolia* accumulated more mineral elements (N, P, K, Ca and Al) than *P. australis*. However, only few or no studies compared the capacities of *A. donax* and *P. australis* in heavy metal accumulation under experimental or controlled environment. Bonanno (2013) compared the trace element bioaccumulation capacities

http://www.aloki.hu ● ISSN 1589 1623 (Print) ● ISSN 1785 0037 (Online)
DOI: http://dx.doi.org/10.15666/aeer/1704_79577972

of the two plant species under field or natural conditions, and the results showed that *P. australis* is a better heavy metal accumulator than *A. donax*. He measured the heavy metals Al, As, Cd, Cr, Cu, Hg, Mn, Ni, Pb, and Zn in *Typha domingensis*, *P. australis* and *A. donax* naturally growing along a stream in Italy. The results showed that the bioaccumulation capacities decreased in the order of root>stem>leaf in *T. domingensis*, and root>leaf>stem in *P. australis* and *A. donax*. Generally the bioaccumulation capacities for *P. australis* and *T. domingensis* were found to be higher than that of *A. donax*. Thus, if the native *P. australis* is more effective in removal of heavy metals than its counterpart *A. donax* in wetlands, it is imperative to promote the former species to eventually replace the notorious invader *A. donax* in wetlands. However, to ascertain this, future research should focus on comparing the heavy metal uptake capacities of the two plant species under controlled/experimental conditions. This is because they are widely distributed in many parts of the country and they both provide similar economic and ecological functions. They are useful as thatching, ornamental and musical-instrument (like flutes) materials and source of energy, and wildlife habitat (Bonanno, 2012; Shuai et al., 2016). However, because of their similar morphology, discrimination between the two species and monitoring their occurrence and their environmental foot prints in the field is difficult.

Methods of monitoring heavy metal uptake by aquatic macrophytes

While many aquatic macrophytes have proven to be valuable for phytoremediation, the process requires continuous monitoring to ensure timely harvest of plant biomass and thier replacement for continuous and effective removal of water contaminants (Carson et al., 2018). Appropriate tool of monitoring is required to determine the heavy metal accumulation in the phytoremediating plant tissues and their health status to avoid metal-induced stress and subsequent death of plant tissues before their harvest and removal (Vassilev et al., 2004). Traditional methods of monitoring heavy metal uptake by plants involve sampling plant tissues and sample preparation for laboratory analysis. For example tree-ring analysis, which involves chemical analysis of samples from successive growth rings, can be done to monitor patterns of heavy metal uptake by plants over years (Lepp, 1975). In the same manner samples of plant roots, stems, and leaves can be analysed in the laboratory to determine the heavy metal uptake ability by plants (Vymazal and Brezinova, 2016). However, for monitoring large areas, traditional surveys involve lots of plant sample collection and preparation, which may be difficult, expensive, too technical, time consuming and poses safety issues on chemical handling and disposal. Sampling of representative plant tissue could also be constrained due to inaccessiblity. Remote sensing is a modern and alternative technology for monitoring such wetland phytoremediating plants. It is also an effective, non-destructive tool for monitoring heavy metal accumulation by wetland plants (Van Deventer and Cho, 2014). Remote sensing can be used to acquire spatial and temporal variations of accumulated heavy metal concentrations over large and inaccessible areas, as opposed to the in-situ traditional methods which are limited to small and accessible areas (Liu et al., 2010).

Monitoring of heavy metal uptake by wetland plants with remote sensing

Remote sensing is the technology of obtaining information about an object without a direct contact to the object under observation. Monitoring of vegetation using remote sensing is possible because vegetation under different conditions and of different

http://www.aloki.hu ● ISSN 1589 1623 (Print) ● ISSN 1785 0037 (Online)
DOI: http://dx.doi.org/10.15666/aeer/1704_79577972

characteristics and quality has unique spectral characteristics in the electromagnetic spectrum (Knipling, 1970). The spectral response properties of vegetation are determined by the biochemical content (e.g. chlorophyll) and anatomical (e.g. canopy architecture) structure of their leaves or crowns (Curran, 1989). All vegetation has a spectral response curve, which is unique to each species. High chlorophyll levels result in increased absorption (reduced reflection) in the red region of the electromagnetic spectrum, and broadening of the absorption pit in the red (660–680 nm) (Horler et al., 1983). It also shifts the red edge reflectance slope (680–760 nm) and the point of maximum slope in the red edge known as the chlorophyll red edge position (REP) towards the longer wavelengths, referred to as a red shift (Horler et al., 1983). Accordingly, decreased chlorophyll results in increased reflectance in the red region, and a shift of the red edge slope and REP towards the shorter wavelengths, which is referred to as a blue shift. Increases in biomass increases reflection in the near-infrared (NIR) region (Rouse Jr., 1974). Various heavy metal concentrations also have significant effects on the spectral reflectance properties of leaves. According to Sridhar et al. (2007), Zn accumulated in plant leaves causes a blue shift in the REP and a decrease in NIR reflectance. Accumulated Cd also results in a blue shift of REP and overall increase of reflectance in the visible region (Sridhar et al., 2007). Lead results in increased reflectance in the NIR region (Clevers et al., 2004). Liu et al. (2010) studied the possibility of using a small scale hand held hyperspectral sensor to estimate heavy metal (Pb, Cu and Zn) concentrations in *P. australis*. The study revealed that heavy metal concentrations affected chlorophyll levels in the plants, which in turn determine the hyperspectral measurements for the plant leaves. It was also found that chlorophyll concentrations for the sampled leaves varied inversely with concentrations of Pb, Cu and Zn, and chlorophyll concentration accounted for about 30% of the variations in the three heavy metals, respectively. Linear combination of normalized band depths at wavelengths 537 (green), 667 (red) and 747 (near infrared) nm were found to explain 82% of the variation of chlorophyll concentration (Liu et al., 2010). Thus it was concluded that it is possible to use laboratory-based hyperspectral data to estimate concentrations of Pb, Cu and Zn in *P. australis* (Liu et al., 2010). In another study, Shakya et al. (2008) also concluded that high concentrations of heavy metals in plants determine their chlorophyll content, which can be measured by field hyperspectral data or hyperspectral images. Research by Li et al. (2008) investigated the biogeochemistry responses of vegetation *Rhus chinensis* Mill in a copper mine area to heavy metal contamination. The results showed that there was a significant correlation between copper concentration in leaves and leaf reflectance. Increased copper concentrations were found to: increase the leaf spectral reflectance by about 5% to 30%, cause a blue shift of about 5 to 15 nm, increase the red edge from 4.5534 to 8.9475 nm and decrease the chlorophyll absorption depth. Thus, remote sensing can be used to differentiate between healthy and stressed vegetation and to determine the level of specific heavy metals in plants. Some plants used for phytoremediation in wetlands like *P. australis* and *A. donax* are morphologically similar, and it is also important to be able to discriminate between such species using remote sensing.

Use of remote sensing to discriminate wetland plant species

Successful management of wetlands requires proper and up to date mapping and discrimination of wetland plants (Hirano et al., 2003; Davranche et al., 2010). While the physical methods of mapping and discriminating wetland vegetation are time

http://www.aloki.hu ● ISSN 1589 1623 (Print) ● ISSN 1785 0037 (Online)
DOI: http://dx.doi.org/10.15666/aeer/1704_79577972

consuming and have accessibility and many other logistical problems, remote sensing can be an effective alternative for such purpose. Discrimination of plant species using remote sensing is possible because different vegetation types reflect differently to electromagnetic radiation. Plant leaves of different plant species have different biophysical and biochemical characteristics, and these affect their leaves' spectral properties, and make it possible to discriminate between different plant species (Kurmar et al., 2001). Extensive research has been done using remote sensing to discriminate between plant species (Adam et al., 2010). For example, Dubula et al. (2016) proved the potential of remote sensing in discriminating invasive plant species in the Klipriviersberg nature reserve in Johannesburg, South Africa. Their research concluded that at both individual level and plot level, the near infrared region of the electromagnetic spectrum could be used to discriminate between *Asparagus laricinus* and other vegetation species in the nature reserve. Pu (2009) used spectrometry to identify 11 forest species. They concluded that two classification algorithms, Artificial Neural network (ANN) and Linear Discriminant Analysis (LDA) were effective in discriminating plant species using selected spectral variables that are linked to water content, pigments and other biochemical.

Even though remote sensing is proved as a practical and cheap method for discriminating plant species, there are some challenges involved when discriminating wetland plant species. It is not easy to detect and discriminate wetland vegetation types using optical remote sensing because of very high spatial and spectral variability, due to very short ecotones between wetland vegetation units (Adam and Mutanga, 2009; Zomer et al., 2009). Thus the selection of the appropriate spatial and spectral resolution and the best process to use to extract the spectral information is of paramount importance (Elhadi et al., 2009). According to the review paper by Adam et al. (2010), hyperspectral remote sensing, especially field spectrometry, is more appropriate and accurate in discrimination of wetland plant species compared to aerial photography and multispectral remote sensing such as Landsat TM and SPOT. This is because hyperspectral sensors have hundreds of narrow continuous spectral bands ranging between 400 to 2500 nm, which make them capable to provide more details on vegetation types (Zomer et al., 2009). In this regard, a research by Smith and Blackshaw (2003) confirmed that plant species discrimination using hyperspectral data yielded more accurate results than that of multispectral data. The research also indicated that the visible (400-700 nm) and the red edge (700-730 nm) bands were the regions significantly useful for plant species discrimination. Schmidt and Skidmore (2003) also concluded that increased spectral resolution improved accuracy in discrimination of vegetation species of similar structure in a wetland. The purpose of their research was to discriminate 27 wetland plant species, including *Phragmites australis* (Cav.) Trin. ex Steud. using field spectrometry. Their results showed that more than 75% of the possible pairs of plant species showed significant differences based on their spectral reflectance measurements. Furthermore, research by Vaiphasa et al. (2005) concluded that field spectral measurements of crown leaves of various mangrove species were efficient in discriminating mangrove species. In their research a field spectrometer, with 2151 bands ranging from 350 to 2500 nm, was used to measure leaf spectral reflectance of 16 mangrove species. Statistical analysis of the spectral measurements indicated that the 16 species were statistically different at most spectral locations. Adam et al. (2012) also used ASD spectrometry measurements to discriminate among four wetland vegetation species, *Cyperus papyrus* L., *P. australis*, *Echinochloa pyramidalis* and

http://www.aloki.hu ● ISSN 1589 1623 (Print) ● ISSN 1785 0037 (Online)
DOI: http://dx.doi.org/10.15666/aeer/1704_79577972

Thelypteris interrupta in Greater St Lucia Wetlands Park in South Africa. Van Deventer and Cho (2014) also proved that field spectroscopy can be a quick and cheap method to assess the health and condition of vegetation affected by Acid Mine Drainage.

Conclusion

Arundo donax L. and *Phragmites australis* (Cav.) Trin. ex Steud., among other macrophytes, are very important in phytoremediation of heavy metal contaminated wetland systems. Their efficiencies in heavy metal uptake have never been compared under same and controlled environment. While the two species could be important phytoremediating plants, determining their efficiency could help their management as weeds, particularly considering the fact that *A. donax* is an infamous invader of the water system in South Africa. It will also help determine the effective plant of choice for phytoremediation in constructed wetlands. Remote sensing could be an effective method for monitoring of heavy metal induced stress in both plant species to facilitate their management before they die and release the contaminants removed from water and accumulated in plant tissue back to the source. Although the two plant species are morphologically similar, remote sensing can also effectively discriminate between them. Future research should compare the heavy metal uptake capacities of the two plant species under controlled/experimental conditions, and determine the best remote sensing analysis method to discriminate between the two species, and monitoring their heavy metal uptake capacities.

REFERENCES

[1] Adam, E., Mutanga, O. (2009): Spectral discrimination of papyrus vegetation (*Cyperus papyrus L.*) in swamp wetlands using field spectrometry. – ISPRS Journal of Photogrammetry and Remote Sensing 64: 612-620. doi:10.1016/j.isprsjprs.2009.04.004.

[2] Adam, E., Mutanga, O., Rugege, D. (2010): Multispectral and hyperspectral remote sensing for identification and mapping of wetland vegetation: a review. – Wetlands Ecology and Management 18: 281-296. doi:10.1007/s11273-009-9169-z.

[3] Adam, E. M., Mutanga, O., Rugege, D., Ismail, R. (2012): Discriminating the papyrus vegetation (*Cyperus papyrus L.*) and its co-existent species using random forest and hyperspectral data resampled to HYMAP. – International Journal of Remote Sensing 33: 552-569. doi:10.1080/01431161.2010.543182.

[4] Adams, J. B., Bate, G. C. (1999): Growth and photosynthetic performance of *Phragmites australis (Cav.) Trin. ex Steud.* in estuarine waters: a field and experimental evaluation. – Aquatic Botany 64(3–4): 359-367. https://doi.org/10.1016/S0304-3770(99)00063-7.

[5] Akcil, A., Koldas, S. (2006): Acid Mine Drainage (AMD): causes, treatment and case studies. – Journal of Cleaner Production 14(12–13): 1139-1145. Available at: https://doi.org/10.1016/j.jclepro.2004.09.006.

[6] Allende, M. L., Bektas, M., Lee, B. G., Bonifacino, E., Kang, J., Tuymetova, G., Chen, W., Saba, J. D., Proia, R. L. (2011): Sphingosine-1-phosphate Lyase Deficiency Produces a Pro-inflammatory Response While Impairing Neutrophil Trafficking. – Journal of Biological Chemistry 286: 7348-7358. doi:10.1074/jbc.M110.171819.

[7] Aminsharei, F., Borghei, S. M., Arjomandi, R., Nouri, J., Pendashteh, A. (2017): Seasonal pollutant removal by lactuca sativa, medicago sativa and Phragmites australis (Cav.) Trin. ex Steud. in constructed wetlands. – Applied ecology and environmental research 15(4): 67-76.

http://www.aloki.hu ● ISSN 1589 1623 (Print) ● ISSN 1785 0037 (Online)
DOI: http://dx.doi.org/10.15666/aeer/1704_79577972

[8] Aryal, R., Nirola, R., Beecham, S., Kamruzzaman, M. (2016): Impact of elemental uptake in the root chemistry of wetland plants. – International Journal of Phytoremediation 18: 936-942. doi:10.1080/15226514.2015.1131239.
[9] Bell, F. G., Bullock, S. E. T., Hälbich, T. F. J., Lindsay, P. (2001): Environmental impacts associated with an abandoned mine in the Witbank Coalfield, South Africa. – International Journal of Coal Geology 45(2): 195-216.
[10] Bello, A. O., Tawabini, B. S., Khalil, A. B., Boland, C. R., Saleh, T. A. (2018): Phytoremediation of cadmium-, lead- and nickel-contaminated water by *Phragmites australis (Cav.) Trin. ex Steud.* in hydroponic systems. – Ecological Engineering 120: 126-133. https://doi.org/10.1016/j.ecoleng.2018.05.035.
[11] Bonanno, G. (2012): *Arundo donax L.* as a potential biomonitor of trace element contamination in water and sediment. – Ecotoxicology and Environmental Safety 80: 20-27. https://doi.org/10.1016/j.ecoenv.2012.02.005.
[12] Bonanno, G. (2013): Comparative performance of trace element bioaccumulation and biomonitoring in the plant species Typha domingensis, *Phragmites australis (Cav.) Trin. ex Steud.* and *Arundo donax L.* – Ecotoxicology and Environmental Safety 97: 124-130. https://doi.org/10.1016/j.ecoenv.2013.07.017.
[13] Bragato, C., Brix, H., Malagoli, M. (2006): Accumulation of nutrients and heavy metals in *Phragmites australis (Cav.) Trin. ex Steud. (Cav.) Trin. ex Steudel* and *Bolboschoenus maritimus (L.) Palla* in a constructed wetland of the Venice lagoon watershed. – Environmental Pollution 144(3): 967-975. https://doi.org/10.1016/j.envpol.2006.01.046.
[14] Bruneau, S. (2017): Wetland Management: A review of policies and practices. – Camrose, Alberta: Battle River Watershed Alliance.
[15] Canavan, K., Paterson, I. D., Hill, M. P. (2017): Exploring the Origin and Genetic Diversity of the Giant Reed, *Arundo donax.* in South Africa. – Invasive Plant Science and Management 10(1): 53-60.
[16] Carson, B. D., Lishawa, S. C., Tuchman, N. C., Monks, A. M., Lawrence, B. A., Albert, D. A. (2018): Harvesting invasive plants to reduce nutrient loads and produce bioenergy: an assessment of Great Lakes coastal wetlands. – Ecosphere 9(6): p.e02320.
[17] Clevers, J. G. P. W., Kooistra, L., Salas, E. A. L. (2004): Study of heavy metal contamination in river floodplains using the red-edge position in spectroscopic data. – International Journal of Remote Sensing 25: 3883-3895. doi:10.1080/01431160310001654473.
[18] Coetzee, H., Winde, F., Wade, P. W. (2006): An Assessment of Sources, Pathways, Mechanisms and Risks of Current and Potential Future Pollution of Water and Sediments in Gold-mining Areas of the Wonderfonteinspruit Catchment. – Report to the Water Research Commission. Water Research Comission.
[19] Curran, P. J. (1989): Remote sensing of foliar chemistry. – Remote sensing of Environment 30(3): 271-278.
[20] Davranche, A., Lefebvre, G., Poulin, B. (2010): Wetland monitoring using classification trees and SPOT-5 seasonal time series. – Remote sensing of environment 114(3): 552-562.
[21] De Villiers, C., Driver, A., Clark, B., Euston-Brown, D., Day, L., Job, N., Helme, N., Van Ginkel, C. E., Glen, R. P., Gordon-Gray, K. D., Cilliers, C. J. (2011): Easy identification of some South African Wetland Plants. – WRC Report No TT 479(10).
[22] Deng, H., Ye, Z., Wong, M. (2004): Accumulation of lead, zinc, copper and cadmium by 12 wetland plant species thriving in metal-contaminated sites in China. – Environmental Pollution 132: 29-40. doi:10.1016/j.envpol.2004.03.030.
[23] Department of Environmental Affairs (2016): National Environmental Management. – Biodiversity Act (10/2004), Alien and Invasive Species Lists, South Africa.
[24] Dubula, B., Tesfamichael, S. G., Rampedi, I. T. (2016): Assessing the potential of remote sensing to discriminate invasive *Asparagus laricinus* from adjacent land cover types. – Cogent Geoscience 2: 1-17. doi:10.1080/23312041.2016.1154650.

http://www.aloki.hu ● ISSN 1589 1623 (Print) ● ISSN 1785 0037 (Online)
DOI: http://dx.doi.org/10.15666/aeer/1704_79577972

[25] Elhadi, M. A., Mutanga, O., Rugege, D., Ismail, R. (2009): July. Field spectrometry of papyrus vegetation (*Cyperus papyrus L.*) in swamp wetlands of St Lucia, South Africa. – In 2009 IEEE International Geoscience and Remote Sensing Symposium 4: IV-260. IEEE.

[26] Elhawat, N., Alshaal, T., Domokos-Szabolcsy, É., El-Ramady, H., Márton, L., Czakó, M., Kátai, J., Balogh, P., Sztrik, A., Molnár, M., Popp, J., Fári, M. G. (2014): Phytoaccumulation potentials of two biotechnologically propagated ecotypes of *Arundo donax* in copper-contaminated synthetic wastewater. – Environmental Science and Pollution Research 21: 7773-7780. https://doi.org/10.1007/s11356-014-2736-8.

[27] Emmanuel, D., Elsie, U., Patience, A. (2014): Phytoremediation of xylene polluted environment, using a macrophyte Commelina benghalensis L. – Asian Journal of Plant Science and Research 4: 1-4.

[28] Frick, C. M., Germida, J. J., Farrell, R. E. (1999): December. Assessment of phytoremediation as an in-situ technique for cleaning oil-contaminated sites. – In technical seminar on chemical spills. Environment Canada 1998: 105a-124a.

[29] Gates, D. M., Keegan, H. J., Schleter, J. C., Weidner, V. R. (1965): Spectral properties of plants. – Applied optics 4(1): 11-20.

[30] Gupta, S. K., Nikhil, K. (2016): Ground Water Contamination in Coal Mining Areas: A Critical Review. – International Journal of Engineering and Applied Sciences (IJEAS) ISSN: 3(2): 2394-3661.

[31] Henderson, L. (2001): Alien Weeds and Invasive Plants — A complete guide to declared weeds and invaders in South Africa. – Plant Protection Research Institute Handbook no. 12, - Agricultural Research Council, Pretoria.

[32] Henderson, L., Cilliers, C. J. (2004): Invasive Aquatic Plants. A guide to the identification of the most important and potentially dangerous invasive aquatic plants in South Africa. – PPRI handbook no. 16.

[33] Hirano, A., Madden, M., Welch, R. (2003): Hyperspectral image data for mapping wetland vegetation. – Wetlands 23(2): 436-448.

[34] Horler, D. N. H., Dockray, M., Barber, J. (1983): The red edge of plant leaf reflectance. – International Journal of Remote Sensing 4: 273-288.

[35] Ilfergane, A. (2016): Investigations on the effects of Typha capensis on male reproductive functions. – Doctoral dissertation, University of the Western Cape.

[36] Kaewtubtim, P., Meeinkuirt, W., Seepom, S., Pichtel, J. (2016): Heavy metal phytoremediation potential of plant species in a mangrove ecosystem in Pattani Bay, Thailand. – Appl Ecol Environ Res 14(1): 367-382.

[37] Kalra, Y. P. (1998): Handbook of Reference Methods for Plant Analysis. – CRC Press. Taylor and Francis Group, Boca Raton, FL.

[38] Kaplan, D. I., Buettner, S. W., Li, D., Huang, S., van Groos, P. G. K., Jaffé, P. R., Seaman, J. C. (2017): In situ porewater uranium concentrations in a contaminated wetland: Effect of seasons and sediment depth. – Applied Geochemistry 85: 128-136.

[39] Knipling, E. B. (1970): Physical and physiological basis for the reflectance of visible and near-infrared radiation from vegetation. – Remote Sensing of Environment 1: 155-159. https://doi.org/10.1016/S0034-4257(70)80021-9.

[40] Kumari, M., Tripathi, B. D. (2015): Efficiency of *Phragmites australis* and *Typha latifolia* for heavy metal removal from wastewater. – Ecotoxicology and Environmental Safety 112: 80-86. doi:10.1016/j.ecoenv.2014.10.034.

[41] Laghlimi, M., Baghdad, B., El Hadi, H., Bouabdli, A. (2015): Phytoremediation mechanisms of heavy metal contaminated soils: a review. – Open journal of Ecology 5(08): 375.

[42] Lambert, A. M., Dudley, T. L., Saltonstall, K. (2010): Ecology and Impacts of the Large-Statured Invasive Grasses *Arundo donax* and *Phragmites australis* in North America. – Invasive Plant Science and Management 3: 489-494. doi:10.1614/IPSM-D-10-00031.1.

http://www.aloki.hu ● ISSN 1589 1623 (Print) ● ISSN 1785 0037 (Online)
DOI: http://dx.doi.org/10.15666/aeer/1704_79577972

[43] Leguizamo, M. A. O., Gómez, W. D. F., Sarmiento, M. C. G. (2017): Native herbaceous plant species with potential use in phytoremediation of heavy metals, spotlight on wetlands—a review. – Chemosphere 168: 1230-1247.
[44] Lepp, N. W. (1975): The potential of tree-ring analysis for monitoring heavy metal pollution patterns. – Environmental Pollution 9(1): 49-61.
[45] Li, Q. T., Yang, F. J., Zhang, B., Zhang, X., Zhou, G. Z. (2008): Biogeochemistry responses and spectral characteristics of *Rhus chinensis Mill* under heavy metal contamination stress. – Journal of Remote Sensing -Beijing 12(2): 290.
[46] Liu, J., Dong, Y., Xu, H., Wang, D., Xu, J. (2007): Accumulation of Cd, Pb and Zn by 19 wetland plant species in constructed wetland. – Journal of Hazardous Materials 147: 947-953. doi:10.1016/j.jhazmat.2007.01.125.
[47] Liu, Y., Chen, H., Wu, G., Wu, X. (2010): Feasibility of estimating heavy metal concentrations in *Phragmites australis.* using laboratory-based hyperspectral data. A case study along Le'an River, China. – International Journal of Applied Earth Observation and Geoinformation 12: S166-S170. https://doi.org/10.1016/j.jag.2010.01.003.
[48] Luo, S., Wang, C., Xi, X., Pan, F., Qian, M., Peng, D., Nie, S., Qin, H., Lin, Y. (2017): Retrieving aboveground biomass of wetland Phragmites australis (common reed) using a combination of airborne discrete-return LiDAR and hyperspectral data. – International Journal of Applied Earth Observation and Geoinformation 58: 107-117.
[49] Lusweti, A., Wabuyele, E., Ssegawa, P., Mauremootoo, J. R. (2011): Invasive plants of East Africa (Kenya, Uganda and Tanzania). – Lucid v. 3.5 key and fact sheets, National Museums of Kenya, Makerere University, BioNET-EAFRINET, CABI and the University of Queensland, keys.lucidcentral.org/keys/v3/EAFRINET. Accessed 3 August 2017.
[50] Masoko, P., Mokgotho, M. P., Mbazima, V. G., Mampuru, L. J. (2008): Biological activities of Typha capensis (Typhaceae) from Limpopo Province (South Africa). – African Journal of Biotechnology 7(20).
[51] Matagi, S., Swai, D., Mugabe, R. (1998): A review of Heavy Metal Removal Mechanisms in wetlands. – African Journal of Tropical Hydrobiology and Fisheries 8(1): 13-25. https://doi.org/10.4314/ajthf.v8i1.1386.
[52] McCarthy, T. S., Humphries, M. S. (2013): Contamination of the water supply to the town of Carolina, Mpumalanga, January 2012. – South African Journal of Science 109: 01-10.
[53] Milton, S. J. (2004): Grasses as invasive alien plants in South Africa: working for water. – South African Journal of Science 100: 69-75.
[54] Mojiri, A., Aziz, H. A., Tajuddin, R. B. M., Gavanji, S., Gholami, A. (2015): Heavy Metals Phytoremediation from Urban Waste Leachate by the Common Reed (*Phragmites australis*). – In: Phytoremediation. Springer, Cham, pp. 75-81. Available at: https://doi.org/10.1007/978-3-319-10969-5_7.
[55] Newete, S. W., Byrne, M. J. (2016): The capacity of aquatic macrophytes for phytoremediation and their disposal with specific reference to water hyacinth. – Environmental Science and Pollution Research 23: 10630-10643. doi:10.1007/s11356-016-6329-6.
[56] Newete, S. W., Erasmus, B. F. N., Weiersbye, I. M., Byrne, M. J. (2016): Sequestration of precious and pollutant metals in biomass of cultured water hyacinth (Eichhornia crassipes). – Environmental Science for Pollution Research 23: 20805-20818. https://doi.org/10.1007/s11356-016-7292-y.
[57] Ochieng, G. M., Seanego, E. S., Nkwonta, O. I. (2010): Impacts of mining on water resources in South Africa: A review. – Scientific Research and Essays 5(22): 3351-3357.
[58] Papazoglou, E. G., Karantounias, G. A., Vemmos, S. N., Bouranis, D. L. (2005): Photosynthesis and growth responses of giant reed (*Arundo donax* L.) to the heavy metals Cd and Ni. – Environment International 31: 243-249. doi:10.1016/j.envint.2004.09.022.

http://www.aloki.hu ● ISSN 1589 1623 (Print) ● ISSN 1785 0037 (Online)
DOI: http://dx.doi.org/10.15666/aeer/1704_79577972

[59] Pilon-Smits, E. (2005): Phytoremediation. – Annu. Rev. Plant Biol. 56: 15-39. - Pollution Bulletin 42(10): 811-816.
[60] Pu, R. (2009): Broadleaf species recognition with in situ hyperspectral data. – International Journal of Remote Sensing 30(11): 2759-2779.
[61] Ramsar Convention Secretariat (2016): An Introduction to the Convention on Wetlands (previously The Ramsar Convention Manual). – Ramsar Convention Secretariat, Gland, Switzerland.
[62] Raskin, I., Smith, R. D., Salt, D. E. (1997): Phytoremediation of metals: using plants to remove pollutants from the environment. – Current opinion in biotechnology 8: 221-226.
[63] Rizwan, M., Ali, S., Qayyum, M. F., Ok, Y. S., Zia-ur-Rehman, M., Abbas, Z., Hannan, F. (2017): Use of Maize (Zea mays L.) for phytomanagement of Cd-contaminated soils: a critical review. – Environmental geochemistry and health 39(2): 259-277.
[64] Rouget, M., Richardson, D. M., Nel, J. L., Le Maitre, D. C., Egoh, B., Mgidi, T. (2004): Mapping the potential ranges of major plant invaders in South Africa, Lesotho and Swaziland using climatic suitability. – Diversity and Distributions 10(5-6): 475-484.
[65] Rouse Jr, J. W. (1974): Monitoring the vernal advancement and retrogradation (green wave effect) of natural vegetation. – Type I Progress Report Number 6, Texas University, Remote sensing center.
[66] Sasmaz, A., Obek, E., Hasar, H. (2008): The accumulation of heavy metals in *Typha latifolia* L. grown in a stream carrying secondary effluent. – Ecological Engineering 33: 278-284. doi:10.1016/j.ecoleng.2008.05.006.
[67] Schmidt, K. S., Skidmore, A. K. (2003): Spectral discrimination of vegetation types in a coastal wetland. – Remote Sensing of Environment 85: 92-108. doi:10.1016/S0034-4257(02)00196-7.
[68] Shakya, K., Chettri, M. K., Sawidis, T. (2008): Impact of Heavy Metals (Copper, Zinc, and Lead) on the Chlorophyll Content of Some Mosses. – Archives of Environmental Contamination and Toxicology 54: 412-421. https://doi.org/10.1007/s00244-007-9060-y.
[69] Sheoran, A. S., Sheoran, V. (2006): Heavy metal removal mechanism of acid mine drainage in wetlands: A critical review. – Minerals Engineering 19: 105-116. doi:10.1016/j.mineng.2005.08.006.
[70] Shuai, W., Chen, N., Li, B., Zhou, D., Gao, J. (2016): Life cycle assessment of common reed (*Phragmites australis* (Cav) Trin. ex Steud) cellulosic bioethanol in Jiangsu Province, China. – Biomass and Bioenergy 92: 40-47. Available at: https://doi.org/10.1016/j.biombioe.2016.06.002.
[71] Shuping, L. S., Snyman, R. G., Odendaal, J. P., Ndakidemi, P. A. (2011): Accumulation and distribution of metals in *Bolboschoenus maritimus* (Cyperaceae), from a South African river. – Water, Air, and Soil Pollution 216(1-4): 319-328.
[72] Smith, A. M., Blackshaw, R. E. (2003): Weed–Crop Discrimination Using Remote Sensing: A Detached Leaf Experiment. – Weed Technology 17(4): 811-820.
[73] Sridhar, B. B. M., Han, F. X., Diehl, S. V., Monts, D. L., Su, Y. (2007): Spectral reflectance and leaf internal structure changes of barley plants due to phytoextraction of zinc and cadmium. – International Journal of Remote Sensing 28: 1041-1054. doi:10.1080/01431160500075832.
[74] US Department of State Geographer (2018): AfriGIS (Pty) Ltd. – Google earth. Image accessed on 9 January 2019.
[75] Usharani, B., Vasudevan, N. (2016): Impact of heavy metal toxicity and constructed wetland system as a tool in remediation. – Archives of environmental and occupational health 71(2): 102-110.
[76] Vaiphasa, C., Ongsomwang, S., Vaiphasa, T., Skidmore, A. K. (2005): Tropical mangrove species discrimination using hyperspectral data: A laboratory study. – Estuarine, Coastal and Shelf Science 65: 371-379. doi:10.1016/j.ecss.2005.06.014.
[77] Van der Merwe, C. G., Schoonbee, H. J., Pretorius, J. (1990): Observations on concentrations of the heavy metals zinc, manganese, nickel and iron in the water, in the

http://www.aloki.hu ● ISSN 1589 1623 (Print) ● ISSN 1785 0037 (Online)
DOI: http://dx.doi.org/10.15666/aeer/1704_79577972

sediments and in two aquatic macrophytes, Typha capensis (Rohrb.) N. E. Br. and *Arundo donax* L., of a stream affected by goldmine and industrial effluents. – Water S. A. 16(2): 119-124.

[78] Van Deventer, H., Cho, M. A. (2014): Assessing leaf spectral properties of *Phragmites australis* impacted by acid mine drainage. – South African Journal of science 110: 1-12.

[79] Vassilev, A., Schwitzguébel, J. P., Thewys, T., Van Der Lelie, D., Vangronsveld, J. (2004): The use of plants for remediation of metal-contaminated soils. – The Scientific World Journal 4: 9-34.

[80] Vymazal, J., Březinová, T. (2015): The use of constructed wetlands for removal of pesticides from agricultural runoff and drainage: a review. – Environment international 75: 11-20.

[81] Vymazal, J., Březinová, T. (2016): Accumulation of heavy metals in aboveground biomass of *Phragmites australis* in horizontal flow constructed wetlands for wastewater treatment: A review. – Chemical Engineering Journal 290: 232-242. doi:10.1016/j.cej.2015.12.108.

[82] Wong, M. H. (2003): Ecological restoration of mine degraded soils, with emphasis on metal contaminated soils. – Chemosphere 50(6): 775-780.

[83] Yang, X., Feng, Y., He, Z., Stoffella, P. J. (2005): Molecular mechanisms of heavy metal hyperaccumulation and phytoremediation. – Journal of Trace Elements in Medicine and Biology 18(4): 339-353. https://doi.org/10.1016/j.jtemb.2005.02.007.

[84] Yang, B., Lan, C. Y., Yang, C. S., Liao, W. B., Chang, H., Shu, W. S. (2006): Long-term efficiency and stability of wetlands for treating wastewater of a lead/zinc mine and the concurrent ecosystem development. – Environmental Pollution 143: 499-512. doi:10.1016/j.envpol.2005.11.045.

[85] Zedler, J. B., Kercher, S. (2004): Causes and consequences of invasive plants in wetlands: opportunities, opportunists, and outcomes. – Critical Reviews in Plant sciences 23(5): 431-452.

[86] Zingelwa, N. S., Wooldridge, J. (2016): Uptake and accumulation of mineral elements from winery and distillery effluents by *Typha latifolia* and *Phragmites australis*. – South African Journal of Enology and Viticulture 30(1): 43-48.

[87] Zomer, R. J., Trabucco, A., Ustin, S. L. (2009): Building spectral libraries for wetlands land cover classification and hyperspectral remote sensing. – Journal of Environmental Management 90: 2170-2177. doi:10.1016/j.jenvman.2007.06.028.

[88] Zwiggelaar, R. (1998): A review of spectral properties of plants and their potential use for crop/weed discrimination in row-crops. – Crop Protection 17(3): 189-206.

http://www.aloki.hu ● ISSN 1589 1623 (Print) ● ISSN 1785 0037 (Online)
DOI: http://dx.doi.org/10.15666/aeer/1704_79577972

SEASONAL PATTERN OF N_2O CONCENTRATIONS AND EMISSIONS IN THE SEWAGE-ENRICHED RIVERS: CASE OF CHAOHU LAKE BASIN IN SOUTHEAST CHINA

YANG, L.B.[1,2] – LI, F.[2*]

[1]*River and Coastal Environment Research Center, Chinese Research Academy of Environmental Sciences, Beijing 100012, China*

[2]*Institute of Geographic Sciences and Natural Resources Research, Chinese Academy of Sciences, Beijing 100101, China*

Both authors contributed equally to this work, in no particular order.

**Corresponding author: LI, F.*
e-mail: lifcas@gmail.com

(Received 23rd Nov 2018; accepted 1st May 2019)

Abstract. Two sewage-enriched urban rivers within Chaohu Lake Basin in Southeast China were selected to study the seasonal variations in Nitrous Oxide (N_2O) concentrations, to improve the information of N_2O concentrations and emissions in the similar areas. The results indicate that N_2O concentrations ranged 16.12~1043.09 nmol/L and averaged 266.27 ± 250.28 nmol/L during the sampling period. N_2O was oversaturated in both rivers ranging 184~12084% (mean 2964%). The significantly higher level of N_2O concentrations and emissions were observed in cold months. It is indicated that the two rivers were net sources of atmospheric N_2O. N_2O emissions ranged 11.32~2920.38 μg $N\text{-}N_2O/m^2/h$ with an overall mean value of 743.57 ± 831.78 μg $N\text{-}N_2O/m^2/h$. A significant negative correlation exists between N_2O concentration and water temperature, which may be regulated by inverse tendencies between temperature and riverine nutrient loadings. Dissolved Oxygen (DO) is a predictor of N_2O in Nanfei River explaining 60% of variability in N_2O; while water temperature and NO_3^- are better predictors of N_2O in Ershibu River explaining 73% of variability in N_2O. The riverine N_2O may be produced by denitrification in Nanfei River while by coupled nitrification-denitrification in Ershibu River.
Keywords: *nitrous oxide, concentration, nitrification, flux, urban river*

Introduction

Nitrous Oxide (N_2O) is one of the most significant greenhouse gases contributing to the destruction of stratospheric ozone and climate change (Ravishankara et al., 2009; Wójcik-Gront et al., 2015; Pauleta, et al., 2019). The atmospheric N_2O has risen from about 270 ppb in the pre-industrial era to 319 ppb in the present, mainly due to human perturbations of the global nitrogen (N) cycle (Holland et al., 2005). As N inputs increase, potentially more N_2O is produced (Bouwman, 1995; Wójcik-Gront et al., 2015). In river networks, more than 0.68 Tg/yr of anthropogenic N inputs were converted to N_2O on the global scale, equivalent to 10% of the anthropogenic N_2O emission rate (Beaulieu et al., 2011; Quick et al., 2019; Luo et al., 2019). Therefore, more and more attentions have been paid to the emissions of N_2O from different sources as accurate information is required to determine the contribution of N_2O to global greenhouse gas fluxes (Khalil et al., 2002; Yang and Lei, 2018).

Among the many natural and anthropogenic N_2O sources, most are biological ones (Short et al., 2013). In aquaculture systems, N_2O can be produced by denitrification under anaerobic conditions, where NO_3^- was converted to N_2O and dinitrogen (N_2)

http://www.aloki.hu ● ISSN 1589 1623 (Print) ● ISSN 1785 0037 (Online)
DOI: http://dx.doi.org/10.15666/aeer/1704_79737985

(Öquist et al., 2004). Under oxic conditions, N_2O is also produced as a by-product of nitrification where ammonium (NH_4^+) was oxidized to nitrite (NO_2^-), and subsequently to NO_3^- (Stein and Yung, 2003). Natural rivers have shown large temporal and spatial variations in their N_2O production and emissions due to the changes of topographic feature and environmental factors (Wilcock et al., 1998; Bansal et al., 2015; Quick et al., 2019). The exact mechanisms of aquatic N_2O production are related to the various specific environmental conditions, such as N species and loads, dissolved oxygen (DO) concentration, pH, and others. The classification of carbon source also influences N_2O emission from denitrification and nitrification. Controlling factors related to N_2O production and emissions in rivers are still needed to fully understand due to lack of *in situ* observation data. Thus, more investigation is needed to determine the underlying mechanism of seasonal variation in N_2O concentration in rivers.

Emissions of N_2O from riverine ecosystems take significant influences on the global climate change, since riverine ecosystems are very sensitive to human activities and often receive high loadings of nutrient and organic matter (Richey et al., 2002; Bansal et al., 2015; Yang and Lei, 2018; Quick et al., 2019). Much work has been dedicated to quantifying N_2O emissions from terrestrial ecosystems; however, emissions of N_2O from rivers and streams have received much less attention and remain a major source of uncertainty in the global N_2O budget. Similar to many developing countries, river N pollution is one of the most critical environmental problems in China (Richey et al., 2002; Yang et al., 2006, 2013; Wang et al., 2007; Luo et al., 2019). The related researches on China's greenhouse gas emission primarily focus on the estuary and coastal areas (Yang et al., 2006; Wang et al., 2007; Liu et al., 2015; Yang and Lei, 2018). However, few studies actually directly measure N_2O fluxes from N enriched rivers, and that information is sparse.

Chaohu Lake is a shallow lake in Southeast China, which has suffered from serious pollution resulting from substantial discharge of urban wastewater and agricultural runoff. It has been reported that, the annual mean concentration of Total Nitrogen (TN) and Total Phosphorus (TP) over 2001-2016 ranged 0.08-24.60 and 0.02-2.46 mg/L, respectively, meanwhile, the lake water quality showed no substantial improvement (Yang et al., 2013; Yang and Lei, 2018). The Nanfei River (NR) and Ershibu River (ER) are two urban tributaries of Chaohu Lake. These two rivers are narrow and short with low flow speed. Large amounts of N-enriched sewage inputs into the two rivers result in highly eutrophic river water. Significantly, small rivers are thought to be hot spots of nitrogen cycling (Alexander et al., 2000; Bansal et al., 2015; Quick et al., 2019) and can remove a large proportion of nutrient inputs (Wollheim et al., 2006; Luo et al., 2019; Quick et al., 2019), hence could be important sites of N_2O emissions. Therefore, this study aimed to determine: (1) the presence and extent of seasonal variations in river water chemistry, dissolved N_2O concentration and emissions in sewage-enriched rivers in the Chaohu Lake region; (2) the potential factors that regulate the seasonal N_2O variability.

Materials and methods

Sites description

The study was carried out in NR and ER, two tributaries of Chaohu Lake. The mean annual temperature and precipitation of this region is 15.5 °C and 950 mm respectively. The NR and ER are small rivers with a total length of 70 and 17 km respectively

http://www.aloki.hu ● ISSN 1589 1623 (Print) ● ISSN 1785 0037 (Online)
DOI: http://dx.doi.org/10.15666/aeer/1704_79737985

(*Table 1*). In this study, the sampling site was set up at the downstream of each river and located at urban areas (*Fig. 1*). The respective mean water depth of the sampling site is 1.8 m and 3.2 m in NR and ER, and the respective mean flow speed is 0.2 and 0.3 m/s. In recent years, the sewage loading of NR and ER have significantly increased as a result of the effects of local development, which may have become atmospheric N_2O sources. Increases in riverine N and organic matter discharge also stimulate microbial processes and associated algae blooming in Chaohu Lake.

Table 1. *Physical characteristics of the study rivers*

River	River length (km)	Mean flow speed (m/s)	Mean water depth (m)	Dominant land use (%)	Sampling location
NR	70	0.2	1.8	Urban (> 70)	Daxing port
ER	17	0.3	3.2	Urban (> 80)	Longtang bridge

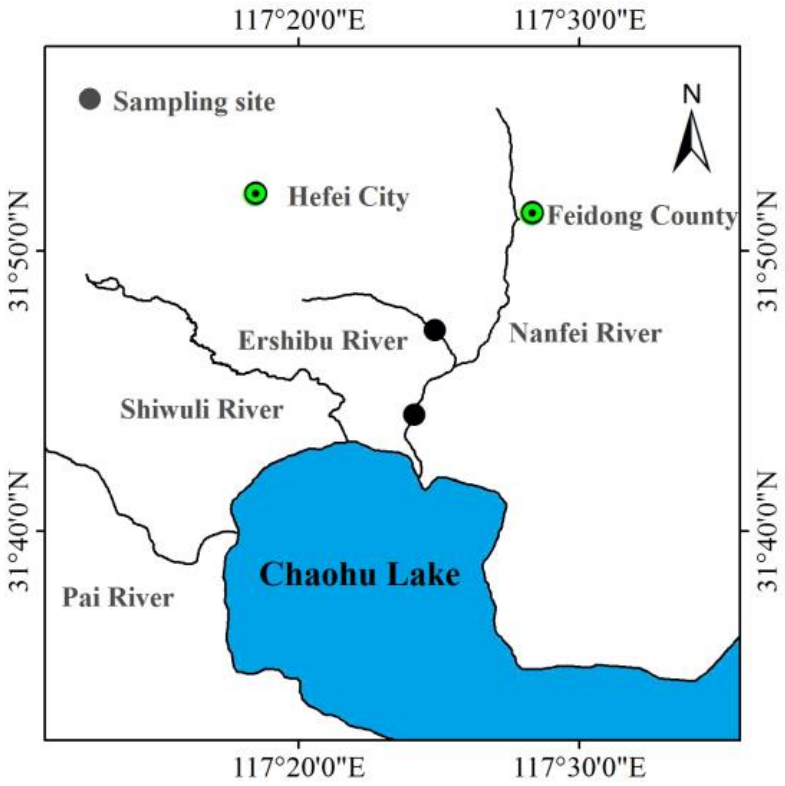

Figure 1. *The location of the sampling rivers and sampling sites*

Sample collection and chemical analysis

Triplicate surface water (0.2 m depth) samples were collected monthly during Jan. and Dec. in 2017 for the measurement of NH_4^+, NO_3^-, TP, BOD_5, COD_{Mn}, SO_4^{2-}, and Cl^-. Dissolved oxygen (DO), pH, and water temperature were measured *in situ* using a portable meter (HQ30D, USA). Samples for dissolved N_2O analysis were collected in 60-ml serum bottles sealed with a butyl-rubber stopper, and preserved after the addition of a few drops of saturated mercuric chloride solution to prevent their biological activities. Water samples were stored in ice box during transport and analyzed within 24 h.

http://www.aloki.hu ● ISSN 1589 1623 (Print) ● ISSN 1785 0037 (Online)
DOI: http://dx.doi.org/10.15666/aeer/1704_79737985

The respective concentration of NH_4^+, NO_3^-, TP, BOD_5, COD_{Mn}, SO_4^{2-}, and Cl^- in water samples was determined according to the standard methodology of GB3838-2002 promulgated by the China central government. The headspace-equilibrium method was used for measurement of initial sample dissolved N_2O concentrations in river water (Huttunen et al., 2002; Liu et al., 2015; Quick et al., 2019; Luo et al., 2019). Twenty milliliters of highly purified N_2 (purity > 99.999%) was injected into the serum bottle using an airtight syringe and a 20-ml water sample was displaced. Bottle headspace N_2O concentrations were directly analyzed using a gas chromatograph (HP5890 II) equipped with an electron capture detector (ECD) after the bottles were vigorously shaken for 4 h. Initial N_2O concentrations (C_w) in water samples were calculated (Johnson et al., 1990; Yang and Lei, 2018). The equilibrium concentration (C_e) of N_2O in river water with atmosphere was calculated using Henry's first law. Dissolved N_2O saturation, expressed in %, was calculated by comparing C_w and C_e.

N_2O emission flux

N_2O emission flux across the water-air interface was estimated using the two-layer model:

$$F = k \times (C_w - C_e) \quad \text{(Eq.1)}$$

where F is the N_2O emission flux (μg $N\text{-}N_2O/m^2/h$); C_w and C_e is the measured and equilibrium concentration of N_2O (nmol/L), respectively; k (cm/h) is the gas transfer coefficient, calculated by the equation accounting for both wind speed and flow speed (Borges et al., 2004; Liu et al., 2015):

$$k = [1 + 1.719(w/h)^{0.5} + 2.58\mu_{10}](S_c/600)^{-1/2} \quad \text{(Eq.2)}$$

where w and h are flow speed ($m\ s^{-1}$) and depth (m) of river water column, respectively; μ_{10} (m/s) is the instantaneous wind speed at the 10 m height; Sc is the Schmidt number for N_2O calculated by the equation proposed firstly by Wanninkhof (1992): $S_c = 2301.1 - 151.1t + 4.7364t^2 - 0.059431t^3$, where t (°C) is in situ river water temperature. In this study, wind speed data was gained from the Hefei Meteorologic Bureau, Anhui Province.

Results

Water chemistry

NH_4^+ and NO_3^- concentrations varied considerably over the sampling time, ranging 1.97~23.75 (mean12.24 ± 5.13) and 0.05~6.98 (mean3.54 ± 4.45) mg/L (*Fig. 2a, b*), respectively. NH_4^+ and NO_3^- concentrations indicated a generally higher level in cold months ($P < 0.001$). Difference in mean NH_4^+ and NO_3^- concentrations was not significant between the two rivers ($P > 0.05$). DO concentration ranged 0.20~7.70 mg/L with an overall mean of 2.61 ± 2.14 mg/L (*Fig. 2c*). In NR, DO concentrations were generally lower than 2 mg/L. Similar to the patterns of NH_4^+, TP concentrations (ranging 0.20~2.37 mg/L, mean 1.16 ± 0.53 mg/L) showed the marked temporal variations and reached the lowest value in July in both rivers (*Fig. 2d*). Water temperature ranged 11.0~33.3°°C (*Fig. 2e*), significantly negatively related with DO ($P < 0.05$). The pH value of river water ranged 6.60~8.56 and decreased dramatically after August (*Fig. 2f*).

http://www.aloki.hu ● ISSN 1589 1623 (Print) ● ISSN 1785 0037 (Online)
DOI: http://dx.doi.org/10.15666/aeer/1704_79737985

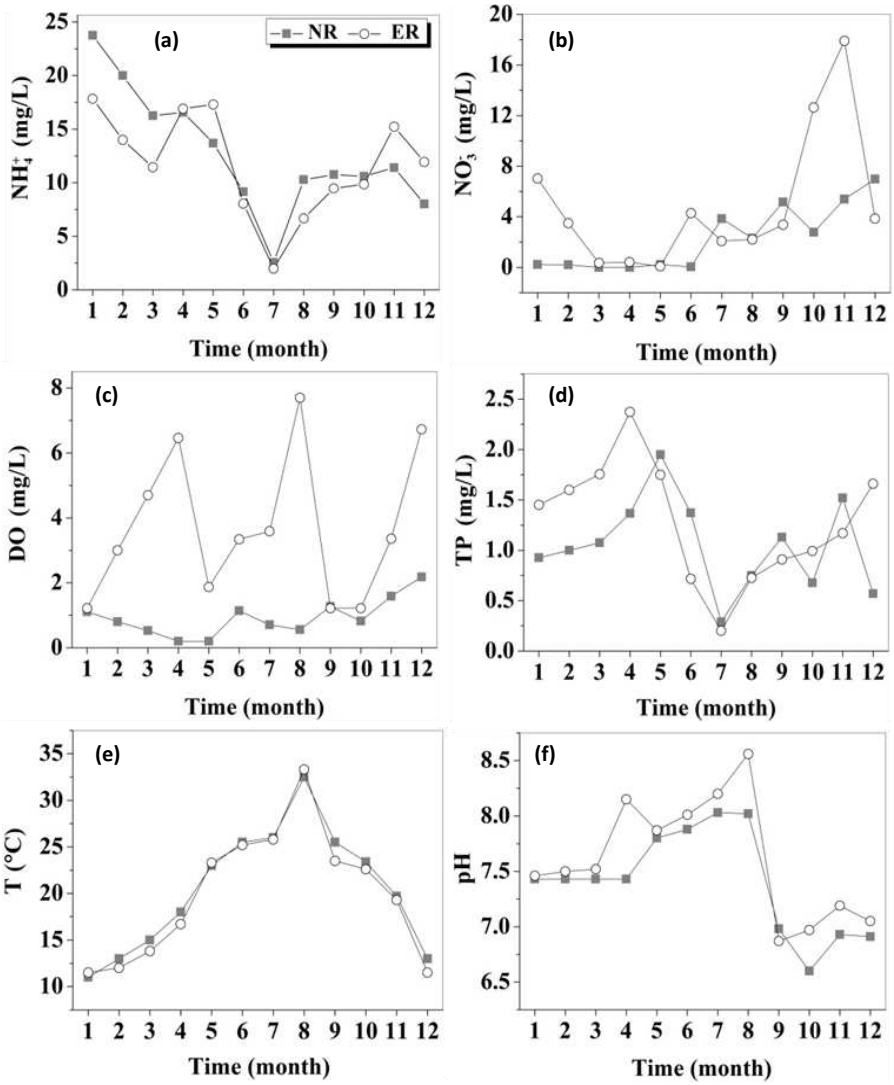

Figure 2. *Seasonal variations in NH_4^+, NO_3^-, DO, TP, water temperature (T), and pH value of Nanfei and Ershibu River*

Monthly concentrations of BOD_5, COD_{Mn}, SO_4^{2-}, and Cl^- in water samples are shown in *Table 2*. BOD_5 and COD_{Mn} concentrations ranged 3.6-23.1 and 7.5-20.4 mg/L, with an overall mean of 9.80 ± 5.37 and 11.97 ± 4.44 mg/L, respectively. Significantly higher BOD_5 and COD_{Mn} concentrations were investigated in spring and winter ($P < 0.001$). SO_4^{2-} and Cl^- concentrations ranged 45.65~332.50 (mean 101.43 ± 79.06) and 28.55~277.14 (mean 107.16 ± 56.57) mg/L, respectively, generally lower in summer.

Compared to other rivers in this region, the NR and ER showed extremely high level of NH_4^+, NO_3^-, TP, BOD_5, COD_{Mn}, SO_4^{2-}, and Cl^- concentrations. The long-term dynamics of water quality in Chaohu river nets were observed over 13 years (Yang et al., 2013; Yang and Lei, 2018), indicating that NH_4^+, COD_{Mn}, and TP concentrations in the Fengle and Hangbu river which drained agricultural runoff averaged 0.25, 0.07, 4.17 mg/L and 0.31, 0.10, 3.47 mg/L, respectively. Based on the latest investigation, the respective mean SO_4^{2-} and Cl^- concentration was 29.8 and 23.5 mg L^{-1} in Fengle River, and 57.1 and 37.9 mg/L in Hangbu River.

http://www.aloki.hu ● ISSN 1589 1623 (Print) ● ISSN 1785 0037 (Online)
DOI: http://dx.doi.org/10.15666/aeer/1704_79737985

Table 2. *Monthly concentrations of BOD_5, COD_{Mn}, SO_4^{2-}, and Cl^- in NR and ER*

River	Conc. mg/L	Sampling time (month)											
		1	2	3	4	5	6	7	8	9	10	11	12
NR	BOD_5	9.7	12.0	13.6	23.1	11	12.8	4.6	4.4	6.4	6.7	7.1	4.6
	COD_{Mn}	16.2	15.0	13.7	20.4	19.7	12.3	10	11.3	9.1	8.3	8.7	7.5
	SO_4^{2-}	73.4	62.6	51.7	79.8	332.5	125.9	71.5	64.5	45.6	316.3	64.2	53.4
	Cl^-	138.9	115.8	92.7	138.9	154.4	115.7	33.2	80.8	65.6	172.8	277.1	196.2
ER	BOD_5	14.7	16.0	17.8	18.0	12.0	7.5	4.0	8.2	6.2	3.6	5.1	5.0
	COD_{Mn}	11.96	10.0	8.7	19.8	15.9	18.2	8.7	8.1	10.2	7.3	8.8	7.6
	SO_4^{2-}	69.6	60.3	51.1	143.2	114.2	168.6	73.98	54.7	52.0	98.5	66.3	60.5
	Cl^-	94.5	82.3	70.1	117.9	110.5	96.9	28.5	58.9	73.5	76.6	86.8	77.0

Dissolved N_2O concentration and emission flux

Overall, N_2O concentration ranged 16.12~143.09 nmol/L and averaged 226.27 ± 250.28 nmol/L (*Fig. 3a, b*). A clear seasonal variation in N_2O concentration was found in each river. Consistent seasonal trends were apparent between rivers. In general, the higher N_2O concentrations were observed in colder months. Difference in mean N_2O concentration was not significant between the two rivers ($P > 0.05$). During the sampling period, both rivers were oversaturated in N_2O with a range of 184~12084% (mean 2964%).

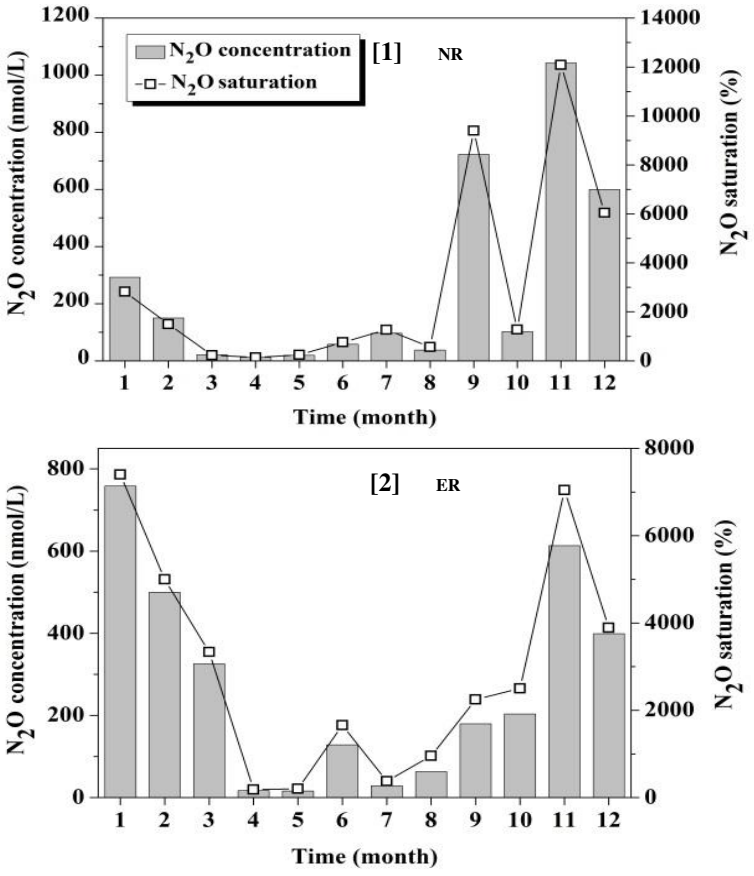

Figure 3. *Seasonal variations in N_2O concentration and percentage saturation*

http://www.aloki.hu ● ISSN 1589 1623 (Print) ● ISSN 1785 0037 (Online)
DOI: http://dx.doi.org/10.15666/aeer/1704_79737985

This study indicates that NR and ER were net sources of N_2O across all the seasons sampled. N_2O emission fluxes also followed a distinct seasonal patter ranging of 11.32~2920.38 μg N-N_2O/m^2/h (mean 743.57 ± 831.78 μg N-N_2O/m^2/h) (*Fig. 4*). Significantly lower N_2O emission fluxes were investigated in summer.

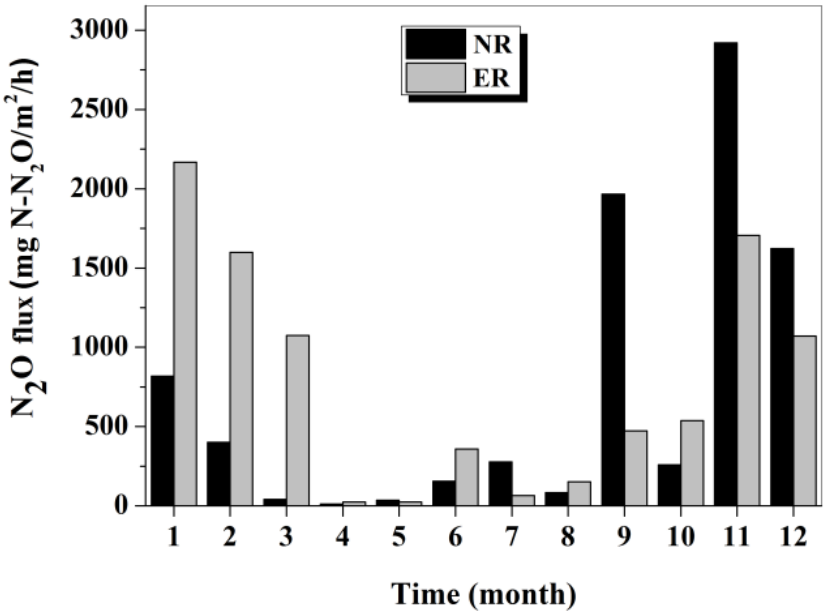

Figure 4. *Seasonal variations in N_2O emission flux*

Discussion

Compared to some literatures on the temporal and spatial variation of water pollution in the Zhegao River of Chaohu Lake basin (Chu et al., 2011; Yang et al., 2013), in which NH_4^+, NO_3^-, and TP showed an annual mean concentration of 1.13, 0.63, and 0.11 mg/L respectively. However, low NO_3^-/Cl^- ratios (ranging 0.000~0.21, mean 0.04) were observed both in NR and ER in this study; this result further indicates that high riverine N concentrations in these rivers can be strongly attributed to the direct discharge of untreated sewage. Based on the measurements, the contribution of N_2O flux in colder seasons accounted for 90% of the annual budget, similar to results from two subtropical reservoirs (Liu et al., 2011, 2015), with lower fluxes of N_2O appearing in summer. However, different seasonal variation patterns on water surface N_2O emissions were also reported from the Three Gorges Reservoir in China (Zhu et al., 2013; Zhao et al., 2012). Some sewage-enriched rivers showed higher dissolved N_2O concentrations and were net atmospheric sources of N_2O. Xin'an Tang river (Taihu Lake basin of China) receiving high untreated sewage inputs indicated high N_2O concentration and emission flux with respective mean value of 0.48 μg N-N_2O/L and 56.1 μg N-N_2O/m^2/h (Xia et al., 2013). The overall mean saturation and emission was 770% and 1.91 mg N-N_2O/m^2/d in the Shanghai city river network (Yu et al., 2013), respectively. The urban rivers in Tianjin city (Haihe basin of China) showed high N_2O concentration and emission rate in winter with respective mean value of 88.9 nmol/L and 71.4 N-N_2O/m^2/h (Hu et al., 2013; Liu et al., 2015). Thus, given the rapid progress of global urbanization, it is urgent to better understand the effect of urban rivers on global N_2O budget.

http://www.aloki.hu ● ISSN 1589 1623 (Print) ● ISSN 1785 0037 (Online)
DOI: http://dx.doi.org/10.15666/aeer/1704_79737985

Seasonal variation in N_2O concentration and its potential control

Seasonal variations in N_2O concentration in two sampling rivers were observed in the study. Generally, the significantly higher N_2O concentration was observed in colder months. It has been reported that, seasonal patterns of trace gas concentration and emission in aquatic systems were governed by seasonal variability in temperatures affecting water availability, production of substrate precursors and microbial activity (Whalen, 2005; Quick et al., 2019). For example, water temperature positively correlated to N_2O saturation and explained 70% of the seasonal variance of N_2O saturation in a large and impounded river (Beaulieu et al., 2010). However, a negative correlation between water temperature and N_2O concentration was investigated in this study ($P = 0.03$) (*Fig. 5*). Some studies (Sun et al., 2013; Liu et al., 2015) also found a similar seasonal pattern in N_2O concentration and emission in the Yellow River estuary. It is indicated that this seasonal pattern of N_2O concentration in the NR and ER was mainly regulated by the inverse tendencies between temperature and riverine nutrient loadings during the study period. Small river discharge and high riverine nitrogen concentration was generally investigated during the cold seasons in this region. This combination of decreased water discharge and increased nutrient loadings is likely to have sustained high N_2O concentration in cold seasons. The correlation between NO_3^- and N_2O concentration was significant in NR but not significant in ER. These results suggested that N_2O may be produced by denitrification in NR while by coupled nitrification-denitrification in ER, which could be further proved by the significant negative correlation between DO and N_2O concentration in NR and significant positive correlation in ER. However, N_2O concentration was not significantly correlated with NH_4^+ and NO_3^- based on the data collected.

It is suggested that none of the environmental variables stood out as a clearly superior predictor of N_2O when considered them alone, though several of them showed some predictive value with respect to dissolved N_2O concentration. Herein, a stepwise multiple regression that include DO, NH_4^+, NO_3^-, TP, BOD_5, COD_{Mn}, water temperature, and pH was conducted to assess predictors of N_2O concentration. The results showed that DO is a better predictor of N_2O in NR explaining 60% of variability in N_2O, indicating N_2O production was limited by DO concentration; while water temperature and NO_3^- are better predictors of N_2O in ER explaining 73% of variability in N_2O, indicating N_2O production was NO_3^- limited. Based on all of the observation data, water temperature and NO_3^- are better predictors of N_2O explaining 43% variability in N_2O. Other investigations also found similar relationships between NO_3^- and N_2O concentration in urban rivers (Wang et al., 2015; Quick et al., 2019). However, Yu et al. (2013) reported that N_2O production was greatly controlled by DO and NH_4^+ level in some urban rivers. As discussed above, river N_2O may be produced by denitrification in NR while by coupled nitrification-denitrification in ER. Meanwhile, we thought that, high NH_4^+ come from the decomposition of organic nitrogen in urban effluents in urban rivers, while NH_4^+ cannot be oxide to NO_3^- rapidly under hypoxic conditions. As a result, river N_2O production was NO_3^- limited based on the data collected.

Uncertainty of N_2O emission flux

There are many models for gas emission estimation. However, the overall accuracy of model-based gas estimation in rivers remains uncertain, since models were developed

http://www.aloki.hu ● ISSN 1589 1623 (Print) ● ISSN 1785 0037 (Online)
DOI: http://dx.doi.org/10.15666/aeer/1704_79737985

in different settings and gas transfer coefficients (k) estimated with these models have not satisfied all field conditions (Kremer et al., 2003; Pauleta et al., 2019). In open waters, k is usually parameterized as a function of wind speed. It is reported that the primary driving mechanism that regulates k is presumed to be near-surface turbulence from low to moderate wind speeds; while at higher winds, bubble-mediated exchange produced by breaking waves may play significant roles on k (Borges et al., 2004). It is also reported that bottom-generated turbulence that is transported to the surface can significantly affect gas transfer especially in deep flowing waters (Nimmo-Smith et al., 1999; Zappa et al., 2003; Luo et al., 2019). Thus, choices of the models for estimation of k took a considerable bearing on the estimated gas emissions. Gas transfer velocity was directly measured in some studies to improve accuracy of estimating N_2O emission, as is however beyond this study.

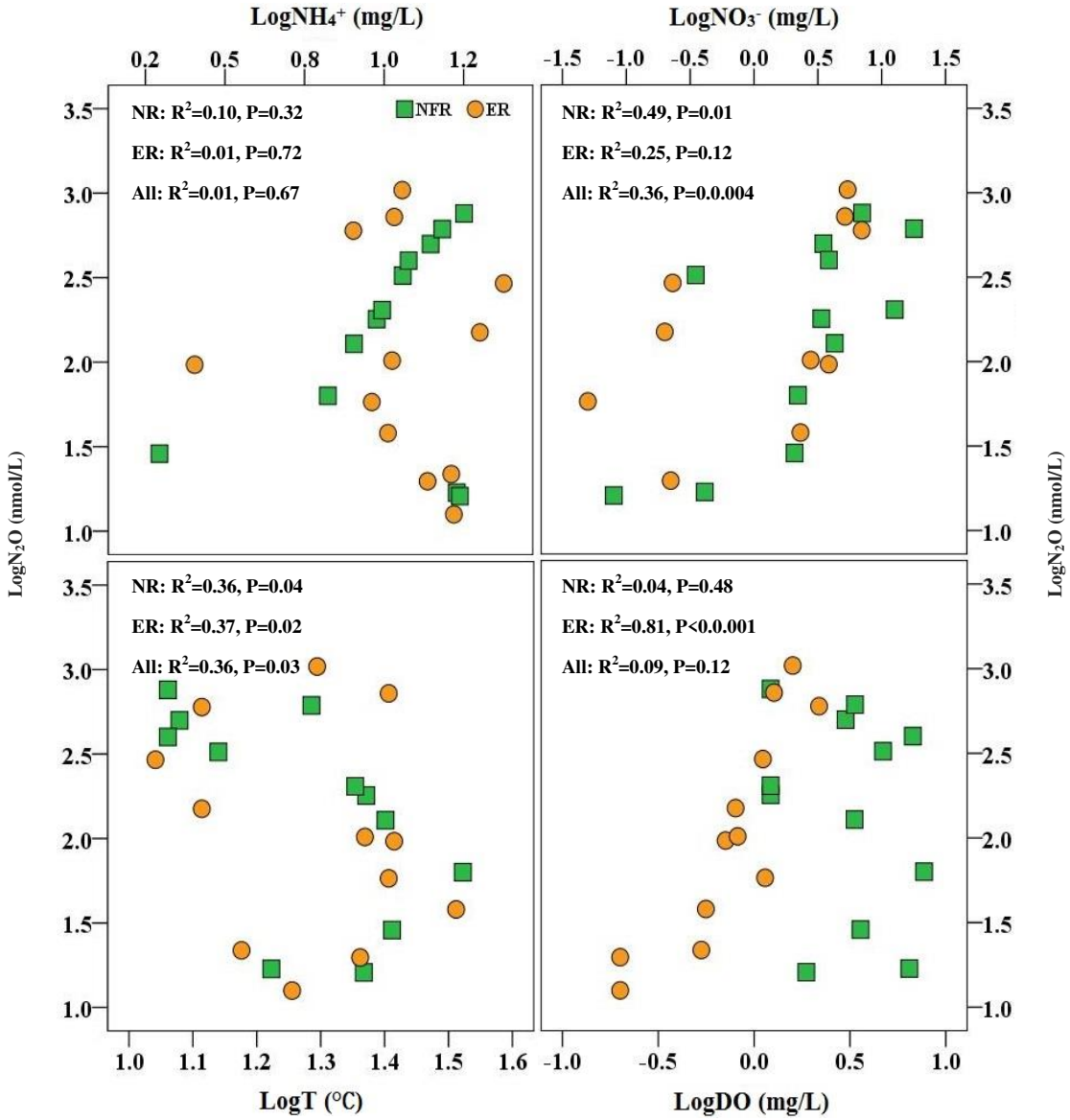

Figure 5. *Simple linear regression analysis of normalized N_2O concentration with (a) normalized NH_4^+, DO, (b) normalized NO_3^-, (c) normalized water temperature (T), and (d) normalized DO for sampling rivers*

http://www.aloki.hu ● ISSN 1589 1623 (Print) ● ISSN 1785 0037 (Online)
DOI: http://dx.doi.org/10.15666/aeer/1704_79737985

Herein, 5 wind-based models (Liss and Merlivat, 1986; Wanninkhof, 1992; Raymond and Cole, 2001; Liu et al., 2015; Yang and Lei, 2018) and 2 wind-currents based models (Borges et al., 2004; Clough et al., 2007; Luo et al., 2019) were selected to compare the disparities in k_{N2O} and eventually N_2O fluxes among models. The results showed wide disparities in gas transfer velocity estimates between different models. Overall, k_{N2O} ranged 0.03~29.05 cm/h and averaged 4.26 ± 4.22 cm/h (*Fig. 6*). LM86a gave the lowest estimates while CL07 gave the highest estimation results. BO04 model expressed by *Equation 2* gave an intermediate k_{N2O} value (mean 4.77 ± 1.61 cm/h) relative to the other selected models. Generally, estimated k_{N2O} using wind-based models indicated lower level than wind-current based model. Thus, studies that applied wind speed value only to estimate N_2O emissions in rivers may be grossly underestimating emissions and their contribution to the global budgets. The results also indicated that providing a range for the model-based N_2O emissions might be more reliable than providing a single flux value by using a single model.

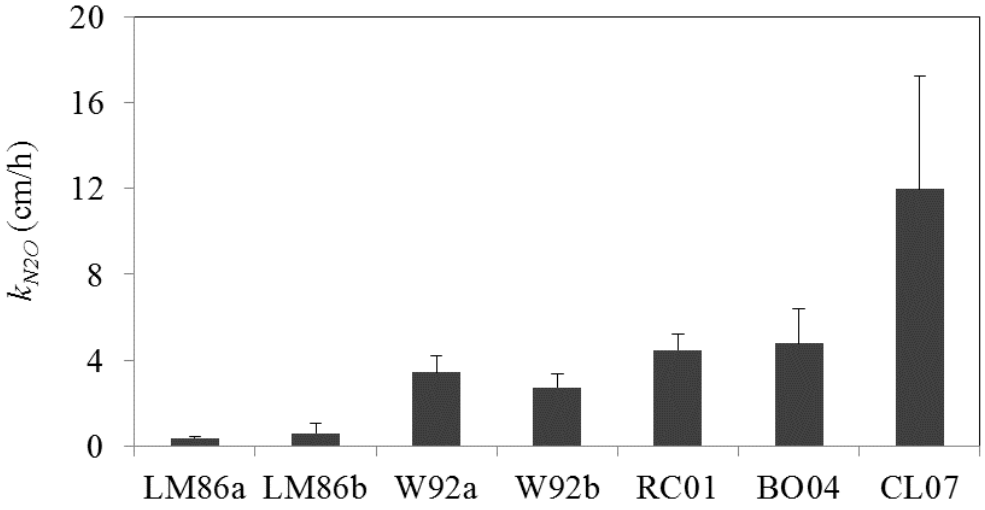

Figure 6. *Comparison of gas transfer velocities estimated*

Conclusions

Seasonal variation in N_2O concentrations and emissions of two urban rivers receiving sewage effluents in Chaohu Lake basin of China was investigated, to provide information on N_2O concentrations and emissions in the similar areas. The sampling rivers were oversaturated in N_2O and were net sources of atmospheric N_2O. Generally, significantly higher N_2O concentrations and emissions were observed during cold seasons. The simple linear regression analysis showed a negative correlation between N_2O concentration and water temperature based on the data collected, which may be regulated by the inverse tendencies between temperature and riverine N loadings during the study period. The results for the predicted production of riverine N_2O showed that DO is a better predictor of N_2O in NR explaining 60% of variability in N_2O, indicating N_2O production was limited by DO concentration; while water temperature and NO_3^- are better predictors of N_2O in ER explaining 73% of variability in N_2O, indicating N_2O production was NO_3^- limited. The riverine N_2O may be produced by denitrification in Nanfei River while by coupled nitrification-denitrification in Ershibu River.

http://www.aloki.hu ● ISSN 1589 1623 (Print) ● ISSN 1785 0037 (Online)
DOI: http://dx.doi.org/10.15666/aeer/1704_79737985

Although further investigation is clearly needed to answer the question of how best to proceed before any unquestionable conclusion can be drawn, deriving quantitative estimates and the relative implications such as those presented in this study, is helpful to advance the policy debate. In the future, impacts of economic activities and land use on the concentration and emission of nitrous oxide in urban nitrogen-enriched rivers would be the crux in the relative study.

Acknowledgements. This study is supported by the Science & Technology Basic Resources Investigation Program of China (No. 2017FY101300) and Foundation of Ethnic Group Culture Research Base of Nanling Corridor, Key Research Institute of Humanities and Social Sciences in Guangxi General Universities (No. 2015KF03). We are also grateful for the help from Prof Kun Lei and Dr Sun Pu in the field sampling.

REFERENCES

[1] Alexander, R. B., Smith, R. A., Schwarz, G. E. (2000): Effect of stream channel size on the delivery of nitrogen to the Gulf of Mexico. – Nature 403: 758-761.
[2] Bansal, S., Chakraborty, M., Katyal, D., Garg, J. K. (2015): Methane flux from a subtropical reservoir located in the floodplains of River Yamuna, India. – Applied Ecology and Environmental Research 13(2). 597-613.
[3] Beaulieu, J. J., Shuster, W. D., Rebholz, J. A. (2010): Nitrous oxide emissions from a large, impounded river: the Ohio River. – Environmental Science and Technology 44: 7527-7533.
[4] Beaulieu, J. J., Tank, J. L., Hamilton, S. K., Wollheim, W. M., Hall, R. O, Mulholland, P. J., Peterson, B. J., Ashkenas, L. R., Cooper, L. W., Dahm, C. N. (2011): Nitrous oxide emission from denitrification in stream and river networks. – Proceedings of the National Academy of Sciences 108: 214-219.
[5] Borges, A. V., Vanderborght, J. P., Schiettecatte, L. S., Gazeau, F., Ferrón-Smith, S., Delille, B., Frankignoulle, M. (2004): Variability of the gas transfer velocities of CO_2 in a macrotidal estuary (the Scheldt). – Estuaries 27: 593-603.
[6] Bouwman, A. F. (1995): Compilation of a global inventory of emissions of nitrous oxide. – PhD thesis, Agricultural University, Wageningen, Netherlands.
[7] Chu, Y., Zhu, J., Xia, S. X., Ma, Y. H., Jiang, L. T., Li, Y., Li, X. C. (2011): Temporal and spatial variation of water pollution in Zhegao River of Chao Lake Basin. – Journal of Soil and Water Conservation 25(4): 243-248.
[8] Clough, T. J., Buckthought, L. E., Kelliher, F. M., Sherlock, R. R. (2007): Diurnal fluctuations of dissolved nitrous oxide (N_2O) concentrations and estimates of N_2O emissions from a spring-fed river: Implications for IPCC methodology. – Global Change Biology 13: 1016-1027.
[9] Holland, E. A., Braswell, B. H., Sulzman, J., Lamarque, J. F. (2005): Nitrogen deposition onto the United States and Western Europe: synthesis of observations and models. – Journal of Applied Ecology 15: 38-57.
[10] Hu, B. B., Tan, Y. J., Wang, D. Q., Deng, H. G.; Lin, Y. J., Yu, Z. J., Chen, Z. L. (2013): Methane and nitrous oxide dissolved concentration and emission flux of Plain River network in winter. – Science China Chemistry 43(7): 919-929.
[11] Huttunen, J. T., Väisänen, T. S., Hellsten, S. K. (2002): Fluxes of CH_4, CO_2, and N_2O in hydroelectric reservoirs Lokka and Porttipahta in the northern boreal zone in Finland. – Global Biogeochemical Cycles 16(1): 1-17.
[12] Johnson, K. M., Hughes, J. E., Donaghay, P. L. (1990): Bottle-calibration static head space method for the determination of methane dissolved in seawater. – Analytical Chemistry 62(21): 2408-2412.

http://www.aloki.hu ● ISSN 1589 1623 (Print) ● ISSN 1785 0037 (Online)
DOI: http://dx.doi.org/10.15666/aeer/1704_79737985

[13] Khalil, M. A. K., Rasmussen, A., Shearer, M. J. (2002): Atmospheric nitrous oxide: patterns of global change during recent decades and centuries. – Chemosphere 47: 807-821.
[14] Kremer, J. N., Nixon, S. W., Buckley, B., Roques, P. (2003): Technique note: conditions for using the floating chamber method to estimate air-water gas exchange. – Estuaries 26(4): 985-990.
[15] Liss, P. S., Merlivat, L. (1986): Air-Sea Gas Exchange Rates: Introduction and Synthesis. – In: Buat-Ménard, P. (ed.) The Role of Air-Sea Exchange in Geochemical Cycling. Springer, Dordrecht, the Netherlands.
[16] Liu, X. L., Liu, C. Q., Li, S. L., Wang, F. S., Wang, B. L., Wang, Z. L. (2011): Spatial-temporal variations of nitrous oxide (N_2O) emissions from two reservoirs in SW China. – Atmospheric Environment 45: 5458-5468.
[17] Liu, X. L., Bai, L., Wang, Z. L., Li, J., Yue, F. J., Li, S. L. (2015): Nitrous oxide emissions from river network with variable nitrogen loading in Tianjin, China. – Journal of Geochemical Exploration 157: 153-161.
[18] Luo, Z. B., Lam, S. K., Fu, H., Hu, S. Y., Chen, D. L. (2019): Temporal and spatial evolution of nitrous oxide emissions in China: assessment, strategy and recommendation. – Journal of Cleaner Production 223: 360-367.
[19] Nimmo-Smith, W. A. M., Thorpe, S. A., Graham, A. (1999): Surface effects of bottom-generated turbulence in a shallow tidal sea. – Nature 400: 251-254.
[20] Öquist, M. G., Nilsson, M., Sörensson, F., Kasimir-Klemedtsson, A., Persson, T., Weslien, P., Klemedtsson, L. (2004): Nitrous oxide production in a forest soil at low temperatures-processes and environmental controls. – FEMS Microbiology Ecology 49: 371-378.
[21] Pauleta, S. R., Carepo, M. S. P., Moura, I. (2019): Source and reduction of nitrous oxide, – Coordination Chemistry Reviews 387: 436-449.
[22] Quick, A. M., Reeder, W. J., Farrell, T. B., Tonina, D., Feris, K. P., Benner, S. G. (2019): Nitrous oxide from streams and rivers: a review of primary biogeochemical pathways and environmental variables. – Earth-Science Reviews 191: 224-262.
[23] Ravishankara, A. R., Daniel, J. S., Portmann, R. W. (2009): Nitrous oxide (N_2O): The dominant ozone-depleting sub-stance emitted in the 21st century. – Science 326(5949): 123-125.
[24] Raymond, P. A., Cole, J. J. (2001): Gas exchange in rivers and estuaries: choosing a gas transfer velocity. – Estuaries 24: 312-317.
[25] Richey, J. E., Melack, J. M., Aufdenkampe, A. K., Ballester, V. M., Hess, L. L. (2002): Outgassing from Amazonian rivers and wetlands as a large tropical source of atmospheric CO_2. – Nature 416: 617-620.
[26] Short, M. D., Peters, G. M., Peirson, W. L., Ashbolt, N. J. (2013): Marine nitrous oxide emissions: an unknown liability for the international water sector. – Environmental science & policy 33: 209-221.
[27] Stein, L. Y., Yung, Y. L. (2003): Production, isotopic composition, and atmospheric fate of biologically produced nitrous oxide. – Annual Review of Earth and Planetary Sciences 31: 329-356.
[28] Sun, Z. G., Wang, L. L., Tian, H. Q., Jiang, H. H., Mou, X. J., Sun, W. L. (2013): Fluxes of nitrous oxide and methane in different coastal Suaeda salsa marshes of the Yellow River estuary, China. – Chemosphere 90: 856-865.
[29] Wang, D. Q., Chen, Z. L., Wang, J., Xu, S. Y., Yang, H. X., Chen, H., Yang, L. Y., Hu, L. Z. (2007): Summer-time denitrification and nitrous oxide exchange in the intertidal zone of the Yangtze estuary. – Estuarine Coastal and Shelf Science 73: 43-53.
[30] Wang, J. N., Chen, N. W., Yan, W. J., Wang, B., Yang, L. B. (2015): Effect of dissolved oxygen and nitrogen on emission of N_2O from rivers in China. – Atmospheric Environment 103: 347-356.

http://www.aloki.hu ● ISSN 1589 1623 (Print) ● ISSN 1785 0037 (Online)
DOI: http://dx.doi.org/10.15666/aeer/1704_79737985

[31] Wanninkhof, R. (1992): Relationship between wind speed and gas exchange over the ocean. – Journal of Geophysical Research 97(C5): 7373-7382.
[32] Whalen, S. C. (2005): Biogeochemistry of methane exchange between natural wetlands and the atmosphere. – Environmental Engineering Science 22: 73-94.
[33] Wilcock, R. J., Nagels, J. W., Mcbride, G. B., Collier, K. J., Wilson, B. T., Huser, B. A. (1998): Characterization of lowland streams using a single-station diurnal curve analysis model with continuous monitoring data for dissolved oxygen and temperature. – New Zealand Journal of Marine and Freshwater Research 32: 67-79.
[34] Wollheim, W. M., Vorosmarty, C. J., Peterson, B. J., Seitzinger, S. P., Hopkinson, C. S. (2006): Relationship between river size and nutrient removal. – Geophysical Research Letters 33: L06410.
[35] Wójcik-Gront, E. (2015): Territorial analysis of agricultural greenhouse gas emission in Poland. – Applied Ecology and Environmental Research 13(2): 417-425.
[36] Xia, Y. Q., Li, Y. F., Li, X. B., Guo, M., She, D. L., Yan, X. Y. (2013): Diurnal pattern in nitrous oxide emissions from a sewage-enriched river. – Chemosphere 92: 421-428.
[37] Yang, H. X., Wang, D. Q., Chen, Z. L., Xu, S. Y. (2006): Elementary research on greenhouse gas emissions in Chongming east intertidal flat of the Changjiang estuary. – Marine Environmental Research 25: 20-23.
[38] Yang, L. B., Lei, K. (2018): Effects of land use on the concentration and emission of nitrous oxide in nitrogen-enriched rivers. – Environmental Pollution 238: 379-388.
[39] Yang, L. B., Lei, K, Meng, W., Fu, G., Yan, W. J. (2013): Temporal and spatial changes in nutrients and chlorophyll-a in a shallow lake, Lake Chaohu, China: an 11-year investigation. – Journal of Environmental Sciences 25(6): 1117-1123.
[40] Yu, J. Z., Deng, H. G., Wang, D. Q., Ye, M. W., Tan, Y. J., Li, Y. J., Chen, Z. L., Xu, S. Y. (2013): Nitrous oxide emissions in the Shanghai river network: implications for the effects of urban sewage and IPCC methodology. – Global Change Biology 19: 2999-3010.
[41] Zappa, C. J., Raymond, P. A., Terray, E. A., Mcgillis, W. R. (2003): Variation in surface turbulence and the gas transfer velocity over a tidal cycle in a macro-tidal estuary. – Estuaries 26(6): 1401-1415.
[42] Zhao, Y., Wu, B. F., Zeng, Y. (2012): Spatial and temporal aspects of greenhouse gas emissions from Three Gorges Reservoir, China. – Biogeosciences Discuss 9: 14503-14535.
[43] Zhu, D., Chen, H., Yuan, X. Z., Wu, N., Gao, Y. H., Wu, Y., Zhang, Y. M., Peng, C. H., Zhu, Q. A., Yang, G., Wu, J. H. (2013): Nitrous oxide emissions from the surface of the Three Gorges Reservoir. – Ecological Engineering 60: 150-154.

http://www.aloki.hu ● ISSN 1589 1623 (Print) ● ISSN 1785 0037 (Online)
DOI: http://dx.doi.org/10.15666/aeer/1704_79737985

CLIMATE CHANGE PERCEPTIONS AND ADAPTIVE ACTIONS BY PASTORAL COMMUNITY ON THE TIBETAN PLATEAU, CHINA

SHARIF, J.[1] – RAFIQ, M. K.[2,3] – RAFIQ, M. T.[4] – AZIZ, R.[5,*] – QAYYUM, A.[6] – SALEEM, A.R.[7] – NISA,W.U.[5] – JENKS, M. A.[8] – LI, Y.[1*]

[1]*School of Philosophy and Sociology, Lanzhou University, Lanzhou 730000, PR China*

[2]*UK Biochar Research Center of Geosciences, The University of Edinburgh, Edinburgh EH9 3FF, UK*

[3]*Rangeland Research Institute, National Agricultural Research Center, 44000 Islamabad, Pakistan*

[4]*Center for Integrated Research in Basic Sciences, International Islamic University, 44000 Islamabad, Pakistan*

[5]*Department of Environmental Science, International Islamic University, 44000 Islamabad, Pakistan*

[6]*Department of Agronomy, University of Haripur, 22620 Haripur, Pakistan*

[7]*Department of Earth and Environmental Sciences, Bahria University, 44000 Islamabad, Pakistan*

[8]*School of Plant Sciences, University of Arizona, Forbes Building, Tucson AZ 85721-0036, USA*

**Corresponding authors*
e-mail: rukhsanda.aziz@iiu.edu.pk, liyongjin@lzu.edu.cn

(Received 9th Dec 2018; accepted 10th Apr 2019)

Abstract. Tibetan plateau is an area of global ecological and cultural significance often called the third pole of the earth, world water towers and roof of the world. The plateau provides forage to 95% of world's total yak population and supports the largest pastoral population (9.8 million) of the globe. The plateau is vulnerable to climate change which threatens grassland resources, watersheds, livestock and pastoral population. As the pastoralists are the key custodians of the plateau, this study examined their climate change perceptions and analyzed their adaptation strategies in Tibetan Plateau, China. The results showed that majority of the pastoralists were aware of the climate change issues in the plateau. It was found that pastoralists have noticed changes in climate variability leading to grassland degradation and poor animal health and productivity. TV Programs about climate change and weather forecast programs were among the key tools for developing pastoral perception about climate change. The demographic characteristic of the pastorals like education, age and household size proved to contribute in the development of climate change perceptions among pastorals ($P \leq 0.05$). The study found that livelihood diversification, having mixed livestock breeds, cultivation of high yielding and drought tolerant forage varieties, grassland fencing and controlled grazing were among the most practiced adaptation strategies in the Plateau. Pastoralists are the key stakeholders of the Plateau. Therefore, their capacity needs improvement to adapt climate effects and work with the government institutions for the betterment of the plateau and their improved livelihood so that it can create win-win situation for pastoralists and government managers as well.
Keywords: *global warming, climatic variability, pasture utilization, mitigation measures, diversification*

Introduction

Global warming is changing climate rapidly, with adverse effects of excessive and uneven rainfall, floods and droughts with impacts on forests, environment, agriculture and humanity. Therefore, climate change is thought as one of the major threats to the earth's environment and to human race. Pastoralism is internationally significant for the

http://www.aloki.hu ● ISSN 1589 1623 (Print) ● ISSN 1785 0037 (Online)
DOI: http://dx.doi.org/10.15666/aeer/1704_79878009

communities it supports, the food stuff and environmental services it provides, the economic benefits it grants to some of the world's areas with the highest poverty rates and the long-lasting civilizations, it has helped survive to this day (Nori and Davies, 2007). Unluckily, threats relating to human populations, development, changes in land use and climate are challenging experts and managers to maintain and conserve these socially, culturally, economically, and ecologically precious assets around the world (Nori and Davies, 2007; Asrat and Simane, 2018).

Adaptation to climate change has been an important research topic, especially in agriculture, ever since climate change has been commonly recognized (Adger et al., 2003). There have been several studies investigating factors that affect adaptation to climate change in agriculture sector (Apata et al., 2009; Bryan et al., 2009; Below et al., 2012; Deressa et al., 2009, 2011; Hassan and Nhemachena, 2008; Seo and Mendelsohn, 2008a, b; Asrat and Simane, 2018; Hyland et al., 2015 and Lasco et al., 2015). Most of them have been conducted in developing economies where agriculture plays an essential role. In Southeast Asian countries, there have been significant variations in the intensity and frequency of extreme weather events associated with the changes in climate. The understanding of adaptation, however, is still limited as far as those countries are concerned (Francisco et al., 2008).

Adaptation to climate change in the perspectives of rural livelihood

Many research findings have highlighted the significance of policies related to climate change adaptation that can involve to deal the climate change issues (Adger et al., 2003; Hulme and Shepherd, 2003; IPCC, 2001, 2014). Adaptation is an approach that helps to manage ecological systems and socio-economic in reference to climate change consequence (Gallopin, 2006; Smit et al., 1999). Adaptation is generally considered as a capability of a society to form social capital in collective way (Adger, 2003). The capability and efficiency of climate change adaptation relies on the vulnerability of people and natural systems to climate adverse effects. The vulnerability "is the susceptibility to be damaged from pressures related with environmental and social change without having any capacity to cope with" (Adger, 2006). Ability to adapt climate change is context specific and varies among nations, communities, social groups and individuals over time (Smit and Wandel, 2006).

To minimize the vulnerability of an individual and a society to changes in climate has close connections with rural livelihood improvements, as poor livelihood is known as a condition and determinant of vulnerability (Tanner and Mitchell, 2008). According to Sen (1999), poverty is linked to inadequate outputs related to health, nutrition and literacy, as well with weaker social relations, insecurity, low self-worth and non-helping attitude. Sen (1999) comments that the basic ability of people improves their ability to question, challenge, propose and control new actions. Poverty has also linkage to social justice and is explained as "an incapability to contribute, due to limited resources" (Whelan, 2007). Thus, a multidimensional viewpoint of poverty highlights a broader picture of deficiency, social variables, relationships and structural aspects (Curwood and Eckerle, 2009; Frye, 2008).

The climate change and livelihood perspectives in the study area

In China, Grasslands occupy two thirds of the Tibetan Plateau's area (Cui and Graf, 2009), and climate change impacts on the plateau ecosystem have already been observed

http://www.aloki.hu ● ISSN 1589 1623 (Print) ● ISSN 1785 0037 (Online)
DOI: http://dx.doi.org/10.15666/aeer/1704_79878009

(Fu et al., 2012). The Tibetan Plateau is sensitive to global climate change because average air temperatures have increased at much higher rates (0.16 °C/decade) than Northern Hemisphere as a whole (Liu and Chen, 2000; Zheng et al., 2002). (IPCC) The Intergovernmental Panel on Climate Change projects that by 2050s, temperatures on plateau will increase more than 3 °C (IPCC, 2007), although precipitation changes on the plateau will likely be variable (Niu et al., 2004; Li and Kang, 2006; Xu et al., 2008).

Tibetan communities are dealing with the highly variable climate and winter snowstorms for many years. Traditionally, to live with the harsh climate, the Tibetan herders have developed a range of sophisticated strategies. These included migratory grazing over time and geographic space, flexibility in migration patterns and underlying social norms (e.g., reciprocity and trust), making use of diverse environment (e.g., seasonal pastures) and plant species, and the exchange of products from livestock and substance essential for daily living through local markets. Diversifying herd composition according to grassland vegetation is also employed to minimize the risk of livestock loss in harsh winters (Miller, 2002). These strategies helped them to lessen the damages during climate hazards and to have an efficient use of grassland resource base.

In the scenario of changes in climate, herder communities on the Tibetan Plateau would like to face more risks due to climate change. In order to improve Tibetan grassland social-ecological systems herders that are highly prone to climate changes should be capable to counter these changes. Governments are required to support and take advantage of adaptation strategies that are already being practice in a proven way further built up ability of herder communities to adapt. Thus, examination of historical adaptation mechanism based on livelihood and associated local institutional facilitators are important for this goal.

Strengthening of institution and changes in policies can support adaptation process by removing or introducing subsides and insurance systems, by supporting and inducing income diversification and early warning systems and other forecasting and crisis-awareness systems. However, it is significant that pastoralist should help to devise these actions. Keeping in view climate change scenario, this study documented the socioeconomic profile of the pastoralists. The study also recorded the climate change perceptions and adaptation strategies by the pastorals. The data generated and recommendations made through this study would help policy makers, scientist and managers to improve grasslands and pastoral livelihood in Tibetan Plateau. The specific objectives of the present study include: i) to document community perception about climate change and the factors responsible develop this perceptions; ii) to document activities adopted by the pastoral communities for climate change adaptation and how they diversify their activities for sustainable livelihood; iii) to document the recommendations made by the pastoralists for improving capacity and efficiency for climate change adaptation.

Materials and methods

Study area

This research study was accomplished in Daiqian Village of Zhuaxixiulong Township of Tianzhu County of Tibetan Autonomous Region of Gansu Province, China and Dawu Village of MaqinGuoluo Prefecture Qinghai Tibetan plateau. The topography of Daiqian village is relatively diversified due to the topographic impact of Maya Snow Mountain to the south and Leigong Mountain to the north. Jinqiang River flows into the

http://www.aloki.hu ● ISSN 1589 1623 (Print) ● ISSN 1785 0037 (Online)
DOI: http://dx.doi.org/10.15666/aeer/1704_79878009

valley from west to east. Different landforms and communities of various plants and grasses are scattered along the river. The Dawu Village is located at Maqin County of Guoluo Prefecture of Qinghai Tibetan Plateau of Qinghai Province (*Fig. 1*). The salient features of the Daiqian Village and Dawu Village have been described in *Table 1*.

Table 1. *Salient features of the selected villages*

Location	1. Daiqian Village: Tianzhu County of Autonomous Region, Tibetan Plateau of Gansu Province, China 2. Dawu village: MaqinCounty of Guoluo Prefecture, Tibetan Autonomous Region, Qinghai Province, China
Geographical location	1. N 37°14′, E 102°35′ 2. N 34°28′11″, E100°12′39″
Elevation	1. 3177 m above sea level 2. 4200 m above sea level
Climate	1. Mean annual temperature, -0.1 °C; Mean annual precipitation, 416 mm 2. Mean annual temperature, -0.6 °C; Mean annual precipitation, 513 mm
Households	1. 120 2. 180
Population	1. 600 2. 1075
Vegetation	1. Alpine meadows 2. Alpine meadows
Major livestock types	1. White Yak, Tibetan sheep and others 2. Yak, Tibetan sheep and others
Livelihood	Mostly dependent on grasslands for grazing their livestock for livelihoods

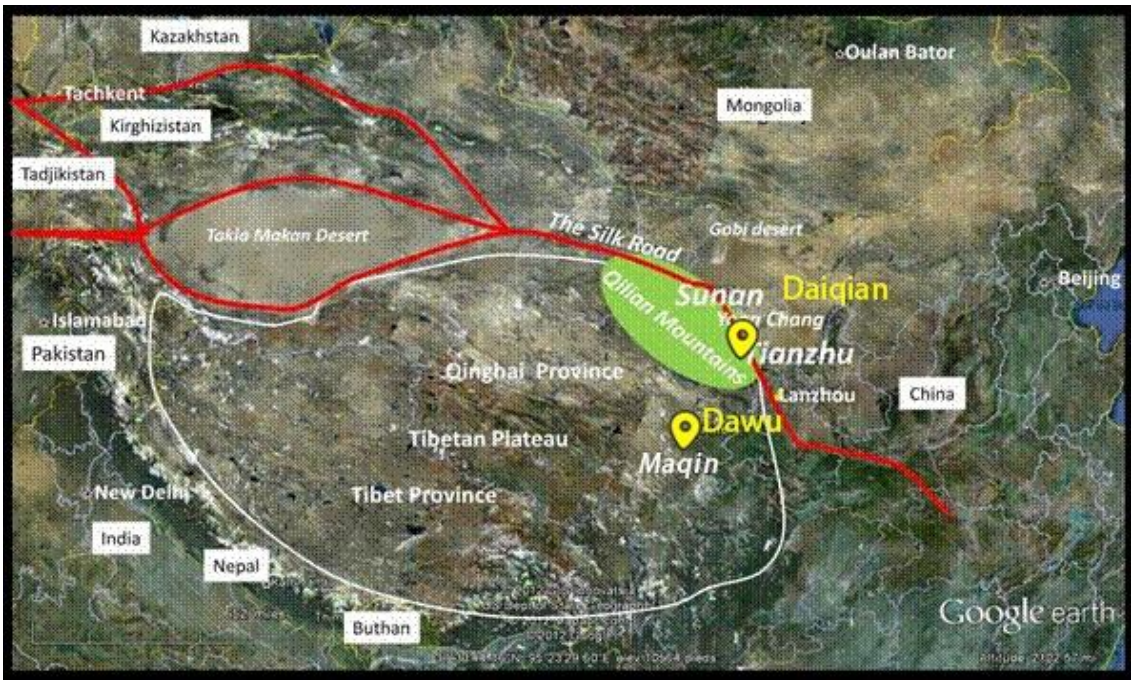

Figure 1. *Study area (Daiqian & Dawu). Red line is showing the Silk Road and green area is showing the Qilian Mountain. (Source: Google Earth®)*

http://www.aloki.hu ● ISSN 1589 1623 (Print) ● ISSN 1785 0037 (Online)
DOI: http://dx.doi.org/10.15666/aeer/1704_79878009

Variation in climate parameters (temperature and precipitation) in study areas

The climate of the study area is cold temperatures and most of precipitations occur in the form of snowfall due to its location at high altitude and dry temperature zone. The last two decades climate data (1991-2012) of the areas (Tianzhou county and Maqin county) is given in *Figure 2*. Along with the variation in annual precipitation of both counties (Tianzhou county and Maqin county) is given in *Figure 3*.

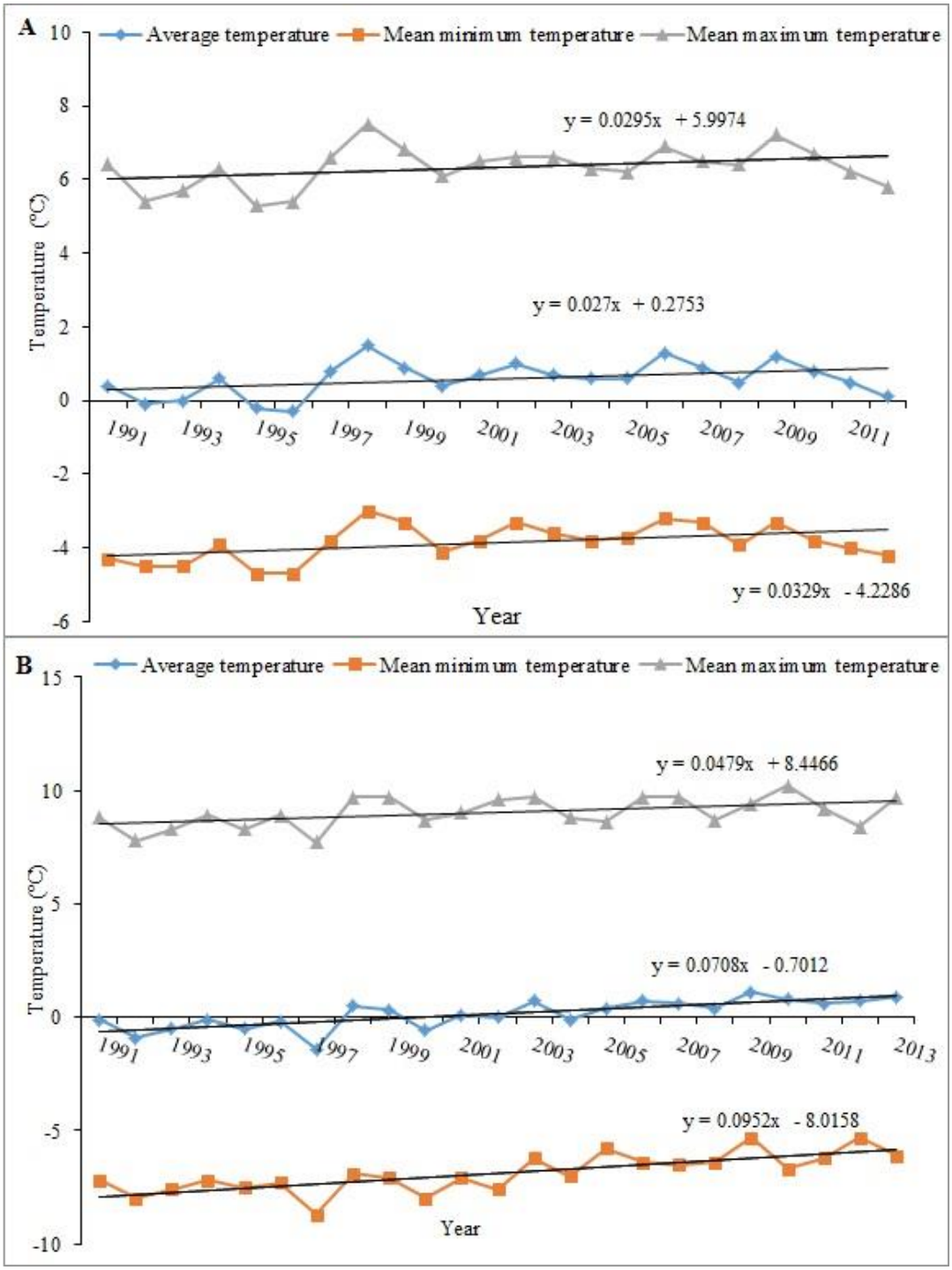

Figure 2. *Variations in annual temperature data. A) Tianzhu County 1991-2011. B) Maqin County during 1991-2013*

http://www.aloki.hu ● ISSN 1589 1623 (Print) ● ISSN 1785 0037 (Online)
DOI: http://dx.doi.org/10.15666/aeer/1704_79878009

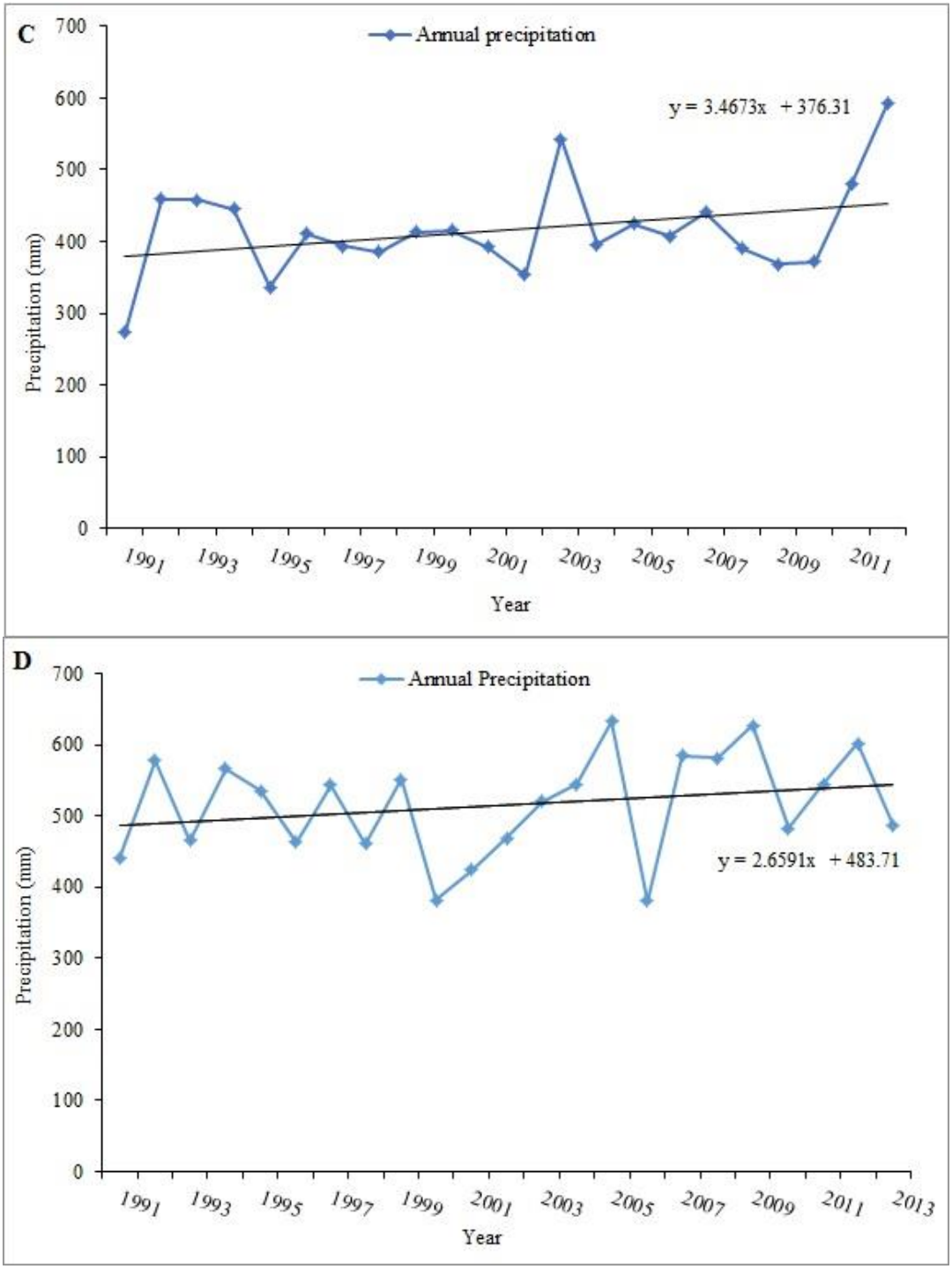

Figure 3. *Variation in annual precipitation data. C) Tianzhu County 1991-2011. D) Maqin County during 1991-2013. (The climate data of Tianzhu County and Maqin County are from http://data.cma.cn/data/cdcdetail/datacode/surf_cli_chn_mul_yer.html, by permission)*

Increasing temperature

Analyses of temperature variability over the last two decades in Tianzhou County have been given in (*Fig. 2A*). A gradual increase in average annual, mean maximum and mean minimum temperatures have been noticed in the study area. The trend line shows

http://www.aloki.hu ● ISSN 1589 1623 (Print) ● ISSN 1785 0037 (Online)
DOI: http://dx.doi.org/10.15666/aeer/1704_79878009

upward trend indicating a gradual increase in annual temperature from 1991-2013. For example, the mean maximum temperature ranges from 5.3 °C in 1995 to 7.5 °C in 1998. Similarly, year 1998 and 1995 had the highest mean minimum temperature -3.0 °C and lowest mean minimum temperature -4.7 °C, respectively. There is a sudden variation in temperature in Tianzhou County. The mean maximum temperature ranged from 7.2 °C in 2009 to 5.8 °C in 2012. In the same way year 2009 and 2012 had the highest mean minimum temperature -3.3 °C and lowest mean minimum temperature -4.2 °C respectively. In Maqin county (*Fig. 2B*) temperature is gradually increasing and is also highly variable. The mean maximum temperature in year 2010 and 2012 is 10.2 °C and 8.4 °C) respectively. In this county in 1997 had the lowest mean minimum temperature -8.3 °C) and 2009 and 2012 had the highest mean minimum temperature -5.3 °C).

Erratic precipitation

A noticeable variation in precipitation patterns over the last 22 years has occurred (*Fig. 3C*). In 1991 annual precipitation was recorded as the lowest 274 mm and in 2012 was recorded as the highest precipitation 592.8 mm during the last 22 years.

In Maqin County (*Fig. 3D*) the variation in annual precipitation is also noticeable. For example year 2005 had the highest annual precipitation 632 mm and year 2006 had the lowest precipitation 380 mm during the last 22 years. The trend line shows an increasing trend both in temperature and precipitation in both of the study areas; however the deviation in the lower or higher case is much prominent that may be due to climate change effects. However the impact of these extreme variations may be much pronounced on grasslands and livestock health that actually helps pastoralists to perceive these variations.

Pasture utilization and animal feeding calendar of a year

The grazing period for animals is from mid-June to mid-August. The summer pastures are far from pastoralists' houses and all of the animals have free access to the pasture for grazing in summer. A generalized pasture utilization and animal feeding calendar of the year is given in *Table 2*.

Table 2. *Major features of livestock production system of study areas*

	January	**February**	**March**	**April**	**May**	**June**	**July**	**August**	**September**	**October**	**November**	**December**
Animal's area	Winter pasture				Summer pasture				Autumn pasture	Winter pasture		
Grazing	-			+	++	+++			+	-		
Supplementation (forage)	Yes									Yes		
Supplementation (concentrates)	Yes											
Milking						Yes						
Calving period					Yes							
Lambing period			Yes									
Wool sales						Yes						
Animal selling period									Yes			
Planting period					Yes							
Harvest									Yes			

-No grazing, +light grazing, ++moderate grazing, +++heavy grazing

http://www.aloki.hu ● ISSN 1589 1623 (Print) ● ISSN 1785 0037 (Online)
DOI: http://dx.doi.org/10.15666/aeer/1704_79878009

Data collection

The data was collected through questionnaire and interviewing (see *Appendix*). 30 households were selected from Daiqian Village while 40 households were selected from Dawu village. The snowball sampling method was applied to approach the respondents. Snowball sampling approach is more appropriate to access the populations which are difficult to locate. Pastoralists often have scattered homes far from one another in the mountains and hilly areas with no proper access. So keeping in view we used snowball sampling method in this research. Interviewing helps scientists to look into the features of a society and know about a particular social fact by respondents own opinion (Dutcher et al., 2004). All interviews with villagers were taken with the help of Chinese interpreters, and all respondents showed their willingness to give interview. The data collected thus was tabulated in excel program.

Data analysis

For the purpose to describe and have a fair understanding about the collected data, data were analyzed using sociological statistic software known as Statistical Product and Service Solutions (SPSS 13.0 version, 2004) and Microsoft Excel. Based on the statistical results of the research conclusions were drawn. Statistical analysis base on best fit model, relying on the null hypothesis (H0) that an effect does not exist whereas the alternative hypothesis (H1) is contrary to that (Field, 2009). The acceptance or declining of the null hypothesis base on the probability value (p-value), that is to be related to the confidence interval around the average value of a tested response variable. A 95% confidence level was considered in this study and then, if the p-value is below or equal to 0.05, the null hypothesis is declined. Descriptive statistics, binomial and chi-square tests were also applied in this data analysis.

Binomial test

To examine whether respondents perceive (category I) or not perceiving (category II) about the statement of climate change perception, we carried out a binomial analysis. This analysis was also used for frequencies for category I and II of the variables "perception", "impacts" as well "adaptations" that have been explained in *Table 3*. Binomial test also examines frequencies of every class of "Yes" and "No". In our research we examined either the frequencies of category I differs from the category II. In this case null hypothesis (H0) was created like "the frequency of category I (Yes) is higher than the frequency of category II (No)".

Chi-square test

In order to better understand the relationship between two categorical variables Pearson Chi-square test was applied. The analysis gives a judgment between the observed frequency level in a category and the expected frequencies by testing perfect random possibility (Field, 2009). A null hypothesis was created "there is no relationship between the two variables" and a substitute hypothesis (H1) describes "there is a relationship between the two variables". There is a key supposition in this analysis that expected frequencies must be more than 5. If every variable has only two categories, we should use Fisher's exact test. The Pearson chi-square tests results are not consistent every time, and can be considered investigative only.

http://www.aloki.hu ● ISSN 1589 1623 (Print) ● ISSN 1785 0037 (Online)
DOI: http://dx.doi.org/10.15666/aeer/1704_79878009

Table 3. *Description of the variables changed to a categorical scale*

Variables	Description	Category I	Category II
Factors for developing climate change perception	The following helped to develop climate change perceptions • Personal observations • Government department • TV programs • Weather forecast	Yes/agree	No/disagree
Awareness of weather	Farmers awareness about the changes in climatic conditions • Temperature is rising • Rainfall is decreasing	Yes	No
Impacts on resources	Are there any adverse effects of climate change on grasslands and livestock? • Grassland degradation • Negative impacts on livestock health • Deaths in livestock	Yes	No
Adaptation	Are they adapting the climate changes? • Water harvesting • Forage cultivation • Good quality seed • Fencing • Controlled grazing • Mixed livestock breed	Yes	No

Results

Displayed results contribute a better insight of pastoralist's perceptions about climate change and their adaptation for these changes. It will help the governments to find the best possible incentives, measures and interventions to improve the adaptation practices and protect the natural, environmental and cultural resource on a sustainable base that has a unique global importance. Firstly, the participant's general demographic characteristics are described; containing gender, age, education, household including their socioeconomic profile about incomes and expenditures. Secondly, perception of the pastoralists including contributing factors leading to develop climate awareness in pastoralist has been described. Thirdly, measures taken by the pastoralists to adopt issues associated to climate change and diversification of livelihood have been discussed. Lastly, the recommendations made by the pastoralists to enhance climate change perception and adoption in Tibetan Plateau have been explained.

Demographic profile of pastoral community

Table 4 shows the demographic profile of the respondent pastoral communities of the Daiqian Village and Dawu Village. The respondents from Daiqian village consists of 66.33% male and 36.37% female while in Dawu village most of the respondent were men 92% and only 8% were the female respondents. The age of the respondents ranges from 30 to 70 years. Majority of the respondent (40%) in Daiqian village belonged to 40-50 years age group as compared the 50% of the Dawu village respondents belonged to age group of 30-40 years. In Daiqian village majority of the respondents (41.9%) got their education up to primary level while in Dawu village majority of the respondent

http://www.aloki.hu ● ISSN 1589 1623 (Print) ● ISSN 1785 0037 (Online)
DOI: http://dx.doi.org/10.15666/aeer/1704_79878009

were illiterate as the 85% of the respondent had no education. The household size of the respondents was divided into less than five members and greater than five family members. In Daiqian village majority of the respondent have family size of the ≤ 5 that counted about 73% while in Dawu about 50% of the respondents were having family member ≤ 5.

Table 4. *Demographic profile of pastoral communities of selected villages*

Variable	Category	Daiqian village	Dawu village
Gender	Male Female Total	19 (66.33%) 11 (36.67%) 30 (100%)	37 (92%) 3 (7.5%) 40 (100%)
Age (years)	30-40 41-50 51-60 61-70	8 (26.66%) 12 (40.0%) 8 (26.67%) 2 (6.66%)	20 (50%) 11 (27.5%) 2 (05.0%) 7 (17.5%)
Education	Illiterate Primary Elementary	12(40%) 13 (41.9%) 5 (16.1%)	34 (85%) 6 (15%) 0
Household size	≤ 5 > 5	22 (73.33%) 8 (25.8%)	21 (52.5%) 19 (47.7%)

Rural household resources and socio-economic characteristics

Rural household resources and socio-economic profile of the respondent communities of Daiqian village and Dawu village have been recorded in *Table 5*. Both of the villages have minimum household size of family members of 03 while on the other hand Dawu village have maximum number of family members up to 09 as compared to 07 members of Daiqian village. The mean pasture land holding size of Daiqian and Dawu is (13 ha) and (33 ha) respectively. The maximum land holding size for pasture is (38 ha) while in Dawu it reached to (133 ha). The mean mobility of the herder in Daiqian and Dawu village was recorded as 3 km. Mean annual income were found in Daiqian (7886 $), that were more in Dawu (8422 $). Similar trend was observed in mean annual expenditures in both villages. Mean livestock number was more in Daiqian as compared to Dawu village.

Table 5. *Rural household resources and socio-economic characteristics of study areas*

	Daiqian				Dawu			
	N	Min	Max	Mean	N	Min	Max	Mean
Household size	30	3	7	4.47	40	3	9	5.38
Land holding (ha) pasture area	30	04	38	13	40	5.3	133	33
Mobility	> 5 km	1	5	3	> 5 km	1	5	3
Annual income ($)	30	2830	15094	7886	40	1146	35631	8422
Annual expenditures ($)	30	1190	11901	6001	40	2496	17968	6874
Livestock	30	50	350	152.47	40	15	458	109.20

http://www.aloki.hu ● ISSN 1589 1623 (Print) ● ISSN 1785 0037 (Online)
DOI: http://dx.doi.org/10.15666/aeer/1704_79878009

Economic profile of the selected respondent communities

Figure 4 explained the economic profile including the income sources and types of various expenditures incurred of the respondent communities of Daiqian and Dawu villages during the year. Major income sources included livestock sale, wool sale, caterpillar fungus sale, subsides and other including labor, sale of milk , dung etc while the major expenditures include buying livestock, daily living (food and other things), medical, livestock feed, vaccination and others. Livestock sale, subsidies were among the major income sources for both of the communities while living and animal feed were among the major expenditures of the respondent communities.

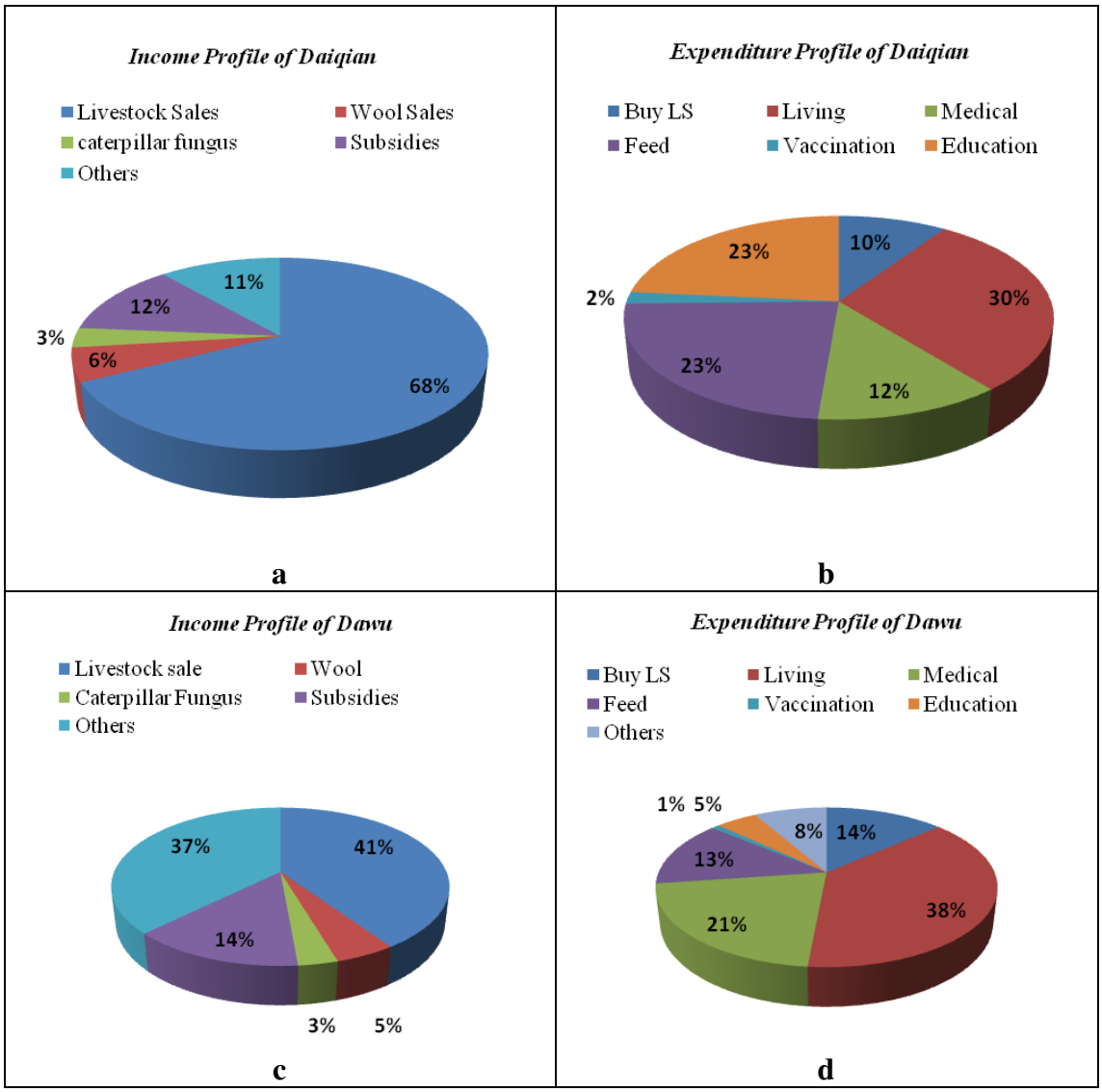

Figure 4. *Income and expenditure profile of the pastoral community*

Pastoralist's perceptions about climate change

The data presented in *Figure 5* has shown the responses of the pastoral communities about climate change perception. Responding to the question whether they know about

http://www.aloki.hu ● ISSN 1589 1623 (Print) ● ISSN 1785 0037 (Online)
DOI: http://dx.doi.org/10.15666/aeer/1704_79878009

climate change or not. 83.3% of the respondents belonging to Daiqian village were aware of the climate change issues while about 16.7% of the respondents were not aware of the climate change phenomenon at all. As compared to Daiqian, the pastoral community of the Dawu was less aware of the climate change. However majority of the respondents of Dawu village75% had the knowledge about climate change while 25% did not have awareness about climate change (*Table 6*).

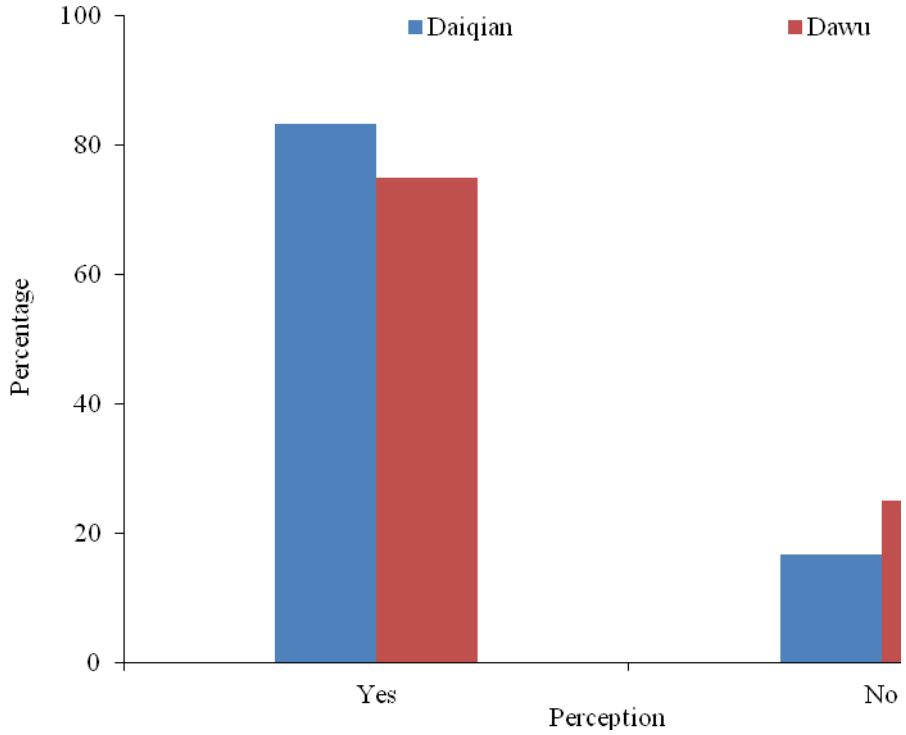

Figure 5. *Pastoralist's perceptions about climate change in selected villages*

Table 6. *Climate change perception and factors for perception development*

Variable	Statement	P value Daiqian	P value Dawu
Knowledge about climate change	Know about climate change	.000	.001
Factors for developing climate change perception	Personal observations	.043	.006
	Government department	.000	.000
	TV programs	1.000	.006
	Weather forecast	.000	.002

Majority of the respondents 72.5% in Dawu village were having a personal experience to judge the climate change issue while only 30% in Daiqian village have examined the climate change through personal observations (*Table 7*). The other factor contributing in the development of climate change awareness among pastoralist included Government Departments, weather forecast program, TV programs and multiple sources. Weather forecast program and TV program jointly contributed in developing perception among 13 (43%) and 16 (40%) of the respondents in Daiqian and Dawu respectively.

http://www.aloki.hu ● ISSN 1589 1623 (Print) ● ISSN 1785 0037 (Online)
DOI: http://dx.doi.org/10.15666/aeer/1704_79878009

Table 7. *Different tools of climate change perceptions among respondents*

Sources of climate change perception	Daiqian	Dawu
	Frequency/percent	Frequency/percent
Personal observation/experience	9 (30.0%)	29 (72.5%)
From government department	2 (6.7%)	3 (7.5%)
Weather forecast	5 (16.7%)	10 (25.0%)
TV program	8 (26.7%)	6 (15.0%)
Multiple sources	15 (50.0%)	11 (27.5%)

Perceived impacts of climate change

After recording the pastoralists knowledge about climate change and tools helping to develop awareness about climate change, next to that pastoralist were asked about the perceived impacts of climate change. *Figure 6* shows, in Daiqian village, most of the participants (18%) perceived changes in climate in the form of rise in annual temperatures in the area (p = .043) while 29% of the respondents perceived changes in climate in the form of low rainfall and rainfall variations (p = .000). The other perceived negative impacts of climate change in Daiqian were low production of the grasslands (12.5%), poor animal health (15%) and death of animals (12.5%) (= .000). On the other side, 17.5 and 15% (p = .000) of the respondent in Dawu village increase in temperature and lower rainfall distribution respectively (*Fig. 6*).

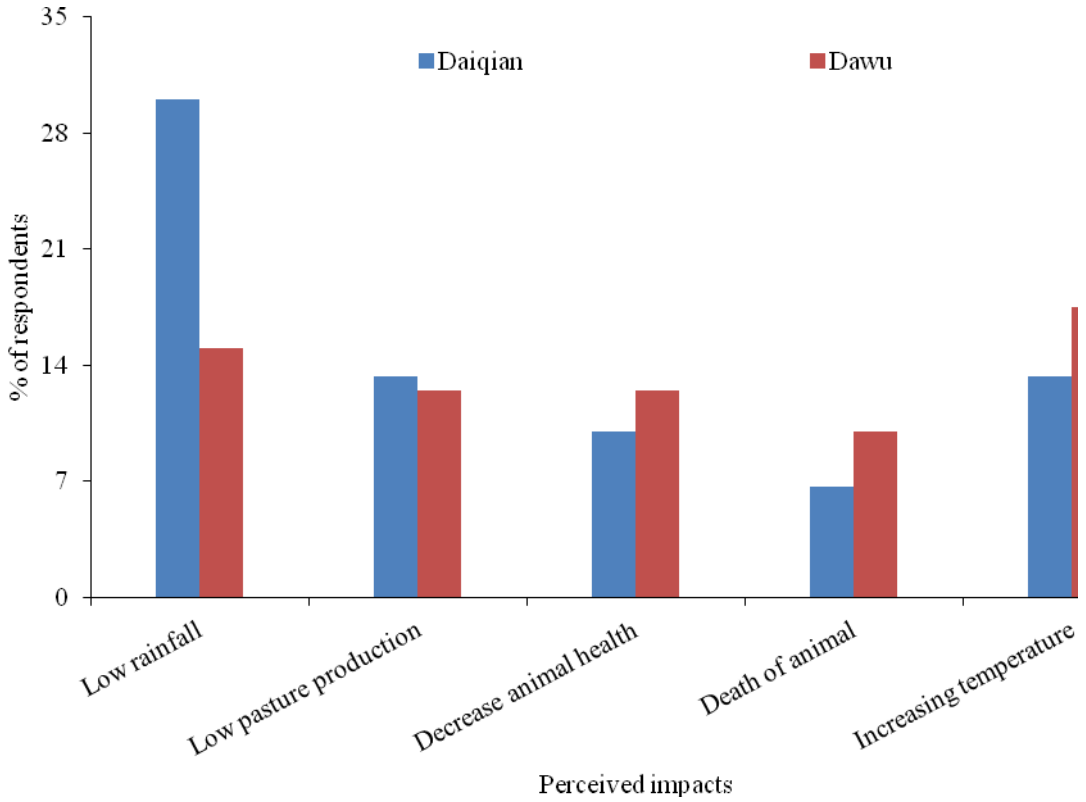

Figure 6. *Perceived impacts of climate change by pastoral communities*

http://www.aloki.hu ● ISSN 1589 1623 (Print) ● ISSN 1785 0037 (Online)
DOI: http://dx.doi.org/10.15666/aeer/1704_79878009

Climate change adaptations

The data about adaptation measures being practiced by the pastoralists have been presented in *Figure 7*. In Daiqian village having mixed livestock was one of practice that being adopted by majority of the respondents of 86.7% ($p = .000$), the having mixed livestock not only helps to utilize the available grassland resources but also can be voided loss in case of any epidemic to one type of livestock. In addition smaller animal can be sold as and when needed due to shorter age of maturity and high prices to sustain the livelihood. In Dawu village about 57.5% were having the mixed livestock. Controlled grazing was being adapted by the respondents (60%) of both of villages equally to minimize the climate impacts on their daily life management scenario, Good quality seed for forage cultivation and fencing to pasture area were also recorded as the strategies to reduce climate change impacts on livelihood of the pastoralists.

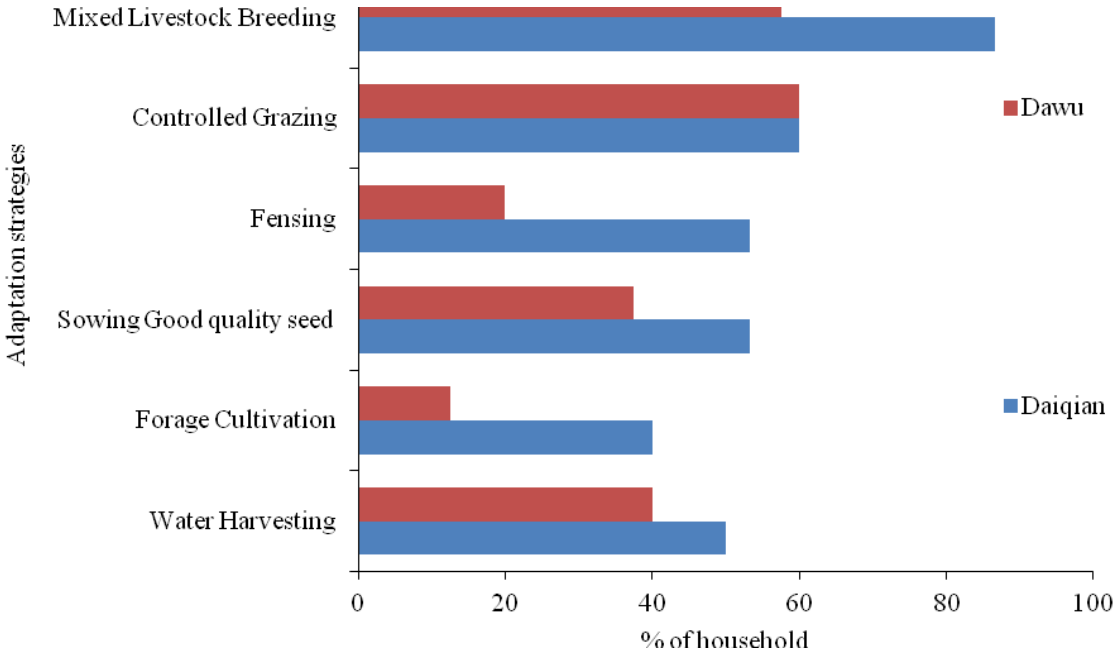

Figure 7. *Climate change adaptation measures by selected communities*

Relationship between demographic factors and climate change perception and adaptation

The demographic factor may have had an effect on the climate change perception, impacts and adaptation. It was tried to expose such relationship through chi-square tests. If these relationships are known, it will be easier to develop sufficient and area specific governmental intervention. *Table 8* describes the results about the relationship is significant or not. The data shows that only the age is one of the significant factors in Daiqian village that may influence their given answers significantly for developing the perception among the pastoralists. Similarly education is Daiqian village could possibly be helpful influencing the knowledge of the respondents about climate perceptions. Similarly household could positively be able to contribute in developing the perception of climate change knowledge in respondents.

http://www.aloki.hu ● ISSN 1589 1623 (Print) ● ISSN 1785 0037 (Online)
DOI: http://dx.doi.org/10.15666/aeer/1704_79878009

Table 8. *Relationship between demographic factors and climate change perception and adaptation*

Daiqian	Knowledge	Impact	Adaptation	**Dawu**	Knowledge	Impact	Adaptation
Gender	.381	.310	.470	Gender	.411	.704	.348
Age	.036*	.748	.375	Age	.471	.641	.441
Education	.063*	.977	.557	Education	.153	.351	.456
House hold size	.757	.275	.927	House hold size	.058*	.331	.468

*Significant relationship P < 0.1

Livelihood diversification

Livelihood diversification is considered as one of the effective tools that not only helps pastoralists to manage climate change effects but also supports sustainable livelihood by enhancing income levels of the pastoralists. While responding about livelihood diversification mixed livestock was considered as one of the major activity in both of the villages because it is not only utilizes the pastures in a better way but sheep and goats can be sold as and when needed to meet the urgent needs (*Fig. 8*). However in Daiqian village about 86.7% of the pastoralists were having mixed livestock to sustain their lives and meet their daily needs where in Dawu only 57.5% were having the mixed livestock. Almost all of the pastoralists were selling wools of their animal to earn some money. In addition collection and selling of caterpillar fungus, labors were also recorded as means to diversify pastoral income in Daiqian and Dawu villages.

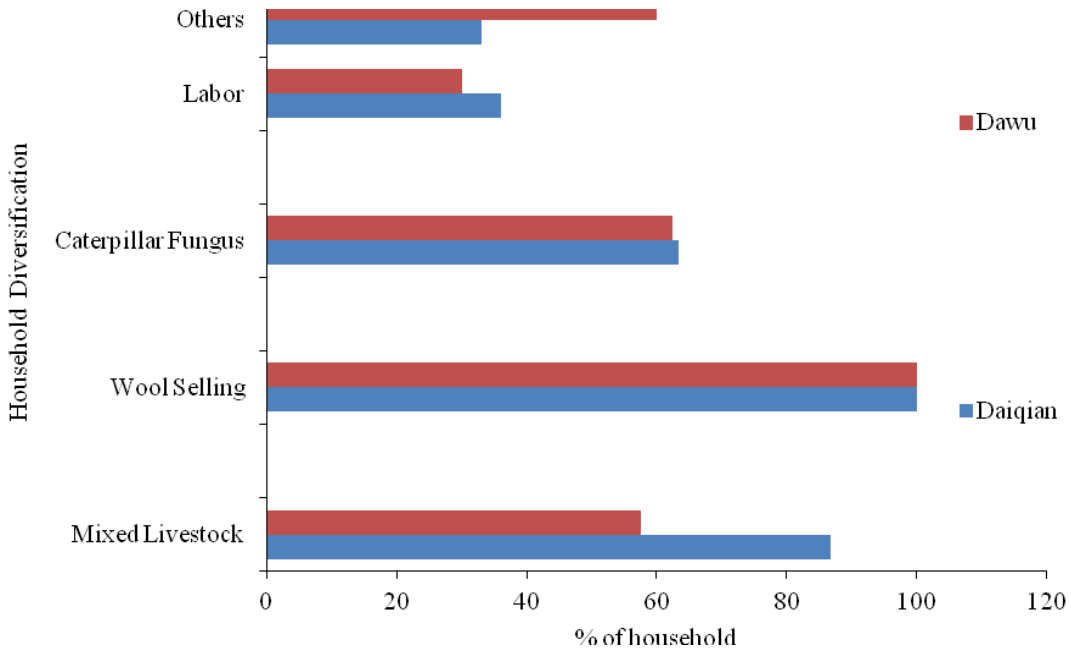

Figure 8. *Livelihood diversification measures by pastorals in Daiqian and Dawu villages*

Institutional set up and government policies

The pastoralists were asked whether they know about the institutional set up and government policies about different sectors in their villages. Responding to the

http://www.aloki.hu ● ISSN 1589 1623 (Print) ● ISSN 1785 0037 (Online)
DOI: http://dx.doi.org/10.15666/aeer/1704_79878009

questions most of pastoralists in villages were aware about pasture management institution and policies *Table 9*. In Daiqian village 56.7% and Dawu village 60% of the villages were aware about the pasture management and related policies. Following to the pasture management, people were aware about the credit organizations in both villages as in Daiqian 46% and Dawu 15%. People in both of the villages were also having more or less information about NGOs, Water management and Agriculture management both villages.

Table 9. *Institutional set up and government policies*

Govt. Policies	Daiqian			Dawu		
	Yes	No	Don't know	Yes	No	Don't know
Water management	26.7%	36.7%	36.7%	55%	37.5%	7.5%
Pasture management	56.7%	6.7%	36.7%	60%	32.5%	7.5%
Agriculture management	10.0%	53.3%	36.7%	7.5%	85.0%	7.5%
Credit organization	46.7%	16.7%	36.7%	15%	77.5%	7.5%
Disaster relief and rescue	40.0%	36.7%	23.3%	77.5%	15.0%	7.5%
NGO's	30.0%	40.0%	30.0%	22.5%	67.5%	10.0%

Key recommendations by pastoralists to mitigate future effects

Pastoralists are the key custodians of the grasslands of the Tibetan Plateau. They can play a significant role in the conservation of this resource base if their opinion is given due consideration and noticed their needs in this regards. Keeping in view it was sought to put a question about their recommendation to not only conserve this resource but this unique diminishing social and cultural heritage of pastoralism (*Table 10*). The majority of the Daiqian respondents (26%) recommended that grassland degradation should be controlled. Secondly they recommended (20%) that their capacity should be built through training about pasture and climate change management as well as similar number of respondents recommended watering points for live stocks. In addition about 16.7% of the respondents suggested developing forage bases and introduction seed of drought and cold tolerant good forage varieties. In the case of Dawu village capacity building for pasture and climate change, establishment of watering points for grazing livestock in the pasture area, development of forage base with introduction of good variety seed were recorded (*Table 10*).

Table 10. *Key recommendations by pastoralists to mitigate future effects*

Recommendations by pastoralists	Daiqian (%)	Dawu (%)
Training of pasture knowledge and climate change scientific management	20.0	17.5
Awareness campaigns	13.3	10.0
The establishment of livestock water points	20	17.5
Strengthening governance about the protection of natural grassland	3.3	10.0
Increase grassland degradation control	26.7	10.0
Development of forage base and cultivate new varieties of drought resistant	16.7	17.5
Infrastructure for drinking water	6.7	5.0
Strengthen meteorological disaster forecast	10.0	17.5

http://www.aloki.hu ● ISSN 1589 1623 (Print) ● ISSN 1785 0037 (Online)
DOI: http://dx.doi.org/10.15666/aeer/1704_79878009

Discussion

Farmer's perceptions about climate change

This study noticed some important findings about the perception. The study found that the participated pastoralists had knowledge about climate changes and its impact on their lives and associated resources. The findings are in line with the results of Thomas (2008) who found that farmers could recognize changes in climate and increased variability in natural climatic conditions due to climate change. In some sense, communication on climate change has been enormously successful. Across nations, almost everyone in study area has heard the issue and many can identify at least some important climate change impacts (Leiserowitz, 2007). In this study, communication way like electronic media, weather forecast information has been noticed as the tool to develop perception of the respondent about climate change. It is therefore, suggested that government institutions and policy makers could use media as a tool for developing climate change perception among masses. The awareness about climate change is related to age thus older pastoralists have better understanding about climate change that may be based on their experience to observe these changes. Pastoralists in Tibetan Plateau indicate a declined precipitation and increased temperatures with a short rainy spell. The comparable findings were reported by several other researchers as (Lema and Majule, 2009; Wongtschowskiet al., 2009; Zampaligréet al., 2013). Pastoral perceptions have been verified by the long term climate data examination that highlighted a decreasing tendency in rainfall pattern with a mild to highly worst drought frequency, and increase in temperature. The findings of (IPCC, 2007) observed a universal shortage in rainfall with increased temperatures along with a hint that there will be higher rainfall occurrence in some areas, while many other areas will receive insufficient rainfall. The Tibetan plateau may fall in the second scenario having low rainfall. However, if local people's native knowledge about prediction of weather changes has been interrupted, this may lead to inefficiency of local mitigation and adaptation strategies (Nyonget al., 2007). Agro-pastoralists understand that change and inconsistency in climatic conditions effects grasslands, water resources, animal vigor and productivity. Actually, the production of agriculture, grasslands and water resource are greatly associated with climatic parameters such as precipitation and temperature. Decline in rainfall causes a reduced pasture production (Lema and Majule, 2009; IUCN, 2010). Increase in temperatures accelerates evapotranspiration rate by plants which leads to condition of drought (IPCC, 2007). Pastoralists' perceptions about the impacts of global change on the pastures have also been noticed by Wongtschowskiet al. (2009) and Zampaligreet al. (2013). They concluded that forage availability, the soil quality and the pastures specie composition (e.g. biodiversity) is affecting by climate change.

Adaptation strategies and livelihood diversification

Transformation in livestock possessions and livestock management systems, are fundamental for adaptation of long term global changes (Deressa et al., 2009). It was noticed that mixed live breed holdings by the pastoralists is one of the major adaptation measures in the area. This can help to not only face issues related to climate aspects but also sustain livelihood prospects. The mix livestock breed helps not only to use different types of forage and livelihood sustainability, as sheep and goats are sold out as and when needed as compared to yak that needs long time for getting more money. For efficient and better adaptation of the impacts of climate change and variability

http://www.aloki.hu ● ISSN 1589 1623 (Print) ● ISSN 1785 0037 (Online)
DOI: http://dx.doi.org/10.15666/aeer/1704_79878009

pastoralists diversify their livestock species, cultivate supplementary forage and practice other measures (*Fig. 9*).

Figure 9. *Pictorial representation of some adaptation and livelihood practices by pastoralists of the selected villages*

The sheep and goat have a significant role in pastoral livestock production system by allowing the pastoralists to fulfill their instant socioeconomically requirements (Malonine, 2006). Diversification by means of forage production not only produces cereals for their own food but also feed for their livestock from crop straw residues. In addition, to perform diversification crop farmers also practice shifting cultivation, enlarge their cropland, and grow superior plant breeds. However, the increased frequency and harsh intensity of climate events (floods, droughts) and the rainfall variations are posing bigger threats to the pastoralists' adaptive capacity (Kandjiet al., 2006). Farmers become more vulnerable to climate changes if they don't have very good ability to adapt climate change effects for their resilience. The pastoralists were of the view that training should be imparted to them for building their capacities to perceive and mitigate climate change issues.

Conclusions

Pastoral perception of climate change and analysis of climate data both showed a decrease in rainfall and an increase in temperatures with a reduction of rainy season in study area. Personal experience and electronic media are main factors for developing climate awareness among local pastoralist, so these should be taken into consideration while launching campaigns and initiatives about climate awareness and adaptation in the plateau. Climate change and deviation have affected the accessibility of natural resources such as pasture, water, livestock production, and livestock health

http://www.aloki.hu ● ISSN 1589 1623 (Print) ● ISSN 1785 0037 (Online)
DOI: http://dx.doi.org/10.15666/aeer/1704_79878009

deterioration. Due to strong negative effects on people's welfare and safety, climate change is a huge risk to pastoral safety. To adapt these impacts of climate change and variability pastoralists shifted from monoculture (yak) of livestock to mixed species (yak + sheep + goats) and diversification of income sources. Adaptation to climate change has to be included in disaster risk reduction policies and should be regularized into land plans policies at national, local and regional levels.

Keeping in view above concluding paragraph following recommendation are made:

- Migration, ethnicity and religious believes could be important factors to develop climate change adaptation among pastorals societies, it is therefore recommended that future studies may be conducted while addressing these parameters.
- Electronic media and weather forecast programs have been indicated by the pastoralist as an effective tool for developing awareness among the pastoralists. Government and policy institutions can strengthen these sources and develop an effective mechanism for their efficient use for developing knowledge about climate change in the area.
- Personal experience and education have a strong relationship with knowledge about climate change, so Government should consider these factors while developing mechanisms
- The development of cottage industry associated to livestock products can help pastorals to improve their livelihood. There are opportunities for organic meet production and its processing, commercial production of caterpillar fungus and cottage industry related to livestock products like wool products and cheese production. All these opportunities can help to improve their livelihood and also can enhance their adaptation to the adverse effects of climate change.
- In order to improve an efficient adaptation to climate change on the bases of long term, planned adaptation is necessary. Therefore, government should offer financial in it will reduce the financial risk for the farmer. But it should be given as a reward on the bases of the pastoralists' performance for adopting good practices for climate and resource conservation.
- Pastoralists are the key custodians of the grasslands of Tibetan Plateau so they should be given a central place while developing policies and initiatives for climate change mitigations and resource restoration in the area.

Acknowledgements. The present study was financed by China Scholarship Council (CSC), China award No. 2014GXZB87, for Master Studies in Environmental Sociology at Lanzhou University, PR-China.

REFERENCES

[1] Adger, W. N. (2003): Social capital, collective action and adaptation to climate change. – Economic Geography 79(4): 387-404.
[2] Adger, W. N. (2006): Vulnerability. – Global Environmental Change 16(3): 268-281.
[3] Adger, W. N., Huq, S., Brown, K., Conway, D., Hulme, M. (2003): Adaptation to climate change in the developing world. – Progress in Development Studies 3(3): 179-195.
[4] Apata, T. G., Samuel, K. D., Adeola, A. O. (2009): Analysis of climate change perception and adaptation among Arable Food Crop farmers in south western Nigeria. – International Association of Agricultural Economists' 2009 Conference, Beijing, China.

http://www.aloki.hu ● ISSN 1589 1623 (Print) ● ISSN 1785 0037 (Online)
DOI: http://dx.doi.org/10.15666/aeer/1704_79878009

[5] Asrat, P., Simane, B. (2018): Farmers' perception of climate change and adaptation strategies in the Dabus watershed, North-West Ethiopia. – Journal of Ecological Processes 7: 7.
[6] Below, T. B., Mutabazi, K. D., Kirschke, D., Franke, C., Sieber, S., Siebert, R., Tscherning, K. (2012): Can farmers' adaptation to climate change be explained by socio-economic household- level variables? – Global Environmental Change 22(1): 223-235.
[7] Bryan, E., Deressa, T. T., Gbetibouo, G. A., Ringler, C. (2009): Adaptation to climate change in Ethiopia and South Africa: options and constraints. – Environmental Science & Policy 12(4): 413-426.
[8] Cui, X. F., Graf, H. F. (2009): Recent land cover changes on the Tibetan Plateau: A Review. – Climatic Change 94(1-2): 47-61.
[9] Curwood, P. D., Eckerle, S. (2009): What is poverty? – Esurio: Journal of Hunger and Poverty 1(2): 9-17.
[10] Deressa, T. T., Hassan, R. M., Ringler, C., Alemu, T., Yesuf, M. (2009): Determinants for farmers' choice of adaptation methods to climate change in the Nile Basin of Ethiopia. – Global Environmental Change 19: 248-255.
[11] Dutcher, D. D., Finley, J. C., Luloff, A. E., Johnson, J. (2004): Landowner perceptions ofprotecting and establishing riparian forests: a qualitative analysis. – Society & Natural Resources 17: 329-342.
[12] Field, A. (2009): Discovering Statistics Using SPSS, Third Ed. – Sage, London.
[13] Francisco, H., Nabangchang, O., Bui, D. T., Yusuf, A. A. (2008): Climate change: impacts, adaptation, and policy in Southeast Asia. – Proceedings of EEPSEA Conference, 13-15 February 2008, Bali, Indonesia.
[14] Frye, I. (2008): What is Poverty? A Qualitative Reflection of People's Experiences of Poverty. – National Labor and Economic Development Institute, Johannesburg, South Africa.
[15] Fu, Y., Grumbine, R. E., Wilkes, A., Wang, Y., Xu, J. C., Yang, Y. P. (2012): Climate change adaptation among Tibetan pastoralists: challenges in enhancing local adaptation through policy support. – Environmental Management 50(4): 607-621.
[16] Gallopín, G. C. (2006): Linkages between vulnerability, resilience, and adaptive capacity. – Global Environmental Change 16(3): 293-303.
[17] Hassan, R., Nhemachena, C. (2008): Determinants of African farmers' strategies for adapting to climate change: multinomial choice analysis. – African Journal of Agricultural and Resource Economics 2(1): 83-104.
[18] Hulme, D., Shepherd, A. (2003): Conceptualizing chronic poverty. – World Development 31(3): 403-423.
[19] Hyland, J. J., Barnes, A., Parkhill, K., Jones, D. L., Williams, A. P. (2016): Farmers' perceptions of climate change: identifying types. – Agric. Hum. Values 33: 323-339.
[20] IPCC (2014): Climate Change 2014: Impacts, Adaptation, and Vulnerability. Part A: Global and Sectoral Aspects. – In: Field, C. B. et al. (eds.) Contribution of Working Group II to the Fifth Assessment Report of the Intergovernmental Panel on Climate Change. Cambridge University Press, Cambridge, UK. http://www.ipcc.ch/report/ar5/wg2.
[21] Intergovernmental Panel on Climate Change (IPCC) (2001): Climate Change 2001: Impacts, Adaptation and Vulnerability. – Cambridge University Press, Cambridge, UK.
[22] Intergovernmental Panel on Climate Change (2007): Regional Climate Projections. – In: Solomon, S., Qin, D., Manning, M., Chen, Z., Marquis, M. et al. (eds) Climate change (2007): the physical science basis. Contribution of Working Group I to the Fourth Assessment Report of the Intergovernmental Panel on Climate Change. Cambridge University Press, Cambridge, UK, pp. 879-886.
[23] IUCN (2010): Building Climate Change Resilience for African Livestock in Sub-Saharan Africa. – The International Union for Conservation of Nature, Eastern and Southern Africa Regional Office, Nairobi.

http://www.aloki.hu ● ISSN 1589 1623 (Print) ● ISSN 1785 0037 (Online)
DOI: http://dx.doi.org/10.15666/aeer/1704_79878009

[24] Kandji, S. T., Verchot, L., Mackensen, J. (2006): Climate Change and Variability in the SahelRegion: Impacts and Adaptation Strategies in the Agricultural Sector. – UNEP/ICRAF, Nairobi, Kenya.
[25] Lasco, R. D., Espaldon, M. L. O. Habito, C. M. D. (2015): Smallholder farmers' perceptions of climate change and the roles of trees and agroforestry in climate risk adaptation: evidence from Bohol, Philippines. – Agroforest Systems 90(3): 521-540. DOI: 10.1007/s10457-015-9874-y.
[26] Lema, M. A., Majule, A. E. (2009): Impacts of climate change, variability and adaptation strategies on agriculture in semi-arid areas of Tanzania: the case of Manyoni District in Singida Region, Tanzania. – African Journal of Environmental Science and Technology 3(8): 206-218.
[27] Li, C. L., Kang, S. C. (2006): Review of studies in climate change over the Tibetan Plateau (in Chinese). – ActaGeographicaSinica 61(3): 327-335.
[28] Liu, X. D., Chen, B. D. (2000): Climatic warming in the Tibetan Plateau during recent decades. – International Journal of Climatology 20(14): 1729-1742.
[29] Leiserowitz, A. (2007): Communicating the Risks of Global Warming: American Risk Perceptions, Affective Images, and Interpretive Communities. – In: Moser, S. C., Dilling, L. (eds.) Creating a Climate for Change: Communicating Climate Change and Facilitating Social Change. Cambridge University Press, Cambridge, pp. 44-63.
[30] Malonine, C. (2006): Les Liens Famille-Troupeau du Ferlo (Sénégal): Témoins de la Dynamique des Systèmesd' Elevage Pastoraux. – Doctoral Thesis. Université Claude Bernard deLyon (Médecine-Pharmacie).
[31] Miller, D. J. (2002): The importance of China's nomads. – Rangelands 24(1): 22-24.
[32] Niu, T., Chen, L. X., Zhou, Z. J. (2004): The characteristics of climate change over the Tibetan Plateau in the last 40 years and the detection of climatic jumps. – Advances in Atmospheric Sciences 21(2): 193-203.
[33] Nori, M., Davies, J. (2007): Change of Wind or Wind of Change? Climate Change, Adaptation and Pastoralism. The World Initiative for Sustainable Pastoralism. – International Union for Conservation of Nature, Nairobi, Kenya.
[34] Nyong, A., Adesina, F., Elasha, B. O. (2007): The value of indigenous knowledge in climate change mitigation and adaptation strategies in the African Sahel. – Mitigation and Adaptation Strategies for Global Change12: 787-797.
[35] Sen, A. (1999): Development as Freedom. – Oxford University Press, Oxford, UK.
[36] Seo, S. N., Mendelsohn, R. (2008a): An analysis of crop choice: adapting to climate change in South American farms. – Ecological Economics 67(1): 109-116.
[37] Seo, S. N., Mendelsohn, R. (2008b): Measuring impacts and adaptations to climate change: a structural Ricardian model of African livestock management. – Agricultural Economics 38(2): 151-165.
[38] Smit, B., Wandel, J. (2006): Adaptation, adaptive capacity and vulnerability. – Global Environmental Change 16(3): 282-292.
[39] Smit, B., Burton, I., Klein, R. J. T., Street, R. (1999): The science of adaptation: a framework for assessment. – Mitigation and Adaptation Strategies for Global Change 4(3): 199-213.
[40] Tanner, T., Mitchell, T. (2008): Entrenchment or enhancement: could climate change adaptation help to reduce chronic poverty? – IDS Bulletin 39(4).
[41] Thomas, R. J. (2008): Opportunities to reduce the vulnerability of dryland farmers in Central and West Asia and North Africa to climate change. – Agriculture, Ecosystems and Environment 126: 36-45.
[42] Whelan, C. T. (2007): Measuring consistent poverty in Ireland. – The Economic & Social Review 38(2): 211-234.
[43] Wongtschowski, M., Verburg, M., Waters-Bayer, A. (2009): What can local innovation contribute to adaptation to climate change? – Paper presented and discussed at the 3rdInternational Conference on Community-Based Adaptation, Dhaka, Bangladesh.

http://www.aloki.hu ● ISSN 1589 1623 (Print) ● ISSN 1785 0037 (Online)
DOI: http://dx.doi.org/10.15666/aeer/1704_79878009

[44] Xiaopen, P., Degang, Z., Changlin, X., Jiangang, C. (2000): The economic comparison on yak production in two types of cold season grassland in Tianzhu, China. – Proceedings of the Third International Congress on Yak Held in Lhasa, P. R. China.
[45] Xu, Z. X., Gong, T. L., Li, J. Y. (2008): Decadal trend of climate in the Tibetan Plateau: regional temperature and precipitation. – Hydrological Process 22(16): 3056-3065.
[46] Zampaligré, N., Dossa, L. H., Schlecht, E. (2013): Climate Change and Variability: Perception and Adaptation Strategies of Pastoralists and Agro-pastoralists across different Zones of Burkina Faso. – Regional Environmental Change 13(5): 18-38.
[47] Zheng, D., Lin, Z. Y., Zhang, X. Q. (2002): Progress in studies of Tibetan Plateau and global environmental change (in Chinese). – Earth Science Frontiers 9(1): 95-102.

APPENDIX

Questionnaire household

CLIMATE CHANGE PERCEPTIONS AND ADAPTIVE ACTIONS BY PASTORAL COMMUNITY ON THE TIBETAN PLATEAU, CHINA

Name of Village _____	Number of Households_____
Community Name _____	Population_____

I. 1. Name of interviewer:_____ 2. Date: _____ 3. Location_____

II. INTERVIEWEE INFORMATION
4. Name:_____ Ethnicity Sex: Male ( ) Female ( ) Age: _____
5. Education level (Iitterate, primary, secondary, higher secondary, university level)
6. Size of Family: _____ Male ( ), Female ( ) Village Name: _____
7. Occupation:
Pastoralist ( ) Farm Income () Private Services ( )
Government Services ( )Business ( ) Day Laborer ( )

III. CLIMATE CHANGE PERCEPTION
8. Do you know about climate change? Yes () No ()
9. If yes How did you know about climate Change issues?
a. Personal Observation and experience
b. From Government Departments
c. Others sources
10. Is there any impact of climate change on pasture resources and you economic conditions? Yes () No ()
11. If Yes describe
_____
_____
12. Do you own land? Yes ( ) No ( )

IV. LIVESTOCK INFORMATION
13. What are livestock resource do you have?

http://www.aloki.hu ● ISSN 1589 1623 (Print) ● ISSN 1785 0037 (Online)
DOI: http://dx.doi.org/10.15666/aeer/1704_79878009

Livestock resources

Type of live stock	Number	Feeding Type		
		Open Grazing	Stall feeding	Both
Yak				
Sheep				
Goat				
Other				

V. PASTURE INFORMATION

14. Do you own on pasture for livestock grazing? Yes ( ) No.( )
15. What type of Pasture? a) Natural b) Artificial
16. On average, how far do the individuals in the community live from the pasture? a. > 1 km ( ) b. 1-5 km ( )c. < 5 km ( )

VI. NATURAL ENVIRONMENT

17. Have you experienced any changes or deviation in weather parameters over the past 20 Years? Yes ( ) No ( )
18. If yes what are negative impacts of climate change on grasslands, livestock etc?

VII. ADOPTION MEASURES

19. Have you adopted any of the following additional techniques?

Techniques	**Yes**	**No**	**Reasons**
Changing of crop/tree species			
Irrigation practices/Water Harvesting Techniques			
Mix cropping/cultivation of forage			
Changing from crops to livestock			
Sowing of good quality seeds			
Fencing of grassland			
Controlled grazing			

VIII. INSTITUTIONAL SETUP

20. Are there any local organizations for
    Water management ( ) Pasture management ( ) Agriculture management ( )
    Agricultural credits ( ) Disaster relief and rescue ( )
    Other organizations (please specify) _____
21. What do you expect/ what should local government do for adopt of CC impact?

_____

_____

http://www.aloki.hu ● ISSN 1589 1623 (Print) ● ISSN 1785 0037 (Online)
DOI: http://dx.doi.org/10.15666/aeer/1704_79878009

INFLUENCE OF SOIL MICROBIAL ACTIVITY AND PHYSICAL PROPERTIES ON SOIL RESPIRATION UNDER MAIZE (*ZEA MAYS* L.)

BOJARSZCZUK, J.* – KSIĘŻAK, J. – GAŁĄZKA, A. – NIEDŹWIECKI, J.

Institute of Soil Science and Plant Cultivation, State Research Institute, Czartoryskich 8 Str., 24-100 Puławy, Poland
(phone: +48-81-478-6796, fax: +48-81-478-6900)

**Corresponding author*
e-mail: jolanta.bojarszczuk@iung.pulawy.pl

(Received 29th Dec 2018; accepted 8th Apr 2019)

Abstract. Soil respiration is an important indicator of soil fertility and biological activity, which has impact on plant yield. The aim of the present study was the evaluation of soil respiration intensity depending on different soil treatment practices in cultivation of maize and to determine the effect of biology activity on soil respiration. The study was based on the long-term field experiment located at the Agricultural Experimental Station at the Institute of Soil Science and Plant Cultivation – State Research Institute in Grabów (Poland). Three objects were included in this research: maize cropped continuously (monoculture) with direct sowing, maize monoculture cropped continuously with full tillage and crop rotation (spring barley, winter wheat, maize) with full tillage. Research indicates that soil respiration depends on cultivation method used before the maize is sown. The analysis showed that soil respiration was correlated with its biological activity and biochemical parameters. The statistically strongest negative correlation was found between soil respiration and evapotranspiration, changes in carbon dioxide concentration and acid phosphatase activity, while strongest positive correlation was found between soil respiration and ammonifying bacteria. The simple regression analysis showed linear relationship between soil respiration and such parameters as: acid phosphatase activity and ammonifying bacteria.
Keywords: *monoculture, tillage practice, microbial and biochemical properties, dehydrogenase activity, acid phosphatase, soil moisture*

Abbreviations: Sr: soil respiration (g $CO_2 \cdot m \cdot h^{-1}$), E: evapotranspiration (g $CO_2 \cdot m \cdot h^{-1}$), ΔCO_2: changes in carbon dioxide concentration, ΔMb: changes in soil moisture, SM: soil moisture (%, v/v), SBD: soil bulk density ($Mg \cdot m^{-3}$), DHA: soil dehydrogenase activity DHA (ug formazan·g DM of soil·24 h^{-1}), AcP: acid phosphatase (ug p-nitrophenol·g DM^{-1} of soil·h^{-1}), AlP: alkaline phosphatase (ug p-nitrophenol·g DM of soil·h^{-1}), B + A: total bacteria and Actinomycetes number (10^7 CFU (colony forming units)·g DM^{-1} (dry matter) of soil, F: total fungi number (10^4 CFU·g DM^{-1} of soil), AM: ammonifying bacteria (10^4 CFU·g DM^{-1} of soil), OLIGO: total oligotrophic bacteria (10^6 CFU·g DM^{-1} of soil), KOP: total copiotrophic bacteria (10^6 CFU·g DM^{-1} of soil)

Introduction

Soil respiration refers to the production of carbon dioxide by soil organisms (Luo and Zhou, 2006). A small part of soil respiration (below 10%) results from the decomposition of resistant organic carbon particles (Hanson et al., 2000; Schlesinger and Andrews, 2000).

Soil capacity to produce CO_2 varies depending on soil structure, season, intensity and quality of agrotechnical tillage, soil water, cultivated plant, fertilizer etc. (Moraru and Rusu, 2012). Soil respiration leads to CO_2 emissions from soil to the atmosphere, in significant amounts for the global carbon cycle (Moraru et al., 2010).

Tillage practices influence soil physical, chemical and biological properties, which in turn may alter plant growth and yield (Czyż, 2011; Feiza et al., 2005; Gus et al., 2008;

http://www.aloki.hu ● ISSN 1589 1623 (Print) ● ISSN 1785 0037 (Online)
DOI: http://dx.doi.org/10.15666/aeer/1704_80118022

Mark and Al-Kaisi, 2004; Moroizumi and Horino, 2002; Natywa et al., 2009; Ozpinar and Cay, 2006; Rashidi and Keshavarzpour, 2009; Ulrich et al., 2006). They also have a significant influence on biological activities (Swędrzyńska et al., 2013; Ghimire et al., 2014) and soil CO_2 efflux (Frank et al., 2006). The soil temperature and its moisture may be affected on soil respiration intensity (Box and Meentemeyer, 1993; Frank et al., 2006; Natywa et al., 2010).

Systems for soil gas measurements offer crucial information regarding production, consumption, and gas transportation, with major implications in quantitative and qualitative assessment of soil respiration and soil aeration (Moraru and Rusu, 2010).

Conventional tillage includes the largest number of soil treatment (Imadi et al., 2016). This method of soil cultivation allows a good aeration of the soil and increases its biological activity (Olesen et al., 2011).

Knowledge about the influence of soil microbial activity and physical properties on soil respiration is insufficient. This indicates a need to conduct research aimed at recognizing and understanding the responses of effect the microbial, biochemical and physical properties on soil efflux under various crop species.

The aim of the present study was evaluation of soil respiration intensity depending on different soil treatment practices and to determine the effect of biology activity on soil respiration.

Materials and methods

Location of experiment

The study was based on the long term field experiment located at the Agricultural Experimental Station (AES) of the Institute of Soil Science and Plant Cultivation – State Research Institute in Grabów (Mazowieckie voivodeship, Poland; 51°23'N; 21°38'E). The experiment has been running since 2004. Experiment involving maize cropped continuously and rotated with other crops. The experimental scheme involved three following treatments:

1. Maize monoculture with direct seeding (zero tillage) (A)
2. Maize monoculture with full ploughing tillage (B)
3. Cultivation in crop rotation with full tillage (C)

Experiment was conducted on a grey brown podsolic soil formed from light loam (USDA soil classification) classified as very good rye complex. The ploughing layer of soil was characterized by low magnesium content, medium potassium content, and high phosphorus content. The size of a plot was 27.0 m^2 at the set-up of the experiment and 21.0 m^2 at harvest. The experiment was established using a long strip design in four replications.

Maize cultivar Delphine, sown at the end of April or at the beginning of May, with a precision seed drill. The fertilization dose of nitrogen amounted to 140 kg $N \cdot ha^{-1}$ (70 + 70 at the six-leaf stage). The doses of phosphorus and potassium for maize were P_2O_5 - 80 $kg \cdot ha^{-1}$ and K_2O - 125 $kg \cdot ha^{-1}$. In the case of crop rotation, all plant species were grown. In all the years of the study, a full dose of manure was used for maize. It was cattle dung containing: 20-22% dry matter, 0.45-0.51% N, 0.12-0.17% P, 0.53-0.59%.

Cv. Antek of spring barley (sown at the first or second decade of April) and cv. Turnia of wheat were seeded. Annual fertilizer rates supplied to barley were 60 N, 35

http://www.aloki.hu ● ISSN 1589 1623 (Print) ● ISSN 1785 0037 (Online)
DOI: http://dx.doi.org/10.15666/aeer/1704_80118022

P_2O_5, and 50 kg ha^{-1} K_2O, and to wheat 120 N, 40 P_2O_5, and 70 kg ha^{-1} K_2O. In order to measure the effects of maize tillage prior to the onset and after termination of the trial we assessed pH in KCl and soil contents (mg per 100 g of soil) of P_2O_5 (CFA method), K_2O (FES method), MgO (AAS method), percentage of total nitrogen (CFA method). The results content yields of maize (plant height, weight of 1000 grains, parameters of maize cobs, plant density of harvest, grain yields of cereals) were published (Księżak et al., 2018).

Soil respiration measurement

Soil respiration (Sr) was measured twice by a model CIRAS-2 apparatus (PP-Systems, USA), portable infrared CO_2 analyzer equipped in Soil CO_2 Flux dynamic closed Chamber. The closed chamber is having a head space volume of 1.17 dm^3, enclose an area of 75.6 cm^2 and was kept inserted into the soil during the measurement. Soil respiration was estimated from the rate of increase in CO_2 in the closed chamber during a 60-s period. The measurements were conducted before sowing of maize (in term 15-25 of April depending on the year of the study) and after harvest (15-25 of October) in four replications. All measurement were done during day time (i.e. 9:00–13:00 a.m.) on rows. Concentration value of carbon dioxide expressed in g $CO_2 \cdot m^2 \cdot h^{-1}$. The measurement range of SRC-1 is 0-9.99 g $CO_2 \cdot m^2 \cdot h^{-1}$. The level of evapotranspiration (E), the differences in carbon dioxide concentration (ΔCO_2), changes in soil moisture (ΔM_B) were also determined.

Soil moisture measurement

The soil moisture (SM, %, v/v) and soil bulky density ($Mg \cdot m^{-3}$) measurements were made on 7 depth level: 0-5, 5-10, 10-15, 15-20, 20-25, 25-30 and 30-35 cm in four replication for each variant of soil tillage, which made by made by weighing and drying method, using cylinders with a volume of 100 cm^3. Soil for the determination of the physical properties was collected during the harvesting of maize for grain. For analysis used mean data of measurement from soil layer 0-30 cm and 30-35 cm.

Soil samples

Soil samples were collected according to Polish Standard PN-ISO 1038-6 (1998). The soil samples in three replicates were taken from the 0-20 cm layer and sieved through a 2 mm sieve and stored in a refrigerator (4 °C) until analysis.

Microbial and biochemical properties

The soil samples were examined for different microorganisms groups. Microbial and biochemical properties analysis was described by Gałązka (2017).

Statistical analysis

Statistical analyses were performed using the Statistica Program PL (10.0). The analysis were carried out using ANOVA method in a proper model for the experimental design. The 95% confidence limit ($P < 0.05$) was chosen to determine the significance of differences between soil respiration and studied parameters of soil chemical and biological properties.

http://www.aloki.hu ● ISSN 1589 1623 (Print) ● ISSN 1785 0037 (Online)
DOI: http://dx.doi.org/10.15666/aeer/1704_80118022

Course of weather conditions were different in the years of study. In Grabów, the total precipitation during the growing period was higher in the first and the second year of the study than the average multi-annual precipitation (by 40 and 33%, respectively) (*Table 1*). In 2010, high precipitation occurred in August and September, while a rain deficit took place in June and July. In 2011, very abundant precipitation was recorded in July (3.5-fold higher than the multi-year average), while a shortage of rainfall occurred in June and August. The third year of the study (2012) was more favourable in terms of the quantity and distribution of precipitations. Same deficits were recorded in May and June (*Table 1*).

Table 1. *Course of weather conditions during the vegetation periods. (Source: Bulletin of State Hydrological and Meteorological Service IMGW-PIB)*

Specification	Year	Month						Sum
		April	May	June	July	August	September	
Rainfalls	**2010**	20.8	114.0	50.7	53.4	155.1	135.7	529.7
	2011	35.9	74.5	52.4	298.8	35.6	3.6	500.8
	2012	37.8	36.5	54.3	81.6	64.2	21.8	296.2
Rainfalls mean from multi-years (mm)		**39.0**	**57.0**	**71.0**	**84.0**	**75.0**	**50.0**	**376.0**
Temperature (°C)	**2010**	9.0	13.9	17.6	21.5	19.9	12.1	15.7
	2011	10.3	13.9	18.5	18.4	18.8	14.7	15.8
	2012	9.6	15.3	17.7	20.9	18.8	14.5	16.1
Temperature mean from multi-years (°C)		**7.7**	**13.4**	**16.7**	**18.3**	**17.3**	**13.2**	**14.4**

Average from years 1871-2000

Results and discussion

Results of the study showed that the highest value of soil respiration, as before sowing as after harvest, was measured under maize cropped in monoculture with full ploughing tillage (C) (*Fig. 1*), while the least one, under maize cropped in the direct sowing system (A). Analysis of variance showed that treatments have significant effect on soil respiration (*Fig. 1*). So that, addition of soil simplification reduced CO_2 emission while addition of soil tillage have influence on soil respiration. The research results obtained by Lamptey et al. (2017) showed that zero-tillage significantly decreased soil respiration compared to conventional tillage. Hryńczuk and Weber (2004) reported higher values of soil respiration in cultivation with full tillage compared to direct sowing. Kordas (2007) and Kordas and Zbroszczyk (2012) reported higher soil biological activity after soil treatment simplification and the least one in traditional cultivation. These authors found that as soil is more simplificated, as biological activity and ability of soil respiration are higher. Analysis showed that higher soil respiration in all cultivation method was recorded after harvest of maize (second term). The differences between terms amounted 25%. Analysis of variance showed that the mean CO_2 emission was significantly influenced by seasons. In the studies by Amos et al. (2005), Lou et al. (2004) and Natywa et al. (2010), the strongest soil respiration activity was at springtime. Wielgosz and Szember (2006) noted a decline in soil respiration in the summer. Amos et al. (2005) and Lou et al. (2004) attributed this result to the increased root respiration as well as to the soil temperature and moisture conditions. Quemada (2001) reported that soil respiration was greatly affected by temperature and

http://www.aloki.hu ● ISSN 1589 1623 (Print) ● ISSN 1785 0037 (Online)
DOI: http://dx.doi.org/10.15666/aeer/1704_80118022

water content. In his study the highest values were obtained in August when high temperatures and water content produced the highest respiration. These results were confirmed also by Frank et al. (2002), Bajracharya et al. (2000) and Mielnick and Dugas (2000). According to Sandor et al. (2011) beginning of summer could also offer good conditions for development of soil microbial biomass which in turn could reach the highest metabolic activity. As Lou et al. (2004) reported high soil temperature is positively correlated with CO_2 flux.

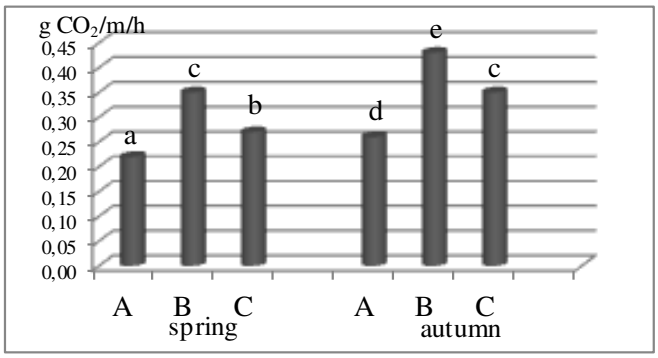

Figure 1. *Soil respiration (Sr) depending on method of soil cultivation (average of the years of the study). Values followed by a different letter are significantly different (P < 0.05)*

The evapotranspiration process was most strongly under maize cropped in monoculture in full tillage, but strongly the least under maize cropped in crop rotation. Significantly higher levels of this parameter were found in date after sowing (*Fig. 2*). The difference between two terms regardless soil tillage amounted to 81%.

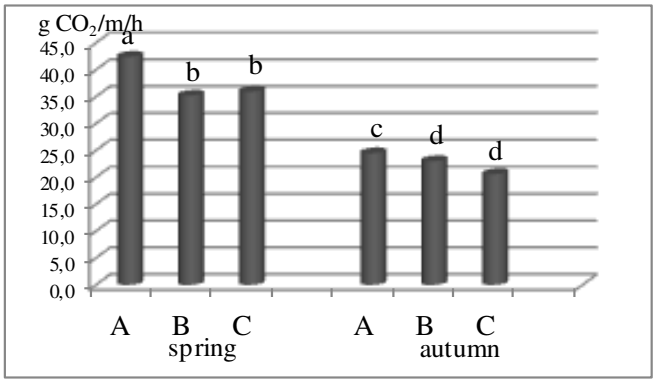

Figure 2. *Evapotranspiration (Sr) depending on method of soil cultivation (average of the years of the study). Values followed by a different letter are significantly different (P < 0.05)*

The differences in carbon dioxide concentration were highest in term after maize sowing. Compared method of soil cultivation, the highest changes in this parameter in both terms were found under maize cropped in monoculture (*Fig. 3*). While the least changes in the changes dioxide concentration were differentiated depend on season. In the first term the least value of this parameter were found under maize cropped in monoculture in full tillage, while in the second term in crop rotation.

http://www.aloki.hu ● ISSN 1589 1623 (Print) ● ISSN 1785 0037 (Online)
DOI: http://dx.doi.org/10.15666/aeer/1704_80118022

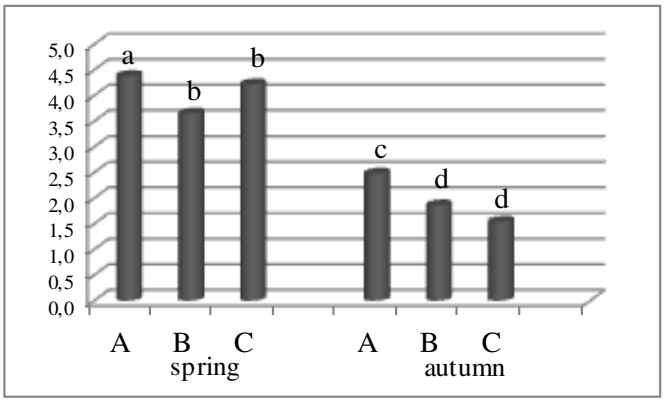

Figure 3. *Changes in carbon dioxide concentration depending on method of soil cultivation (ΔCO_2). Values followed by a different letter are significantly different ($P < 0.05$)*

The highest changes in soil moisture were recorded under maize cropped in direct sowing, while the smallest one in crop rotation (*Fig. 4*). A significant variability was recorded in the changes in soil moisture between method of soil cultivation. In the studies of Lamptey et al. (2017) soil water content increased under no-tillage soils compared with conventional treatment. According to Cook and Orchad (2008) to compare the effect on respiration, a measure of the soil-water status is required.

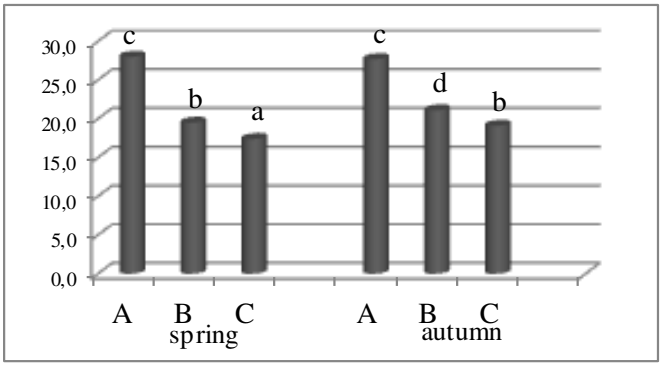

Figure 4. *Changes in soil moisture (ΔMB) depending on method of soil cultivation. Values followed by a different letter are significantly different ($P < 0.05$)*

The soil respiration was correlated with its biological activity and biochemical parameters (*Table 2*). The statistically strongest negative correlation was found between soil respiration and evapotranspiration (-0.495), changes in carbon dioxide concentration (-0.493) and acid phosphatase activity (-0.683), while strongest positive correlation was found between soil respiration and ammonifying bacteria (0.598).

Statistical analysis revealed also that no linear relationship was found between soil respiration and such parameters as: evapotranspiration and changes in carbon dioxide concentration (*Fig. 5a, b*) and biochemical parameters as: soil dehydrogenase activity and acid phosphatase activity (*Figs. 6* and *7*). According to Cook and Orchad (2008) to compare the effect on respiration, a measure of the soil-water status is required.

http://www.aloki.hu ● ISSN 1589 1623 (Print) ● ISSN 1785 0037 (Online)
DOI: http://dx.doi.org/10.15666/aeer/1704_80118022

Dehydrogenase and phosphatase activities are good indicators of changes of soil parameters and widely used microbial parameters of soil biology (Wolińska et al., 2013). Phosphatase can be a good indicator of the mineralization potential of organic phosphorus and soil biological activity. In the studies of Gałązka et al. (2017) the dehydrogenase activity was is in correlation with the increased number of the most examined groups of microorganisms.

Table 2. *The Pearson's correlation coefficient of soil respiration and selected microbiological, chemical and biochemical parameters*

Parameter	Sr	E	ΔCO_2	ΔMb	SM_1	SBD_1	SM_2	SBD_2
Sr	-	**-0.495**	**-0.493**	-0.141	0.242	-0.085	-0.174	0.164
E	**-0.495**	-	**0.788**	0.175	0.111	-0.010	0.100	-0.028
ΔCO_2	**-0.493**	**0.788**	-	0.051	0.236	-0.029	0.237	-0.158
ΔMb	-0.141	0.175	0.051	-	-0.004	0.096	0.003	-0.004
SM_1	0.242	0.111	0.236	-0.004	-	-	-	-
SBD_1	-0.085	-0.010	-0.029	0.096	-	-	-	-
SM_2	-0.174	0.100	0.237	0.003	-	-	-	-
SBD_2	0.164	-0.028	-0.158	-0.004	-	-	-	-
DEH	-0.348	-0.189	-0.323	0.422	-0.086	0.177	-0.208	0.077
AcP	**-0.684**	0.383	0.237	**0.542**	0.266	0.273	0.150	-0.105
AlP	0.182	0.353	0.302	-0.029	0.192	0.101	0.186	-0.320
B + A	0.264	**-0.624**	**-0.667**	0.000	-0.120	0.235	-0.142	-0.208
F	0.027	-0.237	-0.336	0.320	**-0.354**	0.384	-0.440	0.036
AM	**0.598**	**-0.612**	**-0.587**	0.040	-0.233	0.104	-0.177	-0.160
OLIGO	0.274	-0.383	**-0.477**	0.083	**-0.486**	0.085	-0.451	-0.040
KOP	-0.013	-0.375	**-0.534**	0.324	**-0.483**	**0.459**	**-0.556**	0.043

Values in bold are statistically significant ($P \leq 0.05$)
Sr: soil respiration (g $CO_2 \cdot m \cdot h^{-1}$), E: evapotranspiration (g $CO_2 \cdot m \cdot h^{-1}$), ΔCO_2: changes in carbon dioxide concentration, ΔMb: changes in soil moisture, SM_1: soil moisture in 0-30 cm soil layer (%, v/v), SBD_1: soil bulk density in 0-30 cm soil layer ($Mg \cdot m^{-3}$), SM_2: soil moisture in 30-35 cm soil layer (%, v/v), SBD_2: soil bulk density in 30-35 cm soil layer ($Mg \cdot m^{-3}$), (DHA: soil dehydrogenase activity DHA (ug formazan·g DM of soil·24 h^{-1}), AcP: acid phosphatase (ug p-nitrophenol·g DM^{-1} of soil·h^{-1}), AlP: alkaline phosphatase (ug p-nitrophenol·g DM of soil·h^{-1}), B + A: total bacteria and Actinomycetes number (10^7), CFU: colony forming units,·g DM^{-1}: dry matter of soil, F: total fungi number (10^4 CFU·g DM^{-1} of soil), AM: ammonifying bacteria (10^4 CFU·g DM^{-1} of soil), OLIGO: total oligotrophic bacteria (10^6 CFU·g DM^{-1} of soil), KOP: total copiotrophic bacteria (10^6 CFU·g DM^{-1} of soil)

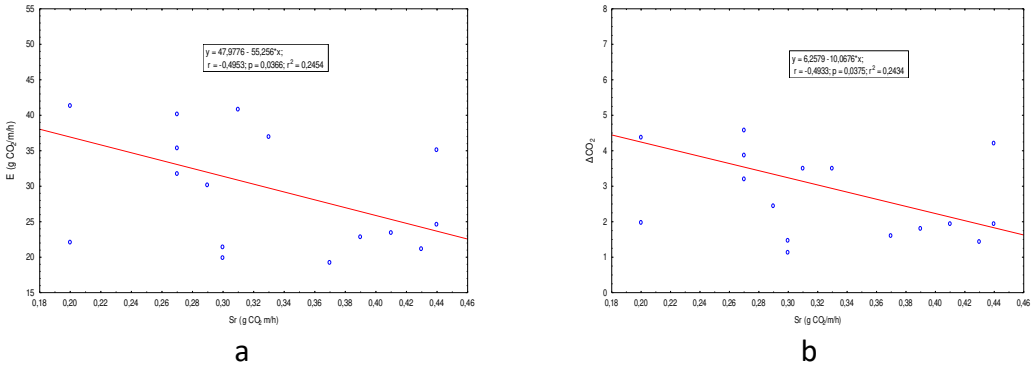

a b

Figure 5. *Relationship between soil respiration (Sr) and (a) evapotranspiration (E), and (b) changes in carbon dioxide concentration soil moisture (ΔCO_2)*

http://www.aloki.hu ● ISSN 1589 1623 (Print) ● ISSN 1785 0037 (Online)
DOI: http://dx.doi.org/10.15666/aeer/1704_80118022

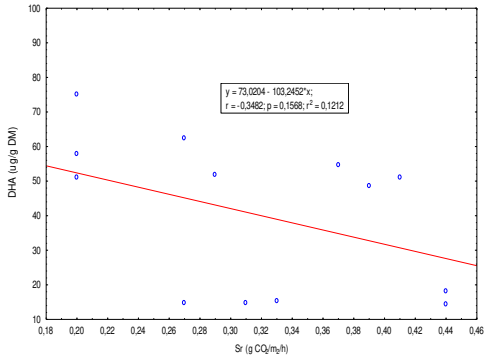

Figure 6. *Relationship between soil respiration (Sr) and soil dehydrogenase activity (DHA)*

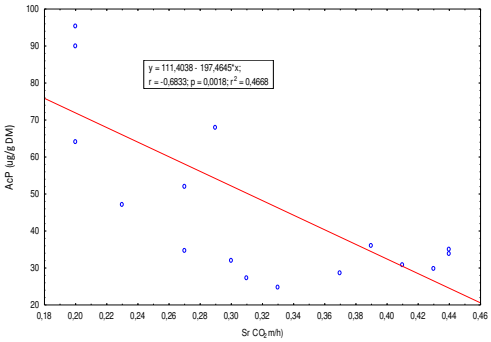

Figure 7. *Relationship between soil respiration (Sr) and acid phosphatase (AcP)*

Soil respiration was not significantly affected by the soil moisture and soil bulk density in 0-30 cm soil layer (*Table 2*). The simple regression analysis showed linear relationship between soil respiration and such parameters as: acid phosphatase activity and ammonifying bacteria (*Figs. 7* and *8*). The strongest relationships was found between soil respiration and acid phosphatase activity, which is confirm by value of coefficient of determination ($R^2 = 47\%$).

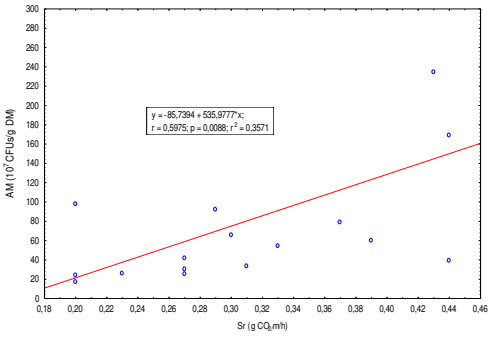

Figure 8. *Relationship between soil respiration (Sr) and ammonifying bacteria (AM)*

The available literature lacks studies on the effect of physical properties on soil respiration. Małecka et al. (2012) found that the no-tillage systems favoured the increase of soil moisture and density, as well as the reduction of capillary water

http://www.aloki.hu ● ISSN 1589 1623 (Print) ● ISSN 1785 0037 (Online)
DOI: http://dx.doi.org/10.15666/aeer/1704_80118022

capacity, especially in the 0-10 cm layer. The studies of Morris et al. (2010) and Raczkowski et al. (2012) indicate the increase in the volume density of soils in the ploughed systems. In own studies, analysis showed that soil bulk density in 0-30 cm soil layer (SBD_1) was significantly affected total copiotrophic bacteria (KOP) (0.459), while soil bulk density in deeper layer (30-35 cm) was not affected any characteristics. Soil moisture in both deep soil layer: 0-30 cm and 30-35 cm (SM_1 and SM_2) was negatively influence on total copiotrophic bacteria (KOP) (-0.483 and -0.556 respectively). Soil moisture in 0-30 cm layer was negatively significantly influence on total fungi number (F) (-0.354) and total oligotrophic bacteria (OLIGO) (-0.486) (*Tab. 2*).

The continuous use of the no-tillage system with crop rotation usually results in an increase of the microbial biomass and decrease in soil respiration, therefore, displaying evident long-term effects on the increase of soil C contents (Valpassos et al., 2001).

Soil respiration refers to microbial decomposition of dead plant residues and soil organic matter (Kuzyakov and Gavrichkova, 2010), which is controlled by soil microbial activities and soil C content. According to Lou et al. (2011) soil microbial activities are influenced by soil physicochemical conditions, such as soil moisture.

Soil moisture was considered by Bonal et al. (2008); Luo and Zhou (2006) and Lou et al. (2011) to be the secondary important factor controlling soil respiration. According to Huang et al. (2014) soil respiration was negatively correlated with soil moisture at high soil moisture content (> 19). According to Zhang et al. (2016) soil respiration was negatively correlated with soil moisture and soil pH. While Chang et al. (2016) reported that soil respiration is mainly controlled by soil temperature and moisture. According to Pietri and Brookers (2009) soil pH also had been proved to be an important factor influencing microbial respiration. The results of Șandor and Opruța (2012) show a relationship between soil moisture and soil respiration. It was suggested (Mielnick and Dugas, 2000) that wet soil at deep depth may counteract the effect of surface dry soil on soil respiration.

Conclusions

The results of soil samples analysis (soil properties and microbial activity) would not provide a complete understanding of the relation between soil properties and soil respiration. However, the values may be used as indicators of changes on soil quality, and parameters such as respiration are sensitive indices to study the effect of crop systems in the soil microbiological environment. Among the studied soil treatments, zero-tillage system exhibited better results for bulk density, soil chemical properties. Our study did not present enough variety to go further in our conclusions, but it confirms the relevance of influence effects between factors.

This study demonstrated that tillage systems under maize influence soil respiration along with soil biochemical, physical and other microbiological properties. Further research is needed to determine the soil respiration in long-time period of field experiment under maize growth in different agricultural management practices.

Acknowledgements. This research did not receive any specific grant from funding agencies in the public, commercial, or not-for-profit sectors.

http://www.aloki.hu ● ISSN 1589 1623 (Print) ● ISSN 1785 0037 (Online)
DOI: http://dx.doi.org/10.15666/aeer/1704_80118022

REFERENCES

[1] Amos, B., Arkebauer, T. J., Doran, J. W. (2005): Soil surface greenhouse gases in an irrigated maize-bazed agroecosystem. – Soil Science Society of America Journal 69: 387-395.

[2] Bajracharya, R. M., Lal, R., Kimble, J. M. (2000): Diurnal and seasonal CO_2-C flux from soil as related to erosion phases in central Ohio. – Soil Science Society of America Journal 64: 286-293.

[3] Bonal, D., Bosc, A., Ponton, S., Goret, J. Y., Burban, B., Gross, P., Bonnefond, J. M., Elbers, J. A. N., Longdoz, B., Epron, D. (2008): Impact of severe dry season on net ecosystem exchange in the neotropical rainforest of French Guiana. – Global Change Biology 14: 1917-1933.

[4] Box, E. O., Meentemeyer, V. (1993): Soil carbon dioxide evolution: environmental controls, world patterns and amounts. – Conference Papers 18 "Geography of organic matter production and decay". IGiPZ PAN, Warszwa, pp. 21-49.

[5] Chang, S. X., Shi, Z., Thomas, R. R. (2016): Soil respiration and its temperature sensitivity in agricultural and afforested poplar plantation systems in northern Alberta. – Biology and Fertility of Soils 52: 629-641.

[6] Cook, F. J., Orchad, V. A. (2008): Relationships between soil respiration and soil moisture – Soil Biology and Biochemistry 40: 1013-1018.

[7] Czyż, E. (2011): Effects of cultivation of maize (*Zea mays* L.) in monoculture and crop rotation on some soil physical properties. – Roczniki Gleboznawcze 62(1): 12-24.

[8] Feiza, V., Irena, D., Danute, S. (2005): Soil Physical and Agrochemical Properties Changes, Weediness and Yield of Crops in Long-Term Tillage Experiment in Lithuania. – Scientific Publication Vol. 48. Agronomy, USAMV, Iasi.

[9] Frank, A. B., Liebig, M. A., Hanson, J. D. (2002): Soil carbon dioxide fluxes in northern semiarid grasslands. – Soil Biology and Biochemistry 34: 1235-1241.

[10] Frank, A. B., Liebig, M. A., Tanaka, D. L. (2006): Management effects on soil CO_2 efflux in northern semiarid grassland and cropland. – Soil & Tillage Research 89: 78-85. DOI: 10.1016/j.still.2005.06.009. www.sciencedirect.com.

[11] Gałązka, A., Gawryjołek, K., Perzyński, A., Gałązka, R., Księżak, J. (2017): Changes in enzymatic activities and microbial communities in soil under long-term maize monoculture and crop rotation. – Polish Journal of Environmental Studies 26: 39-46.

[12] Ghimire, R., Norton, J. B., Stahl, P. D., Norton, U. (2014): Soil microbial substrate properties and microbial community responses under irrigated organic and reduced-tillage crop and forage production systems. – PLoS ONE 9: e103901.

[13] Gus, P., Rusu, T., Bogdan, I. (2008): Factors which impose completing preserving effects of minimum soil tillage systems on arable fields situated on slopes. – 5th International Symposium-Soil Minimum Tillage System, Risoprint, Cluj-Napoca 1: 155-161.

[14] Hanson, P. J., Edwards, N. T., Garten, C. T., Andrews, J. A. (2000): Separating root and soil microbial contributions to soil respiration: a review of methods and observations. – Biogeochemistry 48: 115-146. https://doi.org/10.1023/A:1006244819642.

[15] Hryńczuk, B., Weber, R. (2004): Impact of tillage on the intensity of microbial transformation in soil and plant yield. – Annales UMCS, Sectio E, Agriculture 59(2): 639-648.

[16] Huang, Z., Yu, Z., Wang, M. (2014): Environmental controls and the influence of tree species on temporal variation in soil respiration in subtropical China. – Plant and Soil 382: 75-87.

[17] Imadi, S. R., Shazadi, K., Gul, A., Hakeem, K. R. (2016): Sustainable Crop Production System. – In: Hakeem, K., Akhtar, M., Abdullah, S. (eds.) Plant, Soil and Microbes. Springer, Cham.

[18] Kordas, L. (2007): Wpływ sposobu uprawy roli i nawożenia azotowego na respirację gleby. – Zeszyty Naukowe UP Wrocław, Inżynieria Rolnicza 552: 6: 65-71.

http://www.aloki.hu ● ISSN 1589 1623 (Print) ● ISSN 1785 0037 (Online)
DOI: http://dx.doi.org/10.15666/aeer/1704_80118022

[19] Kordas, L., Zbroszczyk, U. (2012): Wpływ systemu uprawy roli i efektywnych mikroorganizmów (EM) na właściwości biologiczne gleby spod pszenicy jarej uprawianej w krótkotrwałej monokulturze. – Fragmenta Agronomica 29(3): 95-102.
[20] Księżak, J., Bojarszczuk, J., Staniak, M. (2018): Comparison of maize yield and soil chemical properties under maize (*Zea mays* L.) grown in monoculture and crop rotation. – Journal of Elementology 23(2): 531-543. DOI: 10.5601/jelem.2017.22.3.1453.
[21] Kuzyakov, Y., Gavrichkova, O. (2010): REVIEW: Time lag between photosynthesis and carbon dioxide efflux from soil: a review of mechanisms and controls. – Global Change Biology 16: 3386-3406.
[22] Lamptey, S., Li, L., Xie, J., Zhang, R., Luo, Z., Cai, L., Liu, J. (2017): Soil respiration and net ecosystem production under different tillage practices in semi-arid Northwest China. – Plant Soil Environment 63(1): 14-21.
[23] Luo, Y., Zhou, X. (2006): Soil Respiration and the Environment. – Academic Press, San Diego. doi.org/10.1016/B978-0-12-088782-8.X5000-1.
[24] Lou, Y., Li, Z., Zhang, T., Liang, Y. (2004): CO_2 emissions from subtropical arable soils of China. – Soil Biology & Biochemistry 36: 1835-1842.
[25] Lou, Y. L., Liang, W. J., Xu, M. G., He, X. H., Wang, Y. D., Zhao, K. (2011): Straw coverage alleviates seasonal variability of the topsoil microbial biomass and activity. – Catena 86: 117-120.
[26] Małecka, I., Swędrzyńska, D., Blecharczyk, A., Dytman–Hagedorn, M. (2012): Impact of tillage systems for pea production on physical, chemical and microbiological soil properties. – Fragmenta Agronomica 29(4): 106-116.
[27] Mark, A. L., Al-Kaisi, M. (2004): Strip-tillage effect seedbed soil temperature and other soil physical properties. – Soil and Tillage Research 8(1-2): 233-249.
[28] Mielnick, P. C., Dugas, W. A. (2000): Soil CO_2 flux in a tallgrass prairie. – Soil Biology & Biochemistry 32: 221-228.
[29] Moraru, P. I., Rusu, T. (2012): Effect of tillage systems on soil moisture, soil temperature, soil respiration and production of wheat, maize and soybean crops. – Journal of Food, Agriculture and Environment 10(2): 445-448.
[30] Moraru, P. I, Rusu, T., Sopterean, M. L. (2010): Soil tillage conservation and its effect on erosion control, water management and carbon sequestration. – In ProEnvironment ProMediu no. 3(6).
[31] Moroizumi, T., Horino, H. (2002): The effects of tillage on soil temperature and soil water. – Soil Science 167(8): 548-559.
[32] Morris, N. L., Miller, P. C. H., Orson, J. H., Froud-Williams, R. J. (2010): The adoption of non-inversion tillage systems in the United Kingdom and the agronomic impact on soil, crops and the environment. A review. – Soil Tillage Research 108: 1-15.
[33] Natywa, M., Majchrzak, L., Sawicka, A. (2009): Effect of soil tillage system on the enzymatic activity in soil and maize yield. – Ekologia i Technika 17(4): 171-177.
[34] Natywa, M., Ambroży, K., Sawicka, A., Wolna-Maruwka, A. (2010): Aktywność respiracyjna i dehydrogenazowa gleby pod uprawą kukurydzy w zależności od różnych dawek nawozu azotowego. – Nauka Przyroda Technologie, Rolnictwo 4(6): #89.
[35] Olesen, J. E., Trnka, M., Kersebaum, K. C., Skjelvåg, A. O., Seguin, B., Peltonen- Sainio, P., Rossi, F., Kozyra, J., Micale, F. (2011): Impacts and adaptation of European crop production systems to climate change. – European Journal of Agronomy 34: 96-112.
[36] Ozpinar, S., Cay, A. (2006): Effect of different tillage systems on the quality and crop productivity of a clay–loam soil in semi-arid north-western Turkey. – Soil Tillage Research 88(1-2): 95-106.
[37] Pietri, J. A., Brookes, P. (2009): Substrate inputs and pH as factors controlling microbial biomass, activity and community structure in an arable soil. – Soil Biology & Biochemistry 41: 1396-1405.

http://www.aloki.hu ● ISSN 1589 1623 (Print) ● ISSN 1785 0037 (Online)
DOI: http://dx.doi.org/10.15666/aeer/1704_80118022

[38] Polish Standard (1998): PN-ISO 10381-6 Quality of Soil. – Collected samples. Principles of collected and kept of soil samples to the microbiological research in laboratory conditions.
[39] Quemada, M. (2001): Soil respiration 1 year after sewage sludge application. – Biology of Fertility of Soils 33: 344-346.
[40] Raczkowski, C. W., Mueller, J. P., Busscher, W. J., Bell, M. C., McGraw, M. L. (2012): Soil physical properties of agricultural systems in a large-scale study. – Soil Tillage Research 119: 50-59.
[41] Rashidi, M., Keshavarzpour, F. (2009): Effect of different tillage methods on grain yield and yield components of maize (*Zea mays* L.). – International Journal of Agriculture and Biology 9(2): 274-277.
[42] Șandor, M., Opruța, C. (2012): The effects of mineral and organic fertilizers on soil respiration in a potato field. – Bulletin UASVM Agriculture 69(2): 122-127.
[43] Șandor, M., Brad, T., Maxim, C., Toader, C. (2011): The influence of selected meteorological factors on microbial biomass and mineralization of two organic fertilizers. – Notulae Botanicae Horti Agrobotanici Cluj Napoca 39: 107-113.
[44] Schlesinger, H. W., Andrews, J. A. (2000): Soil respiration and the global carbon cycle. – Biogeochemistry 48: 7-20. https://doi.org/10.1023/A:1006247623877.
[45] Swędrzyńska, D., Małecka, I., Blecharczyk, A., Swędrzyński, A., Starzyk, J. (2013): Effects of various long-term tillage system on some chemical and biological properties in soil. – Polish Journal of Environmental Studies 22(6): 1835-1844.
[46] Ulrich, S., Hofmann, B., Tischer, S., Christen, O. (2006): Influence of Tillage on Soil Quality in a Long-Term Trial in Germany. – In: Horn, R. et al. (eds.) Soil Management for Sustainability. IUSS, Catena Verlag, Reiskirchen, pp. 110-116.
[47] Valpassos, M. A. R., Cavalcante, E. G. S., Cassiolato, A. M. R, Alves, M. C. (2001): Effects of soil management systems on soil microbial activity, bulk density and chemical properties. – Pesquisa Agropecuária Brasileira 36(12): 1539-1545.
[48] Wielgosz, E., Szember, A. (2006): Wpływ wybranych roślin na liczebność i aktywność drobnoustrojów glebowych. – Annales UMCS, Sectio E 61: 107-119.
[49] Wolińska, A., Stepniewska, Z., Szymańska, E. (2013): Dehydrogenase activity of soil microorganisms and the total DNA level in soil of different use. – Journal of Agricultural Science and Technology B3: 613-622.
[50] Zhang, Y., Yan, Y., Fu, X., Yang, J., Zhang, S., Xu, S., Tang, Z., Li, Z., Lu, S. (2016): Responses of soil microbial respiration to plantations depend on soil properties in subtropical China. – Journal of Integrative Agriculture 15(6): 1376-1384.

http://www.aloki.hu ● ISSN 1589 1623 (Print) ● ISSN 1785 0037 (Online)
DOI: http://dx.doi.org/10.15666/aeer/1704_80118022

NATURAL REGENERATION DYNAMICS OF WOODY PLANTS IN THE MARANTACEAE FORESTS OF YOKO RESERVE AND ITS SURROUNDINGS

MBANGILWA, M. M.[1] – JIANG, L.C.[1*] – MBAYU, M. F.[2] – TAMBWE, L. E.[3] – BBIDJO, T. V.[4] – NSHIMBA, S. H.[2]

[1]*Key Laboratory of Sustainable Forest Ecosystem Management-Ministry of Education, School of Forestry, Northeast Forestry University, Harbin 150040, China*

[2]*University of Kisangani, Kisangani, DR Congo*

[3]*Higher Institute of Agronomic Studies, Bengamisa, DR Congo*

[4]*Higher Education Institute of Bunia, Bunia, DR Congo*

**Corresponding authors*
e-mail: jlichun@nefu.edu.cn

(Received 6th Jan 2019; accepted 3rd May 2019)

Abstract. Forest areas occupied by Marantaceae show a significant regeneration deficit because of the bulk of foliar and subterranean biomass of these herbaceous plants. The present study evaluates the regeneration dynamics (< 10 cm diameter) of Marantaceae forests by counting and identifying pre-existing regrowth, then their subsistence rate, and finally comparing the potential of regeneration with that of mixed wood forests and that of the *Gilbertiodendron dewevrei* forests (De Wild.) J Leonard. At a confidence level of 95%, a highly significant difference ($F = 120.40$, $p < 2.2e\text{-}16$***) is observed between the averages. These averages are 68.36 ± 40.19 in the Marantaceae of Biaro, 105, 24 ± 84 in the Marantaceae of Yoko Forest Reserve, 435.8 ± 147.3 in the mixed forests and 620, 16 ± 175.55 in the *G. dewevrei* forests at (De Wild.) J Leonard. In addition, regeneration of Marantaceae has a very high mortality rate averaging at 23.22%. This pre-existing deficit and the high mortality rate significantly affects the forest dynamics of the Yoko Forest Reserve and its surroundings. The clear-cut technique of the aboveground and underground biomass of Marantaceae tested during this study is essential for any development of these herbaceous groups, it has increased by an average of $23.5 \pm 7.43\%$ in the plots of 2 m².

Keywords: *aboveground, underground, biomass, Gilbertiodendron dewevrei, Biaro*

Introduction

Regeneration is a vital process in forest ecosystems. It is at the base of the balance and demography of the plant population and the rejuvenation of the stand following the disappearance of mature trees by windfall or exploitation. These populations of the future result either from pre-existing regrowth or vegetative potential, or from pre-existing seeds or edaphic seminal potential, and finally, seeds arriving from the outside after opening of the cover or external potential (Alexander, 1982, 1989; N'dja et al., 2010).

Two meanings are attributed to the expression of natural regeneration. The first expresses the process in which the tropical forest reproduces itself naturally. It refers to the meaning of dynamics. The second, which is often used by foresters, corresponds to all the seedlings, strands and seedlings existing in a stand. It refers to the statistics of regeneration potential in a forest stand (Oldeman, 1990; Puig et al., 1989, 1992; Puig, 2001). More than 10% of the forests in the Yoko Forest Reserve are infested with

http://www.aloki.hu ● ISSN 1589 1623 (Print) ● ISSN 1785 0037 (Online)
DOI: http://dx.doi.org/10.15666/aeer/1704_80238035

Marantaceae herbaceous plants. In that zone the regeneration of woody trees seems very limited. The foliage biomass of these herbaceous species is screened to limit the substantial penetration of the luminous flux into the soil and their very perennial rhizomes in the basements constitute real obstacles to the flowering of the seedlings in an area intended for sustainable conservation forest resources.

This study evaluates the dynamics of regeneration at counting thresholds (< 10 cm) of Marantaceae forests by counting and identification, then their mortality rate, and finally, compares the regeneration potential of these herbaceous plants with that of mixedwood forests and that of *Gilbertiodendron dewevrei* forests (De Wild.) J Leonard on the same topological sequence.

Materials and methods

Study area

The present study was conducted in the forests around Kisangani, specifically in the Yoko Forest Reserve located in the Tshopo province, the community of Bakumu-Mangongo, Ubundu territory and more particularly in experimental plots of Biaro (*Fig. 1*), in east of the Democratic Republic of Congo.

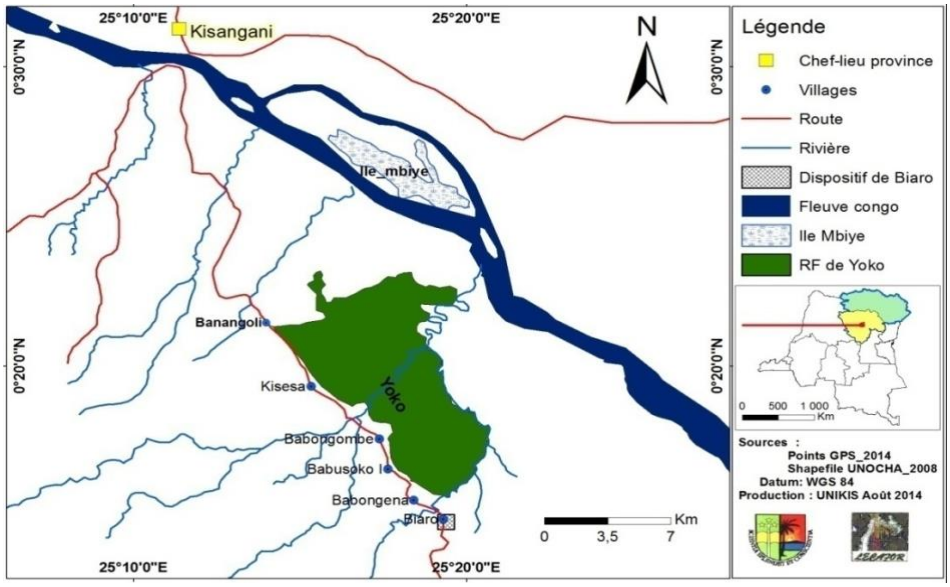

Figure 1. *Location of the Yoko Forest Reserve and the Biaro plots*

It is governed by the ordinance n° 52/104 of the 28/02/1959 of the Ministry of the Environment, Nature Conservation and Sustainable development. It is a private property of the Congolese Institute for the Conservation of Nature accordance to the ordinance - law no. 75-023 of July 1975 of the Ministry of the Environment establishing a public company of the State for the purpose of managing certain public environmental institutions as modified and supplemented by the ordinance-law n° 78-190 of May 05, 1988.

The Yoko Forest Reserve is located on North longitude: 00° 17’ 59” and East: 025° 17’ 4” between 400 and 500 m altitude. The Biaro device is located ± 10 km south of the Yoko Forest Reserve on North Longitude 00° 12.27’ 1” and East 025° 20.0’ 4” between 420-530

http://www.aloki.hu ● ISSN 1589 1623 (Print) ● ISSN 1785 0037 (Online)
DOI: http://dx.doi.org/10.15666/aeer/1704_80238035

m. The average temperature is 25 °C and the annual average rainfall is 1750 mm. It is located between 23 and 45 km points of the road and the Kisangani-Ubundu railway. The Yoko River, which crosses this concession, divides it into two blocks, of which the North block with 3,370 ha and the South block with 3,605 ha represent an overall area of 6,975 ha (Lomba and Ndjele, 1998). Vegetation in the reserve is composed of mixed forest, sometimes sparse, forests of Marantaceae and rattan, monodominant forests of *Gilbertiodendron dewevrei* (De Wild.) J. Leonard, and secondary forests (Lomba, 2012).

Methods

The equipment used consists of a vernier caliper to measure seedling diameters, metric ribbons to size plots and study plots, a GPS to collect geographic coordinates. The biological material is made from consisted of woody seedlings less than 10 cm in diameter. Full counting and identification of vegetative potential at counting threshold of diameter < 10 cm was carried out in the 50 m² plots stratified in 10 m² plots in the Marantaceae of the Yoko Forest Reserve and Biaro. To compare the pre-existing regrowth potential of Marantaceae with that of *Gilbertiodendron dewevrei* (De Wild.) J. Léonard and mixedwood forests, plots of identical size were delineated in these stands. The geographical coordinates of the sites in study are shown in *Table 1*.

Table 1. *Coordinates and altitudes of the study areas*

Study areas	Informations	Altitude (m)
Marantaceae Forest RF Yoko	N00° 18' 42.6'' E025° 17' 31.0''	435
Marantaceae Forest of Biaro	N00° 12' 05.9'' E025° 17' 20.05''	456
Mixed forest	N00° 18' 27.9'' E025° 17' 40.4''	466
Gilbertiodendron dewevrei Forest	N00° 18' 02.2'' E025° 17' 49.9''	456

Assisted regeneration was tested in the Marantaceae of the Yoko Forest Reserve. The technique consisted of clear cutting of aboveground biomass and rhizome extirpation in plots of 40 m² stratified in 2 m² plots. All seedlings were counted and marked. Two months later, a recount was done.

Data processing was based on the few botanical characterization indices (Doucet, 2003):

$$\text{Relative frequency of a species} = \frac{frequency\ of\ a\ species}{\sum frequencies\ of\ all\ species} \times 100 \quad \text{(Eq.1)}$$

$$\text{Abundance (\%)} = \frac{Number\ of\ individuals\ of\ the\ species}{Number\ of\ individuals\ of\ all\ species} \times 100 \quad \text{(Eq.2)}$$

$$\text{Dominance (\%)} = \frac{Basal\ area\ of\ the\ species}{Total\ basal\ area} \times 100 \quad \text{(Eq.3)}$$

$$\text{Relative importance: } I_r = \frac{D_r + D_{or} + F_r}{3} \quad \text{(Eq.4)}$$

http://www.aloki.hu ● ISSN 1589 1623 (Print) ● ISSN 1785 0037 (Online)
DOI: http://dx.doi.org/10.15666/aeer/1704_80238035

The annual mortality rate (March 2013 - March 2014) is evaluated from the Madron relationship (1993): $TM(\%) = 100x[1 - Nt/No]^(1/t)$, where: TM = mortality rate, t = duration of the calculation period, N_0 = starting workforce and N_t = number of survivors after t years. Four plots of 200 m² divided into plots of 100 m² were delimited in the East, West and South of the forest reserve of Yoko Biaro were followed.

The comparison of the averages was done by the ANOVA test. As for the ANOVA, Tukey's post-hoc test at $p < 0.05$ was used to detect the differences between the different averages taken two by two. The Shapiro-Wilk test was used initially to check the normality of the data. The comparison of the two averages was done by Student's t-test. The comparison of the proportions between the diameter classes was carried out with the test of $\chi^2 = \sum_{i=1}^{k} \frac{(ni-ti)^2}{ti}$., where ni = number of individuals observed in class i; t_i = number of theoretical individuals in class i; k = class number of the qualitative variable ($k \geq 2$) and i = class number of the qualitative variable ($1 \leq I \leq k$).

The different tests and their significance were provided by the R version 2.10.0 software.

Results

Potential for woody seedlings of Marantaceae, mixedwood and Gilbertiodendron dewevrei forests (De Wild.) J. Léonard

The average densities of woody seedlings at counting thresholds of < 10 cm diameter, for a 95% confidence interval in Marantaceae forests, mixedwood forests and *Gilbertiodendron dewevrei* (De Wild.) J. Leonard forests are arranged in descending order (*Fig. 2*): 69.36 ± 40.19 6 < 105.24 ± 89 < 435.8 ± 147.39 < 620.16 ± 170.55 respectively, in the Marantaceae of the Yoko (MarRFY), the Marantaceae of Biaro (MarBia), the mixed forests and the forests to *Gilbertiodendron dewevrei* (De Wild.) J. Leonard (FDM and FDG).

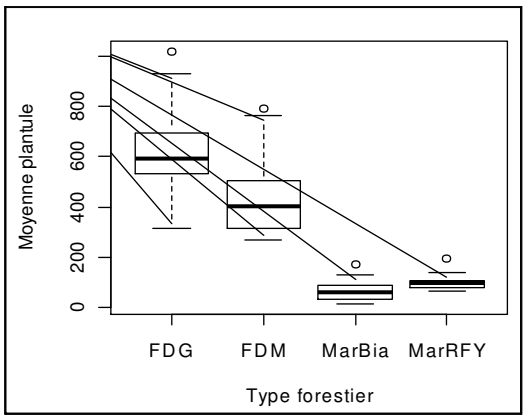

Figure 2. *Dispersion of seedling density values of Marantaceae, mixedwood and Gilbertiodendron dewevrei forests (De Wild.) J. Léonard*

The highly significant difference is observed between the different groups (F = 120.40, $p < 2.2e-16$***), and is not significant between the Yoko Forest Reserve of Marantaceae and the Biaro forest of Marantaceae (Tukey: $p > 0.05$), highly significant

http://www.aloki.hu ● ISSN 1589 1623 (Print) ● ISSN 1785 0037 (Online)
DOI: http://dx.doi.org/10.15666/aeer/1704_80238035

between Marantaceae and mixedwood forests and between Marantaceae and *Gilbertiodendron dewevrei* forests (De Wild.) J. Leonard (Tukey: $p < 0.01$).

Mortality rate in Marantaceae forests

The mortality rate is studied in the East, West and South Marantaceae of the Yoko Forest Reserve and at Biaro (*Table 2*). In each site, two plots of 10 m² were monitored. A count was made in each plaza on March 10, 2012 and a recount on March 10, 2013.

Table 2. *Mortality rate of woody seedlings in Marantaceae forests*

Site	Number of seedlings		
	2012	**2013**	**Mortality rate (%)**
Ouest Marantaceaa RF Yoko 1	136	73	46.32
Ouest Marantaceaa RF Yoko 2	136	116	14.71
East Marantaceaa RF Yoko 1	44	26	40, 91
East Marantaceaa RF Yoko 2	94	66	29.79
South Marantaceaa RF Yoko 1	93	62	29.79
South Marantaceaa RF Yoko 2	115	93	19.13
Biaro 1 Marantaceaa	130	104	20
Biaro 2 Marantaceaa	64	61	20
Average	101.5 ± 34.26	75.14 ± 28.53	23.22 ± 12.26

The mortality rate varies from one site to another. It is higher in the Marantaceae of the Yoko Forest Reserve where it varies from 46.32% to 4.71% whereas it varies from 20.00% to 4.69% in Biaro.

Specific richness and index of importance of woody seedlings

The species richness and the importance index (*Table 3*) calculated in the different sites on equivalent areas equal to 2,500 m².

Table 3. *Temperament and index of importance of woody seedlings of Marantaceae forests*

Species	Temperament	De r (%)	Dor (%)	Fr (%)	IVI
North Mar					
Barteria nigritaina Hooker	TO	10.75	35.02	10.73	56.51
Aidia micrantha (K. Schum.) F. White	TO	9.84	10.32	9.82	29.98
Scaphopetalum thonneri De Wild. & Th. Dur.	TO	9.61	3.02	9.61	22.24
Pycnanthus angolensis (Welw.) Exell	HNP	4.58	5.43	4.58	14.59
Staudtia kamerunensis Warb	TO	5.03	3.27	5.03	13.33
Marantaceae: Eastern Forest Reserve of Yoko					
Xylia ghesquierei Robyns	HNP	10.8	8.03	10	28.83
Staudtia kamerunensis Warb	TO	8.33	7.16	8.3	23.79
Campylospemum sp	TO	7.41	2.47	7.41	17.29
Trilepisium madagascariense DC	TO	6.17	2.25	6.17	14.59
Pycnanthus angolensis (Welw.) Exell	HNP	5.56	1.6	5.56	12.72

http://www.aloki.hu ● ISSN 1589 1623 (Print) ● ISSN 1785 0037 (Online)
DOI: http://dx.doi.org/10.15666/aeer/1704_80238035

Marantaceae: Western Forest Reserve of Yoko					
Myrianthus preussii Engler	HP	3.7	7.74	44.58	56.02
Scaphopetalum thonneri De Wild. & Th. Dur.	TO	13.51	8.05	13.51	35.07
Pycnanthus angolensis (Welw.) Exell	HNP	8.5	8.95	8.5	25.95
Turraeanthus africanus (Welw.) Pellegr.	TO	9.37	5.98	9.37	24.72
Trilepisium madagascariense DC	TO	5.66	2.12	5.66	13.44
Marantaceae: Western Forest Reserve of Yoko					
Scaphopetalum thonneri De Wild. & Th. Dur.	TO	14.99	9.97	14.73	39.69
Rinorea oblongifolia (C.H. Wright) Marquand ex Chipp	HNP	8.89	13.81	9.5	32.19
Olax gambecola Bailon	TO	4.73	7.65	4.65	17.03
Alchornea floribunda Mull. Arg	HNP	4.54	3.13	4.56	12.23
Aidia micrantha (K. Schum.) F. White	TO	3.55	3.97	3.49	11.01
Marantaceae Biaro					
Thomandersia hensii De Wild. & Th. Dur.	TO	16.67	26.34	21.66	64.67
Rinorea oblongifolia (C.H. Wright) Marquand ex Chipp	HNP	5.07	4.55	6.69	16.31
Petersianthus macrocarpus (P. Beauv.) Liben	TO	3.86	5.8	5.1	14.76
Aidia micrantha (K. Schum.) F. White	TO	3.86	5.69	4.78	14.33
Olax gambecola Bailon	TO	3.14	4.21	4.14	11.49

HNP = non-pioneering heliophile, TO = shade tolerant, HP = pioneer heliophile, Dr = relative density, Dor = relative dominance, Fr = Relative frequency, IVI = importance index

The most important woody seedlings vary from one site to another: *Barteria nigritiana* Hooke (IVI = 56.51) is more important in the northern *Marantaceae*, *Xylia ghesquierei* Robyns (IVI = 28.83) in the Marantaceae of the East, *Myrianthus preussii* Engler (IVI = 56.02) in the western Marantaceae, *Scaphopetalum thonneri* De Wild & Th Dur (IVI = 39.69) in the southern Marantaceae and *Thomandersia hensii* De Wild. & Th Dur (IVI = 64.67) is more important in the Marantaceae of Biaro.

The majority of regenerating seedlings in Marantaceae forests are shade tolerant (TO) species. Some light species appear intermittently in the sites (*Pycnanthus angolensis* (Welw.) Warb., *Rinorea oblongifolia (C.H Wild) Marquand ex Chipp, Xylia ghesquierei* Robyns *and Alchornea floribunda Mull.* Arg.

Diametric distribution dynamics of seedlings in Marantaceae forests

Diameter frequencies (*Table 4*) by seedling neck diameter class were measured in the Marantaceae of the North, South, East and West of the Yoko Forest Reserve and in Biaro on equivalent areas of 500 m^2 stratified in 5 plots (10 m × 10 m).

The frequency of seedlings per diameter class in five sites is low in classes > 1-1 cm, it goes up a notch in classes 1-2 cm, then an asymmetrical decrease begins to be observed from classes 2-3 cm. The independence test χ^2 applied to compare the diametric structures indicates that there is a "site" effect, ($\chi^2 = 308.81$, df = 32, $p < 0.01$). Calculating the contributions (%) of χ^2 from each diameter class to the total χ^2 statistic shows that the classes (1-2, 2-3, > 1-1, 3-4, 6-7 and 4-5) contribute the most to this difference.

Residue analysis shows that in classes (1-2 cm), the size of southern Marantaceae individuals is larger and contributes the most to the significant difference of χ^2 total obtained. The numbers of the Northern Marantaceae classes 2-3, 4-5 and 6-7 are larger

http://www.aloki.hu ● ISSN 1589 1623 (Print) ● ISSN 1785 0037 (Online)
DOI: http://dx.doi.org/10.15666/aeer/1704_80238035

and contribute the most to the significant difference of χ^2 total obtained. In classes (> 1-1) the numbers of western Marantaceae are larger and contribute the most to the significant difference of χ^2 total obtained. In the class (3-4), the number of Marantaceae de Biaro individuals is larger and contributes the most to the significant difference of χ^2 total obtained. To correctly interpret the degeneracy observed in the diameter classes, the frequencies of the five most important species were followed (*Fig. 3*).

Table 4. *Seedling frequency by site and diameter class (cm)*

Dbh (cm)	MarRFYE	MarRFYW	MarRFYS	MarRFYN	MarBia
>1-1	64	97	38	58	48
1-2	142	197	325	110	74
2-3	32	57	54	109	63
3-4	14	58	26	46	50
4-5	17	9	15	35	26
5-6	18	8	21	24	16
6-7	10	5	5	23	17
7-8	7	5	10	12	6
8-9	11	6	11	12	11
Average	35 ± 43.79	49.11 ± 65.57	56.11 ± 102.01	47.46 ± 38.13	47.67 ± 38.13
CV (%)	125.1	131.87	181.78	79.99	70.04

MarRFYN = Marantaceae North Yoko Forest Reserve, MarRFYE = Yoko Forest Reserve East Marantaceae, MarRFYW = Marantaceae West Yoko Forest Reserve, MarRFYS = South Marantaceae Yoko Forest Reserve, MarBia = Marantaceae of Biaro

It is observed that shade tolerants (TO), which are mainly larger (*Table 3*), show a positive asymmetry for the most part. This is the case of *Barteria nigritiana* Hooker, *Scaphopetalum thonnerii* De Wild & Th. Dur, *Campylospermum sp*, *Trilepisium madagascariense* DC, *Turraeanthus africanus* (Welw. Ex C.DC.) Pellegr, *Olax Gambecola* Bailon, *Thomandersia hensii* De Wild. & Th. Dur. The species *Aidia micrantha* (K. Schum.) F. White has, in addition to the structure with positive asymmetry, an irregular frequency. It is the same for *Petersianthus macrocarpus* (P. Beauv.) Liben.

Non-pioneer heliophiles (HNP) exhibit variable behavior, sometimes a right-handed distribution or an irregular distribution. This is the case of *Pycnanthus angolensis* (Welw.) Warb. A symmetrically positive structure is also observed in *Rinorea oblongifolia* (C.H. Wright) Marquand ex Chipp and *Myrianthus preussii* Engler, the only pioneering heliophile *Alchornea floribunda* Mull. Arg presents, unlike all other species, an increase of the numbers in the initial classes > 1-1 cm and 1-2 cm, which decreases appreciably subsequently, from the intermediate classes. Finally, *Xylia ghesquierei* Robyns is the only species that has the classical L-shaped structure. A large number of individuals are observed in the initial classes, whereas it decreases as the diameter increases. It is the only species with good regeneration.

Assisted regeneration

The assisted regeneration (*Table 5*) was followed in 10 plots of 2 m² divided into two plots in the West, East and South sites of the Yoko Forest Reserve and Biaro.

http://www.aloki.hu ● ISSN 1589 1623 (Print) ● ISSN 1785 0037 (Online)
DOI: http://dx.doi.org/10.15666/aeer/1704_80238035

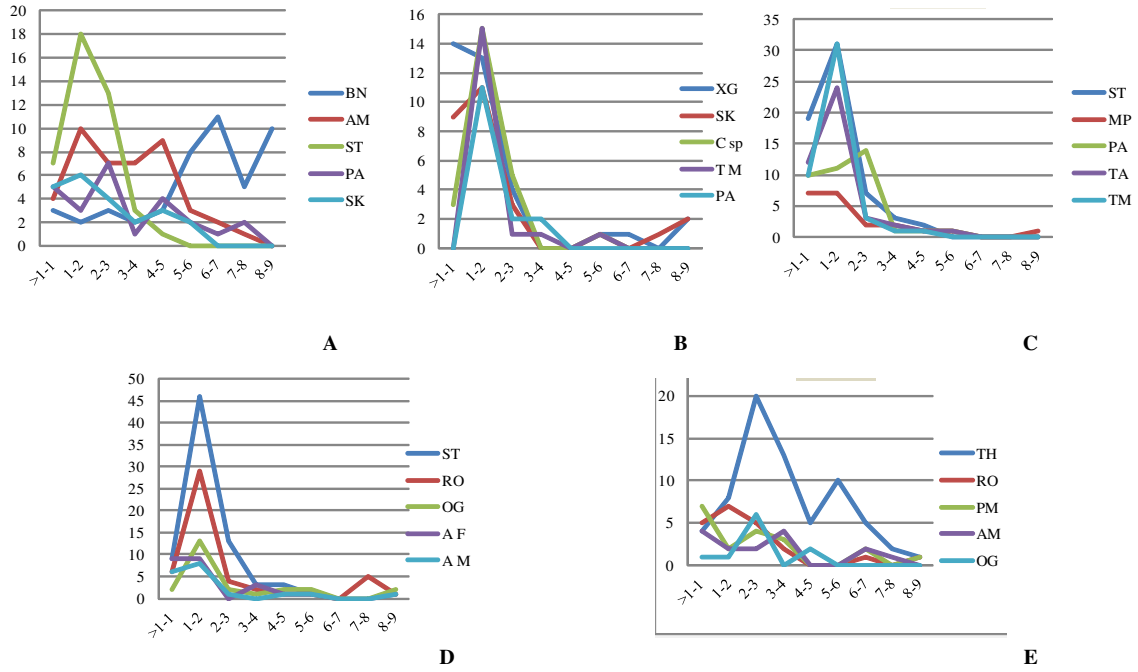

Figure 3. *Distribution dynamics of woody seedlings (diameter < 10 cm) by diameter class of the most important species in Marantaceae forests. (A = Marantaceae North Yoko Forest Reserve, B = Marantaceae East Yoko Forest Reserve, C = Marantaceae West Yoko Forest Reserve, D = Marantaceae South Yoko Forest Reserve, E = Biaro Marantaceae, BN = Barteria nigritiana, MA = Aidia micrantha, ST = Scaphopetalum thonnerii, SK = Staudtia kamerunensis, PA = Pycnanthus angolensis, XG = Xylia ghesquierii, C sp = Campylospermum sp, MP = Myrianthus preussii, TA = Turraeanthus africanus TM = Trilepisium madagascariense, RO = Rinorea oblongifolia = OG: Olax gambecola, AF = Alchornea floribunda TH = Thomandersia hensii PM = Petersianthus macrocarpus)*

Table 5. *Regenerative potential (number of seedlings) before and after clearing of the Marantaceae*

Quadrant	Number of seedlings before thinning	Number of seedlings after thinning	Number of growing seedlings
I	5	30	25
II	19	37	18
III	6	36	30
IV	18	37	19
V	4	39	35
VI	13	33	20
VII	7	31	24
VIII	21	55	34
IX	4	20	19
X	11	25	14
Averages	10.8 ± 43.51	28.9 ± 7.69	23.5 ± 7.43

After clear-cutting of Marantaceae biomass, the number of woody seedlings increased from an average of 10.8 ± 43.51 to 23.5 ± 7.43 for a confidence level of 95%.

http://www.aloki.hu ● ISSN 1589 1623 (Print) ● ISSN 1785 0037 (Online)
DOI: http://dx.doi.org/10.15666/aeer/1704_80238035

The mean independence t-test indicates a highly significant difference between the initial density of the seedlings before clear-cutting and the density of newly planted seedlings after clearcutting ($t = 4.2257$, $df = 18$, $p < 0.0005131$***).

Discussion

Regenerative dynamics, mortality rate and neck diameter structure of seedlings in Marantaceae forests

The regeneration of woody plants in forests at Marantaceae is very low. For a confidence level of 95%, the average is 105.24 ± 89 woody seedlings in the Marantaceae of the Yoko Forest Reserve. This average is nearly 5 times less than that of the forests of *Gilbertiodendron dewevrei* (De Wild.) J. Leonard and 4 times lower than that of mixed forests. A lower average (47.67 ± 36.13) was observed in the Marantaceae of Biaro. It is 9 times less than that of *J. dewevrei* (De Wild.) J. Léonard forests and 6 times less inferior to that of mixed forests. A highly significant difference is observed between the different groups (Anova: $F = 120, 40$, $p < 2.2e\text{-}16$***). Considered in pairs, Tukey's post-hoc comparison of multiple averages test showed a highly significant difference between Marantaceae forests and *J. dewevrei* (De Wild.) J. Leonard forests and between them mixed forests ($p < 0.05$***).

In addition, an insignificant difference is observed between the Marantaceae of the Yoko Forest Reserve and the Marantaceae of Biaro ($p > 0.05$). Similar results were observed in Odzala where the regeneration density was very low, ie 10 to 70 stems per 100 m² was observed in the dense Marantaceae forests and 804 to 984 stems per 100 m² in the dry Marantaceae dry forests (Gillet et al., 2008). This deficit justifies the ability of these herbaceous plants to easily dominate the acquired space to the detriment of woody regeneration for long periods (Lejoly, 1996; Kouka, 2004; Gillet et al., 2008).

Several factors allow Marantaceae to compete with other plants to form persistent monodominant shrubs, namely, (i) the production of a dense leaf layer, (ii) the rapid recovery of rhizomes after each disturbance. These powerful branched rhizomes allow them, from a single strain, to extend considerably the scale of their vegetative apparatus and thus to occupy vast spaces, (iii) they arouse the underground competition and the competition for the light with young plants and (iv) their clonal growth (De Foresta, 1990; Brncic, 2002; Vande Weghe, 2004). This resource rivalry prevents the growth of seedling potential and is the cause of a significant mortality rate of 23.23% on average in the Marantaceae of the Yoko Forest Reserve and Biaro.

The inhibition impact of these herbaceous plants does not only affect ligneous plants. In Odzala, Bruguière et al. (2000) and Mbayu (2009) observed a decrease in density of small primates at the same time of 40% with 2.99 troops per km (all species combined). The heaviest monkeys, *Lophocebus albigena* (white-cheeked mangabe) and *Cercopithecus nictitan* (monkey-hog), which preferentially use high forest layers, were more sensitive to canopy opening. Therefore, these impacts suggest that colonization of Marantaceae in a forest area negatively and non-discriminatorily impacts all diversity and may even block the regeneration process (Nepstad et al., 1991).

The frequency degeneration of the pre-existing regrowth in the Marantaceae of the Yoko Forest Reserve and Biaro attests that there is a net "site" effect ($\chi^2 = 308.81$, $dof = 32$, $p < 0.05$). Residue analysis after χ^2 total showed some classes contributed significantly to this difference, this is the case of classes 1-2 cm in the South, 2-3 cm, 4-

http://www.aloki.hu ● ISSN 1589 1623 (Print) ● ISSN 1785 0037 (Online)
DOI: http://dx.doi.org/10.15666/aeer/1704_80238035

5 cm and 6-7 cm and the class > 1-1 cm west of Yoko Forest Reserve and 3-5 cm class in Biaro. In all cases, it is observed that the extreme classes 1-1 cm, 4-5 cm and 8-9 cm have a low density compared to the intermediate classes 1-2 cm and 3-4 cm). This positive asymmetry distribution suggests a weak regeneration apparently related to disturbances in the environment (Puig, 2001). Such a structure is different from the structure observed in humid dense forests where the frequencies of individuals in classes ranging from 1 to 10 follow the exponential type law (Puig, 1989 et al, Puig, 1992; N'dja, 2010).

The 5 most important species that were tracked for frequency in the diametric classes showed that shade-tolerant species (TOs) had a positive asymmetric structure. This is the case of *Barteria nigritiana* DC, *Scaphopetalum thonnerii* DC, *Campilospermum sp*, *Trilepisium madagascariense* DC, *Turraeanthus africanus* (Welwc ex C.DC.) Pellegr., *Olax gambecola* Muell. Arg, *Thomandersia hensii* De Wild. & Th. Dur. The species *Aidia micrantha* (K. Schum.) F. White has in addition to the bell structure, an irregular structure. The irregular structure is also observed for the species *Petersianthus macrocarpus* (P. Beauv.) Liben. On the other hand, non-pioneer heliophiles (HNP) show a very variable behavior, sometimes an irregular structure, this is the case of *Pycnanthus angolensis* (Welw.) Excell, sometimes a positive asymmetric structure in *Rinorea oblongifolia* (CHWright) Marquant ex Chipp, *Myrianthus preussii* Engler and *Alchornea floribunda* Mull. Arg. have, unlike other heliophiles, an increase in numbers in the initial classes>1-1 cm and 1-2 cm which decrease significantly from intermediate classes. The species *Xylia ghesquierei* Robyns is the only species with an exponential-like structure characteristic of dense moist forest species (Rollet, 1974).

The analysis of the structure of a tropical rainforest shows this structural variability according to species, genera or families. This variation reflects in most cases the temperament of the species (Puig, 2001). This behavior is explained by the fluctuation of the luminous flux in the mass of Marantaceae leaves. The ligneous trees show variable behavior in the light. At a young age, they have specific peculiarities relating to their growth and gregariousness. This behavior would lead to types of structures much more varied than the general structure of the L-shaped stand more or less erect, truncated or asymmetric bell, S more or less stretched, or having a spread distribution and almost independent of the diameter (Puig, 1992).

Light plays a fundamental role in the germination of the seminal potential of the soil and the growth of pre-existing recruits. The variations in its intensity and the composition of its spectrum influence the growth, production and productivity of forest ecosystems and indirectly its structure. The decrease in intensity that occurs varies depending on the canopy, the leaf motion and the angle of incidence of the sun's rays (Hall et al., 1981; Puig et al., 1989; Clark, 1990).

Assisted regeneration in Marantaceae forests

Forests in Marantaceae are considered ecosystems whose regeneration and evolution are extremely slow and deficient due to the almost inextricable coverage of their surface leaf masses and rhizomes in the soil (Brugière et al., 2000; Brncic, 2002). Nevertheless, the clear-cut regeneration of aboveground and underground biomass of these giant herbaceous plants in a few plots during this study increased the density of pre-existing recruits. Overall, for all species combined, an increase in woody seedlings averaged 23.5 ± 7.4%. This increase suggests that the seminal potential of the soil that was

http://www.aloki.hu ● ISSN 1589 1623 (Print) ● ISSN 1785 0037 (Online)
DOI: http://dx.doi.org/10.15666/aeer/1704_80238035

dormant beneath the Marantaceae mass of leaves found an optimal luminous flux that allowed it to begin germination (Rey, 1997).

Assisted regeneration was tested in the Marantaceae in Congo Brazza by Gillet in (2013) in order to reinvigorate the deficient regeneration of pre-existing heliophilous species inventoried and identified and then cleared of neighboring competing vegetation. Similarly, nursery seedlings were introduced to maintain linear density in all 4 m. This silviculture has resulted in remarkable performances. The species *Canarium schweinfurhii* Engl, *Ricinodendron heudoloti*i (Baillon) Pierre ex Hecke, *Terminalia superba* Engler & Diels *Nauclea diderrichii* (De Wild. & T. Durand) Sea, followed for a year, showed an average growth of between 124 cm and 154 cm. The most successful planted species was *Triplochiton scleroxylon* K. Schum, which grew at a height of 95 cm in a single year.

Numerous interventions based on silvicultural improvement for the management of natural stands have been carried out. These are natural forest interventions in which the silviculturist sought to promote the growth of valuable species in order to valorize and order the forest for its good management (Dupuy, 1989). In Yangambi in the Tshopo Province, several tests were carried out by INERA since colonial times. However, as everywhere in Africa, methods for natural regeneration with more than one canopy opening provided very uncertain results because of the variability of application conditions, the problem of light dosing, the costs of the work, the number of intervention and spread of work over time. But these operations, which remain the only way to develop dense tropical forests, have been abandoned in the process (CTFT, 1989).

In this study, testing of assisted regeneration in Marantaceae forests was not intended to favor any category of species. It was essentially a question of observing the behavior of the potential of the pre-existing recrudescence of the seminal potential in the face of light. The results showed that the forests at Marantaeae abound with an important seminal potential that was waiting for light to initiate their germination. In addition, the potential for pre-existing regrowth exhibited an optimal growth performance after the addition of the luminous flux for two less tests. But it will be necessary to point out that for this prosperous regeneration, it will have to go beyond the carpet of the herbaceous plants which approach them thus to try to slow their development by an optimal closure of the tree cover (Gillet, 2003).

Conclusion

The impact of Marantaceae forests on woody regeneration in the Yoko Forest Reserve and surrounding area is significant. These herbaceous plants substantially inhibit the regeneration and growth of the potential of pre-existing recrudescence and seminal potential. This impact results in a significant reduction in the density of woody seedlings compared with mixed forests and *Gilbertiodendron dewevrei* (De Wild.) J. Leonard forests. In addition, under the conditions of highly increased competition, growing recruits have a significant mortality rate of around 23.22% on average. The few species that regenerates in these herbaceous Marantaceae are mostly shade tolerant and some heliophiles with a structure unfortunately bell or irregular attesting a weak regeneration.

The assisted regeneration test carried out in this study allowed the penetration of an optimal luminous flux which triggered the germination of the seminal potential and

http://www.aloki.hu ● ISSN 1589 1623 (Print) ● ISSN 1785 0037 (Online)
DOI: http://dx.doi.org/10.15666/aeer/1704_80238035

stimulated the growth of pre-existing recruits. This silvicultural technique is the means of management to reinvigorate regeneration in the Marantaceae forests of the forest reserve.

For future research conducted in and around the Yoko Forest Reserve, we suggested that:

- Studies of permanent assisted regeneration are undertaken based on species growth and silviculture of fast-growing species is practiced and assisted in infested areas.
- Soil and dynamics studies on the annual rate of occupation of the herbaceous species are initiated and conducted.
- Anthracological studies are densified and systematically deepened in the different forest groupings of the Yoko Forest Reserve and surrounding areas to understand the history of the stands in the region.

Agroforestry techniques are popularized and monitored in the riparian communities of the Yoko Forest Reserve and surrounding areas. This integrated land management practice will help contain the practices of clearing that favor the proliferation of hegemonic herbs throughout the region to the detriment of forest dynamics.

REFERENCES

[1] Alexander, D. Y. (1982): Study of the illumination of the undergrowth of a dense humid forest evergreen (Tai, Ivory Coast). – Acta Oecologica, Oecol. Gener 4(30): 407-447.

[2] Alexander, D. Y. (1989): Dynamics of Natural Regeneration in Dense Forest of Ivory Coast. Study and Theses. – ORSTOM, Paris.

[3] Brncic, T. (2002): Ecology and patch dynamics of Megaphrynium macrostachym (Beth) M. Read (Marantaceae) in the south-west Central African Republic. – Doctoral Thesis. Oxford Forestry Institute and Linacre College, Oxford.

[4] Brugière, D., Bougras, S., Gautier-Hion, A. (2000): Forest dynamics and the colonization process-extinction: fauna-flora relationships in the Marantaceae forests of Odzala National Park. – Ecofac Report 2000: 1-10.

[5] Clark, D. B. (1990): The Role of Disturbance in the Regeneration of Neotropical Moist Forests. – In: Bawa, K., Hadley, M. (eds.) Reproductive Ecology of Tropical Forest Plants. Parthenon, Nashville, TN, pp. 291-305.

[6] CIRAD-CTFT - FRA. 1989. Forester's Memento. Paris: Ministry of Cooperation and Development, 1266 p. (Rural Techniques in Africa) ISBN 2-11-084874-X

[7] De Foresta, H. (1990): Origin and Evolution of Intramayambian Savannahs (R. P. Congo). – In: Lafranchi, R., Schwartz, D. (eds). II. Contributions of Forest Botany. ORSTOM, Paris, pp. 326-335.

[8] Doucet, J. L. (2003): The delicate alliance of forest management and biodiversity in the forests of central Gabon. – PhD Thesis, University Faculty of Agricultural Sciences of Gembloux, Belgium.

[9] Dupuy, B. (1998): Bases for silviculture in tropical moist tropical forest. – Forafri Series, 1998, Document CIRAD-Forêt, Montpellier, pp 1-10.

[10] Gillet, J. F., Missamba-Lola, A. P., Ngalouo, B. (2008): Analysis Report Dynamic Forest Component. – CIB FFEM project “Monitoring the dynamic forest program - agroforestry - wildlife inventories” under the FFEM grant under the financing agreement No CCG 1071.01 A.

[11] Hall, J. B., Swaine, M. D. (1981): Distribution and Ecology of Vascular Plants in a Tropical Rain Forest. Forest Vegetation in Ghana. – W. Junk, The Hague.

http://www.aloki.hu ● ISSN 1589 1623 (Print) ● ISSN 1785 0037 (Online)
DOI: http://dx.doi.org/10.15666/aeer/1704_80238035

[12] Kouka, L. A. (2004): Regeneration of woody species in forest of Odzala National Park (Congo-Brazzaville). – Acta Botanica Gallica 151(1-3): 293-309.
[13] Lejoly, J. (1996): Use of transect methods for the study of biodiversity in the Ngotto Forest Conservation Area (RCA). – Technical Report: ECOFAC Project, Agreco-CTFT.
[14] Lomba, B.L., Ndjele, M-B. (1998): Using the transect method for the study of phytodiversity in the Yoko Reserve (Ubundu, DR Congo). – Annals (11), Fac. Sci. UNIKIS, 35-46 pp.
[15] Lomba, B. L. (2012): Systems of aggregation and diametric structures according to the temperaments of some species in the permanent devices of Yoko and Biaro (Ubundu, Orientale Province, R. D. Congo). – Thesis F. Sc, University of Kisangani.
[16] Madron, D. L. (1993): Mortality, chablis and the role of holes in sylvigenesis before and after exploitation on the Paracou, French Guiana forestry study system. Ph.D. thesis. – ENGREF Nancy / CIRAD-Forest, 203 pp. - annexes.
[17] Mbayu, M. F. (2009): Comparative distribution of Laccosperma secundiflorum (P. Beauv.) Wendl, Eremospatha haullevilleana De Wild. and E. cabrae De Wild. In the REAFOR system of the Yoko Forest Reserve (Eastern Province) DR Congo. – DEA, F. Sc., University of Kisangani.
[18] N'dja, J. K., Ake-Assi, E., Tiebre, M. S. (2010): Plant biodiversity and speed of regeneration of the Sanaimbo classified forest (Côte d'Ivoire). – Science & Nature 7(2): 195-206.
[19] Nepstad, D., Uhl, C., Serrão, E. A. S. (1991): Recuperation of a degraded Amazonian landscape: forest recovery and agricultural restoration. – Amb. 20: 248-255.
[20] Oldeman, R. A. A. (1990): Forest: Elements of Silvology. – Springer-Verlag, Berlin.
[21] Puig, H. (1992): Forest regeneration. – Adventure Collection, Paris.
[22] Puig, H., Forget, P. M., Sist, P. (1989): Dissemination and regeneration of some trees in the Guyana tropical forest. – Bulletin of French Society 136, Actualité.
[23] Puig. H. (2001): Humid Dense Tropical Forest. – Belin, Paris.
[24] Rey, B. (1997): Consideration of forest dynamics in the context of multifunctional management of woodlands. – XI World Forestry Congress 2: 10, Antalya, Turkey, 13-22 October.
[25] Rollet, B. (1969): Natural regeneration in dense evergreen lowland forest of Venezuelan Guiana. – Woods and Forests of Tropics 124: 19-38.
[26] Vande Weghe, J. P. (2004): Forests of Central Africa, Nature and Man. – Ecofac, Tielt Belgium.

http://www.aloki.hu ● ISSN 1589 1623 (Print) ● ISSN 1785 0037 (Online)
DOI: http://dx.doi.org/10.15666/aeer/1704_80238035

METAL LEVELS IN WATER AND THE MUSCLE TISSUE OF FISHES IN THE CACHORROS RIVER, SÃO LUÍS ISLAND, STATE OF MARANHÃO, BRAZIL

SANTOS, D. C. C.[1] – AZEVEDO, J. W. J.[2,3] – FERREIRA, H. R. S.[4] – FRANÇA, V. L.[1] – SOARES, L. S.[1] – PINHEIRO, J. R. JR.[2] – REBÊLO, J. M. M.[3] – SILVA, M. H. L.[3] – CASTRO, A. C. L.[1,2*]

[1]Programa de Pós-Graduação em Saúde e Ambiente, Universidade Federal do Maranhão (UFMA), Av. dos Portugueses, 1966, 65085-580, São Luís, Maranhão, Brasil (phone: +55-98-3272-8563)

[2]Departamento de Oceanografia e Limnologia, Universidade Federal do Maranhão (UFMA), Av. dos Portugueses, 1966, 65085-580, São Luís, Maranhão, Brasil (phone: +55-98-3272-8561)

[3]Programa de Pós-Graduação em Biodiversidade e Biotecnologia da Amazônia Legal – Rede Bionorte, Doutorado, Universidade Federal do Maranhão (UFMA), Av. dos Portugueses, 1966, 65085-580, São Luís, Maranhão, Brasil (phone: +55-98-3272-8563)

[4]Programa de Pós-Graduação em Oceanografia, Mestrado, Universidade Federal do Maranhão – UFMA, Av. dos Portugueses, 196665085-580, São Luís, Maranhão, Brasil (phone: +55-98-3272-8563)

**Corresponding author*
e-mail: alec@ufma.br; phone: +55-98-3272-8563

(Received 9th Jan 2019; accepted 22nd Feb 2019)

Abstract. The present study evaluates physicochemical variables, perform a microbiological analysis as well as determine heavy metal concentrations in the water and muscle tissue of fishes from the Cachorros River. The analysis of metal concentrations in the estuarine water revealed high levels of Fe and Al, with values above the limits established by Brazilian legislation. The concentration of total coliforms and thermotolerant coliforms tended to be higher in the rainy season. Regarding metal concentrations in the muscle tissue of fishes, high levels of Pb and Cd were found, especially in carnivorous and detritivorous species, with values above the limits established by national legislation. Two-factor analysis of variance revealed that only Pb demonstrated a significant interaction between seasonality and the feeding habits of the fish fauna, with higher concentrations of this metal in the dry season among detritivorous species in comparison to herbivorous species. The present findings demonstrate the contamination pattern that has been occurring in the Cachorros River, as evidenced by the concentration of trace metals in both the water and muscle tissue of fishes, which are an important source of protein as well as an economic resource for the population of this river basin.
Keywords: *estuarine fish, metal levels, microbiological contamination, physicochemical variables, health risk*

Introduction

A large portion of the world's population lives in urban centers near estuarine coastlines, which places anthropogenic pressure on water resources due to the demands and wastes of such populations (Cunha et al., 2005; Carmo et al., 2011; Barbosa, 2006). It is estimated that approximately 75% of the world's population will be living within 160 km of a coastline by the year 2025 (Moura, 2009). Thus, urbanization and

http://www.aloki.hu ● ISSN 1589 1623 (Print) ● ISSN 1785 0037 (Online)
DOI: http://dx.doi.org/10.15666/aeer/1704_80378047

industrialization have made the issue of the contamination of aquatic environments increasingly critical (Simões, 2007; Curcho, 2009). In Brazil, disorderly urbanization, the increase in the population and the indiscriminate construction over of natural areas have led to progressive environment degradation, which is directly associated with the health status of populations that reside around affected areas (Sanches Filho et al., 2013).

Estuaries and coastal regions are often used for the disposal of urban and industrial effluents, leading to the contamination of freshwater and marine life by diverse pollutants. From the public health standpoint, the degree of contamination of these ecosystems poses a risk to the river communities that use such water for the purposes of aquaculture, recreational fishing and leisure activities (Castro, 2009).

Pollution by trace metals constitutes a major source of contamination in aquatic environments. These elements are non-biodegradable and tend to accumulate in the tissues of living organisms, the consequences of which include the decimation of the biota and the intoxication of living beings throughout the food chain, which can eventually reach humans (Castro et al., 1999). Trace metals are chemically highly reactive, which explains the difficulty in finding these metals in their pure state in nature, since concentrations are normally very low and associated with other chemical elements.

Estuarine pollution can be evaluated by an analysis of trace metals found in the water, sediment and aquatic organisms. The characteristics of teleost fish, such as the rate at which they accumulate metals, abundance, sampling ease and adequate size for tissue analysis, make these organisms effective indicators of pollution in estuarine environments.

According to Lins et al. (2010), the close relationship between water quality and numerous illnesses that affect populations is widely known. It is therefore necessary to determine the source, mechanism of action and consequences of contaminants in aquatic environments. Exposure to industrial waste can affect human health in the form of headaches, nausea, skin irritation and lung irritation as well as serious reductions in neurological and hepatic functions (Moraes and Jordão, 2002). Thus, there is a need for research directed at the acquisition of knowledge regarding the environmental transformations that stem from the contamination of aquatic ecosystems as well as implications regarding the health of surrounding communities to assist in decision-making processes and the formulation of effective management policies.

The aims of the present study were to evaluate physicochemical variables, perform a microbiological analysis and determine heavy metal concentrations in the water and muscle tissue of fishes from the Cachorros River in the city of São Luís, state of Maranhão, Brazil.

Materials and methods

A large part of the watersheds on São Luis island concentrate industrial activities developed in the city of São Luís, state capital of Maranhão in northeastern Brazil. The Cachorros River is the largest estuarine river basin in the southeastern portion of the island, covering an area of 63.7 km² (*Fig. 1*), most of which is in the rural zone and near large industrial enterprises, such as the Itaqui Port Complex, ENESA and VALE, as well as smaller enterprises, such as slaughterhouses and mining activities. The river empties into the Coqueiro Strait in front of the ALUMAR port, where materials used in

http://www.aloki.hu ● ISSN 1589 1623 (Print) ● ISSN 1785 0037 (Online)
DOI: http://dx.doi.org/10.15666/aeer/1704_80378047

the production of aluminum (bauxite, coke, tar, coal and lye) are unloaded and alumina loading operations occur (Castro, 2009).

The estuary of the river is considered extremely important to the populations of the villages Parnauaçu, Cajueiro, Porto Grande, Limoeiro and Taim that conduct fishing activities and use the estuary for other purposes, such as navigation and recreation (Carvalho, 2011). The watershed also has mineral reserves for use in civil construction, such as sand and clay, which supply the internal market. However, mineral extractions are in need of greater control in terms of public power, as these raw materials are removed without planning or authorization (Castro and Pereira, 2012).

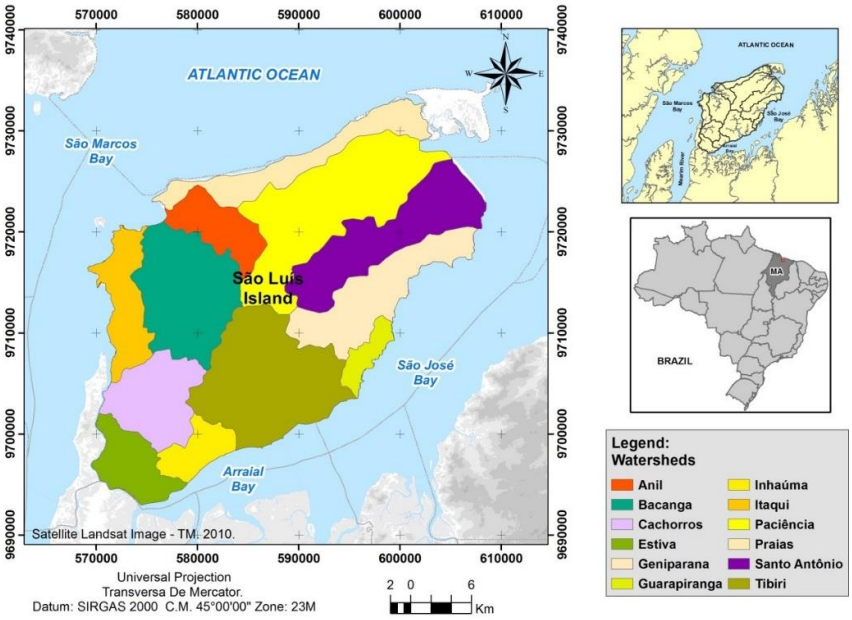

Figure 1. *Map of watersheds on São Luís Island, Maranhão, Brazil*

The evaluation of water quality involved the determination of physicochemical variables, a microbiological analysis and the determination of concentrations of heavy metals (Al, Fe, Zn, Cu, Cd and Pb). Four sampling campaigns were conducted in the rainy and dry seasons. Sampling was performed bimonthly from April to November 2014 at three points spatially distributed along the salinity gradient (*Fig. 2*). The coordinates of the sampling points were determined using of a Global Positioning System: Point 1 – 0571470/9704228; Point 2 – 0574746/9704786; and Point 3 – 0576841/9704838.

At each sampling point, water temperature (°C), pH, dissolved oxygen ($mg.L^{-1}$) and conductivity ($mS.cm^{-1}$) were recorded using a HANNA HI 9828 multi-parameter kit. Turbidity (UNT) was determined using a HANNA HI 93703 turbidimeter and water transparency (cm) was determined using a SECCHI disc. Water samples were also collected 50 cm from the surface in duly labeled 500-mL glass recipients for the subsequent determination of dissolved metals. Nitric acid (1 mL) was added to each sample to maintain the physicochemical properties of the water (APHA, 2012). The samples were placed in a cooler with ice and transported to the lab for storage under refrigeration. For the subsequent analyses, an aliquot (100 mL) was removed from each sample and placed on a hot plate for chemical digestion until reaching a volume of

http://www.aloki.hu ● ISSN 1589 1623 (Print) ● ISSN 1785 0037 (Online)
DOI: http://dx.doi.org/10.15666/aeer/1704_80378047

20 mL. Five mL of nitric acid were added every 15 min to facilitate the digestion. The samples were diluted to 100 mL with de-ionized water and filtered with a fiberglass filter with a porosity of 0.45 μm. Readings were performed in an atomic absorption spectrophotometer with a graphite furnace (SpectrAA24OZ). Other water quality variables were determined following the Standard Methods for the Examination of Water and Wastewater (APHA, 2012). The collection methods and preservation of the samples followed the ABNT NBR 9897 and ABNT NBR 9898 guidelines, which stipulate the conditions for the sampling of domestic and industrial liquid effluents, sediments and water samples from receiving bodies of water.

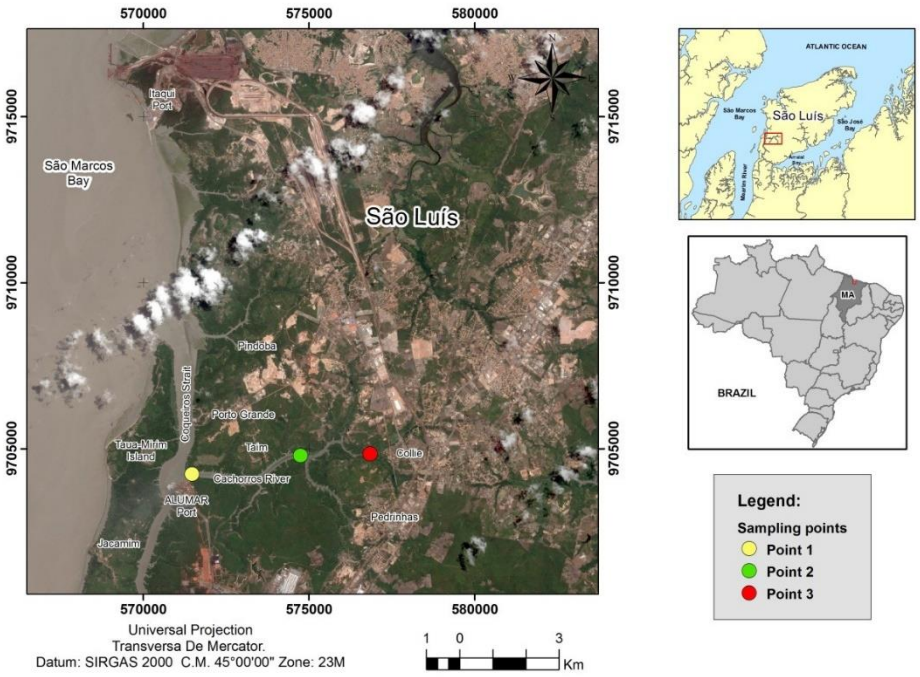

Figure 2. *Map of sampling points*

For the microbiological analysis, water samples were collected approximately 50 cm from the surface, placed in sterilized beakers with a capacity of 250 mL and transferred in coolers to the Microbiology Lab of the Federal University of Maranhão (Brazil). The multiple tube method was used for the determination of the most probable number (MPN) of total and thermotolerant coliforms as well as the identification of *Escherichia coli* following the methods established by the American Public Health Association (APHA, 2005).

Fish species were acquired from local fishermen, stored in plastic packages and transported under refrigeration to the lab. The muscle tissue was removed and weighed to form five replicates of approximately 4 g each. The samples were dehydrated for 24 h at 105 °C and digested with nitric acid + water ($HNO_3 + H_2O$) (1:1) and 150 μL of octanol ($C_8H_{18}O$) following the recommendations proposed by Carvalho et al. (2000). The extracts were analyzed at the Soil Lab of Maranhão State University (Brazil) using atomic absorption spectrophotometry for the trace metals Al, Fe, Zn, Cu, Cd and Pb. The determination of the elemental concentrations was performed through analyses of the ash obtained by dry digestion after complete decomposition of the muscle tissue, as

http://www.aloki.hu ● ISSN 1589 1623 (Print) ● ISSN 1785 0037 (Online)
DOI: http://dx.doi.org/10.15666/aeer/1704_80378047

adapted from Jones and Case (1990) and Perkin-Elmer (1973). The solutions were analyzed in an inductively coupled plasma atomic emission spectrophotometer (model 720-ES, VARIAN). Specific calibration curves were used for each element and all analyses were conducted in triplicate. The blank reading was performed ten times to calculate the quantification limit (LQ) and the detection limit (LD) of the equipment, which were calculated considering the mean white signal plus 10 times the standard deviation (SD) for LQ and the mean white signal plus 3 times standard deviation (SD) to LD,, according to definition and criteria established by the IUPAC (1997). The entire analytical procedure was tested for both measurement precision and accuracy in order to assess the degree of reliability which can be allocated to the data generated by this investigation. The precision of the method was established by a calculation of the between assay variation coefficients from data of ten independent analyses.

One-way analysis of variance (ANOVA) was used for the spatiotemporal comparison of the variables. In cases of significant values, Tukey's test was used for the association between sampling months and points. Levene's test was used to assess the equality of variances. Feeding habits of the species were defined based on information in Fishbase (Froese and Pauly, 2009) and two-way ANOVA was employed to determine possible associations between the concentration of metals in the muscle tissue of the fishes and both local seasonality and trophic level.

Results and discussion

The distribution of dissolved metals in estuarine environments depends on the behavior of physicochemical variables and their controlling mechanisms. Many studies have demonstrated that the partition of trace metals between particulate and dissolved phases depends on factors such as pH, salinity, temperature, redox potential, dissolved organic carbon and the composition of suspended particulate matter (Hatje et al., 2003). The samples from the Cachorros River demonstrated quite homogenous physicochemical aspects on the spatial scale, with no statistically significant differences among the sampling points (ANOVA; $p > 0.05$). On the temporal scale, a differentiation pattern was found for nearly all physicochemical variables ($p < 0.05$). These differences mainly occurred when comparing the rainy months (April and June) to the dry months (September and November). *Tables 1* and *2* display descriptive statistics and the results of Tukey's test for the physicochemical variables in the study area on both temporal and spatial scales, respectively.

Table 1. *Mean and standard deviation (± SD) values and coefficient of variation (CV) for physicochemical variables in Cachorros River according to sampling month*

Variable	April		June		September		November	
	Mean ± SD	CV	Mean ± SD	CV	Mean ± SD	CV	Mean ± SD	CV
Water temperature (°C)	29.9 ± 0.17^{a}	0.58	29.3 ± 0.15^{b}	0.52	28.7 ± 0.2^{c}	0.69	28.2 ± 0.51^{c}	1.02
pH	7.9 ± 0.16^{abc}	2.09	7.9 ± 0.11^{abc}	1.44	8.2 ± 0.21^{b}	2.53	7.8 ± 0.29^{c}	0.74
Conductivity (mS/cm)	29.0 ± 2.71^{a}	9.35	19.3 ± 1.01^{b}	5.26	43.1 ± 3.49^{c}	7.98	49.1 ± 0.06^{c}	3.60
Salinity	17.9 ± 1.91^{a}	10.71	29.1 ± 1.31^{b}	4.5	27.6 ± 2.48^{b}	8.99	32.3 ± 1.27^{b}	6.19
Total dissolved solids (mg/L)	14.6 ± 1.46^{a}	10.00	40.2 ± 29.8^{a}	74.07	21.7 ± 1.83^{a}	8.46	31.4 ± 2.89^{a}	3.69
Transparency (cm)	58.0 ± 11.26^{a}	19.43	13.3 ± 7.57^{b}	56.79	$51{,}0 \pm 10.53^{a}$	20.66	32 ± 1.15^{ab}	39.03
Dissolved oxygen (mg/L)	5.2 ± 0.44^{abc}	8.46	5.4 ± 0.35^{abc}	6.57	4.3 ± 1.03^{b}	23.75	6.6 ± 12.49^{c}	9.10

Same letters on same line indicate statistical equality and different letters indicate significant differences

http://www.aloki.hu ● ISSN 1589 1623 (Print) ● ISSN 1785 0037 (Online)
DOI: http://dx.doi.org/10.15666/aeer/1704_80378047

Table 2. *Mean and standard deviation (± SD) values and coefficient of variation (CV) for physicochemical variables in Cachorros River according to sampling point*

Variable	POINT 1		POINT 2		POINT 3	
	Mean ± SD	CV	Mean ± SD	CV	Mean ± SD	CV
Water temperature (°C)	29.1 ± 0.70 [a]	2.42	29.1 ± 0.75 [a]	2.57	28.9 ± 0.79 [a]	2.74
pH	8.1 ± 0.21 [a]	2.53	8.0 ± 0.22 [a]	2.74	7.9 ± 0.09 [a]	1.21
Conductivity (mS/cm)	37.2 ± 13.70 [a]	36.82	35.3 ± 14.05 [a]	39.73	32.8 ± 12.85 [a]	39.11
Salinity	28.3 ± 5.79 [a]	20.45	26.8 ± 6.52 [a]	24.29	24.9 ± 6.36 [a]	25.51
Total dissolved solids (mg/L)	35.6 ± 24.48 [a]	68.71	20.0 ± 9.18 [a]	45.79	25.3 ± 11.04 [a]	43.65
Transparency (cm)	35.5 ± 26.75 [a]	75.36	43.0 ± 25.47 [a]	59.23	37.2 ± 10.37 [a]	27.84
Dissolved oxygen (mg/L)	5.9 ± 0.81 [a]	13.6	5.4 ± 0.98 [a]	18.08	4.8 ± 1.07 [a]	22.37

In the water column, concentrations of dissolved trace metals tend to vary by several orders of magnitude due to the large number of variables involved in the dynamics of the process, such as daily and seasonal variations in water flow, local discharges of urban and industrial effluents, variations in pH and redox conditions, detergent concentrations, salinity and temperature (Förstner and Wittmann, 1983). Despite these variations, the determination of concentrations of dissolved metals in water is a useful tool for the evaluation of the degree of contamination of a given ecosystem that has been employed by researchers throughout the world (Garbarino et al., 1995; Hurley et al., 1995, 1998; Marjanovic et al., 1995; Watras et al., 1995; Smith et al., 1996; Mastrine et al., 1999).

The analysis of metals in the estuarine water of Cachorros River revealed Fe and Al with values higher than the limits established by Brazilian legislation throughout all sampling months and points. The concentration of Cu was high at all sampling points only in September. Concentrations of Pb, Cr and Cd remained below the detection limit throughout the study (*Table 3*).

Table 3. *Concentrations of heavy metals ($mg.L^{-1}$) in Cachorros River (limits established by CONAMA Resolution 357/05 in bold)*

Month	Sampling point	Heavy metals ($mg.L^{-1}$)						
		Pb	Cr	Cd	Fe	Zn	Al	Cu
April	P1	< 0.01	< 0.01	< 0.005	0.108	< 0.01	0.409	< 0.005
	P2	< 0.01	< 0.01	< 0.005	0.11	< 0.01	0.386	< 0.005
	P3	< 0.01	< 0.01	< 0.005	0.158	< 0.01	0.487	< 0.005
June	P1	< 0.01	< 0.01	< 0.005	0.807	< 0.01	1.51	< 0.005
	P2	< 0.01	< 0.01	< 0.005	0.365	< 0.01	0.585	< 0.005
	P3	< 0.01	< 0.01	< 0.005	0.433	< 0.01	1.05	< 0.005
September	P1	< 0.01	< 0.01	< 0.005	0.0409	0.0105	0.0775	0.0276
	P2	< 0.01	< 0.01	< 0.005	0.429	< 0.01	0.371	0.0222
	P3	< 0.01	< 0.01	< 0.005	0.114	< 0.01	0.109	0.0192
November	P1	< 0.01	< 0.01	< 0.005	0.819	< 0.01	0.967	< 0.005
	P2	< 0.01	< 0.01	< 0.005	0.349	< 0.01	0.633	< 0.005
	P3	< 0.01	< 0.01	< 0.005	0.732	< 0.01	1.2	< 0.005
Limit - CONAMA Resolution 357/05		**0.21**	**1.1**	**0.04**	**0.3**	**0.12**	**0.1**	**0.005**

http://www.aloki.hu ● ISSN 1589 1623 (Print) ● ISSN 1785 0037 (Online)
DOI: http://dx.doi.org/10.15666/aeer/1704_80378047

Total and thermotolerant coliforms ranged from 23 to 2400 MPN.100 mL^{-1}, with the highest values in June (rainy season). *E. coli* was also detected in June, extending through to September at all sampling points. *E. coli* was only detected at Point 3 in November and was absent from all sampling points in April (*Table 4*).

Table 4. *Most probable number (MPN) of total and thermotolerant coliforms and identification of E. coli throughout sampling months and points*

Sampling month/points	MPN/100 ml of total coliforms	MPN/100 ml of thermotolerant coliforms	*Escherichia coli*
April			
1	9.3×10^1	9.3×10^1	Absent
2	2.4×10^2	2.4×10^2	Absent
3	1.1×10^3	1.1×10^3	Absent
June			
1	2.4×10^3	2.4×10^3	Present
2	2.4×10^3	2.4×10^3	Present
3	2.4×10^3	2.4×10^3	Present
September			
1	9.3×10^1	9.3×10^1	Present
2	2.3×10^1	2.3×10^1	Present
3	2.4×10^2	2.4×10^2	Present
November			
1	2.3×10^1	2.3×10^1	Absent
2	2.3×10^1	2.3×10^1	Absent
3	4.6×10^2	4.6×10^2	Present

According to Schenone et al. (2014), fishes are good indicators of pollution by trace metals and can be used for the identification of the potential risk for human consumption. Fishes living in polluted waters can accumulate toxic trace metals through the food chain to levels that can compromise human health.

The determination of the concentration of metals in the muscle tissue of fishes caught in Cachorros River revealed Mn and Cd only in the dry season, occurring in three species. Mn was only detected in *M. curema*, whereas concentrations of Cd were found in the muscle tissue of both *C. acoupa* and *S. herzbergii* at levels above the limit established by Collegiate Board Resolution 42/13, which imposes greater restrictions in comparison to other Brazilian resolutions. Levels of Zn and Cu were higher, but below the limits established by Brazilian legislation. Zn was found in all species sampled and Cu was found in all except *G. luteus* and *M. curema*. Higher concentrations of these elements were found in the rainy season. Pb was the only metal analyzed with values above the limits established by all Brazilian legislation, with significantly higher values in the dry season for all species.

Although there are no national laws regulating the concentrations of Fe or Al in the muscle tissue of fishes, high values were found in both the rainy and dry seasons. Fe levels were highest in *G. luteus* and *C. microlepidotus* in the rainy season, whereas the highest level in the dry season was found in *M. curema*, with concentrations twofold higher in comparison to the other species. It was not possible to analyze Al in the rainy season, but the results were notably high in the dry season, especially for *M. curema* and *C. microlepidotus*, both of which had concentrations greater than 180.0 mg.kg^{-1} (*Table 5*).

http://www.aloki.hu ● ISSN 1589 1623 (Print) ● ISSN 1785 0037 (Online)
DOI: http://dx.doi.org/10.15666/aeer/1704_80378047

Table 5. *Concentrations of trace metals in different fish species caught in Cachorros River in rainy and wet seasons (limits established by Brazilian legislation in bold); Feeding habit: D – detritivorous; C – carnivorous; H – herbivorous*

Season	Species	Concentration of metals mg.kg^{-1}							
		Mn	**Zn**	**Pb**	**Fe**	**Al**	**Cu**	**Cd**	**Feeding habit**
Rainy	*P. nodosu*	0	3.6	0.7	4.7	-	6.3	0	D
	S. herzbergii	0	9.5	0.0	9.3	-	1.9	0	D
	G. luteus	0	17.5	0.0	27.1	-	0	0	D
	C. microlepidotus	0	7.3	0.0	28.6	-	2.6	0	C
	M. curema	0	10.3	0.0	4.9	-	0	0	H
Dry	*C. acoupa*	0	5.7	6.4	6.2	69.2	0.04	0.09	C
	C. microlepidotus	0	3.6	8.4	5.1	185.8	0.56	0	C
	S. herzbergii	0	8.5	10.2	5.2	22.2	0.38	0.06	D
	M. curema	0.04	5.0	5.7	14.4	361.9	4.1	0	H
Legislated limit (mg.kg^{-1})		**-**	**50.0[b]**	**2.0[a.b]**	**-**	**-**	**30.0[b]**	**1.0[a.b]**	
				0.30[c]				**0.05[c]**	

[a]ANVISA, Ordinance n° 685, August 27, 1998
[b]BRASIL, Decree n° 55.871, March 26, 1965
[c]Collegiate Board Resolution Nº 42 from 2013

Two-way ANOVA was used to determine significant differences in metal concentrations in the muscle tissue of fishes as a function of season (dry and rainy) and feeding habit (detritivorous, carnivorous and herbivorous). The only significant interaction between factors regarded Pb, as concentrations of this metal were higher in the dry season in detritivorous species in comparison to herbivorous species (*Table 6*).

Table 6. *Results of two-factor ANOVA for evaluation of concentration of Pb as function of season and feeding habit*

Pb (mg.kg^{-1})					
	SumSqrs	**df**	**MeanSqr**	**F**	**p**
Season	126.2	1	126.2	162.7	0.00104
Feeding habit	9.41	2	4.705	6.066	0.08827
Interaction	23.48	2	11.74	15.14	0.02707
Within	2.327	3	0.7756		
Total	139	8			

Knowledge on seasonal variability in the concentration of trace metals in the water and muscle tissue of fishes in estuarine environments is extremely useful to understanding the effects of human actions on transitional ecosystems and the toxicological impact on populations that depend on these fishing resources. Marine fishes constitute an important source of protein and are a representative component of the human diet for a multitude of people who live in the rural zones of coastal cities (Mziray and Kimirei, 2016). The gradual increase in industrialization and urban expansion of the Industrial District of the city of São Luís, which potentiates the

http://www.aloki.hu ● ISSN 1589 1623 (Print) ● ISSN 1785 0037 (Online)
DOI: http://dx.doi.org/10.15666/aeer/1704_80378047

introduction of undesirable amounts of pollutants in the aquatic environment, underscores the need for studies on the determination and quantification of trace metals in different compartments and trophic levels of the aquatic biota.

Besides industrial expansion, the estuarine region of Cachorros River is submitted to other forms of environmental pressure, such as domestic sewage, effluents from agricultural activities and livestock farming and the extraction of sand. However, according to Coimbra (2003), these factors have less importance when compared to the potential risks of contamination due to industrial activities, which affect the quality of aquatic ecosystems, posing potential risks to organisms and an important portion of the local human population that depends on fishing resources as a source of income and food.

Conclusion

The physicochemical variables of the water (temperature, pH, salinity and dissolved oxygen) only demonstrated temporal differences, thereby confirming seasonality as the determinant factor of such variations.

Concentrations of Al and Fe were high in both the water and muscle tissue of the fishes analyzed, although such concentrations could be attributed to natural processes, such as the breakdown of rocks and the transport of soils.

Concentrations of Cu and Pb were high in the water and muscle tissue of fishes, respectively, which raises concerns regarding the potential for the biomagnification of these elements and serious public health risks.

The interaction of season and feeding habits was significant with regard to the concentration of Pb in detritivorous species.

Escherichia coli in the water in June, September and November reveals contamination of a fecal origin due to the absence of adequate sanitation in the rural communities surrounding the Cachorros River.

Besides, further studies are needed to evaluate the extent of heavy metal contamination in sediment and other structures such as gills and liver, as well as whether feeding behavior, habitat preferences and life history patterns could influence heavy metal in fish. This study suggests a contamination of water resource due to the anthropogenic sources and a competent surveillance and monitoring program becomes extremely necessary to any attempt of managing the coastal areas in urbanized regions.

Acknowledgements. This study received financial support from the Fundação de Amparo à Pesquisa e ao Desenvolvimento Científico e Tecnológico do Maranhão (FAPEMA).

REFERENCES

[1] APHA (2005): Standard Methods for the Examination of Water and Wastewater. – APHA; AWWA; WEF, Washington.

[2] APHA (2012): Standard Methods for the Examination of Water and Wastewater. 22th Ed. – American Public Health Association (APHA); American Water Works Association (AWWA); Water Environment Federation (WEF), Washington.

[3] Barbosa, F. G. (2006): Variações temporais e espaciais de nutrientes dissolvidas e metais traço na área portuária da cidade do Rio Grande (Estuário Lagoa dos Patos - RS).

http://www.aloki.hu ● ISSN 1589 1623 (Print) ● ISSN 1785 0037 (Online)
DOI: http://dx.doi.org/10.15666/aeer/1704_80378047

Dissertação (Mestrado em Oceanografia Física, Química e Geológica) – Universidade Federal do Rio Grande, Rio Grande.

[4] Carmo, C. A., Abessa, D. M. S., Neto, J. G. M. (2011): Metais em águas, sedimentos e peixes coletados no Estuário de São Vicente-SP, Brasil. – O Mundo da Saúde 35(1): 64-70.

[5] Carvalho, F. C. (2011): Gestão do território, lugar e conflitos socioambientais: o caso da usina termelétrica Porto do Itaqui em São Luís, MA. – Dissertação (Mestrado em Geografia) - Universidade de Brasília, Brasília.

[6] Carvalho, G. P., Cavalcante, P. R. S., Castro, A. C. L., Rojas, M. O. A. I. (2000): Preliminary assessment of heavy metals levels in Mytella falcata (Bivalvia, Mytilidae) from Bacanga River Estuary, São Luis, State of Maranhão, Northeastern Brazil. – Rev. Brasil. Biol. 60(1): 11-16.

[7] Castro, A. C. L., Garcia, M. R. S., Cavalcante, P. R. S. (1999): Avaliação dos níveis de Cu e Zn no tecido muscular de Mugil gaimardianus (pisces, osteichthyes) no estuário do rio Tibiri. – Boletim do Laboratório de Hidrobiologia 12: 23-47.

[8] Castro, H. F. R., Pereira, E. D. (2012): Cartografia geológico-geotécnica da bacia hidrográfica do rio dos Cachorros. – Revista Geonorte. v. 3. n.4.

[9] Castro, J. K. C. (2009): Avaliação de impactos ambientais causados por metais-traço em água, sedimento, material biológico, na Baía de São Marcos, São Luís, Maranhão. – Tese (Doutorado em Química), Universidade Federal da Paraíba, João Pessoa.

[10] Coimbra, A. G. (2003): Distribuição de metais pesados em moluscos e sedimentos nos manguezais de Coroa Grande e da Enseada das Garças, Baía de Sepetiba, RJ. – Tese de Mestrado. Universidade Federal Fluminense - UFF.

[11] Cunha, A. C., Cunha, H. F. A., Souza, J. A., Nazaré, A. S., Pantoja, S. (2005): Monitoramento de Águas Superficiais em Rios Estuarinos do Estado do Amapá sob Poluição Microbiológica. Bol. Mus. Para. Emílio. Goeldi. – Sér. Ciências Naturais 9(4): 191-199.

[12] Curcho, M. R. S. M. (2009): Avaliação de micro e macroelementos tóxicos (Cd, Hg e Pb) e ácidos graxos, peixes disponíveis comercialmente para consumo em Cananéia e Cubatão, Estado de São Paulo. – Dissertação (Mestrado em Ciências), Universidade de São Paulo, São Paulo.

[13] Förstner, U., Wittmann, G. T. W. (1983): Metal Pollution in the Aquatic Environment. – Springer, New York.

[14] Froese, R., Pauly, D. (eds.) (2016): FishBase. – World Wide Web electronic publication. www.fishbase.org, version (06/2016).

[15] Garbarino, J. R., Hayes, H. C., Roth, D. A., Antweiler, R. C., Rinton, T. I., Taylor, H. E. (1995): Heavy Metals in the Mississippi River. – US Geological Survey, Reston.

[16] Hatje, V., Apte, S. C., Hales, L., Birch, G. F. (2003): Dissolved trace metal distributions in Port Jackson estuary (Sydney Harbour), Australia. – Marine Pollution Bulletin 46: 719-730.

[17] Hurley, J. P., Cowell, S. E., Shafer, M. M., Hughes, P. E. (1998): Tributary loading of mercury to lake Michigan: importance of seasonal events and phase partitioning. – The Science of the Total Environment 213: 129-137.

[18] Hurley, P. J., Benoit, J. M., Babiarz, C. L., Shafer, M. M., Andren, A. W., Sullivan, J. R., Hammond, R., Webb, D. A. (1995): Influences of watershed characteristics on mercury levels in Wisconsin rivers. – Environmental Science and Technology 29: 1867-1875.

[19] Jones, J. B., Case, V. W. (1990): Sampling, Handling and Analyzing Plant Tissue Samples. – In: Westerman, R. L. (ed.) Soil Testing and Plant Analysis. 3rd ed. Soil Science Society of America, Madison, WI, pp. 389-427.

[20] Lins, J. A. P. N., Kirschnik, P. G., Queiroz, V. S., Círio, S. M. (out./dez. 2010): Uso de peixes como biomarcadores para monitoramento ambiental aquático. – Rev. Acad., Ciênc. Agrár. Ambient. 8(4): 469-484.

http://www.aloki.hu ● ISSN 1589 1623 (Print) ● ISSN 1785 0037 (Online)
DOI: http://dx.doi.org/10.15666/aeer/1704_80378047

[21] Marjanovic, P., Miloradov, M., Cukic, Z. (1995): Heavy Metals in the Danube River Yugoslavia. – In: Salomons, W., Förstner, U., Mader, P. (eds.) Heavy Metals: Problems and Solutions. Springer, Berlin, pp. 301-321.
[22] Mastrine, J. A., Bonzongo, J.-C. J., Lyons, W. B. (1999): Mercury concentrations in surface waters from fluvial systems draining historical precious metals mining areas in southeastern U.S.A. – Applied Geochemistry 14: 147-158.
[23] Moraes, D. S. L., Jordao, B. Q. (2002): Degradação de recursos hídricos e seus efeitos sobre a saúde humana. – Rev. Saúde Pública 36(3). http://www.scielosp.org/scielo.php?script=sci_arttext&pid=S0034-89102002000300018&lng=pt&nrm=iso>. Acessos em 04 out. 2013.
[24] Moura, J. F. (2009): O boto-cinza (Sotalia guianensis) como sentinela da saúde dos ambientes costeiros: estudo das concentrações de mercúrio no estuário Amazônico e costa norte do Rio de Janeiro. – Dissertação (Mestrado em Ciências) - FIOCRUZ, Escola Nacional de Saúde Pública, Rio de Janeiro.
[25] Mziray, P., Kimirei, I. A. (2016): Bioaccumulation of heavy metals in marine fishes (Siganus sutor, Lethrinus harak, and Rastrelliger kanagurta) from Dar es Salaam Tanzania. – Regional Studies in Marine Science 7: 72-80. DOI: 10.1016/j.rsma.2016.05.014.
[26] Sanches Filho, P. J., Fonseca, V. K., Holbig, L. (2015): Avaliação de metais em pescado da região do Pontal da Barra, Laguna dos Patos, Pelotas-RS. – Ecotoxicol. Environ. Contam 8(1): 105-111. DOI: 10.5132/eec.2013.01.015.
[27] Schenone, N. F., Avigliano, E., Goessler, W., Cirelli, A. F. (2014): Toxic metals, trace and major elements determined by ICPMS in tissues of Parapimelodus valenciennis and Prochilodus lineatus from Chascomus Lake, Argentina. – Microchemical Journal 112: 127-131.
[28] Simões, E. C. (2007): Diagnóstico ambiental em manguezais dos complexos estuarinos da Baixada Santista e da Cananéia - São Paulo, no tocante a metais e compostos organoclorados. – Dissertação (Mestrado em Ciências) - Universidade de São Paulo, São Carlos.
[29] Smith, S., Chen, M. H., Bailey, R. G., Willians, W. P. (1996): Concentration and distribution of copper and cadmium in water, sediments, detritus, plants and animals in a hardwater lowland river. – Hydrobiologia 341: 71-80.
[30] Watras, C. J., Morrison, K. A., Bloom, N. S. (1995): Mercury in remote Rocky Mountain lakes of Glacier National Park, Montana, in comparison with other temperate North American regions. – Canadian Journal of Fisheries and Aquatic Sciences 52: 1220-1228.

http://www.aloki.hu ● ISSN 1589 1623 (Print) ● ISSN 1785 0037 (Online)
DOI: http://dx.doi.org/10.15666/aeer/1704_80378047

SOIL ANALYSIS, SPECIES COMPOSITION AND CARBON DYNAMICS OF *ABIES PINDROW* FOREST OF DIR KOHISTAN, PAKISTAN

UDDIN, R.[1,3*] – ANSARI, L.[1] – AHMAD, A.[2,3] – ULLAH, S.[3] – MUNIR, M.[4] – SHER, K.[5]

[1]*Department of Forestry and Range Management, Pir Mahir Ali Sha Arid Agriculture University Rawalpindi 46000, Pakistan*

[2]*Department of Forest Sciences, Beijing Forestry University Beijing 100083, China*

[3]*Department of Forestry, Shaheed Benazir Bhutto University Sheringal Dir Upper 18000, Pakistan*

[4]*Department of Botany, University of Veterinary and Animal Sciences Ravi Campus, Pattoki, Pakistan*

[5]*Department of Botany, Shaheed Benazir Bhutto University Sheringal Dir Upper 18000, Pakistan*

**Corresponding author*
e-mail: rahman0944@gmail.com

(Received 22nd Jan 2019; accepted 8th Mar 2019)

Abstract. This study highlighted the structure, species composition and biomass carbon stock in the *Abies Pindrow* dominant community in Dir Kohistan, temperate region of Pakistan. The results showed that stem density varied between 3 ha^{-1} in *Acer ceasium* to 273 ha^{-1} in *Abies pindrow*, with a total stand density of 350 trees ha^{-1}. The importance value index (IVI) varied between 2.27 (*Acer ceasium)* and 62.22 (*Abies pindrow*). The mean basal area was recorded at 132.15 m^2 ha^{-1}. The average stem volume was measured at 120 m^3 ha^{-1}. The mean stem and total tree biomass carbon was 639 and 967 t ha^{-1} respectively. Similarly, the understory vegetation and litter, dead wood and cone biomass carbon was found 1.43 t ha^{-1} and 12.02 t ha^{-1} respectively. Soil carbon (0-30 cm) was calculated by using Walkey-Black methods multiplied by mean soil bulk density measurements. The average soil organic carbon was calculated 70.75 t ha^{-1}. The Total average carbon stock of the community was calculated at 568.63 t ha^{-1}. These results provide the evidence that, *Abies Pindrow* dominant community has a greater potential of sequestering carbon. Upon proper carbon management the ecosystem might be included in the carbon trading of Kyoto protocol.
Keywords: *soil, temperate region, structural attributes, growing stock, biomass, carbon, Kumrat Valley*

Introduction

Forests sequester and accumulate more carbon than any other terrestrial ecosystem and are a significant natural 'brake' on climate change (Pan et al., 2011; Espírito-Santo et al., 2014; Manan et al., 2018). Forest biomass contained a significant amount of carbon and can accumulate continuous carbon through their life spin (IPCC, 2006; Ahmad et al., 2014, 2015). Various anthropogenic activities e.g. industrialization, deforestation, forest degradation and burning of fossil fuel, has caused an increase in the level of carbon in the atmosphere and disrupted the global carbon cycle (Sharma and Rai, 2007; Ahmad et al., 2014; Manan et al., 2018). However, nature has its own mechanism of sequestering and storing the carbon in its "reservoirs" or "sinks''. The removal of carbon for decreasing the CO_2 level is need of the time (Wani et al., 2014, 2016). Forest plays an important role in

http://www.aloki.hu ● ISSN 1589 1623 (Print) ● ISSN 1785 0037 (Online)
DOI: http://dx.doi.org/10.15666/aeer/1704_80498058

the global carbon cycle as carbon sinks of the terrestrial ecosystem (Coulston et al., 2015; Calfapitera et al., 2015). Forest contained about 4 billion ha of the globe with 861 ± 66 Pg stock carbon (Wani et al., 2014; FAO, 2015).

The Intergovernmental Panel on Climate Change (IPCC) identified five carbon pools of the forest ecosystem, namely the above-ground biomass, below-ground biomass, litter, woody debris and soil organic matter (Nizami, 2012). Among all the carbon pools, the above-ground biomass constitutes the major portion of the carbon pool (Ahmad et al., 2014). Estimating the amount of forest biomass is very crucial for monitoring and estimating the amount of carbon that is lost or emitted, as well the forest's potential to sequester and store carbon (Ahmad et al., 2018; Manan et al., 2018; Saeed et al., 2019). The IPCC and the Kyoto protocol (KP) identified forest as one of the important tool for the mitigating climate change through managing forest carbon for climate change strategy (Hosonuma et al., 2012). Concerns regarding the climate change mitigation, the international community stresses on the national and regional monitoring of forest carbon under the IPCC proposed guidelines (Böttcher et al., 2008).

Pakistan, being a member, to the IPPC and KP, the measurement of periodic and annual budgeting of the stored carbon in their forest is their obligation. In Pakistan various researcher outline the carbon stock of different forest like in temperate region (Ahmad et al., 2014; Ahmad et al., 2015; Ahmad and Nizami, 2015; Manan et al., 2018; Ahmad et al., 2018), in subtropical region (Nizami, 2012; Manan et al., 2018; Amir et al., 2018) and in planted forest. However, the carbon stock potential as well the species composition of the dominant Abies Pindrow community is not worked out yet. Looking into consideration this study was designed with the objectives to figure out the soil analysis, forest structure, species composition and biomass carbon of the *Abies pindrow* forest of Dir Kohistan, Pakistan.

Materials and methods

Study area and research design

Dir Kohistan is located to the North West side of Khyber Pakhtunkhwa province Pakistan. Geographically Dir Kohistan is mountainous with elevation ranges from 2000 to 6000 m (Ahmad et al., 2018). The *Abies pindrow* community occurred with in elevation range of 2500 to 3000 m along with latitude 35° 34' to 35° 43' and longitude72° 10' to 72° 16'. The mean annual precipitation in area ranges from 1000 to 1500 mm, while the mean temperature ranges from 0.6 to 25 °C (Ahmad and Nizami, 2015). Geologically most of the rocks are diorites, nitrites, and schist is the principle types of rocks. The underground rocks are mostly quartzite, schist, shale, slate, and granites. Soil is rich in organic matters and acidic in nature (Ahmad and Nizami 2015; Ahmad et al., 2018). For the related data collection, 14 sample plots, each of size 0.1 ha were laid out randomly in the forest (*Table A1* in the *Appendix*). The species composition and their related attributes, the growing stock, and biomass carbon in the respective pools were assessed (*Fig. 1*).

Species composition and related attributes

The species composition and their related attributed like stem density, relative density, basal area, relative basal area, frequency, relative frequency and importance value index were measured using *Equations 1-6* given below.

http://www.aloki.hu ● ISSN 1589 1623 (Print) ● ISSN 1785 0037 (Online)
DOI: http://dx.doi.org/10.15666/aeer/1704_80498058

$$\textbf{Density (D)} = \frac{\text{Total number of individual of a species in all the sample plots}}{\text{Total number of sample plots taken}} \quad \text{(Eq.1)}$$

$$\textbf{Relativedensity (D3)} = \frac{\text{Total No,individual of a species in all quadrates}}{\text{Total No.of individuals of all species in all quadrates}} \times 100 \quad \text{(Eq.2)}$$

$$\textbf{Average cover per species, (C)} = \frac{\text{Total cover (square feet) of a species}}{\text{Number of plants of a species}} \quad \text{(Eq.3)}$$

$$\textbf{Relative Cover of Species (C3)} = \frac{\text{TotalCoverSqftofallPlantsofallSpp}}{\text{TotalCoverSqftofallPlantsOfallSpecies}} \quad \text{(Eq.4)}$$

$$\textbf{Frequency (F)} = \frac{\text{Number of quadrats of occurrence of a species}}{\text{Total number of quadrats used by sampling}} \times 100 \quad \text{(Eq.5)}$$

$$\textbf{RelativeFrequency (F3)} = \frac{\text{Frequency of a species}}{\text{Total frequency of all species}} \times 100 \quad \text{(Eq.6)}$$

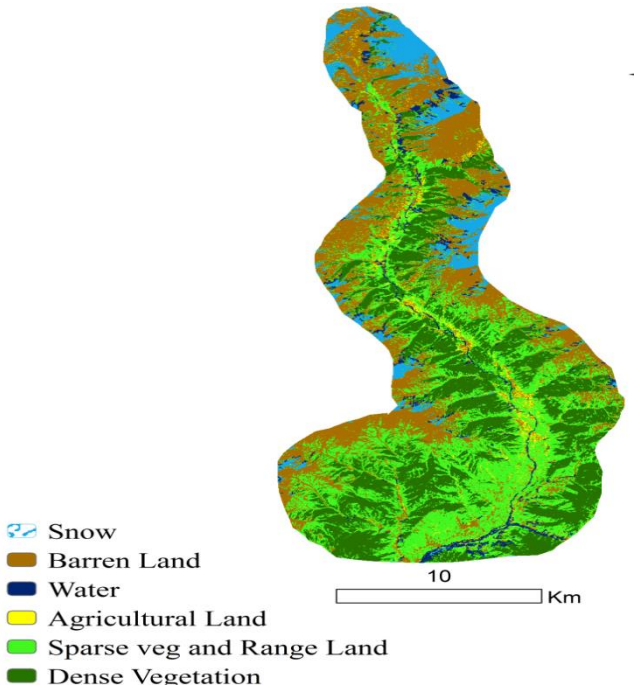

Figure 1. *Study area*

Importance value index (IVI)

In mixed forest, data of density, cover and frequency of a species do not give a clear data about the main species. It was estimated by adding the value of relative cover, relative density, and relative frequency and to dividing it by 3 given the importance value index (IVI) of the species. IVI for a forest stand were calculated as the total of the relative density, relative frequency and relative cover (Curtis, 1959).

$$\text{I.V.I} = \frac{\text{D3} + \text{C3} + \text{F3}}{3} \quad \text{(Eq.7)}$$

http://www.aloki.hu ● ISSN 1589 1623 (Print) ● ISSN 1785 0037 (Online)
DOI: http://dx.doi.org/10.15666/aeer/1704_80498058

Biomass carbon estimation

For upper storey vegetation biomass carbon, in each plot diameter and tree height was measured. The stem volume was measured from the relationship of diameter (cm) and height (m) following formula:

$$\text{Tree volume } (m^3) = \pi/4d^2 \times h \times FF \quad \text{(Eq.8)}$$

Stem biomass (kg) was calculated from the relationship of stem volume (m^3) and basic wood density (Kg/m^3). Basic wood density was sourced from available literature (Haripriya, 2000; Ahmad et al., 2014; Manan et al., 2018,). The following formula was used to estimate stem biomass:

$$\text{Stem biomass (kg)} = \text{Stem volume } (m^3) \times \text{Wood density } (Kg/m^3) \quad \text{(Eq.9)}$$

To estimate total biomass, biomass expansion factor was used. The BEF ratio of 1.51 for conifers and 1.55 for broad leaved was used to find out total biomass of a tree (Haripriya, 2000; Ahmad et al.,2018; Manan et al., 2018).

$$\text{Total biomass (Kg)} = \text{Stem biomass (Kg)} \times BEF \quad \text{(Eq.10)}$$

For the measurement of understory vegetation, dead wood, cone, and litter biomass carbon, sub plots each of 1 m^2 size were laid out. From the each sub plot, the understory vegetation was harvested destructively and dead wood, cone and litter were collected and their fresh weight was measured. The collected samples were oven dried for 48 h at 72 °C and their dry weight was taken as their biomass (Ahmad and Nizami, 2015; Ahmad et al., 2018; Manan et al., 2018).

The carbon values were assessed from the biomass of the respective pools. The conversion factor of 0.5 was used to convert biomass into carbon that has been used widely around the Globe (Brown and Lugo, 1982; Malhi et al., 2004; Nizami, 2012; Ahmad et al., 2014; Amir et al., 2018; Saeed et al., 2019). For soil carbon assessment, soil samples were collected from each plot at the depth of 30 cm. The soil organic carbon was measured following (Walkely, 1934). The soil carbon in t ha^{-1} was assessed from the soil bulk density, depth increment and soil organic carbon following (Ahmad and Nizami, 2015; Saeed et al., 2018; Ahmad et al., 2018).

Results and discussion

Species composition and growing stock

The results regarding the species composition and related attributed are given in *Table 1*. The results clearly figure out that *Abies pindrow* is the dominant tree species with the maximum species compositional attributes while the minimum values for these attributes were recorded for *Acer cesium*. Over all the results showed that the stem density varied between 3 ha^{-1} (*Acer caesium*) and 276 ha^{-1} (*Abies pindrow*) with a total stem density of 350 trees ha^{-1}. The results of frequency in *Table 1* explained that along with *Abies pindrow*, *Taxus baccata* and *Picea smithiana* were found throughout the community. Regarding the growing stock (volume m^3 ha^{-1}) details are given in *Table 2*. The results in *Table 2* showed that the total growing stock in the community was

http://www.aloki.hu ● ISSN 1589 1623 (Print) ● ISSN 1785 0037 (Online)
DOI: http://dx.doi.org/10.15666/aeer/1704_80498058

recorded at 1720 m^3 ha^{-1}. Regarding the relationship between basal area (m^2 ha^{-1}) and growing stock (m^3 ha^{-1}), the results in *Figure 2* showed a strong positive linear correlation with R^2 value of 0.98. The highly positive correlation of basal area and growing stock indicated that growing stock is the function of basal area (Nizami, 2012; Ahmad et al., 2014; Ahmad and Nizami, 2015; Saeed et al., 2019; Amir et al., 2018).

Table 1. *Species composition and related attributes*

Species	D ha^{-1}	RD %	BA ha^{-1}	RB %	F %	RF %	IVI
Abies pindrow	276	77.23	112.39	85.12	100.00	27.31	63.22
Taxus baccata	35	10.64	3.61	2.78	100	27.14	13.52
Picea smithiana	25	7.56	11.02	8.08	100	27.14	14.26
Acer caesium	3	0.65	0.53	0.33	28.57	5.83	2.27
Juglans regia	8	2.17	2.09	1.34	42.85	8.69	4.06
Platanus orientalis	4	1.11	2.51	1.66	21.42	4.04	2.27
Total	350	100.00	132.15	100.00		100.00	100.00

D = Density, RD = Relative density, BA = Basal area, RB = Relative basal area, F = Frequency, RF = Relative frequency, IVI = Importance value index

Table 2. *Volume and biomass carbon of upper storey vegetation*

Species	Volume m^3 ha^{-1}	Stem biomass t ha^{-1}	Total tree biomass t ha^{-1}	Carbon stock t ha^{-1}	Percentage
Abies pindrow	1425	528	800	400	82.64
Taxus baccata	54	20	30	15	3.08
Picea smithiana	164	60	94	47	9.66
Acer caesium	8	3	5	2	0.46
Juglans regia	31	11	18	9	1.83
Platanus orientalis	37	14	21	11	2.20
Total	1720	636	967	484	100

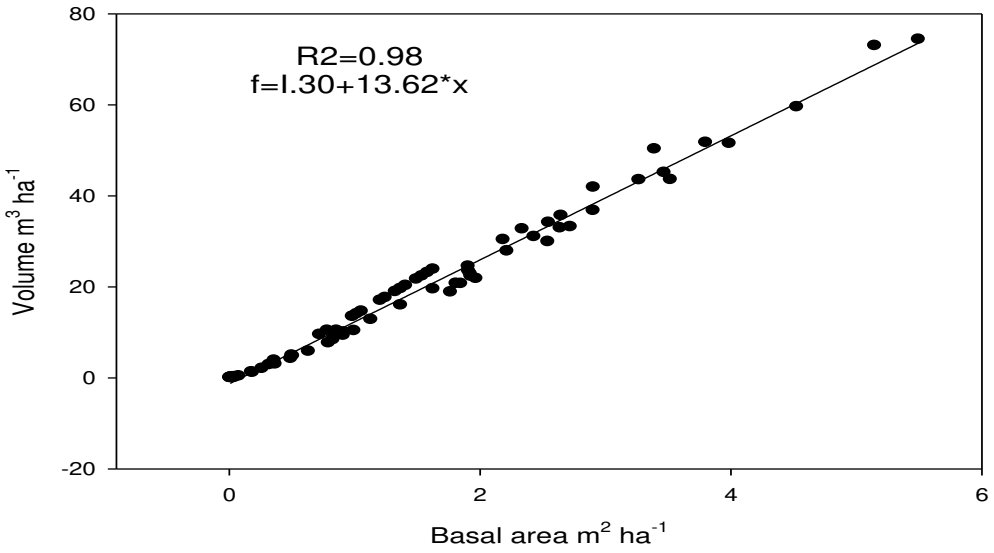

Figure 2. *Relationship between volume (m^3 ha^{-1}) and basal area m^2 ha^{-1}*

http://www.aloki.hu ● ISSN 1589 1623 (Print) ● ISSN 1785 0037 (Online)
DOI: http://dx.doi.org/10.15666/aeer/1704_80498058

Biomass carbon

The total tree biomass value varied between 5 and 800 t ha^{-1} (*Table 2*) with overall value of 967 t ha^{-1}. The relationship of basal area (m^2 ha^{-1}) and biomass is presented in *Figures 3* and *4*. The value of R^2 suggested a very strong correlation between basal area and biomass. The basal area and biomass have a functional relationship and with increase in the basal area the biomass also increases (Nizami, 2012; Saeed et al., 2018). Under storey vegetation were mostly consist of grasses, forbs and shrubs. The average biomass of under storey vegetation was 2.87 t ha^{-1}. The biomass carbon of the upper story vegetation was 484 t ha^{-1}. In the total tree biomass carbon, the contribution of *Abies pindrow* was 82.64%. In the under storey vegetation, the mean carbon stock was 1.43 t ha^{-1}. Similarly, the carbon stock in litter, dead wood and cones was recorded as 12.02 t ha^{-1}. The soil carbon varied from 52.13 to 81.78 t ha^{-1} (*Table 3*) with mean value of 70.74 t ha^{-1} (*Table 4*).

Table 3. *Soil bulk density and soil organic carbon stock tons* ha^{-1}

Plot	Bulk density (0-15 cm)	Bulk density (15-30 cm)	SOM %	SOM %	Total SOM%	T otal SOC%	SOC tons ha^{-1}
1	1.01	1.05	3.14	0.98	4.12	2.38	73.07
2	1.009	1.04	3.39	1.19	4.58	2.65	80.46
3	1.009	0.93	3.16	1.02	4.18	2.42	73.43
4	0.99	1.03	2.84	1.02	3.86	2.23	66.52
5	0.91	1	2.34	0.94	3.28	1.90	52.13
6	0.99	0.89	2.54	0.78	3.32	1.92	57.21
7	1	1.05	3.68	1.02	4.7	2.72	81.78
8	0.99	0.95	3.78	0.94	4.72	2.73	81.34
Total	7.908	7.94	24.87	7.89	32.76	18.95	565.94

Table 4. *Total carbon stock in forest ecosystem*

S. No	Carbon pools	Average carbon stock (tons ha^{-1})
1	Upper storey vegetation carbon stock	484
2	Under storey vegetation carbon stock	1.43
3	Litter, dead wood and cones carbon stock	12.02
4	Soil carbon stock	70.74
Total average carbon stock		568.63

Overall the results in *Table 4* showed that the *Abies pindrow* community stored 568.63 t ha^{-1} carbon. The upper storey vegetation hold maximum carbon followed by soil, whereas the understory vegetation hold the minimum carbon. In compression the current carbon values in the biomass gives higher estimates from the reported values from Himalayan temperate regions (Sharma et al., 2010, 2011; Wani et al., 2014). This higher value might be the results of the presences of larger tree particularly of *Abies pindrow*. We found trees up to 150 cm in diameter that resulted in the maximum carbon value in the community. However, the soil carbon was found low from the reported value of Sharma et al. (2011) and Wani et al. (2014). This may be due to the

http://www.aloki.hu ● ISSN 1589 1623 (Print) ● ISSN 1785 0037 (Online)
DOI: http://dx.doi.org/10.15666/aeer/1704_80498058

management practices. The forest are managed forest and during management operations the dead wood are removed from the forest floor and upon the removal of the deadwood the forest floor have little deadwood stuff, resulting low soil carbon (Barbati et al., 2007).

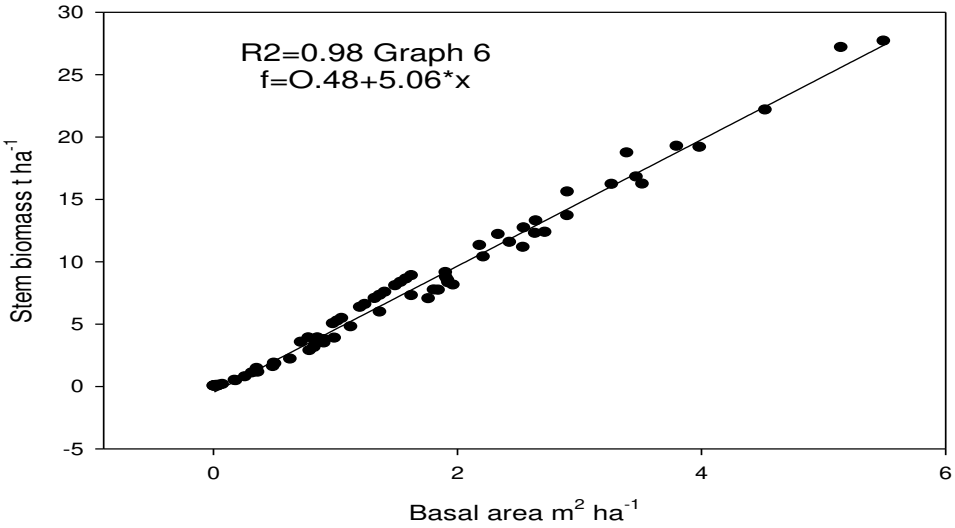

Figure 3. *Relationship between stem biomass (t ha^{-1}) and basal area m^2 ha^{-1}*

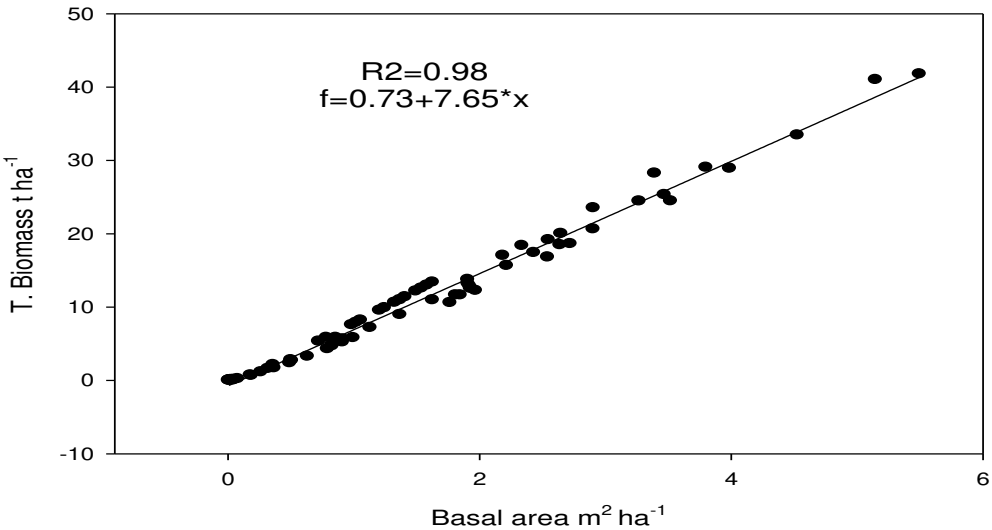

Figure 4. *Relationship between stem biomass (t ha^{-1}) and basal area m^2 ha^{-1}*

Soil carbon stock

Soil carbon in tons ha^{-1} was calculated from the relation of soil organic carbon (SOC %), Soil bulk density (gm/cm^3) and thickness of horizon (cm). Soil carbon was estimated by the use of different chemical solution like M K_2 Cr_2O_7 and H_2SO_4. Composite soil samples were collected at 0-15 and 15-30 cm depths from each inventory plot, using an auger. Soil carbon concentration (g C/g of soil) was established using the Walkey-Black titration method. Data collection for desired objectives was

http://www.aloki.hu ● ISSN 1589 1623 (Print) ● ISSN 1785 0037 (Online)
DOI: http://dx.doi.org/10.15666/aeer/1704_80498058

recorded using standard procedures (FAO, 2005). The result of study showed that soil organic carbon stock decrease with increasing soil depth. The high value of organic carbon content showed that there is fast decomposition rate in forest litter in suitable environment. The soil organic carbon is affected due to different environmental factors geographic location along with slope. The average soil organic carbon was 70.75 ± 11.26 t ha^{-1} with average soil bulk density 0.99 ± 0.032 was recorded.

Soil PH

Soil pH was measured by using soil pH meter (Mc Lean, 1982). The average pH was recorded 6.19 ± 0.12 the minimum soil pH was recorded 5.93 while maximum was 6.33 with coefficient variance. The result of the study shows that the soil was strongly acidic.

Conclusion

The presented finding in this study revealed that the *Abies pindrow* community having the greater carbon sequestration potential. However, the forest faces greater pressure in term of grazing, fuel wood collection and timber harvest. In this regard activities like Reduction in timber harvest, promotion of aforestation, reforestation, and the development of Hydropower should be imitated from the preservation and conservation of the forest.

REFERENCES

[1] Ahmad, A., Nizami, S. M. (2015): Carbon stocks of different land uses in the Kumrat valley, Hindu Kush Region of Pakistan. – Journal of Forest Research 26: 57-64.

[2] Ahmad, A., Nizami, S. M., Marwat, K. B., Muhammad, J. (2015): Annual accumulation of carbon in the coniferous forest of Dir Kohistan: An inventory based estimate. – Pakistan Journal of Botany 47: 115-118.

[3] Ahmad, A., Liu, Q. I. J., Nizami, S. M., Mannan, A., Saeed, S. (2018): Carbon emission from deforestation, forest degradation and wood harvest in the temperate region of hindukush himalaya, pakistan between 1994 and 2016. – Land Use Policy 78: 781-790. DOI: https://doi.org/10.1016/j.landusepol.2018.07.009.

[4] Ahmad, A., Mirza, S. N., Nizami, S. M. (2014): Assessment of biomass and carbon stocks in Coniferous forest of Dir Kohistan, KPK. – Pakistan Journal of Agriculture Sciences 51: 335-340.

[5] Amir, M., Liu, X., Ahmad, A., Saeed, S., Mannan, A., Atif, M., M. (2018): Patterns of biomass and carbon allocation across chronosequence of chir pine (Pinus roxburghii) forest in Pakistan: inventory-based estimate. – Advances in Meteorology Article ID 3095891. https://doi.org/10.1155/2018/3095891.

[6] Barbati, A., Corona, P., Marchetti, M. (2007): A forest typology for monitoring sustainable forest management: the case of European forest types. – Plant Biosystems 141: 93-103.

[7] Böttcher, H., Kurz, W. A., Freibauer, A. (2008): Accounting of forest carbon sink and sources under a future climate protocol-factoring out past disturbance and management effects on age-class structure. – Environmental Science & Policy 11: 669-686.

[8] Brown, S., Lugo A. E. (1982): The storage and production of organic matter in tropical forest and their role in global carbon cycle. – Biotropicia 14: 161-187.

http://www.aloki.hu ● ISSN 1589 1623 (Print) ● ISSN 1785 0037 (Online)
DOI: http://dx.doi.org/10.15666/aeer/1704_80498058

[9] Calfapietra, C., Barbati, A., Perugini, L., Ferrari, B., Guidolotti, G., Quatrini, A., Corona, P. (2015): Carbon mitigation potential of different forest ecosystems under climate change and various managements in Italy. – Ecosystem Health & Sustainability 1: 1-9.

[10] Coulston, J. W., Wear, D. N., Vose, J. M. (2015): Complex forest dynamics indicate potential for slowing carbon accumulation in the southeastern United States. – Scientific Reports 5: 8002. https://doi.org/10.1038/srep08002. https://www.nature.com/articles/srep08002# supplementary- information.

[11] Curtis, J. T. (1959): The vegetation of Wisconsin: an ordination of plant communities: – University of Wisconsin Press, Madison, WI.

[12] Espírito-Santo, F. D. B., Gloor, M., Keller, M., Malhi, Y., Saatchi, S., Nelson, B., Junior, R. C. O., Pereira, C., Lloyd, J., Frolking, S., Palace, M., Shimabukuro, Y. E., Duarte, V., Mendoza, A. M., López- González, G., Baker, T. R., Feldpausch, T. R., Brienen, R. J. W., Asner, G. P., Boyd, D. S., Phillips, O. L. (2014): Size And frequency of natural forest disturbances and the Amazon forest carbon balance. – Nature Communication 5: (3434).

[13] FAO. (2005). Global Forest Resource Assessment Rome, Italy.

[14] FAO (2015): Global Forest Resources Assessment. FAO Forestry Paper No. 1. – FAO, Rome.

[15] Haripriya, G. (2000): Estimates of biomass in Indian forests. – Biomass & Bioenergy 19: 245-258.

[16] Hosonuma, N., Herold, M., de Sy, V., de Fries, R. S., Brockhaus, M., Verchot, L., Angelsen, A., Romijn, E. (2012): An assessment of deforestation and forest degradation drivers in developing countries. – Environmental Research Letters 7: 1-12.

[17] IPCC (2006): Intergovernmental Panel on Climate Change (IPCC) Guidelines for National Greenhouse Gas. – IPCC, Geneva.

[18] McLean, E. O. (1982). Soil pH and lime requirement. Methods of soil analysis. Part 2. Chemical and microbiological properties, (methodsofsoilan2), 199-224.

[19] Malhi, Y. B. T., Phillips, O. L., Almeida, S., Alvarez, E., Arroyo, L., Chave, J., CzimczikI, C. I., Fiore, A. D., Higuchi, N., Killeen, T. J., Laurance, S. G., Laurance, W. F., Lewis, S. L., Montoya, L. M., Lloyd, J. (2004): The above-groundcoarse wood productivity of 104 Neotropical forest plots. – Global Change Biology 101: 563-559.

[20] Mannan, A., Feng, Z., Ahmad, A., Liu, J., Saeed, S., Mukete, B. (2018): Carbon dynamics with land use change in Margallah Hills National Park, Islamabad (Pakistan) from 1990 to 2017. – Applied Ecology and Environmental Research 16(3): 3197-3214.

[21] Nizami, S. M. (2012): The inventory of the carbon stocks in sub tropical forests of Pakistan for reporting under Kyoto Protocol. – Journal of Forestry Research 23: 377-384.

[22] Pan, Y., Birdsey, R. A., Fang, J., Houghton, R., Kauppi, P. E., Kurz, W. A., Phillips, O. L., Shvidenko, A., Lewis, S. L., Canadell, J. G. et al. (2011): A large and persistent carbon sink in the world's forests. – Science 333: 988-993.

[23] Saeed, S., Sun, Y., Beckline, M., Chen, L., Lai, Z., Mannan, A., Ahmad, A., Shah, S., Amir, M., Ullah, T., Khan, A., Akbar, F. (2018): Altitudinal gradients and forest edge effect on soil organic carbon in chinese fir (*Cunninghamia Lanceolata*): a study from Southeastern China. – Applied Ecology and Environmental Research 17(1): 745-757.

[24] Saeed, S., Sun, Y., Beckline, M., Chen, L., Zhang, B., Ahmad, A., Mannan, A., Khan, A., Iqbal, A. (2019): Forest edge effect on biomass carbon along altitudinal gradients in Chinese Fir Cunninghamia lanceolata): a study from Southeastern China. – Carbon Management. DOI: 10.1080/17583004.2018.1537517.

[25] Sharma, C. M., Baduni, N. P., Gairola, S., Ghildiyal, S. K., Suyal, S. (2010): Treediversityand carbon stocks of some major forest types of Garhwal Himalaya, India. – Forest Ecology & Management 260: 2170-2179. https://doi.org/10.1016/j.foreco.2010.09.014.

[26] Sharma, C. M., Gairola S., Baduni N. P., Ghildiyal S. K., Sarvesh, S. (2011): Variation in carbon stocks on different slope aspects in seven major types of temperate region of Garhwal Himalaya. – India Journal of Biosciences 36(4): 701-708.

http://www.aloki.hu ● ISSN 1589 1623 (Print) ● ISSN 1785 0037 (Online)
DOI: http://dx.doi.org/10.15666/aeer/1704_80498058

[27] Sharma, P., Rai, S. (2007): Carbon sequestration with land-use cover change in a Himalayan Watershed. – Geoderma 139: 371-378.
[28] Walkey, A., Black, I. A. (1934): An examination of the Degtjareff method for determining soil organic matter, and a proposed modification of the chromic acid titration method. – Soil Sciences 37: 29-38.
[29] Wani, A. A., Joshi, P., Singh, O., Bhat, J. (2014): Estimating soil carbon storage and mitigation under temperate coniferous forests in the southern region of Kashmir Himalayas. – Mitigation and Adaptation Strategies for Global Change 19: 1179-1194.
[30] Wani, A. A., Joshi, P. K., Singh, O., Shafi, S. (2016): Multi-temporal forest cover dynamics in Kashmir Himalayan region for assessing deforestation and forest degradation in the context of REDD+ policy. – Journal of Mitigation Science. 13: 1431-1441. https://doi.org/10.1007/ s11629-015-3545-3.

APPENDIX

Table A1. *Geographic position and elevation of each plot*

Plot no	Elevation ft	Latitude	Longitude
1	8030	35° 34'.09"	72° 10'.28"
2	8050	35° 34'.15"	72° 10'.35"
3	8082	35° 34'.23"	72° 10'.38"
4	8098	35° 35'.33"	72° 11'.44"
5	8127	35° 35'.55"	72° 11'.58"
6	8160	35° 36'.45"	72° 12'.09"
7	8198	35° 37'.55"	72° 12'.58"
8	8221	35° 39'.38"	72° 13'.34"
9	8240	35° 39'.53"	72° 13'.51"
10	8267	35° 40'.09"	72° 14'. 04"
11	8289	35° 40'.50"	72° 14'.49"
12	8308	35° 41'.44"	72° 15'.22"
13	8345	35° 42.51"	72° 15'.51"
14	8431	35° 43'.15"	72° 16'.35"

Table A2. *Soil bulk density and soil organic carbon stock tons ha^{-1}*

Plot	Bulk density (0-15 cm)	Bulk density (15-30 cm)	SOM%	SOM%	Total SOM%	T SOC%	SOC tons ha^{-1}
1	1.01923	1.05769	3.14	0.98	4.12	2.38	73.0724
2	1.009615	1.04808	3.39	1.19	4.58	2.65	80.4647
3	1.009615	0.93269	3.16	1.02	4.18	2.42	73.4372
4	0.99038	1.03846	2.84	1.02	3.86	2.23	66.5235
5	0.91346	1	2.34	0.94	3.28	1.90	52.1372
6	0.99038	0.89423	2.54	0.78	3.32	1.92	57.2171
7	1	1.05769	3.68	1.02	4.7	2.72	81.7865
8	0.99038	0.95192	3.78	0.94	4.72	2.73	81.3448
Mean	0.99038	0.99759	3.10	0.98	4.095	2.37	70.7479
SD	0.03291	0.06372	0.51	0.11	0.5757	0.33	11.2661
Std error	0.01163	0.02253	0.18	0.04	0.2035	0.11	3.98318
Variance	0.00108	0.00406	0.26	0.01	0.3314	0.11	126.925
CV %	3.32292	6.3883	16.5	11.6	14.057	14.05	15.9243

http://www.aloki.hu ● ISSN 1589 1623 (Print) ● ISSN 1785 0037 (Online)
DOI: http://dx.doi.org/10.15666/aeer/1704_80498058

CLOSED LANDFILL HEAVY METAL CONTAMINATION DISTRIBUTION PROFILES AT DIFFERENT SOIL DEPTHS AND RADIUSES

OTHMAN, R.[1*] – MOHD LATIFF, N. H.[1] – BAHARUDDIN, Z. M.[1] – HASHIM, K. S. H. Y.[2] – LUKMAN HAKIM MAHAMOD, L. H.[3]

[1]*International Institute for Halal Research and Training (INHART) Department of Landscape Architecture, Kulliyyah of Architecture and Environmental Design (KAED), International Islamic University Malaysia, 53100 Kuala Lumpur, Malaysia*

[2]*Department of Urban & Regional Planning, Kulliyyah of Architecture and Environmental Design (KAED), International Islamic University Malaysia, 53100 Kuala Lumpur, Malaysia*

[3]*Department of Quantity Surveying, Kulliyyah of Architecture and Environmental Design (KAED), International Islamic University Malaysia, 53100 Kuala Lumpur, Malaysia*

[*]*Corresponding author*
e-mail: rashidi@iium.edu.my; phone: +60-126-644-772; fax: +60-361-964-864

(Received 24th Jan 2019; accepted 3rd May 2019)

Abstract. Various types of wastes are the main sources of heavy metal within a landfill system including metal waste components such as food cans, scrap metal, household hazardous waste and electronic waste such as batteries and old computers. The procedure that occurs inside the waste cells quickens that procedure for substantial metal draining from the waste component. This study comparing soil samples taken from four different sites in Selangor of closed non-sanitary (Sungai Kembong) and sanitary (Ampar Tenang, Air Hitam and Kubang Badak) landfills at different depths (0-30 cm, 30-60 cm and 60-90 cm) and radiuses (5-10 m, 10-15 m and 15-20 m), for ten heavy metals (Al, Cr, Mn, Fe, Co, Ni, Cu, Zn, Cd and Pb) to find the risk of heavy metal movement from the upper layer cell into the deeper layer. The data were analysed using ICP-MS (Perkin Elmer NexION 300X). Al and Fe displayed higher concentration at most of the sites with different volume of concentration at different depth and radius. Most of the sites consistently showed higher contamination in deeper soil than the upper layer of the soil.
Keywords: *urban pollution, landfill, inorganic pollutant, laterite soil, leachate, municipal solid waste*

Introduction

It is estimated that approximately 0.5 to 4.5 kg of solid waste per person per day is produced at different regions of the world (Bakare et al., 2005; Swati et al., 2014). Land degradation, which caused by human activities, creates significant adverse effects on the environments and ecosystems worldwide (Thomaz and Luiz, 2012; Bai et al., 2013; Li et al., 2013; Chen et al., 2015). Thus, solid waste becomes an important and emerging environmental problem. The most common ways to manage such waste disposal are landfills and incinerators. At the time being, it is up to 95% total of municipal solid waste (MSW) collected is disposed of in landfills worldwide (El-Fadel, 1997; Swati, 2014). Landfilling is the major MSW disposal method used in modern cities (Wong, 2015).

Due to the problems of environmental pollution and the shortage of urban land, landfill becomes a major issue in any urban management in the world (Hoornweg and Bhada, 2012). As consequences, ex-landfills are turned into another beneficial alternative to the urban population. At present, there were 143 closed landfills in Malaysia

http://www.aloki.hu ● ISSN 1589 1623 (Print) ● ISSN 1785 0037 (Online)
DOI: http://dx.doi.org/10.15666/aeer/1704_80598067

(SWCorp, 2017). The number of the closed landfills had increased each year from 115 in 2003 to 131 in 2012 and it has been expected to become 296 when all the existing landfills closed their operation in 2020 (Simis et al., 2016). For the time being, there are about 160 operating landfills and 143 closed landfills, which make altogether 303 landfills in total that, are available in Malaysia. It has been expected more than 70.0% of the future ex-landfills to be located in urban areas and become the major concern of the local population within the ex-landfill areas (Chun-Yang and Talib, 2006).

Based on Act 672 under Solid Waste and Public Cleansing Management Act 2007, every ex-landfill must undergo waste recovery through new technology such as waste to energy facilities, construction and demolition recovery facilities, organic waste facilities, landfill closure, and integrated waste management. However, the existence of the ex-landfill within the neighbourhood reported creating issues of foul odours, leachate, and landfill gas pollution. The local communities have reported it and they claimed to have declined health and quality of life (Simis and Awang, 2015). These concerns probably have become more pragmatic when recent intensive studies demonstrated the increment of human health risk caused by exposure to toxic chemicals, such as dioxins and related compounds, and heavy metals in these dumping sites (Agusa et al., 2003; Minh et al., 2003).

Landfills containing hazardous materials are under critical observation today for potential hazards, resulting in the need for thorough risk analyses along with the soil and groundwater that have been contaminated with chemicals leaching from landfills. Several reports have been published which are documented on the leachate characterization and its effect on groundwater pollution (Boels and Fleming, 1993), but little information is available on the effect of landfills on soil contamination and its toxicological effects. Damaging human activities cause pollution. Thus, more information and assessment of land pollution are needed to overcome the problems occurred (Kardanpour et al., 2015; Mahmoud and El-Kader, 2015).

Based on the previous study, most organic chemical substances will eventually either be degraded through biochemical reactions in the landfill or be leached out of the landfill with water movement. However, the majority of heavy metals will remain in the landfill because heavy metal migration is very limited compared to the number of metals accumulated in the landfill (Oygard et al., 2004; Riber et al., 2005), especially in anaerobic processes. The slow movement of heavy metals is the result of heavy metals being subjected to strong sorption on soil particles, precipitation under anaerobic conditions, and chelation with inorganic and organic ligands in landfills (Bozkurt et al., 1999, 2000). Heavy metals occur naturally at low concentrations in soils. They are considered soil contaminants due to their widespread occurrence, as well as their acute and chronic toxicity (Youn-Joo, 2004).

High concentrations of heavy metal such as As, Cd, Cu, Pb, and Zn in soils have often been reported in a number of countries. It was reported by Bhattacharya (2012), that no significant adverse impacts of As upon human health in Bangladesh, India, and China. It is claimed that millions of people are potentially at risk from As poisoning. Similar to As, Cd accumulation in the offal of grazing animals in New Zealand and Australia made it unsuitable for human consumption. Besides, it affected access to meat products to overseas markets (Loganathan et al., 2008). There are also concerned about the urban development of horticultural sites which contained toxic levels of heavy metals in soils that resulting from excessive use of fungicides and herbicides (Pietrzak and Uren, 2011).

http://www.aloki.hu ● ISSN 1589 1623 (Print) ● ISSN 1785 0037 (Online)
DOI: http://dx.doi.org/10.15666/aeer/1704_80598067

Materials and methods

Study area description

Twelve points at 4 different sites of closed landfill located at Selangor, Malaysia namely; Ampar Tenang sanitary landfill (2°49'13.3"N 101°40'47.6"E), Sungai Kembong non-sanitary landfill (2°53'08.8"N 101°49'17.0"E), Air Hitam sanitary landfill (2°52'22.4"N 101°38'53.8"E) and Kubang Badak sanitary landfill (3°23'01.6"N 101°24'54.2"E) were selected for this study. The site selection was based on the types of the landfill and the size of the landfill located in Selangor state. *Table 1* indicates the landfill sites info with the area covered, wasted collected, total year of operation and the current status of the landfill studied.

Table 1. *Selected landfill sites with the area covered, waste collected per day, total year operation and current status*

LANDFILL SITES	AREA (ACRE)	WASTE COLLECTED (TONE/DAY)	TOTAL YEAR OPERATION	CURRENT STATUS	SOURCE
Air Hitam Sanitary Landfill	100	1500	16	Closed	Othman et al. (2016)
Kubang Badak Sanitary Landfill	30	400	10	Closed	Yahaya et al. (2016)
Ampar Tenang Sanitary Landfill	10	100	9	Closed	Yusoff et al. (2013)
Kampung Sungai Kembong Inert Waste	38.5	83	5	Closed	Yahaya et al. (2016)

Soil sampling

Soil samples were collected at different points (0-200 mm depth, approx. 1000 g) were taken by using soil auger (Eijkelkamp Agrisearch). The soil then was sealed in a polyethylene bag and labelled. The soil was dried in an oven for 70ºC for 3 days to a week depending on the moistness of the soil. Then samples were ground by using agate mortar until becoming small particles. Then it was sieved using a 2 mm mesh to remove stones and plant materials. Then samples were stored at room temperature before being digested using Microwave Digestion Ethos D (Milestone, 2001). Heavy metals, Al, Cr, Mn, Fe, Co, Ni, Cu, Zn, Cd, and Pb were then analysed by using ICP-MS (Perkin Elmer NexION 300X).

Determination of Heavy Metals in Soils

0.5 g of soil samples were accurately weighed into a container made of PFA perfluoroalkoxy polymer and digested through a microwave digestion system using the digestion method as described by Zhao et al. (1994). Soil samples were air-dried and sieved. Soil samples were passed through a 2 mm sieve and ready for further analysis. Dried and the ground sample was mixed with 10 ml of concentrated nitric acid (HNO_3 65%) and digested. Acid was added for each soil samples and then the digestion tubes were placed in a rotor segment by using a torque wrench. The segments were inserted into the microwave cavity and connected with the temperature sensor. The mixture temperature was adjusted to ±175ºC and 1,200 Watt of power for 30 minutes using Microwave Digestion (Milestone Start D) as detailed in Method US EPA 3051. The digestion was completed after the last solution was clear and no brownish fumes

http://www.aloki.hu ● ISSN 1589 1623 (Print) ● ISSN 1785 0037 (Online)
DOI: http://dx.doi.org/10.15666/aeer/1704_80598067

were released from the digestion vessel tubes. When digestion was completed, samples were removed and diluted. The soil digests were adjusted to the final volume of 50 mL with deionized water. This solution is further 1:1 diluted for the analysis of components by ICP-MS and divided into triplicate each into 15 ml tubes.

Data analysis

All the experiments were carried out in triplicates and data presented as mean values of three independent replicates. Data were further analysed using analysis of variance (ANOVA). Statistical analysis for all experiments was performed by using SAS through factorial analysis of variance followed by Tukey's test with significant different at $P<0.0001$.

Results and discussion

Ampar Tenang sanitary landfill

The results in *Fig. 1* showed heavy metal concentration in a closed sanitary landfill with a radius of 5 to 10 m, 10 to 15 m and 15 to 20 m at different depth 0 to 30 cm, 30 to 60 cm and 60 to 90 cm of Ampar Tenang sanitary landfill.

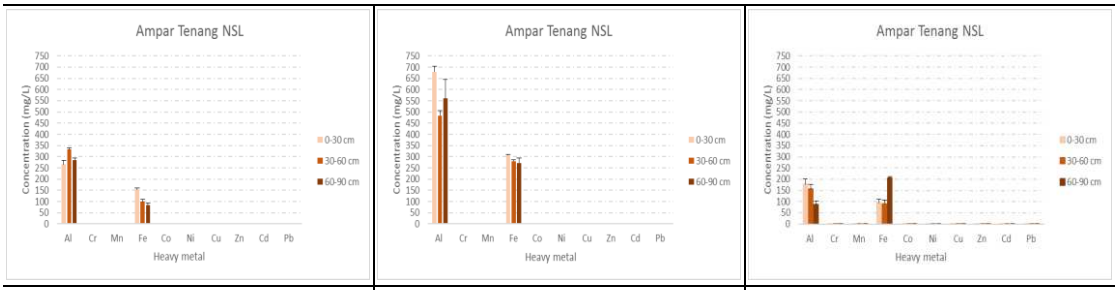

Figure 1. *The pattern of 10 heavy metal concentration depicted Ampar Tenang sanitary landfill at different soil depths (0-30 cm, 30-60 cm, and 60-90 cm) and radiuses (A: 5-10 m, B: 10-15 m and C: 15-20 m) of the closed landfill*

Results of heavy metal showed that Al and Fe concentration is higher at all point of Ampar Tenang landfill. Among the analysed heavy metals, Al and Fe concentration at radius 10 to 15 m had the highest concentrations. Each showed 679.088 mg/kg, 483.627 mg/kg and 560.437 mg/kg for Al while 306.678 mg/kg, 280.216 mg/kg and 272.183 mg/kg for Fe. Concentration for the radius 5 to 10 m and 15 to 20 m also almost equal within each depth. The heavy metal concentration at radius 15 to 20 m showed Al range between 87.711 mg/kg and 177.155 mg/kg while for Fe the concentration range between 90.317 mg/kg and 204.819 mg/kg. Meanwhile, radius 5 to 10 m showed Al concentration higher than Fe concentration. Each at 265.645 mg/kg, 332.441 mg/kg, and 284.904 mg/kg for Al and 152.911 mg/kg, 99.968 mg/kg and 84.924 mg/kg for Fe.

Sungai Kembong non-sanitary landfill

The results in *Fig. 2* showed heavy metal concentration in a closed non-sanitary landfill with a radius of 5 to 10 m, 10 to 15 m and 15 to 20 m at different depth 0 to

http://www.aloki.hu ● ISSN 1589 1623 (Print) ● ISSN 1785 0037 (Online)
DOI: http://dx.doi.org/10.15666/aeer/1704_80598067

30 cm, 30 to 60 cm and 60 to 90 cm of Sungai Kembong non-sanitary landfill. Results of heavy metal showed that Al and Fe concentration is higher at all point of Sungai Kembong landfill. Among the analysed heavy metals, Fe concentration at radius 15 to 20 m showed 364.243 mg/kg, 534.058 mg/kg and 559.114 mg/kg. Fe concentration at radius 15 to 20 m and 5 to 10 m also showed high concentrations. Each showed 170.397 mg/kg, 316.408 mg/kg and 436.530 mg/kg for radius 15 to 20 m while 337.625 mg/kg, 342.236 mg/kg and 289.030 mg/kg for radius 5 to 10 m. The Al concentration showed the highest reading for radius 5 to 10 m at 160.216 mg/kg, 185.739 mg/kg and 239.069 mg/kg compared to Al concentration at radius 10 to 15 m and radius 15 to 20 m. For radius 10 to 15 m, the concentration for Al range between 160.216 mg/kg, 185.739 mg/kg and 239.069 mg/kg. Meanwhile, for radius 15 to 20 m showed a range between 28.183 mg/kg and 43.081 mg/kg.

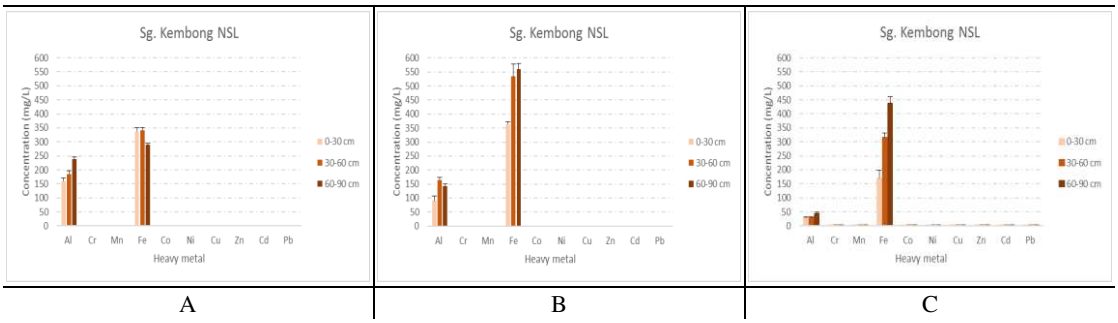

Figure 2. *The pattern of 10 heavy metal concentration depicted Sungai Kembong non-sanitary landfill at different soil depths (0-30 cm, 30-60 cm, and 60-90 cm) and radiuses (A: 5-10 m, B: 10-15 m and C: 15-20 m) of the closed landfill*

Air Hitam sanitary landfill

The results in *Fig. 3* showed heavy metal concentration in a closed non-sanitary landfill with a radius of 5 to 10 m, 10 to 15 m and 15 to 20 m at different depth 0 to 30 cm, 30 to 60 cm and 60 to 90 cm of Air Hitam sanitary landfill. Results of heavy metal showed that Al and Fe concentration is higher at all point of Air Hitam landfill. Among the analysed heavy metals, Al concentration at the radius 10 to 15 m showed the highest concentration. Each showed 235.604 mg/kg and 460.756 mg/kg and 422.434 mg/kg. Meanwhile, radius 5 to 15 m and 15 to 20 m showed 87.317 mg/kg, 75.733 mg/kg and 68.102 mg/kg for radius 5 to 10 m and 19.247 mg/kg, 42.861 mg/kg and 28.097 mg/kg for radius 15 to 20 m. For Fe concentration, the highest concentration depicted by radius 15 to 20 m; 523.195 mg/kg at 0 to 30 cm depth. Fe concentration at radius 10 to 15 m showed almost equal concentration at a different depth. Each showed 337.115 mg/kg, 270.938 mg/kg and 330.970 mg/kg. Meanwhile for radius 5 to 10 m, Fe concentration showed lower concentration at 107.231 mg/kg, 137.143 mg/kg and 136.536 mg/kg for each different depth.

Kubang Badak sanitary landfill

The results in *Fig. 4* showed heavy metal concentration in a closed sanitary landfill with a radius of 5 to 10 m, 10 to 15 m and 15 to 20 m at different depth 0 to 30 cm, 30 to 60 cm and 60 to 90 cm of Kubang Badak sanitary landfill. Results of heavy metal showed that Al and Fe concentration is higher at all point of Kubang Badak landfill.

http://www.aloki.hu ● ISSN 1589 1623 (Print) ● ISSN 1785 0037 (Online)
DOI: http://dx.doi.org/10.15666/aeer/1704_80598067

Among the analysed heavy metals, Fe concentration depicted the highest concentration at the radius 15 to 20 m, 10 to 15 m as well as radius 5 to 10 m of the radius. Each showed 471.797 mg/kg, 260.469 mg/kg and 103.413 mg/kg at radius 15 to 20 m; 676.043 mg/kg, 618.660 mg/kg and 524.594 mg/kg at radius 10 to 15 m and 255.221 mg/kg, 268.966 mg/kg and 353.415 mg/kg at radius 5 to 10 m. However, Al concentration showed the highest concentration depicted by radius 10 to 15 m and 5 to 10 m. Each showed 359.564 mg/kg, 407.121 mg/kg and 289.186 mg/kg at radius 10 to 15 m while 332.316 mg/kg, 391.556 mg/kg and 342.372 mg/kg at radius 5 to 10 m. Meanwhile, Al concentration at radius 15 to 20 m showed 172.183 mg/kg, 121.184 mg/kg and 91.807 mg/kg. Other heavy metal despite Al and Fe showed the lowest concentration at all radius and depth.

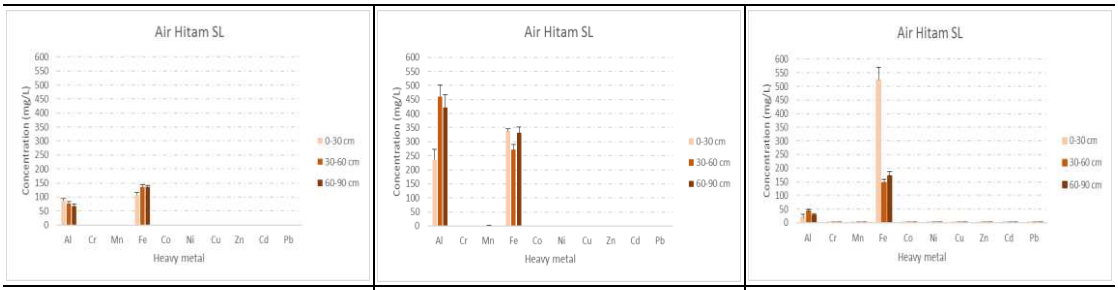

Figure 3. *The pattern of 10 heavy metal concentration depicted Air Hitam sanitary landfill at different soil depths (0-30 cm, 30-60 cm, and 60-90 cm) and radiuses (A: 5-10 m, B: 10-15 m and C: 15-20 m) of the closed landfill*

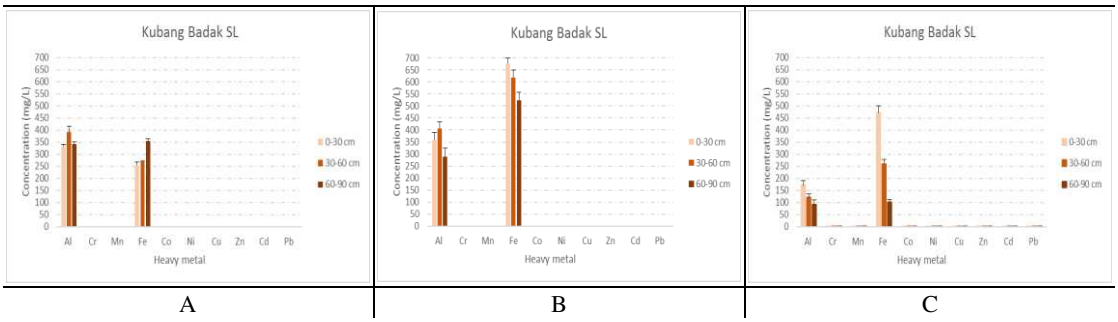

Figure 4. *The pattern of 10 heavy metal concentration depicted Kubang Badak sanitary landfill at different soil depths (0-30 cm, 30-60 cm, and 60-90 cm) and radiuses (A: 5-10 m, B: 10-15 m and C: 15-20 m) of the closed landfill*

Analysis of variance confirmed the findings by exhibiting highly significant differences (P<0.0001) between the radius, depth, and heavy metal concentration at three different radiuses, three different depths, and ten heavy metals concentration. This clearly demonstrates that environmental factors and landfill area background can have an important influence on the accumulation of certain heavy metal and its content. Al and Fe concentration showed the highest pattern on all 4 closed landfill sites. Research by Elwali et al. (2008), showed that the most common heavy metal contaminations at the landfill area vary from iron (Fe), cadmium (Cd), copper (Cu), zinc (Zn) and nickel (Ni). Furthermore, various studies reveal very high contaminants levels in the

http://www.aloki.hu ● ISSN 1589 1623 (Print) ● ISSN 1785 0037 (Online)
DOI: http://dx.doi.org/10.15666/aeer/1704_80598067

groundwater underneath the non-engineered waste disposal sites in Selangor (Bahaa-eldin et al., 2010; Suratman and Sefie, 2010; Taha et al., 2011). The subsurface soils were considerably polluted by heavy metals where wastes were dumped directly on top of the unlined natural formation (Mohd et al., 2013). This is probably the reason for the high concentration of the river alluvium soil beneath the landfill that has the highest metal concentrations of Cu, Zn and Pb (Elwali et al., 2008). Based on the shallow and fluctuation of the periodic water table, water infiltration during the rainy season, acidic soil environment and local groundwater flow direction were the main reasons that enhanced the contamination migration through the soil formation into the groundwater (Elwali et al., 2008). Although the contamination present in the solid waste applied a significant impact on the groundwater, it has to be stressed that different metals behaved differently. Heavy metal binding properties of these soil constituents differ with the charges of the soil material and the ionic valences. As a result, different depths of the sample soil from landfill depict different capability of heavy metal binding. In addition, the rate and amount of pollutant penetration through the soil is also influencing the concentration of heavy metal present in the landfill environment.

Conclusions

The effects of the heavy metals content and composition, radiuses, depths and localities interactions have not been studied in the landfill area. Despite significant results in our understanding of heavy metals contamination distribution profiles at different soil depths and radiuses at closed landfill area, type of soil, the control mechanisms regulating the type of heavy metals distribution and accumulation and soil chemical reaction still remain an enigma. Each factor had an effect on the heavy metals content and profile; however, the most influential factor appeared to be a type of soil. Recommendations for future researches are by identifying the key factors controlling heavy metals distribution and accumulation in a different type of soils a greater understanding of landfill pollution mechanism in response to interactions with environmental factors will emerge.

Acknowledgements. The research was supported by the Ministry of Higher Education Malaysia (MOHE) and International Islamic University Malaysia (IIUM) under research grant PRIGS18-021-0021.

REFERENCES

[1] Agusa, T., Kunito, T., Nakashima, E., Minh, T. B., Tanabe, S., Subramanian, A., Viet, P. H. (2003): Preliminary on trace element contamination in dumping sites of municipal wastes in India and Vietnam. – Journal de Physique IV 107: 21-24.

[2] Bahaa-eldin, E., Rahim, A., Yusoff, I., Samsudin, A. R., Yaacob, W. Z. W., Rafek, A. G. M. (2010): Deterioration of groundwater quality in the vicinity of an active open-tipping site in West Malaysia. – Hydrogeology Journal 18: 997-1006.

[3] Bai, X. Y., Wang, S. J., Xiong, K. N. (2013): Assessing spatial-temporal evolution processes of karst rocky desertification land: indications for restoration strategies. – Land Degradation & Development 24: 47-56.

[4] Bakare, A. A., Mosuro, A. A., Osibanjo, O. (2005): An in vivo evaluation of induction of abnormal sperm morphology in mice by landfill leachates. – Mutation Research-Genetic Toxicology and Environmental 582: 28-34.

http://www.aloki.hu ● ISSN 1589 1623 (Print) ● ISSN 1785 0037 (Online)
DOI: http://dx.doi.org/10.15666/aeer/1704_80598067

[5] Bhattacharya, S., Gupta, K., Debnath, S., Ghosh, U. C., Chattopadhyay, D., Mukhopadhyay, A. (2012): Arsenic bioaccumulation in rice and edible plants and subsequent transmission through food chain in Bengal basin: a review of the perspectives for environmental health. – Toxicological & Environmental Chemistry 94: 429-44.
[6] Boels, D., Fleming, G. (1993): Chemical time bombs from landfills: appraisal and Modelling. – Land Degradation & Rehabilitation 4: 399-405.
[7] Bozkurt, S., Moreno, L., Neretnieks, I. (1999): Long term fate of organics in waste deposits and its effect on metal release. – Science of the Total Environment 228: 135-152.
[8] Bozkurt, S., Moreno, L., Neretnieks, I. (2000): Long term process in waste deposits. – Science of the Total Environment 250: 101-121.
[9] Chen, X. W., Tsz-Fung, W. J., Mo, W. Y., Man, Y. B., Wang-Wai, N. C., Wong, M. H. (2015): Ecological Performance of the Restored South East New Territories (SENT) Landfill in Hong Kong (2000–2012). – Land Degradation & Development 1: 1-13.
[10] Chun-Yang, S. Y., Talib, M. (2006): Overview of brownfields in Malaysia. – Engineer Bulletin. Kuala Lumpur: Institute of Engineering Malaysia.
[11] El-Fadel, M., Findikakis, A. N., Leckie, J. O. (1997): Environmental impacts of solid waste landfilling. – Journal of Environmental Management 50: 1-25.
[12] Elwali, B-E. E. A. R., Yusoff, I., Samsudin, A. R., Yaacob, W. Z. W., Ghani, M. R. A. (2008): Heavy metal contamination of soil beneath a waste disposal site at Dengkil, Selangor, Malaysia. – Soil and Sediment Contamination 17: 449-466.
[13] Hoornweg, D., Bhada-Tata, P. (2012): What A Waste: A Global Review of Solid Waste Management. – Urban Development Series Knowledge Papers. No. 15. The World Bank.
[14] Kardanpour, Z., Jacobsen, O. S., Esbensen, K. H. (2015): Local versus field scale soil heterogeneity characterization - a challenge for representative sampling in pollution studies. – Soil 1: 695-705.
[15] Li, X. L., Gao, J., Brierley, G., Qiao, Y. M., Zhang, J., Yang, Y. W. (2013): Rangeland degradation on the Qinghai–Tibet Plateau: implications for rehabilitation. – Land Degradation & Development 24: 72-80.
[16] Loganathan, P., Hedley, M. J., Grace, N. D. (2008): Pasture soils contaminated with fertilizer derived cadmium and fluoride: livestock effects. – Reviews of Environmental Contamination and Toxicology 192: 29-66.
[17] Mahmoud, E., El-Kader, N. A. (2015): Heavy metal immobilization in contaminated soils using phosphogypsum and rice straw compost. – Land Degradation & Development 26: 819-824.
[18] Minh, N. H., Minh, T. B., Watanabe, M., Kunisue, T., Shinsuke, I., Tanabe, S., Sakai, S., Subramanian, A., Sasikumar, K., Viet, P. H., Tuyen, B. C., Tana, T. S., Prudente, M. S. (2003): Open dumping site in Asian developing countries: a potential source of polychlorinated dibenzo-p-dioxins and polychlorinated dibenzofurans. – Environmental Science and Technology 37: 1493-1502.
[19] Mohd, A. S. N., Yusoff, S., Piaw, C. Y. (2013): Soil chemistry and pollution study of a closed landfill site at Ampar Tenang, Selangor, Malaysia. – Waste Management & Research: the Journal of the International Solid Wastes and Public Cleansing Association, ISWA 31(6): 599-612.
[20] Othman, R., Ali, Q. A. M., Ramya, R. (2016). Contamination composition of Fe, Mn and Al at 8 different profiles of solid waste disposal areas in Malaysia. – International Journal of Environmental Science and Development 7(5): 395-398.
[21] Oygard, J. K., Mage, A., Gjengedal, E. (2004): Estimation of the mass-balance of selected metals in four sanitary landfills inWestern Norway, with emphasis on the heavy metal content of the deposited waste and the leachate. – Water Research 38: 2851-2858.
[22] Pietrzak, U., Uren, N. (2011): Remedial options for copper contaminated vineyard soils. – Soil Research 49: 44-55.

http://www.aloki.hu ● ISSN 1589 1623 (Print) ● ISSN 1785 0037 (Online)
DOI: http://dx.doi.org/10.15666/aeer/1704_80598067

[23] Riber, C., Fredriksen, G. S., Christensen, T. H. (2005): Heavy metal content of combustible municipal solid waste in Denmark. – Waste Management & Research 23: 126-132.
[24] Simis, M., Awang, A. (2015): Planning for Ex-Landfill Redevelopment: Assessing What Community Have in Mind. – Asian Social Science 11(15): 136.
[25] Simis, M., Awang, A., Arifin, K. (2016): From Ex-landfill to Public Park: Impact on Local Community's Quality of Life and Living Environment. – Procedia-Social and Behavioral Sciences 222: 763-771.
[26] Suratman, S., Sefie, A. (2010): Groundwater contamination at landfill sites in Selangor. – IAH, Krakow 2205-11.
[27] Swati, Ghosh, P., Das, M. T., Thakur, I. S. (2014): *In vitro* toxicity evaluation of organic extract of landfill soil and its detoxification by indigenous pyrene-degrading *Bacillus* sp. ISTPY1. – International Biodeterioration & Biodegradation 90: 145-151.
[28] SWCorp (2017): Solid Waste Management and Public Cleansing Corporation. – Personal interview: Top Management Official.
[29] Taha, M. R., Yaacob, W. Z. W., Samsudin, A. R., Yaakob, J. (2011): Groundwater quality at two landfill sites in Selangor, Malaysia. – Bulletin of the Geological Society of Malaysia 57: 13-18.
[30] Tengku Ibrahim, T. N. B., Othman, F., Mahmood, N. Z. (2017): Assessment of water quality of Sembilang River receiving effluent from controlled municipal solid waste (MSW) landfill in Selangor. – International Technical Postgraduate Conference, IOP Conference Series: Materials Science and Engineering 210.
[31] Thomaz, E. L., Luiz, J. C. (2012): Soil loss, soil degradation and rehabilitation in a degraded land area in Guarapuava (Brazil). – Land Degradation & Development 23: 72-81.
[32] Wong, M. H., Chan, Y. S. G., Zhang, C., Wang-Wai, N. C. (2015): Comparison of pioneer and native woodland species growing on top of an engineered landfill, Hong Kong: restoration program. – Land Degradation & Development 2380.
[33] Yahaya, N. S., Lim, C. S., Taha, M. R., Pereira, J. J. (2016): Exposure of municipal solid waste disposal sites to climate related geohazards: Case study of Selangor. – Bulletin of the Geological Society of Malaysia 62: 57-63.
[34] Youn-Joo, A. (2004): Soil ecotoxicity assessment using cadmium sensitive plants. – Environmental Pollution 127: 21-26.
[35] Yusoff, I., Alias, Y., Yusof, M., Ashraf, M. A. (2013): Assessment of pollutants migration at Ampar Tenang landfill site, Selangor, Malaysia. – Science Asia 39: 392-409.
[36] Zhao, F., McGrath, S. P., Crosland, A. R. (1994): Comparison of three wet digestion methods for determination of plant sulphur by inductively coupled plasma atomic emission spectroscopy (ICP-AES). – Communications in Soil Science and Plant Analysis 25: 407-418.

http://www.aloki.hu ● ISSN 1589 1623 (Print) ● ISSN 1785 0037 (Online)
DOI: http://dx.doi.org/10.15666/aeer/1704_80598067

STUDY ON HEAVY METAL CONTAMINATION DISTRIBUTION AT ACTIVE LANDFILL AT DIFFERENT DEPTHS AND RADIUSES

OTHMAN, R.[1*] – MOHD LATIFF, N. H.[1] – BAHARUDDIN, Z. M.[1] – HASHIM, K. S. H. Y.[2] – LUKMAN HAKIM MAHAMOD, L. H.[3]

[1]*International Institute for Halal Research and Training (INHART) Department of Landscape Architecture, Kulliyyah of Architecture and Environmental Design (KAED), International Islamic University Malaysia, 53100 Kuala Lumpur, Malaysia*

[2]*Department of Urban & Regional Planning, Kulliyyah of Architecture and Environmental Design (KAED), International Islamic University Malaysia, 53100 Kuala Lumpur, Malaysia*

[3]*Department of Quantity Surveying, Kulliyyah of Architecture and Environmental Design (KAED), International Islamic University Malaysia, 53100 Kuala Lumpur, Malaysia*

[*]*Corresponding author*
e-mail: rashidi@iium.edu.my; phone: +60-126-644-772; fax: +60-361-964-864

(Received 24th Jan 2019; accepted 3rd May 2019)

Abstract. Landfilling is more preferable in Malaysia compared to another disposal method due to low cost, and availability of land. Other than solid waste, the percolation of water into the landfill leads to leachate formation. The migration of waste in leachate form may accelerate the heavy metal contamination of the soil one of the major concerns in landfilling. This study aimed in comparing soil samples taken from five different sites in Selangor of inert waste (Sungai Kertas, Kuang and Dengkil) and sanitary (Tanjung Dua Belas and Jeram) landfills at different depths (0-30 cm, 30-60 cm and 60-90 cm) and radiuses (5-10 m, 10-15 m and 15-20 m), for ten heavy metals (Al, Cr, Mn, Fe, Co, Ni, Cu, Zn, Cd and Pb) to find the risk of heavy metal movement from the upper layer cell into the deeper layer of the soil block. All the data were analysed using ICP-MS (Perkin Elmer NexION 300X). Al and Fe displayed high concentration at most of the sites especially at the deeper depth of the soil.
Keywords: *urban pollution, landfill, active sanitary landfills, inorganic pollutant, leachate, municipal solid waste*

Introduction

According to Agamuthu et al. (2014) and Yusoff et al. (2013), there is a total of about 251 landfills of different sizes and ages recognized officially in Malaysia. Out of these, 111 were closed and 150 are active landfills. These active landfills include 77 open dumpsites, 49 open-tipping sites, 19 landfills without leachate treatment, 10 landfills with leachate treatment, and 6 are sanitary (engineered). In Malaysia, proper disposal of solid waste at sanitary landfills constitute only a small portion of a whole and was built recently compared to open dumps which constitute around 90% of all the waste disposal sites (Agamuthu and Fauziah, 2011; Sharifah and Latifah, 2013).

Selangor as one of the most developed states in Malaysia has produced the highest MSW per capita due to the high standard of living (Agamuthu, 2001; Leete, 2002). Studies reported that Selangor is responsible for one-third of the total amount of solid waste generated in Malaysia with 3,923 tons daily (Riber et al., 2005; Ismail and Manaf, 2013; Sharifah and Latifah, 2013). Twelve landfill sites from a total of 20 landfill sites in Selangor (closed and operating) are considered as open dumpsites with level 0 sanitary

http://www.aloki.hu ● ISSN 1589 1623 (Print) ● ISSN 1785 0037 (Online)
DOI: http://dx.doi.org/10.15666/aeer/1704_80698077

classification, which generate the highest risk of contamination and leachate migration. In addition, all 20 landfills are located in 5 main river basins where the Sungai Selangor Basin has the highest number of operating landfills (three) and four closed landfills. The classification is as followings; Level 0: Open dumping; Level I: Controlled tipping; Level II: Sanitary landfill with a bund and daily soil cover; Level III: Sanitary landfill with leachate recirculation system; and Level IV: Sanitary landfill with leachate treatment facilities.

Sanitary landfilling and open dumping are commonly known across the world as disposal of municipal solid waste (MSW) method. Sanitary landfilling is predominantly practiced in developed nations while open dumping is common in low-income and developing nations (Yahaya, 2016). An open dump is a primitive and non-sanitary waste disposal site where indiscriminate wastes are improperly tipped or dumped in a pre-existing hole or on the side of a hill without proper maintenance (Agamuthu, 2001; Blight, 2008). As an alternative, a sanitary landfill utilizes the principles of engineering to ensure the protection of the environment and public health while providing safe long-term disposal of solid wastes (American Society of Civil engineers, 1959). In Malaysia, municipal solid waste is disposed of in both the newer sanitary landfills and older open dumps.

The increasing of waste generation due to this municipal solid waste, however, shortens the span of a landfill. Thus, more and more new areas have to be converted into disposal sites. The negative impacts of MSW landfill on the environment cause a wide range of concern. It includes the risk of explosion, odor problem, leachate seeping into surface and groundwater system, as well as, soil contamination due to heavy metal sourced from disposed waste (Fauziah and Agamuthu, 2005). Contaminated soil remediation is reported as one of the most expensive technologies in environmental management.

Based on the previous study, most organic chemical substances will eventually either be degraded through biochemical reactions in the landfill or be leached out of the landfill with water movement. However, the majority of heavy metals will remain in the landfill because heavy metal migration is very limited compared to the number of metals accumulated in the landfill (Øygard et al., 2004; Riber et al., 2004), especially in anaerobic processes. The slow movement of heavy metals is the result of heavy metals being subjected to strong sorption on soil particles, precipitation under anaerobic conditions, and chelation with inorganic and organic ligands in landfills (Bozkurt et al., 1999, 2000). Heavy metal contamination is mainly due to the subsequent migration of leachate from and within the landfill's waste cell. The natural process taking place within the boundaries of the waste cells accelerate the process of heavy metal leaching from the waste component. Various types of wastes are the main sources of heavy metal within a landfill system. This includes metal waste components such as food cans and scrap metal and the indiscriminate dumping of household hazardous waste and electronic waste such as batteries and old computer. The release of heavy metal into the adjacent environment is a serious environmental concern and a threat to public health and safety.

Material and methods

Study area description

Five active landfill sites (3 non-sanitary landfills and 2 sanitary landfills) located at Selangor, Malaysia namely; Sungai Kertas non-sanitary landfill (3°15'52.5"N

http://www.aloki.hu ● ISSN 1589 1623 (Print) ● ISSN 1785 0037 (Online)
DOI: http://dx.doi.org/10.15666/aeer/1704_80698077

101°41'05.1"E), Kuang non-sanitary landfill (3°15'31.4"N 101°33'50.0"E), Dengkil non-sanitary landfill (2°52'12.2"N 101°38'54.1"E), Tanjung Dua Belas sanitary landfill (2°43'48.9"N 101°36'21.7"E) and Jeram sanitary landfill (3°11'23.8"N 101°21'54.3"E) were selected for this study. The site selection was based on the types of the landfill and the size of the landfill located in Selangor state. *Table 1* indicates the landfill sites info with the area covered, wasted collected, total year of operation and the current status of the landfill studied.

Table 1. *Selected landfill sites with the area covered, waste collected per day, total year operation and current status*

Landfill Sites	Area (Acre)	Waste Collected (Tone/Day)	Total Year Operation	Current Status	Source
Kampung Sungai Kertas Inert Waste	14.19	130	7	Active	Othman et al. (2016)
Kuang Inert Waste Landfill	27	50	11	Active	Tengku Ibrahim et al. (2017)
Dengkil Inert Waste Landfill	145	400	25	Active	Othman et al. (2016)
Tanjung 12 Sanitary Landfill	160	1000	20	Active	Yahaya et al. (2016)
Jeram Sanitary Landfill	160	2500	16	Active	Othman et al. (2016)

Soil sampling

Soil samples were collected at different points (0-200 mm depth, approx. 1000 g) were taken by using soil auger (Eijkelkamp Agrisearch). The soil then was sealed in a polyethylene bag and labeled. The soil was dried in an oven for 70ºC for 3 days to a week depending on the moistness of the soil. Then samples were ground by using agate mortar until becoming small particles. Then it was sieved using a 2 mm mesh to remove stones and plant materials. Then samples were stored at room temperature before being digested using Microwave Digestion Ethos D (Milestone, 2001). Heavy metals, Al, Cr, Mn, Fe, Co, Ni, Cu, Zn, Cd, and Pb were then analysed by using ICP-MS (Perkin Elmer NexION 300X).

Heavy metals digestion and analysis

0.5 g of soil samples were accurately weighed into a container made of PFA perfluoroalkoxy polymer and digested through a microwave digestion system using the digestion method as described by Zhao et al. (1994). Soil samples were air-dried and sieved. Soil samples were passed through a 2 mm sieve and ready for further analysis. Dried and the ground sample was mixed with 10 ml of concentrated nitric acid (HNO_3 65%) and digested. Acid was added for each soil samples and then the digestion tubes were placed in a rotor segment by using a torque wrench. The segments were inserted into the microwave cavity and connected with the temperature sensor. The mixture temperature was adjusted to ±175ºC and 1,200 Watt of power for 30 minutes using Microwave Digestion (Milestone Start D) as detailed in Method US EPA 3051. The digestion was completed after the last solution was clear and no brownish fumes were released from the digestion vessel tubes. When digestion was completed, samples

http://www.aloki.hu ● ISSN 1589 1623 (Print) ● ISSN 1785 0037 (Online)
DOI: http://dx.doi.org/10.15666/aeer/1704_80698077

were removed and diluted. The soil digests were adjusted to the final volume of 50 mL with deionized water. This solution is further 1:1 diluted for the analysis of components by ICP-MS and divided into triplicate each into 15 ml tubes.

Data Analysis

All the experiments were carried out in triplicates and data presented as mean values of three independent replicates. Data were further analysed using analysis of variance (ANOVA). Statistical analysis for all experiments was performed by using SAS through factorial analysis of variance followed by Tukey's test with significant different at $P<0.0001$.

Results and discussion

Sungai Kertas Inert Waste non-sanitary landfill

The results in *Fig. 1* showed heavy metal concentration in an active non-sanitary landfill with a radius of 5 to 10 m, 10 to 15 m and 15 to 20 m at different depth 0 to 30 cm, 30 to 60 cm and 60 to 90 cm of Sungai Kertas non-sanitary landfill. Results of heavy metal showed that Al and Fe concentration is higher at all point of Sungai Kertas landfill.

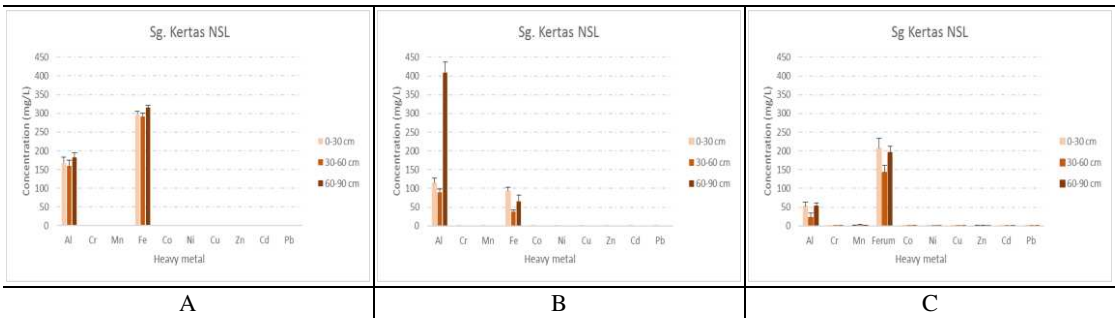

Figure 1. *The pattern of 10 heavy metal concentration depicted Sungai Kertas non-sanitary landfill at different soil depths (0-30 cm, 30-60 cm, and 60-90 cm) and radiuses (A: 5-10 m, B: 10-15 m and C: 15-20 m) of the active landfill*

Among the analyzed heavy metals, Al had the highest concentrations up to 409.786 mg/kg within active non-sanitary soil heavy metal concentration. Compared altogether between these three radiuses of Sungai Kertas non-sanitary landfill, the heavy metal concentration at radius 5 to 10 m showed the highest result for Fe; 297.023 mg/kg, 291.954 mg/kg and 314.758 mg/kg. The lowest results showed by Al at radius 15 to 20 m; 52.089 mg/kg, 22.256 mg/kg and 53.188 mg/kg meanwhile Fe at radius 10 to 15 m showed 93.175 mg/kg, 38.714 mg/kg and 65.584 mg/kg.

Kuang Inert Waste non-sanitary landfill

The results in *Fig. 2* showed heavy metal concentration in an active non-sanitary landfill with a radius of 5 to 10 m, 10 to 15 m and 15 to 20 m at different depth 0 to 30 cm, 30 to 60 cm and 60 to 90 cm of Kuang non-sanitary landfill. Results of heavy metal showed that the highest concentration is depicted by Fe. The concentration is

http://www.aloki.hu ● ISSN 1589 1623 (Print) ● ISSN 1785 0037 (Online)
DOI: http://dx.doi.org/10.15666/aeer/1704_80698077

higher at the centre and the middle point of Kuang landfill. Compared altogether between these three radius of Kuang non-sanitary landfill, heavy metal concentration showed the highest result for Fe at the radius 15 to 20 m; 593.954 mg/kg, 546.171 mg/kg and 570.699 mg/kg and radius 10 to 15 m; 433.383 mg/kg, 235.407 mg/kg and 230.230 mg/kg. The lowest results showed by Al at radius 10 to 15 m; 22.311 mg/kg, 36.557 mg/kg and 32.934 mg/kg well as radius 5 to 10 m; 44.811 mg/kg, 29.436 mg/kg and 36.277 mg/kg.

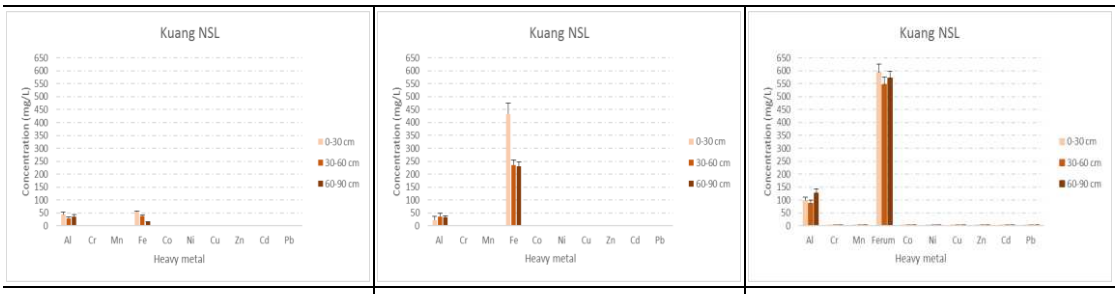

Figure 2. *The pattern of 10 heavy metal concentration depicted Kuang non-sanitary landfill at different soil depths (0-30 cm, 30-60 cm, and 60-90 cm) and radiuses (A: 5-10 m, B: 10-15 m and C: 15-20 m) of the active landfill*

Dengkil Inert Waste non-sanitary landfill

The results in *Fig. 3* showed heavy metal concentration in an active non-sanitary landfill with a radius of 5 to 10 m, 10 to 15 m and 15 to 20 m at different depth 0 to 30 cm, 30 to 60 cm and 60 to 90 cm of Dengkil non-sanitary landfill. Results of heavy metal showed that the highest concentration is depicted by Al. The concentration is higher at radius 10 to 15 m of Dengkil landfill.

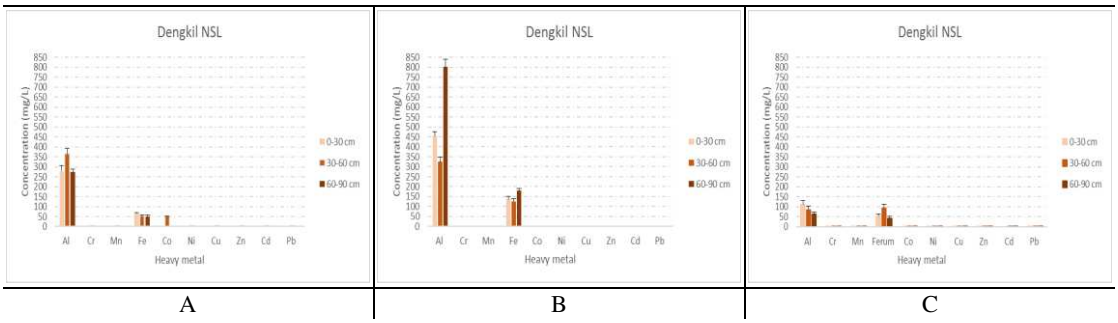

Figure 3. *The pattern of 10 heavy metal concentration depicted Dengkil non-sanitary landfill at different soil depths (0-30 cm, 30-60 cm, and 60-90 cm) and radiuses (A: 5-10 m, B: 10-15 m and C: 15-20 m) of the active landfill*

Compared altogether between these three radiuses of Dengkil non-sanitary landfill, heavy metal concentration showed the highest result for Al at radius 10 to 15 m; 455.457 mg/kg, 325.270 mg/kg and 800.804 mg/kg followed by radius 5 to 10 m; 278.700 mg/kg, 364.215 mg/kg and 275.386 mg/kg. The lowest results showed by Fe at all point. The highest concentration for Fe showed by radius 10 to 15 m;

http://www.aloki.hu ● ISSN 1589 1623 (Print) ● ISSN 1785 0037 (Online)
DOI: http://dx.doi.org/10.15666/aeer/1704_80698077

137.191 mg/kg, 126.688 mg/kg and 178.860 mg/kg followed by radius 15 to 20 m; 54.143 mg/kg, 93.842 mg/kg and 41.216 mg/kg then radius 5 to 10 m; 65.457 mg/kg, 52.985 mg/kg and 51.282 mg/kg. There is a concentration of Co that showed up to 52.985 mg/kg at 30-60 cm depth for radius 5 to 10 m.

Tanjung Dua Belas sanitary landfill

The results in *Fig. 4* showed heavy metal concentration in an active sanitary landfill with a radius of 5 to 10 m, 10 to 15 m and 15 to 20 m at different depth 0 to 30 cm, 30 to 60 cm and 60 to 90 cm of Tanjung Dua Belas sanitary landfill. Results of heavy metal showed that the highest concentration is depicted by Fe and Al. The concentration is higher at radius 10 to 15 m of Tanjung Dua Belas landfill. Compared altogether between these three radiuses of Tanjung Dua Belas sanitary landfill, heavy metal concentration showed the highest result for Al at radius 10 to 15 m; 85.182 mg/kg, 159.445 mg/kg and 567.264 mg/kg followed by Fe; 113.967 mg/kg, 161.552 mg/kg and 321.409 mg/kg. The radius 15 to 20 m concentration also lead by Al and Fe. Each showed 133.694 mg/kg, 120.739 mg/kg, 137.235 mg/kg for Al concentration and 170.976 mg/kg, 83.036 mg/kg and 162.968 mg/kg for Fe concentration. Meanwhile, at a radius 5 to 10 m, the concentration showed almost equal between Al and Fe. Al concentration at radius 5 to 10 m; 104.207 mg/kg, 138.692 mg/kg and 136.317 mg/kg followed by Fe; 120.165 mg/kg, 106.395 mg/kg and 103.827 mg/kg.

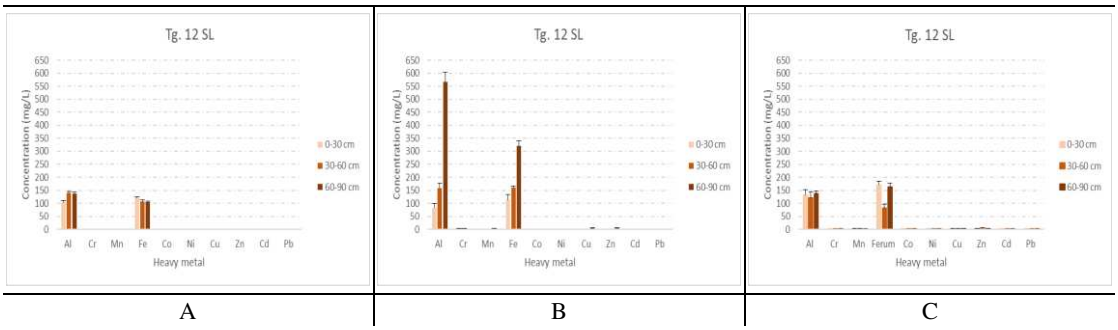

A B C

Figure 4. *The pattern of 10 heavy metal concentration depicted Tanjung Dua Belas sanitary landfill at different soil depths (0-30 cm, 30-60 cm, and 60-90 cm) and radiuses (A: 5-10 m, B: 10-15 m and C: 15-20 m) of the active landfill*

Jeram sanitary landfill

The results in *Fig. 5* showed heavy metal concentration in an active sanitary landfill with a radius of 5 to 10 m, 10 to 15 m and 15 to 20 m at different depth 0 to 30 cm, 30 to 60 cm and 60 to 90 cm of Jeram sanitary landfill. Results of heavy metal showed that the highest concentration is depicted by Fe and Al. The concentration is higher at the radius 15 to 20 m of Jeram landfill. Compared altogether between these three radiuses of Jeram sanitary landfill, heavy metal concentration showed the highest result for Al and Fe at radius 15 to 20 m; each at 219.009 mg/kg and 232.830 mg/kg for 0 to 30 cm depth. Followed by Fe at radius 10 to 15 m; 239.127 mg/kg for 30 to 60 cm depth. Meanwhile, for Al and Fe concentration at radius 5 to 10 m showed almost equal readings at all depth. Each showed 32.632 mg/kg, 82.432 mg/kg and 52.744 mg/kg for Al and 104.709 mg/kg, 168.297 mg/kg and 151.001 mg/kg for Fe.

http://www.aloki.hu ● ISSN 1589 1623 (Print) ● ISSN 1785 0037 (Online)
DOI: http://dx.doi.org/10.15666/aeer/1704_80698077

Analysis of variance confirmed the findings by exhibiting highly significant differences (P<0.0001) between the radius, depth, and heavy metal concentration at three different radiuses, three different depths, and ten heavy metals concentration. This clearly demonstrates that environmental factors and landfill area background can have an important influence on the accumulation of certain heavy metal and its content. Al and Fe concentration showed the highest pattern on all 4 active landfill sites. This might probably cause by the transportation of metals that may vary between relatively unpolluted systems and disturbed or polluted systems as well as the site context. Particulate transport is dominant in unpolluted systems where metal inputs are principally from the erosion of watershed substrates (Elder, 1989).

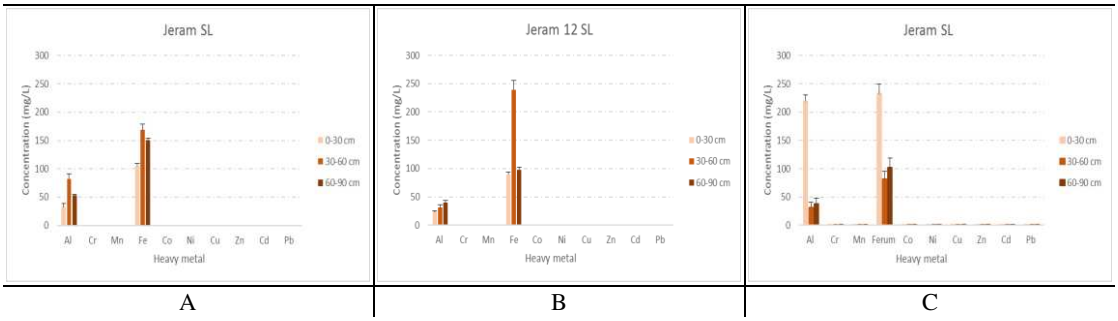

Figure 5. *The pattern of 10 heavy metal concentration depicted Jeram sanitary landfill at different soil depths (0-30 cm, 30-60 cm, and 60-90 cm) and radiuses (A: 5-10 m, B: 10-15 m and C: 15-20 m) of the active landfill*

In disturbed or polluted systems, for example, those affected by acid-mine drainage, point sources commonly deliver metals in a soluble phase or associated with organic matter, and the proportion of dissolved metals and their bioavailability tends to be higher (Solomons and Förstner, 1984). Leachate is still being produced even though most of the non-sanitary landfills in Selangor have been closed or still operating. This leachate production still occurs and badly affect the nearest water system and soil due to the location of the landfills near the water system as a source of water to the local residents. Therefore, environmental factors and landfill area background can have an important influence on the accumulation of certain heavy metal and its content. There are high contaminants levels in the groundwater underneath the non-engineered waste disposal sites in Selangor. The rate and amount of pollutant penetration through the soil is also influencing the concentration of heavy metal present in the landfill environment and finally lead to different capability depiction of heavy metal binding in the soil.

Conclusions

It can be summarised that heavy metal contents in Sungai Kertas non-sanitary landfill, Kuang non-sanitary landfill, Dengkil non-sanitary landfill, Tanjung Dua Belas sanitary landfill and Jeram sanitary landfill were accumulated by high Al and Fe. A few of the landfills had been exposed to Cr, Mn, Zn, Co, and Cu below 5.0 mg/kg. They are Sungai Kertas non-sanitary landfill, Dengkil non-sanitary landfill and Tanjung Dua Belas sanitary landfill. Kuang non-sanitary landfill and Jeram sanitary landfill showed only Al and Fe contaminations. In other words, there are particular locations as well as

http://www.aloki.hu ● ISSN 1589 1623 (Print) ● ISSN 1785 0037 (Online)
DOI: http://dx.doi.org/10.15666/aeer/1704_80698077

depth and radius where specific heavy metals signature accumulates with high concentration levels and some with low level. This raises the importance and needs for an effective potential model system for future research to investigate in depth the environmental factors such as the type of soil and waste that influence heavy metals profile and distribution or controlling heavy metals accumulation.

Acknowledgements. The research was supported by the Ministry of Higher Education Malaysia (MOHE) and International Islamic University Malaysia (IIUM) under research grant PRIGS18-021-0021.

REFERENCES

[1] Agamuthu, P. (2001): Solid waste: Principles and management, with Malaysian case studies. – University of Malaya Press 395.
[2] Agamuthu, P., Fauziah, S. H. (2011): Challenges and issues in moving towards sustainable landfilling in a transitory country, Malaysia. – Waste Management & Research, The Journal of the International Solid Wastes and Public Cleansing Association ISWA 29(1): 13-19.
[3] Agamuthu, P., Yee, C. W., Rahedah, S., Nithyarubini, T., Boon Tien, L., Jayanthi, B. (2014): Enhancement of landfill methane oxidation using different types of organic wastes. – Environmental Earth Science 73(5): 2489-2496.
[4] American Society of Civil Engineers, ASCE (1959): Sanitary Landfill Manual of Practice. – ASCE, New York USA 61.
[5] Blight, G. E. (2008): Slope failures in municipal solid waste dumps and landfills: a review. – Waste Management and Research 26(5): 448-463.
[6] Bozkurt, S., Moreno, L., Neretnieks, I. (1999): Long term fate of organics in waste deposits and its effect on metal release. – Science of the Total Environment 228: 135-152.
[7] Bozkurt, S., Moreno, L., Neretnieks, I. (2000): Long term process in waste deposits. – Science of the Total Environment 250: 101-121.
[8] Elder, J. F. (1989): Metal biogeochemistry in surface-water systems—A review of principles and concepts: U.S. – Geological Survey Circular 1013: 43.
[9] Fauziah, S. H., Agamuthu, P. (2005): Pollution Impacts of MSW Landfill Leachate. – Malaysian Journal of Science 24: 31-37.
[10] Ismail, S. N. S., Manaf, L. A. (2013): The challenge of future landfill: A case study of Malaysia. – Journal of Toxicology and Environmental Health Sciences 5(6): 86-96.
[11] Leete, R. (2005): Selangor's Human Development: Progress and Challenges. – United Nations Development Programme (UNDP) http://dspace.cigilibrary.org/jspui/handle/123456789/20421.
[12] Othman, R., Ali, Q. A. M., Ramya, R. (2016): Contamination composition of Fe, Mn and Al at 8 different profiles of solid waste disposal areas in Malaysia. – Int. Journal of Environ. Science and Dev 7(5): 395-398.
[13] Øygard, J. K., Mage, A., Gjengedal, E. (2004): Estimation of the mass-balance of selected metals in four sanitary landfills inWestern Norway, with emphasis on the heavy metal content of the deposited waste and the leachate. – Water Res 38: 2851-2858.
[14] Riber, C., Fredriksen, G. S., Christensen, T. H. (2005): Heavy metal content of combustible municipal solid waste in Denmark. – Waste Management & Research 23: 126-132.
[15] Saheri, S., Mir, M. A., Basri, N. E. A., Mahmood, N. Z., Begum, R. A. (2012): Life cycle assessment for solid waste disposal options in Malaysia. – Polish Journal of Environmental Studies 21(5): 1377-1382.
[16] Sharifah, N. S. I., Latifah, A. M. (2013): The challenge of future landfill: A case study of Malaysia. – Journal of Toxicology and Environmental Health Sciences 5(6): 86-96.

http://www.aloki.hu ● ISSN 1589 1623 (Print) ● ISSN 1785 0037 (Online)
DOI: http://dx.doi.org/10.15666/aeer/1704_80698077

[17] Simmons, R. W., Pongsakul, P., Saiyasitpanich, D., Klinphoklap, S. (2004): Cadmium contamination of soil and rice in a case study location in Thailand: Impliations for public health and potential management options. – International Symposium on Phytoremediation Technology.
[18] Tarmudi, Z., Abdullah, M. L., Tap, A. O. M. (2012): An overview of municipal solid wastes generation in Malaysia. – JurnalTeknologi 51(1): 1-15.
[19] Tengku Ibrahim, T. N. B., Othman, F., Mahmood, N. Z. (2017): Assessment of water quality of Sembilang River receiving effluent from controlled municipal solid waste (MSW) landfill in Selangor. – International Technical Postgraduate Conference IOP Conference Series: Materials Science and Engineering 210.
[20] Yahaya, N. S., Choun, S. L., Taha, M. R., Joy, J. P. (2016): Exposure of municipal solid waste disposal sites to climate related geohazards: Case study of Selangor. – Bulletin of the Geological Society of Malaysia 62: 57-63.
[21] Yusoff, I., Alias, Y., Yusof, M., Ashraf, M. A. (2013): Assessment of pollutants migration at Ampar Tenang landfill site, Selangor, Malaysia. – Science Asia 39: 392-409.
[22] Zhao, F., McGrath, S. P., Crosland, A. R. (1994): Comparison of three wet digestion methods for determination of plant sulphur by inductively coupled plasma atomic emission spectroscopy (ICP-AES). – Communications in Soil Science and Plant Analysis 25: 407-418.

http://www.aloki.hu ● ISSN 1589 1623 (Print) ● ISSN 1785 0037 (Online)
DOI: http://dx.doi.org/10.15666/aeer/1704_80698077

THE INFLUENCE OF URBAN PARK GREEN SPACES, PLANT MATERIAL SPECIFICATIONS AND SPATIAL DESIGN ORGANIZATION AND PATTERN TOWARDS CARBON SEQUESTRATION RATE

OTHMAN, R.[1*] – SUID, S.[1] – MOHD NOOR, N. F.[1] – BAHARUDDIN, Z. M.[1] – HASHIM, K. S. H. Y.[2] – LUKMAN HAKIM MAHAMOD, L. H.[3]

[1]International Institute for Halal Research and Training (INHART) Department of Landscape Architecture, Kulliyyah of Architecture and Environmental Design (KAED), International Islamic University Malaysia, 53100 Kuala Lumpur, Malaysia

[2]Department of Urban & Regional Planning, Kulliyyah of Architecture and Environmental Design (KAED), International Islamic University Malaysia, 53100 Kuala Lumpur, Malaysia

[3]Department of Quantity Surveying, Kulliyyah of Architecture and Environmental Design (KAED), International Islamic University Malaysia, 53100 Kuala Lumpur, Malaysia

[*]Corresponding author
e-mail: rashidi@iium.edu.my; phone: +60-126-644-772; fax: +60-361-964-864

(Received 24th Jan 2019; accepted 3rd May 2019)

Abstract. Urban parks planning and management is a crucial issue in the context of the urban environment and community development by creating space for social interactions, recreation, aesthetics and provide natural habitats. Apart from that, the value of the ecological functions such as air purification, storm water regulation and carbon storage are also crucial for biodiversity conservation within the urban context. This study provides a case study of the quantification of carbon sequestration rate by a selected urban park with a hybrid design landscape setting in Putra Heights, Mukim Damansara, Selangor. The carbon sequestration rate was calculated by biomass equations, using field data inventory, measurements, plan analysis and survey data analysis. This study aimed to discuss the influence of urban park green spaces, plant materials specifications and spatial design organization and pattern towards carbon sequestration rate. The significant outcome of this study is the determination of key factors that influenced the Carbon Sequestration Rate. This study proved that higher plants specification plays an important role in sequestering more carbon. The larger green area also contributes to higher carbon sequestration rate. These findings will become a novel landscape design approach to neutralize carbon emission with cost-effective and environmentally friendly.
Keywords: *carbon emission, air pollution, green technology, landscape design, urban landscape*

Introduction

Recently, urban greenery systems have been promoted as a climate change mitigation method (Velasco et al., 2016) as urban vegetation reduces the carbon dioxide (CO_2) concentration of the atmosphere through photosynthesis and by carbon storage via plant growth. The greatest available green spaces for city residents are urban parks (Ehnat, 2011; Gratani et al., 2016). Urban parks have been identified as one of the most important components of cities and had an evolving role in the life of city residents. Urban parks help decrease carbon emission levels in cities (Sadeghian, 2013). Trees act as a sink for CO_2 by fixing carbon during photosynthesis and storing carbon as biomass (Nowak, 2013). According to Shahidan (2015), plants can filter heat and reduce radiation thus cooling off the urban environment. Therefore, urban park due to its

http://www.aloki.hu ● ISSN 1589 1623 (Print) ● ISSN 1785 0037 (Online)
DOI: http://dx.doi.org/10.15666/aeer/1704_80798088

conditions that are covered with plants is more likely beneficial to reduce urban heat island effect. Urban heat island effect is caused by the large areas of heat-absorbing surfaces, in a combination of high energy use in cities (Sadeghian, 2013).

However, the rapid wave of urbanization in recent decades foresees the high potential for increasing energy demand and severe environmental concerns, simultaneously. Furthermore, it is expected that by 2020, 3 quarters of the Malaysian population will be living in urban areas (Tenth Malaysia Plan, 2010). According to the Department of Statistics Malaysia (2011), in tandem with Malaysia's rapid development, the proportion of urban population increased to 71.0 percent in 2010 compared with 62.0 percent in 2000. One of the state in Malaysia with a high level of urbanization was Selangor with 91.4 percent. A significant increase in the urban population in a short span of time creates various problems, especially environmental problems. Air and noise pollutions are generally considered as a major concern in urban areas.

The recent study by Shahbaz et al. (2015) found strong causal links between urbanization and energy consumption in Malaysia. Therefore, there is a possibility that the urbanization also has direct or indirect relation with carbon dioxide emission. Thus, having an urban park will help to mitigate climate change by functioning as a carbon sink to reduce air pollutant level and sequestering atmospheric CO_2. Carbon sequestration is defined as a method or process of moderating carbon dioxide in the atmosphere to stop it from being polluted (Singh, 2013). This method will contribute to mitigating global warming as it will capture and store carbon dioxide gas in a particular process (Rackley, 2010).

Although the impacts of urban trees thus have been studied rather extensively, at least through urban air quality models, there is a suggestion that research specifically on urban parks has been limited so far (Pataki et al., 2011; Yin et al., 2011). The case study for this research is Putra Heights Neighbourhood Park (*Fig. 1*) with hybrid design landscape setting located at Selangor, Malaysia. Thus, the objective of this research is to assess the influence of urban park green spaces, plant materials specifications and spatial design organization and pattern towards carbon sequestration rate.

Material and methods

Study area description

Selected site study area (*Fig. 1*) located at Neighborhood Park, Putra Heights, Mukim Damansara, Daerah Petaling, Selangor (3°01'13.1"N 101°34'31.7"E), a rapidly urbanized and populated city surrounded by highly developed residential areas with the Light Rail Transit (LRT) and ELITE highway located nearby. With the overall park area of 10.45 acres, this urban park serves as a recreational park to the surrounding neighbourhood area.

Site inventory and plan analysis

The first method applied was through site inventory and analysis. The girth of each plants species was measured conventionally at the breast height (GBH) i.e. near about 1.32 m above the ground surface as well as overall plants heights (Moumita, 2015). For calculating the total built-up area and green area of the park, the base map of Putra Heights Neighborhood Park was obtained from the authority. Plan analysis was

http://www.aloki.hu ● ISSN 1589 1623 (Print) ● ISSN 1785 0037 (Online)
DOI: http://dx.doi.org/10.15666/aeer/1704_80798088

conducted to determine the overall park design structure, planting composition and also spatial design organization and pattern. Apart from that, the bill of quantities of landscape plants was also retrieved in order to identify the exact quantity of the plant materials and to identify the plant specifications including the overall height and breast height diameter of plants for determination of age. Next, the current carbon sequestration rate (CSR) on every planting species was calculated using the carbon calculator formula stated in *Table 1* below. In calculating the carbon sequestration rate of the selected site study area, there are few matters needed to be considered as the rate for carbon sequestration vary greatly depending on a few factors such as tree species, age/stage of tree, composition/density of tree, location/condition of the tree and type of soil (Othman, 2016).

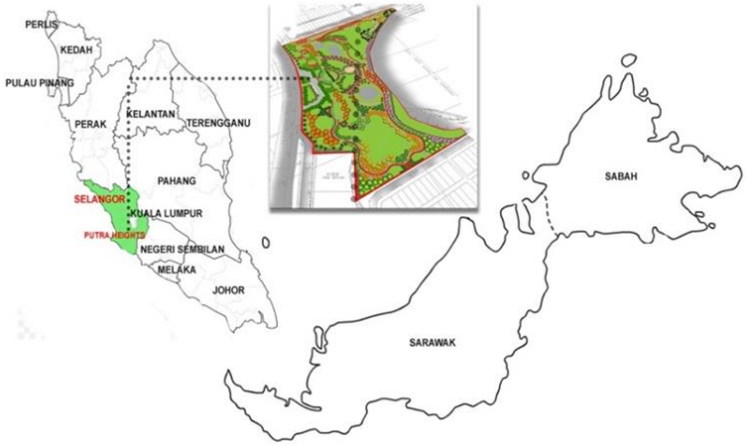

Figure 1. *Base map showing the study area located at Putra Heights Neighbourhood Park, Selangor, Malaysia*

Table 1. *The formula to calculate carbon sequestration rate (CSR)*

CSR formula for tree and shrub	CSR formula for turf, climber and groundcover
Total Green Weight (TGW): $0.25D^2H$ (1.2)	Total Dry Weight (TDW): 0.56 x area (m^2)
Total Dry Weight (TDW): TGW x 0.725	Total Carbon Weight (TCW): TDW x 0.427
Total Carbon Weight (TCW): TDW x 0.5	Total CO_2 Weight (TCO_2W): TCW x 3.6663
Total CO_2 Weight (TCO_2W): TCW x 3.6663	D = Diameter of the trunk; H = Height of the tree

Results and discussion

Carbon Sequestration Rate at Putra Heights Neighbourhood Park

Tables 2-6 and *Fig. 2* portrayed the amount of CO_2 sequestered by different types of plant's categories and species. The carbon sequestration value for all planting species from each planting categories was then calculated. The highest amount of carbon sequestration rate is from the turf category (*Axonopus compressus*). The total amount of CO_2 sequestered by this turfing species is 31530 $kgCO_2e$ compared to other plants categories such as trees (11438.83 $kgCO_2e$), orchard trees (272.80 $kgCO_2e$), palms (1264.57 $kgCO_2e$) and shrubs (943.19 $kgCO_2e$). From *Table 1*, it can be depicted that tree species of Samanea saman sequestered the highest total amount of CO_2 of

http://www.aloki.hu ● ISSN 1589 1623 (Print) ● ISSN 1785 0037 (Online)
DOI: http://dx.doi.org/10.15666/aeer/1704_80798088

1937.93 kgCO_2e. Meanwhile, Neodypsis leptocheilos ranked as the highest sequester agent for palm category with the amount of 427.32 kgCO_2e. Eugenia oleana has been classified as the highest sequester agent under shrubs categories that sequestered 692.06 kgCO_2e.

Table 2. *Carbon sequestration rate produced by trees at Putra Heights Neighbourhood Park*

No	Species	Overall Height (Feet)	Trunk Diameter (Inch)	Quantity (Nos)	Age	tCO_2e/ unit	Total CO_2e (kg)
1.	*Agathis borneensis*	13.12	1.82	33	5.4	0.001	48.03
2.	*Azadirachta excelsa*	22.97	6.97	40	5.4	0.037	1494.91
3.	*Bucida molineti*	32.81	7.11	36	6	0.050	1799.78
4.	*Caesalpinia ferrea*	19.69	4.77	14	5.6	0.014	202.56
5.	*Cinnamomum iners*	19.69	4.87	35	5.6	0.015	527.85
6.	*Cratoxylum formosum*	16.4	4.01	25	6	0.008	198.72
7.	*Dalbergia latifolia*	19.69	4.83	35	5.2	0.016	559.15
8.	*Eugenia grandis*	32.81	5.01	50	6	0.025	1241.15
9.	*Fagraea fragrans*	19.69	3.55	27	5.6	0.008	216.37
10.	*Hopea odorata*	22.97	3.59	35	5.6	0.010	334.62
11.	*Mesua ferrea*	19.69	3.11	11	5.6	0.006	67.65
12.	*Pongamia pinnata*	26.25	4.84	47	5.6	0.020	933.37
13.	*Samanea saman*	32.81	8.2	34	7	0.057	1937.93
14.	*Saraca cauliflora*	19.69	3.76	10	5.6	0.009	89.90
15.	*Schizolobium parahyba*	29.53	7.42	20	5.6	0.053	1050.11
16.	*Spathodea campanulata*	16.4	5.31	34	6	0.014	473.90
17.	*Tristaniopsis whiteana*	16.4	2.54	28	5.6	0.003	95.68
18.	*Xanthostemon chrysanthus*	19.69	2.63	38	5.6	0.004	167.14
							11438.83

Table 3. *Carbon sequestration rate produced by orchard trees at Putra Heights Neighbourhood Park*

No	Species	Overall Height (Feet)	Trunk Diameter (Inch)	Quantity (Nos)	Age	tCO_2e/ unit	Total CO_2e (kg)
1.	*Artocarpus altilis*	13.12	4.97	3	5	0.0117	35.17
2.	*Averrhoa bilimbi*	13.12	2	5	5	0.0019	9.49
3.	*Averrhoa carambola*	13.12	2.83	5	5	0.0038	19.00
4.	*Euphoria malaiense*	13.12	2.28	3	5	0.0025	7.40
5.	*Garcinia mangostana*	13.12	1.98	10	5	0.0019	18.60
6.	*Lansium domensticium*	13.12	2.34	5	5	0.0026	12.99
7.	*Mangifera indica*	13.12	3.61	22	5	0.0062	136.06
8.	*Spondias cytherea*	13.12	3.46	6	5	0.0057	34.09
							272.80

Table 4. *Carbon sequestration rate produced by palms at Putra Heights Neighbourhood Park*

No	Species	Overall Height (Feet)	Trunk Diameter (Inch)	Quantity (Nos)	Age	tCO_2e/ unit	Total CO_2e (kg)
1.	*Cocos nucifera 'dwarf'*	11.48	6.67	10	8	0.012	115.46
2.	*Livistonia rotundifolia*	26.25	7.08	10	8	0.030	297.46
3.	*Neodypsis leptocheilos*	13.12	6.93	30	8	0.014	427.32
4.	*Ptychosperma macarthurii*	11.48	3.54	14	5	0.005	72.85
5.	*Wodyetia bifurca*	14.76	8.38	15	8	0.023	351.48
							1264.57

http://www.aloki.hu ● ISSN 1589 1623 (Print) ● ISSN 1785 0037 (Online)
DOI: http://dx.doi.org/10.15666/aeer/1704_80798088

Table 5. *Carbon sequestration rate produced by shrubs at Putra Heights Neighbourhood Park*

No	Species	Overall Height (Feet)	Trunk Diameter (Inch)	Quantity (Nos)	Age	tCO_2e/ unit	Total CO_2e (kg)
1.	*Eugenia oleana*	8.2	2	700	6	0.0010	692.06
2.	*Raphis multifida*	3.94	1	105	5	0.0001	14.96
3.	*Murraya paniculata*	2.95	1	240	5	0.0001	25.61
4.	*Bougainvillea*	2.95	1	300	5	0.0001	32.01
5.	*Codiaeum variegatum*	2.95	1	180	5	0.0001	19.21
6.	*Dracaena marginata 'bicolor'*	3.28	1	80	5	0.0001	9.49
7.	*Duranta erecta 'gold'*	2.95	1	475	5	0.0001	50.68
8.	*Hibiscus rosa sinensis*	3.28	1	264	5	0.0001	31.32
9.	*Ixora cultivar*	3.28	1	320	5	0.0001	37.96
10.	*Osmoxylum lineare*	2.95	1	280	5	0.0001	29.88
							943.19

Table 6. *Carbon sequestration rate produced by turf at Putra Heights Neighbourhood Park*

No	Species	Area (m^2)	Total CO_2e (kg)
1.	*Axonopus compressus*	35,970	31530.00
			31530.00

Figure 2. *Planting plan at Putra Heights Neighbourhood Park*

From *Fig. 3,* it can be depicted that the highest value represents as an effective agent to sequester carbon is from turf category (31530 $kgCO_2e$). The amount is tremendously high compared to other planting categories. At this particular site, turfing category

http://www.aloki.hu ● ISSN 1589 1623 (Print) ● ISSN 1785 0037 (Online)
DOI: http://dx.doi.org/10.15666/aeer/1704_80798088

(*Axonopus compressus*) acts as a dominant Carbon Sequestration Rate (CSR) agent which contribute the highest CSR value due to the large coverage area for planted turfing. Meanwhile, trees category has become the second highest CSR agent that sequester 11438.83 $kgCO_2e$, followed by palms (1264.57 $kgCO_2e$), shrubs (943.19 $kgCO_2e$) and the least CSR value represented by orchard tree category which sequestered 272.80 $kgCO_2e$ of carbon dioxide.

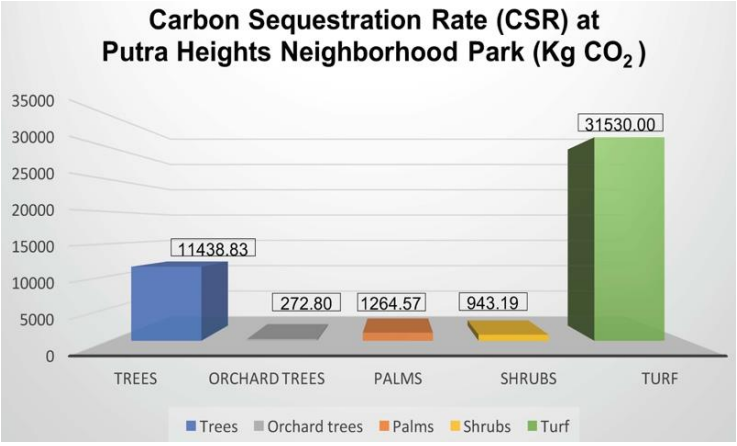

Figure 3. *Carbon sequestration rate produced by a different type of planting category at Neighbourhood Park, Putra Heights*

Total Park Area, Green Area and Built Up Area of Neighbourhood Park

In calculating the total park area, green area and built-up area of the park, the base map is obtained from the authorities (*Fig. 4*). The summary of the findings is presented in *Table 7*. According to *Table 7*, it can be found that the total park area is 42,288 m^2, covered majority by a green area with the percentage of 87% (36760 m^2) and covered only 13% with the built-up area (5528 m^2). According to *Table 8*, the green area consists of soft landscape plantings which categorized as trees, palms, shrubs and turfing while the built-up area consists of the parking area, hard landscape components such as pedestrian walkways, jogging track, open plaza, wakaf, courts and children playground. Putra Heights Neighborhood Park is perceived to have a greener area than built up area.

This formula is created in order to identify the minimum amount of carbon sequestration rate required in every 1meter square. For example, Malaysia's carbon emission is predicted at around 285.73 million tonnes by the year 2020 (Safaai et al., 2011):

$$\frac{285.73\ million\ tonnes}{330{,}803\ km^2} = \frac{x}{1\ km^2} \qquad \text{(Eq.1)}$$

1km^2 x 285730000 tonnes km^2 = x (330,803 km^2)

x = 285730000 tonnes km^2 / 330803 km^2

x = 863.746 tonnes per km^2 / 1000000

1m^2 = 0.000863 tonnes / 0.863 kg CO_2

http://www.aloki.hu ● ISSN 1589 1623 (Print) ● ISSN 1785 0037 (Online)
DOI: http://dx.doi.org/10.15666/aeer/1704_80798088

From the calculation above, every 1 m^2 of Malaysia should sequester minimum of 0.863 $kgCO_2$ emissions. Next, the amount will be multiplied by the total area of the site. Hence, Putra Heights Neighbourhood Park sequestered 1.077 Kg CO_2 for every 1 m^2, which is more than the amount of CO_2 that it should sequester.

Figure 4. *Distribution of total park area, green area and built up*

Table 7. *Components of Putra Heights Neighbourhood Park*

	Area (m^2)	Percentage (%)
Total built-up area	**5,528**	**13**
Parking Area	1055	2.48
Hard Landscape Elements:		
Pedestrian walkways	2000	4.70
Jogging track	730	1.72
Reflexology path	90	0.21
Open plaza	325	0.76
Wakaf/Gazebo	96	0.23
Basketball & futsal court	732	1.72
Children playground	500	1.18
Total green area	**36760**	**87**
Trees and palms	690	1.63
Shrubs	100	0.24
Turfing	35970	85.13
Total Park Area	**42288**	**100**

http://www.aloki.hu ● ISSN 1589 1623 (Print) ● ISSN 1785 0037 (Online)
DOI: http://dx.doi.org/10.15666/aeer/1704_80798088

Table 8. *Distribution of plant's category and quantity, carbon sequestration rate value and CO_2 sequestered per m^2*

Plant's Category	Plant's Quantity	CSR Value ($kgCO_2e$)	CO_2 Sequestered per m^2 ($kgCO_2$)
Trees	552 nos	11438.83	0.270
Orchard trees	59 nos	272.80	0.006
Palms	79 nos	1264.57	0.030
Shrubs	2944 nos	943.19	0.022
Turf	35970 m^2	31530.00	0.746
Total CSR		**45449.39**	**1.077**
Total park area – 42288 m^2			

Factors Influencing Total Carbon Sequestration Rate

Results showed that different planting specification contributes to the different amount of carbon sequestration rate even though there are from the same plant's category. According to Mandal et al. (2016), the effect of carbon sequestration varies from the plant species, for instance, parks with trees and shrubs have the most efficient carbon sequestration effect. Therefore, the findings proved that higher plants specification contributes to greater CSR value. For example, as the trees grow older, the tree trunk becomes taller and the trunk diameter becomes bigger, the greater carbons are being absorbed by the plants provided with the plants are being maintained and taken care with the proper landscape maintenance practice applied. Apart from that, planting quantity also has interrelated to influence the total carbon sequestration rate. Results proved that planting with larger quantity and higher specifications have a greater capability to sequester the higher amount of carbon dioxide. The difference between the ability of each plants category to sequester carbon differs greatly as referring back to *Table 3.*

Furthermore, from the findings, it is also revealed that a larger green area contributes to the higher value of carbon sequestration rate. Therefore, the percentage allocated for the green area has very much influence on the total carbon sequestration rate. The larger green area, the higher value of CSR will be obtained. At this site study area, by referring back to the *Figure 3*, it is clearly seen that green area covered majority from the total park area with 87% allocated for the green area as compared to only 13% allocated for a built-up area. Thus, this percentage of green area covered mostly by turf planting had influenced the total carbon sequestration rate of the park. This assumption is supported by Almeida et al. (2018), stated that urban parks are critical components within the metabolism of cities as well as the core scenes for open-air leisure communal activities. Thus, the concerns for designing a contemporary urban park must consider the size and quality of the green areas aiming to improve the air quality conditions of the nearby urban settlement. On the other hand, landscape design setting or spatial design organization also influence the total carbon sequestration rate. Putra Heights Neighbourhood Park portrayed hybrid design landscape setting with the combination of linear design and curvilinear design landscape planting. Most of the trees, palms and shrubs were organized to be planted in a combination of linear and curvilinear planting according to its spatial functionality.

In summary, it can be concluded that there are key factors that influence the carbon sequestration rate and optimization in applying these factors can contribute to the optimum value of carbon sequestration rate in urban parks.

http://www.aloki.hu ● ISSN 1589 1623 (Print) ● ISSN 1785 0037 (Online)
DOI: http://dx.doi.org/10.15666/aeer/1704_80798088

i. Planting quantity and specifications.
ii. Percentage of green area and built up area.
iii. Landscape design setting / spatial design organization.

Thus, this will become new design guidelines to the researchers, landscape architects and designer to consider before they start designing any open space or urban parks.

Conclusions

In urban parks, trees are considered as a green belt asset and function as sinks for excess CO_2 in the atmosphere. Trees played an important role in contributing to environmental change and many studies aware of the role of trees in urban environments. Carbon storage of urban trees can lead to a thorough understanding of the ability of urban trees in global carbon that relating to greenhouse emissions. From the findings of the present study, it is clearly shown that urban park green spaces, plant materials specifications and spatial design organization and pattern have greatly influenced the carbon sequestration rate in urban parks. From the context of this site study area, a higher percentage of the green area has much influenced to contribute greater CSR value. Furthermore, plant materials with higher specifications and larger quantities also contribute to the higher carbon sequestration rate. Besides, by having a hybrid design landscape setting also helps in optimizing the CSR value. Consideration of the optimization of these three key factors in designing or enhancing the existing urban parks will help to sequester optimum value or carbon sequestration rate. Thus, by applying these key factors as design guidelines during the design stage or before starting any developments will help the researchers, landscape architects and designers. By having an urban park with an optimum value of carbon sequestration rates will help to strengthen the ecosystem services, therefore, alleviating urban heat island and global warming. These findings will become a novel landscape design guideline to improve environmental quality with cost-effective and environmental friendly. Correlation between plant material group and type of design can be indicative of the carbon sequestration rate. In other words, there is a particular design where specific plant material group sequester high level of carbon. Thus for future research, this raises the importance and need for an effective potential model system to investigate in depth the environmental factors, type of design and plant material group that influence or controlling carbon sequestration rate.

Acknowledgements. The research was supported by the Ministry of Higher Education Malaysia (MOHE) and International Islamic University Malaysia (IIUM) under research grant MOHE18-001-0001.

REFERENCES

[1] Almeida, C. M. V. B., Mariano, M. V., Agostinho, F., Liu, G. Y., Giannetti, B. F. (2018): Exploring the potential of urban park size for the provision of ecosystem services to urban centres: A case study in São Paulo, Brazil. – Building and Environment 144: 450-458.
[2] Department of Statistics, Malaysia (2011): Population Distribution and Basic Demographic Characteristic Report.

http://www.aloki.hu ● ISSN 1589 1623 (Print) ● ISSN 1785 0037 (Online)
DOI: http://dx.doi.org/10.15666/aeer/1704_80798088

[3] Ehnat, T., Hill, F., Lincoln, L. Y., Menke, K., Town, O., Proctor, R. F. (2011): Neighborhood Business District. – Strategic Urban Forest Management Plan, (Washington Department of Natural Resources): 1-124.
[4] Gratani, L., Varone, L., Bonito, A. (2016): Urban forestry & urban greening carbon sequestration of four urban parks in Rome. – Urban Forestry & Urban Greening 19: 2014-2016.
[5] Mandal, R. A., Jha, P. K., Dutta, I. C., Thapa, U., Karmacharya, S. B. (2016): Carbon sequestration in tropical and subtropical plant species in collaborative and community forests of Nepal. – Advances in Ecology. http://dx.doi.org/10.1155/2016/1529703.
[6] Moumita, D., Ambarish, M. (2015): Carbon sequestration potential, its correlation with height and girth of selected trees in the Golapbag Campus, Burdwan, West Bengal, India. – Indian Journal of Scientific Research 10(1): 53-57.
[7] Nowak, D. J., Crane, D. E. (2013): Carbon storage and sequestration by urban trees in the USA. – Environmental Pollution 116: 381-389.
[8] Othman, R., Abu Kassim, S. Z. (2016): Assessment of plant materials carbon sequestration rate for horizontal and vertical landscape design. – International Journal of Environmental Science and Development 7(6): 410-414.
[9] Pataki, D. E., Carreiro, M. M., Cherrier, J., Grulke, N. E., Jennings, V., Pincetl, S. (2011): Coupling biogeochemical cycles in urban environments: Ecosystem services, green solutions, and misconceptions. – Frontiers in Ecology and the Environment 9(1): 27-36.
[10] Rackley, S. A. (2010): Carbon capture and storage. – Butterwoth-Heinemann Publication, United States of America, pp. 42-49.
[11] Sadeghian, M. M., Vardanyan, Z. (2013): The benefits of urban parks, a review of urban research. – Journal of Novel Applied Sciences: 231-237.
[12] Safaai, N. S. M., Noor, Z. Z., Hashim, H., Ujang, Z., Talib, J. (2011): Projection of CO_2 emissions in Malaysia. – Environmental Progress and Sustainable Energy 30(4): 658-665.
[13] Shahbaz, M., Mallick, H., Mahalik, M. K., Sadorsky, P. (2016): The role of globalization on the recent evolution of energy demand in India: Implications for sustainable development. – Energy Economics 55: 52-68.
[14] Shahidan, M. F. (2015): Potential of individual and cluster tree cooling Effect performances through tree canopy density model evaluation in improving urban microclimate. – Current World Environment 10(2): 398-413.
[15] Singh, U. (2013): Carbon capture and storage: An effective way to mitigate global warming. – Current Science 105(7): 914-922.
[16] Tenth Malaysia Plan. (2010): The Economic Planning Unit. – Prime Minister's Department, Putrajaya, 1-451.
[17] Velasco, E., Roth, M., Norford, L., Molina, L. T. (2016): Landscape and urban planning does urban vegetation enhance carbon sequestration? – Landscape and Urban Planning 148: 99-107.
[18] Yin, S., Shen, Z., Zhou, P., Zou, X., Che, S., Wang, W. (2011): Quantifying air pollution attenuation within urban parks: An experimental approach in Shanghai, China. – Environmental Pollution 159(8-9): 2155-2163.

http://www.aloki.hu ● ISSN 1589 1623 (Print) ● ISSN 1785 0037 (Online)
DOI: http://dx.doi.org/10.15666/aeer/1704_80798088

ESTIMATION OF CARBON SEQUESTRATION RATE OF URBAN PARK WITH LINEAR AND CURVILINEAR DESIGN LANDSCAPE SETTING

OTHMAN, R.[1*] – SUID, S.[1] – MOHD NOOR, N. F.[1] – BAHARUDDIN, Z. M.[1] – HASHIM, K. S. H. Y.[2] – LUKMAN HAKIM MAHAMOD, L. H.[3]

[1]*International Institute for Halal Research and Training (INHART) Department of Landscape Architecture, Kulliyyah of Architecture and Environmental Design (KAED), International Islamic University Malaysia, 53100 Kuala Lumpur, Malaysia*

[2]*Department of Urban & Regional Planning, Kulliyyah of Architecture and Environmental Design (KAED), International Islamic University Malaysia, 53100 Kuala Lumpur, Malaysia*

[3]*Department of Quantity Surveying, Kulliyyah of Architecture and Environmental Design (KAED), International Islamic University Malaysia, 53100 Kuala Lumpur, Malaysia*

[*]*Corresponding author*
e-mail: rashidi@iium.edu.my; phone: +60-126-644-772; fax: +60-361-964-864

(Received 24th Jan 2019; accepted 3rd May 2019)

Abstract. The need for urban parks became greater as cities expanded and the urban population rapidly grew. Therefore, having an urban park can facilitate a reduction in GHG emissions by alleviating some of the impacts of this dense development. Trees in the urban parks are an important factors reducing the amount of carbon dioxide accumulated in the urban area. The carbon sequestration rate was calculated with biomass equations, using field data collection, measurements and survey data analysis. This study aimed to calculate, predict and compare carbon sequestration rate of plant materials with linear and curvilinear design landscape setting. The decisive outcome of this study are the optimization of carbon sequestration rate by selecting the right plant material specifications with suitable landscape design setting. The findings revealed that the curvilinear design landscape setting sequesters more carbon per m^2 than linear design landscape setting. Plants with bigger girth and larger quantities contribute to sequestering greater carbon compared to smaller girth and fewer trees. These findings will become a green practice approached towards building a sustainable environment with better design solutions.
Keywords: *carbon stock, air pollution, green technology, phytosequestration, urban landscape design*

Introduction

Urban parks have been viewed as an important component of the urban fabric that benefits for community development by providing space for recreation and leisure. From a social perspective, green spaces provide health and a range of recreational and psychological benefits, create environmental awareness and encourage positive actions toward climate change (Pataki et al., 2011; Demuzere et al., 2014). A study conducted in Helsinki, Finland, indicated that nearly all (97%) city residents participate in some outdoor recreation during the year (Sadeghian and Vardanyan, 2013). Thus, the need for urban parks become greater as cities expanded and the urban population rapidly grew. According to Department of Statistics Malaysia (2011), in tandem with Malaysia's rapid development, the proportion of urban population increased to 71.0 percent in 2010 and this growth is expected to continue as total population increased over the years. One of the state in Malaysia with a high level of urbanization was Selangor with 91.4 percent.

http://www.aloki.hu ● ISSN 1589 1623 (Print) ● ISSN 1785 0037 (Online)
DOI: http://dx.doi.org/10.15666/aeer/1704_80898101

A significant increase in the urban population in a short span of time creates various problems, especially environmental problems. Therefore, under the Paris Agreement, in accordance with decisions of the United Nations Framework Convention on Climate Change (UNFCCC) (Biennial Update Report to the UNFCCC, 2015), Malaysia has committed to reducing its greenhouse gas (GHG) emissions intensity of GDP by 45% by 2030 relative to the emissions intensity of GDP in 2005. Alternative ways that have been further studied to reduce these greenhouse effects in the atmosphere is through carbon sequestration technology (Wiedman et al., 2007). Carbon sequestration is the process through which CO_2 from the atmosphere is absorbed naturally through photosynthesis by the plants (Pandya et al., 2013). Trees in urban parks play an important role in the urban environment by sequestering a substantial amount of carbon dioxide from the atmosphere. Urban trees in air pollution reduction, mentioning their effects in terms of intercepting atmospheric particles and absorbing various gaseous pollutants (Yin et al., 2011). In both neighborhoods, the trees with the highest carbon stocks and sequestration rates are generally located along the main roads and in public parks (Velasco et al., 2016). Although the impacts of urban trees thus have been studied rather extensively, at least through urban quality models, there is a suggestion that research specifically on urban parks has been limited so far (Pataki et al., 2011; Yin et al., 2011). Hence, this study aimed to estimate, predict and compare carbon sequestration rate produced by plant materials through linear and curvilinear design landscape setting at two selected urban parks in Selangor. The chosen case studies for this research is differentiated between two urban parks with different landscape settings, which are linear and curvilinear design landscape setting.

Materials and Method

The first method of this study used field data collection through site inventory and analysis to estimate total carbon sequestration rate Two selected urban parks in Selangor with different landscape design settings were chosen as site studies which are Putra Heights Linear Park (3°01'13.1"N 101°34'31.7"E, linear design landscape setting) and Subang Jaya Urban Forest Park (3°03'19.0"N 101°34'15.0"E, curvilinear design landscape setting) (*Fig. 1*).

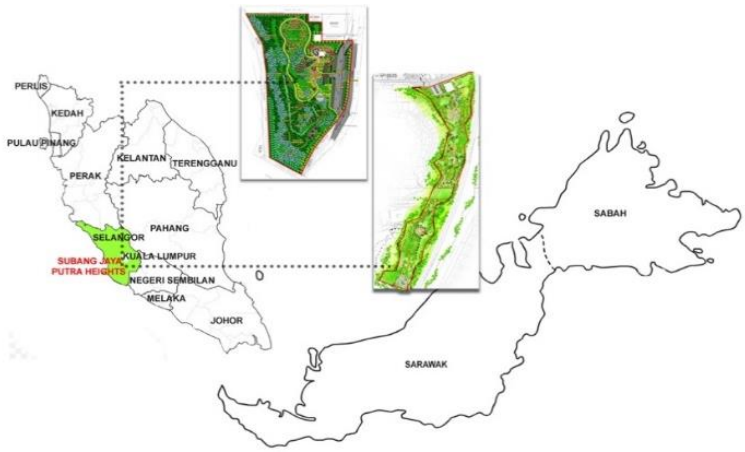

Figure 1. *Base map showing Subang Jaya Urban Forest Park with curvilinear design (left) and Putra Heights Linear Park (right), Selangor, Malaysia*

http://www.aloki.hu ● ISSN 1589 1623 (Print) ● ISSN 1785 0037 (Online)
DOI: http://dx.doi.org/10.15666/aeer/1704_80898101

Both sites were selected for inventory and analysis process in acquiring data needed. Besides, for calculating the total green area and built up area of the selected site studies, the site plan for both urban parks was obtained from the authorities. Whereas, for calculating the exact numbers of trees and detailed plants specifications on site, bill of quantities is also collected from the authorities. The data needed in this study including plants specifications such as overall plant's heights, trunk diameter, plant's age, plant's quantity and area of the plants (for climbers and turfing). Next, the current carbon sequestration rate (CSR) on every planting species was calculated using the carbon calculator formula stated in *Table 1*.

Table 1. *The formula to calculate carbon sequestration rate (CSR)*

CSR formula for tree and shrub	CSR formula for turf, climber and groundcover
Total Green Weight (TGW): $0.25D^2H$ (1.2)	Total Dry Weight (TDW): 0.56 x area (m^2)
Total Dry Weight (TDW): TGW x 0.725	Total Carbon Weight (TCW): TDW x 0.427
Total Carbon Weight (TCW): TDW x 0.5	Total CO_2 Weight (TCO_2W): TCW x 3.6663
Total CO_2 Weight (TCO_2W): TCW x 3.6663	D = Diameter of the trunk; H = Height of the tree

Results and Discussions

Carbon sequestration rate at Putra Heights Linear Park (linear design landscape setting)

Fig. 2 showed the planting plan at Putra Heights Linear Park which depicted linear design landscape planting. *Tables 2-4* portrayed the amount of CO_2 that sequestered by different types of plant species categorized under tree, shrub and turfgrass at Putra Heights Linear Park.

Figure 2. *Planting Plan of Putra Heights Linear Park located in Selangor, Malaysia*

http://www.aloki.hu ● ISSN 1589 1623 (Print) ● ISSN 1785 0037 (Online)
DOI: http://dx.doi.org/10.15666/aeer/1704_80898101

Table 2. *Carbon sequestration rate produced by trees at Linear Park, Putra Heights*

NO	SPECIES	OVERALL HEIGHT (feet)	TRUNK DIAMETER (Inch)	QUANTITY (Nos)	AGE	tCO_2e /unit	TOTAL CO_2e (kg)
1.	*Agathis borneensis*	9.84	1.57	110	1.6	0.0027	301.57
2.	*Cratoxylum cochinchinense*	13.12	1.97	55	2	0.0046	253.23
3.	*Eucalyptus deglupta*	9.84	1.97	55	2	0.0035	189.93
4.	*Eugenia grandis*	9.84	1.57	25	1.6	0.0027	68.54
5.	*Fagraea fragrans*	9.84	1.57	16	1.6	0.0027	43.86
6.	*Filicium decipiens*	9.84	1.77	50	1.8	0.0031	154.87
7.	*Gardenia carinata*	9.84	1.57	165	1.6	0.0027	452.36
8.	*Hopea odorata*	13.12	1.77	325	1.8	0.0041	1342.19
9.	*Lagerstroemia langkawiensis*	9.84	1.57	50	1.6	0.0027	137.08
10.	*Melaleuca leucadendron*	13.12	1.97	60	2	0.0046	276.26
11.	*Michelia champaca*	11.48	1.57	65	1.6	0.0032	207.90
12.	*Pongamia pinnata*	9.84	1.57	30	1.6	0.0027	82.25
13.	*Samanea saman*	22.97	4	131	4	0.0166	2176.79
14.	*Tristaniopsis whiteana*	9.84	1.57	46	1.6	0.0027	126.11
15.	*Xanthostemon chrysanthus*	9.84	1.57	25	1.6	0.0027	68.54
16.	*Cynometra cauliflora*	9.84	1.57	28	1.6	0.0027	76.76
17.	*Garcinia mangostana*	9.84	1.57	21	1.6	0.0027	57.57
18.	*Mangifera indica*	9.84	1.57	43	1.6	0.0027	117.89
19.	*Nephelium lappaceum*	9.84	1.57	37	1.6	0.0027	101.44
20.	*Phyllanthus acidus*	9.84	1.57	32	1.6	0.0027	87.73
21.	*Azadirachta exelsa*	9.84	1.57	38	1.6	0.0027	104.18
22.	*Cinnamomum iners*	9.84	1.57	35	1.6	0.0027	95.95
23.	*Cratoxylum formosum*	9.84	1.57	38	1.6	0.0027	104.18
24.	*Mesua ferrea*	9.84	1.57	53	1.6	0.0027	145.30
25.	*Acacia auriculiformis*	32.81	10	20	10	0.0356	712.05
26.	*Dyera costulata*	32.81	10	13	10	0.0356	462.83
27.	*Hevea brasiliensis*	32.81	10	42	10	0.0356	1495.31
28.	*Koompassia excelsa*	32.81	10	7	10	0.0356	249.22
							9691.89

Table 3. *Carbon sequestration rate produced by shrubs at Linear Park, Putra Heights*

NO	SPECIES	OVERALL HEIGHT (feet)	TRUNK DIAMETER (Inch)	QUANTITY (Nos)	AGE	tCOe /unit	TOTAL COe (kg)
1	*Eugenia oleana*	3.28	1	600	1	0.0006	355.92
2	*Murraya paniculata*	1.48	0.5	5000	1	0.0001	334.58
							690.49

Table 4. *Carbon sequestration rate produced by turfgrass at Linear Park, Putra Heights*

NO.	SPECIES	AREA (M^2)	QUANTITY	TOTAL COe (kg)
1	*Axonopus compresus*	96300	96300	84430.00
2	*Zoysia matrella*	18000	18000	15780.00
				100,210.00

http://www.aloki.hu ● ISSN 1589 1623 (Print) ● ISSN 1785 0037 (Online)
DOI: http://dx.doi.org/10.15666/aeer/1704_80898101

The highest amount of CO_2 sequestered by *Axonopus compressus* at 100,205.17 $kgCO_2e$. This amount is substantially high as compared to the other planting categories which are from tree and shrub category, sequestered at 9691.89 $kgCO_2e$ and 690.49 $kgCO_2e$, respectively. The main reason for this turfgrass becomes a dominant CSR agent because of the large coverage area planted with turfing at this particular site. Thus, it can be concluded that larger turfing area contributes to the greater amount of CO_2 that can be sequestered at one time. The tree species that sequestered the highest total amount of carbon at this site is *Samanea saman* (2176.79 $kgCO_2e$). The high CSR value of this species compared to the other tree species is due to higher plants specification used such as taller in height, bigger in trunk diameter, planted in larger quantity and had an older age (*Table 2*). According to Othman et al. (2016), the effect of carbon sequestration varies from the plant species, for instance, parks with trees and shrubs have the most efficient carbon sequestration effect. Meanwhile, *Eugenia oleana* ranked as the highest sequester agent for a shrub with the amount of 355.92 $kgCO_2e$. This value is slightly higher from the other one shrub species which is *Murraya paniculata* with the sequestered amount of 334.58 $kgCO_2e$. From *Table 3*, it can be clearly seen that even though the quantity of shrub for *Murraya paniculata* has a greater number planted on site (5000 nos), the total CSR value for this plant is still lower than *Eugenia oleana* which was only planted at 600 nos on site. Therefore, this finding revealed that plants specifications such as overall height and trunk diameter have very much influenced the total CSR percentage.

Fig. 3 indicates the relationship between planting categories and the total amount of carbon sequestration rate from each category. It can be depicted that the highest CSR value is from turfing category, followed by trees and shrubs category.

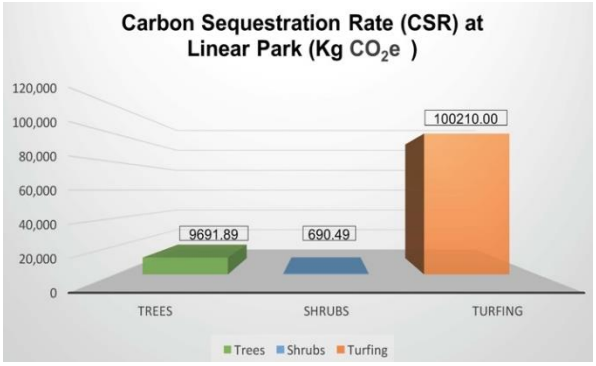

Figure 3. *Carbon sequestration rate based on planting categories at Putra Heights Linear Park (linear design landscape setting)*

Table 5 tabulated in detail distribution of plant's category, plant's quantity and CSR value obtained from each category. With the total numbers of 1615 nos of trees, 5600 nos of shrubs and 114,300 m^2 of planted turfing, the overall total of CO_2 sequestered by all plants in this site is 110,592.38 $kgCO_2e$.

Carbon sequestration rate at Subang Jaya urban forest park (curvilinear design landscape setting)

Fig. 4 illustrates the planting plan at Subang Jaya urban forest park which represents curvilinear design landscape setting. *Tables 6-11* showed the current carbon

http://www.aloki.hu ● ISSN 1589 1623 (Print) ● ISSN 1785 0037 (Online)
DOI: http://dx.doi.org/10.15666/aeer/1704_80898101

sequestration rate obtained at Subang Jaya urban forest park (curvilinear design landscape setting) based on plants categories and the total amount of CO_2 sequestered by each plant. It can be concluded that the highest value represented as an effective CSR agent to sequester carbon is from turfgrass category, which named *Axonopus compressus* and *Zoysia matrella* with the sequestered amount of 24,190 $kgCO_2e$ and 350 $kgCO_2e$, respectively.

Table 5. *Distribution of plant's quantity and carbon sequestration rate by plant's category*

Plant's Category	Plant's Quantity	CSR Value/ ($kgCO_2e$)
Trees	1615 nos	9,691.89
Shrubs	5600 nos	690.49
Turfing	114300 m^2	100,210.00
Total CSR ($kgCO_2e$)		**110,592.38**

Figure 4. *Planting plan of Subang Jaya urban forest park, Selangor*

At this particular plant's category, *Axonopus compressus* has become a dominant CSR agent because of the quantity planted is tremendously high compared to *Zoysia matrella.* Thus, this finding proved that quantities of the plant have very much influence on the CSR value. The total amount of carbon sequestration rate produced by turfgrass at this site is 24,540 $kgCO_2e$. The amount is tremendously high as compared to the other planting categories such as trees (2781.28 $kgCO_2e$), palm (170.84 kg CO_2e) and

http://www.aloki.hu ● ISSN 1589 1623 (Print) ● ISSN 1785 0037 (Online)
DOI: http://dx.doi.org/10.15666/aeer/1704_80898101

tall shrubs (518.59 $kgCO_2e$) categories. Besides, for the shrubs and climbers categories have the same CSR value which is 310 $kgCO_2e$ each. The tree species that sequestered the highest amount of CO_2 is known as *Hopea odorata* (274.06 $kgCO_2e$) whereas for the palm species is *Livistonia rotundifolia* (170.84 $kgCO_2e$). Apart from that, as for the tall shrubs category, *Murraya paniculata* has the highest amount of CO_2 sequestered. *Labisia pumila* (90 $kgCO_2e$) and *Tristellateia australasiae* (100 $kgCO_2e$) have ranked the highest contributor of carbon sequestration for shrubs and climbers categories.

Table 6. *Carbon sequestration rate produced by trees at Subang Jaya Urban Forest Park*

NO	Species	Overall Height (Feet)	Trunk Diameter (Inch)	Quantity (Nos)	Age	tCO_2e/unit	Total CO_2e (kg)
1.	*Cinnamomum inners*	9.84	2	20	2	0.0036	71.18
2.	*Dillenia indica*	9.84	2	15	2	0.0036	53.39
3.	*Evatamia divaricata*	6.56	2	15	2	0.0024	35.59
4.	*Fragraea fragrans*	11.48	2	35	2	0.0042	145.33
5.	*Gardenia carinata*	9.84	2	30	2	0.0036	106.78
6.	*Mechelia champaka*	9.84	2	20	2	0.0036	71.18
7.	*Melia indica*	8.2	2	15	2	0.0030	44.49
8.	*Mimosup elengi*	8.2	2	20	2	0.0030	59.32
9.	*Casia fistula*	9.84	1.97	15	1.6	0.0043	64.75
10.	*Jacaranda obtusifolia*	9.84	1.97	20	1.97	0.0035	70.12
11.	*Langerstomia speciosa*	9.84	1.97	20	1.97	0.0035	70.12
12.	*Plumeriarubra*	8.2	2	15	2	0.0030	44.49
13.	*Tabeibuia rosea*	8.2	2	30	2	0.0030	88.98
14.	*Xanthostemon chrysanthus*	8.2	1.8	30	1.8	0.0027	80.08
15.	*Andira enermis*	9.84	1.97	30	1.97	0.0035	105.17
16.	*Cratoxylum cochichinensis*	11.48	3	42	3	0.0062	261.60
17.	*Dipterocarpuschartaceus*	8.2	2	25	2	0.0030	74.15
18.	*Dyeracostulata*	9.84	2	16	2	0.0036	56.95
19.	*Eucalyptus deglupta*	11.48	3	40	3	0.0062	249.14
20.	*Neobalanocarpusheimii*	9.84	2	15	2	0.0036	53.39
21.	*Hopea odorata*	11.48	2	66	2	0.0042	274.06
22.	*Melaleuca cajuputi*	9.84	1.97	25	1.97	0.0035	87.64
23.	*Mesua ferrea*	9.84	2	30	2	0.0036	106.78
24.	*Pentaspadon motley*	8.2	1.6	20	1.6	0.0024	47.46
25.	*Pometia pinnata*	9.84	1.97	20	1.97	0.0035	70.12
26.	*Shorea leprosula*	9.84	1.97	35	1.97	0.0035	122.70
27.	*Stercula foetida*	8.2	1.6	16	1.6	0.0024	37.96
28.	*Tectona grandis*	8.2	1.6	30	1.6	0.0024	71.18
29.	*Tristaniopsis whiteana*	9.84	2	40	2	0.0036	142.37
30.	*Eurycoma longifolia*	3.28	1	25	1	0.0006	14.83
							2781.28

Table 7. *Carbon sequestration rate produced by palm at Subang Jaya Urban Forest Park*

NO	Species	Overall Height (Feet)	Trunk Diameter (Inch)	Quantity (Nos)	Age	tCO_2e /unit	Total CO_2e (kg)
1.	*Livistonia rotundifolia*	13.12	4	18	4	0.0095	170.84
							170.84

http://www.aloki.hu ● ISSN 1589 1623 (Print) ● ISSN 1785 0037 (Online)
DOI: http://dx.doi.org/10.15666/aeer/1704_80898101

Table 8. *Carbon sequestration rate produced by tall shrubs at Subang Jaya Urban Forest Park*

NO	Species	Overall Height (Feet)	Trunk Diameter (Inch)	Quantity (Nos)	Age	tCO2e /unit	Total CO2e (kg)
1.	*Gardenia jasminoides*	1.64	1	300	1	0.00030	88.98
2.	*Jasminium sambac*	1.31	1	350	1	0.00024	82.92
3.	*Murraya paniculata*	1.64	1	350	1	0.00030	103.81
4.	*Acalypha siamensis*	1.31	1	400	1	0.00024	94.77
5.	*Bougainvillea spectabilis*	1.31	1	100	1	0.00024	23.69
6.	*Durantha erecta Gold*	1.31	1	400	1	0.00024	94.77
7.	*Leucophyllum frutescens*	1.64	1	100	1	0.00030	29.66
							518.59

Table 9. *Carbon sequestration rate produced by shrubs at Subang Jaya Urban Forest Park*

NO.	Species	Area (m^2)	Quantity	Total CO_2e (kg)
1.	*Pandanus anaryllifolius*	33.33	100	30.00
2.	*Costus woodsonii*	33.33	100	30.00
3.	*Clinacanthu snutans*	50	300	40.00
4.	*Cosmos caudafusi*	50	300	40.00
5.	*Gynura procumbens*	50	300	40.00
6.	*Labisia pumila*	100	300	90.00
7.	*Orthosiphon aristatus*	50	300	40.00
				310.00

Table 10. *Carbon sequestration rate produced by climbers at Subang Jaya Urban Forest Park*

NO.	Species	Area (m^2)	Quantity	Total CO_2e (kg)
1.	*Vallaris glabra*	66.67	400	60.00
2.	*Portulaca grandifolia*	21.67	130	20.00
3.	*Thunbergia grandifolia*	50	300	40.00
4.	*Tristellateia australasiae*	110	660	100.00
5.	*Quisqualis indica*	50	300	40.00
6.	*Ophiopogon jaburan*	53.33	320	50.00
				310.00

Table 11. *Carbon sequestration rate produced by turfgrass at Subang Jaya Urban Forest Park*

NO.	Species	Area (m^2)	Quantity	Total CO_2e (kg)
1.	*Axonopus compressus*	27591	27591	24190.00
2.	*Zoysia matrella*	400	400	350.00
				24540.00

Fig. 5 showed the relationship between planting categories and the total amount of carbon sequestration rate from each category at Subang Jaya urban forest park. It can be depicted that the highest CSR value is from turfing category, followed by trees, tall shrubs, shrubs, climbers and palm category. At this particular period of time, turfing has become the dominant CSR agent due to the large coverage area for turfing. *Table 12*

http://www.aloki.hu ● ISSN 1589 1623 (Print) ● ISSN 1785 0037 (Online)
DOI: http://dx.doi.org/10.15666/aeer/1704_80898101

tabulated distribution of plant's category, quantities and the CSR value that sequestered from each planting category. With the total number of 775 nos trees, 18 nos palm, 2000 nos tall shrubs, 366.66 m^2 of shrubs, 351.67 m^2 of climbers and 27,991 m^2 of turfing, total carbon sequestration rate for this particular site is 28,630.71 $kgCO_2e$.

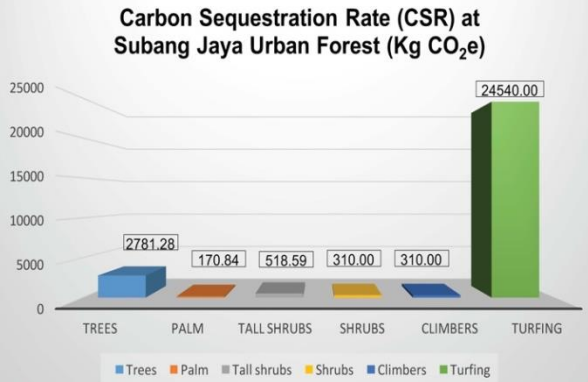

Figure 5. *Carbon sequestration rate based on planting categories at Subang Jaya urban forest park (curvilinear design landscape setting)*

Table 12. *Distribution of plant's category, plant's quantity, andcarbon sequestration rate value*

Plant's Category	Plant's Quantity	CSR Value/ $KgCO_2e$
Trees	775 nos	2781.28
Palms	18 nos	170.84
Tall Shrubs	2000 nos	518.59
Shrubs	366.66 m^2	310.00
Climbers	351.67 m^2	310.00
Turfgrass	27991 m^2	24,540.00
Total CSR ($kgCO_2e$)		**28,630.71**

Total Park Area, Green Area and Built Up Area

Fig. 6 illustrated the total park area, green area and built up area for both selected site studies. It has been found that the green area for Putra Heights linear park (114300 m^2) is enormously larger than Subang Jaya urban forest park (25,446.63 m^2). From the results, it can be concluded that a larger green area contributes to the greater value of carbon sequestration rate.

Fig. 7 showed the comparison of carbon sequestration rate obtained at Putra Heights linear park (linear design landscape setting) and Subang Jaya urban forest park (curvilinear design landscape setting). From the bar graph shown, it can be clearly seen that the Putra Heights linear park (110592.38 $kgCO_2e$) had sequestered more carbon compared to Subang Jaya urban forest park (28630.71 $kgCO_2e$). There are many factors contribute to this difference which will be explained on the next page.

Comparison of Carbon Sequestration Rate for Linear and Curvilinear Design Landscape Setting

Table 13 portrayed comparison between Putra Heights linear park character and Subang Jaya urban forest park character. There are four categories considered in doing

http://www.aloki.hu ● ISSN 1589 1623 (Print) ● ISSN 1785 0037 (Online)
DOI: http://dx.doi.org/10.15666/aeer/1704_80898101

this assessment, which are a green area, landscape design setting, plant's category and quantity and also means trees specification. From the tabulated results, it is shown that Putra Heights linear park possessed higher amount in terms of green area, plant's category, and quantity and also mean trees specifications. Therefore, these factors have very much influenced the total CSR rate.

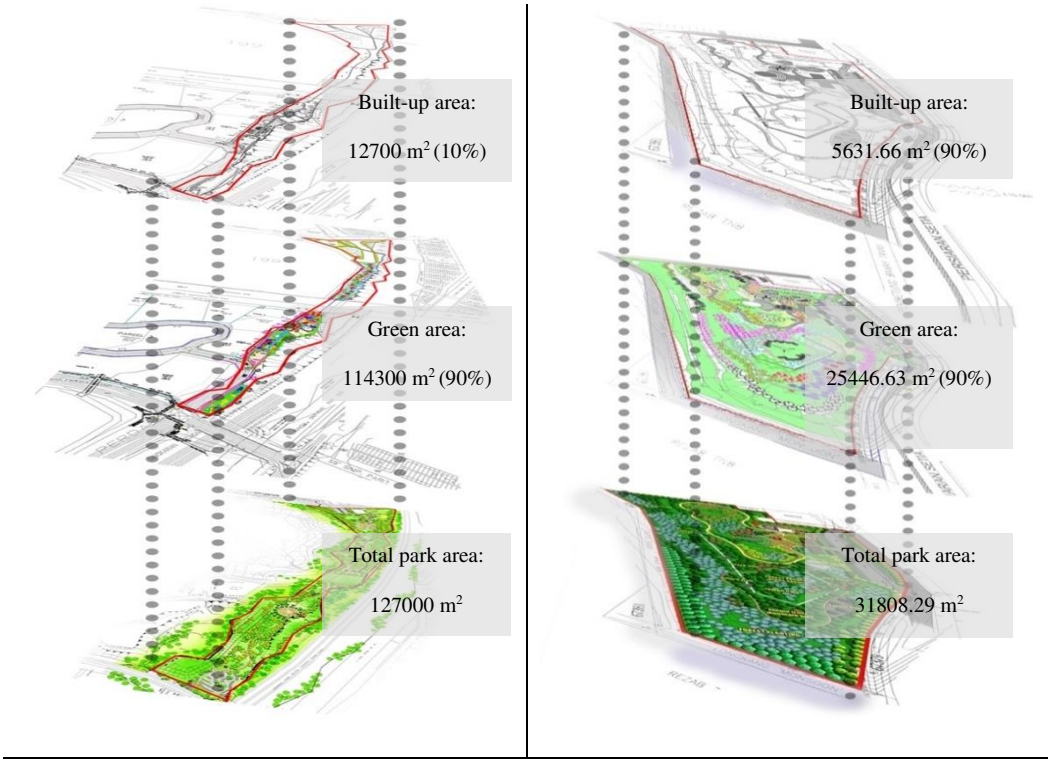

Figure 6. *Distribution of total park area, green area and built up area for both urban parks*

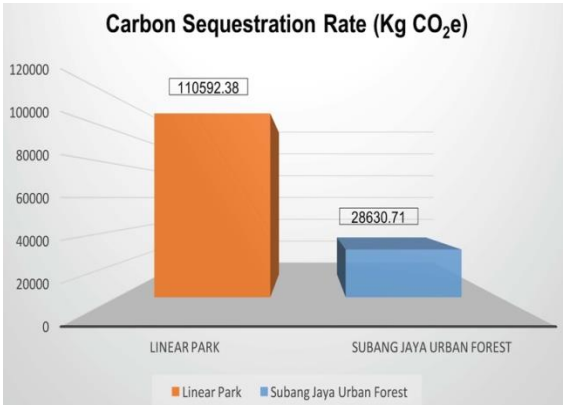

Figure 7. *Carbon sequestration rate based on planting categories at Subang Jaya Urban Forest Park (curvilinear design landscape setting)*

Optimizing the Carbon Sequestration Rate

According to Safaai et al. (2011), Malaysia's carbon emission is predicted at around 285.73 million tonnes by the year 2020. With the total land area of 330,803 km^2, every

http://www.aloki.hu ● ISSN 1589 1623 (Print) ● ISSN 1785 0037 (Online)
DOI: http://dx.doi.org/10.15666/aeer/1704_80898101

1 m^2 of Malaysia should sequester minimum of 0.863 $kgCO_2e$ emissions. Next, the amount will be multiplied by the total area of the site. *Table 14* showed the distribution of total CSR and CO_2 sequestered per m^2 for both urban parks according to planting categories. Surprisingly, Subang Jaya curvilinear urban forest park sequestered 0.9 $kgCOe/m^2$, which is higher than Putra Heights linear park. Therefore, this finding revealed that curvilinear design landscape setting contributes to the greater amount of CO_2 sequestered per m^2. Both urban parks sequestered more than the amount of CO_2 that it should sequester. Apart from that, the amount of CO_2 sequestered per m^2 for trees category of Subang Jaya curvilinear urban forest park (0.09 $kgCO_2e$) is higher even though the total quantity of trees is lower compared to Putra Heights linear park (0.08 $kgCO_2e$). There are a few factors affected such as planting distance and spatial design organization. The total amount of CO_2 sequestered per m^2 for turfing category is nearly equal for both parks.

Table 13. *Comparison between Putra Heights linear park and Subang Jaya urban forest park landscape design setting*

	Putra Heights Linear Park	**Subang Jaya Urban Forest Park**
Green area (m^2)	114,300.00 m^2	25,446.63 m^2
Landscape design setting	Linear design	Curvilinear design
Plant's category & quantity	Trees – 1615 nos Shrubs – 5600 nos Turfing – 114,300 m^2	Trees – 775 nos Palm – 18 nos Tall shrubs – 2000 nos Shrubs – 366.66 m^2 Climbers – 351.67 m^2 Turfing – 24,540m^2
Trees specification	Overall height – 14 ft Trunk diameter – 2.92 inch Age – 2.9 years	Overall height – 9.24ft Trunk diameter – 1.98 inch Age – 2 years

Table 14. *Distribution of total CSR and CO_2 Sequestered per m^2 for both site studies area*

	Total CSR ($kgCO_2e$)	**CO_2 Sequestered per m^2 ($kgCO_2e$)**
Putra Heights Linear Park		
Total Park Area = 127,000 m^2		
Trees (1615 nos)	**110,592.38**	**0.871**
Shrubs (5600 nos)	9,691.89	0.076
Turfing (114,300 m^2)	690.49	0.005
	100,210.00	0.789
Subang Jaya Urban Forest Park		
Total Park Area = 31,808.29 m^2		
Trees (775 nos)	**28,630.71**	**0.900**
Palm (18 nos)	2781.28	0.087
Tall Shrubs (2000 nos)	170.84	0.003
Shrubs (366.66 m^2)	518.59	0.016
Climbers (351.67 m^2)	310.00	0.010
Turfing (27,991 m^2)	310.00	0.010
	24,540.00	

http://www.aloki.hu ● ISSN 1589 1623 (Print) ● ISSN 1785 0037 (Online)
DOI: http://dx.doi.org/10.15666/aeer/1704_80898101

Conclusions

Plants in urban parks are important agents that sequester the CO_2 emission of the earth atmosphere. Thus, the sequestration of carbon by urban trees and other vegetation plays an important role in mitigating climate change and have a high potential in reducing urban air pollution. Carbon sequestration rates differ based on the species of tree, planting quantity and specifications, type of plant materials group, percentage of green area and built up area as well as landscape design setting or spatial design organization. Therefore, by selecting the appropriate planting materials with suitable landscape design setting will contribute to sequestering greater value or carbon sequestration rate. It can be concluded that curvilinear design landscape setting sequester more CO_2 per m^2 compared to the linear design landscape setting. Thus, the selection of landscape design settings also plays an important role in contributing to the higher CSR value. Moreover, a higher percentage of the green area has much influenced in contributing to the greater CSR value. By selecting the right plant materials with higher specifications and larger quantities will also contribute to the optimum value of carbon sequestration rate in urban parks. Therefore, having an urban park with an optimum value of carbon sequestration rates will help to strengthen the ecosystem services, as a result, alleviating urban heat island and global warming. These findings will become a green practice approached towards building a sustainable environment with better design solutions. Thus, for future research, the environmental factors such as locality, type of soil and seasonal climatic variation may have influenced the carbon sequestration rate. Clearly, a further study utilizing plant material grown under different environmental conditions is required to confirm this hypothesis.

Acknowledgements. The research was supported by the Ministry of Higher Education Malaysia (MOHE) and International Islamic University Malaysia (IIUM) under research grant MOHE18-001-0001.

REFERENCES

[1] Biennial Update Report to the UNFCCC (2015): Framework Convention On Climate Change In December 2015. – Ministry Of Natural Resources and Environment Malaysia, 1-174.

[2] Demuzere, M., Orru, K., Heidrich, O., Olazabal, E., Geneletti, D., Orru, H., Bhave, A. G., Mittal, N., Feliu, E., Faehnle, M. (2014): Mitigating and adapting to climate change: Multi-functional and multi-scale assessment of green urban infrastructure. – Journal of environmental management 146C: 107-115.

[3] Department of Statistics, Malaysia. (2011): Population Distribution and Basic Demographic Characteristic Report.

[4] Othman, R., Abu Kassim, S. Z. (2016): Assessment of plant materials carbon sequestration rate for horizontal and vertical landscape design. – International Journal of Environmental Science and Development 7(6): 410-414.

[5] Pandya Ishan, Y., Salvi, H., Chahar, O., Vaghela, N. (2013): Quantitative Analysis on Carbon Storage of 25 Valuable Tree Species of Gujrat, Incredible India. – Indian J. Sci. Res. 4(1): 137-141.

[6] Pataki, D. E., Carreiro, M. M., Cherrier, J., Grulke, N. E., Jennings, V., Pincetl, S., Pouyat, R., Whitlow, T., Zipperer, W. (2011): Coupling biogeochemical cycles in urban environments: Ecosystem services, green solutions, and misconceptions. – Frontiers in Ecology and the Environment 9(1): 27-36.

http://www.aloki.hu ● ISSN 1589 1623 (Print) ● ISSN 1785 0037 (Online)
DOI: http://dx.doi.org/10.15666/aeer/1704_80898101

[7] Sadeghian, M. M., Vardanyan, Z. (2013): The Benefits of Urban Parks, a Review of Urban Research. – Journal of Novel Applied Sciences: 231-237.
[8] Safaai, N. S. M., Noor, Z. Z., Hashim, H., Ujang, Z., Talib, J. (2011): Projection of CO_2 emissions in Malaysia. – Environmental Progress and Sustainable Energy 30(4): 658-665.
[9] Velasco, E., Roth, M., Norford, L., Molina, L. T. (2016): Landscape and Urban Planning Does urban vegetation enhance carbon sequestration? – Landscape and Urban Planning 148: 99-107.
[10] Wiedman, T., Minx, J. (2007): The Carbon Trust Helps UK Businesses Reduce their Environmental Effect. – Ecological Economic Research Trend, Library of Congress Cataloging-In-Publication Data, Nova Science Publisher, pp.1-11.
[11] Yin, S., Shen, Z., Zhou, P., Zou, X., Che, S., Wang, W. (2011): Quantifying air pollution attenuation within urban parks: An experimental approach in Shanghai, China. – Environmental Pollution 159(8-9): 2155-2163.

http://www.aloki.hu ● ISSN 1589 1623 (Print) ● ISSN 1785 0037 (Online)
DOI: http://dx.doi.org/10.15666/aeer/1704_80898101

ASSESSING SPATIAL DISTRIBUTION AND IMPACT FACTORS OF FINE PARTICULATE MATTER ($PM_{2.5}$) AND NITROGEN DIOXIDE (NO_2) BY COMBINING HIGH-RESOLUTION GEOGRAPHICAL CENSUS DATA, AND METEOROLOGICAL DATA IN HEBEI PROVINCE, CHINA

YAO, S. Y.[1] – QIAO, B. S.[1] – YU, X. T.[1] – LIU, C.[2*] – SUN, W.[3] – ZHANG, F.[4] – CAO, Y. M.[5] – LI, Z. Y.[6] – PENG, Z. R.[7,8] – WANG, Y.[3]

[1]*School of Traffic and Transportation, Shijiazhuang Tiedao University, Shijiazhuang 050043, China*

[2]*College of Architecture and Urban Planning, Tongji University, Siping Rd. 1239, Shanghai 200082, China*

[3]*The Third Institute of Surveying and Mapping of Hebei Province, Shijiazhuang 050032, China*

[4]*Environmental Monitoring Center of Hebei Province, Shijiazhuang 050030, China*

[5]*Hebei Zhengrun Environmental Technology Co.,Ltd, Shijiazhuang 050051, China*

[6]*College of Resources and Environmental Sciences, Shijiazhuang College, Shijiazhuang 050035, China*

[7]*School of Naval Architecture, Ocean and Civil Engineering, Shanghai Jiaotong University, Shanghai 200240, China*

[8]*Department of Urban and Regional Planning, University of Florida, P. O. Box 115706, Gainesville, FL 32611-5706, USA*

**Corresponding author*
e-mail: liuchao1020@gmail.com

(Received 29th Jan 2019; accepted 10th Apr 2019)

Abstract. This paper was the first to employ land use regression (LUR) with high-resolution geographical census data for Hebei, one of the most severely polluted regions in China, to evaluate its spatial distribution characteristics of $PM_{2.5}$ and NO_2 concentrations and identify influencing factors. To develop the LUR model, $PM_{2.5}$ and NO_2 concentrations recorded at 53 sites in Hebei were selected as dependent variables. Independent variables include buffer-related and location-based factors. At first, 169 independent variables were chosen in total. Then pre-processing of bivariate correlation was performed to prevent multicollinearity. Lastly, step-wise regression was processed to identify the impacting factors. Different to other cities which have been studied like Shanghai or Beijing, we find that the results showed that PM2.5 and NO2 concentrations were positively correlated with the industrial pollution sources in a buffer area. NO_2 concentrations displayed significant negative correlations with forestland within the distance of 1 km and from the coastline. This study showed that the introduction of high-resolution geographical data into the LUR model significantly improved the fitting. More importantly, our study identified industries within a 9 km-buffer as important influencing factors in Hebei and was also consistent with empirical observations. It provided data on effective buffers to support future policy-making and designations of residential areas.
Keywords: *land use regression, fine particulate matter, air pollution*

Introduction

Fine particulate matter with a diameter of less than 2.5 μm ($PM_{2.5}$) and nitrogen dioxide (NO_2) have been recognized as causes of adverse health effects (Duki et al., 2003; Roswall et

http://www.aloki.hu ● ISSN 1589 1623 (Print) ● ISSN 1785 0037 (Online)
DOI: http://dx.doi.org/10.15666/aeer/1704_81038120

al., 2017; Chen et al., 2018; Yin et al., 2017). Empirical studies have shown a significant increase in the proportion of related diseases in regions affected by air pollution (Shekarrizfard et al., 2016; Su et al., 2008). Research by the World Health Organization (WHO) has shown that outdoor pollution caused 3.0 million extra deaths in 2012 (WHO, 2016). After three decades of rapid economic development, China has become the world's second largest economy (Morrison et al., 2015). At the same time, China is suffering from serious air pollution (Chambers et al., 2015; Chan et al., 2008; He et al., 2016; Hu et al., 2015; Wang et al., 2013; Fengwen et al., 2015; Song et al., 2017). There are emerging studies from various perspectives under pressures of urban and social development (Liu et al., 2017), but interdisciplinary research linking urban land use pattern, air pollution and meteorology at the regional level in China is lacking.

Many studies in Europe and North America have shown that land use patterns directly and indirectly influence air pollutant concentrations, and the optimization of land use patterns is feasible to alleviate air pollution problems (Briggs et al., 2000). In order to optimize land use, it is necessary to understand the impacts of its various influencing factors. There are numerous approaches to the quantitative assessment of the influence of land use on air pollution, such as diffusion models (Ciocănea et al., 2013) (for example, land use regression [LUR]), numerical simulations of the atmosphere (Chen et al., 2009), inversion of MODIS remote sensing images (Wu et al., 2016; Yao et al., 2017), and artificial neural network models (Jerret et al., 2005; Lu et al., 2003), etc. Jedynska et al. (2015) and Liang et al. (2016) respectively applied the LUR model on relationship of air pollutants, land use variables in Oslo, The Netherlands, Munich/Augsburg, and Catalonia of Europe and Houston of USA.

Among these tools, LUR has been proved to be feasible and appropriate of regions of China and other areas worldwide (Hoek et al., 2008; Ross et al., 2007). Therefore, LUR was chosen as the method to study spatial influencing factors in air pollution in this paper. As of the study areas, Hebei Province was selected because it is one of the most polluted area in China and worldwide, and in-depth research is needed to understand its pollution characteristics (He et al., 2016; Zhang et al., 2016).

LUR models are important methods for studying the relation between the spatial distribution of air pollutants and elements of geographical space. Usually, an LUR model is built by constructing a regression equation to analyze factors affecting air quality, in which data for air pollutant concentrations serve as the dependent variable while data for socioeconomic, land use, and meteorological factors, etc., serve as the independent variables.

After the Chinese government established national networks for monitoring air pollutants in 2013, relevant studies using LUR models gradually increased in number. Some researchers employed an LUR model to study land use and air pollution levels in Shanghai, one of the largest megacities in China (Liu et al., 2016; Meng et al., 2015). Although, Meng et al. (2015) was the first to combine aerosol optical depth (AOD), meteorological information and the land use regression (LUR) model to predict ground PM10 levels on high spatiotemporal resolution. However, in their studies, the resolution of land use data is not high.

Previous studies showed that the Beijing–Tianjin–Hebei region is one of the most seriously areas affected by the pollutant haze in China (Wang et al., 2015b; Gang et al., 2014; He et al., 2018). Beijing and Tianjin are two of the most important cities in China. Beijing is the capital of China, and Tianjin is an important municipality directly under the jurisdiction of the central government. Both cities have a high degree of urbanization and high levels of financial industry. Although the level of urbanization in Hebei Province is not high, its industry is dominated by steel and coal. The sources of pollution are therefore different, and the spatial patterns and influencing factors of pollution are also potentially different.

http://www.aloki.hu ● ISSN 1589 1623 (Print) ● ISSN 1785 0037 (Online)
DOI: http://dx.doi.org/10.15666/aeer/1704_81038120

Some researchers have pointed out that the impact of motor vehicle exhaust emissions on the atmosphere is the most significant pollution source in Beijing and Tianjin, whereas in Hebei Province industry is the most notable contributor (Yang et al., 2018; Wang et al., 2017).

By the end of 2012, the total coal consumption of Hebei Province reached 271 million tons, which was much higher than the combined consumption of Beijing and Tianjin. Among 74 major cities in China, pollution by $PM_{2.5}$ in seven Hebei cities is the most serious (Wang et al., 2013).

An LUR model has been used to analyze the spatial distribution and influencing factors of air pollutants in Tianjin and Beijing and good results have been achieved (Chen et al., 2010; Wu et al., 2014). However, an LUR model has not been employed in Hebei Province alone in any recent researches. Because of the heavy industry-based industrial structure and complex geographical and meteorological environment, we focused exclusively on Hebei and used high-resolution land use data to employ LUR for the identification of influencing factors.

The purpose of this study is to conduct Land use Regression model to analyze the relationship between spatial characteristic and air pollutants in Hebei province. In comparison with previous studies, this paper improved both data fineness and model integrity in cooperation with multiple local and international institutes. Firstly, high-resolution (1 × 1 m) land use data from national geographical census data were used. Secondly, we set 20 buffer distances to refine the influencing factors that significantly influenced the concentrations of air pollutants. Finally, this study introduced meteorological data as a variable for a more comprehensive analysis on air pollution problems.

Data and methodology

Hebei Province was chosen as the study area because it is the most polluted region of China (Lu et al., 2015). In contrast to Beijing and Tianjin, Hebei has a more complex and diverse geographical environment and a much larger area. Furthermore, Hebei is relatively less urbanized and has more heavy industries. Hebei's unique characteristics need customized research designs, and it is necessary to conduct separate studies in Hebei alone. When we developed our LUR model, the $PM_{2.5}$ and NO_2 concentrations at 53 air quality monitoring sites were selected as separate dependent variables, and various influencing indicators (e.g., meteorological factors, land use types, road area, population density, monitoring enterprises, pollution sources, elevation, etc.) were selected as independent variables. The LUR model was analyzed with a statistical package (SPSS) and geographic information system (GIS) software (ArcGIS 10.1). A flow chart of the study is shown in *Figure 1*.

Research area

Hebei Province is a coastal province adjacent to two megacities in northern China, namely, Beijing and Tianjin. The Beijing–Tianjin–Hebei region is also one of China's largest urban agglomerations. Hebei consists of 11 cities, and its land area is approximately 188,500 km^2. The Yanshan and Taihang Mountains lie to its north and west respectively and the Bohai Sea lies to its northeast Hebei, as illustrated in *Figures 2* and *3*. At the end of 2014, the gross domestic product (GDP) of Hebei reached 2942.12 billion renminbi (RMB), its population was 73.83 million, and its average population density was 392 inhabitants/km^2 (National Bureau of Statistics, 2015).

http://www.aloki.hu ● ISSN 1589 1623 (Print) ● ISSN 1785 0037 (Online)
DOI: http://dx.doi.org/10.15666/aeer/1704_81038120

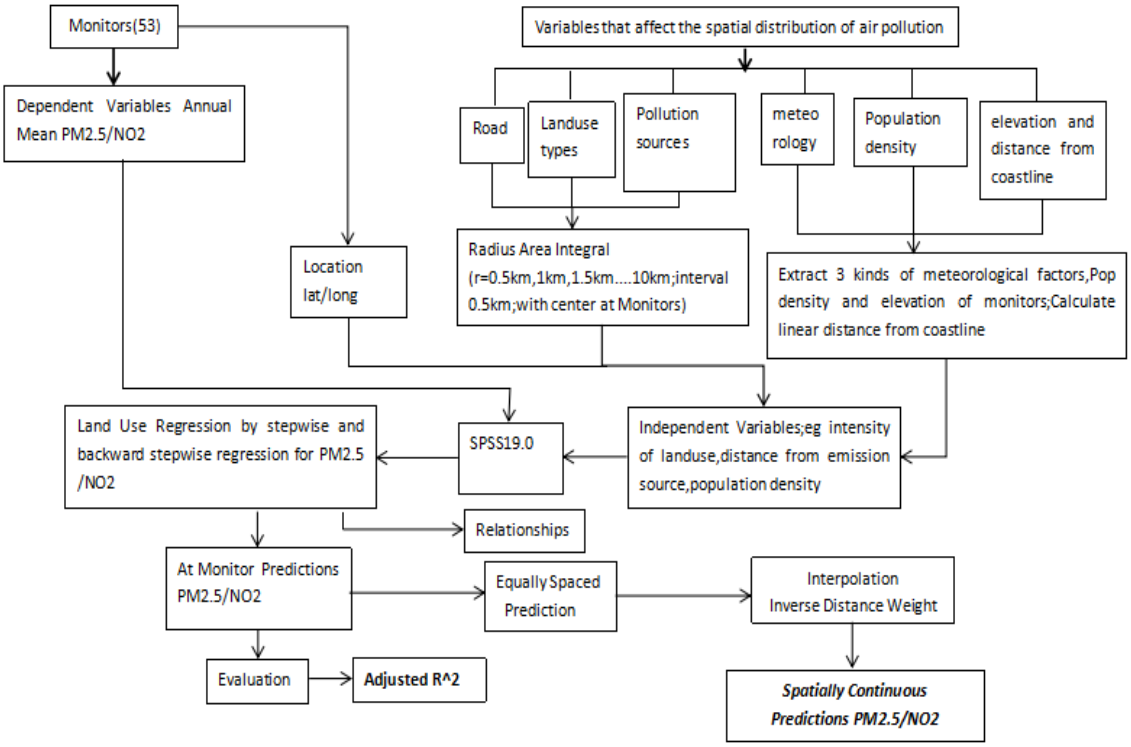

Figure 1. *Flow chart of our study*

The annual temperature at meteorological monitoring sites in Hebei Province in 2014 ranged is 13°C (Climate Bulletin of 2014 in Hebei Province), and the average wind speed is 2.5 m/s, calculated from data for 20 national meteorological monitoring stations in Hebei in 2014. The average wind speed in southern and western areas is lower than that in northern and eastern areas because the Taihang and Yanshan mountains to the west and north of Hebei block the prevailing northerly winds in winter.

LUR model setting

Dependent variables: $PM_{2.5}$ and NO_2

Hebei Province started to report $PM_{2.5}$ concentrations in 2012. In this study, we extracted hourly monitoring data for $PM_{2.5}$/NO_2 concentrations from the official website of China Environmental Monitoring Station (http://www.cnemc.cn) during the period from March 22, 2014 to March 22, 2015. In total, one-year observations from 53 national air quality monitoring sites in 11 cities of Hebei were collected, and the average annual values of $PM_{2.5}$ and NO_2 concentrations were used as dependent variables.

Independent variables

Independent variables were divided into buffer-related and location-based variables, of which the latter were specific to the 53 air quality monitoring sites. The buffer-related variables are comprised of six land use types, road areas, and the numbers of pollution-emitting industries in different buffer areas around each monitoring site, which were calculated for 20 different buffer distances (from 0.5 km to 10 km at

http://www.aloki.hu ● ISSN 1589 1623 (Print) ● ISSN 1785 0037 (Online)
DOI: http://dx.doi.org/10.15666/aeer/1704_81038120

intervals of 500 m) from each monitoring site. Furthermore, the location-based variables included the longitude, latitude, distance from the monitoring site to the coastline, population density, and elevation, as well as meteorological elements, including air pressure, wind speed, temperature, precipitation, and relative humidity. In the LUR model, 169 independent variables were used, and each independent variable is described as follows.

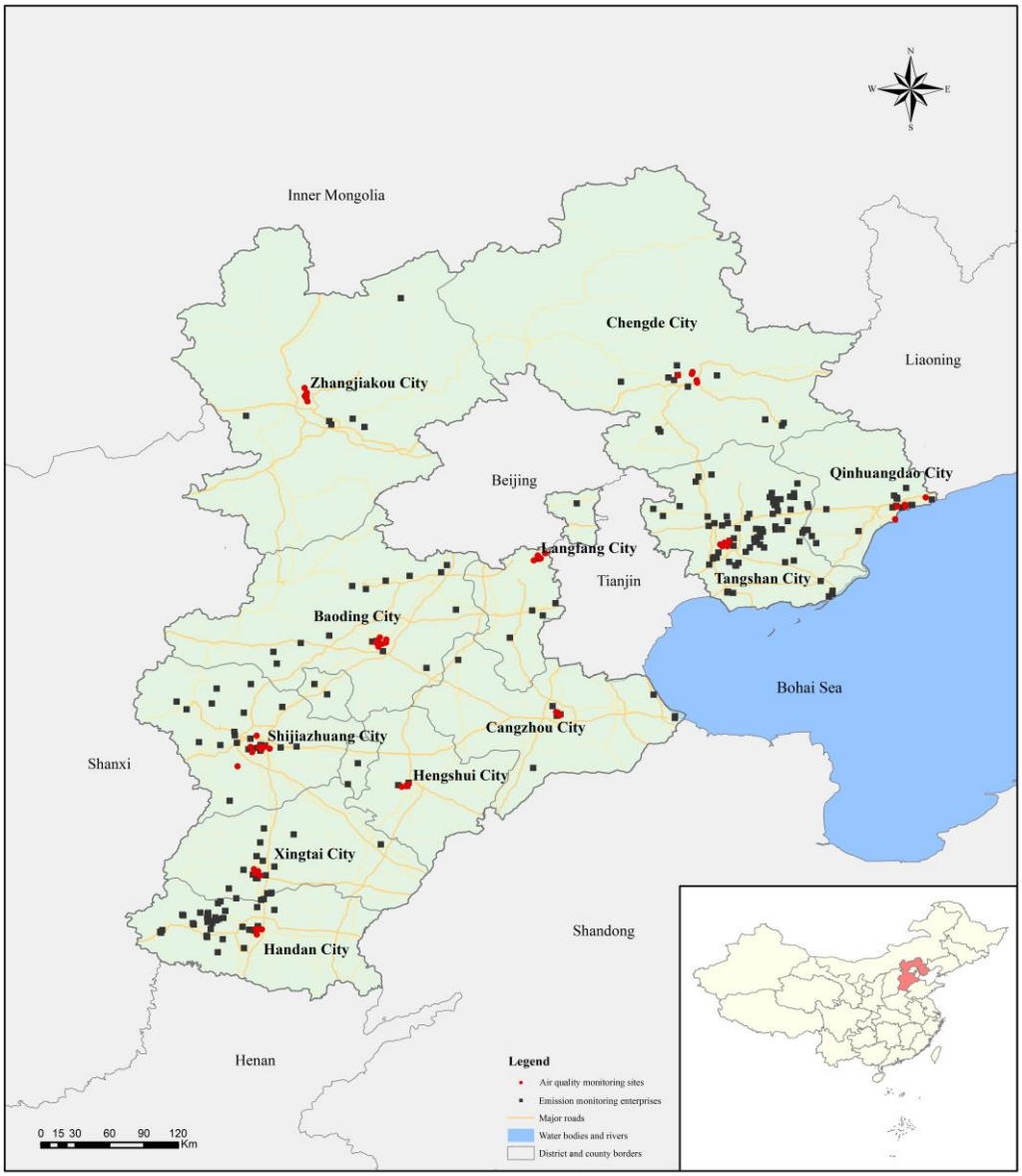

Figure 2. *Study area and monitor distributions*

Land use

The six land use types adopted are comprised of building land (including workplaces, residences, educational institutions, and buildings used for entertainment), forest land, farmland, bodies of water (rivers and lakes), greenhouses, and garden land. (A greenhouse is defined as a heating facility used to cultivate plants.) The areas occupied

http://www.aloki.hu ● ISSN 1589 1623 (Print) ● ISSN 1785 0037 (Online)
DOI: http://dx.doi.org/10.15666/aeer/1704_81038120

by each land use in each buffer zone were calculated separately. The land use data were derived from national geographical census data for Hebei Province with high resolution (1 × 1 m), which were collected by the Hebei Bureau of Geoinformation (http://www.hebsm.gov.cn/) in 2015. The variables were denoted as the land use type plus buffer distance as follows: build_buffer distance, fore_buffer distance, farm_buffer distance, wat_buffer distance, ghl_buffer distance, and gar_buffer distance. The explanation of abbreviation is shown in *Table A3* in the *Appendix*.

Figure 3. *Study area and ridgelines distributions*

Road areas

The areas of all road types in the different buffer zones in km^2 were calculated. The road area data were derived from high-resolution national geographical census data for Hebei Province from the Hebei Bureau of Geoinformation (http://www.hebsm.gov.cn/). The road types included national roads, provincial roads, county roads in rural areas, expressways, arterial streets, sub-arterial streets, and local streets in urban areas. We did not separate these road types in detail but uniformly calculated the areas of all types of roads in different buffer zones, which were denoted as rdar_buffer in this paper.

http://www.aloki.hu ● ISSN 1589 1623 (Print) ● ISSN 1785 0037 (Online)
DOI: http://dx.doi.org/10.15666/aeer/1704_81038120

Population density

Population density data in inhabitants/km^2 were extracted from the database of China's population distribution provided by the Data Center for Resources and Environmental Sciences, Chinese Academy of Sciences. We used the GIS to extract the raster values of the 53 air quality monitoring sites in Hebei Province as population density variables from the population distribution dataset for the Chinese population grid (1 × 1 km), which was calculated by Fu et al. (2013). In comparison with the census data, the above-mentioned data have higher resolution and are better for revealing spatial differences in population density, because the relative error is kept under 10% (Fu et al., 2010).

Distance to the coastline

The straight-line distance (m) between each air quality monitoring site and the nearest coastline was measured on a map of Hebei Province with the GIS. The measurement of the distance to the coastline served to determine the effects of the deposition of pollutants in the sea and the dilution of pollutants by sea breezes.

Geographical features of air quality monitoring sites

The geographical coordinates of each air quality monitoring site (including its longitude and latitude) were recorded, which were obtained from the Environmental Monitoring Center of Hebei Province. Elevations were extracted from the data of a digital elevation model of Hebei with a worldwide resolution of 30 m.

Industrial sources of air pollution

This study considered 241 enterprises that carried out national emission monitoring in Hebei Province in 2015, as listed on the website of the Ministry of Environmental Protection of China, as shown in *Figure 2* (http://www.zhb.gov.cn/). These included waste gas, coal, and thermal power plants, etc. We counted the number of these enterprises within each buffer zone, which was included as an independent variable in the model.

Meteorological data

We extracted meteorological data for 20 national meteorological monitoring stations in Hebei Province from the official website of the China Meteorological Administration. The mean values of five variables (air pressure, temperature, precipitation, wind speed, and relative humidity) in one year were calculated. By means of the kriging interpolation algorithm in ArcGIS 10.1, the values of the five classes of meteorological data for each air pollution monitoring site were taken as independent variables.

Statistical analysis

Pre-processing was performed to solve problems arising from multicollinearity between independent variables. Firstly, a bivariate (Pearson) correlation test was used to calculate the absolute strength of the correlation between all variables and the measured $PM_{2.5}$/NO_2 concentrations. Secondly, for land use factors, from two independent variables between which the correlation coefficient was greater than 0.6, only the

http://www.aloki.hu ● ISSN 1589 1623 (Print) ● ISSN 1785 0037 (Online)
DOI: http://dx.doi.org/10.15666/aeer/1704_81038120

variable with a stronger correlation with the dependent variables was employed in the LUR model. In addition, the longitude, latitude, wind speed, population density, precipitation, pressure, temperature, and altitude were added directly to the LUR model.

After the pre-processing step, stepwise backward multiple regression methods were employed to test the remaining variables for their correlations with $PM_{2.5}$ and NO_2 concentrations. The adjusted R^2 and residuals were used to evaluate the goodness of model fitting. The global Moran's index and Durbin–Watson index were employed to test the assumption that the regression residuals were spatially independent. In the application of GIS model, Moran's (Anselin, 1983) and Durbin-Watson (Mcauliffe, 2015) indexes are generally used for spatial autocorrelation test of data.

Results and discussion

Descriptive characteristics of $PM_{2.5}$ and NO_2 concentrations

The average $PM_{2.5}$ and NO_2 concentrations at the 53 air quality monitoring sites in Hebei Province were 83.64 ± 29.45 μg/m^3 and 47.18 ± 12.10 μg/m^3, respectively. *Figure 4a* shows an inverse distance weighting (IDW) interpolation map derived from the annual average values of $PM_{2.5}$ concentrations. *Figure 4b* shows an IDW interpolation map derived from the annual average values of NO_2 concentrations. The maps indicate that the concentrations in the southwest were higher than those in other areas. In addition, there were significant differences in concentration between the north and south of Hebei along the Yanshan mountains. Areas under severe air pollution were mainly concentrated in the south of Hebei for both $PM_{2.5}$ and NO_2.

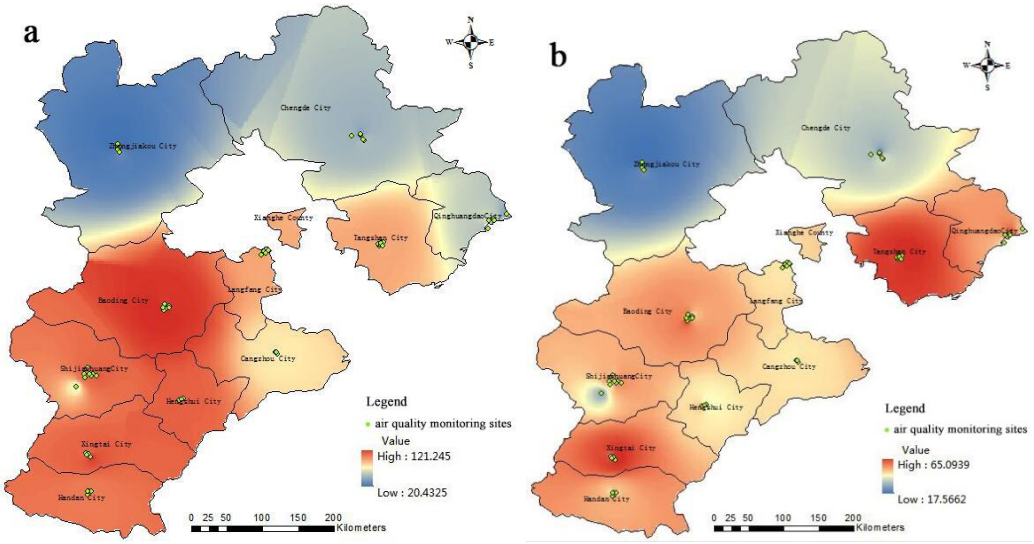

***Figure 4. a** Interpolation map of $PM_{2.5}$ concentrations (μg/m^3) based on observational data. **b** Interpolation map of NO_2 concentrations (μg/m^3) based on observational data*

Results of pre-processing for multicollinearity

There were initially a total of 169 indicator variables in this study; after filtering for multicollinearity between the influencing factors with reference to the modelling method proposed by Wu et al. (2014), 20 influencing factors remained for $PM_{2.5}$

http://www.aloki.hu ● ISSN 1589 1623 (Print) ● ISSN 1785 0037 (Online)
DOI: http://dx.doi.org/10.15666/aeer/1704_81038120

concentrations (*Table 1*) and 19 influencing factors remained for NO_2 concentrations (*Table 1*), which were added to the LUR model at the outset.

Table 1. *Screening of optimal correlation factors for bivariate correlation analysis with $PM_{2.5}$/NO_2 concentration*

$PM_{2.5}$		**NO_2**	
Influencing factors	**Correlation coefficient**	**Influencing factors**	**Correlation coefficient**
Longitude	−0.39**	Distance to the coastline	−0.28*
Latitude	−0.75**	Latitude	−0.44**
Population density	0.52**	Population density	0.52**
Elevation	−0.73**	Elevation	−0.76**
Wind speed	−0.51**	Wind speed	−0.46**
Temperature	0.77**	Temperature	0.41**
Air pressure	0.75**	Relative humidity	0.61**
Precipitation	−0.30*	Air pressure	0.72**
Farmland_0.5 km	0.31*	Road area_0.5 km	0.34*
Building land_0.5 km	0.52**	Forest land_1 km	−0.73**
Farmland_3 km	0.28*	Road area_1 km	0.43**
Farmland_3.5 km	0.31*	Emission monitoring enterprises_3.5 km	0.37**
Water_3.5 km	−0.37**	Emission monitoring enterprises_4 km	0.37**
Emission monitoring enterprises_3.5 km	0.34*	Garden land_5 km	−0.42**
Emission monitoring enterprises_4 km	0.33*	Building land_5 km	0.63**
Forest land_6 km	−0.70**	Emission monitoring enterprises_8.5 km	0.76**
Building land_9 km	0.78**	Water_10 km	0.36**
Emission monitoring enterprises_7.5 km	0.48**	Farmland_10 km	0.26*
Farmland_10 km	0.58**	Road area_10 km	0.66**
Road area _10 km	0.62**	-	-

**Significant correlation at level of $p < 0.01$. *Significant correlation at level of $p < 0.05$

LUR model results

$PM_{2.5}$ concentration modeling results

The adjusted R^2 in the regression model was 0.96 and the F-statistic was 157.71 ($p < 0.01$), which indicates that the LUR model had good fitness (*Table A1* in the *Appendix*). The value of the Durbin–Watson test statistic was 1.954, which indicates that there was no autocorrelation in the residual sequence. Eight independent variables were finally entered into the LUR model, namely, air pressure, precipitation, temperature, wind speed, longitude, elevation, farmland_500 m, and pollution-emitting industries within the 7.5 km buffer zone. The standardized regression coefficients for air pressure and precipitation were 0.94 and 0.23, respectively, which indicates that they

http://www.aloki.hu ● ISSN 1589 1623 (Print) ● ISSN 1785 0037 (Online)
DOI: http://dx.doi.org/10.15666/aeer/1704_81038120

were positively correlated with $PM_{2.5}$ concentrations. In contrast, the standardized regression coefficients for temperature and wind speed were -0.62 and -0.15, respectively, which indicates that they were negatively correlated with $PM_{2.5}$ concentrations. The results also show that the area of farmland within the 500 m buffer zone and emission monitoring enterprises within the 7.5 km buffer zone (Emission monitoring enterprises_7.5 km) were included as significant predictor variables, with standardized regression coefficients of 0.07 and 0.10, respectively. This indicates that the emission source of waste gas enterprises is the main contributor to the concentration of $PM_{2.5}$ pollutants, and the wind speed is the main factor to alleviate $PM_{2.5}$ pollution, which is similar to the conclusions of relevant study (Guan et al., 2017; Liu et al., 2018). Longitude and elevation were also influencing factors negatively correlated with $PM_{2.5}$ concentrations, with standardized regression coefficients of -1.14 and -0.29.

The final model explains 96% of the variation in the measured $PM_{2.5}$ concentrations. There was no apparent bias in the model, as shown in *Figure 5a* and *b*. The results for spatial autocorrelation are shown in *Figure 5c*. The z-score was 0.74, which is less than the critical value of 1.96, which means the probability that the residuals resulted from random factors is greater than 0.95. The value of Moran's index of 0.056 further indicates that there was no autocorrelation and justifies the assumption that errors were spatially independent.

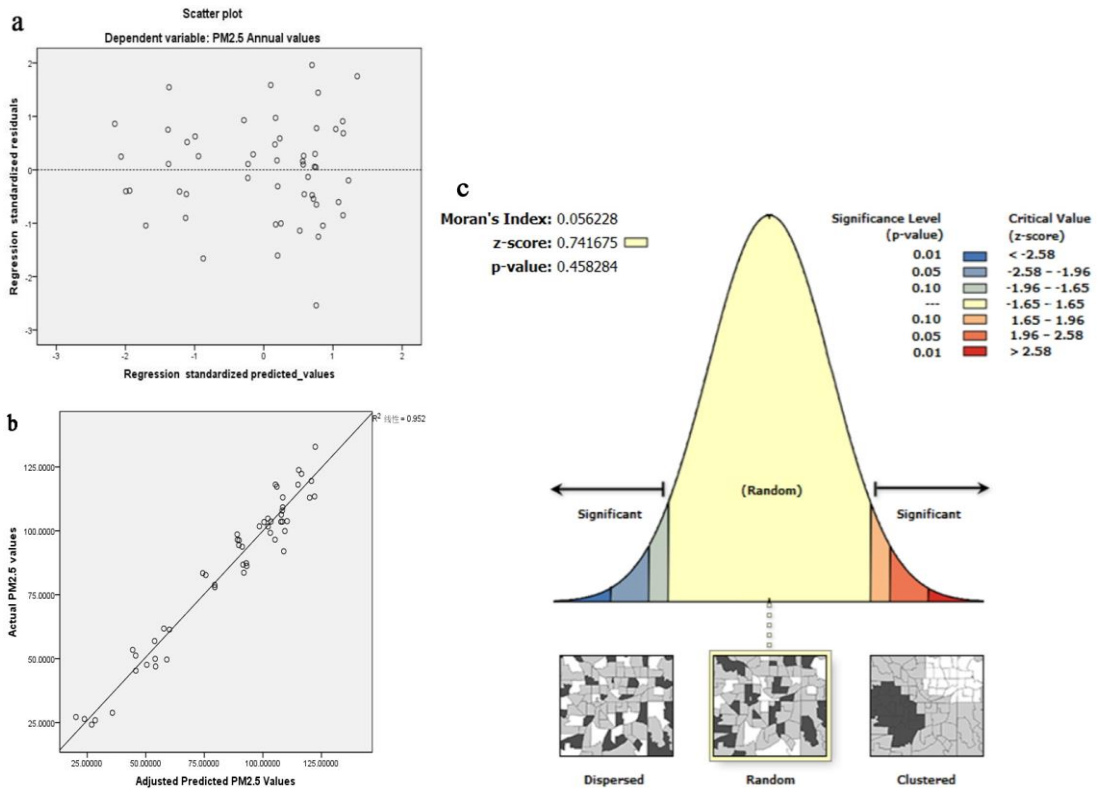

***Figure 5. a** Plot of residuals versus predicted $PM_{2.5}$ values. **b** Plot of monitored versus predicted $PM_{2.5}$ values ($\mu g/m^3$). **c** Results of spatial autocorrelation test for LUR residuals*

An interpolation map of measured values of $PM_{2.5}$ concentrations is shown in *Figure 4a*, and an interpolation map of LUR predictions of $PM_{2.5}$ concentrations is shown in *Figure 6a*. From these two figures, we can conclude that there existed

http://www.aloki.hu ● ISSN 1589 1623 (Print) ● ISSN 1785 0037 (Online)
DOI: http://dx.doi.org/10.15666/aeer/1704_81038120

significant heterogeneity in the spatial distribution of $PM_{2.5}$ concentrations in Hebei Province. The variables of longitude and elevation were negatively correlated with $PM_{2.5}$ concentrations. Correspondingly, the LUR model results show that western areas were more heavily polluted than eastern areas and that southern areas were more heavily polluted than northern areas. The regression coefficients for the number of emission monitoring enterprises within the 7.5 km buffer zone and farmland within the 500 m buffer zone show that these variables were positively correlated with $PM_{2.5}$ concentrations.

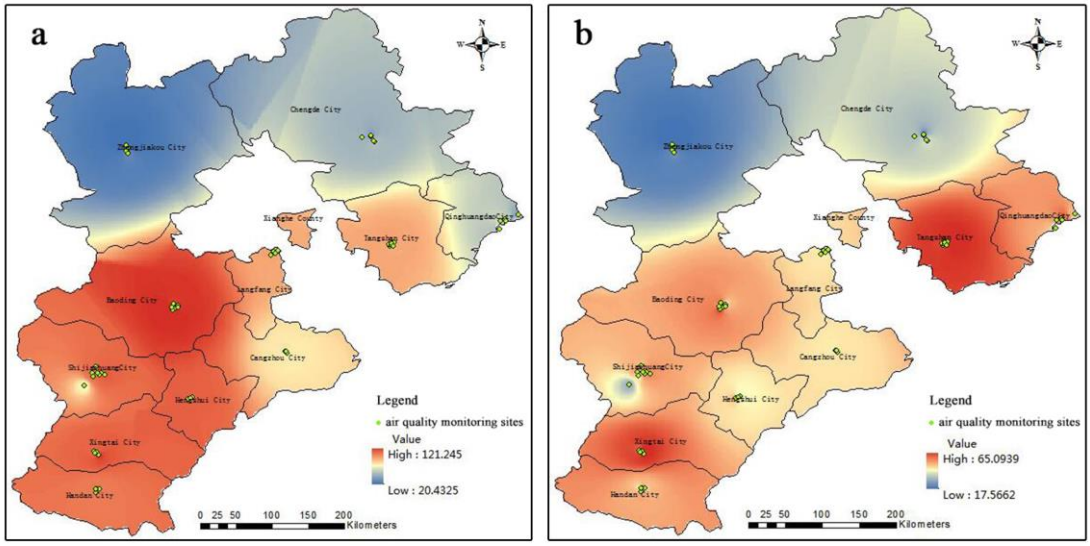

Figure 6. a *LUR predictions of $PM_{2.5}$ concentrations ($\mu g/m^3$).* ***b*** *LUR predictions of NO_2 concentrations ($\mu g/m^3$)*

This is due to the following reasons. Firstly, industrial emissions of air pollutants make a great contribution to $PM_{2.5}$ concentrations (Rohde et al., 2015). Secondly, the destruction of the soil structure and surface vegetation cover of farmland by human farming processes (Bogman et al., 2005; Goossens, 2004; Pattey et al., 2012) and the burning of biomass lead to the increases in $PM_{2.5}$ concentrations (Cheng et al., 2014). Therefore, we conclude that $PM_{2.5}$ concentrations are influenced by meteorological factors, certain land uses, and heavy industries.

Spatial distribution of NO_2 concentrations and influencing factors

NO_2 is the main air pollutant indicator that originates from transportation. In this study, we also developed an LUR model for NO_2 for comparison with the features of $PM_{2.5}$ pollution. The adjusted R2 in the regression model was 0.81 and the F-statistic was 25.31 ($p < 0.01$), which indicates that the LUR model was also highly predictive for NO_2 concentrations (*Table A2* in the *Appendix*). The value of the Durbin–Watson test statistic was 2.08, which is very close to 2, indicating that there was no autocorrelation in the residual sequence. Finally, nine independent variables were entered into the model, namely, distance to the coastline, latitude, forest land within the 1 km buffer zone, emission monitoring enterprises within the 8.5 km buffer zone, area of water within the 10 km buffer zone, wind speed, temperature, air pressure, and relative humidity.

http://www.aloki.hu ● ISSN 1589 1623 (Print) ● ISSN 1785 0037 (Online)
DOI: http://dx.doi.org/10.15666/aeer/1704_81038120

An interpolation map of measured values of NO_2 concentrations is shown in *Figure 4b*, and an interpolation map of LUR predictions of NO_2 concentrations is shown in *Figure 5b*.

The main similarity was that for both $PM_{2.5}$ and NO_2 the number of emission monitoring enterprises and air pressure had a positive influence on pollution levels. There were also differences between the two models. In general, land uses were more influential in the NO_2 model than in the $PM_{2.5}$ model, whereas meteorological factors were more significant in the $PM_{2.5}$ model than in the NO_2 model. A possible reason is that $PM_{2.5}$ remains suspended for a longer time and could be transported over longer distances with the help of meteorological conditions in comparison with NO_2 (Liu et al., 2016). NO_2 is considered to be a local pollutant and is thus more influenced by local land uses (Liu et al., 2016). The results of the NO_2 model differed from those of the $PM_{2.5}$ model. Unlike the LUR model results for $PM_{2.5}$, the distance to the coastline and latitude affected NO_2 pollution but were not entered into the $PM_{2.5}$ model. Secondly, wind speed, temperature, and relative humidity were positively correlated with NO_2 concentrations but negatively correlated with $PM_{2.5}$ concentrations. Thirdly, forest land was helpful for NO_2 pollution reduction but did not exhibit significant effects in decreasing $PM_{2.5}$ concentrations. Besides, the adjusted R^2 for the NO_2 regression was lower than that for the $PM_{2.5}$ model.

There is a negative correlation between wind speed and NO_2 concentration in *Table 1*. This suggests that without being influenced by anything else, the higher the wind speed, the more favorable is the diffusion of NO_2 concentration. But in the LUR model, the influence factor coefficient of wind speed is negative, this may be because the influence of wind speed on NO_2 concentration may be interfered by other factors.

Discussion

A comparison was carried out with LUR results for similar regions. Owing to the lack of specialized research in Hebei Province using LUR, we chose previous studies of the Beijing–Tianjin–Hebei region as a whole to compare our results. Each study had a specific combination of influencing variables for the prediction of $PM_{2.5}$ concentrations, as shown in *Table 2*.

The results of the comparison showed that this study displayed the best fitness and the highest adjusted R^2. The primary reason was that Hebei Province and the cities of Beijing and Tianjin have distinct economic structures. Beijing and Tianjin are two of the most highly developed cities of China, with high levels of urbanization and much fewer polluting industries. Therefore, the fitness of the LUR model was lower when Beijing–Tianjin–Hebei as a whole was considered as the study region and the spatial characteristics were assumed to be the same in the model.

In all three sets of results, elevation was a common variable and was negatively correlated with $PM_{2.5}$ concentrations. Emission monitoring enterprises played an important role both in this study and in the model used by Gang et al. (2016), which had buffer zones of 9 km and 10 km, respectively. This consistency indicates that the influence of pollution-emitting industries on $PM_{2.5}$ concentrations was significant.

Our study was the first to consider the impacts of meteorological factors on pollutant levels. Our model showed that meteorological factors were even more significant for predicting $PM_{2.5}$ concentrations, and hence a comprehensive LUR including meteorological factors is valuable and more convincing.

http://www.aloki.hu ● ISSN 1589 1623 (Print) ● ISSN 1785 0037 (Online)
DOI: http://dx.doi.org/10.15666/aeer/1704_81038120

Table 2. *Comparison of LUR results for $PM_{2.5}$ concentrations for the Beijing–Tianjin–Hebei region*

Authors	Study area	Buffers	Adjusted R^2	Influencing variables in the model
Our study	Hebei Province	0–10 km total, 20 different buffers, interval 500 m	0.96	Pressure, longitude, precipitation, temperature, elevation, wind speed, emission monitoring enterprises_9 km, farmland_0.5 km
Xu et al. (2016)	Beijing–Tianjin–Hebei region	0–10 km total, 22 different buffers	0.81	Temperature, elevation, emission monitoring enterprises_10 km, water_10 km
Jian-Sheng et al. (2017)	Beijing–Tianjin–Hebei region	100, 200, 300, 500, 1000, 2000, 3000, 5000 m	0.81	Elevation, water_2 km, relative humidity

Conclusions

Our LUR models indicate that the $PM_{2.5}$ and NO_2 concentrations in Hebei Province had significant spatial heterogeneity, and that the $PM_{2.5}$ and NO_2 concentrations in southern cities were higher than in northern cities.

In contrast to relevant research studies in Europe, America, and other areas in China, the distribution of $PM_{2.5}$ and NO_2 concentrations in Hebei Province is affected by pollution-emitting industries, whereas the road network is not the most significant variable. This is because Hebei is a developing region, whereas other areas of the Beijing–Tianjin–Hebei region are already developed. Specifically, Beijing's per capita GDP reached 99,995 RMB and the per capita GDP of Tianjin reached 105,231 RMB, whereas the per capita GDP of Hebei was only 39,984 RMB (National Bureau of Statistics, 2015).

In general, the model results for $PM_{2.5}$ concentrations demonstrate a gradually decreasing tendency from west to east, and the pollutant concentration is lower near the coastline than inland, which can be attributed to the influence of the onshore monsoon. The effect of dilution by sea breezes is consistent with the conclusions of a study performed in Shanghai (Liu et al., 2016).

The results show that the rational planning of land uses, such as the designation of land as industrial land or as green space, plays an important role in mitigating air pollution and can effectively reduce $PM_{2.5}$ and NO_2 concentrations.

Our study was the first to use high-resolution geographical data to study Hebei Province as the sole study area. Furthermore, our models made significant improvements with the use of meteorological factors, which were usually not incorporated into traditional LUR models. The results indicate the importance of meteorological factors. In addition, we identified the most distinctive characteristic of the spatial patterns of pollution in Hebei in comparison with developed cities, namely, the effective buffers around polluting industry. Our findings can be utilized for the planning of residential land and the design of buffers around heavily polluting industry and can help to reveal the land use factors with the greatest influences on $PM_{2.5}$ and NO_2 concentrations.

Some limitations of the LUR models used in this study should be recognized. Firstly, the total number of national monitoring stations in Hebei Province used in this study was 53. Although this conforms to the number of monitoring sites (40–80)

http://www.aloki.hu ● ISSN 1589 1623 (Print) ● ISSN 1785 0037 (Online)
DOI: http://dx.doi.org/10.15666/aeer/1704_81038120

recommended by Hoek et al. (2008), most monitoring sites were located in urban areas and there was a lack of rural monitoring sites. Secondly, our study was limited by the availability of refined variables, including land use types, pollutant emission sources, real-time meteorological data, and transportation emission data. This is a common constraint that also existed in previous studies.

Further studies should be performed with more monitoring site data and more dynamic variables. In addition, empirical observations are needed to support our findings, such as the impact of buffers around industry, meteorological impacts, etc. As the most severely polluted region in China, Hebei Province needs more comprehensive study from an interdisciplinary perspective to identify the relevant problems, reasons, and solutions.

Acknowledgements. This study was supported by the Hebei Province Natural Science Fund (Grant No. D2016210008). This study was supported by the National Natural Science Foundation of China (51308358), the Hebei Province Natural Science Fund (D2016210008), the Science and Technology Department of Hebei Province (18390324D), the Science and Technology Bureau of Shijiazhuang City (181130034A).

REFERENCES

[1] Anselin, L. (1983): Spatial processes, models and applications. – Economic Geography 59(3): 322-325.

[2] Bogman, P., Cornelis, W., Rollé, H., Gabriels, D. (2005): Prediction of TSP and PM10 emissions from agricultural operations in Flanders, Belgium. – Proceedings of the 14th International Conference “Transport and Air Pollution”, Graz, Austria, June.

[3] Briggs, D. J., Collins, S., Elliott, P., Fischer, P., Kingham, S., Lebret, E., Pryl, K., Van Reeuwijk, H., Smallbone, K., Van Der Veen, A. (1997): Mapping urban air pollution using GIS: a regression-based approach. – International Journal of Geographical Information Science 11(7): 699-718.

[4] Chambers, S. D., Wang, F., Williams, A. G., Deng, X., Zhang, H., Lonati, G., Crawford, J., Griffiths, A. D., Ianniello, A., Allegrini, I. (2015): Quantifying the influences of atmospheric stability on air pollution in Lanzhou, China, using a radon-based stability monitor. – Atmospheric Environment 107: 233-243.

[5] Chan, C. K., Yao, X. (2008): Air pollution in mega cities in China. – Atmospheric Environment 42(1): 1-42.

[6] Chen, H., Bai, S., Eisinger, D. S., Niemeier, D., Claggett, M. (2009): Predicting near-road PM2.5 concentrations: comparative assessment of CALINE4, CAL3QHC, and AERMOD. – Transportation Research Record: Journal of the Transportation Research Board 2123(1): 26-37.

[7] Chen, J., Zhou, C., Wang, S., Hu, J. (2018): Identifying the socioeconomic determinants of population exposure to particulate matter (PM 2.5) in China using geographically weighted regression modeling. – Environmental Pollution 241: 494-503.

[8] Chen, L., Bai, Z., Kong, S., Han, B., You, Y., Ding, X., Du, S., Liu, A. (2010): A land use regression for predicting NO2 and PM10 concentrations in different seasons in Tianjin region, China. – Journal of Environmental Sciences 22(9): 1364-1373.

[9] Cheng, Z., Wang, S. X., Fu, X., Watson, J. G., Jiang, J. K., Fu, Q. Y., Chen, C. H., Xu, B. Y., Yu, J. S., Chow, J. C. (2014): Impact of biomass burning on haze pollution in the Yangtze River Delta, China: A case study of summer in 2011. – Atmospheric Chemistry & Physics Discussions 14(9): 4573-4585.

http://www.aloki.hu ● ISSN 1589 1623 (Print) ● ISSN 1785 0037 (Online)
DOI: http://dx.doi.org/10.15666/aeer/1704_81038120

[10] Ciocănea, A., Dragomirescu, A. (2013): Modular ventilation with twin air curtains for reducing dispersed pollution. – Tunnelling & Underground Space Technology Incorporating Trenchless Technology Research 37(6): 180-198.
[11] Duki, M. I., Sudarmadi, S. S., Kawada, T., Tri, T. A. (2003): Effect of air pollution on respiratory health in Indonesia and its economic cost. – Archives of Environmental Health an International Journal 58(3): 135-143.
[12] Fengwen, W., Tian, L., Jialiang, F., Huaiyu, F., Zhigang, G. (2015): Source apportionment of polycyclic aromatic hydrocarbons in PM2.5 using positive matrix factorization modeling in Shanghai, China. – Environ Sci Process Impacts 17(1): 197-205.
[13] Gang, L., Jingying, F., Dong, J., Wensheng, H., Donglin, D., Yaohuan, H., Mingdong, Z. (2014): Spatio-temporal variation of PM2.5 concentrations and their relationship with geographic and socioeconomic factors in China. – International Journal of Environmental Research & Public Health 11(1): 173-186.
[14] Gang, X. U., Jiao, L., Xiao, F., Zhao, S., Zhang, X. (2016): Applying land use regression model to estimate spatial distribution of PM_(2.5) concentration in Beijing-Tianjin-Hebei region. – Journal of Arid Land Resources & Environment 2016(10): 116-120.
[15] Gilbert, N. L., Goldberg, M. S., Bernardo, B., Brook, J. R., Michael, J. (2005): Assessing spatial variability of ambient nitrogen dioxide in Montréal, Canada, with a land-use regression model. – Journal of the Air & Waste Management Association 55(8): 1059-1063.
[16] Goossens, D., Riksen, M. (2004): Wind Erosion and Dust Dynamics at the Commencement of the 21st Century. – In: Goossens, D., Riksen, M. (eds.) Wind Erosion and Dust Dynamics: Observations, Simulations, Modelling. ESW Publications, Wageningen, pp. 7-13.
[17] Guan, Q., Cai, A., Wang, F., Yang, L., Xu, C., Liu, Z. (2017): Spatio-temporal variability of particulate matter in the key part of Gansu Province, Western China. – Environmental Pollution 230: 189-198.
[18] He, G., Fan, M., Zhou, M. (2016): The Effect of Air Pollution on Mortality in China: Evidence from the 2008 Beijing Olympic Games. – Social Science Electronic Publishing, New York.
[19] He, Q., Bo, H. (2018): Satellite-based high-resolution PM 2.5 estimation over the Beijing-Tianjin-Hebei region of China using an improved geographically and temporally weighted regression model. – Environmental Pollution 236:1027-1037..
[20] Hoek, G., Beelen, R., Hoogh, K. D., Vienneau, D., Gulliver, J., Fischer, P., Briggs, D. (2008): A review of land-use regression models to assess spatial variation of outdoor air pollution. – Atmospheric Environment 42(33): 7561-7578.
[21] Hu, J., Ying, Q., Wang, Y., Zhang, H. (2015): Characterizing multi-pollutant air pollution in China: Comparison of three air quality indices. – Environment International 84: 17-25.
[22] Jedynska, A., Hoek, G., Wang, M., Eeftens, M., Cyrys, J., Beelen, R., Cirach, M., Nazelle, A. D., Keuken, M., Visschedijk, A. (2015): Spatial variations of levoglucosan in four European study areas. – Science of the Total Environment 505: 1072-1081.
[23] Jerrett, M., Arain, A. P., Beckerman, B., Potoglou, D., Sahsuvaroglu, T., Morrison, J., Giovis, C. (2005): A review and evaluation of intraurban air pollution exposure models. – J Expo Anal Environ Epidemiol 15(2): 185-204.
[24] Jian-Sheng, W. U., Wang, X., Jia-Cheng, L. I., Yuan-Jie, T. U. (2017): Comparison of models on spatial variation of PM_(2.5) concentration: a case of Beijing-Tianjin-Hebei region. – Environmental Science. DOI: 10.13227/j.hjkx.201611114.
[25] Liang, Z., Zou, B., Xin, F., Luo, Y., Wan, N., Shuang, L. (2016): Land use regression modeling of PM2.5 concentrations at optimized spatial scales. – Atmosphere 8(1): 1.
[26] Liu, C., Henderson, B. H., Wang, D., Yang, X., Peng, Z. R. (2016): A land use regression application into assessing spatial variation of intra-urban fine particulate matter (PM 2.5)

http://www.aloki.hu ● ISSN 1589 1623 (Print) ● ISSN 1785 0037 (Online)
DOI: http://dx.doi.org/10.15666/aeer/1704_81038120

and nitrogen dioxide (NO 2) concentrations in City of Shanghai, China. – Science of the Total Environment 565: 607-615.

[27] Liu, M., Huang, Y., Jin, Z., Ma, Z., Liu, X., Zhang, B., Liu, Y., Yu, Y., Wang, J., Bi, J. (2017): The nexus between urbanization and PM2.5 related mortality in China. – Environmental Pollution 227: 15.

[28] Liu, W., Liu, Q., Liu, W. X., Yu, S. Y., Wang, X., Xu, Y. S., Liu, Y., Tao, S. (2018): Oxidative potential of ambient PM2.5 in the coastal cities of the Bohai Sea, Northern China: seasonal variation and source apportionment. – Environmental Pollution 236: 514-528.

[29] Lu, W. Z., Fan, H. Y., Lo, S. M. (2003): Application of evolutionary neural network method in predicting pollutant levels in downtown area of Hong Kong. – Neurocomputing 51(2): 387-400.

[30] Mcauliffe, R. E. (2015): Durbin–Watson Statistic. – In: Mcauliffe, R. E. (ed.) The Blackwell Encyclopedia of Management. Vol. 8: Managerial Economics. Blackwell, Hoboken, NJ.

[31] Meng, X., Fu, Q., Ma, Z., Chen, L., Zou, B., Zhang, Y., Xue, W., Wang, J., Wang, D., Kan, H. (2015): Estimating ground-level PM 10 in a Chinese city by combining satellite data, meteorological information and a land use regression model. – Environmental Pollution 208(Pt A): 177.

[32] Morrison, W. M. (2015): China's Economic Rise: History, Trends, Challenges, and Implications for the United States. – Congressional Research Service Reports 7-5700, www.crs.gov, RL33534.

[33] National Bureau of Statistics (2015): Hebei Economic Yearbook. – China Statistics Press, Beijing.

[34] Pattey, E., Qiu, G. (2012): Trends in primary particulate matter emissions from Canadian agriculture. – Journal of the Air & Waste Management Association 62(7): 737-747.

[35] Rohde, R. A., Muller, R. A. (2015): Air pollution in China: mapping of concentrations and sources. – Plos One 10(8): e0135749.

[36] Ross, Z., Jerrett, M., Ito, K., Tempalski, B., Thurston, G. D. (2007): A land use regression for predicting fine particulate matter concentrations in the New York City region. – Atmospheric Environment 41(11): 2255-2269.

[37] Roswall, N., Raaschou-Nielsen, O., Ketzel, M., Gammelmark, A., Overvad, K., Olsen, A., Sørensen, M. (2017): Long-term residential road traffic noise and NO 2 exposure in relation to risk of incident myocardial infarction - a Danish cohort study. – Environmental Research 156: 80-86.

[38] Shekarrizfard, M., Faghih-Imani, A., Dan, L. C., Goldberg, M., Ross, N., Eluru, N., Hatzopoulou, M. (2016): Individual exposure to traffic related air pollution across land-use clusters. – Transportation Research Part D Transport & Environment 46: 339-350.

[39] Song, C., Lin, W., Xie, Y., He, J., Xi, C., Wang, T., Lin, Y., Jin, T., Wang, A., Yan, L. (2017): Air pollution in China: Status and spatiotemporal variations. – Environmental Pollution 227: 334-347.

[40] Su, J. G., Brauer, M., Ainslie, B., Steyn, D., Larson, T., Buzzelli, M. (2008): An innovative land use regression model incorporating meteorology for exposure analysis. – Science of the Total Environment 390(2): 520-529.

[41] Wang, J., Zimei, H. U., Chen, Y., Chen, Z., Shiyuan, X. U. (2013): Contamination characteristics and possible sources of PM10 and PM2.5 in different functional areas of Shanghai, China. – Atmospheric Environment 68(2): 221-229.

[42] Wang, L., Zhang, N., Liu, Z., Sun, Y., Ji, D., Wang, Y. (2015): The Influence of Climate Factors, Meteorological Conditions, and Boundary-Layer Structure on Severe Haze Pollution in the Beijing-Tianjin-Hebei Region during January 2013. – Advances in Meteorology 2014(7): 1-14.

http://www.aloki.hu ● ISSN 1589 1623 (Print) ● ISSN 1785 0037 (Online)
DOI: http://dx.doi.org/10.15666/aeer/1704_81038120

[43] Wang, S., Zhou, C., Wang, Z., Feng, K., Hubacek, K. (2017): The characteristics and drivers of fine particulate matter (PM 2.5) distribution in China. – Journal of Cleaner Production 142(4): 1800-1809.
[44] Wheeler, A. J., Smith-Doiron, M., Xu, X., Gilbert, N. L., Brook, J. R. (2008): Intra-urban variability of air pollution in Windsor, Ontario—Measurement and modeling for human exposure assessment. – Environmental Research 106(1): 7-16.
[45] WHO (2016): World Health Statistics 2016. Monitoring Health for the SDGs. – WHO, Geneva.
[46] Wu, J., Li, J., Jian, P., Li, W., Xu, G., Dong, C. (2014): Applying land use regression model to estimate spatial variation of PM 2.5 in Beijing, China. – Environmental Science & Pollution Research 22(9): 7045-7061.
[47] Wu, J., Yao, F., Li, W., Si, M. (2016): VIIRS-based remote sensing estimation of ground-level PM2. 5 concentrations in Beijing–Tianjin–Hebei: a spatiotemporal statistical model. – Remote Sensing of Environment 184: 316-328.
[48] Yang, G., Huang, J., Li, X. (2018): Mining sequential patterns of PM2. 5 pollution in three zones in China. – Journal of Cleaner Production 170: 388-398.
[49] Yao, F., Si, M., Li, W., Wu, J. (2017): A multidimensional comparison between MODIS and VIIRS AOD in estimating ground-level PM2.5 concentrations over a heavily polluted region in China. – Science of the Total Environment 618: 819-828.
[50] Yin, H., Pizzol, M., Xu, L. (2017): External costs of PM2.5 pollution in Beijing, China: Uncertainty analysis of multiple health impacts and costs. – Environmental Pollution 226: 356.
[51] Zhang, Y., Lin, Y., Cai, J., Liu, Y., Hong, L., Qin, M., Zhao, Y., Ma, J., Wang, X., Zhu, T. (2016): Atmospheric PAHs in North China: spatial distribution and sources. – Science of the Total Environment 565: 994-1000.

APPENDIX

Table A1. *Regression results of Hebei $PM_{2.5}$ LUR model*

Model parameter	Unit	Unstandardized coefficient β	Standardized coefficient β	p-values
Constant	−	1472.79	−	< 0.01
Air pressure	hPa	0.95	0.94	< 0.01
Longitude	°	−19.34	−1.14	< 0.01
Precipitation	mm	0.09	0.23	< 0.01
Temperature	°C	−8.39	−0.62	< 0.01
Farmland_500 m	km2	33.1	0.07	0.02
Elevation	m	−0.03	−0.29	< 0.01
Wind speed	m/s	−10.05	−0.15	< 0.01
Emission monitoring enterprises_7.5 km	N	1.7	0.1	< 0.01
Adjusted R2	0.96			
Durbin–Watson statistic	1.95			
F-values	157.71			p < 0.01

http://www.aloki.hu ● ISSN 1589 1623 (Print) ● ISSN 1785 0037 (Online)
DOI: http://dx.doi.org/10.15666/aeer/1704_81038120

Table A2. *Regression results of Hebei NO_2 LUR model*

Model parameter	Unit	Unstandardized coefficient β	Standardized coefficient β	p-values
Constant	−	-1500.62	−	< 0.01
Distance to coastline	km	0.20	1.88	< 0.01
Latitude	°	19.11	2.14	< 0.01
Forest land_1 km	km2	−3.28	−0.20	0.073
Water_10 km	km2	0.88	0.20	0.082
Emission monitoring enterprises_8.5 km	N	2.93	0.48	< 0.01
Wind speed	m/s	14.17	0.51	0.04
Temperature	°C	6.09	1.09	0.04
Air pressure	hPa	0.40	0.96	0.02
Relative humidity	%	4.56	1.35	0.02
Adjusted R2	0.81			
Durbin–Watson statistic	2.08			
F-values	25.31			p < 0.01

Table A3. *Explanation of abbreviations of land use*

Abbreviation for land use data	Description
build_buffer	The area of building land in a circular area centered on a monitoring station
fore_buffer	The area of forest in a circular area centered on a monitoring station
farm_buffer	The area of farmland in a circular area centered on a monitoring station
wat_buffer	The area of water in a circular area centered on a monitoring station
ghl_buffer	Greenhouse area in a circular area centered on a monitoring station
gar_buffer	Garden area in a circular area centered on a monitoring station

http://www.aloki.hu ● ISSN 1589 1623 (Print) ● ISSN 1785 0037 (Online)
DOI: http://dx.doi.org/10.15666/aeer/1704_81038120

EFFECTS OF SPRAYING ZINC FERTILIZER ON THE PHYSIOLOGICAL AND PHOTOSYNTHETIC CHARACTERISTICS OF MILLET PLANTS (*SETARIA ITALICA L.*) AT DIFFERENT GROWTH STAGES

CAO, M. L.[1] – LI, Y. X.[1] – DU, H. L.[2*]

[1]*College of Agricultural Science, Shanxi Agricultural University, Taigu, Shanxi 030801, People's Republic of China*

[2]*College of Arts and Sciences, Shanxi Agricultural University, Taigu, Shanxi 030801, People's Republic of China*

**Corresponding author*
e-mail: duhuiling66@163.com

(Received 1st Feb 2019; accepted 16th May 2019)

Abstract. Pot experiments were conducted from May 2017 to October of 2017 at the cultivation base of the Resource and Environment College of the Shanxi Agricultural University in China. The physiological and photosynthetic characteristics of different cultivars treated with different Zn concentrations at different growth stages were investigated to determine the optimum spraying period and spraying concentration of Zn fertilizer ($ZnSO_4 \cdot 7H_2O$) in Millet plants (*Setaria italica* L.). Results showed that spraying low Zn concentrations (20, 40, and 60 $mg \cdot L^{-1}$) solutions decreased the malondialdehyde content, Ci (intercellular CO_2 concentration), and qN (non-photochemical quenching coefficient) but increased antioxidant enzymatic activities, pigment content, photosynthetic gas exchange parameters (except Ci), and chlorophyll fluorescence parameters (except qN). By contrast spraying high Zn concentration (80 and 100 $mg \cdot L^{-1}$) showed opposite effects. Moreover, 'Jingu 21' (susceptible variety, conventional cultivar) showed more remarkable variation higher than 'Zhangzagu10' (resistant variety, hybrids). Thus, low Zn concentration promoted plant growth, while high Zn concentration inhibited plant growth, which was most pronounced during the Millet booting stage. The optimal conditions were booting period and 40 $mg \cdot L^{-1}$ of Zn. Thus, a theoretical basis for the efficient use of Zinc Fertilizer in Millet is provided.
Keywords: *foxtail millet, growth stage, zinc fertilizer, antioxidant enzyme activity, photosynthetic gas exchange parameters, chlorophyll fluorescence parameters*

Introduction

Zinc is an essential element in human health and an indispensable trace element in animal and plant growth (Gartler et al., 2013). As the only metal element to be simultaneously present in six enzymes, Zn plays an important regulatory role in plant photosynthesis, protein and nucleic acid metabolism, auxin metabolism, biofilm stability, and cell division (Prasad and Hagemeyer, 1999; Kabata-Pendias and Pendias, 2001). In recent years, plants have taken away substantial amount of nutrients from the soil because of the growing area of crops and the gradually increased yield (Feng, 2010). In addition, the amount of organic fertilizer applied in the field has generally declined (Mutegi et al., 2012), and trace elements could not be replenished in time. Thus, the available Zn in the soil gradually decreased with the passage of time. This phenomenon resulted in the prevalent deficiency of Zn in crops (Carroll and Loneragan, 1968; Alloway, 2009). Zn deficiency can cause dwarf plants, short internodes, suppression of leaf expansion and elongation, leaflets, twisted leaves, and wrinkled leaf margins. Albino corn seedlings and stiff Miller of rice seedlings are due to Zn

http://www.aloki.hu ● ISSN 1589 1623 (Print) ● ISSN 1785 0037 (Online)
DOI: http://dx.doi.org/10.15666/aeer/1704_81218138

deficiency (Rengel et al., 1998; Singh and Yashbir, 2017). At present, the application of Zn fertilizer to crops is the safest, most convenient, and effective approach to augment the micronutrient Zn deficiency in humans. This process can also effectively improve the symptoms of Zn deficiency in crops (Noulas et al., 2018). However, excessive application of Zn will inhibit the growth of crops, cause poisoning (Mateos-Naranjo et al., 2014), and can lead to toxicity, such as nutrient imbalances, growth inhibition, leaf chlorosis, and photosynthesis impairment (Todeschini et al., 2011; Cambrollé et al., 2012).

Photosynthesis is an important factor in plant growth and an indicator to assess plant growth status (Moss and Musgrabe, 1971; Silveira and Carvalho, 2016). Chlorophyll fluorescence is an effective tool to sense and assess the impact of Zn on the photosynthetic apparatus, and this tool has been used extensively to investigate the effects of various substances in crops (Appenroth et al., 2001; Prasad et al., 2001; Frankart et al., 2002; Drinovec et al., 2004). Zn plays a significant role in the regulation of the stomatal aperture, which accounts for the possible role of Zn in maintaining a high K content in the guard cells (Sharma et al., 1995). Cambrollé et al. (2013) showed that an appropriate Zn concentration (60 mmol/L) could increase the net photosynthetic rate (Pn), but greater external Zn concentration (90–130 mmol/L) could negatively affect plant growth probably because of the recorded decline in the Pn. This process may be linked to the adverse effect of Zn on the photosynthetic electron transport.

Various grain industries have received increasing attention because of the improved human dietary structure (Ardiea et al., 2015). The millet (*Setaria italica* L.) originated from China and is an important strategic food crop in the country (Guo et al., 2018; Yuan et al., 2017). The millet is a traditional drought-resistant crop (Bai et al., 2009; Andersen and Nepal, 2017) and the preferred crop in drought-scarce areas in northern China. The main components of millet, including starch, protein, lipid, vitamins, and minerals, satisfy the various dietary needs of the human body (Usha et al., 1996). Low Zn availability affects crop yield and food production worldwide, and this phenomenon has led to the more efficient use of Zn in agriculture. The application of Zn fertilizer is an effective measure to increase nutrient Zn (Genty et al., 1989; Bouis and Welch, 2010; Gibson, 2006), but the safety of Zn to foxtail millet is ambiguous.

Studies on Zn fertilizers are mostly concentrated on rice (Jamalomidi et al., 2006), wheat (Khoshgoftarmanesh et al., 2006; Hacisalihoglu et al., 2003), and other crops (Gunes, 1996; Hu, 1991), but few reports have focused on millet production (Zong, 2011; Guo, 2014). In this experiment, millet was used to study the effects of different Zn concentrations on the growth of millet under different stages. Moreover, the optimal combination of conditions for the growth of millet was determined to provide a theoretical basis for the reasonable application of Zn fertilizer on millet.

Materials and methods

Site and plant materials

The pot experiments were conducted from May 2017 to October of 2017 at the cultivation base of the Resource and Environment College of Shanxi Agricultural University (37°42′ N, 112°55′ E) in Shanxi, China. The area has a mean annual temperature of 9.9 °C and a frost-free period of 176 days. The precipitation is concentrated, and the mean annual rainfall is 462.9 mm. The plant materials were ‘Zhangzagu 10’ (provided by the Zhangjiakou Academy of Agricultural Sciences of

http://www.aloki.hu ● ISSN 1589 1623 (Print) ● ISSN 1785 0037 (Online)
DOI: http://dx.doi.org/10.15666/aeer/1704_81218138

Hebei Province, China.) and 'Jingu 21' (provided by the Institute of Millet Research, Shanxi Academy of Agricultural Sciences, China). The soil used was calcareous soil, with pH value of 8.51, organic matter content of 21.02 g/kg, alkali nitrogen content of 52.37 mg/kg, available phosphorus content is 21.98 mg/kg, available potassium content of 21.98 mg/kg, total N content of 1.180 g/kg, total P content of 1.261 g/kg, and total K content of 20.18 g/kg. The seeds were sown on May 31, 2017. After 20 days of thinning out the seedlings, five seedlings were left in each pot.

Treatment details and allocation

The experiment was conducted in a completely random design. The seeds of 'Zhangzagu 10' and 'Jingu 21' were separately sown in pots with a diameter of 32 cm and a height of 26 cm under normal water content, and each pot was filled with 10 kg of soil, the cultivation temperature was 22-35℃, relative humidity of atmosphere was 70-80%. The seeds were normally watered daily after germination to ensure the normal growth of the seedlings (by weighing method, the Moisture field was maintained at 13%-15%). Different concentrations of $ZnSO_4 \cdot 7H_2O$ solution were sprayed at the seedling stage (SL, 35 d after planting), booting stage (BT, 60 after planting), flowering stage (FE, 70 d after planting), and filling stage (FL, 90 d after planting). A control (no Zn application) was set simultaneously, and each treatment was repeated thrice. The Zn concentrations sprayed were 0, 20, 40, 60, 80, and 100 $mg \cdot L^{-1}$, and the corresponding samples were labeled as CK, Zn1, Zn2, Zn3, Zn4, and Zn5. After 7 days of Zn treatment, the physiological and photosynthetic characteristics were measured.

Determination of antioxidant enzyme activity

Fresh plant leaves (0.1 g) were placed in an ice-cooled mortar, and 1 $mg \cdot L^{-1}$ of 50 mM phosphate buffer (pH 7.8) was added. The leaves were ground on ice, transferred to a 1.5 mL centrifuge tube, and centrifuged at 12000 $\times g$ for 15 min at 4 °C. The supernatant was extracted to determine the superoxide dismutase (SOD), peroxidase (POD), and catalase (CAT) activities.

The SOD activity was determined using the nitroblue tetrazolium (NBT) photoreduction method (Gao, 2006). First, the NBT reaction solution was configured. The solution consisted of 50 mM phosphate buffer (pH 7.8), 13 mM L-methionine, 0.075 mM NBT, 0.002 mM riboflavin, and 0.01 mM EDTA. Then, 5 mL of the reaction solution was added to the blank and control tubes. A portion of 50 μL of the supernatant was taken from the test tube and mixed with 5 mL of the reaction solution. The control and test tubes were illuminated for 20 min under 4000 lx light conditions at 25 °C. The absorbance of the irradiated solution was measured at 560 nm, and a non-irradiated complete reaction mixture served as a control. The result was calculated by inhibiting 50% of the NBT photochemical reduction as an enzyme unit. SOD activity was presented as the number of units per gram of fresh weight (U/g FW).

The POD activity was determined by the guaiacol method (Gao, 2006). The supernatant (5 μL) was mixed with 3 mL of the reaction solution containing 3 mL of 0.1 mM phosphate buffer (pH 6.0), 28 μL of 30% H_2O_2, and 19 μL of guaiacol (0.1%). The absorbance of the complete reaction mixture was measured at 470 nm, and the 0.1 mM phosphate buffer (pH 6.0) served as a control. The change in absorbance every 3 min indicated the POD activity.

http://www.aloki.hu ● ISSN 1589 1623 (Print) ● ISSN 1785 0037 (Online)
DOI: http://dx.doi.org/10.15666/aeer/1704_81218138

The CAT activity was determined by the UV absorption method (Gao, 2006). The supernatant (50 μL) was mixed with 3 mL of the reaction solution containing 2.7 mL of Tris-HCl buffer (pH 7.0) and 50 μL of 200 mM H_2O_2. The absorbance of the complete reaction mixture was measured at 240 nm. The decrease of 0.1 by A240 in 1 min was the enzymatic activity unit.

Determination of lipid peroxidation

The MDA content was determined by the thiobarbituric acid (TBA) spectrophotometry method (Zhao et al., 1994). Fresh plant leaves (0.4 g) were placed in an ice-cooled mortar, and 5 mL of 0.1% trichloroacetic acid was added. The leaves were ground on ice, and 5 mL of 0.5% TBA was added. The ground leaves were transferred to a 15 mL centrifuge tube. After boiling in water for 15 min, the leaves were cooled to room temperature and centrifuged at 3000 $\times g$ for 15 min. The absorbance of the supernatant was measured at 560 nm and 600 nm.

Determination of photosynthetic pigment content

The pigment contents of the leaves were determined using acetone extraction. Fresh plant leaves (0.1 g) were extracted in 10 mL of acetone (80%, v/v) and stored in the dark for 24 h (Gao, 2006). The absorbance of the supernatant was measured at 470, 646, and 663 nm (*Eqs.1-3*).

$$Ca = 12.21A663 - 2.81A646 \quad \text{(Eq.1)}$$

$$Cb = 20.13A646 - 5.03A663 \quad \text{(Eq.2)}$$

$$Cx.c = (1000A470 - 3.27Ca - 104Cb)/229 \quad \text{(Eq.3)}$$

Determination of photosynthetic gas exchange parameters

The Pn, transpiration rate (Tr), intercellular CO_2 concentration (Ci), and stomatal conductance (Gs) were measured using a CI-340 portable photosynthesis system (CID Bio-Science, Inc., USA, *Fig. 1*). The seedlings with uniform growth were randomly selected from each pot, and the photosynthetic gas exchange parameters were measured at 9:00–11:00 am on the 7th day after spraying the $ZnSO_4 \cdot 7H_2O$ solution. Photosynthetically active radiation (PAR) at the leaf surface was approximately 1000 ± 50 μmol/m^2/s. The temperature in the leaf chamber was 38 ± 2 °C, and ambient CO_2 concentration was 420 ± 30 μmol/mol.

Figure 1. *CI-340 portable photosynthesis system*

http://www.aloki.hu ● ISSN 1589 1623 (Print) ● ISSN 1785 0037 (Online)
DOI: http://dx.doi.org/10.15666/aeer/1704_81218138

Determination of chlorophyll fluorescence parameters

Actual photochemical efficiency (ΦPSII), photosynthetic electron transport rate (ETR), photochemical quenching coefficient (qP), non-photochemical quenching coefficient (qN), and maximum photochemical efficiency (Fv/Fm) were measured using a portable chlorophyll fluorometer PAM-2500 (Walz, Germany, *Fig. 2*). Prior to measurements, the leaves were first treated in the dark for 30 min, and a beam of measurement light (less than 0.1 μmol) was irradiated on the fully dark-adapted leaves to obtain the initial fluorescence Fo. Then, saturated pulsed light (8000 μmol $m^{-2}s^{-1}$) was turned on to obtain the maximum fluorescence Fm under dark adaptation (Marwood et al., 2001). Afterward, the endogenous actinic light (600 μmol $m^{-2}s^{-1}$) was turned on. When the actual primary light energy capture efficiency ΦPSII had stabilized, the action light was turned off, and the far-infrared light was illuminated (Schreiber et al., 1986, 2003). The ETR was automatically calculated by the instrument (Mayer et al., 2008). The different parameters were calculated as follows (*Eqs.4-7*):

$$Fv / Fm = (Fm - Fo) / Fm \quad \text{(Eq.4)}$$

$$\Phi PSII = (Fm' - Ft) / Fm' \quad \text{(Eq.5)}$$

$$qP = (Fm' - Ft) / (Fm' - Fo') \quad \text{(Eq.6)}$$

$$qN = 1 - (Fm' - Fo') / (Fm - Fo) \quad \text{(Eq.7)}$$

Statistical analysis

The data were plotted using Microsoft Excel and analyzed by ANOVA using SPSS 17.0. Duncan's test ($P < 0.05$) were used to determine the significance of differences between treatment means.

Results

Effect of Zn on the antioxidant enzymatic activity of foxtail millet

After Zn treatment, protective enzymes SOD, POD, and CAT in both cultivars increased first and then decreased with the increase in Zn concentration, and the level of change in these enzymes differed between the cultivars and among periods (*Figs. 3-5*). Among the three protective enzymes, Zn treatment of the same cultivars reached maximum effect in Zn2 and reached a significant level compared with the control ($P < 0.05$). However, in 'Zhangzagu10', no significant difference in CAT was found between the control and Zn2 treatment during the SL stage (*Fig. 3*). However, the three enzymatic activities were lower in Zn4 than in CK, and the change was more obvious after Zn5 treatment. *Figures 3-5* show that Zn treatment of the two millet varieties was most obvious at the BT stage.

Compared with CK, during the BT stage, after 7 days of Zn2 treatment, the SOD, POD, and CAT activities of 'Jingu 21' increased by 28.2%, 61.1%, and 35.1%, respectively. By contrast, the corresponding values of 'Zhangzagu 10' increased by 11.3%, 15.5%, and 10.6%. After 7 days of Zn5 treatment, compared with CK, the SOD, POD, and CAT activities of 'Jingu 21' decreased by 17.2%, 20.4%, and 16.8%' respectively, while those of 'Zhangzagu 10' were reduced by 11.7%, 12.1%, and 12.6%' respectively (*Figs. 3-5*).

http://www.aloki.hu ● ISSN 1589 1623 (Print) ● ISSN 1785 0037 (Online)
DOI: http://dx.doi.org/10.15666/aeer/1704_81218138

Figure 2. *Portable chlorophyll fluorometer PAM-2500*

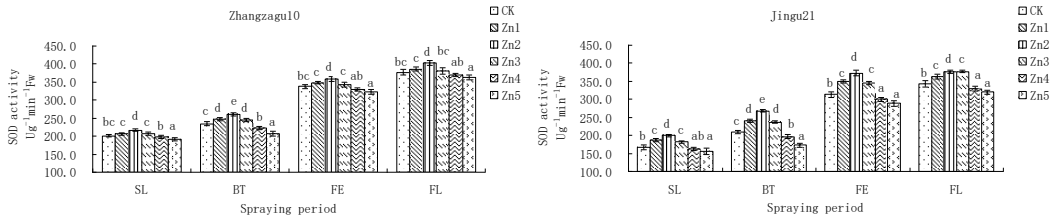

Figure 3. *Effects of Zn on the superoxide dismutase (SOD) activity in the leaves of 'Zhangzagu 10' and 'Jingu 21' at the different growth stages*

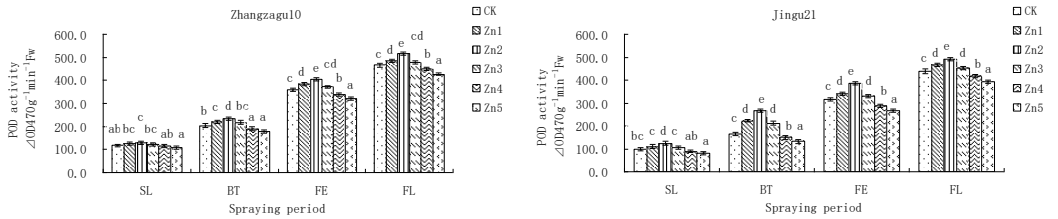

Figure 4. *Effects of Zn on peroxidase (POD) activity in the leaves of 'Zhangzagu 10' and 'Jingu 21' in the different growth stages*

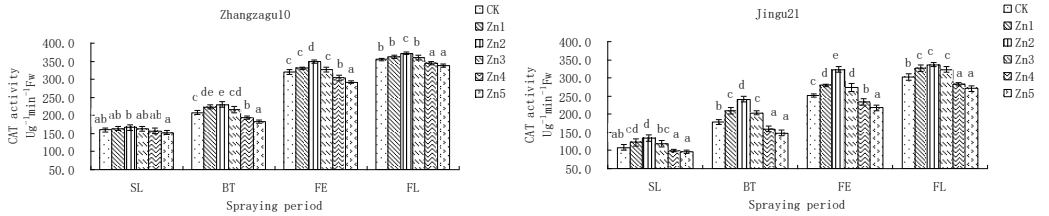

Figure 5. *Effects of Zn on the catalase (CAT) activity in the leaves of 'Zhangzagu 10' and 'Jingu 21' at the different growth stages*

http://www.aloki.hu ● ISSN 1589 1623 (Print) ● ISSN 1785 0037 (Online)
DOI: http://dx.doi.org/10.15666/aeer/1704_81218138

Effect of Zn on the MDA content of foxtail millet

The trend of MDA was opposite to that of the protective enzyme activity. The MDA decreased first and then increased with the increase in Zn concentration. MDA content reached minimum in Zn2 and then gradually increased until Zn4 treatment, during which the MDA content was higher than that in CK. *Figure 4* shows that the MDA content had the greatest impact during the BT stage.

Compared with CK, after 7 days of Zn2 treatment, the MDA activities of 'Jingu 21' in SL, BT, FE, and FL were decreased by 26.0%, 35.9%, 15.4% and 13.3%, respectively, while those of 'Zhangzagu10' were reduced by 14.2%, 16.7%, 11.7% and 10.7%, respectively (*Fig. 6*).

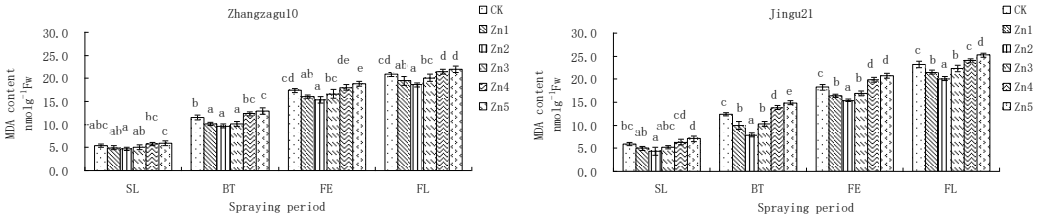

Figure 6. *Effects of Zn on the malondialdehyde (MDA) content in the leaves of 'Zhangzagu 10' and 'Jingu 21' at the different growth stages*

Effect of Zn on the pigments of foxtail millet

The average amounts of pigments in the leaves as affected by spraying period and spraying concentrations are presented in *Tables 1* and *2*. The pigment contents in the leaves of foxtail millet increased with increasing Zn concentrations until Zn2. However, the pigment contents declined at Zn4 and Zn5 treatments, and the levels were even lower than those of the CK. Although both cultivars showed similar trends in the different stages, the degrees of increase or decrease of chlorophyll contents in the cultivars were not identical. Chlorophyll a, chlorophyll b, chlorophyll, and carotenoid were most affected by Zn treatment during the BT stage.

Compared with CK, during the BT stage, after 7 days of Zn2 treatment, the chlorophyll a, chlorophyll b, chlorophyll, and carotenoid of 'Jingu 21' increased by 27.1%, 36.7%, 28.9%, and 9.7%, respectively, while those of 'Zhangzagu 10' increased by 13.3%, 27.8%, 15.9%, and 8.0%, respectively.

In addition to the carotenoid during SL of 'Jingu 21', these pigments reached significant levels. After 7 days of Zn5 treatment, compared with CK, chlorophyll a, chlorophyll b, chlorophyll, and carotenoid of 'Jingu 21' decreased by 11.6%, 31.3%, 15.3%, and 7.7%, respectively, while those of 'Zhangzagu 10' declined by 6.5%, 23.5%, 9.6%, and 6.5%, respectively. These values almost reached significant levels (*Tables 1* and *2*).

Effect of Zn on the photosynthetic gas exchange parameters of foxtail millet

After Zn treatment, the Pn, Gs, and Tr in both cultivars increased first and then decreased with the increase of Zn concentration. The change in these indices differed between cultivars and among periods (*Figs. 7-9*).

http://www.aloki.hu ● ISSN 1589 1623 (Print) ● ISSN 1785 0037 (Online)
DOI: http://dx.doi.org/10.15666/aeer/1704_81218138

Among these three indices, Zn treatment reached maximum effect in Zn2 and then gradually decreased. From the Zn4 treatment, these indices were lower than CK and reached a significant level between treatments. *Figures 7-9* show that the Zn treatment of the two millet varieties was most obvious during BT.

Table 1. *Effects of Zn on the pigment contents in the leaves of 'Zhangzagu 10' at the different growth stages*

Cultivar	Period	Treatment	Chlorophyll a (mg/gFw)	Chlorophyll b (mg/gFw)	Chlorophyll (mg/gFw)	Carotenoid (mg/gFw)
'Zhangza 10'	SL	CK	9.66 ± 0.18c	3.77 ± 0.17b	13.43 ± 0.11c	1.40 ± 0.04ab
		Zn1	10.13 ± 0.05d	4.07 ± 0.12cd	14.21 ± 0.17e	1.47 ± 0.04c
		Zn2	10.40 ± 0.09e	4.21 ± 0.03d	14.62 ± 0.10f	1.47 ± 0.03c
		Zn3	9.99 ± 0.07d	3.97 ± 0.11c	13.96 ± 0.04d	1.42 ± 0.01bc
		Zn4	9.35 ± 0.10b	3.47 ± 0.09a	12.82 ± 0.19b	1.36 ± 0.05ab
		Zn5	9.14 ± 0.10a	3.27 ± 0.11a	12.41 ± 0.10a	1.35 ± 0.02a
	BT	CK	16.39 ± 0.09c	3.59 ± 0.12c	19.99 ± 0.20c	4.19 ± 0.09c
		Zn1	17.48 ± 0.12d	3.99 ± 0.15d	21.47 ± 0.08d	4.42 ± 0.07de
		Zn2	18.57 ± 0.06e	4.59 ± 0.08e	23.17 ± 0.12e	4.53 ± 0.06e
		Zn3	17.28 ± 0.17d	3.96 ± 0.16d	21.24 ± 0.12d	4.33 ± 0.09d
		Zn4	15.60 ± 0.13b	3.20 ± 0.13b	18.81 ± 0.14b	4.05 ± 0.06b
		Zn5	15.33 ± 0.11a	2.75 ± 0.13a	18.08 ± 0.12a	3.92 ± 0.04a
	FE	CK	16.46 ± 0.11c	3.71 ± 0.10bc	20.16 ± 0.16c	4.79 ± 0.05c
		Zn1	17.14 ± 0.06e	3.92 ± 0.13c	21.06 ± 0.11d	4.97 ± 0.08de
		Zn2	17.48 ± 0.09f	4.43 ± 0.07d	21.92 ± 0.16e	5.04 ± 0.06e
		Zn3	16.97 ± 0.07d	3.85 ± 0.12c	20.82 ± 0.09d	4.91 ± 0.06d
		Zn4	16.03 ± 0.11b	3.51 ± 0.15ab	19.54 ± 0.16b	4.65 ± 0.10b
		Zn5	15.76 ± 0.03a	3.36 ± 0.19a	19.11 ± 0.17a	4.52 ± 0.04a
	FL	CK	16.10 ± 0.07c	3.38 ± 0.03b	19.49 ± 0.10c	4.06 ± 0.04b
		Zn1	16.42 ± 0.06de	3.54 ± 0.07bc	19.97 ± 0.10e	4.14 ± 0.06bc
		Zn2	16.56 ± 0.17e	3.75 ± 0.12c	20.31 ± 0.10f	4.23 ± 0.07c
		Zn3	16.32 ± 0.06d	3.43 ± 0.09b	19.75 ± 0.15d	4.12 ± 0.03bc
		Zn4	15.85 ± 0.03b	3.30 ± 0.12ab	19.15 ± 0.14b	4.02 ± 0.01ab
		Zn5	15.59 ± 0.12a	3.13 ± 0.23a	18.71 ± 0.11a	3.93 ± 0.11a

Values are mean ± SE (n = 3). Different letters in the same column indicate significant difference at the $P < 0.05$ level by Duncan's new multiple range test. SL, BT, FE, and FL represent the seedling, booting, flowering, and filling stages, respectively

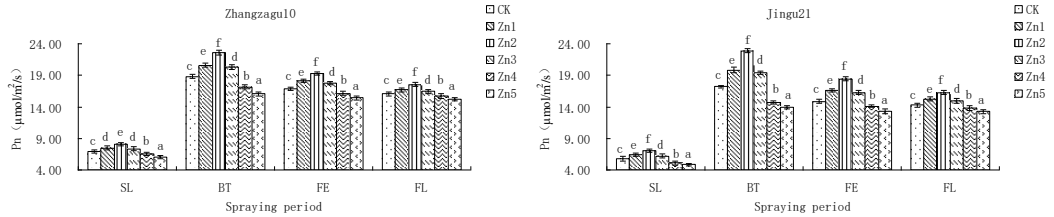

Figure 7. *Effects of Zn on the net photosynthesis rate (Pn) in the leaves of 'Zhangzagu 10' and 'Jingu 21' at the different growth stages*

http://www.aloki.hu ● ISSN 1589 1623 (Print) ● ISSN 1785 0037 (Online)
DOI: http://dx.doi.org/10.15666/aeer/1704_81218138

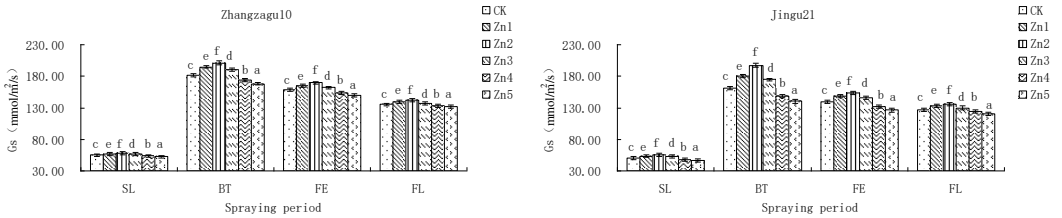

Figure 8. *Effects of Zn on stomatal conductance (Gs) in the leaves of 'Zhangzagu 10' and 'Jingu 21' at the different growth stages*

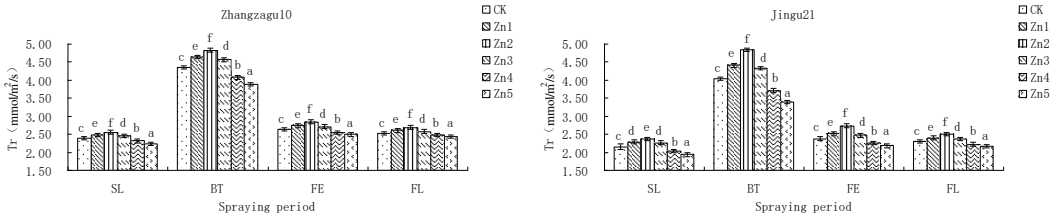

Figure 9. *Effects of Zn on transpiration rate (Tr) in the leaves of 'Zhangzagu 10' and 'Jingu 21' at the different growth stages*

During the BT stage, compared with CK, after 7 days of Zn2 treatment, the Pn, Gs, and Tr of 'Jingu 21' increased by 33.1%, 22.4%, and 20.0%, respectively, while those of 'Zhangzagu 10' increased by 19.9%, 10.5%, and 10.7%, respectively. After 7 days of Zn5 treatment, compared with CK, the Pn, Gs, and Tr of 'Jingu 21' decreased by 19.1%, 13.1%, and 16.0%, respectively, while those of 'Zhangzagu 10' declined by 14.6%, 7.7%, and 11.1%, respectively (*Figs. 7-9*).

As the Zn concentration increased, Ci decreased first and then increased, which was opposite to the trend of Pn. Among the different Zn treatments for the same period, the reduction of Zn2 treatment was the most obvious. *Figure 8* shows that, after Zn treatment, Ci had the greatest impact during the BT stage.

Compared with the control, after 7 days of Zn2 treatment, the Ci of 'Jingu 21' during SL, BT, FE, and FL decreased by 16.9%, 23.7%, 18.3%, and 13.8% respectively, while those of 'Zhangzagu 10' declined by 11.2%, 16.4%, 13.7%, and 9.5%, respectively (*Fig. 10*). During BT, the Ci of Jingu 21 was as follows: Zn5 > Zn4 > CK > Zn3 > Zn2 > Zn1. 'Zhangzagu 10' had the same trend. Although 'Zhangzagu 10' and 'Jingu 21' showed similar trends in the different concentrations, the degrees of increase or decrease in Ci for the cultivars were not same.

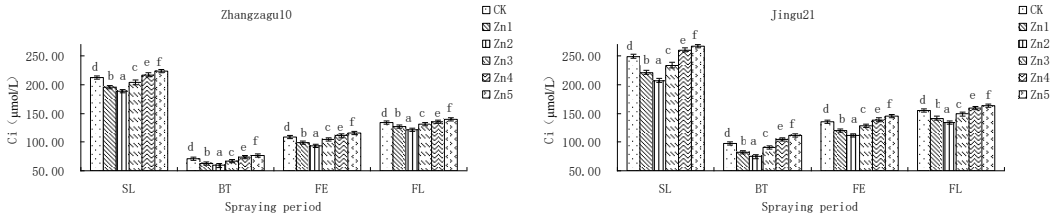

Figure 10. *Effects of Zn on intercellular CO_2 concentration (Ci) in the leaves of 'Zhangzagu 10' and 'Jingu 21' at the different growth stages*

http://www.aloki.hu ● ISSN 1589 1623 (Print) ● ISSN 1785 0037 (Online)
DOI: http://dx.doi.org/10.15666/aeer/1704_81218138

Table 2. *Effects of Zn on the pigment contents in the leaves of 'Jingu 21' at the different growth stages*

Cultivar	Period	Treatment	Chlorophyll a (mg/gFw)	Chlorophyll b (mg/gFw)	Chlorophyll (mg/gFw)	Carotenoid (mg/gFw)
'Jingu 21'	SL	CK	7.36 ± 0.11c	2.38 ± 0.16bc	9.74 ± 0.16c	1.31 ± 0.09ab
		Zn1	8.02 ± 0.12d	2.60 ± 0.32c	10.62 ± 0.25d	1.38 ± 0.13ab
		Zn2	8.36 ± 0.09e	2.95 ± 0.13d	11.32 ± 0.12e	1.42 ± 0.03b
		Zn3	7.86 ± 0.05d	2.56 ± 0.14c	10.41 ± 0.19d	1.34 ± 0.05ab
		Zn4	7.02 ± 0.09b	2.17 ± 0.07ab	9.19 ± 0.16b	1.27 ± 0.01a
		Zn5	6.66 ± 0.09a	1.95 ± 0.17a	8.61 ± 0.09a	1.26 ± 0.08a
	BT	CK	15.51 ± 0.07c	3.57 ± 0.14c	19.08 ± 0.12c	3.84 ± 0.03c
		Zn1	17.28 ± 0.04e	4.03 ± 0.07d	21.30 ± 0.11e	4.08 ± 0.05d
		Zn2	19.71 ± 0.12f	4.88 ± 0.03e	24.60 ± 0.14f	4.22 ± 0.03e
		Zn3	16.98 ± 0.07d	3.95 ± 0.10d	20.93 ± 0.10d	4.01 ± 0.09d
		Zn4	14.14 ± 0.07b	2.96 ± 0.10b	17.10 ± 0.08b	3.68 ± 0.08b
		Zn5	13.71 ± 0.03a	2.45 ± 0.05a	16.16 ± 0.02a	3.55 ± 0.01a
	FE	CK	16.18 ± 0.05c	2.25 ± 0.07bc	18.43 ± 0.12c	4.27 ± 0.07bc
		Zn1	17.56 ± 0.16e	2.49 ± 0.16c	20.05 ± 0.27e	4.47 ± 0.09de
		Zn2	18.18 ± 0.14f	2.83 ± 0.18d	21.00 ± 0.09f	4.58 ± 0.10e
		Zn3	17.06 ± 0.10d	2.39 ± 0.23c	19.46 ± 0.20d	4.41 ± 0.10cd
		Zn4	15.41 ± 0.05b	2.10 ± 0.13c	17.51 ± 0.17b	4.12 ± 0.08ab
		Zn5	14.82 ± 0.07a	1.95 ± 0.07a	16.77 ± 0.13a	3.99 ± 0.06a
	FL	CK	15.91 ± 0.08c	2.11 ± 0.23abc	18.01 ± 0.15c	3.55 ± 0.07bc
		Zn1	16.44 ± 0.16d	2.27 ± 0.28bc	18.71 ± 0.17d	3.66 ± 0.08cd
		Zn2	16.91 ± 0.05e	2.41 ± 0.23c	19.32 ± 0.22e	3.77 ± 0.10d
		Zn3	16.28 ± 0.05d	2.19 ± 0.17abc	18.47 ± 0.18d	3.62 ± 0.06c
		Zn4	15.39 ± 0.12b	2.04 ± 0.08ab	17.43 ± 0.19b	3.46 ± 0.05ab
		Zn5	14.87 ± 0.13a	1.86 ± 0.05a	16.73 ± 0.16a	3.37 ± 0.01a

Values are mean ± SE (n = 3). Different letters in the same column indicate significant difference at the $P < 0.05$ level by Duncan's new multiple range test. SL, BT, FE, and FL represent the seedling, booting, flowering, and filling stages, respectively

Effect of Zn on the chlorophyll fluorescence parameters of foxtail millet

Tables 3 and *4* show that the chlorophyll fluorescence parameters of foxtail millet increased with increasing Zn concentrations until Zn2. Then, at the Zn4 and Zn5 treatments, the chlorophyll fluorescence parameters declined, even lower than those at CK, except the values of qN. These indicators showed the greatest impact on millet during BT and had greater effect on 'Jingu 21' than 'Zhangzagu 10'.

During BT, compared with CK, after 7 days of Zn2 treatment, the Fo, Fm, Fv/Fm, and Fv/Fo of 'Jingu 21' increased by 5.5%, 42.5%, 11.4%, and 50.4%, respectively, while those of 'Zhangzagu 10' increased by 4.9%, 27.6%, 7.6%, and 30.9%, respectively. After 7 days of Zn5 treatment, compared with CK, the Fo, Fm, Fv/Fm, and Fv/Fo of 'Jingu 21' decreased by 6.7%, 18.5%, 6.4%, and 18.3%, respectively, while those of 'Zhangzagu 10' declined by 5.2%, 13.9%, 4.3% and 13.1%, respectively (*Tables 3* and *4*).

http://www.aloki.hu ● ISSN 1589 1623 (Print) ● ISSN 1785 0037 (Online)
DOI: http://dx.doi.org/10.15666/aeer/1704_81218138

Table 3. *Effects of Zn on chlorophyll fluorescence parameters of 'Zhangzagu 10' in the different growth stages*

Cultivar	Period	Treatment	Fo	Fm	Fv/Fm	Fv/Fo	Y2	ETR	qP	qN
'Zhangza 10'	SL	CK	0.226c	0.866c	0.738c	2.824c	0.214bc	69.3c	0.431c	1.144c
		Zn1	0.231d	0.935e	0.753e	3.041e	0.227de	71.8e	0.450d	1.063b
		Zn2	0.235e	0.978f	0.760f	3.159f	0.233e	74.5f	0.466e	0.982a
		Zn3	0.231d	0.913d	0.747d	2.958d	0.219cd	70.8d	0.443d	1.068b
		Zn4	0.222b	0.808b	0.726b	2.647b	0.206b	67.5b	0.409b	1.197d
		Zn5	0.217a	0.767a	0.717a	2.537a	0.196a	65.6a	0.386a	1.295e
	BT	CK	0.240c	0.803c	0.701c	2.341c	0.231c	68.2c	0.451c	1.049d
		Zn1	0.248d	0.916e	0.729d	2.697d	0.250d	72.1e	0.489e	0.881b
		Zn2	0.252e	1.024f	0.754e	3.063e	0.266e	74.9f	0.521f	0.751a
		Zn3	0.246d	0.895d	0.726d	2.646d	0.244d	71.1d	0.478d	0.911c
		Zn4	0.233b	0.738b	0.684b	2.169b	0.211b	64.7b	0.413b	1.152e
		Zn5	0.228a	0.691a	0.670a	2.035a	0.201a	62.7a	0.383a	1.237f
	FE	CK	0.236c	0.842c	0.719c	2.562c	0.219c	71.1c	0.441c	0.932d
		Zn1	0.242d	0.941e	0.743e	2.896e	0.234e	74.3e	0.464d	0.842b
		Zn2	0.246e	1.042f	0.764f	3.236f	0.244f	77.0f	0.497e	0.777a
		Zn3	0.240d	0.911d	0.736d	2.795d	0.227d	73.3d	0.460d	0.874c
		Zn4	0.231b	0.785b	0.705b	2.394b	0.205b	68.3b	0.412b	0.995e
		Zn5	0.226a	0.749a	0.698a	2.307a	0.195a	66.5a	0.398a	1.045f
	FL	CK	0.224c	0.872c	0.744c	2.899c	0.200c	71.9c	0.439c	0.866d
		Zn1	0.228d	0.933e	0.756e	3.093e	0.211d	73.7e	0.455d	0.828b
		Zn2	0.232e	1.002f	0.768f	3.314f	0.217e	75.0f	0.472e	0.779a
		Zn3	0.226d	0.914d	0.752d	3.031d	0.205cd	72.9d	0.452d	0.841c
		Zn4	0.221b	0.830b	0.734b	2.758b	0.194b	70.4b	0.430b	0.897e
		Zn5	0.218a	0.797a	0.727a	2.664a	0.185a	68.9a	0.411a	0.948f

Values are mean ± SE (n = 3). Different letters in the same column indicate significant difference at the $P < 0.05$ level by Duncan's new multiple range test. SL, BT, FE, and FL represent the seedling, booting, flowering, and filling stages, respectively

Compared with the CK, during the BT stage, after 7 days of Zn2 treatment, the Y2, ETR, and qP of 'Jingu 21' increased by 30.9%, 17.8%, and 23.1%, respectively, while those of 'Zhangzagu 10' increased by 15.0%, 9.9%, and 15.5%, respectively. After 7 days of Zn5 treatment, compared with those at CK, the Y2, ETR, and qP of 'Jingu 21' decreased by 25.8%, 10.2%, and 17.5%, respectively, while those of 'Zhangzagu 10' declined by 12.8%, 8.1%, and 15.2%, respectively (*Tables 3* and *4*).

After Zn treatment, the qN in both cultivars increased first and then decreased with increase in Zn concentration, and the level of change differed between cultivars and among periods, which was opposite to the trend of qP. In this index, the Zn treatment of the same cultivars reached the minimum effect in Zn2 and gradually increased. The levels of both cultivars from the Zn4 treatment were both lower than those in CK and reached significant levels with each treatment. *Tables 3* and *4* show that Zn treatment of the two millet varieties was most obvious during the BT stage.

Compared with CK, after 7 days of Zn2 treatment, the qN of 'Jingu 21' during SL, BT, FE, and FL decreased by 20.6%, 33.5%, 28.6%, and 13.7% respectively, while

http://www.aloki.hu ● ISSN 1589 1623 (Print) ● ISSN 1785 0037 (Online)
DOI: http://dx.doi.org/10.15666/aeer/1704_81218138

those of 'Zhangzagu 10' declined by 14.2%, 28.4%, 16.6%, and 10.0%, respectively (*Tables 3* and *4*). During the BT stage, the qP of 'Jingu 21' was as follows: Zn5 > Zn4 > CK > Zn3 > Zn2 > Zn1, and 'Zhangzagu 10' showed a similar trend.

Table 4. *Effects of Zn on the chlorophyll fluorescence parameters of 'Jingu 21' at the different growth stages*

Cultivar	Period	Treatment	Fo	Fm	Fv/Fm	Fv/Fo	Y2	ETR	qP	qN
'Jingu 21'	SL	CK	0.230c	0.881c	0.739c	2.828c	0.201c	72.3c	0.422c	1.162d
		Zn1	0.236d	0.966e	0.755d	3.086d	0.222d	77.2e	0.454d	1.014b
		Zn2	0.241e	1.010f	0.762e	3.197e	0.250e	80.9f	0.487e	0.922a
		Zn3	0.235d	0.949d	0.753d	3.041d	0.217d	75.7d	0.449d	1.051c
		Zn4	0.222b	0.786b	0.718b	2.546b	0.188b	68.6b	0.387b	1.278e
		Zn5	0.218a	0.726a	0.699a	2.328a	0.175a	66.4a	0.365a	1.379f
	BT	CK	0.242c	0.794c	0.696c	2.285c	0.208c	70.6c	0.451c	1.026d
		Zn1	0.250d	0.953e	0.737e	2.809e	0.257e	79.0e	0.505e	0.803b
		Zn2	0.255e	1.132f	0.775f	3.436f	0.273f	83.2f	0.556f	0.682a
		Zn3	0.248d	0.918d	0.730d	2.701d	0.244d	76.9d	0.493d	0.849c
		Zn4	0.230b	0.697b	0.669b	2.024b	0.175b	65.2b	0.399b	1.195e
		Zn5	0.226a	0.647a	0.651a	1.868a	0.155a	63.5a	0.372a	1.290f
	FE	CK	0.236c	0.823c	0.713c	2.485c	0.213c	73.1c	0.448c	0.917d
		Zn1	0.244d	0.955e	0.745e	2.922e	0.236e	77.9e	0.490e	0.790b
		Zn2	0.248e	1.097f	0.774f	3.422f	0.259f	81.5f	0.542f	0.655a
		Zn3	0.241d	0.911d	0.736d	2.781d	0.227d	75.9d	0.480d	0.824c
		Zn4	0.230b	0.746b	0.692b	2.247b	0.190b	69.1b	0.405b	1.028e
		Zn5	0.224a	0.699a	0.679a	2.114a	0.181a	67.0a	0.387a	1.113f
	FL	CK	0.229c	0.910c	0.748c	2.976c	0.205c	71.1c	0.441c	0.858d
		Zn1	0.235d	1.007e	0.767e	3.289e	0.221e	74.7e	0.464d	0.775b
		Zn2	0.239e	1.087f	0.780f	3.547f	0.236f	78.2f	0.519e	0.741a
		Zn3	0.233d	0.976d	0.761d	3.187d	0.214d	72.7d	0.459d	0.797c
		Zn4	0.224b	0.841b	0.733b	2.747b	0.195b	68.8b	0.423b	0.921e
		Zn5	0.221a	0.800a	0.724a	2.621a	0.184a	66.7a	0.403a	0.995f

Values are mean ± SE (n = 3). Different letters in the same column indicate significant difference at the $P < 0.05$ level by Duncan's new multiple range test. SL, BT, FE, and FL represent the seedling, booting, flowering, and filling stages, respectively

Discussion

Effects of Zn on the physiological characteristics

Although Zn is a micronutrient necessary for photosynthesis and plant growth at low concentration, Zn becomes toxic when its concentration reaches a threshold level (Cunha et al., 2008; Lin and Aarts, 2012). Jat et al. (2007) reported that Zn activates several antioxidant enzymes, such as SOD, POD, and CAT. Saeed et al. reported that SOD, POD, and CAT and free radical scavenging activities in cut-flowers remained maximum with the medium dose of Zn (6 mg Zn kg^{-1}). Thus, Zn applied at 6-8 mg kg^{-1} imparted greater beneficial effects on growth, production, vase life quality, and antioxidative activities in gladiolus cut flower and further higher application rates

http://www.aloki.hu ● ISSN 1589 1623 (Print) ● ISSN 1785 0037 (Online)
DOI: http://dx.doi.org/10.15666/aeer/1704_81218138

rendered non-significant improvement (Tariq et al., 2013). In this study, 40 $mg \cdot L^{-1}$ of $ZnSO_4 \cdot 7H_2O$ significantly increased the SOD, POD, and CAT activities of 'Jingu 21' and 'Zhangzagu 10' at different stages. However, 80 $mg \cdot L^{-1}$ of $ZnSO_4 \cdot 7H_2O$ resulted in SOD, POD, and CAT activities lower than those of CK (*Figs. 3-5*). Moreover, 40 $mg \cdot L^{-1}$ of $ZnSO_4 \cdot 7H_2O$ significantly decreased the MDA content, but 80 $mg \cdot L^{-1}$ of $ZnSO_4 \cdot 7H_2O$ increased the MDA content higher than that of CK (*Fig. 6*).

Zn plays an important role in the anti-lipid peroxidation of millet. The suitable Zn concentration can alleviate the peroxidation of membrane lipids and improve the antioxidant activity of foxtail millet (Kakade et al., 2009; Maurya and Kumar, 2014; Hajiboland and Beiramzadeh, 2008). Therefore, the application of a suitable concentration of Zn to foxtail millet will help improve its resistance to stress. The mechanism of the effect of Zn on energy metabolism needs further study.

Effects of Zn on pigments

Pigment is the most important part of photosynthesis. This parameter can reflect the ability of plant light energy conversion to a certain extent, and it will also protect the normal operation of photosynthetic apparatus to some extent (Nouet et al., 2011). The main factors in the pigments are chlorophyll and carotenoids, and Zn can prevent the oxidation of pigments (Cakmak 2000; Cherif et al., 2010). Pongrac et al. (2009) reported that an appropriate amount of Zn can increase the chlorophyll content of leaves, but excessive Zn reduces the chlorophyll content of leaves. This experiment shows that low concentration of Zn can increase the pigment content, while high concentration treatment will inhibit the pigment content. In 'Jingu 21', the pigment content was as follows Zn2 > Zn1 > Zn3 > CK > Zn4 > Zn5, and 'Zhangzagu 10' showed a similar trend (*Tables 1* and *2*). Excessive Zn affected the growth of the seedlings, causing a significant decrease in photosynthetic pigment content and yellowing of the leaves. This phenomenon may be due to the antagonistic effect of Zn and iron metabolism in plants, and the excessive Zn content inhibited the absorption of iron by plants (Wirén et al., 1996). Thus, an appropriate amount of Zn concentration can effectively increase the pigment content of the leaves (Kumar and Arora, 2000) and delay the rapid senescence of the foxtail millet.

Effects of photosynthetic gas exchange parameters

Photosynthesis plays a very important role in plants. This process is the source of plant yield, which is related to plant growth and development. This process involves photoreaction and carbon reaction to convert carbon dioxide and water into organic matter and oxygen, which are the basis for plant survival (Baron et al., 1995; Yruela, 2005). The Pn, Gs, Tr, and Ci are important indicators to affect the photosynthesis. Fernàndez-Martínez et al. (2014) reported that the photoprotective and antioxidant responses were enhanced with increasing Zn concentration, but high Zn concentration produced high toxicity levels for both clones and resulted in impaired biomass production, photochemical processes, and photosynthesis. The results showed that Zn treatment could increase Pn, Gs, and Tr and reached maximum levels in Zn2, gradually decreased. From the Zn4 treatment, these three indices were both lower than those at CK, but Ci showed an opposite trend of Pn (*Figs. 7-10*). Although the trends are similar at all times, but the degrees of increase or decrease were not the same. In summary, Zn had a regulatory effect on plant photosynthesis and exhibits different effects depending

http://www.aloki.hu ● ISSN 1589 1623 (Print) ● ISSN 1785 0037 (Online)
DOI: http://dx.doi.org/10.15666/aeer/1704_81218138

on the application concentration, period, and crop type (Sidhu, 2016; Camargo Gai et al., 2017).

Effects of chlorophyll fluorescence parameters

The chlorophyll fluorescence parameter is a set of variables or constant values used to describe the photosynthesis mechanism and photosynthetic physiological state of plants. This parameter reflects the "inherent" characteristics of plants and regarded as an intrinsic probe to study the relationship between plant photosynthesis and environment (Lahive et al., 2012). Information on the donor side, receptor side, and reaction center of PSII can be obtained using the chlorophyll fluorescence induction kinetics curve (Appenroth et al., 2001; Wen et al., 2002). Fv/Fm represents the primary light energy conversion efficiency of PSII. Previous studies suggested that Fv/Fm is a sensitive indicator of plant photoinhibition under stress conditions. This ratio is a measure of the maximum ability of primary light energy capture, reflecting the potential maximum photosynthetic abilities of plants (Krivosheeva et al., 1996). Fv/Fo represents the potential activity of PSII, which is more sensitive in reflecting changes in photon conversion efficiency during leaf senescence (Krivosheeva et al., 1996). In this study, the Fv/Fm and Fv/Fo values increased first and then decreased with the change in Zn concentration, indicating that low Zn concentration can enhance photosynthesis, but high Zn concentration can cause photoinhibition of foxtail millet or damage PSII complex. Y2 reflects the quantum conversion efficiency of photosynthetic electron transport and is the efficiency of PSII light energy capture in case of PSII reaction center shutdown (Longstaff et al., 2002). ETR reflects the apparent electron transfer efficiency under actual light intensity conditions (Longstaff et al., 2002). The results of this experiment indicate that as the Zn concentration increases, Y2 and ETR increased and then decreased. This phenomenon indicated that the low Zn concentration can enhance photosynthesis, but high Zn concentration inhibition of photosynthesis decreased the actual quantum yield of the PSII photosynthetic reaction center (*Tables 3* and *4*).

Photochemical quenching (qP) reflects the quantity of light energy absorbed by the PSII antenna pigment for photochemical electron transport. This parameter is a measure of the oxidation state of the original electron acceptor (QA). This parameter represents the proportion of the open part of the PSII reaction center, which can reflect the electron transfer rate of the electron photosynthetic chain and its efficiency in CO_2 fixation (Mu et al., 2016). Under the experimental conditions, 40 $mg \cdot L^{-1}$ of $ZnSO_4 \cdot 7H_2O$ significantly increased the qP of 'Jingu 21' and 'Zhangzagu 10' in different stages. However, from 80 $mg \cdot L^{-1}$ of $ZnSO_4 \cdot 7H_2O$, the qP was lower than that of the control (*Tables 3* and *4*). This result indicated that the low Zn concentration strengthened the electron transfer activity of PSII, while high Zn concentration decreased the open part of the PSII reaction center, which hindered the photosynthetic electron transfer. The parameter qN reflects the portion of the light energy dissipated in the form of heat that cannot be used for photosynthetic electron transport in the light absorbed by the PSII antenna (Mu et al., 2016; Mikulic and Beardall, 2014). The results showed that qN increased first and then decreased with the increase in Zn concentration. This parameter indicated that Zn concentration had an inhibitory effect on the heat loss of millet light energy. This process is beneficial to the accumulation of dry matter in foxtail millet.

http://www.aloki.hu ● ISSN 1589 1623 (Print) ● ISSN 1785 0037 (Online)
DOI: http://dx.doi.org/10.15666/aeer/1704_81218138

Conclusions

In summary, low Zn concentration could promote plant growth and enhance plant antioxidant capacity and photosynthesis. However, high Zn concentration inhibited plant growth and leaf photosynthesis. 'Jingu 21' changed more than 'Zhangzagu10'. The combination of optimal Zn spraying period and spraying concentration for the foxtail millet growth was BT and 40 $mg \cdot L^{-1}$ of Zn. Thus, a theoretical basis for the safe application of Zn fertilizer on foxtail millet is provided.

The study did not test a larger number of genotypes cultivars and more soil fertility conditions because of the limited experimental conditions. The numbers of test materials and test sites were not sufficiently comprehensive. Multiple materials, multiple points, and multiple years of tests are required to provide a clear direction for the subsequent research.

Acknowledgements. This work was financially supported by the Key Research and Development Project of Shanxi Province (201603D221007-2).

REFERENCES

[1] Alloway, B. J. (2009): Soil factors associated with zinc deficiency in crops and humans. – Environ. Geochem. Hlth. 31: 537-548.
[2] Andersen, E. J., Nepal, M. P. (2017): Genetic diversity of disease resistance genes in foxtail millet (Setaria italica, L.). – Plant Gene 10: 8-16.
[3] Appenroth, K. J., Stöckel, J., Srivastava, A., Strasser, R. J. (2001): Multiple effects of chromate on the photosynthetic apparatus of Spirodela polyrhiza as probed by OJIP chlorophyll a fluorescence. – Environmental Pollution 115: 49-64.
[4] Ardiea, S. W., Khumaida, N., Nur, A., Fauziah, N. (2015): Early identification of salt tolerant foxtail millet (Setaria italica L. Beauv). – Procedia Food Science 3: 303-312.
[5] Bai, Q., Chai, M., Gu, Z., Cao, X., Li, Y., Liu, K. (2009): Effects of components in culture medium on glutamate decarboxylase activity and c-aminobutyric acid accumulation in foxtail millet (Setaria italica L.) during germination. – Food Chemistry 116: 152-157.
[6] Baron, M., Arellano, J. B., Lopez-Gorge, J. (1995): Copper and photosystem II: a controversial relationship. – Physiol Plant 94: 174-180.
[7] Bouis, H. E., Welch, R. M. (2010): Biofortification a sustainable agricultural strategy for reducing micronutrient malnutrition in the global South. – Crop Sci 50: S20–S32. http://dx.doi.org/10.2135/cropsci2009.09.0531.
[8] Cakmak, I. (2000): Tansley review No. 111. Possible roles of zinc in protecting plant cells from damage by reactive oxygen species. – New Phytologist 146(2): 185-205.
[9] Camargo Gai, A. P., dos Santos, D. S., Vieira, E. A. (2017): Effects of zinc excess on antioxidant metabolism, mineral content and initial growth of Handroanthus impetiginosus (Mart. ex DC.) Mattos and Tabebuia roseoalba (Ridl.) Sandwith. – Environmental and Experimental Botany 144: 88-99.
[10] Cambrollé, J., Mancilla-Leyton, J. M., Munoz-Valles, S., Luque, T., Figueroa, M. E. (2012): Zinc tolerance and accumulation in the salt-marsh shrub Halimione portulacoides. – Chemosphere 86: 867-874.
[11] Cambrollé, J., Mancilla-Leytón, J. M., Munoz-Vallés, S., Figueroa-Luque, E., Luque, T., Figueroa, M. E. (2013): Evaluation of zinc tolerance and accumulation potential of the coastal shrub Limoniastrum monopetalum (L.) Boiss. – Environmental and Experimental Botany 85: 50-57.

http://www.aloki.hu ● ISSN 1589 1623 (Print) ● ISSN 1785 0037 (Online)
DOI: http://dx.doi.org/10.15666/aeer/1704_81218138

[12] Carroll, M. D., Loneragan, J. F. (1968): Response of plant species to concentrations of zinc in solution. I. Growth and zinc content of plants. – Aust. J. Agr. Res. 19: 859-868.
[13] Cherif, J., Derbel, N., Nakkach, M., Bergmannc, H., Jemala, F., Lakhdar, Z. B. (2010): Analysis of in vivo chlorophyll fluorescence spectra to monitor physiological state of tomato plants growing under zinc stress. – Journal of Photochemistry and Photobiology B: Biology 101(3): 332-339.
[14] Cunha, K. C. V., Nascimento, C. W. A., Pimentel, R. M. M., Accioly, M. A., Silva, A. J. (2008): Cadmium and zinc availability, accumulation and toxicity in maize grown in a contaminated soil. – Rev. Bras. Ciênc. Solo 32: 1319-1328.
[15] Drinovec, L., Drobne, D., Jerman, I., Zrimec, A. (2004): Delayed fluorescence of Lemna minor: a biomarker of the effects of copper, cadmium, and zinc. – Bulletin of Environment Contamination and Toxicology 72: 896-902.
[16] Feng, J. (2010): The Characteristics of Migration of Cu and Zn in Different Black Soil Farmland. – Northeast Forestry University, Heilongjiang (in Chinese).
[17] Fernàndez-Martínez, J., Zacchini, M., Fernández-Marín, B., García-Plazaola, J. I., Fleck, I. (2014): Gas-exchange, photo- and antioxidant protection, and metal accumulation in I-214 and Eridano Populus sp. clones subjected to elevated zinc concentrations. – Environmental and Experimental Botany 107: 144-153.
[18] Frankart, C., Eullaffroy, P., Vernet, G. (2002): Photosynthetic responses of Lemna minor exposed to xenobiotics, copper, and their combinations. – Ecotoxicology and Environment Safety 53: 439-445.
[19] Gao, J. (2006): Plant Physiology Experiments Guidance. – Higher Education Press, Beijing (in Chinese).
[20] Gartler, J., Robinson, B., Burton, K., Clucas, L. (2013): Carbonaceous soil amendments to biofortify crop plants with zinc. – Science of the Total Environment 465: 308-313.
[21] Genty, B., Briantais, J.-M., Baker, N. R. (1989): The relationship between the quantum yield of photosynthetic electron transport and quenching of chlorophyll fluorescence. – Biochimica et Biophysica Acta - Molecular Cell Research 990: 87-92.
[22] Gibson, R. S. (2006): Zinc: the missing link in combating micronutrient malnutrition in developing countries. – Proc. Nutr. Soc. 65: 51-60.
[23] Gunes, A., Inal, A., Alpaslan, M. (1996): Effect of salinity on stomatal resistance, proline and mineral composition of pepper. – J. Plant Nut. 19: 389-396.
[24] Guo, J. (2014): Effects of Different Concentrations and Different Mineral Elements Filling of Spraying on Physiological Characteristics and Yield of Millet. – Shanxi Agricultural University, Taigu (in Chinese).
[25] Guo, M., Wang, Y., Yuan, X., Dong, S., Wen, Y., Song, X., Guo, P. (2018): Responses of the antioxidant system to fluroxypyr in foxtail millet (Setaria italica, L.) at the seedling stage. – Journal of Integrative Agriculture 17(3): 554-565.
[26] Hacisalihoglu, G., Hart, J. J., Wang, Y.-H., Cakmak, I., Kochian, L. V. (2003): Zinc efficiency is correlated with enhanced expression and activity of Cu/Zn superoxide dismutase and carbonic anhydrase in wheat. – Plant Physiol. 131: 595-602.
[27] Hajiboland, R., Beiramzadeh, N. (2008): Growth, gas exchange and function of antioxidant defense system in two contrasting rice genotypes under Zn and Fe deficiency and hypoxia. – Acta Biol. Szegediensis 52 (2): 283-294.
[28] Hu, H., Sparks, D. (1991): Zinc deficiency inhibits chlorophyll synthesis and gas exchange in 'Stuart' pecan. – Hort Science 26: 267-268.
[29] Jamalomidi, M., Esfahani, M., Carapetian, J. (2006): Zinc and salinity interaction on agronomical traits, chlorophyll and proline content in lowland rice (Oryza sativa, L.) genotypes. – Pak. J. Biol. Sci. 9: 1315-1319.
[30] Jat, R. N., Khandelwal, S. K., Gupta, K. N. (2007): Effect of foliar application of urea and zinc sulphate on growth and flowering parameters in African marigold (Tagetes erecta Linn.). – J. Ornam. Hort. 10 (4): 271-273.

http://www.aloki.hu ● ISSN 1589 1623 (Print) ● ISSN 1785 0037 (Online)
DOI: http://dx.doi.org/10.15666/aeer/1704_81218138

[31] Kabata-Pendias, A., Pendias, H. (2001): Trace Elements in Soils and Plants. – CRC Press, Boca Ratón, FL.
[32] Kakade, D. K., Rajput, S. G., Joshi, K. I. (2009): Effect of foliar application of 'Fe' and 'Zn' on growth, flowering and yield of China aster (Callistephus chinensis LNees). – Asian, J. Hort. 4(1): 138-140.
[33] Khoshgoftarmanesh, A. H., Shariatmadari, H., Karimian, N., Khajehpour, M. R. (2006): Responses of wheat genotypes to zinc fertilization under saline soil conditions. – J. Plant Nut. 29: 1543-1556.
[34] Krivosheeva, A., Tao, D. L., Ottander, C., Wingsle, G., Dube, S. L., Öquist, G. (1996): Cold acclimated and photoinhibition in scots pine. – Planta 200: 296-305.
[35] Kumar, P., Arora, J. S. (2000): Effect of micronutrients on gladiolus. – J. Ornam. Hort. New Ser. 3(2): 91-93.
[36] Lahive, E., O'Halloran, J., Jansen, M. A. K. (2012): Frond development gradients are a determinant of the impact of zinc on photosynthesis in three species of Lemnaceae. – Aquatic Botany 101: 55-63.
[37] Lin, Y. F., Aarts, M. G. M. (2012): The molecular mechanism of zinc and cadmium stress response in plants. – Cell. Mol. Life Sci. 69: 3187-3206.
[38] Longstaff, B. J., Kildea, T., Runcie, J. W., Cheshire, A., Dennison, W., Hurd, C. L., Kana, T., Raven, J. A., Larkum, A. W. D. (2002): An in situ study of photosynthetic oxygen exchange and electron transport rate in the marine macroalga Ulva lactuca (Chlorophyta). – Photosynth. Res. 74: 281-293.
[39] Marwood, C., Solomon, K., Greenberg, B. (2001): Chlorophyll fluorescence as a bioindi cator of effects on growth in aquatic macrophytes from mixtures of polycyclic aromatic hydrocarbons. – Environmental Toxicology and Chemistry 20: 890-898.
[40] Mateos-Naranjo, E., Castellanos, E. M., Perez-Martin, A. (2014): Zinc tolerance and accumulation in the halophytic species Juncus acutus. – Environmental and Experimental Botany 100: 114-121.
[41] Maurya, R., Kumar, A. (2014): Effect of micronutrients on growth and corm yield of gladiolus. – Plant Arch. 14 (1): 529-533.
[42] Mayer, J. E., Feiffer, W. H. P., Beyer, P. (2008): Biofortified crops to alleviate micronutrient malnutrition. – Curr. Opin. Plant Biol. 11: 166-170.
[43] Mikulic, P., Beardall, J. (2014): Contrasting ecotoxicity effects of zinc on growth and photosynthesis in a neutrophilic alga (Chlamydomonas reinhardtii) and an extremophilic alga (Cyanidium caldarium). – Chemosphere 112: 402-411.
[44] Moss, D. N., Musgrave, R. B. (1971): Photosynthesis and Crop Production. – Advances in Agronomy 23: 317-336.
[45] Mu, T., Du, H., Zhang, F., Li, Z., Jing, X., Tian, G. (2016): Effect of exogenous selenium on foxtail millet chlorophyll fluorescence characteristic. – Chinese Agricultural Science Bulletin 32(36): 73-77 (in Chinese).
[46] Mutegi, E. M., Kung'u, J. B., Muna, M., Pieter, P., Mugendi, D. N. (2012): Complementary effects of organic and mineral fertilizers on maize production in the smallholder farms of Meru South District, Kenya. – Agricultural Sciences 3(2): 221-229.
[47] Nouet, N., Motte, P., Hanikenne, M. (2011): Chloroplastic and mitochondrial metal homeostasis. – Trends in Plant Science 16(7): 395-404.
[48] Noulas, C., Tziouvalekas, M., Karyotis, T. (2018): Zinc in soils, water and food crops. – Journal of Trace Elements in Medicine and Biology. https://doi.org/10.1016/j.jtemb.2018.02.009.
[49] Pongrac, P., Zhao, F., Razinger, J., Zrimec, A., Regvar, M. (2009): Physiological responses to Cd and Zn in two Cd/Zn hyperaccumulating Thlaspi species. – Environmental and Experimental Botany 66: 479-486.
[50] Prasad, M., Malec, P., Waloszek, A., Bojko, M., Strzalka, K. (2001): Physiological responses of Lemna trisulca, L. (duckweed) to cadmium and copper bioaccumulation. – Plant Science (Limerick) 161: 881-889.

http://www.aloki.hu ● ISSN 1589 1623 (Print) ● ISSN 1785 0037 (Online)
DOI: http://dx.doi.org/10.15666/aeer/1704_81218138

[51] Prasad, M. N. V., Hagemeyer, J. (eds.) (1999): Heavy Metal Stress in Plants: From Molecules to Ecosystems. – Springer, Berlin.
[52] Rengel, Z., Romheld, V., Marschner, H. (1998): Uptake of zinc and iron by wheat genotypes differing in tolerance to zinc deficiency. – J Plant Physiol 152: 433-438.
[53] Schreiber, U., Schliwa, U., Bilger, W. (1986): Continuous recording of photochemical and non-photochemical chlorophyll fluorescence quenching with a new type of modulation fluorometer. – Photosynthesis Research 10: 51-62.
[54] Schreiber, U., Walz, H., Kolbowski, J. (2003): Propagation of spatial variations of chlorophyll fluorescence parameters in dandeloin leaves induced by spot laser heating. – PAM News 1: 1-18.
[55] Sharma, P. N., Tripathi, A., Bisht, S. S. (1995): Zinc requirement for stomatal opening in cauliflower. – Plant Physiol. 107: 751-756.
[56] Sidhu, G. P. S. (2016): Physiological, biochemical and molecular mechanisms of zinc uptake, toxicity and tolerance in plants. – J. Global Biosci. 5(9): 4603-4633.
[57] Silveira, J. A. G., Carvalho, F. E. L. (2016): Proteomics, photosynthesis and salt resistance in crops: an integrative view. – Journal of Proteomics 143: 24-35.
[58] Singh, A., Yashbir, S. S. (2017): Effect of green manures and zinc fertilizer sources on DTPA-extractable zinc in soil and zinc concentration in basmati rice plants at different growth stages. – Pedosphere. DOI: http://dx.doi.org/10.1016/S1002-0160(17)60442-9.
[59] Tariq, S., Imran, H., Ghulam, J., Nadeem, A. A. (2013): Zinc augments the growth and floral attributes of gladiolus, and alleviates oxidative stress in cut flowers. – Scientia Horticulturae 164: 124-129.
[60] Todeschini, V., Lingua, G., D'Agostino, G., Carniato, F., Roccotiello, E., Berta, G. (2011): Effects of high zinc concentration on poplar leaves: a morphological and biochemical study. – Environ. Exp. Bot. 71: 50-56.
[61] Usha, A., Sripriya, G., Chandra, T. S. (1996): The effect of fermentation on the primary nutrients in foxtail millet (Setaria italica). – Food Chemistry 56: 381-384.
[62] Wen, X. G., Qiu, N. W., Lu, Q. T., Lu, C. M. (2002): Enhanced thermo tolerance of photosystem II in salt-adapted plants of the halophyte Artemisia anethifolia. – Planta 220: 486-497.
[63] Wirén, N., Marschner, H., Romheld, V. (1996): Roots of iron-efficient maize also absorb phytosiderophore-chelated zinc. – Plant Physiology 111(4):1119-1125.
[64] Yruela, I. (2005): Copper in plants. – Braz. J. Plant Physiol. 17: 145-146.
[65] Yuan, X. Y., Zhang, L., Huang, L., Yang, H., Zhong, Y., Ning, N., Wen, Y., Dong, S., Song, X., Wang, H., Guo, P. (2017): Spraying Brassinolide improves Sigma Broad tolerance in foxtail millet (Setaria italica L.) through modulation of antioxidant activity and photosynthetic capacity. – Scientific Report 7: 1-9.
[66] Zhao, S., Xu, C., Zou, Q., Meng, Q. (1994): Improvements of method for measurement of Malondialdehvde in plant tissues. – Plant Physiology Communications 30(3): 207-210 (in Chinese).
[67] Zong, X. (2011): Effects of Foliar Application of Zinc on Millet. – Agricultural University of Hebei (in Chinese).

http://www.aloki.hu ● ISSN 1589 1623 (Print) ● ISSN 1785 0037 (Online)
DOI: http://dx.doi.org/10.15666/aeer/1704_81218138

MINERAL COMPOSITION OF MORINGA OLEIFERA LEAF MEAL (MOLM) AND THE RESPONSES OF ROSS 308 BROILERS TO MOLM SUPPLEMENTATION

MODISAOJANG-MOJANAGA, M. M. C. – OGBUEWU, I. P.* – MOKOLOPI, B. G. – OGUTTU, J. W. – MBAJIORGU, C. A.

Department of Agriculture and Animal Health, University of South Africa
Private Bag X6, Florida 1710, Johannesburg, South Africa

**Corresponding author*
e-mail: dr.ogbuewu@gmail.com, ogbueip@unisa.ac.za

(Received 13th Feb 2019; accepted 29th Mar 2019)

Abstract. A 42-day study was designed to determine the mineral composition of *Moringa oleifera* leaf meal (MOLM) and the response of Ross 308 broilers to dietary MOLM supplementation. Day-old Ross 308 broiler chicks (n = 500) were allotted to five treatments in completely randomized design with each group replicated five times with each replicate having 20 chicks. Birds received diets supplemented with MOLM at 0, 25, 50, 75 and 100 g/kg feed, respectively and assigned T1, T2, T3, T4 and T5. MOLM level that supported optimum variables was modelled using the quadratic function. At day 42, three birds per replicate were slaughtered to evaluate carcass and organ yields. Results of mineral assay indicate that MOLM was high in calcium, sodium, potassium, sulphur and iron. Daily feed intake (FI), average daily gain (ADG) and feed conversion ratio were the same among the groups with the exception of starter broilers on diet T1 that had higher ADG ($p < 0.05$) than those on the other diets. Final live weight (FLW), mortality and gizzard weight were influenced ($p < 0.05$) by MOLM supplementation. MOLM supplementation had no effect on other parameters measured. MOLM supplementation at 39.98 and 35.80 g/kg feed supported optimum FLW and ADG at starter phase and 46.88 g/kg feed MOLM supported optimum FLW at finisher phase. In conclusion, MOLM is a good source of nutrients and suitable for production of enhanced cut parts in broiler chickens.
Keyword: *alternative feedstuffs, broilers, optimization, production outputs, South Africa*

Introduction

The development of the broiler industry as a means of bridging the food and nutrition insecurity gap in most countries has been attracting great attention (Dieye et al., 2010). Unfortunately, the growth of the broiler sector in most developing countries are constrained by the spiralling feed cost due to rising prices of feed ingredients particularly protein supplements (Abbas, 2013). This spiralling feed cost is having negative impacts on the feed supply chain as well as the quality of the compounded rations. This rising price of feeds has been partly attributed to the competition between humans and animals for protein and energy concentrates. Therefore, it has become imperative that the potential of alternative protein feedstuffs that are not in direct competition with humans be fully harnessed in broiler nutrition (Ogbuewu et al., 2015, 2019). One of the best-suited alternative plant protein feed raw material for broiler feeding in the developing countries is the leaf of Moringa plant.

Moringa oleifera belongs to the family Moringaceae and thrives well during severe drought and heat. *Moringa oleifera* is one of commonest specie among the 14 species in the family and grows to a height of 7–12 m. It is native to India, but thrive well in the tropics (Nsofor et al., 2012). The leaves of moringa plant are high in essential amino acids, protein, minerals, vitamin A and fibre (Ustundag and Ozdogan, 2015) and could

http://www.aloki.hu ● ISSN 1589 1623 (Print) ● ISSN 1785 0037 (Online)
DOI: http://dx.doi.org/10.15666/aeer/1704_81398150

be incorporated in broiler feed. In addition, *M. oleifera* leaf meal contains 2.4% ether extract, 25.4% crude protein, 17.4% crude fibre and 5.9% ash (Alnidawi et al., 2016) as against 18.8% ether extract, 42.8% crude protein, 20% crude fibre and 5.5% ash in (Banaszkiewicz, 2000). *Moringa oleifera* leaf therefore is lower in protein than soybean but much higher in ash (minerals) value thus supporting the earlier reports of Ustundag and Ozdogan (2015) that *M. oleifera* leaf can partially substitute soybean and fishmeal in broiler rations without negative impacts of production data while lessening the prize of feed (Ebenebe et al., 2012). In addition, research has established that *M. oleifera* leaves are abundant in water and fat-soluble vitamins as well as lutein and β-carotene (Igwilo et al., 2014; Saini et al., 2014). Evidence also exists that *M. oleifera* leaf is a storehouse for a variety of essential bioactive elements such as saponins, flavonoids, and phenols among others (Saini et al., 2016).

Feeding trial conducted by Kakengi et al. (2007) in chickens fed *M. oleifera* leaf meal revealed enhanced feed and dry matter intake hence showing the palatability of the *M. oleifera* leaf meal based diets to the chickens. In view of this observation, other authors (Onu and Aniebo, 2011; Onunkwo and George, 2015) fed broilers diet containing 10% MOLM and noticed to boost feed utilization and weight gain in comparison with birds fed 0% MOLM. In experiment conducted in native chickens, Gadzirayi et al. (2012) observed reduced feed consumption and enhanced growth rate in birds that received MOLM at 5% as a substitute for soybean meal (SBM) when compared with the group fed SBM alone as the main protein source. Increased egg production and egg mass in laying hens fed 20% MOLM has been documented (Kakengi et al., 2007). Also, improved growth rate and blood constituents in goats and fish fed MOLM have been reported (Paul et al., 2013; Jiwuba et al., 2017).

Several publications have been documented on the use of Moringa leaves as a feed resource for livestock and poultry (Gadzirayi et al., 2012; Paul et al., 2013; Onunkwo and George, 2015; Jiwuba et al., 2017). However, there is no comprehensive data on the mineral assay of moringa leaves and such knowledge will allow farmers to optimize the nutritional value of this plant in animal production. Hence, it has become important to investigate the mineral constituents of leaf meal of *Moringa oleifera* plant and their influence on the production characteristics of meat typed chickens. The objectives of this feeding trial therefore, was to determine the mineral content of *M. oleifera* leaf meal and the effect of its supplementation on production physiology of Ross 308 broilers. The *M. oleifera* leaf meal supplementation level that supported optimum performance in Ross 308 broilers were also reported.

Materials and methods

Study site and preparation of Moringa oleifera leaf meal

The study was performed in a private broiler farm located at Plot 519 Zuurbekom, Gauteng province, South Africa in the months of December 2017 to January 2018. Gauteng province is located at the Highveld of South Africa and lies between latitude 26° 11' 42.8856" S and longitude 28° 2' 2.716" E. Fresh and tender leaves of *M. oleifera* were harvested in Grootfontein, a village near Polokwane in Limpopo province of South Africa and air-dried for 3-5 days to a moisture level of about 10%. Thereafter, the dried leaves were milled and stored in unused feedbags for determination of mineral content and diet formulation.

http://www.aloki.hu ● ISSN 1589 1623 (Print) ● ISSN 1785 0037 (Online)
DOI: http://dx.doi.org/10.15666/aeer/1704_81398150

Mineral analysis

The mineral values were determined in triplicates in the Department of Animal Science Laboratory, North-West University-Mafikeng Campus, South Africa as described by AOAC (2000). The mineral constituents determined were calcium (Ca), phosphorus (P), potassium (K), magnesium (Mg), sodium (Na), sulphur (S), iron (Fe), chromium (Cr) and manganese (Mn).

Experimental procedures

Day-old Ross 308 broiler chicks (n = 500) were allotted to five treatments in completely randomized design with five replications with each replicate having 20 chicks. Birds received commercial mash diets (*Table 1*) supplemented with MOLM at 0, 25, 50, 75 and 100 g/kg feed, respectively and tagged T1, T2, T3, T4 and T5. Birds were procured from the National Chicks' Hatcheries located in the Boschkop area of East of Pretoria, Gauteng province, South Africa. The floor of each pen was swept, scrubbed with a strong brush, thereafter cleaned with water and later disinfected with Virkon® S. Pens were left open for several days after cleaning with Virkon® S as to break the breeding cycle of the pathogens that may have escaped the actions of the disinfectant. The floor of each of the pen was covered to a depth of 7 cm with fresh sawdust under a deep litter management system. The drinkers, feeders, and accessories were assembled and carefully positioned 7 days before the chicks arrived. In addition, pens were heated for 24 h via an infrared light before the chicks arrived. The starter diet (21.0% crude protein) and grower diet (19.0% crude protein) were formulated according to NRC (1994) standard to meet the nutrient requirements of the experimental birds. Feed and water were offered ad libitum and the investigation lasted for 42 days. All the biosecurity measures conformed to the rules and guidelines of the Ethics Committee of the University of South Africa and the South African Animal Disease Act 35, of 1984.

Table 1. *Nutrient content of the diets used in the experiment*

Nutrient* (%)	Starter (0-21 days)	Grower (22–42 days)
Crude protein	21.0	19.0
Lysine	1.30	1.15
Methionine	0.58	0.5
Moisture	12.0	12.0
Fat	2.5	2.5
Fibre	5.0	6.0
Calcium	1.2	1.2
Phosphorus	0.6	0.55

*As illustrated in feed label

Data collection

The initial live weights (LWs) of broiler chicks in each pen were taken at the beginning of the study and weekly thereafter to obtain the weekly LW and weight difference. The mean LW of birds on each pen was determined by dividing total LW by the number of birds in the pen. Feed consumption was determined by subtracting the leftover feed in the feeding trough the following morning from the quantities of feed

http://www.aloki.hu ● ISSN 1589 1623 (Print) ● ISSN 1785 0037 (Online)
DOI: http://dx.doi.org/10.15666/aeer/1704_81398150

offered daily to the birds. Average daily gain in each pen was computed as the quotients of the LW at the end of the study less the live weights at the start of the study and the period the investigation lasted. Feed conversion ratio (FCR) was determined as the quotient of FI and ADG. At 42 days, 15 birds were chosen from each treatment, denied of feed for 12 h and thereafter, slaughtered to assess the carcass and organ weights. The carcass, organ and cut parts were weighed and expressed as a percentage of the live weight and carcass weight respectively following the procedures of Chukwukaelo et al. (2018).

Data analysis

Data collected were subjected to one-way analysis of variance (ANOVA), and differences in means where significant F-test ($p < 0.05$), Duncan's multiple range test (Duncan, 1955) method was used to separate the means (SPSS 24.0 package). The supplementation related responses in growth and production parameters to MOLM in Ross 308 broilers were modeled using the following quadratic optimization equation:

$$Y = a + b_1x + b_2x^2$$

where Y = growth indices (LW, FI, ADG, FCR and mortality), carcass, dressing percent, cut parts (breast, thigh and drumstick) or organ (liver, heart and gizzard) weight; a = the Y intercept; b = coefficient of quadratic optimization equation; x = MOLM supplementation levels and $-b_1 / 2b_2 = x$ value for optimum response. The quadratic equation was fitted to the experimental data by means of the nonlinear model procedure of SPSS 24.0. The choice of the quadratic regression model is because it fitted the model and the probability level for significance is 5%.

Results

Nutrient composition of experimental diet and MOLM

The results of the nutrient content of the treatment diets are shown in *Table 1*. The crude protein levels were 21.0% for the starter mash and 19.0% for the grower mash. *Table 2* presents the mineral composition of MOLM. The mineral content of the MOLM contains appreciable levels of beneficial minerals, including calcium, phosphorus, magnesium, sodium, potassium, iron, sulphur, chromium and manganese showing that MOLM is a source of mineral for livestock. The coefficient of variation (CV) values across sample measurements for the minerals were higher and ranged from 61.35–81.70%.

Growth performance of starter broilers

Table 3 presents the growth indices of starter Ross 308 broilers fed with diets supplemented with varying levels of MOLM. Broilers fed diet T1 recorded the highest FLW of 833 g, which was significantly different from birds on diets supplemented with MOLM at 25, 50, 75 and 100 g/kg feed. ILW and DFI had similar ($p > 0.05$) value in the groups. ADG decreased ($p < 0.05$) steadily with increasing supplementation levels of MOLM. Birds on diet T1 (0 g MOLM/kg feed) had better FCR when compared with birds that received diets supplemented with MOLM at 25, 50, 75 and 100 g/kg feed,

http://www.aloki.hu ● ISSN 1589 1623 (Print) ● ISSN 1785 0037 (Online)
DOI: http://dx.doi.org/10.15666/aeer/1704_81398150

however, the difference was not significant ($p > 0.05$). Mortality rate was significantly ($p < 0.05$) higher for birds on diet T1 when compared with birds fed the other four diets.

Table 2. *Macro and micro mineral composition of MOLM (mg/kg)*

Parameters	Mean ± SD	CV (%)
Calcium	2687.41 ± 188.68	70.20
Phosphorus	120.73 ± 8.68	71.85
Magnesium	250.00 ± 17.88	71.51
Sodium	968.02 ± 6.03	62.32
Potassium	734.59 ± 45.10	61.35
Iron	316.98 ± 31.68	73.73
Sulphur	1144.09 ± 87.52	76.44
Chromium	3.21 ± 0.26	81.7
Manganese	12.52 ± 0.14	67.18

SD – Standard deviation; CV – Coefficient of variations

Table 3. *Growth indices of starter broilers (1-3 weeks) fed MOLM supplemented diets*

MOLM Level	ILW (g)	FLW (g)	DFI (g)	ADG (g)	FCR	Mortality (%)
0 g/kg feed	40.73	833.87[a]	34.59	37.77[a]	2.29	3.00[a]
25 g/kg feed	39.64	771.56[b]	32.46	34.85[b]	2.40	0.00[c]
50 g/kg feed	40.10	770.49[b]	32.80	34.78[b]	2.40	0.00[c]
75 g/kg feed	40.03	748.72[b]	32.86	33.75[b]	2.43	1.00[b]
100 g/kg feed	39.39	728.30[b]	31.19	32.81[b]	2.41	0.00[c]
Mean	39.98	770.59	32.78	34.79	2.39	0.80
SD	0.51	39.60	1.22	1.86	0.06	1.30
CV (%)	1.28	5.13	3.70	5.35	3.96	-
SEM	0.23	17.71	0.54	0.83	0.03	0.58
p-value	0.06	0.01	0.06	0.02	0.14	0.02

Means with the same letters within column differed statistically at $p < 0.05$, ILW – initial live weight, FLW – final live weight, DFI – daily feed intake, ADG – average daily gain, FCR – feed conversion ratio, SD – standard deviation, CV – coefficient of variation, SEM – standard error of the mean

Growth performance of finisher broilers

The result of growth indices of finisher Ross 308 broilers fed with diets supplemented with varying levels of MOLM as shown in *Table 4*. Higher FLW ($p > 0.05$) was reported control birds fed MOLM at 0 g/kg feed than those fed diets supplemented with MOLM at 25, 50, 75 and 100 g/kg feed. Broilers fed MOLM supplemented diet at 0, 25, 50 and 100 g/kg feed had comparable ($p > 0.05$) ILW, DFI, and ADG values. Birds fed MOLM supplemented diet at 75 g/kg feed had the best FCR, although the difference was not significant ($p > 0.05$) compared with the groups fed the other four diets. Birds on 0 g/kg feed MOLM had the highest mortality ($p < 0.05$) when compared to the birds supplemented with 25, 50, 75 and 100 g/kg feed MOLM.

http://www.aloki.hu ● ISSN 1589 1623 (Print) ● ISSN 1785 0037 (Online)
DOI: http://dx.doi.org/10.15666/aeer/1704_81398150

Table 4. *Growth indices of finisher broilers (4–6 weeks) fed MOLM supplemented diets*

MOLM Level	ILW (g)	FLW (g)	DFI (g)	ADG (g)	FCR	Mortality (%)
0 g/kg feed	763.87	3000.40[a]	124.57	74.76	1.54	5.00[a]
25 g/kg feed	761.56	2848.40[b]	122.69	69.70	1.40	0.00[b]
50 g/kg feed	760.49	2761.20[b]	122.16	69.65	1.63	0.00[b]
75 g/kg feed	768.72	2729.33[b]	123.38	69.36	1.31	2.00[b]
100 g/kg feed	768.30	2699.26[b]	121.90	70.17	1.41	0.00
Mean	764.59	2807.72	122.94	70.73	1.46	1.40
SD	4.60	121.30	1.07	2.27	0.13	2.19
CV (%)	5.13	4.32	0.87	3.21	8.66	156.48
SEM	5.71	55.25	0.48	1.02	0.06	0.98
p-value	0.610	0.038	0.75	0.82	1.14	0.02

Means with the same letters within column differed statistically at $p < 0.05$, ILW – initial live weight, FLW – final live weight, DFI – daily feed intake, ADG – average daily gain, FCR – feed conversion ratio, SD – standard deviation, CV – coefficient of variation, SEM – standard error of the mean

Relative carcass and organ weight of finisher broilers

The performance in terms of the relative weights of the carcass and organs are presented in *Table 5.* Birds fed diet with MOLM at 0 g/kg feed had higher live weight ($p < 0.05$) than those on diets supplemented with MOLM at 25, 50, 75 and 100 g/kg feed. Birds on diet with MOLM at 0 g/kg feed had higher non-significant ($p > 0.05$) carcass weight than those on diets with MOLM at 25, 50, 75 and 100 g/kg feed. Although, broilers on diets with MOLM at 75 g/kg feed returned the highest non-significant dressing percent ($p > 0.05$) relative to the birds on the other four diets. Cut parts and organ weights of broilers fed MOLM supplemented diets at 25, 50, 75 and 100 g/kg feed had the same values.

Table 5. *Relative carcass and organ weight values of finisher broilers fed MOLM supplemented diets*

Parameters	MOLM inclusion (g/kg feed)					Mean	SD	CV	SEM	P-value
	0	25	50	75	100					
LW (g)	3000.40[a]	2848.40[b]	2761.20[b]	2729.33[b]	2699.26[b]	2807.72	121.30	4.32	55.25	0.0384
CW (g)	2911.53	2778.93	2690.53	2659.60	2637.86	2735.69	112.01	4.09	50.09	0.1128
BW (%CW)	27.26	25.54	30.02	25.27	27.42	27.10	1.90	7.00	0.85	0.3960
DW (%CW)	16.81	17.11	18.02	18.65	18.64	17.85	0.85	4.78	0.38	0.5208
TW (%CW)	21.23	22.83	22.90	23.73	23.66	22.87	1.01	4.49	0.45	0.6315
HW (%LW)	3.01	1.94	2.28	2.08	2.04	2.27	0.43	19.01	0.19	0.0828
LW (%LW)	9.26	9.76	10.13	10.46	10.54	10.03	0.53	5.27	0.24	0.9785
GW (%LW)	7.87[b]	9.19[a]	8.56[ab]	8.56[ab]	10.21[a]	8.88	0.88	9.89	0.39	0.2358
DP (%)	97.04	97.56	97.42	97.45	97.71	97.44	0.25	0.25	0.11	0.0781

Means in the same row sharing the same superscript are significant ($p < 0.05$). LW – live weight, CW – carcass weight, BW- breast weight, DW – drumstick weight, TW – thigh weight, HW – heart weight, LW – liver weight, GW – gizzard weight, DP – dressing percent, SD – standard deviation, CV – coefficient of variation, SEM – standard error of the mean

http://www.aloki.hu ● ISSN 1589 1623 (Print) ● ISSN 1785 0037 (Online)
DOI: http://dx.doi.org/10.15666/aeer/1704_81398150

Optimization functions

The results of the effect MOLM supplementation on FLW and ADG in Ross 308 broilers are presented in *Tables 6* and *7*. FLW and ADG were optimized at 2538.4 – 173.97 MOLM + 21.756 $MOLM^2$, $r^2 = 0.8994$ and 79.334 – 5.8806 MOLM + 0.8214 $MOLM^2$, $r^2 = 0.8960$ respectively in starter broilers while FLW was optimized at 3173.7 – 200.36 MOLM + 21.371 $MOLM^2$, $r^2 = 0.9928$ in finisher broilers.

Table 6. *Quadratic analysis of the effect of MOLM on FLW and ADG in starter broilers*

Variables	Formula	r^2	x-value	y-value	P-value
FLW	$Y = 2538.4 – 173.97x + 21.756x^2$	0.8994	39.98	2190.63	0.0100
ADG	$Y = 79.334 – 5.8806x + 0.8214x^2$	0.8960	35.80	68.81	0.0200

Table 7. *Quadratic analysis of the effect of MOLM on FLW in finisher broilers*

Variable	Formula	r^2	x-value	y-value	P-value
FLW	$Y = 3173.7 – 200.36x + 21.371x^2$	0.9928	46.88	2704.09	0.0384

Discussion

The objective of this feeding investigation was to determine the responses of Ross 308 broilers to commercial diets (starter and grower) mash supplemented with varying levels of MOLM. The starter diet contained crude protein level of 21.0% while grower contained crude protein level of 19.0% with similar levels of other essential nutrients that satisfied the bird's nutrient demands as endorsed by NRC (1994) for poultry.

Minerals are vital in poultry nutrition because they serve as cofactors for several biological processes. Calcium, an important mineral for bone growth, muscle, and neurological functions are high in MOLM with the order of macro mineral level being calcium (2687.41 mg/kg) > sodium (968.02 mg/kg) > potassium (734.59 mg/kg) > magnesium (250.00 mg/kg) > phosphorus (120.73 mg/kg) as determined in the current study. These observations are in harmony to the value recorded by Sena et al. (1998). Furthermore, the calcium, potassium, magnesium and phosphorus values determined herein were lower in general than the corresponding values of 16046.7, 17450, 2833.8 and 4827.4 mg/kg published by Olson et al. (2016) in Mexico. Freiberger et al. (1998) and Yaméogo et al. (2011) have noticed a higher calcium value (14,400 to 35,126 mg/kg) than the value determined in this experiment, and is therefore not clear what is responsible for this wide difference. Noteworthy too was the fact that the sodium content (117.4 mg/kg) reported by Olson et al. (2016) was about 99% units lower to what was determined in this experiment. These variations may be associated with such factors as soil composition, agro climatic condition, plant age and stage of maturity of the leaves, digestion protocols and analyzing techniques used as observed by Melesse et al. (2012) and Mbah et al. (2012). Phosphorus is another important macro mineral needed for rapid bone growth in meat-typed chickens. Such rapid bone growth requires adequate calcium and phosphorus supply (Williams et al., 2000).

Inadequate supply of both or one of the minerals as a result of the deficiency or excess of one of them interferes with homeostasis of the second one (Kebreab and Vitti, 2005), resulting in reduced growth rate and bone mineralization (Hurwitz et al., 1995).

http://www.aloki.hu ● ISSN 1589 1623 (Print) ● ISSN 1785 0037 (Online)
DOI: http://dx.doi.org/10.15666/aeer/1704_81398150

The analysed leaf meal contained small amounts of phosphorus; however, this was not a problem since the leaves were used as protein supplement for broilers. The study plant also contains appreciable quantities of iron and sulphur. This high iron content could explain the improved blood values in chickens fed MOLM based diets (Ustundag and Ozdogan, 2015; Alnidawi et al., 2016) since they are needed for haemoglobin formation. Noteworthy is that MOLM has moderate potential as a good source of dietary minerals (calcium, potassium, sodium, iron, and sulphur) in animal nutrition. High sulphur content (1144.09 mg/kg) recorded in the current study for MOLM was in agreement with Lyon et al. (2017) who reported that *Moringa oleifera* tree has an exceptional power to take up and store in the leaves mineral sulphur, even when grown on soils with low in sulphur. The health and medical benefits of this finding is that MOLM may be used to enhance productivity in animals fed low sulphur diets. The coefficient of variation of mean mineral values as observed in the current study was high, thus suggesting that the means could not serve as reference mineral value for MOLM in the study location.

The results reveal that the final live weight of starter broilers on the control birds was significantly higher than the groups on diets supplemented with MOLM at 25, 50, 75 and 100 g/kg feed, but lower than the reference live weight of 929 g recorded for 21-day-old unsexed Ross 308 broilers (www.aviagen.com). Factors such as enhanced nutrition and improved housing conditions may have explained the observed disparity in starter phase. The present result showed that MOLM supplementation up to the rate of 100 g/kg feed showed no adverse influence on feed consumption. This compared favourably with the result of Divya et al. (2014) who also noticed non-significantly reduced feed intakes in broilers fed *Moringa oleifera* leaf meal based rations. This finding indicate that the level of MOLM supplemented in the current study is acceptable to the birds. However, the reason for the acceptability is not known. Although, one possible reason is anti-nutritional factors as similarly observed by Makkar and Becker (1996). The non-significant reduction in average daily gain as observed for birds fed MOLM supplemented diets in the current feeding investigation was similar to value recorded in broilers by Divya et al. (2014). There was no significant MOLM effects on feed to gain ratio in the present feeding investigation. The result of the percentage mortality revealed that MOLM supplementation significantly influenced mortality rate ($p < 0.05$) with birds on control experiencing the highest rate. Mortality was significantly low in treatment groups relative to the control group and this observation may be because of high levels of phytochemical compounds in moringa leaves, which have been reported to have medicinal and pharmacological property such as antiprotozoal, antibacterial and antifungal effect as well as immune stimulating actions in animals (Sharma and Paliwal, 2013). Furtherance to this, the coefficient of variation of mean growth performance values were small, indicating that the reported means could be used as reference value for broilers fed diets with varying supplementation levels of MOLM in the study location.

The non-significant carcass weight and dressing percent at 25, 50, 75 and 100 g/kg feed supplementation rates can be attributed to high quality of the MOLM supplemented diets and enhanced nutrient utilisation by the broilers (Hassan et al., 2016). The result of the weights of breast, drumstick and thigh suggested that MOLM supplementation positively influenced the development of the cut parts but did not maintain progressive pattern, which is in agreement with the earlier findings published by Hassan et al. (2016). This observation has shown the suitability of MOLM

http://www.aloki.hu ● ISSN 1589 1623 (Print) ● ISSN 1785 0037 (Online)
DOI: http://dx.doi.org/10.15666/aeer/1704_81398150

supplemented diets for enhanced cut parts development and production in broilers and therefore may be recommended for broiler production. The slight enlargement on the size of the liver of broilers fed MOLM supplemented diets at 25–100 g/kg feed could be linked to enhanced activity of this organ in a bid to detoxify the antinutritional factors that may be present in the experimental diet (Igwilo et al., 2007). The weight of gizzard at 25 and 100 g/kg feed was significantly increased and this corroborated with works of Ayssiwede et al. (2011), who recorded higher gizzard weights in indigenous chickens fed MOLM based diets. In addition, the coefficient of variation of mean carcass and organ parts were narrow, suggesting that the means could serve as standard value for Ross 308 broilers fed MOLM supplemented diets in the study region.

The results of the quadratic function showed that no single MOLM supplementation level optimized FLW and ADG in the current feeding experiment. The quadratic function showed that all the significant parameters had very high (89.6–99.3%) coefficients of determination (r^2). Handful of studies has used a quadratic model to ascertain the optimal levels of feed that supported optimum performance variables in chickens (Okoro et al., 2016 a, b). However, information on the use of quadratic analysis to determining the MOLM supplementation level that supported optimum production parameters in Ross 308 broilers is lacking in the literature. The results of the quadratic function in the current study corroborate the results of Okoro et al. (2016a, b) who observed that no single feed inclusion level optimized all production parameters in chickens. The results of this feeding experiment revealed that for starter broilers, FLW and ADG was statistically optimized at 39.98 and 35.80 g/kg feed respectively. However, the value of 39.98 g/kg feed MOLM that optimized final live weight at the starter phase was 6.9 g/kg lower than the value of 46.88 g/kg that optimized the final live weight at the finisher phase. The observed difference is expected since the starter diet was high in protein (21.0%) than the finisher diet (19.0%), thus the birds on the starter phase will tend to take less diet to meet their daily protein requirements when supplemented with MOLM which are reported to contains 25.4–42.8% crude protein by Banaszkiewicz (2000) and Alnidawi et al. (2016). The high r^2 value recorded for the FLW and ADG revealed the high strength of relationship of the two variables using the quadratic analysis. These observations have practical application when supplementing diets with MOLM for FLW and ADG in Ross 308 broilers as to reduce the wastage of feed supplements. The significant optimization influence on FLW and ADG n implied that their values could be predicted at a given quantity of MOLM supplemented in the broiler diet.

Conclusion

The information provided in the current investigation further support the potential of *Moringa oleifera* leaves as an alternative non-conventional protein feed resource in broiler chicken diets. Importantly, this is useful for smallholder poultry farmers who are compelled by the high prices of conventional protein feed resource such as soybean meal to rely on such alternative protein source for enhancing the productivity of their animals. In addition, *Moringa oleifera* leaves are good sources of minerals and is suitable for cut parts development and production of enhanced cut parts in the broiler chickens. It is therefore, recommended that supplementation rate of 100 g/kg feed MOLM may be well accepted by the Ross 308 broiler chickens.

http://www.aloki.hu ● ISSN 1589 1623 (Print) ● ISSN 1785 0037 (Online)
DOI: http://dx.doi.org/10.15666/aeer/1704_81398150

REFERENCES

[1] Abbas, T. E. (2013): The use of Moringa oleifera in poultry diets. – Turkish Journal of Veterinary and Animal Science 37: 492-496.
[2] Alnidawi, N. A. A., Ali, H. F. M., Abdelgayed, S. S., Ahmed, F. A., Farid, M. (2016): Moringa oleifera leaves in broiler diets: effect on chicken performance and health. – Food Science and Quality Management 56: 40-48.
[3] AOAC (2000): Official Methods of Analysis of AOAC International (17th Ed.). – AOAC, Washington, DC.
[4] Ayssiwede, S. B., Dieng, A., Bello, H., Chrysostome, C. A. A. M., Hane, M. B., Mankor, A., Dahouda, M., Houinato, M. R., Hurnick, J. R., Missohou, A. (2011): Effects of Moringa oleifera (Lam.) leaves meal incorporation in diets on growth performances, carcass characteristics and economics results of growing indigenous Senegal chickens. – Pakistan Journal of Nutrition 10: 1132-1145.
[5] Banaszkiewicz, T. (2000): Nutritive value of newrape cultivars stated in the tests for broiler chickens. – Thesis University of Podlasie 61: 1-99.
[6] Chukwukaelo, A. K., Aladi, N. O., Okeudo, N. J., Obikaonu, H. O., Ogbuewu, I. P., Okoli, I. C. (2018): Performance and meat quality characteristics of broilers fed fermented mixtures of grated cassava roots and palm kernel cake as replacement for maize. – Tropical Animal Health and Production 50: 485-493. DOI: 10.1007/s11250-017-1457-7.
[7] Dieye, P. N., Missohou, N. A., Faye, A. (2010): L'aviculture familiale: Un levier pouraméliorer les revenus des éleveurspauvres au Sud du Sénégal. – In: Faye, B, Duteurtre, G. (eds.) L'élevage, richesse des pauvres. Editions Quae, Paris, pp. 191-201.
[8] Divya, A. B., Mandal, A., Biswas, A., Yadav, A. S., Biswas, A. K. (2014): Effect of dietary Moringa oleifera leaves powder on growth performance, blood chemistry, meat quality and gut microflora of broiler chicks. – Animal Nutrition and Feed Technology 14: 349-357.
[9] Duncan, D. B. (1955): Multiple range and multiple F-test. – Biometrics 11: 1-42.
[10] Ebenebe, C. I., Umegechi, C. O., Aniebo, B. O. (2012): Comparison of haematological parameters and weight changes of broiler chicks fed different levels of Moringa oleifera diet. – International Journal of Agriculture and Biosciences 1: 23-25.
[11] Freiberger, C., Vanderjagt, D., Pastuszyn, A., Glew, S., Mounkaila, G., Millson. M., Glew, R. H. (1998): Nutrient content of the edible leaves of seven wild plants from Niger. – Plant Foods for Human Nutrition 53: 57-69.
[12] Gadziravi, C. T., Masamha. B. J. F., Mupangwa, J. F., Washaya, S. (2012): Performance of broiler chickens fed on mature Moringa oleifera in supplement to soybean meal. – International Journal of Poultry Sciences 11: 5-10.
[13] Hassan, H. M. A., El-Moniary, M. M., Hamouda, Y., El-Daly, E. F., Youssef, A. W., Abd El-Azeem, N. A. (2016): Effect of different levels of Moringa oleifera leaves meal on productive performance, carcass characteristics and some blood parameters of broiler chicks reared under heat stress conditions. – Asian Journal of Animal and Veterinary Advance 11: 60-66.
[14] Hurwitz, S., Plavnik, I., Shapiro, A., Wax, E., Talpaz, H., Bar, A. (1995): Calcium metabolism and requirements of chickens are affected by growth. – Journal of Nutrition 125: 2679-2686.
[15] Igwilo, I. O., Oloyode, O. B., Enemor, V. H. A. (2007): Nutrient composition and the effects of processing on Canavalian ensiformis seed. – International Journal of Agriculture, Food Systems 1: 48-50.
[16] Igwilo, I. O., Ezeonu, F. C., Ezekwesili-Ofili, J. O., Igwilo, S. N., Nsofor, C. I., Abdulsalami, M. S., Obi, E. (2014): Anti-nutritional factors in roots of a local cultivar of Moringa oleifera (Lam). – Pakistan Journal of Biological Sciences 17: 114-117.

http://www.aloki.hu ● ISSN 1589 1623 (Print) ● ISSN 1785 0037 (Online)
DOI: http://dx.doi.org/10.15666/aeer/1704_81398150

[17] Jiwuba, P. C., Ahamefule, F. O., Ogbuewu, I. P., Ikwunze, K. (2017): Blood chemistry and haematology of West African dwarf Goats fed Moringa oleifera leaf meal (MOLM) in their diet. – Comparative Clinical Pathology. DOI: 10.1007/s00580-017-2434-2.
[18] Kakengi, A. M. V., Kaijage, J. T., Sarwatt, S. V., Mutayoba, S. K., Shem, M. N., Fujihara, T. (2007): Effect of Moringa oleifera leaf meal as a substitute for sunflower seed meal on performance of laying hens in Tanzania. – Livestock Research for Rural Development 19(8). http://www.lrrd.org/lrrd19/8/kake19120.htm.
[19] Kebreab, E., Vitti, D. M. S. S. (2005): Mineral Metabolism. – In: Dijkstra, J., Forbes, J. M., France, J. (eds.) Quantitative Aspects of Ruminant Digestion and Metabolism. CAB International, Wallingford, UK, pp. 469-486.
[20] Lyons, G., Gondwe, C., Banuelos, G., Mendoza, C., Haug, A., Christophersen, O., Ebert, A. W. (2017): Drumstick tree (Moringa oleifera) leaves as a source of dietary selenium, sulphur and pro-vitamin A. – Acta Horticulturae 1158: 287-292.
[21] Makkar, H. P. S., Becker, K. (1996): Nutritional value and whole and ethanol antinutritional components of extracted Moringa oleifera leaves. – Animal Feed Science Technology 63: 211-228.
[22] Mbah, B. O., Eme, P., Paul, A. E. (2012): Effect of drying techniques on the proximate and other nutrient composition of Moringa oleifera leaves from two areas in eastern Nigeria. – Pakistan Journal of Nutrition 11(11): 1044-1048.
[23] Melesse, A., Steingass, H., Boguhn, J., Schollenberger, M., Rodehutscord, M. (2012): Effects of elevation and season on nutrient composition of leaves and green pods of Moringa stenopetala and Moringa oleifera. – Agroforestry Systems 86: 505-518.
[24] NRC (1994): Nutrient Requirements of Poultry. 9th Revised Ed. – National Academy of Science Press, Washington, DC.
[25] Nsofor, C. I., Igwilo, I. O., Avwemoya, F. E., Adindu, C. S. (2012): The effects of feeds formulated with Moringa oleifera leaves in the growth of the African catfish, Clarias gariepinus. – Research and Reviews in Bioscience 6: 121-126.
[26] Ogbuewu, I. P., Mbajiorgu, C. A. (2019): Potential of leaf and seed meals of tropical plants in chicken diet: effect on spermatozoa and egg production. – Tropical Animal Health and Production 51: 267-277.
[27] Ogbuewu, I. P., Emenalom, O. O., Okoli, I. C. (2015): Alternative feedstuffs and their effects on blood chemistry and haematology of rabbits & chickens: a review. – Comparative Clinical Pathology 26(2): 277-286.
[28] Okoro, V. M. O., Mbajiorgu, C. A., Mbajiorgu, E. F. (2016a): Semen quality characteristics of Koekoek breeder cocks influenced by supplemental inclusion levels of onion and garlic mixture at 35–41 weeks of age. – Revista Brasileira de Zootecnia 45: 433-440.
[29] Okoro, V. M. O., Nwokeocha, A. C. C., Ijezie, C. O., Mbajiorgu, C. A., Mbajiorgu, E. F. (2016b): Effect of varying dietary supplemental inclusion levels of onion and garlic on semen quality characteristics of Hubbard white breeder broiler cocks aged 35-41 weeks old. – Indian Journal of Animal Research 50: 922-929.
[30] Olson, M. E., Sankaran, R. P., Fahey, J. W., Grusak, M. A., Odee, D., Nouman, W. (2016): Leaf protein and mineral concentrations across the "Miracle Tree" Genus Moringa. – PLoS One 11(7): e0159782.
[31] Onu, P. N., Aniebo, A. O. (2011): Influence of Moringa oleifera leaf meal on the performance and blood biochemistry of starter broilers. – Nigerian International Journal of Food, Agriculture and Veterinary Science 1: 38-44.
[32] Onunkwo, D. N., George, O. S. (2015): Effects of Moringa oleifera leaf meal on the growth performance and carcass characteristics of broiler birds. – Journal of Agriculture and Veterinary Science (IOSR-JAVS) 8: 63-66.
[33] Paul, L. T., Fowler, F. A., Barry, R. J., Watts, S. A. (2013): Evaluation of Moringa oleifera as a dietary supplement on growth and reproductive performance in Zebra fish. – Journal of Nutritional Ecology and Food Research 1: 322-328.

http://www.aloki.hu ● ISSN 1589 1623 (Print) ● ISSN 1785 0037 (Online)
DOI: http://dx.doi.org/10.15666/aeer/1704_81398150

[34] Saini, R. K., Shetty, N. P., Giridhar, P. (2014): Carotenoid content in vegetative and reproductive parts of commercially grown Moringa oleifera Lam. cultivars from India by LC–APCI–MS. – European Food Research and Technology 238: 971-978.
[35] Saini, R. K., Sivanesan, I., Young-Soo, K. (2016): Phytochemicals of Moringa oleifera: a review of their nutritional, therapeutic and industrial significance. – 3. Biotech 6(203): 1-14.
[36] Sena, L. P., Vanderjagt, D. J., Rivera, C., Tsin, A. T. C., Muhamadu, I., Mahamadou, O., Millson, M., Pastuszyn, A., Glew, R. H. (1998): Analysis of nutritional components of eight famine foods of the Republic of Niger. – Plant Foods for Human Nutrition 52: 17-30.
[37] Sharma, V., Paliwal, R. (2013): Isolation and characterization of saponins from Moringa oleifera (Moringaceae) pods. – International Journal of Pharmaceutical Sciences 5: 179-183.
[38] SPSS (2007): SPSS Statistical software 17.0.978-156827-401-0.
[39] Ustundag, A. O., Ozdogan, M. (2016): Using Moringa oleifera in poultry nutrition. – Journal of Agriculture Faculty of Ulundag University 30: 195-201.
[40] Williams, B., Waddington, D., Solomon, S., Farquharson, C. (2000): Dietary effects on bone quality and turnover, and Ca and P metabolism in chickens. – Research Veterinary Science 69: 81-87.
[41] Yaméogo, C., Bengaly, M., Savadogo, A., Nikiema, P., Traore, S. (2011): Determination of chemical composition and nutritional values of Moringa oleifera leaves. – Pakistan Journal of Nutrition 10: 264-268.

http://www.aloki.hu ● ISSN 1589 1623 (Print) ● ISSN 1785 0037 (Online)
DOI: http://dx.doi.org/10.15666/aeer/1704_81398150

LINKING LAND USE CHANGES TO VARIATION IN SURFACE WATER QUALITY: EVIDENCE FROM 36 CATCHMENTS IN IRAN

MAHMOODI, M.[1] – HONARMAND, M.[1*] – NASERI, F.[1] – MOHAMMADI, S.[1]

[1]*Department of Ecology, Institute of Science and Technology and Environmental Sciences, Graduate University of Advanced Technology, Kerman, Iran*

**Corresponding author*
e-mail: mehonarmand167@yahoo.com

(Received 13th Feb 2019; accepted 24th May 2019)

Abstract. In this article, the response of surface water quality to land use/land cover changes studied. We investigate the impact of land use changes on quality of water during three decades in the Razavi Khorasan Province of Iran. Detecting of LULC changes has done using Landsat satellite images belonging to the years 1987 (TM), 2001 (ETM^+) and 2015 (OLI). In the study area based on RS and GIS standard techniques, sixteen land use classes were defined: barren, rocky, residential, swamp, water, dunes, salt marsh, irrigated cultivation, garden, dry farming, desert, good rangeland, medium rangeland, poor rangeland, wooded rangeland, and watercourse. Also, the water quality data from 1987 to 2015 in the stream gauge station located at the outlet of the 36 catchments analyzed. In this study, 13 parameters included K, Cl, Ca, Mg, Na, CO_3, HCO_3, SO_4, EC, pH, TDS, SAR, and Hardness investigated. After removing variance, non-parametric tests performed and trends of water quality variables in the time series evaluated. Then, using a multivariate linear regression model was trying to link water quality variables to land use changes. Results demonstrated that the models estimate water quality parameters with an acceptable degree of accuracy (P-value < 0.05) except calcium, potassium, carbonate, and bicarbonate. The results showed the relationship between land use and the water quality indicators that can be applied in environmental protection and land use planning.
Keywords: *sustainable development, remote sensing, regression model, Landsat satellite, GIS*

Introduction

Ecological and human health directly affect by water attribute and for this reason, the quality of water is as important as its quantity (Zamani et al., 2013). In the past few decades, surface water characteristics deteriorated in numerous countries. The major environmental worry is the deterioration of stream water quality due to unsustainable activities of human (Chen and Lu, 2014). Also, the quality of water is momentous to assess the health of a watershed and to make necessary management decisions to control current and future pollution (Walling and Fang, 2003). Water carries the particles from the land, as flows from the land surface and be enriched with different kinds of contaminants when flows from various types of land use (Tong, 1990). Rivers are vulnerable to land use and land cover (LULC) change and ubiquitous exploitation (Withers and Jarvie, 2008; Vörösmarty et al., 2010) and comprehending the relationship between land use and surface water quality is essential for effective water management (Ding et al., 2015).

Watershed is a topographic region of natural space that encompasses the correlation of water, its physical appearance, along with the related movement of elements connected with water resources usage. Thus, the best unit for water-related research at the regional scale is catchment (Li et al., 2012). The relevance between the quality of water in rivers and land use, despite its significance for the watershed, is not well described (Ding et al., 2016). Many studies derived that a significant relationship exists

http://www.aloki.hu ● ISSN 1589 1623 (Print) ● ISSN 1785 0037 (Online)
DOI: http://dx.doi.org/10.15666/aeer/1704_81518169

between the water quality parameters and land use and land cover at a basin scale (Kibena et al., 2014; du Plessis et al., 2014), while others demonstrated that are dependent on the depth of studies (Miserendino et al., 2011; Dabrowski et al., 2013; Namugize et al., 2018). Because of its reiterative data, digital format appropriate for processing, and precise geo-referencing approaches, satellite imagery is the most common data source for detection and mapping of land use changes (Minaei and Kainz, 2016). LULC change detection has become the main usage of RS data, due to repetitive coverage at short intervals and consistent image quality (Joorabian Shooshtari et al., 2012).

In relation to ecology, deforestation, desertification, urbanization, sustainable management of natural resources, identifying and modelling the impacts of weather events and climate change, etc land use change is monitored (Rafiee et al., 2009). Geographic Information System (GIS) provides many various methods to analyze and evaluate land use changes. These methods developed by using Remote Sensing (RS) and image processing techniques. For example, in the Beijing, (in China) (Wu et al., 2006) applied a combination of GIS and RS to find land use changes and found a significant increase in urban areas and a decline in rangeland from 1986 to 2001. Or in another research, in the north-western coastal region of Egypt from 1987 to 2001, (Shalaby and Tateishi, 2007) monitored land use changes used the post-classification method and maximum likelihood technique to generate the maps, detect land use changes and report on the effects of development projects in tourism and agriculture on vegetation cover region. In the west of Nile River (Egept), (Abd El-Kawy et al., 2011) applied Post-classification comparisons to investigate land use changes. And numerous similar studies conducted using GIS and RS combinations.

To specify whether the measured values of a variable increase or decrease during a period, generally trend analysis apply. Many methods are available for the quantification and detection of trends: regression analysis, T-tests, graphical methods, etc. Trend analysis method for water quality data should consider some of the specifications generally found in the water quality data (Zamani et al., 2013). Seasonality, non-normality, missing values, outliers, autocorrelation, and dependence on other variables such as river flow are some of these specifications (Zamani et al., 2013). (Esterby, 1996) provided a comprehensive review of statistical approaches that are using for trend analysis of water quality time series.

The intricate relationships of land use, water quality in various geographical regions under different scales are yet to be clarified, although there are some studies on the impacts of land use on water quality. The common procedures for predicting water quality in river basins based on land use types are still developmental. In a study, Huang explained the major participants to the increase of nutrients and sediments in freshwater ecosystems are increasing in agricultural and civil areas (Huang et al., 2016). Results in another study by (Mello et al., 2018), showed that organic matter and nitrogen were more influenced by the riparian zone composition, while fecal coliforms, phosphorus, sediment, and dissolved oxygen were affected by land use types at the watershed scale (Shi et al., 2017) in their research found that the land use composition in a riparian area is a superior predictor of water quality than in the whole basin, while (Zhou et al., 2012) showed that land use types at the basin scale can better account for the variability in river water quality.

Iran is among the arid and semi-arid countries of the world, and in most of its areas, there is a water shortage problem. Khorasan Razavi, besides the problem of water

http://www.aloki.hu ● ISSN 1589 1623 (Print) ● ISSN 1785 0037 (Online)
DOI: http://dx.doi.org/10.15666/aeer/1704_81518169

shortage, has a problem with reducing water quality. As it follows from the review of previous studies, one of the factors of long-term change in water quality is the change in land use. However, according to the authors' information, in Khorasan Razavi Province, no research has been undertaken for linking the spatial and temporal changes in land use and quality of water. The purpose of this study is to answer three basic questions. First of all, is land use change in Khorasan Razavi province significant? Second, do these land use changes affect the quality of surface water resources? And eventually, are these changes in water quality predictable and can be modelled?

Material and methods

Study area and data description

Razavi Khorasan province with an area of 117966 km^2, located between 56° 13′ 40″ to 61° 17′ 07″ eastern longitudes and 33° 51′ 16″ to 37° 42′ 18″ north latitudes in the northeast of Iran (*Fig. 1*).

Figure 1. *Geographical location of Razavi Khorasan Province in Iran*

Two kinds of data applied in this research: land use data and water quality data. To study the dynamics of land use, it is needful to have maps that reflect the status of land cover at various periods. In this study, we used a set of Landsat satellite images from TM (1987), ETM$^+$ (2001) and OLI (2015) sensors to obtain land use maps of Khorasan Razavi Province. For complete coverage of the province in each year, 12 images (Overall 36) were used (*Table 1*). *Figure 2* shows the final image of 1987, which is a combination of 12 Landsat 5 images. For the 2001 image, the combination of 12 Landsat 7 images and for the 2015 image, the combination of 12 Landsat 8 images used (*Figs. 3* and *4,* respectively).

http://www.aloki.hu ● ISSN 1589 1623 (Print) ● ISSN 1785 0037 (Online)
DOI: http://dx.doi.org/10.15666/aeer/1704_81518169

Table 1. *Satellite images applied over the study period (each year 12 images, overall 36)*

Number		Date of frames			Spatial resolution (m)
Row	Path	TM	ETM +	OLI	
35	158	1987/06/27	2001/07/11	2015/06/24	30
36	158	1987/06/27	2001/07/27	2015/06/24	30
37	158	1987/06/27	2001/06/25	2015/06/24	30
34	159	1987/06/18	2001/05/31	2015/06/15	30
35	159	1987/06/18	2001/05/31	2015/06/15	30
36	159	1987/06/18	2001/05/31	2015/06/15	30
34	160	1987/06/25	2001/07/09	2015/06/22	30
35	160	1987/06/25	2001/07/09	2015/06/22	30
36	160	1987/06/25	2001/06/23	2015/06/22	30
34	161	1987/06/16	2001/05/29	2015/06/29	30
35	161	1987/06/16	2001/06/30	2015/06/29	30
36	161	1987/06/16	2001/06/30	2015/06/29	30

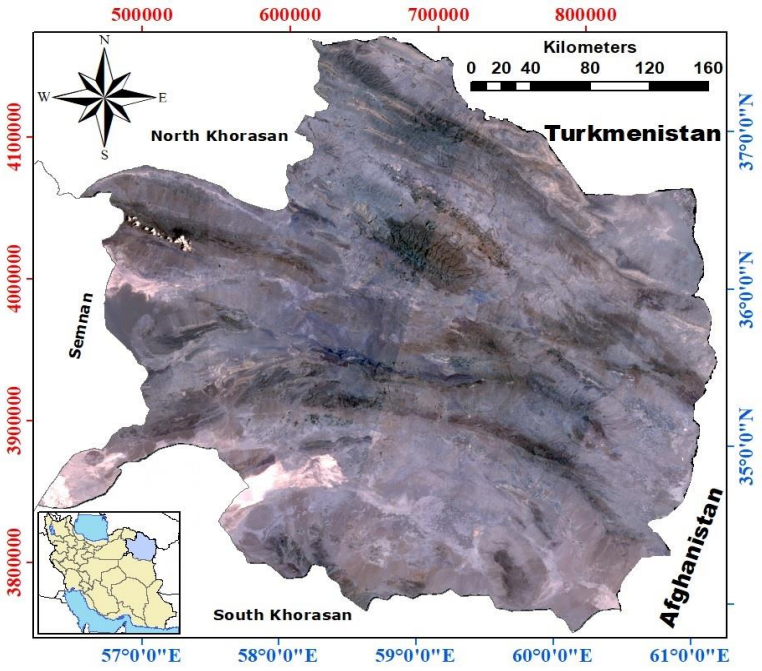

Figure 2. *Image of 1987 (the result of combining 12 Landsat 5 images)*

This study was performed to apply the river-basin based approach to analyze possible statistical and spatial correlations of LULC on the surface water quality. In this province, there are 70 hydrometric stations located at the outlet of the watersheds (*Fig. 5*). For this study, 36 stations with complete data of surface water quality in the years studied selected (*Table 2*). The water quality data for the period of 1987-2015 obtained from the Iran Water Resources Research Organization. This organization is a repository for water quality, quantity, chemical and physical data. Water quality variables, including calcium (Ca), potassium (K), chlorides (Cl), carbonate (CO_3), bicarbonates (HCO_3), magnesium (Mg), sulphate (SO_4), sodium (Na), electrical

http://www.aloki.hu ● ISSN 1589 1623 (Print) ● ISSN 1785 0037 (Online)
DOI: http://dx.doi.org/10.15666/aeer/1704_81518169

conductivity (EC), potential of hydrogen (pH), sodium adsorption ratio (SAR), total dissolved solids (TDS), and total hardness (TH) were chosen. The data is measured on these stations daily. Since the changes in water quality due to land use changes do not change over a day, therefore, the multi-day average of these data was used in this study.

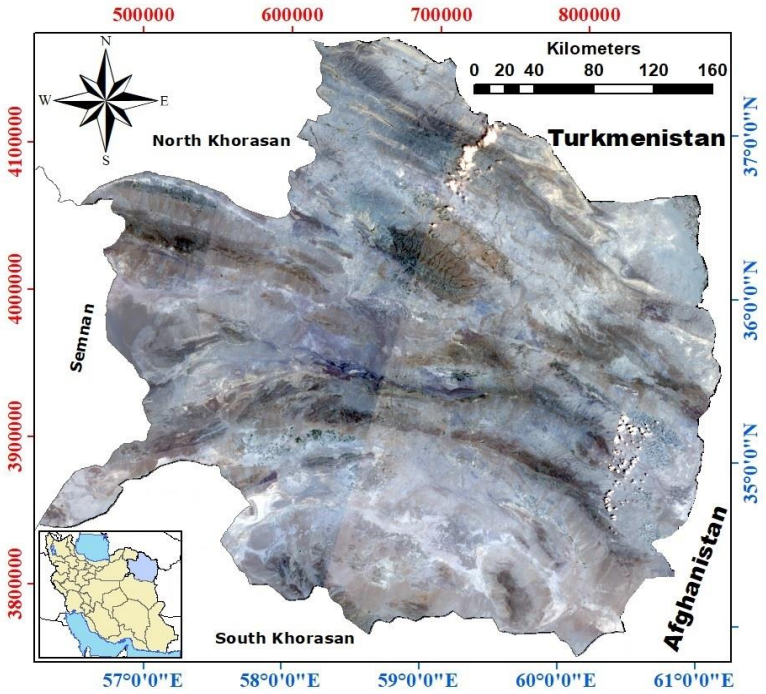

Figure 3. *Image of 2001 (the result of combining 12 Landsat 7 images)*

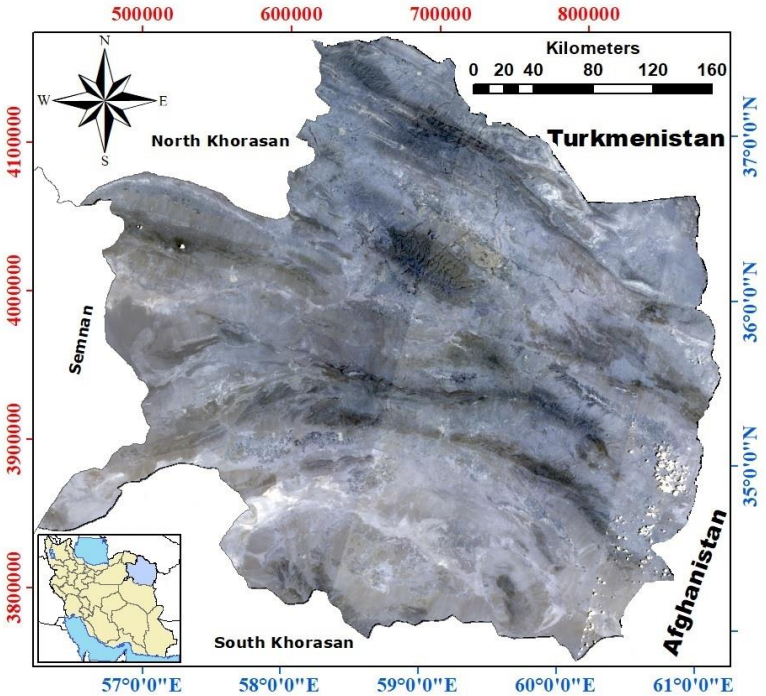

Figure 4. *Image of 2015 (the result of combining 12 Landsat 8 images)*

http://www.aloki.hu ● ISSN 1589 1623 (Print) ● ISSN 1785 0037 (Online)
DOI: http://dx.doi.org/10.15666/aeer/1704_81518169

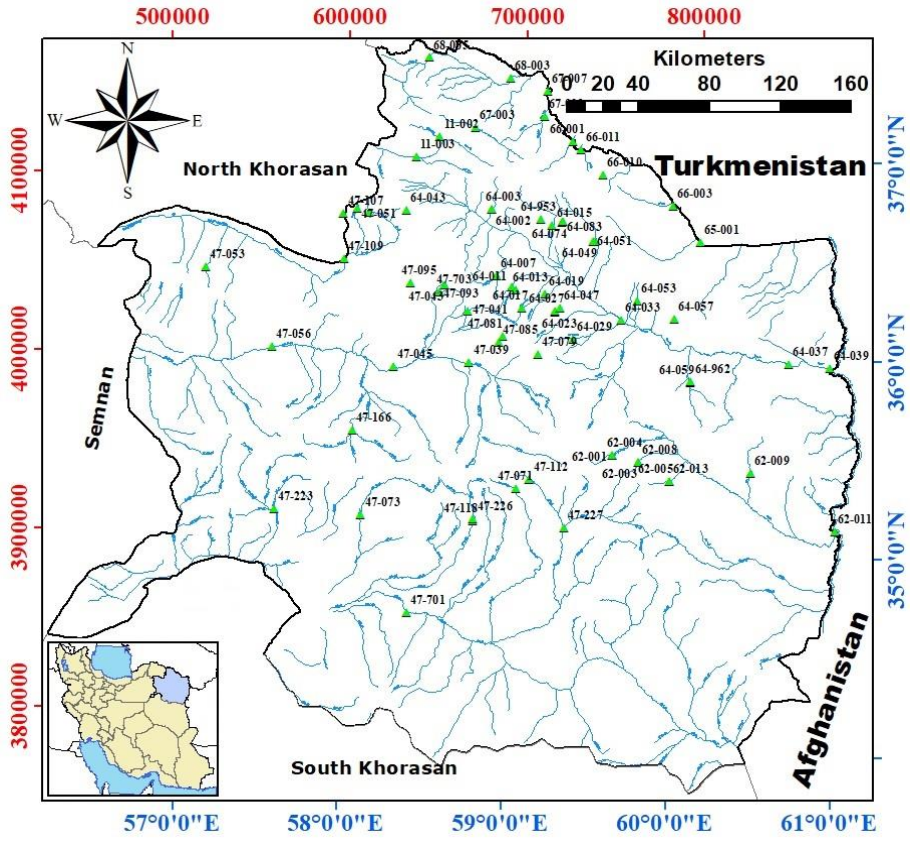

Figure 5. *Location of water quality gauge stations and river network in study area*

Table 2. *Water quality monitoring sites and its characteristics*

Row	Station code	Area (km^2)	Latitude	Longitude	Row	Station code	Area (km^2)	Latitude	Longitude
1	47041	152	36.32250	58.85694	19	64017	68	36.33472	59.19667
2	47043	111	36.45806	58.71194	20	64019	203	36.40028	59.33972
3	47071	76	35.42000	59.13361	21	64023	116	36.30944	59.40278
4	47073	805	35.30444	58.16694	22	64027	74	36.31472	59.40111
5	47079	29	36.09639	59.28889	23	64029	140	36.17167	59.51167
6	47081	53	36.19083	59.07417	24	64033	9074	36.25167	59.64528
7	47085	109	36.16083	59.04694	25	64037	15964	36.00500	60.85611
8	47093	82	36.42361	58.68083	26	64039	16427	35.97528	61.10889
9	47095	491	36.47444	58.49861	27	64043	41	36.84000	58.47750
10	47166	1180	35.73306	58.12083	28	64047	310	36.32750	59.43222
11	62001	273	35.57806	59.73639	29	64049	432	36.65972	59.66611
12	62003	121	35.53639	59.89556	30	64059	235	35.93528	60.23806
13	62009	505	35.46278	60.59361	31	65001	838	36.64111	60.33111
14	64003	240	36.83639	59.02000	32	66001	228	37.16944	59.54167
15	64007	277	36.32222	59.04083	33	66003	847	36.82694	60.16806
16	64011	49	36.44333	59.13306	34	67001	1239	37.30139	59.36694
17	64013	40	36.42694	59.15750	35	67003	81	37.25111	58.92500
18	64015	497	36.75139	59.38667	36	68005	943	37.61500	58.64028

http://www.aloki.hu ● ISSN 1589 1623 (Print) ● ISSN 1785 0037 (Online)
DOI: http://dx.doi.org/10.15666/aeer/1704_81518169

Long-term land use change detection

To find the impact of land use changes on water quality trends, land use changes during the study period investigated (Worrall and Burt, 1999). Using Erdas Imagine 2014 software and RS data, the LULC changes in Razavi Khorasan Province between the years of 1987, 2001 and 2015 were determined in the manner described below.

In the present study, in spite of the positive results of the research experience that used the Maximum likelihood method for categorization (Al-Ahmadi and Hames, 2009), three different supervised classification techniques including Maximum likelihood, Mahalanobis Distance, and Minimum Distance are applied for the classification of Landsat 8 (image of 2015). All non-thermal bands of the images used to generate spectral signatures for classification. For further separating and identifying the phenomena, false-colour images generated (Khoi and Murayama, 2010). These produced images helped to distinguish various types of land use in the study area.

The first step in performing a supervised classification method was to define areas used as training samples for each class. Using random point generation tool in ArcGIS, reference points randomly generated and the accuracy of the classification verified (Jensen, 2015). For this goal, the following steps were employed: first, using a GPS, 200 points were specified for the images of 2015, and after that, the actual ground points compared with the classified maps. Then, by applying GCP (ground control points) and visual interpretation, the overall accuracy assessment of the classified maps of 2015 (three maps that were prepared by the Maximum likelihood, Mahalanobis Distance, and Minimum Distance methods) determined (Schulz et al., 2010). The admitted RMSE between any two dates should not be more than 0.5 pixels (Lunetta and Elvidge, 1998), so the acceptable RMSE between the two images considered less than 0.5 pixels. The results of these three methods were compared and the best method for the classification was chosen.

Following the classification of imagery from the individual years, to specify changes in land use between the intervals (1987–2001 and 2001–2015), Post-Classification Comparison method applied (Erdogan et al., 2015). The post-classification technique supply 'from–to' change information and so, the type of LULC changes that occurred can be easily determined (Yuan et al., 2005). By applying extension X tools in ArcGIS 10.3, the extent of each land use types determined. Also, the transition matrix obtained by cross-tabulating the maps of 1987, 2001, and 2015. This matrix generally reported in the land use change detection studies (Dewan and Yamaguchi, 2009; Monteiro et al., 2011).

The area of watersheds for each of hydrometric stations delineated by applying ArcGIS software and it used as a foundation map for the analysis. Then the layers of the watershed used to clip 1987, 2001, and 2015 LULC coverage allowing calculation of the effective land uses. For analyzing the spatial distribution of various land use category and land cover transformation, the cross-tabulation method performed. Finally, using cross tabulations in ArcGIS software (Spatial Analyst Tools > Zonal > Tabulate Area), maps of land cover classes compared with each other, as the maps of 1987 and 2001, 2001 and 2015 crossed and aspects of changes extracted.

Long-term trend analysis of water quality

At hydrometric stations, water quality data are measured daily. In this study, given the fact that water quality data may change over the course of a few days due to short-

http://www.aloki.hu ● ISSN 1589 1623 (Print) ● ISSN 1785 0037 (Online)
DOI: http://dx.doi.org/10.15666/aeer/1704_81518169

term or local changes, the multi-day average data was used to study the changes in surface water quality. According to *Table 1*, Landsat 5 images were captured in 1987 between June 16th and June 27th (12 days). Similarly, Landsat 7 images were captured in 2001 between May 29 and July 27 (63 days) and Landsat 8 images in 2015 between June 15 and June 29th (15 days). Therefore, the water quality data of the aforementioned days were averaged and used in subsequent calculations.

For example, in 1987, for the TDS parameter, there are 12 data in each sub-basin (12 days). The average of these 12 data was considered as the value of the TDS parameter in 1987 in each sub-basin. This was done for all 36 sub-basins and the TSD parameter value was obtained in 1987 (36 data for the TDS parameter in 1987). Also in 2001, for the TDS parameter, there are 63 data in each sub-basin (63 days). The average of these 63 data was considered as the value of the TDS parameter in 2001 in each sub-basin. This was done for all 36 sub-basins and the TSD parameter value was obtained in 2001 (36 data for the TDS parameter in 2001). The same way, in 2015, for the TDS parameter, there are 15 data in each sub-basin (15 days). The average of these 15 data was considered as the value of the TDS parameter in 2015 in each sub-basin. This was done for all 36 sub-basins and the TSD parameter value was obtained in 2015 (36 data for the TDS parameter in 2015). The same method was used for other parameters. Considering that 13 parameters were evaluated in this study, 1404 numbers were obtained for modelling.

The Mann-Kendall and Seasonal Kendall tests are the most common trend tests in hydro-meteorological studies for non-normal variables. While, the linear regression and analysis of covariance are some of the parametric methods, which is used for normally distributed variables (Zamani et al., 2013; Sheikhy Narany et al., 2017). We assessed the normality of data by means of the Kolmogorov-Smirnov and Shapiro-Wilk tests and then the appropriate method for trend test was chosen (Pratt and Chang, 2012).

Simulation and predicting of water quality data

The null hypothesis was water quality is not related to the land use changes at a watershed scale and the statistical analysis employed to test it. A rejected null hypothesis reveals that "there is a relationship between land use changes and water quality". In SPSS software, Spearman's rank correlation analysis applied to finding the relationships between land use types (as an independent variable) and water quality in the 36 hydrometric stations (as a dependent variable) (Tong and Chen, 2002).

For modelling, at first, the amount of land use area in 36 sub-basins extracted using ArcGIS software from the attribute table of each layer. Since some of the land use does not exist in all sub-basin so in modelling, was not used. For example, there is a poor rangeland area in all 36 sub-basins. According to the maps of 1987, 2001, and 2015, 108 land use values (for poor rangeland) are obtained. These data considered as parameter x and water quality data as a parameter y. But for land use that does not exist in all sub-basin (for example, residential land), the number of data for modelling would be less and may reduce correlation and not be used in modelling.

It is difficult and time-consuming to thoroughly analyze the data of one variable at a time. Because of identifying the relevance of the variables, the multivariate statistics are useful and apply for reducing the number of components in a dataset. Thus, the multivariate linear regression model used to investigate the statistical relationships of land use changes and water quality variables to making model. For this purpose, different types of land use as independent variables (Range, Garden, Residential, etc.)

http://www.aloki.hu ● ISSN 1589 1623 (Print) ● ISSN 1785 0037 (Online)
DOI: http://dx.doi.org/10.15666/aeer/1704_81518169

and changes in each factor of the surface water quality considered as a dependent variable (TDS, EC, pH, etc). After reducing the number of factors, modelling done with fewer parameters and further simulation of surface water quality performed.

By using relationships between land use types in 1987, 2001, and 2015, the linear regression models created and applied for predicting land use types in the future. The time interval between the selected images for studying land use changes for the years 1987, 2001, and 2015 is 14 years. In order to make a more accurate estimate of land use changes, the time interval for the prediction of variations was chosen 14 years, so that the resulting data would be maximally consistent. Then, by using the regression model that provided for predicting water quality, and the area of land use predicted in 2029, each water quality parameter was simulated.

Results

Satellite imagery data were analysed with digital image processing methods and spatial analysis techniques to detect spatial-temporal changes in land use. A multitemporal Landsat satellite dataset formed the basis for the change detection procedure. The overall accuracy assessment of the classified maps of 2015 that were prepared by the Maximum likelihood, Mahalanobis Distance, and Minimum Distance methods was 87.3, 83.7, and 78.5, respectively. So, by applying the supervised maximum likelihood classification technique, the images classified (Schulz et al., 2010). Land use maps of Khorasan Razavi Province for the years 1987, 2001 and 2015 showed in *Figures 6, 7* and *8,* respectively.

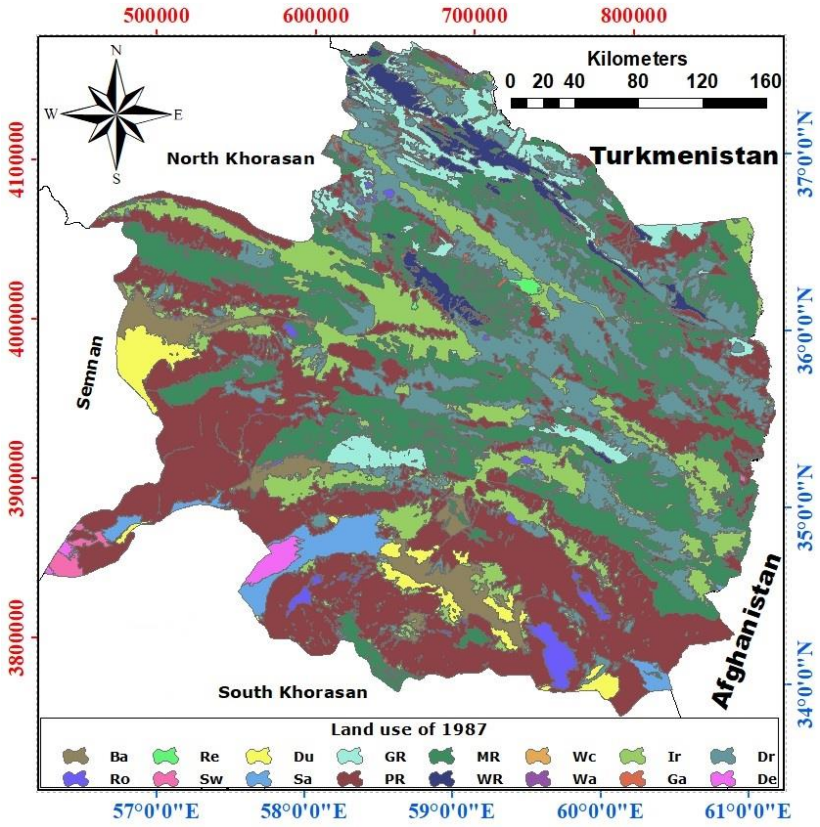

Figure 6. *Land use maps of Khorasan Razavi Province for the year 1987*

http://www.aloki.hu ● ISSN 1589 1623 (Print) ● ISSN 1785 0037 (Online)
DOI: http://dx.doi.org/10.15666/aeer/1704_81518169

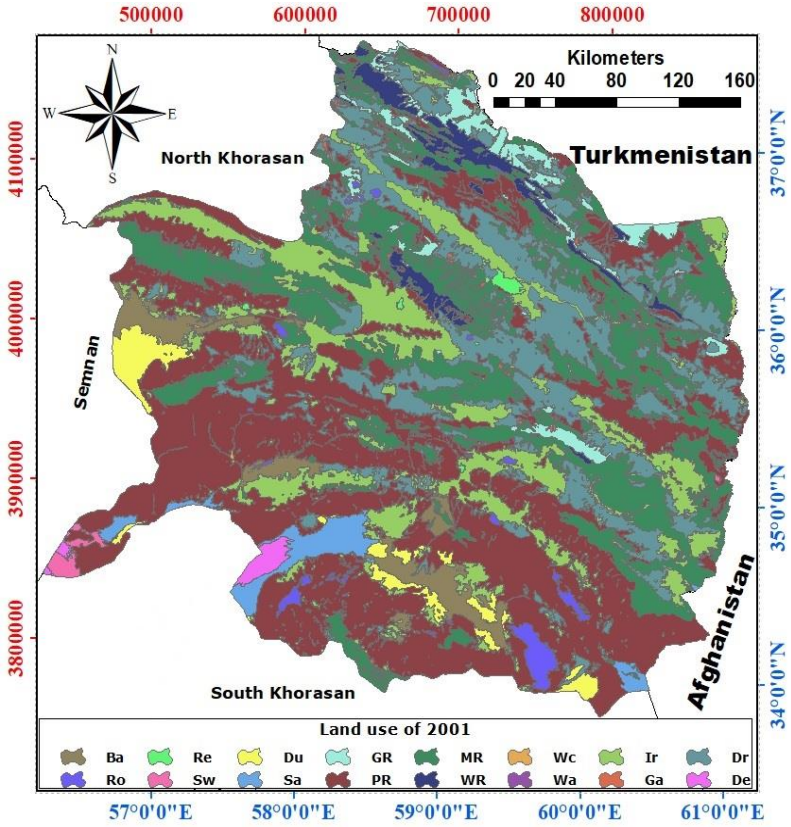

Figure 7. *Land use maps of Khorasan Razavi Province for the year 2001*

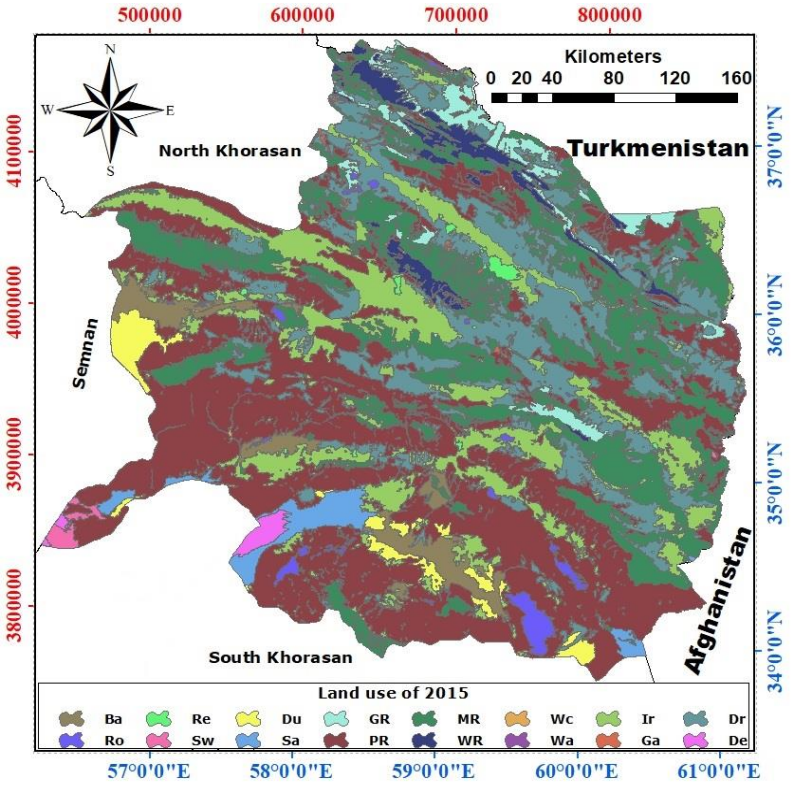

Figure 8. *Land use maps of Khorasan Razavi Province for the year 2015*

http://www.aloki.hu ● ISSN 1589 1623 (Print) ● ISSN 1785 0037 (Online)
DOI: http://dx.doi.org/10.15666/aeer/1704_81518169

In the Khorasan Razavi Province identified sixteen land use classes included: Barren (Ba), Rocky (Ro), Residential (Re), Swamp (Sw), Water (Wa), Dunes (Du), Salt marsh (Sa), Irrigated cultivation (Ir), Garden (Ga), Dry farming (Dr), Desert (De), Good rangeland (GR), Medium rangeland (MR), Poor rangeland (PR), Wooded rangeland (WR), Watercourse (Wc). The coverage of each land use class gave as the area (km^2) and percentage (%) for the years of 1987, 2001 and 2015 (*Table 3*).

Table 3. *Distribution of land use classes in 1987, 2001 and 2015*

Land use	1987		2001		2015	
	(km^2)	(%)	(km^2)	(%)	(km^2)	(%)
Barren	3716.2	3.2	3638.7	3.1	3638.7	3.1
Rocky	1325.9	1.1	1325.9	1.1	1325.9	1.1
Residential	380.5	0.3	477.1	0.4	569.9	0.5
Swamp	403.4	0.3	402.1	0.3	400.4	0.3
Water	1.3	0.0	5.0	0.0	23.8	0.0
Dunes	2470.6	2.1	2437.8	2.1	2318.6	2.0
Salt marsh	2139.9	1.8	2121.9	1.8	2121.9	1.8
Irrigated cultivation	14371.7	12.2	15042.1	12.8	15135.7	12.8
Garden	946.4	0.8	947.3	0.8	947.6	0.8
Dry farming	18229.3	15.5	18243.5	15.5	18606.4	15.8
Desert	567.7	0.5	567.7	0.5	566.7	0.5
Good rangeland	5296.1	4.5	3024.4	2.6	3057.3	2.6
Medium rangeland	27989.7	23.7	24195.1	20.5	22783.8	19.3
Poor rangeland	36879.4	31.3	42330.6	35.9	43295.5	36.7
Wooded rangeland	3093.3	2.6	3052.2	2.6	3019.3	2.6
Watercourse	154.4	0.1	154.4	0.1	154.4	0.1
Total	117966.0	100	117966.0	100	117966.0	100

In Khorasan Razavi Province, between 1987 and 2001, the highest incremental changes in the percentage of land use area were 378, 125 and 115 related to water area, residential and poor range, respectively. The maximum of incremental changes in the area was 5449 km^2 (poor range), 670 km^2 (irrigated cultivation) and 96 km^2 (residential). Also, the maximum decreasing changes in the area were 3794 km^2, 2271 km^2, and 77 km^2 related to medium range, good range, and barren, respectively. In this area, during 2001-2015, the highest incremental changes in the percentage of land use area were 473, 119 and 102 percent related to water area, residential and dry farming, respectively. The maximum of incremental changes in the area were 961 km^2 (poor range), 362 km^2 (dry farming) and 92 km^2 (residential). Also, the highest decreasing changes related to medium range (1411 km^2), dunes (119 km^2) and wooded rangeland (32 km^2), respectively.

In ArcGIS software, using land use maps of Razavi Khorasan province (1987, 2001 and 2015) and the surface of 36 catchments, land use changes in the watershed of hydrometric stations extracted. Thus, a total of 108 land use maps were prepared. Using linear regression models (*Table 4*), land use changes in the years 2029 estimated (*Table 5*).

http://www.aloki.hu ● ISSN 1589 1623 (Print) ● ISSN 1785 0037 (Online)
DOI: http://dx.doi.org/10.15666/aeer/1704_81518169

Table 4. *Equations for predicting land use area. "y" is area (km^2) and "x" is time (year)*

Row	Land use	R^2	Equation
1	Barren	0.7500	y = -2.7659x + 9,199.1016
2	Rocky	1.0000	y = 1,325.9000
3	Residential	0.9999	y = 6.7630x – 13,057.0028
4	Swamp	0.9941	y = -0.1071x + 616.3520
5	Water	0.8697	y = 0.8038x – 1,598.4082
6	Dunes	0.9027	y = -5.4279x + 13,270.1455
7	Salt marsh	0.7500	y = -0.6411x + 3,410.7148
8	Irrigated cultivation	0.8403	y = 27.2867x – 39,750.8704
9	Garden	0.9164	y = 0.0408x + 865.4379
10	Dry farming	0.7781	y = 13.4683x – 8,590.3179
11	Desert	0.7500	y = -0.0357x + 638.6401
12	Good rangeland	0.7390	y = -79.9566x + 163,785.8109
13	Medium rangeland	0.9347	y = -185.9272x + 397,029.9174
14	Poor rangeland	0.8599	y = 229.1433x – 417,680.5879
15	Wooded rangeland	0.9959	y = -2.6445x + 8,346.4889
16	Watercourse	1.0000	y = 154.4400

Table 5. *Estimate of land use changes in study area, 2015-2029 (km^2)*

Land use	Ba	Ro	Re	Sw	Wa	Du	Sa	Ir	Ga	Dr	De	GR	MR	PR	WR	Wc	Total (2015)
Ba	3553	0	2	0	0	0	0	83	0	1	0	0	0	0	0	0	3639
Ro	0	1326	0	0	0	0	0	0	0	0	0	0	0	0	0	0	1326
Re	0	0	570	0	0	0	0	0	0	0	0	0	0	0	0	0	570
Dr	0	0	51	0	1	0	0	151	3	18400	0	0	0	0	0	0	18606
Sw	0	0	0	403	0	0	0	0	0	0	0	0	0	0	0	0	403
Wa	0	0	0	0	24	0	0	0	0	0	0	0	0	0	0	0	24
Ga	0	0	8	0	1	0	0	0	944	0	0	0	0	0	0	0	953
Du	0	0	0	0	0	2284	0	18	0	0	0	0	17	0	0	0	2319
Sa	0	0	0	0	0	0	2104	6	1	0	0	0	0	10	0	0	2122
Ir	10	0	23	0	0	0	0	15089	6	0	0	0	0	0	0	2	15130
PR	0	0	11	0	2	0	0	373	0	70	0	0	42828	2	0	6	43291
De	0	0	0	0	0	0	0	0	0	0	568	0	0	0	0	0	568
GR	0	0	0	0	0	0	0	0	0	0	0	1746	472	839	0	0	3057
MR	0	0	4	0	0	0	0	107	0	127	0	0	4077	18468	0	0	22784
WR	0	0	0	0	0	0	0	0	0	0	0	0	0	40	2979	0	3019
Wc	0	0	0	0	0	0	0	2	0	0	0	0	0	0	0	152	154
Total (2029)	3564	1326	669	403	28	2284	2104	15830	954	18598	568	1746	47394	19360	2979	160	117966

Ba: Barren, Ro: Rocky, Re: Residential, Sw: Swamp, Wa: Water, Du: Dunes, Sa: Salt marsh, Ir: Irrigated cultivation, Ga: Garden, Dr: Dry farming, De: Desert, GR: Good rangeland, MR: Medium rangeland, PR: Poor rangeland, WR: Wooded rangeland, Wc: Watercourse

Because of identifying the relevance of the variables, the multivariate statistics are useful and so apply for reducing the number of components in a dataset. Based on the

http://www.aloki.hu ● ISSN 1589 1623 (Print) ● ISSN 1785 0037 (Online)
DOI: http://dx.doi.org/10.15666/aeer/1704_81518169

findings, among the 16 types of land use, eight items showed the highest correlation. The eight items were Residential, Irrigated cultivation, Garden, Dry farming, Good rangeland, Medium rangeland, Poor rangeland, and Wooded rangeland.

Using Pearson correlation analysis, the correlation coefficient of these eight land use parameters versus water quality parameters were investigated. Results showed in *Table 6*.

Table 6. *Results of Pearson correlation analysis for change in LULC area to change of water quality variables*

Physico-chemicals	Parameters	Re	Ir	Ga	Dr	GR	MR	PR	WR
Ca	Pearson correlation	.866**	.504	.626**	.593**	.689**	.566**	.549**	.430*
	Sig. (2-tailed)	.005	.114	.000	.001	.002	.000	.005	.025
	N	8	11	33	26	17	36	24	27
Mg	Pearson correlation	.902**	.242	.453**	.309	.508*	.356*	.383	.423*
	Sig. (2-tailed)	.002	.474	.008	.125	.038	.033	.065	.028
	N	8	11	33	26	17	36	24	27
Na	Pearson correlation	.853**	.052	.642**	.219	.734**	.239	.393	.294
	Sig. (2-tailed)	.007	.880	.000	.282	.001	.160	.057	.137
	N	8	11	33	26	17	36	24	27
K	Pearson correlation	.761*	.476	.862**	.600**	.629**	.604**	.696**	.367
	Sig. (2-tailed)	.028	.139	.000	.001	.007	.000	.000	.060
	N	8	11	33	26	17	36	24	27
Cl	Pearson correlation	.872**	.042	.662**	.202	.736**	.215	.373	.272
	Sig. (2-tailed)	.005	.903	.000	.321	.001	.208	.073	.170
	N	8	11	33	26	17	36	24	27
CO_3	Pearson correlation	-.291	-.284	-.109	-.144	-.164	-.099	-.161	.019
	Sig. (2-tailed)	.484	.397	.545	.484	.529	.566	.451	.925
	N	8	11	33	26	17	36	24	27
HCO_3	Pearson correlation	.954**	.832**	.747**	.665**	.582*	.657**	.720**	.402*
	Sig. (2-tailed)	.000	.001	.000	.000	.014	.000	.000	.037
	N	8	11	33	26	17	36	24	27
SO4	Pearson correlation	.857**	.246	.539**	.387	.611**	.420*	.446*	.432*
	Sig. (2-tailed)	.007	.467	.001	.051	.009	.011	.029	.024
	N	8	11	33	26	17	36	24	27
EC	Pearson correlation	.888**	.182	.679**	.357	.740**	.379*	.493*	.409*
	Sig. (2-tailed)	.003	.592	.000	.073	.001	.023	.014	.034
	N	8	11	33	26	17	36	24	27
pH	Pearson correlation	-.969**	-.909**	-.839**	-.804**	-.765**	-.783**	-.845**	-.420*
	Sig. (2-tailed)	.000	.000	.000	.000	.000	.000	.000	.029
	N	8	11	33	26	17	36	24	27
TDS	Pearson correlation	.888**	.182	.679**	.357	.740**	.379*	.493*	.409*
	Sig. (2-tailed)	.003	.592	.000	.073	.001	.023	.014	.034
	N	8	11	33	26	17	36	24	27
SAR	Pearson correlation	.641	.018	.500**	.180	.704**	.205	.367	.276
	Sig. (2-tailed)	.087	.958	.003	.378	.002	.231	.078	.164
	N	8	11	33	26	17	36	24	27
Thard	Pearson correlation	.898**	.446	.595**	.506**	.653**	.513**	.520**	.447*
	Sig. (2-tailed)	.002	.169	.000	.008	.004	.001	.009	.019
	N	8	11	33	26	17	36	24	27

Re: Residential, Ir: Irrigated cultivation, Ga: Garden, Dr: Dry farming, GR: Good rangeland, MR: Medium rangeland, PR: Poor rangeland, WR: Wooded rangeland

http://www.aloki.hu ● ISSN 1589 1623 (Print) ● ISSN 1785 0037 (Online)
DOI: http://dx.doi.org/10.15666/aeer/1704_81518169

Using the data in *Table 6* and the linear regression model, each water quality parameter was modelled (*Table 7*). The general formula was the linear equation including "y = (variable*x) + constant". The 'x' parameter value selected based on the highest correlation, in *Table 6*. For example, for predicting the parameter magnesium (Mg) the highest correlation belongs to residential land use ($R^2 = 0.902$), so the area of the residential land use used as 'x'. No models were available to predict the amount of potassium. Then, using the linear regression model was trying to estimate water quality variables in the years 2029 (*Table 8*). Results demonstrated that except calcium (Ca), Carbonate (CO_3) and Bicarbonate (HCO_3), the models estimate all other water quality variables with an acceptable degree of accuracy (P-value < 0.05).

Discussion and conclusions

One of the objectives of this study was to investigate the significance of land use change. The results showed that changes in the direction of a significant decline in good rangeland and a significant increase in poor rangeland that is in agreement with the findings by (Farazmand et al., 2018).

In the present study, three different supervised classification techniques including Maximum likelihood, Mahalanobis Distance, and Minimum Distance are applied for the classification. Results showed that the Maximum likelihood method gave the best results and that is in agreement with results found in other environments by Al-Ahmadi and Hames (2009) and Schulz et al. (2010).

The basic goal of this study was to linking LULC changes to surface water quality variation by using GIS and RS technique. Current methods of estimating water quality in river basins based on land-use patterns are still developing. In this study, we used 36 basins as a case study to consider the relationships between land use and water quality. The relation between water quality and land use types could be different at the various scales of rivers. However, through the analysis of the correlation between water quality variables and various land use types, different land cover patterns that could affect water quality can be recognized.

Table 7. *Linear regression models for physic-chemicals and LULC*

Water quality variables	Model summary				
	Constant	Variable	t	R	Sig.
Ca	2.487	4.521E-5	1.569	0.299	0.129
Mg	2.235	0.000	2.296	0.501	0.036
Na	2.402	0.000	2.815	0.567	0.012
K	-	-	-	-	-
Cl	1.353	0.000	2.143	0.472	0.048
CO_3	0.006	-2.59E-7	-0.782	0.155	0.442
HCO_3	3.557	4.823E-7	0.733	0.131	0.469
SO4	1.973	0.000	3.753	0.559	0.001
EC	691.375	0.058	2.770	0.570	0.014
pH	8.028	-4.22E-7	-2.663	0.664	0.026
TDS	308.124	0.041	2.558	0.772	0.043
SAR	0.499	0.000	2.897	0.587	0.010
Total hardness	29.671	0.003	2.535	0.542	0.018

y = (variable * x) + constant

http://www.aloki.hu ● ISSN 1589 1623 (Print) ● ISSN 1785 0037 (Online)
DOI: http://dx.doi.org/10.15666/aeer/1704_81518169

Table 8. *Estimated surface water quality variables in the year 2029*

Row	Station code	Ca	Mg	Na	K	Cl	CO_3	HCO_3	SO4	EC	pH	TDS	SAR	Total hardness
1	47041	-	2.2	2.4	-	1.4	-	-	2.0	697.7	8.0	312.6	1.5	225.1
2	47043	-	2.3	2.5	-	1.4	-	-	2.1	746.7	8.0	347.3	1.5	232.7
3	47071	-	2.3	2.5	-	1.4	-	-	2.0	724.2	8.0	331.4	1.5	229.2
4	47073	-	2.5	2.7	-	1.6	-	-	2.2	850.6	8.0	420.7	1.7	248.8
5	47079	-	2.3	2.4	-	1.4	-	-	2.0	709.7	8.0	321.1	1.5	227.0
6	47081	-	2.3	2.4	-	1.4	-	-	2.0	709.0	8.0	320.6	1.5	226.9
7	47085	-	2.3	2.5	-	1.4	-	-	2.1	740.7	8.0	343.0	1.5	231.8
8	47093	-	2.3	2.5	-	1.4	-	-	2.0	719.3	8.0	327.8	1.5	228.5
9	47095	-	2.4	2.5	-	1.5	-	-	2.1	770.4	8.0	364.0	1.6	236.4
10	47166	-	2.2	2.4	-	1.4	-	-	2.0	691.4	8.0	308.1	1.5	224.1
11	62001	-	2.5	2.6	-	1.6	-	-	2.2	834.4	8.0	409.2	1.7	246.3
12	62003	-	2.4	2.6	-	1.5	-	-	2.1	788.6	8.0	376.8	1.6	239.2
13	62009	-	2.2	2.4	-	1.4	-	-	2.0	691.4	8.0	308.1	1.5	224.1
14	64003	-	2.3	2.5	-	1.4	-	-	2.0	735.6	8.0	339.4	1.5	231.0
15	64007	-	2.4	2.6	-	1.5	-	-	2.1	793.6	8.0	380.4	1.6	240.0
16	64011	-	2.2	2.4	-	1.4	-	-	2.0	697.8	8.0	312.7	1.5	225.1
17	64013	-	2.3	2.4	-	1.4	-	-	2.0	704.7	8.0	317.6	1.5	226.2
18	64015	-	2.4	2.6	-	1.6	-	-	2.2	810.6	8.0	392.4	1.7	242.6
19	64017	-	2.3	2.5	-	1.4	-	-	2.1	736.4	8.0	340.0	1.5	231.1
20	64019	-	2.5	2.7	-	1.7	-	-	2.3	866.0	8.0	431.6	1.8	251.2
21	64023	-	2.3	2.5	-	1.5	-	-	2.1	751.8	8.0	350.9	1.6	233.5
22	64027	-	2.4	2.5	-	1.5	-	-	2.1	761.5	8.0	357.7	1.6	235.0
23	64029	-	2.4	2.5	-	1.5	-	-	2.1	774.4	8.0	366.8	1.6	237.0
24	64033	-	4.8	5.0	-	3.9	-	-	4.6	2194.4	7.8	1370.6	4.0	457.4
25	64037	-	5.9	6.0	-	5.0	-	-	5.6	2803.3	7.7	1801.1	5.1	551.9
26	64039	-	5.9	6.0	-	5.0	-	-	5.6	2803.3	7.6	1801.1	5.1	551.9
27	64043	-	2.2	2.4	-	1.4	-	-	2.0	691.4	8.0	308.1	1.5	224.1
28	64047	-	2.6	2.8	-	1.7	-	-	2.3	906.7	8.0	460.4	1.8	257.6
29	64049	-	2.4	2.6	-	1.5	-	-	2.1	781.0	8.0	371.5	1.6	238.0
30	64059	-	2.4	2.5	-	1.5	-	-	2.1	760.0	8.0	356.6	1.6	234.8
31	65001	-	2.9	3.0	-	2.0	-	-	2.6	1063.3	8.0	571.1	2.1	281.9
32	66001	-	2.3	2.5	-	1.5	-	-	2.1	756.9	8.0	354.4	1.6	234.3
33	66003	-	2.6	2.7	-	1.7	-	-	2.3	875.1	8.0	438.0	1.8	252.7
34	67001	-	2.5	2.7	-	1.6	-	-	2.3	856.1	8.0	424.5	1.7	249.7
35	67003	-	2.4	2.6	-	1.6	-	-	2.2	812.9	8.0	394.0	1.7	243.0
36	68005	-	2.3	2.5	-	1.5	-	-	2.1	753.5	8.0	352.0	1.6	233.8

Our results proposed that Garden, Irrigated cultivation and Residential land uses can be a parameter affecting the water quality in the study area. Also, results represented that an overview of the relationship between land use and water quality could provide a combination of large-scale investigations and multivariate statistical techniques. The research showed that the concentration of Electricity Conductivity (EC), Sodium Adsorption Ratio (SAR) and Total Hardness (TH) varied in various sub-basins. Results

http://www.aloki.hu ● ISSN 1589 1623 (Print) ● ISSN 1785 0037 (Online)
DOI: http://dx.doi.org/10.15666/aeer/1704_81518169

demonstrated that in 8 out of 13 models can estimate water quality variables with a correlation coefficient of 60%, approximately.

The relevance of land use changes and water quality parameters is complex and site-specific, while the correlation coefficients vary among sub-basin. These results add to the body of research studies accomplished by (Du Plessis et al., 2014) in South Africa, (Wan et al., 2014) in China, (Kibena et al., 2014) in Zimbabwe and (Maimaitijiang et al., 2015) in the USA.

The findings of this research assist policymakers and watershed managers in developing catchment management plans to effectively protect water quality conditions. Therefore, figuring out the effects of changes in LULC is serious for retaining a favourite level of water quality and for restoring water quality in affected areas. However, consequence researches in similar environments can inform that changes in land use and land management practices are initial factors responsible for the variation of receiving water quality. One of the most regular approaches to test these relationships is to develop statistical correlations between water chemistry and current land use in the drainage basins of surface-water sampling points (Wayland et al., 2002). Considering the limitations of this study, the results are only valid in the study area. However, the results and methodology in this study still have implications for water quality management and land use planning in the future for the study area.

Recommendations

The results of this study propose that land use change is one of the main parameters causing water quality changes. It is suggested for making model use additional layers of parameters such as geomorphology, geology, soil, etc. to increase the accuracy and the coefficient of determination. Further study with a better design of spatial and temporal sampling regime may better clarify the complex nature of the relationship between land use and water quality. Future research for linking the finding of hydrological processes with different pollutant transfer processes is needed. Also, to obtain superior data on the linkages between land use patterns and water quality parameters, a water sampling point per sub-basin is required, as well as an increase in monitoring sites, so that information on smaller sub-catchments will be available.

Acknowledgements. The authors would like to thank the Khorasan Razavi Regional Water Authority for supplying funding for this PhD research (Contracted Number KOE-92075). We would further like to thank TAMAB for providing water quality datasets. We also thank the Kerman Graduate University of Advanced Technology for the structural support; and appreciate the classmate for helping with the statistical analyzing the water quality data.

REFERENCES

[1] Abd El-Kawy, O. R., Rød, J. K., Ismail, H. A., Suliman, A. S. (2011): Land use and land cover change detection in the western Nile delta of Egypt using remote sensing data. – Applied Geography 31: 483-494.

[2] Al-Ahmadi, F. S., Hames, A. S. (2009): Comparison of four classification methods to extract land use and land cover from raw satellite images for some remote arid areas, Kingdom of Saudi Arabia. – Journal of King Abdul-Aziz University 20(1): 167-191.

http://www.aloki.hu ● ISSN 1589 1623 (Print) ● ISSN 1785 0037 (Online)
DOI: http://dx.doi.org/10.15666/aeer/1704_81518169

[3] Chen, J., Lu, J. (2014): Effects of land use, topography and socio-economic factors on river water quality in a mountainous watershed with intensive agricultural production in east China. – PLoS One 9. DOI: 10.1371/journal.pone.0102714.
[4] Dabrowski, J. M., de Klerk, L. P. (2013): An assessment of the impact of different land use activities on water quality in the upper Olifants River catchment. – Water SA 39(2): 231-244.
[5] Dewan, A. M., Yamaguchi, Y. (2009): Land use and land cover change in Greater Dhaka, Bangladesh: using remote sensing to promote sustainable urbanization. – Applied Geography 29: 390-401.
[6] Ding, J., Jiang, Y., Fu, L., Liu, Q., Peng, Q., Kang, M. (2015): Impacts of Land use on surface water quality in a subtropical river basin: a case study of the Dongjiang River Basin, South-eastern China. – Water-Open Access Journal 7: 4427-4445.
[7] Ding, J., Jiang, Y., Liu, Q., Hou, Z., Liao, J., Fu, L., Peng, Q. (2016): Influences of the land use pattern on water quality in low-order streams of the Dongjiang River basin, China: a multi-scale analysis. – Science of the Total Environment 551-552: 205-216.
[8] Du Plessis, A., Harmse, T., Ahmed, F. (2014): Quantifying and predicting the water quality associated with land cover change: a case study of the Blesbok Spruit Catchment, South Africa. – Water 6(10): 2946-2968.
[9] Erdogan, N., Nurlu, E., Guvensen, A., Erdem, U. (2015): Land use/land cover change detection for environmental monitoring in Turkey: a case study in Karaburun Peninsula. – Journal of Environmental Protection and Ecology 16: 252-263.
[10] Esterby, S. R. (1996): Review of methods for the detection and estimation of trends with emphasis on water quality applications. – Hydrological Processes 10: 127-149.
[11] Farzamand, A., Arzani, H., Javadi, S. A., Sanadgol, A. A. (2018): Determining the factors affecting rangeland suitability for livestock and wildlife grazing. – Applied Ecology and Environmental Research 17(1): 317-329.
[12] Huang, Z., Han, L., Zeng, L., Xiao, W., Tian, Y. (2016): Effects of land use patterns on stream water quality: a case study of a small-scale watershed in the Three Gorges Reservoir Area, China. – Environmental Science and Pollution Research 23(4): 3943-3955.
[13] Jensen, J. R. (2015): Introductory Digital Image Processing: A Remote Sensing Perspective. 4rd Ed. – Prentice Hall, Upper Saddle River, NJ.
[14] Joorabian Shooshtari, S. H., Hosseini, S. M., Esmaili-Sari, A., Gholamalifard, M. (2012): Monitoring land cover change, degradation, and restoration of the Hyrcanian forests in northern Iran (1977-2010). – International Journal of Environmental Sciences 3: 1038-1056. DOI: 10.6088/ijes.2012030133012.
[15] Khoi, D. D., Murayama, Y. (2010): Forecasting areas vulnerable to forest conversion in the Tam Dao national park region, Vietnam. – Remote Sensing 2: 1249-1272.
[16] Kibena, J., Nhapi, I., Gumindoga, W. (2014): Assessing the relationship between water quality parameters and changes in landuse patterns in the Upper Manyame River, Zimbabwe. – Physics and Chemistry of the Earth, Parts A/B/C 67-69(0): 153-163.
[17] Li, Y. L., Liu, K., Li, L., Xu, Z. X. (2012): Relationship of land use/cover on water quality in the Liao River basin, China. – Procedia Environmental Sciences 13: 1484-1493.
[18] Lunetta, R. S., Elvidge, C. D. (1998): Remote Sensing Change Detection. – Ann Arbor Press, Chelsea, MI.
[19] Maimaitijiang, M., Ghulam, A., Sandoval, J. S. O., Maimaitiyiming, M. (2015): Drivers of land cover and land use changes in St. Louis metropolitan area over the past 40 years characterized by remote sensing and census population data. – International Journal of Applied Earth Observation and Geoinformation Part B 35: 161-174.
[20] Mello, K., Valente, R., Randhir, T., Dos Santos, A., Alberto Vettorazzi, C. (2018): Effects of land use and land cover on water quality of low-order streams in Southeastern Brazil: watershed versus riparian zone. – Catena 167: 130-138.

http://www.aloki.hu ● ISSN 1589 1623 (Print) ● ISSN 1785 0037 (Online)
DOI: http://dx.doi.org/10.15666/aeer/1704_81518169

[21] Minaei, M., Kainz, W. (2016): Watershed land cover/land use mapping using remote sensing and date mining in Gorganrood, Iran. – International Journal of Geo-Information 5: 57. DOI: 10.3390/ijgi5050057.
[22] Miserendino, M. L., Casaux, R., Archangelsky, M., Di Prinzio, C. Y., Brand, C., Kutschker, A. M. (2011): Assessing land-use effects on water quality, in-stream habitat, riparian ecosystems and biodiversity in Patagonian northwest streams. – Science of the Total Environment 409(3): 612-624.
[23] Monteiro, A. T., Fava, F., Hiltbrunner, E., Marianna, G. D., Bocchi, S. (2011): Assessment of land cover changes and spatial drivers behind loss of permanent meadows in the lowlands of Italian Alps. – Landscape and Urban Planning 100: 287-294.
[24] Namugize, J., Jewitt, G., Graham, M. (2018): Effects of land use and land cover changes on water quality in the uMngeni river catchment, South Africa. – Physics and Chemistry of the Earth, Parts A/B/C 105: 247-264.
[25] Pratt, B., Chang, H. (2012): Effects of land cover, topography, and built structure on seasonal water quality at multiple spatial scales. – Journal of Hazardous Materials 209: 48-58.
[26] Rafiee, R., Mahiny, A. S., Khorasani, N. (2009): Assessment of changes in urban green spaces of Mashad city using satellite data. – International Journal of Applied Earth Observation and Geoinformation 11: 431-438.
[27] Schulz, J. J., Cayuela, C., Echeverria, C., Salas, J., Rey Benayas, J. M. (2010): Monitoring land cover change of the dryland forest landscape of Central Chile 1975-2008. – Applied Geography 30: 436-447.
[28] Shalaby, A., Tateishi, A. (2007): Remote sensing and GIS for mapping and monitoring land cover and landuse changes in the north-western coastal zone of Egypt. – Applied Geography 27: 28-41.
[29] Sheikhy Narany, T., Zaharin Aris, A., Sefie, A., Keesstra, S. (2017): Detecting and predicting the impact of land use changes on groundwater quality, a case study in Northern Kelantan, Malaysia. – Science of the Total Environment 599-600: 844-853.
[30] Shi, P., Zhang, Y., Li, Z., Li, P., Xu, G. (2017): Influence of land use and land cover patterns on seasonal water quality at multi-spatial scales. – Catena 151: 182-190.
[31] Tong, S. T. Y. (1990): The hydrologic effects of urban land use: a case study of the Little Miami River Basin. – Landscape & Urban Planning 19: 99-105.
[32] Tong, S. T. Y., Chen, W. (2002): Modelling the relationship between land use and surface water quality. – Journal of Environmental Management 66: 377-393.
[33] Vörösmarty, C. J., McIntyre, P. B., Gessner, M. O., Dudgeon, D., Prusevich, A., Green, P., Glidden, S., Bunn, S. E., Sullivan, C. A., Liermann, C. R. (2010): Global threats to human water security and river biodiversity. – Nature 467: 555-561.
[34] Walling, D. E., Fang, D. (2003): Recent trends in the suspended sediment loads of the world's rivers. – Global and Planetary Change 39: 111-126.
[35] Wan, R., Cai, S., Li, H., Yang, G., Li, Z., Nie, X. (2014): Inferring land use and land cover impact on stream water quality using a Bayesian hierarchical modeling approach in the Xitiaoxi River Watershed, China. – Journal of Environmental Management 133(0): 1-11.
[36] Wayland, K. G., Hyndman, D. W., Boutt, D., Pijanowski, B. C., Long, D. T. (2002): Modeling the impact of historical land uses on surface-water quality using groundwater flow and solute-transport models. – Lakes & Reservoirs: Research and Management 7: 189-199.
[37] Withers, P. J., Jarvie, H. P. (2008): Delivery and cycling of phosphorus in rivers: a review. – Science of the Total Environment 400: 379-395.
[38] Worrall, F., Burt, T. P. (1999): The impact of land-use change on water quality at the catchment scale: the use of export coefficient and structural models. – Hydrology 221: 75-90.

http://www.aloki.hu ● ISSN 1589 1623 (Print) ● ISSN 1785 0037 (Online)
DOI: http://dx.doi.org/10.15666/aeer/1704_81518169

[39] Wu, Q., Li, H., Wang, R., Paulussen, J., He, Y., Wang, M., Wang, B., Wang, Z. (2006): Monitoring and predicting land use change in Beijing using remote sensing and GIS. – Landscape and Urban Planning 78: 322-333.
[40] Yuan, E., Kali Sawaya, K. E., Loeffelholz, B. C., Bauer, M. E. (2005): Land cover classification and change analysis of the Twin Cities (Minnesota) Metropolitan Area by multi-temporal Landsat remote sensing. – Remote Sensing Environment 98: 317-328.
[41] Zamani, M., Sadoddin, A., Garizi, A. Z. (2013): Assessing land cover/land use change and its impacts on surface water quality in the Ziarat catchment, Golestan Province-Iran. – Hydrology Current Research - Open Access Journal 4: 1-5.
[42] Zhou, T., Wu, J., Peng, S. (2012): Assessing the effects of landscape pattern on river water quality at multiple scales: a case study of the Dongjiang River watershed, China. – Ecological Indicators 23: 166-175.

http://www.aloki.hu ● ISSN 1589 1623 (Print) ● ISSN 1785 0037 (Online)
DOI: http://dx.doi.org/10.15666/aeer/1704_81518169

SOME CHEMICAL, NUTRITIONAL AND MINERAL PROPERTIES OF DRIED JUNIPER (*JUNIPERUS DRUPACEA* L.) BERRIES GROWING IN TURKEY

ODABAŞ-SERİN, Z.* – BAKIR, O.

Kahramanmaraş Sütçü Imam University, Faculty of Forestry, Department of Forest Industry Engineering, 46040 Kahramanmaraş, Turkey

**Corresponding author*
e-mail: zehra@ksu.edu.tr; phone: +90-344-300-1780; fax: +90-344-300-1712

(Received 18th Feb 2019; accepted 8th Apr 2019)

Abstract. Berries of *Juniperus drupacea* L. are important non-wood product used in traditional pekmez (fruit concentrate) production in Turkey. In this article, some chemical, nutritional and mineral properties of dried mature *J. drupacea* berries are reported. The materials were collected from Kahramanmaraş and Adana Provinces (Turkey). The results are given in the order of Kahramanmaraş and Adana; total dry matter 92.89 and 93.30%, water soluble dry matter 62.40 and 57.07%, protein 2.06 and 3.74%, lipid 5.49 and 3.84 g/100g, pH 5.53 and 5.65, titretable acidity 0.38 and 0.52%, K 14.5 and 17.3 g/kg, Ca 890.5 and 794.7 mg/kg, Na 67.0 and 68.1 mg/kg, Mg 439.2 and 543.6 mg/kg, Fe 33.8 and 65.8 mg/kg, Cu 4.4 and 5.5 mg/kg, Zn 16.5 and 18.1 mg/kg and finally Mn 4.7 and 5.1 mg/kg. In addition, holocellulose (carbohydrate) was determined as 14.29 and 16.01%, lignin (phenolic compounds) as 16.94 and 18.98% and ash (inorganic constituents) content as 4.00 and 3.38%. The soluble content of toluen/acetone/ethyl alcohol, hot water and cold water for Kahramanmaraş samples were 31.18, 67.08 and 60.74%. They were 37.56, 63.36 and 55.81% for specimens from Adana. The berries from Kahramanmaraş showed higher lipid, soluble solid, Ca and ash contents than those from Adana.
Keywords: *Syrian juniper, refractometer, protein, lipid, functional foods*

Introduction

One of the juniper species in Turkey is *J. drupacea* which naturally grows in Mediterranean countries such as Turkey, Syria, Lebanon and Greece. Within this general distribution area, in the mountainous parts of the Eastern and Central Mediterranean regions of Turkey, it has a significant distribution between 600 and 1750 m altitude (Gültekin, 2014). It covers 958.423 ha which is 4.29% of the total forest area of country (OGM, 2015).

In Turkey, from the fruits of *J. drupacea* "pekmez" (fruit concentrate) is produced traditionally by the local people and used to treat asthma and bronchitis. It is an important foodstuff for people with high energy needs, mainly consumed in the winter months (Seca et al., 2015; Güneş et al., 2017).

Functional nutritional science has been very important nowadays. As average life expectation and healthcare costs rice, the people has investigated to become healthier and improve the quality of life. Functional foods may be "an essential macronutrient, or an essential micronutrient. While a macronutrient (e.g. carbohydrates, fats, and proteins) must be ingested in large amounts in human diet, a micronutrient (e.g. vitamins or minerals) must be consumed in certain trace amounts. Bioactive compounds are considered as the source of functional food effectiveness. Bioactive compounds can be categorized as "phenolic compounds, proteins, peptides and lipids, and carbohydrates (Martirosyan and Singh, 2015).

http://www.aloki.hu ● ISSN 1589 1623 (Print) ● ISSN 1785 0037 (Online)
DOI: http://dx.doi.org/10.15666/aeer/1704_81718178

Leaves, fruits, seeds and wood parts of junipers contain considerable chemical components. So, it takes important places in medicine, pharmacology and food industry. Juniper species are very miscellaneous and have been subject of researches by many scientists for it's oil, protein, reduced sugar, mineral, essential oil, phenolic compound content and antioxidant - antimicrobial activity properties (Nasri et al., 2011; Jalal et al., 2014; Hosseinihashemi, 2017; Salamon et al., 2017; Miceli et al., 2018).

Although there are many works about *J. drupacea* fruit concentrate (Özdemir et al., 2004; Akıncı et al., 2004; Kocakulak, 2007; İzgi, 2011), less studies related to its dried fruit physical, chemical and mineral features are provided with. In the present study, some chemical (holocellulose, lignin, toluene-acetone-ethyl alcohol solubility, hot-cold water solubility and ash content), nutritional (total dry matter, water soluble dry matter, protein, lipid, pH, titretable acidity) and mineral (K, Ca, Na, Mg, Fe, Cu, Zn ve Mn) components of dried mature fruit are identified.

Materials and methods

Materials

In this study, mature ripe juniper berries obtained from Kahramanmaraş-Andırın (KM) and Adana-Kozan (AA) in Eastern Mediterranean Region were used as experimental materials (*Figure 1*). The samples were collected in 2014, February-March and the information related to the places samples taken are given in *Table 1* and *Figure 2*. Thirty berries were collected from each of the 30 randomly selected trees and a total of 900 berries were collected in each province. The collected samples were then dried in the laboratory environment under open air conditions. The dried samples were broken and seeds removed, later the remaining parts were grinded in the Willey-mill, sieved and preserved in glass jars.

Methods

The methods used to identify the main chemical components of the juniper berry: Holocellulose, lignin and ash content was determined according to Wise's chlorite method (Wise and Karl, 1962), TAPPI T222om-02 (2002) and TAPPI T211om-02 (2002) standards, respectively. Solubility properties, including toluene-acetone-ethyl alcohol (4:1:1, w/w) and cold - hot water solubilities were determined according to TAPPI T204cm-97 (1997) and TAPPI T207cm-99 (1999), respectively.

Methods for determining nutritional properties of *J. drupacea* berries are: Total dry matter was determined by drying the samples to a constant weight in a 65^{o}C oven (AOAC, 1990). Soluble solid and pH values of the extract from the berries were determined by using a Hanna HI96801 refractometer and a pH meter (IFJU, 1968a, 1968b). Protein was calculated from the percentage of nitrogen found by using the Kjeldahl method (TS4895 EN ISO3188). Lipid content and titratable acidity of the samples were determined by the soxhlet extraction method, with hexane (AOAC, 1984) and by the titration method with, 0.1 N NaOH (IFJU, 1968c), respectively. All chemical analysis results were calculated relative to oven dry sample weight.

To determine the mineral components of juniper berry the samples were burned with HNO_3 (65%) and H_2O_2 (35%) solution in a microwave. Then, the absorbance of the extract was determined with the Atomic Absorbance Spectrophotometer, Perkin Elmer

http://www.aloki.hu ● ISSN 1589 1623 (Print) ● ISSN 1785 0037 (Online)
DOI: http://dx.doi.org/10.15666/aeer/1704_81718178

Optima 2100DV ICP-OES coupled with AS93 auto sampler. The mineral content was calculated with a standard curve.

To evaluate the significant differences between the mean values of each of the properties, independent-samples t-test analyses (ISTTA) were used. All statistical analyses were conducted by means of SPSS Statistics software, and the results were considered significant at $p \leq 0.05$.

Figure 1. *Juniperus drupacea tree, leaf and fruit (Kocakulak, 2007)*

Table 1. *Information for locations where juniper berries collected*

Location	Latitude	Longitude	Altitude (m)
Kahramanmaraş-Andırın	37º45'	36º42'	943
Adana-Kozan	37º38'	35º50'	895

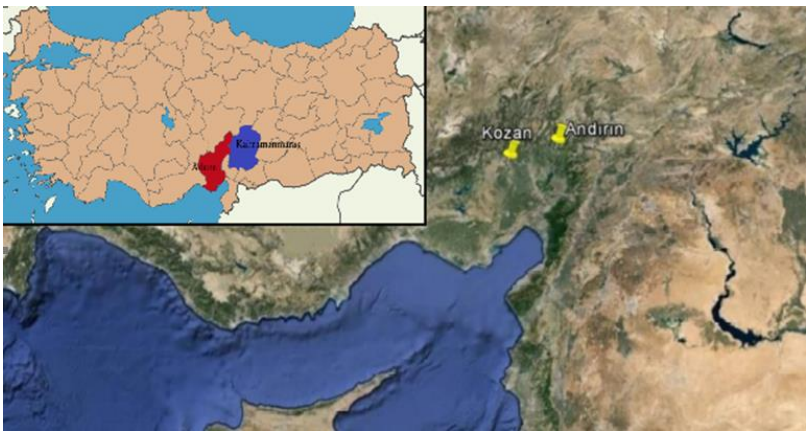

Figure 2. *Geographical location of the study area in Turkey*

Results and discussion

The main chemical, nutritional and mineral composition of *J. drupacea* dried berries are shown in *Tables 1, 2 and 3*, respectively. In order to compare the provided results, the properties of juniper berries from Akseki-Antalya (AY) from Western Mediterranean Region are also shown in *Table 2* and *Table 3*. In addition to these, related properties of carob bean and raisins are given in the same tables, respectively.

http://www.aloki.hu ● ISSN 1589 1623 (Print) ● ISSN 1785 0037 (Online)
DOI: http://dx.doi.org/10.15666/aeer/1704_81718178

Table 2. *Dried J. drupacea berries' main chemical components and their ratios*

Component (%)	Determination			Literature	
	KM berries	AA berries	Mean	Softwoods (Kırcı, 2006)	Hardwoods (Kırcı, 2006)
Holocellulose	14.29 (0.38) b	16.01 (0.31) a	15.15	63 - 70	72 - 82
Lignin	16.94 (0.40) b	18.98 (0.33) a	17.96	25 - 32	18 - 26
Toluene/acetone/alcohol solubility	31.18 (0.32) b	37.56 (0.45) a	34.37	1 - 5.8	1 - 6.2
Hot water solubility	67.08 (0.14) a	63.36 (0.37) b	65.22	1 - 5	1 - 8
Cold water solubility	60.74 (0.26) a	55.81 (0.41) b	58.28	0.5 - 4	0.2 - 4
Ash	4.00 (0.25) a	3.38 (0.05) b	3.69	0.2 - 0.5	0.2 - 0.7

*KM= Kahramanmaraş, AA= Adana, AY= Antalya
**Values given in parentheses indicate (±) standard deviations
***Different letters in the same line represent statistical differences at the 95% confidence level

Table 3. *Nutritional properties of J. drupacea dried berries*

Content	Determination			Literature	
	KM berries	AA berries	Mean	AY Berries (Akıncı et al., 2004)	Carob bean (Karcıer and Artık, 1995)
Total dry matter (%)	92.89 (0.11) b	93.30 (0.00) a	93.10	76.57	91.60
Soluble solid (%)	62.40 (0.11) a	57.07 (0.09) b	59.74	33.68	64.68
Protein (%)	2.06 (0.04) b	3.74 (0.03) a	2.90	2.45	4.05
Lipid (%)	5.49 (0.09) a	3.84 (0.03) b	4.67	4.28	-
pH	5.53 (0.03) b	5.65 (0.00) a	5.59	5.77	5.53
Titretable acidity (%, SSA)	0.38 (0.02) b	0.52 (0.01) a	0.45	-	0.72

*KM: Kahramanmaraş, AA: Adana, AY: Antalya
**Values given in parentheses indicate (±) standard deviations
***Different letters in the same line represent statistical differences at the 95% confidence level

Chemical and nutritional properties of J. drupacea dried berries

The major chemical components of natural lignocellulosic materials are holocellulose (total carbohydrate), lignin (phenolic compounds), ash (total inorganic constituents) and a very small fraction of so-called extractives (Fengel and Wegener, 1989; Chen, 2014). All these substances have an important place in human nutrition.

The average results and standard deviations of main chemical components of juniper berry from KM and AA are given in *Table 2*, the results of nutritional properties are given in *Table 3*. Juniper berry is a hard nut and cannot be consumed as a fresh fruit. So, general chemical properties of main components for softwoods and hardwoods are also given in *Table 2*.

As indicated in *Table 2*, the holocellulose mean ratio for juniper berry is 15.15% and this value is quite less than that in both softwood and hardwoods. With regard to lignin amount juniper samples (17.96%), it showed hardwood characteristics. Phenolic substances have important contributions to human health. These compounds have been reported to play an effective role in preventing cancer and cardiovascular diseases by preventing free radical formation in the body (Gil et al., 2000). The results also showed that fruits from AA junipers have more lignin (18.98%), in other words, more phenolic compounds than those from KM (16.94%).

It is possible to remove waxes, oils, resins, photosterols, non-volatile hydrocarbons, low molecular weight carbohydrates, salts and other water soluble components present

http://www.aloki.hu ● ISSN 1589 1623 (Print) ● ISSN 1785 0037 (Online)
DOI: http://dx.doi.org/10.15666/aeer/1704_81718178

in the sample with neutral organic solvents (TAPPI T204cm-97, 1997). According to the results obtained, the solubility content of toluene/acetone/ ethyl alcohol (34.37%) and the hot water (65.22%) - cold water (58.28%) of the samples were found to be fairly high when compared to softwood and hardwoods.

The ash content of juniper berry samples was determined as 3.69%. This value found to be 2.51 g/100g for Antalya samples, 2.40% for raisins and 2.5% for carob bean (Karkacıer and Artık, 1995; Akıncı et al., 2004; Kalkan et al., 2012). According to all these values, the amount of ash in KM and AA junipers berry found to be rather high.

When nutritional property mean values in *Table 3* compared, soluble solid content was 62.40% for the berries from KM and 57.07% for AA samples. This value has been reported as 33.68% for AY juniper berry and 64.68% for carob bean (Karkacıer and Artık, 1995; Akıncı et al., 2004). The highness of this value is desirable. Accordingly, KM and AA soluble dry matter is 77.4% higher than AY specimen, and shows similarity to that from carob fruit.

Considering *Table 3*, the protein (3.74%), pH (5.65) and titratable acidity (0.52%) values of AA samples were higher than those for samples from KM as 2.06%, 5.53 and 0.38%, respectively. The lipid amount of KM samples was found to be 43% higher than that from AA. According to data from literature survey, the value for protein was found as: AY juniper berries 2.45%, *J. communis* L. berries 4.28% and carob bean 4.05% (Karcıer and Artık, 1995; Akıncı et al., 2004; Bacém, 2018). According to results from the present work, titretable acidity value for juniper berries (0.45%SSA) is more acidic than carob bean (0.72%SSA).

Mineral composition of J. drupacea dried berries

Minerals have important place in human nutrition. The importance of these minerals, also known as trace elements, has been well understood in recent years, since when missed, causes diseases and major disorders in the human body (Bittencourt, 2018).

Mineral content and their ratio in KM and AA juniper berries are given in *Table 4*.

Table 4. *Mineral composition of J. drupacea dried berries*

Mineral composition	Determination			Literature	
	KM berries	AA berries	Mean	AY berries (Akıncı et al., 2004)	Raisins (Kalkan et al., 2012)
K (g/kg)	14.5 (b)	17.3 (a)	**15.9**	10.0	7.5
Ca (mg/kg)	890.5 (a)	794.7 (b)	**842.6**	1063.0	500.0
Na (mg/kg)	67.0 (b)	68.1 (a)	**67.6**	84.8	20.0
Mg (mg/kg)	439.2 (b)	543.6 (a)	**491.4**	477.0	70.0
Fe (mg/kg)	33.8 (b)	65.8 (a)	**49.8**	15.4	18.8
Cu (mg/kg)	4.4 (b)	5.5 (a)	**4.95**	29.2	3.2
Zn (mg/kg)	16.5 (b)	18.1 (a)	**17.3**	13.9	2.2
Mn (mg/kg)	4.7 (b)	5.1 (a)	**4.9**	9.0	-

*KM: Kahramanmaraş, AA: Adana, AY: Antalya

**Letters in parentheses represent statistical differences at the 95% confidence level

Results showed that the amount of K (17.3 g/kg), Na (68.1 mg/kg), Mg (543.6 mg/kg), Fe (65.8 mg/kg), Cu (5.5 mg/kg), Zn (18.1 mg/kg) ve Mn (5.1 mg/kg) from AA are higher than those in KM samples. In contrast, only the amount of Ca (890.5 mg/kg) in KM berries is higher than that in AA (794.7 mg/kg).

http://www.aloki.hu ● ISSN 1589 1623 (Print) ● ISSN 1785 0037 (Online)
DOI: http://dx.doi.org/10.15666/aeer/1704_81718178

When the mean values of the results considered, KM and AA berries contain more K, Mg, Fe and Zn than AY berries and raisins. Inci et al. (2016) reported that *Juniperus communis* berries contained 61.2 g/kg K, 1.90 mg/kg Mg, 80.12 mg/kg Fe, 15.31 mg/kg Mn, 18.80 mg/kg Zn and 19.94 mg/kg Cu. When we compared berries of *J. drupacea* and *J. communis*, it is seen that *J. communis* berries has a higher mineral content.

Conclusion

When the data obtained within the scope of the study considered, it can be mentioned that juniper berries collected from Kahramanmaras Province, found to be more oily, with more soluble solids, extractive matter (hot and cold water solubility), ash and calcium content than those from Adana Province samples. However, dried berries from Adana Province contains more holocellulose, lignin, protein and mineral matters (K, Na, Mg, Fe, Cu, Zn, Mn).

When the data obtained within the scope of the study considered, it can be mentioned that juniper berry is a good source of minerals. It contains especially a fine ratio of Fe.

Acknowledgements. This study was supported by Kahramanmaraş Sütçü İmam University, BAP Department with project number 2015 / 2-33LAP.

REFERENCES

[1] Akıncı, İ., Özdemir, F., Topuz, A., Kabas, O., Çanakçı, M. (2004): Some physical and nutritional properties of Juniperus drupacea fruits. – J of Food Eng. 65: 325-331.
[2] AOAC (1984): Official Method. – 14th ed. Arlintong, VA, AOAC.
[3] AOAC (1990): Official Method. – 17th ed. Washington, DC, USA: Association of Official Analytical Chemists.
[4] Bacém, I. A. R. (2018): Composição química e atividade biológica de bagas do Zimbro (Juniperus communis L.). – Master Thesis, Instituto Politécnico de Bragança, 67p, Bragança.
[5] Bittencourt, J. A. (2018): The power of carbohydratesi proteins, and lipids. – Fourth Edition, CreateSpace.
[6] Chen, H. (2014): Biotechnology of lignocellulose theory and practice. – ISBN: 978-94-007-6897-0, Springer, 510p.
[7] Fengel, G., Wegener, G. (1989): Wood chemistry, ultrastructure, reactions. – Walter de Gruyter. Berlin, New York, 611pp.
[8] Gil, M. I., Tomas-Barberan, F. A., Hess-Pierce, B., Holcroft, D. M., Kader, A. A. (2000): Antioxidant activity of pomegranate juice and its relationship with phenolic composition and processing. – J Agric Food Chem. 48: 4581-4589.
[9] Gültekin, H. C. (2014): Plant production techniques of important forest trees (conifers, leafy trees). – Republic of Turkey Ministry of Forestry and Water Management, Forest Management, Poplar and Rapidly Growing Forest Trees Research Institute. Publication Nr.271, İzmit, Turkey, 337pp.
[10] Güneş, S., Savran, A., Paksoy, A. Y., Koşar, M., Çakılcıoğlu, U. (2017): Ethnopharmacological survey of medicinal plants in Karaisalı and its surrounding (Adana-Turkey). – J of Herb Med. 8: 68-75.

http://www.aloki.hu ● ISSN 1589 1623 (Print) ● ISSN 1785 0037 (Online)
DOI: http://dx.doi.org/10.15666/aeer/1704_81718178

[11] Hosseinihashemi, S. K., Dadpour, A., Lashgari, A. (2017): Antioxidant activity and chemical composition of Juniperus excelsa ssp. polycarpos wood extracts. – Nat Prod Res. 31(6): 681-685.
[12] IFJU Analyses (1968a): Determination of soluble solids. – Nr.8. 21p.
[13] IFJU Analyses (1968b): Determination of measurement of pH value. – Nr.11, 2p.
[14] IFJU Analyses (1968c): Determination of titratable acid. – Nr.3, 4p.
[15] Inci, H., Ozdemir, G., Şengül, A. Y., Söğüt, B., Nursoy, H., Şengül, T. (2016): Using juniper berry (Juniperus communis) as a supplement in Japanese quail diets. – R Brasç Zootec. 45(5): 230-235.
[16] İzgi, N. (2011): Determination of composition of homemade andız molasses, rheological characteristics, antioxidant and antimicrobial activities. – Namık Kemal University, Graduate School of Natural and Applied Sciences, Department of Food Engineering, MSc Thesis, Tekirdağ, Turkey.
[17] Jalal, F., Wassim, A., Issam, H. A. M. (2014): Chemical composition of essential oil extracted from syrian juniper berries (Juniperus drupacea L.). – Int. J of Agric Res. 9(3): 158-163.
[18] Kalkan, N. N., Öz, M. H., Cangı, R. (2012): Determination of some physical-chemical properties and production techniques of Saruç. – J of Food and Feed Sci - Tech. 12: 11-18.
[19] Karkacıer, M., Artık, N. (1995): Determination of physical properties, chemical composition and extraction conditions of carob bean (Ceratonica siliqua L.). – The J of Food 20(3): 131-136.
[20] Kırcı, H. (2006): Pulp industry lecture notes. – Karadeniz Technical University, Forest Faculty Publication, Trabzon, Turkey.
[21] Kocakulak, E. (2007): Researches on the essential oils of Juniperus drupacea Lab. – Gazi University, Institute of Health Sciences, PhD Thesis, Ankara, Turkey.
[22] Martirosyan, D. M., Singh, J. (2015): A new definition of functional food by FFC: what makes a new definition unique? – Funct Foods in Health and Dis. 5(6): 209-223.
[23] Miceli, N., Marino, A., Köroğlu, A., Cacciola, F., Dugo, P., Mondello, L., Taviano, M. F. (2018): Comparative study of the phenolic profile, antioxidant and antimicrobial activities of leaf extracts of five Juniperus L. (Cupressaceae) taxa growing in Turkey. – Nat Prod Res. 1-6.
[24] Nasri, N., Tlili, N., Elfalleh, W., Cherif, E., Ferchichi, A., Khaldi, A., Triki, S. (2011): Chemical compounds from Phoenician juniper berries (Juniperus phoenicea). – Nat Prod Res. 25(18): 1733-1742.
[25] OGM (2015): The presence of Turkey's forests-2012. – Republic of Turkey General Directorate of Forestry, Ankara, Turkey, 31pp.
[26] Özdemir, F., Topuz, A., Gölükçü, M., Şahin, H. (2004): A study on improving process techniques of Juniperis drupacea's fruit pekmez. – The J of Food 29(1): 33-40.
[27] Salamon, I., Ibraliu, A., Kryvtsova, M., Petruska, P. (2017): Essential oil of common juniper (Juniperus communis L.) in Albania. – Sci. Bull. Uzhhorod Univ. (Ser. Biol.). 43: 72-75.
[28] Seca, A. M. L., Pinto, D. C. G. A., Silva, A. M. S. (2015): The Current Status of Bioactive Metabolites from the Genus Juniperus. – In: Bioactive Phytochemicals: Perspectives for Modern Medicine Vol.3, Daya Publishing House, 365-407.
[29] TAPPI T204cm-97 (1997): Solvent extractives of wood and pulp. – Tappi Press, Atlanta, GA.
[30] TAPPI T207cm-99 (1999): Water solubility of wood and pulp. – Tappi Press, Atlanta, GA.
[31] TAPPI T211om-02 (2002): Ash in wood, pulp, paper and paperboard: combustion at 525 oC. – Tappi Press, Atlanta, GA.
[32] TAPPI T222om-02 (2002): Acid-insoluble lignin in wood and pulp. – Tappi Press, Atlanta, GA.

http://www.aloki.hu ● ISSN 1589 1623 (Print) ● ISSN 1785 0037 (Online)
DOI: http://dx.doi.org/10.15666/aeer/1704_81718178

[33] TS 4895 EN ISO 3188 (1998): Starches and derived products - determination of nitrogen content by the Kjeldahl method-titrimetric method. – Turkish Standards Institution.
[34] Wise, E. L., Karl, H. L. (1962): Cellulose and hemicelluloses in pulp and paper science and technology. – In: Earl, C. L. (ed.) Vol. 1: Pulp. McGraw Hill-Book Co., New York.

http://www.aloki.hu ● ISSN 1589 1623 (Print) ● ISSN 1785 0037 (Online)
DOI: http://dx.doi.org/10.15666/aeer/1704_81718178

EXPERIMENTAL STUDY OF THE IMPACT OF THE VEGETABLE COLD STORE FLOOR LOCATION ON HEAT EXCHANGE WITH THE SOIL

SOKOLOWSKI, P.* – NAWALANY, G.

Department of Rural Building, Faculty of Environmental Engineering, University of Agriculture in Krakow, al. Mickiewicza 24/28, 30-059 Krakow, Poland
(e-mail: kbw@urk.edu.pl; phone: +48-12-662-4009)

**Corresponding author*
e-mail: p.sokolowski@urk.edu.pl

(Received 18th Feb 2019; accepted 10th Apr 2019)

Abstract. The paper analyses the impact of location of the vegetable cold store floor in relation to the ground level on heat exchange with the soil. The scope includes the analysis of indoor and outdoor temperature and soil temperature under the cold store and its surrounding, specification and adaptation of the cold store heat exchange model with soil, calculations for chosen variants in non-stationary conditions and a comparative analysis of cold store heat exchange with soil and soil temperature in chosen solutions. The paper used the results of field studies conducted in a cold store located in southern Poland. The said building was used to store carrots from 1 October to 30 June. Three calculation variants were used in order to determine in detail the impact of the chosen factors on heat exchange between the cold store and soil. The calculations were made based on the elementary balances method in WUFI®plus software. The calculation model was validated based on the results of field studies of indoor and outdoor temperature and soil temperature in 5 measurement lines at the depth of 0.05, 0.50, 1.00 and 1.50 m. The obtained validation results showed a very high correlation of measurement data and calculated data and an absence of significant differences. The calculation results for 3 variants showed statistically significant ($p < 0.05$) differences in both soil temperature and heat exchange with the soil.
Keywords: *cooling chamber, energy management, energy efficiency, microclimate, ground temperature*

Introduction

In order to preserve an adequate commercial, nutritional and biological quality, the picked fruit should be stored at a precisely specified temperature, humidity and with an appropriate gas composition and lighting in the store (Sun et al., 2004; Zhihang et al., 2006). Appropriate storage is intended mainly to reduce the intensity of microbiological, chemical, physical and biological processes causing unfavourable quality changes of the product (Łapczyńska-Kordon and Krzysztofik, 2008; Mazzeo et al., 2015). Such processes include breathing, transpiration, change of chemical composition, ripening and ageing, and damage caused by various pathogens. Changes in the fruit chemical composition take place at a various rate depending on many factors such as cultivation, fruit species and variety and, most of all, storage conditions (Wu et al., 2012; Phillips et al., 2016). Active cooling and controlled storage atmosphere is used to reduce the risk of deterioration of quantitative and qualitative factors (Liu et al., 2010; Ambaw et al., 2013; East et al., 2013). Other methods of preservation include application of edible coats, potentially not hazardous to humans, the main purpose of which is inter alia to prevent the fruit discoloration and to destroy harmful bacteria. The main benefit of such treatment is a significant extension of the shelf life of stored products (Soliva-Fortuny and Martin-Belloso, 2003; Albanese et al., 2007).

http://www.aloki.hu ● ISSN 1589 1623 (Print) ● ISSN 1785 0037 (Online)
DOI: http://dx.doi.org/10.15666/aeer/1704_81798189

The heat exchange with soil is an issue that is well known and described in the literature. The studies in this area were conducted by inter alia Radoń et al. (2014), Nawalany et al. (2014, 2017), Aresti et al. (2018), Janssen (2002) and Deru (2001). Due to a large accumulation potential of soil, partially earth-sheltered buildings have a reduced demand for heating and cooling energy in comparison to non-earth-sheltered buildings, assuming the functional and spatial solutions in such buildings are similar (Dronkelaar et al., 2014).

The paper aimed at determining the impact of cold store floor location relative to the ground level on heat exchange between the floor and the soil.

Materials and methods

The field studies were conducted in a vegetable cold store in southern Poland. The said cold store has a set of rooms, with the manipulation area located at the head of the row of two cold rooms. The sorting and packing areas are located in the northern part of the building, and the cold rooms in the south-eastern and south-western part. The total building area is 232 m^2, including 58 m^2 of sorting and packing areas, 96 m^2 of right-hand cold room and 78 m^2 of left-hand cold room. The building has a steel frame structure on a 30-cm wide concrete foundation located 1.0 m below the ground level. Important for the heat exchange with the soil is the fact that the foundation is not thermally insulated. The chamber floors are made of 10-cm thick cement screed and feature a 4-cm thick thermal insulation of hard EPS. An organoleptic soil examination showed that the cold store surrounding includes a 40-cm thick humus layer, with a 1.5-m thick layer of silty clay below it. The outside walls and ceiling of the chambers are made of sandwich panels, comprising steel sheets galvanized and painted on both sides, and a 15-cm thick EPS core. Polyurethane foam was used at the joints of panels to eliminate thermal bridges.

The storage cycle in the examined facility lasted from 15 October to 30 June, with a technological interruption from 1 July to 30 September. The optimum temperature was kept by a 20 kW refrigerating unit. The cold rooms' dimensions were adapted to multiples of box pallets in which carrots were kept. The distance between the box pallets and walls and between the box pallet rows were 10 cm to 30 cm and 5 cm to 10 cm, respectively.

The field studies were conducted between 1 May 2009 to 30 June 2011, and the period from 1 May 2010 and 30 April 2011 was used for this paper. The studies included continuous measurements of indoor and outdoor air temperature and floor temperature at 1-hour intervals. The temperature was measured by twenty-two APATOR TOP 168 sensors based on a PT100 platinum resistor (0.1°C measurement resolution, 0.1°C measurement error). The sensors were connected to an HP 34970A recorder. The measurement results were used to validate the calculation model that was used in this paper. *Figure 1* shows the building layout and location of the measurement points.

Three calculation variants were applied to study the impact of cold store floor location relative to the ground level on the indoor microclimate and soil temperature under the cold store and in its surrounding: variant 1 - floor on the ground level, variant 2 - floor elevated +0.75 m above the ground level, variant 3 - floor sunk -0.75 m below the ground level. The simulation was conducted in WUFI®plus software which allows for calculating in a non-stationary approach using the method of elementary balances.

http://www.aloki.hu ● ISSN 1589 1623 (Print) ● ISSN 1785 0037 (Online)
DOI: http://dx.doi.org/10.15666/aeer/1704_81798189

Prior to the calculation analysis, the software was validated based on actual measuring data. The starting point for the model validation was to build a discrete geometrical model divided into balance-differential elements. The model included measuring points corresponding to their actual location in the field-studied facility (*Fig. 2*).

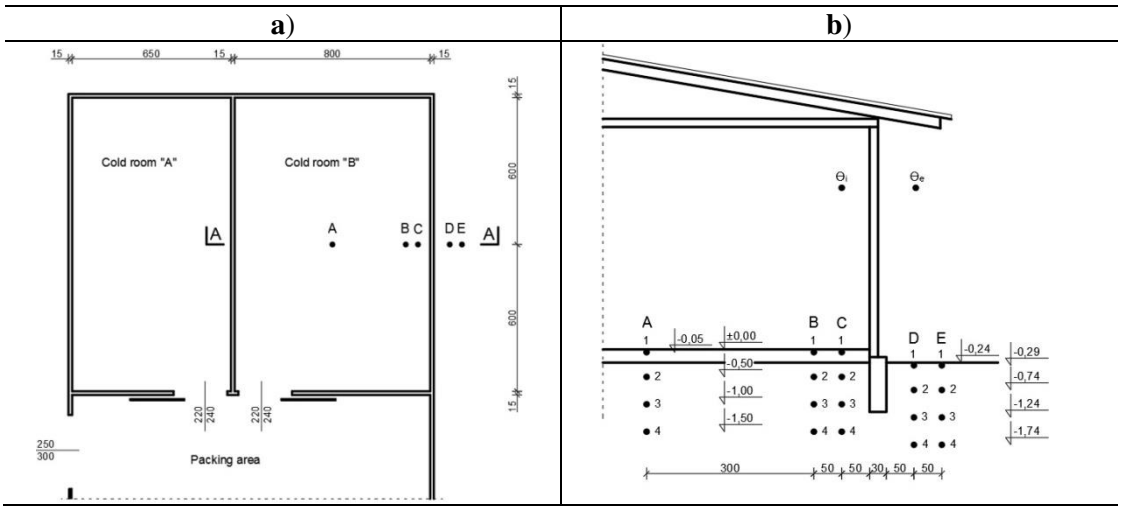

Figure 1. *Location of measurement points in the cold store: (a) plan; (b) section A - A: A, B, C, D, E - measuring lines, A1 - A4, B1 - B4, C1 - C4, D1 - D4, E1 - E4 - soil temperature measurement points, Θi, Θe - air temperature measurement points*

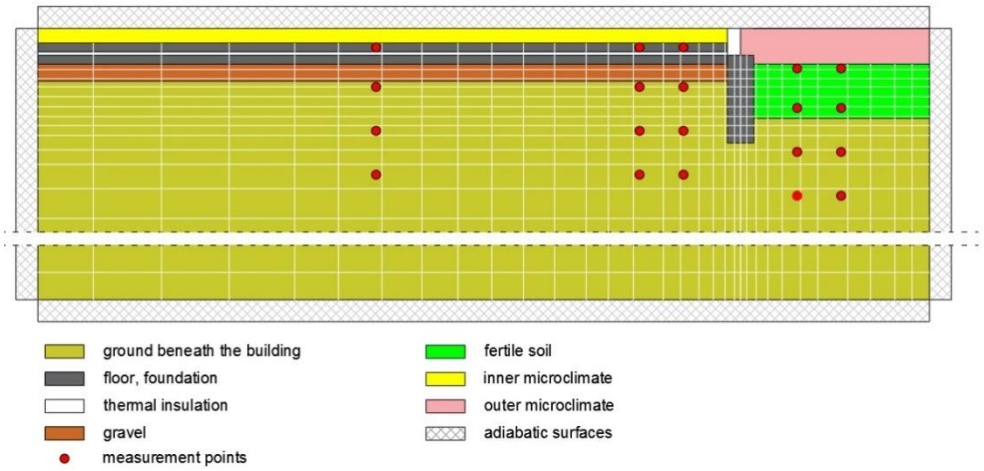

Figure 2. *Section of the modelled facility with division network and layout of soil temperature calculation points (model from WUFI®plus software)*

The physical parameters of the construction materials and soil used in the calculation model for validation are presented in *Table 1*. The minimum indoor air temperature used in calculations was $\Theta_{i,min}$ = 0°C, maximum indoor air temperature $\Theta_{i,max}$ = 4°C, minimum indoor air relative humidity $Rh_{i,min}$ = 80%, and maximum indoor air relative humidity $Rh_{i,max}$ = 99%. The natural air change was assumed at 0.3 h^{-1} and infiltration at 0.2 h^{-1}. The variant calculation analysis was based on climatic data for a typical

http://www.aloki.hu ● ISSN 1589 1623 (Print) ● ISSN 1785 0037 (Online)
DOI: http://dx.doi.org/10.15666/aeer/1704_81798189

meteorological year (TRY) for Krakow, Poland, available in the WUFI®plus software database. Correlation analysis was performed for results obtained from all the measuring points, based on the Spearman's Rank Test (the data distribution was not normal). The data distribution normality was tested previously using the Shapiro-Wilk Test.

Table 1. *Physical parameters of the soil and construction materials used in the calculations*

Specification		Unit	Value
clay	bulk density	kg·m-3	1600
	heat capacity	J·kg-1·K-1	1000
	thermal conductivity	W·m-1·K-1	1.80
humus	bulk density	kg·m-3	1800
	heat capacity	J·kg-1·K-1	1260
	thermal conductivity	W·m-1·K-1	0.90
styrofoam	bulk density	kg·m-3	20
	heat capacity	J·kg-1·K-1	1500
	thermal conductivity	W·m-1·K-1	0.04
concrete	bulk density	kg·m-3	2300
	heat capacity	J·kg-1·K-1	1000
	thermal conductivity	W·m-1·K-1	2.30
gravel	bulk density	kg·m-3	1800
	heat capacity	J·kg-1·K-1	840
	thermal conductivity	W·m-1·K-1	0.90

Results

Results of experimental studies

The indoor air temperature during the storage period (15 October - 30 June) was kept between 0.0°C and 4.0°C. During the technological interruption from the beginning of July to the end of September the indoor microclimate in the cold store changed passively depending on the outdoor microclimate; this caused the indoor temperature to increase to 15.3°C in August. The maximum outdoor air temperature in that period was 22.3°C. The indoor temperature fell abruptly in the last week of September after the cooling system had been activated to ensure the optimum temperature from the first day of the storage period - that is 1 October. From 1 October to 6 December the indoor air temperature was kept again at 4.0°C, with small, short-term drops. The drops were caused by a decrease of the outdoor air temperature and were in the 0.2 - 0.8°C range. In winter the average indoor air temperature in the cold store was in the 1.0 - 1.6°C range, and in the remaining months it was near 4.0°C (*Fig. 3*).

The floor temperature analysis in point A1 showed 4.2°C on the last day of the storage period. On the first day of the next storage cycle, the floor temperature was 11.6°C and decreased gradually. It was that in the analysed calculation variant determined the time necessary to reduce the floor temperature to the value from the end of the storage period is 18 days.

In points C1, B1 and A1 located in the soil under the cold store, the annual soil temperature amplitude was in the 13.9 - 14.3°C range. A larger impact of the soil on the stabilisation of thermal conditions is visible at the depth of 1.5 m. At the depth of 0.50 m, the annual temperature fluctuations were reduced almost twofold compared to the depth of 0.05 m. The impact of the cold store on the soil temperature decreases with depth. In points located in the facility surrounding, the annual soil temperature

http://www.aloki.hu ● ISSN 1589 1623 (Print) ● ISSN 1785 0037 (Online)
DOI: http://dx.doi.org/10.15666/aeer/1704_81798189

amplitude was from 14.5°C (point D2) to 15.1°C (point E2), and in points under the cold store it was from 7.5°C (A2), 6.5°C (B2) and 6.6°C in C2 (*Fig. 4*).

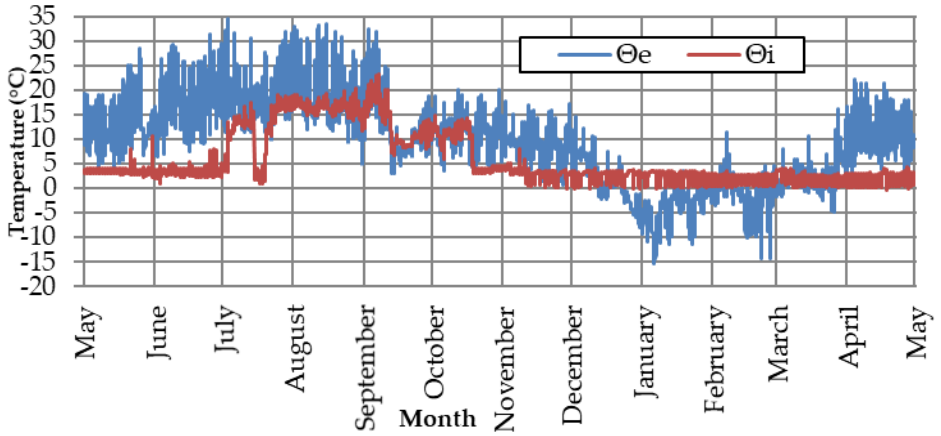

Figure 3. *Outdoor (Θe) and indoor (Θi) air temperature*

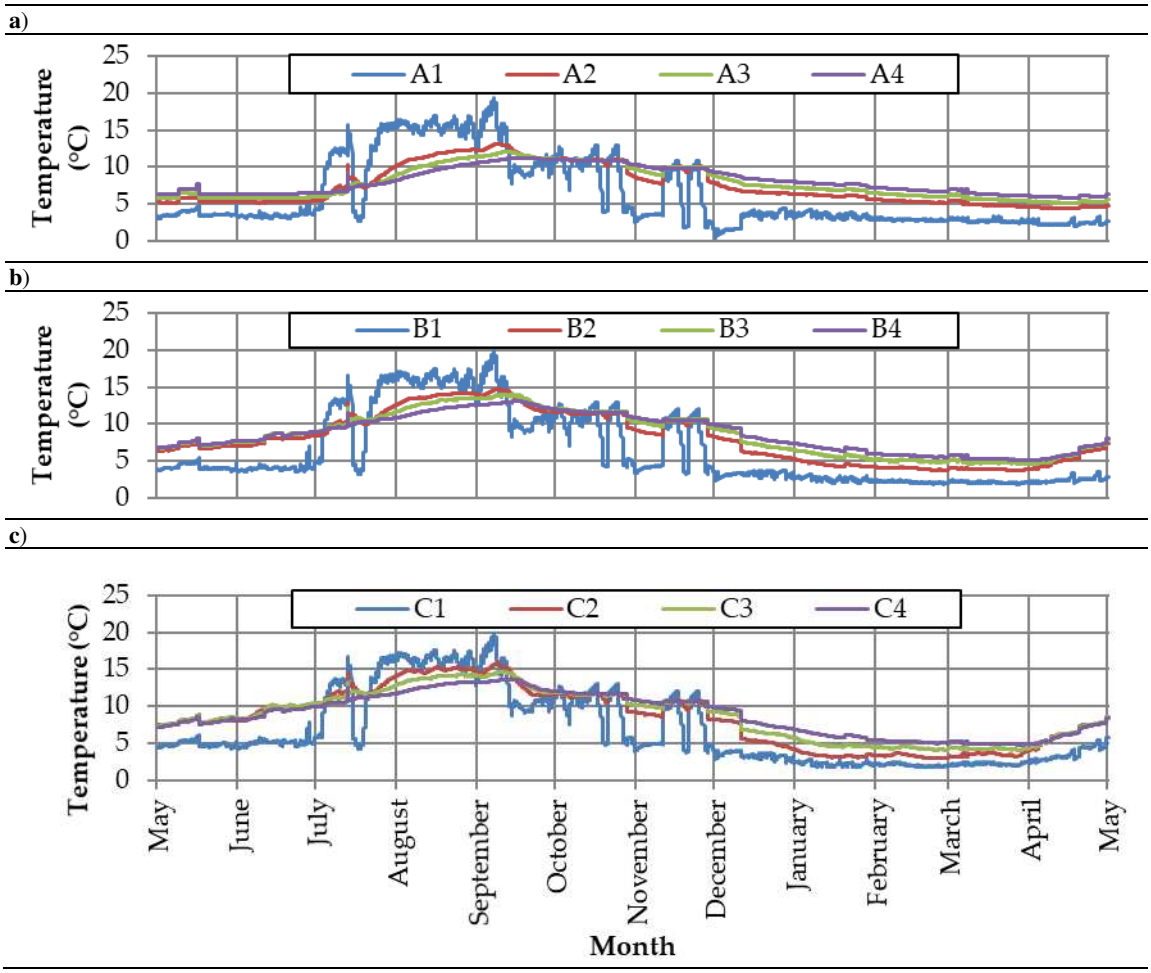

Figure 4. *Measured soil temperatures in lines A, B and C: (a) temperature points A1 (0.05m), A2 (0.50 m), A3 (1.00 m) A4 (1.50 m); (b) points B1 (0.05 m), B2 (0.50 m), B3 (1.00 m), B4 (1.50 m); (c) points C1 (0.05 m), C2 (0.50 m), C3 (1.00 m) and C4 (1.50 m)*

http://www.aloki.hu ● ISSN 1589 1623 (Print) ● ISSN 1785 0037 (Online)
DOI: http://dx.doi.org/10.15666/aeer/1704_81798189

The soil temperature in the cold store surrounding depended on the indoor and outdoor air temperature. The annual soil temperature amplitude in point E1 was 29.4°C, and at the depth of 1.5 m in the same measuring line (E4) it was 9.2°C. The calculation results showed the highest soil temperature in the measuring point E1 in June (18.8°C), and the lowest soil temperature (-10.6°C) was recorded in January in the same measuring point (*Fig. 5*).

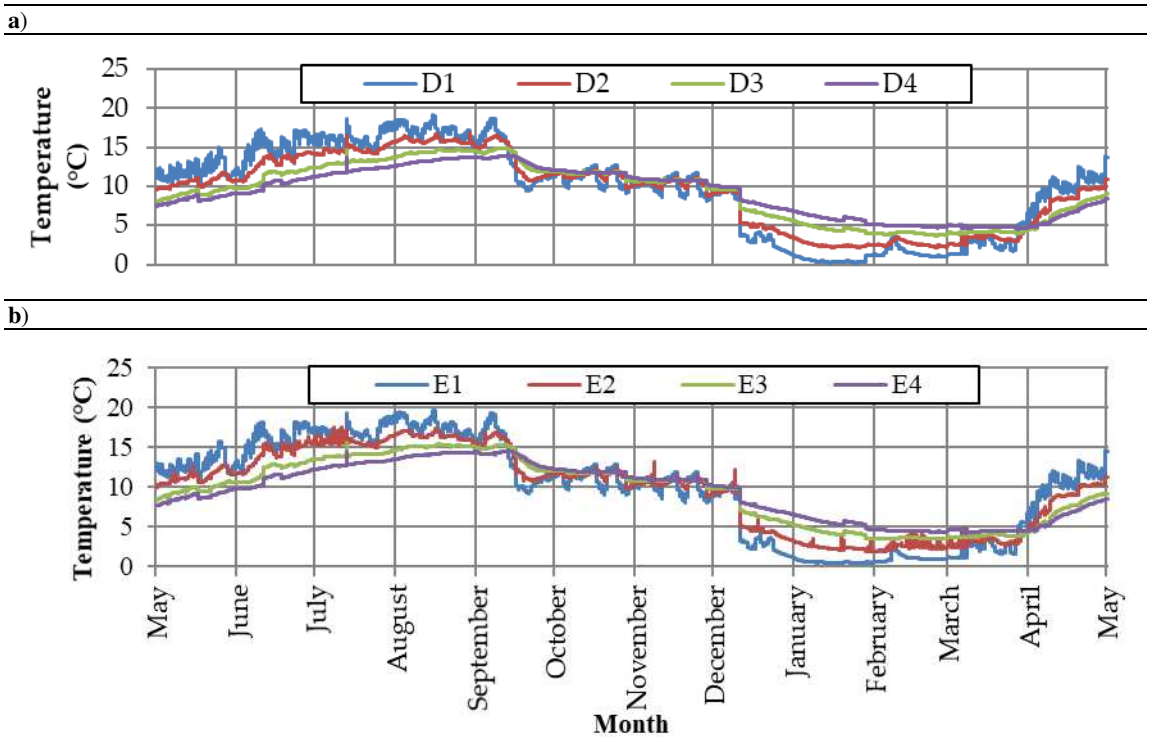

Figure 5. *Measured soil temperatures in lines D and E: (a) temperature points D1 (0.05m), D2 (0.50 m), D3 (1.00 m) D4 (1.50 m); (b) points E1 (0.05 m), E2 (0.50 m), E3 (1.00 m), E4 (1.50m)*

Results of generalising calculations

The calculation model was validated based on measured temperature inside and outside the cold store. In relation to the soil temperature, the measured temperature was a boundary condition of the third kind. The initial soil temperature was assumed at 8.8°C, which corresponds to the average annual outdoor air temperature for Krakow (TRY).

The highest correlation coefficient (0.95 - 0.99) was determined for measuring points E2, E3, E4, D2, D3, D4, C2, C3, C4, B2, B3, B4, A2, A3 and A4. Consequently, the conformity of calculation and measurement data at the depth of 0.50 m, 1.00 m and 1.50 m can be considered full. In the case of points E1 and D1, located 0.05 m below the ground level, and A1, B1 and C1 located under the floor, the correlation coefficient was 0.85 - 0.88, so the conformity of measurement and calculation data should be considered very high (*Fig. 6* and *Fig. 7*).

It should be emphasised that in winter the actual soil temperature at the depth of 0.10 m differed from the calculated values by 11.2°C in line E and 11.0°C in line D. The reason was the impossibility to account for the snow cover. The differences occurred, however,

http://www.aloki.hu ● ISSN 1589 1623 (Print) ● ISSN 1785 0037 (Online)
DOI: http://dx.doi.org/10.15666/aeer/1704_81798189

only for a short time and were not significant for the entire period of study. The statistical significance of differences was tested using the Kruskal-Wallis ($p < 0.05$) test.

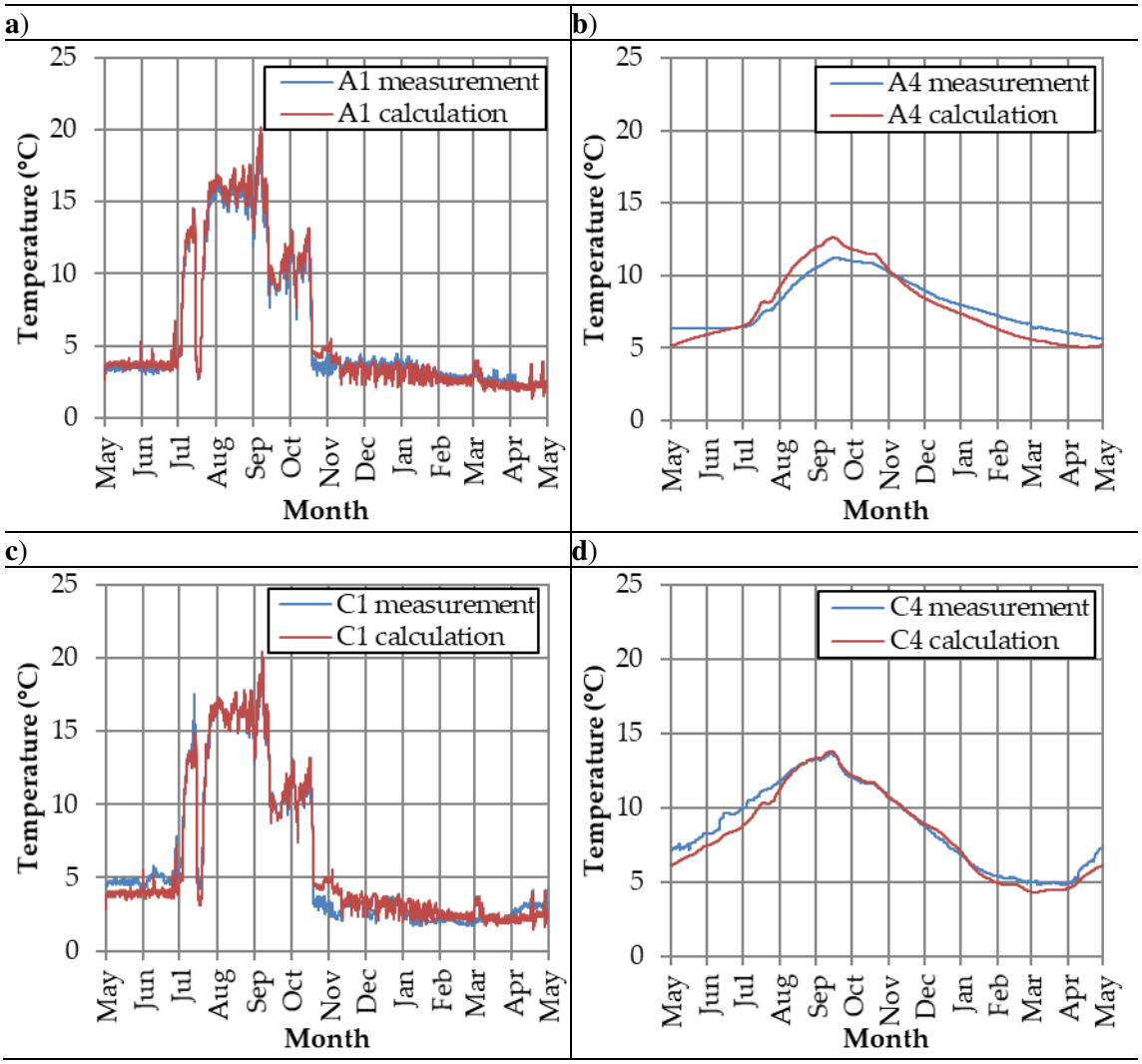

Figure 6. *Calculated and actual soil temperature: (a) A1; (b) A4; (c) C1; (d) C4*

The analysis of heat exchange intensity between the indoor air and the soil for the cold store with the floor at the ground level (variant 1) showed that the soil share in the total cold store energy balance was 16.6%. The highest energy gains from the soil were discovered in October (478.5 kWh). As a result of technological interruption in the summer, there was an intensive heat flow to the soil in July (588.1 kWh). The location of the cold store floor +0.75 m above the ground level (variant 2) reduced the soil share in the energy management to 8.2% relative to variant 1. The energy demand for cooling was 4920.5 kWh, and for heating 682.7 kWh. The analysis of variant with the floor -0.75 m under the ground level indicated that such variant significantly increases the soil share in the cold store energy balance relative to variant 1. During one year the soil share in the cold store energy balance for variant 3 was 32.8%. Similar to the two previously discussed variants, the highest heat gains were in October (891.5 kWh). The analysis of the balance of heat exchange with soil indicated high energy gains of 2054.6 kWh (*Fig. 8*).

http://www.aloki.hu ● ISSN 1589 1623 (Print) ● ISSN 1785 0037 (Online)
DOI: http://dx.doi.org/10.15666/aeer/1704_81798189

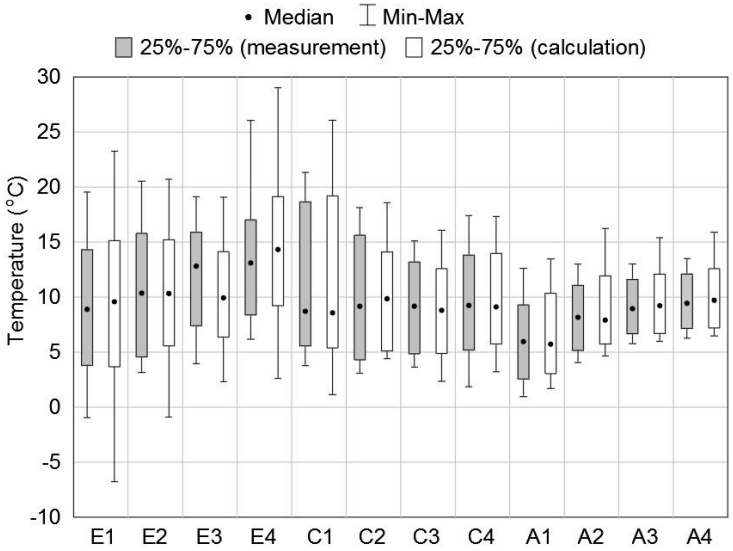

Figure 7. *Statistical agreement of the measured and calculated data, E1 – E4; C1 – C4; A1 – A4 – floor and ground temperature measurement points*

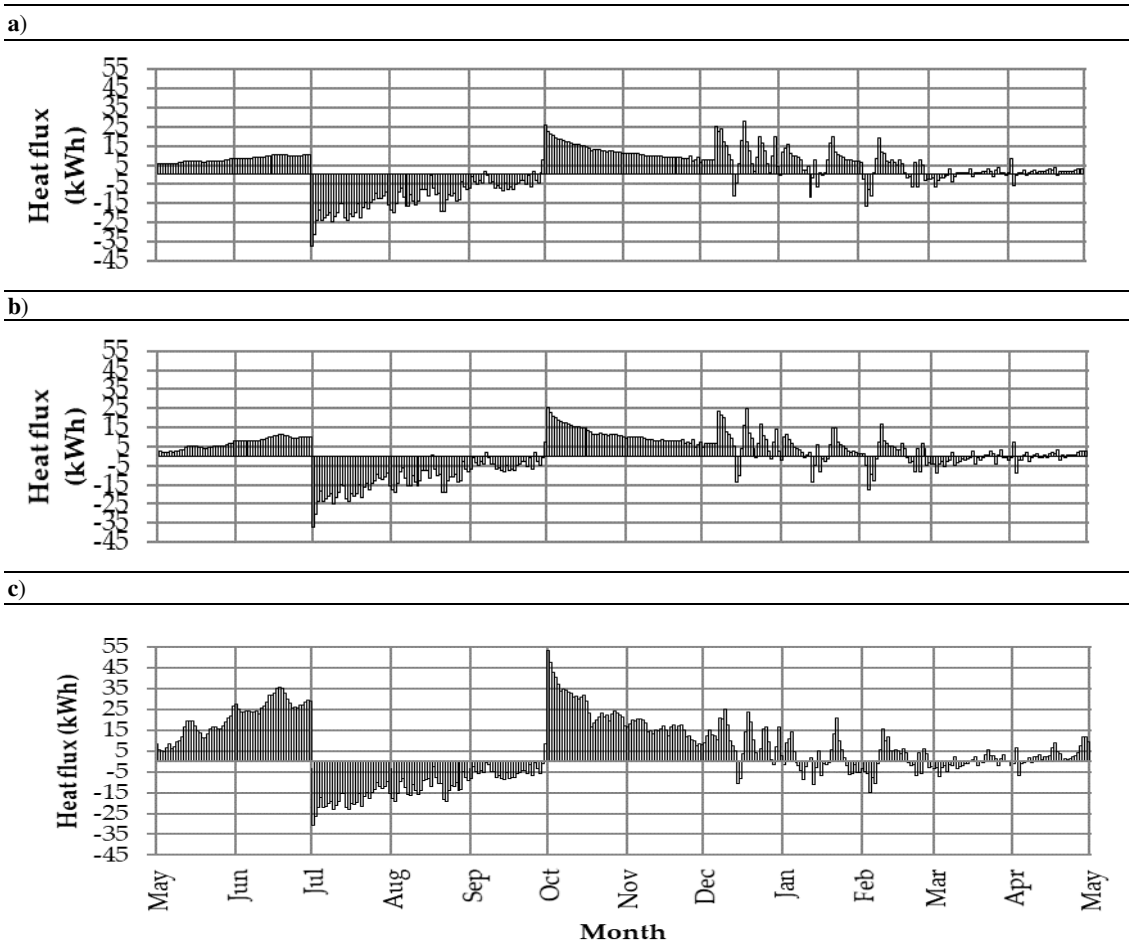

Figure 8. *Heat exchange between the cold store and soil: (a) variant 1; (b) variant 2; (c) variant 3*

http://www.aloki.hu ● ISSN 1589 1623 (Print) ● ISSN 1785 0037 (Online)
DOI: http://dx.doi.org/10.15666/aeer/1704_81798189

The highest dynamics of heat exchange with the soil was determined in variant 3, with a 3-month cooling period from 1 October to 30 June and a 3-month technological interruption from 1 July to 30 September. The annual amplitude of the heat stream flowing through the soil in that period was 4849.4 kWh. The least soil share in the total cold store energy balance was found in variant 2 with the floor elevated +0.75 above the ground level (*Table 2*). The swap of the floor level relative to the ground level affects the decrease of the soil temperature under the cold store even by 4.0°C. Similar to the soil temperature, the data deviated from the normal distribution also in case of the cold store-soil exchange. The analysis of the significance of differences between the individual variants indicated that all the examined solutions significantly affect the heat exchange between the cold store and soil.

Table 2. *Calculation results of the heat exchange between the cold store and soil and the cold store energy demand for heating and cooling, annual balance for all variants*

	Variant 1	**Variant 2**	**Variant 3**
Heat gains from the ground (kWh·rok^{-1})	2259.1	1876.1	3452.0
Heat losses to the ground (kWh·rok^{-1})	-1319.7	-1417.7	-1397.4
Participation of the ground in cold store energy balance throughout the year (%)	16.6	8.2	32.8
Energy demand and for cooling (kWh·rok^{-1})	5141.4	4920.5	5745.5

The results show that the cold store floor elevated +0.75 m above the ground level decreases the cooling energy demand by 220.9 kWh per year compared to the variant with the floor at the ground level. The floor located below the ground level seems to be the least favourable option as it significantly increases the cooling energy demand. It should be noted that such a relationship occurs as a result of a unique storage technology. There is a 9-month storage period in the examined cold store, and the technological interruption takes place in the summer.

Discussion

The obtained generalising results of the simulation can be accepted as reliable and universal for all buildings of this type. Numerical analysis is one of the most accurate and frequently used methods in science (Janssen et al., 2004; Radoń et al., 2014; Nawalany et al., 2017; Dong, 2017; Bambara and Athienitis, 2018). However, the authors have not encountered such analysis for a vegetable cold store. Compared to other agricultural buildings, for example a greenhouses, a cold store has a significantly higher share of soil in the total energy balance of the building. In greenhouses, the soil share in the total energy balance is about 5% (Nawalany et al., 2014). The results presented in this paper indicate that in a cold store such a value is 16.6% in the case of the floor on the ground level. The studies (Bambara and Athienitis, 2018; Hyung-Kweon et al., 2018) indicate the need to verify the impact of the cold store thermal insulation at various floor location variants on the intensity of heat exchange with the soil and the soil share in the total energy balance of the building. An adequate building insulation can lead to even a 5-fold decrease of the soil share in energy gains and losses of the building (Nawalany et al., 2017; Dong, 2017).

http://www.aloki.hu ● ISSN 1589 1623 (Print) ● ISSN 1785 0037 (Online)
DOI: http://dx.doi.org/10.15666/aeer/1704_81798189

Conclusions

The studies show that the cold store floor location has a significant impact on the heat exchange with the soil. When a cold store is partially earth-sheltered (floor 0.75 m below the ground level), the heat flow from soil increases even by 16.2% compared to the variant with the floor at the ground level. A floor elevated above the ground level (+ 0.75 m) decreases the heat flow from the soil by 8.4% compared to the variant with the floor at the ground level. The variants with the floor above and below the ground level significantly affect the cold store energy balance. The share of the foundation and floor in a partially earth-sheltered cold store is 32.8%, and 8.2% in an elevated cold store (+ 0.75 m). Significant differences can also be observed in the cooling energy demand. The most favourable variant is the one with the elevated floor in which the cooling energy demand is 4920.5 kWh/year. The least favourable variant is the one with the floor -0.75 m below the ground level as it increases the cooling energy demand to 5745.5 kWh/year.

REFERENCES

[1] Albanese, D., Cinquanta, I., Di Matteo, M. (2007): Effects of an innovative dipping treatment on the cold storage of minimally processed Annurca apples. – Food Chemistry 105: 1054-1060.

[2] Ambaw, A., Delele, M. A., Defraeye, T., Ho, Q. T., Opara, L. U., Nicolai, B. M., Verboven, P. (2013): The use of CFD to characterize and design post-harvest storage facilities: Past, prezent and future. – Computers and Electronics in Agriculture 93: 184-194.

[3] Aresti, L., Christodoulides, P., Florides, G. (2018): A review of the design aspects of ground heat exchangers. – Renewable and Sustainable Energy Reviews 92: 757-773.

[4] Bambara, J., Athienitis, A. K. (2018): Energy and Economic Analysis for greenhouse Ground Insulation Design. – Energies 11(11): 3218. doi:10.3390/en11113218.

[5] Deru, M. (2001): Ground-Coupled Heat and Moisture Transfer from Buildings. – Ph.D. Dissertation, Colorado State Univeristy, Fort Collins, CO.

[6] Dong, C. (2017): Heat Loss via Concrete Slab Floors in Australian Houses. – Procedia Engineering 205: 108-115.

[7] van Dronkelaar, C., Costola, D., Mangkuto, R. A., Hensen, J. L. M. (2014): Heating and cooling energy demand in underground buildings: potential for saving in various climates and functions. – Energy and Buildings 71: 129-136.

[8] East, A. R., Smale, N. J., Trujillo, F. J. (2013): Potential for energy cost savings by utilising alternative temperature control strategies for controlled atmosphere stored apples. – International Journal of Refrigeration 36: 1109-1117.

[9] Hyung-Kweon, K., Geum-Choon, K., Jong-Pil, M., Tae-Seok, L., Sung-Sik, O. (2018): Estimation of Thermal Performance and Heat Loss in Plastic Greenhouses with and without Thermal Curtains. – Energies 11(3): 578. https://doi.org/10.3390/en11030578.

[10] Janssen, H. (2002): The influence of soil moisture transfer on building heat loss via the ground. – Ph.D. Dissertation, Departement Burgerlijke Bouwkunde. Katholieke Universiteit Leuven.

[11] Janssen, H., Cormeliet, J., Hens, H. (2004): The influence of soil moisture transfer on building heat loss via the ground. – Building and Environment 39: 825-836.

[12] Łapczyńska-Kordon, B., Krzysztofik, B. (2008): Wpływ sposobów i czasu przechowywania na wybrane właściwości fizyczne jabłek. – Inżynieria Rolnicza 2(100): 179-185.

http://www.aloki.hu ● ISSN 1589 1623 (Print) ● ISSN 1785 0037 (Online)
DOI: http://dx.doi.org/10.15666/aeer/1704_81798189

[13] Liu, Y., Langer, V., Hogh-Jensen, H., Egelyng, H. (2010): Life Cycle Assessment of fossil energy use and greenhouse gas emissions in Chinese pear production. – Journal of Cleaner Production 18: 1423-1430.
[14] Mazzeo, T., Paciulli, M., Chiavaro, E., Visconti, A., Pellegrini, N. (2015): Impact of the industrial freezing process on selected vegetables - Part II. Colour and bioactive compounds. – Food Research International 75: 89-97.
[15] Nawalany, G., Bieda, W., Radoń, J., Herbut, P. (2014). Experimental study on development of thermal conditions in ground beneath a greenhouses. – Energy and Buildings 69: 103-111.
[16] Nawalany, G., Radon, J., Bieda, W., Sokolowski, P. (2017): Influence of selected factors on heat exchange with the ground in a greenhouse. – Transactions of the ASABE 60(2): 479-487.
[17] Phillips, K. M., Council-Troche, A., McGinty, R. C., Rasor, A. S., Tarrago-Trani, M. T. (2016): Stability of vitamin C in fruit and vegetable homogenates stored at different temperatures. – Journal of Food Composition and Analysis 45: 147-162.
[18] Radoń, J., Bieda, W., Lendelova, J., Pogran, S. (2014): Computational model of heat exchange between dairy cow and bedding. – Computers and Electronics in Agriculture 107: 29-37.
[19] Soliva-Fortuny, R., Martin-Belloso, O. (2003): New advances in extending the shelf life of fresh-cut fruits: a review. – Trends in Food Science & Technology 14: 341-353.
[20] Sun, D.-W., Wang, L. (2004): Experimental investigation of performance of vacuum cooling for commercial large cooked meat joints. – Journal of Food Engineering 61(4): 527-532.
[21] Wu, Z. S., Zhang, M., Wang, S. (2012): Effects of high pressure argon treatments on the quality of fresh-cut apples at cold storage. – Food Control 23: 120-127.
[22] Zhang, Z., Sun, D.-W. (2006): Effect of cooling methods on the cooling efficiencies and qualities of cooked broccoli and carrot slices. – Journal of Food Engineering 77(2): 320-326.

http://www.aloki.hu ● ISSN 1589 1623 (Print) ● ISSN 1785 0037 (Online)
DOI: http://dx.doi.org/10.15666/aeer/1704_81798189

SPATIOTEMPORAL CHARACTERISTICS AND THE INTERSPECIFIC COMPETITION OF PHYTOPLANKTON IN TIEGANG RESERVOIR (CHINA)

SONG, Y. L.[1] – ZHU, J.[2] – WANG, L.[3] – TAO, Y.[4]– GAO, J.S.[1] –ZHANG, J. S.[1*]

[1]*School of Civil and Environment Engineering, Harbin Institute of Technology, Shenzhen 518055, China*

[2]*School of Architectural and Environmental Engineering, Shenzhen Polytechnic, Shenzhen 518055, China*

[3]*Shenzhen Water Quality Testing Center, Shenzhen 518055, China*

[4]*Graduate School at Shenzhen, Tsinghua University, Shenzhen 518055, China*

**Corresponding author*
e-mail: 562045128@qq.com

(Received 19th Feb 2019; accepted 1st May 2019)

Abstract. Chlorophyll a concentration [ρ(Chla)] in phytoplankton is used to understand algal biomass and the primary productivity of a water body. To investigate the seasonal dynamics of [ρ(Chla)] and their relationship with environmental factors Tiegang Reservoir at Guangdong China, continuous observation and analysis was carried out from April 2013 to June 2014. The distribution of algae had an obvious spatial heterogeneity, and the ρ(Chla) gradual increased from the southeast to the northwest of the reservoir. From April to early December 2013 and from late April to June 2014, the dominant algae was cyanobacteria. In other months, bacillariophyta were dominant. Chlorophyta were at a low level throughout the year. Multivariate analysis showed that water temperature (WT) was the primary driving factor of the spatio-temporal distribution of algae. The main environmental factors of cyanobacteria, bacillariophyta and chlorophyta were greatly different. Single environmental factors such as WT, total organic carbon (TOC), nitrate nitrogen (NO_3--N), and chemical oxygen demand (COD) were significantly related to the competitiveness of cyanobacteria and bacillariophyta. And they can be used as early warning indexs for cyanobacteria and diatom blooms. The dual synergistic effects of WT and other environmental factors on the competitiveness of cyanobacteria and bacillariophyta were analyzed. A combination of environmental factors at high risk for cyanobacteria or diatoms were found.
Keywords: *chlorophyll a, environment factors, seasonal variation, multivariate analysis, interspecific competitiveness*

Introduction

Shenzhen is the most densely populated city in mainland China. At the beginning of its establishment, the total population was 320,000 (Liu et al., 2013; Gu and Ma, 2013; Qin et al., 2014; Ng et al., 2011; Zhou et al., 2011). As of the end of 2016, the actual population had increased to 18 million, and the population density reached 9,015 persons/km, ranking first among the cities in mainland China. The influx of a large immigrant population placed unprecedented pressure on the water supply system and seriously polluted the water environment (Liu et al., 2013; Gu and Ma, 2013; Qin et al., 2014; Ng et al., 2011; Zhou et al., 2011). Although Shenzhen is located in the subtropical region, no large rivers or lakes exist in the territory. Therefore, rich rainfall cannot be effectively gathered, resulting in scarce water resources. So Shenzhen is experiencing a serious water shortage (Güneralp and Seto, 2008; Liu and Ma, 2011). In

http://www.aloki.hu ● ISSN 1589 1623 (Print) ● ISSN 1785 0037 (Online)
DOI: http://dx.doi.org/10.15666/aeer/1704_81918217

2015, nearly 90% of the city's drinking water needed to be imported from the Pearl River. Shenzhen water supply system is mainly composed of overseas water diversion engineering and local reservoirs. There are nearly 168 reservoirs in Shenzhen. After arriving at Shenzhen, overseas water was firstly stockpiled in local reservoirs and then was supplied to nearby water works. Therefore, water quality of those reservoirs has played an important role to the city's drinking water security. And how to ensure the safety of drinking water and to meet the people's increasing requirement for the quality of drinking water became important topics in the construction of ecological civilization in Shenzhen (Liu et al., 2013; Li et al., 2015; Lu et al., 2015).

Chl-a is an important pigment for the photosynthesis of phytoplankton (Liu et al., 2013; Li et al., 2015; Lu et al., 2015) and an important medium for absorbing and transmitting light energy. In environmental science, the concentration of chl-a in phytoplankton is used to understand algal biomass (Eisner et al., 2016; Tebbs et al., 2013; Bowes et al., 2012; Wainger et al., 2016) and the primary productivity (Lee et al., 2015; Mantyla et al., 2008; Bott et al., 2006; Morin et al., 1999) of a water body. Chl-a is used to evaluate the nutritional status (Qin et al., 2014; Naeher et al., 2016; Bell et al., 2014; Terauchi et al., 2014) of the water environment. The traditional chl-a detecting method is breaking the algal cell wall by grinding, repeatedly thawing or using microwave methods, and the total chl-a concentration is then detected by spectrophotometry (Pyo et al., 2016) without distinguishing the different algae. According to the difference of fluorescence characteristics of algae, the chl-a concentration of cyanobacteria, chlorophyta and bacillariophyta can be detected by PAM (pulse-amplitude modulation) chlorophyll fluorometer (Jakob et al., 2005; Beecraft et al., 2017; Ruth et al., 2010), which can reflect the algal biomass and provide strong technical support for studying the community structure of algae.

Reservoir is a typical non-stable water body that is influenced by nature and humans, and its hydrodynamic and ecological characteristics are distinct from those of a natural lake (Teeter et al., 2001). Tiegang Reservoir is the largest water supply reservoir in Shenzhen. Shenzhen has promoted water quality in recent years to improve the water pollution situation of the reservoir, but the total nitrogen (TN) level is still seriously above the standard, and the water quality is poor (grade V) (Zhu et al., 2018; Qin et al., 2014). To date, few studies on Tiegang Reservoirs are available, and most of them are focused on water quality, while studies of the algae community structure and seasonal changing pattern are lacking. Our research group carried out continuous monitoring of the chl-a concentration of cyanobacteria, chlorophyta and bacillariophyta and their main environmental factors from April 2013 to June 2014. The temporal and spatial distribution characteristics and evolution of chl-a in algae were analyzed, the high risk areas and periods of algal blooms were identified, and the relationship between environmental factors and algae was studied. This study provides technical support to explore the mechanism of algal blooms, to ensure the safety of drinking water and to improve the ecological civilization of water.

Materials and methods

The layout of the study area and sampling sites

There were a total of 10 sampling sites in Tiegang Reservoir (*Fig. 1*): the No. 1 site is near the inlet of Xili Reservoir, No. 2 is near the intake point of the water plant, No. 3 and No. 4 are in the running water area in the middle east reservoir (where water flow

http://www.aloki.hu ● ISSN 1589 1623 (Print) ● ISSN 1785 0037 (Online)
DOI: http://dx.doi.org/10.15666/aeer/1704_81918217

velocity is fast), No. 5 and No. 6 are in the dead water area (where water flow velocity is slow), No. 7 is near the water intake point of Shiyan Reservoir, No. 8 is in the running water area in the western reservoir, No. 9 is near the Jiuwei River, and No. 10 is near the Liaokeng River. For each sampling site, the samples were collected within 3 layers from top to bottom; the surface layer is the water layer approximately 10 cm below the surface, the transparent layer is the water layer corresponding to the depth of the transparency measurement, and the bottom layer is the water layer approximately 10 cm above the sediment.

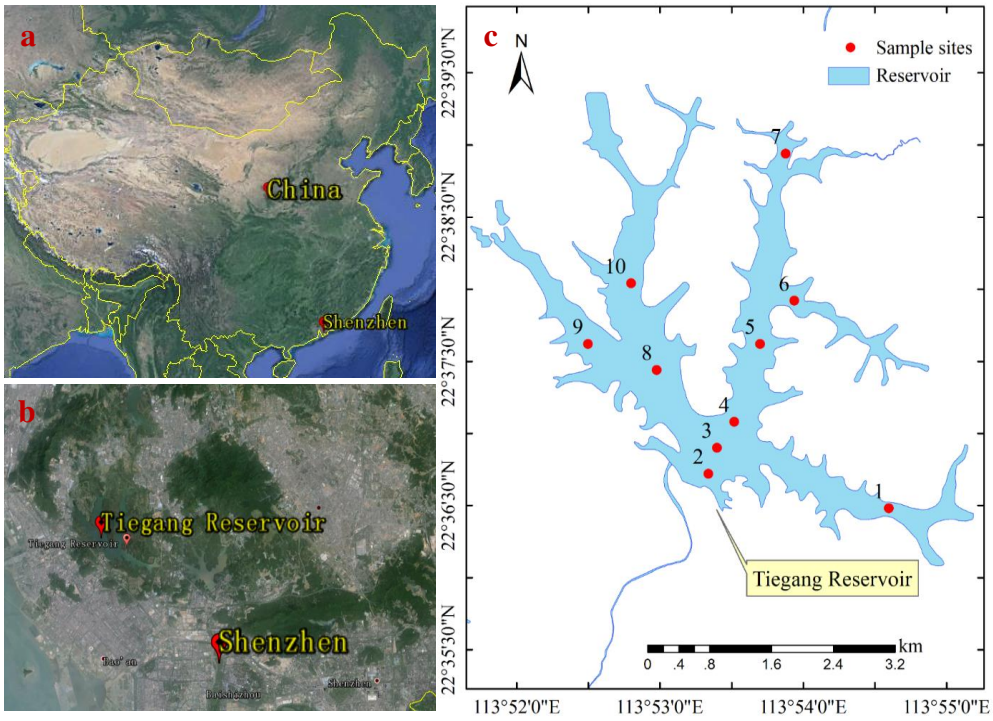

Figure 1. *The sampling sites at Tiegang Reservoir*

Sampling and analysis

The samples were collected using a ZPY-1 water collector and stored separately. The water samples were transferred to the laboratory within 2 h after collected and they were preservated at 4 °C. The chemiluminescence detection of the permanganate index (COD_{Mn}) and determination of ρ(Chla), total organic carbon (TOC), total nitrogen (TN), total phosphorus (TP), ammonia nitrogen (NH_4^+-N), nitrate nitrogen (NO_3^--N), iron (Fe) and silicate were carried out within two days. Chl-a was measured by using a modulated fluorometer (WALZ Phyto-PAM, Germany) that was periodically calibrated by acetone extraction spectrophotometry. The depth of the water, WT, pH, DO and turbidity were measured in-site using a multi-parameter water quality analyzer (YSI 6600V2, USA). The transparency (SD) was measured in-site using a secchi disk. COD was measured by the acidic potassium permanganate method; TP was determined by ammonium molybdate spectrophotometry (Shimadzu UV-2700 Ultraviolet-Visible Spectrophotometer, Japan); silicate was determined by silicon molybdenum blue spectrophotometry (Shimadzu UV-2700 Ultraviolet-Visible Spectrophotometer, Japan); TN, NH_4^+-N and NO_3^--N were analyzed by a flow analyzer (AMS-Alliance-Futura,

http://www.aloki.hu ● ISSN 1589 1623 (Print) ● ISSN 1785 0037 (Online)
DOI: http://dx.doi.org/10.15666/aeer/1704_81918217

French); and TOC was determined using a TOC analyzer (GE-Siever 5310C). The meteorological data, including temperature, air pressure, humidity, rainfall, evapoproportion n and sunshine hours, were provided by the Shenzhen National Climate Observatory. Three parallel samples were measured for each monitoring sample, and then the average value was taken as the final result.

Climatic periods

According to the weather characteristics, sampling time was divided into five periods. Pre-rainy period (PRP) was from April to June 2013 and 2014. Latter rainy period (LRP) was from July to September 2013. High temperature and rain free period (HTRFP) was from October to November 2013. Winter drought period (WDP) was from December 2013 to February 2014. Temperature jump period (TJP) was March 2013.

Data processing

The bivariate relationship between ρ(Chla) and the environmental factors was analyzed by Pearson correlation analysis on SPSS20. *Values in bold are different from 0 with a significance level alpha = 0.05. **Values in bold are different from 0 with a significance level alpha = 0.01. Time and space factors on environment factor and ρ(Chla) was analyzed by one-way ANOVA and two-way ANOVA that performed with SPSS20. The comprehensive correlation between the ρ(Chla) of the algae and the environmental factors was carried out using canonical correspondence analysis (CCA) on XLSTAT2010. The distribution chart of algal chl-a was generated on ArcMap10.2 by the Kriging interpolation method based on the mean of the ρ(TChla) of several months at each sampling site in the corresponding climatic period. Other graphics were prepared via using Origin9.0.

Results and discussion

Spatio-temporal evolution pattern of chl-a

Spatio-temporal evolution pattern of total chl-a

Figure 2 shows the seasonal changing pattern of ρ(TChla) in Tiegang Reservoir. The highest ρ(TChla) of Tiegang Reservoir in the sampling period was 145.06 μg L^{-1}, which appeared on the surface layer of the No. 9 sampling site on June 17, 2013. The peak period of chlorophyll a in Taihu Lake of China is from July 1 to 10 every year (Liu et al., 2019). Compared with Taihu Lake, the peak period of algae in Tiegang Reservoir is 2-3 weeks earlier. This is mainly because Tiegang Reservoir is located in the subtropical zone and its temperature is higher than that in the Taihu Lake Basin. The lowest ρ(TChla) was 4.72 μg L^{-1}, which appeared on the bottom layer of the No. 1 sampling site on January 27, 2014. The mean value was 38.53 μg L^{-1}, which was significantly higher than the value of 16.84 μg L^{-1} for the upstream reservoir - Xili Reservoir and lower than the value of 52.03 μg L^{-1} for the downstream reservoir - Shiyan Reservoir in the same period. These results indicate that the quality of the water from the Dongjiang River was significantly deteriorated after storage and transfer in the cascade reservoirs, and the water body had evolved from an oligotrophic state to a mesotrophic state.

http://www.aloki.hu ● ISSN 1589 1623 (Print) ● ISSN 1785 0037 (Online)
DOI: http://dx.doi.org/10.15666/aeer/1704_81918217

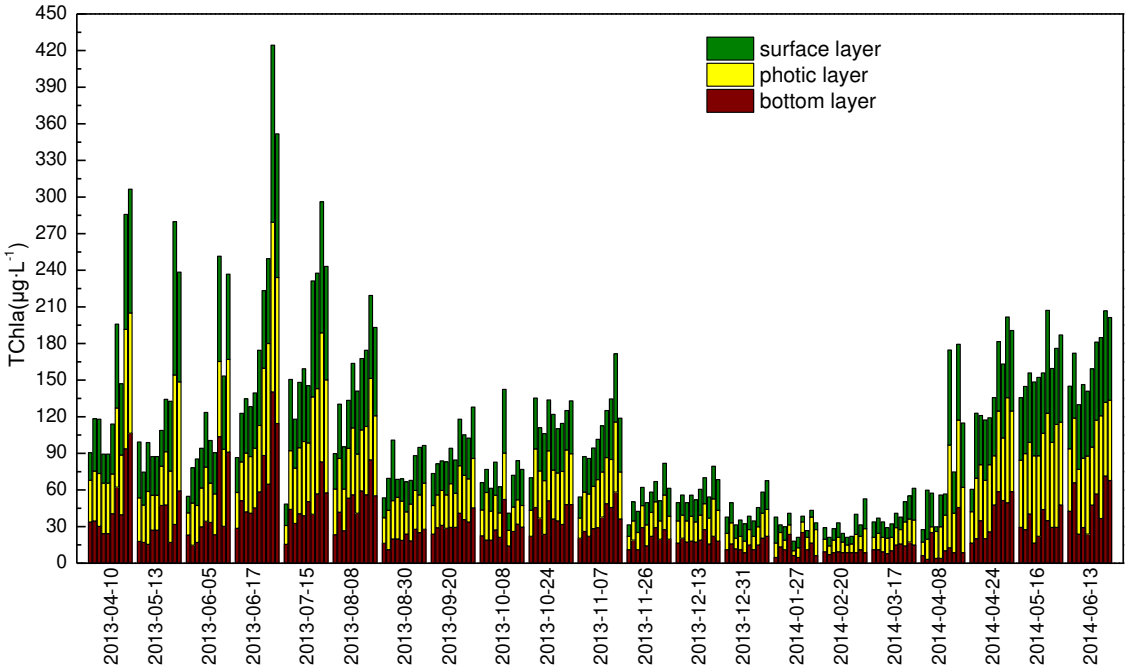

Figure 2. *Annual trend in total chl-a concentration. There are 10 columns every month and each column from left to right represents sampling sites 1 to sampling sites 10*

The temporal heterogeneity of chl-a in the algae of Tiegang Reservoir was evident: the algae began anabiosis in the temperature rising period in March 2013. The ρ(TChla) increased rapidly in April 2013 and reached 67.43 μg L^{-1} on June 17, 2013, which was the highest level for the year. From July to August 2013, the ρ(TChla) remained high, began to decline in September and remained at a medium concentration level in November, with an average value of ρ(TChla) in this period of 33.29 μg L^{-1}. From December 2013 to February 2014, the ρ(TChla) was at the lowest level of the whole year due to the low temperature, and the average value of ρ(TChla) in this period was 14.26 μg L^{-1}. From March to April 2014, the ρ(TChla) increased sharply due to the increased temperature and runoff pollution from the average of 14.4 μg L^{-1} on March 17 to 35.10 μg L^{-1} on April 8th. From May to June 2014, the reservoir again entered the high algae laden period.

The spatial heterogeneity of chl-a in the algae during the rainy season was obvious, especially from April 10 to August 8, 2013. The ρ(TChla) of the No. 9 and No. 10 sampling sites was approximately 1.5-2 times that of other sampling sites because these sites were close to the Jiuwei River and Liaokeng River and were affected by river basin pollution. From August 30 to September 20, 2013, at the end of the rainy season, the spatial heterogeneity of ρ(TChla) decreased because the pollutants in the watershed were rinsed by the heavy rainfall from April to July 2013, resulting in a significant decrease in the intensity of pollution. In August and September, although there was still heavy rainfall, the concentration of pollutants from the runoff was significantly reduced, and the concentration of algae in the inlet area from the rivers to the reservoir was also reduced due to dilution by the runoff. The spatial heterogeneity of ρ(TChla) at each sampling site in the periods of high temperature and rain free, winter drought and temperature jump was not clear. On April 8, 2014, with the arrival of the new rainy season, the ρ(TChla) of the No. 9 and No. 10 sampling sites in the northwest of the

http://www.aloki.hu ● ISSN 1589 1623 (Print) ● ISSN 1785 0037 (Online)
DOI: http://dx.doi.org/10.15666/aeer/1704_81918217

reservoir was significantly increased, and the spatial heterogeneity of the ρ(TChla) in the reservoir was again observed.

The chlorophyll-a of algae has a certain spatial heterogeneity in the vertical direction. The distribution pattern of ρ(TChla) is the transparent layer > the surface layer > the bottom layer. The deeper the water, the more obvious this pattern became. At a water depth of 3-5 m, the algae showed a distribution pattern of the transparent layer > the surface layer > the bottom layer. At a water depth of 5-8 m, the ρ(TChla) of the bottom layer decreased rapidly, and its differences between the surface layer or transparent layer became enlarged. At a water depth of 8-15 m, the mean ρ(TChla) of the bottom layer was only approximately 3/5 that of the transparent layer. The spatial heterogeneity of chl-a in the vertical direction in a natural water body is mainly caused by the stratification of light and the water temperature (Nishijima et al., 2016). The deeper the water body, the greater the difference of the water temperature and light between the different water layers is and the more obvious the difference of ρ(TChla) should be. The ρ(TChla) of Tiegang Reservoir did not show a large difference between the bottom layer and the surface layer as in natural deep lake reservoirs, mainly because Tiegang Reservoir is a typical unstable water body affected by artificial water, with fast water flow and frequent exchange. This was especially true for the sampling sites at the intake points of the water plant and the downstream reservoir, which were 3-6 m under the water surface, thus promoting water exchange in the vertical direction and reducing the spatial heterogeneity of the algae in the vertical direction.

Spatio-temporal evolution pattern of chl-a and community structure of phytoplankton

Figure 3 shows the seasonal changing pattern of the chl-a concentration of cyanobacteria, chlorophyta and bacillariophyta in the surface layer, the transparent layer and the bottom layer of the water body. During the monitoring period, the mean value of the ρ(Chla) of cyanobacteria was 22.74 μg L^{-1}; the highest value was 98.95 μg L^{-1} in the surface layer of the No. 9 sampling site on June 17, 2013, and the lowest value was 1.57 μg L^{-1} in the bottom layer of the No. 1 sampling site on December 31, 2013. The highest monthly average was 43.98 μg L^{-1} in July 2013, and the lowest monthly average was 4.43 μg L^{-1} in January 2014. The mean value of the ρ(Chla) of bacillariophyta was 11.53 μg L^{-1}; the highest value was 49.27 μg L^{-1} in the transparent layer of the No. 10 sampling site on April 10, 2013, and the lowest value was 3.15 μg L^{-1} in the bottom layer of the No. 1 sampling site on January 27, 2014. The highest monthly average was 22.63 μg L^{-1} in April 2013, and the lowest monthly average was 4.18 μg L^{-1} in January 2014. The mean value of the ρ(Chla) of chlorophyta was 4.54 μg L^{-1}; the highest value was 18.66 μg L^{-1} in the surface layer of the No. 9 sampling site on June 17, 2013, and the lowest value was 0.18 μg L^{-1} in the bottom layer of the No. 2 sampling site on January 27, 2014. The highest monthly average was 9.24 μg L^{-1} in June 2013, and the lowest monthly average was 1.18 μg L^{-1} in February 2014.

The changing pattern of the ρ(Chla) of cyanobacteria was essentially the same as that of ρ(TChla) described in the previous section: rising in the early rainy season in 2013, reaching the highest level in June-August, decreasing to a lower level in September-November, reaching the lowest level in December 2013-March 2014 and rapidly rising in early April 2014 to reach a high in June 2014. Compared with the same period of the previous year, the ρ(Chla) of cyanobacteria was increased by 30%-50% from May to June in 2014, indicating that the diversity of algae in the reservoir decreased, and the risk of a cyanobacteria bloom further intensified. The ρ(Chla) of bacillariophyta reached

http://www.aloki.hu ● ISSN 1589 1623 (Print) ● ISSN 1785 0037 (Online)
DOI: http://dx.doi.org/10.15666/aeer/1704_81918217

a maximum at March-April each year, which was slightly decreased in May-July and remained low from August to early October. From late October to early December, due to the sharp decrease of cyanobacteria, the interspecific competition was weakened; thus, the ρ(Chla) of bacillariophyta rose again. In late December to February, due to the cold weather, the ρ(Chla) of bacillariophyta was reduced again and was at the lowest level of the year. The ρ(Chla) of chlorophyta was relatively low, showing the overall characteristic of being high in the summer and autumn and low in the winter and spring.

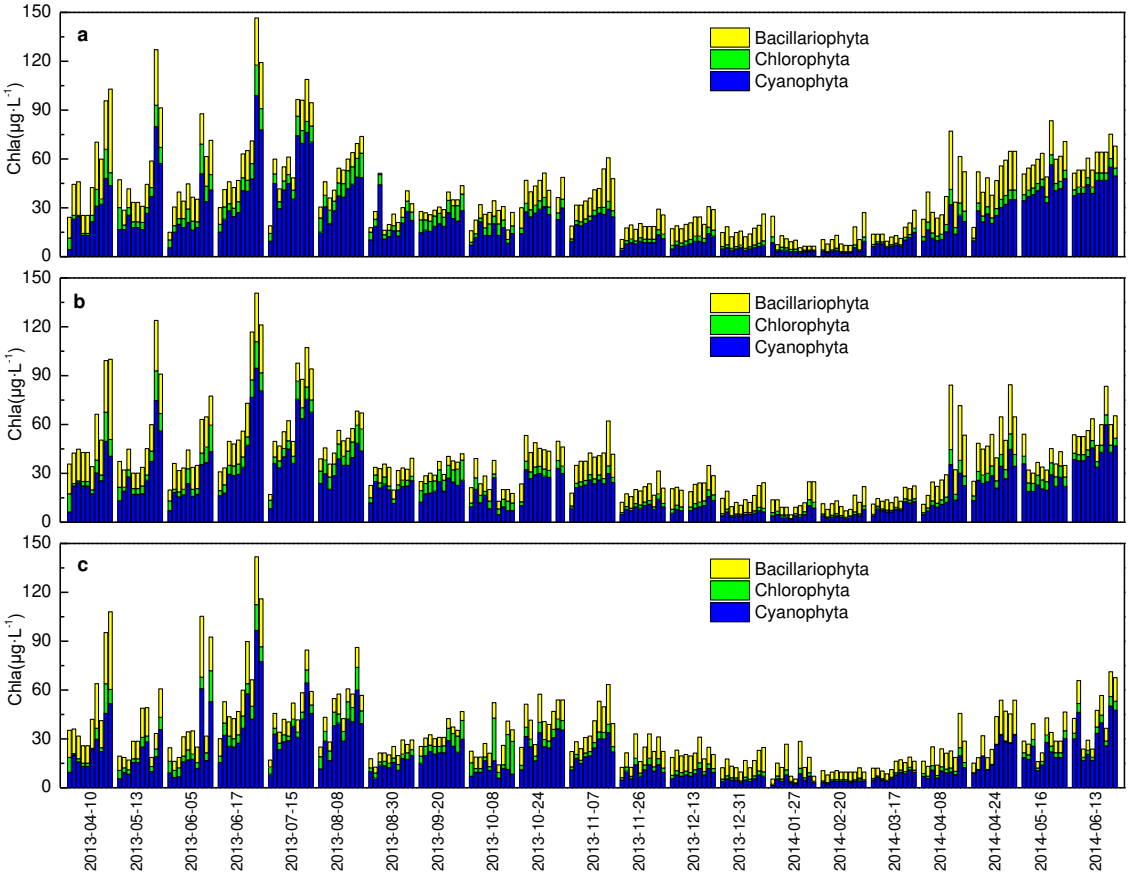

Figure 3. *Annual trend in chl-a concentration of cyonophyta, chlorophyt and bacillariophyta:* ***a*** *surface layer;* ***b*** *photic layer;* ***c*** *bottom layer. There are 10 columns every month and each column from left to right represents sampling sites 1 to 10*

Figure 4 shows the changing pattern of the algae population structure. The dominance of cyanobacteria in Tiegang Reservoir was apparent, accounting for 27.21%-72.58%, with an average of 54.49%. Bacillariophyta dominated in the winter and spring, accounting for 16.27%-61.82%, with an average of 34.17%. Chlorophyta was always at a low level, accounting for 7.21%-17.03% for the entire monitoring period, with an average of 11.38%. From April 2013 to July 2013, the proportion of cyanobacteria gradually increased from 49.28% to 72.58% and was maintained at approximately 65% until October. After December 2013, cyanobacteria rapidly decreased until the loss of dominance in December and finally reached the minimum in February 2014. In March 2014, cyanobacteria began to recover and reached 53.83% in late April to become dominant again; then, the proportion quickly rose to 71.28% in

http://www.aloki.hu ● ISSN 1589 1623 (Print) ● ISSN 1785 0037 (Online)
DOI: http://dx.doi.org/10.15666/aeer/1704_81918217

June. The changing trend of bacillariophyta was the opposite of that of cyanobacteria, which decreased from 43.41% in April 2013 to 16.27% in July 2013 and remained low in August-September. In October, the proportion of bacillariophyta rebounded rapidly to 46.99% at the end of December, becoming the dominant algae; this dominance was maintained until the beginning of April 2014 and reached a peak in February-March 2014. This was followed by a rapid decline under the impact of cyanobacteria recovery, falling to 21.47% in June 2014. The proportion of chlorophyta was low throughout the year, showing no obvious changing pattern in the proportion throughout the year. Compared with the same period of the previous year, the proportion of cyanobacteria in Tiegang Reservoir was increased in May-June 2014, and the proportions of bacillariophyta and chlorophyta decreased with the decreased diversity of algae. The algal population structure is a measure of the ecological diversity and stability of the water body (Pinckney et al., 2017; Tachibana et al., 2017; Tian et al., 2017). Tiegang Reservoir was dominated by cyanobacteria; the algal structure was relatively simple, with poor diversity, and the risk of a cyanobacteria bloom was rising.

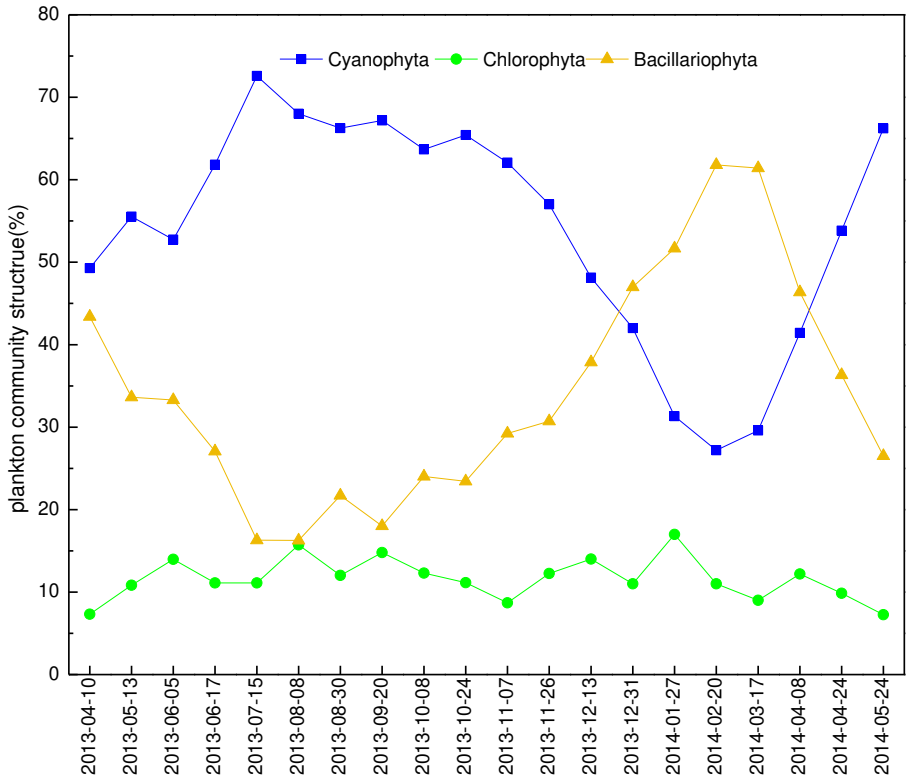

Figure 4. *Community structure of phytoplankton in Tiegang Reservoir*

Identification of the high risk area of an algal bloom

Tiegang Reservoir has a large capacity and a high spatial heterogeneity of ρ(Chla), showing the overall characteristic of gradual increases from the southeast to the northwest of the reservoir area (*Fig. 5*). From the perspective of time, the northwest and northeastern reservoir areas in the early rainy season and the northwest reservoir area in the late rainy season were at high risk of a cyanobacteria bloom, and the reservoir areas near the No. 9 and No. 10 sampling sites had a mild algal bloom in June-July 2013.

http://www.aloki.hu ● ISSN 1589 1623 (Print) ● ISSN 1785 0037 (Online)
DOI: http://dx.doi.org/10.15666/aeer/1704_81918217

There is a moderate risk of cyanobacteria bloom in the northeastern reservoir area in the late rainy season and the northwest reservoir area in the high temperature and dry period. The winter drought period and temperature jump period showed no risk of cyanobacteria bloom.

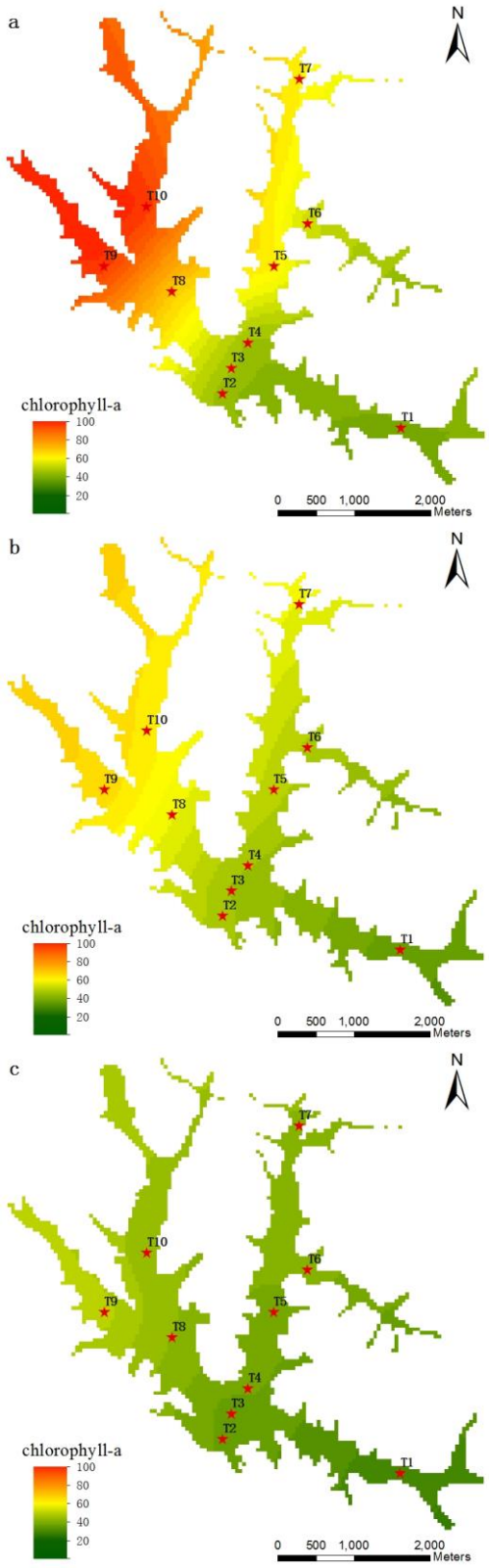

http://www.aloki.hu ● ISSN 1589 1623 (Print) ● ISSN 1785 0037 (Online)
DOI: http://dx.doi.org/10.15666/aeer/1704_81918217

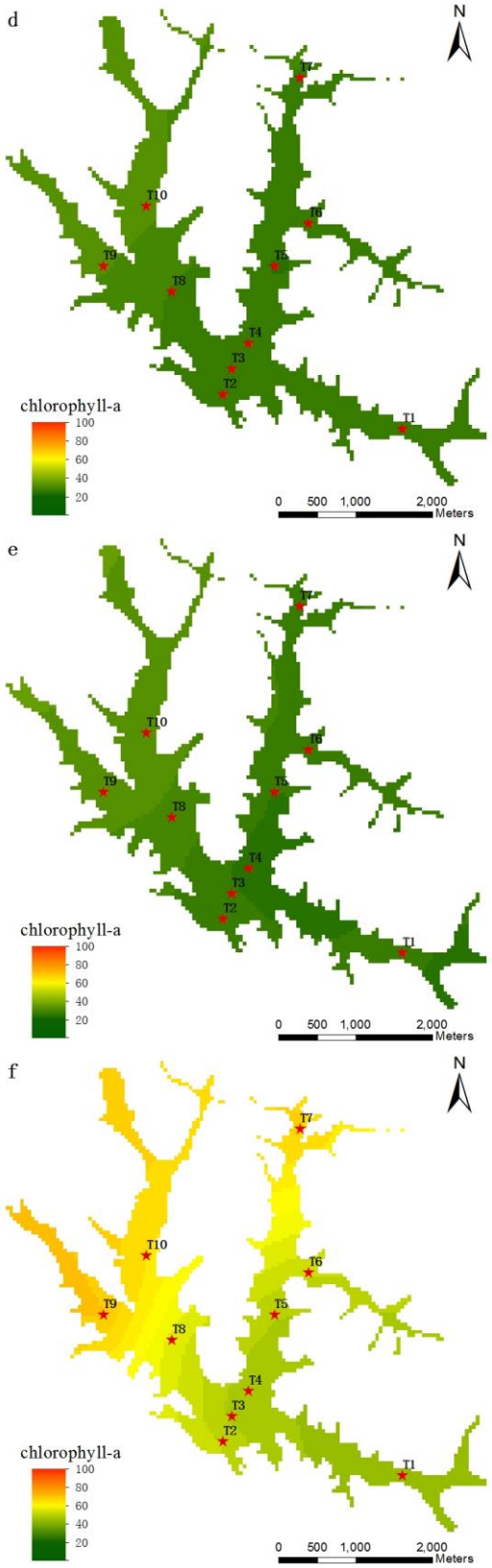

Figure 5. *Chl-a chart in different climatic period at Tiegang Reservior.* ***a*** *2013 pre-rainy period;* ***b*** *2013 latter rainy period;* ***c*** *2013 high temperature and rain free period;* ***d*** *2013 winter drought period;* ***e*** *2014 temperature rising period;* ***f*** *2014 pre-rainy period*

http://www.aloki.hu ● ISSN 1589 1623 (Print) ● ISSN 1785 0037 (Online)
DOI: http://dx.doi.org/10.15666/aeer/1704_81918217

From the perspective of space, the No. 1 sampling site was at the inlet of Tiegang Reservoir from the Xili Reservoir, whose ρ(TChla) was 4.72-55.01 μg L^{-1}, with an average of 21.13 μg L^{-1}. The water quality was relatively good, and the algae concentration was low. The No. 2 sampling site was close to the water intake point from Tiegang Reservoir for the water plant. Because of the daily water supply to the water plant, the water exchange was most frequent in the No. 2 sampling site; therefore, the growth of algae was inhibited, with a mean ρ(TChla) value of 25.14 μg L^{-1}, showing good water quality. The No. 1 and No. 2 sampling sites were essentially free of algal blooms. The No. 3 and No. 4 sampling sites were located in the center of the reservoir, with good hydrodynamic conditions, whose mean values of ρ(TChla) were 28.50 μg L^{-1} and 28.16 μg L^{-1}, respectively, showing a relatively low risk of algal bloom. The No. 5 and No. 6 sampling sites were located in the dead water area, whose mean values of ρ(TChla) were 32.63 μg L^{-1} and 31.83 μg L^{-1}, respectively, showing a moderate risk of algae bloom in the rainy season. This was especially true for the No. 5 sampling site in June 2013, with a ρ(Chla) of 104.88-122.43 μg L^{-1}, showing a sign of mild algal bloom. The No. 7 sampling site was at the inlet from Tiegang Reservoir to the Shiyan Reservoir, whose ρ(TChla) was 4.07-96.17 μg L^{-1}, with a mean value of 69.01 μg L^{-1}, showing a moderate risk of algal bloom in the rainy season. The No. 9 and No. 10 sampling sites were close to the entry from the Jiuwei River and Liaokeng River, whose mean values of ρ(TChla) were 53.50 μg L^{-1} and 67.01 μg L^{-1}, respectively. The maximum values of ρ(TChla) were 145.06 μg L^{-1} and 119.62 μg L^{-1} in June 2013, respectively. Except for the winter dry storage period and the temperature rising period, the No. 9 and No. 10 sampling sites were at moderate or high risk of algal bloom in all other months, and the water supply safety was threatened, which needs to be addressed. The No. 8 sampling site was located at the intersection of the No. 9 and No. 10 sampling site waters, whose average annual ρ(Chla) was 39.42 μg L^{-1}, also showing a certain risk of algal bloom in the rainy season. Overall, most areas of Tiegang Reservoir are already in a mesotrophic state, and some areas are in the transition to a eutrophic state.

Multivariate analysis of chl-a and environmental factors

Pearson correlation analysis of chl-a and water quality factors

Table 1 shows the relationship between chl-a and water quality factors in the flood and drought seasons. The main correlation factors of cyonophyta, chlorophyt and bacillariophyta in different periods were different. The main correlation factors of cyanobacteria in descending order of the absolute value of the correlation coefficient for the rainy season were WT > transparency > turbidity > N:P > TP > silicate > TOC, in which transparency, N:P and silicate were negatively correlated. The main correlation factors of cyanobacteria in descending order of the absolute value of the correlation coefficient for the drought season were TOC > WT > NO_3^--N > TN > Fe > N:P, in which the NO_3^--N, TN, Fe and N:P were negatively correlated. The main correlation factors of bacillariophyta in descending order of the absolute value of the correlation coefficient for the rainy season were WT > TP > TN > TOC > NO_3^--N, in which the WT and TOC were negatively correlated. The main correlation factors of bacillariophyta in descending order of the absolute value of the correlation coefficient for the drought season were silicate > N:P > TN > transparency > NO_3^--N > Fe, in which N:P, TN, transparency, NO_3^--N and Fe were negatively correlated. The main

http://www.aloki.hu ● ISSN 1589 1623 (Print) ● ISSN 1785 0037 (Online)
DOI: http://dx.doi.org/10.15666/aeer/1704_81918217

correlation factors of chlorophyta in descending order of the absolute value of the correlation coefficient for the rainy season were COD > transparency > TOC > NO_3^--N > DO > WT, in which transparency and NO_3^--N were negatively correlated. The main correlation factors of chlorophyta in descending order of the absolute value of the correlation coefficient for the drought season were TOC > WT > TP > N:P > pH > COD, in which N:P was negatively correlated. In general, the correlations between the three algae and the water quality factors in the drought season were significantly higher than those in the rainy season. This likely occurs because the algae concentration was significantly decreased by the dilution effect of the heavy rainfall (Bernal-Brooks et al., 2016) in a short time during the rainy season, leading to strong fluctuations in the chl-a concentration; therefore, the correlation with water quality factors was reduced.

Table 1. *Pearson correlation coefficients between chl-a and water quality factors*

Period	Phytoplankton	DO	pH	WT	SD	Turbidity	COD	TOC	Silicate	NO_3^--N	TN	TP	N:P	Fe
Rainy season	Cyanophyta	0.047	-0.008	**0.418****	**-0.393****	**0.360****	0.152	**0.233***	**-0.261***	-0.042	0.132	**0.284****	**-0.310****	-0.105
	Bacillariophyta	-0.176	-0.080	**-0.562****	0.127	0.022	-0.183	**-0.403****	-0.195	**0.354****	**0.454****	**0.475****	**-0.238***	-0.135
	Chlorophyta	**0.308****	**0.213***	**0.273****	**-0.445****	0.142	**0.536****	**0.339****	**0.253***	**-0.322****	0.002	-0.075	-0.007	0.023
	Total Algae	0.013	-0.004	-0.028	**-0.283****	**0.271***	0.114	0.062	-0.209	0.052	**0.286****	**0.350****	**-0.294****	-0.115
Drought season	Cyanophyta	0.124	**0.398****	**0.651****	-0.251	-0.078	0.133	**0.778****	**0.425****	**-0.618****	**-0.616****	**0.274****	**-0.442****	**-0.513****
	Bacillariophyta	**0.224****	**0.309****	**0.268****	**-0.400****	0.085	0.049	**0.434****	**0.478****	**-0.396****	**-0.460****	**0.263****	**-0.461****	**-0.369****
	Chlorophyta	0.178	**0.502****	**0.695****	**-0.474****	-0.013	**0.475****	**0.758****	**0.465****	**-0.390****	**-0.414****	**0.601****	**-0.541****	**-0.388****
	Total Algae	0.181	**0.428****	**0.601****	**-0.361****	-0.015	0.160	**0.750****	**0.501****	**-0.615****	**-0.613****	**0.343****	**-0.515****	**-0.511****
Whole time	Cyanophyta	0.041	0.157	**0.659****	**-0.323****	**0.208****	**0.270****	**0.600****	-0.129	**-0.215****	0.134	0.161	-0.187	**-0.242****
	Bacillariophyta	-0.073	0.087	0.165	-0.141	0.005	0.024	0.085	-0.029	0.145	**0.378****	**0.350****	**-0.236****	**-0.226****
	Chlorophyta	0.196	**0.266****	**0.663****	**-0.389****	0.016	**0.491****	**0.626****	0.100	**-0.352****	0.095	0.029	-0.050	-0.146
	Total Algae	0.034	0.169	**0.590****	**-0.315****	0.176	**0.259****	**0.521****	-0.083	-0.154	**0.213****	**0.215****	**-0.203****	**-0.250****

Rainy season was from April to September 2013 and April to July 2014. Drought season was from October 2013 to March 2014. *Significant at the 0.05 level. **Significant at the 0.01 level. DO-dissolved oxygen. WT: water temperature, SD: transparency, COD: chemical oxygen demand, TOC: total organic carbon, TN: total nitrogen, NO^{3-}: N-nitrate nitrogen, TP: total phosphorus, N: P-the proportion of TN to TP

In particular, in the rainy season, the WT was positively correlated to cyanobacteria, with a correlation coefficient of 0.418, and was negatively correlated to bacillariophyta, with a correlation coefficient of -0.562. It was found that rising temperatures (1.4 – 6.8 °C) could increase cyanobacteria growth rates and increase cyanobacteria bloom occurrences (Davis et al., 2009; Wu et al., 2014; O Neil et al., 2012). The optimum temperature for microcytic species are 30–33 °C (Mowe et al., 2017). Fadel et al. (2015) investigated a freshwater reservoir in the Mediterranean and found that when the WT exceeded 25 °C, the cyanobacteria represented by microcystis began to multiply. It was found that the suitable temperature for the growth of bacillariophyta was 10–25 °C (Mitrovic et al., 2010), and the maximum growth rate occurred at 20 °C, and the growth rate of bacillariophyta was inhibited and the biomass began to decrease when the WT exceeded 25 °C (Jung et al., 2013). The WT of Tiegang Reservoir was 22.46–32.79 °C in the rainy season, with an average of 29.44 °C, and reached 28 °C in May. The higher WT is beneficial to the growth and reproduction of cyanobacteria, and it somehow inhibits the growth of bacillariophyta, which allows the cyanobacteria to gain an advantage over bacillariophyta. Therefore, the WT was positively correlated with cyanobacteria and negatively correlated with bacillariophyta in the rainy season. In the rainy season, the concentration of cyanobacteria was positively correlated with turbidity and negatively correlated with transparency, indicating that the rapid increase of

http://www.aloki.hu ● ISSN 1589 1623 (Print) ● ISSN 1785 0037 (Online)
DOI: http://dx.doi.org/10.15666/aeer/1704_81918217

cyanobacteria in the rainy season increased the water turbidity while reducing the water transparency and light intensity. The photosynthesis of algae is limited with reduced light intensity in a water body. However, some cyanobacteria have pseudo-vacuoles, which can float up to the surface water layer where the light intensity is higher, and they will subsequently not be inhibited by the weakening of light. Bacillariophyta are more widely distributed in the middle layers of water, and the high turbidity and low light intensity of the water body will therefore more significantly affect the growth of bacillariophyta. In the rainy season, TN was significantly correlated with bacillariophyta, and TP showed a certain correlation with both bacillariophyta and cyanobacteria, indicating that nitrogen and phosphorus are the important factors for algae growth. Tiegang Reservoir is a nitrogen-contaminated reservoir, with total nitrogen levels up to 1.64 mg L^{-1}, a surface water quality of grade V, and TP levels as low as 0.024 mg L^{-1}, belonging to the surface water quality of grade II. For algal growth, TN is relatively abundant, and TP is relatively scarce, and phosphorus is a limiting nutrient for algal growth. The N: P of Tiegang Reservoir in the rainy season and drought season was 69 and 54, respectively, and the N: P showed a negative correlation with cyanobacteria and bacillariophyta, indicating that a high N: P was not favorable for the growth of algae. This result is consistent with the findings of Smith (1983), who proposed the "N: P law" based on the study of 17 lakes; that is, cyanobacteria blooms can easily outbreak when N: P is lower than 29. The WT in the drought season was still the main influencing factor for all three algae, especially for chlorophyta and cyanobacteria, with correlation coefficients as high as 0.695 and 0.651, respectively. All three algae in the drought season showed significant negative correlations with water quality factors, including NO_3^--N, TN and Fe. There were two main reasons for this phenomenon. On the one hand, the ρ(Chla) of algae in the drought season significantly decreased with decreased temperature. On the other hand, water is lacking in the drought season, and the reservoir was operating at low water level; thus, the concentrations of water quality factors, including NO_3^--N and TN increased slightly. The transparency was negatively correlated with the three algae at each period to varying degrees, indicating that the growth of algae in the reservoir was not conducive to the transparency of the water body. The correlations between DO and the three algae in each period were not obvious because Tiegang Reservoir is a typical artificial water transfer and supply reservoir, with a highly frequent water exchange and a low stability of the water body. The average concentrations of dissolved oxygen in the rainy season and drought season were 8.89 and 9.12 mg L^{-1}, respectively, which are sufficient to meet the needs of algal growth.

Pearson correlation analysis of chl-a with the meteorological and hydrodynamic factors

Table 2 shows the correlation of chl-a with the meteorological factors and hydrodynamic factors in the flood and drought seasons. On the same day, the collected hydrodynamic factors and meteorological factors should be the same, and the data characteristics were different from those of water quality factors. Therefore, their correlations with the chl-a were analyzed separately. *Table 2* shows that there were significant differences in the main correlated factors of different algae in the same period and the same algae at different periods. The main correlated factors of different algae in different periods were different. In the rainy season, the main correlated factors of cyanobacteria in descending order of the absolute value of the correlation coefficient

http://www.aloki.hu ● ISSN 1589 1623 (Print) ● ISSN 1785 0037 (Online)
DOI: http://dx.doi.org/10.15666/aeer/1704_81918217

were WT > evapoproportion n > pressure > runoff > sunshine hours > hydraulic retention times (HRT). The main correlated factors of bacillariophyta in descending order of the absolute value of the correlation coefficient were temperature > evapoproportion n > sunshine hours > runoff > HRT > pressure. The main correlated factor of chlorophyta was temperature. In the drought season, the main correlated factors of cyanobacteria in descending order of the absolute value of the correlation coefficient were water evapoproportion n > temperature. The main correlated factors of bacillariophyta in descending order of the absolute value of the correlation coefficient were evapoproportion n > pressure > temperature. The main correlated factors of chlorophyta in descending order of the absolute value of the correlation coefficient were humidity > evapoproportion n > pressure. Temperature showed a significant positive correlation with cyanobacteria and a significant negative correlation with bacillariophyta, which was consistent with the effect of WT on cyanobacteria and bacillariophyta. Rainfall is the main driving force of watershed pollution entering the reservoir. The rainwater washed the organic matter and nitrogen/phosphorus nutrient salt deposits from the watershed surface into the reservoir in the form of ground surface runoff (Abell and Hamilton, 2015). The runoff in the early rainy season showed a significant negative correlation with cyanobacteria and a negative correlation with bacillariophyta. The runoff in the late rainy season showed a slight negative correlation with all three algae. This occurs because the proportion of organic matter and nutrient salts in the runoff of the early rainy season were high, which could increase the organic matter and nutrient salts in the reservoir and promote the growth and reproduction of cyanobacteria. The water quality of the runoff in the late rainy season was better, which was mainly due to the increased amount of water in the reservoir, which diluted the organic matter, nutrient salts and algae. In the rainy season, HRT was highly negatively correlated with cyanobacteria, indicating that, in order to inhibit the excessive reproduction of cyanobacteria during the rainy season, the reservoir management department can reduce the water retention time by increasing the water supply and reducing the water level of the reservoir to prevent a cyanobacteria bloom. The pressure was negatively correlated with all three algae to different degrees, but the results do not indicate that the pressure has a significant direct effect on algal growth. This is mainly due to the significant negative correlation between air pressure and air temperature in meteorological regularity. Pearson correlation analysis also showed that the correlation coefficients of air temperature and air pressure in the flood and drought seasons were -0.859 and -0.936, respectively.

Canonical correspondence analysis (CCA) of chl-a and environmental factors

Canonical correspondence analysis of the relationship of the water quality, meteorological factors and hydrodynamic factors with algae ρ(Chla) in the rainy season and the drought season was carried out to investigate the comprehensive effects of the environmental factors on the growth of algae in the flood and drought seasons (*Fig. 6*). The arrow in the figure indicates the environmental factor, and the length of the arrow indicates the correlation between the algae and this environmental factor. The angle between the arrow line and the ordination axis indicates the correlation between this environmental factor and the ordination axis, and the smaller the angle is, the closer the correlation is. The quadrant of the arrow indicates the positive or negative correlation between the environmental factor and the ordination axis. In the rainy season, cyanobacteria, chlorophyta and bacillariophyta were located in the fourth, first and

http://www.aloki.hu ● ISSN 1589 1623 (Print) ● ISSN 1785 0037 (Online)
DOI: http://dx.doi.org/10.15666/aeer/1704_81918217

second quadrants, respectively; in the drought season, cyanobacteria, chlorophyta and bacillariophyta were located in the second, fourth and first quadrants, respectively, indicating that the growth patterns of the three algae were different, and the environmental factors influencing the three algae varied widely. The eigenvalues of F1 and F2 in the rainy season were 0.022 and 0.008, respectively, and the explanatory rates were 72.61% and 27.39%, respectively. The eigenvalues of F1 and F2 in the drought season were 0.024 and 0.009, respectively, and the explanatory rates were 73.10% and 26.90%, respectively.

Table 2. *Pearson correlation coefficients between chl-a and hydrodynamic/meteorological factors*

Period	Phytoplankton	AT	BP	Humidity	SHD	EC	RV	TR	HRT
Rainy season	Cyanophyta	**0.401****	**-0.391****	-0.103	**0.336****	**0.392****	**0.323****	-0.108	**-0.258***
	Bacillariophyta	**-0.484****	**0.327****	0.189	**-0.386****	-0.129	-0.104	**-0.212***	0.347
	Chlorophyta	0.108	-0.064	-0.049	0.069	-0.096	-0.018	0.039	-0.095
	Total Alage	0.047	-0.157	-0.009	0.099	0.205	0.122	-0.143	-0.064
Drought season	Cyanophyta	**0.564****	**-0.352****	-0.138	0.009	**0.401****	-0.082	-0.118	-0.172
	Bacillariophyta	0.071	0.069	**-0.315****	0.102	**0.323****	**-0.233***	-0.130	-0.077
	Chlorophyta	**0.589****	**-0.387****	**-0.450****	**0.503****	**0.651****	**-0.299****	**-0.377****	**-0.315****
	Total Alage	**0.462****	**-0.251***	**-0.255***	0.102	**0.464****	-0.172	-0.168	-0.176
Whole time	Cyanophyta	**0.689****	**-0.723****	**0.513****	0.038	-0.015	**0.335****	**0.343****	0.049
	Bacillariophyta	**0.272***	**-0.200***	**0.254****	**-0.262****	-0.107	-0.047	0.076	**0.326****
	Chlorophyta	0.108	-0.064	-0.049	0.069	-0.096	-0.018	0.039	-0.095
	Total Alage	**0.608****	**-0.637****	**0.494****	-0.048	-0.059	**0.266****	**0.310****	0.142

Rainy season was from April to September 2013 and April to July 2014. Drought season was from October 2013 to March 2014. AT: air temperature, BP: barometric pressure, SHD: sunshine duration, EC: evaporation capacity, RV: runoff volume, TR: total rainfall, HRT: hydraulic retention time. *Significant at the 0.05 level. **Significant at the 0.01 level

Figure 6 shows that the environmental factors with the highest correlation degree to algae were the meteorological factors, including the temperature, sunshine hours, pressure and evaporation, indicating that the spatio-temporal distribution and evolution of algae are mainly driven by changes in climate. Panels a and b show that the strongest environmental factor associated with algae in the rainy season and the drought season was WT, followed by air temperature, indicating that temperature is the primary driving factor for algal growth in Tiegang Reservoir. The environmental factors showing the maximum projection on the F1 axes of the two panels were both WT; thus, the F1 axis mainly reflects the change in WT. The number of sunshine hours and the amount of evaporation in both figure a and figure b showed positive correlations with algae. Light is the essential condition for the photosynthesis of algae, and the increase of sunshine hours is beneficial to the increase of algal biomass. The amount of evaporation reflects the loss of the reservoir water from liquid to gas; the greater the amount of evaporation is, the more the loss of the reservoir water due to evaporation, resulting in increased algal concentration. Air pressure was negatively correlated with algae and was highly opposite to temperature in figure a and figure b since pressure was negatively correlated with temperature in the meteorological regularity; thus, pressure was indirectly negatively correlated with algae, which does not indicate that pressure has a direct causal relationship with algal growth. The hydrodynamic factor HRT reflects the length of residence time of water in the reservoir, which was significantly correlated with algae in both figure a and figure b. This negative correlation was especially significant for

http://www.aloki.hu ● ISSN 1589 1623 (Print) ● ISSN 1785 0037 (Online)
DOI: http://dx.doi.org/10.15666/aeer/1704_81918217

cyanobacteria, indicating that frequent water exchange could inhibit the growth of algae. This finding is consistent with the result of the Pearson correlation analysis. TOC and COD represent the contents of organic matter in the water, whereas TN, ammonia nitrogen, nitrate nitrogen and TP reflect the contents of nutrient salts in the water. The TOC, COD, TN, ammonia nitrogen, nitrate nitrogen and TP were moderately correlated with algal concentration ns in figure a and figure b. Silicate was more closely related to algae in the rainy season, and the correlation in the drought season was not obvious. In the drought season, Fe was highly correlated with the F1 axis because Fe is an essential element of algal photosynthesis and metabolism and has an important effect on the biomass and growth rate of algae, especially bacillariophyta (Sugie et al., 2013; Okumura et al., 2013; Russo et al., 2015).

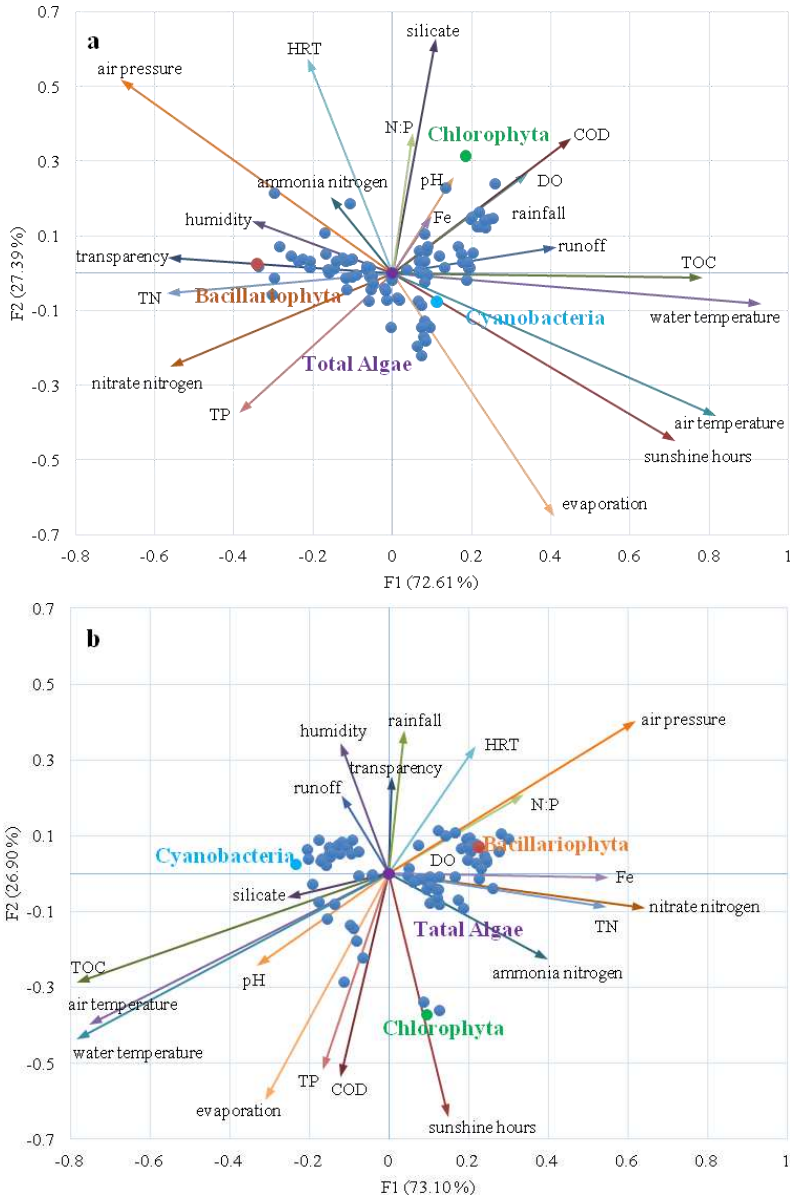

Figure 6. *Canonical correspondence analysis of environmental factors and phytoplankton:* ***a*** *rainy period;* ***b*** *drought period. The light blue, green, yellow and purple dots, respectively, represent cyanobacteria, chlorophyta, bacillariophyta and total algae; the dark blue dots indicate the sampling sites; and the arrows indicate the environmental factors*

http://www.aloki.hu ● ISSN 1589 1623 (Print) ● ISSN 1785 0037 (Online)
DOI: http://dx.doi.org/10.15666/aeer/1704_81918217

Influence of environmental factors on the competitiveness of cyanobacteria and Bacillariophyta

Effects of single environmental factors on the competitiveness of cyanobacteria and Bacillariophyta

Chl-a proportions of cyanobacteria and diatom were used to characterize the competitiveness of cyanobacteria and bacillariophyta, thus describing the potential for growth and eruption. When the chl-a proportion was less than 40%, it meant that the outbreak risk was low. When the chl-a proportion reached 40%~60%, it meant that they had slight risk of outbreaks. When the chl-a proportion were more than 60%, it meant that they were at high risk of outbreaks.

Figure 7 shows when WT was lower than 17 °C, the proportion of cyanobacteria was between 30~40%, and the advantage was not obvious. With the increase of WT, the competitiveness of cyanobacteria increased gradually. When the WT was 21.5 °C, the proportion of cyanobacteria and bacillariophyta were both equal to 48%. The two were equal in competitiveness. There was a high risk of cyanobacteria blooming. When WT reached 28.8 °C, the proportion of cyanobacteria was over 60%, which completely occupied the dominant position. When WT exceeded 30 °C, the cyanobacteria proportion raised to 70%~80%, reaching the highest level. The linear fitting formula of cyanobacteria competitiveness and WT was calculated as *Equation 1*. When WT was below 17.2 °C, the diatom proportion was higher than 60%. Bacillariophyta occupied a dominant position. As the water temperature raised, the diatom proportion decreased gradually. When WT was 21.5 °C, the proportion of cyanobacteria and diatom was both 48%. When WT exceeded 24.3 °C, the diatom proportion fell below 40%, completely losing the dominant position. When WT exceeded 32 °C, the diatom proportion dropped to 10~15%, reaching the lowest level in the whole year. The linear fitting formula of diatom competitiveness and WT was calcuated as *Equation 2*.

$$[\text{Chla-cyanophyta}] = 11.94 + 1.68\text{WT}, R^2 = 0.81 \quad \text{(Eq.1)}$$

$$[\text{Chla-bacillariophyta}] = 107.60 - 2.76\text{WT}, R^2 = 0.49 \quad \text{(Eq.2)}$$

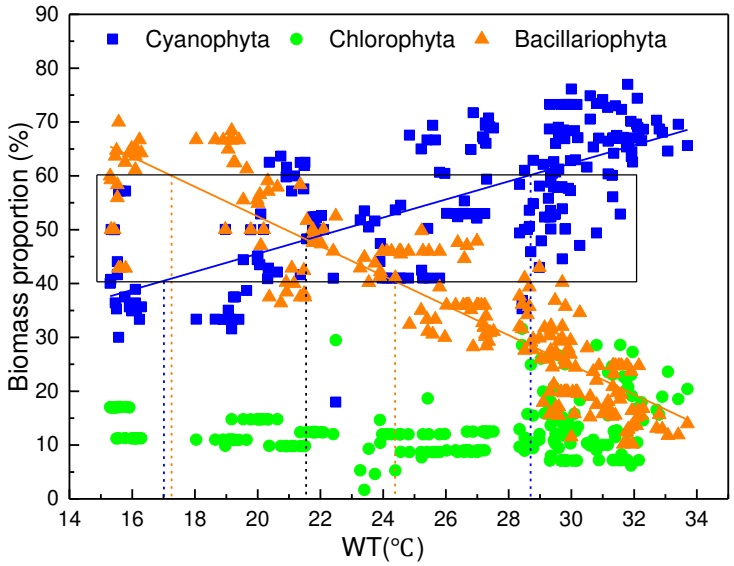

Figure 7. *Effects of WT on the competitiveness of cyanobacteria and bacillariophyta*

http://www.aloki.hu ● ISSN 1589 1623 (Print) ● ISSN 1785 0037 (Online)
DOI: http://dx.doi.org/10.15666/aeer/1704_81918217

Figure 8 shows when TOC was below 2.25 mg/L, the proportion of cyanobacteria was between 30~40%, and its advantage was not obvious. With the increase of TOC, the competitiveness of cyanobacteria increased gradually. When TOC was 2.62 mg/L, the proportion of cyanobacteria and bacillariophyta were both equal to 48%. The two were equal in competitiveness. When TOC reached 4.21 mg/L, the proportion of cyanobacteria was more than 60%, which fully occupied the dominant position. When TOC exceeded 5.0 mg/L, the cyanobacteria proportion raised to 65%~75%, reaching the highest level in the year. The linear fitting formula of cyanobacteria competitiveness and TOC was calculated as *Equation 3*.

When TOC was below 1.70 mg/L, the diatom proportion was higher than 60%. Diatom occupied a dominant position. With the increasing of TOC, the proportion of diatom decreased gradually. When TOC was 2.62 mg/L, the proportion of cyanobacteria and bacillariophyta was both 48%. When TOC exceeded 3.29 mg/L, the diatom proportion fell below 40%, completely losing dominance. When TOC exceeded 4.52 mg/L, the diatom proportion falls to 10%~20%, reaching the lowest level of the year. The linear fitting formula of diatom competitiveness and TOC was calculated as *Equation 4*.

$$[\text{Chla-cyanophyta}] = 26.11 + 8.22\text{TOC}, R^2 = 0.54 \quad \text{(Eq.3)}$$

$$[\text{Chla-bacillariophyta}] = 82.09\text{-}12.89\text{TOC}, R^2 = 0.69 \quad \text{(Eq.4)}$$

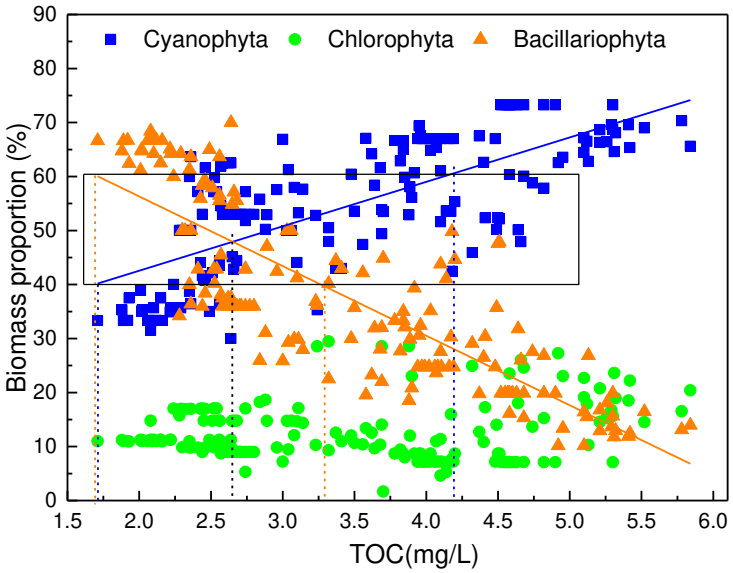

Figure 8. *Effects of TOC on the competitiveness of cyanobacteria and bacillariophyta*

Figure 9 shows when NO_3^--N was below 0.82 mg/L, the proportion of cyanobacteria was between 60~75%, taking full advantage. With the increasing of NO_3^--N, the competitiveness of cyanobacteria declined gradually. When NO_3^--N was 1.28 mg/L, the proportion of cyanobacteria and bacillariophyta were both equal to 46%. The two were equal in competitiveness. When NO_3^--N reached 1.53 mg/L, the proportion of cyanobacteria fell below 40%. Cyanobacteria completely lost dominance. The linear fitting formula of cyanobacteria competition and NO_3^--N was calculated as *Equation 5*.

http://www.aloki.hu ● ISSN 1589 1623 (Print) ● ISSN 1785 0037 (Online)
DOI: http://dx.doi.org/10.15666/aeer/1704_81918217

When NO_3^--N was below 0.82 mg/L, the diatom proportion was below 30%, and the competitiveness was very low. With the increasing of NO_3^--N, the proportion of diatom raised gradually. When NO_3^--N was 1.28 mg/L, the proportion of cyanobacteria and bacillariophyta was both 48%. When NO_3^--N exceeded 1.4 mg/L, diatom occupied the dominant position. The linear fitting formula of diatom competition and NO_3^--N was calculated as *Equation 6*.

$$[\text{Chla-cyanophyta}] = 82.97 + 27.93\ NO_3^-\text{-N},\ R^2 = 0.28 \quad \text{(Eq.5)}$$

$$[\text{Chla-bacillariophyta}] = -2.59\text{-}39.04\ NO_3^-\text{-N},\ R^2 = 0.30 \quad \text{(Eq.6)}$$

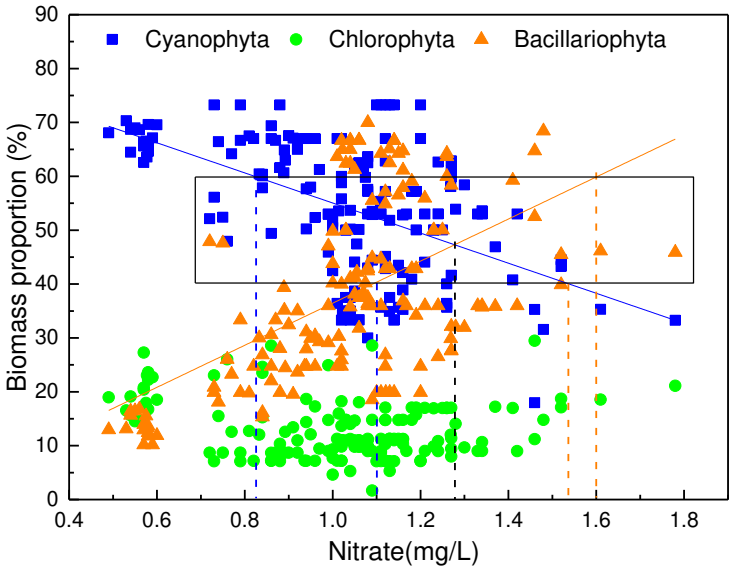

Figure 9. *Effects of NO_3^--N on the competitiveness of cyanobacteria and bacillariophyta*

Figure 10 shows when COD was 1.20~1.50 mg/L, the proportion of cyanobacteria and bacillariophyta was 30%~72%. When COD was 1.38 mg/L, the proportion of cyanobacteria and bacillariophyta were both equal to 49%. The competition between them was fierce and neither had obvious advantages. With the increase of COD, the dominance of bacillariophyta declined while the dominance of cyanobacteria increased. When COD was 1.82 mg/L, the proportion of bacillariophyta dropped below 40%, losing dominance, while the proportion of cyanobacteria rose further. When COD was 2.55 mg/L, the proportion of cyanobacteria was over 60%. Cyanobacteria completely occupied the dominant position, while the diatom proportion dropped to about 20%. From *Figure 9,* it can be found that the competitiveness of cyanobacteria is significantly higher than that of diatoms at lower nutrient saline levels. With the increase of nutrient concentration, the competitiveness of bacillariophyta increased significantly. This validates the research results of Onur. Cyanobacteria cell sizes are much smaller than diatom cells. Therefore the higher nutrient affinity and growth rate of the small s Cyanobacteria makes them better competitors (Onur et al., 2012). The linear fitting formula of blue-green algae competitiveness and COD was calculated as *Equation 7*. The linear fitting formula of diatom competitiveness and COD was calculated as *Equation 8*.

http://www.aloki.hu ● ISSN 1589 1623 (Print) ● ISSN 1785 0037 (Online)
DOI: http://dx.doi.org/10.15666/aeer/1704_81918217

$$[\text{Chla-cyanophyta}] = 36.14 + 9.44\text{COD}, R^2 = 0.17 \quad \text{(Eq.7)}$$

$$[\text{Chla-bacillariophyta}] = 73.42\text{-}18.15\text{COD}, R^2 = 0.31 \quad \text{(Eq.8)}$$

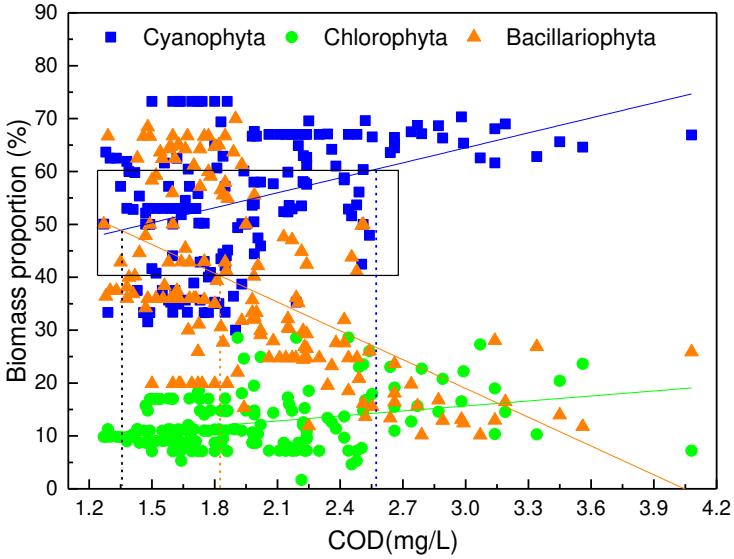

Figure 10. *Effects of COD on the competitiveness of cyanobacteria and bacillariophyta*

Therefore, environmental factors such as WT, TOC, NO_3^--N and COD were closely related to the competitiveness of cyanobacteria and bacillariophyta. So they can be used as an early warning index for algal bloom. WT 22 °C can be used as a primary WT threshold of cyanobacteria. When WT was more than 22 °C, the diatom dominance decreased, and the predominance of cyanobacteria rose rapidly. WT 28 °C can be used as the secondary WT threshold of cyanobacteria. When WT was over 28 °C, and the predominance of cyanobacteria was over 60%, and cyanobacteria blooming was most likely to occur. Similarly, the primary TOC threshold of cyanobacteria was 2.8 mg/L, and the secondary TOC threshold was 4.2 mg/L. The primary NO_3^--N threshold of cyanobacteria was 1.25 mg/L, and the secondary NO_3^--N threshold was 0.85 mg/L. The primary COD threshold of cyanobacteria was 1.25 mg/L, and the t secondary COD threshold was 2.55 mg/L.

Analysis of the effects of dual environmental factors on the competitiveness of cyanobacteria and bacillariophyta

The effects of single environmental factors on the competitiveness of cyanobacteria and bacillariophyta were analyzed in the previous section (*Figs. 11–14*). However, in the real environment of the reservoir, the growth of algae was influenced by synergistic effect of many environmental factors. WT was the most important environmental factor. Therefore, the dual synergistic effects of WT and other environmental factors on the competitiveness of cyanobacteria and bacillariophyta were further analyzed. Bubble charts were used and bubble size indicated the proportion of chl-a to cyanobacteria or bacillariophyta, which represented the competitiveness of cyanobacteria and bacillariophyta.

http://www.aloki.hu ● ISSN 1589 1623 (Print) ● ISSN 1785 0037 (Online)
DOI: http://dx.doi.org/10.15666/aeer/1704_81918217

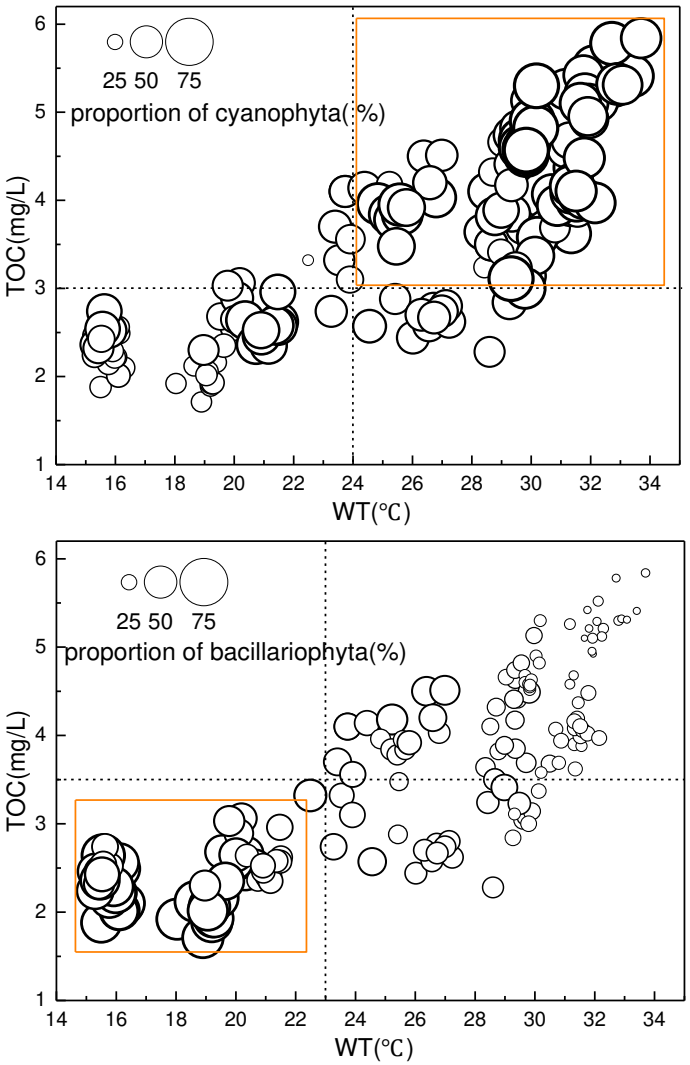

Figure 11. *Combined effects of WT and TOC on the competitiveness of cyanobacteria and bacillariophyta*

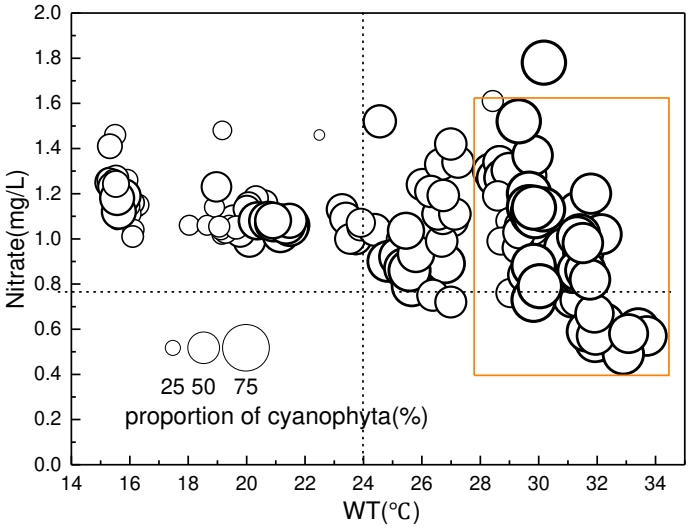

http://www.aloki.hu ● ISSN 1589 1623 (Print) ● ISSN 1785 0037 (Online)
DOI: http://dx.doi.org/10.15666/aeer/1704_81918217

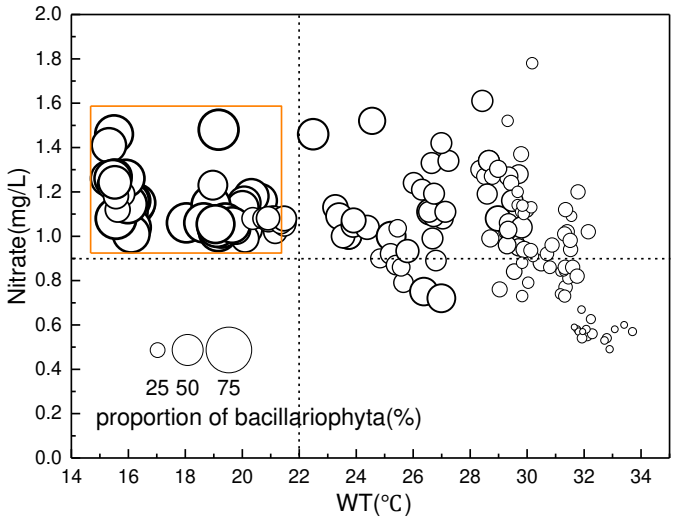

Figure 12. *Combined effects of WT and NO_3^--N on the competitiveness of cyanobacteria and bacillariophyta*

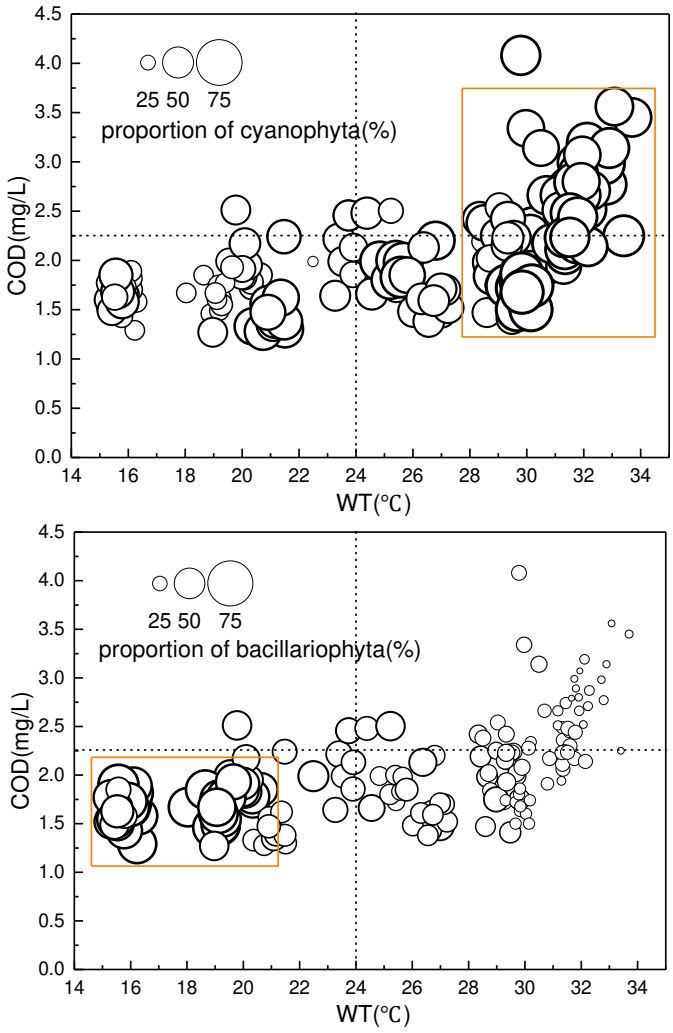

Figure 13. *Combined effects of WT and COD on the competitiveness of cyanobacteria and bacillariophyta*

http://www.aloki.hu ● ISSN 1589 1623 (Print) ● ISSN 1785 0037 (Online)
DOI: http://dx.doi.org/10.15666/aeer/1704_81918217

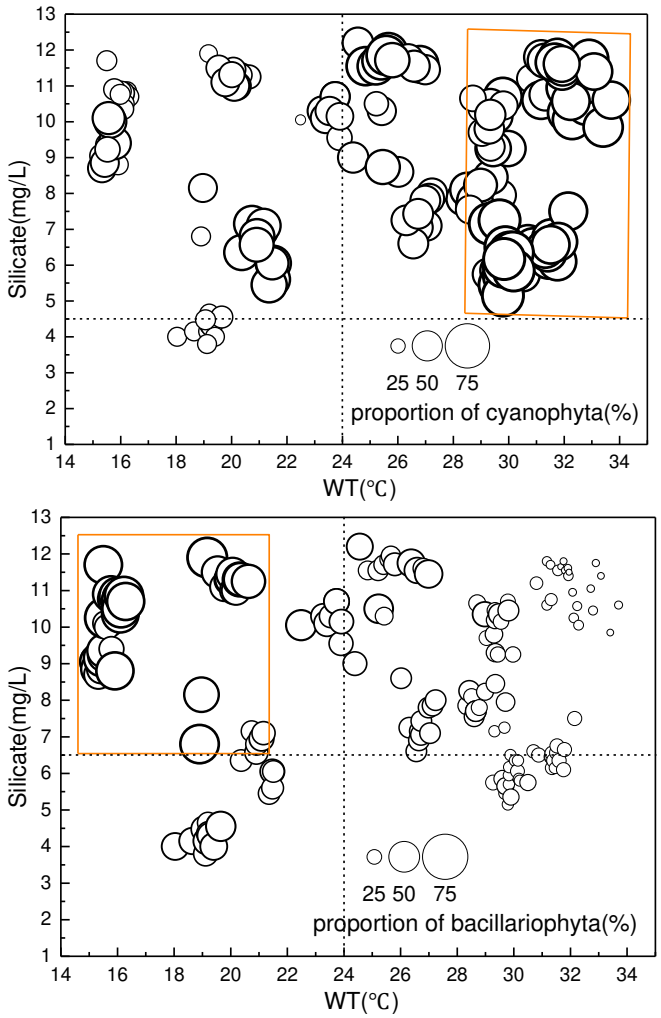

Figure 14. *Combined effects of Silicate and NO_3^--N on the competitiveness of cyanobacteria and bacillariophyta*

A combination of environmental factors at high risk for cyanobacteria or diatoms were found. WT (24.5~33.5 °C) and TOC (3.2~5.8 mg/L) were high risk factors for cyanobacteria outbreaks. WT (15.5~21.5 °C) and TOC (1.5~3.3 mg/L) were high risk factors for bacillariophyta outbreaks. WT (28.5~33.5 °C) and NO_3^--N (0.5~1.5 mg/L) were high risk factors for cyanobacteria outbreaks. WT (15.5~21.5 °C) and NO_3^--N (1.0~1.5 mg/L) were high risk factors for bacillariophyta outbreaks. WT (28.5~33.5 °C) and COD (1.7~3.5 mg/L) were high risk factors for cyanobacteria outbreaks. WT (15.5~20.5 °C) and COD (1.2~1.9 mg/L) were high risk factors for bacillariophyta outbreaks. WT (28.5~33.5 °C) and Silicate (5.0~11.8 mg/L) were high risk factors for cyanobacteria outbreaks. WT (15.5~20.5 °C) and Silicate (6.5~12.0 mg/L) were high risk factors for bacillariophyta outbreaks.

Conclusions

1) During the monitoring period, the average connection of algae [ρ(TChla)] in Tiegang Reservoir was 38.81 μg L^{-1}, which was in a mesotrophic state. The mean

http://www.aloki.hu ● ISSN 1589 1623 (Print) ● ISSN 1785 0037 (Online)
DOI: http://dx.doi.org/10.15666/aeer/1704_81918217

ρ(Chla) values of cyanobacteria, bacillariophyta and chlorophyta were 22.74, 11.53 and 4.54 μg L^{-1}, respectively. From late December 2013 to early 2014, bacillariophyta was the dominant algae (46.37–61.81%), cyanobacteria was dominant in all other periods (48.13–72.58%), and chlorophyta was low throughout the entire year (7.25–14.80%). Compared with the same period of the previous year, the proportion of cyanobacteria was increased in the period of May-June 2014, and the proportions of bacillariophyta and chlorophyta decreased with the decreased diversity of algae, leading to the increased risk of a cyanobacteria bloom.

2) The temporal changing pattern of ρ(Chla) in Tiegang Reservoir is as follows: the early rainy season > the late rainy season > the high temperature and no rain period > the temperature rising period > the autumn and winter water storage period. The distribution of ρ(Chla) in the vertical direction is as follows: the transparent layer > the surface layer > the bottom layer. The spatial changing pattern of ρ(Chla) is a gradual increase from southeast to northwest. The No. 9 and No. 10 sampling sites are at the entry of the runoff to the reservoir, whose ρ(Chla) were significantly higher than that in other reservoir areas. The water quality of the No. 2 sampling site at the intake point of the water plant was good. The northwest reservoir area is at high risk of an algal bloom.

3) Pearson correlation analysis and CCA analysis showed that the spatio-temporal distribution of algae was mainly driven by changes in climate, for which the WT was the primary driving factor. The main environmental factors for cyanobacteria, bacillariophyta and chlorophyta were greatly different. Cyanobacteria is mainly associated with WT, TOC, sunshine hours, runoff and HRT; bacillariophyta is mainly associated with WT, silicate, TN, TP and HRT; and chlorophyta are mainly associated with TOC, COD, WT, NO_3^--N and sunshine hours.

4) Influence of environmental factors on the competitiveness of cyanobacteria and bacillariophyta was analyzed. Single environmental factors such as WT, TOC, NO_3^--N, and COD were significantly related to the competitiveness of cyanobacteria and bacillariophyta. The linear fitting formula of cyanobacteria competitiveness and environmental factors were calculated. The dual synergistic effects of WT and other environmental factors on the competitiveness of cyanobacteria and bacillariophyta were analyzed. A combination of environmental factors with high risk of cyanobacteria and diatom outbreaks was proposed.

Acknowledgements. This study was founded by the Special Funds for Public Industry Research Projects of the National Ministry of Water Resources (201301047) and Shenzhen Science and Technology Innovation Project (JCYJ20140508155916418).

REFERENCES

[1] Abell, J. M., Hamilton, D. P. (2015): Biogeochemical processes and phytoplankton nutrient limitation in the inflow transition zone of a large eutrophic lake during a summer rain event. – Ecohydrology 8: 243-262.

[2] Beecraft, L., Watson, S. B., Smith, R. E. H. (2017): Multi-wavelength pulse amplitude modulated fluorometry (Phyto-PAM) reveals differential effects of ultraviolet radiation on the photosynthetic physiology of phytoplankton pigment groups. – Freshwater Biology 62: 72-86.

http://www.aloki.hu ● ISSN 1589 1623 (Print) ● ISSN 1785 0037 (Online)
DOI: http://dx.doi.org/10.15666/aeer/1704_81918217

[3] Bell, P. R. F., Elmetri, I., Lapointe, B. E. (2014): Evidence of large-scale chronic eutrophication in the great barrier reef: quantification of chlorophyll a thresholds for sustaining coral reef communities. – AMBIO 43: 361-376.
[4] Bernal-Brooks, F. W., Sánchez Chávez, J. J., Bravo Inclán, L. et al. (2016): The algal growth-limiting nutrient of lakes located at Mexico's Mesa Central. – Journal of Limnology 75: 169-178.
[5] Bott, T. L., Montgomery, D. S., Arscott, D. B., Dow, C. L. (2006): Primary productivity in receiving reservoirs: links to influent streams. – Journal of the North American Benthological Society 25: 1045-1061.
[6] Bowes, M. J., Gozzard, E., Johnson, A. C. et al. (2012): Spatial and temporal changes in chlorophyll-a concentrations in the River Thames basin, UK: are phosphorus concentrations beginning to limit phytoplankton biomass? – Science of the Total Environment 426: 45-55.
[7] Davis, T. W., Berry, D. L., Boyer, G. L., Gobler, C. J. (2009): The effects of temperature and nutrients on the growth and dynamics of toxic and non-toxic strains of Microcystis during cyanobacteria blooms. – Harmful Algae 8: 715-725.
[8] Eisner, L. B., Gann, J. C., Ladd, C. et al. (2016): Late summer/early fall phytoplankton biomass (chlorophyll a) in the eastern Bering Sea: spatial and temporal variations and factors affecting chlorophyll a concentrations. – Deep Sea Research Part II: Topical Studies in Oceanography 134: 100-114.
[9] Fadel, A., Atoui, A., Lemaire, B. J., Vinçon-Leite, B., Slim, K. (2015): Environmental factors associated with phytoplankton succession in a Mediterranean reservoir with a highly fluctuating water level. – Environmental Monitoring and Assessment 187: 1-14.
[10] Gu, P., Ma, X. (2013): Investigation and analysis of a floating population's settlement intention and environmental concerns: a case study in the Shawan River Basin in Shenzhen, China. – Habitat International 39:170-178.
[11] Güneralp, B., Seto, K. C. (2008): Environmental impacts of urban growth from an integrated dynamic perspective: a case study of Shenzhen, South China. – Global Environmental Change 18: 720-735.
[12] Jakob, T., Schreiber, U., Kirchesch, V. et al. (2005): Estimation of chlorophyll content and daily primary production of the major algal groups by means of multiwavelength-excitation PAM chlorophyll fluorometry: performance and methodological limits. – Photosynth Res 83: 343-61.
[13] Jung, S. W., Youn, S. J., Shin, H. H. et al. (2013): Effect of temperature on changes in size and morphology of the marine diatom, Ditylum brightwellii (West) Grunow (Bacillariophyceae). – Estuarine, Coastal and Shelf Science 135: 128-136.
[14] Lee, Y. J., Matrai, P. A., Friedrichs, M. A. M. et al. (2015): An assessment of phytoplankton primary productivity in the Arctic Ocean from satellite ocean color/in situ chlorophyll-a based models. – Journal of Geophysical Research Oceans 120: 6508.
[15] Li, T., Wang, N., Li, S. (2015): Preliminary investigation of radon concentration in surface water and drinking water in Shenzhen City, South China. – Radiation Protection Dosimetry 167: 59-64.
[16] Liu, L., Ma, X. (2011): Integrated river basin management in rapidly urbanizing areas: a case of Shenzhen, China. – Frontiers of Environmental Science & Engineering in China 5: 243-254.
[17] Liu, X., Feng, J. F., Wang, Y. Q. (2019) Chlorophyll a predictability and relative importance of factors governing lake phytoplankton at different timescales. – Science of the Total Environment 648: 472-480.
[18] Liu, Z. H., Wang, Y. L., Li, Z. H., Peng, J. (2013): Impervious surface impact on water quality in the process of rapid urbanization in Shenzhen, China. – Environmental Earth Sciences 68: 2365-2373.

http://www.aloki.hu ● ISSN 1589 1623 (Print) ● ISSN 1785 0037 (Online)
DOI: http://dx.doi.org/10.15666/aeer/1704_81918217

[19] Lu, S., Zhang, H., Sojinu, S. O., Liu, G. et al. (2015): Trace elements contamination and human health risk assessment in drinking water from Shenzhen, China. – Environmental Monitoring and Assessment 187(1): 4220.
[20] Mantyla, A. W., Bograd, S. J., Venrick, E. L. (2008): Patterns and controls of chlorophyll-a and primary productivity cycles in the Southern California Bight. – Journal of Marine Systems 73: 48-60.
[21] Mitrovic, S. M., Hitchcock, J. N., Davie, A. W., Ryan, D. A. (2010): Growth responses of Cyclotella meneghiniana (Bacillariophyceae) to various temperatures. – Journal of Plankton Research 32: 1217-1221.
[22] Molisani, M. M., Becker, H., Barroso, H. S., Hijo, C. A. et al. (2011): The influence of Castanhao reservoir on nutrient and suspended matter transport during rainy season in the ephemeral Jaguaribe River (CE, Brazil). – Braz J Biol 73: 115-23.
[23] Morin, A., Lamoureux, W., Busnarda, J. (1999): Empirical models predicting primary productivity from chlorophyll a and water temperature for stream periphyton and lake and ocean phytoplankton. – Freshwater Science 18: 299-307.
[24] Mowe, M. A. D., Porojan, C., Abbas, F., Mitrovic, S. M. et al. (2017): Corrigendum to Rising temperatures may increase growth rates and microcystin production in tropical Microcystis species. – Harmful Algae 63: 205-206.
[25] Naeher, S., Suga, H., Ogawa, N. O. et al. (2016): Compound-specific carbon and nitrogen isotopic compositions of chlorophyll a and its derivatives reveal the eutrophication history of Lake Zurich (Switzerland). – Chemical Geology 443: 210-219.
[26] Ng, C. N., Xie, Y. J., Yu, X. J. (2011): Measuring the spatio-temporal variation of habitat isolation due to rapid urbanization: a case study of the Shenzhen River cross-boundary catchment, China. – Landscape and Urban Planning 103: 44-54.
[27] Nishijima, W., Umehara, A., Sekito, S. et al. (2016): Spatial and temporal distributions of Secchi depths and chlorophyll a concentrations in the Suo Nada of the Seto Inland Sea, Japan, exposed to anthropogenic nutrient loading. – Science of the Total Environment 571: 543-550.
[28] O Neil, J. M., Davis, T. W., Burford, M. A., Gobler, C. J. (2012): The rise of harmful cyanobacteria blooms: the potential roles of eutrophication and climate change. – Harmful Algae 14: 313-334.
[29] Okumura, C., Rahman, M. A., Takimoto, A., Hasegawa, H. (2013): Effect of nitrate on the determination of iron concentration in phytoplankton culture medium by liquid scintillation counting (LSC) method using 55Fe as radioisotope tracer. – Journal of Radioanalytical and Nuclear Chemistry 296: 1295-1302.
[30] Onur, K., Dietmar, S., Frank, P. (2012): Role of phytoplankton cell size on the competition for nutrients and light in incompletely mixed systems. – Journal of Theoretical Biology 300: 330-343.
[31] Pinckney, J. L., Quigg, A. S., Roelke, D. L. (2017): Interannual and seasonal patterns of estuarine phytoplankton diversity in Galveston Bay, Texas, USA. – Estuaries and Coasts 40: 310-316.
[32] Pyo, J., Ha, S., Pachepsky, Y. A., Lee, H. et al. (2016): Chlorophyll-a concentration estimation using three difference bio-optical algorithms, including a correction for the low-concentration range: the case of the Yiam reservoir, Korea. – Remote Sensing Letters 7: 407-416.
[33] Qin, H. P., Su, Q., Khu, S. T. (2014): Water quality changes during rapid urbanization in the Shenzhen River catchment: an integrated view of socio-economic and infrastructure development. – Sustainability 6(10): 7433-7451.
[34] Russo, A. D. P. G., de Souza, M. S., Mendes, C. R. B. et al. (2015): Photophysiological effects of Fe concentration gradients on diatom-dominated phytoplankton assemblages in the Antarctic Peninsula region. – Journal of Experimental Marine Biology and Ecology 466: 49-58.

http://www.aloki.hu ● ISSN 1589 1623 (Print) ● ISSN 1785 0037 (Online)
DOI: http://dx.doi.org/10.15666/aeer/1704_81918217

[35] Smith, V. H. (1983): Low nitrogen to phosphorus ratios favor dominance by blue-green algae in lake phytoplankton. – Science 221: 669-671.
[36] Sugie, K., Nishioka, J., Kuma, K. et al. (2013): Availability of particulate Fe to phytoplankton in the Sea of Okhotsk. – Marine Chemistry 152: 20-31.
[37] Tachibana, A., Nishibe, Y., Fukuda, H. et al. (2017): Phytoplankton community structure in Otsuchi Bay, northeastern Japan, after the 2011 off the Pacific coast of Tohoku Earthquake and tsunami. – Journal of Oceanography 73: 55-65.
[38] Tebbs, E. J., Remedios, J. J., Harper, D. M. (2013): Remote sensing of chlorophyll-a as a measure of cyanobacterial biomass in Lake Bogoria, a hypertrophic, saline–alkaline, flamingo lake, using Landsat ETM+. – Remote Sensing of Environment 135: 92-106.
[39] Teeter, A. M., Johnson, B. H., Berger, C. et al. (2001): Hydrodynamic and sediment transport modeling with emphasis on shallow-water, vegetated areas (lakes, reservoirs, estuaries and lagoons). – Hydrobiologia 444: 1-23.
[40] Terauchi, G., Tsujimoto, R., Ishizaka, J., Nakata, H. (2014): Preliminary assessment of eutrophication by remotely sensed chlorophyll-a in Toyama Bay, the Sea of Japan. – Journal of Oceanography 70: 175-184.
[41] Tian, W., Zhang, H., Zhao, L. et al. (2017): Phytoplankton diversity effects on community biomass and stability along nutrient gradients in a Eutrophic Lake. – International Journal of Environmental Research 14: 1-15.
[42] van Ruth, P. D., Ganf, G. G., Ward, T. M. (2010): The influence of mixing on primary productivity: A unique application of classical critical depth theory. – Progress in Oceanography 85: 224-235.
[43] Wainger, L., Yu, H., Gazenski, K., Boynton, W. (2016): The relative influence of local and regional environmental drivers of algal biomass (chlorophyll-a) varies by estuarine location. – Estuarine, Coastal and Shelf Science 178: 65-76.
[44] Wu, Y., Li, L., Gan, N., Zheng, L. et al. (2014): Seasonal dynamics of water bloom-forming Microcystis morphospecies and the associated extracellular microcystin concentrations in large, shallow, eutrophic Dianchi Lake. – Journal of Environmental Sciences 26: 1921-1929.
[45] Zhou, H., Shi, P., Wang, J., Yu, D., Gao, L. (2011): Rapid urbanization and implications for river ecological services restoration: case study in Shenzhen, China. – Journal of Urban Planning & Development 137: 121-132.
[46] Zhu, D. W., Wu, S. Z., Han, J. C. (2018): Evaluation of nutrients and heavy metals in the sediments of the Heer River, Shenzhen, China. – Environmental Monitoring and Assessment 190(7): 380.

http://www.aloki.hu ● ISSN 1589 1623 (Print) ● ISSN 1785 0037 (Online)
DOI: http://dx.doi.org/10.15666/aeer/1704_81918217

THE EFFECT OF NOVEL AND FAMILIAR PREDATOR CUES ON PREY VIGILANCE AND FORAGING BEHAVIORS IN THE GREATER KHINGAN MOUNTAINS, INNER MONGOLIA, CHINA

MPEMBA, H.[1#] – FAN, Y.[1#] – MACLEOD, K. J.[2,3] – WEN, D.[1] – JIANG, G.[1*]

[1]*Feline Research Center of State Forestry and Grassland Administration, College of Wildlife Resources, Northeast Forestry University*
26 Hexing Road, Harbin, Heilongjiang 150040, P.R. China

[2]*Department of Ecosystem Science and Management, Pennsylvania State Univ., Forest Resources Building, University Park, PA 16802, USA*

[3]*Department of Biology, Lund University, Sölvegatan 37, 223 62 Lund, Sweden*

[#]*Contributed equally*

[*]*Corresponding author*
e-mail: jgshun@126.com; phone: +8613895712963

(Received 23rd Feb 2019; accepted 1st May 2019)

Abstract. During periods of predation risk, prey adopt antipredator behaviours to maximise chances of survival, such as increased vigilance, reduced foraging time, shifting to safe habitat, and group formation. To effectively balance resource acquisition and antipredator behavior, prey animals make use of cues within their environment that provide them accurate information about the realistic threat of predation. Using camera traps, we tested vigilance and feeding behavioural responses of two naturally occurring ungulate species roe deer and moose to cues from naturally occurring brown bear and novel Amur tiger predators. We found that roe deer and moose vigilance and feeding behaviours were not affected by either visual or olfactory cues from predators, suggesting that ungulates in this system do not respond differently to novel predator cues. There are a number of potential explanations for this surprising lack of response to any predator cues: a) habituation to uninformative cues is important; b) ungulates might have relied more heavily on other cue types, such as auditory cues, or cues in combination; and, c) constraints on dispersal and/or resources may result in prey being forced to remain in high risk food patches, and continued prioritization of feeding over vigilance. We therefore, recommend that in the future studies regarding cues should involve a combination of cues at a similar location to increase predation risk to the animals to maximise prey response. To our knowledge, this is the first study to lay out the foundation of the ecological influences of captive Amur tiger on prey behaviors in the wild environment.
Keywords: *predators, ungulates, fear ecology, camera trap, antipredator, hanma, vigilance, foraging*

Introduction

Under predation risk, prey adopt predation avoidance behaviours to maximise their chances of survival (Blumstein, 2006), such as increased vigilance, change of foraging time, shifting to safe habitat, and group formation (Creel and Christianson, 2008; Li et al., 2011; Kuijper et al., 2014). Vigilance behaviors - which can be explained as the time a prey animal spends being alert, actively scanning for predators, and fleeing (Brown and Kotler, 2004; Creel and Christianson, 2008; Creel et al., 2014) - help prey animals adjust to predation risk (Li et al., 2011) through prioritizing predator recognition (Brown and Kotler, 2004). Predation risk determines the habitat pattern to be used by most prey species (Laundré et al., 2001; Hernández and Laundré, 2005), due to the fact that the presence of large predators builds a “landscape of fear” (Laundré et

http://www.aloki.hu ● ISSN 1589 1623 (Print) ● ISSN 1785 0037 (Online)
DOI: http://dx.doi.org/10.15666/aeer/1704_82198234

al., 2001) meaning that prey perceive risk differently in different habitats and act and distribute themselves accordingly (Hernández and Laundré, 2005; Brook et al., 2012).

Prey species trade off activities such as foraging, moving between patches, mating, and vigilance behaviours – how this unfolds can have substantial effects on prey species life history trajectories (Lima and Bednekoff, 1999; Eccard et al., 2017). This balance of behaviours is likely to be skewed more towards antipredator behaviours in high predation risk habitat, with vigilance taking a higher priority (Blumstein, 2003). The optimal foraging theory states that under high risk conditions, foraging time is minimised (Lima and Bednekoff, 1999; Eccard and Liesenjohann, 2008). For example, under high predation pressure from predators like wolves (*Canis lupus*) and Lynx (*Lynx lynx*) (Eccard et al., 2017), ungulate species decrease foraging and increase vigilance (Eccard et al., 2017). This shows how fear effects can shape individual behaviours and even community significantly even than direct killing (Creel and Christianson, 2008; Creel et al., 2014).

In order to effectively balance resource acquisition and antipredator behavior (Brown and Cowan, 2000; Brown and Kotler, 2004), prey animals make use of cues within their environment that provide them accurate information about the realistic threat of predation (Hemmi and Pfeil, 2010). For example, experimental manipulation of apex predator cues, such as visual and odor cues or both, reduces foraging behaviors carried out by the dottyback fish, *Pseudochromis fuscus* (Palacios et al., 2016). In most cases predator odour cue results in minimized foraging activity (Nersesian et al., 2012) or total prey avoidance of the area (Apfelbach et al., 2005; Kats and Dill, 2016). In mammalian species, the use of predator odour cues may be especially prevalent given the importance of olfactory cue use in intraspecific communication (Wikenros et al., 2017). For example, roe deer *Capreolus pygargus* respond to lynx odour (urine) cue by either staying vigilant or avoiding predation risk areas (Eccard et al., 2017). In terms of informational content, however, predator visual cues may elicit stronger responses because they reveal immediate risk (Noell, 2013; Chamaillé-Jammes et al., 2014).

To improve our understanding of how the ecological community is structured, it is wise to learn how prey species assess and respond to risk from predators (Blumstein et al., 2000). Our previous work (submitted) has shown that predator cues alter the incidence of ungulate species in a landscape. However, ungulates do still exist in landscapes where perceived predation risk is high (i.e., in the presence of predator cues). Here, we test if these predator cues (visual and odour) result in altered prey behavior. We hypothesise that in the presence of cues, ungulates will display a) increased vigilance, and b) reduced foraging, in line with the findings of previous studies (Bridges, 2002; Brown and Kotler, 2004; Apfelbach et al., 2005; Nersesian et al., 2012; Creel et al., 2014; Cremona et al., 2014; Beauchamp, 2015; Olson et al., 2015; Eccard et al., 2017). We also test whether there is a difference in ungulate response to familiar and novel predators (Brown bear and Amur tiger, respectively). Prey that is not familiar with a predator (novel predator) due to lack of experience or non-evolutionary history might not respond or show a weak response (Banks and Dickman, 2007; Smith et al., 2008; Sih et al., 2010). Therefore, since there is no evidence for Amur tiger to have historically lived in the study area we would expect no or weak response from the prey to tiger cues. Since there are plans to train and rewild the Amur tiger (Wang et al., 2018), it is useful to know well about its ecological influence on prey foraging and vigilance behaviors. Lastly, we also test differences in response to cues between ungulates of different size classes (roe deer, and moose). As it is suggested that small

http://www.aloki.hu ● ISSN 1589 1623 (Print) ● ISSN 1785 0037 (Online)
DOI: http://dx.doi.org/10.15666/aeer/1704_82198234

and large body sizes mammal respond differently to predation risk (Riginos, 2015; Rogers, 2016); hence, we predict size-differences in predator response. This study will help our understanding of whether and how the presence of predator cues in an environment may further influence ungulate behavioural trade-offs beyond the differential use of the landscape, with possible consequences for fitness and population dynamics.

Material and methods

Study area

The study was conducted in Hanma National Nature Reserve, near to a small town of Genhe, Inner Mongolia, North East China (*Fig. 1*) (51°20′02″–51°49′48″N, 122°23′34″–122°52′46″E) (Guo et al., 2017) between July 2016 and July 2017. The National Forestry Administration Unit owns the reserve which is located in the Greater Khingan Mountains, being run as a nature reserve. Hanma has a total area of 1073 km^2, with no or very low human disturbance due to its distance from human settlements (Zhai Penghui, 2015; Guo et al., 2017). Habitat, vegetation and wildlife composition are described elsewhere (Zhai Penghui, 2015; Guo et al., 2017).

Experimental design and treatments

Design

In the current study, we tested the behavioural responses of two naturally occurring ungulate species roe deer (*Capreolus pygargus*) and moose (*Alces alces)*) to cues from naturally occurring brown bear (*Ursus arctos*) and a novel Amur tiger (*Panthera tigris tigris*) predators. We divided the study site into grids, randomly created using the fishnet method in ArcGIS 9.3 (Krivoruchko, 2011), which encompassed 2 different types of cue treatments.

Three grids contained visual cues: one grid containing cues of Amur tiger, one grid containing cues of brown bear, and a separate control grid. Treatments were kept separate in order to avoid cue treatment at one camera site affecting the behaviour of ungulates at nearby camera sites that may be of different treatments. The grid plot sizes were quantified as 3.2 km × 3.2 km, and each grid had 18 camera traps including control, 54 in total. Note that because brown bears are native in this habitat, we cannot conclusively confirm that our control grids contained no bear cues; however, as bears occur at low density in this area (Guo et al., 2017), we are confident that at least, our treatment increased perceived predator density in this area.

An odour cue experiment was initially designed in the same way (one grid containing tiger odour, and a control grid). However, after arriving at the site, we found some area (parts of the tiger odour cue experiment/group) were flooded with water and others with too big mountains with a dense forest harsh to be accessed. Due to this setback, we redesigned the tiger odour cue experiment with both of the two grids containing both treatment (tiger odour cue) and control in each half (See *Figure 1*) in order to set each treatment grid with its control over similar environmental conditions. Here, grid plots were smaller in size, i.e. (1.6 km × 1.6 km) compared to that of visual cues experiment due to the same logistical constraints. Each grid had eight camera traps, i.e. (8 x tiger feces, 8 x controls) × 2, making a total of 32 camera traps for the odour cue experiment.

http://www.aloki.hu ● ISSN 1589 1623 (Print) ● ISSN 1785 0037 (Online)
DOI: http://dx.doi.org/10.15666/aeer/1704_82198234

In the assigned grids, we deployed a total of 86 camera traps (LTL ACORN scouting camera; Ltl 5210 5MP & Ltl 5210A 12MP, and Nighthawk Bestguarder SG-990V infrared sensor trigger self-timer digital camera). Cameras were set at least 1 km apart, and the positioning for each individual camera was decided based on different animal signs such as trails, droppings and near water sources. We set all the cameras with a video mode to record 20 seconds at an interval of 5 seconds when triggered.

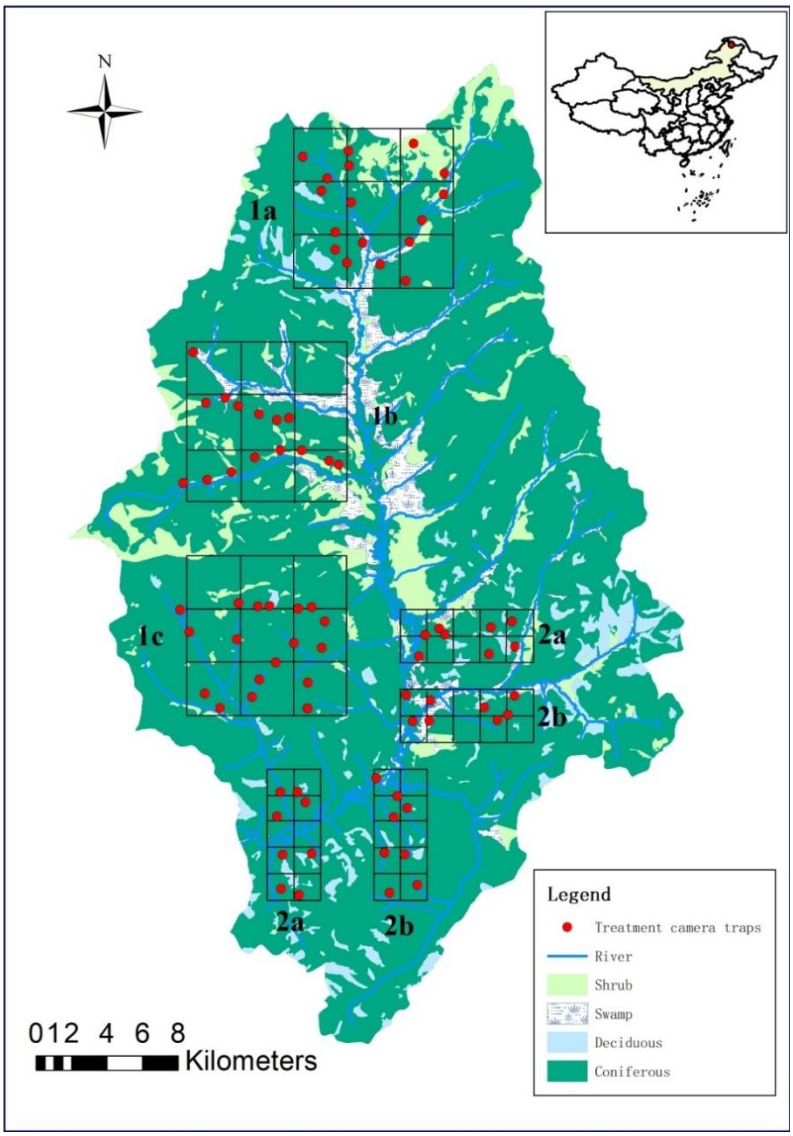

Figure 1. *A map indicating the location of the experimental area and different types of surrounding habitats. The number 1 represent visual cue experiment (i.e., 1a- tiger, 1b- bear, 1c- control), and number 2 represent the odour cue experiment (i.e., 2a- tiger, 2b- control). Tiger visual (1a) includes a 100 cm x 100 a 2D picture of standing tiger printed on a canvas which is tied to two opposite trees, with a camera tied to one of the trees; with everything similar at the bear visual (1c). For the control visual (1c), a canvas similar in settings as tiger and bear visual cues was printed to mimic the environment and tied to two opposite trees with a camera tied to one of the trees to record visitation incidences. The Grids in 2 (a&b) represent the tiger order cue experiment, a plastic bottle filled with tiger feces (i.e., 2a groups) and then a camera tied on a nearby tree to record the visitation rate; the same was done to odour cue control filled with soil (2b) groups*

http://www.aloki.hu ● ISSN 1589 1623 (Print) ● ISSN 1785 0037 (Online)
DOI: http://dx.doi.org/10.15666/aeer/1704_82198234

Visual cue experiment

Predator visual cues (a life-size photo of a standing tiger, bear or vegetation like control were printed on a canvas; *Figure 2*. following studies by (Li et al., 2011; Fischer et al., 2017) were printed on canvas at a size of 100 cm x 100 cm. The canvas was suspended between two opposite standing trees at each camera site. Cameras were tied ~50 cm from the ground one of the trees to record animal behaviours (i.e., the camera faced away from the visual cue, in the direction of approaching ungulates).

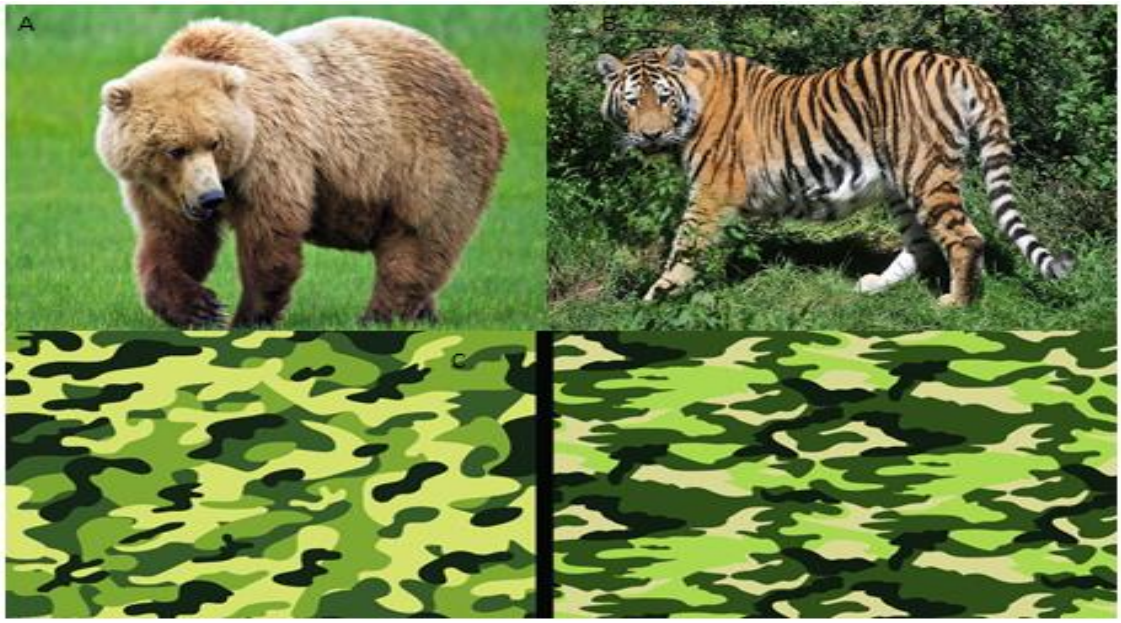

Figure 2. *Visual cues treatment and control. A- Is a brown bear photo representing bear visual cue, B- is Amur tiger photo reprinting tiger visual cue, and C- which is vegetation/habitat like photo represent control visual cue. They were both hanged on two different trees and a camera tied on one of the trees to record ungulates behavioral responses*

Odour cue experiment

As predator odour cue, we used Amur tiger fresh feces from Harbin Siberian Tiger Park, transferred into 150 ml plastic bottles (*Figure 3B*) which had small holes around to produce the odour. Feces were collected no more than one week before deployment and in the interim stored in laboratory refrigerators at -20°C to avoid quality loss. Bottles were tied to trees ~50 cm above ground opposite the camera trap and in the focus of the camera to record animal behavioural responses. As a control, we used soil which was filled in the same 150 ml plastic bottles and tied on the tree at the same settings as the odour cues (*Figure 3A*). Due to unavailability of fresh bear feces, we, unfortunately,, could not involve bear odour cues in this experiment.

Data collection

Cameras were deployed for 1 year, after which SD cards were collected, and cues were removed. Behavioural data were collected from the resulting videos using focal sampling and all occurrence methodology (Altmann, 1974; Martin et al., 1993; Margulis, 2016). For this study the behavioral data extracted were– vigilance and

http://www.aloki.hu ● ISSN 1589 1623 (Print) ● ISSN 1785 0037 (Online)
DOI: http://dx.doi.org/10.15666/aeer/1704_82198234

foraging behaviours for ungulates which triggered the camera to record). All recordings which were activated inside 30 minutes of one another and contained similar animals were considered one visit. Ungulate species that were detected included roe deer, musk deer (*Cervus elaphus*), red deer, wild boar (*Sus scrofa*), and moose; however, due to low numbers, we only considered roe deer and moose further.

Figure 3. *Odour cue treatment and control; A- Represent a plastic bottle (150ml) field with Amur tiger odour cue control (soil), and B is the same bottle filled with Amur tiger odour cue (feces). All the bottles were similar, just differing in contents. The camera was located in front or nearby the bottler to be able to record animal behavioral responses when around the odour cue or control*

Behavioral coding, description, and classification

We classified behaviours into five main components following Heijtel and van Hooft (2014), Meng et al. (2008), and Li et al. (2011), to include vigilance and feeding behaviours (*Table 1*).

Table 1. *Behavioral classification used in this study*

Behavior	Description/definition
Vigilant - VG	Animal keeps a careful watch or looks for possible danger occurrence within the habitat. Usually, the eyes are wide open. It includes behaviors as stare, stand while head up, smell while staring, walk while head up, walk while turning head, turn head, turn ears, alert, stand, listen and turn the body
Feeding - FD	The animal is feeding/eating or drinking. It involves behaviors like forage, walk while foraging, water drinking, and suckling
Locomotion - LO	The animal is moving without any accompanying behaviors; it includes actions as walk, jump, trot, run and swim
Communication - CO	Animal express behaviors that help others to know their presence and also marking their territories. It includes behaviors like the smell, sniff, walk while smelling, rub and rub against a tree

We included other behaviours such as communication and locomotion in separate groups because we did not have explicit predictions about how predator cues might influence these behaviours and because we decided to focus on the foraging/vigilance trade off. Our analyses focused on feeding and vigilance behaviours, as the trade-off between anti-predator behaviour (vigilance) and self-maintenance behaviour (foraging)

http://www.aloki.hu ● ISSN 1589 1623 (Print) ● ISSN 1785 0037 (Online)
DOI: http://dx.doi.org/10.15666/aeer/1704_82198234

is a key life-history concern in response to predation risk (Brown, 1999). We included other behaviours such as communication and locomotion in separate groups because we did not have explicit predictions about how predator cues might influence these behaviours and because we decided to focus on the foraging/vigilance trade off.

Statistical methods

From our camera traps, we obtained a total of 193 records from cameras in the visual cues experiment, and 399 records from cameras in the olfactory cues experiment. For the purposes of statistical analyses, we excluded records from species that had too few records overall, or where records were from too few cameras to be representative (N=41 records from musk deer (from only 2 cameras), in the visual cues experiment; N=15 musk deer and N=5 wild boar in the olfactory cues experiment). We also excluded records from moose in the analysis of the visual cues experiment, as all control records were from a total of only 2 cameras. As a result, analyses of the visual experiment consisted of 142 records of roe deer, and analyses of the olfactory cue experiment consisted of 209 records of roe deer and 170 records of moose.

The effects of predator cues (visual and olfactory) on the proportion time ungulates spent being vigilant (as defined in *Table 1*) and time spent feeding (as defined in *Table 1*) were tested using generalized linear mixed models using the *lme4* package in R (Team, 2015). For analyses of both the visual and olfactory cue experiments, the proportion of time spent vigilant/feeding was constructed as a paired column (created using the *cbind* function in R). The paired column containing time spent vigilant/time spent feeding in one column, and total time spent doing other behaviours (i.e., the total time the animal was recorded, minus the time spent vigilant/feeding) as a second column. This allowed us to account for variation in the total time recorded. Experimental treatment (in the case of the visual cue experiment: control, tiger cue, bear cue; in the case of the olfactory cue experiment: control, tiger cue) was set independent variable. Also included was the number of days the camera had been active at the time of recording (i.e., days treatment was in place) (this variable was logged to improve normality and scaling). Camera ID was set as a random term to account for non-independence of multiple records from the same camera. As the visual cue experiment contained the only deer, species was not included as a variable in this analysis. In the analysis of the olfactory cue experiment, an interaction term treatment*species was included as an explanatory variable to test whether treatment effects differed between species.

Results

Visual predator cue experiment

There was no effect of visual predator cue treatments on roe deer vigilance behaviour (treatment $X^2_2 = 0.15$, P = 0.93), or feeding (treatment $X^2_2 = 2.81$, P = 0.25) (*Figure 4*). Post-hoc analysis (Tukey test) revealed that there was no difference in proportion time spent vigilant or feeding specifically between the two predator cue treatments (tiger and bear visual cues: vigilance Z = 0.08, P = 0.99; feeding Z = -1.55, P = 0.27). Vigilant and feeding behaviours also were not predicted by the length of time (days) the camera and treatment had been in place (days camera activity vigilance: $X^2_1 = 2.45$, P = 0.12; feeding $X^2_1 = 0.79$, P = 0.37).

http://www.aloki.hu ● ISSN 1589 1623 (Print) ● ISSN 1785 0037 (Online)
DOI: http://dx.doi.org/10.15666/aeer/1704_82198234

Olfactory predator cue experiment

We observed a significant interactive effect of treatment and species on time investment in vigilance behaviour (treatment*species X^2_1 = 22.8, P < 0.001). Post-hoc analysis (Tukey test) revealed that this effect was driven by roe deer having a higher base vigilance rate (i.e. were more vigilant than moose under the control treatment: Z = 3.56, P < 0.01) but a lower vigilance rate under the predator treatment, tiger odour (Z = -3.15, P < 0.01) (*Figure 5a*).

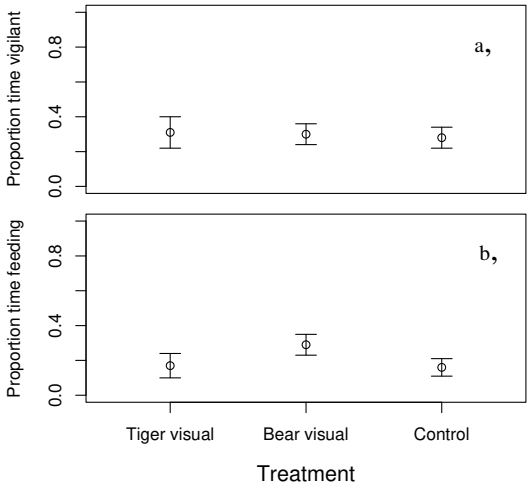

Figure 4. *The presence of predator visual cues did not influence time investment in a) vigilance and b) feeding behaviour in roe deer*

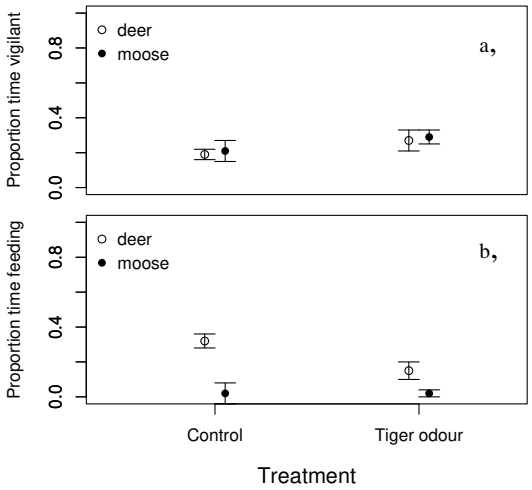

Figure 5. *Predicted effects from a model accounting for days of camera activity of predator odour treatment on a) vigilance and b) feeding in roe deer (open circles) and moose (filled circles). Effects of treatment differed significantly between species in both cases, but responses to predator odour within species were not statistically significant in both cases*

This interactive result suggests that moose responded more strongly to tiger odour. However, within-species effects of treatment were not significant, according to post-hoc tests (roe deer Z = 1.05, P = 0.72; moose Z = -2.05, P = 0.17).

http://www.aloki.hu ● ISSN 1589 1623 (Print) ● ISSN 1785 0037 (Online)
DOI: http://dx.doi.org/10.15666/aeer/1704_82198234

We also observed a significant interactive effect of treatment and species on time investment in feeding (treatment*species $X^2_1 = 49.12$, $P < 0.001$) (*Figure 5b*). Post-hoc analysis (Tukey test) revealed that this effect was driven by differences between roe deer and moose feeding rates under the control treatment (moose feeding rate significantly lower, $Z = 5.94$, $P < 0.001$) (*Figure 6*). There was no significant difference between roe deer and moose in feeding rates under the predator cue treatment ($Z = -0.3$, $P = 0.99$). Again, within-species effects of treatment were not significant, according to post-hoc tests (roe deer $Z = 1.95$, $P = 0.21$; moose $Z = -2.25$, $P = 0.11$).

Both vigilance and feeding behaviours were significantly predicted by the length of time (days) the camera and treatment had been in place (days camera activity, vigilance: $X^2_1 = 164.34$, $P < 0.001$; feeding $X^2_1 = 11.86$, < 0.001).

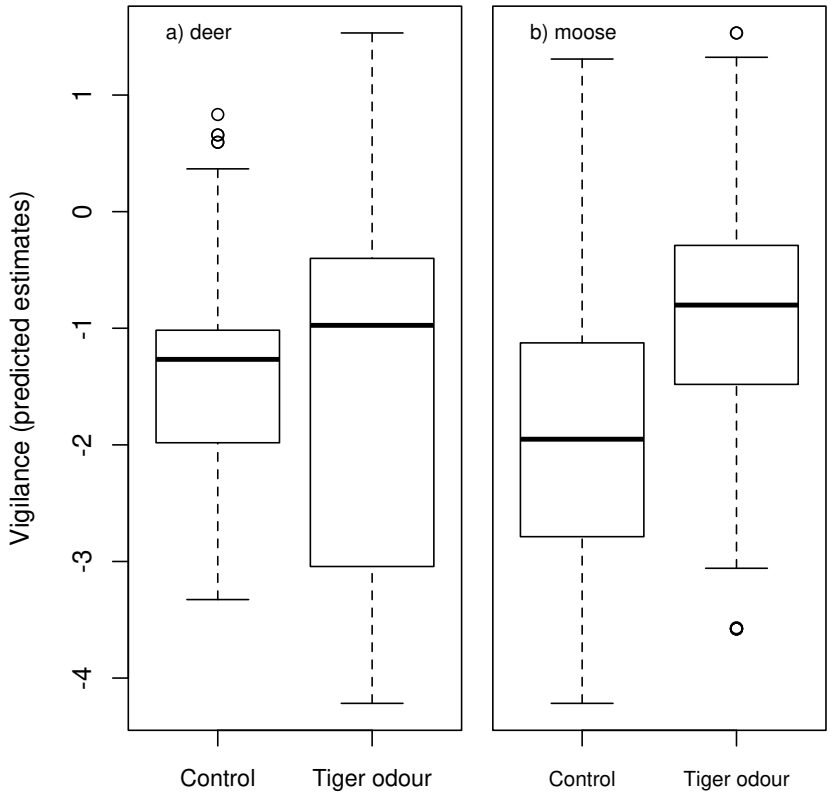

Figure 6. *Predicted effects from a model accounting for days of camera activity of predator odour treatment on vigilance behaviour in a) roe deer and b) moose. Effects of treatment differed significantly between species, with moose showing a stronger response than roe deer, though the strength of responses to predator odour within species was not statistically significant*

Discussion

Predator cues alter the incidence of prey species in a landscape, which is likely to have cascading effects on population dynamics throughout the system in line with hypotheses based on the "landscape of fear" (Suraci et al., 2016). Predator cues reduce prey species incidence in areas where predation risk is perceived as high: but prey species do continue to use high risk areas, albeit at lower levels. Understanding how behaviour changes where they do exist in those landscapes is important to gain a fuller

http://www.aloki.hu ● ISSN 1589 1623 (Print) ● ISSN 1785 0037 (Online)
DOI: http://dx.doi.org/10.15666/aeer/1704_82198234

picture of the effects of predation risk on individual level fitness and population dynamics. In this study we tested the effects of visual and olfactory cues on ungulate vigilance and feeding behaviour tradeoffs, and show no significant changes in either vigilance or feeding behaviour according to predator-cue treatment, contrary to our hypotheses and previous work showing increased vigilance at the expense of feeding in a number of prey species (Creel et al., 2014; Cremona et al., 2014; Beauchamp, 2015; Olson et al., 2015; Eccard et al., 2017). The familiarity of the predator also had no effect on ungulate behavior. We suggest that these results indicate that when prey animals exist in high risk environments (perhaps due to constraints associated with dispersal, or food patch availability), they may display higher selectivity in cue use (i.e. ignoring cues that may be inaccurate) in order to maximise energy intake (Lima and Bednekoff, 1999; Eccard et al., 2017). Additionally, our results reveal differences in how species (roe deer and moose) respond towards predator cues, potentially because body size may effect on how species respond to predation risk (Rogers, 2016; Venter et al., 2017).

Ungulates did not reduce feeding and increase vigilance in the presence of predator cues

Prey animals use cues within their environment to inform their time allocation to antipredator and other behaviours (McCoy et al., 2012). Based on this, we expected that in the presence of predator cues, ungulates would increase their time spent vigilant, and decrease time spent foraging, in order to maximise survival in a perceived high risk environment. However, we found that roe deer and moose vigilance and feeding behaviours were not affected by either visual or olfactory cues from predators (*Figure 4*). There are a number of potential explanations for this surprising lack of response to predator cues, that we will consider in turn: a) habituation to uninformative cues is important, b) ungulates may rely more heavily on other cue types, such as auditory cues, or cues in combination, and c) constraints on dispersal resulting in prey forced to remain in high risk food patches and continued prioritization of feeding over vigilance.

First, it is possible that ungulates habituated to the cues presented over time as they learned that the cue was not actually associated with a live predator and did not pose a real threat. Using up to date and accurate information is essential since as suggested by (Karban et al., 2016) it becomes more costly to keep responding to unreliable cues, responding correctly to precise information enhances animal fitness. Our visual cue model accounted for the length of treatment and showed no effect of how long the treatment was deployed, where we might have expected to see a stronger response initially which declined when animals habituated. We, therefore, cannot conclusively say that this is why we see no overall effect of predator cues on behavior in response to visual cues. However, in the context of the olfactory cue, investment in both vigilance and feeding behaviours were significantly predicted by the length of time (days) the camera and treatment had been in place. The strong effect of length of treatment in the odour treatment is essential; it means that they stopped responding once the cue was out of date. This is strongly adaptive; animals do not want to keep using cues that are out of date because then they are wasting opportunities and energy based on wrong information (Karban et al., 2016). Perhaps they are choosier and more discriminatory in how they use cues to alter behaviours related to energy use/consumption, similar to what suggested by (Venter et al., 2006) that different animals respond differently to different threats (predator odour cues included).

http://www.aloki.hu ● ISSN 1589 1623 (Print) ● ISSN 1785 0037 (Online)
DOI: http://dx.doi.org/10.15666/aeer/1704_82198234

Second, cues that influence habitat use and behaviour may be different; perhaps ungulates rely more on auditory cues, which may contain more accurate and up-to-date information, to adjust their behaviour. We think that we were not able to see the effect because (from the previous submitted study) we saw that these species are already using the landscape differently, so perhaps it might be that those using these areas have already adjusted their behaviours. Venter et al. (2017) suggested that ungulates depend less on visual cues when searching for food (relative to movement behaviors), possibly because it is easier to incorporate auditory cues while foraging with head down, than visual cues, which require the cessation of foraging to lift the head. Auditory cues may also be more likely to be accurate and up-to-date than olfactory cues (Shelton and Kumar, 2010). The effectiveness of olfactory/chemical cues varies with different factors such as weather, seasons, the frequency of use, amount of concentration, and food availability (Elmeros et al., 2011). Another reason might be odour cues might be less effective during harsh winter which characterizes the study area for most parts of the year. To make these cues more effective we in the future we suggest similar to (Knapp et al., 2004; Andreassen et al., 2005) that they should be used in combination with another cue at the same area to pose more risk to the area.

Ungulates did not respond differently to novel/familiar predator cues

The introduction of a novel predator in an area can have a significant impact on prey species, particularly if prey species do not respond appropriately to novel predator cues, or if there is a learning period (Dunlop-Hayden and Rehage, 2011; Polo-Cavia and Gomez-Mestre, 2014; Carthey et al., 2017). Given that in a previous study (submitted) in the same system novel predator visual cues influenced the incidence of prey species (incidence was more strongly predicted by familiar predator cue presence), we predicted that ungulates might similarly respond less strongly behaviourally to cues from a novel predator (Amur tiger) than to cues from a familiar one (brown bear) (Smith et al., 2008; Saxon-Mills et al., 2018). However, our results show no difference in the amount of time spent vigilant or feeding between the two predator cues treatments (tiger and bear visual cues), i.e., ungulates showed the same lack of response to both novel and familiar predator cues. This is different from what would have normally expected that ungulates (roe deer in this case) would have responded strongly to at least native bear cues and less to a novel tiger cue; but this result is similar to a study showing that mosquitos and flagfish failed to differentiate a chemical cue that comes from a novel predator (Cichlid) (Dunlop-Hayden and Rehage, 2011). It is possible that the fine-scale differentiation of native and novel predators depends on specific cues used by such prey (Dunlop-Hayden and Rehage, 2011), or potentially cues in combination (for example visual + chemical at the same place): Amo et al. (2004) also revealed that lizard increase more the antipredator behavior once exposed to combined cues (visual and chemical) of their snake predator might respond well to cues once they are combined. As well, Elmeros et al. (2011) found that chemical cues did don't repel deer unless integrated directly within the food.

Ungulates did not respond differently to novel/familiar predator cues

The olfactory predator cue had a significant interactive effect with ungulate species on time allocation on vigilance behaviour, driven by roe deer being more vigilant than moose under control conditions, but having a reduced response to the predator treatment, tiger odour (*Figure 5a*). We also observed a significant interactive effect of

http://www.aloki.hu ● ISSN 1589 1623 (Print) ● ISSN 1785 0037 (Online)
DOI: http://dx.doi.org/10.15666/aeer/1704_82198234

treatment and species on time investment on feeding behavior (*Figure 5b*). It is necessary for prey to allocate time wisely for feeding in order to avoid predation risk at the same avoiding the effect of staying vigilant (e.g., poor fitness, malnourishment) (Lima and Bednekoff, 1999). It was primarily driven by the difference of feeding rate between roe deer and moose at the control treatment, with moose showing a significant lower feeding rate at the control treatment (*Figure 7*).

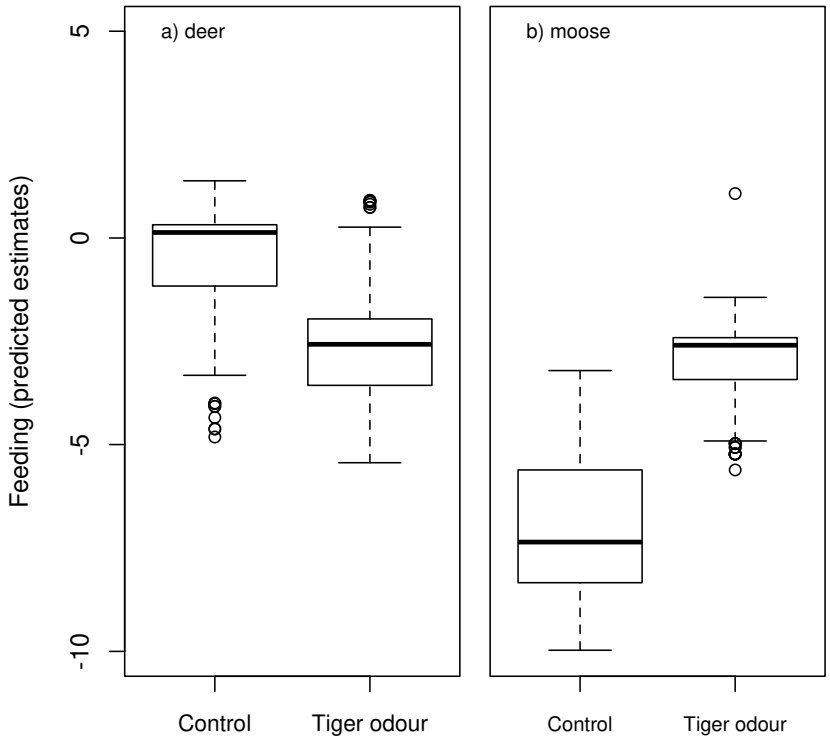

Figure 7. *Predicted effects from a model accounting for days of camera activity of predator odour treatment on feeding in a) roe deer and b) moose. Effects of treatment differed significantly between species, with moose showing a significantly lower feeding rate under control treatment than roe deer; the responses to predator odour within species were not statistically significant*

Nevertheless, treatment showed no significant effects within-species, partly may be due to the differences in the sense of odour cue perception (Padodara and Jacob, 2014) within these two species. It is possible that species like roe deer, due to their higher vulnerability to a greater number of potential predators (Rogers, 2016), are more vigilant under any circumstances, with the predator cue evoking a lessened response given that they are already at a reasonably high level of vigilance (beyond which, the benefits of increased vigilance may be minimal). Conversely, the stronger response of moose was surprising, since we would expect larger species to be less responsive to risk compared to those of smaller body size (Riginos, 2015), because large body species are a) less likely to be targeted by predators, and b) affected more by lack of food availability than predation risk. Our results emphases the importance of considering different prey species separately when investigating the effects of predation risk and cue use, as ecological and life history differences are likely to contribute to different outcomes of risk.

http://www.aloki.hu ● ISSN 1589 1623 (Print) ● ISSN 1785 0037 (Online)
DOI: http://dx.doi.org/10.15666/aeer/1704_82198234

Conclusions

We have successfully shown that both familiar (brown bear) and novel (Amur tiger) cues have no significant influence on ungulates (roe deer and moose) vigilance and foraging behaviors in our study system. Also, our results demonstrate that when prey animals occur in a fearful environment due to limitations of factors like food availability, mating, and dispersal; they display selectivity or even ignore cue use so as to maximise energy intake (Lima and Bednekoff, 1999; Eccard et al., 2017). Likewise, our results tell the differences in how species respond towards predator risk, that small body size animals (roe deer) are potentially at high risk from various predators compared to large size (moose) which are mostly limited by food (foraging) (Rogers, 2016; Venter et al., 2017). Our results also indicate that due to differences in historical background, it is essential to consider each species differently when considering predation risk or cue use effects of different prey species. We further recommend that in the future studies regarding cues can involve a combination of cues (example; visual and order) at the same location to increase predation risk to the animals and see their response. Lastly, to our best level of understanding, this is the first study to lay out the foundation on the ecological influences of captive Amur tiger on prey behaviors in the wild environment.

Acknowledgements. This work was funded by the Fundamental Research Funds for the Central Universities (2572017PZ14), the fund from the National Key Programme of Research and Development, Ministry of Science and Technology (2016YFC0503200), and National Nature Science Foundation of China (NSFC 31872241; 31572285). We thank Benjamin Jarrett for providing his helpful comments on statistical methodology, Bao Heng, Zhai Penghu and Liu Yan for their support during fieldwork. Lastly, thanks to the entire Hanma National Nature Reserve staff for their outstanding support during fieldwork. This work is part of the principal author PhD work.

REFERENCES

[1] Altmann, J. (1974): Observational study of behavior: sampling methods. – Behaviour 49(3): 227-266.

[2] Amo, L., López, P., Martín, J. (2004): Wall lizards combine chemical and visual cues of ambush snake predators to avoid overestimating risk inside refuges. – Animal Behaviour 67(4): 647-653.

[3] Andreassen, H. P., Gundersen, H., Storaas, T. (2005): The effect of scent-marking, forest clearing, and supplemental feeding on moose-train collisions. – The Journal of wildlife management 69(3): 1125-1132.

[4] Apfelbach, R., Blanchard, C. D., Blanchard, R. J., Hayes, R. A., McGregor, I. S. (2005): The effects of predator odors in mammalian prey species: a review of field and laboratory studies. – Neuroscience & Biobehavioral Reviews 29(8): 1123-1144.

[5] Banks, P. B., Dickman, C. R. (2007): Alien predation and the effects of multiple levels of prey naiveté. – Trends in ecology & evolution 22(5): 229-230.

[6] Beauchamp, G. (2015): Animal vigilance: monitoring predators and competitors. – Academic Press.

[7] Blumstein, D. T. (2003): Flight-initiation distance in birds is dependent on intruder starting distance. – The Journal of Wildlife Management: 852-857.

[8] Blumstein, D. T. (2006): The multipredator hypothesis and the evolutionary persistence of antipredator behavior. – Ethology 112(3): 209-217.

http://www.aloki.hu ● ISSN 1589 1623 (Print) ● ISSN 1785 0037 (Online)
DOI: http://dx.doi.org/10.15666/aeer/1704_82198234

[9] Blumstein, D. T., Daniel, J. C., Griffin, A. S., Evans, C. S. (2000): Insular tammar wallabies (Macropus eugenii) respond to visual but not acoustic cues from predators. – Behavioral Ecology 11(5): 528-535.
[10] Bridges, C. M. (2002): Tadpoles balance foraging and predator avoidance: effects of predation, pond drying, and hunger. – Journal of Herpetology: 627-634.
[11] Brook, L. A., Johnson, C. N., Ritchie, E. G. (2012): Effects of predator control on behaviour of an apex predator and indirect consequences for mesopredator suppression. – Journal of applied ecology 49(6): 1278-1286.
[12] Brown, G. E., Cowan, J. (2000): Foraging trade-offs and predator inspection in an Ostariophysan fish: switching from chemical to visual cues. – Behaviour 137(2): 181-195.
[13] Brown, J. S. (1999): Vigilance, patch use and habitat selection: foraging under predation risk. – Evolutionary Ecology Research 1(1): 49-71.
[14] Brown, J. S., Kotler, B. P. (2004): Hazardous duty pay and the foraging cost of predation. – Ecology letters 7(10): 999-1014.
[15] Carthey, A. J., Bucknall, M. P., Wierucka, K., Banks, P. B. (2017): Novel predators emit novel cues: a mechanism for prey naivety towards alien predators. – Scientific reports 7(1): 16377.
[16] Chamaillé-Jammes, S., Malcuit, H., Le Saout, S., Martin, J.-L. (2014): Innate threat-sensitive foraging: black-tailed deer remain more fearful of wolf than of the less dangerous black bear even after 100 years of wolf absence. – Oecologia 174(4): 1151-1158.
[17] Creel, S., Christianson, D. (2008): Relationships between direct predation and risk effects. – Trends in Ecology & Evolution 23(4): 194-201.
[18] Creel, S., Schuette, P., Christianson, D. (2014): Effects of predation risk on group size, vigilance, and foraging behavior in an African ungulate community. – Behavioral Ecology 25(4): 773-784.
[19] Cremona, T., Crowther, M. S., Webb, J. K. (2014): Variation of prey responses to cues from a mesopredator and an apex predator. – Austral ecology 39(7): 749-754.
[20] Dunlop-Hayden, K., Rehage, J. S. (2011): Antipredator behavior and cue recognition by multiple Everglades prey to a novel cichlid predator. – Behaviour 148(7): 795-823.
[21] Eccard, J. A., Liesenjohann, T. (2008): Foraging decisions in risk-uniform landscapes. – PLoS One 3(10): e3438.
[22] Eccard, J. A., Meißner, J. K., Heurich, M. (2017): European roe deer increase vigilance when faced with immediate predation risk by Eurasian Lynx. – Ethology 123(1): 30-40.
[23] Elmeros, M., Winbladh, J. K., Andersen, P. N., Madsen, A. B., Christensen, J. T. (2011): Effectiveness of odour repellents on red deer (Cervus elaphus) and roe deer (Capreolus capreolus): a field test. – European journal of wildlife research 57(6): 1223-1226.
[24] Fischer, S., Oberhummer, E., Cunha-Saraiva, F., Gerber, N., Taborsky, B. (2017): Smell or vision? The use of different sensory modalities in predator discrimination. – Behavioral Ecology and Sociobiology 71(10): 143.
[25] Guo, K., Liu, H., Bao, H., Hu, J., Wang, S., Zhang, W., Zhao, Y., Jiang, G. (2017): Habitat selection and their interspecific interactions for mammal assemblage in the Greater Khingan Mountains, northeastern China. – Wildlife Biology: 00261.
[26] Heijtel, M. G., van Hooft, W. (2014): Camera trapping the wolf (Canis lupus) population in Białowieża Primeval Forest, Poland.
[27] Hemmi, J. M., Pfeil, A. (2010): A multi-stage anti-predator response increases information on predation risk. – Journal of Experimental Biology 213(9): 1484-1489.
[28] Hernández, L., Laundré, J. W. (2005): Foraging in the 'landscape of fear'and its implications for habitat use and diet quality of elk Cervus elaphus and bison Bison bison. – Wildlife Biology 11(3): 215-220.

http://www.aloki.hu ● ISSN 1589 1623 (Print) ● ISSN 1785 0037 (Online)
DOI: http://dx.doi.org/10.15666/aeer/1704_82198234

[29] Karban, R., Orrock, J. L., Preisser, E. L., Sih, A. (2016): A comparison of plants and animals in their responses to risk of consumption. – Current opinion in plant biology 32: 1-8.
[30] Kats, L. B., Dill, L. M. (2016): The scent of death: Chemosensory assessment of predation risk by prey animals. – Écoscience 5(3): 361-394.
[31] Knapp, K. K., Yi, X., Oakasa, T., Thimm, W., Hudson, E., Rathmann, C. (2004): Deer-vehicle crash countermeasure toolbox: a decision and choice resource. – http://www.deercrash.org/toolbox/finalreport.pdf.
[32] Krivoruchko, K. (2011): Spatial statistical data analysis for GIS users. – Esri Press Redlands.
[33] Kuijper, D. P., Verwijmeren, M., Churski, M., Zbyryt, A., Schmidt, K., Jędrzejewska, B., Smit, C. (2014): What cues do ungulates use to assess predation risk in dense temperate forests? – PLoS One 9(1): e84607.
[34] Laundré, J. W., Hernández, L., Altendorf, K. B. (2001): Wolves, elk, and bison: reestablishing the" landscape of fear" in Yellowstone National Park, USA. – Canadian Journal of Zoology 79(8): 1401-1409.
[35] Li, C., Yang, X., Ding, Y., Zhang, L., Fang, H., Tang, S., Jiang, Z. (2011): Do Pere David's deer lose memories of their ancestral predators? – PLoS One 6(8): e23623.
[36] Lima, S. L., Bednekoff, P. A. (1999): Temporal variation in danger drives antipredator behavior: the predation risk allocation hypothesis. – The American Naturalist 153(6): 649-659.
[37] Margulis, S. (2016): Sampling Animal Behavior: Animal Behavior Society Workshop. – Available online.
[38] Martin, P., Bateson, P. P. G., Bateson, P. (1993): Measuring behaviour: an introductory guide. – Cambridge University Press.
[39] McCoy, M. W., Touchon, J. C., Landberg, T., Warkentin, K. M., Vonesh, J. R. (2012): Prey responses to predator chemical cues: disentangling the importance of the number and biomass of prey consumed. – PloS one 7(10): e47495.
[40] Meng, X., Yang, Q., Feng, Z., Xu, H., Perkins, G. C., Feng, J., Zhang, D. (2008): Seasonal behavioral patterns of captive alpine musk deer (Moschus sifanicus): Rut and pre-rut comparisons. – Biologia 63(4): 594-598.
[41] Nersesian, C. L., Banks, P. B., McArthur, C. (2012): Behavioural responses to indirect and direct predator cues by a mammalian herbivore, the common brushtail possum. – Behavioral Ecology and Sociobiology 66(1): 47-55.
[42] Noell, S. (2013): Effects of brown bear (Ursus arctos) odour on the patch choice and behaviour of different ungulate species. – Swedish University of Agricultural Sciences.
[43] Olson, R. S., Haley, P. B., Dyer, F. C., Adami, C. (2015): Exploring the evolution of a trade-off between vigilance and foraging in group-living organisms. – Royal Society open science 2(9): 150135.
[44] Padodara, R., Jacob, N. (2014): Olfactory Sense in Different Animals. – Indian Journal of Veterinary Science 2: 1-14.
[45] Palacios, M., Warren, D. T., McCormick, M. I. (2016): Sensory cues of a top-predator indirectly control a reef fish mesopredator. – Oikos 125(2): 201-209.
[46] Polo-Cavia, N., Gomez-Mestre, I. (2014): Learned recognition of introduced predators determines survival of tadpole prey. – Functional Ecology 28(2): 432-439.
[47] Riginos, C. (2015): Climate and the landscape of fear in an African savanna. – Journal of Animal Ecology 84(1): 124-133.
[48] Rogers, H. (2016): Influence of temperature and predation risk on herbivore micro habitat choice in a South African savanna. – Swedish University of Agricultural Sciences, Epsilon Archive for Student projects.
[49] Saxon-Mills, E. C., Moseby, K., Blumstein, D. T., Letnic, M. (2018): Prey naïveté and the anti-predator responses of a vulnerable marsupial prey to known and novel predators. – Behavioral Ecology and Sociobiology 72(9): 151.

http://www.aloki.hu ● ISSN 1589 1623 (Print) ● ISSN 1785 0037 (Online)
DOI: http://dx.doi.org/10.15666/aeer/1704_82198234

[50] Shelton, J., Kumar, G. P. (2010): Comparison between auditory and visual simple reaction times. – Neuroscience & Medicine 1(1): 30-32.
[51] Sih, A., Bolnick, D. I., Luttbeg, B., Orrock, J. L., Peacor, S. D., Pintor, L. M., Preisser, E., Rehage, J. S., Vonesh, J. R. (2010): Predator–prey naïveté, antipredator behavior, and the ecology of predator invasions. – Oikos 119(4): 610-621.
[52] Smith, G. R., Boyd, A., Dayer, C. B., Winter, K. E. (2008): Behavioral responses of American toad and bullfrog tadpoles to the presence of cues from the invasive fish, Gambusia affinis. – Biological Invasions 10(5): 743-748.
[53] Suraci, J. P., Clinchy, M., Dill, L. M., Roberts, D., Zanette, L. Y. (2016): Fear of large carnivores causes a trophic cascade. – Nature Communications 7: 10698.
[54] Team, R. C. (2015): R: A language and environment for statistical computing [Internet]. – Vienna, Austria: R Foundation for Statistical Computing; 2015.
[55] Venter, O., Brodeur, N. N., Nemiroff, L., Belland, B., Dolinsek, I. J., Grant, J. W. (2006): Threats to endangered species in Canada. – AIBS Bulletin 56(11): 903-910.
[56] Venter, J. A., Prins, H. H., Mashanova, A., Slotow, R. (2017): Ungulates rely less on visual cues, but more on adapting movement behaviour, when searching for forage. – PeerJ 5: e3178.
[57] Wang, Q., Liu, D., Holyoak, M., Jia, T., Yang, S., Liu, X., Kong, X., Jiang, G. (2018): Innate preference for native prey and personality implications in captive Amur tigers. – Applied Animal Behaviour Science 210: 95-102.
[58] Wikenros, C., Jarnemo, A., Frisén, M., Kuijper, D. P., Schmidt, K. (2017): Mesopredator behavioral response to olfactory signals of an apex predator. – Journal of ethology 35(2): 161-168.
[59] Zhai Penghui, L. Y., Li, Z. S. (2015): The Current Situation and Evaluation of the Biodiversity of Hanma National Nature Reserve. – China Academic Journal Electronic House.

http://www.aloki.hu ● ISSN 1589 1623 (Print) ● ISSN 1785 0037 (Online)
DOI: http://dx.doi.org/10.15666/aeer/1704_82198234

PERCEIVED INDOOR ENVIRONMENTAL QUALITY OF HOSPITAL WARDS AND PATIENTS' OUTCOMES: A STUDY OF A GENERAL HOSPITAL, MINNA, NIGERIA

ALFA, M. T.* – ÖZTÜRK, A.

Department of Architecture, Cyprus International University, Haspolat, via Mersin 10, Turkey

**Corresponding author*
e-mail: mohammedtalfa@yahoo.com, malfa@ciu.edu.tr

(Received 24th Feb 2019; accepted 24th May 2019)

Abstract. The objective of this study was to assess patients' perceptions of the indoor environment of wards in a hospital in terms of architectural design, thermal comfort, indoor air quality (IAQ), lighting and acoustical parameters. The study attempted to determine the factors influencing the perceived indoor environmental quality (PIEQ) and explored the relationships between the perceived importance of indoor environmental quality (PI-IEQ) and health recovery, health satisfaction and therapeutic ambience of the hospital. A field study of the indoor environmental quality (IEQ) of 4 wards in the General hospital at Minna, Niger state, Nigeria was conducted, and responses from 271 patients were obtained. Structural equation modelling was employed for data analysis. The research identified the six IEQ factors that influenced PIEQ as architectural design features, thermal comfort, adaptive opportunities, lighting, IAQ and acoustics aspects. PIEQ had a positive influence on a ward being perceived as conducive for wellbeing. It was observed that health satisfaction had the most significant and positive influence on PI-IEQ. The second most positive influence was health recovery. Therapeutic ambience also had a positive influence on PI-IEQ but this was not significant.
Keywords: *architectural design, thermal comfort, adaptive opportunities, lighting, indoor air quality, acoustics, health recovery, health satisfaction, hospital ward*

Introduction

Indoor environmental quality (IEQ) as one of the features of green buildings and the sustainable environment has been drawing much attention, due to its high impact on the behaviour of the building users. An assessment of the (IEQ) of buildings is essential in determining success and failure. Buildings are designed and constructed to be occupied by people and the requirements for their occupancy must be made a prerequisite for their comfort. Therefore, the significance of sustaining better (IEQ) in buildings including hospital buildings should be a concern for architects, planners and stakeholders.

For buildings such as healthcare facilities, the issue of maintaining health and comfort should not be overlooked. In the practice of nursing, a healthy environment has been noted as having significant impacts on the health of the patient. This conforms to Al-Rajhi et al.'s (2010) notion who describe hospitals as diagnostic human treatment environments where activities such as care promotion, health education, training and research is undertaken. A hospital environment that contributes to healing does not only add to the patient's wellbeing, but also the wellbeing of the healthcare workers. It has been posited by Zborowsky and Kreitzer (2008) that hospital buildings which are comprised of adequate indoor environmental quality would attract, retain, and enhance the patient's healing process as well as the worker's efficiency. Therefore, a hospital facility should be designed to accommodate the maximum benefit to the occupants, namely patients, their family members, visitors, and healthcare workers. As such, the

http://www.aloki.hu ● ISSN 1589 1623 (Print) ● ISSN 1785 0037 (Online)
DOI: http://dx.doi.org/10.15666/aeer/1704_82358259

indoor environmental quality of a hospital facility is essential for its occupants. A poor (IEQ) create stressful feelings on the occupants' perception of their environment.

Similarly, research has shown that poor (IEQ) is associated with a negative impact on the occupants' physical and psychological health (Mahbob et al., 2011; Sadek and Nofal, 2013). Additionally, Sadek and Nofal (2013) remark that the impact of (IEQ) on patient's satisfaction affects psychological and physical dispositions. Thus, the design and settings of the indoor environment of hospitals should be designed to foster the emotional needs of patients, their families, and staff (Salonen et al., 2013).

The awareness for a healthy and comfortable work environment in buildings has not yet taken root or informed the design of healthcare facilities. This is because the pressure to create sustainable buildings has given more attention to the environmental aspects of the built form, and less to the health and wellbeing of occupants. Researchers, however, have begun to understand the need to focus on the sustainable environment for occupants (Smith and Pitt, 2011), and this should be the same for hospital facilities. Therefore, this paper identifies the influence of each factor affecting PIEQ and explores its relationship with health recovery, health satisfaction and therapeutic ambience on PI-IEQ.

Background

Architectural design features

Features of the hospital's architectural design include room size, design and furniture. Room size (dimensions, area and volume) is an essential factor that can affect the perception of patients. The design includes the shape of the walls, floor and ceiling. According to Kembel et al. (2014), hospital design and spatial configuration have an impact on patient recovery. Similarly, Scholz et al. (2019) suggest that room design influences patients' healing outcomes. For example, furniture in the hospital room, in particular flexible furniture has been shown to play a crucial role in meeting various health and recovery requirements (Huisman et al., 2012). Furniture criteria include type, design, postural comfort and ergonomics (Biancheri and Landi, 2017). In the context of health care settings, there are limited studies that have investigated the relationships between the spatial environment and patient recovery processes (Bosch and Lorusso, 2019). Other authors suggest that the configuration of the plan and the size of the hospital rooms may facilitate patient interaction and support medical care activities (Alfonsi et al., 2014; Mourshed and Zhao, 2012).

Thermal comfort

A thermally comfortable and healthy indoor environment for patients is essential for their optimum recovery. Thermal comfort describes the condition of the mind in terms of temperature satisfaction in a defined environment (ASHRAE, 2004a). Two important schools of thought exist in thermal convenience research; the heat balance approach (Fanger, 1970) and the adaptive thermal comfort approach (de Dear et al., 2013). Fanger (1970) introduced the concepts of the predicted mean vote (PMV) and predicted percentage of dissatisfied (PPD), which have been incorporated into the international standards (ISO, 2005) and ASHRAE (2004b). The adaptive principle opined that 'humans react in such a way that tends to lean towards ensuring that their comfort is reestablished when changes which affect their comfort level' occur (Nicol et al., 2012). The idea of adaptive thermal convenience, based on the adaptive principle and outcomes

http://www.aloki.hu ● ISSN 1589 1623 (Print) ● ISSN 1785 0037 (Online)
DOI: http://dx.doi.org/10.15666/aeer/1704_82358259

of several field studies, has been incorporated into ASHRAE (2004b) and CEN 15251 (2007). Several studies have investigated the physical quantities that affect the indoor thermal comfort of wards and also the effects of thermal comfort on patients (Khalid et al., 2019; Sadrizadeh et al., 2018; Shi et al., 2018; Verheyen et al., 2011). Such researches were carried out in naturally ventilated (NV) and air-conditioned (AC) wards using the heat balance approach and adaptive comfort models. Over time, studies have revealed that no specific temperature is ideal for people living in a particular building enclosure. However, although 20-24 °C has been judged as the range that is acceptable for healthy daily living, priority must be given to personal preferences or sentiments expressed by individuals. The level of activities and the choice of clothes also impacts on the thermal comfort of an individual (Djongyang et al., 2010; Gou et al., 2018; Kamalha et al., 2013).

Research outcomes related to indoor thermal comfort deals with the thermal environment acceptability of hospital wards and their level of compliance with global best practices (Khodakarami and Nasrollahi, 2012). Khalid et al. (2019) showed that the wellbeing of patients largely depends upon their preferences in terms of thermal comfort and air quality, and this should be considered. For example, the assessment of thermal comfort in a Belgian healthcare facility is set at 95% despite 29% of the thermal surrounding not being in accordance with ASHRAE design ranges of temperature and relative humidity (Verheyen et al., 2011). This situation implies that the environmental conditions of hospital patient rooms recommended by ASHRAE are sometimes very tough for patients to adapt to and suggests that perhaps the range of environmental parameters should be broadened.

Studies have shown that sensation, comfort and preferences in tropical countries are at variance with global standards (ASHRAE, 2007; ISO, 2005), which implies that thermal tolerance confronted in warm, humid season is greater, due to adaptation and acclimatisation (Anam, 2018). Therefore, greater efforts aimed at improving relevant and contextual thermal comfort that can consider varied outcomes, preferences and adaptation measures, for non-air conditioned spaces in tropical locations are required. Additionally, humans strive better under a cooler temperature that higher temperature (USEPA, 2015). This indicates that a relative rise in temperature also leads to the corresponding vaporisation of particulate matter from indoor components including furniture, fittings and building materials thereby limiting indoor thermal quality (Toftum, 2010). A varied number of factors impact room temperature ranging from fenestration opening that can increase thermal challenges during summer (Norbäck and Nordström, 2008). The architectural decision to design a well-ventilated in-patient ward, by utilising the outdoor environment should be of principal consideration in tropical countries. Accurate and adequate fenestration for ventilation and positioning of ceiling fans should also be evaluated and considered.

Lighting

The indoor environments of hospital buildings are highly demanding, with ambient parameters that are dependent upon use patterns, activities and specific sanitary needs. As a result, guaranteeing adequate comfort conditions becomes a more important and pressing issue than energy consumption (Ulrich et al., 2008), which has been regarded as a crucial factor for designing healing environments (Huisman et al., 2012). A well-designed healing environment in healthcare can have a significant impact on health outcomes including reducing errors and infections (Joseph, 2006), improving patients'

http://www.aloki.hu ● ISSN 1589 1623 (Print) ● ISSN 1785 0037 (Online)
DOI: http://dx.doi.org/10.15666/aeer/1704_82358259

moods (Beute and Kort, 2014) and stress (Ulrich, 1991). Also, colour and lighting play a major part in the perceived health outcomes of patients (Dalke, 2006) in addition to adequate soundscape environments (Mackrill et al., 2014). This is achieved by providing high window-to-wall ratios that enhance daylighting parameters and result in visual comfort and energy savings in patients' rooms.

Improper use of roller shutters may darken the room to the detriment of health and wellbeing. Daylighting conditions, indoor illuminance levels and visibility from the room to the outside should be key considerations for work on energy retrofitting of hospitals (Calama-González et al., 2019). Choi et al. (2012) identified a significant relationship between indoor daylight environments and a patient's average length of stay in a hospital room. The study revealed that in addition to the seasonal weather factor, indoor illuminance and luminance ratios could potentially influence the design of hospital spaces. Benedetti et al. (2001) highlight the antidepressant effect of daylighting on occupants and conclude that direct exposure to natural sunlight may reduce a patient's length of stay in hospitals. Likewise, Raanaas et al. (2012) reveal that having views through the windows as opposed to partially or blocked views may help alleviate stress and shorten patients' stay in hospitals.

Indoor air quality

Hospitals represent a uniquely complex environment that differs from other commercial or residential buildings, given that its occupants are at a higher risk of health symptoms such as eye irritation, headaches, coughs, colds, dizziness, asthma, respiratory and cardiovascular diseases (Eames et al., 2009; Pérez-Padilla et al., 2010; Verde et al., 2015). Environmental microbes can contaminate the patient care environment and complicate recovery if users develop infections from common infectious agents. Therefore, good ventilation performance is important to achieve minimal exposure to infectious airborne microbes (Leung and Chan, 2006; Verde et al., 2015). Consequently, hospitals should be regarded as high-performance buildings in terms of environmental and air quality to enhance staff efficiency and maintain patients' healing process (Leung and Chan, 2006; Shrivastava et al., 2013; Verde et al., 2015; Wan et al., 2011).

Achieving clean indoor air quality within hospitals is important and requires a good understanding of how the ventilation systems, indoor occupants, type of medical activities, building materials, as well as spatial and seasonal variations affect indoor air pollution levels (Erdogan et al., 2010; Jung et al., 2015; Nimlyat and Kandar, 2015; Verde et al., 2015). Fenestration within the hospital building can allow for the inflow of polluted air from outdoor sources into the indoor environment of the hospitals. Likewise, evaporation of particulate matter from furniture, water and infiltration of radon and other gases from underlying soil and bedrock also contributes to the pollution of the indoor environment (John et al., 2010). Other factors that may contribute to poor IAQ include poor cleaning practices, poor moisture control (e.g. water leaks or persistent damp surfaces), human occupancy (e.g. odours) and poor building maintenance (Paevere et al., 2008).

Acoustics

The sound environment is a vital part of the overall environmental ecosystem, and sounds beyond the acceptable decibel level is unwanted (usually referred to as noise) and can be seen as a major environmental stressor in the clinical surrounding (Xie et al.,

http://www.aloki.hu ● ISSN 1589 1623 (Print) ● ISSN 1785 0037 (Online)
DOI: http://dx.doi.org/10.15666/aeer/1704_82358259

2009). The impact of sensory stimuli such as sound and light is a critical challenge in creating a suitable environment in hospital settings for patients and operators. Research has shown that noise in the hospital environment can inhibit sleep and patient's recovery (Gardner et al., 2009; Hofhuis et al., 2012; Monsén and Edéll-Gustafsson, 2005; Waye et al., 2013; Xie et al., 2009). This suggests that unpleasant or distressing sounds impact negatively on the rate of recovery of patients in the hospital and in some extreme cases worsen the health condition of the patients. This includes psychological and physiological effects such as altered memory, increased agitation, aggressive behaviour, depression, anxiety, psychiatric disorders and deciphering speech difficulties (Elmenhorst et al., 2012; Helton et al., 2009; Joseph and Ulrich, 2007; Ryherdet al., 2008; Short et al., 2011). According to Frumkin and Louv (2007), it could be argued that people are closely attached to the natural world, which suggests that contact with nature is beneficial to health and wellbeing. As such, nature sounds may also be introduced in the environment as a positive distraction, which has been shown to have a significant influence on patients' clinical and behavioural outcomes (Pati and Nanda, 2011; Shepley, 2006).

Adaptive opportunities

Adaptive opportunities as defined by Nicol et al. (2012) are 'the chances created by structures for occupants to provide adequate comfort themselves such as windows, blinds, fans, etc.' The feedback approach suggested by Nicol and Humphreys (1973), relating to deductions from research on thermal comfort field surveys, targets feelings of high temperature or cold as a significant function of the comfort control system. And also further opined that poor sensation conditions the occupants to evolve basic measures, mitigation and modification that helps to stabilise the system. This approach to thermal comfort is generally termed an adaptive model (Nicol et al., 2012).

Adaptive actions cover the physiological, social and behavioural dimensions that enable occupants to start depending on their thermal environment (Yan et al., 2017; Kim et al., 2018). Such adaptive actions, among others, include switching on fans, opening a window, switching on the air conditioners and so on. An adaptive approach to thermal comfort targets the behaviour of the occupants who try to achieve their comfort. Brager et al. (2004) defined the imperatives of individual control, as an avenue to enhance the performance and promote the thermal satisfaction of the users. Gou, Lau, and Chen (2012) evaluated the occupants' dimension of management on the comparative note against building use studies (BUS) benchmarking system. Their study reveals a significant correlation between occupants' control of heating, cooling and ventilation with the thermal comfort, overall comfort and productivity, which are important components of IEQ.

Theoretical predictions

Based on the literature review on the various dimension of IEQ and exploratory factor analysis (EFA), the factors that influence PIEQ were identified, and a model was developed to explore the influence of PIEQ on patient's perception of a ward being conducive. The model also explored the influence of health satisfaction, health recovery and therapeutic ambience on PI-IEQ of the hospital. The final research model (*Fig. 1*) and hypotheses are proposed as follows.

http://www.aloki.hu ● ISSN 1589 1623 (Print) ● ISSN 1785 0037 (Online)
DOI: http://dx.doi.org/10.15666/aeer/1704_82358259

Hypotheses

Hypothesis 1 (H1): Patient satisfaction is enhanced with an enhanced level of PIEQ.

Hypothesis 2 (H2): An enhanced level of PIEQ of ward leads to an enhanced level of perception of the ward as being conducive for wellbeing.

Hypothesis 3 (H3): Health satisfaction, health recovery and therapeutic ambience has a positive influence of PI-IEQ.

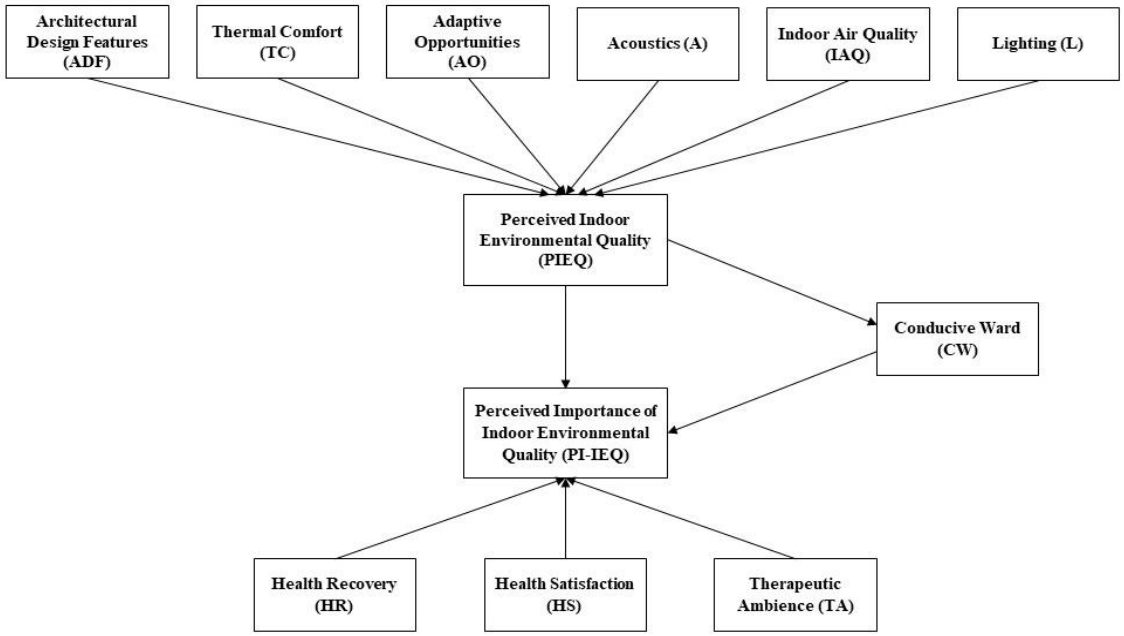

Figure 1. *Research model*

Research methods

The study area

This study is carried out in Minna, Niger State, which is the twelfth largest state in Nigeria. As demonstrated in *Figure 2,* Minna is situated at latitude 9°37' North and longitude 6°33' East. The northeast part of the city has a rock outcrop that acts as a physical constraint to development. Minna is 200 Kilometres from Abuja, the federal capital and covers 100,000 Hectares of land at the present development (Minna Master Plan, 1979). This increased the population of about 200,000 in 1991 to about 552,000 in 2017 (Sulyman et al., 2017). Minna as a city lies in North Central Nigeria, and it is in the Savannah region of the country. The average mean precipitation is 1,334 mm (52.52 inches) and the highest mean monthly rainfall is in September (300 mm or 11.7 inches), and the mean monthly temperature is between 33 and 27 °C (Nimet, 2010). Minna, in common with other cities in Nigeria experience both dry and rainy seasons. The dry season starts in October and lasts until April and has a strong north east trade wind known as the Harmattan wind or tornadoes. The wind is cool, dry, hazy and dusty. It brings about a cold environment with dryness. The rainy season starts at the end of April and lasts until mid-October and has a south west trade wind which brings about a warm, heavy wind that brings on the rain.

http://www.aloki.hu ● ISSN 1589 1623 (Print) ● ISSN 1785 0037 (Online)
DOI: http://dx.doi.org/10.15666/aeer/1704_82358259

The study was conducted among the patients of general hospital Minna, Niger state in Nigeria. The collection of field data for this study was carried out in four selected wards of the general hospital. The questionnaire survey was conducted in four wards, namely the amenity ward, surgical ward, pediatric ward and emergency ward. The studied wards were located in different parts of the hospital (*Fig. 3*).

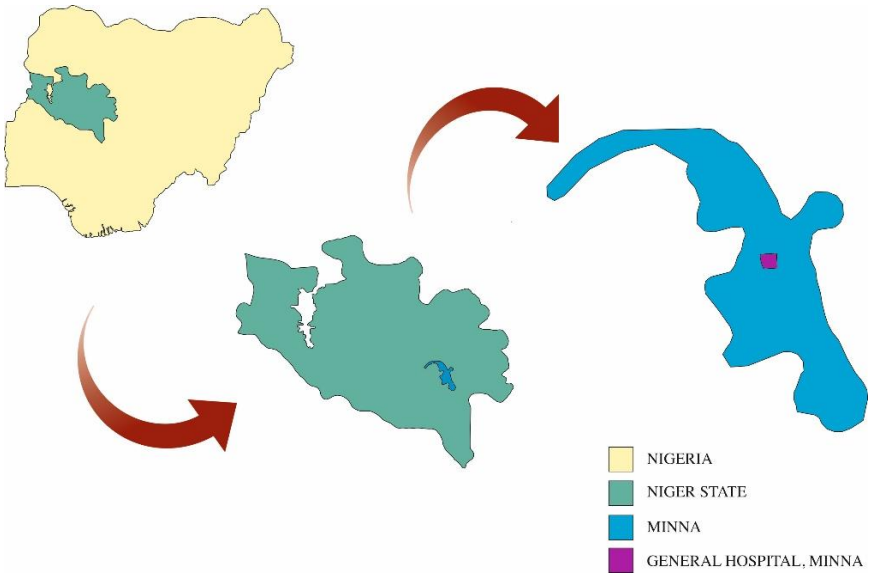

Figure 2. *Showing the map of Minna, Niger State, Nigeria*

Figure 3. *Existing site layout of general hospital Minna*

Objective and subjective data collection

Parameters such as temperature, relative humidity, illuminance, sound and CO_2 were recorded within each ward throughout the day using DrDAQ (USB) CO122/133 and REED SD – 9901. DrDAQ (USB) CO122/133 was used to measure temperature,

http://www.aloki.hu ● ISSN 1589 1623 (Print) ● ISSN 1785 0037 (Online)
DOI: http://dx.doi.org/10.15666/aeer/1704_82358259

illuminance level and sound intensity level (Temperature range 0–70 °C, accuracy ± 0.3 °C, Light Intensity range 0 – 100 and sound level range 55–100dBA, accuracy ± 5dBA) while REED SD – 9901 was used to measure relative humidity and carbon dioxide concentration (Relative Humidity range 5 – 95%, accuracy ± 3%, Carbon dioxide range 0–4000 ppm, accuracy). The data loggers were placed on a table in the middle of the ward 1 m above the floor.

Questions related to each of the dimensions of the indoor environment (architectural design features, thermal, adaptive opportunity, lighting, acoustic and IAQ) were included in terms of adequacy, satisfaction, conduciveness and importance. A seven-point Likert-type scale was used to measure adequacy, satisfaction, conduciveness and importance. 300 questionnaires were distributed in four different wards on different days, during the period from February 2018 to April 2018. Out of 300 questionnaires distributed, only 280 were returned. Nine of the questionnaires were not used due to being incomplete. Therefore, a total of 271 questionnaires were used for the analysis.

Data analysis

Evaluating indoor conditions by means of surveys alongside measuring campaigns is a widely used approach that has been extensively tested (De Giuli et al., 2013; Sattayakorn et al., 2017; Verheyen et al., 2011). The objective data was collected using the above instruments and were compared to the recommended standards. The analysis of the patients' responses was carried out using SPSS version 23.0 and SmartPLS 3.0 version, frequently used for structural equation modelling (SEM) to test the fitness, estimate flexibility, and predicting both observed and latent variable influences on each other in a particular model.

Results and analysis of the objective data

The scientific measurement of the various climatic factors which affects the IEQ in the hospital ward was carried out using the identified instruments as shown in *Table 1*. These factors are temperature, relative humidity, sound, lighting and CO_2. The temporal resolution of the measurements from this study has been displayed in the *Appendix*. However, the measurement for illumination and light intensity in the various wards surveyed was pegged at between 6am and 8pm. This is so based on the noticeable challenge of power inefficiency in the study area. Nigeria has a serious energy supply deficit and this often applied to all class of infrastructure in the country (Olatunji et al., 2018). On the basis of this argument, the readings and measurements taken in the study area between 6am and 8pm is an aggregate of analysis between both natural and artificial lightning system, however beyond 8:00pm, lightening is basically dependent on artificial lightning which made reading difficult to examine because of the dearth in power supply, hence, the research considered lightening measure at periods when natural lighting can be relied upon in d absence of the artificial lightning. The outcomes of these measurements are included in *Table 2,* which presents the various averages shown on the table for temperature, relative humidity, sound, lighting and CO_2. The analysis shows that the average daily temperature for the various hospital wards examined were 33.8 °C for the surgical ward, 31.5 °C for the emergency ward, 34.1 °C in the amenity ward and 32.3 °C in the paediatric ward. The recommended standard of temperature ranges is between 23-26 °C (ASHRAE, 2006) and 24-33 °C (British Standards Institution, 2007).

http://www.aloki.hu ● ISSN 1589 1623 (Print) ● ISSN 1785 0037 (Online)
DOI: http://dx.doi.org/10.15666/aeer/1704_82358259

Table 1. *IEQ mobile measurement station logger. (Source: Author's analysis, 2018)*

IEQ element	Instrument model	Resolution	Range	Accuracy
Air temperature	Mastech MS8209	0.1 °C @25 °C	0-70 °C	± 0.3 °C
Relative humidity	Mastech MS8209	0.10%	5 – 95%	± 3%
Light intensity	DrDAQ (USB) CO122/133	0.1	0 – 100	Manually calibrated
Sound level	DrDAQ (USB) CO122/133	1 dBA	55 – 100dBA	± 5 dBA
Carbon dioxide (CO_2)	REED SD – 9901	1 ppm	0 – 4000ppm	± 5%(> 1000 ppm)

Table 2. *Objectives measurements averages*

Month	Wards	Temp (°C)	RH (%)	Sound (dBA)	Lighting (lux)	CO_2 (ppm)
February	Surgical	33.8	55.5	43.5	371	510
	Emergency	31.5	55.0	44.9	402	496
	Amenity	34.1	54.9	46.1	410	495
	Pediatric	32.3	54.6	46.2	420	517
March	Surgical	33.8	54.5	43.8	403	490
	Emergency	33.6	54.9	45.1	397	498
	Amenity	33.9	55.2	45.7	399	487
	Pediatric	33.4	54.5	45.0	391	506
April	Surgical	34.1	54.1	43.8	402	497
	Emergency	34.0	54.8	45.0	402	493
	Amenity	33.0	54.6	46.0	403	506
	Pediatric	32.6	54.7	45.2	412	490

Temp = temperature; RH = relative humidity

Furthermore, the average daily minimum and maximum temperatures range from 23.1 °C and 33.4 °C within the various wards examined between February, March and April. It was observed that the weather condition of the city and the internal environment of the hospital wards examined differ considerably given the temperature recorded within the chosen month. This suggests that such wards will require an external input in terms of artificial ventilation to help make the internal environment of the hospital wards conducive for patients who are treated for various medical conditions.

Another indoor element examined in the measurement is the relative humidity of the hospital wards. The analysis shows that the average daily relative humidity of the hospital wards within February, March and April ranges from an average daily range from 41.2 to 68.2% daily within the months sampled. The average relative humidity of the wards measured is presented as 55.5% for the surgical ward, 55.0% for the emergency ward, 54.9% in the amenity ward and 54.6% in the pediatric ward. However the recommended guideline for relative humidity by ASHRAE (2004a) is 30-60%. Based on the data presented, relative humidity in the selected wards is within the recommended standard.

The sound level and acoustic properties of the hospital wards were also measured in the for the four wards sampled for this research. The measurement shows that the surgical ward has a daily average sound decibel of 43.5 dBA, the emergency ward is

http://www.aloki.hu ● ISSN 1589 1623 (Print) ● ISSN 1785 0037 (Online)
DOI: http://dx.doi.org/10.15666/aeer/1704_82358259

44.9 dBA, the amenity ward is 46.1 dBA, and the paediatric ward is 46.2 dBA. This shows that most of the hospital wards are relatively noisy and unconducive for the patients. The daily sound level of the wards was measured at 26.6 dBA minimum and 69.7 dBA maximum. However, the recommended sound level should not exceed 40 dBA (WHO, 1999) and 60 dBA (ASHRAE, 2007). From the sound measurement carried out, it shows that the highest level of noise is recorded in the afternoons of February across the hospital wards. This situation shows a serious challenge for design as most of the wards are expected to be designed in such a way that these high noise levels are properly managed in order to achieve a good level of comfort for the patients.

The lighting conditions of the wards were also examined between February-April. The analysis shows that the surgical ward has a daily average light intensity of 371 lux, the emergency ward is 402 lux, Amenity ward is 410 lux, and the paediatric ward is 420 lux. However, the recommended guideline is 100-225 lux (CIBSE, 1989). This shows that most of the hospital wards are bright during the day time and are above the recommended standard.

The particulate matter is another element of the indoor air quality that was measured in this research. The measurement of the particulate matter shows a daily minimum of 258 ppm and 750 ppm. The measurement further showed that the surgical ward has a daily average CO_2 of 510 ppm, the emergency ward is 496 ppm, amenity ward is 495 ppm, and the paediatric ward is 517 ppm. This measurement given the daily measures shows that the level of CO_2 is within the acceptable range recommended of > 700 ppm (ASHRAE, 2010; British Standards Institution, 2007)

Structural equation model

Structural Equation Modeling (SEM) approaches are a second-generation multivariate technique that has been widely employed for investigating or testing the research model of several studies (Fornell and Bookstein, 1982). Using SEM is similar to the employment of Multiple Regression Analysis (Ali et al., 2018). In addition, SEM is used to predict the influence of the independent variable on the dependent variable of a particular research model. A two-stage analysis was conducted under the structural equation model in this study, first the assessment of the measurement model and secondly evaluating the structural model (Anderson and Gerbing, 1982).

Content validity

The content validity of the survey questionnaire in this current study was investigated in two ways. First, the questionnaire items were adopted from studies which has been used and tested. Second, the draft of the survey questionnaire was re-evaluated by some professionals in the field under the study to ensure content validity.

Internal consistency

The internal consistency of the constructs was tested using Cronbach's alpha (α). The general accepted reliability or internal consistency of the constructs should be greater or equal to 0.70 (Hair et al., 2010). As indicated in *Table 3*, the Cronbach alpha ranges from 0.75 to 0.972 indicating high internal consistency. The skewness and Kurtosis indices are also presented in *Table 3*, to assess the normality of the data. Lei and Lomax (2005) suggest less than an absolute value |2.3| for both skewness and kurtosis indices to ensure adequate data normality.

http://www.aloki.hu ● ISSN 1589 1623 (Print) ● ISSN 1785 0037 (Online)
DOI: http://dx.doi.org/10.15666/aeer/1704_82358259

Table 3. *Summary of exploration factor analysis (EFA) results*

Constructs	Item descriptions	Factor loadings	Kurtosis	Skewness
Acoustics (A)	AVE = 0.953., CR = 0.976 and α = 0.952			
AI	Satisfaction with the noise level	0.970	0.519	-1,346
A2	Satisfaction with noise privacy	0.982	0.577	-1,380
Adaptive opportunities (AO)	AVE = 0.681., CR = 0.864 and α = 0.757			
AO1	Satisfaction with the freedom to switch the ceiling fans on/off	0.692	-0.576	-0.925
AO2	Satisfaction with the freedom to open/close the window shutters	0.885	-0.407	-0.936
AO3	Satisfaction with the freedom to switch the fluorescent lamps on/off	0.884	-0.082	-0.996
Conducive ward (CW)	AVE = 0.972., CR = 0.986 and α = 0.972			
CW1	How conducive is the ward for the wellbeing	0.985	-1.810	-0.168
CW2	How can you rate the level of conduciveness of the ward	0.987	-1.731	-0.211
Architectural design features (ADF)	AVE = 0.895., CR = 0.962 and α = 0.942			
ADF1	Adequacy of openings in the ward	0.936	-0.854	-0.817
ADF2	Satisfaction with ward layout	0.955	-0.660	-0.855
ADF3	Satisfaction with a hospital bed (furniture)	0.948	-0.604	-0.888
Health recovery (HR)	AVE = 0.926., CR = 0.962 and α = 0.921			
HR1	Satisfaction with Health Recovery rate	0.967	-1,159	-0.257
HR2	Satisfaction with Health Recovery	0.958	-1,106	-0.251
Health satisfaction (HS)	AVE = 0.923., CR = 0.960 and α = 0.916			
HS1	How do you perceive the Overall health satisfaction within the ward?	0.961	-0.854	-0.817
HS2	How do you rate the overall Health satisfaction	0.960	-0.660	-0.855
Indoor air quality (IAQ)	AVE = 0.943., CR = 0.971 and α = 0.940			
IAQ1	Satisfaction with air quality	0.966	0.725	-1,388
IAQ2	Satisfaction with air exchange rate	0.976	0.453	-1,389
Lighting (L)	AVE = 0.908., CR = 0.952 and α = 0.900			
L1	Satisfaction with the amount of daylight	0.942	-0.892	-0.597
L2	Satisfaction with visibility or with the amount of light	0.964	-0.787	-0.722
Perceived importance of indoor environmental quality (PI-IEQ)	AVE = 0.853., CR = 0.921 and α = 0.830			
	How do you perceive the importance of IEQ	0.941	-1,106	-0.251
	How do you rate the perceived importance of IEQ	0.906	-0.787	-0.722
Perceived indoor environmental quality (PIEQ)	AVE = 0.927., CR = 0.962 and α = 0.922			
	Overall satisfaction with the Perceived IEQ of the ward	0.965	0.483	-1,332
	How do you rate the perceived IEQ of the ward	0.961	0.802	-1,424
Therapeutic ambience (TA)	AVE = 0.769., CR = 0.869 and α = 0.705			
TA1	How do you perceive Therapeutic ambience of the hospital ward	0.841	1,523	-1,161
TA2	How do you perceive the Therapeutic ambience of the hospital environment	0.912	0.422	-0.962
Thermal comfort (TC)	AVE = 0.972., CR = 0.986 and α = 0.972			
TC1	Satisfaction with temperature	0.985	-1,810	-0.168
TC2	Satisfaction with relative humidity	0.987	-1,731	-0.211

Convergent validity

Average variance extracted (AVE) composite reliability (CR) and factor loadings were used to measure convergent validity. Each factor loading is expected to be above a

http://www.aloki.hu ● ISSN 1589 1623 (Print) ● ISSN 1785 0037 (Online)
DOI: http://dx.doi.org/10.15666/aeer/1704_82358259

0.70 threshold (Kurfali et al., 2017). All factors loadings were above 0.60. The recommended AVE values should be more than 0.5 while CR values exceed 0.7 for accepted convergent validity (Hair et al., 2010). As indicated in *Table 3*, AVE value ranges from 0.681 to 0.972 while CR value ranges from 0.869 to 0.986, suggesting significant level of approval (Sarstedt et al., 2014).

Discriminant validity

The discriminant validity is said to be attained if the square root of the Average Variance Extracted (AVE) for individual constructs are higher than the inter-factor correlation between the construct in the model (Chin, 1998; Hair et al., 2010; Kurfali et al., 2017) as boldly shown in the diagonal cells in *Table 4*. The general results in *Table 5* were within the endorsed values. The general results satisfy the discriminant validity recommendation of the model construct.

Table 4. *Correlation matrix of the constructs*

	A	AD	CW	ADF	HR	HS	IAQ	L	PI-IEQ	PIEQ	TA	TC
A	**0.976**											
AD	0.255	**0.825**										
CW	0.137	0.300	**0.986**									
ADF	0.260	0.609	0.341	**0.946**								
HR	0.185	0.049	0.254	0.215	**0.962**							
ADF	0.220	0.580	0.347	0.478	0.184	**0.961**						
IAQ	0.096	0.094	0.047	0.119	0.059	0.124	**0.971**					
L	0.120	0.421	0.300	0.564	0.318	0.531	0.150	**0.953**				
PI-IEQ	0.136	0.428	0.357	0.565	0.379	0.533	0.142	0.446	**0.924**			
PIEQ	0.331	0.661	0.528	0.642	0.215	0.628	0.298	0.486	0.557	**0.963**		
TA	0.082	0.128	0.110	0.199	0.099	0.226	0.106	0.145	0.116	0.076	**0.877**	
TC	0.137	0.300	0.340	0.341	0.254	0.347	0.047	0.300	0.357	0.528	0.110	**0.986**

Diagonal elements are square roots of AVE (in bold)
A = Acoustics, AD = Adaptive opportunity, CW = Conducive ward, ADF = Architectural design features, HR = Health recovery, IAQ = Indoor air quality, L = Lightning, PI-IEQ = Perceived importance of indoor environmental quality, PIEQ = Perceived indoor environmental quality, TA = Therapeutic Ambience, TC = Thermal comfort

Evaluation of structural model and hypotheses

Generally, the CFI, NFI values are expected to be 0.9 and RMSEA $\leq$ 0.08 and SRMSR $\leq$ 0.05 (Hooper et al., 2008; Wong et al., 2014) to indicate a good model fit. As indicated in *Table 5*, the statistical results shown Chi-square/degree of freedom (χ^2/df) = 2.804, CFI = 0.964, RMSEA = 0.0432, P-value = 0.002, NFI = 0.950, and SRMSR = 0.0454. This suggested that the model for this current study has a good fit.

As indicated in *Table 6* and *Figure 4,* the result from the hypothesis H4, H12, H2, and H7 were all supported. That is Architectural design features ($\beta = 0.263$, $p = 0.022 > 0.05$), Thermal comfort ($\beta = 0.304$, $p = 0.000 < 0.05$), Adaptive opportunity ($\beta = 0.268$, $p = 0.010 < 0.005$) and indoor air quality ($\beta = 0.209$, $p = 0.002 < 0.05$) have a positive influence on the Perceived Indoor Environmental Quality of the studied hospital wards. However, H1 and H8 were not supported. Thus, Acoustics ($\beta = 0.122$,

http://www.aloki.hu ● ISSN 1589 1623 (Print) ● ISSN 1785 0037 (Online)
DOI: http://dx.doi.org/10.15666/aeer/1704_82358259

p = 0.109 > 0.05) and lighting (β = 0.087, p = 0.375 > 0.05) also have no significant effect on perceived indoor environmental quality. Furthermore, Hypotheses, H9 and H10 were supported. The Perceived Indoor Environmental Quality was positive and had a significant influence on the conducive ward (β = 0.502, p = 0.000 < 0.05) and the perceived importance of indoor environmental quality (β = 0.268, p = 0.048 < 0.05). Also, H3 was not supported. That is, the conducive ward ((β = 0.048, p = 0.600 > 0.05) has no significant ınfluence on the perceived importance of indoor environmental quality.

Table 5. *Confirmatory factor analysis*

Fit indices	Recommended value	Research model
Chi square/degree of freedom (χ^2 /df)	≤ 3.00	2.804
P-value	≤ 0.05	0.002
Comparative fit index (CFI)	≥ 0.90	0.964
Normed fit index (NFI)	≥ .90	0.950
Standardized root mean square residual (SRMSR)	≤ 0.05	0.0454
Root mean square error of approximation (RMSEA)	≤ 0.08	0.0432

In addition, Hypotheses H5 and H6 were supported. Indicating that, Health Recovery (β = 0.223, p = 0.011 < 0.05) and Health Satisfaction (β = 0.264, p = 0.015 < 0.05) has a positive influence on the perceived importance of the indoor environmental quality. However, Hypothesis, H11 was not supported. This suggests that Therapeutic Ambience (β = 0.025, p = 0.761 > 0.005) has no significant influence on the perceived importance of indoor environmental quality. Lastly 59.4%, 34.9% and 25.2% of the variance in the perceived indoor environmental quality, perceived importance of indoor environmental quality and conducive ward are explained respectively as presented in *Figure 4.*

Table 6. *Summarised structural modelling results*

	Hypotheses	Path coefficient	T statistics	P values	Decision
H1	A - > PIEQ	0.122	1.605	0.109	Not supported
H2	AO - > PIEQ	0.268	2.577	0.010**	Supported
H3	CW - > PI-IEQ	0.048	0.525	0.600	Not supported
H4	ADF - > PIEQ	0.263	2.303	0.022**	Supported
H5	HR - > PI-IEQ	0.223	2.556	0.011**	Supported
H6	HS - > PI-IEQ	0.264	2.432	0.015**	Supported
H7	IAQ - > PIEQ	0.209	3.124	0.002**	Supported
H8	L - > PIEQ	0.087	0.889	0.375	Not supported
H9	PIEQ - > CW	0.502	7.048	0.000**	Supported
H10	PIEQ - > PI-IEQ	0.268	1.981	0.048**	Supported
H11	TA - > PI-IEQ	0.025	0.305	0.761	Not supported
H12	TC - > PIEQ	0.304	4.611	0.000**	Supported

Significant at **p < 0.05

http://www.aloki.hu ● ISSN 1589 1623 (Print) ● ISSN 1785 0037 (Online)
DOI: http://dx.doi.org/10.15666/aeer/1704_82358259

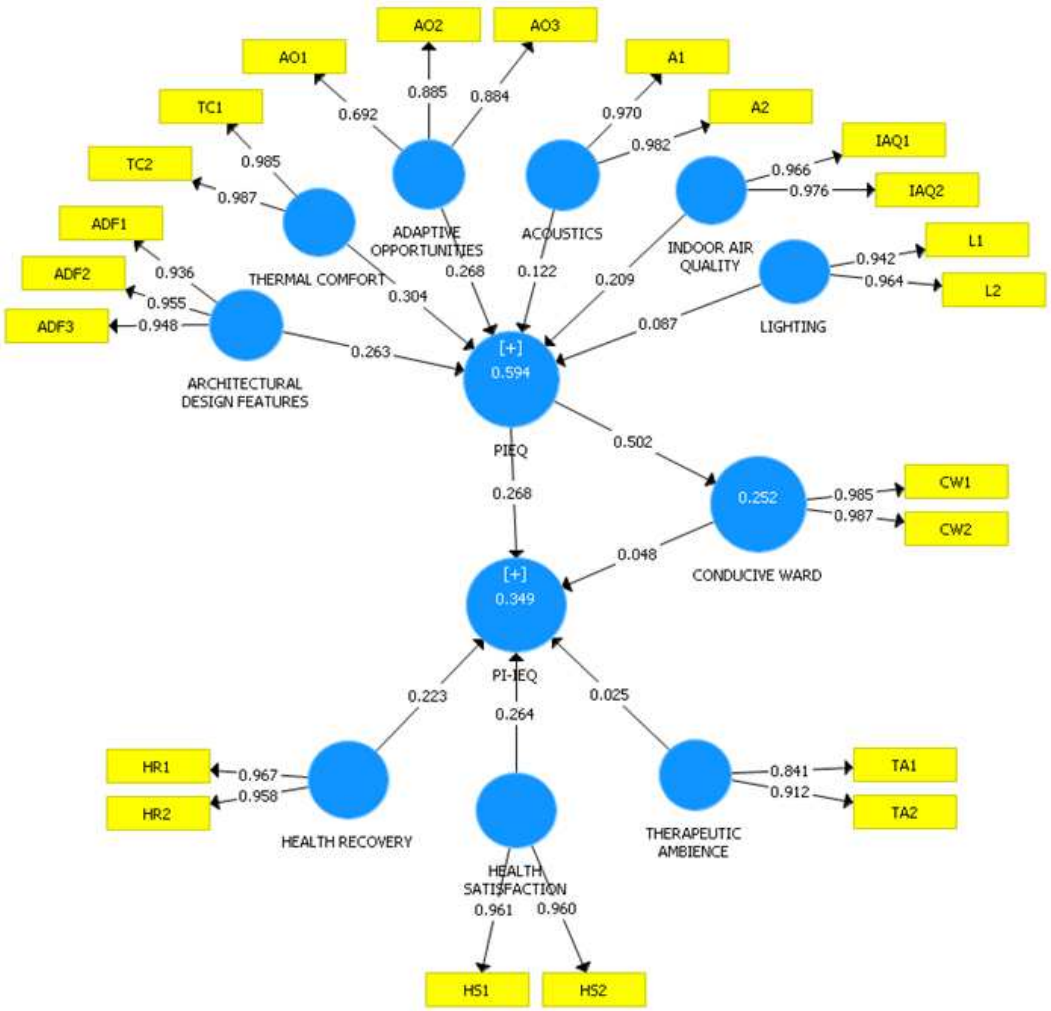

Figure 4. *Structural model evaluation*

Discussion

The six factors that influence PIEQ were consistent with the findings obtained from the literature review. Several types of research conducted indicate that patient's perception significantly relied on design features and ambient attributes (air quality, temperature, daylight, acoustics and artificial lighting) in hospital wards (Ghalib,2018; Gou et al., 2018; Iyendo et al., 2016; Salonen et al., 2013).

In this study, Adaptive opportunity in the context of IAQ and lighting includes the freedom to switch the ceiling fans, freedom to open/close the window shutter and freedom to switch fluorescent lamps. The provision of opportunities to control the patient's indoor environment improved the thermal and visual comfort and satisfaction with IAQ (Fisk, 2000). Occupants attempt to restore their thermal comfort by responding consciously or unconsciously to the thermal environment (Nicol and Humphreys, 2002) and by adjusting the personal environment conditions by opening/closing windows or switching fans on/off (de Dear and Brager, 1998).

Architectural design features were the third most influencing factor on PIEQ in this study (*Fig. 5*). Architectural design features in ward play an important role and health satisfaction of patients (Bosch and Lorusso, 2019; Devlin and Arneill, 2003; Douglas

http://www.aloki.hu ● ISSN 1589 1623 (Print) ● ISSN 1785 0037 (Online)
DOI: http://dx.doi.org/10.15666/aeer/1704_82358259

and Douglas, 2004). The beds in the studied wards are fixed and unable to be adjusted by the patients. A flexible bed that could be adjusted to the different comfort level of the patient contributes to the conducive space. The spaces between the beds are not sufficient for patients to move around and for staff to treat patients. The layout of the wards contributes to the health satisfaction of the patients depending on the arrangement of the beds in the ward (Bosch and Lorusso, 2019; Liu et al., 2018; Schweitzer et al., 2004). The number and size of opening influence the temperature, ambient air, and lighting in the ward which effect on the perception of the patients.

Figure 5. *Interior views of the selected wards*

In this study, visual comfort influence on patients in the wards is positive but not significant. Daylight levels in a ward depend upon the size of several windows, and their orientation and location within the building (*Fig. 6*). The orientation of the wards is the same, and also the acoustics of the wards was observed to have a positive influence on PIEQ which was not significant.

Interestingly, in this study, thermal conditions had the highest influence on PIEQ. As per Frontczak and Wargocki (2011), thermal comfort was accorded greater importance compared to visual and acoustic comfort and IAQ by the occupants, and it had a higher degree of influence on the overall satisfaction with IEQ compared to other indoor environmental factors. Studies have reported that temperature had the most influence on patients' perceptions of healing environments (De Giuli et al., 2013). All the selected wards in this study depend on the combination of cross-ventilation and the use of ceiling fans.

Conducive and comfortable wards that meet the needs of patients facilitate recovery and health satisfaction (Doyle et al., 2013; Hughes, 2008; Lim et al., 2019; Reiling et al., 2008). It was observed from this study that the higher the PIEQ, the higher the perception of the wards being perceived conducive. Rarely have researchers

http://www.aloki.hu ● ISSN 1589 1623 (Print) ● ISSN 1785 0037 (Online)
DOI: http://dx.doi.org/10.15666/aeer/1704_82358259

investigated the influence of health recovery, health satisfaction and therapeutic ambience on PI-IEQ. Interestingly, this study revealed that Health satisfaction had the most positive influence, followed by heath recovery. Moreover, therapeutic ambience had a positive influent but not significant.

Figure 6. *Exterior views of the selected wards*

Summary

Comfortable thermal environment helps to maintain patients' mood and improves the healing of patients. From the objective survey, the high temperature levels increases toxins rate from building materials and also reduce the recovery rate of the patients in the wards (Kameel and Khalil, 2003). This may increase the lenght of stay of the patients in the wards. Sound level affects comfort and well-being of patients according to Cunha and Silva (2015). The level of noise in this current study can lead to increase in the use of drugs, cardiovascular disease, sleep disruption and hearing loss of the patients. A similar study conducted in Nigeria revealed that most of the indoor environmental quality factors were either above or below the recommended standards (Nimlyat and Kandar, 2015). Temperature and lighting were above the recommended standard in the previous study.

On the other hand, the subjective survey indicated that thermal comfort had the highest influence on the perceived indoor environmental quality in this study. This conforms to the findings of other studies conducted in the tropics (De Giuli et al., 2013; Sattayakorn et al., 2017). Most patients in this study were not satisfied with the adequacy of openings, layout and bed space which contributes to the indoor environment as also reported in a study by De Giuli et al. (2013). Architectural design features such as layout, bed space and openings had significant influence on the PIEQ, as architecture has a role to play in IEQ of buildings (Biancheri and Landi, 2017;

http://www.aloki.hu ● ISSN 1589 1623 (Print) ● ISSN 1785 0037 (Online)
DOI: http://dx.doi.org/10.15666/aeer/1704_82358259

Alfonsi et al., 2014; Mourshed and Zhao, 2012). Patients chose health satisfaction over health recovery and therapeutic ambience as factors influencing PI-IEQ. This implies that, health satisfaction is more important to the patient followed by the health recovery.

Conclusions, implications and limitations

In this study, objective physical measurements and a questionnaire based subjective survey were conducted to investigate the IEQ of four different wards in the General hospital at Minna, Nigeria. Objective measurements of IEQ include temperature, humidity, acoustics, air quality and illuminance. The measurement was recorded daily for three months. Two hundred and seventy-one (271) questionnaires were retrieved from the patients in different wards during the recording period.

From the Objective measurement, temperature, relative humidity, illuminance and sound level were all above recommended guidelines of WHO, British standards and ASHRAE. On the other hand, results from the subjective survey indicated that thermal comfort, adaptive opportunity, architectural features, air quality, lighting and acoustics positively affect the PIEQ. However, Acoustics and lighting do not have a significant influence on PIEQ in this study. An improved PIEQ of patients significantly increases the level of conduciveness of ward and also PI-IEQ of the ward. It was observed that health satisfaction health recovery and therapeutic ambience had a positive influence on PI-IEQ respectively.

Nigeria, being the most populous nation in Africa, has a large number of cases of widespread communicable diseases and an increasing population of more than 190 million. More than 30,000 Nigerians spend $1 billion annually on medical tourism because of the state of health services (Nigeria Investment Promotion Commission, 2019). With a need for more hospitals and proposals to add more wards to the existing hospitals to meet the growing demand of healthcare services, focus need to be accorded by health practitioners and architects to the design of hospital wards. This study added to the existing knowledge of healing environments, in terms of the outcome of the patient's perception of the hospital ward, particularly through PIEQ and PI-IEQ.

The objective data analysis was limited, as data was collected within three months of the dry season. There will be a need for data collection throughout the year in order to understand the role of other influential factors that may affect PIEQ evaluation in hospital buildings in general. Architectural design features were only limited to layout, the opening of windows and furniture (bed). Other design features such as material finishes, landscape elements, bed spaces etc. should be studied in detail to ascertain how they influence the PIEQ.

Acknowledgements. The authors are grateful to Niger state ministry of health for the permission of using general hospital Minna as a case study.

REFERENCES

[1] Alfonsi, E., Capolongo, S., Buffoli, M. (2014): Evidence based design and healthcare - an unconventional approach to hospital design. – Ann Ig 26(2): 137-43.

[2] Ali, F., Rasoolimanesh, S. M., Sarstedt, M., Ringle, C. M., Ryu, K. (2018): An assessment of the use of partial least squares structural equation modeling (PLS-SEM) in

http://www.aloki.hu ● ISSN 1589 1623 (Print) ● ISSN 1785 0037 (Online)
DOI: http://dx.doi.org/10.15666/aeer/1704_82358259

hospitality research. – International Journal of Contemporary Hospitality Management 30(1): 514-538.

[3] Al-Rajhi, S., Ramaswamy, M., Al-Jahwari, F. (2010): IAQ in hospitals - better health through indoor air quality awareness. – Proceedings of the Tenth International Conference Enhanced Building Operations, Kuwait, October 26-28, 2010.

[4] Anam, S. I. (2018): Assessment of thermal comfort of non-airconditioned in-patient hospital wards in Dhaka during warm, humid periods. – Dissertation submitted in partial fulfillment of the requirements for the degree of master of architecture. Department of Architecture Bangladesh University of Engineering and Technology Dhaka, Bangladesh.

[5] Anderson, J. C., Gerbing, D. W. (1982): Some methods for respecifying measurement models to obtain unidimensional construct measurement. – Journal of Marketing Research 19(4): 453-460.

[6] ASHRAE (2004a): Standard 90.1-2004, Energy Standard for Buildings Except Low Rise Residential Buildings. – American Society of Heating, Refrigerating and Air-Conditioning Engineers, Inc, Atlanta, GA.

[7] ASHRAE (2004b): Thermal Environmental Conditions for Human Occupancy, Vol. 55. – American Society of Heating, Refrigerating and Air-Conditioning Engineers, Atlanta, GA.

[8] ASHRAE (2006): Refrigeration. – American Society of Heating, Refrigerating and Air-Conditioning Engineers, Atlanta, GA.

[9] ASHRAE (2007): ASHRAE Applications Handbook. Atlanta, USA. – American Society of Heating, Refrigeration, and Air-conditioning Engineers, Inc, Atlanta, GA.

[10] ASHRAE (2010): ANSI/ASHRAE 62.1 - 2010. Atlanta, USA. – American Society of Heating, Refrigeration, and Air-conditioning Engineers, Inc, Atlanta, GA.

[11] Benedetti, F., Colombo, C., Barbini, B., Campori, E., Smeraldi, E. (2001): Morning sunlight reduces length of hospitalization in bipolar depression. – Journal of Affective Disorders 62(3): 221-223.

[12] Beute, F., de Kort, Y. A. (2014): Salutogenic effects of the environment: review of health protective effects of nature and daylight. – Applied Psychology, Health and Well-Being 6(1): 67-95.

[13] Biancheri, R., Landi, S. (2017): Gender and healthcare environments: a proposal of gender-sensitive methodology for improving the environmental quality in the existing heritage. Territorio della Ricerca su Insediamenti e Ambiente. – Rivista Internazionale di Cultura Urbanistica 17: 69-82.

[14] Bosch, S. J., Lorusso, L. N. (2019): Promoting patient and family engagement through healthcare facility design: a systematic literature review. – Journal of Environmental Psychology.

[15] Brager, G., Paliaga, G., De Dear, R. (2004): Operable windows, personal control and occupant comfort. – ASHRAE Transactions 110: 17-35.

[16] British Standards Institution (2007): BS EN 15251: Indoor Environmental Input Parameters for Design and Assessment of Energy Performance of Buildings Addressing Indoor Air Quality, Thermal Environment, Lighting and Acoustics. – British Standard Institution, London.

[17] Calama-González, C. M., León-Rodríguez, Á. L., Suárez, R. (2019): Daylighting performance of solar control films for hospital buildings in a Mediterranean climate. – Energies 12(3): 489.

[18] CEN 15251 (2007): Indoor Environmental Input Parameters for Design and Assessment of Energy Performance of Buildings Addressing Indoor Air Quality, Thermal Environment, Lighting and Acoustics. – CEN, Brussels, Belgium.

[19] Chin, W. W. (1998): The partial least squares approach to structural equation modeling. – Modern Methods for Business Research 295(2): 295-336.

http://www.aloki.hu ● ISSN 1589 1623 (Print) ● ISSN 1785 0037 (Online)
DOI: http://dx.doi.org/10.15666/aeer/1704_82358259

[20] Choi, J. H., Beltran, L. O., Kim, H. S. (2012): Impacts of indoor daylight environments on patient average length of stay (ALOS) in a healthcare facility. – Building and Environment 50: 65-75.
[21] CIBSE (1989): Lighting Guide: Hospitals and Healthcare Buildings. – CIBSE, London.
[22] Cunha, M., Silva, N. (2015): Hospital noise and patients' wellbeing. – Procedia-Social and Behavioral Sciences 171: 246-251.
[23] Dalke, H., Little, J., Niemann, E., Camgoz, N., Steadman, G., Hill, S., Stott, L. (2006): Colour and lighting in hospital design. – Optics & Laser Technology 38(4-6): 343-365.
[24] de Dear, R. J., Akimoto, T., Arens, E. A., Brager, G., Candido, C., Cheong, K. W. D. Toftum, J. et al. (2013): Progress in thermal comfort research over the last twenty years. – Indoor air 23(6): 442-461.
[25] de Dear, R., Brager, G. S. (1998): Developing an adaptive model of thermal comfort and preference. – ASHRAE Transactions 104(1): 145-167.
[26] De Giuli, V., Zecchin, R., Salmaso, L., Corain, L., De Carli, M. (2013): Measured and perceived indoor environmental quality: Padua Hospital case study. – Building and Environment 59: 211-226.
[27] Devlin, A. S., Arneill, A. B. (2003): Health care environments and patient outcomes: A review of the literature. – Environment and Behavior 35(5): 665-694.
[28] Djongyang, N., Tchinda, R., Njomo, D. (2010): Thermal comfort: A review paper. – Renewable and Sustainable Energy Reviews 14(9): 2626-2640.
[29] Douglas, C. H., Douglas, M. R. (2004): Patient-friendly hospital environments: exploring the patients' perspective. – Health Expectations 7(1): 61-73.
[30] Doyle, C., Lennox, L., Bell, D. (2013): A systematic review of evidence on the links between patient experience and clinical safety and effectiveness. – BMJ Open 3(1): e001570.
[31] Eames, I., Tang, J. W., Li, Y., Wilson, P. (2009): Airborne transmission of disease in hospitals. – Journal of the Royal Society Interface. DOI: 10.1098/rsif.2009.0407.focus.
[32] Elmenhorst, E. M., Pennig, S., Rolny, V., Quehl, J., Mueller, U., Maaß, H., Basner, M. (2012): Examining nocturnal railway noise and aircraft noise in the field: Sleep, psychomotor performance, and annoyance. – Science of the Total Environment 424: 48-56.
[33] Erdogan, M. S., Yurtseven, E., Erginöz, E., Vehid, S., Köksal, S., Yüceokur, A. A. (2010): Total volatile organic compounds (TVOC), carbon monoxide (CO), carbon dioxide (CO2) concentrations in the hospital building of a medical faculty in Istanbul, Turkey. – Emergency 20: 23.
[34] European Standard (2008): UNE-EN 15251:2008. Indoor environmental input parameters for design and assessment of energy performance of buildings addressing indoor air quality, thermal environment, lighting and acoustics. – Aenor 1-52. https://doi.org/10.1520/E2019-03R13.Copyright.
[35] Fanger, P. O. (1970): Thermal comfort. Analysis and applications in environmental engineering. – Thermal comfort. Analysis and applications in environmental engineering.
[36] Fisk, W. J. (2000): Health and productivity gains from better indoor environments and their relationship with building energy efficiency. – Annual Review of Energy and the Environment 25(1): 537-566.
[37] Fornell, C., Bookstein, F. L. (1982): Two structural equation models: LISREL and PLS applied to consumer exit-voice theory. – Journal of Marketing Research 19(4): 440-452.
[38] Frontczak, M., Wargocki, P. (2011): Literature survey on how different factors influence human comfort in indoor environments. – Building and Environment 46(4): 922-937.
[39] Frumkin, H., Louv, R. (2007): The powerful link between conserving land and preserving health. – Land Trust Alliance Special Anniversary Report 2007: 1-5.
[40] Gardner, G., Collins, C., Osborne, S., Henderson, A., Eastwood, M. (2009): Creating a therapeutic environment: a non-randomised controlled trial of a quiet time intervention for patients in acute care. – International Journal of Nursing Studies 46(6): 778-786.

http://www.aloki.hu ● ISSN 1589 1623 (Print) ● ISSN 1785 0037 (Online)
DOI: http://dx.doi.org/10.15666/aeer/1704_82358259

[41] Ghalib, A. (2018): Enhancing Inclusive Design in Emergency Department Waiting Areas: A Mixed Methods Architectural Study of Five Toronto Hospitals. – http://openresearch.ocadu.ca/id/eprint/2409.
[42] Gou, Z., Lau, S. S. Y., Chen, F. (2012): Subjective and objective evaluation of the thermal environment in a three-star green office building in China. – Indoor and Built Environment 21(3): 412-422.
[43] Gou, Z., Gamage, W., Lau, S., Lau, S. (2018): An investigation of thermal comfort and adaptive behaviors in naturally ventilated residential buildings in tropical climates: a pilot study. – Buildings 8(1): 5.
[44] Hair, J. F., Black, W. C., Babin, B. J., Anderson, R. E. (2010): Multivariate data analysis (7th Ed.). – Prentice Hall, Upper Saddle River, NJ.
[45] Helton, W. S., Matthews, G., Warm, J. S. (2009): Stress state mediation between environmental variables and performance: the case of noise and vigilance. – Acta Psychologica 130(3): 204-213.
[46] Hofhuis, J. G., Langevoort, G., Rommes, J. H., Spronk, P. E. (2012): Sleep disturbances and sedation practices in the intensive care unit—a postal survey in the Netherlands. – Intensive and Critical Care Nursing 28(3): 141-149.
[47] Hooper, D., Coughlan, J., Mullen, M. (2008): Structural equation modelling: guidelines for determining model fit. – Electronic Journal on Business Research Methods 6(1): 53-60.
[48] Hughes, R. G. (2008): Tools and strategies for quality improvement and patient safety. In Patient safety and quality: an evidence-based handbook for nurses. – Agency for Healthcare Research and Quality, Rockville, Maryland.
[49] Huisman, E. R., Morales, E., van Hoof, J., Kort, H. S. M. (2012): Healing environment: a review of the impact of physical environmental factors on users. – Building and Environment 58: 70-80.
[50] ISO 7730 (2005): Ergonomics of the thermal environment—analytical determination and interpretation of thermal comfort using calculation of the PMV and PPD indices and local thermal comfort criteria. – Management 3: 605-615. https://www.sis.se/api/document/preview/907006/.
[51] Iyendo, T. O., Uwajeh, P. C., Ikenna, E. S. (2016): The therapeutic impacts of environmental design interventions on wellness in clinical settings: a narrative review. – Complementary Therapies in Clinical Practice 24: 174-188.
[52] John, G., Clements-Croome, D., Howe, J. (2010): A conceptual approach to determine optimal indoor air quality: a mixture experiment method. – Proceeding of the CLIMA Conference, Held in Antalya, Turkey, 9-12 May, 2010, pp. 193-203.
[53] Joseph, A. (2006): The Impact of the Environment on Infections in Healthcare Facilities. – Center for Health Design, Concord, CA.
[54] Joseph, A., Ulrich, R. (2007): Sound Control for Improved Outcomes in Healthcare Settings. – Center for Health Design, Concord, CA.
[55] Jung, C. C., Wu, P. C., Tseng, C. H., Su, H. J. (2015): Indoor air quality varies with ventilation types and working areas in hospitals. – Building and Environment 85: 190-195.
[56] Kamalha, E., Zeng, Y., Mwasiagi, J. I., Kyatuheire, S. (2013): The comfort dimension; a review of perception in clothing. – Journal of Sensory Studies 28(6): 423-444.
[57] Kameel, R., Khalil, E. E. (2003): Energy efficiency, air quality, and comfort in air-conditioned spaces. – ASME 2003 International Design Engineering Technical Conferences and Computers and Information in Engineering Conference (pp. 775-782). American Society of Mechanical Engineers.
[58] Kembel, S. W., Meadow, J. F., O'Connor, T. K., Mhuireach, G., Northcutt, D., Kline, J. et al. (2014): Architectural design drives the biogeography of indoor bacterial communities. – PloS One 9(1): e87093.

http://www.aloki.hu ● ISSN 1589 1623 (Print) ● ISSN 1785 0037 (Online)
DOI: http://dx.doi.org/10.15666/aeer/1704_82358259

[59] Khalid, W., Zaki, S. A., Rijal, H. B., Yakub, F. (2019): Investigation of comfort temperature and thermal adaptation for patients and visitors in Malaysian hospitals. – Energy and Buildings 183: 484-499.
[60] Khodakarami, J., Nasrollahi, N. (2012): Thermal comfort in hospitals–A literature review. – Renewable and Sustainable Energy Reviews 16(6): 4071-4077.
[61] Kim, J., Zhou, Y., Schiavon, S., Raftery, P., Brager, G. (2018): Personal comfort models: predicting individuals' thermal preference using occupant heating and cooling behavior and machine learning. – Building and Environment 129: 96-106.
[62] Kurfali, M., Arifoglu, A., Tokdemir, G., Pacin, Y. (2017): Adoption of e-Government services in Turkey. – Computers in Human Behavior 66: 168-178.
[63] Lei, M., Lomax, R. G. (2005): The effect of varying degrees of nonnormality in structural equation modeling. – Structural Equation Modeling 12(1): 1-27.
[64] Leung, M., Chan, A. H. (2006): Control and management of hospital indoor air quality. – Medical Science Monitor 12(3): SR17-SR23.
[65] Lim, E., Wynaden, D., Heslop, K. (2019): Changing practice using recovery-focused care in acute mental health settings to reduce aggression: A qualitative study. – International Journal of Mental Health Nursing 28(1): 237-246.
[66] Liu, Y., Wang, Z., Zhang, Z., Hong, J., Lin, B. (2018): Investigation on the indoor environment quality of health care facilities in China. – Building and Environment. DOI: 10.1016/j.buildenv.2018.05.054.
[67] Mackrill, J., Jennings, P., Cain, R. (2014): Exploring positive hospital ward soundscape interventions. – Applied Ergonomics 45(6): 1454-1460.
[68] Mahbob, N. S., Kamaruzzaman, S. N., Salleh, N., Sulaiman, R. (2011): A correlation studies of indoor environmental quality (IEQ) towards productive workplace. – 2nd International Conference on Environmental Science and Technology IPCBEE, Vol. 6. IACSIT Press, Singapore.
[69] Minna Master Plan (1979): The Capital City of Niger State. Town Planning Division, Ministry of Housing and Environment, Niger State. – Final Report. Prepared by Max Lock Group, Nig. Ltd. https://wedc-knowledge.lboro.ac.uk/details.html?id = 8324.
[70] Monsén, M. G., Edéll-Gustafsson, U. M. (2005): Noise and sleep disturbance factors before and after implementation of a behavioural modification programme. – Intensive and Critical Care Nursing 21(4): 208-219.
[71] Mourshed, M., Zhao, Y. (2012): Healthcare providers' perception of design factors related to physical environments in hospitals. – Journal of Environmental Psychology 32(4): 362-370.
[72] Nicol, J. F., Humphreys, M. A. (1973): Thermal comfort as part of a self-regulating system. – Building Research & Practice 1(3): 174-179.
[73] Nicol, J. F., Humphreys, M. A. (2002): Adaptive thermal comfort and sustainable thermal standards for buildings. – Energy and Buildings 34(6): 563-572.
[74] Nicol, F., Humphreys, M., Roaf, S. (2012): Adaptive Thermal Comfort: Principles and Practice. – Routledge, Abingdon.
[75] Nigeria Investment Promotion Commission (2019): https://www.nipc.gov.ng/overview-healthcare. – Accessed on 15th January, 2019.
[76] Nigeria Meteorological Agency (2010): Nigeria Climate Review Bulletin. – http://www.nimetng.org/uploads/publication/2010%20Climate%20Review.pdf. Accessed on 19th March 2019.
[77] Nimlyat, P. S., Kandar, M. Z. (2015): Appraisal of indoor environmental quality (IEQ) in healthcare facilities: A literature review. – Sustainable Cities and Society 17: 61-68.
[78] Norbäck, D., Nordström, K. (2008): Sick building syndrome in relation to air exchange rate, CO 2, room temperature and relative air humidity in university computer classrooms: an experimental study. – International Archives of Occupational and Environmental Health 82(1): 21-30.

http://www.aloki.hu ● ISSN 1589 1623 (Print) ● ISSN 1785 0037 (Online)
DOI: http://dx.doi.org/10.15666/aeer/1704_82358259

[79] Olatunji, O., Akinlabi, S., Oluseyi, A., Abioye, A., Ishola, F., Peter, M., Madushele, N. (2018): Electric power crisis in nigeria: a strategic call for change of focus to renewable sources. – IOP Conference Series: Materials Science and Engineering 413(1): 012053.
[80] Paevere, P., Brown, S., Leaman, A., Luther, M., Adams, R. (2008): Indoor environment quality and occupant productivity in the CH2 building. – SB08: Proceedings of the 2008 International Scientific Committee World Sustainable Building Conference (pp. 222-229).
[81] Pati, D., Nanda, U. (2011): Influence of positive distractions on children in two clinic waiting areas. – HERD: Health Environments Research & Design Journal 4(3): 124-140.
[82] Pérez-Padilla, R., Schilmann, A., Riojas-Rodriguez, H. (2010): Respiratory health effects of indoor air pollution. – The International Journal of Tuberculosis and Lung Disease 14(9): 1079-1086.
[83] Raanaas, R. K., Patil, G. G., Hartig, T. (2012): Health benefits of a view of nature through the window: a quasi-experimental study of patients in a residential rehabilitation center. – Clinical Rehabilitation 26(1): 21-32.
[84] Reiling, J., Hughes, R. G., Murphy, M. R. (2008): The impact of facility design on patient safety. In Patient safety and quality: An evidence-based handbook for nurses. – Agency for Healthcare Research and Quality (US).
[85] Ryherdet, E., West, J. E., Busch-Vishniac, I., Waye, K. P. (2008): Evaluating the hospital soundscape. – Acoust. Today 4(4): 22-29.
[86] Sadek, A. H., Nofal, E. M. (2013): Effects of indoor environmental quality on occupant satisfaction in healing environments. – Proceedings of the 1st Conference of the Egyptian Affiliation of International Building Performance Simulation Association, Towards Sustainable and Green Life, June, 2013, Cairo, Egypt.
[87] Sadrizadeh, S., Stensson, S., Marashian, S., Walker, I., Holmberg, S. (2018): Airborne bacteria inactivation in a hospital ward by ultraviolet irradiation. – The 4th International Conference on building Energy & Environment (COBEE 2018). February 5-9 2018; Melbourne, Australia.
[88] Salonen, H., Lahtinen, M., Lappalainen, S., Nevala, N., Knibbs, L. D., Morawska, L., Reijula, K. (2013): Design approaches for promoting beneficial indoor environments in healthcare facilities: a review. – Intelligent Buildings International 5(1): 26-50.
[89] Sarstedt, M., Ringle, C. M., Hair, J. F. (2014): PLS-SEM: looking back and moving forward. – Long Range Planning 47(3): 132-137. https://doi.org/10.1016/j.lrp.2014.02.008.
[90] Sattayakorn, S., Ichinose, M., Sasaki, R. (2017): Clarifying thermal comfort of healthcare occupants in tropical region: a case of indoor environment in Thai hospitals. – Energy and Buildings 149: 45-57.
[91] Scholz, R., Hönning, A., Seifert, J., Spranger, N., Stengel, D. (2019): Effectiveness of architectural separation of septic and aseptic operating theatres for improving process quality and patient outcomes: a systematic review. – Systematic Reviews 8(1): 16.
[92] Schweitzer, M., Gilpin, L., Frampton, S. (2004): Healing spaces: elements of environmental design that make an impact on health. – Journal of Alternative & Complementary Medicine 10(Supplement 1): S-71.
[93] Shepley, M. M. (2006): The role of positive distraction in neonatal intensive care unit settings. – Journal of Perinatology 26(S3): S34.
[94] Shi, Z., Qian, H., Zheng, X., Lv, Z., Li, Y., Liu, L., Nielsen, P. V. (2018): Seasonal variation of window opening behaviors in two naturally ventilated hospital wards. – Building and Environment 130: 85-93.
[95] Short, A. E., Short, K. T., Holdgate, A., Ahern, N., Morris, J. (2011): Noise levels in an Australian emergency department. – Australasian Emergency Nursing Journal 14(1): 26-31.
[96] Shrivastava, S. R., Shrivastava, P. S., Ramasamy, J. (2013): Airborne infection control in healthcare settings. – Infection Ecology & Epidemiology 3(1): 21411.

http://www.aloki.hu ● ISSN 1589 1623 (Print) ● ISSN 1785 0037 (Online)
DOI: http://dx.doi.org/10.15666/aeer/1704_82358259

[97] Smith, A., Pitt, M. (2011): Sustainable workplaces and building user comfort and satisfaction. – Journal of Corporate Real Estate 13(3): 144-156.
[98] Sulyman, A. O., Abd'razack, N. T. A., Medayese, S. O. (2017): Ecological footprint of housing in Minna, Nigeria. – Journal of Applied Sciences & Environmental Sustainability 3(7): 68-84.
[99] Toftum, J. (2010): Central automatic control or distributed occupant control for better indoor environment quality in the future. – Building and Environment 45(1): 23-28.
[100] Ulrich, R. S. (1991): Effects of interior design on wellness: Theory and recent scientific research. – Journal of Health Care Interior Design 3(1): 97-109.
[101] Ulrich, R. S., Zimring, C., Zhu, X., DuBose, J., Seo, H. B., Choi, Y. S. et al. (2008): A review of the research literature on evidence-based healthcare design. – HERD: Health Environments Research & Design Journal 1(3): 61-125.
[102] USEPA (US Environmental Protection Agency) (2015): Connectivity of streams and wetlands to downstream waters: a review and synthesis of the scientific evidence. – USEPA, Washington, DC.
[103] Verde, S. C., Almeida, S. M., Matos, J., Guerreiro, D., Meneses, M., Faria, T. et al. (2015): Microbiological assessment of indoor air quality at different hospital sites. – Research in Microbiology 166(7): 557-563.
[104] Verheyen, J., Theys, N., Allonsius, L., Descamps, F. (2011): Thermal comfort of patients: Objective and subjective measurements in patient rooms of a Belgian healthcare facility. – Building and Environment 46(5): 1195-1204.
[105] Wan, G. H., Chung, F. F., Tang, C. S. (2011): Long-term surveillance of air quality in medical center operating rooms. – American Journal of Infection Control 39(4): 302-308.
[106] Waye, K. P., Elmenhorst, E. M., Croy, I., Pedersen, E. (2013): Improvement of intensive care unit sound environment and analyses of consequences on sleep: an experimental study. – Sleep Medicine 14(12): 1334-1340.
[107] Wong, W. S., Lam, H. M. J., Chow, Y. F., Chen, P. P., Lim, H. S., Wong, S., Fielding, R. (2014): The effects of anxiety sensitivity, pain hypervigilance, and pain catastrophizing on quality of life outcomes of patients with chronic pain: a preliminary, cross-sectional analysis. – Quality of Life Research 23(8): 2333-2341.
[108] World Health Organization (WHO) (1999): Guidelines for Community Noise (Berglund, B., Lindvall, T., Schwela, D. H. eds.). – World Health Organization, Geneva.
[109] Xie, H., Kang, J., Mills, G. H. (2009): Clinical review: the impact of noise on patients' sleep and the effectiveness of noise reduction strategies in intensive care units. – Critical Care 13(2): 208.
[110] Yan, D., Hong, T., Dong, B., Mahdavi, A., D'Oca, S., Gaetani, I., Feng, X. (2017): IEA EBC Annex 66: Definition and simulation of occupant behavior in buildings. – Energy and Buildings 156: 258-270.
[111] Zborowsky, T., Kreitzer, M. J. (2008): Creating optimal healing environments in a health care setting. – Minnesota Medicine 91(3): 35-38.

APPENDIX

Indoor air temperature in the selected hospitals wards in Minna (monthly averages)

Month	Ward	Variables	6-8 am	8-10 am	10-12 pm	12-2 pm	2-4 pm	4-6 pm	6-8 pm	8-10 pm	10-12 am	12-2 am	2-4 am	4-6 am
February	Surgical	Temp. (°C)	27.9	30.9	32.9	33.8	39.7	36.8	35.1	34.4	32.6	30.6	28.7	27.9
	Emergency		28.0	31.8	29.4	30.7	39.2	32.3	32.1	31.4	28.4	26.6	25.7	23.7
	Amenity		28.5	32.1	36.9	39.9	38.7	38.4	39.4	36.3	33.1	30.0	28.2	29.4
	Pediatric		28.3	30.4	27.9	28.7	39.9	31.3	31.2	30.3	28.4	27.6	26.9	24.7

http://www.aloki.hu ● ISSN 1589 1623 (Print) ● ISSN 1785 0037 (Online)
DOI: http://dx.doi.org/10.15666/aeer/1704_82358259

March	Surgical	Temp. (°C)	29.3	31.4	33.9	34.7	38.9	37.3	35.2	34.3	32.6	31.6	28.7	28.7
	Emergency		29.3	31.2	33.4	34.5	39.9	37.1	35.7	34.6	32.9	30.9	28.9	27.2
	Amenity		29.3	31.7	32.8	34.2	39.5	36.8	36.7	34.4	32.5	31.9	29.1	28.2
	Pediatric		29.3	31.5	33.6	35.2	39.7	37.5	35.9	33.9	29.3	31.7	28.6	28.2
April	Surgical	Temp. (°C)	28.9	31.7	32.9	35.2	40.7	38.4	36.4	35.3	33.1	31.0	28.2	27.4
	Emergency		29.9	31.9	32.6	35.9	39.7	37.1	35.4	33.3	31.1	32.0	28.4	28.2
	Amenity		28.3	30.8	31.9	35.7	38.9	38.3	36.2	34.3	32.1	31.4	28.1	27.1
	Pediatric		28.9	31.1	32.7	35.9	38.7	37.4	35.4	35.1	33.1	31.0	28.2	26.4

Relative humidity in the selected hospitals wards in Minna (monthly averages)

Month	Ward	Variables	6-8 am	8-10 am	10-12 pm	12-2 pm	2-4 pm	4-6 pm	6-8 pm	8-10 pm	10-12 am	12-2 am	2-4 am	4-6 am
February	Surgical	R.H. (%)	58.3	52.1	47.2	42.6	44.4	48.4	50.1	55.5	60.2	68.3	62.1	61.1
	Emergency		54.0	53.8	47.1	42.2	44.2	47.3	51.1	56.1	61.4	67.6	63.7	61.2
	Amenity		54.2	51.1	47.5	41.9	44.7	47.4	51.4	56.3	61.1	68.0	63.2	61.6
	Pediatric		55.1	54.4	47.7	41.7	44.9	47.3	51.2	56.3	61.5	67.4	63.4	61.9
March	Surgical	R.H. (%)	57.3	52.4	48.9	41.7	43.9	41.3	51.2	54.3	61.6	67.6	64.7	61.4
	Emergency		57.7	53.2	48.4	41.5	43.6	42.1	51.7	54.6	60.9	68.2	64.9	62.5
	Amenity		57.6	52.7	48.8	42.2	43.5	42.5	51.6	55.4	61.5	67.9	65.1	62.5
	Pediatric		57.9	51.5	49.1	41.2	43.7	42.3	51.9	54.9	61.3	67.7	64.6	62.1
April	Surgical	R.H. (%)	58.6	52.7	48.9	41.2	45.5	42.4	51.4	50.3	59.5	67.0	64.2	63.8
	Emergency		58.2	52.9	48.6	41.9	45.5	42.1	51.4	50.3	60.1	67.5	64.4	63.7
	Amenity		58.3	52.8	47.9	41.7	45.2	42.3	51.2	50.3	59.9	67.4	64.1	63.9
	Pediatric		58.7	52.1	47.7	41.5	45.1	42.4	51.4	50.1	60.1	67.8	64.2	64.3

Noise level in the selected hospital wards in Minna (monthly averages)

Month	Ward	Variables	6-8 am	8-10 am	10-12 pm	12-2 pm	2-4 pm	4-6 pm	6-8 pm	8-10 pm	10-12 am	12-2 am	2-4 am	4-6 am
February	Surgical	(dBA)	26.6	47.7	52.1	58.4	60.4	60.6	58.6	47.0	44.4	35.3	30.0	27.3
	Emergency		27.1	48.7	53.1	60.4	62.7	61.1	59.6	49.2	46.4	34.3	31.3	28.3
	Amenity		28.1	47.4	49.1	61.7	64.1	62.0	50.3	48.1	46.6	34.9	31.1	28.7
	Pediatric		26.3	48.6	50.7	63.2	65.7	66.1	55.3	49.3	45.1	36.4	32.2	29.3
March	Surgical	(dBA)	26.3	47.6	58.7	66.2	69.7	64.1	58.3	49.3	46.1	39.4	31.1	27.4
	Emergency		26.1	48.7	57.6	68.7	69.2	65.3	56.1	48.7	45.2	36.1	32.1	26.1
	Amenity		25.1	49.7	56.6	68.4	69.2	68.3	58.1	50.7	44.2	35.1	31.3	29.2
	Pediatric		26.1	47.9	59.6	66.7	67.2	65.3	59.1	51.7	47.2	37.1	32.4	26.2
April	Surgical	(dBA)	26.7	47.4	59.2	68.7	62.1	63.0	58.4	49.1	41.6	39.9	36.4	27.6
	Emergency		28.7	49.4	58.2	66.7	62.9	64.0	60.4	51.1	43.6	37.9	34.7	28.4
	Amenity		29.3	48.6	58.7	68.2	64.7	66.1	59.3	48.3	44.1	38.4	35.1	27.1
	Pediatric		27.7	48.9	59.2	69.7	66.1	68.0	58.4	49.1	45.6	39.9	35.4	27.6

Light intensity level in the selected hospital wards in Minna (monthly averages)

Month	Ward	Variables	6-8 am	8-10 am	10-12 pm	12-2 pm	2-4 pm	4-6 pm	6-8 pm
February	Surgical	(lux)	296	300	336	380	470	442	310
	Emergency		300	305	340	381	500	451	332

http://www.aloki.hu ● ISSN 1589 1623 (Print) ● ISSN 1785 0037 (Online)
DOI: http://dx.doi.org/10.15666/aeer/1704_82358259

	Amenity		307	310	342	387	510	462	341
	Pediatric		315	320	351	392	520	466	354
March	Surgical	(lux)	303	310	388	383	495	471	311
	Emergency		280	289	367	385	505	473	312
	Amenity		285	291	359	372	506	480	313
	Pediatric		266	273	369	366	508	462	315
April	Surgical	(lux)	306	310	388	380	495	465	310
	Emergency		291	299	399	385	505	475	312
	Amenity		300	305	395	386	500	478	313
	Pediatric		309	315	405	390	510	480	325

Level of CO_2 concentration in the selected hospital wards in Minna (monthly averages)

Month	**Ward**	**Variables**	**6-8 am**	**8-10 am**	**10-12 pm**	**12-2 pm**	**2-4 pm**	**4-6 pm**	**6-8 pm**	**8-10 pm**	**10-12 am**	**12-2 am**	**2-4 am**	**4-6 am**
February	Surgical	(ppm)	520	600	686	710	680	512	580	470	450	390	330	310
	Emergency		530	605	690	721	640	531	450	482	445	385	328	271
	Amenity		535	610	692	730	640	542	435	461	412	377	316	260
	Pediatric		538	620	701	750	665	586	427	484	434	367	321	285
March	Surgical	(ppm)	518	610	698	723	675	521	471	462	452	388	325	258
	Emergency		513	608	687	733	645	533	461	475	440	397	320	264
	Amenity		522	612	695	725	641	548	440	458	431	382	313	280
	Pediatric		519	627	709	740	668	589	433	477	441	375	316	272
April	Surgical	(ppm)	515	610	678	703	650	485	440	430	422	360	310	290
	Emergency		511	615	674	711	610	515	435	422	428	350	307	275
	Amenity		518	605	685	715	625	508	445	433	412	345	303	298
	Pediatric		516	621	673	700	638	520	405	415	410	330	301	281

http://www.aloki.hu ● ISSN 1589 1623 (Print) ● ISSN 1785 0037 (Online)
DOI: http://dx.doi.org/10.15666/aeer/1704_82358259

SEED CHEMICAL COMPOSITION OF ENDEMIC PLANT *FRAXINUS ORNUS* SUBSP. *CILICICA*

TONGUÇ, F.

Isparta Applied Sciences University, Faculty of Forestry, Isparta, Turkey
(e-mail: fatihtonguc@isparta.edu.tr; phone: +90-246-211-3989; fax: +90-246-211-3948)

(Received 25th Feb 2019; accepted 15th May 2019)

Abstract. The present study was conducted to determine the biochemical characteristics of *Fraxinus ornus* subsp. *cilicica*, seeds, an endemic tree species of Turkey. Seeds were collected from three provenances (Düziçi-Osmaniye, Andırın-Kahramanmaraş, Pozantı-Adana). Seed reserve composition (total soluble sugars, reducing sugars, carotenoids, xanthophylls, total soluble proteins, total tocopherol, total soluble phenolics, flavanoids and oil content) and seed fatty acids contents were examined. Total soluble sugars content and total tocopherol contents of seed among provenances did not differ significantly but other seed constituents were different among provenances. The highest amount of fatty acids present in *F. ornus* subsp. *cilicica* seeds were linoleic and oleic acids. The present study is the first report dealing with various aspects of seed composition and should provide valuable information for this endemic species.
Keywords: *fatty acids, manna ash, taurus flowering ash, oil content, provenance*

Introduction

Fraxinus ornus (L.) (Oleaceae), also known as Manna ash (Fraxigen, 2005), can be used for numerous purposes for example, afforestation/reforestation of deforested areas, urban landscape design, forest restoration and manna production. Manna refers to white or faded yellow sugary substance that dried exudates collected from diverse natural sources and used in several locations around the world as a traditional sweet, emergency food or traditional medicine to treat trivial diseases (Harrison, 1950). Manna production for many years was the source of mannitol used as nutritive sweetener (Debord et al., 1987; Wisselink et al., 2002). Mannas have been known from the earliest times, particularly in Asia Minor, where some mannas are still regularly used in the preparation of local sweets.

Fraxinus ornus subsp. *cilicica* (Lingelsh) Yalt., localy named as Taurus flowering ash, is an endemic tree species of Turkey. The species has ornamental value because of its flower, foliage and interesting crown form (Dirr and Heuser, 1987). This species is an insect-pollinated tree (Verdú et al., 2007), fruits are winged, elongated and single seeded samaras borne in clusters (Bonner, 2008). It is distributed on southern parts of Turkey, mostly on Taurus and Amanos mountains in the East. Taurus flowering ash could reach 8-10 m height and sometimes reach up to 20 m height (Yaltirik, 1978; Browicz, 1982; Yilmaz and Tonguç, 2009). Taurus flowering ash mostly found in karstic areas on sunny southern slopes and grows from 350 m to 1500 m above sea level. Throughout its natural distribution areas, it is scattered generally as individual trees and rarely as clusters and groups. *F. ornus* subsp. *cilicica* wood is used to make shovel handles and therefore scattered populations of this species are under the threat of illegal harvest (Yilmaz and Tonguç, 2013a). However, there are no special conservation programs for the tree species in Turkey. In the last decades, there is an increasing awareness in using native local trees for reforestation and urban planting studies (Grey and Deneke, 1992; Ürgenç, 1998).

http://www.aloki.hu ● ISSN 1589 1623 (Print) ●ISSN1785 0037 (Online)
DOI: http://dx.doi.org/10.15666/aeer/1704_82618269

Forestry activities are long-term investments, therefore use of high quality seeds are critical to have successful seedling establishment. Factors in relation to the provenance and genetic diversity among the populations together with variety within origins should be taken into consideration because field performance of the seeds obtained from different origins of the same species might be varied greatly (Evans, 1982; Duryea, 1985). Though high quality seeds have fundamental importance for success in plantation forestry, chemical properties are yet more important. The term of high quality seeds for reforestation and urban planting studies refers to not only provenance but more importantly chemical composition of the seeds (Ayaz et al., 2011). While many studies deal with seed size, seed dispersal and seed size and seedling establishment, research on seed reserve contents of forest trees has been started studying recently (Brancalion et al., 2008; Soriano et al., 2011; Ataíde et al., 2013).

Although some studies on the seed morphology and physiology (Yilmaz and Tonguç, 2009; Yilmaz and Tonguç, 2013b) and seed fatty acid and mineral content (Ayaz et al., 2011) of endemic *Fraxinus ornus* subsp. *cilicica* species were carried out, there is no detailed studies on the seed chemical composition. The purpose of the present study was to obtain information regarding to the chemical composition of *F. ornus* subsp. *cilicica* seeds collected from three different provenances.

Material and methods

Seed collection

Fraxinus ornus subsp. *cilicica* seeds were collected from three provenances; Düziçi-Osmaniye, Andırın-Kahramanmaraş and Pozantı-Adana. The seeds were collected in October 2016 at least from 10 individual trees and were packed and transported to the laboratory. Seeds were air dried and 400 seeds were taken and seed wings were removed before the analysis. Taurus ash seed morphologies were analyzed in detail previously among the provenances and therefore they were not included in the present study (Yilmaz and Tonguç, 2009, 2013a). Seed provenances and their locality properties were given in *Table 1* and *Figure 1*.

Table 1. *Seed provenances and their localities used in the study*

Provenances	Latitude	Longitude	Altitude (m)	Mean annual rainfall (mm)	Mean annual temperature (°C)
Adana (Pozantı)	37°22’	34°53’	1150	916.9	11.1
Kahramanmaraş (Andırın)	37°32’	36°18’	950	1477.2	14.2
Osmaniye (Düziçi)	37°16’	36°30’	1400	1362.9	11.2

Biochemical analyses

All chemicals were purchased either from Merck-Millipore (Darmstadt, Germany) or Sigma-Aldrich Chemical Co. (St Louis, USA). Spectrophotometric measurements were made on a T80 spectrophotometer (PG Instruments, UK). Total soluble and reducing sugars were extracted as described by Tonguç et al. (2012). The total soluble sugars content was determined by the phenol sulfuric acid assay (DuBois et al., 1956) and the reducing sugars content was determined by Somogyi method (Somogyi, 1952). Glucose was used as standard and the results were expressed as mg/g dry weight. Total

http://www.aloki.hu ● ISSN 1589 1623 (Print) ●ISSN1785 0037 (Online)
DOI: http://dx.doi.org/10.15666/aeer/1704_82618269

carotenoids and xanthophylls contents were determined according to Association of Official Analytical Chemists (AOAC) (AOAC, 1984). 10 ml of acetone-hexane (4:6) solvent was added to 1.0 g pulverized seed samples and the mixture was shaken at 15 minutes and the upper phase was washed twice with 20% NaCl solution. Two phases were separated, and the aliquots were taken from the upper phase and read on a spectrophotometer at 436 and 474 nm wavelengths. The protein extraction was performed according to the method of Larson and Beevers (1965) and the total soluble protein content was determined following Hartree method (Hartree, 1972). Bovine serum albumin (BSA) was used as standard. Total tocopherol content was determined according to modified Emmerie-Engel method (Baker et al., 1980). Standard curve was prepared using α-tocopherol. Total soluble phenolics and flavonoid contents of the seeds were determined following procedures of Sakanaka et al. (2005). Standart curve was prepared using (+)-catechin solution and the results were expressed as mg/g dry weight.

The oil content and fatty acid composition of the seeds were determined using Nuclear magnetic resonance (NMR, Bruker mq-one, USA) and Gas chromatography (GC, Perkin Elmer Auto System XL, USA), respectively. The oil samples (50-100 mg) were extracted and converted to its fatty acid methyl esters (FAME) by the method of Maquard (1987). GC-MS analysis was performed as described by Tonguç and Erbaş (2012). Total free fatty acids content of seeds (%) was determined as oleic acid equivalents.

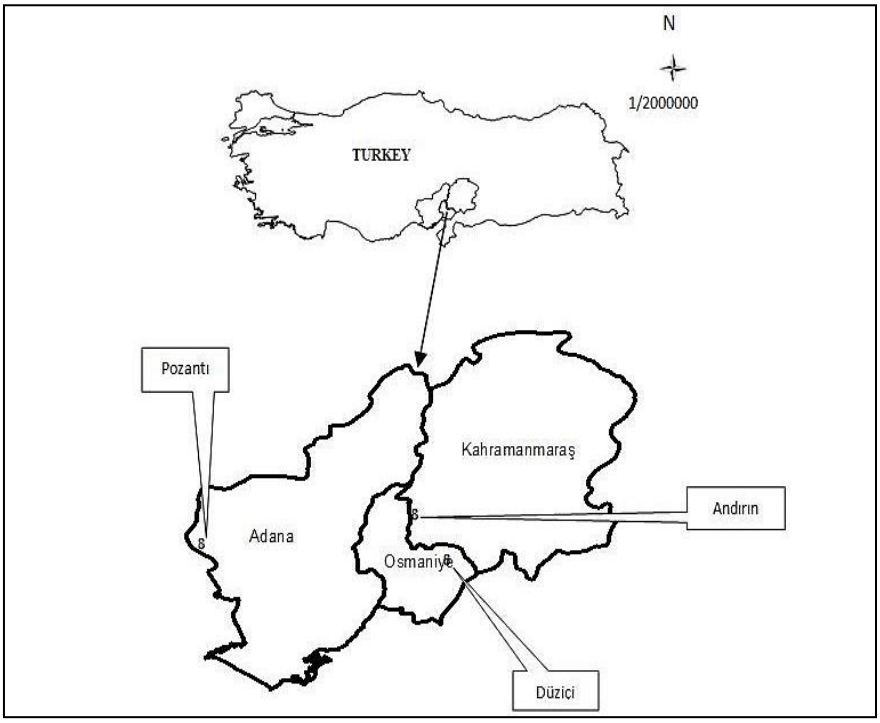

Figure 1. *Location map of seed collection sites*

Statistical analysis

Chemical compositions of provenances were measured 3 times independently and results were analyzed with the analysis of variance (ANOVA). To determine differences between the means, Duncan's Multiple Range test was performed.

http://www.aloki.hu ● ISSN 1589 1623 (Print) ●ISSN1785 0037 (Online)
DOI: http://dx.doi.org/10.15666/aeer/1704_82618269

Results and Discussion

Total of nine parameters related to seed reserves as well as fatty acids compositions were measured to determine chemical composition of *F. ornus* subsp. *cilicica* seeds from 3 provenances. The highest reducing sugars content was found from seeds collected from Adana (146.32 mg/g) followed by Kahramanmaraş (141.29 mg/g) and Osmaniye (138.52 mg/g), however reducing sugars content of the seeds collected from Kahramanmaraş and Osmaniye did no differ significantly. On the other hand, total soluble sugars contents was not statistically significant among the provenances (*Table 2*).

The highest total carotenes (0.894 mg/g) and xanthophylls (0.586 mg/g) contents were obtained from seeds collected in Osmaniye. Unlike reducing sugars content, *F. ornus* subsp. *cilicica* seeds from Osmaniye provenance had higher carotene (0.894 mg/g) and xanthophylls (0.586 mg/g) contents than *F. ornus* subsp. *cilicica* seeds collected from Adana and Kahramanmaraş.

Table 2. *Chemical composition of F. ornus subsp. cilicica seeds from different origins*

Provenance	Reducing sugars (mg/g)	Total soluble sugars (mg/g)	Carotenes (mg/g)	Xanthophyll (mg/g)	Total Soluble proteins (mg/ml)	Total tocopherol (mg/g)	Total soluble phenolics (mg/g)	Flavonoids (mg/g)	Total oil content (%)
Adana	146.32a*	200.24	0.776b*	0.517c**	10.06b*	76.16	5.95a*	2.22a*	23.83c**
Kahramanmaraş	141.29ab	199.96	0.763b	0.556b	9.10b	76.94	5.35b	2.18a	28.42a
Osmaniye	138.52b	199.52	0.894a	0.586a	11.47a	76.48	4.70c	1.89b	25.18b

The values on the same row followed by the same letter are not significantly different at $p<0.05$

Total soluble protein content was also differed significantly between the seed sources. Protein content was not significantly differed between Adana and Kahramanmaraş (*Table 2*). The highest protein content among the seeds was observed in Osmaniye provenance (11.47 mg/ml) and the lowest protein content was found in seeds from Kahramanmaraş (9.10 mg/ml).

Total tocopherol content of *F. ornus* subsp. *cilicica* seeds were close to each other and varied between 76.16-76.94 mg/g. While seeds from Adana had lower tocopherol content than the seeds from Kahramanmaraş and Osmaniye provenances, the difference was not statistically significant.

Total soluble phenolics content was significantly differed among the provenances and changed between 4.70-5.95 mg/g, and the highest soluble phenolics content was observed from the seeds collected from Adana provenance. Total flavanoid content ranged between 1.89-2.24 mg/g among the seed sources and was different between Osmaniye and Adana-Kahramanmaraş provenances.

Total oil content was also measured and statistically different variations were found among the seeds collected from Adana, Kahramanmaraş and Osmaniye provenances. Seeds from Kahramanmaraş had the highest oil content (28.42%) while seeds from Adana (23.83%) and Osmaniye (25.18%) had lower oil contents.

Fatty acid compositions of *F. ornus* subsp. *cilicica* seeds from different seed provenances were also examined. GC/MS analysis revealed 3 major fatty acids (C16:0 palmitic acid, C18:1 oleic acid, C18:2 linoleic acid) and 5 minor fatty acids (C16:1 hexenoicacid, C17:0 heptadecanoic acid, C18:0 stearic acid, C18:3 linolenic acid). Detected fatty acids accounted more than 97% of total fatty acids found in *F. ornus*

http://www.aloki.hu ● ISSN 1589 1623 (Print) ●ISSN1785 0037 (Online)
DOI: http://dx.doi.org/10.15666/aeer/1704_82618269

subsp. *cilicica* seeds. Majority of the fatty acids were unsaturated fatty acids and linoleic and oleic acids constituted the majority of the unsaturated fatty acids. Palmitic acid had the highest amount among the saturated fatty acids (*Table 3*).

Seeds contain carbohydrates, proteins and lipids as reserve molecules and they are usually accumulated as insoluble large macromolecules (Vidigal et al., 2016). These macromolecules are the fundamental constituent of seed biomass and are the source of energy playing important roles for the seedling during germination, early development and survival (Soriano et al., 2011; Wahid and Bounoua, 2013; Zhao et al., 2018). During the germination enzymatic pathways are activated upon imbibition to convert these molecules into smaller soluble units for energy production and synthesis of new molecules (Bewley et al., 2013). Other molecules, such as vitamins, carotenoids and xanthophylls, are also present in seeds in varying amounts. Presence of these molecules protects seeds from enzymatic and non-enzymatic lipid peroxidation during the storage and germination (Priestley, 1986). Information on chemical composition of seeds belong to wild species is scarce therefore some chemical parameters were determined for *F. ornus* subsp. *cilicica* seeds in the present study.

Table 3. *Fatty acid contents (%) of F. ornus subsp. cilicica seeds*

Fatty Acid		RT*	Seed Provenance		
			Adana	Kahramanmaraş	Osmaniye
C16:0	Palmitic acid	24.564	11.69	8.88	11.36
C16:1C7	7-hexenoic acid	25.234	0.31	0.75	1.24
C16:1C9	9-hexenoic acid	27.013	0.16	0.24	1.55
C17:0	Heptadecanoic acid	29.408	0.32	0.25	0.95
C18:0	Steraic acid	32.780	2.65	1.99	3.05
C18:1	Oleic acid	33.408	24.73	17.50	19.12
C18:2	Linoleic acid	34.916	57.56	66.67	56.33
C18:3	Linolenic acid	37.193	0.60	0.95	0.70

*Retention time

It has been reported that type and amount of seed reserves have influence on germination rate, germination percentage or both (Zhao et al., 2018). Different reserves have different influence on germination for example protein content was positively correlated with germination percentage in different tree speceies (Brancalion et al., 2006; Soriano et al., 2011; Wahid and Bounoua, 2013), yet total soluble sugars content was not have influence on germination percentage in *Pinus pinaster* (Wahid and Bounoua, 2013) and did not significantly different among the seeds of the different populations. Oilseed species such as sunflower and safflower seeds showed significant reduction of protein and oil reserves during the germination and early seedling growth, but total soluble sugars and reducing sugars did not decreased significantly (Tonguç et al., 2012; Erbaş et al., 2016). Seed germination parameters have been studied previously (Yilmaz and Tonguç, 2013a,b) but we did not investigate type of the reserves used during the germination and early seedling growth. Different species use different reserves for germination and *F. ornus* subsp. *cilicica* seeds are rich in sugars, proteins and lipids and their role in germination should be investigated further to ascertain their role during germination and seedling growth.

Environmental factors and seed provenances may influence seed morphology and reserve composition. In a previous stduy, seed morphologies of *F. ornus* subsp. c*ilicica* trees colleceted from 8 provenances were described (Yilmaz and Tonguç, 2009). While

http://www.aloki.hu ● ISSN 1589 1623 (Print) ●ISSN1785 0037 (Online)
DOI: http://dx.doi.org/10.15666/aeer/1704_82618269

there were differences among the seed morphologies depending on provenances, only the mean temperature had influence on samara width among the studied parameters. In the present study, mean temperature of Kahramanmaraş was different to have an influence on seed morphology. Total soluble sugars and tocopherol amounts did not differ significantly between provenances, but other reserves of the seeds showed significant differences among the provenances. (*Table 2*). Effects of precipitation on seed lipid, protein and sugar contents on 19 tree species were reported. Lower rainfall increased seed protein content of 12 species while it reduced sugar content of seeds in 2 species. Lipid content of 5 species decreased and one species showed increased lipid content out of 19 tree species in Mexico (Soriano et al., 2011). Phenolics and flavonoids in the seeds have major roles for protecting plant species against insect feeding, herbivory and abiotic stresses such as drought, temperature flactuations, lipid peroxidation (Mierziak et al., 2014). Caratenoids and xhanthophylls are present in photosynthetic tissues and in seeds and protect plants from oxidative damage. Caratenoids in plant seeds also involved in abscisic acid production and seed dormancy (Howit and Pogson, 2006). Tocopherols are also present in seeds and their major role is the prevention of lipid peroxidation during seed storage and germination (Sattler et al., 2004). In the present study, amount of caratenoids and xanthophylls, and total phenolics and flavanoids was different among the seeds from the provenances, suggesting different mechanisms may have involved in the accumulation of these compounds. We have studied effects of storage temperature and seed moisture content of *F. ornus* subsp. *cilicica* seeds collected from 5 provenances (Yilmaz et al., 2014) but their effects on seed storability have not been investigated. The present study will be helpful to investigate seed storage compounds and seed storability of *F. ornus* subsp. *cilicica* seeds.

The present study is a preliminary study to determine some seed reservers of *F. ornus* subsp. c*ilicica* seeds and was conducted one year therefore it was not possible to identify. Influence of environmental factors on seed reserve composition at present. Multi year studies must be conducted to deliminate effects of environmental factors on seed reserve composition.

Seed fatty acid composition have also been investigated. Majority of fatty acids were mono and poly unsaturated fatty acids in *F. ornus* subsp. *cilicica* seeds. GC/MS analysis revealed 97% of fatty acids present in seeds therefore there are other undetected fatty acids and their amounts and types should be investigated further. Lajara et al. (1990) and Bozan and Kaplan (2007) stated that fatty acid profiles are affected by temperature, plant species, genotype and environmental conditions. Differences in fatty acid compositions might be due to lower altitude of seed source and therefore the warmer climate of Kahramanmaraş compared to other provenances (*Tables 1, 3*). Similar results were reported by Ayaz et al. (2011) that provenances in the cooler temperatures were tended to deposit higher levels of oleic acid for *Fagus orientalis* seeds.

Conclusion

The present study was conducted to quantify different seed reserves and chemical constituents in *F. ornus* subsp. *cilicica* seeds. Seed reserves such as seed oil content and 8 other seed reserves involving in different features of seed life and seed fatty acid contents have been investigated. Seven compounds present in seeds were differently accumulated in seeds dependeing on seed source. Total soluble sugars and total

http://www.aloki.hu ● ISSN 1589 1623 (Print) ●ISSN1785 0037 (Online)
DOI: http://dx.doi.org/10.15666/aeer/1704_82618269

tocopherol contents among the provenances were not different. Eight different fatty acids have been detected in *F. ornus* subsp. *cilicica* seeds and majority of fatty acids were unsaturated fatty acids. Previous studies revealed that seed reserve accumulation depends on many factors such as environment and maternal plants, and seed provenances differ in their germination capabilities. Further studies would be necessary to conduct to investigate type of reserves accumulated in different seasons and used during the seed germination and their effects on germination capability among different seed provenaces of *F. ornus* subsp. *cilicica* seeds.

REFERENCES

[1] AOAC (1984): Official Methods of Analysis, Association of Official Analytical Chemists. – 14th ed. Washington DC.

[2] Ataíde, G. D. M., Borges, E. E. D. L., Guimarães, V. M., Flores, A. V., Bicalho, E. M. (2013): Alterations in seed reserves of *Dalbergia nigra* ((Vell.) Fr All. Ex Benth.) during hydration. – Journal of Seed Science 35: 56-63.

[3] Ayaz, F. A., Glew, R. H., Turna, I., Güney, D., Chuang, L. T., Chang, Y. C., Andrews, R., Power, L., Presley, J., Torun, H., Şahin, N. (2011): *Fagus orientalis* (Oriental beechnut) seeds are a good source of essential fatty acids, amino acids and minerals. – Food 5: 48-51.

[4] Baker, H., Frank, O., DeAngelis, B., Feingold, S. (1980): Plasma tocopherol in man at various times after ingesting free or acetylated tocopherol. – Nutrition Reports International 21(4): 531-536.

[5] Bewley, J. D., Bradford, K., Hilhorst, H., Nonogaki, H. (2013): Environmental regulation of dormancy and germination. – In: Seeds. Springer, New York, NY.

[6] Bonner, F. T. (2008): Storage of Seed. – In: Bonner, F. T., Karrfalt, R. P. (eds.) The Woody Plant Seed Manual. Agriculture Handbook 727, USDA Forest Service.

[7] Bozan, B., Karakaplan, U. (2007): Antioxidants from laurel (*Laurus nobilis* L.) berries: influence of extraction procedure on yield and antioxidant activity of extracts. – Alimentaria 36(3): 321-328.

[8] Brancalion, P. H., Tay, D., Rodrigues, R. R., Novembre, A. D., Cunha, L. D. (2006): Seed imbibition of five Brazilian native tree seeds. – Acta Horticulturae 771: 77-81.

[9] Browicz, K. (1982): Chorology of Trees and Shrubs in South-West Asia and Adjacent Regions. – Polish Scientific Publishers, Poznan.

[10] Debord, B., Lefebvre, A. M., Guyot-Hermann, J., Bouche, H. R., Cuyot, J. C. (1987): Study of different forms of mannitol: Comparative behaviour under compression. – Drug Development and Industrial Pharmacy 13(9-11): 1533-1546.

[11] Dirr, M. A., Heuser, C. W. (1987): The reference Manual of Woody Plant Propagation. – Varsity Press, Athens, GA.

[12] DuBois, M., Gilles, K. A., Hamilton, J. K. (1956): Colorimetric method for determination of sugars and related substances. – Analytical Chemistry 28: 350-356.

[13] Duryea, M. L. (1985): Evaluating Seedling Quality: Principles, Procedures and Predictive Abilities of Major Tests. – Forest Research Labarotory, Oregon State University, Corvallis.

[14] Erbaş, S., Tonguç, M., Karakurt, Y., Şanli, A. (2016): Mobilization of seed reserves during germination and early seedling growth of two sunflower cultivars. – Journal of Applied Botany and Food Quality 89: 217-222.

[15] Evans, J. C. (1982): Plantation Forestry in the Tropics. – Claridon Press, Oxford, UK.

[16] Fraxigen (2005): Ash Species in Europe: Biological Characteristics and Practical Guidelines for Sustainable Use. – UK: Oxford Forestry Institute, University of Oxford, Oxford.

http://www.aloki.hu ● ISSN 1589 1623 (Print) ●ISSN1785 0037 (Online)
DOI: http://dx.doi.org/10.15666/aeer/1704_82618269

[17] Grey, G. W., Deneke, F. J. (1992): Urban Forestry. – Krieger Publishing, Florida, USA.
[18] Harris, H. C., McWilliam, J. R., Mason, W. K. (1978): Influence of temperature on oil content and composition of sunflower seed. – Australian Journal of Agricultural Research 29: 1203-1212.
[19] Harrison, S. G. (1950): Manna and its sources. – Kew Bulletin 5(3): 407-417.
[20] Hartree, E. F. (1972): Determination of protein: A modification of the Lowry method that gives a linear photometric response. – Analytical Biochemistry 48(2): 422-427.
[21] Howitt, C. A., Pogson, B. J. (2006): Carotenoid accumulation and function in seeds and non-green tissues. – Plant, Cell & Environment 29(3): 435-445.
[22] Lajara, J. R., Diaz, U., Quidiello, R. D. (1990): Definite influence of location and climatic conditions on the fatty acid composition of sunflower seed oil. – Journal of the American Oil Chemists' Society 67(10): 618-623.
[23] Larson, L. A., Beevers, H. (1965): Amino acid metabolism in young pea seedlings. – Plant Physiology 40: 424-432.
[24] Maquard, R. (1987): Qualitätsanalytik im Dienste der Ölpflanzenzüchtung. – Fat Science Technology 89: 95-99.
[25] Mierziak, J., Kostyn, K., Kulma, A. (2014): Flavonoids as important molecules of plant interactions with the environment. – Molecules 19(10): 16240-16265.
[26] Priestley, D. A. (1986): Seed Aging: Implications for Seed Storage and Persistence in the Soil. – Ithaca, NY.
[27] Sakanaka, S., Tachibana, Y., Okada, Y. (2005): Preparation and antioxidant properties of extracts of japanese persimmon leaf tea (kakinoha-cha). – Food Chemistry 89(4): 569-575.
[28] Sattler, S. E., Gilliland, L. U., Magallanes-Lundback, M., Pollard, M., DellaPenna, D. (2004): Vitamin E is essential for seed longevity and for preventing lipid peroxidation during germination. – The Plant Cell 16(6): 1419-1432.
[29] Somogyi, M. (1952): Notes on sugar determination. – Journal of Biological Chemistry 195: 19-23.
[30] Soriano, D., Orozcosegovia, A., Márquezguzmán, J., Kitajima, K., Buen, A. G., Huante, P. (2011): Seed reserve composition in 19 tree species of a tropical deciduous forest in Mexico and its relationship to seed germination and seedling growth. – Annals of Botany 107: 939-951.
[31] Tonguç, M., Erbaş, S. (2012): Evaluation of fatty acid compositions and some seed characters of common wild plant species of Turkey. – Turkish Journal of Agriculture and Forestry 36: 673-679.
[32] Tonguç, M., Elkoyunu, R., Erbaş, S., Karakurt, Y. (2012): Changes in seed reserve composition during germination and initial seedling development of safflower (*Carthamus tinctorius* L.). – Turkish Journal Biology 36: 107-112.
[33] Ürgenç, S. (1998): Ağaçlandırma Tekniği. – İstanbul Üniversitesi, Orman Fakültesi Yayinlari, No: 3994/441, Istanbul.
[34] Verdú, M., Spanos, K., Čaňová, I., Slobodník, B., Paule, L. (2007): Similar gender dimorphism in the costs of reproduction across the geographic range of *Fraxinus ornus*. – Annals of Botany 99(1): 183-191.
[35] Vidigal, D. S., Marques, A. C., Willems, L. A., Méndez-Vigo, B., Hilhorst, H. W., Bentsink, L., Picó, F. X., Alonso-Blanco, C. (2016): Altitudinal and climatic associations of seed dormancy and flowering traits evidence adaptation of annual life cycle timing in *Arabidopsis thaliana*. – Plant, Cell and Environment 39(8): 1737-1748.
[36] Wahid, N., Bounoua, L. (2013): The relationship between seed weight, germination and biochemical reserves of maritime pine (*Pinus pinaster* Ait.) in Morocco. – New Forests 44: 385-397.
[37] Wisselink, H. W., Weusthuis, R. A., Eggink, G., Hugenholtz, J., Grobben, G. J. (2002): Mannitol production by lactic acid bacteria: a review. – International Dairy Journal 12(2-3): 151-161.

http://www.aloki.hu ● ISSN 1589 1623 (Print) ●ISSN1785 0037 (Online)
DOI: http://dx.doi.org/10.15666/aeer/1704_82618269

[38] Yaltirik, F. (1978): *Fraxinus* L. – In: Davis, P. H. (ed.) Flora of Turkey and the East Aegean Islands. Edinburgh University Press, Vol. 6, Edinburgh.
[39] Yilmaz, M., Tonguç, F. (2009): Fruit and seed size variability of *Fraxinus ornus* subsp. *cilicica*. – International Journal of Natural and Engineering Sciences 3(3): 122-125.
[40] Yilmaz, M., Tonguç, F. (2013a): Effects of temperature on the germination of *Fraxinus ornus* subsp. *cilicica* seeds. – Dendrobiology 69: 111-115.
[41] Yilmaz, M., Tonguç, F. (2013b): Dormancy level and dormancy-breaking pretreatments in seeds of *Fraxinus ornus* subsp. *cilicica*, an endemic to Turkey. – Propagation of Ornamental Plants 13(1): 40-45.
[42] Yılmaz, M., Tonguç, F., Ok, T. (2014): Storage effects of *Fraxinus ornus* subsp. *cilicica* seeds on seed viability and germination, an endemic tree in Turkey. – Süleyman Demirel Üniversitesi Orman Fakültesi Dergisi Seri A 15(1): 15-20.
[43] Zhao, M., Zhang, H., Yan, H., Qiu, L., Baskin, C. C. (2018): Mobilization and role of starch, protein, and fat reserves during seed germination of six wild grassland species. – Frontiers in Plant Science 9(234): 1-11.

http://www.aloki.hu ● ISSN 1589 1623 (Print) ●ISSN1785 0037 (Online)
DOI: http://dx.doi.org/10.15666/aeer/1704_82618269

DYNAMICS OF LANDSCAPE CHANGE IN A MOUNTAINOUS RIVER BASIN: A CASE STUDY OF THE BHAGIRATHI RIVER, WESTERN HIMALAYA

GAUR, T.[1] – SINHA, A.[1] – ADHIKARI, B. S.[1] – RAMESH, K.[1,2*]

[1]*Wildlife Institute of India, Dehradun 248001, Uttarakhand, India*

[2]*Faculty of Forestry, University of British Columbia, Vancouver, Canada*

**Corresponding author*
e-mail: ramesh@wii.gov.in; phone: +91-941-297-1678

(Received 27th Feb 2019; accepted 1st May 2019)

Abstract. Riverine systems are influenced by historical and current land use practices linked to alterations in the riparian zone across multiple scales. This study aims to explore the trend of spatiotemporal land cover changes and configuration along a major headstream of the river Ganges in India. Geo-spatial tools were used to quantify the changes in the landscape across a time span of 22 years. Landscape configuration was quantified by applying class level metrics using the software FRAGSTATS. A loss of 18.3% and 5.5% in the dense forest class was perceived in the upland and the riverine areas respectively aided by conversion of large contiguous forests into smaller isolated patches. Markov analysis showed that the forests in the landscape still possess inherent resilience capacity as indicated by a probability of 47% conversion of open forest class to dense forest class in future based on current land-use practices. Land cover changes and forest fragmentation can have inevitable impacts on ecological functioning and species persistence. Monitoring these changes is fundamental in planning future strategies for riverine landscape management. The present study underpins the utility of remote sensing and GIS in building useful baseline data for inaccessible mountainous landscapes at both local and regional scales.
Keywords: *Bhagirathi basin, fragmentation, landscape change, landscape-level assessment, riverine landscape*

Introduction

Natural riverine landscapes are classic examples of ecotonal habitats characterized by a high level of heterogeneity. Multiple interactive pathways operating across various spatiotemporal scales determine the dynamic structure and function of these terrestrial-aquatic continuum habitats (Steel et al., 2010). River form linear corridor features in the landscapes they traverse; montane river systems characteristically being single-thread channels bordered by a narrow band of native riparian vegetation (Ward et al., 2002). Riverine forests grow along the riverbanks and their structural composition is unique and highly influenced by the river's fluvial activities (Naiman et al., 1993). They provide multiple ecosystem services (Tomscha et al., 2017; Sutfin et al., 2016); providing habitats to diverse organisms (Dybala et al., 2019) and maintaining a network of dispersal corridors (Naiman et al., 2005). Riverine forests support high densities and diversities of migratory birds by providing a critical habitat and the only edge cover available to them during migration (Naiman et al., 1993; Gergel et al., 2007).

Forests are losing their resilience capacity at an increasing rate, often irreversibly due to large-scale changes occurring at an unprecedented rate (Wilson, 1992). Forest fragmentation is a global concern, effects of which are well documented in climatic, biophysical and hydrological cycles (Ramanathan et al., 2005), biodiversity and associated ecosystem services (Xu et al., 2009). Fragmentation has impacts on the overall health of the

http://www.aloki.hu ● ISSN 1589 1623 (Print) ● ISSN 1785 0037 (Online)
DOI: http://dx.doi.org/10.15666/aeer/1704_82718289

forest ecosystem. Forest loss and changes in forest configuration impedes the survival of the forest dependent species (Villard et al., 1999; Bogaert et al., 2011). India is endowed with a forest cover of 21.34% (FSI, 2015) of its total landmass and is ranked tenth in the world in terms of the extent of forest cover (FAO, 2010). Although, escalating human population is increasing dependence on forested landscapes for space and resources leading to the degradation of forests, fragmentation being a major corollary (Roy and Roy, 2010). In the state of Uttarakhand, anthropogenic pressure has led to dwindling of forest cover with a loss of 268 km^2 area in a span of two (2013-2015) years (FSI, 2015) with individual case studies from different districts providing strong evidences in the same line (Rawat and Kumar, 2015; Rawat et al., 2013).

Hence, it is critical to assess the current condition of vegetation in a landscape for its conservation and designing future restoration programs (Egbert et al., 2002; He et al., 2005). Discerning the patterns of vegetation change within a landscape can provide a basis for future monitoring and addressing its management (Gould, 2000). Remote sensing offers the best tool to analyze, map, and monitor ecosystem patterns and processes. It facilitates possible data archives from present time to over several decades back due to its potential for observing the Earth's surface at different times (Ety and Rashid, 2019; Xie et al., 2008). Change is an inherent characteristic of a landscape driven by natural and anthropogenic drivers shaping its structure, function and dynamics. Detecting change is an important aspect for studying landscapes that are dynamic and continuously changing, where change is 'an alteration in the surface components of the vegetation cover' (Milne, 1988) or 'a spectral/spatial movement of a vegetation entity over time' (Lund, 1983).

This study aims to explore the use of geo-spatial tools in monitoring landscape changes for inaccessible areas in mountainous terrains across spatial and temporal scales. Advanced tools like FRAGSTATS (McGarigaI and Marks, 1994; Neel et al., 2004) and simulation models using Markov analysis were used to understand patterns of forest fragmentation and predicting future scenarios in the backdrop of current land-use patterns. The study is intended to a comparative understanding of Land-Use and Land-Cover (LULC) change and forest fragmentation events in riverine stands in contrast to the entire river basin.

Materials and methods

Study area

The river Ganga is the largest and longest river of India and a lifeline to millions of humans (supporting > 40% of the total population; sustaining 520 people per sq. km) (Census of India, 2001). It is also listed among 'the top 10 rivers of the world at risk' because of over-extraction of water resources (Wong et al., 2007). The mountainous catchment of the river Ganga is formed by the two Himalayan rivers - the Bhagirathi and the Alaknanda. The study area i.e. the Bhagirathi basin spreads across three administrative districts of Garhwal region viz., Tehri, Pauri, and Uttarkashi in the state of Uttarakhand, Western Himalaya (*Fig. 1*). We focused our study along the river stretch between Gaumukh, the origin of the Gangotri glacier (30°55'37.35"N lat. and 79°4'46.98"E long.) and Rishikesh (30°05'12.94"N lat. and 78°16'3.40"E long.), where the river enters the plains encompassing an elevational range of 4100 to 330 m above sea level. Due to enormous hydro-power potential, many operational and proposed hydro-electric projects exist enroute the Bhagirathi River (Rajvanshi et al., 2012). The characteristic species representing various vegetation types include *Shorea robusta, Mallotus philippensis, Acacia catechu, Bauhinia variegata, Toona ciliata, Celtis*

http://www.aloki.hu ● ISSN 1589 1623 (Print) ● ISSN 1785 0037 (Online)
DOI: http://dx.doi.org/10.15666/aeer/1704_82718289

australis, Pinus roxburghii, Alnus nepalensis, Pinus wallichiana, Populus ciliata, Cedrus deodara and *Betula utilis* in association with a large number of shrubs and herbaceous flora. The climate of the state of Uttarakhand is primarily temperate except for the plains, with temperatures ranging from below 0 to 43 °C with an annual rainfall of 1550 mm (Government of Uttarakhand, 2014).

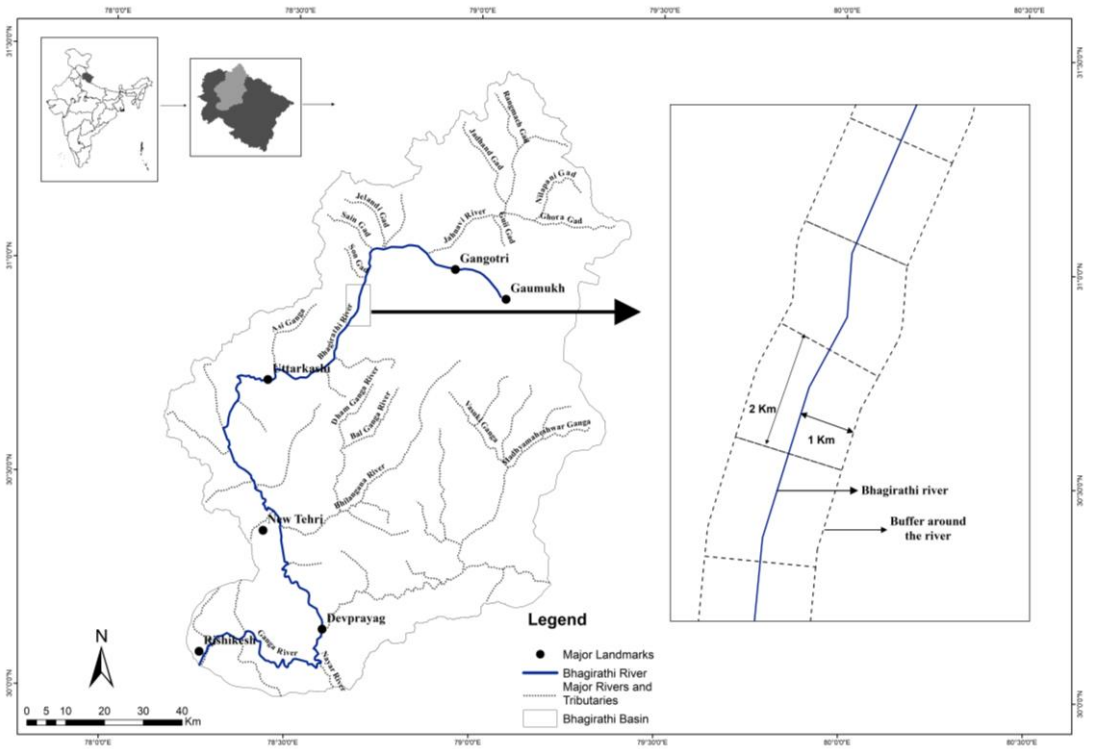

Figure 1. *Location of Bhagirathi river basin in the state of Uttarakhand in India and diagrammatic sketch (right side) represents the cross-section of riverine buffer (2 km long and 1 km wide) on either side along the Bhagirathi river*

Data procurement and processing

Past studies on LULC changes have been carried out by using remote sensing data sets (Halmy et al., 2015), such as MODIS (Alhamdan et al., 2017), Landsat (Osgouei and Kaya, 2017) and SPOT (McCarthy et al., 2018). Since, Landsat offers optimum spatial and spectral resolutions and multi-temporal archives to understand the changes over space and time, it is best suited for this study. Cloud-free Landsat satellite data of 30 m spatial resolution was downloaded from USGS Earth Explorer (www.earthexplorer.usgs.gov) for the month of May for the years 1993 and 2015. The imageries of the path and row 146/38 and 146/39 were subsequently mosaiced for further image interpretation (*Table 1*). Preprocessing was performed in Erdas Imagine 2013 and ArcGIS 10.1 before classifying the images, including radiometric correction and topographic normalization. Normalization algorithms aided in removing albedo variations and topographic effects associated with remote sensing data acquired for mountainous regions. To remove topographic effects resulting from the position of the sun and angle of terrain, an algorithm called Minnaert correction was used (Allen, 2000; Ge et al., 2008).

http://www.aloki.hu ● ISSN 1589 1623 (Print) ● ISSN 1785 0037 (Online)
DOI: http://dx.doi.org/10.15666/aeer/1704_82718289

Table 1. *Details of the Landsat satellite images used as the primary dataset for spatiotemporal LULC change analysis and forest fragmentation*

Landsat 5 (1993)			Landsat 8 (2015)		
Bands	**Spectral resolution (µm)**	**Spatial resolution (m)**	**Bands**	**Spectral resolution (µm)**	**Spatial resolution (m)**
B1- Blue	0.45-0.52	30	B1- Coastal	0.43-0.45	30
B2- Green	0.52-0.60	30	B2- Blue	0.45-0.51	30
B3- Red	0.63-0.69	30	B3- Green	0.53-0.59	30
B4- NIR (Near infrared)	0.76-0.90	30	B4- Red	0.64-0.67	30
B5- MIR (Middle infrared)	1.55-1.75	30	B5- NIR (Near infrared)	0.85-0.88	30
B6- Thermal infrared	10.40-12.50	120	B6- SWIR 1 (Short wave infrared)	1.57-1.65	30
B7- MIR (Middle infrared)	2.08-2.35	30	B7- SWIR 2 (Short wave infrared)	2.11-2.29	30
			B8- Pan (Panchromatic)	0.50-0.68	15
			B9- Cirrus	1.36-1.38	30
			B10- TIRS 1 (Thermal infrared sensor)	10.6-11.19	100
			B11- TIRS 2 (Thermal infrared sensor)	11.5-12.51	100

A reconnaissance field survey was undertaken before classifying the image and ground truth points were collected during subsequent field surveys across the entire river basin. Processed False Color Composite (using the spectral band combination of Near-infrared, Red and Green) for the years 1993 and 2015 were classified using unsupervised classification (ISODATA technique) beginning with 100 classes and then decreasingly grouping together into eight land cover classes namely, dense forest, open forest, shrubland, grassland, agriculture, barren land, river and snow. To validate the remotely sensed data, ground truth points were gathered from on ground surveys and Google Earth generated points to improve accuracy of classified LULC images. The classification accuracy for the images of the two years was measured using the agreement between predicted and observed (field validation points) categories of a dataset, while correcting for agreement that occurs by chance (Jenness and Wynne, 2005). It made use of overall accuracy (OA) of the model in terms of both predictive model and field surveyed sample points, to correct for chance agreement between the both. Around 270 ground truth points collected through extensive field surveys aided in improving the classification accuracy.

Landscape configuration and temporal change

We calculated the area under the eight land cover classes in ArcGIS 10.1 to understand current landscape configuration of the Bhagirathi river basin along with

http://www.aloki.hu ● ISSN 1589 1623 (Print) ● ISSN 1785 0037 (Online)
DOI: http://dx.doi.org/10.15666/aeer/1704_82718289

temporal change across a period of two decades. Markov chain prediction using IDRISI GIS Analysis in TerrSet software was performed to develop the probability matrix for future transitions resulting from the cross-tabulation between the earlier and later times' land cover images. This matrix calculates the probability of a given class pixel to change into any other class or stay the same in the next time period. In a Markov Chain transition, the probability $p(y_t)$ that a phenomenon exists in state a_j if it was in state a_i at a previous time is denoted by the following equation:

$$p\langle y_t = a_j | y_{t-1} = a_i \rangle$$

A landscape is characterized by various land-use and land-cover configurations which is dynamic over time, hence depicts a Markov Chain matrix that encapsulates multiple transitions:

$$\underline{P} = [p_{ij}] = \begin{bmatrix} p_{11}, p_{12} \ldots p_{1n} \\ p_{21}, p_{22} \ldots p_{2n} \\ p_{n1} p_{n2} p_{nn} \end{bmatrix}$$

where $\underline{P} = [p_{ij}]$ is the probability of transitioning from one state i to a different state j or to multiple states (i_1, i_2,...i_j) (Wilson et al., 2018).

FRAGSTATS 4.2.1 was used to quantify the spatiotemporal changes in the structural characteristics reflecting the ecological process and consequent pattern in the landscape. We used class-level metrics to understand the status of forested areas at two scales, for the entire landscape and the riverine buffer (considering a distance of 1 km on either side). We investigated the change in forest class across the landscape using patch density (PD), largest patch index (LPI) and percentage of the landscape (PLAND) under the patch area metrics, the area of the patch (AREA MN) under the shape metrics, clumpiness index (CLUMPY) and aggregation index (AI) under the interspersion metrics. PD is expressed as the number of patches on a per unit area basis and is considered as general index of spatial heterogeneity of the entire class in a landscape mosaic. LPI at the class level quantifies the percentage of total landscape area comprised by the largest patch and is a simple measure of dominance. PLAND quantifies the proportion of particular patch type of a class in a landscape and approaches zero when the class becomes increasingly rare in the landscape. Area MN or mean patch size is a measure of fragmentation in a landscape as the smaller the mean patch size the more fragmented is the focal class in a landscape. Both AI and CLUMPY are calculated from adjacency matrix which means a single, compact patch type is achieved when the AI approaches maximum value while clumpiness index values varies between -1 to + 1 indicating maximum disaggregation or aggregation of the focal patch type (McGarigal and Marks, 1995). For further insights regarding changes in the riverine forest stands, we also analyzed patch properties along both the banks of the Bhagirathi river.

A total of 123 units of 2 km length each were created on the river (linear shapefile) with the aid of the Split tool in ArcGIS10.1 (*Fig. 1*). Thereafter, the Buffer tool was used to create a buffer of 1 km width on both sides of the river. Hence, we created 123 segments of 2 km^2 area on both sides of the river for performing FRAGSTATS analyses in the riverine buffer. With a special focus on understanding the pattern of forest fragmentation in these narrow linear habitats, we used class-level FRAGSTATS analyses. Metrics used for this analysis were identical to those used for comprehending spatiotemporal pattern of forest structure in the entire landscape for enabling a comparative understanding.

http://www.aloki.hu ● ISSN 1589 1623 (Print) ● ISSN 1785 0037 (Online)
DOI: http://dx.doi.org/10.15666/aeer/1704_82718289

Results

Landscape configuration and temporal change

The entire river basin comprised of a total area of 11389 km^2. The overall accuracy of the classified images for the years 2015 and 1993 were 85.1% and 87.2%, respectively. The LULC pattern for the year 2015 indicated 24.1% of the land under dense forest class followed by, open forest (24.3%), shrubland (3.1%), grassland (5.6%), agriculture land (4.5%), barren land (7.1%), river (0.6%) and snow cover (30.6%). The dense forest markedly declined (18.3%) across the time span of 22 years, although the overall area under forests has relatively not undergone much change (*Table 2*). The open forest class showed an increase (18.3%) in the entire river basin. Agriculture class (increase of 2.5%) was found uniformly distributed in the entire landscape barring higher altitudes with a significant concentration along the rivers (*Fig. A1* in the *Appendix; Table 2*). The buffer of a width of 1 km encompassing an area of 409.9 km^2 varied in composition, although it reflected almost similar trends of landscape change as of the entire basin (*Table 2*).

Table 2. *An area-wise comparative analysis of spatiotemporal change (increase depicted as positive [+] and loss as negative [-]) of land cover between 1993 and 2015 in Bhagirathi basin (total area = 11389 km^2) and 1 km buffer along both the sides of Bhagirathi river (total area = 490.9 km^2)*

Land cover class	Basin			Buffer		
	1993	2015	% Change	1993	2015	% Change
	Area (km^2)	Area (km^2)		Area (km^2)	Area (km^2)	
Dense forest	4830.9	2746.2	-18.3	201.7	174.7	-5.5
Open forest	683.8	2768.1	18.3	55.9	109.7	11.0
Shrubland	508.4	358.7	-1.3	59.8	7.9	-10.6
Grassland	672.8	636.4	-0.3	67.7	52.7	-3.1
Agriculture	226.2	507.7	2.5	15.1	45.9	6.3
Barren land	1136.7	814.2	-2.8	62.2	54.3	-1.6
Snow	3282.0	3486.9	1.8	3.8	5.0	0.2
River	48.5	70.8	0.2	24.8	40.8	3.3

The study area depicted a decline in dense forest areas across the entire Bhagirathi basin (4830.9 km^2 to 2746.2 km^2) as well as in the riverine buffer (201.7 km^2 to 174.7 km^2) (*Table 2*). There was a substantial increase in the open forest class in both buffer areas and entire basin, whereas shrubland decreased significantly in the riverine buffer (10.6%). The area under river class increased markedly from 48.5 km^2 (1993) to 70.8 km^2 (2015) owing to land submergence by the Tehri dam, which became operational in the year 2008 and is conspicuous in the map (*Fig. A1*). Area under shrubland and grassland categories decreased across time, remarkably in the riverine buffer (Shrubland-10.6%, Grassland-3.1%). Agricultural land increased across the entire basin, comparatively more in the riverine areas. The riverine buffer units (*Fig. 2; Table A1* in the *Appendix*) depict the similar trends where dense forest showed mostly a negative change while open forest and river showed a positive change across a span of 22 years.

http://www.aloki.hu ● ISSN 1589 1623 (Print) ● ISSN 1785 0037 (Online)
DOI: http://dx.doi.org/10.15666/aeer/1704_82718289

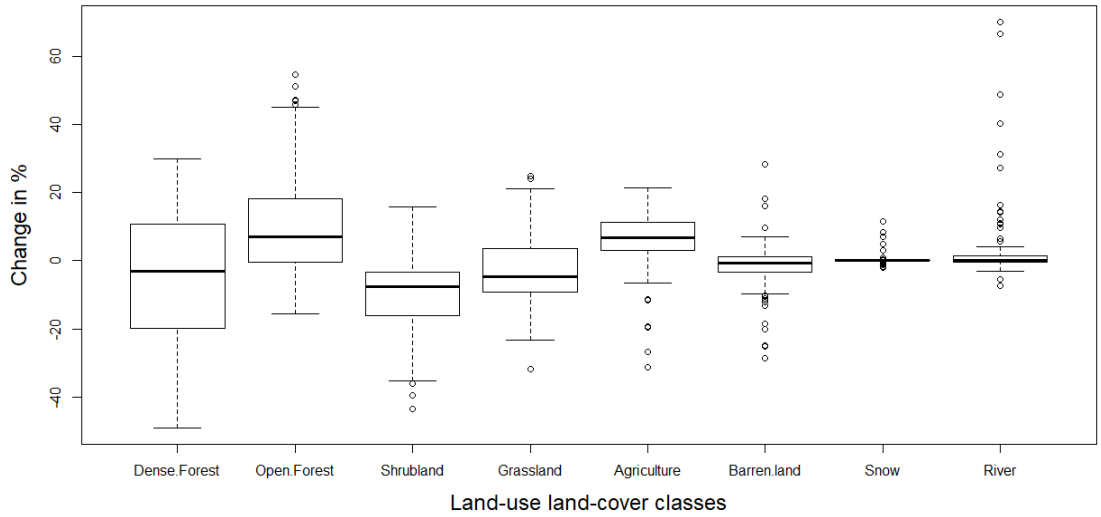

Figure 2. *Box and whisker plot illustrating the area-wise percentage change of Land use/Land cover categories from the years 1993 to 2015 in the 123 riverine buffer units (4 km^2 area) along both the banks of the Bhagirathi River*

Results of Markov analysis reveal that areas under open forest in the entire Bhagirathi basin still hold an equal probability (0.47) of reverting back to dense forest and vice-versa by the year 2037 (*Fig. 3*) depending on the current land-use practices. Area under grassland showed a significant probability of getting converted into open forest (40%). The probabilities of shrubland getting converted to open forest and vice-versa are comparatively similar and smaller in magnitude, while the probability of desertification (conversion of open forest into barren land) was found to be negligible (2%).

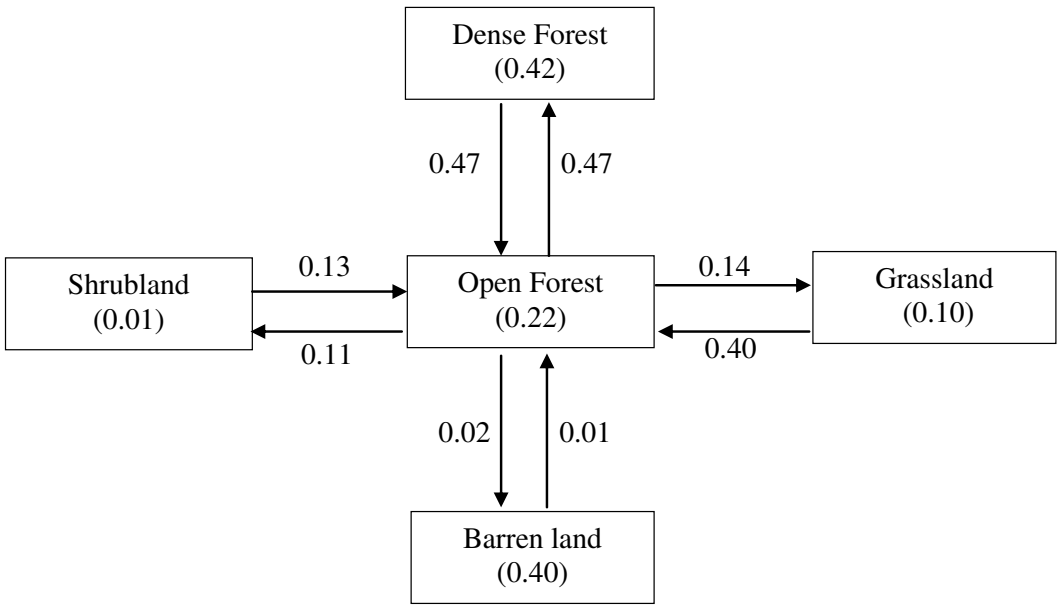

Figure 3. *Land cover/Land use transition probabilities as predicted for the year 2037 (22 years) using Markov analysis (values within box denotes self-replacement probability and values on arrows are their transition probabilities to other land-cover classes)*

http://www.aloki.hu ● ISSN 1589 1623 (Print) ● ISSN 1785 0037 (Online)
DOI: http://dx.doi.org/10.15666/aeer/1704_82718289

Forest integrity and intactness

Results of FRAGSTATS analysis indicate fragmentation events with an increase in the number of patches (1993: 30166 and 2015: 31978) and patch density (1993: 2.65 patches km^{-2}, 2015: 2.81 patches km^{-2}) and decrease in the Large Patch Index (LPI; 1993: 46.0% and 2015: 40.1%) for the forested areas in the Bhagirathi basin. Patch density is a fundamental aspect of landscape pattern and serves as a general index of spatial heterogeneity of the entire landscape mosaic. LPI essentially quantifies the percentage of total landscape area comprised by the largest patch and is a simple measure of dominance. The river basin has undergone a drastic increase in patch density with decreasing LPI in the basin, indicating the disintegration of existing forest patches into smaller fragments.

Proportion of Landscape (PLAND) values decreased in the dense forest class from 42.5% (1993) to 24.1% (2015) while simultaneously increasing in the open forest class from 6.0% to 24.3%, providing evidence for the process of conversion of dense forest to open forest (*Table 3*). Values for Aggregation Index (AI) has decreased moderately in the dense forest type indicating decrease in intactness. In contrary, AI values increased for the open forest class hinting towards decreasing distance between neighbouring patches of this class. The overall status of forests in the Bhagirathi basin portrayed more patchiness in the dense forest class with patches of open forest getting clustered together with time.

Table 3. *Comparative analysis of forest fragmentation using class metrics (dense forest and open forest) between the years 1993 and 2015 in the Bhagirathi basin*

Forest type	Year	PLAND (%)	NP	PD (number of patches/km^2)	LPI (%)	AREAMN (km^2)	CLUMPY	AI (%)
Dense	1993	42.49	44952	3.96	34.44	10.74	0.82	89.92
	2015	24.12	119856	10.43	1.9	2.29	0.65	73.4
Open	1993	6.02	109691	9.66	0.01	0.62	0.47	50.22
	2015	24.31	60486	5.32	4.41	4.57	0.68	75.65

NP: Number of Patches, PD: Patch Density, LPI: Large Patch Index, PLAND: Proportion of Landscape, AREA MN: Area Mean: CLUMPY: Clumpiness Index, AI: Aggregation Index

Although it is useful to consider forest fragmentation at the landscape level, the quality of the forest is best realized when focusing on a single habitat type i.e. smaller geographic extent. The forest communities along riverbanks are central elements of riverine landscapes undergoing maximum interactions at the terrestrial-aquatic interface. Results of FRAGSTATS analyses for 123 units along both the banks of the Bhagirathi river were noteworthy for the riverine forest cover (*Fig. 4*). There was minimal change in the patch density in the units 1-3 (*Fig. 4*) which belong to the high-altitude areas forming treeline, consisting stands of *Cedrus deodara* which have remained relatively intact temporally. This can be owing to the inaccessibility of these areas due to their remoteness and also because this forested land is protected under the Gangotri National Park. A similar trend exists for units 110-123, which lie around the town of Rishikesh where riverine stands comprise of late successional species like *Holoptelea integrifolia* and *Haldina cordifolia* which are well established and less prone to disintegration. Temporal fluctuations in patch density showed spatial patterns with

http://www.aloki.hu ● ISSN 1589 1623 (Print) ● ISSN 1785 0037 (Online)
DOI: http://dx.doi.org/10.15666/aeer/1704_82718289

three distinct peaks. Increase in patch density in the higher elevation river reaches can be owed to the natural riverine vegetation in this belt (units from 15-30). Forest community here comprises of *Alnus nepalensis* and *Populus ciliata* both of which are early successional species and grow well on eroding slopes and open flat sites, respectively. LPI has considerably been constant across the entire riverine stretch (*Fig. 4*) with a little increase around the submergence zone of Tehri dam followed by an increase in patch density (units around 40-60) depicting the afforestation activities near Tehri dam in an area of 138.4 km^2 under Forest Department plantation scheme raised in the year 2010-11.

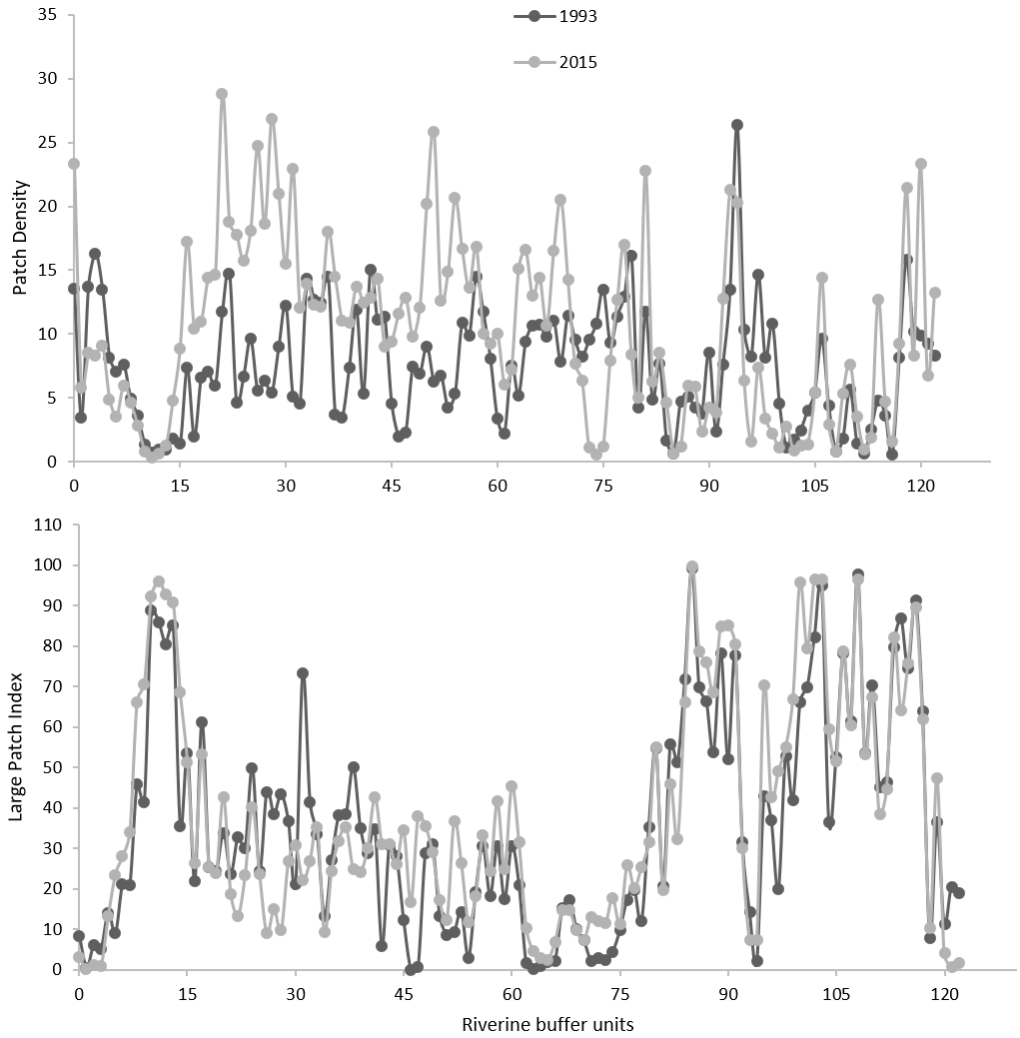

Figure 4. *Graphs comparing fragmentation events of the years 1993 and 2015 for two class level indices. (a) Patch density and (b) large patch index for forest class in the 123 riverine buffer units (2 km long and1 km wide) along both the banks of the Bhagirathi river*

Discussion

Spatiotemporal landscape change has been studied for varied applications including planning and management of urban sprawl (Vani and Prasad, 2019), understanding dynamics of vegetation cover change (Kaur et al., 2019), forest connectivity for wildlife (Areendran et al., 2017) and watershed planning and management (Wilson et al., 2018).

http://www.aloki.hu ● ISSN 1589 1623 (Print) ● ISSN 1785 0037 (Online)
DOI: http://dx.doi.org/10.15666/aeer/1704_82718289

Riverine landscapes are fragile and dynamic in nature (Miles et al., 2004) and consist of plant species with narrow distribution ranges (Silva et al., 2008) which renders the characteristics of riverine vegetation to be markedly different in structure and function. This makes the riverine ecosystem more vulnerable to extreme events and natural disasters, and thus, an important landscape to understand and manage (Stella and Bendix, 2019). The Himalayan river systems are undergoing major modifications through changes in land use, climate and water resource development (Rajvanshi et al., 2012; Manel et al., 2000). A similar study was found useful for knowledge-based future land management practices in the Upper Awash basin, Ethiopia where river basins and sub-basins were considered as focal area to study the extent and the rate of landscape change (Shawul and Chakma, 2019). Our study is a pioneering attempt of landscape-level assessment, ascertaining forest fragmentation patterns by select metrics across a time-span of two decades containing a substantial amount of riparian stands, which are otherwise not protected by law (Roy et al., 2013). Results highlight considerable conversion of dense forest into open forest characterized by the proliferation of much smaller, less connected forest patches in the studied landscape. Although rates of forest fragmentation were found to be appreciable, the forests of the landscape exhibited marked resilience capacity as portrayed by the results of the Markov transition probability matrix (*Fig. 2*). A remote-sensing-based analysis of the forest cover in the Western Himalaya during the years 1985–2005 also indicated significant degradation in the forest cover during two decades as depicted by our study (Roy and Rathore, 2019).

The composition and spatial configuration of the landscape matrix have multiple cascading effects mediated by disproportionate edge and area ratios which can profoundly affect dispersal- colonization dynamics (Dunning et al., 1992; Gascon et al., 1999) and habitat use (Antongiovanni and Metzger, 2005; Norton et al., 2000) of animals. The magnitude of change in select landscape matrices used to quantify patterns of landscape composition and configuration can influence ecological communities dependent on these forest patches (Donovan, 1997; Rodewald and Bakermans, 2006). In our study, the decrease in the LPI in the basin with rise in the number of patches highlights internally driven dynamics within patches themselves (Woodroffe and Ginsberg, 1998; Chen et al., 1995). Results of Fragstats analysis brings forth the fact that patches under the dense forest category are undergoing isolation with time whereas patches of open forest are clumping together (*Table 2*). Fragmented vegetation reduces overall plant species richness, encourages edge species and discourages interior forest species (Solbrig, 1992), hence modifying the entire structure of communities (Haddad et al., 2015). Intact large patches of natural vegetation persist in areas protected by legal restrictions and forests in inaccessible terrains (high-altitude region) (*Fig. 3*). In future, patch level analyses can be performed to comprehend the underlying factors that have resulted in the distinct spatial patterns observed in the forest.

The Ganga basin has the highest dam density (1/18 of the river channel being dammed) followed by Brahmaputra (1/35 km) and the Indus (1/36 km) in the Indian Himalayan Region (Pandit and Grumbine, 2012). Due to the development of Tehri dam, Koteshwar hydropower plant and Kotli-Bhel hydropower project (under development in Bhagirathi basin), approximately 68.03 km (31%) of the Bhagirathi river is being diverted, whereas 85.4 km^2 (39%) of the riverine area has been submerged (Rajvanshi et al., 2012). Dams alter the natural flow of rivers and streams, thus changing the temperature and chemical composition of water which determines the distribution of riverine tree species (Bergkamp et al., 2000). A large number of dams along the course

http://www.aloki.hu ● ISSN 1589 1623 (Print) ● ISSN 1785 0037 (Online)
DOI: http://dx.doi.org/10.15666/aeer/1704_82718289

of the Bhagirathi river has resulted in modification of the native riverine vegetation owing to altered micro-climatic regimes and afforestation activities by Forest Department around the Tehri region highlighted by an increase in the LPI in this region (*Fig. 3*). Landslides are common in montane river networks and cause considerable loss to riverine forest stands on a regular basis. Hence, quantifying the landscape change in the riverine buffer is concerning in the backdrop of vulnerability to natural disasters.

Over the last several decades, riverine buffers have been employed as a conservation tool in an attempt to maintain natural processes and functions in running-water ecosystems and consequently protect native aquatic organisms (Richardson et al., 2005; Marczak et al., 2010; Kuglerová et al., 2014). Their biodiversity values render them as hotspots for adaptation to climate change in the near future (Das, 2014; Pandey et al., 1999). The current study is useful in filling the information gap for remote terrains, features predominant in the Himalaya, which are poorly researched due to inaccessibility. Such understanding is required for realization of the vulnerability of these systems, which are ever dynamic, and thus, necessitates the need to conduct the study at a broader scale of time and space.

Conclusion

India is endowed with a magnificent river basin network; water resources having an overriding influence on the socio-economic development of the country. This necessitates the establishment of baseline information for monitoring these systems and for developing local and national policies for guiding conservation programmes. Riverine landscapes are one of the most human-dominated areas eliciting increased developmental activities in and around the river. Dams which have comparatively larger-scale consequences, require machinery and manpower for building and maintenance, steering rapid growth of cities and settlements around; accelerating the process of habitat loss and forest fragmentation in riverine areas. Given their high productivity values and increasing degradation rates, periodic monitoring of forest fragmentation dynamics and change in land cover needs to be documented systematically and at regular time intervals. The use of satellite imageries with higher spatial/spectral resolution can aid in identifying the underlying drivers of landscape change and substantially add to such initiatives to better understand the magnitude and direction of landscape change and forest fragmentation. Delineating the rate of change from one class to another and using more comprehensive fragmentation index including patch-level analysis can aid in understanding the trends of future land use/land cover conversion to determine the resilience of these important riverine systems.

Riverine forests are fragile and have immense bio-diverse and socio-economic significance. Hydrologic alteration caused by river regulation alters the vital processes which establish and maintain riverine vegetation. The site-specific ecological consequences of natural and human induced changes remain challenging to predict and address. This is often associated with the difficulty in delineation of riparian buffers from the remaining landscape. Identifying intact forest patches of enhanced biodiversity values along the river can substantially aid in effective management and conservation. The overall trends that emerge from our study give a synoptic view of landscape change and forest fragmentation processes which can be beneficial in navigating conservation efforts towards biodiversity management at a large scale, and particularly in difficult mountain terrains predominant in the Himalaya. There is a dire need to conduct

http://www.aloki.hu ● ISSN 1589 1623 (Print) ● ISSN 1785 0037 (Online)
DOI: http://dx.doi.org/10.15666/aeer/1704_82718289

scientific studies on the flora and fauna of such fragmented habitats. The research can further be upgraded by understanding the underlying drivers of landscape change and potential causes of the forest fragmentation. Hence, a combination of both anthropogenic and climatic drivers can give us a holistic understanding of the actual causes underlying the fragmentation of riverine landscape features in the future. Pertinent research aiming to understand the role of fragmented vegetation in species conservation and devising novel approaches of possible restoration programmes for such fluvial landscapes is vital for future conservation.

Acknowledgements. The authors are thankful to the Department of Science and Technology, Government of India for financial assistance under the grant (SERB No: F. No. SERB/SR/SO/PS/06/2010). Thanks are due to the Uttarakhand forest department and Dr. V. B Mathur, Dr. P. K Mathur, Dr. G. S Rawat and Dr. S. Sathyakumar, Wildlife Institute of India for their support. We are grateful to Kevin Moore and Kamna Pokhariya for their assistance in analyzing the remote sensing data.

REFERENCES

[1] Alhamdan, M. Z., Oduor, P., Flores, A. I., Kotikot, S. M., Mugo, R., Ababu, J. (2017): Evaluating land cover changes in Eastern and Southern Africa from 2000 to 2010 using validated Landsat and MODIS data. – International Journal of Applied Earth Observation and Geoinformation 62: 8-26.

[2] Allen, T. R. (2000): Topographic normalization of Landsat Thematic Mapper data in three mountain environments. – Geocarto International 15: 15-22.

[3] Areendran, G., Raj, K., Mazumdar, S., Sharma, A. (2017): Land use and land cover change analysis for Kosi River wildlife corridor in Terai Arc Landscape of Northern India: Implications for future management. – Tropical Ecology 58(1).

[4] Antongiovanni, M., Metzger, J. P. (2005): Influence of matrix habitats on the occurrence of insectivorous bird species in Amazonian forest fragments. – Biological Conservation 122: 441-451.

[5] Bergkamp, G., McCartney, M., Dugan, P., McNeely, J., Acreman, M. (2000): Dams, Ecosystem Functions and Environmental Restoration. – Thematic Review II (1) prepared as an input to the World Commission on Dams, Cape Town.

[6] Bogaert, J., Barima, Y. S., Iyongo, W. M. L., Bamba, I., Mama, A., Toyi, M., Lafortezza, R. (2011): Forest Fragmentation: Causes, Ecological Impacts and Implications for Landscape Management. – In: Li, C. et al. (eds.) Landscape Ecology in Forest Management and Conservation. Challenges and Solutions for Global Change, Springer, Berlin, pp. 273-296.

[7] Census of India (2001): Government of India: New Delhi, India. – http://censusindia.gov.in/ [accessed on 23 August 2017].

[8] Chen, J., Franklin, J. F., Spies, T. A. (1995): Growing-season microclimatic gradients from clearcut edges into old-growth Douglas-fir forests. – Ecological Applications 5: 74-86.

[9] Das, S. (2014): Ganga - Our Endangered Heritage. – In: Sanghi, R. (ed.) Our National River Ganga. Springer International Publishing, Switzerland, pp. 45-71.

[10] Donovan, T. M., Jones, P. W., Annand, E. M., Thompson, F. R. (1997): Variation in local-scale edge effects: mechanisms and landscape context. – Ecology 78: 2064-2075.

[11] Dunning, J. B., Danielson, B. J., Pulliam, H. R. (1992): Ecological processes that affect populations in complex landscapes. – Oikos 65: 169-175.

http://www.aloki.hu ● ISSN 1589 1623 (Print) ● ISSN 1785 0037 (Online)
DOI: http://dx.doi.org/10.15666/aeer/1704_82718289

[12] Dybala, K. E., Matzek, V., Gardali, T., Seavy, N. E. (2019): Carbon sequestration in riparian forests: a global synthesis and meta-analysis. – Global Change Biology 25: 57-67.
[13] Egbert, S. L., Park, S., Price, K. P. (2002): Using conservation reserve program maps derived from satellite imagery to characterize landscape structure. – Computer and Electronics in Agriculture 37: 141-56.
[14] Ety, N. J., Rashid, M. S. (2019): Spatiotemporal variability of erosion and accretion in Ganges River using GIS and RS: a comparative study overlapping Rennell's map of 1760s. – Environment, Development and Sustainability. https://doi.org/10.1007/s10668-019-00317-4.
[15] FAO (2010): Global forest resource assessment. – Food and Agriculture Organization of the United Nations. http://www.fao.org/docrep/013/i1757e/i1757e.pdf.
[16] FSI (2015): India State of Forest Report. – Forest Survey of India, Ministry of Environment, Forest & Climate Change, Kaulagarh Road, Dehradun. http://fsi.nic.in/forest-report-2015.
[17] Gascon, C., Lovejoy, T. E., Bierregaard Jr, R. O., Malcolm, J. R., Stouffer, P. C., Vasconcelos, H. L., Laurance, W. F., Zimmerman, B., Tocher, M., Borges, S. (1999): Matrix habitat and species richness in tropical forest remnants. – Biological Conservation 91: 223-229.
[18] Ge, H., Lu, D., He, S., Xu, A., Zhou, G., Du, H. (2008): Pixel-based Minnaert correction method for reducing topographic effects on a Landsat 7 ETM+ image. – Photogrammetric Engineering and Remote Sensing 74: 1343-1350.
[19] Gergel, S. E., Stange, Y., Coops, N. C., Johansen, K., Kirby, K. R. (2007): What is the Value of a good map? An example using high spatial resolution imagery to aid Riparian restoration. – Ecosystems 10: 688-702.
[20] Gould, W. (2000): Remote sensing of vegetation, plant species richness, and regional biodiversity hotspots source. – Ecological Applications 10: 1861-1870.
[21] Government of Uttarakhand (2014): Uttarakhand action plan on climate change- 'Transforming Crisis into Opportunity'. – http://www.moef.gov.in/sites/default/files/Uttarakhand%20SAPCC.pdf.
[22] Haddad, N. M., Brudvig, L. A., Clobert, J., Davies, K. F., Gonzalez, A., Holt, R. D., Lovejoy, T. E., Sexton, J. O., Austin, M. P., Collins, C. D., Cook, W. M. (2015): Habitat fragmentation and its lasting impact on Earth's ecosystems. – Science Advances 1: e1500052.
[23] Halmy, M. W. A., Gessler, P. E., Hicke, J. A., Salem, B. B. (2015): Land use/land cover change detection and prediction in the north-western coastal desert of Egypt using Markov- CA. – Applied Geography 63: 101-112.
[24] He, C., Zhang, Q., Li. Y. (2005): Zoning grassland protection area using remote sensing and cellular automata modeling- a case study in Xilingol steppe grassland in northern China. – Journal of Arid Environments 63: 814-26.
[25] Jenness, J., Wynne, J. J. (2005): Cohen's Kappa and classification table metrics 2.0: An ArcView 3. extension for accuracy assessment of spatially explicit models. – Open-File Report of 2005-1363. US Geological Survey, Southwest Biological Science Center, Flagstaff, AZ.
[26] Kaur, A., Ghosh, S., Das, S. K. (2019): Satellite image-based land use/land cover dynamics and forest cover change analysis (1996-2016) in Odisha, India. – Asian Journal of Water, Environment and Pollution 16(1): 25-39.
[27] Kuglerová, L., Ågren, A., Jansson, R., Laudon, H. (2014): Towards optimizing riparian buffer zones: ecological and biogeochemical implications for forest management. – Forest Ecology and Management 334: 74-84.
[28] Lund, H. G. (1983): Change: now you see it - now you don't! – Proceedings of the International Conference on Renewable Resource Inventories for Monitoring Changes and Trends, Oregon State University, Corvallis, OR, USA 211-213.

http://www.aloki.hu ● ISSN 1589 1623 (Print) ● ISSN 1785 0037 (Online)
DOI: http://dx.doi.org/10.15666/aeer/1704_82718289

[29] Manel, S., Buckton, S. T., Ormerod, S. J. (2000): Testing large-scale hypotheses using surveys: the effects of land use on the habitats, invertebrates and birds of Himalayan rivers. – Journal of Applied Ecology 37: 756-770.
[30] Marczak, L. B., Sakamaki, T., Turvey, S. L., Deguise, I., Wood, S. L., Richardson, J. S. (2010): Are forested buffers an effective conservation strategy for riparian fauna? An assessment using meta-analysis. – Ecological Applications 20: 126-134.
[31] McCarthy, M. J., Radabaugh, K. R., Moyer, R. P., Muller-Karger, F. E. (2018): Enabling efficient, large-scale high spatial resolution wetland mapping using satellites. – Remote Sensing of Environment 208: 189-201.
[32] McGarigaI, K., Marks, B. J. (1994): FRAGSTATS: Spatial Pattern Analysis. Programme for Quantifying Landscape Structure. – Forest Science Department, Oregon State University, Corvallis.
[33] McGarigal, K., Marks, B. J. (1995): FRAGSTATS: Spatial Pattern Analysis Program for Quantifying Landscape Structure. – Gen. Tech. Rep. PNW-GTR-351. Portland, OR Department of Agriculture, Forest Service, Pacific Northwest Research Station 122: 351.
[34] Miles, L., Grainger, A., Phillips, O. (2004): The impact of global climate change on tropical forest biodiversity in Amazonia. – Global Ecology and Biogeography 13: 553-565.
[35] Milne, A. K. (1988): Change direction analysis using Landsat imagery: a review of methodology. – Proceedings of the IGARSS'88 Symposium, Edinburgh, Scotland, ESA 1: 541-544.
[36] Naiman, R. J., Decamps, H., Pollock, M. (1993): The role of Riparian corridors in maintaining regional biodiversity. – Ecological Applications 3: 209-212.
[37] Naiman, R. J., Decamps, H., McClain, M. E. (2005): Riparian Ecology, Conservation, and Management of Streamside Communities. – Elsevier Academic Press, San Diego, California, USA.
[38] Neel, M. C., McGarigal, K., Cushman, S. A. (2004): Behavior of class-level landscape metrics across gradients of class aggregation and area. – Landscape Ecology 19: 435-455.
[39] Norton, M. R., Hannon, S. J., Schmiegelow, F. K. A. (2000): Fragments are not islands: patch vs. landscape perspectives on songbird presence and abundance in a harvested boreal forest. – Ecography 23: 209-223.
[40] Osgouei, P. E., Kaya, S. (2017): Analysis of land cover/use changes using Landsat 5TMdata and indices. – Environmental Monitoring and Assessment 189(4): 136.
[41] Pandey, S. K., Singh, A. K., Hasnain, S. I. (1999): Weathering and geochemical processes controlling solute acquisition in Ganga headwater–Bhagirathi river, Garhwal Himalaya, India. – Aquatic Geochemistry 5: 357-379.
[42] Pandit, M. K., Grumbine, R. E. (2012): Potential effects of ongoing and proposed hydropower development on terrestrial biological diversity in the Indian Himalaya. – Conservation Biology 26: 1061-1071.
[43] Rajvanshi, A., Arora, R., Mathur, V. B., Sivakumar, K., Sathyakumar, S., Rawat, G. S., Johnson, J. A., Ramesh, K., Dimri, N. K., Maletha, A. (2012): Assessment of Cumulative Impacts of Hydroelectric Projects on Aquatic and Terrestrial Biodiversity in Alaknanda and Bhagirathi Basins, Uttarakhand. – Technical Report, Wildlife Institute of India, Dehradun.
[44] Ramanathan, V., Chung, C., Kim, D., Bettge, T., Buja, L., Kiehl, J. T., Washington, W. M., Fu, Q., Sikka, D. R., Wild, M. (2005): Atmospheric brown clouds: impacts on south Asian climate and hydrological cycle. – Proceedings of National Academy of Sciences 102: 5326-5333.
[45] Rawat, J. S., Kumar, M. (2015): Monitoring land use/cover change using remote sensing and GIS techniques: a case study of Hawalbagh block, district Almora, Uttarakhand, India. – The Egyptian Journal of Remote Sensing and Space Sciences 18: 77-84.

http://www.aloki.hu ● ISSN 1589 1623 (Print) ● ISSN 1785 0037 (Online)
DOI: http://dx.doi.org/10.15666/aeer/1704_82718289

[46] Rawat, J. S., Biswas, V., Kumar, M. (2013): Changes in land use/cover using geospatial techniques-A case study of Ramnagar town area, district Nainital, Uttarakhand, India. – The Egyptian Journal of Remote Sensing and Space Sciences 16: 111-117.
[47] Richardson, J. S., Naiman, R. J., Swanson, F. J., Hibbs, D. E. (2005): Riparian communities associated with Pacific Northwest headwater streams: assemblages, processes, and uniqueness. – Journal of the American Water Resources Association 41: 935-947.
[48] Rodewald, A. D., Bakermans, M. H. (2006): What is the appropriate paradigm for riparian forest conservation? – Biological Conservation 128: 193-200.
[49] Roy, A., Rathore, P. (2019): Western Himalayan Forests in Climate Change Scenario. – In: Navalgund, R. R. et al. (eds.) Remote Sensing of Northwest Himalayan Ecosystems. Springer, Singapore, pp. 265-283.
[50] Roy, P. S., Roy, A. (2010): Land use and land cover change in India: a remote sensing & GIS perspective. – Journal of the Indian Institute of Science 90: 489-502.
[51] Roy, P. S., Murthy, M. S. R., Roy, A., Kushwaha, S. P. S., Singh, S., Jha, C. S., Behera, M. D., Joshi, P. K., Jagannathan, C., Karnatak, H. C., Saran, S. (2013): Forest fragmentation in India. – Current Science 105: 774-780.
[52] Shawul, A. A., Chakma, S. (2019): Spatiotemporal detection of land use/land cover change in the large basin using integrated approaches of remote sensing and GIS in the Upper Awash basin, Ethiopia. – Environmental Earth Sciences 78(5): 141.
[53] Silva, T. S., Costa, M. P., Melack, J. M., Novo, E. M. (2008): Remote sensing of aquatic vegetation: theory and applications. – Environmental Monitoring and Assessment 40: 131-145.
[54] Solbrig, O. T. (1992): The IUBS-SCOPE-UNESCO programme of research in biodiversity. – Ecological Applications 2: 131-8.
[55] Steel, E. A., Hughes, R. M., Fullerton, A. H., Schmutz, S., Young, J. A., Fukushima, M., Muhar, S., Poppe, M., Feist, B. E., Trautwein, C. (2010): Are we meeting the challenges of landscape-scale riverine research? A review. – Living Reviews in Landscape Research 4: 1-60.
[56] Stella, J. C., Bendix, J. (2019): Multiple Stressors in Riparian Ecosystems. In: Sabater, S. et al. (eds.) Multiple Stressors in River Ecosystems – Elsevier, Amsterdam, pp. 81-110.
[57] Sutfin, N. A., Wohl, E. E., Dwire, K. A. (2016): Banking carbon: a review of organic carbon storage and physical factors influencing retention in floodplains and riparian ecosystems. – Earth Surface Processes and Landforms 41: 38-60.
[58] Tomscha, S. A., Gergel, S. E., Tomlinson, M. J. (2017): The spatial organization of ecosystem services in river-floodplains. – Ecosphere 8: e01728.
[59] Vani, M., Prasad, P. R. C. (2019): Assessment of spatio-temporal changes in land use and land cover, urban sprawl, and land surface temperature in and around Vijayawada city, India. – Environment, Development and Sustainability. https://doi.org/10.1007/s10668-019-00335-2.
[60] Villard, M. A., Trzcinski, M. K., Merriam, G. (1999): Fragmentation effects on forest birds: relative influence of woodland cover and configuration on landscape occupancy. – Conservation Biology 13: 774-783.
[61] Ward, J. V., Malard, F., Tockner, K (2002): Landscape ecology: a framework for integrating pattern and process in river corridors. – Landscape Ecology 17: 35-45.
[62] Wilson, C. O., Liang, B., Rose, S. J. (2018): Projecting future land use/land cover by integrating drivers and plan prescriptions: the case for watershed applications. – GIS Science & Remote Sensing 56(4): 511-535.
[63] Wilson, E. (1992): The Diversity of Life. – W. W. Norton & Company, New York.
[64] Wong, C. M., Williams, C. E., Pittock, J., Collier, U., Schelle, P. (2007): World's Top Ten Rivers at Risk. – WWF International, Gland, Switzerland. assets.panda.org/downloads/worldstop10riversatriskfinalmarch13.pdf.

http://www.aloki.hu ● ISSN 1589 1623 (Print) ● ISSN 1785 0037 (Online)
DOI: http://dx.doi.org/10.15666/aeer/1704_82718289

[65] Woodroffe, R., Ginsberg, J. R. (1998): Edge effects and the extinction of populations inside protected areas. – Science 280: 2126-2128.
[66] Xie, Y., Sha, Z., Yu, M. (2008): Remote sensing imagery in vegetation mapping: a review. – Journal of Plant Ecology 1: 9-23.
[67] Xu, J., Grumbine, R. E., Shrestha, A., Eriksson, M., Yang, X., Wang, Y. U. N., Wilkes, A. (2009): The melting Himalayas: cascading effects of climate change on water, biodiversity and livelihoods. – Conservation Biology 24: 520-530.

APPENDIX

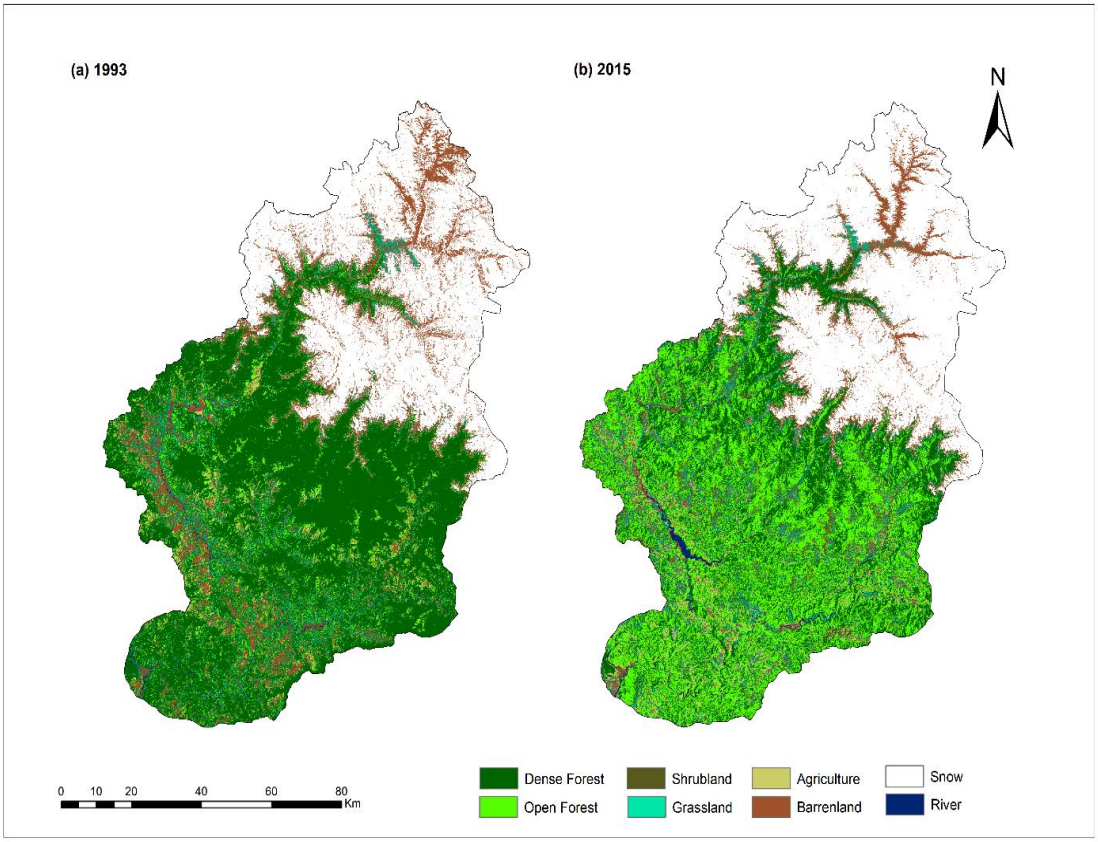

Figure A1. *Land cover maps depicting temporal change (a: 1993 and b: 2015) in the eight land cover types namely, dense forest, open forest, shrubland, grassland, agriculture, barren land, snow and river) of the Bhagirathi basin.*

http://www.aloki.hu ● ISSN 1589 1623 (Print) ● ISSN 1785 0037 (Online)
DOI: http://dx.doi.org/10.15666/aeer/1704_82718289

Table A1. *Percentage landscape change of eight land cover classes from 1993 to 2015 in the 123 buffer unit (area = 4 km^2 each) s along the river Bhagirathi*

Buffer units	Dense forest	Open forest	Shrubland	Grassland	Agriculture	Barren land	Snow	River
1	-16.3	-1.3	-16.4	4.9	13.0	16.0	0.0	0.2
2	0.1	-0.3	-0.2	0.4	0.0	-11.5	11.5	0.0
3	0.9	-3.2	-1.3	-3.3	0.0	-1.6	8.5	0.0
4	-11.0	-7.6	-3.6	8.7	1.0	5.4	7.1	0.0
5	-0.8	-9.9	-3.3	6.2	0.6	2.2	5.0	0.0
6	22.6	-15.7	-2.9	-9.6	0.9	1.6	3.0	0.0
7	12.5	-10.1	-5.1	4.7	0.9	-3.4	0.5	0.0
8	14.0	-7.7	-4.3	-1.9	2.5	-3.5	1.0	0.0
9	10.3	-8.0	-4.5	2.4	2.5	-2.7	0.0	0.0
10	21.3	-10.9	-5.6	-8.7	3.1	0.7	0.0	0.0
11	11.3	-7.1	-6.2	-2.7	3.2	-0.1	0.2	1.4
12	10.8	-3.6	-2.6	-6.2	1.0	-1.3	0.0	1.8
13	11.2	-2.2	-3.7	-5.4	2.0	-2.2	0.0	0.2
14	4.6	0.2	-2.4	-3.3	2.1	-1.4	0.0	0.1
15	-6.2	8.2	-3.2	-0.9	3.3	-1.7	0.0	0.6
16	-9.8	10.0	-6.8	-1.5	6.3	-0.1	-0.4	2.4
17	-3.0	4.0	-9.2	-0.2	9.4	-2.8	-2.1	4.0
18	-9.5	8.4	-10.6	2.7	10.6	-2.7	-1.0	2.1
19	-4.1	0.3	-5.9	7.9	4.9	-4.6	-0.7	2.1
20	5.5	-4.9	-12.4	4.3	12.2	-6.3	-1.8	3.4
21	9.5	-9.7	-15.1	12.0	13.4	-10.3	-1.1	1.4
22	4.9	-6.8	-18.8	16.5	12.2	-9.8	-0.9	2.6
23	-1.4	-6.5	-2.8	10.6	2.4	-3.2	0.4	0.5
24	-16.1	5.1	-5.8	11.3	6.8	-1.9	0.0	0.6
25	-13.1	-0.8	-3.3	15.2	4.2	-1.5	0.0	-0.8
26	-7.4	0.4	-6.6	10.4	8.5	-5.9	0.0	0.6
27	-20.0	1.6	5.2	11.0	5.2	-2.1	0.0	-0.9
28	-18.9	-0.5	6.9	11.2	0.2	1.4	0.0	-0.2
29	-28.8	0.5	-1.0	24.8	5.0	-0.4	0.0	0.0
30	-23.7	16.4	-7.4	7.9	7.4	-0.4	0.0	-0.3
31	-22.1	23.9	-9.7	3.3	3.6	1.0	0.0	-0.1
32	-24.5	1.8	1.1	17.3	3.2	0.9	0.0	0.1
33	-21.9	0.8	13.5	17.5	-11.5	1.1	0.0	0.6
34	-14.0	11.6	10.1	16.9	-19.7	-3.7	0.0	-1.3
35	-21.7	16.5	15.8	24.1	-26.8	-8.5	0.0	0.7
36	-21.9	17.8	6.3	16.4	-19.4	1.1	0.0	-0.4
37	-29.4	22.8	-3.7	21.2	-11.2	0.6	0.0	-0.3
38	-31.5	9.7	1.5	18.5	-0.9	2.9	0.0	-0.1
39	-15.3	5.8	0.0	4.2	2.9	3.2	0.0	-0.7
40	-9.5	14.9	-8.6	-4.9	5.1	4.6	0.0	-1.6
41	19.0	-7.3	-10.8	-6.1	4.7	1.1	0.1	-0.8
42	-5.4	2.6	-6.6	7.7	3.2	-0.9	0.0	-0.5

http://www.aloki.hu ● ISSN 1589 1623 (Print) ● ISSN 1785 0037 (Online)
DOI: http://dx.doi.org/10.15666/aeer/1704_82718289

43	27.4	11.0	-22.3	-19.4	4.5	-0.4	0.0	-0.9
44	15.2	2.5	-15.9	-6.5	3.7	1.0	0.0	-0.1
45	23.5	-9.1	-7.5	6.4	-5.0	-7.8	0.0	-0.6
46	28.7	1.5	-9.4	-9.5	5.2	-18.5	0.0	2.0
47	29.9	15.6	-7.1	-1.8	-31.3	-6.3	0.0	1.0
48	18.0	18.5	-13.4	3.2	-2.8	-24.8	0.0	1.3
49	20.5	6.2	-11.6	-4.1	7.1	-11.0	0.0	-7.2
50	-0.7	8.6	-13.8	5.3	3.2	-3.2	0.0	0.5
51	18.4	-0.7	-22.2	3.7	5.0	-2.9	0.0	-1.3
52	16.0	4.5	-6.7	-8.0	8.5	-13.3	0.0	-1.1
53	26.8	-2.1	-12.0	-8.9	4.6	-5.5	0.0	-2.8
54	21.2	2.3	-23.2	-5.6	13.5	-6.9	0.0	-1.3
55	20.3	9.9	-43.6	-1.2	21.3	-6.0	0.0	-0.7
56	26.5	-8.4	-22.1	-3.8	6.7	1.9	0.0	-0.9
57	25.2	-2.7	-23.6	-4.1	5.8	1.7	0.0	-2.3
58	12.5	13.5	-22.6	-18.3	14.0	2.4	0.0	-1.6
59	25.6	3.6	-20.7	-15.7	8.9	1.3	0.0	-3.0
60	8.1	15.2	-20.1	-4.6	4.8	-2.7	0.0	-0.7
61	3.3	9.2	-14.4	-6.1	4.4	4.5	0.1	-1.1
62	8.2	15.1	-30.6	-10.6	10.6	7.0	0.0	0.2
63	10.7	12.8	-30.8	-7.3	15.8	-2.5	0.0	1.2
64	17.3	2.7	-36.2	-4.7	16.7	2.3	0.0	2.1
65	9.3	7.2	-43.4	-9.9	13.0	18.1	0.0	5.7
66	7.5	0.4	-32.8	3.8	9.8	-0.8	0.0	12.0
67	10.9	4.5	-35.1	-3.5	14.4	-0.8	0.0	9.6
68	12.1	-10.7	-22.1	-5.4	7.4	4.3	0.0	14.5
69	11.7	-7.0	-25.9	-14.2	17.6	3.7	0.0	14.1
70	10.4	-4.7	-24.1	-9.3	14.3	-2.9	0.0	16.3
71	3.2	10.1	-39.4	-22.2	10.9	6.3	0.0	31.2
72	19.3	8.6	-35.3	-8.4	-1.1	-10.3	0.0	27.3
73	6.7	7.1	-27.9	-13.4	-0.5	-12.2	0.0	40.3
74	3.4	2.4	-24.0	-21.5	-5.3	-25.1	0.0	70.1
75	-2.2	2.5	-10.0	-21.9	-6.4	-28.6	0.0	66.6
76	-2.2	5.5	-18.5	-17.0	3.4	-20.0	0.0	48.8
77	0.3	11.7	-9.4	-2.6	3.2	2.3	0.0	-5.4
78	3.7	7.1	-20.1	0.3	14.8	-7.3	0.0	1.5
79	7.0	6.8	-21.8	-0.4	14.6	-8.6	0.0	2.4
80	2.4	5.9	-16.9	-0.7	8.7	-3.3	0.0	3.8
81	-39.0	38.0	-8.8	-5.6	8.7	0.1	0.0	6.6
82	-10.9	9.3	-11.3	-6.9	8.9	0.1	0.0	10.8
83	-22.0	12.7	-3.7	-1.0	3.7	0.7	0.0	9.6
84	-17.6	4.2	-7.7	-6.2	11.2	5.0	0.0	11.1
85	-9.3	12.3	-8.5	-5.3	9.1	-0.5	0.0	2.2
86	-33.8	41.9	-2.7	-8.2	3.7	-0.2	0.0	-0.7
87	-13.2	24.8	-15.1	-11.7	18.0	-2.3	0.0	-0.5
88	-7.8	21.4	-10.8	-12.5	16.2	-6.6	0.0	0.0

http://www.aloki.hu ● ISSN 1589 1623 (Print) ● ISSN 1785 0037 (Online)
DOI: http://dx.doi.org/10.15666/aeer/1704_82718289

89	8.8	0.8	-5.6	-2.0	7.0	-8.7	0.0	-0.3
90	-10.6	29.9	-9.5	-21.8	12.1	-0.7	0.0	0.5
91	7.6	-0.3	-5.6	-12.6	10.5	0.5	0.0	-0.2
92	18.2	-5.9	-13.3	-15.2	20.0	-4.0	0.0	0.1
93	13.5	-9.1	-14.3	-2.0	17.4	-4.6	0.0	-1.0
94	-2.7	13.1	-16.7	-5.4	19.9	-7.2	0.0	-0.9
95	-11.9	27.2	-16.9	-12.0	19.2	-6.6	0.0	1.0
96	-17.1	38.8	-11.7	-23.2	14.3	-2.3	0.0	1.1
97	-18.5	28.1	-7.2	-12.3	10.1	-1.8	0.0	1.5
98	-20.7	54.8	-13.3	-31.9	14.4	-3.3	0.0	0.1
99	-35.7	39.1	-3.0	-8.8	8.0	-0.8	0.0	1.3
100	-23.8	22.3	-1.0	-5.7	4.5	0.4	0.0	3.3
101	-29.6	34.0	-1.5	-7.1	5.2	-0.9	0.0	0.0
102	-32.7	42.6	-2.0	-12.1	4.5	-0.5	0.0	0.3
103	-32.6	40.2	-4.6	-8.7	6.8	-1.3	0.0	0.2
104	-21.6	29.2	-2.7	-12.5	8.1	-0.4	0.0	-0.1
105	-19.7	28.1	-2.5	-16.6	11.0	-0.5	0.0	0.1
106	-11.7	17.5	-3.8	-12.7	11.0	0.7	0.0	-1.1
107	-28.0	27.9	-3.9	-8.4	13.8	-1.4	0.0	0.0
108	-15.0	21.6	-6.9	-18.7	19.1	0.4	0.0	-0.5
109	-44.7	47.2	-3.8	-5.5	7.3	-0.2	0.0	-0.2
110	-45.3	46.0	-2.8	-4.9	7.3	-0.1	0.0	-0.3
111	-35.8	32.2	-6.3	-1.6	11.3	0.4	0.0	-0.2
112	-49.0	42.8	-4.8	-4.9	13.4	2.9	0.0	-0.4
113	-45.6	41.8	-3.8	-3.7	10.7	0.6	0.0	0.1
114	-44.4	45.2	-2.1	-3.4	4.7	0.1	0.0	0.0
115	-39.2	35.0	-1.6	-6.8	11.1	1.5	0.0	0.0
116	-46.2	46.9	-1.9	-6.3	7.2	1.7	0.0	-1.5
117	-48.7	51.3	-1.2	-3.1	3.0	-0.6	0.0	-0.7
118	-38.3	43.0	-2.0	-14.0	11.7	0.7	0.0	-1.1
119	-16.4	17.3	-12.2	-9.3	15.7	6.5	0.0	-1.6
120	-19.2	16.7	-9.9	-10.1	15.8	7.0	0.0	-0.4
121	-9.1	6.5	-11.1	-6.8	10.5	9.7	0.0	0.3
122	-2.9	-5.5	-10.9	4.9	-2.7	16.2	0.0	0.9
123	-6.7	-11.2	-24.2	9.5	2.9	28.2	0.0	1.5

http://www.aloki.hu ● ISSN 1589 1623 (Print) ● ISSN 1785 0037 (Online)
DOI: http://dx.doi.org/10.15666/aeer/1704_82718289

YIELD OF WHEAT IS INCREASED THROUGH IMPROVING THE CHEMICAL PROPERTIES, NUTRIENT AVAILABILITY AND WATER PRODUCTIVITY OF SALT AFFECTED SOILS IN THE NORTH DELTA OF EGYPT

SOROUR, S. GH.[1] – AIAD, M. A.[2] – AHMED, A. A.[1] – HENASH, M. I. A.[1] – METWALY, E. M.[1] – ALHARBY, H.[3] – BAMAGOOS, A.[3] – HOSSAIN, A.[4] – BARUTCULAR, C.[5] – SANEOKA, H.[6] – EL SABAGH, A.[1*]

[1]*Agronomy Department, Faculty of Agriculture, Kafrelsheikh University, 33516 Kafrelsheikh, Egypt*

[2]*Soils, Water and Environment Research Institute, Agriculture Research Center, 33717 Kafr Elsheikh, Egypt*

[3]*Department of Biological Sciences, Faculty of Science, King Abdulaziz University, 21589 Jeddah, Saudi Arabia*

[4]*Bangladesh Wheat and Maize Research Institute, Nashipur, Dinajpur-5200, Bangladesh*

[5]*Department of Field Crops, Faculty of Agriculture, Cukurova University, Turkey*

[6]*Laboratory of Plant Nutritional Physiology, Graduate School of Biosphere Science, Hiroshima University, Japan*

**Corresponding author*
e-mail: ayman.elsabagh@agr.kfs.edu.eg

(Received 18th Feb 2019; accepted 1st May 2019)

Abstract. The lysimeter experiment was carried out twice in consecutive two years (2014-15 and 2015-16) at Sakha Agricultural Research Station, Kafrelsheikh, Egypt to study the effect of three irrigation levels water (i.e., 100, 110 and 120% field capacity (FC), two rates of gypsum (G) (i.e., 50 and 100% G) and three sources of nitrogen (90 kg nitrogen (N), 10 t compost (C) and 7.5 t C + 45 kg N (CN) fed^{-1} (fed = 4200 m^2)) on grain yield of wheat, water relations and soil chemical properties. Water consumptive use (WCU) was markedly increased due to the increase of the level of irrigation, rate of gypsum (G) and CN source (7.5 t C + 45 kg N fed^{-1}). Irrigation with water amount equal to 120% FC recorded the highest values of WCU 1433 and 1570 m^{3}fed^{-1} in both seasons. Water productivity (kg grain m^{-3} water) for either water application (WA) in both seasons or WCU in the second season was decreased by increasing level of irrigation from 100 to 120% FC in the second season, while the inverse was true for WCU in the first season. The highest mean values of water productivity for WCU 1.816 and 1.791 kg m^{-3} were obtained with the irrigation level of 120% FC in the first season and 100% FC in the second season, respectively. Gypsum rate and N source have an effect on the productivity of irrigation water (WP) for WA and WCU, where the highest mean values for both the two irrigations efficiency were recorded under 100% G requirements and CN (7.5 t C + 45 kg N fed^{-1}). The interaction of 110% FC × 100% G × 7.5 t C + 45 kg N fed^{-1} produced the highest values of WP for WA (1.245 and 1.374 kg grain m^{-3} WA) in both seasons. Grain yield fedd.$^{-1}$ was increased significantly with the irrigation level from 100 to 120% FC in both seasons, G rate and CN source. Grain yield (GY) did not differ significantly due to the levels of irrigation water between 120 and 110% FC in both years. Application of 100% G and 7.5 t C + 45 kg N fed^{-1} at any irrigation level were among those treatments having high GY, being insignificant. The mean values of electrical conductivity (acidity; ECe) and soil sodicity (SARe) were affected by irrigation treatments, G rates and nitrogen sources. A stronger reduction in soil ECe and SARe were recorded under the irrigation level of 120%FC, 100% G and 10 t compost in both seasons. While the soils ECe and SARe were increased by application of chemical N fertilizer alone or with compost. Therefore, it can be concluded that irrigation with water amount equal to 110 or 120% FC, 100% G requirements and 7.5 t C and 45 kg N fed^{-1} was the best treatment for getting high GY, improving the soil chemical properties, nutrients availability and increasing the water productivity of salt-affected soil in North Delta of Egypt.

http://www.aloki.hu ● ISSN 1589 1623 (Print) ● ISSN 1785 0037 (Online)
DOI: http://dx.doi.org/10.15666/aeer/1704_82918306

Keywords: *irrigation, lysimeter, soil salinity, soil sodicity, gypsum*

Abbreviations: C: compost; CN: carbon & nitrogen; ECe: electrical conductivity (soil salinity); FC: field capacity; fed.: feddan (fed = 4200 m^2); G: Gypsum; GY: grain yield K: potassium; N: nitrogen; OM: organic matter; P: phosphorus; SARe: sodium adsorption ratio (soil sodicity); t: ton; WA: water applied; WCU: water consumptive use

Introduction

Wheat (*Triticum aestivum*, L.) is a vital cereal across the globe and it is the most widely grown food cereal crop and its demand is increasing with the increasing population (Hossain et al., 2018; Jahan et al., 2019). It is considered a strategic crop and has played a major role on the national economy and it is one of the widely adapted cereals, grown in different environments (Barutcular et al., 2017; Yildirim et al., 2018). In Egypt, it is also the main food crop, as the current production of wheat does not meet the consumption demand. Recently US' Foreign Agricultural Service (FAS) in Cairo estimated that the wheat production in Egypt reaches 8.45 million metric tons (MMT) in the year in 2018-19, which was 4.3% higher than 2017-18 (Egypt Today, 2018; IndexMundi, 2018). Although in the year 2017, 60.2% of Egypt's total wheat consumption was imported. Concerning wheat consumption, FAS Cairo forecasts Egypt's total wheat consumption in the marketing year (MY) 2018-19 was 20 MMT, which was 1.5% more than the MY 2017-18 (Egypt Today, 2018; IndexMundi, 2018). Therefore, it is confirmed that the demand for wheat in Egypt is increasing day by day, but domestic production could not meet the current demand. As a result, to meet the food security of increasing population, the government of Egypt has taken several initiatives such as increase the area of production, development of high yield potential and stress resistance wheat cultivars, and also to find out improved management practices for reduction the imported percentage to be less than 50% (McGill et al., 2015; IndexMundi, 2018).

Wheat production depends on several factors including environmental condition, cultivars and management factors, such as irrigation and soil fertility. Among the management approaches, irrigation and fertilization and their interaction are considered the most important factors for increasing wheat production (Shaaban, 2006). For example, application of one irrigation increases the yield of wheat by more than 40%, whereas two to three irrigations with proper water and fertilizer management practices increase wheat yield by 50-100% (Hossain et al., 2006). However, to assist the efficient water use, plant-soil-water positive and negative interaction should be well understood under various environmental conditions, particularly in arid and semi-arid regions, where irrigation water is limit due to lack of rainfall (Musick et al., 1994; Wiedenfeld, 2000; Halitigil et al., 2000).

On the other hand, as Egypt is situated under the arid and semi-arid region of the Mediterranean environment, heat, drought and salinity are the major abiotic stress which decreases the productivity of wheat (Al-Naggar et al., 2015a, b; Abdelaal et al., 2018). Among the abiotic stresses, salinity is the most important one that adversely affects the productivity and quality of wheat through altering the physiological and biochemical activity of plants (Otu et al., 2018; Yassin et al., 2019) by accelerating osmotic stress and ion cytotoxicity in plants' cell (Chen and Jiang, 2010; Islam et al., 2011). It is anticipated that the consequence of soil salinity may be increased in future due to the scarcity of annual rainfall, rising of sea water, irrigation with saline water,

http://www.aloki.hu ● ISSN 1589 1623 (Print) ● ISSN 1785 0037 (Online)
DOI: http://dx.doi.org/10.15666/aeer/1704_82918306

excessive use of fertilizers and absence of a good drainage system, particularly in the Mediterranean environment (El-Hendawy et al., 2005).

Therefore, to improve or reclaim the sodic soil for sustainable crop production, it is important for replacing the most of the Na^+ by the most favourable Ca^{++} followed by removal/leaching of salts derived by the reaction of the amendment from sodic soil. While many chemical compounds such as amendments are known in this respect of effective salts reclamation. For example, amendments directly or indirectly supply soluble Ca^{++} and improve the soil productivity by escaping Na^+ from saline soils. Sodic soil reclamation by using amendment will largely depend on the nature of the soil, effectiveness and cost considerations. Among the amendments, gypsum ($CaSO_4$-$2H_2O$) is a typical soil amendment, which replaces Na^+ ions by the calcium (Ca^{++}) ions (Hanay et al., 2004).

However, the presence of organic matter (OM) through the management of crop residues, using different types of organic manures in the soil is a fundamental option for maintaining soil fertility and productivity. It improves the physical properties, biological activity, water holding capacity and soil's aeration for better seed germination and seedling stand establishment (Edwards and Hailu, 2011). Considering the above important issues for the sustainability of crops production, the research was aimed to study the effect of different requirements of irrigation water, soil amendments and nitrogen fertilization on wheat yield, water relations and some soil chemical properties.

Materials and methods

Location and duration of the study

The lysimeter study was established during the wheat grown season of 2014-15 and 2015-16 at Sakha Agricultural Research Station, Kafr ElSheikh-Egypt. The location lies in 134 km north Cairo, Egypt under North Delta-Egypt. The location is situated at 31°07'N latitude and 30°57'E longitude. The study aimed to study the effect of irrigation water level, soil amendments and nitrogen fertilizer sources on wheat yield, water relations and some soil chemical properties.

Physical and chemical properties of lysimeters' soil

Soils in the North Delta of Egypt are characterized by saline and sodic. For determination of soils' chemical and physical soil properties, soil samples were taken from each lysimeter at the depth of 0-15, 15-30, 30-45 and 45-60 cm before sowing and after harvesting in both seasons (*Table 1).* Soil reaction (pH) was determined according to Cottenie et al. (1982), electrical conductivity (ECe) according to Page (1982) and sodium adsorption ratio (SAR) was calculated. Soil OM status was estimated though Walkally Black method according to Hesse (1971). Available N and K were determined according to Jackson (1967). Phosphorus (P) availability was observed according to Olsen et al. (1954), by following sodium bicarbonate method. Mechanical soil analysis was determined according to the international pipette method (Piper, 1950). Gypsum requirement was calculated according to Schoonover method (1952). Soil bulk density was measured by using the core sampling technique as described by Campbell (1994). The chemical composition of compost used in the study is amiable in *Table 2.* The

http://www.aloki.hu ● ISSN 1589 1623 (Print) ● ISSN 1785 0037 (Online)
DOI: http://dx.doi.org/10.15666/aeer/1704_82918306

lysimeters were fertilized with 15.5 kg P_2O_5 feddan^{-1} in the form of calcium superphosphate (15.5% P_2O_5) during soil preparation.

Table 1. *Physical and chemical properties of the lysimeters' soil recorded before sowing during the 2014-15 season*

Properties	Soil depth (cm)				
	0-15	**15-30**	**30-45**	**45-60**	**Mean**
Particle size (%)					
Sand	13.35	14.72	12.5	16.33	14.23
Silt	26.89	28.58	27.3	27.85	27.66
Clay	59.76	56.7	60.2	55.82	58.12
Texture class	Clay	Clay	Clay	Clay	Clay
Soil moisture (%)					
Field capacity	42.65	40.2	39.83	38.45	40.28
Wilting point	22.87	20.65	19.89	19.36	20.69
Available water	19.78	19.55	19.94	19.09	19.59
Bulk density (kg m^{-3})	1.21	1.26	1.31	1.34	1.28
Chemical properties					
pH (1:2.5)	8.36	8.45	8.54	8.67	8.51
ECe (dS m^{-1})	5.84	6.46	7.19	8.89	7.1
SAR (%)	11.83	13.03	14.23	15.76	13.71
OM (%)	1.76	1.54	1.45	1.15	1.48
Available N (mg kg^{-1})	36.21	31.87	26.45	18.96	28.37
Available P (mg kg^{-1})	9.28	8.92	8.56	8.19	8.74
Available K (mg kg^{-1})	365	348	297	248	314.5
Gypsum requirements (meq 100 g^{-1} soil)	2.3				

Table 2. *The chemical composition of compost used in the experiment*

EC dS/m	pH 1:5	Total N %	C %	C/N ratio	OM %	Total P%	Total K%	Fe ppm	Zn ppm	Mn ppm	Moisture %
3.76	8.23	1.79	29.78	16.64	51.34	1.68	1.28	142	51	132	26.80

Meteorological information during growing seasons

The meteorological data on mean monthly temperature, relative humidity, wind speed and pan evaporation as well as rainfall in both seasons (2014-15 and 2015-16) from Sakha Station were recorded and presented in *Table 3*.

Experimental treatments and design

Treatments of the present study were arranged in a split-split plot design and repeated four times in both seasons. Where main plots were arranged in levels of irrigation, sub-plots were in rates of gypsum (G) and sub-sub-plots were in sources of nitrogen. Irrigation was done five times at all irrigation treatments: first irrigation was done at each of sowing, the second was tillering, third at jointing, fourth at heading and final one (fifth irrigation) were done at milking stages. Irrigation treatments were started

http://www.aloki.hu ● ISSN 1589 1623 (Print) ● ISSN 1785 0037 (Online)
DOI: http://dx.doi.org/10.15666/aeer/1704_82918306

after the sowing irrigation. Amounts of applied irrigation water were equal to 100, 110 and 120% of field capacity (FC) in the root zone (0-60 cm depth) of the plants. The second and third irrigation were increased 10 and 20% than FC as leaching requirement. Gypsum (G) requirements were used in two rates, i.e., 2.21 and 4.42 t fed^{-1} (for maintaining 50 and 100% G requirements). Nitrogen (N) sources were 90 kg N (N), 10 t compost (C) and 7.5 t C + 45 kg N (CN) fed^{-1}.

Table 3. *Mean monthly of temperature, relative humidity, wind speed and pan evaporation as well as rainfall quantity in both seasons*

Month	Temperature (°C)		Relative humidity (%)		Wind speed (km day^{-1})		Pan-evaporation (mm $month^{-1}$)		Rainfall (mm $month^{-1}$)	
	2014-15	2015-16	2014-15	2015-16	2014-15	2015-16	2014-15	2015-16	2014-15	2015-16
November	19.05	19.41	74.15	75.60	67.3	70.3	277	319	24.60	52.40
December	15.99	14.03	76.05	77.90	46.03	57.9	172	250	5.70	25.00
January	12.63	12.38	74.60	74.05	70.80	69.2	271	252	52.55	43.21
February	13.35	15.97	74.75	69.05	72.91	58.8	290	252	38.80	-
March	17.19	18.05	70.59	69.90	87.64	63.2	323	359	6.25	13.2
April	18.17	24.33	63.40	61.70	95.70	87.1	607	594	23.90	-

Experimental procedure and data collection

Seeds of wheat variety 'Sids 13' was seeded by hand in rows 12.5 cm a part at the rate of 50 kg seeds fed^{-1}, sown on 18 and 23 November in both years (2014 and 2015 seasons), respectively. While each lysimeter was included 8 rows. Phosphorus (P) and potassium (K) fertilizers were added according to the recommended doses of North Delta area of Egypt. For the source of N, fertilizer urea (46% N) was applied in two equal splits, before sowing irrigation and at the tillering stage. G and C were added before planting. The different agricultural practices were done as recommended. At harvest (158 and 154 days after sowing), the central of 6 rows were harvested and threshed to determine grain and straw yield. The weight of GY was adjusted to 14.5% moisture content.

Water measurements

Amount of irrigation water applied (WA) was measured by a portable pump equipped with a water meter for each lysimeter. Amount of irrigation water applied (WA) was determined according to Phocaides (2001) as follows:

$$WA = \frac{FC - \theta_1}{100} \times BD \times DS \qquad \text{(Eq.1)}$$

where, WA: water applied (cm^3); FC: soil moisture percentage at field capacity; Θ_1: soil moisture percentage before irrigation; BD: bulk density (g cm^{-3}) and DS: soil layer (cm).

Water consumptive use by growing plants was calculated based on soil moisture depletion (SMD) according to Israelsen and Hansen (1962):

http://www.aloki.hu ● ISSN 1589 1623 (Print) ● ISSN 1785 0037 (Online)
DOI: http://dx.doi.org/10.15666/aeer/1704_82918306

$$Cu = SMD = \sum_{i=1}^{i=4} \frac{\theta_2 - \theta_1}{100} x Dbi\ x\ Di\ x\ 4200 \quad \text{(Eq.2)}$$

where, Cu: water consumptive use (m^3/fed.) in the effective root zone; Θ_2: soil moisture percentage after irrigation; Θ_1: soil moisture percentage before next irrigation; Dbi: soil bulk density (g cm^{-3}); Di: soil layer depth (cm) and i: number of soil layer (1-4).

Soil moisture (%) was determined by drying the soil samples at 105 °C to constant weight and the moisture content was calculated according to Singh (1980).

Water productivity (WP) was calculated as the ratio of GY with the amount of irrigation water applied (PIW) and water consumptive use (PW) according to Ali et al. (2007) as follows:

$$PIW = \frac{\text{Yield (kg/ feddan)}}{\text{Applied water } (m^3 / \text{feddan})} \quad \text{(Eq.3)}$$

$$PW = \frac{\text{Yield (kg/ feddan)}}{\text{water consumpitive use } (m^3 / \text{feddan})} \quad \text{(Eq.4)}$$

Statistical analysis

Data in the present study were arranged and all statistical analysis was subjected to analysis according to Gomez and Gomez (1984) by using "MSTATC" computer software package. Treatment means were compared by Duncan's Multiple Range Test at 5% level of significance (Duncan, 1955).

Results and discussion

Seasonal water applied

Applied seasonal water (WA) consisted of two sources such as irrigation water delivered to lysimeter and effective rainfall. In both seasons, the total amounts of the effective rainfall were recorded 446 and 393 m^3 fed^{-1}, respectively (*Table 3*). At the same irrigation treatment, lysimeters of all combinations between gypsum rates and nitrogen sources were received an equal amount of irrigation during the growing season.

Figure 1 shows that the amounts of WA from sowing to harvesting of wheat were gradually increased by increasing the level of irrigation from 100 to 120% FC in both seasons. Wheat plants irrigated with the water amounts equal to 120% FC recorded the highest values of WA 2320 and 2207 m^3 fed^{-1} (55.24 and 52.54 cm) in the two seasons, while the 100% FC recorded the lowest levels of WA i.e., 2095 and 1972 m^3 fed^{-1} (49.88 and 46.95 cm) in both growing seasons, respectively. Such increased in the amount of WA by increasing irrigation level may be attributed to a considerable increase in vegetative growth and leaf area, which resulted in greater transpiration and in turn water requirement. These findings are in close harmony with the findings of Hossain et al. (2006), Sarker et al. (2007), Inamullah et al. (2011) and El-Agrodi et al. (2016).

Seasonal water consumptive use

Data in *Table 4* show that the amount of water lost as evapotranspiration (seasonal water consumptive use, WCU) was increased by increasing irrigation level in the two

http://www.aloki.hu ● ISSN 1589 1623 (Print) ● ISSN 1785 0037 (Online)
DOI: http://dx.doi.org/10.15666/aeer/1704_82918306

seasons. WCU was markedly increased by an increasing the amount of irrigation water from 100 to 120% FC in both seasons. The irrigation level of 120% FC recorded the highest values of WCU followed by 110 and 100% FC. As the soil moisture level increased the water consumptive use was increased due to more improved growth and perhaps luxury consumptive of water. Also, this may be due to an increase in leaching water by increasing the amount of water applied than field capacity.

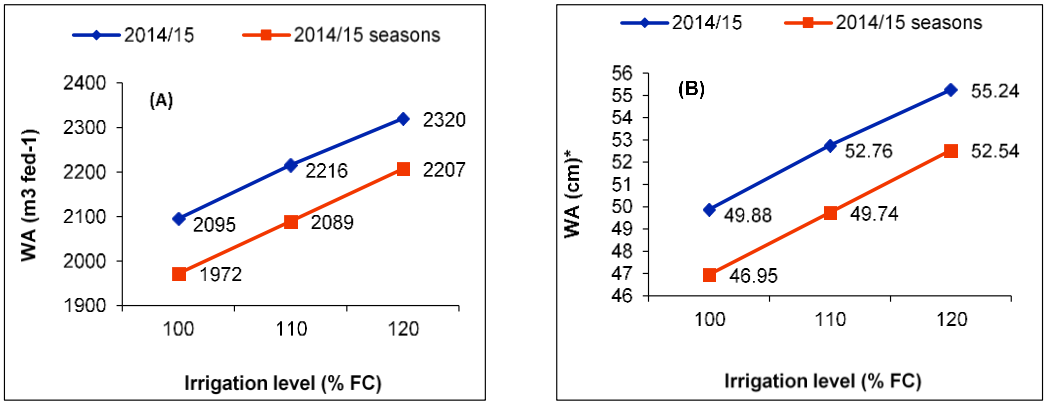

** Fed=feddan= 4200 m2= 0.42 h

* 1 cm water = 42 m^3 fed^{-1}

Figure 1. *WA in m^3 fed^{-1} (A) and in cm (B) as affected by irrigation level in both seasons*

Incorporation of gypsum in the soil at the rate of 4.42 t fed^{-1}(100% of requirements) resulted in the greater WCU than the rate of 2.21 t fed^{-1} (50% of requirements) in both seasons. This may be due to more water applied for leaching the exchangeable sodium.

Source of N had a substantial effect on WCU in both seasons. Whereas, application of 7.5 t C + 45 kg N fed^{-1} (CN) exceeded the application of 90 kg N (N) or 10 t compost fed^{-1} (C) alone in WCU in both seasons. Nitrogen sources were arranged in descending order CN > N > C in this trait in both seasons. While, the application of C and chemical N fertilizer (urea), enhanced the availability of the nutrients in the soil solution. The available nutrients might have helped in enhancing leaf area, which thereby resulted in higher transpiration and more water consumptive.

The interaction between irrigation levels and gypsum rate exerted a substantial effect on WCU. Data show that WCU was increased by increasing each of irrigation level and G rate alone or together in both seasons.

The highest values of WCU 1454 and 1587 m^3 fed^{-1} were recorded by the irrigation level of 120% FC along with 100% G requirements, while the lowest ones 1349 and 1391 m^3 fed^{-1} were recorded by the irrigation level of 100% FC along with 50% G requirements in both seasons. The integration between chemical nitrogen (45 kg N fed^{-1}) and C fertilizer (7.5 t compost fed^{-1}) along with the irrigation level of 120% FC consumed greater water than the irrigation level of 100% FC and 10 t C fed^{-1} in both seasons (*Table 4*). The second order of interaction (irrigation level × G rate × nitrogen source) had a markedly effect on WCU (*Table 4*).

Increasing irrigation level and G rate increased WCU at the same nitrogen source. However, application of both compost and chemical N (7.5 t C + 45 kg N fed^{-1}), resulted in a markedly increased in WCU, as compared with application 90 kg N or 10 t compost fed^{-1} alone at the same combination of irrigation level and G rate. Wheat plants

http://www.aloki.hu ● ISSN 1589 1623 (Print) ● ISSN 1785 0037 (Online)
DOI: http://dx.doi.org/10.15666/aeer/1704_82918306

received 120% FC WA, 100% G and 7.5 t C + 45 kg N fed^{-1} recorded the highest values of WCU (1491 and 1603 m^3 fed^{-1}), while those received 100% FC WA, 50% G and 7.5 t C fed^{-1} recorded the lowest ones (1344 and 1394 m^3 fed^{-1}) in both seasons. Results demonstrated that water consumptive use increased as soil moisture content was highly maintained by increasing amount of water applied due to increasing leaching requirements. Also, the higher frequent irrigation provides a chance for more water consumption, ultimately resulted in increasing plant transpiration and evaporation from the soil surface. These results are in great harmony with those obtained by Ali et al. (2007).

Table 4. *Water consumptive use (WCU), WP for WA and WCU and GY of wheat as affected by levels of irrigation, the rate of gypsum and nitrogen source in both seasons*

Irrigation level	Gypsum rate	N source fed^{-1}	WCU (m^3 fed^{-1})		WP for WA (kg grain m^{-3} water)		WP for WCU (kg grain m^{-3} water)	
			2014-15	2015-16	2014-15	2015-16	2014-15	2015-16
100% FC			1370	1415	1.724	1.787	1.129	1.283
110% FC			1398	1491	1.779	1.755	1.122	1.229
120% FC			1433	1570	1.816	1.754	1.125	1.249
	50%		1379	1473	1.766	1.749	1.103	1.234
	100%		1422	1510	1.78	1.782	1.146	1.289
		90 kg N	1396	1491	1.763	1.795	1.114	1.282
		10 t compost	1378	1471	1.673	1.639	1.156	1.154
		7.5t C + 45 kg N	1427	1514	1.885	1.862	1.217	1.339
100% FC		90 kg N	1367	1415	1.697	1.809	1.489	1.297
100% FC		10 t compost	1351	1391	1.636	1.66	1.056	1.172
100% FC		7.5t C + 45 kg N	1393	1439	1.839	1.891	1.223	1.379
110% FC		90 kg N	1395	1490	1.769	1.793	1.113	1.279
110% FC		10 t compost	1373	1472	1.674	1.617	1.037	1.139
110% FC		7.5t C + 45 kg N	1427	1512	1.894	1.855	1.217	1.342
120% FC		90 kg N	1428	1570	1.822	1.784	1.121	1.269
120% FC		10 t compost	1410	1549	1.707	1.64	1.037	1.151
120% FC		7.5t C + 45 kg N	1462	1591	1.921	1.839	1.211	1.326
100% FC	50%		1349	1391	1.704	1.782	1.098	1.257
100% FC	100%		1391	1438	1.744	1.791	1.159	1.308
110% FC	50%		1375	1476	1.782	1.738	1.106	1.229
110% FC	100%		1421	1506	1.776	1.771	1.138	1.228
120% FC	50%		1412	1553	1.813	1.726	1.104	1.215
120% FC	100%		1454	1587	1.819	1.783	1.141	1.282
	50%	90 kg N	1375	1476	1.767	1.791	1.099	1.265
	50%	10 t compost	1358	1451	1.667	1.611	1.025	1.119
	50%	7.5t C + 45 kg N	1403	1493	1.866	1.844	1.184	1.317
	100%	90 kg N	1417	1507	1.758	1.799	1.128	1.298
	100%	10 t compost	1397	1490	1.678	1.667	1.061	1.189
	100%	7.5t C + 45 kg N	1451	1534	1.904	1.879	1.249	1.361
100% FC	50%	90 kg N	1344	1394	1.691	1.803	1.085	1.274
100% FC	50%	10 t compost	1332	1372	1.629	1.637	1.036	1.139
100% FC	50%	7.5t C + 45 kg N	1374	1407	1.791	1.905	1.172	1.359
100% FC	100%	90 kg N	1389	1435	1.703	1.814	1.129	1.32
100% FC	100%	10 t compost	1370	1410	1.643	1.684	1.075	1.204
100% FC	100%	7.5t C + 45 kg N	1415	1470	1.886	1.877	1.274	1.399

http://www.aloki.hu ● ISSN 1589 1623 (Print) ● ISSN 1785 0037 (Online)
DOI: http://dx.doi.org/10.15666/aeer/1704_82918306

110% FC	50%	90 kg N	1369	1476	1.798	1.791	1.111	1.265
110% FC	50%	10 t compost	1351	1460	1.672	1.59	1.019	1.112
110% FC	50%	7.5t C + 45 kg N	1406	1492	1.876	1.834	1.189	1.309
110% FC	100%	90 kg N	1420	1504	1.739	1.795	1.115	1.292
110% FC	100%	10 t compost	1395	1483	1.676	1.643	1.055	1.167
110% FC	100%	7.5t C + 45 kg N	1448	1531	1.912	1.875	1.245	1.374
120% FC	50%	90 kg N	1412	1557	1.811	1.778	1.102	1.255
120% FC	50%	10 t compost	1392	1522	1.7	1.606	1.019	1.107
120% FC	50%	7.5t C + 45 kg N	1433	1579	1.93	1.793	1.192	1.283
120% FC	100%	90 kg N	1443	1582	1.832	1.79	1.139	1.283
120% FC	100%	10 t compost	1427	1576	1.714	1.674	1.054	1.195
120% FC	100%	7.5t C + 45 kg N	1491	1602	1.912	1.886	1.229	1.369

Generally, WCU values were greater in the second season than in the first season (*Table 4*). This may be due to increase temperature and decrease relative humidity at the most growing months in the second seasons, which increased evaporation and transpiration and in turn more water consumptive.

Water productivity

GY per unit of applied irrigation water (WA) or water consumptive use (WCU) in kg grain m^{-3} water were used to determine water productivity. Data in *Table 4* show that WP (kg grain m^{-3} water) for either WA in both seasons or WCU in the second season was decreased by increasing irrigation level from 100 to 120% FC. The inverse was true in WP for WCU in the first season. The WP for WA and WCU was increased by increasing the gypsum (G) rate in both seasons. Application of 7.5 t C along with 45 kg N fed^{-1} recorded the highest values of WP for WA and WCU followed by 90 kg N and 10 t compost fed^{-1} alone in the two seasons. Incorporation of 100% G requirements and integration of compost with chemical nitrogen resulted in an increase in WP for WA and WCU through increasing GY in both seasons.

The first and second order of interaction had a substantial effect on WP for WA and WCU in both seasons. The relative ranking of the interaction among irrigation level, G rate and nitrogen source in was WP for WA and WCU inconsistent in both seasons. The interaction of 110% FC × 100% G × 7.5 t compost + 45 kg N fed^{-1} produced the highest values of WP for WA (1.245 and 1.374 kg grain m^{-3} WA), while the interaction of 110% FC × 50% G × 10 t compost fed^{-1} produced the lowest values (1.019 and 1.112 kg grain m^{-3} WA) in the two seasons. The interaction of 120% FC × 100% G × 7.5 t compost + 45 kg N fed^{-1} produced the highest values of WP for WCU (1.922 and 1.886 kg grain m^{-3} WCU) in both seasons. However, the lowest value of WP for WCU was 1.629 kg grain m^{-3} WCU recorded from the interaction of 100% FC × 50% G × 10 t compost fed^{-1} in the first seasons, while the interaction of 110% FC × 50% G × 10 t compost fed^{-1} recorded the lowest value 1.590 kg grain m^{-3} WCU in the second season. Results of the present study could be attributed to the great differences between GY of wheat as well as differences between water applied and water consumed also confirmed by the findings of Ali et al. (2007), Liu et al. (2013), Ali (2016) and El-Shawy et al. (2017).

http://www.aloki.hu ● ISSN 1589 1623 (Print) ● ISSN 1785 0037 (Online)
DOI: http://dx.doi.org/10.15666/aeer/1704_82918306

Grain yield

Grain yield fed^{-1} was significantly increased by increasing the level of irrigation from 100 to 120% FC in both seasons (*Table 5*). While no significant difference was recorded for GY due to the levels of irrigation water of 120 and 110% FC in both seasons. This may be due to the increase in growth and yield components. In this connection, adequate water not only allowed the wheat plant to increase photosynthetic rate but also give extra time to translocate the carbohydrates in grains, which enhanced grain size and ultimately causes higher GY. This trend in agreement with Ali et al. (2007), Liu et al. (2013); Ali (2016) and Abdrabbo et al. (2016) and Rashwan et al. (2016). The high rate of G (100%) out yielded the low rate (50%) in GY in both seasons. This trend could enhance with Abdel-Fattah (2012), and Hafez et al. (2015). The combination of compost and chemical nitrogen resulted in a significant increase in GY compared with each of the two sources alone in both seasons. Application of organic (compost) and chemical N fertilizer to wheat enhanced the availability of nutrients in the soil solution. The available nutrients might have helped in the stimulation of various physiological processes including cell division and cell elongation of internodes resulting in more tillers formation, leaf numbers and photosynthetic area (leaf area), which resulted in more photosynthetic production and consequently increased dry matter accumulation and GY. Similar results were reported by Ayadi et al. (2012), Yousef et al. (2014), Mehasen et al., 2015), Abd El-Lattief (2016) and Gharib et al. (2016).

Table 5. *Grain yield, soil salinity (EC) and sodium adsorption ratio (SAR) after wheat harvest as affected by irrigation level, gypsum rate and nitrogen source in both seasons*

Irrigation level	Gypsum rate	N source fed^{-1}	Grain yield (t fed^{-1})		EC (ds m^{-1})		SAR (%)	
			2014-15	2015-16	2014-15	2015-16	2014-15	2015-16
100% FC			2.364 b	2.529 b	6.40	6.07	13.35	12.09
110% FC			2.489 ab	2.618 ab	6.05	5.73	11.91	11.29
120% FC			2.604 a	2.756 a	5.77	5.36	11.49	11.17
	50%		2.438 b	2.576 b	6.21	5.86	12.48	12.11
	100%		2.533 a	2.692 a	5.93	5.57	12.02	10.92
		90 kg N	2.462 b	2.676 a	6.30	6.07	12.64	12.00
		10 t compost	2.305 c	2.41 b	5.82	5.73	11.93	11.11
		7.5t C+45 kg N	2.691 a	2.816 a	6.10	5.36	12.18	11.44
100% FC		90 kg N	2.319 de	2.558 cd	6.70	6.46	13.66	12.48
100% FC		10 t compost	2.21 e	2.31 e	6.11	5.75	13.03	11.79
100% FC		7.5t C+45 kg N	2.563 bc	2.72 abc	6.39	6.00	13.37	11.99
110% FC		90 kg N	2.466 cd	2.671 bc	6.32	5.98	12.33	11.91
110% FC		10 t compost	2.299 de	2.379 de	5.81	5.41	11.73	10.97
110% FC		7.5t C+45 kg N	2.703 ab	2.803 ab	6.02	5.79	11.68	11.01
120% FC		90 kg N	2.6 abc	2.8 ab	5.89	5.69	11.94	11.60
120% FC		10 t compost	2.406 cde	2.541 cd	5.54	5.00	11.04	10.59
120% FC		7.5t C+45 kg N	2.808 a	2.926 a	5.89	5.38	11.48	11.33
100% FC	50%		2.3 c	2.48 c	6.56	6.16	13.51	12.48
100% FC	100%		2.428 bc	2.578 bc	6.24	5.98	13.19	11.69
110% FC	50%		2.453 b	2.567 bc	6.20	5.86	12.29	12.11
110% FC	100%		2.526 ab	2.669 ab	5.89	5.59	11.53	10.47
120% FC	50%		2.563 ab	2.681 ab	5.88	5.56	11.64	11.75
120% FC	100%		2.646 a	2.83 a	5.66	5.15	11.33	10.60

http://www.aloki.hu ● ISSN 1589 1623 (Print) ● ISSN 1785 0037 (Online)
DOI: http://dx.doi.org/10.15666/aeer/1704_82918306

	50%	90 kg N	2.431 cd	2.641 bc	6.41	6.16	12.89	12.52
	50%	10 t compost	2.265 d	2.337 d	5.99	5.86	12.24	11.73
	50%	7.5t C+45 kg N	2.62 ab	2.749 ab	6.23	5.56	12.32	12.09
	100%	90 kg N	2.493 bc	2.711 ab	6.19	5.98	12.40	11.47
	100%	10 t compost	2.345 cd	2.483 cd	5.64	5.59	11.62	10.50
	100%	7.5t C+45 kg N	2.763 a	2.883 a	5.96	5.15	12.04	10.80
100% FC	50%	90 kg N	2.273 de	2.513b-f	6.82	6.58	13.68	12.93
100% FC	50%	10 t compost	2.17 e	2.246 f	6.29	5.78	13.23	12.08
100% FC	50%	7.5t C+45 kg N	2.456 b-e	2.681a-d	6.56	6.11	13.52	12.45
100% FC	100%	90 kg N	2.365 cde	2.603b-e	6.57	6.33	13.53	12.03
100% FC	100%	10 t compost	2.251 de	2.374 def	5.92	5.72	12.83	11.52
100% FC	100%	7.5t C+45 kg N	2.669 abc	2.759abc	6.22	5.89	13.22	11.53
110% FC	50%	90 kg N	2.462 b-e	2.643b-e	6.52	6.11	12.86	12.66
110% FC	50%	10 t compost	2.259 de	2.322ef	5.96	5.49	12.21	11.77
110% FC	50%	7.5t C+45 kg N	2.637 abc	2.736abc	6.12	5.98	11.80	11.91
110% FC	100%	90 kg N	2.47 b-e	2.699 a-d	6.12	5.85	11.80	11.15
110% FC	100%	10 t compost	2.338 cde	2.437 c-f	5.65	5.32	11.24	10.16
110% FC	100%	7.5t C+45 kg N	2.769 ab	2.871 ab	5.91	5.59	11.59	10.11
120% FC	50%	90 kg N	2.557 a-d	2.769 abc	5.90	5.78	12.02	11.98
120% FC	50%	10 t compost	2.366 cde	2.444 c-f	5.73	5.22	11.28	11.36
120% FC	50%	7.5t C+45 kg N	2.765 ab	2.831 ab	6.02	5.68	11.63	11.90
120% FC	100%	90 kg N	2.643 abc	2.831 ab	5.89	5.60	11.86	11.22
120% FC	100%	10 t compost	2.446 b-e	2.638 b-e	5.34	4.78	10.80	9.82
120% FC	100%	7.5t C+45 kg N	2.851 a	3.021 a	5.75	5.07	11.33	10.76

Means of each factor in grain yield columns designated by the same latter are not significantly different at 5% level using DMRT

All the first and second order interactions had a significant effect on GY in both seasons. Increasing irrigation level and G rate along with compost and nitrogen together substantially increased GY. Application of 100% G and 7.5 t compost + 45 kg N fed^{-1} at any irrigation level were among those treatments having high GY, being insignificant, in both seasons. These results go with those reported by Attia et al. (2013), Abdel-Fattah, 2012), Hafez et al. (2015) and Gharib et al. (2016).

Salinity and sodicity

Salinity (ECe) and sodicity (SARe) of the soil after harvesting as affected by irrigation level, G rate, nitrogen source and their interactions under wheat crop are shown in *Table 5*. The initial value of ECe before the experiment was 7.10 dS m^{-1} (*Table 1*). Data show that the values of salinity and sodicity were decreased after harvesting compared with those before the beginning of experiment at any studied treatment in both seasons. Increasing irrigation level, G rate and compost alone resulted in a substantially decrease salinity and sodicity of soil after harvesting. Data show that application N fertilizer alone or with compost increased these traits compared with compost alone at any combination between irrigation and G in both seasons. The lowest values of ECe (5.34 and 4.78 dS m^{-1}) and SARe (10.80 and 9.82%) were obtained from the irrigation level of 120% FC, 100% G and 7.5 t compost fed^{-1} in both seasons.

Application of 10 t compost alone with 100% G reduced Ec greater than 16% at any irrigation level in both seasons (*Figs. 2* and *3*). The highest values of reduction percentage 24.8 and 32.7% were recorded by the interaction of 120% FC × 100% G × 10 t compost fed^{-1} in the two seasons. The application of G and compost had a positive effect on the soil

http://www.aloki.hu ● ISSN 1589 1623 (Print) ● ISSN 1785 0037 (Online)
DOI: http://dx.doi.org/10.15666/aeer/1704_82918306

properties and the present investigations have addressed the combined effect of compost and G on the saline-sodic soils under semi-arid conditions. The effect of G application on saline-sodic soil reclamation have shown that the soil receiving G at higher rate since it removes the greatest amount of Na^+ from the soil columns and causes a substantial decrease in soil electrical conductivity (EC) and sodium adsorption ratio (SAR) (Hamza and Andrrson, 2003; Rasouli et al., 2013).

Application of 10 t compost alone with 100% gypsum reduced SAR greater than 18% at irrigation levels of 110 and 120% FC in both seasons (*Figs. 2* and *3*). The highest values of reduction percentage 21.2 and 28.4% were recorded by the interaction of 120% FC × 100% gypsum × 10 t compost fed^{-1} in the two seasons.

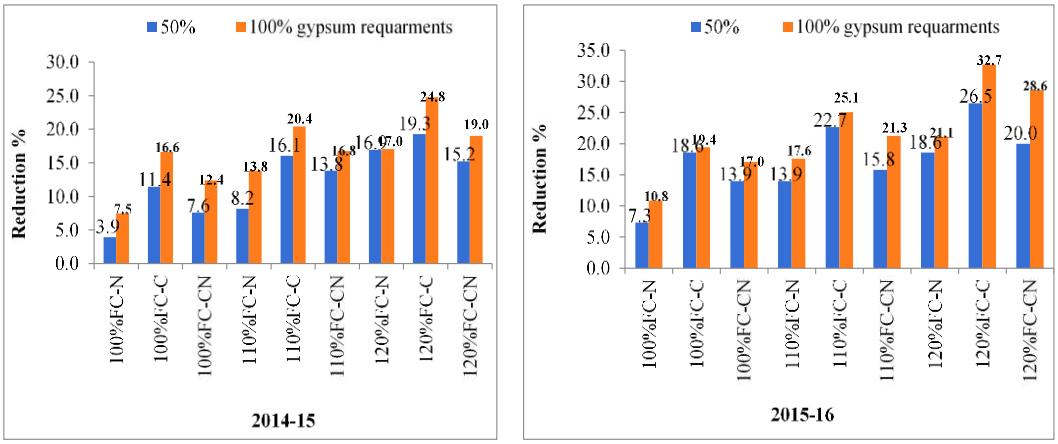

Figure 2. *The percent reduction of EC after harvest based on its initial value (7.10) as affected by the interaction of irrigation level, gypsum rate and nitrogen source in both seasons*

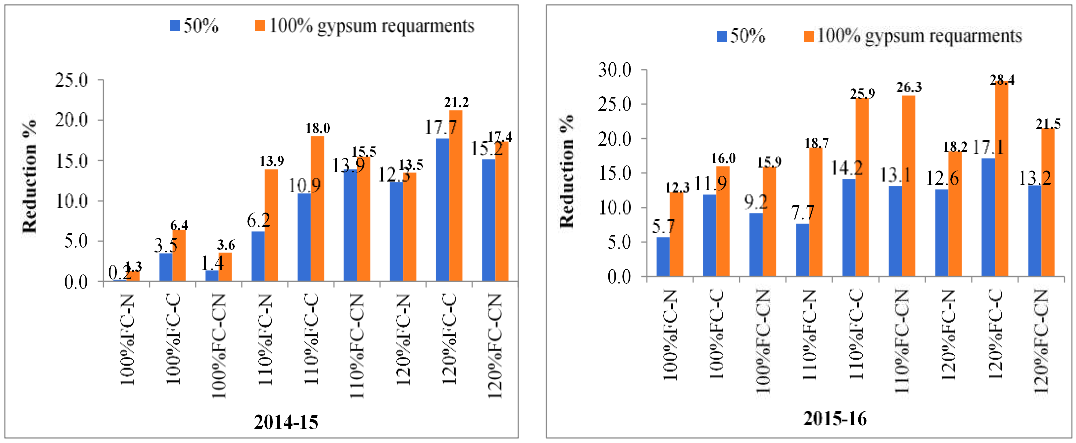

Figure 3. *The percent reduction of SAR after harvest based on its initial value (13.71) as affected by the interaction of irrigation level, gypsum rate and nitrogen source in both seasons*

Conclusion

In summary, it can be concluded that irrigation with water amount equal to 110 or 120% FC, 100% G requirements and 7.5 t C and 45 kg N fed^{-1} was the best treatment for getting high GY, improve the soil chemical properties, nutrients availability and increase water productivity of salt-affected soil in North Delta of Egypt.

http://www.aloki.hu ● ISSN 1589 1623 (Print) ● ISSN 1785 0037 (Online)
DOI: http://dx.doi.org/10.15666/aeer/1704_82918306

Disclaimer. We hereby declare that the manuscript contains no material which has been accepted for the award of any degree or diploma in any university and that, to the best of our knowledge and belief, the review contains no copy of any material previously published or written by another person except where due reference is made in the text.

REFERENCES

[1] Abd El-Lattief, E. A. (2014): Effect of integrated use of farmyard manure (FYM) and chemical fertilizers (NPK) on productivity of bread wheat under arid conditions. – International Journal of Advanced Research in Engineering and Applied Sciences 3(12): 22-27.

[2] Abdel-Fattah, M. K. (2012): Role of gypsum and compost in reclaiming saline sodic soils. – IOSR Journal of Agriculture and Veterinary Science 1(3): 30-38.

[3] Abdelaal, A. A. K., Omara, I. R., Hafez, M. Y., Samar, M. E., EL Sabagh, A. (2018): Anatomical, biochemical and physiological changes in some Egyptian wheat cultivars inoculated with Puccinia graminis F. sp. Tritici. – Fresenius Environmental Bulletin 27(1): 296-305.

[4] Abdrabbo, M. A. A., Hashem, F. A., Abou-Hadid, A. F. (2016): Irrigation requirements for some bread wheat cultivars. – Journal of Agricultural Science and Research 3(1): 23-40.

[5] Ali, F. T. (2016): The effect of different deficit irrigation strategies on yield, quality, and water-use efficiencies of wheat under semi-arid conditions. – Agricultural Water Management 167: 1-10.

[6] Ali, M. H., Hoque, M. R., Hassan, A. A., Khair, A. (2007): Effect of deficit irrigation on yield water productivity and economic returns of wheat. – Agricultural Water Management 92(3): 151-161.

[7] Al-Naggar, A. M. M., Sabry, S. R. S., Atta, M. M. M., El-Aleem, O. M. A. (2015a): Effects of salinity on performance, heritability, selection gain and correlations in wheat (*Triticum aestivum* L.) doubled haploids. – Scientia Agriculturae 10(2): 70-83.

[8] Al-Naggar, A. M. M., Sabry, S. R. S., Atta, M. M. M., El-Aleem, O. M. A. (2015b): Field screening of wheat (*Triticum aestivum* L.) genotypes for salinity tolerance at three locations in Egypt. – Journal of Agriculture and Ecology Research International 4(3): 88-104.

[9] Attia, A. N. E., Seadh, S. E., Sharshar, M. S. E., Genedy, M. S. (2013): Comparative studies on number of irrigations, planting methods and nitrogen levels for wheat in north Delta soils. – Journal of Plant Production, Mansoura University 4(7): 1139-1148.

[10] Ayadi, S., Karmous, C., Hammami, Z., Tamani, N., Trifa, Y., Esposito, S., Rezgui, S. (2012): Genetic variability of nitrogen use efficiency components in Tunisian improved genotypes and landraces of durum wheat. – Agriculture Science Research Journal 2(11): 591-601.

[11] Barutcular, C., EL Sabagh, A., Koç, M., Ratnasekera, D. (2017): Relationships between grain yield and physiological traits of durum wheat varieties under drought and high temperature stress in Mediterranean conditions. – Fresenius Environmental Bulletin 26(6): 4282-4291.

[12] Chen, H., Jiang, J. G. (2010): Osmotic adjustment and plant adaptation to environmental changes related to drought and salinity. – Environmental Reviews 18: 309-319.

[13] Campbell, D. J. (1994): Determination and Use of Bulk Density in Relation to Soil compaction. – In: Ouwerkerk, C. van, Soane, B. D. (eds). Soil Compaction in Crop Production. Elsevier, London.

[14] Cottenie, A., Verloo, M., Velghe, G., Kiekon, L. (1982): Biological and Analytical Aspects of Soil Pollution. – Lab. of Analytical Agro. State Univ., Gent.

[15] Duncan, B. D. (1955): Multiple range and multiple F-test. – Bionetrics 11: 1-42.

http://www.aloki.hu ● ISSN 1589 1623 (Print) ● ISSN 1785 0037 (Online)
DOI: http://dx.doi.org/10.15666/aeer/1704_82918306

[16] Edwards, S., Hailu, A. (2011): How to Make Compost and Use. – In: Ching, L. L., Edwards, S., Scialabba, N. E. (eds.) Climate Change and Food Systems Resilience in Sub-Saharan Africa. FAO, Italy, pp. 379-436.
[17] Egypt Today (2018): Egypt's wheat production to increase 4.3% YoY in 2018/19: FAS. – Sunday May 13, 2018. https://www.egypttoday.com/Article/3/49959/Egypt%E2%80%99s-wheat-production-to-increase-4-3-YoY-in-2018.
[18] El-Agrodi, M. W. M., Saied, M. M., Ahmed, G. L., Khalifa, T. S. H. (2016): Effect of soil moisture depletion and nitrogen levels on wheat (*Triticum aestivum,* L.). – Journal of Soil Science and Agricultural Engineering, Mansoura University 7(2): 169-178.
[19] El-Hendawy, S. E., Hu, Y., Yakout, G. M., Awad, A. M., Hafiz, S. E., Schmidhalter, U. (2005): Evaluating salt tolerance of wheat genotypes using multiple parameters. – European Journal of Agronomy 22: 243-253.
[20] El-Shawy, E.E., El Sabagh, A., Mansour, M., Barutcular, C. (2017): A comparative study for drought tolerance and yield stability in different genotypes of barley (*Hordeum vulgare* L.). – Journal of Experimental Biology and Agricultural Sciences 5(2):151-162.
[21] Gharib, H., Hafez, E., EL Sabagh, A. (2016): Optimized potential of utilization efficiency and productivity in wheat by integrated chemical nitrogen fertilization and simulative compounds. – Cercetari Agronomice in Moldova 2(166): 5-20.
[22] Gomez, K. A., Gomez, K. A. (1984): Statistical Procedures for Agricultural Research. 1st Ed. – John Wiley and Sons, New York.
[23] Hafez, E. M., Abou Khadrah, A., Sorour, S. Gh. R., Yousef, A. R. (2015): Comparison of agronomical and physiological nitrogen use efficiency in three cultivars of wheat as affected by different levels of N-sources. – Proc. 13th International Conf. Agron., Fac. of Agric., Benha Univ., Egypt, 9-10 September, pp. 130-145.
[24] Halitligil, M. B., Akın, A., Bilgin, N., Deniz, Y., Öğretir, K., Altınel, B., Işık, Y. (2000): Effect of nitrogen fertilization on yield and nitrogen and water use efficiencies of winter wheat (durum and bread) varieties grown under conditions found in Central Anatolia. – Biology and Fertility of Soils 31(2): 175-182.
[25] Hamza, M. A., Anderson, W. K. (2003): Responses of soil properties and grain yields to deep ripping and gypsum application in a compacted loamy sand soil contrasted with a sandy clay loam soil in Western Australia. – Australian Journal of Agricultural Research 54: 273-282.
[26] Hanay, A., Buyuksonmez, F., Kiziloglu, F. M., Canbolat, M. Y. (2004): Reclamation of saline-sodic soils with gypsum and MSW compost. – Compost Science & Utilization 12: 175-179.
[27] Hesse, P. R. (1971): A Text Book of Soil Chemical Analysis. – John Murray Ltd., London.
[28] Hossain, M. A., Rashid, M. H., Rahman, M. S., Biswas, S. K. (2006): Interaction of irrigation levels and fertilizer doses on wheat production in Bangladesh. – Bangladesh Journal of Agricultural Engineering 17(1-2): 1-8.
[29] Hossain, M. M., Hossain, A., Alam, M. A., EL Sabagh, A., Khandakar Faisal Ibn Murad, Haque, M. M., Muriruzzaman, M., Islam, M. Z., Das, S., Barutcular, C., Kizilgeci, F. (2018): Evaluation of fifty spring wheat genotypes grown under heat stress condition in multiple environments of Bangladesh. – Fresen. Environ. Bull. 27: 5993-6004.
[30] Inamullah, A., Farhan U. K., Iftikhar, H. K. (2011): Environmental effect on wheat phenology and yields. – Sarhad Journal of Agriculture 27(3): 395-402.
[31] Index Mundi (2018): Egypt wheat production by year. – https://www.indexmundi.com/agriculture/?country=eg&commodity=wheat&graph=production.
[32] Islam, M. S., Akhter, M. M., El Sabagh, A., Liu, L. Y., Nguyen, N. T., Ueda, A., Masaoka. Y., Saneoka, H. (2011): Comparative studies on growth and physiological

http://www.aloki.hu ● ISSN 1589 1623 (Print) ● ISSN 1785 0037 (Online)
DOI: http://dx.doi.org/10.15666/aeer/1704_82918306

responses to saline and alkaline stresses of Foxtail millet ('Setaria italica'L.) and Proso millet (*Panicum miliaceum* L.). – Australian Journal of Crop Science 5(10): 1269 -1277

[33] Israelsen, D. W., Hansen, V. E. (1962): Flow of Water into and through Soil Irrigation Principles and Practices. 3rd Ed. – John Wiley and Sons Inc., New York.

[34] Jahan, M. A. H. S., Hossain, A., Jaime, A., Da Silva, T., EL Sabagh, A., Rashid, M. H., Barutçular, C. (2019): Effect of naphthaleneacetic acid on root and plant growth and yield of ten irrigated wheat genotypes. – Pakistan Journal of Botany 51(2): 451-459.

[35] Jackson, M. L. (1967): Soil Chemical Analysis. – Prentice Hall, New Delhi.

[36] Liu, X., Shao, L., Sun, H., Chen, S., Zhang, X. (2013): Responses of yield and water use efficiency to irrigation amount decided by pan evaporation for winter wheat. – Agricultural Water Management 129: 173-180.

[37] McGill, J., Prikhodko, D., Sterk, B., Talks, P. (2015): Egypt: Wheat Sector Review. – FAO Investment Centre. Country Highlights (FAO) Eng No. 21. http://www.fao.org/3/a-i4898e.pdf.

[38] Mehasen, S. A. S., Badawy, S. A., Abdullah S. S. (2015): Influence of bio and mineral nitrogen fertilizers on productivity of some bread wheat varieties. – Journal of Food Agriculture and Environment 13(2): 162-167.

[39] Musick, J. T., Jones, G. R., Stewart, B. A., Dusek, D. A. (1994): Water-yield relationships for irrigated and dry land wheat in the US southern plains. – Agronomy Journal 86: 980-986.

[40] Olsen, S. R., Cale, C. V., Watenable, F. S., Deann, L. A. (1954): Estimation of Available Phosphorus in Soil by Extraction with Sodium Bicarbonate. – US Dept. of Agric., Washington, DC.

[41] Out, H., Celiktas, V., Duzenli, S., Hossain, A., El Sabagh, A. (2018): Germination and early seedling growth of five durum wheat cultivars (*Triticum durum* desf.) is affected by different levels of salinity. – Fresenius Environmental Bulletin 27(11): 7746-7757.

[42] Page, A. L. (ed.) (1982): Methods of Soil Analysis. Part 2: Chemical and Microbiological Properties. 2nd Ed. – American Society of Agronomy, Inc. Soil Sci. Soc. of Am. Inc., Madison, WI.

[43] Phocaides, A. (2001): Handbook on Pressurized Irrigation Techniques. – Food and Agriculture Organization of the United Nations, Rome.

[44] Piper, C. S. (1950): Soil and Plant Analysis. – Inter Science Publication, New York.

[45] Rashwan, E., Mousa, A., El-Sabagh, A., Barutçular, C. (2016):Yield and quality traits of some flax cultivars as influenced by different irrigation intervals. – Journal of Agricultural Science 8 (10): 226-240.

[46] Rasouli, F., Poya, A. K., Karimian, N. (2013): Wheat yield and physicohemical properties of a sodic soil from semi-arid area of Iran as affected by applied gypsum. – Geoderma 193-194: 246-225.

[47] Sarker, K. K., Sarker, A. Z., Malaker, P. K., Roy, K. C., Islam, D. (2007): Comparative study on water requirement and economic return of wheat and boro rice. – Journal of Bangladesh Society for Agricultural Science and Technology 4(3&4): 45-48.

[48] Schoonover, W. R. (1952): Examination of Soils for Alkali. – University of California Extension Service, Berkeley, CA.

[49] Shaaban, S. M. (2006): Effect of organic and inorganic nitrogen fertilizer on wheat plant under water regime. – Journal of Applied Sciences Research 2: 650-656.

[50] Singh, R. A. (1980): Soil Physical Analysis. – Kalyans, New Delhi, pp. 81-82.

[51] Wiendenfeld, R. P. (2000): Water stress during different sugarcane growth periods on yield and response to N fertilization. – Agricultural Water Management 43(2): 173-182.

[52] Yassin, M., Mekawy, A. M., EL Sabagh, A., Islam, M. S., Hossain, A., Barutcular, C., Alharby, H., Bamagoos, A., Liu, L., Ueda, A., Saneoka, H. (2019): Physiological and biochemical responses of two bread wheat (*Triticum aestivum* L.) genotypes grown under salinity stress. – Applied Ecology and Environmental Research 17(2): 5029-5041.

http://www.aloki.hu ● ISSN 1589 1623 (Print) ● ISSN 1785 0037 (Online)
DOI: http://dx.doi.org/10.15666/aeer/1704_82918306

[53] Yildirim, M., Barutçular, C., Hossain, A., Koç, M., Dizlek, H., Akinci, C., Toptaş, I., Basdemir, F., Islam, M. S., EL Sabagh, A. (2018): Assessment of The Grain Quality of Wheat Genotypes Grown Under Multiple Environments Using GGE Biplot Analysis. – Fresenius Environmental Bulletin 27(7): 4830-4837.

[54] Yousaf, M., Fahad, S., Shah, A. N., Shaaban, M., Khan, M. J., Sabiel, S. A. I., Ali, S. A. I., Wang, Y., Osman, K. A. (2014): The effect of nitrogen application rates and timing of first irrigation on wheat growth and yield. – International Journal of Agricultural Innovation and Research 2(4): 645-653.

http://www.aloki.hu ● ISSN 1589 1623 (Print) ● ISSN 1785 0037 (Online)
DOI: http://dx.doi.org/10.15666/aeer/1704_82918306

WHEAT (*TRITICUM AESTIVUM* L.) PRODUCTION UNDER DROUGHT AND HEAT STRESS – ADVERSE EFFECTS, MECHANISMS AND MITIGATION: A REVIEW

EL SABAGH, A.[1*] – HOSSAIN, A.[2] – BARUTÇULAR, C.[3] – ISLAM, M. S.[4] – AWAN, S. I.[5] – GALAL, A.[1] – IQBAL, M. A.[6] – SYTAR, O.[7] – YILDIRIM, M.[8] – MEENA, R. S.[9] – FAHAD, S.[10] – NAJEEB, U.[11] – KONUSKAN, O.[12] – HABIB, R. A.[13] – LLANES, A.[14] – HUSSAIN, S.[15] – FAROOQ, M.[16] – HASANUZZAMAN, M.[17] – ABDELAAL, K. H.[18] – HAFEZ, Y.[18] – CIG, F.[19] – SANEOKA, H.[20]

[1]*Department of Agronomy, Faculty of Agriculture, University of Kafrelsheikh, Egypt*

[2]*Wheat Research Center, Bangladesh Agricultural Research Institute Dinajpur-5200, Bangladesh*

[3]*Department of Field Crops, Faculty of Agriculture, University of Çukurova, Turkey*

[4]*Department of Agronomy, Hajee Mohammad Danesh Science and Technology University, Bangladesh*

[5]*Department of Plant Breeding and Molecular Genetics, Fac. of Agric., University of Poonch, Rawalakot, Pakistan*

[6]*Department of Agronomy, University of the Poonch Rawalakot (AJK), Pakistan*

[7]*Department of Plant Physiology, Faculty of Agrobiology and Food Resources, Slovak University of Agriculture,Tr. A. Hlinku 2, 949 76 Nitra, Slovakia*

[8]*Department of Field Crops, Faculty of Agriculture, Dicle University, Diyarbakir, Turkey*

[9]*Deapartment of Agronomy, Inistitute of Agricultural Sciences, BHU Varanasi (UP)-221 005, India*

[10]*Agriculture Department, The University of Swabi, Khyber Paktunkhwa, Pakistan*

[11]*Queensland Alliance for Agriculture and Food Innovation, Centre for Crop Science, the University of Queensland,, Toowoomba, QLD 4350, Australia*

[12]*Department of Field Crops, Faculty of Agriculture, Mustafa Kemal University, Hatay, Turkey*

[13]*Institute of Pure and Applied Biology, Bahauddin Zakariya University, Multan, Pakistan*

[14]*Plant Physiology Laboratory, Department of Natural Sciences, FCEFQyN, Universidad Nacional de Río Cuarto, Río Cuarto X5800, Argentina*

[15]*Department of Agronomy, University of Agriculture, Faisalabad ,38040, Punjab-Pakistan*

[16]*Department of Crop Sciences, College of Agricultural and Marine Sciences, Sultan Qaboos University, Al-Khoudh-123, Oman*

[17]*Department of Agronomy, Faculty of Agriculture, Sher-e-Bangla Agricultural University, Dhaka-1207,Bangladesh*

[18]*EPCRS Excellence Center, Plant Pathology and Biotechnology Lab., Agriculture Botany Department, Faculty Agriculture, Kafrelsheikh University, 33516, Egypt*

[19]*Department of Field Crops, Faculty of Agriculture, Siirt University, Turkey*

[20]*Pant nutritional physiology, Graduate School of Biosphere Science, Hiroshima University, Japan*

[*]*Corresponding author*
e-mail: ayman.elsabagh@agr.kfs.edu.eg

(Received 18th Feb 2019; accepted 1st May 2019)

APPLIED ECOLOGY AND ENVIRONMENTAL RESEARCH 17(4):8307-8332.
http://www.aloki.hu ● ISSN 1589 1623 (Print) ● ISSN 1785 0037 (Online)
DOI: http://dx.doi.org/10.15666/aeer/1704_83078332

Abstract. Heat and drought stresses are the most important abiotic factors that reduce crops productivity by affecting various physiological and biochemical processes. Thus, selecting cultivars with better drought or heat stress tolerance or breeding for stress tolerance will be helpful in enhancing crop productivity under harsh environments. This review elaborates the physiological basis of high temperature and drought stress tolerance in wheat which can be used as selection criteria in wheat breeding program. In addition, some agronomic selection criteria which are valid and useful in selecting stress tolerant wheat species and cultivars. The review also discussed the valid usage of stress tolerance indices (such as mean productivity (MP), geometric mean productivity (GMP), yield index (YI), yield stability index (YSI), relative productivity (RP%), stress susceptibility index (SSI), and the tolerance index (TOL)) to scan the genotypes against drought and heat stress. Beside these, exogenous application of stress signaling compounds, osmolytes, or certain inorganic salts play a vital role for alleviating adverse effects of abiotic stresses for sustainable wheat production. In addition, applications for soil amendments will also helpful in increasing wheat crop productivity under stressful conditions. All these strategies may be helpful to meet the food demands of the increasing population.
Keywords: *wheat, drought, heat stress, stress tolerance indices, agronomic approaches*

Abbreviations: AsA, ascorbic acid; CAT, catalase; DRI, drought resistance index; ES, early sowing; GB, glycine betaine; GMP, geometric mean productivity; GY, grain yield; HSI, heat susceptibility index; MP, mean productivity; LS, late sowing; OS, optimum sowing; POX, peroxidase; RH, relative humidity; %RP, relative performance; SSI, stress susceptibility index; Se, selenium; SA, salicylic acid; STIs, stress tolerance indices; TOL, tolerance index; YE, Yeast extract; YI, yield index; YSI, yield stability index

Introduction

Wheat (*Triticum aestivum* L.) is one of the leading cereals and used as a staple food for 1.2 billion people worldwide (Afzal et al., 2015; Iqbal et al., 2018). To feed the increasing population, the global demand for wheat is expected to increase up to 40% by 2050 to meet the food security (Rosegrant and Agcaoili, 2010; Abdelaal et al., 2018; Jahan et al., 2019). In view of the global climate change, drought ,salinity and heat stresses are the major abiotic constraints for wheat productivity and adversely affects the yield and quality through altering the physiological activity (Kosina et al., 2007; Otu et al., 2018; Yassin et al., 2019). Short or long-term exposure to heat and drought stresses can significantly affect the growth and yield, particularly at sensitive growth stages (Prasad et al., 2008). Hoegh – Guldberg et al. (2018) estimated that due to climate change and 2-3°C rise in global temperature, losses of wheat yield will increase by up to 30% by 2050. As water availability is a major factor limiting crop production in many parts of the world, the management practices focus on enhancing water use efficiency of the future crops (Majid et al., 2017). In addition, drought tolerance traits must be incorporated in crops anticipating the climate changing scenario (EL-Shawy et al., 2017). To cope climate change, selection of suitable varieties as well as optimization of irrigation water are needed for maintaining sustainable food supplies (Bernardi, 2011).

Various approaches are suggested to overcome crop losses due to drought and heat stresses such as stress management practices, breeding for developing stress-tolerant cultivars, use of physiological mechanisms in developing stress tolerant cultivars and exogenous use of chemicals which improve stress tolerance (Farooq et al., 2011; Hossain and Teixeira da Silva, 2012, 2013). Since most of the modern wheat varieties are not sufficiently tolerant to drought and heat (Alghabari et al., 2015), development of wheat cultivars that are tolerant to drought and heat is one of the main challenges for wheat breeders around the world (EL Sabagh et al., 2018a). The present review aimed to assess the current status of knowledge of the physiological basis of stress tolerance in plants, the applicability of this knowledge in developing stress tolerant crop cultivars,

http://www.aloki.hu ● ISSN 1589 1623 (Print) ● ISSN 1785 0037 (Online)
DOI: http://dx.doi.org/10.15666/aeer/1704_83078332

limitations or deficiencies in understanding mechanism of stress tolerance, and efficiency of different approaches in mitigating adverse effects of drought and heat stress on plants. In other words, the main objective of the present review is to rationalize the physiological breeding for drought and heat stress tolerance in wheat. This will help in deciding future directions in developing high yielding wheat cultivars under heat and drought stress conditions.

Impacts of drought and heat stress on phenology, growth, and productivity of wheat

A temperature above or below the optimum can hamper the growth and development of wheat crop by influencing various processes such as uptake of water and nutrients, however, such effects may vary with plant developmental stages (Wahid et al., 2007). Under high temperature, the crop completes its life cycle relatively faster which ultimately lead to decrease the final biomass and yield (Rahman et al., 2009; Nahar et al., 2010; Hakim et al., 2012; Hossain et al., 2009, 2011, 2012a, b, c, 2013, 2017,2018). In the Sub-Tropical region of South-Asia such as Pakistan, India, Bangladesh, delayed planting significantly reduces the days to maturity and grain filling period and grain yield of wheat (Mahboob et al., 2005). Similarly, Barutcular et al. (2016b, c; Yıldırım et al.,2018) noticed that delayed planting cause the exposure of wheat plants to high temperature and moisture stress that resulted in a reduction in growth and yield of wheat. In view of these reports, it is suggested that efforts should focus on identifying drought and heat resistant ideotypes and selection should be based on yield traits to increase the economic yield under heat and drought stress conditions. However, traits responsible for drought and/or heat resistance in wheat are not well defined. Drought tolerance in crop species can be defined as the ability of crop cultivar to produce satisfactory harvestable yield under water deficit conditions (Basu et al., 2016). However, yield stability is better to stress tolerance indicator under heat stress or water stress conditions (Fleury et al., 2010). In addition, a little progress has been made in identifying key mechanisms associated with high yield and stress tolerance against high temperature and drought stress (Ogbaga et al., 2018).

Drought and heat stress in relation to sowing time

Days to germination

Seed germination in wheat is one of the most critical growth stages that influence initial plant population, stand establishment, and finally yield of wheat under stress condition (Almansouri et al., 2001). Environmental factors such as seed-bed soil moisture, temperature, as well as seed vigour/quality, play an important role in seed germination and stand establishment of the crops (Khajeh-Hosseini et al., 2003). Since soil moisture availability and temperature both regulate seed germination, lower moisture and/or low soil temperature hinder or delay seed germination which results in unequal seedling establishment and ultimately reduce the final grain yield of crops (Hampson and Simpson, 1990; Hossain et al., 2012). Generally, in the arid and semi-arid region, seed germination in spring wheat occurs at the range of air and soil temperature of 20-30°C (Hossain et al., 2012a,b,c). However, late sown (LS) wheat crop takes longer time to germinate than sown at optimum sowing in temperate region (like Russia), due to reduced soil moisture and low temperature (<12°C) (Hossain and Teixeira da Silva, 2012; Hossain et al., 2012b; *Fig. 1*).

http://www.aloki.hu ● ISSN 1589 1623 (Print) ● ISSN 1785 0037 (Online)
DOI: http://dx.doi.org/10.15666/aeer/1704_83078332

The impact of heat stress in combination with deficit soil moisture (drought stress) is the most critical to impact seed germination than the individual stress (Al-Karaki et al., 2007; Hossain et al., 2013). Similarly, Hossain and Teixeira da Silva (2012) found significant differences in days to germination among the three wheat varieties in OS (optimum sowing) and LS (late sowing) conditions (*Fig. 2*). They found that the days to germination were increased by 25 to 50% in late sown condition due to a low temperature at germination, while under OS, all varieties showed no variation in germination time (*Fig. 3*; Hossain and Teixeira da Silva, 2012). Likewise, while conducting a field experiment Chakrabarti et al. (2011) reported that air temperature greater than 15°C is appropriate for seed germination and seedling stand establishment of spring wheat.

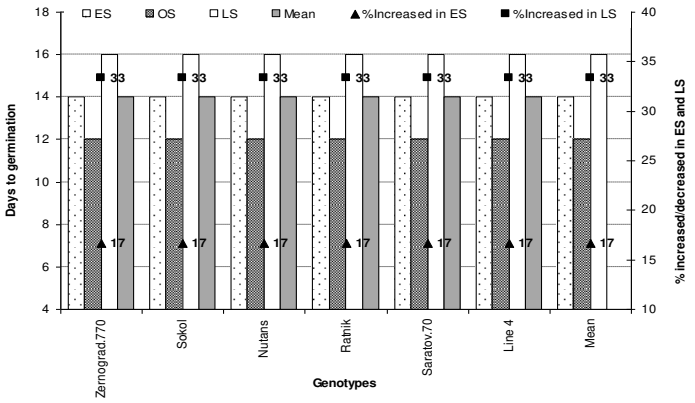

Figure 1. *Days to start germination of wheat and barley as influenced by low temperature in early sown and high temperature with drought stress in late sown condition in the arid region of south-eastern Russia; ES, early sowing; OS, optimum sowing; LS, late sowing (Source: Hossain et al., 2012b)*

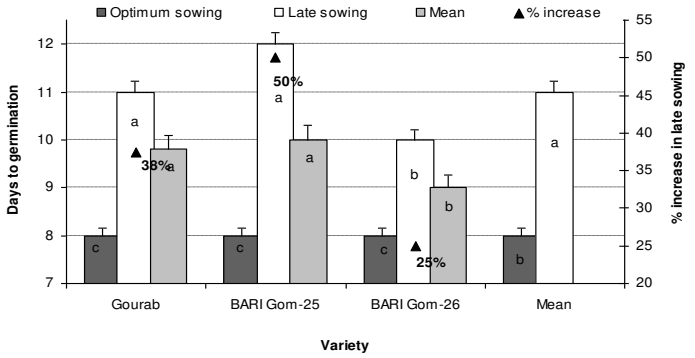

Figure 2. *Days to seed germination of three wheat varieties as influenced by late sown heat stress conditions in the north-western part of Bangladesh (Source: Hossain and Teixeira da Silva, 2012)*

Days to booting

The reproductive stages are the most sensitive to high temperature and drought stress (Foolad, 2005). Heat stress induced by late sowing of wheat reduced days to booting by 4-14% in variety 'Shatabdi', 'BARI Gom 27 and 'BARI Gom 28' in the north-western part of Bangladesh (Hossain and Teixeira da Silva, 2012; Hossain et al., 2017; *Fig. 4*). Similarly,

http://www.aloki.hu ● ISSN 1589 1623 (Print) ● ISSN 1785 0037 (Online)
DOI: http://dx.doi.org/10.15666/aeer/1704_83078332

Hakim et al. (2012) noticed that days to maturity in different wheat cultivars were significantly decreased under late sown condition (LS) as compared to optimum sowing (OS), which was probably due to heat stress at the reproductive phase. These reports suggested that number of days to attain specific phenological stage are affected by the change in sowing date and alterations in soil moisture availability and prevailing temperature. However, such effects were lesser for drought and heat stress tolerant wheat cultivars (Hassanuzzaman et al., 2013).

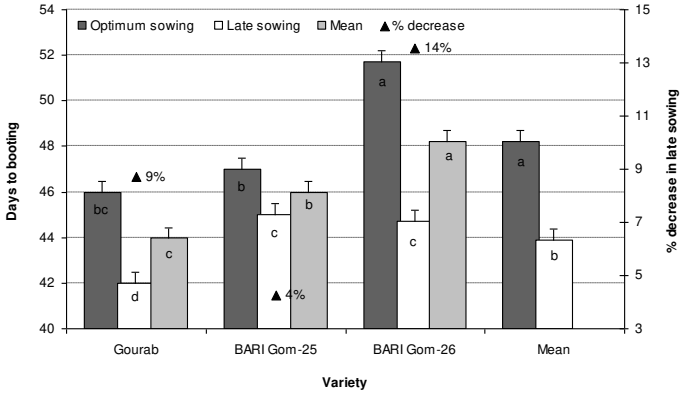

Figure 3. *Days to booting of wheat varieties as influenced by very late sown heat stress conditions in north-western part of Bangladesh. (Source: Hossain and Teixeira da Silva, 2012)*

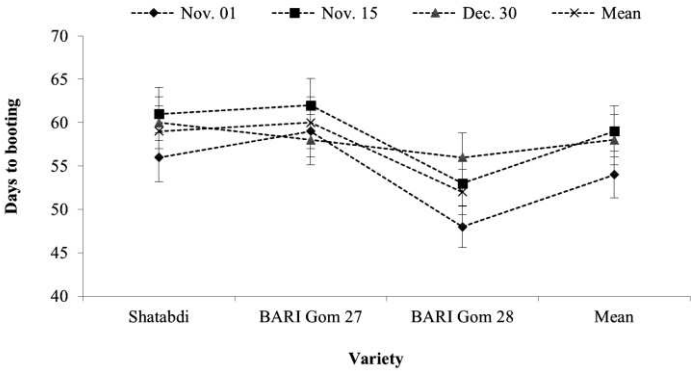

Figure 4. *Number of days to booting in three wheat varieties when sown on three different dates in North-Western Bangladesh (Source: Hossain et al., 2017)*

Days to first awn development

Ear emergence or first visble awn developmental stage is sensitive to heat stress. For example, Foolad (2005) reported that heat stress is most detrimental to wheat crops at the first awn development stage and this heat sensitivity in wheat continues up to 10 to 15 days after flowering. Hossain and Teixeira da Silva (2012) found a considerable genetic variation in days to first visible awn in late sowing wheat genotypes (*Fig. 5*). They further added that such variation in first awn development was associated with degree of sensitivity to heat stress.

Similarly, Reynolds et al. (2000) reported a reduction in the crop growth period in response to the shortage of favourable resources under heat stress, resulting in low total plant biomass, finally low grain yield. Nahar et al. (2010) also found a decrease in the life span of

http://www.aloki.hu ● ISSN 1589 1623 (Print) ● ISSN 1785 0037 (Online)
DOI: http://dx.doi.org/10.15666/aeer/1704_83078332

wheat under late sown induced heat stress condition in Bangladesh. In their study, in late sown condition, the maximum temperature at vegetative and reproduction phases were 25 to 27°C and 30 to 32°C, respectively. However, under environmental condition of south-eastern part of Russian, Hossain et al. (2012b) observed that wheat and barley genotypes took a long time until the first visible awn in early sowing as compared to optimum and late sowing, due to the delay of germination and a long period of vegetative growth due to the low of temperature *(Fig. 6).* They also reported that days to first awn visible was reduced by 19 to 25% (*Fig. 6*) in late sowing conditions, due to high temperature in combined with drought stress (Hossain et al., 2012b). From these reports, it is clear that soil moisture availability and high temperature shorten the time to visible awn, which might have been due to the adverse impact on plant metabolism and available resources.

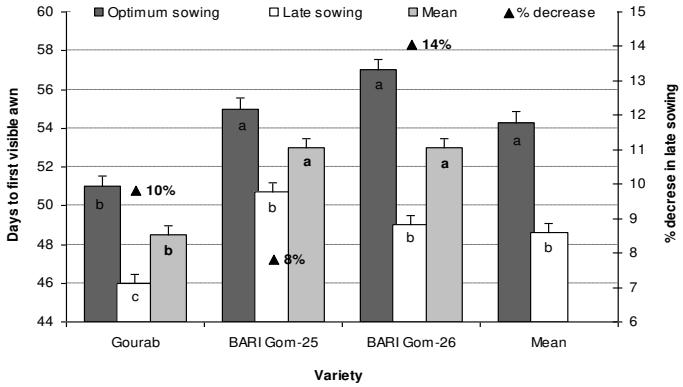

Figure 5. *Number of days to the first visible awn of wheat varieties sown at different dates. Due to different sowing times, wheat plants become exposed to different temperatures at a specific growth stage (Source: Hossain and Teixeira da Silva, 2012)*

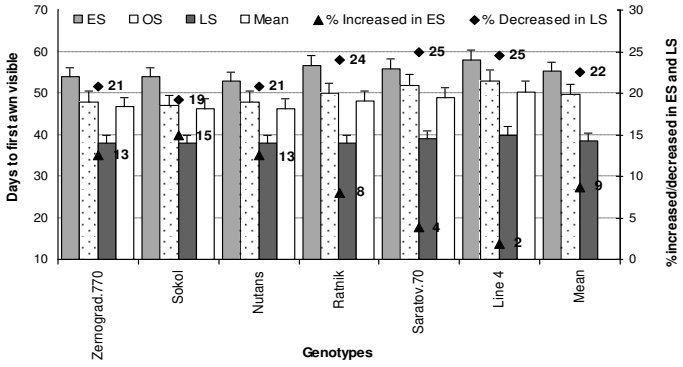

Figure 6. *Days to first awn visible of wheat and barley is influenced by low-temperature at early sown and high temperature with drought stress at late sown condition in the south-eastern part of Russia (Source: Hossain et al., 2012b)*

Days to anthesis

Development of flowers with visible mature anthers is called anthesis stage in wheat. Flowering is regulated by temperature, duration of light and dark (photoperiodic) and plant vigour. Change in temperature alters the time of flowering in wheat plants by changing sowing time. It has been observed that anthesis time can be modulated by

http://www.aloki.hu ● ISSN 1589 1623 (Print) ● ISSN 1785 0037 (Online)
DOI: http://dx.doi.org/10.15666/aeer/1704_83078332

15-20 days (Reynolds and Trethowan, 2007; Prasad et al., 2008). By optimizing sowing date, the temperature at the anthesis stage can be modulated in wheat plants which may favour fertilization. In the environmental condition of Bangladesh, Hossain and Teixeira da Silva (2012) carried out a field research in north-western part of Bangladesh with three wheat varieties sown at optimum (OS) and late sowing (LS) conditions and observed that all evaluated wheat varieties took less time to anthesis, due to the harmful effect of high temperature and drought and all varieties decreased the life span from 10 to 21% to complete anthesis (*Fig. 7*).

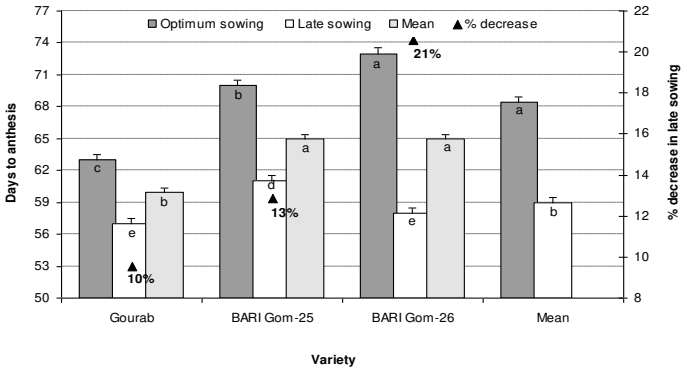

Figure 7. *Days required to anthesis of wheat varieties are influenced by the very late sown heat stress condition in the climatic condition of north-western Bangladesh (Source: Hossain and Teixeira da Silva, 2012)*

Similar results were also reported by Ubaidullah et al. (2006), who found that late sown wheat faced adverse effect of high temperature (25-33°C) stress at a reproductive stage under the condition of Pakistan that ultimately leads to decrease the yield of wheat. However, heat stress tolerant wheat cultivars had a lesser impact on yield. These reports suggested that exposure of wheat plants to episodes of high temperature at the initial stage of reproductive phase cause yield losses due to either shortening of plant growth period or due to adverse effects of high temperature on fertilization, or grain filling process. It is already well established that high temperature affects meiosis and gametogenesis in anthers which results in poor development of pollen grain and hence fertilization.

Days of physiological maturity

Under stress condition, most of the crops try to finish their developmental phases within a shorter period of time (Hakim et al., 2012; Hossain et al., 2012a,b,c, 2013). Araus et al. (2007) argued that environmental factors such as temperature and drought accelerate the time to reach different growth stages of wheat but this effect may vary with the type of cultivar and stress imposition at the specific phenological stage. Ubaidullah et al. (2006) found that heading, grain-filling and physiological maturity period of wheat crops in Pakistan were significantly different with the change in sowing time. Similarly, Prasad et al. (2008) found that late-sown spring wheat took fewer days to anthesis, grain-filling, and physiological maturity due to exposure to heat stress in India. The effect of heat stress on late-sown heat wheat crops was also confirmed by Hossain and Teixeira da Silva (2012) (*Fig. 8*) in the north-western climate condition of

http://www.aloki.hu ● ISSN 1589 1623 (Print) ● ISSN 1785 0037 (Online)
DOI: http://dx.doi.org/10.15666/aeer/1704_83078332

Bangladesh, where they observed that a temperature >30°C during grain-filling forced late-sown crop to mature earlier than the crop sown at the optimum time. These reports suggested that detailed understanding of differential sensitivity to varying temperature and soil moisture availability induced by different sowing times in different agro-ecological zones is necessary for selection of superior wheat genotypes.

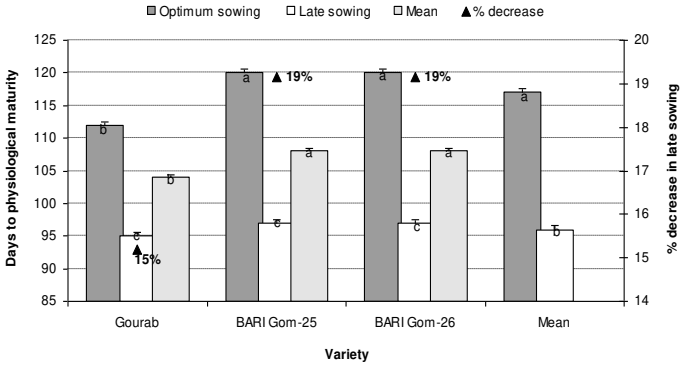

Figure 8. *Required days to physical maturity of three wheat varieties are influenced by very late sown heat stress conditions of north-western Bangladesh (Source: Hossain and Teixeira da Silva, 2012)*

Growth and development of wheat as affected by drought and heat stress

High temperatures along with low moisture availability particularly in late sown crop reduced the growth and yield of spring wheat in different agro-ecological regions of the world including the arid and semi-arid region of the Mediterranean environment. Heat stress in late sown induced accelerate leaf senescence, abscission of the shoot and cause poor root growth (Vollenweider and Gunthardt-Goerg, 2005; Martiniello and Teixeira da Silva, 2011). These reports suggested that the adverse effect of heat stress due to late sowing reduced the wheat growth and yield by affecting vegetative growth traits that are translated in to yield. Understanding the effects of heat and soil moisture availability on these agronomic traits and its relationship with wheat yield will help in devising management strategies to overcome this problem.

Plant population of wheat in relation to stress tolerance

Plant population of field crops generally depends on seed rate, genotypes, germination percentage and seed-bed environment, especially soil moisture and temperature (Khajeh-Hosseini et al., 2003; Hossain et al., 2013). Similarly, Wazid et al. (2004), Hossain et al. (2012a,b,c) and Mumtaz et al. (2015) observed that the number of plants m^{-2} was higher in early sown wheat genotypes followed by optimum sowing and late sowing. Planting density was strongly influenced by the availability of soil moisture and favourable temperature at germination. They also reported that plants m^{-2} reduced by 12-70% in late sowing due to low temperature and low soil moisture. Al-Karaki et al. (2007) reported that the combined effect of high air temperature and drought was critical for reducing the per cent seed germination, finally plant population was lower under combined stresses than the individual stress. Hampson and Simpson (1990) and Hossain et al. (2012b; *Fig. 9*) reported that soil moisture deficit postpones the germination rate of wheat, causes unequal plants per unit area, and finally reduce the

http://www.aloki.hu ● ISSN 1589 1623 (Print) ● ISSN 1785 0037 (Online)
DOI: http://dx.doi.org/10.15666/aeer/1704_83078332

seed yield and quality of wheat. Although above-mentioned reports suggested that temperature variation during seed germination affect plant density which results in lower yield, there are published reports which demonstrated that plant density 80-400 plants/m^2 did not show any change in yield because of other factors such as tillering (Fischer et al., 2019).

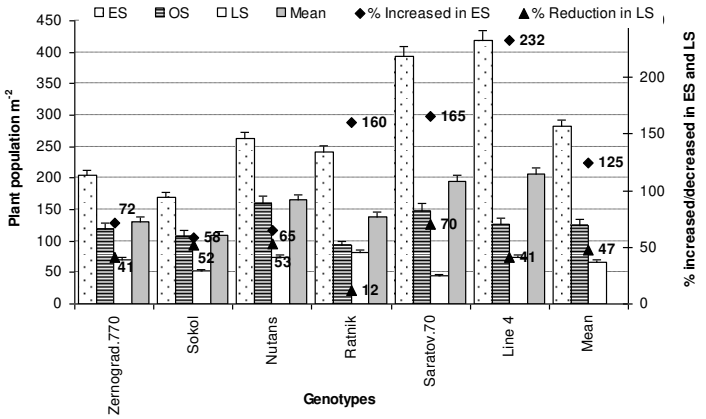

Figure 9. *Plants m^{-2} of all wheat & barley genotypes is affected by low (early sowing) and high temperature with drought (late sowing) in the environmental condition of south-eastern part of Russia (Source: Hossain et al., 2012b)*

However, the yield of spring wheat cultivars with erect growth habit planted at higher altitude is highly sensitive to plant density and row spacing. In addition, yield sensitivity to plant density and row spacing is moderate in winter wheat. However, at low soil moisture availability, optimum plant density become reduced (Fischer et al., 2019).

Tillering capability of wheat under heat and drought stresses

Wheat tillers generally grow from the axils of the main shoot leaves, the potential numbers of tillers depend on the type of species or its genetic makeup and prevailing temperature (Hossain et al., 2012a,b). Shifting in sowing dates (early or late sown) change temperature at a specific plant reduced the number of tillers (Patil et al., 2001; Singh and Pal, 2003; Subhani, 2010). While assessing the impact of different planting dates on tillering in wheat in a two-year experiment in Pakistan, Mumtaz et al. (2015) reported that late sowing reduced the number of tillers. They further added that the reduction in the number of tillers per unit area is positively associated with an increased temperature at the tillering stage. Upadhyay et al. (2015) stated that numbers of effective tillers were significantly superior for crop sown on 20th November followed by 10th December, to late sown on 30th October. The effective number of tillers decreased with early and delayed sowings, due to environmental stresses (Herbek and Lee, 2009; Hossain et al., 2012b; *Fig. 10*). Although a substantial amount of evidence is available that number of tillers per unit area is co-determined by cultivar characteristics, agronomic practice such as sowing date and environmental factors mainly thermal conditions, developing general consensus on phenological responses to changing sowing dates as climate warming is not an easy task because of different genetic makeup of different wheat cultivars.

http://www.aloki.hu ● ISSN 1589 1623 (Print) ● ISSN 1785 0037 (Online)
DOI: http://dx.doi.org/10.15666/aeer/1704_83078332

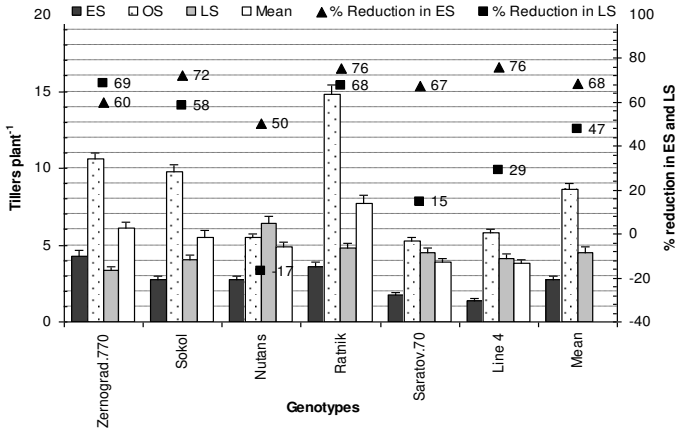

Figure 10. *Tillers plant^{-1} of all wheat and barley genotypes is influenced by low-temperature stress in early sowing and high temperature combine with drought in late sowing conditions (Source: Hossain et al., 2012b)*

Dry matter partitioning of wheat and barley genotypes as influenced by high-temperature

Under favourable environment, 80 to 90% of the carbohydrates is translocated to the grain and rest of 10 to 20% is reserve to wheat plant's (Spiertz and Vos, 1985). Ahamed et al. (2010) found that dry matter partitioning and yield in five wheat varieties was influenced by the heat stress (30 to 32°C) under late sowing. Hossain et al. (2012b; *Fig. 11*) found that most of the existing spring wheat and barley genotypes in the south-eastern part of Russia were highly sensitive to high temperature and drought in late sown condition, whereas in early sowing generally rainfed spring wheat and barley face low-temperature stress. Despite a higher plant population in early sowing, tillers production plant^{-1} was low due to low-temperature stress. This caused 10 to 42% reduction in dry biomass of early-sown crop. While, the late sown crop suffered 57 to 81% reduction in dry biomass due to high temperature (with low soil moisture and low relative humidity in air) that ultimately affected rate of seed germination (*Fig. 9*), tillers plant^{-1} (*Fig. 10*), and grain yield (Reynolds et al., 2000; Hossain et al., 2012b; *Fig. 11*).

Gupta et al. (2002) found the maximum dry weight in wheat genotypes under optimum sown conditions as compared to those of late sown conditions. The late sown wheat genotypes faced unfavourable conditions during germination to reproductive stages that ultimately lead to decreased final biomass accumulation of wheat cultivars. Similarly, Jat et al. (2013) found the maximum dry matter at optimum sown crops as compared to late sown crops. Ahamed et al. (2010) conducted an experiment with five wheat varieties ('Sourav', 'Pradip', 'Sufi', 'Shatabdi' and 'Bijoy') under two sowing times (at November 30 and December 30) and found the highest dry matter partitioning in 'Shatabdi' under heat stress environment but 'Prodip' and 'Sufi' produced the lowest dry matter partitioning, which indicated that dry matter partitioning of a genotype fully depend on genetic makeup of the specific variety. Similarly, Khichar and Niwas (2007) reported that delayed sowing resulted in a decrease in biomass and grain yields, due to the unfavourable environment during late sown conditions, especially high temperature and water deficit. Mondal et al. (2016) also reported that optimizing of sowing date can significantly enhance biomass yield of wheat. These reports suggested that

http://www.aloki.hu ● ISSN 1589 1623 (Print) ● ISSN 1785 0037 (Online)
DOI: http://dx.doi.org/10.15666/aeer/1704_83078332

environmental factors affect plant metabolism associated with translocation of photo-assimilates from source to sink.

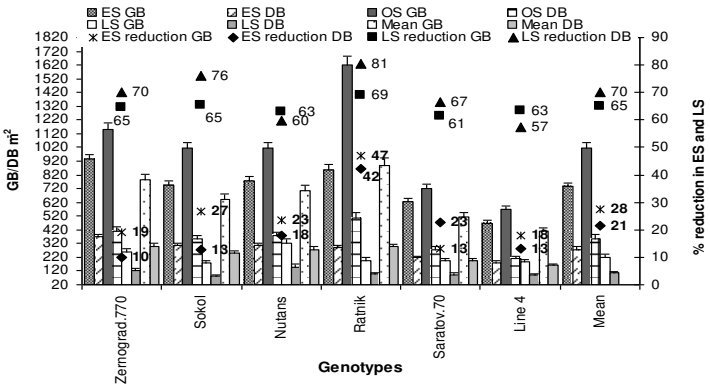

Figure 11. *Dry and green biomass of rainfed spring wheat and barley are affected by in early sowing low-temperature stress and heat stress in combination with drought stress in late sowing conditions in south-eastern part of Russia. GB-green biomass and DB-dry biomass (Hossain et al., 2012b)*

Plant height of wheat and barley genotypes as affected by high-temperature stress

Hossain et al. (2012b) observed a significant genotypic and environmental effect on the height of wheat genotypes under early and late sown conditions (*Fig. 12*). They also found that plant height in early and late sowing was lower, due to low-temperature in early sowing, while high temperature combined with drought in late sowing (Hossain et al., 2012b; *Fig. 12*). It is suggested that prevailing temperature at early growth stage regulated plant height probably through gibberellic acid biosynthesis or GA signaling response pathway.

Yield and yield attributes of wheat genotypes influenced by heat and drought stress

Tillers m^{-2}, spikes m^{-2}, grains $spike^{-1}$, number of fertile tillers m^{-2}, 1000-grain weight, spike length, spike weight, stem weight and awn length in wheat are considered most important yield contributing characters that are positively correlated with final grain weight of wheat and thus are the most important parameter for screening wheat genotypes in breeding programs (Forgone, 2009). However, drought and heat are the two significant environmental factors that limiting crop productivity through influencing the yield attributes of wheat (Prasad et al., 2008). However, interaction of environmental and genetic factors has a significant role in obtaining high productivity as reported by Shahin and Valiollah (2009). Maralian et al. (2010) observed that tillering and heading stages were sensitive to drought, and can reduce up to 37% grain yield. Mirbahar et al. (2009) reported that drought stress significantly decreased the spike length, spikelets per spike, grains $spike^{-1}$ and 1000-grain weight of wheat. The maximum reduction in all traits was observed in terminal drought, while post- and pre-flowering drought significantly influenced the 1000-grain weight (Abdoli et al., 2013).

Grain yield of wheat genotypes is strongly influenced by heat stress. Hossain and Teixeira da Silva (2012) found that the grain yield of wheat varieties significantly decreased when sown late compared with optimum sowing time (*Fig. 13*). Similarly, Barutçular et al. (2017) reported that cultivation of wheat under heat stress conditions

http://www.aloki.hu ● ISSN 1589 1623 (Print) ● ISSN 1785 0037 (Online)
DOI: http://dx.doi.org/10.15666/aeer/1704_83078332

recorded significantly lower grain yield. The inhibited kernel weight at maturity was the result of high temperature which shortened the grain filling period (Wardlaw, 2002). The grain yield reduction in wheat was associated with delayed sowing, which exposed the reproductive phase of plants to high temperature (Mostafa et al., 2009). Menshawy (2007) found that delayed sowing reduced the grain yield by shortening the grain filling process, and kernels achieved maturity before completion of filling.

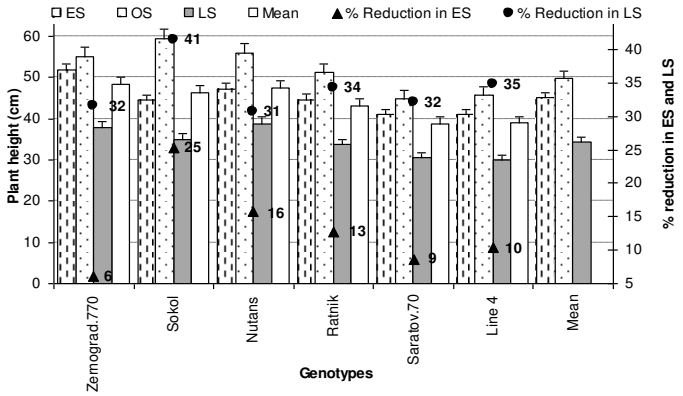

Figure 12. *Plant height (cm) of wheat and barley genotypes is influenced by low-temperature stress in early sowing and high temperature combine with drought stress in late sowing conditions (Hossain et al., 2012b)*

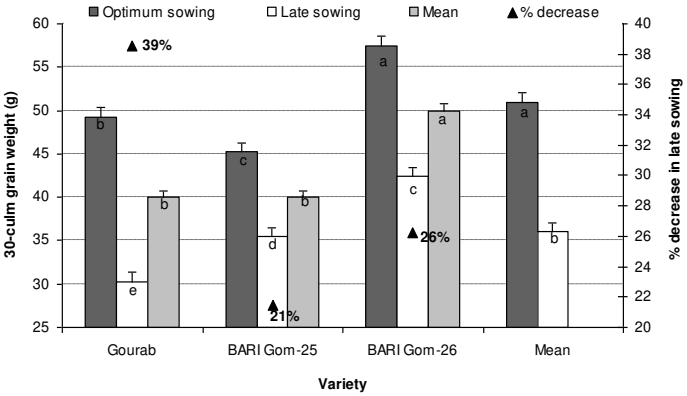

Figure 13. *Grain yield of wheat varieties is influenced by late sown heat stress condition (Hossain and Teixeira da Silva, 2012)*

Stone and Nicolas (1994) reported that high temperature during grain filling reduced grain weight and pre-anthesis decreased the grain number in wheat (Wardlaw et al., 1989; Wardlaw and Moncur, 1995). Subedi et al. (2007) found variation in grain yield and yield attributes among wheat genotypes grown at delay sowing comparing optimum sowing could be attributed through hampering of grain filling process that is high temperatures arisen at late sown wheat shortened the grain filling period.

The occurrence of drought stress along with the high temperature in the arid region is the most frequent after heading and grain filling that remarkably influences grain yield of wheat crop (Balla et al., 2011; Saleh, 2011). Hozayn and El-Monem (2010) reported that the decrease in growth and yield attributes of wheat might be due to water stress

http://www.aloki.hu ● ISSN 1589 1623 (Print) ● ISSN 1785 0037 (Online)
DOI: http://dx.doi.org/10.15666/aeer/1704_83078332

during grain filling stage; while Zeidan et al. (2009) associated grain yield reduction in wheat with drought-induced photosynthetic inhibition.

Physiological and biochemical traits

High-temperature and water availability influence the photosynthetic capacity of plants including wheat (Chaves et al., 2009; Efeoglu et al., 2009). Chlorophyll content and stem reserves are very sensitive to high-temperature (Mohammadi et al., 2009). Singh (2009) observed the variation in the thermo-tolerance and physiological traits of wheat varieties under high-temperature stress. Hence, leaf chlorophyll content could be used as an indicator to determine the performance of the photosynthetic rate and reflect the photosynthetic potential (Hussain et al., 2018). Li et al. (2006) found that drought tolerance in wheat genotypes was associated with leaf chlorophyll content. Xia (2012) reported that heat, as well as drought stress tolerance, was positively associated with photosynthetic capacity. Recently, Ogbaga et al. (2018) suggested that developing thermos-tolerance in photosynthetic machineries such as in rubisco or rubisco activase will result in enhanced crop productivity. Stay-green plants have been used to select for yield stability and a selection criterion for heat stress tolerance in wheat (Joshi et al., 2007; Christopher et al., 2008). Reynolds and Trethowan (2007) reported that leaf chlorophyll content or stay-green was correlated with the leaf transpiration efficiency, which enhances the water use efficiency (WUE) under drought stress conditions. The studies on the stay-green trait of wheat genotypes are largely elusive (Rehman et al., 2009) and are yet to be evaluated for their association with stress tolerance in the wheat (Cao et al., 2015). Yeganehpoor et al. (2016) noticed that grain yield had a significant positive correlation with leaf area and chlorophyll content. Furthermore, chlorophyll content can simultaneously enhance grain yield, and plants with large leaves and higher chlorophyll content can also produce higher grain yield. These reports suggested that the amount of chlorophyll regulates the light harvesting capacity of plants which is sensitive to both heat and drought stress. In addition, photosynthetic pigment sensitivity to abiotic stresses is cultivar specific in wheat, thus could be used as selection criteria for selecting tolerant cultivars.

The reduction in the CO_2 assimilation rate in drought-stressed plants is mainly due to the reduction in leaf stomatal conductance (Chaves et al., 2009). Therefore, stomatal conductance could be used as a reliable indicator of growth rate responses to drought stress at the whole plant or canopy level (Munns et al., 2010). However, metabolism limitation to photosynthesis in drought or heat stressed plants are also well established. For example, the reduction in photosynthesis is the result of adverse effects on the metabolic process that lead to growth inhibition, stomatal closure with consecutive reduction of transpiration (Yordanov et al., 2003). Similarly, Zhang et al. (2009) reported that the soluble carbohydrate content was lower in stressed plants than that of well-watered wheat plants. Araus et al. (2007) reported that leaf physiological aspects such as water potential, chlorophyll content, photosynthetic rate, stomatal conductance, and transpiration rate are associated with the physiological adaptation of crops to environmental stress. Increase in transpiration lowers the plant water status which affects cell division and cell enlargement. For example, Manivannan et al. (2007) suggested that water deficit can significantly reduce leaf area development in wheat genotypes by arresting the cell enlargement. Similarly, Almeselmani et al. (2011) reported that relative water content (RWC) indicates the water status of the cells and have a positive correlation with production and stress tolerance. However, transpiration

http://www.aloki.hu ● ISSN 1589 1623 (Print) ● ISSN 1785 0037 (Online)
DOI: http://dx.doi.org/10.15666/aeer/1704_83078332

through stomates regulates leaf or canopy temperature. For instance, when transpiration rate is low in wheat plants under drought stress conditions, the canopy temperatures of plants at both vegetative and anthesis stages were higher than in plants under control conditions (Siddique et al., 2000). Balota et al. (2007) proposed that low canopy temperature can be used as a selection criterion for drought tolerance in wheat.

Reactive oxygen species (ROS) are generated in chloroplast, mitochondria and in the cytoplasm upon explore to heat and drought stresses and can cause membrane damage (Larkindale and Knight, 2002). The reduction in the activity of ROS scavenging enzymes has been found under drought conditions (Ahmadi and Baker, 2001). Maria et al. (2008) reported that water deficit could significantly reduce phenoloxidase activity of wheat plants, however, such effect is lesser in stress tolerant genotypes. Although an increase in activities of one or more than two ROS scavenging enzymes may have a role in inducing stress tolerance, it is not necessary that higher activities of ROS scavenging enzymes are associated with stress tolerance. Membrane damage due to ROS generation can be assessed by measuring the extent of lipid peroxidation or leaf electrolyte leakage. Under stress, cellular membrane permeability of plants become increased and often correlated with reduced growth of wheat (Iqbal, 2009). The heat tolerant cultivars had lower leaf electrolyte leakage under heat stress (Thiaw and Hall, 2004) and selection based on low leaf electrolyte leakage can be used as selection criteria for enhancing heat and drought tolerance. Proline accumulation enhances membrane stability under heat or drought stress conditions (Ashraf and Foolad, 2007). The accumulation of proline with high rate in leaves under stressed occurs during the grain filling phase under moderate stress and the role of proline is correlated to a protective action against stress (Zhu et al., 2004). Sugar alcohols enhance the stability of membranes and protein to high-temperature denaturation (Heber and Santarius, 1973).

Correlation among yield attributes and stress tolerance

In the previous section, some physiological indicators for heat and drought stress have discussed. However, agronomic traits and their derived parameters can also be used as selection criteria in the breeding program. Here we describe the importance of agronomic criteria in brief. The relationship between the stress tolerance indices (STIs) and grain yield (GY) can be used to screen the wheat genotypes that are suitable to grow under stress conditions. A positive relationship between GY and each of (stress tolerance indices) MP, GMP, YI, YSI, and RP% were observed (Khan and Kabir, 2014). Mitra (2001) suggested that a significant correlation between GY and STIs of a genotype is suitable to grow under heat stress conditions. Such correlations also hold true for other stresses such as drought. Toorchi et al. (2012) and Khalili et al. (2012) reported that GY was positively correlated with each of GMP, MP, YI, and YSI under heat stress conditions.

The mean values of drought resistance index (DRI) are used for characterizing drought and heat stress tolerance and adaptation of genotypes to stress conditions. Drought stress index (DSI) was negatively correlated with grain yield under cool supplement irrigation. Moreover, heat stress index (HSI) was also positively correlated with grain yield under warm conditions inferring that heat stress was more effective for grain yield than drought stress under the warm environment. The higher values of DRI indicated more tolerance in wheat genotypes under stress environments and might be used as stress tolerant index (STI) in wheat breeding programs (EL-Shawy et al., 2017; Barutçular et al., 2016a, 2017). Since modern wheat varieties are not sufficiently

http://www.aloki.hu ● ISSN 1589 1623 (Print) ● ISSN 1785 0037 (Online)
DOI: http://dx.doi.org/10.15666/aeer/1704_83078332

stressed tolerant, developing cultivars tolerant to heat is challenging for wheat breeders (Timsina and Connor, 2001). Rahman et al. (2009) found that stress resistance genotype had a higher value (%) of relative performance (RP %). Similarity, compared with RP% at late sown condition (high temperature and drought) genotype 'Nutans' (57%) performed better than 'Saratov.70' (18%), while at early sowing low-temperature stress condition, genotype 'Zernograd.770' (74%) was highly resistant to low-temperature stress and 'Saratov.70' (27%) was recorded as heat sensitive (Hossain and Teixeira da Silva, 2012; *Fig. 14*).

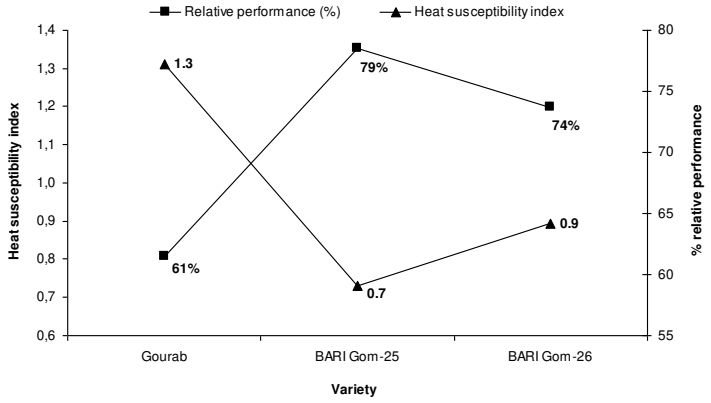

Figure 14. *Relative performance (%) and heat susceptibility index of three wheat varieties in very late heat stress condition, as compared with optimum sowing (Hossain and Teixeira da Silva, 2012)*

Similarly, Hossain et al. (2012a) found that three genotypes had SSI higher than 1.0 under late sowing condition (high temperature) indicating susceptible to stress, while other two genotypes (SSI <1, indicating tolerant to high temperature in combined with drought) (*Fig. 15*). A number of researchers suggested that stress tolerance indices (STIs), stress tolerance (TOL) (Rosielle and Hamblin, 1981), mean productivity (MP) (Clarke and McCaig, 1982), geometric mean productivity (GMP) (Ramirez and Kelly, 1998), stress susceptibility index (SSI) (Fischer and Maurer, 1978), and STI (Fernandez, 1992) can be used to identify high-yielding varieties with improved tolerance to stress.

Approaches to enhance drought and heat stress tolerance in wheat

Development and selection of wheat genotypes are aimed at enhancing yield under existing climatic conditions. Various strategies including seed dressing/coating, seed soaking, and foliar application of plant growth regulators, osmoprotectants and antioxidants have been used to enhance stress tolerance in wheat plants. Moreover, another organic compound like yeast extract (YE) is a natural source of several growth substances that positively effect to mitigate the deleterious influence of drought stress (Hammad and Ali, 2014). Barnett et al. (1990) found that YE has a significant role in regulating vegetative and reproductive growth of plant under stress condition. Nagodawithana (1991) found that exogenous application of amino acids or yeast on wheat lead to a significant improvement in all growth traits under stress conditions compared to control. El-Nabarawy (2001) reported that amino acids or yeast play a significant role in the synthesis of chlorophyll content. Furthermore, Wanas (2002)

http://www.aloki.hu ● ISSN 1589 1623 (Print) ● ISSN 1785 0037 (Online)
DOI: http://dx.doi.org/10.15666/aeer/1704_83078332

recorded that the yeast improved the chlorophyll while delayed the degradation and senescence in plants. Osmoregulators protect plants through osmotic adjustment by maintaining membrane integrity, protecting the macromolecular structure, and stabilization of proteins and enzymes (Ashraf and Foolad, 2007; Hayat et al., 2012). There are several reports indicating that abiotic stress triggers the accumulation of proline in plant tissues (Slama et al., 2014). Moreover, exogenous application of proline caused an increase in endogenous level in plants subjected to water stress conditions and induced plant tolerance (Ashraf and Foolad, 2007; Ali et al., 2008). Glycine betaine (GB) plays an essential role in the protection of photosynthetic apparatus from photo-damage (Zhao et al., 2007), and involvement of GB in the regulation of the activities of antioxidant enzymes has been reported by Wang et al. (2010).

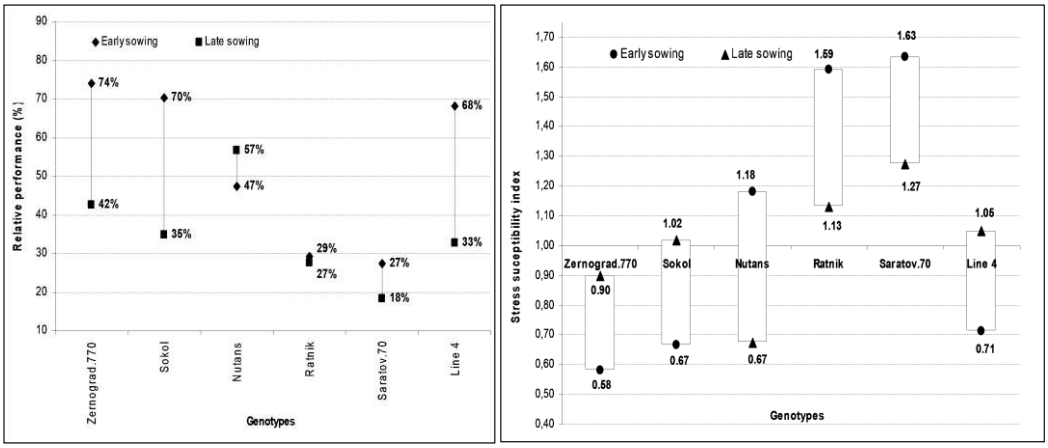

Figure 15. *Relative yield performance (%) and stress susceptibility index of different genotypes under ES-early sowing and LS-late sowing (Source: Hossain et al., 2012a)*

In addition to osmoprotectants, antioxidants are also being used to regulate stress tolerance such as salicylic acid, ascorbic acid etc. Salicylic acid (SA) is useful for the establishment of systemic acquired resistance in plants (Larkindale and Huang, 2005). Ascorbic acid (AsA), is an antioxidant that plays a beneficial role in cell growth and division, differentiation and metabolism in plants (Athar et al., 2009). Xu et al. (2015) observed that foliar application of AsA ameliorates the adverse effects of drought stress by controlling the stomatal closure, nutrient uptake, total chlorophyll content, protein synthesis, transpiration, photosynthesis, and plant growth. Bakry et al. (2012) applied AsA aiming to control pattern of growth and development coupled with improvement of systemic tolerance against different stressful environments of plants and they reported that AsA enhances plants growth to survive under stress conditions by changing plant structure and function.

Recently, selenium (Se) has been reported to counteract with the detrimental effects of various environmental stresses such as excess water stress (Wang et al., 2010), chilling (Hussain et al., 2016a,b), submergence (Hussain et al., 2016c) and high-temperature stress (Djanaguiraman et al., 2010). It may regulate water status (Kuznetsov et al., 2003), and increase biomass production (Nawaz et al., 2013) by the activation of antioxidant apparatus of water-stressed plants (Hasanuzzaman and Fujita, 2011).

http://www.aloki.hu ● ISSN 1589 1623 (Print) ● ISSN 1785 0037 (Online)
DOI: http://dx.doi.org/10.15666/aeer/1704_83078332

Conclusion and future prospect

The drought and heat stresses may occur simultaneously under natural environments and cause huge crop losses. Thus, selecting cultivars with better drought or heat stress tolerance or breeding for stress tolerance will help in developing stress tolerant cultivars to enhance crop productivity under harsh environmental conditions. The present review synthesizes and elaborates the physiological basis of high temperature and drought stress tolerance in wheat which can be used as selection criteria in wheat breeding program. In addition, some agronomic selection criteria which are valid and useful in selecting stress tolerant wheat cultivars. In addition, to mitigate the adverse effects of these stresses on wheat, optimization of production technology package especially sowing dates, selection of appropriate irrigation at critical growth stages, and/or development of drought and heat-tolerant cultivars will help to sustain grain yield production. Application of natural bio-stimulants, especially amino acids lead to overcome the damaging effects and consequently lead to enhance the growth and yield of wheat under stress environments. In addition, exogenous application of signaling compounds, osmolytes, and certain inorganic salts play a significant role in alleviating stress. Any suitable combinations of these management strategies can enhance stress tolerance of wheat in the Mediterranean environment and similar eco-regions elsewhere. Beside these approaches, applications for soil amendments will also helpful in increasing wheat crop productivity under stressful environments. The review also discussed a positive and negative correlation between (grain yield) GY and stress tolerance indices (such as mean productivity (MP), geometric mean productivity (GMP), yield index (YI), yield stability index (YSI), relative productivity (RP%), stress susceptibility index (SSI), and the tolerance index (TOL)) to scan the genotypes against drought and heat stress. In the future, stress adversities might be minimized by improving tolerance in genotypes and by adopting better agronomic strategies. In the present review, field phenotyping for heat and drought stress tolerance in wheat discussed at length which is based on visual scoring, weighing biomass, stress tolerance indices and physiological traits. However, such practices are time consuming and labor intensive. With the advent of artificial intelligence, robotics, communication and immage processing large number of studies are focused on high throughput phenotyping using spectral sensors and algorithms to assess in depth genotypic variation at specific growth stages. Such advance phenoimic approaches not only helped in identifying physiological responses of crops to drought and heat stress, it will aid in developing stress tolerant crop cultivars. Global interest will increase in this area of research in future for agricultural sustainability.

Conflict of interests. Authors declared no conflict of interests.

REFERENCES

[1] Abdoli, M., Saeidi, M., Jalali-Honarmand, S., Mansourifar, S., Eghbal-Ghobadi, M. E. (2013): Evaluation of some physiological and biochemical traits and their relationships with yield and its components in some improved wheat cultivars under post-anthesis water deficit. – Environmental Stresses in Crop Sciences. 6(1): 47-63. [In Persian with English Summary].

http://www.aloki.hu ● ISSN 1589 1623 (Print) ● ISSN 1785 0037 (Online)
DOI: http://dx.doi.org/10.15666/aeer/1704_83078332

[2] Abdelaal, Kh. A. A., Omara, I. R., Hafez, M. Y., Samar, M. E., EL Sabagh, A. (2018): Anatomical, Biochemical and Physiological Changes in Some Egyptian Wheat Cultivars Inoculated with Puccinia gramini f. sp. tritici f. sp. tritici f.sp. tritici. – Fresenius Environmental Bulletin 27(1): 296-305.
[3] Afzal, M. I., Muhammad, A. I., Zahid, A. C. (2015): Triggering growth and boosting economic yield of late-sown wheat (*Triticum aestivum* L.) with foliar application of allelopathic water extracts. – World Journal of Agricultural Sciences 11(2): 94-100.
[4] Ahamed, K. U., Nahar, K., Fujita, M. (2010): Sowing date mediated heat stress affects the leaf growth and dry matter partitioning in some spring wheat (*Triticum aestivum* L.) cultivars. – The IIOAB Journal 1(3): 1-9.
[5] Ahmadi, A., Baker, D. A. (2001): The effect of water stress on grain filling processes in wheat. – Journal of Agricultural Science 136: 257-269.
[6] Alghabari, F., Ihsan, M. Z., Hussain, S., Aishia, G., Daur, I. (2015): Effect of Rht alleles on wheat grain yield and quality under high temperature and drought stress during booting and anthesis. – Environmental Science and Pollution Research 20: 15506-15515.
[7] Ali, Q., Ashraf, M., Shahbaz, M., Humera, H. (2008): Ameliorating effect of foliar applied proline on nutrient uptake in water stressed maize (*Zea mays* L.) plants. – Pakistan Journal of Botany 40: 211-219.
[8] Al-Karaki, G. N., Al-Ajmi, A., Othman, Y. (2007): Seed germination and early root growth of three barley cultivars as affected by temperature and water stress. – American-Eurasian Journal of Agricultural and Environmental Science 2(2): 112-117.
[9] Almansouri, M., Kinet, J. M., Lutts, S. (2001): Effect of salt and osmotic stresses on germination in durum wheat (*Triticum durum* Desf.). – Plant and Soil 231: 243-254.
[10] Almeselmani, M., Abdullah, F., Hareri, F., Naaesan, M., Ammar, M. A., Kanbar, O. Z., Saud, A. (2011): Effect of drought on different physiological characters and yield component in different Syrian durum wheat varieties. – Journal of Agricultural Science 3: 127-133.
[11] Araus, J., Ferrio, J., Buxo, R., Voltas, J. (2007): The historical perspective of dry land agriculture: lessons learned from 10000 years of wheat cultivation. – Journal of Experimental Botany 58(2): 131-145.
[12] Ashraf, M., Foolad, M. R. (2007): Roles of glycine betaine and proline in improving plant abiotic stress resistance. – Environmental and Experimental Botany 59: 206-216.
[13] Athar, H. R., Khan, A., Ashraf, M. (2009): Inducing salt tolerance in wheat by exogenously applied ascorbic acid through different modes. – Journal Plant Nutrition 32: 1799-1817.
[14] Bakry, A. B., Abdelraouf, R. E., Ahmed, M. A., El Karamany, M. F. (2012): Effect of drought stress and ascorbic acid foliar application on productivity and irrigation water use efficiency of wheat under newly reclaimed sandy soil. – Journal of Applied Scientific Research 8(8): 4552-4558.
[15] Balla, K., Rakszegi, M., Li, Z. G., Bekes, F., Bencze, S., Veisz, O. (2011): Quality of winter wheat in relation to heat and drought shock after anthesis. – Czech Journal of Food Science 29: 117-128.
[16] Balota, M., Payne, W. A., Evett, S. R., Lazar, M. D. (2007): Canopy Temperature Depression Sampling to Assess Grain Yield and Genotypic Differentiation in Winter Wheat. – Crop Science 47: 1518-1529.
[17] Barnett, J. A., Payne, R. W., Yarrow, D. (1990): Yeast Characteristics and Identification. – second ed. Press, Cambridge Univ., London, UK, 1012 p.
[18] Barutçular, C., EL Sabagh, A., Konuskan, O., Saneoka, H., Yoldash, K. M. (2016a): Evaluation of maize hybrids to terminal drought stress tolerance by defining drought indices. – Journal of Experimental Biology and Agricultural Sciences 4: 610-616.
[19] Barutcular, C., Yıldırım, M., Koç, M., Akıncı, C., Tanrıkulu, A., EL Sabagh, A., Saneoka, H., Ueda, A., Islam, M. S., Toptas, I., Albayrak, O., Tanrikulu, A. (2016b):

http://www.aloki.hu ● ISSN 1589 1623 (Print) ● ISSN 1785 0037 (Online)
DOI: http://dx.doi.org/10.15666/aeer/1704_83078332

Quality traits performance of bread wheat genotypes under drought and heat stress conditions. – Fresenius Environmental Bulletin 25(12a): 6159-6165.

[20] Barutcular, C., Yildirim, M., Koc, M., Akinci, C., Toptac, I., Albayrak, O., Tanrikulu, A., El Sabagh, A. (2016c): Evaluation of SPAD chlorophyll in spring wheat genotypes under different environments. – Fresenius Environmental Bulletin 25(4/2016a): 1258-1266.

[21] Barutçular, C., EL Sabagh, A., Koç, M., Ratnasekera, D. (2017): Relationships between Grain Yield and Physiological Traits of Durum Wheat Varieties under Drought and High Temperature Stress in Mediterranean Conditions. – Fresenius Environmental Bulletin 26(4): 4282-4291.

[22] Basu, S., Ramegowda, V., Kumar, A., Pereira, A. (2016): Plant adaptation to drought stress. – F1000Research, 5, F1000 Faculty Rev-1554. doi:10.12688/f1000research.7678.1.

[23] Bernardi, M. (2011): Understanding user needs for climate services in agriculture. – Bulletin, Volume 60(2). <http://www.wmo.int/pages> (Accessed on 06 April 2019).

[24] Cao, X., Mondal, S., Cheng, D. (2015): Evaluation of agronomic and physiological traits associated with high temperature stress tolerance in the winter wheat cultivars. – Acta Physiologiae Plantarum 37: 90. doi:10.1007/s11738-015-1835-1836.

[25] Chakrabarti, B., Singh, S. D., Nagarajan, S., Aggarwal, P. K. (2011): Impact of temperature on phenology and pollen sterility of wheat varieties. – Australian Journal of Crop Science 5(8): 1039-1043.

[26] Chaves, M. M., Maroco, J. P., Pereira, J. S. (2003): Understanding plant response to drought- from genes to the whole plant. – Functional Plant Biology 30: 239-264.

[27] Christopher, J. T., Manschadi, A. M., Hammer, G. L., Borrell, A. K. (2008): Stay green wheat for Australia's changing dry environment. – In: Appels, R., Eastwood, R., Lagudah, E., Langridge, P., Mackay, M., McIntyre, L., Sharp, P. (eds.) 11th International wheat genetics symposium 2008—Proceedings, vol 1. Sydney University Press, Sydney, pp 119-120.

[28] Clarke, J. M., McCaig, T. N. (1982): Evaluation of techniques for screening for drought resistance in wheat. – Crop Science 22(3): 503-506.

[29] Djanaguiraman, M., Prasad, P. V. V., Seppanen, M. (2010): Selenium protects sorghum leaves from oxidative damage under high temperature stress by enhancing antioxidant defense system. – Plant Physiology and Biochemistry 48(12): 999-1007.

[30] Efeoglu, B., Terzioglu, S. (2009): Photosynthetic responses of two wheat varieties to high temperature. – European Asia Journal of Biological Science 3: 97-106.

[31] El-Nabarawy, M. A. (2001): Mitigation of dark induced senescence. 1 – By some amino acids. – Annals of Agriculture Science Moshtohor University 39(1): 225-232.

[32] EL Sabagh, A., Hossain, A., Barutçular, C., Anjorin, F., Islam, M. S., Ratnasekera, D., Kizilgeçi, F., Yadav, G. S., Yıldırım, M., Saneoka, H. (2018a): A revıew on varıous factors whıch affectıng sustaınable maıze (*Zea mays* l.) productıon under drought stress. – Journal of Experimental Biology and Agricultural Sciences 5(6): 779-794.

[33] EL-Shawy, E. E., EL Sabagh, A., Mansour, M., Barutcular, C. (2017): A comparative study for drought tolerance and yield stability in different genotypes of barley (*Hordeum vulgare* L.). – Journal of Experimental Biology and Agricultural Sciences 5(2): 151-162.

[34] Farooq, M., Bramley, H., Palta, J. A., Siddique, K. H. (2011): Heat stress in wheat during reproductive and grain-filling phases. – Critical Review of Plant Science 30: 491-507.

[35] Fernandez, G. C. J. (1992): Effective selection criteria for assessing stress tolerance. – In: Kuo, C. G. (ed.) Proc. Int. Sym. Adaptation of Vegetables and Other Food Crops in Temperature and Water Stress, Publication, Tainan, Taiwan.

[36] Fischer, R. A., Maurer, R. (1978): Drought resistance in spring wheat cultivars. I. Grain yield response. – Australian Journal of Agricultural Research 29: 897-907.

http://www.aloki.hu ● ISSN 1589 1623 (Print) ● ISSN 1785 0037 (Online)
DOI: http://dx.doi.org/10.15666/aeer/1704_83078332

[37] Fischer, R. A., Ramos, O. M., Monasterio, I. O., Sayre, K. D. (2019): Yield response to plant density, row spacing and raised beds in low latitude spring wheat with ample soil resources: An update. – Field Crops Research 232: 95-105.
[38] Fleury, D., Jefferies, S., Kuchel, H., Langridge, P. (2010): Genetic and genomic tools to improve drought tolerance in wheat. – Journal of Experimental Botany 61(12): 3211-3222.
[39] Foolad, M. R. (2005): Breeding for abiotic stress tolerances in tomato. – In: Ashraf, M., Harris, P. J. C. (eds.) Abiotic Stresses: Plant resistance through breeding and molecular approaches, The Haworth Press Inc., New York, USA. p. 613-684.
[40] Forgone, A. G. (2009): Physiological indicators of drought tolerance of wheat. – Biology PhD Program. University of Szeged Faculty of Science and Informatics Department of plant Biology, Szeged.
[41] Gupta, N. K., Shukla, D. S., Pande, P. C. (2002): Interaction of yield determining parameters in late sown wheat genotypes. – Indian Journal of Plant Physiology 7(3): 204-269.
[42] Hakim, M. A., Hossain, A., Teixeira da Silva, J. A., Zvolinsky, V. P., Khan, M. M. (2012): Yield, protein and starch content of 20 wheat (*Triticum aestivum* L.) genotypes exposed to high temperature under late sowing conditions. – Journal of Scientific Research 4(2): 477-489.
[43] Hammad, S. A. R., Ali, O. A. M. (2014): Physiological and biochemical studies on drought tolerance of wheat plants by application of amino acids and yeast extract. – Annals of Agricultural Science 59(1): 133-145.
[44] Hampson, C. R., Simpson, G. M. (1990): Effect of temperature, salt and osmotic potential on early growth of wheat (*Trticum aestivum* L.). I. Germination. – Canadian Journal of Botany 68: 524-528.
[45] Hasanuzzaman, M., Fujita, M. (2011): Selenium pretreatment upregulates the antioxidant defense and methylglyoxal detoxification system and confers enhanced tolerance to drought stress in rapeseed seedlings. – Biological Trace Element Research 143(3): 1758-1776.
[46] Hasanuzzaman, M., Nahar, K., Alam, M., Roychowdhury, R., Fujita, M. (2013): Physiological, biochemical, and molecular mechanisms of heat stress tolerance in plants. – International Journal of Molecular Sciences 14(5): 9643-9684.
[47] Hayat, S., Hayat, Q., Alyemeni, M. N., Wani, A. S., Pichtel, J., Ahmad, A. (2012): Role of proline under changing environments: A review. – Plant Signaling and Behavior 7: 1-11.
[48] Heber, U., Santaius, K. A. (1973): Cell death by cold and heat and resistance to extreme temperature. Mechanisms of hardening and dehardning. – In: Prechts, H., Christophersen, J., Hensel, H., Larcher, W. (eds.) Temperature and life. pp: 232-263.
[49] Herbek, J., Lee, C. (2009): A Comprehensive Guide to Wheat Management in Kentucky. – U.S. Department of Agriculture, M. Scott Smith, Director, Cooperative Extension Service, University of Kentucky College of Agriculture, Lexington, and Kentucky State University, Frankfort. <http://www.uky.edu/Ag/GrainCrops/ID125Section2.htm> (Last accessed 13 February 2018). (Last accessed 24 May 2019).
[50] Hoegh-Guldberg, O., Jacob, D., Taylor, M., Bindi, M., Brown, S., Camilloni, I., Diedhiou, A., Djalante, R. (2018): Impacts of 1.5ºC global warming on natural and human systems. – In: Global Warming of 1.5°C an IPCC special report on the impacts of global warming of 1.5°C above pre-industrial levels and related global greenhouse gas emission pathways, in the context of strengthening the global response to the threat of climate change. Chapter 3. Intergovernmental Panel on Climate Change. International Institute for Applied Systems Analysis (IIASA) - Schlossplatz 1 - A-2361 Laxenburg, Austria. Available link: http://pure.iiasa.ac.at/id/eprint/15518/.
[51] Hossain, M. M., Hossain, A., Alam, M. A., EL Sabagh, A., Khandakar Faisal Ibn Murad, Haque, M. M., Muriruzzaman, M., Islam, M. Z., Das, S., Barutcular, C., Kizilgeci, F.

http://www.aloki.hu ● ISSN 1589 1623 (Print) ● ISSN 1785 0037 (Online)
DOI: http://dx.doi.org/10.15666/aeer/1704_83078332

(2018): Evaluation of fifty spring wheat genotypes grown under heat stress condition in multiple environments of Bangladesh. – Fresen. Environ. Bull. 27: 5993-6004.

[52] Hossain, A., Sarker, M. A. Z., Saifuzzaman, M., Akhter, M. M., Mandal, M. S. N. (2009): Effect of sowing dates on yield of wheat varieties and lines developed since 1998. – Bangladesh Journal of Progressive Science and Technology 7(1): 5-8.

[53] Hossain, A., Sarker, M. A. Z., Hakim, M. A., Lozovskaya, M. V., Zvolinsky, V. P. (2011): Effect of temperature on yield and some agronomic characters of spring wheat (*Triticum aestivum* L.) genotypes. – International Journal Agricultural Research Innovation and Technology 1(1): 44-54.

[54] Hossain, A., Teixeira da Silva, J. A. (2012): Phenology, growth and yield of three wheat (*Triticum aestivum* L.) varieties as affected by high temperature stress. – Notulae Scientia Biologicae 4(3): 97-106.

[55] Hossain, A., Teixeira da Silva, J. A., Lozovskaya, M. V., Zvolinsky, V. P., Mukhortov, V. I. (2012a): High temperature combined with drought affect rainfed spring wheat and barley in south-eastern Russia: yield, relative performance and heat susceptibility index. – Journal of Plant Breeding and Crop Science 4(11): 184-196.

[56] Hossain, A., Teixeira da Silva, J. A., Lozovskaya, M. V., Zvolinsky, V. P. (2012b): High temperature combined with drought affect rainfed spring wheat and barley in South-Eastern Russia: I. Phenology and growth. – Saudi Journal of Biological Sciences 19(4): 473-487.

[57] Hossain, A., Teixeira da Silva, J. A., Lozovskaya, M. V., Zvolinsky, V. P. (2012c): The Effect of High Temperature Stress on the Phenology, Growth and Yield of Five Wheat (*Triticum aestivum* L.) Genotypes. – The Asian and Australasian Journal of Plant Science and Biotechnology 6(1): 14-23.

[58] Hossain, A., Teixeira da Silva, J. A. (2013): Wheat production in Bangladesh: its future in the light of global warming. – AoB Plants published online January 8, 2013, 5: pls042 (Annals of Botany Company). doi: 10.1093/aobpla/pls042.

[59] Hossain, A., Sarker, M. A. Z., Saifuzzaman, M., Teixeira da Silva, J. A., Lozovskaya, M. V., Akhter, M. M. (2013): Evaluation of growth, yield, relative performance and heat susceptibility of eight wheat (*Triticum aestivum* L.) genotypes grown under heat stress. – International Journal of Plant Production 7(3): 615-636.

[60] Hossain, A., Islam, M. R., Rahman, K. A. M. M., Rashid, M. H., Anwari, A. (2017): Comparative performance of three wheat (*Triticum aestivum* L.) varieties under heat stress. – International Journal of Natural and Social Sciences 4(3): 26-42.

[61] Hozayn, M., El-Monem, A. A. (2010): Alleviation of the potential impact of climate change on wheat productivity using arginine under irrigated Egyptian agriculture. – Opions Méditerranéennes 95: 95-100.

[62] Hussain, S., Khan, F., Hussain, H. A., Nie, L. (2016a): Physiological and biochemical mechanisms of seed priming-induced chilling tolerance in rice cultivars. – Frontiers in Plant Science. doi: 10.3389/fpls.2016.00116.

[63] Hussain, S., Khan, F., Cao, W., Geng, M. (2016b): Seed priming alters the production and detoxification of reactive oxygen intermediates in rice seedlings grown under sub-optimal temperature and nutrient supply. – Frontiers in Plant Science doi: 10.3389/fpls.2016.00439.

[64] Hussain, S., Yin, H., Peng, S., Khan, F. A., Khan, F., Huang, J., Cui, K., Nie, L. (2016c): Comparative transcriptional profiling of primed and non-primed rice seedlings under submergence stress. – Frontiers in Plant Science. doi: 10.3389/fpls.2016.01125.

[65] Hussain, H. A., Hussain, S., Khaliq, A., Ashraf, U., Anjum, S. A., Men, S., Wang, L. (2018): Chilling and Drought Stresses in Crop Plants: Implications, Cross Talk, and Potential Management Opportunities. – Frontiers in Plant Science. doi: 10.3389/fpls.2018.00393.

http://www.aloki.hu ● ISSN 1589 1623 (Print) ● ISSN 1785 0037 (Online)
DOI: http://dx.doi.org/10.15666/aeer/1704_83078332

[66] Iqbal, S. (2009): Physiology of Wheat (*Triticum aestivum* L.) Accessions and the Role of Phytohormones under Water Stress. – Ph.D. Thesis, Fac. of Biological Sci., Quaid-i-azam Univ., Islamabad, pp. 83-154.
[67] Iqbal, M. A., Imtiaz, H., Muzammil, H. S., Essa, A., Zahoor, A. (2018): Probing profitability of irrigated and rainfed bread wheat (*Triticum aestivum* L.) crops under foliage applied sorghum and moringa extracts in Pakistan. – Custos e Agronegocio 14(2): 2-16.
[68] Jahan, M. A. H. S., Hossain, A., Jaime, A., Da Silva, T., EL Sabagh, A., Rashid, M. H., Barutçular, C. (2019): Effect of Naphthaleneacetic Acid on Root and Plant Growth and Yield of Ten Irrigated Wheat Genotypes. – Pakistan Journal of Botany 51(2): 451-459.
[69] Jat, L. K., Singh, S. K., Latre, A. M., Singh, R. S., Patel, C. B. (2013): Effect of dates of sowing and fertilizer on growth and yield of wheat (*Triticum aestivum* L.) in an Inceptisol of Varanasi. – Indian Journal Agronomy 58(4): 611-614.
[70] Joshi, A. K., Chand, R., Arun, B., Singh, R. P., Ortiz, R. (2007): Breeding crops for reduced-tillage management in the intensive, rice-wheat systems of South Asia. – Euphytica 153(1-2): 135-151.
[71] Khajeh-Hosseini, M., Powell, A. A., Bingham, I. J. (2003): The interaction between salinity stress and seed vigour during germination of soybean seeds. – Seed Science Technology 31: 715-725.
[72] Khalili, M., Naghavi, M. R., Pour Aboughadareh, A. R., Talebzadeh, S. J. (2012): Evaluating of drought stress tolerance based on selection indices in spring canola cultivars (*Brassica napus* L.). – Journal of Agricultural Science 4(11): 78-85.
[73] Khan, A. A., Kabir, M. R. (2014): Evaluation of spring wheat genotypes (*Triticum aestivum* l.) for heat stress tolerance using different stress tolerance indices. – Cercetari Agronomice in Moldova 47(4): 49-63. doi: 10.1515/cerce-2015-0004.
[74] Khichar, M. L., Niwas, R. (2007): Thermal effect on growth and yield of wheat under different sowing environments and planting systems. – Indian Journal Agricultural Research 41(2): 92-96.
[75] Kosina, P., Reynolds, M. P., Dixon, J., Joshi, A. (2007): Stakeholder perception of wheat production constraints, capacity building needs and research partnerships in the developing countries. – Euphytica 157: 475-483.
[76] Kuznetsov, V. V., Kholodova, V. P., Kuznetsov, V. V., Yagodin, B. A. (2003): Selenium regulates the water status of plants exposed to drought. – Doklady Biological Sciences 390: 266-268.
[77] Larkindale, J., Knight, M. R. (2002): Protection against heat stress induced oxidative damage in Arabidopsis involves calcium, abscisic acid, ethylene, and salicylic acid. – Plant Physiology 128: 682-695.
[78] Larkindale, J., Huang, B. (2005): Effects of abscisic acid, salicylic acid, ethylene and hydrogen peroxide in thermos-tolerance and recovery for creeping bent-grass. – Plant Growth Regulator 47: 17-28.
[79] Li, R. H., Guo, P. G., Baum, M., Grando, S., Ceccarelli, S. (2006): Evaluation of chlorophyll content and fluorescence parameters as indicators of drought tolerance in barley. – Agriculture Science in China 5(10): 751-757.
[80] Mahboob, A. S., Arain, M. A., Khanzada, S., Naqvi, M. H., Dahot, M. U., Nizamani, N. A. (2005): Yield and quality parameters of wheat genotypes as affected by sowing dates and high temperature stress. – Pakistan Journal of Botany 37(3): 575-584.
[81] Majid, M. A., Islam, M. S., Sabagh, A. E. L., Hasan, M. K., Barutcular, C., Ratnasekera, D., Islam, M. S. (2017): Evaluation of growth and yield traits in corn under irrigation regimes in sub-tropical climate. – Journal of Experimental Biology and Agricultural Science 5(2):143-150.
[82] Manivannan, P., Jaleel, C. A., Sankar, B., Kishore, K. A., Somasundaram, R., Alagu, Lakshmanan, G. M., Panneerselvam, R. (2007): Growth, biochemical modifications and

http://www.aloki.hu ● ISSN 1589 1623 (Print) ● ISSN 1785 0037 (Online)
DOI: http://dx.doi.org/10.15666/aeer/1704_83078332

proline metabolism in Helianthus annuus L. as induced by drought stress. – Colloids Surf. B: Biointerf. 59: 141-149.

[83] Maralian, H., Ebadi, A., Didar, T. R., Haji-Eghrari, B. (2010): Influence of water deficit stress on wheat grain yield and proline accumulation rate. – African Journal of Agricultural Reserach 5(4): 286-289.

[84] Maria, A. M., Gendy, A. A., Selim, A. H., Abd El-All, A. M. (2008): Response of wheat plants grown under water stress in relation to Jasmonic acid. – Minufiya Journal of Agricultural Research 33(6): 1355-1375.

[85] Martiniello, P., Teixeira da Silva, J. A. (2011): Physiological and bio–agronomical aspects involved in growth and yield components of cultivated forage species in Mediterranean environments: A review. – European Journal of Plant Science and Biotechnology 5 (Special Issue 2): 64-98.

[86] Menshawy, A. M. M. (2007): Evaluation of some early bread wheat genotypes under different sowing dates:1 Earliness characters. – Fifth plant breeding conference (May). Egypt Journal of Plant Breeding 11(1): 25-40.

[87] Mirbahar, A. A., Markhand, G. S., Mahar, A. R., Abro, S. A., Kanhar, N. A. (2009): Effect of water stress on yield and yield components of wheat (*Triticum aestivum* L.) varieties. – Pakistan Journal of Botany 41(3): 1303-1310.

[88] Mitra, J. (2001): Genetics and genetic improvement of drought resistance in crop plants. – Current Science 80: 758-762.

[89] Mondal, S., Singh, R. P., Mason, E. R., Huerta-Espino, J., Autrique, E., Joshi, A. K. (2016): Grain yield, adaptation and progress in breeding for early-maturing and heat-tolerant wheat lines in South Asia. – Field Crops Research 192: 78-85.

[90] Mostafa, H. A. M., Hassanein, R. A., Khalil, S. I., El-Khawas, S. A., El-Bassiouny, H. M. S., El-Monem, A. A. (2009): Effect of arginine or putrescine on growth, yield and yield components of late sowing wheat. – Journal of Applied Scientific Reserach 6: 177-183.

[91] Mumtaz, M. Z., Aslam, M., Nasrullah, H. M., Akhtar, M., Ali, B. (2015): Effect of Various Sowing Dates on Growth, Yield and Yield Components of Different Wheat Genotypes. – American-Eurasian Journal of Agricultural and Environmental Science 15(11): 2230-2234.

[92] Munns, R., James, R. A., Sirault, X. R. R., Furbank, R. T., Jones, H. G. (2010): New Phenotyping Methods for Screening Wheat and Barley for Beneficial Responses to Water Deficit. – Journal of Experimental Botany 61(13): 3499-3507.

[93] Nagodawithana, W. T. (1991): Yeast Technology. – Universal foods corporation Milwaukee, Wisconsin. Van Nostrand Reinhold, New York, 273 p.

[94] Nahar, K., Ahamed, K. U., Fujita, M. (2010): Phenological variation and its relation with yield in several wheat (*Triticum aestivum* L.) cultivars under normal and late sown mediated heat stress condition. – Notulae Scientia Biologicae 2(3): 51-56.

[95] Ogbaga, C. C., Stepien, P., Athar, H. U. R., Ashraf, M. (2018): Engineering Rubisco activase from thermophilic cyanobacteria into high-temperature sensitive plants. – Critical Reviews in Biotechnology 38(4): 559-572.

[96] Out, H., Celiktas, V., Duzenli, S., Hossain, A., El Sabagh, A. (2018): Germination and early seedling growth of five durum wheat cultivars (*Triticum durum* desf.) is affected by different levels of salinity. – Fresenius Environmental Bulletin 27(11): 7746-7757.

[97] Patil, K. S., Durga, D. V., Phadnawis, B. N., Shivankar, R. S., Rathod, T. H. (2001): Effect of sowing dates on biomass production of wheat cultivars. – Annals of Plant Physiology 14(2): 115-119.

[98] Prasad, P. V. V., Pisipati, S. R., Ristic, Z., Bukovnik, U., Fritz, A. K. (2008): Impact of nighttime temperature on physiology and growth of spring wheat. – Crop Science 48: 2372-2380.

http://www.aloki.hu ● ISSN 1589 1623 (Print) ● ISSN 1785 0037 (Online)
DOI: http://dx.doi.org/10.15666/aeer/1704_83078332

[99] Rahman, M. M., Hossain, A., Hakim, M. A., Kabir, M. R., Shah, M. M. R. (2009): Performance of wheat genotypes under optimum and late sowing condition. – International Journal of Sustainable Crop Production 4(6): 34-39.
[100] Ramirez-Vallejo, P., Kelly, J. D. (1998): Traits related to drought resistance in common bean. – Euphytica 99(2): 127-136.
[101] Rehman, A., Habib, I., Ahmad, N., Hussain, M., Khan, M. A., Farooq, J., Ali, M. A. (2009): Screening wheat germplasm for heat tolerance at terminal growth stage. – Plant Omics 2(1): 9-19.
[102] Reynolds, M. P., Delgado, M. I., Gutiérrez–Rodríguez, M., Larqué–Saavedra, A. (2000): Photosynthesis of wheat in a warm, irrigated environment. I: Genetic diversity and crop productivity. – Field Crops Research 66: 37-50.
[103] Reynolds, M. P., Trethowan, R. M. (2007): Physiological interventions in breeding for adaptation to abiotic stress. – In: Spiertz, J. H. J. (ed.) Scale and complexity in plant systems research, gene-plant-crop relations. Springer, Dordrecht, the Netherlands. pp. 129-146.
[104] Rosegrant, M. W., Agcaoili, M. (2010): Global food demand, supply, and price prospects to 2010. – International Food Policy Research Institute, Washington, D.C. USA.
[105] Rosielle, A. A., Hamblin, J. (1981): Theoretical aspect of selection for yield in stress and non-stress environment. – Crop Science 21: 943-946.
[106] Saleh, S. H. (2011): Performance, correlation and path coefficient analysis for grain yield and its related traits in diallel crosses of bread wheat under normal irrigation and drought conditions. – World Journal of Agricultural Science 7: 270-279.
[107] Shahin, Y., Valiollah, R. (2009): Effects of row spacing and seeding rates on some agronomical traits of spring canola (*Brassica napus* L.) cultivars. – Journal of Central European Agriculture 10(1): 115-122.
[108] Siddique, B. M. R., Hamid, A., Islam, M. S. (2000): Drought stress effect on water relation of wheat. – Botanical Bulletin of Academia Sinica 41: 35-39.
[109] Singh, S., Pal, M. (2003): Growth, yield and phenological response of wheat cultivars to delayed sowing. – Indian Journal of Plant Physiology 8(3): 277-286.
[110] Singh, S. (2009): Variation in physiological traits for thermos-tolerance in wheat. – Indian Journal of Plant Physiology 14: 407-412.
[111] Slama, I., Rejeb, K. B., Rouached, A., Jdey, A., Rabhi, M., Talbi, O., Debez, A., Savouré, A., Abdelly, C. (2014): Presence of proline in salinized nutrient solution reenforces the role of this amino acid in osmoregulation and protects lipid membrane peroxidation in *Arabidopsis thaliana*. – Australian Journal of Crop Science 8: 1367-1372.
[112] Spiertz, J. H. J., Vos, J. (1985): Grain growth of wheat and its limitations by carbohydrate and nitrogen supply. – In: Day, W., Atkin, R. K. (eds.) Wheat growth and modeling. Plenum press, New York. p. 129-141.
[113] Stone, P. J., Nicolas, M. E. (1994): Wheat cultivars vary widely in their responses of grain yield and quality to short periods of post anthesis heat stress. – Australian Journal of Plant Physiology 21: 887-900.
[114] Subedi, K. D., Ma, B. L., Xue, A. G. (2007): Planting Date and Nitrogen Effects on Grain Yield and Protein Content of Spring Wheat. – Crop Science 47: 36-44.
[115] Subhani, R. (2010): Effect of temperature on development and grain formation in spring wheat. – Pakistan Journal of Botany 42(2): 899-906.
[116] Tarchoun, N., M'hamdi, M., Teixeira da Silva, J. A., Mehouachi, T. (2012): Approaches to evaluate the sensitivity of hot pepper floral structures to low night temperature. – European Journal of Horticultural Science 77(2): 78-83.
[117] Thiaw, S., Hall, A. E. (2004): Comparison of selection for either leaf electrolyte-leakage or pod set in enhancing heat tolerance and grain yield of cowpea. – Field Crops Research 86: 239-253.
[118] Timsina, J., Connor, D. J. (2001): The productivity and sustainability of rice-wheat cropping systems: issues and challenges. – Field Crop Research 69: 93-132.

http://www.aloki.hu ● ISSN 1589 1623 (Print) ● ISSN 1785 0037 (Online)
DOI: http://dx.doi.org/10.15666/aeer/1704_83078332

[119] Ubaidullah, R., Mohammad, T., Hafeezullah, A. S., Nassimi, A. W. (2006): Screening of wheat (*Triticum aestivum* L.) genotypes for some important traits against natural terminal heat stress. – Pakistan Journal of Biological Science 9: 2069-2075.
[120] Upadhyay, R. G., Ranjan, R., Negi, P. S. (2015): Influence of sowing dates and varieties on productivity of wheat under mid Himalayan region of Uttarakhand. – International Journal of Tropical Agriculture 33(2): 1905-1909.
[121] Vollenweider, P., Gunthardt–Goerg, M. S. (2005): Diagnosis of abiotic and biotic stress factors using the visible symptoms in foliage. – Environmental Pollution 137: 455-465.
[122] Wahid, A., Gelani, S., Ashraf, M., Foolad, M. R. (2007): Heat tolerance in plants: An overview. – Environmental and Experimental Botany 61: 199-233.
[123] Wanas, A. L. (2002): Response of faba bean (*Vicia faba,* L.) plants to seed soaking application with natural yeast and carrot extracts. – Annals of Agricultural Science Moshtohor University 40(1): 83-102.
[124] Wang, G. P., Zhang, X. Y., Li, F., Luo, Y., Wang, W. (2010): Over accumulation of glycine betaine enhances tolerance to drought and heat stress in wheat leaves in the protection of photosynthesis. – Photosynthetica 48: 117-126.
[125] Wardlaw, I. F., Dawson, I. A., Munibi, P. (1989): The tolerance of wheat to high temperatures during reproductive growth: II. Grain development. – Australian Journal of Agricultural Research 40: 15-24.
[126] Wardlaw, I. F., Moncur, L. (1995): The response of wheat to high temperature following anthesis. I. The rate and duration of kernel filling. – Australian Journal of Plant Physiology 22: 391-397.
[127] Wardlaw, I. F. (2002): Interaction between drought and chronic high temperature during kernel filling in wheat in a controlled environment. – Annals of Botany 90: 469-476.
[128] Wazid, A., Hussain, A., Ahama, A., Ahamad, A. R., Ibrahim, A. M., Mussaddique, M. (2004): Effect of sowing date and plant population on biomass, grain yield and yield components of wheat. – International Journal of Agriculture and Biology 6: 1003-1005.
[129] Xia, Y. (2012): Photosynthesis-related physiological responses of field-grown maize to plant density and nitrogen stress during vegetative and reproductive stages. – Ph.D. Dissertation. Purdue University.
[130] Xu, Y., Xu, Q., Huag, B. (2015): Ascorbic acid mitigation of water stress-inhibition of root growth in association with oxidative defense in tall fescue (*Festuca arundinacea* Schreb.). – Frontiers in Plant Science 6(807): 1-14.
[131] Yassin, M., Mekawy, A. M., EL Sabagh, A., Islam, M. S., Hossain, A., Barutcular, C., Alharby, H., Bamagoos, A., Liu, L., Ueda, A., Saneoka, H. (2019): Physiological and biochemical responses of two bread wheat (*Triticum aestivum* L.) genotypes grown under salinity stress. – Applied Ecology and Environmental Research 17(2): 5029-5041.
[132] Yeganehpoor, F., Salmasi, S. Z., Kolvanagh, J. S., Golezani, K. G., Dastborhan, S. (2016): Changes in growth, chlorophyll content and grain yield of Coriander (*Coriandrum sativum* L.) in response to water stress, chemical and biological fertilizers and salicylic acid. – International Journal of Advanced Biological and Biomedical Research 5(1): 228-236.
[133] Yıldırım, M., Barutçular, C., Hossain, A., Koç, M., Dizlek, H., Akinci, C., Toptaş, I., Basdemir, F., Islam, M. S., EL Sabagh, A. (2018): Assessment of The Grain Quality of Wheat Genotypes Grown Under Multiple Environments Using GGE Biplot Analysis. – Fresenius Environmental Bulletin 27(7): 4830 - 4837.
[134] Yordanov, I., Velikova, V., Tsonev, T. (2003): Plant responses to drought and stress tolerance. – Bulgarian Journal of Plant Physiology pp. 187-206.
[135] Zeidan, E. M., El-Hameed, A., Bassiouny, A. H., Waly, A. A. (2009): Effect of irrigation intervals, nitrogen and organic fertilization on yield, yield attributes and crude protein content of some wheat cultivars under newly reclaimed saline soil conditions. – Proc. of

http://www.aloki.hu ● ISSN 1589 1623 (Print) ● ISSN 1785 0037 (Online)
DOI: http://dx.doi.org/10.15666/aeer/1704_83078332

the 4th Conf. on Recent Technol. in Agric. November 3-5, 2009, Cairo, Giza, Egypt. pp: 298-307.

[136] Zhang, J., Dell, B., Conocono, E., Waters, I., Setter, T., Appels, R. (2009): Water deficits in wheat: fructan exohydrolase (1-FEH) mRNA expression and relationship to soluble carbohydrate concentrations in two varieties. – New Phytologist 181: 843-850.

[137] Zhao, X. X., Liang, C., Fang, Y., Wang, Y. Q., Wang, W. (2007): Effect of glycinebetaine on function of thylakoid membranes in wheat flag leaves under drought stress. – Biologia Plantarum 51(3): 584-588.

[138] Zhu, L. H., van de Peppel, A., Li, X. Y., Welander, M. (2004): Changes of leaf water potential and endogenous cytokinins in young apple trees treated with or without paclobutrazol under drought conditions. – Scientia Horticulturae 99(2): 133-141.

http://www.aloki.hu ● ISSN 1589 1623 (Print) ● ISSN 1785 0037 (Online)
DOI: http://dx.doi.org/10.15666/aeer/1704_83078332

SEED PRIMING WITH GLYCINE BETAINE IMPROVE SEED GERMINATION CHARACTERISTICS AND ANTIOXIDANT CAPACITY OF WHEAT (*TRITICUM AESTIVUM* L.) SEEDLINGS UNDER WATER-STRESS CONDITIONS

AHMED, N. – ZHANG, Y. – YU, H. – GABAR, A. – ZHOU, Y. – LI, Z. – ZHANG, M.*

Engineering Research Center of Plant Growth Regulator, Ministry of Education College of Agronomy and Biotechnology, China Agricultural University, Beijing 100193, China (phone: (86)-1062733049)

**Corresponding author*
e-mail: zmc1214@163.com

(Received 1st Mar 2019; accepted 1st May 2019)

Abstract. Water-stress is one of the most adversarial environmental constraints limiting wheat growth and productivity. Seed priming is a promising approach to alleviate the adverse effects of water-stress on seed germination and early seedling establishment. In the current study, we evaluated the effectiveness of Glycine-betaine (GB) to improve seed germination and early seedling establishment of Wheat (Cultivar: Jimai-22) under water-stress conditions. The current study was conducted at the Engineering Research Centre of Plant Growth Regulator, College of Agronomy and Biotechnology, China Agricultural University, Beijing, China, during the year 2018-19. Water-stress significantly reduced seed germination characteristics, shoot/root fresh weight and dry matter accumulation, and relative water content (RWC). Moreover, water-stress aggressively increased the production of Proline, soluble sugars, Hydrogen peroxide (H_2O_2), and Malondialdehyde (MDA) and showed higher electrolyte leakage and reduced membrane stability. However, seed priming with GB significantly alleviated adversities of water-stress on seed germination characteristics and early seedling growth attributes; the effects were more pronounced with GB 50 and 100 mM seed treatment. Seed priming with GB counteracted the overaccumulation of proline, soluble sugars, H_2O_2, and MDA content and increased membrane stability and reduced electrolyte leakage with higher activity of antioxidant enzymes under water-stress treatment. Water-stress tolerance augmented by GB priming might be related to higher antioxidant activity and reduced reactive oxygen species (ROS) accumulation and lipid peroxidation, eventually lower electrolyte leakage and higher membrane stability, all these salient features of GB enhanced survival capability of wheat seedlings under water-stress conditions. The study is a valuable validation for enhancing water-stress tolerance via GB priming, which is of broad-spectrum interest for sustainable agriculture production.
Keywords: *seed treatment, Glycine betaine, seedling vigor, osmolyte accumulation, water-stress tolerance*

Introduction

Water-stress is a serious agronomic problem worldwide and is one of the most important factors reducing crop productivity (Farooq et al., 2012; Li and Liu, 2016). Successful and uniform seed germination is essential for healthy plant growth and development to enhance productivity potential as well as the quality of crop production (Conrath et al., 2006; Cheng et al., 2018). Uneven and delayed seed germination often result in poor seedling establishment. Therefore, it is essential to enhance seed germination and seedling vigor under osmotically stressed conditions. Seed germination and emergence are the primary steps in successful seedling development and crop productivity. Seed germination is defined as a sequence of events that start with the imbibition of dry seeds and that terminate with the elongation of the embryonic radicle (Bewley, 1997; Wolny et al., 2018).

http://www.aloki.hu ● ISSN 1589 1623 (Print) ● ISSN 1785 0037 (Online)
DOI: http://dx.doi.org/10.15666/aeer/1704_83338350

Generally, seeds start the germination process under optimal environmental conditions (i.e., sufficient or optimal water, oxygen and temperature). However, seeds under sub-optimal conditions, such as water stress, salinity, and extreme temperatures, showed uneven germination and poor seedling development (Mahmood et al., 2009; Jisha et al., 2013; Nawaz et al., 2013; Hussain et al., 2016). Extensive research efforts have been carried out in order to improve the crop performance under water deficit conditions. Nevertheless, water deficit is still a major limitation to crop growth and productivity. Typically, seed germination and early seedling growth are less tolerant to environmental fluctuations as compared to mature plants. Thus, soil moisture stress during early growth may result in high mortality rates, leading to reduced crop performance (Chachar et al., 2016).

To enhance seed germination rate and seedling vigor under adverse environmental conditions. The pretreatment of seeds called seed priming is widely practiced in agriculture. Suitable priming treatment enhances seed germination and boosts seedling vigor in different crops. Research demonstrated that variety of chemicals shown potential to act under specific conditions as a defense priming agent against a range of different abiotic stresses (Beckers and Conrath, 2007), such chemicals includes: amino acids; Proline, Glycine-Betaine (Moustakas et al., 2011), hormones; Salicylic acid, Abscisic acid (Srivastava et al., 2010; Nazar et al., 2015), reactive oxygen-nitrogen–sulfur species (Seabra and Oliveira, 2016), mineral priming; Selenium, Calcium chloride (Iqbal et al., 2015) and even water; hydro-priming (Iqbal et al., 2015).

GB priming is an effective strategy to improve seed germination, emergence, and seedling growth of several crop plants, especially under stress conditions (Farooq et al., 2008; Atta et al., 2013; Zhang et al., 2014; Rakshit and Singh, 2018). GB could ameliorate the adversities of oxidative stress by detoxification of ROS both directly or by enhancing the activities of ascorbate peroxidase (APX), glutathione (GSH) and GSH/GSSG, Ascorbate (AsA), mono-dehydro-ascorbate reductase (MDHAR), dehydroascorbate reductase (DHAR), glutathione reductase (GR), glutathione peroxidase (GPX), catalase (CAT), and glyoxalase I (Gly I) in the different crops under adverse environmental conditions (Hasanuzzaman et al., 2014; Gupta and Thind, 2015). For example, Cheng et al. (2018) reported that GB priming increased the chilling stress tolerance of Cotton at the seedling stage, exhibited a higher net photosynthetic rate, improved antioxidant enzyme activity, and lower hydrogen peroxide content and less damage to the cell membranes. Water-stress significantly hindered seed germination and seedling growth, reduced starch metabolism, RWC, and increased cell electrolyte leakage. However, seed priming with GB improved the germination rate, root and shoot length, seedling fresh and dry weights, leaf and root scores, RWC, soluble sugars, and a-amylase activity as compared to unprimed seeds of Maize under chilling stress (Farooq et al., 2008). Similar improvements were also noted for Turfgrass under different stress conditions such as drought, salinity, and temperature (Zhang et al., 2014).

Seed priming has potential to promote uniform and synchronized seedling emergence and enhance the capability of seedlings to establish under unfavorable environmental conditions. Physiologically, seed priming strengthened the antioxidant activities of CAT, POD, SOD, and APX and as well as promoted the accumulation of compatible solutes including reducing sugar, proline, soluble sugars, free amino acids, and soluble proteins contents (Zhang et al., 2015). As a result, seed priming reduced lipid peroxidation and stabilized the cell membranes integrity, resulting in increased stress

http://www.aloki.hu ● ISSN 1589 1623 (Print) ● ISSN 1785 0037 (Online)
DOI: http://dx.doi.org/10.15666/aeer/1704_83338350

tolerance under water-deficit or excessive soil moisture environments (Zhang et al., 2015).

Seed priming with GB could play a significant role during germination and early seedling growth of wheat. Therefore, it is crucial that this method should be employed in wheat production to improve water-stress tolerance by seed priming with GB. In this study, we examined the effects of GB seed priming with different concentrations of GB to optimize suitable concentration and evaluate its effectiveness to improve wheat seed germination and seedlings development under water-stress conditions. We ensured that 50 to 100 mM concentrations of GB for seed priming 12 h were more advantageous for uniform and synchronised seed germination and successful seedling growth. For further insight into the phenomenon, we investigated the activities of different antioxidant enzymes directly involved in detoxification of ROS, triggered by water-stress.

Material And Methods

Growing conditions and treatment details

This study was conducted at the Engineering Research Center of Plant Growth Regulator, College of Agronomy and Biotechnology, China Agricultural University, Beijing, China, during the year 2018-19. The present study was aimed to evaluate the effect of GB seed priming on wheat seed germination and early seedling growth. Wheat (*Triticum aestivum* L.) cultivar "Jimai-22" was used in the current study. Jimai-22 is an inbreed hexaploid wheat cultivar, which is mostly planted by the wheat farmers in North China Plan (Li et al., 2015). To eradicate contamination during seed priming, wheat seeds of uniform size were surface-sterilized with 3% NaClO for 10 minutes. All the glassware and hydroponic solution used in this study were autoclaved before to use. The seed-priming treatments were hydro-priming (HP; distilled water), chemical priming (GB: 10, 25, 50 and 100 mM), and a non-primed control (NP) included for comparison. Wheat seeds were primed in the dark at 25ºC for 12 h with constant gentle shaking in a mechanical shaker. The proportion of seed weight to volume of priming solution was maintained as (w/v) was 1:5 (Hussain et al., 2016). After 12 h of priming treatment, the primed seeds were washed thoroughly with deionized water for 4-5 times, to remove priming agent from the surface of the seeds. The primed seeds were surface-dried using blotting paper and placed to an air- drying oven at 25°C for 48 h to minimize the moisture content to <10%. The experiment was designed in Completely Randomized Design (CRD) with three replications. After achieving required seed moisture content, 20 seeds per replicate were placed in 12.5 cm Petri dish on a double layer of filter paper No.102, moistened with 10 ml of distilled water considered as well-water (control) or with 10 ml of 10% PEG-6000 solution (water-stress). During the experiment, 10 ml of autoclaved distilled water or 10% (w/v) PEG-6000 solution was added to each petridish after every 24 h to maintain constant moisture. The radicle protrusion at 1 mm was recorded as the criterion for germination (Guo et al., 2017). The experiment was conducted in a controlled room (Environmental Growth Chamber, China Agricultural University, Beijing), which was set to maintain 22/18°C (day/night), 60% relative humidity, 12-h photoperiod, and 650 $\mu molm^{-2}$ s^{-1} photosynthetically active radiation at the canopy level. Seedlings kept for eight days under stressed and non-stressed conditions. Growing media solution was changed after every 48 h; the number of seeds germinated after every 12 h was recorded and final germination percentage was calculated when there was no more germination in reach treatment

http://www.aloki.hu ● ISSN 1589 1623 (Print) ● ISSN 1785 0037 (Online)
DOI: http://dx.doi.org/10.15666/aeer/1704_83338350

(day-4). All the seedlings were harvested after eight days of planting, five seedlings from each replicate were used for the root and shoot fresh and dry weight measurements, while the rest of seedlings were wrapped in an aluminum foil and exposed to liquid nitrogen and saved to -80°C for further biochemical studies.

Seed germination characteristics

The following germination characteristics were recorded according to AOSA (1983).
Final germination %

$$(G) = \frac{total\ seeds\ germinated}{total\ \ seeds\ planted} \times 100 \quad \text{(Eq.1)}$$

Germination rate index

$$(\mathrm{GRI}) = (\frac{G1}{1} + \frac{G2}{2} + \frac{G3}{3} + \cdots \frac{Gi}{i}) \quad \text{(Eq.2)}$$

where G1 is the germination percentage on day 1, G2 is the germination percentage on day 2; and so on.
Seedling Vigour Index

$$(\mathrm{SVI}) = \text{shoot lenghth} + \text{root length} \times \mathrm{G} \quad \text{(Eq.3)}$$

Root and shoot length measurement

Fifteen seedlings from each treatment were randomly collected (five for each replicate) for the measurement of the root and shoot length (by using a Vernier caliper) at the 8th day of planting.

Plant growth and biomass accumulation

For the measurement of fresh weight and dry matter accumulation, shoot, and root were separated and weighed for their fresh weight. The shoot/root dry weight was recorded in milligrams after drying in hot air oven (SANYO, Model, MOV-202, Japan) at 80°C ± 5°C for 72 hours. All the related traits were recorded after eight days of planting.

Relative water content (RWC)

The RWC was calculated by using leaves from randomly selected plants; the leaves were cut into about one cm discs and weighed to get fresh weight (FW). Later these leaf discs were soaked in distilled water for 4 h and turgid weight (TW) was recorded, leaves discs were then dried in an oven till constant weight at 80°C to obtain the dry weight (DW). RWC was calculated as

$$\mathrm{RWC\%} = \frac{FW-DW}{\mathrm{TW-DW}} \times 100 \quad \text{(Eq.4)}$$

Malondialdehyde (MDA) and Hydrogen peroxide (H_2O_2) content

Determination of lipid peroxidation in wheat seedlings was done by, Thiobarbituric acid (TBA) test, which determines MDA as an end product of lipid peroxidation (Heath

http://www.aloki.hu ● ISSN 1589 1623 (Print) ● ISSN 1785 0037 (Online)
DOI: http://dx.doi.org/10.15666/aeer/1704_83338350

and Packer, 1968). Plant material (500 mg) was homogenized in 5 ml of 0.1% (w/v) Trichloroacetic acid (TCA) solution. The homogenate was centrifuged at 10000× g for 20 min, and 0.75 ml of the supernatant was added to 1.5 ml of 0.5% (w/v) TBA in 20% TCA. The mixture was incubated in boiling water for 30 min, and then reaction stopped by placing the reaction tubes in an ice bath. Then the samples tubes were centrifuged at 10000×g for 5 min, and the absorbance of the supernatant was recorded at 532 nm by using UNICO UV-2800AH spectrophotometer (UNICO Instrument Co. Ltd., Shanghai). The value for non-specific absorption at 600 nm was subtracted. The following equation was used to calculate MDA concentration using its absorption coefficient (ε) and expressed as μmol Malondialdehyde g^{-1} fresh weight:

$$\text{MDA } (\mu\text{mol } g^{-1} \text{ FW}) = [(A532 - A600) \times Vt \times 1000/\varepsilon] \times Wt \quad \text{(Eq.5)}$$

where ε is the specific extinction coefficient (=155 mM cm^{-1}), Vt is the volume of total extract and Wt is the fresh weight of leaf sample, A600 and A532 is the absorbance at 600 and 532 nm wavelength.

The H_2O_2 concentration was determined according to Alexieva et al. (2001). 500 mg of wheat seedlings (shoot) samples were homogenized in an ice bath with 5 ml of 0.1% (w/v) TCA. The homogenate was centrifuged at 10000×g for 20 min, and 0.5 ml of the supernatant was added to 0.5 ml of 10 mM potassium phosphate buffer (pH 7.0) and 1 ml of 1Molar potassium iodide (KI). The absorbency of the supernatant was recorded on Spectrophotometer at 390 nm. The content of H_2O_2 was given on a standard curve.

Electrolyte leakage, and membrane stability index

Leaf membrane damage was estimated by the recording of electrolyte leakage (EL) as reported by Bajji et al. (2002) with slight modifications. Plant material (500 mg) washed with distilled water and then placed in 15 ml test tubes with 10 ml of deionized water and incubated for 4 h at 25°C. Subsequently, the electrical conductivity (EC) of the samples (R1) was recorded on the EC meter (DDS-12A; Shanghai Kangyi Co., Ltd., Shanghai, China). The samples were then autoclaved at 120°C for 20 minutes, cooled at room temperature and the final conductivity (R2) was recorded on the EC meter. The EL was defined as follows:

$$EL\% = \frac{R1}{R2} \times 100 \quad \text{(Eq.6)}$$

However, Membrane stability index (MSI) was calculated by using the following equation:

$$MSI\% = \frac{1-R1}{R2} \times 100 \quad \text{(Eq.7)}$$

Antioxidant enzymes extraction and assays

Antioxidant enzymes extraction was performed as described in Seckin et al. (2010) with slight modifications. Shoots of wheat seedlings were collected at the 8th day of planting, and immediately placed into liquid nitrogen, then stored at -80°C until used. Approximately 500 mg of leaf sample was rapidly extracted in a pre-chilled mortar on an ice bath with five mL of ice-cold 50 mM sodium phosphate buffer (pH 7.8)

http://www.aloki.hu ● ISSN 1589 1623 (Print) ● ISSN 1785 0037 (Online)
DOI: http://dx.doi.org/10.15666/aeer/1704_83338350

containing 1 mM disodium diammonium acetate (EDTA-Na_2), 1% (w/v) polyvinyl pyrrolidone (PVPP) and 10 mmol / L magnesium chloride. Samples were centrifuged at 12,000×g for 25 min, and the supernatant was used for the determination of antioxidant enzymes activities. Likewise, catalase (CAT, EC 1.11.1.6) activity was estimated by monitoring the initial rate of disappearance of H_2O_2 by using spectrophotometer at 240 nm wavelength according to Cakmak and Horst (1991). Meanwhile, the activity of superoxide dismutase (SOD, EC 1.15.1.1) was determined using the method of Xue et al. (2008). Thus, the peroxidase activity (POD, EC 1.11.1.7) was determined by the guaiacol oxidation method (Nakano and Asada, 1981).

Osmolyte accumulation

Free proline content in shoots of wheat seedlings was extracted with 3% sulfosalicylic acid and centrifuged at 12,000×g. An aliquot was mixed with glacial acetic acid and acidic ninhydrin for 30 minutes at 100°C. The reaction was terminated in an ice bath, and chromophore was extracted with five mL of toluene. The chromophore-containing toluene was warmed to room temperature, and absorbance was recorded on a spectrophotometer at 520 nm (Bates et al., 1973).

Total soluble sugars were extracted from the shoots samples previously stored at -80°C. 500 mg of shoot sample with 5 ml distilled water incubated in hot-water bath at 100°C for 20 minutes, the extract were centrifuged at 12,000×g for 10 min; supernatant was transferred to 15 ml tube, and again 5 ml of distilled water was added into the sample tube and extraction was repeated, supernatants were collected together. The supernatant was mixed with anthrone reagent, heated for 7 min, the reaction was terminated by placing reaction tubes in an ice bath for 10 min and the absorbance was recorded on Spectrophotometer at 625 nm. Total soluble sugars content was recorded according to the method elaborated by Morris (1948) and expressed as mg g^{-1} fresh weight.

Statistical analysis

Statistical analysis and data computations were made using Microsoft Excel 2016 (Microsoft Corporation, Redmond, WA, USA) and Statistix 8.1 (Analytical Software, Tallahassee, USA). Significantly different treatment means were separated using the least significant difference (LSD at 0.05) test.

Results

Seed germination ability, synchronization and seedling characteristics

The seed germination response was varied among different water-stress and priming treatments (*Fig. 1*). Water-stress significantly arrested seed germination. However, seeds primed with distilled water (HP) as well as with different concentrations of GB had better seed germination percentage as compared to NP seeds under well-water and water-stress conditions. The maximum final seed germination % was recorded in seeds primed with GB 50 and 100 mM and had 13% higher seed germination % as compare to non-primed (NP) seeds under well-water conditions. Whereas under water-stress, a similar trend was observed and GB had maximum seed germination of 80% as compared to NP seeds of only 64%.

http://www.aloki.hu ● ISSN 1589 1623 (Print) ● ISSN 1785 0037 (Online)
DOI: http://dx.doi.org/10.15666/aeer/1704_83338350

The germination rate index presented in *Fig. 1*, was also affected by water-stress and priming treatments; the higher germination rate was noted in response to GB priming treatments followed by HP. However, NP showed least germination index both under well-water and water-stress conditions.

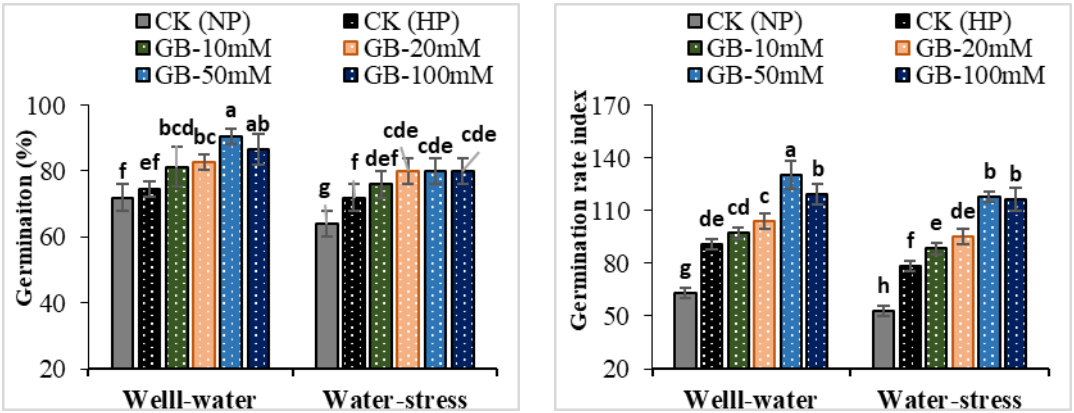

Figure 1. *Effect of different seed priming treatments on seed germination (a) and germination rate index (b) of wheat seeds under well-water (non-stressed) and water-stress (PEG-10%) condition. Control non-primed; CK (NP), Control hydro-primed; CK (HP), Glycine-betaine primed denotes GB. All values represent means ± standard deviations (SD) of three replicates. Bars showing the same letters are not significantly different at P ≤ 0.05 as determined by LSD test*

Shoot, root length

Under well-water conditions, the length of shoot and root was higher in primed seeds as compared to NP seeds. However, water-stress significantly affected seedling's shoot and root morphological characters (*Figs. 2 and 3*).

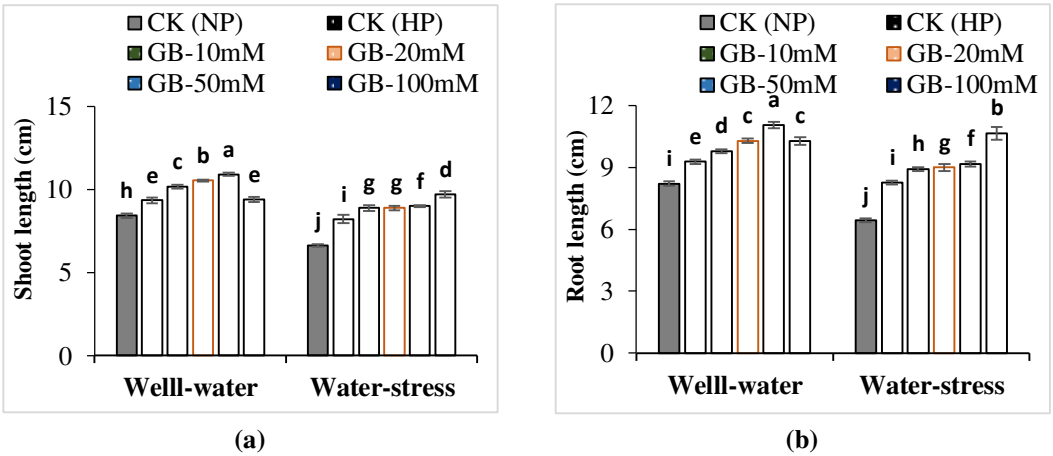

Figure 2. *Effects of different seed priming treatments on shoot length (a) and root length (b) of wheat seedlings under well-water and water-stress conditions. Control non-primed; CK (NP), Control hydro-primed; CK (HP), Glycine-betaine primed denotes GB. All values represent means ± standard deviations (SD) of three replicates. Bars showing the same letters are not significantly different at P ≤ 0.05 as determined by LSD test*

http://www.aloki.hu ● ISSN 1589 1623 (Print) ● ISSN 1785 0037 (Online)
DOI: http://dx.doi.org/10.15666/aeer/1704_83338350

Under well-water treatment seeds primed with GB 50 mM showed contrasting results in term of shoot and root length and showed 29 and 35% higher shoot and root length as compared to NP seeds, however, HP seeds also had significant difference of 11 and 13% higher shoot and root length as compared to NP seeds under well-water treatment. Under water-stress, seeds primed with GB 100mM showed better seedling character in term of the shoot and root length and had 36 and 66% higher shoot and root length as compared to seedlings of NP seeds under water-stress conditions.

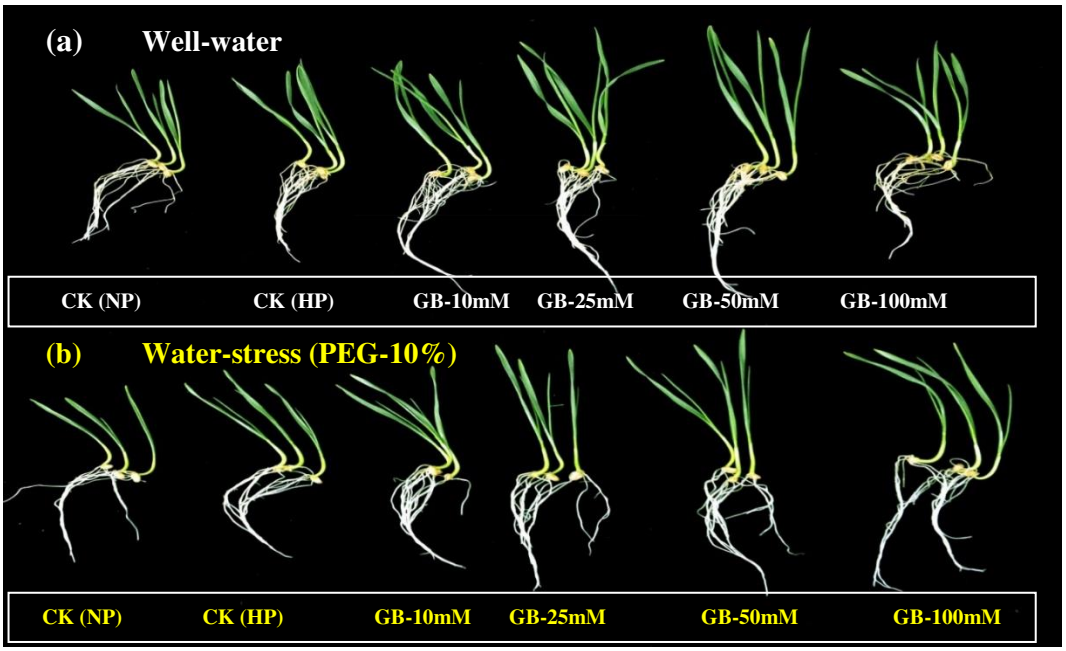

Figure 3. *Effects of different seed priming treatments on morphological characteristics of wheat seedlings under well-water (a) and water-stress (PEG-10) (b) conditions. Control non-primed; CK (NP), Control hydro-primed; CK (HP), Glycine-betaine primed denotes GB*

Shoot, root fresh weight, and dry matter accumulation

The response of wheat seedlings with respect to shoot and root fresh weight and dry matter accumulation were varied among different water and priming treatments (*Fig. 4*). The maximum shoot and root fresh weight were noted in 25 and 50 mM of GB primed seeds as compared to rest of GB, HP and NP primed seeds, however, under water-stress conditions seeds primed with GB 50 and 100 mM showed better performance as compared to seedlings of HP and NP treatments. Under the water-stress condition, NP demonstrated diminishing growth of the seedlings along with a significant decrease in dry weight of shoot and root (*Fig. 4*). Similar to seedling fresh weight, the dry weight of seedlings was also higher in 25 and 50 mM GB primed seeds and under well-water treatment. However, GB 50 and 100 mM were more effective under water-stress treatment and had higher dry matter accumulation as compared to HP and NP seeds.

Seedling vigor index

In the current study, water-stress significantly reduced the seedling vigor index as compared to the well-water treatment (*Fig. 5*). Irrespective of water-stress effects, seeds primed with GB significantly increase the seedling vigor index as compared to HP and

http://www.aloki.hu ● ISSN 1589 1623 (Print) ● ISSN 1785 0037 (Online)
DOI: http://dx.doi.org/10.15666/aeer/1704_83338350

NP seed treatments. The more prominent increase in seedling vigor was revealed by GB 100 mM seed priming followed by 50, 25 and 10 mM under water-stress treatment.

Shoot relative water content (RWC)

There was a significant reduction in shoot RWC under water-stress as compared to well-water treatment (*Fig. 5*). Seed priming either with HP or GB considerably enhanced shoot RWC in water-stress treatment. The seedlings originating from the NP or HP seeds suffered a more significant decline in shoot RWC under water-stress treatment. However, seed priming with GB 50 and 100 mM significantly increased 4.7 and 3.8 % higher shoot RWC as compared to seedlings originated from NP seeds under water-stress treatment.

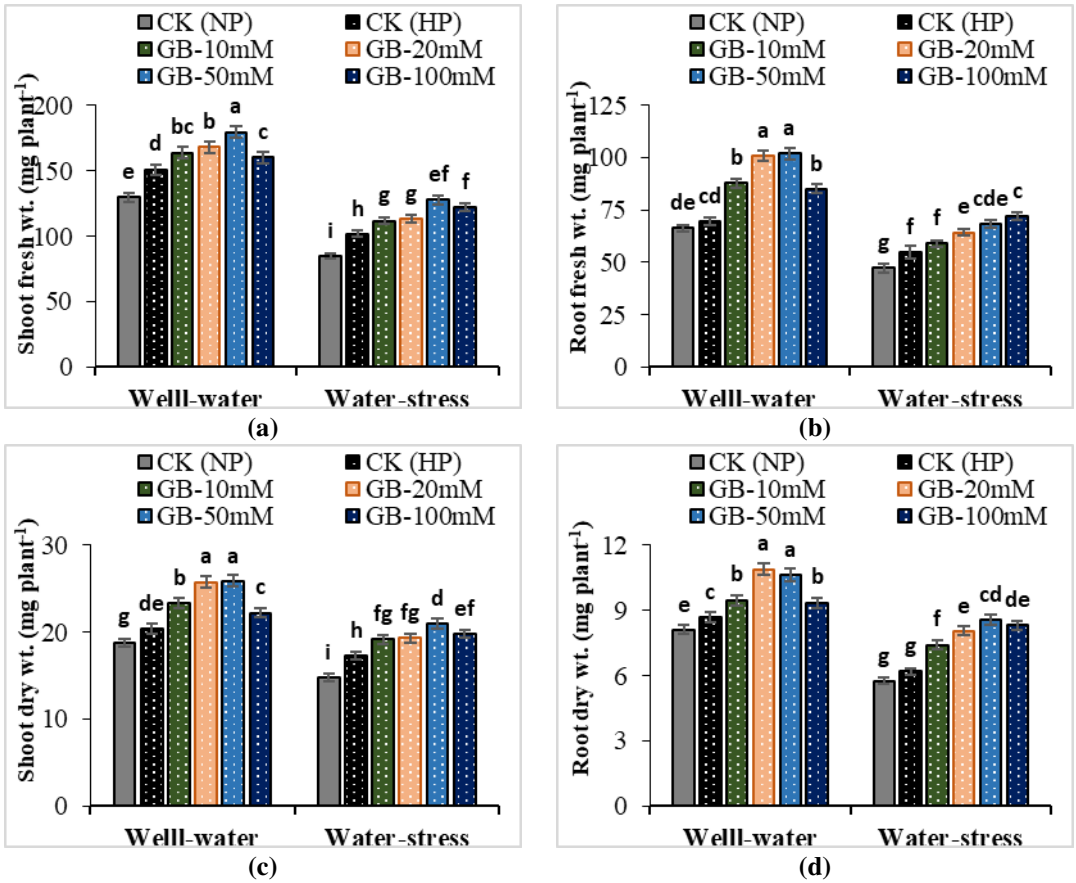

Figure 4. *Effects of different seed priming treatments on the shoot and root fresh (a and b) and dry (c and d) weight of wheat seedlings grown under well-water and water-stress conditions. Control non-primed; CK (NP), Control hydro-primed; CK (HP), Glycine-betaine primed denotes GB. All values represent means ± standard deviations (SD) of three replicates. Bars showing the same letters are not significantly different at $P \leq 0.05$ as determined by LSD test*

Lipid peroxidation and ROS accumulation

The rate of lipid peroxidation was recorded in term of MDA accumulation, induced by PEG-stress was found to be dependent upon water-stress treatment (*Fig. 6*). Under well-water conditions, the MDA accumulation was almost similar in all wheat seedlings originated from either NP, HP or GB treated seeds. Upon exposure to PEG stress, the

http://www.aloki.hu ● ISSN 1589 1623 (Print) ● ISSN 1785 0037 (Online)
DOI: http://dx.doi.org/10.15666/aeer/1704_83338350

MDA accumulation was increased in all priming treatments; however, in the seedlings of GB primed seeds, the increase was lower than that of NP and HP seed priming treatments.

The response of wheat seedlings originated from NP, HP and GB primed seeds were varied among water-stress treatments, and exposure to water-stress all priming treatments showed a significant increase in H_2O_2 accumulation (*Fig. 6*). However, all the seeds either primed with different concentrations of GB or primed with distilled water (HP) showed lower accumulation of H_2O_2 and presented better performance as compared to seedlings of NP seeds under water-stress condition. The seedlings from the seeds treated with 100 mM showed 18% lower H_2O_2 content compared with seedlings of NP seeds under water-stress treatment respectively.

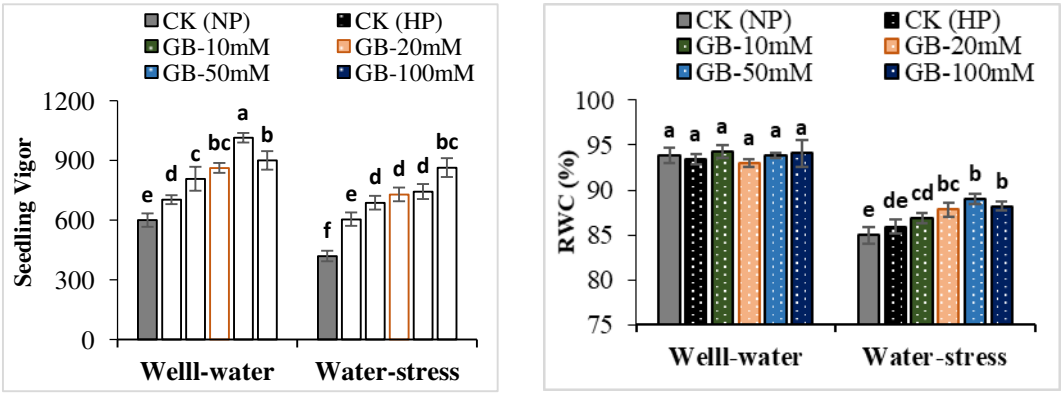

Figure 5. *Effects of different seed priming treatments on seedlings vigor (a) and RWC (b) of wheat seedlings grown under well-water and water-stress conditions. Control non-primed; CK (NP), Control hydro-primed; CK (HP), Glycine-betaine primed denotes GB. All values represent means ± standard deviations (SD) of three replicates. Bars showing the same letters are not significantly different at $P \leq 0.05$ as determined by LSD test*

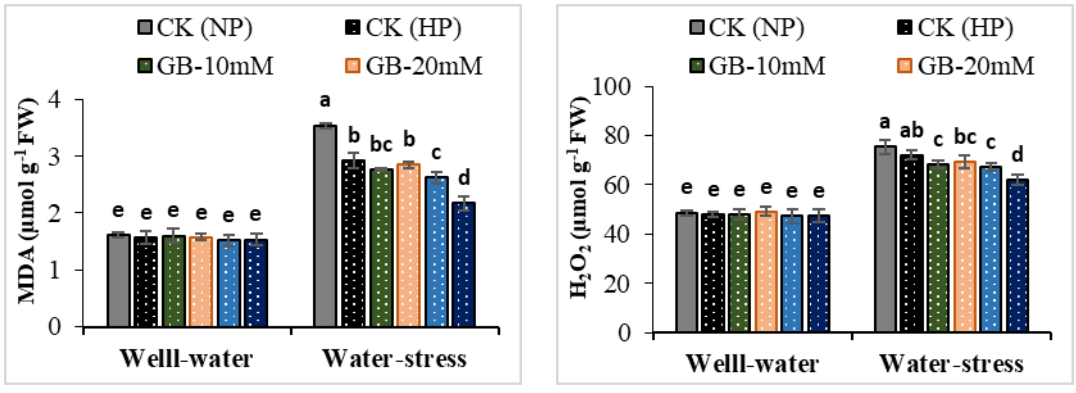

Figure 6. *Effects of different seed priming treatments on MDA (a) and H_2O_2 (b) content in wheat seedlings grown under well-water and water-stress conditions. Control non-primed; CK (NP), Control hydro-primed; CK (HP), Glycine-betaine primed denotes GB. All values represent means ± standard deviations (SD) of three replicates. Bars showing the same letters are not significantly different at $P \leq 0.05$ as determined by LSD test*

http://www.aloki.hu ● ISSN 1589 1623 (Print) ● ISSN 1785 0037 (Online)
DOI: http://dx.doi.org/10.15666/aeer/1704_83338350

Membranes stability index and electrolyte leakage

Cellular membrane stability is reciprocal to electrolyte leakage, the higher electrolyte leakage, the lower membrane stability. Membrane stability was not changed among different priming treatments and had lower electrolyte leakage under well-water conditions. However, under water-stress treatment cellular membrane stability was significantly reduced as elucidated from a significant increase in electrolyte leakage in the wheat seedling originated from either primed or non-primed seeds (*Fig. 7*).

The most damaging effects of water-stress were observed in wheat seedlings originated from NP seeds as increased electrolyte leakage and lower membrane stability index values under water-stress (*Fig. 7*). However, seed priming either with GB or with water significantly reduced electrolyte leakage and increased cellular membrane stability index under water-stress treatment. The most contrasting results were obtained by seed priming with GB 25 to 100 mM concentrations and found lower electrolyte leakage and higher membrane stability index in wheat seeding originated from the seeds primed with high concentrations of GB and grown under water-stress conditions.

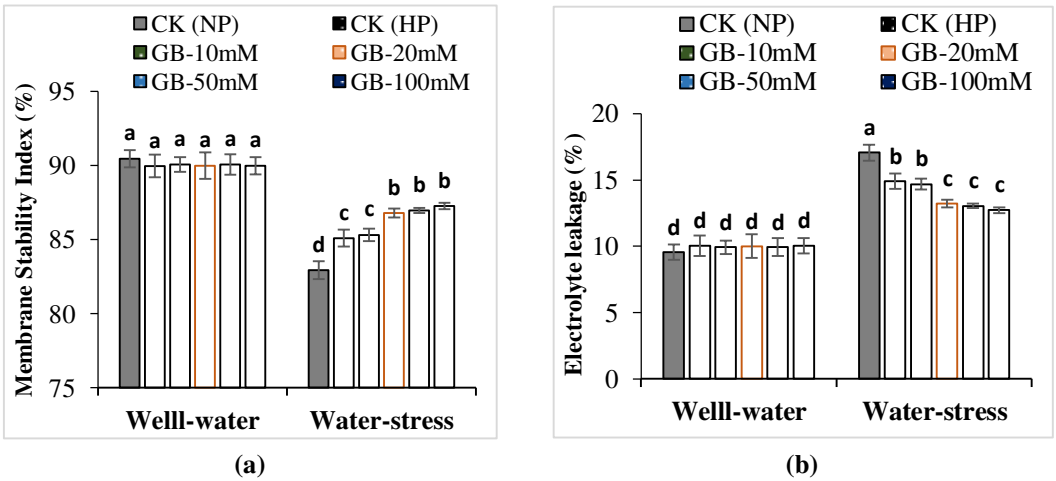

Figure 7. *Effects of different seed priming treatments on membrane stability index (a) and electrolyte leakage (b) of wheat seedlings grown under well-water and water-stress conditions. Control non-primed; CK (NP), Control hydro-primed; CK (HP), Glycine-betaine primed denotes GB. All values represent means ± standard deviations (SD) of three replicates. Bars showing the same letters are not significantly different at P ≤ 0.05 as determined by LSD test*

Activities of antioxidant enzymes

The activities of antioxidant enzymes (CAT, POD and SOD) were significantly higher in osmotically stressed seedlings and significant variation was recorded among different priming treatments, whereas, under well-water conditions, the activities of CAT, POD and SOD in the seedlings of GB and HP primed seeds were almost similar to seedlings of NP seeds (*Fig. 8*). Under the water-stress condition, the CAT activity was increased significantly in the seedlings of GB 50 and 100 mM primed seeds as compared to HP and NP seedlings. The activities of POD under water-stress, the seeding originated from GB 100 and 25 mM primed seeds showed 19 and 14% higher POD activity as compared to seedlings of NP seeds. However, seedlings originated

http://www.aloki.hu ● ISSN 1589 1623 (Print) ● ISSN 1785 0037 (Online)
DOI: http://dx.doi.org/10.15666/aeer/1704_83338350

from 100mM GB and HP seeds showed 43% and 13% higher SOD activity as compared to seedlings of NP seeds under water-stress treatment (*Fig. 8*).

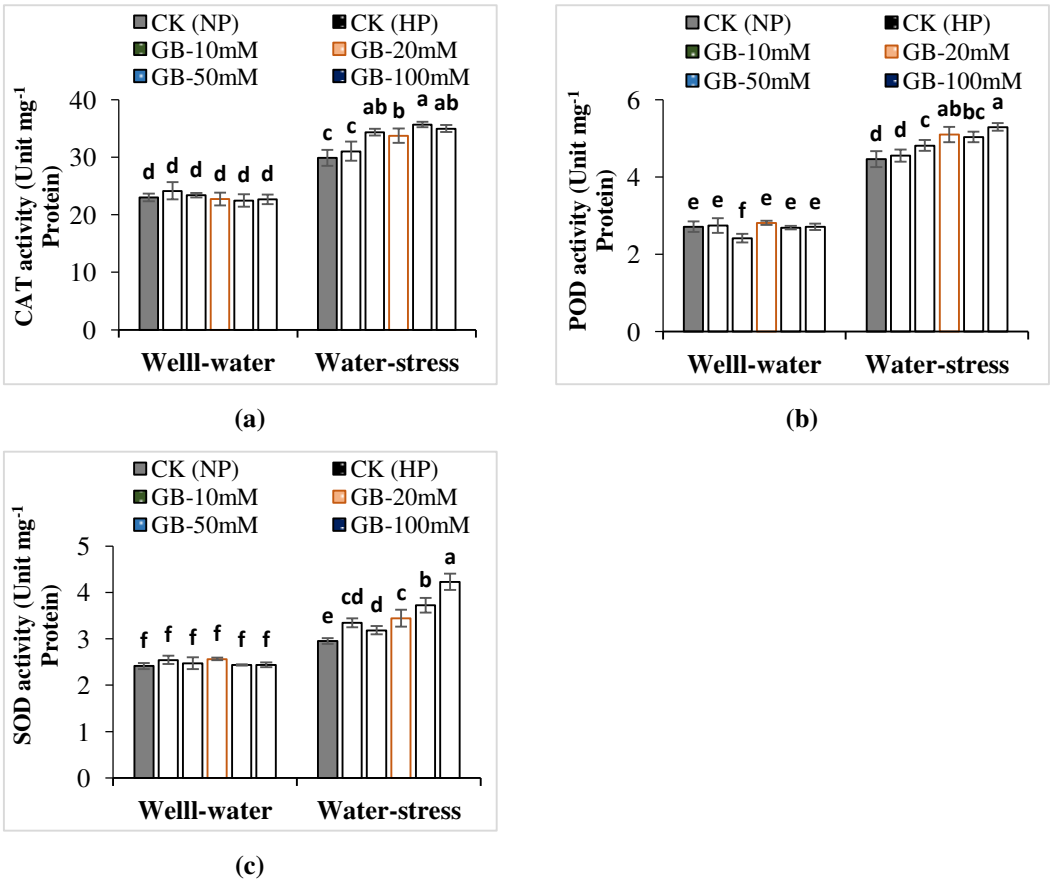

Figure 8. *Effects of different seed priming treatments on the activities of antioxidant enzymes; catalase (CAT) (a), Peroxidase (POD) (b) and superoxide dismutase (SOD) (c), in wheat seedlings grown under well-water and water-stress conditions. Control non-primed; CK (NP), Control hydro-primed; CK (HP), Glycine-betaine primed denotes GB. All values represent means ± standard deviations (SD) of three replicates. Bars showing the same letters are not significantly different at P ≤ 0.05 as determined by LSD test*

Osmolytes accumulation

The results represent proline and soluble sugars contents in wheat seedlings under well-water and water-stress treatments are presented in *Fig. 9*. The accumulation of proline and soluble sugars significantly enhanced by water-stress; for instance, there was an approximately 6-fold increase in the proline content of water-stressed seedlings of NP seeds as compared to NP seedlings of well-water treatment. In addition, the proline content remarkably decreased with seed priming treatments. Moreover, 33 and 44% lower proline accumulation were recorded in the seedlings originated from GB 50 and 100 mM primed seeds as compared to the seedlings of NP seeds under water-stress treatment. Similarly, the accumulation of soluble sugars content in wheat seedling was higher in water-stressed seedlings; however, more pronounced accumulation of soluble sugars was recorded in the seedlings of NP seeds. Seed priming significantly altered soluble sugars accumulation and 28 to 27% lower soluble sugars were accumulated in

http://www.aloki.hu ● ISSN 1589 1623 (Print) ● ISSN 1785 0037 (Online)
DOI: http://dx.doi.org/10.15666/aeer/1704_83338350

seedlings originated from GB 50 and 100 mM primed seeds planted in water-stress treatment (*Fig. 9*).

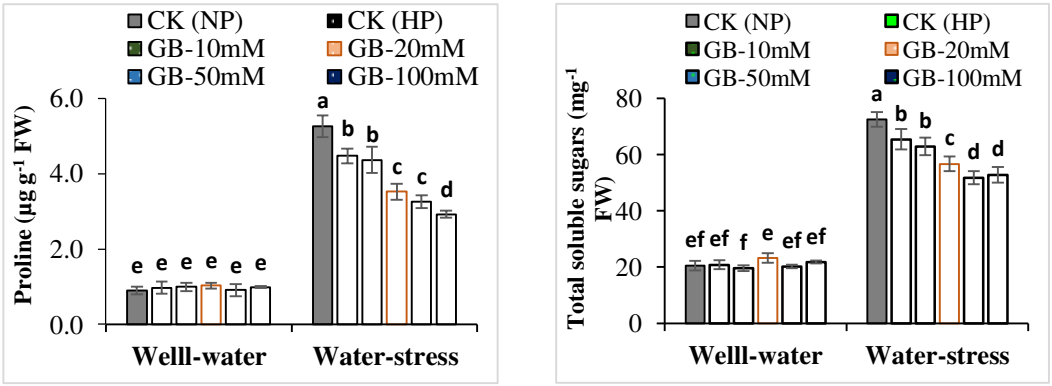

Figure 9. *Effects of different seed priming treatments on proline (a), and total soluble sugars (b) content in wheat seedlings grown under-well-water and water-stress conditions. Control non-primed; CK (NP), Control hydro-primed; CK (HP), Glycine-betaine primed denotes GB. All values represent means ± standard deviations (SD) of three replicates. Bars showing the same letters are not significantly different at P ≤ 0.05 as determined by LSD test*

Discussion

Results of this study revealed that seed treatment with an appropriate agent and its concentration could invigorate wheat seeds, subsequent in greater germination ability and better seedling establishment and higher seedling fresh weight and dry matter accumulation under well-water and water deficit conditions (*Figs. 1 to 4*). In the current study, faster and more synchronized and uniform seed germination and seedlings emergence were recorded with seed priming, as indicated by higher germination %, germination index (*Fig. 1*), shoot and root length (*Fig. 2*), fresh weight or dry matter accumulation (*Fig. 4*), and seedling vigor index (*Fig. 5*). Water-stress induced deleterious effects on seed germination and seedling growth were alleviated by seed treatment with GB, this improvement in synchronized seed germination and better seedlings establishment could be attributed from higher antioxidant activity and Maintainance of cellular membrane integrity. Our results are in agreement with the previous finding with Safflower, cotton, Turfgrass, and Wheat (Zhang et al., 2014; Salama et al., 2015; Alasvandyari et al., 2017; Cheng et al., 2018). Uniform and synchronized seed germination and early seedling establishment are the most critical stages for any crop. Water deficit may severely reduce seed germination capability, uniformity and dry matter accumulation (Jisha et al., 2013; Nawaz et al., 2013; Hussain et al., 2016). Consequently, the advantages of seed priming may be more helpful under sub-optimal soil water conditions compared with more favorable soil moisture conditions (Farooq et al., 2008; Mahmood et al., 2009; Zhang et al., 2014).

Water-stress induced growth decline has been previously reported by many researchers in different crops: Turfgrass (Zhang et al., 2014), Rice (Farooq et al., 2008) Sorghum (Zhang et al., 2015) and Wheat (Nawaz et al., 2013; Guo et al., 2017). Water-stress-induced reduction in plant growth and development is mainly attributed to a reduction in plant water potential, leaf RWC, photosynthesis and dry matter

http://www.aloki.hu ● ISSN 1589 1623 (Print) ● ISSN 1785 0037 (Online)
DOI: http://dx.doi.org/10.15666/aeer/1704_83338350

accumulation (Farooq et al., 2012). Our findings revealed that inhibitory effects of water-stress could be ameliorated by seed priming with GB appropriate concentration, our results demonstrated that seedling originated from seeds, primed with GB 50 and 100 mM had better shoot RWC under water-deficit conditions and had the ability to reduce adversities of water-stress (*Fig. 5*). The decline in RWC showed a loss of turgor, which restricted water availability necessary for proper plant growth and development. Water-stress tolerance is substantially associated with tissue water potential and antioxidant system, exogenous application of GB significantly reduced adversities of water-stress in seedlings of fine grain aromatic rice and improved leaf water potential and had higher antioxidant activity and better photosynthetic ability under water-deprived conditions (Farooq et al., 2008; Wani et al., 2013).

The cellular membrane stability was significantly affected by the overproduction of H_2O_2, and MDA content, which elucidated from the higher release of electrolytes from the cells under water-stress conditions. Furthermore, water-stress stimulated overproduction of H_2O_2 and MDA content in wheat seedlings (*Fig. 6*) represents a well-known indicator of oxidative stress. However, seed priming with GB alleviated adversities of water-stress, which were manifested in term of substantially improved membrane stability index, as noted from lower electrolyte leakage (*Fig. 7*) and reduced H_2O_2 and MDA production. Higher ion leakage and MDA production are considered as indicators of oxidative stress (Mahajan and Tuteja, 2005; Farooq et al., 2012). The oxidative stress often arises from the overaccumulation of ROS, especially H_2O_2. Overproduction of H_2O_2 is toxic to cellular structure and macromolecules, impairing normal cellular activities (Das and Roychoudhury, 2014; Mittler, 2017). The overproduction of ROS in plants is managed by a variety of antioxidant enzymes and lipids and water-soluble macromolecules. Of these antioxidant enzymes (CAT, POD, and SOD) are the key components of ROS scavenging mechanism under oxidative stress conditions (Das and Roychoudhury, 2014; Lou et al., 2015; Xu et al., 2018). Our results suggested that the activities of antioxidant enzymes significantly triggered in wheat seedling originated from the seeds treated with GB (*Fig. 8*). This increase in activities of antioxidant enzymes and reduced ROS mediated injuries in wheat seedlings as evident from the association between H_2O_2 and MDA and antioxidant enzymes system under water-stress but not under well-water conditions.

It is well-established phenomena that proline and soluble sugars content in plant tissues enhanced by a variety of environmental stress including water-stress (He et al., 2011; Wei et al., 2015). Accumulations of these osmolytes in maize hybrids were increased with the severity of drought stress (Anjum et al., 2017). Water-stress significantly triggered the accumulation of proline and soluble sugars in this study (*Fig. 9*). Our results revealed that seed priming with GB reduced overproduction of proline and soluble sugars under water-stress. The effects of GB seed priming on proline accumulation under water can be interpreted based on the argument that higher accumulation of endogenous proline does not contribute to the osmotic adjustment in plants under water-stress conditions (Borgo et al., 2015). Lower accumulation of endogenous proline in wheat seedlings are also reported in GB primed seeds under salinity stress (Salama et al., 2015). Moreover, higher accumulation of soluble sugars adversely affects plant physiological and biochemical activities in a concentration-dependent manner (Aldesuquy et al., 2012; Sami et al., 2016).

http://www.aloki.hu ● ISSN 1589 1623 (Print) ● ISSN 1785 0037 (Online)
DOI: http://dx.doi.org/10.15666/aeer/1704_83338350

Conclusion

The results of the present study elucidated that the seed priming with GB did not simply accelerated germination-related processes but was also involved in other specific mechanisms that improved the seedling vigor and allowed the wheat seedlings to cope with the oxidative stress induced by water-stress. Increase in activities of antioxidants as governed by GB based seed priming can protect the degradation of enzymes from water- stress-induced ROS production and maintained cellular membranes stability. In addition to protecting from oxidative stress, GB seed priming was also involved in regulation of endogenous accumulation of proline and soluble sugars, RWC and antioxidant system in wheat seedlings, which may also be a remarkable demonstration of enhanced seed germination characteristics and seedling vigor under stressful environment.

Acknowledgements. This research was supported by National Key Research and Development Program of China (Grant No. 2017YFD0300410), and Introduction of International Advanced Agricultural Science and Technology Program of Ministry of Agriculture (Grant No. 2011-G19).

REFERENCES

[1] Alasvandyari, F., Mahdavi, B., Hosseini, S. M. (2017): Glycine betaine affects the antioxidant system and ion accumulation and reduces salinity-induced damage in safflower seedlings. – Archives of Biological Sciences 69(1): 139-147.
[2] Aldesuquy, H. S., Abbas, M. A., Hamed, S. A. A., Elhakem, A. H., Alsokari, S. S. (2012): Glycine betaine and salicylic acid induced modification in productivity of two different cultivars of wheat grown under water stress. – Journal of Stress Physiology & Biochemistry 8(2): 72-89.
[3] Alexieva, V., Sergiev, I., Mapelli, S., Karanov, E. (2001): The effect of drought and ultraviolet radiation on growth and stress markers in pea and wheat. – Plant, Cell and Environment 24(12): 1337-1344.
[4] Amedea, B., Seabra, C., Oliveira, H. (2016): How nitric oxide donors can protect plants in a changing environment: what we know so far and perspectives. – AIMS Molecular Science 3(4): 692-718.
[5] Anjum, S. A., Ashraf, U., Tanveer, M., Khan, I., Hussain, S., Shahzad, B., Zohaib, A., Abbas, F., Saleem, M. F., Ali, I., Wang, L. C. (2017): Drought induced changes in growth, osmolyte accumulation and antioxidant metabolism of three maize hybrids. – Frontiers in Plant Science 08: 1-12.
[6] AOSA (1983): Seed Vigour Testing Handbook. USA: Contribution, Association of Official Seed Analysis and SCST. – Available at: https://www.analyzeseeds.com/product/seed-vigor-testing-handbook-2017/ (Accessed: 19 February 2019).
[7] Atta, B. M., Mahmood, T., Trethowan, R. M. (2013): Relationship between root morphology and grain yield of wheat in north-western NSW, Australia. – Australian Journal of Crop Science 7(13): 2108-2115.
[8] Bajji, M., Kinet, J. M., Lutts, S. (2002): The use of the electrolyte leakage method for assessing cell membrane stability as a water stress tolerance test in durum wheat. – Plant Growth Regulation 36(1): 61-70.
[9] Bates, L. S., Waldren, R. P., Teare, I. D. (1973): Rapid determination of free proline for water-stress studies. – Plant and Soil 39(1): 205-207.
[10] Beckers, G. J., Conrath, U. (2007): Priming for stress resistance: from the lab to the field. – Current Opinion in Plant Biology 10(4): 425-431.
[11] Bewley, J. D. (1997): Seed Germination and Dormancy. – The Plant cell 9(7): 1055-1066.

http://www.aloki.hu ● ISSN 1589 1623 (Print) ● ISSN 1785 0037 (Online)
DOI: http://dx.doi.org/10.15666/aeer/1704_83338350

[12] Borgo, L., Marur, C. J., Vieira, L. G. E. (2015): Effects of high proline accumulation on chloroplast and mitochondrial ultrastructure and on osmotic adjustment in tobacco plants. – Acta Scientiarum. Agronomy 37(2): 191-199.
[13] Cakmak, I., Horst, W. J. (1991): Effect of aluminium on lipid peroxidation, superoxide dismutase, catalase, and peroxidase activities in root tips of soybean (Glycine max). – Physiologia Plantarum 83(3): 463-468.
[14] Chachar, M. H., Chachar, N. A., Chachar, Q., Mujtaba, S. M., Chacahr, S., Chachar, Z. (2016): Physiological Characterization of Six Wheat genotypes for drought tolerance. – International Journal of Research – Granthaalayah 4(2): 184-196.
[15] Cheng, C., Pei, L. M., Yin, T. T., Zhang, K. W. (2018): Seed treatment with glycine betaine enhances tolerance of cotton to chilling stress. – The Journal of Agricultural Science: 1-10.
[16] Conrath, U., Beckers, G. J. M., Flors, V., García-Agustín, P., Jakab, G., Mauch, F., Newman, M.-A., Pieterse, C. M. J., Poinssot, B., Pozo, M. J., Pugin, A., Schaffrath, U., Ton, J., Wendehenne, D., Zimmerli, L., Mauch-Mani, B. (2006): Priming: getting ready for battle. – Molecular Pant-Microbe Interactions 19(10): 1062-1071.
[17] Das, K., Roychoudhury, A. (2014): Reactive oxygen species (ROS) and response of antioxidants as ROS-scavengers during environmental stress in plants. – Frontiers in Environmental Science 2: 1-13.
[18] Farooq, M., Aziz, T., Hussain, M., Rehman, H., Jabran, K., Khan, M. B. (2008): Glycinebetaine improves chilling tolerance in hybrid maize. – Journal of Agronomy and Crop Science 194(2): 152-160.
[19] Farooq, M., Basra, S. M. A., Wahid, A., Cheema, Z. A., Cheema, M. A., Khaliq, A. (2008): Physiological role of exogenously applied glycinebetaine to improve drought tolerance in fine grain Aromatic Rice (Oryza sativa L.). – Journal of Agronomy and Crop Science 194: 325-333.
[20] Farooq, M., Hussain, M., Wahid, A., Siddique, K. H. M. (2012): Drought stress in plants: An overview. – In: Aroca, R. (ed.) Plant responses to drought stress: 1-33.
[21] Guo, Q., Wang, Y., Zhang, H., Qu, G., Wang, T., Sun, Q., Liang, D. (2017): Alleviation of adverse effects of drought stress on wheat seed germination using atmospheric dielectric barrier discharge plasma treatment. – Scientific Reports 7(1): 1-14.
[22] Gupta, N., Thind, S. K. (2015): Improving photosynthetic performance of bread wheat under field drought stress by foliar applied glycine betaine. – Journal of Agricultural Science and Technology 17(1): 75-86.
[23] Hasanuzzaman, M., Alam, M. M., Rahman, A., Hasanuzzaman, M., Nahar, K., Fujita, M. (2014): Exogenous proline and glycine betaine mediated upregulation of antioxidant defense and glyoxalase systems provides better protection against salt-induced oxidative stress in two rice (Oryza sativa L.) varieties. – BioMed research international 2014: 1-17.
[24] He, C., Zhang, W., Gao, Q., Yang, A., Hu, X., Zhang, J. (2011): Enhancement of drought resistance and biomass by increasing the amount of glycine betaine in wheat seedlings. – Euphytica 177(2): 151-167.
[25] Heath, R. L., Packer, L. (1968): Photoperoxidation in isolated chloroplasts. – Archives of Biochemistry and Biophysics 125(1): 189-198.
[26] Hussain, S., Khan, F., Cao, W., Wu, L., Geng, M. (2016): Seed priming alters the production and detoxification of reactive oxygen intermediates in rice seedlings grown under sub-optimal temperature and nutrient supply. – Frontiers in plant science 7(4): 1-13.
[27] Iqbal, M., Hussain, I., Liaqat, H., Ashraf, M. A., Rasheed, R., Rehman, A. U. (2015): Exogenously applied selenium reduces oxidative stress and induces heat tolerance in spring wheat. – Plant Physiology and Biochemistry 94: 95-103.
[28] Jisha, K. C., Vijayakumari, K., Puthur, J. T. (2013): Seed priming for abiotic stress tolerance: an overview. – Acta Physiologiae Plantarum 35(5): 1381-1396.

http://www.aloki.hu ● ISSN 1589 1623 (Print) ● ISSN 1785 0037 (Online)
DOI: http://dx.doi.org/10.15666/aeer/1704_83338350

[29] Li, Q., Bian, C., Liu, X., Ma, C., Liu, Q. (2015): Winter wheat grain yield and water use efficiency in wide-precision planting pattern under deficit irrigation in North China Plain. – Agricultural Water Management 153: 71-76.
[30] Li, X., Liu, F. (2016): Drought stress memory and drought stress tolerance in plants: Biochemical and molecular basis. – In: Drought stress tolerance in plants, Vol 1. Switzerland 2016: 616.
[31] Lou, Y., Yang, Y., Hu, L., Liu, H., Xu, Q. (2015): Exogenous glycinebetaine alleviates the detrimental effect of Cd stress on perennial ryegrass. – Ecotoxicology 24(6): 1330-1340.
[32] Mahajan, S., Tuteja, N. (2005): Cold, salinity and drought stresses: An overview. – Archives of Biochemistry and Biophysics 444(2): 139-158.
[33] Mahmood, T., Ashraf, M., Shahbaz, M. (2009): Does exogenous application of glycinebetaine as a pre-sowing seed treatment improve growth and plants grown under water deficit conditions? – Pakistan Journal of Botany 41(3): 1291-1302.
[34] Mittler, R. (2017): ROS Are Good. – Trends in Plant Science 22(1): 11-19.
[35] Morris, D. L. (1948): Quantitative determination of carbohydrates with dreywood's Anthrone reagent. – Science 107(2775): 254-255.
[36] Moustakas, M., Ilektra, S., Kouna, T., Antonopoulou, C. I., Therios, I. (2011): Exogenous proline induces soluble sugar accumulation and alleviates drought stress effects on photosystem II functioning of Arabidopsis thaliana leaves. – Plant Growth Regulation 65(2): 315-325.
[37] Nakano, Y., Asada, K. (1981): Hydrogen peroxide is scavenged by ascorbate-specific peroxidase in spinach chloroplasts. – Plant and Cell Physiology 22(5): 867-880.
[38] Nawaz, F., Ashraf, M. Y., Ahmad, R., Waraich, E. A. (2013): Selenium (Se) seed priming induced growth and biochemical changes in wheat under water deficit conditions. – Biological Trace Element Research 151(2): 284-293.
[39] Nazar, R., Umar, S., Khan, N. A., Sareer, O. (2015): Salicylic acid supplementation improves photosynthesis and growth in mustard through changes in proline accumulation and ethylene formation under drought stress. – South African Journal of Botany 98: 84-94.
[40] Rakshit, A., Singh, H. B. (2018): Advances in Seed Priming. – 1st edition, Singapore: Springer Singapore.
[41] Salama, K. H. A., Mansour, M. M. F., Al-Malawi, H. A. (2015): Glycinebetaine priming improves salt tolerance of wheat. – Biologia (Poland) 70(10): 1334-1339.
[42] Sami, F., Yusuf, M., Faizan, M., Faraz, A., Hayat, S. (2016): Role of sugars under abiotic stress. – Plant Physiology and Biochemistry 109: 54-61.
[43] Seckin, B., Turkan, I., Sekmen, A. H., Ozfidan, C. (2010): The role of antioxidant defense systems at differential salt tolerance of Hordeum marinum Huds. (sea barleygrass) and Hordeum vulgare L. (cultivated barley). – Environmental and Experimental Botany 69(1): 76-85.
[44] Srivastava, A. K., Lokhande, V. H., Patade, V. Y., Suprasanna, P., Sjahril, R., D'Souza, S. F. (2010): Comparative evaluation of hydro-, chemo-, and hormonal-priming methods for imparting salt and PEG stress tolerance in Indian mustard (Brassica juncea L.). – Acta Physiologiae Plantarum 32(6): 1135-1144.
[45] Wani, S. H., Singh, N. B., Haribhushan, A., Mir, J. I. (2013): Compatible solute engineering in plants for abiotic stress tolerance - Role of glycine betaine. – Current Genomics 14: 157-165.
[46] Wei, L., Wang, L., Yang, Y., Liu, G., Wu, Y., Guo, T., Kang, G. (2015): Abscisic acid increases leaf starch content of polyethylene glycol-treated wheat seedlings by temporally increasing transcripts of genes encoding starch synthesis enzymes. – Acta Physiologiae Plantarum 37(10): 1-6.
[47] Wolny, E., Betekhtin, A., Rojek, M., Braszewska-Zalewska, A., Lusinska, J., Hasterok, R. (2018): Germination and the early stages of seedling development in brachypodium distachyon. – International Journal of Molecular Sciences 19(10): 1-14.

http://www.aloki.hu ● ISSN 1589 1623 (Print) ● ISSN 1785 0037 (Online)
DOI: http://dx.doi.org/10.15666/aeer/1704_83338350

[48] Xu, Z., Sun, M., Jiang, X., Sun, H., Dang, X., Cong, H., Qiao, F. (2018): Glycinebetaine biosynthesis in response to osmotic stress depends on jasmonate signaling in Watermelon suspension cells. – Frontiers in plant science 9: 1-14.

[49] Xue, G. P., McIntyre, C. L., Glassop, D., Shorter, R. (2008): Use of expression analysis to dissect alterations in carbohydrate metabolism in wheat leaves during drought stress. – Plant Molecular Biology 67(3): 197-214.

[50] Zhang, Q., Rue, K., Mueller, J. (2014): The effect of glycinebetaine priming on seed germination of six turfgrass species under drought, salinity, or temperature stress. – HortScience 49(11): 1454-1460.

[51] Zhang, F., Yu, J., Johnston, C. R., Wang, Y., Zhu, K., Lu, F., Zhang, Z., Zou, J. (2015): Seed priming with polyethylene glycol induces physiological changes in sorghum (Sorghum bicolor L. moench) seedlings under suboptimal soil moisture environments. – PLoS ONE 10(10): 1-15.

http://www.aloki.hu ● ISSN 1589 1623 (Print) ● ISSN 1785 0037 (Online)
DOI: http://dx.doi.org/10.15666/aeer/1704_83338350

AT-SITE RAINFALL FREQUENCY ANALYSIS USING PARTIAL DURATION SERIES AND ANNUAL MAXIMUM SERIES: A CASE STUDY

AHMAD, I.[1,2*] – KHAN, D. A.[2] – ALMANJAHIE, IBRAHIM M.[1] – CHIKR-ELMEZOUAR, Z.[1] – LAKSACI, A.[1]

[1]*Department of Mathematics, College of Science, King Khalid University, 61413 Abha, Kingdom of Saudi Arabia*
(phone: +966-17-241-7734, fax: +966-17-241-7637)

[2]*Department of Mathematics and Statistics, Faculty of Basic and Applied Sciences, International Islamic University, 44000 Islamabad, Pakistan*

**Corresponding author*
e-mail: ishfaq.ahmad@iiu.edu.pk; phone: +966-59-681-7557

(Received 1st Mar 2019; accepted 17th May 2019)

Abstract. At-site Rainfall Frequency Analysis (RFA) is a crucial tool for designing of water related infrastructures. Partial Duration Series (PDS) and Annual Maximum Series (AMS) are the most popular techniques for RFA. PDS is capable of including more extreme events as compared to the AMS. Keeping in view the importance of at site RFA, in this study we identify suitable statistical model that best represent PDS and AMS extracted from daily rainfall records of 25 years in the vastly growing city, Rawalpindi, Pakistan. The most commonly used statistical distributions in RFA such as Generalized Pareto (GPA), Generalized Extreme Value (GEV), Generalized Logistic (GLO), and Pearson Type-3 (PE-3) distributions are used in this study. The parameters of these distributions are estimated by method of linear moments (LM). Anderson-Darling (A-D) testing criterion along with L-moment ratio diagram have been used to determine the best fit probability distribution. The findings of our study suggest that GEV as the best fit statistical distribution for PDS while GLO for AMS. Moreover, in this study we have also estimated quantiles for the best fitted probability distributions. The results revealed that PDS sample outperforms than AMS for various return periods. These estimates can be used in designing of water-related infrastructures such as culverts, bridges and other hydrological structures in the city.
Keywords: *frequency factor, goodness-fit test, linear moments, quintile estimation*

Introduction

Nowadays, climate change is one of the main challenge for mankind. Global warming occurs due to multiple changes in the climate such as changes in the intensity, duration, frequency and timing of extreme events including bolstering lengthening droughts, heat waves and occurrence of more precipitation. Like other countries worldwide, in Pakistan also, due to abrupt changes in the climate, several extreme changes in the weather have been observed in the form extreme rainfalls, droughts, irregular floods, glacier melting, sea-level rising, etc. (Rasul et al., 2012). In Pakistan, global warming has also putting severe impacts on hydrological parameters leading to cause an increase in precipitation for arid region including Rawalpindi city of Pakistan (Hassan et al., 2017). These heavy rains due insufficient water resources management cause flash floods in the city. Resulting disasters damage the economy of the country and create problems for citizens. In worst circumstances these disasters cause disruption of normal services like health care livelihoods and also loss of human lives. Reduction in flood risk, the mitigation of resulting damages is possible by human actions on the fluvial system, such as the

http://www.aloki.hu ● ISSN 1589 1623 (Print) ● ISSN 1785 0037 (Online)
DOI: http://dx.doi.org/10.15666/aeer/1704_83518367

construction of reservoirs, culverts and other protection measures. Rainfall Frequency analysis using different probability models is one of the randomising approaches which could be used to estimates future rainfall with certain probability in order to mitigate the losses mentioned above. However, relatively small samples of annual maximum rainfall series put some limitations to the degree of statistical sophistication that can be engaged during at-site frequency analysis. The data of extreme events must reflect the variations expected in the quantity of interest. However, the values of many hydrological and hydrometeorological data vary in time giving alternating sequences of large and small values. So, usually, the larger values are greater than the mean values and make clusters in short time period followed by smaller values or null values sometimes. In the result of such temporal pattern, we get the typical configuration of a succession of exceedances over a specified threshold. The number and magnitude of such exceedances can be modeled by probability modeling. Such series are known as partial duration series (Naghettini, 2016).

For this study we have carried out RFA using two commonly known methods i.e. Annual Maximum Series (AMS) and Partial Duration Series (PDS) for the daily rainfall records of the city Rawalpindi, Pakistan. Rawalpindi is located in the north-south of the sub-mountainous region of the province Punjab. In recent decades, abrupt fluctuations in rainfall patterns are being observed particularly in northern Photohar regions. In the past years due to heavy rainfalls i.e., 1981, 1988, 1997, 2001, several tributaries have been affected badly in the city. A total of 11 major small tributaries of rain water pass through the city including the famous Lai-Nullah. The intensity amount of rainfall caused the water level of Lai-Nullah (the famous rainfall tributary in the city) particularly, other tributaries to rise remarkably and gave raise to heavy floods in the city. In the result of these floods, 74 human lives were lost, around 400,000 people were affected, 742 cattle heads were perished, 1,087 houses were completely 2,448 partially were demolished. The flash flood which drove by the monsoon rain in 2001 turn into a loss of US$ 250 million (Rasul et al., 2004). There are many factors causing this situation in these tributaries such as the illegal constructions along with these tributaries has squeezed the space for smooth flow of sewage rainwater collection of debris and also other construction materials being dumped in these rain water tributaries resulting in the rise of rainfall water to a precarious level. The accurate modeling in the form of at-site frequency analysis of these heavy rainfalls is of immense importance to mitigate future losses. Rainfall frequency analysis (RFA) with the passage of time is getting more attention worldwide. Extensive research works are being carried out in various parts of the world. According to Lang et al. (1999) two techniques, PDS and AMS are commonly used techniques in rainfall frequency analysis. AMS consists of single value, the maximum value per year of the daily records while PDS consists of all well-defined maximum peaks above a certain threshold level (Beguería, 2005). The dilemma in RFA is to select the proper series among AMS and PDS. The most regular objection with respect to use of annual maximum series is that it uses only one peak value in a year. On some occasions, the second largest event in a data may be greater than many AM events of the other years. On contrary, PDS modeling represents a complete description of extreme events (heavy rainfalls or floods), particularly when the issue of short length of data is under consideration (Lang et al., 1999). Fischer and Schuman (2014) explained that PDS modeling provide comparatively more data series per year as compared to AMS. The substitute makes possible to analyze events which are extreme still higher than annual maxima of others years and are not incorporated in the AMS technique. Lang et al. (1999) proposed to consider PDS modeling as a compromise between AMS analysis and classical

http://www.aloki.hu ● ISSN 1589 1623 (Print) ● ISSN 1785 0037 (Online)
DOI: http://dx.doi.org/10.15666/aeer/1704_83518367

time series modeling. A lot of studies are available around the globe address different aspects of PDS and AMS modeling techniques (see for example Nagy et al., 2017), where they discussed the technical questions concerning the use of the partial duration series (PDS) within the domain of flood frequency analysis while the study of Chang et al. (2015) presented a comparison of AMS and PDS for derivation of rainfall intensity-duration-frequency relationships in peninsular Malaysia. Berton et al. (2018) discussed the Improving peak flow estimation across the United States by using PDS. Agilan et al. (2017) proposed non-stationary rainfall intensity-duration-frequency relationship with a comparison between AMS and PDS. Gado and Nguyen (2016) presented regional estimation of floods for ungauged sites using scaling approach partial duration series. Vrban et al. (2018) evaluated the Stormwater Infrastructure using PDS and AMS Models. Guru and Ramakar (2016) presented a study on flood estimation in Mahanadi river system, India using PDS. Olsson (2019) debated the short-duration rainfall extremes in Sweden with a regional analysis paradigm. Pham et al. (2013) discussed the statistical properties of PDS with a case study of North New Zealand. Alahmadi et al. (2014) proposed the best fit distribution for PDS of daily rainfall in Madinah, western Saudi Arabia. Karim et al. (2017) evaluated the AMS and PDS for estimating frequency of small floods for 24 gauging stations in the Great Barrier Reef (GBR) lagoon catchments in north-eastern Australia. Keeping in view the importance of PDS frequency analysis, we have compared the performance of PDS frequency analysis with AMS frequency for Rawalpindi city, Pakistan.

Objectives of the study

- To provide comparative at-site rainfall frequency analysis of Rawalpindi city of Pakistan using PDS and AMS modeling techniques.
- To determine the best fit probability distribution for PDS and AMS and estimate their parameters using robust estimation method of L-moments
- Finally, to estimate the quantiles of the best fit probability distribution under PDS and AMS paradigms.

Materials and methods

Data description

The daily rainfall data for length of 25 years of Rawalpindi City, Pakistan is being retrieved from Pakistan Meteorology department. The data is measured in millimeters (mm). Each normal year contains 365 values of daily rainfall while a leap year contains 366 values. We have total of 9131 values with minimum value of 0 mm and maximum of 592 mm. There are total 6 leap years during the study period from 1990 to 2014. Each value has been recorded during 24 h in the city. The average rainfall during 25 years is 53.52 mm with a standard deviation of 24.041 mm. The distribution of daily rainfall is positively skewed with sharp peak. The basic statistics of the study sample is given in *Table 1*.

Table 1. *Summary statistics of basic data for the time period from 1990 to 2014*

Number of values	Minimum value (mm)	Maximum value (mm)	Mean value (mm)	Standard deviation (mm)	Coefficient of skewness	Coefficient of kurtosis
9131	0	592	53.52	24.041	13.137	83.780

http://www.aloki.hu ● ISSN 1589 1623 (Print) ● ISSN 1785 0037 (Online)
DOI: http://dx.doi.org/10.15666/aeer/1704_83518367

Preliminary trend analysis

Preliminary trend analysis is also very important to know about the nature of the data. In order to identify the random behaviour of the time series test of serial correlation could be applied. This test must be applied before applying Mann-Kedall's (MK) test. MK test is normally applied for serially uncorrelated series. If a series is found to be serially correlated, we must do prewhitening to make it serially uncorrelated. The test statistic is given in *Equation 1* and its confidence interval is given in *Equation 2*.

$$R = \frac{1/(n-1)\sum_{t=1}^{n-1}(y_t - \bar{y_t})(y_{t+1} - \bar{y_t})}{1/n\sum_{t=1}^{n-1}(y_t - \bar{y_t})} \quad \text{(Eq.1)}$$

$$\frac{\{-1-1.645\sqrt{n-2}\}}{n-1} \leq R \leq \frac{\{-1+1.645\sqrt{n-2}\}}{n-1} \quad \text{(Eq.2)}$$

where R shows lag-1 correlation while $\bar{y}_t$ represents the average of the time series, n is the number of data points in the time series. The general rule is that if lag-1 correlation co-efficient R is found to be present in the interval as shown in *Equation 2*, we say that there is no significant correlation and declare that the desired series is free from serial correlation at given level of significance otherwise not. The Mann- Kendall's Test, also known as Kendall's tau statistic denoted by "S" by *Equation 3* is applied to find significance and direction of the trend. The null hypothesis will be that series at h with independent and identically distributed observations with two side alternative hypothesis. The constraints for the test are that k j ≤ n j ≠ k.

The test statistic "S" is defined as

$$S = \sum_{k=1}^{n-1}\sum_{j=k+1}^{n}\mathrm{sgn}(y_j - y_k), \quad \text{(Eq.3)}$$

where

$$\mathrm{sgn}(y_j - y_k) = \begin{Bmatrix} +1 \ if \ (y_j - y_k) > 0 \\ 0 \ if \ (y_j - y_k) = 0 \\ -1 \ if \ (y_j - y_k) < 0 \end{Bmatrix}$$

where y_k y_j represent the rank of the data. For the time series with mean of 0 and identical distribution, variance of S statistic can be calculated as in *Equation 4* (Adamowski and Bougadis, 2003):

$$V(S) = \frac{\left\{n(n-1)(2n+5) - \sum_{h=1}^{n} t_h(h)(h-1)(2h+5)\right\}}{18} \quad \text{(Eq.4)}$$

http://www.aloki.hu ● ISSN 1589 1623 (Print) ● ISSN 1785 0037 (Online)
DOI: http://dx.doi.org/10.15666/aeer/1704_83518367

where t_h shows the summation of t, equal to number of tied values to the extent of c. For sample size more than 10, the above statistic follows normal distribution, as given in *Equation 5*. We can calculate the Z statistic as

$$z = \begin{Bmatrix} \frac{s-1}{\sqrt{\mathrm{var}(s)}} if\ s \geq 0 \\ 0 if\ s = 0 \\ \frac{s+1}{\sqrt{\mathrm{var}(s)}} if\ s \leq 0 \end{Bmatrix}, \quad \text{(Eq.5)}$$

After calculating the above statistic, we can compare it with standard normal variate at specified level of significance. The S statistic not only determine the significance of the test but also the direction of the trend. For example, a positive value shows an upward trend while a negative value shows downwards trend in the data. The exact value of slope in the time series could be determined with the help of Sen's estimator, with an assumption that there is a linear trend in the data. It is also a nonparametric method used to find the change per unit time. To find the slope, first we calculate the statistic $Qi\ from\ M\ pairs$ of the given time series as shown below in *Equation 6:*

$$Q_i = \frac{y_j - y_k}{j-k}, \quad \text{(Eq.6)}$$

for i = 1, 2, 3,……..,M; where *"i"* indicates the *ith* pair of the data. The data point at *j*th time should be larger than the data point at *k*th time. The next step is finding the median value of these M values of *Qi*. This median value shows our required Sen's estimator. There are two cases: the first one is that if *M* is odd, the median value is given in *Equation 7:*

$$Q_{median} = Q_{\frac{m+1}{2}} \quad \text{(Eq.7)}$$

Second, if *M* is even, the median value is given in *Equation 8:*

$$Q_{median} = \frac{1}{2}\left[Q_{\frac{M}{2}} + Q_{\frac{M}{2}+1} \right], \quad \text{(Eq.8)}$$

Formation of annual maximum series (AMS) and partial duration series (PDS)

From the basic data of daily rainfall of 25 years we want to formulate two series, such as Partial Duration Series (PDS) and Annual Maximum Series (AMS) for further analysis. The AMS consists of single value, the maximum value in the whole year. It is largest value among 365 values while, PDS consists of all well-defined maximum peaks above a certain threshold level (Beguería, 2005). Selection of threshold is one of the major complexities in the PDS modeling. It turns out that there is, in the state of the art, no universal and unambiguous rule for the selection of the threshold which incorporates as much information as desirable without compromising the independence requirement between occurrences over time. The selection of threshold has direct impact on the analysis. The problem of the selection of threshold is also discussed extensively by

http://www.aloki.hu ● ISSN 1589 1623 (Print) ● ISSN 1785 0037 (Online)
DOI: http://dx.doi.org/10.15666/aeer/1704_83518367

Rosbjerg and Madsen (1992). They compared different methods to define the threshold level based on certain values of frequency factor *K*. This method presents a predefined frequency factor *K*, can be written as in *Equation 9:*

$$Threshold = E\{1\} + (K).S(1) \quad \text{(Eq.9)}$$

where E {I} and S {I} are, the mean and the standard deviation of the basic data.

To enhance the usage of PDS modeling among the practitioners, it is required to develop a practice-oriented guidelines (Rasmussen et al., 1994). Meeting the independence condition for the set of selected peaks is a prerequisite in frequency analysis of PDS. In terms of computation, PDS modeling is more complicated than the AMS modeling. According to extreme value theory, along with fundamental assumptions of independence and identical distribution, PDS modeling also requires that number of peaks above threshold to follow Poisson process while the peaks themselves follow GPD (Cunnane, 1979). Once the series satisfies the basic assumptions, the next step is to determine the best fit probability distribution. Therefore, we study most commonly used distributions for frequency analysis in this study such as GLO, GEV, GPD, PE3.

Selection of estimation method

Linear moments (LM) estimation technique has been adopted in this study to estimate the parameters of the statistical models. In case of extreme values present in the data series LM method is advantageous over the conventional moments method (Ahmad et al., 2015). Estimates of the conventional moments methods are not robust in quality and do not provide reliable estimates for the probability distributions with three or more parameters. The method of maximum likelihood (MLE) is considered as one of the efficient parameters estimation approach. It gives the least variance of the estimated parameters but it suffers from serious disadvantage of giving biased estimates with small samples especially if the numbers of parameters are large (Ahmad et al., 2016a, b, 2017). The method of LM corresponding to probability weighted moments (PWMs) are variants of the method of moments which provide a different way to summarize the data set. LM are summary statistics for probability distributions and data sample. Measure of location, dispersion, skewness, kurtosis and other descriptive statistics can be obtained through LM. To compute LM, we consider linear combination of ordered statistics. For instance, X_1, X_2, X_3, ... X_r, *be* the random sample of magnitude r, with cumulative distribution function $F(X)$ and quantile function $X(F)$.

Let $X(1:r) \leq X(2:r) \leq \ldots \leq X(r:r)$ be the order statistics of a random sample. For random variable X, the rth population L-moment as explained by (Hosking, 1990) can be written as in *Equation 10:*

$$\lambda_r = \frac{1}{r}\sum_{k=0}^{r-1}(-1)^k \binom{r-1}{k} E(X_{r-k:r}) \quad \text{(Eq.10)}$$
$$r = 1, 2, \ldots\ldots$$

In *Equation 10* λ_r is a linear function of the expected order statistics. The L-moment ratios are also very important. These can be defined as in *Equations 11-13:*

http://www.aloki.hu ● ISSN 1589 1623 (Print) ● ISSN 1785 0037 (Online)
DOI: http://dx.doi.org/10.15666/aeer/1704_83518367

$$\tau = \frac{\lambda_2}{\lambda_1} \quad \text{(Eq.11)}$$

$$\tau_3 = \frac{\lambda_3}{\lambda_2} \quad \text{(Eq.12)}$$

$$\tau_4 = \frac{\lambda_4}{\lambda_2} \quad \text{(Eq.13)}$$

where τ is a measure of L-coefficient of variation (L-Cv), τ_3 τ_4 are L-skewness and L-Kurtosis, respectively. In general sample linear moments are estimated utilizing the sample obtained from the large set of data. In this study we have also obtained the sample moments using the sample of the large set of daily rainfall records of 25 years of Rawalpindi city. The r_{th} sample L-moments as suggested by Hosking (1990) are given in *Equation 14:*

$$l_r = \frac{1}{r} r \sum_{i=1}^{n} \left[\sum_{j=0}^{r-1} \frac{(-1)^j \binom{r-1}{j} \binom{i-1}{r-1-j} \binom{n-1}{j}}{\binom{n}{r}} \right] X_{i:n} \quad \text{(Eq.14)}$$

$$r = 1, 2, 3, \ldots\ldots$$

The sample L-ratios are defined in *Equation 15:*

$$t = \frac{\ell_2}{\ell_1},\ t_3 = \frac{\ell_3}{\ell_2}\ \ t_4 = \frac{\ell_4}{\ell_2} \quad \text{(Eq.15)}$$

where ℓ1 is sample measure of location, *"t"* is sample measure of CV, t_3 t_4 are the sample skewness and Kurtosis based on LM respectively. These measures are used to identify the distribution from which the sample is drawn. Additionally, these measures are used in the estimation of parameters when distribution is fitted to a sample by equating the sample L-moments to corresponding population L-moments.

Goodness of fit criteria

Another fundamental step in rainfall frequency analysis after selection of efficient robust estimation method is the selection of best fit statistical models. For the selection of best fit statistical model, we have standard criteria, i.e. Akaik Information Criterion (AIC) and Bayesian Information Criterion (BIC), but do not work efficiently in the presence of small sample data. These criteria fail to produce efficient results with asymmetric probability distribution that commonly encountered in extreme events applications. Therefore, in this study we have used Anderson - Darling (A-D) test to verify whether or not a sample belongs to specific population. This test statistics is a modified form of the Kolmogorov Smirknove (K-S) test. This testing criterion is considered to be better than K-S testing criterion as it gives more weight to the tails in the highly skewed distributions. This test also considers specific distribution in the calculation process of critical values. Baldassarre and Montanari (2009) suggested using

http://www.aloki.hu ● ISSN 1589 1623 (Print) ● ISSN 1785 0037 (Online)
DOI: http://dx.doi.org/10.15666/aeer/1704_83518367

A-D testing criterion as a goodness of fit test for small sample data. Similar suggestions are found in Onoz and Bayazit (1995). The mathematical form of A-D testing criterion can be defined by the formula given in *Equation 16:*

$$A^2 = -n - \frac{1}{n}\sum_{i=1}^{n}(2i-1) \\ [\ln F(Xi) + \ln(1 - F(1 - F(X_{n-i+1}))) \quad \text{(Eq.16)}$$

In *Equation 16* "n" is the size of the sample, $X_{i,s}$ are the observed data values arranged in an ascending order $F_{(X)_i}$ is the expected distribution function. The larger value of the test statistic will show more discrepancy between expected and empirical distribution function, hence would lead us to reject the null hypothesis. L-moment ratio diagram has also been adopted as an expedient tool for the selection of candidate distribution (Ahmad et al., 2015). These diagrams represent a theoretical relationship between the L-skewness τ_3 and the L-kurtosis τ_4 of different probability distribution. The sample ratio of L-skewness and L-kurtosis goes near to the most appropriate distribution in the diagram.

Basic assumptions of the data

PDS and AMS analysis requires that the data must fulfill the fundamental assumptions of statistical hydrology such as randomness, independence, homogeneity and stationarity. Assumption of randomness uncovers, either the given sample is drawn at random from the population. If the data fulfills the assumption, it implies that the sample values are the realization of a random variable (Naghettini, 2016). NERC (1975) proposed a nonparametric test for checking randomness by considering the number of turning points present in the sample for a given time period. A turning point may be defined as a peak or a trough in a time series plot of the data. Underlying intuitive idea behind the test is that if there are too many or few turning points in the data, then the sample would be declared as possibly non-random. The numbers of turning points "p" is a purely random process of N observations with mean variance mentioned in *Equations 17* and *18:*

$$E(p) = \frac{2(N-2)}{3} \quad \text{(Eq.17)}$$

$$Var(p) = \frac{16N-29}{90} \quad \text{(Eq.18)}$$

This approximation is available in literature for large sample (Yule, 1950). It has been proposed that the resulting variable "t" follows normal distribution for larger size. Therefore, under the null-hypothesis of randomness the standardized test statistic, $(t = \frac{p-E(p)}{\sqrt{var(p)}})$, follows normal distribution.

For fulfillment of independence assumption, we used Wald and Wolfowitz test. The assumption of independence implies that not a single sample value could affect the occurrence or non-occurrence of any other sample value present in the data. Generally, the AMS is expected to follow the assumption of independence, while strong dependence is expected for PDS. In any case, the assumption of independence must be checked before further analysis. Wald and Wolfowitz (1943) suggested a non-parametric test for this purpose. Let $\{x_1, x_2, \ldots, x_n\}$ describe a sample of size N from X,

http://www.aloki.hu ● ISSN 1589 1623 (Print) ● ISSN 1785 0037 (Online)
DOI: http://dx.doi.org/10.15666/aeer/1704_83518367

while $\{x_1', x_2', \ldots, x_N'\}$ is the sequence of differences of any ith sample value from the sample mean $\bar{x}$.

The test statistic is calculated using R, E (R) $\widehat{Sr}$ given in *Equations 19-21:*

$$R = \sum_{i=1}^{N-1} x_i' x_{i+1}' + x_1' x_N', \quad \text{(Eq.19)}$$

$$E(R) = \frac{s_2}{N-1} \quad Var(R) = \frac{s_2^2 - s_4}{N-1} + \frac{s_2^2 - 2s_4}{(N-1)(N-2)} - \frac{s_2^2}{(N-1)^2} \quad \text{(Eq.20)}$$

where:

$$\widehat{s_r} = \sum_{i=1}^{N} (x_i')^r \quad \text{(Eq.21)}$$

For large sample under true null hypothesis of independence, Wald and Wolfowitz (1943) found that this test statistic follows a normal distribution as mentioned in *Equation 22*.

$$t = \frac{R - E(R)}{\sqrt{var(R)}} \quad \text{(Eq. 22)}$$

The assumption of homogeneity implies that all elements of the sample data belong to a single common population. However, considering mean values or total of values makes easier to detect the heterogeneities. The assumption of homogeneity is generally checked through a non-parametric test developed by Mann-Whitney (1947). For a given sample $\{x_1, x_2, x_3, \ldots\ldots, x_n\}$, of size N, one has to split the data in two sub samples of size N_1 $\{x_1, x_2, x_3, \ldots\ldots, x_{N1}\}$, N_2 $\{x_1, x_2, x_3, \ldots\ldots, x_{N2}\}$ sizes such that $N_1 + N_2 = N$ (with approximately equal subsamples). Once the splitting of the data is done the second step is to rank the entire sample in ascending order by noting the rank order say (m) of each element also from which subsample belongs to. The basic idea behind the test is that if the given sample is not homogenous, the sum of ranking orders of the elements belonging to first subsample would be consistently higher or lower than the sum of ranking orders of elements of the second subsample (Naghettini, 2016).

The Mann–Whitney test statistic can be written in the form mentioned in *Equations 23* and *24*.

$$V_1 = N_1 N_2 + \frac{N_1 (N_1 + 1)}{2} - R_1 \quad \text{(Eq.23)}$$

$$V_2 = N_1 N_2 - V_1 \quad \text{(Eq.24)}$$

where R_1 indicates the sum of ranks of all elements from first subsample. If both of the subsamples are larger than 20, the null hypothesis is true such that the given sample is homogenous, Mann-Whitney (1947) showed that V follows a normal distribution with mean: $E[V] = \frac{N_1 N_2}{2}$; variance: $VAR(V) = \frac{N_1 N_2 (N_1 + N_2 + 1)}{N_2}$; Hence, the require statistic for the Mann–Whitney test will be written as: $t = \frac{V - E(V)}{\sqrt{var(V)}}$, which follows a standard normal distribution.

The notion of stationarity implies that some basic properties of the observed sample as well as relevant functional form of the probability distribution and its parameters do not change with respect to time. Non-stationarity might be in form of monotonic trend

http://www.aloki.hu ● ISSN 1589 1623 (Print) ● ISSN 1785 0037 (Online)
DOI: http://dx.doi.org/10.15666/aeer/1704_83518367

as well as abrupt change in the data at some time interval. It is to be noted that a non-stationary series is always non-homogenous but non- homogenous series is not necessarily stationary (Naghettini, 2016).

In order to verify the assumption of stationarity, a non-parametric test named Spearman's rank correlation coefficient is used. It is a statistical dependence between two variables, one is the ordered ranks say (m_t) of the observed sample in ascending order while the other one is the time indices $T_t = 1,2, \ldots . N$. It reveals the monotonic trend which is not restricted to only linear as in case of conventional correlation coefficient. It also depicts the nonlinear correlation between the ranks' orders say (m_t) of the observed sample and the time indices $T_t = 1,2, \ldots . N$. It is written as in the following form given in *Equation 25*.

$$r_s = 1 - \frac{6\sum_{t=1}^{N}(m_t - T_t)^2}{N^3 - N} \quad \text{(Eq.25)}$$

The corresponding test statistic is written in *Equation 26:*

$$t = r_s\sqrt{\frac{N-2}{1-r_s^2}} \quad \text{(Eq.26)}$$

Assumptions of partial duration series analysis

For PDS sample, it is required that it must fulfills the assumption of Poison process. Bogeria (2005) discovered that the original daily rainfall series did not adjust to a Poisson process at lower threshold level, however the study showed that the tendency towards the Poisson process was increased as the level of threshold increases. For at-site frequency analysis, Cunnane (1979) proposed Fisher testing criterion given in *Equation 28* to test Poisson process states that the number of peaks values exceeding certain threshold level must conforms to a Poisson Process with mean such as *Equation 27*.

$$p = \frac{e^{-\mu}\mu^x}{x!} \quad \text{(Eq.27)}$$

A test of Poisson assumption can be piloted on observed series of peaks exceeding the certain threshold level. Fisher test statistics is based on the equation given in *Equation 28*. This statistics is utilized for the verification of PD series.

$$R = \sum\frac{(ni - \lambda)^2}{\lambda} \quad \text{(Eq.28)}$$

In the equation above ni represents the number of peaks above at certain threshold in a year, λ is the mean number of peaks exceeding certain threshold level. In the literature this testing criterion has been used for the verification of Poisson assumption. Under the true null hypothesis, statistics R is distributed as chi-square distribution with the confidence limits as $\chi^2_{\alpha/2}(t-1) < R < \chi^2_{1-\alpha/2}(t-1)$. These confidence limits verify either data series to follow the Poisson distribution. If, test statistics R lies within the upper and lower confidence limits then the PDS will be considered to follow Poisson process. If the classical PDS model comprises the assumption of Poisson process then

http://www.aloki.hu ● ISSN 1589 1623 (Print) ● ISSN 1785 0037 (Online)
DOI: http://dx.doi.org/10.15666/aeer/1704_83518367

the exceedances may follow exponential distribution. However, in recent years numerous researches have emphasized that the peaks in PDS modeling follow GPD (see for example Hosking Wallis, 1987; Madsen and Rosbjerg, 1994). Few other research studies have proved that peaks in PDS may also follow distributions other than GPD (for example see Rasmussen et al., 1991).

Results and discussion

Preliminary trend analysis is also very important to know about the nature of the data. In this study, we have carried out the trend analysis using monthly and overall precipitation series of 25 years of data of Rawalpindi city from 1990 to 2014. There are total thirteen variables including one for overall daily rainfall (raw) data and remaining twelve for monthly data. We implemented two non-parametric methods for trend analysis. In other words, Mann-Kendall (MK) test procedure is used to find the significance of the trend while Sen's slope estimator to find change per unit time. The MK test will help to find not only the significance of the trend but also direction of the trend with an assumption of linear trend. Before applying Mann-Kendall's test for significance of the trend, we also implemented lag-1 serial correlation test to determine either we need some prewhitening of the data or not. The data of Rawalpindi station on monthly basis as well as overall data did not show any lag-1 serial correlation among the successive values. This implies that we do not need any prewhitening of given time series. The given series can be used for further trend significance. The bold value in *Table 2* shows the presence of significant trends. All months shows insignificant trends except the month of March. Three months such as Month of January, June and November show negative insignificant trends. Overall data also indicate that the trend is insignificant positive trend. Further, we can also notice that the trend in monsoon season (July to September) is positive insignificant.

Table 2. *Trend analysis in monthly rainfall and daily rainfall data from 1990 to 2014*

Jan	Feb	Mar	Apr	May	Jun	Jul	Aug	Sep	Oct	Nov	Dec	Overall
-0.01	0.047	**0.127**	0.081	0.05	-0.022	0.014	0.017	0.022	0.018	-0.03	0.005	0.021

Formation of partial duration (PDS) and annual maximum series (AMS)

For AMS frequency analysis, maximum value per year is considered. For the length of 25 years data we have only 25 values, whereas, in PDS, exceedances above certain threshold level are considered. For PDS different samples were selected utilizing different values of *K* (frequency factor) in objective formula.

The size of the sample in PDS is associated with the value of frequency factor (*K*). A slight increase in the value of K reduces the sample to a large extent as shown in *Table 3*. A sample of size 126 was obtained using 3.5 as frequency factor. Similarly, the sample of size 96, 58 were obtained using 4 and 5 as K values in the objective formula. For PDS sample to be used for further analysis is necessary to follow the assumption of Poisson process. Therefore, all the samples of PDS given in *Table 3* were tested for Poisson process. The results are given in *Table 4* based on 99% and 95% confidence interval.

http://www.aloki.hu ● ISSN 1589 1623 (Print) ● ISSN 1785 0037 (Online)
DOI: http://dx.doi.org/10.15666/aeer/1704_83518367

Table 3. *Frequency factor and number of exceedances using objective formulation*

Frequency factor (K)	PDS sample size
K = 3.5	126
K = 4	96
K = 5	58

Table 4. *The assumption of Poisson distribution for partial duration series*

K	R	C.I (1%)	Decision	C.I (5%)	Decision
3.5	12.49	9.02 < R < 45.559	Accepted	12.401 < R < 39.36	Accepted
4.5	5.82	9.02 < R < 45.559	Rejected	12.401 < R < 39.36	Rejected

Table 4 shows that a sample of size 126 was obtained using value of 3.5 for *K* in the objective formula which fulfills the assumption of Poisson process both at 99% confidence interval 95% confidence interval. The value of the statistic falls in the confidence interval which supports that the PDS sample from this frequency factor is following Poisson process assumption. Whereas, rest of the sample do not fulfills the assumption of Poisson process. For further rainfall frequency analysis we will consider only the sample with frequency factor = 3.5. For AMS analysis we have 25 values while for PDS analysis we have 126 values for further analysis.

Fundamental assumptions are essential before carrying out formal RFA. Therefore, we have tested both samples, i.e. PDS and AMS for randomness, Independence, homogeneity and stationarity. *Table 5* presents that the values of test statistics *t* for different assumptions at 5% level of significance. The calculated values of the said test statistic are less than the critical value of 1.96, therefore it can be suggested that both series are random, independent, homogenous and stationary. Thus it is concluded that both series are suitable for further RFA.

Table 5. *Results of fundamental assumptions for PDS AMS*

Series	Randomness*	Independence*	Homogeneity*	Stationarity*
PDS	$\hat{t} = 1.80$; Since $\lvert\hat{t}\rvert < Z_{1-\frac{\alpha}{2}} = 1.96$ Do not reject H_0	$\hat{t} = 1.48$; Since $\lvert\hat{t}\rvert < Z_{1-\frac{\alpha}{2}} = 1.96$ Do not reject H_0	$\hat{t} = -0.153$; Since $\lvert\hat{t}\rvert < Z_{1-\frac{\alpha}{2}} = 1.96$ Do not reject H_0	$\hat{t} = -0.3279$; Since $\lvert\hat{t}\rvert < t_{1-\alpha/2,(N-2)} = 0.687$ Do not reject H_0
AMS	$\hat{t} = 1.29$; Since $\lvert\hat{t}\rvert < Z_{1-\frac{\alpha}{2}} = 1.96$ Do not reject H_0	$\hat{t} = -0.412$; Since $\lvert\hat{t}\rvert < Z_{1-\frac{\alpha}{2}} = 1.96$ Do not reject H_0	$\hat{t} = -1.22$; Since $\lvert\hat{t}\rvert < Z_{1-\frac{\alpha}{2}} = 1.96$ Do not reject H_0	$\hat{t} = 1.419$; Since $\lvert\hat{t}\rvert < t_{1-\alpha/2,(N-2)} = 1.66$ Do not reject H_0

*5% level of significance

To find the best distribution for both samples, we considered most commonly used distributions for at-site frequency analysis. The goodness of fit of these distributions is evaluated using the most common goodness of fit criteria, i.e., AD and L-moment ratio diagram. Based on the AD testing criterion and the L-moment ratio diagram, the best fitted probability distribution for PDS sample was the GEV while for the AMS sample the GLO distribution. In case of AD testing criterion, the smallest test statistics values

http://www.aloki.hu ● ISSN 1589 1623 (Print) ● ISSN 1785 0037 (Online)
DOI: http://dx.doi.org/10.15666/aeer/1704_83518367

would be considered as the best fitted and will be ranked one. As shown in *Table 6,* the best fitted probability distribution is GEV that ranked one in case of PDS sample whereas, GLO in case of AMS. The ratio of sample L-skewness and L-Kurtosis is shown with symbol "+". The closeness of symbol "+" to the curve in the diagram declares the distribution as best fitted for sample at hand. It is apparent from *Figures 1* and *2* that GEV distribution is the best fitted for PDS while GLO for AMS. The outputs of the graphs validated the mathematical results obtained from AD testing criterion.

Table 6. *Determination of best fit probability distribution for PDS AMS*

Distributions	PD Series (n = 126)		AM series (n = 25)	
	AD	Rank	AD	Rank
GEV	0.29438	1st	0.49	2nd
PE-3	5.5266750	4th	6.11	4th
GLO	3.57	2nd	0.47	1st
GPD	3.646	3rd	2.92	3rd

The next step in RFA after declaration of the best fitted probability distribution is the quantiles estimation. Quantile estimation provides estimates to ensure a resilience hydrological structure. Therefore, we constructed a *Table 7* that consists of quantiles estimates for various return periods. These estimates are computed for PDS and AMS samples separately and further their standard errors are given in parenthesis. These standard errors will assure the robustness and efficiency of PDS and AMS samples. The relationship between return periods and occurrence of an extreme event is established through notion of a geometric random variable (waiting time until an extreme event occurs) using mathematical expression: $E(X) = T = 1/p$, which is in fact the mean of the geometric random variable (average time for occurrence of an extreme event, for example exceeding of water flow above certain level of a hydrological structure), where p is the probability of occurrence or exceedance for T year return period. Suppose we have a return period of ten-years, the corresponding probability of exceedance is calculated using above equation as 0.1 and the probability of non-exceedance as 0.9. The corresponding quantile estimates based on the best fitted distribution (GEV for PDS) is 129.64 mm, which implies that in next ten-year, the daily rainfall in the city would exceed 129.64 mm once on the average with a probability of 0.1. These quantiles could be used for planning of water-related emergencies, sustainable water resource management, construction of better flood design estimates in the form of culverts, bridges other hydrological structures in the city. The quantile estimation for AMS series showed significant variation in magnitude as compared to PDS for various return periods. Further, to identify the best technique between AMS and PDS, we calculated the standard errors of these quantiles estimates at different return periods. These standard errors are given in parenthesis as shown in *Table 7*. The standard errors of PDS sample are significantly smaller than AMS sample. It implies that PDS sample outperforms than AMS sample at different return periods which strengthens the use of PDS in the current study. Comparisons of AMS and PDS extreme events have also indicated that for all return periods PDS give more consistent, efficient and robust predictions of extreme rainfall than AMS. The predicted magnitude based on PDS are also more closer to the historical records as compared to AMS. The quantiles estimates

http://www.aloki.hu ● ISSN 1589 1623 (Print) ● ISSN 1785 0037 (Online)
DOI: http://dx.doi.org/10.15666/aeer/1704_83518367

for different return periods are helpful to construct a variety of hydrological infrastructures such as bridges, culverts and others in the city

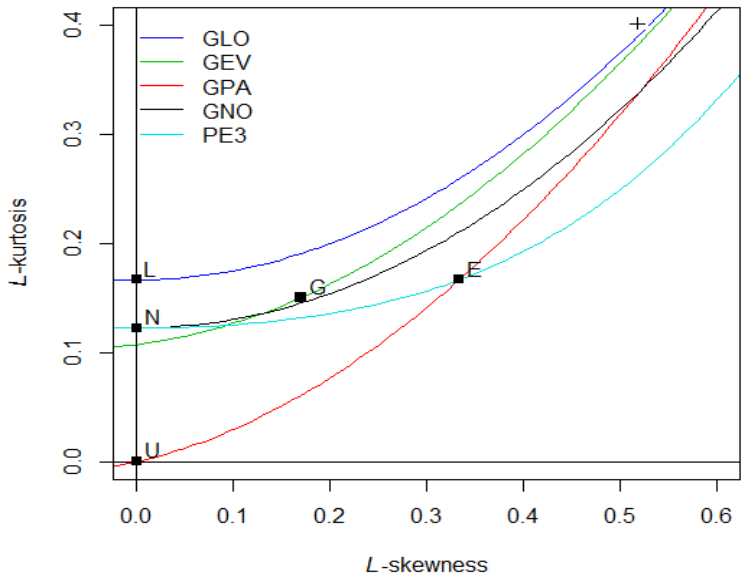

Figure 1. *L moment ratio diagram for AMS sample*

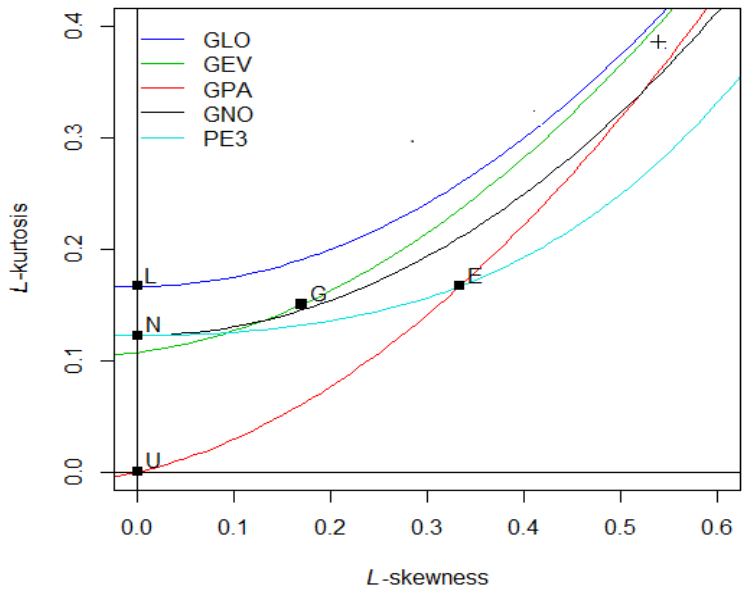

Figure 2. *L moment ratio diagram for PDS sample*

Table 7. *Quantile estimates for different return periods*

	Best fitted distribution	**5**	**10**	**100**	**1000**
		****80%**	**90%**	**99%**	**99.9%**
PDS	GEV	98.072 (0.346)	129.64 (0.245)	308.77(0.175)	720.52 (0.179)
AMS	GLO	172.0268 (0.742)	230.08 (0.641)	594.74 (0.442)	1591.07 (0.318)

**Probability of non-exceedances

http://www.aloki.hu ● ISSN 1589 1623 (Print) ● ISSN 1785 0037 (Online)
DOI: http://dx.doi.org/10.15666/aeer/1704_83518367

Conclusions

In this study, we conducted rainfall frequency analysis in the fast growing city Rawalpindi, Pakistan by extracting two series such as PDS and AMS from daily rainfall data measured in millimeters for a period of 25 years (1990-2014). The selection of best sample between PDS and AMS had always been a dilemma in rainfall frequency analysis. This study also provided a comparative analysis of these two techniques. After preliminary trend analysis, for PDS sample extraction we used objective method. The size of the sample for PDS was higher than AMS. After extraction of the required samples, we implemented the most common probability distributions used in statistical hydrology to check the best fit. For this purpose two GOF criteria such as Anderson Darling (A-D) test and L-moment ratio diagram were implemented. The analysis revealed that GEV was best fit for PDS while GLO for AMS. In this study we also found quantiles estimates using the parameters of the best probability distributions for both series. The predicted values based on quantile estimation for AMS series showed significant variation in magnitude as compared to PDS for various return periods. The standard errors of quantile estimates based on these techniques revealed that PDS was better than AMS. PDS would be a more reasonable and effective choice for such type of frequency analysis. Our results are also analogous to the outcomes of earlier studies (e.g., Fischer and Schuman, 2014; Alahmadi et al., 2014; Karim et al., 2017) where PDS technique outperformed than AMS.

Thus we can conclude that the results obtained using PDS sample were generally preferable for at-site quantile estimation. The findings from this study could be implemented in selection of better design criteria for flood management, particularly flood protection measures in the city. This study could also be extended for rainfall frequency analysis in the other areas of Pakistan with similar geomorphologic hydrological characteristics.

Acknowledgements. Authors are very grateful to deanship of scientific research at King Khalid University, Abha, Saudi Arabia for the financial support through General Research Program under project number GRP-133-40.

Conflict of interests. Authors have no conflict of interests on publication of this paper in Applied Ecology and Environmental Research (AEER) journal.

REFERENCES

[1] Adamowski, K., Bougadis, J. (2003): Detection of trends in annual extreme rainfall. – Hydrological Processes 17(18): 3547-3560.

[2] Agilan, V., Umamahesh, N. V. (2017): Non-stationary rainfall intensity-duration-frequency relationship: a comparison between annual maximum and partial duration series. – Water Resources Management 31(6): 1825-1841.

[3] Ahmad, I., Fawad, M., Abbas, A., Saghir, A. (2016a): Probability modelling of low flows at different sites of Indus basin in Pakistan using L-moments and TL-moments. – Pakistan Journal of Science 68(1): 86-93.

[4] Ahmad, I., Fawad, M., Mahmood, I. (2015): At-site flood frequency analysis of annual peak stream flows in Pakistan using robust estimation methods. – Polish Journal of Environmental Studies 24(6).

http://www.aloki.hu ● ISSN 1589 1623 (Print) ● ISSN 1785 0037 (Online)
DOI: http://dx.doi.org/10.15666/aeer/1704_83518367

[5] Ahmad, I., Fawad, M., Akbar, M., Abbas, A., Zafar, H. (2016b): Regional frequency analysis of annual peak flows in Pakistan using linear combination of order statistics. – Polish Journal of Environmental Studies 25(6): 1-10.
[6] Ahmad, I., Yasin, M., Fawad, M., Saghir, A. (2017): Regional frequency analysis of Low flows using L. moments for Indus Basin, in Pakistan. – Pakistan Journal of Science 69(1): 75-83.
[7] Alahmadi, F., Rahman, N. A., Abdulrazzak, M. (2014): Evaluation of the best fit distribution for partial duration series of daily rainfall in Madinah, western Saudi Arabia. – Proceedings of the International Association of Hydrological Sciences 364: 159-163.
[8] Baldassarre, G. D., Montanari, A. (2009): Uncertainty in river discharge observations: a quantitative analysis. – Hydrology Earth System Sciences 13(6): 913-921.
[9] Beguería, S. (2005): Uncertainties in partial duration series modeling of extremes related to the choice of the threshold value. – Journal of Hydrology 303(1): 215-230.
[10] Berton, R., Rahmani, V. (2018): Improving peak flow estimation across the United States by using partial duration series. –AGU Fall Meeting Abstracts #H41M-2279.
[11] Chang, K. B., Lai, S. H., Othman, F. (2015): Comparison of annual maximum and partial duration series for derivation of rainfall intensity-duration-frequency relationships in peninsular Malaysia. – Journal of Hydrologic Engineering 21(1): 0501-513.
[12] Cunnane, C. (1979): A note on the Poisson assumption in partial duration series models. – Water Resources Research 15(2): 489-494.
[13] Fischer, S., Schumann, A. (2014): Comparison between Classical Annual Maxima and Peak over Threshold Approach Concerning Robustness. – Universitätsbibliothek Dortmund.
[14] Gado, T. A., Nguyen, V. T. V. (2016): Regional estimation of floods for ungauged sites using partial duration series and scaling approach. – Journal of Hydrologic Engineering 21(12): 04016044.
[15] Guru, N., Jha, R. (2016): Flood estimation in Mahanadi river system, India using partial duration series. – Georisk: Assessment and Management of Risk for Engineered Systems and Geohazards 10(2): 135-145.
[16] Hassan, I., Ghumman, A. R., Ghazaw, Y., Abdel-Maguid, R. H., Samreen, B. (2017): Climate change impact on precipitation in arid areas of Pakistan. – Int. J. Water Resour. Arid Environ. 6: 80-88.
[17] Hosking, J., Wallis, J. (1987): Parameter quantile estimation for the generalized pareto distribution. – Technimetrics 29(3): 339-349.
[18] Hosking, J. R. M. (1990): L-moments: Analysis and estimation of distributions using linear combinations of order statistics. – Journal of the Royal Statistical Society: Series B (Methodological) 52(1): 105-124.
[19] Karim, F., Hasan, M., Marvanek, S. (2017): Evaluating annual maximum and partial duration series for estimating frequency of small magnitude floods. – Water 9(7): 481-488.
[20] Lang, M., Ouarda, T. B. M. J., Bobee, B. (1999): Towards operational guidelines for over-threshold modeling. – Journal of Hydrology 225(3): 103-117.
[21] Madsen, H., Rosbjerg, D., Harremoës, P. (1994): PDS-modelling regional Bayesian estimation of extreme rainfalls. – Hydrology Research 25(4): 279-300.
[22] Mann, H. B, Whitney, D. R (1947): On the test of whether one of two random variables is stochastically larger than the other. – Ann Math Stat 18: 50-60.
[23] Naghettini, M. (2016): Fundamentals of Statistical Hydrology. – Springer, Berlin.
[24] Nagy, B. K., Mohssen, M., Hughey, K. F. D. (2017): Flood frequency analysis for a braided river catchment in New Zealand: comparing annual maximum and partial duration series with varying record lengths. – Journal of Hydrology 547: 365-374.
[25] NERC (1975): Flood Studies Report. Vol 1. – National Environmental Research Council, London.

http://www.aloki.hu ● ISSN 1589 1623 (Print) ● ISSN 1785 0037 (Online)
DOI: http://dx.doi.org/10.15666/aeer/1704_83518367

[26] Olsson, J., Södling, J., Berg, P., Wern, L., Eronn, A. (2019): Short-duration rainfall extremes in Sweden: a regional analysis. – Hydrology Research. https://doi.org/10.2166/nh.2019.073.
[27] Önöz, B., Bayazit, M. (1995): Best-fit distributions of largest available flood samples. – Journal of Hydrology 167(1-4): 195-208.
[28] Pham, H. X., Shamseldin, A. Y., Melville, B. (2013): Statistical properties of partial duration series: Case study of North Island, New Zealand. – Journal of Hydrologic Engineering 19(4): 807-815.
[29] Rasmussen, P., Ashkar, F., Rosbjerg, D., Bobee, B. (1994): The POT Method for Flood Estimation: A Review. – In: Hiper, K. W. (ed.) Stochastic and Statistical Methods in Hydrology and Environmental Engineering. Springer, Dordrecht.
[30] Rasul, G., Sixiong, Z., Qingcun, Z. (2004): A diagnostic study of record heavy rain in twin cities Islāmābad-Rāwalpindi. – Advances in Atmospheric Sciences 21(6): 976-988.
[31] Rasul, G., Mahmood, A., Sadiq, A., Khan, S. I. (2012): Vulnerability of the Indus delta to climate change in Pakistan. – Pakistan Journal of Meteorology 8(16): 89-107.
[32] Rosbjerg, D., Madsen, H. (1992): On the choice of threshold level in partial duration series. – Nordic Hydrological Conference Alta, NHP-Report 30: 604-615.
[33] Vrban, S., Wang, Y., McBean, E. A., Binns, A., Gharabaghi, B. (2018): Evaluation of stormwater infrastructure design storms developed using partial duration and annual maximum series models. – Journal of Hydrologic Engineering 23(12).
[34] Wald, A., Wolfowitz, J. (1943): An exact test for randomness in the non-parametric case based on serial correlation. – The Annals of Mathematical Statistics 14(4): 378-388.
[35] Yule, G. Y., Kendall, M. G. (1950): An Introduction to the Theory of Statistics. – Charles Griffin and Co., London.

http://www.aloki.hu ● ISSN 1589 1623 (Print) ● ISSN 1785 0037 (Online)
DOI: http://dx.doi.org/10.15666/aeer/1704_83518367

DETERMINATION OF 17 ELEMENTS IN FREE-RANGE HEN EGGS WITH ICP-MS

KILIÇ ALTUN, S.[1*] – PAKSOY, N.[2] – DİNÇ, H.[3] – DURMAZ, H.[1]

[1]*Harran University, Veterinary Faculty, Department of Food Hygiene and Technology 63200 Şanlıurfa, Turkey*

[2]*Harran University, Veterinary Faculty, Department of Biochemistry, 63200 Şanlıurfa, Turkey*

[3]*Harran University, Veterinary Faculty, Department of Pharmacology and Toxicology 63200 Şanlıurfa, Turkey*

**Corresponding author*
e-mail: skilicaltun@harran.edu.tr; phone: +90-414-318-2676

(Received 27th Feb 2019; accepted 15th May 2019)

Abstract. The egg is a widely consumed food material with the higher nutritional value obtained from poultry. It contains almost all the nutrients needed by metabolism, therefore, the biological value of an egg is high. The aim of this study is to determine the levels of eighteen elements in free-range hen eggs. Eggs (n=217) were collected from February 2017 to September 2017 in the spring, summer and autumn seasons from towns near the Syrian border. The ICP-MS method was used to determine the Na, Mg, K, Ca, Cr, Mn, Fe, Co, Ni, Cu, Zn, Se, Ti, As, Cd, Tl and Pb elements levels in the study. The most abundant elements were Na and K ranging between 248.12-7755 mg/kg and 80.25-4235 mg/kg, respectively. When the element levels of the free-range hen egg samples were examined, it was seen that there was a statistical difference between the seasons while the samples were contaminated with As on an average of 1131.25 µg/kg when the toxic element levels were examined. It was concluded that the element content of free-range hen eggs produced in this region was affected by seasonal changes.
Keywords: *free-range hen eggs, ICP-MS, macro element, micro element, toxic element*

Introduction

Occupation and income status of a society influences nutritional habits and thereby human health. Due to easily accessible, the widely available food source of hen eggs, which are basic food ingredients, consumed a lot in the worldwide. Hen egg has important nutritional value and contributes significantly to a healthy diet with its' high-quality proteins, vitamins, fats, and minerals (Domingo, 2014). A medium-sized egg includes 78 kcal, consisting of 6.5 g of protein, 2.3 g monounsaturated fat on an average. Most of the lipids of the egg are in the form of lipoproteins found in egg yolk as well as proteins located in all parts of the egg (Kovacs-Nolan et al., 2005; Domingo, 2014). It also includes dietary cholesterol, unsaturated fatty acids, and minerals (Fernandez, 2012). In continents surveyed by Food and Agriculture Organization of the United Nations, per capita egg consumption in 2009 varied from 2.3 kg in Africa to 12.7 kg in Europe (FAO, 2012). According to the Central Association of Egg Producers of Turkey (YUM-BIR), Turks consume 200 chicken eggs per person per year (YUM-BIR, 2015).

In recent years consumers began to prefer free-range hen eggs although the yolk color of free-range eggs was lower than that of battery-reared hen eggs (Kucukkoyuncu et al., 2017). Instead of battery-reared system eggs owing to the common wisdom that free-range hen eggs have preferable nutritional quality. In the free-range system, hens

http://www.aloki.hu ● ISSN 1589 1623 (Print) ● ISSN 1785 0037 (Online)
DOI: http://dx.doi.org/10.15666/aeer/1704_83698380

have opportunity pasture foraging in around. A close relationship with the environment may cause to be exposed to contaminants (Van Overmeire et al., 2006). And even free-range hen eggs are expected good bio-indicators of the contaminants of the environment in where the hen's pasture (Chang et al., 1989). Despite this well- known view, home-produced foods like free-range hen eggs are not analyzed to any convenience check by a routine program. Monitoring the levels of the macro, trace, and potentially toxic elements are one of the aspects of the food and also environmental quality. Macro and trace elements are found naturally and essential for throughout life (Esposito et al., 2016). But toxic elements such as Pb, Cd, As known to be toxic and have maximum limits by European Commission in some foods but not for eggs (European Commission Regulation, EC No 1881, 2006). The European Food Safety Authority has reported that the environmental pollutants such as toxic element detected in free-range hen eggs that pasture outdoors and more exposed to environmental contamination were higher than those detected in battery-reared hen eggs (EFSA Scientific Report—update of the monitoring of levels of dioxins and PCBs in food and feed, 2012). Actually, a close relationship with the soil identifies higher levels of Co, Zn, Pb in free-range hen eggs (de Freitas et al., 2013).

Şanlıurfa is located along the Syrian border and has four districts on the borderline. These are; Akçakale, Birecik, Harran, and Suruç. In these districts, that they are close of the Syrian war which is ongoing for a long time, the possible transition of toxic element contaminants from the environment to the local consumers and even to the food chain are not existing. The design of this paper focuses on the content of thirteen essential elements (Na, Mg, K, Ca, Cr, Mn, Fe, Co, Cu, Zn, Se, Ni, Ti) and four toxic elements (As, Pb, Tl, Cd) in fresh eggs of free-range hen eggs which should be bio-indicator of pollution. To the best of our knowledge, this study provides the first seasonal variation of elements in free-range hen eggs worldwide. The aims were for (1) an evaluation of concentrations of elements, (2) a vision of seasonal variations, and (3) indication of cautious risk affects.

Material and Methods

Samples

A total of 217 fresh eggs from free ranged hens were used as study material. The samples were separated depending on the seasonal variations as

i) 60 eggs collected in the spring season.
ii) 73 eggs collected in the summer season.
iii)84 eggs collected in the autumn season.

The samples were collected from home producers from Akçakale, Birecik, Harran, Suruç between March to October 2017 as shown in *Figure 1*. They were transported to the laboratory and stored at 4^{o}C until analyses.

Sample preparation and analytical procedures

Egg samples were homogenized by taking into 50 ml sterile falcon tubes. Whole equipment was previously kept for one night in 10% HNO_3 and then washed with ultrapure water to eliminate possible contamination of elements. One g of the homogenized egg samples were mineralized acid digestion with 6 ml HNO_3 65% (v/v) (Merck, Germany) and 2 ml H_2O_2 30% (v/v) (Merck, Germany) in PTFE vessels of

http://www.aloki.hu ● ISSN 1589 1623 (Print) ● ISSN 1785 0037 (Online)
DOI: http://dx.doi.org/10.15666/aeer/1704_83698380

Mars Xpress (CEM Corporation) microwave system as described in the literature (Esposito et al., 2016). Subsamples were treated as the following procedure; up to 120ºC for 7 min 1600 W and constant 5 min, up to 160ºC for 5 min 1600 W and constant 5 min, up to 210ºC for 20 min 1600 W and constant 5 min. The same procedure was done for every blank sample (1 ml ultrapure water). After the cooling stage to room temperature (22-23ºC), the subsamples were diluted to 50 ml with ultrapure water (MES MP Mini pure, Turkey).

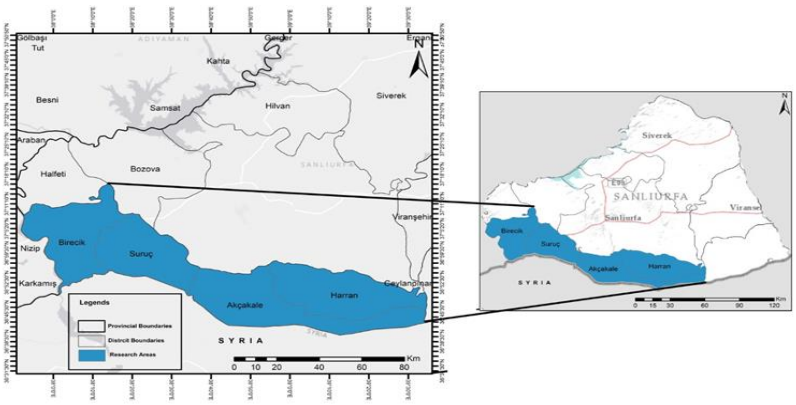

Figure 1. *Map of the study area*

Elemental analyses were done by Inductively Coupled Plasma Mass Spectrometer (ICP-MS) (Agilent 7500ce with an Octopole Reaction System) equipped with a nebulizer (Agilent, Japan), autosampler (Cetac ASX-520), and spray chamber.

All analytical method were performed according to the method of UNI EN 15763: 2010 preferably modified. The following isotopes were measured: $^{23}Na^{+}$, $^{24}Mg^{+}$, $^{39}K^{+}$, $^{44}Ca^{+}$, $^{52}Cr^{+}$, $^{55}Mn^{+}$, $^{56}Fe^{+}$, $^{59}Co^{+}$, $^{63}Cu^{+}$, $^{66}Zn^{+}$, $^{78}Se^{+}$, $^{75}As^{+}$, $^{206}Pb^{+}$, $^{60}Ni^{+}$, $^{48}Ti^{+}$, $^{205}Tl^{+}$, $^{111}Cd^{+}$.

Quality controls were assured to confirm the accuracy of the analytical procedure with the reference materials (NIST SRM 1515 Apple Leaves). The limit of detection and quantification were calculated as three and ten times.

Analyses of certified reference material allowed an assessment of accuracy and precision over a range of element concentrations. Certified values indicated that monitored levels correlated well with certified levels as shown in *Table 1*.

Statistical Analysis

For testing the normality of the data, the Shapiro-Wilk test was performed. In order to compare normal non-dispersive variables in more than two independent groups, Kruskal Wallis and All Pairwise Multiple Comparison tests were used. Spearman Rank Correlation Coefficient was used in testing the relations between numerical variables. For descriptive statistics, mean ± standard deviation values for numerical variables are given. Values of $P<0.05$ was considered as statistically significant. All statistical analyses were performed in order to verify the existence or not of significant differences between the samples. SPSS for Windows version 24.0 package program (SPSS Inc., Chicago, USA) was used for statistical analysis. When the concentration of the element was below the limit of quantification (LOQ) that value did not participate in the statistic.

http://www.aloki.hu ● ISSN 1589 1623 (Print) ● ISSN 1785 0037 (Online)
DOI: http://dx.doi.org/10.15666/aeer/1704_83698380

Table 1. *Element concentrations in certified reference material (NIST SRM 1515 Apple Leaves)*

Element	Certified data (mg/kg)	Our data (mg/kg)	Recovery (%)
Na	10.0	9.96	99.6
Mg	10.0	9.95	99.5
K	10.0	9.98	99.8
Ca	10.0	10.2	102
Cr	10.0	9.95	99.5
Mn	10.0	9.90	99.0
Fe	10.0	10.4	104
Co	10.0	9.93	99.3
Cu	10.0	9.99	99.9
Zn	10.0	9.97	99.7
Se	10.0	9.96	99.6
Ti	10.0	10.1	101
As	10.0	9.97	99.7
Pb	10.0	10.3	103
Ni	10.0	10.4	104
Tl	10.0	9.95	99.5
Cd	10.0	10.5	105

Results and Discussion

The concentration of Sodium, Magnesium, Potassium, Calcium, Chromium, Manganese, Iron, Cobalt, Copper, Zinc, Selenium, Arsenic, Lead, Nickel, Titanium, Talium, Cadmium in the egg samples are listed in *Table 2*, which reports mean and standard deviation in different seasons and *Table 3* reports median and quartiles of free-range hen eggs. Box plot analyses of groups of data was shown in *Figure 2*.

Table 2. *Comparison of concentrations of elements between seasons*

Element	Positive sample (n)	Spring (Mean ± SD)	Positive sample (n)	Summer (Mean ± SD)	Positive sample (n)	Autumn (Mean ± SD)
Na (mg/kg)	60	1278.08 ±324.27	73	4329.86 ±1460.72	84	1707.73 ±384.32
Mg (mg/kg)	60	246.15 ±31.44	73	143.54 ±25.57	84	157.76 ±17.47
K (mg/kg)	60	1035.92 ±342.37	73	1953.67 ±775.17	84	1964.9 ±437.86
Ca (mg/kg)	60	1067.33 ±219.75	73	490.53 ±167.6	84	560.54 ±111.96
Cr (µg/kg)	13	543.92 ±35.38		<LOQ		<LOQ
Mn (µg/kg)	34	709.41 ±152.94		<LOQ	6	576.16 ±35.38
Fe (mg/kg)	60	39.9 ±12.79	73	112.01±25.76	84	45.65 ±8.88
Co (µg/kg)		<LOQ		<LOQ		<LOQ
Cu (µg/kg)	14	974.12 ±850.27	73	9904.66 ±4004.7	84	2012.95 ±365.29
Zn (mg/kg)	60	32.34 ±7.44	60	11.80 ±6.50	84	22.77 ±4.59
Se (µg/kg)	60	7354.92 ±2972.93	38	9875.39 ±4522.55	84	11834.66 ±3624.58
Ti (µg/kg)	60	3940.1 ±578.65	35	3021.57 ±353.47	84	2125.68 ±247.91
As (µg/kg)	3	841.66 ±263.45	1	2545	4	990.25 ±70.35
Pb (µg/kg)		<LOQ		<LOQ		<LOQ
Ni (µg/kg)	20	140.25 ±109.45		<LOQ		<LOQ
Tl (µg/kg)		<LOQ		<LOQ		<LOQ
Cd (µg/kg)		<LOQ		<LOQ		<LOQ

http://www.aloki.hu ● ISSN 1589 1623 (Print) ● ISSN 1785 0037 (Online)
DOI: http://dx.doi.org/10.15666/aeer/1704_83698380

Table 3. *Values of median, 25th, and 75th variance for essential elements in free-range hen eggs*

	Spring			Summer			Autumn		
	Quartile 1	**Median**	**Quartile 3**	**Quartile 1**	**Median**	**Quartile 3**	**Quartile 1**	**Median**	**Quartile 3**
Na(mg/kg)	1068.76	1234.68	1417.49	3202.50	4137.50	5655.00	1510.40	1763.60	1954.40
Mg(mg/kg)	223.07	241.39	262.26	126.35	144.35	158.80	147.33	157.53	166.73
K (mg/kg)	846.30	997.43	1179.55	1549.00	1848.00	2502.50	1831.00	2020.00	2177.50
Ca(mg/kg)	878.75	1095.00	1217.25	360.25	489.25	611.50	522.00	558.00	601.00
Fe (mg/kg)	32.89	39.12	46.82	93.15	104.68	121.53	39.74	45.32	50.10
Cu (µg/kg)	137.50	824.05	1895.85	7290.00	9027.50	13525.00	1796.00	2026.25	2251.50
Zn(mg/kg)	26.80	33.01	36.86	6.55	11.19	15.03	20.62	22.447.50	25.45
Se (µg/kg)	5048.30	6522.85	8820.85	6510.00	8668.75	12702.50	9935.00	11505.00	14555.00

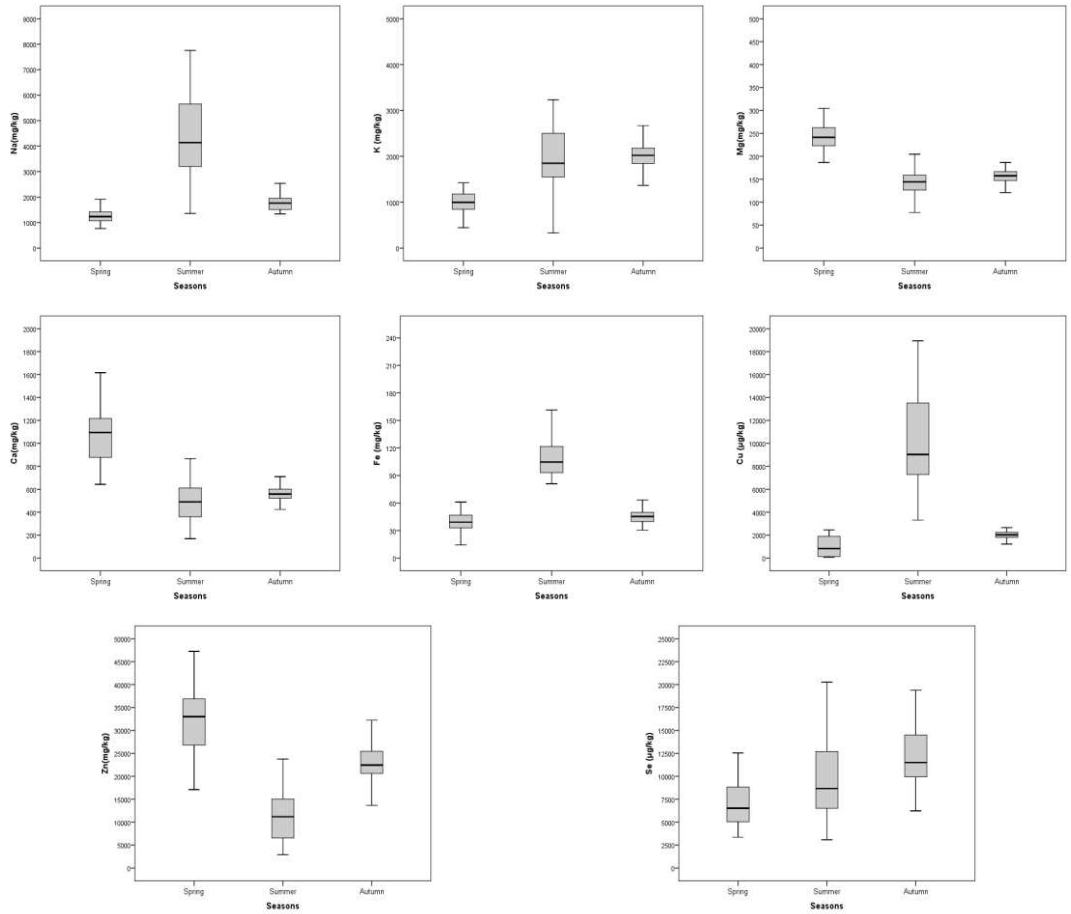

Figure 2. *Box plot of essential elements in free-range hen eggs*

In the present study the sodium content of free-range hen eggs showed an average level of 1278.08 mg/kg in the spring season; this is relatively low when compared with the mean level (1707.73 mg/kg) in the autumn season and also very low when compared with the mean level (4329.86 mg/kg) in the summer season. *Table 4* shows the

http://www.aloki.hu ● ISSN 1589 1623 (Print) ● ISSN 1785 0037 (Online)
DOI: http://dx.doi.org/10.15666/aeer/1704_83698380

comparison of the levels of elements reported in the different samples of home-grown hen and free-range hen eggs with previous literature. In the literature, the sodium content of eggs showed a mean level of 1149 mg/kg; this is lowly especially compared with the present study (Rubio et al., 2017).

Magnesium concentration of spring, summer, and autumn seasons in free-range hen eggs showed mean levels of 246.15, 143.54, 157.76 mg/kg, respectively. In the literature, a lower value have been reported in Canary Islands (87.5 mg/kg), while value as high as has been found in home-produced eggs from Brazil (674 mg/kg) (de Freitas et al., 2013).

The average levels of potassium detected in free-range hen eggs were 1034.92 mg/kg in spring, 1953.67 mg/kg in summer, and 1964.9 mg/kg in the autumn season. These values are high, especially when compared with the reported data in the literature (Rubio et al., 2017, 2018).

These latter tables report calcium concentrations of 1067.33 mg/kg in spring season while the value is higher than both summer (490.53 mg/kg) and autumn (560.54 mg/kg) seasons. The concentrations in our samples were also comparable to that reported in free-range hens egg from the Island of Tenerife with a mean level of 231 mg/kg (Rubio et al., 2018).

The average level of chromium in the spring season (543.92 μg/kg) is much higher than that detected in both summer (<LOQ) and autumn (<LOQ) season. In the spring, due to the fact that the chromium element is detected in egg samples, agricultural activities in the region are intense and pesticides and foliar fertilizers are generally applied in spring.

The manganese is one of the most abundant elements in the earth crust. The manganese mean content in the spring season (709.41 μg/kg) was higher than the mean content in autumn season (576.16 μg/kg) and in free-range hen eggs in United Kingdom (0.277 mg/kg) (Siddiqui et al., 2011). The iron mean content in the spring season (39.9 mg/kg) was lower than the values found in summer season (112.01 mg/kg) but similar to that analyzed in autumn season (45.65 mg/kg). The mean concentration of iron determined in free-range hen eggs proved to be far higher than the levels reported in eggs in the Island of Tenerife (7.62 mg/kg) (Rubio et al., 2018) and parallel with eggs in Brazil (114 μg/g) (de Freitas et al., 2013).

In the present study, the average level of copper was significantly increased from 974.12 to 9904.66 μg/kg between spring season to summer season afterward in the autumn season the mean copper content was 2012.95 μg/kg. The change rule of the concentration of copper was similar to iron.

The average concentration of Zinc in free-range hen eggs in spring season (32.34 mg/kg) was significantly higher than both summer (11.80 mg/kg) and autumn (22.77 mg/kg) season and was 10-fold higher than reported in fresh cage-reared hens eggs from Canary Islands (Rubio et al., 2017).

The average level of selenium in free-range hens eggs was increased from 7354.92 to 11834.66 between spring to autumn season and marginally higher than found in eggs from residential backyards in Italy (Esposito et al., 2016).

Arsenic is a micropollutant which can be easily detected in the soil, water, fertilizer, and industrial wastes. Long term exposures, arsenic is accumulated in metabolism and should because chronic diseases (Hashemi et al., 2018). The mean concentration of arsenic in free-range hen eggs was 841.66 μg/kg in the spring season, 2545 μg/kg in the summer season, and 990.25 μg/kg in the autumn season.

http://www.aloki.hu ● ISSN 1589 1623 (Print) ● ISSN 1785 0037 (Online)
DOI: http://dx.doi.org/10.15666/aeer/1704_83698380

Table 4. *Comparison of the levels of elements reported in the different samples of home-grown hen and free-range hen eggs*

Element	Rubio et al. (2017)	Rubio et al. (2018)	Esposito et al. (2016)	Grace and MacFarlane (2016)	De Freitas et al. (2013)	Van Overmeire et al. (2006)	Fakayode and Olu-Owolabi (2003)	Hashemi et al. (2018)	This study Spring	This study Summer	This study Autumn
Na (mg/kg)	1149±96.2	1290±154							1278.08 ± 324.27	4329.86±1460.72	1707.73±384.32
Mg (mg/kg)	87.5±26.1	103±13			674±138				246.15±31.44	143.54 ± 25.57	157.76±17.47
K (mg/kg)	491±217	712±135							1035.92±342.37	1953.67±775.17	1964.9±437.86
Ca (mg/kg)	174±83.3	231±56							1067.33±219.75	490.53±167.6	560.54±111.96
Cr (µg/kg)	170±240	50.0±90.0	8.0±9.0					1621	543.92±35.38	<LOQ	<LOQ
Mn (µg/kg)	100±110	140±70	360±142		1500±600	313.98			709.41±152.94	<LOQ	576.16±35.38
Fe (mg/kg)	5.49±4.10	7.62±2.7			114±30		23.20		39.9±12.79	112.01±25.76	45.65±8.88
Co (µg/kg)	<LOQ	<LOQ	4.0±2.0		19100±12500	5.15	10		<LOQ	<LOQ	<LOQ
Cu (µg/kg)	2220±1100	1780±780	679±128	750	2900±500	603.64	780		974.12±850.27	9904.66±4004.7	2012.95±365.29
Zn (mg/kg)	3.37±1.73	5.03±1.4	15.75±4.05	11.3	65.3±20.3	11.543	13.75		32.34±7.44	11.80±6.50	22.77±4.59
Se (µg/kg)			313±147		600±200	272.97			7354.92±2972.93	9875.3±4522.5	11834.6±3624.5
Ti (µg/kg)									3940.1±578.65	3021.5±353.4	2125.6±247.9
As (µg/kg)			7.0±4.0	30	21.5±8.5	15.95			841.66±263.45	2545	990.2±70.3
Pb (µg/kg)	20±20	30±20	19±28	90	89±245	68.56	590		<LOQ	<LOQ	<LOQ
Ni (µg/kg)	50±30	30±20	96±97			36.58	30		140.25 ± 109.45	<LOQ	<LOQ
Tl (µg/kg)			10±22			0.69			<LOQ	<LOQ	<LOQ
Cd (µg/kg)	<LOQ	<LOQ	3±3	1	0.6±0.5	0.53	70	13	<LOQ	<LOQ	<LOQ

http://www.aloki.hu ● ISSN 1589 1623 (Print) ● ISSN 1785 0037 (Online)
DOI: http://dx.doi.org/10.15666/aeer/1704_83698380

The reported concentrations of arsenic in egg samples from Italy (Esposito et al., 2016), Australia (Grace and MacFarlane, 2016), Brazil (de Freitas et al., 2013) were 7.0, 30, and 21.5 μg/kg, respectively. The finding of this study is very high than the reported concentrations of arsenic in egg samples from different countries.

The mean value of nickel from Canary Island (Rubio et al., 2018), Italy (Esposito et al., 2016), and Turkey (Uluözlü et al., 2009) were 30, 96, and 90 μg/kg, respectively. These levels are lower than our study (140.25 μg/kg).

Element content in the free-range hen eggs in the spring season

The mean concentration and standard deviation of each element analyzed in the spring season are shown in *Table 5*. Sodium (1278.08 mg/kg) was the most abundant macro-element analyzed in the highest proportion in free-range hen egg samples, followed by Ca>K>Mg.

Table 5. *Descriptive statistics of essential elements for the spring season*

Elements	Akçakale	Birecik	Harran	Suruç
Na (mg/kg)	1280.7±152.97	1440.38±435.26	1244.67±266.59	1146.58±333.55
Mg (mg/kg)	236.3±25.72	254.7±33.09	248.43±39.06	245.17±26.33
K (mg/kg)	1073.22±167.25	1378.47±419.25	936.3±137.13	755.68±222.36
Ca (mg/kg)	979.97±211.01	1029.67±191.62	1074.1±210.94	1185.6±230.29
Fe (mg/kg)	39.27±11.72	41.86±9.36	41.22±18.52	37.26±10.37
Cu (μg/kg)	104.73±46.35	929.56±796.22	719.11±512.22	1729.1±1058.9
Zn (mg/kg)	28.90±6.85	31.06±5.28	32.18±7.15	37.21±8.22
Se (μg/kg)	7426.73±1208.47	11655.05±1955.3	5761.96±743.91	4575.93±774.25

The major trace element found in egg samples was selenium (7354.92 μg/kg), followed by Cu>Mn>Ti>Cr>Ni>Fe>Zn>Co. Arsenic (841.66 μg/kg) was the most abundant toxic element found in three free-range hen eggs; Pb, Tl, Cd levels were below the limit of quantification in all samples in the spring season.

Element content in the free-range hen eggs in the summer season

The mean concentration and standard deviation of each element analyzed in the summer season are shown in *Table 6*. The most abundant macroelement in the free-range hen eggs was sodium (4329.86 mg/kg), followed by K>Ca>Mg. As for the trace elements, copper (9904.66 μg/kg) was the most notable in the egg samples, followed by Se>Ti>Fe>Zn. The Cr, Mn, Co and Ni levels were below the limit of quantification in all samples in the summer season. The detected levels of Co and Cd were below the quantification limit. Arsenic (2545 μg/kg) was the most abundant toxic element found in 1 free-range hen egg; Pb, Tl, Cd levels were below the limit of quantification in all samples in the summer season.

Element content in the free-range hen eggs in the autumn season

The mean concentration and standard deviation of each element analyzed in autumn season are shown in *Table 7*. Potassium (1964.90 mg/kg) was the most abundant macro-element analyzed in the highest proportion in egg samples, followed by Na>Ca>Mg. The major trace element found in egg samples was selenium (11834.66 μg/kg),

http://www.aloki.hu ● ISSN 1589 1623 (Print) ● ISSN 1785 0037 (Online)
DOI: http://dx.doi.org/10.15666/aeer/1704_83698380

followed by Ti>Cu>Mn>Fe>Zn. Co and Ni levels were below the limit of quantification in all samples in the autumn season. Arsenic (990.25 µg/kg) was the most abundant toxic element found in 4 free-range hen egg. The detected levels of Pb, Tl and Cd were below the quantification limit in the autumn season.

Table 6. *Descriptive statistics of essential elements for the summer season*

Elements	Akçakale	Birecik	Harran	Suruç
Na (mg/kg)	4195.5±969.41	5775.25±352.97	4142.97±370.31	2598.79±685.53
Mg (mg/kg)	155.15±19.87	141.31±24.37	136.66±15.39	131.76±34.43
K (mg/kg)	2006.99±385.34	2707.8±562.41	1764.94±229.93	1071.89±579.56
Ca (mg/kg)	570.69±177.35	463.68±111.54	421.13±167.73	450.91±143.39
Fe (mg/kg)	119.27±28.21	129.81±20.66	94.94±8.54	100.51±18.19
Cu (µg/kg)	9568.25±2581.11	14020.5±872.72	9079.53±705.53	5192.65±1501.68
Zn (mg/kg)	13.76±4.74	8.22±3.65	10.25±6.34	10.38±5.373.66
Se (µg/kg)	11117.12±4557.47	5320±2857.78	9170.77±2760.29	7160±0

Table 7. *Descriptive statistics of essential elements for the autumn season*

Element	Akçakale	Birecik	Harran	Suruç
Na (mg/kg)	1727.77±463.76	1965.72±174.47	1602.34±190.34	1378.14±443.87
Mg (mg/kg)	163.11±15.74	159.19±15.69	153.88±21.54	155.26±16.49
K (mg/kg)	1965.73±467.98	2129.5±239.09	2058±301.55	1586.44±579.32
Ca (mg/kg)	582.32±74.77	534.16±73.04	584.38±133.5	561.13±157.71
Fe (mg/kg)	46.45±9.19	41.97±5.34	50.88±8.71	45.33±11
Cu (µg/kg)	2189.9±267.48	2248.8±240.94	1880.1±235.71	1596.88±319.51
Zn (mg/kg)	23.10±3.385	21.50±3.47	23.90±7.02	23.44±3.13
Se (µg/kg)	8765.17±2472.89	10570.33±1635.91	14309.25±2485.36	13750.22±4963.94

Correlation between elements

Correlation between elements in free-range hen eggs samples was shown in *Table 8* for the spring season, *Table 9* for the summer season, and *Table 10* for the autumn season.

Table 8. *The correlations between the of essential elements in the spring season*

	Mg	K	Ca	Ti	Fe	Cu	Zn	Se
Na	.236	.584**	-.608**	-.580**	-.291*	.262	-.684**	.397**
Mg	1.000	.087	.136	.206	.227	.305	.066	.066
K		1.000	-.338**	-.366**	.076	.196	-.427**	.732**
Ca			1.000	.986**	.671**	-.196	.919**	-.366**
Ti				1.000	.644**	-.103	.903**	-.388**
Fe					1.000	.134	.644**	.001
Cu						1.000	-.066	-.240
Zn							1.000	-.428**

Notes: Spearman correlation test, *P<0.05, **P<0.01

http://www.aloki.hu ● ISSN 1589 1623 (Print) ● ISSN 1785 0037 (Online)
DOI: http://dx.doi.org/10.15666/aeer/1704_83698380

Table 9. *The correlations between the essential elements in the summer season*

	Mg	K	Ca	Ti	Fe	Cu	Zn	Se
Na	0.157	.907**	0.061	0.014	.470**	.964**	0.028	-0.287
Mg	1	0.197	.525**	.376*	.346**	0.163	.447**	0.242
K		1	0.227	-0.054	.626**	.906**	0.099	-0.204
Ca			1	.673**	.562**	0.171	.912**	0.073
Ti				1	0.304	0.027	.621**	0.403
Fe					1	.533**	.392**	0.193
Cu						1	0.138	-0.308
Zn							1	-0.115

Notes: Spearman correlation test, *P<0.05, **P<0.01

Table 10. *The correlations between the elements in autumn season*

	Mg	K	Ca	Ti	Fe	Cu	Zn	Se
Na	.379**	.538**	-.355**	.036	-.180	.642**	-.379**	-.394**
Mg	1.000	.235*	.006	.219	.139	.230*	-.007	-.196
K		1.000	-.131	.153	.093	.532**	.004	-.179
Ca			1.000	.804**	.502**	-.084	.819**	.116
Ti				1.000	.416**	.319**	.679**	-.224*
Fe					1.000	.013	.431**	.058
Cu						1.000	.047	-.624**
Zn							1.000	.105

Notes: Spearman correlation test, *P<0.05, **P<0.01

In spring season, very strong correlations were detected between CaxTi, CaxZn, TixZn, and also strong correlations were detected between NaxZn, NaxCa, KxSe, CaxFe, TixFe, FexZn as shown in *Table 7*. Interestingly there wasn't a correlation between elements with Mg, so further studies required.

In the summer season, very strong correlations were detected between NaxK, NaxCu, CaxZn, KxCu. Strong correlations were found between KxFe, CaxTi, TixZn as shown in *Table 9*. In autumn season, very strong correlations were detected between CaxTi, CaxZn, and strong correlation between NaxCu, TixZn, CuxSe as shown in *Table 10*. A correlation between CaxZn were detected in all seasons thus it means that the season is not influencing this very strong correlation.

Conclusion

In this study, the element levels of eighteen elements in the free-range hen egg samples were examined by means of ICP-MS. Free-range hen eggs are an acceptable source of essential elements, in particular, of Na, Mg, K, Ca, Cu, Fe, Zn, and Se. The presence of Cr in the spring season, Cu in the summer season and Se in all seasons in our samples may be related to a geographic source. Finally, the lack of data on the presence of some Ti in free-range hen eggs does not allow comparisons. It was seen that there was a statistical difference between the seasons so it was concluded that the

http://www.aloki.hu ● ISSN 1589 1623 (Print) ● ISSN 1785 0037 (Online)
DOI: http://dx.doi.org/10.15666/aeer/1704_83698380

element content of free-range hen eggs produced in this region was affected by seasonal changes.

Compilation of these data may serve to understand the element composition and to define the reference levels of macro, trace and toxic elements to be used in food safety assessments of free-range hen eggs produced in an area near the Syrian border because it was determined that eight samples of free-range hen eggs were contaminated with As on an average of 1131.25 μg/kg when the toxic element levels were examined. It is important to regularly monitoring the levels of toxic elements in free-range hen eggs for assessing the risk of long-term exposure.

Acknowledgements. The authors acknowledge the Harran Scientific Research Project Department of the Harran University for funding this study with the project number of 17113. This paper was presented at 1st International Veterinary Biochemistry and Clinical Biochemistry Congress which took place on April 12-15, 2018, in Hatay/Turkey.

REFERENCES

[1] Central Association of Egg Producers of Turkey (YUM-BIR) (2015): https://www.yum-bir.org/UserFiles/File/Veriler2016.pdf.
[2] Chang, R., Hayward, D., Goldman, L., Harnly, M., Flattery, J., Stephens, R. (1989): Foraging animals as biomonitors for dioxin contamination. – Chemosphere 19: 481-486.
[3] de Freitas, R., Ramos, N. L., Batista, B. L., Barbosa Jr., F. (2013): Toxic and essential elements in conventional and home-produced eggs by ICP-MS analysis. – Food Additives & Contaminants Part B Surveillance 6(1): 30-35.
[4] Domingo, J. L. (2014): Health risks of human exposure to chemical contaminants through egg consumption: a review. – Food Research International 56: 159-165.
[5] EFSA (2012): Scientific Report—update of the monitoring of levels of dioxins and PCBs in food and feed. – Europian Food Safety Authority Journal 10(7): 2832.
[6] Esposito, M., Cavallo, S., Chiaravalle, E., Miedico, O., Pellicanò, R., Rosato, G., Baldi, L. (2016): Trace elements in free-range hen eggs in the Campania region (Italy) analyzed by inductively coupled plasma mass spectrometry (ICP-MS). – Environmental Monitoring and Assessment 188(6): 326-334.
[7] European Commission Regulation (EC) No 1881 (2006). – Of 19 December 2006 setting maximum levels for certain contaminants in foodstuffs. – Official Journal of the European Union L364: 5-24.
[8] Fakayode, S. O., Olu-Owolabi, I. B. (2003): Trace metal content and estimated daily human intake from chicken eggs in Ibadan, Nigeria. – Archives of Environmental Health: An International Journal 58(4): 245-251.
[9] Fernandez, M. L. (2012): Rethinking dietary cholesterol. – Current Opinion in Clinical Nutrition & Metabolic Care 15(2): 117-121.
[10] Food and Agriculture Organization of the United Nations (FAO) (2012): World Egg Day. – www.fao.org/ag/againfo/home/en/news_archive/2012_World_Egg_Day_2012.html.
[11] Grace, E. J., MacFarlane, G. R. (2016): Assessment of the bioaccumulation of metals to chicken eggs from residential backyards. – Science of the Total Environment 563: 256-260.
[12] Hashemi, M., Sadeghi, A., Dankob, M., Aminzare, M., Raeisi, M., Miri, H. H., Saghi, M. (2018): The impact of strain and feed intake on egg toxic trace elements deposition in laying hens and its health risk assessment. – Environmental Monitoring and Assessment 190(9): 540-552.

http://www.aloki.hu ● ISSN 1589 1623 (Print) ● ISSN 1785 0037 (Online)
DOI: http://dx.doi.org/10.15666/aeer/1704_83698380

[13] Kovacs-Nolan, J., Phillips, M., Mine, Y. (2005): Advances in the value of eggs and egg components for human health. – Journal of Agricultural and Food Chemistry 53(22): 8421-8431.
[14] Kucukkoyuncu, E., Okur, A. A., Tahtabicen, E., Korkmaz, F., Samli, H. E. (2017): Comparing quality of free range and battery cage eggs. – European Poultry Science 81: 1-7.
[15] Rubio, C., Paz, S., Ojeda, I., Gutiérrez, A. J., González-Weller, D., Hardisson, A., Revert, C. (2017): Dietary intake of metals from fresh cage-reared hens' eggs in Tenerife, Canary Islands. – Journal of Food Quality 2017: 1-11.
[16] Rubio, C., Ojeda, I., Gutierrez, A. J., Paz, S., González-Weller, D., Hardisson, A. (2018): Exposure assessment of trace elements in fresh eggs from free-range and home-grown hens analysed by inductively coupled plasma optical emission spectrometry (ICP-OES). – Journal of Food Composition and Analysis 69: 45-52.
[17] Siddiqui, I., Nazami, S. S., Ahmed Khan, F., Bhutto, S., Tahir, M., Munshi, A. B., Syed, N. (2011): Determination of some heavy metals in hen eggs using ICP-AES technique. – Pakistan Journal of Biochemistry & Molecular Biology 44(4): 133-136.
[18] Uluozlu, O. D., Tuzen, M., Mendil, D., Soylak, M. (2009): Assessment of trace element contents of chicken products from Turkey. – Journal of Hazardous Materials 163(2-3): 982-987.
[19] Van Overmeire, I., Pussemier, L., Hanot, V., De Temmerman, L., Hoenig, M., Goeyens, L. (2006): Chemical contamination of free-range eggs from Belgium. – Food Additives and Contaminants 23(11): 1109-1122.

http://www.aloki.hu ● ISSN 1589 1623 (Print) ● ISSN 1785 0037 (Online)
DOI: http://dx.doi.org/10.15666/aeer/1704_83698380

RESEARCH ON THE DRIVING FACTORS OF ENERGY CARBON FOOTPRINT IN LIAONING PROVINCE USING RANDOM FOREST ALGORITHM

SUN, Q.

Business School, Shandong University of Technology
No.88, Gongqingtuan West Road, Zibo City, Shandong Province, China
(e-mail: yssunqiang@163.com; phone: +86-151-6608-3805)

(Received 7th Mar 2019; accepted 3rd May 2019)

Abstract. Rapid development of economy has obviously promoted the growth of carbon emission, which causes the ecological environment more fragile. How to calculate the energy carbon footprint and explore tradeoff between energy and environment becomes further significance. This study examines energy carbon footprint in Liaoning Province. The main goal of this study is to calculate the energy carbon footprint using random forest algorithm and verify the performance of random forest algorithm. The study first examines factors of energy carbon emissions and implicates calculating method of energy carbon footprint. Subsequently random forest algorithm is developed in calculating energy carbon footprint. The results show that the calculated results of random forest algorithm is close to the actual value and the trend of change is basically similar to the actual value. Furthermore, the performance of random forest algorithm is compared with Partial Least Squares algorithm. The relative error and average relative error of random forest algorithm are both less than Partial Least Squares algorithm.
Keywords: *carbon footprint, LMDI, energy efficiency, low carbon economy, energy structure, strategies*

Introduction

An ecosystem is an open system, in which many basic substances are continuously cycled. Ecosystem has the capacity to maintain stability via self-regulation. However, when strong pressures on the ecosystem go beyond its threshold level, the ecosystem loses self-regulation ability and the ecosystem structure will be damaged (Ginestet et al., 2013; Tao et al., 2014; Chen et al., 2018). In an age of limited resources and destructive ecology, the idea of ecological civilization should give close attention to build a safe ecological environment (Yasar and Kalfa, 2012).

Carbon footprint which refers to the overall emissions of greenhouse gases can be analyzed by life cycle assessment and comes from the concept of ecological footprint (An and Xue, 2017; Sun, 2017). It is applied to measure the energy using and reveal the trends on climate change and atmospheric environment (Hertzberg and Schreuder, 2016). Current research is focused on the assessment of the carbon footprint model and the approach to reduce carbon footprint (Mancini et al., 2016; Qi et al., 2018; Long et al., 2018). Also many factors are mentioned to reduce the carbon footprint (David et al., 2009; Sovacool and Brown, 2010). Besides, some methods such as input-output model, theoretical modeling, objective program method, profit-maximized carbon cycle model (Dominic et al., 2008; Kenny and Gray, 2009). Studies have shown that carbon accounting standards for the production and consumption-based so that newly industrialized countries face a serious carbon leakage (Sun and Zhou, 2016). The carbon footprint of the developed countries has been seriously underestimated. Therefore, it is recommended to consume carbon footprint accounting system as a benchmark by the rules of regional trade agreements, eliminate carbon leakage and promote equitable global range of carbon emission reduction targets.

http://www.aloki.hu ● ISSN 1589 1623 (Print) ● ISSN 1785 0037 (Online)
DOI: http://dx.doi.org/10.15666/aeer/1704_83818394

The aim of this paper is to develop a random forest algorithm model for calculating the energy carbon footprint in Liaoning Province and identify the main driving factors of carbon emission. The reminder of this paper is structured as follows: after the introduction section, section 2 describes the method of energy carbon footprint, random forest algorithm and model fitting evaluation model. Results are given in Section 3 and discussion is given in Section 4. Finally, the conclusions are summarized in Section 5.

Material and methods

Energy carbon footprint

Based on the actual situation of energy consumption and economic development and taking into account the availability of data, the following categories were chosen for the calculation of carbon footprints: raw coal, coke, crude oil, petrol, diesel oil, black mineral oil and natural gas. Raw coal referred to the coal obtained after the removal of dirt and iron pyrite from the run-of-mine (rom) coal. Coke referred to the solid substance obtained after carbonation of coking coal at a high temperature (Chelgani et al., 2016; Bergthorson, 2018). Crude oil was the mineral oil comprised of the polymer from natural hydrocarbon source. The black mineral oil was the black sticky residue obtained from the distillation of crude oil, or its mixture with lighter components. It was mainly used as the fuel for the steam boiler and other heating furnaces, large slow diesel oil fuel, or other industrial fuels (Romijn, 2011; Pragya et al., 2017; Dalir et al., 2018).

According to the standard coal, the content of carbon emitted from the energy can be calculated clearly. Given the 2006 IPCC Guidelines for National Greenhouse Gas Inventories published by Intergovernmental Panel on Climate Change (IPCC) advice, the carbon footprint of energy consumption in China was computed (Druckman and Jackson, 2009; Ohimain, 2012; Affuso and Hite, 2013). In addition, the coefficient of each fuel conversion, the standard coal identified in China 2015 List of Greenhouse Gases, as well as the way to compute carbon footprint and carbon emission are as follows:

$$f_{CE} = \sum_i \frac{44}{12} \cdot \beta_i \cdot \varepsilon_i \cdot Q_i \cdot V_i \cdot q_i \cdot 10^{-3} \quad \text{(Eq.1)}$$

where

- f_{CE} is carbon footprint emitted from all kinds of energy.
- β_i is the conversion factor of i type of energy which was achieved by transforming the fuel into energy (TJ) in accordance with the net calorific value.
- ε_i is the transforming coefficient for i kind of energy into standard coal Which was the benchmarking for transforming a variety of energies into standard coal.
- Q_i is the consumed amount of i type energy.
- V_i is carbon emission factor of i type energy.
- q_i is the carbon oxidation ratio of i type energy.
- 10^{-3} is the unit conversion coefficient.
- $\frac{44}{12}$ is the conversion coefficient between carbon and CO_2.

http://www.aloki.hu ● ISSN 1589 1623 (Print) ● ISSN 1785 0037 (Online)
DOI: http://dx.doi.org/10.15666/aeer/1704_83818394

The conversion factor of standard coal was identified in the General Principle for Computing Comprehensive Energy Consumption (GB/T2589-2008). The carbon emission factor, carbon oxidation ratio and energy conversion factor were identified in IPCC National List of Greenhouse Gases (2006). More detailed information of the conversion parameters is shown in *Table 1*.

Table 1. *Parameters of calculating carbon footprint*

Energy	ε_i **(kg kg^{-1})**	V_i **(kg J^{-1})**	q_i **(%)**	β_i **(TJ g^{-1})**
Raw coal	0.7143	25.8	0.90	26.7
Coke	0.9714	29.2	0.90	28.2
Crude oil	1.4286	20.0	0.98	42.3
Petrol	1.4714	20.2	0.98	43.0
Diesel oil	1.4571	20.2	0.98	43.0
Black mineral oil	1.4286	21.1	0.98	40.4
Natural gas	12.1430	15.3	0.99	48.0

Random forest algorithm

Random forest (RF) algorithm is a nonlinear modeling tool which proposed by Leo Breiman (Zhou and Qiu, 2018). It is a useful method to prevent the nonlinear approximation of statistical relationships problems among different variables (Abellán et al., 2018). This method is widely used in cancer analysis, data biology, astronomy, and other fields of discriminate analysis and feature selection (Dalir et al., 2018; Kamińska, 2018). But it is nearly used in calculating energy carbon footprint and few studies reported the use of the RF algorithm in energy carbon footprint applications.

RF algorithm begins with bootstrap sampling method, random vector θ comprise the combined model:

$$h(X,\theta_m), m = 1,2,\text{L},M \quad \text{(Eq.2)}$$

X is the input variable, θ_m is the independent and identically distributed random vector. If the output variable is Y, then the original is (X,Y). The predicted sequence $\{h(\text{X},\theta_1), h(\text{X},\theta_2),\cdots, h(\text{X},\theta_m)\}$ will be obtained by training of m times and this result can be constructed predictive model prediction and eventually results:

$$\overline{h}(X) = (1/M)\cdot\sum_{m=1}^{M} h(\text{X},\theta_m) \quad \text{(Eq.3)}$$

The prediction can be obtained vector $h(\text{X})$ of the extrapolation error mean:

$$EMSE = EX,Y(\text{Y}-h(\text{X})) \quad \text{(Eq.4)}$$

It has its inherent characteristics of random forests. When the number of trees in the forest tends to infinity, there is:

$$E_{X,Y}\left(Y-\alpha v_k h\left(X,\theta_k\right)\right)^2 \to E_{X,Y}\left(Y-E_\theta h\left(X,\theta_k\right)\right)^2 \quad \text{(Eq.5)}$$

http://www.aloki.hu ● ISSN 1589 1623 (Print) ● ISSN 1785 0037 (Online)
DOI: http://dx.doi.org/10.15666/aeer/1704_83818394

For all θ, then:

$$\mathrm{PE}^{*}\left(forset\right) \le \rho\,\mathrm{PE}^{*}\left(tree\right) \quad \text{(Eq.6)}$$

$$\mathrm{PE}^{*}\left(tree\right) = E_{\theta}E_{X,Y}\left(Y - h(\mathrm{X},\theta)\right)^{2} \quad \text{(Eq.7)}$$

ρ is weight-related between the $Y - h(\mathrm{X},\theta)$ and reaming $Y - h(\mathrm{X},\theta)$, θ is independent.

Realization of random forests is as follows:

Drawn n_{tree} from the original sample by bootstrap. Each sample has not been able to get a sample consisting out-of-bag (OOB) as the test sample.

Set of raw data variables *P*, in each tree each node randomly selects M_{try} feature, and then select the best branches.

In random forest, the choice of the parameters M_{try} is in accordance with $M_{try} = P/3$.

Using the effect of the model to evaluate the residual mean square of OOB prediction. As shown in the following formula:

$$MSE_{OOB} = \frac{\sum_{1}^{m}\left(y_i - \hat{y}_i^{\,OOB^2}\right)}{n} \quad \text{(Eq.8)}$$

$$R_{RF}^{2} = 1 - MSE_{OOB} / \hat{\sigma}_{y}^{2} \quad \text{(Eq.9)}$$

- y_i is the actual value of the output variable of the OOB.
- $\hat{y}_i^{\,OOB^2}$ is the corresponding forecast value.
- $\hat{\sigma}_{y}^{2}$ is the variance of the predictive value of the OOB.

Study area

Liaoning Province is located in the south of Northeast China, bordering on the Huanghai Sea and Bohai Sea in the south, and acrossing the Yangtze River from the North Korea, as shown in *Fig. 1*. It is the gateway to the northeast and the eastern part of Inner Mongolia Autonomous Region of China. Liaoning Province is an important old industrial base in China and is one of the provinces with a relatively complete industrial category. The land area of Liaoning Province is 148,000 square kilometers, the mainland coastline is 2,292 kilometers long and the offshore waters cover an area of 68,000 square kilometers. It is a key area for grain production, animal husbandry, fisheries, high-quality fruits and a variety of special products. At present, there are 39 major categories, 197 medium-sized and 500 small-sized industries in Liaoning Province. With superior location and convenient transportation, Liaoning Province is an important gateway to the northeast area and an important gateway to the Eurasian Continental Bridge. It is an area with relatively developed infrastructure such as transportation and electric power.

http://www.aloki.hu ● ISSN 1589 1623 (Print) ● ISSN 1785 0037 (Online)
DOI: http://dx.doi.org/10.15666/aeer/1704_83818394

Liaoning Province is located in the northern margin of the Pacific Rim. It has excellent geological mineralization conditions and is rich in mineral resources. More than 110 minerals have been discovered, of which 66 have been proved. The magnesite of Liaoning Province is an advantageous mineral in the world, with a reserve of 2.56 billion tons and about 25% of the world. Minerals with advantages in the country include boron, iron, diamond, talc, jade and so on. The minerals with comparative advantages are mainly coal, coalbed methane, natural gas, gold and silver.

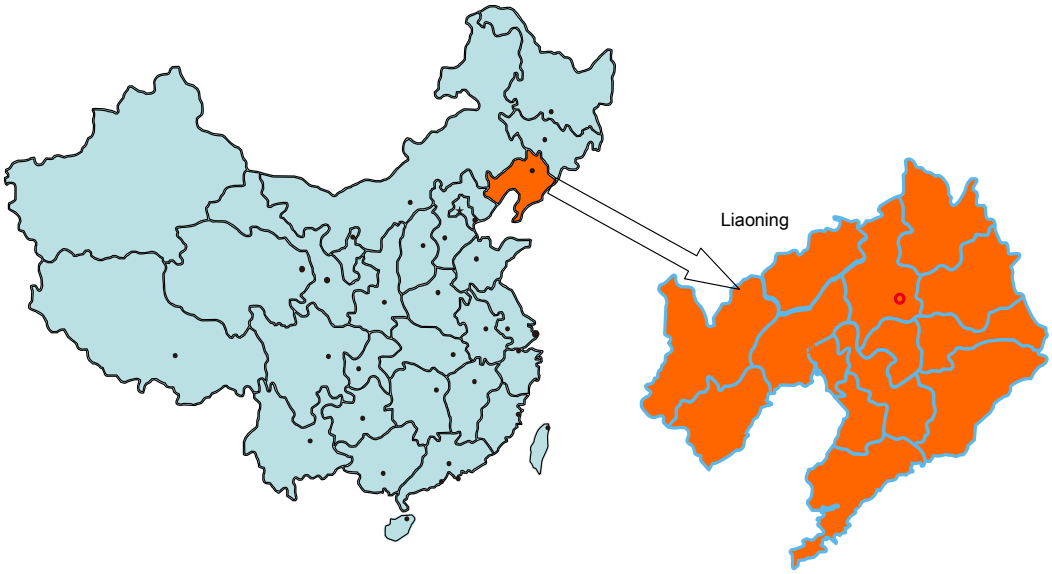

Figure 1. *Location of Liaoning province in China*

In this study, Liaoning Province is chosen to analyze the energy carbon footprint characteristics. First, Laioning Province is listed among the circular economy in 2008. The energy carbon emission should be slowed down dramatically to fulfill the development of circular economy. The circular economy is to reach the harmonious circulation of the economic system and the natural ecosystem through the waste reduction and resource harmlessness in the economic development. The basic principles of circular economy are reduction, reuse, and resource utilization. It is the fundamental change in the traditional growth model of mass production, mass consumption and mass abandonment. Circular economy is a production activity process that comprehensively utilizes energy and waste in accordance with the method of sustainable development under the guidance of sustainable development.

Liaoning Province is a major province of heavy chemical industry with large resource consumption and environmental pollution. Under the traditional economic development mode, the excessive development of resources has increasingly affected economic development and social progress. The depletion of resources is to force transformation to circular economy in Liaoning Province.

Second, as a province depended on nature resources, Liaoning Province is highly similar to other resource-based provinces in industrial transition. Third, because of the vulnerable environments pollution, location and regional characteristics, Liaoning Province deserve to be studied.

http://www.aloki.hu ● ISSN 1589 1623 (Print) ● ISSN 1785 0037 (Online)
DOI: http://dx.doi.org/10.15666/aeer/1704_83818394

Data acquisition

Liaoning is a resource-dependent province, while the most common used are raw coal, coke, crude oil, petrol, diesel oil, black mineral oil and natural gas. In this section, these seven kinds of different energy are chosen to calculate the energy carbon footprint. Raw coal refers to the coal after screening to remove the meteorite, pyrite and so on from the ground or underground. Coke is a kind of solid fuel which is made by high temperature dry distillation of coal, which has high calorific value and is mostly used for iron making. Crude oil is crude oil that is directly extracted from oil wells. It is a dark brown or dark green viscous liquid or semi-solid combustible material composed of various hydrocarbons. Petrol, diesel oil and black mineral oil are liquid oil produced by crude oil.

The energy consumption data used in this section was mainly retrieved from China Statistical Yearbook, China Energy Statistical Yearbook, China Forestry Statistical Yearbook, China Agriculture Statistical Yearbook, and Liaoning Statistical Yearbook published from 1998 to 2016. Part of the data was obtained from the Liaoning provincial government website and Liaoning Statistical Bureau website. The part of the data, which was missing, was compensated by the method of moving averages. Year 1998 was considered as the benchmark, to avoid the influence of price level variations.

Fig. 2 shows energy consumption in Liaoning Province from 1998 to 2016. It is shown that the energy consumption is a increasing trence.

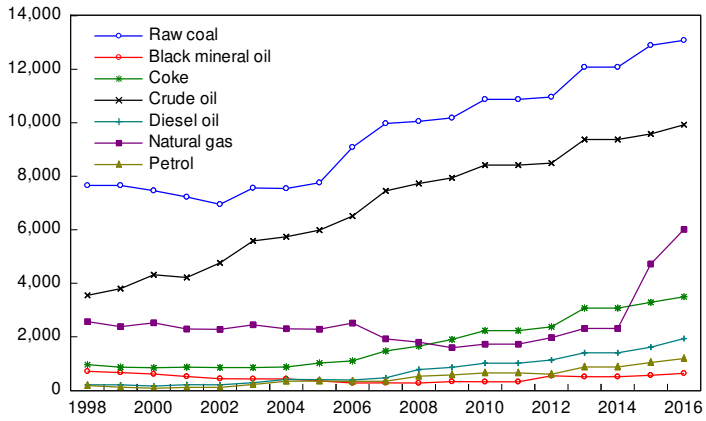

Figure 2. *Energy consumption in Liaoning Province from 1998 to 2016 (unit: million tons)*

Results

Evaluation results of carbon footprint

According to the calculating method of energy carbon footprint mentioned above, the normalized energy carbon footprint and energy carbon capacity as well as energy carbon surplus in Liaoning Province from 1998 to 2016 are figured up. *Fig. 3* shows the carbon footprint (10^4 ton) in Liaoning from1998 to 2016. As shown in *Fig. 3*, the overall carbon footprint in Liaoning Province increased by 236.768% with an annual rate of 13.154% from 410.164 million tons in 1998 to 971.139 million tons in 2016. Energy carbon footprint caused by coal has been the dominant part of energy carbon footprint. Since 2003, the carbon footprint of energy consumption has started a new round of rapid growth. In the period of national economy rapid developing, while

http://www.aloki.hu ● ISSN 1589 1623 (Print) ● ISSN 1785 0037 (Online)
DOI: http://dx.doi.org/10.15666/aeer/1704_83818394

accelerating the process of urbanization and a series of external factors driven by the energy consumption continues to rise. The promotion and use of natural gas as well as the rapid growth of private cars has further increased the energy requirements and consumption in Liaoning Province. The carbon footprint of energy consumption in Liaoning Province is mainly influenced by the social and economic factors. To grasp the dynamic change trend of future energy consumption is of great significance to the implementation of sustainable development in Liaoning Province.

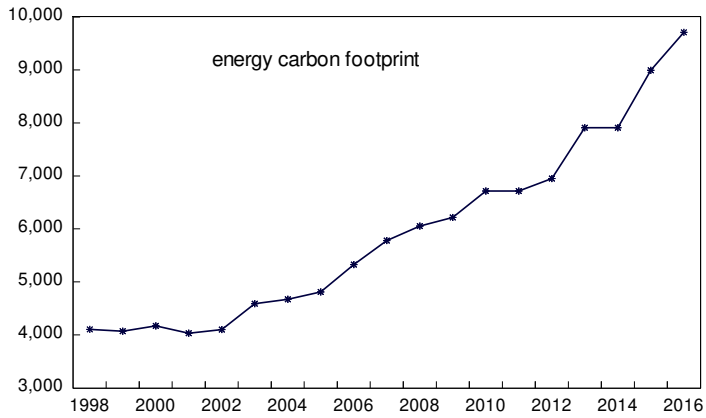

Figure 3. *Carbon footprint in Liaoning from 1998 to 2016 (unit: million tons)*

Fig. 4 shows the each energy carbon footprint in Liaoning from 1998 to 2016.

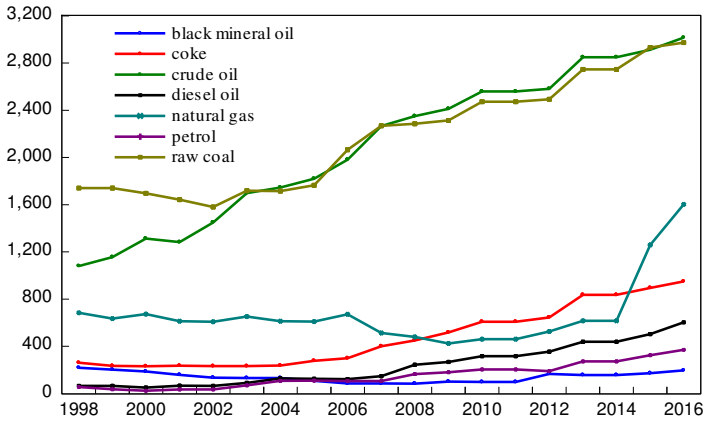

Figure 4. *Carbon footprint of each energy in Liaoning from 1998 to 2016 (unit: million tons)*

It is clear that energy structure of carbon footprint in Liaoning Province is relative stable. The proportions of the raw coal and crude oil have decreased and the proportion of the natural gas increased gradually. The main sources of greenhouse gases on a global approach include consumption of fossil fuels and primary energy. Coal combustion is one of the most important ways of pollution. Primary energy structure dominated by coal, which is impossible to get a complete change in the short term coupled with relatively outdated coal mining technology and refining our processing methods. It has increased the pressure on the government for environmental protection. This will give our global greenhouse gas control and a tremendous challenge.

http://www.aloki.hu ● ISSN 1589 1623 (Print) ● ISSN 1785 0037 (Online)
DOI: http://dx.doi.org/10.15666/aeer/1704_83818394

Evaluation results of random forest algorithm

The major application of the random forest algorithm in this study was to calculate carbon footprint. Thus, the training dataset was selected from the statistical report from Chinese official bulletin. Then the sampling size and feature number were determined based on the principle of minimal error. And the results were generated with the training dataset with specific sampling size and feature. After a comparison of parameters and multiple simulation experiments, a set of optimal parameters is obtained. Finally, according to the simulation process, the simulation experiment is carried out with this set of parameters: M_{try} is 4 and n_{tree} is 600. The result of random forest algorithm is shown in *Fig. 5.*

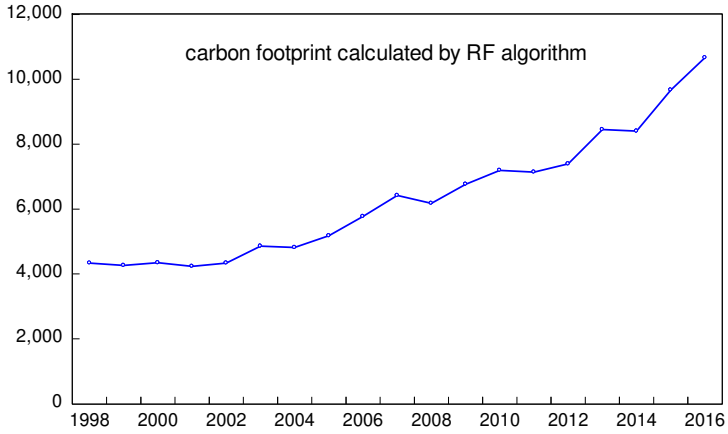

Figure 5. *Carbon footprint calculated by random forest algorithm*

Fig. 6 shows the calculation results of carbon footprint of Liaoning Province by each algorithm.

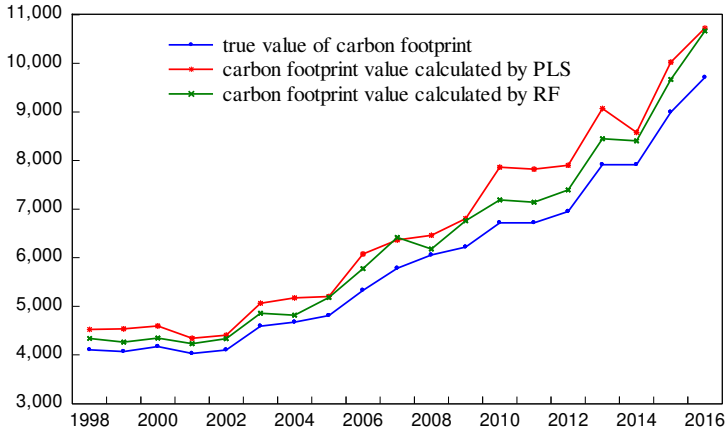

Figure 6. *Comparison of algorithm accuracy*

It can be seen from *Fig. 6* that the calculated results of random forest and PLS are both close to the actual value, and the trend of change is basically similar. However, the value calculated by PLS algorithm is higher than random forest algorithm and the actual

http://www.aloki.hu ● ISSN 1589 1623 (Print) ● ISSN 1785 0037 (Online)
DOI: http://dx.doi.org/10.15666/aeer/1704_83818394

value, which indicating that random forest algorithm has higher accuracy. Besides, random forest algorithm has a high accuracy comparing to the linear regression or logistic regression. The main reason of the high accuracy is generated by the random nature in both sampling size and feature. The other reason of the high accuracy is the application of bootstrap method in the algorithm.

Fig. 7 shows the absolute error of each algorithm and *Fig. 8* shows the relative error of each algorithm in calculating the carbon footprint of Liaoning Province.

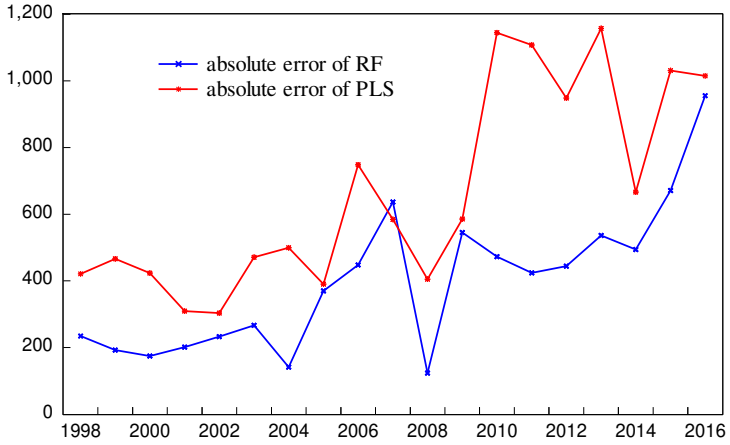

Figure 7. *Absolute error of each algorithm*

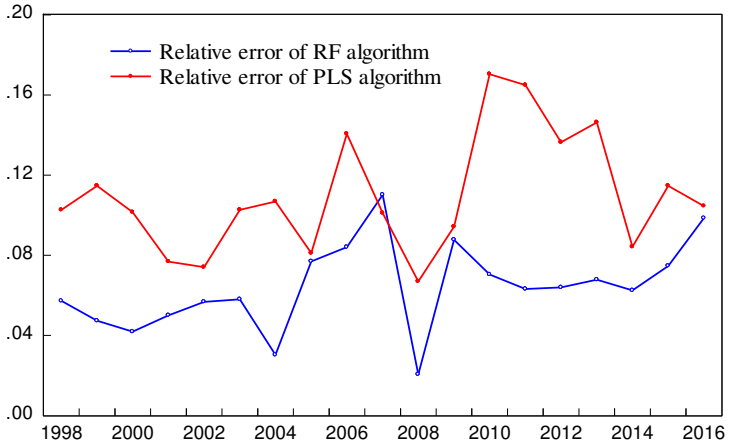

Figure 8. *Relative error rate of each algorithm*

It can be seen from *Fig. 8* that the random forest model has little relative error with the actual value of energy carbon footprint. The relative error of the PLS algorithm is larger and the relative error is at most 0.1704. The relative error of random forest algorithm is less than PLS algorithm, with the largest relative error being 0.1101 and the smallest being only 0.0204. In addition, from the aspect of average relative error, the average relative error of random forest algorithm is 0.0643, while the average relative error of PLS algorithm is 0.1097, which also verifies the superiority of random forest algorithm in reducing the computational error. Thus the results of *Fig. 7* and *Fig. 8* are consistent with the accuracy evaluation of the reflected algorithm.

http://www.aloki.hu ● ISSN 1589 1623 (Print) ● ISSN 1785 0037 (Online)
DOI: http://dx.doi.org/10.15666/aeer/1704_83818394

Sensitive analysis of random forest algorithm

Random forest algorithm is mainly to select the appropriate parameter values by OOB errors. The relationship between M_{try} and OOB error was shown in *Fig. 9*. It is shown that when M_{try} is 2, the OOB error reaches a peak value of 0.000181. When M_{try} value is 7, a minimum of OOB error is 0.000071. With M_{try} increments, OOB error has ups and downs but overall tends to increase.

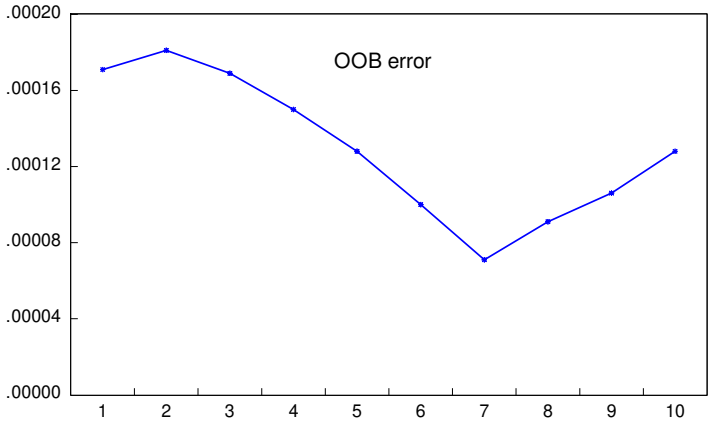

Figure 9. *Relationship between the number of split variables and OOB error*

Discussion

Driving factors of energy carbon footprint

The LMDI (Logarithmic Mean Divisia Index) decomposition method is an empirical research method proposed by Ang et al. in 1998 to decompose and measure energy carbon footprint factors. This method extends the Kaya identity and uses the log-average formula to solve the problem. The elements are decomposed and can effectively eliminate the residuals (Branger and Quirion, 2015). Introducing it into this study, it is conducive to the decomposition of energ carbon footprint driving factors. Considering the complexity of energ carbon footprint systems, the openness and availability of economic data, the influencing factors of energy carbon footprint (Y) is devided into energy structure (X1), energy efficiency (X2), energy intensity (X3) and economic development (X4). The energy carbon footprint factors are decomposed through LMDI, as shown in *Fig. 10*.

The energy structure effect is further exceeded than that of energy effiency, which are the major contributor to the increase in energy carbon footprint. Energy intensity and economic development can curtail the increase in energy carbon footprints. In particular, the energy intensity effect was reduced from -0.1157 to -1.3189. The economic development effect was reduced from -0.0064 to -0.1329. It means that adjusting energy structure can reduce energy carbon footprints and particularly alleviate dependence on primaryenergy. And the use of new energy and the development of green energy can also alleviate thegreenhouse effect.

Based on the accumulative effects of energy carbon footprint factors, the energy structure and energy intensity effects contribute the most to the increase in energy carbon footprint, which is shown in *Fig. 11*.

http://www.aloki.hu ● ISSN 1589 1623 (Print) ● ISSN 1785 0037 (Online)
DOI: http://dx.doi.org/10.15666/aeer/1704_83818394

Duro (2006) provide a methodology for decomposing international inequalities in per capita CO_2 emissions into Kaya (multiplicative) factors which indicated that energy intensity have made a less significant contribution to energy carbon footprint. This paper demonstrate energy intensity effects contribute the most to the increase in energy carbon footprint. In fact, energy intensity is truly affected the energy carbon footprint. This paper is the continuation of energy carbon footprint driving factors.

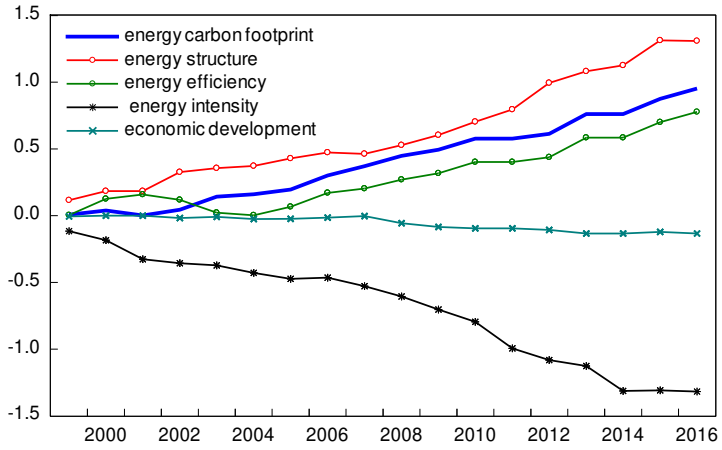

Figure 10. *Factor decomposition of carbon footprint in Liaoning*

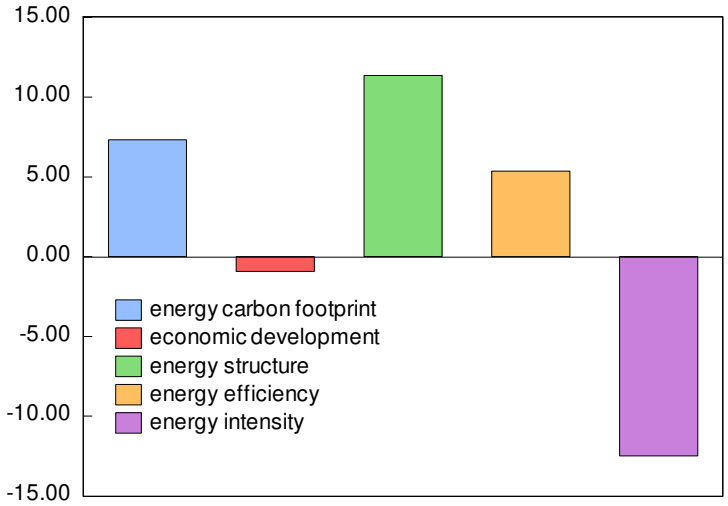

Figure 11. *Cumulative effect of energy carbon footprint*

Besides, Liu (2007) analyzes the change of industrial carbon emissions from 36 industrial sectors in China over the period 1998–2005 and the industrial carbon emissions are decomposed into carbon emissions coefficients of heat and electricity, energy intensity, industrial structural shift, industrial activity and final fuel shift. The overwhelming contributors to the change of China's industrial sectors' carbon emissions in the period 1998–2005 were the industrial activity and energy intensity. This paper also verifed that energy intensity was contribute the most to the increase in energy carbon footprint, which indicated the accuracy of LMDI.

http://www.aloki.hu ● ISSN 1589 1623 (Print) ● ISSN 1785 0037 (Online)
DOI: http://dx.doi.org/10.15666/aeer/1704_83818394

Strategies to decrease carbon footprint

The random forest algorithm used for calculating energy carbon footprint in Liaoning Province reveals the dynamic mechanism and trance of energy carbon footprint. The result of random forest algorithm shows that carbon footprint of energy carbon footprint grow rapidly. This dynamic mechanism also provides a theoretical support and data basis for the growth of carbon footprint and the transformation of economic development model. The conclusion is that the economic development of the rapid increase in carbon footprint played a crucial role. Based on empirical results, combined with the national conditions and development of advanced foreign experience, it proposes relevant measures to mitigate the carbon footprint growth and development of low-carbon economy recommendations. The following recommendations should be taken into consideration so as to decrease the carbon footprint and promote the national economy for sustainable development.

Increase energy efficiency and develop low-carbon economy

Much effort should be made to optimize the energy structures, reduce environmental pollution, develop the green energy, accelerate the modernization of enterprises, increase the quality of economic growth, and finally create a new pattern to develop economy. At the same time, the low-carbon concepts such as green lifestyles, green manufacturers should be advocated and the public awareness of environmental protection should be heightened.

A collaborative reverse logistics network should be established

The reverse logistics can be outsourced to those third-party reverse logistics enterprises for expertise. Thus it can be exploited to increase the management efficiency, decrease resource consumption and reduce the management risks. A prompt product recalling system should be built and the renewable materials should be recommended to achieve the environmental protection.

Design products in an eco-friendly way

The effect on environment and resources should be completely considered in the life cycle of products. And the waste rate of products should be decreased in order to reduce the adverse effect of products on the environment and maximize the resource utilization rates. Meanwhile, renewable resources and secondary energy should be used to slow down exhaustion of resources and ensure sustainable supply of resources.

Conclusions

The goal of this study has been to gain an understanding of the calculation of energy carbon footprint in Liaoning Province. We characterized the energy categories for the calculation of carbon footprints: raw coal, coke, crude oil, petrol, diesel oil, black mineral oil and natural gas. The empirical model subsequently used to calculate the energy carbon footprint in Liaoning Province. In order to evaluate the performance of random forest algorithm, the PLS algorithm is compared with the models proposed in this paper. The results showed that random forest algorithm not only can control parameter deviations, but also it can enhance the precision and accuracy of algorithm.

http://www.aloki.hu ● ISSN 1589 1623 (Print) ● ISSN 1785 0037 (Online)
DOI: http://dx.doi.org/10.15666/aeer/1704_83818394

The utility of random forest algorithm and results proposed in this paper can be extended by examining the energy carbon footprint of the other regions and countries.

As guidance for the future research, the random forest algorithm addressed in this paper can be enhanced to identify the main environmental and social driving factors of energy carbon footprint in Liaoning Province. It could be highly helpful for public sector to formulate energy policies. Besides, random forest algorithm can be used to deal with the other environmental and social numerical problems.

REFERENCES

[1] Abellán, J., Carlos, J., Mantas, C. J., Castellano, J. G., Moral-García, S. (2018): Increasing diversity in random forest learning algorithm via imprecise probabilities. – Expert System with Aplications 18(12): 228-243.

[2] Affuso, E., Hite, D. (2013): A model for sustainable land use in biofuel production: An application to the state of Alabama. – Energy Economics 37(5): 29-39.

[3] An, J., Xue, X. X. (2017): Life-cycle carbon footprint analysis of magnesia products. – Resources, Conservation and Recycling 119(4): 4-11.

[4] Bergthorson, J. M. (2018): Recyclable metal fuels for clean and compact zero carbon power. – Progress in Energy and Combustion Science 68(9): 169-196.

[5] Branger, F., Quirion, P. (2015): Reaping the carbon rent: Abatement and overall location profits in the European cement industry, insights from an LMDI decomposition analysis. – Energy Economics 47(7): 189-205.

[6] Chelgani, S. C., Matin, S. S., Hower, J. C. (2016): Explaining relationships between coke quality index and coal properties by Random Forest method. – Fuel 182(10): 754-760.

[7] Chen, B. L., Yang, Z. X., Ma, G. P., Kong, D., Xiong, W., Wang, J., Zhu, Y., Xia, Y. (2018): Heteroatom-doped porous carbons with enhanced carbon dioxide uptake and excellent methylene blue adsorption capacities. – Microporous and Mesoporous Materials 257(2): 1-8.

[8] Dalir, F., Motlagh, M. S., Ashrafi, K. (2018): A dynamic quasi comprehensive model for determining the carbon footprint of fossil fuel electricity: a case study of Iran. – Journal of Cleaner Production 188: 362-370.

[9] Dominic, C. Y., Raymond, R. T., Denny, K. S. (2008): Carbon and footprint-constrained energy planning using cascade analysis technique. – Energy 33(10): 1480-1488.

[10] Druckman, A., Jackson, T. (2009): The carbon footprint of UK household 1990-2004: A socio-economically disaggregated, quasi multi-regional input output model. – Ecological Economics 68(7): 2066-2077.

[11] Duro, J. A., Padilla, E. (2006): International Inequalities in per capita CO_2 Emissions: A Decomposition Methodology by Kaya Factors. – Energy Economics 28(2): 170-187.

[12] Ginestet, S., Marchio, D., Morisot, O. (2013): Improvement of buildings energy efficiency: comparison, operability and results of commissioning tools. – Enegy Conversion and Management 76(12): 368-376.

[13] Hertzberg, M., Schreuder, H. (2016): Role of atmospheric carbon dioxide in climate change. – Energy and Environment 27(6-7): 785-797.

[14] Kamińska, J. A. (2018): The use of random forests in modelling short-term air pollution effects based on traffic and meteorological conditions: A case study in Wrocław. – Journal of Environmental Management 217(7): 164-174.

[15] Kenny, T. K., Gray, N. F. (2009): Comparative performance of six carbon footprint models for use in Ireland. – Environmental Impact Assessment Review 29(1): 1-6.

[16] Liu, L. C., Fan, Y., Wu, G., Wei, Y.-M. (2007): Using LMDI method to analyze the change of China's industrial emissions from final fuel use:an empirical analysis. – Energy Policy 35(11): 5892-5900.

http://www.aloki.hu ● ISSN 1589 1623 (Print) ● ISSN 1785 0037 (Online)
DOI: http://dx.doi.org/10.15666/aeer/1704_83818394

[17] Long, Y., Dong, L., Yoshikuni, Y., Li, Z. L. (2018): Evaluation of energy related household carbon footprints in metropolitan areas of Japan. – Ecological modelling 377: 16-25.
[18] Mancini, M. S., Galli, A., Niccolucci, V., Lin, D., Bastianoni, S., Wackernagel, M., Marchettini, N. (2016): Ecological Footprint: refining the carbon footprint calculation. – Ecological Indicators 61(2): 390-403.
[19] Ohimain, E. I. (2012): The benefits and potential impacts of household cooking fuel substitution with bio-ethanol produced from cassava feedstock in Nigeria. – Energy for Sustainable Development 16(3): 352-362.
[20] Pragya, N., Sharma, N., Devnekar, A. S. (2017): Estimation of carbon emissions/savings incurred by wasteland and abandoned cropland-conversion from plantation of biofuel producing perennial tree species - Case study of India. – Global Ecology and Conservation 11(7): 158-164.
[21] Qi, Z. Q., Gao, C. K., Na, H. M., Ye, Z. (2018): Using forest area for carbon footprint analysis of typical steel enterprises in China. – Resources, Conservation and Recycling 132(5): 352-360.
[22] Romijn, H. A. (2011): Land clearing and greenhouse gas emissions from Jatropha biofuels on African Miombo Woodlands. – Energy Policy 39(10): 5751-5762.
[23] Sovacool, B. K., Brown, M. A. (2010): Twelve metropolitan carbon footprints: A preliminary comparative global assessment. – Energy Policy 38(9): 4856-4869.
[24] Sun, Q., Zhou, X. Z. (2016): Dynamic analysis of regional carbon footprint coupling and influencing factors. – Oxidation Communications 39(2): 1462-1477.
[25] Sun, Q. (2017): Research on the influencing factors of reverse logistics carbon footprint under sustainable development. – Environmental Science and Pollution Research 24(29): 22790-22798.
[26] Tao, Z. D., Tao, G., Jin, H., Yi, X., Jin, F. (2014): Trends and spatial distribution of embedded carbon Footprints in China. – Energy and Environment 25(5): 915-930.
[27] Wood, D., Giri, J. N., Mokhatab, S. (2009): Asian versus Global Strategies for Energy Fairness and Reduced Carbon Footprint -The Promise of the CDM. – Energy and Environment 20(3): 387-398.
[28] Yasar, Y., Kalfa, S. M. (2012): The effects of window alternatives on energy efficiency and building economy in high-rise residential buildings in moderate to humid climates. – Enegy Conversion and Management 64(12): 170-181.
[29] Zhou, Y. M., Qiu, G. P. (2018): Random forest for label ranking. – Expert Systems with Applications 112(12): 99-109.

http://www.aloki.hu ● ISSN 1589 1623 (Print) ● ISSN 1785 0037 (Online)
DOI: http://dx.doi.org/10.15666/aeer/1704_83818394

ANALYSIS OF AGRICULTURAL DEVELOPMENT PLANNING IN LOW HILLY RED SOIL REGION BASED ON PLANTING STRUCTURE

WANG, X.-L.

School of Economics and Management, Zhejiang University of Water Conservancy and Electric Power, Hangzhou, 310018 Zhejiang, China

(Received 8th Mar 2019; accepted 21st May 2019)

Abstract. The main aim of this study is to increase the income of farmers, and to further elaborate the development of low hilly red soil resources and cultivate industries with regionalized agricultural characteristic. By performing principal component analysis of the main agricultural products and determining the influencing factors of the main agricultural products in the low hilly red soil in the region of Jinhua and three key agricultural planting areas, the following conclusion can be drawn: we should expand the scale of land management, improve the basic construction of irrigation and water conservancy, promote the development of agricultural land consolidation projects, and implement the construction of agricultural ecological protection, so as to improve agricultural output and improve agricultural production performance.
Keywords: *the income of farmers, industrial layout, the potential of land resources, Zhejiang Province, agricultural production performance*

Introduction

With the rapid development of Zhejiang's economy, the situation surrounding land resources is becoming increasingly tense (Song, et al., 2012), the contradiction between people and land is becoming more and more prominent, the speed of agricultural development is slowing down, the comparative benefits of agriculture are declining, and the influence of land is growing over the industrial and agricultural production of Zhejiang Province and the sustainable development of the national economy (Zhang, 2011). It leads to some important influencing factors as the foundation of the national economy, agriculture is the basis and precondition for the existence and development of other industries such as commercial trade and crafts. (Gao, 2006). The potential method to accelerate the development of land reserved resources has become an important engine for promoting Zhejiang's economic development (Lü et al., 2000).

In the hilly areas of Zhejiang Province, the low hilly red soil is spread over most of the province's cities. For a long time, due to the long-term unreasonable management of low hilly red soil, single operation, deforestation, unreasonable land reclamation, excessive mining and quarrying (Shen et al., 2013), out-of-control population growth, combined with harsh climatic conditions (serious drought) and the inherent vulnerability of low-valve red soil ecosystems, make the above-mentioned huge advantages and potentials of low hilly red soil not only fully exerted, but also initiate various resources and ecological environment degradation processes (Chen, 2004). On the contrary, it is becoming more and more serious, and the contradiction between people and land is becoming more and more prominent (Zhang, 2013). At present, the development of low hilly red soil agriculture faces the following problems:

First, people increase their land demand, and the contradiction between people and land is prominent (Dai, 2005). The per capita cultivated land and agricultural labor force is extremely limited, the quality is poor, and the development investment is large. With

http://www.aloki.hu ● ISSN 1589 1623 (Print) ● ISSN 1785 0037 (Online)
DOI: http://dx.doi.org/10.15666/aeer/1704_83958415

the development of the market economy, it only pays attention to economic opening, but neglects the comprehensive development of resources (Zeng et al., 2006). The phenomenon of arable land abandonment is quite common, and the encroachment and pollution of cultivated land in the development zone is also increasing (Zhang, 2014). The serious slippage of grain production, coupled with the rapid growth of the population, the contradiction between the reverse development of man and land is quite sharp, and agriculture is shrinking.

Second, the agricultural structure is unreasonable and the advantages of the hills have not been realized. In terms of landform and landscape composition, Zhejiang Province has the characteristics of "seven mountains (Deng and Zhang, 2003), one water and two fields", with mountains and hills as the main body, and low hilly red soil areas accounting for about 38% of Zhejiang Province. In the use of land resources, the long-term implementation of the cropping industry as the main food-centred single unreasonable agriculture "model" is only concentrated on the valley plains, mountains and inter-valley valleys (Ni, 1982), basins and low hills. The relatively intensive agricultural operation was carried out in the gently-sloping section of the (Taiwan) area, while the vast mountains and hills in Zhejiang Province were basically idle or insufficient due to extensive management.

Third, the soil resources are degraded and the ecological environment is seriously damaged. The long-term unreasonable development and utilization of resources, combined with harsh climatic conditions, especially severe seasonal rains and droughts, as well as special soil and site characteristics, have led to and exacerbated Zhejiang Province, especially in the densely populated low-lying red soil agricultural areas. Soil erosion and fertility declined, and other processes of soil and agro-ecosystem degradation occurred as well. Therefore, strengthening the management and development of low hilly red soil and improving the agricultural output of low hilly red soil region are effective ways to improve the agricultural benefits of Zhejiang Province.

The low hilly soil region is affected by natural conditions such as topography, climate, parent material and hydrology, and human production activities. It has obvious regional characteristics. Different soil textures and physical and chemical properties determine the development and utilization of land by humans. By understanding the characteristics of various planting types, soil resources development can be rationalised and a stable and virtuous cycle of the soil system can be achieved. Taking the acceleration of agriculture and rural modernization as the starting point focus should be on increasing farmers' income (Jong, 2001), taking market as the guide and relying on science and technology to develop low hilly red soil resources and cultivating industries with regionalized agricultural characteristic. According to the objective needs of social and economic development and regional nature, social, economic, technological and ecological conditions, close focus should be on adapting to the new requirements of agricultural development, facing the needs of the province's internal and external markets, giving play to regional advantages, accelerating the adjustment of agricultural industrial structure, planting agricultural products that can meet market demand, and developing and managing low-lying red soil resources. It is of great practical significance to analyze the planting structure of agricultural products in the low hilly red soil region. This study is based on overall planning, keeping the social economic and ecological benefits unified, adapting to local conditions, maintaining the characteristics of land and agricultural utilization, safe production, efficiency, optimizing resources,

http://www.aloki.hu ● ISSN 1589 1623 (Print) ● ISSN 1785 0037 (Online)
DOI: http://dx.doi.org/10.15666/aeer/1704_83958415

comprehensive development and other principles, in the main distribution area of low hill red soil in Zhejiang Province.

Materials and methods

Literature review

China was one of the first countries to conduct land type research. As early as the 5th century BC, there were records of land type division. According to records, Zhou Li in the Warring States Period divided the land of the country into five categories: Shanlin, Kawasaki, Hill, Wenyan and Yuan. According to the topography, the "People in the Pipeline" divides the national land into three categories: "Putian", "Hill" and "Mountain". The determination of land type is very comprehensive.

(1) About land type division

Since the 1930s, many countries have conducted various investigations and studies on land types and land resource utilization in order to increase grain production and comprehensive development and utilization of land. Former Soviet geographer Berger published his book on "The Soviet Landscape Geography Zone" is a comprehensive exposition of landscape geography, the idea of comprehensive research on land and a systematic theoretical summary of the comprehensive features of land from a geographical perspective.

In the late 1950s, with the full development of China's natural zoning work, some geographers conducted land type surveys and cartographic studies at different scales. For example, Yan Qinshang's research (Yan, 2012; Rawat et al., 2019) on landscape mapping in the Kangding, Jiulong, and Yajiang areas of the Tibetan area, such as Isachinko, etc.; Yang Newzhang's to the west of the Tolahai River in the Qaidam Basin and the Malcommi in western Sichuan Research on the natural landscape of the Yaluolin area.

Since the 1990s, land type research has begun to be combined with practical work, and the scope has gradually focused on small and medium-sized areas. At the same time, significant progress has been made in land cover change and landscape ecology. The main researches of this period were the followings: Zhang (2000), Wang et al. (2000), Junior et al. (2019), Yang (2001), etc. applied remote sensing images, multi-source remote sensing data and other image data to the extraction of land types. Papers by Liu (1990), Shen (1992), Jiao et al. (2005), Liu and Li (2009), Khanchoul and Boubehziz (2019) studied the land types and mappings of the Oasis area in the Hexi Corridor, the agro-pastoral interlaced zone, the hilly area and the Loess Plateau in the arid regions. Liu Wei (2004), Yang et al. (2002), Fu et al. (2001), Liu and Chen (2002), Dali and Kamarudin (2018), proposed corresponding theoretical methods and zoning schemes for China's ecological zoning research. Wang et al. (2001), Cai (2001), Wang and Bao (1999) discussed scales for land use/land cover change, driving force by investment intensity of manpower and physical resources, the social economic output level, the intensity of natural disasters disturbance and educational level of workers.

(2) Indicators on the classification of land types

As early as the early 1960s, some developed countries (Xie et al., 2008) and some international organizations (Huang and Cai, 2005) began to use the relevant indicator

http://www.aloki.hu ● ISSN 1589 1623 (Print) ● ISSN 1785 0037 (Online)
DOI: http://dx.doi.org/10.15666/aeer/1704_83958415

system to evaluate economic and social development issues in macroeconomic and social research.

From the perspective of evaluation indicators, after the 1970s, the selection of representative indicator systems (Chen and Tao, 2000) to comprehensively evaluate various issues has become an indispensable and important means in modern management. Yu (2002) and others examined the issue from the point of view of developed agriculture, civilized farmers, affluent rural areas and good environment, Chen et al. (1993), etc. from the status of agriculture in macroeconomics and society, the living standards and quality of farmers, modern technology in agricultural production, application and agricultural production efficiency; Jiang (1997) observed procedures from production efficiency, management level, modern technology application and rural living standards; and other aspects of agricultural modernization, rural industrialization and rural urbanization (Cheng, 1999). The evaluation index system of agricultural modernization has been constructed in terms of output and socio-economic culture (Liang and Wenshun, 2019). Xu and Wu (1994), Tao (2018) and others established five aspects of system structure macro standards, production efficiency, agricultural production technology standards, comprehensive benefits and farmers' living standards (Xia and Li, 2000); Zhang Yuwu et al. established county-level eco-agricultural indicator system from three aspects: resource utilization evaluation, structural evaluation and functional benefit evaluation. Huang et al. (1995), Ma Kangyu, Gu Jianmin and others established an assessment indicator system for high-yield, high-quality and high-efficiency agriculture. Sun et al. (1995) and others have established a comprehensive evaluation index system for ecological agriculture from the aspects of system structure, system function and system efficiency, high yield, high efficiency, benign circulation and sustainable development, resource utilization, ecological function benefit, economic function benefit and social benefit (Ilyas et al., 2019).

From the indicator system, the number of specific indicators range from a few to dozens. Peng (1994) used nine indicators when evaluating the agro-ecological development of the central and sub-tropical agriculture in eastern China and the agro-ecological types of the county; Li et al. (2005) used 34 indicators for the evaluation of the agricultural ecosystem in Fujian Province; Qin Huibao was in the hilly area (Zhou et al., 2017; Asghar et al., 2018). The evaluation of village-level eco-agricultural systems used 26 indicators (Xia, 2013; Wali et al., 2018).

(3) Study on low hilly red soil and classification

The research on the development and utilization of low-hill red soil is firstly the discussion of resource characteristics (Huang et al., 2014; Ogunyele et al., 2018). As a comprehensive low-hill and gentle slope resource of comprehensive natural economic geography complex, the use of low-hill and gentle slope resources varies from vertical to horizontal (Shen et al., 2013). The vertical space difference mainly reflects the characteristics of altitude sunshine hours, temperature, precipitation (Huang and Tang, 2015) and other significant differences in climate resources. From the perspective of horizontal space differences (Wang and He, 2005), it mainly reflects the obvious differences in development costs, significant differences in natural geography and socio-economic conditions (Jia, 2016).

Secondly, the research focuses on the development potential of low hilly red soil resources. From the perspective of environmental analysis, land degradation, vegetation

http://www.aloki.hu ● ISSN 1589 1623 (Print) ● ISSN 1785 0037 (Online)
DOI: http://dx.doi.org/10.15666/aeer/1704_83958415

cover, soil fertility, soil erosion, and small watershed management are the main problems in the low hilly red soil region (Fang et al., 2010). Geostatistical method was used to study the spatial and temporal variability of soil fertility in the subtropical low hilly red soil region of China (Yin, 2006), and the effects of different utilization methods on soil fertility were analyzed and discussed. The development potential was mainly related to area, aspect, slope and land use. Factors such as status, altitude, and soil texture were also associated (Deng et al., 2017). Taking the typical low hilly red soil region in the Fuyang area of Hunan Province as the research area, the seasonal intercropping of soil moisture content in the long-term experimental plots of different fertilizer ratios in red soil dryland in low hilly areas (Pang, 2015) and its relationship with meteorological factors were studied (Chai, 1997). The variation of soil moisture in typical red soil areas was analyzed.

There is also agricultural planting research in the low hilly red soil region (Shi et al., 2018). The existing low hilly red soil industry development is mainly based on fisheries, forestry, conversion town construction land and ecological agriculture (Wu, and Chen, 2016). There are also test forests in the low hilly red soil area with a number of tree species, and the tree species with good economic and ecological benefits are screened out, which provides a basis for the rational development of low hilly red soil and intensive management of forestry (Wang et al., 2017). Based on the research of the basic characteristics of red soil in Poyang Lake and surrounding economic zones, it is pointed out that the layout of red soil is unreasonable in development and utilization, the production is simple (Bao et al., 2006), the level of forestry production is very low, and the cultivation of cultivated land is lacking, resulting in low yield and instability (Han et al., 2013), soil erosion and other issues.

In summary, for more than a century, domestic and foreign scholars have conducted various researches on land types for different research purposes, with different research techniques and means, so that they gradually mature in theory and method with the development of science and technology. With progress, I began to make extensive use of computer technology (Wang and Tao, 2012). China's research on the quantitative evaluation of agro-ecosystems is mainly focused on the evaluation of the establishment of the indicator system. There is still a lot of room for the understanding of the system as a whole and for the study of multi-level and multi-dimensional systems (Xu et al., 2016). In addition to improving agricultural soil infrastructure, improving agricultural infrastructure, and changing agricultural processing logistics (Chen et al., 2005) and branding, modern agricultural management practices, such as refined agriculture and facility agriculture, are inevitable for low-hill red soil (Ma and Wang, 2010). Regional agricultural development puts forward new requirements. Based on the type of land planting, this paper establishes a more comprehensive and scientific evaluation system of agricultural development, and applies land type planning better in land evaluation research. How to improve the agricultural planting structure in the low hilly regions? The development of the red soil region provides a direction.

Research methods

Since the last century, scientists from all fields have conducted extensive research on land resource changes and cover from their respective disciplines, and have shown a trend of multi-disciplinary cooperation (She, 2014). Principal component research is a core issue in the change of land resource utilization. The main component refers to the main cause of changes in land resource utilization. Since principal component research

http://www.aloki.hu ● ISSN 1589 1623 (Print) ● ISSN 1785 0037 (Online)
DOI: http://dx.doi.org/10.15666/aeer/1704_83958415

plays a very important part in the simulation of land resource utilization change (Jia et al., 2001), it has attracted the attention of many scholars at the beginning. Some scholars have analyzed the spatial and temporal changes of land resource utilization in China by establishing mathematical models (Xu, 2017), using principal component analysis models to evaluate the level of cultivated land use in Chongqing, and discovering the inadequacies of land resource utilization in Chongqing and exploiting the land resources of the city. Suggested countermeasures occurred soon. Some scholars have used principal component analysis to evaluate the use of cultivated land in Changsha City, and put forward relevant suggestions on agricultural planting varieties and development directions to promote the effective use of cultivated land in Changsha (Zhu et al., 2018). Based on these studies, this paper intends to use the principal component analysis method to analyze the agricultural development strategy of low hilly red soil region, and provide reference for agricultural planting varieties and categories.

(1) Principle of principal component analysis

Principal component analysis is a common method of data processing. Principal component analysis mainly uses the main factors in a set of data to analyze (Shi and Han, 2013), and transforms many research variables involved in evaluation and analysis into several external variables that have major influences, reducing the complexity of the research. Since 1901, the British mathematician Pearson introduced the principal component and the variables involved in the evaluation (Li and Ye, 2001), this method has been gradually promoted, and after long-term evolution and development, principal component analysis has been applied in data analysis in many fields.

Principal Component Analysis (PCA) (Zhang and Liu, 1995) is a comprehensive method of data dimensionality reduction. Its principle is to transform a series of related index variables into several main principal component index variables by statistical analysis to replace the original complex variables (Liu, 1998). Its mathematical model is a random vector group M = (M1,…,Mr). After orthogonal transformation, the transformed matrix N is obtained. In the matrix N, the components (Lu, 2000) are linearly independent, and the variance of the first component of N is the largest, the second is the next.

(2) Steps of principal component analysis

The steps of principal component analysis are as follows:

The first step is to suppose that there are A research areas, and the original sample matrix X of the B selection index is as follows (*Eq. 1*):

$$X = (Xij)\ A*B,\ i = 1, 2,...\ A,\ j = 1, 2,..., B \quad \text{(Eq.1)}$$

The second step is to compute the correlation matrix Rb*b, its eigenvalue 1 b 0 and the normalized eigenvector ej. The principal component Ti is obtained as follows (*Eq. 2*):

$$Ti = Xej \quad \text{(Eq.2)}$$

http://www.aloki.hu ● ISSN 1589 1623 (Print) ● ISSN 1785 0037 (Online)
DOI: http://dx.doi.org/10.15666/aeer/1704_83958415

In the third step, the contribution of the j principal component variance is 85%~95%, and the first Q principal component T1, T2,... Tq, then the principal component Q can be used to reflect the information of the original B indicators. The contribution rate formula (*Eq. 3*) is as follows:

$$a = \sum_{i=1}^{q} a_j \quad \text{(Eq.3)}$$

The fourth step is to get the comprehensive score W for agricultural planting in different regions (*Eq. 4*).

$$W = aX_1 + bX_2 + \ldots + xX_x \quad \text{(Eq.4)}$$

where X represents the eigenvector of eigenvalues; a and B are standardized data of original index.

Results

In order to further improve the benefit of comprehensive exploitation and utilization of red soil resources in low hilly areas, and to improve the ecological environment, agricultural productivity and soil and water conservation capacity of red soil areas in low hilly areas, the internal driving factors of red soil management and development in low hilly areas in Zhejiang Province were studied.

Research area

The low hilly red soil defined by the Zhejiang Provincial Reclamation Bureau refers to the hilly red soil area with the lower limit of the slope (Zhang, 2001), 250 m in the north, 300 m in the east and the middle, and 350 m in the south. In addition to Jiaxing City, the remaining 10 cities in the province are distributed.

The scope of this study is Jinhua City, located in the eastern half of the Jinyu Basin in Zhejiang Province. It belongs to the mid-subtropical region and is a key area for the development of low hill red soil in Zhejiang Province, including Wucheng District, Jindong District and Lanxi City under the jurisdiction of Jinhua City. Dongyang City, Yongkang City, Wuyi County, Pujiang County, and Chun'an County have a total of 8 counties and cities.

Low-hill red soil is most widely distributed (Wu and Chen, 1995) and characteristic in the area of Jinhua City in Zhejiang Province. There are a total of 16.3814 million units (mu) of land, including 2,911.3 thousand mu of low hilly red soil, accounting for 17.77% of the total land area. The soil types are roughly divided into three categories: red sand soil, purple sand soil and yellow gluten mud, which are distributed at the bottom of the Jinyu Basin. Low hilly red soil resources, due to its unique natural conditions, have become the main potential of agricultural development in Zhejiang Province. In the low hilly red soil area of Jinhua City, the improved soil methods such as land modification, green manure cultivation and straw returning to the field have been continuously applied. The crops such as tea and fruits have developed rapidly, the income of farmers has increased, the income from agricultural efficiency has increased significantly, and the social economy has continued to develop in general. This study

http://www.aloki.hu ● ISSN 1589 1623 (Print) ● ISSN 1785 0037 (Online)
DOI: http://dx.doi.org/10.15666/aeer/1704_83958415

uses the agricultural production resource data of the counties and cities under Jinhua City to analyze and evaluate the development and utilization potential of low hilly red soil, and provide decision-making basis for better utilization of low hilly red soil resources.

Index selection

The establishment of the indicator system in practical application is not necessarily based on a certain theory. It is often necessary to use a variety of theories in combination. The key is to meet certain research purposes and tasks, so that the indicator system can fully reflect the status and substance of the system. The scientific nature of the indicator system ultimately depends on the extent to which the researcher understands the system. In order to improve the functions of the sustainable indicator system, in the construction of the indicator system and the selection of indicators, according to the principles of science, comparability, operability, and simplicity should be selected by the principal component analysis indicators. In the establishment of indicators, the main areas of Jinhua City are considered. The existing agricultural planting structure data, first, the area planted with crops, and the second is the crop yield. Through the data of two types in recent years, the total area of crops, food crops, grains, beans are finally selected. Indicators such as vegetables, potatoes, rapeseed, medicinal herbs, watermelon, mulberry, tea, citrus, peach, and other fruits were selected to explore the laws of agricultural planting in Jinhua City, and better guide agricultural planting and industrial development.

Data collection and audit

The statistical yearbook of Jinhua City in 2014 was selected as the data source (Zhang, 2001), and the data of agricultural planting area in the study area was selected as the research data of affecting the development of low hilly red soil.

In order to ensure the quality of the data and lay a foundation for further analysis, it is necessary to audit the statistical data. The completeness and accuracy of the original data obtained from the direct investigation shall be examined. Audit integrity is mainly to check whether the unit or individual is missing, whether the survey items or indicators are completed and so on. The accuracy of audit is mainly to check the embodiment of the survey data in the objective truth of statistical information.

Sample descriptive statistics

Based on the sown area data of grain (*Table 1*) and main cash crops (*Table 2*) in Jinhua City, this paper analyzes the main driving factors of the development of red soil in hilly area by quantitative method, and summarizes the change law of utilization and quality of red soil in hilly area, so as to guide the management and development of red soil in hilly area better, and realize the cultivated land while increasing the productivity of red soil in hilly area. High efficiency and sustainable utilization provide scientific basis for the sustainable development of regional social economy.

Discussion

According to the local economic and social development needs and the suitability orientation of low hilly red soil, according to local conditions and overall arrangement,

http://www.aloki.hu ● ISSN 1589 1623 (Print) ● ISSN 1785 0037 (Online)
DOI: http://dx.doi.org/10.15666/aeer/1704_83958415

the rational utilization direction is determined, and the principle of "agriculture is suitable, forestry is suitable, garden is suitable" is adhered to, so as to give full play to the comprehensive benefits of low hilly red soil resources.

Table 1. *Agricultural acreage of low hilly red soil region in Jinhua city in 2014 (unit: hectare)*

	Total area	Grain	Cereals	Beans	Potatoes	Rape	Medicinal materials	Vegetable	Watermelon
Jinhua	56439	28287	22233	3047	3007	4877	10	8402	1703
Wuyi	30644	18565	14835	2025	1705	2677	142	5356	817
Pujiang	23928	13564	8800	2343	2421	2790	77	4184	844
Panan	17454	8164	2455	1471	1945	107	4502	3355	660
Lanxi	47065	23069	16817	4141	2111	9089	119	5600	1027
Dongyang	46613	31321	24381	3860	3080	1467	2082	5707	971
Yiwu	30684	17464	11068	3029	3367	1027	94	7277	1124
Yongkang	19298	12984	10529	1148	1307	497	121	2603	831
Total	272125	153418	111118	21064	18943	22531	7147	42484	7977

Table 2. *Planting area of mulberry orchard in hilly red soil region of Jinhua city in 2014 (unit: hectare)*

	Mulberry	Tea	Orange	Peach	Other fruits
Jinhua	9	1975	3001	959	6345
Wuyi	862	6411	501	166	1949
Pujiang	173	2215	340	50	3048
Panan	246	5078	6	76	772
Lanxi	1038	1232	1630	464	9817
Dongyang	342	3176	615	205	3488
Yiwu	116	727	968	489	3633
Yongkang	368	249	951	287	3776
Total	3154	21063	8012	2696	32828

Index description

All the indicators included factors such as grain, vegetables, fruits and other cash crops, as shown (*Table 3*), for their mean, maximum, minimum and standard deviation.

Index principal component extraction

Taking Wucheng District, Jindong District, Lanxi City, Dongyang City, Yongkang City, Wuyi County, Pujiang County and Pan'an County under the jurisdiction of Jinhua City as the samples, taking the standardized data in the tables as the evaluation data, using SPSS statistical analysis software to process the data, the correlation coefficient matrix of the indices and the characteristics of the matrix are obtained. The information of eigenvalue, variance contribution rate and factor load matrix are extracted by principal component analysis, which contains a lot of information of original variables. After factor analysis of the standardized data in the table, the correlation coefficient matrix, variance of each eigenvalue, cumulative contribution rate and factor load matrix are transformed.

http://www.aloki.hu ● ISSN 1589 1623 (Print) ● ISSN 1785 0037 (Online)
DOI: http://dx.doi.org/10.15666/aeer/1704_83958415

Table 3. *Descriptive statistics of main crops in sample counties (unit: hectare)*

	Case number	Minimum	Maximum	Average value	Standard deviation
Total area	8	17454	56439	34015.625	14377.12199
Grain	8	8164	31321	19177.25	7928.8857
Cereal	8	2455	24381	13889.75	7221.53934
Beans	8	1148	4141	2633	1076.8365
Potatoes	8	1307	3367	2367.875	729.6127
Rape	8	107	9089	2816.375	2960.57451
Medicinal materials	8	10	4502	893.375	1616.06258
Vegetable	8	2603	8402	5310.5	1930.62262
Watermelon	8	660	1703	997.125	319.16742
Mulberry	8	9	1038	394.25	365.16014
tea	8	249	6411	2632.875	2152.50482
orange	8	6	3001	1001.5	943.03234
Peach	8	50	959	337	298.99164
Other fruits	8	772	9817	4103.5	2808.93254
Case number	8				

Factor analysis

The total planting area of crops, grain crops, cereals, legumes, potatoes, rapeseed, medicinal materials, vegetables, watermelon, mulberry, tea, fruit trees, citrus, peach and other 14 variables as the analysis indicators have a certain degree of representativeness, the specific situation is shown in *Table 3*. After the above variables are put into SPSS statistical analysis software, the correlation coefficient matrix between the original variables and the correlation analysis results are obtained. From the correlation coefficient matrix, different degrees of correlation were revealed among the 14 influencing factors, and the correlation coefficients among other factors are in different distribution states.

Table 4 shows the common degree of variables of the 14 primitive variables. The index of variable commonality can reflect the degree of dependence of multiple variables on all common factors extracted. From *Table 4*, except for variables X1, X2, X9, X10, X12 greater than 90%, the common degree of all other variables are less than 90%, but higher than 65%, which fully shows that the common factor we extracted can contain most of the information of the original variables, the extraction result will be very satisfactory.

According to the requirements of principal component analysis, as long as the eigenvalue is greater than 1, and the cumulative contribution rate is higher than 80%, it can become the principal component. From the column of the eigenvalues and variance cumulative contribution rate (*Table 5*), we can see that the first three cumulative contribution rates have reached 84.076%. Therefore, the three principal components selected in this study are the first, second and third three common factors. The variance contribution rate of the three principal components after rotation is given in the factor load matrix. From this contribution rate, we can see that although the contribution rate of the three common factors after rotation has changed, the total cumulative variance contribution rate of the three factors has not changed, it is still 84.076%.

http://www.aloki.hu ● ISSN 1589 1623 (Print) ● ISSN 1785 0037 (Online)
DOI: http://dx.doi.org/10.15666/aeer/1704_83958415

Table 4. *Common degree of variables*

	Initial	Extract
X_1	1.000	.977
X_2	1.000	.902
X_3	1.000	.807
X_4	1.000	.804
X_5	1.000	.802
X_6	1.000	.869
X_7	1.000	.561
X_8	1.000	.848
X_9	1.000	.942
X_{10}	1.000	.932
X_{11}	1.000	.648
X_{12}	1.000	.921
X_{13}	1.000	.883
X_{14}	1.000	.875

Table 5. *Cumulative contribution of eigenvalue and variance*

Component	Initial eigenvalue			Extraction of sum of squares		
	Total	Variance%	Cumulative %	Total	Variance %	Cumulative %
1	7.763	55.451	55.451	7.763	55.451	55.451
2	2.271	16.224	71.675	2.271	16.224	71.675
3	1.736	12.401	84.076	1.736	12.401	84.076
4	.898	6.413	90.489			
5	.666	4.758	95.246			
6	.522	3.727	98.974			
7	.144	1.026	100.000			
8	0.0000000000000004488	0.000000000000003206	100.000			
9	0.0000000000000008075	0.0000000000000006218	100.000			
10	0.0000000000000006023	0.0000000000000004302	100.000			
11	0.0000000000000003404	0.0000000000000002431	100.000			
12	-0.0000000000000003773	-0.0000000000000002695	100.000			
13	-0.0000000000000001603	-0.0000000000000001145	100.000			
14	-0.0000000000000004554	-0.0000000000000003253	100.000			

According to the previous results, because the contribution rate of the first common factor is especially large, the common factor (the first principal component) in the index X1 total crop area, X2 grain crop area, X3 grain area, X4 legume area, X8 vegetable area, X9 watermelon area and other indicators, these are mainly planting food crops and vegetables (*Table 6*). Cultivated land, therefore, farmland in Jinhua City plays a larger role, so we need to focus on the management and development of cultivated land.

The second common factor (the second principal component) is evident in the index X5 potato area, X6 rape area, X10 mulberry area, X12 orchard area, X13 citrus area, X14 peach orchard area and other indicators. Among these six indicators, four are mainly reflected in economic forest and fruit products, therefore to strengthen, economic forest and fruit development still needs to be obtained.

http://www.aloki.hu ● ISSN 1589 1623 (Print) ● ISSN 1785 0037 (Online)
DOI: http://dx.doi.org/10.15666/aeer/1704_83958415

The third public factor (the third principal component) is obvious in the index X11 tea garden area, X7 medicinal materials planting area, and has a direct relationship with the characteristic agricultural industry in Jinhua, especially in Pan'an County, the development of Chinese medicinal materials is beneficial and needs to be concerned. To sum up, the factors covered by these three principal components also agree with the previous qualitative analysis.

Table 6. *Factor load matrix*

	Component		
	One	**Two**	**Three**
X_1	.948	.053	.274
X_2	.851	-.003	.422
X_3	.822	.053	.357
X_4	.788	.178	.389
X_5	.599	-.605	.276
X_6	.670	.645	-.057
X_7	-.511	-.244	.490
X_8	.850	-.319	.155
X_9	.892	-.333	-.191
X_{10}	.003	.939	.224
X_{11}	-.401	.059	.696
X_{12}	.496	.778	-.263
X_{13}	-.049	.876	-.338
X_{14}	-.212	.851	-.326

Analysis

Land use zoning is one of the main basis for determining land use and adopting specific land use measures. Through the use of land division, various agricultural production layouts can be reasonably arranged, that is, rationally planning the production sectors such as plantation, forestry, animal husbandry, and the spatial distribution of various production categories in various industries in order to obtain a certain area. Planting should involve as much quality agricultural products as possible on the land to achieve the best economic benefits and comprehensive social benefits. The layout of agricultural production in a region is inseparable from two conditions: the land type structure of the region and the hydrothermal conditions of the region, that is, the land quality level of the region. On the basis of the regional land quality level, according to the land type structure, reasonable determination of the local production development direction, combined with the appropriate utilization, transformation and protection measures, will greatly promote the production and ecological protection of the region. Therefore, in the basic soil of the above-mentioned evaluation results of land planting structure, to provide scientific theoretical and practical basis for promoting the efficient development of agriculture, combined with the local economic situation, the agricultural development strategy of the low hilly red soil region of Jinhua City is summarized in the followings:

http://www.aloki.hu ● ISSN 1589 1623 (Print) ● ISSN 1785 0037 (Online)
DOI: http://dx.doi.org/10.15666/aeer/1704_83958415

(1) Traditional agriculture such as grain in the low hilly red soil region

The agricultural land in the low hilly red soil area of Jinhua City plays a relatively large part (Liao et al., 2017), has a long development time, and has many development projects. It is suitable for long-term stable development and enhances the level of low hilly red soil development. As shown in *Figure 1,* Dongyang City, Jinhua City and Lanxi are the county-level administrative units with the largest grain planting area (*Fig. 1*). The low hilly red soil areas in these blocks are relatively flat, the agricultural supporting facilities are more comprehensive, and the agricultural basic conditions are better compared to other areas. More obvious benefits can be generated in the development of cultivated land. In the plain area, the slope is slow, the human activity is the strongest, and the land use diversity is the most abundant. According to the potential of soil resources and crop varieties it is required to optimize production system management, achieve intensive farmland management, develop precise agriculture, and ensure efficient use of resources. Dry land that can be realized by artificial water diversion can be transformed into paddy fields, which can not only obtain higher yield and economic income than dry farming, but also reduce soil erosion, improve soil properties and increase nutrient accumulation. Strengthening the production of food crops is the basis for the development of agriculture, the premise of agricultural industrialization, and the necessary condition for the rapid and stable economic development of Jinhua City.

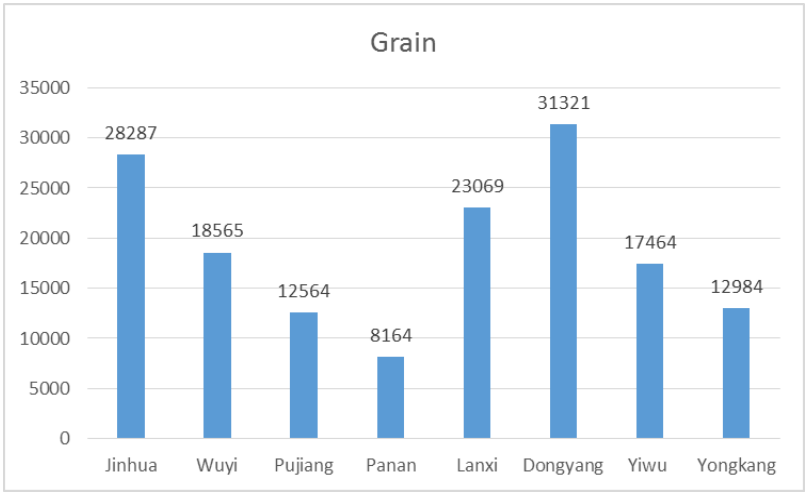

Figure 1. *The grain sown area of each county in Jinhua city (unit: hectare)*

(2) Economic forest fruit production in the low hilly red soil region

It is suggested to focus on and support local specialty products such as tea, camellia oil and citrus. The rapeseed planting area in Lanxi City, Jinhua City and Pujiang County ranks in the top three, and the citrus planting area in Jinhua City, Lanxi City, Yiwu City and Yongkang City is larger compared to other areas (*Figs. 2* and *3*). The economic forestry and fruit industry in Jinhua City has not formed a local regional brand, and there are no local agricultural regional brands such as Changshan Huyou, Yuhuan Wendan and Xianju Yangmei. The quality of citrus, tea and camellia products in Jinhua is not lost to foreign products (Yang et al., 2019). It has a long history and a good industrial foundation. On the basis of analyzing the status quo of land use distribution,

http://www.aloki.hu ● ISSN 1589 1623 (Print) ● ISSN 1785 0037 (Online)
DOI: http://dx.doi.org/10.15666/aeer/1704_83958415

correctly understand the suitability of regional topographic conditions and the characteristics of soil types, the rational layout of land use in the region can be explored, the land use structure can be optimized, and optimal allocation and intensive use of low hilly soil resources can be provided. In the next stage of low hilly-red soil management development it is suggested to focus on strengthening the development of economic crops and economic forest fruit, improve agricultural output, build local brand agriculture, and improve the comparative benefits of low hilly red soil governance development.

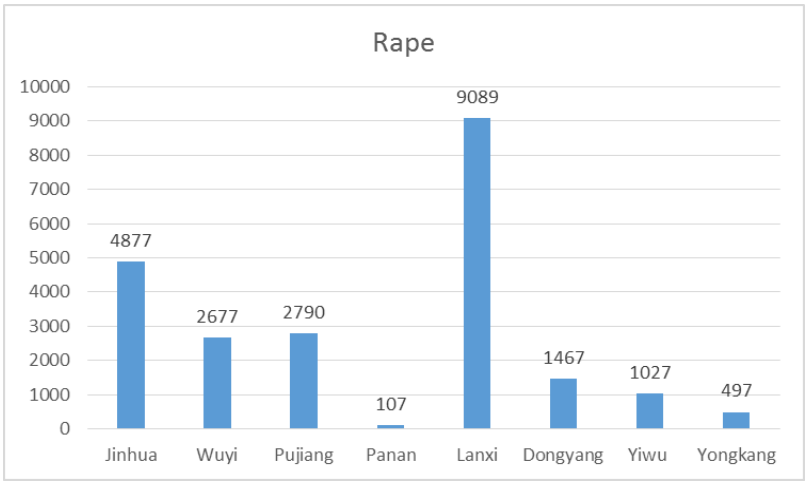

Figure 2. *Rape planting area of each county in Jinhua city (unit: hectare)*

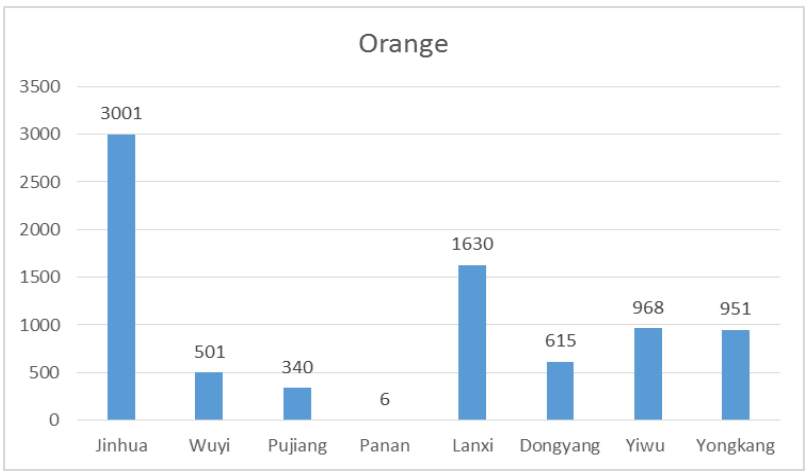

Figure 3. *Orange planting area of each county in Jinhua city (unit: hectare)*

(3) The development of Jinhua characteristic agriculture in the low hilly red soil region

The unique natural conditions such as topography, land and water have created a distinctive geographical environment, forming a regional brand of agricultural products such as Jinhua bergamot and Chun'an Chinese herbal medicine. The tea planting area in Wuyi County, Chun'an County and Dongyang City ranks in the top three in the city (*Figs. 4* and *5*). Most of Jinhua City's medicinal materials are planted in Chun'an

http://www.aloki.hu ● ISSN 1589 1623 (Print) ● ISSN 1785 0037 (Online)
DOI: http://dx.doi.org/10.15666/aeer/1704_83958415

County and Dongyang City, and there are Chinese herbal medicines in Chun'an. In the trading market, the Dapanshan National Chinese Herbal Medicine Nature Reserve has promoted the cultivation of medicinal materials in the adjacent Dongyang City. Jinhua City should focus on supporting the development of characteristic agriculture. Under certain technical, economic and ecological environment conditions, the existing red soil resources that can be exploited and utilized can be rationally developed, and the characteristic agricultural industries should be upgraded through technical measures such as agriculture, water conservancy and biology. The completion of the characteristic agricultural product industry has expanded the production scale, optimized the variety structure, improved the product grade, increased the added value of agricultural products, and fully exerted the social benefits of the project (Yu and Wu, 2018).

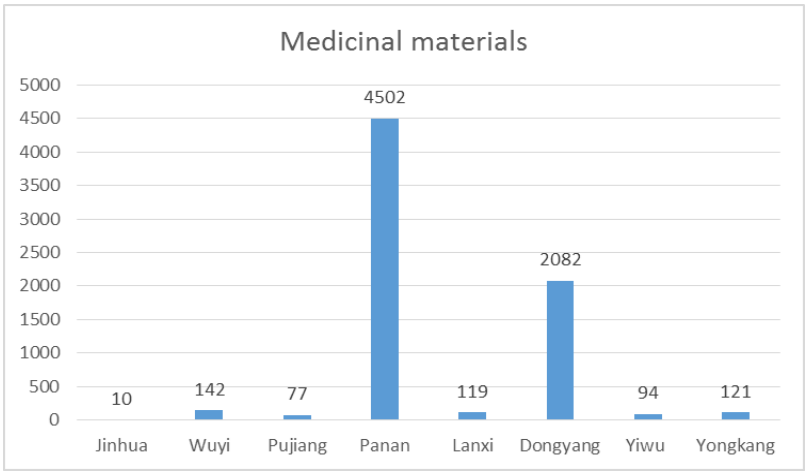

Figure 4. *Medicinal herbs area of each county in Jinhua city (unit: hectare)*

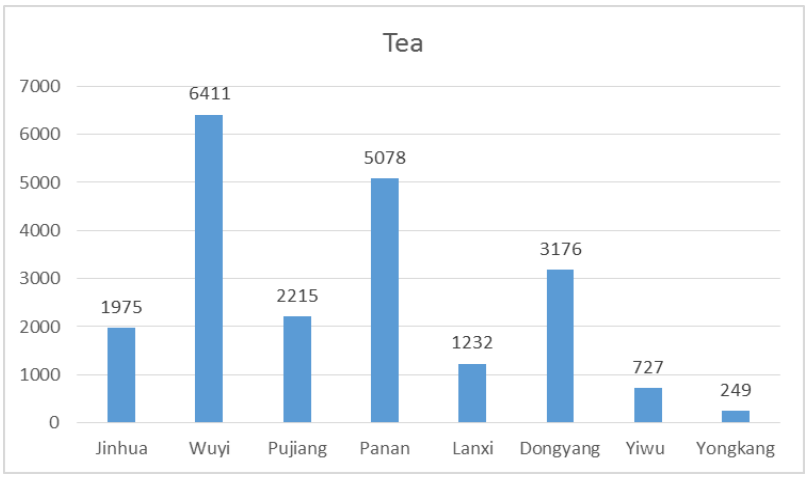

Figure 5. *Tea planting area of each county in Jinhua city (unit: hectare)*

Conclusion

This study is based on overall planning, keeping the social economic and ecological benefits unified, adapting to local conditions, maintaining the characteristics of land and agricultural utilization, safe production, efficiency, optimizing resources, comprehensive

http://www.aloki.hu ● ISSN 1589 1623 (Print) ● ISSN 1785 0037 (Online)
DOI: http://dx.doi.org/10.15666/aeer/1704_83958415

development and other principles, and it involves the main distribution area of low-hill red soil in Zhejiang Province. The planting structure was analyzed and it was considered that the rational layout of different landform units was strengthened and the potential of land resources was fully explored. It is necessary to actively develop precision agriculture in the plain area and reduce the occupation of construction land on low hilly red soil. Low-mountain hilly areas should vigorously develop a complex ecosystem of forest and fruit combination, so that grain should be grainy, forest should be forested, fruit should be fruitful, and rational layout should be achieved to achieve the best ecological, economic and environmental effects.

In the next stage of the development of low-hill red soil governance, Jinhua City was regarded as a model project of low hilly red soil agriculture, which involves the followings: (1) Expanding the scale of land management for farmers. Fully understand the importance and urgency of large-scale operation of low hilly red soil land, changing the concept of land use (Le et al., 2017), transforming the economic development mode, and adjust and optimize the economic structure. Strengthening planning guidance, tapping the potential of stocks of low hilly red soil, and increasing the scale of land use. Speeding up the transformation of land to large-scale utilization and improving the land use efficiency of low hilly red soil. (2) Improving the construction of farmland water conservancy infrastructure. In the development of characteristic agriculture in the low hilly red soil region, it is necessary to promote the construction and management of farmland water conservancy projects in the low hilly red soil region, and to increase the end-canal system reform in large and medium-sized irrigation districts, and accelerate the construction of small-scale drainage facilities. It is appropriate to take the form of incentives and subsidies to fully mobilize the enthusiasm of farmers to build farmland water conservancy projects.

(3) Promoting the development of agricultural land consolidation projects. Through the method of finishing low hilly red soil area, the low hilly red soil resources are levelled and the water conservancy facilities, field protection forests, and field roads in the development area are constructed. Reaching Tian Chengfang, the canal is connected, the road is connected, the forest is net, and the irrigation is carried out. The requirements of the row have led to a significant improvement in farmland production conditions. Continuously increasing the effective arable land area and improving the comprehensive agricultural production conditions are also suggested.

(4) Implementing agro-ecological protection projects in low hilly red soil areas, improving the management methods for various types of funds for ecological compensation, incorporating ecological protection indicators for low hilly red soil into comprehensive evaluation system for economic and social development and establishing a comprehensive evaluation system for leading cadres, inspiring internal motivation of the cadres and the masses at all levels to protect the ecological environment. Finally, we will improve the comprehensive agricultural production conditions, change the agricultural planting structure, and achieve the goal of improving agricultural output value and improving agricultural production performance.

In the future the planting structure will be analyzed further and more effective agricultural development planning will be proposed, which will not be limited in low hilly red soil region, but other regions will also be involved to provide reference for further studies.

http://www.aloki.hu ● ISSN 1589 1623 (Print) ● ISSN 1785 0037 (Online)
DOI: http://dx.doi.org/10.15666/aeer/1704_83958415

REFERENCES

[1] Asghar, Z., Ali, W., Nasir, A., Arshad, A. (2018): Atmospheric monitoring for ambient air quality parameters and source apportionment of city Faisalabad, Pakistan. – Earth Sciences Pakistan 2(1): 01-04.
[2] Bao, Y., Hu, Z. Q., Bai, Y. (2006): Application of principal component cluster analysis in land use ecological security assessment. – Transactions of the Chinese Society of Agricultural Engineering 22(8): 87-90.
[3] Cai, Y. l. (2001): Research on land use/land cover change: seeking a new comprehensive approach. – Geographical Research 20(6): 645-652.
[4] Chai, J. (1997): Quantitative research on the status of agricultural industrialization. – Agricultural Technology & Economy 3: 4-7.
[5] Chen, A. (2004): The choice and exploration of ecological agriculture road—a study on the countermeasures of land resources utilization and sustainable development in the low hilly red soil region of Zhejiang Province. – Journal of Finance and Economics 5: 19-23.
[6] Chen, C., Yan, X., He, Y. B. (2005): Principal component analysis of ecological agriculture model in red soil region of Southeast China. – Resources and Environment in the Yangtze Basin 14(2): 193-197.
[7] Chen, Y. H., Cao, C. G., Zhang, S. B. (1993): Study on ecological agriculture model of farmers in hilly areas. – Chinese Journal of Eco-Agriculture 1(4): 43-51.
[8] Chen, Y. Q., Tao, Tao. (2000): On the evaluation index of sustainable agriculture. – Journal of Agricultural Modernization 21(5): 271-275.
[9] Cheng, Z. Q. (1999): Shanghai agricultural sustainable development index system and its evaluation. – Agricultural Technology & Economy 1: 39-43.
[10] Dai, Y. Z. (2005): Development and utilization of superior resources in reserve resources of cultivated land in Zhejiang Province. – Zhejiang Land Resources 7: 44-47.
[11] Dali, N. M., Kamarudin, K. S. N. (2018): The effect of cosurfactant in CO_2 absorption in water-in-oil emulsion. – Environment & Ecosystem Science 2(2): 42-46.
[12] Deng, R., Zhang, Z. Q. (2003): The impact of China's entry into the world trade organization on China's animal husbandry industry. – Journal of Beijing Agricultural College 18(1): 36-42.
[13] Deng, Y., Cai, C., Xia, D., Ding, S., Chen, J., Wang, T. (2017) Soil Atterberg limits of different weathering profiles of the collapsing gullies in the hilly granitic region of southern China Solid Earth, 8 (1), 499–513.
[14] Fang, W., Chen, X. M., Du, Y. J. (2010): Dynamic changes of red soil moisture in low hilly areas and its influencing factors. – Transactions of the Chinese Society of Agricultural Engineering 26(1): 67-72.
[15] Fu, B. J., Liu, G. H., Chen, L. (2001): China's ecological zoning scheme. – Chinese Journal of Ecology 21(1): 1-6.
[16] Gao, K. Y. (2006): Investigation and Evaluation of Red Soil Resources in Low Hills of Zhejiang Province. – Zhejiang University, Hangzhou.
[17] Han, X. Y., Jing, Y. S., Li, G. (2013): Redundancy analysis of meteorological factors for soil moisture change on low hilly red soil slope. – Chinese Journal of Ecology 32(9): 2368-2374.
[18] Huang, J., Bao, G. J., Lin, L. (2014): Spatial differences in the development of hilly and low slope mountain in Yunnan Province and its countermeasures. – Acta Agriculturala Sinica 4(10).
[19] Huang, Q. Y., Cai, Y. L. (2005): A review of several land use change models in China. – China Land Science 19(5): 25-30.
[20] Huang, W. X., Ma, K. Y., Gu, J. M. (1995): Rural modernization index system and its popularization and application. – Jiangsu Agricultural Sciences (3): 2-5.

http://www.aloki.hu ● ISSN 1589 1623 (Print) ● ISSN 1785 0037 (Online)
DOI: http://dx.doi.org/10.15666/aeer/1704_83958415

[21] Huang, Y. D., Tang, X. H. (2015): Research on land use functional zoning in Quanzhou City based on principal component-cluster analysis. – Journal of Hainan Normal University (Natural Science Edition) (4): 443-447.
[22] Ilyas, M., Ali, M. A., Awan, A. N., Haider, S., Shahid, A. (2019): Estimation of noise levels in the road side parks and study of its impacts on health of visitors in Faisalabad. – Earth Sciences Pakistan 3(1): 14-22.
[23] Jia, Q. H. (2016): Microclimate characteristics and soil water dynamics simulation in low hilly red soil region. – Nanjing University of Information Science & Technology.
[24] Jia, X. C., Wang, S. Q., Wang, J. R. (2001): Research on sustainable development and utilization of Fangxiadian small watershed. – Contemporary Ecological Agriculture (z2): 97-100.
[25] Jiang, X. Q. (1997): Discussion on the evaluation index system of sustainable development of design agriculture. – China Rural Economy 6: 39-40.
[26] Jiang, Y. X. (1963): Preliminary study on habitat types of Miyaluo and Maerkang Alpine forests in Western Sichuan. – Forestry Science 8(4): 321-335.
[27] Jiao, F., Wen, Z. M., Li, R. (2005): Evaluation of land type structure at county scale in loess hilly region (Ansai). – Soil and Water Conservation Research 12(1): 000030-131.
[28] Jong, S. M. D., Hornstra, T., Maas, H. G. (2001): An integrated spatial and spectral approach to the classification of Mediterranean land cover types: the SSC method. – International Journal of Applied Earth Observations & Geoinformation 3(2): 176-183.
[29] Junior, J. J. M., Silva, E. A., Reis, A. L. D. A., Santos, J. P. M. S. (2019): Dynamical spatial modeling to simulate the forest scenario in Brazilian dry forest landscapes. – Geology, Ecology, and Landscapes 3(1): 46-52.
[30] Khanchoul, K., Boubehziz, S. (2019): Spatial variability of soil erodibility at El Hammam Catchment, Northeast of Algeria. – Environment & Ecosystem Science 3(1): 17-25.
[31] Le, K., Yao, J. Z., Li, Z., Ke, Z. (2017): Preparation, characterization and photocatalytic activity of novel CeO2 loaded porous alkali-activated steel slag-based binding material. – International Journal of Hydrogen Energy 42(27): 17341-17349.
[32] Li, Q. S., Ye, X. J. (2001): A study on the evaluation method of the sustainable development rate of agriculture ecosystems. – Chinese Journal of Ecology 21(5): 695-700.
[33] Li, Y. C., Jia, Z., Song, N. P. (2005): Evaluation of agro-ecosystem structure of different types of farmers and herdsmen in the farming-pastoral ecotone. – Journal of Sichuan Agricultural University 26(1): 76-80.
[34] Liang, Z., Wenshun, W. (2019): Parametric architectural design based on optimization algorithm. – Engineering Heritage Journal 3(1): 13-17.
[35] Liao, X. F., Xiao, W. J., Xie, G. (2017): Study on soil physical and chemical properties of typical small watershed in karst area of low-mountain and hilly area in Northeast Yunnan—taking Gaoqianghe small watershed as an example. – Hubei Agricultural Sciences 56(22).
[36] Liu, D. L., Li, B. C. (2009): Classification and mapping of land types in small watersheds of the Loess Plateau—a case study of Shanghuang test area in Guyuan City. – Eco Economy (1): 32-33.
[37] Liu, J. L. (1998): Factor analysis method for natural ecosystem evaluation factors of natural villages in the Huang-Huai-Hai Plain. – Chinese Journal of Ecology (3): 11-15.
[38] Liu, W. (2004): Study on the new methodology of mesoscale earth observation system supporting China's comprehensive natural geographical regionalization. – Journal of Geographical Sciences 23(6): 1-9.
[39] Liu, Y. H. (1990): Land types of oasis in Hexi Corridor and their development and utilization: a case study of Dunhuang and Wuwei. – Resources and Environment in Arid Areas 52-60.
[40] Liu, Y. S., Chen, B. M. (2002): Research on China's sustainable development and land use/cover change. – Geographical Research 21(3): 324-330.

http://www.aloki.hu ● ISSN 1589 1623 (Print) ● ISSN 1785 0037 (Online)
DOI: http://dx.doi.org/10.15666/aeer/1704_83958415

[41] Lu, J. B. (2000): Sustainability of agricultural ecosystem and its evaluation index. – Journal of Ecology 19(2): 56-58.
[42] Lü, X. N., Lu, Y. B., Wang, R. C. (2000): Numerical evaluation of fertility of red soil in Zhejiang low hill. – Chinese Journal of Soil Science 31(3): 107-110.
[43] Ma, W. X., Wang, Jun, W. (2010): Research on leading industry selection in yichun state-owned forest region based on principal component analysis. – Forestry Economics 10: 45-49.
[44] Ni, S. X. (1982): Recent research on the study of natural geographical division in the geography of the Soviet Union. – Geographical Research 1(1): 95-102.
[45] Ogunyele, A. C., Obaje, S. O., Akingboye, A. S. (2018): Lithostructural relationships and petrogenetic affinities of the basement complex rocks around Okpella, Southwestern Nigeria. – Earth Sciences Malaysia 2(1): 29-36.
[46] Pang, W. (2015): Study on Energy Balance Characteristics and Evapotranspiration Model of Paddy Field in Low Hilly Red Soil Region. – Nanjing University of Information Science & Technology, Nanjing.
[47] Peng, T. B. (1994): Study on the Genesis and Development Mechanism of Agro-Ecological Types in the Eastern Central Asia Tropical Region. – Science Press, Beijing.
[48] Rawat, K. S., Kumar, R., Singh, S. K. (2019): Topographical distribution of cobalt in different agro-climatic zones of Jharkhand state, India. – Geology, Ecology, and Landscapes 3(1): 14-21.
[49] She, T. T. (2014): Reconstruction Technology of Low-Yield Bamboo in Low Hilly Red Soil Area. – Central South University of Forestry and Technology, Changsha.
[50] Shen, Y. C. (1992): Discussion on the structure of land resources and the rational land use of agriculture, forestry and animal husbandry—a case study of Hexi Corridor in Gansu Province. – Resources and Environment in Arid Areas (2): 1-8.
[51] Shen, Z. W., Zhang, J. J., Zhang, X. (2013): Soil characteristics of low hilly red soil region in Zhejiang Province. – Bulletin of Science and Technology 7: 72-77.
[52] Shi, C., Han, L. D. (2013): Ecological security evaluation of land resources in Jinhua City. – Hunan Agricultural Sciences (5): 135-138.
[53] Shi, Z., Yang, J., Li, Z. W. (2018): Comprehensive control of soil and water loss in low-mountain and hilly areas of southern red soils. – Journal of Soil and Water Conservation 32(1): 6-9.
[54] Song, M. Y., Wang, S. Y., Wei, L. L. (2012): Research on the development and utilization of low slope land resources in Zhejiang Province—from the perspective of industrial construction land. – Journal of Henan Institute of Education (Natural Science) 21(3): 52-54.
[55] Sun, H. L., Qi, W., Gu, W. (1986): Principles and indicators system for comprehensive evaluation of ecological agriculture benefits. – Journal of Agricultural Modernization 7(3): 26-29.
[56] Tao, S. (2018): Evaluation of technology innovation in Hubei Province. – Engineering Heritage Journal 2(2): 09-10.
[57] Wali, E., Phil-Eze, P. O., Nwankwoala, H. O. (2018): Saltwater-freshwater wetland ecosystem and urban land use change in Port Harcourt Metropolis, Nigeria. – Earth Sciences Malaysia 2(1): 01-07.
[58] Wang, H., Tao, Z. F. (2012): Research on evaluation method of land intensive use. – Earth 9: 99-99.
[59] Wang, J., Dong, G. R., Li, W. J. (2000): Research on hierarchical selection of desertification land types using remote sensing information decision tree method. – Journal of Desert Research 20(3): 243-247.
[60] Wang, M. Z., He, Y. Q. (2005): Application of low hill red soil development model. – Journal of Huazhong Agricultural University (2): 146-152.
[61] Wang, S. Y., Liu, J. Y., Zhang, Z. X. (2001): Analysis of temporal and spatial characteristics of land use in China. – Acta Geographica Sinica 56(6): 631-639.

http://www.aloki.hu ● ISSN 1589 1623 (Print) ● ISSN 1785 0037 (Online)
DOI: http://dx.doi.org/10.15666/aeer/1704_83958415

[62] Wang, X. L., Bao, Y. H. (1999): Discussion on the research methods of land use dynamic change. – Progress in Geography 18(1): 81-87.
[63] Wang, Y. J., Pu, L., Liu, Z. Y. (2017): Ecological security assessment of land use in arid area based on principal component fuzzy evaluation analysis. – China Manganese Industry 35(3): 158-161.
[64] Wu, Z. L., Chen, Y. H. (1995): Research on comprehensive evaluation and regulation of agricultural ecosystem. – Chinese Journal of Applied Ecology s1: 98-104.
[65] Wu, Z. L., Chen, Y. H. (2016): Comprehensive evaluation index system of agricultural ecosystem and its weight. – Chinese Journal of Eco-Agriculture 4(2): 28-31.
[66] Xia, D. D. (2013): Investigation and enlightenment of follow-up management of red soil project. – Zhejiang Modern Agriculture 2013: 42-43.
[67] Xia, J. G., Li, T. X. (2000): Application of principal component analysis in the evaluation of cultivated land quality. – Journal of Southwest Agricultural University 13(2): 51-55.
[68] Xie, Z. L., Xu, X. G., Sun, Q. (2008): Land cover change prediction based on patch-dynamics model—Taking Beijing as an example. – Journal of Peking University: Natural Science 44(3): 452-458.
[69] Xu, B. S., Wu, Yu. jun. (1994): Research on comprehensive evaluation system of agricultural modernization level in Shanghai suburbs. – Journal of Agricultural Modernization 15(1): 28-31.
[70] Xu, W. (2017): Research on scientific planning method of land resources development and utilization in Jinhua. – China Real Estate 20.
[71] Xu, Y. H., Pan, Y. C., Liu, Y. (2016): Temporal and spatial differentiation of cultivated land intensive use level in Hainan Province. – Journal of Capital Normal University (Natural Science Edition) 37(4): 78-84.
[72] Yan, Q. S. (2012): Natural landscape of Kangding, Jiulong and Yajiang in Xikang Province—a case study of mountain geography. – Acta Geographica Sinica (Z1): 43-48.
[73] Yang, Q. H., Qi, J. W., Sun, Y. J. (2001): Research on high-resolution satellite remote sensing data in the dynamic monitoring of land use. – Remote Sensing of Land and Resources 4: 20-26
[74] Yang, Q. Y., Zheng, D., Wu, S. H. (2002): Research on ecological regional system in China. – Advances in Natural Science 12(3): 65-69.
[75] Yang, Y. X., Li, H., Zheng, W. K., Yun, B., Liu, Z. M., Zhang, J. J. (2019): Experimental study on calcining process of secondary coated ceramsite solidified chromium contaminated soil. – Science of Advanced Materials 11(2): 208-214.
[76] Yin, G. Q. (2006): Analysis on the necessity and function of development and utilization of low hilly red soil. – Zhejiang Water Resources Science & Technology 2: 29-30.
[77] Yu, J. S. (2002): The index system and development path choice for Shanghai to take the lead in realizing agricultural modernization. – Shanghai Rural Economy 1: 14-16.
[78] Yu, J., Wu, J. (2018): The Sustainability of Agricultural Development in China: The Agriculture–Environment Nexus. Sustainability 10 (1): 1776-1195.
[79] Zeng, W., Chen, X. P., Wang, W. (2006): Spatial variability and distribution of nutrients in low hilly red soil based on geostatistics and GIS: a case study of low hill red soil in Longyou County. – Zhejiang Forestry Science and Technology 26(3): 1-6.
[80] Zhang, H. (2011): Research on Evaluation Standards of Land Intensive Use in Zhejiang Development Zone. – Zhejiang University, Hangzhou.
[81] Zhang, J. L., Liu, L. D. (1995): Evaluation of comprehensive benefits of agroforestry ecosystem in Jiangtan. – Chinese Journal of Ecology 15(4): 442-449.
[82] Zhang, M. (2000): Study on the landscape pattern and evolution of fragile ecological environment in Yulin area. – Geographical Research 19(1): 30-36.
[83] Zhang, S. J. (2014): Remote Sensing Evaluation and Change Analysis of Ecological Environment in Low Hilly Red Soil Ecologically Fragile Area of Zhejiang Province. – Zhejiang University, Hangzhou.

http://www.aloki.hu ● ISSN 1589 1623 (Print) ● ISSN 1785 0037 (Online)
DOI: http://dx.doi.org/10.15666/aeer/1704_83958415

[84] Zhang, X. Y., Zhu, X. Y., Wang, W. (2013): Evaluation of cultivated land development potential in low hilly red soil region based on remote sensing and GIS. – Transactions of the Chinese Society of Agricultural Engineering 24(3): 114-118.
[85] Zhang, Z. Q. (2001): Principal component analysis of influencing factors of China's grain production system. – Journal of Beijing Agricultural College 16(1): 65-68.
[86] Zhou, S. X., Chen, L. L., Liu, L. (2017): Temporal and spatial evolution characteristics of agro-ecosystem adaptability in the southern hilly region under the background of global change: a case study of Hengyang Basin. – Chinese Journal of Eco-Agriculture 25(2): 147-156.
[87] Zhu, W., Wang, E., Hou, Y., Xian, L., Ashraf, M. A. (2018): Hybrid filtering optimization method for denoising contaminated spot images at near-sea-surface intervals. – Journal of Coastal Research: Journal of Coastal Research 82: 70 - 7.

http://www.aloki.hu ● ISSN 1589 1623 (Print) ● ISSN 1785 0037 (Online)
DOI: http://dx.doi.org/10.15666/aeer/1704_83958415

INFLUENCE OF ENVIRONMENTAL REGULATION ON THE GROWTH OF TOTAL FACTOR PRODUCTIVITY—AN EMPIRICAL RESEARCH BASED ON CHINA'S PROVINCIAL PANEL DATA

WANG, Y.* – HAO, C. – ZHANG, Z.

School of Economics and Management, Xi'an University of Technology, Xi'an, PR China

**Corresponding author*
e-mail: wangyan@xaut.edu.cn

(Received 8th Mar 2019; accepted 21st May 2019)

Abstract. Previous researches tended to ignore the influence of environmental regulation on technical efficiency, and in this sense, the total factor productivity is easy to be overestimated. This paper establishes the translog stochastic frontier production function model, includes environmental regulation into technical inefficiency equation, calculates the total factor productivity and its composition in China (including eastern, central and western regions) from 1995 to 2015, and also makes an analytical comparison with the value not considering environmental regulation. The results show that: (1) the investment on industrial pollution control and SO_2 emission intensity will significantly promote technology inefficiency, thus exerting a negative impact on economic growth; (2) environmental regulation slows down the growth rate of total factor productivity in China and all of its regions; (3) Considering the environmental regulation, technical efficiency is improved significantly and becomes the major drive behind the grow of total factor productivity, while technological progress, scale efficiency and the allocation efficiency show setback; (4) In terms of different regions, the growth rate of total factor productivity is the fastest in the east of China, and the slowest in the central region. Drives behind the growth of total factor productivity in each region are distinct.
Keywords: *technical efficiency; economic growth; driving force; environmental factor; computing method*

Introduction

The report of the 19th National Congress pointed out that "China's economy has been transitioning from a phase of rapid growth to a stage of high-quality development," so the country should shift from the extensive growth, which focuses on speed and scale, to intensive growth, which emphasizes efficiency. In the new stage, economic growth should not be judged merely by speed, and the quality should be regarded as the key. Over the past 30 years, due to the limitation of productivity, China's economic growth has been based on "high investment, high consumption and high emissions", which although promoted a high speed of economic development, has brought serious environmental pollution at the same time. Global Environmental Performance Index (EPI) ranked China the 109th in 180 participating countries and regions in 2016, which reflects that China's environmental situation is apparently not optimistic. Because of this, the century government has attached great importance to energy conservation and pollution emission, pointing out in "The Thirteenth Five-Year Plan" the target of "greatly improving the efficiency of exploiting energy resources, effectively controlling energy consumption, the total amount of carbon emissions, and greatly reducing major pollution emissions". The realization of this goal cannot be separated from enacting and implementing environmental regulation, the constant

http://www.aloki.hu ● ISSN 1589 1623 (Print) ● ISSN 1785 0037 (Online)
DOI: http://dx.doi.org/10.15666/aeer/1704_84178434

strengthening of which constitutes an inevitable trend of China's economic and social development (Barla and Perelman, 2005; Thanh and Do, 2018).

Total factor productivity, as a critical basis for measuring the quality of economic growth, has attracted wide attention from scholars. Finding a way to improve the contribution of the total factor productivity to economic growth has become a top priority for China's high-quality growth (Cai and Zhou, 2017; Sufiyan et al., 2018). Is it possible to achieve a win-win situation between environmental pollution control and economic growth? Chen (2017) and Abija and Nwankwoala (2018) found that the current establishment and enforcement of environmental regulation in China had a certain inhibitory effect on economic growth for it continuously expands the social welfare cost. It has become an urgent and significant problem in China to formulate a rational environmental regulation to promote total factor productivity. Based on this, this paper discusses the influence of environmental regulation of the growth of total factor productivity through a theoretical perspective.

Literature review

In terms of the influence of environmental regulation on total factor productivity, there are three representative views abroad: first, environmental regulation will have a negative impact on total factor productivity. Granderson and Prior (2013) and Anan (2019) analyzed and tested the influence of environmental regulation on the efficiency of the fossil fuel generation industry in the United States and its total factor productivity, and they pointed out that the increased regulatory intensity of sulfur dioxide emissions resulted in a significant growth in the costs of generating electricity, thus limiting the increase of total factor productivity in the power sector. Research conducted by Aklin (2016) demonstrated that environmental regulation would push production costs of enterprises upward, and that relatively intensified environmental regulation might lead to wrong strategic development decisions for enterprises and deviation from their original development track. This would inhibit technological progress and promotion of productivity. The empirical test results of Zárate-Marco and Vallés-Giménez also proved the above ideas, which they referred to as "following the costs theory" Second (Zárate-Marco and Vallés-Giménez, 2015), environmental regulation will promote the improvement of total factor productivity. Scholars including Klemetsen et al. (2016; Xu, 2018) and Cherkashin et al. (2015) stated that the total factor productivity under the influence of environmental regulation was higher than traditional total factor productivity, and they explained this conclusion by the Potter Hypothesis, arguing that the purpose of moderate environmental regulation was to reduce the negative impact of the environment, which could stimulate the "innovation compensation" effect, promote technological innovation, and make up costs generated by or even beyond the environmental regulation, Guo et al. (2015) conducted sample studies in refineries of Los Angeles from 1990 to 2009, finding that despite the high costs of environmental regulation in the region, the total factor productivity witnessed significant improvement. Brolund and Lundmark (2017) and Gautam et al. (2019), with the aim of exploring whether environmental laws and regulations affected the productivity and technological changes of European paper industry, conducted empirical studies by taking the total factor productivities of the paper industry in eight European countries from 1993 to 2009 as dependent variables, and the intensity of environmental regulation of various pollutants as independent variables. Results showed

http://www.aloki.hu ● ISSN 1589 1623 (Print) ● ISSN 1785 0037 (Online)
DOI: http://dx.doi.org/10.15666/aeer/1704_84178434

that the management of nitrogen oxides was related with the improvement of total factor productivity in the following period. Third, the influence of environmental regulation on total factor productivity is uncertain. This view holder believed that various factors such as production scale, industrial characteristics, environmental regulation policy and tools selection made the direction and degree of the influence uncertain (Naso et al., 2017; Zulkapli et al., 2018). Qu (2015) employed the data of Quebec manufacturing sector from 1996 to 2008, and they found that the environmental regulation was negatively related to total factor productivity in the same period, but when the model took lagged variables into consideration, the Potter Hypothesis took effect and they became positively related. Ravetti et al. (2016) believed that no evidence showed that environmental regulation policy had an obvious and continuous effect on innovation, and they found through further empirical tests that environmental regulation had little effect on green technology innovation of enterprises.

Domestic researches on the relationship between environmental regulation and total factor productivity started relatively late, and focused mainly on the influence of environmental regulation on technological progress and technical efficiency. Wang and Sheng (2015), starting from the internal relationship between environmental pollution and China's industrial growth, constructed the total factor productivity limited by environmental regulation, and decomposed it into technological progress and technical efficiency by Malmquist-Luenberger (ML) index method. They found that there was a positive relationship between environmental regulation and technological progress. Liu et al. (2016) and Baharuddin and Samsudin (2018) employed the slack based measure (SBM) directional distance function and the ML index to investigate factors affecting Global Trade Finance Program (GTFP) in China's 29 provinces (cities), and results displayed that appropriate market environment regulations could improve productivity via stimulating technological innovation. Li et al. (2017), with the panel data of China's 30 provinces (cities) from 2005 to 2014, conducted empirical tests on the effect of environmental tax on enterprises' technological progress. Tests results showed that the influence of environmental tax intensity on technological progress was notably positive. Lv et al. (2017) calculated the green total factor productivity of 28 sub-sectors of China's manufacturing industry using data envelopment analysis (DEA)-Malmquist index method, which further verified the relationship between environmental regulation and the green total factor productivity of manufacturing industry. They found that technological progress constituted the core drive for the improvement of the manufacturing industry, and that environmental technology efficiency was generally lower.

The above literature demonstrates that scholars have made fruitful achievements in the study of the relationship between environmental regulation and total factor productivity, but there still exist several problems: first, despite the fact that the DEA method has been used to incorporate environmental factors into the productivity analysis framework to calculate the total factor productivity, potential effects caused by random error are not considered. Second, the study of environmental regulation and total factor productivity is mainly limited to the relationship between environmental regulation and technological progress or technical efficiency. The relationship between environmental regulation and specific components of all factor productivity is not included. Third, the majority of the previous researches start from the micro and macro perspective of environmental regulation and total factor productivity, with little focus on regional studies. In view of the above situation, this paper under the random frontier

http://www.aloki.hu ● ISSN 1589 1623 (Print) ● ISSN 1785 0037 (Online)
DOI: http://dx.doi.org/10.15666/aeer/1704_84178434

framework intends to incorporate environmental regulation into technical inefficiency, constructs the economic growth accounting equation with the total amount of energy consumption, capital and labor force as production factors, and calculates the value of total factor productivity and its decomposition part, the result of which will be contrasted with the one made without considering environmental regulation. This way, the internal structure and the drive behind the influence of environmental regulation on total factor productivity growth will be explored. In addition, given that the significant difference of resource distribution, industrial structure and development stage in distinct regions of China, which makes it different the influence of environmental regulation on total factor productivity, this paper divides China into eastern, central and western regions[1] so as to measure the difference of the total factor productivities growth between diverse regions, thus providing theoretical basis for the coordinated growth of total factor productivity in various regions.

Materials and methods

Stochastic frontier model

Existed literatures adopted two methods to build the production frontier, that is, the non-parametric Data Envelopment Analysis (DEA) and the parameter stochastic frontier analysis (SFA). This paper intends to use SFA to calculate the total factor productivity, which has the following advantages over DEA: first, the error structure of SFA constitutes a composite form, which takes into consideration the influence of both technical inefficiency and random factors on efficiency, while the production frontier constructed by DEA is non-random, which attributes all deviations to technical inefficiency, and this may not coincide with the reality; second, SFA can measure efficiency and analyze the factors that affect it at the same time, while DEA must adopt the two steps; third, SFA, with statistical properties, is capable of conducting statistical tests of parameters and models, which DEA fails to achieve; Four, the SFA measures the absolute efficiency, which is convenient for comparison and analysis of different units. In contrast, DEA calculates relative efficiency, which is 1 for all units, making it difficult to compare and analyze these effective units. Therefore, this paper adopts the stochastic frontier model, and the basic form of the empirical model is as follows (*Eq. 1*):

$$Y_{it} = f[x_{it}, \ \beta]\exp(v_{it} - u_{it}) \quad \text{(Eq.1)}$$

In the above formula, i represents the province, t indicates time, Y means output, $f(x_{it},\beta)$ indicates production frontier, x represents input factor, and β is the parameter to be estimated. $(v_{it} - u_{it})$ is a composite error structure, in which v_{it} represents random disturbance variable, u_{it} indicates the technical inefficiency of production and they are independent of each other.

[1]The eastern, central and western regions in China in this paper are divided as follows: the eastern region includes Beijing, Tianjin, Hebei, Liaoning, Shanghai, Jiangsu, Zhejiang, Fujian, Shandong, Guangdong, Hainan and Guangxi. The central region includes Shanxi, Inner Mongolia, Jilin, Heilongjiang, Anhui, Jiangxi, Henan, Hubei and Hunan. The western region includes Chongqing, Sichuan, Guizhou, Yunnan, Shaanxi, Gansu, Qinghai, Ningxia and Xinjiang.

http://www.aloki.hu ● ISSN 1589 1623 (Print) ● ISSN 1785 0037 (Online)
DOI: http://dx.doi.org/10.15666/aeer/1704_84178434

In actual production activities, although the related factors of environmental regulation cannot be directly included in the production equation, it may exert influence on the total factor productivity by affecting the technical inefficiency. Neglecting these factors will result in the inaccuracy of estimated results. In this sense, the following technical inefficiency regression equation is established as follows (*Eq. 2*):

$$u_{it} = \delta_0 + \delta_i Z_{it} \tag{Eq.2}$$

δ_0 is a constant term, Z_{it} indicates the factor affecting technical inefficiency, δ_i represents estimated coefficient of the factor, which, when positive, indicates that the factor restrain the promotion of technical efficiency, and vice versa.

Selection of production function and decomposition of total factor productivity

Early classical economists regard labor and capital as the main factors affecting economic output, and natural resources are often considered to be able to replace each other or be substituted by other productive factors. This is not consistent with the actual situation in which a large number of non-renewable resources are required in the process of production. In 2016, China surpassed the United States in the consumption of renewable energy, ranking the first in the world, and the total energy consumption in China accounted for 23% that of the world. Massive energy consumption has brought serious environmental pollution and climate change (Xiao et al., 2017; Kumar and Kumar, 2018). Therefore, research regarding economic growth in China cannot overlook the input of energy elements in the production process. This paper intends to employ capital (K), labor force (L) and energy (E) to jointly construct the production function Y = f (K, L, E).

Compared with the Cobb Douglas production function (C-D), the translog production function is inclusive and easier to estimate, which can better avoid the deviation caused by misspecification of production functions (Wang and Qi, 2017; Onwuka et al., 2019). In addition, considering the substitution effect between input factors, whether the technological progress is neutral or the technological progress should all be reflected in the model, this paper selects the time-varying model of translog production function.

$$\begin{aligned}
&\ln y_{it} = \ln f[x_{it}(t), t] + (v_{it} - u_{it}) \\
&= \beta_0 + \beta_l \ln L_{it} + \beta_k \ln K_{it} + \beta_e \ln E_{it} + \beta_t t + \beta_{kl} \ln K_{it} \ln L_{it} + \beta_{ke} \ln K_{it} \ln E_{it} + \beta_{le} \ln L_{it} \ln E_{it} \\
&+ \beta_{kle} \ln K_{it} \ln L_{it} \ln E_{it} + \beta_{kt} t \ln K_{it} + \beta_{lt} t \ln L_{it} + \beta_{et} t \ln E_{it} + \beta_{t^2} t^2 + \beta_{l^2} \ln^2 L_{it} + \beta_{k^2} \ln^2 K_{it} \\
&+ \beta_{e^2} \ln^2 E_{it} + v_{it} - u_{it}
\end{aligned} \tag{Eq.3}$$

According to Solow (1957), the growth of total factor productivity was output growth deduct input growth. He believed that technological progress was the same factor as total factor productivity, and did no segmentation research on total factor productivity. Kumbhakar and Lovell (2000) further decomposed the growth of total factor productivity into four factors: technological progress (△TP), technological efficiency change (△TE), scale efficiency change (△SE) and allocation efficiency change (△AE), which provided a new way for the in-depth study of economic growth pattern. Based on this, this paper decomposes total factor productivity into the following four parts.

http://www.aloki.hu ● ISSN 1589 1623 (Print) ● ISSN 1785 0037 (Online)
DOI: http://dx.doi.org/10.15666/aeer/1704_84178434

(1) The rate of technological progress. It reflects the technological progress of production frontiers, representing the output with the change of time under the condition of constant input elements. Taking log of formula (*Eq. 3*) and taking derivatives of t can generate the following formula (*Eq. 4*):

$$\Delta TP = \frac{\partial f}{\partial t} = \beta_t + \beta_{lt} \ln L_{it} + \beta_{kt} \ln K_{it} + \beta_{et} \ln E_{it} + 2\beta_{t^2} t \quad \text{(Eq.4)}$$

(2) The rate of technical efficiency change. The index refers to, under the same factor input and technology level, the ratio of actual output and frontier output (maximum output) with the changes of time (*Eq. 5*).

$$\Delta TE = -\frac{du_{it}}{dt} = \frac{TE_{it}}{TE_{it-1}} - 1 \quad \text{(Eq.5)}$$

(3) The rate of scale efficiency change. Scale efficiency refers to the changes of output according to the increase of factor input with the enlargement of production scale. There are three kinds of situations, that is, the increase, decrease and unchanged scale efficiency. The formula for the rate of scale efficiency change (*Eq. 6*) is shown below:

$$\begin{aligned} \Delta SE &= (E-1)\sum_j \frac{E_j}{E}\dot{x}_j = (f_l + f_k + f_e - 1) \\ &\times \left(\frac{f_l}{f_l+f_k+f_e} \times \dot{L} + \frac{f_k}{f_l+f_k+f_e} \times \dot{K} + \frac{f_e}{f_l+f_k+f_e} \times \dot{E}\right) \end{aligned} \quad \text{(Eq.6)}$$

According to the *Equation 3:*

$$f_l = \frac{\partial f}{\partial l} = \beta_l + \beta_{el} \ln E_{it} + \beta_{lk} \ln K_{it} + \beta_{elk} \ln E_{it} \ln K_{it} + \beta_{lt} t + 2\beta_{l^2} \ln L_{it}$$

$$f_k = \frac{\partial f}{\partial k} = \beta_k + \beta_{ek} \ln E_{it} + \beta_{lk} \ln L_{it} + \beta_{elk} \ln E_{it} \ln L_{it} + \beta_{kt} t + 2\beta_{k^2} \ln K_{it}$$

$$f_e = \frac{\partial f}{\partial e} = \beta_e + \beta_{el} \ln L_{it} + \beta_{ek} \ln K_{it} + \beta_{elk} \ln L_{it} \ln K_{it} + \beta_{el} t + 2\beta_{e^2} \ln E_{it}$$

(4) The rate of allocation efficiency change. This mainly examines the contribution of factor structure changes to total factor productivity in the production process under given frontier technological level. The equation is as follows (*Eq. 7*):

$$\begin{aligned} \Delta AE &= \sum_j [(\frac{E_j}{E} - s_j) \times \dot{x}_j] = (\frac{f_l}{f_l + f_k + f_e} - \frac{L}{L+K+E}) \times \dot{L} \\ &+ (\frac{f_k}{f_l + f_k + f_e} - \frac{K}{L+K+E}) \times \dot{K} + (\frac{f_e}{f_l + f_k + f_e} - \frac{E}{L+K+E}) \times \dot{E} \end{aligned} \quad \text{(Eq.7)}$$

The empirical study of the early stochastic frontier model is carried out in two steps. First, the maximum likelihood estimation is made to the frontier production function to obtain the coefficients of the explanatory variables. Then the regression equation is

http://www.aloki.hu ● ISSN 1589 1623 (Print) ● ISSN 1785 0037 (Online)
DOI: http://dx.doi.org/10.15666/aeer/1704_84178434

reconstructed by separating out the technical inefficiencies and other exogenous explanatory variables of non-factor inputs. However, there still exist the following problems: first, it is necessary to assume that there is no correlation between the exogenous factors and the input factors, the omission of these variables will result in deviation of the technical efficiency in the first step estimation. If the first step is biased, the estimation of coefficient of the technical efficiency equation in the second step will also witness deviation. Second, the stochastic frontier model often assumes that the distribution of the invalid term is the same, but in the second step technical efficiency regression equation, the technical efficiency term is changed with the different external variables, which forms a contradiction (Chen and Zhang, 2016). In contrast, one-step method can avoid these problems. Wang and Schmidt (2002) verified that one step method was superior to the two-steps method by Monte Carlo simulation. In this sense, this paper, for the purpose of attaining more accurate conclusions, employs the maximum likelihood method and one-step regression estimation method. In addition, this paper first assumes that the distribution of the technical invalid term is a truncated normal distribution, because compared with the exponential distribution and the half-normal distribution, it is more flexible. and this hypothesis will be tested later.

Variables selection and data description

According to the constructed stochastic frontier model, this paper adopts K, L and E as input variables and gross domestic product (GDP) as output variables. As for K, the capital stock, according to the estimation results of Shan (2008), through the perpetual inventory method, the data is expanded to 2015 under the assumption of 10.96% capital depreciation rate. The price level is converted to that of the year 1995 according to the corresponding Price Indices of Investment in Fixed Assets. The calculation method of the labor force (L) is the number of the employees at the end of the year in each province multiplied by the average wage of employees, which are handled according to the consumer price index in 1995 as the base period. GDP is based on the retail price index in 1995.

Variables representing environmental regulation are numerous, and in order to comprehensively investigate the impact of different types of environmental regulation on total factor productivity, this paper chooses to measure environmental regulations by environmental pollution control investment (invadd), the number of environmental regulations (fg) and the emission intensity of industrial SO_2 (strs). As the most basic embodiment of the government's environmental regulation, the investment in environmental pollution control is calculated as follows: (the actual pollution control input of the year / total industrial output value) × 1000. As for the variable of environmental regulations number, referring to Cole et al. (2008), the intensity of environmental regulation could be examined by the number of environmental regulations and administrative penalties related to environmental protection. The emission of industrial SO_2 can reflect the enterprise's efforts to improve the environment under the government's environmental regulations (Barla and Perelman, 2005). In addition, taking into consideration other factors that may affect the total factor productivity, this paper selects the economic development level (ag) and the urbanization rate (urban) as control variables, in which the former is measured by the per capita GDP, to be specific, by GDP deflator with the year 1995 as the base period, while the latter variable is evaluated by the ratio of the urban population to the total population in each province at the end of the year (Yuan et al., 2017).

http://www.aloki.hu ● ISSN 1589 1623 (Print) ● ISSN 1785 0037 (Online)
DOI: http://dx.doi.org/10.15666/aeer/1704_84178434

In this paper, 30 provinces (cities) and autonomous regions (excluding Tibet) in China are used as samples, and the interval is from 1995 to 2015. The data is collected from China Statistical Yearbook, China Energy Statistical Yearbook and China Environment Yearbook (1996-2017).

Discussion

This paper employs the stata14.0 software calculate the stochastic frontier regression of the translog production function. In model 2, results were estimated by introducing environmental regulation into the technical inefficiency equation and performing a one-step regression with the production efficiency equation. Considering that the focus of this paper is to study the influence of environmental regulation on the total factor productivity, modules in the technical invalid equation without factors related to environmental regulation are also estimated (model 1), which makes it possible to further explore the difference of the total factor productivity with and without considering the environmental regulation (Xiong et al., 2017).

The estimation results (*Table 1*) show that the two models have achieved sound regression results, indicating that the stochastic frontier set in this paper is reasonable. In model 1 and model 2, the coefficients of capital, labor and energy factors are positive and constitute at least 10% of the significant level, which means the influence of these three factors on economic growth is positive, but the contribution of capital and labor factors is greater than that of energy factors. Compared with model 1, the regression coefficient of model 2 is more significant. In addition, the value of γ in the two models is close to 1, which indicates that the phenomenon of production inefficiency exists generally in all provinces in China, and that the method of analyzing the trans-logarithm stochastic frontier of technical invalid term to study the dynamic state of total factor productivity with environmental regulation is necessary and reliable.

Table 1. *Estimation results*

Estimation of production efficiency equation					
Variables	**Model 1**	**Model 2**	**Variables**	**Model 1**	**Model 2**
lnk	1.5453***	1.6980***	lntl	0.005	-0.0004
lnl	0.4381*	0.4945**	lnte	-0.0252***	-0.0182***
lne	0.0868*	0.1844*	lnkle	0.0037	0.0044*
t	-0.2548***	-0.2664***	lnk^2	-0.1646***	-0.1838***
lnkl	0.2151***	0.2074***	lnl^2	-0.1290***	-0.1158***
lnke	0.0844**	0.0712*	lne^2	0.027	0.0410*
lnle	-0.1165**	-0.1269***	t^2	-0.0032***	-0.0026***
lntk	0.0322***	0.0344***	Constant	-3.265***	-3.3818***
Estimation of technical invalid equation					
Variables	**Model 1**	**Model 2**	**Variables**	**Model 1**	**Model 2**
lnag	2.7879	-0.1192***	Loglikelihood	436.666	492.683
lnurban	-9.9672***	-0.1511***	γ	0.694	0.627
lninvadd		0.0208**	Constant	-4.322***	1.010***
lnfg		0.0097			
lnstrs		0.0272*			

*, **and *** represent, respectively, the significant level of 10%, 5% and 1%. γ indicates the ratio of invalid term variance to the entire stochastic error term variance, which reflects the importance of invalid term to the entire stochastic error term

http://www.aloki.hu ● ISSN 1589 1623 (Print) ● ISSN 1785 0037 (Online)
DOI: http://dx.doi.org/10.15666/aeer/1704_84178434

The regression coefficient of related indicators of environmental regulation is estimated by the technical inefficiency, which is the result of the industrial pollution control investment and industrial SO_2 emission intensity, as an explanatory variable. From the regression results, the industrial pollution control investment is more significant in the form of technical invalidity as the 1% increase in the proportion of the investment to the industrial added-value would lead to 2.08% growth in the technical invalidity, which is not conducive to economic growth (Mut, 2018). This coincides with the "following the costs theory" of environmental regulation. The coefficient of industrial SO_2 emission intensity is positive, which can be understood as the emission of pollutants in the production process out of enterprises' own interests. This indicates that in the future actions of saving energy and reducing emission, enterprises' emission of SO_2 should be controlled more strictly. The coefficient of the number of environmental legislation published by local governments is 0.0097, but the statistical test value is not significant. Moreover, the coefficients of per capita GDP and urbanization rate are notably negative, indicating that the level of regional economic development and urbanization are favorable for the improvement of technical efficiency (Hajikhani, 2017).

The conclusion of stochastic frontier analysis tends to rely on the function form of the model, and in order to ensure that the model is correct, this paper carries out a likelihood ratio test, in the broad sense, for the translog form of the production function, and the existence of technical inefficiency and technological progress, the statistic is $\lambda = -2\ln[L(H_0)/L(H_1)]$, with $L(H_0)$, $L(H_1)$ as the likelihood function value of the original hypothesis and the alternative hypothesis respectively. If the null hypothesis is established, the test statistic λ obeys the Mixed Chi-square Distribution, and the degree of freedom is the number of the constrained variables. Test results are shown in *Table 2*.

Table 2. *Test results of hypothetical model*

Original hypothesis	$L(H_0)$	λ	Critical value	Test results
$H_0: \beta_{k^2} = \beta_{l^2} = \beta_{e^2} = \beta_{t^2} = \beta_{kl} = \beta_{ke} = \beta_{el} = \beta_{kle} = \beta_{kt} = \beta_{lt} = \beta_{et}$	312.22	360.82	24.72	Refusal
$H_0: \beta_t = \beta_{t^2} = \beta_{kt} = \beta_{lt} = \beta_{et} = 0$	246.21	492.84	15.09	Refusal
$H_0: \gamma = \mu = \eta = 0$	429.98	126.30	15.09	Refusal
$H_0: \beta_{kt} = \beta_{lt} = \beta_{et} = 0$	396.78	191.70	11.34	Refusal

The unlimited log likelihood is $L(H_1) = 492.63$, and the significance level of critical value is 1%

The first original hypothesis indicates that all the interaction items and square term coefficients in the production function are zero, which means that employing the C-D production function is enough, and that no translog form is needed *(Table 2)*; the second original hypothesis assumes that all the time dependent variables in the model are zero, that is, there exists no frontier technological progress; the third original hypothesis is designed to test the existence of the technical inefficiency. When γ is zero, it shows that the proportion of the variance of the technical inefficiency to the variance of stochastic error term is zero, and it is completely not necessary to consider this term. If μ is zero, the technical inefficiency obeys a half-normal distribution rather than a truncated normal distribution. When η is zero, there is no need considering the time-

http://www.aloki.hu ● ISSN 1589 1623 (Print) ● ISSN 1785 0037 (Online)
DOI: http://dx.doi.org/10.15666/aeer/1704_84178434

varying effect of the technical inefficiency. The last original hypothesis indicates that if the interaction coefficients of time and the three factors are all zero, the technological progress is not Hicks-neutral (Pascual-Córdova, 2018). From the test results, all the zero hypotheses are rejected, which proves that it is reasonable to use the translog form of production function, with the technical inefficiency objectively existing.

Results

According to the regression results of the stochastic frontier model (*Table 3*), the growth rate of total factor productivity can be estimated. At the same time, in order to understand the influence of the environmental regulation, when added the technical inefficiency, on the total factor productivity more clearly, this paper will combine the two situations of considering and not considering the environmental regulation and give an analysis of the two cases according to the regions divided above (eastern, central and western regions of China) to explore the differences between the regional total factor productivity growth (Huang et al., 2017).

When not considering the environmental regulation, although the starting points of economic development is distinct, the total factor productivity (TFP) of the eastern, central and western regions have achieved rapid growth, with the average growth rate of 5.15%, 3.99% and 4.19%, respectively. TFP growth is the fastest in the eastern region, and the slowest in the central region. The total factor productivity of all regions decline significantly in 2006, which is related to the deterioration of the macroeconomic situation in China, such as the stock market turbulence in China, the rising price of crude oil and the hit of domestic export enterprises. In the following years, the gap of TFP growth rate in the three major regions has been gradually narrowed, and the central and western regions had a tendency to catch up with the eastern region. After the inclusion of environmental regulation factors in the technical inefficiency, the growth rate of TFP in the three regions slow down, with the average growth rate of 3.68%, 2.52% and 2.76% respectively, and the central and western regions even take on a negative growth. In the majority of years, the growth rate of TFP is still the highest in the eastern region, and the central region, as the lowest in terms of the average growth rate of TFP, the largest decline also appears after the inclusion of environmental regulation (Perozo, 2016). Since China's reform and opening up, the economic development in the central region is ordinary, and its second and third industries starts late. With the promotion of "the rise of central China strategy", some manufacturing industries and heavy chemical industries of high energy consumption and pollution have achieved development first. However, due to the restrictions of capital and technology as well as relatively relaxed environmental policies, the environmental regulation was "selectively ignored", which, while promoting the economic development in the region, aggravated the problem of environmental pollution (Qu and Xi, 2012). The western region is vast and rich in resources. With the implementation of the strategy of "developing the west", its late-mover advantages gradually become noticeable, forming the trend of catching up with the developed areas. Even in the times of the macroeconomic situation deterioration in China, it still maintained the rising momentum. However, the rapid growth of the area is mainly dependent on its rich resources, and pollutant emission increased rapidly in the development process, leading to the poor TFP growth rate when considering environmental regulation.

http://www.aloki.hu ● ISSN 1589 1623 (Print) ● ISSN 1785 0037 (Online)
DOI: http://dx.doi.org/10.15666/aeer/1704_84178434

Table 3. *TPF growth in China's regions with and without considering environmental regulation over 1995-2015 (in %)*

Year	TPF growth without environmental regulation			TPF growth with environmental regulation		
	East	Central	West	East	Central	West
1995-1996	1.876	0.647	1.717	0.291	0.142	0.391
1996-1997	2.000	0.482	0.633	1.077	-1.319	-0.725
1997-1998	2.259	-0.457	-0.366	2.002	-0.875	-1.639
1998-1999	3.826	0.859	0.581	2.387	-1.935	-1.712
1999-2000	4.057	1.276	0.608	3.507	-1.062	-1.341
2000-2001	4.214	1.679	1.398	5.163	2.652	2.431
2001-2002	5.282	2.169	2.200	5.598	2.250	0.991
2002-2003	4.733	2.838	2.915	3.900	2.845	2.463
2003-2004	5.742	3.744	3.670	5.185	2.084	1.344
2004-2005	5.687	3.726	4.157	4.090	3.233	2.817
2005-2006	-2.844	-3.417	3.969	-5.309	-3.781	2.894
2006-2007	2.208	5.185	4.704	3.722	2.809	3.815
2007-2008	6.411	5.698	4.974	4.915	4.312	3.761
2008-2009	6.797	6.106	5.828	4.937	4.604	4.424
2009-2010	7.641	6.838	7.013	6.105	5.839	6.537
2010-2011	7.333	7.379	7.018	3.637	6.545	5.722
2011-2012	8.312	7.735	7.371	4.816	5.588	5.388
2012-2013	8.746	9.037	7.847	5.021	3.397	4.530
2013-2014	9.172	8.661	8.331	5.567	6.498	5.818
2014-2015	9.498	9.526	9.201	6.917	6.478	7.384
Average	5.147	3.986	4.188	3.676	2.515	2.764

In order to explore the influence of environmental regulation on the decompositions of total factor productivity and regional differences after including environmental regulation in technical inefficiency, this paper further analyzes the TFP growth rate by decomposing it into four parts: technological progress (△TP), technical efficiency change (△TE), scale efficiency change (△SE) and allocation efficiency change (△AE). This is much closer to the essence of the growth of total factor productivity. It can be seen from *Table 4* that when not considering the environmental regulation, the technological progress of the three regions shows a positive growth trend, and it has become the major source of the total factor productivity growth (*Table 4*), while the contribution of the technical efficiency change is very small or even negative, which is similar to the conclusions of produced by Wang et al. (2006), Tian et al. (2011). After considering the environmental regulation, the technical efficiency change in the three regions has been obviously improved, with the average value of the eastern region rising from -0.02% to 1.61%, and the central and western regions increasing to 2.14% and 2.08% respectively, which constitutes the main driving force of the TFP growth. In contrast, the technological progress in all regions slows down, in which technological progress growth rate in the eastern region becomes slower although it is still growing. The technological retreat in the central and western regions is more obvious, with the western region most severely affected. The average value of the technological progress

http://www.aloki.hu ● ISSN 1589 1623 (Print) ● ISSN 1785 0037 (Online)
DOI: http://dx.doi.org/10.15666/aeer/1704_84178434

in the western region falls from 1.5% to -0.79%, and this index shows negative growth every year from 1995 to 2008. It is not difficult to find that the eastern coastal areas is often close to the production frontier or directly on the frontiers, so a large part of the increase in productivity demonstrates the forward movement of the frontiers, that is, technological progress (Perozo, 2016). However, in the underdeveloped areas like the central and western regions, due to the lack of inner drive of technological progress, production relies on technology introduction and simple imitation, and the increase in productivity takes more of the form of the improvement in technical efficiency.

The research result also shows that the growth rate of scale efficiency demonstrates a declining trend in the western, central and eastern regions regardless of the influence of environmental regulation. However, after taking into consideration the environmental regulation, the growth rate of scale efficiency in the three regions all shows a decrease, with the average growth rate in the eastern region falling most dramatically from 1.1% to 0.45%, during which period there even exist diseconomies of scale. This is related to the overdependence on the increase of production factor input in the process of economic development, which leads to the decrease of the marginal output of the production factors and the loss of the scale efficiency. The change of the scale efficiency of the central and western regions reflects a relatively strong positive effect, indicating that the two regions are in the stage of scale economy (Jamali, 2016). The growth rate of the scale efficiency in the west region is generally higher than that in the central region, indicating that western region has an obvious advantage in terms of scale efficiency, which is a main factor that makes up for the difference of growth of total factor productivity against other regions. In addition, the allocation efficiency of production factors was ignored in the documents in the past, but this paper finds out that the efficiency allocation is an objective existence after calculation, and there is a continuous and obvious fluctuation of the allocation efficiency in different regions over the past 20 years (Yu, 2019). Without taking environmental regulation into consideration, the average growth rates of allocation efficiency in eastern, central and western regions are -0.40%, -0.44% and 0.77%. The allocation efficiency of the three regions declines if taking environmental regulation into account, and the average growth rate of western region, which is the most affected region, declines from 0.77% to -0.17%. This indicates that environmental regulation cannot optimize the allocation of resources.

In general, if taking the technical inefficiency resulted by environmental regulation into consideration, the growth of total factor productivity will slow down in most years, and the growth rate will decrease progressively in eastern, western and central regions, and the sources of the growth of total factor productivity will be different. Eastern region has more obvious advantage of technical progress, and the change rate of scale efficiency is the main reason that stops the growth of total factor productivity in this region. The total factor productivity declines in western region mainly because the range of technical efficiency improved is smaller than the falling range of technical progress and allocation efficiency. The total factor productivity in central region is the lowest, the technical efficiency was improved in the period of analysis, but the returns to scale, allocation efficiency and technical progress all declined to some extent, all these factors resulted in the decrease of the growth of TFP. Therefore, when calculating the total factor productivity, if the impact that environmental regulation exerts on productivity (technical efficiency) is ignored, the total factor productivity of our country is likely to be overestimated, and the related policy suggestions will be misleading to some extent.

http://www.aloki.hu ● ISSN 1589 1623 (Print) ● ISSN 1785 0037 (Online)
DOI: http://dx.doi.org/10.15666/aeer/1704_84178434

Table 4. *TFP growth's decomposition in China's regions with and without considering environmental regulation over 1995-2015 (in %)*

Year	TFP growth's decomposition without considering environmental regulation												TFP growth's decomposition with considering environmental regulation											
	△SE			△AE			△TP			△TE			△SE			△AE			△TP			△TE		
	East	Central	West	East	Central	West	East	Central	West	East	Central	West	East	Central	West	East	Central	West	East	Central	West	East	Central	West
1995-1996	0.454	0.595	1.224	-0.775	-0.941	2.159	2.032	-0.359	-1.823	0.164	1.353	0.157	-0.035	0.326	1.165	-1.379	-1.829	0.922	-0.006	-2.429	-4.247	1.711	4.074	2.551
1996-1997	0.461	0.695	1.232	-0.899	-0.684	0.499	2.289	-0.067	-1.395	0.149	0.537	0.297	-0.030	0.414	1.152	-1.260	-1.628	-0.472	0.242	-2.128	-3.822	2.125	2.023	2.417
1997-1998	0.560	0.737	1.372	-0.935	-1.648	-0.492	2.638	0.418	-0.978	-0.003	0.037	-0.268	0.003	0.404	1.327	-0.506	-1.660	-0.730	0.541	-1.713	-3.418	1.964	2.094	1.181
1998-1999	0.631	0.738	1.318	0.248	-1.007	-0.081	2.900	0.766	-0.538	0.047	0.362	-0.118	0.051	0.451	1.282	0.628	-0.965	-0.661	0.778	-1.402	-2.999	0.930	-0.018	0.665
1999-2000	0.623	0.693	1.385	0.377	-0.765	-0.121	3.033	1.064	-0.137	0.024	0.284	-0.519	0.054	0.392	1.380	0.910	-1.033	-0.273	0.922	-1.120	-2.618	1.620	0.699	0.170
2000-2001	0.714	0.851	1.494	0.251	-0.641	-0.110	3.268	1.299	0.234	-0.019	0.171	-0.221	0.140	0.596	1.482	1.032	-0.304	0.067	1.127	-0.895	-2.267	2.864	3.255	3.149
2001-2002	0.862	1.044	1.338	1.094	-0.442	0.467	3.379	1.463	0.564	-0.052	0.103	-0.169	0.258	0.775	1.229	2.003	0.076	0.037	1.253	-0.711	-1.925	2.084	2.110	1.650
2002-2003	0.925	1.250	1.488	0.245	-0.172	0.631	3.546	1.639	0.771	0.017	0.121	0.025	0.282	0.903	1.341	0.579	-0.434	0.082	1.445	-0.482	-1.653	1.595	2.859	2.692
2003-2004	1.171	1.592	1.493	0.845	0.172	0.692	3.689	1.801	0.981	0.037	0.179	0.504	0.518	1.202	1.341	1.061	-0.202	-0.037	1.631	-0.247	-1.380	1.976	1.330	1.420
2004-2005	1.359	1.896	1.672	0.437	-0.258	0.909	3.919	2.105	1.161	-0.027	-0.018	0.415	0.643	1.426	1.514	0.167	-0.704	0.264	1.902	0.096	-1.129	1.378	2.415	2.169
2005-2006	-0.322	1.752	1.902	-6.801	-7.576	0.480	4.144	2.562	1.446	0.135	-0.156	0.141	-0.985	1.102	1.787	-8.646	-6.750	0.101	2.228	0.525	-0.821	2.093	1.342	1.828
2006-2007	1.556	1.957	1.857	-3.680	0.317	0.715	4.521	2.954	1.730	-0.188	-0.043	0.402	0.825	1.305	1.684	-2.007	-2.334	0.177	2.541	1.002	-0.509	2.363	2.836	2.463
2007-2008	1.469	2.100	1.793	0.117	0.278	0.789	4.890	3.415	2.081	-0.065	-0.095	0.312	0.784	1.403	1.536	-0.975	-1.654	-0.278	2.915	1.490	-0.141	2.191	3.073	2.644
2008-2009	1.666	2.357	2.214	0.029	0.165	1.164	5.320	3.949	2.512	-0.217	-0.364	-0.063	0.892	1.561	1.914	-1.253	-1.664	0.033	3.344	2.027	0.292	1.954	2.681	2.184
2009-2010	1.764	2.248	2.355	0.340	0.377	1.538	5.701	4.424	2.900	-0.162	-0.212	0.221	0.989	1.465	1.950	-0.765	-1.713	-0.104	3.736	2.525	0.727	2.144	3.562	3.964
2010-2011	1.614	2.314	2.430	-0.231	0.354	1.232	6.067	4.812	3.236	-0.117	-0.100	0.120	0.858	1.622	2.076	-2.165	-0.686	-0.071	4.132	2.927	1.112	0.812	2.681	2.605
2011-2012	1.732	2.149	2.705	0.218	0.456	1.008	6.462	5.255	3.626	-0.100	-0.125	0.031	0.959	1.412	2.266	-1.452	-1.227	-0.434	4.532	3.369	1.539	0.777	2.034	2.018
2012-2013	1.674	2.051	2.745	0.239	1.261	1.139	6.820	5.868	4.086	0.013	-0.142	-0.124	0.957	1.146	2.218	-1.200	-1.823	-0.754	4.890	3.941	2.014	0.374	0.133	1.051
2013—2014	1.605	1.750	2.838	0.361	0.742	1.144	7.166	6.181	4.522	0.040	-0.011	-0.174	0.934	1.146	2.247	-0.939	-0.701	-0.799	5.225	4.271	2.474	0.347	1.782	1.895
2014—2015	1.427	1.701	2.754	0.612	1.135	1.661	7.463	6.605	4.956	-0.003	0.085	-0.170	0.863	1.000	2.145	-0.334	-0.942	-0.481	5.503	4.671	2.923	0.885	1.748	2.797
Average	1.097	1.523	1.881	-0.395	-0.444	0.771	4.462	2.808	1.497	-0.016	0.098	0.040	0.448	1.003	1.652	-0.825	-1.409	-0.171	2.444	0.786	-0.792	1.609	2.136	2.076

http://www.aloki.hu ● ISSN 1589 1623 (Print) ● ISSN 1785 0037 (Online)
DOI: http://dx.doi.org/10.15666/aeer/1704_84178434

Figure 1 compares the two change curves of the total factor productivity in China between 1995 and 2015 (with and without considering environmental regulation), the growth rate of total factor productivity declines in most years if taking environmental regulation into consideration. The total factor productivity that takes environmental regulation into consideration can reflect the performance of green economy growth and indicates that environmental regulation results in technical inefficiency during the development of China's economy, and therefore deters the growth rate of total factor productivity. This goes against the 'the theory of Innovation Compensation" proposed by many scholars in recent years and conforms to the "the theory of Compliance Cost" proposed by scholars at early phase. It indicates that environmental regulation forces enterprises to occupy productive investment, and enterprises will suffer private cost increase to meet environmental requirements and will reduce the production efficiency. This will exert negative effects on China's economic development and deter the growth of total factor productivity in the long run (Alkin, 2016).

Figure 2 makes decomposition of the sources of growth of total factor productivity with environmental regulation considered. It can be figured out that technical efficiency contributes the most. The growth rate of cutting-edge technique progress is negative before 2004, but turns positive gradually after 2004. The change of scale efficiency exerts positive influence on the growth rate of total factor productivity, but the influence is not obvious. It is worth noting that the growth rate of allocation efficiency is negative in most times, and it is an important factor that restricts the growth of total factor productivity.

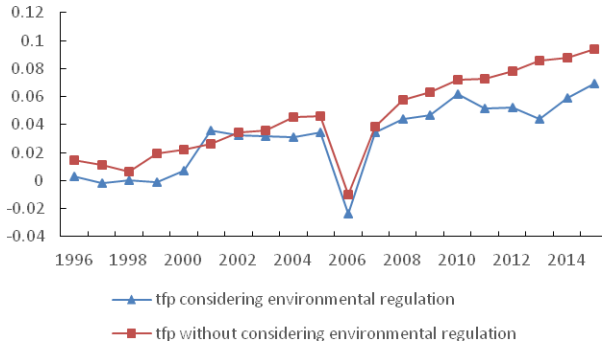

Figure 1. *TPF growth in China with and without considering environmental regulation over 1995-2015(in %)*

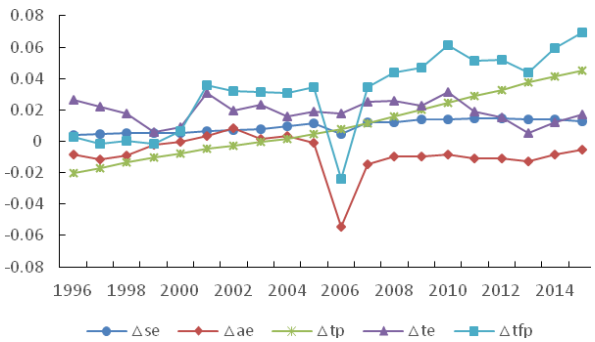

Figure 2. *TFP growth and its decomposition in China considering environmental regulation over 1995-2015(in %)*

http://www.aloki.hu ● ISSN 1589 1623 (Print) ● ISSN 1785 0037 (Online)
DOI: http://dx.doi.org/10.15666/aeer/1704_84178434

Conclusion

In this paper, the authors constructs the translog stochastic frontier production function model, brings the index of correlation of environmental regulation into the equation of technical inefficiency to make maximum likelihood estimation, worked out the growth rate and compositions of total factor productivity in China as a whole and Eastern, Central and Western regions from 1995 to 2015, and makes a comparison analysis of the total factor productivity without considering the environmental regulation. The main conclusions are as follows:

(1) Total factor productivity slows down when taking environmental regulation into technical inefficiency. The investment of industrial pollution control and emission intensity of industrial SO_2 all result in technical inefficiency, and are harmful to the improvement of total factor productivity. The influence of the number of environmental legislation published by local governments is not obvious. This indicates that there are still numerous things to be done to achieve China's win-win situation between environment and economy. Governments should carry out functional environmental regulations and manage the implementation of these regulations properly based on local resources and pollution status of local environment during the process of economic development. For enterprises that discharge pollutants out of their own benefits, government should fully arouse enterprises' enthusiasm and initiative of energy conservation and emission reduction to form an incentive and restraint mechanism of energy conservation and emission reduction.

(2) After taking environmental regulation into consideration, technical efficiency change becomes the main source of the growth of total factor productivity, technological progress slows down and the decline of growth of total factor productivity is closely related to the negative growth of allocation efficiency. The majority part of the eastern regions have been in the diseconomy of scale, so for these provinces, it is more important to improve the efficiency of resource utilization and the introduction and application of advanced technology to drive the progress of frontier technology rather than to expand the input and scale.

(3) The difference of total factor productivity growth rate in various regions of China has gradually narrowed in recent years, with the central and western regions even surpassing the eastern region, but it still shows obvious regional characteristics. After considering the environmental regulation, there exist differences in the reasons for the decrease of total factor productivity in various regions. Therefore, when formulating the environmental regulation, practical and feasible measures should be adopted through taking into account the differences in resources endowment, industrial structure and development stages of various regions.

Therefore, in the future, we should properly improve our environmental regulation system and adopt flexible forms of environmental regulation to ensure the positive impact of TFP on the environment.

REFERENCES

[1] Abija, F. A., Nwankwoala, H. O. (2018): Characterization of aquifers in parts of Abia State Southeastern Nigeria. – Earth Sciences Pakistan 2(1): 18-22.

[2] Aklin, M. (2016): Re-exploring the trade and environment nexus through the diffusion of pollution. – Environmental & Resource Economics 64(4): 663-682.

http://www.aloki.hu ● ISSN 1589 1623 (Print) ● ISSN 1785 0037 (Online)
DOI: http://dx.doi.org/10.15666/aeer/1704_84178434

[3] Anan, H. S. (2019): Contribution to the paleontology, stratigraphy and paleo-biogeography of some diagnostic Pakistanian Palaeogene foraminifer in the Middle East. – Earth Sciences Pakistan 3(1): 23-28.
[4] Baharuddin, D., Samsudin, M. D. M. (2018): Effect of pH and moisture content on current density of impressed current cathodic protection: response surface methodology study. – Environment & Ecosystem Science, 2(2): 15-19.
[5] Barla, P., Perelman, S. (2005): Sulphur emissions and productivity growth in industrialised countries. – Annals of Public & Cooperative Economics 76(2): 275-300.
[6] Brolund, J., Lundmark, R. (2017): Effect of environmental regulation stringency on the pulp and paper industry. – Sustainability 9(12): 2323.
[7] Cai, W. G., Zhou, X. L. (2017): Dual effect of Chinese environmental regulation on green total factor productivity. – Economist 9: 27-35.
[8] Chen, L. (2017): Dual nature of environmental regulation: restraining or promoting technological progress—evidence from Wuhan City circle. – Science & Technology Progress and Policy 34(12): 43-48.
[9] Chen, Y., Zhang, J. (2016): Carbon emission, green total factor productivity and economic growth. – The Journal of Quantitative & Technical Economics 8: 47-63.
[10] Cherkashin, I., Demidova, S., Kee, H. L. (2015): Firm heterogeneity and costly trade: a new estimation strategy and policy experiments. – Journal of International Economics 96(1): 18-36.
[11] Cole, M. A., Elliott, R. J. R., Shanshan, W. U. (2008): Industrial activity and the environment in China: an industry-level analysis. – China Economic Review 19(3): 393-408.
[12] Gautam, A., Batra, R., Singh, N. (2019): A study on use of rice husk ash in concrete. – Engineering Heritage Journal 1(1): 01-04.
[13] González, L. C. (2016): Efecto de la cachaza más roca fosfatada enriquecida con microorganismos sobre la disponibilidad, absorción de P y el crecimiento del maíz en dos tipos de suelo. – Revista de la Facultad de Agronomia de la Universidad del Zulia 33(1).
[14] Granderson, G., Prior, D. (2013): Environmental externalities and regulation constrained cost productivity growth in the US electric utility industry. – Journal of Productivity Analysis 39(3): 243-257.
[15] Guo, D., Bose, S., Alnes, K. (2015): Employment implications of stricter pollution regulation in China: theories and lessons from the USA. – Environment Development & Sustainability 19(2): 549-569.
[16] Hajikhani, S. (2017): 8. The effect of planting date and applications herbicide on the population, weed dry matter and grain yield of chintzy beans. – Revista de la Facultad de Agronomia de la Universidad del Zulia 34(3).
[17] Huang, N, Jiang, Y. J., Liu, R. C., Li, B. O., Zhang, Z. Y. (2017): A predictive model of permeability for fractal-based rough rock fractures during shear. – Fractals 25(5). https://doi.org/10.1142/S0218348X17500517.
[18] Jamali, F. (2016): 5. Effects of planting distance and weeding regime on green bean (Phaseolus vulgaris L.) growth and yield. – Revista de la Facultad de Agronomia de la Universidad del Zulia 33(3).
[19] Klemetsen, M. E., Bye, B., Raknerud, A. (2016): Can direct regulations spur innovations in environmental technologies? A study on firm-level patenting. – Scandinavian Journal of Economics 120(2): 338-371.
[20] Kumar, R., Kumar, V. (2018): A review of phylogeography: biotic and abiotic factors. – Geology, Ecology, and Landscapes 2(4): 268-274.
[21] Kumbhakar, S. C., Lovell, C. A. K. (2000): Stochastic frontier analysis. – Cambridge University Press, Cambridge.
[22] Li, X. J., Du, W., Wang, X. F. (2017): Environmental tax system and green development: based on the perspective of technological progress. – Modern Economic Science 39(4): 117-123.

http://www.aloki.hu ● ISSN 1589 1623 (Print) ● ISSN 1785 0037 (Online)
DOI: http://dx.doi.org/10.15666/aeer/1704_84178434

[23] Liu, H. W., Zheng, S. L., Zuo, W. T. (2016): The influence mechanism of environmental regulation on TFP of enterprises. – Science Research Management 37(5): 33-41.
[24] Lv, K. J., Cheng, Y., Fan, B. J. (2017): The relations study on environmental regulation and green total factor productivity of China's manufacturing industry. – Ecological Economy 33(4): 49-52.
[25] Mut, Z. (2018): 3. Evaluation of hay yield and quality traits of oat genotypes grown at different locations. – Revista de la Facultad de Agronomia de la Universidad del Zulia 35(2).
[26] Naso, P. (2017): The porter hypothesis goes to China: spatial development. Environmental regulation and productivity. – CIES Research Paper Series 53-2017, Centre for International Environmental Studies, The Graduate Institute.
[27] Onwuka, O. S., Ezugwu, C. K., Ifediegwu, S. I. (2019): Assessment of the impact of onsite sanitary sewage system and agricultural wastes on groundwater quality in Ikem and its environs, south-eastern Nigeria. – Geology, Ecology, and Landscapes 3(1): 65-81.
[28] Pascual-Córdova, G. (2018): 1. Indicadores de calidad del suelo en el agroecosistema caña de azúcar (Saccharum spp.). – Revista de la Facultad de Agronomia de la Universidad del Zulia 35(1).
[29] Perozo, J. V. (2016): 6. Germinación de embriones somáticos de Psidium guajava L. en envases de cultivo con ventilación forzada. – Revista de la Facultad de Agronomia de la Universidad del Zulia 33(2).
[30] Qu, X. E. (2015): Industry characteristics, environmental regulation and productivity growth—Based on the test of the "Porter Hypothesis". – Soft Science 2015-02.
[31] Qu, X. E., Xi, Y. (2012): Total factor productivity in China under the dual regulation of the resourses and the environment—Empirical analysis based on the data of 1996-2009. – Journal of Business Economics 1(5): 89-96.
[32] Ravetti, C., Theoduloz, T., Valacchi, G. (2016): Energy, trade and innovation: the tragedy of the locals. – CIES Research Paper 41-2016. Centre for International Environmental Studies, The Graduate Institute.
[33] Shan, H. J. (2008): Reestimating the capital stock of China: 1952~2006. – The Journal of Quantitative & Technical Economics 10: 17-31.
[34] Solow, R. M. (1957): Technical change and the aggregate production function. – Review of Economics & Statistics 39(3): 554-562.
[35] Sufiyan, I., Zakariya, R., Yacoob, R., Idris, M. S., Idris, N. M. (2018): SWAT subbasins parameters and flood risk simulations using 3d in Terengganu watershed. – Earth Sciences Malaysia 2(2): 10-15.
[36] Thanh, L. D., Do, P. V. (2018): Streaming current induced by fluid flow in porous media. – Earth Sciences Malaysia 2(1): 22-28.
[37] Tian, Y. H., He, S. B., Hu, S. Q. (2011): Re-estimation of China's regional total factor productivity growth under environment regulation: 1998–2008. – China Industrial Economics 1: 47-57.
[38] Wang, H. J., Schmidt, P. (2002): One-step and two-step estimation of the effects of exogenous variables on technical efficiency levels. – Journal of Productivity Analysis 18(2): 129-144.
[39] Wang, J., Sheng, P. F. (2015): Does environmental management reduce Chinese industrial total-factor productivity: a study based on modified directional distance function. – Industrial Economics Research 5: 31-39.
[40] Wang, W., Qi, L. Q. (2017): Volatility and heterogeneity of total factor productivity growth in China's equipment manufacturing industry. – The Journal of Quantitative & Technical Economics 10: 111-127.
[41] Wang, Z. G., Gong, L. T., Chen, Y. Y. (2006): China's regional differences in technical efficiency and the decomposition of total factor productivity growth (1978-2003). – Social Sciences in China 2: 55-66.

http://www.aloki.hu ● ISSN 1589 1623 (Print) ● ISSN 1785 0037 (Online)
DOI: http://dx.doi.org/10.15666/aeer/1704_84178434

[42] Xiao, X. J., Yang, G. (2017): China energy situation analysis in 2016 and prospects in. – Energy of China 39(3): 5-12.
[43] Xiong, Y. Q., Han, M. A., Romanovski, V. G. (2017): The maximal number of limit cycles in perturbations of piecewise linear Hamitonian systems with two saddles. – International Journal of Bifurcation and Chaos 27(8).
[44] Xu, D. (2018): Research on brand construction and development of agricultural products in Guizhou. – Engineering Heritage Journal 2(2): 19-24.
[45] Yu, M. (2019): Impact of environmental regulation on green innovation practice of food enterprises: regulating effect of environmental awareness of different executives. – Revista de la Facultad de Agronomia de la Universidad del Zulia 36(1).
[46] Yuan, Q., Chen, C. S., Yang, H. W. (2017): Existence of positive solutions for a Schrödinger-Poisson system with bounded potential and weighted functions in R3. – Boundary Value Problems (2017): 151.
[47] Zárate-Marco, A., Vallés-Giménez, J. (2015): Environmental tax and productivity in a decentralized context: new findings on the Porter hypothesis. – European Journal of Law & Economics 40(2): 313-339.
[48] Zulkapli, M. F., Rashid, N. M., Sokri, M. N. M., Nasri, N. (2018): Study on optical properties of graphene-Tio2 nanocomposite as photoanodes layer in dye sensitized solar cell (DSSC). – Environment & Ecosystem Science 2(2): 39-41.

http://www.aloki.hu ● ISSN 1589 1623 (Print) ● ISSN 1785 0037 (Online)
DOI: http://dx.doi.org/10.15666/aeer/1704_84178434

CALCULATION AND POLICY RESPONSES OF THERMAL POWER CARBON EMISSIONS IN 1995-2015 IN SHAANXI PROVINCE, CHINA

WANG, X. H. – LI, G.

School of Humanity and Social Sciences of Xi'an University of Posts and Telecommunications, Xi'an, Shaanxi 710121, China

**Corresponding author*
e-mail: wxh2324@126.com

(Received 8th Mar 2019; accepted 21st May 2019)

Abstract. Thermal power industry is a key area of China's energy conservation and emission reduction. Using the national recommendation method, we calculated the carbon emissions data of Shaanxi's thermal power in the 1995-2015 period, and analyzed the response to environmental management policies. The policy response selects energy industry development and environmental governance as the endogenous variables, and uses the methods of co-integration and error correction model to analyze the long-term ensuring future equilibrium and short-term impact mechanism for the three. Based on variance decomposition, this paper refines the contribution of dynamic energy industry development and environmental governance to thermal power carbon emissions. The research shows that the carbon emission of thermal power in Shaanxi province rose from 1891.63×10^4 t in 1995 to the peak of 11086.14×10^4 t in 2010, and then the improvement of energy efficiency has brought a downward trend of carbon emissions. Energy industry development and environmental governance can negatively effect carbon emissions from thermal power plants. In the long run, carbon emissions from thermal power plants can be gradually reduced. The contribution of the two variables is about 5% and 6% respectively, which has great room for improvement.
Keywords: *energy industry development, environmental governance, call mechanism, efficiency improvement, pollution reduction*

Introduction

Using the heat generated from coal and other combustion-based methods to produce electricity, thermal power generation is the main source of power in China and one of the main CO2 emission sources. At present, the thermal power industry has become a key area of national energy conservation and emission reduction. China's thermal power enterprises are mainly concentrated in Jiangsu, Shandong, Shaanxi and several other, and Shaanxi in 2010 became the first batch of the country's low carbon experimental development province, therefore, the measurement of thermal power carbon emission in Shaanxi province can provide effective data basis for the management of regional energy saving and emission reduction (Nas and Talebian-Kiakalaieh, 2017; Majumder et al., 2019).

In the current research, the calculation of carbon emission of thermal power is mainly expressed as "energy consumption method", that is to sum up energy consumption, and calculate carbon emission volume in combination with various energy carbon emission factors (Licht et al., 2018; Pazand and Hezarkhani, 2018). "Energy consumption law" can be used to estimate the carbon emissions of the industry better, but this method is limited to static research, neglects the carbon emission in the process of power transmission from the thermal power industry and the process of desulfurization, which eventually leads to the leakage calculation of carbon emissions

http://www.aloki.hu ● ISSN 1589 1623 (Print) ● ISSN 1785 0037 (Online)
DOI: http://dx.doi.org/10.15666/aeer/1704_84358448

(Bergthorson, 2018; Joseph et al., 2019). Therefore, it is necessary to improve the carbon emission research systematically and dynamically.

In 2013, the State Development and Reform Commission of China issued the Guidelines for the Accounting Methods and Reporting of Greenhouse Gas Emissions by China's Power Generation Enterprises (Trial Implementation) to determine the emission standards of air pollutants in thermal power plants. Based on the national development and Reform Commission's guidance method, this paper calculates the thermal power carbon emission data in Shaanxi province in 1995-2015, probes the response relationship of relevant policies to thermal power carbon emissions, and analyzes its long-term equilibrium and short-term impact mechanism to provide reference for future environmental management policy formulation (Ma et al., 2017; Sufiyan et al., 2018).

Shaanxi, also known as Qin, is located between the eastern longitude 105°29'–111°15' and northern latitude 31°42'–30°35'. It has jurisdiction over 10 prefecture-level cities, such as Xi'an, Xianyang, Yan'an and Hanzhong, and is an important hub connecting eastern, central, northwestern and southwestern China. The topography of Shaanxi includes mountains, highlands, plains and basins (*Fig. 1*). The total area is 205 thousand and 800 km^2. The forest coverage rate was 43.06%. The Yellow River basin covers an area of 133 thousand and 300 km^2, and the Yangtze River Basin has an area of 72 thousand and 300 km^2 (Velea et al., 2009; Rajput et al., 2019). The annual average temperature of the province is 13.6 centigrade; the annual precipitation is 598.1 mm.

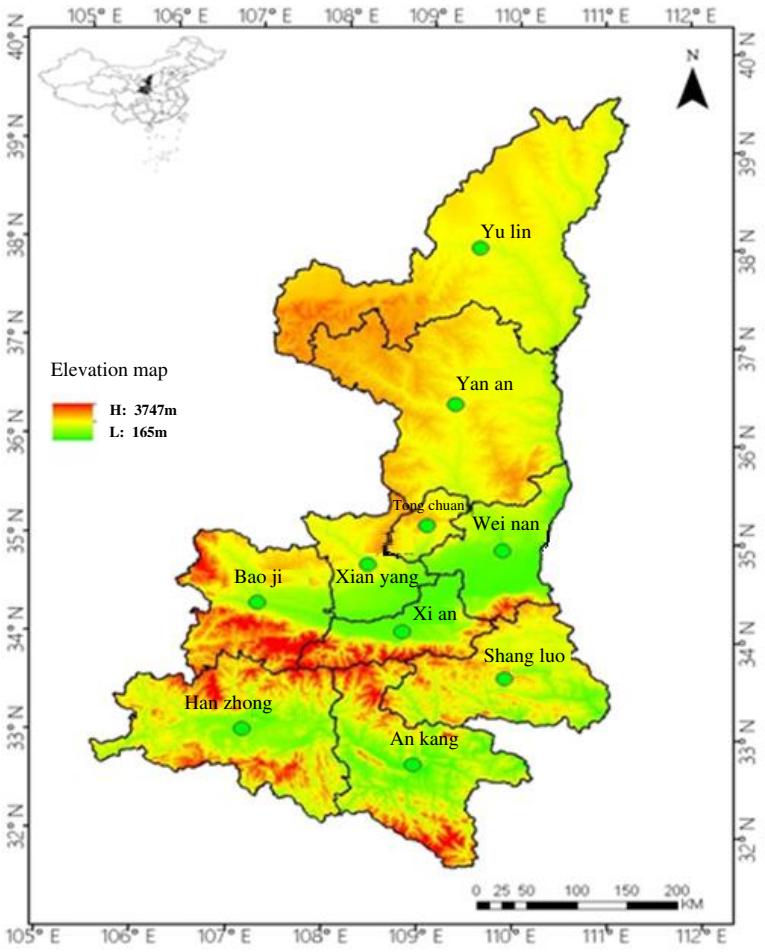

Figure 1. *Elevation map of the Shaanxi Province*

http://www.aloki.hu ● ISSN 1589 1623 (Print) ● ISSN 1785 0037 (Online)
DOI: http://dx.doi.org/10.15666/aeer/1704_84358448

Methodology

Calculation of carbon emission in thermal power

The Accounting Methods and Reporting Guidelines for Greenhouse Gas Emissions from China's power generation enterprises (Trial Implementation) regulates that the total amount of greenhouse gas emissions from power generation enterprises is equal to the emission of fossil fuel combustion in the boundary of the enterprise, the discharge of the desulfurization process and the emissions generated by the net purchase and use of electricity. Among them,

$$E_{energy\ consumption} = \sum AD_i \times EF_i \quad \text{(Eq.1)}$$

$$E_{desulfurization\ process} = \sum CAL \times EF \quad \text{(Eq.2)}$$

$$E_{electricity\ purchase} = \sum AD \times EF \quad \text{(Eq.3)}$$

In *Equations 1, 2* and *3,* AD_i is the level of i energy activity, which is expressed in the calorific value (Atimtay, 2003; Kumar et al., 2017; Kumar, 2018), EF_i is the i emission factor; CAL is the consumption of carbonate in the process of desulfurization; EF is the emission factor of carbonate in the desulfurizer. Based on the real situation of thermal power generation in China, the desulfurizer is limestone, its carbonate content is 90% by default, and the carbon emission factor is 0.44. 2 thousand and 700 tons of limestone is consumed at 100 million kW h of power generation. AD is the purchase of electricity, and error factor (EF) is the emission factor.

Vector autoregression and vector error correction model construction

(1) Vector autoregressive model and error correction model

Vector autoregressive models are often used to predict interconnected time series systems and to analyze the dynamic effects of random disturbances on variable systems. The expression is:

$$Y_t = A_1 Y_{t-1} + A_2 Y_{t-2} + \cdots A_p Y_{t-p} + BX_t + \varepsilon_t, \quad t = 1,2,\cdots T \quad \text{(Eq.4)}$$

Among them, Y_t is a vector of k endogenous variable; X_t is a d dimension exogenous variable vector; p is a lag order; T is a sample number; ε_t is a k dimension error vector, A_1, A_2 A_p, B is an estimated coefficient matrix.

However, the defect of vector autoregressive model is that it cannot describe the relationship between synchronous variables, and the error correction model can deal with this problem better.

$$\Delta Y_t = \alpha ECM_{t-1} + \sum_{i=1}^{p-1} \Gamma_i \Delta Y_{t-i} + \varepsilon_t \quad \text{(Eq.5)}$$

Among them, ECM_{t-1} is the error correction term, α is the adjustment coefficient, and the influence coefficient of Γ_i is ΔY_{t-i}'s short term fluctuation on ΔY_t.

http://www.aloki.hu ● ISSN 1589 1623 (Print) ● ISSN 1785 0037 (Online)
DOI: http://dx.doi.org/10.15666/aeer/1704_84358448

(2) Selection and treatment of index

In the field of environmental governance, energy industry technology upgrading and industrial pollution control are the main strategies for energy conservation and emission reduction (Valiani et al., 2016; Jamil et al., 2018). As the electricity belongs to the energy industry, in order to better reflect the corresponding management, the energy industry investment (EIS) and the industrial pollution control investment (IPS) are selected to represent the status quo of the development of energy industry and the status of environmental governance respectively, and the endogenous variables of the thermal power carbon emission (CES) model are constructed (Reddy and Momoh, 2016; Ali et al., 2018).

According to the selection index, *Equation 4*: $Y = \begin{bmatrix} CES \\ EIS \\ IPS \end{bmatrix}$, $X = 0$. In order to reduce the large fluctuation of data, the natural logarithms of CES, EIS and IPS sequences are taken respectively. The *X, Y, t* value substitution (*Eq. 4*) can be obtained:

$$\begin{bmatrix} LCES \\ LEIS \\ LIPS \end{bmatrix}_t = \begin{bmatrix} a_0 \\ a_1 \\ a_3 \end{bmatrix} + \begin{bmatrix} b_{11} & b_{12} & b_{13} \\ b_{21} & b_{22} & b_{23} \\ b_{31} & b_{32} & b_{33} \end{bmatrix} \begin{bmatrix} LCES \\ LEIS \\ LIPS \end{bmatrix}_{t-1} + \begin{bmatrix} c_{11} & c_{12} & c_{13} \\ c_{21} & c_{22} & c_{23} \\ c_{31} & c_{32} & c_{33} \end{bmatrix} \begin{bmatrix} LCES \\ LEIS \\ LIPS \end{bmatrix}_{t-2} + \begin{bmatrix} \hat{\varepsilon}_0 \\ \hat{\varepsilon}_1 \\ \hat{\varepsilon}_2 \end{bmatrix}_t \quad \text{(Eq.6)}$$

Results, analysis and discussion

The data of thermal power consumption, the average low calorific value of energy and electricity purchased are derived from the《Shaanxi statistical yearbook》. The unit calorific value carbon content data comes from the provincial carbon emission accounting guide and Intergovernmental Panel on Climate Change (IPCC) standard. Some energy data and the average emission factor of regional power grid are derived from "The guide to China's carbon emissions accounting". Among them, the average emission factor of the northwest regional power grid is 0.977 kg/KW h, Over the years, the investment in Shaanxi's energy industry and investment in industrial pollution control came from the National Bureau of statistics of China (Salem, 2018; Hossain et al., 2019).

Empirical results and analysis

(1) Carbon emission of thermal power in Shaanxi

The results of thermal power carbon emission calculation in Shaanxi Province from 1995 to 2015 are in *Table 1*. The carbon emission of thermal power in Shaanxi Province has been increasing since 1995 until the turning point of 2010. The emission reached its peak of 11086.14×10^4 t in 2010, which is due to the 190.52×10^8 KW h increase of

http://www.aloki.hu ● ISSN 1589 1623 (Print) ● ISSN 1785 0037 (Online)
DOI: http://dx.doi.org/10.15666/aeer/1704_84358448

the thermal power generation in 2010 compared with the previous year. The amount of raw coal used for thermal power generation increased from3949.22 × 10^4 t in 2009 to 4850 × 10^4 t, and then dropped to4107.56 × 10^4 t in 2011 (Boutabba and Lardic, 2016; Shrestha and Baral, 2018).

Table 1. *The carbon emission of thermal power generation in Shaanxi Province (unit: 10^4 t)*

Time	Emission value	Time	Emission value	Time	Emission value
1995	1891.63	2002	3312.53	2009	8177.14
1996	2177.56	2003	4350.98	2010	11086.14
1997	2471.41	2004	5148.33	2011	9206.80
1998	2589.26	2005	5014.09	2012	9428.29
1999	2701.68	2006	5805.92	2013	9445.80
2000	2737.83	2007	6296.26	2014	9502.33
2001	2902.70	2008	7134.40	2015	9533.27

At the same time, according to the composition of Shaanxi's thermal power carbon emissions (*Fig. 2*), we can also see in the purchase of electric power plate, Shaanxi's purchase of electricity carbon emissions also reached a maximum of 1608.92 × 10^4 t in 2010 (Moon and Seo, 2016). Since 2011, the purchase of electricity has been blank, which has led to the historical peak of Shaanxi's thermal power carbon emissions in 2010.

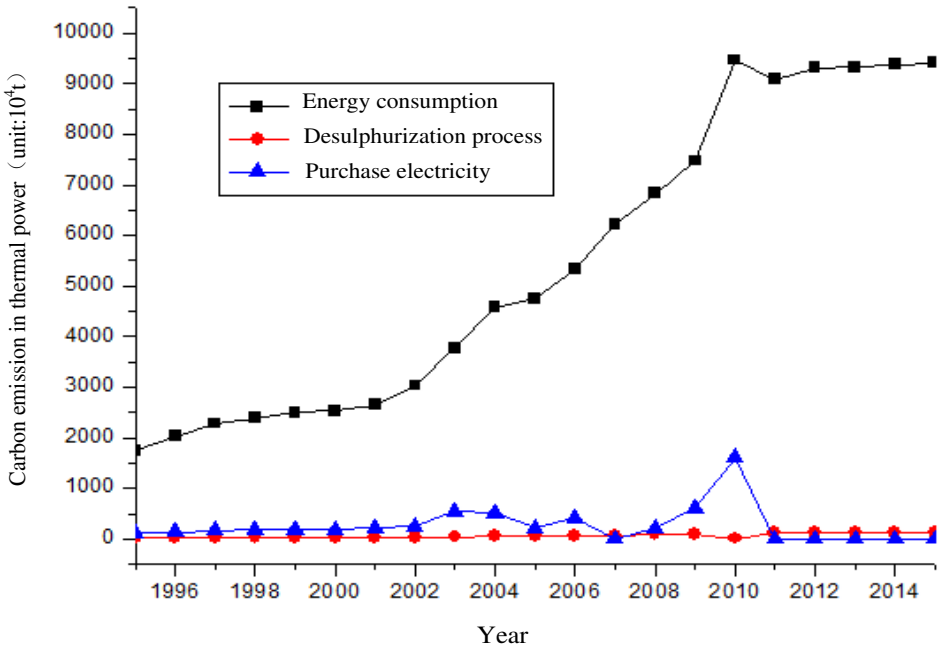

Figure 2. *Carbon emission from Shaanxi Province*

In the comparison of three components of thermal power carbon emissions, energy consumption becomes the key source of carbon emissions again (Moon and Shin, 2017). The total amount of carbon emissions in the desulfurization process is the lowest,

http://www.aloki.hu ● ISSN 1589 1623 (Print) ● ISSN 1785 0037 (Online)
DOI: http://dx.doi.org/10.15666/aeer/1704_84358448

and the purchase of electricity has been kept low before 2009. In 2010, the purchase of electricity in Shaanxi province increased sharply, followed by a state of "0" in the following years.

For the fluctuation of carbon emission in Shaanxi thermal power industry, the reason is the policy changes (Deleidi, 2017). In the plan of "11th Five-Year" from 2005 to 2010, carbon emission reduction in Shaanxi province is to by the means of "optimize the development of thermal power enterprises", the main measures are to actively improve the power generation technology and to the reduce the coal consumption during the process of power generation. During that period, thermal power generation or province is the main form of power generation (Kalshian, 2016). In the period of "12th Five-Year", the plan clearly proposes to vigorously develop hydropower, wind power and solar power, and carries out the project of "gasification Shaanxi" in an all-round way. So the standard coal consumption per unit energy consumption and thermal power supply were reduced by 16% and 13% on the basis of 2010. In 2011-2015, thermal power generation continued to increase, but carbon emission is under control, indicating that thermal power energy efficiency has been improved. At the same time, the improvement of clean energy production capacity, such as hydropower, has also contributed to the efficiency of carbon emission reduction.

Taking hydroelectric power as an example, the generation of hydropower in Shaanxi Province increased five times from 25.43×10^8 KW˙h in 1995 to112.98×10^8 KW˙h in 2014. The generation of wind power in 2015 was 28×10^8 KW˙h. Average utilization hours of power generation in 2015 were 281 h less than the previous year, 499 h for hydropower, 210 h for wind power and 354 h less for thermal power (Bloom et al., 2016). Therefore, the improvement of energy efficiency and the rapid construction of clean energy such as water conservancy and wind power have promoted the low-carbon development of Shaanxi electric power industry.

In a comprehensive view, although the power generation capacity of hydropower and wind power is increasing annually, the proportion of the total amount of electricity generated by these powers is very small compared with the amount of thermal power generated. The thermal power occupies 90% of the power generation, so currently the thermal power is main the power production in Shaanxi. In 2015, the total installed capacity of China's power generation was149000×10^4 KW, and the total installed capacity of thermal power was 101150×10^4 KW. It is predicted that the total installed capacity of thermal power generation in China will increase to 200000×10^4 KW and 380000×10^4 KW by 2020 and 2050, among which thermal power is also predicted to reach 124650×10^4 KW and 154700×10^4 KW in each year. The increase of the capacity cannot be separated from the capital investment of the country, so in the environment management, the investment in the energy industry and the treatment of industrial pollution will play key roles in the carbon emissions in the related industries (Taylor, 2009).

Model verification and analysis

(1) Model parameter estimation

The stability of time series data is the precondition to ensure the validity of the model. Automatic Direction Finder (ADF) method is used to test the stability of data by unit root (*Table 2*). In the selection of lag order, the optimal lag period is determined to be 2 order based on Chichi information criterion (AIC) and Schwartz criterion (SC).

http://www.aloki.hu ● ISSN 1589 1623 (Print) ● ISSN 1785 0037 (Online)
DOI: http://dx.doi.org/10.15666/aeer/1704_84358448

Table 2. *ADF stability test*

Variable	ADF statistics	1% critical value	5% critical value	10% critical value	P value	Conclusion
LCE	-0.636	-2.700	-1.961	-1.607	0.2361	Unstable
ΔLCE	-2.910	-2.700	-1.961	-1.607	0.0097	Stable
LEI	-1.602	-2.700	-1.961	-1.607	0.1088	Unstable
ΔLEI	-3.692	-2.700	-1.961	-1.607	0.0018	Stable
LIP	-0.9613	-2.700	-1.961	-1.607	0.2236	Unstable
ΔLIP	-4.299	-2.700	-1.961	-1.607	0.0005	Stable

From *Table 2* we can see that *LCES*, *LEIS* and *LIPS* of the ADF statistics are greater than 10%, which contain unit roots and non-stationary sequences. But the test values of the first difference are less than 1% of the critical value, the difference sequence does not contain the unit root, so the difference sequence is stable, and the data series conforms to the requirement of the construction model. The statistical software EViews7.2 is used to build the model. The result of operation data is substituted (*Eq. 6*), and the vector auto regression model is:

$$\begin{bmatrix} LCES \\ LEIS \\ LIPS \end{bmatrix}_t = \begin{bmatrix} 3.047 \\ -4.290 \\ 0.990 \end{bmatrix} + \begin{bmatrix} 0.596 & 0.319 & 0.109 \\ 0.946 & 0.819 & -0.152 \\ 0.813 & 0244 & 0.167 \end{bmatrix} \begin{bmatrix} LCES \\ LEIS \\ LIPS \end{bmatrix}_{t-1}$$

$$+ \begin{bmatrix} -0.216 & -0.200 & 0.033 \\ -0.117 & -0.163 & 0.095 \\ -0.410 & 0.059 & 0.301 \end{bmatrix} \begin{bmatrix} LCES \\ LEIS \\ LIPS \end{bmatrix}_{t-2} + \begin{bmatrix} \hat{\varepsilon}_0 \\ \hat{\varepsilon}_1 \\ \hat{\varepsilon}_2 \end{bmatrix}_t \quad \text{(Eq.7)}$$

The model (*Eq. 7*) is a variable system of carbon emissions, energy industry development and environmental governance of thermal power plants in Shaanxi. The AR root test of the model is based on the principle that the reciprocal of the model with all the characteristic roots of the model is less than 1. From *Figure 3* we can find that the model has 6 characteristic roots, and the reciprocal of all the eigenvalues of the model is in the unit circle, so the model is stable.

Meanwhile, according to the residual synchronization correlation matrix between variables, we can test the variables have mutual influence, and the correlation coefficients of *LCES* and *LEIS*, *LIPS* are 0.6071 and 0.4259 respectively (Bloch et al., 2012; Rojamary and Uma, 2017). Therefore, in order to explore the response mechanism between the energy industry development, environmental governance and thermal power carbon emission, we need to further cointegration test of the residual sequence of model (*Eq. 7*), in order to understand whether there is a long-term equilibrium relationship between the three variables. The real economic data are often caused by the "unbalanced process", the long-term equilibrium relationship can not reflect the short-term change. So we need to build vector error correction model to analyze what kind of short-term effects the variables will have if they deviate from equilibrium relations.

http://www.aloki.hu ● ISSN 1589 1623 (Print) ● ISSN 1785 0037 (Online)
DOI: http://dx.doi.org/10.15666/aeer/1704_84358448

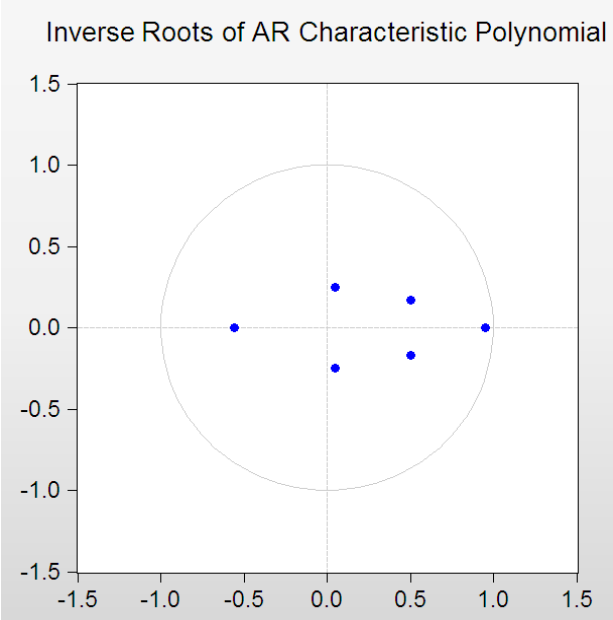

Figure 3. *Unit circle and characteristic root*

(2) Response mechanism of thermal power carbon emissions

Pseudo regression is likely to occur in nonstationary sequences. Johansen cointegration test is used to verify multiple variables, and whether there is a stable relationship between variables (*Table 3*).

Table 3. *Johansen co-integration test*

Number of equations	Characteristic value	Trace statistics	5% critical value	P value	Conclusion
0	0.8225	35.9189	29.7971	0.0087	Refuse
Up to 1	0.3044	6.53111	15.4847	0.6327	Accept
Up to 2	0.0211	0.36107	3.84147	0.5479	Accept

Table 3 shows a co-integration relationship at the 5% level, indicating a long-term equilibrium between energy industry development and environmental governance, and thermal carbon emissions. The cointegration equation is as follows:

$$LCES = 0.3470LEIS - 0.1225LIPS \quad \text{(Eq.8)}$$
$$\text{Standard deviation} = (0.0249) \qquad (0.0252)$$

According to cointegration equation, the elastic coefficient of energy industry development to thermal power carbon emission is 0.3470, that is, the investment of energy industry increases by 1%, the carbon emission of thermal power increases by about 0.35%, and the treatment of environmental pollution is negative (Oluleye et al., 2018 ; Li et al., 2013). It shows that the investment of industrial pollution control can effectively reduce the carbon emissions of thermal power enterprises. At the same time, the error correction term can be constructed based on the cointegration equation (*Eq. 8*) and the error correction model is established (*Table 4*).

http://www.aloki.hu ● ISSN 1589 1623 (Print) ● ISSN 1785 0037 (Online)
DOI: http://dx.doi.org/10.15666/aeer/1704_84358448

Table 4. *Error correction model coefficient vector statistics*

Error correction	D(LCES)	D(LEIS)	D(IPS)
CointEq1	-0.4445	2.0404	-0.0995
D((LCES)-1)	0.3750	-0.7096	1.6479
D((LCES)-2)	0.1972	-0.8650	0.4596
D((LEIS) -1)	0.0163	0.3469	-0.0187
D((LEIS) -2)	-0.1912	0.0351	0.4608
D((IPS) -1)	-0.0544	-0.0020	-0.8466
D((IPS) -2)	-0.1293	-0.0729	-0.5882
C	2.9200	0.6578	39.0031

A vector error correction model (*Eq. 9*) is established from *Table 4:*

$$\begin{bmatrix} D(LCES) \\ D(LEIS) \\ D(LIPS) \end{bmatrix} = \begin{bmatrix} 2.920 \\ 0.658 \\ 39.003 \end{bmatrix} + \begin{bmatrix} 0.375 & 0.016 & -0.054 \\ -0.710 & 0.347 & -0.002 \\ 1.648 & -0.019 & -0.847 \end{bmatrix} \begin{bmatrix} D(LCES) \\ D(LEIS) \\ D(LIPS) \end{bmatrix}_{t-1} + \begin{bmatrix} 0.197 & -0.191 & 0.129 \\ -0.865 & 0.035 & -0.073 \\ 0.460 & 0.461 & -0.588 \end{bmatrix} \begin{bmatrix} D(LCES) \\ D(LEIS) \\ D(LIPS) \end{bmatrix}_{t-2} + \begin{bmatrix} -0.445 \\ 2.040 \\ -0.100 \end{bmatrix} (LCES_t - 0.347LEIS + 0.123LIPS) + \hat{\varepsilon}_t \quad \text{(Eq.9)}$$

Equation 9 the error correction model consists of two parts: one is the short-term effect of itself and other variables, and the other is the effect of deviating from the long-term equilibrium relationship. Among them, -0.445, 2.040 and -0.100 respectively indicate that the carbon emission of thermal power, the development of energy industry and the environmental governance will deviate in the speed and direction from the long-term cointegration. Judging from the absolute value, the development of the energy industry has the fastest speed (Kang et al., 2018; Jiang et al., 2018; Raja, 2017). From the view of direction, the investment of thermal power carbon emissions and the environmental governance have a negative adjustment effect on the cointegration relationship.

Based on the research object of this paper, the error correction model of thermal power carbon emission is emphatically analyzed. Its determinant is:

$$\begin{aligned} D(LCES) = & -0.4445*(LCES(-1) - 0.3470*LEIS(-1) + 0.1225*LIPS(-1) - 5.1705) \\ & + 0.3750*D(LCES(-1)) + 0.1972*D(LCES(-2)) + 0.01630*D(LEIS(-1)) \\ & - 0.1912*D(LEIS(-2)) - 0.0544*D(LIPS(-1)) - 0.1294*D(LIPS(-2)) + 2.9200 \end{aligned} \quad \text{(Eq.10)}$$

From *Equation 10,* we can judge energy industry development and environmental governance can negatively adjust carbon emissions from thermal power plants. Investment in energy industry construction can improve the level of technological

http://www.aloki.hu ● ISSN 1589 1623 (Print) ● ISSN 1785 0037 (Online)
DOI: http://dx.doi.org/10.15666/aeer/1704_84358448

productivity, and industrial pollution investment directly promotes the control of various pollution sources. *IPS* lag difference coefficient is - 0.0544 and - 0.1294 respectively, indicating that short-term fluctuations in environmental management can reduce the amount of carbon emissions from thermal power plants. The impact of *EIS* on carbon emissions of thermal power is not stable, but from the view of impact coefficient, it can inhibit carbon emissions.

(3) Analysis of contribution

Co-integration analysis and error correction model estimate the long term equilibrium and short-term impact mechanism between the development of energy industry and environmental governance and the carbon emissions in thermal power plants from a static point of view. The impulse response function can help us understand the dynamic characteristics of the development of the energy industry, environmental governance and the response of thermal power to carbon emissions better.

Figure 4 shows the results of impulse response of carbon emission from thermal power to the energy industry development and environmental governance respectively. The horizontal axis represents the lag period of impact, the vertical axis represents the amount of carbon emissions, the solid line represents the impulse response function, and the dotted line represents the deviation band of positive and negative double standard deviation. According to *Figure 4,* the response of thermal power carbon emissions to energy industry development and environmental governance are similar, reaching the highest value in the second phase. Energy industry investment keeps declining from the third phase until the sixth phase to reach the stability, showing the trend of convergence. Environmental governance has a response fluctuation in the third and fourth periods, and tends to be stable and convergent after the fifth phase. It shows that the development of energy industry and environmental control in Shaanxi Province are effective in the long run, and the carbon emission of thermal power can be slowed down step by step. Variance decomposition is used to analyze the contribution of each structural shock to the change of thermal power carbon emissions (*Table 5*), so as to evaluate the contribution of different variables.

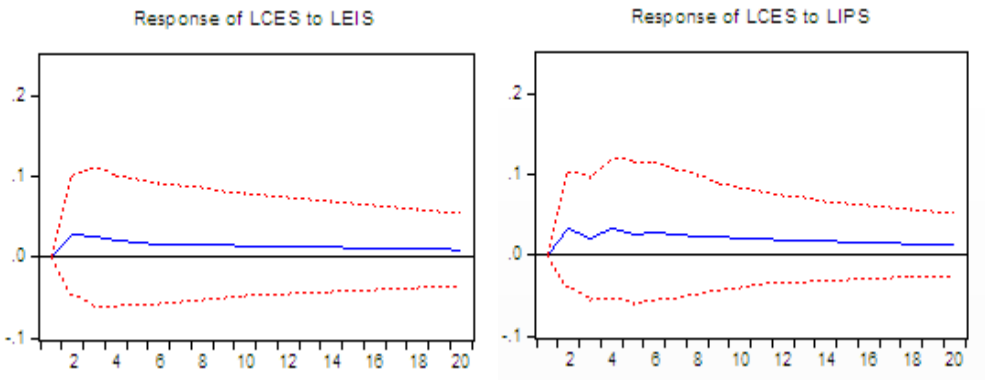

Figure 4. *Impulse response of thermal power carbon emissions to energy industry development and environmental governance*

As can be seen from *Table 5,* the interference response of thermal power carbon emission itself shows the trend of decreasing, and the contribution degree of energy

http://www.aloki.hu ● ISSN 1589 1623 (Print) ● ISSN 1785 0037 (Online)
DOI: http://dx.doi.org/10.15666/aeer/1704_84358448

industry development and environmental governance is increasing gradually in the ninth phase. From the second to the fourth, the contribution of the energy industry is higher than the environmental governance, and the improving of energy efficiency can reduce the carbon emissions rapidly. However, due to the phase nature of the technology renewal, the contribution of the energy industry is slowed down from the fifth stage; the contribution of the two is 5% and 6% respectively in the 20 phase. It shows that the development of energy industry and the intensity of environmental pollution control have certain explanatory to the fluctuation of carbon emissions from thermal power plants, which have a greater room for improvement.

Table 5. *Variance decomposition*

Phases	Variance contribution		
	LCES	*LEIS*	*LIPS*
1	100.0000	0.0000	0.0000
2	94.5204	2.7914	2.6882
3	93.4209	3.7777	2.8015
4	92.0112	4.1107	3.8780
5	91.4399	4.2839	4.2762
6	90.8427	4.4295	4.7279
7	90.4889	4.5483	4.9628
8	90.1787	4.6484	5.1729
9	89.9582	4.7307	5.3111
10	89.7720	4.7995	5.4284
15	89.2392	5.0082	5.7524
20	88.9946	5.1045	5.9009

Conclusions

Economic development depends on the drive of power and energy. Based on the estimated carbon emission values of thermal power in Shaanxi province in 1995-2015, combined with the investment of energy industry and environment governance, the VCE model is constructed to explore the long-term equilibrium and short-term fluctuation response mechanism between the three variables. The following conclusions are drawn:

(1) Shaanxi thermal power carbon emission keeps rising from 1995 until 2010. Because of the drastically increase of the amount of raw coal used in thermal power in 2010, thermal power carbon emissions reaches the peak in the recent 20 years. The development of hydropower, wind power, solar power generation and the reduction of standard coal consumption have promoted the low carbon industry in Shaanxi province.

(2) There is a long-term co-integration relationship between energy industry development, environmental governance and thermal power carbon emissions. Energy industry development and environmental governance can negatively adjust thermal power carbon emissions.

(3) In terms of contribution rate, the contribution rate of energy industry development and environmental governance has gradually increased. The contribution rate of industrial pollution control investment is slightly higher than that of energy industry investment. Therefore, in the future development of Shaanxi thermal power

http://www.aloki.hu ● ISSN 1589 1623 (Print) ● ISSN 1785 0037 (Online)
DOI: http://dx.doi.org/10.15666/aeer/1704_84358448

industry, we should adjust the energy structure, make full use of non-fossil energy, and actively optimize and upgrade of industrial structure.

(4) Increase investment in wind power and hydropower to reduce environmental pollution caused by thermal power generation.

Generally speaking, most scholars use the energy consumption method to calculate the carbon emission of thermal power, that is, the energy consumption of thermal power is multiplied by the energy carbon emission factor. On the basis of "energy consumption", this paper takes the desulfurization process and the carbon emission of power transmission into consideration. So it is relatively comprehensive. Industrial pollutants include waste water, waste gas, solid waste, noise and so on, due to the lack of part of the waste gas treatment data, this paper uses the total investment of industrial pollution control to construct the error correction model. Since the average proportion of investment in waste gas control in 2004-2015 was 49.72%, in 2013 and 2014 the annual waste gas investment accounted for 77%, the total investment in environment governance can represent the objective impact of waste gas treatment. Meanwhile, the electricity consumption of specific industries is an important basis for carbon emission reduction of thermal power plants. Based on the analysis of industrial macro data, this paper will further explore the main emission reduction paths of thermal power carbon emissions.

Acknowledgements. This paper is sponsored by The National Natural Science Foundation of China (41501093); and Sponsored by Social Science Planning Project of Shaanxi Province (2016R022).

REFERENCES

[1] Ali, W., Nasir, M. S., Nasir, A., Rashid, H., Ayub, I., Gillani, S. H., Latif, M. J. (2018): Assessment of carbon footprints in terms of CO_2 of diesel generator, Pakistan. – Earth Sciences Pakistan 2(1): 15-17.

[2] Atimtay, A. T. (2003): A global outlook to the carbon dioxide emissions in the world and emission factors of the thermal power plants in Turkey. – Water Air & Soil Pollution Focus 3(5-6): 335-345.

[3] Bergthorson, J. M. (2018): Recyclable metal fuels for clean and compact zero-carbon power. – Progress in Energy & Combustion Science 68: 169-196.

[4] Bloch, H., Rafiq, S., Salim, R. (2012): Coal consumption CO_2, emission and economic growth in China: empirical evidence and policy responses. – Energy Economics 34(2): 518-528.

[5] Bloom, D. E., Chatterji, S., Kowal, P. (2015): Macroeconomic implications of population ageing and selected policy responses. – Lancet 385(9968): 649.

[6] Boutabba, M. A., Lardic, S. (2016): EU emissions trading scheme, competitiveness and carbon leakage: new evidence from cement and steel industries. – Annals of Operations Research 255(1): 47-61.

[7] Deleidi, M. (2017): Post Keynesian endogenous money theory: a theoretical and empirical investigation of the credit demand schedule. – Journal of Post Keynesian Economics (2): 1-25.

[8] Hossain, M. S., Karlson, M., Neset, T. S. (2019): Application of gis for cyclone vulnerability analysis of Bangladesh. – Earth Sciences Malaysia 3(1): 25-34.

[9] Jamil, F., Arshad, R., Ali, M. A. (2018): Design, fabrication and evaluation of rotary hot-air dryer for the value addition of fruit waste. – Earth Sciences Pakistan 2(2): 07-11.

http://www.aloki.hu ● ISSN 1589 1623 (Print) ● ISSN 1785 0037 (Online)
DOI: http://dx.doi.org/10.15666/aeer/1704_84358448

[10] Jiang, S., Lian, M., Lu, C., Gu, Q., Ruan, S., Xie, X. (2018): Ensemble prediction algorithm of anomaly monitoring based on big data analysis platform of open-pit mine slope. – Complexity 2018.
[11] Joseph, O. T., Adeoti, O. O., Olufemi, A. A. (2019): Study of the phytodiversity along Antorun Reservoir, near Ogbomoso, Nigeria. – Environment & Ecosystem Science 3(1): 1-12.
[12] Kalshian, R. (2016): Introduction: Energy versus emissions: the big challenge of the new millennium. – Journal of International Consumer Marketing 26(1): 58-74.
[13] Kang, L., Du, H. L., Zhang, H., Ma, W. L. (2018): Systematic research on the application of steel slag resources under the background of big data. – Complexity 2018. https://doi.org/10.1155/2018/6703908.
[14] Kumar, M., Mao, Y., Wang, Y., Qiu, T., Chenggen, Y., Zhang, W. (2017): Fuzzy theoretic approach to signals and systems: static systems. – Information Sciences 418: 668-702.
[15] Kumar, R. (2018): Comparison of instruction scheduling and register allocation for MIPS and HPL-PD architecture for exploitation of instruction level parallelism. – Engineering Heritage Journal 2(2): 04-08.
[16] Li, G., Chen, M. (2013) Intertwined phenomenon of a kind of dynamical systems. – Advances in Difference Equations 2013(1): 265.
[17] Licht, S., Wu, H. J., Hettige, C. (2018): STEP cement: solar thermal electrochemical production of CaO without CO_2 emission. – Chemical Communications 48(48): 6019-6021.
[18] Ma, X. J., Wang, Y., Wang, C. (2017): Low-carbon development of China's thermal power industry based on an international comparison: review, analysis and forecast. – Renewable & Sustainable Energy Reviews 80: 942-970.
[19] Majumder, S. C., Islam, K., Hossain, M. M. (2019): State of research on carbon sequestration in Bangladesh: a comprehensive review. – Geology, Ecology, and Landscapes 3(1): 29-36.
[20] Moon, G. H., Seo, J. Y. (2017): Dynamic mechanism between economic shocks and adjustments to loan portfolio weight: evidence from South Korean banks. – Journal of the Asia Pacific Economy 4: 1-19.
[21] Moon, T., Shin, D. H. (2017): Forecasting model of construction cost index based on VECM with search query. – KSCE Journal of Civil Engineering 11: 1-9.
[22] Nas, A., Talebian-Kiakalaieh, A. (2017): Reduction of CO_2 emission by INCAM model in Malaysia biomass power plants during the year 2016. – Waste Manage 73: 256-264.
[23] Oluleye, G., Allison, J., Kelly, N. (2018): An optimisation study on integrating and incentivising thermal energy storage (TES) in a dwelling energy system. – Energies 11(5): 1095.
[24] Pazand, K., Hezarkhani, A. (2018): Predictive Cu porphyry potential mapping using fuzzy modelling in Ahar–Arasbaran zone, Iran. – Geology, Ecology, and Landscapes 2(4): 229-239.
[25] Raja, B. (2017): Some properties of hypergeometric functions for Sakaguchi type functions. – Revista de la Facultad de Agronomia de la Universidad del Zulia 34(4).
[26] Rajput, K., Gupta, A., Arus, H. (2019): Re-cycle of e-waste in concrete by partial replacement of coarse aggregate. – Engineering Heritage Journal. DOI: 10.26480/gwk.01.2019.05.08.
[27] Reddy, S. S., Momoh, J. A. (2016): Minimum emissions optimal power flow in wind-thermal power system using opposition based bacterial dynamics algorithm. – 2016 Power and Energy Society General Meeting, IEEE. DOI: 10.1109/PESGM.2016.7741635.
[28] Rojamary, T., Uma, K. P. (2017): A stochastic model for the cost analysis of a system with two components for the loss of manpower threshold. – Revista de la Facultad de Agronomía 34(2).

http://www.aloki.hu ● ISSN 1589 1623 (Print) ● ISSN 1785 0037 (Online)
DOI: http://dx.doi.org/10.15666/aeer/1704_84358448

[29] Salem, R., Bahadorijahromi, A., Mylona, A. (2018): Comparison and evaluation of the potential energy, carbon emissions, and financial impacts from the incorporation of CHP and CCHP systems in existing UK hotel buildings. – Energies 11(5): 1219.
[30] Shrestha, A., Baral, S. (2018): Socioeconomic factors affecting awareness and adaption of climate change: a case study of Banke District Nepal. – Earth Sciences Malaysia 2(2): 20-24.
[31] Sufiyan, I., Zakariya, R., Yaacob, R. (2018): Delineation of flood risk zones and 3D modeling In Terengganu River catchment using GIS and SWAT. – Environment & Ecosystem Science 2(2): 01-05.
[32] Taylor, J. B. (2009): The financial crisis and the policy responses: an empirical analysis of what went wrong. – NBER Working Papers 21(2-3): 341-364.
[33] Valiani, S., Tahouni, N., Panjeshahi, M. H. (2016): Optimization of pre-combustion capture for thermal power plants using pinch analysis. – Energy 119: 950-960.
[34] Velea, S., Dragos, N., Serban, S. (2009): Biological sequestration of carbon dioxide from thermal power plant emissions, by absorption in microalgal culture media. – Romanian Biotechnological Letters 14(4): 4485-4500.

http://www.aloki.hu ● ISSN 1589 1623 (Print) ● ISSN 1785 0037 (Online)
DOI: http://dx.doi.org/10.15666/aeer/1704_84358448

DESIGNING AN INTELLIGENT GREENHOUSE MONITORING SYSTEM BASED ON THE INTERNET OF THINGS

CAI, W.[1*] – WEN, X.[1] – TU, Q.[1]

School of Civil and Transportation Engineering, Ningbo University of Technology, Ningbo 315211, Zhejiang, China
(e-mails: wenxiaodong@nbut.cn, tuqiuky@163.com)

**Corresponding author*
e-mail: caiwei@nbut.edu.cn

(Received 8th Mar 2019; accepted 21st May 2019)

Abstract. With the development of the Internet, the development of the Internet of Things (IoT) has also been promoted. The IoT is a network of "objects and objects connected." The IoT is based on cloud computing platforms and wireless networks. It acquires data based on sensor groups and conducts decision analysis to change the behavior control and feedback of objects, such as the greenhouse monitoring system studied in this paper. The IoT has subverted the traditional agricultural production model, from the agricultural farming model to the "smart agriculture" production-operation-sales model, which provides a direction for the sustainable development of agriculture in China at this stage. Based on the IoT and Zig Bee wireless sensor network technology, this paper designs a general scheme of an intelligent greenhouse control system based on IoT technology. The greenhouse control strategy was studied using IoT technology and fuzzy adaptive PID control algorithm. The experimental simulation was carried out with MATLAB software. The simulation results show that the optimal control of greenhouse temperature is achieved. The temperature in the greenhouse is always maintained at 16.5 °C -23.0 °C, and the humidity value is always maintained at 68.2% RH-89.3% RH. The test verified that the paper can achieve the expected effect for the greenhouse.
Keywords: *cloud computing platforms, smart agriculture, fuzzy adaptive PID, Zig Bee, MATLAB software*

Introduction

The Internet of Things (IoT) is a new technology that connects every object in a system to make it a whole. Integrating IoT technology into greenhouse control systems can make greenhouse monitoring systems more intelligent and coordinated. The main components of the IoT have the following parts. (1) Storage analysis (Buscheck et al., 2012; Zakeri and Syri, 2015; Dickinson et al., 2017; Patle et al., 2019), the server can receive and display the collected data in real time, and give corresponding processing analysis according to different application environments to achieve effective decision-making. (2) Network transmission (Wertheim et al., 2014; Hale et al., 2016; Choudhari et al., 2018), in order to achieve remote operation of the IoT, the collected information must pass through the sensor gateway and then transmitted to the remote server. (3) Information collection (Timonen et al., 2014; Joseph et al., 2019), in the monitoring area, we should deploy a variety of sensors to collect different data information in the environment, and send data through the transmitting device to form a wireless network. (4) Intelligent control (Kazmierkowski, 2014; Yoh-Han et al., 2016; Li et al., 2017; Jurkowski et al., 2015) combines its module with other controllers to achieve system control. After receiving the sent control command, different submodules will cooperate with each other. (5) Environment (Yahya et al., 2018), the collection and transmission of information is usually done through the environment, first of all, to perceive the

http://www.aloki.hu ● ISSN 1589 1623 (Print) ● ISSN 1785 0037 (Online)
DOI: http://dx.doi.org/10.15666/aeer/1704_84498464

surrounding environment, and then adjust the information through the corresponding control equipment. IoT technology is the product of the development of new generation information technology, and has been highly valued and widely used in wireless communication applications.

The IoT is generally combined with Zig Bee wireless sensor network technology (Espinosafaller, 2012), which is a short-range, low-rate wireless communication technology. The name of Zig Bee comes from the body language of the bees. When the bees find pollen, they will dance in a zig-zag motion. Through this splay, the message of the pollen's position and distance will be transmitted to the companion. It was formerly known as "Home RF Lite" or "Fire Fly" communication technology for wireless communication at close range (Yusof et al., 2015; Hithnawi et al., 2016; Tianlei, 2019). Zig Bee has the characteristics of small size, low energy consumption, short delay, large network capacity and strong stability. It can be easily integrated into various devices and is suitable for various intelligent control areas (Zheng et al., 2018). Zig Bee's network/security layer is responsible for providing LG WPAN with Zig Bee wireless network formation, network protection and information management services, and defines some common application function interfaces, defining appropriate service interfaces for the application layer to ensure stable operation of the MAC layer (Messo et al., 2013; Jang et al., 2015; Kasim et al., 2019). The application framework layer mainly contains application support layers, Zig Bee device objects, objects provided by the manufacturer, and is used to provide some common application framework models for Zig Bee applications (Fan et al., 2011; Nkwuda et al., 2019). Based on the IoT architecture, Zig Bee wireless sensor network technology has been applied to the greenhouse.

The greenhouse is also called glasshouse. Its main function is to plant crops and to maintain the function of heat preservation and light transmission. In the spring and winter seasons, there are some crops that are not suitable for growing. The greenhouse can artificially provide a growing environment for crops, which in turn increases crop yields. The variety of greenhouses can be divided into many different types depending on the roofing materials, lighting supplies, appearance and heating conditions. From the structure of the greenhouse, it should be a confined space and able to maintain temperature, while also having the function of facilitating ventilation and reducing temperature. Today's modern greenhouses use the computer control system to achieve intelligent control of environmental factors in the greenhouse, which improves the growth environment for crop growth. The greenhouse mainly uses sunshade materials to build some or all of the outer shells, and can build corresponding greenhouses for their crops in cold seasons or in climates where crop growth is not suitable (Messelink, 2014; Snipen, 2015; Azeem et al., 2018).

The main factors affecting the growth and development of crops are: temperature, moisture, light, air, biological factors, etc. (Vakilian and Massah, 2017). These factors do not exist alone, but have a close relationship with each other. The growth of crops is often affected by environmental integration. Crop growth is often affected by complex environments. Among them, factors such as temperature and humidity are the most important, and the stability of the greenhouse ecological environment is maintained by controlling them to maintain the environment in which crops are suitable for growth.

Based on the IoT architecture and Zig Bee wireless sensor network technology (Zhang et al., 2018a; Okpoli, 2019), this paper designs a general scheme of intelligent greenhouse control system based on IoT technology. The application of IoT technology

http://www.aloki.hu ● ISSN 1589 1623 (Print) ● ISSN 1785 0037 (Online)
DOI: http://dx.doi.org/10.15666/aeer/1704_84498464

and fuzzy adaptive PID control algorithm combined with greenhouses to analyze the characteristics of greenhouse environmental factors. Just as the above mentioned temperature, moisture, illumination, etc. were verified, the main control parameters in the greenhouse environment were determined. According to the control characteristics of the main factors, the control schemes of various environmental factors in the greenhouse were designed, and the corresponding mathematical models were established. The greenhouse temperature control strategy was studied (Zhang et al., 2018b; Sunny et al., 2018). The experimental test verified that the system design can achieve the expected effect of the greenhouse. Then, based on the characteristics of non-linearity and large hysteresis of greenhouse temperature, a fuzzy adaptive PID controller is designed. According to the actual requirements of greenhouse temperature, the PID parameters are adjusted online to achieve optimal control of greenhouse temperature (Zou, 2018). The simulation results show that the algorithm has good effectiveness in the temperature control process.

Proposed method

Fuzzy PID control algorithm

The greenhouse monitoring system is a group of 15 greenhouses and a complex monitoring system for monitoring the environment. In terms of monitoring, there are mainly indoor temperature, humidity and light. It is also necessary to monitor the multi-parameter complex data such as moisture, pH and even air content in the soil, temperature and humidity of plant foliage. In the control, there are many devices such as fans, heating pipes, sunshades and humidifiers, which need to participate in the environmental change process of the greenhouse.

The fuzzy PID control algorithm can adjust the scale factor, integral factor and differential factor of the conventional PID control in real time according to the pre-designed fuzzy rules to adjust the environmental parameters of the greenhouse. The main core is the PID control method, and the fuzzy control is the method of continuously adjusting the PID parameters.

In practical engineering applications, the most commonly used controller design is the PID controller. It is mainly composed of the proportional coefficient k_p, the integral coefficient k_i and the differential coefficient k_d. The structure of the fuzzy PID controller is shown in *Figure 1*.

Among them, $r(t)$ is the set value of the system, $y(t)$ is the actual measured value of the system, $e(t)$ is the difference between the system set value and the measured value of the system, that is, the deviation, which is generally used as the input of the PID controller, and its calculation formula (*Eq. 1*) is:

$$e(t) = r(t) - y(t) \tag{Eq.1}$$

The output expression of the PID controller (*Eq. 2*) is:

$$u(t) = K_p e(t) + K_I \int_0^t e(\tau) dx + K_D \frac{de(t)}{dt} \tag{Eq.2}$$

http://www.aloki.hu ● ISSN 1589 1623 (Print) ● ISSN 1785 0037 (Online)
DOI: http://dx.doi.org/10.15666/aeer/1704_84498464

In the above formula, K_P represents the proportional gain, K_I represents the integral gain, and K_D represents the differential gain. The PID controller adjusts the size of these three parameters to meet the requirements of the control system. According to the fuzzy control process, the precise quantity is transformed into the membership function of the fuzzy set by means of quantization and fuzzification. Fuzzification, by definition, converts the input space of the input domain observation into a mapping in the fuzzy set, essentially finding the fuzzy set membership function of the numerical domain corresponding to the concept.

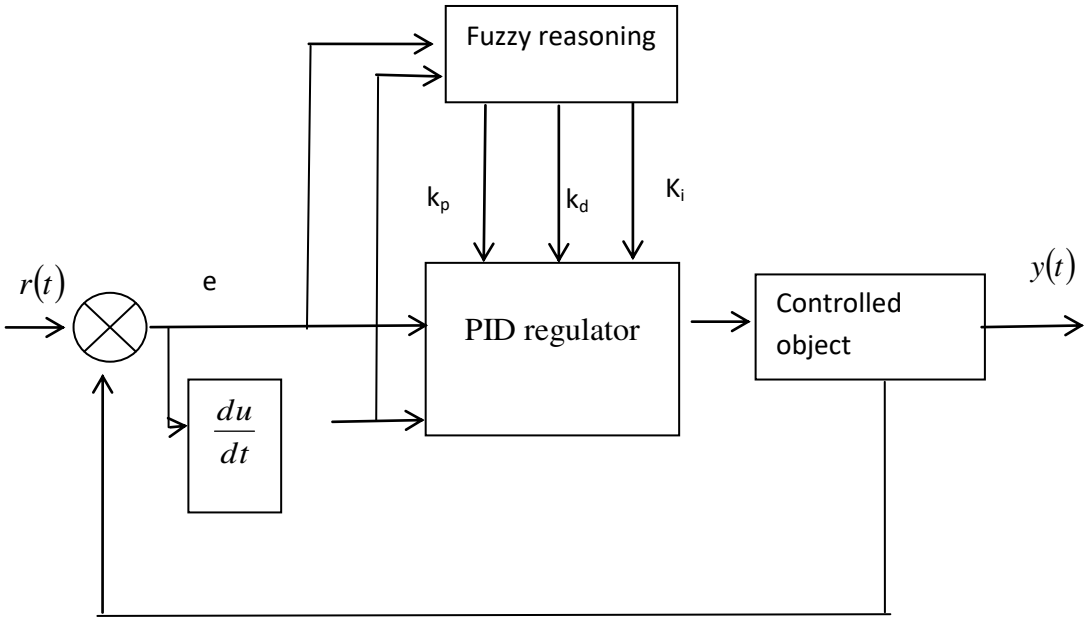

Figure 1. *Fuzzy PID structure diagram*

The tuning of PID parameters must consider the role and mutual influence of proportional integral differential coefficients in different corresponding stages. The traditional PID parameter adjustment experience shows that:

(1) When the deviation is large, a larger proportional coefficient should be taken to ensure the acceleration response speed of the system; in order to avoid the differential saturation caused by excessive deviation change, the control effect is out of range, and the differential coefficient change should be made smaller; The system response is over-adjusted, resulting in integral saturation, and the integral action should be removed;

(2) When the deviation and deviation change rate are medium, take a small proportional coefficient to prevent overshoot, and the integral differential coefficient should take the median value;

(3) When the deviation is small, a smaller proportional coefficient should be taken to ensure that no overshoot is generated, and a larger integral coefficient is taken to improve the dynamic characteristics of the system. The differential coefficient becomes smaller when the rate of change of the deviation is large, and becomes larger when the rate of change of the deviation is small.

(4) When the rate of change of the deviation is large, the smaller the proportional coefficient, the slower the response speed, and the greater the integral strain.

http://www.aloki.hu ● ISSN 1589 1623 (Print) ● ISSN 1785 0037 (Online)
DOI: http://dx.doi.org/10.15666/aeer/1704_84498464

Radial basis function (RBF) neural network data fusion

RBF network belongs to a multilayer forward network. When the BP network is used for function approximation, the weight is adjusted by the negative gradient descent method. This method of adjusting the weight has the disadvantages of slow convergence and local minimum. Since the BP neural network corrects the weight by the gradient descent method in the process of function approximation, this correction method has a slow convergence speed and easily converges to the local minimum point, which has certain limitations. RBF neural networks are superior to BP neural networks in terms of approximation ability, classification ability and learning speed.

The most commonly used RBF is a Gaussian function with two adjustable parameters, the center position and the variance b (the width parameter of the function). When using such a function, there are three sets of tunable parameters (parameters to be trained) of the entire network, that is, the center position, variance, and weight of the output unit of each basis function. Usually, the number of nodes in the hidden layer is selected as the number of training samples, and each node has a center vector of a RBF, which is the input vector of the training sample. Its network structure is shown in *Figure 2.*

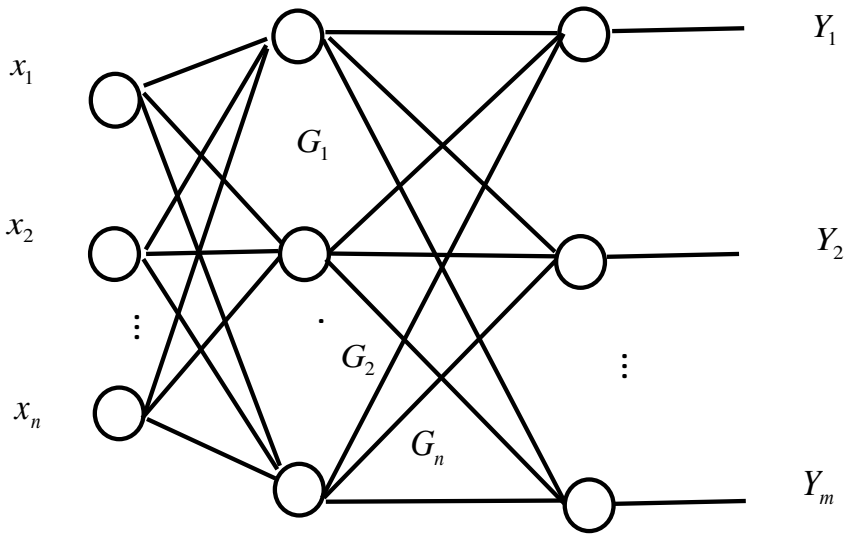

Figure 2. *RBF neural network structure*

The transfer function of the hidden layer node is Gauss function: $f(x) = \exp(-x^2/b) = \exp(-\delta^2 K/b)$, where the parameter *b* controls the effect of the width of the bell-shaped Gaussian curve.

The center value of the Gaussian function of each hidden layer node is $C_K = |C_{K1}, C_{K2}, ..., C_{Kn}|$, $K = 1,2,...N$, and the net input of the hidden node is defined as the Euclidean distance between the input $\boldsymbol{X}$ and the RBF center vector of the hidden node (*Eq. 3*), namely:

$$\delta_K = \|X - C_K\|^2 = \sum_{i=1}^{n} (x_i - C_{Ki})^2 \quad K = 1,2,...N \qquad \text{(Eq.3)}$$

http://www.aloki.hu ● ISSN 1589 1623 (Print) ● ISSN 1785 0037 (Online)
DOI: http://dx.doi.org/10.15666/aeer/1704_84498464

The output $y_K = f(\delta_K)$ of the hidden layer node represents the extent to which the input mode leaves the center of the RBF represented by the implicit node. The final output layer of the network is a linear combination of the output of the hidden layer node. The output of the node j is: $Y_j = \sum_{K=1}^{N} w_{Kj} \cdot Z_K - \theta = W_j \cdot Z$, where $W_j = [w_{1j}, w_{2j}, \ldots, w_{Nj}]$ is the weight of the output layer and $Z = [z_1, z_2, ..., z_N]$ is the hidden layer output.

The learning process of the RBF network is divided into two phases. In the first stage, the center value C_k and the normalization constant of the Gaussian kernel function of each node of the hidden layer are determined according to all the input samples; in the second stage, the weight of the output layer is obtained by the least square method according to the sample.

In this paper, the RBF neural network model with soil temperature, humidity and soil moisture change per unit time as inputs can effectively predict soil moisture trends and deep soil water content.

Mathematical model of the controlled object

The greenhouse monitoring system is a complex system that comprehensively monitors environmental factor changes and enables the actuator to automatically adjust in real time to the required control algorithms.

In the environmental data monitored by greenhouses, the environmental factors required to monitor crops are multifaceted. The greenhouse group used in this paper consists of 20 large greenhouses. When the actuators act, the environmental parameters change slowly. The greenhouse monitoring system is a multi-parameter, time-varying, nonlinear and hysteresis system. When the system is large, it is inevitable that the external interference factors will increase. The influence of interference factors should be considered, and the parameters such as temperature and humidity, illumination and carbon dioxide that are easy to monitor are directly controlled. The parameters of the equipment that affect each parameter are changed in real time to achieve real-time balance, so that the internal environmental parameters of the greenhouse can promote the growth of plants. This project is a greenhouse group mainly planting peach trees. The growth of peach trees is mainly affected by temperature. Therefore, this chapter takes temperature as an example to illustrate, and other factors are referenced. According to the actual experience of the subject, taking temperature as an example, in the greenhouse temperature, the opening degree of the heating pipe plays the most important role in the temperature inside the greenhouse. At the same time, the plastic film in the greenhouse has the function of heat preservation and heat insulation, and the greenhouse will exhibit convective heat transfer characteristics when the heat changes, and when the temperature changes in a greenhouse, the plastic film has a function of heat storage. When the set temperature value becomes lower and the valve opening degree of the heating pipe is decreased, the hysteresis of slow heat dissipation is exhibited. Because of the large area of the greenhouse, it shows a certain inertia, so it includes the inertia lagging link. Therefore, the transfer function G(s) of the controlled object of the temperature control system of the greenhouse is defined (*Eq. 4*) as the following form:

$$G_{(S)} = \frac{Ke^{-\tau s}}{Ts + 1} \quad \text{(Eq.4)}$$

http://www.aloki.hu ● ISSN 1589 1623 (Print) ● ISSN 1785 0037 (Online)
DOI: http://dx.doi.org/10.15666/aeer/1704_84498464

The characteristics of the controlled object can be described by three parameters: K (static gain), τ (lag time), and T (time constant).

The static gain K refers to the ratio of the system output to the system input when the system reaches a steady state. It does not change due to other changes. It is only related to the controlled object and is a sign indicating the stability of the controlled object. The larger the K, the worse the stability, and the smaller the K, the stronger the stability.

The lag time τ represents a dynamic parameter describing the hysteresis, and it takes a long time for the controlled quantity to change as the input variable changes.

The time constant T reflects the degree of change of the output variable from the initial state to the steady state after the input signal is applied, reflecting the fast and slow characteristics of the dynamic process of the controlled object (Lu et al., 2019).

Discretization algorithm

The idea of discretization algorithm is to discretize continuous attributes into classification attributes, which provides an important way for the conversion between different types of data. In practical applications, the data set to be clustered contains both continuous attribute data and classification attribute data. But unfortunately, most of the existing algorithms can only process the data of the classification attribute, or the data of the classification attribute is more suitable than the data of the continuous attribute. In order to adapt to this situation, it is required to discretize the data of continuous attributes.

There are many advantages to the discretization of continuous attributes: discretization results reduce the need for storage space in subsequent processing algorithms; discretized data is the specification and simplification of the original data, easier to understand and use; continuous attribute discretization method can be effective to improve the accuracy of data analysis, thus enhancing the robustness to data noise.

Discretization of continuous attributes is a process of transforming quantitative data into qualitative data (Deng, 2019). Firstly, several segmentation points are set in the range of the continuous attribute, then the range of the continuous attribute is divided into discrete intervals, each sub-interval corresponds to a discrete value, and finally the original data is updated to a discrete value. The discretization problem is described as follows:

A decision table is a knowledge expression system consisting of a quad $S=(U,A,V,f)$, where $U=\{x_1,x_2,...,x_n\}$ is the domain and $A=C\bigcup\{d\}$ is the property set. $C=\{a_1,a_2,...,a_m\}$ and $\{d\}$ are the condition attribute set and the decision attribute set respectively, and $C\bigcap\{d\}=\Phi$, V is a set of attribute value ranges, and f is a map of $U\times A\to V$, which represents the value of each object in U on each attribute.

Suppose that for a conditional attribute $a\in C$ and a value field of $V_a=[l_a,r_a]$, where there is a set of points $l_a=c_0^a<c_1^a<c_2^a<...c_{ka}^a<c_{ka+1}^a=r_a$, then this set of points divides the conditional attribute range into: $V_a=[c_0^a,c_1^a)\bigcup[c_1^a,c_2^a)\bigcup....\bigcup[c_{ka}^a,c_{ka+1}^a)$. Here each $[c_i^a,c_{i+1}^a)$ is called an interval, each c_{ka}^a is called a breakpoint, and the set of all breakpoints on the attribute ***a*** constitutes a breakpoint set $Q^a=\{c_{ka}^a\}(I\le k\le m)$ of the attribute a. The ultimate goal of discretization is to find a suitable set Q of breakpoints

http://www.aloki.hu ● ISSN 1589 1623 (Print) ● ISSN 1785 0037 (Online)
DOI: http://dx.doi.org/10.15666/aeer/1704_84498464

for all continuous properties. Therefore, $Q = \bigcup Q^a \left(a \in C\right)$ defines a new decision table $S^p = \left(U, A, V^p, f^p\right)$, and for $\vee x \in U$, $i \in \{0,...k_a\}, f^p\left(x,a\right) = i \leftrightarrow f\left(x,a\right) \in \left[c_i^a, c_{i+1}^a\right]$.

The process of discretization of continuous attributes is the process of dividing the range of continuous attributes by using the selected breakpoints. Suppose that an attribute has r attribute values, and then there are $r-1$ breakpoints on this attribute. As the number of attribute values increases, the number of breakable points will increase with the value of the attribute. The process of selecting breakpoints is the process of merging attribute values. The discretization process of continuous attributes can reduce information redundancy and reduce the size of data, thus reducing the requirement for storage space. The discretization of the data can also reduce the complexity of subsequent processing data.

Evaluating the success of a discretization algorithm can be considered from the following three aspects: (1) The completeness of discretization. A successful discretization algorithm needs to be able to discretize multiple continuous attributes because the data set may contain more than one continuous attribute, so the discretization algorithm must be able to handle all of the continuous attributes in the data set rather than selectively processing some of the continuous attributes. (2) The degree of simplicity of discretization results. The number of discretized intervals should be as small as possible. If the number of breakpoints is too large, the recurrence of the data processed by the subsequent algorithm will be increased. (3) The degree of consistency of the data. Discretized results should maintain the original data as much as possible, minimizing the rate of information loss.

Experiments

After completing the software design of the greenhouse remote intelligent control system, the corresponding system debugging is carried out. The successful PC software interface is connected with the corresponding hardware device to test each control function module in the greenhouse to verify the feasibility of the overall system design. This article uses a PC with Windows 10 operating system as the host, and the target is the Tiny6410 development board. Firstly, you need to install the VMware10.0 virtual machine on your PC and then install your own Linux system in the virtual machine. Network training and simulation were carried out using the MATLAB software in the computer to control the temperature, moisture, the concentration of CO_2 and illumination intensity in the greenhouse environment. Compare the data collected by the smart system sensor with the data measured by the humidity meter (Yi, 2018).

Discussion

This paper gives an overall framework considering the limitations of current equipment, the structure of the greenhouse site, and the needs of reality. The greenhouse site is mainly composed of data collection and video surveillance; the server is composed of a data server, a video server and a server, and the three can be on the same server; the client actually refers to the customer and the agricultural monitoring service network that is open to the public (Zeng, 2018). The greenhouse site is connected to the server through a mobile network, and the client and server interact through the Internet, as shown in *Figure 3*.

http://www.aloki.hu ● ISSN 1589 1623 (Print) ● ISSN 1785 0037 (Online)
DOI: http://dx.doi.org/10.15666/aeer/1704_84498464

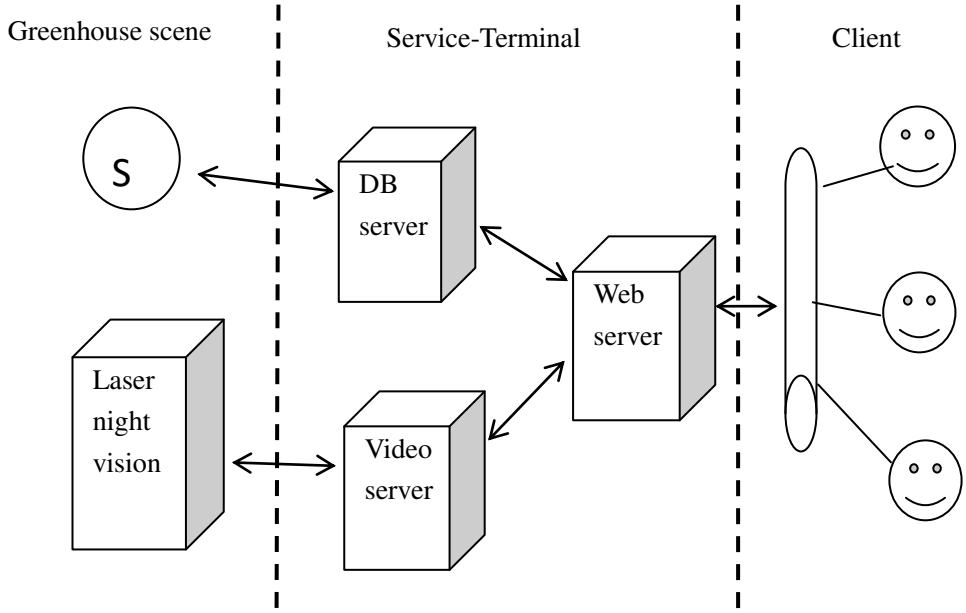

Figure 3. *Overall system framework*

The main environmental factors affecting crop growth in the microclimate environment of greenhouses are temperature, humidity, solar radiation, and carbon dioxide concentration (Shan, 2018). This test mainly collected detailed test parameter values for meteorological conditions such as temperature, humidity, CO_2 concentration and illumination intensity in the greenhouse. Among them, a routing node is set up between each module, which can be regarded as a "data transmission transfer station". When the distance between the module and the coordinator is far, this may result in no way to transmit data. At this time, the routing node plays a role of relaying, providing convenient data transmission channels through the node to ensure the integrity of system data transmission. Therefore, the setting of the node not only ensures the stability of the system control process, but also increases the transmission distance of the data (Zhang et al., 2017).

In order to verify the feasibility of the system, when collecting data on the greenhouse environmental factors, before the experiment, taking into account the accuracy of the reference values, it is necessary to accurately test each sensor module. Various types of sensors are installed in different corners of the laboratory to ensure the integrity of data collection anywhere in the laboratory. When detecting the received data, in order to more intuitively observe the trend of the data, one of the sensors collects the data interface, and the detected value obtained by the interface is compared with the data collected by the actual engineering instrument, thereby verify the validity of the data collection (Lu, 2018). During the interval of every half hour, data of 6 groups of different time periods are collected, and the collected data is detected, and the average value of the data is compared with the actual collected data. The data comparison results are shown in *Tables 1* and *2*.

According to the experimental data comparison analysis table, it can be seen that the temperature sensor used in the laboratory has a temperature error range of ± 0.3 °C compared with the industrial meter, and the humidity sensor used in the laboratory has a humidity error range of -0.6–1.1% RH compared to the industrial instrument. Through

http://www.aloki.hu ● ISSN 1589 1623 (Print) ● ISSN 1785 0037 (Online)
DOI: http://dx.doi.org/10.15666/aeer/1704_84498464

the comparison of experimental data, the temperature and humidity sensor measurement error is within a reasonable range, and the data collected by the sensor can be verified to have reliability characteristics.

Table 1. *Comparison of light intensity data*

Serial number	Temperature collected by the sensor °C	Temperature measured by the temperature meter °C	Temperature error value °C
1	17.6	17.7	-0.1
2	19.2	19.1	0.1
3	20.4	20.6	-0.2
4	21.7	21.5	0.2
5	21.7	21.9	-0.2
6	23.2	22.9	0.3

Table 2. *Comparison of humidity data*

Serial number	Humidity collected by the sensor %RH	Humidity measured by humidity meter %RH	Humidity error value %RH
1	41.1	40.4	0.7
2	49.1	48.6	0.5
3	56.8	55.7	1.1
4	68.4	67.8	0.6
5	70.3	71.1	-0.8
6	76.5	77.2	-0.7

For the design of the illumination sensor, an LED light device is used to measure the light intensity in the laboratory. Six sets of data were taken for analysis. The average of the six sets of data was compared with the data collected by the light intensity measuring instrument in the actual project. The results of the comparative analysis of the light intensity data are shown in *Table 3*.

Table 3. *Comparison of light intensity data*

Serial number	Light intensity collected by the sensor Lx	Data measured by the illuminometer Lx	Error Lx	Relative error %
1	1103	1099	4	0.36
2	1356	1321	35	2.58
3	2689	2660	29	1.72
4	4780	4705	75	1.57
5	6643	6556	87	1.31
6	12453	12343	110	0.88

From the comparison of the above experimental data, it can be seen that the light intensity data collected by the sensors in the laboratory is between 0.36 and 2.58% than the light intensity of the actual engineering light intensity equipment. Therefore, the effectiveness of the data collected by this sensor is indicated.

http://www.aloki.hu ● ISSN 1589 1623 (Print) ● ISSN 1785 0037 (Online)
DOI: http://dx.doi.org/10.15666/aeer/1704_84498464

Similarly, the CO_2 data will also be valid, so the data acquisition is available, and then the experimental results of the fuzzy adaptive PID controller are tested experimentally, and the pre-designed control system is applied to the greenhouse for experiments. In the aspect of temperature and humidity control, the fuzzy adaptive PID control method is introduced. Since the humidity and temperature control design are similar, the temperature is taken as an example for detailed design, and the illumination is controlled by the upper and lower limit values.

For the regulation of temperature and humidity in the greenhouse, a half-year follow-up test was conducted, and the test time was 08:30-15:00 every day. Through the parameter setting module in the system, the crop is set to a temperature range of 19 to 23 °C and a humidity range of 60–90% RH. According to its variation in the growth cycle, the ideal temperature setting is 20 °C, and the ideal humidity setting is 80% RH. In the parameter setting module, the value of the greenhouse degree is determined, and the value is input into the system, and after the corresponding saving process is performed, the intelligent control module is operated. In the one-week tracking test, the data collection interval is 30 min. The data collected on any day is selected for experimental analysis. The changes in greenhouse environmental factor parameter values are shown in *Table 4*.

Table 4. *Indoor environmental parameter values*

Serial number	Time	Temperature value °C	Humidity value %RH	Sunlight illumination lx	CO_2 concentration ppm
1	8:30	19.0	82.3	4312	1312
2	9:00	19.5	82.1	4641	1411
3	9:30	20.1	79.8	5123	1091
4	10:00	20.4	77.2	6001	901
5	10:30	20.7	78.8	9137	721
6	11:00	20.8	76.9	10011	901
7	11:30	21.2	77.8	12404	1047
8	12:00	21.5	80.9	13115	1109
9	12:30	22.1	82.6	10132	1216
10	13:00	23.0	79.3	11478	1110
11	13:30	22.4	77.8	10014	1921
12	14:00	21.1	76.9	9311	1104
13	14:30	20.1	80.2	8121	1114
14	15:00	19.5	83.1	7123	1220

It can be seen from *Table 4* that the temperature value in the greenhouse is always within the range of 16.5-23.0 °C in different time periods, and the humidity value is always kept within the range of 68.2–89.3% RH. According to the data collected from the outdoor, the indoor and outdoor temperature and humidity are compared, and the indoor and outdoor temperature comparison results are shown in *Figure 4*.

The dotted line represents the outdoor temperature change, the solid line represents the indoor temperature, and the blue line represents the temperature set value of 20 °C. It can be seen from the analysis in *Figure 4* that the error range between the indoor temperature change trend and the set value can be kept within ± 4 °C, while the indoor

http://www.aloki.hu ● ISSN 1589 1623 (Print) ● ISSN 1785 0037 (Online)
DOI: http://dx.doi.org/10.15666/aeer/1704_84498464

temperature is affected by the outdoor temperature. The increase of the outdoor temperature causes the indoor temperature to increase. A sudden drop in the outdoor temperature causes a decrease in the indoor temperature.

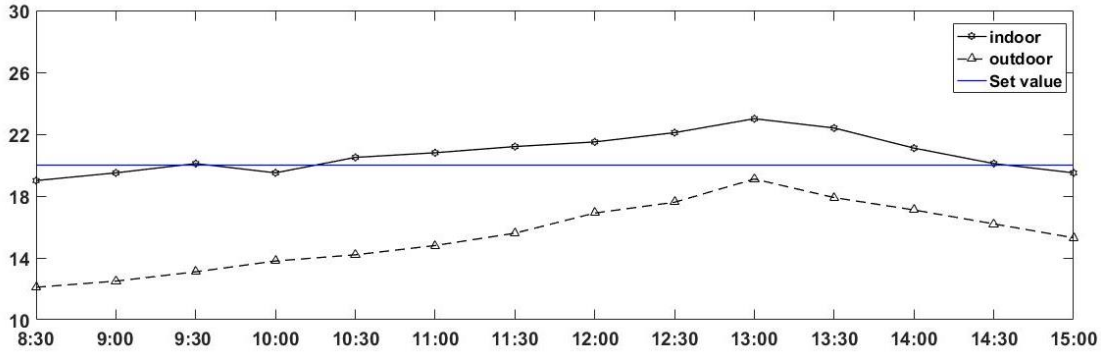

Figure 4. *Comparison of indoor and outdoor temperature*

The indoor humidity comparison results are shown in *Figure 5.*

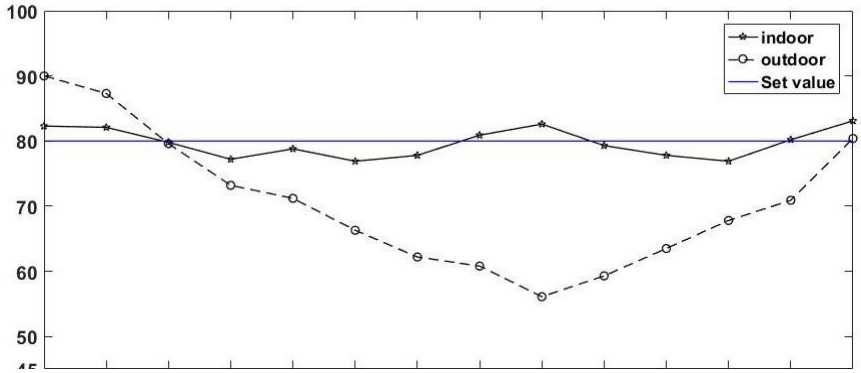

Figure 5. *Comparison of indoor and outdoor humidity*

The blue straight line is set to 80% R, the dotted line is the outdoor humidity, and the solid line is the indoor humidity. It can be seen from the analysis in *Figure 5* that the error range between the change of indoor humidity and the set value is kept at ± 10% RH, the error of humidity can be kept within the set ideal error range. The indoor temperature is increasing when the outdoor humidity is lowered.

Through the comparative analysis of the experimental data, the fuzzy adaptive PID control algorithm can respond to the environmental changes in the system in time, so that the environmental factor control process can have good performance indicators and meet the good control effect.

Conclusions

Greenhouse cultivation in agriculture has brought convenience to improve people's living standards, and has been rapidly promoted and applied. Environmental factors such as temperature, humidity, light intensity, and CO_2 concentration in the greenhouse

http://www.aloki.hu ● ISSN 1589 1623 (Print) ● ISSN 1785 0037 (Online)
DOI: http://dx.doi.org/10.15666/aeer/1704_84498464

planting environment have a great impact on crop production. Timely and effective monitoring of these environmental factors will greatly promote production. At the earliest, only the manual monitoring and control methods can be used for greenhouse environmental management. With the development of automation technology and computer technology, monitoring technology has gradually developed and is now applied to the IoT. In this regard, in the framework of the IoT, the Zig Bee node with sensors is placed in the greenhouse to collect data, and the required environmental data is collected in real time. The Zig Bee node self-organizes to form a wireless sensor network, which is passed through the Zig Bee node. Control information is passed to the controller of the actuator to control changes in environmental variables. It mainly monitors environmental parameters such as temperature, humidity, CO_2 concentration and light intensity in greenhouses, as well as remote control of water pump, exhaust, lighting and other equipment in the greenhouse. Finally, based on the characteristics of the greenhouse environment, the mathematical model of the greenhouse was established and the final model optimization was carried out. The mathematical model was established in MATLAB, and the performance of the designed controller was verified by simulation. The simulation experiments show that the fuzzy adaptive PID control algorithm is superior to the conventional PID control algorithm and pure fuzzy control algorithm in the dynamic performance index of system control, and is controlled by the following greenhouse cultivation.

Temperature and humidity control strategy

For example, in the low temperature environment in winter, the principle of controlling the temperature and then controlling the humidity should be followed. After the indoor temperature has reached a certain level, then the humidity is adjusted to meet the set requirements. If the humidity is high and the temperature is low, heating and heat preservation are the main factors. The dehumidification operation can only be achieved when the temperature rises to a specific value. In the summer when the temperature is high, the principle of controlling the humidity and then controlling the temperature should be followed. When the humidity is too low, you should turn on the humidifying device. When the temperature is too high, you need to measure the relative humidity in the room when you need to start the cooling device. The cooling device can only be started when the humidity value is less than a certain setting range.

Light intensity control strategy

The ideal value of the light intensity in the greenhouse is 20,000 to 70,000 lx. The specific implementation scheme is: (1) When the light intensity is greater than 70000 lx, open the outer shade net and close the inner shade net; (2) When the light intensity is between 20000 and 70,000 lx, if the external shading is turned off, the inner shading remains unchanged; if the external shading is turned on, the inner shading is turned off. (3) When the light intensity is less than 20000 lx, the inner and outer shade nets are closed; (4) When the light intensity is below 5000 lx and the time is between 8am and 17pm, turn on the fill light.

It can be seen that the Internet of Things will become a new “smart agriculture” production-operation-sales model, which is subversive to the traditional agricultural tillage. It is conducive to the sustainable development of agriculture in China at the present stage.

http://www.aloki.hu ● ISSN 1589 1623 (Print) ● ISSN 1785 0037 (Online)
DOI: http://dx.doi.org/10.15666/aeer/1704_84498464

Acknowledgements. The authors thank the editor and anonymous reviewers for their helpful comments and valuable suggestions. This research was supported by Zhejiang Provincial Natural Science Foundation of China under Grant No. LY15E080016 and funded by Beijing Key Lab of Heating, Gas Supply, Ventilating and Air Conditioning Engineering (No. NR2015K07). Programs supported by Ningbo Natural Science Foundation (No. 2016A610113).

Author contributions. Conceptualization: W. C.; Methodology: X. D. W.; Validation: W. C. and Q. T.; Writing—original draft preparation: W. C.; Writing—review and editing: Q. T. and X. D. W.

Conflict of interests. There are no potential competing interests in our paper, and all authors have seen the manuscript and approved to submit it to your journal. We confirm that the content of the manuscript has not been published or submitted for publication elsewhere.

Declarations. Ethical approval and consent to participate: Approved. Consent for publication: Approved. Availability of supporting data: We can provide the data.

REFERENCES

[1] Azeem, N., Arslan, C. H., Rashid, H., Sattar, A. (2018): Comparative study of hospital waste management practices at different health care units in district Faisalabad for the development of improvement strategies. – Earth Sciences Pakistan 2(2): 16-21.
[2] Buscheck, T. A., Sun, Y., Chen, M. (2012): Active CO_2 reservoir management for carbon storage: Analysis of operational strategies to relieve pressure buildup and improve injectivity. – International Journal of Greenhouse Gas Control 6(1): 230-245.
[3] Choudhari, P. P., Nigam, G. K., Singh, S. K., Thakur, S. (2018): Morphometric based prioritization of watershed for groundwater potential of Mula River basin, Maharashtra, India. – Geology, Ecology, and Landscapes 2(4): 256-267.
[4] Deng, Y. (2019): Numerical simulation of the effect of protection layer mining on the underlying strata. – Acta Microscopica 28(1).
[5] Dickinson, J. S., Buik, N., Matthews, M. C. (2017): Aquifer thermal energy storage: Theoretical and operational analysis. – Géotechnique 59(3): 249-260.
[6] Espinosafaller, F. J. (2012): A ZigBee Wireless sensor network for monitoring an aquaculture recirculating system. – Journal of Applied Research & Technology 10(3): 380-387.
[7] Fan, C., Wen, Z., Wang, F. (2011): A middleware of Internet of Things (IoT) based on Zigbee and RFID. – IET International Conference on Communication Technology and Application, pp. 732-736.
[8] Hale, G., Kapan, T., Minoiu, C. (2016): Crisis transmission in the global banking network. – IMF Working Papers 16(91): 1.
[9] Hithnawi, A., Li, S., Shafagh, H. (2016): CrossZig: combating cross-technology interference in low-power wireless networks. – International Conference on Information Processing in Sensor Networks, IEEE Press.
[10] Jang, H. J., Park, C. Y., An, J. S. (2015): Effects of a 2 nm thick Al 2 O 3, buffer layer in metal auxiliary electrode on lifetime and stable operation of large-area organic light emitting diodes. – Organic Electronics 24: 51-56.
[11] Joseph, O. T., Adepoju, A. A., Olufemi, A. (2019): Biodiversity: overexploited but underutilized natural resource for human existence and economic development. – Environment & Ecosystem Science 3(1): 26-34.
[12] Jurkowski, T. P., Ravichandran, M., Stepper, P. (2015): Synthetic epigenetics—towards intelligent control of epigenetic states and cell identity. – Clinical Epigenetics 7(1): 1-12.
[13] Kasim, S., Hassan, R., Zakaria, Z. (2019): Re-engineering in confinement method. – Engineering Heritage Journal 3(1): 18-19.
[14] Kazmierkowski, M. (2014): Advanced and intelligent control in power electronics and drives. – Industrial Electronics Magazine IEEE 8(3): 72-72.

http://www.aloki.hu ● ISSN 1589 1623 (Print) ● ISSN 1785 0037 (Online)
DOI: http://dx.doi.org/10.15666/aeer/1704_84498464

[15] Li, G., Miao, W., Jiang, G. (2017): Intelligent control model and its simulation of flue temperature in coke oven. – Discrete and Continuous Dynamical Systems - Series S (DCDS-S) 8(6): 1223-1237.
[16] Lu, D., Feng, L., Jie, P. (2019): Solar cells various appearance defects automatic simultaneous detection system of the greenhouses. – Acta Microscopica 28(1).
[17] Lu, D., Huang, X., Zhang, G., Zheng, X., Liu, H. (2018): Trusted device-to-device based heterogeneous cellular networks: a new framework for connectivity optimization. – IEEE Transactions on Vehicular Technology 67(11): 11219-11233.
[18] Messelink, G. J. (2014): Persistent and emerging pests in greenhouse crops: is there a need for new natural enemies. – IOBC/WPRS Bulletin 102: 143-150.
[19] Messo, T., Jokipii, J., Puukko, J. (2013): Determining the value of DC-link capacitance to ensure stable operation of a three-phase photovoltaic inverter. – IEEE Transactions on Power Electronics 29(2): 665-673.
[20] Nkwuda, N. G., Theophine, M. A., Okogwu, O. I. (2019): Impacts of rock mineralization and poor sanitary system on borehole waters quality and the health implications. – Earth Sciences Pakistan 3(1): 10-13.
[21] Okpoli, C. C. (2019): High resolution magnetic field signatures over akure and its environs, Southwestern Nigeria. – Earth Sciences Malaysia 3(1): 09-17.
[22] Patle, G. T., Sikar, T. T., Rawat, K. S., Singh, S. K. (2019): Estimation of infiltration rate from soil properties using regression model for cultivated land. – Geology, Ecology, and Landscapes 3(1): 1-13.
[23] Shan, P. F., Lai, X. P. (2018): Numerical simulation of the fluid–solid coupling process during the failure of a fractured coal–rock mass based on the regional geostress. – Transport in Porous Media 124(3): 1061-1079.
[24] Snipen, L. G. (2015): Predicting plant height of greenhouse grown crops with a polynomial growth rate model. – Biometrical Journal 40(3): 295-311.
[25] Sunny, A. A., Omowumi, A., Chris, O. A. (2018): Improved magnetic data analyses and enhancement techniques for lithological and structural mapping around Akure, Southwestern Nigeria. – Earth Sciences Malaysia 2(1): 16-21.
[26] Tianlei, W. (2019): Nonlinear control strategies and planning for underactuated overhead cranes. – Engineering Heritage Journal 3(1): 09-12.
[27] Timonen, J., Lääperi, L., Rummukainen, L. (2014): Situational awareness and information collection from critical infrastructure. – International Conference on Cyber Conflict IEEE, pp. 157-173.
[28] Vakilian, K. A., Massah, J. (2017): A farmer-assistant robot for nitrogen fertilizing management of greenhouse crops. – Computers & Electronics in Agriculture 139: 153-163.
[29] Wertheim, J. O., LeighBrown, A. J., Hepler, N. L. (2014): The global transmission network of HIV-1. – Journal of Infectious Diseases 209(2): 304.
[30] Yahya, N., Aziz, F., Enriquez, M. A. O., Aizat, A., Jaafar, J., Lau, W. J., Yusof, N., Salleh, W. N. W., Ismail, A. F. (2018): Preparation and characterization of Lafeo3 Using dual-complexing agents for photodegradation of humic acid. – Environment & Ecosystem Science 2(2): 30-34.
[31] Yi, L. (2018): 3. Difference analysis of economic factors on per capita education level between the ethnic provinces and the western region. – Argos 35(68).
[32] Yoh-Han, P., Phillips, S., Sobajic, D. (2016): Neural-net computing and the intelligent control of systems. – International Journal of Control 56(2): 263-289.
[33] Yusof, K. H., Seman, N., Jamaluddin, M. H. (2015): Design of ultra wideband 3 dB coupled-line coupler and 90° power divider with zig-zag-shaped slot for wireless communication applications. – Wireless Personal Communications - An International Journal 84(4): 2599-2611.
[34] Zakeri, B., Syri, S. (2015): Electrical energy storage systems: a comparative life cycle cost analysis. – Renewable & Sustainable Energy Reviews 42(C): 569-596.

http://www.aloki.hu ● ISSN 1589 1623 (Print) ● ISSN 1785 0037 (Online)
DOI: http://dx.doi.org/10.15666/aeer/1704_84498464

[35] Zeng, J. (2018): A cellular automata model to simulate micro-characteristics of tunnel traffic flow. – Acta Microscopica 27(4).
[36] Zhang, W., Yang, J., Fang, Y., Chen, H., Mao, Y., Kumar, M. (2017): Analytical fuzzy approach to biological data analysis. – Saudi Journal of Biological Sciences 24(3): 563-573.
[37] Zhang, X. G., Liu, L. S., Wu, Y. H., Cui, Y. G. (2018a): Existence of infinitely solutions for a modified nonlinear Schrodinger equation via dual approach, electron. – Differential Equations 147: 1-15.
[38] Zhang, X. Q., Liu, L. S., Zou, Y. M. (2018b): Fixed-point theorems for systems of operator equations and their applications to the fractional differential equations. – Journal of Function Spaces 2018.
[39] Zheng, S. D., Zhao, W., Zhang, L., Li, J., X., Ashraf, M. A. (2018) Experimental study on the influence of footstep motion on resuspension of particles in small box. Journal of Intelligent & Fuzzy Systems. 35 (4): 4097-4105.
[40] Zou, Y. M. (2018): Positive solutions for a fractional boundary value problem with a perturbation term. – Journal of Function Spaces 2018.

http://www.aloki.hu ● ISSN 1589 1623 (Print) ● ISSN 1785 0037 (Online)
DOI: http://dx.doi.org/10.15666/aeer/1704_84498464

FRONT SYSTEMS AND SUSPENDED SEDIMENT DYNAMICS OF LINGDINGYANG BAY IN THE SUMMER, PEARL RIVER ESTUARY, SOUTH CHINA

WEI, H. – ZHU, L.*

School of Civil Engineering and Transportation, South China University of Technology, GuangZhou 510641, China
(e-mail: 772365131@qq.com – H. Wei)

**Corresponding author*
e-mail: lszhu2000@vip.163.com

(Received 8th Mar 2019; accepted 21st May 2019)

Abstract. Lingdingyang (LDY) is an important navigation waterway for the Pearl River delta (PRD), and an important passage for fresh water and sediments entering the sea. The data and hydrological information, including SSC, current, water level, and bed sediment was collected on July 6-7, 2005 to analyze its characteristics, and sediment transport. The data was entered into a hydrodynamic simulation model used to characterize the processes of sedimentation and morphological evolution of the Pearl River estuary (PRE). LDY was divided into three sub-areas dominated by (1) west shoal area, (2) jet flow area, and (3) saline water area. Navigation engineering and other human activities result in an increase of deposition rate. These characteristics can be greatly accelerated by human activities. Field data and model results indicate that the front system, composed of the shear front and tide incursion front, has an important impact on sedimentation.
Keywords: *fresh water, a hydrodynamic simulation model, navigation engineering, deposition rate, silting characteristics*

Introduction

The Pearl River delta in southern China is one of the most complex deltas in world. It is a typical river network delta including three converging rivers and eight outlets emptying to the sea (Allen et al., 1980; Daniel et al., 2018). The three rivers are the West River (WR), North River (NR) and East River (ER). The eight outlets are the Humen (HM), Jiaomen (JM), Hongqimen (HQM), Hengmen (HM), Modaomen (MDM), Jitimen (JTM), Hutiaomen (HTM), and Aimen (AM). Humen and Aimen are tidal-dominated estuaries. The other six are fluvial-dominated mouths. Humen, Jiaomen, Hongqimen and Henmen, also called the eastern four mouths, empty into the tidal-dominated estuary of Lingdingyang (LDY) bay. LDY is characterized by three shoals and two channels, which refer to the West, Central, and East shoals, and the East, and West channels (Ren et al., 2001; Nwankwoala, 2019). The west shoal is an important buffer between Lingdingyang bay and the eastern three river mouths (JM HQM and HM). It is also a water passage carrying sediment from the three river mouths and a protecting barrier for the Lingding navigation channel.

Tides of LDY belongs to irregular semidiurnal mixing tides, low tides and high tides occurring two times a day, with a tidal coefficient of 0.94 ~ 1.77. The LDY tidal range is less than 2 m, and due to the influence of the trumpet shaped topography, increasing tidal range from outer bay to head. Because of runoff, the tidal range descends from HUM to HM. Outer sea area, greatly affected by tide, ebb duration is approximately equal to flood duration. River outlet, affected by runoff, ebb duration is

http://www.aloki.hu ● ISSN 1589 1623 (Print) ● ISSN 1785 0037 (Online)
DOI: http://dx.doi.org/10.15666/aeer/1704_84658484

longer than that of the flood. The flood and ebb duration ratio, is 0.93 ~ 1.26 in dry season, 1.05 ~ 1.55 in wet season.

An estuary is a semi-enclosed coastal body of water, which is connected to the open sea, extending to a river to the limit of tidal influence, and within which sea water is diluted with fresh water derived from land drainage (Cameron et al., 1963 ; Van Maren et al., 2016; Dalrymple et al., 1992; Dai et al., 2013, 2012; 2011a; Rahim et al., 2018). The estuary acts as a filter between the land and the ocean (Dai et al., 2011b), and sediment traps, retaining a proportion of their river and marine borne sediment load in the intertidal zone (Dellwig et al., 2000; Sharjeel et al., 2019).

Dynamics of estuarine suspended sediments are very complex and strongly variable over time scales ranging from seconds to years (Dyer et al., 1988). In tidal estuaries, fine sediment dynamics is often related to the Mechanism of turbidity maximum zone (Fettweis et al., 2012; Ferriera et al., 1997; Grabemann et al., 1997; Hume and Herdendorf, 1988; Omini and Akpang, 2018). Subsequently, many literatures studied mainly TMZ and its response to estuarine forces (Jalón-Rojas et al., 2017, 2015; Jia et al., 2013; Chen et al., 1999; Largier, 1992; Shi, 2010). Another important process is estuarine front system, which has been given more attentions to since 1990's (Williams et al., 2015; Li, 2004; Qiao, 2018). Fronts may exert control on the surface and water column sediment and pollutant partitioning and also on the distribution and persistence of bed load transport pathways (Li et al., 2003). Both estuarine circulation and tidal asymmetry are of great importance to the fine sediment processes (Lick et al., 1994), and the two processes are very obvious in front system.

Previous research on sediments of LDY has involved the development of a mathematical tidal model (Lick et al., 1995), physical model (Lu et al., 2005), ground sampling surveys and theoretical analysis (Le Hir et al., 2001; Pinckney and Dustan, 1990; Pritchard, 1967). Estuarine front is an important dynamical process, which exerts an influence on sedimentation (Reeves and Duce, 2001; Sarwar et al., 2019). According to dynamics, there are four types fronts in LDY, tidal intrusion front, head land front, oblique plume front, and shoal front (Ren et al., 2010).

As there are enough gradients of density and velocity in waters, the fronts would be formed. Shelf saline water intruding there that make the difference of sediment dynamic process and sediment grain distribution in spatial, i.e. coarse, fine, and fairly coarse from upper to lower regions (Ren et al., 2006; Sarker et al., 2019).

According to geomorphology, LDY can be divided into three geo-systems, tide inlet of HM (Northwest LDY), fluvial dominated area (West LDY), shelf saline water area (south LDY) (Duck and Wewetzer, 2001). The boundary of these power structures is the interface between two kinds of fronts, namely the continental shelf front and shear front.

This paper focuses on the characteristics and sedimentation, as well as impacts of recent silting. Our goal was to understand the processes associated with front system and human activity leading to sedimentation during the wet season (Jiang et al., 2018). The LDY is dominated by runoff and most sediment comes from eastern outlets of PRD during the wet season. The system of shoals and channels plays an important role in sediment transportation and front systems also result from the geography of the system (Savenije, 2006). Human activity has an enormous impact on sedimentation and this is reflected in system evolution.

http://www.aloki.hu ● ISSN 1589 1623 (Print) ● ISSN 1785 0037 (Online)
DOI: http://dx.doi.org/10.15666/aeer/1704_84658484

Materials and methods

Morphology

LDY is a funnel-shaped estuary located on the east side of the PRD (*Fig. 1*). The width of bay head is 4 km, width of bay mouth is 65 km, longitudinal length is 60 km, and total area 2100 km^2.

The West shoal is located in the west side of the Lingding navigation channel. It receives water and sediments from Hengmen, Hongqimen, Jiaomen, and its area is 185 km^2. In the 1940's, floods scoured out the underwater levee, which gradually eroded then become the North branch. The North branch plays an important role in sediment transportation between the South branch and the Lingding channel (*Fig. 2*). The North branch acts as a flood diversion channel during the flood season, accelerates the flood discharge, and reduces flood pressure on Hongqimen and Henmen. The depths of North branch, South branch, and Lingding channel are 3-5 m, 7-8 m and 15 m respectively. Using the method of dynamic geomorphology, the channel system of the shoal can be divided into flood-dominated channels (flood channel) and ebb-dominated channels (ebb channel) in part B of *Figure 1*. During the dry season, tidal dynamics dominates the shoal, and the net transportation of sediments differs in the two channel types. In the wet season, the entire shoal is dominated by river dynamics and the net transportation of sediments seaward is consistent among the channels. Because the main river bifurcates easterly, the river dynamics weaken. The middle and lower segments evolve from an ebb channel to a flood channel in part B of *Figure 1*.

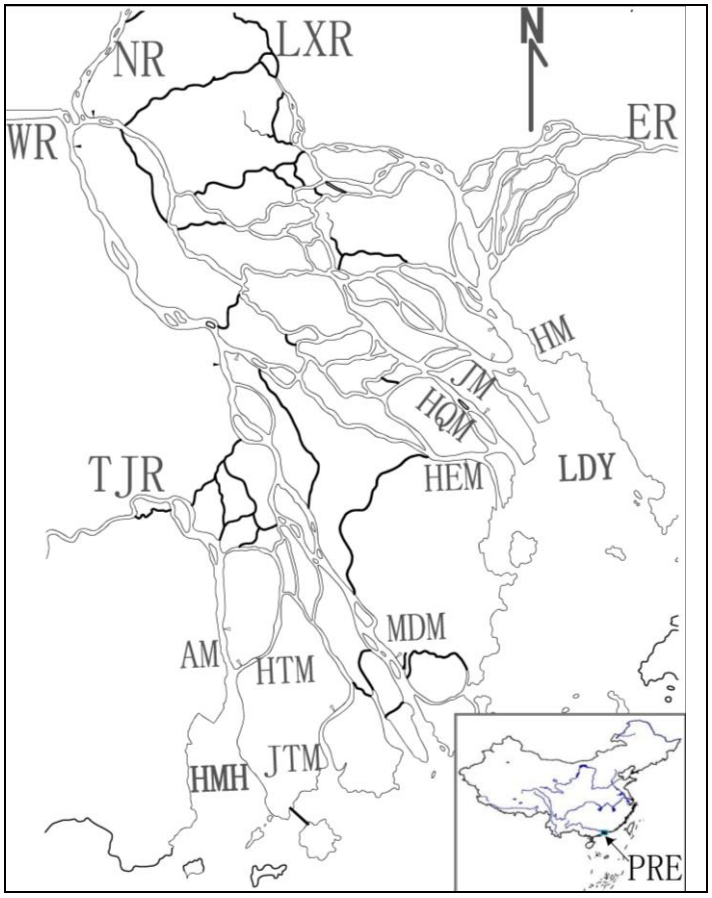

Figure 1. *Sketch of PRE*

http://www.aloki.hu ● ISSN 1589 1623 (Print) ● ISSN 1785 0037 (Online)
DOI: http://dx.doi.org/10.15666/aeer/1704_84658484

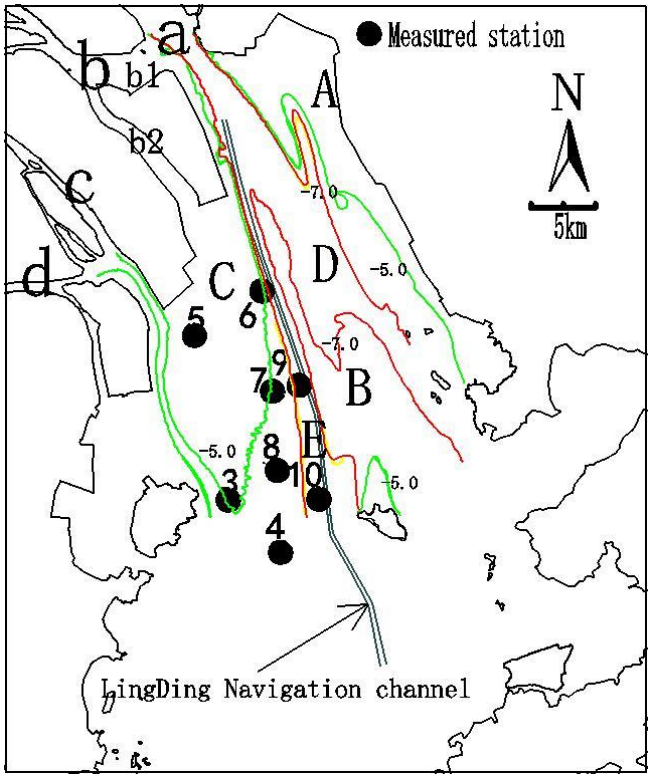

Figure 2. *Sketch and measured station of study area (A: East tidal flat, B: Central tidal flat, C: West tidal flat, D: East channel, E: West channel; a: Humen, b: Jiaomen, c: Hongqimen, d: Hengmen, b1: north branch, b2: south branch)*

Hydrology and sediment

The Pearl River has a mild subtropical monsoon climate with relatively abundant precipitation. Mean annual rainfall is 1526 mm and this is concentrated in 9 months which, together, account for 80% of the annual rainfall. SSC of the Pearl River is the lowest of the seven major China rivers. However, sediment transport capacity from runoff is large. Average sediment transport capacity is 85.7 million tons, which is the third largest amount for China rivers. The average SSC of Gaoyao station of West River is 0.320 kg/m^3.

PRE has an irregular semidiurnal tide, and the tidal range is small. The mean tidal range is 1.60 m and the maximum tidal range is 3.36 m. The PRE is a typical weak tidal estuary. Flood tide (current that moves toward shore) duration lasts 7 h and 20 min and mean ebb duration lasts 5 h and 30 min. The flood tide duration during the wet season is shorter than that in the dry season.

LDY is a micro-tidal estuary. With a funnel-shaped topography, the tidal energy converges and tidal range increases from mouth to head. Average ranges of Chiwan, Sanbanzhou, and Dahu stations were 1.36 m, 1.59 m, and 1.69 m respectively. Tides are irregular semidiurnal mixed with ebbing and flooding twice a day. SSC during the wet season is larger than that of dry season, and SSC varies with ebb and flood (*Table 1*). In the wet season, fine sand is the major component of bed sediment at Hongqimen and Jiaomen. Particle size at these two outlets ranges between 0.1 mm and 0.5 mm, which occupies 90% of the total. The bed sediment of Humen is composed of medium coarse sand with a median particle diameter of 0.244 mm.

http://www.aloki.hu ● ISSN 1589 1623 (Print) ● ISSN 1785 0037 (Online)
DOI: http://dx.doi.org/10.15666/aeer/1704_84658484

Table 1. *SSC of eastern four outlets (unit, kg/m^3)*

Outlet name	Season	Flood		Ebb	
		Average	Maximum	Average	Maximum
Henmen	Dry season	0.029	0.071	0.031	0.059
	Wet season			0.570	0.670
Hongqimen	Dry season	0.021	0.050	0.021	0.034
	Wet season			0.720	0.830
Jiaomen	Dry season	0.044	0.110	0.035	0.074
	Wet season			0.420	0.610
Humen	Dry season	0.083	0.160	0.074	0.130
	Wet season	0.130	0.190	0.200	0.310

Data

We used the data of the second phase project of Zhongshan port. Synchronous hydrology sediment testing was completed by the hydrology and Water Resources Survey Bureau of the Yangtze River Water Conservancy Committee.

The survey period included tidal cycles from July 6 to July 7 in 2005. Fourteen boats are used for fixed-point measures, and measured items included velocity, SSC, and salinity. Three water level stations were established. The scale of the topographic survey was 1:5000. *Figure 2* shows the sites of the measuring stations and bed sediment sample points.

Hydrological testing at fixed stations was done by using a conventional current meter that was fixed to a boat. SSC samples were obtained by using the 2000 CC horizontal type sampler once per hour. If the depth was greater than 5 m, we used the six point method (surface, 0.2 h, 0.4 h, 0.6 h, 0.8 h, bottom), or the three point method (0.2 h, 0.6 h, 0.8 h).

Suspended particles were analyzed using a centrifugal sedimentation particle size distribution instrument. We sampled bed sediments for particle size analysis using a cone type sampler, ensuring that the dry weight exceeded 50 g. The distance between two samples sites is less than 3 km. Analysis of bed sediment was done with a sonic vibration automatic sieving particle size analyzer and wide particle size analyzer. Salinity was determined using an electrode salinometer.

Mathematical model

The paper used Delft3D to model current, salinity, sediments. Delft Hydraulics has developed a unique, fully integrated computer software suite for a multi-disciplinary approach and 3D computations for coastal, river and estuarine areas.

It can carry out simulations of flows, sediment transports, waves, water quality, morphological developments and ecology. It has been designed for experts and non-experts alike. The Delft3D suite is composed of several modules, grouped around a mutual interface, while being capable to interact with one another. Delft3D-FLOW, which this manual is about, is one of these modules. Delft3D-FLOW is a multi-dimensional (2D or 3D) hydrodynamic (and transport) simulation program which calculates non-steady flow and transport phenomena that result from tidal and meteorological forcing on a rectilinear or a curvilinear, boundary fitted grid.

http://www.aloki.hu ● ISSN 1589 1623 (Print) ● ISSN 1785 0037 (Online)
DOI: http://dx.doi.org/10.15666/aeer/1704_84658484

In order to model the hydrodynamics and cohesive sediments, a model covering the eight outlets and outer sea was established. The computed area was divided into 2050000 cells. The smallest side length in these cells was 10 m, and the largest was 1000 m. It is depth chart of LDY (*Fig. 3*). The model setup is shown in the following figure (*Fig. 4*), Model correction in the following figure (*Fig. 5*). It is the main modelling parameters for cohesive sediments (*Table 2*).

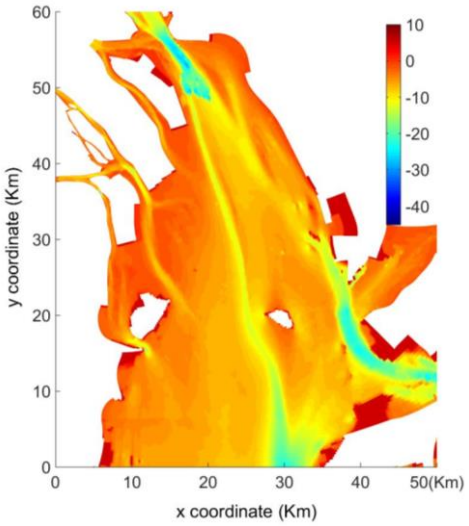

Figure 3. *Depth chart of LDY*

Table 2. *Model parameters for cohesive sediments*

Parameter	Number	Units
Setting velocity	0.06-0.20	mm/s
Bed shear stress of sedimentation	0.30-.0.50	N/m^2
Bed shear stress of erosion	0.55-0.80	N/m^2
Erosion parameter	1.2e-4--1.8e-4	$kg/m^2/s$
Initial layer thickness	0.1	m

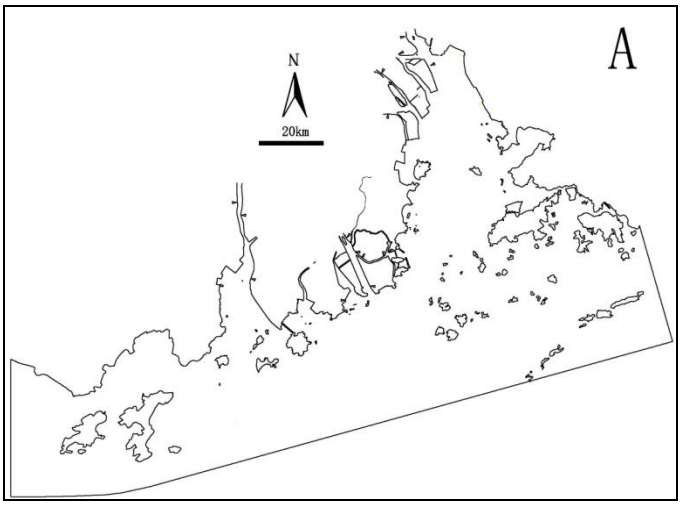

http://www.aloki.hu ● ISSN 1589 1623 (Print) ● ISSN 1785 0037 (Online)
DOI: http://dx.doi.org/10.15666/aeer/1704_84658484

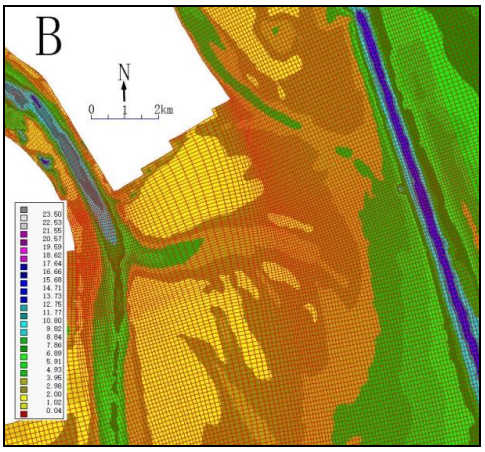

Figure 4. *Model area (A) and local grid configuration (B)*

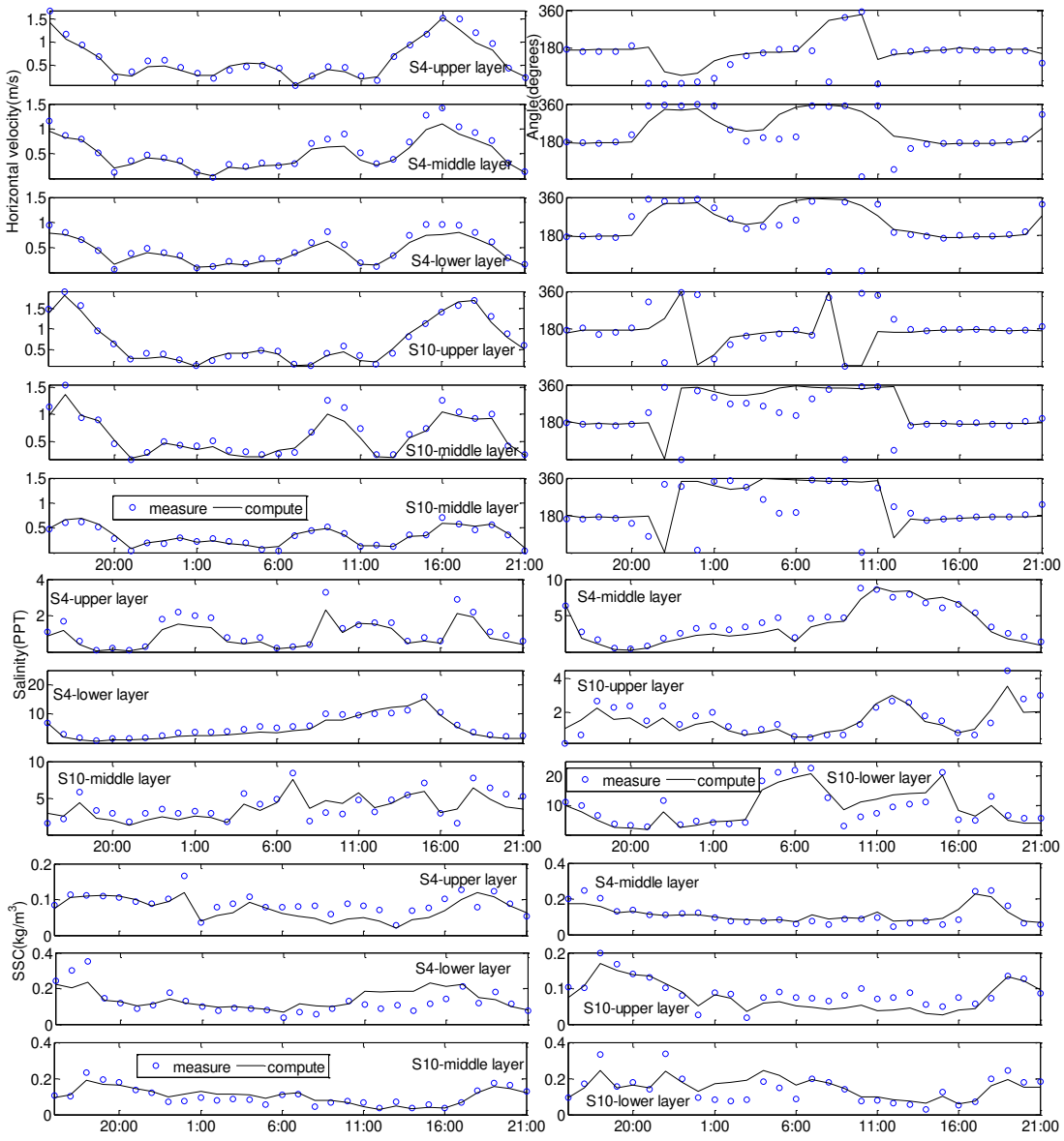

Figure 5. *Model calibration figures*

http://www.aloki.hu ● ISSN 1589 1623 (Print) ● ISSN 1785 0037 (Online)
DOI: http://dx.doi.org/10.15666/aeer/1704_84658484

Results

Hydrodynamic characters

In wet season, LDY is dominated by discharge from runoff, and Salinity of LYD except a small south fraction is zero. The chart of modeling current field of model is shown in *Figure 6*. In flood tide duration, the velocity is very small in LDY, even no flood tide current in outlets. But, the ebb tide flow is very large, reaching above 1.0 m s^{-1} (*Fig. 6*).

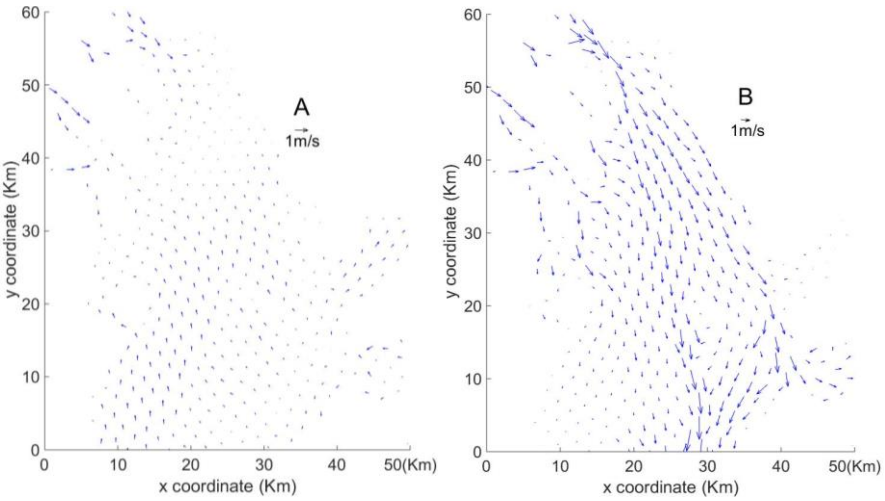

Figure 6. *Current field of model (A: flood tide, B: ebb tide)*

High saline water from continental shelf intruders along both sides of Hong Kong Island to LDY, and salinity of lower layer accounts for over 30‰ (*Fig. 7*). The tide intrusion front (also tide intrusion front) comes into being due to the large gradient of salinity and density. However, because of the difference of velocity and landforms due to shoal and trough in west shoal border zone of LDY, another front is generated.

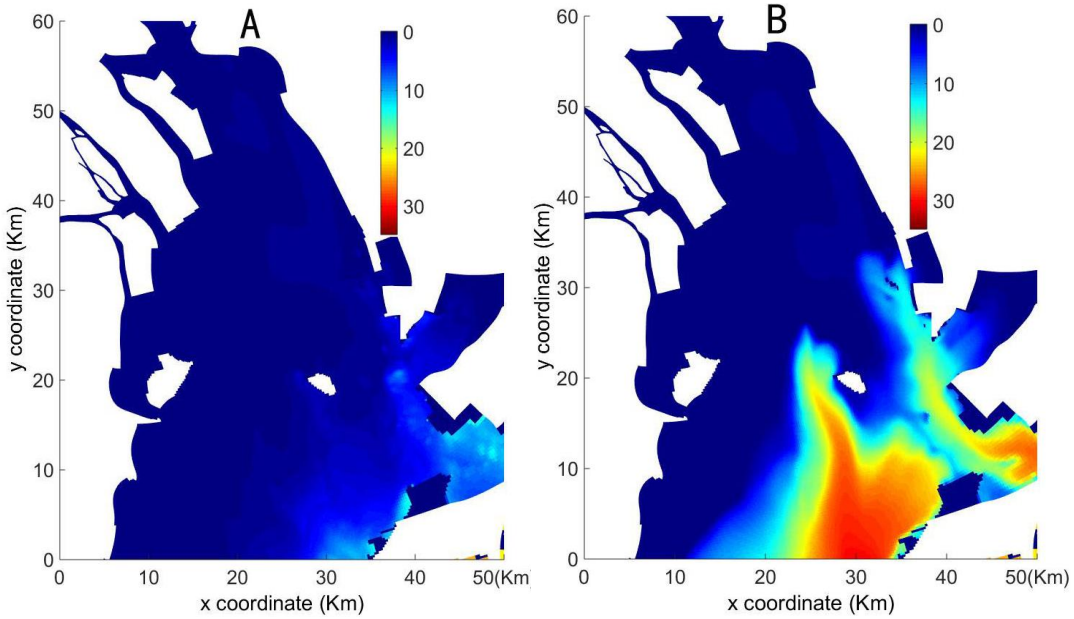

http://www.aloki.hu ● ISSN 1589 1623 (Print) ● ISSN 1785 0037 (Online)
DOI: http://dx.doi.org/10.15666/aeer/1704_84658484

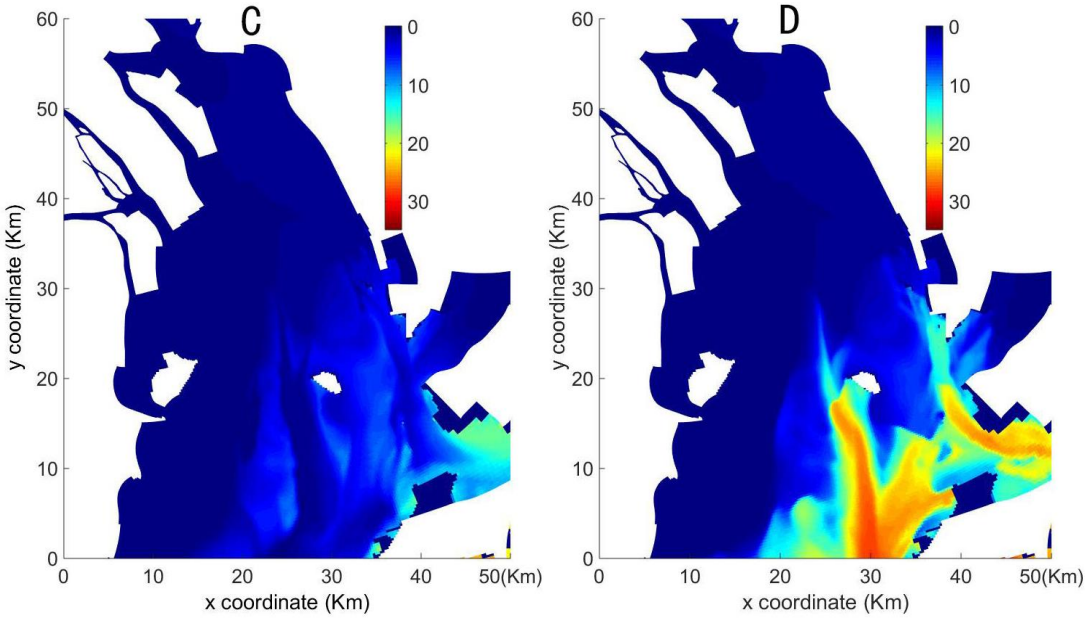

Figure 7. *Salinity charts (‰; A: surface, flood, B: bottom, flood, C: surface, ebb, D: bottom, ebb)*

Based on the analysis above, the LDY can be divided into three type sub-areas of dynamic sedimentation, west area, jet-flow area, salt water area (*Fig. 8*). The west area is dominated by discharge from JM, HQM, HM, and flow seaward along West shoal into outer sea. Salt water area refers to the southeast of LDY, and the main characteristic is high salinity and density, resulting in three dimensionality of flow. Large part area of LDY is affected by jet-flow (Shilun, 1994) due to ebb current from HUM. The jet-flow structure is complicated, and evolves into plume flow in the end of jet-flow, which is suffered from salt water from middle and lower layer due to continental shelf water intrusion. So, fresh water from HUM flow seaward through upper layer.

Three dynamical structures interact through front (*Figs. 9* and *10*), resulting in control of water and sediment movement, also control the stability of main channel and sedimentation balance. According to the salinity, these dynamical structures correspond to three water mass, the fresh water, diluted water and sea water. The core part of the estuary is controlled by diluted water.

The diluted water mass is under the action of runoff discharge, and develops seaward in flood season. During the dry season, it recedes deeper into the land. In the dry season, the length of diluted water can reach 83 km, while the flood season is below 40 km. In above section of stagnation point, the kinetic is barotropic, and the net material is to transport seaward. In lower section of stagnation point, the pressure is baroclinic, and net material transport landward.

According to the surveying data, LDY is dominated by seaward flow. The velocity is faster and the duration is longer during the ebb period than in flood tide. The velocity of the middle and lower layers is greater than the surface downstream from the West shoal during the flooding period. During ebb, the surface velocity is the greatest. During both flood and ebb, the surface velocity upstream is greatest in surface, middle and bottom layers. Because flows from Lingding channel, North branch, and South branch of

http://www.aloki.hu ● ISSN 1589 1623 (Print) ● ISSN 1785 0037 (Online)
DOI: http://dx.doi.org/10.15666/aeer/1704_84658484

Jiaomen converge in the West shoal, surface velocity increases seaward during ebb. The majority of LDY was dominated by freshwater. Their middle and bottom layers were dominated by highly saline water from the shelf in the summer, especially during the flood period. The bottom maximum salinities of stations 4, 10 and 9 were, respectively, 22‰, 17.1‰, and 7.8‰ during the flood period, and the salinity of the rest stations was zero. *Figure 7B* and *D,* illustrates the lower layer salinity of the lower section of the LDY. During the flood period, a salt wedge intrudes landward, and the salinity structure is highly stratified. This is referred to as the "tide inrush front" (Simpson and Turrell, 1986; Oyedotun, 2019).

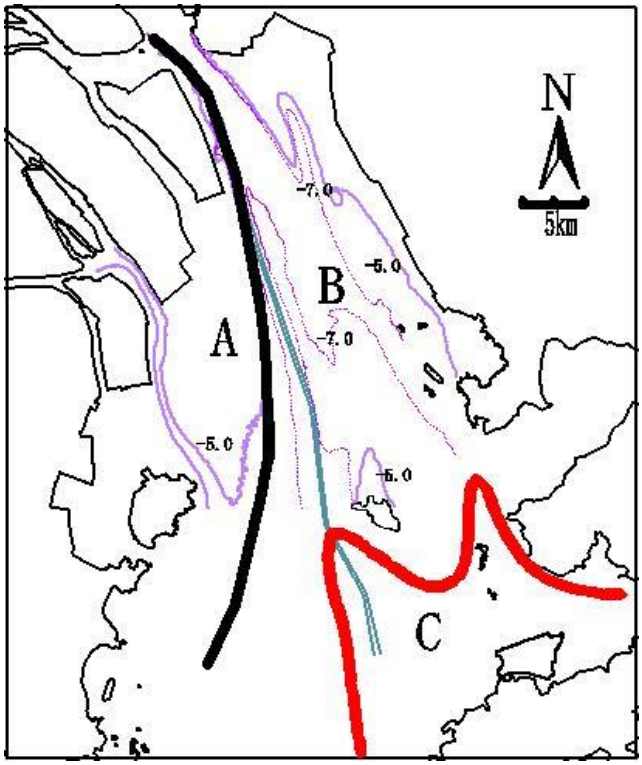

Figure 8. *Dynamical subarea (the black broad line, estuarine front, the red broad line tide intrusion front, also saline wedge, A: fluvial area, B: jet-flow area, C: saline water area)*

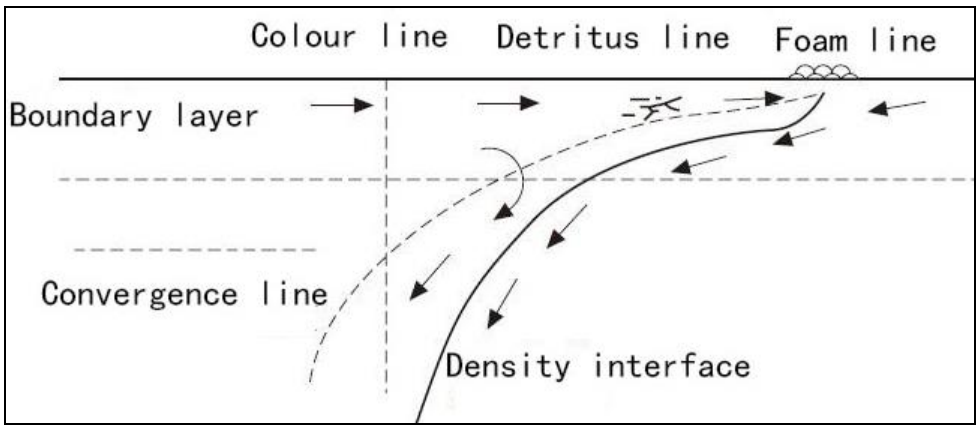

Figure 9. *Schematic diagram of a vertical section perpendicular to a frontal convergence zone. (After Klemas and Polis, 1977; Ferrier, 1997)*

http://www.aloki.hu ● ISSN 1589 1623 (Print) ● ISSN 1785 0037 (Online)
DOI: http://dx.doi.org/10.15666/aeer/1704_84658484

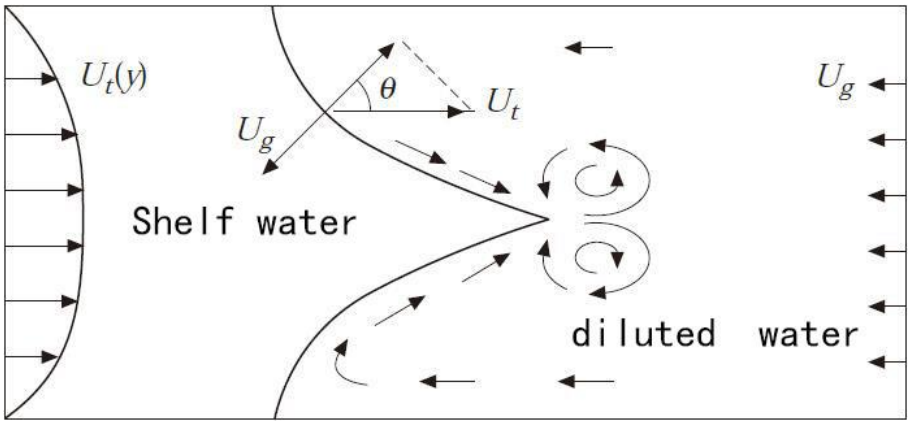

Figure 10. *Schematic illustration of the interaction of tidal intrusion front with the lateral shear to produce a V-shaped front with a single point convergence at the apex and attendant gyres. (After Simpson and Turrell, 1986; Ferrier, 1997)*

Front system and suspended sediment transportation

Sediments, moving from river to sea, must pass through three hydrodynamic sections. The three sections are the river, near mouth, and estuary. The downstream limit of the river section is the tidal limit (Sanshanjiao), the near mouth section is the area between the tide limit and the tidal current limit (near the 21st Stream). The estuary section is the area between the tidal current limit and the front of the shelf water (near Hong Kong). These three sections play important roles in sediment transportation and deposition. When flow enters the tidal limit, the flow will be surfing from the reaction force of the tide and the longitudinal gradient of surface level will flatten out and flow velocity will decrease (Nouaim et al., 2019). As a result, the relative coarse silt group of suspended sediments will settle on the bed and because the transportation force has decreased, the coarse sand and gravel will be deposited. Field data regarding the first settlement ratio is not available but in the Yangtse River estuary, 10-15% of suspended sediment will be deposited on the bed (Simpson and Nunes, 1981). Sediment that enters the estuary section suffers from bidirectional flow during flood and ebb periods. Sediment that is temporarily deposited on the bed during floods erodes due to ebb currents. Flow, which enters the West shoal, diffuses on the shoal surface, velocity declines and sediments deposit on the bed. The two flows from the West shoal and west channel converge at the edge of the West shoal and form a shear front (*Figs. 11* and *12*). Because of significant salt water invasion into the LDY from the middle and bottom layers, tide invasion fronts become important in the southeast area of LDY. Sediments in the front will settle again. According to the July 2005 data, about 3% of the total suspended sediment deposits, and the majority of the bed load is trapped. The ancient riverbed sand can be transported to the estuary from human agitation resulting from sand mining. SSC chart is shown in *Figure 11,* which show clearly transportation trend of suspended sediments in three water mass.

The silting content is high, and Mean percent content of stations 1, 5, 6, 7, 8 is respectively 73.8%, 70%, 68.2%, 66.9% and 66.5%, indicating that the percentage of silt decreases seaward (*Table 3*). Average silt percentage of stations 9 and 10 was 65.5% and 66.1%, respectively, which is less than that of the West shoal. Silt content of suspended matter decreases seaward indicating that coarse sediments settle gradually

http://www.aloki.hu ● ISSN 1589 1623 (Print) ● ISSN 1785 0037 (Online)
DOI: http://dx.doi.org/10.15666/aeer/1704_84658484

during the transportation process, and suspended sediment becomes bed load. Surface velocity at ebb of stations 5, 6, and 4 increased longitudinally and the mean silt content decreased. Median diameter of bed sediment decreases seaward. Median particle diameters at stations 6, 7, 8 and 4 were 0.071 mm, 0.068 mm, 0.026 mm, and 0.026 mm, respectively. The latitudinal change rule of median diameter and percentage of sand in bed sediment is related to the longitudinal variation. Median diameter and percentage of sand decreased from the West shoal to the west channel. *Figure 12* is the SSC section of west channel, which illustrate that suspended sediments is transported through the upper layer of salt water area. Front systems and sediments transportation are shown in *Figures 13* and *14*.

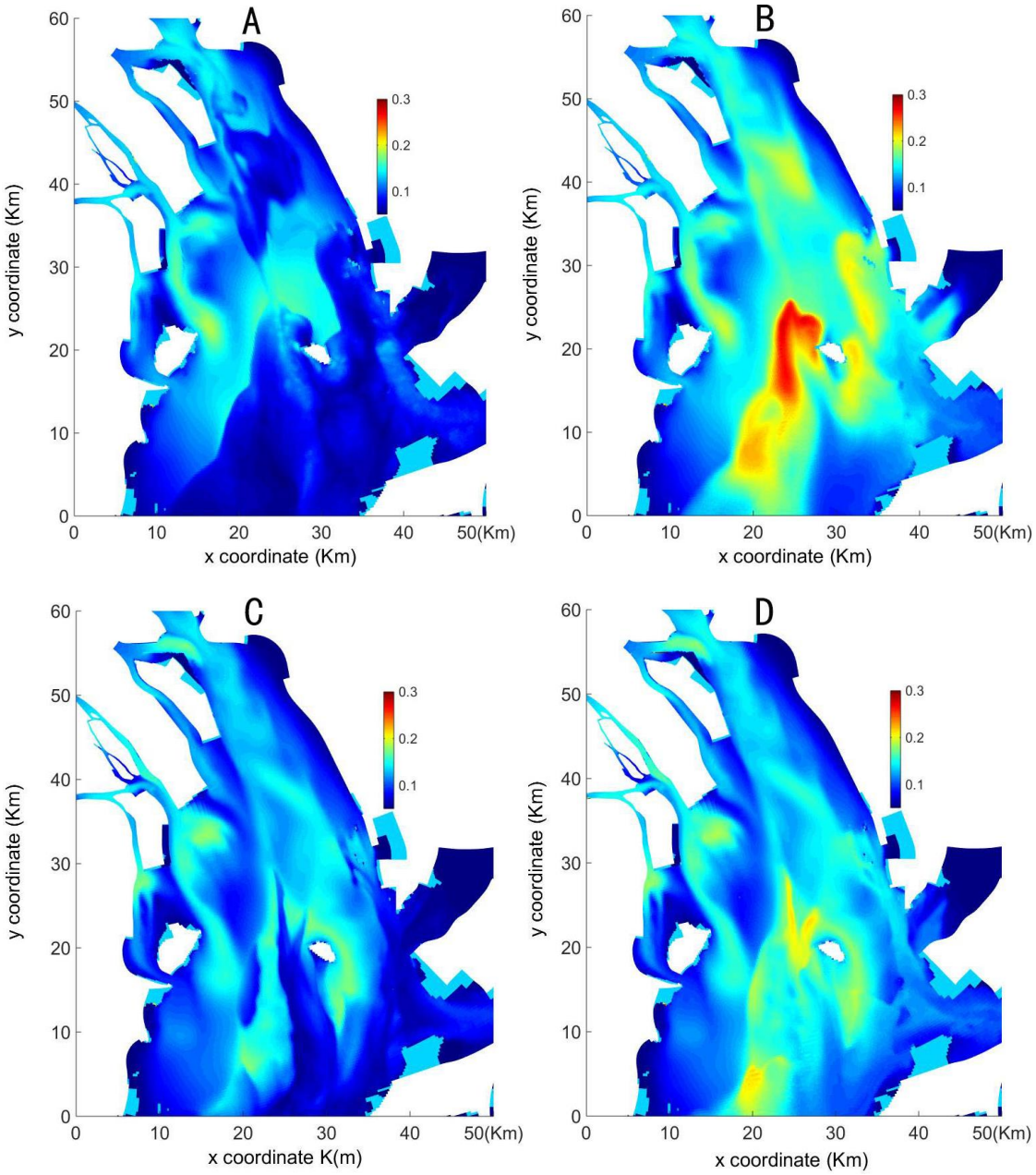

Figure 11. *SSC chart (kg/m^3, A: flood, upper layer; B: flood, lower layer; C: ebb, upper layer, D: ebb, lower layer)*

http://www.aloki.hu ● ISSN 1589 1623 (Print) ● ISSN 1785 0037 (Online)
DOI: http://dx.doi.org/10.15666/aeer/1704_84658484

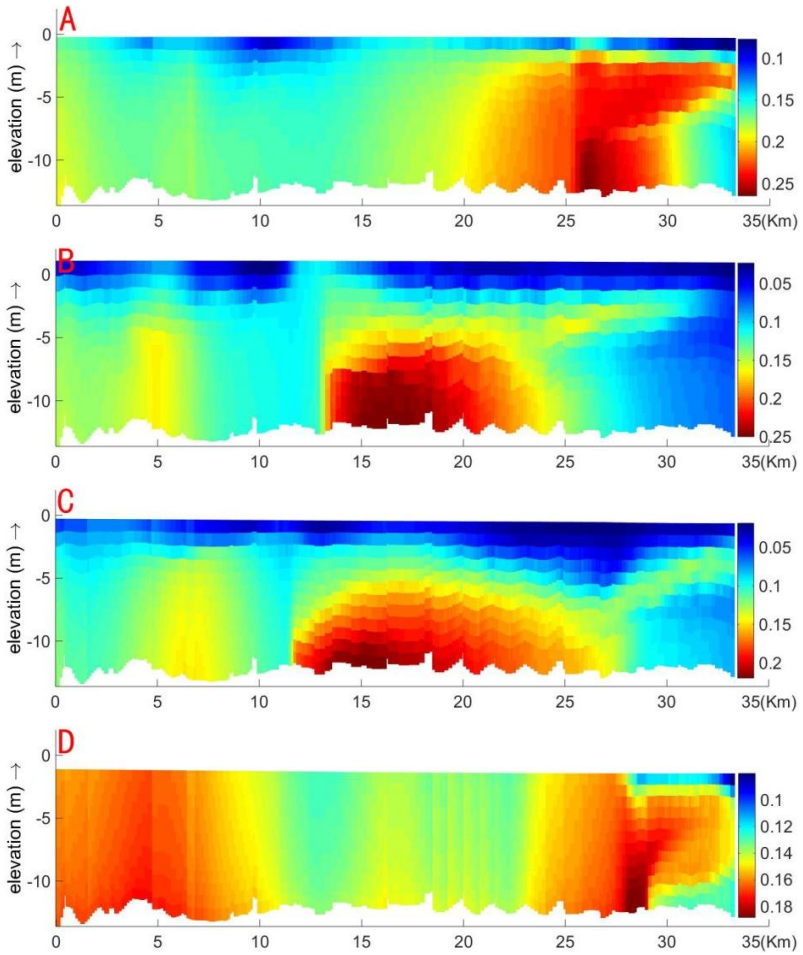

Figure 12. *SSC section of Lingding navigation channel (A: flood period, B: flood slack, C: ebb period, D: ebb slack)*

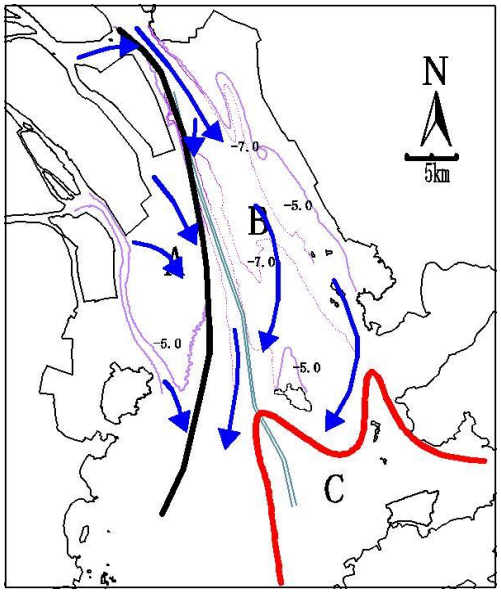

Figure 13. *Front systems and sediments transportation (blue arrow: transportation orientation of cohesive sediment)*

http://www.aloki.hu ● ISSN 1589 1623 (Print) ● ISSN 1785 0037 (Online)
DOI: http://dx.doi.org/10.15666/aeer/1704_84658484

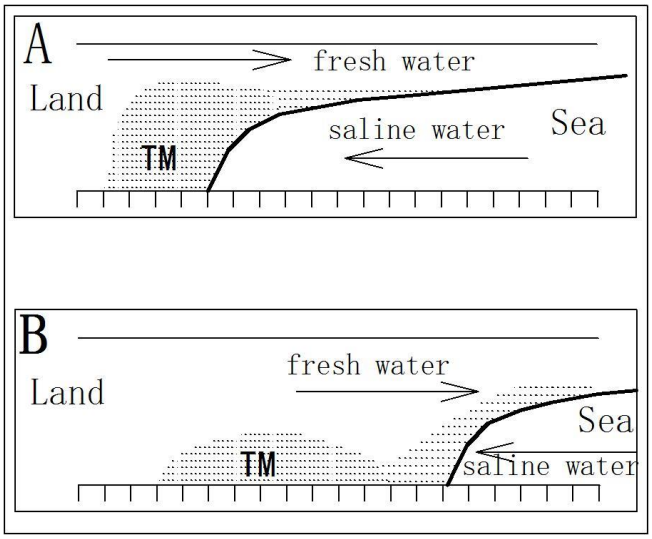

Figure 14. *Conceptual model of estuarine circulation and sediment transportation (A: flooding tide, B: ebbing tide; TM: turbidity maximum)*

Table 3. *Percentages of fine sand and clay in suspended sediment*

Items		1	5	6	7	8	4	9	10
Silt	Mean	73.8	70.0	69.3	68.2	66.9	66.5	65.5	66.1
	Max	87.3	67.7	72.4	74.9	70.6	76.0	65.5	67.4
	Min	62.0	59.6	57.4	57.4	56.8	52.1	51.8	51.4
Clay	Mean	26.2	30.0	30.7	31.8	33.1	33.5	34.5	33.9
	Max	38.0	40.4	42.6	42.6	43.2	47.9	48.2	48.6
	Min	12.7	32.3	27.6	25.1	29.4	24.0	34.5	32.6

Action of front systems on sedimentation

Estuaries are located in the transition zone between rivers and the sea, and have zones or fronts which have significant impacts on sedimentation and pollutants. There are at least three types of fronts in LDY: tidal intrusion, headland, and shoal fronts (Talke et al., 2009). Based on charts of currents, landforms, and measured data, we propose the use of shear front instead of shoal front. The physical significance of a shear front is clearer than that of a shoal front. *Figure 7* shows that there is salt wedge southeast of the LDY, which varies with ebb and flood (Yang, 2018). In fact, this is the tide intrusion front. Therefore, the tide intrusion front and the shear front become the main front system of the LDY. Fronts are formed by several mechanisms, including tidal intrusion, axial convergence, advective flow, and flow separation. Fronts act as temporary barriers, inhibit exchange of water masses, and entrap free particulate materials. We suggest that, in terms of suspended sediment transport through and within estuaries that are characterized by fronts, such features should be considered as "sieves" in the estuarine sediment transfer system (Townend, 2005). The "sieve" or trapping function for sediment is achieved by front systems of the estuary. Sediment transport characteristics of shear fronts include: (1) in a northerly direction, the surface water and sediments move downward, while in deeper water the sediments move upward; and (2)

http://www.aloki.hu ● ISSN 1589 1623 (Print) ● ISSN 1785 0037 (Online)
DOI: http://dx.doi.org/10.15666/aeer/1704_84658484

in a westerly direction, the surface water and sediments move into the channels, while in deeper water the sediments move into the shoals (Townend, et al., 2000). Therefore, the shear fronts between the shoals and the channel act as a barrier affecting the sediment deposition into the deep channel from the shoals (Uncles and Stephens, 1993). Fronts play an important role as barriers, traps, and filters for sediments. Sediments from the North branch will be trapped in an area near the shear front. The sedimentation rate of the region with 3-6 m depth is greater than in the region with depths > 6 m. But, the shear front of the West shoal also has an erosion effect. During ebb periods, double-spiral circulation forms on both sides of the shear front, and, driven by longitudinal current, flows seaward with velocity greater than 1.0 m/s. The spiral flow will effectively scour the bed near the Lingding navigation channel. The secondary spiral flow associated with the front had the greatest influence on the lateral distribution of finer grains and the least influence on the lateral distribution of coarser grains (Uncles et al., 2006). So, the sedimentation rate of areas with 6-8 m depths is less than that of areas where the depth < 6 m (*Fig. 15*).

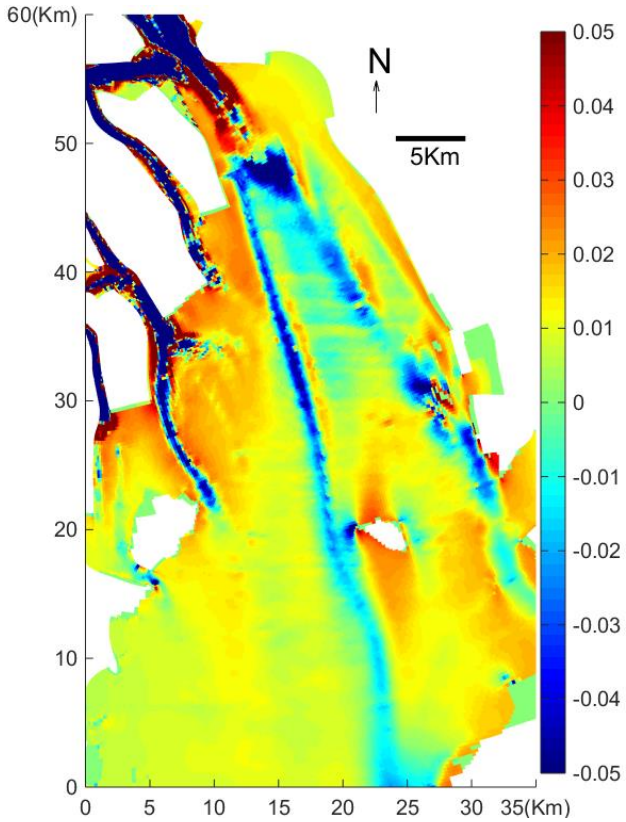

Figure 15. *Depositional thickness of suspended sediment (m, half a year, from model result)*

The tide intrusion front is located southeast of the LDY and varies with ebb and flood. The front penetrates landward under the water during flood, and the salinity structure is highly stratified. In addition, the front retreats seaward during ebb period. The formation and development of the tide intrusion front is opposite to that of the shear front. The functions of the tide intrusion front are similar to that of the shear front, which provides a barrier, filters, and traps material. However, the transportation function of this front is easy to underestimate. The West shoal is an important passage

http://www.aloki.hu ● ISSN 1589 1623 (Print) ● ISSN 1785 0037 (Online)
DOI: http://dx.doi.org/10.15666/aeer/1704_84658484

for fresh water, sediments, and pollutants. Materials from land are transported to sea along the front. The tide intrusion front also possesses the function of transportation, not by transport landward under water, but also transport seaward by the fresh water of the middle and top layers (Yang, 2018).

Discussion

Natural sediment sinks have been removed in many estuaries and tidal basins, and the resulting loss in accommodation space likely led to an increase in the suspended sediment concentration (Winterwerp et al., 2013). However, channel deepening also leads to higher SSC levels (Kang et al., 2018; Wu et al., 2003). Larger engineers such as reclamation, port construction, result in a reduction of the tidal prism, leading to smaller tidal flow velocities in the tidal channels, thereby promoting sediment deposition (Zhifu, 1995). Human activities have got attentions in Pearl River estuary (Zhifu, 1994) and Yangtze River estuary.

Economic development and human activity have had a large impact on the LDY estuary. The main human activities of LDY include reclamation, port construction, mining of bed sand, and channel dredging. The reclamation area includes 204 km^2, which is 17% of the total area. Bed sand harvesting is up to 200 million m^3, which is equivalent to 8% of the capacity of LDY.

Human removal of bed sediment for building construction has deepened the riverbed. After 2000, large-scale projects such as construction of the Lingding navigation channel and construction of the Nansha port near the West shoal will increase SSC. Because the front system of the West shoal can trap river-borne and sea-borne sediment, the sedimentation rate has increased after 2000 (*Table 4*). Although there were no human construction projects on the West shoal, the indirect impact of upstream and downstream projects on sedimentation has been significant.

Table 4. *Sedimentation rate of west shoal*

Year	Depth	Area (km^2/a)	Volume (Ten th. m^3/a)	Sed. rate (cm/a)
2000~2005	> -2	0.3763	15.46	0.60
	-2~-3	0.2987	41.82	1.00
	-3~-4	0.5881	100.45	3.40
	-4~-5	0.0023	128.03	5.00
	-5~-6	-0.3921	125.79	4.30
	-6~-7	-0.7358	24.84	1.10
	-7~-8	0.1593	26.4	3.00
1986~2000	> -2	-0.064	3.71	0.10
	-2~-3	0.4292	9.06	0.20
	-3~-4	0.1072	41.48	1.60
	-4~-5	0.052	52.84	2.10
	-5~-6	-0.0257	52.24	1.70
	-6~-7	-0.5246	29.4	1.10
	-7~-8	-0.2024	-13.86	-1.80

http://www.aloki.hu ● ISSN 1589 1623 (Print) ● ISSN 1785 0037 (Online)
DOI: http://dx.doi.org/10.15666/aeer/1704_84658484

Conclusion

The LDY is a complex tidal bay, which has two main front systems, tide intrusion front and shear front. These two front systems divided the LDY into three dynamics area, west shoal area, jet-flow area, salinity water area. Sediment transport and deposition processes of the three areas differ (Dager, 2017). Silting characteristics include shoal silting and channel deepening. Sediment transportation and sedimentation are subject to front systems, which sedimentary facies is corresponding to. Human activities such as river estuary regulation and channel dredging increase SSC, which leads to promote sediment deposition. The amount of sediment deposition has greatly increased since 2000.

It can be seen that human activities such as estuary regulation and river dredging are important factors for increasing sediment deposition, and the increasing sediment deposition will make the imbalance of sediment transport more prominent. In order to improve navigation conditions and reduce siltation under sluice gates, measures such as drainage, mechanical dragging and tidal scouring can be taken.

Acknowledgements. The study was supported by the Natural Science Foundation (41406005). We thank the hydrology and water resources survey bureau of the Yangtze River Water Conservancy Committee, which completed the work of field observation. We thank LetPub for its linguistic assistance during the preparation of this manuscript.

REFERENCES

[1] Allen, G. P., Salomon, J. C., Bassoullet, P., Du Penhoat, Y., De Grandpre, C. (1980): Effects of tides on mixing and suspended sediment transport in macrotidal estuaries. – Sediment Geol 26: 69-90.

[2] Cameron, G., Prichard, D. (1963): Estuaries. – In: Hill, M. N. (ed.) The Sea. Wiley, New York, pp. 306-324.

[3] Chen, J., Li, D., Chen, B., Hu, F., Zhu, H., Liu, C. (1999): The processes of dynamic sedimentation in the Changjiang Estuary. – Journal of Sea Research 41(1-2): 129-140.

[4] Dager, M. R. (2017): 1. Composición de la materia orgánica, pH, intercambio catiónico y textura de cinco suelos ubicados entre 670 y 1600 msnm en la cuenca del río Maracay, Venezuela. – Revista de la Facultad de Agronomia de la Universidad del Zulia 34(2).

[5] Dai, Z. J., Du, J. Z., Zhang, X. L., Su, N., Li, J. F. (2011a): Variation of riverine matrial loads and environmental consequences on the Changjiang estuary in recent decades. – Environmental Science and Technology 45: 223-227.

[6] Dai, Z. J., Du, J. Z., Chu, A., Zhang, X. L. (2011b): Sediment characteristics in the North Branch of the Yangtze Estuary based on radioisotope tracers. – Environmental Earth Sciences 62: 1629-11634.

[7] Dai, Z., Chu, A., Stive, M. J., Yao, H. (2012): Impact of the Three Gorges Dam overruled by an extreme climate hazard. – Natural Hazards Review 13(4): 310-316.

[8] Dai, Z. J., Chu, A., Li, W. H., Li, J. F., Wu, H. L. (2013): Has suspended sediment concentration near the mouth bar of the Yangtze (Changjiang) Estuary been declining in recent years? – Journal of Coastal Research 29(4): 809-818.

[9] Dalrymple, R. W., Zaitlin, B. A., Boyd, R. (1992): Estuarine facies models; conceptual basis and stratigraphic implications. – Journal of Sedimentary Research 62(6): 1130-1146.

http://www.aloki.hu ● ISSN 1589 1623 (Print) ● ISSN 1785 0037 (Online)
DOI: http://dx.doi.org/10.15666/aeer/1704_84658484

[10] Daniel, G. I., Henry, O. U., Ayodeji, B. B., Silas, M. Y. (2018): Land suitability analysis for the production of Cocoyam Inbenue State, Nigeria. – Earth Sciences Malaysia 2(2): 25-30.
[11] Dellwig, O., Hinrichs, J., Hild, A., Brumsack, H. J. (2000): Changing sedimentation in tidal flat sediments of the southern North Sea from the Holocene to the present: a geochemical approach. – Journal of Sea Research 44: 195-208.
[12] Duck, R. W., Wewetzer, S. F. K. (2001): Impact of frontal systems on estuarine sediment and pollutant dynamics. – The Science of the Total Environment 266: 23-31.
[13] Dyer, K. R. (1988): Fine Sediment Particle Transport in Estuaries. – In: Dronkers, J., van Leussen, W. (eds.) Physical Process in Estuaries. Springer, Berlin, pp. 427-445.
[14] Ferriera, G. J., Anderson, M. (1997): A multi-disciplinary study of frontal systems in the Tay Estuary, Scotland. – Estuarine, Coastal and Shelf Science 45: 317-336.
[15] Fettweis, M., Monbaliu, J., Baeye, M., Nechad, B., Van den Eynde, D. (2012): Weather and climate induced spatial variability of surface suspended particulate matter concentration in the North Sea and the English Channel. – Methods Oceanogr 3(4): 25-39.
[16] Grabemann, I., Uncles, R. J., Krause, G., Stephens, J. A. (1997): Behaviour of turbidity maxima in the Tamar (UK) and Weser (FRG) estuaries. – Estuar. Coast. Shelf Sci. 45: 235-246.
[17] Hume, T. M., Herdendorf, C. E. (1988): A geomorphic classification of estuaries and its application to coastal resource management—a New Zealand example. – Ocean Shoreline Manag 11(3): 249-274.
[18] Jalón-Rojas, I., Schmidt, S., Sottolichio, A. (2015): Turbidity in the fluvial Gironde Estuary (southwest France) based on 10-year continuous monitoring: sensitivity to hydrological conditions. – Hydrology and Earth System Sciences 19(6): 2805-2819.
[19] Jalón-Rojas, I., Schmidt, S., Sottolichio, A. (2017): Comparison of environmental forcings affecting suspended sediments variability in two macrotidal, highly-turbid estuaries. – Estuarine, Coastal and Shelf Science 198: 529-541.
[20] Jia, L. W., Pan, S. Q., Wu, C. Y. (2013): Effects of the anthropogenic activities on the morphological evolution of the Modaomen Estuary, Pearl River Delta, China. – China Ocean Engineering 27(6): 795-808.
[21] Jiang, S., Lian, M., Lu, C., Gu, Q., Ruan, S., Xie, X. (2018): Ensemble prediction algorithm of anomaly monitoring based on big data analysis platform of open-pit mine slope. – Complexity 2018.
[22] Kang, L.; Du, H. L.; Du, X.; Wang, H. T.; Ma, W. L.; Wang, M. L.; Zhang, F. B. (2018): Study on dye wastewater treatment of tunable conductivity solid-waste-based composite cementitious material catalyst. – Desalination and Water Treatment 125: 296-301.
[23] Largier, J. L. (1992): Tidal intrusion fronts. – Estuaries 15(1): 26-39.
[24] Le Hir, P., Ficht, A., Jacinto, R. S., Lesueur, P., Dupont, J. P., Lafite, R., Cugier, P. (2001): Fine sediment transport and accumulations at the mouth of the Seine estuary (France). – Estuaries 24(6): 950-963.
[25] Li, C. C. (2004): Estuarine Process and Evolution Pattern in South China. – Science Press, Beijing 9: 80-91.
[26] Li, M. G., Shi, Z., Qin, C. R. (2003): Three dimensional suspended sediment movement simulation of the Ligdingyang Bay. – Shuili Xuebao 4: 51-56.
[27] Lick, W., Lick, J., Ziegler, C. (1994): The resuspension and transport of fine-grained sediments in Lake Erie. – Journal of Great Lakes Research 20(4): 599-612.
[28] Lick, W., Xu, Y. J., McNeil, J. (1995): Resuspension properties of sediments from the Fox, Saginaw, and Buffalo Rivers. – Journal of Great Lakes Research 21(2): 257-274.
[29] Lu, Y. J., Li, H. L., Wang, H. C., Zuo, L. Q. (2005): Back silting and regulation of waterway with sand bar in strong tidal estuary. – Shuili Xuebao (Journal of Hydraulic Engineering) 36(12): 1450-1456.

http://www.aloki.hu ● ISSN 1589 1623 (Print) ● ISSN 1785 0037 (Online)
DOI: http://dx.doi.org/10.15666/aeer/1704_84658484

[30] Nouaim, W., Chakiri, S., Rambourg, D., Karaoui, I., Ettaqy, A., Chao, J., Allouza, M., Razoki, B., Yazidi, M., Hmidi, F. E. (2019): Mapping the water erosion risk in the Lakhdar river basin (central High Atlas, Morocco). – Geology, Ecology, and Landscapes 3(1): 22-28.
[31] Nwankwoala, H. O. (2019): Geoethics as an emerging discipline: perspectives, ethical challenges and prospects. – Earth Sciences Malaysia 3(1): 01-08.
[32] Omini, E. O., Akpang, O. M. (2018): Cavity detection under re-enforced concrete floor using ground penetration radar. – Engineering Heritage Journal 2(2): 11-18.
[33] Oyedotun, T. D. T. (2019): Land use change and classification in Chaohu Lake catchment from multi-temporal remotely sensed images. – Geology, Ecology, and Landscapes 3(1): 37-45.
[34] Pinckney, J., Dustan, P. (1990): Ebb-tidal fronts in Charleston Harbor, South Carolina: physical and biological characteristics. – Estuaries 13(1): 1-7.
[35] Pritchard, D. W. (1967): What is an Estuary: Physical Viewpoint. – In: Lauff, G. H. (ed.) Estuaries. American Association for the Advancement of Science, Washington, pp. 3-5.
[36] Qiao, F. (2018): The study on the integration of green architecture and appropriate technology. – Engineering Heritage Journal 2(2): 01-03.
[37] Rahim, Y., Khan, M. S., Mughal, S. (2018): Petrography of sandstone of the Lumshiwal Formation from eastern Hazara, Khyber Pakhtunkhwa, Pakistan: implications for provenance, diagenesis and environments of deposition. – Earth Sciences Pakistan 2(2): 01-06.
[38] Reeves, A. D., Duck, R. W. (2001): Density fronts: Sieves in the estuarine sediment transfer system? – Physics and Chemistry of the Earth, Part B: Hydrology, Oceans and Atmosphere 26(1): 89-92.
[39] Ren, J., Bao, Y., Lin, W. Q. (2001): Analyseson water and suspended sediment fluxes in ling ding yang estuary of Zhu Jiang River mouth. – Journal of Tropical Oceanography 3: 31-40.
[40] Ren, J., Wu, C. C., Bao, Y. (2006): Dynamic structure of Humen estuary of the Pearl River. – Acta Scientiarum Naturalium Universitatis Sunyatseni 45(3): 105-109.
[41] Ren, J., Zeng, X. Z., Jia, L. W. (2010): Mechanism study of retrogressive erosion in the lower Reach of Dongjiang River. – Advances in Water Science 21(1): 84-88.
[42] Sarker, M. K. U., Majumder, A. K., Haque, M. Z., Hossain, M. S., Nayeem, A. A. (2019): Assessment of inland water quality parameters of Dhaka City, Bangladesh. – Environment & Ecosystem Science 3(1): 13-16.
[43] Sarwar, M. T., Hui, Z. H., Maqbool, A. (2019): Causes and control measures of urban air pollution in China. – Environment & Ecosystem Science 3(1): 35-36.
[44] Savenije, H. H. (2006): Salinity and Tides in Alluvial Estuaries. – Elsevier, Amsterdam.
[45] Sharjeel, A., Anwar, S., Nasir, A., Rashid, H. (2019): Design, development and performance of optimum water softener. – Earth Sciences Pakistan 3(1): 23-28.
[46] Shi, J. Z. (2010): Tidal resuspension and transport processes of fine sediment within the river plume in the partially-mixed Changjiang River estuary, China: a personal perspective. – Geomorphology 121: 133-151.
[47] Shilun, Y. (1994): Statistical regularity of particle size parameters and hydrodynamic explanation in Yangtse River estuary. – Sediment Research 3: 23-31.
[48] Simpson, J. H., Nunes, R. A. (1981): The tidal intrusion front: an estuarine convergence zone. – Estuarine and Coastal Shelf Science 13: 257-266.
[49] Simpson, J. H., Turrell, W. R. (1986): Convergent Fronts in the Circulation of Tidal Estuaries. – In: Wolfe, D. A. (ed.). Estuarine Variability. Academic Press, New York.
[50] Talke, S. A., Swart, H. E., Schuttelaars, H. M. (2009): Feedback between residual circulations and sediment distribution in highly turbid estuaries: an analytical model. Cont. – Shelf Res 29: 119-135.
[51] Townend, I. (2005): An examination of empirical stability relationships for UK estuaries. – Journal of Coastal Research 21(5): 1042-1053.

http://www.aloki.hu ● ISSN 1589 1623 (Print) ● ISSN 1785 0037 (Online)
DOI: http://dx.doi.org/10.15666/aeer/1704_84658484

[52] Townend, I., Wright, A., Price, D. (2000): An investigation of the gross properties of UK estuaries. – Modelling Estuary Morphology and Process. Report prepared by the EMPHASYS Consortium for the Estuaries Research Programme Phase 1, MAFF Project FD1401.
[53] Uncles, R. J., Stephens, J. A. (1993): The freshwater-saltwater interface and its relationship to the turbidity maximum in the Tamar Estuary, United Kingdom. – Estuaries and Coasts 16(1): 126-141.
[54] Uncles, R. J., Stephens, J. A., Law, D. J. (2006): Turbidity maximum in the macro-tidal, highly turbid Humber Estuary, UK: flocs, fluid mud, stationary suspensions and tidal bores. – Estuar. Coast. Shelf Sci. 67: 30-52.
[55] Van Maren, D. S., Oost, A. P., Wang, Z. B., Vos, P. C. (2016): The effect of land reclamations and sediment extraction on the suspended sediment concentration in the Ems Estuary. – Marine Geology 376: 147-157.
[56] Williams, J., Lee, G. H., Shin, H. J., Dellapenna, T. (2015): Mechanism for sediment convergence in the anthropogenically altered microtidal Nakdong Estuary, South Korea. – Marine Geology 369: 79-90.
[57] Winterwerp, J. C., Wang, Z. B., Van Braeckel, A., Van Holland, G., Kösters, F. (2013): Man-induced regime shifts in small estuaries—I: a comparison of rivers. – Ocean Dyn 63(11-12): 1293-1306.
[58] Wu, J., Zhang, S., Ren, L. (2003): Field observations of current and suspended sediment concentration during sediment disposal in the Changjiang (Yangtze) Estuary. – Acta Oceanologica Sinica 25(4): 91-103.
[59] Yang, B., Luo, Y., Jeng, D., Feng, J., Huhe, A. (2018a): Experimental studies on initiation of current-induced movement of mud. – Applied Ocean Research 80: 220-227.
[60] Yang, B., Gao, F. P., Jeng, D. S. (2018b): Failure mode and dynamic response of a double-sided slope with high water content of soil. – Journal of Mountain Science 15(4): 859-870.
[61] Zhifu, Y. (1994): The frontal classification and its influence on sedimentation in lingdingyang, zhu jiang river estuary. – Journal of Tropical Marine 13: 25-32.
[62] Zhifu, Y. (1995): A study on notable features of sedimentary dynamics in Lingdingyang estuary of Zhujiang River. – Tropicoceanology 14(2): 76-82.

http://www.aloki.hu ● ISSN 1589 1623 (Print) ● ISSN 1785 0037 (Online)
DOI: http://dx.doi.org/10.15666/aeer/1704_84658484

ENVIRONMENTAL FACTORS AFFECTING THE SPATIOTEMPORAL DISTRIBUTION OF *DECAPTERUS MARUADSI* IN THE WESTERN GUANGDONG WATERS, CHINA

YU, J.[1] – LIU, Z.-N.[1,2] – CHEN, P.-M.[1] – YAO, L.-J.[3*]

[1]South China Sea Fisheries Research Institute, Chinese Academy of Fishery Sciences/Guangdong Provincial Key Laboratory of Fishery Ecology and Environment/Scientific Observing and Experimental Station of South China Sea Fishery Resources and Environment, Ministry of Agriculture and Rural Affairs/Guangdong Engineering Technology Research Center of Marine Recreational Fishery/Key Laboratory of Marine Ranching Technology, CAFS, Guangzhou 510300, China

[2]College of Marine Science, Shanghai Ocean University, Shanghai 201306, China

[3]Department of Optoelectronic Engineering, College of Science and Engineering, Jinan University, Guangzhou 510632, China

**Corresponding author*
e-mail: constancecarson15@gmail.com

(Received 8th Mar 2019; accepted 21st May 2019)

Abstract. *Decapterus maruadsi* is a small pelagic fish and is of great significance to the ecosystems in the northern South China Sea. We collected and analyzed the data recorded by the fishing vessels in the western Guangdong waters in winter and summer and remote sensing data including sea surface temperature (SST), chlorophyll a concentration (Chl a) and sea level anomalies (SLA) from 2011 to 2015, using generalized additive model (GAM). Results showed that the catch per unit effort (CPUE) of *D. maruadsi* in the western Guangdong waters had a significant positive linear correlation with longitude, and the *D. maruadsi* populations were concentrated in the east of the study area. The total explanation of *D. maruadsi* CPUE in GAMs was 47.40%, among which, the factors year, month, lunar phase, latitude, Chl a, SLA and water depth explained 9.30%, 13.50%, 6.50%, 1.90%, 1.70%, 4.60%, and 9.90%, respectively. The *D. maruadsi* populations in the study were concentrated in the area of latitude 21°N, Chl a 0.1- 0.5 $mg \cdot m^{-3}$, SLA -0.05 m and water depth 80 m. Results of this work will help in understanding the environmental factors affecting *D. maruadsi* distribution in the western Guangdong waters.

Keywords: *generalized additive model, environmental factors, habitat suitability index (HSI), fisheries, main spawning habitats*

Introduction

Decapterus maruadsi, a pelagic fish in the family Carangidae (Perciformes), lives in warm waters, and is widely distributed along the coasts of Southeast China (Deng et al., 1991). It is one of the major species captured by pelagic trawls and light luring seine fishing vessels (Zheng et al., 2014; Thanh and Do, 2018). *D. maruadsi* has a short lifespan and fast growth and reproduction rate, and as an R-selected species, it is susceptible to fishing intensity and marine environment (Chen et al., 2003; Dai, 2017; Austin et al., 2018). The populations of *D. maruadsi* in the northern South China Sea shifted towards younger age and smaller size due to overfishing since the 1990s (Lu, 2000; Chen and Qiu, 2009). But the *D. maruadsi* resource is beginning to recover due to summer fishing moratorium and other fishery industry restructuring policies in recent years (Chen et al., 2010; Geng et al., 2018; Abija and Nwankwoala, 2018). As a small

http://www.aloki.hu ● ISSN 1589 1623 (Print) ● ISSN 1785 0037 (Online)
DOI: http://dx.doi.org/10.15666/aeer/1704_84858499

pelagic fish, *D. maruadsi* has an important impact on the ecosystem output of the northern South China Sea (Chen and Qi, 2009). The sea area off western Guangdong is one of the main spawning habitats for *D. maruadsi* in the northern South China Sea (Chen et al., 2003), so it is of great significance to investigate the temporal and spatial distribution of this species in this area. At present, the existing studies on *D. maruadsi* are mostly focused on its biology (Jiang, 2012; Huang, 1995; Da, 2017), resource assessment (Chen and Qiu, 2003; Jamil et al., 2018), etc. Acoustic assessments indicate that carangid fish such as *D. maruadsi* along the east coast of Peninsular Malaysia are concentrated at 40-60 m below the ocean surface (Hashim, 2017; Tao, 2018). The studies that assessed the relationship between *D. maruadsi* fisheries and environmental factors in the northern South China Sea in different seasons based on the habitat suitability index (HSI) model indicated that chlorophyll a (Chl a) concentration is the determinant of the distribution of *D. maruadsi* fisheries in spring. In recent years, due to the increase in offshore fishing intensity, changes in ecological environment and climate, the resource stock and spatial distribution of many marine species have changed, which has a profound impact on fish habitats and ecosystems. Therefore, evaluating the correlation between *D. maruadsi* distribution and marine environmental factors in western Guangdong is important for the sustainable development of fisheries.

The relationship between fishery resources and marine environment is very complicated, as it is non-linear and non-additive (Stenseth et al., 2002, 2004; Dingstor et al., 2007; Tianlei, 2019), and the use of different observational scales can cause large differences in results (Fauchald et al., 2000). Therefore, it is crucial to choose a suitable method for quantitative analysis of the relationship between fishery resources and the marine environment. As the nonparametric extensions of generalized linear models (GLMs), generalized additive models (GAMs) provide flexible method for uncovering the nonlinear relationship between response and predictor variables (Hastie and Tibshirani, 1990; Jegatheesan and Zakaria, 2018), and thus are suitable for exploring the nonlinear relationship between fishery resources and marine environment (Stoner, 2001; Agenbag, 2003). GAMs not only can be used for different species or different seas, but also can be combined with a variety of environmental factors to better reveal the relationship between environmental factors and the variation, spatial distribution, temporal distribution of fishery resources (Venables et al., 2004; La et al., 2016; Bacha et al., 2017). The studies based on GAMs have shown that zooplankton biomass and the location of oceanic fronts have an impact on the distribution of *Clupea harengus* in the vicinity of the Shetland Islands (Maravelias et al., 1997). The spatial distribution of *Loligo spp.* and *Tachysurus* in the Arabian Sea was well predicted based on the data of sea surface temperature (SST), chlorophyll a (Chl a) concentration, photosynthetically active radiation (PRA) and sea level anomalies (SLA) in the study of Solanki (2017). The interaction between upwelling index, year and latitude had a great influence on the spatial distribution of sardines in Mauritanian waters (Bacha et al., 2017; Abdullah and Rahim, 2018). Wang et al. (2018) reported that prey density, water depth, bottom water temperature and distance to shore had a great influence on the distribution of Chinese white dolphin in western Pearl River Estuary.

In this study, generalized additive models (GAMs) were used to quantitatively analyze the main environmental factors affecting the spatiotemporal distribution of *D. maruadsi*, and to explore the formation mechanism of *D. maruadsi* fishery in the western Guangdong waters, and to provide a theoretical basis for fishery management and marine protected area planning under climate changes.

http://www.aloki.hu ● ISSN 1589 1623 (Print) ● ISSN 1785 0037 (Online)
DOI: http://dx.doi.org/10.15666/aeer/1704_84858499

Materials and methods

Data collection

Fishery data

The data of *D. maruadsi* resource were from the observational records of large-scale light-luring seine fishing vessels in western Guangdong waters (19.75° to 21.75°N, 111.25°E to 113.75°E) in January, February, August and September from 2011 to 2015. The data (including working time, voyage, longitude, latitude and fish catch) were generated at a spatial resolution of 0.5° × 0.5° in latitude and longitude (one fishing area), and summarized by day (*Fig. 1*).

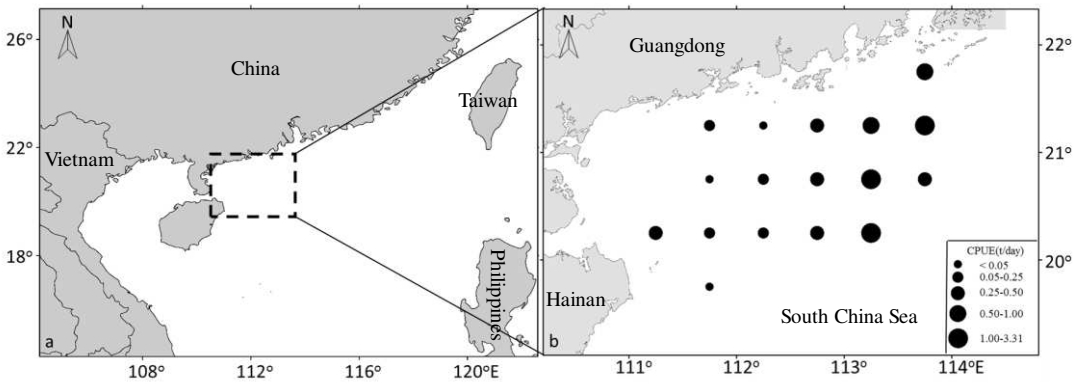

Figure1. *Distribution of D. maruadsi CPUE in western Guangdong waters*

Environmental data

The remote sensing data including chlorophyll a concentration (Chl a), sea surface temperature (SST) and sea level anomalies (SLA) were used in this study. Among them, Chl a and SST were from MODIS Aqua Level 3 data products (https://oceancolor.gsfc.nasa.gov), with a temporal resolution of one day and a spatial resolution of 4 km. SLA data were from CTOH/LEGOS website (https://www.aviso.altimetry.fr/en/home.html) with a temporal resolution of one day and a spatial resolution of 0.25°. Water depth data were acquired from Google Earth, with a spatial resolution of 70 m (Jaimes, 2017).

Data processing

CPUE (catch per unit effort) calculation (Campbel, 2004)

$$CPUE = \frac{c}{f} \quad \text{(Eq.1)}$$

where, CPUE is the average daily *D. maruadsi* catch by a vessel (unit: tons per day), c is daily *D. maruadsi* catch in a 0.5° × 0.5° fishing grid (unit: tons), *f* is the number of operations in a 0.5° × 0.5° fishing grid (days).

http://www.aloki.hu ● ISSN 1589 1623 (Print) ● ISSN 1785 0037 (Online)
DOI: http://dx.doi.org/10.15666/aeer/1704_84858499

Remote sensing data fusion (Fu et al., 2009)

The remote sensing data (Chl, SST and SLA) of the study area were extracted and merged using the formula as follows:

$$Average_j = \frac{\sum_{i=1}^{m} value(i)_j}{m} \quad \text{(Eq.2)}$$

where, $Average_j$ is the mean value of fused environmental data (Chl, SST and SLA) in fishing grid j, j is a 0.5°×0.5° fishing grid, m is the number of pixels of environmental data (Chl, SST, SLA) in fishing grid j, $Value(_i)$ is the value of a single pixel in fishing area j.

GAM analysis

Generalized additive models (GAM) focus on exploring data nonparametrically, compared to generalized linear models (Feng, 2007; Sudhakaran et al., 2018). In order to avoid excessive computation and over-fitting, the linear correlation between *D. maruadsi* CPUE and each predictor variable was measured according to Pearson correlation coefficient R before GAM was constructed (Li, 2007; Le, 2017). When $R > 0.5$, the predictor variable has a linear relationship with *D. maruadsi* CPUE, and should be removed from the model. The R mgcv package was used to fit the GAM (Wood, 2004, 2011). The general form of the model can be written as:

$$g(\mu) = \beta + f_1(x_1) + \cdots + f_i(x_i) + \varepsilon \quad \text{(Eq.3)}$$

where $g(\mu)$ is the link function, which is the logarithm of CPUE + 1; β is the intercept term; f is a smooth function, i is the number of predictor variables, ε is the error term. The GAM procedure uses smoothing splines s( ).

Diagnosis of GAM

The predictor variables influencing *D. maruadsi* CPUE that should be incorporated into the model were identified applying a stepwise GAM and according to Akaike Information Criterion (AIC) (Shih, 2014; Franco et al., 2018). Models were built by adding in new terms and seeing how much they improved the fit, and by dropping terms that did not degrade the fit significantly. The influence of the predictors was assessed via F-test and chi-square test (Quinn and Deriso, 1999). AIC was calculated as follows (Venables, 2004):

$$AIC = \theta + 2df\delta$$

where θ is the deviance, df is the effective degree of freedom, and δ is the variance.

Violin plot

A violin plot, similar to a box plot with a rotated kernel density plot on each side, simultaneously reflects the statistical features (maximum, minimum, median, and upper and lower quartiles) and distribution of a set of data (Hintze, 1998). The violin plot was made using the ggplot2 package in R software from *D. maruadsi* CPUE in winters

http://www.aloki.hu ● ISSN 1589 1623 (Print) ● ISSN 1785 0037 (Online)
DOI: http://dx.doi.org/10.15666/aeer/1704_84858499

(January and February) and summers (August and September). Since the average CPUE differed greatly, the ordinate was scaled logarithmically. Then the violin plot was used to analyze the difference in *D. maruadsi* CPUE between winters and summers in western Guangdong waters (Cortez, 2016).

Results

Linear correlation analysis between D. maruadsi CPUE and the influencing factors

Pearson correlation analysis on *D. maruadsi* CPUE and the factors influencing it including year, month, lunar phase, longitude (Lon), latitude (Lat), SST, Chl a, SLA and water depth (*Table 1*) showed that seven of the factors (month, lunar phase, longitude, latitude, SST, Chl a, SLA and depth) were significantly correlated with *D. maruadsi* CPUE ($P < 0.05$), and the correlation coefficient between longitude and CPUE was greater than 0.5 ($R > 0.5$), indicating that longitude had a strong positive linear correlation with *D. maruadsi* CPUE. Therefore, longitude was removed from the GAM.

Table 1. *Pearson correlation coefficient of Decapterus maruadsi CPUE and Impact factors*

Factors	Cor	P-value
Year	-0.067	0.345
Month	0.292	$2.514*10^{-5}$
Lunar phase	-0.146	0.038
Lon	0.535	$2.678*10^{-16}$
Lat	0.205	0.003
SST	0.261	$1.830*10^{-4}$
Chl a	-0.167	0.018
SLA	-0.178	0.012
Depth	-0.163	0.021

Analysis of longitudinal distribution of *D. maruadsi* CPUE (*Fig. 2*) revealed that the maximum values of *D. maruadsi* CPUE within longitude 115.25°E - 113.75°E were 0.56 t/d, 1.00 t/d, 1.00 t/d, 3.00 t/d, 30.20 t/d and 18.00 t/d, respectively. The upper quartile of *D. maruadsi* CPUE increased with longitude increasing from 112.25°E to 113.75°E. The median value and lower quartile of *D. maruadsi* CPUE also increased with longitude increasing from 111.75°E to 113.75°E. There were fewest data at 111.25°E and most data113.25 °E. To sum up, *D. maruadsi* CPUE value showed a general decreasing trend from east to west in the study area, and the high CPUE values were concentrated within 113.25°E-113.75°E.

Environmental effects on D. maruadsi CPUE based on GAM analysis

The GAM was built by adding in the temporal, spatial and environmental factors stepwise and seeing how much they improved the fit. The temporal, spatial and environmental variables included in the model were year, month, lunar phase, latitude, Chl a, SLA and depth (*Table 2*). The GAM could explain 47.40% of the variability in *D. maruadsi* CPUE in total, and the residual degrees of freedom was 185.23.

http://www.aloki.hu ● ISSN 1589 1623 (Print) ● ISSN 1785 0037 (Online)
DOI: http://dx.doi.org/10.15666/aeer/1704_84858499

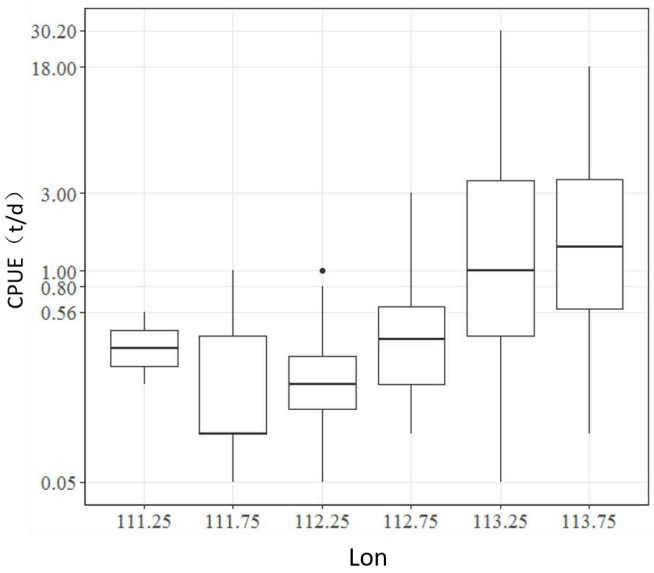

Figure 2. *Box plot of longitudinal distribution of D. maruadsi CPUE*

Table 2. *Generalized additive models (GAMs) fitted to D. maruadsi CPUE and analysis of deviance*

Factors	Residual degree of freedom	AIC value	Cumulative of deviance explained
Log(CPUE + 1) = NULL	200.00	16.34	0.00
Log(CPUE + 1) = s(Year)	196.28	4.16	9.30%
Log(CPUE + 1) = s(Year) + s(Month)	193.73	-23.09	22.80%
Log(CPUE + 1) = s(Year) + s(Month) + s(Lunar phase)	191.87	-37.14	29.30%
Log(CPUE + 1) = s(Year) + s(Month) + s(Lunar phase) + s(Lat)	191.08	-40.88	31.20%
Log(CPUE + 1) = s(Year) + s(Month) + s(Lunar phase) + s(Lat) + s(Chl a)	190.24	-44.22	32.90%
Log(CPUE + 1) = s(Year) + s(Month) + s(Lunar phase) + s(Lat) + s(Chl a) + s(SLA)	190.24	-54.73	37.50%
Log(CPUE + 1) = s(Year) + s(Month) + s(Lunar phase) + s(Lat) + s(Chl a) + s(SLA) + s(Depth)	185.23	-83.23	47.40%
Log(CPUE + 1) = s(Year) + s(Month) + s(Lunar phase) + s(Lat) + s(Chl a) + s(SLA) + s(Depth) + s(SST)	184.21	-82.33	47.70%

The contribution of each factor included in GAMs to *D. maruadsi* CPUE indicated their influence on *D. maruadsi* CPUE (*Table 3*). Among them, the most influential factor was month, which explained 13.50% of the variability in *D. maruadsi* CPUE, followed by depth, year, lunar phase, SLA, latitude, Chl a, which explained 9.9%, 9.30%, 6.50%, 4.60%, 1.90%, and 1.70% of the variability in *D. maruadsi* CPUE respectively. The *F* test and Chi-squared test showed that after SST was added into the model, it did not degrade the fit significantly ($P > 0.05$), while *AIC* value increased, suggesting that SST had no significant effect on *D. maruadsi* CPUE, so it was removed from the model.

http://www.aloki.hu ● ISSN 1589 1623 (Print) ● ISSN 1785 0037 (Online)
DOI: http://dx.doi.org/10.15666/aeer/1704_84858499

Table 3. *Statistical significance and contribution of the factors in GAM*

Factors	Degree of freedom	P-value	F-test	Chi-square test	Contribution of selected variables
Year	3.69	$1.35*10^{-3}$	$6.71*10^{-4}$	$4.51*10^{-4}$	9.30%
Month	1.00	$1.92*10^{-6}$	$6.02*10^{-7}$	$1.70*10^{-7}$	13.50%
Lunar phase	1.91	$2.80*10^{-4}$	$1.88*10^{-4}$	$1.27*10^{-4}$	6.50%
Lat	1.72	$1.30*10^{-2}$	0.02	0.02	1.90%
Chl a	1.00	$1.76*10^{-2}$	0.03	0.03	1.70%
SLA	2.76	$1.47*10^{-3}$	$5.47*10^{-4}$	$4.20*10^{-4}$	4.60%
Depth	2.71	$7.32*10^{-7}$	1.61 6	$4.31*10^{-7}$	9.90%
SST	1.00	0.317	0.32	0.32	0.30%

Relationship between *D. maruadsi* CPUE and the influencing factors (*Fig. 3*). Among all temporal factors, the year factor showed a positive effect in 2011-2013 and 2014-2015 (*Fig. 3a*) and a negative effect in 2013-2014, with no significant change in the confidence interval (*Fig. 3b*). From January to February, and from August to September, *D. maruadsi* CPUE increased monotonously over time; the width of the confidence interval decreased between different seasons (from February to August), and increased within the same seasons (January to February, August to September). *D. maruadsi* CPUE monotonously decreased with lunar phase changing from 1 to 15, and monotonously increased with lunar phase changing from 15 to 30 (*Fig. 3c*), with no significant change in the confidence interval.

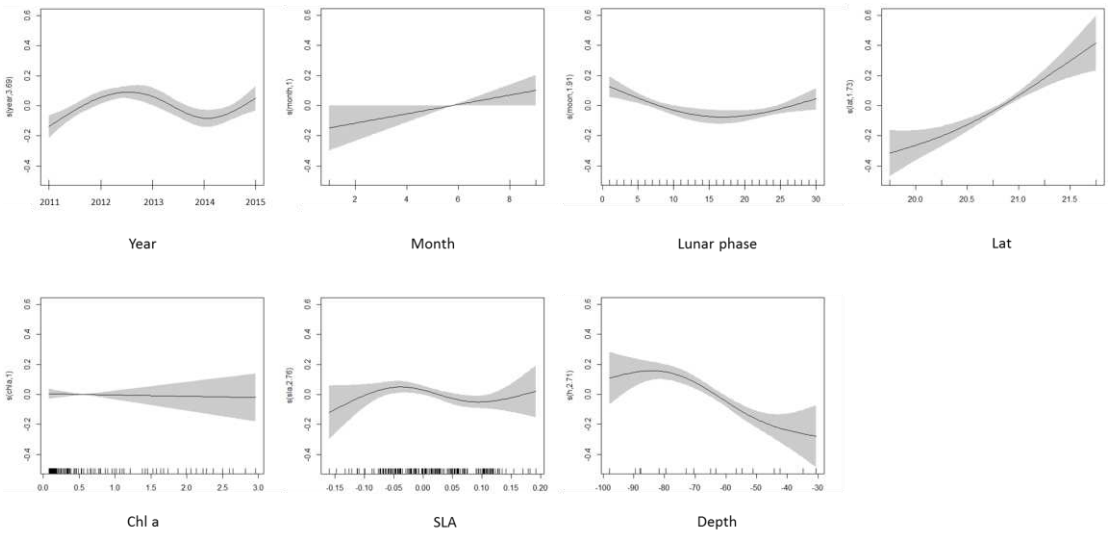

Figure 3. *Effects of different factors on D. CPUE from GAM analysis. The shadow area indicates the 95% confidence intervals. Rug plots on the x-axis indicate data density*

D. maruadsi CPUE increased monotonically with latitude increasing from 20°N to 21.5°N (*Fig. 3d*). The width of the confidence interval decreased within 20.5°N - 21.0°N, suggesting increased reliability of the estimation. The width of the confidence interval increased within 20.0°N -20.5°N and 21.0°N -21.5°N suggesting decreased reliability of the estimation.

http://www.aloki.hu ● ISSN 1589 1623 (Print) ● ISSN 1785 0037 (Online)
DOI: http://dx.doi.org/10.15666/aeer/1704_84858499

D. maruadsi CPUE changed little with Chl a increasing (*Fig. 3e*). The data were concentrated within Chl a range of 0.1-0.5 $mg \cdot m^{-3}$, and the narrow confidence interval indicated high reliability of the estimation. With Chl a increasing in the range of 0.5-3.0 $mg \cdot m^{-3}$, the amount of data decreased, the width of confidence interval increased, indicating the reliability of the estimation decreased. It showed the effect of SLA on *D. maruadsi* CPUE (*Fig. 3f*). With SLA increasing from -0.15 to -0.05 m, *D. maruadsi* CPUE increased, and the width of confidence interval decreased. As SLA increased from -0.05 to 0.10 m, *D. maruadsi* CPUE decreased, the confidence interval became narrower, indicating the reliability of the estimation increased. As SLA increased from 0.10 to 0.20 m, *D. maruadsi* CPUE increased again, while the confidence interval became broader, and the reliability of the estimation decreased. The data were concentrated within SLA range of -0.8 to 0.13 m. It showed the effect of water depth on *D. maruadsi* CPUE (*Fig. 3g*). In detail, *D. maruadsi* CPUE increased with depth increasing from 30 to 80 m, while the width of confidence interval increased, indicating that the reliability of the estimation increased. With water depth increasing from 80 to 100 m, *D. maruadsi* CPUE declined, while the width of confidence interval increased, indicating that the reliability of the estimation reduced.

Seasonal variation in D. maruadsi CPUE

According to GAM analysis, the effect of the month factor which was most influential to *D. maruadsi* CPUE was further analyzed. The fishing vessels were operated in the sea area within 19.75°-21.75°N and 111.25°-113.75°E in January, February, August and September every year. Our data revealed that *D. maruadsi* CPUE was high in summer, with a maximum value of 18.00. t/d, a median value of 1.28 t/d, a minimum value of 0.00 t/d, and the abnormally high value in summer was 30.20 t/d. *D. maruadsi* CPUE was low in winter, with a maximum value of 1.25 t/d, a median of 0.20 t/d, and a minimum value of 0.00 t/d. Comparing the kernel density distribution plots of *D. maruadsi* CPUE between summer and winter, we found that the distribution of *D. maruadsi* CPUE in summer was discrete, with a peak value around 0.60, and that in winter was concentrated, with a peak value around 0.20. All the maximum value, upper quartile, median, and lower quartile of *D. maruadsi* CPUE in summer were higher than in winter (*Fig. 4*).

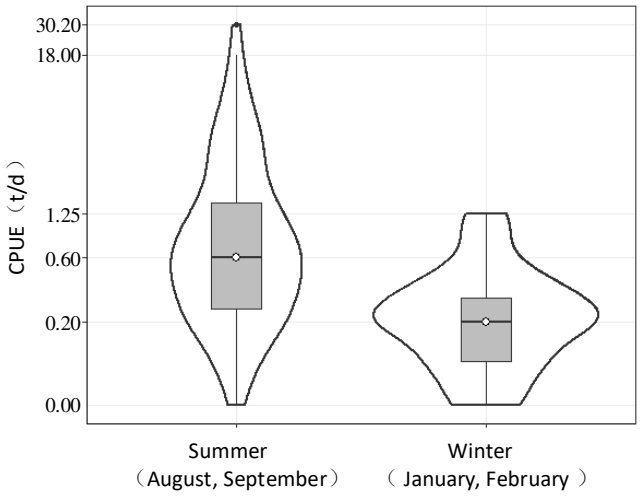

Figure 4. *Violin plot of CPUE distribution of Decapterus maruadsi in summer and winter*

http://www.aloki.hu ● ISSN 1589 1623 (Print) ● ISSN 1785 0037 (Online)
DOI: http://dx.doi.org/10.15666/aeer/1704_84858499

Discussion

Relationship between D. maruadsi CPUE and temporal/spatial factors

GAMs analyze the relationship between response and predictor variables based on data model. They possess obvious advantages in analyzing the highly nonlinear and non-monotonic relationship between response and predictor variables, and can be used to reveal the unknown ecological relationships in fishery (Hastie et al., 1999; La et al., 2016; Bacha et al., 2017). Among all the factors included in GAM, the month factor made the greatest contribution to the GAM, up to13.50% (*Table 3*). There was an obvious seasonal variation in *D. maruadsi* resources in western Guangdong waters, and its CPUE was higher in summer (August and September) than in winter (January and February) (*Fig. 3b*). Studies have shown that the spawning period of *D. maruadsi* begins at the end of winter and ends in summer (Chen et al., 2003; Wu, 2000). Previous studies on *D. maruadsi* in the Beibu Gulf and the Taiwan Strait indicates that summer is an important season for *D. maruadsi* to fatten up (Huang, 1995; Yang, 2016). *D. maruadsi* populations are able to increase during summer fishing moratorium (SFM) in June and July, and then gradually decrease from August to November due to the continuous high-intensity fishing in this period, resulting in significant difference in *D. maruadsi* CPUE between winter and summer.

The year factor explained 9.30% of the variability in *D. maruadsi* CPUE (*Table 3*). *D. maruadsi* CPUE fluctuated during 2011-2015 (*Fig. 3a*), and the decrease in 2014 was probably due to the unusually late summer monsoon season in the South China Sea in this year (Yuan, 2014). As an R-selected species, it is susceptible to environmental influence (Chen et al., 2003; Yan et al., 1987). The reduced fishing intensity during summer moratorium from June to July (Zhu, 2009; Qu, 2018), and the increased primary productivity caused by the upwelling in western Guangdong waters (Song, 2012) provide favorable conditions for the replenishment of *D. maruadsi* resources. It is widely accepted that summer winds may be the reason for the strong upwellings in the study area from June to July (Xie, 2016). The summer monsoon in the South China Sea in 2014 started unusually late, which might delay the occurrence of upwelling in this area, as a result, the *D. maruadsi* resources were not sufficiently replenished. In 2015, the summer monsoon in South China Sea occurred at the usual time (Si et al., 2016), and thus the *D. maruadsi* resources were able to recover during moratorium, so its CPUE in 2015 was higher than in 2014.

Lunar phase explained 6.50% of the deviance of the model (*Table 3*). The relationship between *D. maruadsi* CPUE and lunar phase was represented by an inverted U-shaped curve, with the minimum CPUE value at lunar phase 15 (*Fig. 3c*), which might be caused by the light luring seine used by the vessels. The moon is at its brightest when full in a month, and the moonlight lowers the attractiveness of light luring seines to cephalopods (Chen et al., 2006; Yan, 2015). As the major catch of light luring seine fishing in western Guangdong waters (Yang et al., 2009), similar results were obtained in *D. maruadsi* in our study. In addition to the influence of moonlight intensity, whether the changes in the marine environment caused by lunar phase have an impact on *D. maruadsi* CPUE needs to be further studied.

Correlation analysis indicated that there was a positive linear correlation between longitude and *D. maruadsi* CPUE in western Guangdong waters (*Table 1*). The violin plot (*Fig. 2*) showed that the maximum value, median value, and the amount of data of *D. maruadsi* CPUE were all higher at longitude 113.25°E-113.75°E. GAM analysis

http://www.aloki.hu ● ISSN 1589 1623 (Print) ● ISSN 1785 0037 (Online)
DOI: http://dx.doi.org/10.15666/aeer/1704_84858499

showed that latitude and *D. maruadsi* CPUE had a high positive correlation near longitude 21°N (*Fig. 3d*). *D. maruadsi* tends to spawn in the areas where seawater is diluted by fresh water, and the spawning season lasts for a long period until the end of summer (Chen et al., 2003; Zhu, 1984). Therefore, *D. maruadsi* population tends to concentrate in the Pearl River estuary in winter and summer. The decreased water depth along coasts may be the factor restricting the positive effect of latitude, increasing the width of confidence interval north of 21°N, and reducing the reliability of the estimation.

Relationship between D. maruadsi CPUE and environmental factors

Among the environmental factors, water depth was the most influential to GAM, and it explained 9.90% of the deviance (*Table 3*). In detail, *D. maruadsi* CPUE increased monotonously with depth increasing from 30 to 80 m, and the reliability of the estimation was higher at depth 50-80 m. With further increase in water depth, *D. maruadsi* CPUE declined monotonously (*Fig. 3g*). *D. maruadsi* is a pelagic fish (Deng, 1991). Acoustic assessments indicate that three carangid species including *D. maruadsi* along the east coast of Peninsular Malaysia are concentrated at depth of 40-60 m, and their density is 0 when water depth exceeds 80 m. The depth of study area is about 0-200 m. While some researchers believe that *D. maruadsi* in this sea area lives at or near the bottom of the sea (Fan, 2018). The GAMs showed that in western Guangdong waters, the high CPUE values of *D. maruadsi* appeared at about 80 m, which might have been affected by light luring seines.

SLA explained 4.6% of the total deviance (*Table 3*). The positive effect of SLA on *D. maruadsi* CPUE peaked at SLA around -0.05 m (*Fig. 3f*), which may be related to oceanic currents (such as eddies, upwelling) in this area. Remote sensing data about sea surface height such as SLA and sea surface height anomaly (SSHA) are the indicators of oceanic currents and density stratification of seawater (Thomas, 2012), and are widely used for eddy identification (Wang, 2015; Yi, 2014; Zhan, 2014). Eddies regulates SST, SSS, and Chl a by a complicated mechanism (Chelton, 2011; Schütte, 2016; He, 2016). The center of anticyclonic eddies in the northeastern Atlantic is characterized by a negative SLA value and a reduced SST and SSS (Schütte, 2016). Along the coasts of the southwest Indian Ocean, the cold eddies have a negative SSHA value at their center, and stir up nutrients from the bottom, resulting in an elevation in Chl a. In the northern South China Sea, the positive effect of eddies on Chl a is stronger than the negative effect of anticyclonic eddies. And the eddies in the northern South China Sea increased seawater Chl a and promoted the transport of Chl a along longitude. In addition, SLA in upwelling region also exhibits a certain pattern. In West Africa, the upwelling center has a negative SLA, decreased SST and elevated Chl a (Nieto, 2017). The eastern Hainan-western Guangdong upwelling in the study area increased the Chl a and primary productivity in the area in summer (Song, 2012; He, 2016). Therefore, it is speculated that the oceanic currents (eddies, upwelling, etc.) at SLA -0.05 m provide favorable conditions for *D. maruadsi,* so that the positive effect of SLA on *D. maruadsi* CPUE reaches the maximum level within this SLA range.

No significant correlation between *D. maruadsi* CPUE and Chl a was observed in this study (*Fig. 3e*), but the data density plot indicated that *D. maruadsi* CPUE was concentrated at Chl a ranging from 0.1 to 0.5 $mg \cdot m^{-3}$, suggesting that *D. maruadsi* tends to live in waters with this range of Chl a. As an indicator of marine phytoplankton, Chl a has an important impact on fishery distribution. The study on the Pacific saury

http://www.aloki.hu ● ISSN 1589 1623 (Print) ● ISSN 1785 0037 (Online)
DOI: http://dx.doi.org/10.15666/aeer/1704_84858499

(*Cololabis saira*) distribution in the northwestern Pacific Ocean based on empirical cumulative distribution function (ECDF) showed that high CPUE occurred when Chl a ranged from 0.4 to 0.6 mg·m^{-3} (Tseng, 2013). The study on yellowfin tuna (*Thunnus albacares*) in the western and central Pacific showed that the tuna tends to live in the waters with Chl a of 0.1-0.6 mg·m^{-3} (Wang, 2016; Kang, 2018). It has been reported that *D. maruadsi* in southern Taiwan Strait prefer to live in the waters with Chl a ranging from 0.2 to 1.0 mg·m^{-3} (Li, 2006). The data density distribution based on GAM analysis in this study revealed a Chl a range suitable for *D. maruadsi* in the western Guangdong waters.

Conclusions

To examine the relative influence of environmental factors on the distribution of *D. maruadsi*, data recorded by the fishing vessels and remote sensing including SST, Chl a and SLA in the western Guangdong waters, were analyzed using GAMs combined with correlation analysis in this study. Results showed that *D. maruadsi* CPUE in western Guangdong waters had a significant positive linear correlation with longitude, showing a general trend of decreasing from east to west. The final model explained 47.40% of the variability in *D. maruadsi* CPUE in total. Among all the factors included in the model, month was most influential to the distribution of *D. maruadsi*, followed by depth, year, lunar phase, SLA and latitude, Chl a and SST. The *D. maruadsi* resources were concentrated in the areas where the latitude was 21°N, Chl a ranged from 0.1 to 0.5 mg·m^{-3}, SLA was -0.05 m and water depth was 80 m. The fishing method (light luring seines) used in this study might affect the conclusions about the effects of lunar phase and water depth on *D. maruadsi* CPUE. Therefore, different fishing methods will be used verify the effects of the two factors in the future work.

Acknowledgements. This study was supported by the following funds: (1) Central Public-interest Scientific Institution Basal Research Fund, CAFS (2018HY-ZD0104), (2) National Key R&D Program of China (2018YFD0900901); (3) Natural Science Foundation of Guangdong Province, China (2018A030313120), (4) State Key Laboratory of Tropical Oceanography, South China Sea Institute of Oceanology, Chinese Academy of Sciences (LTO1806).

REFERENCES

[1] Abdullah, N. A., Rahim, F. (2018): Distinctiveness and potentials of two flowering roadside hedgerows, Turnera ulmifolia and Melastoma malabathricum as benefecial plants for insects. – Environment & Ecosystem Science 2(2): 06-10.
[2] Abija, F. A., Nwankwoala, H. O. (2018): Characterization of aquifers in parts of Abia State Southeastern Nigeria. – Earth Sciences Pakistan 2(1): 18-22.
[3] Agenbag, J. J., Richardson, A. J., Demarcq, H. et al. (2003): Estimating environmental preferences of South African pelagic fish species using catch size- and remote sensing data. – Progress in Oceanography 59(2): 275-300.
[4] Austin, O. E., Ebuka, A. O., Zanders, A. C. C., Joseph, I. N. (2018): Seismic analysis of the transgressive systems tracts (TSTS) of the Niger Delta. – Earth Sciences Malaysia 2(2): 16-19.
[5] Bacha, M, Jeyid. M. A., Vantrepotte, V. et al. (2017): Environmental effects on the spatio-temporal patterns of abundance and distribution of Sardina pilchardus and

http://www.aloki.hu ● ISSN 1589 1623 (Print) ● ISSN 1785 0037 (Online)
DOI: http://dx.doi.org/10.15666/aeer/1704_84858499

sardinella off the Mauritanian coast (North-West Africa). – Fisheries Oceanography 8(5): 12-25.

[6] Campbell, R. A. (2004): CPUE standardisation and the construction of indices of stock abundance in a spatially varying fishery using general linear models. – Fisheries Research (Amsterdam) 70(2-3): 0-227.

[7] Chelton, D. B., Samelson, R. M. (2011): The influence of nonlinear mesoscale eddies on near-surface oceanic chlorophyll. – Science 334(6054): 328.

[8] Chen, G. B., Qiu, Y. S. (2003): Study on growth, mortality and reasonable utilization of *Decapterus maruadsi* in northern continental shelf waters of South China Sea. – Journal of Applied of Oceanography 22(4): 457-464.

[9] Chen, G. B., Li, Y. Z., Chen, P. M. A. (2003): study on spawning ground of blue mackerel scad (decapterus maruadsi) in continental shelf waters of Northern South China Sea. – Journal of Tropical Oceanography 22(6): 22-28.

[10] Chen, X. J., Tian, S. Q., Qian, W. G. (2006): Effect of moon phase on the jigging rate of *Ommastrephes bartrami* in the North Pacific. – Marine Fisheries 28(2): 136-140.

[11] Chen, Z. Z., Qiu, Y. S. (2009): Assessment of the food-web structure, energy flows, and system attribute of northern South China Sea ecosystem. – Acta Ecologica Sinica 30(18): 4855-4865.

[12] Chen, Z. Z., Lin, Z. J., Qiu, Y. S. (2010): Evaluation of sustainability of fisheries resources for South China Sea based on the AHP. – Journal of Natural Resources 25(2): 249-257.

[13] Cortez, A. (2016): 3. Variabilidad espacio temporal de la precipitación en el estado Guárico, Venezuela. – Revista de la Facultad de Agronomia de la Universidad del Zulia 33(3).

[14] Dai, J. G., Chen, Z. Z., Hunag, Z. R., Xu, Y. W., Sun, M. S., Zhang, K., Jiang, Y. E. (2017): Otolith morphology of Decapterus maruadsi in the continental shelf of northern South China Sea. – Journal of Applied of Oceanography 36(3): 417-426.

[15] Deng, J. Y. (1991): Marine Biology. – China Agriculture Press, Beijing.

[16] Dingstor, G. E., Ciannelli, L., Chan, K. S. et al. (2007): Density dependence and density independence during the early life stages of four marine fish stocks. – Ecology 88(3): 625-634.

[17] Fan, J. T., Huang, Z. R., Xu, Y. W., Sun, M. S., Chen, G. B., Chen, Z. Z. (2018): Habitat model analysis for decapterus maruadsi in northern South China Sea based on remote sensing data. – Transactions of Oceanology and Limnology 3: 142-147.

[18] Fauchald, P., Skarsfjord, H., Erikstad, K. E. (2000): Scale-dependent predator-prey interactions: the hierarchical spatial distribution of seabirds and prey. – Ecology 81(3): 773-783.

[19] Franco, G. H., Macancela, N. A., Gavín-Quinchuela, T., Carrión-Mero, P. (2018): Participatory socio-ecological system: Manglaralto-Santa Elena, Ecuador. – Geology, Ecology, and Landscapes 2(4): 303-310.

[20] Fu, D. Y., Pan, D. L., Ding, Y. Z., Zou, J. H. (2009): Quantitative study of effects of the sea chlorophyll-a concentration by typhoon based on remote-sensing. – Acta Oceanologica Sinica 31(3): 46-56.

[21] Geng, P., Zhang, K., Chen, Z. Z. Xu, Y. W., Sun, M. S. (2018): Interannual change in biological traits and exploitation rate of Decapterus maruadsi in Beibu Gulf. – South China Fisheries Science 14(6): 1-9.

[22] Hashim, M., Aziz, M. F. H. A., Hassan, R. B. et al. (2017): Assessing target strength, abundance, and biomass for three commercial pelagic fish species along the east coast of peninsular Malaysia using a split-beam echo sounder. – Journal of Coastal Research 33(6).

[23] Hastie, T. J., Tibshirani, R. J. (1990): Generalized Additive Models. – Chapman and Hall, London, pp. 236-351.

http://www.aloki.hu ● ISSN 1589 1623 (Print) ● ISSN 1785 0037 (Online)
DOI: http://dx.doi.org/10.15666/aeer/1704_84858499

[24] He, Q., Zhan, H., Cai, S. et al. (2016): Eddy effects on surface chlorophyll in the northern South China Sea: mechanism investigation and temporal variability analysis. – Deep Sea Research Part I: Oceanographic Research Papers S0967063715301230.
[25] Hintze, J., Nelson, R. (1998): Violin plots: a box plot-density trace synergism. – The American Statistician 52(2): 4.
[26] Huang, M. Z. (1995): Feeding habits of Decafterus maruadsi in Taiwan Strait. – Journal of Applied of Oceanography (4): 399-406.
[27] Jaimes, E. J. (2017): 2. Capacidad de carga y presión de uso de la tierra en cuatro sectores de la sub-cuenca del río Déleg, Provincia del Cañar, Ecuador. – Revista de la Facultad de Agronomia de la Universidad del Zulia 34(3).
[28] Jamil, F., Arshad, R., Ali, M. A. (2018): Design, fabrication and evaluation of rotary hot-air dryer for the value addition of fruit waste. – Earth Sciences Pakistan 2(2): 07-11.
[29] Jegatheesan, J., Zakaria, Z. (2018): Stress analysis on pressure vessel. – Environment & Ecosystem Science 2(2): 53-57.
[30] Jiang, R. J., Xu, H. X., Jin, H. W., Zhou, Y. D., He, Z. T. (2012): Feeding habits of blue mackerel scad Decapterus maruadsi Temminck et Schlegel in the East China Sea. – Journal of Fisheries of China 36(2): 216-227.
[31] Kang, L., Du, H. L., Zhang, H., Ma, W. L. (2018): Systematic research on the application of steel slag resources under the background of big data. – Complexity. doi.org/10.1155/2018/6703908.
[32] La Mesa, M., La Mesa, G., Catalano, B. et al. (2016): Spatial distribution pattern and physical-biological interactions in the larval notothenioid fish assemblages from the Bransfield Strait and adjacent waters. – Fisheries Oceanography 25(6): 624-636.
[33] Le, K., Yao, J. Z., Li, Z., Ke, Z. (2017): Preparation, characterization and photocatalytic activity of novel CeO2 loaded porous alkali-activated steel slag-based binding material. – International Journal of Hydrogen Energy 42(27): 17341-17349.
[34] Li, X. D. (2006): Monthly variability in the catchability of chub macherel and round scad and its relationship with environmental seasonality in the southern Taiwan Strait. – Xiamen University, Xiamen, pp. 40-72.
[35] Lu, Z. B., Dai, Q. S. (2000): An estimation of resources of chub mackerel, round scad and other pelagic fish stocks in the Taiwan Strait and the adjacent waters. – Journal of Fishery Sciences of China 7(1): 41-45.
[36] Maravelias, C. D., Reid, D. G. (1997): Identifying the effects of oceanographic features and zooplankton on prespawning herring abundance using generalized additive models. – Marine Ecology Progress 147(1-3): 1-9.
[37] Nieto, K., Mélin, F. (2017): Variability of chlorophyll-a concentration in the Gulf of Guinea and its relation to physical oceanographic variables. – Progress in Oceanography 151: 97-115.
[38] Qu, Y. N., Pei, Z. B., Yang, S. T. (2018): Legal consideration on China's summer marine fishing moratorium system: in the perspective of venables sustainable development. – Ocean Development and Management 9.
[39] Quinn, T. J., Deriso, R. B. (1999): Quantitative Fish Dynamic. – Oxford University Press, New York, pp. 124-256.
[40] Schütte, F., Brandt, P., Karstensen, J. (2016): Occurrence and characteristics of mesoscale eddies in the tropical northeast Atlantic Ocean. – Ocean Science 12(3): 663-685.
[41] Shih, C., Chen, Y., Hsu, C. (2014): Modeling the effect of environmental factors on the ricker stock-recruitment relationship for north pacific albacore using generalized additive models. – Terrestrial Atmospheric & Oceanic Sciences 25: 581-590.
[42] Si, D., Liu, Y. J., Shao, X., Wang, Y. J. (2016): Anomalies of oceanic and atmospheric circulation in 2015 and their impacts on climate in China. – Meteorological Monthly 42(4): 481-488.

http://www.aloki.hu ● ISSN 1589 1623 (Print) ● ISSN 1785 0037 (Online)
DOI: http://dx.doi.org/10.15666/aeer/1704_84858499

[43] Solanki, H. U., Bhatpuria, D., Chauhan, P. (2017): Applications of generalized additive model (GAM) to satellite-derived variables and fishery data for prediction of fishery resources distributions in the Arabian Sea. – Geocarto International 32(1): 14.
[44] Song, X., Lai, Z., Ji, R., Chen, C., Zhang, J., Huang, L., Yin, J., Wang, Y., Lian, S. Zhu, X. (2012): Summertime primary production in northwest South China Sea: interaction of coastal eddy, upwelling and biological processes. – Continental Shelf Research 48(5): 110-121.
[45] Stenseth, N. C., Mysterud, A., Ottersen, G. et al. (2002): Ecological effects of climate fluctuations. – Science 297(5585): 1292-1296.
[46] Stoner, A. W., Manderson, J. P., Pessutti, J. P. (2001): Spatially explicit analysis of estuarine habitat for juvenile winter flounder: combining generalized additive models and geographic information systems. – Marine Ecology Progress 213(4): 253-271.
[47] Sudhakaran, M., Ramamoorthy, D., Savitha, V., Balamurugan, S. (2018): Assessment of trace elements and its influence on physico-chemical and biological properties in coastal agroecosystem soil, Puducherry region. – Geology, Ecology, and Landscapes 2(3): 169-176.
[48] Tao, S. (2018): Evaluation of technology innovation in Hubei Province. – Engineering Heritage Journal 2(2): 09-10.
[49] Thanh, L. D., Do, P. V. (2018): Streaming current induced by fluid flow in porous media. – Earth Sciences Malaysia 2(1): 22-28.
[50] Thomas, A. C., Strub, P. T., Weatherbee, R. A. et al. (2012): Satellite views of Pacific chlorophyll variability: comparisons to physical variability, local versus nonlocal influences and links to climate indices. – Deep Sea Research Part II Topical Studies in Oceanography 77-80(10): 99-116.
[51] Tianlei, W. (2019): Nonlinear control strategies and planning for underactuated overhead cranes. – Engineering Heritage Journal 3(1): 09-12.
[52] Tseng, C. T., Su, N. J., Sun, C. L. et al. (2013): Spatial and temporal variability of the Pacific saury (Cololabis saira) distribution in the northwestern Pacific Ocean. – Ices Journal of Marine Science 70(5): 991-999.
[53] Venables, W. N., Dichmont, C. M. (2004): GLMs, GAMs and GLMMs: an overview of theory for applications in fisheries research. – Fisheries Research 70(2-3): 315-333.
[54] Wang, J., Chen, X., Chen, Y. (2016): Spatio-temporal distribution of skipjack in relation to oceanographic conditions in the west-central Pacific Ocean. – International Journal of Remote Sensing 37(24): 6149-6164.
[55] Wang, X. X., Chen, T., Li, M., Wang, X. H., Wang, Y. Z. (2018): Relationships between environmental factors and the distribution of Indo-Pacific humpback dolphins (Sousa chinensis) in the western Pearl River Estuary, China. – Acta Ecologica Sinica 38(03): 934-944.
[56] Wang, Z., Li, Q., Sun, L. et al. (2015): The most typical shape of oceanic mesoscale eddies from global satellite sea level observations. – Frontiers of Earth Science 9(2): 202-208.
[57] Wood, S. N. (2004): Stable and efficient multiple smoothing parameter estimation for generalized additive models. – J. Amer. Statist. Ass. 99: 673-686.
[58] Wood, S. N. (2011): Fast stable restricted maximum likelihood and marginal likelihood estimation of semiparametric generalized linear models. – Journal of the Royal Statistical Society (B) 73(1): 3-36.
[59] Wu, Z. Q., Qiu, S. Y., Yang, S. Y. (2000): Characters of reproductive biology of six pelagic fishes in Minnan-Taiwan bank fishing ground. – Marine Science Bulletin 19(2): 25-29.
[60] Xie, L. L., Zong, X. L., Yin, X. F., Li, M. (2016): The interannual variation and long-term trend of Qiongdong Upwelling. – Oceanologia et Limnologia Sinica 47(1): 43-51.

http://www.aloki.hu ● ISSN 1589 1623 (Print) ● ISSN 1785 0037 (Online)
DOI: http://dx.doi.org/10.15666/aeer/1704_84858499

[61] Yan, L., Zhang, P., Yang, L., Yang, B. Z., Chen, S., Li, Y. N., Tan, Y. G. (2015): Effect of moon phase on fishing rate by light falling-net fishing vessels of *Symplectoteuthis oualaniensis* in the South China Sea. – South China Fisheries Science 3: 16-21.
[62] Yan, Y. M., Lu, Z. B., Dai, Q. S. (1987): Study on growth characteristics of round scad in Minzhong and Mindong fishing grounds. – Journal of Zoology 22(5): 8-13.
[63] Yang, L., Zhang, X. F., Tan, Y. G., Zhang, P. (2009): The catch composition of light falling-net fishing and its impact on fishery resources in the northern South China Sea. – South China Fisheries Science 5(4): 41-46.
[64] Yang, L., Cao, W. Q., Lin, Y. S., Chen, Y. H., Lin, Z. J., Wang, X. H. (2016): Preliminary study on feeding habits and trophic niche of nine economic fish species in Beibu Gulf in summer. – Journal of Tropical Oceanography 35(2): 66-75.
[65] Yi, J., Du, Y., He, Z. et al. (2014): Enhancing the accuracy of automatic eddy detection and the capability of recognizing the multi-core structures from maps of sea level anomaly. – Ocean Science 10(1): 39-48.
[66] Yuan, Y., Liu, Y. J., Wang, Y. J., Wang, P. L. (2014): Main characteristics and possible causes for the climate in China during the spring of 2014. – Meteorological Monthly 41(10): 1292-1297.
[67] Zhan, P., Subramanian, A. C., Yao, F. et al. (2014): Eddies in the Red Sea: a statistical and dynamical study. – Journal of Geophysical Research Oceans 119(6): 3909-3925.
[68] Zheng, Y. J., Li, J. S., Zhang, Q. Y., Hong, W. S. (2014): Research progresses of resource biology of important marine pelagic food fishes in China. – Journal of Fisheries of China 38(1): 149-160.
[69] Zhu, D. L., Song, H. T., Bo, Z. L., Wu, Z. J. (1984): A study on mackerel and round scadfishing ground off Zhejiang coast in the summer-autumn season. – Marine Science Bulletin 3(2): 64-72.
[70] Zhu, Y. G. (2009): Research on the Effects of China's Summer Fishing Moratorium - A Perspective of Institutional Analysis. – Ocean University of China, Qingdao, pp. 89-95.

http://www.aloki.hu ● ISSN 1589 1623 (Print) ● ISSN 1785 0037 (Online)
DOI: http://dx.doi.org/10.15666/aeer/1704_84858499

EFFECTS OF ELEVATED ATMOSPHERIC CO_2, O_3 AND SOIL PHENANTHRENE ON SOIL ENZYME ACTIVITIES AND MICROBIAL BIOMASS

DONG, D.[1] – SHI, C.[1*] – YAN, S.[1] – ASHRAF, M. A.[2]

[1]*School of Biological Engineering, Huainan Normal University, Huainan 232001, China*

[2]*School of Environmental Studies, China University of Geosciences, Wuhan 430074, China*

**Corresponding author*
e-mail: traceypage3311@gmail.com

(Received 8th Mar 2019; accepted 21st May 2019)

Abstract. This paper aimed to investigate the effects of elevated [CO_2], [O_3] or [$CO_2 + O_3$] on soil physicochemical properties, microbial biomass and soil enzyme activities in phenanthrene-added and -unadded soils. The results showed that elevated [CO_2] increased the dissolved organic carbon (DOC), total phosphorus (TP), available phosphorus (AP), total potassium (TK), total carbon (TC), and nitric nitrogen (NN) contents to some extent in phenanthrene-untreated soils, which contrary to the elevated [O_3], and thus differentially promoted the contents of microbial biomass carbon (MBC), microbial biomass nitrogen (MBN) as well as activities of soil protease (PRA), sucrase (SA), acid phosphatase (APA) and neutral phosphatase (NPA) in the soils. The elevated [O_3] increased ratios of MBC/MBN, and led to the decrease of the activities of PRA, APA and NPA to some extent. However, to some extent, [$CO_2 + O_3$] alleviated the inhibition of the soil microbial biomass and soil enzyme activities by [O_3] elevation and basically did not change the tendency of the soil physicochemical properties, microbial biomass and enzyme activities, but their contents in phenanthrene-added soils compared with the phenanthrene-untreated soils. Therefore, the alteration of soil microbial biomass and soil enzyme activities can be used for assessment of the effects of elevated atmospheric CO_2, O_3 or phenanthrene-polluted soil on the soil microbial systems.

Keywords: *open top chamber (OTC), phenanthrene-added soils, elevated [CO_2], elevated [O_3], soil physicochemical properties*

Introduction

For the past few years, the continuous increase of CO_2 and O_3 concentration in the atmosphere and global climate change have attracted wide attention of the whole society (Wang et al., 2014). The research results show that elevated atmospheric CO_2 concentration significantly affects the land ecological system through improving the plant photosynthesis changes of plant root secretion and soil microbial community composition and the quantity, flow and distribution of carbon and nitrogen in soil, and the size of soluble carbohydrate pool indirectly changes the physical and chemical properties of soil, so as to affect the alteration of soil microbial ecosystem (Xu et al., 2013; Sulman et al., 2014; Manna et al., 2012).

O_3 is a naturally occurring photochemical oxidant in the troposphere of the Earth, and a major component of greenhouse gases and photochemical smog. Higher O_3 levels can have negative effects on plants. O_3 enters plant tissue thorough stomata, and can reduce stomatal conductance, and then inhibits photosynthesis and nutrient absorption, and finally reduces plant biomass and crop yield (Díaz-de-Quijano et al., 2012; Zhang et al., 2011). Under the stress of O_3, changes in plant root secretions might also change the physical and chemical properties of soil, and reduce soil microbial biomass carbon and nitrogen, and potentially change the rhizosphere microbial community, nutritional status

http://www.aloki.hu ● ISSN 1589 1623 (Print) ● ISSN 1785 0037 (Online)
DOI: http://dx.doi.org/10.15666/aeer/1704_85018512

and soil enzyme activity (Wu et al., 2012; Haesler et al., 2014; Cheng et al., 2014; Veeraragavan et al., 2018).

Soil enzymes are involved in the material circulation, energy flow and degradation of organic pollutants in soil, and changes in their activity can reflect the strength and direction of various biochemical processes in soil. The microbial biomass is very sensitive to environmental factors, and is always applied to monitor the scale and activity of soil microbial community (Lou et al., 2011). Therefore, soil microbial biomass and soil enzyme activity have been developed into ecological indicators for evaluating soil environmental quality (Han et al., 2016; Tripathi et al., 2007; Kumar and Jaafar, 2018), and have been applied to evaluate the alteration of soil microecological environment under atmospheric CO_2 and O_3 pollution conditions (Li et al., 2010; Rozuki et al., 2018).

People usually adopt free-air CO_2 enrichment (FACE) or Open top chamber (OTC) system to investigate the elevated atmospheric CO_2 and O_3 concentration influence on plant and soil microbial system (Wu et al., 2012; Formánek et al., 2014). The study found that elevated atmospheric CO_2 and O_3 concentration can change the plant population composition, and then affect plant chemistry (Booker et al., 2005; Johnson and Pregitzer, 2007), and increases the content of phenolic substances (Li et al., 2008; Sen et al., 2018), and finally indirectly change soil chemical characteristics and induce changes in soil microbial functional diversity, biomass and enzyme activity (Xu et al., 2013; Huang et al., 2013; Wu et al., 2015). As a representative of polycyclic aromatic hydrocarbons pollutants, the phenanthrene (PHE) is gradually accumulated in the soil with a low-dose superposition. Its potential ecological risk of soil pollution has been widely concerned (Zhang et al., 2018).

At present, most researches about the change of soil–plant system under elevated CO_2 and O_3 conditions, are to simulate impact and evaluation of a single elevated CO_2 and O_3 on ecosystem safety, while there are few researches on the combined conditions of the two (Tian et al., 2011; Ren et al., 2014), especially on the effect of soil phenanthrene on soil enzyme activity under the condition of atmospheric CO_2 and O_3 rising. Based on OTC platform, under the condition of CO_2, O_3, $CO_2 + O_3$ increase, the research build micro universe soil - green vegetable potted simulation system to discuss the change of soil protease, polyphenol oxidase, phosphatase, urease and invertase as well as the change of soil microbial biomass with or without adding phenanthrene (López-Hernández, 2018), which was aimed to obtain the future elevated atmospheric CO_2 and/or O_3 micro ecological impact on the soil.

Materials and methods

Test platform and processing mode

The test platform is located in Xianlin Campus of Nanjing University (118°57′36.15″E, 31°7′23.99″N). The platform includes 4 air chambers. One is connected to the normal atmosphere. One has 200 ppm more CO_2 concentration than normal atmosphere. One has 50 ppb O_3 concentration than normal atmosphere. One control the compound increase of CO_2 and O_3 concentration. The air chamber is octagon with 2 m of diameter and 2.8 m of height. CO_2 was provided by Du Wa Guan (Q/JB-THB002, Beijing Tianhai Industry Co., Ltd). CO_2 was purchased by Nanjing Tianze Gas Co., Ltd with 99.9% of purity. O_3 is produced by O_3 generator (NPF 10/W, Shandong Tianze). CO_2 and O_3 (gas was controlled by valves and flow meter) mixed

http://www.aloki.hu ● ISSN 1589 1623 (Print) ● ISSN 1785 0037 (Online)
DOI: http://dx.doi.org/10.15666/aeer/1704_85018512

with normal atmosphere by axial flow fan (SFG-2, Shanghai Jia Bao) into the bottom of the chamber. And then the gas entered the chamber through holes (0.5 cm of diameter) on the bottom of the chamber and the stainless steel plate in the middle of the chamber. The gas then entered that outer atmosphere through the opening at the top of the gas chamber. The gas replacement frequency should ensure than the gas will be replaced 3~4 times per minute in the chamber. CO_2 concentration was monitored by CO_2 detector (Li-7000, Li-Cor, USA), and O_3 concentration was monitored by O_3 detector (Model 205, 2B Co., USA). CO_2 was injected into the gas chamber all the times, and the injection time of O_3 was from 9 am to 5 pm (except rainy days).

In July 2014, the soil with 100 ppm of exo-phenanthrene and the soil without adding phenanthrene were prepared. In June 2017, the concentration of phenanthrene in the contaminated soil was measured at about 30 ppm. Meanwhile, these aged soils were divided into flowerpots (10 kg/pot). Fertilizer (2 g/pot, N:P:K = 1:1:1) was added, and then turned over, and mixed well. Then 10 green vegetable seeds were planted. Finally the flowerpots without adding phenanthrene were transferred to 4 chambers in OTC which were ambient[Amb], [CO_2], [O_3] and [$CO_2 + O_3$] representing the normal atmosphere, high CO_2, high O_3 and mixed increase of CO_2 and O_2.

At the same time, the soil polluted by phenanthrene was also transferred to the 4 air chambers represented by [Amb] + [PHE], [CO_2] + [PHE], [O_3] + [PHE] and [$CO_2 + O_3$] + [PHE]. 3 pots were prepared for each treatment. After germination, the seeding began to grow for another week. Each flowerpot kept 3 seedlings with same size. They were replenished regularly with the same amount of deionized water. Soil samples were collected after 30 days for the detection and analysis of the following indicators.

Determination of physical and chemical properties of soil

The method of Shi Cuie and teammates (Shi et al., 2015) was referenced to determine the physical and chemical properties.

Determination of soil microbial biomass carbon (MBC) and microbial biomass nitrogen (MBN)

Soil MBC and MBN were measured by chloroform fumigation - K2SO4 extraction (Shi et al., 2015). The content of organic carbon and total N in the extraction solution (Multi C/N 3100, Jena) were determined by TOC analyzer. The calculation methods of MBC and MBN are as follows. MBC = EC/0.45, MBN = EN/0.45, EC, EN were the differences of organic carbon or total nitrogen between the fumigated and non-fumigated soil leaching solution (Liu et al., 2014), and 0.45 is the proportion coefficient of the extracted biomass after chloroform fumigation (Iqbal et al., 2010). The carbon nitrogen ratio of microorganisms was expressed as MBC/MBN.

Determination of soil enzyme activity

Soil enzyme activity was determined by indanone colorimetry in accordance with the method of Guan (1986). 1 mg NH_2-N produced by 1 g soil after 24 h was defined as 1 mg NH_2-N$\cdot g^{-1}\cdot 24\ h^{-1}$ for soil protease (PRA) activity. Sucrose enzyme (SA) was determined by 3,5-dinitrosalicylic acid colorimetry. 1 g glucose produced by 1 g soil after 24 h was defined as 1 mg glucose$\cdot g^{-1}\cdot 24\ h^{-1}$. Urease activity (UA) was determined by sodium phenol - sodium hypochlorite colorimetric method. 1 μg NH_3-N produced by 1 g soil after

http://www.aloki.hu ● ISSN 1589 1623 (Print) ● ISSN 1785 0037 (Online)
DOI: http://dx.doi.org/10.15666/aeer/1704_85018512

24 h under 37 °C was defined as 1 μg NH_3-N·g^{-1}·24 h^{-1}. The activity of polyphenol oxidase (POA) was determined by using purple gallic acid colorimetry. 1 g purple gallic acid colorimetry produced by 1 g soil after 2 h was defined as 1 mg PG·g^{-1}·2 h^{-1}. The activity of soil acid phosphatase (APA) and neutral phosphatase (NPA) were determined by disodium phenyl phosphate. 1 mg P_2O_5 produced by 100 g soil after 2 h under 37 °C was defined as 1 mg P_2O_5·100 g^{-1}·2 h^{-1}.

Data processing

Raw data were sorted out by Excel 2003. SPSS 20.0 was applied for statistical analysis. Variance analysis was used to test the differences between the factors, and SNK method was used for multiple comparisons between the two factors.

Results and analysis

Effects of the rising of CO_2 and O_3 in atmosphere and phenanthrene in soil on physical and chemical properties of soil

With the increase of CO_2 or/and O_3 in OTC, the content alteration of NN, TP, TK and TC in the soil without adding phenanthrene soil presents a trend of [CO_2] > [Amb] > [CO_2 + O_3] > [O_3]. The trend of content alteration of AN, DON, TN and DOC was [CO_2] > [CO_2 + O_3] > [Amb] > [O_3]. The trend of content alteration SWC and AP was [CO_2] > [CO_2 + O_3] > [O_3] > [Amb], while the decline of pH value was as the trend of [O_3] > [CO_2 + O_3] > [Amb] > [CO_2] (*Table 1*).

Table 1. *Effects of elevated atmospheric CO_2 or/and O_3 on soil physicochemical properties of phenanthrene-added and unadded soils*

Treatments	NN/mg·g^{-1}	TP/mg·kg^{-1}	TK/mg·g^{-1}	TC/mg·g^{-1}	AN/mg·g^{-1}	TN/mg·g^{-1}
Amb	9.98±1.12ab	404.65±45.90bc	10.78±1.89ab	13.14±1.20a	0.77±0.10 bc	1.28±0.20a
CO_2	13.72±2.61b	463.33±47.09c	11.40±1.31b	14.70±2.32ab	0.93±0.12bc	1.50±0.21a
O_3	5.87±1.57a	293.50±23.07a	6.78±0.70a	12.30±1.30a	0.56±0.12a	1.23±0.19a
CO_2+O_3	8.43±1.13a	370.60±50.00abc	9.71±1.02ab	12.89±1.31a	0.83±0.12bc	1.40±0.18a
Amb+phenanthrene	10.07±2.01ab	435.40±50.00bc	10.51±1.91ab	15.90±2.43ab	0.89±0.13bc	1.37±0.22a
CO_2+phenanthrene	13.84±2.02b	583.70±42.95d	11.01±2.01ab	16.70±1.02b	0.97±0.14c	1.60±0.15a
O_3+phenanthrene	8.08±1.45a	332.90±50.00ab	8.95±1.03ab	12.50±2.13a	0.70±0.11ab	1.24±0.20a
CO_2+O_3+phenanthrene	8.61±1.12a	429.25±44.99bc	10.87±2.06b	13.61±1.34ab	0.81±0.11bc	1.45±0.18a

Treatments	DON/mg·g^{-1}	DOC/mg·g^{-1}	AP/mg·g^{-1}	SWC/%	pH
Amb	16.45±2.40ab	33.54±4.00b	7.76±1.21a	21.77±3.06a	6.11±1.50a
CO_2	18.25±2.05ab	72.36±10.34d	20.81±3.97c	28.36±3.51a	5.78±1.00a
O_3	14.23±1.50a	20.70±2.56a	12.27±1.96ab	24.49±4.00a	6.35±1.65a
CO_2+O_3	16.57±2.21ab	44.74±4.67c	14.12±1.98b	24.90±3.50a	6.17±1.11a
Amb+phenanthrene	17.56±1.92ab	49.07±5.35c	18.77±1.94c	25.35±4.00a	6.02±1.03a
CO_2+phenanthrene	21.70±4.13b	82.97±10.12e	13.91±2.11b	27.20±3.55a	5.85±0.76a
O_3+phenanthrene	16.26±1.50ab	27.07±4.01ab	10.82±0.88ab	25.03±2.62a	6.33±1.13a
CO_2+O_3+phenanthrene	16.97±2.32ab	49.92±5.05c	10.52±1.97ab	25.40±1.92a	6.19±1.10a

SWC: Soil water content; TP: Total phosphorus; TC: Total carbon; TN: Total nitrogen; TK: Total K; AN: NH_4^+-N: NN: NO_3—N; AP: Available P; DOC: Dissolved organic carbon; DON: Dissolved organic nitrogen. Values represent mean ± SD, n = 3. Different small letters in the same column represent significant differences at 0.05 level. The same as follows

The increase of CO_2 or/and O_3 also induced the change of physical and chemical properties of the soil with adding phenanthrene. In the soil with adding phenanthrene,

http://www.aloki.hu ● ISSN 1589 1623 (Print) ● ISSN 1785 0037 (Online)
DOI: http://dx.doi.org/10.15666/aeer/1704_85018512

the content trend of NN, TP, TK, TC, AN and DON was [CO_2] + [PHE] > [Amb] + [PHE] > [CO_2 + O_3] + [PHE] > [O_3] + [PHE]. The content alteration of TN, SWC and DOC was [CO_2] + [PHE] >[CO_2 + O_3] + [PHE] > [Amb] + [PHE] > [O_3] + [PHE], while the soil pH alteration was [O_3] + [PHE] > [CO_2 + O_3] + [PHE] > [Amb] + [PHE] > [CO_2] + [PHE].

The results also indicated that the contents of NN, TP, AN, DON, TK, TC and TN in the soil with adding phenanthrene were slightly higher than that of the soil without adding phenanthrene (*Table 1*). Therefore, the increase of atmospheric CO_2 or/and O_3, as well as the pollution of phenanthrene in soil, induced the change of physical and chemical properties of the experimental soil to some extent.

Effects of rising of CO_2, O_3 in atmosphere and phenanthrene in soil on soil microbial biomass

The change of soil microbial biomass carbon (MBC) and nitrogen (MBN) in the soil without adding phenanthrene was [CO_2] > [CO_2 + O_3] > [Amb] > [O_3]. Multiple comparison results showed that compared with [Amp], CO_2 injection induced a significant increase in MBC and MBN content ($P < 0.05$), while only O_3 injection induced a significant decrease in MBN content ($P < 0.05$). The carbon nitrogen ratio (MBC/MBN) of microbial biomass showed a trend of [O_3] > [CO_2 + O_3]> [CO_2] > [Amb]. Multiple comparison results showed that only [O_3] induced significant increase in MBC/MBN compared with [Amb] ($P < 0.05$).

In the soil with adding phenanthrene, the content change of MBC and MBN was [CO_2] + [PHE] > [Amb] + [PHE] > [CO_2 + O_3] + [PHE] > [O_3] + [PHE]. Multiple comparison results suggested that compared with [Amb] + [PHE], [O_3] + [PHE] induced a significant decrease in MBC and MBN ($P < 0.05$), while no significant change was observed in other treatment groups. Under normal atmospheric conditions, MBC and MBN in soil with adding phenanthrene increased by 47% and 45% ($P < 0.05$) respectively compared with that of the soil without adding phenanthrene (*Table 2*). MBC/MBN presented an alteration trend of [O_3] + [PHE] > [CO_2] + [PHE] > [Amb] + [PHE] > [CO_2 + O_3] + [PHE], while the changes within the treatment groups was not significant ($P > 0.05$).

Table 2. *Effect of elevated atmospheric CO_2 and/or O_3 on contents of carbon and nitrogen of microbial biomass and ratio of microbial biomass carbon/nitrogen in phenanthrene-added and -unadded soils*

Treatments	MBC/mg·kg^{-1}	MBN/mg·kg^{-1}	MBC/MBN
Amb	50.42±7.8a	7.08±1.02b	7.11±0.10ab
CO_2	83.36±7.39c	10.69±1.12c	7.82±0.54b
O_3	46.52±4.18a	4.81±1.03a	9.68±0.19c
CO_2+O_3	57.69±10.01ab	7.3±1.02b	7.88±0.29b
Amb+phenanthrene	73.9±10.06bc	10.29±1.02c	7.16±0.38ab
CO_2+phenanthrene	86.55±7.2c	11.52±1.01c	7.56±1.00b
O_3+phenanthrene	54.19±5.04a	7.08±1.04b	7.88±0.46b
CO_2+O_3+phenanthrene	60.52±11ab	9.78±1.01c	6.16±0.40ab

MBC: Microbial biomass carbon; MBN: Microbial biomass nitrogen; MBC/MBN: ratio of microbial biomass carbon/nitrogen

The results of multivariate analysis of variance showed suggested that the effects of different treatment groups [CO_2], [CO_2 + O_3], [Amb] and [O_3], (Pascual-Córdova, 2018)

http://www.aloki.hu ● ISSN 1589 1623 (Print) ● ISSN 1785 0037 (Online)
DOI: http://dx.doi.org/10.15666/aeer/1704_85018512

as well as the soil treatment model with adding phenanthrene and the model without adding phenanthrene on soil microbial biomass carbon and nitrogen were extremely significant ($P < 0.05$). At the same time, the interaction between different treatment groups and two soil treatment models had no significant influence on soil microbial biomass carbon and nitrogen.

Effects of rising of CO_2, O_3 in atmosphere and phenanthrene on soil enzyme activity

The alteration trends in the activity of soil protease (PRA), invertase (SA), urease (UA), (Espinoza, 2017) polyphenol oxidase (POA) and acidic phosphatase (APA) under the condition of increase of atmospheric CO_2 or and O_3 without adding phenanthrene was like $[CO_2] > [CO_2 + O_3] > [Amb] > [O_3]$ that was consistent with the alteration trends of MBC and MBN in soil. Multiple comparison results showed that, compared with [Amb], only the injection of O_3 induced significant decrease of APA ($P < 0.05$), and only the injection of CO_2 induced significant increase of SA ($P < 0.05$). However, there was no significant difference between UA or POA in each treatment group ($P > 0.05$). Meanwhile, NPA showed a trend of $[CO_2] > [Amb] > [CO_2 + O_3] > [O_3]$, and CO_2 injection induced significant increase of NPA ($P < 0.05$) (*Fig. 1*).

In the soil with adding phenanthrene, with the increase of CO_2 or/and O_3, the alteration trend of PRA, SA, UA, POA, APA and NPA was all $[CO_2]$ + [phenanthrene] > [Amb] + [PHE] > $[CO_2 + O_3]$ + [PHE] > $[O_3]$ + [PHE] which was same as the trend of MBC and MBN. Multiple comparison results showed that, compared with [Amb] + [PHE], $[O_3]$ + [PHE] induced significant decline of PRA ($P < 0.05$), and significant increase of NPA ($P < 0.05$), while the $[O_3]$ + [PHE] and $[CO_2 + O_3]$ + [PHE] induced significant decrease of SA ($P < 0.05$). In addition, under normal atmospheric conditions, the PRA, SA and APA activity in soil with adding phenanthrene increased by 53%, 37% and 30% respectively compared with that in soil without adding phenanthrene. The activity of UA and POA increased in soil with adding phenanthrene, but the trend was not significant ($P > 0.05$).

The results of multifactorial variance analysis showed that the effects of $[CO_2]$, $[CO_2 + O_3]$, [Amb] and $[O_3]$ had significant influence on PRA, SA, UA, APA, NPA ($P < 0.05$), while had few influences on POA ($P > 0.05$) (Jaimes, 2017). The two soil groups with and without adding phenanthrene had significant influences on PRA, APA and NPA ($P < 0.05$), while had few influences on SA, UA and POA ($P > 0.05$). Meanwhile, interaction within different treatment groups and two soil treatment models had bare influence on PRA, SA, UA, POA, APA and NPA.

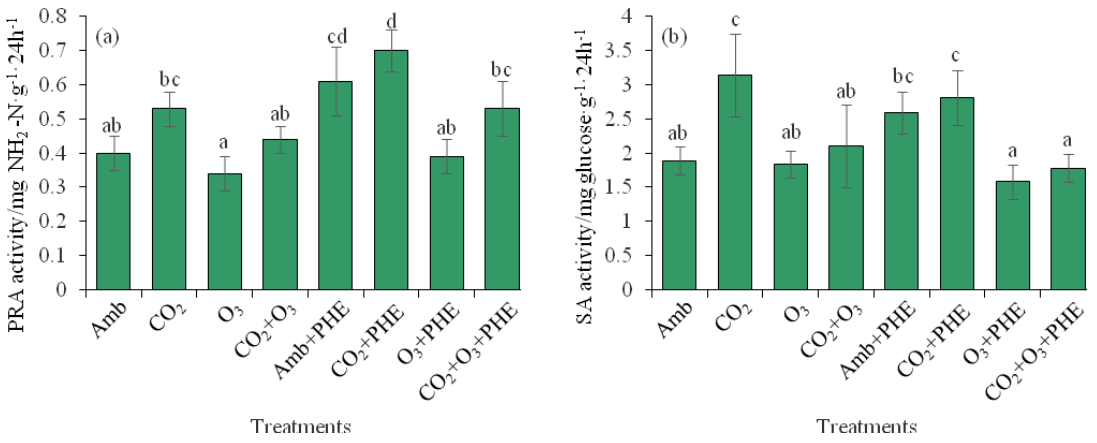

http://www.aloki.hu ● ISSN 1589 1623 (Print) ● ISSN 1785 0037 (Online)
DOI: http://dx.doi.org/10.15666/aeer/1704_85018512

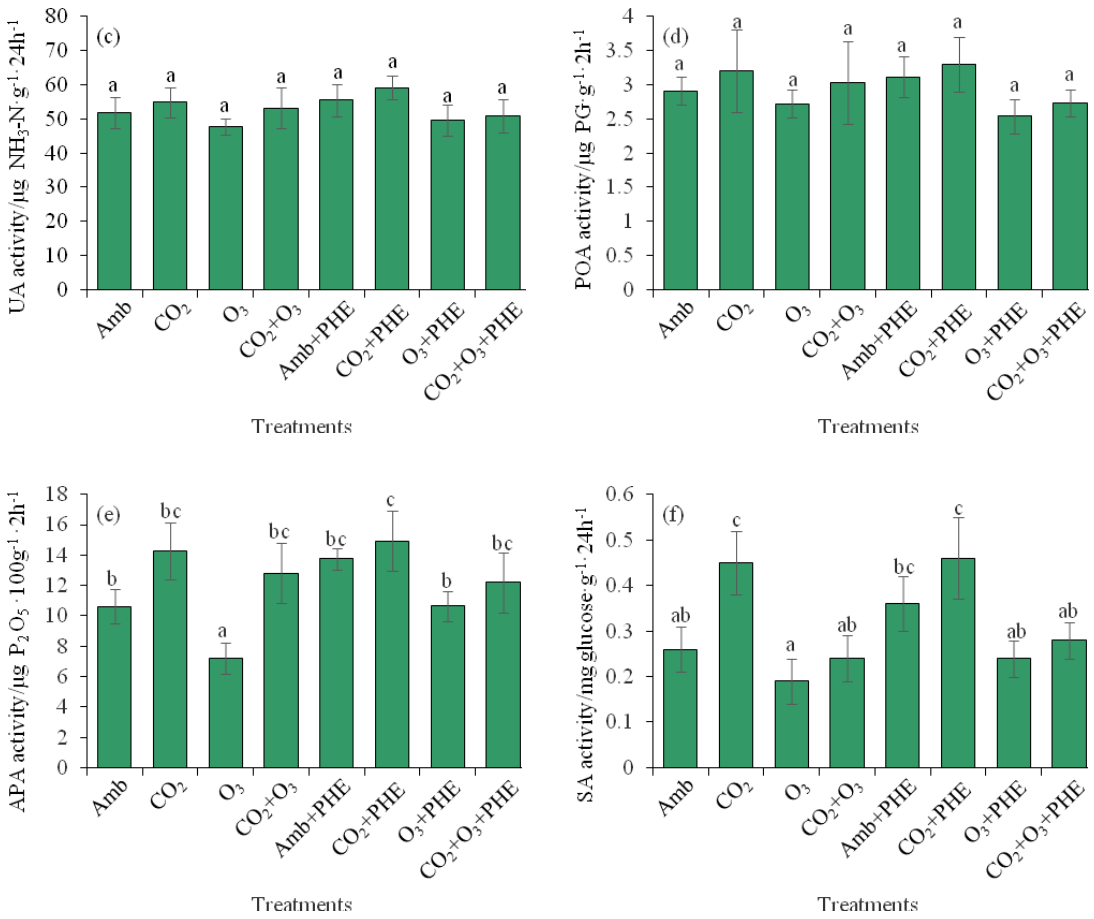

Figure 1. *Effect of elevated atmospheric CO_2 and/or O_3 on soil enzymatic activities in phenanthrene-added and -unadded soils. (PRA: Protease; SA: Sucrase; UA: Urease; POA: Phenol oxidase; APA: Acid phosphatase; NPA: neutral phosphatase)*

Discussion

Elevated atmospheric CO_2 or/and O_3 induce changes in the physical and chemical properties and enzyme activity of soil without adding phenanthrene

In this experiment, and OTC platform was used to build a soil-vegetable pot simulation system, and the changes of soil physical and chemical properties and soil enzyme activities under the elevated environment of CO_2 or/and O_3 were studied (Dager, 2017). The results showed that the increase of [CO_2] induced the increase of physical and chemical indicators such as NN, TP, TK, TC, DOC, AP, and MBC and MBN in the soil without adding phenanthrene, and the alteration trend was [CO_2] > [Amb]. Meanwhile, it was also found that soil enzyme activities such as NPA, PRA, SA and APA showed similar alteration trend. It was speculated that the increase of [CO_2] promoted the above soil physical and chemical indicators and soil enzyme activity. Studies have reported that the increase of atmospheric CO_2 concentration can promote the photosynthesis of plants, and improve the biomass and secretion of roots, and change the material composition of roots into soil (Xu et al., 2013; Sulman et al., 2014; Sunny et al., 2018). The increase of atmospheric CO_2 can also improve total organic carbon content and rhizospheric carbon availability through the metabolism of

http://www.aloki.hu ● ISSN 1589 1623 (Print) ● ISSN 1785 0037 (Online)
DOI: http://dx.doi.org/10.15666/aeer/1704_85018512

plants, which lead to the increase of the soil microbial biomass C, N and microbial activity (Tian et al., 2011; Ren et al., 2014; Shrestha and Baral, 2018). Changes in soil microorganism amount induced changes in soil enzyme activities such as PRA, SA, UA, POA, APA and NPA (Ren et al., 2014; Larson et al., 2002; Mahmood et al., 2018). Therefore, in this experiment, the increase of [CO_2] improved soil NN, TP, TK, TC, DOC, AP and other physical and chemical indicators, and MBC and MBN probably through promoting photosynthesis of vegetables and the synthesis and output of root secretions, and then induced the increase the soil enzyme activity of NPA, PRA, SA and APA (*Tables 1* and *2*).

It was also found that the increase of [O_3] decreased the physical and chemical indicators and enzyme activity of the above soil, and they showed a decline trend of [O_3] < [Amb]. Meanwhile, the increase of [O_3] also led to the increase of MBC/MBN ratio of microorganisms (*Table 2*). Studies have reported that the increase of atmospheric O_3 concentration can close the stomata of leaves and restrict the entering of CO_2 into the leaf tissue, thus reducing the photosynthetic rate and the carbohydrate content in plants (Chen et al., 2012; Anan, 2019). Increased O_3 concentration can reduce root secretions and change the types of secretions (Díaz-de-Quijano et al., 2012; Hu et al., 2011). It can also reduce the metabolism of soil microorganism C and the content of N, and increase the ratio of MBC/MBN (Li et al., 2014), which indirectly interferes with soil nutrients, rhizosphere microecological environment and soil enzyme activity (Johnson and Pregitzer, 2007; Huang et al., 2013; Cheng et al., 2011; Xu et al., 2013; Qiao, 2018). It was speculated that the rise of [O_3] reduces and changes the vegetables root secretion through inhibiting photosynthesis of green vegetables, and changed the soil C and N metabolism to some extent, and leads to abnormal changes in physical and chemical indicators such as NN, AN, TP, AP, TK, DOC, DON and MBC, MBN, which indirectly inhibits the activity of soil enzymes such as NPA, PRA, APA and NPA (*Tables 1* and *2*).

The results also showed that the soil enzyme activity of NN, AN, TN, AP, TP, TK, TC, DOC, DON and MBC, MBN, and NPA, PRA, SA, UA, POA, APA showed a trend of [CO_2 + O_3] > [O_3] (*Tables 1* and *2*). [CO_2] might reduce the damage of [O_3] to the leaf tissue of vegetables and the interference of physiological and biochemical process such as photosynthesis on the leaf tissue of vegetables, thus indirectly inducing the increase of soil physical and chemical indicators such as TP, TK, AN, AP, DOC, DON, and MBC, MBN, as well as enzyme activities such as APA, NPA and PRA. The correlation mechanism remains to be further discussed.

Elevated atmospheric CO_2 or/and O_3 induce changes in the physical and chemical properties and enzyme activities of the soil with adding phenanthrene

Phenanthrene is one of the typical polycyclic aromatic hydrocarbon pollutants in soil. Studies on the effects of atmospheric CO_2 or/and O_3 increase on the microecological environment of the phenanthrene polluted soil have not been reported (Olivares et al., 2017). The results of this study showed that [CO_2] increased the physical and chemical indicators (NN, AN, TP, AP, TC, DOC, DON, etc.), and MBC, MBN, and the soil enzyme activities of NPA, PRA, SA and APA. The alteration trend of above indicators was [CO_2] + [PHE] > [Amb] + [phenanthrene]. It was also found that the increase of [O_3] decreased the above soil physical and chemical indicators and enzyme activity, and showed the trend of [O3] + [PHE] < [Amb] + [PHE]. Therefore, the alteration trend of [CO_2] + [PHE] > [Amb] + [PHE] > [O_3] + [PHE] showed by the above indicators was

http://www.aloki.hu ● ISSN 1589 1623 (Print) ● ISSN 1785 0037 (Online)
DOI: http://dx.doi.org/10.15666/aeer/1704_85018512

consistent with the soil with adding phenanthrene. The direct effects of CO_2 and O_3 on the leaf tissue of vegetables might promote or interfere with the secretion of root substances through affecting the photosynthesis of leaves, thus causing the change of coil microecological environment (Wang et al., 2014; Cheng et al., 2011; Gautam et al., 2019). Soil phenanthrene affect directly on the root system of vegetables, and its target organs are different from CO_2 and O_3. Therefore, in the same CO_2 and O_3 exposure environment, the addition of phenanthrene to soil only changed the size of physical and chemical indicators but did not change its alteration trend (*Table 1*).

It was also found that [CO_2 + O_3] could alleviate the inhibition of [O_3] on the physical and chemical indicators and enzyme activity of the above mentioned soil, and its alteration trend of [CO_2 + O_3] + [PHE] > [O_3] + [PHE] was consistent with the that in soil without adding phenanthrene. The potential mechanism might be related to the alleviation of CO_2 on damage of O_3 to vegetables or the reduction of inhibition effect of O_3 on photosynthesis of vegetables. The interaction between soil pollution and atmospheric CO_2 or/and O_3 increase is a complex process, and its microscopic mechanism remains to be further studied.

Conclusion

(1) In the soil without adding phenanthrene, the increase of [CO_2] induced the increase of physical and chemical indicators, NN, TP, TK, TC, DOC and AP, and MBC, MBN, as well as soil enzyme activities of NPA, PRA, SA, APA with a trend of [CO_2] > [Amb]. The increase of [O_3] decreased the above soil physical and chemical indicators and enzyme activity ([Amb] > [O_3]), while increased the ratio of soil microorganism MBC/MBN. [CO_2 + O_3], to some extent, decreased the inhibition effect of [O_3] on soil microbial biomass and enzyme activity, and also released the stimulating effect of [CO2] increase on soil microbial biomass and enzyme activity.

(2) In the soil with adding phenanthrene, [CO_2] increased physical and chemical indicators, NN, AN, TP, AP, TC, DOC, DON and the ratio MBC/MBN with a rising trend of [CO_2] + [PHE] > [Amb] + [PHE]. [O_3] exposure decreased the above indicators and enzyme activities ([Amb] + [PHE] > [O_3] + [PHE]). [CO_2 + O_3] + [PHE] could alleviate the inhibition effect of [O_3] + [PHE] on those indicators and enzyme activities. These trends were basically consistent with the alteration trend in soil without adding phenanthrene. Moreover, the interaction within [CO_2], [CO_2 + O_3], [Amb], [O_3] and the two soil treatment models groups had no significant impact on MBC, MBN, PRA, SA, UA, POA, APA, NPA, the reason of which might be that CO_2 and O_3 directly affect of leaf tissue of cabbage, while the soil phenanthrene directly affect the root system of cabbage. The increase of CO2 or/and O2 might play an indirect role with soil phenanthrene through affecting photosynthesis of leaves and secretion of root system of cabbage, and only changed the value of physical and medical while did not change its trend. Its microscopic mechanism remains to be further studied.

Acknowledgements. This study was financially supported by the National Natural Science Funds Fund (Grant 31501461), the project of top-notch personnel cultivation in Colleges and Universities of Anhui Province (gxfx2017091) and the Key Research and Development Project of Anhui Province (Grant 1804a07020122, Grant 1704f0704067).

http://www.aloki.hu ● ISSN 1589 1623 (Print) ● ISSN 1785 0037 (Online)
DOI: http://dx.doi.org/10.15666/aeer/1704_85018512

REFERENCES

[1] Anan, H. S. (2019): Contribution to the paleontology, stratigraphy and paleo-biogeography of some diagnostic Pakistanian Paleogene foraminifer in the Middle East. – Earth Sciences Pakistan 3(1): 23-28.

[2] Booker, F. L., Prior, S. A., Torbert, H. A., Fiscus, E. L., Pursley, W. A., Hu, S. J. (2005): Decomposition of soybean grown under elevated concentrations of CO_2 and O_3. – Global Change Biology 11(4): 685-698.

[3] Chen, X. M., Liu, J. X., Deng, Q., Yan, J. H., Zhang, D. Q. (2012): Effects of elevated CO_2 and nitrogen addition on soil organic carbon fractions in a subtropical forest. – Plant and Soil 357(1-2): 25-34.

[4] Cheng, L., Booker, F. L., Burkey, K. O., Tu, C., Shew, H. D., Rufty, T. W., Fiscus, E. L., Deforest, J. L., Hu, S. (2011): Soil microbial responses to elevated CO_2 and O_3 in a nitrogen-aggrading agroecosystem. – PLoS ONE 6(6): 1-11.

[5] Cheng, Z., Wang, X. K., Shang, H. (2014): Ozone effects on soil microbial community of rice investigated by ^{13}C isotope labeling. – Environmental Science 35(10): 3911-3917 (in Chinese).

[6] Dager, M. R. (2017): Composición de la materia orgánica, pH, intercambio catiónico y textura de cinco suelos ubicados entre 670 y 1600 msnm en la cuenca del río Maracay, Venezuela. – Revista de la Facultad de Agronomia de la Universidad del Zulia 34(2): 53-60.

[7] Díaz-de-Quijano, M., Schaub, M., Bassin, S., Volk, M., Peñuelas, J. (2012): Ozone visible symptoms and reduced root biomass in the subalpine species *Pinus uncinata* after two years of free-air ozone fumigation. – Environmental Pollution 169: 250-257.

[8] Espinoza, Y. (2017): Efecto del sistema labranza sobre la estructura y fracciones de carbono y nitrógeno del suelo y su impacto en el desarrollo del cultivo de maíz. – Revista de la Facultad de Agronomia de la Universidad del Zulia 34(4): 94-100.

[9] Formánek, P., Rejšek, K., Vranová, V. (2014): Effect of elevated CO_2, O_3, and UV radiation on soils. – The Scientific World Journal 2014(4): 1-8.

[10] Gautam, A., Batra, R., Singh, N. (2019): A study on use of rice husk ash in concrete. – Engineering Heritage Journal 1(1): 01-04.

[11] Guan, S. Y. (1986): Soil enzymes and their research methods. – China Agriculture Press, Beijing, pp. 274-300 (in Chinese).

[12] Haesler, F., Hagn, A., Engel, M., Schloter, M. (2014): Impact of elevated atmospheric O_3 on the actinobacterial community structure and function in the rhizosphere of European beech (*Fagus sylvatica* L.). – Frontiers in Microbiology 5: 1-12.

[13] Han, W., Kemmitt, S. J., Brookes, P. C. (2016): Soil microbial biomass and activity in Chinese tea gardens of varying stand age and productivity. – Soil Biology and Biochemistry 39(7): 1468-1478.

[14] Hu, Z. H., Li, C. Z., Chen, S. T., Li, H. M., Yang, Y. P., Shen, S. H. (2011): Effects of elevated ozone concentration on CO_2 emission from soil-winter wheat system. – Environmental Science 32(1): 46-50 (in Chinese).

[15] Huang, Y. Z., Wang, F., Zhong, M., Sui, L. H., Wu, W. (2013): Effects of elevated ozone on carbon, nitrogen content and soil enzymes activities in a winter wheat field. – Asian Journal of Ecotoxicology 8(6): 871-878 (in Chinese).

[16] Iqbal, J., Hu, R. G., Feng, M. L., Lin, S., Malghani, S., Ali, I. M. (2010): Microbial biomass, and dissolved organic carbon and nitrogen strongly affect soil respiration in different land uses: a case study at Three Gorges Reservoir Area, South China. – Agriculture, Ecosystems & Environment 137(3-4): 294-307.

[17] Jaimes, E. J. (2017): Capacidad de carga y presión de uso de la tierra en cuatro sectores de la sub-cuenca del río Déleg, Provincia del Cañar, Ecuador. – Revista de la Facultad de Agronomia de la Universidad del Zulia 34(3): 75-81.

http://www.aloki.hu ● ISSN 1589 1623 (Print) ● ISSN 1785 0037 (Online)
DOI: http://dx.doi.org/10.15666/aeer/1704_85018512

[18] Johnson, R. M., Pregitzer, K. S. (2007): Concentration of sugars, phenolic acids, and amino acids in forest soils exposed to elevated atmospheric CO_2 and O_3. – Soil Biology and Biochemistry 39(12): 3159-3166.
[19] Kumar, M., Jaafar, J. (2018): Preparation and characterization of TiO_2 nanofiber coated PVDF membrane for softdrink wastewater treatment. – Environment & Ecosystem Science 2(2): 35-38.
[20] Larson, J. L., Zak, D. R., Sinsabaugh, R. L. (2002): Extracellular enzyme activity beneath temperate trees growing under elevated carbon dioxide and ozone. – Soil Science Society of America 66(6): 1848-1856.
[21] Li, G. M., Shi, Y., Chen, X. (2008): Effects of elevated CO_2 and O_3 on phenolic compounds in spring wheat and maize leaves. – Bulletin of Environmental Contamination and Toxicology 81(5): 436-439.
[22] Li, S., Zheng, Y. F., Wu, R. J., Yin, J. F., Xu, J. X. (2014): Research progress on plant vegetative growth and protection under ozone pollution stress. – Journal of Agricultural Science and Technology 16(1): 117-124 (in Chinese).
[23] Li, X. F., Han, S. J., Guo, Z. L., Shao, D. K., Xin, L. H. (2010): Changes in soil microbial biomass carbon and enzyme activities under elevated CO_2 affect fine root decomposition processes in a Mongolian oak ecosystem. – Soil Biology and Biochemistry 42(7): 1101-1107.
[24] Liu, C., Liu, Y. K., Jin, G. Z. (2014): Seasonal dynamics of soil microbial biomass in six forest types in Xiaoxing'an Mountains, China. – Acta Ecologica Sinica 32(2): 451-459 (in Chinese).
[25] López-Hernández, D. (2018): Áreas superficiales específicas y parámetros asociados en suelos venezolanos con diferentes grados de pedogénesis. – Revista de la Facultad de Agronomia de la Universidad del Zulia 35(3): 111-116.
[26] Lou, Y., Liang, W., Xu, M., He, X., Wang, Y., Zhao, K. (2011): Straw coverage alleviates seasonal variability of the topsoil microbial biomass and activity. – Catena 86(2): 117-120.
[27] Mahmood, S., Kazmi, S. T., Ali, S. S. (2018): Comparison of drinking water bottles of different countries along with Zamzam water, Pakistan. – Earth Sciences Pakistan 2(1): 05-14.
[28] Manna, S., Singh, N., Singh, V. P. (2012): Effect of elevated CO_2 on degradation of azoxystrobin and soil microbial activity in rice soil. – Environmental Monitoring and Assessment 185(4): 2591-2906.
[29] Olivares, B., Cortez, A., Lobo, D., Parra, R., Rey, J., Rodríguez, M. (2017): Evaluación de la vulnerabilidad agrícola a la sequía meteorológica en diferentes localidades de Venezuela. – Revista de la Facultad de Agronomía 34(1): 103-129.
[30] Pascual-Córdova, G. (2018): Indicadores de calidad del suelo en el agroecosistema caña de azúcar (Saccharum spp.). – Revista de la Facultad de Agronomia de la Universidad del Zulia 35(1): 98-104.
[31] Qiao, F. (2018): The study on the integration of green architecture and appropriate technology. – Engineering Heritage Journal 2(2): 01-03.
[32] Ren, X. W., Tang, J. Y., Liu, J. C., He, H. J., Dong, D., Cheng, Y. X. (2014): Effects of elevated CO_2 and temperature on soil enzymes of seedlings under different nitrogen concentrations. – Journal of Beijing Forestry University 36(5): 44-53 (in Chinese).
[33] Rozuki, N. F. A., Tajuddin, M. H., Yusof, N. (2018): Effect of different solvent on asymmetric polysulfone (Psf) membranes for CO_2/CH_4 separation. – Environment & Ecosystem Science 2(2): 11-14.
[34] Sen, B., Goswami, S., Devi, G., Sarma, H. P., Bind, A. (2018): Valorization of Adenanthera pavonina seeds as a potential biosorbent for lead and cadmium removal from single and binary contaminated system. – Geology, Ecology, and Landscapes 2(4): 275-287.

http://www.aloki.hu ● ISSN 1589 1623 (Print) ● ISSN 1785 0037 (Online)
DOI: http://dx.doi.org/10.15666/aeer/1704_85018512

[35] Shi, C. E., Gao, Y., Wang, Y. L., Xu, X. N., Huang, B. (2015): Soil microbial biomass and enzyme activities in *Pinus massoniana* forest infected by pine wood nematode. – Chinese Journal of Ecology 34(4): 1046-1051 (in Chinese).
[36] Shrestha, A., Baral, S. (2018): Socioeconomic Factors affecting awareness and adaption of climate change: a case study of Banke District Nepal. – Earth Sciences Malaysia 2(2): 20-24.
[37] Sulman, B. N., Phillips, R. P., Oishi, A. C., Shevliakova, E., Pacala, S. W. (2014): Microbe-driven turnover offsets mineral-mediated storage of soil carbon under elevated CO_2. – Nature Climate Change 4(12): 1099-1102.
[38] Sunny, A. A., Omowumi, A., Chris, O. A. (2018): Improved magnetic data analyses and enhancement techniques for lithological and structural mapping around Akure, southwestern Nigeria. – Earth Sciences Malaysia 2(1): 16-21.
[39] Tian, R., Zhou, H., Huang, J., Zhu, J. G., Yin, Y., Sun, Y. Y., Wang, X. R., Guo, H. Y. (2011): Effect of elevated atmospheric CO_2 concentration on the soil enzymes and microbial communities under stress of Cd pollution. – Journal of Nanjing University (Natural Sciences) 47(6): 712-717 (in Chinese).
[40] Tripathi, S., Chakraborty, A., Chakrabarti, K., Bandyopadhyay, B. K. (2007): Enzyme activities and microbial biomass in coastal soils of India. – Soil Biology and Biochemistry 39(11): 2840-2848.
[41] Veeraragavan, S., Duraisamy, R., Mani, S. (2018): Prevalence and seasonality of insect pests in medicinally important plant Senna alata L. under tropical climate in the Coromandel Coast of India. – Geology, Ecology, and Landscapes 2(3): 177-187.
[42] Wang, Y. X., Song, Q. L., Frei, M., Shao, Z. S., Yang, L. X. (2014): Effects of elevated ozone, carbon dioxide, and the combination of both on the grain quality of Chinese hybrid rice. – Environmental Pollution 189: 9-17.
[43] Wu, F. F., Zheng, Y. F., Wu, R. J., Wang, J. Q., Li, P. (2015): Effects of ozone fumigation and depressed solar irradiance on soil microbial functional diversity in winter wheat rhizosphere. – Acta Ecologica Sinica 35(12): 3949-3958 (in Chinese).
[44] Wu, W., Huang, Y. Z., Li, M. S., Yu, F. M., Zhong, M., Sui, L. H., Hao, X. W. (2012): Effects of elevated ozone on quantity of ammonium-oxidizing bacteria, ammonia-oxidizing achaea and nitrobacteria in wheat field soil. – Journal of Agro-Environment Science 31(1): 491-497.
[45] Xu, L., Zheng, Y. F., Wu, R. J., Xu, J. X. (2013): A review on impacts of elevated near-earth storey ozone concentration to above and below ground parts of crops. – Crops 5: 18-24 (in Chinese).
[46] Xu, M. Y., He, Z. L., Deng, Y., Wu, L. Y., Nostrand, J. D. V., Hobbie, S. E., Reich, P. B., Zhou, J. Z. (2013): Elevated CO_2 influences microbial carbon and nitrogen cycling. – BMC Microbiology 13(1): 1-11.
[47] Zhang, W. W., Niu, J. F., Wang, X. K., Tian, Y., Yao, F. F., Feng, Z. Z. (2011): Effects of ozone exposure on growth and photosynthesis of the seedlings of *Liriodendron chinense* (Hemsl.) Sarg, a native tree species of subtropical China. – Photosynthetica 49(1): 29-36.
[48] Zhang, Y. F., Wu, J. H., Song, L., Song, Y. G., Yang, M., Wang, N. B., Han, J. B., Guan, D. M. (2018): Source apportionment and ecological risk assessment of PAHs in surface sediments from the Liaodong Bay, northern China. – Acta Oceanologica Sinica 37(4): 12-21.

http://www.aloki.hu ● ISSN 1589 1623 (Print) ● ISSN 1785 0037 (Online)
DOI: http://dx.doi.org/10.15666/aeer/1704_85018512

EVALUATION OF ECOLOGICAL CIVILIZATION DEVELOPMENT IN THE POST-OLYMPIC TIMES

YANG, P.[1] – SHENG, X.[1*] – ZHAO, Y.[2] – ZHU, L.[3]

[1]*Management School, Beijing Union University, Beijing 100101, China*
(e-mail: 963450574@qq.com – P. Yang)

[2]*School of Applied Science and Technology, Beijing Union University, Beijing 100101, China*
(e-mail: 1447502494@qq.com)

[3]*College of Business and Public Management, West Chester University, West Chester 19383 PA, USA*
(e-mail: xzhu@wcupa.edu)

**Corresponding author*
e-mail: shengxiaojuan@buu.edu.cn

(Received 8th Mar 2019; accepted 21st May 2019)

Abstract. As a major sport event attracting global attention, the Olympic Games reflect the overall national strength, and highlight the international influence and competitiveness of the host country. As the competitive events have a requirement for the environment of the host country, which is a good opportunity to improve the ecological civilization of the host country. Beijing 2008 Olympic Games has played an important role in improving the ecological environment of Beijing. With the approaching of the Winter Olympics in 2022, we have ushered in new opportunities to promote the construction of Beijing's ecological civilization. Taking Beijing's ecological civilization as the research subject, we construct the evaluation index system of the index of ecological civilization, and use the coefficient of variation method to determine the weight of the index. It evaluates Beijing's ecological civilization from five aspects: growth quality, environmental protection, environmental quality, resource utilization and environmental governance. It is concluded that the index of Beijing's ecological civilization is on the rise as a whole. It has a significant impact on the construction of ecological civilization, and the measures taken by the government are ready for the successful hosting of the 2022 Winter Olympic Games.
Keywords: *ecological environment, host country, Beijing, evaluation index system, comprehensive national strength*

Introduction

The Olympic Games held every four years are the most influential international event in the world; it is of great consequences and will bring far-reaching significance for any hosting country. The 2008 Beijing Olympic Games not only promoted the economic development of various industries (Kang et al., 2017; Ogunyele et al., 2018), but also improved the urban ecological environment. On the occasion of the Olympics Games, Beijing municipal government carried out environmental protection activities such as increasing green areas, reducing emissions and pollution to further promote ecological development (Geisendorf and Klippert, 2017; Khanchoul et al., 2018). A report delivered at the 19th National Congress stated that we must realize that lucid waters and lush mountains are invaluable assets and we should have a strong commitment to socialist ecological civilization and work to develop a new model of modernization with humans developing in harmony with nature. The concept of ecological civilization has continuously penetrated into all aspects of China's social and economic development. To be better prepared for the 2022 Winter Olympics, we should not only maintain steady economic growth, but also

http://www.aloki.hu ● ISSN 1589 1623 (Print) ● ISSN 1785 0037 (Online)
DOI: http://dx.doi.org/10.15666/aeer/1704_85138525

maintain a good environmental quality (Zhou et al., 2018; Nawaz et al., 2018). As the capital of China, Beijing must play a leading role in the construction of an ecological civilization.

The term building an ecological civilization is proposed concerning China's construction, while foreign research mainly focuses on environmental aspects of resource utilization, environment and sustainable development. International organizations, foreign governments and scholars at home and abroad have constructed a number of sustainable development evaluation index systems from different perspectives. So far, there are four versions namely EPI2008, EPI2010, EPI2012 and EPI2014. Foreign researches on the ecological environment have been relatively complete, providing a good foundation for us. Eco-civilization is a concept with Chinese characteristics, which is of great significance to the sustainable development of China. Since the successful completion of the 2008 Beijing Olympic Games, more attention has been paid to the ecological environment (Shen, 2018). Chinese scholars have provided new strategies for environmental improvement (Fernando, 2016; Arslan et al., 2018) from the perspective of behavioral science. From the perspective of green ecological planning and economy, they have found that new urban planning can promote the construction of resource-based cities (Guan, 2016). Eighteen evaluation indicators were selected from water carrying capacity, land carrying capacity, atmospheric environmental carrying capacity, energy carrying capacity and environmental carrying capacity. An index system of carrying capacity of urban resources and environmentally friendly living in ecological civilization (Zhang et al., 2017; Kumar, 2018) was established. The model method of ecological benefit and trade-off in circular economy practice was also provided, as well as the development of regional ecological industry (Sun et al., 2017). For China's rapid urbanization, Guiyang and Port, as typical eco-civilized cities, provide an ideal laboratory to develop a hybrid model of carbon emissions and energy consumption (Fang et al., 2017; Liang and Wenshun, 2019), and provide policy guidance for the port to promote the construction of ecological civilization from the perspective of PECC (Li, et al., 2018). Not only should we pay attention to the education of ecological civilization, but also to the regional ecological innovation in China (Yu et al., 2016). Scholars have established a comprehensive evaluation model of ecological civilization education in Colleges and universities (Ping et al., 2018; Suhaili and Samsudin, 2018), and selected 30 provinces. The level of regional ecological innovation was evaluated, and the factors influencing regional ecological innovation in China (Chen et al., 2017; Rajendran and Mohsin, 2018) were obtained.

To sum up, scholars at home and abroad have inherited rich experience and achieved fruitful research results. Because of different research directions, there is no uniform standard for evaluation index. Most of the studies at home and abroad focus on the macro level of environment and city, without considering the impact of major historical events on ecological civilization. Based on this, this paper takes Beijing as the research object, evaluates the development of ecological civilization after the Olympic Games, and predicts the ecological civilization of the Olympic Games in 2022, which is also the starting point and innovation of this paper.

Materials and methods

Evaluation of research thought of ecological civilization

Ecological civilization is the inevitable requirement for the harmonious coexistence of man and nature. It is a synthesis of eco-politics, eco-economy, eco-environment, eco-culture

http://www.aloki.hu ● ISSN 1589 1623 (Print) ● ISSN 1785 0037 (Online)
DOI: http://dx.doi.org/10.15666/aeer/1704_85138525

and eco-system. On the basis of previous studies, this paper draws lessons from the existing index system, relevant policies and the actual situation of Beijing, constructs the evaluation index system of ecological civilization, which can better measure the ecological civilization index of Beijing (Serpe, 2018; Madhav et al., 2018). In order to establish a harmonious development between human and nature, there are five secondary indicators, namely, growth quality, environmental protection, environmental quality, resource utilization and environmental governance. Each secondary indicator has corresponding three-level indicators, totaling 27 three-level indicators. The ecological civilization index is calculated more scientifically from five different aspects. Based on scientific principles and from the practical point of view of the construction of ecological civilization, this paper takes Beijing and 16 regions as the research objects, adopts the time series data of Beijing from 2009 to 2016 and the panel data of air quality of each region, carries out the comprehensive evaluation of ecological civilization, and predicts the ecological civilization index of the 2022 Winter Olympic Games. By comparing the air quality of different regions (Lee, 2016), the regional disparities and shortcomings in the process of ecological civilization construction in Beijing and other regions are analyzed, the main influencing factors of ecological civilization in Beijing are revealed, and the direction of efforts is determined (Lee et al., 2016; Raj and Prabhakaran, 2018), so as to provide a better living environment for the hosting of the Winter Olympic Games.

Construct an evaluation index system and weight determination

The scientific indicator system is crucial for the objective evaluation of ecological civilization. The quality of indicators directly affects the scientific nature and accuracy of results of ecological civilization evaluation. Based on the scientific nature of indicators (Marinelli, 2018), the availability of data, the comparability of regional data, the measurability of results, and the principles of predictability, an ecological civilization indicator system is constructed. It is necessary to consider the new elements arising from the 2008 Olympic Games. In the light of the resource-constrained objectives set out in the 12th Five-Year Plan Outline for National Economic and Social Development and the 13th Five-Year Plan Outline for National Economic and Social Development (Oglu Nasirov, 2018), the 19th National Congress put forward the socialist ecological concept. The General Office of the State Council issued the Evaluation and Evaluation System for the Objectives of Ecological Civilization Construction and Green Hair. On the basis of the exhibition index system and the "Three-year Action Plan for Winning the Blue Sky and Defending the War" issued by the State Council, as well as the existing research results on ecological civilization at home and abroad, the index system of ecological civilization in Beijing is constructed.

According to the connotation of ecological civilization and the design principle of the index system, the three-level index system is constructed, and the comprehensive evaluation index system is progressive step by step (Sun et al., 2016). The whole index system is divided into three levels, the first level is the target level and the general goal; the second level is the factor level, which is the factor influencing the overall goal. The ecological civilization index of the target level is divided into five elements, namely, growth quality, ecological protection, air quality, resource utilization and environmental governance; the third level is the index level, which is composed of 27 indicators. In the total index system, there are 11 absolute indexes and 16 relative indexes. Among them, there are 20 positive indicators and 5 negative indicators. This paper takes Beijing as the research object., the evaluation data comes from Beijing Statistical Yearbook 2009-

http://www.aloki.hu ● ISSN 1589 1623 (Print) ● ISSN 1785 0037 (Online)
DOI: http://dx.doi.org/10.15666/aeer/1704_85138525

2016, Statistical Yearbook 2009-2016 of Beijing Municipal Environmental Protection Bureau, Statistical Yearbook 2009-2016 of Beijing Water Affairs Bureau, Annual Report on Ecological Civilization of Beijing Environmental Protection Bureau in 2009-2016, Statistical Yearbook of Beijing Municipal Bureau of Landscape Architecture 2009-2016 and other relevant statistical yearbooks (Song et al., 2016). Because some data are not available, the method of interpolation is used to calculate the missing data.

The determination of index weight is a key factor in the evaluation of ecological civilization index (*Table 1*). The weight of the index affects the scientific nature of the evaluation results. According to the nature of the evaluation indicators (Zhang et al., 2016), the evaluation indicators are divided into two categories: positive indicators and negative indicators. The positive indicator is the indicator that the bigger the value, the better, and the negative index is just the opposite. Considering the characteristics of ecological civilization, research needs and actual situation, this paper will use the variable coefficient in the objective weighting method to determine the weight of each index. The weights of each indicator are calculated as shown in *Table 1*.

Table 1. *Weight of each indicator in the indicator system*

Grade 1 indicator	Grade 2 indicators	Weight	Grade 3 indicators	Nature	Weight
ECI	Growth quality	0.220892487	GDP per capita (yuan/person)	Positive	0.031709382
			Urban per capita disposable income (yuan)	Positive	0.038115002
			Rural per capita disposable income (yuan)	Positive	0.032653215
			Contribution of tertiary industry to regional GDP growth (%)	Positive	0.039223131
			R&D fund investment (%)	Positive	0.019192412
			Urbanization rate (%)	Positive	0.019983622
	Ecological protection	0.131205615	Forest coverage rate (%)	Positive	0.03765499
			Living wood growing stock (10,000 m^3)	Positive	0.035318786
			Proportion of nature reserve in urban area (%)	Positive	0.043285846
			Urban green coverage ratio (%)	Positive	0.032408979
			Forest coverage rate (%)	Positive	0.035415529
			Per capita park green space (m^2/person)	Positive	0.025207522
	Environment quality	0.212767028	Chemical oxygen demand (10,000 tons)	Negative	0.044148014
			Ammonia nitrogen emissions (10,000 tons)	Negative	0.058856794
			Sulfur dioxide emissions (10,000 tons)	Negative	0.039333396
			Soot emissions (10,000 tons)	Negative	0.037713962
			Mean noise of regional environment (%)	Negative	0.035089344
			Mean noise of trunk roads (%)	Negative	0.02527412
	Resource utilization	0.22308159	Comprehensive utilization rate of general industrial solid wastes (%)	Positive	0.03247559
			Comprehensive utilization rate of hazardous waste (%)	Positive	0.033620128
			Per capita water resources (100 million m^3/person)	Positive	0.036348532
			Per capita water consumption (10,000 m^3/person)	Positive	0.058662852
	Environmental governance	0.21205328	Sewage treatment rate (%)	Positive	0.038919427
			Harmless treatment rate of domestic garbage	Positive	0.023913285
			Proportion of environmental pollution prevention investment in GDP (%)	Positive	0.054794877
			Proportion of pollution reduction investment in GDP (%)	Positive	0.041328738
			Proportion of natural ecological protection investment in GDP (%)	Positive	0.049352524

http://www.aloki.hu ● ISSN 1589 1623 (Print) ● ISSN 1785 0037 (Online)
DOI: http://dx.doi.org/10.15666/aeer/1704_85138525

As can be seen from *Table 1,* Beijing's ecological civilization is evaluated from these five aspects (Glenys, 2017). Among grade 2 indicators, growth quality, environmental quality and resource utilization account have a large weight ratio, which is due to reasonable and effective policies implemented by government. The weight of ecological protection is relatively small. It is because the areas of Beijing, nature reserves and forests will not have major changes in years to come, and the amount of change is too small to adjust (Sun, 2018). The Grade 3 indicators of chemical oxygen demand, ammonia nitrogen emissions, sulfur dioxide emissions, the proportion of nature reserves in urban areas, urban green coverage, and proportion of natural ecological protection investment in GDP have a large weight. In the construction of ecological civilization, we should pay attention to the indicators with greater weight and make an improvement from these aspects.

Determination of ECI

ECI of Beijing and the secondary indicators are calculated by multiplying weight of each indicator by the standardized value. Obviously, the greater the value of the ecological civilization index, the higher the level of ecological civilization, and vice versa. The overall ecological civilization index of Beijing is obtained, which is shown (*Table 2*).

Table 2. *Beijing's ecological civilization index*

Year	Growth quality	Ecological protection	Environmental quality	Resource utilization	Environmental governance	ECI
2009	0.03922313	0.02045288	0.08077432	0.00000000	0.09824335	0.23869369
2010	0.07110915	0.04160665	0.07450494	0.00280862	0.03632017	0.22634952
2011	0.07561496	0.04427208	0.04787827	0.00682093	0.03983102	0.21441726
2012	0.08672186	0.07112219	0.05467986	0.01083324	0.04797150	0.27132865
2013	0.09715975	0.10403975	0.07935489	0.01725294	0.09678202	0.39458935
2014	0.10784921	0.17770485	0.10218744	0.02327141	0.09116103	0.50217394
2015	0.13754789	0.19842073	0.13413917	0.03049357	0.10792734	0.60852870
2016	0.13818652	0.19448334	0.19970982	0.03891943	0.11762759	0.68892669

Results

(1) The ECI shows a trend of decreasing first and then rising (*Fig. 1*).

The ecological index from 2009 to 2011 has slightly decreased. The main reason is that the implementation measures lag behind; as hosting the Olympic Games require financial expenditures in all aspects, many factories were put into production after the Olympic Games to increase positive growth in a timely manner, which emitted a large amount of pollutants, resulting in a decline in the ecological index (Zhang, 2017).

The ECI continued to grow from 2012 to 2016. The main reason is that 2012 is the most crucial year for the implementation of the 12th Five-Year Plan for the prevention and control of dangerous pollutants and solid pollutants. Beijing has fully implemented the environmental management system for solid wastes, actively explored the management model of hazardous wastes from social sources, and fully safeguarded the environmental safety of the capital. Secondly, the number of nature reserves has

http://www.aloki.hu ● ISSN 1589 1623 (Print) ● ISSN 1785 0037 (Online)
DOI: http://dx.doi.org/10.15666/aeer/1704_85138525

increased, resource utilization has become more rationalized, and the government has invested a large amount of money to manage the environment.

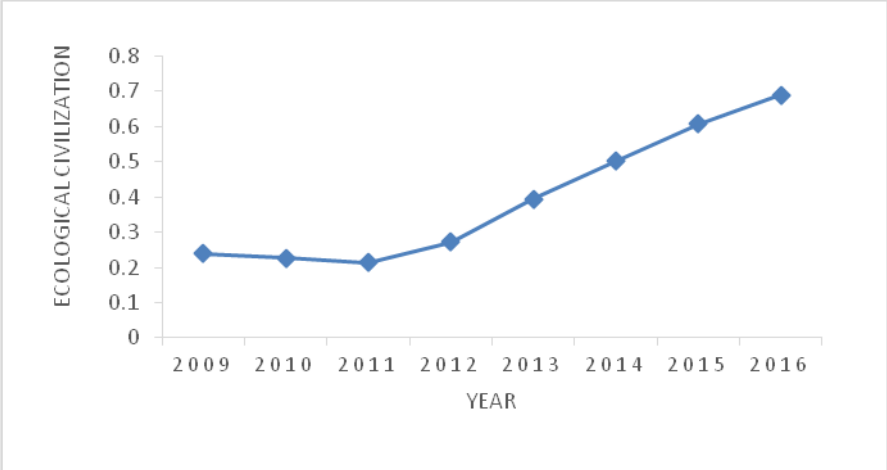

Figure 1. *ECI of Beijing after 2008 Olympic Games*

(2) The growth quality index first grew at a faster rate, then increased slowly, and finally tended to be stable (*Fig. 2*).

Beijing's growth quality index is growing steadily. The main reason is that Beijing has actively expanded domestic demand and deepened supply-side structural reforms for the past eight years. The overall economy is stable and positive. Secondly, as a capital city, Beijing is a place that many people yearn for, and a large number of people swarmed into Beijing. In order to solve the employment problem, Beijing government has continued to promote the adjustment of industrial structure, accelerated the construction of science and technology innovation centers, and increased the disposable income of residents. Science and technology innovation has become a new engine of economic growth, and Beijing's investment in testing and research and development has been increasing. As a result, the Beijing's quality growth index is growing steadily (Zhang, 2018).

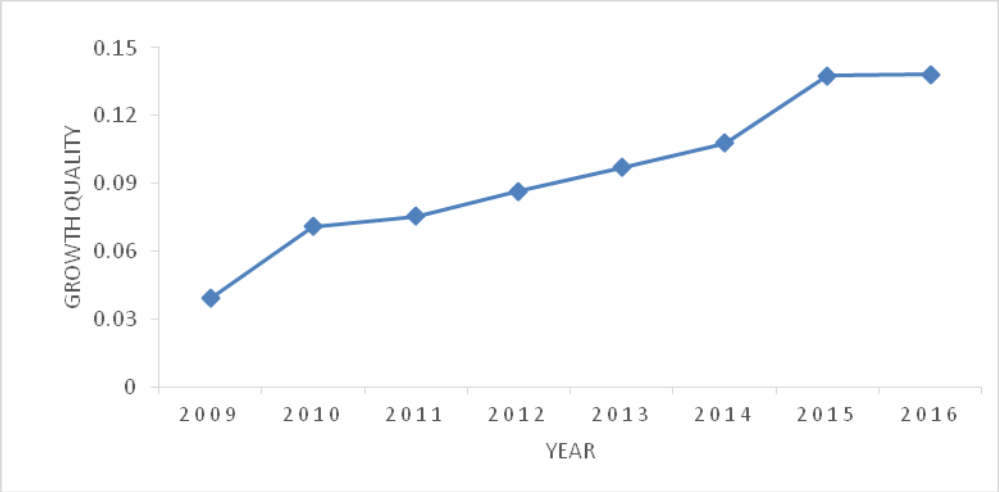

Figure 2. *Growth quality index of Beijing after 2008 Olympic Games*

http://www.aloki.hu ● ISSN 1589 1623 (Print) ● ISSN 1785 0037 (Online)
DOI: http://dx.doi.org/10.15666/aeer/1704_85138525

(3) The ecological protection index is growing steadily (*Fig. 3*).

In 2009-2015, the ecological protection index grew steadily, and it did not change too much in 2016. It was mainly because that the stationarity of Beijing area, forest coverage rate and the proportion of nature reserves in urban areas increased. Furthermore, Beijing government implemented construction projects of nature reserves protection, developed biodiversity protection action plans; and finally, urban greening coverage has been increasing thanks to the construction of national environmental protection model urban areas, ecological zones, and ecological civilization pilot areas.

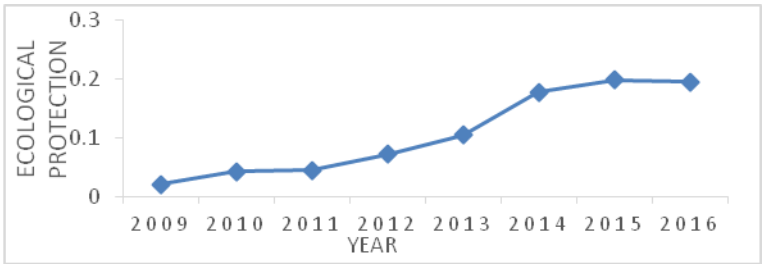

Figure 3. *Ecological protection index of Beijing after 2008 Olympic Games*

(4) The environmental quality index declined firstly and then rose (*Fig. 4*).

The environmental quality of Beijing continued to decline during 2009-2011, which was mainly due to construction of a large amount of infrastructure and the investment of a large amount of funds. Besides, the shutdown of a few heavy industries led to a decline in the economic level. In the post-Olympic period, in order to make the economy grow as before, the manufacturing industry resumed production and emitted a large amount of pollutants.

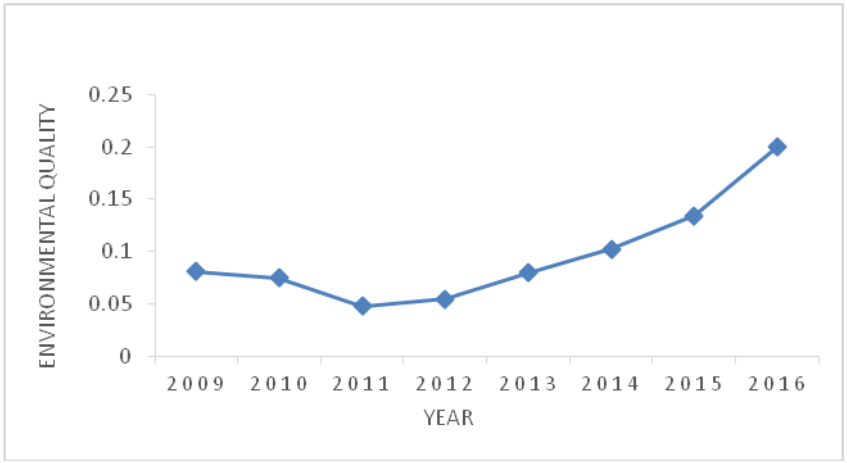

Figure 4. *Environmental quality index of Beijing after 2008 Olympic Games*

The environmental quality began to increase year by year during 2012-2016. The main reason is that the Environmental Protection Agency has significantly enhanced the prevention and control of atmospheric pollution, pollution reduction and air pollution prevention and control (Feng et al., 2018); secondly, pollution reduction efforts

http://www.aloki.hu ● ISSN 1589 1623 (Print) ● ISSN 1785 0037 (Online)
DOI: http://dx.doi.org/10.15666/aeer/1704_85138525

continued to be maintained, and air cleaning activities were carried out; finally, unified management was implemented on heavy air pollution (Hao et al., 2019).

(5) Resource utilization index continued to increase (*Fig. 5*).

The resource utilization index has increased year by year during 2009-2016. Firstly, it was because the solid waste environmental management system was fully implemented and industrial pollution prevention strategies and means were optimized from multiple angles. Secondly, solid waste supervision was strengthened to promote industrial pollution reduction, and the utilization rate of industrial solid waste has increased. Finally, the process will be improved if the pollutants were substandard, so the sewage treatment rate continued to increase.

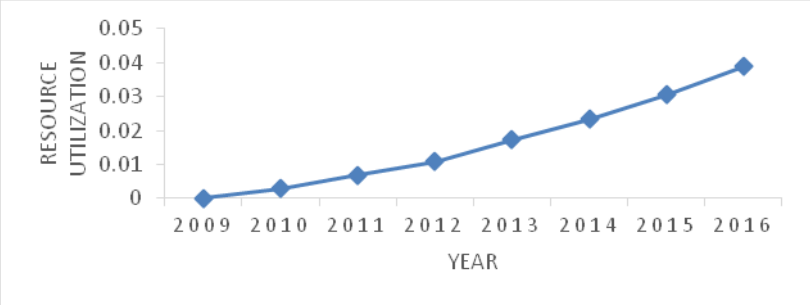

Figure 5. *Resource utilization index of Beijing after 2008 Olympic Games*

(6) The environmental governance index dropped sharply first, then increased year by year, and finally stabilized (*Fig. 6*).

The environmental management in 2009-2010 dropped drastically. It was mainly due to project expenditure in terms of pollution prevention in 2009 and less investment in similar projects in 2010. Besides, major pollutant emission reduction projects were invested in 2009, and the budget for similar projects in 2010 decreased (Pu, 2019)

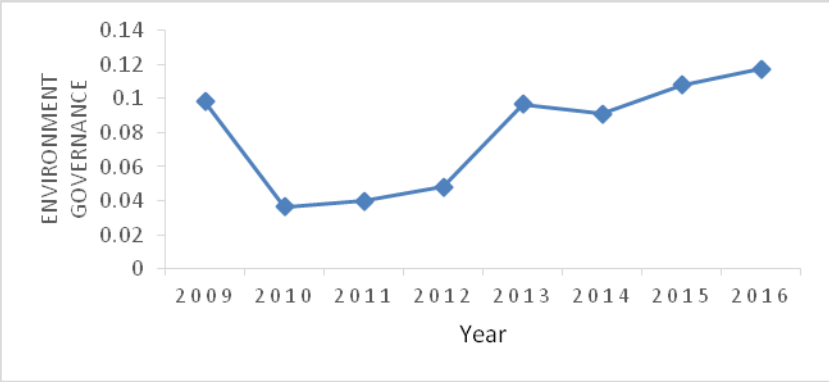

Figure 6. *Environmental governance index of Beijing after 2008 Olympic Games*

It remained on a slow-growth path in the 2010-2012 and 2013-2016 periods, but achieved rapid growth from 2012 to 2013, which was mainly due to the implementation of the 2013-2016 Clean Air Action Plan. Besides, the unliquidated funds that in the previous year were paid (Wang et al., 2019).

http://www.aloki.hu ● ISSN 1589 1623 (Print) ● ISSN 1785 0037 (Online)
DOI: http://dx.doi.org/10.15666/aeer/1704_85138525

Discussion

In this paper, we use the quadratic fit to predict and present a relatively smooth curve. If a fitting is used, a regression straight line will be made, which makes a large error for the result. At this time, a quadratic fitting is required to obtain a quadratic regression equation, making the prediction result more accurate and reliable. The 2009-2016 data will be used to predict the growth quality, ecological protection, environmental quality, resource utilization, environmental quality and ecological civilization index of the 2022 Winter Olympics. The forecast trend is shown (*Fig. 7*).

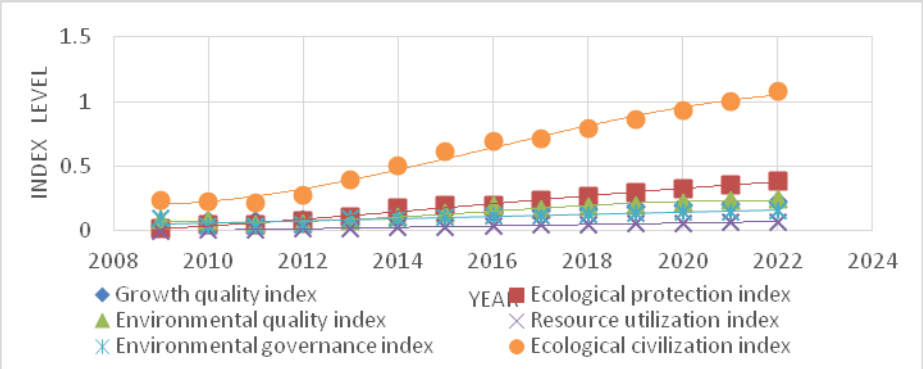

Figure 7. *Prediction map of various indicators in Beijing*

It can be seen from *Figure 7* that the growth quality, ecological protection, environmental quality, resource utilization, and environmental quality index increase in the 2022 Winter Olympics. Therefore, Beijing's ECI has also been increasing year by year. Compared with the ECI of 1.077 in 2020 and 0.717 in 2017, the ECI in the 2022 Winter Olympics increase significantly. Therefore, we believe that the predicted ECI can be achieved if we implement protection policies and improve public awareness of environmental protection.

Conclusions and suggestions

Conclusions

(1) Major events such as the Olympic Games have a major impact on the construction of ecological civilization

There are obvious differences in the index of ecological civilization before and after the Olympic Games. The index of ecological civilization has increased significantly after the Olympic Games, which shows that the Olympic Games have a significant impact on the construction of ecological civilization (Chang, 2018).

In order to successfully hold the Olympic Games, the government has adopted effective policies and the index of ecological civilization has increased, which shows that the policy has a great impact on the development of ecological civilization. The economic and ecological development of each region cannot be separated from the regional characteristics and policy impact of each region, which makes the ecological index and air quality index of Beijing and each region improved.

http://www.aloki.hu ● ISSN 1589 1623 (Print) ● ISSN 1785 0037 (Online)
DOI: http://dx.doi.org/10.15666/aeer/1704_85138525

The Olympic Games is an undertaking that our country has spent a lot of money to accomplish. It is not only to enhance our international status and influence, but also to promote the rapid development of all aspects of our country. The Olympic Games have received the attention of the media from all walks of life, forcing us to issue relevant policy documents, to pay attention to the construction of ecological civilization, and to take the Olympic Games as an important opportunity to promote the coordinated development of ecology and economy.

(2) Get prepared for the 2022 Winter Olympics

According to the prediction of air quality in Beijing and various regions, the 2022 Winter Olympics will be held in Yanqing District, Beijing, which has laid a good foundation for ecological construction. The ECI and air quality index will reach the ecological environment indicators required for hosting the Olympic Games.

Therefore, before the coming of the Winter Olympic Games in 2022, we must take measures to protect the environment, improve the quality of the environment, and pay attention to the construction of ecological civilization, so as to leave a good impression on the people of the world.

Suggestions

With the end of the 2008 Summer Olympics, Beijing's ecological civilization has shown a trend of continuous growing of ecological civilization index and the air quality index so far, but there are also some shortcomings. This paper makes the following suggestions for reference.

(1) Enhance protection and improve the effectiveness of environmental policy implementation

It can be seen from the chart of ECI that the ecological civilization index has dropped significantly after the 2008 Olympic Games. Therefore, in preparing for the 2022 Winter Olympics, we must avoid the occurrence of similar problems, and adopt a long-term mechanism to build an ecological civilization. We cannot rely on temporary management and control, otherwise, it will happen again. Firstly, we should develop effective and targeted measures at regular intervals: environmental pollution control actions; secondly, we will promote the application of new clean energy, prevent and control from the source to reduce tail gas pollution; and finally, develop coordinated development strategy between humans and nature to achieve green development (Hu, 2018).

We should carry out the development strategy of ecological civilization from the following four aspects: in the aspect of eco-economy, vigorously develop tourism and rationally develop local natural resources; in the aspect of ecological environment, we should attach great importance to forestry construction and constantly strengthen the project of benefiting people and increasing green; in the aspect of ecological life, we should save water, reduce waste discharge and improve the rate of waste water treatment; and in the aspect of ecological system. To implement the Party's guidelines and establish a sound ecological environment supervision system. In order to achieve the win-win situation of economic and social development and ecological environment protection, a compound ecological and social system with virtuous circle of economy, society and nature is established.

http://www.aloki.hu ● ISSN 1589 1623 (Print) ● ISSN 1785 0037 (Online)
DOI: http://dx.doi.org/10.15666/aeer/1704_85138525

(2) Enhance public awareness of ecological protection and enhance environmental responsibility

We are about to usher in the 2022 Winter Olympics, combined with the socialist ecological concept put forward by the 19th National Congress of CPC, it is a good opportunity for us to strengthen the education of environmental awareness, to put forward the idea of ecological protection, and to achieve it through practice. A series of specific measures can be taken (Chen et al., 2018). For example, the government can conduct environmental education first, so that citizens can establish environmental awareness, form the concept of common development between man and nature in the mind, and secondly, vigorously promote environmental protection knowledge through the influence of the news media. Everyone protects the environment, increases participation in environmental protection issues, and promotes ecological development. Finally, lectures or seminars to protect the environment can be held to raise the awareness of citizen protection. This will enhance the sense of responsibility for environmental protection in the whole society and make the ecological civilization construction of the 2022 Winter Olympics better.

Acknowledgements. This work was supported by Funding of Beijing Philosophical and Social Science Program (No.13JGC123), Funding of Humanities and Social Sciences General Project of the Ministry of Education (No.16YJC630121), Funding of Talents Developing Strategy Plan of Beijing Union University (No. BPHR2018ES02).

REFERENCES

[1] Arslan, C. H., Sattar, A., Cuong, D. M., Khan, F. U. H., Nasir, A., Bakhat, Z., Ilyas, F. (2018): Study of spatial and temporal variability of arsenic in groundwater due to drain by using GIS. – Earth Sciences Pakistan 2(2): 22-24.

[2] Chang, H., Wang, Z., Li, Y., Chen, G. (2018): Dynamic analysis of a bistable bi-local active memristor and its associated oscillator system. – International Journal of Bifurcation and Chaos 28(08): 1850105.

[3] Chen, C., Xu, J., O'Regan, D., Fu, Z. (2018): Positive solutions for a system of semipositone fractional difference boundary value problems. – Journal of Function Spaces. https://doi.org/10.1155/2018/6835028.

[4] Chen, J., Cheng, J., Dai, S. (2017): Regional eco-innovation in China: an analysis of eco-innovation levels and influencing factors. – Journal of Cleaner Production 153(1): 1-14.

[5] Fang, K., Dong, L., Ren, J., Zhang, Q., Han, L., Fu, H. (2017): Carbon footprints of urban transition: tracking circular economy promotions in Guiyang, China. – Ecological Modelling 365: 30-44.

[6] Feng, M., Li, P., Sun, S. (2018): Symmetric positive solutions for fourth-order n-dimensional m-Laplace systems. – Boundary Value Problems 2018(1): 63.

[7] Fernando, S. (2016): Consumer behavior and sustainable development in china: the role of behavioral sciences in environmental policymaking. – Sustainability 8(9): 897.

[8] Geisendorf, S., Klippert, C. (2017): The effect of green investments in an agent-based climate-economic model. – Environmental Modeling & Assessment 22(1): 1-21.

[9] Glenys, A. (2017): Labor performance and the stability of administrative personnel contracted in the school of medicine at the University of Zulia. – Argos 34(66).

[10] Guan, H.-L. (2016): Analysis of new urban planning based ecological economics. – Open House International 41(3): 102-106.

http://www.aloki.hu ● ISSN 1589 1623 (Print) ● ISSN 1785 0037 (Online)
DOI: http://dx.doi.org/10.15666/aeer/1704_85138525

[11] Hao, M., Lu, C., Li, Y. (2019): Simulation experiment study on adhering sand casing well full-waveform characteristics. – Acta Microscopica 28(2).
[12] Hassanpour, M. (2018): Semeiology of Iranian commercial and cultural photomontage posters after the revolution. – Argos 35(71).
[13] Hu, B., Ma, W. X., Xia, T., Zhang, L. (2018): Nonlinear integrable couplings of a generalized super Ablowitz-Kaup-Newell-Segur hierarchy and its super bi-Hamiltonian structures. – Mathematical Methods in the Applied Sciences 41(4): 1565-1577.
[14] Jing, G. (2018): Application of traditional cultural elements in modern urban public art landscape design. – Argos 35(71).
[15] Kang, H., Jung, S. H., Park, D. (2017): Development of an ecological impact assessment model for dam construction. – Landscape and Ecological Engineering 13(1): 15-31.
[16] Khanchoul, K., Saaidia, B., Altschul, R. (2018): Variation in sediment concentration and water discharge during storm events in two catchments, Northeast of Algeria. – Earth Sciences Malaysia 2(2): 01-09.
[17] Kumar, R. (2018): Comparison of instruction scheduling and register allocation for MIPS and HPL -PD architecture for exploitation of instruction level parallelism. – Engineering Heritage Journal 2(2): 04-08.
[18] Lee, B. X., Kjaerulf, F., Turner, S., Cohen, L., Donnelly, P. D., Muggah, R. et al. (2016): Transforming our world: implementing the 2030 agenda through sustainable development goal indicators. – Journal of Public Health Policy 37(1): 13-31.
[19] Lee, M. S. (2016): Global health promotion efforts for achieving the UN 2030 agenda for Sustainable Development, UN 2030. – Korean Journal of Health Education and Promotion 35(4): 1-18.
[20] Li, J., Jiang, B., Lin, N. (2018): A study on the influence mechanism of port environmental carrying capacity. – The Asian Journal of Shipping and Logistics 34(3): 191-197.
[21] Liang, Z., Wenshun, W. (2019): Parametric architectural design based on optimization algorithm. – Engineering Heritage Journal 3(1): 13-17.
[22] Madhav, S., Ahamad, A., Kumar, A., Kushawaha, J., Singh, P., Mishra, P. K. (2018): Geochemical assessment of groundwater quality for its suitability for drinking and irrigation purpose in rural areas of Sant Ravidas Nagar (Bhadohi), Uttar Pradesh. – Geology, Ecology, and Landscapes 2(2): 127-136.
[23] Marinelli, M. (2018): How to build a 'beautiful China' in the Anthropocene. The political discourse and the intellectual debate on ecological civilization. – Journal of Chinese Political Science 23(3): 365-386.
[24] Nawaz, A., Arshad, F., Khurshid, F. (2018): Evaluation of low cost environment friendly natural extracts for the purification of drinking water. – Earth Sciences Pakistan 2(1): 23-25.
[25] Oglu Nasirov, A. Y. (2018): Importance of silk road in the international trade. – Argos 35(70).
[26] Ogunyele, A. C., Obaje, S. O., Akingboye, A. S. (2018): Lithostructural relationships and petrogenetic affinities of the basement complex rocks around Okpella, Southwestern Nigeria. – Earth Sciences Malaysia 2(1): 29-36.
[27] Ping, R., Liu, X., Liu, J. (2018): Research on construction of indicator system for evaluation of the ecological civilization education in Chinese universities. – Cognitive Systems Research 52: 747-755.
[28] Pu, X., Guo, D., Zhao, Y. (2019): Dual diagnostic method for fracture morphology of thermal coalbed methane reservoir. – Acta Microscopica 28(2).
[29] Raj, N. J., Prabhakaran, A. (2018): Lineaments of Kodaikanal-Palani massif, Southern Granulitic Terrain of Tamil Nadu, India: a study using SRTM DEM and LANDSAT satellite's OLI sensor's FCC. – Geology, Ecology, and Landscapes 2(3): 188-202.

http://www.aloki.hu ● ISSN 1589 1623 (Print) ● ISSN 1785 0037 (Online)
DOI: http://dx.doi.org/10.15666/aeer/1704_85138525

[30] Rajendran, Y., Mohsin, R. (2018): Emission due to motor gasoline fuel in reciprocating lycoming O -320 engine in comparison to aviation gasoline fuel. – Environment & Ecosystem Science 2(2): 20-24.
[31] Serpe, C. (2018): The right to education-a key to social-economic development. – Argos 35(68).
[32] Shen, L. (2018): Rural toilet reform: the current situation, problems and countermeasures-based on the survey of 944 farmers. – Argos 35(68).
[33] Song, M., Guan, Y., Wang, J, Zhao, J. (2016): Evaluation of urban industrial ecological transformation in China. – Clean Technologies & Environmental Policy 18(8): 1-14.
[34] Suhaili, M. Z., Samsudin, M. D. M. (2018): Utilization of wastewater for corrosion prevention of carbon steel pipe using single chamber microbial fuel cells. – Environment & Ecosystem Science 2(2): 47-52.
[35] Sun, H. (2018): Analysis on group behavior of college students based on cellular automation. – Argos 35(68).
[36] Sun, L., Li, H., Dong, L., Fang, K., Ren, J., Geng, Y. et al. (2016): Eco-benefits assessment on urban industrial symbiosis based on material flows analysis and emergy evaluation approach: a case of Liuzhou city China. – Resources, Conservation and Recycling 119: 78-88.
[37] Sun, X., Gao, L., Ren, H. (2018): China's progress towards sustainable land development and ecological civilization. – Landscape Ecology 33(10): 1647-1653.
[38] Wang, Q., Zhang, C., Liao, G., Wang, X. (2019): Influence of distribution width on early-age hydration and setting behaviors of calcium aluminate cement at 20 °C. – Acta Microscopica 28(2).
[39] Yu, Y., Wu, W., Zhang, T., Liu, Y. (2016): Environmental catching-up, eco-innovation, and technological leadership in China's pilot ecological civilization zones. – Technological Forecasting & Social Change 112: 228-236.
[40] Zhang, M., Liu, Y., Wu, J., Wang, T. (2018): Index system of urban resource and environment carrying capacity based on ecological civilization. – Environmental Impact Assessment Review 68: 90-97.
[41] Zhang, W., Yang, J., Fang, Y., Chen, H., Mao, Y., Kumar, M. (2017): Analytical fuzzy approach to biological data analysis. – Saudi Journal of Biological Sciences 24(3): 563-573.
[42] Zhang, X., Wang, Y. et al. (2016): Evaluating the trends of China's ecological civilization construction using a novel indicator system. – Journal of Cleaner Production 133: 910-923.
[43] Zhang, X., Wu, J., Liu, L., Wu, Y., Cui, Y. (2018): Convergence analysis of iterative scheme and error estimation of positive solution for a fractional differential equation. – Mathematical Modelling and Analysis 23(4): 611-626.
[44] Zhou, X., Liang, X., Du, X., Zhao, J. (2018): Structure based user identification across social networks. – IEEE Transactions on Knowledge and Data Engineering 30(6): 1178-119.

http://www.aloki.hu ● ISSN 1589 1623 (Print) ● ISSN 1785 0037 (Online)
DOI: http://dx.doi.org/10.15666/aeer/1704_85138525

EVALUATION OF ECOLOGICAL CIVILIZATION IN MEGACITIES

ZHAO, Y.[1] – SHENG, X.[2*] – YANG, P.[2] – ZHU, L.[3]

[1]*School of Applied Science and Technology, Beijing Union University, Beijing 100101, China*
(e-mail: 1447502494@qq.com)

[2]*Management School, Beijing Union University, Beijing 100101, China*
(e-mail: 963450574@qq.com – P. Yang)

[3]*College of Business and Public Management, West Chester University, West Chester 19383 PA, USA*
(e-mail: xzhu@wcupa.edu)

**Corresponding author*
e-mail: shengxiaojuan@buu.edu.cn

(Received 8th Mar 2019; accepted 21st May 2019)

Abstract. General Secretary Xi Jinping clearly pointed out in the report of the Nineteenth Party Congress that speeding up the reform of ecological civilization system and building ecological civilization are the millennium plan for the sustainable development of the Chinese nation. The ecological problems of mega-cities are related to the sustainable development of economy and society. Because the radiation area of mega-cities is relatively wide, the geographical environment of various city regions is different, and so is the functional orientation, the selection of evaluation criteria and evaluation indicators is particularly important in the evaluation process. Based on the perspective of mega-city functional areas and combining it with the urban development planning of Beijing, this paper discusses the evaluation of ecological civilization in mega-cities, constructs the evaluation index system of ecological civilization index, and uses the coefficient of variation method of objective empowerment method to determine the index weight, and evaluates the ecological civilization of each functional area in Beijing from three aspects: growth quality, ecological protection and air quality. It can be concluded that the index of ecological civilization in Beijing shows an upward trend as a whole, each functional area presents different characteristics, and the implementation of policies has a significant impact on the construction and development of ecological civilization.

Keywords: *urban development, functional areas, judgement standard, coefficient variation, sustainable development*

Introduction

At present, China's rapid development is facing the ecological dilemma brought about by economic development and social transformation. In the Amendment to the Constitution of the People's Republic of China adopted in 2018, ecological civilization was written into the Constitution, which had a higher legal status and had stronger legal effects (Lai, 2013; Nwankwo and Nwankwoala, 2018). It was written into the Party Constitution and Constitution, which made the idea of ecological civilization a vivid manifestation of the will of the state. With the improvement of urbanization level, people pay more and more attention to ecological problems (Yan, 2017; Yang et al., 2018b, c; Sufiyan et al., 2018). The number of megacities is rising, and the proportion of GDP and total population is expanding. Therefore, the evaluation of ecological civilization in megacities is particularly important. As a typical megacity, Beijing's ecological civilization building is related to the image of

http://www.aloki.hu ● ISSN 1589 1623 (Print) ● ISSN 1785 0037 (Online)
DOI: http://dx.doi.org/10.15666/aeer/1704_85278540

the country and the capital, and it relates to the quality of the city and the welfare of the people.

As the center of human activities and social civilization, the city has further reduced the living standards of human beings and hindered the sustainable development of urban ecosystems at the expense of severe environmental degradation and enormous ecological environmental pressures (Liu et al., 2014; Yilmaz, 2018; Azeem et al., 2018). Chinese government promotes ecological civilization in the "13th five year plan" (2016-2020) period. As a result, ecological impacts become highlighted in the national circular economy practices (Sun et al., 2016; Nkwuda et al., 2019). According to official statistics, 70% of China's population will live in cities in 2030, and China's urbanization will have a great development. The report points out that China's urbanization draws on the theory of ecological modernization and uses "sustainability" and "governance" and "ecological civilization". It is very meaningful to see that the rise in the research on ecological civilization can be attributed to this decision (Muldavin, 2015; Xu, 2018).

The national strategy of building an ecological civilization is not simply to focus on environmental issues, but to create a new "five-pronged" civilization based on a new historical orientation. Turning to ecological civilization, realizing national strategy, and benefiting and leading the world with China's program of ecological civilization, education is not only an important starting point, but the only way. The research and construction of the education evaluation index system of China's efficient ecological civilization will provide a new method (Ping, 2018; Kasim et al., 2019). Low-carbon m & a is a new mode of merger and acquisition under the ecological civilization education (Tian, 2017; Dali and Kamarudin, 2018). The historical assessment and future prediction of ecological security (Yang et al., 2018a) and the study on the establishment of safety factor system model for the construction of water ecological civilization (Zhang, 2017; Baharuddin and Samsudin, 2018) are also very important. Regional landscape-ecological studies have acquired a special topicality as they assure efficient environmental conservation and sustainable use of natural resources. A landscape-ecological analysis was performed based on four basic integral indices: (1) ecological potential, (2) ecological stability, (3) ecological load and (4) ecological tension (Muradyan and Asmaryan, 2015; Emeh and Igwe, 2018). Urban ecological vulnerability is measured on the basis of ecological sensitivity and resilience based on the concept analysis of vulnerability. GIS-based multicriteria decision analysis (GIS-MCDA) methods are used, supported by the spatial analysis tools of GIS, to define different levels of vulnerability for areas of the urban ecology. These areas are further classified into different types of regulatory zones. In this way, five types of vulnerability areas have been classified as follows: very low vulnerability, low vulnerability, medium vulnerability, high vulnerability and very high vulnerability (Zhang et al., 2015; Karaoui et al., 2018).

The establishment of ecological civilization evaluation index plays a decisive role in evaluating the level of ecological civilization in a region. Different scholars, according to different practical significance to put forward the index system of different, consider URECC evaluation index system (Zhang et al., 2018) and the index system of people-oriented EC (Zhang et al., 2016), which are for the overall, different areas have different characteristics, establish a comprehensive index of regional ecological civilization in China, the regional ecological civilization construction is particularly important to carry on the scientific and objective evaluation (Liu et al.,

http://www.aloki.hu ● ISSN 1589 1623 (Print) ● ISSN 1785 0037 (Online)
DOI: http://dx.doi.org/10.15666/aeer/1704_85278540

2016). Understanding the link between ecological civilization and performance assessment will help to better monitor the level of ecological civilization (Tan et al., 2014).

In summary, scholars have inherited rich experience and have rich research results, covering a wide range of areas, and the evaluation indicators vary widely. For megacities, they should pay attention to regional differences, different functional areas, existing natural resources, economic conditions, etc. Different, then the role played is different. The division of functional areas has given us a new perspective on the study of Beijing's ecological civilization. On this basis, we can conduct ecological civilization evaluation from the perspective of functional areas and explore the ecological civilization of Beijing's functional areas.

According to the ecological civilization evaluation of the functional areas, we can see that the division of the functional areas of Beijing has, to a certain extent, rationalized the management system of the functional areas and the administrative area. Each function area has its own characteristics, is of great significance in resource integration, urban space expansion and urban efficiency. This is the key point for the future development of Beijing's ecology, and it is also the research entry point and academic innovation of this paper.

Methodology

Construction of Beijing's ecological civilization evaluation system

Overall evaluation ideas

Beijing Regional Statistical Yearbook officially divided functional areas from 2011. Based on this, from the perspective of the practice of ecological civilization construction, the four functional areas of Beijing are taken as the basic unit, the panel data of various functional areas in Beijing from 2011 to 2016 (12th Five-Year Plan and 18th National Congress periods) are selected to carry out comprehensive evaluation of the level of ecological civilization, compare and analyze the pattern characteristics and existing deficiencies of various functional areas in Beijing during the process of ecological civilization construction, and reveal the main influencing factors of ecological civilization in various functional areas of Beijing to determine what we should work on in the future.

Building an indicator system

Based on the 13th Five-Year Plan for Economic and Social Development, the Assessment System for Ecological Civilization Construction and the Green Development Indicator System, and the existing research results at home and abroad, the index system of ecological civilization index the various functional areas in Beijing will be built.

According to the connotation of ecological civilization and the design principle of index system, a set of three-level superposition and layered recursive comprehensive evaluation index system is constructed. However, due to the lack of indicators in each district and the data released by the National Bureau of Statistics, the indicators were adjusted. The target ecological civilization index (ECI) is divided into three elements, namely, growth quality, ecological protection, and air quality (*Table 1*).

http://www.aloki.hu ● ISSN 1589 1623 (Print) ● ISSN 1785 0037 (Online)
DOI: http://dx.doi.org/10.15666/aeer/1704_85278540

Table 1. *ECI System of functional areas in Beijing*

Grade 1 indicator	Grade 2 indicators	Grade 3 indicators	Unit	Nature
Ecological civilization	Growth quality	GDP per capita	10,000 yuan/person	Positive
		Urban per capita disposable income	Yuan	Positive
		R&D	10,000 yuan	Positive
		Urbanization rate	%	Positive
	Ecological protection	Woody plant cover rate	%	Positive
		Proportion of wetland area in urban area	%	Positive
		Forest stock	10,000 m^3	Positive
		Forest coverage rate	%	Positive
		Harmless disposal rate of household garbage	%	Positive
	Air quality	Annual average concentration of SO2	mcg/m3	Negative
		Annual average concentration of NO2	mcg/m3	Negative
		Annual average concentration of inhalable particulate matter	mcg/m3	Negative
		Average annual concentration of fine particles (PM2.5)	mcg/m3	Negative

Data source and evaluation method

The evaluation data of the ECI in Beijing and various districts come from Beijing Statistical Yearbook, Statistical Yearbook of Beijing Municipal Environmental Protection Bureau, Statistical Yearbook of Beijing Water Affairs Bureau, Statistical Yearbook of Beijing Municipal Bureau of Landscape Architecture and related statistical yearbooks. This paper uses the ecological civilization index to evaluate the ecological civilization. The specific process of the ecological civilization index evaluation is as follows.

(1) Build an original indicator data matrix

Suppose there are m evaluation indicators, n years, forming the original indicator data matrix:

$$Xij = (Xij)m \times n(0 \leq i \leq m; 0 \leq j \leq n) \quad \text{(Eq.1)}$$

In *Equation 1,* Xij refers to the i-th indicator, and the index value of the j-th year.

(2) Data standardization processing method

Since the attributes of the ecological civilization evaluation index are inconsistent with the measurement unit, in order to make calculation by a unified method, the data needs to be dimensionlessly standardized. According to the nature of the evaluation indicators, the evaluation indicators are divided into two categories: positive indicators and negative indicators (Rojamary and Uma, 2017). The standardization method is:

http://www.aloki.hu ● ISSN 1589 1623 (Print) ● ISSN 1785 0037 (Online)
DOI: http://dx.doi.org/10.15666/aeer/1704_85278540

Positive indicator:

$$Z = \frac{Yij - y\min j}{Yj\max - yj\min} \quad (i = 1,2,\ldots,n;j = 1,2,\ldots,n) \qquad \text{(Eq.2)}$$

Negative indicator:

$$Z = \frac{Ymaxj - yij}{Yj\max - yj\min} \quad (i = 1,2,\ldots,n;j = 1,2,\ldots,n) \qquad \text{(Eq.3)}$$

wherein: *Yj*max and *Ymin*j the maximum and minimum of X_{ij} indicator, the decision matric is Zij after standardized processing, this allows the data of the decision matrix to be processed.

(3) Determination of the weight of evaluation indicators

Considering the characteristics of ecological civilization and the needs and practice of the research, this paper will use the coefficient of variation method in the objective weighting method to determine the weight of each indicator. The method is:

$$Wi = \frac{Vi}{\sum_{i=I}^{m} Vi}, \quad Vi = \frac{\sigma i}{Zi} \qquad \text{(Eq.4)}$$

wherein: σ is the standard deviation of the i-th indicator, Z is the average of the i-th indicator, and V is the coefficient of variation of the i-th indicator. W refers to the weight of the i-th indicator (*Table 2*). In the process of calculating the weights, Beijing is given a weight as a whole, and the weights of each indicator are calculated.

Table 2. *Weights of indicators in the indicator system*

Grade 1 indicator	Grade 2 indicators	Weight	Grade 3 indicators	Weight
Ecological civilization	Growth quality	0.326289465	GDP per capita (10,000 yuan/person)	0.104145517
			Urban per capita disposable income (Yuan)	0.074994926
			R&D (10,000 yuan)	0.17295373
			Urbanization rate	0.02682463
	Ecological protection	0.539946483	Woody plant cover rate %	0.060229909
			Proportion of wetland area in urban area	0.262925633
			Forest stock	0.060981161
			Forest coverage rate	0.059912983
			Harmless disposal rate of household garbage (calculated by amount of garbage clean-up %)	0.021883686
	Air quality	0.139531838	Annual average concentration of SO2 (mcg/m3)	0.028731574
			Annual average concentration of NO2 (mcg/m3)	0.048975187
			Annual average concentration of inhalable particulate matter (mcg/m3)	0.047048155
			Fine particles (PM2.5) annual average concentration (mcg/m3)	0.030392911

http://www.aloki.hu ● ISSN 1589 1623 (Print) ● ISSN 1785 0037 (Online)
DOI: http://dx.doi.org/10.15666/aeer/1704_85278540

(4) Determination of ECI

$$Rij = \sum_{i=1}^{m} Zij * Wi \quad \text{(Eq.5)}$$

In the *Equation 5,* R represents the ecological civilization index. Based on this formula, the ecological civilization index Rij and Grade 2 indicators of various regions in Beijing can be calculated (*Table 3*). The data of each functional area is an average of the indexes of the districts and counties belonging to each functional area, so that it is convenient to compare the differences between the functional areas of Beijing.

Table 3. *Beijing ecological civilization index*

Functional areas	Year	Growth quality	Ecological protection	Air quality	Ecological civilization index
Core functional area of the capital	2011	0.119255327	0.022013989	0.023623497	0.164892814
	2012	0.130016473	0.022071368	0.040681712	0.192769553
	2013	0.139937143	0.022128748	0.048013585	0.210079476
	2014	0.152639386	0.021973004	0.051775002	0.226387392
	2015	0.195048883	0.021973004	0.084733885	0.301755772
	2016	0.217907123	0.029584236	0.100050385	0.347541743
	Average growth rate	12.81%	6.09%	33.47%	16.08%
Urban functional expansion area	2011	0.190150847	0.080596187	0.024212684	0.294959718
	2012	0.189436944	0.082054262	0.041580443	0.313071649
	2013	0.187391939	0.08387603	0.036968568	0.308236538
	2014	0.216492554	0.083149692	0.032664156	0.332306402
	2015	0.230943838	0.083914856	0.07591888	0.390777574
	2016	0.287175331	0.295023757	0.102029288	0.684228376
	Average growth rate	8.59%	29.63%	33.33%	18.33%
New urban development area	2011	0.02879102	0.103577099	0.012504876	0.144872995
	2012	0.040611046	0.12173979	0.041620135	0.203970971
	2013	0.053229603	0.130241314	0.044855477	0.228326395
	2014	0.103008569	0.134186654	0.045694723	0.282889946
	2015	0.067694893	0.134538993	0.080870658	0.283104544
	2016	0.073536103	0.367488963	0.102416706	0.543441773
	Average growth rate	20.63%	28.82%	52.29%	30.27%
Ecological conservation development area	2011	0.022149826	0.166664689	0.088081247	0.276895762
	2012	0.023950504	0.1731915	0.103474282	0.300616286
	2013	0.025388707	0.183889776	0.108132201	0.317410685
	2014	0.027361617	0.198585163	0.10685063	0.33279741
	2015	0.028947303	0.192690473	0.139155322	0.360793098
	2016	0.031826831	0.462821252	0.155781064	0.650429147
	Average growth rate	7.52%	22.66%	12.08%	18.63%

http://www.aloki.hu ● ISSN 1589 1623 (Print) ● ISSN 1785 0037 (Online)
DOI: http://dx.doi.org/10.15666/aeer/1704_85278540

Result analysis and discussion

Dongcheng and Xicheng districts in Beijing have been identified as "the core functional area of the capital"; the four districts of Chaoyang, Haidian, Fengtai and Shijingshan are the "urban functional expansion areas" in Beijing; the "New Urban Development Area" include Fangshan, Tongzhou, Daxing, Shunyi and Changping districts; Mentougou, Pinggu, Huairou, Miyun and Yanqing are Ecological Conservation Development Area.

Index changes

Core functional area of the capital

Growth quality has the greatest influence on the ecological civilization index. It is related to the characteristics of the core functional area of the capital (*Fig. 1*). The core functional area of the capital are the highest level of urbanization of Beijing, gather most of the city-level and some important district-level commercial centers, and economic level is higher than other regions; the ecological protection index is the lowest and tends to be stable, mainly because its plant cover rate and forest coverage are not high; the effect of air quality on ecological civilization is on the rise. Based on this, the regional positioning of the core functional area of the capital is highlighted to promote financial service industry and a national business district, and to strengthen efforts for air quality control, in doing so, it is more conducive to promoting the ecological civilization level of the core functional area.

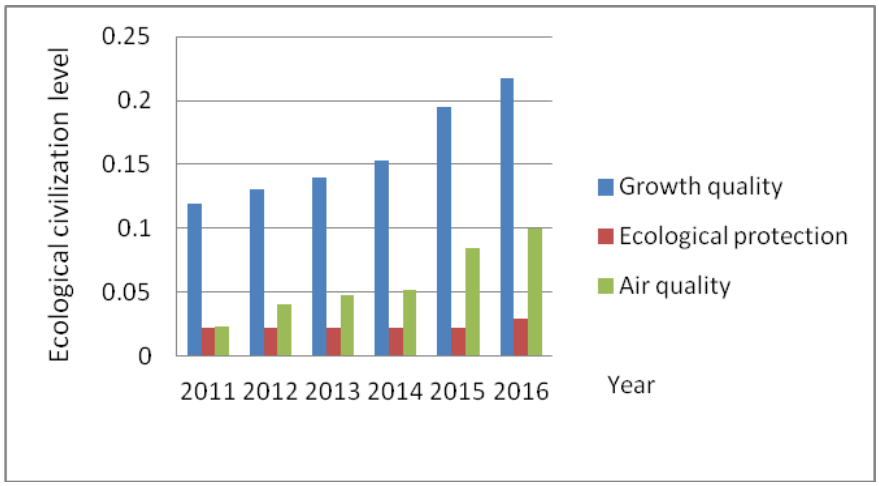

Figure 1. *Comparison of ECI in capital core functional areas*

Urban functional expansion area

The quality growth index of the urban functional expansion area continues to rise, and the quality growth index is the main influencing factor affecting the urban functional expansion area. Overall, the ecological protection index tends to be stable, the air quality index rises, and the urban function expansion area covers the Zhongguancun Science and Technology Park, and the important functional areas such as Beijing Central Business District (*Fig. 2*). It is a main area for the development of commercial and high-end industries in the metropolitan area with high level of economy

http://www.aloki.hu ● ISSN 1589 1623 (Print) ● ISSN 1785 0037 (Online)
DOI: http://dx.doi.org/10.15666/aeer/1704_85278540

and large population, and an important area that reflects Beijing's modern economy and the function of international exchanges.

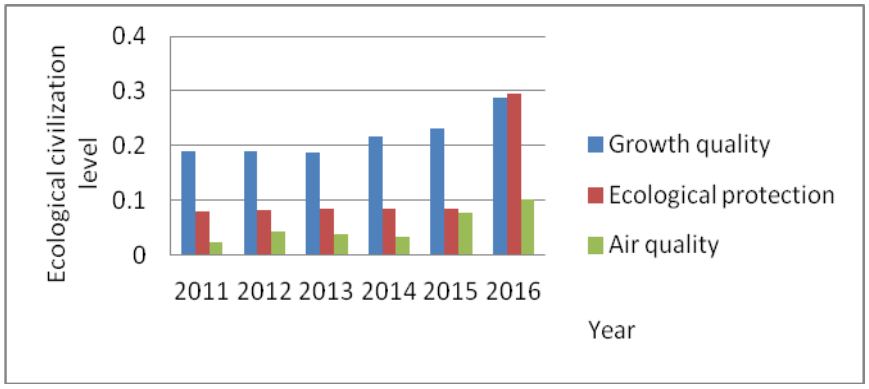

Figure 2. *Comparison of ECI in urban functional expansion areas*

New urban development area

It can be seen from *Figure 3* that the ecological protection index is the main influencing factor of the ecological civilization of the new urban development area, because the urban development new area is the main carrier of Beijing's high-tech industries, modern manufacturing and modern agriculture, and is the future development of Beijing's economic center and future cities (*Fig. 3*). Although the growth quality and the air quality index are inferior to the ecological protection index, the index has shown an upward trend over time (Olivares, 2017). We should introduce talents while maintaining the ecological environment, create a good business environment, and continuously improve the air quality.

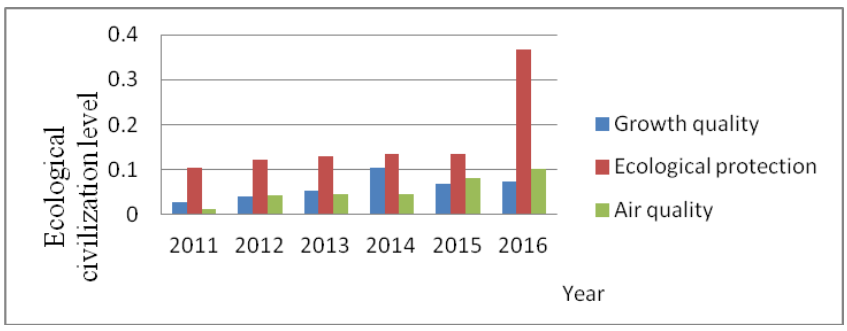

Figure 3. *Comparison of ECI in new urban development area*

Ecological conservation development area

The ecological protection and air quality index in the ecological conservation development area ranked first. It can be seen that ecological protection has always been a major factor affecting the ecological conservation development area, mainly because the ecological conservation development area is Beijing's ecological barrier and water source protection site, the environmentally friendly industrial base, and also an ideal space for Beijing citizens to take a leisurely life (Jaimes, 2017; Higuchi, 2017) (*Fig. 4*). We must strengthen the construction of ecological protection.

http://www.aloki.hu ● ISSN 1589 1623 (Print) ● ISSN 1785 0037 (Online)
DOI: http://dx.doi.org/10.15666/aeer/1704_85278540

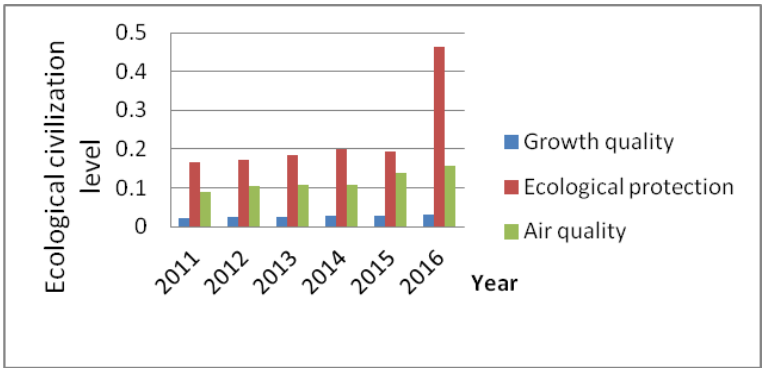

Figure 4. *Comparison of ECI in ecological conservation development area*

Change in growth rate

Comparison of functional areas under the same indicator

From 2011 to 2016, the air quality index had the highest growth rate in core functional area of the capital, urban function development area, and urban development new area, indicating that during the "Twelfth Five-Year Plan" and the implementation of the spirit of the 18th National Congress, air pollution control has made significant achievements (*Fig. 5*). The ecological protection index had the highest growth rate in the ecological conservation development area, indicating that the ecological conservation zone adapts to local conditions and develops its own advantages (Guevara-Hernández, 2018).

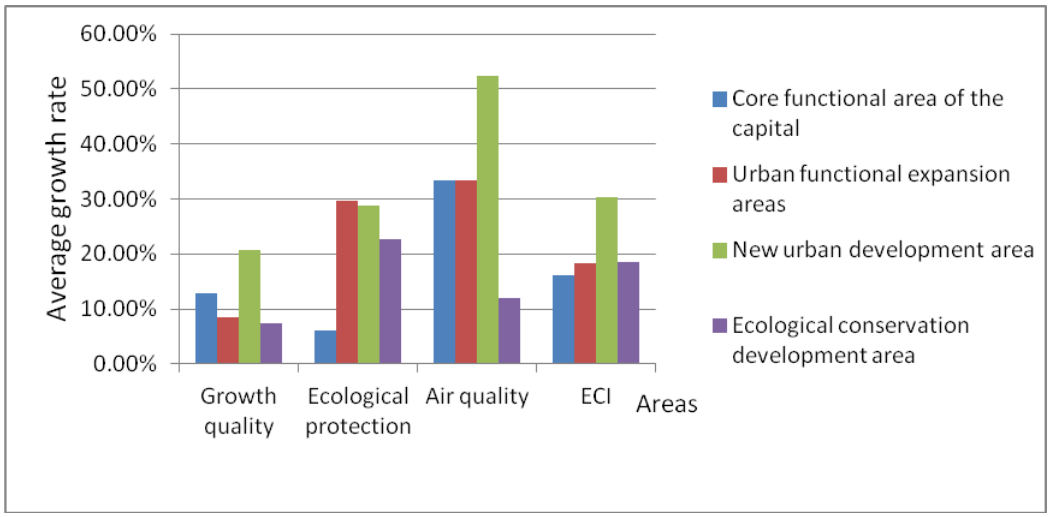

Figure 5. *Growth rate of various indicators in functional areas in 2011-2016*

Comparison of growth rate indicators for the same functional areas

From 2011 to 2016, the air quality index, ecological civilization index and growth quality index of the new urban development area have the highest growth rate (*Fig. 6*). The Outline of the Plan for Coordinated Development for the Beijing-Tianjin-Hebei Region released in 2015 pointed out that the core of promoting the coordinated development of Beijing-Tianjin-Hebei is to orderly relocate all non-essential functions

http://www.aloki.hu ● ISSN 1589 1623 (Print) ● ISSN 1785 0037 (Online)
DOI: http://dx.doi.org/10.15666/aeer/1704_85278540

from Beijing. Fangshan District is located in the southwest of the Beijing-Tianjin-Hebei region, shouldering the responsibility of "connection between inside and outside" (Naustdalslid, 2014). The economic and ecological development of Fangshan District has driven the development of new urban development area. Due to the promotion of policy or development needs, the development of new urban development area from 2011 to 2016 was extremely fast.

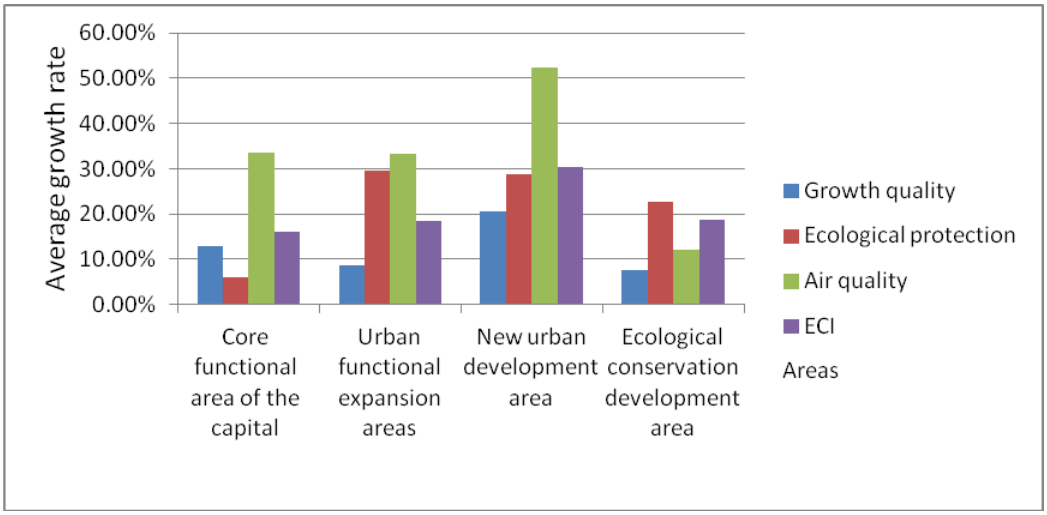

Figure 6. *Growth rate of various indicators in functional areas in 2011-2016*

Analysis of the factors affecting the development of ecological civilization in various functional areas

It can be seen from *Figures 1–4* that in 2016, apart from the core functional area of the capital, the ecological protection index of the other three areas increased rapidly, even surpassing the main influencing factors affecting these areas (Pechurkin and Somova, 2014; Olivares, 2017). This is mainly because 2016 is a crucial year for all kinds of people-benefit projects and green projects for Beijing, and Beijing has achieved fruitful results in ecological protection in 2016. At the same time, it can be seen that the ecological protection in the core functional area of the capital is currently in a state of saturation, and it is not suitable for large-scale tree planting (Mendoza, 2018; Jaimes, 2017).

Conclusions and suggestions

Conclusions

(1) The development of ecological civilization presents different characteristics in different functional areas

From the main influencing factors of various functional areas, quality growth is the main factor in the capital functional core area and urban functional expansion area, which is mainly related to the characteristics of these two areas, namely, high economic level and dense population (Higuchi, 2017); Ecological protection is the main influencing factor of urban development new area and ecological conservation area. The ecological environment and air quality of these two areas are excellent, with abundant

http://www.aloki.hu ● ISSN 1589 1623 (Print) ● ISSN 1785 0037 (Online)
DOI: http://dx.doi.org/10.15666/aeer/1704_85278540

forest resources and sparse population. Different functional areas present different characteristics, so we need to manage functional areas according to local conditions.

(2) The implementation of policies significantly affects the construction and development of ecological civilization

The impact of policies on the development of ecological civilization is enormous. With the conclusion of Beijing's people-benefit projects in 2016, except the core functional area of the capital in 2016, the ecological protection index of the other three areas has made a great leap forward. The development of various functional areas is inseparable from the development of other functional areas. The introduction of the Outline of the Plan for Coordinated Development for the Beijing-Tianjin-Hebei Region has driven economic development of new urban development area and brought changes to air quality. The implementation of policies will be more targeted and effective in improving the problems in the ecological civilization.

(3) Functional areas not optimally positioned

From the perspective of vertical time evolution, the level of ecological civilization in the four functional areas of Beijing is constantly improving. However, from the analysis of the horizontal dimension, urban functional expansion areas and ecological conservation development area have the highest level of ecological civilization, followed by new urban development area and core functional area of the capital. The core functional area of the capital is the most important carrier of the capital's function and "four services". However, the air quality index of the core functional area of the capital is not high, which will affect the impression of the capital and the people's healthier and more comfortable life.

Suggestions

(1) Develop regional ecological civilization according to local conditions

According to the development goals of Beijing's functional areas, we will vigorously implement the regional coordinated development strategy and give full play to the advantages and potentials of each region (Guevara-Hernández, 2018). There is no one-size-fits-all approach to technology and model, specific conditions require concrete analysis, and we should develop regional ecological civilization in accordance with local conditions. The capital functional core area and the urban function development area have developed rapidly. We should focus on quality growth, while the urban development new area and the ecological conservation development area are characterized by geographical marginality and abundant natural resources, and they have great advantages and potential in air quality and ecological protection. We will always adhere to the principle of developing regional ecological civilization according to local conditions to improve the level of ecological civilization.

(2) Ecological civilization driven by policies

Since the 18th National Congress of the Communist Party of China, the CPC Central Committee with Comrade Xi Jinping as the core has attached great importance to the construction of ecological civilization and environmental protection, and emphasized that promoting a green development mode and lifestyle is an inevitable requirement for

http://www.aloki.hu ● ISSN 1589 1623 (Print) ● ISSN 1785 0037 (Online)
DOI: http://dx.doi.org/10.15666/aeer/1704_85278540

implementing the new development concept. It is necessary to put ecological civilization construction in a prominent position of the whole work. Relevant national laws and regulations such as the Opinions on Accelerating the Construction of Ecological Civilization and other laws have been successively released. We cannot be a giant of ideas and a dwarf in action. We must implement the policy, strengthen the intensity of supervision, and constantly improve the level of ecological civilization in China.

(3) Build an ecological civilization evaluation system for megacities based on the main functional areas

This paper provides an ecological civilization evaluation from the perspective of functional areas, and provides a new idea for the construction of the evaluation system based on the main functional areas theory. The main functional area theory has gradually become the main basis for the development of ecological civilization throughout the country. The reason is that the evaluation of the functional areas is in line with the national macro requirements, and closely follows the footsteps of economic and social construction. It has both practical significance and referential significance.

(4) Promote mutual development

The shortcomings of ecological conservation development area are mainly focused on quality growth. Governments at all levels should have a series of special policy support for the ecological conservation development area. These policies are essential for the development of these regions. Since the ecological conservation development area is Beijing's ecological barrier and water conservation site, it should be compensated as much as possible in the form of policies, for example, funding for the construction of tourist attractions, the giving living subsidies to people who live in the area.

Acknowledgements. This work was supported by Funding of Beijing Philosophical and Social Science Program (No. 13JGC123), Funding of Humanities and Social Sciences General Project of the Ministry of Education (No. 16YJC630121), Funding of Talents Developing Strategy Plan of Beijing Union University (No. BPHR2018ES02).

REFERENCES

[1] Azeem, N., Arslan, C. H., Rashid, H., Sattar, A. (2018): Comparative study of hospital waste management practices at different health care units in district Faisalabad for the development of improvement strategies. – Earth Sciences Pakistan 2(2): 16-21.

[2] Baharuddin, D., Samsudin, M. D. M. (2018): Effect of pH and moisture content on current density of impressed current cathodic protection: response surface methodology study. – Environment & Ecosystem Science 2(2): 15-19.

[3] Dali, N. M., Kamarudin, K. S. N. (2018): The effect of cosurfactant in CO_2 absorption in water-in-oil emulsion. – Environment & Ecosystem Science 2(2): 42-46.

[4] Emeh, C., Igwe, O. (2018): Effect of environmental pollution on susceptibility of sesquioxide-rich soils to water erosion. – Geology, Ecology, and Landscapes 2(2): 115-126.

http://www.aloki.hu ● ISSN 1589 1623 (Print) ● ISSN 1785 0037 (Online)
DOI: http://dx.doi.org/10.15666/aeer/1704_85278540

[5] Guevara-Hernández, F. (2018a): Actores y estrategias de la innovación tecnológica en la producción de maíz en Chiapas, México. – Revista de la Facultad de Agronomia de la Universidad del Zulia 35(2).
[6] Guevara-Hernández, F. (2018b): Análisis comparativo energético-económico del agroecosistema maíz bajo prácticas convencionales y de conservación en la región Frailesca, Chiapas, México. – Revista de la Facultad de Agronomia de la Universidad del Zulia 35(3).
[7] Higuchi, A. (2017): Socio-economic characteristics and attitudes of organic and non-organic consumers in Lima, Peru. – Revista de la Facultad de Agronomia de la Universidad del Zulia 34(4).
[8] Jaimes, E. J. (2017): Capacidad de carga y presión de uso de la tierra en cuatro sectores de la sub-cuenca del río Déleg, Provincia del Cañar, Ecuador. – Revista de la Facultad de Agronomia de la Universidad del Zulia 34(3).
[9] Jiang, S., Lian, M., Lu, C., Gu, Q., Ruan, S., Xie, X. (2018): Ensemble prediction algorithm of anomaly monitoring based on big data analysis platform of open-pit mine slope. – Complexity. https://doi.org/10.1155/2018/1048756.
[10] Karaoui, I., Arioua, A., Idrissi, A. E. A., Hssaisoune, M., Nouaim, W., Ouhamchich, K. A., Elhamdouni, D. (2018): Assessing land use/cover variation effects on flood intensity via hydraulic simulations: a case study of Oued El Abid watershed (Morocco). – Geology, Ecology, and Landscapes 2(2): 73-80.
[11] Kasim, S., Hassan, R., Zakaria, Z. (2019): Re-engineering in confinement method. – Engineering Heritage Journal 3(1): 18-19.
[12] Kumar, M., Mao, Y., Wang, Y., Qiu, T., Chenggen, Y., Zhang, W. (2017): Fuzzy theoretic approach to signals and systems: static systems. – Information Sciences 418: 668-702.
[13] Lai, X., Liu, G., Wang, H. (2013): Evaluation and analysis of DEA efficiency in construction of ecological civilization of Jiangsu Province. – Disaster Advances 6: 102-108.
[14] Liu, G., Yang, Z., Chen, B., Ulgiati, S. (2014): Emergy-based dynamic mechanisms of urban development, resource consumption and environmental impacts. – Ecological Modelling 271: 90-102.
[15] Liu, M., Liu, X., Yang, Z. (2016): An integrated indicator on regional ecological civilization construction in China. – International Journal of Sustainable Development and World Ecology 23(1): 53-60.
[16] Mendoza, J. L. L. H. (2018): Economic analysis of the use of commercial biofertilizers in the cultivation of sorghum. – Revista de la Facultad de Agronomia de la Universidad del Zulia 35(4).
[17] Muldavin, J. (2015): Using cities to control the countryside: an alternative assessment of the China National Human Development Report 2013. – Development & Change 46(4): 993-1009.
[18] Muradyan, V. S., Asmaryan, S. G. (2015): Applying landscape-ecological concept and gis modelling for assessing and mapping of ecological situation of mountainous landscapes (on the case of Syunik Marz, Armenia). – Geocarto International 30(10): 1077-1091.
[19] Naustdalslid, J. (2014): Circular economy in China—the environmental dimension of the harmonious society. – International Journal of Sustainable Development & World Ecology 21(4): 303-313.
[20] Nkwuda, N. G., Theophine, M. A., Okogwu, O. I. (2019): Impacts of rock mineralization and poor sanitary system on borehole waters quality and the health implications. – Earth Sciences Pakistan 3(1): 10-13.
[21] Nwankwo, C., Nwankwoala, H. O. (2018): Gully erosion susceptibility mapping in Ikwuano local government area of Abia State using GIS techniques. – Earth Sciences Malaysia 2(1): 08-15.

http://www.aloki.hu ● ISSN 1589 1623 (Print) ● ISSN 1785 0037 (Online)
DOI: http://dx.doi.org/10.15666/aeer/1704_85278540

[22] Olivares, B. O. (2017): Caracterización socioeconómica y modos de producción de la comunidad agrícola indígena Kashaama, Anzoátegui, Venezuela. – Revista de la Facultad de Agronomia de la Universidad del Zulia 34(2).
[23] Pechurkin, N. S., Somova, L. A. (2014): Anthropogenic civilization: from socioeconomic to environmental instability. – Herald of the Russian Academy of Sciences 84(1): 47-51.
[24] Ping, R., Xi, L., Liu, J. W. (2018): Research on construction of indicator system for evaluation of the ecological civilization education in Chinese universities. – Cognitive Systems Research 52: 747-755.
[25] Rojamary, T., Uma, K. P. (2017): A stochastic model for the cost analysis of a system with two components for the loss of manpower threshold. – Revista de la Facultad de Agronomía 34(2).
[26] Sufiyan, I., Zakariya, R., Yacoob, R., Idris, M. S., Idris, N. M. (2018): SWAT subbasins parameters and flood risk simulations using 3D in Terengganu watershed. – Earth Sciences Malaysia 2(2): 10-15.
[27] Sun, L., Li, H., Dong, L., Fang, K., Ren, J., Geng, Y. et al. (2016): Eco-benefits assessment on urban industrial symbiosis based on material flows analysis and emergy evaluation approach: a case of Liuzhou City, China. – Resources Conservation and Recycling 119: 78-88.
[28] Tan, K. H., Shi, L., Tseng, M. L., Cui, W. J. (2014): Managing the indirect effects of environmental regulation and performance measurement. – Industrial Engineering & Management Systems 13(2): 148-153.
[29] Tian, M., Yan, S., Peng, H. (2017): Research on the differences of ecological efficiency of low-carbon M&A among enterprises under the education of ecological civilization. – Eurasia Journal of Mathematics Science and Technology Education 13(8): 5233-5245.
[30] Xu, D. (2018): Research on brand construction and development of agricultural products in Guizhou. – Engineering Heritage Journal 2(2): 19-24.
[31] Yan, C., Dai, H., Guo, W. (2017): Evaluation of ecological environmental quality in a coal mining area by modelling approach. – Sustainability 9(8): 1-13.
[32] Yang, B., Gao, F. P., Jeng, D. S. (2018a). Failure mode and dynamic response of a double-sided slope with high water content of soil. – Journal of Mountain Science 15(4): 859-870.
[33] Yang, B., Luo, Y., Jeng, D., Feng, J., Huhe, A. (2018b). Experimental studies on initiation of current-induced movement of mud. – Applied Ocean Research 80: 220-227.
[34] Yang, Q., Liu, G., Hao, Y., Coscieme, L., Zhang, J., Jiang, N. et al. (2018c): Quantitative analysis of the dynamic changes of ecological security in the provinces of China through emergy-ecological footprint hybrid indicators. – Journal of Cleaner Production 184: 678-695.
[35] Yilmaz, H. (2018): Economic and environmental analysis of pesticide use for sustainable barley (Hordeum vulgare L.) production in Turkey. – Revista de la Facultad de Agronomia de la Universidad del Zulia 35(1).
[36] Zhang, M., Liu, Y., Wu, J., Wang, T. (2018): Index system of urban resource and environment carrying capacity based on ecological civilization. – Environmental Impact Assessment Review 68: 90-97.
[37] Zhang, X. (2017): Study on the construction of the security element system model of water ecological civilization construction. – Agro Food Industry Hi-Tech 28(3): 679-683.
[38] Zhang, X., Wang, Z., Lin, J. (2015): GIS-based measurement and regulatory zoning of urban ecological vulnerability. – Sustainability 7(8): 9924-9942.
[39] Zhang, X., Wang, Y., Qi, Y., Wu, J., Liao, W., Shui, W. et al. (2016): Evaluating the trends of China's ecological civilization construction using a novel indicator system. – Journal of Cleaner Production 133: 910-923.
[40] Zhou, X., Liang, X., Du, X., Zhao, J. (2018): Structure based user identification across social networks. – IEEE Transactions on Knowledge and Data Engineering 30(6): 1178-119.

http://www.aloki.hu ● ISSN 1589 1623 (Print) ● ISSN 1785 0037 (Online)
DOI: http://dx.doi.org/10.15666/aeer/1704_85278540

STUDY ON HYDROGEN PRODUCTION OYF BIO-OIL CATALYTIC REFORMING BY CHARCOAL CATALYST

ZHANG, Y.

College of Chemical Engineering, Guangdong University of Petrochemical Technology, Maoming 525000, China
(e-mail: 280512356@qq.com; fax: +86-066-8298-1080)

(Received 8th Mar 2019; accepted 21st May 2019)

Abstract. In this study Charcoal was used as a primary bio-oil steam reforming catalyst. The performance of the catalyst was investigated. The dynamic parameters of the first order dynamic equation were calculated. The stability of charcoal was also examined. The results indicated that first, when reforming temperatures were lower than 700 °C, the bio-oil contents in the outlet dry gas were very high. This indicated unsuitability for further catalytic reforming over a metal catalyst. Second, the catalytic activity of charcoal became very significant under high temperature conditions (≥ 800 °C); thus, the apparent activation energy of the first order kinetic rate constant is 56.98 kJ/mol, and the pre-exponential factor is $1.58 \times 10^4 s^{-1}$. Third, the bio-oil contents in the outlet dry gas varied from a decrease to a slight increase in the first 2 h under a catalytic reforming temperature of 900 °C, a WHSV (weight hourly space velocity) of 2.6 h^{-1}, a bio-oil feeding rate of 47.02 g/h, and a S/B (mass steam-to-bio-oil) ratio of 2. Overall, the charcoal exhibited an excellent bio-oil removal rate (conversion > 99.6%) and the bio-oil contents in the outlet dry gas were lower than 1.89 g/Nm^3, hence signifying suitability for further reforming over metal catalysts.
Keywords: *catalyzer, stability, char, gas cleaning, steam reforming process*

Introduction

Interest in the hydrogen economy is increasing due to its potential applications in hydrogen fuel cell vehicles and fuel cell power generation (Li et al., 2018). Currently, the main hydrogen production processes are catalytic reforming of naphtha, light hydrocarbons and methane (Zhou et al., 2017a), while coal gasification is also widely used (Zhang, 2018; Daniel et al., 2018). However, the sustainable energy development can be realized only by using renewable energy as raw material to produce hydrogen (Bizkarra et al., 2018; Hossain et al., 2019). In this regard, steam reforming of bio-oil has been reported in many journals (Beatriz et al., 2018; Asghar et al., 2018). Bio-oil is produced by rapid pyrolysis of biomass. And its main components include alcohol, furan, acid, sugar, phenol, ketone and aldehyde (Arandia et al., 2018; Ilyas et al., 2018). The catalytic reforming of bio-oil mainly depends on the catalytic capacity of the catalyst for steam reforming reaction ($C_nH_mO_k + (n - k)\ H_2O = (n + m/2 - k)\ H_2 + nCO$) and water gas shift reaction ($CO + H_2O = H_2 + CO_2$). When bio-oil is reformed at high temperature, the Boudoard reaction ($2CO = C + CO_2$) and partial thermal decomposition of bio-oil may occur simultaneously (Zhou et al., 2017b).

Preliminary economic analysis shows that bio-oil steam reforming for hydrogen production is profitable in the current market (Czernik and French, 2014; Omini and Akpang, 2018). However, bio-oil catalytic reforming for hydrogen production is still facing many technical difficulties in order to become a commercially mature technology. Zeng et al. (2015) and Rajput et al. (2019) reported that carbon deposition on catalyst supports leads to low purity hydrogen in gas products. Li et al. (2017) proposed that a significant challenge in bio-oil hydrodeoxygenation was the

http://www.aloki.hu ● ISSN 1589 1623 (Print) ● ISSN 1785 0037 (Online)
DOI: http://dx.doi.org/10.15666/aeer/1704_85418553

deactivation of coke deposits on zeolite catalysts. Wu et al. (2008) proposed dolomite catalyst with low cost to be chosen as the first-order catalyst for tar steam reforming, and then methane and tar are further reformed on nickel metal catalyst (Zhang et al., 2017). This technological process can protect the metal catalyst from quick deactivation and the economic loss could be reduced efficiently (Li et al., 2008). This technological process can effectively prevent the rapid deactivation of nickel metal catalysts and reduce economic losses (Cho et al., 2014; Yahya et al., 2018). However, since the calcined dolomite is easy to break up under the impact of air flow, powder dolomite may cause the resistance of the catalyst bed to rise sharply (Thakkar et al., 2016).

The research on catalytic reforming of tar over charcoal during biomass gasification can be used as a reference for steam reforming of bio-oil (El-Rub et al., 2008; Masri and Samsudin, 2018). Char itself has some activity for biomass tar conversion (Nestler et al., 2016), and its conversion activity is affected by surface area (Mun et al., 2010), pore size and ash composition (Zanzi et al., 1996). The coke deposited on the charcoal will block the pore and reduce the surface area, thus reducing the activity of the charcoal. However (Morishita et al., 2002), coke can also be consumed by gaseous products such as steam and carbon dioxide, and its deactivation can be suppressed by generating new pores (Hosokai et al., 2005; Sharma and Yadav, 2018). Furthermore, char catalysts would have low costs and be simply burned/gasified to recover the energy of the char without the need of often expensive regeneration after deactivation (Li, 2007). Hence, choosing a char catalyst as the primary steam reforming catalyst is more promising (Kai et al., 2018). It is important to study the catalytic activity and stability of the char catalysts for bio-oil conversion.

In this study, char is used as a primary steam reforming catalyst (Min et al., 2011; Naidu et al., 2018). The catalytic performance of the catalyst for bio-oil catalytic steam reforming under different operating conditions was studied. The stability of the charcoal catalyst was also investigated. The kinetic parameters were calculated by using the first-order kinetic equation (Qian and Kumar, 2015).

Materials and Methods

Test material

Bio-oil was produced by rapid pyrolysis of sawdust with fluidizer N_2 in the temperature range of 450 to 500 °C. The reactor used was a fluidized bed designed by East China University of Technology (Shanghai, China). Bio-oil components were determined by a gas chromatography-mass spectrometry. The results are shown in *Table 1*.

Properties of char

The commercial charcoal was supplied by Shanghai Canature Environmental Products Co., Ltd. (Shanghai, China). Elemental analysis of dried samples showed that it contained C 74.09%, O 17.51%, H 4.80%, S 0.018% and N 0.1%. Industrial analysis showed that ash content was 3.48%.

Before the catalytic test, the commercial biomass charcoal was heated to 900 °C at a heating rate of 27 K/min under the condition of air isolation, and the temperature was maintained for 30 min. *Table 2* shows the elemental analysis and ash content of the treated charcoal samples. Elemental C, N, and H analyses were performed using an

http://www.aloki.hu ● ISSN 1589 1623 (Print) ● ISSN 1785 0037 (Online)
DOI: http://dx.doi.org/10.15666/aeer/1704_85418553

elemental analyzer, Elementar Vario EL III (Langenselbold, Germany). A sulfur analysis was accomplished on a Coulomb sulfur analyzer, CLS-2 (Jiangsu Jiangfen Electric Instrument Co. Ltd., Jiangyan, China). The composition of ash was determined *via* Sequential X-ray fluorescence spectrometry, (XRF-1800, Thermofisher, Beijing, China). The char samples were screened to the particle sizes of 1 mm to 2 mm.

Installation and procedure for experiment

As shown (*Fig. 1*), the catalytic reforming was performed in a fixed-bed reactor made of stainless steel. The height and diameter of the reactor are 800 mm and 20 mm respectively. The reaction pressure is atmospheric. The char catalysts were placed in the middle of the fixed-bed tube and the fixed bed was heated by an electric heating furnace equipped with a temperature control device. The nitrogen purged the system prior to the reactor heating. Bio-oil and water were fed into the reactor at a constant rate by two separate metering pumps. The reaction products were first condensed by tap water, then by ice-water mixtures, and the condensate was collected in liquid containers. The non-condensed components of the product gases were determined using an online gas analyzer (Gasboard-3100, Cubic Optoelectronics Co., Ltd., Wuhan, China) and the gas flow rate was measured using a soap membrane flow-meter (Agilent technologies Co., Ltd., Santa Clara, USA). When the feed is finished, the reactor is cooled to room temperature by nitrogen flow with a flow rate of 0.6 L/min, then the char catalysts are collected and weighed.

Table 1. *Components of bio-oil*

Name	Area (%)	Name	Area (%)
Acetaldehyde	2.81	2-methyl-2-Pentenal	0.28
Methanol	5.83	Phenol	1.23
Acetone	1.27	Unknown	0.48
Unknown	0.49	2-Hydroxy-3-methyl-2-Cyclopenten-1-one	1.22
2-Pentanone	0.33	2-methyl-Phenol	0.78
Pentane	0.16	2-methoxy-Phenol	0.85
Formic acid	0.86	4-methyl-Phenol	1.48
Unknown	2.18	3,4-dimethyl-Phenol	0.45
Acetic acid	20.34	2-methoxy-4-methyl-Phenol	0.98
1-hydroxy-2-Propanone	11.49	1,2-Benzenediol	3.44
Propanoic acid	0.81	4-ethyl-2-methoxy-Phenol	0.36
3-hydroxy-2-Butanone	1.25	3-methoxy-1,2-Benzenediol	0.21
1-(acetyloxy)-2-Butanone	1.83	4-hydroxy-Benzenemethanol	0.76
2-methyl-Pentanal	0.83	2,6-dimethoxy-Phenol	1.21
Propanoic acid,2-oxo-, methyl ester	0.52	2-methoxy-4-(1-propenyl)-Phenol	0.10
Unknown	0.78	Vanillin	0.16
Furfural	2.15	1,2,4-Trimethoxybenzene	0.52
2-Cyclopenten-1-one	0.36	Unknown	0.20
2-Butanone	0.77	1-(4-hydroxy-3-methoxy phenyl)-Ethanone	0.18
1-(acetyloxy)-2-Propanone	0.46	1,2,3-trimethoxy-5-methyl-Benzene	0.19
2-methyl-2-Cyclopenten-1-one	0.27	1-(4-hydroxy-3-methoxy phenyl)-2-Propanone	0.22
Butyrolactone	0.30	D-Mannoheptulose	0.91
2(5H)-Furanone	1.04	2,6-dimethoxy-4-(2-propenyl)-Phenol	0.60
2-hydroxy-2-Cyclopenten-1-one	0.44	D-Allose	23.68
5-methyl-2(5H)-Furanone	0.21	1-(4-hydroxy-3,5-dimethoxyphenyl)-Ethanone	0.45
5-methyl-2-Furancarboxaldehydehyde	0.42	1,1'-butylidenebis-Benzene	0.49
3-methyl-2-Cyclopenten-1-one	0.38		

http://www.aloki.hu ● ISSN 1589 1623 (Print) ● ISSN 1785 0037 (Online)
DOI: http://dx.doi.org/10.15666/aeer/1704_85418553

Table 2. *Elemental analysis and ash composition of the ultimate charcoal samples*

Ultimate analysis (wt.%, dry basis)							
C	91.03	O	2.766	H	1.05		
S	0.024	N	0.14	Ash	4.99		
Ash composition (%)							
K_2O	8.3240	MgO	12.3426	CaO	57.2088	SiO_2	8.1264
SO_3	2.0576	Fe_2O_3	2.6929	P_2O_5	4.6305	MnO	0.0736
Al_2O_3	1.4948	SrO	0.5573	TiO_2	0.1616	CuO	0.1614
ZnO	0.0739	Cl	0.1273	ZrO_2	0.1286	Na_2O	1.6748
NiO	0.0717	BaO	0.0475	Cr_2O_3	0.0269	Rb_2O	0.0100
Co_2O_3	0.0062	Y_2O_3	0.0017				

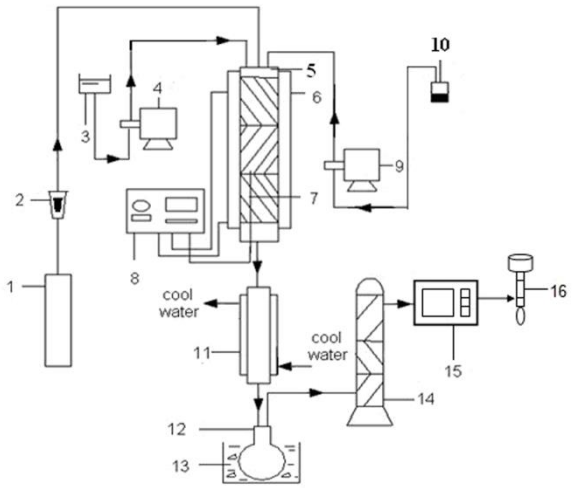

Figure 1. *Schematic diagram of experimental device; 1) Nitrogen cylinder, 2) Gas flow indicator, 3) Water, 4) Meterflow pump I, 5) Fixed bed reactor, 6) Heating tube, 7) Thermocouple, 8) Temperature controller, 9) Meterflow pump II, 10) bio-oil, 11) Condenser, 12) Liquid collector, 13) Ice-water bath, 14) Drying tower, 15) GC, and 16) soap membrane flow-meter*

Analysis of bio-oil in liquid condensate

TOC (Total Organic Carbon) method was used to analyze liquid products. Liquid products can be divided into water-soluble and non-water-soluble substances, namely light hydrocarbons and heavy hydrocarbons, and oxygenates. Both fractions were called 'tars.' Although the water-soluble tar was a complex mixture of organic compounds, phenol represented the "average" tar compound. The tar yield determination was made in the same manner as previously indicated by Corella et al. (1991).

Experimental data evaluation

The conversion of bio-oil was calculated from their mass inlet and outlet as shown in *Equation 1:*

http://www.aloki.hu ● ISSN 1589 1623 (Print) ● ISSN 1785 0037 (Online)
DOI: http://dx.doi.org/10.15666/aeer/1704_85418553

$$X = \frac{F_{in} - F_{out}}{F_{in}} \times 100 \quad \text{(Eq.1)}$$

where X (%) is the bio-oil conversion, F_{in} (g) is the total mass of the inlet bio-oil, and F_{out} (g) is the total mass of the outlet bio-oil.

The main property selected for determining the suitability of further catalytic steam reforming over a metal catalyst was the bio-oil contents in the outlet dry gas (Y). It was defined as the ratio of the mass flow rate of bio-oil (g/min) over the flow rate of dry gas (Nm^3/min) in an outlet as shown in *Equation 2:*

$$Y = F_{out} / \text{(Total vol. of non-condensed gaseous products except for } Nm^3) \quad \text{(Eq.2)}$$

The residence time (s) in the catalyst bed were defined as *Equation 3:*

$$t = \frac{\varepsilon \times V_{char}}{Q_{in,T}} \quad \text{(Eq.3)}$$

where ε (dimensionless) was the bed porosity of the catalyst (with a value of 0.38 in), V_{char} was the volume (L) of char in the bed, and $Q_{in,\,T}$ was the total inlet flow rate (L/s) of N_2, bio-oil, and water vapor under reactor temperature. The $Q_{in,\,T}$ was calculated by the equation for the state of ideal gas, as shown in *Equation 4:*

$$Q_{in,T} = \frac{1000 \times F_{inlet,n} \times R \times T}{P} \quad \text{(Eq.4)}$$

where $F_{\text{inlet,n}}$ (mol/s) was the total inlet molar flow rate of N_2, bio-oil, and water vapor, R = 8.314 (J/mol/K), T (K) is the reactor temperature, and P = 101325 (Pa).

Results and discussion

Effect of catalytic reforming temperature

The effects of catalytic reforming temperatures in the range from 600 to 900 °C on the dry gas composition, bio-oil conversion, and bio-oil contents in the outlet dry gas were investigated while the N_2 flow rate, WHSV (Weight hourly space velocity), feeding rate of bio-oil, and S/B (mass steam-to-bio-oil ratio) were fixed at 30 mL/min, 5.2 h^{-1}, 47.02 g/h, and 2, respectively. As can be seen from *Table 3,* as expected, the concentration of hydrogen in the gaseous product and the bio-oil conversion increased with the catalytic reforming temperature, while the concentration of carbon dioxide in the gaseous product and the bio-oil content in the outlet dry gas decreased. Comparing the results with that of Wang et al. (2007), it can be seen that the catalytic activity of the char catalyst is higher than the C12A7-O^-/18% Mg catalyst at 600 to 700 °C. This indicated that the char catalyst had good catalytic performance for the bio-oil conversion. However, comparison with the results of Wang et al. (Wang et al., 1998) found that the total concentration of H_2 and CO was about 80% over the commercial catalysts of the UCI G-90C and ICI 46-series. Nevertheless, the total composition of H_2 and CO was lower than 64% over the char catalyst at 800 to 900 °C. A reason for this was because the concentration of CH_4 in the gaseous product was high. This indicated

http://www.aloki.hu ● ISSN 1589 1623 (Print) ● ISSN 1785 0037 (Online)
DOI: http://dx.doi.org/10.15666/aeer/1704_85418553

that the char catalyst had limited effects on the CH_4 transformation (Yang et al., 2019). When the temperature was lower than 700 °C, the bio-oil contents in the outlet dry gas was very high, and therefore is not suitable for further catalytic steam reforming over the metal catalyst. The catalytic activity of char became very prominent at high temperatures (≥ 800 °C). The bio-oil conversion was higher than 80% and the bio-oil contents in the outlet dry gas became much lower, though the technological parameters should be further optimized to reduce the bio-oil contents in outlet dry gas.

Table 3. *Effects of catalytic reforming temperatures on dry gas composition and bio-oil conversion as well as bio-oil contents in outlet dry gas*

Temperature (°C)	Dry gas composition (vol.%)				Bio-oil	
	H_2	CO	CH_4	CO_2	Conversion (wt.%)	In outlet dry gas (g/Nm^3)
600	0.33	6.14	17.45	76.09	49.00	2664.44
700	12.24	10.84	21.79	55.13	62.65	1105.79
800	18.62	19.50	27.93	33.95	82.22	237.50
900	45.85	18.36	11.34	24.45	93.87	53.25

Kinetic aspects of catalytic reforming

From the previous sections it was found that the catalytic activity of char became very significant at high temperatures above 800 °C. The temperature and char dosage effects on the bio-oil conversion were studied in the temperature range of 800 to 900 °C and the char dosage range of 9 to 18 g.

A first order kinetic equation is used to calculate the kinetic parameters (*Eq. 5*), for the overall bio-oil catalytic reforming reactions:

$$\frac{dF}{dt} = -kF \qquad \text{(Eq.5)}$$

where F (mol/s) is the molar flow rate of bio-oil at the reactor inlet and k is the apparent kinetic constant.

To verify plug flow conditions in the fixed bed, the longitudinal or axial dispersion coefficient (D), which characterizes the degree of back mixing during the flow, needed to be calculated. This coefficient is used in the dimensionless Peclet number (Pe) to determine the type of flow, according to *Equation 6:*

$$Pe = \frac{v \times L}{D} \qquad \text{(Eq.6)}$$

$Pe \rightarrow 0$ large dispersion, hence the use of a mixed flow; $Pe \rightarrow \infty$ negligible dispersion, hence the use of a plug flow, where L is the length of the bed (units) and m and v are the average actual fluid velocity (m/s).

The Peclet number was very high (approximately 1.81×10^4), hence the plug flow conditions can be assumed. Under the plug flow conditions, the first-order kinetic equation can be integrated according to *Equation 7*:

http://www.aloki.hu ● ISSN 1589 1623 (Print) ● ISSN 1785 0037 (Online)
DOI: http://dx.doi.org/10.15666/aeer/1704_85418553

$$\ln(\frac{F_{in}}{F_{out}}) = kt \quad \text{(Eq.7)}$$

The slopes of those lines were calculated by a linear regression to give the apparent kinetic constant, *k*, under the catalytic gasification temperature of 800 °C, 850 °C, and 900 °C as shown in *Figure 2*.

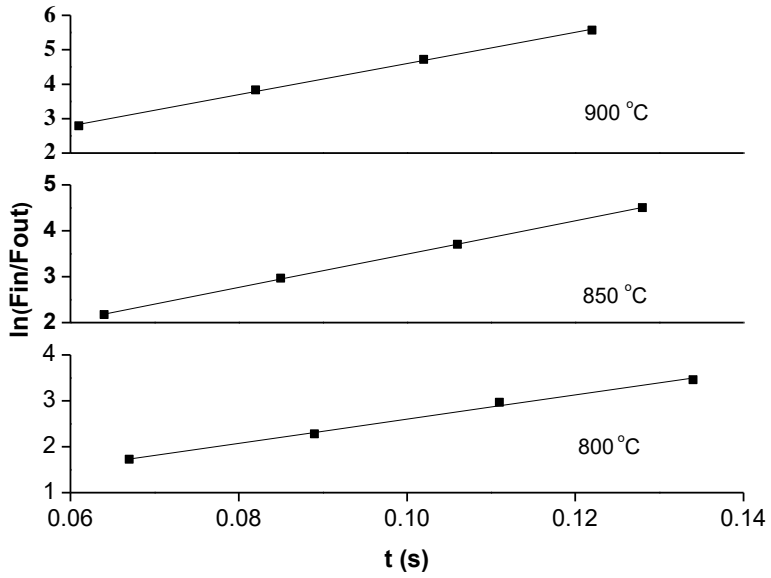

Figure 2. *Effects of the residence time in the catalyst bed on ln(Fin/Fout) under catalytic gasification temperature of 800 °C, 850 °C, and 900 °C. (Dosage of char rose from 9 to 18 g at a rate of 3 g, feeding rate of bio-oil was 47.02 g/h and S/B was 2)*

The apparent rate constant of the bio-oil conversion over char was estimated according to the Arrhenius' law, seen in *Equation 8*. The estimated apparent activation energy of char was assumed to be constant in the studied temperature range (800 to 900 °C).

$$k = k_0 e^{(-E_a/RT)} \quad \text{(Eq.8)}$$

where k_0 is the apparent frequency factor, s^{-1} and E_a are the apparent activation energy (J/mol).

The Arrhenius plots and Cremer-Constable diagram of the catalytic gasification (800 to 900 °C) are shown in *Figure 3*. The slopes and intercepts of the line were calculated by a linear regression to give the apparent activation energies (E_a) of 56.98 KJ/mol and the pre-exponential factors (k_0) of 1.58×10^4 s^{-1} for a catalytic reforming with the char catalyst. It would be interesting to compare the results with the results of other researchers. However, research on the bio-oil conversion kinetic parameters for the biomass char could not be found. Only a comparison with tar reduction was made (Shan et al., 2018). The Charcoal in this work gave lower apparent activation energies (E_a) values in comparison to several different chars (85.8 KJ/mol for sorbent-free coal char (Shamsi et al., 1996), 61 KJ/mol (El-Rub et al., 2008), 81.2 KJ/mol for foster wheeler

http://www.aloki.hu ● ISSN 1589 1623 (Print) ● ISSN 1785 0037 (Online)
DOI: http://dx.doi.org/10.15666/aeer/1704_85418553

char (Shamsi et al., 1996), BASF (58 KJ/mol) (Aznar, 1998), and G1-25 S (58 KJ/mol) (Aznar, 1998). And it gives pre-exponential factors (k_0) higher than the commercial biomass char (1.0×10^4 s^{-1}) (El-Rub et al., 2008), and foster wheeler char (1.30×10^4 s^{-1}) (Shamsi et al., 1996). Therefore, bio-oil can be considered an easier removal than tar either from biomass gasification or coal gasification.

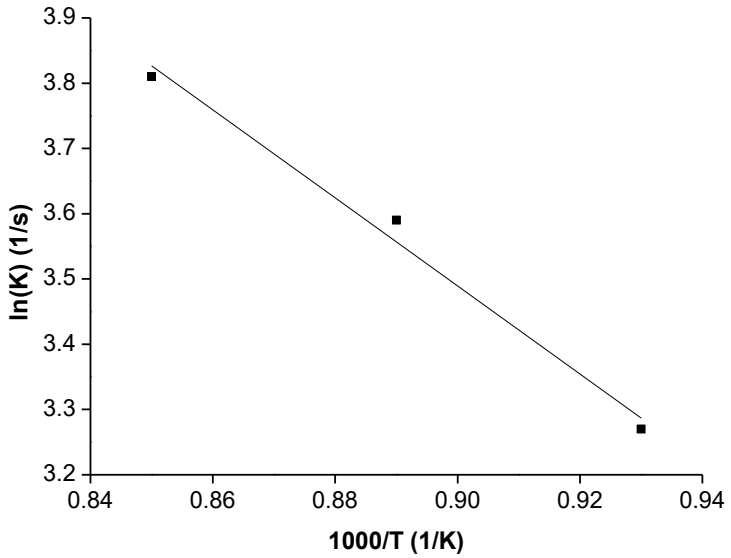

Figure 3. *The relationship between apparent reaction rate constant and temperature according to Arrhenius' law*

Stability of the char catalyst on bio-oil catalytic reforming

From the previous sections it was found that the bio-oil contents in the outlet dry gas was low under the catalytic reforming conditions, with a catalytic temperature of 900 °C, N_2 flow rate, 30 mL/min, WHSV, 2.6 h^{-1}, a feeding rate of bio-oil, 47.02 g/h and S/B of 2. It was suitable for further catalytic steam reforming over the metal catalyst (Mengping et al., 2018). However, the stability of the char catalyst should be well understood (Chang et al., 2018). Thus, dry gas composition, bio-oil conversion, bio-oil contents in outlet dry gas, char waste, and the weight percentage of char consumed were studied as a function of time (Li et al., 2019). The experimental results (*Table 4*) show that the increase in time resulted in the bio-oil contents of outlet dry gas to vary from decreasing to a slight increase, whereas the bio-oil conversion varied from increasing to a slight reduction (Zhang et al., 2018). These phenomena indicated that as time increased from 0.5 h to 1 h, the char catalyst was consumed by steam and CO_2, which produced new pores. In contrast, more alkali metals, such as CaO and K_2O (*Table 2*), which have a better catalytic performance on the bio-oil gasification (Wang et al., 2018), were exposed on the char surface so that the catalytic performance of char increased. However, as the reaction time increased, more char catalysts are deactivation for sticking together. When the reaction time increased from 0.5 to 1 h, the weight percentage of char catalyst consumption increased from 9.51 to 12.22%, which confirmed that the char catalyst was consumed by steam and CO_2 (Kang et al., 2017). As the reaction time increased from 1 h to 2 h, the weight percentage of char consumed decreased to 4.02%, which indicated that the coke deposition increased. All in all, the

http://www.aloki.hu ● ISSN 1589 1623 (Print) ● ISSN 1785 0037 (Online)
DOI: http://dx.doi.org/10.15666/aeer/1704_85418553

char catalyst exhibited an excellent bio-oil removal rate (bio-oil conversion > 99.6%) in the first 2 h. Aznar (1999) has confirmed in his work that in order to avoid deactivation of the catalyst by coke, the tar content in the gas product must be less than 2 g/Nm^3. In this work, the bio-oil contents of the outlet dry gas were lower than 1.89 g/Nm^3 in the first 2 h, thus it is suitable for further catalytic steam reforming over a metal catalyst. The CO_2 and H_2 concentrations showed similar trends of a small increase, whereas both the CO and CH_4 concentrations decreased as the reaction time rose. From the dry gas composition point of view, it is suitable for hydrogen production.

When the experiment was performed in nearly 3 h, the water-metering pump could not feed water into the reactor because of the high pressure in the reactor. This was caused by char catalysts sticking together. A further study should include understanding on the reason for char sticking together and how to reduce such.

Table 4. *Stability of char catalyst*

Time (h)	Dry gas composition (vol.%)				Bio-oil		Char waste	
	H_2	CO	CH_4	CO_2	Conversion (wt.%)	In the outlet dry gas (g/Nm^3)	g	wt.%
0.5	51.69	15.88	8.90	23.53	99.62	1.89	1.69	9.51
1	52.74	14.25	8.80	24.20	99.91	0.38	2.31	12.22
2	54.35	13.12	7.64	24.89	99.89	0.47	0.74	4.02

Reason for char sticking together and methods to overcome it

There are three possible reasons for char sticking together, (1) the char catalysts tended to slag because of high alkali content and lower fusion temperatures, (2) as the char catalyst was consumed by steam and CO_2, the framework of char collapsed, and (3) carbon deposition between the char catalysts. If char stickiness was mainly caused by slagging, the char catalyst would have a slower sticking rate under lower catalytic temperatures. To verify whether char sticking together was caused by slagging, a test was performed under the catalytic reforming conditions with a catalytic temperature of 800 °C, N_2 flow rate, 30 mL/min, WHSV, 1.9 h^{-1}, feeding rate of bio-oil, 35 g/h and a S/B of 2. The experimental results indicated that water also could not be fed into the reactor through the water-metering pump after 118 min. Lower reaction temperatures caused char to stick faster, which indicated that slagging could not be the main factor causing the char to stick together. It is known that char catalysts always stick at the top of the char bed, which is near to the inlet of the reactor, and only a very small part of char stick together. Therefore, it is believed that the temperature at the top of the char bed is much lower than 900 °C for the continuously feeding thus carbon was formed. In other words, bio-oil and water need to be preheated. Prior to being fed into the catalytic reforming reactor, bio-oil, water, and N_2 were preheated at 800 °C. The catalytic reforming test was performed under conditions that were identical to the previous sections. The result shows that char sticking together and char collapsing were not found. This confirmed that char sticking together was caused only by carbon deposition between the char catalysts and preheating the bio-oil. It also confirmed that water was an effective method to overcome the char from sticking together.

http://www.aloki.hu ● ISSN 1589 1623 (Print) ● ISSN 1785 0037 (Online)
DOI: http://dx.doi.org/10.15666/aeer/1704_85418553

Conclusions

(1) When catalytic gasification temperatures were lower than 700 °C, the bio-oil contents in the outlet dry gas were very high. Reforming product was not suitable for further catalytic steam reforming over a metal catalyst. The catalytic activity of char catalysts became very prominent at high temperatures (≥ 800 °C).

(2) The first order kinetic rate constant of char for bio-oil conversion, in the temperature range of 800 to 900 °C, was found to have an apparent activation energy (E_a) of 56.98 KJ/mol and a pre-exponential factor (k_0) of 1.58×10^4 s^{-1}.

(3) Bio-oil contents in the outlet dry gas varied from decreasing to a slight increase in the first 2 h under the catalytic gasification conditions with a catalytic temperature of 900 °C, WHSV, 2.6 h^{-1}, feeding rate of bio-oil of 47.02 g/h and S/B of 2. In comparison, bio-oil conversions vary from increasing to a slight reduction. All in all, the char catalyst exhibited an excellent bio-oil removal rate (bio-oil conversion > 99.6%) and the bio-oil contents in the outlet dry gas were lower than 1.89 g/Nm^3, thus it was suitable for further catalytic steam reforming over a metal catalyst.

(4) The feeding materials temperature should be allowed to achieve the designed reaction temperature before reaching the char catalysts, to block the char catalysts from sticking together.

In the study of catalytic reforming of biomass pyrolysis oil for hydrogen production, only a small number of catalysts have been studied. It is necessary to study in depth the catalysts suitable for the reforming of biomass pyrolysis oil for hydrogen production with good selectivity, high activity and long life. In this way, the research on hydrogen production from Bio-oil reforming catalyzed by activated carbon will make progress in the future.

Acknowledgements. This work is supported by the Natural Science Foundation of China No. 21506087.

REFERENCES

[1] Arandia, A., Remiro, A., García, V. et al. (2018): Oxidative steam reforming of raw bio-oil over supported and bulk Ni catalysts for hydrogen production. – Catalysts 8(8): 322.

[2] Asghar, Z., Ali, W., Nasir, A., Arshad, A. (2018): Atmospheric monitoring for ambient air quality parameters and source apportionment of city Faisalabad, Pakistan. – Earth Sciences Pakistan 2(1): 01-04.

[3] Aznar, M. P. (1998): Commercial steam reforming catalysts to improve biomass gasification with steam–oxygen mixtures. Catalytic tar removal. – Industrial & Engineering Chemistry Research 37(7): 2668-2680.

[4] Bizkarra, K., Barrio, V. L., Gartzia-Rivero, L. et al. (2018): Hydrogen production from a model bio-oil/bio-glycerol mixture through steam reforming using Zeolite L supported catalysts. – International Journal of Hydrogen Energy. https://doi.org/10.1016/j.ijhydene.2018.11.079.

[5] Chang, H., Wang, Z., Li, Y. X., Chen, G. R. (2018): Dynamics analysis of a bistable bi-local active memristor and its associated oscillator system. – International Journal of Bifurcation and Chaos 28(08).

[6] Cho, M. H., Mun, T. Y., Choi, Y. K. et al. (2014): Two-stage air gasification of mixed plastic waste: olivine as the bed material and effects of various additives and a nickel-plated distributor on the tar removal. – Energy 70(3): 128-134.

http://www.aloki.hu ● ISSN 1589 1623 (Print) ● ISSN 1785 0037 (Online)
DOI: http://dx.doi.org/10.15666/aeer/1704_85418553

[7] Corella, J., Aznar, M. P., Delgado, J. et al. (1991): Steam gasification of cellulosic wastes in a fluidized bed with downstream vessels. – Industrial & Engineering Chemistry Research 30(10): 2252-2262.
[8] Czernik, S., French, R. (2014): Distributed production of hydrogen by auto-thermal reforming of fast pyrolysis bio-oil. – International Journal of Hydrogen Energy 39(2): 744-750.
[9] Daniel, G. I., Henry, O. U., Ayodeji, B. B., Silas, M. Y. (2018): Land suitability analysis for the production of Cocoyam Inbenue State, Nigeria. – Earth Sciences Malaysia 2(2): 25-30.
[10] El-Rub, Z. A., Bramer, E. A., Brem, G. (2008): Experimental comparison of biomass chars with other catalysts for tar reduction. – Fuel 87(10-11): 2243-2252.
[11] Hayashi, J. I., Iwatsuki, M., Morishita, K. et al. (2002): Roles of inherent metallic species in secondary reactions of tar and char during rapid pyrolysis of brown coals in a drop-tube reactor. – Fuel 81(15): 1977-1987.
[12] Hosokai, S., Hayashi, J. I., Shimada, T. et al. (2005): Spontaneous generation of tar decomposition promoter in a biomass steam reformer. – Chemical Engineering Research & Design 83(9): 1093-1102.
[13] Hossain, M. S., Karlson, M., Neset, T. S. (2019): Application of GIS for cyclone vulnerability analysis of Bangladesh. – Earth Sciences Malaysia 3(1): 25-34.
[14] Ilyas, M., Ali, M. A., Awan, A. N., Haider, S., Shahid, A. (2019): Estimation of noise levels in the road side parks and study of its impacts on health of visitors in Faisalabad. – Earth Sciences Pakistan 3(1): 14-22.
[15] Kai, W., Shengzhe, Z., Yanting, Z., Jun, R., Liwei, L., Yong, L. (2018): Synthesis of porous carbon by activation method and its electrochemical performance. – Int. J. Electrochem. Sci 13(11): 10766-10773.
[16] Kang, L., Zhang, Y. J., Zhang, L., Zhang, K. (2017): Preparation, characterization and photocatalytic activity of novel CeO_2 loaded porous alkali-activated steel slag-based binding material. – International Journal of Hydrogen Energy 42(27): 17341-17349.
[17] Li, C. Z. (2007): Some recent advances in the understanding of the pyrolysis and gasification behaviour of Victorian brown coal. – Fuel 86(12): 1664-1683.
[18] Li, C., Li, S., Tian, Q. (2019): Microbial attachment behavior and pollutant removal performance of modified quartz sand. – Acta Microscopica 28(2).
[19] Li, W. Z., Yan, Y. J., Li, T. C. et al. (2008): Preparation of hydrogen via catalytic gasification of residues from biomass hydrolysis with a novel high strength catalyst. – Energy & Fuels 22(2): 1233-1238.
[20] Li, Y., Zhang, C. S., Liu, Y. G. et al. (2017): Coke formation on the surface of Ni/HZSM-5 and Ni-Cu/HZSM-5 catalysts during bio-oil hydrodeoxygenation. – Fuel 189: 23-31.
[21] Li, Y., Cheng, H., Wang, J., Wang, Y. (2018): Dynamic analysis of unilateral diffusion Gompertz model with impulsive control strategy. – Advances in Difference Equations 2018(1): 32.
[22] Masri, E., Samsudin, M. D. M. (2018): Optimization performance of biological cathodic protection system using organic waste. – Environment & Ecosystem Science 2(2): 25-29.
[23] Min, Z. H., Yimsiri, P., Asadullah, M. et al. (2011): Catalytic reforming of tar during gasification. Part II. Char as a catalyst or as a catalyst support for tar reforming. – Fuel 90(7): 2545-2552.
[24] Mun, T. Y., Seon, P. G., Kim, J. S. (2010): Production of a producer gas from woody waste via air gasification using activated carbon and a two-stage gasifier and characterization of tar. – Fuel 89(11): 3226-3234.
[25] Naidu, M. T., Premavani, D., Suthari, S., Venkaiah, M. (2018): Assessment of tree diversity in tropical deciduous forests of Northcentral Eastern Ghats, India. – Geology, Ecology, and Landscapes 2(3): 216-227.

http://www.aloki.hu ● ISSN 1589 1623 (Print) ● ISSN 1785 0037 (Online)
DOI: http://dx.doi.org/10.15666/aeer/1704_85418553

[26] Nestler, F., Burhenne, L., Amtenbrink, M. J. et al. (2016): Catalytic decomposition of biomass tars: the impact of wood char surface characteristics on the catalytic performance for naphthalene removal. – Fuel Processing Technology 145: 31-41.
[27] Omini, E. O., Akpang, O. M. (2018): Cavity detection under re-enforced concrete floor using ground penetration radar. – Engineering Heritage Journal 2(2): 11-18.
[28] Shan, P. F., Lai, X. P. (2018): Numerical simulation of the fluid-solid coupling process during the failure of a fractured coal-rock mass based on the regional geostress characteristics. – Transport in Porous Media 124(3): 1061-1079.
[29] Park, J., Lee, Y., Ryu, C. (2016): Reduction of primary tar vapor from biomass by hot char particles in fixed bed gasification. – Biomass and Bioenergy 90: 114-121.
[30] Qian, K. Z., Kumar, A. (2015): Reforming of lignin-derived tars over char-based catalyst using Py-GC/MS. – Fuel 162: 47-54.
[31] Rajput, K., Gupta, A., Arushi (2019): Re-cycle of e-waste in concrete by partial replacement of coarse aggregate. – Engineering Heritage Journal 1(1): 05-08.
[32] Shamsi, A. (1996): Catalytic and thermal cracking of coal-derived liquid in a fixed-bed reactor. – Industrial & Engineering Chemistry Research 35(4): 1251-1256.
[33] Sharma, D., Yadav, K. D. (2018): Application of rotary in-vessel composting and analytical hierarchy process for the selection of a suitable combination of flower waste. – Geology, Ecology, and Landscapes 2(2): 137-147.
[34] Thakkar, M., Makwana, J. P., Mohaty, P. et al. (2016): In bed catalytic tar reduction in the autothermal fluidized bed gasification of rice husk: extraction of silica, energy and cost analysis. – Industrial Crops and Products 87: 324-332.
[35] Valle, B., Aramburu, B., Benito, P. L. et al. (2018): Biomass to hydrogen-rich gas via steam reforming of raw bio-oil over Ni/La_2O_3-αAl_2O_3 catalyst: effect of space-time and steam-to-carbon ratio. – Fuel 216: 445-455.
[36] Wang, D., Czernik, S., Chornet, E. (1998): Production of hydrogen from biomass by catalytic steam reforming of fast pyrolysis oils. – Energy & Fuels 12: 19-24.
[37] Wang, K., Zhou, S. Z., Zhou, Y. T., Ren, J. et al. (2018): Synthesis of porous carbon by activation method and its electrochemical performance. – International Journal of Electrochemical Science 13(11): 10766-10773.
[38] Wang, Z. X., Pan, Y., Dong, T. et al. (2007): Production of hydrogen from catalytic steam reforming of bio-oil using C12A7-O-based catalysts. – Applied Catalysis A: General 320(3): 24-34.
[39] Wu, C., Huang, Q., Sui, M. et al. (2008): Hydrogen production via catalytic steam reforming of fast pyrolysis bio-oil in a two-stage fixed bed reactor system. – Fuel Processing Technology 89(12): 1306-1316.
[40] Xing, M. P., Shen, H., Wang, Z. (2018): H∞ synchronization of semi-Markovian jump neural networks with randomly occurring time-varying delays. – Complexity 2018: 16. DOI: 10.1155/2018/8094292.
[41] Yahya, N., Aziz, F., Enriquez, M. A. O., Aizat, A., Jaafar, J., Lau, W. J., Yusof, N., Salleh, W. N. W., Ismail, A. F. (2018): Preparation and characterization of Lafeo3 using dual-complexing agents for photodegradation of humic acid. – Environment & Ecosystem Science 2(2): 30-34.
[42] Yang, Y. X., Li, H., Zheng, W. K., Bai, Y., Liu, Z. M., Zhang, J. J. (2019): Experimental study on calcining process of secondary coated ceramsite solidified chromium contaminated soil. – Science of Advanced Materials 11(2): 208-214.
[43] Zanzi, R., Sjostrom, K., Bjornbom, E. (1996): Rapid high-temperature pyrolysis of biomass in a free-fall reactor. – Fuel 75(5): 545-550.
[44] Zeng, D. W., Xiao, R., Zhang, S. et al. (2015): Bio-oil heavy fraction for hydrogen production by iron-based oxygen carrier redox cycle. – Fuel Processing Technology 139: 1-7.

http://www.aloki.hu ● ISSN 1589 1623 (Print) ● ISSN 1785 0037 (Online)
DOI: http://dx.doi.org/10.15666/aeer/1704_85418553

[45] Zhang, J., Xia, J. W., Sun, W., Zhuang, G. G., Wang, Z. (2018): Finite-time tracking control for stochastic nonlinear systems with full state constraints. – Applied Mathematics and Computation 338: 207-220.
[46] Zhang, S., Song, Y., Song, Y. C. et al. (2016): An advanced biomass gasification technology with integrated catalytic hot gas cleaning. Part III: Effects of inorganic species in char on the reforming of tars from wood and agricultural wastes. – Fuel 183: 177-184.
[47] Zhang, W. P., Yang, J. Z., Fang, Y. L., Chen, H. Y., Mao, Y. H., Kumar, M. (2017): Analytical fuzzy approach to biological data analysis. – Saudi Journal of Biological Sciences 24(3): 563-573.
[48] Zhang, Y. H. (2018): In-situ IR study for elucidating the adsorption cracking mechanism of toluene over calcined olivine catalyst. – International Journal of Hydrogen Energy 43: 15835-15842.
[49] Zhou, D., Gao, F., Breaz, E., Ravey, A., Miraoui, A. (2017a): Degradation prediction of PEM fuel cell using a moving window based hybrid prognostic approach. – Energy 138: 1175-1186.
[50] Zhou, D., Al-Durra, A., Gao, F., Ravey, A., Matraji, I., Godoy Simões, M. (2017b): Online energy management strategy of fuel cell hybrid electric vehicles based on data fusion approach. – Journal of Power Sources 366(31): 278-291.

http://www.aloki.hu ● ISSN 1589 1623 (Print) ● ISSN 1785 0037 (Online)
DOI: http://dx.doi.org/10.15666/aeer/1704_85418553

EFFECT OF LATERAL EARTH RESISTIVITY CHANGES ON EARTH SURFACE POTENTIAL AROUND DC GROUNDING ELECTRODES

MA, C.[1,3*] – LIU, L.[1] – SUN, L.[2] – ZHAO, S.[2]

[1]*State Key Laboratory of Alternate Electrical Power System With Renewable Energy Sources (North China Electric Power University), Changping District, Beijing 102206, China (e-mail: alian0220224@163.com – L. Liu)*

[2]*School of Electrical Engineering, Northeast Electric Power University, Jilin 132012, Jilin, China (e-mails: sunlinedu@163.com – L. Sun, 649425903@qq.com – S. Zhao)*

[3]*School of Electrical and Electronic Engineering, North China Electric Power University, Beijing, China*

**Corresponding author*
e-mail: machenglian@neepu.edu.cn

(Received 8th Mar 2019; accepted 21st May 2019)

Abstract. In the trial stage of Xiluodu-Zhexi ± 800 kV HVDC project, grounding current trough DC electrode incurred severe DC bias in substation transformers near the Jinsi electrode, indicating further research on the factors influencing such DC bias problem and since vertical and lateral change of soli resistivity could be one of the main factors, their mechanisms should be studied. Besides a normal layered earth resistivity model, a complex model was established to simulate forms of lateral resistivity changes according to measured soil resistivity data at the site of Jinsi electrode. Then ESP was calculated with finite element method and the effect of lateral change on ESP and its characteristics was analyzed. Later, an assumed case example demonstrated the error of DC bias estimation caused by such ESP distortion. The results suggest the distance from DC electrode to the lateral change interface influences ESP distortion the most, and a high resistivity region in shallow layers at 5 km from DC electrode could incur a relative error of 25.9% in DC bias estimation. The grounding location and impact assessment has indicated that the measurement range of the earth resistivity should be investigated.
Keywords: *DC bias, mechanisms, finite element method, converter station, transformer substation*

Introduction

In the trial stage of XiluoduWestern Zhejiang ± 800 kV High Voltage Direct Current (HVDC) project, grounding current trough Direct Current (DC) electrode incurred severe DC bias in substation transformers near Jinsi electrode (Yang et al., 2018). During the trial stage of March 28, 2014, the measured DC bias current of some transformer neutral point is more than 10 A while the grounding current of the grounding electrode is only 500 A (Kazerooni et al., 2016a; Wali et al., 2018). According to the rated transmission power XiluoduWestern Zhejiang ± 800 kV HVDC project, the grounding current of the grounding electrode can reach 5000 A during full load operation with single pole. Due to the transformer DC bias current is linear with the ground current, the 5000 A ground current will produce 100200 A DC bias current in the substation transformer near the grounding electrode, which may threat the safety of the power system and transformer (Kang et al., 2018). Although a large number of DC transmission projects have been successfully constructed and put into operation, the problem of DC bias in XiluoduWestern Zhejiang Ultra High Voltage Direct Current

http://www.aloki.hu ● ISSN 1589 1623 (Print) ● ISSN 1785 0037 (Online)
DOI: http://dx.doi.org/10.15666/aeer/1704_85558568

(UHVDC) Project shows that the influence factors and mechanism of DC bias have not been fully understood in the study of grounding electrode effect.

The influence assessment of grounding electrode on DC bias of transformer is based on the establishment of power grid model, Earth resistivity model, and the network topology. The accuracy of the former depends on power grid parameters. The latter depends on the mastery of the stratified data of the earth's resistivity and the differential data of the transverse and longitudinal directions. The problem belongs to the geodetic and geodetic problems in the field of Geophysics (Mousavi and Bonmann, 2017; Kazerooni et al., 2016b; Austin et al., 2018). In the grounding location selection and its impact assessment of HVDC and UHVDC, selection and design of grounding electrode are only based on the comprehensive calculation of the earth resistivity from several dozens of measuring points near the electrode. The ground potential is calculated by horizontal homogeneous layered earth resistivity model with the measured data of ground resistivity. The influence of grounding electrode current on the dc bias of transformer is evaluated. The influence of the lateral variation factors of the earth resistivity is not considered. Compared with uniform distribution of the earth resistivity, the research result of geomagnetic storm induced electric field shows that within 1000 km around the earth resistivity lateral variation interface, the surface potential always changes. When the change frequency of geomagnetic storm surface current is 0.03 Hz, the electric field increases at 70% near the low conduction proximity interface (Hussein and Ali, 2017; Arslan et al., 2018). Compared with the influence of geomagnetic storms, geomagnetic storms have greater impact scale and mainly consider the distribution of geoelectric field along the transmission line. Although the effect of DC grounding electrode current is relatively small, usually in the range of 100 km, it is necessary to consider the potential distribution of the circular area with the earth electrode as the center. In theory, the grounding electrode current penetrates the earth deeper, and the lithosphere structure of China is the most complicated in the world (Choi et al., 2018; Moon et al., 2017; Liu and Liu, 2017; Wang et al., 2015; Okpoli and Ehinmitan, 2019). Therefore, in the site selection and impact assessment of ground electrode, it is very complicated to clarify the influencing factors and mechanism of the electrode site resistivity.

Whether the serious DC bias problem in Xiluodu-western Zhejiang UHVDC Project is influenced by the earth structure around the Jinsi electrode, or the resistivity of the deep earth, due to the lack of detailed magnetotelluric data of the earth, there is no inference at present. However, the test report on soil resistivity of Jinsi electrode in Xiluodu-western Zhejiang UHVDC Project shows that, the soil structure of electrode surrounding and the horizontal uniformity of shallow soil has a great influence on the surface potential distribution. The related papers are also discussed (Wei-Li and Liu, 2013). In this paper, according to the test data of soil resistivity in the site selection and design of Jinsi grounding electrode, and the types of lateral variation of soil resistivity reported in the test report, the earth resistivity model and surface potential algorithm considering lateral variation of earth resistivity are established (Zhou et al., 2016; Kasim et al., 2019). The influence of the width, depth, resistivity, distance from interface to ground electrode on the surface potential distribution around the electrode site and its characteristics are studied. According to the influence characteristics, the mechanism of serious DC bias caused by Jinsi grounding electrode is revealed, which provides basis for site selection of UHVDC grounding electrode and resistivity test scheme.

http://www.aloki.hu ● ISSN 1589 1623 (Print) ● ISSN 1785 0037 (Online)
DOI: http://dx.doi.org/10.15666/aeer/1704_85558568

According to the earth resistivity data near the Jinsi grounding electrode of Xiluodu-Western Zhejiang UHVDC project, based on the lateral variation of the resistivity between the faults in the soil structure and the shallow-layer resistance, a model of the earth resistivity considering lateral variation is proposed. The surface potential distribution near grounding electrode is calculated by finite element method. The influence of lateral variation on surface potential distribution and its characteristics are compared and analyzed with different soil parameters. The error of the DC bias current caused by the change of the uneven potential distribution of the earth's transverse resistivity distribution is analyzed with an example. The conclusions provide a theoretical reference for accurate estimation of DC bias level and site selection of grounding electrode in practical engineering.

Materials and methods

Horizontal homogeneous layered earth resistivity model

Earth resistivity of Jinsi grounding electrode is obtained by 87 measuring points near the electrode with conventional symmetrical quadrupole method, 4 measuring lines of Controlled Source Audiofrequency Magnetotelluric (CSAMT) and 3 measuring points of Magnetic Tube (MT). Based on the 6 layer earth resistivity model, a horizontal homogeneous layered earth resistivity model is proposed and shown in *Figure 1,* and the parameters of each layer are shown in *Table 1*.

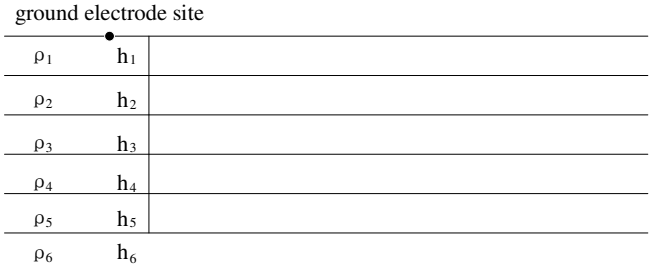

Figure 1. *Layered earth resistivity model*

Table 1. *Parameters of layered earth resistivity around electrode*

Layer	Depth（m）	Resistivity（Ω·m）
1	0 - 45	50
2	45 - 155	250
3	155 - 300	2500
4	300 - 600	400
5	600 - 2000	1500
6	> 2000	4000

A composite model considering the lateral variation of earth resistivity

The above horizontal homogeneous earth resistivity model is a common model for the calculation of surface potential at present. The earth resistivity test of Jinsi electrode

http://www.aloki.hu ● ISSN 1589 1623 (Print) ● ISSN 1785 0037 (Online)
DOI: http://dx.doi.org/10.15666/aeer/1704_85558568

covers only 1 km^2 range, and the results of some measurement points reflect the earth fracture and high and low resistance mixed in this area. To study the influence of the lateral variation of the earth resistivity on the surface potential of ground electrode (Liu et al., 2018; Rajput et al., 2019), a composite geodetic resistivity model considering lateral variation based on the type of horizontal change reflected by the resistivity test has been proposed and shown in *Figure 2*.

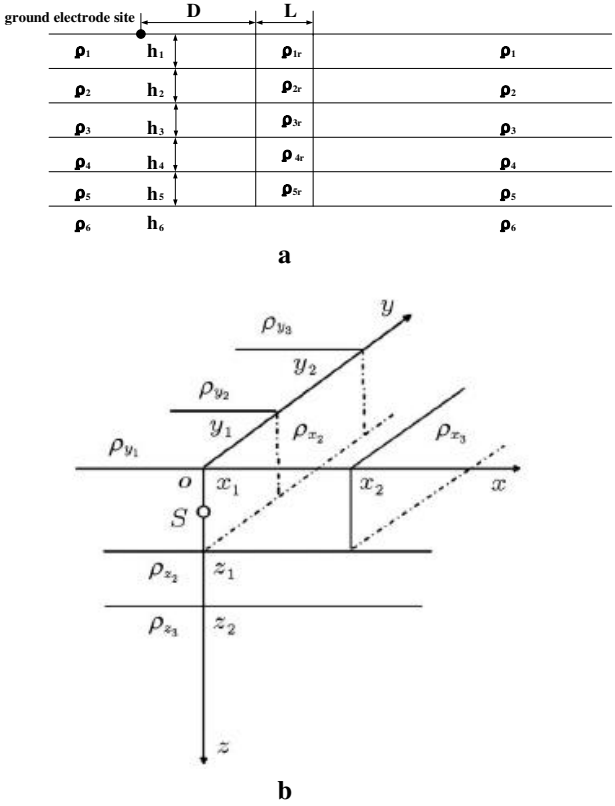

Figure 2. *Complex earth resistivity model concerning resistivity lateral change*

Ground surface potential model DC around ground electrode

Grounding current from electrode formed a constant DC current field. The differential equations of the current field can be represented as follows (*Eqs. 1* and *2*):

$$\nabla \times \vec{E} = 0 \tag{Eq.1}$$

$$\nabla \cdot \vec{J} = -\frac{\partial \rho}{\partial t} \tag{Eq.2}$$

Auxiliary equation is (*Eqs. 3* and *4*):

$$\vec{J} = \sigma \vec{E} \tag{Eq.3}$$

$$\vec{E} = -\nabla V \tag{Eq.4}$$

http://www.aloki.hu ● ISSN 1589 1623 (Print) ● ISSN 1785 0037 (Online)
DOI: http://dx.doi.org/10.15666/aeer/1704_85558568

where, E is electric field intensity (V/m), J is current density (A/m2), ρ is charge density (C/m3), σ is conductivity (S/m), and V is electric potential (V).

In the field except the current source, the equation (*Eq. 5*) of the current field can be expressed as:

$$\nabla^2 \cdot V = 0 \quad \text{(Eq.5)}$$

In this paper, the finite element software Ansys is proposed to calculate the surface potential distribution of Jinsi grounding electrode. Based on the three-dimensional composite Earth resistivity model established above, the lateral variation of Earth resistivity should be considered when analyzing the influence mechanism of earth resistivity lateral change on ground surface potential. Three-dimensional problem is transferred into two-dimensional finite element problem. Based on the measured resistivity lateral difference type, to solve the surface potential by axisymmetric analysis with 2D Quad 230 unit, decouple network, input load data and boundary condition (Birchfield et al., 2016; Zulkapli et al., 2018).

External boundary condition (*Eq. 6*) is:

$$V = 0 \quad \text{(Eq.6)}$$

At the air interface (*Eq. 7*):

$$\frac{dV}{dn} = 0 \quad \text{(Eq.7)}$$

where n is exterior normal direction (*Eqs. 8* and *9*), and resistivity adjacent soil interface can be obtained:

$$V_i = V_j \quad \text{(Eq.8)}$$

$$\frac{1}{\rho_i}\frac{dV_i}{dn} = \frac{1}{\rho_j}\frac{dV_j}{dn} \quad \text{(Eq.9)}$$

The earth surface potential affects up to dozens of km or greater (Harrison and Anderson, 2016; Barsainya and Rawat, 2017; Rezaei-Zare et al., 2016; Boteler and Bradley, 2016; Pan et al., 2016; Boteler and Pirjola, 1998; Viljanen et al., 2004; Baharuddin and Samsudin, 2018). Since the rated earth current is 5000 A, this paper selected 150 km as the distance between grounding electrode and 0 potential boundary. Moreover, the Jinsi grounding electrode is double-ring body structure. The polar ring is 1140 m in the east-west direction, 480 m in the north and south, 3.5 m in depth and 0.326 Ω in the grounding resistance. Because the size of the grounding electrode is far less than the influence range of its surface potential, treat the grounding electrode to a point power supply (Zhu and Overbye, 2015; Prabhakaran and Raj, 2018).

Select the rectangular coordinate system, x refers to the north, y refers to the East, z is vertical to ground. The model is shown in *Figure 3*. In *Figure 3,* six boundary interfaces for the rectangular structure of the earth model are shown. The arrow reflects a possible flow of the grounding current at the inner and side boundary of the earth conductor. The lateral difference of resistivity may exist inside the conductor, thus

http://www.aloki.hu ● ISSN 1589 1623 (Print) ● ISSN 1785 0037 (Online)
DOI: http://dx.doi.org/10.15666/aeer/1704_85558568

changing the flow direction of the grounding current to the earth (Zhang et al., 2018). The truncated boundary is selected far away from the zone of resistivity sudden change. It is considered that there is no lateral difference, and the grounding current flow into and out of the model horizontally (Lewicki, 2007; Bernabeu, 2015; Barakat et al., 2018).

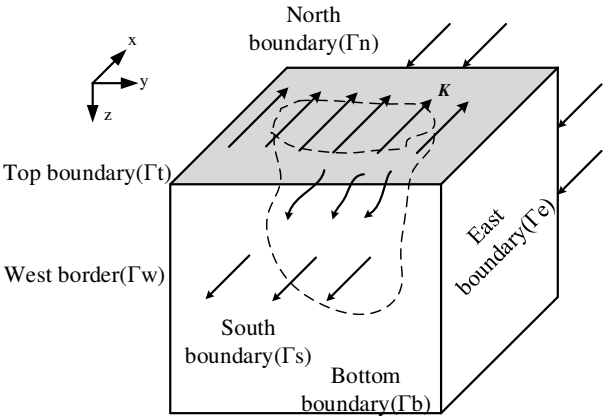

Figure 3. *Sketch of earth conductivity model*

In this paper, the type of earth resistivity lateral difference should be considered, when analyzing the mechanism of the influence of lateral variation of earth resistivity on ground electrode. According to the resistivity lateral difference type from the experiment, parameters as shown in *Table 2*. In *Table 2,* the scheme 1~4 simulate 4 kinds of fracture situations, because the earth resistivity is generally less than 200 Ω•m in the fracture area, the value here is 150 Ω•m (Guo et al., 2017). The scheme 5~8 simulate the high and low resistance of surface layer, and the values of shallow-layer high resistance is 1000 Ω•m and 5000 Ω•m.

Table 2. *Parameter scenarios to simulate different soil resistivity lateral changes*

Scheme	1	2	3	4	5	6	7	8
D(m)	800	800	5000	800	800	800	800	5000
L(m)	200	200	200	1000	1000	1000	2000	1000
ρ_{1r}(Ω·m)	150	150	150	150	1000	5000	1000	1000
ρ_{2r}(Ω·m)	150	150	150	150	1000	5000	1000	1000
ρ_{3r}(Ω·m)	150	150	150	150	2500	2500	2500	2500
ρ_{4r}(Ω·m)	150	150	150	150	400	400	400	400

Results and discussion

Analysis of the influence of the lateral variation of earth resistivity on the surface potential

In this paper, two kinds of Earth resistivity models are proposed, and by using Ansys, the distribution of surface potential of the Jinsi grounding electrode is calculated, based on the 8 scenarios of earth resistivity lateral variation. The results are shown in *Figures 4* and *5*. In *Figures 4* and *5,* (a) is the potential distribution within 50 km. In

http://www.aloki.hu ● ISSN 1589 1623 (Print) ● ISSN 1785 0037 (Online)
DOI: http://dx.doi.org/10.15666/aeer/1704_85558568

order to observe the difference of local potential distribution and its influence, (b) is the enlarged display of the surface potential distribution change near the place where the earth resistivity lateral change happens, and (b) is corresponded to the calculated result in (a). In the figure, the curve "0" corresponds to the surface potential distribution in the horizontal homogeneous layered earth resistivity model, and the other curves correspond to the resistivity lateral change plans (*Table 2*). In the scheme 1~4, the surface potential distribution near the Jinsi ground electrode are shown in *Figure 4*.

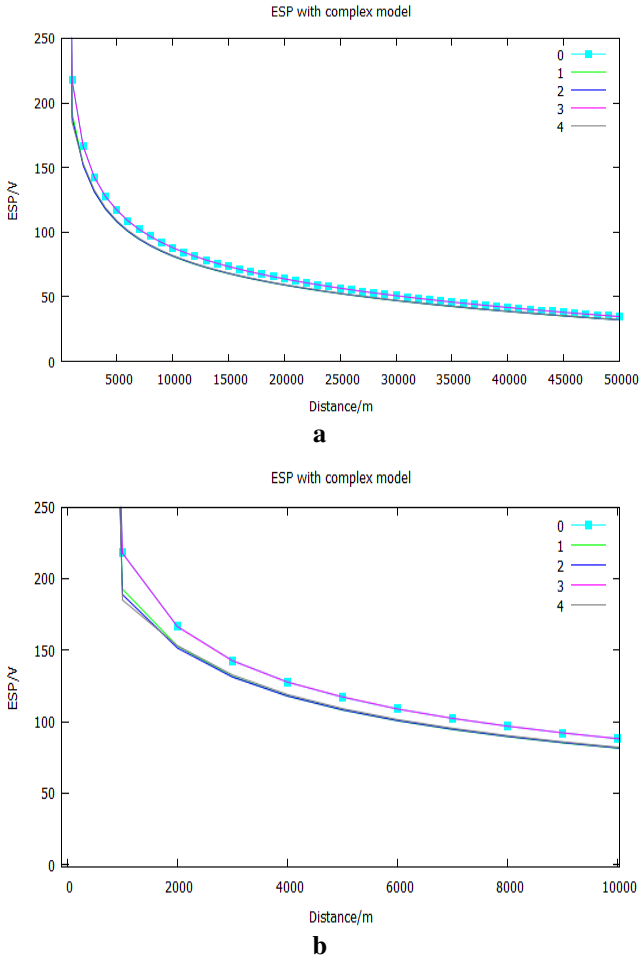

Figure 4. *Earth conductivity model ESP around Jinsi electrode under resistivity lateral change scenarios 1-4*

As *Figure 4a* shows the surface potential from the grounding electrode to the fracture interface is overall reduction. Compared with the curve 0, the surface potential of the curve 1 is obviously reduced, and the curve 3 is almost coincided with the curve 0. Because the curve 1 is fractured at 800 m, the curve 3 is fractured at 5000 m. The rest of the parameters are the same. This indicates that the closer the fracture interface to the ground electrode, the more significant lateral resistivity change effects on the surface potential. And the fracture in a far position has little effect on the earth surface potential. Moreover, the depth or width parameters among the 3 types of breakages shown in the curves 1, 2, and 4 are different. But the location of the fracture is 800 m, and the surface

http://www.aloki.hu ● ISSN 1589 1623 (Print) ● ISSN 1785 0037 (Online)
DOI: http://dx.doi.org/10.15666/aeer/1704_85558568

potential of the 3 types are similar. This shows that the distance between the fracture interface and the ground electrode has a greater influence on the surface potential distribution than the depth and width.

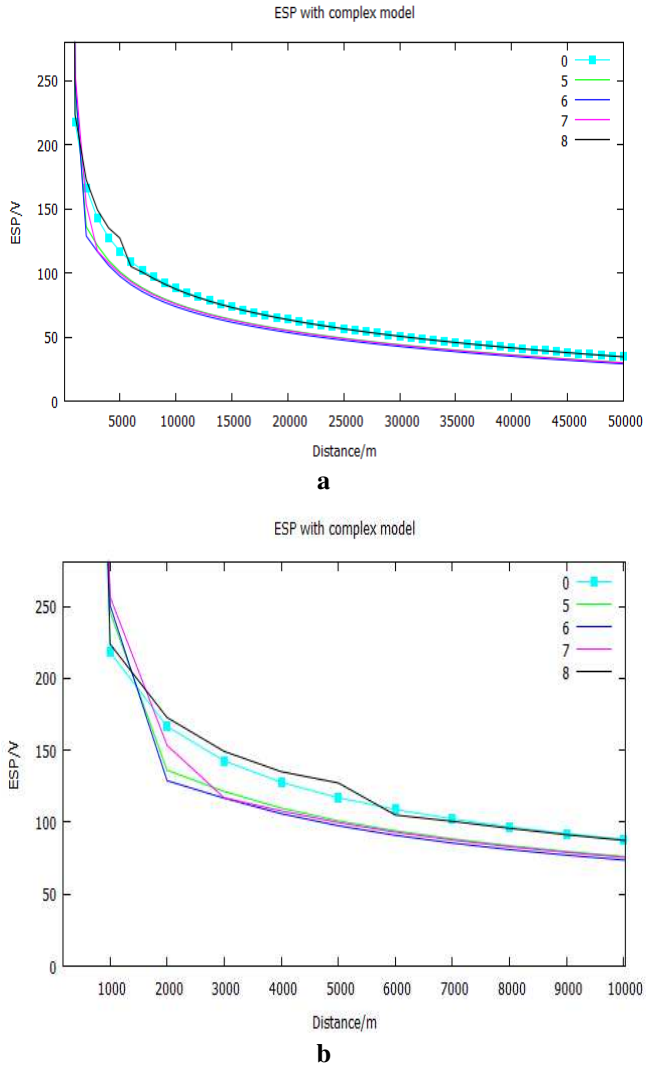

Figure 5. *ESP around Jinsi electrode under resistivity lateral change scenarios 5-8 (b)*

Near the fracture position, the surface potential dropping of the curves 1, 2, and 4 are different (*Fig. 4b*). The curve 4 is lower than the curve 1. This indicates that the greater the width of the fracture, the greater the decrease of the surface potential caused by the influence. The curve 2 is lower than the curve 1. This indicates that the deeper the depth of the fracture is, the greater the decrease of the surface potential caused by its influence.

In the earth resistivity lateral variation case 5-8, the surface potential distribution around the Jinsi grounding electrode is shown in *Figure 5*.

Comparing with the horizontal homogeneous layered situations, when considering the resistivity lateral variation caused by the high and low resistance mixture in the surface layer, in front of the high resistance area, the surface potential rises (*Fig. 5a*).

http://www.aloki.hu ● ISSN 1589 1623 (Print) ● ISSN 1785 0037 (Online)
DOI: http://dx.doi.org/10.15666/aeer/1704_85558568

And behind the high resistance area, the surface potential drops, and the surface potential drops significantly in the area with high resistance. Comparing with the width and resistivity of the high resistance area, the distance between the interface and the grounding electrode has a greater influence on the surface potential.

In curves 5, 6 and 7, surface potential from the front section of the curve near the high resistance region are different. The surface potential uplift of the front section of the curve 6 is slightly higher than that of the curve 5 (*Fig. 5b*). The surface potential behind the high resistance region is slightly lower than that of the curve 5. The higher resistance in high resistance area, the greater the surface potential drops, and the greater the influence on the overall surface potential distribution. Comparing the curves 5 and 7, it can be seen that the greater the width of the high resistance region is, the greater the surface potential drops in the region, and the greater the effect on the overall surface potential. It is noteworthy that the contrast curves 8 and 0 can be seen, when the surface layer high resistance area is far from the grounding electrode, although the surface potential distribution of the high resistance area will not be significantly affected, there will still be obvious surface potential rise in front of the interface, and intensify the surface potential drop in the surface layer high resistance area. Compared with the curve 0, the surface potential drop between 5 and 6 km in the curve 8 is 14 V.

The effect of Lateral change of earth resistivity on the intensification of magnetic bias current

The results of the above calculation and analysis show that, the lateral change of the earth resistivity will cause a significant change in the surface potential around the grounding electrode. Considering the influence of the grounding current, the DC bias current of the nearby power grid is directly affected by the surface potential distribution (Liu et al., 2016). Therefore, it is necessary to investigate the influence of the potential distribution change on the magnetic current of the nearby power grid. Taking case 8 in *Table 2* as an example, and the analysis shows that comparing with the earth resistivity homogeneous stratified model, the intensification of lateral resistivity variation on the bias current of the power grid.

Power grid model and parameters

Since there is no accurate earth resistivity data of the Jinsi grounding electrode at present, it is assumed that there is a power grid containing four 500 kV substations, and the substations distribute along the grounding electrode, numbered respectively with A, B, C and D. The distances of each transformer to the ground electrode are 5 km, 10 km, 15 km and 20 km. Two sets of single-phase autotransformer are used in each substations. The high voltage and middle voltage windings of the transformer are 0.238 Ω and 0.097 Ω. The grounding resistance of the substation is 0.2 Ω. The transmission lines between the substations are four split conductors. The single phase DC resistance of the wire is 0.0187 Ω/km. Its equivalent DC circuit is shown in *Figure 6*. DC is the neutral grounding equivalent DC potential of the surrounding AC substations under the influence of DC grounding current from grounding electrode (Babazadeh et al., 2017; Shetye and Overbye, 2015; Rezaei-Zare, 2015; Kovan and De Leon, 2016).

http://www.aloki.hu ● ISSN 1589 1623 (Print) ● ISSN 1785 0037 (Online)
DOI: http://dx.doi.org/10.15666/aeer/1704_85558568

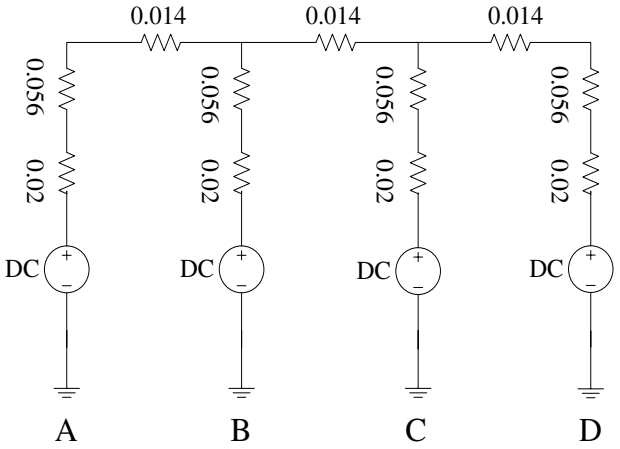

Figure 6. *DC bias circuit of the AC network*

Calculation results and analysis

According to the comparative analysis above, the surface potential distribution is calculated by selecting the earth resistivity parameters from scheme 01 and 8 in *Table 2*. The surface potential calculation results of each substation are shown in *Table 3* (Aboura and Touhami, 2017; Marti and Yin, 2015).

Table 3. *ESP distributions under two scenarios (V)*

Distance	5 km	10 km	15 km	20 km
Scheme1	117.01	88.039	73.465	63.840
Scheme8	127.22	87.387	73.086	63.554

By using the node voltage method, the DC bias current of the transformer in the AC network from *Figure 6* is calculated according to the earth surface potential corresponding to the two cases in *Table 3*. The result of the calculation is shown in *Table 4*. The positive value indicates the current flows from the earth to the neutral point (Girgis and Vedante, 2015; Rezaei-Zare, 2015).

Table 4. *DC bias currents in substations (A)*

Transformer substation	A	B	C	D
Scheme1	113.74	6.80	-43.54	-76.93
Scheme8	143.17	-4.60	-52.89	-85.45

The results of the calculation in *Table 4* show that, comparing with the horizontal homogeneous layered earth resistivity model, the change of surface potential distribution caused by the high resistance of surface layer between 5 and 6 km from the grounding electrode. It leads to the bias current increase of some substations in the power grid. Influenced by it, the bias current of substation A, C and D are obviously increased, and the growth rates are 25.9%, 21.5% and 11.1%.

http://www.aloki.hu ● ISSN 1589 1623 (Print) ● ISSN 1785 0037 (Online)
DOI: http://dx.doi.org/10.15666/aeer/1704_85558568

It can be seen that the change of surface potential distribution caused by lateral variation of earth resistivity will significantly affect the DC bias current level across the grid. However, the surface layer high resistance area is located between substation A and B, it is the horizontal changing area, the potential difference between the two sides of the substation is increased. And the bias current will flow across the entire power gird, this surface potential distribution change will cause the bias current increase of distant substation C and D (Wu et al., 2014; Gilbert, 2015; Boteler, 2015; Kwon et al., 2017; Zhou et al., 2016).

Conclusions

In this paper, a composite model of earth resistivity considering lateral variation is established. The influence mechanism of the earth resistivity lateral variation on the surface potential is analyzed. It is revealed that the earth resistivity measurement is not elaborate and the data are inaccurate during the site selection and impact assessment of the grounding electrode at present. The conclusions are as follows:

(1) When calculating surface potential caused by grounding current of earth electrode, comparing with calculation results from the horizontal homogeneous layered earth resistivity model, the resistivity lateral change caused by the earth fracture and high and low resistance mixture of surface conducting layer, will significantly affect the scale and distribution of surface potential. The scale of its influence is most affected by the distance between the lateral variation interface to the grounding electrode, The influence of distant fracture can be neglected, but far from the shallow high resistance region will have a greater potential drop in the region, the front curve of ground electric potential rise significantly, and it can not be neglected in the surface potential distribution calculation.

(2) In the calculation of DC bias, the accurate calculation of ESP is the key, and the calculation shows that the variation of ground potential caused by lateral variation of earth resistivity will increase the bias current of the entire power grid when the nearby power grid goes through the lateral resistivity variation area. And because the bias current will circulate in the grid, the change of ground potential in local area will cause the increase of the bias current in a larger region, and if the comprehensive value horizontal homogeneous layered earth resistivity model is adopted, the large error will appear, and the surface layer high resistance at 5 km in the example will cause the substation bias estimated value to be 25.9% lower.

(3) Because of the lateral variation of the resistivity at a distance can also cause a significant change in the surface potential distribution, which affects the magnetic current level of the surrounding grid, considering that the distance between the boundary surface and the grounding electrode is the primary influencing factor, and the lateral variation of the 5 km outside the electrode site can still make a large error in the estimation of the bias current. So at present, the resistivity measurement in the range of the grounding electrode location can not satisfy the requirement of the bias current estimation, and the range of the resistivity measurement should be considered in the siting stage of the grounding pole. The lateral variation of earth resistivity has a great effect on the surface potential distribution, and its scale is related to the range of fracture width, depth, lateral variation, distance to grounding electrode and the level of resistivity change.

http://www.aloki.hu ● ISSN 1589 1623 (Print) ● ISSN 1785 0037 (Online)
DOI: http://dx.doi.org/10.15666/aeer/1704_85558568

In addition, due to the analysis of the influence mechanism of earth resistivity lateral variation on surface potential, only considering the two-dimensional resistivity model of the Earth, the three-dimensional problem is converted into two-dimensional finite element analysis, and the actual earth resistivity is changed in the three-dimensional land space, which may have a greater effect on the distribution of ground potential. This impact needs to be further studied.

Acknowledgements. This work was supported by National Key R&D Program of China (2016YFC0800100); Project Supported by National Natural Science Foundation of China (51677068, 51577060).

REFERENCES

[1] Aboura, F., Touhami, O. (2017): Effect of the GICs on magnetic saturation of asymmetric three-phase transformer. – IET Electric Power Applications 11(7): 1306-1314.
[2] Arslan, C. H., Sattar, A., Cuong, D. M., Khan, F. U. H., Nasir, A., Bakhat, Z., Ilyas, F. (2018): Study of spatial and temporal variability of arsenic in groundwater due to drain by using GIS. – Earth Sciences Pakistan 2(2): 22-24.
[3] Austin, O. E., Ebuka, A. O., Zanders, A. C. C., Joseph, I. N. (2018): Seismic analysis of the transgressive systems tracts (TSTS) of the Niger Delta. – Earth Sciences Malaysia 2(2): 16-19.
[4] Babazadeh, D., Muthukrishnan, A., Mitra, P. (2017): Selection of DC voltage controlling station in an HVDC grid. – Electric Power Systems Research 144: 224-232.
[5] Baharuddin, D., Samsudin, M. D. M. (2018): Effect of Ph and moisture content on current density of impressed current cathodic protection: response surface methodology study. – Environment & Ecosystem Science 2(2): 15-19.
[6] Barakat, A., Khellouk, R., Jazouli, A. E., Touhami, F., Nadem, S. (2018): Monitoring of forest cover dynamics in eastern area of Béni-Mellal Province using ASTER and Sentinel-2A multispectral data. – Geology, Ecology, and Landscapes 2(3): 203-215.
[7] Barsainya, R., Rawat, T. K. (2017): Novel realization of GIC based wave digital filters using Al-Alaoui transform. – Alexandria Engineering Journal. DOI: 10.1016/j.aej.2017.03.010.
[8] Bernabeu, E. E. (2015): Single-Phase transformer harmonics produced during geomagnetic disturbances: theory, modeling, and monitoring. – IEEE Transactions on Power Delivery 30(3): 1323-1330.
[9] Birchfield, A. B., Gegner, K. M., Xu, T. (2016): Statistical considerations in the creation of realistic synthetic power grids for geomagnetic disturbance studies. – IEEE Transactions on Power Systems 99: 1-1.
[10] Boteler, D. H. (2015): The evolution of Québec earth models used to model geomagnetically induced currents. – IEEE Transactions on Power Delivery 30(5): 2171-2178.
[11] Boteler, D. H., Bradley, E. (2016): On the interaction of power transformers and geomagnetically induced currents. – IEEE Transactions on Power Delivery 31(5): 2188-2195.
[12] Boteler, D. H., Pirjola, R. (1998): The complex-image method for calculating the magnetic and electric fields produced at the surface of the Earth by the auroral electrojet. – Geophysical Journal International 132(1): 31-40.
[13] Choi, D. H., Lee, S. H., Son, G. T. (2018): Planning of HVDC System Applied to Korea Electric Power Grid. – Journal of Electrical Engineering & Technology 13(1): 105-113.

http://www.aloki.hu ● ISSN 1589 1623 (Print) ● ISSN 1785 0037 (Online)
DOI: http://dx.doi.org/10.15666/aeer/1704_85558568

[14] Gilbert, J. L. (2015): Simplified techniques for treating the ocean–land interface for geomagnetically induced electric fields. – Electromagnetic Compatibility IEEE Transactions on 57(4): 688-692.
[15] Girgis, R. S., Vedante, K. B. (2015): Impact of GICs on power transformers: overheating is not the real issue. – IEEE Electrification Magazine 3(4): 8-12.
[16] Guo, M., Xue, Y., Gao, Z., Zhang, Y., Dou, G., Li, Y. (2017): Dynamic analysis of a physical SBT memristor-based chaotic circuit. – International Journal of Bifurcation and Chaos 27(13): 1730047.
[17] Harrison, C. W., Anderson, P. I. (2016): Characterization of grain-oriented electrical steels under high DC biased conditions. – IEEE Transactions on Magnetics 52(5): 1-4.
[18] Hussein, A. A., Ali, M. H. (2017): Fuzzy logic controlled variable resistor for suppressing GIC in transformers. – Iet Generation Transmission & Distribution 11(6): 1494-1501.
[19] Kang, L.; Du, H. L.; Du, X.; Wang, H. T.; Ma, W. L.; Wang, M. L.; Zhang, F. B. (2018): Study on dye wastewater treatment of tunable conductivity solid-waste-based composite cementitious material catalyst. – Desalination and Water Treatment 125: 296-301.
[20] Kasim, S., Hassan, R., Zakaria, Z. (2019): Re-engineering in confinement method. – Engineering Heritage Journal 3(1): 18-19.
[21] Kazerooni, M., Zhu, H., Overbye, T. (2016a): Transmission system geomagnetically induced current model validation. – IEEE Transactions on Power Systems 99: 1-1.
[22] Kazerooni, M., Zhu, H., Overbye, T. J. (2016b): Improved modeling of geomagnetically induced currents utilizing derivation techniques for substation grounding resistance. – IEEE Transactions on Power Delivery 99: 1-1.
[23] Kovan, B., De Leon, F. (2016): Mitigation of geomagnetically induced currents by neutral switching. – Power Delivery IEEE Transactions on 30(4): 1999-2006.
[24] Kwon, D., Kim, Y., Moon, S. (2017): Modeling of HVDC system to improve estimation of transient DC current and voltages for AC line-to-ground fault—an actual case study in Korea. – Energies 10(10): 1543.
[25] Lewicki, J. (2007): Equivalent circuits of transformers with distorted and asymmetricalcurrents and supply voltages and with regard to magnetizing current. – IEEE International Symposium on Industrial Electronics IEEE Xplore 2: 820-826.
[26] Liu, F. (2018): Rough maximal functions supported by subvarieties on Triebel–Lizorkin spaces. – Revista de la Real Academia de Ciencias Exactas, Físicas y Naturales. Serie A. Matemáticas 112(2): 593-614.
[27] Liu, L. G., Wei, K., Ge, X. N. (2015): GIC in future large-scale power grids: an analysis of the problem. – IEEE Electrification Magazine 3(4): 52-59.
[28] Liu, Y. P., Liu, H. C. (2017): Influence of endurance tests on space charge distribution of 160 kV HVDC XLPE cable. – Journal of Electrical Engineering & Technology 12(1): 302-309.
[29] Marti, L., Yin, C. (2015): Real-time management of geomagnetic disturbances: Hydro One's eXtreme space weather control room tools. – Electrification Magazine IEEE 3(4): 46-51.
[30] Moon, B. S., Ko, B., Choi, J. S. (2017): The study on the efficient HVDC capacity considering extremely low probability of 765 kV double circuit transmission lines trip. – Journal of Electrical Engineering & Technology 12.
[31] Mousavi, S. A., Bonmann, D. (2017): Analysis of asymmetric magnetization current and reactive power demand of power transformers due to GIC. – Procedia Engineering 202: 264-272.
[32] Okpoli, A. O., Ehinmitan, D. (2019): Geological and lithologigal mapping of part of Igarra Schist belt using integrated geophysical method. – Earth Sciences Pakistan 3(1): 01-09.
[33] Pan, Z., Zhang, L., Wang, X. (2016): HVDC ground return current modeling in AC systems considering mutual resistances. – IEEE Transactions on Power Delivery 31(1): 165-173.

http://www.aloki.hu ● ISSN 1589 1623 (Print) ● ISSN 1785 0037 (Online)
DOI: http://dx.doi.org/10.15666/aeer/1704_85558568

[34] Prabhakaran, A., Raj, N. J. (2018): Mapping and analysis of tectonic lineaments of Pachamalai hills, Tamil Nadu, India using geospatial technology. – Geology, Ecology, and Landscapes 2(2): 81-103.
[35] Rajput, K., Gupta, A., Arushi (2019): Re-cycle of e-waste in concrete by partial replacement of coarse aggregate. – Engineering Heritage Journal 1(1): 05-08.
[36] Rezaei-Zare, A. (2015a): Reactive power loss versus GIC characteristic of single-phase transformers. – IEEE Transactions on Power Delivery 30(3): 1639-1640.
[37] Rezaei-Zare, A. (2015b): Enhanced transformer model for low- and mid-frequency transients—Part II: validation and simulation results. – IEEE Transactions on Power Delivery 30(1): 316-325.
[38] Rezaei-Zare, A., Marti, L., Narang, A. (2016): Analysis of three-phase transformer response due to GIC using an advanced duality-based model. – IEEE Transactions on Power Delivery 31(5): 2342-2350.
[39] Shetye, K., Overbye, T. (2015): Modeling and analysis of GMD effects on power systems: an overview of the impact on large-scale power systems. – IEEE Electrification Magazine 3(4): 13-21.
[40] Viljanen, A., Pulkkinen, A., Amm, O. (2004): Fast computation of the geoelectric field using the method of elementary current systems and planar Earth models. – Annales Geophysicae 22(1): 101-113.
[41] Wali, E., Phil-Eze, P. O., Nwankwoala, H. O. (2018): Saltwater–freshwater wetland ecosystem and urban land use change in Port Harcourt Metropolis, Nigeria. – Earth Sciences Malaysia 2(1): 01-07.
[42] Wang, J., Gao, C., Duan, X. (2015): Multi-field coupling simulation and experimental study on transformer vibration caused by DC bias. – Journal of Electrical Engineering & Technology 10(1): 176-187.
[43] Wei-Li, W. U., Liu, L. G. (2013): Long-distance transmission system voltage sensitivity research of geoelectric field due to magnetic storm. – Science Technology & Engineering 2013(16).
[44] Wu, W. L., Liu, L. G., Liu, C. M. (2014): Voltage stability in a long-distance power transmission system impacted by the geoelectric field due to a geomagnetic disturbance. – Earth Science Informatics 7(3): 173-185.
[45] Yang, B., Luo, Y., Jeng, D., Feng, J., Huhe, A. (2018): Experimental studies on initiation of current-induced movement of mud. – Applied Ocean Research 80: 220-227.
[46] Zhang, X., Liu, L., Wu, Y., Cui, Y. (2018): Existence of infinitely solutions for a modified nonlinear schrodinger equation via dual approach. – Electronic Journal of Differential Equations 147: 1-15.
[47] Zhou, D., Zhang, K., Ravey, A., Gao, F., Miraoui, A. (2016): On-line estimation of lithium polymer batteries state-of-charge using particle filter based data fusion with multi-models approach. – IEEE Transactions on Industry Applications 52(3): 2582-2595.
[48] Zhu, H., Overbye, T. J. (2015): Blocking device placement for mitigating the effects of geomagnetically induced currents. – IEEE Transactions on Power Systems 30(4): 2081-2089.
[49] Zulkapli, M. F., Rashid, N. M., Sokri, M. N. M., Nasri, N. (2018): Study on optical properties of graphene-TiO2 nanocomposite as photoanodes layer in dye sensitized solar cell (DSSC). – Environment & Ecosystem Science 2(2): 39-41.

http://www.aloki.hu ● ISSN 1589 1623 (Print) ● ISSN 1785 0037 (Online)
DOI: http://dx.doi.org/10.15666/aeer/1704_85558568

DYNAMIC SIMULATION OF URBAN GREEN SPACE EVOLUTION BASED ON CA-MARKOV MODEL-A CASE STUDY OF HEXI NEW TOWN OF NANJING CITY, CHINA

SHEN, S.[1*] – CHEN, L.[1] – FAN, C.[2] – GAO, Y.[2]

[1]*College of Landscape Architecture, Nanjing Forestry University, 210037 Nanjing, China*

[2]*School of Architecture, Tsinghua University, 100084 Beijing, China*

**Corresponding author*
e-mail: shensg@njfu.edu.cn

(Received 8th Mar 2019; accepted 21st May 2019)

Abstract. Based on the SPOT-5 images in 2004 and 2010 and SPOT-6 images in 2016 on the northern region of Hexi new town of Nanjing, the urban green space pattern of 2022 was predicted using the CA-Markov model. On this basis, four landscape indexes were used to analyze the evolution of green landscape pattern in the study area from 2004 to 2022. The results showed that the spatial accuracy of urban green space simulated by CA-Markov model was as high as 87.23%, and the Kappa index was 0.8533, which means high reliability. It is predicted that the scale of urban green space in the northern region of Hexi new town will continue to increase in 2016-2022, accounting for 17.28%, and the patch area of the dominant green space will keep increasing. The number of green patches NP and complexity LSI show a downward trend, the green landscape begins to become orderly, the fragmentation is lessening, the green space network system is gradually formed, and the spatial layout of urban green space tends to be reasonable. The simulation results can provide decision-making basis for the dynamic control of urban green space of Hexi new town of Nanjing.
Keywords: *the spatial accuracy of urban, Kappa index, the number of green patches, landscape index, the remote sensing image data*

Introduction

Since the beginning of the 21st century, with the advancement of global urbanization, China has been in the stage of urban space expansion driven by rapid urbanization. However, with the extensive and inefficient urbanization of land, the urban natural ecosystem is degrading, which further restricts the sustainable development of cites (Weber and Puissant, 2003; Daniel et al., 2018). Therefore, the land use and land cover change research has become a frontier and hot topic of global change research (Mooney et al., 2013; Ismail et al., 2019), and its importance is increasingly prominent in the study of global environmental change and sustainable development (Blumstein and Thompson, 2015; Mahmood et al., 2018). In urban planning, strengthening the control of green space layout can optimize the living environment and reduce the impact of urban development on the natural ecosystem. With the continuous development of the construction of the green space system, the intervention of its layout is a dynamic approach process, so the dynamic simulation method can effectively guide the planning of urban green space layout.

In recent years, the cellular automata model (CA) and the Markov model (Markov) are important predictive models in the field of land use dynamic simulation. The cellular automata, as a discrete grid dynamics model, has strong spatial computing ability and spatiotemporal coupling characteristics, which can effectively simulate complex spatiotemporal change processes (White and Engelen, 1993; Al-shalabi et al., 2013; Anan,

http://www.aloki.hu ● ISSN 1589 1623 (Print) ● ISSN 1785 0037 (Online)
DOI: http://dx.doi.org/10.15666/aeer/1704_85698581

2019). The Markov model was a prediction method created by A. Markov in 1940s, and it is also called Markov chain. The Markov chain is an analytical tool that can predict the future trends of variables (Paul et al., 2016). The Markov model was used by Hulst to solve the problem of vegetation ecological prediction (Hulst, 1979), and was also used by Balzter and Pastor to analyze vegetation changes (Balzter, 2000; Pastor et al., 2005; Xu, 2018).

At present, cellular automata model and Markov model have been widely used in land use change prediction. Markov model has great advantages in studying time evolution, but it is weak in spatial computing ability, while CA model has strong spatial computing ability (Liu and Chen, 2002). Therefore, the CA-Markov model, which combines the two methods, can simulate the land use change from both quantitative and spatial aspects (Halmy et al., 2015). It is more and more widely used (Weng, 2002; Ye, 2007), and has achieved better prediction results (Guan et al., 2011; Moghadam and Helbich, 2013; Anputhes et al., 2016). In addition, the CA-Markov model is mainly used to study large-scale land use change, and there are a few dynamic simulation studies on open space or green infrastructure in foreign countries (Mitsova et al., 2016; Joseph et al., 2019). However, there are few dynamic simulation studies on urban green space expansion.

Compared with the simulation of dynamic change of construction land, the simulation of dynamic change of green space has two characteristics: (1) The green space has its own spreading process, because with the green plant growth, it will increase the vegetation coverage. (2) Another characteristic of green space expansion is that it is obviously influenced by human activities, for example, both sides of the new road and the waterfront space are highly adaptable to the green space layout. In this paper, CA-Markov model is applied to green space simulation, because the model can simulate the suitable green space spread phenomenon, this is an attempt and breakthrough for the study of green space (Lin, 2018a; Sarker et al., 2019). Using this method to study the law of spatial expansion of green space in the process of urbanization is not only helpful to forecast the law of green space development, but also to provide targeted optimization measures for urban green space layout. However, this study is particularly important for the control and optimization of green space layout in China's rapidly urbanized areas (Pascual-Córdova, 2018).

This paper takes the northern region of Hexi of Nanjing as the research area, takes the SPOT images of 2004, 2010 and 2016 as the land use information source, using CA-Markov model to construct the conversion rules of urban green space micro-land cells in the cellular automaton model and then use logistic regression model to construct a comprehensive evaluation model of urban green space expansion (Asgari, 2018). In this way, the spatial change of urban green space in the study area in 2022 is predicted and the landscape indexes is used to analyze the evolution characteristics of the overall green space landscape pattern in the study area from 2004 to 2022. The results can provide reference for the dynamic regulation of green space expansion in fast urbanized areas (Liu, 2018; Bind et al., 2018). At the same time, it also explores the scientific way of urban green space planning and construction, and explores new methods for the layout of urban green space.

Research data and methods

Overview of the study area

Nanjing Hexi new town is located in the southwest of Nanjing main city zone. According to the temporal evaluation, it is divided into three regions: the north, the middle

http://www.aloki.hu ● ISSN 1589 1623 (Print) ● ISSN 1785 0037 (Online)
DOI: http://dx.doi.org/10.15666/aeer/1704_85698581

and the south. The study area is the northern region of Hexi new town of Nanjing (*Fig. 1*), which is located on the west side of Nanjing main city zone, with Yangtze River in the west, external Qinhuai River in the east, Sancha River in the north, and Yingtian Avenue in the south, with a total area of 27.74 km^2. The study area and its surrounding areas have rich natural and cultural landscapes such as Qingliang Mountain park, Stone park, Mochou lake park, Gulin park and Peach garden scenic belt and so on.

In recent years, Hexi new town of Nanjing has successfully hosted a series of major international and domestic events, such as the 10th National Games of China, China EU summit, Asian Youth Games, the Summer Youth Olympic Games, Nanjing International Marathon and World Speed Roller Skating Championships. At present, Hexi new town has become a city center with great potential for development, beautiful living environment and first-class functional quality in Nanjing.

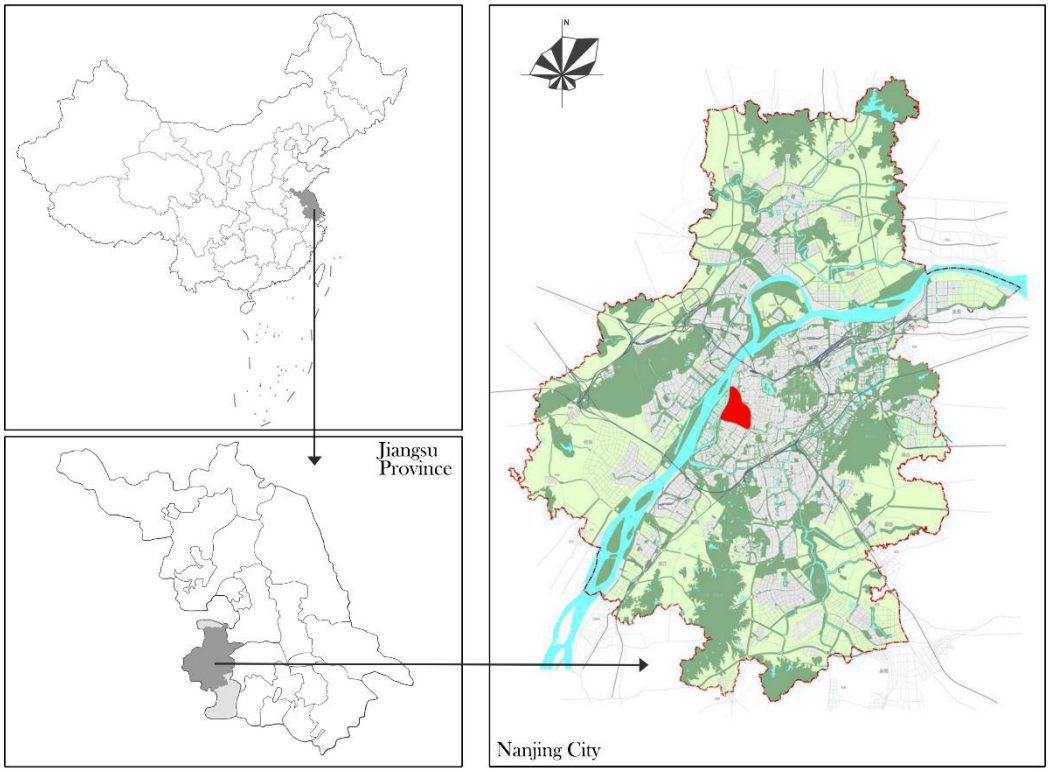

Figure 1. *Study area*

Research data and preprocessing

The remote sensing data used was three SPOT images covering the study area, including two SPOT-5 images (the acquisition time is June 2004 and June 2010, and spatial resolution is 2 m), and one SPOT-6 image (the acquisition time is July 2016, and spatial resolution is 2 m). Based on 1:25,000 topographic map, Gaussian Kriging projection (Xi'an 80 coordinate system, and central meridian 120°E) was selected, and geometric accurate correction was carried out for SPOT images by two polynomial correction methods (the root mean square error is within 0.5 pixels). According to the first class classification standard in "LUCC (Land-Use and Land-Cover Change) Classification System" of the Chinese Academy of Sciences and "Technical

http://www.aloki.hu ● ISSN 1589 1623 (Print) ● ISSN 1785 0037 (Online)
DOI: http://dx.doi.org/10.15666/aeer/1704_85698581

Regulations for Land Use Investigation" in China, combined with the characteristics of the study area, the land use types of the study area were divided into five categories: water area, urban green space, urban road land, urban construction land, and open land (unused land). Based on the field survey data and the existing sample database, the remote sensing interpretation marks in the study area were established (Lin, 2018b; Naidu et al., 2018). The three images were supervised and classified by Maximum Likelihood (ML) in Easy Feature software and ARCGIS software, and the classification results were manually revised. Using field survey data, Google Earth image and Ovi interactive map, 100 points were randomly selected to evaluate the classification map. The overall accuracy of the image classification maps in 2004, 2010 and 2016 was 95%, 96% and 97% respectively, which met the requirements of remote sensing interpretation accuracy. In ARCgis, the spatial distribution map of land use in the study area in 2004, 2010 and 2016 was formed.

CA-Markov prediction model construction

The CA-Markov model has both the predictive ability of Markov model and the advantage of cellular automata model in simulating the spatial changes of complex systems (Kamusoko et al., 2009). With the support of IDRISI software, the data probability transformation matrix in the study area is added to the cellular automata model. In the model, the transfer area and probability of each land use type were generated by Markov chain, and the image set of land use transfer suitability was created by logistic regression model. Finally, the future land use situation was simulated by CA cellular automata combined with transfer probability and transfer suitability atlas (Hu et al., 2013) (*Fig. 2*).

It should be pointed out that according to the principle of urban planning, the water and construction land cannot be converted between each other in study area. In addition, the time interval between remote sensing images is equal to 6 years, so each period of the change is iterated the same 6 times.

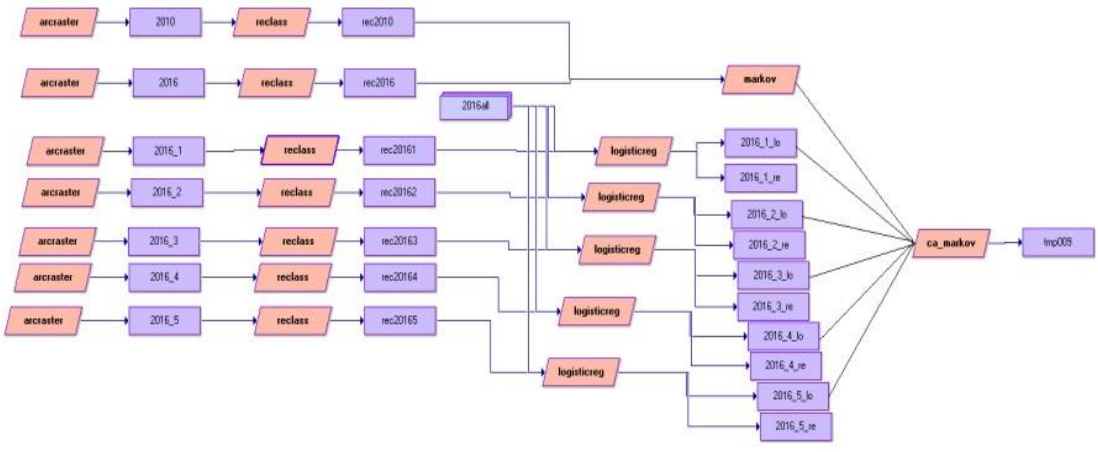

Figure 2. *The flow chart of urban green space simulated dynamically by CA-Markov model*

In this study, the dynamic simulation prediction of urban green space was realized based on the CA-Markov model. It should be carried out on the premise of ensuring the accuracy of the model, and the experimental periods were 2004, 2010 and 2016, with a

http://www.aloki.hu ● ISSN 1589 1623 (Print) ● ISSN 1785 0037 (Online)
DOI: http://dx.doi.org/10.15666/aeer/1704_85698581

time interval of 6 years. The prediction process was achieved through 2 steps. The first was the data accuracy test (Zuo et al., 2014) and spatial data test (Han et al., 2016). That was to say, the green space data and distribution in 2016 were predicted by the images from 2004 to 2010, and compared with the measured green space data in 2016, so as to test the feasibility and accuracy of this method. If the accuracy met the requirements, the second part was studied, that was the data and distribution of green space in 2022 were predicted through the 2010-2016 image data (Jiménez et al., 2016).

The specific steps were as follows: (1) According to the land use classification results of remote sensing images in the study area in 2004 and 2010, the transfer area matrix and transfer probability matrix of land use in 2004-2010 were obtained by Markov model. (2) The land change suitability image in 2004-2010 was made by using Logistic regression model. (3) Using CA-Markov model, the land use distribution map of 2010 was superimposed on the road network of 2016. On this basis, the land use transfer probability matrix and transfer suitability image set from 2004 to 2010 were used to predict the green land data and its distribution in 2016 (Huang, 2019). The proximity filter was set to 5 × 5. (4) In order to test the reliability of simulation results, the accuracy of the CA-Markov model should be verified. The land use classification map in 2010 was used as the initial image to predict the distribution of urban green space in 2016, and the predicted value in 2016 was compared with the actual value. In this paper, area accuracy (*Eq. 1*) and spatial accuracy (*Eq. 2*) are used to compare their consistency. In *Equation 1,* m_{iy} and m_{ix} are respectively the simulated area and the actual area of the i land, the higher of the E1 numerical value, the better the consistency between the simulated area and the actual area. In *Equation 2,* c_{iy} is the grid number of i land in the land use simulation map, and c_{ix} is the grid number of I class land in the land use actual map at the same location as c_{iy}. The same meaning, the higher of the E2 numerical value, the higher the spatial precision. In this study, it was feasible that *E2* was set to 85%. (5) According to the above (1)-(4) steps, the land use distribution map of 2016 was taken as the initial image, and the land use classification results of 2010 and 2016 remote sensing images in the study area were used to generate transfer probability matrix and land change suitability image set to predict the spatial distribution of green space in the study area in 2022.

$$E1 = \left\{1 - \frac{\left|m_{iy} - m_{iy}\right|}{m_{ix}}\right\} \times 100\% \quad \text{(Eq.1)}$$

$$E2 = \frac{c_{iy}}{c_{ix}} \times 100\% \quad \text{(Eq.2)}$$

Urban green space landscape index acquisition

Landscape index is used to quantitatively analyze the characteristics of landscape pattern (Riitters et al., 1995). In the landscape index analysis, four indexes of number of patches (NP), landscape shape index (LSI), the proportion of the largest patch to the landscape area (LPI) and Shannon diversity index (SHDI) were selected as the characteristic indexes reflecting landscape pattern (Zhang et al., 2014; Wu et al., 2016) (*Table 1*). The vector land use map was transformed into raster map by ArcGIS, and the

http://www.aloki.hu ● ISSN 1589 1623 (Print) ● ISSN 1785 0037 (Online)
DOI: http://dx.doi.org/10.15666/aeer/1704_85698581

vector diagram was transformed into Arc Grid format data with a size of 10 m ×10 m, and the above landscape indexes were calculated by Fragstats 4.2 software.

Table 1. *Main landscape index and its ecological significance*

Index type	Index name	English abbreviation	Application scale	Ecological significance
Density and diversity index	Number of plaques	NP	Type/landscape	It reflects the total number of patches reflecting the patch type in the landscape, which is positively correlated with the degree of fragmentation of the landscape. Generally, the larger the NP, the higher the degree of fragmentation, the smaller the NP, and the lower the broken degree
Shape index	Landscape shape index	LSI	Type/landscape	It reflects the shape complexity of the overall landscape. The closer the LSI to 1, the simpler the overall landscape. The larger the LSI is, the more complex it is
Area index	The proportion of the largest patch to the landscape area	LPI	Type/landscape	It reflects the degree of plaque concentration and the dominant type of landscape
Diversity standard	Shannon diversity index	SHDI	Landscape	It reflects the change of the quantity and proportion of landscape components. In the landscape composed of multiple components, when the proportion of each component is equal, the diversity index is the highest

Results and analysis

Change of land use structure in the study region in 2004-2016

Based on the classification results of ARCGIS, all kinds of land use scale is shown in *Table 2*, and the mutual transformation of each land use type is complicated (*Fig. 3*). It can be seen that in 2004-2016: (1) The scale of construction land has been decreasing. This is mainly because in the process of urban construction, road and green space have been increasing, reducing the projection area of construction land. (2) The scale of roads increases first and then decreases because a large number of new roads have been added between 2004 and 2010, but the road green space has not been improved during this period. Between 2010 and 2016, the road green space has been gradually improved. With the increase of road green coverage, the roads are covered with greenery. (3) The scale of urban green space has increased rapidly. From 2004 to 2016, the scale of green space has been expanding and a green network system along the river and road has been formed. (4) During this period, the scale of open land (unused land) declined, mainly because a lot of wasteland was changed to construction land. (5) The size of water area changes little, indicating that the water system is well preserved.

CA-Markov model constructed for prediction test

Based on the CA-Markov urban green space prediction model constructed in *Figure 2,* the distribution and scale of green space and all kinds of land in 2016 were

http://www.aloki.hu ● ISSN 1589 1623 (Print) ● ISSN 1785 0037 (Online)
DOI: http://dx.doi.org/10.15666/aeer/1704_85698581

predicted by using data from 2004 to 2010 (Wang, 2019). The results are shown in *Figure 4* and *Table 2*. The predicted results were only 5% less than the measured data in 2016, the data precision E of simulated green space was 87.23%, and the spatial precision kappa coefficient was 0.8533, indicating that it was feasible to use CA-Markov model to predict the dynamic change of green space (*Fig. 4*). Therefore, it was reliable to use this method to predict the size and layout of urban green space in 2022 by using the actual measurement of urban green space in 2010 and 2016.

Table 2. *Statistics of all kinds of land use scale (unit: km^2)*

	Land used for building	Road	Green space	River system	Open space	Total
2004 actual measurement	19.32	2.81	1.52	1.79	2.31	27.74
2010 actual measurement	18.09	3.81	2.65	1.72	1.48	27.74
2016 actual measurement	17.73	3.55	4.20	1.73	0.54	27.74
2016 premeasurement	17.66	3.91	3.97	1.70	0.50	27.74
2022 premeasurement	17.28	3.48	4.79	1.73	0.46	27.74

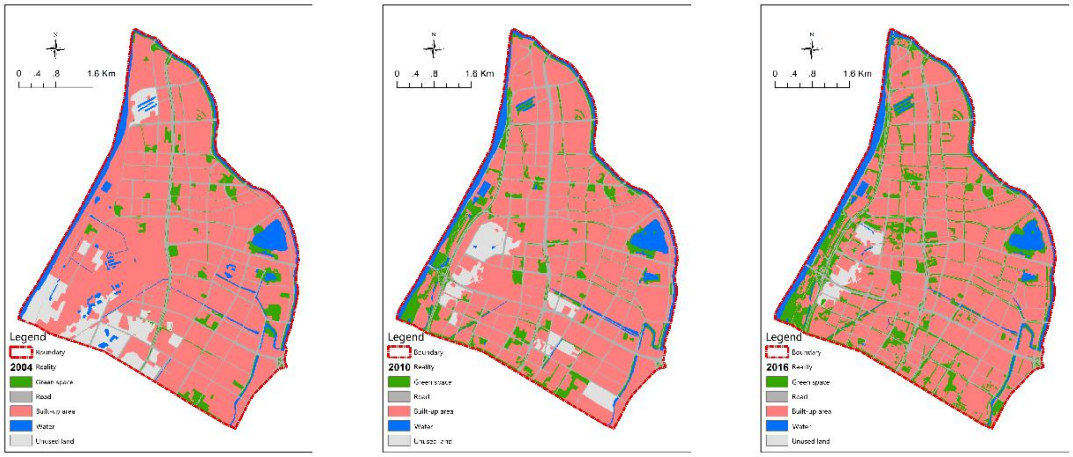

(a) 2004 **(b) 2010** **(c) 2016**

Figure 3. *Results of remote sensing image classification in the study area*

Prediction of urban green space change trend in 2022

According to the land use change prediction of CA-Markov model (*Table 2* and *Fig. 5*), in 2010-2016, on the whole, the change range of all kinds of land was smaller than the previous 12 years from 2004 to 2016. The urban green space will continue to improve in 2016-2022, and the scale will continue to increase. According to the forecast, the greening level of the riverside park of the Yangtze River and key roads will be higher than 2016, the width of green bandwidth will be further improved, the overall scale will be increased from 4.20 km^2 in 2016 to 4.79 km^2, but the improvement of

http://www.aloki.hu ● ISSN 1589 1623 (Print) ● ISSN 1785 0037 (Online)
DOI: http://dx.doi.org/10.15666/aeer/1704_85698581

green space network will make the construction land and road (projected area) scale of the study area continue to decline, and the overall scale of both will be reduced by about 0.59 km^2 (Yanyan et al., 2019).

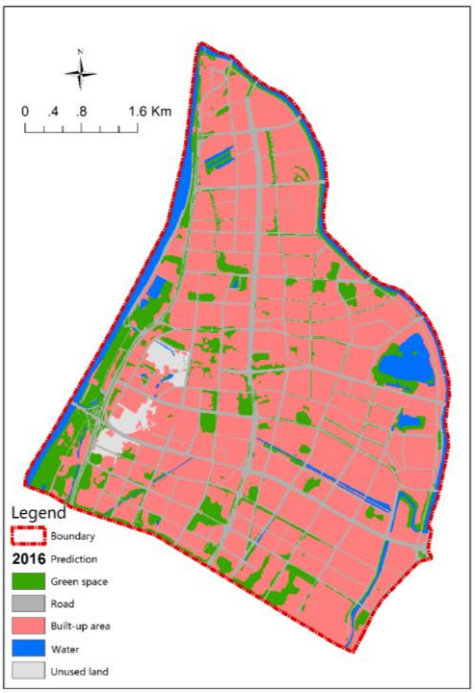

Figure 4. *Prediction of green space distribution in 2016 based on remote sensing image data in 2004 and 2010*

Figure 5. *Prediction of green space distribution in 2022 based on remote sensing image data in 2004 and 2010*

http://www.aloki.hu ● ISSN 1589 1623 (Print) ● ISSN 1785 0037 (Online)
DOI: http://dx.doi.org/10.15666/aeer/1704_85698581

Green space landscape pattern analysis in 2004-2022

Based on the measured land use distribution maps of 2004, 2010 and 2016 and the predicted land use distribution maps of 2022, 16 landscape indexes of four periods were calculated (*Table 3*). From *Table 3* it can be seen that the number of patches of green space NP and the complexity LSI are on the rise, which indicates that the fragmentation and disorder degree of green space landscape in the study area became more and more serious between 2004 and 2016, and the mutual relationship between green space and all kinds of land became complex, and the degree of mosaic increased (Yu, 2019). From 2016 to 2022, the number of patches NP and complexity LSI of green space show a downward trend, the landscape of green space starts to become orderly, the fragmentation is reduced, and the green space network system is gradually formed. The landscape shape index (LPI) shows an increasing trend, indicating that the patch area of green space with dominant effect increases all the time (Perdomo-Valentín, 2016). Shannon diversity index (SHDI) increases slightly, indicating that the heterogeneity of urban green space decreases and presents a trend of balanced distribution, and the spatial layout of urban green space tends to be reasonable (Ebrahimian, 2017).

Table 3. *Landscape pattern analysis in 2004-2022*

Year	Green Space NP	Green space LSI	Green space LPI	Total SHDI
2004 actual measurement	598	23.3065	0.1347	1.03
2010 actual measurement	674	34.1506	0.3674	1.10
2016 actual measurement	802	46.9604	0.4323	1.08
2022 premeasurement	715	44.152	0.4648	1.11

Conclusions and discussion

Based on the remote sensing image data of 2004 and 2010, the spatial distribution of urban green space in the northern area of Hexi new town of Nanjing in 2016 and 2022 was simulated and predicted by using CA-Markov model. The evolution of green space landscape pattern in the study area was analyzed by using four landscape indices. The following conclusions can be drawn:

(1) In this study, based on CA-Markov model and GIS and RS technologies, taking the spatial transformation of construction land, road, green space, water system and open land (unused land) as the research objects, the CA-Markov model was used to predict the scale and distribution of urban green space in northern region of Hexi new town of Nanjing in 2022. The predicted results in 2016 obtained by the experiment show that the simulation accuracy is up to 87.23% and the Kappa index is 0.8533, indicating that the proposed conversion rules are feasible and the predicted model has high reliability. It also shows that the CA-Markov model can not only predict urban land use change, but also predict the future development of urban green space. The results can provide decision support for the dynamic regulation of urban green space.

(2) From 2004 to 2016, the area of green space in the study area has increased year by year. There are two main reasons for this result: first, due to the impact of urban

http://www.aloki.hu ● ISSN 1589 1623 (Print) ● ISSN 1785 0037 (Online)
DOI: http://dx.doi.org/10.15666/aeer/1704_85698581

planning and construction, green space was mainly transformed from the unused land of the study area, the unused land was reduced from 2.31 km^2 in 2004 to 0.50 km^2 in 2016; another reason is that along with the roadside trees grow up, the coverage area of road greening is also gradually increased. Therefore, the scale of green space in the study area increased from 1.52 km^2 in 2004 to 3.97 km^2 in 2016, and the scale of green space will continue to increase gradually in the future.

(3) According to the change of the landscape index from 2004 to 2016, the green space in the study area has undergone a process from disorderly development to orderly development, and the layout of green space has also changed from plaque fragmentation to system network. Therefore, the spatial layout of urban green space system will become more and more reasonable.

(4) This study is an attempt to introduce CA-Markov model into the dynamic simulation of urban green space, hoping to provide a method for dynamic regulation of urban green space. However, this study is only based on the size and distribution of urban green space in 2004, 2010 and 2016 to dynamically simulate the changes of urban green space in the future. The impact of the adjustment of urban planning, the occurrence of major events and other policy changes on the construction of green space has not been considered, which may lead to greater errors in the prediction of urban green space. Therefore, in the further study, different scenarios can be set to formulate constraints, so as to make the simulation results more reasonable.

Acknowledgments. The authors acknowledge the National Natural Science Foundation of China (Grant: 31570703); Top-notch Academic Programs Project of Jiangsu Higher Education Institutions (No. PPZY2015A063); Advanced analysis and testing center of Nanjing Forestry University.

Conflict of interests. The authors declare no conflict of interests.

REFERENCES

[1] Al-shalabi, M., Billa, L., Pradhan, B. (2013): Modeling urban growth evolution and land-use changes using GIS based cellular automata and SLEUTH models: the case of Sana'a metropolitan city, Yemen. – Environment Earth Sciences 70(1): 425-437.

[2] Anan, H. S. (2019): Contribution to the paleontology, stratigraphy and paleo-biogeography of some diagnostic Pakistanian paleogene foraminifer in the Middle East. – Earth Sciences Pakistan 3(1): 23-28.

[3] Anputhes, M., Janmaat, J. A., Nicol, C. F. (2016): Modeling spatial association in pattern based land use simulation models. – Journal of Environmental Management 181: 465-476.

[4] Asgari, A. (2018): Methods for breaking Chinese lantern (Physalis alkekengi L.) seed dormancy. Laboratory and greenhouse studies. – Revista de la Facultad de Agronomia de la Universidad del Zulia 35(2).

[5] Balzter, H. (2000): Markov chain model for vegetation dynamics. – Ecological Modeling 126: 139-154.

[6] Bind, A., Goswami, L., Prakash, V. (2018): Comparative analysis of floating and submerged macrophytes for heavy metal (copper, chromium, arsenic and lead) removal: sorbent preparation, characterization, regeneration and cost estimation. – Geology, Ecology, and Landscapes 2(2): 61-72.

[7] Blumstein, M., Thompson, J. R. (2015): Land-use impacts on the quantity and configuration of ecosystem service provisioning in Massachusetts, USA. – Journal of Applied Ecology 52(8): 1009-1019.

http://www.aloki.hu ● ISSN 1589 1623 (Print) ● ISSN 1785 0037 (Online)
DOI: http://dx.doi.org/10.15666/aeer/1704_85698581

[8] Daniel, G. I., Henry, O. U., Ayodeji, B. B., Silas, M. Y. (2018): Land suitability analysis for the production of Cocoyam Inbenue State, Nigeria. – Earth Sciences Malaysia 2(2): 25-30.
[9] Ebrahimian, H. (2017): Water and energy productivity in sprinkler irrigation systems under using groundwater. – Revista de la Facultad de Agronomia de la Universidad del Zulia 34(4).
[10] Gautam, A., Batra, R., Singh, N. (2019): A study on use of rice husk ash in concrete. – Engineering Heritage Journal 1(1): 01-04.
[11] Guan, D. J., Li, H. F., Inohae, T. (2011): Modeling urban land use change by the integration of cellular automaton and Markov model. – Ecological Modelling 222: 3761-3772.
[12] Halmy, M. W. A., Gessler, P. E., Hicke, J. A. (2015): Land use/land cover change detection and prediction in the north-western coastal desert of Egypt using Markov-CA. – Applied Geography 63: 101-112.
[13] Han, W. T., Guo, C. C., Zhang, L. Y. (2016): Classification method of land cover and irrigated farm land use based on UAV remote sensing in irrigation. – Transactions of the Chinese Society for Agricultural Machinery 47(11): 270-277.
[14] Hu, X. L., Xu, L., Zhang, S. (2013): Land use pattern of Dalian City, Liaoning Province of Northeast China based on CA-Markov model and multi-objective optimization. – Chinese Journal of Applied Ecology 24(6): 1652-1660.
[15] Huang, Q. (2019): Application of ADAS multi-sensor vision simulation system for tree recognition in urban garden environment. – Revista de la Facultad de Agronomia de la Universidad del Zulia 36(1).
[16] Hulst, R. (1979): On the dynamics of vegetation: Markov chains as models of succession. – Vegetation 40: 3-14.
[17] Ismail, I., Husain, M. L., Satyanarayana, B., Ibrahim, S., Zakaria, R. (2019): Root density analysis and wave attenuation ability of Rhizophora species at Kemaman, Terengganu. – Earth Sciences Malaysia 3(1): 18-24.
[18] Jiménez-Chavarría, M., Rodríguez-Arrieta, A., Salas-Fumero, F., Retana-Salazar, A. P. (2016): Descripción ultraestructural de la hoja de tres especies De Aráceas (Araceae) con características hidrofóbicas. – Acta Microscopica 25(2).
[19] Joseph, O. T., Adepoju, A. A., Olufemi, A. (2019): Biodiversity: overexploited but underutilized natural resource for human existence and economic development. – Environment & Ecosystem Science 3(1): 26-34.
[20] Kamusoko, C., Aniya, M., Adi, B. (2009): Rural sustain-ability under threat in Zimbabwe: Simulation of future land use/cover changes in the Bindura district based on the Markov-cellular automata model. – Applied Geography (29): 435-447.
[21] Lin, X. (2018a): Early warning of forest carbon sink market risk from the perspective of law. – Argos 35(69).
[22] Lin, X. (2018b): Performance evaluation of forest carbon sink in China based on principal component analysis. – Argos 35(69).
[23] Liu, J. S., Chen, Y. G. (2002): GIS-based cellular automata models and researches on spatial complexity of man-land relationship. – Geographical Research 21(2): 155-162.
[24] Liu, W. (2018): Mutual reference and integration of ecological documentaries and ecological feature films. – Argos 35(70).
[25] Mahmood, S., Kazmi, S. T., Ali, S. S. (2018): Comparison of drinking water bottles of different countries along with Zamzam water, Pakistan. – Earth Sciences Pakistan 2(1): 05-14.
[26] Mitsova, D., Shuster, W., Wang, X. (2011): A cellular automata model of land cover change to integrate urban growth with open space conservation. – Landscape & Urban Planning 99(2): 141-153.

http://www.aloki.hu ● ISSN 1589 1623 (Print) ● ISSN 1785 0037 (Online)
DOI: http://dx.doi.org/10.15666/aeer/1704_85698581

[27] Moghadam, H. S., Helbich, M. (2013): Spatiotemporal urbanization processes in the megacity of Mumbai, India: a Markov chains-cellular automata urban growth model. – Applied Geography 40: 140-149.
[28] Mooney, H. A., Duraiappah, A., Larigauderie, A. (2013): Evolution of natural and social science interactions in global change research programs. – PNAS 110(Suppl 1): 3665-3672.
[29] Naidu, M. T., Premavani, D., Suthari, S., Venkaiah, M. (2018): Assessment of tree diversity in tropical deciduous forests of Northcentral Eastern Ghats, India. – Geology, Ecology, and Landscapes 2(3): 216-227.
[30] Pascual-Córdova, G. (2018): Indicadores de calidad del suelo en el agroecosistema caña de azúcar (Saccharum spp.). – Revista de la Facultad de Agronomia de la Universidad del Zulia 35(1).
[31] Pastor, J., Sharp, A., Wolter, P. (2005): An application of Markov model to the dynamics of Minnesota's. – Journal of Forest Research 35: 3011-3019.
[32] Paul, D., Wagner, S., Murty, B., Balaji, N. (2016): Dynamic integration of land use changes in a hydrologic assessment of a rapidly developing Indian catchment. – Science of the Total Environment 539: 153-164.
[33] Perdomo-Valentín, O. (2016): Ecoconciencia y ecoactividad para la naturación urbana en estudiantes de postgrado en agricultura de México. – Revista de la Facultad de Agronomia de la Universidad del Zulia 33(4).
[34] Riitters, K. H., O'Neill, R. V., Hunsaker, C. T. (1995): A factor analysis of landscape pattern and structure metric. – Landscape Ecology 10(1): 23-39.
[35] Sarker, M. K. U., Majumder, A. K., Haque, M. Z., Hossain, M. S., Nayeem, A. A. (2019): Assessment of inland water quality parameters of Dhaka City, Bangladesh. – Environment & Ecosystem Science 3(1): 13-16.
[36] Wang, Y. (2019): Influencing factors of water-saving irrigation technology used by vegetable growers from the perspective of cost-benefit. – Revista de la Facultad de Agronomia de la Universidad del Zulia 36(1).
[37] Weber, C., Puissant, A. (2003): Urbanization pressure and modeling of urban growth: Example of the Tunis metropolitan area. – Remote Sensing of Environment 86(1/2): 341-352.
[38] Weng, Q. H. (2002): Land use change analysis in the Zhujiang Delta of China using satellite remote sensing, GIS and stochastic modelling. – Journal of Environmental Management 64: 273-284.
[39] White, R., Engelen, G. (1993): Cellular automata and fractal urban form: A cellular modeling approach to the evolution of urban land use patterns. – Environment and Planning A 25(8): 1175-1199.
[40] Wu, W., Xu, L. P., Zhang, M. (2016): Impact of landscape metrics on grain size effect in different types of patches: a case study of Wuxi City. – Acta Ecologica Sinica 36(9): 2740-2749.
[41] Xu, D. (2018): Research on brand construction and development of agricultural products in Guizhou. – Engineering Heritage Journal 2(2): 19-24.
[42] Yanyan, D., Fuwen, D., Yue, L. (2019): Effect of sewage load on microenvironment and sludge reduction efficiency of situ biofilm sludge reduction system. – Acta Microscopica 28(2).
[43] Ye, B. Y., Bai, Z. K. (2007): Simulating land use/cover changes of Nenjiang County based on CA-Markov model. – Computer and Computing Technologies in Agriculture 58: 319-327.
[44] Yu, M. (2019): Impact of environmental regulation on green innovation practice of food enterprises: regulating effect of environmental awareness of different executives. – Revista de la Facultad de Agronomia de la Universidad del Zulia 36(1).

http://www.aloki.hu ● ISSN 1589 1623 (Print) ● ISSN 1785 0037 (Online)
DOI: http://dx.doi.org/10.15666/aeer/1704_85698581

[45] Zhang, X. L., Qu, Y. H., Ren, Y. Y. (2014): Correlative analysis among pedodiversity, land use diversity and the other related ecological indexes. – Ecology and Environmental Sciences 23(6): 923-931.
[46] Zuo, T., He, L., Zhang, J. M. (2014): Dynamic change in coastal soil salinization based on the CA-Markov Model. – Resources Science 36(6): 1298-1305.

http://www.aloki.hu ● ISSN 1589 1623 (Print) ● ISSN 1785 0037 (Online)
DOI: http://dx.doi.org/10.15666/aeer/1704_85698581

THE EFFECTS OF SALT AND ALKALINE STRESS ON THE FOURWING SALTBUSH (*ATRIPLEX CANESCENS* (PURSH) NUTT.) STRESS

ZHANG, T.* – HE, K. N. – ZHANG, Z. Z.

College of Soil and Water Conservation, Beijing Forestry University, Beijing 100083, China

Key Laboratory of State Forestry Administration on Soil and Water Conservation, Beijing Forestry University, Beijing 100083, China

**Corresponding author*
e-mail: whitneylogan6017@gmail.com

(Received 8th Mar 2019; accepted 21st May 2019)

Abstract. *Atriplex canescens* is a C_4 fodder shrub that is excellent for phytore-mediation in saline-alkali environments. However, little is known about the response of this shrub species to salt and alkaline stress and its underlying physiological adaptive mechanisms. In this study, we treated 8-week-old *A. canescens* seedlings in the lab with neutral salt (NS) (1:1 molar ratio of NaCl to Na_2SO_4, pH 6.65-6.95) and alkali salt (AS) (1:1 molar ratio of $NaHCO_3$ to Na_2CO_3, pH 9.75-10.12) at five concentrations (0-400 mM). Our results showed that individual *A. canescens* seedlings could maintain growth under certain ranges of both NS stress and AS stress. These findings suggest that AS can more strongly inhibit *A. canescens* seedlings than can NS. This result was attributed to a decrease in photosynthetic ability and damage to Na^+/K^+ homeostasis under alkali salinity. Differences were evident in the NS and AS treatments for almost all of the considered parameters.
Keywords: *adaptive mechanism, concentration, chlorophyll, photosynthesis, environmental science*

Introduction

Primary and secondary soil salinization and alkalization are well-known constraints against the sustainable development of agriculture and land conservation, as they are critical environmental factors that can inhibit plant productivity (Flowers, 2004; Kalaji et al., 2016; Ogunyele et al., 2018). Natural salt-alkalinized soils are driven by various cations, such as Na^+, K^+, Ca^{2+} and Mg^{2+}, and various anions, such as Cl^-, SO_4^{2-}, HCO_3^- and CO_3^{2-} (Läuchli and Lüttge, 2002; Nwankwo and Nwankwoala, 2018). Based on salt characteristics, two types of stresses can be incurred from salt-alkalinized soils. Neutral salt (NS) stress, which is induced by a high amount of NS such as NaCl and Na_2SO_4. And alkali salt (AS) stress, which is caused by $NaHCO_3$ and Na_2CO_3 (Shi and Yin, 1993; Jamil et al., 2018). AS stress can impact plants more severely than deleted NS stress (Shi and Yin, 1993; Gong et al., 2014; Nkwuda et al., 2019). Furthermore, plants growing in salt-alkalinized soils are affected by both NS and AS.

Salinity can exert osmotic and toxic effects on plants, consequently damaging the photosynthetic process and impeding plant growth (Benzart Maali et al., 2012; Kumar, 2018). High-salt environments can disrupt ionic homeostasis in plant tissues. The re-establishment of both ionic balance and osmotic adjustment is a key functional mechanism for plant survival under NS stress (Li et al., 2003; Tianlei, 2019). Compared to that of NS stress, the higher pH value of AS stress can impose greater effects on plants, probably because the alkalinity of saline soils can severely disrupt both ionic and pH homeostases in plant tissues (Yang et al., 2008; Rajendran and Mohsin, 2018).

http://www.aloki.hu ● ISSN 1589 1623 (Print) ● ISSN 1785 0037 (Online)
DOI: http://dx.doi.org/10.15666/aeer/1704_85838598

Therefore, plants under AS stress may suffer not only from ion toxicity and physiological drought but also from alkaline stress in high-pH environments. To resist AS stress, plants must allocate higher amounts of energy to regulate the pH in their roots to maintain intracellular ionic balance (Yang et al., 2007; Sufiyan et al., 2018).

Due to the high adaptability of halophytes to saline and alkaline environments, many studies have examined the physiological responses of these types of plants to salt stress (Maali Benzart et al., 2014). Many studies have found that moderate salt solutions can stimulate net photosynthetic rates (Pns) (i.e., the highest rates of net photosynthesis ar found in plants under moderate salt concentrations). For example, the growth rate of the C_3 perennial halophyte shrub *Atriplex portulacoides* peaked at 200 mM NaCl concentrations (Redondo-Gómez et al., 2007; Madhav et al., 2018). Halophytes can survive in saline environments by employing the following mechanisms: enhancing photosynthetic ability, reducing Na^+ concentrations in the cytosol and using Na^+ as an osmoregulator to maintain cellular ion homeostasis, as well as improving water status via osmotic adjustment by producing compatible solutes (Shabala et al., 2014; Flowers et al., 2015). For instance, *Puccinellia tenuiflora* can limit Na^+ influx to maintain a high K^+/Na^+ ratio in the shoots (Niu et al., 2016; Raj and Prabhakaran, 2018). However, studies on the effects of salt stress on plants have mainly focused on NS environments dominated by NaCl. Few studies have investigated the impact of alkaline stress on halophytes and their underlying mechanisms, which may have implications for better utilization and restoration of salt-alkalinized soil.

Furthermore, recent studies have typically used herbs and crops, including *Chloris virgate*, *P. tenuiflora*, *Kochia sieversiana*, wheat, oats and tomato, to investigate the effects of salt and alkaline stress on plants (Yang et al., 2008). However, how halophytes are affected by salt and alkaline stress and the way they physiologically respond in saline and alkaline environments are not well understood. The saline-alkali region in Northwest China also experiences long periods of drought, gale-force winds and dust. Therefore, shrubs have great implications in land restoration and local economies, as shrubs cannot be replaced by herbs and crops due to the lack of ecological functions, such as disrupting wind and preventing erosion, of those two plant types. The C_4 perennial evergreen shrub *Atriplex canescens*, which belongs to the Chenopodiaceae family, is native to xeric and saline deserts in North America. Due to its strong resistance to drought (annual rainfall of 90-350 mm), salinity（soil salinity of 0.5-1.5%, and cold (elevation of 500-3500 m) (Glenn and Brown, 1999; Kong, 2013), this species is well naturalized and adapted to a wide range of environments. It is widely used as fodder and screens and for preventing soil erosion and soil recovery (Peterson et al., 1987; Benzarti et al., 2013). This shrub species was introduced to China in 1990 and has shown the ability to maintain high levels of photosynthesis and growth rates throughout a wide range of NaCl concentrations (Pan et al., 2016). Therefore, *A. canescens* represents an excellent phytoremediation plant in saline-alkali environments (Benzarti et al., 2013). However, it is not clear whether the photosynthesis and growth of *A. canescens* differ between AS and NS environments. In this study, we conducted a controlled experiment by simulating neutral and alkali soil salt conditions along a concentration gradient from 0 to 400 mM in order to compare the different effects of NS and AS on the growth and physiological response of *A. canescens*. To understand the different impact of salt and alkaline stress on their plants and their physiological response traits, we tested the following three hypotheses:

1. AS more strongly inhibits plant growth than does NS.

http://www.aloki.hu ● ISSN 1589 1623 (Print) ● ISSN 1785 0037 (Online)
DOI: http://dx.doi.org/10.15666/aeer/1704_85838598

2. AS more strongly inhibits plant photosynthetic ability than does NS.
3. The Na^+ and K^+ contents in *A. canescens* seedlings are more strongly influenced by AS than by NS.

Materials and methods

Experimental treatments

Plant materials

We collected seeds of *A. canescens* from the Academy of Agriculture and Forestry Sciences, Qinghai University, China. The seeds were treated with H_2SO_4 and distilled water and then were germinated in washed sand under dark conditions for 8 days in a greenhouse. A total of 100 plastic pots were used to house the germinated *A. canescens* seeds; the size of each pot was 10 cm × 10 cm × 10 cm. Each pot was filled with 1 kg of washed soil (1.36 g/cm^3 of soil bulk density) and contained 2 seedlings. The seedlings were watered with 1/2-strength Hoagland nutrient solution at 2-day intervals until a suitable soil moisture content (19.96 ± 1.32%, 79.64% percentage of field capacity) was reached. We examined the relationship between the diurnal variation in soil water and seedling growth and defined the suitable soil moisture content as that at which the highest plant growth rates occurred. The climatic conditions of the greenhouse included a temperature of 27.5 ± 1.5 °C/19.0 ± 1.5 °C (day/night) and a photoperiod of 16 h/8 h (light/dark). We controlled the photosynthetically active radiation (PAR) to be 800 μmol m^{-2} s^{-1} and the relative humidity to be 60 ± 2.5%.

Design of simulated salt and alkali conditions

The northwestern inland saline-alkali area in China is characterized by a low annual precipitation (43.5 mm) and a very high intensity of solar radiation (2940 KJ cm^{-2}). The soil salts are mainly composed of NaCl, Na_2SO_4, $NaHCO_3$ and Na_2CO_3. Accordingly, we simulated the NS conditions by mixing NaCl and Na_2SO_4 at a molar ratio of 1:1. To simulate the AS conditions, we mixed $NaHCO_3$ and Na_2CO_3 at a molar ratio of 1:1. Under each salt condition, five levels of soil solution salt concentrations were applied: 80, 160, 240, 320, and 400 mmol L^{-1} (mM).

Stress treatment

A total of 72 uniform 8-week-old seedlings (36 pots) were selected and randomly divided into 12 sets. Each set consisted of 3 pots, and each pot contained two plants. One set was used to measure the initial size of the seedlings at the beginning of the treatment, and one set was used as a control group during the whole treatment. Five sets were used for AS stress treatments, while the other five sets were used for NS stress treatments.

By using the soil solution's salt concentrations, soil bulk density and soil moisture content data, we calculated the quantity of the four different salts added to each treatment. One fifth of the salt quantity were added to the plants along with 200 mL 1/2-strength Hoagland nutrient solution between 17:30 and 18:30 every day for five days until the salt quantity reached the desired level. After the desired salt concentrations in the soil were met, the treatments continued for 20 days in the greenhouse. And the soil

http://www.aloki.hu ● ISSN 1589 1623 (Print) ● ISSN 1785 0037 (Online)
DOI: http://dx.doi.org/10.15666/aeer/1704_85838598

moisture contents in all pots were kept constant at 19.96 ± 1.32% throughout the whole experiment.

Measurement of parameters

Growth

Shoot and root relative growth rates (RGRs) were measured. After the experiment, we harvested the whole plants, separated the shoots from the roots and then dried the tissue at 80 °C for 48 h. We calculated the RGR of both the shoots and roots in accordance with the methods of Kingsbury et al. (1984) as follows: RGR = (ln DM_1-ln DM_0)/D, where DM_1 denotes the dry mass at the end of the stress treatment, DM_0 refers to the initial dry mass at the beginning of the stress treatment, and DM is the total treatment duration in days.

Photosynthesis

To measure the photosynthetic ability of the plants, the Pn, stomatal conductance (Gs), transpiration rate (Tr) and chlorophyll (chl) content were measured. Before harvesting the plants, we selected a total of three fully expanded leaves on the upper, middle and lower parts of the seedlings for measuring their Pn, Gs and Tr under a light intensity of 1000 μmol m^{-2} s^{-1} by using an Li-6400 portable photosynthesis system (LiCor, Lincoln, NE, USA) between 10:00 and 11:00. For each leaf, three replicate measurements were performed for each parameter. The same leaves used for measuring Pn were used for measuring leaf area and chl content. We used a photo scanner (CS4200F; Canon, Inc., Tokyo, Japan) to estimate the leaf area. The water use efficiency (WUE) was calculated as the Pn/Tr ratio. The chl a (Chla), chl b (Chlb) and carotenoids (Car) were extracted by using acetone, and their contents were determined with a spectrophotometer (UV-6100PCS; Mapada Instruments, Co., Ltd., Shanghai, China) at 440-, 654-, and 663-nm wavelengths, respectively. Their concentrations were calculated in accordance with the equations (Lichtenthaler, 1987).

Na^+, K^+ concentrations

The roots, stems and leaves were carefully separated and rinsed with deionized water, after which they were dried in an oven at 80 °C for 72 h. The Na^+ and K^+ ions were extracted from the dried tissues by using 100 mM acetic acid at 90 °C for at least 2 h. The extractions were then transferred to a water bath, cooled and filtered, after which the cation accumulation was determined by using a flame spectrophotometer (Model 410 Flame; Sherwood Scientific, Ltd., Cambridge, UK) (Bao et al., 2016). Three replicates were used per measurement.

Statistical analysis

One-way analysis of variance (ANOVA) was performed for each measurement by using SPSS statistical software (Ver. 19.0, SPSS, Inc., Chicago, IL, USA). Duncan's multiple range test (DMRT) was used to identify significant differences among the means at a significance level of $P < 0.05$. All the acquired data were presented as the average values and their standard errors (SEs).

http://www.aloki.hu ● ISSN 1589 1623 (Print) ● ISSN 1785 0037 (Online)
DOI: http://dx.doi.org/10.15666/aeer/1704_85838598

Results

In total, 66 seedlings (1 set of control treatment, 5 sets of NS treatment and 5 sets of AS treatment) were analysed. The mean height of the *A. canescens* seedlings was 12.26 ± 1.90 cm and 10.43 ± 1.21 cm under NS and AS conditions (0-400 mM), respectively, after 20 days.

Effects of NS and AS on the growth of A. canescens seedlings

The growth of *A. canescens* seedlings under the AS treatment differed from that under the NS treatment at the same level of salinity (*Fig. 1*). A moderate NS concentration (i.e., 160 mM) caused a growth peak for both the shoots and roots. When the NS concentration reached 240 mM or greater (< 400 mM), the shoot growth rates did not significantly differ from those under the non-saline conditions. Under AS conditions, the peak growth of the both the shoots and roots occurred at the lowest AS concentration (80 mM). Further increases in the AS concentrations considerably reduced the growth rates, especially for the root RGR above the AS concentration of 240 mM, which had already significantly inhibited root growth.

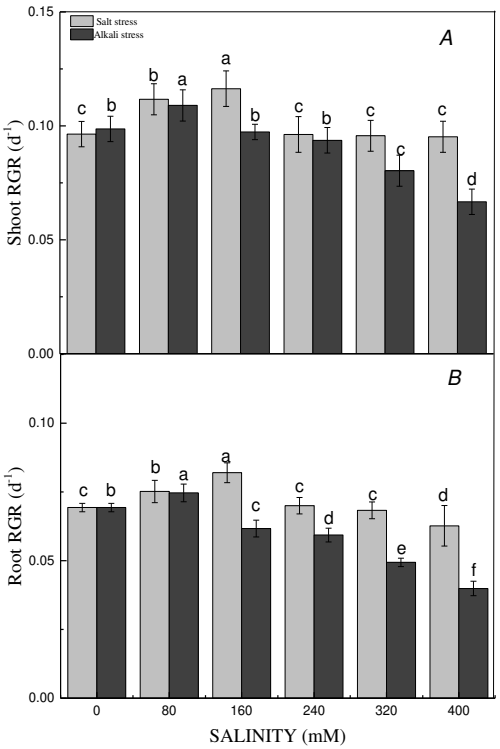

Figure 1. *The mean relative growth rates (RGRs) of the shoots (A) and roots (B) of A. canescens seedlings under different neutral salt (NS) and alkali salt (AS) concentrations (0-400 mM) after 20 days. The error bars indicate the 95% confidence intervals of the means. Different letters in the same panel indicate significant differences at $P < 0.05$ according to the Duncan test*

Effects of NS and AS on photosynthetic ability of A. canescens seedlings

The variation in leaf Pn as salinity increased under AS conditions differed from that under NS conditions (*Fig. 2*). The Pn significantly and continuously increased as

http://www.aloki.hu ● ISSN 1589 1623 (Print) ● ISSN 1785 0037 (Online)
DOI: http://dx.doi.org/10.15666/aeer/1704_85838598

salinity increased under NS conditions. Moderate AS concentrations increased the Pn; however, compared with that of the control, the Pn decreased dramatically when the AS concentration reached 320 mM or above. NS concentrations of 160 mM and AS concentrations of 80 mM resulted in highest leaf Gs values. The leaf Gs gradually decreased as salinity further increased. However, *A. canescens* seedlings subjected to NS and AS conditions presented different leaf Ci contents. When exposed to NS, the Ci continuously decreased as the salt concentration increased in NS treatment, and similar trend was observed under AS conditions. Furthermore, under AS conditions, after reaching the lowest content at 240 mM, the Ci sharply increased at 320 mM. Correspondingly, leaf WUE was significantly reduced at 160 mM but gradually increased as the salinity concentration increased. At salinity concentrations of 320 mM, the leaf WUE was higher under NS conditions than under AS conditions.

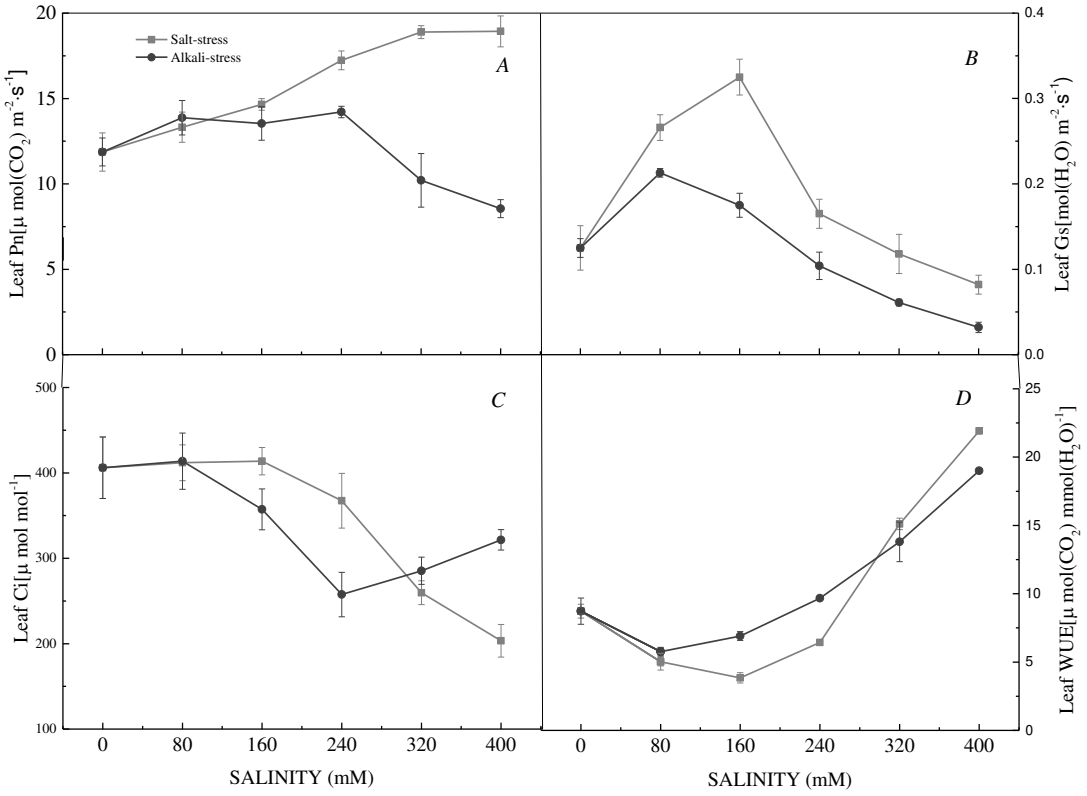

Figure 2. *Mean leaf net photosynthetic rate (Pn) (A), leaf stomatal conductance (Gs) (B), leaf intercellular CO_2 concentration (Ci) (C), and leaf water use efficiency (WUE) (D) of A. canescens seedlings under different NS and AS concentrations (0-400 mM) after 20 days. The error bars indicate the 95% confidence intervals of the means*

The leaf chl contents of the *A. canescens* seedlings under AS conditions were lower than those under NS conditions ($P < 0.05$) (*Table 1*). Leaves produced more Chla, Chlb and Car as the NS concentration increased (*Table 1*). At 400 mM NS, the leaf Chla and Chlb contents were 52% and 44% higher than those under non-saline soil conditions, respectively. However, the Chla, Chlb and Car of leaves responded differently to AS stress than to NS stress. The leaf chl content slightly increased as the AS concentration increased but significantly decreased at the AS concentration of 320 mM. Leaf Car were

http://www.aloki.hu ● ISSN 1589 1623 (Print) ● ISSN 1785 0037 (Online)
DOI: http://dx.doi.org/10.15666/aeer/1704_85838598

not affected by AS concentrations less than 320 mM; however, the Car increased at AS concentrations of 400 mM. The ratio of leaf Chla and Chlb increased as NS concentrations increased but decreased as AS concentrations increased.

Table 1. *The mean contents of photosynthetic pigments (Chl – chlorophyll, Car – carotenoids) [g kg^{-1} of fresh matter (FM)] in A. canescens seedlings under different NS and AS concentrations (0-400 mM) after 20 days*

Treatment	Salinity concentration [mM]	Chla [mg g^{-1} of dry matter (DM)]	Chlb [mg g^{-1} of DM]	Chla/Chlb	Car [mg g^{-1} of DM]
Control	0	1.42 ± 0.07 c	0.43 ± 0.01 b	3.30 ± 0.07 b	0.35 ± 0.01 b
NS	80	1.66 ± 0.21 c	0.47 ± 0.04 b	3.53 ± 0.12 b	0.35 ± 0.02 b
	160	1.85 ± 0.09 b	0.51 ± 0.02 b	3.62 ± 0.06 a	0.38 ± 0.06 a
	240	1.90 ± 0.14 b	0.54 ± 0.07 b	3.51 ± 0.11 b	0.39 ± 0.07 a
	320	1.99 ± 0.03 b	0.56 ± 0.06 a	3.55 ± 0.08 b	0.40 ± 0.05 a
	400	2.16 ± 0.12 a	0.62 ± 0.05 a	3.48 ± 0.05 b	0.41 ± 0.01 a
Control	0	1.42 ± 0.07 b	0.43 ± 0.01a	3.30 ± 0.07 a	0.35 ± 0.01b
AS	80	1.49 ± 0.05 b	0.44 ± 0.03a	3.38 ± 0.06 a	0.38 ± 0.06 b
	160	1.52 ± 0.06 a	0.45 ± 0.01 a	3.37 ± 0.11a	0.38 ± 0.07 b
	240	1.55 ± 0.11 a	0.43 ± 0.04 a	3.29 ± 0.03 a	0.39 ± 0.04 b
	320	1.29 ± 0.13 c	0.38 ± 0.07 b	3.14 ± 0.07 b	0.37 ± 0.01 b
	400	1.09 ± 0.01 c	0.35 ± 0.03 b	2.86 ± 0.08 c	0.47 ± 0.05 a

In each column, different letters indicate significant differences at $P < 0.05$ according to the Duncan test

Effects of NS and AS on the Na^+/K^+ of A. canescens seedlings

The Na^+ and K^+ contents in *A. canescens* seedlings were differently influenced by AS than by NS. The Na^+ content in the leaves, stems and roots under AS conditions was higher than that under NS conditions, with the exception of the roots in which the AS concentrations of 320 and 400 mM significantly inhibited root Na^+ absorption. At 400 mM NS, the leaf, stem, and root Na^+ contents were approximately 17.25-, 14.89- and 3.86-fold higher than those of the control plants, respectively. Compared with NS stress, AS stress had a more profound effect on reducing the K^+ content in all plant organs.

Under NS conditions, the K^+ content in shoot tissue remained relatively constant as salinity increased, whereas the root K^+ content decreased as salinity increased. Similarly, the K^+ content significantly decreased in the leaves and the roots as the AS concentration increased (*Fig. 3D-F*). The Na^+/K^+ ratios in the leaves and stems significantly increased as salinity increased, and a larger magnitude of increase occurred under NS conditions than under AS conditions. However, in the roots, the Na^+/K^+ ratio peaked at 240 mM under both NS and AS conditions, but the ratio decreased thereafter as the NS concentration increased (*Fig. 3G-I*).

Discussion

The RGR reflects the life-sustaining activities of plants and how they respond to stress (Wang et al., 2015). Our results showed that *A. canescens* can adjust to NS stress and AS stress. However, higher AS stress more strongly inhibits plant growth, which confirms our first hypothesis. We found that the growth rates peaked at moderate NS concentrations (160 mM), and growth was maintained in non-saline environments at NS

http://www.aloki.hu ● ISSN 1589 1623 (Print) ● ISSN 1785 0037 (Online)
DOI: http://dx.doi.org/10.15666/aeer/1704_85838598

concentrations up to 400 mM. Similarly, Pan et al. (Pan et al., 2016) reported that *A. canescens* grew better under 100 mM NaCl conditions than under non-saline conditions; however, the salinity level at which the peak growth occurred was lower than the level we recorded in our experiments (100 mM vs. 160 mM). This finding might be attributed to the salt mixtures (i.e., NaCl and Na_2SO_4) that we used (Qiu et al., 2003). In contrast, growth was inhibited by external AS treatment (> 320 mM). Previous reports have also shown greater deleterious effects from alkaline stress than salt stress on other plant species, such as *Aneurolepidium chinense*, *Chloris virgate*, *Suaeda corniculata*, (Shi and Wang, 2005; Yang et al., 2007, 2008). The different influence of both kinds of stress on plant growth might be due to the different underlying mechanisms. Plant survival in AS soil relies not only on the ability to address ion toxicity and low water potential but also on the ability to tolerate high pH (Shi and Wang, 2005; Yang et al., 2007, 2008). Adjustments of the pH outside the roots may represent another key physiological mechanism of alkalinity resistance. Under high AS conditions, a high pH around the roots could disrupt the governing ion balance and nutrient supplies; this disruption could lead to the inhibition of transmembrane electrochemical potential gradients in the root cells, which would negatively impact photosynthetic parameters and growth. Moreover, our results also demonstrated that the different responses of the photosynthetic ability (Shabala et al., 2014), ion homeostasis and osmotic adjustment capacity of the *A. canescens* seedlings represented the mechanisms that drove the stronger growth inhibition under AS conditions than under NS conditions (*Fig. 1*).

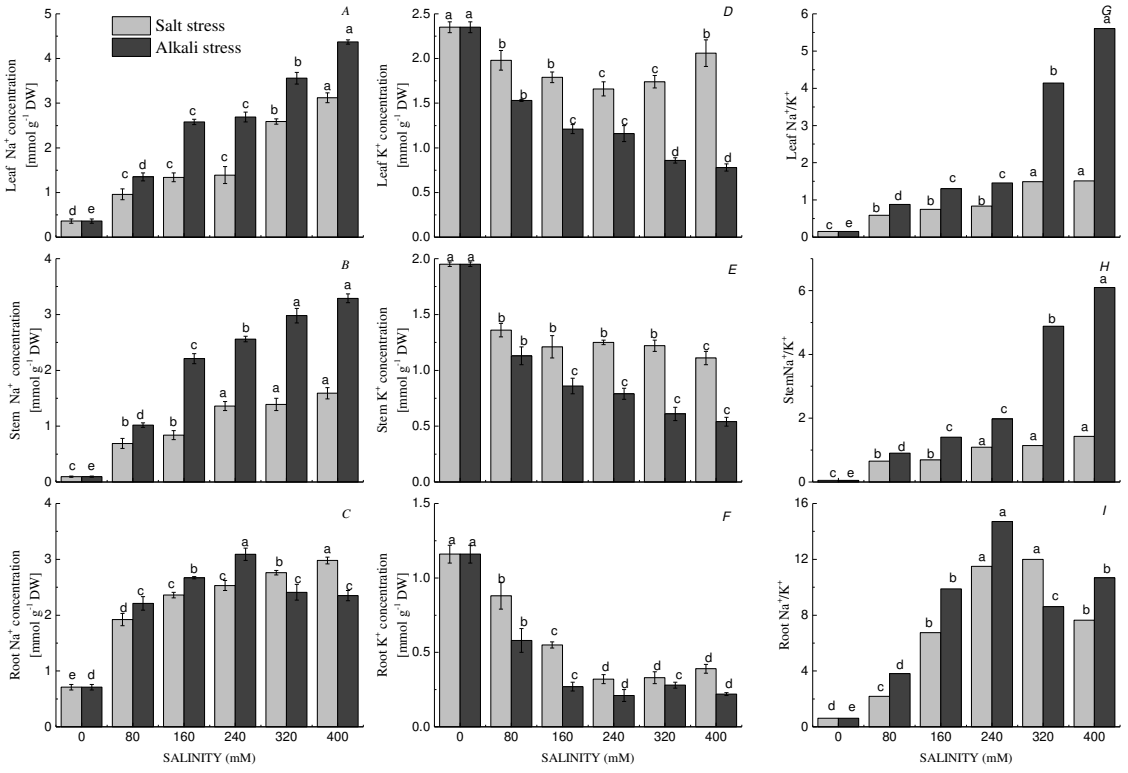

Figure 3. *The mean Na^+ and K^+ contents and Na^+/K^+ ratios in the leaves (A, D, G), stems (B, E, H) and roots (C, F, I) of A. canescens seedlings under different NS and AS concentrations (0-400 mM) after 20 days. The error bars indicate 95% confidence intervals of the means. Different letters in the same panel indicate significant differences at $P < 0.05$ according to the Duncan test*

http://www.aloki.hu ● ISSN 1589 1623 (Print) ● ISSN 1785 0037 (Online)
DOI: http://dx.doi.org/10.15666/aeer/1704_85838598

Plants must spend energy to adapt and exhibit resistance to stressful environments. The amount of energy spent directly depends on the photosynthetic ability (Wellburn and Lichtenthaler, 1984). The different growth rates of the *A. canescens* seedlings under the different treatments were basically the result of the Pn (Wang et al., 2004). In the present study, the Pn of the *A. canescens* seedlings significantly increased as both NS and AS concentrations increased, with the exception of that at 320 and 400 mM AS (Tsutsumi et al., 2015). This finding indicated that the *A. canescens* seedlings strongly tolerated more than just salt and alkaline stress (Shi and Wang, 2015). However, the AS more strongly inhibited the Pn of the plants than did the NS, which is in line with our second hypothesis.

The responses of the Pn might be mediated by the photochemical process, resistance to gas exchange and the assimilatory system. Under moderate stress, *A. canescens* seedlings can increase cyclical electron transport (Bukhov and Carpentier, 2004) and photorespiration (Parida and Das, 2005) as mechanisms for protection against salinity. Furthermore, *A. canescens* seedlings can cope with excessive salt by decreasing their stomatal aperture to increase leaf WUE and carboxylation (Guy et al., 1980; Megdiche et al., 2008). Our results showed that the Gs first increased but then decreased as salinity increased. In contrast (Ma et al., 2012) reported that the Pn and Gs of *Zygophyllum xanthoxylum* were positively correlated. This correlation might be due to the different properties of C_3 and C_4 plants (Yang et al., 2017). Moderate Na^+ concentrations may promote the C_4 photosynthesis of *A. canescens* by facilitating the activity of photosystem II (PSII), converting pyruvate to phosphoenolpyruvate, as well as other biochemical processes in the photosynthetic pathway (Chaves et al., 2011; Kronzucker et al., 2013). In this study, we also found that the contents of Chla, Chlb and Car increased as the NS concentration increased. Under moderate stress, the *A. canescens* seedlings might accumulate photosynthetic pigments and metabolically regulate chl to adapt to NS or AS conditions. In addition, Car are not only photosynthetic pigments but also endogenous antioxidants. Apart from the photosynthetic function of Car, they can also prevent membrane lipid peroxidation (Yang et al., 2008). In contrast to the stimulating effects of the high levels of neutral salinity on the Pn, high concentrations of AS significantly reduced the Pn. This result might be due to the dual effects of stimulation and inhibition caused by the AS (Zhao et al., 2013). At AS concentrations of 320 mM, the inhibitory effects gradually strengthened as salinity increased and exceeded the stimulatory effects. High pH values may injure the photosynthetic system, possibly inhibiting the transmembrane electrochemical potential of PSII. The sudden increase in Ci also indicated a damaged photosynthetic system when the AS concentrations reached 320 mM or greater (Yang et al., 2012). This Ci enhancement at AS concentrations of 320 mM was probably caused by non-stomatal limitations in accordance with the Farquhar gas exchange model. For example, limiting Rubisco carboxylase activity and destroying chloroplast structure could explain the reductions in the Pn, causing Ci to increase (Bethke and Drew, 1992; James et al., 2006). Salinity induces a wide range of perturbations in terms of chl concentration and chloroplast structure (Abdelkader et al., 2007). In our study, the reduced chl content after an initial increase as the AS concentration increased might also indicate a stronger inhibitory impact of AS compared with NS on chl synthesis, and Mg^{2+} precipitation (Shi and Zhao, 1997). Furthermore, Chlb is an important component of the light-harvesting complex. The decrease in Chlb in our results might also impair the light-harvesting complex structure and function, consequently weakening the light

http://www.aloki.hu ● ISSN 1589 1623 (Print) ● ISSN 1785 0037 (Online)
DOI: http://dx.doi.org/10.15666/aeer/1704_85838598

absorption ability of the chloroplasts. To summarize the above results, the inhibition of *A. canescens* seedling growth under AS conditions might result from a decrease in the Pn, which might be due to non-stomatal limitations and lower chl concentrations caused by a high pH (Zhao et al., 2014).

In saline soil, Na^+ is considered a major toxic ion. Low Na^+ and high K^+ contents in plant cells are preconditions to the maintenance of enzymatic processes (Munns and Tester, 2008). Thus, maintaining a relatively constant intracellular Na^+/K^+ homeostasis is crucial for plants to acclimate to salinity stress conditions (Zhu, 2003; Tang et al., 2014). In the present study, the Na^+ content was higher and the K^+ content was lower under AS conditions than under NS conditions (Volkov, 2015). The Na^+/K^+ ratios increased along the salinity gradient. However, compared with the AS treatment, the NS treatment resulted in Na^+/K^+ ratios that remained relatively constant as salinity increased. This finding confirmed our third hypothesis that AS more strongly influenced the Na^+ and K^+ contents in *A. canescens* seedlings than did NS (Zhang, 2013). The increased accumulation of Na^+ and decreased accumulation of K^+ represent mechanisms for adapting to salinity in *Atriplex* (Bajji et al., 1998; Bose et al., 2015; Ma et al., 2016). In the present study, the growth of *A. canescens* seedlings was positively affected by NS despite the increased Na^+ content, which might be attributed to two physiological processes. First, ion compartmentation enables plants to sequester a large quantity of excess Na^+ into epidermal bladder cells to avoid ion toxicity in organelles (Flowers and Colmer, 2008; Ding et al., 2010; Shabala, 2011, 2014). Second, *A. canescens* is capable of transporting K^+ instead of Na^+ from the roots to the stem or from the stem to the leaves to maintain a relatively constant cytosolic Na^+/K^+ ratio in the shoots (Flowers and Colmer, 2008; Pan et al., 2016). In contrast, under AS conditions, the over-accumulation of Na^+ had adverse impact on the *A. canescens* seedlings. This finding might be related to reduced Na^+ sequestration within vacuoles and weakened control over Na^+ transport within plant tissues driven by high pH values (Chen et al., 2009). These phenomena can thus lead to a significant increase in Na^+ concentration and can disrupt ionic balance in tissues. Furthermore, AS can also neutralize the number of protons and weaken the establishment of Na^+/H^+ antiporters in the plasma membrane, leading to the failure of Na^+ compartmentation (Munns and Tester, 2008; Pan et al., 2016). Our results further showed that the AS environment more strongly impeded the ability of plants to maintain K^+ uptake than did the NS environment. Similarly, excess Na^+ competes with K^+ uptake in many species. This phenomenon can inhibit K^+-dependent metabolic process, such as the induction of the photosynthetic ATPase enzyme, and can inhibit the participation of K^+ during carbohydrate biosynthesis, consequently resulting in oxidative stress (Munns and Tester, 2008; Flowers et al., 2015; Volkov, 2015). We demonstrated that the disrupted K^+ and Na^+ homeostasis due to the high pH value is probably responsible for the inhibited growth and reduced Pn of *A. canescens* seedlings in AS environments.

Conclusion

Our results indicated that *A. canescens* seedlings can adapt to NS stress and AS stress though strengthening the photosynthetic ability and maintaining ionic homeostasis capacity. However, at higher concentrations (> 240 mM), alkali salinity more strongly inhibited plant performance than did neutral salinity, and the change was associated with a decrease in photosynthetic ability and damage to Na^+/K^+ homeostasis under

http://www.aloki.hu ● ISSN 1589 1623 (Print) ● ISSN 1785 0037 (Online)
DOI: http://dx.doi.org/10.15666/aeer/1704_85838598

alkali salinity. *A. canescens* as an exotic tree species can used to achieve the ecological recovery and city afforestation for moderate salinization areas of northwest China. In this study, we compared the growth responses of *Atriplex canescens* to salt and alkaline stress under an optimal soil water condition. In the future, experiments may be conducted under different soil water conditions.

Acknowledgements. This study was funded by "Research and demonstration on saline-alkali land afforestation in Qaidam basin" (grant number 2014-NK-A4-4).

Conflict of interests. The authors declare that they have no conflict of interest.

Compliance with ethical standards. This article does not contain any studies with human participants or animals performed by any of the authors. Informed consent was obtained from all individual participants included in the study.

REFERENCES

[1] Abdelkader, A. F., Aronsson, H., Solymosi, K. et al. (2007): High salt stress induces swollen prothylakoids in dark grown wheat and alters both prolamellar body transformation and reformation after irradiation. – J Exp Bot 58: 2553-2564.

[2] Al-Turki, T. A., Omer, S., Ghafoor, A. (2000): A synopsis of the genus *Atriplex* L. (Chenopodiaceae) – Feddes Repert 111: 261-293.

[3] Araùjo, Desilveira, S. A. M., Silveira, Almeida, J. A. G. et al. (2006): Salinity tolerance of halophyte *Atriplex nummularia* L. grown under increasing NaCl levels. – Revista Brasileira de Engenharia Agricola e Ambiental. –Agriambi 10: 65-66.

[4] Ayala, F., O'Leary, J. W., Schumaker, K. S. (1996): Increased vacuolar and plasma membrane H^+-ATPase activities in *Salicornia bigelovii Torr.* in response to NaCl. – Journal of Experimental Botany 47(1): 25-32.

[5] Bajji, M., Kinet, J. M., Lutts, S. (1998): Salt stress effects on roots and leaves of *Atriplex halimus* L. and their corresponding callus cultures. – Plant 137: 131.

[6] Bao, A. K., Du, B. Q., Touil, L. et al. (2016): Co-expression of tonoplast Cation/H^+ antiporter (NHX) and H^+-pyro phosphatase (H^+-PPase) from xerophyte *Zygophyllum xanthoxylum* improves alfalfa plant growth under salinity, drought, and field conditions. – Plant Biotechnol. J. 14: 964-975.

[7] Ben Hassine, A., Ghanem, M. E., Bouzid, S., Lutts, S. (2008): An inland and a coastal population of the Mediterranean xero-halophyte species *Atriplex halimus* L. differ in their ability to accumulate proline and glycinebetaine in response to salinity and water stress. – J. Exp. Bot 59: 1315-1326.

[8] Benzarti, M., Ben Rejeb, Debez, A. et al. (2013): Environmental and Economical Opportunities for the Valorisation of the Genus *Atriplex:* New Insights. – In: Hakeem, K., Ahmad, P., Ozturk, M. (eds.) Crop Improvement. – Springer, New York, pp. 441-457.

[9] Benzarti, M., Rejeb, K. B., Debez, A. et al. (2012): Photosynthetic activity and leaf anti oxidative responses of *Atriplexportulacoides*– subjected to extreme salinity. – Acta Physiologiae Plantarum 34: 1679-1688.

[10] Benzarti, M., Rejeb, K. B., Messedi, D. et al. (2014): Effect of high salinity on *Atriplex portulacoides*: growth, leaf water relations and solute accumulation in relation with osmotic adjustment. – South African Journal of Botany 95: 70-77.

[11] Bethke, P. C., Drew, M. C. (1992): Stomatal and non-stomatal components to inhibition of photosynthesis in leaves of *Capsicum annuum* during progressive exposure to NaCl salinity. – Plant Physiol 99: 219-226.

http://www.aloki.hu ● ISSN 1589 1623 (Print) ● ISSN 1785 0037 (Online)
DOI: http://dx.doi.org/10.15666/aeer/1704_85838598

[12] Bose, J., Rodrigo-Moreno, A. Lai et al. (2015): Rapid regulation of the plasma membrane H^+-ATPase activity is essential to salinity tolerance in two halophyte species, *Atriplex lentiformis* and *Chenopodium quinoa*. – Ann. Bot 115: 48181.
[13] Bouchenak, F., Henri, P., Bebrebiha, F. Z. et al. (2012): Differential responses to salinity of two *Atriplex halimus* populations in relation to organic solutes and antioxidant systems involving thiol reductases. – J. Plant Physiol 169: 1445-1453.
[14] Bukhov, N., Carpentier, R. (2004): Alternative photosystem I-driven electron transport routes: mechanisms and functions. – Photosynthesis Research 82: 17-33.
[15] Campbell, S. A., Nishio, J. N. (2000): Iron deficiency studies of sugar beet using an improved sodium bicarbonate-buffered hydroponics growth system. – J. Plant Nutr 23: 741-757.
[16] Chaves, M. M., Costa, J. M., Saibo, N. M. (2011): Recent advances in photosynthesis under drought and salinity. – Adv. Bot. Res. 57: 49-104.
[17] Chen, W., Cui, P., Sun, H. et al. (2009): Comparative effects of salt and alkaline stresses on organic acid accumulation and ionic balance of sea buckthorn (*Hippophaer hamnoides* L). – Industrial Crops & Products 30(3): 351-358.
[18] Debez, A., Koyro, H. W., Grignon, C. et al. (2008): Relationship between the photosynthetic activity and the performance of *Cakile maritima* after long-term salt treatment. – Physiol Plant 133(2): 373-385.
[19] Ding, F., Yang, J. C., Yuan, F. et al. (2010): Progress in mechanism of salt excretion in recreto halopytes. – Front. Biol 5(2): 164-170.
[20] Elshma, S. (1996): Comparative effect of sodium carbonate, sodium sulphate, and sodium chloride on the growth and related metabolic activities of pea plants. – J. Plant Nutr 19: 717-728.
[21] Flowers, T. J. (2004): Improving crop salt tolerance. – J. Exp. Bot 55: 307-319.
[22] Flowers, T. J., Colmer, T. D. (2008): Salinity tolerance in halophytes. – New Phytol 179: 945-963.
[23] Flowers, T. J., Galal, H. K., Bromham, L. (2010): Evolution of halophytes: multiple origins of salt tolerance in land plants. – Funct. Plant Biol 37: 604-612.
[24] Flowers, T. J., Munns, R. Colmer, T. D. (2015): Sodium chloride toxicity and the cellular basis of s alt tolerance in halophytes. – Ann. Bot 115: 419-431.
[25] Ge, Y., Li, J. D. (1990): A preliminary study on the effects of halophytes on salt accumulation and desalination in the soil of Songnen Plain, northeast China. – Acta Pratacult Sin 70-76.
[26] Ghoulam, C., Foursy, A., Fares, K. (2002): Effects of salt stress on growth, inorganic ions and proline accumulation in relation to osmotic adjustment in five sugar beet cultivars. – Environ Exp Bot 47: 39-50.
[27] Glenn, E. P., Brown, J. J. (1999): Effects of soil salt levels on the growth and water use efficiency of *Atriplex canescens* (Chenopodiaceae) varieties in drying soil. – Am. J. Bot 85: 10-16.
[28] Glenn, E. P., Pfister, R., Briwn, J. J. et al. (1996): Na and K accumulation and salt tolerance of *Atriplex canescens* (Chenopodiaceae) genotypes. – Am. J. Bot 83: 997-1005.
[29] Glenn, E. P., Olsen, M., Frye, R. et al. (2010): How much sodium accumulation is necessary for salt tolerance in subspecies of the halophyte *Atriplex canescens.* – Plant Cell Environ 17: 711-719.
[30] Gong, B., Zhang, C. J., Li, X. et al. (2014): Identification of NaCl and $NaHCO_3$ stress responsive proteins in tomato roots using iTRAQ-based analysis. – Biochem. Biophys. Res. Commun 446: 417-422.
[31] Guy, R. D., Reid, D. M., Krouse, H. R. (1980): Shifts in carbon isotope ratios of two C3, halophytes under natural land artificial conditions. – Oecologia 44: 241-247.

http://www.aloki.hu ● ISSN 1589 1623 (Print) ● ISSN 1785 0037 (Online)
DOI: http://dx.doi.org/10.15666/aeer/1704_85838598

[32] Hamdia, M., Shaddad, H. M. A., Ellogamad, A. (1996): Comparative effect of sodium carbonate, sodium sulphate, and sodium chloride on the growth and related metabolic activities of pea plants. – J. Plant Nutr 19(5): 717-728.
[33] Hao, G. Y., Lucero, M. E., Sanderson, S. C. et al. (2013): Polyploidy enhances the occupation of heterogeneous environments through hydraulic related trade-offs in *Atriplex canescens* (Chenopodiaceae). – New Phytol 197: 970-978.
[34] Hassine, A. B., Lutts, S. (2010): Differential responses of saltbush *Atriplex halimus* L. exposed to salinity and water stress in relation to senescing hormones abscisic acid and ethylene. – J. of Plant Physiol 167: 1448-1456.
[35] Hassine, A. B., Ghanem, Bouzid, S. et al. (2008): An inland and a coastal population of the Mediterranean xero-halophyte species *Atriplex halimus* L. differ in their ability to accumulate proline and glycine betaine in response to salinity and water stress. – J. Exp. Bot 59: 1315.
[36] James, R. A., Munns, R., Caemmerer, S. V. et al. (2016): Photosynthetic capacity is related to the cellular and subcellular partitioning of Na^+, K^+ and Cl^- in salt-affected barley and durum wheat. – Plant Cell Environ 29: 2185-2197.
[37] Jamil, F., Arshad, R., Ali, M. A. (2018): Design, fabrication and evaluation of rotary hot-air dryer for the value addition of fruit waste. – Earth Sciences Pakistan 2(2): 07-11.
[38] Kalaji, H. M., Jajoo, A. et al. (2016): Chlorophyll a fluorescence as a tool to monitor physiological status of plants under abiotic stress conditions. – Acta Physiol. Plant 38: 102. https://doi.org/10.1007/s11738-016-2113-y.
[39] Kawanabe, S., Zhu, T. C. (1991): Degeneration and conservation of *Aneurolepidium* chinense grassland in Northern China. – J. Jap. Grassland Soc 37: 91-99.
[40] Kingsbury, R. W., Epstein, E. et al. (1984): Physiological responses to salinity in selected lines of wheat. – Plant Physiol 74: 417-423.
[41] Kong, D. S. (2013): Morphological characteristics and eco-physiological adaptability of *Atriplex canescens*: a review. – Chin. J. Ecol 32: 210-216.
[42] Kronzucker, H. J., Coskun, D., Schulze, L. M. et al. (2013): Sodium as nutrient and toxicant. – Plant Soil 369: 1-23.
[43] Kumar, R. (2018): Comparison of instruction scheduling and register allocation for MIPS and HPL -PD architecture for exploitation of instruction level parallelism. – Engineering Heritage Journal 2(2): 04-08.
[44] Li, P. H., Zhang, H. Wang, B. S. (2003): Ionic homeostasis of plant under salt stress. – Acta Bot Boreal-Occident Sin 23: 1810.
[45] Lichtenthaler, H. K. (1987): Chlorophylls and carotenoids: pigments of photosynthetic biomembranes. – Methods in Enzymology 148: 350-382.
[46] Ma, Q., Yue, L. J., Zhang, J. L. et al. (2012): Sodium chloride improves photosynthesis and water status in the succulent xerophyte *Zygophyllumx anthoxylum*. – Tree Physiol 32: 4-13.
[47] Ma, Q., Bao, A. K., Chai, W. W. et al. (2016): Transcriptomic analysis of the succulent xerophyte Zygophyllum xanthoxylumin response to salt treatment and osmotic stress. – Plant Soil 402(1-2): 343-361.
[48] Madhav, S., Ahamad, A., Kumar, A., Kushawaha, J., Singh, P., Mishra, P. K. (2018): Geochemical assessment of groundwater quality for its suitability for drinking and irrigation purpose in rural areas of Sant Ravidas Nagar (Bhadohi), Uttar Pradesh. – Geology, Ecology, and Landscapes 2(2): 127-136.
[49] Marttnez, J. P., Lutts, S., Schanck, A. et al. (2004): Is osmotic adjustment required for water-stress resistance in the Mediterraneanshrub *Atriplex halimus* L? – Plant Physiol 161: 10411.
[50] Megdiche, W., Hessini, K., Gharbi, F. et al. (2008): Photosynthesis and photosystem 2 efficiency of two salt-adapted halophytic seashore *Cakilemaritima* ecotypes. – Photo-synthetica 46: 410-419.

http://www.aloki.hu ● ISSN 1589 1623 (Print) ● ISSN 1785 0037 (Online)
DOI: http://dx.doi.org/10.15666/aeer/1704_85838598

[51] Munns, R., Tester, M. (2008): Mechanisms of salinity tolerance. Annu. Rev. – Plant Biol 59: 651-681.
[52] Nemat-Alla, M. M., Khedr, A. H. A., Serag, M. M. et al. (2011): Physiological aspects of tolerance in *Atriplexhalimus* L. to NaCl and drought. – Acta Physiol. Plant 33: 547-557.
[53] Niu, S. Q., Li, H. R., Paré, P. W. et al. (2016): Induced growth promotion and higher salt tolerance in the halophyte grass *Puccinellia tenuiflora* by beneficial rhizobacteria. – Plant & Soil 407(1-2): 1-14.
[54] Nkwuda, N. G., Theophine, M. A., Okogwu, O. I. (2019): Impacts of rock mineralization and poor sanitary system on borehole waters quality and the health implications. – Earth Sciences Pakistan 3(1): 10-13.
[55] Nwankwo, C., Nwankwoala, H. O. (2018): Gully erosion susceptibility mapping in Ikwuano local government area of Abia State using GIS techniques. – Earth Sciences Malaysia 2(1): 08-15.
[56] Ogunyele, A. C., Obaje, S. O., Akingboye, A. S. (2018): Lithostructural relationships and petrogenetic affinities of the basement complex rocks around Okpella, Southwestern Nigeria. – Earth Sciences Malaysia 2(1): 29-36.
[57] Ortiz-Dorda, J., Martinez-Mora, C., Correal, E. et al. (2005): Genetic structure of *Atriplex halimus* populations in the Mediterranean Basin. – Ann Bot 95: 827-834.
[58] Pan, Y. Q., Guo, H., Wang, S. M. et al. (2016): The photosynthesis, Na^+/K^+ homeostasis and osmotic adjustment of *Atriplex canescensin* response to salinity. – Frontiers in Plant Science 7(848).
[59] Parida, A. K., Das, A. B. (2005): Salt tolerance and salinity effects on plants: a review. – Ecotoxicology and Environmental Safety 60: 324-349.
[60] Peterson, J. L., Ueckert, D. N., Potter, R. L. et al. (1987): Ecotypic variation in selected fourwing saltbush populations in western Texas. – J. Range Manage. Arch 40: 361-366.
[61] Qiu, N., Lu, Q., Lu, C. (2003): Photosynthesis, photosystem II efficiency and the xanthophyll cycle in the salt-adapted halophyte *Atriplex centralasiatica*. – New Phytologist 159: 479-486.
[62] Raj, N. J., Prabhakaran, A. (2018): Lineaments of Kodaikanal-Palani massif, Southern Granulitic Terrain of Tamil Nadu, India: a study using SRTM DEM and LANDSAT satellite's OLI sensor's FCC. – Geology, Ecology, and Landscapes 2(3): 188-202.
[63] Rajendran, Y., Mohsin, R. (2018): Emission due to motor gasoline fuel in reciprocating lycoming O -320 engine in comparison to aviation gasoline fuel. – Environment & Ecosystem Science 2(2): 20-24.
[64] Redondo-Gómez, S., Figueroa, M. E. (2007): Growth and photosynthetic responses to salinity of the salt-marsh shrub *Atriplex portulacoides*. – Annals of Botany 100: 55-63.
[65] Roosta, H. R., Karimi, H. R. (2002): Effects of alkali-stress on ungrafted and grafted cucumber plants using two types of local squash as rootstock. – J. Plant Nutr 35: 1843-1852.
[66] Sa, R. L., Liu, J. H., Liu, W. et al. (2004): Cation-responsive mechanisms of Oats to alkaline stress. – Acta Agron. Sin 40: 362-368.
[67] Sergey, S. (2013): Learning from halophytes: physiological basis and strategies to improve abiotic stress tolerance in crops. – Ann. Bot 112: 1209-1221.
[68] Shabala, S., Mackay, A. (2011): Ion transport in halophytes. – Adv. Bot. Res 57: 151-199.
[69] Shabala, S., Bose, J., Hedtich, R. (2014): Salt bladders: do they matter? – Trends Plant Sci 19: 687-691.
[70] Shi, D. C., Sheng, Y. (2005): Effect of various salt-alkaline mixed stress conditions on sunflower seedlings and analysis of their stress factors. – Environ Exp Bot 54: 8-21.
[71] Shi, D. C., Wang, D. (2005): Effects of various salt-alkali mixed stresses on *Aneurolepidium* chinense (Trin.) Kitag. – Plant Soil 271: 15-26.

http://www.aloki.hu ● ISSN 1589 1623 (Print) ● ISSN 1785 0037 (Online)
DOI: http://dx.doi.org/10.15666/aeer/1704_85838598

[72] Shi, D. C., Yin, L. J. (1993): Difference between salt (NaCl) and alkaline (Na_2CO_3) stresses on *Puccinellia tenuiflora* (Griseb.) Scribn. et Merr. plants. – Acta Bot. Sin. 35: 144-149.
[73] Shi, D. C., Zhao, K. F. (1997): Effects of NaCl and Na_2CO_3 on growth of *Puccinelliatenuiflora* and on present state of mineral elements in nutrient solution. – Actapratacu. Sin 6: 51-61.
[74] Sufiyan, I., Zakariya, R., Yaacob, R. (2018): Delineation of flood risk zones and 3D modeling in Terengganu River catchment using GIS and SWAT. – Environment & Ecosystem Science 2(2): 01-05.
[75] Tang, X. L., Mu, X., Wang, H. et al. (2014): Global plant-responding mechanisms to salt stress: physiological and molecular level sand implications in biotechnology. – Crit. Rev. Biotechnol 35: 425-437.
[76] Tanji, K, K. (2002): Salinity in the Soil Environment. – In: Läuchli A., Lüttge U. (eds.) Salinity: Environment - Plants - Molecules. Springer, Dordrecht, pp. 21-51.
[77] Tianlei, W. (2019): Nonlinear control strategies and planning for underactuated overhead cranes. – Engineering Heritage Journal 3(1): 09-12.
[78] Tsutsumi, K., Yamada, N. et al. (2015): Differential accumulation of glycine betaine and choline monooxygenase inbladder hairs and lamina leaves of *Atriplexgmelini* under high salinity. – Plant Physiol 176: 101-107.
[79] Volkov, V. (2015): Salinity tolerance in plants. Quantitative approach to ion transport starting from halophytes and stepping to genetic and proteinengineering for manipulating ion fluxes. – Front. Plant Sci 6: 873.
[80] Wang, P., Guo, Q., Wang, Q., Zhou, X. R. et al. (2015): PtAKT1 maintains selective absorption capacity for K^+over Na^+ in halophyte *Puccinellia tenuiflora* under salt stress. – Acta Physiol. Plant 37: 100.
[81] Wang, S., Wan, C., Wang, Y. et al. *(2004):* The characteristics of Na^+, K^+ and free proline distribution in several drought-resistant plants of the Alxa Desert, China. – Journal of Arid Environments 56: 525-539.
[82] Wellburn, A. R., Lichtenthaler, H. (1984): Formulae and Program to Determine Total Carotenoids and Chlorophylls A and B of Leaf Extracts in Different Solvents. – In: Sybesma C. (ed.) Advances in Photosynthesis Research. Advances in Agricultural Biotechnology. Vol 2. Springer, Dordrecht, pp. 9-12.
[83] Yan, K., Shao, H. (2013): Physiological adaptive mechanisms of plants grown in saline soil and implications for sustainable saline agriculture in coastal zone. – Acta Physiol. Plant 35: 2867-2878.
[84] Yang, C., Chong, J., Li, C. et al. (2007): Osmotic adjustment and ion balance traits of an alkali resistant halophyte *Kochia sieversiana*, during adaptation to salt and alkali conditions. – Plant and Soil 294: 263-276.
[85] Yang, C. W. (2009): Comparative effects of salt-stress and alkali-stress on the growth, photosynthesis, solute accumulation, and ion balance of barley plants. – Photosynthetica 47: 79-86.
[86] Yang, C. W., Chong, J., Li, C. et al. (2007): Osmotic adjustment and ion balance traits of an alkali resistant halophyte *Kochia sieversiana* during adaptation to salt and alkali conditions. – Plant Soil 294: 263-276.
[87] Yang, C. W., Jianaer, A., Li, C. Y. et al. (2008): Comparison of the effects of salt-stress and alkali-stress on photosynthesis and energy storage of an alkali-resistant halophyte *Chloris virgate*. – Photosynthetica 46: 273-278.
[88] Yang, C. W., Zhao, N., Xu, C. M. et al. (2012): Regulation of ion homeostasis in rice subjected to salt and alkaline stresses. – Aust. J. Crop Sci 6: 724-731.
[89] Zhang, J. F., Song, Y. M., Xing, S. J. et al. (2002): Saline soil amelioration and forestation techniques. – Journal of Northeast Forestry University 30(6): 124-129.

http://www.aloki.hu ● ISSN 1589 1623 (Print) ● ISSN 1785 0037 (Online)
DOI: http://dx.doi.org/10.15666/aeer/1704_85838598

[90] Zhang, W. P., Yang, J. Z., Fang, Y. L., Chen, H. Y., Mao, Y. H., Kumar, M. (2017): Analytical fuzzy approach to biological data analysis, – Saudi Journal of Biological Sciences 24(3): 563-573.
[91] Zhang, X., Wei, L., Wang, Z. et al. (2013): Physiological and molecular features of *Puccinellia tenuiflora* tolerating salt and alkaline-salt stress. – J. Integr. Plant Biol 55: 262-276.
[92] Zhao, Y. Y., Lu, Z., He, L. (2014): Effects of saline-alkaline stress on seed germination and seedling growth of *Sorghum bicolor* (L.) Moench. – Appl. Biochem. Biotech 173: 1680-1691.
[93] Zhu, J. K. (2003): Regulation of ion homeostasis under salt stress. – Plant Biol 6: 441-445.
[94] Zhu, J. K. (2014): Plant salt tolerance. – Trends Plant Sci 6: 66-71.

http://www.aloki.hu ● ISSN 1589 1623 (Print) ● ISSN 1785 0037 (Online)
DOI: http://dx.doi.org/10.15666/aeer/1704_85838598

SOIL WATER REPELLENCY IN CHINA AND ISRAEL: SYNTHESIS OF OBSERVATIONS AND EXPERIMENTS

LIU, F.* – ZHAN, Y.*

Faculty of Forestry, Central South University of Forestry and Technology
Changsha, Hunan 410004, China

**Corresponding authors*
e-mail: Liufl680@126.com; phone: +86-1597-4170-413 (Liu, F.)
e-mail: 752523727@qq.com; phone: +86-1597-4219-341 (Zhan, Y.)

(Received 8th Mar 2019; accepted 21st May 2019)

Abstract. Study of soil water repellency (SWR) has been very systematized in Europe and America but underdeveloped in Asia. This study aims to comprehensively and systematically analyze SWR in China and Israel, and to contribute to the knowledge on SWR in the world. We collected all documents about SWR that were published in China. Research sites were all over the China and typical areas of Israel. 4647 datasets were obtained from these documents. We have done a rounded analysis based on the influencing factors like soil type, soil depth, land type, interference type. Through the data collection and analysis, we found most of the soil in China and Israel is water-repellent, and almost all of the soil types are water-repellent. However, most of the soil types only have low water repellency. The level of soil water repellency of different soil types is different. The soil in forest ecosystem generally has a higher water repellency than that in the non-forest ecosystem. SWR will increase after the interference of water or fire, and the effect of water is more significant. The results provide theoretical basis for soil improvement and vegetation restoration in China and Israel even the World.
Keywords: *water repellency, fire disturbance, soil type, forest ecosystem, external disturbance*

Introduction

Soil water repellency has perplexed people for almost one century. Soil water repellency is mainly caused by organic hydrophobic matter which originated from plants, external disturbance, and microbial activities, resulting soil hard to be wetted or wet soil difficult to be wetted again after drying. It is pervasive and prevalent to evaluate SWR by Bisdom classification (1993) (Bisdom et al., 1993; Sunny et al., 2018), using water drop penetration time (WDPT): wettable soil (<5 s), good for wettability; slightly water repellent (5-60 s), decreasing water holding capacity (Doerr et al., 2000; Hossain et al., 2019); strongly water repellent (60-600 s), resulting uneven water infiltration and potential risk to groundwater polluted (Bogner et al., 2008; Ali et al., 2018); severely water repellent (600-3600 s), and extremely water repellent (>3600 s), causing severe soil erosion, environmental damage, and economic loss (Craswell and Lefroy, 2001; Sharjeel et al., 2019).

The climate of China and Israel are different, there is no Mediterranean climate in China. China and Israel are completely different in rainfall characteristics but both of their water resources are uneven distribution. SWR is an important index in soil health evaluation system. The water conservation capacity of soil is weak because of the SWR; this lead to the water cannot be conservation well by soil. China and Israel are facing available water crisis. There have no researches evaluated the soil quality of China and Israel according to the SWR. Our research filled the gap and supplied data of SWR of China and Israel for world SWR database. And our research can also provide reference to soil quality evaluate in other areas.

http://www.aloki.hu ● ISSN 1589 1623 (Print) ● ISSN 1785 0037 (Online)
DOI: http://dx.doi.org/10.15666/aeer/1704_85998614

China, as a principle Asian country, the SWR researches began in the 1990s (Ebelhar et al., 2008; Tao, 2018). The scientists paid little attention on the correlative studies which started late and lacked of deep research. Only a few simple introductions that lacked of standard, unified and comprehensive analysis could be found in the existing documents discussing about SWR determination methods (Crockford et al., 1991; Liang and Wenshun, 2019), the influential factors of desert SWR (Dahlgren et al., 2008) and the influences of fire disturbance on forest SWR (Chesworth et al., 2008) etc. All terrains types and agrotypes could be discovered in China where had a large range of altitude (-154-8844.43 m), a high precipitation disparity of different regions (5.9-1600 mm), different climate and a big regional heterogeneity. Israel has typical Mediterranean climate and the research of SWR in desert soil in Israel is developed. The comprehensive and objective research on Chinese and Israel SWR hasn't been reported.

By collecting the existing research data, for the first time, the Chinese and Israel's SWR records were combined and analyzed, and unified the calibration of the data unit and classification by utilizing various international standards. Research 1) the overall distribution characteristics of Chinese and Israel's SWR; and 2) the integrated characteristics of Chinese and Israel's SWR.

Materials and Methods

The database

This study had collected and sorted out all published SWR documents in China. The data screening work had complied with the following requirements: (1) The experiment design had no obvious flaws. This study did not probe into the uncertainty of different measurement, only took WDPT as a measurement and quantitative index of SWR. (2) Include WDPT measurement data. (3) The properties of the variables in the experiment were related to the temporal or spatial distribution patterns, the control experiment variables like the contact angle between soil and water were excluded. We extracted original information such as geographic information (longitude, latitude, altitude and so on), time (experimental time), land use (vegetation cover type, vegetation type, vegetation composition etc.), soil information (soil type, soil depth etc.), and interference (interference types) from each document. Moreover, some literature data were published in the form of pictures. According to the ordinary way, we intercepted these pictures and employed image analysis software (DigitizeIt, version 1.5.8 http://www.digitizeit.de/) to digitize the data and recover it to the raw data. Great efforts were devoted to data standardized after extraction: (1) WDPT data was unified in second. (2) As for the researches did not mention the specific experiment time, we could reasonably calculate the experiment time according to the data published time. (3) The classification of the land use and ecological regions were based on Hou Hsioh-yu's classification of natural ecological regions in China in 1988. (4) The identification and classification of soil types referred to the soil classification system of the Food and Agriculture Organization of the United Nations (FAO). Compared the soil samples with the data in Chinese Soil Database and the World Soil Database on the basis of the soil background and soil name of those sampling sites to identify the standard names, then contrasted with FAO 85 and FAO 90 to screen and determine the accurate classification of the sample soil by the FAO standard.

http://www.aloki.hu ● ISSN 1589 1623 (Print) ● ISSN 1785 0037 (Online)
DOI: http://dx.doi.org/10.15666/aeer/1704_85998614

In this study, we arranged 4647 data regarding with all SWR data in China and Israel. At first, We mapped and visualized the spatial and temporal distribution of WDPT data there (*Fig. 1, Fig. S1*). The research sites were across Chinese provinces in the western, northern, central, southern area and Israel and the research time were span from the earliest WDPT reports in 2009 to 2016.

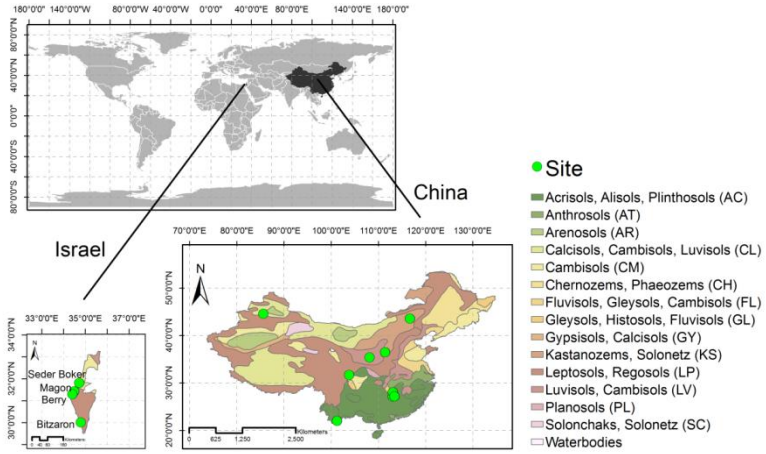

Figure 1. *Geographic distributions and sites of data collected. The map on the top is the location of sampling countries in the world. Two maps below are location and Soil backgrounds of sampling sites in China and Israel. Green points represent the location of the sampling sites of data. The background of the soil type distributions were obtainable from the FAO web page (http://www.fao.org/AG/agL/agll/wrb/soilres.stm), to process soil map backgrounds using ArcGIS9.3 at a scale of 1:25 000 000(WRB2003). The soil classification follows world reference base for soil resources (FAO 1990)*

4 different environment gradients were set: (1) Land use, including forest (n=970) and non - forest (grassland and farmland, n=3673), had 8 different natural ecological periods and more than 20 forest types such as Cunninghamia lanceolata plantation, Pinus massoniana plantation and Schima superba mixed forest (*Table 1*). (2) Soil type, contained 8 soil types, that were Aeolian soils (n=288), Calcisols (n=72), Red earth (n=62), Red-yellow earth (n=260), Gray-brown desert soil (n=100), Yellow-brown earth (n=3529), Castano-cinnamon soil (n=44), Regosols (n=288) (*Table 2*). (3) Soil depth, can be reduced to 2 levels, topsoil (0-5cm, n=4439) and subsoil (depth> 5cm, n=204). (4) Processing gradients, no processing (n=3807), sewage irrigation (n=528), fire disturbance (n=308).

Statistical analysis

In this study, WDPT data were logarithmically (Log10WDPT) normalized. We divided the data into five grades according to the SWR grading standards: wettable (<5 s), slightly water repellent (5-60 s), strongly water repellent (60-600 s), severely water repellent (600-3600 s), extremely water repellent (>3600 s). The data were differentiated by different environmental factors (such as land use, soil type, soil depth and interference type) and the impacts of different environmental factors on SWR were analyzed. We sorted the data with Microsoft Excel 2010 at first, and did the further description and analysis job with IBM SPSS Statistics21.0, finally drew the charts with Origin8.0.

http://www.aloki.hu ● ISSN 1589 1623 (Print) ● ISSN 1785 0037 (Online)
DOI: http://dx.doi.org/10.15666/aeer/1704_85998614

Table 1. *Land use, location and additional details about data collection*

Category	Natural ecological zone*	Site	Content	Reference
Forests	Eastern subtropical evergreen broad - leaved forest ecological zone	Gaojian forest in Zhuzhou city,Huangfeng bridge forest in Zhuzhou City Youxian County, Zhaoshan demonstration area in Xiangtan city	*Chinese fir* plantation, *Pinus massoniana* plantation, Pinus massoniana and coniferous and broad-leaved mixed forest; *Sassafras fir* wood mixed forest; *Liquidambar formosana* secondary forest; *Pinus massoniana* mixed forest; *Schima superba* mixed forest; *Pinus massoniana*	
	Western transitional tropical, tropical monsoon rain forest ecological zone	Tropical rainforest ecological station, Chinese Academy of Sciences Xishuangbanna Tropical Botanical Garden	Tropical original seasonal rain forest, artificial rubber forest	
	others	Berry, Bitzaron, Magon, Seder Boker	Economic forest	
Grassland & Farmland	Warm temperate forest grassland, clustered grass grassland ecological zone	Tielongwan forest in Yichuan County	*Populus davidiana*, *Artificial Pinus tabulaeformis, Hippophae rhamnoides, yellow thorns, pear seabuckthorn mixed forest, Robinia pseudoacacia, Agropyron,* etc.	
	Temperate dwarf semi - arid desert ecological zone	Manas River Basin in Xinjiang Uygur Autonomous Region	Economic forest, no forest land	
	Temperate forest grassland, clustered grass grassland ecological zone	Yangcao sample site	Temperate grassland	

Hou Hsioh-yu, (Chinese vegetation and its geographical distribution) .Ann. Missouri BOT.GARD.1983

Table 2. *Soil types and standardizing according to Food and Agriculture Organization (FAO) in China (or Israel)*

Category	FAO	Chinese soil
Aeolian soils	Arenosols	Aeolian soils
Calcisols	Calcisols	
Red earths	Ferralic Cambisols; Haplic Alisols	Torrid red soils; Latosolic red earths; Red earths; Yellow earths
Red-yellow earth	Haplic alisols; haplic acrisols; Ferralic Cambisols	Latosolic red earths; Red earths; Yellow earths; Latosols; Torrid red soils
Gray-brown desert soil	Haplic Calcisols; Calcaric Fluvisols	Brown caliche soils; Gray desert soils; Gray-brown desert soils; Irrigated silting soils; Irrigated desert soils
Yellow-brown earths	Haplic luvisols; albic luvisols; eutric ambisols; dystric ambisols; ferric luvisols	Yellow-brown earths; Brown earths; Dark-brown earths; Gray-cinnamon soils; Mountain meadow soils
Castano-cinnamon soils	Kastanozems	Castanozems; Castano-cinnamon soils
Regosols	Regosols	

Data Availability

All data generated or analysed during this study are included in Supplementary Information files.

http://www.aloki.hu ● ISSN 1589 1623 (Print) ● ISSN 1785 0037 (Online)
DOI: http://dx.doi.org/10.15666/aeer/1704_85998614

Results

SWR

China and Israel soil WDPT was (median) 7 s, from 0.503-4990.84 s (*Fig. 2, Table S1*). Most soils had water repellency (75.96%) in which slightly water-repellent soil predominated (58.22%), followed by no water-repellent soil (close to 24.04% of the total), strong water repellency and severe water repellency soil added up to 17.49%, and few extremely water-repellent soil (0.26%) (*Fig. 3, Table S2*).

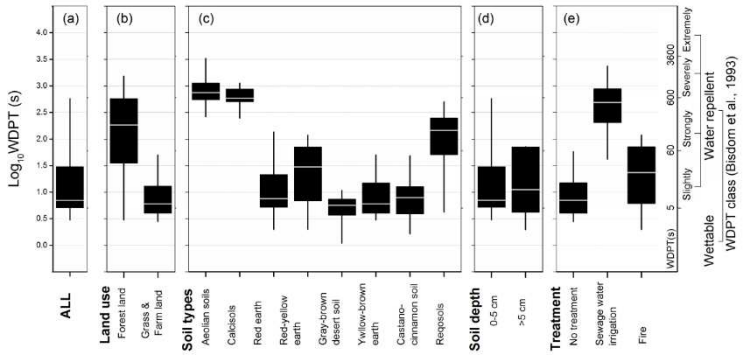

Figure 2. *Distribution of soil water repellency characteristics in China and Israel. WDPT data were standardized into Log_{10}, SWR was divided into five levels according to WDPT (Bisdom et al., 1993): wettable soil(WDPT<5 s), slightly water repellent(WDPT range 5−60 s), strongly water repellent (WDPT range 60−600 s), severely water repellent (WDPT range 600−3600 s), extremely water repellent (WDPT>3600s). (a)Summary distribution characteristics of SWR; (b)−(e)SWR distribution along different environmental gradients: (b)land use, (c)soil type, (d)soil depth, (e)treatment. In the boxplot, the line within the box represents the median, the lower boundary of each box means the first quartile (25^{th} percentile), while the upper boundary is the third quartile (75^{th} percentile) of the distribution. The lower the upper error bars are the 1^{st} and 99^{th} percentile value in the distribution, respectively*

SWR distribution

Most Chinese soils were slightly water-repellent, but they showed different SWR differentiation characteristics under different gradients of land use, soil type, soil depth and disturbance type (*Fig. 2, Fig. 3*).

In different land uses, the forest ecosystem SWR was stronger than grassland and farmland ecosystem SWR. The forest ecosystem soil WDPT ranged from 0.9 s to 4988.8 s with nearly half of the soils showed strong water repellency (WDPT median value was 183.831 s and the strong water repellent soil accounted for 45.77%). The non-forest soil WDPT was in the range of 0.5 s to 350 s with most soils showed a slight water repellency (WDPT median value was 6 s and the slightly water-repellent soil accounted for 67.76%) (*Table S1, Table S2*).

The SWR differentiation characteristics of different soil types was significant, especially the Aeolian soils, Calcisols and Regosols (The WDPT median values were 740.876 s, 580.694 s and 144.273 s, respectively). Most Aeolian soils showed severely water repellency (61.11%), Calcisols mainly showed strong soil water repellent and severely soil water repellent (55.56% and 44.44%), and the Regosols mainly were strong water repellent (69.44%).

http://www.aloki.hu ● ISSN 1589 1623 (Print) ● ISSN 1785 0037 (Online)
DOI: http://dx.doi.org/10.15666/aeer/1704_85998614

The rest soils (Gray-brown desert soil, Yellow-brown earth, Red earth, Castano-cinnamon soil, Red-yellow earth) were slightly water-repellent (The WDPT median values were 5.649, 6, 7.534, 7.877, 29.825 s), occupied 58%, 68.09%, 66.13%, 63.64%, and 42.69%. The cumulative percentage of the slight water repellency were 100%, 95.66%, 88.71%, 97.73%, and 62.69%. As for the SWR of different soil depth, the overall topsoil (0-5 cm)WDPT was less than subsoil (> 5 cm) (The WDPT median values were 7 s and 11.077 s), but the topsoil SWR showed a greater variation than subsoil. The subsoil SWR was obviously the strong water repellency, the topsoil sometimes was severely water repellency or even extremely water repellency. The topsoil WDPT ranged from 0.503 s to 4990.84 s, covering wettable, slightly water repellent, strongly water repellency, severely water repellency and even extremely water repellency (occupied 23.81%, 58.98%, 12.12%, 4.82%, and 0.27%, respectively), mainly showed the slight water repellency (the cumulative percentage was 82.79%). The subsoil WDPT ranged from 0.902 s to 95.266 s with the wettable and slightly water repellency accounted for 28.92% and 41.67%, respectively, but the characteristics of severe water repellency were more obvious than the topsoil (29.41%, the cumulative percentage was 100%).

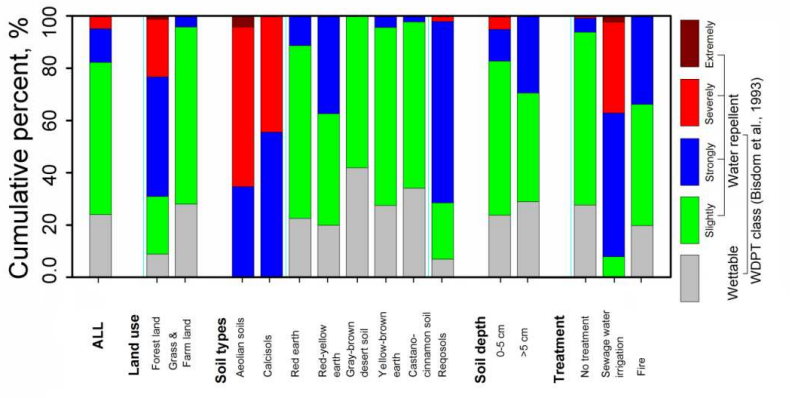

Figure 3. *Cumulative percentage distribution of five levels of SWR along different gradients. Gray bars mean wettable soil; green bars represent slight water repellency; blue bars mean strong water repellency; red bars are severe water repellency; while brown bars stand for extreme water repellency*

Under different process gradients (no processing, sewage irrigation and fire), no processing soil showed slight soil water repellent (the WDPT median value was 7 s, ranged from 0.503 s to 1225.211 s, slightly soil water repellent occupied 66.14%, the cumulative percentage was 93.85%). Sewage irrigation had the greatest impact on SWR and definitely will cause SWR (wettable soil account for 0%). The soil under sewage irrigation (The WDPT median value was 485.584 s, ranged from 6.315 s to 4990.84 s) showed strongly soil water repellency (54.92%, cumulative percentage of 62.88%) and severely soil water repellency (34.85%, cumulative percentage of 97.73%) and a few extremely soil water repellency (2.27%).

The soil after fire disturbance (the WDPT median value is 23.183 s, ranged from 0.902 s to 369.766 s) might not cause SWR (wettable soil accounted for 19.81%), most were slightly water repellent (46.43%), and partially strongly water repellency (33.77%), without severely water repellency and extremely water repellent soil (0%).

http://www.aloki.hu ● ISSN 1589 1623 (Print) ● ISSN 1785 0037 (Online)
DOI: http://dx.doi.org/10.15666/aeer/1704_85998614

Discussions

Synthesis

Existing researches tended to measure SWR at specific sites through a single experiment or long-term monitoring. The choice of sites most depended on the research contents, for example, some researches specifically concentrated in the regions where the distribution of SWR were common and the climate was arid and semi-arid Mediterranean climate areas (e.g. Germany, Spain and California). Some researches chose the humid forest of Central Europe (Buczko et al., 2002; Hubbert and Oriol, 2005; Khanchoul and Boubehziz, 2019). The researches that study the SWR in large scale area were few. China has a vast territory; some regions are humid (South Central) and some are arid and semi-arid regions (West and North). China and Israel faced frequent droughts and the crisis of reclaimed water and available water in recent years (Medina, 2010; Joseph et al., 2019). Most soils in China and Israel showed SWR, mainly were slightly water repellent and contained different degrees (the range of WDPT were 0.503 s-4990.84 s). For example, it could be seen from the SWR reports about the Mediterranean climate region (semi-arid zone) that some researchers suggested that the soils were slightly water-repellent with the WDPT ranged from 10 s to 30 s (Mataix-Solera et al., 2007), and some other researchers found that the forest soil in the Mediterranean climate region was strong water repellency and even extremely water repellency (Crockford et al., 1991; Wahl, 2008; Oyedotun, 2018). In this study, we sampled all SWR researches which could represent the SWR in China.

Characterization

Soil as a giant container and complicate system, it currently focuses on the causes of SWR (such as fire or hydrophobic organic matter) (Jiménez-Pinilla et al., 2016; Siteur et al., 2016), predicts and simulates the emergence of SWR through some leading factors, such as land type, litter type, soil properties, operation mode, microbe activity, seasonal variation, etc. (Buczko et al., 2007; Schmitt et al., 2010; Jordán et al., 2013; Cesarano et al., 2016), and compares and improves the research methods (Doerr, 1998; Wahl, 2008; Sharma and Yadav, 2018). But the previous researches were always just a single experiment report, no one described SWR integratedly and from different gradients. In this study, the SWR distribution situation and distribution pattern were described from four perspectives: land use, soil type, soil depth and interference type.

There were more comparative studies about the impact of land use on SWR than others. Previous studies suggested that the bare land or wilderness would show extreme water repellency, while the soils under vegetation showed less significant, SWR could be limited by vegetation cover type and availability of litter (Arcenegui et al., 2007; Zavala et al., 2009). The influence of different vegetation cover types on SWR had great different, this result was same as our research. It universally accepted that grass and farmland which were generally wettable soil and slightly water-repellent soil showed less severity water repellency than forest that usually showed strong water repellency as well as severe water repellency and even some serious water repellency (Mataix-Solera et al., 2007; Buczko et al., 2007; Verheijen and Cammeraat, 2007; Kořenková et al., 2015; Walden et al., 2015). Human disturbance, such as different farming methods did not seem to be the cause of these differences (Malvar et al., 2016), different soil organic contents (SOC) of different land types might be the reason. There was a significant positive correlation between SOC and SWR (r2=0•74, p=0•01), and the soil with SOC

http://www.aloki.hu ● ISSN 1589 1623 (Print) ● ISSN 1785 0037 (Online)
DOI: http://dx.doi.org/10.15666/aeer/1704_85998614

content higher than 8.06% might have SWR. There were different views in some researches. By comparing three different land uses (eucalyptus, grassland and shrub) in Australia, it was found that the diversity of SWR was independent of soil properties such as SOC content and composition, that might be caused by inducing a small amount of hydrophobic compounds from the trees. However, eucalyptus seemed to be a significant tree species in terms of SWR. Compared with other species, the eucalyptus SWR had a greater variation range and a more complex dynamic change process (Rodríguez-Alleres and Benito, 2011; Santos et al., 2013). And SWR might vary according to different forest types, for example, pure forest exhibited relatively low SWR when compared with mixed forest (Buczko et al., 2002, 2005). Deciduous broad-leaved forest showed a higher SWR when compared to coniferous forest (Gimbel et al., 2016). Some studies assumed that SWR might be irrelevant to forest types (Wahl, 2008). However, they suggested that the diversity in humus brought about different levels of SWR. For example, the humus species of mixed and deciduous broad-leaved forests were more complex and the surface soil humus was thicker than pure forest and coniferous forest (Buczko et al., 2002, 2005; Wahl et al., 2005). On the other hand, the higher SWR may be accompanied by the humus form of "ecologically less favorable" (e.g. moder and mor-like forms) (Sevink et al., 1989; Scott and Wyk, 1990; Crockford et al., 1991; Imeson et al., 1992).

Different soil types played an important role in SWR diversity, and the SWR might be the loopholes in soil system operation. Therefore, it was overgeneralization to study and explain the causes of SWR and predict the variation trend only from the individual soil properties. This study described the SWR distribution patterns of 8 different soil types (Aeolian soils, Calcisols, Regosols, Red earth, Red-yellow earth, Yellow-brown earth, Gray-brown desert soil, Castano-cinnamon soil) that were common in China and Israel. Aeolian soils and Calcisols, the two most serious water-repellent soil types were typical sandy soils with poor water holding capacity and widely distributed in arid and semi-arid areas (Zhenghu et al., 2007; Chesworth et al., 2008). Regosols which considered to be "taxonomic rest group" exhibited serious SWR, its particle size was between sand and clay (Meek et al., 2008). Other soil types were slightly water repellent and some strongly water repellent. Among them, Red earth (Alisols), Red-yellow earth (Acrisols), Yellow-brown earth (luvisols) belonged to mafic soils, the difference between them were the different properties and the development of the parent rock and the initial rock (Lal and Stewart, 2011), higher clay content, stronger acidity and the water holding capacity, limited agricultural use. They were usually forested areas and some low intensity pasture (Yu, 1997; Ebelhar et al., 2008; Dahlgren et al., 2008). Gray-brown desert soil was a typical Fluvisols that was adaptable for xerophytes. It usually possessed the features of sedimentary soils in lakes and seas that might exhibit low pH, high aluminum and salt content (Paz et al., 2008). Castano-cinnamon soil with relatively high humus content was a typical grassland soil (Spaargaren, 2008). The study on integrated report of different soil types had been done little so far, and the existing studies usually was a small sample (dozens of samples), small scale (covers few soil types), focusing on the nature of soil as well as trying to explain and forecast the SWR from a single perspective, and so on. The few existing studies made a comparison among several particular soil types, such as Regosol in the semi-arid regions of the Mediterranean was more prone to SWR than Luvisol (Arcenegui et al., 2007). Cambisols and Podsols in broad-leaved and coniferous forests in northern Europe (Jutland and Denmark) were strong water-repellent soil (Wahl, 2008). Most Cambreeol

http://www.aloki.hu ● ISSN 1589 1623 (Print) ● ISSN 1785 0037 (Online)
DOI: http://dx.doi.org/10.15666/aeer/1704_85998614

and Leptosol in the European mountains were slightly water-repellent soils and little parts were strongly water-repellent soil, Luvisol and Regosols were slightly water-repellent and strongly water-repellent soil, Fluvisols were slightly water-repellent soil (Kořenková et al., 2015). Most of the studies focused on the influence of different soil properties on SWR, and tried to explain the differences of SWR in different soil types (Mirbabaei et al., 2013). The focused soil properties were concentrated on the soil texture, SOC, pH, moisture content, the role of clay particle, soil elements content, etc., but there were different opinions about the dominant factor. In this study, Aeolian soils, Calcisols and Regosols from arid and semi-arid areas had a higher sediment concentration, the clay content was lower and water repellent was most significant comparing with the remaining five soils. It had been widely believed that soils from forest or farmland systems which were rich in sediment concentration were more likely to exhibit SWR. SWR might be positively correlated with sediment concentration, and there was a negative correlation with clay content, but the magnitude of correlation was still controversial (Mirbabaei et al., 2013; Kořenková et al., 2015). However, there were reports that SWR (South Africa) negatively correlated with sediment concentration (Scott, 2000), and different amounts of sediment in the same soil type were not significantly associated with SWR (Dekker and Ritsema, 1994; Wahl, 2008) and so on. Similar to the reports of different land uses, SOC was also considered to be the cause of SWR differences in different soil uses. Mafic soils which widely distributed in the south-central part of China had a large amount of cosmid content, low SOC and pH content and showed slightly water repellent. The previous studies concluded that SOC content positively correlated with SWR (Buczko et al., 2002; Mirbabaei et al., 2013; Kořenková et al., 2015), however, it also been suggested that SOC was not the main cause of SWR (Wahl, 2008; Vogelmann et al., 2010), pH which negatively correlated with SWR was the dominant property of SWR differences, and we could alleviate SWR by increasing the soil pH (Ritsema et al., 1998; Hurraß and Schaumann, 2006; Mataix-Solera et al., 2007; Mirbabaei et al., 2013; Kořenková et al., 2015).

Most of the SWR research would first assume that the soil humus had a huge impact and effect, their research often focused on topsoil (0-5 cm) (Santos et al., 2013; Bachmann et al., 2016; Robichaud et al., 2016). However, most of these studies drew conclusions from a single experiment, it often could not verify all SWR changes in topsoil and subsoil (>5 cm) by this single experiment. SWR occurred mainly in topsoil which was more prone to produce strong or stronger water repellency than subsoil according to previous studies (Reeder and Jurgensen, 1979; Wahl, 2008; Robichaud et al., 2016). By analyzing the SWR distribution pattern along different depths in different areas, vegetation cover types and soil types, it had been found that topsoil had a great SWR variation, covering strongly water repellency, severely water repellency and extremely water repellency (17.21%), but the median value of WDPT was less than subsoil, and although subsoil didn't show severely water repellency and extremely water repellency, the probability of SWR was greater than topsoil (29.4%). Therefore, it might be incomplete that most studies had found SWR might decrease with increasing soil depth (Barrett and Slaymaker, 1989; Doerr et al., 2000; Walden et al., 2015; Malvar et al., 2016), the gradient variation and trend of SWR along different soil layer depth might be more complicated than the existing researches.

Many studies suggested that fire interference was the main reason of SWR and would exacerbate SWR (Reeder and Jurgensen, 1979; DeBano, 2000; Doerr et al., 2000; Jordán et al., 2013; Jiménez-Pinilla et al., 2016). More than 40% of SWR was due to

http://www.aloki.hu ● ISSN 1589 1623 (Print) ● ISSN 1785 0037 (Online)
DOI: http://dx.doi.org/10.15666/aeer/1704_85998614

fire disturbance (Reeder and Jurgensen, 1979), hence a large number of experiments designed with different fire intensities to measure the forest soil SWR, investigate the response of forest types, structures, soil infiltration capacity and runoff rate after fire disturbance (Robichaud et al., 2016), so as to guide forest management, forest soil protection and restoration, forest reconstruction after fire, etc. However, it had found that the fire did not always lead to SWR by integrating the fire interference experiments data, appropriate small fire might not affect SWR (wettable soil 27.71%), the maximum WDPT caused by fire even less than the WDPT of no interference soil (369.766 and 1225.211 s). In contrast to fire, sewage irrigation might be a more serious problem for SWR, especially in China and Israel where droughts, reclaimed water and available water crises occurred frequently (Medina, 2010). Irrigation with sewage would be common in the future, especially in arid and semi-arid areas where available water was short. Unlike fire interference, sewage irrigation would certainly cause SWR (wettable soil 0%), and far more serious. This might be related to the ingredients of sewage. It had been found that diluted soapy water could accelerate the wetting rate of the water repellent soil at the beginning, but when the moisture was slowly lost, the soil that added the surfactant showed even more severe water repellency than before (Jamison, 1943). Various cationic, anionic, non-ionic substances could humidify soil faster (Cisar et al., 2000), but the surface-active substances would increase soil hydrophobicity after being wet (Adhikari and Chakrabarti, 1976). In addition, sewage irrigation also increased the biological activity and abundance of soil organisms (Barkle et al., 2000), which might also be responsible for increasing SWR (Bond and Harris, 1964).

Summary and Conclusions

Through full sampling analysis of SWR in China and Israel, it had found that SWR were widespread in China, but most were only slightly water-repellent. Only a small part of the soil had strong water repellency or stronger water repellency. The main factors affecting SWR were soil type, soil depth, land use, type of disturbance, etc. There was a significant difference in SWR between different soil types, due to different soil properties. The order of SWR is Aeolian soils > Calcisols > Regosols > Red-yellow earth > Red earth > Yellow-brown earth > Castano-cinnamon soil > Gray-brown desert soil. SWR tended to decrease with the increase of soil depth, and the external disturbance had a great influence on the water repellency of topsoil, and had little effect on subsoil. There was a significant difference in SWR between different land use, and there was a significant SWR in forest ecosystems compared with grassland and farmland. A certain intensity of fire interference and sewage irrigation would exacerbate the water repellent in the soil, in which the impact of sewage irrigation on SWR was more significant, the SWR would increase with the increase of fire intensity. The reasons for different SWR will be worth studying in the future. The results of this study filled the gaps in the evaluation of the overall water repellency of soils in China and Israel, and summarized the factors affecting SWR, which would provide the basis for soil improvement and ecological restoration in China and even the world.

Acknowledgements. This study was financially supported by the National Natural Science Foundation of China (No. 31470659), the forestry public industry scientific research project (No: 201504301).

http://www.aloki.hu ● ISSN 1589 1623 (Print) ● ISSN 1785 0037 (Online)
DOI: http://dx.doi.org/10.15666/aeer/1704_85998614

REFERENCES

[1] Adhikari, M., Chakrabarti, G. (1976): Contribution of natural and microbial humic acids to water repellency in soil. – Journal of the Indian Society of Soil Science: 217-219.
[2] Ali, W., Nasir, M. S., Nasir, A., Rashid, H., Ayub, I., Gillani, S. H., Latif, M. J. (2018): Assessment Of Carbon Footprints In Terms Of Co2 Of Diesel Generator, Pakistan. – Earth Sciences Pakistan 2(1): 15-17.
[3] Arcenegui, V., Mataix-Solera, J., Guerrero, C., Zornoza, R., Mayoral, A. M., Morales, J. (2007): Factors controlling the water repellency induced by fire in calcareous Mediterranean forest soils. – European Journal of Soil Science 58: 1254-1259.
[4] Bachmann, J., Krueger, J., Goebel, M. O., Heinze, S. (2016): Occurrence and spatial pattern of water repellency in a beech forest subsoil. – Journal of Hydrology and Hydromechanics 64: 100-110.
[5] Barkle, G. F., Stenger, R., Singleton, P. L., Painter, D. J. (2000): Effect of regular irrigation with dairy farm effluent on soil organic matter and soil microbial biomass. – Australian Journal of Soil Research 38: 1087-1097.
[6] Barrett, G., Slaymaker, O. (1989): Identification, characterization, and hydrological implications of water repellency in mountain soils, southern British Columbia. – Catena 16: 477-489.
[7] Bisdom, E. B. A., Dekker, L. W., Schoute, J. F. Th. (1993): Water repellency of sieve fractions from sandy soils and relationships with organic material and soil structure. – Geoderma 56: 105-118.
[8] Bogner, C., Wolf, B., Schlather, M., Huwe, B. (2008): Analysing flow patterns from dye tracer experiments in a forest soil using extreme value statistics. – European Journal of Soil Science 59: 103-113.
[9] Bond, R., Harris, J. (1964): The influence of the microflora on the physical properties of soils. I. Effects associated with filamentous algae and fungi. – Australian Journal of Soil Research 2: 111-122.
[10] Buczko, U., Bens, O., Fischer, H., Hüttl, R. F. (2002): Water repellency in sandy luvisols under different forest transformation stages in northeast Germany. – Geoderma 109: 1-18.
[11] Buczko, U., Bens, O., Hüttl, R. F. (2005): Variability of soil water repellency in sandy forest soils with different stand structure under Scots pine (Pinus sylvestris) and beech (Fagus sylvatica). – Geoderma 126: 317-336.
[12] Buczko, U., Bens, O., Hüttl, R. F. (2007): Changes in soil water repellency in a pine–beech forest transformation chronosequence: Influence of antecedent rainfall and air temperatures. – Ecological Engineering 31: 154-164.
[13] Butzen, V., Seeger, M., Marruedo, A., de Jonge, L., Wengel, R., Ries, J. B., Casper, M. C. (2015): Water repellency under coniferous and deciduous forest - Experimental assessment and impact on overland flow. – Catena 133: 255-265.
[14] Cesarano, G., Incerti, G., Bonanomi, G. (2016): The Influence of Plant Litter on Soil Water Repellency: Insight from 13C NMR Spectroscopy. – PloS one 11: e0152565.
[15] Chesworth, W., Camps Arbestain, M., Macías, F., Spaargaren, O. (2008): Calcisols. – In: Chesworth, W. (ed.) Encyclopedia of Soil Science. Springer Netherlands: 79-80.
[16] Cisar, J. L., Williams, K. E., Vivas, H. E., Haydu, J. J. (2000): The occurrence and alleviation by surfactants of soil-water repellency on sand-based turfgrass systems. – Journal of Hydrology 231-232: 352-358.
[17] Craswell, E. T., Lefroy, R. D. B. (2001): The role and function of organic matter in tropical soils. – Nutrient Cycling in Agroecosystems 61: 7-18.
[18] Crockford, H., Topalidis, S., Richardson, D. (1991): Water repellency in a dry sclerophyll eucalypt forest—measurements and processes. – Hydrological Processes 5: 405-420.
[19] Dahlgren, R. A. (2008): Acrisols. – In: Chesworth, W. (ed.) Encyclopedia of Soil Science. Springer Netherlands: 22-24.

http://www.aloki.hu ● ISSN 1589 1623 (Print) ● ISSN 1785 0037 (Online)
DOI: http://dx.doi.org/10.15666/aeer/1704_85998614

[20] DeBano, L. F. (2000): Water repellency in soils: a historical overview. – Journal of Hydrology 231-232: 4-32.
[21] DeBano, L. F. (2000): The role of fire and soil heating on water repellency in wildland environments: a review. – Journal of Hydrology and Hydromechanics 231-232: 195-206.
[22] Dekker, L. W., Ritsema, C. J. (1994): How water moves in a water repellent sandy soil: 1. Potential and actual water repellency. – Water Resources Research 30: 2507-2517.
[23] Doerr, S. H. (1998): On standardizing the 'Water Drop Penetration Time' and the 'Molarity of an Ethanol Droplet' techniques to classify soil hydrophobicity: A case study using medium textured soils. – Earth Surface Processes and Landforms 23: 663-668.
[24] Doerr, S. H., Shakesby, R. A., Walsh, R. P. D. (2000): Soil water repellency: its causes, characteristics and hydro-geomorphological significance. – Earth-Science Reviews 51: 33-65.
[25] Ebelhar, S. A., Chesworth, W., Paris, Q., Spaargaren, O. (2008): Luvisols. – In: Chesworth, W. (ed.) Encyclopedia of Soil Science. Springer Netherlands: 440-442.
[26] Fang, N. F., Wang, L., Shi, Z. H. (2017): Runoff and soil erosion of field plots in a subtropical mountainous region of China. – Journal of Hydrology 552: 387-395.
[27] Gimbel, K. F., Puhlmann, H., Weiler, M. (2016): Does drought alter hydrological functions in forest soils? – Hydrology and Earth System Sciences 20: 1301-1317.
[28] Hossain, M. S., Karlson, M., Neset, T. S. (2019): Application Of Gis For Cyclone Vulnerability Analysis Of Bangladesh. – Earth Sciences Malaysia 3(1): 25-34.
[29] Hubbert, K. R., Oriol, V. (2005): Temporal fluctuations in soil water repellency following wildfire in chaparral steeplands, southern California. – International Journal of Wildland Fire 14: 439-447.
[30] Hurraß, J., Schaumann, G. E. (2006): Properties of soil organic matter and aqueous extracts of actually water repellent and wettable soil samples. – Geoderma 132: 222-239.
[31] Imeson, Dr. A. C., Verstraten, Dr. J. M., van Mulligen, Dr. E. J., Sevink, Dr. J. (1992): The effects of fire and water repellency on infiltration and runoff under Mediterranean type forest. – Catena 19: 345-361.
[32] Jamison, V. C. (1943): The slow reversible drying of sandy surface soils beneath citrus trees in central Florida. – Soil Science Society of America Journal 7: 36-41.
[33] Jiménez-Pinilla, P., Doerr, S. H., Ahn, S., Lozano, E., Mataix-Solera, J., Jordán, A., Zavala, L. M., Arcenegui, V. (2016): Effects of relative humidity on the water repellency of fire-affected soils. – Catena 138: 68-76.
[34] Jordán, A., Zavala, L. M., Mataix-Solera, J., Doerr, S. H. (2013): Soil water repellency: Origin, assessment and geomorphological consequences. – Catena 108: 1-5.
[35] Joseph, O. T., Adeoti, O. O., Olufemi, A. A. (2019): Study Of The Phytodiversity Along Antorun Reservoir, Near Ogbomoso, Nigeria. – Environment & Ecosystem Science 3(1): 1-12.
[36] Khanchoul, K., Boubehziz, S. (2019): Spatial Variability Of Soil Erodibility At El Hammam Catchment, Northeast Of Algeria. – Environment & Ecosystem Science 3(1): 17-25.
[37] Kořenková, L., Šimkovic, I., Dlapa, P., Juráni, B., Matúš, P. (2015): Identifying the origin of soil water repellency at regional level using multiple soil characteristics: The White Carpathians and Myjavska pahorkatina Upland case study. – Soil and Water Research 10: 78-89.
[38] Lal, R., Stewart, B. A. (2011): World soil resources and food security. – CRC Press.
[39] Liang, Z., Wenshun, W. (2019): Parametric Architectural Design Based On Optimization Algorithm. – Engineering Heritage Journal 3(1): 13-17.
[40] Malvar, M. C., Prats, S. A., Nunes, J. P., Keizer, J. J. (2016): Soil Water Repellency Severity and its Spatio-Temporal Variation in Burnt Eucalypt Plantations in North-Central Portugal. – Land Degradation & Development 27: 1463-1478.
[41] Mataix-Solera, J., Arcenegui, V., Guerrero, C., Mayoral, A. M., Morales, J., González, J., García-Orenes, F., Gómez, I. (2007): Water repellency under different plant species in a calcareous forest soil in a semiarid Mediterranean environment. – Hydrological Processes 21: 2300-2309.

http://www.aloki.hu ● ISSN 1589 1623 (Print) ● ISSN 1785 0037 (Online)
DOI: http://dx.doi.org/10.15666/aeer/1704_85998614

[42] Medina, M. A. (2010): Global Water Crisis and Climate Change. – Journal of Hydrologic Engineering 15: 167-170.
[43] Meek, B. D., Chesworth, W., Spaargaren, O. (2008): Regosols. – In: Chesworth, W. (ed.) Encyclopedia of Soil Science. Springer Netherlands: 605-606.
[44] Mirbabaei, S. M., Shahrestani, M. S., Zolfaghari, A., Abkenar, K. T. (2013): Relationship between soil water repellency and some of soil properties in northern Iran. – Catena 108: 26-34.
[45] Oyedotun, T. D. T. (2018): X-ray fluorescence (XRF) in the investigation of the composition of earth materials: a review and an overview. – Geology, Ecology, and Landscapes 2(2): 138-154.
[46] Paz, C. G. (2008): Fluvisols. – In: Chesworth, W. (ed.) Encyclopedia of Soil Science. Springer Netherlands: 281-282.
[47] Reeder, C. J., Jurgensen, M. F. (1979): Fire-induced water repellency in forest soils of upper Michigan. – Canadian Journal of Forest Research 9: 369-373.
[48] Ritsema, C. J., Dekker, L. W., Nieber, J. L., Steenhuis, T. S. (1998): Modeling and field evidence of finger formation and finger recurrence in a water repellent sandy soil. – Water Resources Research 34: 555-567.
[49] Robichaud, P. R., Wagenbrenner, J. W., Pierson, F. B., Spaeth, K. E., Ashmun, L. E., Moffet, C. A. (2016): Infiltration and interrill erosion rates after a wildfire in western Montana, USA. – Catena 142: 77-88.
[50] Rodríguez-Alleres, M., Benito, E. (2011): Spatial and temporal variability of surface water repellency in sandy loam soils of NW Spain under Pinus pinaster and Eucalyptus globulus plantations. – Hydrological Processes 25: 3649-3658.
[51] Santos, J. M., Verheijen, F. G. A., Tavares Wahren, F., Wahren, A., Feger, K.-H., Bernard-Jannin, L., Rial-Rivas, M. E., Keizer, J. J., Nunes, J. P. (2013): Soil Water Repellency Dynamics in Pine and Eucalypt Plantations in Portugal – A High-resolution Time Series. – Land Degradation & Development 27: 1334-1343.
[52] Sblackwell, P. (2000): Management of water repellency in Australia, and risks associated with preferential flow, pesticide concentration and leaching. – Journal of Hydrology 231-232: 384-395.
[53] Schmitt, A., Glaser, B., Borken, W., Matzner, E. (2010): Organic matter quality of a forest soil subjected to repeated drying and different re-wetting intensities. – European Journal of Soil Science 61: 243-254.
[54] Scott, D. F., Wyk, D. B. V. (1990): The effects of wildfire on soil wettability and hydrological behaviour of an afforested catchment. – Journal of Hydrology 121: 239-256.
[55] Scott, D. (2000): Soil wettability in forested catchments in South Africa; as measured by different methods and as affected by vegetation cover and soil characteristics. – Journal of Hydrology 231: 87-104.
[56] Sevink, J., Imeson, A. C., Verstraten, J. M. (1989): Humus form development and hillslope runoff, and the effects of fire and management, under Mediterranean forest in NE-Spain. – Catena 16: 461-475.
[57] Sharjeel, A., Anwar, S., Nasir, A., Rashid, H. (2019): Design, Development And Performance Of Optimum Water Softener. – Earth Sciences Pakistan 3(1): 23-28.
[58] Sharma, D., Yadav, K. D. (2018): Application of rotary in-vessel composting and analytical hierarchy process for the selection of a suitable combination of flower waste. – Geology, Ecology, and Landscapes 2(2): 137-147.
[59] Siteur, K., Mao, J., Nierop, K. G. J., Rietkerk, M., Dekker, S. C., Eppinga, M. B. (2016): Soil Water Repellency: A Potential Driver of Vegetation Dynamics in Coastal Dunes. – Ecosystems 19: 1210-1224.
[60] Spaargaren, O. (2008): Kastanozems. – In: Chesworth, W. (ed.) Encyclopedia of Soil Science. Springer Netherlands: 421-423.

http://www.aloki.hu ● ISSN 1589 1623 (Print) ● ISSN 1785 0037 (Online)
DOI: http://dx.doi.org/10.15666/aeer/1704_85998614

[61] Sunny, A. A., Omowumi, A., Chris, O. A. (2018): Improved Magnetic Data Analyses And Enhancement Techniques For Lithological And Structural Mapping Around Akure, Southwestern Nigeria. – Earth Sciences Malaysia 2(1): 16-21.
[62] Tao, S. (2018): Evaluation Of Technology Innovation In Hubei Province. – Engineering Heritage Journal 2(2): 09-10.
[63] Verheijen, F. G. A., Cammeraat, L. H. (2007): The association between three dominant shrub species and water repellent soils along a range of soil moisture contents in semi-arid Spain. – Hydrological Processes 21: 2310-2316.
[64] Vogelmann, E. S., Reichert, J. M., Reinert, D. J., Mentges, M. I., Vieira, D. A., de Barros, C. A. P., Fasinmirin, J. T. (2010): Water repellency in soils of humid subtropical climate of Rio Grande do Sul, Brazil. – Soil and Tillage Research 110: 126-133.
[65] Wahl, N. A., Wöllecke, B., Bens, O., Hüttl, R. (2005): Can forest transformation help reducing floods in forested watersheds? Certain aspects on soil hydraulics and organic matter properties. – Physics and Chemistry of the Earth, Parts A/B/C 30: 611-621.
[66] Wahl, N. A. (2008): Variability of Water Repellency in Sandy Forest Soils under Broadleaves and Conifers in north-western Jutland/Denmark. – Soil and Water Research 3: S155–S164.
[67] Walden, L. L., Harper, R. J., Mendham, D. S., Henry, D. J., Fontaine, J. B. (2015): Eucalyptus reforestation induces soil water repellency. – Soil Research 53: 168-177.
[68] Yu, T. R. (1997): Chemistry of Variable Charge Soils. – Oxford University Press.
[69] Zavala, L. M., González, F. A., Jordán, A. (2009): Intensity and persistence of water repellency in relation to vegetation types and soil parameters in Mediterranean SW Spain. – Geoderma 152: 361-374.
[70] Zhenghu, D., Honglang, X., Zhibao, D., Gang, W., Drake, S. (2007): Morphological, physical and chemical properties of aeolian sandy soils in northern China. – Journal of Arid Environments 68: 66-76.

APPENDIX

SUPPORTING INFORMATION

Table S1. *Statistical analysis of Log10WDPT along different gradients*

		N	Median	Mean	SD	SE for Mean	Min.	Max.
All		4643	0.845	1.152	0.717	0.011	−0.298	3.698
Vegetation Class	Forest land	970	2.264	2.086	0.844	0.027	−0.045	3.698
	Grass & Farm land	3673	0.778	0.905	0.413	0.007	−0.298	2.544
Soil type	Aeolian soils	288	2.870	2.911	0.311	0.018	2.281	3.698
	Calcisols	72	2.764	2.771	0.188	0.022	2.315	3.083
	Red earth	62	0.877	1.039	0.528	0.067	0.198	2.557
	Red-yellow earth	260	1.475	1.335	0.609	0.038	−0.045	2.568
	Gray-brown desert soil	100	0.752	0.664	0.298	0.030	−0.298	1.150
	Yellow-brown earth	3529	0.778	0.912	0.414	0.007	0.000	2.544
	Castano-cinnamon soil	44	0.896	0.895	0.406	0.061	0.000	1.791
	Regosols	288	2.159	1.992	0.592	0.035	0.097	2.867
Soil depth	0-5cm	4439	0.845	1.153	0.722	0.011	−0.298	3.698
	>5cm	204	1.044	1.128	0.590	0.041	−0.045	1.979
Disturbance Class	No treatment	3807	0.845	0.940	0.478	0.008	−0.298	3.088
	Sewage water irrigation	528	2.686	2.590	0.509	0.022	0.800	3.698
	Fire	308	1.365	1.306	0.603	0.034	−0.045	2.568

http://www.aloki.hu ● ISSN 1589 1623 (Print) ● ISSN 1785 0037 (Online)
DOI: http://dx.doi.org/10.15666/aeer/1704_85998614

Table S2. *Percentage and cumulative percentage of five WDPT classes ((Bisdom et al., 1993)*

			Total	WDPT Class				
				Wettable	Slightly	Strongly	Severely	Extremely
ALL		N	4643	1116	2703	598	214	12
		%		24.04	58.22	12.88	4.61	0.26
		Cumulative%		24.04	82.25	95.13	99.74	100.00
Vegetation Class	Forest land	N	970	86	214	444	214	12
		%		8.87	22.06	45.77	22.06	1.24
		Cumulative%		8.87	30.93	76.70	98.76	100.00
	Grass & Farm land	N	3673	1030	2489	154		
		%		28.04	67.76	4.19	0.00	0.00
		Cumulative%		28.04	95.81	100.00	100.00	100.00
Soil type	Aeolian soils	N	288			100	176	12
		%		0.00	0.00	34.72	61.11	4.17
		Cumulative%		0.00	0.00	34.72	95.83	100.00
	Calcisols	N	72			40	32	
		%		0.00	0.00	55.56	44.44	0.00
		Cumulative%		0.00	0.00	55.56	100.00	100.00
	Red earth	N	62	14	41	7		
		%		22.58	66.13	11.29	0.00	0.00
		Cumulative%		22.58	88.71	100.00	100.00	100.00
	Red-yellow earth	N	260	52	111	97		
		%		20.00	42.69	37.31	0.00	0.00
		Cumulative%		20.00	62.69	100.00	100.00	100.00
	Gray-brown desert soil	N	100	42	58			
		%		42.00	58.00	0.00	0.00	0.00
		Cumulative%		42.00	100.00	100.00	100.00	100.00
	Yellow-brown earth	N	3529	973	2403	153		
		%		27.57	68.09	4.34	0.00	0.00
		Cumulative%		27.57	95.66	100.00	100.00	100.00
	Castano-cinnamon soil	N	44	15	28	1		
		%		34.09	63.64	2.27	0.00	0.00
		Cumulative%		34.09	97.73	100.00	100.00	100.00
	Regosols	N	288	20	62	200	6	
		%		6.94	21.53	69.44	2.08	0.00
		Cumulative%		6.94	28.47	97.92	100.00	100.00
Soil depth	0-5cm	N	4439	1057	2618	538	214	12
		%		23.81	58.98	12.12	4.82	0.27
		Cumulative%		23.81	82.79	94.91	99.73	100.00
	>5cm	N	204	59	85	60		
		%		28.92	41.67	29.41	0.00	0.00
		Cumulative%		28.92	70.59	100.00	100.00	100.00
Disturbance Class	No treatment	N	3807	1055	2518	204	30	
		%		27.71	66.14	5.36	0.79	0.00
		Cumulative%		27.71	93.85	99.21	100.00	100.00
	Sewage water irrigation	N	528		42	290	184	12
		%		0.00	7.95	54.92	34.85	2.27
		Cumulative%		0.00	7.95	62.88	97.73	100.00
	Fire	N	308	61	143	104		
		%		19.81	46.43	33.77	0.00	0.00
		Cumulative%		19.81	66.23	100.00	100.00	100.00

http://www.aloki.hu ● ISSN 1589 1623 (Print) ● ISSN 1785 0037 (Online)
DOI: http://dx.doi.org/10.15666/aeer/1704_85998614

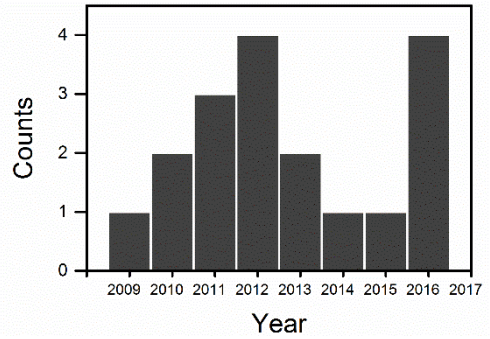

Figure S1. *Temporal distribution of soil water repellency about data collection*

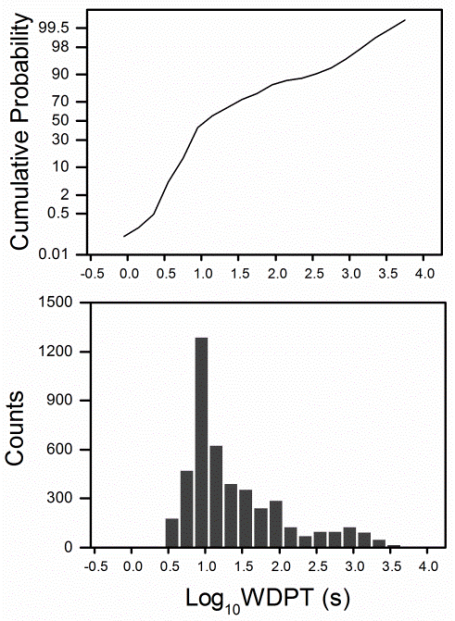

Figure S2. *Summary frequency distribution and cumulative probability characteristics of Log10 WDPT (s)*

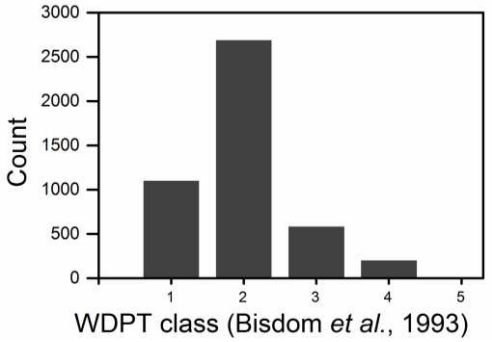

Figure S3. *Summary frequency distribution characteristics of five WDPT classes (Bisdom et al., 1993). 1: wettable soil (WDPT<5 s); 2:slightly water repellent (WDPT range 5−60s); 3:strongly water repellent (WDPT range 60−600s) 4:severely water repellent (WDPT range 600−3600s) 5:extremely water repellent (WDPT>3600s)*

http://www.aloki.hu ● ISSN 1589 1623 (Print) ● ISSN 1785 0037 (Online)
DOI: http://dx.doi.org/10.15666/aeer/1704_85998614

ON DILEMMAS AND SOLUTIONS FOR THE ISSUES OF HIGH SEAS MARINE PROTECTED AREAS DURING THE BBNJ NEGOTIATION

WANG, Y.

East China University of Political Science and Law
No. 1575 Wan Hangdu Road, 200042 Shanghai, China

(Received 8th Mar 2019; accepted 21st May 2019)

Abstract. This study aims to discuss the dilemmas and solutions for the issues of high seas marine protected areas during the BBNJ negotiation. It expounds the dilemmas of BBNJ negotiations on the issue of MPAs (such as there is no single universally agreed definition of MPAs, the selection criteria for MPAs are still not clear and no clear consensus on the designation process of MPAs), analyzes the reasons for dilemmas of MPAs in the process of BBNJ negotiations and proposes the solutions of main issues in the process of BBNJ negotiations. The result of this research is that MPAs, as a breakthrough to the traditional marine management tools, are becoming an important means for the international community to protect marine biodiversity. Finally, it concluded that after dealing with dilemmas of lack of definition, unclear selection criteria and disputes over the governance model, the negotiation of the issue of MPAs in ABNJ will inevitably reach a reasonable institutional framework, and further promote marine biodiversity protection.
Keywords: *marine biological diversity, global governance model, international instrument, marine resources, alternative management approach*

Introduction

Since the end of 20th century, MPAs, as alternative management approach of marine resources, have been proposed to remedy the defect of traditional marine management methods and to be established in large numbers. Among them, those established on the high seas or other areas beyond national jurisdiction are collectively referred to as marine protected areas beyond national jurisdiction (hereinafter referred to as "ABNJ marine protected areas"). While emphasizing the protection of the marine environment, ABNJ marine protected areas usually restrict the rights of countries to exploit and utilize marine resources to a certain extent. During the four Pre-committee meetings and the first BBNJ Intergovernmental Conference in 2018, as an important part of the ILBI, the issue of ABNJ marine protected areas has induced an intense debate between countries or groups of countries concerned. The purpose of this research is to discuss the dilemmas and solutions during the BBNJ negotiation for the issue of High Seas Marine Protected Areas.

Methods

Dilemmas of BBNJ negotiations on the issue of MPAs

At its 47th meeting, the Preparatory committee adopted the recommendations, which clearly stated that the text of ILBI would set out objectives of area-based management tools, including marine protected areas, relationship to measures under relevant instruments, frameworks and bodies, process, implementation, monitoring, and review (Afonso et al., 2018; Sufiyan et al., 2018). Most countries expressed their positions and

http://www.aloki.hu ● ISSN 1589 1623 (Print) ● ISSN 1785 0037 (Online)
DOI: http://dx.doi.org/10.15666/aeer/1704_86158629

suggestions regarding the definitions of MPAs, objectives and principles, criteria, governance, and institutional mechanisms. By sorting out the positions of all sides, we can conclude that the current BBNJ negotiations are mainly facing the following dilemmas:

There is a dispute on the definitions for MPAs

Given that the definition of MPAs is the logical starting point for other issues related, it should be clear in the negotiations. Whether the ILBI defines the MPAs in ABNJ or not and its general definition leads to contention among parties.

With regard to this issue, some states supported that the ILBI should be based on existing concepts, such as the definition of the CBD Technical Expert Group on Marine and Coastal Protected Areas or the IUCN's definition of MPAs. Others suggested that the MPA definition should be sufficiently broad to encompass specific types of conservation and impact restrictions, for example, High Seas Alliance favored adapting CBD and IUCN definitions, also including cultural values. However, the North-East Atlantic Fisheries Commission (NEAFC) underscored that ABMTs by RFMOs are functioning well and that the ILBI should enhance harmony between tools of different sectoral bodies, rather than define ABMTs (Alger and Dauvergne, 2017; Khanchoul et al., 2018). It is noteworthy that Costa Rica suggested a working concept of MPAs as "a clearly defined geographic space recognized, dedicated and managed through legal and other effective means to achieve the conservation of biodiversity, ecosystem services, and other cultural values."

The selection criteria for MPAs are still not clear

The so-called selection criteria for designing marine protected areas mainly refer to which scientific standard should be introduced to estimate the level of biodiversity, in order to further evaluate whether an area needs to protect and what the extent of protection should be deleted. The selection criteria for MPAs are vital to determine the location and geographic scope of MPAs, constituting a basis for the establishment of ABNJ marine protected areas.

Many countries proposed to draw lessons from the EBSA (ecologically or biologically significant marine areas) criteria, and CBD guidelines on MPA networks (Ayer et al., 2018; Ilyas et al., 2018). Others noted that criteria would vary depending on the regional circumstances and should include, inter alia, biological productivity and/or diversity (Ban et al., 2017; Rahim et al., 2018). In addition, countries called for establishing MPAs in vulnerable areas and important areas for certain species (Cabral et al., 2017; Abdullah and Rahim, 2018). The positions of countries on this issue were dispersed, and the main dispute lies in which scientific criteria should be introduced into the ILBI.

However, the preparatory committee just listed the criteria which belong to existing criteria that countries proposed during the discussion. Thus, there were still a lack of unified selection criteria for MPAs finally and the issue of selection criteria would be further discussed at the intergovernmental conferences.

http://www.aloki.hu ● ISSN 1589 1623 (Print) ● ISSN 1785 0037 (Online)
DOI: http://dx.doi.org/10.15666/aeer/1704_86158629

No clear consensus on the designation process of MPAs

In the substantive recommendations, the preparatory committee summarized the proposal, consultation on and assessment of the proposal, decision-making as the issue of the designation process.

In terms of the proposal, the dispute on the issue is whether the international organizations can be authorized to submit a proposal for the establishment of MPAs, but the preparatory committee did not explain it in the recommendations. Some countries supported that state parties, other organizations, even a scientific and technical body can propose to establish MPA (Carr et al., 2017; Sarwar at al., 2018). Other countries consider that the proposal of MPAs should be put forward by state parties individually or jointly, but they did not mention whether international organizations can enjoy the right to submit proposals. For example, the EU highlighted that proposals to designate or recognize MPAs should come from state parties, individually or as a group. Though Japan, Argentina and Sweden had the generally same position as the EU, they emphasized on adequate communication with stakeholders prior to the proposal (Dias et al., 2017; Majumder et al., 2019). The US also underscored lack of clarity regarding who can submit proposals (Duarte et al., 2017).

With respect to consultation on and assessment of the proposal, a major point of dispute is whether ILBI needs to establish an independent global body to decide on proposed MPAs. For this issue, the US, supported by Canada and Australia, favored referring to a "scientific process," rather than a "scientific committee," providing input to "policy making," instead of a policy-making "body" (Feng et al., 2017). By contrast, most of the countries called for creating a scientific subsidiary body to technically assess proposals (Ferrari et al., 2018). Hence, no consensus has been reached on the establishment of a new scientific body at the global level.

In respect of decision-making, divisions mainly lie in whether establish a decision-making body or entitle existing regional institution to decide on MPAs proposals. The African Group, supported by the EU, called for global-level, consensus-based decision-making on ABMTs (Area-Based Management Tools) or MPAs (Gonson et al., 2017; Nouaim et al., 2019). However, Australia preferred a regional action-oriented process, including regional decision-making and Norway, supported RFMOs and the ISA designating and implementing MPAs (Havermans et al., 2018). Moreover, the Russian Federation opposed the creation of a new global mechanism for creating ABMTs and Norway noted lack of consensus on creating a new organization for establishing ABMTs during the fourth session of the preparatory committee (Hughes and Grant, 2017). To sum up, there are many countries opposed the global mechanism for MPAs.

Discussion

Analysis of the reasons for dilemmas of MPAs in the process of BBNJ negotiations

There is no single universally agreed definition of MPAs

As an instrument for marine biodiversity conservation and sustainable use, MPAs have been receiving increasing attention from policymakers. A reasonable concept of marine protected areas should include at least three elements: clear objectives, scope, and management measures. But there is a lack of a definition accepted by most countries in the international community.

http://www.aloki.hu ● ISSN 1589 1623 (Print) ● ISSN 1785 0037 (Online)
DOI: http://dx.doi.org/10.15666/aeer/1704_86158629

At the level of the global treatise, no conventions clearly defined the concept of MPAs in their text, but there are several related concepts similar to MPAs. For example, according to the Convention on Biological Diversity (CBD), "protected areas" means a geographically defined area which is designated or regulated and managed to achieve specific conservation objectives (Jabou and Smith, 2018). But the concept of "protected areas" is different from the concept of "marine protected areas", especially the concept of "marine protected areas beyond national jurisdiction". In 2004, the CBD conference of the parties adopted the Decision VII/5, defined "marine and coastal protected areas" as "an area within or adjacent to the marine environment, together with its overlying waters and associated flora, fauna, and historical and cultural features, which has been reserved by legislation or other effective means, including custom, with the effect that its marine and/or coastal biodiversity enjoys a higher level of protection than its surroundings". However, the definition of "marine and coastal protected areas" is still a broad concept that includes "historical and cultural features", which remains further discussion for applying to ILBI. The Convention Concerning the Protection of the World Cultural and Natural Heritage which has been ratified by 193 states parties, defined the "natural heritage" as "natural features consisting of physical and biological formations or groups of such formations, which are of outstanding universal value from the aesthetic or scientific point of view; geological and physiographical formations and precisely delineated areas which constitute the habitat of threatened species of animals and plants of outstanding universal value from the point of view of science or conservation; natural sites or precisely delineated natural areas of outstanding universal value from the point of view of science, conservation or natural beauty." It can be seen that the concept of "natural heritage" not only emphasizes the protection of the habitat of threatened species but also the value of aesthetic. Hence, a definition of MPAs is absent at the level of global treatise.

At the level of regional frameworks or bodies, The International Convention for the Prevention of Pollution from Ships, 1978 (MARPOL 78) that was developed by the International Maritime Organization (IMO), defining the "Special Areas" as "a sea area where for recognized technical reasons in relation to its oceanographical and ecological condition and to the particular character of its traffic the adoption of special mandatory methods for the prevention of sea pollution by oil is required" (Kay and Butenschön, 2018). In 1991, IMO introduced a new concept called "Particular Sensitive Sea Area (PSSA)" to protect the marine environment and ecosystem (Laffoley and Freestone, 2017). Moreover, in 2011, the Council of the international seabed authority proposed an environmental management plan in the area of the Clarion-Clipperton Zone to protect the biodiversity and ecosystem structure. In this plan, the international seabed authority adopted the term of "Area of Particular Environmental Interest (APEI)", which refers to "protect biodiversity and ecosystem structure and function by a system of representative seafloor areas closed to mining activities." As the report of Secretary-General pointed, a number of expressions are used to refer to the various area-based management tools presently in use, include: "special areas"; "specially protected areas"; "marine protected areas"; "spatial and temporal closures" in the fisheries context; "particularly sensitive sea areas" in the shipping context; "sanctuaries"; and "reserves" (Lambert et al., 2017). Thus, there is no single universally agreed definition of MPAs and the above definitions or concepts similar to "marine protected areas" at the global or regional level cannot be viewed as the concept of MPAs essentially, but they may only offer references for the ILBI.

http://www.aloki.hu ● ISSN 1589 1623 (Print) ● ISSN 1785 0037 (Online)
DOI: http://dx.doi.org/10.15666/aeer/1704_86158629

The reasons for lacking a universally accepted definition for MPAs, in my opinion, mainly are as follows:

First, the history of MPAs is relatively short, which leads to the understanding of countries to MPA is still in its infancy. The global extent of MPAs only really began to increase significantly from the late 1970s, notably with the declaration of the Great Barrier Reef Marine Park in Australia (Lathrop et al., 2017). Furthermore, the proportion of marine protected areas to the total ocean area increased from only 0 to 3% between 1960 and 2013, compared with less than 1% in 1990 (Madrigal et al., 2017). While MPAs in ABNJ emerged later and the first Pelagos Sanctuary, which is designated in 1999 and is not absolutely located in the high seas. It can be seen that the management tool of MPAs not only has a relatively short history, but the process of development is slow, which leads to the lack of a more unified understanding of MPA among countries. For instance, even though the US with the world's largest exclusive economic zone and has established over 1700 MPAs, its definition of MPAs is different from the definition used by the World Conservation Union (IUCN) (Mazaris, 2017).

Second, MPAs can be classified into different types according to their purpose, which may easily cause some misalignment of understanding in different countries. In fact, MPAs can be further divided into 5 different types, each of them is: (1) MPAs for purpose of fishery management and resources conservation; (2) the marine development zone for purpose of ecosystem or habitat conservation; (3) MPAs for purpose of marine biodiversity conservation; (4) MPAs for purpose of rare or endangered species preservation; (5) MPAs for tourism, entertainment, education and scientific research. Moreover, the International Union for Conservation of Nature (IUCN) divided MPA into six types, depending on their objectives: (1) Strict Nature Reserve/Wilderness Area; (2) National Park; (3) Natural Monument; (4) Habitat/Species Management Area; (5) Protected Landscape/Seascape; (6) Managed Resource Protected Area (Mcneill et al., 2018). Consequently, some countries may have only established the single type of MPAs mentioned above, while others may have established several different types of MPAs at the same time, resulting in an inconsistent understanding of MPAs among countries.

Finally, there are still a few countries in the world have the capacity to establish and manage MPAs effectively. Most countries are too inexperienced to establish MPAs, especially the large-scale MPAs. According to statistics, there are more than 70 countries in the world including China, Indian and Canada, whose area of MPAs is less than 1% of their exclusive economic zones, while just only 14 countries' MPAs account for more than 10% of their exclusive economic zones. In addition, according to statistics, it can also be concluded that countries with the capacity and experience in establishing very large MPAs are just limited to several countries, such as Australia, Russia, the US, New Zealand, the United Kingdom and France (Mrema, 2017). Judging from the current practice, the four "high seas MPAs" are only a short period of 5 to 15 years, which is slightly short-lived and the actual effect is not obvious. However, MPAs established by the ILBI are precisely those large-scale pelagic marine protected areas, so most countries are in fact lack of experience in setting up such MPAs and not to reach an agreement on the definition of MPAs.

A variety of selection criteria have made ILBI difficult to choose and coordinate

On the premise of defining MPAs, it's necessary to further define the selection criteria for MPAs. At present, the existing selection criteria for MPAs mainly include

http://www.aloki.hu ● ISSN 1589 1623 (Print) ● ISSN 1785 0037 (Online)
DOI: http://dx.doi.org/10.15666/aeer/1704_86158629

scientific criteria for identifying ecologically or biologically significant marine areas (EBSA), guidelines on designating a "particularly sensitive sea area" (PSSA), vulnerable marine ecosystems (VME) criteria, the general design guidelines for area of particular environmental interest (APEI), key biodiversity areas (KBA) adopted by IUCN and etc. The ILBI would eventually choose a set of selection criteria, but now there are at least 7 set of selection criteria with different elements that make the ILBI difficult to choose and coordinate.

From the regional organizations or bodies of these selection criteria, different types of selection criteria are proposed and implemented by different international organizations that they have seldom interaction with each other. From the emphasis of these selection criteria, different priorities lead to the different selection criteria. For instance, the criteria of VME pays the more attention to the ecological damages caused by deep-sea fisheries. Thus, the FAO proposed a distinct standard from the EBSA, named “Functional significance of the habitat” which is to protect habitats that are necessary for the survival, function, spawning/reproduction or recovery of fish stocks. In addition, the application scope and the amounts of the region selected by these criteria are also different. The VME has been adopted by some regional fishery management organizations, such as NEAFC, CCAMLR, NAFO GFCM, SEAFO and SPRFMO. Currently, IMO has also designated 17 particularly sensitive sea areas around the world, most of which are located within national jurisdiction. The EBSA description work is also constantly updated and deepened, 71 out of 279 ecologically or biologically significant areas (EBSAs) are located in ABNJ, covering 21% of total surface area of ABNJ (Nikitine et al., 2018). It can be seen that the inconsistencies and even coincidences in the scope of different selection criteria have made it difficult for ILBI to determine the selection criteria.

Given that the ILBI should coordinate the relationship of different selection criteria for MPAs or other area-based management tools and prevent duplication, the negotiations of the ILBI are actually facing the dual difficulty in choosing and coordinating the selection criteria. In fact, the relationship between choosing and coordinating is like the two sides of the coin. It is manifested that when making the final decision on the issue of selection criteria, it is necessary to make trade-offs between existing criteria and avoid conflicts with existing criteria. Therefore, the situation of dual difficulty faced in determining the selection criteria is an important reason for the delay in reaching a consensus on this issue during the BBNJ negotiations.

MPAs in ABNJ will impose a significant impact on some states’ fishery interests

The designation process is directly related to the management model of MPAs. In the third session of the preparatory committee, Chair Duarte proposed focusing on three options: a global model, a hybrid model and a regional and sectoral model (Pereira et al., 2018). Specifically, the states with skeptical and negative views on the global model are Australia, New Zealand, Norway, Iceland, Russia, Canada and the Pacific small island developing States (PSIDS). These states undoubtedly all advocated the leading role of regional organizations in the establishment of ABNJ marine protected areas and considered that excessive intervention from the global level should be reduced or avoided. The regional and sectoral model means to essentially authorize the regional fisheries management organizations (RFMO) the decision-making powers for initiating and managing a high seas MPA. However, whether the regional fisheries management organizations or bodies actually establish an ABNJ marine protected area in accordance

http://www.aloki.hu ● ISSN 1589 1623 (Print) ● ISSN 1785 0037 (Online)
DOI: http://dx.doi.org/10.15666/aeer/1704_86158629

with the ILBI depends on the will of the all contracting parties of the organizations and their internal decision-making rules.

At present, there are many regional fisheries management organizations, including the Commission for the Conservation of Antarctic Marine Living Resources (CCAMLR), Northwest Atlantic Fisheries Organization (NAFO), the North East Atlantic Fisheries Commission (NEAFC), the South East Atlantic Fisheries Organization (SEAFO), The South Pacific Regional Fisheries Management Organization (SPRFMO), the North Pacific Fisheries Commission (NPFC), the Western and Central Pacific Fisheries Commission (WCPFC), the Southern Indian Ocean Fisheries Agreement (SIOFA), the General Fisheries Commission for the Mediterranean (GFCM) and etc.

The current governance model of high seas fisheries is mainly relied on regional fisheries management organizations and there are 20 regional fishery management organizations with mandate, covering the main fishing areas of the global ocean. In respect to the number of the contracting parties, members of the CCAMLR currently include 24 States and the European Union, NAFO has 12 Contracting Parties, the NEAFC has 5 contracting parties and 5 non- cooperating contracting parties, the SEAFO has 7 contracting parties, the SPRFMO has currently 15 Members, the NPFC has 8 contracting parties, the WCPFC has 26 contracting parties, the SIOFA has 9 contracting parties and the GFCM has 24 contracting parties. To sum up, despite the WCPFC has the largest number of the contracting parties among the regional fisheries management organizations mentioned above, but it only has the 26 contracting parties. Among the countries that do not approve of the global model, Norway, Iceland, Russia and Canada are all members of NAFO, while Norway, Iceland and Russia are also parties to NEAFC (Wu, 2018). Therefore, the leadership of establishing the high seas MPAs is easily controlled by the RFMO that is represented by a few states.

From the states with skeptical and negative attitude to the global model, their capture production of fisheries usually depends heavily on the single region under the management of the RFMO. For example, Norway, Iceland, Russia and Canada are all the contracting parties of the NAFO, while Norway, Iceland and Russia are also the members of the NEAFC at the same time. Australia and New Zealand are both contracting parties of the WCPFC and the SPRFMO. According to the statistics of FAO in 2016, total capture production of Norway is 203,8810 tons in the area of Northeast Atlantic, accounting for 92% of its annual total capture production; It is worth noting that the geographic scope of FAO fishing area 27 is the same to the areas of the NEAFC Convention. Furthermore, all the capture production of Iceland in 2016 come from the area of Northeast Atlantic; The capture production of Canada in the Northwest Atlantic is 663,680 tons, accounting for 78% of its annual total capture production; In addition, the capture production of New Zealand in the Northwest Pacific is 421,646 tons, accounting for 99% of its annual total capture production (Plassjohnson et al., 2017). However, as the country with the highest capture production of fisheries in the world, China’s marine fisheries production in 2016 was 15,331,960 tons, but the 97% of the total annual production came from the Northwest Pacific. According to the "13th Five-Year Plan" issued by the Ministry of Agriculture in 2017, by the end of 2016, the total production of China's far-off ocean fisheries was 1.99 million tons, including 1.32 million tons of high seas fisheries. Hence, China’s fishery production on the high seas only accounts for 8% of its annual marine capture production and the fishing area

http://www.aloki.hu ● ISSN 1589 1623 (Print) ● ISSN 1785 0037 (Online)
DOI: http://dx.doi.org/10.15666/aeer/1704_86158629

of China in Northwest Pacific is not entirely within the scope of regional fisheries management organizations.

From the decision-making mechanism of the relevant regional fisheries organizations, the NEAFC and the SPRFMO, which are composed mainly of states with negative attitude to the global model as mentioned above, provided for their respective decision-making mechanisms. According to the NEAFC Convention, decisions of the Commission shall be taken by a simple majority or by a two-thirds majority (Postaire et al., 2017). The SPRFMO Convention provided that decisions by the Commission shall be taken by consensus (Schulze et al., 2017). It can be concluded that the decision-making mechanism of regional fisheries management organizations has an obvious dependence on the will of the members. When the contracting parties hold different or opposing positions on the proposals, the regional fisheries management organizations will not effectively make a decision and implement it. Furthermore, the Objection Procedure is also prevalent in regional fisheries organizations, as long as members formally raise objections during the decision-making process of regional fisheries management organizations. This procedure has led regional fisheries organizations to reach the consensus of all members so as to a better compliance. Therefore, if the ILBI authorizes the RFMO the autonomy to establish MPAs, it is the same as granting the minority contracting parties of these RFMO the right to establish MPAs.

The establishment of the high seas MPAs will inevitably impose restrictions on the fishing activities, for example, the conservation measures of the Ross Sea established in 2016 provided for "fishing activities are prohibited within the MPA" (Soares and Lucas, 2018). Thus, the states whose fishery productions highly depend on the single region under the management of the RFMO do not hope it adopts the decision to establish MPA. To this end, from external relations, these fishing nations of the RFMO will emphasize the role of RFMO in the BBNJ negotiations and tend to retain their respective autonomies in establishing the ABNJ marine protected areas. From the internal relations of the RFMO, these states will also make full use of the decision-making mechanism in order to minimize the impact of MPAs on their fishing interests.

Results

The solutions of main issues in the process of BBNJ negotiations

The ILBI should clarify the definition of MPAs on the basis of existing definitions

The definition of MPAs not only should be clarified in the process of BBNJ negotiations but also defined in the ILBI. As an important newly emerging marine management measure, the concept of MPAs is not clearly defined in the existing international conventions, including the UNCLOS and there is no universally accepted concept of MPAs in the international community. When the UNCLOS was enacted between 1973 and 1982, marine biodiversity beyond national jurisdiction did not attract the attention of all countries, leaving many gaps in the Convention. Thus, the legal and institutional frameworks that govern marine biodiversity in areas beyond national jurisdiction (ABNJ) are widely perceived as inadequate for ensuring the long-term health and equitable use of the living resources of this vast area and the ILBI should fill the gaps of UNCLOS (Solovyev et al., 2017). Therefore, before creating an MPA system in the ILBI, country participants must agree on what they understand by this term.

http://www.aloki.hu ● ISSN 1589 1623 (Print) ● ISSN 1785 0037 (Online)
DOI: http://dx.doi.org/10.15666/aeer/1704_86158629

According to the definition of IUCN, it comprises both legal approaches and other approaches; it can be applied in three-dimensional scope of protection, including not only the intertidal zone or the sub-tidal zone of the ocean, but also the seabed environment within this scope; the protection objectives are also broad, including historical and cultural features (Urra et al., 2018). Strictly speaking, the historical and cultural features of the IUCN's definition are not consistent with the objective of protecting marine biodiversity. The definition of protected areas in CBD is an ambiguous definition that does not specify the objectives and management methods of MPAs, and whether the nature of the management methods adopted is a "no-take" MPAs. The OSPAR Commission established by the Convention for the Protection of the Marine Environment of the North-East Atlantic (OSPAR Convention) defined the "marine protected areas" as "an area within the maritime area for which protective, conservation, restorative or precautionary measures, consistent with international law have been instituted for the purpose of protecting and conserving species, habitats, ecosystems or ecological processes of the marine environment." Despite the definition of the OSPAR Commission has the elements of objectives, geographic scope and management measures, but it is not clear whether this definition includes MPAs established in the seabed area. However, the MPA networks of the North-East Atlantic are so far consisted by 7 high seas MPAs and 5 of them are located in the seamount or mid-ocean ridge areas (Young and Friedman, 2018). Hence, the ILBI should determine whether the geographic scope of MPAs' definition includes the seabed areas.

In conclusion, the definitions of MPAs mentioned above are more or less unreasonable when applied to the ILBI, so it is difficult to directly copy the existing definitions of MPAs to the ILBI. The intergovernmental conference on an ILBI under the UNCLOS on the conservation and sustainable use of the marine biological diversity of areas beyond national jurisdiction needs to specify the definition of MPA. First, the ILBI should make clear the geographic scope of MPAs' definition, especially whether the scope should include the international seabed areas. Second, the ILBI should set up specific objectives and take proper account of whether the objectives should comprise the characteristic and historical features. Third, it needs to be further clarified whether the management measures in the ILBI should be defined in a general or enumerated way (Tagle, 2018).

The selection criteria for MPAs in the ILBI should draw lessons from the existing criteria

The possible ways to cope with the dual difficulty that ILBI faced in determining the selection criteria is to draw lessons from the existing criteria and provide for the inclusive criteria for the ILBI. Thus, its necessary to make a comparative analysis of the existing selection criteria.

According to the statistics of the *Table 1*, despite different organizations have their selection criteria, but the most of the selection criteria are similar and the nine selection criteria mentioned in have almost covered the existing selection criteria for MPAs in the international community. First, most of the definitions of 9 selection criteria in the were clearly defined in Resolution A.982(24) adopted by the 24th Assembly of the IMO, while the remaining selection criteria are defined in decision IX/20 adopted by the conference of the parties to the convention on biological diversity at its 9th meeting. Second, only the operational guidelines for the Implementation of the World Heritage Convention includes the criteria of "historical geomorphological importance". However,

http://www.aloki.hu ● ISSN 1589 1623 (Print) ● ISSN 1785 0037 (Online)
DOI: http://dx.doi.org/10.15666/aeer/1704_86158629

the so-called "historical geomorphological importance" refers to "the property represents major stages of earth's history, including the record of life, significant on-going geological processes in the development of landforms, or significant geomorphic or physiographic features" (Bokuniewicz and Jang, 2018). Hence, the criteria of the historical geomorphological importance, in fact, should be excluded when the ILBI set out the selection criteria for MPAs.

Table 1. *Correspondence between the CBD EBSA criteria and other international criteria used by IGOs and NGOs (i.e. Birdlife and IUCN) mentioned in this manuscript. Correspondence is indicated by either a check where it exists, an X where it doesn't, or a? where there is uncertainty or the criteria suite is under review (Tommasi et al., 2017)*

Organization	CBD	FAO	IMO	UNESCO	RAMSAR	Birdlife	IUCN
Site criteria	EBSA	VME	PSSA	WHS	RAMSAR	IBA	KBA
Year	2008	2009	2005	1977(first version)	2004	**early 1980s**	2016
Uniqueness or rarity	✓	✓	✓	✓	✓	✓	✓
Special importance for life history stages of species	✓	✓	✓	✓	✓	✓	✓
Importance to threatened or endangered species	✓	✓	✓	✓	✓	✓	✓
Vulnerability, fragility, sensitivity or slow recovery	✓	✓	✓	**X**	**?**	**X**	**?**
Productivity	✓	**X**	✓	✓	**X**	**X**	**?**
Biodiversity	✓	**X**	✓	✓	✓	**X**	**?**
Naturalness	✓	**X**	✓	✓	✓	**X**	**?**
Structure	**X**	✓	✓	**X**	**X**	**X**	**?**
Historical geomorphological importance	**X**	**X**	**X**	✓	**X**	**X**	**X**

Third, the criteria of "Uniqueness or rarity", "Special importance for life history stages of species" and "Importance to threatened or endangered species" are all stipulated in the existing selection criteria lists and the criteria of "Biodiversity" and "Naturalness" are also adopted by four selection criteria. Hence, these criteria have been accepted by the international community. Fourth, 15 specific selection criteria were listed in the recommendations of the preparatory committee, of which five are beyond the scope of the existing criteria, namely "Representativeness", "Dependency", "Connectivity", "Ecological processes" as well as "Economic and social factors." These five selection criteria need to be further discussed during the intergovernmental conferences. Finally, no matter what selection criteria are adopted by the ILBI, the activities of identifying MPAs are in fact the scientific exercise, which should not be regarded as bringing about any potential management measures and any obligations to establish MPAs. Therefore, the issue of selection criteria for MPAs under the ILBI should be strictly distinguished from the establishment, management, review of MPAs, so that it can continue to be the scientific exercise and provide references for the establishment of MPAs.

To sum up, under the premise of the scientific activities, the ILBI should coordinate the different existing criteria and draw lessons from the regional practice, providing for a set of comprehensive and unified selection criteria for the high seas MPAs.

http://www.aloki.hu ● ISSN 1589 1623 (Print) ● ISSN 1785 0037 (Online)
DOI: http://dx.doi.org/10.15666/aeer/1704_86158629

The ILBI should adopt the global model for the high seas MPAs

The adoption of the General Assembly resolution evinces a growing recognition within the international community that the regime governing the marine biodiversity in ABNJ is no longer fit for purpose, and that further action to develop a legal and institutional framework is necessary (Wang et al., 2018). The global model has obvious advantages compared with the hybrid model or regional and sectoral model.

First, a treaty shall not create either obligations or rights for a third State without its consent in pursuant to Article 34 of Vienna Convention on the Law of Treaties and this provision is also considered to be a customary international law rule. Therefore, the management measures of MPAs adopted by regional organizations or institutions cannot generally create obligations for third states without its consent. The number of Parties in each regional organization or institution under the regional model is far less than those of a universally representative global convention. Hence, the MPAs in ABNJ under the regional model will not be able to directly restrict non-Parties, which will result in the management measures of MPAs cannot be universally observed and regional model have deficiencies in the general principles of international law.

Second, a regional and sectoral model is unable to take unified actions at the global level and are likely to further deepen the fragmentation of marine biodiversity protection beyond national jurisdictions, thus making cooperation and coordination between different regions or sectors more difficult. On the one hand, the ILBI is facing the status quo of "divided governance" between the water column and the international seabed areas, which further leads to possibly apply different governance rules to living resources and mineral resources beyond national jurisdiction. But in the world of the deep sea, minerals and organisms are usually inseparable, that is, they are two aspects of one thing and should be managed as a whole (Tapia et al., 2018). Consequently, the application of different rules is inconsistent with the laws of nature, artificially increasing the difficulties of coordination and may to a certain extent reduce the effectiveness of marine biodiversity protection. On the other hand, if the ILBI were to adopt a regional model and authorize the regional bodies to establish, manage and review the high seas MPAs, the laws of nature that ocean creatures and their communities are moving all the time is also ignored. Thus, the approaches by dividing the marine ecosystem into different areas are no help to protect the marine biological diversity and further deepens the degree of fragmentation of existing international frameworks.

Third, apart from deepening fragmentation of international frameworks, a regional and sectoral model cannot provide the basis of international law for the establishment of MPAs in areas beyond national jurisdiction. In addition, a regional and sectoral model easily leads to a crisis of trust. For example, in the process of establishing the Ross Sea protected areas, Russia, Ukraine, China and other states raised doubts about the legal capacity of CCAMLR in establishing MPAs and lacking a definition of MPA at the annual CCAMLR conference. In 2012 and 2013, Russia even pointed that it would refuse further negotiations if the two issues were not resolved (Shoda et al., 2017). Moreover, in 2014, Russia submitted a working paper "Marine Protected Areas in the Antarctic Treaty System" to the Antarctic Treaty Consultative Meeting (ATCM) and stated that "Taking into account that seven countries of those which have signed the Antarctic Treaty and the CCAMLR Convention have earlier declared territorial claims to Antarctica, Russia is obliged to consider the potential possibility that an MPA may be used as an instrument to establish geopolitical control over southern polar regions over

http://www.aloki.hu ● ISSN 1589 1623 (Print) ● ISSN 1785 0037 (Online)
DOI: http://dx.doi.org/10.15666/aeer/1704_86158629

which territorial claims were made earlier" (Botte, 2017). It can be seen that the legitimacy of the high seas MPAs is vulnerable to be challenged when the regional model is not authorized at the global level. The non-contracting parties of the RFMO may concern about their freedoms on the high seas which will be imposed further restrictions by the RFMO.

Final, the main purpose of a hybrid model is to provide guidance and legal basis for regional bodies or the RFMO through the ILBI, which cannot avoid the defects of the regional model mentioned above. Moreover, as a compromise, the effectiveness of a hybrid model is difficult to guarantee and the relationship between a global framework and regional organizations is not easy to put in order. If we can solve this problem, hybrid model may be a good choice.

To sum up, the advantages of the global model are obvious, and it is foreseeable that ILBI should finally establish a global governance model for MPAs.

Conclusion

As a breakthrough to the traditional marine management tools, MPAs are becoming an important means for the international community to protect marine biodiversity. The negotiation of the issue of MPAs in ABNJ will, after dealing with dilemmas of lack of definition, unclear selection criteria, and disputes over the governance model, inevitably reach a reasonable institutional framework, and further promote marine biodiversity protection. The above is only a preliminary discussion on this issue. In the future, specific planning and implementation measures are needed to make this problem better solved.

REFERENCES

[1] Abdullah, N. A., Rahim, F. (2018): Distinctiveness And Potentials Of Two Flowering Roadside Hedgerows, Turnera Ulmifolia And Melastoma Malabathricum As Benefecial Plants For Iinsects. – Environment & Ecosystem Science 2(2): 06-10.

[2] Afonso, P., Schmiing, M., Fontes, J., Tempera, F., Morato, T., Santos, R. S. (2018): Effects of marine protected areas on coastal fishes across the n, mid-north atlantic. – Journal of Sea Research 138: 34-47.

[3] Alger, J., Dauvergne, P. (2017): The politics of pacific ocean conservation: lessons from the pitcairn islands marine reserve. – Pacific Affairs 90(1): 29-50.

[4] Ayer, A., Fulton, S., Caamal-Madrigal, J. A., Espinoza-Tenorio, A. (2018): Halfway to sustainability: management lessons from community-based, marine no-take zones in the mexican caribbean. – Marine Policy 93: 22-30.

[5] Ban, N. C., Davies, T. E., Aguilera, S. E., Brooks, C., Cox, M., Epstein, G., Evans, L. S., Maxwell, S. M., Nenadovic, M. (2017): Social and ecological effectiveness of large marine protected areas. – Global Environmental Change 43: 82-91.

[6] Bokuniewicz, H., Jang, S. G. (2018): Dredging intensity: a spatio-temporal indicator for managing marine resources. – Environmental Management 62(5): 1-8.

[7] Botte, E. (2017): Exploiting the sea. annalisa marzano, harvesting the sea. the exploitation of marine resources in the roman mediterranean (oxford studies on the roman economy; oxford 2013). – Journal of Roman Archaeology 28: 684-687.

[8] Cabral, R. B., Gaines, S. D., Johnson, B. A., Bell, T. W., White, C. (2017): Drivers of redistribution of fishing and non-fishing effort after the implementation of a marine protected area network. – Ecological Applications 27(2): 416-428.

http://www.aloki.hu ● ISSN 1589 1623 (Print) ● ISSN 1785 0037 (Online)
DOI: http://dx.doi.org/10.15666/aeer/1704_86158629

[9] Carr, M. H., Robinson, S. P., Wahle, C., Davis, G., Kroll, S., Murray, S., Schumacker, E. J., Williams, M. (2017): The central importance of ecological spatial connectivity to effective coastal marine protected areas and to meeting the challenges of climate change in the marine environment. – Aquatic Conservation Marine & Freshwater Ecosystems 27(2): 6-29.
[10] Dias, M. P., Bond, A. L., Carneiro, A. P. B., Lascelles, B., Small, C., Gonzã Lezsolã, S. J. (2017): Using globally threatened pelagic birds to identify priority sites for marine conservation in the south atlantic ocean. – Biological Conservation 211: 76-84.
[11] Duarte, F., Doherty, G., Nakazawa, P. (2017): Redrawing the boundaries: planning and governance of a marine protected area—the case of the exuma cays land and sea park. – Journal of Coastal Conservation 21(2): 265-271.
[12] Feng, C., Xu, M., Feng, C., Wettberg, E. J. B. V., Kang, M. (2017): The complete chloroplast genome of primulina and two novel strategies for development of high polymorphic loci for population genetic and phylogenetic studies. – Bmc Evolutionary Biology 17(1): 224.
[13] Ferrari, R., Marzinelli, E. M., Ayroza, C. R., Jordan, A., Figueira, W. F., Byrne, M., Malcolm, H. A., Williams, S. B., Steinberg, P. D. (2018): Large-scale assessment of benthic communities across multiple marine protected areas using an autonomous underwater vehicle. – Plos One 137(1): 1-11.
[14] Gonson, C., Pelletier, D., Alban, F., Giraud-Carrier, C., Ferraris, J. (2017): Influence of settings management and protection status on recreational uses and pressures in marine protected areas. – Journal of Environmental Management 200: 170-185.
[15] Havermans, C., Seefeldt, M. A., Held, C. (2018): A biodiversity survey of scavenging amphipods in a proposed marine protected area: the filchner area in the weddell sea, antarctica. – Polar Biology 41(18): 1-20.
[16] Hughes, K. A., Grant, S. M. (2017): The spatial distribution of antarctica's protected areas: a product of pragmatism, geopolitics or conservation need? – Environmental Science & Policy 72: 41-51.
[17] Ilyas, F., Arif, M., Iftikhar, A., Sattar, A., Cuong, D. M., Ilyas, M., Parveen, A. (2018): Indigenous Vesicular Mycorrhizal Fungi Effect on Maize Under Different Textures. – Earth Sciences Pakistan 2(2): 12-15.
[18] Jabour, J., Smith, D. (2018): The ross sea region marine protected area: can it be successfully managed? – Ocean Yearbook Online 32(1): 190-205.
[19] Kay, S., Butenschön, M. (2018): Projections of change in key ecosystem indicators for planning and management of marine protected areas: an example study for european seas. – Estuarine Coastal & Shelf Science 201(3): 129-136.
[20] Khanchoul, K., Saaidia, B., Altschul, R. (2018): Variation in Sediment Concentration and Water Disharge During Storm Events in Two Catchments, Northeast of Algeria. – Earth Sciences Malaysia 2(2): 01-09.
[21] Laffoley, D., Freestone, D. (2017): A world of difference - opportunities for applying the 1972 world heritage convention to the high seas. – Aquatic Conservation Marine & Freshwater Ecosystems 27(6): 78-88.
[22] Lambert, C., Virgili, A., Pettex, E., Delavenne, J., Toison, V., Blanck, A., Ridoux, V. (2017): Habitat modelling predictions highlight seasonal relevance of marine protected areas for marine megafauna. – Deep Sea Research Part II Topical Studies in Oceanography 141: 262-274.
[23] Lathrop, R. G., Bognar, J., Buenaventura, E., Ciappi, M., Green, E., Belton, T. J. (2017): Establishment of marine protected areas to reduce watercraft impacts in barnegat bay, new jersey. – Journal of Coastal Research 78: 277-286.
[24] Madrigal-Ballestero, R., Albers, H. J., Capitán, T., Salas, A. (2017): Marine protected areas in costa rica: how do artisanal fishers respond? – Ambio 46(4): 1-10.

http://www.aloki.hu ● ISSN 1589 1623 (Print) ● ISSN 1785 0037 (Online)
DOI: http://dx.doi.org/10.15666/aeer/1704_86158629

[25] Majumder, S. C., Islam, K., Hossain, M. M. (2019): State of research on carbon sequestration in Bangladesh: a comprehensive review. – Geology, Ecology, and Landscapes 3(1): 29-36.
[26] Mazaris, A. D. (2017): Manifestation of maritime piracy as an additional challenge for global conservation. – Marine Policy 77(Complete): 171-175.
[27] Mcneill, A., Clifton, J., Harvey, E. S. (2018): Attitudes to a marine protected area are associated with perceived social impacts. – Marine Policy 94(3): 106-118.
[28] Mrema, E. (2017): Introduction: protecting the global commons. – Georgetown Journal of International Affairs 18(1): 3-5.
[29] Nikitine, J., Wilson, A. M. W., Dawson, T. P. (2018): Developing a framework for the efficient design and management of large scale marine protected areas. – Marine Policy 94: 196-203.
[30] Nouaim, W., Chakiri, S., Rambourg, D., Karaoui, I., Ettaqy, A., Chao, J., Allouza, M., Razoki, B., Yazidi, M., Hmidi, F. E. (2019): Mapping the water erosion risk in the Lakhdar river basin (central High Atlas, Morocco). – Geology, Ecology, and Landscapes 3(1): 22-28.
[31] Omini, E. O., Akpang, O. M. (2018): Cavity Detection Under Re-Enforced Concrete Floor Using Ground Penetration Radar. – Engineering Heritage Journal 2(2): 11-18.
[32] Pereira, J. M., Krüger, L., Oliveira, N., Meirinho, A., Silva, A., Ramos, J. A., Paiva, V. H. (2018): Using a multi-model ensemble forecasting approach to identify key marine protected areas for seabirds in the portuguese coast. – Ocean & Coastal Management 153: 98-107.
[33] Plassjohnson, J., Mcquaid, C., Porri, F. (2017): Top-down effects on intertidal mussel populations: assessing two predator guilds in a south african marine protected area. – Marine Ecology Progress 411(6): 149-159.
[34] Postaire, B., Gélin, P., Bruggemann, H., Pratlong, M., Magalon, H. (2017): Population differentiation or species formation across the indian and the pacific oceans? an example from the brooding marine hydrozoanmacrorhynchia phoenicea. – Ecology & Evolution 7(20): 8170-8186.
[35] Qiao, F. (2018): The Study On The Integration Of Green Architecture And Appropriate Technology. – Engineering Heritage Journal 2(2): 01-03.
[36] Rahim, Y., Khan, M. S., Mughal, S. (2018): Petrography Of Sandstone Of The Lumshiwal Formation From Eastern Hazara, Khyber Pakhtunkhwa, Pakistan: Implications For Provenance, Diagenesis And Environments Of Deposition. – Earth Sciences Pakistan 2(2): 01-06.
[37] Sarwar, M. T., Hui, Z. H., Maqbool, A. (2019): Causes And Control Measures Of Urban Air Pollution In China. – Environment & Ecosystem Science 3(1): 35-36.
[38] Schulze, A., Grimes, C. J., Rudek, T. E. (2017): Tough, armed and omnivorous: hermodice carunculata (annelida: amphinomidae) is prepared for ecological challenges. – Journal of the Marine Biological Association of the United Kingdom 97: 1-6.
[39] Shoda, S., Lucquin, A., Ahn, J. H., Hwang, C. J., Craig, O. E. (2017): Pottery use by early holocene hunter-gatherers of the korean peninsula closely linked with the exploitation of marine resources. – Quaternary Science Reviews 170: 164-173.
[40] Soares, M. D. O., Lucas, C. C. (2018): Towards large and remote protected areas in the south atlantic ocean: st. peter and st. paul´s archipelago and the vitória-trindade seamount chain. – Marine Policy 93: 101-103.
[41] Solovyev, B., Spiridonov, V., Onufrenya, I., Belikov, S., Chernova, N., Dobrynin, D., Gavrilo, M., Glazov, D., Krasnov, Y., Mukharamova, S., Pantyulin, A., Platonov, N., Saveliev, A., Stishovm M., Tertitski, G. (2017): Identifying a network of priority areas for conservation in the arctic seas: practical lessons from Russia. – Aquatic Conservation Marine & Freshwater Ecosystems 27(Supplement S1): 30-51.

http://www.aloki.hu ● ISSN 1589 1623 (Print) ● ISSN 1785 0037 (Online)
DOI: http://dx.doi.org/10.15666/aeer/1704_86158629

[42] Sufiyan, I., Zakariya, R., Yacoob, R., Idris, M. S., Idris, N. M. (2018): SWAT Subbasins Parameters and Flood Risk Simulations Using 3d In Terengganu Watershed. – Earth Sciences Malaysia 2(2): 10-15.
[43] Tagle, V. (2018): Characterization of two natural sorbents for the evaluation of metal contamination in water. – Acta Microscopica 27(3).
[44] Tapia-Monsalve, R., Newsome, S. D., Sanchez-Hernandez, J. C., Bozinovic, F., Nespolo, R., Sabat, P. (2018): Terrestrial birds in coastal environments: metabolic rate and oxidative status varies with the use of marine resources. – Oecologia: 1-9.
[45] Tommasi, D., Stock, C. A., Hobday, A. J., Methot, R., Kaplan, I. C., Eveson, J. P., Holsman, K., Miller, T. J., Gaichas, S., Gehlen, M., Pershing, A., Vecchi, G. A., Msadek, R., Delworth, T., Eakin, C. M., Haltuch, M. A., Séférian, R., Spillman, C. M., Werner, F. E. (2017): Managing living marine resources in a dynamic environment: the role of seasonal to decadal climate forecasts. – Progress in Oceanography 152: 15-49.
[46] Urra, J., Rueda, J. L., Marina, P., Antit, M., Salas, C. (2018): Populations of commercial molluscs within a highly biodiverse marine protected area of the northern alboran sea (w mediterranean): preferential habitats, seasonal dynamics and importance for artisanal fisheries. – Thalassas An International Journal of Marine Sciences 34(4): 1-11.
[47] Wang, Z., Wang, X., Wang, J. (2018): Recent advances in antibacterial and antiendotoxic peptides or proteins from marine resources. – Marine Drugs 16(2): 57.
[48] Wu, L. (2018): A Review of 300,000 Foreign Students Plan of Japan over the Past Decade (2008-2017): Analysis based on International Students in Japan by JASSO. – Argos 35(71).
[49] Young, M., Friedman, A. (2018): Biodiversity beyond national jurisdiction: regimes and their interaction. – AJIL Unbound 112: 123-128.

http://www.aloki.hu ● ISSN 1589 1623 (Print) ● ISSN 1785 0037 (Online)
DOI: http://dx.doi.org/10.15666/aeer/1704_86158629

EFFECTS OF PROCESS PARAMETERS ON MICROARC OXIDATION FILM LAYERS OF POROUS TITANIUM

FAN, X. P.

Panzhihua University, Panzhihua, Sichuan, PR China
e-mail: fanxingping123@163.com

(Received 8th Mar 2019; accepted 21st May 2019)

Abstract. In order to better understand the specific effect of process parameters on porous titanium micro-arc oxidation coating. In this paper, TiO_2 membrane layer was prepared on porous titanium matrix with 67 % porosity by microarc oxidation method (MAO), which use a phosphoric acid solution as electrolyte. The samples were characterized using XRD and SEM. The results showed that the samples prepared under the experimental parameters of 350 V and 30 min had a good surface morphology and could provide a higher specific surface area. After soaking in SBF for 7 days, the formation of hydroxyapatite (HA) can be induced, indicating that porous titanium after micro-arc oxidation modification has good biological activity.
Keywords: *phosphoric acid, hydroxyapatite, carbon dioxide film, process parameters, biological activity*

Introduction

Titanium (Ti) and its alloys are widely used as hard tissue repair materials in clinics owing to their high biocompatibility (Choi and Kim, 2016; Nune et al., 2016; Thanh and Do, 2018). However, their far larger elastic moduli and the mismatched mechanical properties compared to human bones would lead to post-implant stress shield and finally to the loosening and failure of implants (Nomura et al., 2005; Shrestha and Baral, 2018). Nevertheless, the emerging porous structures can efficiently improve the mechanical properties of Ti to the levels of human bone tissues. Moreover, porous Ti has high biocompatibility, and (Hao, 2018) its unique structures are favorable for the body fluid transmission and tissue regeneration / reconstruction and accelerate the healing process. (Zhang et al., 2017). Generally, a higher porosity offers a larger space for tissue growth, which is favorable for the inward growth of peripheral cells and the growth of new bones and strengthens the bio-fixation with bone tissues (Wen et al., 2001; Ali et al., 2018).

However, Ti is a biologically inert material that can hardly bind with bone tissues to form bone bonding (Wang et al., 2014; Rahim et al., 2018), which limits its further application in the medical field (Das et al., 2016; Qiao, 2018). Thus, surface modification is required to improve the biological performances of porous Ti. The emerging microarc oxidation surface modification in recent years can be used to prepare porous ceramic coating layers on surfaces of Ti and thereby to largely improve its properties (Chien et al., 2017; Gautam et al., 2019). The phases and morphology largely affect the bioactivity of porous ceramic films (Zhao et al., 2014), but there is rare research on microarc oxidation coating of porous Ti. Thus, the microarc oxidation technology was used to prepare porous coatings on the porous Ti matrix. The effects of anode voltage and oxidation time on the surface morphology and phases of the coatings were systematically studied (Chen et al., 2017; Dali and Kamarudin, 2018). The findings offer some reference for subsequent research.

http://www.aloki.hu ● ISSN 1589 1623 (Print) ● ISSN 1785 0037 (Online)
DOI: http://dx.doi.org/10.15666/aeer/1704_86318641

Materials and Method

Preparation of porous Ti

The 300-mesh commercial pure Ti powder and NH_4HCO_3 (granularity=100-300 μm) as the pore-forming agent were mixed at the mass fraction ratio of 1:1, uniformly stirred, and placed (Zhang et al., 2018; Masri and Samsudin, 2018) into a mold, which was pressed by a miniature hydraulic press at the pressure of 80 MPa. The molded specimens were preserved in an ordinary muffle furnace at 100ºC for 5 h in order to completely remove the pore-forming agent, then heated to 1300ºC in a vacuum sintering furnace (< 10^{-3} MPa), heat-preserved for 2 h and naturally cooled, forming the porous Ti substrate.

Preparation of surface TiO_2 films on porous Ti via microarc oxidation

The sintered porous Ti was cut into sheets (Φ10 mm × H2 mm), which were ultrasonically washed with ethanol and deionized water and then dried. (Zhang et al., 2018). The porous Ti sheets were used as the anode, graphite sheets as the cathode, and a 0.5 mol/L H_3PO_4 solution as the electrolytic solution in the microarc oxidation experiments at the time of 5 - 30 min and voltage of 250-450 V. When the electrolytic solution was controlled below 30ºC, porous Ti MAO films were formed and the oxidized specimens were washed in distilled water and dried.

Characterization of TiO_2 films

Morphology was observed under a Quanta200 scanning electron microscope (SEM) and phases were analyzed under an X'Pert Pro MPD X-ray diffractometer (XRD).

Bioactivity experiments

A simulated body fluid (SBF) was made according to the composition by Tadashi Kokubo. The specimens after the above microarc oxidation were soaked in the SBF at 37ºC. The SBF was changed once every day. After 7 days, the specimens were taken out, rinsed with deionized water and air-dried.

Results and discussion

Effects of electrode voltage

Effects on the surface morphology of microarc oxidized film layers

The figure below (*Fig. 1*) shows the surface morphology of the oxidized films prepared after 30 min of oxidation at different electrode voltages. Clearly, (Kang et al., 2017) numerous fine micropores (1-2 μm) were formed on surfaces at the constant voltage of 250 V (*Fig. 1a*). At the voltage of 300 V, however, the specimen surfaces were uneven, with irregularly-shaped heaves in some places and irregular porous surfaces in other places, and the micropores were minor, unevenly-sized and nonuniformly distributed *(Fig. 1b*). At the voltage of 350 V, the surface oxidation films were rough, and the number of micropores significantly increased, but the sizes and distributions were uniform, and the pore sizes were enlarged to 4 - 6 μm (*Fig. 1c*). At the voltage of 450 V, the micropores on their surface oxidation films were significantly enlarged, but the numbers considerably decreased, and a part of the micropores fused

http://www.aloki.hu ● ISSN 1589 1623 (Print) ● ISSN 1785 0037 (Online)
DOI: http://dx.doi.org/10.15666/aeer/1704_86318641

and the walls were broken *(Fig. 1d*). The above results suggest that the pores in the surface films are gradually enlarged and the numbers decline along with the increase of electrode voltage.

This was because due to the overly low voltage, the resulting oxidation films were very thin and weak and could be easily punctured, (Kai et al., 2018; Babaranti et al., 2019) and together with the low discharge quantity, the resulting micropores were large in number and small in size. At high voltage, the enlarged discharge channels due to intense discharge led to the enlarged pores. Thus, when constant-voltage 250 V was applied, the low voltage, small discharge and gentle surface reactions made it easier to puncture the surface thin films, and consequently, a large number of small-sized micropores were formed. At voltage 300 V (Yang et al., 2019), the relatively low voltage and small discharge decelerated the metal surface oxidation, and thus decreased the numbers of micropores on the oxidation films. The slow oxidation led to less heat release and nonuniform oxidation, and irregular convexes and irregular micropores were formed on the oxidation film layers. As the electrode voltage rose to 350 V, the voltage and discharge increased and the metal surface oxidation was quickened, (Zeng et al., 2018) which led to the increased amount of uniformly-distributed micropores on the oxidation films. At the voltage of 450 V, the excessive voltage led to intense discharge, while the released high-energy caused micropore melting and enlarged the discharge channels and micropores.

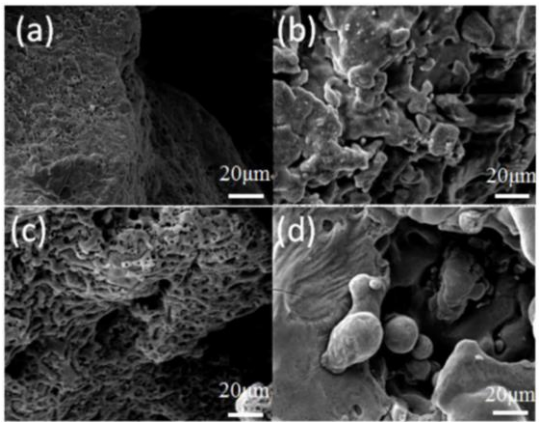

Figure 1. *Surface morphology of specimen under different voltage treatment (a) 250V; (b) 300V; (c) 350V; (d) 450V*

Moreover, (Sheng et al., 2018) the film thickening or densening reduced the conductivity, thereby decelerated the metal surface oxidation and decreased the amount of micropores on the oxidation film layers (Zhu et al., 2008; Pazand and Hezarkhani, 2018). At the electrode voltage of 450 V, evident cracks appeared at the oxidation film surfaces and between pores (*Fig. 1d*). The possible reason was that at higher voltage, the discharge quantity increased and the melting led to the formation of more oxides, (Tang et al., 2019) but during the sudden cooling under the action of external electrolytic solutions, the melts gradually clustered together rather than slowly dispersing or solidifying, leading to the formation of internal stress inside the structures. As the microarc oxidation proceeded, (Xiao, 2019) the inner stress was gradually intensified and finally was macroscopically embodied as local forced cracking on the oxidation films, which explained the formation of microcracks.

http://www.aloki.hu ● ISSN 1589 1623 (Print) ● ISSN 1785 0037 (Online)
DOI: http://dx.doi.org/10.15666/aeer/1704_86318641

According to the basic principles of microarc oxidation, as the microarc oxidation reaction proceeds, the electrode voltage, after exceeding the critical level, will puncture the relatively weak parts on the surfaces of the anode specimens. At the early stage of microarc oxidation, the newly- formed oxide layer is very weak and is likely to be first penetrated, and the short-term overly high temperature subjects the locally-discharged anode to splashed melting, forming current channels for discharge, and after a certain period of external cooling, the penetrated oxidation film layer and the current channels are all reserved. At the same place of puncturing, the new matrix is oxidized into a new oxidation film layer, and the weak parts are punctured again. Thereby, this procedure circulates and consequently the oxidation film layer accumulates and thickens, forming a porous film structure on specimen surfaces in which large pores cover small pores (*Fig. 1c*). In this structure, the film layers and the matrix are mutually inlayed and bond more firmly, which also enlarge the specific surface areas. After 30 min of oxidation, when the constant voltage is 350 V, porous microarc oxidation films with rough surfaces and more micropores are formed on specimen surfaces, and the large pores in the micropores cover the small pores. Under this condition, the specific surface areas are the largest, and the oxidation film layers bond firmly with the matrix. It is deduced that microarc oxidation for surface processing of porous Ti would form the most ideal microarc oxidation films under this condition.

Effects of electrode voltage on the phases of the microarc oxidation films

The following figure shows the XRD images of the surface oxidation films formed from microarc oxidation at different electrode voltages. Clearly, the diffraction peaks of Anatase TiO_2 are very obvious (*Fig. 2*), suggesting the surface oxidation films formed from microarc oxidation under different conditions are all rich in Anatase TiO_2, (Selvaraj, 2017) which is the major component of the oxidation film layers.

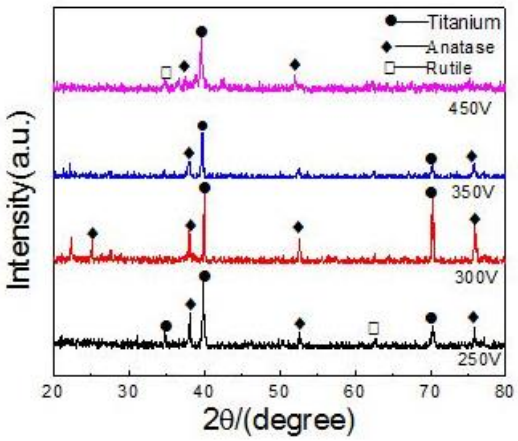

Figure 2. *X-ray diffraction (XRD) patterns of microarc oxide film with different electrode voltage*

Moreover, the diffraction peaks of the base material -- pure Ti are also very strong, but the peaks of Rutile TiO_2 are very weak and only appear at a part of the electrode voltages. These XRD results imply the major phase of the oxidation films formed under different oxidation conditions is anatase TiO_2, and Rutile TiO_2 did appear under certain

http://www.aloki.hu ● ISSN 1589 1623 (Print) ● ISSN 1785 0037 (Online)
DOI: http://dx.doi.org/10.15666/aeer/1704_86318641

conditions, but no rules concerning its concentration were found. This is because rutile TiO_2 has higher activation energy than anatase TiO_2, and the conversion from anatase TiO_2 to rutile TiO_2 relies on very high temperature. Thus, the reason why the rutile TiO_2 concentration did not increase with the rising electrode voltage was deduced. Specifically, the temperature during the microarc oxidation was controlled by the cooling in an ice-water mixture, which was hard to reach the high-temperature needed for the formation of rutile TiO_2. As a result, in the surface oxidation film layers after the microarc oxidation under different conditions, the rutile TiO_2 concentration did not change regularly and was very low.

Effects of time

Effects of time on surface morphology of microarc oxidized films

The figure below shows the surface morphology (×500) of the oxidation films prepared under electrode voltage of 350 V and different time durations (*Fig. 3*). Compared with the blank group (*Fig. 3a*), when the microarc oxidation proceeded under the constant voltage of 350 V, surface porous film layers were formed and the surface roughness was significantly intensified with the reaction time prolonged from 5 to 30 min. At this magnification factor, the specimen surfaces after 5 min of oxidation became rough and contained numerous fine micropores (*Fig. 3*). The surface roughness decreased after 15 to 30 min of oxidation. After 30 min of oxidation, porous film layers containing numerous evenly-distributed and large-sized pores were evidently formed (*Fig. 3d*). Clearly, the numbers and sizes of micropores in the film layers both changed at the same electrode voltage and after different durations of oxidation.

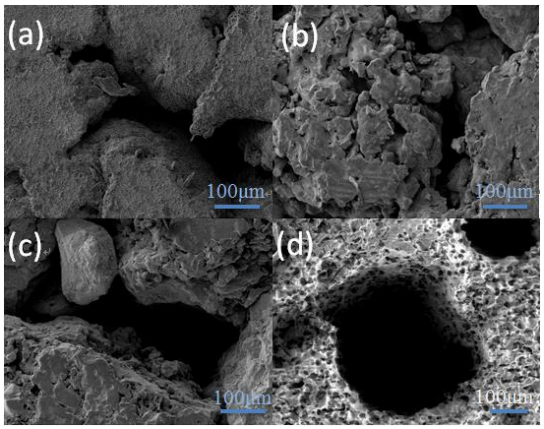

Figure 3. *Low ploid morphology (500 ×) of microarc oxide film surface at different oxidation times*
(a) 5 min; (b) 15min; (c) 25 min; (d) 30 min

The figure below shows the surface morphology (×3000) of the oxidation films prepared under the same electrode voltage of 350 V and different time durations (*Fig. 4*). During the microarc oxidation at the constant voltage of 350 V, very rough porous oxidation film layers were formed after 5 min of oxidation, which contained numerous micropores below 5 μm and were obviously melted (*Fig. 4a*). After 15 min of oxidation, the surface roughness decreased significantly and the numbers of micropores decreased, and the porous film layers contained size-varying and unevenly-distributed

http://www.aloki.hu ● ISSN 1589 1623 (Print) ● ISSN 1785 0037 (Online)
DOI: http://dx.doi.org/10.15666/aeer/1704_86318641

micropores, and the pore sizes decreased, the small pores were in size of ~ 500 nm and the large pores were about 3 μm (*Fig. 4b*). After 25 min of oxidation, the surface oxidation film layers were relatively even, and the sizes (1-2 μm) and distribution of micropores were relatively uniform (*Fig. 4c*). After 30 min, the surface oxidation films were very regular and formed a complete porous structure of small pores in large pores, but the micropores significantly decreased in number and considerably enlarged to about 6 μm (*Fig. 4d*). Clearly, with the prolonging of time before 25 min, the surface roughness gradually decreased, and the micropore distribution in the oxidation film layers became uniform, but the pore sizes decreased slowly. At about 30 min, the micropores were significantly enlarged in size and obviously decreased in numbers, and the porous layer structure of small pores in large pores was the most regular. Thus, at a constant voltage of 350 V was applied, the porous oxidation film layers formed from the micro-arc oxidation were optimized when the oxidation time was 30 min.

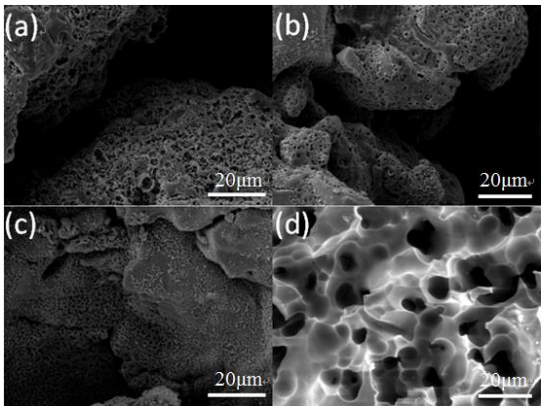

Figure 4. *The surface of the micro-arc oxide film has a high multiple morphology(3000 ×) (a) 5 min at different oxidation times; (b) 15min; (c) 25 min; (d) 30 min*

According to the fundamental principles of oxidation, at the early stage of reaction after 5 min of oxidation, a weak oxidation film layer that could be easily punctured was first formed on the surfaces of the base material. At the voltage of 350 V, the discharge and energy were very large, but the corresponding discharge channels were very small, and numerous fine-sized micropores were formed. However, the instant high-energy release would melt the walls of a part of the surface fine micropores, locally forming large-sized micropores (*Fig. 4a*). With the oxidation time prolonged from 15 to 25 min, the oxidation film layers thickened, reducing conductivity and making the films unpuncturable, but the residual discharge channels were gradually narrowed. The micropores formed at this moment decreased in size, while the residual energy accumulated inside the porous layer structures and would not easily released, leading to the gradual decrease of surface roughness (*Fig. 4b,c*). After 30 min of oxidation, due to the small discharge channels and the gradual energy accumulation, the relatively high energy caused the ablation of film layers and the consequent local melting of micropore walls, forming a smaller amount of larger-sized micropores. At this moment, the oxidation, dissolution and solidification speeds were relatively balanced and thus, regular porous layer surfaces with large pores containing small pores were formed (*Fig. 4a*). It was deduced that as the oxidation time was prolonged, surface ablation would be intensified and thereby more micropores were melted, and consequently, the

http://www.aloki.hu ● ISSN 1589 1623 (Print) ● ISSN 1785 0037 (Online)
DOI: http://dx.doi.org/10.15666/aeer/1704_86318641

oxidation film layers might be punctured and locally shed (Yan et al., 2010). Thus, the time of microarc oxidation should be controlled within a reasonable range.

Effects of time on the phases of the microarc oxidation film layers

The figure below (*Fig. 5*) shows the XRD images of the surface oxidation films formed from different time durations of microarc oxidation. Clearly, the diffraction peaks of Anatase TiO2 are very obvious (*Fig. 5*), suggesting the surface oxidation films formed from different time durations of microarc oxidation are all rich in anatase TiO_2, which is the major phase of the oxidation film layers.

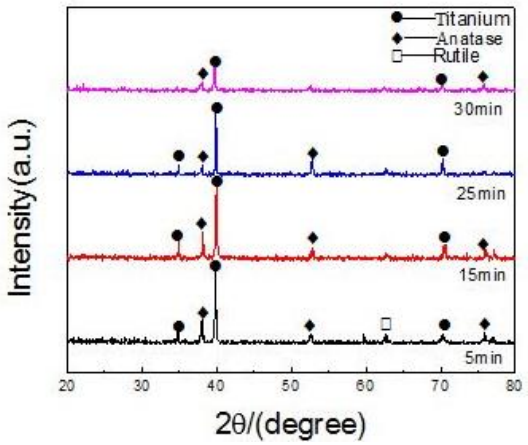

Figure 5. *XRD patterns of microarc oxide films at different oxidation times*

Effects of modification on bioactivity

The figure below (*Fig. 6*) shows the morphology of porous Ti (30 min of oxidation at 350 V, or without oxidation) after soaking in SBF for 7 days. After the non-oxidized porous Ti was soaked in the SBF, new substances were formed (*Fig. 6a*), but in the oxidized porous Ti, the surfaces were fully covered by a sediment after 7 days of mineralization (*Fig. 6b*). XRD patterns confirm this sediment is apatite (*Fig. 7*).

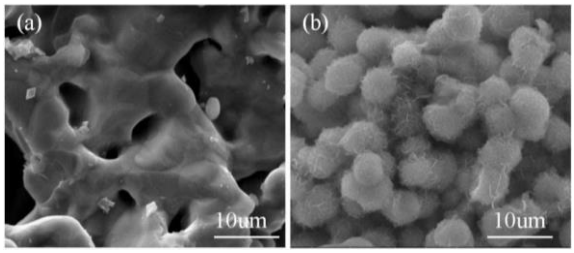

Figure 6. *Morphology of biomimetic mineralization of SEM(a) and(b) before and after microarc oxidation after 7 days of soaking in SBF with porous titanium oxidized by 350V voltage, respectively*

Microarc oxidation, also called plasma electrolysis oxidation or anode sparkle oxidation, is a relatively convenient technique to prepare oxide layers on metal surfaces. Compared with common anode oxidation, its major difference is the higher oxidation

http://www.aloki.hu ● ISSN 1589 1623 (Print) ● ISSN 1785 0037 (Online)
DOI: http://dx.doi.org/10.15666/aeer/1704_86318641

voltage. After microarc oxidation, surface coatings can form on porous metals or irregularly-shaped metals that have complex geometric morphology. The principle of this method in activating Ti and its alloys is attributed to the effect of microstructures on biological reactions. Chen et al. (2010) created different crystal forms of TiO_2 coatings atop β Ti alloys by regulating the microarc oxidation voltage and investigated the effects of crystal forms on osteoblast growth.

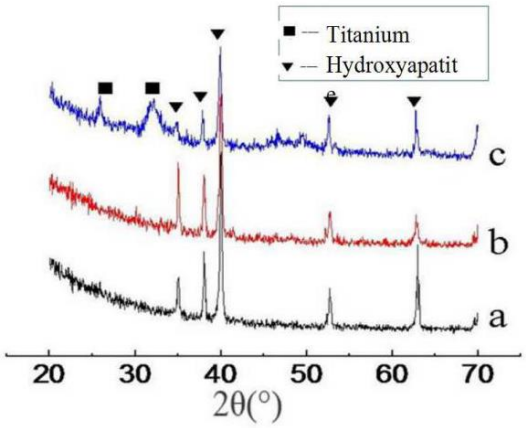

Figure 7. *XRD map of different samples*
a) Porous titanium prepared by vacuum sintering; b) is a sample of porous titanium that has not been treated with microarc oxidation after being soaked in SBF for 7 days; c) is a porous titanium after microarc oxidation (voltage 350V, oxidation time 30 min) and then soaked in SBF for 7 days

They found the TiO_2 after microarc oxidation possessed the bioactivity and Ca deposition ability like cells. Bayati et al. (2010) found with the increasing oxidation voltage, the surface pore sizes and roughness both significantly increased, but the number of pores first rose and then declined, while the contact angle first decreased and then enlarged. Furthermore, the variation of hydrophilicity was caused by mainly two factors, including the existence of surface oxidation films and the variation of specific surface (Yang et al., 2019). Since we conducted microarc oxidation on surfaces of porous Ti, the oxidation parameters were different from those of dense Ti. Firstly, the films formed under our experimental conditions were all porous and were TiO_2 films, and these film microstructures were favorable for the formation of the precipitate HA. Secondly, the hierarchical microstructures formed from porous Ti oxidation increased the specific surface areas and hydrophilicity. The enlarged specific surface areas enhanced the specific surface energy and surface activity of porous Ti, which created more sites for apatite nucleation. The more hydrophilic surfaces were more likely to contact and bind with polar ions in SBF, which accelerated the apatite nucleation and crystallization. The different mineralization results in our study can be explained from two reasons. The first reason is the change of surface morphology, since the increase in pore number and specific surface area offer more sites for the nucleation of precipitates. The second reason might be related to the phases of post-oxidation surface film layers. The above analysis suggests the surface activity can be enhanced by surface-modifying the porous Ti through microarc oxidation. Thus, microarc oxidation may be used to modify the surface activation of porous Ti.

http://www.aloki.hu ● ISSN 1589 1623 (Print) ● ISSN 1785 0037 (Online)
DOI: http://dx.doi.org/10.15666/aeer/1704_86318641

Conclusions

(1) When the time of oxidation was constant, the pores in the surface oxidation film layers gradually increased in size and decreased in number with the increment of electrode voltage. The oxidized film layers contained both rutile TiO_2 and anatase TiO_2.

(2) When the voltage was constant, with the prolonging of oxidation time within 5 and 25 min, the surface roughness gradually decreased, the micropores on the oxidation film layers became uniformly-distributed and decreased slowly in size. At about 30 min, the micropores were significantly enlarged in size and obviously decreased in number, and the porous layer structure of small pores in large pores was the most regular. The oxidation film layers were mainly composed of anatase TiO_2.

(3) After 30 min of oxidation at voltage 350 V, the oxidized film layers on pore walls of porous Ti became uniform micropore structures in pore size of ~ 6 μm, and these structures had large specific surface areas, which were the optimal experimental parameters under the tested conditions.

(4) The porous Ti modified by microarc oxidation induced apatite generation and was more bioactive compared with the porous Ti surface without microarc oxidation.

In the future, when the porous Ti micro-arc oxidation film is applied in specific fields, all the parameters in this paper can provide beneficial value.

Aknowledgements. This study was funded by Panzhihua University Doctor Foundation (0210600011).

REFERENCES

[1] Ali, W., Nasir, M. S., Nasir, A., Rashid, H., Ayub, I., Gillani, S. H., Latif, M. J. (2018): Assessment Of Carbon Footprints In Terms Of Co2 Of Diesel Generator, Pakistan. – Earth Sciences Pakistan 2(1): 15-17.

[2] Babaranti, O., Horn, S., Jowett, T., Frew, R. (2019): Isotopic signatures in Mytilus galloprovincialis and Ulva latuca as bioindicators for assessing discharged sewage effluent in coastal waters along Otago Peninsula, New Zealand. – Geology, Ecology, and Landscapes 3(1): 53-64.

[3] Bayati, M. R., Molaei, R., Kajbafvala, A., Zanganeh, S., Zargar, H. R., Janghorban, K. (2010): Ivestigation on hydrophilicity of micro-arc oxidized TiO_2 nano/micro-porous layers. – Electrochim acta 55: 5786-92.

[4] Chen, H. T., Chung, C. J., Yang, T. C., Chiang, I. P., Tang, C. H., Chen, K. C., He, J. L. (2010): Osteoblast growth behavior on micro-arc oxidizedβ-titanium alloy. – Surf coat tech 205: 1624-9.

[5] Chen, L., Tang, M., Chen, C., Chen, M., Luo, K., Xu, J., Zhou, D., Wu, F. (2017): Efficient bacterial inactivation by transition metal catalyzed auto-oxidation of sulfite. – Environmental Science & Technology 51(21): 12663-12671.

[6] Chien, C. S., Hung, Y. C., Hong, T. F., Wu, C. C., Kuo, T. Y., Lee, T. M., Liao, T. Y., Lin, H. C., Chuang, C. H. (2017): Preparation and characterization of porous bioceramic layers on pure titanium surfaces obtained by micro-arc oxidation process. – Applied Physics A: Materials Science and Processing 123(3): 204-303.

[7] Choi, J. W., Kim, N. (2015): Clinical application of three-dimensional printing technology in craniofacial plastic surgery. – Archives of Plastic Surgery 42(3): 267-277.

[8] Dali, N. M., Kamarudin, K. S. N. (2018): The Effect of Cosurfactant In Co2 Absorption In Water – In – Oil Emulsion. – Environment & Ecosystem Science 2(2): 42-46.

http://www.aloki.hu ● ISSN 1589 1623 (Print) ● ISSN 1785 0037 (Online)
DOI: http://dx.doi.org/10.15666/aeer/1704_86318641

[9] Das, I., Chattopadhyay, S., Mahato, A., Kundu, B., De, G. (2016): Fabrication of a cubic zirconia nanocoating on a titanium dental implant with excellent adhension, hardness and biocompatibility. – RSC Advances 6(64): 59030-59038.
[10] Gautam, A., Batra, R., Singh, N. (2019): A Study On Use Of Rice Husk Ash In Concrete. – Engineering Heritage Journal 1(1): 01-04.
[11] Hao, M. (2018): Numerical Simulation of Borehole Acoustic Field of Adhering Sand Casing Well. – Acta Microscopica 27(4): 305-308.
[12] Kai, W., Shengzhe, Z., Yanting, Z., Jun, R., Liwei, L., Yong, L. (2018): Synthesis of porous carbon by activation method and its electrochemical performance. – Int. J. Electrochem. Sci 13(11): 10766-10773.
[13] Kang, L., Zhang, Y. J., Zhang, L., Zhang, K. (2017): Preparation, characterization and photocatalytic activity of novel CeO2 loaded porous alkali-activated steel slag-based binding material. – International Journal of Hydrogen Energy 42(27): 17341-17349.
[14] Masri, E., Samsudin, M. D. M. (2018): Optimization Performance Of Biological Cathodic Protection System Using Organic Waste. – Environment & Ecosystem Science 2(2): 25-29.
[15] Nomura, N., Kohama, T., Oh, I. H., Hanada, S., Chiba, A., Kanehira, M., Sasaki, K. (2005): Mechanical properties of porous Ti-15-Mo-3Al compacts prepared by powder sintering. – Materials Science & Engineering C 25: 330-335.
[16] Nune, K. C., Kumar, A., Murr, L. E., Misra, R. D. (2016): Interplay between self-assembled structure of bone morphogenetic protein-2 (BMP-2) and osteoblast functions in three-dimensional titanium alloy scaffolds: stimulation of osteogenic activity. – Journal of Biomedical Materials Research Part A 104(2): 517-532.
[17] Pazand, K., Hezarkhani, A. (2018): Predictive Cu porphyry potential mapping using fuzzy modelling in Ahar–Arasbaran zone, Iran. – Geology, Ecology, and Landscapes 2(4): 229-239.
[18] Qiao, F. (2018): The Study On The Integration Of Green Architecture And Appropriate Technology. – Engineering Heritage Journal 2(2): 01-03.
[19] Rahim, Y., Khan, M. S., Mughal, S. (2018): Petrography Of Sandstone Of The Lumshiwal Formation From Eastern Hazara, Khyber Pakhtunkhwa, Pakistan: Implications For Provenance, Diagenesis And Environments Of Deposition. – Earth Sciences Pakistan 2(2): 01-06.
[20] Selvaraj, P. (2017): Segregation of Degradable and Non Degradable using Sensor. – Revista de la Facultad de Agronomia de la Universidad del Zulia 34(3): 306-312.
[21] Sheng, J., Su, J., La, P., Ren, J., Ma, J., Shi, Y., Song, Y. (2018): Progress of In-Situ Study on Mechanical Properties for Micro/Nano-Structured Alloy. – Journal of Nanoelectronics and Optoelectronics 13(5): 637-645.
[22] Shrestha, A., Baral, S. (2018): Socioeconomic Factors Affecting Awareness And Adaption Of Climate Change: A Case Study Of Banke District Nepal. – Earth Sciences Malaysia 2(2): 20-24.
[23] Tang, Y., Li, L., Wang, C., Chen, M., Feng, W., Zou, X., Huang, K. (2019): Real-time detection of surface deformation and strain in recycled aggregate concrete-filled steel tubular columns via four-ocular vision. – Robotics and Computer-Integrated Manufacturing 59: 36-46.
[24] Thanh, L. D., Do, P. V. (2018): Streaming Current Induced By Fluid Flow In Porous Media. – Earth Sciences Malaysia 2(1): 22-28.
[25] Wang, F. H., Zhang, S. S., Shu, J. Y., Gao, Y. (2014): Effects of surface modifacation titanium implants on the osseointegration. – Chinese Journal of Tissue Engineering Research 18(52): 8491-8497.
[26] Wen, C. E., Mabuchi, M., Yamada, Y., Shimojima, K., Chino, Y., Asahina, T. (2001): Processing of biocompatible porous Ti and Mg. – Sctipta Materialia 45(10): 1147-1153.
[27] Xiao, F. (2019): Multi-sensor data fusion based on the belief divergence measure of evidences and the belief entropy. – Information Fusion 46: 23-32.

http://www.aloki.hu ● ISSN 1589 1623 (Print) ● ISSN 1785 0037 (Online)
DOI: http://dx.doi.org/10.15666/aeer/1704_86318641

[28] Yan, F. Y., Shi, Y. L., Mo, W. Y. (2010): Influence of oxidation time on micro-arc oxidation coating on titanium substrate. – Surface technology 39(4): 42-44.
[29] Yang, Y. X., Li, H., Zheng, W. K., Yun, B., Liu, Z. M., Zhang, J. J. (2019): Experimental Study on Calcining Process of Secondary Coated Ceramsite Solidified Chromium Contaminated Soil. – Science of Advanced Materials 11(2): 208-214.
[30] Zeng, L., Guo, X. P, Zhang, G. A., Chen, H. X. (2018): Semiconductivities of passive films formed on stainless steel bend under erosion-corrosion conditions. – Corrosion Science 144: 258-265.
[31] Zhang, Y. Y., Li, Y. A., Bai, C. G. (2017): Microstructure and Oxidation Behavior of Si–MoSi2 Functionally Graded Coating on Mo Substrate. – Ceramics International 43(8): 6250-6256.
[32] Zhang, Y., Ni, W., Li, Y. (2018): Effect of siliconizing temperature on microstructure and phase constitution of Mo–MoSi2 functionally graded materials. – Ceramics International 44(10): 11166-11171.
[33] Zhao, Q. M., Cheng, L., Liu, Z. T., Zhao, J. J. (2014): Surface characteristics of Zinc-TiO_2 coatings prepared via micro-arc oxidation. – Composite Interfaces 21(6): 585-593.
[34] Zhu, R. F., Wang, Z. G., Xiao, G. Y., Li, S., Lu, Y., Hanawa, T., Kobayashi, M. (2008): Effect of electrode voltage on microstructure and performance of micro-arc oxidized ceramic film on surface of pure titanium. – Journal of the chinese ceramic society 36(5): 631-635.

http://www.aloki.hu ● ISSN 1589 1623 (Print) ● ISSN 1785 0037 (Online)
DOI: http://dx.doi.org/10.15666/aeer/1704_86318641

RATIONALITY OF RESIDENTIAL PLANNING BASED ON THE EFFECT ANALYSIS OF WIND ENVIRONMENT

HUANG, J. Z. – CAO W. W. – TAN, L. W. – YONG, X.*

School of Civil Engineering, Architecture, and Environment, Xihua University
Chengdu 610039, China

**Corresponding author*
e-mail: xiangyong@mail.xhu.edu.cn

(Received 8th Mar 2019; accepted 21st May 2019)

Abstract. Among most existing residential areas, the planning designs mainly focus on the function rationality and environment beautification, but neglect the effects of residential layout on micro-climate environment. This work simulated the wind environment with different residential planning schemes using computational fluid. Then, the results of different monsoon environments were analyzed. Taking the planning scheme in Kazi Wanzhen, Urumqi as a case study, the overall rate of calm wind was higher than 50% with the calm wind in winter up to 92%. It shows that the environmental effect of winter monsoon was the worst. Therefore, the original layout was optimized based on the current development strength by simulating the wind environment in this work. After optimization, the rate of calm wind in all four seasons decreased by more than 10%. This result shows that the wind environment can be improved by dislocated and disclosed layout with an opening at windward side and leeward side. Therefore, the deterioration of wind environment can be relieved to improve the living environment and the overall micro-climate.

Keywords: *micro-climate, computational fluid dynamics, winter monsoon, wind speed velocity, the rate of calm wind*

Introduction

In recent years, people have found it important to lead the natural wind surrounding the urban area to the city when solving air pollution. The wind can be led by optimizing urban layout and constructing a natural ventilation corridor. In fact, wind field plays an important role in spreading and diluting pollutants in the air. In terms of residential areas, using wind environment is technically feasible to improve the air quality by optimizing residential planning with natural ventilation.

For a long time, residential planning has emphasized living comfort, convenience, security, beauty, energy preservation, environment protection, etc. People have not paid enough attention to the micro-climate environment up until now. The most newly-built residential areas have rational functions and complete environmental landscape and facilities with convenience. However, the irrational layouts of these areas have caused poor ventilation with air pollutants. Especially in the megacities with severe air pollution, such a problem can be more obvious. Therefore, the residential planning in urban area should focus on the effects of building layout on micro-climate environment. At present, it has become a grand new task and challenge to feasibly improve the living quality by maximizing the improvement of residential ventilation through building layout.

http://www.aloki.hu ● ISSN 1589 1623 (Print) ● ISSN 1785 0037 (Online)
DOI: http://dx.doi.org/10.15666/aeer/1704_86438654

Materials and Methods

Research status

There have been some research achievements about evaluating the atmospheric thermal environment with CFD at home and abroad. The studies by Oke (1973) and Summers (1965) show that the strength and location of a heat island have a certain relation with wind speed. Natural ventilation can relieve urban heat island effect and decrease air pollution (Summers, 1965; Oke, 1973; Junior et al., 2019). Dabberdt and Hoydysh (1991) made thumbnail models of street canyons in different scales for wind tunnel experiment. This study compares the distribution of wind speed field in different wind directions (Dabberdt and Hoydysh, 1991; Choudhari et al., 2018). Stathopoulos and Baskaran (1996) stimulated a wind field of a single high-level building and that of a block, respectively, for wind tunnel experiments. These studies test the simulation results (Stathopoulos and Baskaran, 1996; Rozuki et al., 2018). Yang and Li (2011) established two simple models of Hong Kong with relatively complex landforms in a small scale. The effects of thermal stratification on the thermal conditions and ventilation were studied according to thermal buoyancy and wind speed (Yang and Li, 2011; Kumar and Jaafar, 2018). Hang et al. (2012) stimulated the pollutant distribution of 9- or 18-row high-level building array in a small scale. This study showed the effects of the height diversity on the pollutant diffusion in the air and the ventilation at pedestrian height in an ideal urban area with high-level buildings. Ouyang and Jiang (2003) found the rules of wind environment and pollutant diffusion in urban areas by data measurement (Ouyang and Jiang, 2003; Tianlei, 2019). Pontiggia et al. (2010) simulated the diffusion of hazardous gas in the city with CFD (Pontiggia et al., 2010; Omini and Akpang, 2018). In 2011, Lin and Liu studied the natural ventilation indoors and in the courtyard of traditional Yi Nationality's settlements in Yunnan by CFD simulation. It analyzes the relationship between various influence factors and the natural ventilation inside and outside of the building (Lin and Liu, 2011; Nkwuda et al., 2019). Wang (2012) studied the diffusion of air pollutant around high-level residential buildings in natural ventilation through wind tunnel test (Wang, 2012; Abija and Nwankwoala, 2018). Yuan et al. (2014) studied the diffusion of hazardous gas in the city with CFD model. In 2014, Huang studied the relationship between village form and rural settlement type in Boyang Lake Bioeconomic Zone and the natural ventilation by CFD simulation. This study further proposed the strategies about natural ventilation in the planning and design of new rural area (Huang, 2014; Sufiyan et al., 2018). With CFD, Peng (2015) stimulated and analyzed the natural ventilation effects inside of two different planes in plate-type and tower-type residential forms, which are common in Jinan. In 2016, Zhang and Jin studied the relationship between village forms and wind monsoon of the typical village clusters in the severe cold Northeast China. Strategies of optimizing the wind environment in these villages are proposed in terms of village form (Zhang and Jin, 2016).

The research status at home and abroad shows that studies on the wind environment in a region start earlier in foreign countries than in China. Such studies were mainly taken by wind tunnel experiment. With the improvement of computer hardware and simulation software, these studies are gradually taken by value simulation with wind tunnel experiment for verification. As the wind fields in different suburbs are interconnected, the overall wind field in a city should be simulated to get the correct wind fields in different suburbs. All of these studies set a foundation to this work.

http://www.aloki.hu ● ISSN 1589 1623 (Print) ● ISSN 1785 0037 (Online)
DOI: http://dx.doi.org/10.15666/aeer/1704_86438654

However, the existing studies with CFD simulation pay little attention to a complete residential area, especially in Western China, which becomes the subject root. Aiming at simulating the wind environment in the residential planning, this work explored the optimal mode of wind environment in a residential area for the layout optimization of residential buildings and the overall improvement of atmospheric environment.

Research methods

With the development of computer technology, digital simulations by computer can provide numerical solution to nonlinear partial differential equations. In other words, various data can be obtained by computational fluid dynamics (CFD) to save substantial experimental cost. As CFD is developing, the simulation of flow fields by computer can replace aerodynamics experiment. In the planning, it is safer and more reasonable to use aerodynamics when urban micro-climate is simulated.

CFD is realized as follows:

(1) Establishment of mathematic model (*Eq.1*, *Eq.2*). It means assigning a flow control equation, selecting a value discretization scheme, setting boundary conditions, etc. This process can be completed with commercial CFD software (i.e., ANSYS FLUENT) (Yuan et al., 2014; Wali et al., 2018). The equation (*Eq.1*) is the most common control equation, Navier-Stokes equation in CFD:

$$\frac{\partial \boldsymbol{Q}}{\partial t}+\frac{\partial \boldsymbol{F}_i}{\partial \boldsymbol{x}_i}-\frac{\partial \boldsymbol{F}_i^{\mathrm{v}}}{\partial \boldsymbol{x}_i}=0 \tag{Eq.1}$$

$$\boldsymbol{Q}=\begin{bmatrix}\rho\\ \rho \boldsymbol{u}_i\\ \rho E\end{bmatrix},\ \boldsymbol{F}_i=\begin{bmatrix}\rho \boldsymbol{u}_i\\ \rho \boldsymbol{u}_i \boldsymbol{u}_j+p\delta_{ij}\\ \rho \boldsymbol{u}_i H\end{bmatrix},\ \boldsymbol{F}_i^{\mathrm{v}}=\begin{bmatrix}0\\ \tau_{ij}\\ \boldsymbol{u}_k \tau_{ki}-\boldsymbol{q}_i\end{bmatrix} \tag{Eq.2}$$

(2) Establishment of geometric model. It means drawing corresponding geometric forms in the computer according to the actual size of buildings, landforms, etc. The geometric model is simplified because the actual geographic shapes are complicated.

(3) Generation of computational grid. It means dispersing the actually continuous flow space into intermittent grid units for discrete solutions to CFD.

(4) Numerical solution to CFD. It is realized by setting the assigned turbulence model, iterative steps, residual criterion for convergence, etc. of the commercial software (Hang et al., 2012).

(5) Analysis of numerical results. After solving CFD, the results are analyzed to ensure the rationality of numerical values. Then, the actual issues are analyzed with rational numerical results to draw the wind field around buildings for modifying the irrational layout of buildings.

Results and Discussion

Analysis on regional situation in the case

Kaziwan Community in the north of Urumqi is taken as the research object due to following three reasons:

http://www.aloki.hu ● ISSN 1589 1623 (Print) ● ISSN 1785 0037 (Online)
DOI: http://dx.doi.org/10.15666/aeer/1704_86438654

(1) Urumqi faces a severe problem of atmospheric environment. Located in the interior of Eurasia far away from the ocean, Urumqi has temperate continental climate with dry air. According to 2015 City Rank of Haze Severity of China, Urumqi ranks at No. 76. The weather statistics show that the annual pm2.5 concentration of Urumqi is 72 μg/m^3 which is much higher than 35 μg/m^3 regulated in Ambient Air Quality Standards released by Ministry of Environmental Protection (Ge et al., 2016).

(2) With a long winter in Urumqi, the environmental problem caused by heating supply is obvious. According to Code for Thermal Design of Civil Building (GB50176), Urumqi is in a severe cold area. The period with monthly lowest temperature ≤-10ºC or daily lowest temperature ≤5ºC is longer than 145 days. Due to the cold weather, the heating supply period is from October to April the next year in Urumqi. The heating period here is longer than other areas, while the fire coal for heating may cause atmospheric pollution and jeopardize the public health.

(3) Enterprises with heavy pollution are concentrated in Kaziwan. There are two cement plants (Xingong Cement Plant and Qingsong Cement Plant) within 1 mile from Kaziwan Community. A large amount of dust, sulfur dioxide, nitric oxide and other pollutants may be generated when producing cement to cause severe environmental pollution and harm the health of residents nearby. Although the government has shut down the enterprises causing heavy pollution, the environment pollution in big cities are still unsolved. The current status of pollution is especially severe in winter due to the fire coal for heating. Reducing pollution sources is an important measure, but self-attenuation of air pollutants is more positive by maximizing the ventilation.

Case overview

Located in Midong District in northeast of the city center of Urumqi, Kaziwan Community covers 55,000 m^2 of land use with a volume fraction index of 3.2 and architectural density of 30.14%. The overall floorage is 190,000 m^2 (including the above ground floor area of 176,000 m^2 and underground floor area of 14,000 m^2).

The overall residential buildings are high level with enclosed building layout. Roads are laid surrounding the community, where pedestrian are separated from traffic. In the southwestern corner, two dotted apartments are built. Greening is concentrated in the center of community, while the greenery landscape distributes in trapezoid. Leisure footpath, hard pavage, featured landscape, green trees, etc. are composed of a rich and lifeful common activity area which provides a pleasant outdoor shared area to residents. The planning scheme creates a modern residential area with healthy biology, beautiful environment and reasonable function layout by integrating the site culture and natural conditions.

Model construction and parameter analysis

Kaziwan Community uses the traditional model of residential layout in northern China which is a typical enclosed layout. This model is a spatial layout with strong closure made of surrounding roads (*Fig. 1a*). For the convenience of model construction, effects of plants were neglected in this work by simplifying the whole community as a solid model composed of buildings. With this model, relatively correct simulation results can be obtained by appropriate parameter adjustment. Moreover, this model has advantages of convenient construction, rapid calculation and good convergence.

http://www.aloki.hu ● ISSN 1589 1623 (Print) ● ISSN 1785 0037 (Online)
DOI: http://dx.doi.org/10.15666/aeer/1704_86438654

A computational grid of Kaziwan Community (*Fig. 1b*) is established with ICEM software with about 1.2 million grids. This calculated quantity can ensure accuracy and realize the optimal calculation process (Nikolopoulou and Lykoudis, 2006).

In this case, the incoming flow direction of wind speed is the speed income when the boundary conditions are set within the computational scope. Based on the meteorological data of Urumqi in recent 50 years, the annual average wind speed in Urumqi is 2.47 ms^{-1} from 1961 to 2003. The wind speed in summer is the fastest, followed by that in spring, autumn and winter in order. The average wind speeds are 3.08 ms^{-1}, 2.94 ms^{-1}, 2.31 ms^{-1} and 1.52 ms^{-1}, respectively, in four seasons. The wind in spring is southeaster and summer and that in autumn and winter is northwester (Le et al., 2017; Fu et al., 2018). The export downstream is the pressure export and the boundary condition on ground is the wall space. The boundary conditions in other parts are symmetrically set. To avoid the result error, the parameters should be further rectified (Jing, 2018).

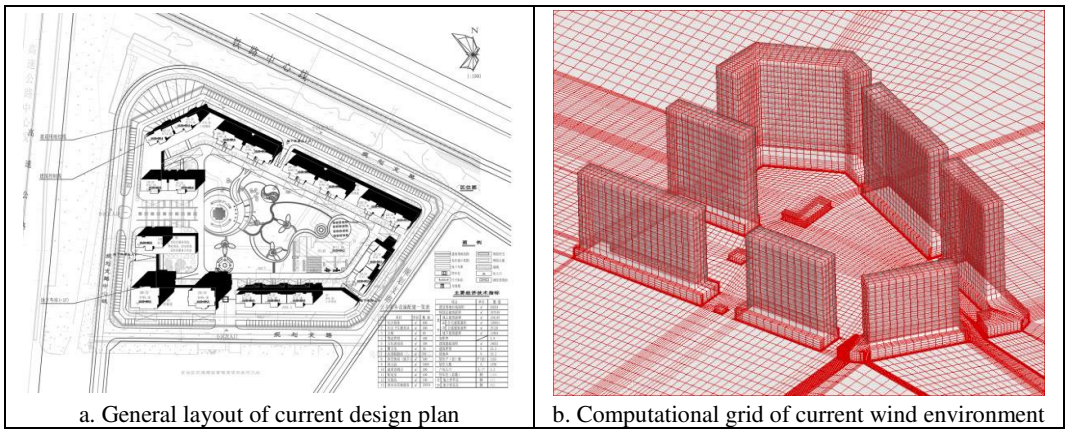

a. General layout of current design plan | b. Computational grid of current wind environment

Figure 1. *Overall appraisal for the current plan of Kaziwan Community and computational grid of wind environment*

Analysis and optimization of research results in the empirical case

The theoretical research shows that the height of 1.5 m is the most obvious thermal inductance for human. The wind speed simulated for this height can intuitively display the comfort and safety in such an environment. Therefore, the wind speed field in the height of pedestrians is simulated by computational fluid mechanics in four seasons. The figures show the simulation results (*Fig. 2 a-d*). Meanwhile, the air pollutant cannot disperse to form a calm zone when the calm rate is lower than 1.04 m/s under 1.5 m as the evaluation criterion. The calm rate is the ratio between this area and the total site area. The higher calm rate means the worse effect of wind environment.

Result analysis of wind speed field in the current plan

The computational results of different monsoon fields in this plan (*Table 1*) show that the calm rates in four seasons are 56.25, 55.32, 55.96 and 91.82%, respectively. The higher the calm rate is, the worse the wind environment will be. Therefore, the monsoon environment in winter is the worst in this case, while that in other three seasons is average. However, the calm rate in all the seasons has been over 50%. Thus, it is urgent to improve the ventilation effect, especially in winter.

http://www.aloki.hu ● ISSN 1589 1623 (Print) ● ISSN 1785 0037 (Online)
DOI: http://dx.doi.org/10.15666/aeer/1704_86438654

According to the distribution of wind speed shown (*Table 1*), the maximum wind speed in winter is 1.17 m/s, 3.17 m/s in spring, 3.27 m/s in summer and 2.71 m/s in autumn. The area with quick wind speed in spring and summer is in three openings in the south and southeast of the area. Moreover, there are also two obvious air channels in the community in autumn. Only in winter, there is no obvious air channel due to the weak wind environment. This is because there is an opening among the buildings towards the wind direction with the maximum wind speed of 3.27 m/s which is lower than the safety threshold of 5 m/s. It is believed that the wind environment formed in this plan is much lower than the standard of windburn. Therefore, this plan with small effects on outdoor activities can satisfy various activities at this site in terms of security (Sheng et al., 2018). Massive annex buildings cause the closure of community environment to the great extent; however, these buildings form a local calm area that is disadvantageous to pollutant dispersion.

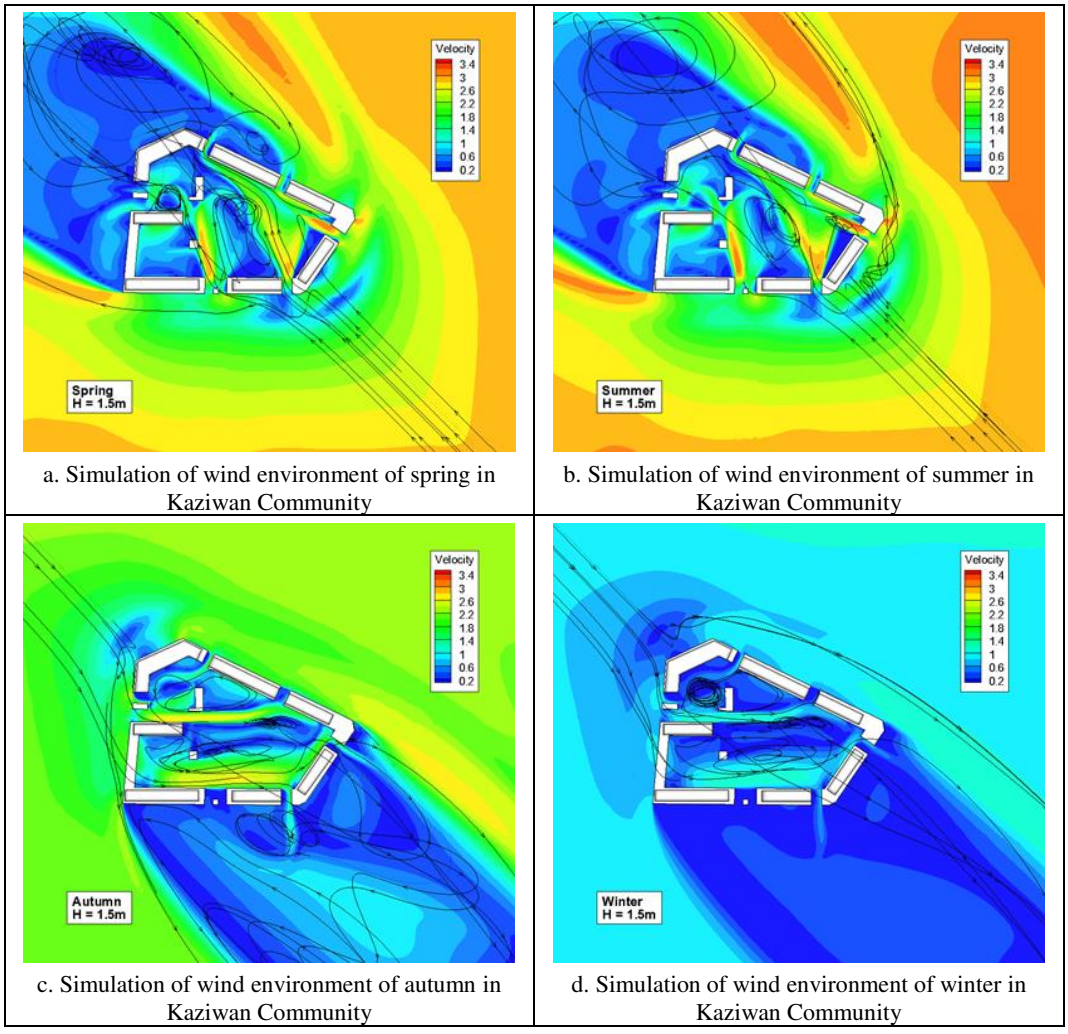

a. Simulation of wind environment of spring in Kaziwan Community

b. Simulation of wind environment of summer in Kaziwan Community

c. Simulation of wind environment of autumn in Kaziwan Community

d. Simulation of wind environment of winter in Kaziwan Community

Figure 2. *Simulation of current plan of four monsoons in Kaziwan Community*

The areas with fast wind speed in winter are in the western entrance and the scenery greenbelt in the south. The maximum wind speed is 1.17 m/s, lower than the speed threshold of 5 m/s. Therefore, this plan with small effects on outdoor activities can

http://www.aloki.hu ● ISSN 1589 1623 (Print) ● ISSN 1785 0037 (Online)
DOI: http://dx.doi.org/10.15666/aeer/1704_86438654

satisfy various activities at this site. It is because the building layout at the northeast corner is vertical to the leading wind direction in winter. The enclosed layout in the north can shield the leading wind in winter. However, such a shield forms a large area of calm wind among the massive enclosed buildings in the north, making pollution more severe (Shan and Lai, 2018).

Table 1. *Simulation results of wind environment in Kaziwan Community*

Current plan	Spring	Summer	Autumn	Winter
Calm rate	56.25%	55.32%	55.96%	91.82%
Maximum wind speed	3.17	3.27	2.71	1.17
Minimum wind speed	0	0.01	0.00	0.00
Building density	0.143	30.14	30.14	30.14

Results analysis on the wind speed fields of four seasons in the optimized plan

The current plan does not cause the windburn but forms an area with severe calm wind, especially in winter. Therefore, adjustment is necessary for this layout to improve the calm wind area in the community during winter to the greatest extent. In this way, the pollutant gathering in the air during winter can be effectively released.

Now, the original plan is optimized with the volume rate and building height constant. The layout is optimized from the traditional enclosure to the dislocated enclosure. In other words, the overall building layout is still enclosed, while the partial layout will be adjusted to plate-type dislocated layout (*Fig. 3a*) to leave a corridor for ventilation for the improvement of wind environment.

With the computational grid established with ICEM (*Fig. 3b*), the computational quantity, 100 W, is the same as the previous plan. The same parameters are set for calculation and simulation.

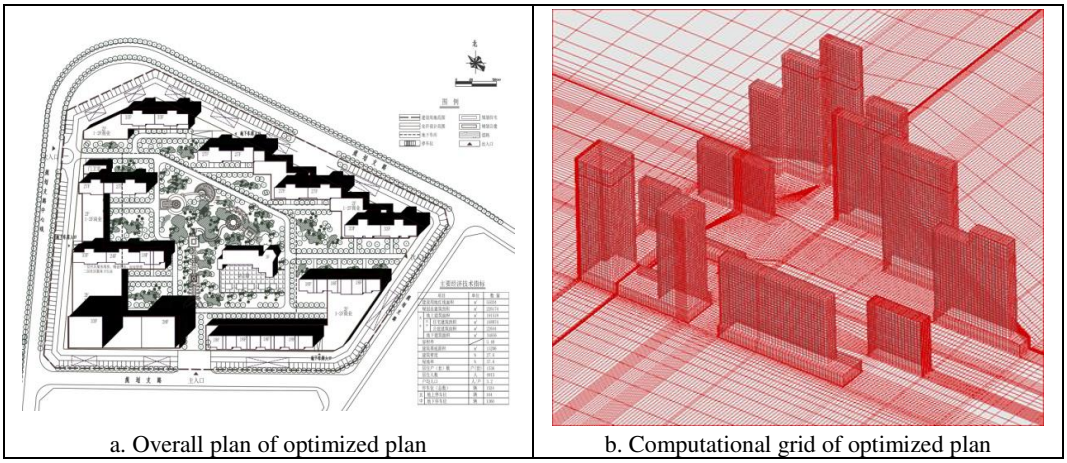

a. Overall plan of optimized plan

b. Computational grid of optimized plan

Figure 3. *Overall evaluation of the optimized plan and the computational grid of wind environment in Kaziwan Community*

For different monsoon speed fields, the optimized plan is simulated in the height of pedestrians in four seasons by computational fluid dynamics. The simulation results are as follows (*Fig. 4a-d and Table 2*).

http://www.aloki.hu ● ISSN 1589 1623 (Print) ● ISSN 1785 0037 (Online)
DOI: http://dx.doi.org/10.15666/aeer/1704_86438654

The figure and the table show that the calm rate in the optimized plan is 40.05, 33.02, 36.35 and 87.27% in spring, summer, autumn and winter, respectively (*Fig. 5, Table 2*). In terms of the environmental effect, the calm rate in winter is still the highest, while that in other three seasons shows small difference. Compared with the current plan, the optimized plan solves the problem of high calm rate. In the optimized plan, the calm rate in every season decreases by about 10%. It shows that the adjustment of building layout will change the wind environment inside of a community to decrease calm rate and improve air quality.

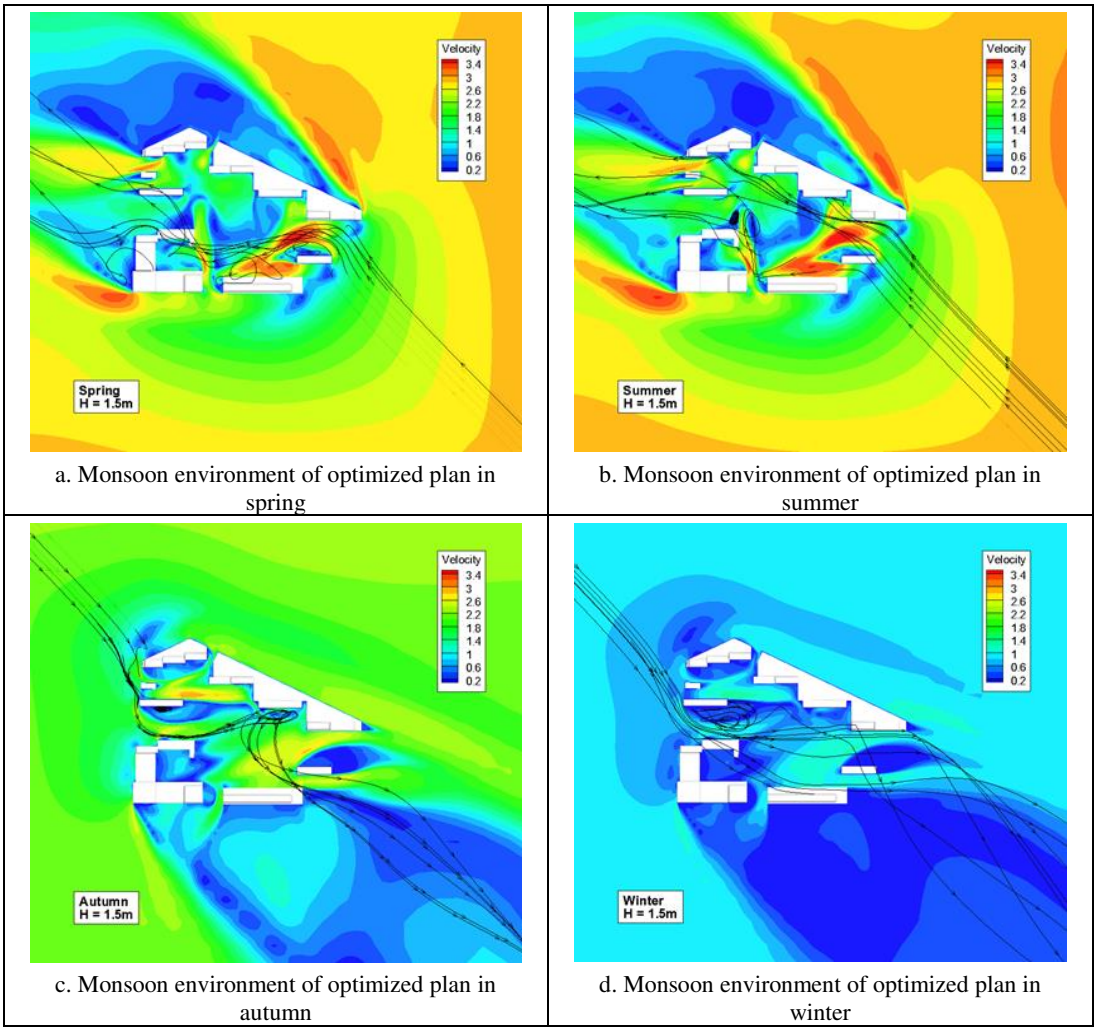

a. Monsoon environment of optimized plan in spring

b. Monsoon environment of optimized plan in summer

c. Monsoon environment of optimized plan in autumn

d. Monsoon environment of optimized plan in winter

Figure 4. *Simulation of monsoon environment in the optimized plan of Kaziwan Community in four seasons*

Table 2. *Simulation results of monsoon environment in the optimized plan*

Optimized plan	Spring	Summer	Autumn	Winter
Calm rate	40.05	33.02	36.35	87.27
Maximum speed	3.54	3.66	2.89	1.27
Minimum speed	0	0.00	0.00	0.00
Building density	31.81	31.81	31.81	31.81

http://www.aloki.hu ● ISSN 1589 1623 (Print) ● ISSN 1785 0037 (Online)
DOI: http://dx.doi.org/10.15666/aeer/1704_86438654

Comparative analysis on the building layout improvement

This work studied the comfort and safety of pedestrians. As the current plan and the optimized plan in this work are the most typical layouts in community design, this research is more persuasive for the future simulation of computational micro-environment with the universal CFD. By comparing the calculation of these two plans, following characteristics can be obtained:

(1) Layout difference between plans

Above computational results show that the changes to current layout significantly decrease the calm rate. It means that the layout has significant effect on wind environment. There are following similarities and differences between the optimized plan and current plan. First, the development strength is almost the same with the volume rate and building height constant. Second, the layout is different. In the optimized plan, the layout changes from the traditional enclosure to dislocated enclosure. In other words, the overall layout is still enclosed with the adjustment of plate-type dislocated layout in partial. This optimized layout leaves a corridor for ventilation for the improvement of wind environment.

(2) Comparative analysis on results

Simulation results show that the wind speed is fast in spring and summer when southeaster prevails. In terms of overall environmental effect, this plan has a large effect on the wind speed field of the whole environment due to the closure. In this plan, a series of calm areas form surrounding high-level buildings, which is disadvantageous to the overall ventilation in the environment. By optimizing this plan, an open corridor forms, making the overall effect of wind environment in the community constant with the external environment. This is advantageous to the ventilation in the community. In terms of internal micro-environment of the community, the wind speed is low in the current plan with only three tiny air flues in incoherency. It is difficult to fluid air exchange with the outside world. After optimization, the overall wind speed in the internal environment is slightly higher with a complete ventilated corridor.

The wind speed in autumn and winter is low when northwester prevails. The difference between internal and external wind speed is significant in the current plan, while the difference is small in the optimized plan. However, the small pattern of internal wind speed field shows that two air flues with high wind speed form near the residential area in the current plan. These flues will make pedestrians uncomfortable in autumn and winter. The optimized plan forms an open air flue in the middle but effectively resist the cold wind due to some random shelter and small enclosure near buildings. Therefore, the optimized plan makes pedestrians more comfortable.

Relation of the internal ventilation with the community and development strength is not strong, while that with the layout pattern is obvious. Dislocated enclosure can more effectively enhance the ventilation effect in the community to improve the overall air quality than surrounding enclosure (Zhang et al., 2018).

Conclusions

By simulating the wind environment in Kaziwan Community of Urumqi and its optimization analysis, following advises are obtained for the reference of creating a comfortable residential environment. First, the problem of severe wind environment due to development strength can be solved by proper layout optimization. Second, the dislocated enclosure can ensure a certain enclosure for heating and leave a ventilation

http://www.aloki.hu ● ISSN 1589 1623 (Print) ● ISSN 1785 0037 (Online)
DOI: http://dx.doi.org/10.15666/aeer/1704_86438654

corridor for the improvement of wind environment (David, 2017). Third, a certain ventilation opening can be left in the building layout at windward side, making the wind enter the community. This opening can optimize the wind environment in the residential area to some extent. Forth, a ventilation opening can be added in partial building layout at leeside to reduce the building separation in the direction of air flue. Therefore, the air flue is continuous in the community for a good circulating wind environment (Lu et al., 2019).

In this work, the wind environment was analyzed with the optimization strategies discussed. The results showed that the planning design of residential area should consider various aspects. Except for the urban esthetics, economic benefits, sunshine spacing and other factors, the wind environment should be optimized to improve the living environment. After optimizing wind environment, the pollutant concentration decreases, and the haze pollution is relieved by accelerating air circulation. Moreover, the green energy preservation can be realized to make a positive effect on human health to some extent (Qi, 2018).

Urban planning is a discipline crossing several disciplines. The impact factors of wind environment cannot be neglected, but more factors should be considered in the actual design. Therefore, the design should be optimized by the analysis technology of wind environment in the basic design principle (Li, 2018). However, as a specific case is taken as background, the conclusion about the layout mode based on the analysis on wind environment effect is only suitable for the case. The university requires further rectification by experiment for different regions.

Acknowledgements. This research was supported by the "Systematic study of prefabricated buildings" grant of Sichuan Provincial Department of Education (NO17ZA0371), supported by "Research on the Collaborative Innovation mechanism of urban government in the new urbanization process" grant of Sichuan science and techonology department, No.2018ZR0146, Postgraduate innovation fund of Xihua University: "Research on the Collaborative Innovation mechanism of urban government in the new urbanization process" (ycjj2018060), "Study on the carrying capacity of urban infrastructure in the construction of new type of urbanization" grant of Ministry of Housing and Urban-Rural Development of the People's Republic of China (NO2016-R2-040).

REFERENCES

[1] Abija, F. A., Nwankwoala, H. O. (2018): Characterization Of Aquifers In Parts Of Abia State Southeastern Nigeria. – Earth Sciences Pakistan 2(1): 18-22.

[2] Choudhari, P. P., Nigam, G. K., Singh, S. K., Thakur, S. (2018): Morphometric based prioritization of watershed for groundwater potential of Mula river basin, Maharashtra, India. – Geology, Ecology, and Landscapes 2(4): 256-267.

[3] Dabberdt, W. F., Hoydysh, W. G. (1991): Street canyon dispersion: sensitivity to block shape and entrainment. – Atmospheric Environment. Part A. General Topics 25(7): 1143-1153.

[4] David, R. C. (2017): 6. Traditional Political Historiography in the Work of Laureano Villanueva. – Argos 34(66).

[5] Fu, H., Li, Z., Liu, Z., Wang, Z. (2018): Research on Big Data Digging of Hot Topics about Recycled Water Use on Micro-Blog Based on Particle Swarm Optimization. – Sustainability 10(7): 2488.

[6] Ge, Q., Zheng, J., Hao, Z., Liu, Y., Li, M. (2016): Recent advances on reconstruction of climate and extreme events in China for the past 2000 years. – Journal of Geographical Sciences 26(7): 827-854.

http://www.aloki.hu ● ISSN 1589 1623 (Print) ● ISSN 1785 0037 (Online)
DOI: http://dx.doi.org/10.15666/aeer/1704_86438654

[7] Hang, J., Li, Y. G., Sandberg, M., Buccolieri, R., Di Sabatino, S. (2012): The influence of building height variability on pollutant dispersion and pedestrian ventilation in idealized high-rise urban areas. – Build Environment 56: 346-360.
[8] Huang, C. (2014): A study on the natural ventilation of rural residential area in Boyang Lake biologic economic zone. – Nanchang: East China Jiaotong University.
[9] Jing, G. (2018): Application of Traditional Cultural Elements in Modern Urban Public Art Landscape Design. – Argos 35(71).
[10] Junior, J. J. M., Silva, E. A., Reis, A. L. D. A., Santos, J. P. M. S. (2019): Dynamical spatial modeling to simulate the forest scenario in Brazilian dry forest landscapes. – Geology, Ecology, and Landscapes 3(1): 46-52.
[11] Kumar, M., Jaafar, J. (2018): Preparation and Characterization Of Tio2 Nanofiber Coated Pvdf Membrane For Softdrink Wastewater Treatment. – Environment & Ecosystem Science 2(2): 35-38.
[12] Le, K., Yao, J. Z., Li, Z., Ke, Z. (2017): Preparation, characterization and photocatalytic activity of novel CeO2 loaded porous alkali-activated steel slag-based binding material. – International Journal of Hydrogen Energy 42(27): 17341-17349.
[13] Li, J. (2018): 2. Income Distribution of Garbage Disposal PPP Project Based on Modified Shapley Value Method. – Argos 35(68).
[14] Lin, C., Liu, J. (2011): A Study on Wind Environment of New-type Traditional Residential Area—Taking Residential Building of Yi Nationality in Yunnan as An Example. – Building Science 27(12): 25-30.
[15] Lu, D., Feng, L., Jie, P. (2019): Solar Cells Various Appearance Defects Automatic Simultaneous Detection System of the Greenhouses. – Acta Microscopica 28(1).
[16] Nikolopoulou, M., Lykoudis, S. (2006): Thermal comfort in outdoor urban spaces: analysis across different European countries. – Building and environment 41(11): 1455-1470.
[17] Nkwuda, N. G., Theophine, M. A., Okogwu, O. I. (2019): Impacts Of Rock Mineralization And Poor Sanitary System On Borehole Waters Quality And The Health Implications. – Earth Sciences Pakistan 3(1): 10-13.
[18] Oke, T. R. (1973): City size and the urban heat island. – Atmospheric Environment 7(8): 769-779.
[19] Omini, E. O., Akpang, O. M. (2018): Cavity Detection Under Re-Enforced Concrete Floor Using Ground Penetration Radar. – Engineering Heritage Journal 2(2): 11-18.
[20] Ouyang, Y., Jiang, W. M. (2003): A Study on Environment Flow Fields in Urban Communities and Wind Tunnel Test for Pollutant Dispersion. – Journal of Nanjing University (Natural Science) (6).
[21] Peng, Y. L. (2015): A strategic study on the optimized design of natural ventilation for high-level buildings in Jinan with CFD simulation. – Shandong University of Architecture and Engineering.
[22] Pontiggia, M., Derudi, M., Alba, M., Scaioni, M., Rota, R. (2010): Hazardous gas releases in urban areas: assessment of consequences through CFD modelling. – Journal of hazardous materials 176(1-3): 589-596.
[23] Qi, X. (2018): 1. Arbitration Mechanism for Intellectual Property Disputes in Free Trade Zone. – Argos 35(68).
[24] Rozuki, N. F. A., Tajuddin, M. H., Yusof, N. (2018): Effect Of Different Solvent On Asymmetric Polysulfone (Psf) Membranes For Co2/Ch4 Separation. – Environment & Ecosystem Science 2(2): 11-14.
[25] Shan, P. F., Lai, X. P. (2018): Numerical Simulation of the Fluid–Solid Coupling Process During the Failure of a Fractured Coal–Rock Mass Based on the Regional Geostress. – Transport in Porous Media 124(3): 1061-1079.
[26] Sheng, J., Su, J., La, P., Ren, J., Ma, J., Shi, Y., Song, Y. (2018): Progress of In-Situ Study on Mechanical Properties for Micro/Nano-Structured Alloy. – Journal of Nanoelectronics and Optoelectronics 13(5): 637-645.

http://www.aloki.hu ● ISSN 1589 1623 (Print) ● ISSN 1785 0037 (Online)
DOI: http://dx.doi.org/10.15666/aeer/1704_86438654

[27] Stathopoulos, T., Baskaran, B. A. (1996): Computer simulation of wind environmental conditions around buildings. – Engineering structures 18(11): 876-885.
[28] Sufiyan, I., Zakariya, R., Yacoob, R., Idris, M. S., Idris, N. M. (2018): SWAT Subbasins Parameters and Flood Risk Simulations Using 3d In Terengganu Watershed. – Earth Sciences Malaysia 2(2): 10-15.
[29] Summers, P. W. (1965): An urban heat island model-its role in air pollution problems with application to Montreal. – First Canadian Conference on Micrometeorology, Toronto 22.
[30] Tianlei, W. (2019): Nonlinear Control Strategies And Planning For Underactuated Overhead Cranes. – Engineering Heritage Journal 3(1): 09-12.
[31] Wali, E., Phil-Eze, P. O., Nwankwoala, H. O. (2018): Saltwater - Freshwater Wetland Ecosystem And Urban Land Use Change In Port Harcourt Metropolis, Nigeria. – Earth Sciences Malaysia 2(1): 01-07.
[32] Wang, J. H. (2012): A Study on Air Pollutant Dispersion Surrounding High-level Residential Buildings in Natural Ventilation. – Chongqing University.
[33] Yang, L., Li, Y. (2011): Thermal conditions and ventilation in an ideal city model of Hong Kong. – Energy and Buildings 43(5): 1139-1148.
[34] Yuan, C., Ng, E., Norford, L. K. (2014): Improving air quality in high-density cities by understanding the relationship between air pollutant dispersion and urban morphologies. – Building and Environment 71: 245-258.
[35] Yuan, C., Ren, C., Ng, E. (2014): GIS-based surface roughness evaluation in the urban planning system to improve the wind environment–A study in Wuhan, China. – Urban Climate 10: 585-593.
[36] Zhang, X. Y., Jin, H. (2016): Optimization study on northeastern village forms based on the improvement of monsoon environment in winter. – Journal of Architecture (10): 83-87.
[37] Zhang, Y. L., Zhao, M. X., Su, J. L., Lu, X., Lv, K. B. (2018): Novel model for cascading failure based on degree strength and its application in directed gene logic networks. – Computational & Mathematical Methods in Medicine, Article ID 8950794. DOI: 10.1155/2018/8950794.

http://www.aloki.hu ● ISSN 1589 1623 (Print) ● ISSN 1785 0037 (Online)
DOI: http://dx.doi.org/10.15666/aeer/1704_86438654

THE EFFECT AND MECHANISM OF URBAN DOMESTIC SEWAGE SECONDARY STERILIZATION BY MICROWAVE

ZHOU, Y. J.

School of Physic and Electronic Engineering, Xianyang Normal University
Xian yang, Shaanxi 712000, China
e-mail: hoozyj@tom.com; phone:+86-1822-0095-253

(Received 8th Mar 2019; accepted 21st May 2019)

Abstract. The interactions between electromagnetic field and the biological system can lead to the change of biological morphology, structure, function and other aspects at the different levels of biological targets. The domestic sewage is secondarily disinfected using continuous electromagnetic waves, the microscopic molecules have a certain dipole-moment and the biological molecular aggregates with dielectric properties of the cell may generate dielectric loss under the effect of the applied electromagnetic field. The thermal effect will be produced by putting the microwave energy into the heat of irregular movement which increases biological system's temperature. Under the influence of an applied electromagnetic field, the membrane potentially undergoes conformational changes that would affect K^+ ion, Na^+ ion channels open and make the voltage-dependant Ca^{2+} ion open, the high concentration of Ca^{2+} ion of the membrane into the cell along the potential gradient, which leads to cell death, resulting in the biological non-thermal effects, the greater the changes of cellular transmembrane voltage, the higher the rate of cell death. The experiment results show that the microwave secondary sterilization has a good sterilizing effect, the method has the advantages of high efficiency, low cost, simple operation, easy automation, without adding any substance and does not produce any secondary pollution, etc.
Keywords: *electromagnetic field, biology system, biological morphology, microscopic molecular, high efficiency*

Introduction

Water is an indispensable natural resource in human production and life, and also an important factor in promoting social development and promoting the progress of civilization. The reform and opening up has made China's economic achievements a great achievement. The people's living standards are getting higher and higher, the urban population is also increasing, the demand for water resources is increasing, and the same domestic sewage discharge is also increasing. China is actually a relatively scarce water resource with low per capita possession, which is a country with severe water shortage.

The application of domestic sewage treatment and reuse technology has historical significance for solving water shortage and environmental pollution. On the one hand, domestic sewage treatment reduces domestic sewage discharge, which is very beneficial to avoid water eutrophication and water pollution caused by water pollution, and greatly reduces the cost of water pollution control. On the other hand, the treatment and reuse of sewage will help people solve the problem of water shortage, and reuse the reused water for urban greening, landscape hydration and road sprinkling, flushing and car washing, industrial, building fire protection and many other aspects. It has had a tremendous impact on agriculture, industry and people's lives, and promoted the sustainable development of society. However, in the past 100 years, urban domestic sewage treatment technology has been in a state of slow progress, lacking technological innovation and innovation (Zhao, 2016; Patle et al., 2019).

http://www.aloki.hu ● ISSN 1589 1623 (Print) ● ISSN 1785 0037 (Online)
DOI: http://dx.doi.org/10.15666/aeer/1704_86558666

Current status of urban domestic sewage

Urban domestic sewage characteristics

Urban domestic sewage contains high levels of suspended solids, such as food residues, grease and other types of domestic waste, which cause the color of the sewage to be heavy. In addition, because there are many organic residues such as food residues contained in urban domestic sewage, when the organic matter rots, it will produce extremely heavy odor and cause the most direct pollution to the environment. In addition, laundry wastewater, because of detergent, generally contains phosphorus and nitrogen. It is easy to cause eutrophication of water bodies. Hospital wastewater may carry a large number of pathogenic microorganisms.

Urban domestic sewage source

Urban domestic sewage mainly comes from wastewater generated by urban residents in daily life. It includes various sewer waste water, washing wastewater, toilet wastewater, hospital sewage, rainwater, etc., which are discharged from living quarters, schools, hospitals, shopping malls, hotels, etc. (Mcleod and Liboff, 1986; Sen et al., 2018). The source is extensive, and the source domestic sewage discharge management is not standardized. The amount produced is large, unstable, and has obvious seasonality.

Urban domestic sewage impact

In general, the hazards of urban domestic sewage at this stage are mainly reflected in the following aspects:

1) The eutrophication of water bodies, with the discharge of domestic sewage, a large amount of organic substances, chemical substances, metal substances, etc., and the increase of chemical substances such as nitrogen and phosphorus substances will pollute the water bodies, resulting in eutrophication of water bodies (Huang, 2000; Yahya et al., 2018). There may even be red tides and the like;
2) Polluted urban environment, some domestic sewage has odor. If it is not treated in time, it will be stinking, directly polluting the urban environment, causing troubles for people's daily life and work. In addition, odor Diffuse can endanger the health of the human body and affect the development of green cities;
3) Affecting groundwater sources. At this stage, due to the complexity of the composition of urban domestic sewage, various chemical substances may be mixed together to produce some chemical reactions, which may cause some toxic substances, if not treated in time (Durney et al., 1988; Suhaili and Samsudin, 2018). It will cause toxic substances to enter the groundwater and urban residents' water, causing residents to poison, directly threatening the life and health and personal safety of urban residents. There are also a large number of pathogenic microorganisms in urban domestic sewage. It poses a great threat to people's health and so on.

Domestic sewage sterilization is an important process to ensure the health and safety of domestic sewage (Lednev, 1991; Kasim et al., 2019). Generally the sterilization methods to water are chlorine, chlorine dioxide, ozone, etc, in which the chlorine is a common method which has the characteristic of low cost, simple process and easy to operate, but the chlorine has powerful oxidation and easy to acting with organic matter

http://www.aloki.hu ● ISSN 1589 1623 (Print) ● ISSN 1785 0037 (Online)
DOI: http://dx.doi.org/10.15666/aeer/1704_86558666

in water to produce halogenated hydrocarbons, chloroform and PCBs that is harmful to people and animals (Zhang, 2002; Tao, 2018). The effect of chlorine dioxide sterilization is better than chlorine and will not easy produce organochloride, but chlorine dioxide is unstable and sensitive to temperature, pressure and light. It is easy to explosive when it meets fire or organics. So it only be produced and used on the spot (Chen and Wang, 2001; Jamil et al., 2018). Ozone has strong oxidation ability, fast, good sterilization effect and not produces odor smell, but the Ozone treatment requires high technique, complicated equipment and high energy (Jin, 1999; Nawaz et al., 2018).

Microwave treatment has unique advantages. The material is heated by way of molecule polarization or ion- conduction effect through microwave. The heated polar molecule or ions rapid motion and orientation in the electromagnetic field which leads to heat by the tearing and mutual friction (Li and Niu, 1990; Austin et al., 2018). Microwave can kill various microorganisms. The thermal effect and mechanism of microwave have been a fact which is widely accepted by people, but there still exists the big dispute to the mechanism of non–thermal effects of electromagnetic (Liboff and Mcleod, 1988; Ismail et al., 2019). The work describes the sterilization effect of microwave to domestic sewage and analyze the phenomena and mechanism of microwave sterilization from the experimental and theoretical (Yang, 2018).

Experiment apparatus and method

It shows the related experimental equipment 1 (*Fig. 1*) and the related experimental equipment 2 (*Fig. 2*).

Figure 1. *The related experimental equipment 1*

The domestic sewage is taken from the domestic sewage well of xianyang normal University living quarters and the water pH's value is 7.3~7.8, the domestic sewage has been treated by bio-oxidation, then be disinfected by microwave, the total amount of bacteria and fecal coliform was decreases with the suspended solids significantly reduce in domestic sewage (Zhou and Zhang, 2000). However, the concentration of the two kinds of germs was still so high that it must be disinfected before discharge. The

http://www.aloki.hu ● ISSN 1589 1623 (Print) ● ISSN 1785 0037 (Online)
DOI: http://dx.doi.org/10.15666/aeer/1704_86558666

continuous microwave is used to disinfect to domestic sewage which has been treated by bio-oxidation in the experiment (Niu et al., 2002). It shows the principle chart of electromagnetic radiation (*Fig. 3*). The microwave frequency is better to be higher (Zhang, 1998), taking into account the depth of penetration and other reasons, the microwave frequency is 2450 MHz and the average power density is 520 MW/cm2 was adopted in this experiment.

Figure 2. *The related experimental equipment 2*

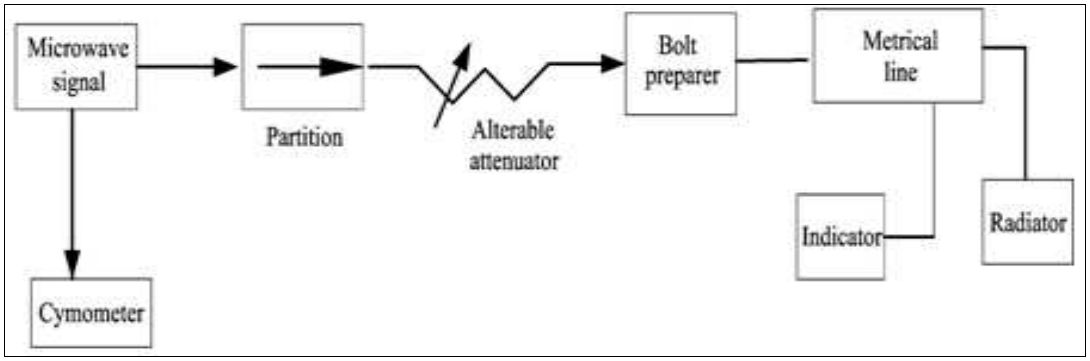

Figure 3. *The principle chart of electromagnetic radiation*

It shows the schematic diagram of domestic sewage sterilization (*Fig. 4*). The diameter of waterpipe is 15 mm; length of 2 m insulated wire wound on a 20 cm long pipeline. The water samples which have different domestic sewage quality were processed by microwave under the identical condition then placed it into incubator about 24 h~48 h (Lu et al., 1996). The plate culture method using detects the number of germs. Three groups constitute a parallel sample contain and each group has three subsets sample. The same water quality domestic sewage as comparison sample, which isn't treatment by microwave. An 828 type pH's apparatuses measure the pH value before and after the sample treated by microwave. It lists the total germs and the corresponding sterilization rate at 40 mins (*Table. 1*). It lists the sterilization rate at

http://www.aloki.hu ● ISSN 1589 1623 (Print) ● ISSN 1785 0037 (Online)
DOI: http://dx.doi.org/10.15666/aeer/1704_86558666

different time (*Table 2*). The temperature in the experiment course is controlled within (25±1) ℃.

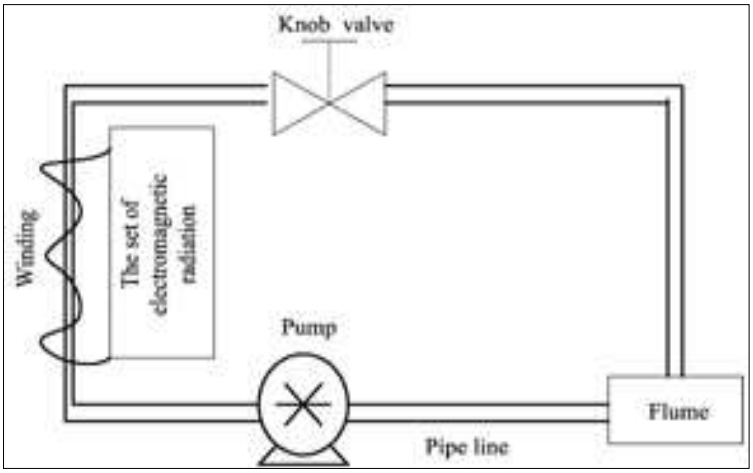

Figure 4. *The schematic diagram of domestic sewage sterilization*

Table 1. *Sterilization effect under different water quality conditions*

Sample number	The sum of bacteria in original sample (Entries/mL)	The sum of bacteria in worked sample (Entries/mL)	The efficiency of kill bacteria / %
1	3.5×10^6	3.5×10^4	99.0
2	4.9×10^6	3.0×10^4	99.3
3	5.3×10^6	3.2×10^4	99.4
4	1.5×10^7	5.1×10^4	99.7

Table 2. *Sterilization effect under different times*

Sample	*t* /min				
	0	10	20	30	40
1	3.2×10^6	1.92×10^6	8×10^5	3.2×10^4	2.56×10^4
2	3.7×10^6	2.294×10^6	8.88×10^5	2.96×10^4	2.59×10^4
3	5.0×10^6	2.85×10^6	1.25×10^6	5×10^4	3×10^4
4	1.9×10^7	1.045×10^7	4.37×10^6	7.6×10^4	4.75×10^4

The result and discussion

The total amount of germs and the sterilization rate of four kinds of water samples disinfected by microwave at 40 mins are listed in *Table 1*. It can be seen from *Table 1* that the sterilization rate of samples 1 to 4 over reaches 99%, but the electromagnetic sterilization effect of sample 4 is better than sample 1. The data in *Table 2* are obtained for samples irradiated by microwave at different time and the trend of the data is the same, that is, with increasing of irradiation time, the higher sterilization rate (Yanyan et al., 2019). However, different samples have different sterilization rate at the same time. For example, it can be seen from sample 1 and sample 2, the efficiency of sterilization rate of sample 1 is about 57% at 20 mins, while the sample 2 is 76% at the same time. The different sterilization rate between samples may be due to, first, different water

http://www.aloki.hu ● ISSN 1589 1623 (Print) ● ISSN 1785 0037 (Online)
DOI: http://dx.doi.org/10.15666/aeer/1704_86558666

samples contained different amounts of bacteria before sterilization. Second, different water samples contained different kinds of bacteria, and thus the electric parameters (permittivity ε, conductivity σ) are different. So microwave energy absorbed is different. In generally, the stronger the microwave energy absorption of bacteria, the better the sterilization rate. If the sample has more fungi, shapeless spores and thermophilric bacteria, then it needs more time to reach the same sterilization effect (Kang, 2018). Therefore, under the same condition, the fewer the sample contained the fungus talked above, the better sterilization effect. The fittest pH value to most bacteria is 7.3~7.8. The pH value of the sample before and after sterilization had been test with 828 type pH's tester. The pH value before sterilization is about 7.4, while after sterilization it is about 7.5. Thus it can be seen that the pH value of sample has slightly changes before and after sterilization, but still between 7.3~7.8. Therefore, the influence brought by the pH value slightly change can be neglected (Li et al., 2019).

Analysis of the mechanism

The mechanism of heating effect

A material may be having many dielectric mechanism or polarization influence. In fact, material loss can be expressed as dielectric loss and conduction loss caused by the electrical conductivity (σ), namely:

$$\varepsilon_{\mathrm{r}}^{''}(\omega) = \varepsilon_{\mathrm{r}}^{''} + \frac{\sigma}{\omega\varepsilon_{\mathrm{O}}} \quad \text{(Eq.1)}$$

Under the action of the electromagnetic wave, the electromagnetic energy is absorbed by material

$$P = \frac{1}{2}\omega\varepsilon_{\mathrm{rd}}^{''}\int_{\mathrm{v}}|E|^2 \mathrm{d}v \quad \text{(Eq.2)}$$

where $\varepsilon_{rd}^{''}$ is dielectric loss of the material, ω is the frequency of electromagnetic wave, and E is the electric field strength.

There exists mass water inside every life body, which distributed in all parts of the living body such as cell membrane, cytoplasm, cell nucleus, cells, tissues, blood and lymph liquid water molecules is polar molecule which has the bigger dipole moment (Cheng and Lin, 1981). At the subcellular level, the orderly biomolecule gathered body also showed significant dielectric properties, such as cell membrane which is bilayer structure dielectric material composed of the lipid molecule. All membrane dipole moments can be fully polarized under the transmembrane resting potential difference and maintain a certain conformation. The force to maintain the conformation of macromolecules primarily is the static electricity of intermolecular and intramolecular (including interaction between dipole and dipole) and other interaction force (for example: van der Waals force). Under the effect of microwave, the negative charges of molecule are distributed again that leads to the change itself of dipole moment and polarization state, which may induce the change of molecule construction. The displace-polarization time of general material establishes needs about 10-16--10-12 s, which can be neglected in microwave scope (microwave priod is 10-9--10-12 s). However, the dipole needs long time which over 10-10 s. For example, water molecules have a strong

http://www.aloki.hu ● ISSN 1589 1623 (Print) ● ISSN 1785 0037 (Online)
DOI: http://dx.doi.org/10.15666/aeer/1704_86558666

intrinsic dipole moment and its relaxation time is 0.25×10-10 s which justly in the scope of microwave, therefore the attenuation effect of water to microwave is bigger than the general material (Zhai et al., 1998), The polarization would appear hysteresis phenomenon which produce the dielectric loss. With the dielectric method of time domain reflection, it has been found that there has significant dielectric loss in the vicinity of 10 MHz when natural DNA was dissolved degeneration (Richard and Stephen, 1998). It can be seen that the thermal effect is more notable at the condition of a higher frequency and a bigger of from the *Equations 1 and 2* under the affection of microwave. These dipoles constantly change from one equilibrium state to another equilibrium state, a molecule dipole would frequently colliding with surrounding other molecules in this course, thus the microwave energy consumed and converted into heat. When the temperature exceeds the temperature of microbes to survive, it will lead to germ death, which is identical to the mechanism of pasteurization (Li, 2018).

The mechanism of non-heating effect

The microwave non-heating mechanism of the body has related discussion (Liu and Wang, 2003), but there is no unified knowledge and many kinds of hypothesis are put forward. Main hypothesis such as cell membrane perforation effect, Ion cyclotron resonance model, Ion parametric resonance model, State parameter representation, an electromagnetism mechanism model ect. The cell membrane perforation effect argues that the cell membrane is a kind of phospholipid bilayer construction which has certain permeability, a certain degree of toughness and a certain charge is absorbed to the surface. Therefore, there has certain potential difference between the inner and outer surface of membrane. The potential difference will be enlarged when an electric field is applied membrane, at this time the permeability of cell membrane also increases. The permeability of cell membrane would dramatic increase and many holes will appear on the membrane which reduces the toughness of membrane when the electric field strength to the critical value. Since the special structure of the cell membrane, it will produce an adaptive adjustment trying to maintain the original way of life, the membrane can control the outside influences within the capacity of the adaptive and the life living with original method (Li et al., 2019). If the outside influences exceed the body's adaptive capacity, which may produce the variations and lead to new existence method. If outside influences exceeded the limit of adaptation, it will destroy the original structure of membrane and lose their function can't be restored, thus cell death. The experiment proves there has clear rift on the cell after the yeast was killed (Jayaran et al., 1994). Though bacterial cell structure is small but there no essential difference of internal structure between general biological cell and bacterial cell. The main effect of electromagnetic wave on the cell is at the cell membrane. Under the condition of resting, the transmembrane resting potential difference of cell membrane is 60~100 mV, which is mount to 107 V/m strong electric field, therefore all dipole moments of the membrane can be full polarization under the strong electric field action. Therefore, it is not hard to understand the electromagnetic field can play significant effect on the membrane (Shan et al., 2018).

With the spherical cell as the research object, the transmembrane voltage Uion is formed due to ion accumulation and transmembrane transport both side of the membrane under the resting state, the Uion value can be calculated from the Goldman's equation (Plonsey and Barr, 2000).

http://www.aloki.hu ● ISSN 1589 1623 (Print) ● ISSN 1785 0037 (Online)
DOI: http://dx.doi.org/10.15666/aeer/1704_86558666

$$U_{\text{ion}} = \frac{RT}{F} \ln \frac{P_{\text{K}}\left[K^{+}\right]_0 + P_{\text{N}_\text{a}}\left[N_{\text{a}}{}^{+}\right]_0 + P_{\text{Cl}}\left[Cl^{-}\right]_0}{P_{\text{K}}\left[K^{+}\right]_{\text{i}} + P_{\text{N}_\text{a}}\left[N_{\text{a}}{}^{+}\right]_{\text{i}} + P_{\text{Cl}}\left[Cl^{-}\right]_{\text{i}}} + \Delta U \quad \text{(Eq.3)}$$

In this state, the membrane permeability to K^+ ion is much larger than Ca^{2+} ion and Na^+ ion. At this moment the ion channels are closed to Ca^{2+} ion and Na^+ ion. Under the applied additional alternating electric field E, the interior cytoplasm and the external medium of the cell as good conductor and the cell membrane as a dielectric. The induced transmembrane voltage UE is superimposed on Uion. According to the classical theory of cell membrane induction electromotive force (Tadej and Damijan, 2000), the induction electromotive force UE is generated on both sides in the cell membrane is

$$U_{\text{E}} = \frac{3}{2} E_{\text{e}}(t) R \cos\alpha \frac{1}{1 + j\omega\tau_{\text{m}}} \quad \text{(Eq.4)}$$

where Ee(t) is outer electric field intensity, R is the cell radius, α is the angle of between the external electric field direction and the axial of ion channels, $\omega = 2\pi f$, f is frequency of the applied electric field, and τ_m is the inductive time constant of membrane that can be expressed through first-order system as:

$$\tau_{\text{m}} = \frac{RC_{\text{m}}}{\frac{2\lambda_{\text{i}}\lambda_{\text{e}}}{\lambda_{\text{i}} + 2\lambda_{\text{e}}} + \frac{R}{d}\lambda_{\text{m}}} \quad \text{(Eq.5)}$$

where Cm is the equivalent capacitance of the cell membrane, λ_i, λ_e and λ_m is respectively the conductivity of inside and outside of cell membrane and the cell membrane, *d* is the average thickness of the membrane (Yang, 2018).

From *Equations 4 and 5*, we know that the amount of change of cell transmembrane potential has relation with the electromagnetic wave field strong and power, has relation with the cell type and size, has relation with the intracellular fluid and extracellular fluid dielectric constant and conductivity (Li, 2018). The external electric field causes the membrane voltage change, thereby enabling the ion permeation rate change of the cell membrane. The ion permeation ratio is direct proportional to the change of membrane voltage caused by the external electric field (Zhang et al., 2004). The studies have shown that Ca^{2+} ion channel is a voltage dependent of membrane. Some kinds of channel activity of K^+ ion and Na^+ ion are relation with Ca^{2+} ion. So the influx of Ca^{2+} ion may also cause the channel open of K^+ ion and Na^+ ion. When the influx volume increasing of Ca^{2+} ion. The influx of Na^+ ion is predominated, while the influx of Ca^{2+} ion can open K^+ channel that is relies on Ca^{2+} ion, which make the outflow of K^+ dominant. Under the action of an applied electromagnetic field, the external electric field, the cell transmembrane potential increases, when the membrane voltage is increased to a certain value so that the voltage-dependent Ca^{2+} ion channels open, the larger concentration of Ca^{2+} ion outside the cell membrane into the cell along the potential gradient (Yang et al., 2018). The experiment and theoretical indicate that the greater the change in cell membrane voltage, the higher the rate of cell death. In addition, from the dielectric properties of the cell membrane to see, the role of the applied voltage causes the inside and outside charge density of cell membrane will

http://www.aloki.hu ● ISSN 1589 1623 (Print) ● ISSN 1785 0037 (Online)
DOI: http://dx.doi.org/10.15666/aeer/1704_86558666

change. The cell membrane surface charge density and the pressure difference between inside and outside of the cell membrane has the following relationship (Gao et al., 2002)

$$\Delta P_{\mathrm{E}} = \frac{\left(\sigma_{\mathrm{i}}^2 + \sigma_0^2\right)}{2\varepsilon_0} + \frac{\sigma_0 \sigma_{\mathrm{i}} r_{\mathrm{i}}}{\varepsilon_0 r_0} \quad \text{(Eq.6)}$$

where σ_i is the surface charge density of the inner surface of cell membrane, σ_0 is the surface charge density of the outer surface of cell membrane, r_i is the curvature radius of the inner membrane, and r_0 is the curvature radius of the outer membrane (Hai et al., 2017).

From *Equation 6*, we know that the greater the surface charge density, the greater the pressure difference between inside and outside of the cell membrane, and thus an impact on the ion channel Open and close (Amit et al., 2017). When the effect of above combination factors exceeds the limits of adaptive of membrane, the original structure of the membrane was destroyed and could not be restored, the cell death, the purpose of sterilization is achieved. The non-heating effect of electromagnetic biological less significant than the thermal effects of electromagnetic biological, it requires a process of accumulation.

Outlook

With the continuous enrichment of material life, people's demand for domestic water is also increasing. The reserves of water resources on the earth are limited and they are non-renewable natural resources (Yanyan et al., 2019). Urban sewage treatment and reuse can effectively solve the shortage of urban water resources, and at the same time reduce environmental pollution, strengthen water recycling and sewage utilization rate, and achieve sustainable development of urban water resources (Kang et al., 2018). Therefore, in the process of treating urban domestic sewage, it is necessary to adhere to the principle of sustainable development and energy conservation and consumption reduction to ensure that urban domestic sewage treatment technologies and treatment processes can meet these requirements in practical applications (Shan et al., 2019).

The microwave sterilization technology can also serve the domestic sewage treatment well. The pathogens such as worm eggs, enteroviruses and pathogenic bacteria can be killed by using the combined action of the biological heating effect and biological non-heating effect. This method is a physics method, there is no obvious chemical treatment, the composition and structure of water was not change and sterilization fast. Compared with traditional domestic sewage treatment and sterilization technologies such as liquid chlorine, chlorine dioxide and ultraviolet sterilization, microwave sterilization technology not only has high sterilization efficiency, no secondary pollution, broad spectrum of sterilization, no noise, no odor, etc. (Yang et al., 2018). All the advantages of the technology, but also have the advantages of stable control system, long service life, low operating cost, excellent energy saving, safe and reliable, easy maintenance, and the ability to provide residual sterilization (Zhang et al., 2017). In order to better promote the technology, the utilization of microwave energy conversion and the expansion of the application range of microwave technology should be paid attention to by the industry. It should popularize the use of the technology on a

http://www.aloki.hu ● ISSN 1589 1623 (Print) ● ISSN 1785 0037 (Online)
DOI: http://dx.doi.org/10.15666/aeer/1704_86558666

large scale, so that the technology can gradually replace some traditional technology and sterilization technology in the future life more efficient, environmentally friendly and more convenient for human production and life (Zhang, 2017).

Acknowledgements. This work was funded by Shaanxi Province Science and Technology Research and Development Program, Grant number 2016JM6053, and was funded by Shaanxi Provincial Department of Education special scientific research project, Grant number 18JK0831, and was funded by the research foundation of Xianyang Normal university, Grant number 14XSYK009, and was funded by Xianyang Normal College Teaching Reform Project, Grant number 201402010, and was funded by Shaanxi University Student Innovation and Entrepreneurship Training Program, Grant number 2510, and was funded by Xianyang Normal University Innovation and Entrepreneurship Training Program, Grant number 2017079.

REFERENCES

[1] Amit, Chandra, R., Ghosh, U. K., Nayak, J. K. (2017): Phycoremediation potential of marine microalga tetraselmis indica on secondary treated domestic sewage for nutrient removal and biodiesel production. – Environmental Science Pollution Research 24(218): 1-8.

[2] Austin, O. E., Ebuka, A. O., Zanders, A. C. C., Joseph, I. N. (2018): Seismic Analysis Of The Transgressive Systems Tracts (TSTS) Of The Niger Delta. – Earth Sciences Malaysia 2(2): 16-19.

[3] Blanchard, J. P., Blackman, C. F. (1994): Clarification and application of an ion parmetric resonance model for magnetic field interactions with biological systems. – Bioelectromagnetics 12: 217-238.

[4] Chen, Y., Wang, X. D. (2001): Using of Ultraviolet Sterilization wastewater treatment. – Chongqing Environmental Science 23(3): 49-51.

[5] Cheng, J. J., Lin, K. C. H. (1981): Acta biophysica sinica. – Beijing: People's Education Publisher 36-40.

[6] Durney, C. H., Rushforth, C. K., Anderson, A. A. (1988): Resonant AC-DC magnetic fields: calculated response. – Bioelectromagnetics 315-336.

[7] Gao, Y. Y., Jiao, Q. Y., Fang, J. Z. H. (2002): Electrical Property of Plant Cell Membrane and its Influence. – Cellular Pressure Acta Biophysica Sinica 18(3): 277-281.

[8] Haiquan, W. U., Zhou, L., Sun, F., Luo, X., Lei, N., Wang, J. (2017): Application of biological enhancement technology on treating urban domestic sewage in alpine regions. – Chinese Journal of Environmental Engineering 11(6): 3511-3517.

[9] Ismail, I., Husain, M. L., Satyanarayana, B., Ibrahim, S., Zakaria, R. (2019): Root Density Analysis And Wave Attenuation Ability Of Rhizophora Species At Kemaman, Terengganu. – Earth Sciences Malaysia 3(1): 18-24.

[10] Jamil, F., Arshad, R., Ali, M. A. (2018): Design, Fabrication And Evaluation Of Rotary Hot-Air Dryer For The Value Addition Of Fruit Waste. – Earth Sciences Pakistan 2(2): 07-11.

[11] Jin, Q. H. (1999): Microwave and chemistry, Beijing. – China Technology Publisher: 13-15.

[12] Kang, L., Du, H. L., Du, X., Wang, H. T., Ma, W. L., Wang, M. L., Zhang, F. B. (2018): Study on dye wastewater treatment of tunable conductivity solid-waste-based composite cementitious material catalyst. – Desalin. Water Treat. 125: 296-301.

[13] Kasim, S., Hassan, R., Zakaria, Z. (2019): Re-Engineering In Confinement Method. – Engineering Heritage Journal 3(1): 18-19.

[14] Lednev, V. V. (1991): Possible mechanism for the influence of weak magnetic field on biological system. – Bioelectromagnetics 12: 71-75.

http://www.aloki.hu ● ISSN 1589 1623 (Print) ● ISSN 1785 0037 (Online)
DOI: http://dx.doi.org/10.15666/aeer/1704_86558666

[15] Li, J. X., Niu, Zh. Q. (1990): The generality of biologic electromagnetism. – Xi'an: Xidain University Publisher: 125-130.
[16] Li, J. (2018): 2. Income Distribution of Garbage Disposal PPP Project Based on Modified Shapley Value Method. – Argos 35(68).
[17] Li, C., Li, S., Tian, Q. (2019): Microbial Attachment Behavior and Pollutant Removal Performance of Modified Quartz Sand. – Acta Microscopica 28(2).
[18] Liboff, R., Mcleod, R. (1988): Kinetics of channel membrane ions in magnetic fields. – Bio-electromagnetics 9: 215-227.
[19] Liu, Y. C. H., Wang, Y. H. (2003): Theoretical Analysis of the Electromagnetic Organism Effect in Killing Bacterium by Electromagnetic Radiation. – Journal of Soochow University (Engineering Science Edition) 23(5): 6-11.
[20] Lu, Z. H. Y., Niu, Z. H. Q., Ma, J. G. (1996): A Study on Killing Germs in Traditional Chinese Medicines by means of Microwaves. – Journal of Microwaves 12(2): 155-158.
[21] Mcleod, R., Liboff, R. (1986): Dynamic characteristics of membrane ions in multifield configurations of low-frequency electromagnetic radiation. – Bioelectro magnetics 7: 177-189.
[22] Nawaz, A., Arshad, F., Khurshid, F. (2018): Evaluation Of Low Cost Environment Friendly Natural Extracts For The Purification Of Drinking Water. – Earth Sciences Pakistan 2(1): 23-25.
[23] Niu, Z. Q., Wang, H. B., Hou, J. Q., Yan, J., Lu, Z. Y. (2002): Basic Theory for the Effects of Electromagnetic wave on Ion Concentration in Cells. – Chinese Journal of Biomedical Engineering 21(6): 552-556.
[24] Patle, G. T., Sikar, T. T., Rawat, K. S., Singh, S. K. (2019): Estimation of infiltration rate from soil properties using regression model for cultivated land. – Geology, Ecology, and Landscapes 3(1): 1-13.
[25] Plonsey, R., Barr, R. C. (2000): Bioelectricity, A Quantitative Approach. – New York: Kluwer Academic 201-235.
[26] Richard, S. L., Stephen, B. (1998): Dielectric studies of chain melting and denaturation in native DNA. – Biochimica Biophysica Acta 1397: 316-324.
[27] Sen, B., Goswami, S., Devi, G., Sarma, H. P., Bind, A. (2018): Valorization of Adenanthera pavonina seeds as a potential biosorbent for lead and cadmium removal from single and binary contaminated system. – Geology, Ecology, and Landscapes 2(4): 275-287.
[28] Shan, P. F., Lai, X. P. (2018): Numerical Simulation of the Fluid–Solid Coupling Process During the Failure of a Fractured Coal–Rock Mass Based on the Regional Geostress. – Transport in Porous Media 124(3): 1061-1079.
[29] Suhaili, M. Z., Samsudin, M. D. M. (2018): Utilization Of Wastewater For Corrosion Prevention Of Carbon Steel Pipe Using Single Chamber Microbial Fuel Cells. – Environment & Ecosystem Science 2(2): 47-52.
[30] Tadej, K., Damijan, M. (2000): Second-order model of membrane electric field induced by alternating external electric fields. – IEEE Transactions on Biomedical Engineering 47(8): 1074-1081.
[31] Tao, S. (2018): Evaluation Of Technology Innovation In Hubei Province. – Engineering Heritage Journal 2(2): 09-10.
[32] Yahya, N., Aziz, F., Enriquez, M. A. O., Aizat, A., Jaafar, J., Lau, W. J., Yusof, N., Salleh, W. N. W., Ismail, A. F. (2018): Preparation And Characterization Of Lafeo3 Using Dual-Complexing Agents For Photodegradation Of Humic Acid. – Environment & Ecosystem Science 2(2): 30-34.
[33] Yang, B., Luo, Y., Jeng, D., Feng, J., Huhe, A. (2018): Experimental studies on initiation of current-induced movement of mud. – Applied Ocean Research 80: 220-227.
[34] Yang, B., Gao, F. P., Jeng, D. S. (2018): Failure mode and dynamic response of a double-sided slope with high water content of soil. – Journal of Mountain Science 15(4): 859-870.

http://www.aloki.hu ● ISSN 1589 1623 (Print) ● ISSN 1785 0037 (Online)
DOI: http://dx.doi.org/10.15666/aeer/1704_86558666

[35] Yanyan, D., Fuwen, D., Yue, L. (2019): Effect of Sewage Load on Microenvironment and Sludge Reduction Efficiency of Situ Biofilm Sludge Reduction System. – Acta Microscopica 28(2).
[36] Zhai, Y. R., Li, J. H., Zhang, H. (1998): Experiment of high physics. – Shenyang: Liaoning University Publisher 101-107.
[37] Zhang, G. C. H. (1998): Cell biology. – Beijing: High Education Publisher 18-61.
[38] Zhang, X. (2002): UV-Desinfection in Wastewater Treatment. – Water and Wastewater Engineering 28(11): 31-34.
[39] Zhang, H. J., Xu, D., Niu, Z. H. Q. (2004): A Response of the Probability Crossing Cell Membrane to the Electromagnetic Wave. – Chinese Journal of Medical Physics 21(3): 179-181.
[40] Zhang, W., Yang, J., Fang, Y., Chen, H., Mao, Y., Kumar, M. (2017): Analytical fuzzy approach to biological data analysis. – Saudi journal of biological sciences 24(3): 563-573.
[41] Zhao, X. F. (2016): Research and application status of urban sewage treatment technology. – Liaoning Chemical 45(10): 1338-1340.
[42] Zhou, W. H., Zhang, J. (2000): Study on the Sterilization Technology of Electromagnetic Pulse. – Journal of Microwaves 16(3): 318-321.

http://www.aloki.hu ● ISSN 1589 1623 (Print) ● ISSN 1785 0037 (Online)
DOI: http://dx.doi.org/10.15666/aeer/1704_86558666

GEOCHEMICAL SIGNATURES OF WATER BODIES AND SOURCES IN THE QINGHAI LAKE AREA, CHINA

LIU, Y.[1,2,3*] – WANG, J.[2,3] – REN, Z.[4] – WANG, H.[2,3]

[1]*East China Normal University, Shanghai 200241, China*

[2]*State Key Laboratory of Simulation and Regulation of Water Cycle in River Basin China Institute of Water Resources and Hydropower Research, Beijing 100038, China*

[3]*Department of Water Resources, China Institute of Water Resources and Hydropower Research, Beijing 100038, China*

[4]*Flathead Lake Biological Station, University of Montana, Polson, MT 59860, USA*

[*]*Corresponding author*
e-mail: liuyang@iwhr.com

(Received 8th Mar 2019; accepted 21st May 2019)

Abstract. The chemical composition of dissolved constituents in aquatic ecosystems is of fundamental importance in regulating chemical and biological dynamics and processes. There are many factors that can determine and affect chemical composition of lakes and rivers. This paper presents fundamental geochemical information for the waters in Qinghai Lake area in China and assesses geochemical patterns, relationships between the elements, and potential mechanisms for these patterns. The concentrations of 30 elements from 16 water samples were measured. The results showed that Ca (8.1-88.9 mg/L), K (5.1-372.7 mg/L), Mg (6.3-1127.0 mg/L), Na (10.0-6459.0 mg/L), and S (4.8-2002.0 mg/L) were the dominant elements in all water samples but exhibited considerable variation among systems. The tributaries had high Ca, relatively low Na+K, and low salinity, indicating rock weathering as the dominant factor determining their geochemistry. The satellite lakes (except the two largest ones) showed low Ca, moderate Na+K and Mg, and low salinity, indicating the combined effects of many factors. Correlation analyses suggested that B, K, Li, Mg, and Na concentrations are determined by evaporation and crystallization and dissolution of sulfate minerals while Al and Fe concentrations are affected mostly by rock weathering.
Keywords: *geology, chemical composition, trace elements, salinity, basin*

Abbreviations: the Buha River: BHR; the Shaliu River: SLR; the Haergai River: HER; the Quanji River: QJR; the Heima River: HMR; the Daotang River: DTR; cluster analysis: CA; coefficient of variation: CV; total dissolved solids: TDS; Qinghai Lake: QL; Moon Lake: ML; Sun Lake: SL; Lanhua Lake: LHL; Ganzihe Lake: GZL; Erhai Lake: EHL; Haiyanwan Lake: HYL; Gahai Lake: GHL

Introduction

Major and trace elements are natural components in aquatic ecosystems worldwide and play important roles in chemical and biological processes (Gaillardet et al., 2003; Bounouira et al., 2013; Qin et al., 2015; Sunny et al., 2018). Some trace elements are commonly required by biota due to their key role in biosynthetic processes and metabolism as cofactors for enzymes (Havig et al., 2015; Daniel et al., 2018). These elements include aluminum (Al), boron (B), chlorine (Cl), chromium (Cr), cobalt (Co), copper (Cu), fluorine (F), iodine (I), iron (Fe), manganese (Mn), molybdenum (Mo), nickel (Ni), selenium (Se), silicon (Si), tin (Sn), vanadium (V), and zinc (Zn) (Çelik and Oehlenschläger, 2007; Tuzen, 2009; Mahmood et al., 2018). However, due to their toxicity, non-degradability, persistence, and bioaccumulation, trace element pollution of

http://www.aloki.hu ● ISSN 1589 1623 (Print) ● ISSN 1785 0037 (Online)
DOI: http://dx.doi.org/10.15666/aeer/1704_86678678

the environment has become one of the most serious global issues in recent years (Tam and Wong, 2000; Cui et al., 2011; Hsieh et al., 2013; Li et al., 2015). Indeed, even bioessential elements will yield toxic effects at high concentrations (Goldhaber, 2003; Anan, 2019).

Major and trace elements are added to an aquatic ecosystem through different pathways, including geological erosion, atmospheric deposition, or anthropogenic sources (Vystavna et al., 2012; Al Abdullah et al., 2014; Shakeri et al., 2014; Xu, 2018). Under natural conditions, the chemical composition of aquatic ecosystems is determined by the weathering of terrigenous minerals, evaporation and crystallization, and precipitation (Négrel et al., 1993; Liang and Wenshun, 2019). Elements originated from rock weathering are transported to downstream water bodies through streams and rivers, carrying the characteristic features of their source's lithology. Upon reaching standing water, evaporation and crystallization are important mechanisms that produce Na-rich and highly saline lakes and ponds, due to sodium's high solubility (Gibbs, 1970). In addition, concentrations of various elements in aquatic systems can be strongly altered by anthropogenic activities, including mining, wastewater discharge, atmospheric deposition, and fertilizer runoff (Yang and Rose, 2005; Yu et al., 2014; Hayzoun et al., 2015; Lynam et al., 2015; Otachi et al., 2015; Baharuddin and Samsudin, 2018). Even remote lakes are not exempt from contamination by the long-range transported trace elements (Battarbee et al., 2009; Elser et al., 2009; Kyllonen et al., 2009). Thus, geochemical signatures of rivers and lakes are determined by and in turn provide important information about the geology of the area, types of rock weathering, anthropogenic activities, biological processes, and atmospheric deposition in drainage basins (Foster and Charlesworth, 1996; Xu et al., 2010; Singh et al., 2015; Walther and Nims, 2015; Wang et al., 2018).

Qinghai Lake, located on the northeastern margin of the Qinghai-Tibet Plateau, is an endorheic brackish lake and the largest natural lake in China. It is also a globally important wetland for biological diversity conservation (Ramsar, 2015; Sarker et al., 2019). However, due to global climate change and human activities, the lake level declined by 4.33 m from 1955 to 2005 and grassland degradation in its catchment has expanded to 37% of the whole watershed area in 2010 (Li et al., 2007, 2009; Chen et al., 2011; Luo et al., 2013). Because of its fragility, sensitivity to global climate change and anthropogenic impacts, and its importance in maintaining ecological security of northeast Qinghai-Tibet Plateau, the Qinghai Lake watershed has recently become an intensive place for research (An et al., 2006; Hao, 2008; Barakat et al., 2018). Furthermore, this area has special hydrological and limnological characteristics. Adjacent to the main lake, there are a number of "satellite lakes"; these are separated from the main lake by barrier dunes and do not receive river or stream inflows (except Erhai Lake, which receives stream inflow). In contrast, the main lake has more than 40 tributaries. Reflecting these differences, Qinghai Lake and the satellite lakes are significantly different from each other in biological, chemical, and hydrologic conditions (Liu et al., 2009; Ao et al., 2014; Meng et al., 2014; Rawat and Singh, 2018). Previous studies of Qinghai Lake have focused on the reconstruction of the region's paleoenvironment and paleoclimate, geology, hydrology, ecological management, hydrobiology, fishery resources, climate change, soil, and sediment geochemistry and have especially emphasized the main lake (Shi et al., 2004; Henderson and Holmes, 2009; Cao and An, 2010; Jin et al., 2010; Liu and Lai, 2013). However, integrated and comparative studies on multi-element geochemistry in the main lake, its satellite lakes,

http://www.aloki.hu ● ISSN 1589 1623 (Print) ● ISSN 1785 0037 (Online)
DOI: http://dx.doi.org/10.15666/aeer/1704_86678678

and tributaries are lacking. Hence, both from a fundamental and an environmental point of view, it is crucial to assess the geochemical signatures of the aquatic ecosystems in Qinghai Lake area. The main objectives of this study were: (1) to document the basic geochemistry of Qinghai Lake, its adjacent lakes, and its inflowing rivers; (2) to identify the geochemical patterns of elements in those systems; (3) to evaluate possible determinant mechanisms causing these differences. The results provide an integrative view of the geochemical characteristics, distribution patterns, and processes of Qinghai Lake area.

Materials and methods

Study area

Qinghai Lake (QL, 36°32′ - 37°15′ N, 99°36′ - 100°47′ E) is a remote endorheic saline lake located at 3194 m above sea level on the Qinghai-Tibet Plateau and lies at a junction of three major climatic systems, the Westerlies, the East Asian, and Indian summer monsoons (An et al., 2012; Chen et al., 2015). It is the largest lake in China with a surface area of 4260 km^2, a catchment area of 29,660 km^2, and an average depth of 21 m. Mean annual precipitation in the basin is 389.1 mm and average annual evaporation is 895.4 mm. Annual mean temperature is -0.3°C with a linear warming rate of 0.28°C /10a. More than 40 rivers and streams flow into Qinghai Lake but most of them are seasonal. There are five main tributaries: the Buha River (BHR), the Shaliu River (SLR), the Haergai River (HER), the Quanji River (QJR), and the Heima River (HMR). Together, these contribute 83% of the total runoff. On the eastern margin of Qinghai Lake there are number of satellite lakes, separated from the main lake by barrier dunes or sand bars (Li et al., 1996). None of the satellite lakes have stream inflows with the exception of Erhai Lake which receives input from the Daotang River (DTR).

Sampling

Field surveys were conducted in late July 2015. A total of 16 water samples was collected, including 10 lake samples and 6 river samples (*Fig. 1*). Of the 10 lake samples, 3 were collected from Qinghai Lake (QL-1, QL-2, and QL-3) and the others were collected from 7 satellite lakes (Moon Lake (ML), Sun Lake (SL), Lanhua Lake (LHL), Ganzihe Lake (GZL), Erhai Lake (EHL), Haiyanwan Lake (HYL), and Gahai Lake (GHL)). Because there was no boat available to reach the center of the lakes, lake water samples were taken from sites about 20-30 m away from the edge of the lakes at depths>50 cm. River water samples were collected in the deepest part of the channel at depths of ~10 cm. All water was filtered through 0.2-μm GF/F filters, stored in 100-ml acid-cleaned polyethylene bottles, fixed with 0.1 ml of concentrated nitric acid, shipped to the laboratory under refrigeration, and frozen until analysis.

Analyses

Element concentrations in the water samples were measured using an Inductively Coupled Plasma Optical Emission Spectrometer (ICP–OES). There were 30 elements measured in total: Ag, Al, As, B, Ba, Be, Bi, Ca, Cd, Co, Cr, Cu, Fe, K, Li, Mg, Mn, Mo, Na, Ni, P, Pb, S, Sb, Se, Si, Sr, Tl, V, and Zn.

http://www.aloki.hu ● ISSN 1589 1623 (Print) ● ISSN 1785 0037 (Online)
DOI: http://dx.doi.org/10.15666/aeer/1704_86678678

Cluster analysis (CA) and Analysis of Variance (ANOVA) were performed to assess general patterns of element concentrations. A Gibbs plot was used to assess the dominant determining mechanisms. Correlation analyses were conducted to identify between-element associations. All the analyses and graphs were done using SPSS 20.0 and ORIGIN 9.2.

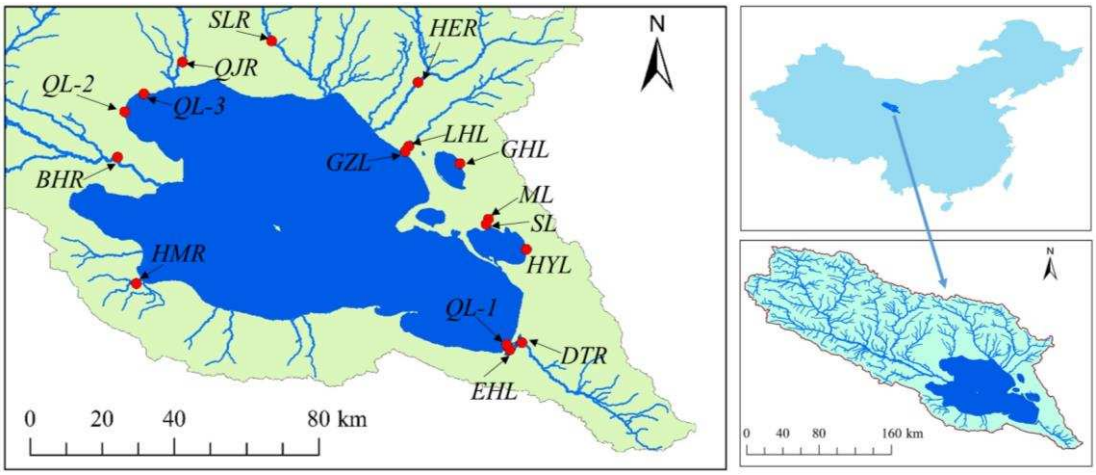

Figure 1. *Study area and sample sites. HMR, DTR, HER, SLR, QJR, and BHR are river sample sites. EHL, HYL, SL, ML, GHL, GZL, LHL, QL-1, QL-2, and QL-3 are lake sample sites*

Results and discussion

Basic geochemical patterns

The concentrations of studied elements in the water samples are shown (*Table 1*). Concentrations of Cr and Sb were below the limits of detection for all sites. Arsenic was detected only in the main lake and the two satellite lakes. P was detected only in five satellite lakes and one tributary (Heima River) with low concentrations (3.8-22.2 μg/L), indicating that the waters in Qinghai Lake area are oligotrophic, especially the main lake. Ca (8.1-88.9 mg/L), K (5.1-372.7 mg/L), Mg (6.3-1127.0 mg/L), Na (10.0-6459.0 mg/L), and S (4.8-2002.0 mg/L) were the dominant elements in all water samples (>1 mg/L, *Table 1*), with a high CV of 88.21%, 209.78%, 132.49%, 158.26%, and 163.37%, respectively. The coefficient of variation (CV) also showed that 22 elements had a CV higher than 50%, which means that most of the element distributions have very high variation.

Cluster Analysis (CA) of the chemical data grouped the samples into four statistically significant clusters: main lake cluster (including HYL and GHL), satellite lake cluster, tributary cluster (excepting DTR), and DTR (*Fig. 2*). DTR was separated from the tributary cluster because of higher concentrations for most elements, which might be caused by intensive anthropogenic activities and low runoff. Based on the ANOVA analysis, the main lake cluster had significantly higher Ag, B, Co, Li, Mg, Na, S, and Ti concentrations ($P<0.05$) than the satellite lake cluster but significantly lower V concentration ($P<0.05$). Compared to the tributary cluster, the main lake cluster had significantly higher concentrations of B, Co, Li, Mg, Na, S, and Ti ($P<0.05$) but significantly lower Al, Ca, Cu, and V concentrations ($P<0.05$). Relative to the tributary cluster, the satellite lake cluster had significantly higher Mg ($P<0.05$) but significantly

http://www.aloki.hu ● ISSN 1589 1623 (Print) ● ISSN 1785 0037 (Online)
DOI: http://dx.doi.org/10.15666/aeer/1704_86678678

lower Ag, Al, Ca, and Cu concentrations ($P<0.05$). HYL and GHL are the two largest satellite lakes and are separated from the main lake by sand bars, which likely allowed some degree of hydrological connectivity. Thus, it is not surprising that GHL and HYL were grouped in the main lake cluster. Nevertheless, GHL had higher concentrations of B, K, Li, Mg, Na, and S than HYL and these concentrations in HYL were higher than in the main lake. Other satellite lakes are surrounded by grassland and are considerably smaller. Their chemical composition is likely to be more easily affected by the terrestrial environment as well as precipitation and in-lake biological processes.

Table 1. *Basic water geochemistry of Qinghai Lake, satellite lakes, and tributaries*

	Main Lake			**Satellite Lakes**							**Tributaries**					
	QL-1	**QL-2**	**QL-3**	**ML**	**SL**	**LHL**	**GZL**	**EHL**	**HYL**	**GHL**	**DTR**	**HMR**	**BHR**	**QJR**	**HGR**	**SLR**
Na (mg/L)	2786.0	3089.0	3333.0	101.6	95.3	24.4	24.8	153.7	4109.0	6459.0	119.1	23.7	23.5	12.2	10.0	34.9
S (mg/L)	696.7	754.7	912.9	4.8	31.3	12.7	5.1	52.4	1036.0	2002.0	53.2	13.5	21.6	6.6	18.0	24.8
Mg (mg/L)	612.7	666.4	714.7	141.6	91.8	39.7	39.7	84.5	892.7	1127.0	65.7	14.5	17.9	6.3	21.5	25.8
K (mg/L)	16.8	28.2	32.4	30.6	39.2	8.3	7.1	15.7	95.8	372.7	10.7	9.8	6.9	6.2	5.1	6.7
Ca (mg/L)	10.7	11.6	11.5	8.1	9.2	29.8	14.1	9.4	10.1	18.1	46.3	88.9	72.4	61.0	83.9	78.0
B (mg/L)	7.6	8.3	8.8	1.3	1.6	0.5	0.5	0.9	10.6	16.1	0.8	0.3	0.4	0.2	0.3	0.3
Tl (mg/L)	11.8	13.6	15.6	2.2	3.0	0.6	0.6	1.4	0.0	0.0	0.9	0.3	0.3	0.1	0.4	0.4
Si (mg/L)	0.1	0.1	--	0.3	1.7	0.7	4.0	0.5	0.1	--	4.3	2.7	2.1	1.3	2.9	2.0
Sr (μg/L)	34.5	41.5	35.9	1178.0	1215.0	246.1	99.4	35.5	38.0	82.0	832.8	311.3	432.0	195.3	252.2	294.2
Li (μg/L)	413.2	468.2	513.1	75.3	94.5	3.0	8.0	43.6	665.7	1516.0	24.9	--	6.3	--	1.0	4.6
Al (μg/L)	45.3	39.4	41.2	53.7	45.5	77.1	66.5	46.0	33.3	50.0	104.0	136.6	138.8	113.1	134.0	140.2
Ba (μg/L)	12.1	12.5	13.1	190.7	212.0	58.6	33.7	4.5	13.8	10.2	40.0	70.7	73.1	54.0	98.2	83.4
Bi (μg/L)	19.1	20.4	15.7	16.0	13.2	13.4	11.5	16.0	16.3	14.8	37.1	11.4	17.6	8.2	38.2	20.0
Se (μg/L)	8.0	28.5	31.8	12.2	32.3	9.0	8.9	11.2	36.9	27.1	8.6	14.8	12.8	15.1	16.2	14.5
Fe (μg/L)	9.6	4.6	4.2	16.9	3.0	12.1	34.2	13.7	3.2	4.8	26.6	8.8	9.2	6.1	14.9	11.7
V (μg/L)	--	0.6	0.9	12.7	14.7	11.6	12.6	13.5	--	--	13.5	13.3	12.3	11.8	12.2	11.6
Ag (μg/L)	9.8	10.0	10.2	4.6	4.0	4.3	5.0	7.2	10.0	11.7	7.8	7.4	8.6	8.3	12.9	12.3
P (μg/L)	--	--	--	6.1	13.1	14.5	3.8	5.1	--	--	--	22.2	--	--	--	--
As (μg/L)	7.9	1.0	--	--	--	--	--	3.8	--	10.2	0.0	--	--	--	--	--
Zn (μg/L)	1.8	3.9	2.0	3.7	0.9	3.5	4.7	2.8	0.9	3.2	4.2	12.9	20.6	2.5	1.7	3.8
Cu (μg/L)	3.7	3.9	3.2	3.2	2.9	2.6	3.5	3.8	3.5	2.3	4.7	6.9	5.4	5.7	4.1	4.5
Pb (μg/L)	2.7	1.7	2.3	1.6	--	4.0	3.8	4.4	--	--	5.6	5.9	3.9	1.5	5.7	2.1
Mn (μg/L)	1.0	2.4	0.7	3.8	0.5	4.5	2.7	1.7	0.0	1.8	17.7	4.4	2.7	0.8	3.9	1.4
Mo (μg/L)	3.9	3.9	3.1	2.3	1.4	2.7	1.1	3.6	4.0	0.2	6.9	1.6	1.6	1.8	6.5	2.3
Co (μg/L)	3.5	3.6	4.2	2.3	2.7	2.0	2.1	2.1	3.4	3.7	2.7	2.6	2.2	3.1	2.7	3.2
Ni (μg/L)	1.1	1.4	1.3	1.5	2.5	1.9	4.4	1.5	1.6	1.0	5.6	3.4	3.2	1.8	3.1	2.7
Cd (μg/L)	0.4	0.6	0.5	0.3	0.2	0.2	0.3	0.3	0.4	0.6	0.3	0.5	0.5	0.8	0.8	0.8
Be (μg/L)	0.0	0.0	--	0.1	0.1	0.1	0.1	0.0	0.0	--	0.1	0.0	0.0	0.0	0.0	0.0
Cr (μg/L)	--	--	--	--	--	--	--	--	--	--	--	--	--	--	--	--
Sb (μg/L)	--	--	--	--	--	--	--	--	--	--	--	--	--	--	--	--

Note: -- is below the minimum detection limit of the instrument

http://www.aloki.hu ● ISSN 1589 1623 (Print) ● ISSN 1785 0037 (Online)
DOI: http://dx.doi.org/10.15666/aeer/1704_86678678

The relative amounts of the dominant elements (Na, K, Ca, and Mg) in the water samples can be seen more clearly in the ternary diagram (*Fig. 3*). The main lake cluster is grouped in the high Na+K sector but with low Mg and Ca. In contrast, the satellite lake cluster was grouped in the middle of the diagram with low Ca but relatively high Mg and Na+K. The tributary waters were very different from the lake waters, situated in a sector with high Ca but relatively low Mg and Na+K. Overall, Ca was the most abundant element in tributaries.

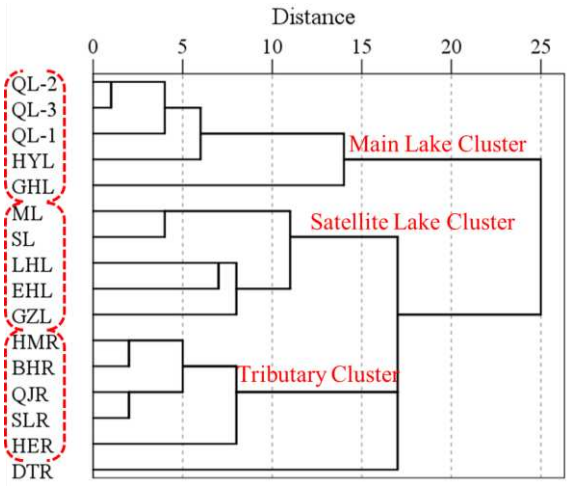

Figure 2. *Cluster dendrogram of the sample sites based on the studied elements*

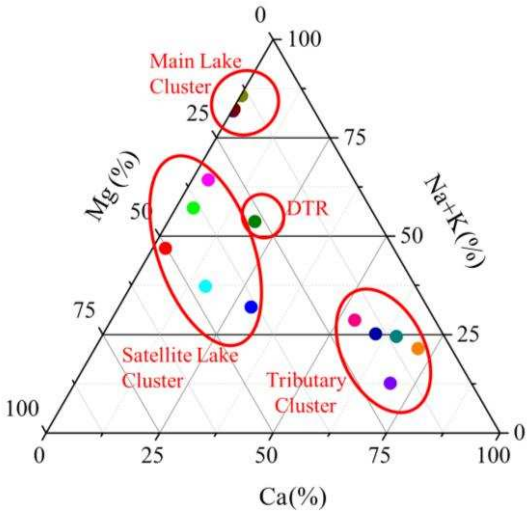

Figure 3. *Ternary diagram of dominant elements in the water samples*

Determinants of water geochemistry

There are three main factors that determine surface water geochemistry: evaporation and crystallization, rock weathering, and precipitation. The relative importance of these factors can assessed via the relationship between total dissolved solids(TDS) and the weight ratio of Na/(Na+Ca). In this model, water with high TDS and high Na (high Na/(Na+Ca)) has chemistry dominated by evaporation and crystallization, while waters

http://www.aloki.hu ● ISSN 1589 1623 (Print) ● ISSN 1785 0037 (Online)
DOI: http://dx.doi.org/10.15666/aeer/1704_86678678

with moderate TDS and high Ca (low Na/(Na+Ca)) are dominated by rock weathering and those with low TDS and high Na are dominated by precipitation. The water samples from Qinghai Lake's tributaries are located in the middle part of the plot (*Fig. 4*), indicating that rock weathering is the dominant factor determining their chemical composition (Ca-rich and moderate salinity) of the tributaries.

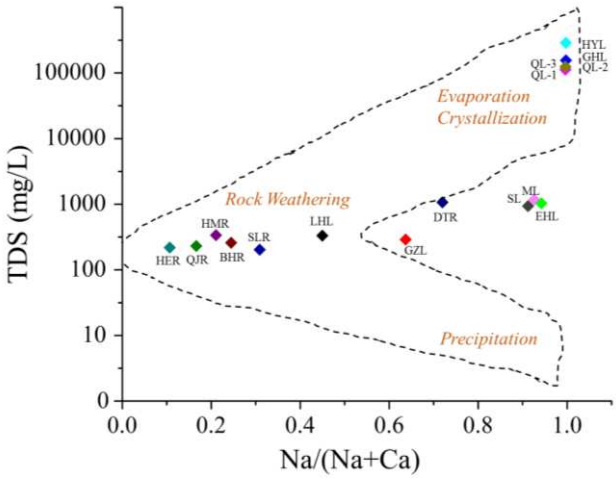

Figure 4. *The relationship between TDS and the weight ratio Na/(Na+Ca) in the water samples (the dash line is cited from Gibbs 1970)*

In contrast, the water samples from the main lake, HYL, and GHL are Na-rich and high in salinity (*Fig. 4*), indicating the evaporation and crystallization are the dominant determining factors for those lakes. Other water samples, which are mostly from the satellite lakes, are located in a zone intermediate between the precipitation end and the evaporation and crystallization end (*Fig. 4*), indicating that combination of factors determines the water geochemistry of the satellite lakes, including evaporation and crystallization, rock weathering, precipitation, hydrology, and biological processes (Shiller, 1997; Zwolsman and Van Eck, 1999).

The relationships between elements

The relationships between elements may provide further insights into their sources or the processes affecting the overall geochemical composition (Mwanamoki et al., 2015). If the elements show high correlation, they likely originated from the same source or are affected by similar mechanisms. *Table 2* shows correlation relationships for the elements that had higher average concentrations (>0.01 mg/L) in the water samples. B, K, Li, Mg, S, and Se all had significantly positive relationships with Na, indicating that they are strongly affected by evaporation and crystallization processes. B, K, Li, Mg, S, and Se also had significantly positive relationships with each other, consistent with joint regulation via interactions with Na solubility during evaporation and crystallization. In contrast, Al and Si had significant relationships with Ca, indicating that they were largely determined by rock weathering. Al and Fe also showed significantly positive relationships with Si, indicating a source associated with silicate weathering. Moreover, there was a significant relationship ($r=0.88$, $P<0.01$) between Ba and Sr. Ba and Sr have

http://www.aloki.hu ● ISSN 1589 1623 (Print) ● ISSN 1785 0037 (Online)
DOI: http://dx.doi.org/10.15666/aeer/1704_86678678

similar geochemical behavior, and their concentrations are largely determined by geological composition of the drainage basin and weathering processes (An et al., 2006; Watmough, 2014; Fu et al., 2018). In the water samples, the main lake cluster had very high S concentrations (697.7-2002.0 mg/L), followed by tributaries (6.6-53.2 mg/L) and satellite lakes (4.8-52.4 mg/L). S also had significantly positive relationships with B, K, Li, Mg, and Na, suggesting that sulfate mineral dissolution is another possible source of these elements in Qinghai Lake regional waters.

Table 2. *Correlations among selected elements in the waters of Qinghai Lake area*

	Al	B	Ba	Bi	Ca	Fe	K	Li	Mg	Na	S	Se	Si	Sr	Tl
Al	1.00														
B	**-0.62**	1.00													
Ba	0.18	-0.47	1.00												
Bi	0.29	-0.11	-0.01	1.00											
Ca	**0.98**	**-0.51**	0.12	0.29	1.00										
Fe	0.20	-0.49	0.00	0.31	0.05	1.00									
K	-0.33	**0.78**	-0.22	-0.14	-0.27	-0.31	1.00								
Li	**-0.52**	**0.97**	-0.41	-0.12	-0.43	-0.44	**0.91**	1.00							
Mg	**-0.65**	**0.99**	-0.48	-0.10	**-0.54**	-0.49	**0.72**	**0.94**	1.00						
Na	**-0.58**	**1.00**	**-0.51**	-0.10	-0.47	-0.48	**0.79**	**0.97**	**0.99**	1.00					
S	**-0.53**	**0.99**	-0.49	-0.10	-0.43	-0.46	**0.85**	**0.99**	**0.97**	**0.99**	1.00				
Se	-0.47	**0.64**	0.00	-0.16	-0.34	**-0.68**	0.43	**0.58**	**0.65**	**0.62**	**0.60**	1.00			
Si	**0.63**	**-0.63**	0.18	0.41	**0.55**	**0.72**	-0.37	**-0.56**	**-0.65**	**-0.61**	**-0.58**	-0.46	1.00		
Sr	0.09	-0.41	**0.88**	0.14	-0.01	0.15	-0.16	-0.35	-0.42	-0.45	-0.43	-0.07	0.27	1.00	
Tl	-0.50	0.42	-0.27	0.00	-0.44	-0.31	-0.12	0.23	0.46	0.39	0.33	0.31	-0.46	-0.25	1.00

Note: Numbers in bold indicate elements that present a significant (P<0.05) coefficient of correlation

Conclusion

This paper reports patterns in the aqueous geochemistry in the main lake, satellite lakes, and tributaries in Qinghai Lake area, including basic water geochemistry information. Our analyses provide an integrated and comparative view of the multi-element geochemistry among different waters in this particular area. The element distributions in the waters varied considerably. In general, the main lake had higher concentrations of most elements than the satellite lakes and the tributaries. However, the two largest satellite lakes showed the highest concentrations of B, K, Li, Mg, Na, and S. The satellite lakes seem to have different degrees of communication with the main lake and with external influences. The geochemical differences among the lakes may necessitate different physiological adjustments among aquatic biota in coping with the geochemical environment. Meanwhile, the low P concentrations that we document indicate the aquatic ecosystems in Qinghai Lake are oligotrophic or ultra-oligotrophic and thus likely sensitive to changes in external nutrient loading, such as inputs from non-point (fertilizer runoff) or point (sewage outfalls) sources. Therefore, further studies with more extensive biological and chemical scope and taken from whole watershed are recommended to better understand the lake basin's spatial geochemistry patterns and consequently to assess the effects of geochemical variations on biological and ecological processes in the aquatic ecosystems in Qinghai Lake area.

http://www.aloki.hu ● ISSN 1589 1623 (Print) ● ISSN 1785 0037 (Online)
DOI: http://dx.doi.org/10.15666/aeer/1704_86678678

Acknowledgements. We are grateful to the anonymous reviewers for the comments. This study was supported by National key research and development program (No. 2018YFC0408103), the Open Fund of State Key Laboratory of Simulation and Regulation of Water Cycle in River Basin, China Institute of Water Resources and Hydropower Research (No. 2016TS01), Hunan Province Science and Technology Major Project (No. 2018SK1010), the Ministerial Science Program of the Ministry of Water Resources (Grant nos. 126301001000160014-2), and Tianjin Province Science and Technology Plan Project (No. 17YFCZZC00210).

REFERENCES

[1] Al Abdullah, J., Michèl, H., Funel, G. B., Féraud, G. (2014): Distribution and baseline values of trace elements in the sediment of Var River catchment, southeast France. – Environmental Monitoring and Assessment 186: 8175-8189.

[2] An, Z. S., Ai, L., Song, Y. G., Colman, S. M. (2006): Lake Qinghai scientific drilling project. – Scientific Drilling 2: 20-22.

[3] An, Z. S., Colman, S. M., Zhou, W., Li, X., Brown, E. T., Jull, A. J., Cai, Y., Huang, Y., Lu, X., Chang, H., Song, Y., Sun, Y., Xu, H., Liu, W., Jin, Z., Liu, X., Cheng, P., Liu, Y., Ai, L., Li, X., Liu, X., Yan, L., Shi, Z., Wang, X., Wu, F., Qiang, X., Dong, J., Lu, F., Xu, X. (2012): Interplay between the westerlies and Asian monsoon recorded in Lake Qinghai sediments since 32 ka. – Scientific Reports 2: 619.

[4] Anan, H. S. (2019): Contribution To The Paleontology, Stratigraphy And Paleo-Biogeography Of Some Diagnostic Pakistanian Paleogene Foraminifer In The Middle East. – Earth Sciences Pakistan 3(1): 23-28.

[5] Ao, H., Wu, C., Xiong, X., Jing, L., Huang, X., Zhang, K., Liu, J. (2014): Water and sediment quality in Qinghai Lake, China: a revisit after half a century. – Environmental Monitoring and Assessment 186: 2121-2133.

[6] Baharuddin, D., Samsudin, M. D. M. (2018): Effect Of Ph And Moisture Content On Current Den sity Of Impressed Current Cathodic Protection: Response Surface Methodology Study. – Environment & Ecosystem Science 2(2): 15-19.

[7] Barakat, A., Khellouk, R., Jazouli, A. E., Touhami, F., Nadem, S. (2018): Monitoring of forest cover dynamics in eastern area of Béni-Mellal Province using ASTER and Sentinel-2A multispectral data. – Geology, Ecology, and Landscapes 2(3): 203-215.

[8] Battarbee, R. W., Kernan, M., Rose, N. (2009): Threatened and stressed mountain lakes of Europe assessment and progress. – Aquatic Ecosystem Health and Management 12: 118-128.

[9] Bounouira, H., Choukri, A., Cherkaoui, E. l., Moursli, R., Chakiri, S., Said, F., Bounakhla, M., Embarch, K. (2013): Geochemical behaviour of major and trace elements in dissolved and particulate phases of the Bouregreg River (Morocco). – Journal of Radioanalytical and Nuclear Chemistry 295: 1067-1083.

[10] Cao, J. J., An, Z. S. (2010): Introduction and progress of the project for technology integration and experimental demonstration of ecological and environmental rehabilitation in Qinghai Lake basin. – Journal of Earth Environment 1: 158-161.

[11] Çelik, U., Oehlenschläger, J. (2007): High contents of cadmium, lead, zinc and copper in popular fishery products sold in Turkish supermarkets. – Food Control 18: 258-261.

[12] Chen, L., Chen, K. L., Liu, B. K., Hou, G. L., Cao, S. K., Han, Y. L., Yang, L., Wu, Y. P. (2011): Characteristics of climate variation in Qinghai Lake basin during the recent 50 years. – Journal of Arid Meteorology 29: 483-487.

[13] Chen, L., Jin, Z., Wan, D., Zhang, F. (2015): Spatial uniformity in the mineralogical and geochemical compositions of surface sediments in Lake Qinghai and their controlling factors. – Limnology 16: 113-125.

http://www.aloki.hu ● ISSN 1589 1623 (Print) ● ISSN 1785 0037 (Online)
DOI: http://dx.doi.org/10.15666/aeer/1704_86678678

[14] Cui, B., Zhang, Q., Zhang, K., Liu, X., Zhang, H. (2011): Analyzing trophic transfer of heavy metals for food webs in the newly-formed wetlands of the Yellow River Delta, China. – Environmental Pollution 159: 1297-1306.
[15] Daniel, G. I., Henry, O. U., Ayodeji, B. B., Silas, M. Y. (2018): Land Suitability Analysis For The Production Of Cocoyam Inbenue State, Nigeria. – Earth Sciences Malaysia 2(2): 25-30.
[16] Elser, J. J., Andersen, T., Baron, J. S., Bergstrom, A. K., Jansson, M., Kyle, M., Nydick, K. R., Steger, L., Hessen, D. O. (2009): Shifts in lake N:P stoichiometry and nutrient limitation driven by atmospheric nitrogen deposition. – Science 326: 835-837.
[17] Foster, I., Charlesworth, S. M. (1996): Heavy metals in the hydrological cycle: trends and explanation. – Hydrological Processes 10: 227-261.
[18] Fu, H., Li, Z., Liu, Z., Wang, Z. (2018): Research on Big Data Digging of Hot Topics about Recycled Water Use on MicroBlog Based on Particle Swarm Optimization. – Sustainability 10: 2488.
[19] Gaillardet, J., Viers, J., Dupré, B. (2003): Trace elements in river waters. – In: Heinrich, D. H., Karl, K. T. (eds.) Treatise on geochemistry. Oxford: Pergamon; p. 225-272.
[20] Gibbs, R. J. (1970): Mechanisms controlling world water chemistry. – Science 170: 1088-1090.
[21] Goldhaber, S. B. (2003): Trace element risk assessment: essentiality vs. Toxicity. – Regulatory Toxicology and Pharmacology 38: 232-242.
[22] Hao, X. (2008): A green fervor sweeps the Qinghai-Tibetan Plateau. – Science 321: 633-635.
[23] Havig, J. R., McCormick M. L., Hamilton, T. L., Kump, L. R. (2015): The behavior of biologically important trace elements across the oxic/euxinic transition of meromictic Fayetteville green lake, new york, usa. – Geochimica et Cosmochimica Acta 165: 389-406.
[24] Hayzoun, H., Garnier, C., Durrieu, G., Lenoble, V., Le Poupon, C., Angeletti, B., Ouammou, A., Mounier, S. (2015): Organic carbon, and major and trace element dynamic and fate in a large river subjected to poorly-regulated urban and industrial pressures (Sebou River, Morocco). – Science of the Total Environment 502: 296-308.
[25] Henderson, A. C. G., Holmes, J. A. (2009): Palaeolimnological evidence for environmental change over the past millennium from Lake Qinghai sediments: a review and future research prospective. – Quaternary International 194: 134-147.
[26] Hsieh, I. T., Mok, H. K., Ko, F. C., Acik, S. (2013): Environmental assessment of trace element bioaccumulation in Sipunculan from seagrass and wetland sediments. – Environmental Monitoring and Assessment 185: 2269-2279.
[27] Jin, Z., You, C., Wang, Y., Shi, Y. (2010): Hydrological and solute budgets of Lake Qinghai, the largest lake on the Tibetan Plateau. – Quaternary International 218: 151-156.
[28] Jin, Z., You, C., Yu, T., Wang, B. (2010): Sources and flux of trace elements in river water collected from the Lake Qinghai catchment, NE Tibetan Plateau. – Applied Geochemistry 25: 1536-1546.
[29] Kyllonen, K., Karlsson, V., Ruoho-Airola, T. (2009): Trace element deposition and trends during a ten year period in Finland. – Science of the Total Environment 407: 2260-2269.
[30] Li, J., Philp, R. P., Pu, F., Allen, J. (1996): Long-chain Alkenones in Qinghai Lake sediments. – Geochimica et Cosmochimica Acta 60: 235-241.
[31] Li, X. Y., Xu, H. Y., Sun, Y. L., Zhang, D. S., Yang, Z. P. (2007): Lake-level change and water balance analysis at Lake Qinghai, west China during recent decades. – Water Resources Management 21: 1505-1516.
[32] Li, X. Y., Ma, Y. J., Xu, H. Y., Wang, J. H., Zhang, D. S. (2009): Impact of land use and land cover change on environmental degradation in Lake Qinghai watershed, northeast Qinghai-Tibet Plateau. – Land Degradation & Development 20: 69-83.

http://www.aloki.hu ● ISSN 1589 1623 (Print) ● ISSN 1785 0037 (Online)
DOI: http://dx.doi.org/10.15666/aeer/1704_86678678

[33] Li, T., Li, X., Zhong, H., Yang, C., Sun, G., Luo, W. (2015): Distribution of trace metals and the benthic foraminiferal assemblage as a characterization of the environment in the north Minjiang River estuary (Fujian, China). – Marine Pollution Bulletin 90: 227-241.
[34] Liang, Z., Wenshun, W. (2019): Parametric Architectural Design Based On Optimization Algorithm. – Engineering Heritage Journal 3(1): 13-17.
[35] Liu, W., Li, X., Zhang, L., An, Z., Xu, L. (2009): Evaluation of oxygen isotopes in carbonate as an indicator of lake evolution in arid areas: the modern Qinghai Lake, Qinghai–Tibet Plateau. – Chemical Geology 268: 126-136.
[36] Liu, X., Lai, Z. (2013): Optical dating of sand wedges and ice-wedge casts from Qinghai Lake area on the northeastern Qinghai-Tibetan plateau and its palaeoenvironmental implications. – Boreas 42: 333-341.
[37] Luo, C. F., Xu, C. J., You, H. Y., Jin, S. H. (2013): Analysis on grassland degradation in Qinghai Lake basin during 2000-2010. – Acta Ecologica Sinica 33: 4450-4459.
[38] Lynam, M. M., Dvonch, J. T., Hall, N. L., Morishita, M., Barres, J. A. (2015): Trace elements and major ions in atmospheric wet and dry deposition across central Illinois, USA. – Air Quality, Atmosphere & Health 8: 135-147.
[39] Mahmood, S., Kazmi, S. T., Ali, S. S. (2018): Comparison Of Drinking Water Bottles Of Different Countries Along With Zamzam Water, Pakistan. – Earth Sciences Pakistan 2(1): 05-14.
[40] Meng, X. L., He, Y. B., Song, Z. Y., Ao, H. Y., Zhang, H., Jiang, X. M. (2014): Structure and spatial distribution patterns of macrozoobenthos in Qinghai Lake area. – Acta Hydrobiologica Sinica 38: 819-827.
[41] Mwanamoki, P. M., Devarajan, N., Niane, B., Ngelinkoto, P., Thevenon, F., Nlandu, J. W., Mpiana, P. T., Prabakar, K., Mubedi, J. I., Kabele, C. G., Wildi, W., Poté, J. (2015): Trace metal distributions in the sediments from river-reservoir systems: case of the Congo River and lake ma Vallée, Kinshasa (democratic republic of Congo). – Environmental Science and Pollution Research 22: 586-597.
[42] Négrel, P., Allègre, C. J., Dupré, B., Lewin, E. (1993): Erosion sources determined by inversion of major and trace element ratios and strontium isotopic ratios in river water: the Congo basin case. – Earth and Planetary Science Letters 120: 59-76.
[43] Otachi, E. O., Plessl, C., Körner, W., Avenant-Oldewage, A., Jirsa, F. (2015): Trace elements in water, sediments and the elongate Tigerfish Hydrocynus Forskahlii (cuvier 1819) from lake Turkana, Kenya including a comprehensive health risk analysis. – Bulletin of Environmental Contamination and Toxicology 95: 286-291.
[44] Qin, D., Jiang, H., Bai, S., Tang, S., Mou, Z. (2015): Determination of 28 trace elements in three farmed cyprinid fish species from northeast china. – Food Control 50: 1-8.
[45] Ramsar, C. O. P. (2015): The list of wetlands of international importance.
[46] Rawat, K. S., Singh, S. K. (2018): Water Quality Indices and GIS-based evaluation of a decadal groundwater quality. – Geology, Ecology, and Landscapes 2(4): 240-255.
[47] Sarker, M. K. U., Majumder, A. K., Haque, M. Z., Hossain, M. S., Nayeem, A. A. (2019): Assessment Of Inland Water Quality Parameters Of Dhaka City, Bangladesh. – Environment & Ecosystem Science 3(1): 13-16.
[48] Shakeri, A., Afrasiabian, A., Rezaei, M., Karimi, M. (2014): Assessment of trace elements contamination in surface sediments of the Bakhtegan Lake, Iran. – Iranian Journal of Science and Technology 38: 75-85.
[49] Shi, J. Q., Qi, H. F., Yang, J. X. (2004): The natural conditions and the present fishery resources situation of Qinghai Lake. – Freshwater Fisheries 34: 3-5.
[50] Shiller, A. M. (1997): Dissolved trace elements in the Mississippi river: seasonal, interannual, and decadal variability. – Geochimica et Cosmochimica Acta 61: 4321-4330.
[51] Singh, V. B., Ramanathan, A., Sharma, P., Pottakkal, J. G. (2015): Dissolved ion chemistry and suspended sediment characteristics of meltwater draining from Chhota Shigri glacier, western Himalaya, India. – Arabian Journal of Geosciences 8: 281-293.

http://www.aloki.hu ● ISSN 1589 1623 (Print) ● ISSN 1785 0037 (Online)
DOI: http://dx.doi.org/10.15666/aeer/1704_86678678

[52] Sunny, A. A., Omowumi, A., Chris, O. A. (2018): Improved Magnetic Data Analyses And Enhancement Techniques For Lithological And Structural Mapping Around Akure, Southwestern Nigeria. – Earth Sciences Malaysia 2(1): 16-21.
[53] Tam, N. F., Wong, Y. S. (2000): Spatial variation of heavy metals in surface sediments of Hong Kong mangrove swamps. – Environmental Pollution 110: 195-205.
[54] Tuzen, M. (2009): Toxic and essential trace elemental contents in fish species from the black sea, turkey. – Food and Chemical Toxicology 47: 1785-1790.
[55] Vystavna, Y., Huneau, F., Sch Fer, J., Motelica-Heino, M., Blanc, G., Larrose, A., Vergeles, Y., Diadin, D., Le Coustumer, P. (2012): Distribution of trace elements in waters and sediments of the Seversky Donets transboundary watershed (Kharkiv region, Eastern Ukraine). – Applied Geochemistry 27: 2077-2087.
[56] Walther, B. D., Nims, M. K. (2015): Spatiotemporal variation of trace elements and stable isotopes in subtropical estuaries: I. Freshwater endmembers and mixing curves. – Estuaries and Coasts 38: 754-768.
[57] Wang, P., Cao, J., Han, Y., Jin, Z., Wu, F., Zhang, F. (2015): Elemental distribution in the topsoil of the Lake Qinghai catchment, NE Tibetan Plateau, and the implications for weathering in semi-arid areas. – Journal of Geochemical Exploration 152: 1-9.
[58] Wang, K., Zhou, S. Z., Zhou, Y. T., Ren, J., Li, W. L., Lan, Y. (2018): Synthesis of Porous Carbon by Activation Method and its Electrochemical Performance. – International Journal of Electrochemical Science 13(11): 10766-10773.
[59] Watmough, S. A. (2014): Calcium, strontium and barium biogeochemistry in a forested catchment and insight into elemental discrimination. – Biogeochemistry 118: 357-369.
[60] Xu, H., Hou, Z., An, Z., Liu, X., Dong, J. (2010): Major ion chemistry of waters in Lake Qinghai catchments, NE Qinghai-Tibet Plateau, china. – Quaternary International 212: 35-43.
[61] Xu, D. (2018): Research On Brand Construction And Development Of Agricultural Products In Guizhou. – Engineering Heritage Journal 2(2): 19-24.
[62] Yang, H., Rose, N. (2005): Trace element pollution records in some UK lake sediments, their history, influence factors and regional differences. – Environment International 31: 63-75.
[63] Yu, Y., Song, J., Duan, L., Li, X., Yuan, H., Li, N. (2014): Sedimentary trace-element records of natural and human-induced environmental changes in the East China Sea. – Journal of Paleolimnology 52: 277-292.
[64] Zwolsman, J. J. G., Van Eck, G. T. M. (1999): Geochemistry of major elements and trace metals in suspended matter of the Scheldt estuary, southwest Netherlands. – Marine Chemistry 66: 91-111.

http://www.aloki.hu ● ISSN 1589 1623 (Print) ● ISSN 1785 0037 (Online)
DOI: http://dx.doi.org/10.15666/aeer/1704_86678678

RESEARCH ON THE OPTIMIZATION OF THE ANALYSIS METHOD OF ECOLOGICAL ENVIRONMENT EMISSION DATA

CHEN, G. B.[1] – LIU, J. M.[2,3,4*]

[1]*Chongqing Key Laboratory of Spatial Data Mining and Big Data Integration for Ecological and Environment, Rongzhi College of Chongqing Technology and Business University Chongqing 401320, P. R. China*

[2]*College of Mathematics and Computer Science, Quanzhou Normal University Quanzhou 362000, Fujian, P. R. China*

[3]*Fujian Provincial Key Laboratory of Data Intensive Computing Quanzhou 362000, Fujian, P. R. China*

[4]*Fujian Provincial Big Data Research Institute of Intelligent Manufacturing Quanzhou 362000, Fujian, P. R. China*

The first two departments contributed equally to this work and are considered co-first departments.

[*]*Corresponding author*
e-mail: liujmcqu19995@163.com

(Received 8th Mar 2019; accepted 21st May 2019)

Abstract. In order to reduce the emission of ecological environment and the pollution of ecological environments and improve the sustainable development of ecological economy, so an improved model of the wavelet (War) based on the improved gravity optimization algorithm (IGSA) is proposed (IGSA-War). The method uses an improved gravitational algorithm to optimize the wavelet, establish an optimization model, and predict the different NOx emissions of coal-fired boilers. Firstly, the grid algorithm is used to initialize the population, and the particle is updated based on the fitness value adaptive decrements inertia weight. Numerical simulation results verify the effectiveness and superiority of the proposed algorithm (López-Hernández, 2018). Then the IGSA is used to optimize the selected hyper-parameters to improve the prediction accuracy and generalization ability of the model; the wavelet model optimizes the noisy emission data to reduce the impact of noise on the system. Finally, taking the discharge of 330 MW coal-fired boiler in a thermal power plant as the research object, the NOx soft measurement model of IGSA-War is established. The simulation results show that the optimization model has high prediction accuracy and generalization ability, and can effectively measure NOx emissions.
Keywords: *nitrogen oxide, gravitational algorithm, wavelet model, IGSA-War, numerical optimization*

Introduction

With the rapid development of chinese economy, ecological deterioration has become an important factor constraining economic development. emissions are in a deteriorating state (Tan and Xia, 2014; Niu et al., 2016; Khanchoul et al., 2018). In order to effectively predict and rationally manage ecological NOx, [something has to be done] thereby reducing NOx emissions and establishing a predictive model of NOx (Lv et al., 2017; Hossain et al., 2019). Artificial intelligence technology is a typical representative of neural network and support vector machine due to its good ability to deal with non-linearity (Li et al., 2003; Zhang et al., 2015; Franco et al., 2018), which can better solve the problem of NOx modeling. In the NOx model prediction process,

http://www.aloki.hu ● ISSN 1589 1623 (Print) ● ISSN 1785 0037 (Online)
DOI: http://dx.doi.org/10.15666/aeer/1704_86798691

the support vector machine (Rashedi et al., 2009; Niu et al., 2014; Nouaim et al., 2019), has received more and more attention in the modeling of NOx emissions due to the lack of over-fitting and generalization of neural networks. The NOx emission prediction problem has complex non-linearity, mufti-dimensional mufti-mode, and few data samples, and needs to solve the problem of structural risk minimization. How to obtain the optimal super-parameter is the key to the accuracy of NOx emission model (Yazdani et al., 2014; Gouthamkumar et al., 2015; Azeem et al., 2018). In fact, the wavelet analysis hyper-parameter adjustment process is also a parameter optimization process. The combustion optimization based on wavelet and optimization technology is an effective way to reduce NOx emissions of boilers (Liu and Niu, 2015; Sharjeel et al., 2019).

Materials and methods

Basic Principles of GSA Algorithm

In the GSA, the position $\{X_i\}, i=1,2,\cdots,N$ of each particle is a feasible solution to the optimization problem, (Pascual-Córdova, 2018) and N is the size of the population, where the position of the i-th particle is $X_i=(x_i^1,x_i^2,\cdots,x_i^s)$, and s is the dimension of the optimization problem. The GSA is based on the fitness value and uses the *Eq.1* to update the quality of the particle:

$$\begin{cases} m_i(t)=\dfrac{fit_i(t)-worst(t)}{best(t)-worst(t)} \\ M_i(t)=\dfrac{m_i(t)}{\sum_{j=1}^{N} m_j(t)} \end{cases} \quad \text{(Eq.1)}$$

where $fit_i(t)$ is the fitness value of the i-th particle; for minimization: $best(t)=\max\limits_{j\in\{1,\cdots N\}} fit_j(t)$, $worst(t)=\min\limits_{j\in\{1,\cdots N\}} fit_j(t)$.

At a specific time t, the gravitational force acting between particle j and particle i is defined as:

$$F_{ij}^d(t)=G(t)\frac{M_i(t)\times M_j(t)}{R_{ij}(t)+\varepsilon}\left(x_j^d(t)-x_i^d(t)\right) \quad \text{(Eq.2)}$$

where M_i and M_j are the masses of the mass points; ε is a smaller constant; $R_{ij}(t)$ is the distance between the mass points; $G(t)$ is the gravitational constant. Then the resultant force acting on the d-th dimension of the i-th particle is:

$$F_i^d(t)=\sum_{j=1,j\neq i}^{N} rank_j F_{ij}^d(t) \quad \text{(Eq.3)}$$

where $rank_j$ is a random number in [0, 1].

Through the law of motion, (Espinoza, 2017) the acceleration of the mass point i in the d dimension at time t:

http://www.aloki.hu ● ISSN 1589 1623 (Print) ● ISSN 1785 0037 (Online)
DOI: http://dx.doi.org/10.15666/aeer/1704_86798691

$$a_i^d(t) = \frac{F_i^d(t)}{M_i(t)} \quad \text{(Eq.4)}$$

In the GSA algorithm, the speed and position of the particle are updated as follows:

$$\begin{cases} v_i^k(t+1) = rank_i \times v_i^k(t) + a_i^k(t) \\ x_i^k(t+1) = x_i^k(t) + v_i^k(t+1) \end{cases} \quad \text{(Eq.5)}$$

where $rank_j$ is a random number in [0, 1].

Improved GSA algorithm

Although the GSA algorithm has better optimization performance, when dealing with some complex optimization problems, GSA still has the disadvantages of premature convergence and easy to fall into the local optimal solution. Therefore, its ability to seek still needs further improvement.

Grid-based algorithm for initializing populations

The first step in the GSA algorithm is to initialize the population. (Jaimes, 2017). A good initial population that covers the entire solution space can help improve the speed of evolution and improve the quality of the solution. If the local solution space containing the global optimal solution is not in the initial group space, and the position update algorithm of the particle cannot extend the coverage space to the region where the global optimal solution is located within a finite number of evolution, premature convergence is not possible. Avoid, it can be seen that the distribution of the initial population individuals directly affects the global convergence performance of the algorithm. The initial population of the original GSA algorithm is randomly distributed, and its coverage space has a large uncertainty. In this paper, the grid algorithm is used to initialize the position group of the particle, so that the initial individual is evenly distributed in the sea, and its expression is as a *Eq.6*:

$$x_i^k = \min(k) + \frac{\max(k) - \min(k)}{n-1} * i \quad \text{(Eq.6)}$$

where: x_i^k represents the k-th component of the i-th (i = 1, 2, ..., N) motion mass points; $\max(k)$, $\min(k)$ are the upper and lower bounds of the k-th component.

It is not difficult to find that the population is initialized by gridding, so that the ergodicity of the population can be improved under the premise of ensuring the randomness of the initial variables, so that the algorithm traverses all possible states, (Dager, 2017) which is beneficial to overcome the general random initialization of the population and the optimization algorithm search. Limitations.

Adaptive weight based on fitness value

In order to further improve the optimization performance of the GSA algorithm and avoid the premature phenomenon appearing in the optimization of complex high-dimensional multi-mode functions, (Olivares et al., 2017) the researchers have carried out a lot of research work and proposed a linear decreasing weight strategy. Although it

http://www.aloki.hu ● ISSN 1589 1623 (Print) ● ISSN 1785 0037 (Online)
DOI: http://dx.doi.org/10.15666/aeer/1704_86798691

is beneficial to improve the optimization performance to a certain extent, (Li and Zhao, 2017; Kumar, 2018) the algorithm does not take into account the fitness value of the optimization problem, and it may reduce the optimization performance when dealing with some complex nonlinear optimization problems. Therefore, based on the linear decreasing inertia weight, this paper proposes an adaptive decreasing inertia weight position update strategy based on the fitness:

$$\begin{cases} t_i = (t_{start} - t_{end}) \frac{maxier - i}{maxiter} + t_{end} \\ \Phi_{fit} = \frac{2}{1 + e^{-\frac{fit_i}{maxiter}}} \\ w_i = \Phi_{fit} * t_i \end{cases} \quad \text{(Eq.7)}$$

where t_{start} and t_{end} are the initial value and the final value, respectively, and $0<t_{end}<t_{start}<1$, $maxier$ and i are the maximum number of iterations of the GSA and the current algebra, respectively, t_i is the linearly decreasing inertia weight, and Φ_{fit} is the fitness value factor whose value fit changes, w_i is an adapt decreasing inertia weight.

Substituting *Eq.7* into equation *Eq.5* to obtain the position update formula of the particle:

$$x_i^k(t+1) = w_i * x_i^k(t) + v_i^k(t+1) \quad \text{(Eq.8)}$$

w_i determines the domain range generated by x_i^k. This range will decrease correspondingly as the search approaches the optimal solution, which will help the GSA to better use prior knowledge to improve the optimization ability of the algorithm.

IGSA optimization steps

Figure 1 shows a flow chart of the improved IGSA algorithm. The specific steps are as follows:

1) Initialization parameters: maximum number of iterations max=1000, population number N=50;
2) The grid algorithm initializes the population;
3) Calculating the fitness value of the population point;
4) update data $\mathrm{G(t)}, \mathrm{best(t)}, \mathrm{worst(t)}$ and $\mathrm{M}_i, i = 1,2,\ldots,N$;
5) Update the resultant force of the particles in all directions according to *Eq.3*;
6) Calculate the velocity of the particle according to *Eq.5*;
7) Update the position of the mass point according to *Eq.7* and *Eq.8*, t_{start} and t_{end} are set to 1 and 0, respectively;
8) Repeat steps (3)~(7) until the stop condition is met.

IGSA performance verification

Complex function optimization has become a research hotspot in the field of optimization algorithms. This paper selects 13 standard functions to evaluate the optimization performance of IGSA. f1~f7 are single-mode functions with only one extreme point. They are mainly used to investigate the execution ability of the algorithm (Chen et al., 2017) and test the optimization precision of the algorithm; f8~f13 is a

http://www.aloki.hu ● ISSN 1589 1623 (Print) ● ISSN 1785 0037 (Online)
DOI: http://dx.doi.org/10.15666/aeer/1704_86798691

multi-modal function, which has a large number of local best advantages, and is a well-recognized function that is well-recognized in the optimization field. Most optimization algorithms often seek to optimize them. Will fall into the local best, they are mainly used to test whether the algorithm has the ability to avoid premature and search for the global optimal solution, except for the minimum value of f8 is -418.9829 × n (n is the dimension of the solution), the other 12 functions. The minimum values are all zero. Reference (Liu et al., 2015; Rajput et al., 2019) describes in detail the range of values for the standard function solution, and points out that the original GSA is superior to PSO, RGA and CFO. This paper will conduct a comparative study of IGSA and the original GSA algorithm (Kang et al., 2017, 2018; Zulkapli et al., 2018).

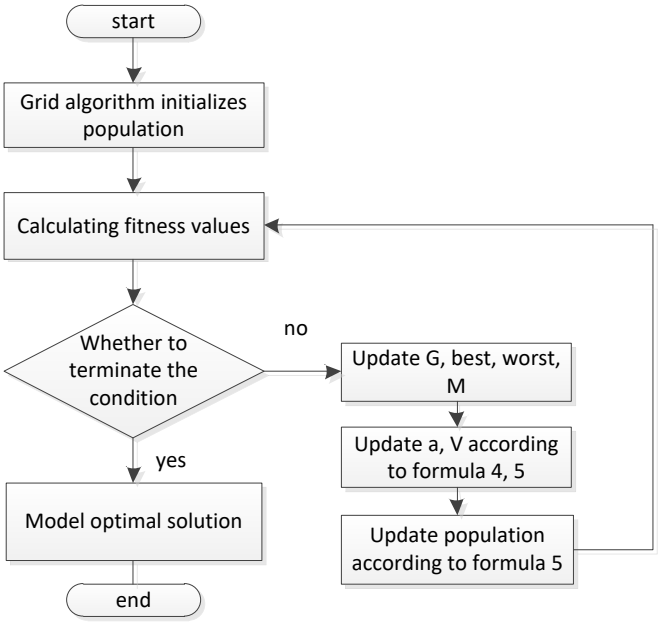

Figure 1. *The program flowchart of IGSA*

In order to effectively reduce the impact of random interference, each runs independently 30 times. *Table 1* gives the statistics data of the average convergence iteration number (CI), average optimal fitness value (Mean) and standard deviation (SD) of the function in 30-dimensional and 50-dimensional cases.

Observe and analyze the optimization results of the 13 standard test functions given in *Table 1*. It is found that for the single-mode function, except for f6, in the three algorithms, (Zhang and Khalique, 2018) whether the function is 30 or 50, the optimization effect of IGSA is the best. And the advantages are obvious; for multi-modal functions, except for f12, the optimization effect of IGSA is the best. Therefore, the superior solution of IGSA has the highest accuracy compared to GSA. At the same time, (Pang et al., 2016) it is found that when n=50, the optimization precision of IGSA is basically close to the accuracy of n=30, which indicates to some extent that the optimization effect of IGSA has not been weakened as the complexity of the problem increases. In comparison, with the increase of the dimension of GSA, most of the optimization effects show a downward trend (*Table 1*).

The standard deviation reflects the robustness of the algorithm, and the average function convergence times C.I. reflects the computational convergence speed of the

http://www.aloki.hu ● ISSN 1589 1623 (Print) ● ISSN 1785 0037 (Online)
DOI: http://dx.doi.org/10.15666/aeer/1704_86798691

algorithm. It can be seen from *Table 1* that ABC and GSA can't always solve the 13 standard functions accurately. It can be clearly observed that the optimization performance of IGSA is more accurate than that of GSA, and the ability to jump out of local extremum is stronger. In terms of optimization speed, the CI index of IGSA is small; from the standard deviation, it can be seen that the GSA is unstable in solving the single-peak and multi-peak continuous functions. Relatively speaking, IGSA is the most stable.

Table 1. *The comparison of performance of 2 algorithms for 13 standard functions with dim=30,50*

Fun	Dim	GSA			IGSA		
		C.I.	Mean	SD	C.I.	Mean	SD
f_1	30	1000	1.9735×10^{-17}	3.1255×10^{-17}	956	0	0
	50	1000	6.8852×10^{-17}	3.8521×10^{-17}	956	0	0
f_2	30	1000	2.3617×10^{-8}	2.4311×10^{-8}	1000	4.5447×10^{-240}	0
	50	1000	1.8237×10^{-6}	3.2107×10^{-6}	1000	8.2777×10^{-240}	0
f_3	30	1000	245.2465	124.1475	956	0	0
	50	1000	1.0389×10^{3}	8.0389×10^{2}	941	0	0
f_4	30	1000	3.4666×10^{-9}	4.6413×10^{-9}	1000	7.2535×10^{-241}	0
	50	1000	3.6869	1.3257	1000	7.1133×10^{-241}	0
f_5	30	1000	26.2523	3.2792	123	6.5915	0.0335
	50	1000	51.2594	1.4218	128	38.7057	0.0319
f_6	30	1000	1.8800×10^{-17}	0.9811×10^{-17}	105	3.1384	0.3688
	50	1000	6.6512×10^{-17}	4.1126×10^{-17}	111	10.1299	0.6813
f_7	30	1000	0.0264	2.2791×10^{-3}	746	1.2265×10^{-5}	3.5151×10^{-5}
	50	1000	0.1206	0.0925	414	4.2318×10^{-5}	2.7627×10^{-5}
f_8	30	1000	-2.7251×10^{3}	72.2457	265	-12763.23	35.3552
	50	1000	-3.733×10^{3}	93.6284	273	-20814.63	44.8538
f_9	30	1000	17.0801	6.0467	385	0	0
	50	1000	36.9129	3.6118	387	0	0
f_{10}	30	1000	3.4686×10^{-9}	2.3746×10^{-9}	741	8.8818×10^{-16}	0
	50	1000	4.9160×10^{-9}	4.2701×10^{-9}	736	8.8818×10^{-16}	0
f_{11}	30	1000	3.9239	0.1092	361	0	0
	50	1000	18.2615	0.4593	357	0	0
f_{12}	30	1000	0.0374	0.0102	103	0.5733	0.2041
	50	1000	0.4460	0.0043	105	0.7983	0.0548
f_{13}	30	1000	1.6696	0.9618	100	0.0055	0.0557
	50	1000	0.2697	0.0612	90	0.0038	0.0871

Ecological emission prediction models

Wavelet prediction model

Wavelet analysis is based on the Fourier transform. However, the problem is that the transformation discards the time information, and the transformation result cannot accurately analyze the occurrence of traffic and related indicators. (Zhang et al., 2017) The general wavelet transform refers to the inner product of the signal x(t) to be analyzed after the basic wavelet function $\psi(t)$ is translated by m and at different scales n.

$$WT_x(n,m) = \frac{1}{\sqrt{a}} x(t)\psi^*\left(\frac{t-m}{n}\right)dt \quad \text{(Eq.9)}$$

http://www.aloki.hu ● ISSN 1589 1623 (Print) ● ISSN 1785 0037 (Online)
DOI: http://dx.doi.org/10.15666/aeer/1704_86798691

$$= \int x(t)\,\psi^{*}_{n,m}(t)dt$$

The equivalent time domain expression is:

$$WT_x(n,m) = \frac{1}{\sqrt{a}}\int x(\omega)\,\psi^{*}\left(\frac{\omega-m}{n}\right)e^{j\omega}dt \quad a>0 \qquad \text{(Eq.10)}$$

Prediction model based on IGSA-War combination

For the predicted emissions to meet the predicted effect, the specific test steps are given here:

When t is used, the actual NOx output of the boiler is O, and the actual discharge amount W_t is St. In order to reduce the suddenness of the emissions and improve the prediction accuracy, the delay D_t and the length L_t of the emissions are mainly used here. Analysis, ie S_t=[D_t, L_t]. In order to effectively deal with the possible occurrence of emission congestion, reasonable queue management is implemented by analyzing the current and past time emissions status to obtain the next-time emission status Z_{t+1}. The following combines the emission state prediction algorithm:

Step 1: Initialize the ecological emission model and its related parameters at the starting time t=0;

Step 2: At time t, the actual emission amount W_t at node O is obtained, and its state vector S_t is obtained, and it is judged according to the IGSA model whether the service is distributed therefrom, if the measurement is satisfied, the process jumps to step 3, otherwise, the process proceeds to step 7;

Step 3: solves the delay D'_{t+1} and the length L'_{t+1} of the service flow at time t+1;

$$\begin{cases} D'_{t+1} = 1-(1-\lambda)\sum_{n=0}^{\infty}\Omega_{m+n+1}((n+1)b-t) \\ L'_{t+1} = (1-\lambda)\sum_{n=0}^{\infty}\Omega_{k+n}(n+1)b \end{cases} \qquad \text{(Eq.11)}$$

where □ is the discharge load size, b is the buffer size, and Ω_{k+n} is the distribution function of the actual emissions.

Step 4: For the fractal and burst characteristics of the actual traffic flow, a wavelet transform is introduced to process the traffic flow. According to the wavelet transform shown in *Eq.11*, the state of the service flow Y_t is determined by the Harr wavelet base (time delay D_t and queue length L_t) is decomposed to obtain the wavelet coefficient $d_j(k)$ and the scale factor $a_j(k)$:

$$\begin{cases} \sqrt{2}a_j(k) = a_{j+1}(2k) + a_j(2k+1) \\ \sqrt{2}d_j(k) = d_{j+1}(2k) + d_j(2k+1) \end{cases} \qquad \text{(Eq.12)}$$

where j is the wavelet decomposition level;

Step 5: Predict the wavelet coefficients according to the IGSA model, and use the inverse wavelet transform to synthesize the delay $D''_{t+1}(t+1)$ and the length$L''_{t+1}(t+1)$;

$$\mu_{t+1} = -\sum_{k=1}^{\xi}\tau_k\mu_{t-1} + \sum_{k=0}^{\delta}\rho_k\mu_{t-k} \qquad \text{(Eq.13)}$$

http://www.aloki.hu ● ISSN 1589 1623 (Print) ● ISSN 1785 0037 (Online)
DOI: http://dx.doi.org/10.15666/aeer/1704_86798691

Step 6: According to step (3) and step (5), the time delay and the captain status information of the actual emissions at time t+1 are performed here. The following fusion operations reduce the prediction error:

$$\begin{cases} D_{t+1} = \phi D'_{t+1} + \varphi D''_{t+1} \\ L_{t+1} = \phi L'_{t+1} + \varphi L''_{t+1} \end{cases} \quad \text{(Eq.14)}$$

wherein, the fusion parameters □ and □ represent the weight distribution of the two prediction results, and can be dynamically adjusted to obtain an optimal result, and 0≤□≤1, 0≤□≤1, □+□=1;

Step 7: Let t=t+1, jump to step (1), and repeatedly calculate the actual emission vector at the next moment until the end;

Step 8: The algorithm ends.

Example simulation and analysis

Data pre-processing evaluation criteria

There is a nonlinear and strong coupling relationship between the main steam flow and its related parameters. Conventional modeling methods are often difficult to accurately establish a mathematical model of the main steam flow of the turbine. When selecting the unit model parameters, based on the magnitude of the correlation between the main steam flow and the thermal parameters, combined with the selected load, the adjusted stage pressure, a section of extraction steam temperature, a section of extraction pressure and high pressure cylinder exhaust pressure Enter the variable and the main steam flow as the output variable. Since the historical training data involves different quantities (power, wind speed and temperature), the data needs to be normalized. The normalization formula is:

$$\hat{x}_i = \frac{x_i - x_{min}}{x_{max} - x_{min}} \quad i = 1,2,\cdots,N \quad \text{(Eq.15)}$$

where $\hat{x}_i$ is the normalized value; $x_{max} = \max(x_i)$; $x_{min} = \max(x_i)$.

For the normalized prediction result y^', the actual prediction value is $y(x) = y'(x_{max} - x_{min}) + x_{min}$.

In order to evaluate the prediction effect of IGSA optimized wavelet model, the normalized MAE, MAPE and RMSE were used to evaluate the model prediction performance. The error formula is

$$\text{MAE} = \frac{1}{N}\sum_{i=1}^{N} |y_i - y_p| \quad \text{(Eq.16)}$$

$$\text{MAPE} = \frac{1}{N}\sum_{i=1}^{N} \frac{|y_i - y_p|}{y_i} * 100\% \quad \text{(Eq.17)}$$

$$\text{RMSE} = \sqrt{\frac{1}{N}\sum_{i=1}^{N}(y_i - y_p)^2} \quad \text{(Eq.18)}$$

http://www.aloki.hu ● ISSN 1589 1623 (Print) ● ISSN 1785 0037 (Online)
DOI: http://dx.doi.org/10.15666/aeer/1704_86798691

where N, y_i ,y_p are the measured, predicted values and the predicted value of the i-th point respectively.

IGSA-War predicts NOx emissions

The IGSA algorithm was used to optimize the parameters of the wavelet model to predict the NOx concentration of a 330 MW pulverized coal drum boiler. The prediction results were compared with the standard GSA, the improved GSA algorithm (IGSA) and the improved GSA and wavelet combination (IGSA-War) optimization method (*Table 2*). In the NOx emission multi-case test, specific data including various operating parameters affecting the combustion characteristics of the boiler, such as power generation load, coal feeder speed, and primary air are shown in *Table 2*.

Table 2. *Part of the original data of boiler operation*

working	load /MW	4 coal feeder speeds /r/m				Secondary wind speed /m/s					Burn out wind opening /%			exhaust temperature /%	Oxygen content /%
		A	B	C	D	AA	AB	BC	CD	DE	OFA up	OFA down	SOFA		
1	329	339	340	413	419	33.1	35	31.7	33.4	32.9	100	100	0	154.6	4.75
2	320.7	328	351	383	386	47.7	49	45.4	48.3	40.1	0	0	0	143.2	6.05
3	319	340	422	454	301	38.7	39.7	36.0	37.8	37.5	50	50	100	150.5	5.70
19	330	335	339	420	418	34.5	38.1	36.5	38	34.6	0	0	100	153.7	4.93

working	Coal quality characteristics /%						Q_{ar} / X10^3 J/kg	One wind speed /m/s				NO_xemission
	C_{ar}	H_{ar}	O_{ar}	C_{ar}	W_{ar}	A_{ar}		I	II	III	IV	mg/m^3
1	58.37	3.81	5.1	1.20	6.4	25	20.29	27.6	29	29	29.4	585.9
2	62.79	3.96	6.48	1.25	10.5	14.50	21.346	29.5	29.8	29.4	28.3	906.15
3	60.47	3.7	5.96	1.24	8.4	19.89	21.021	29.3	27.6	28.3	28	624.65
19	58.37	3.81	5.1	1.21	6.4	25	20.29	28.3	28.4	28.9	28.7	627.5

The IGSA is used to optimize the penalty coefficient C and the kernel function parameter σ^2 in the wavelet, and the optimized wavelet model is used to predict the NOx emissions. Using IGSA to optimize the wavelet model parameters, set the IGSA population size to 50. In the 19 sets of conditions in *Table 3*, select 3 to 17 sets of data for training optimization modeling, and 1 and 2 groups as prediction data to verify Optimized performance of IGSA.

The value of the optimal model parameters (C, σ^2) obtained by IGSA is (655, 184). This group of parameters is used to predict the regression data of 1 and 2 sets of prediction data and another 17 sets of training data, and simultaneously with the other three methods. The model is compared experimentally, and the prediction error is shown in *Figure 2* below. *Table 3* shows the relative error (RE) of the four prediction methods for predicting NOx emissions.

Table 3. *Precision analysis of forecast results of 4 algorithms for testing set*

working	NOx value	GSA	RE(%)	IGSA	RE(%)	IGSA-War	RE(%)
1	585.9	596.0512	1.7326	581.1867	0.8045	589.0208	0.5326
2	906.15	911.5982	0.6012	901.9478	0.4637	908.0396	0.2085

http://www.aloki.hu ● ISSN 1589 1623 (Print) ● ISSN 1785 0037 (Online)
DOI: http://dx.doi.org/10.15666/aeer/1704_86798691

From *Figure 3* and *Table 3*, we can see that the IGSA optimizes the wavelet model parameters, and then the prediction accuracy based on the optimized parameters is higher than that of the GSA, IGSA, and IGSA-War optimization models. That is, IGSA-War can compare with GSA, IGSA, IGSA-War finds better model parameters.

Comparison of models considering the existence of noise

Random noise is added to the ecological emissions in *Figure 1* to test the robustness. The noise emission prediction results and prediction errors of IGSA-War are shown in *Figures 3 and 4*.

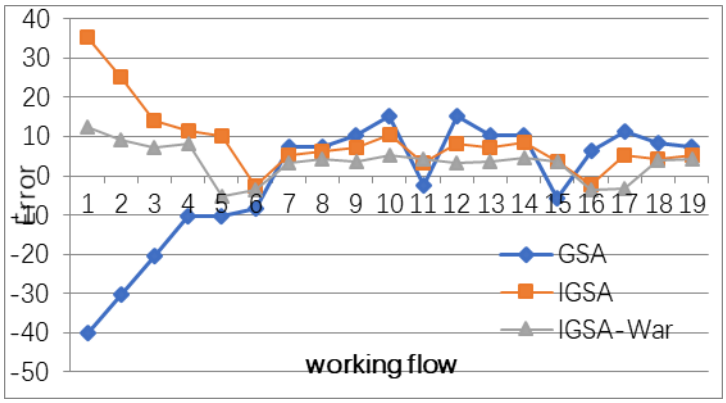

Figure 2. *Error curve between prediction value s and true values of 4 algorithms*

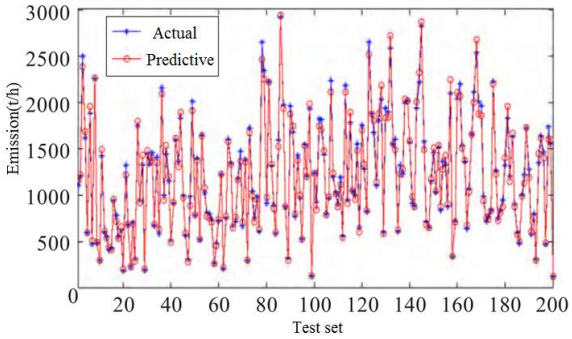

Figure 3. *Prediction in the test data set*

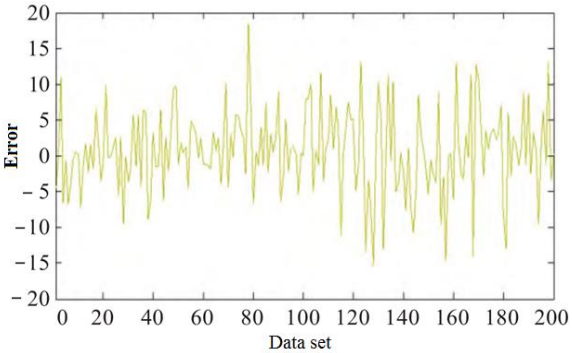

Figure 4. *Error in the test data set*

http://www.aloki.hu ● ISSN 1589 1623 (Print) ● ISSN 1785 0037 (Online)
DOI: http://dx.doi.org/10.15666/aeer/1704_86798691

For noise emission prediction (*Fig. 3*), IGSA-War also obtains an ideal prediction effect, and the prediction error is controlled within an effective range (Khanchoul and Boubehziz, 2019). This is because IGSA-War comprehensively weighs the principle of structural risk minimization and empirical risk minimization, so that the model has certain Anti-noise ability, can adapt to the characteristics of complex and variable, noisy ecological environment changes. The data set is used as the test set, and the other data is used as the training set. The experimental results once again prove the effectiveness of IGSA-War for ecological emission prediction (*Fig. 4*).

Conclusion

The characteristics of NOx emissions from ecological emissions are affected by many factors, and the impact relationship is complicated. The prediction and control of NOx emissions are difficult. This paper uses IGSA-War to establish a NOx emission prediction model. In order to improve the prediction accuracy and generalization ability of IGSA, an improved gravitational search algorithm is used to optimize the model parameters of wavelet selection. Taking a 330 MW pulverized coal fired boiler as a test object, the IGSA algorithm is used to optimize the super-parameters of the wavelet and establish a prediction model of NOx emissions. By using the relevant data collected by the DCS as training samples and test samples, the model is trained and tested. Experiments show that the IGSA-optimized wavelet NOx emission prediction model has better accuracy and stronger generalization ability.

Acknowledgements. This work supported by Chongqing Municipal Education Commission Science and Technology Project (KJQN201802101); Doctoral high school talent training project (RC2016003); Chongqing Graduate Scientific Research Innovation Project (CYB17131); Nature Science Research Programme of the Education Department of Fujian Province (No.JAT160410).

REFERENCES

[1] Azeem, N., Arslan, C. H., Rashid, H., Sattar, A. (2018): Comparative Study Of Hospital Waste Management Practices At Different Health Care Units In District Faisalabad For The Development Of Improvement Strategies. – Earth Sciences Pakistan 2(2): 16-21.

[2] Chen, C., Song, H., Yang, H. (2017): Liouville type theorems for stable solutions of p-Laplace equation in RN. – Nonlinear Analysis 160: 44-52.

[3] Dager, M. R. (2017): Composición de la materia orgánica, pH, intercambio catiónico y textura de cinco suelos ubicados entre 670 y 1600 msnm en la cuenca del río Maracay, Venezuela. – Revista de la Facultad de Agronomia de la Universidad del Zulia 34(2): 53-60.

[4] Espinoza, Y. (2017): Efecto del sistema labranza sobre la estructura y fracciones de carbono y nitrógeno del suelo y su impacto en el desarrollo del cultivo de maíz. – Revista de la Facultad de Agronomia de la Universidad del Zulia 34(4): 94-100.

[5] Franco, G. H., Macancela, N. A., Gavín-Quinchuela, T., Carrión-Mero, P. (2018): Participatory socio-ecological system: Manglaralto-Santa Elena, Ecuador. – Geology, Ecology, and Landscapes 2(4): 303-310.

[6] Gouthamkumar, N., Sharma, V., Naresh, R. (2015): Disruption based gravitational search algorithm for short term hydrothermal scheduling. – Expert Systems with Applications 42(20): 7000-7011.

http://www.aloki.hu ● ISSN 1589 1623 (Print) ● ISSN 1785 0037 (Online)
DOI: http://dx.doi.org/10.15666/aeer/1704_86798691

[7] Hossain, M. S., Karlson, M., Neset, T. S. (2019): Application Of Gis For Cyclone Vulnerability Analysis Of Bangladesh. – Earth Sciences Malaysia 3(1): 25-34.
[8] Jaimes, E. J. (2017): Capacidad de carga y presión de uso de la tierra en cuatro sectores de la sub-cuenca del río Déleg, Provincia del Cañar, Ecuador. – Revista de la Facultad de Agronomia de la Universidad del Zulia 34(3): 75-81.
[9] Kang, L., Zhang, Y. J., Zhang, L., Zhang, K. (2017): Preparation, characterization and photocatalytic activity of novel CeO2 loaded porous alkali-activated steel slag-based binding material. – International Journal of Hydrogen Energy 42(27): 17341-17349.
[10] Kang, L., Du, H. L., Du, X., Wang, H. T., Ma, W. L., Wang, M. L., Zhang, F. B. (2018): Study on dye wastewater treatment of tunable conductivity solid-waste-based composite cementitious material catalyst. – Desalination and Water Treatment 125: 296-301.
[11] Khanchoul, K., Saaidia, B., Altschul, R. (2018): Variation in Sediment Concentration and Water Disharge During Storm Events in Two Catchments, Northeast of Algeria. – Earth Sciences Malaysia 2(2): 01-09.
[12] Khanchoul, K., Boubehziz, S. (2019): Spatial Variability Of Soil Erodibility At El Hammam Catchment, Northeast Of Algeria. – Environment & Ecosystem Science 3(1): 17-25.
[13] Kumar, R. (2018): Comparison Of Instruction Scheduling And Register Allocation For Mips And Hpl -Pd Architecture For Exploitation Of Instruction Level Parallelism. – Engineering Heritage Journal 2(2): 04-08.
[14] Li, G. Q., Niu, P. F., Zhang, W. P. (2003): Model NOx emissions by least squares support vector machine with tuning based on ameliorated teaching–learning-based optimization. – Chemometrics and Intelligent Laboratory Systems 126: 11-20.
[15] Li, X. Y., Zhao, Q. L. (2017): A new integrable symplectic map by the binary nonlinearization to the super AKNS system. – Journal of Geometry and Physics 121: 123-137.
[16] Liu, C., Niu, P. F. (2015): Enhanced shuffled frog-leaping algorithm for solving numerical function optimization problems. – Journal of Intelligent Manufacturing 29(5): 1133-1153.
[17] Liu, P. F., Liu, C., Li, G. Q. (2015): Investigation on Multi-model Modeling Method of Steam Turbine Heat Rate. – Acta Metrologica Sinica 36(3): 251-255.
[18] López-Hernández, D. (2018): Áreas superficiales específicas y parámetros asociados en suelos venezolanos con diferentes grados de pedogénesis. – Revista de la Facultad de Agronomia de la Universidad del Zulia 35(3): 111-116.
[19] Lv, Y., Feng, H., Ting, T. (2017): A dynamic model for the bed temperature prediction of circulating fluidized bed boilers based on least squares support vector machine with real operational data. – Energy 124(4): 284-294.
[20] Niu, P. F., Wang, P. K., Li, G. Q. (2014): Modeling and Optimization of NOx for Coal-fired Boilers by Free Search Algorithm and Support Vector Machine. – Acta Metrologica Sinica 35(6): 626-630.
[21] Niu, P. F., Ma, Y. P., Zhang, J. (2016): Utility Boilers NOx Combustion Optimization Based on Relevance Vector Machine. – Acta Metrologica Sinica 37(2): 191-196.
[22] Nouaim, W., Chakiri, S., Rambourg, D., Karaoui, I., Ettaqy, A., Chao, J., Allouza, M., Razoki, B., Yazidi, M., Hmidi, F. E. (2019): Mapping the water erosion risk in the Lakhdar river basin (central High Atlas, Morocco). – Geology, Ecology, and Landscapes 3(1): 22-28.
[23] Olivares, B., Cortez, A., Lobo, D., Parra, R., Rey, J., Rodríguez, M. (2017): Evaluación de la vulnerabilidad agrícola a la sequía meteorológica en diferentes localidades de Venezuela. – Revista de la Facultad de Agronomía 34(1): 103-129.
[24] Pang, Z. H., Liu, G. P., Zhou, D., Sun, D. (2016): Data-based predictive control for networked nonlinear systems with network-induced delay and packet dropout. – IEEE Transactions on Industrial Electronics 63(2): 1249-1257.

http://www.aloki.hu ● ISSN 1589 1623 (Print) ● ISSN 1785 0037 (Online)
DOI: http://dx.doi.org/10.15666/aeer/1704_86798691

[25] Pascual-Córdova, G. (2018): Indicadores de calidad del suelo en el agroecosistema caña de azúcar (Saccharum spp.). – Revista de la Facultad de Agronomia de la Universidad del Zulia 35(1): 98-104.
[26] Rajput, K., Gupta, A., Hi, A. (2019): Re-Cycle Of E-Waste In Concrete By Partial Replacement Of Coarse Aggregate. – Engineering Heritage Journal 1(1): 05-08.
[27] Rashedi, E., Nezanudmdi-pour, H., Saryazdi, S. (2009): GSA: A Gravitational Search Algorithm. – Information Sciences 179(13): 2232-2248.
[28] Sharjeel, A., Anwar, S., Nasir, A., Rashid, H. (2019): Design, Development And Performance Of Optimum Water Softener. – Earth Sciences Pakistan 3(1): 23-28.
[29] Tan, P., Xia, J. (2014): Modeling and optimization of NOX emission in a coal-fired power plant using advanced machine learning methods. – Energy Procedia 61: 377-380.
[30] Yazdani, S., Nezanudmdi-pour, H., Kamyab, H. (2014): A gravitational search algorithm for multimodal optimization. – Swarm and Evolutionary Computation 14: 1-14.
[31] Zhang, W. P., Zhao, W. L., Niu, P. F. (2015): Forecasting of Turbine Main Steam Flow Based on Rough Sets and Least Squars Support Vector Machine Regression. – Acta Metrologica Sinica 36(1): 43-47.
[32] Zhang, W., Ma, L., Zhang, T. (2017): Discrete-time mean-field stochastic H 2/H∞ control. – Journal of Systems Science and Complexity 30(4): 765-781.
[33] Zhang, L., Khalique, C. (2018): Classification and bifurcation of a class of second-order odes and its application to nonlinear PDES. – Discrete & Continuous Dynamical Systems-Series S 11(4).
[34] Zulkapli, M. F., Rashid, N. M., Sokri, M. N. M., Nasri, N. (2018): Study On Optical Properties Of Graphene-Tio2 Nanocomposite As Photoanodes Layer In Dye Sensitized Solar Cell (Dssc). – Environment & Ecosystem Science 2(2): 39-41.

http://www.aloki.hu ● ISSN 1589 1623 (Print) ● ISSN 1785 0037 (Online)
DOI: http://dx.doi.org/10.15666/aeer/1704_86798691

COUPLING STUDY OF ECONOMIC VALUE, ECOLOGICAL VALUE AND SOCIAL VALUE OF FORESTS

ZHAO, X. – YUE, S.*

Northeast Forestry University College of Economics and Management
26 Hexing Rd, Xiangfang Qu, Haerbin Shi, Heilongjiang Sheng, China
(e-mail: 229335982@qq.com)

**Corresponding author*
e-mail: yueshngzhi@126.com

(Received 8th Mar 2019; accepted 21st May 2019)

Abstract. This paper uses potential function to build a coupling model: firstly, it divides forest value into three subsystems including economic value, ecological value, and social value, and set the index according to their characteristics; then it studies empirically the coupling relationship among economic value, ecological value, and social value of forest in China from 2008 to 2016. The results show that from 2008 to 2016, the overall coordination among economic value, ecological value, and social value of forest in China is poor while the overall trend is continuous growing, and ecological value of forest has a higher weight. In the future, China should pay attention to the development, protection and utilization of ecological forest value to achieve their sustainable development.

Keywords: *sustainable development, overall coordination, coupling model, subsystem, environmental science*

Introduction

Forests are the larges ecosystems on land, supporting the humanity's important mission of sustainable development, regulation of ecological balance, and development of low-carbon economy (Li and Zhao, 2017). With the changes in current social environment and natural economic environment, human beings traditional use pattern of forest could no longer meet the needs of modern economic development.

On the one hand, the sustainable growth of the forestry industry economy is inseparable from the demand for forest resources; on the other hand, the deteriorating ecological environment and people's demand for a better society require us to protect the only remaining forest resources. In terms of the products and functions provided by forest, it can not only provide ecological services such as water conservation, carbon fixation and oxygen production, and air purification, etc. but also develop tourism; it is also a major production materials for the manufacturing industry, promoting economic development (Chen et al., 2017). For this reason, ways to develop forest resources and maximize their own value is of particular importance. Should we protect forest ecological environment or develop forestry economic industry? And what is the

http://www.aloki.hu ● ISSN 1589 1623 (Print) ● ISSN 1785 0037 (Online)
DOI: http://dx.doi.org/10.15666/aeer/1704_86938712

relationship between these two? This issue has become one of the key forest issues for scholars' research. From the perspective of value, Deng et al. (2002) use "shadow engineering" and other methods to study the value of water conservation in the forest ecosystem in the upper reaches of the Yangtze River, Zhang and Khalique (2018) showing that the annual economic value of water conservation in the forest ecosystem is 160.6179 billion yuan (equivalent to a quarter of the GDP in that region in 1999), and the forest ecosystem is so effective for human beings that the country should pay attention to and protect the ecological value of forest. Through the evaluation method combining quality and value, Zhang et al. (2007) and Shrestha and Baral (2018) use shadow engineering approach, market value approach, and production cost, etc. to quantitatively study the service value of forest ecosystem in Gansu Province. The results show that the economic value of water conservation in the forest ecosystem in Gansu is 256 million yuan/a; the economic value of forest-maintained soil is 4.748 billion yuan/a; the value of forest purified water is 248 million yuan/a; the value of CO_2 fixation is 11.532 billion yuan/a; the value of O_2 release is 13.124 billion yuan/a; the value of SO_2 absorption is 388 million yuan/a; the value of dust retention is 15.639 billion yuan/a; and the value of forest ecological service function in Gansu Province is 44.712 billion yuan, accounting for 23.19% of the province's GNP. These help to see visually the important role of the ecological value of forest, requiring formulation of more reasonable operation model to achieve sustainable development of ecological economy. Pang et al. (2016), Cong et al. (2017) and Austin et al. (2018) use distributed measurement to evaluate the service value of forest ecosystem in Helan Mountain National Nature Reserve in Ningxia. The results show that the total value of forest ecological service function in that region in 2015 was 1.68708 billion yuan/a, accounting for 6.68% of the gross output value of agriculture, forestry, animal husbandry, sideline production, and fishery in Ningxia Autonomous Region in 2014; while the total forest area of the nature reserve accounts for 3.03% of the land area of Ningxia Autonomous Region, indicating that forest ecosystem can not only provide forestry by-product value but also has huge ecological value. Wang et al. (2015) take the analysis of increasing demand for tourism in national forest parks as well as the ecological environment and tourist needs of the scenic spot as background, use choice experiment method and conditional Logit model to empirically analyze the main attributes of Shenyang National Forest Park and evaluate its economic value (Zhang et al., 2017). The results show that vegetation coverage, water clarity, garbage quantity, and crowding degree all have significant impact on the recreation effect. The current economic value of the scenic spot is 27.3 yuan per person, however, when vegetation coverage increases by 10% every time, the economic value of the park will increase 30 yuan; when water clarity improves 0.5 m every time, the economic value of the park will increase 24 yuan; when garbage quantity increase 5 pieces every 20 m^2, the economic value of the park will decrease 20 yuan (Olivares et al., 2017). It can be seen that changing the ecological environment plays an important role in improving the

http://www.aloki.hu ● ISSN 1589 1623 (Print) ● ISSN 1785 0037 (Online)
DOI: http://dx.doi.org/10.15666/aeer/1704_86938712

economic and social benefits of national forest parks. Wang et al. (2015) and Ali et al. (2018) start from the perspective of producers to calculate the recreational value of 39 forest parks in Qinling via marginal opportunity cost method. The results show that the total value of forest recreation is 21.63 billion yuan while the ecological value of forest itself accounts for 74.12%, showing that the ecological function of forest itself can better promote the development of forest tourism. From the perspective of theoretical innovation, Liu and Huang (2007) and Jamil et al. (2018) make theoretical innovation from interest-orientation principle, public product theory, and spillover benefit correction theory to coordinate the relationship between forestry ecological benefits and economic benefits; they also propose to rely on market mechanism to adjust the average level of profit by government imputing certain profit parameters to the market so that both forestry activities with or without lumbering can achieve social average profit. Based on complex system theory, Dong and Zhang (2013) use gray correlation evaluation model, and take the calculation method of slope correlation to build a coupling model of the forestry industry and the forest ecosystem; they also take Yichun Shuangfeng Forestry Bureau as an example (Marina et al., 2013; Gautam et al., 2019), and conduct experimental study to find that the degree of coupling between forestry industry and forest ecosystem in that area is 0.47, thus further draw the conclusion that the relationship between forestry industry development and forest ecosystem in that area is moderate and their relevant impact is general (Liao and Zhang, 2017; Tao, 2018). It can be seen that the researches on forest value by Chinese and foreign experts and scholars stays on the basis of comparison to obtain the ratio of the ecological value of the forest to the total value or the differences between the social value of forest and the income that is already earned, while they do not involve the degree of relationship among the three or the content of coordination relationship. This study conducts an empirical study by building a coupling relationship model of the economic value, ecological value, and social value of forest (Dong et al., 2017), trying to explain the coordination relationship among the three major values of forest and provide a theoretical basis for specifying the future development of forest value.

Materials and Methods

Coupling, in physics, refers to the phenomenon in which two or more systems or two forms of motion connect by impact on each other through various interactions, and such dynamic phenomenon is also called coupling effect. The coordination degree of coupling effect is related to dynamic cycle operation of the whole system; at the same time (Zhang, 2016; Dali and Kamarudin, 2018), it can also reflect the coordination state of the development of things that strong coordination means good development while discordance or conflict means development degeneration or stagnation. Coupling effect has been widely used in many fields including sociology, ecology, and economics, etc. based on its characteristics (Wu et al., 2014; Sarwar et al., 2019). This study applies this

http://www.aloki.hu ● ISSN 1589 1623 (Print) ● ISSN 1785 0037 (Online)
DOI: http://dx.doi.org/10.15666/aeer/1704_86938712

concept to analyze the coordination relationship and dynamic development relationship among social value, economic value, and ecological value of forest, providing a theoretical basis for future forest value enhancement and forest sustainable development. The premise of presenting the efficacy of economic value, ecological value, and social value of forest is to build a potential function based on coupling effect. Assume U1 represents the economic value subsystem of forest, U2 represents the ecological value subsystem of forest, U3 represents the social value subsystem of forest (Zhou et al., 2018; Babaranti et al., 2019), and u_{ij} represents the observation value of the jth statistical indicator in subsystem i, then the potential function of subsystem i, subsystem j, and subsystem z is (*Eq.1*):

$$U_i = \sum_{j=1}^{n} \omega_{ij}\mu_{ij}\,, U_j = \sum_{i=1}^{m} \omega_{ij}\mu_{ij}\,, U_z = \sum_{j=1}^{n} \omega_{zj}\mu_{zj} \quad \text{(Eq.1)}$$

where μ_{ij} represents the normalized value of the jth statistical indicator in subsystem i. The normalized processing formulae for this value include positive normalization and negative normalization, respectively (*Eq.2*):

$$\begin{aligned} \mu_1 &= \left[\mu_{ij} - \min \mu_{ij} / \max \mu_{ij} - \min \mu_{ij}\right] \times 0.9 + 0.1 \\ \mu_2 &= \left[\min \mu_{ij} - \mu_{ij} / \max \mu_{ij} - \min \mu_{ij}\right] \times 0.9 + 0.1 \end{aligned} \quad \text{(Eq.2)}$$

ω_{ij} represents the weight of the jth statistical indicator in subsystem i, and meets the following condition (*Eq.3*):

$$\sum_{j=1}^{n} \omega_{ij} = 1, \sum_{i=1}^{m} \omega_{ij} = 1 \quad \text{(Eq.3)}$$

Based on the coupling model built by potential function, the generalized expression of the n-dimensional coupling degree model is (*Eq.4*):

$$H_n = n\left(U_1 U_2 U_3 \cdots U_n / \prod\left(U_i + U_j + U_z\right)\right)^{\frac{1}{n}} \quad \text{(Eq.4)}$$

Since the subsystems involved in this study are economic value, social value, and ecological value of forest, the coupling models of the following three subsystems can be derived (*Eq.5*):

$$H_3 = 3(U_1 U_2 U_3 / \prod(U_1 + U_2 + U_3))^{\frac{1}{3}} \quad \text{(Eq.5)}$$

where H represents the direct coupling degree of each subsystem (Pascual-Córdova, 2018). The value range is [0, 1]. Higher H value means higher coupling degree of each

http://www.aloki.hu ● ISSN 1589 1623 (Print) ● ISSN 1785 0037 (Online)
DOI: http://dx.doi.org/10.15666/aeer/1704_86938712

subsystem, better coordination among systems, and benign and healthy development of the whole system; and lower H value means lower coupling degree of each subsystem, worse coordination among systems, and stagnant or degraded development of the whole system.

In order to further measure the overall coordination degree and efficacy coordination of the system (Yang et al., 2019; Majumder et al., 2019), we also need to formulate a coupling coordination function to measure the coupling degree among economic value, social value, and ecological value of forest in China. The expression formula of D the coupling coordination function is (*Eq.6*):

$$D:\begin{cases} T = (H \times C) \times k \\ C = \alpha U_1 + \beta U_2 + \gamma U_3 \end{cases} \quad \text{(Eq.6)}$$

where T represents the coupling coordination degree among economic value subsystem, social value subsystem, and ecological value subsystem of forest; H represents the degree of coupling among the subsystems; C represents the coordination coefficient among the subsystems; k, α, β, and γ are parameters; k is a constant quantity value of 0.5; α, β, and γ are determined in accordance with the degrees of importance of the economic value, social value, and ecological value of forest in total value of forest. This study first assumes the values of α, β and γ are 0.33 - in equally important position.

In accordance with the coupling relationship among economic value, social value, and ecological value of forest, such coupling relationship can be divided into three categories: sound development, moderate development and slow development; and the coordination degree can be divided into five levels: excellent coordination, good coordination, moderate coordination, weak coordination, and poor coordination. The details are shown in *Table 1*.

Results

Based on the existing research and the principles of scientificity, reliability, systematicness, availability, and measurability, etc., this study selects appropriate measurement index, uses the combination of qualitative and quantitative methods to express the data, and conducts a comparative study of index data to achieve accurate measurement results with more reference valuable. The evaluation system designed in this study includes three subsystems, namely economic value of forest, ecological value of forest and social value of forest. Economic value of forest is mainly reflected in the two aspects including economic benefit and economic structure.

http://www.aloki.hu ● ISSN 1589 1623 (Print) ● ISSN 1785 0037 (Online)
DOI: http://dx.doi.org/10.15666/aeer/1704_86938712

Table 1. *Classification relationship of forest value coordination degree*

Category	Grade	Coordination degree (T)	Relationship	Meaning
Sound development	Excellent coordination	0.8<T≤1	U1>U2>U3	Highly coordinated development, economic value > ecological value > social value
			U2>U1>U3	Highly coordinated development, ecological value > economic value > social value
			U3>U1>U2	Highly coordinated development, social value > economic value > ecological value
			U3>U2>U1	Highly coordinated development, social value > ecological value > economic value
			U1>U3>U2	Highly coordinated development, economic value > social value > ecological value
			U2>U3>U1	Highly coordinated development, ecological value > social value > economic value
	Good coordination	0.6<T≤0.8	U1>U2>U3	Sound coordinated development, economic value > ecological value > social value
			U2>U1>U3	Sound coordinated development, ecological value > economic value > social value
			U3>U1>U2	Sound coordinated development, social value > economic value > ecological value
			U3>U2>U1	Sound coordinated development, social value > ecological value > economic value
			U1>U3>U2	Sound coordinated development, economic value > social value > ecological value
			U2>U3>U1	Sound coordinated development, ecological value > social value > economic value
Moderate development	Moderate coordination	0.4<T≤0.6	U1>U2>U3	Moderate coordinated development, economic value > ecological value > social value
			U2>U1>U3	Moderate coordinated development, ecological value > economic value > social value
			U3>U1>U2	Moderate coordinated development, social value > economic value > ecological value
			U3>U2>U1	Moderate coordinated development, social value > ecological value > economic value
			U1>U3>U2	Moderate coordinated development, economic value > social value > ecological value
			U2>U3>U1	Moderate coordinated development, ecological value > social value > economic value

http://www.aloki.hu ● ISSN 1589 1623 (Print) ● ISSN 1785 0037 (Online)
DOI: http://dx.doi.org/10.15666/aeer/1704_86938712

Category	Grade	Coordination degree (T)	Relationship	Meaning
Slow development	Weak coordination	0.2<T≤0.4	U1>U2>U3	Weak coordinated development, economic value > ecological value > social value
			U2>U1>U3	Weak coordinated development, ecological value > economic value > social value
			U3>U1>U2	Weak coordinated development, social value > economic value > ecological value
			U3>U2>U1	Weak coordinated development, social value > ecological value > economic value
			U1>U3>U2	Weak coordinated development, economic value > social value > ecological value
			U2>U3>U1	Weak coordinated development, ecological value > social value > economic value
	Poor coordination	0<T≤0.2	U1>U2>U3	Poor coordinated development, economic value > ecological value > social value
			U2>U1>U3	Poor coordinated development, ecological value > economic value > social value
			U3>U1>U2	Poor coordinated development, social value > economic value > ecological value
			U3>U2>U1	Poor coordinated development, social value > ecological value > economic value
			U1>U3>U2	Poor coordinated development, economic value > social value > ecological value
			U2>U3>U1	Poor coordinated development, ecological value > social value > economic value

http://www.aloki.hu ● ISSN 1589 1623 (Print) ● ISSN 1785 0037 (Online)
DOI: http://dx.doi.org/10.15666/aeer/1704_86938712

Economic benefit is objective expression of the total amount of forest economy, mainly in five aspects: (1) total output value of forestry industry, namely the sum of the value created by various production and processing based on forestry industry; (2) contribution rate of forestry industry, namely the ratio of the total output value increase of forestry in national GDP growth; (3) the central government's investment amount in the development of forestry economy, namely state's funds for ecological construction, ecological compensation, and forest disaster management; (4) investment amount of local finance in forestry economic development, namely local governments' construction capital for forestry economic development, and (5) ecological construction and protection funds, namely the central and local governments' total ecological compensation that is absorbed because of the ecological benefits of forestry industry.

Forestry economic structure shows the resource allocation of forestry resource elements in various industries, and the industrial structure of forestry is an important factor to promote the development of forestry economy. This study chooses the structural proportions of various industries in forestry industry to reflect if the forestry industry structure is reasonable. By referring to the evaluation system of forest ecological status in Specifications for Assessment of Forest Ecosystem Services in China and National Level Criteria and Indicators of Sustainable Forest Management in China, this study's selection of forest ecological index mainly reflects the ecological basis, ecological structure, forest health, and ecological protection of forest. Ecological basis of forest mainly focuses on three aspects: (1) forest coverage rate, namely the proportion of forest area on land, the degree of greening of land, and the abundance of ecological resources in China; (2) the amount of forest reserves, namely the total amount of various kinds of forest wood in the forests; and (3) afforestation area, the sum of national afforestation area each year. Ecological structure reflects the accumulation of each forest species. Forest health mainly investigates disaster situation of forests. The indicator system of ecological protection function is established based on the indicator system of ecological service of forest. As there are multiple methods to estimate the value of ecological service of forest, and the measurement of some physical quantities cannot be objective and accurate, this study chooses the construction situation of ecological protection projects of forest to reflect the service function of forest. The first is the natural forest protection project. Natural forest has natural advantages that artificial forest cannot match, including great biodiversity, strong self-recovering ability and adaptability to environment and anti-disaster ability. It can better exert forests' functions of water conservation, climate regulation, and biodiversity increase, therefore the construction area of natural forest protection project can reflect the ecological benefits of forests. The second is the project of returning farmland to forests. This project is one of the important national policies for implementing the western development strategy in China. It can improve soil erosion and desert wasteland; at the same time, number of its acres can also be used as a basis for national subsidy. The third is the sand control project. It can improve wind prevention and sand fixation of forest to further reflect the ecological

http://www.aloki.hu ● ISSN 1589 1623 (Print) ● ISSN 1785 0037 (Online)
DOI: http://dx.doi.org/10.15666/aeer/1704_86938712

service value of wind prevention and sand fixation of forest. The fourth is the shelter forest system project. It can resist natural disasters, protect infrastructure and production, improve the environment, maintain ecological peace, and reduce pollution, etc. In accordance with different protection purposes, we can establish various forests with ecological service functions such as water conservation forest, soil and water conservation forest, and landscape shelter forests, etc. Therefore the construction area of shelter forest can be regarded as an important indicator that reflects the ecological protection function. The fifth is the area of nature reserve. This can be taken as an indicator that has impact on the biodiversity of forest. The sixth is the value of forestry ecological service. This is the value of forestry ecological service that has formed industrial activities in the tertiary industry of forestry, e.g. recreation in forest, soil and water conservation, carbon sequestration, and conservation of biodiversity, etc. For social value of forest, as its accounting system is not complete and there are no national accounting indicators, this study integrates the existing literature research and divides the social value of forest in three aspects - value of people's livelihood, value of tourism, and value of culture. Value of people's livelihood uses the number of forestry employees and their average salary to reflect the beneficial contribution of forestry economic development to society. Value of tourism uses the tourism and leisure service value of forestry for reflection. And value of culture reflects the abstract value of forest. Therefore, this study chooses the approximate forest park area and popularity index of forest park to alternatively reflect the cultural value of the forest (Meza, 2018).

Since there is a certain difference in the importance of indicators in different systems, the indicators need to be weighted before coupling analysis. At present, the weighted analysis methods (e.g. expert investigation and analytic hierarchy process) used by most scholars have strong subjectivity; therefore the obtained index weights may have some errors. This study uses objective weighting method and entropy method based on the variation coefficient of objective things to weight each indicator. Specific steps are as follows:

(1) Standardize the index by standardized formula (*Eq.7*):

$$y_i = x_i - \bar{x}/s \tag{Eq.7}$$

where y represents the value after standardization and s is standard deviation with the formula as (*Eq.8*):

$$s = \sqrt{\frac{1}{n-1}\sum_{i=1}^{n}(x_i - \bar{x})^2} \tag{Eq.8}$$

$\bar{x}$ is the average of the variables with the calculation formula as (*Eq.9*):

$$\bar{x} = \frac{1}{n}\sum_{i=1}^{n} x_i \tag{Eq.9}$$

http://www.aloki.hu ● ISSN 1589 1623 (Print) ● ISSN 1785 0037 (Online)
DOI: http://dx.doi.org/10.15666/aeer/1704_86938712

After standardization, different data variables have the same variance and mean value, so they can be directly compared.

(2) Calculate the proportion of the standardized values in the subsystem, a_{ij} represents the proportion of indicator j in subsystem i in the standardized subsystem, and u_{ij} represents the standardized value of indicator j in subsystem i, the formula is (*Eq.10*):

$$a_{ij} = u_{ij} / \sum_{i=1}^{n} u_{ij} \quad \text{(Eq.10)}$$

The entropy value p_j of indicator j in subsystem i can be calculated in accordance with the formula (*Eq.11*):

$$p_j = -k \sum_{i=1}^{n} a_{ij} \ln a_{ij}, k = \frac{1}{\ln(n)} > 0 \quad \text{(Eq.11)}$$

where k is coordinating parameter.

(3) Calculate the variation coefficient l of indicator j in subsystem i, the formula is (*Eq.12*):

$$l_j = 1 - p_j/m - g_p, \ (g_p = \sum_{j=1}^{m} p_j) \quad \text{(Eq.12)}$$

(4) The calculation formula for the weight ω_j of indicator j in subsystem i is (*Eq.13*):

$$\omega_j = l_j / \sum_{j=1}^{m} l_j, \ j = 1, 2, 3 \cdots, m \quad \text{(Eq.13)}$$

The weights of the indicators in each system calculated with this method are shown in *Table 2.*

Discussion

As an important resource asset, forest can not only provide timber and other plant assets for the development of national economy and people's life, but also functions as an important environmental asset and the largest environmental carrier on land with a basic status in developing low-carbon economy and ecological civilization; meanwhile, as an important part of terrestrial ecosystem, forest is also the habitat of biodiversity, playing the role of water conservation, soil conservation, wind prevention and sand fixation, and climate regulation and change, etc. while functioning as the important site to absorb carbon dioxide and sulfur dioxide (Hernández, 2019). It undertakes two major missions of optimizing environment and promoting production. General Secretary Xi Jinping also proposes that we need both valuable assets, and more importantly, lucid waters and lush mountains; after all, lucid waters and lush mountains are invaluable assets.

http://www.aloki.hu ● ISSN 1589 1623 (Print) ● ISSN 1785 0037 (Online)
DOI: http://dx.doi.org/10.15666/aeer/1704_86938712

Table 2. *Index setting and index weight*

Subsystem	Primary index	Secondary index	Unit	Weight
Economic value of forest U1	Economic benefit level U11	Total output value of forestry industry U111	100 million yuan	0.031
		Contribution rate of forestry industry U112	%	0.016
		The central government's investment amount U113	100 million yuan	0.022
		Investment amount of local finance U114	100 million yuan	0.031
		Ecological construction and protection funds U115	100 million yuan	0.019
	Economic structure U12	Proportion of the output value of the primary industry U121	%	0.048
		Proportion of the output value of the secondary industry U122	%	0.018
		Proportion of the output value of the tertiary industry U123	%	0.044
Ecological value of forest U2	Ecological basis U21	Forest coverage rate U211	%	0.079
		The amount of forest reserves U212	10,000 m^3	0.079
		Afforestation area U213	hectare	0.092
	Ecological structure U22	Natural forest quantity U221	10,000 m^3	0.030
		Plantation quantity U222	10,000 m^3	0.079
	Forest health U23	Area of forest fire U231	hectare	0.025
		Area of pests and diseases in forest U232	hectare	0.035
	Ecological protection function U24	Natural forest protection project U241	hectare	0.051
		Project of returning farmland to forests U242	hectare	0.021
		Sand control project U243	hectare	0.037
		Shelter forest system project U244	hectare	0.033
		The area of nature reserve U245	hectare	0.034
		Value of forestry ecological service U246	100 million yuan	0.032
Social valueU3	Value of people's livelihood U31	Employed populationU311	person	0.018
		Average annual salary of in-service employees U312	100 million yuan	0.033
	Tourism value of forest U32	Recreation value of forest U321	100 million yuan	0.041
	Cultural value of forest U33	Area of forest park U331	hectare	0.028
		Popularity index of forest park U332	%	0.016

Therefore, it is an inevitable choice for forestry sustainable development to implement win-win development of forestry with coordination of economic, social and ecological environment, and maximize the economic value, social value and ecological value of forest on the basis of adhering to the virtuous cycle of ecological environment.Under this

http://www.aloki.hu ● ISSN 1589 1623 (Print) ● ISSN 1785 0037 (Online)
DOI: http://dx.doi.org/10.15666/aeer/1704_86938712

development trend, this study chooses the original data in China Forestry Statistical Yearbook from 2008 to 2016 for coupling degree analysis, trying to indicate the direction for future sustainable development of forestry in China through the research results in addition to analyzing the relationship among the three major values of forests (Shan and Lai, 2018).

First, the original data is standardized; then the weight of each index system is calculated by "entropy weight method" and the calculation result is brought into the potential function to obtain the values of economic value, ecological value and social value of forest; finally, coupling model and coupling coordination model are used to calculate the final results shown in *Tables 3 and 4*.

Table 3. *2008 to 2016 calculation result of coupling value H*

2008	2009	2010	2011	2012	2013	2014	2015	2016
0.724	0.729	0.877	0.926	0.948	0.781	0.861	0.796	0.841

Table 4. *2008 to 2016 calculation result of coupling coordination value T*

2008	2009	2010	2011	2012	2013	2014	2015	2016
0.048	0.064	0.077	0.084	0.105	0.153	0.155	0.189	0.203

Table 3 is the coupling values of the economic value, ecological value and social value of forest. In accordance with the coupling degree indicator H described above, the value range is 0 to 1, higher value means higher coupling degree, and conversely, lower value means lower coupling degree. It can be seen from the data in *Table 3* that the coupling degree among economic value, ecological value and social value of forest is high with the average value of all values reaching 0.83, proving the great influence among the economic value, ecological value and social value of forest; the coupling degree increased year by year from 2008 to 2012, showing that the country has made basic achievements in forestry construction since the reform and opening up, a series of initiatives such as the construction of six major ecological protection projects, development of forest tourism, rapid development of the forestry tertiary industry, and continuous implementation of national policy to change desertification have made the value of forest more and more prominent, and the values of forest are moving toward healthy and good development trend steadily.

It can be seen from *Table 4* that the coupling coordination value T of the economic value, ecological value and social value of forest in China from 2008 to 2016 also shows an increasing trend year by year; however, if graded by coordination degree, the coordination differences from 2008 to 2015 were basically in the same level while the

http://www.aloki.hu ● ISSN 1589 1623 (Print) ● ISSN 1785 0037 (Online)
DOI: http://dx.doi.org/10.15666/aeer/1704_86938712

coordination degree in 2016 was weaker with one level up compared with the previous, but the value was not high. The biggest increase was in 2013, this is mainly because since the 18th CPC National Congress, General Secretary Xi Jinping has put forward a series of important speeches on promoting the construction of ecological civilization and made a series of important instructions and profound discussions, while forest, as a main part and important resource of ecosystem on land, is an important ecological guarantee for the survival and development of human beings. Under such background, State Forestry Administration organized experts to prepare Outline of State Forestry Administration's Plan for Promoting Ecological Civilization Construction, which clearly defined the national ecological red line, requiring the forest stock volume of no less than 20 billion cubic meters, so the afforestation area in 2013 increased by 504,270 thousand hectares compared with 2012. However, the growth rate of the ecological value indicators of forest in 2014 decreased compared with that in 2013, resulting in the least increase in the coupling coordination value in 2014. From an overall perspective, the development of the economic value, ecological value and social value of forest in China is transiting from incoordination to coordination. From the perspective of the system's potential function, as shown in the following table (*Table 5*), the ecological value of forest is also significantly higher than the economic value and social value of forest (Wang, 2019).

Table 5. *Potential functions of sub-systems of forest*

Year	**Economic value of forest**	**Ecological value of forest**	**Social value of forest**
2008	0.05890141	0.1270031	0.01534795
2009	0.05427371	0.1832762	0.02660406
2010	0.0795104	0.1457341	0.04059887
2011	0.09396559	0.1296828	0.04896527
2012	0.1177569	0.149074	0.06672682
2013	0.1300533	0.3863547	0.07166745
2014	0.1411518	0.3171471	0.08459407
2015	0.1475089	0.4659078	0.09828729
2016	0.1569462	0.4499682	0.1201707

The following figure shows the variation curves of the potential function of economic value, ecological value and social value subsystems of forest (*Fig. 1*). It can be seen that since 2009, the forestry economic value in China has increased year by year and the social value has also increased, showing that Chinese forestry keeps developing and the social economy is also growing. The reason is that on one hand, the output value of the forestry industry is increasing year by year, and contributions of the secondary industry and tertiary industry are increasing; on the other hand, the level of urbanization is increasing and the per capita income of forestry people rises as well. The curve of ecological value

http://www.aloki.hu ● ISSN 1589 1623 (Print) ● ISSN 1785 0037 (Online)
DOI: http://dx.doi.org/10.15666/aeer/1704_86938712

of forest is more fluctuating, showing an inverted U-shape development. The rising of ecological value curve in 2009 indicates increasing carrying capacity of forest environment, and this is inseparable from the afforestation area and forestry ecological construction in that year.

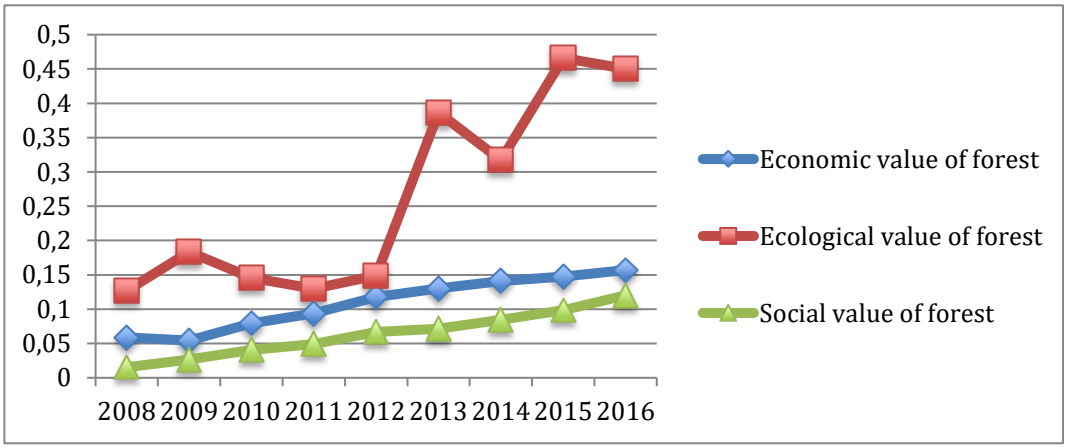

Figure 1. *Variation curves of the potential function of subsystems of forest value*

There was an inflection point in 2011 with the minimum of 0.129. The reason may be related to the forestry development policy in recent years such as the reform of collective forest property right system. In addition, forest is a complex system integrating the primary industry (forest management, etc.), the secondary industry (wood processing, etc.), and tertiary industry (ecological service construction, etc.), increase in the primary industry can promote the development of tertiary industry, and efforts in ecological construction can also increase the output value of the primary industry. For the output value of forestry industry in the past few years, the output value of the second industry was the largest in 2011, while such increase would inevitably lead to excessive exploitation and utilization of forest resources, resulting in imbalanced forest resource structure. This, together with an increase in the damage area of forest and decrease in the construction of ecological protection, will inevitably lead to degradation of forest ecosystem and the lowest ecological value of forest.

In addition, when studying the weight of each subsystem, the author finds that the weight of each indicator in subsystems of forest value is higher than other indicators, and their rankings are higher; therefore, the author adjusts the parameters in the coordination function with the adjusted ratio of $\alpha:\beta:\gamma = 4:21:1$, and takes them into the coupling coordination model to obtain *Table 6*.

It can be seen from the data in *Table 6* that the coupling coordination degree among subsystems of forest value showed a fluctuating rise from 2008 to 2016, and it increased by one level from 2013 with the highest increase. The reason is that in 2011, the State Council held Working Conference on National Natural Forest Resources Protection

http://www.aloki.hu ● ISSN 1589 1623 (Print) ● ISSN 1785 0037 (Online)
DOI: http://dx.doi.org/10.15666/aeer/1704_86938712

Project, and State Forestry Administration actively implemented the spirit of the conference and held Work Arrangement Conference on the 2nd Phase of National Natural Forest Resources Protection Project, requiring to further implement the forest management subsidy and related social insurance subsidy policies; meanwhile, State Forestry Administration also issued *Twelfth Five-Year Plan for Forestry Development*, which affirmed the achievements of forestry construction during the Eleventh Five-Year Plan period, pointed out the three major goals of forestry construction (i.e., to build a sound forestry ecosystem, a developed forestry industry system, and a prosperous ecological and cultural system) to achieve scientific development and sustainable development of forestry, took construction of ecological civilization as the primary task of developing forestry, and clearly gave forestry five main functions including ecological function, economic function, social function, carbon sink function and cultural function, and set the main indicators for forestry development during the Twelfth Five-Year Plan period.

Table 6. *2008 to 2016 calculation result of coupling coordination degree T after adjusting coefficient*

2008	2009	2010	2011	2012	2013	2014	2015	2016
0.081	0.114	0.115	0.112	0.133	0.261	0.242	0.321	0.330

Therefore, under such policy, the coupling coordination indicator of forest values rose greatly from 2012 and increase in the ecological value of forest played a crucial role (Zhang et al., 2017). The reason for fall in 2014 was that the afforestation area in 2014 was 550.45 million hectares less than that in 2013, at the same time, the construction area of natural forest protection project and the area of sand control project were also less than in 2013, and slow growth of forest ecological construction caused slow increase in the ecological value of forest and reduced coupling coordination degree among forest values (Martínez, 2019). To sum up, it can be seen from the above that the development of ecological value of forest plays an important role in the development of the entire forestry economy, and insisting on implementation of afforestation, development of six major forestry projects, and development of forest recreation value is an inevitable choice for China to develop forestry economy as well as a necessary condition for sustainable development of forestry (Asgari, 2018).

To reflect the role of the ecological value of forest in the total value of forest more clearly, the coupling coordination degree T' after adjusting coefficients is compared with the coupling coordination degree T before adjustment (*Fig. 2*).

http://www.aloki.hu ● ISSN 1589 1623 (Print) ● ISSN 1785 0037 (Online)
DOI: http://dx.doi.org/10.15666/aeer/1704_86938712

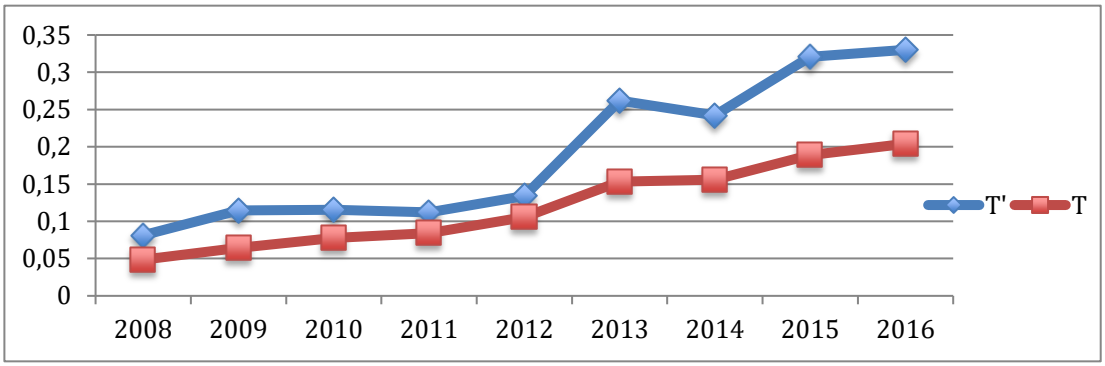

Figure 2. *Comparison analysis of coupling coordination degree after adjusting coefficient*

It can be seen clearly that from 2012, the ecological value of forest greatly increased the coupling coordination degree among the total values of forest, having better function in coordination and development of subsystems.

Conclusion

This study uses potential function and the coupling effect in physics to build a coupling model, conducts research on the economic value, ecological value and social value of forest from the quantitative point of view, and builds indicator systems from nine perspectives respectively including economic benefit, economic structure, ecological basis, ecological structure, forest health condition, ecological protection function, value of people's livelihood, tourism value of forest, and cultural value of forest (Zeng et al., 2018); it also studies the coupling relationship among economic value, ecological value and social value of forest in China from 2008 to 2016 and draws the following conclusions:

(1) The overall coordination degree among economic value, ecological value and social value of forest in China is poor. The coordination degree of all samples was at the level of poor coordination before 2016 and entered into the level of weak coordination after 2016 (Lu et al., 2019). Both levels belong to the state of slow and uncoordinated development, but the ecological value of forest always accounted for a higher proportion than economic value and social value. Therefore, China should continue to adhere to the construction of ecological civilization, improve the ecological environment of forest, and enhance the level of coordination degree of forest values.

(2) From the perspective of national policies, in 2011, State Forestry Administration promulgated the Twelfth Five-Year Plan for forestry and began to implement the 2nd Phase of National Natural Forest Resources Protection Project, having an important impact on the promotion of the ecological value of forest. After 2012, the coordination degree among forest values also improved faster than before and gradually developed to the upper level. This also shows that the promotion of the ecological value of forest can

http://www.aloki.hu ● ISSN 1589 1623 (Print) ● ISSN 1785 0037 (Online)
DOI: http://dx.doi.org/10.15666/aeer/1704_86938712

more effectively promote the economic value and social value of forest so that the relationship among forest values would become more harmonious, and developing the ecological value of forest is an important measure to achieve sustainable development of forest in future.

(3) From the perspective of the index weight of subsystems, what impacts greatly on the weights of index systems is mainly concentrated in the ecological value subsystem of forest with afforestation area accounting for the largest proportion. Therefore, China should adhere to afforestation and restore forest ecological barrier. Secondly, the value of forest tourism has increased year by year with its weight also higher compared with the index in other social value subsystems. This shows that with the development of society, people have better payment ability and increasing recognition that forest tourism can bring more physical and mental pleasure. People's willingness to return to nature and close to nature rises, and the income of national forest tourism also rises continuously. Development of forest tourism can promote the overall increase of the social value and economic value of forest. From the economic structure of forestry industry, with the increasing output value of the tertiary industry of forestry, the potential function value of economic value of forest also increases year by year, showing that the tertiary industry of forest and the economic value of forest are positively related, and active development of the tertiary industry of forest will help improve the economic and ecological value of forest.

(4) By adjusting the parameters of the coupling coordination model, we can clearly see the impact of the ecological value of forest on the overall forest value coordination model. However, increase in only the ecological basis and ecological protection function of forest is not enough to improve the ecological value of forest and exert the ecological benefits of forest, and the country must give certain financial support. Although the country started pilots for ecological benefit subsidy in 2001 and provided certain ecological construction investment every year, ecological subsidy still accounted for a small proportion, not enough to compensate the speed of ecological damage. Therefore, China should promulgate relevant laws and regulations, follow the principle of "whoever benefits shall pay" and "whoever damages shall compensate", and charge certain ecological compensation fee from the direct beneficiaries and direct wrongdoers of forest ecology to increase forest ecological compensation funds, improve social awareness of ecological construction and environmental protection, and promote sustainable development of forests (Zhang et al., 2017).

Forest ecological protection work is a systematic project that needs the participation of the whole people. It needs the strength of the people to complete. Therefore, if we want to achieve the protection of forest ecological resources, we must do a good job in propaganda, enhance the awareness of the importance of forest protection, let them fully realize the importance of forest ecological resources protection, consciously participate in the ranks of forest ecological resources protection.

http://www.aloki.hu ● ISSN 1589 1623 (Print) ● ISSN 1785 0037 (Online)
DOI: http://dx.doi.org/10.15666/aeer/1704_86938712

Acknowledgements. This work was supported by Humanity and Social Science foundation of Ministry of Education of China 16YJA630072.

REFERENCES

[1] Ali, W., Nasir, M. S., Nasir, A., Rashid, H., Ayub, I., Gillani, S. H., Latif, M. J. (2018): Assessment Of Carbon Footprints In Terms Of Co2 Of Diesel Generator, Pakistan. – Earth Sciences Pakistan 2(1): 15-17.
[2] Asgari, A. (2018): 1. Methods for breaking Chinese lantern (Physalis alkekengi L.) seed dormancy. Laboratory and greenhouse studies. – Revista de la Facultad de Agronomia de la Universidad del Zulia 35(2).
[3] Austin, O. E., Ebuka, A. O., Zanders, A. C. C., Joseph, I. N. (2018): Seismic Analysis Of The Transgressive Systems Tracts (TSTS) Of The Niger Delta. – Earth Sciences Malaysia 2(2): 16-19.
[4] Babaranti, O., Horn, S., Jowett, T., Frew, R. (2019): Isotopic signatures in Mytilus galloprovincialis and Ulva latuca as bioindicators for assessing discharged sewage effluent in coastal waters along Otago Peninsula, New Zealand. – Geology, Ecology, and Landscapes 3(1): 53-64.
[5] Chen, C., Song, H., Yang, H. (2017): Liouville type theorems for stable solutions of p-Laplace equation in RN. – Nonlinear Analysis 160: 44-52.
[6] Cong, R. Z., Wang, B., Gu, J. C., Niu, X., Hu, T. H. (2017): Evaluation of forest ecosystem services values of Helan Mountain National Nature Reserve, Ningxia. – Journal of Arid Land Resources and Environment 31(11): 136-140.
[7] Dali, N. M., Kamarudin, K. S. N. (2018): The Effect of Cosurfactant In Co2 Absorption In Water – In – Oil Emulsion. – Environment & Ecosystem Science 2(2): 42-46.
[8] Deng, K. M., Shi, P. L., Xie, G. D. (2002): Water conservation of forest ecosystem in the upper reaches of Yangtze River and its benefits. – Resources Science 24(06): 68-73.
[9] Dong, P. W., Zhang, X. (2013): Measurement study on system coupling between forestry and forest ecosystems. – China Soft Science (11): 178-184.
[10] Dong, W., Tian, S. Y., Li, Y. (2017): Dynamic trend of forestry eco-economic development: theoretical model and regional differences. – East China Economic Management 31(11): 44-50.
[11] García-Nieto, A. P., García-Llorente, M., Iniesta-Arandia, I., Martín-López, B. (2013): Mapping forest ecosystem services: From providing units to beneficiaries. – Ecosystem Services: 126-138.
[12] Gautam, A., Batra, R., Singh, N. (2019): A Study On Use Of Rice Husk Ash In Concrete. – Engineering Heritage Journal 1(1): 01-04.
[13] Hernández, C. (2019): Evaluating the Efficiency of Rice Plant Growth. – Revista de la Facultad de Agronomia de la Universidad del Zulia 36(1).
[14] Jamil, F., Arshad, R., Ali, M. A. (2018): Design, Fabrication And Evaluation Of Rotary Hot-Air Dryer For The Value Addition Of Fruit Waste. – Earth Sciences Pakistan 2(2): 07-11.
[15] Li, X. Y., Zhao, Q. L. (2017): A new integrable symplectic map by the binary nonlinearization to the super AKNS system. – Journal of Geometry and Physics 121: 123-137.
[16] Liao, B., Zhang, Z. G. (2017): The empirical measurement of coupling from indicators to indexes of forestry ecological security. – Resources Science 39(9): 1777-1791.
[17] Liu, D. Q., Huang, Q. (2007): Theoretical investigation and innovation of coordinating forestry ecological benefits and economic benefits. – Public Finance Research (11): 25-27.

http://www.aloki.hu ● ISSN 1589 1623 (Print) ● ISSN 1785 0037 (Online)
DOI: http://dx.doi.org/10.15666/aeer/1704_86938712

[18] Lu, D., Feng, L., Jie, P. (2019): Solar Cells Various Appearance Defects Automatic Simultaneous Detection System of the Greenhouses. – Acta Microscopica 28(1).
[19] Majumder, S. C., Islam, K., Hossain, M. M. (2019): State of research on carbon sequestration in Bangladesh: a comprehensive review. – Geology, Ecology, and Landscapes 3(1): 29-36.
[20] Martínez, R. (2019): Experiments to Improve Sugarcane Production in Cuba. – Revista de la Facultad de Agronomia de la Universidad del Zulia 36(1).
[21] Meza, N. M. (2018): 2. Evaluación de características de calidad de clones promisorios y variedades de papa (Solanum tuberosum L.). – Revista de la Facultad de Agronomia de la Universidad del Zulia 35(2).
[22] Olivares, B., Cortez, A., Lobo, D., Parra, R., Rey, J., Rodríguez, M. (2017): Evaluación de la vulnerabilidad agrícola a la sequía meteorológica en diferentes localidades de Venezuela. – Revista de la Facultad de Agronomía 34(1): 103-129.
[23] Pang, Z. H., Liu, G. P., Zhou, D., Sun, D. (2016): Data-based predictive control for networked nonlinear systems with network-induced delay and packet dropout. – IEEE Transactions on Industrial Electronics 63(2): 1249-1257.
[24] Pascual-Córdova, G. (2018): Indicadores de calidad del suelo en el agroecosistema caña de azúcar (Saccharum spp.). – Revista de la Facultad de Agronomia de la Universidad del Zulia 35(1): 88-95.
[25] Sarwar, M. T., Hui, Z. H., Maqbool, A. (2019): Causes And Control Measures Of Urban Air Pollution In China. – Environment & Ecosystem Science 3(1): 35-36.
[26] Shan, P. F., Lai, X. P. (2018): Numerical Simulation of the Fluid–Solid Coupling Process During the Failure of a Fractured Coal–Rock Mass Based on the Regional Geostress. – Transport in Porous Media 124(3): 1061-1079.
[27] Shrestha, A., Baral, S. (2018): Socioeconomic Factors Affecting Awareness And Adaption Of Climate Change: A Case Study Of Banke District Nepal. – Earth Sciences Malaysia 2(2): 20-24.
[28] Tao, S. (2018): Evaluation Of Technology Innovation In Hubei Province. – Engineering Heritage Journal 2(2): 09-10.
[29] Wang, E. D., Li, L., Wei, J. H. (2015): Economic value evaluation of resources and management attributes for forest parks using choice experiments. – Resources Science 37(01): 193-200.
[30] Wang, W. J., Hu, X. X., Zhao, M. (2015): Forest recreation value estimation based on producer perspective. – Statistics and Decision 3: 14-17.
[31] Wang, Y. (2019): Influencing Factors of Water-saving Irrigation Technology Used by Vegetable Growers from the Perspective of Cost-benefit. – Revista de la Facultad de Agronomia de la Universidad del Zulia 36(1).
[32] Wu, S., Yan, X. D., Zhang, L. J. (2014): The relationship between forest ecosystem energy and forest ecosystem service value in China. – Acta Geographica Sinica 69(03): 334-342.
[33] Yang, Y. X., Li, H., Zheng, W. K., Yun, B., Liu, Z. M., Zhang, J. J. (2019): Experimental Study on Calcining Process of Secondary Coated Ceramsite Solidified Chromium Contaminated Soil. – Science of Advanced Materials 11(2): 208-214.
[34] Zeng, D., Qiu, Y., Peng, S., Chen, C., Zeng, J., Zhang, S., Xiao, R. (2018): Enhanced hydrogen production performance through controllable redox exsolution within CoFeAlO x spinel oxygen carrier materials. – Journal of Materials Chemistry A 6(24): 11306-11316.
[35] Zhang, C., Ren, Z. Y., Gao, M. X., Yan, W. H. (2007): The forest ecosystem services and their valuation in Gansu Province. – Journal of Arid Land Resources and Environment 21(08): 147-151.
[36] Zhang, C. H. (2016): Developing situations of forestry in Xinjiang Province based on the time series & PCA. – Journal of Arid Land Resources and Environment 30(02): 58-62.

http://www.aloki.hu ● ISSN 1589 1623 (Print) ● ISSN 1785 0037 (Online)
DOI: http://dx.doi.org/10.15666/aeer/1704_86938712

[37] Zhang, W., Ma, L., Zhang, T. (2017): Discrete-time mean-field stochastic H 2/H∞ control. – Journal of Systems Science and Complexity 30(4): 765-781.
[38] Zhang, W., Yang, J., Fang, Y., Chen, H., Mao, Y., Kumar, M. (2017): Analytical fuzzy approach to biological data analysis. – Saudi journal of biological sciences 24(3): 563-573.
[39] Zhang, Y., Li, Y., Bai, C. (2017): Microstructure and oxidation behavior of Si–MoSi2 functionally graded coating on Mo substrate. – Ceramics International 43(8): 6250-6256.
[40] Zhang, L., Khalique, C. (2018): Classification and bifurcation of a class of second-order odes and its its application to nonlinear PDES. – Discrete & Continuous Dynamical Systems-Series S 11(4).
[41] Zhou, D. M., Al-Durra, A., Matraji, I., Ravey, A., Gao, F. (2018): Online Energy Management Strategy of Fuel Cell Hybrid Electric Vehicles: A Fractional-Order Extremum Seeking Method. – Transactions on Industrial Electronics 65(8): 6787-6799.

http://www.aloki.hu ● ISSN 1589 1623 (Print) ● ISSN 1785 0037 (Online)
DOI: http://dx.doi.org/10.15666/aeer/1704_86938712

FACTORS AFFECTING ADMINISTRATIVE AND ORGANIZATIONAL SUCCESS IN THE TURKEY'S FORESTRY

KÖSE, M.[1] – DAŞDEMİR, I.[2*] – YURDAKUL EROL, S.[3] – YILDIRIM, H.-T.[3]

[1]*Çanakkale Onsekiz Mart University, Bayramiç Vocational School, Çanakkale, Turkey (e-mail: muratkose@comu.edu.tr)*

[2]*Bartın University, Faculty of Forestry, Bartın, Turkey*

[3]*İstanbul University Cerrahpaşa, Faculty of Forestry, İstanbul, Turkey (e-mail: secily@istanbul.edu.tr, htezcan@istanbul.edu.tr)*

**Corresponding author*
e-mail: isdasdemir@hotmail.com

(Received 6th Mar 2019; accepted 3rd May 2019)

Abstract. This study was dealt with aiming to examine the most important factors (education and self-development, administrative competence, success mentality, motivation and rewarding) affecting administrative and organizational success in the forest resource management of Turkey. For this purpose, four different questionnaires were applied to the total of 565 interviewees related to the forestry section of the Ministry of Forestry and Water Affairs and four different interest groups (employees, subject experts, related institutions and nongovernmental organizations representatives) in nine geographical regions of Turkey. To gather data about the subject and to reach the results, face to face interviews were conducted with interest groups, a questionnaire was applied. The layered-simple random sampling method was used as a sampling method. All obtained data were used as material. The research data were evaluated with descriptive statistics, it was inspected with the Kruskal-Wallis H-Test whether the thoughts of the interviewees related to the most important factors affecting administrative and organizational success differ according to the regions, and the departments, the position and the experience. The different groups were determined by the Duncan Test. Accordingly, most of the interviewees think that the undergraduate education, prevocational and in-service training are inadequate and that they need the most social and economic comprehensive information in the management of forest resources. Middle and upper level managers have the opportunity to further develop themselves, as the duration of experience increases, the administrative competence about forest resources management increases, but scientific studies and research results related to forestry are mostly not followed. The majority of the interviewees correctly identified administrative and organizational success in forestry, determined the most important factors affecting success as organizational and administrative factors and found that there was little or no relationship between success and reward. To increase the success in the forestry, the employees should participate in decisions and the success should be measured and evaluated objectively and numerically in the form of institutional success. According to the results, some suggestions were put forward for development of forest resources management.

Keywords: *forest resource management, education, administrative competence, success mentality, motivation and rewarding, Turkey*

Introduction

Sustainability and multiple utilization principles in forest resources management form the basis of contemporary forestry approach (Aktan, 2013; Lorincova et al., 2016; Albuquerque da Silva et al., 2016; Sanchez Badini et al., 2018). Many issues such as sustainable forest management, participatory management, conflict management, certification, carbon management and strategic management come to the fore in the field of forestry all over the world (Wibowo and Giessen, 2015; Kim et al., 2016). Human

http://www.aloki.hu ● ISSN 1589 1623 (Print) ● ISSN 1785 0037 (Online)
DOI: http://dx.doi.org/10.15666/aeer/1704_87138735

resources is the key factor to fulfill the innovations in those mentioned fields and provide sustainability in forestry and sustainability couldn't be ensured unless sufficient development is achieved in terms of human resources (Pinstrup-Andersen et al., 1998; Szaro et al., 2000). Considering the multifunctional services of forests in the planning and management processes are gradually becoming important in terms of conservation, development and expansion of the forest lands within the context of sustainable management (Baynes et al., 2015; Miteva et al., 2015). Parallel to this approach human resources, particularly the technical staff, has an important role in utilizing forest resources, actualizing new approaches in forestry and achieving the goals of forestry policy (Krott, 2005; Mendes, 2006). In other words, it is impossible to determine and implement effective policies, to solve numerous problems and to achieve sectoral progress without solving the problems of human resources in forestry (Hasanagas, 2014; Wibowo and Giessen, 2015).

Conserving the forest lands and providing the society with forest products sustainably are the duties, which are assigned through the constitution and the legislation, of the forestry organization in Turkey. Fulfillment of this duty as precisely as possible makes it obligatory for the organization to be dispersed and nature compatible (Toksoy et al., 2011). The country-wide problems such as complicated organizational structure, political oppression over the forestry organization and the employees, unequal distribution of human resources to central and provincial units, various unjust appointment and promotion issues are of the main factors that affect human resources (Özdönmez et al., 1998; Gümüş, 2014). Considering the issues listed above for Turkey, it can be clearly observed how essential it is to provide the employees, particularly the technical staff, with job satisfaction. In other words, human resources require to be managed well to ensure sustainable forest resources management. Within this context, it is seen that the concepts such as education, motivation, organizational and administrative success become prominent with regard to sustainable forest resources management (Torres-Rojo et al., 2016; Tumbach et al., 2018).

The characteristics of the forestry practices and the duties of the forestry organization require the staff that is to be employed in the field be specialized in terms of training and education (Kaplan, 1998; Hansman et al., 2016). The organizational structure which is established for the performance of forestry practices also diversifies the training and education of the personnel (Özdönmez et al., 1998). Meanwhile, the absence of a widespread and well-organized education system is a common obstacle against properly benefiting from educated staff for many countries. Although developing countries possess 50% of the whole world's forest lands, they employ only a small proportion of professional foresters and technicians (Schmithüsen, 1983; Elands et al., 2004; MacDicken et al., 2015). On the other hand, when forestry is analyzed in terms of human resources in developed countries, it is seen that training and development of the staff is among the mostly emphasized issues (Imamura, 1982; Hajjar and Oldekop, 2018). Therefore, the importance of well-trained and educated professional human resources for the sake of sustainable forest resources management can be clearly observed.

Monitoring the moral and physical needs of the employees, providing the work environment that meet their goals and expectations, ensuring the consistency among the organizational goals and staff goals in order to enhance motivation and improve labor productivity are considered as basic management processes not only for the motivation of the employees but also for the achievement of organizational goals (Gümüş and Beşir, 2012; Lyons et al., 2016). The most effective motivation tools are determined as

http://www.aloki.hu ● ISSN 1589 1623 (Print) ● ISSN 1785 0037 (Online)
DOI: http://dx.doi.org/10.15666/aeer/1704_87138735

satisfying wages, appreciation, job security, promotion and work satisfaction (Wiley, 1997; Burns and Giessen, 2016). In this regard, the motivation of the employees of the organization in parallel with the job satisfaction among them is crucially important when organizational success and the achievement of future goals are considered.

Forestry organization is an economic organization with public responsibilities, goals and duties to achieve (Daşdemir, 1998). Before determining the factors that affect success in this organization, it is necessary to identify what success means for it. In general, success for an organization is a multi-dimensional concept according to contemporary management approach and can be identified as the level of qualitative and quantitative achievement in scheduled activities, duties and goals with the interactive cooperation of all components of the system (Daşdemir, 1996; Akal, 2005). Despite it is possible to measure success in absolute and relative terms; it is possible to mention about different kinds of success such as economic success, technical success, biological and biophysical success, administrative and organizational success etc. Administrative and organizational success mostly related with organizational, environmental and human factors. The administrative dimension of success is a factor of production that actualizes the administration function. The core of this production factor is human, in other words, the administrators. Accordingly, administrators are responsible for the achievement of organizational goals by combining the efforts of the employees with the other resources within a process that consists of activities such as planning, decision making, organizing, leading, coordinating and supervising. Then, the characteristics that administrators should bear, emerge as the factors that form the most crucial dimension of organizational success. These factors affect the administrative success and hence are dependent on the environmental, organizational and administrative ones (Daşdemir, 1998).

Forestry in Turkey is based on public administration and public property. The institutions which are responsible for forest resources management in Turkey are the General Directorate of Forestry (GDF), the General Directorate of Nature Conservation and National Parks (GDNCNP) and the General Directorate of Combating Desertification and Erosion (GDCDE) under the Ministry of Forestry and Water Affairs (MFWA). The forestry organization, which is responsible for sustainable forest resources management, needs not only an ideal organizational structure but also employees with sufficiency and performance in order to achieve organizational goals and success. For this reason, it is important to identify the factors that affect the administrative and organizational success of the employees.

Therefore, this study aims to evaluate sustainable forest resources management efficiency, training, knowledge and supervision levels of the employees that work as administrators and technical staff in the forestry organization in Turkey. The study also aims to evaluate the administrative and organizational success mentality of the staff, their motivation level, motivation-success relation, measures to take in order to improve success and success measuring system. While evaluating the mentioned issues, the study considers the attitudes of four different interest groups which are the employees, experts, related institutions and nongovernmental organizations (NGO) representatives. The study has been conducted throughout the country among 565 participants including administrators and technical staff who work in forestry sector (GDF, GDNCNP and GDCDE) of the Ministry of Forestry and Water Affairs, and experts, related institutions and NGO representatives. The study has been carried out through interviews and questionnaires. The results are thought to contribute to sustainable forest resources

http://www.aloki.hu ● ISSN 1589 1623 (Print) ● ISSN 1785 0037 (Online)
DOI: http://dx.doi.org/10.15666/aeer/1704_87138735

management, human resources management, administrative and organizational success of forestry organization.

Material and Method

Material

The study has been carried out among the sample group that consists of the employees working in the forestry sector (GDF, GDNCNP and GDCDE) of the MFWA. The provinces (İstanbul, İzmir, Antalya, Adana, Bolu, Trabzon, Erzurum, Şanlıurfa and Ankara) with intense forestry activities have been included to represent the nine geographical regions of Turkey.

Participants belonging to four different interest groups, which are the employees, experts, related institutions and NGO representatives, from the cities listed above have been interviewed and questionnaires have been applied in order to evaluate the factors that affect administrative and organizational success in Turkish forestry sector. Four different interview and questionnaire forms had been prepared for each interest group. The questions in the forms are generally as follows: (1) The sufficiency of the education and the opportunity of self-development, (2) Administrative competence of the employees, (3) Success mentality and (4) Motivation. Similar and different questions were asked for each interest group in the questionnaire forms. The forms include both open-ended and closed-end questions. All kinds of qualitative and quantitative data obtained from research on four different interest groups and literature review are the main materials of the study.

Data Collection Method

The population of the study consists of the technical staff and administrators working in central and provincial units of forestry organization of the MFWA (N=4704) (MFWA, 2016). The number of employees within the scope of this study was calculated using the following formula (*Eq.1*) related to the sample size in measurable groups (Orhunbilge, 2000; Daşdemir, 2016);

$$n \geq \frac{Z^2 \times N \times p \times q}{N \times D^2 + Z^2 \times p \times q} \qquad \text{(Eq.1)}$$

where n is the size of the sample, Z is reliability coefficient (Z=1.96 for 95 % of confidence level), N is the size of the population (N=4704), p is the existence possibility of the measured feature in the population, q is absence possibility of the measured feature in the population (p=0.5; q=0.5 a) and D is acceptable sampling error (0.05).

According to this, n was calculated as 355 and so the minimum number of the interviewees was determined. The minimum number of the participants to be interviewed for each region was calculated by multiplying the number of the employees in each region with the calculated n/N coefficient which represents that each layer has been sampled in proportion to its percent. On the other hand, the number 355 was exceeded and 463 participants, who are technical staffs and administrators, were interviewed during the study (*Table 1*).

The interviewee and the questionnaire participants were selected randomly in each region. Thus, stratified-simple random sampling method was utilized in the study.

http://www.aloki.hu ● ISSN 1589 1623 (Print) ● ISSN 1785 0037 (Online)
DOI: http://dx.doi.org/10.15666/aeer/1704_87138735

As well as the staffs in the forestry organization, a survey research was carried out on 32 representatives of related institutions (municipal authorities, forestry faculties, provincial directorate of agriculture etc.), 37 NGO representatives (the Chamber of Forest Engineers, the Foresters' Association of Turkey, the Foundation for the Promotion and Protection of the Environment and Cultural Heritage, forestry cooperatives, Village Headmen Association, Forestry Union etc.) and 33 experts who have scientific studies on forest resources management or who have been working in forestry organization as administrator for many years and have knowledge on administration of forestry organization and restructuring. Since the actual numbers of other interest groups in each region were small, the survey was conducted in full field (on all their numbers) in each region. Therefore, the sample sizes of other interest groups are equal to their actual numbers. Thus, a total of 565 participants from the four different interest groups were interviewed (*Table 1*).

Table 1. *Numbers of the interviewed participants for all interest groups*

Regions	Staffs in Forestry Organization												Institutions	NGO	Experts	General Total
	GDF		GDNCNP		GDCDE		Center of the MFWA		Total Staff	General						
										Sample						
	Staff	Sample	Staff	Sample	Staff	Sample	Staff	Sample		Technical staffs	Adminis-trators	Total				
Marmara (İstanbul)	721	62	73	9					794	57	14	71	7	10	10	98
Aegean (İzmir)	693	59	57	5					750	38	26	64	3	4	3	74
Western Mediterranean (Antalya)	335	27	30	3					365	15	15	30	4	5	4	43
Eastern Mediterranean (Adana)	459	49	30	15					489	48	16	64	4	4	3	75
Western Black Sea (Bolu)	680	68	34	4					714	32	40	72	2	2	2	78
Eastern Black Sea (Trabzon)	364	30	20	4					384	15	19	34	2	2	1	39
Central Anatolia (Ankara)	692	65	79	6	48	5	54	4	873	47	33	80	6	10	10	106
Eastern Anatolia (Erzurum)	187	20	21	3					208	8	15	23	2			25
Southeastern Anatolia (Şanlıurfa)	89	18	38	7					127	13	12	25	2			27
TOTAL	4220	398	382	56	48	5	54	4	4704	273	190	463	32	37	33	565

The interviews were conducted in 2016. A pretesting was applied for the questionnaire. In the pretesting process, the attitudes of the participants about the questionnaire, the convenience of the questionnaire forms, the clarity of the questions and missing parts were determined, questionnaire form was rearranged. Then the participants were informed about the importance of the subject and the questionnaires were conducted through face to face meetings.

Data Evaluation Method

The data which are mostly qualitative and obtained from four different interest groups' questionnaire survey have been identified and digitized as variables in *Table 2*.

http://www.aloki.hu ● ISSN 1589 1623 (Print) ● ISSN 1785 0037 (Online)
DOI: http://dx.doi.org/10.15666/aeer/1704_87138735

The data was evaluated through descriptive statistics, the Kruskal–Wallis (K-W) H Test and the Duncan's Test and the results were shown in tables. The software Excel-2010 and SPSS (22.0 version) were utilized to evaluate the data.

Results

General Results on Participants and Evaluations

A total of 565 people from four interest groups located in 9 geographical regions in Turkey were interviewed and questionnaires were conducted during this study. 463 of them work as manager and technical staff in the forestry organization. 59% of the participants of the questionnaire are engineers, 11% are forest chiefs, 2% are deputy director of forest enterprises, 2% are managers of forest enterprises, and 24% are branch managers, deputy director or directors of regional directorates of forestry. Also, 52% of the *experts*, number of which is 33, work under the MFWA, 42% are academicians from faculties of forestry and 6% are retired forest engineers. 28% of the 32 participants from *related organization representatives* are the employees of municipalities or various ministries, 53% are of forestry faculties, 19% are of other institutions related to forestry such as General Directorate of State Hydraulic Works (DSI) and General Directorate of Highways (TCK) etc. 34% of these mentioned participants are technical staff, 13% are administrators and 53% are academicians. On the other hand, 51% of the 37 participants, who are *NGO representatives*, are either the members of the Chamber of Forest Engineers or the Foresters' Association, 8% are the members of unions and 41% are the members of foundations etc. related to forestry. 68% of them are members, 32% are either managers or deputy managers.

The educational status, the administrative task duration and experience for the 463 participants who work as administrators and technical staff in the forestry sector across Turkey are indicated in *Table 3*.

Considering the *Table 3*, it can be understood that most of the questionnaire participants (65%) have been working in their current administrative positions between 0-5 years. The rate of those who have been working in the same administrative position more than 11 years is 13%. In other words, 87% of the staff working as administrators have worked in their position maximum for 10 years. Whereas 51% of the survey participants have a 20-year job experience, 49% of the participants have an experience of 21 years or more. 73% of the participants have a bachelor's degree in forest engineering. Only 24% of them have either master or Ph.D. degree while 3% are graduates of some other faculties. This is an important progress in training qualified administrators and technical staff. Approximately 70% of the participants who were consulted as experts are either graduates of two different faculties or have graduate degree (master or Ph.D.).

Sufficiency of Education and Opportunity of Self-Improvement

In this part of the study, the employees in the forestry sector and the experts on organizational structure and administration were asked their attitudes about the sufficiency of the education received in forestry faculties on forest resources management, the sufficiency of the prevocational training, in-service training and human resources development activities provided by the forestry organization.

http://www.aloki.hu ● ISSN 1589 1623 (Print) ● ISSN 1785 0037 (Online)
DOI: http://dx.doi.org/10.15666/aeer/1704_87138735

Table 2. *Identification of the variables*

Category	No	Definition of Variable	Definition of Scale	Unit	Scale
Training Competence and Self-Improvement	1	Sufficiency of undergraduate forestry education on forest resources management	Not all =1, Slightly s= 2, Moderately = 3, Very = 4, Extremely = 5	--	1-5
	2	Sufficiency of prevocational training	Not all =1, Slightly s= 2, Moderately = 3, Very = 4, Extremely = 5	--	1-5
	3	Sufficiency of in-service training	Not all =1, Slightly s= 2, Moderately = 3, Very = 4, Extremely = 5	--	1-5
	4	Knowledge requirement in the management of forestry activities	Basic knowledge=1; Technical Knowledge=2; Biological and ecological knowledge =3; Social and economic knowledge=4	--	1-4
	5	Sufficiency of opportunity for self-improvement in administrative and technical issues	Not all =1, Slightly s= 2, Moderately = 3, Very = 4, Extremely = 5	--	1-5
Administrative Sufficiency	6	Sufficiency of personal knowledge in administrative and technical issues	Not all =1, Slightly s= 2, Moderately = 3, Very = 4, Extremely = 5	--	1-5
	7	Sufficiency of superiors' knowledge in administrative and technical issues	Not all =1, Slightly s= 2, Moderately = 3, Very = 4, Extremely = 5	--	1-5
	8	Sufficiency of subordinates' knowledge in administrative and technical issues	Not all =1, Slightly s= 2, Moderately = 3, Very = 4, Extremely = 5	--	1-5
	9	Sufficiency of technical staff's knowledge in administrative and technical issues	Not all =1, Slightly s= 2, Moderately = 3, Very = 4, Extremely = 5	--	1-5
	10	Sufficiency on legislative knowledge	Not all =1, Slightly s= 2, Moderately = 3, Very = 4, Extremely = 5	--	1-5
	11	Following research and development activities	Yes = 3, Moderately= 2, No =0	--	0-3
Success Mentality	12	Mentality of administrative and organizational success	1- Achieving the goals through efficient use of resources 2- Fulfilling the need of society regarding forest resources 3-Producing highest output from the least input 4-Other 5-Producing the highest amount of goods and services through the market demand 6-Profit maximization	The percentages of four interest groups (%)	(0-81)
	13	Most important factors affecting success	1- Organizational and administrative factors 2- Social factors 3- Technical factors 4- Other factors 5- Ecological and geographical factors 6- Physical factors 7- Economic and financial factors	Percentages of staff and experts' attitudes (%)	(0-73)
	14	Attitudes on success measurement	1-Assessment and Evaluation Unit that will be established under Ministry or General Directorate should measure the organizational success by using some objective criteria and depending on the records of the organizations 2-The success of the staff should be measured by examination and supervision system that will be managed by an expert commission 3-Other 4-Register managers should measure the success by scoring the staff utilizing criteria of standard forms.	Percentages of staff and experts' attitudes (%)	(3-67)
Motivation and Reward	15	Relationship between the success and designation, promotion, premium, being appreciated and being rewarded	Negative relation = -1; Not any relation= 0; Low-level positive relation= 1; High-level positive relation= 2	--	-1- (+2)
	16	Opportunities of raising the motivation / success of staff	1- The attitudes of the staff should be considered and they should participate in decision-making processes 2- Premium should be paid 3-Staff should be appreciated 4-Other 5-Designation should be made in accordance with the preference of the staff 6-Staff should be promoted 7-Staff should be joined to national and international vocational trips	Percentages of staff and experts' attitudes (%)	(0-55)

http://www.aloki.hu ● ISSN 1589 1623 (Print) ● ISSN 1785 0037 (Online)
DOI: http://dx.doi.org/10.15666/aeer/1704_87138735

Table 3. *Educational status, administrative task duration and experience of the participant staff*

Features	Category	Years	Staff	
			Frequency (N)	Percentage (%)
Administrative Task Duration	1	Less than 5	301	65
	2	6-10	100	22
	3	More than 11	62	13
	Total		463	100
Vocational Experience (Career Duration)	1. Low	Less than 10	121	26
	2. Medium	11-20	117	25
	3. High	21-30	185	40
	4. Very High	More than 31	40	9
	Total		463	100
Education	Undergraduate		339	73
	Graduate		111	24
	Get degree from two Undergraduate Programs		13	3
	Total		463	100

Besides, those working as administrators (on planning, organization, operation, and supervision) and technical staff were also asked what kind of knowledge background they require mostly and their attitudes on the opportunity of self-improvement. The attitudes of the participants were evaluated and the results were indicated in *Table 4*. The question, whether the attitudes of the employees differ depending on the regions, departments, position and job experience or not was tested through statistical analyses as well (*Table 5*).

Sixty-four percent of the participants who work for forestry organization and 73% of the experts define *the sufficiency of the education received in forestry faculties on forest resources management* as "moderately sufficient" (*Table 4*). As it is indicated in *Table 5*, the region, department and position have no significant effect on their attitude. However, as for job experience, 95% of reliability level makes a significant difference. It has been observed that less experienced employees (0-10 years of experience) generally define the sufficiency of the education received in forestry faculties on forest resources management as "slightly sufficient" and "moderately sufficient" whereas those with medium, high and quite high experience (≥11 years) mostly define as "reasonably sufficient".

Forty-six percent of the employees find *the prevocational training provided by the organization* "moderately sufficient" (*Table 4*). At this point, the attitudes of the employees differ depending on the region with a reliability level of 99% whereas their attitudes have differences in terms of the position, department and experience with a reliability level of 95%. While those who work in İstanbul, Şanlıurfa, Adana, Antalya and İzmir generally find prevocational training "slightly sufficient", the staff work in Ankara, Bolu, Trabzon and Erzurum mostly find "moderately sufficient". When the departments are considered, those working at the General Directorate of Forestry (GDF) and the General Directorate of Nature Conservation and National Parks (GDNCNP) define training as "slightly sufficient" and "moderately sufficient". On the other hand, the employees working at the General Directorate of Combating Desertification and Erosion (GDCDE) find the mentioned training "moderately sufficient" and "very sufficient". Engineers also find the prevocational training provided by the organization "slightly sufficient" and "moderately sufficient" whereas operation chiefs, assistant

http://www.aloki.hu ● ISSN 1589 1623 (Print) ● ISSN 1785 0037 (Online)
DOI: http://dx.doi.org/10.15666/aeer/1704_87138735

operation managers, operation managers, branch managers, district managers and their assistants mostly find it "moderately sufficient". When job experience is considered, less experienced staff and those with medium experience (0-20 years) define their attitude as "hardly sufficient" and "moderately sufficient" whereas those with high and quite high experience (≥21 years) generally define it as "moderately sufficient" (*Table 5*).

Table 4. *Participants' attitudes on sufficiency of the education and opportunity of self-improvement*

Attitudes	Scale	Percentages of attitudes (%)	
		Staff	Experts
1. Sufficiency of undergraduate education on forest resources management	a) Not all	6	0
	b) Slightly	20	9
	c) Moderately	64	73
	d) Very	8	15
	e) Extremely	2	3
2. Sufficiency of prevocational training	a) Not all	8	-
	b) Slightly	38	-
	c) Moderately	46	-
	d) Very	7	-
	e) Extremely	1	-
3. Sufficiency of in-service training	a) Not all	4	-
	b) Slightly	22	-
	c) Moderately	60	-
	d) Very	13	-
	e) Extremely	1	-
4. Knowledge requirement in the management of forestry activities	a) Basic knowledge (biology, physics, chemistry, mathematics, statistics etc.)	2	0
	b) Technical knowledge (construction, transportation, cadastre, watershed management etc.)	18	0
	c) Biological and ecological knowledge (ecology, entomology, silviculture, afforestation etc.)	30	18
	d) Social and economic knowledge (economy, business administration, production-marketing, finance, planning, law, public relations etc.)	50	82
5. Opportunity for self-improvement in administrative and technical issues	a) Not all	3	0
	b) Slightly	19	9
	c) Moderately	57	70
	d) Very	19	18
	e) Extremely	2	3

On the other hand, when *the sufficiency of the in-service training* is considered, 92% of the employees (60+22+4) find it "moderately sufficient", "slightly sufficient" and "not sufficient" (*Table 4*). The attitudes of the employees regarding this matter differ depending on the position with a reliability level of 99% and on the region, department and experience with a reliability level of 95%. Those working in İstanbul, Adana, Antalya, İzmir, Ankara, Bolu, Trabzon and Erzurum define the sufficiency of the in-service training and human resources development activities as "moderately sufficient" whereas those who work in Şanlıurfa mostly define it as "slightly sufficient". When the department is considered, employees at the GDF state "slightly sufficient" and "moderately sufficient" while the employees at the GDNCNP and the GDCDE generally state "moderately sufficient" and "very sufficient". Those working as engineers, forest chiefs and managers of forest enterprises generally state their attitudes

http://www.aloki.hu ● ISSN 1589 1623 (Print) ● ISSN 1785 0037 (Online)
DOI: http://dx.doi.org/10.15666/aeer/1704_87138735

as "slightly sufficient" and "moderately sufficient". However, deputy managers of forest enterprises, branch managers, directors and deputy directors of regional forest directorates define their attitude as "moderately sufficient" and "very sufficient". Similarly, employees with less, medium and high experience (0 -30 years) find related activities of the organization "slightly sufficient" and "moderately sufficient". Those with quite high experience (≥31 years), on the other hand, generally find the activities "moderately sufficient" and "very sufficient" (*Table 5*).

Table 5. *Difference among the attitudes of employees about sufficiency of education and opportunity of self-improvement depending on the region, department, position and experience*

Attitudes	Kruskal-Wallis H-Test Results			Identify differences by Duncan Test (Groups and in-group components are ranked as to their significance level)			
	Criteria	Khi-square value	SD	Groups with significant differences			
				No	Component of the groups	$\overline{X}$	N
1. Sufficiency of undergraduate education on forest resources management	There is no significant difference with respect to region, department and position					--	--
	Experience	10.30*	3	1	Staff with low experience (0 -10 years)	2.63	121
				2	Staff with medium, high and very high experience (≥11 years)	2.86	342
2. Sufficiency of prevocational training	Region	29.55**	8	1	İstanbul, Şanlıurfa, Adana, Antalya, İzmir	2.38	254
				2	Ankara, Bolu, Trabzon, Erzurum	2.74	209
	Department	7.94*	2	1	GDF, GDNCNP	2.58	458
				2	GDCDE	3.40	5
	Position	14.69*	5	1	Engineer	2.43	273
				2	Forest chief, deputy manager of forest enterprise, manager of forest enterprise, branch manager, deputy manager and manager of regional directorate	2.72	190
	Experience	9.72*	3	1	Staff with low and medium level experience (0 -20 years)	2.43	238
				2	Staff with high and very high experience (≥21 years)	2.67	225
3. Sufficiency of in-service training	Region	18.49*	8	1	Şanlıurfa	2.44	25
				2	İstanbul, Adana, Antalya, İzmir Ankara, Bolu, Trabzon, Erzurum	2.89	438
	Department	8.46*	2	1	GDF	2.81	405
				2	GDNCNP, GDCDE	3.23	58
	Position	18.87**	5	1	Engineer, Forest Chief, Manager of Forest Enterprise	2.88	332
				2	Deputy manager of forest enterprise, Branch manager, Deputy manager and manages of regional directorate	3.11	131
	Experience	8.65*	3	1	Staff with low, medium, high experience (0 -30 years)	2.81	423
				2	Staff with very high experience (≥31 years)	3.05	40
4. Knowledge requirement in the management of forestry activities	There is no significant difference with respect to region, department, position and experience.					--	--
5. Opportunity for self-improvement in administrative and technical issues	There is no significant difference with respect to department and experience.					--	--
	Region	25.28**	8	1	İstanbul, Ankara, Şanlıurfa, Adana, İzmir	2.86	304
				2	Bolu, Trabzon, Erzurum, Antalya	3.17	159
	Position	23.59**	5	1	Engineer, forest chief, branch manager	3.04	436
				2	Manager and deputy manager of forest enterprise and regional directorate	3.40	27

* is significant at 0.05 confidence level; ** is significant at 0.01 confidence level

http://www.aloki.hu ● ISSN 1589 1623 (Print) ● ISSN 1785 0037 (Online)
DOI: http://dx.doi.org/10.15666/aeer/1704_87138735

The complexity of tasks and responsibilities of national forestry organization and the overload job definition of forest engineers who work as land managers makes the importance of the education and training critical for Turkish forestry. The findings showed that both the undergraduate education and vocational education should be developed especially in the context of social and economic aspect. Also the training program's sufficiency is considered lower by GDF's staff than the others. The main reason of this result depends on the diversity of work, work load, task and responsibilities and also the size of organizational structure of GDF. Thus the priority should be given to this institute. This could affect both the personal and organizational performance.

Fifty percent of the employees working in forestry sector and 82% of the experts state that they mostly require social and economic (economics, management, production-marketing, accounting, planning, law and public relations etc.) knowledge background when they are asked *"What kind of knowledge background do you require mostly with your position in the management of forestry activities (planning, organization, operation, and supervision)?"* (*Table 4*). The difference of region, department, position and experience do not significantly affect the employees' attitude related to that aspect (*Table 5*).

Fifty-seven percent of the employees and 70% of the experts answer the question *"Do you find the opportunity for self-improvement in your profession and technical issues?"* as "moderately sufficient" (*Table 4*). The difference in department and experience do not significantly affect the employees' attitude related to the subject. However, it has been observed that the attitude of the employees differ depending on the region and position with a reliability level of 99%. According to the scores of Duncan's test which was applied in order to find the difference among the groups, it has been found out that employees in İstanbul, Ankara, Şanlıurfa, Adana and İzmir generally state that self-development opportunity is "slightly" and "moderately sufficient". However, those working in Bolu, Trabzon, Erzurum and Antalya answer the same question as "moderately sufficient" and "very sufficient". On the other hand, engineers, forest chiefs and branch managers state this aspect as "moderately sufficient" whereas managers and deputy managers of forest enterprises and regional forest directorates state it as "moderately sufficient" (*Table 5*).

Self-improvement is also another important factor that affects the organizational success. It was found out that the self-improvement opportunities were commented in different levels by the regions. Especially the participants of the regions with higher development level such as Istanbul and Ankara expressed that they have lower level of related opportunities. The evaluation of this result in human resources management policies could support the regional level activities. The other interesting finding showed that the level of considering the sufficiency of self-improvement opportunities increase by the position. The reason of this result could be the differences between the duty places and conditions of the staff at different organizational levels. In this context, the staff with lower position level should be supported as a general policy.

Results Related to Administrative Competence

In this part of the study, the employees that work as administrator and technical in the forestry organization were asked to consider the sufficiency of themselves, their subordinates, superiors and technical staff about forest resources management, legislative knowledge and also their attitudes about following the research and

http://www.aloki.hu ● ISSN 1589 1623 (Print) ● ISSN 1785 0037 (Online)
DOI: http://dx.doi.org/10.15666/aeer/1704_87138735

development activities and outputs. Related results were indicated in *Table 6*. The question whether the attitudes of the employees relating the issue differ depending on the regions, departments, position and experience were tested through statistical analyses as well and the results were indicated in *Table 7*.

Table 6. *Employees' attitudes on their administrative competence*

Attitudes	Scale	Percentages of attitudes (%) Staff
1. Sufficiency of personal knowledge in administrative and technical issues	a) Not all	1
	b) Slightly	8
	c) Moderately	60
	d) Very	28
	e) Extremely	3
2. Sufficiency of superiors' knowledge in administrative and technical issues	a) Not all	3
	b) Slightly	17
	c) Moderately	60
	d) Very	18
	e) Extremely	2
3. Sufficiency of subordinates' knowledge in administrative and technical issues	a) Not all	3
	b) Slightly	29
	c) Moderately	60
	d) Very	7
	e) Extremely	1
4. Sufficiency of technical staff's knowledge in administrative and technical issues	a) Not all	1
	b) Slightly	18
	c) Moderately	68
	d) Very	12
	e) Extremely	1
5. Sufficiency on legislative knowledge	a) Not all	0
	b) Slightly	10
	c) Moderately	52
	d) Very	34
	e) Extremely	4
6. Following research and development activities	a) Yes	12
	b) No	26
	c) Moderately	62
7. Reason of not following research and development activities sufficiently	a) I don't care	1
	b) I care, however I don't have enough time	42
	c) I'm not of interest	8
	d) The research results aren't applied	23
	e) I don't believe in researches and find them insufficient	8
	f) Other	18

As it can be concluded from *Table 6*, 60% of the employees working in forestry organization find themselves "moderately sufficient" in forest resources management. The difference of department has no significant effect on the employees' attitudes related to the subject. However, when region and experience are considered, significant effect on the attitude can be seen with a reliability level of 99% and this rate is 95% when position is considered. Those who work in İstanbul, Ankara, Erzurum and Şanlıurfa find themselves "moderately sufficient" in forest resources management, whereas those working in Bolu, Trabzon, Adana, Antalya and İzmir state their competence as "very sufficient" (*Table 7*). As for their position, engineers, forest chiefs

http://www.aloki.hu ● ISSN 1589 1623 (Print) ● ISSN 1785 0037 (Online)
DOI: http://dx.doi.org/10.15666/aeer/1704_87138735

and managers of forest enterprises define themselves as "moderately sufficient" while deputy manager of forest enterprises, branch managers, managers and deputy managers of regional directorate mostly find themselves "very sufficient". Besides, less experienced employees and those with medium experience (0-20 years) evaluate themselves to be "moderately sufficient" and those with high and quite high experience (≥21 years) find themselves "very sufficient" (*Table 7*).

Table 7. *Differences of participants' attitudes on administrative competence depending on region, department, position and experience*

Attitudes	Kruskal-Wallis H-Test Results			Identify differences by Duncan Test (Groups and in-group components are ranked as to their significance level)			
	Criteria	Khi-square value	SD	Groups with significant differences			
				No	Component of the groups	$\bar{X}$	N
1. Sufficiency of personal knowledge in administrative and technical issues	There is no significant difference with respect to department					--	--
	Region	21.00**	8	1	İstanbul, Ankara, Erzurum, Şanlıurfa	3.07	199
				2	Bolu, Trabzon, Adana, Antalya, İzmir	3.34	264
	Position	14.00*	5	1	Engineer , forest chief, manager of forest enterprise	3.21	332
				2	Deputy manager of forest enterprise, branch manager, manager and deputy manager of regional directorate	3.50	131
	Experience	47.89**	3	1	Staff with low and medium experience (0 -20 years)	3.03	238
				2	Staff with very high experience (≥21 years)	3.52	225
2. Sufficiency of superiors' knowledge in administrative and technical issues	There is no significant difference with respect to region and department.					--	--
	Position	12.64*	5	1	Engineer, manager and deputy manager of forest enterprise, branch manager	2.87	400
				2	Forest chief, manager and deputy manager of regional directorate	3.27	63
	Experience	14.64**	3	1	Staff with low experience (0 -10 years)	3.21	121
				2	Staff with medium and very high experience (≥11 years)	2.94	342
3. Sufficiency of subordinates' knowledge in administrative and technical issues	There is no significant difference with respect to region, department, position and experience					--	--
4. Sufficiency of technical staff's knowledge in administrative and technical issues	There is no significant difference with respect to region, department, position and experience					--	--
5. Sufficiency on legislative knowledge	There is no significant difference with respect to region and department					--	--
	Position	24.56**	5	1	Engineer, forest chief, manager of forest enterprise	3.28	332
				2	Deputy manager of forest enterprise, branch manager, manager and deputy manager of regional directorate	3.59	131
	Experience	33.68**	3	1	Staff with low, medium and high experience (0-30 years)	3.27	423
				2	Staff with very high level experience (≥31 years)	3.68	40
6. Following research and development activities	There is no significant difference with respect to region, department, position and experience					--	--

Sixty percent of the participant employees working in the forestry organization think that their superiors are "moderately sufficient" in forest resources management (*Table 6*). The attitudes of the participants do not indicate a significant difference depending on region and department with a reliability level of 95%. However, when position and experience are considered a significant difference is observed in terms of

http://www.aloki.hu ● ISSN 1589 1623 (Print) ● ISSN 1785 0037 (Online)
DOI: http://dx.doi.org/10.15666/aeer/1704_87138735

reliability levels of 95% and 99% respectively. Engineers, managers and deputy managers of forest enterprises, and branch managers generally define their superiors "slightly sufficient" or "moderately sufficient". Forest chiefs, managers and deputy managers of regional forest directorates on the other hand, generally find their superiors "moderately sufficient" or "very sufficient". On the other hand, less experienced employees (0-10 years) in forest resources management generally find their superiors "moderately sufficient" or "very sufficient". Employees with medium, high and quite high experience (≥11 years) think that their superiors are "moderately sufficient" or "slightly sufficient" (*Table 7*). It can be understood that the higher job experience levels that the employees have mean the less competence attitude on their superiors.

Sixty percent of the participants define their subordinates as "moderately sufficient" when their attitude is asked about forest resources management (*Table 6*). Region, department, position and experience difference do not have a significant effect on the attitudes of participants (*Table 7*).

When they are asked about the technical staff, 68% of the participants working in the forestry sector think that they are "moderately sufficient" in forest resources management (*Table 6*). Region, department, position and experience difference do not have a significant effect on the attitudes of participants (*Table 7*). Most of the participants find not only themselves but also their superiors - subordinates and technical staff "moderately sufficient" in forest resources management related issues.

The results showed that the staff defines themselves, their superiors and subornitaes and also the technical staff moderately sufficient in terms of aspects regarding forest resources management. This could be a prominent issue in terms of success of the organization. Determination of the related insufficiencies and their reason could have priority for the forestry sector in Turkey. Thus the key solutions could be designed for improving sustainability of forest resources. Also it was found out that the focus group should be engineers and forest chiefs who are at the lowest position and have much more task and workload. Besides both the managers, land managers and technical staff should be supported about their managerial ability related forest resources.

When the participants are asked as *"How sufficient is your knowledge about the law, regulations and instructions etc. related to your position-department?"* 52% of them define themselves as "moderately sufficient" on legislative knowledge. 34% state that they are "very sufficient" (*Table 6*). Region and department difference do not have a significant effect on the attitudes of participants. However, when their position and experience are considered, a significant difference can be observed with a reliability score of 99%. While engineers, forest chiefs and managers of forest enterprises find themselves "moderately sufficient" and "very sufficient" on legislative, deputy managers of forest enterprises, branch managers, managers and deputy managers of regional forest directorates mostly state that they are "very sufficient" (*Table 7*). Particularly mid-level and senior managers such as branch manager, managers and deputy managers of regional forest directorates define themselves as more sufficient on legislative knowledge when compared with the rest of the employees is both ordinary and necessary. Employees with less, medium and high job experience (0-30 years) find themselves "moderately sufficient" and "very sufficient". Those with a quite high job experience (≥31 years) define themselves as "very sufficient" on legislative knowledge (*Table 7*). It can be stated that the more experienced the employees become, the more sufficient they find themselves on legislative knowledge, which is a realistic situation.

http://www.aloki.hu ● ISSN 1589 1623 (Print) ● ISSN 1785 0037 (Online)
DOI: http://dx.doi.org/10.15666/aeer/1704_87138735

When they are asked as *"Are you able to follow scientific studies and researches related to forestry?"* 12% of the participants answer "Yes"; 26% "No" and 62% "Partially" (*Table 6*). It is observed that the participants (42%) whose answer is "No" or "Partially", give the answer *"I care about them but I am too busy"* as an excuse for not being able to follow research and development activities and their outputs. The second most commonly (23%) given excuse is *"I don't follow because I don't find them applicable"*. As it can be concluded here, 65% (42+23) of the employee state that they are not able to follow research and development activities and their outputs because they do not have enough time or they do not follow them because of not believing the activities to be applicable. No significant difference depending on region, department, position and experience can be found related to the subject (*Table 7*).

It was found out that the staff evaluated their legal knowledge sufficiency at a high level. This is a favorable situation in terms of Turkish Forestry because there are lots of problems derived from application of legislations and the sufficiency of the technical staff about legislative issues makes the forestry organization stronger. However, the level of following research and development activities is low. The interaction between research and decision making and also implementation processes of forestry play critical role on organizational success. This potential should be developed by effective mechanisms to strengthen the managerial process of Turkish forestry.

Results Related to Success Mentality

The attitude of the managers, technical staff and the experts about administrative success, most important factors affecting success and success measurement systems were questioned at this part. Related institution representatives and the representatives from NGOs were also asked about their thoughts on administrative success in forestry. The results were given in the *Table 8*. Besides, the question, whether participants' thoughts differ depending on region, department, position and experience was statistically analyzed and results were given in *Table 9*.

Seventy-for percent of the employees working in forestry sector, 76% of the experts, 63% of related institution representatives and 81% of NGO representatives replied the question *"How do you identify administrative and organizational success in forestry?"* as *"achieving the goals through efficient use of resources"*. The answer by NGO representatives with the highest rate and accuracy indicates how conscious they are about the issue (*Table 8*). Region, department and position difference has no significant effect on the participants' thoughts. However, experience has an effect with a 99% reliability score. According to the Duncan's test score which was performed to find out which group is different, it is understood that the answer *"achieving the goals through efficient use of resources"* is more common among those with medium job experience (11-20 years) when compared with the answers of those with less, high and quite high job experience (0-10 years and ≥21 years) (*Table 9*).

Fifty-six percent of the employees and 73% of the experts identify "organizational and administrative factors such as organizational structure, administrative competence, number of the staff and their level of education as *"the most important factors affecting success"* (*Table 8*). No significant difference depending on region, position and experience can be found related to the subject (*Table 9*) but, a significant difference is found depending on departments with a reliability score of 95%. According to Duncan's test results, employees working at the GDF and the GDCDE are more likely to identify

http://www.aloki.hu ● ISSN 1589 1623 (Print) ● ISSN 1785 0037 (Online)
DOI: http://dx.doi.org/10.15666/aeer/1704_87138735

"organizational and administrative factors" as "the most important factors affecting success" when compared with those working at the GDNCNP (*Table 9*).

The understanding of success of technical staff is toward achieving the goals through efficient use of resources. The common understanding about organizational success could contribute to coordination and cooperation in the forestry organization. Besides the participants evaluated organizational and administrative factors as the most important factor that affects the organizational success. The forest organization's structure is very complex and had changed many times in the historical period. This situation is seen as the source of many forestry-related problems. Also it is seen that it has effect on organizational success. Thus forming an effective organizational structure and administrative system seem to be a prominent aspect in terms of increasing the success of the organization.

Table 8. *Attitudes of participants about administrative success in forestry*

Attitudes	Scale	Percentages of attitudes (%)			
		Staff	Experts	Representatives of Related Institutions	Representatives of NGOs
1. Mentality of administrative and organizational success	a) Maximization of profit	1	0	3	0
	b) Maximization of goods and services production	2	3	3	3
	c) Producing highest output from the least input	6	0	6	5
	d) Achieving the goals through efficient use of resources	74	76	63	81
	e) Producing the highest amount of goods and services through the market demand	3	3	10	0
	f) Fulfilling the need of society regarding forest resources	7	12	6	0
	g) Other	7	6	9	11
2. Most important factors affecting success	a) Physical factors (forest area, forest stock, forest productivity, road density etc.)	4	3	-	-
	b) Economic and financial factors	4	0	-	-
	c) Socio-economic factors	18	15	-	-
	d) Technical factors (technical knowledge, number of machines etc.)	7	0	-	-
	e) Organizational and administrative factors (organizational structure, efficiency of managers, number and training of staff etc.)	56	73	-	-
	f) Ecological and geographical factors (location, climate, soil etc.)	5	9	-	-
	g) Other	6	0	-	-
2. Attitudes on success measurement of forestry organization	a) Assessment and Evaluation Unit that will be established under Ministry or General Directorate should measure the organizational success by using some objective criteria and depending on the records of the organizations.	49	67	-	54
	b) Register managers should measure the success by scoring the staff utilizing criteria of standard forms.	10	3	-	6
	c) The success of the staff should be measured by examination and supervision system that will be managed by an expert commission	27	24	-	24
	d) Other	14	6	-	16

http://www.aloki.hu ● ISSN 1589 1623 (Print) ● ISSN 1785 0037 (Online)
DOI: http://dx.doi.org/10.15666/aeer/1704_87138735

Forty-nine percent of the employees, 67% of the experts and 54% of the NGO representatives stated that organizational success should be considered when they were asked about *"success measurement system for organizational structure success (performance)"* (*Table 8*). No significant difference depending on region, department, position and experience can be found relating to this issue *(Table 9*).

Table 9. *Difference of participants' attitudes on administrative success mentality depending on region, department, position and experience*

Attitudes	Kruskal-Wallis H-Test Results			Identify differences by Duncan Test (Groups and in-group components are ranked as to their significance level)			
	Criteria	Khi-square value	SD	Groups with significant differences			
				No	Component of the groups	$\overline{X}$	N
1. Mentality of administrative success in forestry	There is no significant difference with respect to region, department and position.					--	--
	Experience	13.78**	3	1	Staff with low, high and very high experience (0 -10 years and ≥21 years)	51.36	346
				2	Staff with medium experience (11-20 years)	64.04	117
2. Most important factors affecting success	There is no significant difference with respect to region, position and experience.					--	--
	Department	6.54*	2	1	GDNCNP	29.34	53
				2	GDF, GDCDE	42.11	410
3. Attitudes on success measurement system	There is no significant difference with respect to region, department, position and experience.					--	--

Success measurement system is an important lack which has direct relations with the performance of staff and whole organization. While improving the system as the participants emphasized objectivity should be the essential principle. In other case the staff would develop a negative attitude towards the organizational justice.

Results Related to Motivation and Reward

Motivation has a great role on employees' willingness of fulfilling their tasks (Newman, 1972). Therefore, to increase the motivation of the employees shall increase the success. In this part of the study, the participants were asked their attitudes about the relationship between the success at work and designation, promotion and reward, what should be done to raise the motivation of the employees and accordingly to increase the success and how the performance measuring system should be within the structure of the organization. The answers by the participants were indicated in *Table 10* and the question whether participants' thoughts differ depending on region, department, position and experience was statistically analyzed (*Table 11*).

Fifty-three percent of the employees answered "there is no relationship", 25% answered "there is a slight positive relationship" and 14% answered "there is an inverse relationship" the question "*Is there a relationship between your success at work and designation, promotion, appreciation, premium and being rewarded?"* The rate of those who find "very close relationship" is just 8%. The answers of the experts for the same question are as follows: 49% "there is a slight positive relationship", 27% "there is no relationship" and 3% "there is an inverse relationship" (*Table 10*). The difference of region and position has no significant effect on the participants' attitudes. However, it has been concluded that different departments (95% reliability) and different job experiences (99% reliability) have a significant effect on the issue. Employees working

http://www.aloki.hu ● ISSN 1589 1623 (Print) ● ISSN 1785 0037 (Online)
DOI: http://dx.doi.org/10.15666/aeer/1704_87138735

at the GDF generally think that there is no relationship between success and promotion or being rewarded whereas, the GDNCNP and the GDCDE employees generally think that there is a slight positive relationship. On the other hand, employees with high and quite high job experience (≥21 years) find no relationship while less and medium-experienced ones (0-20 years) generally think that there is a slight positive relationship (*Table 11*).

Table 10. *Participants' attitudes about motivation and reward*

Attitudes	Scale	Percentages of attitudes (%)			
		Staff	Experts	Representatives of Related Institutions	Representatives of NGOs
1. Relationship between the success and designation, promotion, premium, being appreciated and being rewarded	a) There is a negative relation	14	3		
	b) There is not any relation.	53	27		
	c) There is a low-level positive relation	25	49		
	d) There is a high-level positive relation	8	21		
2. Opportunities of raising the motivation / success of staff	a) Premium should be paid	15	18	13	5
	b) Staff should be promoted	5	3	0	0
	c) Designation should be made in accordance with the preference of the staff	7	0	3	0
	d) Staff should be appreciated	14	18	3	8
	e) The attitudes of the staff should be considered and they should participate in decision-making processes	42	55	72	65
	f) Staff should be joined to national and international vocational trips	4	0	3	0
	g) Other	13	6	6	22

Forty-two percent of the employees, 55% of the experts, 72% of the relevant institution representatives and 65% of the NGO representatives answered the question *"What should be done in order to raise the motivation/increase the success of the employees in forestry sector?"* as "their attitudes should be considered and they should participate in decision-making processes" (*Table 10*). This approach was found to be dominant in all interest groups. No significant difference depending on region, department, position and experience can be found relating to this issue (*Table 11*).

This is one of the very critical results of the study. As the staff mentioned without contacting the success with designation, promotion, premium, being appreciated and being rewarded then the system could be evaluated as unjust by the staff. Also it's understood that the staff evaluated participation in decision making process and consideration of their attitudes as the main factor in rising the motivation and success. It should be considered in the context of national level policies on both decision making process and human resources management. Providing active participation of the staff would also support the participatory management mechanism which is also a lack for Turkish forestry. This result could also be a starting point of the new researches regarding administration and organizational behavior related studies for the country and the similar countries.

http://www.aloki.hu ● ISSN 1589 1623 (Print) ● ISSN 1785 0037 (Online)
DOI: http://dx.doi.org/10.15666/aeer/1704_87138735

Table 11. *Difference of participants' attitudes about motivation and reward depending on region, department, position and experience*

Attitudes	Kruskal-Wallis H-Test Results			Identify differences by Duncan Test (Groups and in-group components are ranked as to their significance level)			
	Criteria	Khi-square value	SD	Groups with significant differences			
				No	Component of the groups	$\overline{X}$	N
1. Relationship between the success and designation, promotion, premium, being appreciated and being rewarded	There is no significant difference with respect to region and position.					--	--
	Department	8.73*	2	1	GDF	0.22	405
				2	GDNCNP, GDCDE	0.57	58
	Experience	12.82**	3	1	Staff with low and medium experience (0 -20 years)	0.37	238
				2	Staff with high and very high experience (≥21 years)	0.11	225
2. Opportunities of raising the motivation / success of staff	There is no significant difference with respect to region, department, position and experience.					--	--

Discussion

The results of the study are important in terms of contribution of related national policy making process. Also the results contribute to analyze regional differences and gives opportunity to focus on local level decisions. Both the national and regional level findings can guide to the countries where the forests are publicly managed. Also the results represent the problems and trends of the forestry organizations that have complex organizational structure and managed centrally. Thus the study contributes to international literature and expresses decision makers in national and regional level managers of forestry organizations which have public institution characteristics.

In the study, the most important factors (education and self-development, administrative competence, success mentality, motivation and rewarding) affecting administrative and organizational success in the forest resource management of Turkey were analyzed and evaluated from the perspectives of staff, experts, representatives of related institutions and NGOs. According to the results, a great majority of the participants' think the undergraduate education is insufficient. However, it is seen that as the task duration increases the belief on the education provided by the faculties be sufficient increases as well. It is known that the rate of courses with socioeconomic content, accordingly socioeconomic aspect, is more important in forestry education and training in countries where modern forestry understanding is dominant (Geray, 1991, 1993; Lorincová et al., 2016). In some of the researches conducted in the country (İnal, 1968; Kalıpsız et al., 1969; Pamay et al., 1973; Çepel, 1984; Daşdemir, 1998), it has been determined that forest engineers mostly need courses with socioeconomic content whereas courses related to management and organization, public relations, decision-making methods and scientific research methods dominate provided education. The rate of the courses with socioeconomic content in the curriculum of forestry education in some of the universities in the USA, Australia and Sweden, differs from 23% to 36% while this rate is only 14 %-17% in Turkey (Elands et al., 2004). Therefore, the education system given in the forest faculties should be rearranged as compatible with contemporary forestry approach by considering the attitudes of all partners on the issue, particularly applied training and courses with socioeconomic content should be focused on.

http://www.aloki.hu ● ISSN 1589 1623 (Print) ● ISSN 1785 0037 (Online)
DOI: http://dx.doi.org/10.15666/aeer/1704_87138735

A large part of the participants' state prevocational and in-service training activities to be insufficient which suggests that prevocational and in-service training activities related to the profession should focus on self-improvement of administrators and technical staff besides being solution-oriented. It is observed that former studies had come a similar conclusion (Yurdakul, 2005; Şenyaz, 2008; Şafak, 2008).

Turkey forestry organization has encountered structural changes for several times due to political decisions that are not based on scientific foundations and that lack of participation principle and consequently the problems with administration, organization, planning, supervision etc. has increased and it has encountered problems in achieving organizational goals. Whereas it is necessary to increase the number of those who actually run the business within this context, it is seen that the number of senior managers had raised and the majority of the staff had gathered at the central organization.

Most of the employees, experts, relevant institution representatives and NGO representatives state that "the employees' attitudes should be considered and they should participate in decision-making processes" when the issue *"What should be done in order to raise the motivation/increase the success of the employees in forestry sector?"* is asked. No significant difference depending on region, department, position and experience can be found related this issue. In a study carried out among the technical staff employed at the İstanbul Regional Directorate of Forestry (Yurdakul Erol, 2017; Yurdakul Erol and Köse, 2017); the most satisfying factor is stated to be "the characteristic of the job to enable someone to do something for others". The second most satisfying component about the occupation is stated to be that "the job gives a chance to be a respectable person in the society". "To be able to find the opportunity to guide people" and "employment security" are also found to be other satisfying points of the occupation. As it can be understood from these results, regarding the employees' attitudes, participation in decision-making processes, the idea of being socially beneficial and the desire to be respected in the society should be used as means of motivation in forestry organization.

Organizational success (performance) is a multi-dimensional concept that indicates the level of achievement to organization goals according to contemporary management approach. Performance measurement systems that are not well designed prevent the organization from successfully adapting to the competitive environment. Because, performance measurement with incorrect methods leads to a reduction in the accuracy of the data that will support the application. In this context, it has been concluded that Measurement and Evaluation Center for Success to be established under Ministry or General Directorate should measure the organizational success by using some objective criteria and depending on the records of the organizations. This shows that the presence of a system based on entirely objective criteria without discrimination (attitudes, beliefs, race etc.) is preferred by the employees. Consequently, success measurement system which will be applied in this manner should form the basis for the institutional structure of forestry organization in Turkey and for promoting organizational success.

Conclusion

To achieve organizational success, determination of related problems by considering both internal and external stakeholders is an essential aspect for Turkish forestry. Also

http://www.aloki.hu ● ISSN 1589 1623 (Print) ● ISSN 1785 0037 (Online)
DOI: http://dx.doi.org/10.15666/aeer/1704_87138735

focusing on differences between the stakeholders and regions supports development of specific and solution-oriented decisions and implementations.

Especially education and training is one of the important factors that affect the organizational success as an instrument. Insufficiency about knowledge on socio-economic issues was found out and then the observed prominent problems were parallel to this content. Besides, the interaction between scientific researches and forestry organization is the other key factor what could have direct affect on improvement of forestry organizations' success. The Turkish forestry experience also showed that the foremost factor that affects organizational success is related with organizational and administrative issues. The role of participatory management and objective performance measurement system was considered as the main components of success in Turkish forestry organization. These issues should be considered in forestry-related national level policy and strategy making processes immediately. Further, focusing on region and local level properties could increase the success of implementations of these policies and strategies.

Acknowledgements. This study was produced in the context of the research project entitled "Development of Alternative Organizational Models for Turkish Forestry" and numbered 10.5301/2014-2017 which was supported by the General Directorate of Forestry and directed by the Marmara Forestry Research Institute.

REFERENCES

[1] Akal, Z. (2005): Performance Measurement and Control in Business (Multiple Performance Indicators). – National Productivity Center, Publication No: 473, 368 p., Ankara (in Turkish).

[2] Aktan, Ü. (2013): Private forestry consulting firms and their effect on forest engineer employment. – Artvin Çoruh University, Graduate School of Natural and Applied Sciences, Department of Forest Engineering, Master Thesis 76 p., Artvin (in Turkish).

[3] Albuquerque da Silva, B., Guerra Gomes, N. M., Skowronski, L., Constantino de Oliveira, M. A., Brito da Costa, R. (2016): Multiple uses of forest resources in small and medium farms in the tropics: Economic and social contributions. – African Journal of Agriculture Research 11(41): 4162-4171.

[4] Baynes, J., Herbohn, J., Smith, C., Fisher, R., Bray, D. (2015): Key factors which influence the success of community forestry in developing countries. – Global Environmental Change 35: 226-238.

[5] Burns, S. L., Giessen, L. (2016): Dismantling comprehensive forest bureaucracies: Direct access, the World Bank, agriculture interests, and neoliberal administrative reform of forest policy in Argentina. – Society and Natural Resources 29(4): 493-508.

[6] Çepel, N. (1984): Relationship between forestry teaching and practice. – İstanbul University, Journal of Faculty of Forestry, Series B 34(1): 34-44. İstanbul (in Turkish).

[7] Daşdemir, İ. (1996): Determination of success levels in state forest enterprises (Example of North-East Anatolia and Eastern Black Sea Regions). – Ministry of Forestry, Eastern Anatolia Forestry Research Institute, Technical Bulletin No: 1, 161 p., Erzurum (in Turkish).

[8] Daşdemir, İ. (1998): Determination of Administrative and Organizational Dimensions of State Forest Districts. – Ministry of Forestry Eastern Anatolia Forestry Research Directorate, Technical Report Publication Number: 3, ISSN 1300-9486, 70 p., Erzurum (in Turkish).

http://www.aloki.hu ● ISSN 1589 1623 (Print) ● ISSN 1785 0037 (Online)
DOI: http://dx.doi.org/10.15666/aeer/1704_87138735

[9] Daşdemir, İ. (2016): Scientific Research Methods. – Nobel Academic Publishing and Consulting, Publication No: 1536, ISBN 978-605-320-442-8, 210 p, Ankara (in Turkish).
[10] Elands, B. H. M., O'Leary, T. N., Boerwinkel, H. W. J., Wiersum, K. F. (2004): Forests as mirror of rural conditions; local views on the role of forests across Europe. – Forest Policy and Economics 6: 469-482.
[11] Geray, A. U. (1991): Where are we at contemporary forestry education? – Chamber of Forest Engineers, Journal of Forest Engineering, February Count: 27-31. Ankara (in Turkish).
[12] Geray, A. U. (1993): Development and problems of forest resources management. I. Forestry Council. – Ministry of Forestry Publication No: 6, Series No: 13, Volume: 3: 137-149. Ankara (in Turkish).
[13] Gümüş, S., Beşir, S. (2012): The effect of motivation on organizational commitment and performance. – Hiperlink, ISBN 978944157513, 143 p., İstanbul (in Turkish).
[14] Gümüş, C. (2014): Effects of forestry policies from ottoman to present on forestry organization and current issues. – II. National Mediterranean Forest and Environment Symposium, 22-24 October, pp.477-489, Isparta (in Turkish).
[15] Hajjar, R., Oldekop, J. A. (2018): Research frontiers in community forest management. – Current Opinion in Environmental Sustainability 32: 119-125.
[16] Hansmann, R., Kilchling, P., Seeland, K. (2016): The effects of regional forest owner organizations on forest management in the Swiss Canton of Lucerne. – Small-scale Forestry 15(2): 159-177.
[17] Hasanagas, N. D. (2014): Managing information in forest policy networks: Distinguishing the influential actors from the "postmen". – Forest Policy and Economics, http://dx.doi.org/10.1016/j.forpol.2014.09.007, Haugaard.
[18] Imamura, K. (1982): Human Resources in Japanese Forestry. – Unasylva No: 135.
[19] İnal, S. (1968): Forestry Higher Education in Turkey. – İstanbul University, Faculty of Forestry Publication No:1210/123, İstanbul (in Turkish).
[20] Kalıpsız, A., Gülen, İ., Tokmanoğlu, T. (1969): Report on education and education problems and solutions of forestry faculty of Istanbul University. – İstanbul (in Turkish).
[21] Kaplan, S. (1998): Are there problems in forestry management? – Forest and Hunting Journal 151: 22. Ankara (in Turkish).
[22] Kim, Y.-S., Bae, J. S., Fisher, L. A., Latifah, S., Afifi, M., Lee, S. M., Kim, I.-A. (2016): Indonesia's Forest Management Units: Effective intermediaries in REDD+ implementation? – Forest Policy and Economics 62: 69-77.
[23] Krott, M. (2005): Forest Policy Analysis. – Springer, ISNB 978-1-4020-3478-7 323 p. Netherlands.
[24] Lorincová, S., Hitka, M., Čambál, M., Szabó, P., Javorčiková, J. (2016): Motivational factors influencing senior managers in the forestry and wood-processing sector in Slovakia. – BioResources 11(4): 10339-10348.
[25] Lyons, K., Wlaters, P., Riddell, E. (2016): The role of faith-based organizations in Environmental governance: The case of Forestry in Solomon Islands. – Journal of Environmental Policy and Planning 18(3): 342-360.
[26] MacDicken, H. G., Sola, P., Hall, J. E., Sabogal, C., Tadoum, M., Wasseige, C. (2015): Global progress toward sustainable forest management. – Forest Ecology and Management 352: 47-56.
[27] Mendes, A. M. S. C. (2006): Implementation analysis of forest programs: some theoretical notes and an example. – Forest Policy and Economics 8(5): 512-528.
[28] MFWA (2016): Staffs records of the Ministry of Forestry and Water Affairs for 2016 year. – Ankara (in Turkish).
[29] Miteva, D. A., Loucks, C. J., Pattanayak, S. K. (2015): Social and environmental impacts of forest management certification in Indonesia. – PLoS ONE 10(7): 1-18.
[30] Newman, W. H. (1972): Management in Business and Public Administration. – Sevinç Printing Press, 529 p., Ankara.

http://www.aloki.hu ● ISSN 1589 1623 (Print) ● ISSN 1785 0037 (Online)
DOI: http://dx.doi.org/10.15666/aeer/1704_87138735

[31] Orhunbilge, A. N. (2000): Sampling Methods and Hypothesis Testing (Review and Expanded Second Edition). – Avcıol Printing & Publishing, 420 p., İstanbul (in Turkish).
[32] Özdönmez, M., Akesen, A., Ekizoğlu, A. (1998): Forestry Management Knowledge. – İstanbul University, Faculty of Forestry Publication No: 4157/457, Dilek Offset Printing, 357 pp., İstanbul (in Turkish).
[33] Pamay, B., Kalıpsız, A., Gülen, İ. (1973): Offers on organizing and working principle of forestry research in Turkey. – İstanbul University, Journal of Faculty of Forestry, Series B, Volume XXIII, Number 2, İstanbul (in Turkish).
[34] Pinstrup-Andersen, P., Pandya-Lorchi, R. (1998): Food security and sustainable use of natural resources: a 2020 vision. – Ecological Economics 26(1): 1-10.
[35] Sanchez Badini, O., Hajjar, R., Kozak, R. (2016): Critical success factors for small and medium forest enterprises: A review. – Forest Policy and Economics 94: 34-45.
[36] Schmithüsen, F. (1983): Human Resources Formation: The Weak Link in Forestry Development. – Unasylva No: 142.
[37] Szaro, R. C., Langor, D., Yapi, A. M. (2000): Sustainable forest management in developing world: science challenges and contributions. – Landscape and Urban Planning 47(3-4): 135-142.
[38] Şafak, İ. (2008): Profile of forest engineers in Aegean region. – Journal of Chamber of Forest Engineers 45(10-11-12): 22-26. Ankara (in Turkish).
[39] Toksoy, D., Bayramoğlu, M., Ayaz, H. (2011): A Research on the organizational and organizational problems of forest engineers in forestry. – Kahramanmaraş Sütçü İmam University, Journal of Natural Sciences, Special Issue: 180-184. Kahramanmaraş (in Turkish).
[40] Torres-Rojo, J. M., Moreno-Sánchez, R., Mendoza-Briseño, M. A. (2016): Sustainable forest management in Mexico. – Curr Forestry Rep 2: 93-105.
[41] Tumpach, C., Dwivedi, P., Izlar, R., Cook, C. (2018): Understanding perception of stakeholder groups about Forestry Best Management Practices in Georgia. – Journal of Environmental Management 213: 374-381.
[42] Wibowo, A., Giessen, L. (2015): Absolute and relative power gains among state agencies in forest related land use politics: The Ministry of Forestry and its competitors in the REDD+ Programme and the One Map Policy in Indonesia. – Land Use Policy 49: 131-141.
[43] Wiley, C. (1997): What motivates employees according to over 40 years of motivation surveys? – International Journal of Manpower 18(3): 263-280.
[44] Yurdakul, S. (2005): Human resources management problems and results in forestry organization (discussing sample cases). – Istanbul University, Journal of Faculty of Forestry, Series A 55(1): 161-185. İstanbul (in Turkish).
[45] Yurdakul Erol, S. (2017): Various evaluations on human resources management in forestry in Turkey and the state of technical forestry staff. – Current Trends in Science and Landscape Management. ISBN 978-954-07-4338-7, St. Kliment Ohridski University Press, Sofia, 543-561.
[46] Yurdakul Erol, S., Köse, M. (2017): Job satisfaction of forestry technical staff: the case of İstanbul Regional Forestry Directorate. – Kastamonu University, Journal of Faculty of Economics and Administrative Sciences 18(1) ICEBSS 2017 Special Issue: 273-286. Kastamonu.

http://www.aloki.hu ● ISSN 1589 1623 (Print) ● ISSN 1785 0037 (Online)
DOI: http://dx.doi.org/10.15666/aeer/1704_87138735

FARMERS' HOUSEHOLD WASTE DISPOSAL BEHAVIOR AND ITS INFLUENCING FACTORS IN DEVELOPING COUNTRIES: EVIDENCE FROM JIANGSU, CHINA

LIU, R.[1] – WANG, Y.[2*]

[1]*School of Economics and Management, Beijing University of Chemical Technology*
Beijing 100029, China
(phone: +86-010-6444-8681; fax: +86-010-6444-8681)

[2]*Department of Aviation Safety Management, Civil Aviation Management Institute of China*
Beijing 100102, China
(phone: +86-010-5622-5603; fax: +86-010-5622-5603)

[*]*Corresponding author*
e-mail: 405279930@qq.com

(Received 8th Mar 2019; accepted 1st May 2019)

Abstract. The improper disposal of household waste is a major reason for the deterioration of rural ecological environment in developing countries. As the main producer of rural household waste, farmers' behavior is very important to solve the problem. Based on the data of 671 surveys in Jiangsu, China, the influencing factors of farmers' household waste disposal behavior and their hierarchical relationships were determined by Logit-ISM model. The study finds that there are 7 factors that significantly affect household waste disposal behavior of farmers, among which Major domestic fuel, Clearance of centralized waste dump site and Neighbor's way of disposing household waste are the surface factors; Identifying capacity for pollutants, Major economic source and Availability of centralized waste disposal facility are the intermediate factors; Fixed-point waste disposal policy and its implementation effect is the deep- rooted factor.
Keywords: *farmer household behavior, Lewin's behavior model, Logit model, ISM method, sorted reachability matrix, interpretative structure model*

Introduction

The construction of ecological civilization has increasingly become a hot topic of common concern to mankind. All countries in the world are committed to exploring the road of harmonious coexistence between human and nature. Due to the dominant position of developed countries, relevant organizations and associations mainly focused on the prevention and control of industrial pollution and urban pollution (Petraru and Gavrilescu, 2010; Gong et al., 2019), and less on rural environmental issues. However, for the vast majority of developing countries, rural areas are the largest hinterland of biological resources, carrying the majority of the country's population. Construction of rural ecological civilization occupies a more fundamental position. In the past, kitchen residues were the main part of rural household waste, which was recycled reasonably, resulting in little pollution to the surrounding environment. In recent years, with the rise of the economy in developing countries, the consumption structure of rural residents has changed greatly. As a result, the composition of rural household waste becomes more complex. Plastic products, electronic waste and other non-decomposable items are becoming more common (Hakami and Seif, 2015; Du et al., 2018). The original self-purification ability of rural areas can hardly play an effective role. The impact of household waste on rural ecological environment is becoming increasingly serious.

http://www.aloki.hu ● ISSN 1589 1623 (Print) ● ISSN 1785 0037 (Online)
DOI: http://dx.doi.org/10.15666/aeer/1704_87378748

This phenomenon is particularly prominent in China. Due to the long-standing views of farmers, it is quite common for waste to be dumped at will, resulting in serious soil pollution (Zeng et al., 2018), water pollution (Zhang et al., 2013) and air pollution (Jin et al., 2006). Ultimately, the health of villagers has been damaged. It can be seen that the control of household waste discharge arbitrarily is a very important task. However, the current rural household waste management method is a government-dominant model, which marginalizes farmers and makes them spectators, passives and even adversaries. It needs to be deeply realized that farmers are not only the producers of household waste, but also the direct victims of the pollution. Farmer should be the core subject of the governance of rural environmental problems. However, previous studies mainly focused on the productive environmental behavior of farmers, and paid less attention to the impact of farmers' daily life behavior on the environment.

This paper analyses the impact of farmers' daily life behavior on the environment from their perspective, which is not only related to the quality of life of 900 million rural populations in China, but also directly affects the sustainable development of China's economy. Meanwhile, as a representative of developing countries, China's rural household waste disposal problem is a microcosm of the same problem in developing countries. This study can provide new ways for other developing countries to promote rural ecological environment construction.

Theoretical basis and variable selection

Theoretical basis

Since the 1960s, the process of industrialization and urbanization has been accelerating. Environmental protection has gradually become a consensus of mankind. Sociological circles have begun to pay close attention to this problem. In 1978, American sociologists Catton and Dunlap published their paper *Environmental Sociology: A New Paradigm*, which clearly pointed out that Environmental Sociology should focus on the interaction between environment and human society. Subsequently, the famous Japanese sociologist Torigoe Hiroyuki emphasized that the subject of environmental pollution is human itself. Meanwhile, Kurt Lewin pointed out that individual behavior is the product of the interaction between individual and environment. He put forward the famous Lewin behavior model, namely $B = F(P, E)$, in which B is human behavior; P is the internal condition and characteristics of an individual, E refers to the external environment. Lewin's behavior model provides a solid theoretical basis for people to explore human behavior including environmental behavior.

Variable selection

With the comprehensive study of scholars, based on Lewin behavior model, this paper analyses the influencing factors of farmers' household waste disposal behavior from the perspectives of personal and environment. Personal factors can be divided into physiological characteristics and psychological characteristics. Physiological characteristics are age, gender and cadre status; psychological characteristics include recognition of fixed-point waste disposal, perception of the surrounding environment, and knowledge of environmental protection. Environmental factors can be divided into family environment, social environment and natural environment. Family environment

http://www.aloki.hu ● ISSN 1589 1623 (Print) ● ISSN 1785 0037 (Online)
DOI: http://dx.doi.org/10.15666/aeer/1704_87378748

includes education environment and business environment; social environment includes propaganda and education, incentive and punishment, policy system, organizational setting, infrastructure and social culture; natural environment in this paper mainly refers to geographical location. Variable selection and measurement are shown in *Table 1*.

Table 1. *Variable selection and measurement*

Variable		Variable measurement and assignment
X1	Sex (Schahn and Holzer, 1990)	Male=0; Female=1
X2	Age(Yang et al., 2017)	18-24 years old=1; 25-34 years old=2; 35-44 years old=3; 45-54 years old=4; 55-64=5
X3	Cadre status(Yang et al., 2017)	Yes=0; No=1
X4	Cognition of the necessity of fixed-point disposal of waste (Bamberg, 2003; Oyekale, 2018)	Absolutely unnecessary=0; Unnecessary=1; Uncertainty=2; Necessary; Extremely necessary=3
X5	Cognition of the hazard of household waste disposal at will (Yokoo et al., 2018)	No influence=0; Less influence=1; Uncertainty=2; Some influence=3; Great influence=4
X6	Satisfaction degree of the sanitary environment of your villages(Wang and Kang, 2019)	Extremely satisfactory=0; Basic satisfactory=1; Uncertainty=2; Dissatisfaction=3; Extremely unsatisfactory=4
X7	Attention to environmental protection information(Arcury, 1990; Estrada et al., 2017)	Attention at all times=0; Constant attention=1; Occasional attention=2; Little attention=4
X8	Identifying capacity for pollutants(Milfont, 2012)	Extremely agree=0; Basic agree=1; Uuncertainty=2; Disapproval=3; Extremely disapproval=4
X9	Family educational level(Poortinga et al., 2003; Ma et al., 2009)	Uneducated=1; Primary=2; Junior=3; Senior/ Secondary=4; College/Undergraduate=5; Graduate and above=6
X10	Family annual income(Dorina, 2016)	Less than 50K=1; 50-100K=2; 100-150K=3; 150-200K=4; 200K or more=5 (1K=1000CNY)
X11	Number of migrant workers(Jiang and Yuan, 2013)	According to the specific data value of the survey
X12	Major domestic fuel(Han et al., 2018)	Coal=Wood=Straw and other wilting crops=0; Liquefied gas=Electricity=1
X13	Major economic source(Ma et al., 2009)	Farming income=0; Wage income=1
X14	Advocacy on the benefits of designated waste disposal(Steg, 2008; Hakami and Seif, 2015)	Frequent publicity=0; Occasional publicity=1; Unclear=2; Seemingly no=3; Completely no=4
X15	Call for fixed-point waste disposal(Miliute-Plepiene et al.,2016; Seacat and Boileau, 2018)	Frequent call=0; Occasional call=1; Unclear=2; Seemingly no=3; No call at all=4
X16	Management of discarding waste at will(Li et al., 2016)	Ignorance=0; Verbal warning=1; Notification of criticism=2; Fine=3
X17	Fixed-point waste disposal policy and its implementation effect(Refsgaard and Magnussen, 2009; D'Amato et al., 2016)	Yes, the implementation effect is good=0; Yes, but the implementation effect is not good=1; Yes, but no specific implementation=2; Not very clear=3; No relevant measures=4
X18	Inspection of fixed-point waste recycling(Hage et al., 2018)	Frequent check=0; Occasional check=1; Unclear =2; As if no check=3; No check at all=4
X19	Setting up of professional waste disposal departments or full-time personnel(Guagnano et al., 1995)	Never=0; Occasionally=1; Always=2
X20	Availability of centralized waste disposal facility (Young et al., 1990; Abbott et al., 2013)	Yes=0; No=1
X21	Distance to centralized waste disposal facilities(Jenkins et al., 2003; Struk, 2017)	Very close=0; Slightly distant=1; Far away=2
X22	Clearance of centralized waste dump site (Kuo and Perrings, 2010; Lee et al., 2017)	Irregular, Long intervals=0;Regular, low frequency=1;Regular, high frequency=2
X23	Neighbor's way of disposing household waste (Videras et al., 2012; Czajkowski et al., 2017)	Throw it in front of or behind the house=Pour into the riverside, roadside or ditch=Open storage=Open burning=Landfill nearby=0; Use waste as fertilizer=Sell off after classification =Transport to designated waste pool=1
X24	Distance to the city center(Huang et al., 2012)	Very close=0;Slightly distant=1;Far away=2

http://www.aloki.hu ● ISSN 1589 1623 (Print) ● ISSN 1785 0037 (Online)
DOI: http://dx.doi.org/10.15666/aeer/1704_87378748

Sample characteristics and research method

Sample characteristics

The data used in this study are from the field survey of 128 administrative villages in 13 cities of Jiangsu. 800 questionnaires were sent out and 726 were recovered. After eliminating the invalid information questionnaire, 671 valid questionnaires remained, with an effective rate of 83.9%. According to the basic characteristics of the sample, 453 were women, accounting for 68%; population under 35 years old accounted for 72%; family members with the highest degree of university or above accounted for 35%; nearly half of the annual family income is 50,000-100,000 CNY. The household waste disposal behavior of sample farmers is shown in *Fig. 1*. Generally speaking, majority of rural households can properly dispose of household waste.

Research method

Logit model

There are two ways for household garbage disposal: random and proper, which belong to the typical binary variables. Therefore, Logit Model should be adopted. The derivation of the model is as follows. The actual reaction variable is y_k, with a value of 0 and 1. Explanatory variables are represented by x_k, and error is represented by ε_k. Assuming that there is a linear relationship between y_k^* and x_k, namely (*Eq. 1*)

$$y_k^* = \alpha + \beta x_k + \varepsilon_k \quad \text{(Eq.1)}$$

There is a critical point c, when $y_k^* > c$, then $y_k=1$, when $y_k^* \leq c$, then $y_k=0$. Assuming that the critical point $c = 0$, the error term ε_k obeys Logistic distribution and its cumulative distribution function is $F(.)$, and p_k is the probability of occurrence of case k, there is (*Eq. 2*):

$$\begin{aligned} p_k = P(y_k = 1 | x_k) &= P[(\alpha + \beta x_k + \varepsilon_k) \rangle 0] \\ &= P(\varepsilon_k \langle \alpha + \beta x_k) \\ &= F(\alpha + \beta x_k) \\ &= \frac{exp(\alpha + \beta x_k)}{1 + exp(\alpha + \beta x_k)} \end{aligned} \quad \text{(Eq.2)}$$

After logarithmic transformation, the above formula can be transformed into *Eq. 3*:

$$ln\left(\frac{p_k}{1 - p_k}\right) = \alpha + \beta x_k \quad \text{(Eq.3)}$$

Among them, p_k is the probability of occurrence of case k. It is a non-linear function consisting of the explanatory variable x_k. When there are N independent variables, the binary regression model and its logarithmic transformation are shown in *Eq. 4* and *Eq. 5*, respectively.

http://www.aloki.hu ● ISSN 1589 1623 (Print) ● ISSN 1785 0037 (Online)
DOI: http://dx.doi.org/10.15666/aeer/1704_87378748

$$p_k = P\left(y_k = 1 \middle| x_{1k}, x_{2k}, ..., x_{nk}\right) = \frac{exp\left(\alpha + \sum_{n=1}^{N} \beta_n x_{nk}\right)}{1 + exp\left(\alpha + \sum_{n=1}^{N} \beta_n x_{nk}\right)} \quad \text{(Eq.4)}$$

$$\ln\left(\frac{p_k}{1 - p_k}\right) = \alpha + \sum_{n=1}^{N} \beta_n x_{nk} \ (k=1, 2... K, n=1, 2... N) \quad \text{(Eq.5)}$$

For this study, p is the probability of household waste disposal properly, 1-p is the probability of household waste disposal randomly; α is the constant of regression equation of various factors; β_i is the coefficient of regression equation of various factors; x_i is a variety of influencing factors; n is the number of influencing factors. Maximum likelihood (ML) is generally used to estimate the parameters. For case i, there is a distribution function (*Eq. 6*):

$$p\left(Y_i\right) = p_i^{Y_i}\left(1 - p_i\right)^{1-Y_i} \quad \text{(Eq.6)}$$

Then the logarithmic likelihood function is (*Eq. 7*):

$$\begin{aligned} l(\beta) &= \sum_{i=1}^{n}\left(Y_i \ln p_i + (1 - Y_i)\ln(1 - p_i)\right) \\ &= \sum_{i-1}^{n}\left(Y_i \ln \frac{p_i}{1 - p_i} + \ln(1 - p_i)\right) \\ &= \sum_{i=1}^{n}\left(Y_i(X_i\beta) - \ln(1 + exp(X_i\beta))\right) \end{aligned} \quad \text{(Eq.7)}$$

In order to estimate the value of β, we can derive the partial derivative of $l(\beta)$ over β and make it equal to 0 (*Eq. 8*):

$$\begin{aligned} \frac{\partial l(\beta)}{\partial \beta_1} &= \sum_{i=1}^{n}\left(Y_i - \frac{X_i\beta}{1 + exp(X_i\beta)}\right) = 0 \\ \frac{\partial l(\beta)}{\partial \beta_j} &= \sum_{i=1}^{n}\left(Y_i - \frac{X_i\beta}{1 + exp(X_i\beta)}\right) X_{ji} = 0, \ j = 2, ..., k \end{aligned} \quad \text{(Eq.8)}$$

ISM method

ISM method can transform vague ideas into well-structured models by using people's knowledge as well as the help of computer (Warfield, 1974). The main steps of ISM method are as follows. Step 1: Drawing the corresponding digraph according to Boolean operation. Then, constructing adjacent matrix A. Where a satisfies *Eq. 9*. Step 2: Establishing the reachable matrix M. Operations are defined as *Eq. 10*. Step 3: Obtaining reduced matrix of reachable matrix. Step 4: The reduced matrix is processed hierarchically, and the interpretative structure model is obtained.

http://www.aloki.hu ● ISSN 1589 1623 (Print) ● ISSN 1785 0037 (Online)
DOI: http://dx.doi.org/10.15666/aeer/1704_87378748

$$a_{ij} = \begin{cases} 1, S_i RS_j, R\ says\ S_i\ has\ a\ relationship\ with\ S_j \\ 0, S_i \overline{RS}_j, \overline{R}\ says\ S_i\ has\ no\ relationship\ with\ S_j \end{cases} \quad \text{(Eq.9)}$$

$$if\ (A+I)^r = (A+I)^{r+1} \neq (A+I)^{r-1}, M = (A+I)^r \quad \text{(Eq.10)}$$

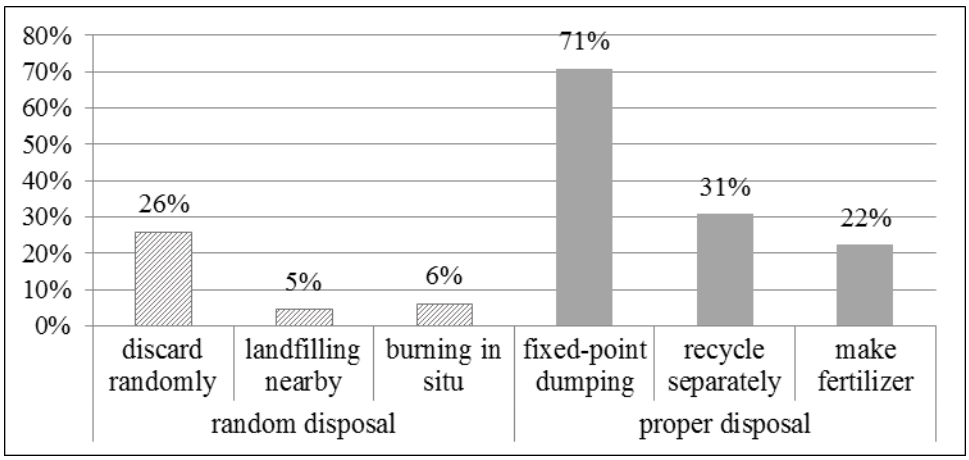

Figure 1. *Household waste disposal behavior of sample farmers*

Results and discussions

Logit model regression results

Firstly, we consider the relationship between all independent variables and dependent variables separately, screen out some variables that may not be meaningful, and then conduct multivariate analysis. Results shown in Model 1 in *Table 2* indicate that variables that may have statistical significance include: X1, X4, X6, X7, X8, X12, X13, X14, X15, X16, X17, X18, X19, X20, X21, X22, X23, and X24. Secondly, after eliminating the insignificant variables, the variables other than X21 and X22 are put into the Logit model according to Forward: LR rules. As shown in Model 2 in *Table 2*, six variables have passed the significance test (*Eq. 11*).

$$y = \ln\left(\frac{p}{1-p}\right) = 0.602 - 0.368 \times X8 + 0.462 \times X12 + 0.623 \times X13 - 0.311 \times X17 - 0.735 \times X20 + 1.516 \times X23 \quad \text{(Eq.11)}$$

The regression results show that: The stronger the identifying capacity for pollutants, the better the household waste can be properly disposed of. Farmers who choose traditional fuels are more likely to dispose waste randomly. Farmers with wages as the main source of livelihood are more inclined to properly dispose of household waste. The village has a fixed-point waste disposal policy and the implementation effect is good, farmers are more likely to show standard waste disposal behavior, and vice versa. Whether there is a centralized waste disposal facility is closely related to the farmers' household waste disposal behavior. If neighbors can take appropriate disposal ways, farmers themselves tend to adopt the similar ways.

http://www.aloki.hu ● ISSN 1589 1623 (Print) ● ISSN 1785 0037 (Online)
DOI: http://dx.doi.org/10.15666/aeer/1704_87378748

Table 2. *Logit model regression results*

Factor	Model1		Model2		Model3	
	B	Sig.	B	Sig.	B	Sig.
X1	0.508***	0.006		0.111		
X2	-0.021	0.874	-	-		
X3	0.001	0.996	-	-		
X4	0.162**	0.015		0.446		
X5	-0.094	0.103	-	-		
X6	-0.287***	0.001		0.716		
X7	-0.337***	0.005		0.338		
X8	-0.347***	0.008	-0.368**	0.015	-0.500	0.006
X9	-0.175	0.118	-	-		
X10	-0.067	0.435	-	-		
X11	0.143	0.180	-	-		
X12	0.957***	0.000	0.462**	0.048	0.562	0.046
X13	1.254***	0.000	0.623***	0.007	0.825	0.002
X14	-0.564***	0.000		0.433		
X15	-0.644***	0.000		0.087		
X16	-0.585***	0.000		0.183		
X17	-0.587***	0.000	-0.311***	0.001	-0.171	0.170
X18	-0.603***	0.000		0.346		
X19	0.843***	0.000		0.797		
X20	-1.880***	0.000	-0.735***	0.005		
X21	-0.694***	0.003				0.231
X22	0.805***	0.000			0.508***	0.003
X23	1.987***	0.000	1.516***	0.000	1.341	0.000
X24	-0.573***	0.000		0.085		

In the above analysis, X20 has passed the significant test, so it is necessary to further test the significance of Distance to centralized waste disposal facilities (X21) and Clearance of centralized waste dump site (X22). Firstly, 546 data are obtained by eliminating the NONE data selected under the variable X20. Then the other five variables selected by multivariate Logit analysis are used as control variables, and X21 and X22 are used as independent variables. As shown in Model 3 in Table 2, X22 passed the significant test. The more timely the disposal of waste centralized dump site is, the more appropriate waste disposal behavior can be promoted. X21 had no significant impact on Y. In conclusion, seven variables, X8, X12, X13, X17, X20, X22 and X23, have significant effects on household waste disposal behavior of farmers.

ISM model analysis results

In order to further determine the logical relationship and hierarchical structure among the seven factors identified above, this paper uses S1, S2, S3, S4, S5, S6 and S7 to represent those seven significant factors, namely Identifying capacity for pollutants (S1), Major domestic fuel (S2), Major economic source (S3), Fixed-point waste disposal policy and its implementation effect (S4), Availability of centralized waste disposal facility (S5), Clearance of centralized waste dump site (S6) and Neighbor's way of disposing household waste (S7). Combining the experience knowledge of experts, the logical relationship among the factors is determined (*Fig. 2a*). V denotes that row elements influence column elements; A indicates that column elements affect row elements; O indicates that there is no relationship between rows and columns. Then, the reachable matrix is obtained (*Fig. 2b*). Seven factors can be divided into three layers.

http://www.aloki.hu ● ISSN 1589 1623 (Print) ● ISSN 1785 0037 (Online)
DOI: http://dx.doi.org/10.15666/aeer/1704_87378748

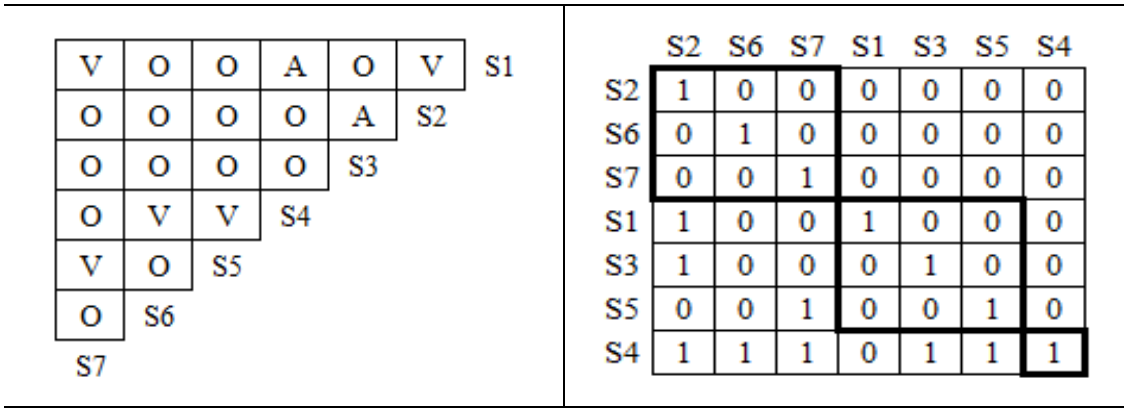

a. b.

Figure 2. *Logical relationship among the factors and sorted reachability matrix*

As can be seen from *Fig. 3*, variables at different levels have different effects on Y. Specifically: At the bottom is S4, which runs through almost all the important parts of the model and becomes the deep-seated root cause of affecting household waste disposal behavior of farmers. S1, S3 and S5 are located in the middle layer, which are important factors affecting Y. Moreover, the influence mode of S3 has certain independence. At the first level are S2, S6, and S7, which have direct impact on farmers' household waste disposal behavior. Meanwhile, S2 is affected by both S1 and S3 from the middle layer, and S7 is affected by S5.

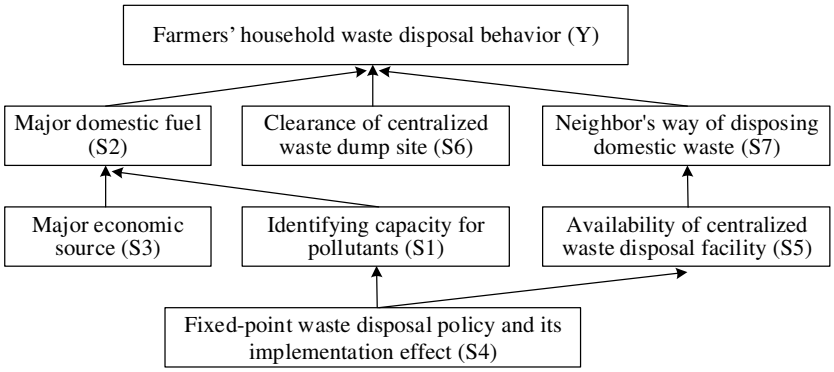

Figure 3. *Interpretative structure model of influencing factors*

Result discussion

As far as the physiological characteristics of farmers are concerned, Age (X2) and Cadre status (X3) have not passed the significant test, which is inconsistent with the research results of Yang et al. (2017). The reason may be that the development of the Internet has reduced the space-time distance, enabling everyone to receive information conveniently and timely, thus reducing the influence of individual differences. In univariate analysis, although Gender (X1) has a certain impact on the dependent variable, the impact of gender is weaker than other factors.

From the regression results of the psychological characteristics of farmers, only Identifying capacity for pollutants (X8) passed the significance test. On the one hand,

http://www.aloki.hu ● ISSN 1589 1623 (Print) ● ISSN 1785 0037 (Online)
DOI: http://dx.doi.org/10.15666/aeer/1704_87378748

Jiangsu paid more attention to the problem of rural household waste disposal. It began to publicize the consequences of waste discarding at will earlier, giving farmers a certain understanding of fixed-point waste disposal. Therefore, the samples have a small difference in the recognition of the relevant factors. On the other hand, the impact of other variables representing farmers' psychological characteristics on Y may have been included in the impact caused by X8, so they failed to pass the significance test. In addition, farmers may have certain psychological pressure when filling in the questionnaires face-to-face. They fail to give an objective assessment of the environment, resulting in the insignificant of X6.

For the family environment, Family educational level (X9) failed to pass the significant test. The reason may be the education situation of rural students in China. In China, schools above junior high school are generally distributed in cities and towns with more developed economy. Rural students need to leave home for a long time, causing them to lack enough opportunities to influence others. Because of the petty farmer idea has not been completely eliminated in China, the improvement of economic conditions will not significantly promote farmers to adopt appropriate waste disposal behavior, resulting in the insignificant of X10. The reason why Number of migrant workers (X11) is not significant is that most families have less migrant workers, and the level of work is not very high.

In terms of social environment, the reason why X19, X14 and X15 are not significant is also because of Jiangsu has attached great importance to rural waste management, narrowing the gap between villages in terms of these factors. Meanwhile, propaganda, education and behavioral management measures can be regarded as part of the policy system. The impact of X14, X15 and X16 on dependent variable may have been included in the impact caused by Fixed-point waste disposal policy and its implementation effect (X17), so these variables have not passed the significance test, which is another possible reason why X19 is not significant.

The reason why Distance to the city center (X24) has not passed the significance test lies in Jiangsu's dense population. On the whole, the geographical space separation between rural and urban areas is not very large, thus the results of questionnaire show little difference in this factor, affecting the result of the significance test.

The intrinsic reasons for the influence of Major domestic fuel (X12) on Y are Major economic source (X13) and Identifying capacity for pollutants (X8). Families whose economic sources are mainly wages are relatively affected by the living habits of urban residents, and more likely to use modern living fuels. Moreover, farmers with wages as their main source of economy are more able to afford modern energy. Besides, the more familiar farmers are with environmental protection knowledge, the more willing they are to adopt pro-environmental behavior (Estrada et al., 2017), and more willing to use less polluted domestic fuels.

The impact of Fixed-point waste disposal policy and its implementation effect (X17) runs through the whole process. If the relevant policies can be promulgated and implemented, it can directly increase investment in waste centralized treatment facilities, increase the frequency of waste pool cleaning, and then promote farmers to adopt appropriate ways of household waste treatment. Meanwhile, X17 can promote the popularization of environmental protection knowledge in a wider range, so that more farmers are aware of the hazards of random disposal of household waste, and have the ability to identify pollutants. Therefore, they are more willing to make environmentally friendly behavior, such as using clean fuels.

http://www.aloki.hu ● ISSN 1589 1623 (Print) ● ISSN 1785 0037 (Online)
DOI: http://dx.doi.org/10.15666/aeer/1704_87378748

Conclusions

Based on Lewin's behavior model and the data of 671 households in Jiangsu, this paper used Logit-ISM model to analyze farmers' household waste disposal behavior and its influencing factors. The results show that seven factors have significant effects on household waste disposal behavior, namely Identifying capacity for pollutants (X8), Major domestic fuel (X12), Major economic source (X13), Fixed-point waste disposal policy and its implementation effect (X17), Availability of centralized waste disposal facility (X20), Clearance of centralized waste dump site (X22) and Neighbour's way of disposing household waste (X23).

The stronger the ability of farmers to discriminate pollutants, the more willing they are to dispose of waste properly. Compared with the areas without fixed-point disposal policy of household waste, those have ones tend to show standardized disposal behaviour of household waste. In areas where centralized waste disposal facilities are available and can be cleaned in time, farmers tend to dispose of household waste properly. Using coal, wood and other traditional energy as main fuel and taking farming as the main source of livelihood have a certain negative impact on farmers' proper waste disposal behavior. Neighbors' disposal of household waste will have a strong assimilation effect on individual's behavior of household waste disposal.

At the same time, there are mutual influences among these seven significant factors. X17 is a deep-seated influencing factor, which has a root effect on farmers' household waste disposal behavior. X8, X13 and X20 are the middle factors. X13 has certain independent impact. X8 and X20 are the nodes that connect the deep factors with surface factors, and play a key intermediary role. X12, X22 and X23 have direct impact, belonging to surface factors.

Based on above conclusions, we put forward the following suggestions: First, establish a long-term mechanism of fixed-point treatment of rural household waste, strengthen the effect of policy implementation. Second, strengthen the propaganda of environmental protection knowledge, especially focusing on the popularization among farmers, and encourage them to replace traditional fuels with clean energy. Third, add waste collection and treatment facilities such as garbage cans, garbage tanks and garbage collection trucks, and clean up these facilities in time. Fourth, set up models, commend and reward villages achieving remarkable results in the treatment of household waste, giving full play to the exemplary driving effect.

Although this paper explored the influencing factors of farmers' household waste disposal behavior in Jiangsu Province and put forward the corresponding countermeasure proposals through qualitative and empirical research, due to time constraints and data acquisition constraints, the research still need to be further investigated. On the one hand, through the case study of typical villages, the impact degree of each influencing factor can be refined with the help of structural equation model, so as to further improve the effectiveness of the policy. On the other hand, future research can be done based on the theory of planned behavior (TPB) in social psychology, or from the perspective of A-B-C theory.

Acknowledgements. This work was supported by the Project funded by China Postdoctoral Science (2019M650456), by the Fundamental Research Funds for the Central Universities (ZY1915, buctrc201804), and by the National Natural Science Foundation of China (71532003).

http://www.aloki.hu ● ISSN 1589 1623 (Print) ● ISSN 1785 0037 (Online)
DOI: http://dx.doi.org/10.15666/aeer/1704_87378748

REFERENCES

[1] Abbott, A., Nandeibam, S., O'Shea, L. (2013): Recycling: Social norms and warm-glow revisited. – Ecological Economics 90: 10-18.
[2] Arcury, T. A. (1990): Environmental attitude and environmental knowledge. – Human organization 49: 300-304.
[3] Bamberg, S. (2003): How does environmental concern influence specific environmentally related behaviors? A new answer to an old question. – Journal of Environmental Psychology 23: 21-32.
[4] Catton, W. R., Dunlap, R. E. (1978): Environmental sociology: A new paradigm. – American Sociologist 13: 41-49.
[5] Czajkowski, M., Hanley, N., Nyborg, K. (2017): Social norms, morals and self-interest as determinants of pro-environment behaviours: The case of household recycling. – Environmental and Resource Economics 66: 647-670.
[6] D'Amato, A., Mancinelli, S., Zoli, M. (2016): Complementarity vs substitutability in waste management behaviors. – Ecological Economics 123: 84-94.
[7] Dorina, G. (2016): Assessing the variables affecting on the rate of solid waste generation and recycling: An empirical analysis in Prespa Park. – Waste Management 48: 3-13.
[8] Du, J., Li, Q., Qiao, F., Yu, L. (2018): Estimation of vehicle emission on mainline freeway under isolated and integrated ramp metering strategies. – Environmental Engineering and Management Journal 17(5): 1237-1248.
[9] Estrada, M., Schultz, P. W., Silva-Send, N., Boudrias, M. A. (2017): The role of social influences on pro-environment behaviors in the San Diego Region. – Journal of Urban Health 94: 170-179.
[10] Gong, D., Tang, M., Liu, S., Xue, G., Wang, L. (2019): Achieving sustainable transport through resource scheduling: A case study for electric vehicle charging stations. – Advances in Production Engineering & Management 14(1): 65-79.
[11] Guagnano, G. A., Stern, P. C., Dietz, T. (1995): Influences on attitude-behavior relationships: A natural experiment with curbside recycling. – Environment and Behavior 27: 699-718.
[12] Hage, O., Sandberg, K., Söderholm, P., Berglund, C. (2018): The regional heterogeneity of household recycling: a spatial-econometric analysis of Swedish plastic packing waste. – Letters in Spatial and Resource Sciences 11: 245-267.
[13] Hakami, B. A., Seif, E. S. S. A. (2015): Household solid waste composition and management in Jeddah City, Saudi Arabia: a planning model. – International Research Journal of Environment Sciences 4: 1-10.
[14] Han, Z., Liu, Y., Zhong, M., Shi, G., Li, Q., Zeng, D., Zhang, Y., Fei, Y., Xie, Y. (2018): Influencing factors of domestic waste characteristics in rural areas of developing countries. – Waste Management 72: 45-54.
[15] Huang, K. X., Wang, J. X., Bai, J. F., Qiu, H. G. (2012): Production of rural domestic solid waste and policy countermeasures. – China Soft Science 9: 72-79.
[16] Jenkins, R. R., Martinez, S. A., Palmer, K., Podolsky, M. J. (2003): The determinants of household recycling: a material-specific analysis of recycling program features and unit pricing. – Journal of Environmental Economics and Management 45: 294-318.
[17] Jiang, T. B., Yuan, J. Z. (2013): The analysis of factors affecting farmers' life trash disposal behavior in the urban and rural balancing development. – Ecological Economy 2013: 161-164.
[18] Jin, Y., Ma, X., Chen, X., Cheng, Y., Baris, E., Ezzati, M. (2006): Exposure to indoor air pollution from household energy use in rural China: the interactions of technology, behavior, and knowledge in health risk management. – Social Science & Medicine 62: 3161-3176.
[19] Kuo, Y. L., Perrings, C. (2010): Wasting Time? Recycling incentives in urban Taiwan and Japan. – Environmental and Resource Economics 47: 423-437.

http://www.aloki.hu ● ISSN 1589 1623 (Print) ● ISSN 1785 0037 (Online)
DOI: http://dx.doi.org/10.15666/aeer/1704_87378748

[20] Lee, M., Choi, H., Koo, Y. (2017): Inconvenience cost of waste disposal behavior in South Korea. – Ecological Economics 140: 58-65.
[21] Li, T., Espínola-Arredondo, A., McCluskey, J. J. (2016): Promoting residential recycling: An alternative policy based on a recycling reward system. – Games 7: 1-18.
[22] Ma, Y., Chen, L., Zhao, X., Zheng, H., Lü, Y. (2009): What motivates farmers to participate in sustainable agriculture? Evidence and policy implications. – International Journal of Sustainable Development & World Ecology 16: 374-380.
[23] Milfont, T. L. (2012): The interplay between knowledge, perceived efficacy, and concern about global warming and climate change: A one-year longitudinal study. – Risk Analysis 32: 1003-1020.
[24] Miliute-Plepiene, J., Hage, O., Plepys, A., Reipas, A. (2016): What motivates households recycling behaviour in recycling schemes of different maturity? Lessons from Lithuania and Sweden. – Resources, Conservation and Recycling 113: 40-52.
[25] Oyekale, A. S. (2018): Determinants of households' involvement in waste separation and collection for recycling in South Africa. – Environment, Development and Sustainability 20: 2343-2371.
[26] Petraru, M., Gavrilescu, M. (2010): Pollution prevention, a key to economic and environmental sustainability. – Environmental Engineering & Management Journal 9: 597-614.
[27] Poortinga, W., Steg, L., Vlek, C., Wiersma, G. (2003): Household preferences for energy-saving measures: A conjoint analysis. – Journal of Economic Psychology 24: 49-64.
[28] Refsgaard, K., Magnussen, K. (2009): Household behaviour and attitudes with respect to recycling food waste–experiences from focus groups. – Journal of Environmental Management 90: 760-771.
[29] Schahn, J., Holzer, E. (1990): Studies of individual environmental concern: The role of knowledge, gender, and background variables. – Environment and Behavior 22: 767-786.
[30] Seacat, J. D., Boileau, N. (2018): Demographic and community-level predictors of recycling behavior: A statewide, assessment. – Journal of Environmental Psychology 56: 12-19.
[31] Steg, L. (2008): Promoting household energy conservation. – Energy Policy 36: 4449-4453.
[32] Struk, M. (2017): Distance and incentives matter: The separation of recyclable municipal waste. – Resources, Conservation and Recycling 122: 155-162.
[33] Videras, J., Owen, A. L., Conover, E., Wu, S. (2012): The influence of social relationships on pro-environment behaviors. – Journal of Environmental Economics and Management 63: 35-50.
[34] Wang, E., Kang, N. (2019): Does life satisfaction matter for pro-environmental behavior? empirical evidence from China general social survey. – Quality & Quantity 53: 449-469.
[35] Warfield, J. N. (1974): Toward interpretation of complex structural models. – IEEE Transactions on Systems, Man, and Cybernetics 4: 405-417.
[36] Yang, R., Long, R., Bai, Y., Li, L. (2017): The influence of household heterogeneity factors on the green travel behavior of urban residents in the East China region. – Sustainability 9: 1-17.
[37] Yokoo, H. F., Kawai, K., Higuchi, Y. (2018): Informal recycling and social preferences: Evidence from household survey data in Vietnam. – Resource and Energy Economics 54: 109-124.
[38] Young, R. D. (1990): Recycling as appropriate behavior: a review of survey data from selected recycling education programs in Michigan. – Resources Conservation & Recycling 3: 253-266.
[39] Zeng, J., Zhou, S., Lv, L., Su, Q., Wang, J. (2018): Soil heavy metal contamination in rural land consolidation areas in the Yangtze River Delta, China. – Journal of Environmental Engineering and Landscape Management 26: 28-37.
[40] Zhang, Y., Gao, Y., Duan, J. (2013): Control mode of rural nonpoint source pollution in Tai Lake Basin, China. – Environmental Engineering & Management Journal 12: 1359-1365.

http://www.aloki.hu ● ISSN 1589 1623 (Print) ● ISSN 1785 0037 (Online)
DOI: http://dx.doi.org/10.15666/aeer/1704_87378748

OPTIMIZATION DECISION ON INFORMAL RECYCLING CHANNEL OF ELECTRIC VECHICLE BATTERIES AND SUPERVISION STRATEGY

GAO, H. – LIU, S. – GONG, D.* – CAO, G.

School of Economics and Management, Beijing Jiaotong University, 100044 Beijing, China

**Corresponding author*
e-mail: dqgong@bjtu.edu.cn

(Received 8th Mar 2019; accepted 1st May 2019)

Abstract. In order to explore the impact of the government' regulatory strategy on the informal recycling channel of electric vehicle batteries, this paper compares and analyzes the evolutionary strategy of the government and the informal recycling channel of electric vehicle batteries group under fixed and dynamic punishment model. The results show that: (1) the dynamic system of replication under the fixed punishment model consists of four saddle points and one central point. The evolution process of the strategy is repetitive and periodic, and cannot reach equilibrium. (2) The dynamic system of replication under the dynamic punishment model consists of four saddle points and one focal point, and the stable Nash equilibrium can be achieved. That is to say, the optimized scenario is valid. (3) In order to improve the probability of the informal recycling channel of electric vehicle batteries choosing the transformation upgrading strategy, improving the legal environmental incomes after the transformation upgrading of the informal recycling channel of electric vehicle batteries group, and reducing the recycling cost of the available components extracted from the waste electric vehicle batteries through formal channels are effective approaches.
Keywords: *dynamic punishment, evolutionary strategy, fixed punishment, recycling channel decision*

Introduction

In recent years, environmental pollution, climate change and energy shortages have caused widespread concern in the world. One of the key factors in aggravating these problems is the transportation industry, which consumes a lot of energy and generates a lot of greenhouse gases (Gong et al., 2019). In order to protect national energy security, alleviate fuel supply conflicts, reduce exhaust emissions, and improve the atmospheric environment, China has proposed a national strategy to vigorously develop new energy vehicles (Zhao et al., 2016). In 2016, China's new energy vehicle sales reached 777,000 units, with a total promotion of more than 1.7 million units, accounting for more than 50% of the global new energy vehicle market. The rapid development of new energy vehicles has also brought about some new problems. It is predicted that the number of power battery scraps will exceed 500,000 tons by 2020, about 20 times the amount recorded in 2016. The contradiction between the development of pure electric vehicle industry and the resource environment is becoming more and more prominent (Li et al., 2014). If the waste power battery is not properly disposed, the potential harmful substances contained in it will cause environmental pollution (Ordoñez et al., 2016). On the other hand, lithium, cobalt, copper and aluminum in the scrapped power battery are recyclable materials, which have extremely high recovery value (Xu et al., 2008; Tan et al., 2015). In fact, China's power battery recycling rate is low. In 2016, China's waste power battery recycling amount was less than 10,000 tons, and the recovery rate was less than 20%. If the power battery recovery rate is still at the current low level, there

http://www.aloki.hu ● ISSN 1589 1623 (Print) ● ISSN 1785 0037 (Online)
DOI: http://dx.doi.org/10.15666/aeer/1704_87498762

will be a large number of used power batteries flowing into private small workshops or abandoned, posing great threat to the ecological environment.

At present, research on used power batteries focuses on the status of recycling, recycling models and the impact of government environmental regulations on recycling strategies. China's recycling process for power batteries is still in the exploratory stage, and recycling technology aiming at recycling manufacturing has not been carried out (Yu et al., 2014). There are no specific measures and equipment guarantees for the production safety and environmental issues involved in the recycling of lithium-ion batteries (Gu et al., 2017). Scholars have done a lot of research on the recycling mode of closed-loop supply chain, for example, Savaskan et al.(2004) considered a decentralized model and a centralized model of a monopolist manufacturer and a retailer, compared and analyzed three modes of manufacturer recycling, retailer recycling and third-party recycling. They found that retailer recycling was the most efficient way. Savaskan et al. (2006) studied the recycling problem from the perspective of the manufacturer's benefit and found that in the homogeneous market, if the competition between retailers is fierce, the manufacturer will adopt the direct recycling model; otherwise, the retailer recycling model will be adopted. De Giovanni et al. (2014) established a two-cycle closed-loop supply chain game model of a monopolist manufacturer and a retailer, and analyzed the corporate, environmental and social benefits of the three modes of manufacturer recycling, retailer recycling and third-party recycling through numerical examples. It was pointed out that only in a small scope, manufacturers outsourcing their recycling business can contribute to corporate, environmental and social benefits. The research on the decision-making problem of power battery recovery mode is still in the initial stage. Liu and Gong (2014) studied the matching behavior of vehicles and batteries in the retailer recycling mode, and analyzed the influencing factors of recycling and the influence degree of various factors. Turner et al. (2016) analyzed and compared of EPR (Extended Producer Responsibility) and EOL (End of life) on recovery rate, recovery efficiency, management cost, etc., and concluded that the effective implementation of EPR is more conducive to the recycling of power batteries. Hong and Yeh (2012) comparative analyzed of retailer recycling and third-party recycling models revealed that retailer recycling models were more effective when third parties are non-profit organizations. Ma et al. (2016) studied on WEEE closed-loop supply chain decision-making problem of mixed channel sales/recycling under government regulation. As China's power battery recycling system is still not perfect, environmental pollution and resource waste in the recycling process are very serious, which will adversely affect the development of the industry (Han et al., 2016). China has no specific legislation on the recycling of new energy vehicle power batteries, and the healthy and sustainable development of the scrapped power battery recycling industry has been restricted (Han et al., 2017). Therefore, the recycling industry is still in the early stages of development, and government intervention is required at this time (Capon et al., 2015). Zhang et al. (2016) pointed out that incentives such as recycling regulatory policies and subsidies are not perfect, resulting in many enterprises power battery recycling interest is very low. Wang and Wu (2017) pointed out that the non-mandatory policy has caused battery manufacturers and OEMs not to plan battery recycling. Wang et al. (2014) studied the effects of four subsidy policy schemes, including direct subsidies, recycling subsidies, research and development subsidies and product subsidies on the recycling of auto parts (Wang et al., 2014; Du et al., 2018). Li

http://www.aloki.hu ● ISSN 1589 1623 (Print) ● ISSN 1785 0037 (Online)
DOI: http://dx.doi.org/10.15666/aeer/1704_87498762

and Mu (2018) analyzed the impact of subsidized 4S stores, OEMs and battery manufacturers on recycling efficiency.

Through the above literature, it is found that there are few studies on the relevant regulatory policies for power battery recycling and the recycling targets are mainly based on formal recycling group. In fact, more than 80% of used power batteries in China have flowed into the informal recycling group. Such groups are spontaneously driven by economic interests, and formal recycling companies lack competitiveness in terms of cost and price. In addition, it is impossible for the government and the informal recycling group to have sufficient information. The two sides cannot be completely rational, and the decisions made can only be completed under bounded rational conditions. Moreover, the government's regulation of recycling vendors is also in its infancy. How the government's incentives for formal and informal recyclers evolved and how the informal recycling community should decide is worth studying.

How to effectively supervise the power recycling industry has become an urgent problem to be solved in the development of circular economy. At present, this issue has not attracted enough attention. The research on reverse recycling of power battery also pays little attention to the informal recycling group. Based on the bounded rationality hypothesis and using the relevant theory of evolutionary game, this paper studies the dynamic game relationship between the informal recycling channel of electric vehicle batteries and the government, and analyzes the stability of different strategies and proposes corresponding management enlightenment.

Evolutionary game model

Model assumptions and description

(1) It is assumed that the participants in the game include the government and the informal recycling channel of electric vehicle batteries, and the two sides of the game are bounded rational.

(2) The informal recycling channel of electric vehicle batteries group consists of n informal recyclers, assuming that n informal recyclers are independent of each other.

(3) There are only two strategies for the government and the informal recycling channel of electric vehicle batteries to participate in the game. The strategies available to the government are {positive regulation, negative regulation}. Positive regulation means the government's punishment measures or subsidy policies for different recycling behaviors of informal recycling channel. Negative regulation means that the government regulatory departments do not supervise and regulate the informal recycling channel groups of electric vehicle batteries. The informal recycling channel groups of electric vehicle batteries have two recycling strategies, the strategies are {transformation upgrading, non-transformation upgrading}. Transformation upgrading strategy means that the informal recycling group of electric vehicle batteries is upgraded into a legal and regular recycling group through technology upgrade, and the non-transformation upgrading strategy means that the informal recycling group of power battery continues to be lucky to recycle through informal recycling channels.

(4) Suppose that the probability of the government choosing the positive regulation strategy is x and the probability of the negative regulation is $1 - x$, meanwhile, the probability of the informal recycling channel of electric vehicle batteries choosing the transformation upgrading strategy is y, and the probability of the non-transformation upgrading strategy is $1 - y$.

http://www.aloki.hu ● ISSN 1589 1623 (Print) ● ISSN 1785 0037 (Online)
DOI: http://dx.doi.org/10.15666/aeer/1704_87498762

(5) The cost and benefit parameters are assumed and explained as follows: C is the recycling cost of the power waste battery that can be utilized without disassembly; C_1 and C_2 are the recycling cost of the available components extracted from the waste electric vehicle batteries through formal channels and informal channels; C_3 is the governance cost that the government needs to pay due to environmental pollution when the informal recyclers choose non-transformation upgrading strategies; α is the proportion of the part of the electric vehicle batteries that does not need to be dismantled; R_1 and R_2 are illegal and legal environmental incomes before and after the transformation upgrading of the informal recycling channel of electric vehicle batteries group; R_3 is the social benefit that the government receives when the informal recycling channel of electric vehicle batteries group choose the transformation upgrading strategy and the government choose the positive regulation strategy; the informal recycling channel of electric vehicle batteries group will receive subsidies from the government when choosing the transformation upgrading strategy, and the subsidy is G; if the informal recycling channel of electric vehicle batteries group chooses the non-transformation upgrading, the probability of being discovered by the government is ε, and the punishment of p is obtained.

According to the above model description and assumptions, the payoff matrix of the government and the informal recycling channel of electric vehicle batteries group evolution game is shown in *Table 1*.

Table 1. *Payoff matrix between the government and the informal recycling channel of electric vehicle batteries group*

The game		**The informal recycling channel of electric vehicle batteries group**	
		Transformation upgrading (y)	**Non-transformation upgrading (1-y)**
The government	Positive regulation (x)	$R_3 - G$ $nR_1 - n\alpha C - n(1-\alpha)C_1 + G$	$R_3 - C_3 + \varepsilon np$ $nR_2 - n\alpha C - n(1-\alpha)C_2 - \varepsilon np$
	Negative regulation (1-x)	0 $nR_1 - n\alpha C - n(1-\alpha)C_1$	$-C_3$ $nR_2 - n\alpha C - n(1-\alpha)C_2$

The model

According to the payoff matrix of the government and the informal recycling channel of electric vehicle batteries group evolution game in *Table 1*, we assume that the expected return of the government's positive regulation strategy is E_{11}, the expected return of negative regulation strategy is E_{12}, and the average expected return of the group is E_1, then we can obtain *Equations 1-3*.

$$E_{11} = x(R_3 - G) + (1-x)(R_3 - C_3 + \varepsilon np) \quad \text{(Eq.1)}$$

$$E_{12} = x \times 0 + (1-x) \times -C_3 \quad \text{(Eq.2)}$$

$$E_1 = yE_{11} + (1-y)E_{12} \quad \text{(Eq.3)}$$

http://www.aloki.hu ● ISSN 1589 1623 (Print) ● ISSN 1785 0037 (Online)
DOI: http://dx.doi.org/10.15666/aeer/1704_87498762

Meanwhile, we assume that the expected return of informal recycling channel of electric vehicle batteries group's transformation upgrading strategy is E_{21}, the expected return of non-transformation upgrading strategy is E_{22}, and the average expected return of the group is E_2, then we can obtain *Equations 4-6*.

$$E_{21} = y(nR_1 - n\alpha C - n(1-\alpha)C_1 + G) + (1-y)(nR_1 - n\alpha C - n(1-\alpha)C_1) \quad \text{(Eq.4)}$$

$$E_{22} = y(nR_2 - n\alpha C - n(1-\alpha)C_2 - \varepsilon np) + (1-y)(nR_2 - n\alpha C - n(1-\alpha)C_{21}) \quad \text{(Eq.5)}$$

$$E_2 = xE_{21} + (1-x)E_{22} \quad \text{(Eq.6)}$$

The complex dynamic equation is actually a dynamic differential equation that describes the frequency or frequency of a particular strategy being used in a population (Friedman, 1991, 1998). So the replication dynamic equation of the government and the informal recycling channel of electric vehicle batteries group evolution game is in the form of *Equation 7*.

$$\begin{cases} \dfrac{dx}{dt} = x(1-x)[nR_1 - nR_2 - n(1-\alpha)(C_1 - C_2) + y(G + \varepsilon np)] \\ \dfrac{dy}{dt} = y(1-y)[R_3 + \varepsilon np - x(G + \varepsilon np)] \end{cases} \quad \text{(Eq.7)}$$

The Jacobian matrix of the evolutionary system of the government and the informal recycling channel of electric vehicle batteries group is in the form of *Equation 8*.

$$J = \begin{vmatrix} (1-2x)[nR_1 - nR_2 - n(1-\alpha)(C_1 - C_2) + y(G + \varepsilon np)] & x(1-x)(G + \varepsilon np) \\ y(1-y)[-x(G + \varepsilon np)] & (1-2y)[R + \varepsilon np - x(G + \varepsilon np)] \end{vmatrix} \quad \text{(Eq.8)}$$

Analysis of equilibrium point of evolutionary game

In order to make the revenue of the government and the informal recycling channel of electric vehicle batteries group more consistent with the reality, this paper considers the following situation: when the government chooses a positive regulation strategy, due to the existence of subsidies and penalties, the benefits of the transformation upgrading of power battery recycling enterprises will be greater than the benefits of non-transformation upgrading; similarly, when the informal recycling channel of electric vehicle batteries group chooses a non-transformation upgrading strategy, the benefits of the positive regulation of the government will be greater than the benefits of the negative regulation. Therefore the following inequalities can be obtained (see *Eq. 9*).

$$\begin{cases} 0 < nR_2 - nR_1 - C_3 + n(C_2 - C_1) < (G + \varepsilon np) \\ 0 < R_3 + \varepsilon np < G + \varepsilon np \end{cases} \quad \text{(Eq.9)}$$

Therefore, the five Nash equilibrium points of the dynamic evolution of the government and the informal recycling channel of electric vehicle batteries group

http://www.aloki.hu ● ISSN 1589 1623 (Print) ● ISSN 1785 0037 (Online)
DOI: http://dx.doi.org/10.15666/aeer/1704_87498762

systems are $(0,0)$, $(1,0)$, $(1,1)$, $(0,1)$ and (x^*, y^*), where $x^* = [nR_2 - nR_1 - n(1-\alpha)(C_2 - C_1)] / (G + \varepsilon np)$, $y^* = (R_3 + \varepsilon np) / (G + \varepsilon np)$. The stability of the five equilibrium points is analyzed by D. Friedman's method for determining the equilibrium point. The analysis results of the five equilibrium points are shown in *Table 2*.

Table 2. *Stability of the dynamic evolution of the government and the informal recycling channel of electric vehicle batteries group evolution*

Equilibrium point	Det(J)	Tr(J)	stability
(0,0)	-	Uncertain	Saddle point
(1,0)	-	Uncertain	Saddle point
(1,1)	-	Uncertain	Saddle point
(0,1)	-	Uncertain	Saddle point
(x^*, y^*)	-	0	Center point

According to the above analysis, the stability of the stability point of the evolutionary game model between the government and the informal recycling channel of electric vehicle batteries group are: the evolutionary state of points $(0,0)$, $(1,0)$, $(1,1)$ and $(0,1)$ are saddle point, and the evolutionary state of point (x^*, y^*) is center point. Since the value of the real part of the feature root corresponding to the center point is zero, we know that (x^*, y^*) is the equilibrium point, but it is not the stable point of evolution. The evolutionary trajectory of the government and the informal recycling channel of electric vehicle batteries group is a closed loop curve without (x^*, y^*). Due to the choice of the initial strategy of both parties and the disturbance in the evolution process, the development of the system will have a certain randomness, which will have a greater impact on environmental protection and social harmony, and also make the management of the government very difficult. The system does not have an evolutionary stability strategy, which may be one of the important reasons why the informal recycling channel of electric vehicle batteries group chooses not to upgrade and lead to environmental pollution.

Optimization model of the evolutionary game

The optimization model

Based on the content of the previous section, we know that the evolutionary behavior of the government and the informal recycling channel of electric vehicle batteries group games under fixed punishment. In fact, in the process of evolutionary game between the two sides, different punishments should be applied to the specific fraudulent behaviors adopted by the informal recycling channel of electric vehicle batteries group. The punishment measures at this time can be called dynamic punishment mechanisms. It is assumed that the punishment measures adopted by the government are directly proportional to the degree to which the informal recycling channel of electric vehicle batteries group adopts a non-transformation upgrading strategy, that is, the punishment value received by the informal recycling channel of electric vehicle batteries group at

http://www.aloki.hu ● ISSN 1589 1623 (Print) ● ISSN 1785 0037 (Online)
DOI: http://dx.doi.org/10.15666/aeer/1704_87498762

this time is changed from p to dynamic $g(y)=(1-y)q$, where q indicates the maximum degree of punishment. After the dynamic punishment measures are taken, the game payoff matrix between the government and the informal recycling channel of electric vehicle batteries group under dynamic punishment mechanism is shown in *Table 3*.

Table 3. *Payoff matrix between the government and the informal recycling channel of electric vehicle batteries group under dynamic punishment mechanism*

The game		The informal recycling channel of electric vehicle batteries group	
		Transformation upgrading (y)	**Non-transformation upgrading (1-y)**
The government	Positive regulation (x)	R_3-G $nR_1-n\alpha C-n(1-\alpha)C_1+G$	$R_3-C_3+\varepsilon ng(y)$ $nR_2-n\alpha C-n(1-\alpha)C_2-\varepsilon ng(y)$
	Negative regulation (1-x)	0 $nR_1-n\alpha C-n(1-\alpha)C_1$	$-C_3$ $nR_2-n\alpha C-n(1-\alpha)C_2$

Based on *Table 3*, we analyze the evolution stability of the government and the informal recycling channel of electric vehicle batteries group under dynamic punishment mechanism. Similar to the fixed punishment mechanism, the dynamic replication equation of the game between the two sides under the dynamic punishment mechanism is in the form of *Equation 10*.

$$\begin{cases} \dfrac{dx}{dt}=x(1-x)[nR_1-nR_2-n(1-\alpha)(C_1-C_2)+y(G+\varepsilon ng(y))] \\ \dfrac{dy}{dt}=y(1-y)[R_3+\varepsilon ng(y)-x(G+\varepsilon ng(y))] \end{cases} \quad \text{(Eq.10)}$$

The equilibrium point after optimization

The Nash equilibrium points of the dynamic evolution of the government and the informal recycling channel of electric vehicle batteries group systems under dynamic punishment mechanism are $(0,0)$, $(1,0)$, $(1,1)$, $(0,1)$ and (x^{**},y^{**}), where $x^{**}=[nR_2-nR_1-n(1-\alpha)(C_2-C_1)]/\ (G+\varepsilon ng(y))$, $y^{**}=(R_3+\varepsilon ng(y))/(G+\varepsilon ng(y))$. The Jacobian matrix of the evolutionary system of the two sides is in the form of *Equation 11*.

$$J_1=\begin{vmatrix} (1-2x)[nR_1-nR_2-n(1-\alpha)(C_1-C_2)+y(G+\varepsilon ng(y))] & x(1-x)(G+\varepsilon ng(y)) \\ y(1-y)[-x(G+\varepsilon ng(y))] & (1-2y)[R+\varepsilon ng(y)-x(G+\varepsilon ng(y))] \end{vmatrix} \quad \text{(Eq.11)}$$

The analysis conditions under the dynamic punishment mechanism are similar to the fixed punishment model, that is, see *Equation 12*.

$$\begin{cases} 0<nR_2-nR_1-n(1-\alpha)(C_2-C_1)<(G+\varepsilon ng(y)) \\ 0<R_3+\varepsilon ng(y)<G+\varepsilon ng(y) \end{cases} \quad \text{(Eq.12)}$$

http://www.aloki.hu ● ISSN 1589 1623 (Print) ● ISSN 1785 0037 (Online)
DOI: http://dx.doi.org/10.15666/aeer/1704_87498762

According to the calculation, the value of the matrix of the determinant corresponding to points $(0,0)$, $(1,0)$, $(1,1)$ and $(0,1)$ are negative, we know that points $(0,0)$, $(1,0)$, $(1,1)$ and $(0,1)$ are saddle points. Substituting point (x^{**}, y^{**}) into formula (11), we can get that the characteristic root of (x^{**}, y^{**}) is a bunch of characteristic negative roots with negative real parts. Point (x^{**}, y^{**}) is the focus of evolutionary stability, and the state of system evolution has asymptotic stability, see *Table 4*.

Table 4. *Stability of the dynamic evolution of the government and the informal recycling channel of electric vehicle batteries group evolution under dynamic punishment mechanism*

Equilibrium point	Det(J)	Tr(J)	stability
(0,0)	-	Uncertain	Saddle point
(1,0)	-	Uncertain	Saddle point
(1,1)	-	Uncertain	Saddle point
(0,1)	-	Uncertain	Saddle point
(x^{**}, y^{**})	-	0	Stable point

Similar to the analysis of evolutionary stability in fixed punishment model, we know that (x^{**}, y^{**}) is the stable equalization point of the system evolution. We can get x^{**}, y^{**} as *Equation 13*.

$$x^{**} = \frac{nR_2 - nR_1 - n(1-\alpha)(C_2 - C_1)}{G + \varepsilon ng(y^{**})}, \quad y^{**} = \frac{R_3 + \varepsilon ng(y^{**})}{G + \varepsilon ng(y^{**})} \qquad \text{(Eq.13)}$$

According to *Equation 13,* we can get x^{**}, y^{**} as *Equation 14*.

$$x^{**} = \frac{2[nR_2 - nR_1 - n(1-\alpha)(C_2 - C_1)]}{G + \sqrt{G^2 + 4(G - R_3)\varepsilon nq}}, \quad y^{**} = 1 + \frac{G - \sqrt{G^2 + 4(G - R_3)\varepsilon nq}}{2\varepsilon nq} \qquad \text{(Eq.14)}$$

According to *Equation 14,* we analyze the influence of the main parameters on the evolutionary equilibrium under the dynamic punishment model. The results of the analysis are as follows:

(1) According to x^{**}, we can get that: $dx^{**}/dn > 0$, $dx^{**}/dR_2 > 0$, $dx^{**}/dC_2 > 0$, $dx^{**}/dR_1 < 0$, $dx^{**}/dC_1 < 0$, $dx^{**}/d\alpha < 0$, $dx^{**}/dG < 0$, $dx^{**}/dR_3 > 0$, $dx^{**}/dR_3 > 0$, $dx^{**}/dq < 0$, $dx^{**}/d\varepsilon < 0$.

(2) According to y^{**}, we can get that: $dy^{**}/dR_3 > 0$, $dy^{**}/dG < 0$, $dy^{**}/dn > 0$, $dy^{**}/d\varepsilon > 0$, $dy^{**}/dq > 0$.

Based on the above analysis, we can get the following conclusion: (1) Number of the informal recycling channel of electric vehicle batteries, the probability of being discovered by the government when the informal recycling channel of electric vehicle batteries group chooses the non-transformation upgrading, the social benefit that the

http://www.aloki.hu ● ISSN 1589 1623 (Print) ● ISSN 1785 0037 (Online)
DOI: http://dx.doi.org/10.15666/aeer/1704_87498762

government receives when the informal recycling channel of electric vehicle batteries group choose the transformation upgrading strategy and the government choose the positive regulation strategy, the maximum degree of punishment and the subsidy when the informal recycling channel of electric vehicle batteries group choose the transformation upgrading strategy will affect the size of x^{**} and y^{**}.

(2) When q and ε increase, x^{**} will decrease, and y^{**} will increase, indicating that the probability that the informal recycling channel of electric vehicle batteries choose the strategic probability of transformation upgrading will increase, and the probability that the government choose the strategic probability of positive regulation will decrease. R_3, G and n have the same effect on the changing trend of x^{**} and y^{**}.

(3) For the government, improving the legal environmental incomes after the transformation upgrading of the informal recycling channel of electric vehicle batteries group, and reducing the recycling cost of the available components extracted from the waste electric vehicle batteries through formal channels can reduce the probability of the government taking positive regulation strategy.

Numerical analysis

We first analyze the evolutionary game between the government and the informal recycling channel of electric vehicle batteries group under the fixed punishment model, the results of the analysis are shown as follows:

The results under the fixed punishment model

(1) When $0 < nR_2 - nR_1 - n(1-\alpha)(C_2 - C_1) < (G + \varepsilon ng(y))$ and $0 < R_3 + \varepsilon ng(y) < G + \varepsilon ng(y)$, the initial probability of the government choosing the positive regulation strategy is x = 0.2, and the initial probability of the informal recycling channel of electric vehicle batteries group choosing transformation upgrading strategy is y = 0.6. The evolutionary game process of the mixed strategy under the fixed punishment mechanism can be shown in *Figure 1*.

It can be seen from *Figure 1* that the evolution process between the government and the informal recycling channel of electric vehicle batteries group under the fixed punishment model is a closed-loop curve with a center cycle. At this time, the game process of both parties is periodic behavior, and there is no stable point.

(2) When $0 < nR_2 - nR_1 - n(1-\alpha)(C_2 - C_1) < (G + \varepsilon ng(y))$ and $0 < R_3 + \varepsilon ng(y) < G + \varepsilon ng(y)$, the initial probability of the government choosing the positive regulation strategy is x = 0.2, and the initial probability of the informal recycling channel of electric vehicle batteries group choosing transformation upgrading strategy is y = 0.2 and y = 0.6, respectively. The evolutionary game process of the strategy that the informal recycling channel of electric vehicle batteries group transformation upgrading strategy under different initial probabilities under the fixed punishment model can be shown in *Figure 2*.

It can be seen from *Figure 2* that the informal recycling channel of electric vehicle batteries group transformation upgrading strategy under the fixed punishment model presents a state of fluctuation, and the fluctuation state is related to the initial probability of the government's strategy, and the fluctuation is larger when the initial strategy of the government's positive regulation is low.

http://www.aloki.hu ● ISSN 1589 1623 (Print) ● ISSN 1785 0037 (Online)
DOI: http://dx.doi.org/10.15666/aeer/1704_87498762

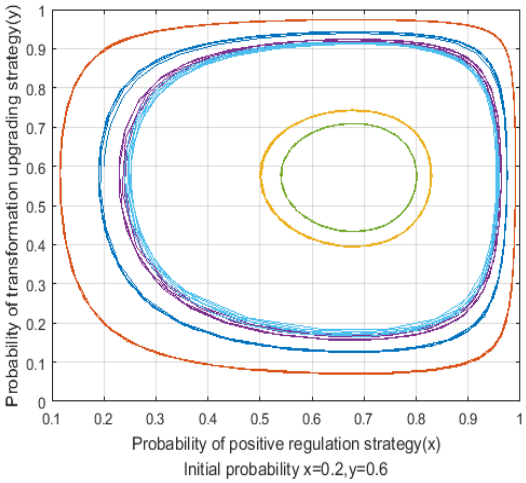

Figure 1. *Hybrid strategy evolution process of the government and the informal recycling channel of electric vehicle batteries group under fixed punishment model*

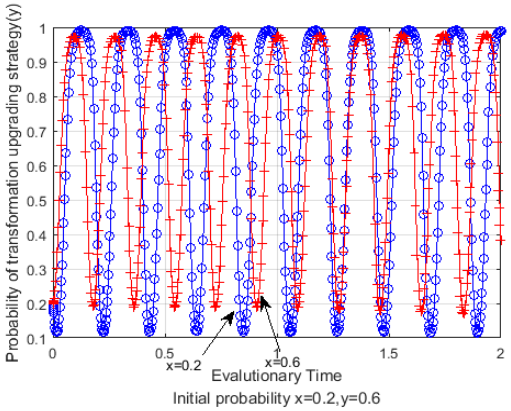

Figure 2. *Evolution process of the informal recycling channel of electric vehicle batteries group's strategy under different initial probabilities under fixed punishment model*

Then we analyze the evolutionary game between the government and the informal recycling channel of electric vehicle batteries group under the dynamic punishment mechanism, the results of the analysis are shown as follows:

The results under the dynamic punishment model

(3) When $0 < nR_2 - nR_1 - n(1-\alpha)(C_2 - C_1) < (G + \varepsilon ng(y))$ and $0 < R_3 + \varepsilon ng(y) < G + \varepsilon ng(y)$, the initial probability of the government choosing the positive regulation strategy is $x = 0.2$, and the initial probability of the informal recycling channel of electric vehicle batteries group choosing transformation upgrading strategy is $y = 0.6$. The evolutionary game process of the mixed strategy under the dynamic punishment model can be shown in *Figure 3*.

It can be seen from *Figure 3* that although the evolution process between the government and the informal recycling channel of electric vehicle batteries group under dynamic penalty model fluctuates, the system will finally converge to the central point,

http://www.aloki.hu ● ISSN 1589 1623 (Print) ● ISSN 1785 0037 (Online)
DOI: http://dx.doi.org/10.15666/aeer/1704_87498762

indicating that the introduction of dynamic punishment model, can gradually stabilize the evolution of the two sides.

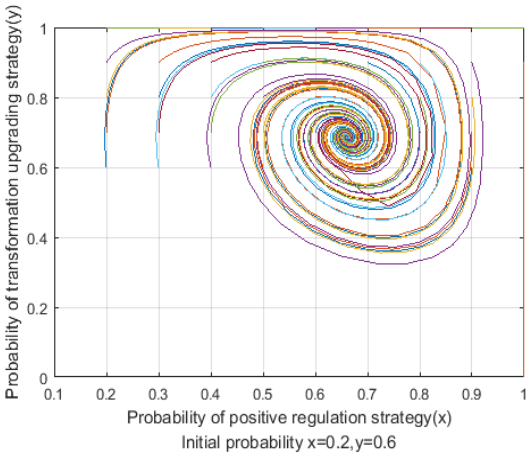

Figure 3. *Hybrid strategy evolution process of the government and the informal recycling channel of electric vehicle batteries group under dynamic punishment model*

(4) When $0 < nR_2 - nR_1 - n(1-\alpha)(C_2 - C_1) < (G + \varepsilon ng(y))$ and $0 < R_3 + \varepsilon ng(y) < G + \varepsilon ng(y)$, the initial probability of the government choosing the positive regulation strategy is $x = 0.2$, and the initial probability of the informal recycling channel of electric vehicle batteries group choosing transformation upgrading strategy is $y = 0.2$ and $y = 0.6$, respectively. The evolutionary game process of the strategy that the informal recycling channel of electric vehicle batteries group transformation upgrading strategy under different initial probabilities under the dynamic punishment model can be shown in *Figure 4*.

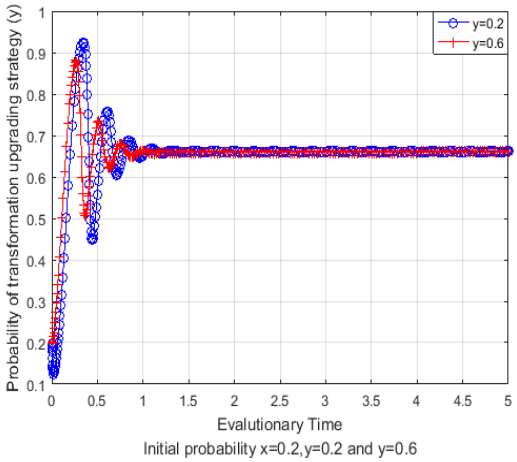

Figure 4. *Hybrid strategy evolution process of the government and the informal recycling channel of electric vehicle batteries group under dynamic punishment model*

It can be seen from *Figure 4* that the strategy of the informal recycling channel of electric vehicle batteries group choose transformation upgrading under the dynamic

http://www.aloki.hu ● ISSN 1589 1623 (Print) ● ISSN 1785 0037 (Online)
DOI: http://dx.doi.org/10.15666/aeer/1704_87498762

punishment model presents a state of volatility. Although the initial stage shows a fluctuating state, it gradually converges with time and finally converges to the central point.

Conclusions

This paper uses evolutionary game theory to explore the strategic choices of the interaction between the government and the informal recycling channel of electric vehicle batteries group. It is found that the evolutionary game model does not have an evolutionary stability strategy under the fixed punishment strategy. Then, the dynamic punishment optimization model is proposed, so that an evolutionary stability strategy emerges in the optimized system, which effectively suppresses the fluctuations in the evolution. When the initial transformation upgrading strategy of the informal recycling channel of electric vehicle batteries group is different, the performance is converged to different equalization values. Increase the upper limit of punishment, the probability of the informal recycling channel of electric vehicle batteries group choosing the transformation upgrading strategy increases.

Based on the above research conclusions, this paper proposes the following management implications. (1) Formulate policies, improve recycling management measures, and gradually improve the support system for power battery recycling. Increase subsidies for formal recycling channels and severely punish informal recycling channels. (2) Learn from the successful experience of developed countries and introduce third-party inspection agencies to assist in management. (3) Relevant enterprises should fulfill the responsibility of electric vehicle batteries, ensure the effective use of power storage batteries and environmental protection, and form a closed-loop management system. (4) Establish a power battery traceability information system to realize the source of power battery can be checked, the direction can be chased, the node can be controlled, and the responsibility can be investigated.

In the research of dynamic punishment mechanism, this paper does not consider the irrational factors of both sides of the game. The next step is to sort out the irrational factors of the two sides of the game under the dynamic punishment mechanism and analyze the impact of the game, and then propose a governance framework of dynamic punishment mechanism. Meanwhile, the simulation of this paper is carried out under the condition of numerical simulation, and the next step can be analyzed in the empirical direction.

Acknowledgements. This paper is supported by MOE (Ministry of Education in China) Project of Humanities and Social Sciences (19YJC630043), National Natural Science Foundation of China (J1824031), the Fundamental Research Funds for the Central Universities (B18RC00070) and Beijing Municipal Bureau of Economy and Information Technology Funds (T17M00070). We appreciate their support very much.

REFERENCES

[1] Capon, A., Gillespie, J., Rolfe, M., Smith, W. (2015): Perceptions of risk from nanotechnologies and trust in stakeholders: a cross sectional study of public, academic, government and business attitudes. – Bmc Public Health 15: 1-13.

http://www.aloki.hu ● ISSN 1589 1623 (Print) ● ISSN 1785 0037 (Online)
DOI: http://dx.doi.org/10.15666/aeer/1704_87498762

[2] Du, J., Li, Q., Qiao, F., Yu, L. (2018): Estimation of vehicle emission on mainline freeway under isolated and integrated ramp metering strategies. – Environmental Engineering and Management Journal 17(5): 1237-1248.
[3] Friedman, D. (1991): Evolutionary games in economics. – Econometrica 59: 637-666.
[4] Friedman, D. (1998): On economic applications of evolutionary game theory. – Journal of Evolutionary Economics 8: 15-43.
[5] Giovanni, P. D., Zaccour, G. (2014): A two-period game of a closed-loop supply chain. – European Journal of Operational Research 232: 22-40.
[6] Gong, D., Tang, M., Liu, S., Xue, G., Wang, L. (2019): Achieving sustainable transport through resource scheduling: a case study for electric vehicle charging stations. – Advances in Production Engineering & Management 14(1): 65-79.
[7] Gu, H., Liu, Z., Qing, Q. (2017): Optimal electric vehicle production strategy under subsidy and battery recycling. – Energy Policy 109: 579-589.
[8] Hao, H., Qiao, Q., Liu, Z., Zhao, F. (2017): Impact of recycling on energy consumption and greenhouse gas emissions from electric vehicle production: the China 2025 case. – Resources, Conservation and Recycling 122: 114-125.
[9] Hong, I., Yeh, J. (2012): Modeling closed-loop supply chains in the electronics industry: a retailer collection application. – Transportation Research Part E 48: 0-829.
[10] Li, L., Zhai, L., Zhang, X., Lu, J., Chen, R., Wu, F., Amine, K. (2014): Recovery of valuable metals from spent lithium-ion batteries by ultrasonic-assisted leaching process. – Journal of Power Sources 262: 380-385.
[11] Li, X., Mu, D. (2018): Recycling price decision and coordinated mechanism of electric vehicle batteries closed-loop supply chain. – Soft Science 5: 1242-129.
[12] Liu, S., Gong, D. (2014): Modelling and simulation on recycling of electric vehicle batteries—using agent approach. – International Journal of Simulation Modelling 13: 79-92.
[13] Ma, Z., Hu, S., Dai, Y. (2016): Decision models for a closed-loop supply chain with hybrid sale collection channels for electrical and electronic equipment under government regulations. – Chinese Journal of Management Science 24: 82-90.
[14] Ordoñez, J., Gago, E. J., Girard, A. (2016): Processes and technologies for the recycling and recovery of spent lithium-ion batteries. – Renewable & Sustainable Energy Reviews 60: 195-205.
[15] Savaskan, R. C., Wassenhove, S. L. (2006): Reverse channel design: the case of competing retailers. – Management Science 52: 1-14.
[16] Savaskan, R. C., Bhattacharya, S., VanWassenhove, L. N. (2004): Closed-loop supply chain models with product remanufacturing. – Management Science 50: 239-252.
[17] Tan, Q., Li, J. (2015): Recycling metals from wastes: a novel application of mechanochemistry. – Environmental Science & Technology 49: 5849-5861.
[18] Turner, J. M., Nugent, L. M. (2016): Charging up battery recycling policies: extended producer responsibility for single-use batteries in the European Union, Canada, and the United States. – Social Science Electronic Publishing 20: 1148-1158.
[19] Wang, W., Wu, Y. (2017): An overview of recycling and treatment of spent LiFePO 4 batteries in China. – Resources, Conservation and Recycling 127: 233-243.
[20] Wang, Y., Chang, X., Chen, Z., Zhong, Y., Fan, T. (2014): Impact of subsidy policies on recycling and remanufacturing using system dynamics methodology: a case of auto parts in China. – Journal of Cleaner Production 74: 161-171.
[21] Xu, J., Thomas, H. R., Francis, R. W., Lum, K. R., Wang, J., Liang, B. (2008): A review of processes and technologies for the recycling of lithium-ion secondary batteries. – Journal of Power Sources 177: 512-527.
[22] Yu, H., Xie, Y., Zhang, T. (2014): Technical progress on power batteries recovery for electric vehicle. – The Chinese Journal of Non-ferrous Metals 24: 448-460.

http://www.aloki.hu ● ISSN 1589 1623 (Print) ● ISSN 1785 0037 (Online)
DOI: http://dx.doi.org/10.15666/aeer/1704_87498762

[23] Zhao, F., Liu, Z., Hao, H., Zhao, S., Zhang, X., Li, J. (2016): Analysis of China's strategy for a stronger automotive country and its implementation pathway. – Forum on Science and Technology in China 8: 45-50.
[24] Zhang, S., Zhang, M., Yu, X., Ren, H. (2016): What keeps Chinese from recycling: accessibility of recycling facilities and the behavior. – Resources Conservation & Recycling 109: 176-186.

http://www.aloki.hu ● ISSN 1589 1623 (Print) ● ISSN 1785 0037 (Online)
DOI: http://dx.doi.org/10.15666/aeer/1704_87498762

EFFECT OF WORKPLACE STATUS ON GREEN CREATIVITY: AN EMPIRICAL STUDY

YANG, Z.* – YE, L. – GUO, M.

School of Economics and Management, Beijing JiaoTong University, Beijing 10044, China

**Corresponding author*
e-mail: 16113169@bjtu.edu.cn

(Received 8th Mar 2019; accepted 1st May 2019)

Abstract. In organizations, green creativity of the employees is an essential part of implementing sustainable development. Our research proposed that workplace status has a significant impact on green creativity. Through an empirical study, we came to the conclusion that an increase in workplace status can lead to green creativity and prosocial motivation mediates the process. Since workplace status promotes the attention for group interests, employees will evaluate their self-worth considering the sustainable development of the environment. Based on the analysis framework of moderated mediation model, this study indicated that organization identification had a positive moderating effect on the relationship between workplace status and green creativity, and it is the boundary condition for workplace status to be effective.
Keywords: *prosocial motivation, organization identification, moderated mediation model, sustainable development, innovation*

Introduction

With the aggravation of environmental problems, researchers in different areas have been studying the issues of global ecosystem protection and sustainable development of the human environment. Responding to environmental challenges, a new manifestation of innovation can bring competitive advantages for organizations (Chen and Chang, 2013). As a result, green creativity has received widespread attention for it enables firms to gain competitive advantages (Gong et al., 2018). The notion of green creativity represents behaviors when companies or individuals propose new ideas for environmental sustainability (Amabile et al., 1996). Among them, natural scientists focus mainly on the technical perspective, which includes how to develop and apply pro-environmental materials and energies (Du et al., 2018; Huppmann et al., 2019), and how to design production models that cause the least harm to the environment (Pombo et al., 2019; Moratis and Melissen, 2019). However, environmental sustainability is ultimately an issue of human behavior, which depends on the complex relationships between individuals, society and natural environment. In other words, it is the interaction of people in the social system with the environment that play a significant role in sustainable development. At the micro level of psychological cognition, green creativity refers to the behavior where individuals generate new ideas to reduce ecological damage, protect natural resources and promote the sustainable development of the economy and the environment (Chen and Chang, 2013). In other words, green creativity reflects the inherent knowledge, beliefs, and value conception systems of an individual or an organization (Song and Yu, 2018; Lichtenfeld et al., 2018). Currently, green creativity has gradually become a research hotspot in social psychology and environmental psychology (Aebischer, 2003; Eisenhandler, 2009; Song and Yu, 2018). Exploring the psychosocial mechanisms of green creativity will not only identify factors

http://www.aloki.hu ● ISSN 1589 1623 (Print) ●ISSN1785 0037 (Online)
DOI: http://dx.doi.org/10.15666/aeer/1704_87638774

that impede positive environmental behavior but also clarify mechanisms that promote positive environmental behavior. In addition, more and more researchers are starting to focus on the social interaction under in an organization context (Song and Yu, 2018).

However, in the perspective of social psychology or environmental psychology, many scholars have discussed the ways of promoting individual green creativity from the aspects of environmental education, suggestion, reinforcement and feedback (Albort-Morant et al., 2016; Zhu et al., 2018; Zhou et al., 2018; Wang et al., 2018). In fact, personality, self-construal, intrinsic motivation and extrinsic motivation will influence social interaction and green creativity (Amabile, 1997; Hennessey and Amabile, 1998; Sawyer, 2017). In recent research, the relationship between organizational situational factors and green creativity are attracting more and more attention, this article will integrate existing research from the perspective of social psychology. Based on the multi-dimensional perspectives such as psychology, society, and culture, will be good for constructing an effective model and institutional design transformation. Therefore, this paper will systematically study the relationship between workplace status and green creativity, with the purpose of providing some reference for future research and policymaking in this field.

In management practice, workplace status as an incentive means widely exists in the design of organizational systems (Djurdjevic et al., 2017). In general, people are eager to gain respect, admiration, and voluntary obedience from other members of the organization (Magee and Galinsky, 2008), and this kind of respect or admiration from others is called workplace status. Status is a concept of sociology, which refers to the universally recognized ranking of individuals in their organization, and the level or grade of a person in an organization. For individuals, workplace status represents the quantity and quality of individuals' valuable resources in the organization (Zinko et al., 2012). Workplace status affects an individual’s resources, development and determines how individuals are restricted in the workplace. As the high value and high demand for workplace status, it is very common for using status as an approach of encouragement. However, how does workplace status affect employee green creativity and the underlying mechanisms are unclear. In terms of influencing factors, little research has paid attention to the internal mediation effect of workplace status on green creativity. Therefore, in this study, we consider how workplace status can contribute to enhancing employees green creativity and explore the boundary conditions for this process.

Research background and hypotheses

Academic research on pro-environmental behavior has a history of nearly 40 years. Green creativity as a representative of pro-environmental behavior is the driving force of sustainable development, therefore every company wants to stimulate the green creativity of its employees more effectively. According to Jia et al. (2018), improving green creativity depends on cooperation between company environmental strategies and corresponding human resource management (HRM) practices. Research on green human resource management mainly focuses on the encouragement of employees to come up with new green ideas and actively participate. The green creativity of employees is of great significance to the sustainable development of enterprises. Therefore, how to effectively stimulate the green creativity of employees in management has received extensive attention.

http://www.aloki.hu ● ISSN 1589 1623 (Print) ●ISSN1785 0037 (Online)
DOI: http://dx.doi.org/10.15666/aeer/1704_87638774

Workplace status and green creativity

Workplace status reflects the respect and admiration in the workplace, and it requires both recognition and good relationships. In order to gain a position in the workplace, a person needs to make great efforts to make their competence recognized. Then, the person must show a friendly attitude to get a warm impression. In general, workplace status represents the social worth of the person and everyone in the organization aim to achieve a high position in the workplace. The social worth will confer the person more useful social resource and access to acquirea positive emotion (Anderson et al., 2015).

Given the complexity of the creative process, social resources and positive emotions may motivate employees to take more participation in green innovation activities. As the high value and high demand for workplace status, it is very common for using status as an approach of encouragement. However, how does workplace status affect employee creativity and the underlying mechanisms are unclear, and little research has paid attention to the internal mediation effect of workplace status on creativity (Song and Yu, 2018). As a result, it is possible to have uncontrollable outcomes in the approach of status encouragement. In other words, the idea is to use status to promote creativity may lead to the opposite result. Based on the interaction theory of creativity, this study explores the mechanism of workplace status on creativity from the perspective of the social interaction generated by green creativity (Wang et al., 2018). In the formation stage of green creativity, the higher workplace status will enhance the interactive relationship in the workplace to activate the internal resources of the organization and promote the transmission of non-redundant information contributing to an internal ecological environment conducive to green innovation (Wrzesniewski et al., 2003). Workplace status is a comprehensive reflection of the ability, prestige, resources, and influence of employees in the workplace. When someone has a high workplace status, it means that he or she will be easier to be recognized and adored. As a result, the person has more probability to believe in his ability and easier to succeed. At the same time, a higher position in the workplace can promote the continuous improvement of green innovative thinking, which is very important to the integration and realization of green ideas. Therefore, this paper assumes that individuals with higher workplace status are more likely to perform green creativity. Based on this, this paper proposed hypothesis 1.

H_1: Workplace status has a positive effect on green creativity.

The mediator role of prosocial motivation

Prosocial motivation refers to encouraging employees to form motivations of benefiting organizations and other members (Grant, 2007), which is a dynamic psychological factor that occurs in social interaction. Since prosocial motivation pays more attention to the interests of others, it shows altruistic behavioral tendencies and cognitive attitudes of respecting others. Workplace status has a significant impact on prosocial motivation for three reasons. First, workplace status reflects the social value of employees in the process of social interaction within the organization and forms an effective social proof in the workplace (Zhu et al., 2018). The prosocial motivation one of the most important internal motivation of individuals meets the value needs of the organization since members of the organization normally have high social expectations for those with high workplace status. Based on the expectation theory, when someone

http://www.aloki.hu ● ISSN 1589 1623 (Print) ●ISSN1785 0037 (Online)
DOI: http://dx.doi.org/10.15666/aeer/1704_87638774

has a higher workplace status, he will have more internal motivation to strive for green innovation.

Second, members with high workplace status have more internal resources and have the obligation to help the organization achieve higher goals. Workplace status is the public's overall evaluation of an individual. In other words, workplace status is a characteristic or trait attributed to a person, which is an intangible capital of the subject (Anderson et al., 2015). Forming prosocial motivation is an effective way for high-level members to achieve organizational goals and this makes workplace status more socially beneficial in the organization.

Third, according to social exchange theory, when employees feel that the organization provides more support, this positive perception will promote green creativity through the mediator role of organizational commitment and job satisfaction. Employees with higher workplace status will pay more attention to the interests of others and have more prosocial behavioral tendencies. In certain circumstances, environmental information in a social situation will trigger people's green creativity intent (Lichtenfeld et al., 2018). Therefore, workplace status will stimulate the prosocial motivation, and then promoting green creativity of the employees. Based on this, we proposed hypothesis 2.

H_2: Prosocial motivation mediates the relationship between workplace status and green creativity.

The moderator role of organization identification

In terms of social perception, recent research indicates the impact of personal beliefs on green creativity. When dealing with environmental issues, people face conflicts between the two goals of achieving enjoyment and following environmental regulations. Therefore, green creativity often means a certain price. Based on the basic premise of cost-benefit, Spanjol et al. (2015) integrated factors such as values, situations, and goals in their theoretical framework. The research for green creativity follows two paths within this framework, one is the external approach, which reduces the cost of pro-environmental decision; the other is the internal approach, which is to strengthen the normative goal and digest the pro-environmental value. Compared with the external approach, the internal approach depends on the corresponding values and the situational factors that can activate such values, so the mechanism of promoting green creativity is very stable (Wang et al., 2018). Within an integrated and diversified framework of green creativity, the role of social perception still exists systematically (Huppmann et al., 2019).

Organization Identification defined as the perception and sense of belonging of individual in an organization has a dramatic impact on employee attitudes, behaviors, and perceptions (Ashforth et al., 2008). According to social identity theory, organizational members have a behavioral tendency to define their social identity according to the social situation they face. Organization identification is a comprehensive reflection of employees' social interaction in the organization and it reflects the cognitive overlap between individual and organization (Farooq et al., 2017). Through this method, an organization's interests can be internalized by employees and organizational success is equivalent to their own success. In other words, organization identification can increase an individual focus on the organization's interests members with a high level oforganization identification may achieve self-positive identity through achieving the organizational goals. This study suggests that organizational

http://www.aloki.hu ● ISSN 1589 1623 (Print) ●ISSN1785 0037 (Online)
DOI: http://dx.doi.org/10.15666/aeer/1704_87638774

identity can enhance the effect of workplace status on green creativity. Therefore, this paper proposes hypothesis 3.

H_3: Organization identification moderates the relationship between workplace status and green creativity.

In summary, in order to further explore the relationship between workplace status and green creativity, this paper establishes a regulated mediation model to reveal the internal mechanism. The model is shown in *Figure 1*.

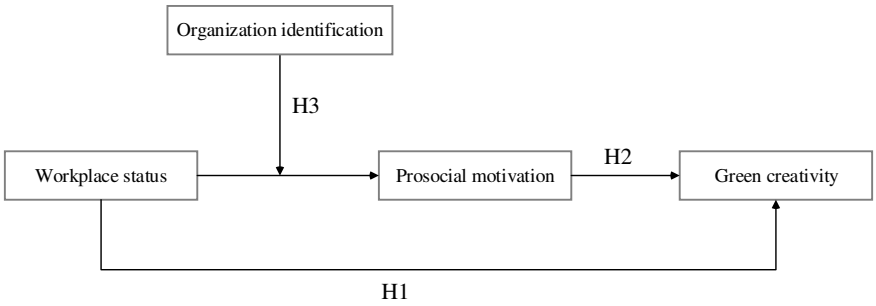

Figure 1. *Theory research model*

Methodology

Data collection

This research mainly aimed at front-line workers in the industry of electricity, telecommunications, and manufacturing. The survey mainly relied on relevant entrusting contact to issue questionnaires and communicated with the responsible persons in detail before the questionnaire. Forty-five companies were selected, and 400 questionnaires were distributed throughout the study. After eliminating invalid questionnaires such as repeated answers and serious missing data, 342 valid questionnaires were obtained (effectiveness 85.4%). Among the employee samples, 54.2% were male; the education level was mainly junior college (66.3%); the age was 26-35 years old (73.7%); the working age was mainly 6 years (36.4%).

The scales used in this study are mature scales widely used in at domestic and abroad areas. Accurate and reliable measurement tools are the basis for exploring green innovative influencing factors and building theoretical models. Recently, researchers havepaid more attention to the scientific and reproducible functionality of behavioral measurement models and have adopted a richer and diverse approach to integrating more effective evaluation structures.

Workplace status is measured based on the 5-question scale developed by Djurdjevic et al. (2017). The paper questionnaire is distributed on-site and the item is like “I enjoy a high status in the workplace”. The prosocial motivation is based on the 4-question scale developed by Grant (2007), measuring items such as “It is important for me to have the opportunity to do my best to help others”. The organization identification is based on the 6-question scale developed by Mael and Ashforth (1992), measuring items such as “The success of the organization is my success”. In addition, we used the model proposed by Chen and Chang (2013) to measure green creativity, and green creativity was measured using the questionnaire in *Table 1*.

http://www.aloki.hu ● ISSN 1589 1623 (Print) ●ISSN1785 0037 (Online)
DOI: http://dx.doi.org/10.15666/aeer/1704_87638774

All English scales were translated into Chinese using the translation-translation back program to maximize the effective understanding of the scale. The scales are all measured by Likert 7 points, from 1 to 7, respectively, indicating that the degree of conformity to the described situation is low to high.The evaluation methods used in the study are self-subjective evaluations of the employees. Therefore, it is necessary to use a rigorous mathematical analysis method to verify the validity of the data.

Table 1. *Measurement items for green creativity (Chen and Chang, 2013)*

No.	Description
1	The members of the green product development project suggest new ways to achieve environmental goals.
2	The members of the green product development project propose new green ideas to improve environmental performance.
3	The members of the green product development project promote and champion new green ideas to others.
4	The members of the green product development project develop adequate plans for the implementation of new green ideas.
5	The members of the green product development project would rethink new green ideas.
6	The members of the green product development project would find out creative solutions to environmental problems.

The framework of moderated mediation model

Mediation models of psychological processes are widely used in the research of organizational behavior because they can reveal the process and mechanism of the influence between variables that get more in-depth results compared with the regression analysis. Applying these models allow us to develop new ideas in theoretical development and explore the possible points of intervention in practice (Shrout and Niall, 2002). In these models, the putative intermediate variables account for the association between independent variables and outcome variables. When the empirical analysis results support the hypothesis proposed by the model, it will provide invaluable information for subsequent experimental research and theoretical exploration (Bollen and Stine, 1990; Mackinnon et al., 2002).

According to Baron and Kenny (1986), a mediation model can be written as:

$$M = i_M + a_X + e_M \quad \text{(Eq.1)}$$

$$Y = i_Y + c'X + bM + e_Y \quad \text{(Eq.2)}$$

In *Equation 1* and *Equation 2*: *i* represents intercept and e represents error, *M* is the mediator between *X* and *Y*, and the indirect effect of this model can be quantified as the product of coefficients *a* and *b*.

In the research of management, psychology and other disciplines, the relationship between two variables is dependent on a third variable is common in many theories. The variables that affect the strength of the relationship between two variables called moderator variables. In other words, a moderation model occurs when the relationship between *X* and *Y* is affected by a moderator variable *Z*. According to Dawson (2014), a moderation model can be written as *Equation 3*.

http://www.aloki.hu ● ISSN 1589 1623 (Print) ●ISSN1785 0037 (Online)
DOI: http://dx.doi.org/10.15666/aeer/1704_87638774

$$Y = i_{1Y} + i_{2Y}Z + c_1X + c_2XZ + e_Y \quad \text{(Eq.3)}$$

When a model contains both mediation variables and moderation variables, it is called a moderated mediation model. According to the basic concepts of the model, a moderated mediation effect occurs when the mediation effect changes with the moderating variable, see in *Figure 2*. Based on previous research (Wang and Preacher, 2015), a moderated mediation model can be written as *Equation 4* and *Equation 5*.

$$M = i_{1M} + i_{2M}Z + a_1X + a_2XZ + e_M \quad \text{(Eq.4)}$$

$$Y = i_{1Y} + i_{2Y}Z + c_1'XZ + c_2'XZ + b_1M + b_2MZ + e_Y \quad \text{(Eq.5)}$$

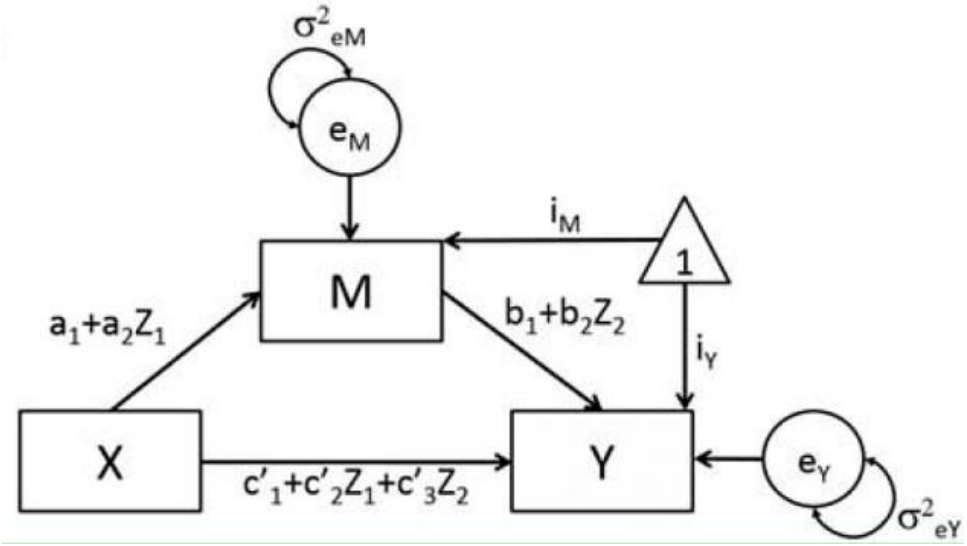

Figure 2. *A moderated mediation model (Wang and Preacher, 2015)*

Results and analysis

Validity and reliability analysis

The exploratory factor analysis and reliability analysis results of the scale are shown in *Table 2* and *Table 3*. From *Table 2*, the interpretable variance of pro-environmentally behaviors is 21.59%, the interpretable variance of organization identification is 19.50%, the interpretable variance of workplace status is 17.06%, and the interpretable variance of prosocial motivation is 14.53%. And greater than 50%. Therefore, this test has good explanatory validity.

It can be seen from *Table 3* that the internal consistency coefficients of all the scales in this study exceeded 0.89, indicating that they all have good measurements.

Descriptive statistics

Table 4 shows the correlation between the various constructs. From the data in the table, the correlation between the variables is good, and the hypothesis is initially supported.

http://www.aloki.hu ● ISSN 1589 1623 (Print) ●ISSN1785 0037 (Online)
DOI: http://dx.doi.org/10.15666/aeer/1704_87638774

Table 2. *Factors, loadings, eigenvalues and explained variance of each factor*

Factor	Items	Loading	Eigenvalue	Variance
Green creativity	GC3	0.861	10.601	21.59%
	GC2	0.820		
	GC4	0.817		
	GC1	0.817		
	GC5	0.687		
	GC6	0.670		
Organization identification	OI4	0.799	1.991	19.50%
	OI2	0.770		
	OI1	0.752		
	OI5	0.751		
	OI3	0.680		
	OI6	0.647		
Workplace status	WP4	0.806	1.530	17.06%
	WP3	0.787		
	WP2	0.784		
	WP5	0.704		
	WP1	0.642		
Prosocial motivation	PM2	0.774	1.140	14.53%
	PM1	0.759		
	PM3	0.759		
	PM4	0.751		

Table 3. *Internal consistencies, mean scores and standard deviations of the scales*

Subscale	Cronbach's alpha	mean score	standard deviation
Green creativity	0.923	6.024	0.921
Organization identification	0.901	5.251	1.270
Workplace status	0.891	4.731	1.189
Prosocial motivation	0.910	5.506	1.130

Table 4. *Inter correlations between subscales*

Subscale	1	2	3	4
1.Green creativity	1	0.591^{**}	0.533^{**}	0.635^{**}
2.Organization identification		1	0.606^{**}	0.611^{**}
3.Workplace status			1	0.618^{**}
4.Prosocial motivation				1

*p <0.05, **p <0.01

Discriminant validity analysis

In order to test the discriminant validity between the main variables, this paper conducts a confirmatory factor analysis of workplace status, prosocial motivation, green creativity, and organization identification. As shown in *Table 5*, compared with the other four competing models, the four-factor model is optimally fitted, and each parameter can reach the fitting standard *($X^2/df=3.66$, NFI=0.96, IFI=0.97, GFI=0.94, RMSEA=0.068, SRMR=0.054)*, indicating that the four variables in this study have good discriminant validity, see in *Figure 3*.

http://www.aloki.hu ● ISSN 1589 1623 (Print) ●ISSN1785 0037 (Online)
DOI: http://dx.doi.org/10.15666/aeer/1704_87638774

Table 5. *Confirmatory factor analysis results*

Model	X^2	df	X^2/df	RMSEA	NFI	IFI	GFI	SRMR
The best one-factor model (WP+PM+GC+OI)	2902.00	189	15.35	0.205	0.88	0.89	0.55	0.099
The best two-factor model A (WP+OI, PM+GC)	2281.79	188	12.14	0.181	0.91	0.92	0.61	0.091
The best two-factor model B (WP, PM+GC+OI)	2377.94	188	12.64	0.185	0.90	0.91	0.60	0.089
The best three-factor model (WP, PM+GC, OI)	1581.18	186	8.50	0.148	0.93	0.94	0.69	0.079
The best four-factor model (WP, PM, GC, OI)	669.38	183	3.66	0.068	0.96	0.97	0.94	0.054

Note: WP=workplace status; PM=prosocial motivation; GC=green creativity; OI=organization identification

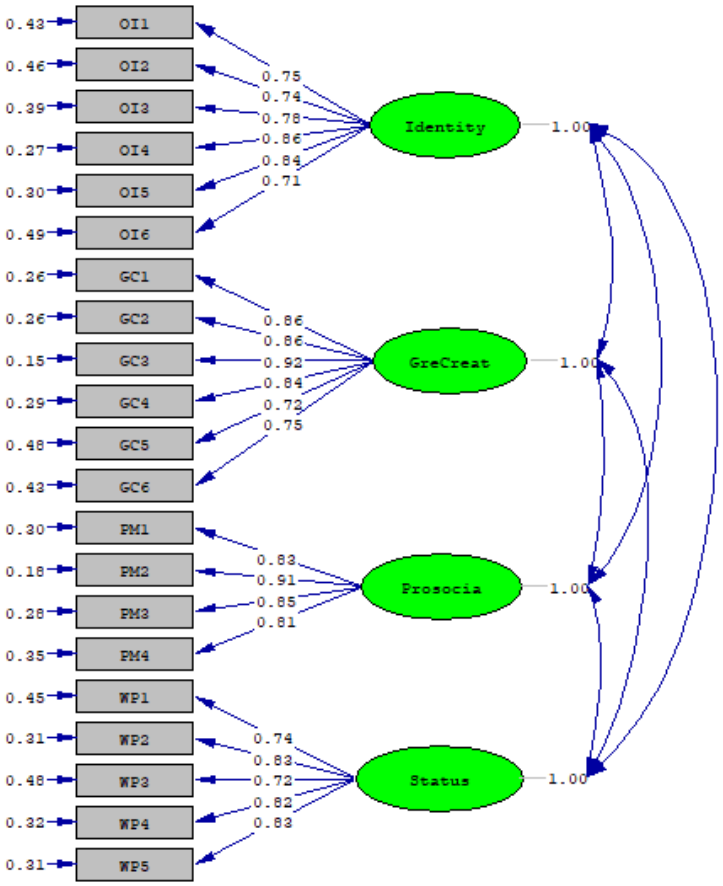

Figure 3. *Validation factor analysis results of the model*

Hierarchical regression analysis

First, we used a method of hierarchical regression analysis to test the mediating effect (Hayes, 2013). After controlling the four variables including age, working years, educational level and technical grade, workplace status still has a significant effect on green creativity, shown in *Table 6*. And we found prosocial motivation partly mediated the relationship between workplace status and green creativity. The regression

http://www.aloki.hu ● ISSN 1589 1623 (Print) ●ISSN1785 0037 (Online)
DOI: http://dx.doi.org/10.15666/aeer/1704_87638774

coefficients with organizational identification were significant that confirmed the moderation effect.

Table 6. *Hierarchical regression analysis*

Variable	Prosocial motivation		Green creativity		
	M1	***M2***	***M3***	***M4***	***M5***
Age	0.023	0.002	-0.064	-0.074	-0.087
Years of working	-0.001	-0.011	0.006	0.006	-0.006
Degree of education	0.126	0.127	0.040	-0.017	0.040
Technical grade	-0.032	0.005	-0.138	-0.123	-0.097
Workplace status	0.613***	0.379***	0.495***	0.216***	0.252***
Prosocial Motivation				0.454***	
organization identification		0.383***			0.398**
interaction term		0.031			0.041***
R^2	0.387	0.478	0.290	0.440	0.406
Adjust R^2	0.378	0.467	0.280	0.430	0.394
$\triangle R^2$	0.371	0.001	0.285	0.149	0.002
$\triangle F$	203.182***	0.763	134.966***	89.262***	1.361

***p< 0.001, **p< 0.01, * p< 0.05

Moderated mediation effect test

In addition, we performed a Bootstrap to get the confidence intervals of the moderated mediation model. With the increase of organizational identification, the correlation coefficient between workplace status and green creativity increased gradually, and the 95% confidence interval does not contain zero, see in *Table 7*. This suggests that organizational identification can moderate the indirect effect between workplace status and green creativity, and the hypothesis H_3 is confirmed. Organizational identification is the boundary condition for workplace status to have an effect on green creativity.

Table 7. *Result of the moderated mediation effect*

Organization Identification	***β***	***Boot SE***	Confidence interval	
			Lower 95%CI	**Lower 95%CI**
1-SD	0.135	0.038	0.067	0.216
1	0.148	0.028	0.099	0.207
1+SD	0.160	0.028	0.112	0.222

Conclusion

In this paper, we proposed a moderated mediation model to explore the relationship between workplace status and green creativity. First, we found workplace status has a significant positive effect on green creativity, and this is very important for the management practices. Second, we confirmed the mediation effect of prosocial motivation, which is an effective complement to the theoretical study of green creativity. In the end, we found organization identification can moderate the indirect effect, and this has a pioneering role in the research of workplace status and green creativity.

http://www.aloki.hu ● ISSN 1589 1623 (Print) ●ISSN1785 0037 (Online)
DOI: http://dx.doi.org/10.15666/aeer/1704_87638774

Acknowledgements. This work was supported by the key project of China's National Social Science Foundation (18AGL012).

REFERENCES

[1] Aebischer, P. (2003): Creative disability/disabled creativity in henry green's 'blindness'. – Studies in the Novel 35: 510-525.
[2] Albort-Morant, G., Leal-Millan, A., Cepeda-Carrion, G. (2016): The antecedents of green innovation performance: A model of learning and capabilities. – Journal of Business Research 69: 4912-4917.
[3] Amabile, T. M. (1997): Motivating creativity in organizations: On doing what you love and loving what you do. – California Management Review 40: 39-58.
[4] Amabile, T. M., Conti, R., Coon, H., Lazenby, J., Herron, M. (1996): Assessing the work environment for creativity. – Academy of Management Journal 39: 1154-1184.
[5] Anderson, C., Hildreth, J. A., Howland, L. (2015): Is the desire for status a fundamental human motive? A review of the empirical literature. – Psychological Bulletin 141: 574-601.
[6] Ashforth, B. E., Harrison, S. H., Corley, K. G. (2008): Identification in organizations: An examination of four fundamental questions. – Journal of Management 34: 325-374.
[7] Baron, R. M., Kenny, D. A. (1986): The moderator–mediator variable distinction in social psychological research: Conceptual, strategic, and statistical considerations. – Journal of Personality and Social Psychology 51: 1173-1182.
[8] Bollen, K. A., Stine, R. (1990): Direct and indirect effects: Classical and bootstrap estimates of variability. – Sociological Methodology 20: 115-140.
[9] Chen, Y.-S., Chang, C.-H. (2013): The determinants of green product development performance: Green dynamic capabilities, green transformational leadership, and green creativity. – Journal of Business Ethics 116: 107-119.
[10] Dawson, J. F. (2014): Moderation in management research: What, why, when, and how. – Journal of Business and Psychology 29: 1-19.
[11] Djurdjevic, E., Stoverink, A. C., Klotz, A. C., Koopman, J., Da, M. V. S., Yam, K. C., Chiang, J. T. (2017): Workplace status: The development and validation of a scale. – Journal of Applied Psychology 102: 1124-1147.
[12] Du J., Li Q., Qiao F., Yu L. (2018): Estimation of vehicle emission on mainline freeway under isolated and integrated ramp metering strategies. – Environmental Engineering and Management Journal 17(5): 1237-1248.
[13] Eisenhandler, S. A. (2009): The greening of creativity and spirituality in 'dooryard' gardeners. – Gerontologist 49: 136-136.
[14] Farooq, O., Rupp, D., Farooq, M. (2017): The multiple pathways through which internal and external corporate social responsibility influence organizational identification and multifoci outcomes: The moderating role of cultural and social orientations. – Academy of Management Journal 60: 954-985.
[15] Gong, D., Liu, S., Tang, M., Ren, L., Liu, J. (2018): Revenue sharing or profit sharing? An internet production perspective. – Advances in Production Engineering & Management 13(1): 81-92.
[16] Grant, A. M. (2007): Relational job design and the motivation to make a prosocial difference. – Academy of Management Review 32: 393-417.
[17] Hayes, A. F. (2013): Introduction to mediation, moderation, and conditional process analysis: A regression-based approach. – Journal of Educational Measurement 51: 335-337.
[18] Hennessey, B. A., Amabile, T. M. (1998): Reward, intrinsic motivation, and creativity. – American Psychologist 53: 674-675.

http://www.aloki.hu ● ISSN 1589 1623 (Print) ●ISSN1785 0037 (Online)
DOI: http://dx.doi.org/10.15666/aeer/1704_87638774

[19] Huppmann, D., Gidden, M., Fricko, O., Kolp, P., Orthofer, C., Pimmer, M., Kushin, N., Vinca, A., Mastrucci, A., Riahi, K., Krey, V. (2019): The message(ix) integrated assessment model and the ix modeling platform (ixmp): An open framework for integrated and cross-cutting analysis of energy, climate, the environment, and sustainable development. – Environmental Modelling & Software 112: 143-156.
[20] Jia, J. F., Liu, H. X., Chin, T. C., Hu, D. Q. (2018): The continuous mediating effects of ghrm on employees' green passion via transformational leadership and green creativity. – Sustainability 10.
[21] Lichtenfeld, S., Maier, M. A., Buechner, V. L., Elliot, A. J. (2018): Ambient green and creativity. – Creativity Research Journal 30: 305-309.
[22] Mackinnon, D. P., Lockwood, C. M., Hoffman, J. M., West, S. G., Sheets, V. (2002): A comparison of methods to test mediation and other intervening variable effects. – Psychological Methods 7: 83-104.
[23] Mael, F., Ashforth, B. E. (1992): Alumni and their alma mater: A partial test of the reformulated model of organizational identification. – Journal of Organizational Behavior 13: 103-123.
[24] Magee, J. C., Galinsky, A. D. (2008): Social hierarchy: The self-reinforcing nature of power and status. – Academy of Management Annals 2: 351-398.
[25] Moratis, L., Melissen, F. (2019): How do the sustainable development goals question rather than inform corporate sustainability? – Resources Conservation And Recycling 141: 253-254.
[26] Pombo, O., Rivela, B., Neila, J. (2019): Life cycle thinking toward sustainable development policy-making: The case of energy retrofits. – Journal Of Cleaner Production 206: 267-281.
[27] Sawyer, R. K. (2017): Creativity research and cultural context: Past, present, and future. – Journal of Creative Behavior 51: 352-354.
[28] Shrout, P. E., Niall, B. (2002): Mediation in experimental and nonexperimental studies: New procedures and recommendations. – Psychological Methods 7: 422.
[29] Song, W. H., Yu, H. Y. (2018): Green innovation strategy and green innovation: The roles of green creativity and green organizational identity. – Corporate Social Responsibility And Environmental Management 25: 135-150.
[30] Spanjol, J., Tam, L., Tam, V. (2015): Employer-employee congruence in environmental values: An exploration of effects on job satisfaction and creativity. – Journal of Business Ethics 130: 117-130.
[31] Wang, L., Preacher, K. J. (2015): Moderated mediation analysis using bayesian methods. – Structural Equation Modeling A Multidisciplinary Journal 22: 249-263.
[32] Wang, X., Zhou, K., Liu, W. (2018): Value congruence: A study of green transformational leadership and employee green behavior. – Frontiers in Psychology 9.
[33] Wrzesniewski, A., Dutton, J. E., Debebe, G. (2003): Interpersonal sensemaking and the meaning of work. – Research in Organizational Behavior 25: 93-135.
[34] Zhou, S., Zhang, D., Lyu, C., Zhang, H. (2018): Does seeing "mind acts upon mind" affect green psychological climate and green product development performance? The role of matching between green transformational leadership and individual green values. – Sustainability 10.
[35] Zhu, Y.-Q., Gardner, D. G., Chen, H.-G. (2018): Relationships between work team climate, individual motivation, and creativity. – Journal of Management 44: 2094-2115.
[36] Zinko, R., Ferris, G. R., Humphrey, S. E., Meyer, C. J., Aime, F. (2012): Personal reputation in organizations: Two-study constructive replication and extension of antecedents and consequences. – Journal of Occupational and Organizational Psychology 85: 156-180.

http://www.aloki.hu ● ISSN 1589 1623 (Print) ●ISSN1785 0037 (Online)
DOI: http://dx.doi.org/10.15666/aeer/1704_87638774

INCENTIVE MECHANISM DESIGN AND SIMULATION OF EMISSION TRADING BASED ON MARKET MAKER SYSTEM

LI, Q. H.* – LI, Y. S. – LI, L. F. – WANG, Y. X.

School of Economics and Management, Beijing Jiaotong University, 100044, Beijing, China
(phone/fax: +86-010-5168-5230)

**Corresponding author*
e-mail: 16113137@bjtu.edu.cn; phone: +86-135-1102-2452

(Received 8th Mar 2019; accepted 1st May 2019)

Abstract. Through model hypothesis and simulation experiment method, this paper demonstrates the behaviour choice of the market maker and emission discharge enterprise after a certain long-term operation with market maker mechanism in the emission trading market under certain pre-defined conditions. Each subject's and overall utility are explored. After analysing the impact of market demand and price difference on market maker trading, the relevant suggestions for introducing the market maker mechanism in the emissions trading market are given.
Keywords: *emission discharge, market maker mechanism, dynamic system, market fluctuations, environment protection*

Introduction

The management of emission rights is an inevitable way to create a harmonious living environment, and it is also a serious issue facing all countries in the world (Du, et al., 2018). International experience shows that emissions trading mechanisms can maximize social benefits while protecting wealth creation, compared to administrative orders and taxation. In a market where market makers participate, the spread (the difference between the asking price and the bid) is not only the price that the market maker provides, which is adjusted according to the change of the market maker's optimal choice (Shen and Starr, 2002), but also a major indicator of the liquidity provided by market makers. It is generally believed that the greater the spread, the greater the risk of holding inventory and thus the lower liquidity (Tarun and Richard, 2001), and vice versa. There are two main theories about the interpretation of the price difference: inventory control theory and reverse selection theory.

The starting point of the inventory control theory is that the market maker must have a certain inventory reserve in order to make the market. Due to the changes in market factors such as interest rates, the market makers will be affected by the uncertainty of the inventory value changes (Gong, et al., 2018). Therefore, the market makers will adjust the ask price and bid price in the quotation to balance inventory risk. The transaction cost problem involved in the spread can be understood by considering the analysis of a neglected problem "foreseeable transaction immediateness" (Demsetz, 1968).

The inverse selection model assumes that there is information asymmetry in the market. There is a market maker and two types of traders in the market: liquid traders and traders with information advantages. Market makers optimize their offers to get the most benefit, that is, by setting a spread to maximize Gains earned by liquidity traders and losses suffered by information advantage traders (Glosten and Milgrom, 1985; Kyle, 1985; Bondarenko, 2001; Calcagno and Lovo, 2006; Zhang and Li, 2011).

http://www.aloki.hu ● ISSN 1589 1623 (Print) ● ISSN 1785 0037 (Online)
DOI: http://dx.doi.org/10.15666/aeer/1704_87758791

From the monopolistic of market makers and the impact of competition on the market, centralized model research shows that the monopolistic expert system on the New York Stock Exchange enables market makers to enhance social welfare because in the scattered market, it partially internalizes the externalities of the spread (Miao, 2006).

From the transparency aspect of information, researchers examined the price display effect in the market maker market and found that in the opaque market, the open spread is large and trading volume is low due to higher search costs, but higher search costs lead to more aggressive pricing strategies, so price discovery speeds are faster in opaque markets (Flood, et al., 1999; Bloomfield and O'Hara, 2000).

In addition, some studies have investigated the aspects of market stability, market maker financing, and locality of market makers. Financial market models were used to test the stability of market makers to the market (Zhu et al., 2009). They assumed that there are two types of investors in the market: fundamental investors and trend investors, market makers acting as liquidity providers and active investors. The research results show that when market makers actively manage their inventory to maximize profits, they do not stabilize the market; and the behavior of market makers depends on the behavior of speculators (Zhu, et al., 2009). The information advantage of local market makers is a very valuable factor in reducing transaction costs (Kedia and Zhou, 2011).

Overall, the research on the market maker system of emission trading at home and abroad is still very imperfect. The Emission trading market should play an active role in pollution control. The market mechanism needs to be improved. The market makers acting as emission trading intermediaries are one of the important components of micro market structures. To introduce market maker trading in the pilot trading phase of China, the most urgent task is to have a complete set of incentives and constraints for market makers to ensure the effectiveness of market makers' behavior. This is also the shortcoming of the current research.

Methods

Since China's emission trading market has not adopted the market maker trading system, this study uses the simulation experiment method to study the trading efficiency of market makers in the emission trading market. The experimental method is one of the main methods for researchers at home and abroad to study emissions trading. In order to reflect the transaction efficiency of the market maker's quotation, the trading system set up by the research institute contains a market maker and a number of emission discharging enterprises. The transactions of the emission discharging enterprises are carried out by the market makers, and the current emission discharge certificates cannot be stored in the conditions of next stage of transaction. Due to the need of market making, the market maker needs to balance the relationship between the current transaction income and the storage cost. under the established supervision, the emission discharge enterprises trade considering the quote of the market maker and its own emission reduction cost. Based on this, this paper explores the long-term behavioral evolution of each participant, studies the transaction efficiency of market makers' quotations in the emission discharge trading market, and provides theoretical guidance for the application of market maker quotation system in China's emissions trading practice.

http://www.aloki.hu ● ISSN 1589 1623 (Print) ● ISSN 1785 0037 (Online)
DOI: http://dx.doi.org/10.15666/aeer/1704_87758791

Hypothesis 1: Each trading entity adjusts its decisions based on their respective profit conditions. In the emission trading system, the amount and quotation of the emission right of the market maker is private information and the quotation setting needs the market maker's information collection of each emission enterprise. Due to the incompleteness of the information, the decision of the market maker and the emission enterprise Behaviors are adjusted only based on the information they have. Under the condition of profit maximization, the profit value can be regarded as the most credible indicator, so it is assumed that each transaction entity adjusts the decision according to their respective profit conditions.

Hypothesis 2: The spread of each period is fixed, but the market maker will adjust the ask price and bid for the next period based on the information of this period. The market makers need to make quotations during making the market. If the price difference is too large, it will damage the interests of the traders, and it is not conducive to the liquidity of the market. In order to standardize the market making behavior of market makers, it is in practice to set the price difference magnitude or upper limit. Therefore, this paper sets a fixed spread and assumes that the spread will remain the same in each period, but the market maker will adjust the bid and bid for the next period based on the information in this period. The model parameters are set as follows:

D - the total market demand of the product, assuming a normal distribution;
D_i - the market demand for the products of enterprise i;
AP - the asking price of the market maker;
BP - the bid of the market maker;
N - the number of emission enterprises;
R_i - the product profit obtained by use of each unit of the emission certificate;
L - the total amount of emission permits available for distribution;
L_i - the number of emission control certificates assigned by each company;
C_i - the cost of abatement of enterprise i, assumed to follow a normal distribution;
Q_i - the trading volume of the emission certificate;
Q_{1i} - the amount of sales of emission control certificates;
Q_{2i} - the purchase amount of the pollutant discharge certificate;
P - the probability of effective supervision;
F - cost of violation punishment.

According to the question, the amount of emission certificates traded by the enterprises is given by *Equations 1* and *2*.

$$Q_{1i}(Sell)=\begin{cases}L_i-D_i, L_i\geq D_i, C_i\geq BP\\ L_i, L_i\geq D_i, C_i\leq BP\\ L_i, L_i\leq D_i, C_i\leq BP\\ 0, \text{else}\end{cases} \quad \text{(Eq.1)}$$

$$Q2i(Buy)=\begin{cases}D_i-L_i, L_i<D_i, R_i>AP, C_i>BP, (D_i-L_i)AP\leq F\times p\\ 0, \text{else}\end{cases} \quad \text{(Eq.2)}$$

Enterprise i's profit model is given by *Equation 3*.

http://www.aloki.hu ● ISSN 1589 1623 (Print) ● ISSN 1785 0037 (Online)
DOI: http://dx.doi.org/10.15666/aeer/1704_87758791

$$\pi^{c}(i)=\begin{cases} D_i \times R_i + (L_i - D_i)BP, C_i \geq BP, L_i \geq D_i \\ D_i \times R_i + L_i \times BP, C_i < BP \\ L_i \times R_i, L_i < D_i, R_i < AP \\ D_i \times R_i - (D_i - L_i)AP, L_i < D_i, R_i \geq AP, C_i \geq BP, (D_i - L_i)AP < p \times F \\ L_i \times R_i, L_i < D_i, R_i \geq AP, C_i \geq BP, (D_i - L_i)AP \geq p \times F \end{cases} \quad \text{(Eq.3)}$$

The market maker's profit model is given by *Equation 4*.

$$\pi^{(M)}=\begin{cases} \sum_{i=1}^{N} \mathrm{Q}_{1i}(AP - BP), Q_{1i} < Q_{2i} \\ \sum_{i=1}^{N} \mathrm{Q}_{2i}(AP - BP) - \sum_{i=1}^{N}(Q_{1i} - Q_{2i})BP, Q_{1i} \geq Q_{2i} \end{cases} \quad \text{(Eq.4)}$$

The total system profit is given by *Equation 5*.

$$\pi^{(s)} = \sum_{i=1}^{N} Q2i(Ci - AP) \quad \text{(Eq.5)}$$

Under normal circumstances, the market price changes with the supply of the two enterprises. Since the two emission enterprises is aware that their respective production will affect the market price, that is, the market price of the product, each enterprise will carefully trade the emission permit.

Proposition 1: Under the condition of complete information, the sufficient condition for the emissions trading is that there is a non-empty emission permit price range which makes $\partial\Pi_1/\partial Q > 0$ and $\partial\Pi_2/\partial Q > 0$.

Proof: The price of the emission permit is set as. Because the rational enterprise aims to maximize the profit, considering that permit trading will cause the change buyer's the marginal emission reduction cost and the market price, the trading is not made, unless the buyer and the seller's profit increment is positive.

According to the profit function, the response curve for deriving the maximum benefit of the emission discharge enterprise is given by *Equations 6* and *7*.

$$Q_1 = \frac{a - bQ_2 - MSC_1 - MCA_1}{2b} \quad \text{(Eq.6)}$$

$$Q_2 = \frac{a - bQ_1 - MSC_2 - MCA_2}{2b} \quad \text{(Eq.7)}$$

The total production is given by *Equation 8*.

$$Q = Q_1 + Q_2 = \frac{2a - MSC_1 - MSC_2 - MCA_1 - MCA_2}{3b} \quad \text{(Eq.8)}$$

Cournot-Nash equilibrium production is given by *Equation 9*.

http://www.aloki.hu ● ISSN 1589 1623 (Print) ● ISSN 1785 0037 (Online)
DOI: http://dx.doi.org/10.15666/aeer/1704_87758791

$$Q_1 = Q_2 = \frac{2a - 2MSC_1 - MCA_1 - MCA_2}{6b} \quad \text{(Eq.9)}$$

At this point, the market price of the product is given by *Equation 10*.

$$P = \frac{a + 2MSC_1 + MCA_1 + MCA_2}{3} \quad \text{(Eq.10)}$$

Emission discharge enterprises are producing under balanced production. It is obvious that emission discharge enterprise 1 will obtain higher profits with lower marginal emission reduction costs. Therefore, in terms of balanced production, the enterprise 2's profit before trade is given by *Equation 11*.

$$\Pi_2 = PQ_2 - \int_0^{Q_2} (MSC_2 + MCA_2)dt \quad \text{(Eq.11)}$$

After trading, the profit of emission discharge enterprise 2 is given by *Equation 12*

$$\Pi_2^* = P^* Q_2 - L_1 P_L - \int_0^{Q_2} MSC_2 dt - \int_0^{Q_2^*} MCA_2 dt \quad \text{(Eq.12)}$$

The conditions for the transaction are : $\Pi_2^* - \Pi_2 \geq 0$. Therefore, the conditions for emission discharge enterprise 2 can be given by *Equation 13*.

$$P_L \leq \frac{(\Delta MCA_1 + \Delta MCA_2)Q_2 + 3\int_{Q_2^*}^{Q_2} MCA_2 dt}{3L_1} \quad \text{(Eq.13)}$$

Similarly, the conditions for the buyer-- emission discharge enterprise 1 to make the trade can be given by *Equation 14*.

$$P_L \geq \frac{(\Delta MCA_1 + \Delta MCA_2)Q_1 + 3\int_{Q_1^*}^{Q_1} MCA_1 dt}{3L_1} \quad \text{(Eq.14)}$$

In summary, the effective conditions of the trade should satisfy *Equation 15*.

$$\frac{(\Delta MCA_1 + \Delta MCA_2)Q_1 + 3\int_{Q_1^*}^{Q_1} MCA_1 dt}{3L_1} \leq P_L \leq \frac{(\Delta MCA_1 + \Delta MCA_2)Q_2 + 3\int_{Q_2^*}^{Q_2} MCA_2 dt}{3L_1} \quad \text{(Eq.15)}$$

Because $MCA_1 \leq MCA_2$, there is a non-empty price set P_L, and the trade will only occur when the price of the emission permit is in this range. In particular, when the marginal emission reduction cost of the enterprise remains unchanged in the short term, it satisfies: $MCA_1 \leq P_L \leq MCA_2$.

In the market environment with asymmetric information, due to the uncertainty of production and operation, the lack of understanding of the needs of the trading parties, etc., the emission discharge enterprises often consider the question of when to buy and

http://www.aloki.hu ● ISSN 1589 1623 (Print) ● ISSN 1785 0037 (Online)
DOI: http://dx.doi.org/10.15666/aeer/1704_87758791

sell, how much to buy and sell, which brings the emissions trading Uncertainty. But at this time, if there is a seller in the market, it can be seen that it provides clear information to the market, because the appearance of selling often means the certainty of the remaining. Conversely, the information conveyed by the buyer is often not clear enough, because the existence of uncertainty tends to increase the demand of the enterprise, resulting in more purchases in the market than real demand. Therefore, the emergence of the seller is a key factor in determining the efficiency of the information asymmetry market.

Proposition 2: Under the asymmetric information environment, the trading volume of emission rights depends on the sales volume of the enterprise.

Proof: It is assumed that under the condition that the price range satisfies the trade occurrence, the probability of the emission discharge enterprise 1 selling the permit is: the probability of not selling is. The smaller the probability value, the stronger the uncertainty of the emission discharge enterprise 1 selling the emission permit. In this regard, the emission discharge enterprise 2 has two strategies: buy, not buy, the strategy matrix is shown in the following *Table 1*.

Table 1. *Strategic matrix of sewage enterprises*

	Sell (p)	**Not sell** ($1-p$)
Buy	$P*Q_1+L_1P_L-\int_0^{Q_1}MSC_1dt$, $P*Q_2-L_1P_L-\int_0^{Q_2}MSC_2dt-\int_0^{Q_2*}MCA_2dt$	$PQ_1-\int_0^{Q_1}MSC_1dt-\int_0^{Q_1*}MSC_1dt$, $PQ_2-\int_0^{Q_2}MSC_2dt-\int_0^{Q_2}MCA_2dt$
Not buy	$PQ_1-\int_0^{Q_1}(MSC_1+MCA_1)dt$, $PQ_2-\int_0^{Q_2}(MSC_2+MCA_2)dt$	$PQ_1-\int_0^{Q_1}MSC_1dt-\int_0^{Q_1*}MSC_1dt$, $PQ_2-\int_0^{Q_2}MSC_2dt-\int_0^{Q_2}MCA_2dt$

Under the two strategies, the expected value functions of the emission discharge enterprises 2 are *Equations 16* and *17*.

$$E(\Pi_{2Buy})=p(P*Q_2-L_1P_L-\int_0^{Q_2}MSC_2dt-\int_0^{Q_2*}MCA_2dt)+(1-p)(PQ_2-\int_0^{Q_2}MSC_2dt-\int_0^{Q_2}MCA_2dt) \quad \text{(Eq.16)}$$

$$E(\Pi_{2Notbuy}=PQ_2-\int_0^{Q_2}(MSC_2+MCA_2)dt \quad \text{(Eq.17)}$$

According to the expected value decision rule, the conditions for the trade should satisfy *Equation 18*.

$$E(\Pi_{2Buy})\geq E(\Pi_{2Notbuy}) \quad \text{(Eq.18)}$$

Inferred that the price generated by the trade is given by *Equation 19*.

$$P_L\leq\frac{(MCA_2*-MCA_2)Q_2+3\int_{Q_2*}^{Q_2}MCA_2dt}{3L_1} \quad \text{(Eq.19)}$$

http://www.aloki.hu ● ISSN 1589 1623 (Print) ● ISSN 1785 0037 (Online)
DOI: http://dx.doi.org/10.15666/aeer/1704_87758791

This price condition is exactly the same as the previous buying condition, that is, as long as the price is in the tradable range, the emission discharge enterprise 2 will certainly buy the emission permit, because the purchasing strategy is always profitable for the emission discharge enterprise 2. Then the key factor restricting the sale and purchase is the probability of the sales of the emission discharge enterprise 1. The greater the probability that the emission discharge enterprise 1 sells, the easier the trade will be generated, conversely, the less likely the trade is. That is: the amount of sales of emission permit is a key factor in determining the volume of emissions trading.

According to Proposition 1 and Proposition 2, whether a market mechanism is effective depends on whether it can make the price in a tradable range and how to form a seller. Based on this analysis, this study compares and analyzes the difference between the market maker's quotation transaction and the current implementation of the emission trading price and the seller's formation mechanism in China.

Data and simulation analysis

For the sake of clarity, it is assumed that there are two emission discharge enterprises in the same region that use the same technology to produce homogeneous products, which have the same marginal social cost (MSC). In terms of quantity, the marginal social cost is equal to the sum of the marginal cost of the production of the emission discharge enterprise (MC) and the marginal external cost of emission caused by the environment (MEC): $MSC = MC + MEC$. Under the conditions of the scale of production, the proportion of input factors, and the fixed level of technology, for the enterprises, the marginal social cost is tilted upwards, because with the increase in production of emission discharge enterprise, the marginal cost of production rises, and with the amount of emission Increase, the harm to the environment also rises. However, due to the different emission reduction technologies adopted, the marginal emission reduction costs (MCA) of the two enterprises are different, and they are respectively MCA_1 and MCA_2. In the short-term, due to the fixed level of emission reduction, the marginal emission reduction cost of emission reduction enterprises should be tilted downwards, because enterprises need to install specific emission reduction equipment when they reduce emissions. When the emission reduction is small, the unit cost will be higher. When the emission reduction is high, the unit cost is reduced accordingly.

It is assumed that the emission discharge enterprises are producing with the goal of maximizing profits, and the target yields of the two enterprises maximizing profits are respectively, and at the same time, because the products are homogeneous, the emission discharge enterprises have the same product demand curve.

Let product price as $P = a - bQ$, Q is the total production of emission discharge enterprise 1 and 2, that is $Q = Q_1 + Q_2$. Then emission discharge enterprise 1's expected income function is *Equation 20*.

$$Max\Pi_1 = PQ_1 - \int_0^{Q_1} (MSC_1 + MCA_1)dt \quad \text{(Eq.20)}$$

Then emission discharge enterprise 2's expected income function is *Equation 21*.

$$Max\Pi_2 = PQ_2 - \int_0^{Q_2} (MSC_2 + MCA_2)dt \quad \text{(Eq.21)}$$

http://www.aloki.hu ● ISSN 1589 1623 (Print) ● ISSN 1785 0037 (Online)
DOI: http://dx.doi.org/10.15666/aeer/1704_87758791

According to the above mathematical model hypothesis, after compiling and running the Fables program, a graphical interface as shown in *Figure 1* will be formed. The parameters of the model are displayed in the dialog box on the left side of the interface, which includes the emission reduction costs set in the previous section. For parameter values such as asking price and bid, the interface box on the right side of the graph is the area showing the result after the program runs.

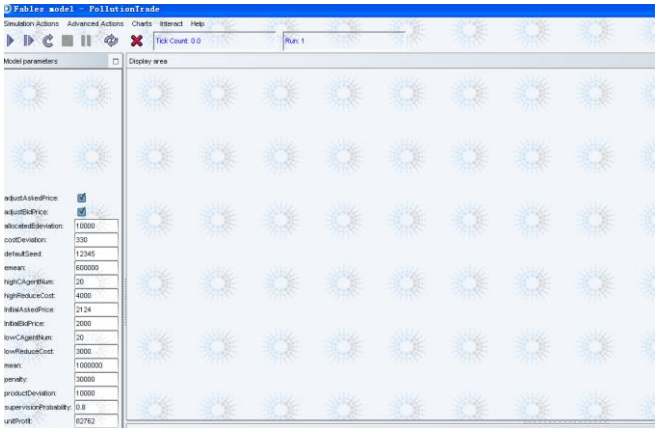

Figure 1. *Running interface of program*

According to the research needs, this study sets four research variables: spread, trading volume, market maker profit, and profit of emission discharge enterprise. The time period is an important factor in the reliability of the reaction simulation results. Therefore, this paper observes the stability of the simulation run for 50 cycles and analyzes the reliability of the indicators. The simulation results are shown in *Figure 2*.

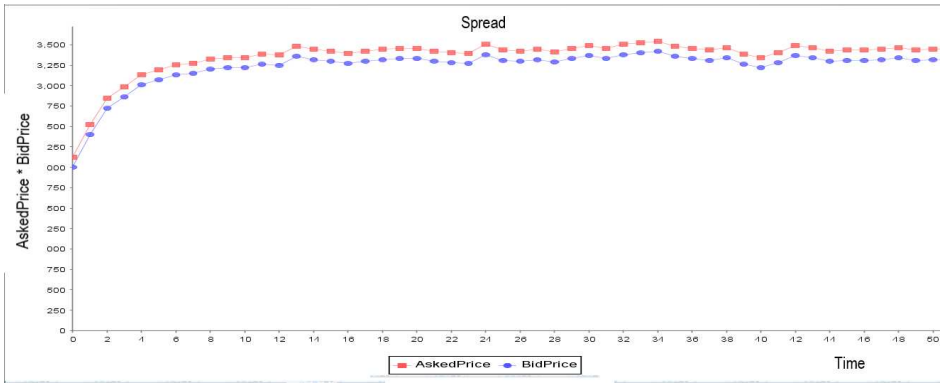

Figure 2. *Simulation diagram of the market maker quotation*

The simulation results of the market maker's quotation in *Figure 2* show that during the 50 cycles of operation, the market maker's quotation and the trend of the price difference are relatively stable, and the volatility of the quotation is small. After about 50 cycles of operation, the quotation increased from the bid of 2,000 yuan/ton and the asking price of 2,124 yuan/ton to the bid of about 3,250 yuan/ton and the asking price of 3,500 yuan/ton, and then stabilized. Through the quote of the market maker, realization of market price discovery mechanism can be enhanced.

http://www.aloki.hu ● ISSN 1589 1623 (Print) ● ISSN 1785 0037 (Online)
DOI: http://dx.doi.org/10.15666/aeer/1704_87758791

The simulation results of the market trading volume in *Figure 3* show that the average market buying and selling volume fluctuates around 6500 as the axis, and the pattern is in good coincidence. This shows that the buyer and the seller are in the same trend, and the market trade are very active. According to the average purchase and sales volume of 6,500, the total trade volume of each period can reach 260,000 units, calculated according to the total allocation of 600,000. The trade ratio is as high as 43%, which will optimize the rational allocation of emission permits. However, as the average fluctuation of the sales volume is small, the volatility of the purchase volume is relatively large, indicating that the large fluctuations in the purchase volume will increase the uncertainty of the market demand for emission permits. as the market organizer. the market maker has a need to have a certain amount of reserves to deal with market risks.

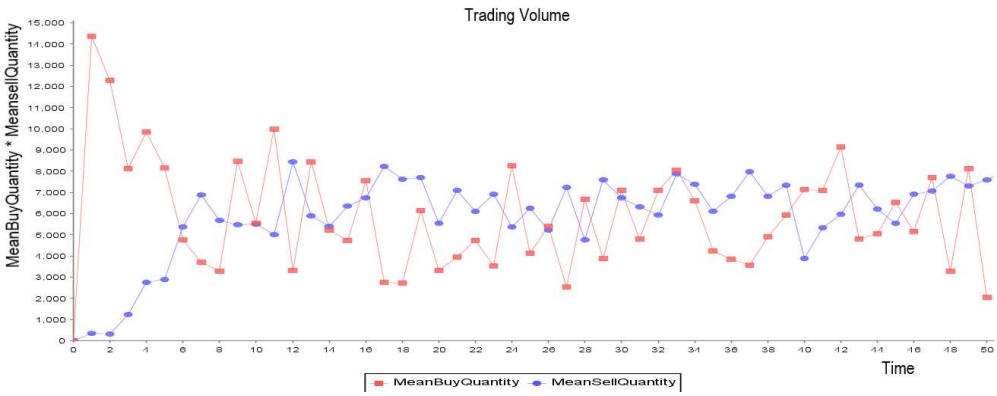

Figure 3. *Simulation diagram of trading volume*

As shown in the simulation results of the market maker's profit in *Figure 4*, in the 50 cycles of operation, the profit of the market maker mainly fluctuates between -5 million and -17.5 million, and the profit fluctuation is large. There are two main reasons for the phenomenon: First, the emission permit is set as not storable, which means that the current permit cannot be used for the next trade. This will bring storage costs and maturity loss risk to the market makers; second, the volume of trading in the company's buying volume fluctuates greatly, which increases the risk of market maker trading.

Figure 4. *Simulation diagram of the market maker profit*

http://www.aloki.hu ● ISSN 1589 1623 (Print) ● ISSN 1785 0037 (Online)
DOI: http://dx.doi.org/10.15666/aeer/1704_87758791

Although the previous simulation results show that the market maker's profit is negative, *Figure 5* shows that the entire emissions trading system has positive returns, and the return value fluctuates between mainly 1 million and 4 million. This indicates that in the case where storage is not allowed, although the market maker suffers a certain loss, the increase in the profit of the emission discharge enterprises and the saving of the emission reduction cost can make up for this loss. Therefore, a comprehensive analysis of the above simulation results shows that market transactions involving market makers increase market efficiency.

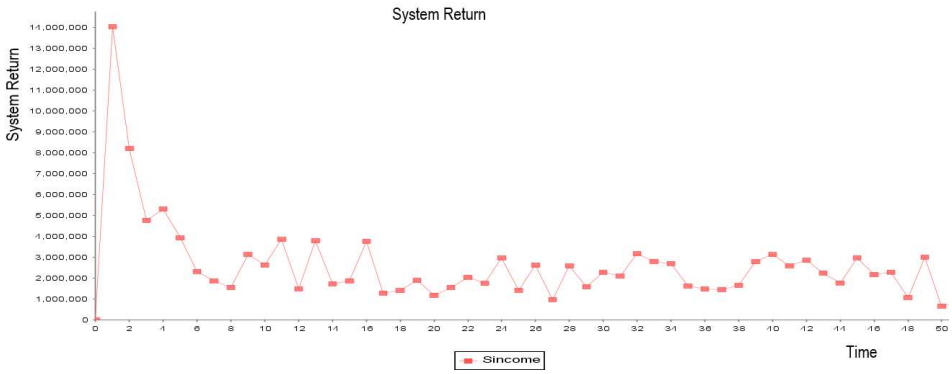

Figure 5. *Simulation diagram of system return*

Results and discussion

In order to understand the performance of the emissions trading market under different market conditions, and to formulate corresponding institutional measures to ensure the operation of the market maker trading market system, this study analyzes the changes in market quotations, system returns and other indicators by changing certain market parameter values and features.

The impact of market demand variance on market maker transactions

When setting the initial value of the simulation, the variance of the market demand variable and the emission right distribution variable is small. This is suitable for the steel industry, which has a small difference between enterprises and a stable market environment. However, in certain industrial environments, or in certain specific environments, market demand changes more severely, and smaller demand variances do not reflect this market change. In addition, in the current allocation of emission rights, the distribution of emission rights often has a higher correlation with the market demand and production volume of the enterprise, and the presence of market power will further aggravate the inequality of the distribution of emission rights.

In order to make the research results more obvious, this study increases the standard deviation of market demand parameters to 10,000, and the standard deviation of emission allocation parameters to 10,000, thus to compare the performance of market makers in different market environments. The simulation results are shown in *Figure 6.*

Figure 6 shows that during the 50 cycles of operation, the volatility of the market maker's quotation increased after the variance increased, although the main quotation range is still concentrated around 3250. The simulation results show that the market

http://www.aloki.hu ● ISSN 1589 1623 (Print) ● ISSN 1785 0037 (Online)
DOI: http://dx.doi.org/10.15666/aeer/1704_87758791

maker's quotation level and spread is greatly affected by the balance of market demand and emission permit allocation.

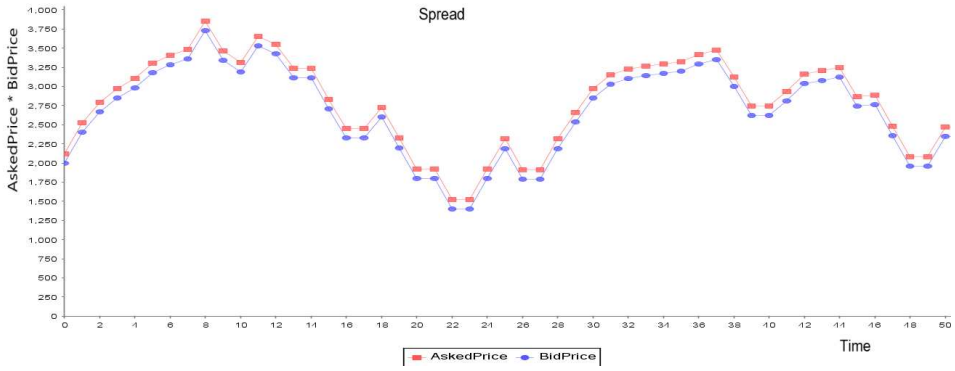

Figure 6. *Simulation diagram of market maker quotation after increasing the variance*

Figure 7 shows that in a drastic market and in the presence of market power, the market's buying and selling volume still have a good coincidence, but the market's trading volume has slightly decreased, and the sales volume is more discrete. The simulation results show that the market trade are in good condition, but the difference between the sales volume and the purchase volume of the market trade becomes larger.

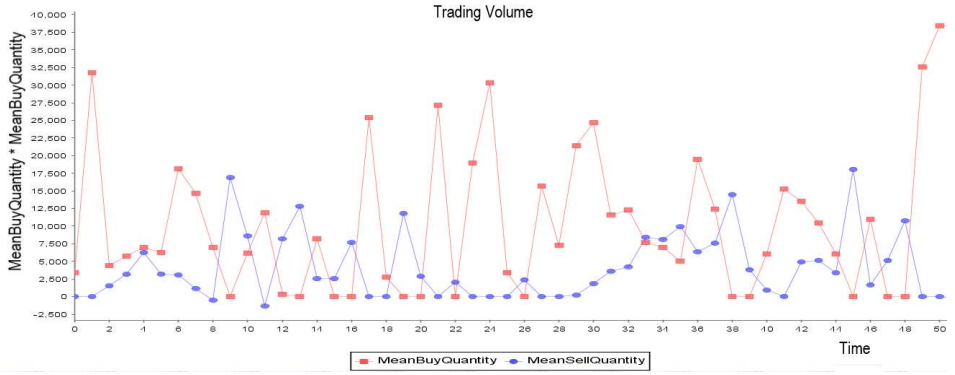

Figure 7. *Simulation diagram of trading volume after increasing the variance*

Figure 8 shows that during the 50 cycles of operation, due to the large fluctuations in the amount of purchases and sales in the market, the profit of market makers also showed strong volatility. But the market makers' profit in some cycles has positive values, which indicates that in the severe market environment, the distribution method of the different emission permits will increase the profit of the market maker.

Figure 9 shows that in the 50 cycles of operation, the system returns are non-negative, and the mean and fluctuation of system benefits are high. The simulation results show that the market demand is uncertain and there is a serious distribution bias. Using market maker transactions can significantly increase the revenue of the entire trading system.

From above simulation analysis it can be seen that under the severe market and the large difference in the market distribution of emission permits, the quotation of market

http://www.aloki.hu ● ISSN 1589 1623 (Print) ● ISSN 1785 0037 (Online)
DOI: http://dx.doi.org/10.15666/aeer/1704_87758791

makers is relatively higher, the system transactions will still maintain a high level, and the system returns are higher. Therefore, it is more suitable to use the market maker market transaction in this environment.

Figure 8. *Simulation diagram of market maker profit after increasing the variance*

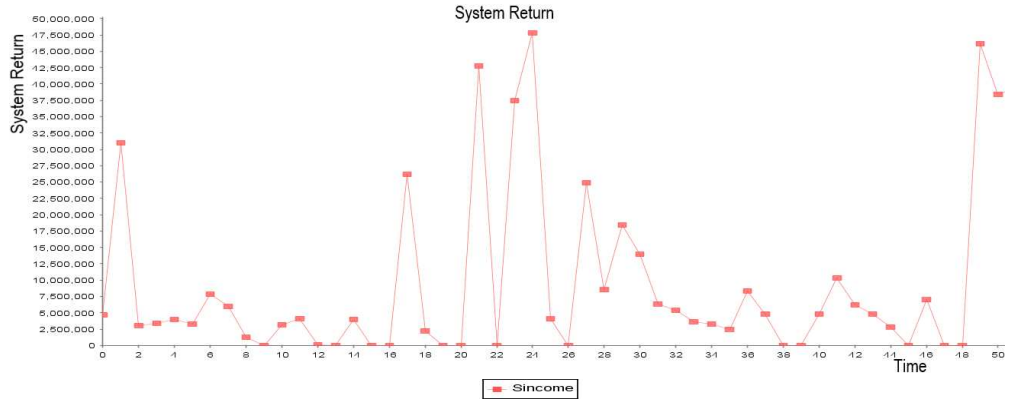

Figure 9. *Simulation diagram of system return profit after increasing the variance*

The effect of spreads on market maker trading

In market maker trading, the price difference is an important factor that restricts the market price and the profit of the market trading entity. In the current financial market, many countries and regions have a clear limit on the price difference of market makers. Therefore, this paper adjusts the spread to compare the impact of the spread on the market for emissions trading.

As shown in *Figures 10* and *11*, the change in the spread during the 50 cycles of operation did not result in large fluctuations in the quoted price of the market maker. However, under the 20% spread, the asking price of the market maker rose to about 3,750, and under the 40% spread, the asking price of the market maker rose to about 4,250. Therefore, the simulation results show that the change in the spread does not change the trend of the quote. However, the change in the price difference will change the absolute value of the market maker's quotation, thus affecting the supply and demand relationship of the market.

http://www.aloki.hu ● ISSN 1589 1623 (Print) ● ISSN 1785 0037 (Online)
DOI: http://dx.doi.org/10.15666/aeer/1704_87758791

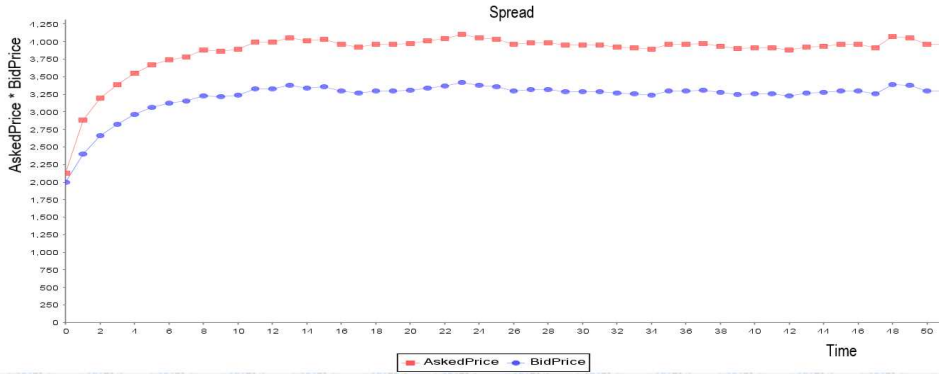

Figure 10. *Simulation diagram of market maker quotation under 20% spread*

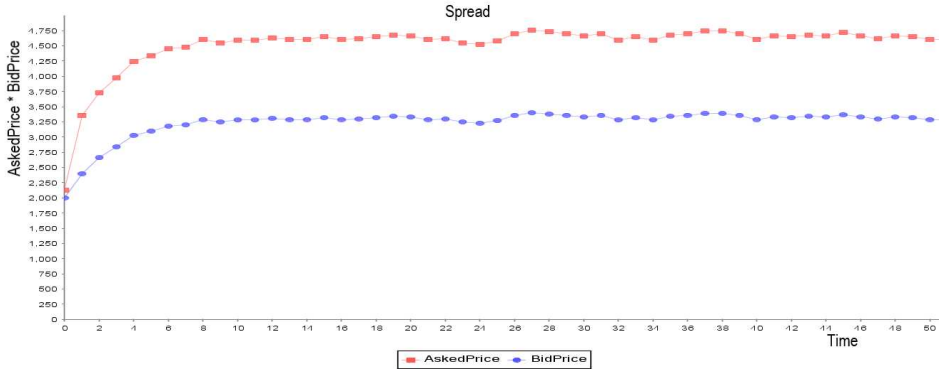

Figure 11. *Simulation diagram of market maker quotation under 40% spread*

As shown in *Figures 12* and *13*, the market's sales volume and purchase volume coincidence are better under different price differences. However, in comparison, under the 40% spread, the market transaction volume is relatively high, indicating that the higher the price difference, the higher the uncertainty of market transactions.

As shown in *Figures 14* and *15*, although the spread of the market maker's offer has increased, the market maker's profit is still negative, and both fluctuate with an axis of -12.5 million. This shows that despite the increase in the spread, the increase in the spread has changed the supply and demand relationship, resulting in fewer purchases. Therefore, the increase in market maker inventory reduces the profit of market makers.

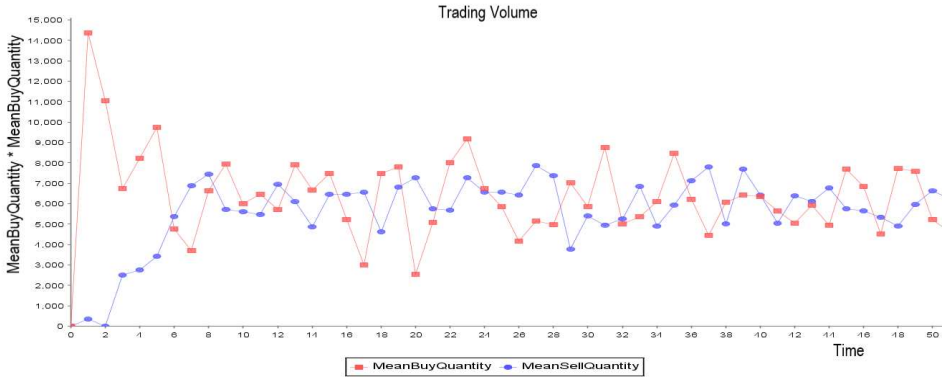

Figure 12. *Simulation diagram of trading volume under 20% spread*

http://www.aloki.hu ● ISSN 1589 1623 (Print) ● ISSN 1785 0037 (Online)
DOI: http://dx.doi.org/10.15666/aeer/1704_87758791

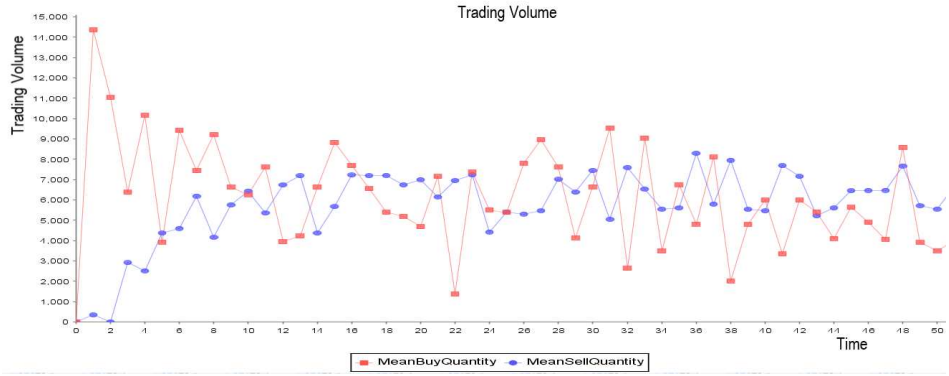

Figure 13. *Simulation diagram of trading volume under 40% spread*

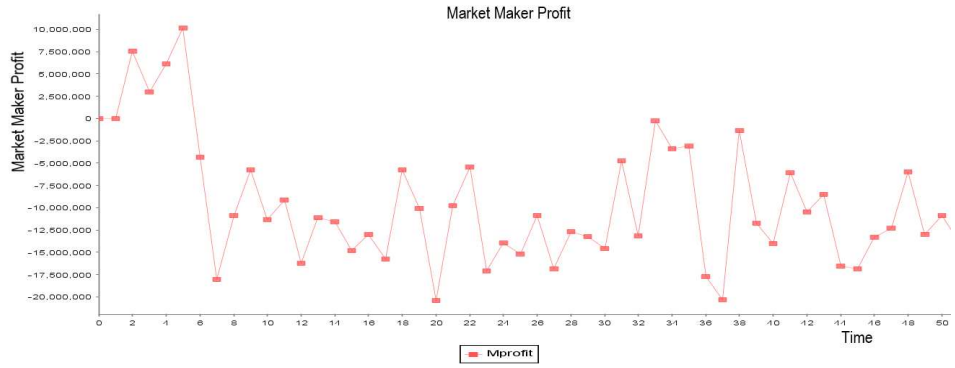

Figure 14. *Simulation diagram of market maker profit under 20% spread*

Figure 15. *Simulation diagram of market maker profit under 40% spread*

As shown in *Figures 16* and *17*, in the 50 operating cycles, the system benefits under the 20% spread have fluctuated near the edge of zero, which has been greatly reduced compared to the previous system benefits. Under the 40% spread, the system returns are all negative, and the average is large, reaching -1 million.

Based on the above analysis, the increase in the spread will reduce the system revenue. Therefore, the market price should be limited in the market maker trading market. According to the analysis of the simulation results, the spread should be controlled within 20%.

http://www.aloki.hu ● ISSN 1589 1623 (Print) ● ISSN 1785 0037 (Online)
DOI: http://dx.doi.org/10.15666/aeer/1704_87758791

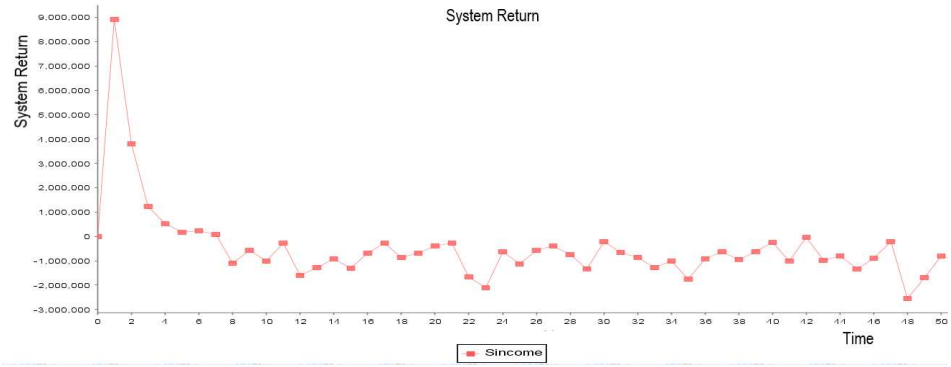

Figure 16. *Simulation diagram of system return under 20% spread*

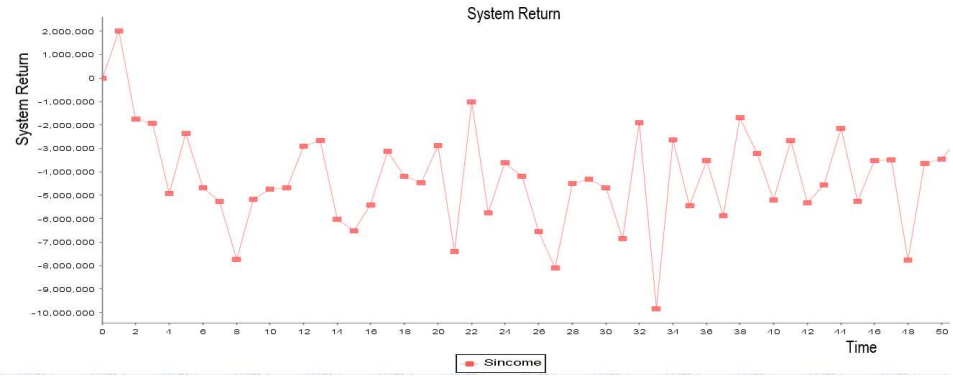

Figure 17. *Simulation diagram of system return under 40% spread*

Conclusions

In the long run, the emissions trading market is in a dynamic system consisting of market makers, emission discharge enterprises, and government. In this paper, we use the simulation experiment method to simulate the operation mode of the emissions trading complex system, and draw the following main conclusions:

First, market maker trading is applicable to a variety of market environments, and can improve the efficiency of the emissions trading system. The simulation results show that regardless of whether the market yield of the products produced by the enterprise is higher or lower, whether it is fluctuating violently or mildly, whether there is market power in the emission permit market, whether the competition of the emission discharge enterprises is fierce, market maker transactions can make Emissions trading volume at a high level, and system revenue is positive.

Second, even if the market for enterprise products fluctuates drastically and there is a large difference in the initial distribution of warrants, market maker transactions are still suitable. Although the quotes of market makers are higher, the system returns are higher.

Third, the increase in the number of emission discharge enterprises will affect the quotation level of market makers, but will not change the trend of market makers' quotations.

http://www.aloki.hu ● ISSN 1589 1623 (Print) ● ISSN 1785 0037 (Online)
DOI: http://dx.doi.org/10.15666/aeer/1704_87758791

Fourth, the increase in the spread will reduce the system revenue, and the market price of the market maker should be limited in the emissions trading market. According to the simulation results, the spread should be controlled within 20%.

Fifth, the adverse environment caused by the introduction of new products, the violent market fluctuations, and the rise of raw materials for products does not hinder the smooth conduct of emissions trading. The market makers can lower the quotation to balance supply and demand, so that the system returns are positive.

In future research, the assumptions could be relaxed in the proposed problem settings to observe their effects on the solutions, so that results could serve the needs of the real world. On the other hand, it is necessary to conduct an study of the behavioral rules of all parties involved in, which would provide a better solution for the parties. Finally, to improve the accuracy of the simulation results, some sophisticated methods can be used to set market demand parameters and emission allocation parameters, in which the set of parameters could be needed.

Acknowledgements. This paper is supported by MOE (Ministry of Education in China) Project of Humanities and Social Sciences (19YJC630043), National Natural Science Foundation of China (J1824031), the Fundamental Research Funds for the Central Universities (B18RC00070) and Beijing Municipal Bureau of Economy and Information Technology Funds (T17M00070). We appreciate their support very much.

REFERENCES

[1] Bloomfield, R., O'Hara, M. (2000): Can transparent markets survive? – Journal of Financial Economics 55(3): 425-59.
[2] Bondarenko, O. (2001): Competing market makers, liquidity provision, and bid–ask spreads. – Journal of Financial Markets 4(3): 269-308.
[3] Calcagno, R., Lovo, S. (2006): Bid-ask price competition with asymmetric information between market makers. – Review of Economic Studies 73(2): 329-355.
[4] Demsetz, H. (1968): The cost of transaction. – Quarterly Journal of Economics 82(1): 33-53.
[5] Du, J., Li, Q., Qiao, F., Yu, L. (2018): Estimation of vehicle emission on mainline freeway under isolated and integrated ramp metering strategies. – Environmental Engineering and Management Journal 17(5): 1237-1248.
[6] Flood, M. D., Huisman, R., Koedijk, K. G. (1999): Quote disclosure and price discovery in multiple-dealer financial markets. – The review of Financial Studies 12(1): 37-59.
[7] Glosten, L. R., Milgrom, P. R. (1985): Bid, ask and transaction prices in a specialist market with heterogeneously informed traders. – Journal of Financial Economics 14(1): 71-100.
[8] Gong, D., Liu, S., Tang, M., Ren, L., Liu, J. (2018): Revenue sharing or profit sharing? An internet production perspective. – Advances in Production Engineering & Management 13(1): 81-92.
[9] Kyle, A. S. (1985): Continuous auction and insider trading. – Econometrica 53(6): 1315-1335.
[10] Kedia, S., Zhou, X. (2011): Local market makers, liquidity and market quality. – Journal of Financial Markets 14(4): 540-567.
[11] Miao, J. A. (2006): Search model of centralized and decentralized trade. – Review of Economic Dynamics 9: 68-92.
[12] Shen, P., Starr, R. M. (2002): Market-makers' supply and pricing of financial market liquidity. – Economics Letters 76(1): 53-58.

http://www.aloki.hu ● ISSN 1589 1623 (Print) ● ISSN 1785 0037 (Online)
DOI: http://dx.doi.org/10.15666/aeer/1704_87758791

[13] Tarun, C., Richard, R. (2001): Market liquidity and trade activity. – The Journal of Finance 56(2): 501-530.
[14] Zhu, M., Chiarella, C., He, X. Z., Wang, D. (2009): Does the market maker stabilize the market? – Physica A: Statistical Mechanics and its Applications 388(15-16): 3164-3180.
[15] Zhang, Y. P., Li, Y. (2011): A probe into the market maker system of China's stock market based on the analysis of the overall welfare and transaction cost of market participants under asymmetric information. – On Economic Problems (9): 91-95.

http://www.aloki.hu ● ISSN 1589 1623 (Print) ● ISSN 1785 0037 (Online)
DOI: http://dx.doi.org/10.15666/aeer/1704_87758791

EFFECT OF LOW CARBON ECONOMY ON ENTERPRISE COMPETITIVENESS: A MULTIPLE MEDIATION MODEL

ZHANG, H. W.

School of Economics and Management, Beijing JiaoTong University, Beijing 10044, China
(e-mail: 16241267@bjtu.edu.cn)

(Received 8th Mar 2019; accepted 1st May 2019)

Abstract. The low-carbon economy is an economic model based on low energy consumption, low pollution and low emissions. According to some research, a low-carbon economy model can have a significant impact on a company's competitiveness. However, there are two different types of views on the relationship between environmental regulation and corporate competitiveness. This study uses a method of testing multiple mediations that can explain many complex internal mechanisms in the field of organizational behavior science. The results show that the low carbon economy has a positive effect on technology innovation, and this effect will influence enterprise competitiveness through sustainable development. We also found that the compound multiple mediation model has an advantage in explaining the problems involved with low carbon economy and enterprise competitiveness.
Keywords: *low energy consumption, sustainable development, CO_2 emissions, technology innovation, enterprise strategic*

Introduction

Low-carbon development is a strategic decision that human beings have to face and seek opportunities under the dual pressure of financial crisis and climate and environmental crisis (Louche et al., 2019; Gong, et al., 2018). It will bring about a series of fundamental changes in the whole economy, society and enterprises. It is not an exaggeration to call it a technological revolution or an industrial revolution. The arrival of the low-carbon era will lead to profound changes in the standards of our enterprises, including value standards and evaluation systems (Niamir et al., 2018). Opportunities of emerging industrial revolution brewing under the development mode of low-carbon economy urgently need the strong support of enterprise strategic planning and thus promote the economic development mode from a high carbon economy to low carbon economy (Barron et al., 2018; Du, et al., 2018).

Low-carbon economy refers to an economic development pattern that achieves a win-win situation for economic and social development and ecological environmental protection (Shimada et al., 2007). Under the guidance of the concept of sustainable development, through technical innovation, system innovation, industrial transformation, new energy development and other means to reduce the high carbon energy consumption of coal, oil, greenhouse gas emissions and so on (Hu et al., 2011). With the increase of the global population and the continued economic growth, the environmental problems and consequences caused by the use of fossil energy and other conventional sources have received more and more attention. Environmental hazards such as exhaust gas pollution, photochemical smog, water pollution and acid rain, as well as global climate change caused by the rise of carbon dioxide concentration in the atmosphere, will cause serious consequences (Foxon, 2011). Therefore, a series of new concepts and policies have emerged, such as carbon footprint, low-carbon economy, low-carbon technology, low-carbon development, low-carbon lifestyle, low-carbon society, low-carbon city and a low-carbon world (Nader, 2009; Liu, 2018; Lefevre et al., 2018; Ervine, 2018).

http://www.aloki.hu ● ISSN 1589 1623 (Print) ● ISSN 1785 0037 (Online)
DOI: http://dx.doi.org/10.15666/aeer/1704_87938803

The arrival of the low-carbon era will lead to profound changes in the standards of our enterprises, including value standards and evaluation systems. Under the guidance of low-carbon economic policies, enterprises must shift from the traditional growth model to directly applying the new century's innovative technology and innovation mechanism and achieving sustainable social development through low-carbon economic model and lifestyle (Tavoni et al., 2012; Li and Sun, 2018; Ropeik, 2017). Opportunities of emerging industrial revolution brewing under the development mode of low-carbon economy urgently need the strong support of enterprise strategic planning and thus promote the economic development mode from a high carbon economy to low carbon economy. From this perspective, the low-carbon economy is both a limitation and an opportunity. Therefore, this study mainly explores the effect of the low-carbon economy on enterprise competitiveness and uses a method of multiple mediation models to reveal the internal mechanism.

Research background and hypotheses

Low carbon economy

The low-carbon economy is an economic model based on low energy consumption, low pollution, and low emissions. The essence of the low-carbon economy is the problem of high energy utilization efficiency and clean energy structure. In the context of global warming, the low-carbon revolution with energy efficiency and low emissions as the core is gradually changing many industrial ecosystems. Therefore, companies must focus on developing low-carbon technologies to seize the opportunities and industry commanding heights.

Tavoni et al. (2012) believe that with the increase in income, the industrial and consumption structures have changed. At the same time, when people began to pay attention to the issue of protecting the environment, the phenomenon of environmental degradation gradually slowed down or even disappeared. Glaser (2003) concluded that CO_2 emissions are in an "N" rather than inverted "U" relationship with economic growth. Smale et al. (2006) believe that in the early stage of industrialization, with the development of the economy and the increase of per capita income, the per capita CO_2 emissions will be at a higher level.

Low-carbon economy and enterprise competitiveness

There are two different types of views on the relationship between environmental regulation and corporate competitiveness. The first perspective is that the implementation of environmental regulations will lead to a decline in the competitiveness of enterprises. The government implements environmental regulations and companies need to add special costs to eliminate pollution and reduce their environmental impact to meet environmental standards. The environmental standards require that the production costs of enterprises will rise sharply, which will directly affect their competitiveness. Healy and Barry (2017) argued that environmental regulation is not only not conducive to technological innovation, but because the entire process of environmental control will cause companies to be forced to transform the original production process, which will have an impact on technological innovation. Garay and Font (2012) pointed out that in order to adapt to environmental regulations, the company's processes are becoming more and more complex, resulting in a large management difficulty, and the management costs

http://www.aloki.hu ● ISSN 1589 1623 (Print) ● ISSN 1785 0037 (Online)
DOI: http://dx.doi.org/10.15666/aeer/1704_87938803

are increasing, eventually resulting in a decline in corporate profits and a decline in competitiveness. Ortiz et al. (2009) showed that as environmental governance costs increase, it is increasingly difficult for individual companies to achieve a win-win situation for both environment and competitiveness. The stricter environmental regulations will inevitably worsen the business conditions of enterprises. At the same time, the benefits of adopting new technologies are not enough to boost the profits of enterprises. While environmental protection regulation improves the overall social welfare, it will lead to a decline in industrial production efficiency, and enterprises pay a higher price for it.

However, other scholars believe that companies will actively seek environmental technology innovation and develop environmental products in response to environmental policies, competitors and consumers (Rijsberman, 2017; Ervine, 2018). As a result, the sustainability of the industry will naturally increase, thus causing the competitiveness to transform and transition around the green. From a dynamic perspective, strict environmental standards will encourage companies to accelerate the pace of product innovation, and encourage enterprises to continuously improve the inefficiency in the production process, and reluctantly. The effective use of resources, through continuous technological innovation, brings about a reduction in pollution and an increase in output, resolving the contradiction between the environment and competitiveness, and achieving a win-win situation in which both economic performance and environmental performance are simultaneously changed. At the same time, this technological innovation will also enable companies that comply with environmental standards to gain a "first mover advantage". Managers should take environmental improvement as an opportunity to add economic value and competitive advantage, and should not only be an annoying cost or threat. Based on this, this paper proposes:

H: Low carbon economy influence enterprise competitiveness through a multiple mediation model, see in Figure 1.

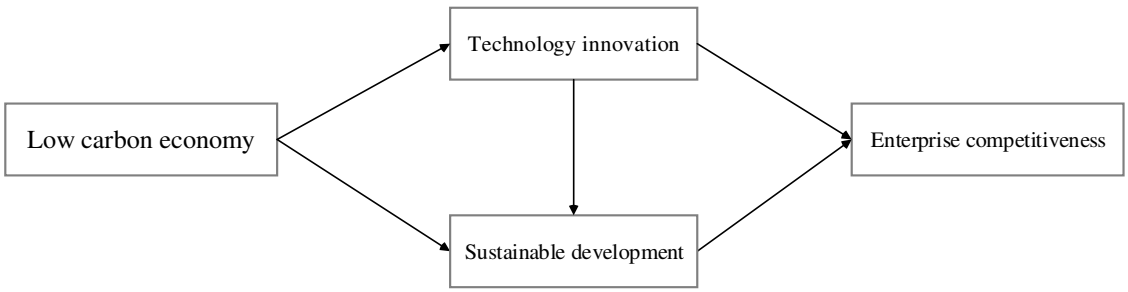

Figure 1. *Theory research model*

Methodology

Sample source

In this paper, we used the multiple mediation models to analyze the relationship between low carbon economy and enterprise competitiveness. First, we selected 42 enterprises in China and got their basic information before the investigation. Then, during the investigation, the managers answered a 20-question questionnaire including all the indicators of this study. The descriptive statistics are in *Table 1*.

http://www.aloki.hu ● ISSN 1589 1623 (Print) ● ISSN 1785 0037 (Online)
DOI: http://dx.doi.org/10.15666/aeer/1704_87938803

Table 1. *Descriptive statistics (n = 42)*

Variable	Low carbon economy	Technology innovation	Sustainable development	Enterprise competitiveness
Low carbon economy	1			
Technology innovation	.639**	1		
Sustainable development	.674**	.751**	1	
Enterprise competitiveness	.641**	.691**	.706**	1

**Correlation is significant at the 0.01 level (double tail)

Multiple mediation model

Ordinary least squares mediation model

The ordinary least squares (OLS) mediation model always present in the form of three regression equations (Preacher and Hayes, 2008):

$$y_i = \beta_{01} + \tau x_i + \varepsilon_{1i} \quad \text{(Eq.1)}$$

$$m_i = \beta_{02} + \alpha x_i + \varepsilon_{2i} \quad \text{(Eq.2)}$$

$$y_i = \beta_{03} + \beta m_i + \tau` x_i + \varepsilon_{3i} \quad \text{(Eq.3)}$$

In these equations (*Eqs. 1–3*), y_i is the dependent variable, m_i is the mediating variable, and x_i is the independent variable. The coefficient between the independent variable and the dependent variable is represented by τ, and $\tau`$ is the coefficient adjusted for the influence of the mediating variable. β_{01}, β_{02}, and β_{03} represent the intercept in the three equations.

To calculate the multiple mediation effects, there are three points to lay the foundation. First, βin the third equation is relating to the dependent variable and the mediating variable. Second, α_i in the second equation is relating to the independent variable and the mediating variable. Third, the product of α and β is the estimator of the indirect effect, and $\tau`$ is the estimator of the direct effect.

The variance of the indirect effect $\sigma^2_{\alpha\beta}$ is based on the variance of α and β, and it is derived using a second-order Taylor series in *Equation 4*:

$$\sigma^2_{\alpha\beta} = \alpha^2\sigma^2_\beta + \beta^2\sigma^2_\alpha + \sigma^2_\alpha\sigma^2_\beta \quad \text{(Eq.4)}$$

If α and β are nonzero values, according to Monte Carlo studies, for a sample size of 100 or more in a simulation model, all three variance estimators appear to have a relative bias of less than 5%. So Confidence limits are constructed in *Equation 5*:

$$\alpha\beta \pm z_{1-\omega/2} \times \sigma_{\alpha\beta} \quad \text{(Eq.5)}$$

where $z_{1-\omega/2}$ is the value on the z-distribution corresponding to the desired Type I error rate, ω.

http://www.aloki.hu ● ISSN 1589 1623 (Print) ● ISSN 1785 0037 (Online)
DOI: http://dx.doi.org/10.15666/aeer/1704_87938803

As the indirect effect is the product of α and β, and the estimates are normally distributed. The distribution of the product is an index to test the indirect effect. In other words, we can test the indirect effect based on $z_\alpha z_\beta$, where $z_\alpha = \alpha / \sigma_\alpha$ and $z_\beta = \alpha / \sigma_\beta$.

The central moments of the process are as follows (*Eqs. 6–9*).

$$Mean: M_1 = \mu = z_\alpha z_\beta \quad \text{(Eq.6)}$$

$$Variance: M_2 = \sigma^2 = z_\alpha^2 + z_\beta^2 + 1 \quad \text{(Eq.7)}$$

$$Skewness: M_3 = \alpha_3 = \frac{6\left(z_\alpha z_\beta\right)}{\left(z_\alpha^2 + z_\beta^2 + 1\right)^{3/2}} \quad \text{(Eq.8)}$$

$$Kurtosis: M_4 = \alpha_4 = \frac{12\left(z_\alpha^2 + z_\beta^2\right) + 6}{\left(z_\alpha^2 + z_\beta^2 + 1\right)^2} \quad \text{(Eq.9)}$$

To get the analytical solution, a Bessel function with a purely imaginary argument is used in *Equation 10*.

$$f\left(z_\alpha z_\beta\right) = \frac{e^{-\left(z_\alpha^2 + z_\beta^2\right)/2}}{\pi}\left[\sum\nolimits_0 K_0 + \left(z_\alpha^2 + z_\beta^2\right)\frac{z_\alpha z_\beta}{2!}\sum\nolimits_2 K_1 + \left(z_\alpha^4 + z_\beta^4\right)\frac{\left(z_\alpha z_\beta\right)^2}{4!}\sum\nolimits_4 K_2 + \left(z_\alpha^6 + z_\beta^6\right)\frac{\left|z_\alpha z_\beta\right|^3}{6!}\sum\nolimits_6 K_3 + \ldots\right] \quad \text{(Eq.10)}$$

In the equation, K is the Bessel function and Σ is a Laurent series in *Equation 11*.

$$\sum\nolimits_r \left(z_\alpha, z_\beta, z_\alpha z_\beta\right) = 1 + \frac{z_\alpha z_\beta z_\alpha z_\beta}{r+1} + \frac{\left(z_\alpha z_\beta z_\alpha z_\beta\right)^2}{\left(r+1\right)^2 2!} + \frac{\left(z_\alpha z_\beta z_\alpha z_\beta\right)^3}{\left(r+1\right)^3 3!} + \ldots \quad \text{(Eq.11)}$$

In the equation, r is the order of the Laurent series in *Equation 12*.

$$\left(r+k\right)^k = \left(r+k\right)\left(r+k-1\right)\ldots\left(r+1\right) \quad \text{(Eq.12)}$$

To calculate the 95% standard normal confidence limits, it used a Standardized Critical Value (SCV). According to Meeker's suggestion (Meeker et al., 1982), it found the Critical Value (CV) in the table, and then convert to the standardized metric of the regression coefficient (α and β) in *Equation 13*.

http://www.aloki.hu ● ISSN 1589 1623 (Print) ● ISSN 1785 0037 (Online)
DOI: http://dx.doi.org/10.15666/aeer/1704_87938803

$$SCV = \frac{CV - z_\alpha z_\beta}{\sqrt{z_\alpha^2 + z_\beta^2 + 1}} \quad \text{(Eq.13)}$$

Parallel multiple mediation model

Parallel multiple mediation model reflects a situation in which multiple variables simultaneously mediate between the independent and dependent variable, see in *Figure 2.*

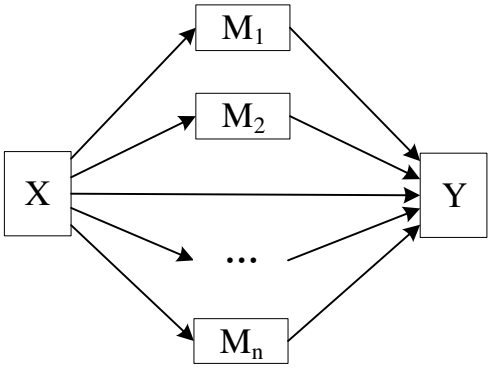

Figure 2. *Parallel multiple mediations model*

The relationship between the dependent variables, independent variables and multiple mediating variables are as follows (*Eqs. 14–16*).

$$Y = \tau X + \varepsilon_X \quad \text{(Eq.14)}$$

$$M_i = \alpha_i X + \varepsilon_i \quad \text{(Eq.15)}$$

$$Y = \sum_{i=1}^{n} \beta_i M_i + \tau` X + \varepsilon \quad \text{(Eq.16)}$$

where i = 1…n, $\tau`$ is the direct effect and τ is the total effect between the dependent variable and independent variable, $\alpha_i \beta_i$ is the indirect effect of each mediation path in *Equation 17*.

$$\tau = \tau` + \sum_{i=1}^{n} \alpha_i \beta_i \quad \text{(Eq.17)}$$

The analysis of parallel multiple mediating effects generally includes three parts: first, the estimation and test of the overall mediating effect; second, the estimation and test of special mediating effects; third, the comparison between the mediating effects.

The total indirect effect is τ - $\tau`$, or $\sum_{i=1}^{n} \alpha_i \beta_i$.

http://www.aloki.hu ● ISSN 1589 1623 (Print) ● ISSN 1785 0037 (Online)
DOI: http://dx.doi.org/10.15666/aeer/1704_87938803

According to Mackinnon's suggestion (Mackinnon et al., 2007), the McGuigan and Langholtz effect size was to test the significance of the total indirect effect in *Equation 18.*

$$t_{N-2} = \frac{\tau - \tau`}{\sqrt{\sigma_{\tau}^2 + \sigma_{\tau`}^2 - 2\rho_{\tau\tau`}\sigma_{\tau}\sigma_{\tau`}}} \quad \text{(Eq.18)}$$

In the equation, σ_{τ} is the standard error of τ, $\sigma_{\tau`}$ is the standard error of $\tau`$, and $\rho_{\tau\tau`}$ is the regression coefficient between $\tau$ and $\tau`$.

Compound multiple mediation model

The compound multiple mediations model is composed of the both parallel and serial mediating path see in *Figure 3*.

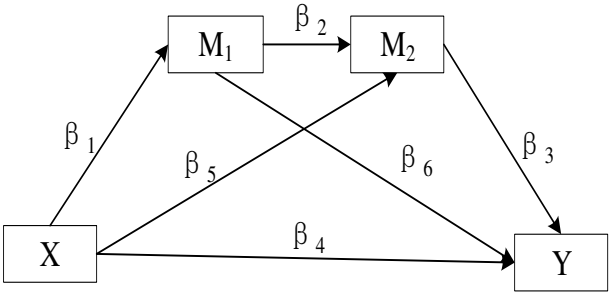

Figure 3 *Compound multiple mediations model*

To test the indirect effect, we need to estimate the following three equations (*Eqs. 19–21*).

$$M_1 = \beta_{01} + \beta_1 + \varepsilon_1 \quad \text{(Eq.19)}$$

$$M_2 = \beta_{02} + \beta_2 M_1 + \beta_5 X + \varepsilon_2 \quad \text{(Eq.20)}$$

$$Y = \beta_{03} + \beta_4 X + \beta_3 M_2 + \beta_6 M_1 + \varepsilon_3 \quad \text{(Eq.21)}$$

Results and analysis

Mediation test

To test the significance of the indirect effect, the multivariate delta method, the unbiased estimate method, and the exact variance estimate method are used. The following is a brief introduction to the principle of these three methods.

Multivariate delta method

As can be seen above, β_1, β_2 and β_3 are the regression coefficients. The product of these three coefficients divides the mediation effect by the estimated standard error. The

http://www.aloki.hu ● ISSN 1589 1623 (Print) ● ISSN 1785 0037 (Online)
DOI: http://dx.doi.org/10.15666/aeer/1704_87938803

derivation of the three estimators of the variance of β_1, β_2 and β_3 are as follows in *Equation 22*.

$$\begin{aligned} s^2_{multi} &= \left[\frac{\partial\beta_1\beta_2\beta_3}{\partial\beta_1}, \frac{\partial\beta_1\beta_2\beta_3}{\partial\beta_2}, \frac{\partial\beta_1\beta_2\beta_3}{\partial\beta_3}\right]\begin{bmatrix} s^2_{\beta 1} & s_{\beta 1\beta 2} & s_{\beta 1\beta 3} \\ s_{\beta 2\beta 1} & s^2_{\beta 2} & s_{\beta 2\beta 3} \\ s_{\beta 3\beta 1} & s_{\beta 3\beta 2} & s^2_{\beta 3} \end{bmatrix}\begin{bmatrix} \frac{\partial\beta_1\beta_2\beta_3}{\partial\beta_1} \\ \frac{\partial\beta_1\beta_2\beta_3}{\partial\beta_2} \\ \frac{\partial\beta_1\beta_2\beta_3}{\partial\beta_3} \end{bmatrix} \\ &= \left[\beta_2\beta_3, \beta_1\beta_3, \beta_1\beta_2\right]\begin{bmatrix} s^2_{\beta 1} & s_{\beta 1\beta 2} & s_{\beta 1\beta 3} \\ s_{\beta 2\beta 1} & s^2_{\beta 2} & s_{\beta 2\beta 3} \\ s_{\beta 3\beta 1} & s_{\beta 3\beta 2} & s^2_{\beta 3} \end{bmatrix}\begin{bmatrix} \beta_2\beta_3 \\ \beta_1\beta_3 \\ \beta_1\beta_2 \end{bmatrix} \\ &= \beta_2^2\beta_3^2 s^2_{\beta 1} + \beta_1^2\beta_3^2 s^2_{\beta 2} + \beta_1^2\beta_2^2 s^2_{\beta 3} + 2\beta_1\beta_2\beta_3^2 s_{\beta 1\beta 2} \\ &\quad + 2\beta_1\beta_2^2\beta_3 s_{\beta 1\beta 3} + 2\beta_1^2\beta_2\beta_3 s_{\beta 2\beta 3} \end{aligned} \tag{Eq.22}$$

In the compound multiple mediation model, β_1, β_2 and β_3 are independent, so the last three items are zero, and the variance in the multivariate delta estimate method is in *Equation 23*.

$$s^2_{multi} = \beta_2^2\beta_3^2 s^2_{\beta 1} + \beta_1^2\beta_3^2 s^2_{\beta 2} + \beta_1^2\beta_2^2 s^2_{\beta 3} \tag{Eq.23}$$

Unbiased estimate method

The unbiased estimate method is based on the work of Goodman (1960). His research gives a suggestion for the calculation of unbiased estimate variance of two independent random variables. Extending his research to this case, the equation is in *Equation 24*.

$$\begin{aligned} s^2_{unbiased} &= \left(\beta_1^2 - s^2_{\beta 1}\right)\left(\beta_2^2 - s^2_{\beta 2}\right)s^2_{\beta 3} + \left(\beta_1^2 - s^2_{\beta 1}\right)\left(\beta_3^2 - s^2_{\beta 3}\right)s^2_{\beta 2} \\ &\quad + \left(\beta_2^2 - s^2_{\beta 2}\right)\left(\beta_3^2 - s^2_{\beta 3}\right)s^2_{\beta 1} + \left(\beta_1^2 - s^2_{\beta 1}\right)s^2_{\beta 2}s^2_{\beta 3} \\ &\quad + \left(\beta_2^2 - s^2_{\beta 2}\right)s^2_{\beta 1}s^2_{\beta 3} + \left(\beta_3^2 - s^2_{\beta 3}\right)s^2_{\beta 1}s^2_{\beta 2} + s^2_{\beta 1}s^2_{\beta 2}s^2_{\beta 3} \\ &= \left(\beta_1^2\beta_2^2 s^2_{\beta 1} - \beta_1^2 s^2_{\beta 2}s^2_{\beta 3} + s^2_{\beta 1}s^2_{\beta 2}s^2_{\beta 3} - \beta_2^2 s^2_{\beta 1}s^2_{\beta 3}\right) + \left(\beta_1^2\beta_3^2 s^2_{\beta 2}\right. \\ &\quad \left. - \beta_1^2 s^2_{\beta 3}s^2_{\beta 2} - \beta_3^2 s^2_{\beta 1}s^2_{\beta 2} + s^2_{\beta 1}s^2_{\beta 2}s^2_{\beta 3}\right) + \left(\beta_2^2\beta_3^2 s^2_{\beta 1} - \beta_2^2 s^2_{\beta 3}s^2_{\beta 1}\right. \\ &\quad \left. - \beta_3^2 s^2_{\beta 2}s^2_{\beta 1} + s^2_{\beta 1}s^2_{\beta 2}s^2_{\beta 3}\right) + \left(\beta_1^2 s^2_{\beta 2}s^2_{\beta 3} - s^2_{\beta 1}s^2_{\beta 2}s^2_{\beta 3}\right) + \left(\beta_2^2 s^2_{\beta 1}s^2_{\beta 3}\right. \\ &\quad \left. - s^2_{\beta 2}s^2_{\beta 1}s^2_{\beta 3}\right) + \left(\beta_3^2 s^2_{\beta 1}s^2_{\beta 2} - s^2_{\beta 3}s^2_{\beta 1}s^2_{\beta 2}\right) + s^2_{\beta 1}s^2_{\beta 2}s^2_{\beta 3} \\ &= \beta_1^2 s^2_{\beta 2}s^2_{\beta 3} + \beta_1^2\beta_3^2 s^2_{\beta 2} + \beta_2^2\beta_3^2 s^2_{\beta 1} - \beta_1^2 s^2_{\beta 2}s^2_{\beta 3} - \beta_2^2 s^2_{\beta 3}s^2_{\beta 1} \\ &\quad - \beta_3^2 s^2_{\beta 1}s^2_{\beta 2} + s^2_{\beta 1}s^2_{\beta 2}s^2_{\beta 3} \end{aligned} \tag{Eq.24}$$

http://www.aloki.hu ● ISSN 1589 1623 (Print) ● ISSN 1785 0037 (Online)
DOI: http://dx.doi.org/10.15666/aeer/1704_87938803

Exact variance estimate method

The exact variance estimate method is also an extension of Goodman's research. In this method, it draws into the square of the coefficient of variation to accomplish the calculation. For variable β_i, the function is in *Equations 25* and *26*.

$$G(b_i) = s_{\beta i}^2 / \beta_i^2 \tag{Eq.25}$$

$$\begin{aligned} s_{exact}^2 &= (\beta_1\beta_2\beta_3)^2 \left[G(\beta_1) + G(\beta_2) + 2G(\beta_3) + 2G(\beta_1)G(\beta_2)G(\beta_3) \right. \\ &\quad \left. + G(\beta_2)G(\beta_3) \right] \\ &= (\beta_1\beta_2\beta_3)^2 \left[\frac{s_{\beta 1}^2}{\beta_1^2} + \frac{s_{\beta 2}^2}{\beta_2^2} + \frac{2s_{\beta 3}^2}{\beta_3^2} + 2 \times \frac{s_{\beta 1}^2}{\beta_1^2} \times \frac{s_{\beta 2}^2}{\beta_2^2} \times \frac{s_{\beta 3}^2}{\beta_3^2} + \frac{s_{\beta 2}^2}{\beta_2^2} \times \frac{s_{\beta 3}^2}{\beta_3^2} \right] \\ &= \beta_2^2\beta_3^2 s_{\beta 1}^2 + \beta_1^2\beta_3^2 s_{\beta 2}^2 + \beta_1^2\beta_2^2 s_{\beta 3}^2 + \beta_1^2 s_{\beta 2}^2 s_{\beta 3}^2 + \beta_2^2 s_{\beta 3}^2 s_{\beta 1}^2 \\ &\quad + \beta_3^2 s_{\beta 1}^2 s_{\beta 2}^2 + s_{\beta 1}^2 s_{\beta 2}^2 s_{\beta 3}^2 \end{aligned} \tag{Eq.26}$$

According to Sobel's suggestion (Sobel, 1982), we calculate the confidence intervals for each method to test the significance of the model in *Equation 27*.

$$95\%\ confidence\ interval = \beta_1\beta_2\beta_3 \pm z_{.975} \left(s_{type}^2 \right)^{1/2} \tag{Eq.27}$$

In the equation above, $z_{.975} = 1.96$, and type is multivariate delta, unbiased or exact. The hypothesis can be confirmed when the 95% confidence interval does not include zero.

Table 2 shows the results for the methods. As the confidence interval of the model did not include zero, the hypothesis of this study was tested.

Table 2. *Results for each method applied to data*

Method	Estimate	Standard error	Test	Hypothesis test result
Joint significance	β_1=0.862	0.071	T=12.074, P<0.001	
	β_2=0.844	0.055	T=15.428, P<0.001	
	β_3=0.589	0.079	T=7.414, P<0.001	Support hypothesis
Multivariate delta method	$\beta_1\beta_2\beta_3$=0.429	0.08	95%Cl=[0.272,0.586]	Support hypothesis
Unbiased estimate method	$\beta_1\beta_2\beta_3$=0.429	0.079	95%Cl=[0.274,0.584]	Support hypothesis
Exact variance estimate method	$\beta_1\beta_2\beta_3$=0.429	0.084	95%Cl=[0.264,0.594]	Support hypothesis
Percentile bootstrap	$\beta_1\beta_2\beta_3$=0.429	—	95%Cl=[0.266,0.577]	Support hypothesis
Bias-corrected bootstrap	$\beta_1\beta_2\beta_3$=0.429	—	95%Cl=[0.279,0.600]	Support hypothesis

Optimal model selection

By the comparison of the three multiple mediation models (see in *Table 3*), we found that the total indirect effect of the compound multiple mediation model was much better than the series multiple mediations model and parallel multiple mediation model. This

http://www.aloki.hu ● ISSN 1589 1623 (Print) ● ISSN 1785 0037 (Online)
DOI: http://dx.doi.org/10.15666/aeer/1704_87938803

indicates that the compound multiple mediation model was more suitable for the practical problem in this study.

Table 3. *Comparison of three multiple mediation models*

Model	Indirect effect	Standard error	Lower 95%CI	Upper 95%CI
Series multiple mediations model	0.177	0.069	0.067	0.327
Parallel multiple mediation model	0.331	0.082	0.177	0.465
Compound multiple mediation model	0.509	0.057	0.407	0.606

Conclusion

In this paper, we proposed a multiple mediation model to explore the relationship between low carbon economy and enterprise competitiveness. The results show that the low-carbon economy has a positive effect on technology innovation, and this effect will influence enterprise competitiveness through sustainable development. We also found that the compound multiple mediation model has more advantage to explain the problems involved with low carbon economy and enterprise competitiveness. Our finding has made an effective supplement to the study of low carbon economy and enterprise competitiveness theory. Therefore, in the future research on enterprise competitiveness, scholars should pay more attention to technological change and sustainable development to adapt to the low-carbon economy. For example, it is very important to explore how to balance the relationship between technological innovation and sustainable development.

REFERENCES

[1] Barron, A. R., Fawcett, A. A., Hafstead, M. A. C., Mcfarland, J. R., Morris, A. C. (2018): Policy insights from the EMF 32 study on U.S. carbon tax scenarios. – Climate Change Economics 9: 1840003.

[2] Du J., Li Q., Qiao F., Yu L. (2018): Estimation of vehicle emission on mainline freeway under isolated and integrated ramp metering strategies. – Environmental Engineering and Management Journal 17(5), 1237-1248.

[3] Ervine, K. (2018): How low can it go? Analysing the political economy of carbon market design and low carbon prices. – New Political Economy 23: 690-710.

[4] Foxon, T. J. (2011): A coevolutionary framework for analysing a transition to a sustainable low carbon economy. – Ecological Economics 70: 2258-2267.

[5] Garay, L., Font, X. (2012): Doing good to do well? Corporate social responsibility reasons, practices and impacts in small and medium accommodation enterprises. – International Journal of Hospitality Management 31: 0-337.

[6] Glaser, M. (2003): Determinants of CO_2 emissions in a small open economy'. – Ecological Economics 45: 133-148.

[7] Gong, D., Liu, S., Tang, M., Ren, L., Liu, J. (2018): Revenue sharing or profit sharing? An internet production perspective. – Advances in Production Engineering & Management 13(1): 81-92.

[8] Goodman, L. A. (1960): On the exact variance of products. – Publications of the American Statistical Association 55: 708-713.

[9] Healy, N., Barry, J. (2017): Politicizing energy justice and energy system transitions: Fossil fuel divestment and a "just transition" – Energy Policy 108: 451-459.

http://www.aloki.hu ● ISSN 1589 1623 (Print) ● ISSN 1785 0037 (Online)
DOI: http://dx.doi.org/10.15666/aeer/1704_87938803

[10] Hu, Z., Yuan, J., Hu, Z. (2011): Study on China's low carbon development in an economy-energy-electricity-environment framework. – Energy Policy 39: 2596-2605.
[11] Lefevre, J., Wills, W., Hourcade, J.-C. (2018): Combining low-carbon economic development and oil exploration in Brazil? An energy-economy assessment. – Climate Policy 18: 1286-1295.
[12] Li, J., Sun, C. (2018): Towards a low carbon economy by removing fossil fuel subsidies? – China Economic Review 50: 17-33.
[13] Louche, C., Busch, T., Crifo, P., Marcus, A. (2019): Financial markets and the transition to a low-carbon economy: Challenging the dominant logics. – Organization & Environment 32: 3-17.
[14] Mackinnon, D. P., Fritz, M. S., Williams, J., Lockwood, C. M. (2007): Distribution of the product confidence limits for the indirect effect: Program PRODCLIN. – Behavior Research Methods 39: 384.
[15] Meeker, W. Q. J., Cornwell, L. W., Aroian, L. A. (1982): The Product of Two Normally Distributed Random Variables. – In: Kennedy, W. J., Odeh, R. E. (eds.) Selected Tables in Mathematical Statistics, Volume VII. American Mathematical Society, Providence, Rhode Island.
[16] Nader, S. (2009): Paths to a Low-Carbon Economy - The Masdar Example. – In: Gale, J., Herzog, H., Braitsch, J. (eds.) Greenhouse Gas Control Technologies 9. Proceedings of the 9th International Conference on Greenhouse Gas Control Technologies (GHGT-9), 16–20 November 2008, Washington DC, USA.
[17] Niamir, L., Filatova, T., Voinov, A., Bressers, H. (2018): Transition to low-carbon economy: Assessing cumulative impacts of individual behavioral changes. – Energy Policy 118: 325-345.
[18] Ortiz, O., Castells, F., Sonnemann, G. (2009): Sustainability in the construction industry: A review of recent developments based on LCA. – Construction & Building Materials 23: 28-39.
[19] Preacher, K. J., Hayes, A. F. (2008): Asymptotic and resampling strategies for assessing and comparing indirect effects in multiple mediator models. – Behavior Research Methods 40: 879-891.
[20] Rijsberman, F. (2017): The key role of the meat industry in transformation to a low-carbon, climate resilient, sustainable economy. – Meat Science 132: 2-5.
[21] Ropeik, D. (2017): Clean energy mind games if policy makers want to accelerate the transition to a low-carbon economy, they should heed the lessons of the decision sciences and take another look at nuclear energy. – Issues in Science and Technology 33: 59-64.
[22] Shimada, K., Tanaka, Y., Gomi, K., Matsuoka, Y. (2007): Developing a long-term local society design methodology towards a low-carbon economy: an application to Shiga Prefecture in Japan. – Energy Policy 35: 4688-4703.
[23] Smale, R., Hartley, M., Hepburn, C., Ward, J., Grubb, M. (2006): The impact of co_2 emissions trading on firm profits and market prices. – Climate Policy 6: 31-48.
[24] Sobel, M. E. (1982): Asymptotic confidence intervals for indirect effects in structural equation models. – Sociological Methodology 13: 290-312.
[25] Tavoni, M., De Cian, E., Luderer, G., Steckel, J. C., Waisman, H. (2012): The value of technology and of its evolution towards a low carbon economy. – Climatic Change 114: 39-57.

http://www.aloki.hu ● ISSN 1589 1623 (Print) ● ISSN 1785 0037 (Online)
DOI: http://dx.doi.org/10.15666/aeer/1704_87938803

EXPLORING THE ALTERNATIVE MODES OF ECO-FRIENDLY EXPRESS FREIGHT TRANSPORT

GAO, H. L.* – ZHANG, M. Q. – ZHANG, Y.

School of Economics and Management, Beijing Jiaotong University, 100044 Beijing, China (phone: +86-158-3119-0158)

**Corresponding author*
e-mail: 16113122@bjtu.edu.cn

(Received 8th Mar 2019; accepted 1st May 2019)

Abstract. Reducing pollutant emissions of transportation is an important strategy for addressing global climate change, high-speed rail (HSR) transport, an eco-friendly mode, neither emits dust, nor emits too much CO_X and NO_X due to the eclectic traction drive. Instead of focusing on passenger transport as most literatures refer to HSR, this paper addresses the strategy of goods movement, and chooses Beijing-Shanghai (B-S) HSR in China as a case study to explore a new freight transport mode to alleviate the increasingly serious environmental pollution problem. After predicting the intercity parcel demand and distribution based on AR-GM and Gravity model, the paper evaluates the supply capacity between cities based on operating schedule. The result shows Origin-Destination Pairs (ODPs) such as Shanghai-Jinan, Shanghai-Beijing, Beijing-Langfang suit for Mixed-train Mode and others such as Beijing-Tianjin, Shanghai-Suzhou, Shanghai-Xuzhou suit for freight-train mode. It concludes that operating high-speed rail freights on a large-scale is feasible and environmentally friendly due to its advantages of energy saving, land saving, low carbon emission. Since alternatives of modes are determined by the time distances, the scale of cities, flow volumes of intercity parcels, Freight-train mode should be adopted between cities with high economic density and large transportation capacity.
Keywords: *forecast, flow, capacity, mode, high speed rail, intercity transport*

Introduction

The issue of global warming and air pollution caused by greenhouse gas emission has drawn the attention of the international community. Transportation growth has become one of main factors that contributing to the negative environmental impacts (Pejić, 2017; Nanaki et al., 2016; Gong et al., 2019). With the economic development, the proportion of transportation in China's national energy consumption is on the rise, making it the second largest energy-consuming industry with heavy tasks of energy conservation and emission reduction. As regulation becomes more stringent, transport companies are more like to choose an eco-friendly mode to cope with the challenge of an internalization of environmental effects (Ferrón-Vílchez, 2015). Among all of the modes, road transport represents, through its characteristic features – high flexibility and accessibility – the mode of transport largely involved in meeting the needs of mobility, though it is answerable for polluting the environment to a significant degree (Mitran et al., 2012; Limbourg and Jourquin, 2009; Du et al.,2018).

It can be seen from *Table 1* that in comprehensive transportation system, railway has the comparative advantage in energy conservation and environmental protection, and is the only transportation can be widely used in large areas to achieve the green environmental protection of "replace oil with electricity". Many scholars believe that introducing freight transport into passenger rail network is one of the important ways to absorb road traffic (Offer et al., 2010; Van Wee et al., 2012; Van Duin et al., 2013). High speed electric trains involve a fully mature technology that can use power

http://www.aloki.hu ● ISSN 1589 1623 (Print) ● ISSN 1785 0037 (Online)
DOI: http://dx.doi.org/10.15666/aeer/1704_88058816

generated by the wind, solar thermal energy and geothermal sources with a carbon footprint of zero. Extensive high-speed rail (HSR) network construction and operation quickly increases the rate of the electrification of the entire railway industry, optimizes the railway energy consumption structure. In fact, HSR not only meets people's growing demand for time-sensitive goods, but also meets the requirements of sustainable development, which shows the strong competitiveness in comparison with other modes of transport.

Table 1. *Comparison of pollutants emission among different transportation mode*

Annual emission (kg/cap)	Rail			Aviation			Truck		
	CO_X	NO_X	SO_X	CO_X	NO_X	SO_X	CO_X	NO_X	SO_X
China	0.031	0.53	4.02	1.76	6.12	9.25	1.81	2.63	4.02
USA	0.17	3.69	11.49	9.62	42.11	26.43	9.9	18.08	11.49
OECD	0.096	1.98	6.45	5.43	22.6	14.86	5.58	9.72	6.47

As shown in *Figure 1,* the mileage of HSR goes up obviously, about 29,000 km in 2018, so does the total income and volume of express industry. In fact, intercity express volume accounts for nearly 70% of the total volume. However, it is difficult to organize and modernize goods transport between large cities (Dablanc, 2007; O'Connor, 2010; Li, et al., 2017; Musolino et al., 2018). Since the two megacities of China, Beijing and Shanghai, connected by HSR in 2011, the transportation and communication between the north and the south of China become more intensive. As economy development depends heavily on transport, investigating the feasibility of coordinating freight and passenger flows using existing and forthcoming rail infrastructure has been a new trend in recent years (Behiri et al., 2018; Talebian and Zou, 2015; Pazour, et al., 2010).

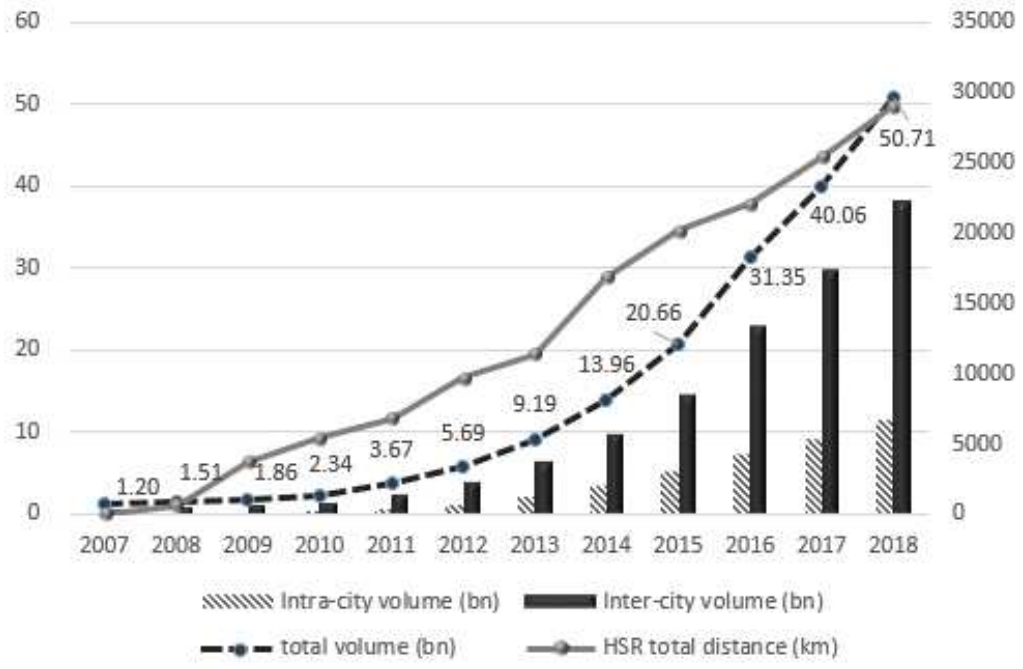

Figure 1. *The development trend of express industry and HSR*

http://www.aloki.hu ● ISSN 1589 1623 (Print) ● ISSN 1785 0037 (Online)
DOI: http://dx.doi.org/10.15666/aeer/1704_88058816

Currently, there is no unified specific definition about high speed freight transportation (Troche, 2005), this paper supposes the modes can be basically divided into two: Mixed-train Mode, using passenger High Speed Train (HST) for freight transportation, including reserving or adding a couple of carriages; Freight-train Mode, adding exclusive high speed freight train or remoulded existing passenger HSTs for freight transport. Generally, compared with conventional transport modes, the main advantage of HSTs is cheaper than aviation and faster than truck. High speed rail is often touted as a means to reduce congestion of passengers transport instead of freight, but this paper offers a new method to quantitatively analyse the feasibility of such a sustainable freight mode and its positive influence to environment.

In the next section, the paper sets out method and algorithm adopted for forecasting Origin-Destination (OD) parcels demand. Section 3 shows a case study of about future freight distribution and the feasibility of adding HSTs on B-S HSR to transport parcels. Section 4 and 5 respectively presents the results and discussion about the adoption of the two modes. Section 6 ends the paper, setting out the conclusion.

Materials and methods

Forecasting demand based on ARMA model

In order to estimate the feasibility of operating high-speed freight on Beijing-Shanghai (B-S) corridor, freight distribution in future should be considered initially. Urban freight demand forecasting has been a crucial part of analysing the quantity of OD flow matrices (Nuzzolo and Comi, 2014; Börjesson, 2014; Jiang et al., 2014; Garrido, 2000), this paper presents a modelling system that tries to point out the freight relation among cities. Auto-Regression Model has been widely used for forecast analysis of time series (Wang, et al., 2013).

The general form of an ARMA model can be listed in *Equation 1* and transformed into *Equation 2*:

$$x_t = \delta_0 + \delta_1 x_1 + \delta_2 x_2 + \cdots + \delta_p x_{t-p} + \tau_m - \theta_1 \varepsilon_1 - \theta_2 \varepsilon_2 - \cdots - \theta_p \varepsilon_{t-q} \quad \text{(Eq.1)}$$

$$(x_t - \mu) - \delta_1 (x_1 - \mu) - \cdots \delta_p (x_{t-p} - \mu) = \varepsilon_t - \theta_1 \varepsilon_1 - \theta_2 \varepsilon_2 - \cdots - \theta_q \varepsilon_{t-q} \quad \text{(Eq.2)}$$

where $\mu = \frac{\delta_0}{1 - \delta_1 - \cdots - \delta_p}$, usually, μ would be estimated by the sample mean $\bar{x} = \frac{1}{N} \sum_1^N x_t$, and the variance will be shown as *Equation 3* if the series is stationary:

$$Var[\bar{x}] = E[\bar{x} - \mu]^2 = \frac{1}{N^2} E\left[\sum_{s=1}^{N} (X_s - \mu) \cdot \sum_{t=1}^{N} (X_t - \mu) \right] = \frac{1}{N^2} \sum_{s=1}^{N} \sum_{t=1}^{N} c_{t-s} \quad \text{(Eq.3)}$$

Assume k = t-s, then c (k) is an even function leads to *Equation 4:*

$$Var[\bar{x}] = \frac{1}{N^2} \sum_{k=-(N-1)}^{N-1} (N - |k| c_k) = \frac{1}{N} \sum_{k=-(N-1)}^{N-1} (1 - \frac{|k|}{N}) c_k \quad \text{(Eq.4)}$$

http://www.aloki.hu ● ISSN 1589 1623 (Print) ● ISSN 1785 0037 (Online)
DOI: http://dx.doi.org/10.15666/aeer/1704_88058816

When the N is large enough, from *Equation 4* it may be expressed as *Equation 5:*

$$Var\left[\bar{x}\right] \approx \frac{1}{N}\sum_{k=-\infty}^{+\infty} c(k) = \frac{\gamma(0)}{N}\left[1+2\sum_{k=1}^{+\infty}\rho(k)\right] = O\left(\frac{1}{N}\right) \quad \text{(Eq.5)}$$

If $\bar{x} \in \left[-2\sqrt{Var\left[\bar{x}\right]}, 2\sqrt{Var\left[\bar{x}\right]}\right]$, the stable series can be considered as a series with a zero mean, if not, a new series $\left\{x_t = x_t - \bar{x}, t = 0, \pm 1, \pm 2, \cdots\right\}$ can be generated as a zero mean stationary sequence.

In order to build a suitable ARMA model, we need to observe the character of partial autocorrelation sequence τ_{kk} and autocorrelation sequence σ_k (*Eq. 6*).

$$\hat{\sigma}(k) = \frac{\frac{1}{N}\sum_{i=1}^{N-|k|} X_i X_{i+|k|}}{\frac{1}{N}\sum_{i=1}^{N} X_i^2}, (k = 0, \pm 1, \pm 2, \cdots) \quad \text{(Eq.6)}$$

If $\hat{\sigma}(k) \sim N\left[0, \frac{1}{N}\left(1+2\sum_{l=1}^{q}\hat{\sigma}_l^2\right)\right], (k > q)$, then $P\left[\left|\hat{\sigma}_k\right| \le \frac{2}{\sqrt{N}}\left(1+2\sum_{i=1}^{q}\hat{\sigma}_i^2\right)^{1/2}\right] = 95.5\%$, thus MA (q) should be established if $\left|\hat{\sigma}_{q+i}\right| \le \frac{2}{\sqrt{N}}\left(1+2\sum_{i=1}^{q}\hat{\sigma}_i^2\right)^{1/2}, i = 1, 2, \cdots M-q$. Similarly, AR (p) should be established if $\tau_{kk} \sim N\left[0, \frac{1}{N}\right], (k > p)$ and $\left|\hat{\tau}_{(p+i)(p+i)}\right| \le \frac{2}{\sqrt{N}}, \left(i = 1, 2, \cdots, M-p\right)$.

For ARMA (p, q), estimated residual sequence $\left\{\varepsilon_t\right\}$ can be estimated as *Equation 7*:

$$\tilde{\varepsilon}_t = x_t - \tilde{\delta}_1 x_{t-1} - \tilde{\delta}_2 x_{t-2} - \cdots - \tilde{\delta}_p x_{t-p} + \hat{\theta}_1\tilde{\varepsilon}_{t-1} + \hat{\theta}_2\tilde{\varepsilon}_{t-2} + \cdots + \hat{\theta}_q\tilde{\varepsilon}_{t-q} \quad \text{(Eq.7)}$$

Residual sum of squares is listed as *Equation 8:*

$$Q = \sum_{i=1}^{N}\tilde{\varepsilon}_i^2 \quad \text{(Eq.8)}$$

The variance of a sequence of residuals can be expressed as *Equation 9:*

$$\tilde{\rho}_\varepsilon^2 = \frac{Q}{N_1 - k} \quad \text{(Eq.9)}$$

N_1 is the number of observations actually used in fitting the model, k is the number of parameters that used in building the model. Akaike Information Criterion (AIC) is

http://www.aloki.hu ● ISSN 1589 1623 (Print) ● ISSN 1785 0037 (Online)
DOI: http://dx.doi.org/10.15666/aeer/1704_88058816

the most popular criterion for identifying the optimal model, which has been used in this paper to find out the suitable model for forecasting the values *Equation 10:*

$$x_m = \delta_0 + \delta_1 T + \delta_2 x_{m-1} + \delta_3 x_{m-2} + \cdots + \delta_p x_{m-p} + \tau_m \quad \text{(Eq.10)}$$

Forecasting demand based on gray model

Liu and Deng (2000) proposed the first-order one-variable gray model (GM (1, 1)) derived from gray system theory, which can be established based on a small amount of incomplete information to describe the fuzzy rule of the development of things in the long term. Since express delivery was only emerging in recent years, which leads to lacking data, the gray model adopted in this paper can help to produce effective results.

We assume the original data sequence is $x^{(0)} = \left(x^{(0)}(1), x^{(0)}(2), \cdots x^{(0)}(n)\right)$, and generate a new sequence: $x^{(1)} = \left(x^{(1)}(1), x^{(1)}(2), \cdots x^{(1)}(n)\right)$, then use accumulated generating operation since $y^{(0)}(m)$ is strictly positive and corresponds to time m. And we can have *Equation 11*:

$$x^{(0)}(m) = x^{(1)}(m) - x^{(1)}(m-1), m = 1, 2, \cdots n-1 \quad \text{(Eq.11)}$$

where $x^{(0)}(1) = x^{(1)}(1)$ $x^{(1)}(m) \in x^{(1)}$. If $n \geq 4$, $x^{(0)}, x^{(1)} \in R^+$, then the GM (1,1) can be expressed by an one-variable, first-order differential equation as *Equation 12:*

$$\frac{dx^{(1)}}{dt} + ax^{(1)} = b \quad \text{(Eq.12)}$$

where a and b are called the development and gray input coefficients respectively. The whitening version of *Equation 5* is shown as $x^{(0)}(m) + az^{(1)}(m) = b$, substitute all values and get *Equation 13*:

$$\begin{aligned} x^{(0)}(2) &= -az^{(1)}(2) + b \\ x^{(0)}(3) &= -az^{(1)}(3) + b \\ x^{(0)}(4) &= -az^{(1)}(4) + b \\ &\cdots \\ x^{(0)}(n) &= -az^{(1)}(n) + b \end{aligned} \quad \text{(Eq.13)}$$

where $z^{(1)}(m)$ is called the background value of $dx^{(1)}/dt$ and is calculated by *Equation 14:*

$$z^{(1)}(m) = \frac{1}{2}\left(x^{(1)}(m) + x^{(1)}(m-1)\right) \quad \text{(Eq.14)}$$

Equation 14 is established based on discrete data and equal spacing in time, by using least-squares method, the coefficients a and b can be obtained as $\begin{bmatrix} a \\ b \end{bmatrix} = \left(B^T B\right)^{-1} B^T x_n$

http://www.aloki.hu ● ISSN 1589 1623 (Print) ● ISSN 1785 0037 (Online)
DOI: http://dx.doi.org/10.15666/aeer/1704_88058816

where $B=\begin{bmatrix} -z^{(1)}(2) & 1 \\ -z^{(1)}(3) & 1 \\ \vdots & \vdots \\ -z^{(1)}(n) & 1 \end{bmatrix}$ and $x_n=\begin{bmatrix} x^{(0)}(2) \\ x^{(0)}(3) \\ \vdots \\ x^{(0)}(n) \end{bmatrix}$, then the values a and b can be solved, $a=\frac{CD-(n-1)E}{(n-1)F-C^2}$, $b=\frac{DF-CE}{(n-1)F-C^2}$, $C=\sum_{k=2}^{n} z^{(1)}(k)$, $D=\sum_{k=2}^{n} x^{(0)}(k)$, $E=\sum_{k=2}^{n} z^{(1)}(k)x^{(0)}(k)$, $F=\sum_{k=2}^{n} z^{(1)}(k)^2$.

Finally, the predicted equation is expressed as *Equation 15:*

$$\hat{x}^{(0)}(m+1)=(x^{(0)}(1)-\frac{b}{a})(1-e^{a})^{-am} \quad \text{(Eq.15)}$$

Matlab has been widely used to solve the research problems related with gray system theory, in this paper, the class-compare verification and remnant verification are used to validate data, then we deal with data by translating the jumping type sequence into monotonic increasing type sequence, and used Matlab R2018b to complete prediction process.

Forecasting distribution of parcels demand between cities

In fact, Auto-Regression Model has been widely used for forecast analysis of time series, and Gray Model is better at dealing with systems that are characterized with poor information and stable trend data. Jia et al. (2016) find the accuracy degree increases obviously after combining two methods together. Based on the prediction express demand results of GM and AR model, a new combination model can be created as *Equation 16:*

$$X_m=\varepsilon_1(\delta_0+\delta_1 T+\delta_2 x_{m-1}+\delta_3 x_{m-2}+\cdots+\delta_p x_{m-p}+\tau_m)+\varepsilon_2\left(x^{(0)}(1)-\frac{b}{a}\right)(1-e^{a})e^{-am} \quad \text{(Eq.16)}$$

where ε_1 and ε_2 are respectively the weight of demand variable based on the accuracy of forecast value of two methods.

This study assumes intercity parcels of every city are delivered through a nationwide network, and focuses on trunk transport and assumes stations of cities as origin and destination nodes, which leads to the formation of ODPs. By modifying the gravity model, the paper builds *Equation 17* to measure the attraction degree ω_{ij} between city i and city j.

$$\omega_{ij}=\frac{\sqrt{POP_i\times GDP_i\times N_i}\times\sqrt{POP_j\times GDP_j\times N_j}}{S_{ij}^2} \quad \text{(Eq.17)}$$

where S_{ij} indicates the minimum high speed rail distance between city i and city j, i = 1,2,……n, j = 1,2,……n, I ≠ j. POP_i, GDP_i and N_i respectively indicates the population, GDP and the average amount of HSTs stop by the station of city i per day.

http://www.aloki.hu ● ISSN 1589 1623 (Print) ● ISSN 1785 0037 (Online)
DOI: http://dx.doi.org/10.15666/aeer/1704_88058816

A case study

Now the paper tries to estimate the feasibility of operating freight trains on Beijing-Shanghai HSR from supply and demand perspective based on the methods shown above.

Demand: attractive amount of parcels distributed on B-S HSR corridor in future

The data used in this section is based on the intercity volume of main cities along B-S HSR from the official website of the cities' post office from 2010 to 2017. In order to forecast the demand of the main cities on B-S HSR corridor in next seven years, AR-GM model has been adopted by using Eviews 8.0 and Matlab R2018b, the accuracy grade of fitted values are shown in *Table 2*.

Table 2. *The accuracy grade of fitted values of main cities*

	Relative error	Variance ratio	Little probability of error	Development coefficient	Accuracy grade
Beijing	0.00081	0.0059	1	-0.0875	First
Tianjin	0.00072	0.1424	1	-0.0340	First
Jinan	0.00018	0.0776	1	-0.0225	First
Nanjing	0.00054	0.1136	1	-0.0455	First
Shanghai	0.00601	0.0301	1	-0.1391	First

It can be seen from *Table 2* that the model is fitting well, the difference and little probability of error reached the "first class" precision. The absolute values of all the development coefficients are smaller than 0.3, which indicates the model is suitable for mid-long term prediction. Therefore, the intercity volume of each city from 2019 to 2025 is shown as follow (*Table 3*).

Table 3. *The forecast of intercity express volume of main cities (mt)*

	2019	2020	2021	2022	2023	2024	2025
Beijing	3.35	3.82	4.33	4.89	5.48	6.13	6.83
Tianjin	0.95	1.09	1.24	1.41	1.59	1.80	2.10
Jinan	0.59	0.72	0.82	1.01	1.15	1.43	1.63
Nanjing	1.01	1.13	1.26	1.40	1.54	1.68	1.83
Shanghai	6.17	7.68	9.38	11.62	14.15	17.59	21.48

As shown in *Table 3*, nowadays only the intercity parcels of Beijing and Shanghai are over 1 mt, but most of main cities will transcend the figure soon. Nanjing owns the lowest express volume growth rate with about 10.5% per year on average, and it will be surpassed by Tianjin in 2022 whose volume will reach 1.41 mt. Beijing's is also lower than national average level recently and the rate will keep dropping based on the consistent policy of emphasis on decentralization made by government, but the amount (6.83 mt) in 2025 will be twice bigger than current volume (3.35 mt). Shanghai, the biggest volume owner, also with the highest average growth rate, 23.10%, has shown

http://www.aloki.hu ● ISSN 1589 1623 (Print) ● ISSN 1785 0037 (Online)
DOI: http://dx.doi.org/10.15666/aeer/1704_88058816

the potential to triple the amount after seven years and dramatically increase to 21.48 mt.

This paper chooses B-S HSR as a case coz if the most crowded HSR in China has space to operate freight train, other HSRs can operate more. The application of method in section 2 leads to the distribution of Origin-Destination Pairs (ODPs) on B-S HSR corridor. The thickness of lines in *Figure 2* indicates the upstream and downstream of ODPs in 2019 and 2025. The different color depths of cities on map indicates numbers of addible HSTs for cities' station.

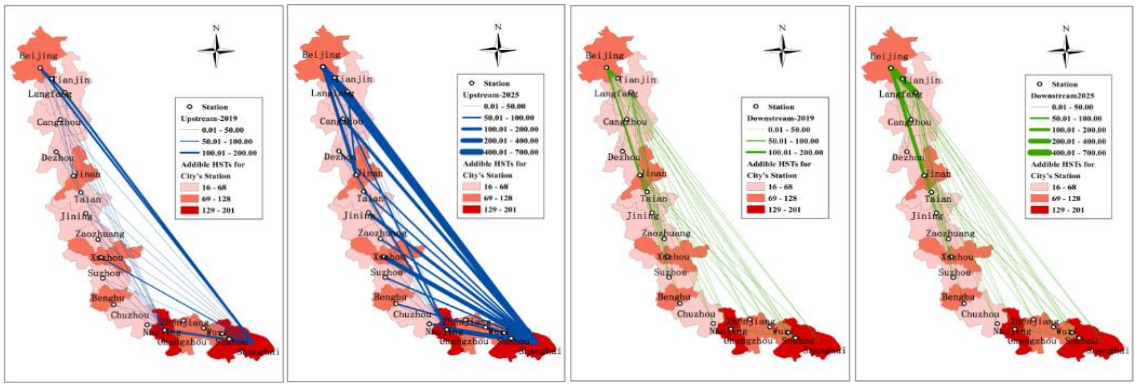

2019-upstream 2025-upstream 2019-downstream 2025-downstream

Figure 2. *ODPs distribution of main cities along B-S HSR corridor*

Most of upstream flows are from Shanghai, which has been more obvious over time. The flow volume from Shanghai to other cities in 2025 will be three times as big as the volume in 2019. Among all the flow of ODPs, the volume of Shanghai-Jinan and Shanghai-Beijing are always at top 2, and both of them have been over 200 kt parcels in 2019. Besides, the number of flows over 100 kt has been raised from 6 in 2019 to 12 in 2025. As for downstream flows, most are relative small and varies slightly, but they can still be double in next seven years. Besides, the top 5 pairs are always Beijing-Tianjin, Beijing-Langfang, Beijing-Jinan, Beijing-Cangzhou, Nanjing-Shang. However, only two pairs of which are over 100 kt in 2019, and the third pair cannot break the line until 2025.

Supply: the addible bullet trains among stations along B-S HSR

This paper believes if China Railway Corportation (CRC) can add more trains to solve the peak congestion, it must own the capacity to add freight trains on workdays if it is necessary. The paper collected the amount of operating trains among 24 stations of B-S HSR from February 9 to March 18 in 2018, which includes the peak time of spring festival and the workdays after. The difference of a high speed station between the peak and workdays indicates that station's capacity of adding freight trains on usual, which has represented by the thickness of line in *Figure 3*.

In general, the densest sheaf of addible trains are among Shanghai city and Jiangsu province. The top of the ODP list is Shanghai-Nanjing, which owns the capacity of adding 50 pairs on usual. And for upstream and downstream addible pairs, there are respectively 13 and 9 ODPs of adding HSTs over 10. Upstream distribution also has similar situation, among all of the cities in northern and southern part, only the ODPs

http://www.aloki.hu ● ISSN 1589 1623 (Print) ● ISSN 1785 0037 (Online)
DOI: http://dx.doi.org/10.15666/aeer/1704_88058816

between Beijing and Nanjing are over 5. Thus, it is feasible for CRC to appropriately add various HSTs based on stations' capacity to transit express parcels on usual.

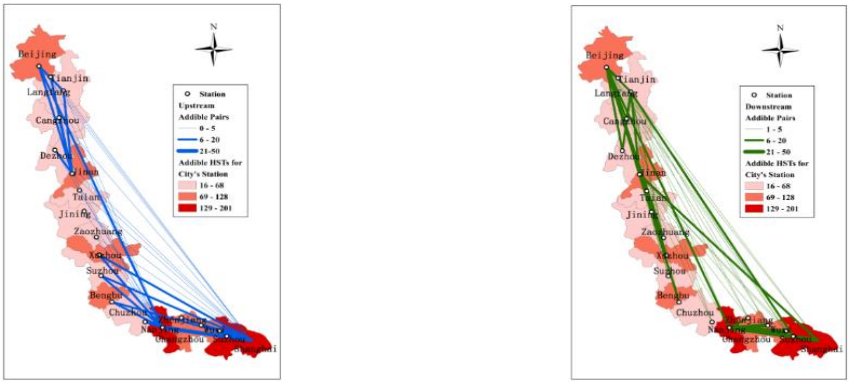

Upstream Downstream

Figure 3. *The supply capacity of high speed stations along B-S HSR corridor*

Results

The optimum alternative of operation mode between cities is determined by demand volume and supply capacity in this paper, we admit that the result will be more convinced if more influential factors are fully considered.

As shown in *Table 4*, those ODPs such as Beijing-Tianjin, Shanghai-Suzhou, Beijing-Jinan, Shanghai-Xuzhou adapt to Freight-train mode because of vast parcels demand and a mass of addible HSTs existing there. Those ODPs like Shanghai-Jinan, Shanghai-Beijing, Beijing-Langfang only have large demand, barely HSTs could be added on usual, so these ODPs suit for adopting Mixed-train mode.

Table 4. *Supply and demand of intercity express volume between cities in 2019*

Origin-destination	Parcels demand (kt)	Addible HSTs	Origin-destination	Parcels demand (kt)	Addible HSTs
Freight train mode			**Mixed-train mode**		
Beijing-Tianjin	320.3	11	Shanghai-Jinan	207.87	1
Tianjin-Beijing	133.55	12	Shanghai-Beijing	196.11	0
Shanghai-Suzhou	127.17	16	Beijing-Langfang	160.22	0
Shanghai-Xuzhou	72.61	8	Shanghai-Tianjin	111.18	0
Shanghai-Wuxi	54.4	7	Shanghai-Nanjing	102.47	1
Beijing-Jinan	54.08	13	Shanghai-Jining	38.08	1
Jinan-Beijing	40.18	14	Nanjing-Jinan	34.31	4
Shanghai-Changzhou	35.79	6	Nanjing-Beijing	32.37	4
Beijing-Cangzhou	30.06	9	Shanghai-Cangzhou	30.91	0
Shanghai-Zhenjiang	26.41	8	Shanghai-Taian	26.41	0

Discussion

The high speed rail freight's emission of dust, NO_X, CO_X, land use and energy consumption are all much lower than truck and air freight, such eco-friendly mode deserves to be applied in a wider scope since environment protection and sustainable development are key issues for the policy-maker (Garau et al., 2011). In fact, Mixed-

http://www.aloki.hu ● ISSN 1589 1623 (Print) ● ISSN 1785 0037 (Online)
DOI: http://dx.doi.org/10.15666/aeer/1704_88058816

train mode has been widely adopted in China, France, Turkey and many other European countries due to the barely extra cost by loading the parcels on the vacant carriage, but the shortcoming is obvious too, for example, the transport capacity is limited and varies too much because of the frequent fluctuation of passenger flow. Particularly, HSTs in China only stop for about 2 min at most stations, which leaves no time for loading or unloading, therefore, such mode can only operate from the departure station to terminal station. Conversely, Freight-train mode does not have the defect and is able to demonstrate bigger advantage and stronger competitiveness in the areas where own large freight demand (Liang et al., 2016).

Interestingly, the cost of Freight-train mode is hardly accepted by both most enterprises and governments when freight demand is low, but if they do not take this mode, it is hard to get more cargo business from freight market. Faced with the considerable investment required for HSR construction, the determination of policy-maker will play an important role in promoting the process of HSR freight, and clearly, Chinese government has shown more ambition on HSR than other countries', which provides more chances for further research into such eco-friendly transport modes.

Conclusion

This paper improves the accuracy of forecasting by combining ARMA and Gray Model, and discusses the feasibility of operating freight on Beijing-Shanghai HSR corridor and offers the solution with reasons for different Origin Destination pairs. Besides, the flow demand of intercity parcels will keep a growth rate vary from 10% to 23% in the next seven years, and the application of high-speed freight, especially the Freight-train mode, will alleviate the severe air pollution and traffic congestion among those big cities.

However, this paper ignores the possibility of operating freight transport on the checking-train at night since the research is based on the daytime schedule. Moreover, "Door to Door" express freight service cannot be accomplished only by HSR, the multimodal transport needs to be considered in future research. Above all, finding the appropriate routes, identifying the potential hub cities for cargo transfer, optimizing the rail network structure to minimize the transport time are all important ways to improve the efficiency and possibility of operating express freight transport. Apparently, we can not take all of the problems into consideration, but we believe focusing on HSR freight helps people make better use of resources and protect environment well.

Acknowledgements. This research was supported by the Fundamental Research Funds for the Central Universities (Grant No. 2018YJS062).

REFERENCES

[1] Behiri, W., Belmokhtar-Berraf, S., Chu, C. (2018): Urban freight transport using passenger rail network: scientific issues and quantitative analysis. – Transp. Res. Part E 115: 227-245.

[2] Börjesson, M. (2014): Forecasting demand for high speed rail. – Transportation Research Part A 70: 81-92.

[3] Dablanc, L. (2007): Goods transport in large European cities: difficult to organize, difficult to modernize. – Transportation Research Part A 41: 280-285.

http://www.aloki.hu ● ISSN 1589 1623 (Print) ● ISSN 1785 0037 (Online)
DOI: http://dx.doi.org/10.15666/aeer/1704_88058816

[4] Du, J., Li, Q., Qiao, F., Yu, L. (2018): Estimation of vehicle emission on mainline freeway under isolated and integrated ramp metering strategies. – Environmental Engineering and Management Journal 17(5): 1237-1248.
[5] Ferrón-Vilchez, V., De la Torre Ruiz, J. M., de Mandojana, O. (2015): How much would environmental issues cost? The internalisation of environmental costs in the European transport industry. – Environmental Engineering and Management Journal 45(9): 2149-2162.
[6] Garau, G., Mandras, G., Schirru, L. (2011): A statistical information system supporting environmental policies. – Environmental Engineering and Management Journal 10 (12): 1903-1910.
[7] Garrido, R. A., Mahmassani, H. S. (2000): Forecasting freight transportation demand with the space-time multinomial probit model. – Transportation Research B 34: 403-418.
[8] Gong, D., Tang, M., Liu, S., Xue, G., Wang, L. (2019): Achieving sustainable transport through resource scheduling: a case study for electric vehicle charging stations. – Advances in Production Engineering & Management 14(1): 65-79.
[9] Jia, S., Xu, T. H., Sun, Z. Z., Li, J. J. (2016): Middle and long-term prediction of ut1-utc based on combination of gray model and autoregressive integrated moving average. – Advances in Space Research 59(3).
[10] Jiang, X., Zhang, L., Chen, X. M. (2014): Short-term forecasting of high-speed rail demand: a hybrid approach combining ensemble empirical mode decomposition and gray support vector machine with real-world applications in China. – Transportation Research Part C 44: 110-127.
[11] Li, G., Jin, F., Jiao, J., Liu, S. (2017): Location characteristics and differentiation mechanism of logistics nodes and logistics enterprises based on points of interest (POI): a case study of Beijing. – J. Geogr. Sci 27: 879-896.
[12] Liang X, Tan K, Whiteing A, Nash C, Johnson, D. (2016): Parcels and mail by high speed rail—comparative analysis of Germany, France and China. – Journal of Rail Transport Planning & Management 6(2):77-88.
[13] Limbourg, S., Jourquin, B. (2009): Optimal rail-road container terminal locations on the European network. – Transportation Research Part E 45 (4): 551-563.
[14] Liu, S., Deng, J. (2000): The range suitable for GM (1,1). – System Engineering Theory and Practice 20(5): 121-124.
[15] Mitran, G., Ilie, S., Tabacu, I., Nicolae, V. (2012): Modeling the impact of road traffic on air pollution in urban environment. Case study: a new overpass in the city of Craiova. – Environ. Eng. Manage. J. 11: 407-412.
[16] Musolino, G., Rindone, C., Polimeni, A., Vitetta, A. (2018): Planning urban distribution center location with variable restocking demand scenarios: general methodology and testing in a medium-size town. – Transp. Policy. DOI: 10.1016/j.tranpol.2018.04.006.
[17] Nanaki, E. A., Koroneos, C. J., Xydis, G. A. (2016): Environmental impact assessment of electricity production from lignite. – Environmental Progress & Sustainable Energy 35: 1868-1875.
[18] Nuzzolo, A., Comi, A. (2014): Urban freight demand forecasting: A mixed quantity/delivery/vehicle-based model. – Transportation Research Part E 65: 84-98.
[19] O'Connor, K. (2010): Global city regions and the location of logistics activity. – Transportation Geography 18: 354-362.
[20] Offer, G. J., Howey, D., Contestabile, M., Clague, R., Brandon, N. P. (2010): Comparative analysis of battery electric, hydrogen fuel cell and hybrid vehicles in a future sustainable road transport system. – Energy Policy 38 (1): 24-29.
[21] Pejić, V., Cedilnik, M., Lisec, A. (2017): Impact on the environment of industrial packaging waste transport. – Environmental Engineering and Management Journal 16 (5): 1155-1160.
[22] Pazour, J. A., Meller, R. D., Pohl, L. M. A. (2010): model to design a national high-speed rail network for freight distribution. – Transportation Research Part A 44: 119-135.

http://www.aloki.hu ● ISSN 1589 1623 (Print) ● ISSN 1785 0037 (Online)
DOI: http://dx.doi.org/10.15666/aeer/1704_88058816

[23] Talebian, A., Zou, B. (2015): Integrated modeling of high performance passenger and freight train planning on shared-use corridors in the US. – Transportation Research Part B: Methodological 82: 114-140.
[24] Troche, G. (2005): High-Speed Rail Freight, Report No: 0512. – KTH Railway Group, Stockholm.
[25] Van Duin, J. H. R., Tavasszy L. A., Quak H. J. (2013): Towards e(lectric)- urban freight: first promising steps in the electric vehicle revolution. – European Transport 54, Paper no. 9.
[26] Van Wee, B., Maat, K., De Bont, C. (2012): Improving sustainability in urban areas: discussing the potential for transforming conventional car-based travel into electric mobility. – European Planning Studies 20 (1): 95-110.
[27] Wang, L., Zhang, W., Lai, M., Xiang, T., Yang, Z., Zhou, B. (2013): Research on the forecasting of electric power demand in Hubei Province based on ARIMA-GM model. – China Rural Water and Hydropower (4): 101-105.

http://www.aloki.hu ● ISSN 1589 1623 (Print) ● ISSN 1785 0037 (Online)
DOI: http://dx.doi.org/10.15666/aeer/1704_88058816

EFFECTS OF BIOCHAR ON THE DIVERSITY AND COMMUNITY STRUCTURE OF SOIL FUNGI IN INTERCROPPING SYSTEM

GUO, X. F.[1,2] – LI, H. S.[2] – HU, Y. M.[2*]

[1]*College of Environmental Science and Engineering, China West Normal University, Nanchong 637009, China*

[2]*College of Resources and Environmental Sciences, South China Agricultural University, Guangzhou 510642, China*

**Corresponding author*
e-mail/phone: ymhu163@163.com/+86-186-8888-2020

(Received 12th Mar 2019; accepted 3rd May 2019)

Abstract. In order to investigate the long-term effects of biochar application on the diversity and community structure of soil fungi, different amount of biochar were applied to the *Machilus pauhoi-Ilex asprella* intercropping system under field conditions. The results showed that biochar significantly increased the pH and the content of organic matter, total nitrogen, total phosphorus, available phosphorus and available potassium in 0-15 cm soils while it had no significant effect on 15-30 cm soil physicochemical properties. The results of species annotation indicated that each biochar treatment increased the relative abundance of *Mortierellomycotina*, *Chytridiomycota*, *Glomeromycota* and *Ascomycota* in 0-15 cm soils. The T2 and T3 treatments increased the abundance of *Ascomycota* in 15-30 cm soils and reduced the abundance of *Basidiomycota*, which were opposite to the results of T1 treatment. At the genus level, in the soil with the depth of 0-15 cm, the application of biochar reduced the relative abundance of *Clitocybula* while significantly increased the relative abundance of *Parascutellinia*, *Glomus*, *Mortierella*, *Funneliformis* and *Plectosphaerella*. In 15-30 cm soils, all biochar treatments increased *Clitocybula* and *Mortierella* relative abundance, but reduced *Glomus* and *Gyroporus* relative abundance. In summary, biochar application has a significant effect on soil physicochemical properties after 3 years of application.
Keywords: *biochar, physicochemical properties, fungal community structure, high-throughput sequencing, RDA analysis*

Introduction

Soil microbes are the basis for material recycling and utilization in ecosystems, and are also a guarantee for ecosystems to maintain stability and normal functioning (Chapin et al., 1997). Soil, as a site for soil microbial activity, has an important impact on microbial composition and activity (Kuramae et al., 2011; Jeanbille et al., 2016). As an important member of soil microbes, fungi play an important role in the decomposition of soil, especially in the degradation of plant residues in the soil (Barbi, et al., 2016). Some soil fungi play a huge role in improving plant stress resistance and maintaining normal plant growth (Mukerji et al., 1996; Filion et al., 1999). Fungi drive the material cycle and energy flow in soil ecosystem. The diversity of soil microbial community structure can reflect the change process of soil environmental quality in advance (Sharma et al., 2010). All soil physical and chemical properties, temperature, moisture, etc., have an effect on soil microbial communities, leading to changes in microbial composition and structure (Alvarado et al., 2010).

Biochar is a stable soil conditioner that biomaterials undergo pyrolysis in a high temperature and oxygen-free environment to form organic carbon-rich (Johannes et al.,

http://www.aloki.hu ● ISSN 1589 1623 (Print) ● ISSN 1785 0037 (Online)
DOI: http://dx.doi.org/10.15666/aeer/1704_88178834

2015). Biochar porosity and adsorption increase soil nutrients and water content (Schulz et al., 2013), providing a direct habitat for soil microbes (Gul et al., 2015). Biochar plays an important role in regulating soil microbial community structure and diversity due to its special physical and chemical properties (Xu et al., 2016; Kolton et al., 2011). Yao et al. (2017) found that the addition of biochar to black soil significantly increased the relative abundance of Guehomyces and reduced the relative abundance of Fusarium. Zheng et al. (2016) found that biochar significantly increased the relative abundance of Zygomycota and Mortierella fungi in paddy soils, and reduced the relative abundance of Penicillium and Cyphellophora fungi degree. In addition, biochar can affect the colonization of mycorrhizal fungi in crop roots. Matsubara et al. (2002) found that adding coconut shell biochar to soil increased the abundance of asparagus root mycorrhizal fungi. Studies have shown that activated carbon components of biochar can be degraded at the beginning of application, providing a source of carbon for microorganisms and promoting microbial growth (Sagrilo et al., 2015; Smith et al., 2010). Kuzyakov et al. (2009) found that biochar-derived carbon in soil microbes decreased by 42.31% after biochar application for 20 months. Over time, the physical and chemical properties of biochar would change, and its long-term interaction with soil particles would create a new soil-biochar system (Jones et al., 2012). However, the current impact on soil microbes after long-term application of biochar is not clear. Therefore, research on the long-term effects of biochar on soil fungi is of great significance.

In this study, the southern red soil was used as the research object, and the effects of biochar on soil physical and chemical properties and fungal community structure after 3 years of biochar application were measured. The changes of soil physical and chemical properties and soil fungal community succession were analyzed. The study aimed to clarify the effects of biochar on fungal communities and explore the relationships between soil properties and soil fungal communities, hoping to provide a theoretical basis for biochar to improve soil biological characteristics.

Material and method

Experimental material

The soil used in this study was the surface soil (0-20 cm soil layer) in the trees garden of South China Agricultural University in Guangzhou, Guangdong province, and the Guangzhou red soil at lower layer, which were mixed according to the soil thickness of the actual woodland. The basic physical and chemical properties of the soil are shown in *Table 1*.

Biochar was supplied by Shaanxi Yixin Bioenergy Technology Development Co., Ltd., and was milled to pass a 3 mm sieve by thermal cracking of discarded fruit tree trunks and branches in a cracking furnace and oxygen-limited environment (450 °C).

Table 1. *Basic physical and chemical properties of soil*

Soil samples	pH	Organic matter (g/kg)	Total N (g/kg)	Total P (g/kg)	Total K (g/kg)	Available N (mg/kg)	Available P (mg/kg)	Available K (mg/kg)
Woodland surface soil	5.65	15.25	0.305	0.248	2.763	19.32	9.95	36.67
Layer red soils	6.05	3.16	0.203	0.165	1.702	11.59	3.20	20.08

http://www.aloki.hu ● ISSN 1589 1623 (Print) ● ISSN 1785 0037 (Online)
DOI: http://dx.doi.org/10.15666/aeer/1704_88178834

The tested plants were 20 cm *Machilus pauhoi* seedlings and 35 cm *Ilex asprella* seedlings, and both plants were selected with good growth and consistency.

Experiment design

This experiment was carried out in outdoor concrete pools in the Resource and Environment College of South China Agricultural University, Guangzhou (N04°09′44.20″, E113°21′57.75″) from 2014 to 2017, with a marine climate of the south subtropical monsoon, a annual average temperature of 21.7 °C and a annual precipitation of 1689.3 mm to 1876.5 mm. The concrete pool has a volume of 1 m × 1 m × 2 m and an area of 2 m^2 (It was about 1 m wide, 2 m long and 1 m deep). There are 12 concrete pools, and each concrete pool serves as a experimental plot. The experiment adopted a randomized block design, and a total of 4 gradients of biochar treatments were set: 0 kg (CK), 1.2 kg (T1), 2.4 kg (T2), 4.8 kg (T3) (the forest charcoal application standard is 12 t/hm^2, which is equivalent to 1.2 kg in this experiment). First, each concrete pool was filled with 80 cm of Guangzhou red soil at the bottom, and then added with the woodland surface soil in the upper part. In 2014, biochar was applied to the surface soil followed by tumbling with tools. Each process was repeated 3 times and all processes were randomly arranged. The soil was pressed to the predetermined height and the conditions of soil were close to that of the actual forest soil. Urea, superphosphate and potassium sulfate was used as N fertilizer, P fertilizer and K fertilizer, respectively, with fertilization ratio at 261:150:181. After conversion according to the number of seedlings, base fertilizer which was composed of 41.76 g urea, 24 g superphosphate and 28.96 g potassium sulphate was added in one concrete pool. Topdressing was carried out with the same fertilizer composition one year later. Each concrete pool was equipped with automatic sprinkler irrigation system. It was irrigated every 3 days at 18:00 in dry season (October-March next year). According to the monthly irrigation allocation, the amount of irrigation was about the average daily rainfall of that monthly rainfall (600 mm). In case of rainy days, the irrigation time was adjusted artificially.

After biochar application, the concrete pools were provided with intercropping system of *Machilus pauhoi* and *Ilex asprella* at a ratio of 9:6. According to the plum planting pattern, the seedlings of *Machilus pauhoi* and *Ilex asprella* were transplanted, as shown in *Figure 1*.

Soil sampling and physical and chemical properties determination

Collection and determination of soil samples: After the seedlings were planted, in March 2017, a 5-point sampling method based on S-shape curve (Smalla et al., 2001) was used to collect soil with the depth of 0-15 cm and 15-30 cm. The five samples from the same depth range were mixed into one. The fresh soil sample was removed from the crop residue and stone by 2 mm sieve, and then divided into two parts. One part was placed in a sterile centrifuge tube and quickly placed in liquid nitrogen for the extraction of soil total DNA and subsequent bioinformatics analysis. The other part was naturally dried in the room and used for the determination of other physical and chemical properties of the soil.

The pH of the soil (water: soil = 2.5:1) was measured with potentiometer. Soil organic matter content was measured by the potassium dichromate volumetric method. Soil total nitrogen mass fraction was determined by Kjeldahl apparatus. Soil total

http://www.aloki.hu ● ISSN 1589 1623 (Print) ● ISSN 1785 0037 (Online)
DOI: http://dx.doi.org/10.15666/aeer/1704_88178834

phosphorus, total potassium, available phosphorus, available potassium, and alkaline nitrogen content were determined according to soil agrochemical analysis methods (Bao, 2000).

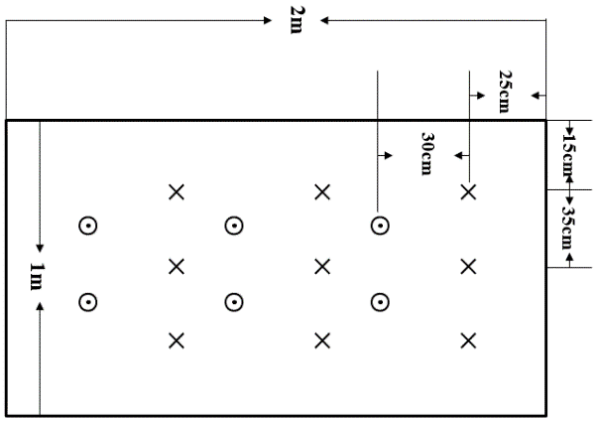

Figure 1. *Experimental planting pattern. (×: Machilus pauhoi; ⊙: Ilex asprella)*

Determination of fungi community structure in the soil

Total DNA extraction and PCR amplification

The total DNA in the soil was extracted using a Power Soil DNA isolation kit (MoBio Laboratories, Inc., Carlsbad, CA, U.S.A.) extraction kit. The integrity and concentration of the extracted DNA were examined using the Qubit 2.0 DNA kit. After passing the assay, the ITS2 region of the total DNA of the fungi was amplified using ITS3 and ITS4 primers (Huang et al., 2006).

Database construction and sequence processing

After purification of the PCR amplification product, all samples were mixed according to the DNA concentration in a ratio of 1:1, and a small fragment library was constructed for Paired-end sequencing using the Illumina (MiSeq PE300) sequencing platform of Guangdong Meige Gene Technology Co., Ltd. According to the similarity threshold of 97%, OTU were divided and clustered with the USEARCH (version 7.1) software for all qualified sequences. The sequence with highest abundance was selected as the representative sequence in each OTU. All representative sequences were species-annotated at the phylum and genus level using the RDP Classifier (classification threshold > 0.8) (Quast et al., 2013).

Data processing and analysis

The Shannon index, Chao1 index and sequencing coverage of samples were calculated using Mothur software (Pitta et al., 2014). Using SPSS software, soil physical and chemical indicators, α diversity of fungi communities and relative abundance of species at different taxonomic levels were analyzed by one-way ANOVA and Multiple comparisons were carried out by Duncan method ($P < 0.05$). The effect of environmental factors on the difference in fungi community structure between samples was analyzed by redundant ordering analysis (RDA). The visualization of RDA is plotted using the "vegan" package of the R software (version 3.3.1).

http://www.aloki.hu ● ISSN 1589 1623 (Print) ● ISSN 1785 0037 (Online)
DOI: http://dx.doi.org/10.15666/aeer/1704_88178834

Results and analysis

Effect of biochar on soil physical and chemical properties

As can be seen from *Table 2*, the application of biochar significantly increased the soil pH in depth of 0-15 cm compared to the control group, while had no significant effect on the pH of soil in 15-30 cm. The contents of soil organic matter and available potassium in the depth of 0-15 cm and 15-30 cm increased with the increase of biochar addition. In general, biochar could significantly increase the content of total nitrogen, total phosphorus and available phosphorus in the soil depth of 0-15 cm, but no significant difference was observed under different biochar additions. In addition, biochar had no significant effect on the content of organic matter, total nitrogen, total phosphorus, total potassium, alkali nitrogen, available phosphorus and available potassium in the soil depth of 15-30 cm. The total nitrogen content of soil as well as total phosphorus, total potassium, alkali nitrogen and available phosphorus in 0-15 cm soil increased first and then decreased with the increase of biochar addition.

Table 2. *Effects of biochar addition on soil physical and chemical properties*

Soil samples	Treatment	pH	Organic matter (g/kg)	Total nitrogen (g/kg)	Total phosphorus (g/kg)	Total potassium (g/kg)	Alkali nitrogen (mg/kg)	Available phosphorus (mg/kg)	Available potassium (mg/kg)
0-15 cm	CK	6.07±0.08a	9.56±2.00a	0.45±0.05a	0.42±0.07a	4.92±1.11a	31.66±5.76a	20.25±7.72a	56.47±11.65a
	T1	6.17±0.01ab	15.9±4.13bc	0.64±0.17b	0.54±0.06b	6.73±1.7ab	43.1±10.24a	28.8±6.53b	80.81±2.67ab
	T2	6.31±0.05ab	17.12±4.15bc	0.65±0.15b	0.49±0.02ab	6.72±0.3ab	43.48±4.12a	25.82±1.58ab	85.59±27.14ab
	T3	6.52±0.07bc	17.99±4.63bc	0.59±0.11ab	0.5±0.08ab	5.12±1.07a	36.81±6.87a	31.33±13.73b	89.67±24.29ab
15-30 cm	CK	6.57±0.08abc	3.77±0.36a	0.20±0.07a	0.26±0.02a	2.47±0.06a	16.02±0.57a	3.32±0.38a	35.53±9.05a
	T1	6.44±0.07ab	4.02±0.5a	0.21±0.01a	0.27±0.03a	2.46±0.2a	16.02±1.51a	3.57±1.38b	34.63±11.11a
	T2	6.47±0.02ab	4.47±1.32ab	0.22±0.03a	0.28±0.01a	2.76±0.2a	19.07±2.58a	3.55±0.76ab	48.62±12.17ab
	T3	6.57±0.03abc	5.63±3.13ab	0.19±0.09a	0.30±0.09ab	2.65±0.59a	16.97±5.5a	8.18±8.85a	69.59±19.1bc

Different letters indicate significant differences ($p < 0.05$) among different treatments.

The OTU of soil samples

A total of 1,193,794 sequences were obtained from 24 soil samples. After optimization, the sequence sequencing amount of each sample was between 40,000 and 55,000. The OTU was clustered at 97% similarity level and the dilution curve of each sample was prepared (*Fig. 2*), and 9,265 OTUs were obtained. The curve gradually becomes flat and the sequencing become saturated, indicating that the library construction was reasonable, and the number of sample sequences was sufficient to reflect the species diversity.

The Venn map can reflect the number of common and unique OTUs between groups or between samples, visually showing the similarity and overlapping between groups or samples. The OTU was analyzed with 97% similarity, and the number of OTUs could also represent the number of strains.

Figure 3 presents the mixed clustering result of the OUT representative sequences of 4 groups of samples in the depth of 0-15 cm and 15-30 cm. It can be seen from *Figure 3* (left) that 744 OTUs can be identified for the soils in the depth of 0-15 cm, of which 440, 448, 545, and 511 OTUs fall in the CK, T1, T2, and T3 communities, respectively. The number of fungi OTUs shared by different treatments was 279. Each treated soil had its unique fungi OTUs, the number of which in CK, T1, T2 and T3 group was 39, 28, 83 and 70, respectively. The number of unique fungi OTUs under T2 and T3

http://www.aloki.hu ● ISSN 1589 1623 (Print) ● ISSN 1785 0037 (Online)
DOI: http://dx.doi.org/10.15666/aeer/1704_88178834

treatments was larger than that of the control group, indicating that the application of biochar could lead to the change of fungi specificity in the soil to a certain extent. Although biochar treatment can increase the unique fungi species in the soil, the increased species varies with the application amount of biochar.

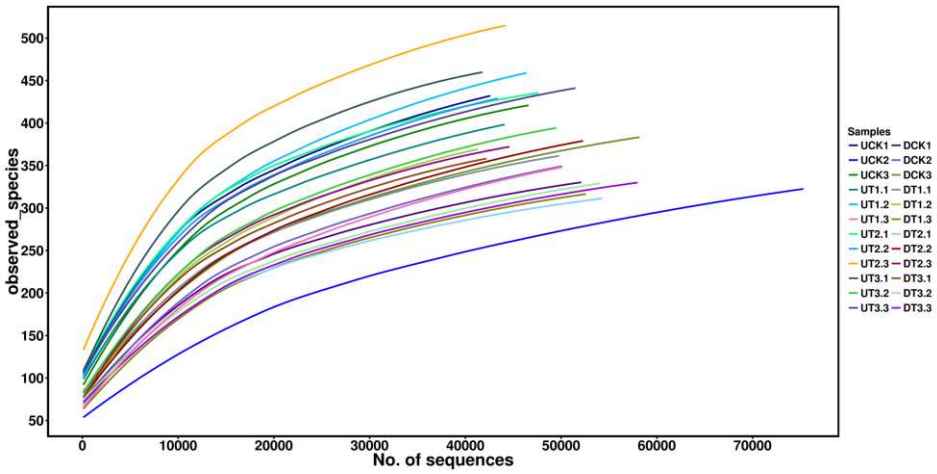

Figure 2. *Rarefaction curve of fungal community in soils. CK, T1, T2 and T3 represent different amounts of biochar, U and D represent soil depths of 0-15 cm and 15-30 cm, respectively*

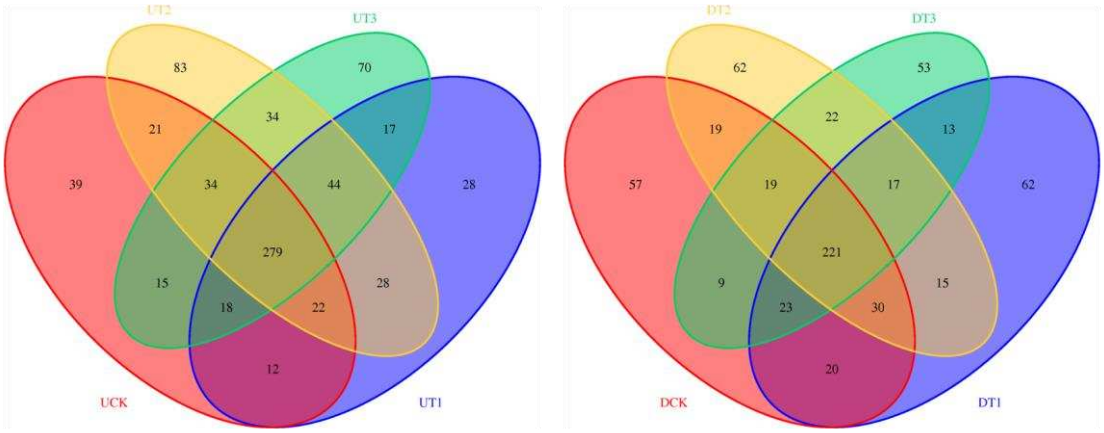

Figure 3. *Venn diagram of fungi in 0-15 cm (left) and 15-30 cm (right) of soil layers with biochar addition*

It can be seen from *Figure 3* (right) that 642 OTUs can be identified in the soils with the depth of 15-30 cm, of which 398, 401, 405, and 377 OTUs fall in the CK, T1, T2, and T3 communities, respectively. The number of fungi OTUs shared by different treatments was 221. Each treated soil had its unique fungi OTUs, the number of which in CK, T1, T2 and T3 group was 57, 62, 62 and 53, respectively. The number of unique fungi OTUs under T1 and T2 treatments was larger than that of the control group, indicating that the application of biochar can lead to the change of fungi specificity in

http://www.aloki.hu ● ISSN 1589 1623 (Print) ● ISSN 1785 0037 (Online)
DOI: http://dx.doi.org/10.15666/aeer/1704_88178834

the soil with the depth of 15-30 cm to a certain extent as well. Although biochar treatment can increase the unique fungi species in the soil, the increased species varies with the application amount of biochar.

Alpha diversity analysis

The Observed species index and the Chao1 index are used to measure the richness of the community in the sample, i.e., the number of single species (the number of OTUs), without involving the abundance of each species in the community. The larger the value is, the richer the species in the sample. Shannon index, Simpson index and PD whole tree reflect the diversity of the community, which is affected by the species richness and species uniformity in the sample community. The larger the value of Shannon index, PD whole tree and Simpson index indicates the higher diversity of the community in the samples.

It can be seen from *Table 3* that in the 0-15 cm soils, the fungi community richness under biochar treatment is higher than that of the control group, which is consistent with the dilution curve. The sequence of chao1 index and the Observed species (OTUs index) were respectively T2 > T1 > T3 > CK and T2 > T3 > T1 > CK; the chao1 index of 15-30 cm soils under each biochar treatment was slightly lower than that of biochar treatment, but the difference was not significant ($P > 0.05$). The difference in Observed species (OTUs index) was also not significant as well. In general, the difference in the abundance of fungi community in the soil with the depth of 15-30 cm was not significant under different treatment conditions.

For different biochar treatment groups, the order of PD whole tree value and Shannon index of soils with the depth of 0-15 cm were T2 > T3 > T1 > CK. T2 had a higher Simpson index than T3, and both T2 and T3 treatment had a higher Simpson index than T1 and CK. The diversity of soil fungi community under charcoal treatment was higher than that of the control group, and it reaches the peak value under T2 treatment. In the 15-30 cm soils, the PD whole tree value, Shannon index and Simpson index under T1 treatment were slightly higher than those of the control group. Overall, there was no significant difference in fungi community diversity among the 15-30 cm soils.

The fungi dominance index of the 0-15 cm soil after T1 treatment was higher than that of the control group while the index after T2 and T3 treatment were smaller than that of control group. For 15-30 cm soils, the conclusions were just the opposite.

Comparing fungal Alpha diversity index of the 0-15 cm soils with that of 15-30 cm soils, it can be seen that in the 0-15 cm soils, except for the dominance index, other indexes were higher than those of 15-30 cm soils.

Table 3. *Alpha diversity index of soil fungal with biochar application treatment*

Soil depth	Treatment	PD whole tree	Chao1 index	Dominance index	Observed species (OTUs index)	Shannon index	Simpson index
0-15cm	CK	18.00±4.36ab	516.74±85.92ab	0.24±0.11ab	363.33±96.13ab	3.54±1.21a	0.76±0.11ab
	T1	18.67±3.06ab	536.85±44.15ab	0.27±0.32ab	387.33±59.58ab	3.91±1.72a	0.74±0.32ab
	T2	22.00±1.73b	566.89±67.11b	0.08±0.03b	451.33±49.08b	5.07±0.48a	0.92±0.03b
	T3	20.00±2.65ab	516.88±34.05ab	0.18±0.12ab	416.00±42.51ab	4.33±0.94a	0.82±0.12ab
15-30cm	CK	16.33±0.58a	460.14±40.35a	0.28±0.04a	327.33±18.5a	3.41±0.23a	0.72±0.04a
	T1	17.00±1.73a	446.53±42.89a	0.26±0.11ab	336.67±37.54a	3.48±0.77a	0.74±0.11a
	T2	16.67±2.52a	441.40±57.63a	0.38±0.04a	333.67±41.2a	3.00±0.21a	0.62±0.04a
	T3	15.67±2.08a	434.77±23.22a	0.29±0.08ab	319.67±32.39a	3.40±0.52a	0.71±0.08a

http://www.aloki.hu ● ISSN 1589 1623 (Print) ● ISSN 1785 0037 (Online)
DOI: http://dx.doi.org/10.15666/aeer/1704_88178834

Soil fungi community structure under different treatments

Relative abundance of fungal in the soil at phylum level under different treatments

Species annotation results showed that 13 of the fungi were detected in the 24 soil samples, including: *Mortierellomycotina*, *Chytridiomycota*, and *Glomeromycota*. *Ascomycota*, *Basidiomycota* and some fungi classified as undetermined. The sequence of relative abundance from high to low was 50.389% of Ascomycota, which was the dominant species, 32.01% of Basidiomycota, 10.17% of *Glomeromycota*, and 1.69% of *Mortierellomycotina*, and 0.62% of *Chytridiomycota*. Their relative abundances together accounted for more than 90% of the annotated species.

It can be seen from *Figure 4* that biochar has different effects on the abundance of different fungi at phylum level in soils with different depth. In 15-30 cm depth soil layer, *Basidiomycota* had the highest relative abundance, and *Ascomycota* ranked the second place. Biochar could increase the relative abundance of *Mortierellomycotina*, *Chytridiomycota*, *Glomeromycota* and *Ascomycota*, all of which peaked the maximum under T2 treatment. However, this phenomenon was not found in 15-30 cm depth soil. In 15-30 cm depth soil layer, the relative abundance of Ascomycota was the highest, followed by *Basidiomycota*. Compared with CK treatment, the abundance of *Ascomycota* increased while the abundance of the *Basidiomycota* decreased after T2 and T3 treatment, which was the opposite to T1 treatment. The decrease degree of the *Glomeromycota* increased with the amount of biochar application. And there was little difference in relative abundance of the *Chytridiomycota* under different treatment.

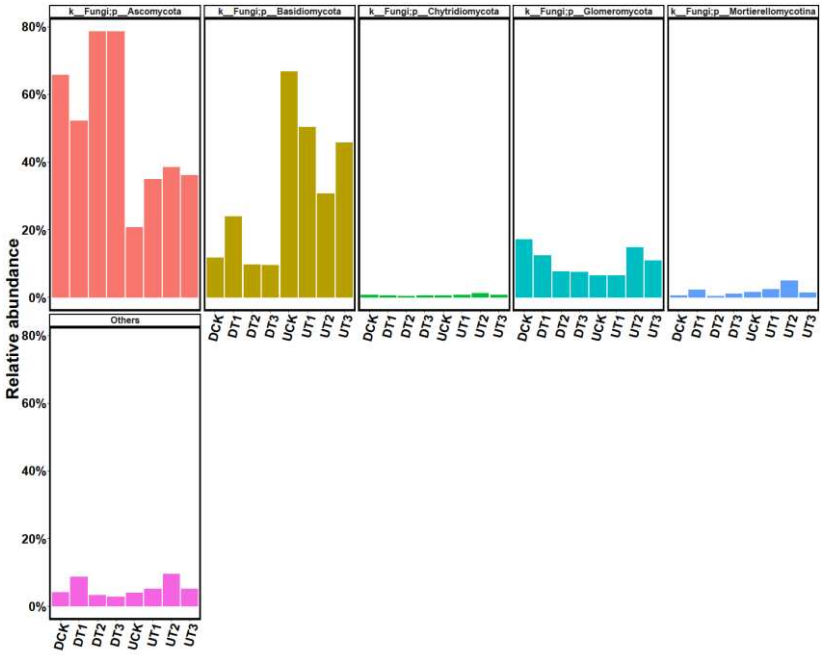

Figure 4. *Relative abundance of fungal communities in soil at phylum level*

Relative abundance of soil fungi at genus level under different treatments

As shown in *Figure 5,* the species annotation results at genus level indicated that the relative abundance of 12 genera was more than 1%. The relative abundance of *Parascutellinia* was the highest, accounting for 42.68% in all the species, followed by

http://www.aloki.hu ● ISSN 1589 1623 (Print) ● ISSN 1785 0037 (Online)
DOI: http://dx.doi.org/10.15666/aeer/1704_88178834

clitocybula, accounting for 32.71%. The relative abundance of these two species was significantly higher than that of other species. In 0-15 cm soil, the application of biochar reduced the relative abundance of *Clitocybula*, which was the smallest under T2 treatment. However, biochar application significantly improved the relative abundance of *Parascutellinia*, *Glomus*, *Mortierella*, *Funneliformis*, *Plectosphaerella*. The relative abundance of *Parascutellinia*, *Glomus*, and *Mortierella* under T2 treatment were the highest, while that of Funneliformis and Plectosphaerella increased with the amount of biochar application.

In 15-30 cm soil, the variation of relative abundance of *Parascutellinia* was consistent with that of soil with the depth of 0-15 cm. The relative abundance of *Clitocybula* and *Mortierella* increased significantly under biochar treatment and peaks the maximum value under T1 treatment. The relative abundance of *Phaeococcomyces* and *Plectosphaerella* were the largest under T2 treatment. However, the relative abundance of *Glomus* and *Gyroporus* decreased under biochar treatment. The relative abundance of *Mycotribulus* and *Ostropa* were not significantly changed under different treatments.

For soils in different depth, the abundance of *Parascutellinia*, *Gyroporus*, *Glomus* and *Phaeococcomyces* in the soils with the depth of 15-30 cm were higher than that in the soils with the depth of 15-30 cm. On the contrary, the 0-15 cm soils containd more *Clitocybula*, *Funneliformis*, *Mortierella*, *Mycotribulus*, *Ostropa*, and *Plectosphaerella*.

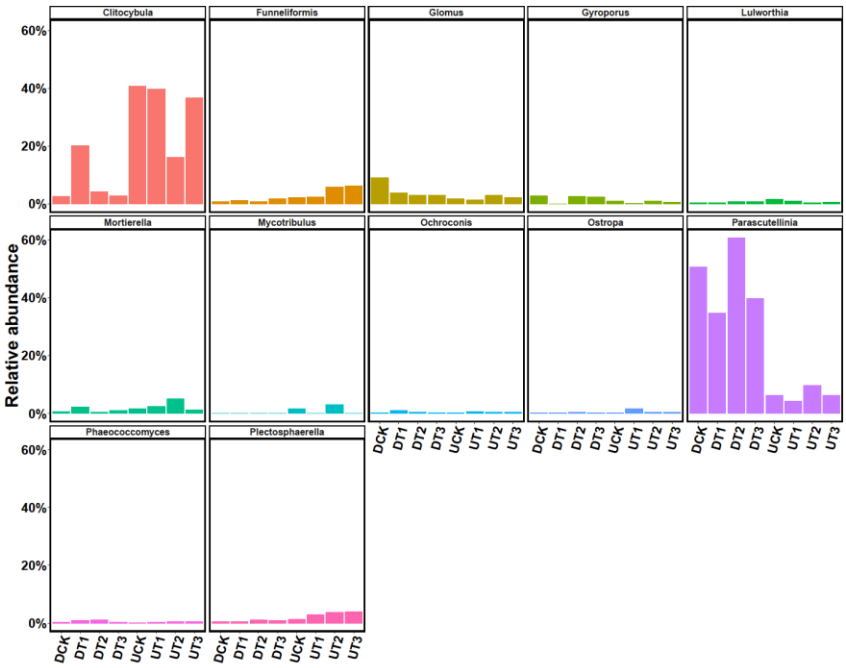

Figure 5. *Relative abundance of fungal communities in soil at genus level*

Cluster analysis on species relative abundance

Cluster analysis on species relative abundance at phylum level

Figure 6 is a species heat map of soil fungi at phylum level. The relative abundances of the species at each level are ranked, and the bacteria in the top 13 are selected (all the species are selected if the number of phylum is less than 13). The heat map is used to

http://www.aloki.hu ● ISSN 1589 1623 (Print) ● ISSN 1785 0037 (Online)
DOI: http://dx.doi.org/10.15666/aeer/1704_88178834

cluster the abundance similarity between different treatments. The similarity and color gradient are used to reflect the difference and similarity of fungal community composition at each level. The darker the red is, the greater the abundance, while darker the blue is, the lighter the abundance. A color patch represents the abundance of a phylum in a sample. In the figure, the horizontal direction is the sample information, and the vertical direction is the species annotation information. The sample clustering tree lies in the upper part and the species clustering tree lies in the left part of the figure.

As can be seen from *Figure 6,* the species in each sample are: Ascomycota, Basidiomycota, Glomeromycota, Mortierellomycotina, and Chytridiomycota, Zoopagomycotina, Mucoromycotina, Arthropoda, Blastocladiomycota, Kickxellomycotina, Entomophthoromycota, Cryptomycota and Annelida. The similarity between UTI and UCK was the highest, and UCK, UT1, and UT3 were also clustered at the top. These three groups had higher abundances of Basidiomycota and Zoopagomycotina, but were far away from UT2, which indicated that, compared with the control group, the effects of T1 and T3 treatment on the fungi community structure of 0-15 cm soil were not obvious while the effect of T2 treatment on soil fungal community structure was significant. UT2 was clustered as a specific group, and, compared to UCK, the red colors corresponding to Mortierellomycotina, Chytridiomycota, Arthropoda, Cryptomycota, Glomeromycota, Mucoromycotina, and Kickxellomycotina in 0-15 cm depth soils under T2 treatment were much darker than other treated samples. However, the color representing Basidiomycota was shallower, indicating that the abundance of fungi community in 0-15 cm soils under T2 treatment was the highest, and the abundance of the above seven fungi could be significantly increased while the abundance of Basidiomycota was reduced.

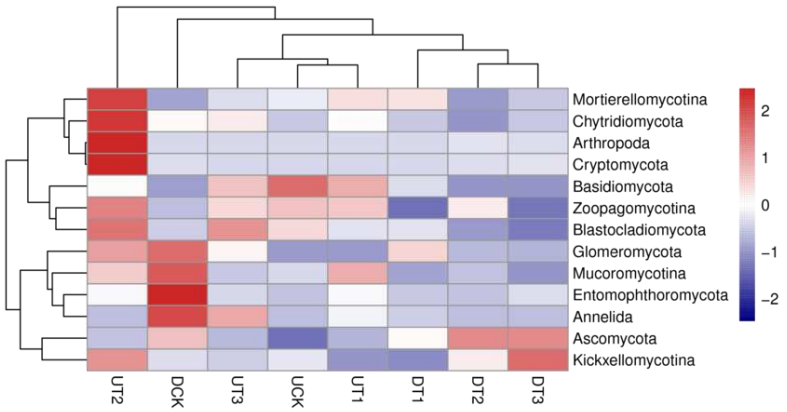

Figure 6. *Thermal map of relative abundance of different fungal phylum in soil. (The sample clustering tree is the clustering tree above and the species clustering tree is the left cluster tree. Similarly hereinafter)*

DT1, DT2 and DT3 are clustered at the top, but they are far away from DCK, indicating that biochar has a great influence on the fungal community structure of 15-30 cm soils. However, different biochar application rates resulted in similar fungi community in 15-30 cm soils. Compared with DCK, the color of *Ascomycota* and *Kickxellomycotina* in the DT2 and DT3 groups were relatively dark while that of *Glomeromycota*, *Mucoromycotina*, *Entomophthoromycota* and *Annelida* was relatively shallow, indicating that the T2 and T3 biochar treatment could increase the abundance

http://www.aloki.hu ● ISSN 1589 1623 (Print) ● ISSN 1785 0037 (Online)
DOI: http://dx.doi.org/10.15666/aeer/1704_88178834

of *Ascomycota* and *Kickxellomycotina* while decrease the abundance of *Glomeromycota*, *Mucoromycotina*, *Entomophthoromycota* and *Annelida*.

It can be seen that the effects of different biochar treatments on the abundance of the same species are different. The same biochar treatment had different effects on the abundance of different types of species. Generally, the biochar treatment could increase the abundance of most fungi communities in 0-15 cm soils to some extent. And the effect of T2 treatment effect was the most obvious. Biochar application could reduce the abundance of most fungi communities in the 15-30 cm soils to some extent. In general, the abundance fungi in 0-15 cm soils were higher than that in 15-30 cm soils, which was consistent with the analysis of the relative abundance distribution in the previous section.

Cluster analysis on species relative abundance at genus level

Figure 7 is a species heat map of soil fungi at genus level. The relative abundances of the species at each level are ranked, and the species in the top 30 are selected (all the species are selected if the number of phylum is less than 30).

As can be seen from *Figure 7,* for different treatments, the clustering result at genus level is consistent with that at phylum level. Comparing the aggregation degree of fungi in 0-15 cm soils under different treatments, it could be found that the abundance of *Ostropa*, *Ochroconis*, *Capnobotryella*, *Muyocopron* and *Hydropisphaera* under T1 and T3 treatment were higher than those under CK treatment. The abundance of most fungi in T3 group were significantly higher than those in CK group, and were also higher than those in other groups. Compared to CK treatment, T1, T2 and T3 treatment had seen more abundant *Funneliformis*, *Plectosphaerella*, *Chaetomella*, *Peziza*, and *Hyaloraphidium*. Nevertheless, CK treatment resulted in higher abundance of *Lulworthia* and *Thamnocephalis*.

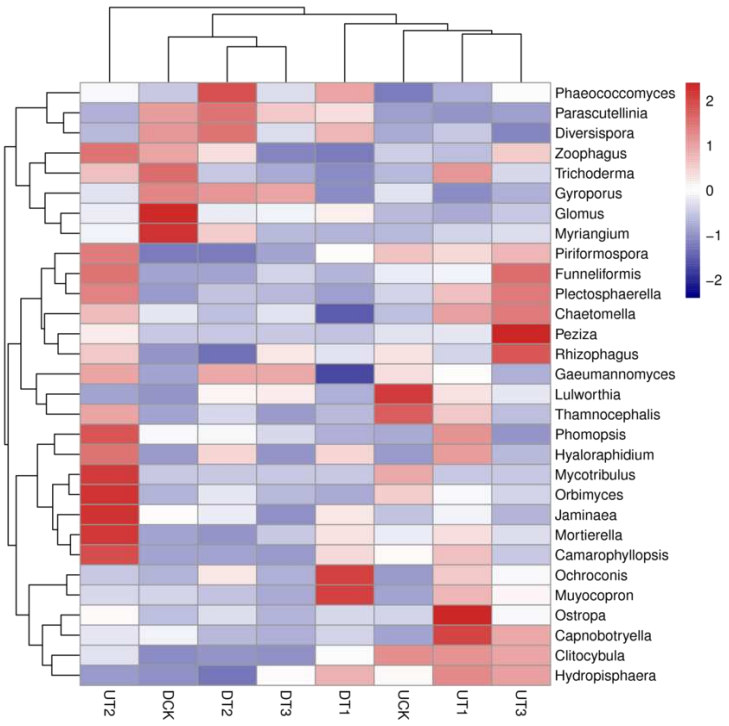

Figure 7. *Thermal map of relative abundance of different fungal genus in soil*

http://www.aloki.hu ● ISSN 1589 1623 (Print) ● ISSN 1785 0037 (Online)
DOI: http://dx.doi.org/10.15666/aeer/1704_88178834

In 15-30 cm soil layer, the abundance of *Glomus*, *Myriangium*, *Capnobotryella*, *Zoophagus*, and *Trichoderma* were relatively low under the treatment of biochar. However, biochar could increase the abundance of certain fungi species. For example, compared with CK, the abundance of *Mortierella*, *Ochroconis*, *Muyocopron*, *Camarophyllopsis*, *Hyaloraphidium*, and *Jaminaea* were relative high under T1 treatment, which indicated that the application of low-dose biochar to the soil could increase the abundance of some fungi in the 15-30 cm soil layer.

Under the various treatments, there was significant difference in the fungi at genus level in 0-15 cm soil layer. The effect of biochar was prominent. The difference of fungi in 15-30 cm soil layer was relatively small.

Correlation between fungi community structure and soil environmental factors

Figure 8 shows the correlation between fungi at the genus level and soil environmental variables. The first and second axes of the RDA ordering accounted for 53.14% and 19.37% of the fungal genus variables, respectively. 0-15 cm soil and 15-30 cm soil samples were clearly separated in the direction of RDA1 axis. In the 0-15 cm soil samples, DCK and DT3 were separated from DT1 and DT2, indicating there was huge difference between T1 and T2 treatment and CK treatment. In the 15-30 cm soil samples, UCK and UT1 were clearly separated from UT2 and UT3, indicating that T2 and T3 treatments were significantly different from CK. In general, compared with soils with different depths, the points of 15-30 cm soils under different treatments were relatively close and concentrated while the points of 15-30 cm soils were far away from each other and the distribution was relatively scattered, indicating that response of fungi abundance to biochar in 0-15 cm soil was more sensitive.

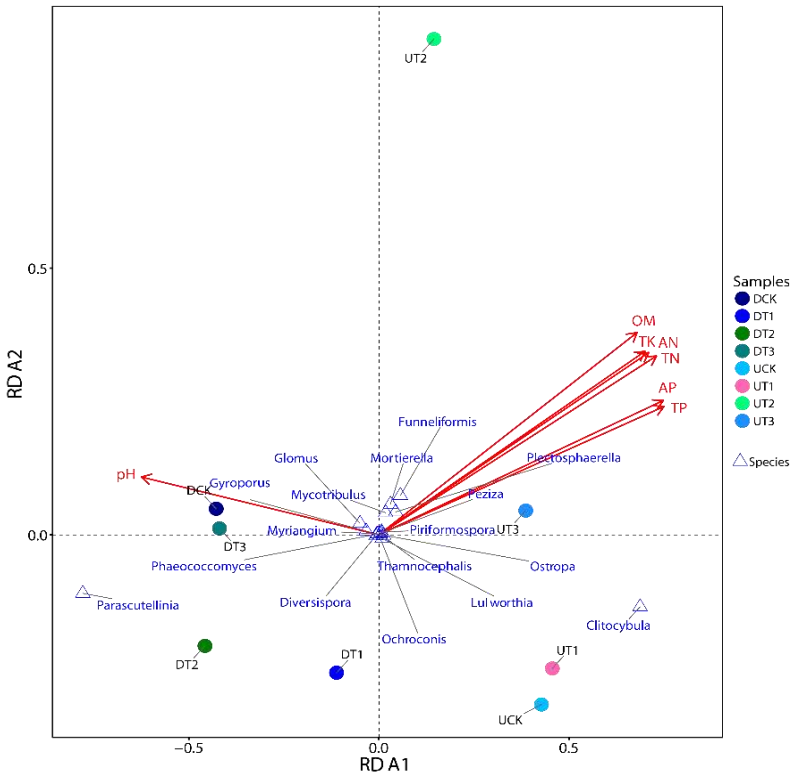

Figure 8. *RDA triplot showing the relationship between the relative abundance of major soil fungal genus in different soil samples and the environmental variables*

http://www.aloki.hu ● ISSN 1589 1623 (Print) ● ISSN 1785 0037 (Online)
DOI: http://dx.doi.org/10.15666/aeer/1704_88178834

There was a significant positive correlation between the content of organic matter, total nitrogen, total phosphorus, total potassium, alkali nitrogen, available phosphorus and available potassium in the soil, but they were negatively correlated with soil pH. The abundance of *Mortierella*, *Funneliformis*, *Plectosphaerella*, *Peziza*, *Piriformospora*, *Ostropa*, *Lulworthia*, *Clitocybula* and *Thamnocephalis* were positively related to content of organic matter, total nitrogen, total phosphorus, total potassium, alkali nitrogen, available phosphorus, and available potassium, while were negatively correlated with soil pH. Among them, the abundance of *Plectosphaerella* had the largest correlation with the content of total phosphorus and available phosphorus, which corresponded to the farthest point from the origin, indicating that it was the most sensitive to the environment. *Piriformospora* was closest to the origin, indicating that it was the least sensitive to the environment. The abundance of *Glomus*, *Mycotribulus*, *Gyroporus*, *Myriangium*, *Phaeococcomyces*, *Parascutellini* were positively related to soil pH, where the *Gyroporus* was the most relevant and *Parascutellinia* was the most sensitive to the environment.

Discussion

After the biochar was applied, the soil microorganisms were directly or indirectly affected by changing the physical and chemical properties of the soil. Most studies had shown that biochar promotes microbial communities (Kolb et al., 2009; Ameloot et al., 2013). In this study, it was clear that after 3 years of application, the physical and chemical properties of the soil had undergone major changes. Soil pH, the content total nitrogen, total phosphorus and available phosphorus were increased. The abundance and diversity of fungi in the soil changed significantly with the application of different amounts of biochar.

From the number of unique fungi OTU and the relative abundance distribution of fungi communities as shown in the Venn diagram (*Figs. 4* and *5*), the application of biochar had changed the original fungal community structure, inhibited the growth of some original fungi species and increased the population of specific microorganisms that are more adaptable to the environment. Biochar had a void structure and a large specific surface area, as a result, the oxygen content was significantly increased as the application of biochar. The soil fungi had both anaerobic and aerobic groups, and their respective abundance was reduced or increased as the change of soil bulk density. The results of Marluthi et al. (2010) also showed that the application of biochar in soil changed the type of carbon source used by soil microbes. There were also differences in the number of fungi species when different amounts of biochar was applied, but the difference was more prominent in 0-15 cm soils than in 15-30 cm soils. The dilution curve also showed that biochar could increase the amount of soil OTUs, which was more significant in 0-15 cm soils, indicating that the effect of biochar on soil fungal community was mainly concentrated in the directly contacted soil layer (0-15 cm) while the impact on the lower soil layer was relatively slight. This might be related to the porosity and large specific surface area of biochar, which could provide a good attachment site and growth environment for soil fungi to promote the growth and reproduction of fungi and avoid predators as well (Thies et al., 2009).

According to the Alpha diversity analysis, biochar treatment could increase the abundance and diversity of soil fungal communities, which reached the maximum value under T2 treatment. When the biochar application rate was high (T3 treatment), the soil

http://www.aloki.hu ● ISSN 1589 1623 (Print) ● ISSN 1785 0037 (Online)
DOI: http://dx.doi.org/10.15666/aeer/1704_88178834

fungal community abundance and diversity did not increase with the increase of the amount of biochar applied. The reason might lie in the fact that the pH of the applewood after carbonization was alkaline, thus adding biochar to the soil would increase the soil pH. It was reported that the higher soil pH could reduce the abundance of soil fungi (Rousk et al., 2010). Biochar with low addition could increase the dominance of fungi in 0-15 cm soil layer, but the effect was not increased as the application rate was increased to T2 and T3. High-volume biochar treatment was not conducive to improving the abundance of soil fungal communities, and the appropriate amount of application was beneficial to the construction of soil micro-ecological environment. Compared with the 15-30 cm soil layer, the fungi abundance and diversity in 15-30 cm soil layer were low, and the difference between the treatments was not obvious. This was also consistent with the OTU quantitative analysis results.

In the soils tested in this experiment, *Mortierellomycotina*, *Chytridiomycota*, *Glomeromycota*, *Ascomycota*, and *Basidiomycota* were dominant species at phylum level. Among them, *Ascomycota* and *Basidiomycota* accounted for more than 80%, which was consistent with previous studies (Roesch et al., 2007). In 0-15 cm soil, the relative abundance of *Mortierellomycotina*, *Chytridiomycota*, *Glomeromycota* and *Ascomycota* under the application of different amounts of biochar were higher than that of control group and were the highest under T2 treatment. Studies have shown that nitrogen application can increase the relative abundance of *Ascomycota* (Paungfoo-Lonhienne et al., 2015), probably because biochar's adsorption to nitrogen fertilizer indirectly increased soil nitrogen content (Clough et al., 2013), thereby increasing the relative abundance of *Ascomycota* in the soil. Different from 0-15 cm soils, the application of biochar could reduce the abundance of certain species, such as *Basidiomycota*, *Glomeromycota*, while increase the abundance of *Ascomycota* in 15-30 cm soils to some extent. This phenomenon was particularly significant under T2 and T3 treatment. It indicated that the dominant fungi in red soil were sensitive to biochar addition. Similarly, at the genus level, biochar also increased the relative abundance of dominant genus such as *Parascutellinia* and *clitocybula*.

Soil chemistry plays an important role in affecting soil microbial community structure (Teague et al., 2011). Previous studies have shown that soil fungi are closely related to many soil physical and chemical properties, such as soil pH (Fierer et al., 2006) and available nitrogen (Frey et al., 2004). Due to the different biological characteristics of the fungi, the soil factors affecting different fungi are also different (Avander et al., 2006). RDA is used to analyze the relationship among environmental factors (pH, soil nutrients), dominant species and different treatments. Due to the composition and structural specificity of biochar, different microbial communities often respond differently to the addition of biochar. In this experiment, the abundance of *Funneliformis*, *Ostropa*, *Piriformospora* and *Plectosphaerella* in soil were positively correlated with the content of organic matter, total nitrogen, total phosphorus, total potassium, alkali nitrogen, and available phosphorus in the soil while were negatively related to soil pH. The abundance of *Glomus*, *Mycotribulus*, and *Gyroporus* were positively correlated with soil pH, where *Gyroporus* had the maximum correlation. In general, neutral and alkaline conditions were considered to be beneficial to bacterial growth but were not conducive to fungi growth (Rousk et al., 2009). Xu et al. (2018) found that soil phosphorus closely affects fungal growth, and insufficient or excessive available phosphorus would inhibit fungi growth and development. In this study, soil total phosphorus and available phosphorus were significantly positively correlated with

http://www.aloki.hu ● ISSN 1589 1623 (Print) ● ISSN 1785 0037 (Online)
DOI: http://dx.doi.org/10.15666/aeer/1704_88178834

Plectosphaerella and *Peziza*, while negatively correlated with *Parascutellinia* and *Phaeococcomyces*, which indicated that the fungi was selective for phosphorus levels, providing a valuable insight into the relationship between fungi diversity and phosphate fertilizer, as well as studies on fungal functional genes (such as genes controlling the phosphorus cycle). In addition, in this study, the interpretation rates of the first and second axes for sample changes were mostly lower than 65.0%, indicating that in addition to the soil physical and chemical indicators analyzed in this study, there might be other soil physical and chemical properties that jointly drove the changes in microbial structure.

The promotion of soil microbial abundance by short-term application of biochar is mainly caused by absorption of soluble carbon in biochar through soil microbe activities (Quilliam et al., 2013). However, although this study has not detected the soluble carbon content of biochar after application, many scholars have shown that the soluble carbon will be depleted by soil microbes within one year (Cheng et al., 2008; Kuzyakov et al., 2009; Wang et al., 2016). In addition, in this study, we found that changes in fungi community structure in soils were closely related to the physical and chemical factors including content of organic matter, total nitrogen, total phosphorus, total potassium, alkali nitrogen, available phosphorus, available potassium, and pH. And these factors were also significantly correlated with the amount of biochar (*Table 3*). In summary, the increase in soil abundance and the change in community structure in this study were indirectly driven by changes in soil physical and chemical properties caused by biochar application.

Conclusions

(1) After 3 years of biochar application, soil pH and nutrient content increased to varying degrees. Especially, soil pH, organic matter and available potassium increased proportionally to the biochar addition. Besides, the nutrient content in the upper layer of soil was significantly higher than that of the lower layer, which illustrated that biochar has a significant long-term effect on soil nutrient retention.

(2) Biochar could increase the amount of soil OTU. Different biochar treatments can lead to specific changes of fungi to a certain extent and increased the abundance and diversity of fungi communities, which reached the maximum value under T2 treatment.

(3) Biochar significantly changed (increased or decreased) the relative abundance of some soil fungi, which was reflected at both phylum and genus level.

(4) RDA analysis showed that the addition of biochar could significantly change the physical and chemical properties of soil pH and nutrient content after 3 a. The changes of these environmental factors further affected the soil fungal community structure. And at different depths, different biochar application addition and soil physical and chemical factors affected the abundance of different fungi species.

Acknowledgements. This research was supported by China West Normal University Doctoral Startup Research Project (412666) and the National Key Research and Development Program of China (2017YFD0800900; 2016YFD0800307).

http://www.aloki.hu ● ISSN 1589 1623 (Print) ● ISSN 1785 0037 (Online)
DOI: http://dx.doi.org/10.15666/aeer/1704_88178834

REFERENCES

[1] Alvarado, S. (2010): Tillage and nitrogen effects on soil physical and chemical properties and microbial community composition of an agricultural soil. – Dementia & Geriatric Cognitive Disorders 30: 71.

[2] Ameloot, N., Neve, S. D., Jegajeevagan, K., Yildiz, G., Buchan, D., Funkuin, Y. N., Prins, W., Bouckaert, L., Sleutel, S. (2013): Short-term CO_2 and N_2O emissions and microbial properties of biochar amended sandy loam soils. – Soil Biology & Biochemistry 57: 401-410.

[3] Avander, W., Javan, V., Smant, W., Boschker, H. T. S., Bloem, J., Kardol, P. W., Hvander, P., Wde, B. (2006): Fungal biomass development in a chronosequence of land abandonment. – Soil Biology & Biochemistry 38: 51-60.

[4] Bao, S. D. (2000): Soil and Agricultural Chemistry Analysis (Third Ed.). – China Agriculture Press, Beijing (in Chinese).

[5] Barbi, F., Prudent, E., Vallon, L., Buee, M., Dubost, A., Legout, A., Marmeisse, R., Fraissinet-Tachet, L., Luis, P. (2016): Tree species select diverse soil fungal communities expressing different sets of lignocellulolytic enzyme-encoding genes. – Soil Biology and Biochemistry 100: 149-159.

[6] Chapin, F. S., Walker, B. H., Hobbs, R. J., Hooper, D. U., Lawton, J. H., Sala, O. E., Tilman, D. (1997): Biotic control over the functioning of ecosystems. – Science 277: 500-504.

[7] Cheng, C. H., Lehmann, J., Thies, J. E., Burton, S. D. (2015): Stability of black carbon in soils across a climatic gradient. – Journal of Geophysical Research Biogeosciences 113: 50-55.

[8] Clough, T. J., Condron, L. M., Kammann, C., Müller, C. (2013): A review of biochar and soil nitrogen dynamics. – Agronomy 3: 275-293.

[9] Fierer, N., Jackson, R. B. (2006): The diversity and biogeography of soil bacterial communities. – Proceedings of the National Academy of Sciences of the United States of America 103: 626-631.

[10] Filion, M., St-Arnaud, M., Fortin, J. A. (1999): Direct interaction between the arbuscular mycorrhizal fungus Glomus intraradices and different rhizosphere microorganisms. – New Phytologist 141: 525-533.

[11] Frey, S. D., Knorr, M., Parrent, J. L., Simpson, R. T. (2004): Chronic nitrogen enrichment affects the structure and function of the soil microbial community in temperate hardwood and pine forests. – Forest Ecology & Management 196: 159-171.

[12] Gul, S., Whalen, J., Thomas, B., Sachdeva, V., Deng, H. (2015): Physico-chemical properties and microbial responses in biochar-amended soils: mechanisms and future directions. – Agriculture Ecosystems & Environment 206: 46-59.

[13] Huang, A. H., Li, J. W., Shen, Z. Q., Wang, X. W., Jin, M. (2006): High-throughput identification of clinical pathogenic fungi by hybridization to an oligonucleotide microarray. – Journal of Clinical Microbiology 44: 3299-3305.

[14] Jeanbille, M., Buã, E., M., Bach, C., Cébron, A., Frey-Klett, P., Turpault, M. P., Uroz, S. (2016): Soil parameters drive the structure, diversity and metabolic potentials of the bacterial communities across temperate beech forest soil sequences. – Microbial Ecology 71: 482-493.

[15] Johannes, L., Stephen, J. (2015): Biochar for environmental management: science, technology and implementation. – Science and Technology; Earthscan 25: 15801-15811(11).

[16] Jones, D. L., Rousk, J., Edwards-Jones, G., DeLuca, T. H., Murphy, D. V. (2012): Biochar-mediated changes in soil quality and plant growth in a three year field trial. – Soil Biology and Biochemistry 45: 113-124.

http://www.aloki.hu ● ISSN 1589 1623 (Print) ● ISSN 1785 0037 (Online)
DOI: http://dx.doi.org/10.15666/aeer/1704_88178834

[17] Kolb, S. E., Fermanich, K. J., Dornbush, M. E. (2009): Effect of charcoal quantity on microbial biomass and activity in temperate soils. – Soil Science Society of America Journal 73: 1173-1181.
[18] Kolton, M., Harel, Y. M., Pasternak, Z., Graber, E. R., Elad, Y., Cytryn, E. (2011): Impact of biochar application to soil on the root-associated bacterial community structure of fully developed greenhouse pepper plants. – Applied and Environmental Microbiology 77: 4924-4930.
[19] Kuramae, E., Gamper, H., Van, V. J., Kowalchuk, G. (2011): Soil and plant factors driving the community of soil-borne microorganisms across chronosequences of secondary succession of chalk grasslands with a neutral pH. – Fems Microbiology Ecology 77: 285-294.
[20] Kuzyakov, Y., Subbotina, I., Chen, H. Q., Bogomolova, I., Xu, X. L. (2009): Black carbon decomposition and incorporation into soil microbial biomass estimated by 14 C labeling. – Soil Biology and Biochemistry 41: 210-219.
[21] Marluthi, S., Ralebitso-Senior, T. K., Rahman, P. K. S. M., Ennis, C. J. (2010): Biochar: impact on soil microbial ecology. – Second Annual Conference: Advancing the Science and Evaluating Biochar Systems. Poster Presented at UK Biochar Reacher Centre, Rothamsted.
[22] Matsubara, Y., Hasegawa, N., Fukui, H. (2002): Incidence of fusarium root rot in asparagus seedlings infected with arbuscular mycorrhizal fungus as affected by several soil amendments. – Journal of the Japanese Society for Horticultural Science 71: 370-374.
[23] Mukerji, K. G. (1996): Concepts in Mycorrhizal Research. – Springer, New Delhi.
[24] Paungfoo-Lonhienne, C., Yeoh, Y. K., Kasinadhuni, N. R., Lonhienne, T. G., Robinson, N., Hugenholtz, P., Ragan, M. A., Schmidt, S. (2015): Nitrogen fertilizer dose alters fungal communities in sugarcane soil and rhizosphere. – Scientific Report 5: 8678.
[25] Pitta, D. W., Parmar, N., Patel, A. K., Indugu, N., Kumar, S., Prajapathi, K. B., Patel, A. B., Reddy, B., Joshi, C. (2014): Bacterial diversity dynamics associated with different diets and different primer pairs in the rumen of Kankrej cattle. – Plos One 9: e111710.
[26] Quast, C., Pruesse, E., Yilmaz, P., Gerken, J., Schweer, T., Yarza, P., Peplies, J., Glöckner, F. O. (2013): The SILVA ribosomal RNA gene database project: improved data processing and webbased tools. – Nucleic Acids Research 41: D590-D596.
[27] Quilliam, R. S., Glanville, H. C., Wade, S. C., Jones, D. L. (2013): Life in the 'charosphere'.-Does biochar in agricultural soil provide a significant habitat for microorganisms? – Soil Biology and Biochemistry 65: 287-293.
[28] Roesch, L. F. W., Fulthorpe, R. R., Riva, A., Casella, G., Hadwin, A. K., Kent, A. D., Daroub, S. H., Camargo, F. A., Farmerie, W. G., Triplett, E. W. (2007): Pyrosequencing enumerates and contrasts soil microbial diversity. – Isme Journal 1: 283-290.
[29] Rousk, J., Brookes, P. C., Bååth, E. (2009): Contrasting soil pH effects on fungal and bacterial growth suggest functional redundancy in carbon mineralization. – Applied & Environmental Microbiology 75: 1589-1596.
[30] Rousk, J., Bääth, E., Brookes, P. C., Lauber, C. L., Lozupone, C., Caporaso, J. G., Knight, R., Fierer, N. (2010): Soil bacterial and fungal communities across a pH gradient in an arable soil. – The ISME Journal 4: 1340-1351.
[31] Sagrilo, E., Rittl, T. F., Hoffland, E., Alves, B. J. R., Mehl, H. U., Kuyper, T. W. (2015): Rapid decomposition of traditionally produced biochar in an oxisol under savannah in northeastern Brazil. – Geoderma Regional 6: 1-6.
[32] Schulz, H., Dunst, G., Glaser, B. (2013): Positive effects of composted biochar on plant growth and soil fertility. – Agronomy for Sustainable Development 33: 817-827.
[33] Sharma, S. K., Ramesh, A., Sharma, M. P., Joshi, O. P., Govaerts, B., Steenwerth, K. L., Karlen, D. L. (2010): Microbial community structure and diversity as indicators for evaluating soil quality, biodiversity, biofuels. – Agroforestry and Conservation Agriculture 5: 317-358.

http://www.aloki.hu ● ISSN 1589 1623 (Print) ● ISSN 1785 0037 (Online)
DOI: http://dx.doi.org/10.15666/aeer/1704_88178834

[34] Smalla, K., Wieland, G., Buchner, A., Zock, A., Parzy, J., Kaiser, S., Roskot, N., Heuer, H., Berg, G. (2001): Bulk and rhizosphere soil bacterial communities studied by denaturing gradient gel electrophoresis: plant-dependent enrichment and seasonal shifts revealed. – Applied and Environmental Microbiology 67: 4742-4751.
[35] Smith, J. L., Collins, H. P., Bailey, V. L. (2010): The effect of young biochar on soil respiration. – Soil Biology and Biochemistry 42: 2345-2347.
[36] Teague, W. R., Dowhower, S. L., Baker, S. A., Haile, N., DeLaune, P. B., Conover, D. M. (2011): Grazing management impacts on vegetation, soil biota and soil chemical, physical and hydrological properties in tall grass prairie. – Agriculture Ecosystems & Environment 141: 310-322.
[37] Thies, J. E., Rillig, M. C. (2009): Characteristics of Biochar: Biological Properties. In: Lehmann, J., Joseph, S. (eds.) Biochar for Environmental Management: Science and Technology. – Earthscan, London, pp. 85-105.
[38] Wang, J., Xiong, Z., Kuzyakov, Y. (2016): Biochar stability in soil: meta-analysis of decomposition and priming effects. – GCB Bioenergy 8: 512-523.
[39] Xu, N., Tan, G. C., Wang, H. Y., Gai, X. (2016): Effect of biochar additions to soil on nitrogen leaching, microbial biomass and bacterial community structure. – European Journal of Soil Biology 741-8.
[40] Xu, S., Liu, J., Song, S., Guo, H. L., Tang, J. J., Yong, J. W. H., Ma, Y., Chen, X. (2018): Arbuscular mycorrhizal fungi influence decomposition and the associated soil microbial community under different soil phosphorus availability. – Soil Biology & Biochemistry 120: 181-190.
[41] Yao, Q., Liu, J. J., Yu, Z. H., Li, Y. S., Jin, J., Liu, X. B., Wang, G. H. (2017): Three years of biochar amendment alters soil physiochemical properties and fungal community composition in a black soil of Northeast China. – Soil Biology and Biochemistry 110: 56-67.
[42] Zheng, J. F., Chen, J. H., Pan, G. X., Liu, X. Y., Zhang, X. H., Li, L. Q., Cheng, K., Zheng, J. W. (2016): Biochar decreased microbial metabolic quotient and shifted community composition four years after a single incorporation in a slightly acid rice paddy from Southwest China. – Science of the Total Environment 571: 206-217.

http://www.aloki.hu ● ISSN 1589 1623 (Print) ● ISSN 1785 0037 (Online)
DOI: http://dx.doi.org/10.15666/aeer/1704_88178834

EVALUATING THE COMPETITIVE ABILITY OF POTATO CULTIVARS WITH WEEDS

NOUROLLAHI, F.[1] – MOHAMMADDOUST-CHAMANABAD, H. R.[1*] – HASSANPANAH, D.[2] – ANVAR, M.[1]

[1]*Department of Agronomy and Plant Breeding, Faculty of Agriculture and Natural Resources University of Mohaghegh Ardabili, Ardabil, Iran*

[2]*Ardabil Agriculture and Natural Resources Research Center, Ardabil, Iran*

[*]*Corresponding author*
e-mail: hr_chamanabad@yahoo.com; phone: +98-915-108-2239

(Received 12th Mar 2019; accepted 22nd May 2019)

Abstract. Using competitive cultivars can be an important integrated weed management (IWM) tool in sustainable agricultural systems and in cultivation of healthy products. Differential competitive ability of 10 potato cultivars was examined in 2015 and 2016 in the research field of the University of Mohaghegh Ardabili, Ardabil, Iran. Experiment was established using a randomized complete block design with three replications. 10 potato cultivars (Caesar, Kennebec, Banba, Markies, Hermes, Marfona, 397097-14, Difla, Satina, Natascha) were observed that has grown with and without natural weed flora. Potato cultivars differed in ability to reduce weed density and weed biomass. In weed conditions, tuber yield ranged from 19.27 in Hermes to 55.56 t ha^{-1} in Satina. Also yield loss ranged from 0 to 38.93%. Satina cultivar had the highest competitive index (CI) and could reduce the weed dry mass by 2 to 3 times more than Hermes as a poor cultivar. In general, the results of this study declare that Satina cultivar was considered as competitive and recommended more for cultivation in Ardabil region than other cultivars. It is more stable than weed, and could have greatly reduce the density and biomass of weed.
Keywords: *competitive ability, potato, healthy hazards, integrated weed management, sustainable agriculture, weed interference*

Introduction

Besides cereal, potato, *Solanum tuberosum* L., is an important crop in the world. Iran has the 13th place in potato production (FAO Statistic, 2016). Potato is the most important crop in the Ardabil area. Ardabil contains 23000 ha of arable land, of which 18500 ha was used for potato production in Iran in 2017, with an average yield of 23.7 t ha^{-1} (IRANSTAT, 2017), but weeds are the main barrier to potato production. Yield loss in potato due to weed interference has been reported 20-30% in Iran (Khalghani, 2010). Few herbicides and modes of action are usually available for use in potato cultivations, so the risk of developing herbicide-resistant weed populations can increase. On the other hand, weed control is one of the main limitations in sustainable agriculture. Efficient weed management is essential for successful organic crop protection, and finding crop cultivars that confer a high degree of competitive ability against weeds are highly desirable (Mason et al., 2006). Although competitiveness has not traditionally been considered a priority for breeding or farmer cultivar choice the challenge of managing herbicide- resistant weed populations, environmental concerns and the unmet needs of organic producers and smallholder farmers has, however, renewed interest in cultural weed control options, including competitive cultivars (Worthington and Rebery-Horton, 2013; Andrew et al., 2015). Many research in cereals have examined how cultivar selection may be used as a mean of weed control by choosing cultivars that are inherently more competitive with, or more tolerant of, commonly

http://www.aloki.hu ● ISSN 1589 1623 (Print) ● ISSN 1785 0037 (Online)
DOI: http://dx.doi.org/10.15666/aeer/1704_88358845

encountered or key weed species (Korres and Froud-Williams, 2002; Worthington and Rebery-Horton, 2013; Lemrele, 2015; Abdollahi and Mohammaddust-Chamanabad, 2017). Some findings presented in complement agronomic and physiological studies of crop- weed interactions in other species such as soybean (Vollman et al., 2010), potato (Nelson and Thoreson, 1981; Love et al., 1995; Khalegi et al., 2007; Colquhoun et al., 2009; Hutchinson et al., 2011; Bashiri-Majd, 2015), tomato (Gonzales-Ponce et al., 1996), canola (Hashem et al., 2010), field pea (Jacob et al., 2016).

There are two aspects of cultivar competitive ability; the ability to compete with weed, is expressed as competitive index (CI) and the ability to tolerate weed interference, is expressed as weed interference tolerance index (WITI). A competitive cultivar (high CI) can maintain high yield in the presence of weeds and can reduce weed biomass or seed production (Tilman, 1987; Goldberg, 1990), while tolerant cultivars only maintain high yield in the presence of weeds. Suppressing weeds is beneficial for weed management in future growing seasons while tolerating weeds is only beneficial in the current growing season. However, the relationship between aspects has not been addressed in potato. According to Cory et al. (2016) it has been reported that pea cultivars that are ranked the highest for AWC were associated with lower weed fecundity, whereas the highest-yielding cultivars generally were those that had the highest CI variation in competitive ability of wheat cultivars (Blackshow, 1994; Lemerle et al., 2001; Mohammaddust-Chamanabad et al., 2014). Abdollahi and Mohammaddust-Chamanabad (2017) also reported positive relationship between the yield of wheat and WITI similarly with CI. Colquhoun (2009) observed that differences in yield among cultivars grown in the presence of weeds suggest differential tolerance of weed competition ability, however, the ability to suppress weeds was similar among cultivars. Khaleghi et al. (2007) reported significant differences among potato cultivars in tolerance of weed presence. According to Bashiri-Majd (2015) late potato cultivars had high competitive ability that produced more yield and reduced weed biomass.

Many long-term studies still conduce on determining cultivars resistance to disease and good combination of traits for logical conditions. While the evaluation of crop cultivars based on competitive ability is necessary. Large genotype by environment interactions may cause difficulties in selecting for competitiveness (Coleman et al., 2001) and selection for competitiveness could be at the expense of other important criteria (Brennan et al., 2001). Nevertheless, within a given climatic zone there appears to be sufficient genetic variation in crop competitive ability (Acciaresi et al., 2001; Coleman et al., 2001) for such selection to be introduced into breeding programs. The over goal of this study was to (1) evaluate the ability potato cultivars to suppress weed density and biomass, (2) rank these cultivars based on competitive ability index, and (3) compare the ability of the same cultivars to maintain tuber yield in the presence of weeds.

Materials and methods

The study was conducted at the Agricultural Research Farm of the University of Mohaghegh Ardabili, Ardabil, Northwestern Iran (longitude 48° 18′ E, latitude 38° 15′ N, 1338 m above sea level) in 2015 and 2016 on loamy clay soil with 1.57% organic matter, and 7.8 pH, EC 1008 μS cm^{-1}. The monthly average air temperatures and total rainfall and long-term averages (1976 to 2014) during the growing season are summarized in *Table 1*. Air temperature and precipitation was different between years compared with the long-term average data. Compared with the long-term averages, air temperatures were

http://www.aloki.hu ● ISSN 1589 1623 (Print) ● ISSN 1785 0037 (Online)
DOI: http://dx.doi.org/10.15666/aeer/1704_88358845

lower during both study years. In 2016, rainfall was generally higher during the studied growing season (May to September) compared to the long-term average in 2015, except for lower precipitation in August.

In both years, treatments were arranged in a randomized complete block design, with three replicates. Ten potato cultivars (Caesar, Kennebek, Banba, Markies, Hermes, Marfona, Difla, Satina and one advanced clone, 397007-14) were grown with and without weed interference. The selections were chosen, based on their differing growth attributes (*Table 2*).

Table 1. *Air temperature and rainfall for 2015 and 2016 growing seasons and Long-term averages (1976-2014) at Ardabil, Iran*

Month	Mean Temperature (°C)			Rainfall (mm)		
	Long term	2015	2016	Long term	2015	2016
May	14.8	8	7.5	34.3	35.7	59.6
June	18.8	12.9	15	48.6	27.7	29.7
July	22.8	17.9	17	26.8	7	14.2
August	26	19.9	19.6	8.1	3.6	0.1
September	25.5	20.4	19.8	5.1	0	1.2
October	23.5	16.9	18.5	10.4	48.9	6.4
November	19.3	13.3	12.2	25.3	58.3	4.8
December	13.3	7.6	7.1	37.5	46.6	40.3
January	7.2	2.5	-1	24.9	13.9	15.4
February	3.9	3.4	0.4	20.5	6.4	3.4
March	4	0.4	7.5	21.3	24.9	1.2

Plots measured 5 by 4.2 m, including 7 potato rows on 60 cm row spacing. Potato seed pieces were hand-planted with 7.5 plants m^{-2} density on May 1, 2015, and 16 May 2016. After the potato emergence, each plot was divided into two equal parts and in one half all weeds were hand-removed during the growing season as weed free plots. Fertilizer was applied at planting (75, 150, 75 kg ha^{-1} NPK) and at tuber initiation (75 kg N ha^{-1}). Supplemental overhead irrigation was supplied to meet crop water demands. Furrow irrigation during the growing season was carried out at the rate of 6000 m^3 ha^{-1} and 10 days.

Data collection included weed density and biomass at end of the season in the weedy plots and tuber yield in all plots. At the end of the season before tuber harvest, weeds were collected from two 0.5×0.6 m quadrates in each weedy plots. Weeds were counted, dried at 75°C for 48 hours and weighed. Potato tuber yield was quantified at season-end by harvesting the three rows in each plot. The following Equations (*Eqs.1 and 2*) were used for the evaluation of the competitive ability (CI) and tolerance ability (WITI) of potato cultivars (Mohammaddust-Chamanabad, 2011).

$$WITI = \frac{(Yp)(YS)}{(\bar{Y}p)^2} \quad \text{(Eq.1)}$$

where Yp is each cultivar yield from the weed free plot, Ys is each cultivar yield from weedy plot. $\bar{Y}$p mean is the average yield of all potato cultivars from the weed free plot.

http://www.aloki.hu ● ISSN 1589 1623 (Print) ● ISSN 1785 0037 (Online)
DOI: http://dx.doi.org/10.15666/aeer/1704_88358845

Table 2. *Traits of potato cultivars used in this study (ECPD, AHDB and PPA 2018)*

S.No.	Popular name	Developing center	Parentage	Year of released	Characteristics								
					Tuber				Botanical Description				
					Shape	Color of skin	Color of flesh	Depth of eyes	Maturity	Height*	Foliage development	Color of flower	Yield potential**
1	Banba	Irish Potato Marketing Ltd	Slaney$_x$Estima	2001	Oval-long	Yellow	Light yellow	Shallow	Early	Medium-tall	Fairly good	White	Very high
2	Caesar	HZPC UK Limited	Monalisax$_x$RopB1178	1990	Oval-long	White to yellow	Yellow	Very shallow-shallow	Intermediate	Medium	Dense	White	Very high
3	Difla	Germicopa-France	Sylvia$_x$cara	1992	Oval	Yellow	White	Shallow-medium	Medium late	Tall	Very good	White	Very high
4	Hermes	GB seed industry	DD 5158$_x$SW 163/55	1973	Round-oval	Yellow	Fairly yellow	Moderately deep	Medium early to medium late	Medium to tall	Fairly good	Red violet	High
5	Kennebek	USDA	((Chippewa$_x$Katahdin)$_x$(3895-13$_x$earlaine))	1941	Round-oval	Pale yellow	White	Shallow	Medium early to medium late	Medium to tall	Good	White	High
6	Markies	Agrico UK ltd	Agria$_x$Fianna	1984	Oval to long oval	Yellow	Pale yellow	Shallow	Late to very late	Tall	Very good to good	White	High
7	Marfona	Agrico UK ltd	Primora$_x$Ko51-123	1975	Round-oval	Yellow	Pale yellow	Rather shallow	Medium early to medium late	Tall	Good	White	Very high
8	Natascha	Marabel$_x$91-050-4	CO.KG,Gmbh	1998	Oval	Yellow	Deep yellow	Shallow	Early	Tall	Good	White	High
9	Satina	Canadian Food Inspection Agency	Puntila$_x$H99/73	1971	Round oval-oval	Yellow	Yellow	Shallow	Medium early	Tall	Rapid-medium	White	Very high
10	397097-14	CIP	397009	-	Round-oval	Yellow	Yellow	Shallow	Intermediate	Tall	Medium	White	High

* Medium (60-70 cm), medium to tall (70- 100cm), Tall (100-150 cm), ** High (40-50 t ha $^{-1}$), very high ($\geq$ 50 t ha $^{-1}$)

http://www.aloki.hu ● ISSN 1589 1623 (Print) ● ISSN 1785 0037 (Online)
DOI: http://dx.doi.org/10.15666/aeer/1704_88358845

$$CI = \left(\frac{Vi}{\bar{V}}\right)/\left(\frac{Di}{\bar{D}}\right) \quad \text{(Eq.2)}$$

where Vi is each cultivar yield from the weedy plot, $\bar{V}$ is the average yield of all potato cultivars from the weedy plot. D_i is weed dry biomass in each potato cultivar and $\bar{D}$ is average weed dry biomass from weedy plots. Relative Yield Loss was calculated as (*Eq.3*):

$$\%Relative\ Yield\ Loss = 100(Yweed\ free - Yweedy)/(\ Yweed\ free) \quad \text{(Eq.3)}$$

Data were subjected to ANOVA, normality was checked using the graphical method in Statistical Package for the Social Sciences (SPSS). Means were separated by Duncan multiple rang test ($P \leq 0.05$). Interaction between treatment and years, as well as between cultivars and weed competition levels were observed for several parameters; therefor, results are presented by year.

Results

Weed density and biomass

The dominant weed species in both years were Turnipweed (*Rapistrum rogosum* L.), Bindweed (*Convolvulus arvensis* L.), common lambsquarters (*Chenopodium album* L.) and red root pigweed (*Amaranthus retroflexus* L.). The cultivars effect was significant for weed density and weed biomass in both years (*Table 3*).

Table 3. *ANOVA for the effect of potato cultivar on weed density and weed biomass*

Source of variation	Mean Square (MS) values			
	2015		2016	
	Weed density		Weed biomass	
Cultivar	94**.3136	4484.41*	11**.154127	**02.10030
Error	867.30	3257.01	23772.97	3657.48
C.V. (%)	43.93	44.71	2.58	30.74

**,* significant at the p≤0.01 and p≤0.05, respectively

Results showed that weed density ranged from 15.6 to 128.9 plant m^{-2} in both years depending on potato cultivar. In both years Satina and Natascha cultivars had the lowest weed density so weed density was lower than 25 plant m^{-2} (*Table 4*). Caesar and Hermes cultivar had the highest weed density. Weed biomass ranged from a minimum of 224.38 for Satina to a maximum of 998.96 for Caesar (*Table 4*). Natascha had consistently a minimum value for weed density in both years. Some cultivars differed substantially in weed biomass among years. For example, Satina, Natascha and Banba had higher ranking in 2015 compared to 2016. Kennebek, Satina, Markies and 397097-14 had higher ranking for weed biomass in 2016 compared to 2015. Results showed that in 2016, all cultivars significantly had less weed biomass. So this may be due to more rainfall in 2016. Regarding the average throughout both year, the highest and the lowest weed biomass was observed in Caesar and Satina cultivars, respectively (*Table 4*).

http://www.aloki.hu ● ISSN 1589 1623 (Print) ● ISSN 1785 0037 (Online)
DOI: http://dx.doi.org/10.15666/aeer/1704_88358845

Table 4. *Potato cultivar weed density and weed biomass in 2015 and 2016*

Cultivar	Weed density (plant/m^2)			Weed biomass (gm^{-2})		
	2015	**2016**	**Mean**	**2015**	**2016**	**Mean**
Caesar	101.0 ^{f}	98.7 ^{c}	99.85	998.96 ^{g}	210.10 ^{bc}	604.5
Kennebek	70.8 ^{def}	84.7 ^{ab}	77.75	738.44 ^{fg}	128.00 ^{a}	433
Banba	61.4 ^{abc}	88.9 ^{ab}	75.15	398.02 ^{ab}	205.64 ^{bc}	302
Markies	89.6 ^{ef}	82.2 ^{ab}	85.9	537.81 ^{ef}	147.38 ^{a}	343
Hermes	102.1 ^{f}	128.9 ^{c}	115.5	741.25 ^{fg}	271.51 ^{c}	506.5
Marfona	85.4 ^{ef}	106.2 ^{c}	95.8	457.60 ^{abc}	222.22 ^{bc}	340
397097-14	87.5 ^{ef}	84.9 ^{ab}	82.2	492.50 ^{def}	150.09 ^{a}	321.5
Difla	34.9 ^{ab}	76.9 ^{ab}	55.9	472.76 ^{def}	302.04 ^{c}	387
Satina	21.9 ^{a}	22.3 ^{a}	22.1	224.38 ^{a}	140.89 ^{a}	182.6
Natascha	15.6 ^{a}	26.3 ^{a}	20.95	343.75 ^{ab}	189.96 ^{bc}	304

In each column, means followed by the same letter do not differ significantly according to a Duncan test performed at $p \leq 0.05$

Potato yield and yield loss

The cultivars effect was significant for potato yield in both years, except for yield in weed free plots in 2015 (*Table 5*). In weed free plots, tuber yield ranged from 29.58 t ha^{-1} for Kennebek cultivar to 57.06 t ha^{-1} for Satina cultivar in 2015 compared with 24.44 t ha^{-1} for Difla cultivar to 38.64 t ha^{-1} for Satina cultivar in 2016 (*Table 6*).

Table 5. *ANOVA for the effect of potato cultivar on yield and competition indices*

Source of variation	2015				2016			
	Yield weed free	**Yield weedy**	**CI**	**WITI**	**Yield weed free**	**Yield weedy**	**CI**	**WITI**
Cultivar	325.730^{ns}	459.517**	2.08**	1.01**	65.303*	56.930*	0.56*	0.17^{ns}
Error	996.304	391.118	0.34	0.21	148.32	202.56	0.29	0.13
C.V. (%)	45.40	87.28	49.77	49.25	57.17	47.18	45.63	38.22

**,* and ns: significant at the $p \leq 0.01$ and $p \leq 0.05$ and non significant, respectively

In weedy plots, tuber yield ranged from 24.33 t ha^{-1} for Hermes cultivar to 55.56 t ha^{-1} for Satina cultivar in 2015 compared with 19.27 t ha^{-1} for Hermes cultivar to 34.53 t ha^{-1} for Satina cultivar in 2016 (*Table 6*). Satina and 397097-14 cultivars had the highest tuber yield in weedy and weed free plots in both years, so their yield loss was down to 9%. In 2015 year, yield loss of Kennebek cultivar was about zero, but it's yield was low too (*Table 6*).

Weed competition indices

The cultivars effect was significant for CI and WITI in both years, except for WITI in 2016 (*Table 5*). Values for CI ranged from 0.31 to 3.15 in 2015 compared with 0.54 to

http://www.aloki.hu ● ISSN 1589 1623 (Print) ● ISSN 1785 0037 (Online)
DOI: http://dx.doi.org/10.15666/aeer/1704_88358845

1.88 in 2016. Results showed that Satina had the highest CI in both years followed by 397097-14 cultivar, so in both cultivar weed biomass were lower and tuber yield was more than the rest (*Tables 4 ,6 and 7*).

Values for WITI ranged from a minimum of 0.36 for Caesar to a maximum of 2.16 for 397097-14 cultivar in 2015. 397097-14 and Satina had higher ranking in this year (*Table 7*). There were no significant variety for WITI value within cultivars in 2016 (*Table 5*).

Table 6. *Potato cultivar yield in weed-free and weedy condition, relative yield loss in 2015 and 2016*

Cultivar	2015			2016		
	$Yield_{wf}$ (t ha^{-1})	$Yield_{w}$ (t ha^{-1})	%YL	$Yield_{wf}$ (t ha^{-1})	$Yield_{w}$ (t ha^{-1})	%YL
Caesar	37.00	29.39 ^{d}	17.74	35.86 ^{ab}	23.38 ^{cd}	27.45
Kennebek	29.58	29.78^{d}	0	29.23 ^{abc}	25.31 ^{ab}	17.02
Banba	47.39	35.39 ^{bc}	23.40	36.76 ^{ab}	25.94 ^{ab}	22.48
Markies	49.72	31.06 ^{c}	31.42	27.47 ^{ef}	27.58 ^{ab}	0.56
Hermes	44.11	24.33 ^{d}	38.93	28.44 ^{def}	19.27 ^{d}	18.77
Marfona	34.44	28. 00 ^{d}	10.01	31.03 ^{abc}	25.60 ^{ab}	6.10
397097-14	48.06	46.00 ^{a}	4.29	36.73 ^{ab}	29.08 ^{ab}	8.31
Difla	57.06	51.22 ^{ab}	10.5	24.44 ^{f}	22.31 ^{d}	8.6
Satina	55.89	55.56 ^{a}	0.14	38.64 ^{a}	34.53 ^{a}	0
Natascha	38.11	34.17 ^{bc}	10.46	30.97 ^{def}	24.74 ^{cd}	5.22

In each column, means followed by the same letter do not differ significantly according to a Duncan test performed at $p < 0.05$, $p < 0.01$

Table 7. *Potato cultivar competition indices in 2015 and 2016*

Cultivar	CI		WITI	
	2015	2016	2015	2016
Caesar	0.31^{g}	1.12 ^{abc}	0.36 ^{d}	0.91
Kennebek	0.62 ^{efg}	1.48 ^{abc}	0.60 ^{d}	0.83
Banba	1.29 ^{bcd}	1.00 ^{def}	0.95 ^{bc}	1.03
Markies	0.62 ^{efg}	1.38^{abc}	0.79 ^{c}	0.88
Hermes	0.44 ^{fg}	0.54 ^{f}	0.52 ^{d}	0.66
Marfona	0.91 ^{bcd}	0.83 ^{ef}	0.49 ^{d}	0.85
397097-14	1.59 ^{b}	1.67 ^{ab}	2.16 ^{a}	1.21
Difla	1.40 ^{bcd}	0.68 ^{ef}	1.13^{bc}	0.62
Satina	3.15 ^{a}	1.88 ^{a}	1.70 ^{ab}	1.43
Natascha	1.54^{bc}	1.12 ^{abc}	0.66^{c}	0.93

In each column, means followed by the same letter do not differ significantly according to a Duncan test performed at $p < 0.05$, $p < 0.01$

To aid in the interpretation of results, potato cultivars were categorized as highly, poorly, and intermediately competitive. Since the lowest weed density, weed biomass, yield loss, and the highest competitive index were recorded in satina in both years (*Tables*

http://www.aloki.hu ● ISSN 1589 1623 (Print) ● ISSN 1785 0037 (Online)
DOI: http://dx.doi.org/10.15666/aeer/1704_88358845

6 and 7) this may be considered highly competitive. Casear and Hermes had the highest weed characteristics and yield loss and the lowest competitive index in both years (*Tables 4, 6 and 7*) thus these may be considered poorly competitive. The rest were not classed as poorly or highly and were considered intermediately competitive (*Figures 1 and 2*).

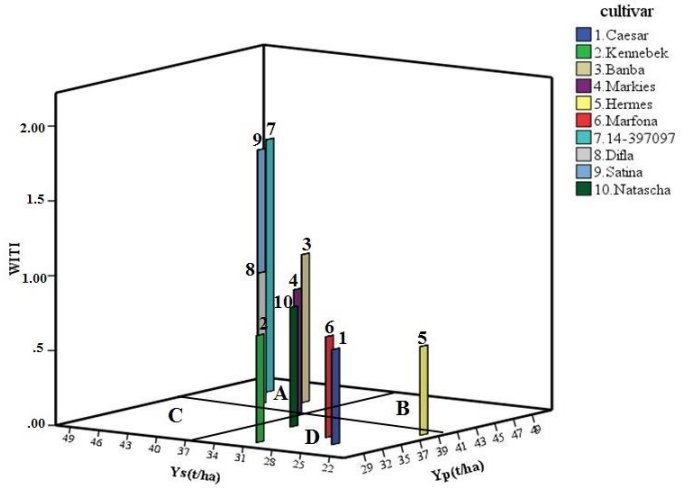

Figure 1. *Three dimensional diagram of WITI index for 10 Potato genotypes based on Potato yield (t ha^{-1}) with weed (Y_s) and without presence of weed (Y_p)*

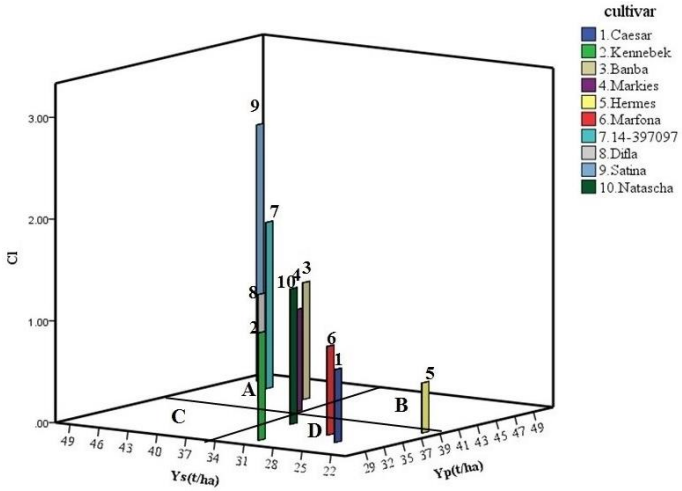

Figure 2. *Three dimensional diagram of CI index for 10 Potato genotypes based on Potato yield (t ha^{-1}) with weed (Y_s) and without presence of weed (Y_p)*

Discussion

Cultivar competitiveness can be expressed as the ability of a cultivar to maintain yield when grown in the presence of weed and can be measured by weed interference tolerance index (WITI) or as one that is able to suppress weed growth, which is measured by competitive index (CI) (Watson et al., 2006). These are important in different production systems. For example, WITI is more suitable for conventional production systems, where

http://www.aloki.hu ● ISSN 1589 1623 (Print) ● ISSN 1785 0037 (Online)
DOI: http://dx.doi.org/10.15666/aeer/1704_88358845

herbicides are used. While in organic systems, CI is important to minimize seed return. However, the relationship between these aspects has not been addressed in potato. In this study, the potato cultivars differed significantly in the suppression weed growth. High CI in Satina caused to reduced weed density and weed biomass and allowed minimizing yield loss. This is in agreement with Watson et al. (2006) who reported barley yield loss and reduced weed seed return when high competitiveness barley cultivars were grown. It has been reported that weed biomass differ through potato cultivars (Nelson and Thoreson, 1981; Love et al., 1995; Khalegi et al., 2007; Hutchinson et al., 2011). Although, Conley et al. (2001) and Colquhoun et al. (2009) reported no differences in weed biomass with six potato cultivars.

Our results showed that Satina cultivar had high CI and, while 397097-14 cultivar had high WITI. Jordan (1993) and Lemerle et al. (2001) stated that CI and WITI might not necessarily be present in the same variety. WITI and CI are traits that differ both genetically and agronomically. CI is often associated with traits including vigorous growth, allelopathic potential, large seedling ground cover, height, canopy structure and overall leaf area (Hansen et al., 2008). 397097-14 is a new cultivar and Satina is an old (released 1971) cultivar. Murphy et al. (2008) reported that modern wheat cultivars were competitiveness than older cultivars. In other words, there is no trade-off among yield and competitive ability.

Potato yield and weed biomass for all cultivars was relatively greater in 2015 than in 2016, this difference between years in weed biomass as well as yield could have been caused by a relatively early rainfall in the seasonal growing conditions in 2015 than in 2016. According to various studies, potato responds to improved moisture conditions (Mazurczyk et al., 2009; Rolbiecki et al., 2009; Zaski, 2011; Karanja et al., 2014).

Conclusion

Potato cultivar competitive ability has a substantial range and can be an important IWM tool or it can be used in conjunction with other IWM tools such as yield loss thresholds and reduction of herbicide hazards. Satina and 397097-14 had highly competitive abilities and can be used in sustainable systems.

REFERENCES

[1] Abdollahi, F., Mohammaddust-Chamanabad, H. R. (2017): The Competitive Response Investigation of 18 Wheat (*Triticum aestivum* L.) Cultivars with Wild Mustard (*Sinapis arvensis*). – Plant Protection 30: 629-638. DOI: 10.22067/jpp.v30i4.50675.

[2] Acciaresi, H. A., Chidichimo, H. O., Sarondon, S. J. (2001): Traits Related to Competitive Ability of Wheat (*Triticum aestivum*) Varieties Against Italian Ryegrass (Lolium multiflorum). – Biological Agriculture and Horticulture 19: 275-286. DOI: 10.1080/01448765.2001.9754930.

[3] AHDB. Agriculture and Horticulture Development Board. (2018): Potato Variety Database. – Retrived from http://varieties.ahdb.org.uk/varieties. Accessed on 14.11.2018.

[4] Andrew, I. K. S., Storkey, J., Sparkes, D. L. (2015): A Review of the Potential for Competitive Cereal Cultivars as a Tool in Integrated Weed Management. – Weed Research 55: 239-248. DOI: 10.1111/wre.12137.

[5] Bashiri-Majd, M. (2015): Evaluation of Potato Cultivars Response to Weed Competition. – Master's Thesis, Buali Sina University, Hamedan, Iran. Retrived from http://ganj-old-irandoc.ac.ir/articles/903685. Accesssed on 14.02.2019.

http://www.aloki.hu ● ISSN 1589 1623 (Print) ● ISSN 1785 0037 (Online)
DOI: http://dx.doi.org/10.15666/aeer/1704_88358845

[6] Blackshaw, R. E. (1994): Differential Competitive Ability of Winter Wheat Cultivars Against Downey Brome. – Agronomy Journal 86: 649-654. DOI: 10.2134/agronj1994.00021962008600040012x.
[7] Brennan, J. P., Lemerle, D., Martin, P. (2001): Economics of Increasing Wheat Competitiveness as a Weed Control Weapon. – Contributed Paper Presented to the 45th annual conference of the Australian Agriculture and Resource Economic Society. Adelaide, 22-25 January 2001, South Australia.
[8] Coleman, R. D., Gill, G. S., Rebetzke, G. J. (2001): Identification of Quantitative Trait Loci for Traits Conferring Weed Competitiveness in Wheat (*Triticum aestivum* L.). – Australian Journal of Agriculture Research 52: 1235-1246. DOI: 10.1071.ARO1055.
[9] Colquhoun, J. B., Konieczka, Ch. M., Rittmeyer, R. A. (2009): Ability of Potato Cultivars to Tolerate and Suppress Weeds. – Weed Technology 23: 287-291. DOI: 10.1614/WT-08-062.1.
[10] Conley, S., Binning, L., Connell, T. (2001): Effect of Cultivar, Row Spacing, and Weed Management on Weed Biomass, Potato Yield, and Net Crop Value. – American Journl of Potato Research 78: 31-37.
[11] Cory, E. J., Eric, N. J., Miles, F. D., Christian, J. W. (2016): Evaluating the Competitive Ability of Semileafless Field Pea Cultivars. – Journal of Weed Science 64: 137-145. DOI: 10/1614/WS-D-15-0011301.
[12] European Cultivated Potato Database (ECPD) (2018): Varieties. – http://europotato.org. Accessed on 20.03.2019.
[13] FAOSTAT. (2016): Food and Agriculture Organization of the United Nations. – Retrived from http://www.faostat.org.
[14] Goldberg, D. E., Miller, T. E. (1990): Effect of Different Resource Additions on Species Diversity in an Annual Plant Comunity. – Journal of Ecology 71: 213-225.
[15] Gonzales-Ponce, R., Zancada, C., Vardugo, M., Salas, L. (1996): Plan Height as a Factor in Competition Between Black Nightshade and Two Horticultural Crops (Tomato and Pepper). – Horticulture Science 71: 453-460. DOI: 10.1080//1462031.6.1996.11515426.
[16] Hashem, A., Borger, C. P. D., Riethmuller, G. (2010): Weed Suppression by Crop Compete. – 17th Australasian weeds conference. New Zealand, 26-30 September, pp. 63-66.
[17] Hutchinson, P. J. S., Beutler, B. R., Fair, J. N. (2011): Hairy Nightshade (*solanum sarranchoides*) Competition with Two Potato Varietes. – Weed Science 59: 37-42. DOI: 10.1614/ws-d-10.00003.1.
[18] IRANSTAT. (2017): Startisical Center of Iran. – Retrieved from http://www.amar.org.ir. Accessed on 25.10.2018.
[19] Jacob, C. E., Johnson, E. N., Dyck, F. D., Willenborg, Ch. J. (2016): Evaluating the competive ability of smile a fless field pea cultivars. – Weed Science 46: 137-145. DOI: 10.1614/WS-D-15-00113.1.
[20] Karanja, A. M., Shasanya, Ch., Makokha, G. (2014): Analysis of Rainfall Variability on Potato Production in Kenya: A Case of Oljoro-orok Division. – Asian Journal of Applied Sciences 2: 447-456.
[21] Khalegi, F., Hejazi, A., Zand, E., Allahdadi, I., Jahedi, A. (2007): Evaluating the Competitive Ability of Potato Cultivars with Weeds. – Applied Entomobgy and Phytopathology journal 75: 95-108.
[22] Khalgani, J. (2010): Research Strategic Plan for Weed Management. – Iranian Research Institute of Plan Protection. Tehran, pp. 331-362.
[23] Korres, N. E., Froud-Williams, R. J. (2002): Effects of Winter Wheat Cultivars and Seed Rate on the Biological Characteristics of Naturally Occurring Weed Flora. – Weed Research 42: 417-428.
[24] Lemerle, D., Gill, G. S., Murphy, C. E., Walker, S. R. (2001): Genetic Improvement and Agronomy for Enhanced Wheat Competitiveness with Weeds. – Australian Journal of Agriculture Research 52: 527-548. DOI: 10 .1071/AR01056.

http://www.aloki.hu ● ISSN 1589 1623 (Print) ● ISSN 1785 0037 (Online)
DOI: http://dx.doi.org/10.15666/aeer/1704_88358845

[25] Lemerle, D., Verbeek, B., Orchard, B. (2015): Ranking the Ability of Wheat Varieties to Complete with *Lolium rigidum*. – Journal Weed Research 41: 197-209. DOI: 10.1046/j.1365-3180.2001.00232.X.
[26] Love, S. L., Eberlein, C. V., Sturk, J. C., Bohi, W. L. (1995): Cultivar and Seed Piece Spacing Effects on Potato Compitiveness with Weeds. – American Potato Journal 72: 197-209. DOI: 10.1007/BF02855036.
[27] Mason, H., Goonewardence, L., Spaner, D. (2008): Competitive Triats and the Stability of Wheat Cultivators in Differing Natural Weed Environment on the Northern Canadian Prairies. – Agriculture Science 146: 21-33. DOI: 10.1017/S0021859607007319.
[28] Mazurczyk, W., Wierzbicka, A., Wroniak, J. (2009): Influence of Optimisation of Irrigation and Nitrogen Fertilisation on some Growth Parameters and Yield of Early Potato Variety. – Infrastructure and Ecology of Rural Areas 3: 91-100. (in Polish).
[29] Mohammaddoust-Chamanabad, H. R. (2011): Introduction to Scientific and Practical Principle of Weed Control. – The Ardabil University Jihad Publications, Ardabil.
[30] Mohammaddust-Chamanabad, H. R., Bakhshi, M., Mohammadnia, S. H. (2014): Evaluation of Weed Tolerace and Competition Indices of Wheat Genotypes. – Iranian Journal of Weed Science 10: 155-166.
[31] Murphy, K. M., Dawson, J. C., Jones, S. S. (2008): Relationship Among Phenotypic Growth Traits, Yield and Weed Suppression in Spring Wheat Landraces and Modern Cultivars. – Field Crops Research 105: 107-115. DOI: 10.1016/j.fcr.2007.08.004.
[32] Nelson, D. C., Thoreson, M. C. (1981): Competition Between Potatoes (*Solanum Tuberosum*) and Weeds. – Weed Science 29: 672-677. DOI: 10.1017/S0431745004025X.
[33] Potato Association of America (PAA) (2018): Potato Varieties. – http://potatoassociation.org/industry/varieties. Accessed on 11.03.2019.
[34] Rolbiecki, S., Rzekanowski, Cz., Rolbiecki, R. (2009): Estimation of Needs and Results of Irrigation of Medium-early Potato in the Vicinity of Bydgoszcz in the Years 2005-2007. – Acta Agrophysica 13: 463-472. (in Polish).
[35] Tilman, D. (1987): On the Meaning of Competition and the Mecanisms of Competitive Superiority. – Journal of functional Ecology 1: 304-315.
[36] Vollman, J., Wagentristl, H., Hartl, W. (2010): The Effects of Simulated Weed Pressure on Early Maturity Soybeans European. – Journal of Agronomy 32: 243-248. DOI: 10.1016/j.eja.2010.01.001.
[37] Watson, P. R., Derksen, D. A., Van Acker, R. C. (2006): The Ability of 29 Barely Cultivars to Compete and Weethstand Competition. – Weed Science 54: 783-792.
[38] Worthington, M., Reberg-Horton, C. (2013): Breeding Cereal Crops for Enhanced Weed Suppression: Optimizing Allelopathy and Competitive Ability. – Chemical Ecology 39: 213-231. DOI: 10.1007/s10886-013-0247-6.
[39] Żarski, J. (2011): Trends of Climate Change Indicators of Irrigation Needs in Plants Region of Bydgoszcz. – Infrastructure and Ecology of Rural Areas 5: 29-37. (in Polish).

http://www.aloki.hu ● ISSN 1589 1623 (Print) ● ISSN 1785 0037 (Online)
DOI: http://dx.doi.org/10.15666/aeer/1704_88358845

INFLUENCE OF SUN AND SHADE ON THE GROWTH, YIELD AND QUALITY OF *VITIS VINIFERA* L. (GRAPES) UNDER SEMI-ARID ENVIRONMENTAL CONDITIONS

AYATULLAH[1] – LEGHARI, S. K.[1*] – SHAUKAT, K.[1] – KHATTAK, M. I.[2] – PANEZAI, M. A.[3] – MARRI, A. A.[4] – ISMAIL, T.[1, 5] – SHAGUFTA[1]

[1]*Department of Botany, University of Balochistan, Quetta, Pakistan*

[2]*Department of Chemistry, University of Balochistan, Quetta, Pakistan*

[3]*Institute of Biochemistry, University of Balochistan, Quetta, Pakistan*

[4]*Department of Statistics, University of Balochistan, Quetta, Pakistan*

[5]*Department of Plant Production and Protection, Kaposvár University, Kaposvár, Hungary*

**Corresponding author*
email: saadbotany@yahoo.com, drsaadullahleghari@gmail.com; phone: +92-81-921-1264

(Received 13th Mar 2019; accepted 24th May 2019)

Abstract. The main objective of this study was to analyse the shade effect on development, productivity and excellence of grape fruits (*Kishmishi* seedless). To attain this, three sun (AM sun, PM sun, Full sun) treatments was linked with those plants growing in three shade treatments (50% shade, 80% shade and 100% shade). Different physical, chemical, ecological and quality factors were evaluated under six diverse treatments. Results showed that 50% shade plant stimulated differences in physiological attributes such as enhanced photosynthesis and augmented leaf area index (LAI), resultant in improved performance than conceivable in direct sun light. Accordingly, grape plants grown under 50% shade produced greater quantity (number) of fruits for example 10,350 individual fruits/plant and greater fruit weights (49 and 12 g fresh and dry weight/fruit respectively) with better fruits quality, than those grown in direct sun light or in 80% and 100% shade. Moreover, 50% shade plants had greater biochemical (nutritional, minerals and vitamin contents) and physiological attribute improvement i.e. greater fruit weight and fruit length which would benefit grower to uphold great grapes yields in long term. Fruit quality assessment (FQA) was calculated and evaluation classes indicated that the 50% shade plant score highest grade point (5) and stood in very good class, followed by AM and PM sun with grade point 3.0 and categorized in moderate class. Other three treated plants (Full sun, 80 and 100% shade) score 2.0 and 1.0 grade points and classified into poor and very poor classes, respectively.
Keywords: *Kishmishi seedless grapes, environmental variables, nutritional, minerals, vitamins and fruit quality assessment*

Introduction

Plant ability to adapt to varying light can be used to change growing circumstances and has the ability to increase crop incomes of primo cane varieties in semi-arid environmental region. The quantity and concentration of light has an important effect on plant growth and development. The quantity of light absorbed by the leaves superficial area as well as the distribution of light influences crop yield. Alkalai-Tuvia et al. (2014) stated that the light excellence and diverse wave length alters fruit color and maturity of fruits. Shade and sunlight are vital feature for plants growth, expansion and physiological characteristics. Two facts to be deliberate for the influence of light on fruits crop comprised: the capture of existing light on plant and the delivery of light

http://www.aloki.hu ● ISSN 1589 1623 (Print) ● ISSN 1785 0037 (Online)
DOI: http://dx.doi.org/10.15666/aeer/1704_88478864

inside plant that outcomes in supreme recital and crops development (Rom, 1991). Ahmed et al. (2016) stated that reducing the absorbance of solar radiation under shade decreases the covering and air temperature as well as transpiration rate in the greenhouse. This therefore decreases the water intake through around 50%, enhances water use efficiency and increases the crop efficiency up to 40%. Approximately consequences of shade on plant growth comprised: plants defence from birds, wind and hail, influence on ecological features (humidity, light and temperature) and augment subtle light that may absorb specific light wavelengths; all of which is subjected to plants growth and development (Stamps, 2009). Alkalai-Tuvia et al. (2014) and Mashabela et al. (2015) reported that the fruit produced in pearl nets shade showed greater fruit weight, pigment contents, ascorbic acid contents and anti-oxidant action. Vendrame et al. (2004) and Jeong et al. (2009) designated that light concentration can affect plants form, flowering, leaf size in both herbaceous and also woody species. Additionally temperature and light can have direct optimistic associations. As light level augmentes beyond of 600 $\mu mol \bullet m^{-2} s^{-1}$ and soil and air temperature exceeded 16 °C and 24 °C, primo canes entered a state of bud dormancy, decreased fruit weight as well as quality (Oliveira et al., 2004). Stamps (1994) documented, that decrease in radioactivity give rise from diverse netting might affect temperature of the environmental air, soil and plant and impact the relative humidity inside shaded structures. This tinted the need for additional investigation to be conducted for the best strength and application of shades to get desired fruit setting and fruits superiority of primo canes. Assumed its complication there are several deliberations that requires to be assessed when determining influences of shade and light on plants growth, development and biological replies. The use of photo selective nets technology is gaining popularity everywhere in the world. This exercise is already general in Europe, particularly in Israel (Fallik et al., 2009; Kong et al., 2013) and other Mediterranean countries (Diaz-Perez, 2014) and in South Africa (Mashabela et al., 2015; Selahle et al., 2015). The usage of shade nets has also become very popular in Serbia due to very high (35–40 °C) temperature in summer season (Ilic et al., 2011, 2015; Milenkovic et al., 2012).

Grapes (*Vitis vinifera* L.) is one of the most cultivated fruit crop not only in the study area but also all-over the world. It have its place in the family Vitaceae and mostly distributed in Asia (app. 40 species), North America (40 species) and Europe (one species) in subtropical, Mediterranean and continental-temperate climatic condition. *V. vinifera* is the only species that attained important commercial attention over time. For agriculturalist's fruits production is a great energy concerning process that offer a wide range of difficulties that could decrease cost-effectiveness and return on investment. Fruits development is a significant feature of cultivation by economic and environmental impacts in the study area (District Mastung, Balochistan, Pakistan). Grapes are usually found growing in full sun. Though, there is no published report about the degree of shade tolerance of these species. Many studies on *Vitis vinifera* L. have been reported on gas exchange (Poni et al., 2014), water-use efficiency (Ghaderi et al., 2011), biochemical changes (Beis and Patakas, 2015), road side dust pollution effect on the growth and total chlorophyll contents in *Vitis vinifera* L. (Leghari et al., 2014), air pollution effect on the leaf morphology of *Vitis vinifera* L. (Leghari and Zaidi, 2013) and biomass distribution (Xiao et al., 2006), in addition to yield and fruit quality (Romero et al., 2015) response to different degrees of drought stress has also been reported. No comprehensive study about the influence of sun and shade on grapes of area has yet been reported. Therefore this investigation aims to calculate in what way

http://www.aloki.hu ● ISSN 1589 1623 (Print) ● ISSN 1785 0037 (Online)
DOI: http://dx.doi.org/10.15666/aeer/1704_88478864

diverse ecological controlled conditions of sun and shade treatments might affect plant growth parameters, productivity and quality traits in economically important fruit crop (Grapes) that is frequently cultivated in study area.

Materials and methods

Study area

In order to evaluate the influence of sun and shade on fruit plant i.e. grapes (*V. vinifera)* plants were grown during April 2017-2018 in the open field. The trials started from April 2018 – October 2018 in an experimental plot situated in the village of district Mastung Balochistan, Pakistan. Geologically, study area district Mastung is hilly area comprising of a sequence of parallel mountains range in north and east, with elevation varying from 934 to 3414 m. a.s.l. and located at 29.8° north latitude, 66.85° east longitude. Soil of the area is mostly calcareous and clay loam and are abstemiously deep thereby reflecting it to be appropriate for agriculture. The average maximum, average minimum and overall average temperatures of the area was noted 44.0, 21.5, and 32.2 °C, respectively (*Table 1*). Mastung district is deliberated as one of the original grapes producing areas of the Balochistan province.

Table 1. *Meteorological data of the study area during growing months (April 2018 – October 2018), study year and last 5 year average data*

Variables	Ave. study period	Study year	Last 5 year ave.	LSD (0.05)
Max. Ave. Tem. (°C)	42.71	34.1	33.1	**0.53**
Min. Ave. Tem. (°C)	19.67	8.3	7.2	**0.04**
Overall Ave. Tem. (°C)	30.8	29.0	28.5	**0.23**
Humidity (%)	25.43	30.4	51.5	**0.01**
Rainfall (mm)	6.47	8.12	106.4	**0.02**

Each value is the mean of three replicates. Ave: average, Max: maximum, Min: minimum

Plant material and field plots

The regional well-known and commercially important grape (*V. vinifera*) variety i.e. *Kishmishi* (seedless) were grown in six lights and shades treatments including: full sun; morning full sun (AM sun); afternoon full sun (PM sun); and 50% shade, 80% shade and 100% shade. Each plot was 7.3 x 1.5 m. Boundaries (1.5 m tall) were constructed of chipboard on the east or west side of the AM sun or PM sun plots, respectively. To retain plant in shade as noon loomed, 0.3 m chipboard overhangs were involved upright to the top of the boundary. Shaded cloth canopies were built above plot to give light intensity level of 50% shade, 80% shade or 100% shade. Each canopy was made with dispersal over a row of seven 1.5 m tall and 1.8 m wide arches. Each arch was prepared with drubbing two 0.5 m length of 1.27 cm EMT channel into the ground, sliding a 1.8 m length of 1.9 cm polyvinyl chloride (PVC) pipe over each piece of channel and then linking PVC pipe at the apex with a 90° elbow connector (All the sun and shade tunnels were locally made) as used by Stanton (2010).

Experimental design and analysis

http://www.aloki.hu ● ISSN 1589 1623 (Print) ● ISSN 1785 0037 (Online)
DOI: http://dx.doi.org/10.15666/aeer/1704_88478864

The trial was arranged in a split-plot design. Six light and shade treatments were the main plots with grapes plants. Every individual set of 6 sun and shade treatment plots was randomized within one of 16 blocks. There was one replication plant per block. So there was a total of 16 replicates for each genotype treatment level as the method used by Stanton (2010). Plant height at implanting time was 35.8 ± 2.30 cm with no significant variations between ecotypes of either species. The plants were grown following the technique usually implemented by the local producers. All the experimental plots were treated with uniform fertilizer and water. During planting year, a total of 0.5 to 1 ounce of nitrogen (N) fertilizer was applied to each plant, depending on soil fertility. In the second year, plants were fertilized with 1 to 1.5 ounces of N per plant. Transmission of fertilizer was done in a circle about 6 to 18 inches from the trunk. The plants were properly watered to found the soil type and climatic condition and kept the soil sufficiently moist without overwatering and gradually decreased watering in mid to late summer. To control different diseases herbicides (2, 4-D) and fungicides (sulfur) were used and to minimize different pests, traps were applied. Only the plants growing vigorously in April 2018 were used for data collection in each treatment. All measurements were conducted in April 2018 and all values presented are averages of untransformed data.

Environmental variables measurements

Light intensity (lux), air temperature relative humidity (%) and soil temperature at a depth of 10-15 cm were measured by a handheld light meter, thermos-hygrometer and soil thermometer, correspondingly from each treatment. The light sensor was held 1.0 - 1.5 m above soil level in each treatment plot. Interpretations were taken at midday and 3 and 6 h earlier and later midday (*Table 2*).

Table 2. *Averages environmental variables under sun and shaded treatments*

Variables	Treatments						LSD (0.05)
	AM sun	PM sun	Full sun	50% shade	80% shade	100% shade	
Air temperature (°C)	28.0	30.0	31.6	30.4	27.5	25.4	0.14
Soil temperature (°C)	20.1	24.2	25.4	24.0	22.5	22.0	0.04
Relative humidity (RH %)	23.0	23.5	21.0	23.0	25.0	27.0	0.15
Light intensity (lux)	811	1030	1250	842	652	610	14.0

Each value is the mean of three replicates

Plant growth variables measurements

Freshly mature, completely extended leaves (90) were detached from each treatment plants for leaf area parameters measurement and photographed. The Leaf area (LA) was determined by the digital image using Image J 1.38x software and graph paper method at the laboratory of botany department university of Balochistan, Quetta and then average was worked out (Leghari and Zaidi, 2013). Plants Leaves were then dried at 70 °C to get leaf dry weight (DW). Specific leaf area (SLA) was calculated as:

$$SLA = LA/DW \quad \text{(Eq.1)}$$

For relative growth rate (RGR, cm cm^{-1} $month^{-1}$) primary pleiotropic branches were selected, their length was measured at the beginning and at the end of the trial.

http://www.aloki.hu ● ISSN 1589 1623 (Print) ● ISSN 1785 0037 (Online)
DOI: http://dx.doi.org/10.15666/aeer/1704_88478864

Pigment analysis

Chlorophyll a & b, total chlorophyll, carotenoid, ratio between chl. a & b, and ratio between total chl. and carotenoid were measured from fresh leaf samples. 2 g of fresh leaves from each treatment were ground in acetone (90% v/v), filtered the extract and made up to final volume of 50 mL. Pigment concentrations in mg g^{-1} fresh weight (fw) were calculated [absorbance (A) of extract at 663, 648 and 470 nm) by the methods described by Lichtenthaler (1987).

$$\text{Chlorophyll a} = [(11.75A663 - 2.35A\ 645) \times 50] / 500 \quad \text{(Eq.2)}$$

$$\text{Chlorophyll b} = [(18.61A645 - 3.96\ A663) \times 50] / 500 \quad \text{(Eq.3)}$$

$$\text{Carotenoids} = [1000A470 - (2.27 \times \text{Chl a}) - (8.14 \times \text{Chl b}) / 227 \times 50] / 500 \quad \text{(Eq.4)}$$

$$\text{Total Chlorophyll} = \text{Chl a} + \text{b} \quad \text{(Eq.5)}$$

Measurement of Chl. fluorescence from leaves at different time intervals

All dimensions of Chl. fluorescence were made by a moveable PAM-2000 fluorimeter (Walz, Effeltrich, Germany). Earlier to the each dimension, the sample leaves were dark adapted for 30 min by leaf-chips. Throughout the trials the position and space from the leaf surface to the end of optic-fiber cable were set aside continual. For initial fluorescence (F0) measurement the weak measuring light was turned on and F0 was noted. To get the maximum fluorescence (Fm) the sample leaf was visible to a 0.1 s saturated flash of about 6000 lmol/m^2/s. the ratio of variable to maximum fluorescence (Fv/Fm) was intended automatically rendering to F0 and Fm calculated [Fv/Fm ¼ (Fm) F0)/Fm]. All dimension of Fm were done by the measuring beam set at a frequency of 600 Hz. Leaf chamber poro-meter (LCpro +) was used to determine the transpiration rate (E, mmol m^{-2} s^{-1} of water vapour), stomatal conductance (Gs, mmol m^{-2} s^{-1} of water vapour or CO^2), Photosynthetically Active Radiation (PAR, µmol photons m^{-2} s^{-1}) and leaf temperature (LT, °C). These factors were measured from five complete, new and completely prolonged leaves on third and fourth pairs from top of each treated plant. These leaves were exposed to a period of dark adaptation for 25 min and then visible to a light pulse of high intensity (2000 µmol photons m^{-2} s^{-1}) by means of chlorophyll fluorimeter (OS-30P) to measure chlorophyll fluorescence, representing the electron transport efficiency of photosystem II (PSII). Chlorophyll fluorescence is shown as the Fv/Fm ratio (no dimension) as a degree of relative quantum yield. Moisture contents were determined by Association of Official Analytical Chemists (AOAC, 1995) procedures. It was done by drying 5.0 gm grapes fruits sample from each treatment in vacuum at 70 °C to continuous mass and moistness was intended a gm water g-100 samples. Color difference meter was used to measure the fruit color and the dimensions were done on 10 separate fruits per replicate (Aleid et al., 2014).

Yield variables

Number Cluster arising from the main stem and fruit density per cluster were counted from 5 randomly nominated plants from each treatment at the end of growing season and lastly pooled to become the number of fruits per plant and average was calculated. Fruit length and diameter was intended from 30 randomly chosen fruits of each plant from each

http://www.aloki.hu ● ISSN 1589 1623 (Print) ● ISSN 1785 0037 (Online)
DOI: http://dx.doi.org/10.15666/aeer/1704_88478864

treatment. The length of each fruit was noted from base of fruits to the tip and diameter (cm) was measured from the centre of each fruit with the help of Vernier Calliper and the average length and diameter of fruit was computed and represented in centimetre. Average weight of fresh and dry fruits were recorded by using electrical balance. The mean of 30 fruits from each site was worked out and expressed in grams.

Total soluble solids (TSS) measurement

Completely mature grape fruit samples were collected from each treatment. Each fruit sample was cut into small pieces and homogenized in a conventional blender in order to obtain the fruit juice. Then, the fruit juice was filtered by using the whatman filter paper no 4. The filtrate was utilized to measure the total soluble solids (TSS). TSS were determined for each fruit samples in three replications using an Atago DR-A1 digital refractometer (Atago Co., Japan) at 20 °C and shown expressed as %. Moisture and fat free samples were analyzed for their Protein, Dietary fibre (DF) and sugar. The Protein content was determined according to method of AOAC 985.29 (1984) and Sowbhagya et al. (2007). The DF contents were recorded by enzymatic and gravimetric method of the Association of Official Analytical Chemists (AOAC) and (Prosky et al., 1988), by the utilization of TDF-100 kit. Beside the test sample, and blank and reference samples were also analyzed at the same time in triplicate for contrast. Carbohydrates were measured with the difference from the total dietary fiber, lipids, protein and ash contents (Chau and Huang, 2003). Sugars level from soaked grapes fruit were measured by water at 85 °C and it was calculated through 3, 5-dinitrosallicylic acid method as designated by Laurey (1997). Overall sugar (Sucrose, glucose, and fructose) contents were noted by high performance liquid chromatography (HPLC) according to the methods of AOAC (1995). Grapes fruit sample were spiked with several mixtures of average sugars (1-5 ppm) to display recovery and the sugar level was noted from highest area of dimension according to the method of Langemeier and Rogers (1995). Contents of the various fruits analyzed were calculated and expressed on fresh weight basis. Various Minerals (Calcium, Iron, magnesium, manganese, phosphorus, potassium, Zinc and Fe) contents were determined through atomic absorption spectrophotometer and expressed by mg/100 g. Different vitamin (B6, E and K) and Ascorbic acid content of fresh fruit were determined by spectrophotometric methods as the method used by Isam Eldin et al. (2017). Potassium permanganate was used as a chromogenic reagent. The absorbance was measured spectrophotometrically at 530 nm. For acidity measurement the pH of fruit juice was noted with a pH meter (model 725p, Istek Co., Seoul, Korea).

$$\text{Acidity (\%)} = [(\text{ml of 0.1 N NaOH}) \times (\text{N NaOH}) \times 0.067 \text{ (malic acid coefficient)} \times 100] / \text{ml sample} \quad \text{(Eq.6)}$$

Fruit quality assessment (FQA)

Raw quality (shape and make, colour and odour, size of fruit, no of fruit per plant) of different sun and shade treated grapes fruits was valued on a scale starting from 1, the minimum value (indicating small shape and make, brownish color and strong/odd odour) to 5, the maximum value (indicating very good shape and make, bluish color and clean odour). Liquor quality (acidity, taste and flavour) was tested by a panel of six experienced judges and values were given from 1, the minimum value (indicating lacking acidity, thin body and poor taste and flavor) to 6, maximum value (indicating

http://www.aloki.hu ● ISSN 1589 1623 (Print) ● ISSN 1785 0037 (Online)
DOI: http://dx.doi.org/10.15666/aeer/1704_88478864

pointed acidity, full taste and very good flavour (unit for both raw and liquor qualities: percentage of score) (Prajapati and Tripathi, 2008; Leghari et al., 2019).

Fruit performance index (FPI) evaluation through fruit quality assessment

For the grapes plant fruit performance index the methods described by Leghari, et al. (2019) and Prajapati and Tripathi (2008) was used. FPI values were calculated by combining the Raw quality fruits and Liquor quality fruits under different sun and shade treatments grapes fruit grown based on character grading (+ or -) fixed to the plant. The principles intended for FPI are specified in *Tables 9* and *10*.

Data analysis

All the collected data was subjected to analysis of variance (ANOVA) using Co-Stat version 6.400 (1998-2008, Co Hort Software). Mean separation was done using the least significant difference test at 0.05 significance level.

Results and discussion

This investigation was not deliberate to measure the hereditary change for light and shade acceptance in the examined species nor it was done to compute the heritability of characters. Nevertheless, the plant species under contrasting natural environments able to change for adaptation to shades and light (Johnson and Cartwright, 2005). In the current investigation there was a fruit crop (grape plant) source-by-treatment dealings and all the results are presented in *Tables 2-10* and *Figs. 1A-F* and *2*.

Meteorological data indicated that the maximum and minimum average temperature in study area during study period and last 5 year average was found 42.71, 34.1 and 33.1 °C and 19.67, 8.3 and 7.2 °C, respectively. Humidity % age was recorded 25.43, 30.4 and 51.5, respectively and Rainfall was found only 6.47 mm and 8.12 mm throughout the study period and study year respectively and last 5year average was 106.4 mm. Significant difference were observed between the periods (study period and study year and last 5 year average) at 0.05 significance level (*Table 1*). Air and soil temperature and light intensity was recorded between 25.4-31.6 and 20.1-25.4 °C, 610-1250 lux, respectively. Maximum air and soil temperature and was found in full sun treatment and minimum in 100% shade and AM sun, respectively. The maximum relative humidity and light intensity was recorded in 100% shade and full sun, while the minimum was found in full sun and 100% shade treatment, respectively. All the investigated variables (air and soil temperature, relative humidity and light intensity) in six different sun and shade treatment were pragmatic significantly different (*Table 2*). Soil temperature shows a very serious role in existence of numerous entities, however in reaction to exchange processes which occur by the soil surface differs. The decrease in soil temperature, noted in 100% shade, was mostly because of the ability of shade soil to steady the native warm air equilibria, the less soil temperature under shade was also noted by Morais et al. (2006). Decreased air temperature noted for grapes plant grown under shade was in agreement with the results reported by Campanha et al. (2005) as they determine that decreased air temperature was mostly due to the reduced straight incidence of solar radiation on coffee canopies. Siebert (2002) also reported that shading decreases soil temperature by decreasing radiant flux reaching the soil and amending the temperature sufficiently at the soil surface thereby shielding the harsh

http://www.aloki.hu ● ISSN 1589 1623 (Print) ● ISSN 1785 0037 (Online)
DOI: http://dx.doi.org/10.15666/aeer/1704_88478864

temperature and delivers a microclimate which alleviate harsh effect of high temperature of soil and air and conserves soil surface humidity.

Current study revealed that the average leaf area (ALA), specific leaf area (SLA), leaf area index (LAI), relative growth rate (RGR) and leaf color in different sun and shade treatments (AM sun, PM sun, Full sun, 50%, 80% and 100% shades) were found in ranged between 27.38-34.7 cm^2, 86.2-107 cm^2/g, 2.8-4.2 m^2 m^{-2}, 10.8-16.8 cm cm^{-1} $month^{-1}$ and -9.8 to -5.7, respectively. The maximum ALA, SLA, LAI and RGR was noted in plant grown under 100% shade, while the minimum was in full sun treatment. Least significant difference (LSD) test indicated that all the plant growth variable (ALA, SLA, LAI, RGR and leaf colour) showed significant variation under different sun and shad treatments at 0.05 significant level (*Table 3*). The variation in ALA, SLA, LAI in different sun and shade treatments were also reported by other researchers (Bote and Struik, 2011; Ilić, 2017) they found differences in leaf parameters in different shade nets. Li et al. (2005) reported that the plant having higher SLA showed greater production and have greater possible RGR than those observed by Poorter and Werf (1998). Robakowski et al. (2003) observed that as the light intensity increased the SLA decreased. In our experiment, lesser SLA was observed from grape plants grown under full sun treatment, which is comparable to the results of Bote and Struik (2011). For 100% shaded grape plants, the increased SLA and the formation of a darker green color were mostly accredited to the higher nitrogen contents found in their leaves. It is probable that the larger SLA and the development of dark green leaf color in shade treatment partially contributed for the higher rate of photosynthesis observed in this condition. McNaughton and Jarvis (1983) reported that greater LAI observed for coffee plants growing in shade designated that these plants have greater possibility for CO_2 integration and dry matter manufacture than un-shaded plant.

Table 3. *Plant leaves and growth variables in response to the sun and shade*

Variables	Treatments						LSD (0.05)
	AM sun	PM sun	Full sun	50% shade	80% shade	100% shade	
ALA (cm^2)	30.24	29.8	27.38	30.57	32.42	34.7	0.12
SLA (cm^2/g)	91.31	90.1	86.2	92.2	96.1	107	0.05
LAI (m^2 m^{-2})	3.0	3.3	2.8	3.2	3.9	4.2	0.02
RGR, (cm cm^{-1} $month^{-1}$)	12.4	12.2	10.8	12.7	14.7	16.8	0.05
Leaf color (value on greenness scale)	-6.1	-6.0	-5.7	-7.2	-8.7	-9.8	0.01

Each value is the mean of three replicates. ALA = average leaf area, SLA = specific leaf area, LAI = leaf area index and RGR = relative growth rate

Photosynthetic pigments including Chl a, b, total chl. and carotenoid contents in the plant leaves of different sun and shade treatments (AM sun, PM sun, Full sun, 50%, 80% and 100% shades) were noted and ranged 1.24-2.47, 0.55-0.85, 1.79, 0.42-0.75 mg/g fw, respectively. The maximum chl a, b, total chl and carotenoids were found in plants grown in 100% shade and minimum in full sun. Statistical analysis of variance showed that all the photosynthetic variables were significantly different among treatments (*Table 4*). Generally shaded leaves have greater total chlorophyll (chl. a & b). Similar observation was recorded by Zoran et al. (2017). They found greater total chlorophyll than the leaves from control plants. Shade growing leaves contain highest

http://www.aloki.hu ● ISSN 1589 1623 (Print) ● ISSN 1785 0037 (Online)
DOI: http://dx.doi.org/10.15666/aeer/1704_88478864

chlorophyll than the leaves exposed to direct sun. Although shaded leaves were not directly exposed to the sunlight they produced additional chl. to capture diffuse radiation to produce the carbohydrates needed for plant to grow. Alkalai-Tuvia et al. (2014) reported that chl. contents of pepper fruits grown under pearl net was significantly higher than that of fruits grown under the black net.

Table 4. *Photosynthetic pigments (mg/g fw) in grapes leaves in response to sun and shade treatments*

Variables	Treatments						LSD (0.05)
	AM sun	PM sun	Full sun	50% shade	80% shade	100% shade	
Chl a (mg/g fw)	1.89	2.0	1.24	1.56	2.21	2.47	0.08
Chl b (mg/g fw)	0.72	0.7	0.55	0.61	0.75	0.85	0.05
Car (mg/g fw)	0.62	0.6	0.42	0.51	0.71	0.75	0.02
Total Chl (mg/g fw)	2.61	2.7	1.79	2.26	2.96	3.32	0.12

Each value is the mean of three replicates: Chl = Chlorophyll; Car= Carotenoids

No. of clusters/plant, No. of fruits/cluster and No. of fruits/plant, in different sun and shade treatments (AM sun, PM sun, Full sun, 50%, 80% and 100% shades) were found in the ranged; 30-45, 160-230, 4960-10350, respectively. All these parameters were noted maximum in 50% shade which followed by full sun, PM sun, AM sun and minimum was in 100% shade. Variation in average fruit length, fruit diameter and average fresh and dry fruit weight (1.60-1.90 cm, 1.27-1.64 cm, 31.7-49.4 g^{-30} and 7.11-12.69 g^{-30}, respectively) were also noted in different treatments. Statistical analysis indicated that all the investigated Yield parameters were significantly different among treatments at 0.05 significance level (*Table 5*). The variation in fruits production and fruit size in different sun and shade treatments was also observed by Bote and Struik (2011). They found weightier and bigger coffee beans that was chiefly influenced by temperature and ripening period. The grapes plants found in direct sun light were grown in environmental conditions that are more likely to lead to plants stress responses, compared with the environmental conditions under which shaded plants are grown. Muschler (2001) who originate similar results, designated that coffee bean size profoundly and reliably increases with increasing shade levels. Similarly, the shade effect on juice taste was also the result of delayed fruit maturation and ripening. Observation recorded by Ilić (2017) are in agreement to the present results. Number and quality of fruit decreases by increasing shade and light level. In Serbia, bell pepper grown in colored nets with 40% or 50% shade had greater total yield as compared to unshaded plants (Ilic et al., 2011). Santana et al. (2012) observed greater yield and better fruits quality for sweet pepper variety grown in photo-selective (red and blue) shading net houses as compared to those obtain from open field. According to Fallik et al. (2009), the peppers grown in arid region under red and yellow shade-nets (30% relative shading in PAR) had a meaningfully higher yield compared to the black nets of the same shading factors, with no effect on fruit size. Miller et al. (2015) reported that the time of shading obviously exaggerated yield by full shade causing the highest reduction as compared to the partial shade. Vaast et al. (2008) reported that the vegetative development has shown to respond to shade intensity as shown in higher vegetative growth under dense (60%) shade in *Terminalia ivorensis* compared to lighter shade (30 to 40%) in *Eucalyptus deglupta.*

http://www.aloki.hu ● ISSN 1589 1623 (Print) ● ISSN 1785 0037 (Online)
DOI: http://dx.doi.org/10.15666/aeer/1704_88478864

Table 5. *Different yield variables of grapes fruits under the influence of sun and shade treatments*

Variables	Treatments						LSD (0.05)
	AM sun	PM sun	Full sun	50% shade	80% shade	100% shade	
No. of clusters/plant	39	41	43	45	34	31	1.02
Fruit density/cluster	188	184	207	230	172	160	7.23
No. of fruit/plant	7332	7544	8901	10350	5848	4960	112.3
Length of fruits (cm)	1.65	1.60	1.63	1.72	1.81	1.90	0.01
Diameter of fruits (cm)	1.38	1.39	1.39	1.64	1.40	1.27	0.04
Weight of fresh fruits (g^{-30})	41.4	43.5	38.7	49.4	36.6	31.7	0.24
Weight of dry fruits (g^{-30})	9.65	9.94	10.11	12.69	8.0	7.11	0.03

Each value is the mean of three replicates

Data regarding photosynthetic variables (Fluorescence ratio (Fv/Fm), ratio between Chlorophyll a & b, ratio between total Chl. and Carotenoid) in different sun and shade treatments including AM sun, PM sun, Full sun, 50%, 80% and 100% shades were found different, which were in range between; 0.57-0.86, 2.25-2.95, 4.17-4.50, respectively. Stomatal conductance, Transpiration rate, Photosynthetically Active Radiation and Leaf temperature) in different sun and shade treatments including AM sun, PM sun, Full sun, 50%, 80% and 100% shades were found statistically different, which were in range between 60-112 mmol m^{-2} s^{-1}, 910-1220 mmol m^{-2} s^{-1}, 344-2280 µmol photons m^{-2} s^{-1} and 23-30 ºC, respectively. The maximum fluorescence (Fv/Fm) ratio, ratio between Chl. a & b, and ratio between total Chl. and Carotenoid, Stomatal Conductance, Transpiration rate, Photosynthetically Active Radiation and Leaf temperature, was found in 50% shade plant and minimum was recorded under 100% shade (*Fig. 1 A-F*). The higher Fv/Fm ratio noted in 50% shade grape plant exhibited the facts that these plants were less stress by the high level of light intensity than those grown in full sun light. Sethar et al. (2002) supported this view indicating Fv/Fm ratio decreases significantly when plant were exposed to the heat stress. The plants grown in full sun or higher irradiation and 100% shade decreased value of Fv/Fm ratio is an indication of the damage of a proportion of a PSII reaction centres this phenomenon called photo-inhibition. Light energy is essential for photosynthesis which is necessary for the plant life. However the excess light can inhibit photosynthesis and lead to photo-oxidative damage of photosynthetic apparatus, thereby reducing the photosynthetic rate of the plant growing in direct sun light (Li et al., 2010). According to Fahl et al. (1994) and Ramalho et al. (2000), the greater value of Fv/Fm observed in shaded leaves might be connected with higher leaf nitrogen contents. Observations recorded by Wang et al. (2017) are also in the agreement to the present results. They found important effect on Light intensity had significant influence on stomatal conductance, transpiration rate and leaf photosynthetic rate, light compensation point and light saturation point (Bellasio and Griffiths, 2014; Li et al., 2007; Ubierna et al., 2013). Therefore, the study of light stress, especially weak light stress, has important practical significance for the maize production.

http://www.aloki.hu ● ISSN 1589 1623 (Print) ● ISSN 1785 0037 (Online)
DOI: http://dx.doi.org/10.15666/aeer/1704_88478864

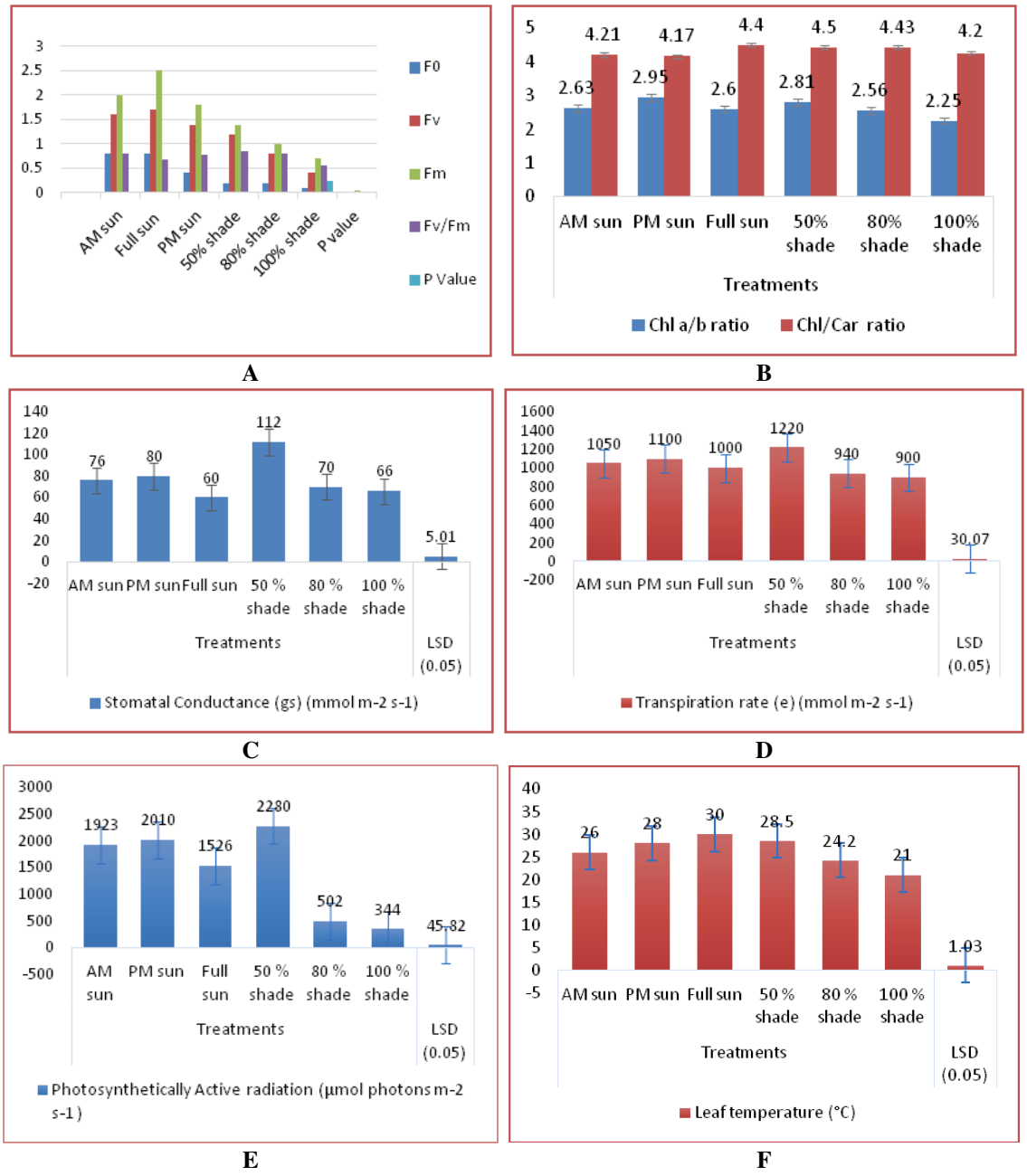

Figure 1. A *Relative level of fluorescence emitted as minimal fluorescence (F0), variable fluorescence (Fv) and the ratio of variable to maximum fluorescence (Fv/Fm) in sun and shaded grapes.* ***B*** *Chlorophyll a/b ratio and total chlorophyll/carotenoid ratio.* ***C*** *Stomatal conductance.* ***D*** *Transpiration rate.* ***E*** *Photosynthetically active radiation.* ***F*** *The leaf temperature of grapes plant under the influence of sun and shade environment*

Ascorbic acid (vitamin C), total sugar, dietary fibre, protein and carbohydrates contents in the fruits of grape plant grown in different sun and shade treatments (AM sun, PM sun, Full sun, 50%, 80% and 100% shades) were found in ranged between 2.0-2.85 mg/100 ml, 13.30-20.04 g/100 g, 0.8-1.94 g/100 g, 0.61-0.80 g/100 g and 17.72-22.0 g/100 g, respectively. The maximum Ascorbic acid, sugar, Protein and Carbohydrates were noted in 50% shade and minimum in 100% shade, while the dietary fibre was

http://www.aloki.hu ● ISSN 1589 1623 (Print) ● ISSN 1785 0037 (Online)
DOI: http://dx.doi.org/10.15666/aeer/1704_88478864

highest in 100% shade and minimum was in full sun treatment (*Table 6*). Topuz-Ozdemir (2007) stated that the vitamin C/ Ascorbic acid content in pepper was affected by cultural practices (genotype and agronomic technique) and on the other hand by the abiotic factors (light and temperature) as stated by López-Marín et al. (2011). Vitamin C development in grapes is connected to glucose metabolism and light induction similarly concentrations of both vitamin C and reducing sugars typically increase as the fruit matures. The similar observation was also noted by other researcher (Ilić, 2017). Mashabela et al. (2015) reported that fruits produced in the pearl nets contain more ascorbic acid at harvest and retain more of it after postharvest storage, perhaps through delayed ripening. Moisture contents and total soluble solids in different sun and shade treated plants were found to range between 73.01-83.1% and 36.24-47.69%, respectively (*Fig. 2*). Statistical analysis indicated that all the examined nutritional variables showed significant variation between the 6 sun and shade treatments at 0.05 significance level (*Table 6*). The highest total carbohydrates was also noted by Miller et al. (2015) in partial shaded apple plant with respect to the full sun and complete shade plant. The highest moisture contents was noted in 100% shade fruits and minimum in full sun, while maximum TSS was recorded in 50% shade and minimum was in full sun (*Fig. 2*). The observations recorded by Ilić (2017) are in contradiction to our findings. He found highest level of TSS (8.03%) in pepper fruits grown in open field.

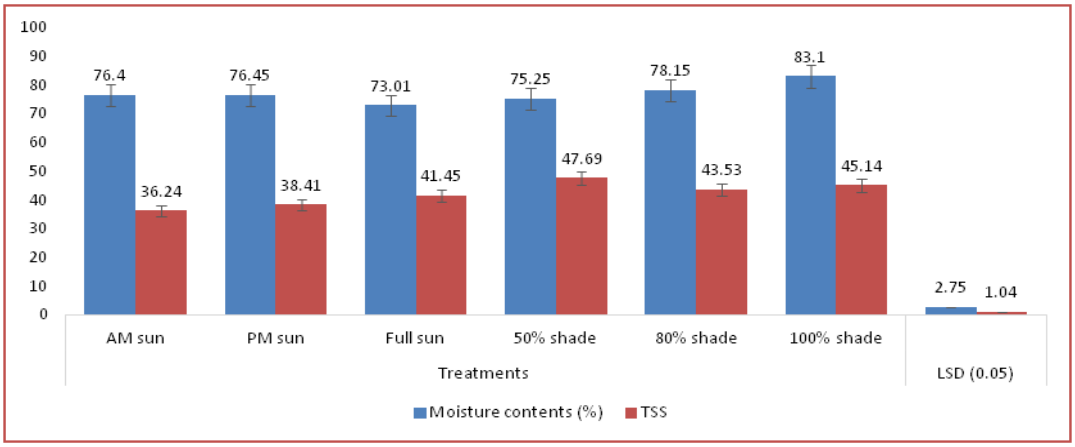

Figure 2. *Moisture contents and TSS (%) in grapes fruits grown in six different sun and shade treatments*

Tables 6. *Variation in nutritional contents in the grape fruits under sun and shade treatments*

Variables	Treatments						LSD (0.05)
	AM sun	PM sun	Full sun	50% shade	80% shade	100% shade	
Ascorbic acid/ Vit. C (mg/100ml)	2.23	2.25	2.41	2.85	2.30	2.0	0.03
Total Sugar (g/100g)	18.2	18.6	19.3	20.1	15.7	13.3	0.22
Dietary Fibre (g/100g)	1.00	1.02	0.8	0.90	1.5	1.94	0.03
Protein (g/100g)	0.73	0.76	0.70	0.80	0.65	0.61	0.02
Carbohydrates (g/100g)	20.3	20.5	20.0	22.0	19.4	17.7	0.02

Each value is the mean of three replicates and Vit; Vitamin

http://www.aloki.hu ● ISSN 1589 1623 (Print) ● ISSN 1785 0037 (Online)
DOI: http://dx.doi.org/10.15666/aeer/1704_88478864

Mineral contents (calcium, iron, magnesium, manganese, phosphorous, potassium, sodium, zinc and Fe) in different sun and shade treatments (AM sun, PM sun, Full sun, 50%, 80% and 100% shades) plants were found varied between 5.1-12.8, 0.21-0.41, 6.2-9.4, 0.061-0.095, 14.04-22.2, 171-199, 1.12-2.7, 0.08-0.09 and 0.095-0.65 mg/100 g, respectively. Almost all the investigated mineral contents was found highest in 50% shade treatment and minimum was recorded in 100% shade and Zinc was found almost similar in all the treatments. Statistical analysis indicated that except zinc all the other mineral were found significantly different in sun and shade treatments and on the other hand Zinc was found non-significant between the treatments at 0.05 significance level (*Table 7*). Morais et al. (2006) showed that shading enhances coffee quality, in terms of biochemical composition, including the contents of caffeine, oil and chlorogenic acid. Vitamins including B6, E and K in grapes fruits under the influence of sun and shade treatments (AM sun, PM sun, Full sun, 50%, 80% and 100% shades) were found in the ranged of 0.04-0.183 mg/100 g, 0.42-1.8 mg/100 g and 7.1-17.2 µg/100 g, respectively. Enhanced vitamin concentration was recorded in grapes grown under 50% shade and minimum in the 100% shade fruits. Significant test indicated that all vitamins showed statistically significant variations among the treatments at 0.05 significance level (*Table 8*). Variation in vitamin contents in grapes fruits might be due to environmental factor.

Table 7. *Variation in minerals contents (mg/100 g) in grape fruits under the influence of sun and shade treatments*

Variables	Treatments						LSD (0.05)
	AM sun	PM sun	Full sun	50% shade	80% shade	100% shade	
Calcium	10.0	11.5	12.0	12.8	8.3	5.1	0.03
Iron	0.37	0.37	0.35	0.41	0.29	0.21	0.03
Magnesium	8.4	8.5	8.4	9.4	7.0	6.2	0.05
Manganese	0.079	0.08	0.084	0.095	0.072	0.061	0.02
Phosphorus	21	20	19.0	22.2	16.0	14.04	0.07
Potassium	192	195	190	199	183	171	1.06
Sodium	2.0	2.0	1.94	2.7	1.54	1.12	0.01
Zinc	0.08	0.08	0.09	0.08	0.08	0.08	Ns
Fe	0.605	0.61	0.648	0.651	0.170	0.095	0.031

Each value is the mean of three replicates

Table 8. *Variation in vitamins contents in grapes fruits under the influence of sun and shade environments*

Variables	Treatments						LSD (0.05)
	AM sun	PM sun	Full sun	50% shade	80% shade	100% shade	
Vitamin B6 (mg/100g)	0.08	0.092	0.08	0.183	0.061	0.04	0.02
Vitamin E (mg/100g)	1.0	1.3	0.92	1.8	0.81	0.42	0.12
Vitamin K (µg /100g)	16.0	16.8	16.5	17.2	10.4	7.71	0.23

Each value is the mean of three replicates

http://www.aloki.hu ● ISSN 1589 1623 (Print) ● ISSN 1785 0037 (Online)
DOI: http://dx.doi.org/10.15666/aeer/1704_88478864

Fruit quality assessment (FQA)

Fruit quality Assessment (FQA) through fruit performance index (FPI) and evaluation classes indicated that the grape plant grown under 50% shade score highest grade point (5) and stand in very good category/class, which followed by AM Sun and PM sun plants with obtaining grade point (3) and fall in moderate categories, while plants of 80 and 100% shade treatment scored lowest grade points (2 and 1) falling in poor and very poor classes, respectively (*Table 9* and *10*). Many other researchers also reported best fruit quality grown under moderate shade as compared to the full sun and completely shaded plants (Stamps, 2009; Ilić et al., 2012, 2015; Morais et al., 2006). Several studies have demonstrated improvement in fruit quality and an increase in commercial fruit production due to the use of colored shading screens (Stamps, 2009; Ilić et al., 2012, 2015). Further, Morais et al. (2006) designated that the quality and size of coffee beans, and the taste of ripened beans were better under shade than in arrangements without shade trees.

Table 9. *Standard of grade point for quality (Prajapati and Tripathi, 2008; Govindaraju et al., 2012; Leghari et al., 2019)*

Valuation classes	Scoring percentage	Grade point
Not recommended	30	0
Very poor	31-40	1
Poor	41-50	2
Moderate	51-60	3
Good	61-70	4
Very good	71-80	5
Excellent	81-90	6
Best	91-100	7

Table 10. *Assessment of grapes fruits according to their quality under sun and shade environmental treatments*

Treatments	Fruit qualities variables								Total plus (+)	Score %	Grade point	Valuation classes
	Raw quality					Liquor quality						
	Shape and make	Color and odor	Size	No. fruit/plant	Obtain scores/20	Acidity	Flavor and taste	Obtain scores/12				
Scale	1-5	1-5	1-5	1-5		1-6	1-6					
AM sun	+++	+++	+++	++++	13	+++	+++	6	19	59.4	3	Moderate
PM sun	+++	+++	+++	++++	13	+++	+++	6	19	59.4	3	Moderate
Full sun	++	++	++	+++	9	+++	+++	6	15	46.9	2	Poor
50% shade	++++	++++	+++	+++++	16	++++	++++	8	24	75.0	5	Very good
80% shade	++	++	+++	++	9	++	++	4	13	40.6	2	Poor
100% shade	++	++	+++	+	8	+	+	2	10	31.3	1	Very poor

http://www.aloki.hu ● ISSN 1589 1623 (Print) ● ISSN 1785 0037 (Online)
DOI: http://dx.doi.org/10.15666/aeer/1704_88478864

Conclusion

The study concludes that grape plants grown in the 50% shade had higher biochemical and physiological potential as compared to the grape plants grown in direct sun light or under 80 and 100% shade. 50% shade grown grapes plants also produce larger, heavier and healthier fruits with better quality. Growing grapes under 50% shade trees would allow other sources of income such as fruits, fuel wood and timber to be produced, it could be socially more acceptable, economically more viable and environmentally more sustainable. We therefore recommended growing grapes under 50% shade. In addition, 50% shade plants serve as an alternative source of income for grapes producers. Nevertheless, highest yields per hectare can be obtained from grapes plants under 50%shade indicating the need for further research on determining proper plant density and the mechanism involved in all enhanced growth and physiological characteristics. On the basis of above facts and figures we support the recommendations of growing grapes under 50% shade and suggest that the future research should be directed toward deterring the development of fungal diseases and increase of grape yield under shaded conditions.

REFERENCES

[1] Ahemd, H. A., Al-Faraj, A. A., Abdel-Ghany, A. M. (2016): Shading greenhouses to improve the microclimate, energy and water saving in hot regions: a review. – Scientia Horticulturae 201: 36-45.

[2] Aleid, S. M., Hassan, B. H., Almaiman, S. A., Al-Kahtani, S. H., Ismail, S. M. (2014): Microbial loads and physicochemical characteristics of fruits from four Saudi date palm tree cultivars: conformity with applicable date standards. – Food and Nutrition Sciences 5(04): 316.

[3] Alkalai-Tuvia, S., Goren, A., Perzelan, Y., Weinberg, T., Fallik, E. (2014): The influence of colored shade nets on pepper quality after harvest-a possible mode-of-action. – Agriculture and Forestry 60: 7-18.

[4] AOAC (1984): Official Methods of Analysis. 4th Ed. – Association of Official Analytical Chemists, Washington, DC.

[5] AOAC (Association of Official Analytical Chemists) (1995): Official Methods of Analysis of AOAC International, 16th Ed. – AOAC International, Gaithersburg, MD.

[6] Bellasio, C., Griffiths, H. (2014): The operation of two decarboxylases, transamination, and partitioning of C4 metabolic processes between mesophyll and bundle sheath cells allows light capture to be balanced for the maize C4 pathway. – Plant Physiology 164(1): 466-480.

[7] Beis, A., Patakas, A. (2015): Differential physiological and biochemical responses to drought in grapevines subjected to partial root drying and deficit irrigation. – European Journal of Agronomy 62: 90-97.

[8] Bote, A. D., Struik, P. C. (2011): Effects of shade on growth, production and quality of coffee (*Coffea arabica*) in Ethiopia. – Journal of Horticulture and Forestry 3(11): 336-341.

[9] Campanha, M. M., Silva, R. H., Freitas, G. B., Martinez, H. E., Gracia, S. L., Fing, F. L. (2005): Growth and yield of coffee plants in agroforestry and monoculture systems in Minas Gerais, Brazil. – Agroforestry Syst 63(1): 75-82.

[10] Chau, C. F., Huang, Y. L. (2003): Comparison of the chemical composition and physicochemical properties of different fibers prepared from the peel of Citrus sinensis L. Cv. Liucheng. – Journal of Agricultural and Food Chemistry 51: 2615-2618.

http://www.aloki.hu ● ISSN 1589 1623 (Print) ● ISSN 1785 0037 (Online)
DOI: http://dx.doi.org/10.15666/aeer/1704_88478864

[11] Díaz-Pérez, J. C. (2014): Bell pepper (*Capsicum annuum* L.) crop as affected by shade level: fruit yield, quality, and postharvest attributes, and incidence of phytophthora blight (caused by *Phytophtora capsici* Leon.). – Journal of Horticultural Science 49: 891-900.
[12] Fahl, J. I., Carelli, M. C., Vega, J., Magalhaes, A. C. (1994): Nitrogen and irradiance levels affecting net photosynthesis and growth of young coffee plants (*Coffea arabica* L.). – Journal of Horticultural Science 69: 161-169.
[13] Fallik, E., Alkalai-Tuvia, S., Perzelan, Y., Aharon, Z., Elmann, A., Offir, Y., Matan, E., Yehezkel, H., Ratner, K., Zur, N., Shahak, Y. (2009): Can colored shade nets maintain sweet pepper quality during storage and marketing. – Acta Horticulturae 830: 37-44. https://doi.org/10.17660/ActaHortic.2009.830.3.
[14] Ghaderi, S., Ramesh, B., Seifalian, A. M. (2011): Fluorescence nanoparticles "quantum dots" as drug delivery system and their toxicity: a review. – Journal of drug targeting 19(7): 475-486.
[15] Ilić, Z. S., Fallik, E. (2017): Light quality manipulation improves vegetable quality at harvest and postharvest: a review. – Environmental and Experimental Botany 139: 79-90.
[16] Ilić, Z. S., Milenkovic, L., Durovka, M., Kapoulas, N. (2011): The effect of color shade nets on the greenhouse climate and pepper yield. – 46th Croatian Symposium of Agricuture, Opatija, Croatia, pp. 529-533.
[17] Ilić, Z. S., Milenković, L., Stanojević, L., Cvetković, D., Fallik, E. (2012): Effects of the modification of light intensity by color shade nets on yield and quality of tomato fruits. – Scientia Horticulturae 139: 90-95.
[18] Ilić, S. Z., Milenković, L., Šunić, L., Cvetković, D., Fallik, E. (2015): Effect of colored shade-nets on plant leaf parameters and tomato fruit quality. – Journal of Science Food and Agriculture 95: 2660-2667.
[19] Isam Eldin, H. E., Mohamed, A. M., Gad-Elkareem, Noh., Elnoor, A. A., Adam Omer, E. A., Alghamdi, Ahmed, M. A. (2017): Comparison of two methods for the determination of vitamin C (ascorbic acid) in some fruits. – American Journal of Chemistry 2(1): 1-7.
[20] Jeong, K. Y., Pasian, C. C., McMahon, M., Tay, D. (2009): Growth of six Begonia species under shading. – The Open Horticulture Journal 2: 22-28.
[21] Johnson, G. R., Cartwright, C. (2005): Genotype × shade effects for western hemlock. – Canadian Journal of Forest Research 35(6): 1496-1501.
[22] Kong, Y., Avraham, L., Perzelan, Y., Alkalai-Tuvia, S., Ratner, K., Shahak, Y., Fallik, E. (2013): Pearl netting affects postharvest quality fruit in 'Vergasa' sweet pepper via light environment manipulation-Scientia. – Horticulturae 150: 290-298. https://doi.org/10.1016/j.scienta.2012.11.029.
[23] Langemeier, J. M., Rogers, D. E. (1995): Rapid method for sugar analysis of doughs and baked products. – Cereal Chemistry 72(4): 349-351.
[24] Laurey, C. (1997): The Cauchy problem for a third order nonlinear Schrödinger equation - nonlinear analysis. – Theory, Methods and Applications 29(2): 121-158.
[25] Leghari, S. K., Zaidi, M. A. (2013): Effect of air pollution on the leaf morphology of common plant species of Quetta City. – Pakistan Journal of Botany 45(S1): 447-454.
[26] Leghari, S. K., Zaid, M. A., Sarangzai¸ A. M. Faheem, M., Shawani, G. R., Ali, W. (2014): Effect of Road Side Dust Pollution on the growth and total chlorophyll contents in *Vitis vinifera* L. (grape). – African Journal of Biotechnology 13(11): 1237-1242.
[27] Leghari, S. K., Akbar, A., Qasim, S., Sami Ullah, Asrar, M., Rohail, H., Ahmed, S., Mehmood, K., Ali, I. (2019): Estimating anticipated performance index and air pollution tolerance index of some trees and ornamental plant species for the construction of green belts. – Polish Journal Environmental Study 28 (3): 1-11.
[28] Lichtenthaler, H. K. (1987): Chlorophylls and carotenoids: pigments of photosynthetic membranes. – Methods in Enzymology 148: 350-382. https://doi.org/10.1016/0076-6879(87)48036-1.

http://www.aloki.hu ● ISSN 1589 1623 (Print) ● ISSN 1785 0037 (Online)
DOI: http://dx.doi.org/10.15666/aeer/1704_88478864

[29] Li, C., Heidt, D. G., Dalerba, P., Burant, C. F., Zhang, L., Adsay, V., Wicha, M., Clarke, M. F., Simeone, D. M. (2007): Identification of pancreatic cancer stem cells. – Cancer Research 67(3): 1030-1037.
[30] Li, H., Yong, Y., Li, B., Jing, R., Lu, C., Li, Z. (2010): Genetic analysis of tolerance to photo-oxidative stress induced by high light in winter wheat (*Triticum aestivum* L.). – Journal of Genet. Genom 37(6): 399-412.
[31] Li, Y., Douglas, A. J., Yongzhong, S. U., Jianyuan, C. I., Tonghui, Z. (2005): Specific leaf area and leaf dry matter content of plants growing in sand dunes. – Bot. Bull. Acad. Sinica. 46: 127-134.
[32] López-Marín, J., González, A., Gálvez, A. (2011): Effect of shade on quality of greenhouse peppers. – Acta Horticulturae 893: 895-900. https://doi.org/10.17660/ActaHortic.2011.893.99.
[33] Mashabela, M. N., Selahle, K. M., Soundy, P., Crosby, K. M., Sivakumar, D. (2015): Bioactive compounds and fruit quality of green sweet pepper grown under different colored shade netting during postharvest storage. – Journal of Food Science 80: 2612-2618. https://doi.org/10.1111/1750 3841.13103.
[34] McNaughton, K. G., Jarvis, P. G. (1983): Predicting effects of vegetation changes on transpiration and evaporation. – Water Deficits and Plant Growth 7: 1-47.
[35] Milenković, L., Ilić, S. Z., Đurovka, M., Kapoulas, N., Mirecki. N., Fallik, E. (2012): Yield and pepper quality as affected by light intensity using color shade nets. – Agriculture and Forestry 58: 19-23.
[36] Miller, S. S., Hott, C., Tworkoski, T. (2015): Shade effects on growth, flowering and fruit of apple. – Journal of Applied Horticulture 17(2): 101-105.
[37] Morais, H., Caramori, P., Ribeiro, A. M., Gomes, J. C., Koguishi, M. S. (2006): Microclimatic characterization and productivity of coffee plants grown under shade of pigeon pea in Southern Brazil. – Pesq. Agropec. Bras. 41(5): 763-770.
[38] Muschler, R. G. (2001): Shade improves coffee quality in a sub-optimal coffee-zone of Costa Rica. – Agroforestry Systems 51(2): 131-139.
[39] Oliveira, P. B., Oliveira, C. M., Monteiro, A. A. (2004): Pruning date and cane density affect primocane development and yield of 'autumn bliss' red raspberry. – J. Amer. Soc. Hort. Sci. Hortsciences 39(3): 520-524.
[40] Poorter, H., van der Werf, A. (1998): Is Inherent Variation in RGR Determined by LAR at Low Irradiance and by NAR at High Irradiance? A Review of Herbaceous Species. – In: Lambers, H. et al. (eds.) Inherent Variation in Plant Growth. Physiological Mechanisms and Ecological Consequences. Backhuys Publishers, Leiden, pp. 309-336.
[41] Poni, S., Merli, M. C., Magnanini, E., Galbignani, M., Bernizzoni, F., Vercesi, A., Gatti, M. (2014): An improved multichamber gas exchange system for determining whole-canopy water-use efficiency in grapevine. – American Journal of Enology and Viticulture 65(2): 268-276.
[42] Prajapati, S. K., Tripathi, B. D. (2008): Anticipated performance index 1 of some tree species considered for green belt development in and around an urban area: a case study of Varaasi city, India. – Journal of Environmental Management 88: 1343.
[43] Prosky, L., Asp, N. G., Schweitzer, T. F., DeVries, W. J., Furda, I. (1988): Determination of insoluble, soluble and total dietary fiber in foods and food products: interlaboratory study. – Journal of the Association of Official Analytical Chemists 71: 1017-1024.
[44] Ramalho, J. C., Pons, T. L., Groeneveld, H. W., Azinheira, H. G., Nunes, M. A. (2000): Photosynthetic acclimation of high light conditions in mature leaves of Coffea arabica L.: role of xanthophylls, quenching mechanisms and nitrogen nutrition. – Aust. J. Plant Physiol. 27(1): 43-51.
[45] Robakowski, P., Montpied, P., Dreyer, E. (2003): Plasticity of morphological and physiological traits in response to different levels of irradiance in seedlings of silver fir (*Abies alba* Mill). – Trees 17(5): 431-441.

http://www.aloki.hu ● ISSN 1589 1623 (Print) ● ISSN 1785 0037 (Online)
DOI: http://dx.doi.org/10.15666/aeer/1704_88478864

[46] Rom, C. R. (1991): Light thresholds for apple tree canopy growth and development. – HortScience 26: 989-992.
[47] Romero, J. G., Ortega, R. (2015): Two globally convergent adaptive speed observers for mechanical systems. – Automatica 60: 7-11.
[48] Santana, J. Q., Balbino, M. A., Tavares, T. R., Bezerra, R. S., Farias, J. G., Ferreira, R. C. (2012): Effect of photo selective screens in the development and productivity of red and yellow sweet pepper. – Acta Horticulturae 956: 493-500. https://doi.org/10.17660/ActaHortic.2012.956.58.
[49] Selahle, K. M., Sivakumar, D., Jifon, J., Soundy, P. (2015): Postharvest responses of red and yellow sweet peppers grown under photo-selective nets. – Food Chemistry 173: 951-956.
[50] Sethar, M. A., Pahoja, V. M., Chachar, Q. (2002): Photosynthetic acclimation of cotton genotypes at higher temperatures. – Asian Journal of Plant Sciences 1: 261-263.
[51] Siebert, S. F. (2002): From shade- to sun-grown perennial crops in Sulawesi, Indonesia: implications for biodiversity conservation and soil fertility. – Biodivers. Conserve 11(11): 1889-1902.
[52] Sowbhagya, H. B., Suma, F. P., Mahadevamma, S., Tharanathan, R. N. (2007): Spent residue from cumin - a potential source of dietary fiber. – Food Chemistry 104(3): 1220-1225.
[53] Stamps, R. H. (1994): Evapotranspiration and Nitrogen Leaching during Leatherleaf Fern Production in Shade Houses. – Florida Dept. Environ. Protection, Palatka, Florida.
[54] Stamps, R. H. (2009): Use of colored shade netting in horticulture. – Hort Science 44: 239-241. http://hortsci.ashspublications.org/content/44/2/239.full.
[55] Stanton, K. M. (2010): Light exposure and shade effects on growth, flowering, and leaf morphology of Spiraea alba du Roi and Spiraea tomentosa L. – Hortscience 45(12): 1912-1916.
[56] Topuz, A., Ozdemir, F. (2007): Assessment of carotenoids, capsaicinoids and ascorbic acid composition of some selected pepper cultivars (*Capsicum annuum* L.) grown in Turkey. – Journal of Food Composition and Analysis 20: 596-602. https://doi.org/10.1016/j.jfca.2007.03.007.
[57] Ubierna, N., Sun, W. E. I., Kramer, D. M., Cousins, A. B. (2013): The efficiency of C4 photosynthesis under low light conditions in Zea mays, Miscanthus x giganteus and Flaveria bidentis. – Plant, Cell and Environment 36(2): 365-381.
[58] Vaast, P., Van Kanten, R., Siles, P., Angrand, J., Aguilar, A., (2008): Biophysical Interactions between Timber Trees and Arabica Coffee in Suboptimal Conditions of Central America. – In: Jose, S., Gordon, A. M. (eds.) Toward Agroforestry Design. Springer, Dordrecht, pp. 133-146.
[59] Vendrame, W., Moore, K. K., Broschat, T. K. (2004): Interaction of light intensity and controlled release fertilization rate on growth and flowering of two New Guinea impatiens cultivars. – Hort. Technology 14: 491-495.
[60] Wang, J., Huang, H., Jia, S., Zhong, X., Li, F., Zhang, K., Shi, Z. (2017): Photosynthesis and Chlorophyll fluorescence reaction to different shade stresses of weak light sensitive maize. – Pakistan Journal of Botany 49(5): 1681-1688.
[61] Xiao, K., Yu, D., Wang, J. (2006): Habitat selection in spatially heterogeneous environments: a test of foraging behaviour in the clonal submerged macrophyte Vallisneria spiralis. – Freshwater Biology 51(8): 1552-1559.
[62] Zoran, S., Ilić, Milenković,1 L., Šunić, L., Barać, S., Mastilović, J., Kevrešan, Ž., Fallik, E. (2017): Effect of shading by colored nets on yield and fruit quality of sweet pepper. – Zemdirbyste-Agriculture 104(1): 53-62.

http://www.aloki.hu ● ISSN 1589 1623 (Print) ● ISSN 1785 0037 (Online)
DOI: http://dx.doi.org/10.15666/aeer/1704_88478864

IMPACT OF BIOCHAR AND ANIMAL MANURE ON SOME BIOLOGICAL AND CHEMICAL PROPERTIES OF SOIL

IRMAK YILMAZ, F.* – ERGUN, Y. A.

Department of Soil Science and Plant Nutrition, Faculty of Agriculture, Ordu University, Ordu, Turkey

**Corresponding author*
e-mail: fundairmak@hotmail.com; phone: +90-452-234-5010; fax: +90-452-226-5269

(Received 15th Mar 2019; accepted 24th May 2019)

Abstract. The aim of this study was to show the relationship between tomato plants grown in soil in different doses of animal manure (AM) and biochar (BC) obtained from hazelnut shell with some soil enzymes, C mineralization, microbial biomass and other soil properties. In this context, 0-5-10-15-20 ton/ha biochar (BC) obtained from hazelnut shell and 5-10-20 ton/ha mature animal manure were applied into the soil. The study repeating 6 times was performed in natural conditions of greenhouse according to the study design of random parcels. Some chemical soil properties (organic material, total N, available P and K) and some soil enzymes of tomato (Lycopersicum esculentum Mill) plant grown in biochar and animal manure applied-soil (dehydrogenase, urease, arylsulfatase and alkaline phosphatase) were identified. Biochar and animal manure applications increased dehydrogenase, urease and arylsulfatase enzyme activities of the soil and it was statistically significant ($p < 0.01$). The activity of alkaline phosphatase enzyme increased but and it was not statistically significant. The biological analyses of the soil showed that the most effective dose varies in each parameter, but it was identified that $BC_5 + AM_5$, $BC_{15} + AM_5$, BC_{20} and AM_{20} doses increased the biological properties. The study showed that biochar and animal manure applications increased the organic material contents of soil and the available macro contents including nitrogen (N), phosphor (P) and potassium (K).
Keywords: *animal manure, nutrition element, biochar, enzyme activity, microbial activity, organic material*

Introduction

The human population increases with a geometric array, and the food demand also rises inevitably at the same speed. The effort to meet the food demand as fast as possible has led to the introduction of a wide range of chemical inputs into the agricultural production processes. Types of chemical manure are a factor accelerating production significantly, however, the destructive aspect for the environment and human health has become a disadvantage in the long term, and the scientists are looking for solutions. Accordingly; organic soil regulators which are compatible with nature, also beneficial for the environment and human health, yielding effective results in agricultural applications in a narrow field, aiming to minimize the use of chemical manure with the same productive capacity for animal and plant production are evaluated. The important preventive measures for food crisis that threatens the future of human life include increasing the amount of organic material in agricultural soils and the use of agricultural methods for the protection, preservation and maintenance of suitable environment for soil organisms. The use of organic manure instead of the chemical manure in organic agriculture helps to increase soil organic materials and microbiological activity. The aim of organic agriculture is to protect the health of the plant, environment, human and animal without causing water, soil and air pollution (Kızılaslan and Olgun, 2012). Besides the natural manuring system, some side products have been tested to improve quality; the most commonly used herbal and woody wastes among these side products are also

http://www.aloki.hu ● ISSN 1589 1623 (Print) ● ISSN 1785 0037 (Online)
DOI: http://dx.doi.org/10.15666/aeer/1704_88658876

preferred to be burnt on agricultural soil for reversible soil recovery without environmental pollution. The aim of this application is to provide available plant nutrition elements and to eliminate environmental pollution caused by woody side products of the residues in agricultural soils by pyrolysis method. The new product containing high carbon and mineral material obtained as a result of pyrolysis of organic substances in the oxygen-free environment or gasification by reduced oxygen is called biochar (Lehmann, 2007), and based on its history, it has been used to support organic manures, and to increase productivity in agricultural soils effectively. Pioneering research on the above-mentioned organic soil regulator were performed for seedling cultivation (Retan, 1915) and soil chemistry (Tyron, 1948). Much earlier than the those researches, waste biomass charcoal was used as a manure in an application carried out in China (Liebig, 1878). Biochar-based researches have been remarkably increased in Japan starting from the first quarter of the 80s (Kishimoto and Sugiura, 1980). Despite of all these researches, global interest in biochar was especially rised in the second quarter of the 2000s, but recognized recently in Turkey. When a biochar rich in organic carbon is burnt, an ash consisting of Ca, Mg and inorganic carbonate is obtained. This high-carbon organic regulator is defined as an aromatic material consisting of six chains of carbon atoms connected to each other without oxygen and hydrogen. Carbon atoms connected to each other without oxygen and hydrogen is considered as advantageous due to absence of more atoms in organic material (Roberts et al., 2009). The highest quality criteria for Biochar includes: high cation exchange capacity, adsorption and low portability of components (Glaser et al., 2002; Liang et al., 2006; McClellan et al., 2007; McLaughlin et al., 2009). The research was conducted to evaluate whether the hazelnut shell without commercial value could be used for other purposes except for fuel in the study region (Central and East Black Sea Region). The aim of the research is to show the relationship between tomato plants grown in soil in different doses of animal manure (AG) and biochar (BC) obtained from hazelnut shell with some soil enzymes, C mineralization, microbial biomass and other soil properties.

Material and method

Study area

The experiment was carried out in the high tunnel greenhouse established in Ordu University experiment area. The study area is located in Ordu province, Altınordu district, Eastern Black Sea Region, Turkey in 2016. The province of Ordu is located between the northern latitudes of 4464031-4551905 with eastern longitudes of 304670-420033 (*Fig. 1*).

Figure 1. *Map shows the location of Ordu University experiment area in the Ordu Province, Turkey*

http://www.aloki.hu ● ISSN 1589 1623 (Print) ● ISSN 1785 0037 (Online)
DOI: http://dx.doi.org/10.15666/aeer/1704_88658876

Materials and methods

In the study performed under the conditions of the greenhouse, soil with clayey texture from a depth of 0-30 was used. As an organic material, the hazelnut shell of Ordu has been transformed into biochar. Production temperature for biochar production is 380 °C; the production time is 270 min (*Fig. 2*). The production continued until the end of the gas outlet, including flammable gases from the system. The mature animal manure was obtained from the farmer in Ordu province Mesudiye district. Alsancak tomato seedling was used as a plant material. Before the experiment was established, some basic physical and chemical analyses of the soil sample were performed (*Table 1.*)

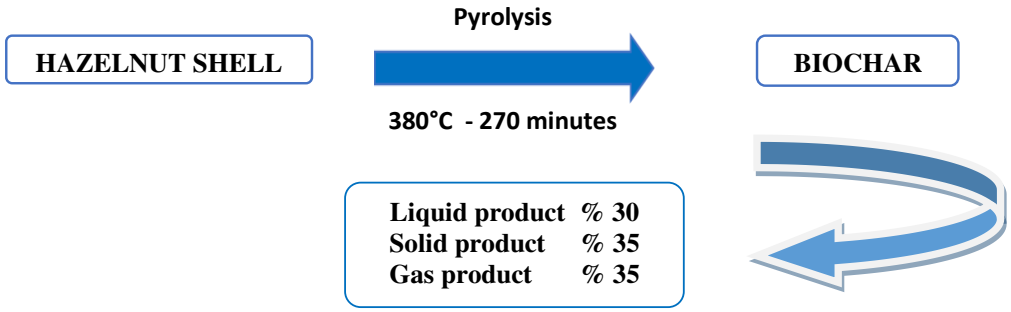

Figure 2. *Biochar pyrolysis process obtained from hazelnut shell (Ronsse et al., 2013)*

Pyrolysis

The process results in the formation of three main products: carbon-rich solid product (biochar), a volatile matter which can further be partially condensed to liquid phase (bio-oil), and the remaining so-called "non-condensable" gases, like CO, CO_2, CH_4, and H_2 (Kambo and Dutta, 2015).

The soil used in the experiment had a clayey structure, having pH value of (6.46) mild acid without saltiness problem. The level of organic material was 1.8%, total N content was 0.045%, P content was 6.7 mg kg^{-1} and K content was 57.1 mg kg^{-1}.

Mature animal manure and biochar, used as organic material, are materials of organic origin, and their properties complement each other. Some chemical and physical properties belonging to the burnt animal manure and biochar used in the experiment is presented in *Table 1*.

Table 1. *Some physical and chemical properties of the soil used in the experiment and biochemical and vermicompost properties*

Material	O.M (%)	C (%)	N (%)	pH	K (mg kg^{-1})	P (mg kg^{-1})	Mg (mg kg^{-1})	Fe (mg kg^{-1})
Soil	1.8	-	0.045	6.46	57.1	6.7	120	8.6
AM		26.4	1.32	7.6	1.24	1.12	-	-
BC		81	1.17	9.24	0.33	-	1690	10.4

Experimental design

In the research, 2 mm grated 2 different organic material (biochar and animal manure) 0-5-10-15-20 ton/ha hazelnut biochar and 5-10-20 ton/ha mature animal

http://www.aloki.hu ● ISSN 1589 1623 (Print) ● ISSN 1785 0037 (Online)
DOI: http://dx.doi.org/10.15666/aeer/1704_88658876

manure doses were used proportionately 6 times according to the study design of random parcels in natural conditions of greenhouse (*Table 2*). In addition, % AM and % BC doses were applied to see the effects alone. After the mixtures were prepared and filled separately in the air dry 3 kg soil flowerpots, they were kept for 24 h in order to stabilize the internal dynamics in the medium. At the end of 24 h, Alsancak tomato seedlings, which is used as a plant material, were planted as 1 seedling per flowerpot. During planting, K_2HPO_4 100 ppm K/pot and 125 ppm P/pot and 100 ppm N/pot manures as $Ca(NO_3)_2$ form were applied as a basic manuring. After this process, all flowerpots are irrigated. Irrigation is performed periodically according to weather conditions and soil humidity. Watering was conducted according to plant water demand. The average temperature during the trial is 22.7 °C degrees. At the end of 1 week, regularly inspected and irrigated plants have begun to grown, each seedling was observed until the flowering period. Plants were harvested during flowering period.

Table 2. *Potted trial applications*

Mediums	
C	Control
(BC_5 + AM_5)	10 gr BC – 10 gr AM
(BC_5 + AM_{10})	10 gr BC – 20 gr AM
BC_{10} + AM_5	20 gr BC – 10 gr AM
(BC_{10} + AM_{10})	20 gr BC – 20 gr AM
(BC_{15} + AM_5)	30 gr BC – 10 gr AM
(BC_{15} + AM_{10})	30 gr BC – 20 gr AM
BC_{20}	40 gr BC
AM_{20}	40 gr AM

Soil physicochemical analyses

Soil samples 2 mm grated were waited and prepared for the analyses in +4 °C refrigerator immediately after, and biological analyses were initiated. To identify the properties of sample soil, the texture was examined by hydrometer method as told by Bouyoucos (1962), soil reaction (pH) and saltiness (EC) by U.S. Salinity Laboratory Staff (1954), organic material by Nelson and Sommers (1982), total nitrogen by Bremner (1965), useful phosphor by Olsen et al. (1954), useful potassium by Knudsen et al. (1982) as told by Müftüoğlu et al. (2012).

Soil biological analyses

For the biological analyses of the soil; CO_2 production was identified by the method told by Isermeyer (1952); microbial biomas-C by Anderson and Domsch (1978), dehydrogenase enzyme activity by Thalmann (1968), urease enzyme activity by Kandeler and Gerber (1988), alkalin phosphatase enzyme activity by Tabatabai and Bremner (1969), arylsulfatase enzyme activity by Tabatabai and Bremner (1970) as told by Schinner et al. (1996). For the organic materials in PH and EC 1:3 ratio organic material-pure water mixture in the study (Gabriels and Verdonck, 1992), organic material was burnt at 550 ± 25 °C for 4 h by the method of Kacar (2009); plant nutrition

http://www.aloki.hu ● ISSN 1589 1623 (Print) ● ISSN 1785 0037 (Online)
DOI: http://dx.doi.org/10.15666/aeer/1704_88658876

element analyses were performed in organic materials by the methods told by Kacar and Kütük (2010).

Statistical analysis

At the end of the study, the variance analysis of the obtained data was performed using the JMP package program and the important results were evaluated according to the LSD test.

Results and discussion

The effect of organic materials on some enzyme activity of the soils

Different doses of biochar and animal manure applications affected and increased the dehydrogenase enzyme activity in the soils favorably; it was found that application are statistically significant at level 1%, and dehydrogenase enzyme activity values of the soils were between 3.16-40.03 mg TPF/g.k.t. The lowest dehydrogenase activity value was in the control application the highest was in $BC_{10} + AM_5$ application (*Fig. 3a*). This application yielded 12.7 fold increase. When the applications into the soil were evaluated numerically, it was observed that the most effective applications were $BC_{10} + AM_5$, $BC_{10} + AM_{10}$, $BC_{15} + AM_5$ and $BC_{15} + AM_{10}$. Single BC_{20} and AM_{20} applications increased dehydrogenase enzyme activity values less than the application comparing BC and AM. The organic materials added to the application have been used as a source of nutrients and energy by microorganisms living in soil.

Paz-Ferreiro et al. declared that (2012) when biochar in different doses obtained from waste sludge is applied to the soil, it increases the activity by 2.8 times compared to the control, however, Park et al. declared that (2011) biochar obtained from the chicken manure increases the dehydrogenase enzyme activity when applied into the soil in increased doses.

The statistical evaluations showed that the effects of the applications on the urease enzyme activity are significant ($p < 0.01$). Biochar and animal manure applications increased urease enzyme activity in soil (0.28), the highest value was obtained for $BC_5 + AM_5$ and $BC_{15} + AM_5$ applications (0.90) (*Fig. 3b*). $BC_5 + AM_5$ and $BC_{15} + AM_5$ applications into the soil increased urease enzyme activity by 3.2 times compared to the control. Kablan (2005) declared that urea, as a substrate source of microorganisms producing urease enzyme, has increased with organic N forms, which are substrates of N content in different organic wastes. Since biochar has a wide C/N ratio, it is subjected to more fragmentation by microorganisms, resulting in the increase of these enzymes. Nannipieri et al. (1990) showed that the final process of urease, which is the organic phase of organic nitrogen mineralization in soil, is the separation of urea and the responsible enzyme is urease (Kablan, 2005). These enzymes are produced by soil microorganisms in order to break down their nutrient materials, then are kept by colloids such as clay and organic material of the soil, and can sustain their activities without being attached to the microorganism cell that produces these enzymes (Aşkın et al., 2004).

Akça and Namlı declared that (2015) after biochar is applied to the tomato plant, the urease enzyme activity is meaningfully and significantly increased by 5% as compared to the control and chemical manual. It was observed that urease enzyme activity of the soil has a significant relationship with important soil properties such as organic

http://www.aloki.hu ● ISSN 1589 1623 (Print) ● ISSN 1785 0037 (Online)
DOI: http://dx.doi.org/10.15666/aeer/1704_88658876

material, soil texture, pH cation exchange capacity, and that the organic wastes added to the soil significantly increase urease enzyme activity (Özdemir et al., 2000). The researches declared that when rapid weatherable organic materials are added into the soil, urease activity may be increased by the stimulation of microbial activity. Moreno et al. (1999) declared that when organic materials are added to the soil, the urease activity increases remarkably. On the contrary, Azam and Malik (1985) reported that organic materials did not affect the urease activity. Biochar and animal manure applications increased arylsulfatase enzyme activity in the soil; arylsulfatase enzyme activity values of the soils were 0.07-0.15 µg *P*- N g.k.t^{-1}. The lowest value was at control application, the highest was at $BC_5 + AG_5$ application; this application yielded 2.2 fold increases. Arylsulfatase enzyme has a key role in S cylce in terms of agricultural aspect. It acts as a catalyst for hydrolisation from assimilable organic S to the inorganic S by the plant, and allows the nutrition element required for plant development to be faster and easier in the inorganic form (Kayıkçıoğlu and Okur, 2013). In a study on tomato plant, the biochar obtained from the litter of poultry in different doses has been applied as an application, and enzyme activities were increased significantly with biochar applications (Akça and Namlı, 2015). In the experimental soils, tomato plant increased arylsulfatase enzyme activity as compared to the control (*Fig. 3c*). Because microbial activity increases in the presence of plant roots, increasing arylsulfatase enzyme activity (Kablan, 2005). Sun et al. (2014) reported that the addition of wood-originated biochar into the sandy agricultural soil does not increase the arylsulfatase enzyme activity too much; however, at the end of approximately 50 years, it contributes several enzymes of biological wastes such as arylsulfatase.

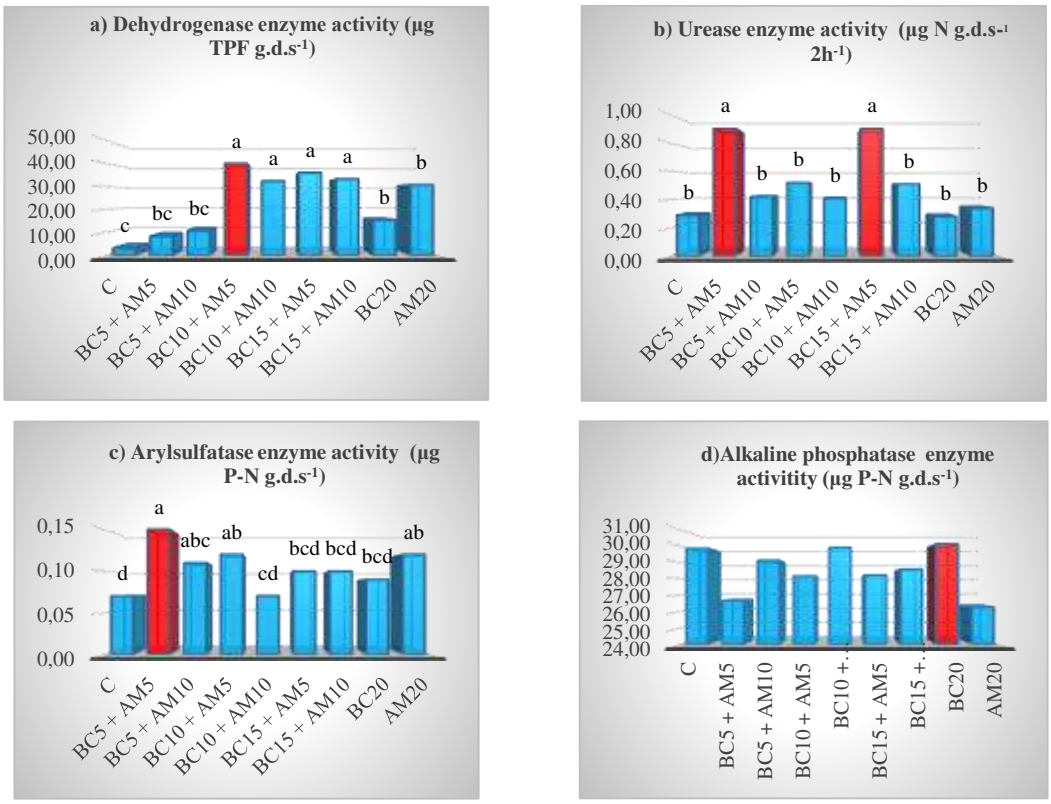

Figure 3. *The effects of biochar and animal manure applied soils on dehydrogenase (a), urease (b), arylsulfatase (c) and alkaline phosphatase (d) enzyme activities (g.d.s : gram dry soil)*

http://www.aloki.hu ● ISSN 1589 1623 (Print) ● ISSN 1785 0037 (Online)
DOI: http://dx.doi.org/10.15666/aeer/1704_88658876

The statistical evaluations showed that the effects of organic wastes on alkaline phosphatase enzyme activity are not significant. However, different doses of biochar and animal manure applications affected the alkaline phosphatase enzyme activity in the soil favorably, and increased numerically; alkaline phosphatase enzyme activity values were between 25.49 and 30.11 (μg *P*- N $g.k.t^{-1}$). The lowest value was at control application, the highest was at BC_{20} application; this application yielded 18% increase (*Fig. 3d*). Phosphor uptake by the plants is performed via the mineralization of the organic phosphor compounds into orthophosphate by phosphatase enzymes. Alkaline phosphotases are secreted only by microorganisms, several bacterial strains produce alkaline phosphotase enzyme (Okur, 1997). It was observed that phosphatase enzyme activity was statistically insignificant, and did not increase in the soils, because if phosphatase is inhibited, PO_4^{-3} synthesis is inhibited and, the formation of orthophosphate acid and alkaline phosphatase enzyme activity of organic phosphor compound is inhibited, meaning that phosphor mineralization is inhibited (Chunderova and Zubets, 1969).

The effect of organic materials on several chemical properties of soils

The effects of biochar and animal manure applications on the organic matter contents of soil are presented in *Table 3*. The statistical evaluations showed that the effects of biochar and animal manure on organic material are significant ($p < 0.05$). The different doses of biochar and animal manure applications increased the organic material content of the soil; the amount of the organic material was increased by 1.80-6.92% (*Table 3*). The lowest value was at control application, the highest was at $BC_{15} + AM_{10}$ application; this application yielded 3.84 fold increase in the organic materials. Mixing of these two materials (organic material and a material with high organic content) in the soil increased the amount of the organic materials in the soil, as expected. Demisie et al. (2014) reported in their study that when the biochar obtained from oak and bamboo is applied into soil, %C value increases between 50 and 286% as compared to the control soil. In agricultural production applications, optimal plant growth in the soil is associated with the physical and chemical indicators of the soil structure.

Analysis of variance for the properties showed that the difference between the mean of at least two groups was statistically significant. The difference between the means shown by the same letter is not significant in its own group.

The most used application to modulate the physical parameters of the soil and maintain its continuity is the addition of organic materials into the soil (Bender et al., 1998). Organic wastes modulate the properties of the soil structure, and provide plant nutrients such as P, K, Ca, Mg, Cu and Zn, especially N. When biochar obtained from poultry is applied to soil of the tomato plant, the value of organic material increases (Akça and Namlı, 2015). Çengel et al. (2009) reported in their study at the organic vineyard region in Manisa that the amount of organic material in the soil with neutral reaction is low; however, additive green manure increase the amount of organic material, and the amount of organic material may yield better results when supported with materials of organic origin. The effects of the application on total N have been found to be significant ($p < 0.01$). Different doses of biochar and animal manure applications increased the % total N amount of the soil; and total N values were between 0.10-0.17% (*Table 3*). The lowest value was at control application, the highest was at $BC_{10} + AM_5$ application; this application yielded 70% increase

http://www.aloki.hu ● ISSN 1589 1623 (Print) ● ISSN 1785 0037 (Online)
DOI: http://dx.doi.org/10.15666/aeer/1704_88658876

Table 3. *The effects of biochar and animal manure applications on the soils organic matter (%), total N, available P and extractable K contents*

Applications	Organic matter (%)	N (%)	P (mg/kg)	K (mg/kg)
Control	1.80 c	0.10 e	2.5d	315 d
$BC_5 + AM_5$	5.10 bc	0.14 bc	3.8 c	408 c
$BC_5 + AM_{10}$	6.07 ab	0.11 de	4.9 bc	373 c
$BC_{10} + AM_5$	6.39 ab	0.17 a	4.3 bc	408. c
$BC_{10} + AM_{10}$	5.72 ab	0.13 cd	4.5 bc	380 c
$BC_{15} + AM_5$	5.30 abc	0.15 ab	6.3 a	554 a
$BC_{15} + AM_{10}$	6.92 a	0.15 abc	4.2 bc	511ab
BC_{20}	6.68 ab	0.16 ab	5.4 ab	477 b
AM_{20}	5.82 ab	0.12 de	4.6 bc	385 c
	LSD ($p < 0.005$) 0.8149	LSD ($p < 0.001$) 0.01028	LSD ($p < 0.001$) 0.65162	LSD ($p < 0.001$) 27.4485

Besides, there has been an effective increase in a short time in test pots with biochar + animal manure. When pine biochar was added into the soil, the useful elements of the material such as N, P, K, Ca, Fe, Mn and Zn increased, biochar plus N application supported plant growth (Sohi et al., 2009; Van Zwieten et al., 2010).

Different doses of biochar and animal manure applications increased the amount of available P in the soil. The available P values are between 2.5-6.3 mg kg in the test soils. The lowest value was at control application, the highest was at $BC_{15} + AM_5$ application (*Table 3*); this application yielded 2,5 fold increase in total N values. This application yielded 1.13 unit increase of the soil pH. According to CFA (California Fertilizer Association, 1995), the highest pH range is 6-7.5 for available phosphor, and the phosphor values in the study were in line with this range. When biochar is applied to soil of the sugar cane, the amount of total phosphor and total dissolved phosphor increase (Alvares-Campos et al., 2018).

Different doses of biochar and animal manure applications increased the amount of available P in the soil; and the values of extractable K in the soil was between 315-554 mg kg^{-1} (*Table 3*). Like 2 other nutrition element contents, the lowest value was at control application, the highest was at $BC_{15} + AM_5$ application; this application yielded 76% increase. The increase of the extractable K value in the soil was thought to be associated with the high extractable K value in the biochar and animal manure. Several researches reported that the amount of extractable K in the soils ranges between 40-150 mg kg^{-1} and no nutrition problem would appear if the extractable K was 150 mg kg^{-1} (Barber, 1985; Namlı et al., 2017).

Conclusion

In general, biochar and manure applications have positive effects on soil biological properties and nutrient content. The statistical evaluation of the enzyme analyses showed that the effects of applications on the enzyme activities of dehydrogenase, urease and arylsulphatase were significant ($p < 0.01$). Dehydrogenase enzyme activity is highest at $BC_{10} + AM_5$ application, urease enzyme activity is highest at $BC_5 + AM_5$ and $BC_{15} + AM_5$ applications, arylsulphatase enzyme activity as well as urease enzyme

http://www.aloki.hu ● ISSN 1589 1623 (Print) ● ISSN 1785 0037 (Online)
DOI: http://dx.doi.org/10.15666/aeer/1704_88658876

activity is highest at $BC_5 + AM_5$ application. The statistical evaluation of alkaline phosphatase enzyme activity showed that the effects of the application was found to be insignificant. And it was identified that the highest numeric increase was at BC_{20} application. When the values of organic material in the soils were evaluated, it was identified that biochar and animal manure applications increased the amount of organic material in the soil as compared to control, and the highest values were obtained in the $BC_{15} + AM_{10}$ application. Mixing of these two materials (organic material and a material with high organic content) in the soil increased the amount of the organic materials in the soil, as expected. When the nutrition contents of the soils were evaluated, biochar and animal manure applications increased the values of total N, available P and extractable K; and the most effective doses were $BC_{10} + AM_5$ application for total N, $BC_{15} + AM_5$ application for available P and extractable K. It is thought that biochar has high C content and therefore C/N ratio is not sufficient by itself and C/N ratio is suitable with organic materials such as animal manure. Because these microorganisms living in soil organic materials because they contain plant nutrients like N and P in terms of their chemical stimulates wealth. As a result, the mineralization of the plant nutrients will be increased with the increase of biological activity in the soil. Due to the high content of biochar, the decomposition rate in the soil is low and it has been shown to be effective for a long time.

REFERENCES

[1] Akça, M. O., Namli, A. (2015): Effects of poultry litter biochar on soil enzyme activities and tomato, pepper and lettuce plants growth. – Eurasian Journal of Soil Science 4(3): 161.

[2] Alvarez-Campos, O., Lang, T. A., Bhadha, J. H., McCray, J. M., Glaz, B., Daroub, S. H. (2018): Biochar and mill ash improve yields of sugarcane on a sand soil in Florida. – Agriculture, Ecosystems & Environment 253: 122-130.

[3] Anderson, T. H., Domsch. K. H. (1978): A physiological method for the quantitative measurement of microbial biomass in soils. – Soil Biology and Chemistry 10: 215-221.

[4] Aşkın, T., Kızılkaya, R., Gülser, C., Bayraklı, B. (2004): Some microbiological properties of campus soils of Ondokuzmayıs University. Ondokuzmayıs Üniversitesi kampus topraklarının bazı mikrobiyolojik özellikleri, O.M.Ü. – Ziraat Fakültesi Dergisi 191: 31-36.

[5] Azam, F., Malik, K. A., Sajjad, M. I. (1985): Transformations in soil and availability to plants of 15 N applied as inorganic fertilizer and legume residues. – Plant and Soil 861: 3-13.

[6] Barber, S. A. (1985): Potassium Availability at the Soil-Root Interface and Factors Influencing Potassium Uptake. – In: Munson, R. D. (ed.) Potassium in Agriculture. ASA-CSSA-SSSA, Madison, WI, USA: 309-324.

[7] Bender, D., Erdal, İ., Dengiz, O., Gürbüz, M., Tarakçıoğlu, C. (1998): The effects of different organic materials on some physical properties of clay soil (Farklı Organik Materyallerin Killi Bir Toprağın Bazı Fiziksel Özellikleri Üzerine Etkisi). – M. Tefik Yeşilsoy International Symposium on Arid Region Soil. 21-24 September, International Agrohydrology Research and Training Center, Menemen-Izmir, pp. 506-511.

[8] Bouyoucos, G. J. (1962): Hydrometer method improved for making particle size analysis of soil. – Agronomy Journal 545: 434-438.

[9] Bremner, J. M. (1965): Total Nitrogen 1. – In: Methods of Soil Analysis. Part 2. Chemical and Microbiological Properties. ASA, Madison, WI, pp. 1149-1178.

http://www.aloki.hu ● ISSN 1589 1623 (Print) ● ISSN 1785 0037 (Online)
DOI: http://dx.doi.org/10.15666/aeer/1704_88658876

[10] California Fertilizer Association (CFA) (1995): Agricultural productions/environmental concerns: new paradigms. – California Plant and Soil Conference, January 10-11.
[11] Çengel, M., Okur, N., Irmak Yılmaz, F. (2009): The effect of green manures and farmyard manure on microbial activity in vineyard soils under organic management (Organik bağ topraklarında yeşil gübre bitkileri ve çiftlik gübresi uygulamalarının topraktaki mikrobiyal aktiviteye etkileri). – Ege University Faculty of Agriculture Journal 46(1): 25-31.
[12] Chunderova, A. I., Zubets, T. (1969): Phosphatase activity in dernopodzolic soils. – Pochvovendenie 11: 47-53.
[13] Demisie, W., Liu, Z., Zhang, M. (2014): Effect of biochar on carbon fractions and enzyme activity of red soil. – Catena 121: 214-221.
[14] Gabriels, R., Verdonck, O. (1992): Method for measuring the water release curve of organic substrats. – Proc. Sym. Artificial Media in Horticulture, pp. 2054-2062.
[15] Glaser, B., Lehmann, J., Zech, W. (2002): Ameliorating physical and chemical properties of highly weathered soils in the tropics with charcoal-a review. – Biology and Fertility of Soils 35(4): 219-230.
[16] Isermeyer, H. (1952): Eine einfache Methode zur Bestimmung der Karbonate im Boden. – Zeitschrift für Planzenernährung, Düngung, Bodenkunde 561(3): 26-38.
[17] Kablan, N. (2005): Effect of different organic wastes on biological properties of soil and maize (Zea mays indendata) rhizosphere (Farklı Organik Atıkların Toprak Ve Mısır (Zea Mays İndendata) Bitkisinin Rizosfer Bölgesindeki Biyolojik Özellikler Üzerine Etkisi). – Yüksek Lisans Tezi Ondokuz Mayıs Üniversitesi Fen Bil. Ens. Toprak Bilimi ve Bitki Besleme Anabilim Dalı. Yayınlanmamış. 40 sf. Samsun.
[18] Kacar, B. (2009): Soil Analysis (Toprak analizleri). Extended Ed. II. – Nobel Publication, Istanbul.
[19] Kacar, B., Kütük, C. (2010): Fertilizer Analysis (Gübre analizleri). – Nobel Publication, Istanbul.
[20] Kambo, H. S., Dutta, A. (2015): A comparative review of biochar and hydrochar in terms of production, physico-chemical properties and applications. – Renewable and Sustainable Energy Reviews 45: 359-378.
[21] Kandeler, E., Gerber, H. (1988): Short-term assay of soil urease activity using colorimetric determination of ammonium. – Biology and Fertility of Soils 6(1): 68-72.
[22] Kayıkçıoğlu, H. H., Okur, N. (2013): Biochemical changes during composting of tannery sludge and assessment of compost quality (Deri sanayi arıtma çamurunun kompostlaştırılması sırasındaki biyokimyasal değişiklikler ve oluşan kompostun kalitesi). – Anadolu Dergisi 22(2): 59-68.
[23] Kishimoto, S., Sugiura, G. (1980): Introduction to Charcoal Making on Sunday. – Sougou Kagaku Shuppan, Tokyo (in Japanese).
[24] Kızılaslan, H., Olgun, A. (2012): Organic agriculture and supports given to organic agriculture in Turkey (Türkiye'de organik tarım ve organik tarıma verilen desteklemeler). – Gaziosmanpaşa Üniversitesi Ziraat Fakültesi Dergisi 29(1): 1-12.
[25] Knudsen, D., Peterson, G. A., Pratt, P. F. (1982): Lithium, Sodium, and Potassium. – In: Methods of Soil Analysis. Part 2. Chemical and Microbiological Properties. ASA, Madison, WI, pp. 225-246.
[26] Lehmann, J. (2007): Bio-energy in the black. – Frontiers in Ecology and the Application 5(7): 381-387.
[27] Liang, B., Lehmann, J., Solomon, D., Kinyangi, J., Grossman, J., O'Neill, B., Skjemstad, J. O., Thies, J., Luizao, F. J., Peterson, J., Neves, E. G. (2006): Black carbon increases cation exchange capacity in soils. – Soil Science Society of America Journal 70: 1719-1730.
[28] McClellan, A. T., Deenik, J., Uehara, G., Antal, M. (2007): Effects of flashed carbonized© macadamia nutshell charcoal on plant growth and soil chemical properties. – American Society of Agronomy Abstracts 80(100): 120.

http://www.aloki.hu ● ISSN 1589 1623 (Print) ● ISSN 1785 0037 (Online)
DOI: http://dx.doi.org/10.15666/aeer/1704_88658876

[29] McLaughlin, H., Anderson, P. S., Shields, F. E., Reed, T. B. (2009): All biochars are not created equal, and how to tell them apart. – Proceedings, North American Biochar Conference, Boulder, Colorado, pp. 1-36.
[30] Moreno, J. L., Hernandez, T., Garcia, C. (1999): Effects of a cadmium-contaminated sewage sludge compost on dynamics of organic matter and microbial activity in an arid soil. – Biology and Fertility of Soils 28: 230-237.
[31] Müftüoğlu, N. M., Türkmen, C., Çıkılı, Y. (2012): Soil and plant fertility analysis (Toprak ve Bitkide Verimlilik Analizleri, Kriter Yayınevi). – Nobel, Ankara.
[32] Namlı, A., Akça, M. O., Akça, H. (2017): The effects of biochars obtained from agricultural wastes on wheat plant growth and some soil properties (Tarımsal atıklardan elde edilen biyokömürün buğday bitkisinin gelişimi ve bazı toprak özellikleri üzerine etkileri). – Toprak Bilimi ve Bitki Besleme Dergisi 5(1): 39-47.
[33] Nannipieri, P., Ceccanti, B., Grego, S. (1990): Ecological significance of the soil biological activity in soil. – Soil Biochemistry 6: 415-471.
[34] Nelson, D. W., Sommers, L. E. (1982): Total Carbon, Organic Carbon and Soil Organic Matter. – In: Page, A. L. et al. (eds.) Methods of Soil Analysis. Part 2: Chemical and Microbiological Properties. ASA-SSSA, Madison, WI, pp. 539-579.
[35] Okur, N. (1997): Soil enzyme lecture notes. Toprak enzimleri ders notları. – Ege Üniversitesi Ziraat Fakültesi Toprak Bölümü, Bornova, İzmir.
[36] Olsen, S. R. (1954): Estimation of Available Phosphorus in Soils by Extraction with Sodium Bicarbonate. – United States Department of Agriculture; Washington.
[37] Özdemir, N., Kızılkaya, R., Sürücü, A. (2000): The effects of different organic wastes on urease enzyme activity of soils (Farklı organik atıkların toprakların üreaz enzim aktivitesi üzerine etkisi). – Ekoloji Çevre Dergisi 10(37): 23-26.
[38] Park, J. H., Choppala, G. K., Bolan, N. S., Chung, J. W., Chuasavathi, T. (2011): Biochar reduces the bioavailability and phytotoxicity of heavy metals. – Plant and Soil 348: (1-2) 439.
[39] Paz-Ferreiro, J., Gascó, G., Gutiérrez, B., Méndez, A. (2012): Soil biochemical activities and the geometric mean of enzyme activities after application of sewage sludge and sewage sludge biochar to soil. – Biology and Fertility of Soils 48(5): 511-517.
[40] Retan, G. A. (1915): Charcoal as a means of solving some nursery problems. – Journal of Forestry 13(1): 25-30.
[41] Roberts, K. G., Gloy, B. A., Joseph, S., Scott, N. R., Lehmann, J. (2009): Life cycle assessment of biochar systems: estimating the energetic, economic, and climate change potential. – Applicational Science & Technology 44(2): 827-833.
[42] Ronsse, F., Van Hecke, S., Dickinson, D., Prins, W. (2013): Production and characterization of slow pyrolysis biochar: influence of feedstock type and pyrolysis conditions. – Gcb Bioenergy 5(2): 104-115.
[43] Schinner, F., Öhlinger, R., Kandeler, E., Margesin, R. (eds.) (1996): Methods in Soil Biology. Springer-Verlag, Berlin.
[44] Sepken, Berber, A., Farasat, S., Namlı, A. (2014): Afforestation effects on soil biochemical properties. – Eurasian Journal of Forest Science 1(1): 25-34.
[45] Sohi, S., Lopez-Capel, E., Krull, E., Bol, R. (2009): Biochar, climate change and soil: a review to guide future research. – CSIRO Land and Water Science Report 5(09): 17-31.
[46] Sun, Y., Gao, B., Yao, Y., Fang, J., Zhang, M., Zhou, Y., Chen, H., Yang, L. (2014): Effects of feedstock type, production method, and pyrolysis temperature on biochar and hydrochar properties. – Chemical Engineering Journal 240. 574-578.
[47] Tabatabai, M. A., Bremner, J. M. (1969): Use of p-nitrophenyl phosphate for assay of soil phosphatase activity. – Soil Biology and Biochemistry 1(4): 301-307.
[48] Tabatabai, M. A., Bremner, J. M. (1970): Arylsulfatase activity of soils. – Soil Science Society of America Journal 34: 225–229.
[49] Thalman, A. (1968): Zur Medhodik der Bestimmung der Dehydrogenase Aktivität im Boden mittels Triphenyltetrazoliumchlorid (TTC). – Landwirtsch. Forsch 21: 249-258.

http://www.aloki.hu ● ISSN 1589 1623 (Print) ● ISSN 1785 0037 (Online)
DOI: http://dx.doi.org/10.15666/aeer/1704_88658876

[50] U.S. Salinity Laboratory Staff (1954): Diagnosis and Improvement of Saline and Saline and Alkali Soils. – Agri. Handbook No. 60. U.S. Salinity Laboratory, Riverside, CA.
[51] Van Zwieten, L., Kimber, S., Morris, S., Downie, A., Berger, E., Rust, J., Scheer, C. (2010): Influence of biochars on flux of N_2O and CO_2 from Ferrosol. – Soil Research 48(7). 555-568.
[52] Von Liebig, J. (1878): Chemische Briefe. – Winter, Heidelberg.

http://www.aloki.hu ● ISSN 1589 1623 (Print) ● ISSN 1785 0037 (Online)
DOI: http://dx.doi.org/10.15666/aeer/1704_88658876

CONSERVATION OF GRASSLAND HABITATS BIODIVERSITY IN THE CONTEXT OF SUSTAINABLE DEVELOPMENT OF MOUNTAIN AREA OF ROMANIA

COJOCARIU, L.[1,2] – COPĂCEAN, L.[1*] – POPESCU, C.[1]

[1]Banat's University of Agricultural Sciences and Veterinary Medicine "King Mihai I of Romania" from Timisoara, 300645, 119, Calea Aradului, Timisoara, Romania (phone: +40-0256-277-009; fax: +40-0256-200-296)

[2]Centre for Mountain Economics, "Costin C. Kiritescu" National Institute for Economic Research, Romanian Academy, 725700, Str. Petreni, nr. 49, Vatra Dornei, jud. Suceava, Romania (phone: +40-3301-10-030; fax: +40-3301-10-030)

[*]Corresponding author e-mail: lorecopacean@yahoo.com; phone:+40-0729-591-651

(Received 17th Mar 2019; accepted 22nd May 2019)

Abstract. The aim of the study was to analyze grassland areas in relation to the activities and financial support schemes dedicated to the conservation of grassland habitats, with a view to sustainable development of Romania's mountainous area. A multitask analysis was carried out: the geomatic approach of pastoral space and its relations with other environmental components, having "localized" results in space and therefore the possibility of intervention "from the general to the specific". The grasslands cover 22.30% of the Romania's mountainous area, a percentage which gives them a special importance. The large number of identified protected areas (770 entities of different categories) support the idea of the high biodiversity of the mountainous area, implicitly of the grassland habitats. One third of grassland areas (36.65%) are included in one or more environmental protection structures. In addition to biodiversity conservation measures imposed by different protected areas, Romania's mountainous area is fully included in the Agro-Environment and Climate and Ecological Agriculture programs, part of the Common Agricultural Policies, which encourages the pursuit of sustainable agriculture, also the protection of biological resources. This study encouraging and sustaining extensive traditional agricultural practices, determines both the maintenance of biodiversity and the diversity of semi-natural grassland habitats.
Keywords: *analysis, geomatics, pasture, protection, financing, management*

Introduction

The political, social, economic and environmental context of the last century has generated changes and, at the same time, complex and synergistic challenges for the real preservation of nature. For example, changes in livestock and the reorganization of agricultural land have a negative and/or positive impact on natural and semi-natural pastures and on traditional landscapes in agriculture, the relationship being possible on the reverse (Baessler and Klotz, 2006; Garnier et al., 2007; Ceballos et al., 2010; Căluşeru et al., 2015). On the other hand, efficient management of grasslands requires the adoption of strategies according to local conditions in order to respond to the context of reality. In this interaction, managers in protected areas and nature conservation institutions, along with the agricultural sector, have a very important role (Balázsi, 2017). In the territory, the installation of protected areas imposes certain rules

http://www.aloki.hu ● ISSN 1589 1623 (Print) ● ISSN 1785 0037 (Online)
DOI: http://dx.doi.org/10.15666/aeer/1704_88778894

and behavior regarding the exploitation of grasslands, which, besides the protection of environmental factors, also aims at preserving biodiversity.

Protected areas, seen as "the key to mitigating climate change, preserving biodiversity, providing ecosystem services and promoting human well-being" (Vega et al., 2017) have seen an upward path in their space-time evolution. Thus, the surface of the globe in the 1990s was "protected" in a proportion of 8.6%, in 2016 this area rising to 14.7% and includes land and estuary ecosystems with the exception of Antarctica (Vega et al., 2017).

The need to set up and extend protected areas is based on a holistic approach, seen at global level and has grown as a result of increased risks generated by climate change (Ruiz-Mallén et al., 2015), concern for the environment (Wandersee et al., 2012), more and more severe deforestation (FAO, 2010) and installation of non-specific or invasive vegetation (Lei et al., 2014), major risks to produce "hydrological" disasters such as floods (Saraswati, 2014) and "unburned" floods, the uncontrolled expansion of urban spaces (McDonald, 2013; López Lambas and Ricci, 2014), in the face of biological formations.

Before 1989, Romania's territory was "protected" by different types of protected areas, at a rate of 4.1% (Iojă et al., 2010). After 2000, interest in protected areas increased significantly; under the pressure of joining the European Union, legislative and normative regulations have been introduced to "extend" the existing protected areas (Geacu et al., 2012). After joining the EU, Romania had to expand its "protected territory" to 17% of the total, making it "joining" the Natura 2000 European Network (Bălteanu et al., 2009).

In 2014, in Romania the protected areas covered 24.84% of the country's territory (protected natural areas, 7% and Natura 2000 sites, 17.84%), being registered: 79 scientific reserves; 13 national parks; 230 monuments of nature; 661 nature reserves, 15 natural parks; 19 Ramsar sites; 3 Biosphere Reserves; 1 World Heritage Site, respectively the Danube Delta (Antonescu et al., 2015).

Declaring a "protected area" has effects on the entire geosystem, depending on its size and profile. There are situations like these (Antonescu et al., 2015): the extension of areas to other areas which do not require protection, initially with other destinations; human settlements located near protected areas are usually underdeveloped and with limited development opportunities, with restricted access to infrastructure, leading to population migration and therefore demographic imbalances.

The management of grasslands from the protected areas is not always economically and socially correlated with the objectives and needs of communities in the deprived areas (Molnár et al., 2016). On the other hand, the "establishment" of the protected areas ensures: preserving biodiversity, attracting european funds and developing projects with multiple benefits, preserving local and regional traditions.

Regarding the use of grasslands in Romania, besides the protective measures imposed by different categories of protected areas, there are several relevant instruments of the Community Agricultural Policy (CAP): direct payments, milk quota, sustainable rural development (Pillar 2 measures) such as investment aid, agri-environmental measures (EMA) and support for mountain areas (Osterburg et al., 2010). Moreover, the CAP has established rules to maintain traditional grassland management through eligibility rules and minimum requirements as a prerequisite for receiving direct payments.

http://www.aloki.hu ● ISSN 1589 1623 (Print) ● ISSN 1785 0037 (Online)
DOI: http://dx.doi.org/10.15666/aeer/1704_88778894

Exploiting grasslands under the socio-economic and cultural conditions of mountain areas in Romania, has long been and is in most cases in line with the principles and rules imposed by the presence of protected areas or CAP policies, not due to "environmental culture", but relied on the basis of financial and technical underdevelopment. Contrary to intensive farming practices, in the mountain environment, through physic-geographic traces and pastoral culture, some of the principles of sustainable agriculture meet, which place the environment and its resources at the forefront.

Concerns about the sustainability of mountain farming and the conservation of grassland habitats' biodiversity are expressed in numerous researches (Öllerer, 2012; Păcurar et al., 2015; Cojocariu et al., 2018), under various theoretical and applicative aspects, context in which the researches presented in this paper are included.

In this context, ***the aim of the study*** was to analyze grassland areas in relation to the activities and financial support schemes dedicated to the conservation of grassland habitats, with a view to sustainable development of Romania's mountainous area. At the same time, we want to answer a number of questions: *"Where are conservation measures applied? What are the relationships between conservation structures? What are the implications for environmental protection in the organization of the geographical space and especially of the agricultural space".*

With the first stage of the documentation on the theme, we have drawn attention to another topical topic, especially in our country, namely the sustainable agriculture, functionally linked to the action of nature conservation. Under these conditions, we attempted to formulate scientifically reasoned answers also to the questions: *"Under what conditions can sustainable agriculture be practiced on the pastures in the mountainous area of Romania?"* or *"Is there financial support for sustainable agriculture?".*

The ***choice of the study area*** was based on the idea that the mountain area, extended over a third of the entire territory of Romania, represents an area with great biological diversity and the most complex ecosystems, but also a "step-by-step" territory for its inhabitants, from socio-economic point of view, despite the availability of natural resources. Of all the natural resources of the mountain range, grasslands can be regarded as "everyone's reach" with minimal operating costs (compared to forests or arable land) available on large and renewable surfaces under appropriate use conditions. These sometimes contradictory aspects have stimulated us and lead us to the deepening and detailed analysis of the pastoral area of Romania's mountainous area, important both at national and European level.

Being a ***multidisciplinary work***, a multitask analysis was carried out: the geomatic approach of pastoral space and its relations with other environmental components, having "localized" results in space and therefore the possibility of intervention "from the general to the specific"; we also analyzed the conditions under which European programs for nature conservation and changes in agricultural practices can be applied. The study draws attention to the conservation status of biodiversity at present and can be used as a basis or model for other research as well as for the development of future strategies for the mountainous area of Romania and the graphic and non-graphic database can be reused, completed or "rearranged" according to new needs.

http://www.aloki.hu ● ISSN 1589 1623 (Print) ● ISSN 1785 0037 (Online)
DOI: http://dx.doi.org/10.15666/aeer/1704_88778894

Work methodology

Study area

The area analyzed in the present paper is equivalent to the Mountain Area defined in the National Rural Development Program 2014 - 2020 - NRDP 2014 – 2020 (MARD, 2019) as being the sum of the areas of the administrative-territorial units (ATU) located at average altitudes greater than or equal to 600 m and of the units located at an altitude of 400-600 m, but with average values of slopes higher than or equal to 15%. Under these conditions, the study area includes the Carpathian area, but also the adjacent areas, Sub-Carpathians, plateaus and high hills (*Fig. 1*).

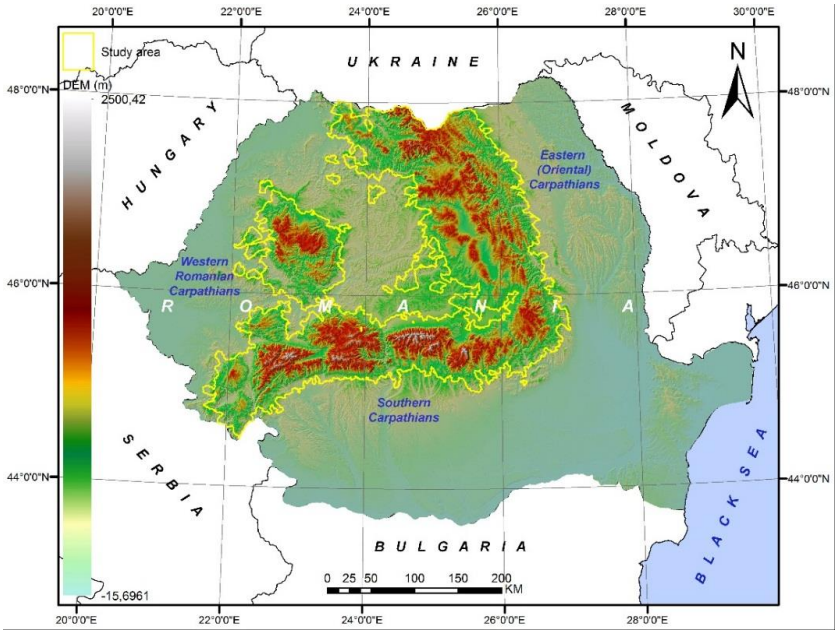

Figure 1. *Location of study area. (processing according to EEA, 2017; MARD, 2019; NACRA, 2019)*

Based on these considerations, the study area with a semi-administrative or semi-physical delimitation comprises 658 ATUs with a total area of 7143943.38 ha (NACRA, 2019), 71439.43 km^2 respectively, being more extensive than the area of the Carpathian Mountains on the territory of Romania, physically and geographically delimited, with the area of 69872 km^2 (Dumitraşcu et al., 2015).

Materials and methods

The four-step systematized research methodology, as well as the materials used in the study, are presented in *Figure 2*. Scientific data and information has been processed and interpreted with the ArcGIS 10.2.1 software, which has also been used to generate cartographic materials.

1. The analysis of grassland surfaces from mountain areas has been based on the Corine Land Cover Database, edition 2012 (EEA, 2012), a program coordinated by the European Environment Agency and part of the Global Monitoring for Environment and Security program, data available on the European Environment Agency website. The database was updated in 2018 by comparison with aerial images (Google Earth

http://www.aloki.hu ● ISSN 1589 1623 (Print) ● ISSN 1785 0037 (Online)
DOI: http://dx.doi.org/10.15666/aeer/1704_88778894

platforme, 2018) and data from the National Institute of Statistics of Romania - Land surface by mode of use, by counties and localities (NIS, 2018).

Of the Corine Land Cover Database (EEA, 2012), a total of 26930 entities (all land use categories) were analyzed, and the "grassland" category, interest in this study, with an area of 1593461.64 ha, included: secondary pastures (code 231), with a total of 4474 entities and a total area of 665494.35 ha and natural grassland (code 321), with a total of 2628 entities and a total area of 503622.83 ha. To the two "clear" categories, we may add pastures and hayfields (including wooded pastures), "recovered" from other categories: agricultural land with significant areas occupied with natural vegetation (code 243), agro-forest land (code 244), and bushy vegetation (code 322, 323, 324).

After the identification and framing of each unit, by means of the "joining" procedure (the Merge command), the map of the grassland distribution in the mountain area was obtained in unitary vector format.

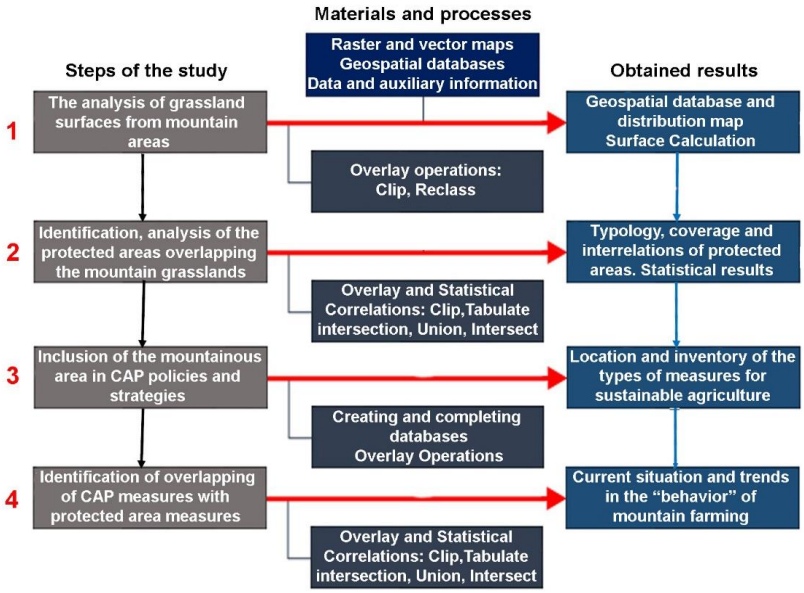

Figure 2. *Methodology of research*

2. The identification and analysis of the protected areas overlapping the grasslands in the mountain area was based on the vector format file with their geometry published on the website of the Ministry of the Environment, in 2017.

In the mountain area, 770 protected areas of different categories were identified, covering a total surface of 4862584.44 ha. Inventory and analysis of protected areas covered all categories of protected sites in the area of interest, both national and international. The "Protected Areas" layer database has been hierarchically structured and categorized.

For each category, we calculated the area and the percentage within the mountain area, and analyzed, as percentage, the situation of the overlapping (*Tabulate Intersection* function), thus calculating the intersection with other areas. Subsequently, the spatial correlation with the grasslands (the *Union* function) was made to determine the "degree and form" of the protection imposed.

3. The inclusion of the mountainous area in CAP policies and strategies was supported by the documentation from NRDP 2014-2020 (MARD, 2019). For each of

http://www.aloki.hu ● ISSN 1589 1623 (Print) ● ISSN 1785 0037 (Online)
DOI: http://dx.doi.org/10.15666/aeer/1704_88778894

the 658 ATUs, we associated descriptive information (database completion) related to applicable programmes in the case of grasslands (Agro-Medium and Climate and Ecologic Agriculture). After spreading the funding strategies, the overall image and regionalization was outlined.

4. The identification of overlapping areas of CAP measures with protected area specific measures was done through multilayer operations, overlapping and unification of the two databases, resulting in the overall situation of supporting sustainable agriculture.

Working procedures in the GIS (Geografic Information Systems) environment were applied according to technical specifications for ArcGIS 10.2.1 software and ESRI documentation.

Results and discussions

Grassland fund from the mountain region of Romania

The grasslands of Romania's mountainous area, one of the most important natural resources, multifunctional and with deep historical references, are "indispensable" to the inhabitants of these areas, being among the few sources of income and can therefore be treated as "support of subsistence".

The grasslands total 1593461.64 ha, respectively 22.30% of the total area of Romania's mountainous area (defined according to MARD, 2019), which are present in all forms and relief units, ranging from river meadows to high mountain areas (*Fig. 3*).

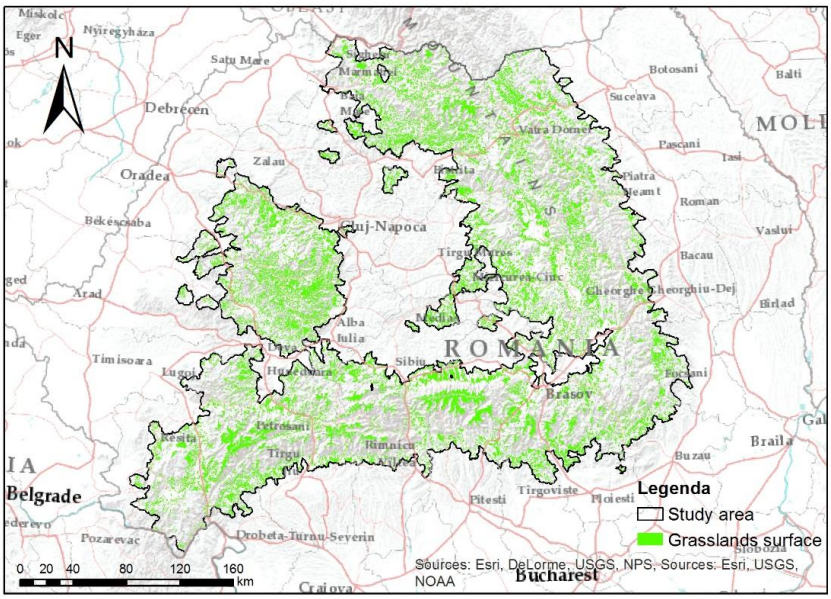

Figure 3. *Distribution of grasslands in the mountainous area of Romania. (processing after EEA, 2012; MARD, 2019)*

Biodiversity conservation structures (Protected areas) in mountain areas, with special reference to the areas used as grasslands

At the level of the mountain area, the protected areas were grouped into 10 categories, presented in *Table 1*.

http://www.aloki.hu ● ISSN 1589 1623 (Print) ● ISSN 1785 0037 (Online)
DOI: http://dx.doi.org/10.15666/aeer/1704_88778894

The statistical data show that Natura 2000 sites have the largest expansion, with 75.62% of the total protected areas, followed by the Protected Areas of National Interest, with a share of 21.45% of the total. Biosphere reserves and Wetlands of international Importance have a reduced share of less than 2% each (*Table 1*).

Table 1. *Type and surface of protected areas from mountain region**

No.	Membership	P.A. type	No. entities	Surface		% of M.A. surface
				ha	% of total P.A.	
1	Natura 2000 Sites	SCI	181	2174706	44.72	30.44
2		SPA	50	1502658	30.9	21.03
3	Protected Areas of National Interest	N.P.	12	298152	6.13	4.17
4		n.p.	10	560572	11.52	7.84
5		M.N.	1	8	0.0001	0.0001
6		S.R.	2	43	0.0008	0.0006
7		N.R.	27	19134	0.42	0.26
8		RONPA	482	164661	3.38	2.30
9	Biosphere Reserves	ROMAB	2	85518	1.76	1.19
10	Wetlands of International Importance	RORMS	3	57127	1.17	0.79

Legend: PA-Protected Areas, MA-Mountain area, SCI-Sites of Community Importance, SPA-Special Protection Areas, NP-National Parks, np-Natural Parks, MN-Monuments of Nature, NR-Natural Reserves from IUCN IV Category, RONPA Natural Reserves, SR-Scientific Reserves, ROMAB-Biosphere Reserves, RORMS-Wetland of International Importance.
* data extracted from the geospatial database published on the website of Ministry of the Environment, 2017

National Parks, declared structures to protect nature's wildlife are materialized in 12 entities (*Table 2*) and are the most "restrictive" structures that "dictate" the conservation measures in overlapping areas, irrespective of the presence of other protection entities (Ministry of the Environment, 2000; Stanciu and Florescu, 2009) and were identified on a small area, 4.17% of total.

Table 2. *National parks superimposed on the mountainous area of Romania**

No.	National Park (NP)	Code	Founded	Location in the mountain area
1	NP Buila Vânturariţa	RONPA0848	2004	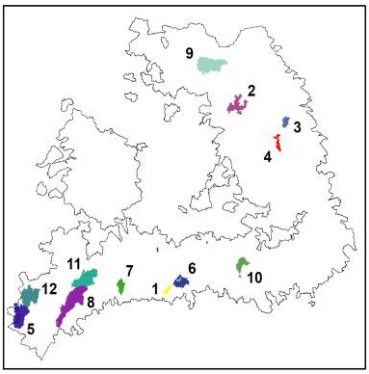
2	NP Călimani	RONPA0009	1990	
3	NP Ceahlău	RONPA0008	1955	
4	NP Cheile Bicazului–Hăşmaş	RONPA0007	1990	
5	NP Cheile Nerei-Beuşniţa	RONPA0003	1990	
6	NP Cozia	RONPA0010	1990	
7	NP Defileul Jiului	RONPA0933	2005	
8	NP Domogled-Valea Cernei	RONPA0001	1990	
9	NP Munţii Rodnei	RONPA0005	1990	
10	NP Piatra Craiului	RONPA0011	1990	
11	NP Retezat	RONPA0002	1988	
12	NP Semenic-Cheile Caraşului	RONPA0012	1990	

* data extracted from the geospatial database published on the website of Ministry of the Environment, 2017

http://www.aloki.hu ● ISSN 1589 1623 (Print) ● ISSN 1785 0037 (Online)
DOI: http://dx.doi.org/10.15666/aeer/1704_88778894

Mathematically, by summing up the areas of all the protected areas, their total area in the mountain area is 4862584.44 ha (68.05%), but in a more detailed analysis, these entities overlap in many cases on the same territory, which invalidates the information and suggests the *Overlay* approach, in which each layer is analyzed in correlation with the others.

Thus, the statistical calculations show that the total area of the protected areas, the horizontal "footprint" on the surface of the mountain area, irrespective of the number of protected areas overlapped vertically, is 2737574.06 ha, which represents 38.32% of the total area of the area mountain.

The results of the spatial correlation of protected areas – grasslands indicate that 584104.86 ha (36.65%) of the total area of mountain grasslands is under the protection of different categories of sites for biodiversity conservation.

Simple visual analysis of the results indicates the "vertical" upgrading of the protected areas on the grassland units, so complex spatial analysis (*Fig. 4*) and statistical analysis (*Table 3*) were required to determine the type and weight of each entity in the combination of "preservation programmes".

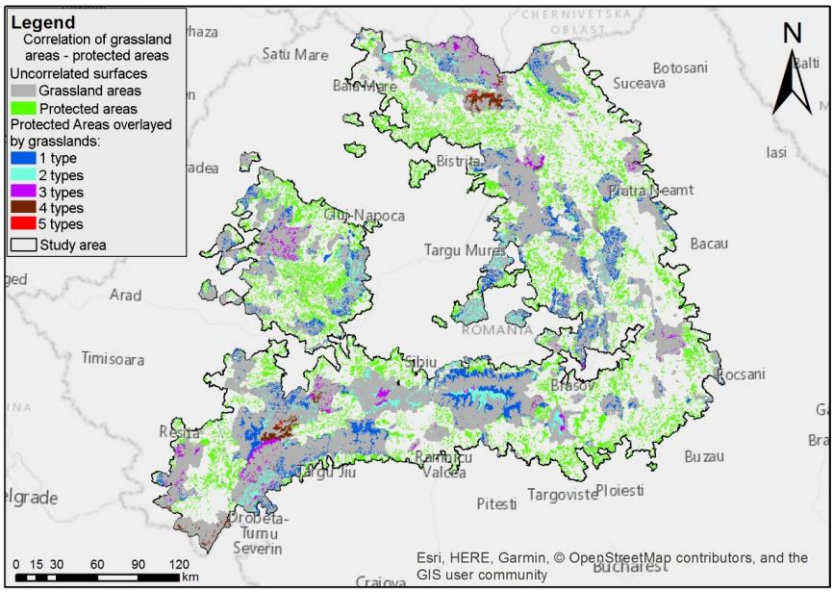

Figure 4. *The correlation of grassland areas with protected areas. (processing after EEA, 2012; Ministry of the Environment, 2017; MARD, 2019)*

From the analysis of the data synthesized in *Figure 4* and *Table 3*, we may remark the following aspects:

- the grasslands are associated only with 27.77% SCIs and SPAs only, 22.96%, these two being the most common in overlapping.
- NP is associated, in most cases, with Natura 2000 sites.
- of the total area of grasslands located in protected areas, there are 15.19% both SCI and SPA areas.
- as share, after SCI and SPA, NP comes into association with other protected areas, in proportions of approx. 5% in each case.
- the grasslands analyzed do not overlap with the category M.N.

http://www.aloki.hu ● ISSN 1589 1623 (Print) ● ISSN 1785 0037 (Online)
DOI: http://dx.doi.org/10.15666/aeer/1704_88778894

Table 3. *Relationship grassland areas – categories of protected areas*

No. of P.A. entities	Category of protected areas*										Affected surface of grasslands**	
	A	B	C	D	E	F	G	H	I	J	ha	%
1										■	162203.66	27.77
								■			980.39	0.17
	■										7.72	0.00
							■				25923.69	4.44
				■							1686.10	0.29
			■								134094.99	22.96
2								■		■	12807.88	2.19
	■									■	6704.55	1.15
							■			■	36944.76	6.33
				■						■	1291.88	0.22
			■							■	88722.75	15.19
			■			■					30.00	0.01
							■	■			11.60	0.00
				■				■			6.51	0.00
			■					■			119.05	0.02
	■		■								0.56	0.00
			■				■				389.22	0.07
			■	■							8.27	0.00
3			■			■				■	21.31	0.00
	■							■		■	6.83	0.00
							■	■		■	4986.35	0.85
				■				■		■	121.16	0.02
			■					■		■	7938.05	1.36
	■						■			■	10.04	0.00
	■		■							■	478.23	0.08
			■				■			■	31892.56	5.46
			■	■						■	23886.57	4.09
			■				■	■			0.17	0.00
4			■			■	■			■	4530.49	0.78
	■						■	■		■	30.28	0.01
			■				■	■		■	5244.40	0.90
			■	■				■		■	2069.25	0.35
			■	■					■	■	27971.18	4.79
			■	■	■					■	14.48	0.00
	■		■				■			■	4.22	0.00
	■		■	■						■	15.47	0.00
5			■			■	■	■		■	62.24	0.01
			■	■				■	■	■	2884.49	0.49
			■	■	■			■		■	1.12	0.00
	■		■	■				■		■	2.20	0.00

Legend: A.P.-Protected area; *Protected area category: A - Natural Reserves from IUCN IV Category (NR), B - Monuments of Nature (MN), C - Special Protection Areas (SPA), D – National Parks (NP), E - Scientific Reserves (SR), F - Wetland of International Importance (RORMS), G - Natural Parks (np), H - Natural Reserves (RONPA), I - Biosphere Reserves (ROMAB), J - Sites of Community Importance (SCI); colored boxes suggest the presence of the protected area; **The figure 0.00 from the column „Affected surface of grasslands" designates surfaces with a percentage of less than 0.001%

The data presented above shows the biological complexity of the Romanian mountainous area, also acknowledged at European level (Mráz and Ronikier, 2016), given by the large number of protected areas (770 entities) and implicitly by the species they protect, irrespective of their location or overlapping.

http://www.aloki.hu ● ISSN 1589 1623 (Print) ● ISSN 1785 0037 (Online)
DOI: http://dx.doi.org/10.15666/aeer/1704_88778894

Therefore, maintaining biodiversity is done through protection measures imposed by the presence of protected areas, but with the association of other independent or functionally related mechanisms: the continuous use of traditional practices, the fact that a substantial part of the region is represented by high nature value agricultural land (Babai and Molnár, 2014) and CAP measures, which will be described below.

Strategies and measures of the Common Agricultural Policy (CAP) applied in the mountain area

The European Union's rural development policy, introduced as the second pillar of the CAP through the Agenda 2000 reform, is co-financed by the European Agricultural Fund for Rural Development (EAFRD) and regional or national funds and was designed to "stimulate" the development of rural areas, with new economic, social and environmental approaches (European Parliament, 2019).

The rural development policy is implemented on the basis of rural development programs designed by the Member States (or their regions). These multiannual programs implement a personalized strategy that responds simultaneously to the specific needs of Member States (or regions). These programs are based on a combination of measures chosen from a "menu" of European measures detailed in the Rural Development Regulation (Regulation (EU) No 1305/2013) and co-financed by the EAFRD (according to the documentation of the Second pillar of the Common Agricultural Policy: rural development policy).

As the present study focuses on the grasslands in the mountainous area of Romania, only the programs that apply to this segment of agriculture (Regulation (EU) No 1307/2013) will be described in the following.

The preservation of high nature value (HNV) agricultural land is essential in the mountain area, for which the NRDP of Romania has introduced and promoted financial support activities and schemes to farmers in HNV areas through the agri-environment and climate measure. *Figure 5* provides descriptive information on the financing strategies applicable to the land used as grassland and the areas where they are applied.

According to the data from the NRDP 2014 – 2020 (MARD, 2019), on approx. 95% of the mountainous area can be used for agro-environment and climate programs and 5% of the area can also be accessed by programs dedicated to Ecologic Agriculture (*Fig. 5*).

High natural value grasslands (HNVs) are spread throughout the mountain area, with funds being allocated to traditional agricultural practices as a compensatory measure for the natural limitation of land productivity due to the pedo-climatic features of the area or as a result of the operation of agricultural work with manual or animal force.

In the central area of the Eastern Carpathians are located grasslands that support the conservation of bird species (*Crex crex)*, in Suceava County (ATU Solca), grasslands that ensure survival and support the preservation of butterflies (*Maculinea* sp.).

Starting from the idea of preserving biodiversity, supported by numerous european and regional research and structures, we consider high natural value grassland to be of great importance, as rural communities depend on the key components of biodiversity and of ecosystem services that are found in non-domestic habitats (Vîntu et al., 2011).

In the view of the European Environment Agency (EEA, 2002), high natural value lands are those areas of high biological diversity on which extensive agriculture is practiced (Öllerer, 2014), also supported by the Live Viva Grass (2019) portal, according to which, in the category of high value pastures natural areas include those

http://www.aloki.hu ● ISSN 1589 1623 (Print) ● ISSN 1785 0037 (Online)
DOI: http://dx.doi.org/10.15666/aeer/1704_88778894

areas where extensive agriculture is practiced, areas with extremely high levels of biodiversity: they support healthy soils and a large number of wild species.

Although between 1947 and 1990 Romania's agriculture was "intensified" under totalitarian policies (Sârbu et al., 2004), large areas of grasslands "survived" these practices, nowadays our country is among the European countries with the highest resources of grasslands rich in "wild" vegetation (Akeroyd and Page, 2011).

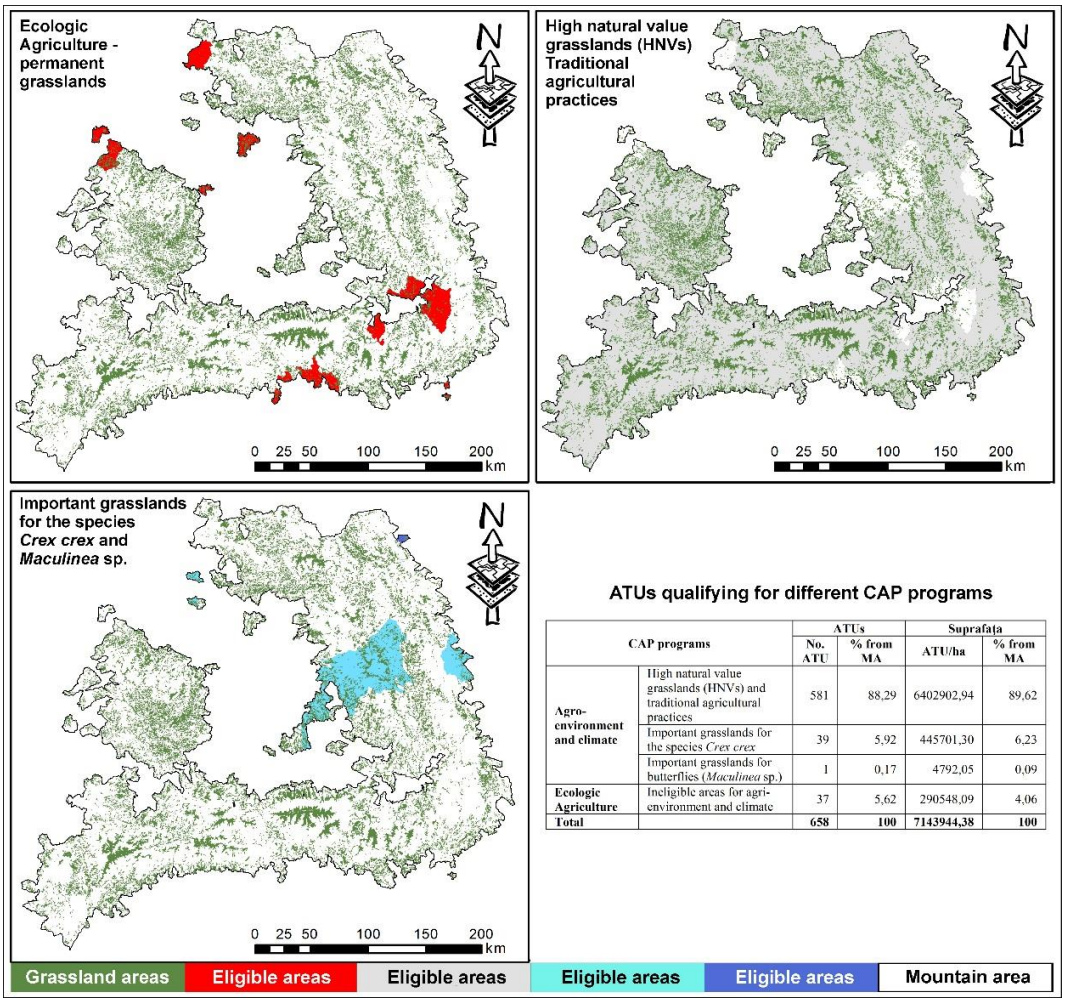

CAP programs		ATUs		Suprafața	
		No. ATU	% from MA	ATU/ha	% from MA
Agro-environment and climate	High natural value grasslands (HNVs) and traditional agricultural practices	581	88,29	6402902,94	89,62
	Important grasslands for the species *Crex crex*	39	5,92	445701,30	6,23
	Important grasslands for butterflies (*Maculinea* sp.)	1	0,17	4792,05	0,09
Ecologic Agriculture	Ineligible areas for agri-environment and climate	37	5,62	290548,09	4,06
Total		658	100	7143944,38	100

Figure 5. *Classification of Romania's mountainous area into the EU's CAP financing programs. (processing after MARD, 2019, list of eligible areas)*

Accessing programs primarily aimed at preserving the biodiversity of habitats and grassland species requires compliance with the requirements for their exploitation in conditions of sustainable "environmentally friendly" agriculture. Considering the fact that a large proportion of the owners and users of grasslands (HNV) in the mountainous area of Romania can receive subsidies through the Agro-Environment and Climate Program (MARD, 2019), these must comply with the conditions imposed by this program on grassland exploitation (*Table 4*).

Among the measures for preserving biodiversity of habitats and species, there is an emphasis on the idea of reducing or eliminating the use of chemical fertilizers. If we analyze the history of Romanian agriculture, chemical fertilization has been for a long

http://www.aloki.hu ● ISSN 1589 1623 (Print) ● ISSN 1785 0037 (Online)
DOI: http://dx.doi.org/10.15666/aeer/1704_88778894

time the "immediate" lever for increasing productivity. Starting from this concept, it is understood that reducing chemical fertilization leads to reduced productivity, but scientific research shows that for high natural value meadows the production of biomass is not affected by the depletion of soil in nutrients (Miladkova et al., 2015).

Table 4. *Agro-environmental and climate requirements for grassland exploitation**

Conditions imposed under the subsidized programs	**Agro-environment and climate**			
	High natural value grasslands (HNV)	**Traditional agricultural practices**	**Grasslands that support the conservation of bird species - *Crex crex***	**Grasslands that support the conservation of butterfly species (*Maculinea* sp.)**
It is necessary	- the traditional use of manure is allowed up to the equivalent of a maximum of 40 kg N n.c./ha, - maximum 1 UVM per hectare, - mowing begins after July 1 (UATs with average altitudes above 600 m) or after June 15 (UAT below 600 m altitude) - compliance with the ban on manure application, - not to apply organic or mineral fertilizers to protective strips.	-	- mowing the meadows after July 31, from the inside of the plot to the outside, - maximum 0,7 UVM per hectare, - the traditional use of manure is allowed up to the equivalent of a maximum of 40 kg N n.c./ha, - a 3-meter-long, non-mowed strip will be left on the edges of each plot (can be mown after 1.09), - compliance with the ban on manure application.	- the traditional use of manure is allowed up to the equivalent of a maximum of 40 kg N n.c./ha, - mowing after 25.08, - grazing is carried out with a maximum of 0.7 UVM per hectare
It is forbidden	- fertilizer and pesticide administration, - groundwater pollution through spillage.	- works with mechanized machinery, - groundwater pollution through spillage.	- works with mechanized machinery, - actions to accelerate natural drainage, - fertilizers and pesticides, - groundwater pollution through spillage.	- fertilizers and pesticides, - works with mechanized machinery, - actions to accelerate natural drainage, - groundwater pollution through spillage

Legend: UVM-large cow unit, * data synthesized according to MARD, 2019

Overlay of grassland areas covered by CAP policies with different protected area categories

Of the total surface area of the grasslands in the mountainous area of Romania, 36.65% is covered by different categories of protected areas (*Table 3, Fig. 4*).

The data from the literature show that the Natura 2000 sites as well as the other categories of protected areas in the Carpathians are also found in the HNV regions (Akeroyd and Page, 2011). In order to identify grasslands covered by protected areas but also eligible for different CAP strategies, applied the multilayer analysis (*Fig. 6*).

As a result of the spatial correlations, more than 90% of the grasslands located in protected areas are also classified as high natural value (HNV) land used by traditional practices, and over approx. 8% of the "protected" grasslands meet the optimal conditions for the *Crex crex* species (*Fig. 6*).

http://www.aloki.hu ● ISSN 1589 1623 (Print) ● ISSN 1785 0037 (Online)
DOI: http://dx.doi.org/10.15666/aeer/1704_88778894

Natura 2000 sites, a pan-european network for nature conservation, also include in Romania priority habitats at community level which required their preservation by setting up Special Areas of Conservation (SAC): SPA sites (established by Romanian Government Decision no. 1284/2007) and SCI sites (set up by the Order of the MMDD no. 776/2007, Romanian Government Decision no. 971/2011).

Natura 2000 sites require special management (Cojocariu et al., 2017) but do not prohibit lucrative activities in favor of grassland biodiversity conservation and seek the adoption of sustainable solutions.

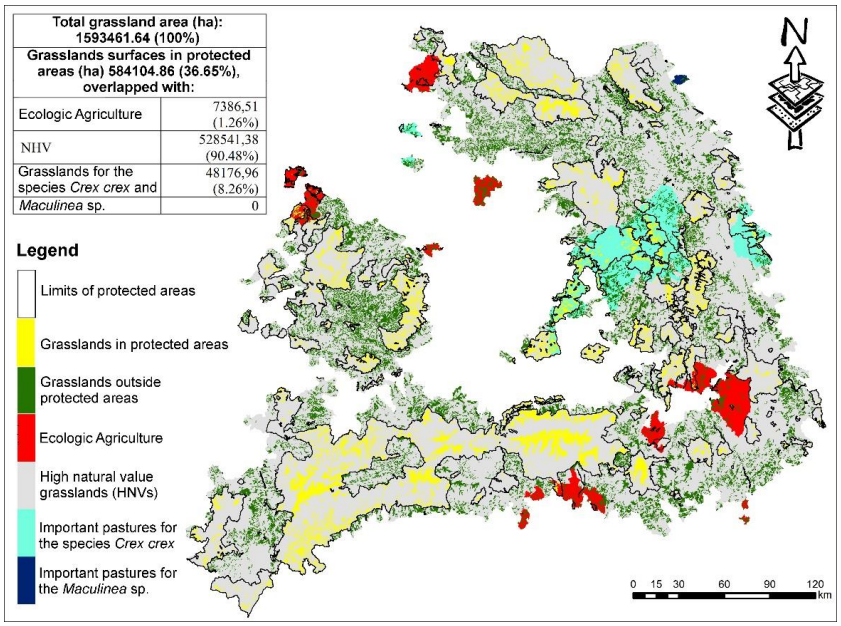

Figure 6. *The correlation of grasslands in protected areas - EU CAP programs. (processing after Ministry of the Environment, 2017; MARD, 2019)*

In order to encourage farmers managing agricultural land within the areas designated as Natura 2000 sites, financial support is expected from Pillar II of the CAP to compensate for the losses suffered.

In addition to the ecoconditionality measures for HNVs summarized in *Table 4*, mountain grassland *users* are also required to comply with a set of minimum conservation measures provided for in the management plan and regulation of the protected area over which they overlap.

Grassland management in protected areas aims to maintain the surface and grassland quality through active management for habitat and species conservation (*Table 5*).

In addition to the general and specific best practice measures for each site, recommended by the management plan, a series of awareness-raising, information and environmental education activities are required in collaboration with local communities and other stakeholders. It is also necessary to inform local communities about the existence and the process of compensation, through EU measures, for the disadvantages suffered by farmers in the mountain area. Therefore, incentives through Agro-Medium, Natura 2000 and conservation projects funded by public funds are very important in preventing mountain abandonment and biodiversity degradation, in the use of ecosystem services and preservation of cultural landscapes (Akeroyd and Page, 2011)

http://www.aloki.hu ● ISSN 1589 1623 (Print) ● ISSN 1785 0037 (Online)
DOI: http://dx.doi.org/10.15666/aeer/1704_88778894

by rural communities. The presence of several instruments can have synergistic effects (Sutcliffe et al., 2015) on the conservation of semi-natural habitats of mountain grasslands. This beautiful mountainous area of Romania still has many natural values that can be promoted and included in the strategies and programs of local communities' development.

Table 5. *Minimum conservation measures in pastures superposed on protected areas*

General measures	
It is necessary	Compliance with the management plan and area regulation with regard to surface use and pastoral activities.
	Maintaining grassland habitats in good conservation status, through grazing and mowing, respecting animal load and grazing and mowing periods.
	Ensure the conditions necessary to maintain the favorable conservation status of grassland habitats as naturally as possible.
	Ensure the conditions necessary to maintain the favorable conservation status of grassland habitats as naturally as possible.
	Maintaining biodiversity to ensure ecological balance of ecosystems and optimal conditions for protected species.
	Preventing the spread and reducing the spread of invasive species on the territory of the protected area.
	Ensuring the necessary conditions for wild fauna species dependent on grassland habitats.
It is forbidden	Intentional killing or capture of wild birds that make their nest in the shrub / trees in the grasslands.
	Damage, destruction of nests and / or harvesting of eggs from nature.
	Deliberate disturbance of wild birds.
	Damage and/or destruction of breeding or resting places of wild animals.
	Harvesting flowers and fruits, harvesting, cutting, uprooting or deliberately destroying wild plants in their natural habitats.

Conclusions

The grasslands cover 22.30% (1593461.64 ha) of the surface area of Romania's mountainous area, a percentage which gives them a special importance for the mountain population being the natural resource with a multifunctional exploitation potential, realizable according to the conditions of sustainable agriculture, traditional practices.

The large number of identified protected areas (770 entities of different categories) support the idea of the high biodiversity of the mountainous area, implicitly of the grassland habitats.

One third of grassland areas (36.65%) are included in one or more environmental protection structures; which again reveals the complexity of ecosystems: the existence of several protected areas overlapping on the same territory means the presence and protection of distinct habitats.

In addition to biodiversity conservation measures imposed by different protected areas, Romania's mountainous area is fully included in the Agro-Environment and Climate and Ecological Agriculture programs, part of the CAP, which encourages the pursuit of sustainable agriculture, also the protection of biological resources. The grasslands, one of the main economic resources of the mountain range, from the point of view of technological restraints, is suitable for a management or extensive management.

The present study, through scientific arguments, promotes and supports the Common Agricultural Policies, adopted at European level and implicitly in Romania, for a

http://www.aloki.hu ● ISSN 1589 1623 (Print) ● ISSN 1785 0037 (Online)
DOI: http://dx.doi.org/10.15666/aeer/1704_88778894

particularly important area in ecological, political, economic, geographical terms, both for Romania and at European level.

Encouraging and sustaining extensive traditional agricultural practices determines both the maintenance of biodiversity and the diversity of semi-natural grassland habitats. In addition to the environmental component, the financial support of grassland owners or users (HNV) also includes a socio-economic component. This is to be understood as an opportunity to obtain income from the inhabitants of these areas as a result of the marketing of agri-food products under the name of "mountain product" (Order no. 31/31.01.2018). This capitalization can be done either in a stand-alone activity or in integrated activities such as agro-tourism.

REFERENCES

[1] Akeroyd, J., Page, N. (2011): Conservation of High Nature Value (HNV) grassland in a farmed landscape in Transylvania, Romania. – Contributii Botanice 46: 57-71.

[2] Antonescu, D., Dumitrascu, M., Geacu, S., Grigorescu, I. (2015): Overview and perspectives of protected natural areas in Romania. – MPRA Paper 68317, University Library of Munich, Germany.

[3] Babai, D., Molnár, Zs. (2014): Small-scale traditional management of highly species-rich grasslands in the Carpathians. – Agriculture, Ecosystems and the Environment (in press).

[4] Baessler, C., Klotz, S. (2006): Effects of changes in agricultural land-use on landscape structure and arable weed vegetation over the last 50 years. – Agriculture, Ecosystems & Environment 115: 43-50.

[5] Balázsi, Á. (2017): Grassland Management in Protected Areas: A Study on the Implementation of the EU Biodiversity Strategy in Certain Post-Communist Countries. – Hacquetia.

[6] Bălteanu, D., Dumitrașcu, M., Ciupitu, D. (2009): România, Ariile naturale protejate, Harta 1:750000. – Editura CD Press, București.

[7] Căluşeru, L. A., Cojocariu, L., Borlea, F., Bordean, D. M., Horablaga, A. (2015): Rural development of mountain areas in Romania, challenges and targets for the year 2020. – SGEM 5(2): 791-798.

[8] Ceballos, G., Davidson, A., List, R., Pacheco, J., Manzano-Fischer, P., Santos-Barrera, G., Cruzado, J. (2010): Rapid decline of a grassland system and its ecological and conservation implications. – PloS one 5(1): e8562. doi:10.1371/journal.pone.0008562.

[9] Cojocariu, L., Căluşeru, A., Horablaga, A., Bostan, C., Bordean, D. M. (2017): Evolution of the development and management of grasslands from Timiș, Romania, included in the ecologic Natura 2000 network. – SGEM 17(54): 307-314.

[10] Cojocariu, L., Bordean, D. M., Copacean, L., Hoancea, L. (2018): Evaluation of the biodiversity protection degree in Romanian Banat by geomatic methods. – SGEM 18(5.1): 369-376.

[11] Dumitraşcu, M., Grigorescu, I., Năstase, M., Dumitraşcu, C. (2015): Sustainable natural landscape management in the Romanian Carpathians. – Recent Advances in Fluid Mechanics and Heat & Mass Transfer: 325-332.

[12] ESRI. Documentation for ArcMap, ArcGIS Desktop. – provided by ESRI. Available at: https://desktop.arcgis.com/en/documentation/.

[13] European Environment Agency (EEA) (2002): High Nature Value Farming Areas, Defining the concept and developing an agri-environmental indicator. – Proceedings of an Expert Meeting 21-22 February 2002, Copenhagen, Annex VI HNV expert meeting proceedings - www.eea.europa.eu/about-us/tenders/.../annex_06.

http://www.aloki.hu ● ISSN 1589 1623 (Print) ● ISSN 1785 0037 (Online)
DOI: http://dx.doi.org/10.15666/aeer/1704_88778894

[14] European Environment Agency (EEA) (2012): Corine Land Cover Database, 2012 Edition. – https://www.eea.europa.eu/data-and-maps/data/external/corine-land-cover-2012.
[15] European Environment Agency (EEA) (2017): Digital Elevation Model (DEM) with spatial resolution at 25 m, Produced using Copernicus data and information funded by the European Union. – EU-DEM layers; owned by the Enterprise and Industry DG (DG-ENTR) and the European Commission. Available at: https://www.eea.europa.eu/data-and-maps/data/copernicus-land-monitoring-service-eu-dem.
[16] European Parliament (2019): Second pillar of the CAP: rural development policy, Fact Sheets on the European Union. Available at: http://www.europarl.europa.eu/factsheets/en/sheet/110/al-doilea-pilon-al-pac-politica-de-dezvoltare-rurala.
[17] Food and Agricultural Organisation of the United Nation (FAO) (2010): Global Forest Resources Assessment, Main report, 2010. – Rome, Italy, 2010. Available at: http://www.fao.org/3/a-i1757e.pdf.
[18] Garnier, E., Lavorel, S., Ansquer, P., Castro, H., Cruz, P., Dolezal, J., Eriksson, O., Fortunel, C., Freitas, H., Golodets, C., Grigulis, K., Jouany, C., Kazakou, E., Kigel, J., Kleyer, M., Lehsten, V., Lepš, J., Meier, T., Pakeman, R., Papadimitriou, M., Papanastasis, V. P., Quested, H., Quétier, F., Robson, M., Roumet, C., Rusch, G., Skarpe, C., Sternberg, M., Theau, J-P., Thébault, A., Vile, D., Zarovali, M. P. (2007): Assessing the Effects of Land-use Change on Plant Traits, Communities and Ecosystem Functioning in Grasslands: A Standardized Methodology and Lessons from an Application to 11 European Sites. – Annals of Botany 99(5): 967-985.
[19] Geacu, S., Dumitraşcu, M., Maxim, I. (2012): The evolution of the natural protected areas Network in Romania. – Romanian Journal of Geography 56(1): 33-41.
[20] Google Earth platform (2018): Satellite images. – https://earth.google.com/web/.
[21] Iojă, C. I., Pătroescua, M., Rozylowicza, L., Popescu, V. D., Vergheleţc, M., Zottac, M. I., Felciucc, M. (2010): The efficacy of Romania's protected areas network in conserving biodiversity. – Biological Conservation 143(11): 2468-2476.
[22] Lei, C., Lin, Z., Zhang, Q. (2014): The spreading front of invasive species in favorable habitat or unfavorable habitat. – J. Differ. Equ. 257: 145-166.
[23] Life Viva Grass (2019): High Nature Value Grasslands. – Available at: https://vivagrass.eu/grasslands/high-nature-value-grasslands/.
[24] López Lambas, M. E., Ricci, S. (2014): Planning and management of mobility in natural protected areas. – Procedia Soc. Behav. Sci. 162: 320-329.
[25] McDonald, R. I. (2013): Implications of Urbanization for Conservation and Biodiversity Protection. – In: Levin, S. A. (ed.) Encyclopedia of Biodiversity, 2nd ed. Academic Press: Amsterdam, The Netherlands, 231-244.
[26] Miladkova, P., Mladek, J., Hejduk, S., Hejcman, M., Cruz, P., Jouany, C., Pakeman, R. J. (2015): High-nature-value grasslands have the capacity to cope with nutrient impoverishment induced by mowing and livestock grazing. – Journal of Applied Ecology 52: 1073-1081.
[27] Ministry of Agriculture and Rural Development of Romania (MARD) (2019): The National Program for Rural Development 2014-2020. – Available at: http://www.madr.ro/docs/dezvoltare-rurala/2019/PNDR-2014-2020-versiunea-IX-aprobata-23-ianuarie-2019.pdf.
[28] Ministry of the Environment (2000): National Strategy for the Conservation of Biodiversity. – Available at: http://www.mmediu.ro/img/attachment/32/biodiversitate-54784ffea5918.pdf.
[29] Ministry of the Environment (2017): Geospatial database with protected area boundaries, information available in vector format, updated on 29.08.2017. – Available at: http://www.mmediu.ro/articol/date-gis/ 434.

http://www.aloki.hu ● ISSN 1589 1623 (Print) ● ISSN 1785 0037 (Online)
DOI: http://dx.doi.org/10.15666/aeer/1704_88778894

[30] Molnár, Z., Kis, J., Vadász, C., Papp, L., Sándor, I., Béres, S., Sinka, G., Varga, A. (2016): Common and conflicting objectives and practices of herders and conservation managers: the need for a conservation herder. – Ecosystem Health and Sustainability 2(4): e01215. doi: 10.1002/ehs2.1215.
[31] Mráz, P., Ronikier, M. (2016): Biogeography of the Carpathians: evolutionary and spatial facets of biodiversity. – Journal of the Linnean Society 119(3): 528-559.
[32] National Agency for Cadastre and Real Estate Advertising (NACRA) (2019): Geospatial vector data. – http://geoportal.ancpi.ro/geoportal/catalog/download/download.page.
[33] National Institute of Statistic of Romania (NIS) (2018): Surface area of the land fund by mode of use, by counties and localities. – Available at: http://statistici.insse.ro:8077/tempo-online/#/pages/tables/insse-table.
[34] Order no. 776/2007 on the declaration of sites of Community importance as an integral part of the European ecological network Natura 2000 in Romania.
[35] Order no. 31/31.01.2018 amending the Annex to the Order of the Minister of Agriculture and Rural Development no. 52/2017 approving the Procedure for checking the conformity of the data contained in the tender dossier in order to grant the right of use of the "mountain product" option and to verify the compliance of the European and national legislation by the economic operators who have obtained the right of use of that mention. – published in the Official Gazette No 133/12.02.2018.
[36] Osterburg, B., Isermeyer, F., Lassen, B., Röder, N. (2010): Impact of economic and political drivers on grassland use in the EU. – Grassland Science in Europe 15: 14-28.
[37] Öllerer, K. (2012): The flora of the Breite woodpasture (Sighişoara, Romania). – Brukenthal Acta Musei 7(3): 589-604.
[38] Öllerer, K. (2014): The ground vegetation management of woodpastures in Romania – Insights in the past for conservation management in the future. – Applied Ecology And Environmental Research 12(2): 549-562.
[39] Păcurar, F., Rotar, I., Pleşa, A., Balázsi, Á., Vidican, R. (2015): Study of the Floristic Composition of Certain Secondary Grasslands in Different Successional Stages as a Result of Abandonment. – Bulletin USAMV series Agriculture 72(1): 193-201.
[40] Regulation (EU) No 1305/2013 of the European Parliament and of the Council of 17 december 2013, on support for rural development by the European Agricultural Fund for Rural Development (EAFRD) and repealing Council Regulation (EC) No 1698/2005. – https://eur-lex.europa.eu/LexUriServ/LexUriServ.do?uri=OJ:L:2013:347:0487:0548:EN:PDF.
[41] Regulation (EU) No 1307/2013 of The European Parliament and of the Council of 17 december 2013 establishing rules for direct payments to farmers under support schemes within the framework of the common agricultural policy and repealing Council Regulation (EC) No 637/2008 and Council Regulation (EC) No 73/2009. Available at https://eur-lex.europa.eu/LexUriServ/LexUriServ.do?uri=OJ:L:2013:347:0608:0670:en:PDF.
[42] Romanian Government Decision no. 971 of 5 October 2011 for amending and completing the Government Decision no. 1.284 / 2007 on the declaration special avifauna protection areas as an integral part of the European ecological network Natura 2000 in Romania. – Issuer: Government of Romania, Published in: Official Monitoring No. 715 of 11 October 2011 - http://www.mmediu.ro/beta/wp-content/uploads/2012/07/2012-07-25_legislatie_arii_protejate_hg971din2011noispanatura2000.pdf.
[43] Romanian Government Decision no. 1284 of 24/10/2007 Published in the Official Gazette, Part I no. 739 of 31/10/2007, on the declaration of Special Aifaunistic Protection Areas as an integral part of the European ecological network Natura 2000 in Romania. – https://www.osrgh.ro/pdf/hotarare-nr-1284-din-24-10-2007.pdf.
[44] Ruiz-Mallén, I., Corbera, E., Calvo-Boyero, D., Reyes-García, D. (2015): Participatory scenarios to explore local adaptation to global change in biosphere reserves: Experiences from Bolivia and Mexico. – Environ - Sci. Policy 54: 398-408.

http://www.aloki.hu ● ISSN 1589 1623 (Print) ● ISSN 1785 0037 (Online)
DOI: http://dx.doi.org/10.15666/aeer/1704_88778894

[45] Saraswati, G. (2014): Development Directives In Disaster-Prone Areas Based on Identification Level Vulnerability Using Geographical Information System Applications in Bogor Regency. – Procedia Soc. Behav. Sci. 135: 112-117.
[46] Sârbu, A., Coldea, G., Negrean, G., Cristea, V., Hanganu, J., Veen, P. (2004): Grasslands of Romania. Final report on National Grassland Inventory 2000-2003. – University of Bucharest & Royal Dutch Society for Nature Conservation.
[47] Stanciu, E., Florescu, F. (2009): Ariile protejate din România, Noţiuni introductive, Editura „Green Steps", Braşov.
[48] Sutcliffe, L., Akeroyd, J., Page, N., Popa, R. (2015): Combining approaches to support High Nature Value Farmland in southern Transylvania, Romania. – Hacquetia 14(1). DOI: 10.1515/hacq-2015-0011.
[49] Vega, J. M., Díaz, A., Nava, J. M., Gallardo, M., Echavarría, P. (2017): Assessing Land Use-Cover Changes and Modelling Change Scenarios in Two Mountain Spanish National Parks. – Environments 4(4): 79.
[50] Vîntu, V., Samuil, C., Rotar, I., Moisuc, A., Razec, I. (2011): Influence of the management on the phytocoenotic biodiversity of some Romanian representative grassland types. – Not Bot Hort Agrobot Cluj 39(1): 119-125.
[51] Wandersee, S. M., An, L., López-Carr, D., Yang, Y. (2012): Perception and decisions in modeling coupled human and natural systems: A case study from Fanjingshan National Nature Reserve. – China. Ecol. Model. 229: 37-49.

http://www.aloki.hu ● ISSN 1589 1623 (Print) ● ISSN 1785 0037 (Online)
DOI: http://dx.doi.org/10.15666/aeer/1704_88778894

SCENARIO SIMULATION OF LAND USE/COVER CHANGE IN FUXIAN LAKE BASIN BASED ON CONVERSION OF LAND USE AND ITS EFFECTS AT SMALL REGION EXTENT MODEL, YUNNAN PROVINCE, CHINA

LI, S. H.[1] – PENG, S. Y.[2*] – JIN, B. X.[3] – ZHOU, J. S.[1] – LI, Y. X.[2]

[1]*Yunnan Provincial Geomatics Centre, Kunming 650034, China*

[2]*College of Tourism & Geographic Sciences, Yunnan Normal University Kunming 650500, China*

[3]*Information Center, Department of Natural Resources of Yunnan Province Kunming 650224, China*

[*]*Corresponding author*
e-mail: frankmei@126.com; phone: +86-13-888-907-693

(Received 18th Mar 2019; accepted 17th May 2019)

Abstract. The construction of land use change model is an important means to deeply understand the cause and process of land use change, forecast the future development trend and analyze its environmental influence. In order to reveal the evolution law of the basin Land Use/Cover Change (LUCC) under the changing situation, based on Conversion of Land Use and its Effects at Small Region Extent model (CLUE-S), two scenarios of natural growth and ecological protection are set up with Fuxian Lake located in Yunnan province, China, as the research area to simulate the LUCC of the basin in 2020. The results show that the CLUE-S model has high reliability to simulate the future Land Use/Land Cover (LULC) change in the basin scale and the high simulation accuracy as a whole, and the Kappa coefficient is all above 0.8; under the scenario of natural change, the ecological lands like forest land, cultivated land, grassland and garden land are decreasing, in which the decrease of forest land is the largest, while the non-ecological lands such as construction piling, building area, structure and road is increasing, and the increase of construction piling is the largest. It is bound to pose a serious threat to the ecological security of the basin; under the scenario of ecological protection, the increase of forest land and water area is the largest, while the cultivated land, grassland, construction piling and garden land are greatly reduced. It shows that the quantity of ecological land increases obviously while the quantity of construction land, planting land and other land which play a restriction on ecological environment protection is decreasing, which will be beneficial to the ecological environment protection of the river basin.
Keywords: *Fuxian Lake basin, CLUE-S, LUCC, scenario simulation, high-altitude plateau lake ecosystem, LULC conversion rules*

Introduction

LULC changes can have a direct or indirect impact on a variety of eco-environmental factors, thus affecting regional and global sustainable development. The study of its dynamic changes is an important subject of global and regional environmental change (Li, 1996; Wijesekara et al., 2012). Analyzing the change characteristics of LULC, revealing the evolution of different space-time scales and predicting future changes are helpful to reveal the process and mechanism of regional ecological environment change under the influence of human society, and thus provide decision-making basis for regional ecological protection and sustainable development.

At present, the main models of LULC change and simulation in academic circles include system dynamics model, CLUE-S model, multi-agent model, Markov model,

http://www.aloki.hu ● ISSN 1589 1623 (Print) ● ISSN 1785 0037 (Online)
DOI: http://dx.doi.org/10.15666/aeer/1704_88958914

CA-markov, FLUS model and so on (Bai, 2000; Duan et al., 2004; Hou et al., 2004; Chu et al., 2005; Liu et al., 2006; Qin et al., 2009; Li et al., 2015; Liu et al., 2017; Hu and Zhang, 2018; Wang et al., 2019). Each model has its own advantages and disadvantages, and the CLUE-S model has obvious advantages in reflecting the gradation, relevance and competitiveness of the LULC change space and is unique in the simulation and optimization of LULC change under policy control (Verburg et al., 2002), thus being widely used in the study of LULC change simulation Cities and urban agglomerations (Peng et al., 2007; Li et al., 2009; Guo et al., 2012; Huang et al., 2012; Liu et al., 2012; Feng et al., 2013; Zhang et al., 2013; Wang et al., 2014; Huang et al., 2015; Jiang et al., 2015; Lu et al., 2015; Xu et al., 2016; Li et al., 2017; Liu et al., 2017; Tian et al., 2019), China's rapid economic growth region (Cai et al., 2004; Tan et al., 2006; Sheng et al., 2008; Lu et al., 2009; Wang et al., 2009; Zhang et al., 2011; Zheng et al., 2014; Han et al., 2015), big city fringe area (Meng et al., 2010), inland arid zone (Zhang et al., 2004; Dai et al., 2013), mountainous area (Peng et al., 2007; Zhu et al., 2010; Gao et al., 2013; Zhao et al., 2014), watershed and lake zone (Bai et al., 2005; Wang et al., 2014; Guo et al., 2016; Li et al., 2016; Sun et al., 2016; Bian et al., 2017; Zhu et al., 2019) village and town (Zhu et al., 2010) and forest park (Li et al., 2016) and so on.

Fuxian Lake is a unique low-latitude and high-altitude plateau lake ecosystem in the world. It is an important international lake to study the mechanism of biodiversity formation. Affected by the East Asian and Southwest monsoon, it is the most sensitive representative lake in response to global change. Favored by experts and scholars at home and abroad, it has become one of the hot spots of the research on international lakes, and it is also one of the plateau lake basin systems with the research value of the most ecological fragile areas in geosciences of China. For this reason, this study takes Fuxian Lake Basin as an example and uses CLUE-S model to carry out LUCC simulation research under different scenarios, so as to reveal the characteristics of land use change with high precision and long time series in plateau lake basin, which has the research value of the most ecological fragile area in the field of geosciences in China. The objective of this study is that the impact and effect of quantification and spatial scales of human decision-making factors on the clue-s model. It is of great significance to study the global change response and biodiversity formation mechanism of the unique low-latitude and high-altitude plateau lake ecosystem in the world. At the same time, it provides guidance for how to effectively implement the land use planning, water source protection, ecological restoration and others of Fuxian Lake basin so as to improve the water environment quality of the river basin.

Materials and Methods

General situation of the study region

Located in the center of the Central Yunnan Basin, Yuxi City, central Yunnan Province, Fuxian Lake is China's largest deep-water freshwater lake, the first large lake in the source of the Pearl River, and is the Nanpanjiang River system. Its geographical location is 24°21′28″- 24°38′00″N and 102°49′12″- 102°57′26″E (*Fig. 1*). As one of the nine plateau lakes in Yunnan Province, Fuxian Lake is the second deep-water lake explored in China and the lake area and water storage amount to the 8th and 3rd in China, respectively (Wang et al., 1998). Because of the particularity of its geographical location and its powerful water supply capacity and recreational value, it is known as

http://www.aloki.hu ● ISSN 1589 1623 (Print) ● ISSN 1785 0037 (Online)
DOI: http://dx.doi.org/10.15666/aeer/1704_88958914

the "plateau pearl" in central Yunnan, serving as an important resource guarantee for the sustainable social and economic development in central Yunnan, the strategic water resource for the regional development of the Pan-Pearl River Delta, as well as the important strategic source of drinking water in the Pearl River Basin and Southwest China (Gao et al., 2013). The water quality of Fuxian Lake is Class I, and is one of the best natural lakes in China.

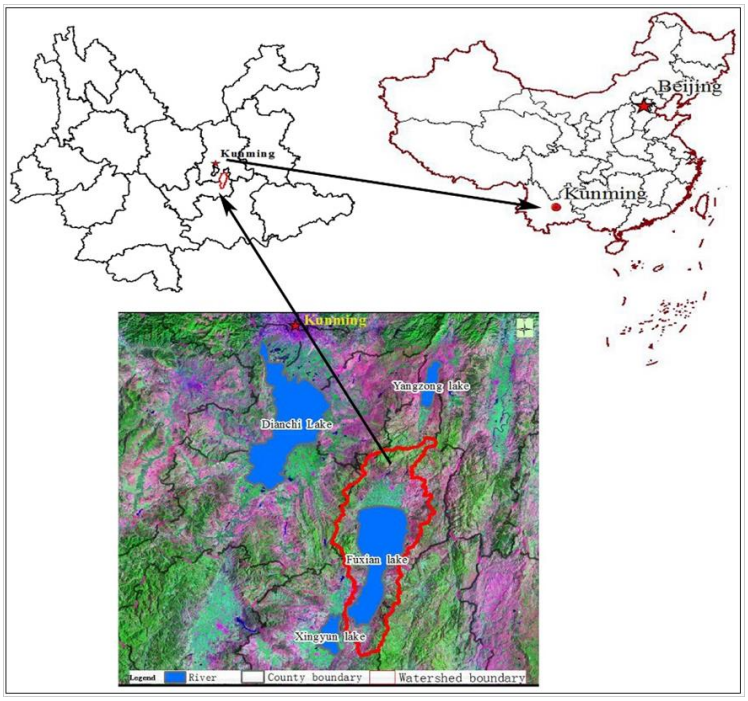

Figure 1. *Location of Fuxian lake watershed*

The vegetation in the basin is mainly secondary vegetation such as grass, shrub and coniferous forest. The population reaches about 160,300, the rural economy mainly comes from crop production, the main food crops include rice, corn, wheat and so on, and economic crops include flue-cured tobacco and rape. The industry is dominated by phosphorus chemical industry, building materials, food processing and aquatic products, of which phosphorus chemical industry is the pillar industry of this area. The land use type of Fuxian Lake Basin has always been dominated by forests and water areas, but with the improvement of the urbanization level of the basin, human activities have increased disturbance on the natural environment, such phenomena as reclamation of lakes, deforestation, over-exploitation of tourism resources, and the rapid increase of functional buildings result in significant change in land coverage types in Fuxian Lake Basin.

Data sources

Because of the obvious seasonal variation of rainfall in Fuxian Lake Basin and the large variation of lake area with season, the remote sensing images of relatively stable lake water level during the dry season from January to March are selected, including 5 phases of high spatial resolution remote sensing image data (*Table 1, Fig. 2*). The reference data are listed in *Table 2*.

http://www.aloki.hu ● ISSN 1589 1623 (Print) ● ISSN 1785 0037 (Online)
DOI: http://dx.doi.org/10.15666/aeer/1704_88958914

Table 1. *Satellite images*

Sensor	Acquired Date	Spatial Resolution	Source
QuickBird	2008-12-18	0.61m	Purchased from remote sensing image agents
WorldView-2	2011-01-29	0.5 m	Purchased from remote sensing image agents
WorldView-2	2014-01-26	0.5 m	Purchased from remote sensing image agents
WorldView-2	2017-03-28	0.5 m	Purchased from remote sensing image agents

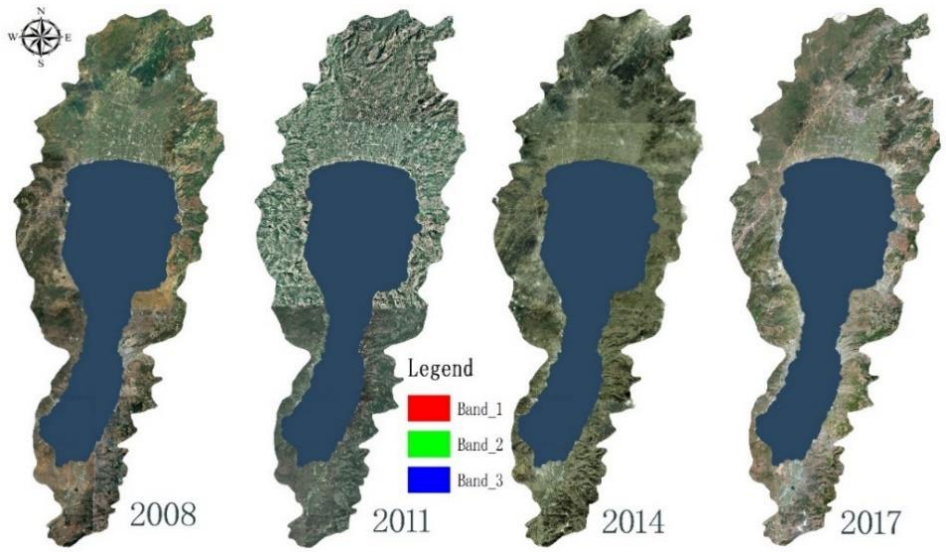

Figure 2. *Remote sensing images in study area*

Table 2. *Supplementary data*

Name	Property and Role	Source
Digital Line Graphic (DLG)	The scale is 1: 10000, including road, river, et al. The reference data sources of orthorectified remote sensing image and Map making of LULC change driving factors	Yunnan Provincial Bureau of Surveying and Mapping
Digital Orthophoto Map (DOM)	0.5m resolution, acquire date 2014. The reference data sources of orthorectified remote sensing image	Yunnan Provincial Bureau of Surveying and Mapping
Digital Elevation Model (DEM)	10 m grid spacing. The reference data sources of orthorectified remote sensing image and the basin's boundary extracted, elevation, slope and slope direction are derived from DEM	Yunnan Provincial Bureau of Surveying and Mapping
GPS and triangle points	GPS C-level points and triangle points of each level measured from 1985 to 2013. The reference data sources of orthorectified remote sensing image	Yunnan Provincial Bureau of Surveying and Mapping
Land use/ Land cover	The product of the first national geographical situation survey in Yunnan Province. The training data and test data for LULC extraction from remote sensing image.	Yunnan Provincial Bureau of Surveying and Mapping
Driving factors	Precipitation, Temperature, population density, GDP of primary Industry, GDP of secondary industry, GDP of tertiary industry.	Statistical Yearbook of Yuxi City (2008, 2011, 2014, 2017)
Driving factors	soil moisture content . The product of the National Geographical state monitoring demonstrative project -Dynamic monitoring for ecological environment in Fuxian lake watershed	Yunnan Provincial Bureau of Surveying and Mapping
Restricted factors	The vector of Fuxian Lake Basin Planning is restricted spatial area of watershed. The 13th Five-Year Plan of Fuxian Lake Basin (2016-2020), which is reference of Scenario construction.	Fuxian Lake Administration Bureau of Yuxi City

http://www.aloki.hu ● ISSN 1589 1623 (Print) ● ISSN 1785 0037 (Online)
DOI: http://dx.doi.org/10.15666/aeer/1704_88958914

Analysis methods

LULC information extraction

The first-class classification system (water area, desert and bare surface, cultivated land, structure, garden land, grassland, forest land, house building, road and construction land) in the general survey contents and indicators of geographical conditions (GDPJ 01-2013) is adopted as a classification system for extracting LULC information of this remote sensing image, and the definition of each type is shown in GDPJ 01-2013. Due to the difference of remote sensing image data sources and time phase, training samples and test samples are collected from the remote sensing images in 2008, 2011, 2014 and 2017, respectively. For each LULC type of images in each phase, 2000 samples are collected, 70% of which are used for training samples and 30% for test samples. The MSORF method (refer to the Reference (Li, 2018) for details) is used to obtain the LULC classification results of the river basin in 2008, 2011, 2014 and 2017. The classification accuracy Kappa is generally 0.8 or more, i.e., 2008 (0.812), 2011 (0.819), 2014 (0.822), and 2017 (0.805). Referring to the current land use map and remote sensing images, the classified data are manually modified to form the final LULC information (*Fig. 3*).

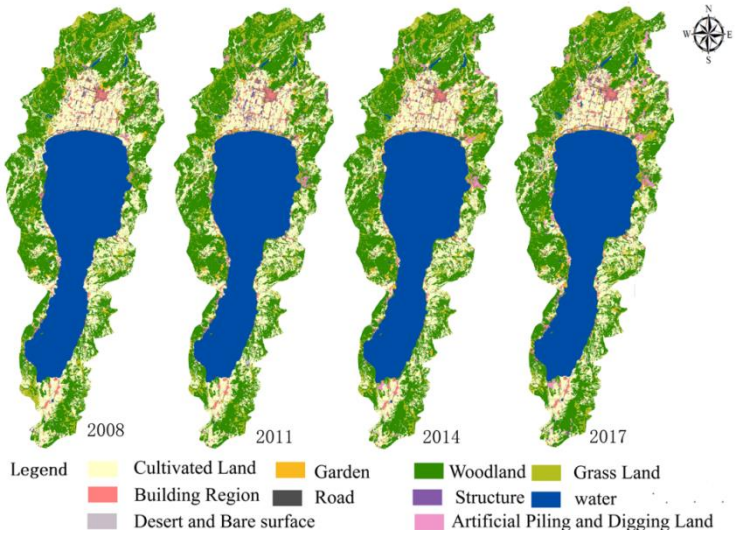

Figure 3. *Classification result of LULC in study area*

In the ArcGIS platform, the LULC classification results were statistically analyzed, and the area change rate of each land type during the study period was obtained to reflect the temporal change characteristics of the LULC (*Table 3*).

Table 3 shows that in 2008-2017, water (W), woodland (WL), cultivated land (CL) and grass land (GL) are the four main types of surface cover. The total area of these four types is 95.00%, 93.89%, 93.43% and 92.50% in 2008, 2011, 2014, 2017, respectively, and Building Region (BR), road (R), garden (G), structure (S), Artificial Piling and Digging Land (APDL), Desert and Bare surface (DB) is 5.00%, 6.11%, 6.57% and 7.50%. The results indicate the area of artificial surface types has increased over years, while that of the natural surface cover types is opposite. The area of artificial excavation land in 2017 is four times of that in 2008. The area of water only decreased 0.03% from 2008 to 2017.

http://www.aloki.hu ● ISSN 1589 1623 (Print) ● ISSN 1785 0037 (Online)
DOI: http://dx.doi.org/10.15666/aeer/1704_88958914

Due to the socio-economic development of the basin and the enhancement of human activities, the LULC type closely related to human economic activities shows a strong growth momentum. Since 2006, due to the implementation of the policy of returning CL to WL and GL, the CL has shown a decreasing trend, and the area of WL has decreased first and then increased. While GL changes little. The main reason is due to natural succession, returning CL to GL, artificial sowing, etc. The area of DB has been changing from increase to decline year by year. The water area remains basically unchanged.

Table 3. *LULC Types Statistics in Fuxian Lake Basin from 2008 to 2017 (area (hm^2), percent (%))*

Year	2008		2011		2014		2017	
LULC type	**Area**	**Percent**	**Area**	**Percent**	**Area**	**Percent**	**Area**	**Percent**
CL	15355.33	22.74	14391.91	21.31	13840.46	20.49	13650.52	20.21
G	496.4	0.74	783.78	1.16	973.87	1.44	958.98	1.42
WL	21947.51	32.50	22596.69	33.46	22472.71	33.28	22029.85	32.62
GL	4924.57	7.29	4643.56	6.88	4940.17	7.32	4880.06	7.23
BR	1368.26	2.03	1465.69	2.17	1486.01	2.20	1608.54	2.38
R	674.57	1.00	732.43	1.08	732.93	1.09	801.09	1.19
S	424.57	0.63	591.36	0.88	443.08	0.66	563.83	0.83
APDL	288.87	0.43	412.46	0.61	703.49	1.04	1017.89	1.51
DB	127.03	0.19	142.81	0.21	100.25	0.15	115.02	0.17
W	21925.16	32.47	21771.58	32.24	21839.30	32.34	21906.48	32.44
Total	67532.27							

Simulation method of LULC change scenarios in the basin

The CLUE-S model (the conversion of land use and its effects at small regional extent) is the improved CLUE model by Verburg et al. (2002). It is a dynamic and small-scale spatial distribution simulation model of LULC change. Its model framework is composed of spatial allocation model and non-spatial demand module. Non-spatial demand module, based on natural and socio-economic analysis, predicts the annual LULC-type demand area of the study region in the future. However, the spatial allocation model is driven by the LULC demand, based on the rasterized spatial data, and allocate the demand change of the annual LULC type according to the LULC conversion rules and the LULC spatial distribution probability, so as to realize the spatial simulation of LULC change. See the CLUE-S operating manual (Verburg and Overmars, 2009; Verburg et al., 2002) for a detailed description.

Scenario construction of LULC change in the basin

The determination of LULC changing situation is based on the rational thought of "if," and "then". If the set conditions are met, what will happen to the future LULC. Therefore, according to relevant policies and development plans such as the *Regulations on the Protection of Fuxian Lake in Yunnan Province* (implemented on September 29, 2016), and the *Protection and Development Plan for Fuxian Lake Basin* (2016-2020), and the *Overall Land Use Planning of Fuxian Lake Basin*, two scenarios such as "natural change" and "ecological protection" are set to simulate the LULC change of Fuxian Lake Basin in 2020.

The natural change scenario is based on the actual number of LULC changes in the Fuxian Lake Basin from 2008 to 2017, assuming that the LULC changes in the Fuxian

http://www.aloki.hu ● ISSN 1589 1623 (Print) ● ISSN 1785 0037 (Online)
DOI: http://dx.doi.org/10.15666/aeer/1704_88958914

Lake Basin are not substantially affected by policy regulation and external policies, and mainly considering the relationship between the natural and socio-economic development indicators and LULC changes, changing with the change rate from 2008 to 2017.

The ecological protection scenario is mainly set according to the contents of the ecological environmental protection planning of the river basin, and the special location and number of ecological lands (water area, forest land, cultivated land and grassland) within the river basin will be adjusted according to the designated and strict requirements of the ecological protection red line. The specific assumption is that the construction land is correspondingly reduced, the water area remains unchanged, the forest land continues to increase, and the forest coverage rate is more than 35% (about 236 square kilometers).

Scenario simulation of LULC changes in the basin based on CLUE-S model

Referring to the CLUE-S model manual and relevant cases and documents, according to the set scenario, the steps of using the CLUE-S model to simulate the LULC change of the basin include the calculation of regression coefficient and land demand, restriction area setting, LULC change driving factor analysis, change matrix setting and other main steps. In order to ensure the reliability and accuracy of the simulation results, the file formed in the above steps must be subject to uniform coordinate and scale, mask, format conversion, etc. before being input into the model, so that the data has a consistent reference system and number of rows and columns, the same coordinate origin and uniform ASCII data format.

(1) Calculation of regression coefficient. The regression parameter file is a file in which the CLUE-S model records the correlation size between each land type and the driving factor calculated by logistic regression analysis. Before calculating the regression coefficient, it is necessary to define the main driving factors of LULC change of the basin. In consideration of the availability and quantification of the data, factors such as the distance from the nearest township center, the distance from the nearest river, the distance from the nearest road, elevation, slope, slope direction, annual average rainfall, annual average temperature, population density, the output value of tertiary industry and soil water content are selected as the driving factors of LULC change of the basin. By means of collinearity analysis, it is found that there is no collinearity among the selected 11 driving factors, and the collinearity coefficient is all less than 0.02, which meets the requirement of model collinearity.

(2) Land use demand in the scenario of basin change. According to the set natural change and ecological protection scenario, combined with the characteristics of CLUE-S model, the demand of LULC type quantity is taken as scenario assumption condition, and input into the model to analyze its influence on the spatial distribution of LULC of the basin. Among them, the cultivated land area, water area and total grain output of the river basin are used as LULC demand files, and the missing year data are supplemented with linear interpolation method. The 2017 simulation of the 2020 demand is based in part on data from previous years using the GM (1,1) model in the DPS. The land use demand for each year are shown in *Table 4*.

In the *Table 4*, Cultivated Land (CL), Woodland (WL), Garden (G), Grass Land (GL), Building Region (BR), Road (R), Structure (S), Artificial Piling and Digging Land (APDL), Water (W), Desert and Bare surface (DB). The bellows is the same.

http://www.aloki.hu ● ISSN 1589 1623 (Print) ● ISSN 1785 0037 (Online)
DOI: http://dx.doi.org/10.15666/aeer/1704_88958914

Table 4. *Land use needs under natural growth and ecological protection scenarios in the Fuxian Lake Basin from 2014 to 2020 (hm^2)*

year / LULC type	2008	2011	2014	2017	2018		2019		2020	
					Natural growth	Ecological protection	Natural growth	Ecological protection	Natural growth	Ecological protection
CL	15355.33	14391.91	13840.46	13650.52	13587.21	11547.04	13523.89	9443.56	13460.58	7340.08
G	496.4	783.78	973.87	958.98	954.02	793.63	949.05	628.27	944.09	462.92
WL	21947.51	22596.69	22472.71	22029.85	21882.23	25379.13	21734.61	28728.42	21586.99	32077.7
GL	4924.57	4643.56	4940.17	4880.06	4860.02	4224.08	4839.99	3568.11	4819.95	2912.13
BR	1368.26	1465.69	1486.01	1608.54	1649.39	1562.34	1690.24	1516.13	1731.09	1469.92
R	674.57	732.43	732.93	801.09	823.82	782.72	846.53	764.36	869.25	745.99
S	424.57	591.36	443.08	563.83	604.08	520.73	644.33	477.63	684.58	434.53
APDL	288.87	412.46	703.49	1017.89	1122.69	678.59	1227.49	339.30	1332.29	0
DB	127.03	142.81	100.25	115.02	119.94	76.68	124.87	38.34	129.79	0
W	21925.16	21771.58	21839.30	21906.48	21928.87	21967.32	21951.27	22028.16	21973.66	22089
Total	67532.27									

(3) Restricted area file setting. The spatially restricted area mainly refers to all kinds of planning areas demarcated by government departments, such as land use planning data, ecological environment protection red line and other planning limitation areas of the basin. In the simulation process, the restricted area will not be changed once being set and directly affects the whole simulation process. The restricted area of this study is mainly the basic farmland protection area in the basin, and the red line area of basin ecological protection in the 13th Five-Year Plan (2016-2020) of water environmental protection in Fuxian Lake Basin (*Fig. 4*).

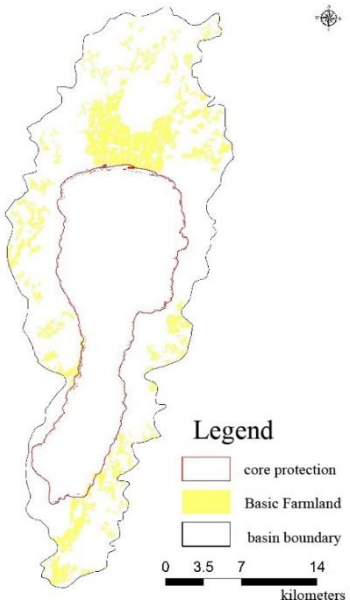

Figure 4. *The restricted spatial area of watershed LULC change simulation under different scenarios*

This file is the restricted area file of the model, but the land use status map is reclassified before the model is input and the value of LULC type must start from 0; the restricted area file is binarized by re-classifying in the same way, that's, water area (0),

http://www.aloki.hu ● ISSN 1589 1623 (Print) ● ISSN 1785 0037 (Online)
DOI: http://dx.doi.org/10.15666/aeer/1704_88958914

forest land (1), building area (2), garden land (3), cultivated land (4), grassland (5), road (6), structure (7), desert and bare land (8), and construction land (9). In the CLUE-S model, the LULC active area, i.e., the unrestricted area, the value will be set to be "0", while the value of the restricted area vwill be set to be "-9998".

(4) Map making of LULC change driving factors. Using the annual LULC information classification results, the road and river data are extracted, and the distance map of each pixel from the nearest river, township center and road is calculated using grid space analysis; rainfall, temperature, population density and economic vector map is made through ArcGIS vector space analysis function; elevation, slope and slope direction are derived from DEM; the extraction algorithm of soil water content based on image (wave band) was used to extract soil water content and make soil water content map, as shown in *Fig. 5*.

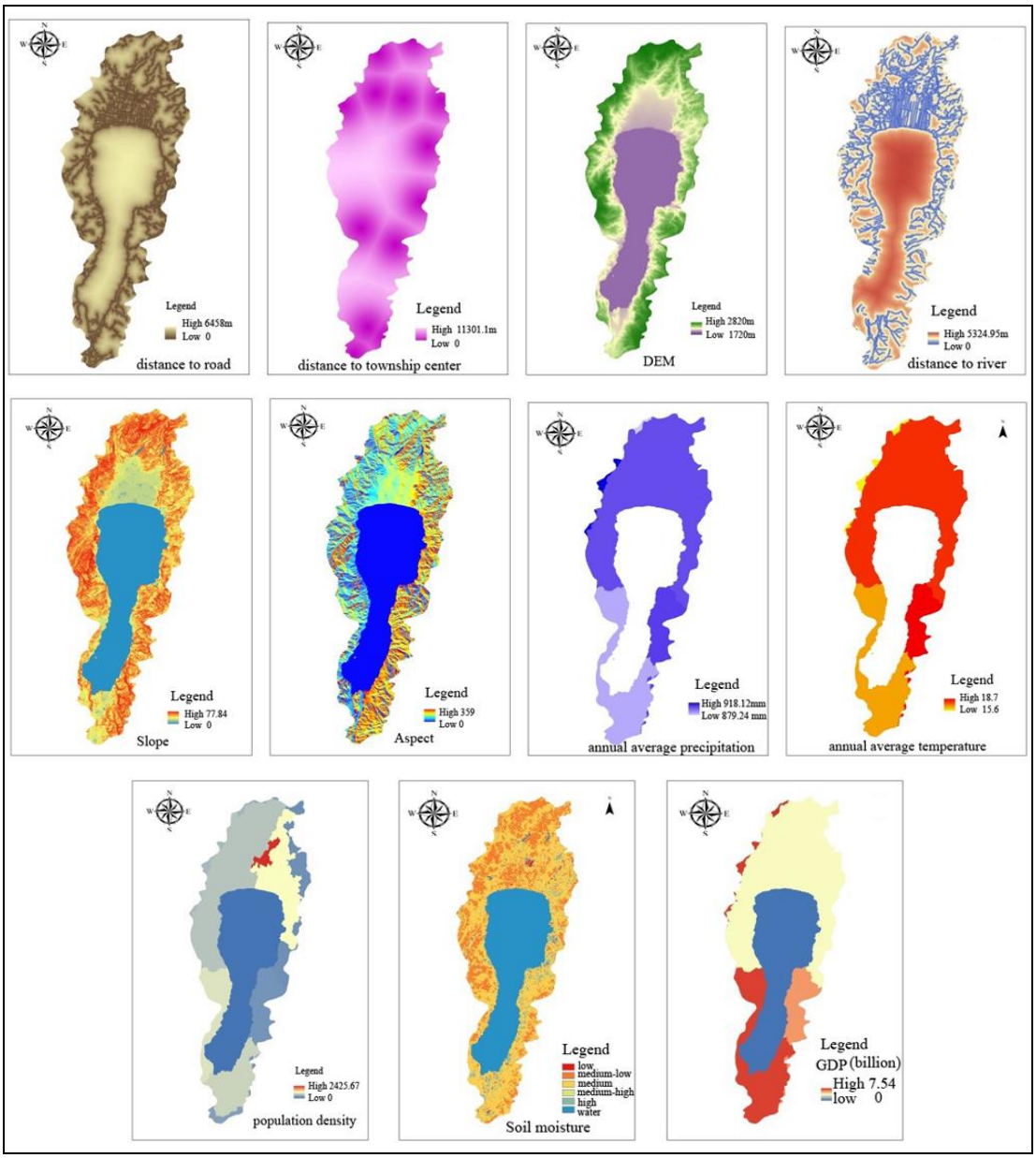

Figure 5. *The driver forces map of land use change*

http://www.aloki.hu ● ISSN 1589 1623 (Print) ● ISSN 1785 0037 (Online)
DOI: http://dx.doi.org/10.15666/aeer/1704_88958914

(5) LULC change matrix setting. The LULC transfer matrix refers to the possibility matrix of mutual conversion between different LULC types according to the set scenario during the research period. Thus, the conversion matrix is set to 10 * 10, the rows representing the period year LULC type, and the columns representing the target year LULC type. If Class A can be conversed to be Class B, it is 1, otherwise it is 0.

(6) Conversion elasticity settings. Conversion elasticity reflects the difficulty with which each LULC type can be converted to another type. Its value ranges from 0 (easy to convert) to 1 (non-convertible). The closer it is to 1, the more stable it is, and the more difficult it is to be changed. The magnitude of the conversion elasticity is generally expressed by transition probability matrix. Using the LULC classification result of the basin, the LULC transition probability matrix for 2008-2011, 2011-2014 and 2014-2017 can be calculated. The values on the diagonal represent the stability of this LULC type, i.e. the conversion elasticity (*Table 5*).

Table 5. *LULC conversion elasticity in watershed from 2008 to 2017*

LULC type	conversion elasticity			
	2008~2011	2011~2014	2014~2017	average
CL	0.93	0.89	0.92	0.91
G	0.89	0.64	0.90	0.81
WL	0.95	0.95	0.96	0.95
GL	0.80	0.72	0.87	0.80
BR	0.98	0.96	0.98	0.97
R	0.97	0.92	0.97	0.95
S	0.79	0.66	0.52	0.66
APDL	0.78	0.55	0.85	0.73
DB	0.44	0.17	0.58	0.40
W	0.99	0.99	0.99	0.99

Table 5 shows that in 2008-2017, the conversion elasticity of all land types fluctuates less and has a higher conversion elasticity. Among them, the conversion elasticity between desert and bare land is the lowest, which is only 0.4, indicating that it is difficult to convert to other places, while the conversion elasticity of other lands is above 0.7, and the water area is the most stable. Because there is a certain band of the conversion elasticity value of each type in the three periods, and the setting of the stability parameter has a great influence on the simulation result, the average value of the three periods is used as the stability parameter among different LULC types in the study area.

(7) Determination of the simulation scale of LULC change in the river basin. In the CLUE-S model, the iteration of spatial allocation is a process in which the demand of LULC type in the research area interacts with the natural, social and economic factors in the grid element, and has obvious scale effect. Under the influence of the same driving factors, taking 10m, 30m, 60m and 100m as the spatial scales of the experiment, the logistic regression analysis models of various spatial scales of each LULC type are constructed, respectively, and the results are described in terms of Area Under Receiver Operating Characteristic (ROC) Curve (AUC) values (*Fig. 6*); then, the simulation results of each spatial scale are compared with the LULC type result map of the actual year to calculate the Kappa value of the land type. The results show that because there are too many pixels on the 10 m grid scale and the calculation amount is too large, the

http://www.aloki.hu ● ISSN 1589 1623 (Print) ● ISSN 1785 0037 (Online)
DOI: http://dx.doi.org/10.15666/aeer/1704_88958914

results cannot be calculated in the Logistic analysis with errors reported and from the AUC curve, the AUC curves at 30 m scale are above the 60 m and 100 m scale curves as a whole. Moreover, the Kappa value and average value of cultivated land, building area, forest land and garden land reach more than 0.9, which is generally higher than other spatial scales, so 30 m * 30 m is chosen as the optimal spatial scale for this simulation.

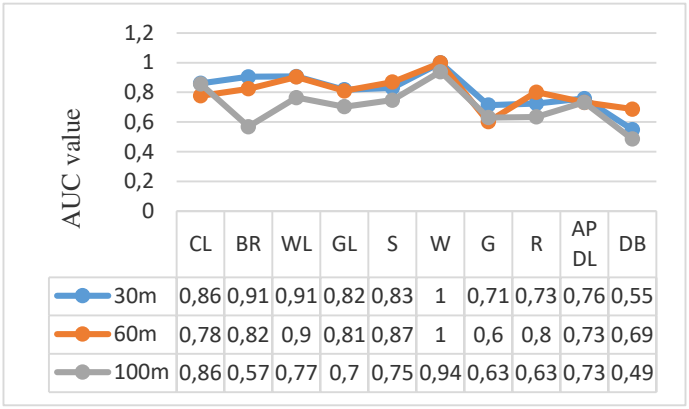

	CL	BR	WL	GL	S	W	G	R	AP DL	DB
30m	0,86	0,91	0,91	0,82	0,83	1	0,71	0,73	0,76	0,55
60m	0,78	0,82	0,9	0,81	0,87	1	0,6	0,8	0,73	0,69
100m	0,86	0,57	0,77	0,7	0,75	0,94	0,63	0,63	0,73	0,49

Figure 6. *The AUC change of muti-scale LULC simulation in watershed*

(8) Simulation of LULC change scenarios in the river basin. Determine the analysis grid size of 30 m * 30 m by using the above-set LULC change simulation parameters, and update the population, rainfall amount, temperature, output value and soil water content by using the selected driving factors with the LULC status chart in 2017 as a reference. According to the set scenario and restriction conditions, the LULC change of Fuxian Lake Basin in 2020 is simulated. The results are shown in *Fig. 7*.

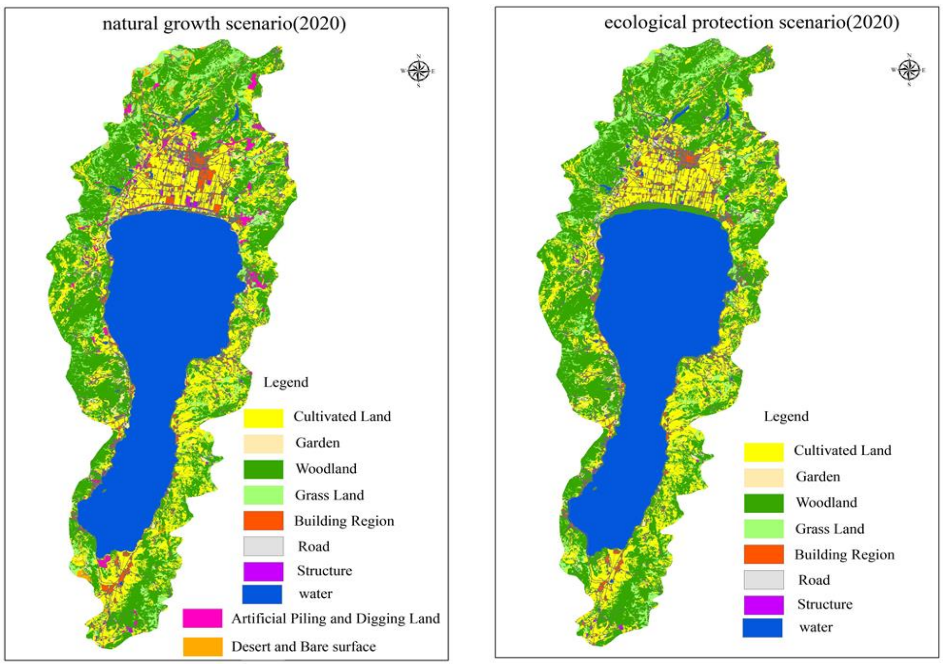

Figure 7. *The results of LULC change simulation under different scenarios in Watershed*

http://www.aloki.hu ● ISSN 1589 1623 (Print) ● ISSN 1785 0037 (Online)
DOI: http://dx.doi.org/10.15666/aeer/1704_88958914

(9) Verification of simulation accuracy. Based on the LULC results of Fuxian Lake in 2008, 2011 and 2014, the time duration is three years to simulate the LULC changes in 2011, 2014 and 2017 in three times. After the simulation is completed, the result files cov all. * 2011, cov _all. * 2014, and cov all. * 2017 are transformed to form a final simulation result (*Fig. 8*).

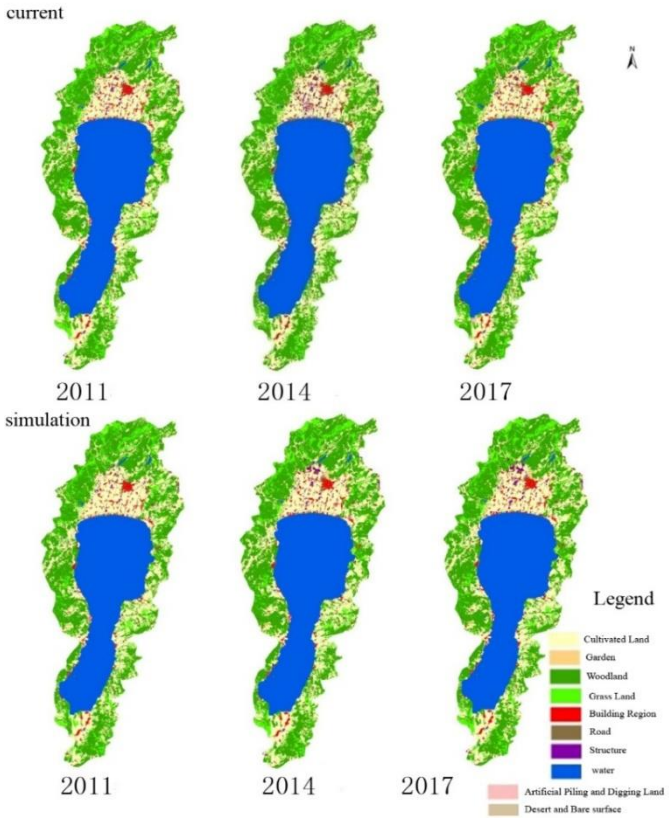

Figure 8. *The Comparison of LULC simulation results with current status map*

It is the most effective method to evaluate the accuracy of the simulation results by comparing the simulation results with the actual LULC graphs in this year (Verberg, 1999). The AUC value and Kappa coefficient of logistic regression analysis are used to verify the accuracy of the simulation results. The simulation results for 2011, 2014, and 2017 are compared with the actual LULC graph for the year to verify the accuracy of the simulation from both spatial and quantitative variations. From the space intersection analysis, the spatial distribution difference of the simulation precision can be obtained, the grid calculation tool is used to subtract the simulation result from the actual result classification graph, and the correct grid number (0-value grid) can be calculated, to obtain Kappa value (*Table 6*).

As can be seen from *Table 6*, the overall simulation accuracy is high, but there is a difference among various land classes. The simulation accuracy of garden land, structure and construction land is relatively low, of which the construction land is the lowest. The Kappa index of the water area and the cultivated land is above 0.9, the water area is above 0.99, which is very high, and the simulation result is almost consistent with the actual result. The results show that the driving factors selected in the study can better explain the spatial change of LULC. Because the garden land, structure,

http://www.aloki.hu ● ISSN 1589 1623 (Print) ● ISSN 1785 0037 (Online)
DOI: http://dx.doi.org/10.15666/aeer/1704_88958914

construction land, desert and bare land are greatly disturbed by human factors, the simulation effect is not very good.

Table 6. *Accuracy verification of simulation result*

LULC type	Kappa			Raster count		
	2011	2014	2017	2011	2014	2017
CL	0.979	0.954	0.924	175542	166530	164556
G	0.750	0.687	0.546	4290	6253	6514
WL	0.993	0.977	0.996	242170	245875	248165
GL	0.984	0.941	0.970	55531	54247	53388
BR	0.940	0.967	0.932	14423	15819	16020
R	0.957	0.908	0.892	7247	7520	7520
S	0.735	0.830	0.649	3586	5537	5862
APDL	0.661	0.664	0.271	2216	3208	3084
DB	0.936	0.774	0.858	1316	1247	1145
W	0.998	0.992	0.996	243982	243630	243660

Analysis of Results

The change characteristics of LULC quantity

The simulation results for 2020 under different scenarios are compared with the 2017 LULC type status chart to analyze the quantitative and spatial changes (*Table 7*).

Table 7 shows that under the natural change scenario, the forest land, farmland, grassland and garden land show a decreasing trend, and the forest land decrease is the largest, while the construction land, building area, structure and road show an increasing trend, and the increase of the construction land is the largest.

Table 7. *Simulation results of LULC type change under different scenario*

LULC type	2017	Natural Growth (2020)	Ecological protection(2020)	Natural Growth change (2020)	Ecological protection Change (2020)
CL	13650.52	13460.58	7340.08	-189.94	-6310.44
G	958.98	944.09	462.92	-14.89	-496.06
WL	22029.85	21586.99	32077.7	-442.86	10047.85
GL	4880.06	4819.95	2912.13	-60.11	-1967.93
BR	1608.55	1731.09	1469.92	122.54	-138.63
R	801.09	869.25	745.99	68.16	-55.1
S	563.83	684.58	434.53	120.75	-129.3
APDL	1017.89	1332.29	0	314.4	-1017.89
DB	115.02	129.79	0	14.77	-115.02
W	21906.48	21973.66	22089	67.18	182.52

According to the spatial distribution of the change, the cultivated land in the village farmland area decrease obviously, while the impervious surface and other land increase, the forest and grass coverage in the phosphate rock area decreases, and other land increases. However, the impervious surface and other land use in the urban area show an increasing trend, while the cultivated land shows a decreasing trend. The numerical and spatial changes of LULC/coverage changes in the basin in natural situation reflect the comprehensive effects of natural and human factors. Along with the improvement of the urbanization level of the river basin, the construction land of the river basin occupies

http://www.aloki.hu ● ISSN 1589 1623 (Print) ● ISSN 1785 0037 (Online)
DOI: http://dx.doi.org/10.15666/aeer/1704_88958914

a large amount of cultivated land, especially the flat area on the north bank (urban area) of Fuxian Lake is the most prominent, which leads to the larger reduction of high-quality cultivated land in the river basin and thus poses a certain threat to the planting level and the safety of grain production in the river basin. At the same time, along with the large increase of other land use in phosphate rock area (desert and bare surface) and impervious surface in urban area promotes surface pollutants to flow into rivers, further aggravating the threat of non-point source pollution to lake-entering rivers, and the forest and grass coverage decreases, which will inevitably pose a serious threat to the ecological security of the river basin.

Under the circumstance of ecological protection, the increase of forest land and water area is the largest, while the cultivated land, grassland, construction land and garden land are greatly reduced. The quantity of ecological land increases obviously, while the quantity of construction land, planting land and other land that restrict the ecological environment protection shows a decreasing trend, which will benefit the ecological environment protection of the river basin. According to the spatial distribution of changes, the other land (desert and bare surface) in the phosphate rock area, the construction land in the urban area, the cultivated land in the village farmland area are greatly reduced, and the forest and grass coverage in the three areas have increased greatly. The result of this change is not only the response of LULC change to the ideal state of the 13th Five-Year Plan on protection the basin, but also the demonstration of the implementation effect of specific policies such as "Four Retreats and Three Returns". This result has greatly increased the forest coverage rate of the basin, and in the core protection area where the pollution source is the most serious, the influence of human activities has been withdrawn, and the ideal state of the natural land types in the core protection area has been realized, forming a natural barrier to the drainage and purification of the lake.

Spatial variation characteristics of LULC

Using the "per category" module of the MCK image comparison tool, the results of scenario simulation are compared with the actual land use in 2014. The results are as shown in the figure. The types of restricted land types such as cultivated land, forestland, garden land, water area, desert and bare land and construction land are mainly analyzed. In the figure, "in one of the maps" indicates the rest of the land types other than this land type, and "in both maps" indicates areas where there is no change in 2014 and 2017, "only in 2014, not in 2017" indicates a reduced area in 2017 relative to 2014, and "only in 2017, not in 2014" refers to the increased area in 2017 relative to 2014.

Fig. 9 shows that from 2008 to 2017, the cultivated land under the natural change scenario was continuously reduced, mainly converted into forest land, garden land and grassland, and a small part was converted into construction land and desert and bare land; but under the ecological protection scenario, the cultivated land also showed the decreasing trend, but the range was smaller than the natural change scenario. The change of the region has been distributed throughout the basin, and for the areas with higher elevation, the part of the cultivated land also has a decreasing trend.

There is a decreasing trend of forest land under natural changes and ecological protection scenarios. It is mainly concentrated in the high altitude area to the north of Fuxian Lake Basin, and the change of forest land within the ecological protection red line is very small.

http://www.aloki.hu ● ISSN 1589 1623 (Print) ● ISSN 1785 0037 (Online)
DOI: http://dx.doi.org/10.15666/aeer/1704_88958914

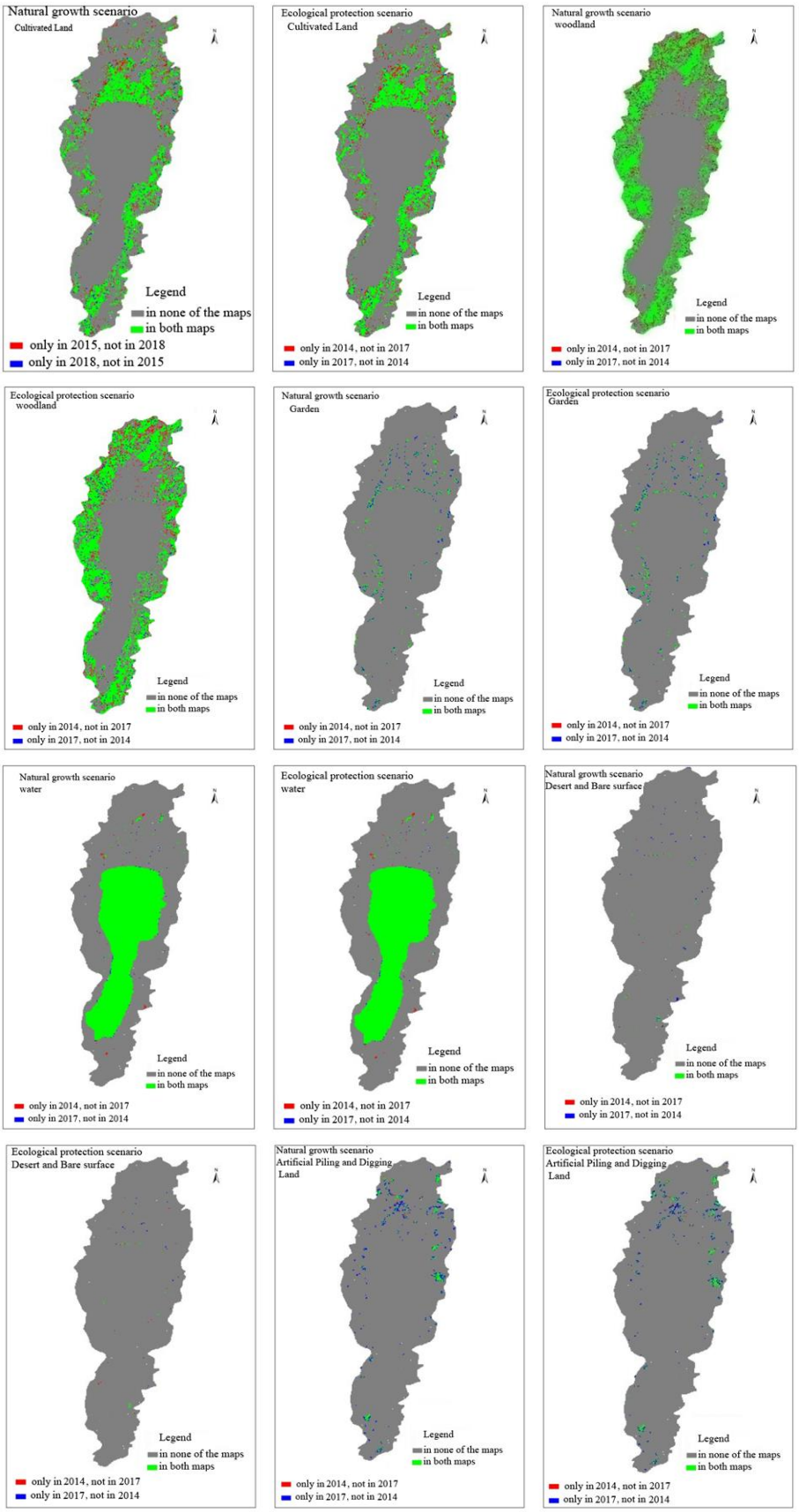

Figure 9. *Spatial distribution of LULC types under different scenarios*

http://www.aloki.hu ● ISSN 1589 1623 (Print) ● ISSN 1785 0037 (Online)
DOI: http://dx.doi.org/10.15666/aeer/1704_88958914

Under the natural change and the ecological protection scenarios, the garden land showed an increasing trend. The garden land area of the natural change scenario increased from 993.28 hectares in 2015 to 1,463.94 hectares, while the ecological protection scenario area increased by 48.68%, which is consistent with the requirements of the ecological protection plan. It is mainly distributed in the middle and low elevation area of the river basin, and in the north and west of the river basin, and it is also the most widely distributed and largest area of the garden land in Chengjiang County.

The distribution of increasing and decreasing water area is close to that of natural change and ecological protection scenarios. The reduced area is the north and northwest of Fuxian Lake Basin, and the waters increase along the edge of the Lake. This fully demonstrates the effectiveness of the policy of returning farmland to lakes and forests in Fuxian Lake Basin.

Under the natural change and ecological protection scenarios, the area of desert, bare land and constructed land all showed an increasing trend. Because the total area of desert, bare land and constructed land is relatively small, but it is an important part of the conversion of ground type, with the highest degree of activity. Although the conversion parameters of the land types are limited in scenario simulation, the general direction of change is unchanged. In the stable change trend, its change area mainly distributes in the urban and rural fringe area with frequent human activities.

Conclusions and Discussion

Conclusions

(1) The CLUE-S model has high reliability to simulate the future LULC change in basin scale. The overall simulation accuracy is high, but there are differences in the simulation accuracy of different land types. The simulation accuracy of the garden land, structure, construction land, desert and bare land disturbed by human factors is relatively low, among which the construction land is the lowest. Kappa index of water area and cultivated land are above 0.9 and water area is above 0.99, which indicates that the driving factors selected in the study could better explain the spatial change of LULC.

(2) Under the natural change scenario, the ecological security of the basin will face serious threats. The forest land, farmland, grassland and garden land is reducing and the decrease of garden land is the largest, while the construction land, building area, structure and road is increasing and the increase of the construction land is the largest. According to the spatial distribution of the change, the cultivated land in the village farmland area decreases obviously, while the impervious surface and other land increase, the forest and grass coverage in the phosphate rock area decreases, and other land increases. However, the impervious surface and other land use in the urban area show an increasing trend, while the cultivated land shows a decreasing trend.

(3) The ecological protection scenario will be beneficial to the ecological environment protection of the river basin. The increase of forestland and water area is the largest, while the cultivated land, grassland, construction land and garden land are greatly reduced. It shows that the quantity of ecological land increases obviously, while the quantity of building land, planting land and other land that restrict the ecological environment protection shows a decreasing trend, which will benefit the ecological environment protection of the river basin. According to the spatial distribution of change, the other lands (desert and bare surface) in the phosphate rock area, the

http://www.aloki.hu ● ISSN 1589 1623 (Print) ● ISSN 1785 0037 (Online)
DOI: http://dx.doi.org/10.15666/aeer/1704_88958914

construction land in the urban area and the cultivated land in the village farmland area are greatly reduced, while the forest and grass coverage in the three areas show a significant increase trend.

Discussion

The CLUE-S model is subjective in setting the transition elasticity of land types according to the land use conversion matrix and the land use conversion probability matrix. How to obtain the objective elastic coefficient of land type conversion needs to be further studied. How to couple other models to realize seamless integration of spatial allocation of spatial and non-spatial modules so as to reach the "equilibrium" state of land use change and economic and social development still is not solved. The CLUE-S model needs to be further studied by coupling with other models.

Acknowledgements. The authors are very grateful to the editor and anonymous referees reviews for their valuable comments and helpful suggestions. In addition, this work is supported by National Natural Science Foundation of P.R. China (A coupling effects study of spatial and temporal process between impervious surface area pattern and soil erosion of Dianchi Lake Basin during fast urbanization, Grant no. 41561086; Future land use/cover simulation and its response mechanism to water quality by coupling human activities and climate change effects in Fuxian lake watershed, Grant no. 41861051, Research on cloud resources auto scaling and load balancing by considering the complexity of spatiotemporal computing, Grant no.41661086), and the National Geographical state monitoring demonstrative project -- "Dynamic monitoring for ecological environment in Fuxian lake watershed" from National Administration of Surveying, Mapping and Geoinformation (file no. 201435).

REFERENCES

[1] Bai, W. Q. (2000): Analysis on land use dynamics of Shenzhen. – Journal of Resources 26(2): 112-116.
[2] Bai, W. Q., Zhang, Y. M., Yang, J. Z., Zhang, Y. L. (2005): Simulation of land use dynamics in the upper reaches of the Dadu river. – Geographical Research 24(2): 206-212.
[3] Bian, Z. H., Ma, X. X., Gong, L. C., Zhao, J., Zeng, C. F., Wang, L. C. (2017): Land use prediction based on CLUE-S model under different non-spatial simulation methods: A case study of the Qinhuai river watershed. – Scientia Geographica Sinica 37(2): 252-258.
[4] Cai, Y. M., Liu, Y. S., Yu, Z. R., Verburg, P. H. (2004): Progress in spatial simulation of land use change: CLUE-S model and its application. – Progress in Geography 23(4): 63-71.
[5] Chu, D., Zhang, Y. L., Zheng, D. (2005): Land use change scenario in Lhasa district using Markov chain model. – Geographical research 24(6): 869-877.
[6] Dai, S. P., Zhang, B. (2013): Land use change scenarios simulation in the middle reaches of the Heihe river basin based on CLUE-S model—A case of Ganzhou district of Zhangye city. – Journal of Natural Resources 28(2): 336-348.
[7] Deng, H., Shao, J. A., Wang, J. L. (2016): Land use driving forces and its future scenario simulation in the Three Gorges Reservoir Area using CLUE-S model. – Acta Geographica Sinica 71: 1981-1997.
[8] Duan, Z. Q., Verburg, P. H., Zhang, F. R., Yu, Z. R. (2004): Construction of a land-use change simulation model and its application in Haidian district, Beijing. – Acta Geographica Sinica 59(6): 1037-1047.
[9] Feng, S. C., Gao, X. H., Gu, J., Kang, J., Guo, L. F., Wu, G. L., Zou, C. (2013): Land use spatial distribution modeling based on CLUE-S model in the Huangshui River Basin. – Acta Ecologica Sinica 33(3): 985-997.

http://www.aloki.hu ● ISSN 1589 1623 (Print) ● ISSN 1785 0037 (Online)
DOI: http://dx.doi.org/10.15666/aeer/1704_88958914

[10] Gao, H. J., Zhang, C. Q., Wang, H. Z., Luo, X. Q. (2013): Simulation of land use change in Karst mountain area based on CLUE-S model. – Science of Surveying and Mapping 41(2): 76-80.
[11] Gao, W., Chen, Y., Xu, M., Guo, H. C., Xie, Y. C. (2013): Trend and driving factors of water quality change in Lake Fuxian (1980-2011). – Journal of Lake Science 25(5): 635-642.
[12] Guo,Y. F., Yu, X. B., Jiang, L. G. (2012): Scenarios analysis of land use change based on CLUE-S model in Jiangxi Province by 2030. – Geographical Research 31(6): 1016-1028.
[13] Guo, H. W., Sun, X. Y., Lian, L. S., Zhang, D. Z., Xu, Y. (2016): Response of water yield function of ecosystem to land use change in Nansi Lake Basin based on CLUE-S model and InVEST model. – Chinese Journal of Applied Ecology 27(9): 2899-2906.
[14] Han, H. R., Yang, C. F., Song, J. P. (2015): Simulation and projection of land-use change in Beijing under different scenarios. – Progress in Geography 34(8): 976-986.
[15] Hou, X. Y., Chang, B., Yu, X. F. (2004): Land use change in Hexi corridor based on CA-Markov methods. – Transactions of the CSAE 20(5): 286-291.
[16] Hu, W., Zhang, B. (2018): Short-term wind power forecast based on back-propagation neural network corrected by Markov chain. – European Journal of Electrical Engineering 20(3): 279-293.
[17] Huang, M., Zhang, X. X., Zhang, J. J., Zhao, Z. Y., Ru, H. (2012): A multi-scale simulation of land use change in Luoyugou watershed based on CLUE-S model. – Resources Science 34(4): 769-776.
[18] Huang, S. (2015): Land use spatial simulation in growth mining city. – China University of Geosciences (Beijing): 79.
[19] Jiang, W. G., Chen, Z., Lei, X., Jia, K., Wu, Y. F. (2015): Simulating urban land use change by incorporating an autologistic regression model into a CLUE-S model. – Journal of Geographical Sciences 25(7): 836-850.
[20] Li, X. B. (1996): A review of the international researches on land use/land cover change. – Acta Geographica Sinica 51(3): 553-557.
[21] Li, X. C., Diao, H. T., Wang, J., Cui, F. B. (2009): Research progress on forecasting method of regional land use demand in China. – Journal of Shandong Agricultural University (Natural Science) 40(4): 655-658.
[22] Li, S. H., Jin, B. X., Wei, X. Y., Jiang, Y. Y., Wang, J. L. (2015): using ca-markov model to model the spatiotemporal change of land use/cover in fuxian lake for decision support. – Surface Science II-4/W2(5): 163-168.
[23] Li, Y., Huang, S. L. (2016): Hydrological responses to land use change under three future scenarios in Luanhe River Basin. – Chinese Journal of Ecology 35(7): 1970-1980.
[24] Li, W., Xie, D. C., Zhang, J. (2016): Application of landscape ecological method in planning environment impact assessment-a case study for east part of Dalian Forest Park. – China Environmental Science 29(6): 605-610.
[25] Li, B., Liu, Y., Zhang, B. (2017): Multi-scenario land use change simulation in Caidian using CLUE-S based on Tietenberg Modeling. – Resources Science 39(9): 1739-1752.
[26] Li, S. H. (2018): Multi-scale spatiotemporal variation of LULC and its relationship to water quality based on high resolution remote sensing image in Fuxian lake watershed. – Phd dissertation, Yunnan Normal university.
[27] Liu, X. P., Li, X., Ai, B., Tao, H. Y., Wu, S. K., Liu, T. (2006): Multi-agent systems for simulating and planning land use development. – Acta Geographica Sinica 61(10): 1101-1112.
[28] Liu, M., Hu, Y. M., Sun, F. Y. (2012): Application of land use model CLUE-S in the planning of central Liaoning urban agglomerations. – Chinese Journal of Ecology 31(2): 413-420.
[29] Liu, J. H., Li, W. F., Zhou, W. Q., Han, L. J., Qian, Y. G., Zhen, X. X. (2017): Simulation and prediction of changes in the landscape patterns of the Beijing-Tianjin-Hebei metropolitan region and their driving mechanisms. – Acta Ecologica Sinica 37(16): 1-10.

http://www.aloki.hu ● ISSN 1589 1623 (Print) ● ISSN 1785 0037 (Online)
DOI: http://dx.doi.org/10.15666/aeer/1704_88958914

[30] Liu, X., Liang, X., Li, X., Xu, X., Ou, J., Chen, Y. M., Li, S. Y., Wang, S. J., Pei, F. S. (2017): A future land use simulation model (FLUS) for simulating multiple land use scenarios by coupling human and natural effects. – Landscape & Urban Planning 168: 94-116.
[31] Lu, R. C., Huang, X. J., Zuo, T. H., Xiao, S. S., Zhao, X. F., Zhang, X. Y. (2009): Land use scenarios simulation based on CLUE-S and Markov Composite Model—A case study of Taihu Lake Rim in Jiangsu Province. – Scientia Geographica Sinica 29(4): 577-581.
[32] Lu, W. T., Dai, C., Guo, H. C. (2015): Land use scenario design and simulation based on Dyna-CLUE model in Dianchi Lake Watershed. – Geographical Research 34(9): 1619-1629.
[33] Meng, J. J., Yan, F., Zhao, C. H. (2010): Land use change simulation on the edge of metropolis-A case study of Changping District in Beijing. – Journal of Basic Science & Engineering 256(22): 6936-6940.
[34] Peng, J., Cai, Y. L., Verburg, P. H. (2007): Scenario simulation of land use and cover change in Karst Mountainous Areas Based on CLU E-S model. – Journal of Agricultural Engineering 23(7): 64-70.
[35] Peng, P., Cai, Y. L., Verburg, P. H. (2007): Simulation of land use/cover change scenarios in Karst mountain areas. – Transactions of the Chinese Society of Agricultural Engineering 23(7): 64-70.
[36] Qin, X. H., Duan, X. J., Li, H., Lu, Y. T. (2009): Urban land expansion simulationm ODEL based on SD and CA- A case study of Nantong city. – Scientia Geographical Sinica 29(3): 439-444.
[37] Sheng, S., Liu, M. S., Xu, C. (2008): Application of CLUE-S model in simulating land use changes in Nanjing metropolitan region. – Chinese Journal of Ecology 27(2): 235-239.
[38] Sun, L. N., Liang, D. M. (2016): Effect of future land use change on hydrology in Dongliaohe basin. – Research of Soil and Water Conservation 23(5): 164-168.
[39] Tan, Y. Z., Wu, C. F., Mu, Y. M., Wang, Q. R., Yu, Z. G. (2006): Simulation of land use spatial pattern change on county scale in the rapid economic development region. – Transactions of the Chinese Society of Agricultural Engineering 22(12): 72-77.
[40] Tian, T. Y., Li, B. S. (2019): Optimization and Simulation of Urban Land Use Pattern Based on the Perspective of Objective Constraint: A Case of Hohhot. – Chinese Agricultural Science Bulletin 35(9): 86-94.
[41] Verburg, P. H., Soepboer, W., Veldkamp, A., Limpiada, R., Espaldon, V., Mastura, S. S. A. (2002): Modeling the spatial dynamics of regional land use: the CLUE-S model. – Environmental Management 30(3): 391-405.
[42] Verburg, P. H., Overmars, K. P. (2009): Combining top-down and bottom-up dynamics in land use modeling: Exploring the future of abandoned farmlands in Europe with the Dyna-CLUE model. – Landscape ecology 24(9): 1167-1181.
[43] Wang, S. M., Dou, H. S. (1998): The annals of Chinese Lake. – Beijing: Science Press 374-377.
[44] Wang, J., Tian, G., Quan, Q., Jiang, J. (2009): Dynamic simulation of land use pattern in Guangzhou based on CLUE-S model. – Chinese Journal of Ecology 29(6): 1257-1262.
[45] Wang, Q., Meng, J. J., Mao, X. Y. (2014): Scenario simulation and landscape pattern assessment of land use change based on neighborhood analysis and auto-logistic model: A case study of Lijiang River Basin. – Geographical Research 33(6): 1073-1084.
[46] Wang, X., Liu, W. L., Zhang, L., Zheng, J. (2014): Landscape Spatial Distribution Modeling Based on CLUE-S Model in the Liaohe Watershed. – Journal of Geo-Information Science 16(6): 925-932.
[47] Wang, B. S., Liao, J. F., Zhu, W., Qiu, Q. Y., Wang, L., Tang, L. N. (2019): The weight of neighborhood setting of the FLUS model based on a historical scenario: A case study

http://www.aloki.hu ● ISSN 1589 1623 (Print) ● ISSN 1785 0037 (Online)
DOI: http://dx.doi.org/10.15666/aeer/1704_88958914

of land use simulation of urban agglomeration of the Golden Triangle of Southern Fujian in 2030. – Acta Ecologica Sinica 39(12): 1-15.

[48] Wijesekara, G. N., Gupta, A., Valeo, C. (2012): Assessing the impact of future land-use changes on hydrological processes in the Elbow River watershed in southern Alberta, Canada. – Journal of Hydrology 412/413: 220-232.

[49] Xu, X. L., Li, X., Xiao, C. J., Ou, M. (2016): Land use layout optimization under different scenarios by using the CLUE-S model. – Acta Ecologica Sinica 36(17): 5401-5410.

[50] Zhang, Y. M., Zhao, S. D., Verburg, P. H. (2004): Scenario analysis of land use change in Horqin Desert and its surrounding area. – Journal of Natural Resources 19(1): 29-37.

[51] Zhang, L. J., Li, W. L., Liu, D., Zhou, D. Y., Verburg, P. H. (2011): Dynamic simulation of the spatial changes of land use in the Ha-Da-Qi Industrial Corridor. – Progress in Geography 30(9): 1180-1186.

[52] Zhang, D. X., Fu, M. C., Tao, J., Hu, L. Z., Yang, X. L. (2013): Scenario simulation of land use change in mining city based on CLUE-S model. – Transactions of the Chinese Society of Agricultural Engineering 29(12): 246-256.

[53] Zhao, G. L., Hu, Y. C. (2014): Study on ecosystem service value changes based on CLUE-S models in Guangxi karst mountainous area. – Research of Soil and Water Conservation 21: 198-203.

[54] Zheng, W. H., Shen, Q. P., Wang, H., Hong, J. K. (2014): Simulating land use change in urban renewal areas: A case study in Hong Kong. – Habitat International 46: 23-34.

[55] Zhou, R., Su, H. L., Wang, X. J., Li, Y. H., Hu, Y. M. (2016): Simulation and accuracy assessment of village land use change based on CLUE-S model. – Resources and Environment in the Yangtze Basin 21(2): 174-180.

[56] Zhou, Z., Tian, N., Zhao, Y. H. (2017): Prediction and Analysis of the Age Population Scale of Compulsory Education in Tianjin based on multi-factor grey prediction model and population estimation algorithm. – Journal of Xinan Normal University (Natural Science) 42(3): 49-55.

[57] Zhu, Z. Q., Liu L. M., Chen, Z. T., Zhang, J. L., Verburg, P. H. (2010): Land-use change simulation and assessment of driving factors in the loess hilly region: A case study as Pengyang county. – Environmental Monitoring and Assessment 164(1-4): 133-142.

[58] Zhu, W. B., Zhang, J. J., Cui, Y. P. (2019): Assessment of territorial ecosystem carbon storage based on land use change scenario: A case study in Qihe River Basin. – Acta Geographica Sinica 74(3): 446-459.

http://www.aloki.hu ● ISSN 1589 1623 (Print) ● ISSN 1785 0037 (Online)
DOI: http://dx.doi.org/10.15666/aeer/1704_88958914

DETERMINATION OF DYNAMIC CRITICAL RAINFALL BASED ON GEOMORPHOLOGICAL INSTANTANEOUS UNIT HYDROGRAPH AND RADIAL BASIS FUNCTION NEURAL NETWORK

WANG, W. S. – MA, X. X.*

College of Water Conservancy & Environmental Engineering, Zhengzhou University, Zhengzhou 450001, China

**Corresponding author*
e-mail: maxx@zzu.edu.cn; phone: +86-136-1371-1818

(Received 18th Mar 2019; accepted 17th May 2019)

Abstract. To disclose the formation mechanism of flash flood disaster, it is necessary to develop a dynamic critical rainfall model that considers all influencing factors. Targeting the Peihe River watershed in China's Henan Province, this paper designs a runoff convergence calculation plan based on the geomorphological instantaneous unit hydrograph (GIUH), and uses the plan to simulate 8 floods in the target watershed. The simulated results were close to the measured data. Next, the GIUH was adopted to predict the critical rainfalls of 16 floods in the target watershed. The radial basis function neural network (RBFNN) was selected to create a dynamic critical rainfall prediction model, with the preceding rainfall, cumulative rainfall and rainfall intensity as the inputs and the critical rainfall of each event as the output. The model was employed to predict the critical rainfalls of 6 historical floods. The results show that the prewarned critical rainfall reached the pass rates of 100% and 83.3%, respectively, for the 1 h and 3 h periods. Hence, that the GIUH can ensure the calculation accuracy despite the lack of data in regions prone to flash flood; the RBFNN-based dynamic critical rainfall prediction model can effectively improve the accuracy of critical rainfall calculation and the flash flood prewarning.
Keywords: *flash flood disaster, prewarning index, concentration model, disaster prevention object, geomorphological parameters*

Introduction

In recent years, the climate change has induced extreme weather conditions across the world, such as the extreme rainfall events. As a result, the flash flood, a rapid flooding in small hilly regions associated with heavy rainfall, became a frequent global disaster with increasing scope of influence (Gruntfest and Handmer, 1999). With complex influencing factors and severe damages, this disaster is difficult to prevent or mitigate, making it the key to flood prevention and mitigation. The critical rainfall is an important parameter in the prewarning and prevention system of flash flood disasters (Li et al., 2014). A pre-warning should be issued when the rainfall is forecasted to reach the critical level, and a warning should be released once the real-time rainfall reaches the critical value. Therefore, the accuracy of critical rainfall is essential to the reduction of casualties and property losses.

Currently, the critical rainfall is mainly determined by the following methods: flash flood guidance (FFG) (WMO, 1994; Villarini et al., 2010; Carpenter et al., 1999; Diagi, 2018; Norbiato et al., 2008; Georgakakos, 2006; Seo et al., 2013; Vizzari et al., 2018; Clark et al., 2014), single-station or regional critical rainfall method based on the characteristic flood-causing rainfall (Chen and Yuan, 2005; Chen et al., 2014), flood-causing flow inversion based on analytical calculation of runoff generation and

http://www.aloki.hu ● ISSN 1589 1623 (Print) ● ISSN 1785 0037 (Online)
DOI: http://dx.doi.org/10.15666/aeer/1704_89158930

convergence (RGC) (Mao, 2016; Ma, 2017), dynamic critical rainfall method based on different soil saturations (Liu et al., 2010; Ye et al., 2014) and the dynamic critical rainfall method based on various influencing factors (Guo et al., 2016). Below is a brief introduction to each of these methods.

The FFG method fully considers such three factors as rainfall, antecedent soil moisture and the underlying surface (Ren, 2015). Firstly, a control section is selected at the prewarning location, and the characteristic flow of the section is computed according to the river section data of the watershed. Next, the design rainfall and other parameters are inputted to the model, and the rainfall-caused flood is simulated through RGC calculation. Finally, the critical rainfalls in different periods at the target location are determined, considering the impacts of antecedent soil moisture on flash flood. Based on a physical mechanism, the FFG method provides dynamic information for prewarning, thanks to its consideration of rainfall, the underlying surface as well as the impacts of soil water content. Thus, this method has been trusted and adopted by most countries in Europe, the Americas and Africa (Georgakakos, 2006). However, the FFG requires professional support platforms and high-quality data on rainfall. In practice, it is very difficult to acquire the parameters of hydrological model, or set up a complete historical flash flood database to verify the flash flood warning.

As for the single-station or regional critical rainfall method based on the characteristic flood-causing rainfall, it is necessary to collect the data on multiple flood-causing rainfalls. Without considering antecedent moisture and spatiotemporal rainfall distribution, this method faces a high calculation error in regions with fewer floods.

By the flood-causing flow inversion based on analytical calculation of RGC, the critical rainfalls in different prewarning periods under dry, general and wet conditions are computed based on the flood-causing flow and the RGC model of the watershed. The real-time prewarning is realized through two steps: estimating the soil water content and the corresponding critical rainfall in each prewarning period, and comparing the estimated value with the forecasted value. The estimation is bound to bring a large error, if the rainwater condition in the region is managed by a single department. What is worse, this method, taking account of only a few factors, ignores the effects of spatiotemporal distribution of rainfall and preceding rainfall on the bottom water of the river.

Following the dynamic critical rainfall method based on different soil saturations, the soil saturation and rainfall of the watershed in each prewarning period are illustrated as a scatter plot, and a straight line of critical prewarning rainfall is drawn in the scatter plot, dividing the state space of soil saturation and the maximum rainfall in each period into two parts. In this way, the critical rainfall for flash flood prewarning changes with the soil saturation in the watershed, laying the basis for dynamic prewarning. Compared with the previous methods, this strategy fully considers the dynamic variation in soil saturation in actual floods. Nevertheless, the soil saturation-based prewarning method will produce a constant critical rainfall after the soil is saturated with water, which goes against the actual situation.

In the dynamic critical rainfall method based on various influencing factors, the critical rainfall of each event is computed according to the measured rainfall process and the watershed RGC model, and the critical rainfall of each event is correlated with the rainfall characteristics of each event, forming the dynamic critical rainfall curve. This method improves the accuracy of critical rainfall calculation to some extent, as it fully considers how the critical rainfall is affected by the time variation of rainfall, the

http://www.aloki.hu ● ISSN 1589 1623 (Print) ● ISSN 1785 0037 (Online)
DOI: http://dx.doi.org/10.15666/aeer/1704_89158930

cumulative rainfall, and the antecedent moisture. However, the calculation accuracy needs to be further improved by differentiating the impact degree of various factors on the critical rainfall.

The watershed RGC calculation is fundamental to the computation of the critical rainfall. The calculation of runoff generation, affected by geographic and geomorphic conditions, directly bears on the flooding of the watershed outlet section, which in turn affects the accuracy of critical rainfall and real-time pre-warning. In the existing rainfall calculation methods, the runoff generation is often computed by inference formula method (Liu et al., 2017; Li, 2016) and hydrograph models of multiple units (e.g. empirical unit, instantaneous unit and geomorphological instantaneous unit (Ye et al., 2013; Wang et al., 2018).

Based on five-point generalization, the flood hydrograph obtained by the inference formula method needs manual calibration, as it deviates from the actual situation in the rising and recession phases. Besides, the effects of the underlying surface (e.g. geomorphic conditions) is not taken into account.

The integrated instantaneous unit hydrograph, integrated empirical unit hydrograph, integrated reference formula and geomorphological instantaneous unit hydrograph are all tools to estimate the flood hydrograph in regions lacking the necessary data. Specifically, the integrated unit hydrograph method firstly analyzes the watersheds with measured data in the study area, derives the relationship between the unit hydrograph and the geographic eigenvalues of the watershed, and then deduces the unit hydrograph of the region lacking the necessary data according to the local geographic eigenvalues and the said relationship. Assuming the linearity and time invariance of the set sum, the unit hydrograph is a function of the natural geographic features of the watershed, but cannot be directly adopted for watersheds lacking necessary data.

The geomorphological instantaneous unit hydrograph (GIUH) can acquire the geomorphic features of the watershed in real time, using digital elevation model (DEM), geographic information system (GIS), remote sensing and other means. In addition, these features are digitalized such that the spatiotemporal effects of human activities can be fully considered in hydrological simulation. The overall consideration ensures that the simulated results are close to the actual situation.

In this paper, the geomorphological features of the target watershed are extracted by ArcGIS, and used to establish a runoff generation model based on the geomorphological instantaneous unit hydrograph proposed by Rodriguez-Iturbe and Valdes (R-V GIUH). Then, the established model was adopted to calculate the critical rainfalls of several rainfall events measured in the watershed. Considering such factors as rainfall intensity, cumulative rainfall and antecedent moisture, the author constructed the dynamic critical rainfall model by the radial basis function (RBF), which discloses the dynamic relationship between critical rainfalls of several floods and various influencing factors. The model was trained into the prediction model by the data of several floods, and applied to forecast the dynamic critical rainfall. The research findings shed new light on the calculation of dynamic critical rainfall.

Materials and methods

Watershed overview

Located in the center of Xinxian County, Xinyang Prefecture, Central China's Henan Province, the Peihe River mainly flows through a mountainous region with huge

http://www.aloki.hu ● ISSN 1589 1623 (Print) ● ISSN 1785 0037 (Online)
DOI: http://dx.doi.org/10.15666/aeer/1704_89158930

elevation difference and complex geomorphic features. The watershed (*Fig. 1*) is covered by yellow brown soil, paddy soil and moisture soil. The climate is relatively humid, with an annual mean rainfall of 1,335 mm. The low vegetation coverage makes the watershed prone to natural disaster and soil erosion. The weather in the watershed could be vastly different from area to area. Thus, heavy rains are commonplace here, leading to severe flash floods. According to statistics, 12 major flash floods has hit the Peihe River watershed since 1949, causing losses of hundreds of million yuan and affecting tens of thousands of people.

In this research, the villages of Xinxian County are selected from the watershed as the objects of disaster prevention. Many of the widely scattered settlements are highly susceptible to flash floods. The villages along the river cann withstand a 20-year flood at the most. Because of the small watershed and short convergence time, the river water will rise above the banks of the rainfall is too intense, causing damages to the villagers.

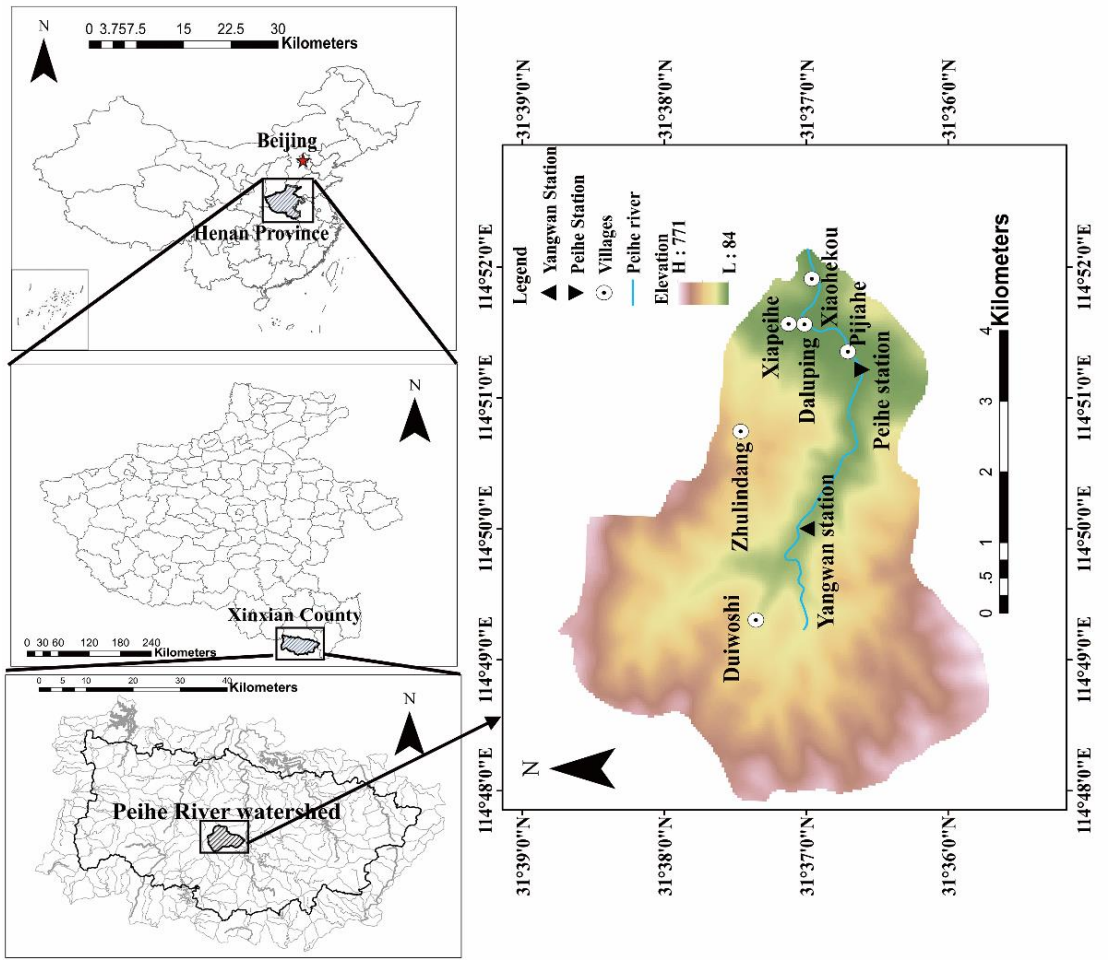

Figure 1. *Overview of the Peihe River watershed*

There is a rainfall station (Yangwan) and a hydrological station (Peihe) in the Peihe River watershed. The two stations observe such items as precipitation, water level and flow rate. The available data cover the heavy rains in flood season over the 32 years between 1982 and 2013. The data period is sufficiently long to have statistical significance, that is, the data can reveal the actual rainfall features in the watershed.

http://www.aloki.hu ● ISSN 1589 1623 (Print) ● ISSN 1785 0037 (Online)
DOI: http://dx.doi.org/10.15666/aeer/1704_89158930

Most of the natural river sections are either V-shaped or U-shaped, with a total catchment area of about 21 km^2. The prewarning water level of the watershed was determined as 97.3 m according to the measured large section data of the Peihe River watershed provided by Henan Provincial Flood Prevention Drought Relief Headquarters and the *2015 Flash Flood Disaster Analysis and Evaluation Report of Xinxian County, Henan Province*. The flow rate corresponding to the prewarning flow, i.e. the prewarning flow, was determined as 92 m^3/s by looking up the water level-flow rate relationship curve of the watershed, which was obtained based on the perennial measured flow rates and water levels.

Geomorphologic instantaneous unit hydrograph proposed by Rodriguez-Iturbe and Valdes (R-V GIUH)

The runoff convergence model of R-V GIUH theory is established based on geomorphic and hydrodynamic parameters of the watershed. The model can reflect the actual geomorphic features with a few easy-to-obtain parameters. In this paper, the general formula proposed by Wen et al. (1991) is adopted to calculate the R-V GIUH of the watershed (*Eq. 1*):

$$R-VGIUH(t)=-\sum_{j=1}^{\Omega}\left\{\lambda_i\left[\sum_{i=1}^{j}\theta_{i,\Omega}(0)A_{ij}\right]e^{-\lambda_j t}\right\} \quad \text{(Eq.1)}$$

where i and j are the orders of rivers ($i \neq j$); λ_i and λ_j are the mean waiting time of order i and order j rivers, respectively; Ω is the order of the river network; $\theta_{i,\Omega}(0)$ is the initial state probability of a order i river in a order Ω river network, i.e. the size ratio of the watershed of the order i river to the watershed of the entire river network; A_{ij} is the correlation coefficient between the mean waiting time λ_i and the state transition probability P_{ij} (P_{ij} is the ratio of the number of order i rivers flowing into order j rivers to the total number of order i rivers; t is time. All these parameters can be calculated based on the geomorphic and hydrodynamic parameters of the watershed.

Extraction and calculation of geomorphic parameters

The river network of the watershed was extracted from the DEM in the study area using the software Geographic Information System (GIS). Then, the Strahler classification (2015) was performed on the extracted river network, yielding the river section data with watershed orders. On this basis, the geomorphic features of each river section in the watershed were determined, including number, length and catchment area, and the river number ratio R_B, river length ratio R_L and area ratio R_A were respectively calculated as follows by the Horton's law (*Eqs. 2-4*):

$$R_B=\frac{N_{i-1}}{N_i}=C, i=1,2,\cdots,\omega \quad \text{(Eq.2)}$$

$$R_L=\frac{\bar{L}_i}{\bar{L}_{i-1}}=C, i=1,2,\cdots,\omega \quad \text{(Eq.3)}$$

http://www.aloki.hu ● ISSN 1589 1623 (Print) ● ISSN 1785 0037 (Online)
DOI: http://dx.doi.org/10.15666/aeer/1704_89158930

$$R_A = \frac{\bar{A}_i}{\bar{A}_{i-1}} = C, i = 1, 2, \cdots, \omega \quad \text{(Eq.4)}$$

where N_i and N_{i-1} are the number of order i rivers and that of order i-1 rivers, respectively; $\bar{L}_i$ and $\bar{L}_{i-1}$ are the mean length of order i rivers and that of order i-1 rivers, respectively; $\bar{A}_i$ and $\bar{A}_{i-1}$ are the mean watershed area that contributes to the runoff of order i rivers and that to the runoff of order i-1 rivers, respectively; C is a constant; ω is the highest order of the river system.

Determination and calculation of hydrodynamic parameters

The hydrodynamic parameters of a watershed include the Manning's roughness coefficient n and the mean river width B. The former was obtained by table look-up according to the local conditions. The latter was generalized as an unknown parameter that varies with the net rainfall intensity i_r. The mean waiting time λ_i of rivers on each order was calculated based on the two parameters. The calculation formulas of n, B and λ_i are as follows (*Eqs. 5-7*):

$$v = 0.665\alpha_\Omega^{0.6}(i_r A_\Omega)^{0.4} \quad \text{(Eq.5)}$$

$$\alpha_\Omega = S^{0.5} / (nB^{2/3}) \quad \text{(Eq.6)}$$

$$\lambda_i = v / (\bar{L}_i \cdot R_L^{i-1}) \quad \text{(Eq.7)}$$

where i_r is the net rainfall intensity of each event; v is the flow rate.

Calculation of critical rainfall of each event

The critical rainfall of each event refers to the critical rainfall in the prewarning period of a flood-causing rainfall event. It is the basis for determining the dynamic critical rainfall for the disaster prevention in the target location. In light of the measured rainfall data, the value of this parameter was obtained by the RGC calculation through the following steps.

(1) The rainfall process from the beginning of rainfall to any time T was intercepted from the rainfall data, the RGC process of the watershed was calculated using the rainfall-runoff correlation map and the R-V GIUH, and the flood hydrograph was derived for the rainfall event.

(2) The peak flow Q_{peak} in this rainfall event was obtained based on the flood hydrograph. If the peak flow is greater than the prewarning flow $Q_{prewarning}$, then the flash flood has occurred. In this case, the rainfall process from the beginning of rainfall to any time T was intercepted again, and Step (1) was repeated until the peak flow is smaller than the prewarning flow.

(3) When the peak flow is smaller than the prewarning flow, the rainfall in the T + 1 period was given a value in ascending order, and the flood process induced by the rainfall in this period was derived. If the peak flow is close to the prewarning flow, then the rainfall in the T + 1 period is the critical rainfall of the event after the rainfall event lasts for a period of T.

http://www.aloki.hu ● ISSN 1589 1623 (Print) ● ISSN 1785 0037 (Online)
DOI: http://dx.doi.org/10.15666/aeer/1704_89158930

(4) The critical rainfalls of different events can be determined by the same method.

RBF-based prediction of dynamic critical rainfall

The RBF neural network (RBFNN) is a RBF-based artificial neural network. With a three-layer feedforward structure, the network has a nonlinear mapping from the input layer to the output layer and a linear mapping from the hidden layer to the output layer. The good nonlinearity enables the RBFNN to approximate any nonlinear function, disclose the intractable regularity in the system, and describes the potential relationship between the predictive index and the influencing factors. Known for its good generalization ability, the network has been successfully applied to nonlinear function approximation, time series analysis, data classification, pattern recognition, system modeling and fault diagnosis. Considering the complex nonlinear relationship between critical rainfall and its influencing factors, the RBFNN is a desirable tool to build the dynamic relationship model about the critical rainfall and the influencing factors. This network can be implemented despite the lack of data in regions suffering from flash floods, as it requires only a few training samples and outputs a unique training outcome.

In this paper, antecedent moisture, cumulative rainfall and rainfall intensity are taken as an input, and the critical rainfall of each event was considered as the output to construct a three-layer neural network. Through the training of the learning samples and the checking of the test samples, the dynamic relationships between the critical rainfall and the influencing factors were established, forming the dynamic critical rainfall prediction model (*Fig. 2*). Mathematical theory of RBFNN is detailed in Zeng et al. (2018).

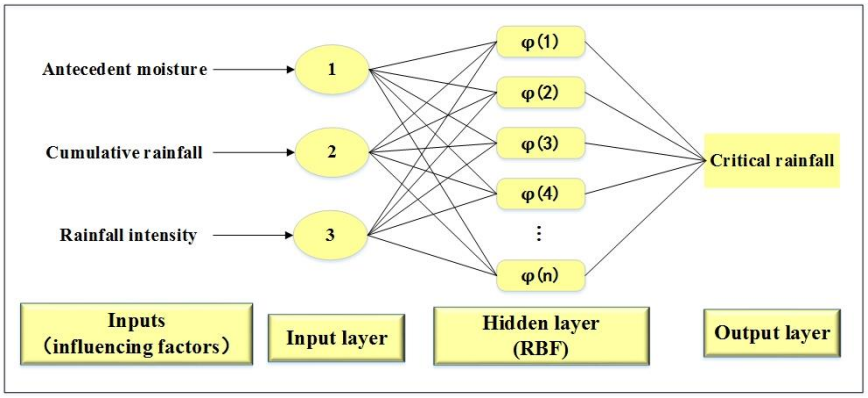

Figure 2. *structure of the dynamic critical rainfall prediction model*

Results

Runoff generation plan

The runoff generation was calculated based on the rainfall-runoff correlation map (*Fig. 3*), which was checked and modified against the 14 typical floods in the Peihe River watershed between 1982 and 2013.

As shown in *Figure 3,* since the 1980s, the actual rainfall-runoff curve in the Peihe River watershed was basically consistent with that in the map, so was the runoff volume. This means the rain and flood data are valid, and the rainfall-runoff correlation map can be adopted for runoff generation calculation.

http://www.aloki.hu ● ISSN 1589 1623 (Print) ● ISSN 1785 0037 (Online)
DOI: http://dx.doi.org/10.15666/aeer/1704_89158930

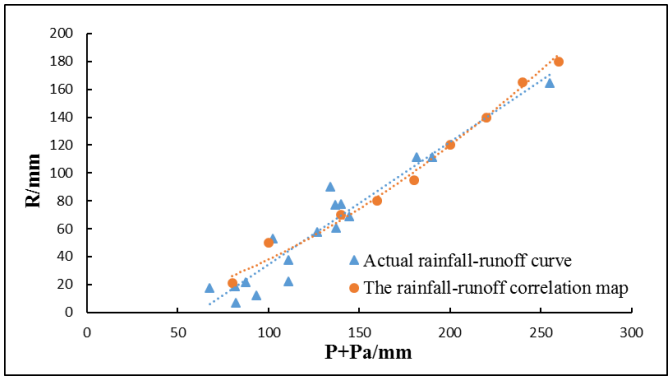

Figure 3. *Rainfall-runoff correlation map of the Peihe River watershed*

Runoff convergence plan

Parameter extraction and model construction

The digital elevation data were downloaded from the Geospatial Data Cloud (http://www.gscloud.cn), with a spatial resolution of 30 m. The data about the Peihe River watershed were processed on ArcMap, producing the river network in the watershed. The network was then divided into four orders by the Strahler classification (*Fig. 4*). The number and total length of rivers in each order were counted (*Table 1*). Next, the watershed was split into several sub-watersheds (*Fig. 5*). The area of each sub-watershed was determined, and the relevant geomorphic parameters were computed by *Equations 2-4* (*Table 1*).

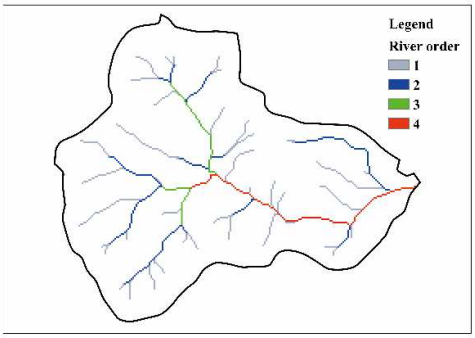

Figure 4. *River network classification*

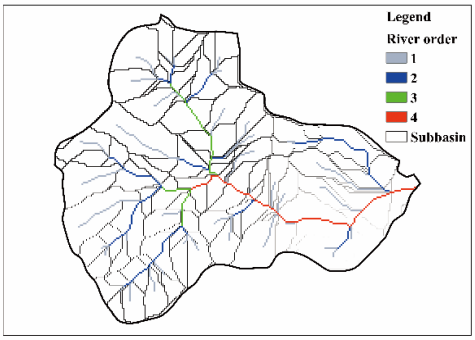

Figure 5. *Vector graph of catchment area*

http://www.aloki.hu ● ISSN 1589 1623 (Print) ● ISSN 1785 0037 (Online)
DOI: http://dx.doi.org/10.15666/aeer/1704_89158930

Table 1. *Geomorphic parameters of the Peihe River watershed*

River order	River numbers	Total length of the river (km)	Average length of the river (km)	Total area of the catchment (km^2)	Average area of the catchment (km^2)	River number ratio	River length ratio	Area ratio
1	47	20.52	0.43	12.20	0.25	3.63	2.57	2.58
2	12	10.20	0.85	4.14	0.34			
3	3	3.45	1.15	1.85	0.61			
4	1	5.10	5.10	2.86	2.86			

The watershed area was acquired as 21.07 km^2 during the extraction of the river network. The area threshold was 0.1 km^2, and the corresponding stream gradient was 13.51%. The Manning's roughness coefficient was determined as 0.025 m by table lookup. The mean river width B was initially determined as 2 m according to the section data extracted on the GIS. On this basis, the value of B was calibrated through the simulation of 4 measured floods. The data of the 4 floods were fitted to obtain the relationship between B and the net rainfall intensity i_r: $B = 0.326\,ln(i_r) + 1.9312$. With these parameters, the R-V GIUH of each flood was derived by (Eq. 1).

Model verification

To verify the applicability of R-V GIUH in regions lacking hydrological data, the R-V GIUH was created based on the parameters of 8 rainfall events measured by Peihe Hydrological Station from 1982 to 2013, and the resulting unit hydrographs were compared with the measured data. *Figure 6* and *Table 2* show the comparison between the simulated results and the measured results of the 8 floods.

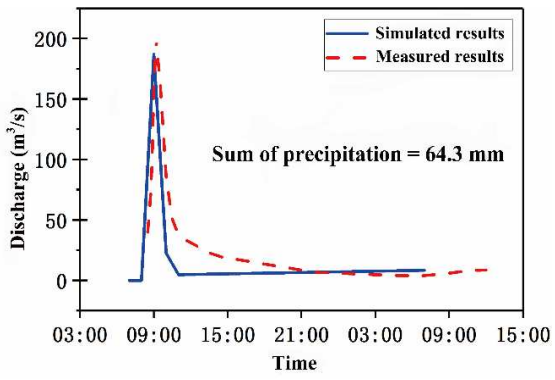

(a) July 19, 1982

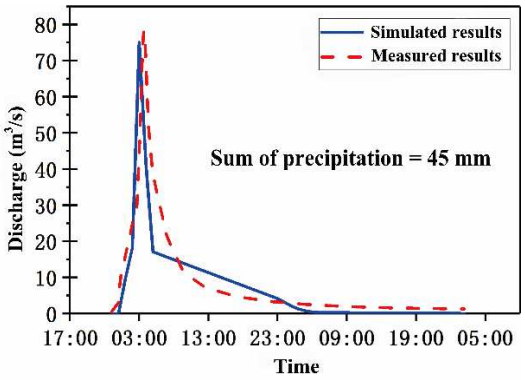

(b) July 17, 1983

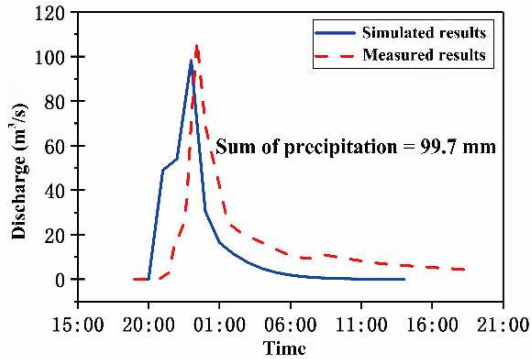

(c) August 8, 1984

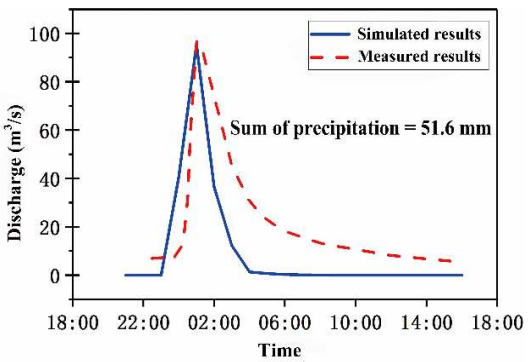

(d) July 17, 1986

http://www.aloki.hu ● ISSN 1589 1623 (Print) ● ISSN 1785 0037 (Online)
DOI: http://dx.doi.org/10.15666/aeer/1704_89158930

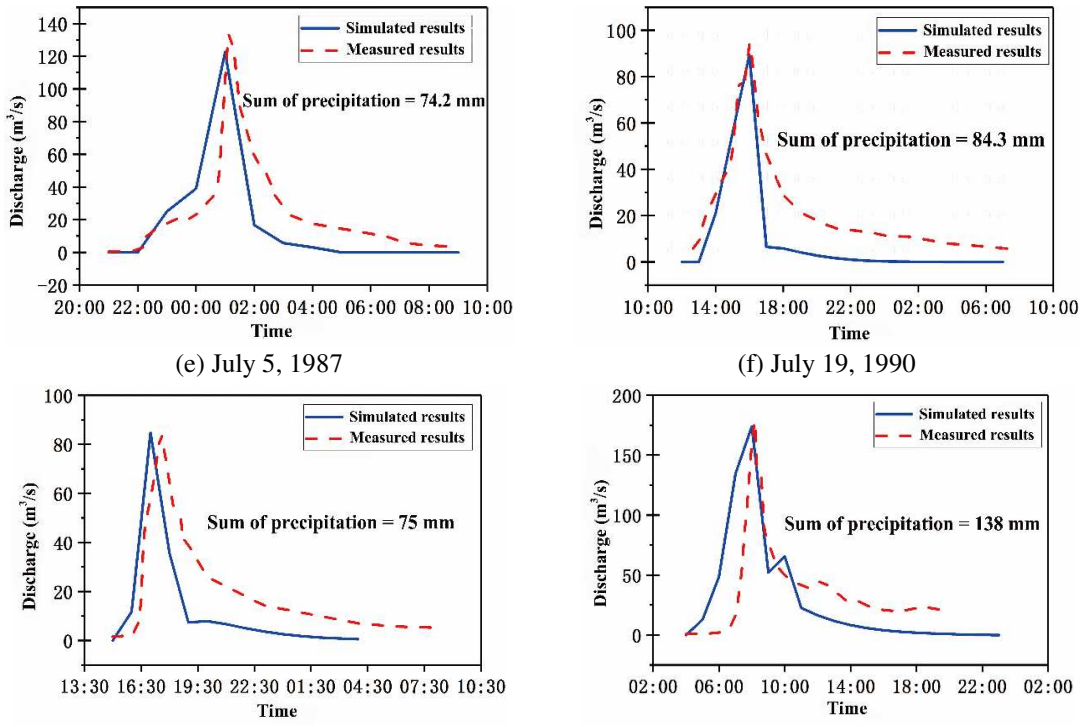

Figure 6. *Comparison between the simulated results and the measured results of the 8 floods*

Table 2. *Comparison between the simulated results and the measured results of the 8 floods*

Flood number	Measured peak/(m^3/s)	Simulated peak/(m^3/s)	Relative error/(m^3/s)	The time error of peak/(min)
July 19, 1982	200	187	-13	18
July 17, 1983	78	75.09	-2.91	40
August 8, 1984	107	98.29	-8.71	25
July 17, 1986	96.6	95.43	-1.17	0
July 5, 1987	133	122.64	-10.36	10
July 19, 1990	94.1	89.6	-4.5	0
July 1, 2007	83.5	84.8	1.3	36
August 16, 2008	178	174.19	-5.81	9

Figure 6 and *Table 2* show that the simulated flood process was basically the same with the measured situation. In the recession phase, the simulated results were slightly faster than the measured results. The minor deviation does not affect the computing accuracy of critical rainfalls, because critical rainfall mainly depends on the peak flow and the situation of the rising phase. Compared with the measured results, the simulated floods rose fast and reached the peak flow early at a low volume. As a result, the simulated critical rainfalls were slightly below the measured values. For safety reasons, the slightly lower critical rainfalls are safer. Overall, the geomorphic-based R-V GIUH model enjoys a high accuracy in runoff generation calculation, and the simulated results are suitable for the simulation of the flood process and the computation of the critical rainfalls.

http://www.aloki.hu ● ISSN 1589 1623 (Print) ● ISSN 1785 0037 (Online)
DOI: http://dx.doi.org/10.15666/aeer/1704_89158930

Analysis of calculated critical rainfall of each event

Two typical prewarning periods, namely 1 h and 3 h, were selected according to the rainstorm features, watershed area and underlying surface of the target region. The critical rainfall of 16 measured floods in the Peihe River between 1982 and 2013 were calculated (*Table 3*). To verify the accuracy of the critical rainfall calculation by R-V GIUH, the critical rainfalls were compared with the actual rainfalls in the prewarning periods to see if flash flood prewarning is necessary, and the prewarning was verified based on whether the actual flow reached the prewarning flow.

Table 3. *Calculated and measured results on critical rainfall of each event*

Prewarning periods	Time	Measured discharge (m^3/s)	Total rainfall of periods (mm)	Critical rainfall (mm)	Prewarned or not	Correct or not
1 h	1982/07/19/09	186	54.4	38.25	Y	√
	1983/09/16/03	73.1	25.8	48.64	N	√
	1984/08/08/23	90.31	36	76.16	N	√
	1985/07/13/08	46.4	25.9	33.29	N	√
	1986/07/18/01	93.86	31.2	29	Y	√
	1987/07/06/01	121.59	36.6	26.72	Y	√
	1988/09/09/01	55	10.6	69.41	N	√
	1990/07/19/16	78.6	29.9	78.82	N	√
	1991/07/03/13	60.7	17.5	23.26	N	√
	1993/06/21/13	37.1	23	21.38	Y	×
	1995/04/22/05	32.1	22.4	81.61	N	√
	1996/07/14/17	104	23.2	16.70	Y	√
	1998/07/02/20	48.1	32.8	29.93	Y	×
	1999/06/27/14	34.4	10.4	56.4	N	√
	2000/06/29/01	59.8	26	84.01	N	√
	2002/06/19/19	101.0	34	33.23	Y	√
3 h	1982/07/19/09	186	58.9	41.66	Y	√
	1983/09/16/03	78.2	37.8	61.1	N	√
	1984/08/08/23	90.31	75	94.7	N	√
	1985/07/13/10	51.8	42.9	39.5	Y	×
	1986/07/18/01	93.86	38.8	33.9	Y	√
	1987/07/06/01	133	45.2	41.6	Y	√
	1988/09/09/01	66.2	22.3	96.4	N	√
	1990/07/19/16	78.6	59.2	91.34	N	√
	1991/07/03/13	60.7	43.6	77.2	N	√
	1993/06/21/13	37.1	45	39.7	Y	×
	1995/04/22/06	45.6	41.6	101.3	N	√
	1996/07/14/17	104	55.5	43.68	Y	√
	1998/07/02/20	48.1	42.3	44.34	N	√
	1999/06/27/14	34.4	25.1	61.7	Y	√
	2000/06/29/02	63	38	98.4	N	√
	2002/06/19/20	147.00	66	57.63	N	√

Y: there is prewarning; N: there is no prewarning; √: the prewarning is correct; ×: the prewarning is incorrect

http://www.aloki.hu ● ISSN 1589 1623 (Print) ● ISSN 1785 0037 (Online)
DOI: http://dx.doi.org/10.15666/aeer/1704_89158930

Table 3 shows that two prewarning based on the 1 h and 3 h critical rainfalls were incorrect, putting the pass rate at 87.5%. The failed cases were analyzed, revealing that the critical rainfalls deviated slightly from the actual rainfalls. The deviation falls within the error tolerance. Overall, the R-V GIUH outputted accurate critical rainfalls.

Dynamic critical rainfall models and accuracy test

According to the disaster-causing mechanism of flash flood, the occurrence of flash flood in a region not only depends on the preceding rainfall, cumulative rainfall and rainfall intensity, but also on rainfall distribution and the bottom water of the river. The latter two factors are already reflected by the cumulative rainfall and the critical rainfall of each event, respectively. Hence, our dynamic critical rainfall model only considers the preceding rainfall (antecedent moisture), cumulative rainfall (the total rainfall from the start to a moment before the prewarning) and rainfall intensity (the rainfall of a period before the prewarning).

In light of the critical rainfall calculation of the said 16 floods, the preceding rainfall, cumulative rainfall and rainfall intensity were taken as the inputs, and the critical rainfall as the output. The first 12 floods were used as calibration samples and the last 4 as test samples. Then, the prediction model was created in different scales through RBFNN training to predict the dynamic critical rainfall. The simulated results are contrasted with the actual results in *Figure 7*.

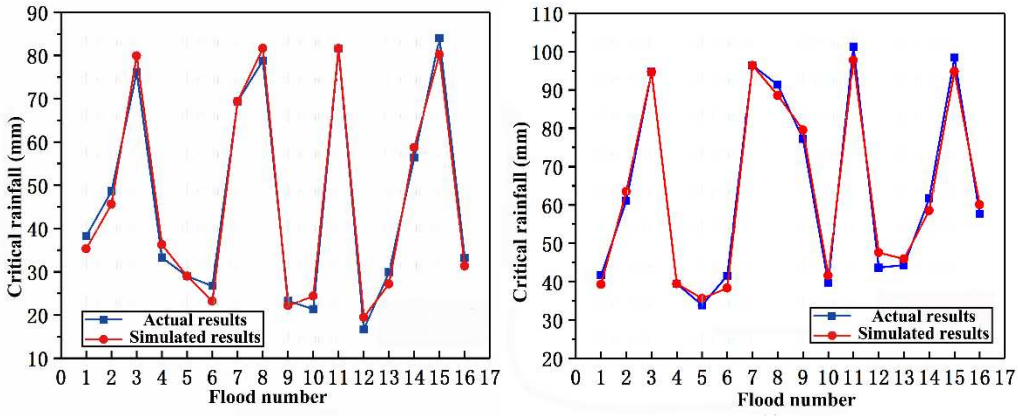

Figure 7. *Simulated results of dynamic critical rainfall prediction*

Figure 7 shows little difference between the simulated and calculated values, indicating that our model is suitable for the prediction of dynamic critical rainfall. To further verify its applicability, the model was adopted to predict the dynamic critical rainfalls of another 6 floods, and the results were also tested by the actual prewarning results (*Table 4*). The flood-causing flow inversion based on analytical calculation of RGC was introduced to determine the static critical rainfalls that only considers the preceding rainfall and to issue prewarning for the 1 h and 3 h periods, aiming to confirm the completeness of our indices and the superiority of our model. The calculated results are listed in *Table 4*.

It can be seen from *Table 4* that all dynamic critical rainfall prewarning for the 1 h period were successful, while five out of the six prewarning for the 3 h period were successful, putting the pass rate at 83.3%. By contrast, the pass rates of static critical

http://www.aloki.hu ● ISSN 1589 1623 (Print) ● ISSN 1785 0037 (Online)
DOI: http://dx.doi.org/10.15666/aeer/1704_89158930

rainfall prewarning were 66.6% and 50%, respectively. In fact, the RBF-based dynamic prediction was more accurate than the contrastive calculation method. To sum up, the R-V GIUH-based critical rainfall prewarning is of high accuracy, and the RBFNN-based dynamic prediction model thus established does well in the forecast of the critical rainfall.

Table 4. *Verification of the results predicted by our dynamic critical rainfall model*

Prewarning periods	Time	Measured discharge (m^3/s)	Total rainfall of periods (mm)	Dynamic critical rainfall prewarning			Static critical rainfall prewarning		
				P_d/mm	Prewarned or not	Correct or not	P_s/mm	Prewarned or not	Correct or not
1 h	2003/07/08/18	137.0	28.7	25.3	Y	√	45.8	N	×
	2004/07/18/06	69.6	19.1	43.4	N	√	67.0	Y	×
	2005/09/02/15	32.7	15	24.5	N	√	47.5	N	√
	2007/07/01/17	66.2	17.1	62.3	N	√	52.0	N	√
	2008/08/16/08	161	38.6	33.2	Y	√	32.1	Y	√
	2010/07/16/21	43.2	20	51.1	N	√	32.1	N	√
3 h	2003/07/08/19	163.00	33	33.4	N	×	63.0	N	×
	2004/07/18/06	69.6	47	76.7	N	√	83.4	Y	×
	2005/09/02/16	46.3	19	27.2	N	√	68.3	N	√
	2007/07/01/18	66.2	32.3	89.5	N	√	75.4	N	√
	2008/08/16/09	178	53	41.7	Y	√	56.7	N	×
	2010/07/16/21	43.2	26	60.4	N	√	56.7	N	√

P_d: the critical rainfall is dynamic; P_s: the critical rainfall is static; Y: there is prewarning; N: there is no prewarning; √: the prewarning is correct; ×: the prewarning is incorrect

Discussion

The critical rainfall is an important tool for the prewarning of flash floods. It is very meaningful to probe into this index. In this paper, the critical rainfall is investigated based on the GIUH and the RBFNN, yielding fruitful results. However, there are some shortcomings with our research. Next, the research findings are compared with the relevant studies in two aspects.

Our research discovers that, while the GIUH-based simulation output close-to-reality flood process, the simulated peak flow appears earlier and smaller than the measured data, causing the underestimation of the critical rainfall. This conclusion agrees well with the research of Tang (2017) and Wang et al. (2018). Meanwhile, the test results in *Table 3* show a good overall accuracy, but the underestimated critical rainfall may lead to wrong prewarning of several floods that do not cause disasters. New solution should be looked for to solve this problem.

Currently, the flash floods can also be simulated by distributed hydrological models, such as the geomorphology-based hydrological model (GBHM) (Liu et al., 2010), the Xin'anjiang (XAJ) model (Ye et al., 2014), the Hydrologic Engineering Center's Hydrological Modeling System (HEC-HMS) model (Liu, 2016; Guan et al., 2017), and the grid XAJ model (Liu et al., 2017). These models can simulate the flood process

http://www.aloki.hu ● ISSN 1589 1623 (Print) ● ISSN 1785 0037 (Online)
DOI: http://dx.doi.org/10.15666/aeer/1704_89158930

more realistically and accurately than the GIUH-based model, and can also be adopted to compute the critical rainfall. Nonetheless, most distributed hydrological models have lots of parameters, which need to be determined by a long series of data. In this respect, the GIUH-based method enjoys certain advantages with relatively few and easy-to-obtain parameters. In future research and applications, the flood computing method should be selected according to the local data.

In addition, the prewarning results of rainfall events differed with time scales, as acquired through the calculation of critical rainfall of each event. For example, the 1998070220 rainfall event was prewarned incorrectly on the 1 h scale and correctly on the 3 h scale, while the 1985071310 rainfall event was prewarned incorrectly on the 3 h scale and correctly on the 1 h scale. The results are consistent with the findings of Guo et al. (2016). Analysis shows that the prewarning effect of short, heavy rainfall is negatively correlated with the time scale. In actual application, the critical rainfalls on different time scales should be considered fully in the prewarning process, such as to reduce false warning and increase prewarning accuracy.

Besides flood computation, the dynamic relationship between the critical rainfall and the influencing factors also bears on the prewarning of flash floods. Many scholars (Liu et al., 2010; Ye et al., 2014; Guan et al., 2017; Guo et al., 2016) have explored this relationship via linear regression and correlation analysis. These methods can output accurate dynamic critical rainfall. However, none of them differentiate between influencing factors on their impact over the critical rainfall. In fact, the influencing factors are simply superimposed in the relevant studies. To further improve the computing accuracy of critical rainfall, this paper sets up the dynamic relationships between critical rainfall and multiple influencing factors based on the RBFNN. The model was proved accurate in prewarning through the analysis on its calibration, test and prediction results. However, the RBFNN, as a black box model, cannot clearly quantify the degree of impact of each influencing factor on the critical rainfall. The prediction results only confirm that the critical rainfall is affected in different degrees by various factors, namely, preceding rainfall, rainfall process and the bottom water of the river, and the relationships between critical rainfall and these factors are complex. To enhance the accuracy of flash flood prewarning and rationalize decision-making for disaster prevention and mitigation, it is necessary to further explore how these factors affect the dynamic variation in critical rainfall.

Conclusions

The geomorphic-based R-V GIUH runoff convergence model has a few easy-to-obtain parameters and requires no detailed hydrological or geomorphic data. It is suitable for computing the runoff convergence of flash flood in regions lacking data on the disaster. Besides, the model can output good results on runoff convergence. In particular, the simulated flow and time of flood peaks in the rising phase, which is important to the determination of critical rainfall, are close to the measured results. As a result, the model can predict the critical rainfall very accurately.

The critical rainfall is jointly determined by such factors as preceding rainfall, cumulative rainfall and rainfall intensity. The RBFNN-based dynamic critical rainfall prediction model is a desirable tool to describe the complex relationship between the critical rainfall and its influencing factors, laying a good basis for accurate prewarning.

http://www.aloki.hu ● ISSN 1589 1623 (Print) ● ISSN 1785 0037 (Online)
DOI: http://dx.doi.org/10.15666/aeer/1704_89158930

REFERENCES

[1] Carpenter, T. M., Sperfslage, J. A., Georgakakos, K. P., Sweeney, T., Fread, D. L. (1999): National threshold runoff estimation utilizing GIS in support of operational flash flood warning systems. – Journal of Hydrology 224: 21-44.
[2] Chen, G. Y., Yuan, Y. M. (2005): Research on analysis and computation method of critical precipitation amount of torrential flood. – Yangtze River 36(12): 40-43.
[3] Chen, Z. L., Huang, G. R., Cheng, G. D. (2014): Research on the calculation methods for critical rainfall of mountain torrent disasters of small watershed. – China Rural Water and Hydropower 6: 82-85.
[4] Clark, R. A, Gourley, J. J, Flamig, Z. L, Hong, Y., Clark, E. (2014): CONUS-wide evaluation of National Weather Service flash flood guidance products. – Weather and Forecasting. https://doi.org/10.1175/WAF-D-12-00124.1.
[5] Diagi, B. E. (2018): Analysis of rainfall trend and variability in Ebonyi state, South Eastern Nigeria. – Environmental and Earth Sciences Research Journal 5(3): 53-57.
[6] Georgakakos, K. P. (2006): Analytical results for operational flash flood guidance. – Journal of Hydrology 317(s1-2): 81-103.
[7] Gruntfest, E., Handmer, J. (1999): Coping with Flash Flood. – Kluwer Academic Publishers, The Netherlands.
[8] Guan, X. X., Yao, X. Y., Shen, J., Song. Y. R., Chu, H. C. (2017): Study on multidimensional dynamic critical rainfall flash flood warning based on distributed model. – Jiangsu Water Resources 12: 42-46.
[9] Guo, K. L., Liang, G. H., He, B. (2016): Dynamic critical precipitation flash flood warning method and its application based on API hydrologic model. – Water Resources and Power 34(12): 74-77.
[10] Li, H. X., Qing, G. H., Wang, X., Miao, R., Liu, Y. F. (2014): Advances in Study on Flash Flood Forecast and Warning. – Journal of China Hydrology 34(5): 14-16.
[11] Li, K. X. (2016); Calculation method of flash flood warning rainfall based on reasoning formula. – Journal of China Hydrology 1: 84-87.
[12] Liu, C. Y., Wu, J. H., Gao, J., Yang, D. M., Liu, Y. M. (2017): Research on calculation method of critical rainfall of flash flood disaster in data deficient region. – China Rural Water and Hydropower 5: 166-169.
[13] Liu, S. Y., Jiang, S. H., Ren, L. L. (2017): Calculation of critical rainfall for early-warning of mountain flood based on distributed hydrological model. – Journal of Hohai University (Natural Sciences) 45(5): 384-390.
[14] Liu, Y. (2016): Research on the Early-Warning System of Mountain Torrent Disaster Dynamic Precipitation Based on the HMS Model - Take Weihai as an Example. – Jinan University, Jinan.
[15] Liu, Z. Y., Yang, D. W., Hu, J. W. (2010): Dynamic Critical Rainfall-Based Torrential Flood Early Warning For Medium-Small Rivers. – Journal of Beijing Normal University (Natural Science) 3: 317-321.
[16] Ma, D. Z. (2017): Research on the Calculation Method of the Critical Rainfall of Flood Disaster in Hexi Inland River Basin. – Lanzhou University, Lanzhou.
[17] Mao, B. P. (2016): Application of the vertically-mixed runoff model to the calculation of the rainfall threshold of flash floods in ungauged basins. – Journal of Basic Science and Engineering 4: 720-730.
[18] Norbiato, D., Borga, M., Espost, S. D., Gaume, E., Anquetin, S. (2008): Flash flood warning based on rainfall thresholds and soil moisture conditions: An assessment for gauged and ungauged basins. – Journal of Hydrology 362(3-4): 274-290.
[19] Ren, C. F. (2015): Research on Early-Warning Indicators of Flash Flood Disaster in Small Watershed in Shandong Province and Its Application. – Shandong University, Jinan.

http://www.aloki.hu ● ISSN 1589 1623 (Print) ● ISSN 1785 0037 (Online)
DOI: http://dx.doi.org/10.15666/aeer/1704_89158930

[20] Sagar, R. C., Srinivas, V. V. (2015): Effect of DEM source on equivalent Horton–Strahler ratio based GIUH for catchments in two Indian river basins. – Journal of Hydrology 528: 463-489.
[21] Seo, D., Lakhankar, T., Mejia, J., Cosgrove, B., Khanbilvardi, R. (2013): Evaluation of operational National Weather Service gridded flash flood guidance over the Arkansas Red River Basin. – J Am Water Resour Assoc 49(6): 1296-1307.
[22] Tang, Y. P. (2017): Research on Critical Rainfall of A Flash Flood Disaster Based on Concentration model of GIUH-Case of Chenjiahe Watershed. – Xi'an University of Technology, Xi'an.
[23] Villarini, G., Krajewski, W. F., Ntelekos, A. A., Georgakakos, K. P., Smith, J. A. (2010): Towards probabilistic forecasting of flash floods: the combined effects of uncertainty in radar-rainfall and flash flood guidance. – Journal of Hydrology 394(1-2).
[24] Vizzari, D., Puntorieri, P., Praticò, F., Fiamma, V., Barbaro, G. (2018): Energy harvesting from solar and permeable pavements: a feasibility study. – Annales de Chimie - Science des Matériaux 42(4): 517-534.
[25] Wang, X. H., Wu, W., Tang, Y. P. Gong, L. Y., Ning, L. Z. (2018): Critical rainfall calculation based on R-V GIUH. – Journal of Northwest A & F University (Natural Science Edition) 7: 147-154.
[26] Wen, K., Li, D. J., Jin, G. S. (1991): Mathematical Simulation of Surface Runoff Process. – Water Resources and Electric Power Press, Beijing, pp. 263-294.
[27] World Meteorological Organization (WMO) (1994): Guide to Hydrological Practices (WMO-No. 168). Fifth Ed. – WMO, Geneva, 2: 765.
[28] Ye, J. Y., Li, Z. J., Wu, Y. T. (2013): Study and application of flash flood warning method for ungauged basins. – Journal of Hydroelectric Engineering 3: 15-19, 33.
[29] Ye, J. Y., Li, Z. J., Chang, L. (2014): Research and application of flash flood early warning method based on dynamic critical precipitation. – Meteorological Monthly 40(1): 101-107.
[30] Zeng, X. Q., Zhen, Z. L., He, J. S., Han, L. X. (2018): A feature selection approach based on sensitivity of RBFNNs. – Neurocomputing 275: 2200-2208.

http://www.aloki.hu ● ISSN 1589 1623 (Print) ● ISSN 1785 0037 (Online)
DOI: http://dx.doi.org/10.15666/aeer/1704_89158930

EXPERIMENTAL STUDY ON PURIFICATION OF POLLUTED RIVER WATER WITH HORIZONTAL SUBSURFACE FLOW CONSTRUCTED WETLANDS OF DIFFERENT FILLERS AND PLANTS

XIAO, L. – LI, J. L. – LV, C. M. – WANG, X. – LIU, J. L*

Urban and Rural Construction Institute, Hebei Agricultural University, Baoding 071001, China

**Corresponding author*
e-mail: hb-ljl@163.com

(Received 18th Mar 2019; accepted 17th May 2019)

Abstract. The Fuhe River in Baoding City is one of the rivers entering Baiyangdian Lake, but its pollution is serious, so improving the water quality of the Fuhe River can not be ignored. In this paper, the horizontal subsurface flow constructed wetland was used to purify the water of Fuhe River, and the pollutant removal effect of ceramsite, crushed stone filler, cyperus alternifolius, Reed and yellow iris plants was analyzed. The results showed that the cyperus alternifolius ceramsite constructed wetland has the best removal effect on COD and TP, its average removal rates are 56.18% and 61.97%, respectively, and its average effluent concentrations are 18.64 mg/L and 0.27 mg/L; the reed ceramsite constructed wetland has the best removal effect on NH_4^+-N, with a rate of 64.00%, respectively, and its average effluent concentration is 0.82 mg/L. The results can provide theoretical reference for improving the water quality of Fuhe River.
Keywords: *Baiyangdian, Fuhe River, horizontal subsurface, plant screening, purification effect, substrate*

Introduction

Xiong'an New Area will be built as an ecological city, in which the river is harmonious with the city. Baiyangdian Lake needs a good ecological environment to meet the requirements of Xiong'an New Area (Xia et al., 2017; Li et al., 2013). At present, the flow of water's environment of Baiyangdian Lake is poor, for which the main pollution source is the water from the Fuhe River into the Lake, so it is very important to control the water of Fuhe River. Currently, constructed wetlands are widely applied to the improvement of polluted water due to its high efficiency, ecology and low investment (Machado et al., 2017; Gagnon et al., 2012).

Fillers and plants play an important role in constructed wetland systems. More and more people begin to study the purification effect of different fillers and plants on constructed wetlands (Leto et al., 2013; Xiong et al., 2015). The constructed wetland designed by Tang et al. (2009) uses a combination of crushed stone and shale to study its purification effect on eutrophic water bodies. The horizontal free surface flow integrated constructed wetland (ICW) concept was proposed by Scholz et al. (2007) and combines that goal of purifying farmland water with the goal of incorporating wetland infrastructure into landscape, with good results achieved after commissioning. Ji et al. (2017) studied the filler and its purification mechanism of constructed wetland sewage treatment system. Hao et al. (2017) conducted a study on the purification efficiency of plant water in constructed wetlands.

Under the background of this study, constructed wetland is used to purify the water quality of Fuhe River, study the effect of wetland on the removal of pollutants in the

http://www.aloki.hu ● ISSN 1589 1623 (Print) ● ISSN 1785 0037 (Online)
DOI: http://dx.doi.org/10.15666/aeer/1704_89318940

river water and the effect of different fillers and plants on the purification effect. In this paper, the polluted river water is taken as the research object, and according to the combination type of different fillers (such as crushed stone and ceramsite) and different plants (cyperus alternifolius, reed and yellow iris), 8 horizontal subsurface constructed wetlands are constructed outdoors to study the purification effect of the river water.

Materials and methods

Raw water quality

The experimental water is taken from the section of Yonghua Bridge, Fuhe River, Baoding City. The water quality of the section for nearly one year is shown in *Table 1*.

Table 1. *Water quality of the section*

pH	DO (mg/L)	Turbidity (NTU)	COD (mg/L)	TP (mg/L)	NH_4^+-N (mg/L)
6-8	0.5-9.0	10-30	30-50	0.6-1.0	1.7-3.0

Construction of experimental device

8 horizontal subsurface flow constructed wetlands are constructed, with the size of the pond as 65 cm × 35 cm × 40 cm and the filling height as 23 cm. They are divided into two group according to the filler, one is ceramsite, other group is crushed stone, the particle diameter of the ceramsite is 10-20 mm, the particle diameter of the crushed stone is 5-10 mm (3 cm), 10-15 mm (10 cm), 15-20 mm (5 cm), and 20-30 mm (5 cm) from the top to the bottom, covering with 5 cm soil on the surface of the filler. According to the principle of strong purifying ability and fast growing to adapt to environment, three kinds of plants are preliminarily selected as wetland plants, such as cyperus alternifolius, reed and yellow iris, with a planting density of 18 plants/square trough. The schematic diagram is shown in *Figure 1*.

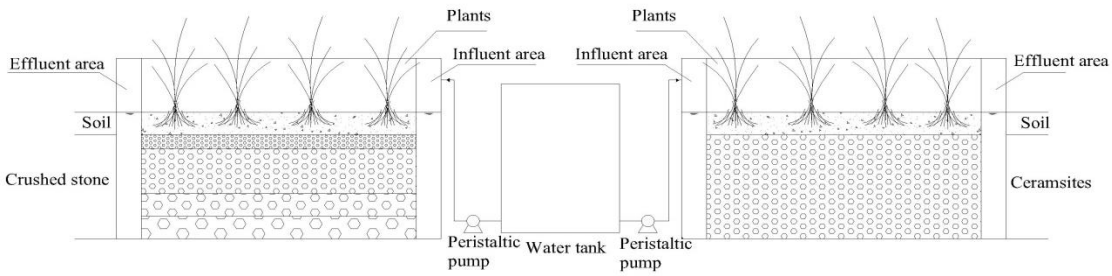

Figure 1. *Schematic diagram of experimental device*

Operation of experimental system

The experimental device adopts continuous water inflow, the hydraulic load is controlled at 0.2-0.4 $m^3/(m^2 \cdot d)$, the hydraulic retention time is 1.5-2.5 d, and the operating water level is located on the soil surface. In order to ensure the stability of water inflow, peristaltic pump is used to quantitatively and constantly supply water to the constructed wetland system. The experimental system lasted 7 months from the

http://www.aloki.hu ● ISSN 1589 1623 (Print) ● ISSN 1785 0037 (Online)
DOI: http://dx.doi.org/10.15666/aeer/1704_89318940

construction of trial operation to the end of operation, and stably ran 3 months after the plant is mature.

Sample collection and testing

Sample collection includes influent and effluent of each wetland. The sample collection frequency is once every three days, and the detection indicators include temperature (T), dissolved oxygen (DO), pH, turbidity, chemical oxygen demand (COD), total phosphorus (TP), ammonia nitrogen (NH_4^+-N), total nitrogen (TN), nitrite nitrogen (NO_2^--N), and nitrate nitrogen (NO_3^-N). The temperature and dissolved oxygen are measured by a dissolved oxygen meter at the sampling site, and the pH is measured by a PH meter. The determination methods of TN and TP are potassium persulfate oxidation-ultraviolet spectrophotometry and anti-spectrophotometric method of potassium persulfate molybdenum antimony oxidation, respectively. Other indicators are measured in the laboratory by the method of national standard.

Results

Removal effect of COD

Figure 2 is a diagram of removal effect of COD by the horizontal subsurface flow constructed wetland system, in which COD concentration of the influent fluctuates little and COD removal is stable. It can be seen from *Figure 2* that the wetland system with plants is better than the blank wetland system in the removal of COD in the water, and among three plants, cyperus alternifolius has the best removal effect on COD, followed by yellow iris and reed. The average effluent COD concentration of cyperus alternifolius ceramsite-bed wetland is 18.64 mg/L, which reaches Class Ⅲ standard of surface water. The average effluent COD concentration of reed, yellow iris and blank ceramisite-bed wetland is 20.86 mg/L, 21.12 mg/L and 24.98 mg/L, and the average effluent COD concentration of cyperus alternifolius, reed, yellow iris and blank crushed stone-bed wetlands is 21.35 mg/L, 23.39 mg/L, 23.73 mg/L and 27.48 mg/L, all of which reach the class IV standard of surface water.

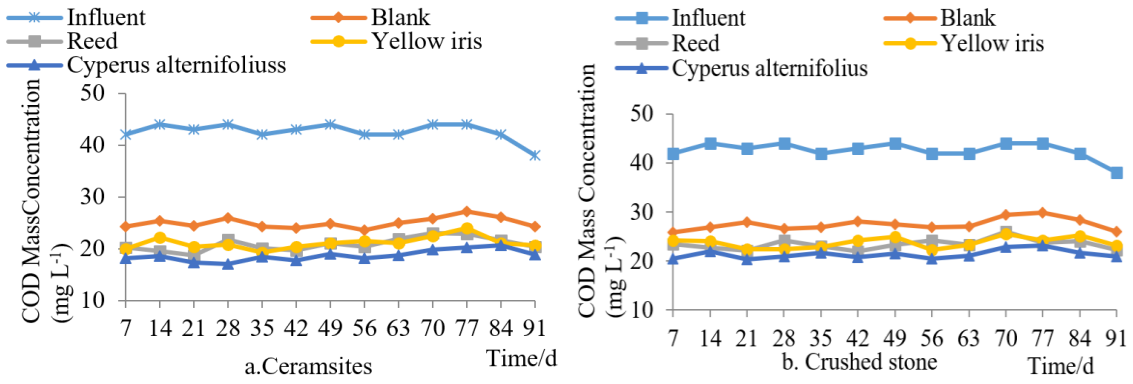

Figure 2. *Removal effect of COD by ceramsite and crushed stone*

In the constructed wetland system, the removal of COD is mainly accomplished by the filtration of substrate and the decomposition of microorganisms. As can be seen from *Figure 2,* compared with the blank wetland group, the removal effect of COD in

http://www.aloki.hu ● ISSN 1589 1623 (Print) ● ISSN 1785 0037 (Online)
DOI: http://dx.doi.org/10.15666/aeer/1704_89318940

the constructed wetland group with plants differs slightly, for which the filtration of the substrate is the main way to remove COD in the constructed wetland system and the proportion of plant absorption and microbial decomposition is relatively small (Kjellin et al., 2007; Albuquerque et al., 2010). From the above results, it can be seen that compared among the three plants, the removal effect of COD in cyperus alternifolius wetland is better than that of the reed wetland and the yellow iris wetland, for which the root system of cyperus alternifolius is stronger than that of the other two wetland plants, its stem and leaf are lush, and its ability to absorb organic pollutants is stronger.

Figure 3 shows the change trend and removal rate of effluent COD of ceramsite-bed and crushed stone-bed constructed wetland systems. It can be seen from *Figure 3* that when the plants are the same, the removal effect of COD by the ceramsite-bed constructed wetland system is better than that of the crushed stone-bed constructed wetland system, for which the surface areas of ceramsite is greater, and under the same hydraulic load, the contact surface between water and ceramsite is more, which increases the absorption of COD by ceramsite and makes the removal rate of COD in ceramsite-bed higher.

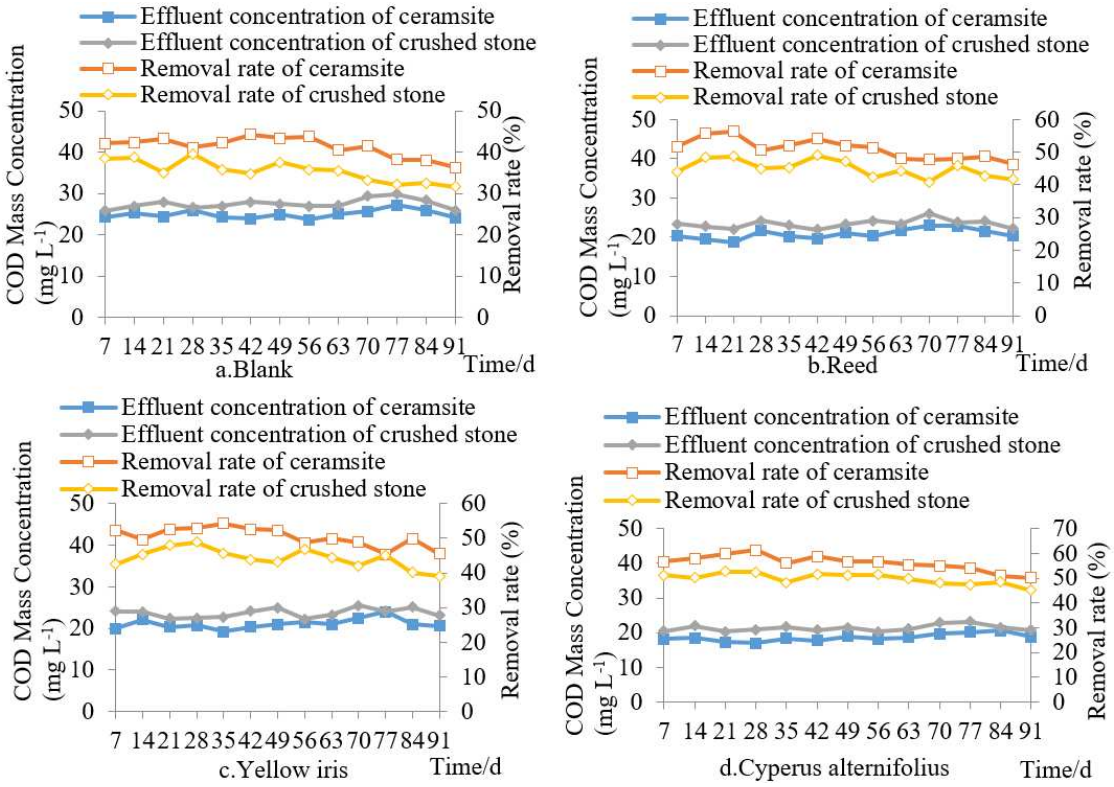

Figure 3. *Comparison of COD removal rate between ceramsite and crushed stone*

It can be seen from *Figure 3* that the removal of COD by the constructed wetland system is relatively uniform and less fluctuating during the operation of the experiment, and the removal rate of the ceramsite-bed wetland and the crushed stone-bed wetland at the later stage of the experiment shows a slow decreasing trend. The reason may be that the plant grows slowly, begins to wither and absorbs less COD, and as the temperature decreases, the activity of microorganisms declines. Meanwhile, with the operation of the experiment, the adsorption of the filler tends to the saturation state, and the

http://www.aloki.hu ● ISSN 1589 1623 (Print) ● ISSN 1785 0037 (Online)
DOI: http://dx.doi.org/10.15666/aeer/1704_89318940

adsorption capacity decreases, resulting in the slowly decreasing trend in the removal rate of COD in wetland system.

Removal effect of TP

Figure 4 shows the removal effect of TP by the wetland system. It can be seen from the figure that the TP concentration of the influent decreases slowly in the later period of the experimental operation, and the TP concentration of effluent in the wetland with plants is lower than the TP concentration of effluent in the blank wetland. Cyperus alternifolius has the best effect on TP removal. The average TP concentration of effluent in cyperus alternifolius ceramsite-bed wetland and cyperus alternifolius crushed stone-bed wetland is 0.27 mg/L and 0.32 mg/L, respectively. Reed and yellow iris has less effect on TP removal. The average TP concentration of effluent in reed ceramsite-bed wetland, yellow iris ceramsite-bed wetland, reed crushed stone-bed wetland and crushed stone-bed wetland is0.30 mg/L, 0.31 mg/L, 0.35 mg/L and 0.34 mg/L, respectively. The blank wetland system also has a certain removal effect on TP. The average TP concentration of effluent is 0.36 mg/L and 0.40 mg/L in the blank ceramsite wetland and the blank crushed stone wetland, respectively.

The removal of phosphorus in constructed wetlands mainly depends on the interaction of plant absorption, adsorption and filtration of substrate and microbial transformation. As can be seen from *Figure 4,* the difference between wetland with plants and blank wetland in removal of TP in water is slight, for which the content of phosphorus absorbed by plant growth accounts for less proportion to the phosphorus removal, and the adsorption and filtration of substrate, which is combined with its Ca, Al, Fe, and others to form precipitates for removal, which accounts for a large proportion (Kotti et al., 2016).

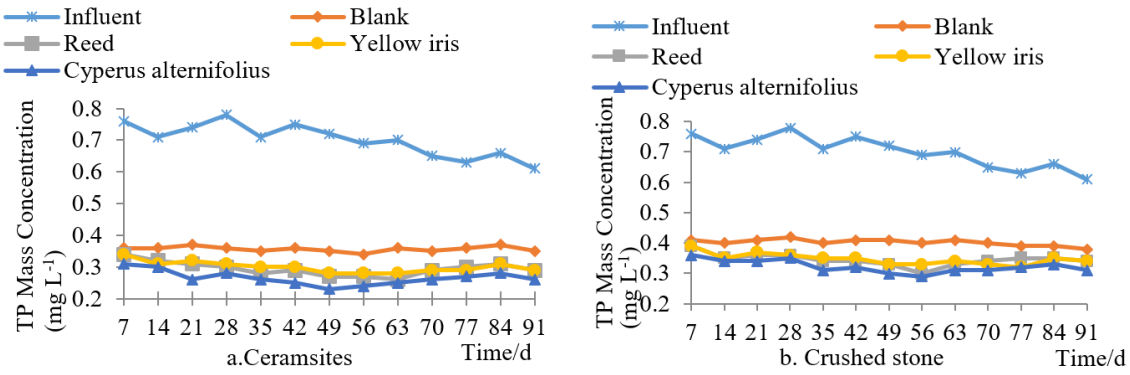

Figure 4. *Removal effect of TP by ceramsite and crushed stone*

Figure 5 shows the change trend and removal rate of effluent TP of ceramsite-bed and crushed stone-bed constructed wetland systems. It can be seen from *Figure 5* that when the plants are the same, the removal effect of TP by the ceramsite-bed constructed wetland system is better than that of the crushed stone-bed constructed wetland system, for which ceramsite is better than crushed stone since its coarse surface is good for the growth of plants and microorganism, and under the same hydraulic load, the contact method between water and ceramsite significantly affects the absorption of TP.

http://www.aloki.hu ● ISSN 1589 1623 (Print) ● ISSN 1785 0037 (Online)
DOI: http://dx.doi.org/10.15666/aeer/1704_89318940

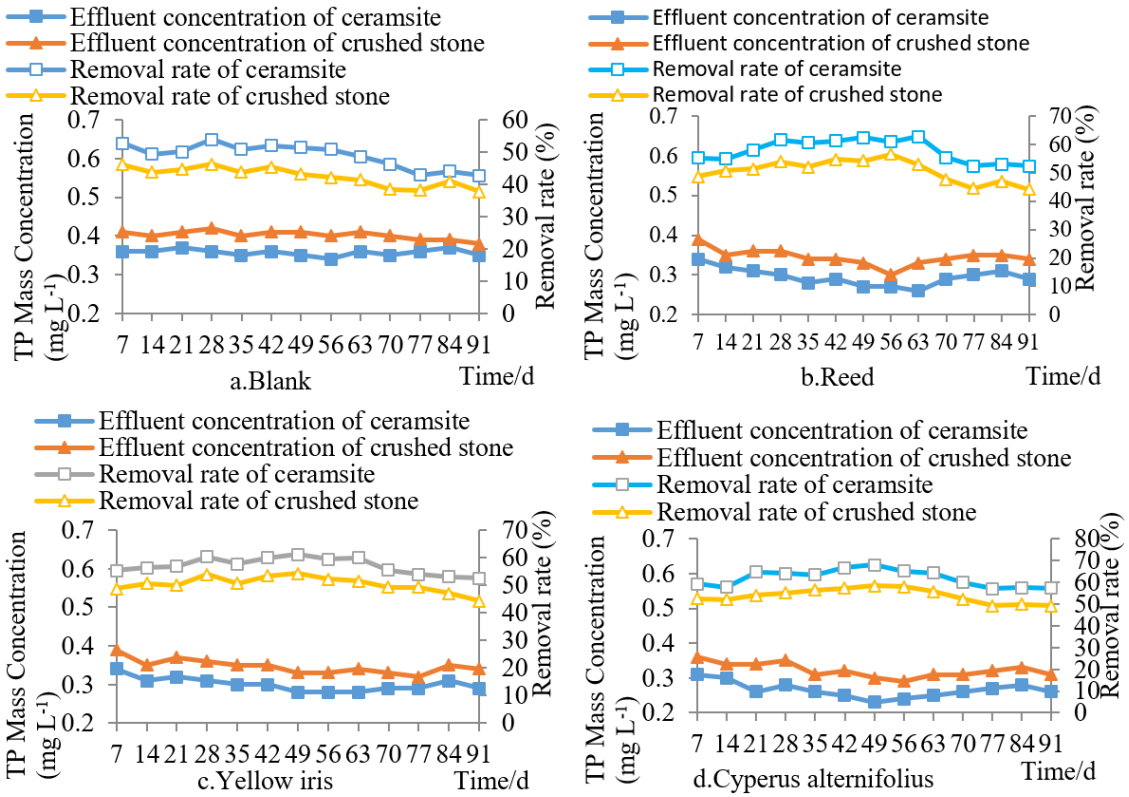

Figure 5. *Comparison of removal rate of TP between ceramsite and crushed stone*

The removal of TP by the constructed wetland system is relatively uniform and less fluctuating during the operation of the experiment, and the removal rate of TP at the later stage of the experiment shows a slow decreasing trend. The reason may be that the plant grows rapidly at the beginning and absorbs more phosphorus, and as the experiments operates, plant grows slowly, begins to wither and absorbs less phosphorus, and even part of the phosphorus in plants is slowly decomposed by microorganisms and released, resulting in the decrease in the removal rate of TP.

Comparing the removal effect of TP between the ceramsite-bed and the crushed stone-bed in *Figure 5,* it is found that the difference between the effluent TP of the ceramsite-bed and the crushed stone-bed with plants is larger than the difference between the blank ceramsite-bed and the blank crushed stone bed. Among them, the difference of the TP concentration of the effluent in the cyperus alternifolius ceramsite-bed wetland and cyperus alternifolius crushed stone-bed wetland is greater than other three experiments, and the reason is that the strong root system of the plants in the wetland system enhances the porosity of the ceramisite, also increases the adsorption of the ceramsite to TP and thus exhibits a strong TP purification capability (Vohla et al., 2011).

Removal effect of NH_4^+-N

As can be seen from *Figure 6,* the NH_4^+-N concentration in the influent gradually increases at the later stage of the experiment. *Figure 6a* shows the removal effect of NH_4^+-N by the constructed wetland system of the ceramsite. As can be seen from the figure, the removal effect of NH_4^+-N by the ceramsite wetland system with plants is

http://www.aloki.hu ● ISSN 1589 1623 (Print) ● ISSN 1785 0037 (Online)
DOI: http://dx.doi.org/10.15666/aeer/1704_89318940

better than that of the blank group. The reed ceramsite-bed wetland has the best effect on NH_4^+-N removal, the average NH_4^+-N concentration of effluent is 0.82 mg/L, while the removal effect of NH_4^+-N by cyperus alternifolius ceramsite-bed wetland and yellow iris ceramsite-bed wetland is similar. The average NH_4^+-N concentration of effluent is 0.95 mg/L and 0.95 mg/L, respectively, while that of blank group is 1.28 mg/L. *Figure 6b* shows the removal effect of NH_4^+-N by the crushed stone-bed constructed wetland system. It can be seen that the removal effect of NH_4^+-N by the crushed stone-bed constructed wetland system with plants is better than that of the blank group; the reed crushed stone-bed constructed wetland has the best effect on NH_4^+-N removal, and its average NH_4^+-N concentration of effluent is 0.99 mg/L, while the removal effect of NH_4^+-N in cyperus alternifolius crushed stone-bed wetland and yellow iris crushed stone-bed wetland is similar with the average NH_4^+-N concentration of effluent as 1.10 mg/L and 1.11 mg/L respectively, while that of blank group is 1.39 mg/L.

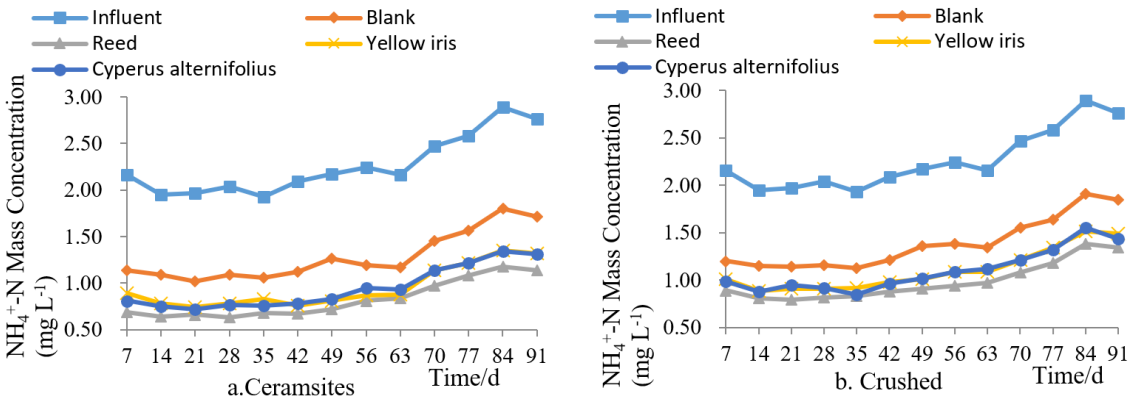

Figure 6. *Removal effect of NH_4^+-N by ceramsite-bed and crushed stone bed*

In the constructed wetland system, the removal of ammonia nitrogen is mainly through the filtration of substrate, the absorption of plants and the nitrification of microorganisms, where nitrification is the main mode, and oxygen supply is a restraint factor affecting nitrification in horizontal subsurface flow constructed wetlands (Vymazal et al., 2007; Saeed et al., 2012). In the experiment, the removal effect of NH_4^+-N by the wetland with plants is much better than that of the blank wetland, and the reason may be that the plants supply most of oxygen for the nitrification reaction through the transportation, release and diffusion of oxygen, strengthening nitrification.

In addition, the root system of the reeds is more developed and its oxygen transport ability is stronger than that of the two plants, so its removal effect of ammonia nitrogen is better.

Figure 7 shows the change trend and removal rate of effluent NH_4^+-N of ceramsite-bed and crushed stone-bed constructed wetland systems. It can be seen from *Figure 7* that the removal of NH_4^+-N by the constructed wetland system is relatively uniform and less fluctuating during the operation of the experiment, and the removal rate at the later stage of the experiment shows a slow decreasing trend. The reason may be that at the later stage the plant grows slowly and has less ability to transport oxygen. At the same time, when the temperature is lower, the activity of nitrifying bacteria and nitrobacteria in the water body will be inhibited to some extent, the nitrification capacity will be

http://www.aloki.hu ● ISSN 1589 1623 (Print) ● ISSN 1785 0037 (Online)
DOI: http://dx.doi.org/10.15666/aeer/1704_89318940

reduced, and the removal rate of $NH4^+$-N will be reduced. It is also possible that with the operation of the experiment, the nitrogen-containing organic matter retained by the filler decomposes in the anaerobic environment at the bottom of the wetland bed, resulting in an increase in the $NH4^+$-N content of the effluent water.

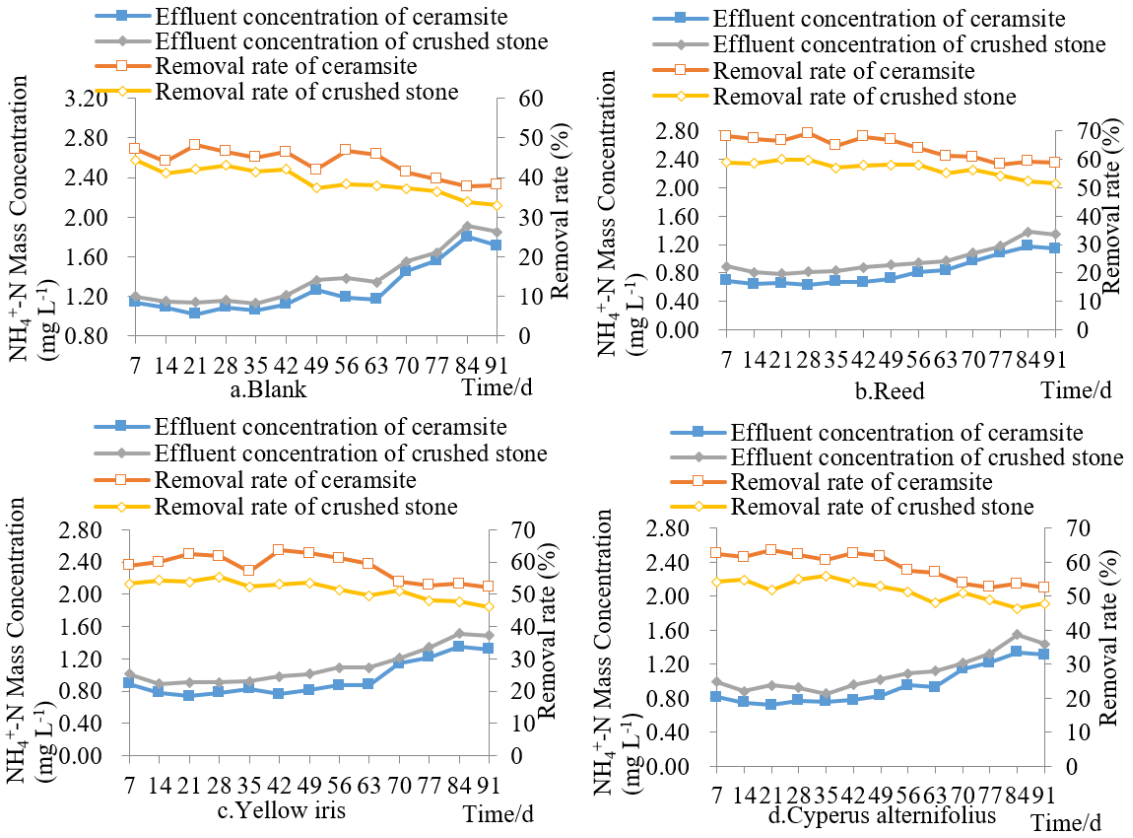

Figure 7. *Comparison of removal rate of NH_4^+-N between ceramsite and crushed stone*

Discussion

From the above experimental results and analysis, it can be seen that the wetland system has good removal effect of pollutants in the water from Fuhe River, and the removal rate tends to decrease slowly in the later stage of the experiment, which has a great effect on the growth cycle of plants. As plants grow rapidly, they will absorb more and more pollutants, which makes the removal rate higher. In the later stage of the experiment, the absorption of pollutants by plants and fillers may reach a saturated state, even release some pollutants, which makes the effluent concentration increase. At end of October, with the decrease in temperature, the life activities of microorganisms are inhibited, the plants begin to wither gradually, with a decrease in the absorption capacity, and the removal rate of pollutants in wetlands gradually decreases.

The removal rate of COD, TP, and NH_4^+-N in ceramsite-bed wetland is higher than that of crushed stone-bed wetland, which is related to the structure of filler. The surface of ceramsite is rough and easy to attach microorganisms, the void ratio is high, and the specific surface area is large, allowing more full contact between the river water and the filler, so its ability of absorbing pollutants is stronger, and the removal rate of pollutants is higher.

http://www.aloki.hu ● ISSN 1589 1623 (Print) ● ISSN 1785 0037 (Online)
DOI: http://dx.doi.org/10.15666/aeer/1704_89318940

Conclusions

The water quality of Fuhe River is improved by purification through the horizontal subsurface flow constructed wetlands, and the effluent water quality reaches the Class IV standard of surface water. Because of the strong adsorption ability of ceramsite, the wetland system with ceramsite as filler is better than the wetland system with crushed stone to remove the pollutants in the water. Cyperus alternifolius ceramsite-bed constructed wetland system has the best effect on COD and TP removal of Fuhe River, with the average removal rate of COD and TP as 56.18% and 61.97%, respectively, and the average concentration of effluent as 18.64 mg/L and 0.27 mg/L, respectively, reaching Class IV water standard of the Environmental Quality Standard for Surface Water (GB3838-2002); the reed ceramsite-bed constructed wetland system has the best effect on NH_4^+-N removal, with the average removal rate as 64% and the average concentration of effluent as 0.82 mg/L, reaching Class Ⅲ water standard of surface water. Blank ceramsite-bed constructed wetland system and blank crushed stone-bed constructed wetland system have less effect on removal of COD, TP and NH_4^+-N, with the average concentration of effluent as 24.98 mg/L and 27.48 mg/L, 0.36 mg/Land 0.40 mg/L, and 1.28 mg/Land 1.39 mg/L, reaching Class V water standard of surface water. This experiment mainly analyzed the purification effect of wetland system on Fuhe River water in summer and autumn. It can extend the test time in future research and analyze the removal effect of pollutants in water by wetland in different seasons.

REFERENCES

[1] Albuquerque, A., Oliveira, J., Semitela, S., Amaral, L. (2010): Evaluation of the effectiveness of horizontal subsurface flow constructed wetlands for different media. – Journal of Environmental Sciences 22(6): 820-825.

[2] Gagnon, V., Chazarenc, F. (2012): Effect of plant species on water quality at the outlet of a sludge treatment wetland. – Water Research 46(16): 5305-5315.

[3] Hao, M. X., Huo, L. L., Wu, S. S. (2017): Research progress on water purification efficiency of plants in artificial wetlands. – Environmental Engineering 35(8): 5-10, 24.

[4] Ji, Z. H., Feng, C. L., Wu, X. F. (2016): Research progress on packing and purification mechanism of sewage treatment system in constructed wetlands. – Chinese Journal of Ecology 35(8): 2234-2243.

[5] Kjellin, J., Anders, W., Håkan, J., Lindahl, A. (2007): Controlling factors for water residence time and flow patterns in Ekeby treatment wetland, Sweden. – Advances in Water Resources 30(4): 838-850.

[6] Kotti, I. P., Sylaios, G. K., Tsihrintzis, V. A. (2016): Fuzzy modeling for nitrogen and phosphorus removal estimation in free-water surface constructed wetlands. – Environmental Processes 3(1S): 65-79.

[7] Leto, C., Tuttolomondo, T., Bella, S. L., Leone, R., Licata, M. (2013): Effects of plant species in a horizontal subsurface flow constructed wetland - phytoremediation of treated urban wastewater with Cyperus alternifolius L. and Typha latifolia L. in the west of Sicily (Italy). – Ecological Engineering 61(19): 282-291.

[8] Li, Y. H., Liu, B. L. (2013): Current status and protection measures of wetland ecological environment in Baiyangdian. – JIANGSU Agricultural Science 41(10): 350-353.

[9] Machado, A. I., Beretta, M., Fragoso, R., Duarte, E. (2017): Overview of the state of the art of constructed wetlands for decentralized wastewater management in Brazil. – Journal of Environmental Management 187: 560-570.

http://www.aloki.hu ● ISSN 1589 1623 (Print) ● ISSN 1785 0037 (Online)
DOI: http://dx.doi.org/10.15666/aeer/1704_89318940

[10] Qin, H. Y., Ouyang, Z. H., Ti, Z. Y., Zhang, F. (2018): Experimental analysis on the optimal proportion of paste filler for a coal mine in China. – Annales de Chimie - Science des Matériaux 42(2): 259-268.
[11] Saeed, T., Sun, G. Z. (2012): A review on nitrogen and organics removal mechanisms in subsurface flow constructed wetlands: dependency on environmental parameters, operating conditions and supporting media. – Journal of Environmental Management 112: 429-44.
[12] Scholz, M., Harrington, R., Carroll, P., Mustafa, A. (2007): The integrated constructed wetlands (ICW) concept. – Wetlands 27(2): 337-354.
[13] Tang, X., Huang, S., Scholz, M., Li, J. (2009): Nutrient removal in pilot-scale constructed wetlands treating eutrophic river water: assessment of plants, intermittent artificial aeration and polyhedron hollow polypropylene balls. – Water, Air, and Soil Pollution 197(1-4): 61-73.
[14] Vohla, C., Bavor, H. (2011): Filter materials for phosphorus removal from wastewater in treatment wetlands. A review. – Ecological Engineering 37(1): 70-89.
[15] Vymazal, J. (2007): Removal of nutrients in various types of constructed wetlands. – Science of the Total Environment 380(1-3): 48-65.
[16] Xia, J., Zhang, Y. Y. (2017): Problems and challenges of building water security in Xiong'an new area. – Bulletin of Chinese Academy of Sciences 32(11): 1199-1205.
[17] Xiong, J. Q., Du, C., Zheng, Y. C. (2015): Effects of plant and matrix matching horizontal flow artificial wetlands on contaminated rivers. – Industrial Water Treatment 35(8): 22-25.

http://www.aloki.hu ● ISSN 1589 1623 (Print) ● ISSN 1785 0037 (Online)
DOI: http://dx.doi.org/10.15666/aeer/1704_89318940

ESTIMATION OF IMPLICIT CARBON IN ENERGY TRADE BETWEEN CHINA AND OTHER COUNTRIES ALONG THE BELT AND THE ROAD BASED ON MULTI-REGIONAL INPUT-OUTPUT MODEL

JIA, X. M.[1,2] – WANG, X. L.[3*]

[1]*School of Management, Xi'an University of Architecture and Technology Xi'an, 710055, China*

[2]*Business College, Xi'an International University Xi'an, 710077, China*

[3]*School of Management, Energy Economics and Management Research Center Xi'an University of Science and Technology, Xi'an, 710054, China*

[*]*Corresponding author*
e-mail: wxllian@sina.com

(Received 18th Mar 2019; accepted 17th May 2019)

Abstract. Considering the transfer of carbon emissions between the countries along the Belt and the Road and the importance of responsibility sharing for carbon emissions to international trade, this paper measures the implicit carbon in the trade between China and other countries along the Belt and the Road by the multi-regional input-output (MRIO) method. The measured results show that the trade between the two sides accounts for 3%~21% of the total carbon emissions in China; China's carbon responsibilities in its trade with the top trade partners along the Belt and the Road differs greatly with responsibility sharing principles; implicit carbon emissions mainly come from industries with relatively high emission intensities; China is advised to adopt the common responsibility mechanism. The research findings shed new light on the estimation of implicit carbon in international trade.
Keywords: *carbon emission, international trade, producer responsibility, consumer responsibility, reduction of carbon emission*

Introduction

Economic development and scientific progress have promoted the international division of labor, affecting the trade circulation of many countries. Typically, commodity production and final consumption occur in different geographic regions. Therefore, a country can reduce domestic production by importing commodities, thereby reducing domestic carbon emissions. This international trade model, while reducing the carbon emissions in consumer countries, causes pollution to rise in producing and exporting countries. The consumer countries should bear the corresponding carbon emission responsibilities. The current responsibility sharing system for carbon emission reduction only highlights the producer responsibility for production-side emissions of each country, that is, a country should be responsible for the greenhouse gases (GHGs) released in the production of commodities for export or domestic consumption. This system fails to consider the responsibility of foreign and domestic consumers for the carbon emissions. Compared with big exporters, large importers need to assume much responsibility for product consumption.

Since joining the World Trade Organization (WTO), China has actively participated in the global division of labor, witnessing a significant growth in the volume of foreign

http://www.aloki.hu ● ISSN 1589 1623 (Print) ●ISSN1785 0037 (Online)
DOI: http://dx.doi.org/10.15666/aeer/1704_89418953

trade.The country has gradually evolved into a major manufacturer in global trade, and won the nickname of the world's factory. From 2001 to 2016, the total import and export volume occupied from 0.51 trillion USD to 3.96 trillion USD (Boamah et al., 2017). The rapid growth in trade is accompanied by the emission of a huge amount of GHG emissions. The 2015 United Nations Climate Change Conference (COP 21) reported that China contributed 20% to the global GHG emissions, most of which originate from the production of export commodities (Cozier, 2016). This means China suffers from the carbon emissions caused by countries importing its commodities, which should be considered in the design of the responsibility sharing system for carbon emission reduction.

In 2013, China, the largest developing country in the world, launched the Belt and Road Initiative, with the aim to deepen the trade exchange with other countries. At present, the trade with the countries along the Belt and the Road occupies an important position in China's international trade. Under the circumstances, it is imperative to China's responsibilities for carbon emission reduction by quantifying the carbon emissions in commodity production and trade and determining the quantity and flow of implicit carbon in trade (Liu et al., 2017; Zhang, 2017; Tu and Ma, 2018).

The implicit carbon in trade is usually estimated by top-down accounting and bottom-up accounting. The former approach is specified in the *IPCC Task Force on National Greenhouse Gas*. This relatively authoritative method requires the classification and decomposition of the carbon emission sources. The latter approach, grounded on enterprise commodities and projects, has certain limitations, as it cannot cover all enterprises or commodities.

The commonly used accounting strategies or carbon emissions can be listed as the emission coefficient method, lifecycle method, and input-output (I-O) method, in light of the research perspective. The emission coefficient method adopts an emission coefficient factor, which is defined as the proportion of air pollutant to all pollutants generated by production activities. For example, Li et al. (2018) employed this method to measure the carbon emissions in the operation phase of a building.

The lifecycle method mainly assess the environmental factors and potential impacts associated with a product or service. Specifically, the related inputs and outputs of a system were recorded, and subjected to correlation analysis. Then, the analysis results are explained through lifecycle assessment, revealing the potential environmental impacts. For instance, Shi (2017) reviewed the development in animal husbandry research fromcarbon emissions to carbon footprint. Bello et al. (2018) calculated the carbon emissions in the lifecycle of buildings, and established a carbon footprint evaluation model for the whole lifecycle of residential buildings. With the aid of lifecycle method, Li (2016) determined the trend and flow of the implicit carbon in China's import and export in the past decade.

The I-O method studies how the commodities of a country affect the environment through international circulation. This strategy can be subdivided into single-regional I-O (SRIO) method, bi-regional I-O (BRIO) method, and multi-regional I-O (MRIO) method. The SRIO treats regions other than the producing country as one entity rather than distinguish between product sources, and assumes that the technology is on the same level at home and abroad. Despite its simplicity, this method cannot measure the consumption of intermediate commodities, or give an accurate depiction of the product flow in global trade. Under the assumption of technical heterogeneity, the BRIO selects different carbon emission factors for different trades. Neither can this method accurately

http://www.aloki.hu ● ISSN 1589 1623 (Print) ●ISSN1785 0037 (Online)
DOI: http://dx.doi.org/10.15666/aeer/1704_89418953

reflect the circulation of intermediate commodities. By contrast, the MRIO fully considers the production and circulation of different industries in different countries, yielding accurate measurement results (Tan et al., 2014). As a result, the MRIO is more widely applied than the other two methods to measure the implicit carbon in international trade.

Diezenbacher et al. (2012) suggested splitting the trade of an enterprise into processing trade and general trade, aiming to prevent the overestimation of implicit carbon in trade by the traditional I-O method (Su and Ang, 2011; Xia et al., 2015). Considering the difference in corporate ownership, Liu et al. (2016) analyzed the implicit carbon of China's trade by extended I-O, and suggested the overlook of corporate heterogeneity will exaggerate the implicit carbon emissions by 20%. Wei and Peng (2017) used the MRIO model to measure the energy sources related to China-US trade between 1995 and 2009, revealing that the exports to the US have become a major emission source to China. Li (2017) estimated the implicit carbon emissions incurred in Chinese and Japanese exports to countries along the Belt and the Road based on the GTAP9 database, discovered the implicit carbon difference in trade between these countries, and attributed the difference to the trade volume, implicit carbon intensity and trade structure of China and Japan. Lan (2015) relied on MRIO to estimate the implicit carbon of China-EU trade, and verified if the bilateral trade causes the flow of EU carbon emissions to China. Sun (2016) measured the implicit carbon in China's export based on the I-O data in 2002, 2005, 2007, 2010 and 2012, concluding that the amount of implicit carbon increased 2.42 times from 471 million tons in 2002 to 1.056 billion tons in 2015. From the angle of intrinsic emissions, Fang and Xu (2013) found that most of the CO_2 generation in China is to satisfy the needs of other countries. Under consumer responsibility, Gao (2016) calculated the implicit carbon of various countries, decomposed the implicit carbon structure, and looked for the causes to difference in carbon emissions through multiple methods. Pan and Wu (2018) measured the implicit carbon of China-Japan trade using the World Input-Output Database (WIOD), pointing out China's deficit of implicit carbon in the trade and the concentration of export implicit carbon in the heavy industry. Yu and Wang (2017) evaluatedthe implicit carbon of trade between China and 36 countries and regions, decomposed the implicit carbon by structural decomposition analysis, and drew the following conclusions: China is faced with a net inflow of implicit carbon and needs to upgrade emission reduction technologies and reduce thecarbon emission intensity.

On the responsibility sharing of carbon emissions, more and more scholars have questioned about the fairness of the current producer responsibility emission reduction model. For instance, Munksgaard (2001) proved that it is difficult for Denmark to achieve its carbon emission reduction target, if the implicit carbon in its export is counted as domestic carbon emissions, as required by the principle of producer responsibility. Using the Trade in Value Added (TiVA) database, Xiao (2016) measured the residual GHG emissions of the producing countries, which arises from the final consumption of commodities in consumer countries, and suggested the consumer countries be the main undertaker of carbon emission responsibilities. Dong et al. (2018) carried out adata envelopment analysis (DEA) on responsibility sharing for implicit carbon in trade among different provinces in China, and divided these provinces into four regions. Comparing producer responsibility and consumer responsibility, Yu and Xu (2017) noted that China will assume fewer responsibilities for emission reduction under consumer responsibility than under producer responsibility. To relieve global

http://www.aloki.hu ● ISSN 1589 1623 (Print) ●ISSN1785 0037 (Online)
DOI: http://dx.doi.org/10.15666/aeer/1704_89418953

environmental pressure, Zhong et al. (2018) came up with an effective strategy for global energy conservation and emission reduction: upgrading production technologies and increasing the proportion of clean energy in total energy consumption. Wang et al. (2017) estimated the carbon emissions of 30 provincial administrative regions in Chinese mainland, discovered obvious net carbon exports from the eastern coast, the southern coast and the Beijing-Tianjin region, and found a clear net carbon transfer from the northwest. Pan et al. (2008) argued that developed countries can manipulate the producer responsibility system and transfer their carbon emissions to developing countries through trade, causing carbon leakage and pushing up global carbon emissions.

Hence, some scholars have proposed to replace the producer responsibility system with consumer responsibility, i.e. including the carbon emissions from the final consumption of self-produced and imported commodities into the total carbon emissions of a country. The consumer responsibility system can mitigate the carbon leakage. However, some problems may occur to the carbon emission efficiency of exporting countries or industries, as the carbon emission responsibility is passed to the final consumers.

In light of the above, this paper selects the major trade partners of China along the Belt and the Road, and employs the MRIO method to calculate the implicit carbon in their trade with China.

Materials and methods

The MRIO model consisting of *n* different countries can be expressed as *Eq.1*:

$$\begin{pmatrix} x_1 \\ x_2 \\ \mathrm{M} \\ x_n \end{pmatrix} = \begin{pmatrix} A_{11} & A_{12} & \mathrm{L} & A_{1n} \\ A_{21} & A_{22} & \mathrm{L} & A_{2n} \\ \mathrm{M} & \mathrm{M} & \mathrm{M} & \mathrm{M} \\ A_{n1} & A_{n2} & \mathrm{L} & A_{nn} \end{pmatrix} \bullet \begin{pmatrix} x_1 \\ x_2 \\ \mathrm{M} \\ x_n \end{pmatrix} + \begin{pmatrix} y_{11} + \sum_{i \neq 1} y_{1i} \\ y_{22} + \sum_{i \neq 2} y_{2i} \\ \mathrm{M} \\ y_{nn} + \sum_{i \neq n} y_{ni} \end{pmatrix} \quad \text{(Eq.1)}$$

where A_{nn} is the direct consumption coefficient of domestic commodities in each country; A_{ij} is the mutual demand between two countries, as reflected by the bilateral trade activities; x_i is the output vector of country i; y_{ii} means country $i$satisfies the domestic demand for commodities; y_{ir} means country i satisfies the demand of country r for commodities, i.e. the final demand. *Eq.1* can be simplified as $X = AX + Y$, and rewritten as $X = (I - A)^{-1}Y$, with X being the world output vector and Y being the final supply vector of each country, including household consumption, government consumption, capital formation and inventory changes.

According to the Kyoto carbon accounting model, the production-side emissions refer to the carbon emissions fromcommodity production in a country, which has nothing to do with the consumption of the commodities. In this case, the total carbon emissions of a country is equivalent to the domestic production emissions. On the contrary, the consumer responsibility system considers both domestic and foreign carbon emissions caused by the final demand as the responsibility of the country. Thus, the consumption-side carbon emissions equalthe domestic emissions plus the foreign emissions.

http://www.aloki.hu ● ISSN 1589 1623 (Print) ●ISSN1785 0037 (Online)
DOI: http://dx.doi.org/10.15666/aeer/1704_89418953

Let $F_w = (f_1, f_2 \cdots f_m)$ be the world's emission intensity vector, with f_1~f_m being the carbon emissions from commodity production in different industries of the country, $Y = (y_1, y_2, \cdots, y_i, \cdots, y_n)$ be the final commodities that meet the foreign demand, with y_2, y_i and y_n being the final demand vectors of the country, and $(I - A)^{-1} = L$ be the Leontief I-O matrix. Based on the MIRO model, the production-side carbon emissions of country i can be described as *Eq.2*:

$$E_i^p = f_i x_i = f_i L Y \quad \text{(Eq.2)}$$

where E_i is the total production-side carbon emissions of country i. The production-side carbon emissions can be further split into those meeting domestic demand and those meeting foreign demand, while the commodities that satisfy foreign demand can be subdivided into intermediate commodities and final commodities. Taking China as country i (i=1), the production-side carbon emissions of China can be expressed as *Eq.3*:

$$E_1^p = f_1 x_{11} + f_1 \sum_{i \neq 1} x_{1i} = f_1 x_{11} + f_1 L_{11} \sum_{i \neq 1} \sum_{r \neq 1} A_{1r} x_{ri} + f_1 L_{11} \sum_{i \neq 1} y_{1i} \quad \text{(Eq.3)}$$

where $L_{11} = (I - A_{11})^{-1}$ is the Leontief I-O matrix of China. Similarly, China's consumption-side carbon emissions are generated across the world to satisfy the country's final demand. In this paper, China's consumption-side emissions refer specifically to the country's carbon emissions from the consumption of the final commodities in countries along the Belt and the Road. Hence, the consumption-side emissions of China can be expressed as *Eq.4*:

$$E_1^c = f_i L y_1 \quad \text{(Eq.4)}$$

China's consumption-side emissions can be broken down into domestic emissions and foreign emissions. The former equals the country's production-side emissions that meets domestic demand, while the latter consists of the carbon emissions from foreign countries, which are generated through the intermediate and final commodities imported by China to satisfy its domestic demand. Thus, *Eq.4* can be rewritten as *Eq.5*:

$$E_1^c = f_1 x_{11} + \sum_{i \neq 1} f_i x_{i1} = f_1 x_{11} + \sum_{r \neq 1} f_r L_{rr} (A_{r1} x_{11} + y_{r1}) + \sum_{r \neq 1} \left(f_r L_{rr} \sum_{i \neq 1, i \neq r} A_{ri} x_{i1} \right) \quad \text{(Eq.5)}$$

where $\sum_{r \neq 1} f_r L_{rr} (A_{r1} x_{11} + y_{r1})$ and $\sum_{r \neq 1} \left(f_r L_{rr} \sum_{i \neq 1, i \neq r} A_{ri} x_{i1} \right)$ are the carbon emissions from direct imports and indirect imports, respectively.

There are three responsibility sharing systems for carbon emissions, namely, producer responsibility, consumer responsibility and common responsibility. The producer responsibility means the producer is responsible for the carbon emissions from the commodities produced within its territory, regardless if the commodities are consumed domestically or overseas. Despite its simplicity, this accounting approach neglects the shift of carbon emissions under trade, and hinders the emission reduction in developing countries with high carbon intensity. The consumer responsibility requires the consumer to assume part of the responsibility for carbon emissions. Compared to the

http://www.aloki.hu ● ISSN 1589 1623 (Print) ●ISSN1785 0037 (Online)
DOI: http://dx.doi.org/10.15666/aeer/1704_89418953

producer responsibility system, this approach can mitigate carbon leakage, andpromote carbon emissions reduction and economic growth in developing countries like China. The common responsibility means both the producer and consumer should be responsible for carbon emissions. Under this system, a country's responsibilities are the sum of the producer's responsibility and the consumer's responsibility. Inspired by Pan et al. (2008), a country's total carbon emissions can be divided into five parts, as shown in *Eq.6*:

$$E = f_1 x_{11} + f_1 L_{11} \sum_{i\neq 1} \sum_{r\neq 1} A_{1r} x_{ri} + f_1 L_{11} \sum_{i\neq 1} y_{1i} + \sum_{r\neq 1} f_r L_{rr} (A_{r1} x_{11} + y_{r1}) + \sum_{r\neq 1} (f_r L_{rr} \sum_{i\neq 1, i\neq r} A_{ri} x_{i1}) \quad \text{(Eq.6)}$$

Under the common responsibility system, China's responsibilities for carbon emissions can be expressed as *Eq.7*:

$$(1-m)(f_1 L_{11} \sum_{i\neq 1} \sum_{r\neq 1} A_{1r} x_{ri} + f_1 L_{11} \sum_{i\neq 1} y_{1i}) + m\left[\sum_{r\neq 1} f_r L_{rr} (A_{r1} x_{11} + y_{r1}) + \sum_{r\neq 1} (f_r L_{rr} \sum_{i\neq 1, i\neq r} A_{ri} x_{i1})\right] \quad \text{(Eq.7)}$$

where *m* is the sharing factor; the first term in the second pair of brackets is the carbon emissions from intermediate commodities produced to meet domestic demand; the second term of the second pair of brackets is the carbon emissions from commodities produced to meet foreign demand; the part in the pair of square brackets is the carbon emissions from imported commodities that meet the domestic demand. The rest of the responsibilities should be borne by other countries along the Belt and the Road. This paper sets the sharing factor to 60%, such that the most able countries take greater shares and that consumers assume part of the responsibilities.

The research data were extracted from the WIOD database, which includes the I-O data of 40 countries and regions across the world. The data of each country is divided into 56 industries. Here, 36 industries are adopted in the global MRIO table according to the *Industrial Classification for National Economic Activities* (GB/T 4754-2017) (*Table 1*).

Table 1. *Industry reclassification summary of multi-area input-output tables in the world*

Code	Name of Product department	Code	Name of Product department
Ag and	Agriculture, forestry, animal husbandry	Au	Automobile, motorcycle manufacturing repair
Mi	Mining industry	Re	Other retail and home repairs
Fo	Food, beverage and tobacco product	Ac	Accommodation and food service activities
Te	Textiles, Apparel and Leather Products	La	Land transport and pipeline transportation
Wo	Wood products and cork products, except	Wt	Water transport activities
Pa	Paper and Printing	Ai	Air transport activities
Pc	Production of coke and refined petroleum	Ta	Other transportation activities
Ch	Chemical manufacturing	Po	Post and Telecommunications
Ru	Rubber and plastic products manufacturing	Fi	Financial industry
Nm	Othernon-metallic mineral products	Re	Real estate activity
Me	Metal manufacturing	Le	Leasing and business services
Ma	Machinery and equipment manufacturing	Sc	Scientific research and technology service
Ee	Electrical equipment manufacturing	Pu	Public administration and defense
Tr	Transportation equipment manufacturing	Ed	Education
Fu	Furniture and other wood products	Hu	Human health and social work activities
Wa	Waste treatment industry	Se	Other service activities
Eh	Electricity, heat, gas and water production	Un	Undifferentiated goods and services
Co	Construction industry	Ex	Extra-territorial organization activities

http://www.aloki.hu ● ISSN 1589 1623 (Print) ●ISSN1785 0037 (Online)
DOI: http://dx.doi.org/10.15666/aeer/1704_89418953

The data on the countries appear both in the WIOD database and on the Belt and Road Portal (www.yidaiyilu.gov.cn/) were downloaded, including but not limited to South Korea, India, Indonesia, Russia, Turkey, Czech Republic, Slovakia, Romania, Greece, Slovenia, Estonia, Bulgaria, Lithuania, Latvia, Croatia, Malta and Cyprus. Among them, the top five trade partners of China, namely, South Korea, India, Indonesia, Russia and Turkey, were selected for further analysis. In terms of trade volume, these countries account for 91.98% of China's trade along the Belt and the Road. Thus, it is suitable to compute the production-side and consumption-side implicit carbon with the data of these countries.

Results and Disscussion

By *Equation (3)*, the production-side implicit carbon emissions of China were computed as 5,408.44 million tons, including 5,248.8 Mt to satisfy domestic demand and 159.64 Mt to satisfy the demand of China's top trade partners along the Belt and the Road. The results show that domestic demand is the main driver of China's production-side carbon emissions.

The implicit carbon emissions to satisfy foreign demand can be further divided into those from intermediate export commodities and those from final export commodities. For the top five trade partners of China along the Belt and the Road, the implicit carbon emissions from intermediate export commodities stood at 7.89 Mt for South Korea, 0.023 Mt for India, 0.21 Mt for Indonesia, 0.59 Mt for Russia and 0.21 Mt for Turkey. Hence, South Korea accounts for 90% of the total volume. *Figure 1* shows the industrial classification of China's implicit carbon emissions from intermediate commodities exported to South Korea. Note that the "Sum" means the total implicit carbon emissions from intermediate commodities exported to the five trade partners.

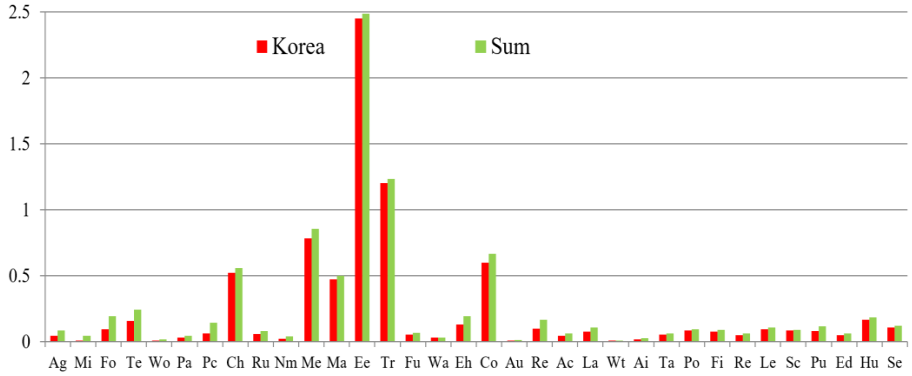

Figure 1. *Industrial classification of China's implicit carbon emissions from intermediate commodities exported to South Korea*

As shown in *Figure 1*, electric equipment production (Ee) generated 2.45 Mt of implicit carbon emissions, about 98% of the total volume of the five trade partners. This industry is clearly the leading contributor to China's implicit carbon emissions from intermediate commodities exported to South Korea, followed by transport equipment production (Tr) (1.20 Mt), metallurgy (Me) (0.79 Mt), construction industry (Co) (0.61 Mt), chemical industry (Ch) (0.52 Mt) and machinery production (Ma) (0.48 Mt).

http://www.aloki.hu ● ISSN 1589 1623 (Print) ●ISSN1785 0037 (Online)
DOI: http://dx.doi.org/10.15666/aeer/1704_89418953

Figure 2 shows the industrial classification of China's implicit carbon emissions from intermediate commodities exported to the other four countries (India, Indonesia, Russia and Turkey). For Russia, the top 4 contributors to the said implicit carbon emissions include coke and refined oil production (Pc) (0.06 Mt), retail goods (Re) (0.053 Mt), electricity and heating (Eh) (0.052 Mt) and construction industry (Co) (0.051 Mt). For Turkey, the top contributors include textile industry (Te) (0.071 Mt), food industry (Fo) (0.021 Mt) and construction industry (Co) (0.010 Mt). For India, the top contributors include chemical industry (ch) (0.003 Mt), textile industry (Te) (0.024 Mt), automobile industry (Au) (0.0024 Mt) and metallurgy (Me) (0.0022 Mt). For Indonesia, the top contributors include food industry (Fo) (0.03 Mt), coke and refined oil production (Pc) (0.02 Mt), electric equipment production (Ee) (0.017 Mt) and metallurgy (Me) (0.015 Mt).

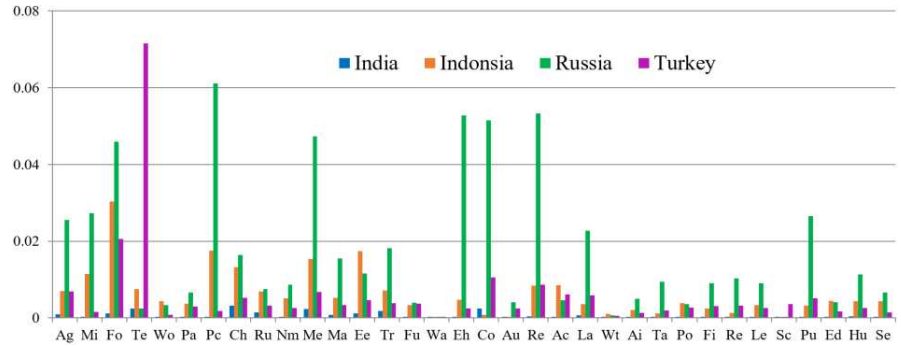

Figure 2. *Industrial classification of China's implicit carbon emissions from intermediate commodities exported to India, Indonesia, Russia and Turkey*

To sum up, the industries that produce high implicit carbon emissions from intermediate export commodities include electric equipment production (Ee), electricity and heating (Eh), metallurgy (Me) and machinery production (Ma), all of which are carbon intensive.

The five trade partners are ranked in descending order as South Korea, India, Indonesia, Russia and Turkey in terms of trade volume with China, and as South Korea, Russia, Indonesia, Turkey and Indiaby carbon emissions. On the implicit carbon emissions from China's intermediate export commodities, Russia comes at the top of the ranking with the volume of 50.98 Mt, followed by South Korea (33.61 Mt), India (27.06 Mt), Indonesia (20.92 Mt) and Turkey (18.15 Mt).

Figure 3 shows the industrial classification of China's implicit carbon emissions from final commodities exported to its top trade partners along the Belt and the Road. It can be seen that 79.95% of the carbon emissions of final exported products come from such industries as electricity and heating (Eh) (70.28 Mt), metallurgy (Me) (14.12 Mt), machinery production (Ma) (15.69 Mt), water transport (Wt) (9.42 Mt) and other transport (Ta) (10.99 Mt).

According to *Equation (5)*, The consumption-side carbon emissions of China, which totals 5,503.89 Mt, are driven by either domestic demand (5,248.8 Mt) and foreign demand (2,282.09 Mt). Thus, most of China's consumption-side carbon emissions (69.70%) originate from domestic demand-driven production. The foreign demand-driven emissions can be further split into those induced by direct import (2,022.28 Mt) and those resulted from indirect trade (259.82 Mt).

http://www.aloki.hu ● ISSN 1589 1623 (Print) ●ISSN1785 0037 (Online)
DOI: http://dx.doi.org/10.15666/aeer/1704_89418953

As shown in *Figure 4*, electric equipment production (Ee) (303.62 Mt) is the leading contributor to China's consumption-side carbon emissions induced by direct import, followed by metallurgy (Me) (220.61 Mt), construction industry (Co) (219.67 Mt), textile industry (Te) (133.51 Mt), chemical industry (Ch) (143.88 Mt) and food industry (Fo) (110.94 Mt). In total, these six industries take up 55.99% of all direct import-induced carbon emissions.

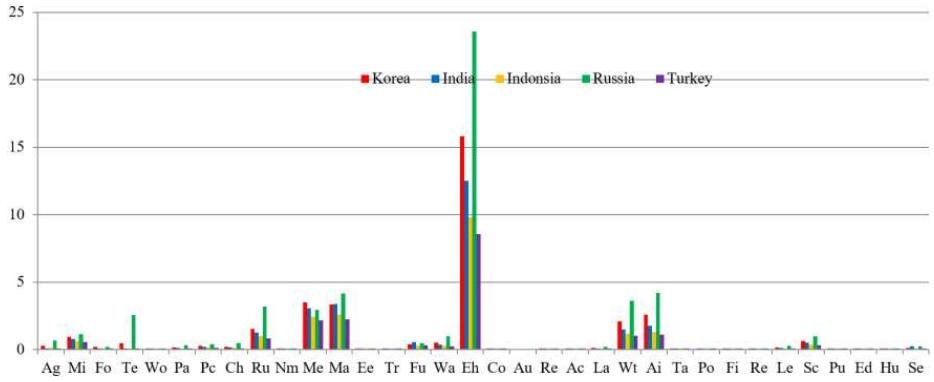

Figure 3. *Industrial classification of China's implicit carbon emissions from final commodities exported to the five trade partners*

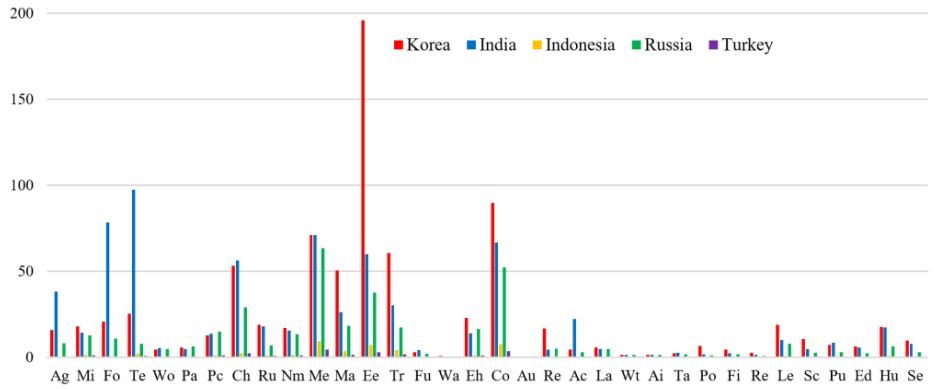

Figure 4. *Industrial classification of China's consumption-side carbon emissions induced by direct import*

The carbon emissions induced by indirect trade refers to those arising from the trade between China and the foreign countries. Coupled with the direct import of intermediate/ final commodities, the indirect trade of commodities determines the final demand of a country in the complex network of global division of labor. For the indirect trade-induced emissions, the leading contributor is electric equipment production (Ee) (52.74 Mt), accounting for 20.30% of the total indirect emissions, followed by metallurgy (Me) (34.34 Mt) (13.22%), coke and refined oil production (Pc) (28.85 Mt) (11.11%), electricity and heating (Eh) (13.47 Mt) (5.52%).

Figure 5 illustrates the calculated responsibilities of China under different sharing principles. As shown in the figure, China needs to assume responsibility for 5,408.44 Mt of carbon emissions in its trade with the countries along the Belt and the Road under the producer responsibility system, 7,503.89 Mt under the consumer

http://www.aloki.hu ● ISSN 1589 1623 (Print) ●ISSN1785 0037 (Online)
DOI: http://dx.doi.org/10.15666/aeer/1704_89418953

responsibility system, and 6,681.91 under the common responsibility system. The responsible amount under the consumer responsibility is 1.39 times that under the producer responsibility, and 1.13 times that under the common responsibility. This is because China imports more commodities from the countries along the Belt and the Road than its export volume to these countries. Comparatively, the common responsibility system is relatively fair, as China needs to assume part of the carbon emissions caused by imported commodities, which is relatively fair.

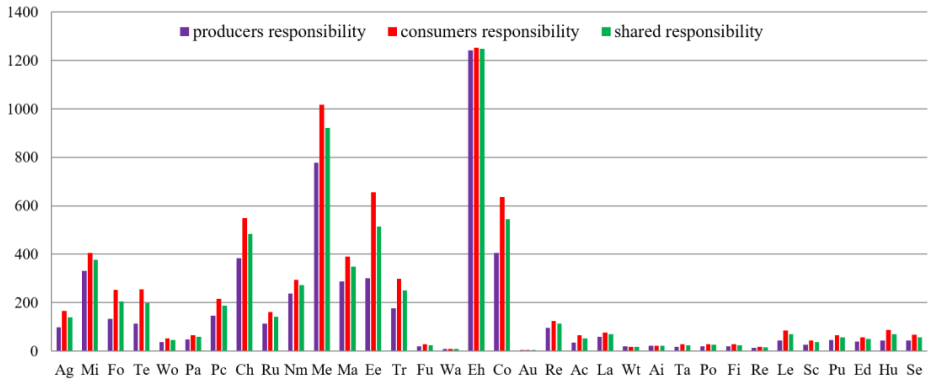

Figure 5. *Responsibility of China under different sharing principles*

The six industries that contribute the most to carbon emissions were selected to analyze their responsibilities under the three sharing principles.

For the leading contributor electricity and heating (Eh), its carbon emission responsibilities will be 1,240.77 Mt, 1,252.49 Mt and 1,247.81 Mt, respectively, under the producer responsibility, consumer responsibility and common responsibility. There is not much difference for this industry under the three sharing principles.

For the second largest emitter metallurgy (Me), its carbon emission responsibilities will be 777.98 Mt, 1,017.96 Mt and 921.97 Mt, respectively, under the producer responsibility, consumer responsibility and common responsibility. The responsible volume under consumer responsibility is 1.31 times that of producer responsibility.

For other large emitters like chemical industry (Ch), electric equipment production (Ee), mining industry (Mi) and machinery production (Ma), the gap between consumer responsibility and producer responsibility in responsible volume is even greater. For these industries, the responsible volume under consumer responsibility is 1.55 times, 2.17 times and 1.22 times that under producer responsibility, respectively.

The huge difference mainly arises from two factors: the industrial difference in carbon emission intensity and the shift in carbon emissions under international trade. For one thing, different industries differ widely in carbon emission intensity. Mining, energy and power industries emit carbon much more intensively than education and scientific research, exerting a high pressure for emission reduction in China. Of course, this also promises a high potential of the country for emission reduction. For another, integration is the main theme of global economic development. This trend brings huge benefits to China's economy. However, it also causes the transfer of carbon emissions, giving the country many unnecessary responsibilities for emission reduction.

http://www.aloki.hu ● ISSN 1589 1623 (Print) ●ISSN1785 0037 (Online)
DOI: http://dx.doi.org/10.15666/aeer/1704_89418953

Conclusion

As the world's largest carbon emitter, China is facing more and more pressure on coping with global climate change. Based on the WIOD database, this paper measures the trade volume between China and its leading trade partners on the Belt and the Road using the MRIO model, revealing the implicit carbon emissions in the trade, and analyzes China's responsibilities for reducing implicit carbon emissions in trade from different perspectives. The main conclusions of this research are as follows:

(1) China's carbon responsibilities in its trade with the top trade partners differs greatly with responsibility sharing principles. The responsible volume under consumer responsibility is much greater than the traditional producer responsibility system. Thus, China and other developing countries should highlight the fairness of responsibility sharing in international negotiations on climate, trying to develop a carbon accounting mechanism favorable to their own rights and interests.

(2) Implicit carbon emissions mainly come from industries with relatively high emission intensities, such as electricity, energy, mining, and chemical industry. All these industries are featured by high energy-consumption and low efficiency. The coal-based energy structure is the fundamental reason for China's high carbon emissions. In future, efforts should be made to increase energy efficiency, increase the proportion of clean energy in the energy structure, and promote the transition towards a clean and efficient consumption structure.

(3) Comparing the different responsibility sharing principles, China is advised to adopt the common responsibility mechanism, which is relatively fair for regions with a large amount of implicit carbon influx.

The future research will clarify China's carbon responsibilities in international trade, assess its emission reduction potential, and allocate the carbon emission responsibilities.

Acknowledgements. Acknowledgements. This work was supported by the Think-tank Program of Education Department in Shaanxi (Nos. 18JT008, 18JT011)., Soft Science Program of Shaanxi Province (Nos. 2019KRM027, 2019KRM109), and National Natural Science Foundation of China (Nos. 71704140, 71804097).

REFERENCES

[1] Bello, M. O., Solarin, S. A., Yen, Y. Y. (2018): The impact of electricity consumption on CO2, emission, carbon footprint, water footprint and ecological footprint: the role of hydropower in an emerging economy. – Journal of Environmental Management 219: 218.

[2] Boamah, K. B., Du, J. G., Bediako, I. A., Boamah, A. J., Abdul-Rasheed, A. A., Owusu, S. M. (2017): Carbon dioxide emission and economic growth of china-the role of international trade. – Environmental Science and Pollution Research 24(14): 13049-13067.

[3] Cozier, M. (2016): The un cop21 climate change conference and the role of ccs. – Greenhouse Gases Science & Technology 5(6): 697-700.

[4] Dietzenbacher, E., Pei, J., Yang, C. (2012): Trade, production fragmentation, and China's carbon dioxide emissions. – Journal of Environmental Economics & Management 64(1): 88-101.

[5] Dong, F., Long, R., Yu, B. (2018): How can China allocate CO2, reduction targets at the provincial level considering both equity and efficiency? Evidence from its Copenhagen Accord pledge. – Resources Conservation & Recycling 130: 31-43.

http://www.aloki.hu ● ISSN 1589 1623 (Print) ●ISSN1785 0037 (Online)
DOI: http://dx.doi.org/10.15666/aeer/1704_89418953

[6] Fang, F., Xu, H. Y. (2013): Carbon Dioxide Emissions Embodied in China's International Trade:Estimation and Analysis Based on Multi-Regional Input-Output Model. – Journal of International Trade (9): 82-91.
[7] Gao, J., Liu, G. G. (2016): Embodied Carbon Emissions Accounting, Structure Decomposition and Allocation of responsibilites in Global Trade: Based on Single-region and Multi-region I-O Methods' Comparison. – Shanghai Journal of Economics 1: 34-43, 70.
[8] Lan, Z. X. (2015): The Estimation of the Implied Carbon Emission of China-EU Bilateral Trade and the Influencing Factors. – Guangdong University of Finance and Economics.
[9] Li, B. (2016): Research on carbon flow and product carbon footprint in export trade. – Beijing Institute of Technology.
[10] Li, Q. R. (2017): China and Japan's calculation of the implied carbon trade in countries along the 'One Belt and One Road'and analysis of influencing factors. – Modern Japan Economics 4: 69-84.
[11] Li, Q., Wen, B., Wang, G. (2018): Study on calculation of carbon emission factors and embodied carbon emissions of iron-containing commodities in international trade of china. – Journal of Cleaner Production 191: 119-126.
[12] Liu, Y., Meng, B., Hubacek, K. (2016): 'Made in China': A reevaluation of embodied CO2, emissions in Chinese exports using firm heterogeneity information. – Applied Energy 184: 1106-1113.
[13] Liu, Y., Tian, Y., Chen, M. (2017): Research on the prediction of carbon emission based on the chaos theory and neural network. – International Journal Bioautomation 21(S4): 339-348.
[14] Munksgaard, J. (2001): CO2 accounts for open economies: producer or consumer responsibility? – Energy Policy 29(4): 327-334.
[15] Pan, J., Phillips, J., Chen, Y. (2008): China's balance of emissions embodied in trade: approaches to measurement and allocating international responsibility. – Oxford Review of Economic Policy 24(2): 354-376.
[16] Pan, A., Wu, X. L. (2018): A Study on Embodied Carbon Emissions in Sino-Japan Trade from the Perspective of GVC Division. – Contemporary Economy of Japan 37(2): 40-52.
[17] Shi, S., Li, C. X., Li, M. T. (2017): Research Progress in the Accounting Method of "Carbon Emission" to "Carbon Footprint" in Animal Husbandry. – Chinese Journal of Population, Resources and Environment 27(6): 36-41.
[18] Su, B., Ang, B. W. (2011): Input-output analysis of CO emissions embodied in trade: The effects of spatial aggregation. – Energy Economics 32(1): 166-175.
[19] Sun, Y. Y. (2016): Research on the Influencing Factors of the Implied Carbon Emission of China's Export Trade. – Dongbei University of Finance and Economics.
[20] Tan, S. L., Qiu, G. Y., Xiong, Y. (2014): New Application of Input-Output Method in Virtual Water Consumption and Trade Research. – Journal of Natural Resources 29(2): 355-364.
[21] Tu, J. Z., Ma, D. L. (2018): A spatial economics perspective on convergence research of carbon emissions performance in China. – International Journal of Heat and Technology 36(3): 962-972.
[22] Wang, A. J., Feng, Z. X., Meng, B. (2017): Measure of Carbon Emission and Carbon Transfer in 30 Provinces of China. – Journal of Quantitative & Technical Economics 34(8): 89-104.
[23] Wei, T., Peng, S. J. (2017): Research on Embodied Energy in China-USA Trade with MRIO Model. – Soft Science 31(8): 39-42, 70.
[24] Xia, Y., Fan, Y., Yang, C. (2015): Assessing the impact of foreign content in China's exports on the carbon outsourcing hypothesis. – Applied Energy 150: 296-307.
[25] Xiao, Y., Zheng, X. D. (2016): Research on the Trade Value-Adding and Carbon Emission Commitment Under Global Value Chain. – Theoretical Exploration 4: 172-176.

http://www.aloki.hu ● ISSN 1589 1623 (Print) ●ISSN1785 0037 (Online)
DOI: http://dx.doi.org/10.15666/aeer/1704_89418953

[26] Yu, T., Wang, W. Z. (2017): Measurement and Decomposition of Implicit Carbon Emissions in China's Foreign Trade. – Ecological Economy 33(7): 37-41.
[27] Yu, X. H., Xu, M. (2017): Research on the Responsibility of China's Industrial Sector for External Trade Carbon Emission from the Perspective of Consumer Responsibility. – Industrial Economic Review 8(1): 18-30.
[28] Zhang, S. E. (2017): Study on dynamic performance modeling for carbon emission of machinofacture system based on mixed space model. – Academic Journal of Manufacturing Engineering 15(2): 87-94.
[29] Zhong, Z. Q., Zhang, X., He, L. Y. (2018): Regional Carbon Emissions Transfer, Embodied Emissions in Trade Per Unit of Value of Trade and Regional Cooperation: Empirical Analysis from 30 Provinces in China. – Journal of International Trade 73(3): 94-104.

http://www.aloki.hu ● ISSN 1589 1623 (Print) ●ISSN1785 0037 (Online)
DOI: http://dx.doi.org/10.15666/aeer/1704_89418953

THE LANDSCAPE EVALUATION SYSTEM OF ECOTOURISM VILLAGES IN QINLING MOUNTAINS

YU, X. H.[1,2*] – WANG, X.[1] – REN, Y. G.[1] – LIU, J. C.[3]

[1]*School of Architecture, Chang'an University, Xi'an 710061, China*

[2]*School of Architecture, Xi'an University of Architectural Science and Technology, Xi'an 710055, China*

[3]*Agile Property Holdings Limited, Xi'an Branch, Xi'an 710061, China*

**Corresponding author*
e-mail: yuxiaohui@chd.edu.cn; phone: +86-029-8233-7365; fax: +86-029-8233-7365

(Received 18th Mar 2019; accepted 17th May 2019)

Abstract. Despite the importance of landscape resources in ecotourism villages, there is no scientific and complete index system for the evaluation of rural ecotourism landscape. This paper attempts to construct an evaluation index system for the ecotourism villages in the Xi'an section of the northern piedmont of Qinling Mountain. Firstly, the preliminary indices and relevant data were collected through field surveys and expert consultation. Next, the weight of each index was determined using the AHP. The conclusion is that: in the criteria layer, the weights of the elements can be ranked as natural elements (A1) > humanistic material elements (A2) > non-material elements (A3); in the factor layer, the weights of the factors under the natural elements can be ranked as ecological environment (B1) > hydro-geomorphic features (B2) > landscape quality (B3), the factors under the humanistic material elements as settlement landscape (B4) > farmland landscape (B6) > road landscape (B5) > facility construction (B7), and the factors under the non-material elements as folk culture (B8) > community participation (B9). Among the 37 indices, the natural disaster frequency (C3), folk culture diversity (C33) and Preservation of traditional residence (C15) were more important than the remaining 34 indices.
Keywords: *ecotourism villages, rural landscape; landscape resources, landscape character assessment, index system, analytical hierarchy process (AHP)*

Introduction

Ecotourism is an important strategy for Chinese villages, as the country has entered a new phase of high-quality development. The quality and sustainability of ecotourism villages are essential to China's pursuit of ecological civilization and rural development. To achieve sustainable development of ecotourism villages, it is a must to evaluate rural landscape resources in a scientific manner.

Among foreign scholars, Ianas (2013) evaluated the landscape in Almăj rural land system between 1990 and 2010. Hogan et al. (2012) estimated the cumulative ecological effect of local landscape changes in south Florida. Gottero and Cassatella (2017) explained the relationship between rural policymakers, agricultural policies and rural landscape through developing and testing key landscape indices. Steinhardt evaluated and planned small and medium rural landscapes on different levels, and applied the fuzzy evaluation theory into the research (Steinhardt, 1998). Gulinck et al. (2001) carried out rural landscape evaluation with three factors (i.e. completeness, diversity, and visual quality) and six indices (i.e. land use suitability, fragmentation degree, species richness, natural restoration potential, and tourism potential).

http://www.aloki.hu ● ISSN 1589 1623 (Print) ● ISSN 1785 0037 (Online)
DOI: http://dx.doi.org/10.15666/aeer/1704_89558968

About the rural landscape evaluation, the Chinese scholars have mainly tackled three issues: ecological evaluation (Xu, 2007; Meng et al., 2011), aesthetic evaluation (Xie, 2004; Petrova et al., 2015) and the evaluation system. There are two widely accepted rural landscape evaluation systems in China. One of them was a human settlement-oriented one proposed by Liu and Wang (2002). This system consists of such three layers as the goal layer, the criteria layer (5 criteria) and the index layer (21 indices). The five factors are habitability, accessibility, compatibility, sensitivity and beauty. The other evaluation system was designed in light of the features of rural landscapes (Xie et al., 2003). Focusing on the social effect, ecological quality and aesthetic effect of rural landscape, this evaluation system has four layers, including a goal layer, a criteria layer (3 criteria), a factor layer (11 factors) and an index layer (31 indices).

To sum up, the foreign studies on rural landscape evaluation mainly concentrate on the ecological effect and aesthetics of a landscape, while also exploring landscape evaluation systems. The domestic studies have designed comprehensive evaluation indices, yet the evaluation systems are still incomplete due to the lack of weight analysis. Considering the previous studies, this paper attempts to construct an evaluation index system for the ecotourism villages in the Xi'an section of the northern piedmont of the Qinling Mountain (hereinafter referred to as the study area). The remainder of this paper mainly deals with data acquisition, index system construction, index weighting, the possible shortcomings and conclusions.

Materials and methods

Rural ecotourism requires a delicate balance between ecotourism and rural life (Yu, 2015). The ecotourism villages should provide services in line with the functions of rural landscape. These services need to cover natural elements (e.g. topography, hydrological conditions, and animal and plant resources), human elements (e.g. settlement environment, service facilities and farmland landscape), as well as non-material cultural elements (e.g. folk culture). For the sustainable development of rural landscape, the following goals should be fulfilled through rural ecotourism: a memorable travel experience of the original life, customs, humane care and unique agricultural landscape in the villages; the development of the villages and the local economy; full demonstration of the functional, aesthetic and ecological values of rural landscape; the coordination between rural development and eco-environmental protection.

Considering the definition of ecotourism villages and the existing index systems for landscape evaluation, this paper sets up an evaluation index system for ecotourism villages in the study area through qualitative and quantitative methods. A total of 75 indices were obtained for rural landscape elements by the investigation. On this basis, each index was rated by experts, and its weight was determined by the analytic hierarchy process (AHP), using data processing software like the SPSS and Matlab.

Data sources

The author investigated 33 towns across the 6 districts/counties (*Fig. 1*) in the study area. A total of 53 villages were identified as ecotourism villages in this region, according to the definitions and functional classifications on the term by various scholars (Dong, 2013; Wu, 2011). Then, the natural, human, social and ecological resources were sorted out in these villages, revealing that the local landscape of

http://www.aloki.hu ● ISSN 1589 1623 (Print) ● ISSN 1785 0037 (Online)
DOI: http://dx.doi.org/10.15666/aeer/1704_89558968

ecotourism villages mainly covers the natural element, the humanistic material element and the non-material element (*Fig. 2*). Among them, the natural element contains ecological environment, hydro-geomorphic features and landscape quality; the humanistic material element includes settlement landscape, road landscape, farmland landscape and facility construction; the non-material element encompasses the folk culture and community participation.

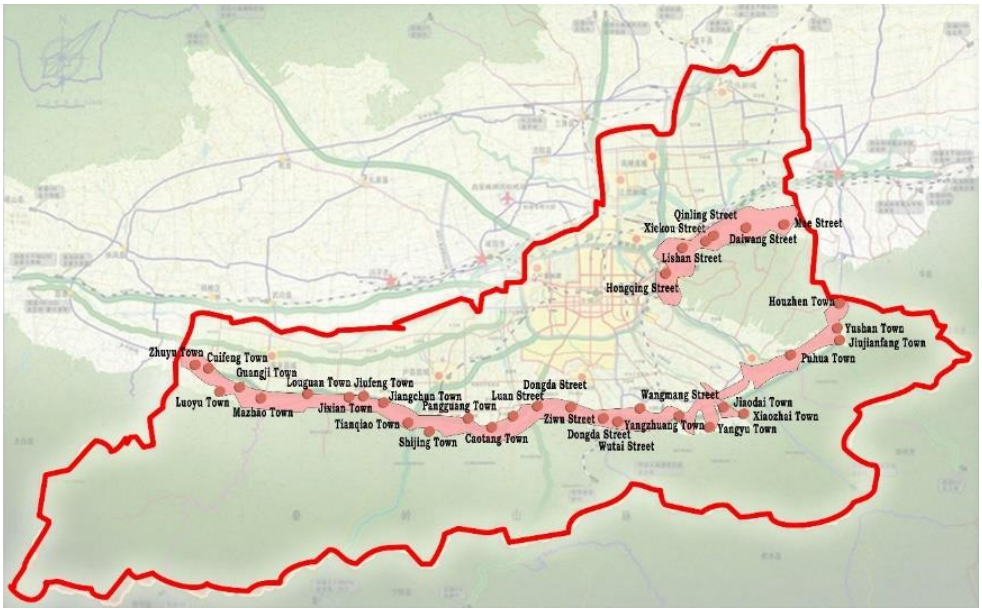

Figure 1. *Towns in the study area*

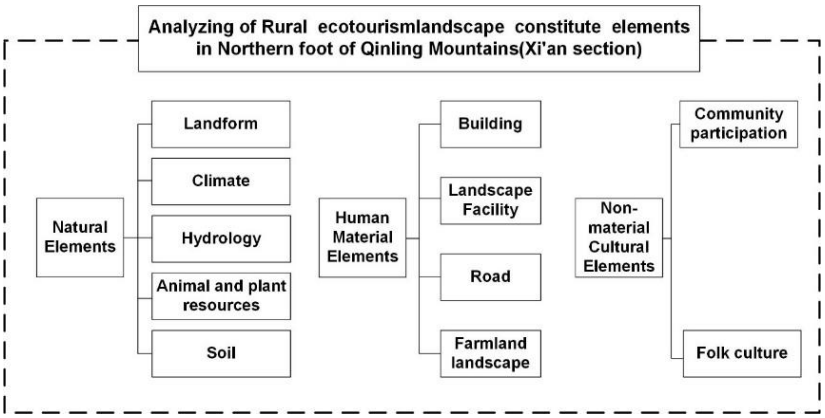

Figure 2. *Elements of rural tourism landscape in the study area*

Structure of the index system

Referring to the relevant studies (Liu and Wang, 2002; Liu and Wu, 2014; Xie et al., 2003), this paper divides the landscape evaluation index system of the ecotourism villages in the study area into four layers according to the landscape features of such villages and the structural features of the research system. From abstract to concrete and from macro to micro, the four layers are respectively the goal layer (G), the criteria layer (C), the factor layer (F) and the index layer (I). As shown in *Figure 3,* the

http://www.aloki.hu ● ISSN 1589 1623 (Print) ● ISSN 1785 0037 (Online)
DOI: http://dx.doi.org/10.15666/aeer/1704_89558968

proposed index system adopts a 1 + 3 + 9 + N (i.e. 1 goal, 3 criteria, 9 factors and N indices) structure, and evaluates the landscape of ecotourism villages from the perspectives of natural, humanistic material and non-material elements.

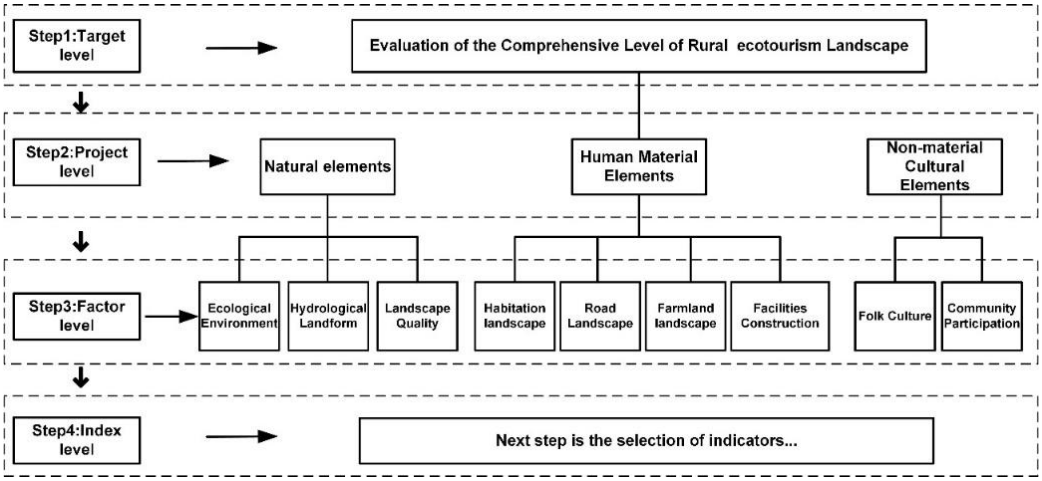

Figure 3. *Structure of landscape evaluation index system of the ecotourism villages*

The first layer is the goal layer (G). This layer specifies the ultimate goal of the index system and reflects the comprehensive level of rural ecotourism landscape in the study area. The second layer is the criteria layer (C). This layer mirrors the status of rural ecotourism landscape in the aspects of natural, humanistic material and non-material elements. The third layer is the factor layer (F). This layer contains 9 factors on the details of the three criteria. The fourth layer is the index layer (I). This layer gives the 37 indices under the 9 factors.

Selection of evaluation indices

The evaluation indices were selected through preliminary selection, screening and correction:

(1) Preliminary selection: A total of 75 indices, more than twice the number of final indices, were selected preliminarily according to the features of rural ecotourism landscape in the study area, the expert opinions and the survey data on local residents. A large number of preliminary indices was designed to ensure the reasonability of the final indices.

(2) Screening: The set of preliminary indices were made into a questionnaire, and rated by experts and scholars in relevant fields. The valid questionnaires were analyzed on the SPSS statistical software. The significance of each index was evaluated by the mean value, and the concentration of expert opinions was determined by the mode percentage and the coefficient of variation. The results are presented in Appendix 2. After two rounds of expert consultation, the 35 indices with a coefficient of variation in [0~0.37] were all retained.

(3) Correction: The index “diversity of riverside greening plants” had large mean value and mode percentage. It was retained after professional discussion. The two indices “perfection of service reception facilities” and “perfection of tourism facilities” were combined into “perfection of tourism service facilities”. Finally, a total of 37 indices were included in the index system (*Table 1*).

http://www.aloki.hu ● ISSN 1589 1623 (Print) ● ISSN 1785 0037 (Online)
DOI: http://dx.doi.org/10.15666/aeer/1704_89558968

Table 1. *List of landscape evaluation indices for ecotourism villages in the study area*

Goal layer G	Criteria layer C	Factor layer F	Index layer I
Landscape evaluation index system for ecotourism villages P	Natural element A1	Ecological environment B1	Forest coverage C1
			Landscape diversity C2
			Natural disaster frequency C3
			Natural landscape beauty C4
		Hydro-geomorphic features B2	Waterbody cleanliness C5
			The diversity of riverside greening plants C6
			Coordination between waterbody and surrounding environment C7
			The diversity of topographical landscapes C8
			Human disturbance in topographical landscape C9
			Accessibility of rural landscape C10
		Landscape quality B3	Uniqueness of rural landscape C11
			The authenticity of rural landscape C12
			Scale and richness of rural tourism resources C13
			Coordination between construction project and surrounding landscape C14
	Humanistic material element A2	Settlement landscape B4	Preservation of traditional residence C15
			The uniqueness of residential building C16
			The overall beauty of settlement space C17
			Coordination between building and landscape C18
		Road landscape B5	Accessibility of road landscape C19
			Effect of street trees on rural ecological landscape C20
			Effect of new roads on rural landscape C21
		Farmland landscape B6	Area ratio of a landscape to farmland C22
			Commercial rate of agricultural products C23
			Continuity of agricultural landscape C24
			Regional features of rural agricultural landscape C25
		Facility construction B7	Waste treatment rate C26
			The perfection of tourist transport facilities C27
			The perfection of infrastructure C28
			The perfection of tourism service facilities C29
			The perfection of tourism safety facilities C30
	Non-material element A3	Folk culture B8	Building materials C31
			Cultural inheritance and retention C32
			Folk culture diversity C33
		Community participation B9	Resident satisfaction C34
			The proportion of community residents in employees C35
			Resident hospitality C36
			A diversity of participated projects C37

http://www.aloki.hu ● ISSN 1589 1623 (Print) ● ISSN 1785 0037 (Online)
DOI: http://dx.doi.org/10.15666/aeer/1704_89558968

Determination of index weights

According to the steps of the AHP, the index weights were determined in a comprehensive manner through questionnaire survey and expert scoring. In total, 13 judgement matrices were set up, 20 questionnaires were sent out, and 10 experts were invited to rate the indices. All returned questionnaires were valid. The elements on each layer were evaluated systematically through pairwise comparison, with respect to their impact on an element above them in the hierarchy. The results of this single hierarchal arrangement include the weights of A relative to P WAi (i = 1, 2, 3), the weights of B relative to A WBi (i = 1, 2, …, 9), the weights of C relative to B WCi (i = 1, 2, …, 37). Finally, the weights of A to P WAi (i = 1, 2, 3) were adopted to check the consistency between the single hierarchal arrangement results on each layer, yielding the final results of index weights.

Evaluation results

Results of single hierarchal arrangement

The single hierarchal arrangement results of the 13 judgement matrices are recorded in *Tables 2–14*.

Table 2. *List of eigenvectors of matrix B1 [C1~C4]*

Matrix B1	Forest coverage C1	Landscape diversity C2	Natural disaster frequency C3	Natural landscape beauty C4	Weight
Forest coverage C1	1	2	1/2	3	0.272
Landscape diversity C2	1/2	1	1/3	2	0.157
Natural disaster frequency C3	2	3	1	5	0.483
Natural landscape beauty C4	1/3	1/2	1/5	1	0.088

Table 3. *List of eigenvectors of matrix B2 [C6~C9]*

Matrix B2	Waterbody cleanliness C5	Diversity of riverside greening plants C6	Coordination between waterbody and surrounding environment C7	The diversity of topographical landscapes C8	Human disturbance in the topographical landscape C9	Weight
Waterbody cleanliness C5	1	2	1/2	6	4	0.285
Diversity of riverside greening plants C6	1/2	1	1/3	3	2	0.150
Coordination between waterbody and surrounding environment C7	2	3	1	6	5	0.430

http://www.aloki.hu ● ISSN 1589 1623 (Print) ● ISSN 1785 0037 (Online)
DOI: http://dx.doi.org/10.15666/aeer/1704_89558968

The diversity of topographical landscapes C8	1/6	1/3	1/6	1	1/2	0.052
Human disturbance in topographical landscape C9	1/4	1/2	1/5	2	1	0.083

Table 4. *List of eigenvectors of matrix B3 [C10~C14]*

Matrix B3	**Accessibility of rural landscape C10**	**Uniqueness of rural landscape C11**	**Authenticity of rural landscape C12**	**Scale and richness of rural tourism resources C13**	**Coordination between construction project and surrounding landscape C14**	**Weight**
Accessibility of rural landscape C10	1	2	1/4	1/6	1/2	0.076
Uniqueness of rural landscape C11	1/2	1	1/4	1/7	1/3	0.051
Authenticity of rural landscape C12	4	4	1	1/2	2	0.263
Scale and richness of rural tourism resources C13	6	7	2	1	1/4	0.288
Coordination between construction project and surrounding landscape C14	2	3	1/2	4	1	0.322

Table 5. *List of eigenvectors of matrix B4 [C15~C18]*

Matrix B4	**Preservation of traditional residence C15**	**Uniqueness of residential building C16**	**Overall beauty of settlement space C17**	**Coordination between building and landscape C18**	**Weight**
Preservation of traditional residence C15	1	6	4	2	0.520
Uniqueness of residential building C16	1/6	1	1/2	1/3	0.081
Overall beauty of settlement space C17	1/4	2	1	1/2	0.140
Coordination between building and landscape C18	1/2	3	2	1	0.260

http://www.aloki.hu ● ISSN 1589 1623 (Print) ● ISSN 1785 0037 (Online)
DOI: http://dx.doi.org/10.15666/aeer/1704_89558968

Table 6. *List of eigenvectors of matrix B5 [C19~C21]*

Matrix B5	Accessibility of road landscape C19	Effect of street trees on rural ecological landscape C20	Effect of new roads on rural landscape C21	Weight
Accessibility of road landscape C19	1	3	5	0.648
Effect of street trees on rural ecological landscape C20	1/3	1	2	0.230
Effect of new roads on rural landscape C21	1/5	1/2	1	0.122

Table 7. *List of eigenvectors of matrix B6 [C22~C25]*

Matrix B6	Area ratio of a landscape to farmland C22	Commercial rate of agricultural products C23	Continuity of agricultural landscape C24	Regional features of rural agricultural landscape C25	Weight
Area ratio of a landscape to farmland C22	1	½	1/4	1/6	0.072
Commercial rate of agricultural products C23	2	1	1/3	1/5	0.114
Continuity of agricultural landscape C24	4	3	1	1/2	0.293
Regional features of rural agricultural landscape C25	6	5	2	1	0.522

Table 8. *List of eigenvectors of matrix B7 [C26~C30]*

Matrix B7	Waste treatment rate C26	Perfection of tourist transport facilities C27	Perfection of infrastructure C28	Perfection of tourism service facilities C29	Perfection of tourism safety facilities C30	Weight
Waste treatment rate C26	1	1/7	1/5	½	1/3	0.052
Perfection of tourist transport facilities C27	7	1	2	5	3	0.440
Perfection of infrastructure C28	5	1/2	1	4	2	0.275
Perfection of tourism service facilities C29	2	1/5	1/4	1	1/2	0.083
Perfection of tourism safety facilities C30	3	1/3	1/2	2	1	0.150

http://www.aloki.hu ● ISSN 1589 1623 (Print) ● ISSN 1785 0037 (Online)
DOI: http://dx.doi.org/10.15666/aeer/1704_89558968

Table 9. *List of eigenvectors of matrix B8 [C31~C33]*

Matrix B8	Building materials C31	Cultural inheritance and retention C32	Folk culture diversity C33	Weight
Building materials C31	1	1/3	1/4	0.117
Cultural inheritance and retention C32	3	1	1/3	0.268
Folk culture diversity C33	4	3	1	0.614

Table 10. *List of eigenvectors of matrix B9 [C34~C37]*

Matrix B9	Resident satisfaction C34	Proportion of community residents in employees C35	Resident hospitality C36	Diversity of participated projects C37	Weight
Resident satisfaction C34	1	4	2	1/2	0.275
Proportion of community residents in employees C35	1/4	1	1/2	1/6	0.074
Resident hospitality C36	1/2	2	1	1/4	0.138
Diversity of participated projects C37	2	6	4	1	0.513

Table 11. *List of eigenvectors of matrix A1 [B1~B4]*

Matrix A1	Ecological environment B1	Hydro-geomorphic features B2	Landscape quality B3	Weight
Ecological environment B1	1	2	4	0.571
Hydro-geomorphic features B2	1/2	1	2	0.286
Landscape quality B3	1/4	1/2	1	0.143

Table 12. *List of eigenvectors of matrix A2 [B4~B7]*

Matrix A2	Settlement landscape B4	Road landscape B5	Farmland landscape B6	Facility construction B7	Weight
Settlement landscape B4	1	3	2	5	0.483
Road landscape B5	1/3	1	1/2	2	0.157
Farmland landscape B6	1/2	2	1	3	0.272
Facility construction B7	1/5	1/2	1/3	1	0.088

http://www.aloki.hu ● ISSN 1589 1623 (Print) ● ISSN 1785 0037 (Online)
DOI: http://dx.doi.org/10.15666/aeer/1704_89558968

Table 13. *List of eigenvectors of matrix A3 [B8~B9]*

Matrix A3	Folk culture B8	Community participation B9	Weight
Folk culture B8	1	2	0.667
Community participation B9	1/2	1	0.333

Table 14. *List of eigenvectors of matrix P [A1~A3]*

Matrix P	Natural element A1	Humanistic material element A2	Non-material element A3	Weight
Natural element A1	1	2	2	0.493
Humanistic material element A2	1/2	1	2	0.311
Non-material element A3	1/2	1/2	1	0.196

Weights of evaluation indices

The 37 indices were subjected to weight analysis by the AHP. The final results are shown in *Table 15*.

Table 15. *List of index weights*

Goal layer	Criteria layer	Factor layer	Single hierarchal arrangement weights	Total hierarchal arrangement weights	Index layer	Single hierarchal arrangement weights	Total hierarchal arrangement weights	Single hierarchal arrangement weights
Landscape evaluation index system for ecotourism villages in the study area	Natural element A1 0.49339	Ecological environment B1	0.571	0.282	Forest coverage C1	0.27197	0.076679	0.2720
					Landscape diversity C2	0.15699	0.044261	0.1570
					Natural disaster frequency C3	0.48289	0.136145	0.4829
					Natural landscape beauty C4	0.08815	0.024853	0.0882
		Hydro-geomorphic features B2	0.286	0.141	Waterbody cleanliness C5	0.28529	0.040216	0.2853
					Diversity of riverside greening plants C6	0.14973	0.021107	0.1497
					Coordination between waterbody and surrounding environment C7	0.43023	0.060648	0.4302
					Diversity of topographical landscapes C8	0.05191	0.007317	0.0519
					Human disturbance in topographical landscape C9	0.08284	0.011677	0.0828

http://www.aloki.hu ● ISSN 1589 1623 (Print) ● ISSN 1785 0037 (Online)
DOI: http://dx.doi.org/10.15666/aeer/1704_89558968

		Landscape quality B3	0.143	0.070	Accessibility of rural landscape C10	0.07632	0.00538	0.0763
					Uniqueness of rural landscape C11	0.0511	0.003602	0.0511
					Authenticity of rural landscape C12	0.26278	0.018522	0.2628
					Scale and richness of rural tourism resources C13	0.28794	0.020296	0.2879
					Coordination between construction project and surrounding landscape C14	0.32186	0.022687	0.3219
	Humanistic material element A2 0.31081	Settlement landscape B4	0.483	0.1500	Preservation of traditional residence C15	0.51952	0.077973	0.5195
					Uniqueness of residential building C16	0.08077	0.012123	0.0808
					Overall beauty of settlement space C17	0.13995	0.021005	0.1400
					Coordination between building and landscape C18	0.25976	0.038987	0.2598
		Road landscape B5	0.157	0.049	Accessibility of road landscape C19	0.64833	0.031635	0.6483
					Effect of street trees on rural ecological landscape C20	0.22965	0.011206	0.2297
					Effect of new roads on rural landscape C21	0.12202	0.005954	0.1220
		Farmland landscape B6	0.272	0.085	Area ratio of landscape to farmland C22	0.07154	0.006047	0.0715
					Commercial rate of agricultural products C23	0.11373	0.009614	0.1137
					Continuity of agricultural landscape C24	0.2928	0.024751	0.2928

http://www.aloki.hu ● ISSN 1589 1623 (Print) ● ISSN 1785 0037 (Online)
DOI: http://dx.doi.org/10.15666/aeer/1704_89558968

					Regional features of rural agricultural landscape C25	0.52193	0.044119	0.5219
		Facility construction B7	0.088	0.027	Waste treatment rate C26	0.05183	0.00142	0.0518
					Perfection of tourist transport facilities C27	0.44011	0.012058	0.4401
					Perfection of infrastructure C28	0.27507	0.007536	0.2751
					Perfection of tourism service facilities C29	0.08303	0.002275	0.083
					Perfection of tourism safety facilities C30	0.14996	0.004109	0.1500
	Non-material element A3 0.1958	Folk culture B8	0.667	0.131	Building materials C31	0.11722	0.015301	0.1172
					Cultural inheritance and retention C32	0.26837	0.035031	0.2684
					Folk culture diversity C33	0.61441	0.080201	0.6144
		Community participation B9	0.333	0.065	Resident satisfaction C34	0.2751	0.017955	0.2751
					Proportion of community residents in employees C35	0.07411	0.004837	0.0741
					Resident hospitality C36	0.13755	0.008977	0.1376
					Diversity of participated projects C37	0.51324	0.033497	0.5132

As shown in the table above, in the criteria layer, the weights of the elements can be ranked as natural elements (A1) > humanistic material elements (A2) > non-material elements (A3); in the factor layer, the weights of the factors under the natural elements can be ranked as an ecological environment (B1) > hydro-geomorphic features (B2) > landscape quality (B3), the factors under the humanistic material elements as settlement landscape (B4) > farmland landscape (B6) > road landscape (B5) > facility construction (B7), and the factors under the non-material element as folk culture (B8) > community participation (B9). Among the 37 indices, the natural disaster frequency C3, folk culture diversity C33 and Preservation of traditional residence C15 were more important than the rest 34 indices.

http://www.aloki.hu ● ISSN 1589 1623 (Print) ● ISSN 1785 0037 (Online)
DOI: http://dx.doi.org/10.15666/aeer/1704_89558968

Discussion

In this research, the indices are selected through field survey and expert consultation, in reference to the previous studies on landscape index system. Besides, the weight of each index was quantified accurately and scientifically using the AHP. Nevertheless, some problems and possible deviations were discovered during the theoretical construction.

First, the AHP is a subjective method that may be biased in the weighting of some qualitative indices.

Second, rural landscape evaluation involves many fields. The selection of indices may not be comprehensive enough due to the limitations of professional knowledge.

Third, the experts involved in this research are all engaged in landscape-related fields; the author did not carry out effective consultations with experts in the fields of ecology, economics, tourism or sociology.

Conclusions

Ecotourism is an important strategy for Chinese villages, as the country has entered a new phase of high-quality development. This paper attempts to design a scientific and effective index system for landscape evaluation of ecotourism villages in the study area. Based on the existing theories on rural landscape evaluation system at home and aboard, the author carried out a field survey and expert consultation to comb the elements of rural ecotourism landscape and determined the weight of each index by the AHP. The following conclusions were drawn from the results and discussion.

This paper sets up a 4-layer index system that evaluates the rural ecotourism landscape from three aspects (i.e. the natural element, the humanistic material element and the non-material element). On this basis, it is necessary to consider the biological impacts of the humanistic material environment, such as the negative effects of settlement landscape, road landscape and facility construction on the biological environment and their indirect impacts on the rational layout of land use in rural planning. Consideration should also be given to the economic impacts of the non-material element, and the effects of landscape index system on agricultural policies and rural housing policies, aiming to create a multi-directional interaction mechanism between ecological, economic, and cultural elements in rural areas.

According to the AHP analysis, in the criteria layer, the weights of the elements can be ranked as natural elements (A1) > humanistic material elements (A2) > non-material elements (A3); in the factor layer, the weights of the factors under the natural elements can be ranked as ecological environment (B1) > hydro-geomorphic features (B2) > landscape quality (B3), the factors under the humanistic material elements as settlement landscape (B4) > farmland landscape (B6) > road landscape (B5) > facility construction (B7), and the factors under the non-material element as folk culture (B8) > community participation (B9). Among the 37 indices, the natural disaster frequency C3, folk culture diversity C33 and Preservation of traditional residence C15 were more important than the rest 34 indices. The natural environment provides the material basis for human survival. There is no time to delay for the protection of the natural environment, facing the severe environmental impacts of human activities. For the study area, the ecotourism villages should rationalize the rural planning, construction and management according to their unique landscape resources and the weights of the proposed indices.

http://www.aloki.hu ● ISSN 1589 1623 (Print) ● ISSN 1785 0037 (Online)
DOI: http://dx.doi.org/10.15666/aeer/1704_89558968

The rural macro-system is involved in the landscape evaluation of ecotourism villages. The future research will improve the rural ecotourism evaluation index system in terms of objective and comprehensive quantification, aiming to provide desirable solutions to rural problems like sustained economic growth, eco-environmental protection and human settlement.

Acknowledgements. This study was supported by the Key Project of the National Natural Science Foundation of China (General Program) (No.51378067), 2016 Shaanxi Province Social Development of Science and Technology Research Plan Project (No.2016SF-417).

REFERENCES

[1] Dong, Y. N. (2013): Study on the Planning of the Typical Eco-Tourism Village in Longnan. A Case of Tianhe in Hui County. – Lanzhou University, Lanzhou.
[2] Gottero, E., Cassatella, C. (2017): Landscape indicators for rural development policies. Application of a core set in the case study of Piedmont region. – Environmental Impact Assessment Review 65: 75-85.
[3] Gulinck, H., Múgica, M., De Lucio, J., Atauri, J. (2001): A framework for comparative landscape analysis and evaluation based on land cover data, with an application in the Madrid region (Spain). – Landscape and Urban Planning 55(4): 257-270.
[4] Hogan, D. M., Labiosa, W., Pearlstine, L., Hallac, D., Strong, D., Hearn, P, Bernknopf, R. (2012): Estimating the cumulative ecological effect of local-scale landscape changes in south Florida. – Environmental Management 49(2): 502-515.
[5] Ianas, A. (2013): Landscape quality assessment in Almaj land rural system from the Mountainous Banat (Romania), during the 1990-2010 period. – Forum Geografic 12(1): 43-51.
[6] Liu, B. Y., Wang, Y. C. (2002): Theoretical base and evaluating indicator system of rural landscape assessment in China. – Chinese Gardens 5: 77-80.
[7] Liu, H. T., Wu, Z. Q. (2014): Theoretical framework of water-city coexistence and its evaluation under the perspective of ecological civilization. – Urban Planning Forum 4: 52-56.
[8] Meng, J. J., Zhou, T., Liu, Y. (2011): Research on regional ecological risk assessment: a case study of Ordos in Inner Mongolia. – Acta Scientiarum Naturalium Universitatis Pekinensis 47(05): 935-943.
[9] Petrova, E. G., Mironov, Y. V., Aoki, Y., Matsushima, H., Ebine, S., Furuya, K., Petrova, A., Takayama, N., Ueda, H. (2015): Comparing the visual perception and aesthetic evaluation of natural landscapes in Russia and Japan: cultural and environmental factors. – Progress in Earth and Planetary Science 2(1): 6.
[10] Steinhardt, U. (1998): Applying the fuzzy set theory for medium and small scale landscape assessment. – Landscape and Urban Planning 41(3): 203-208.
[11] Wu, Y. C. (2011): Study on the Development of Rural Tourism in Western Hunan. – Beijing Forestry University, Beijing.
[12] Xie, H. (2004): Preliminary researches on the functional evaluation of rural landscape. – Acta Ecologica Sinica 24(9): 1988-1993.
[13] Xie, H. L., Liu, L. M. (2003): Research advance and index system of rural landscape evaluation. – Chinese Journal of Ecology 22(6): 97-101.
[14] Xie, H. L., Liu, L. M., Zhao, Y. W. (2003): Studies on the indicator system of rural landscape evaluation and evaluating method. – Research of Agricultural Modernization 2: 95-98.
[15] Xu, Y. Q. (2007): Evaluation of ecological carrying capacity based on ecological footprint model in Beijing. – Resources Science 5: 37-42.
[16] Yu, X. Y. (2015): Multidimensional development pattern of the eco-towns. – Journal of Liaoning Medical College (Social Science Edition) 13(01): 4-6.

http://www.aloki.hu ● ISSN 1589 1623 (Print) ● ISSN 1785 0037 (Online)
DOI: http://dx.doi.org/10.15666/aeer/1704_89558968

AN EMPIRICAL ANALYSIS ON THE RELATIONSHIP BETWEEN GREEN ECONOMY AND INFLATION IN CHINA

LYU, Y. F.

School of Banking & Finance, University of International Business and Economics
Beijing 100029, China
(e-mail: 283420976@qq.com; phone: +86-178-1209-6625)

(Received 18th Mar 2019; accepted 17th May 2019)

Abstract. Targeting the 21 port provinces of China, this paper constructs a panel vector autoregressive (PVAR) model to explore the dynamic relationship between China's green economy and inflation, and to verify whether China's green economy has a negative effect on inflation. Both the global Malmquist-Luenberger (GML) index and the Malmquist-Luenberger (ML) index, which represent the production efficiency under pollution, were adopted to measure China's green economy. It is assumed that the green economy and inflation interact with each other through the output gap, which is associated with pollution, the side-effect of production. The calculated results were tested by impulse response analysis. The final conclusion goes that China's green economy has a weak but long-lasting negative effect on inflation. In other words, China's green economy can alleviate the inflation. Thus, China should speed up pollution control and green economy development to control inflation.
Keywords: *port provinces, global Malmquist-Luenberger (GML) index, Malmquist-Luenberger (ML) index, monetary policy, panel vector autoregressive (PVAR) model*

Introduction

In recent years, the Chinese economy has entered a "new normal" stage, which is characterized by a balanced and manageable growth. According to the National Bureau of Statistics, China's GDP increased 6.6% to RMB 900.309 billion yuan from 2017 to 2018, about 0.1% higher than expected. The fast growth resulted in a hike in China's consumer price index (CPI), an indicator of inflation rate, posing a huge challenge to further economic development (*Figure 1*).

Recent years have also seen growing awareness of global warming across the world. Both the public and the governments are paying more and more attention to the environmental issues induced by global warming. The World Meteorological Organization (WMO) reported that the global mean temperature from January to October in 2018 was 0.98±0.1℃ higher than that before the industrial revolution, making 2018 the fourth warmest year on record. If El Niño occurs in the near future, 2019 may be even warmer than 2018 (NOAA, 2019).

Against this backdrop, it is imperative to strike a balance between economic growth and pollution control, even though many countries used to prioritize economic gains over the environmental benefits and perceive the two factors as contradictory. In other words, special efforts should be paid to develop a green economy, which generates output while reducing pollution, aiming to curb global warming. The official definition of green economy is "one that results in improved human well-being and social equity, while significantly reducing environmental risks and ecological scarcities (UNEP, 2011).

Considering the above, this paper examines whether the development of China's green economy has relieved inflation. It is assumed that China's green economy can suppress the pollution in production, and thus the inflation rate. This hypothesis was

http://www.aloki.hu ● ISSN 1589 1623 (Print) ● ISSN 1785 0037 (Online)
DOI: http://dx.doi.org/10.15666/aeer/1704_89698983

tested with the data from the 21 port provinces in China. Meanwhile, a panel vector autoregressive (PVAR) model was employed to study the dynamic relationship between China's green economy and inflation rate.

The port provinces were targeted in this research because they are both transport hubs and industrial centers. In the past three decades, the main coastal economic zones have concentrated 70% of the industries above designated size in China (Chen, 2016). The rapid industrial development, coupled with economic growth, lead to various environmental problems, such as water pollution and land-based wastes (e.g. domestic waste and industrial waste) (Yan et al., 2018). As a result, the port provinces are more polluted than the rest of provinces in the country. Taking SO_2 emissions as an example (*Figure 2*), more SO_2 was emitted in the port provinces than other Chinese provinces in 2016.

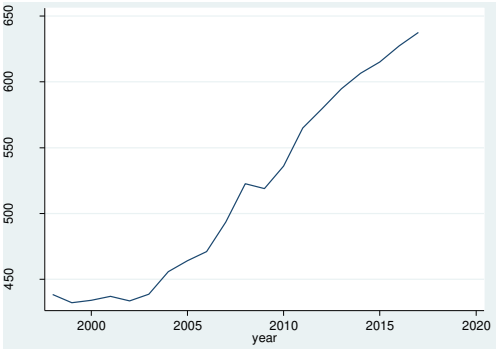

Figure 1. *The variation in China's CPI over time (Data source: The National Bureau of Statistics of China)*

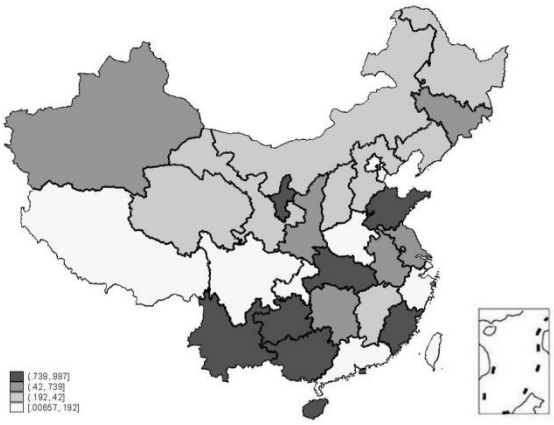

Figure 2. *The distribution of SO2 emissions across China in 2016 (Data source: The National Bureau of Statistics of China)*

Through an impulse response analysis, it is confirmed that the green economy of each port province has a negative effect on inflation. Note that the term "port provinces" refers to provincial administrative regions in Chinese mainland that contains riverside and/or seaside port cities.

The contributions and limitations of this research can be summed up as: (1) The author disclosed the dynamic relationship between China's green economy and the

http://www.aloki.hu ● ISSN 1589 1623 (Print) ● ISSN 1785 0037 (Online)
DOI: http://dx.doi.org/10.15666/aeer/1704_89698983

macroeconomic variable of inflation; (2) It is verified that the green economy interacts with inflation through the output gap, and that China's green economy has a negative impact on inflation, making it possible to control pollution and inflation at the same time; (3) The conclusions are backed up firmly by the actual data from the 21 port provinces in China, which are more polluted than the other Chinese provinces; (4) Due to the lack of a widely accepted way to measure the size of China's green economy, there might be statistical errors in the calculation of the global Malmquist-Luenberger (GML) index or the Malmquist-Luenberger (ML) index; (5) Some biases may exist in the construction of capital stock and output variables.

The remainder of this paper is organized as follows: Section 2 reviews the previous studies on China's green economy and inflation; Section 3 introduces the main variables and estimation methods in our research; Section 4 empirically analyzes the dynamic relationship between China's green economy and inflation, measures China's green economy with its GML index, and tests the robustness by the ML index; Section 5 wraps up this paper with several conclusions.

Materials and methods

Relationship between inflation and output gap

Much research has been done to disclose the relationship between inflation and output gap. For instance, the Phillips curve (1958) reflects the negative correlation between the inflation rate and the unemployment rate, while the New Keynesian Phillips curve (NKPC) reveals the intrinsic causal link between economic output and inflation (Taylor, 1980; Calvo, 1983).

In addition, Jarociński and Lenza (2018) employed a Bayesian dynamic factor model to estimate the output gap in the Eurozone and illustrated the model's predictive power of inflation. With the aid of discrete and continuous wavelet transforms, Tiwari et al. (2014) explored the relationship between inflation and output gap in France, suggesting that the inflation rate can be predicted by economic output in the short and medium terms. Justiniano et al. (2013) confirmed the significant correlation between output gap and inflation through the analysis of the economic data of the US from 1954 to 2009. Based on the NKPC and hybrid NKPC, Bian and Hu (2016) designed the sticky information Phillips curve (SIPC) and double sticky Phillips curve (DSPC) for China, and proved the significance of output gap coefficients in the models, thus validating the Phillips curve.

Measure of China's green economy

There is not yet a widely accepted way to accurately measure the green economy, despite repeated attempts to do so. This is partially attributable to the significant country differences in the status and policies of green economy. On China's green economy, the existing research methods can be divided into four categories: data envelopment analysis (DEA) (Guo et al., 2017; Bao, 2017; Marino et al., 2017; Wang and Zhao, 2017; Yan, 2017, 2018; Shen et al., 2017; Han et al., 2018; Song, 2018), the stochastic impacts by regression on population, affluence and technology (STIRPAT) (Wang, 2017; He, 2017), the logarithmic mean Divisia index (LMDI) model (Wang and Feng, 2018; Chen, 2018), and the GML/ML index.

http://www.aloki.hu ● ISSN 1589 1623 (Print) ● ISSN 1785 0037 (Online)
DOI: http://dx.doi.org/10.15666/aeer/1704_89698983

Coupling the DEA and the directional distance function (DDF), the ML index was modified from the Malmquist index (Chung et al., 1997), which is traditionally calculated from the output distance between different technologies. Compared with the Malmquist index, the ML index is still applicable when undesired outputs like CO_2 emissions or pollution are considered. The index was adopted by Li et al. (2018) to measure the carbon productivity of 36 industrial sectors in from 2003 to 2015. However, the ML still has certain shortcomings, such as the inability to solve linear prediction, non-transferability and additivity.

In 2010, the ML index was further improved by Oh into the GML index. Since then, the GML index has been widely adopted to measure economic output. For example, Emrouznejad and Yang (2016) employed the GML index to evaluate China's manufacturing industry between 2004 and 2012, and built a framework to measure the industrial eco-efficiency in terms of CO_2 emissions. Based on the GML index, Lei et al. (2017) constructed a carbon-weighted economic development indicator for 30 Chinese provinces between 1998 and 2014, and evaluated the economic performance of the carbon emissions-aware economy. Ren et al. (2018) relied on the GML index to incorporate undesirable outputs into the measurement of total factor productivity (TFP) for 11 coastal regions of China between 2006 and 2014, and assessed the efficiency of China's marine economy under environmental constraints. With the aid of the GML index, Pan et al. (2018) designed a measure of the green economy of 30 provinces in China between 1999 and 2016, and evaluated the provincial green economic development. In this paper, the GML index proposed by Oh (2010) is taken as a measure of China's green economy.

The effects of China's green economy

Several scholars have studied the drivers and impacts of China's green economy. Among them, Zeng et al. (2017) built a structural vector autoregressive (SVAR) model to analyze the dynamic relationship between carbon subsidy price, stock price and energy price in Beijing between 2014 and 2015. Lin and Zhu (2017) created a PVAR model to investigate the relationship between urbanization, industrial structure, energy density and carbon density in 30 Chinese provinces between 2000 and 2015. Ouyang and Li (2018) probed into the dynamic relationship between energy consumption, M2 money supply, credit, income, and stock price from Q1, 1996 to Q4, 2015. Using the panel data of 30 Chinese provinces between 1998 and 2014, Lei et al. (2017) investigated the dynamic relationship between the industrial structure, energy structure, low carbon index, foreign direct investment (FDI) and trade, using the PVAR model. In fact, the PVAR is the most frequently used model for the dynamic relationship between China's green economy and other variables. Thus, this model was selected for our research.

The price impact of China's green economy has long been a research hotspot. For example, Zeng et al. (2014) found that, while other factors are under control, land pollution induces a net loss of 31% in the value of nearby plots. On the provincial data in 2001~2010, Leng and Du (2016) verified the positive correlation between energy price distortion and haze pollution in China. Zhang (2018) suggested that the pollution control costs of key monitoring enterprises in China has a significant causal effect on the marginal cost and price of multi-product enterprises.

Drawing from the previous research, the author assumed that pollution, as an externality, will affect the production output, and thus the price (Mas-Colell et al., 1995).

http://www.aloki.hu ● ISSN 1589 1623 (Print) ● ISSN 1785 0037 (Online)
DOI: http://dx.doi.org/10.15666/aeer/1704_89698983

The price change will in turn cause changes in inflation. On the one hand, the mitigation of pollution, a side-effect of production, drags down the output of the whole society and pushes up the marginal production cost, resulting in economic losses (Xi et al., 2013). On the other hand, pollution control also affects the marginal cost of enterprises, e.g. the cost of power generation is influenced by effective energy policies (Zhang et al., 2007; Bianco et al., 2017; Borchiellini et al., 2017; Silvestro et al., 2017; Domenico et al., 2018). In other words, the overall societal cost is subjected to the impacts of externalities. Being a developing country, China tends to suffer greater loss in economic output, which stems from pollution control, than developed countries (Maradan and Anatoli, 2005). Hence, the PVAR model is selected here to study the dynamic relationship between China's green economy and price changes, i.e., inflation.

Methodology of main variables

ML index

The ML index was proposed by Chung et al. (1997) and modified by Oh (2010) to overcome suboptimal properties. In this paper, this index is employed in the robustness test. The ML index of country *i* can be defined by two contemporaneous continuous reference vectors, as in *Equation (1)*:

$$ML^S(x^t, y^t, b^t, x^{t+1}, y^{t+1}, b^{t+1}) = \frac{1+D^s(x^t, y^t, b^t)}{1+D^s(x^{t+1}, y^{t+1}, b^{t+1})} \quad \text{(Eq.1)}$$

where, D^s is the DDF. The DDF can be defined by the synchronous technology set (P^s) in *Equation (2)*:

$$D^s(x, y, b) = \max\{\beta \mid (y+\beta y, b-\beta b\} \in P^S(x)\}, \quad s=t, \quad t+1 \quad \text{(Eq.2)}$$

If the production activity achieves higher output and lower externalities in year *t+1*, then $ML^s > 1$ and production efficiency increases. Otherwise, $ML^s < 1$ and the production efficiency declines. So in *Equation (3)*:

$$ML^t(x^t, y^t, b^t, x^{t+1}, y^{t+1}, b^{t+1}) \neq ML^{t+1}(x^t, y^t, b^t, x^{t+1}, y^{t+1}, b^{t+1}) \quad \text{(Eq.3)}$$

The ML index can also be defined as the geometric mean of two consecutive periods, as in *Equation (4)*:

$$\begin{aligned} ML^{t,t+1}(x^t, y^t, b^t, x^{t+1}, y^{t+1}, b^{t+1}) &= \left[\frac{1+D^t(x^t, y^t, b^t)}{1+D^t(x^{t+1}, y^{t+1}, b^{t+1})} \times \frac{1+D^{t+1}(x^t, y^t, b^t)}{1+D^{t+1}(x^{t+1}, y^{t+1}, b^{t+1})}\right]^{1/2} \\ &= \frac{1+D^t(x^t, y^t, b^t)}{1+D^{t+1}(x^{t+1}, y^{t+1}, b^{t+1})} \times \left[\frac{1+D^{t+1}(x^t, y^t, b^t)}{1+D^t(x^t, y^t, b^t)} \bullet \frac{1+D^{t+1}(x^{t+1}, y^{t+1}, b^{t+1})}{1+D^t(x^{t+1}, y^{t+1}, b^{t+1})}\right]^{1/2} \\ &= \frac{TE^{t+1}}{TE^t} \times \left[TG_t^{t,t+1} \bullet TG_{t+1}^{t,t+1}\right]^{1/2} \\ &= EC^{t,t+1} \times TC^{t,t+1} \end{aligned} \quad \text{(Eq.4)}$$

http://www.aloki.hu ● ISSN 1589 1623 (Print) ● ISSN 1785 0037 (Online)
DOI: http://dx.doi.org/10.15666/aeer/1704_89698983

where, TE^s is technical efficiency of period s; $TG^{t, t+1}$ is the technical gap between periods t and $t+1$; $EC^{t, t+1}$ is the variation in technical efficiency gap between periods t and $t+1$; $TC^{t,t+1}$ is the variation in technical boundary gap between periods t and $t+1$. Obvious, $EC^{t,t+1}>1$ indicates an increase in technical efficiency, and $EC^{t,t+1} < 1$ indicates the opposite; $TC^{t, t+1}>1$ means the technical boundary increases with the growth in output and the reduction of externalities.

GML index

The GML index can be defined in *Equation (5)*:

$$GML^{t,t+1}(x^t, y^t, b^t, x^{t+1}, y^{t+1}, b^{t+1}) = \frac{1+D^G(x^t, y^t, b^t)}{1+D^G(x^{t+1}, y^{t+1}, b^{t+1})} \quad \text{(Eq.5)}$$

where, D^G is the DDF. The DDF can be defined by the global technology set (P^G) in *Equation (6)*:

$$D^G(x, y, b) = \max\{\beta \,|\, (y+\beta y, b-\beta b\} \in P^G(x)\} \quad \text{(Eq.6)}$$

If production activities achieve higher output and lower externalities, then $GML^{t,t+1} >1$ and productivity increases. Otherwise, $GML^{t, t+1}<1$ and productivity decreases. The GML index can be broken down in *Equation (7)*:

$$\begin{aligned} GML^{t,t+1}(x^t, y^t, b^t, x^{t+1}, y^{t+1}, b^{t+1}) &= \frac{1+D^G(x^t, y^t, b^t)}{1+D^G(x^{t+1}, y^{t+1}, b^{t+1})} \\ &= \frac{1+D^t(x^t, y^t, b^t)}{1+D^{t+1}(x^{t+1}, y^{t+1}, b^{t+1})} \times \left[\frac{(1+D^G(x^t, y^t, b^t))/(1+D^t(x^t, y^t, b^t)}{1+D^G(x^{t+1}, y^{t+1}, b^{t+1})/(1+D^{t+1}(x^{t+1}, y^{t+1}, b^{t+1}))} \right] \\ &= \frac{TE^{t+1}}{TE^t} \times \left[\frac{BPG^{t,t+1}_{t+1}}{BPG^{t,t+1}_{t}} \right] \\ &= EC^{t,t+1} \times BPC^{t,t+1} \end{aligned} \quad \text{(Eq.7)}$$

where, TE^s is technical efficiency of period s; $EC^{t, t+1}$ is the variation in technical efficiency gap between periods t and $t+1$; $BPG^{t,t+1}$ is the optimal practice gap between the synchronous technology boundary and the global technology boundary.

Output gap

The potential output can either be estimated from the time series data of actual output or be determined by the production function. The former approach needs to detrend the data and extrapolate growth rates. However, the estimation is too simple to derive the exact amount of potential output. The latter method mainly considers the factor utilization and the impact of technical progress on output, revealing the supply-side of potential output. The production function method has been adopted by many scholars (Guo and Jia, 2004).

In this paper, the production function method is selected to measure the potential output, such as to determine the output gap of each port province in China. Firstly, the

http://www.aloki.hu ● ISSN 1589 1623 (Print) ● ISSN 1785 0037 (Online)
DOI: http://dx.doi.org/10.15666/aeer/1704_89698983

aggregate production function was estimated based on the data on the actual output, labor and capital stock, laying the basis for acquiring the TFP. The Cobb-Douglas production function is adopted in *Equation (8)*:

$$Y_t = AK_t^{\alpha} L_t^{\beta} \quad \text{(Eq.8)}$$

where, Y_t is the actual output; L_t is the actual labor; K_t *i*s the capital stock; α and β are the output elasticities for capital and labor, respectively. Taking the natural logarithm on both sides of *Equation (8)*, we have *Equation (9)*:

$$\ln Y_t = \ln A + \alpha \ln K_t + \beta \ln L_t \quad \text{(Eq.9)}$$

If the production has constant scale of returns, then $\alpha + \beta = 1$. In this case, a double logarithmic model can be constructed in *Equation (10)*:

$$\ln(Y_t / L_t) = \ln A + \alpha \ln(K_t / L_t) + \gamma_t \quad \text{(Eq.10)}$$

The TFP can be obtained from the residual term of this regression (γ_t). Secondly, the TFP was decomposed by the Hodrick–Prescott (HP) filter, and the potential employment was estimated under the potential output in *Equation (11)*:

$$L_t^{Potential} = L_{St} \times Tr_{p,t} \times (1 - NAWRU_t) \quad \text{(Eq.11)}$$

where, L_{St} is the number of people in the working age; $Tr_{p,t}$ is the trend participation rate; $NAWRU_t$ is the unemployment rate induced by non-wage factors. Thirdly, the potential output was established from the estimated TFP trend, potential employment and potential output. Finally, the output gap was determined as the difference between the estimated output and the potential output.

Research data and calculation results

Research data

The 21 port provinces in China were taken as the research objects. As shown in *Table 1*, some of these provinces have both riverside and seaside port cities, and some have either riverside or seaside port cities.

The annual data of these provinces in 2006~2015 were collected to reduce the regression bias in PVAR model estimation. The annual data were selected for three reasons: the large-scale changes in macroeconomic variables are unlikely to occur within a monthly or quarterly range (Beetsma et al., 2008), the macroeconomic variables may change systematically under the expectation effect, which is more prevalent in shorter time windows, and the annual data do not contain any potential seasonal effect.

Calculation of the GML index

The GML index was computed by the method of Oh (2010) according to the annual data of the 21 provinces in 2006~2015. The following variables were covered in the computing process.

http://www.aloki.hu ● ISSN 1589 1623 (Print) ● ISSN 1785 0037 (Online)
DOI: http://dx.doi.org/10.15666/aeer/1704_89698983

(i) The desirable output: the annual GDP of the 21 port provinces. This variable was converted into a constant price by the GDP deflator (unit: RMB 100 million yuan). Data source: CEInet Statistics Database.

(ii) The undesirable output: the annual SO_2 emissions (unit: ton) and wastewater discharge (unit: ton). Data source: The National Bureau of Statistics of China.

(iii) The inputs of production technology: the inputs were measured by three indices, namely, capital stock (unit: RMB 100 million yuan), labor force (unit: 10,000 people) and energy consumption (unit: TCE).

The capital stock was calculated by the method of Shan (2008), who computed the capital stock of China and its provinces in 1952~2006 using the perpetual inventory method (PIM). The PIM assumes that the relative efficiency is geometrically decreasing, while the reset rate is constant. Here, the calculation formula of the capital stock can be expressed in *Equation (12)*:

$$K_t = (1-\delta)K_{t-1} + I_t / P_t \quad \text{(Eq.12)}$$

where, K_{t-1} is the capital stock of the year t-1; δ is the economic depreciation rate; I_t is the investment amount in year t; P^t is the investment price index used to convert the investment amount into constant price. Here, the investment amount is measured by the fixed capital formation amount of each province, which comes from the China Economic and Trade Network, while the investment price index of each province was extracted the CEInet Statistics Database. Under the PIM assumption, the economic depreciation rate of the 21 provinces was set to 10.96%.

Table 1. *List of 21 port provinces in China*

No.	Province	Type	No.	Province	Type	No.	Province	Type
1	Anhui	Riverside	8	Hebei	Seaside	15	Liaoning	Seaside
2	Chongqing	Riverside	9	Heilongjiang	Riverside	16	Shandong	Riverside and seaside
3	Fujian	Seaside	10	Henan	Riverside	17	Shanghai	Riverside and seaside
4	Guangdong	Riverside and seaside	11	Hubei	Riverside	18	Sichuan	Riverside
5	Guangxi	Riverside and seaside	12	Hunan	Riverside	19	Tianjin	Seaside
6	Guizhou	Riverside	13	Jiangsu	Riverside and seaside	20	Yunnan	Riverside
7	Hainan	Seaside	14	Jiangxi	Riverside	21	Zhejiang	Riverside and seaside

Data source: Chinese Ministry of Transport

In addition, the labor force in each province was obtained by adding up the urban residents employed in the public sector, in the private sector, and self-employed, without considering the employment of rural residents. The employment data before 2008 were drawn from the China Stock Market & Accounting Research (CSMAR) Database, and those after 2008 were extracted from the National Bureau of Statistics of China. The provincial data on annual energy consumption were also downloaded from the CSMAR database.

http://www.aloki.hu ● ISSN 1589 1623 (Print) ● ISSN 1785 0037 (Online)
DOI: http://dx.doi.org/10.15666/aeer/1704_89698983

Calculation of the output gap

The annual output gap of each port province in 2006~2015 was calculated by the method of Guo and Jia (2004), using the following variables:

(i) The actual output: the annual GDP of each port province.

(ii) The actual labor force: the annual urban labor force of each province.

(iii) The capital stock: this variable was computed the same as in the preceding subsection.

(iv) $L_{St} \cdot Tr_{p,t}$: the number of people in the working age multiplied by the trend value.

(v) $NAWRU_t$: the number of laborers divided by the total number of people involved in social and economic activities. The latter was defined as the sum of the number of laborers and the number of registered unemployed urban residents. The data were collected from the National Bureau of Statistics of China.

(vi) Constant return on scale: The assumption that the scale of return is constant was verified by the Wald test. The original hypothesis H_0 can be expressed as $\alpha + \beta = 1$. The test results are listed in *Table 2* below.

Table 2. *The results of the Wald test*

H_0	x^2 (1)	P>x^2
α+β=1	1.17	0.2803

The results in *Table 2* show that the P-value is greater than 0.05, revealing the validity of the original hypothesis. Thus, the production mode of China's economy was considered as having constant returns to scale between 2006 and 2015.

PVAR model

The PVAR model was established to analyze the relationship between China's green economy and the inflation rate. The variables were treated as endogenous and interdependent. To reflect the real interaction between the variables, the lag term of all variables was included in the model. The basic form of the PVAR model is established as *Equation (13)*:

$$y_{it} = \alpha_0 + \sum_{l}^{L} \alpha_l y_{i,t-l} + I_i + T_t + \mu_{it} \quad \text{(Eq.13)}$$

where, y_{it} is the column vector containing endogenous variables; i is the serial number of port provinces; t is the year; L is the post-order; I_i is the individual effect vector; T_t is the time effect vector; μ_{it} is a random disturbance term (i.e. the white noise).

The individual effect vector does not change with time, and the right side of *Equation (13)* contains the lag term of the dependent variables. Thus, the mean differencing was adopted to prevent the estimation bias from potential endogeneity. More specifically, the forward-mean-differencing method was adopted to remove the fixed effect in the model (Arellano and Bover, 1995). Besides, the generalized method of moments (GMM) was used to obtain a consistent estimator of the coefficient of the explanatory variable, with the lag term of the explanatory variables as the instrumental variables. Furthermore, an impulse response analysis was conducted through Monte-Carlo simulation.

http://www.aloki.hu ● ISSN 1589 1623 (Print) ● ISSN 1785 0037 (Online)
DOI: http://dx.doi.org/10.15666/aeer/1704_89698983

Results

The dynamic relationship between GML index and inflation

Basic regression

Considering the negative correlation between pollution and the GML, it is assumed that the GML has a negative effect on the CPI. The orthogonal impact response function is the disturbance term of the Cholesky decomposition. By exogenous nature, the Cholesky decomposition variables can be ranked as output gap (*outgap*), China's green economy (*GML*) and inflation (*CPI*). The regression model can thus be established as *Equation (14)*:

$$y_{it} = (outgap_{it}, GML_{it}, CPI_{it})^T \quad \text{(Eq.14)}$$

Prior to the regression, the Fisher-Phillips-Perron (PP) test, the Im-Pesaran-Shin (IPS) test and the Levin-Lin-Chu (LLC) test were carried out, proving that the level values of all variables can be directly used for the regression of the PVAR model. The level values of all variables rejected the null hypothesis at a significance level of 1%, that is, the level values of all variables do not possess unit roots, and all sequences are stationary. Moreover, the optimal lag order (2) was determined by the Akaike information criterion (AIC), Bayesian information criterion (BIC) and Hannan & Quinn information criterion (HQIC). The test results are shown in *Table 3* below.

Table 3. *The results on the optimal lag order*

Lag	AIC	BIC	HQIC
1	6.18901	7.04927	6.53857
2	4.62324*	6.16506*	5.23567*
3	4.63834	6.81804	5.46838

Note: ***, ** and * stand for the significance levels of 1%, 5% and 10%, respectively

As such, the PVAR (2) model was selected for our research.

Impulse response analysis

Through Cholesky decomposition, the author analyzed the interaction between China's green economy and inflation, after excluding the effects of other endogenous variables. Since the data run from 2006 to 2015, a total of 10 years, the impact duration was divided into 10 periods. The impulse response function (IRF) graph of the CPI to the GML was obtained through 1,000 random Monte-Carlo simulations.

Robustness test

Basic regression

The same analysis was performed using the ML index, assuming that the ML also has a negative impact on the CPI. The variables were the same as those in the analysis based on the GML. In the ML-based analysis, the PVAR model was still adopted, and the Cholesky decomposition variables were still ranked as the output gap (*outgap*),

http://www.aloki.hu ● ISSN 1589 1623 (Print) ● ISSN 1785 0037 (Online)
DOI: http://dx.doi.org/10.15666/aeer/1704_89698983

China's green economy (*ML*) and inflation (*CPI*). Thus, the regression model is parallel to *Equation (13)*.

Prior to the regression, the PP-Fisher test, IPS test and LLC test were conducted as well, and the optimal lag order (3) was determined by the AIC, BIC and HQIC criteria. These results are displayed in *Table 4* below.

Table 4. *The results on the optimal lag order*

Lag	AIC	BIC	HQIC
1	6.00907	6.86933	6.35863
2	9.7832	11.325	10.3956
3	2.53134*	4.71105*	3.36139*

Note: ***, ** and * stand for the significance levels of 1%, 5% and 10%, respectively

As such, the PVAR (3) model was selected for our research.

Impulse response analysis

The IRF graph of the CPI to the ML was obtained through 1,000 random Monte-Carlo simulations.

Discussion

As shown in *Figure 3*, the effect of the GML on the CPI was not observable at the start, decreased in the first period, and slightly increased in the second period. After that, the effect continued to decline until the fourth period, and then tended to be stable through the tenth period. Overall, China's green economy has a weak negative effect on inflation in the long run, which agrees with our hypothesis.

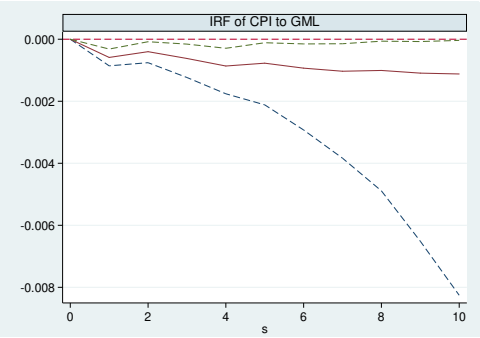

Figure 3. *The IRF graph of the CPI to the GML (Note: The red line is the impulse response curve; the green dotted line stands for the points in the confidence interval of 5%; the blue dotted line stands for the points in the confidence interval of 95%)*

As shown in *Figure 4*, the effect of the ML on the CPI was not observable at the start, decreased in the first period, and slightly increased in the second period. After that, the effect continued to decline until the fourth period, and then tended to be stable through the tenth period. In general, China's green economy has a weak negative effect on inflation in the long run.

http://www.aloki.hu ● ISSN 1589 1623 (Print) ● ISSN 1785 0037 (Online)
DOI: http://dx.doi.org/10.15666/aeer/1704_89698983

To sum up, China's green economy has a weak but long-lasting negative effect on inflation. In other words, China's green economy can alleviate the inflation.

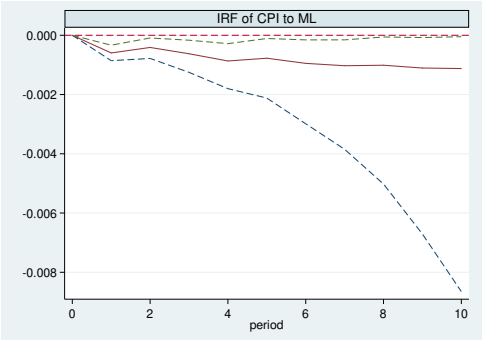

Figure 4. *The IRF graph of the CPI to the ML (Note: The red line is the impulse response curve; the green dotted line stands for the points in the confidence interval of 5%; the blue dotted line stands for the points in the confidence interval of 95%)*

Conclusions

Targeting the most polluted 21 port provinces in China, this paper attempt to disclose the dynamic relationship between China's green economy and inflation, and verify the hypothesis that China's green economy can alleviate the inflation through the output gap. Specifically, a PVAR model was constructed to explore the relationship, and the result was tested by impulse response analysis. It is proved that China's green economy has a causal relationship with inflation, whether it is calculated by the GML or the ML. The final conclusion goes that China's green economy has a weak but long-lasting negative effect on inflation. In other words, China's green economy can alleviate the inflation. Thus, the pollution is positively correlated with inflation.

In light of the findings, China should speed up pollution control and green economy development, such as to complete the 2020 climate targets ahead of schedule and lay the foundation for implementing the 2030 climate targets. Meanwhile, proper monetary policy should be rolled out to enhance the suppression effect of green economy over inflation.

The conclusion about the relationship between the green economy and inflation could indicate that the green economy can be a good signal for monetary policy. So further studies about the analysis of effects of monetary policy signalling within green economy over the clarity of central bank communication could be recommended.

REFERENCES

[1] Arellano, M., Bover, O. (1995): Another look at the instrumental variable estimation of error-components models. – Journal of Econometrics 68(1): 29-51.

[2] Bao, Z. B. (2017): Construction of the evaluation system of regional agricultural circular economy and TOPSIS application. – Environmental and Earth Sciences Research Journal 4(1): 12-16.

[3] Beetsma, R., Giuliodori, M., Klaassen, F. (2008): The effects of public spending shocks on trade balances and budget deficits in the European Union. – Journal of the European Economic Association 6(2-3): 414-423.

http://www.aloki.hu ● ISSN 1589 1623 (Print) ● ISSN 1785 0037 (Online)
DOI: http://dx.doi.org/10.15666/aeer/1704_89698983

[4] Bian, Z., Hu, H. (2016): Sticky Prices, Sticky Information and Chinese Phillips Curve. – The Journal of World Economy 4: 22-43.
[5] Bianco, V., Piazza, G., Scarpa, F., Tagliafico, L. A. (2017): Energy, economic and environmental assessment of the utilization of heat pumps for buildings heating in the Italian residential sector. – International Journal of Heat and Technology 35(S1): S117-S122.
[6] Blundell, R., Bond, S. (1998): Initial conditions and moment restrictions in dynamic panel data models. – Journal of econometrics 87(1): 115-143.
[7] Borchiellini, R., Corgnati, S. P., Becchio, C., Delmastro, C., Bottero, M. C., Dell'Anna, F., Acquaviva, A., Bottaccioli, L., Patti, E., Bompard, E., Pons, E., Estebsari, A., Verda, V., Santarelli, M., Leone, P., Lanzini, A. (2017): The Energy Center Initiative at Politecnico di Torino: Practical experiences on energy efficiency measures in the municipality of Torino. – International Journal of Heat and Technology 35(S1): S196-S204.
[8] Calvo, G. A. (1983): Staggered prices in a utility-maximizing framework. – Journal of Monetary Economics 12(3): 383-398.
[9] Chen, L. (2016): Marine Pollution, Preventing and Treating Status and Its Countermeasures in China. – Environmental Protection 5(65): 1674-1021.
[10] Chen, J. (2018): Estimation and factor decomposition of carbon emissions in China's tourism sector. – Problems of Sustainable Development 13(2): 91-101.
[11] Chung, Y. H., Färe, R., Grosskopf, S. (1997): Productivity and undesirable outputs: a directional distance function approach. – Journal of Environmental Management 51(3): 229-240.
[12] Davis, J. S., Fujiwara, I., Wang, J. (2018): Dealing with time-inconsistency: Inflation targeting vs. exchange rate targeting. – Working paper Australian National University.
[13] Domenico, G., Carla, C. G., Margherita, M. (2018): Integrated urban regeneration policy and soft mobility planning for transport energy-saving. – Instrumentation Mesure Métrologie 17(4): 527-547.
[14] Emrouznejad, A., Yang, G. L. (2016): CO2 emissions reduction of Chinese light manufacturing industries: A novel RAM-based global Malmquist–Luenberger productivity index. – Energy Policy 96: 397-410.
[15] Emrouznejad, A., Yang, G. L. G. R. (2018): A novel inverse DEA model with application to allocate the CO2 emissions quota to different regions in Chinese manufacturing industries. – Journal of the Operational Research Society: 1-12.
[16] Guo, Q., Jia, J. (2004): Estimating Potential Output and the Output Gap in China. – Economic Research Journal 5: 31-39.
[17] Guo, X. (2017): Applying the dynamic DEA model to evaluate the energy efficiency of OECD countries and China. – Energy 134: 392-399.
[18] Han, Y., Long, C., Geng, Z., Zhang, K. (2018): Carbon emission analysis and evaluation of industrial departments in China: An improved environmental DEA cross model based on information entropy. – Journal of environmental management 205: 298-307.
[19] He, Z., Xu, S., Shen, W., Long, R., Chen, H. (2017): Impact of urbanization on energy related CO2 emission at different development levels: Regional difference in China based on panel estimation. – Journal of cleaner production 140: 1719-1730.
[20] Jarociński, M., Lenza, M. (2016): An Inflation-Predicting Measure of the Output Gap in the Euro Area. – Journal of Money, Credit and Banking 50(6): 1189-1224.
[21] Justiniano, A., Primiceri, G. E., Tambalotti, A. (2013): Is there a trade-off between inflation and output stabilization? – American Economic Journal: Macroeconomics 5(2): 1-31.
[22] Lei, M. (2017): Carbon-weighted economic development performance and driving force analysis: Evidence from China. – Energy Policy 111: 179-192.
[23] Leng, Y., Du, S. (2016): Energy Price Distortion and Haze Pollution: The Evidence from China. – Industrial Economics Research 1: 71-79.

http://www.aloki.hu ● ISSN 1589 1623 (Print) ● ISSN 1785 0037 (Online)
DOI: http://dx.doi.org/10.15666/aeer/1704_89698983

[24] Li, H., Shi, J. F. (2014): Energy efficiency analysis on Chinese industrial sectors: An improved Super-SBM model with undesirable outputs. – Journal of Cleaner Production 65: 97-107.
[25] Li, W. (2018): Historical growth in total factor carbon productivity of the Chinese industry-A comprehensive analysis. – Journal of Cleaner Production 170: 471-485.
[26] Lin, B., Zhu, J. (2017): Energy and carbon intensity in China during the urbanization and industrialization process: A panel VAR approach. – Journal of Cleaner Production 168: 780-790.
[27] Love, I., Zicchino, L. (2006): Financial development and dynamic investment behavior: Evidence from panel VAR. – The Quarterly Review of Economics and Finance 46(2): 190-210.
[28] Maradan, D., Vassiliev, A. (2005): Marginal costs of carbon dioxide abatement: empirical evidence from cross-country analysis. – Revue Suisse d'Economie et de Statistique 141(3): 377.
[29] Marino, C., Nucara, A., Nucera, G., Pietrafesa, M. (2017): Economic, energetic and environmental analysis of the waste management system of Reggio Calabria. – International Journal of Heat and Technology 35(S1): S108-S116.
[30] Mas-Colell, A., Whinston, M. D., Green, J. R. (1995): Microeconomic Theory. Vol. 1. – New York: Oxford university press.
[31] NOAA National Centers for Environmental Information, State of the Climate (2018): Global Climate Report for Annual 2018.
[32] Oh, D. H. (2010): A global Malmquist-Luenberger productivity index. – Journal of Productivity Analysis 34(3): 183-197.
[33] Ouyang, Y., Li, P. (2018): On the nexus of financial development, economic growth, and energy consumption in China: New perspective from a GMM panel VAR approach. – Energy Economics 71: 238-252.
[34] Pan, W., Pan, W., Hu, C., Tu, H., Zhao, C., Yu, D., Xiong, J., Zheng, G. (2019): Assessing the green economy in China: An improved framework. – Journal of Cleaner Production 209: 680-691.
[35] Phillips, A. W. (1958): The relation between unemployment and the rate of change of money wage rates in the United Kingdom, 1861-1957. – Economica 25(100): 283-299.
[36] Ramey, V. A. (2011): Identifying government spending shocks: It's all in the timing. – The Quarterly Journal of Economics 126(1): 1-50.
[37] Ren, W. (2018): Evaluation of China's marine economic efficiency under environmental constraints—an empirical analysis of China's eleven coastal regions. – Journal of Cleaner Production 184: 806-814.
[38] Shan, S. (2008): Reestimating the Capital Stock of China:1952-2006. – The Journal of Quantitative & Technical Economics 25(10): 17-31.
[39] Shen, Z., Balezentis, T., Chen, X., Valdmanis, V. (2018): Green growth and structural change in Chinese agricultural sector during 1997–2014. – China Economic Review 51: 83-96.
[40] Silvestro, F., Bagnasco, A., Lanza, I., Massucco, S., Vinci, A. (2017): Energy efficient policy and real time energy monitoring in a large hospital facility: A case study. – International Journal of Heat and Technology 35(S1): S221-S227.
[41] Song, S. L. (2018): Application of gray prediction and linear programming model in economic management. – Mathematical Modelling of Engineering Problems 5(1): 46-50.
[42] Soon, S. V., Baharumshah, A. Z., Wohar, M. E. (2018): Exchange rate pass-through in the Asian countries: does inflation volatility matter? – Applied Economics Letters 25(5): 309-312.
[43] Taylor, J. B. (1980): Aggregate dynamics and staggered contracts. – Journal of Political Economy 88(1): 1-23.

http://www.aloki.hu ● ISSN 1589 1623 (Print) ● ISSN 1785 0037 (Online)
DOI: http://dx.doi.org/10.15666/aeer/1704_89698983

[44] Tiwari, A. K., Oros, C., Albulescu, C. T. (2014): Revisiting the inflation–output gap relationship for France using a wavelet transform approach. – Economic Modelling 37: 464-475.
[45] United Nations Environment Programme (2011): Towards a green economy: Pathways to sustainable development and poverty eradication.
[46] Wang, Q., Zeng, Y. E., Wu, B. W. (2016): Exploring the relationship between urbanization, energy consumption, and CO2 emissions in different provinces of China. – Renewable and Sustainable Energy Reviews 54: 1563-1579.
[47] Wang, Y., Zhang, C., Lu, A., Li, L., He, Y., Tojo, J., Zhu, X. (2017): A disaggregated analysis of the environmental Kuznets curve for industrial CO2 emissions in China. – Applied Energy 190: 172-180.
[48] Wang, J., Zhao, T. (2017): Regional energy-environmental performance and investment strategy for China's non-ferrous metals industry: a non-radial DEA based analysis. – Journal of Cleaner Production 163: 187-201.
[49] Wang, J., Zhao, B., Wang, S., Yang, F., Xing, J., Morawska, L., Ding, A., Kulmala, M., Kerminen, V. M., Kujansuu, J., Wang, Z., Ding, D., Zhang, X., Wang, H., Tian, M., Petäjä, T., Jiang, J., Hao, J. (2017): Particulate matter pollution over China and the effects of control policies. – Science of The Total Environment 584: 426-447.
[50] Wang, M., Feng, C. (2018): Decomposing the change in energy consumption in China's nonferrous metal industry: An empirical analysis based on the LMDI method. – Renewable and Sustainable Energy Reviews 82: 2652-2663.
[51] Yan, Q. (2017): Economic and technical efficiency of the biomass industry in China: A network data envelopment analysis model involving externalities. – Energies 10(9): 1418-1437.
[52] Yan, Q. (2018): Energy–economy–environmental (3E) performance of Chinese regions based on the data envelopment analysis model with mixed assumptions on disposability. – Energy & Environment 29(5): 664-684.
[53] Yan, D., Zhang, H., Fu, D. (2018): Survey on ship pollution source. – Ship Science and Technology 40(11): 9-12.
[54] Yang, X., Teng, F., Wang, G. (2013): Incorporating environmental co-benefits into climate policies: a regional study of the cement industry in China. – Applied Energy 112: 1446-1453.
[55] Zeng, X., Chen, Y., Miao, Z. (2014): The Impacts of Contamination on the Price of Adjacent Land: An Empirical Study in Wuhan Downtown Area. – China Land Sciences 28(11).
[56] Zeng, S., Nan, X., Liu, C., Chen, J. (2017): The response of the Beijing carbon emissions allowance price (BJC) to macroeconomic and energy price indices. – Energy Policy 106: 111-121.
[57] Zhang, Q., Tian, W., Wei, Y., Chen, Y. (2007): External costs from electricity generation of China up to 2030 in energy and abatement scenarios. – Energy Policy 35(8): 4295-4304.
[58] Zhang, W., Li, K., Zhou, D., Gao, H. (2016): Decomposition of intensity of energy-related CO2 emission in Chinese provinces using the LMDI method. – Energy Policy 92: 369-381.
[59] Zhang, Z. (2018): Environmental regulation, price transfer and pollution burden of Chinese manufacturers: evidence based on pollution fees of key monitoring firms. – Industrial Economics Research 4: 65-75.
[60] Zhang, L. P., Zhou, P. (2018): A non-compensatory composite indicator approach to assessing low-carbon performance. – European Journal of Operational Research 270(1): 352-361.

http://www.aloki.hu ● ISSN 1589 1623 (Print) ● ISSN 1785 0037 (Online)
DOI: http://dx.doi.org/10.15666/aeer/1704_89698983

MEASUREMENT OF REGIONAL ENVIRONMENTAL EFFICIENCY IN CHINA BASED ON THE SUPER-EFFICIENCY SBM MODEL

ZHOU, X. B.[1] – CHEN, L. L.[2] – FAN, H. Y.[2] – CHEN, H. T.[2] – ZENG, R. S.[2] – ZHANG, S. F.[2*] – CHEN, S. F.[2]

[1]*School of Economics & Management, Northwest University, Xi'an 710069, China*

[2]*College of Statistics and Mathematics, Zhejiang Gongshang University, Hangzhou 310018, China*

**Corresponding author*
e-mail: zhshangfeng@163.com; phone +86-571-2800-8096

(Received 18th Mar 2019; accepted 17th May 2019)

Abstract. This paper measures the regional environmental efficiency in China by using the super-efficiency slacks-based measure (SBM). It calculates the environmental efficiency in the presence and absence of the environmental pollution variable respectively, and compares the calculation results of the super-efficiency SBM model with the Banker & Charnes & Cooper's (BCC) model, one of the traditional data envelopment analysis (DEA) models. By analyzing the environmental efficiencies in all provinces, it analyzes the slack variables to determine in which direction each region should improve. The results show that the addition of the environmental pollution variable has resulted in significant declines in the efficiencies of provinces with DEA inefficiencies. Among the four regions, the eastern one has the highest environmental efficiency, the western region comes next and the northeastern and central regions are the last ones. There are also some economically developed provinces with low environmental efficiency, and different inefficient provinces need to be improved in different directions.
Keywords: *DEA, regional environmental efficiency, pollution variable, BCC model, slacks-based measure*

Introduction

The continuous environmental deterioration around the world has become a key factor constraining the sustainable development of all countries in the world. Finding a way to prevent further deterioration of the environment has become a significant issue of concern for the global academic community and governments. For China, the increasingly serious environmental problems have also turned into a major issue affecting China's overall economic development and become a "bottleneck" in its sustainable development path. Therefore, studying how to improve environmental efficiency more effectively is of great significance for promoting the scientific frontier development and helping the government achieve energy conservation and emission reduction targets.

Environmental efficiency is a crucial measure of the environmental conditions in a country (or region). There is still no universal agreement on the definition of environmental efficiency, but it is generally divided into two categories. The first defines the ratio of economic aggregate to environmental load as environmental efficiency (Beukes et al., 2010; Halkos and Tzeremes, 2013; Wang et al., 2007; Zhang, 2008). The environmental load refers to the carrying capacity of the external environment when humans are conducting economic activities, e.g. the carrying capacity of energy, land, general resources, water resources and forest resources, etc. The second definition

http://www.aloki.hu ● ISSN 1589 1623 (Print) ● ISSN 1785 0037 (Online)
DOI: http://dx.doi.org/10.15666/aeer/1704_89859005

focuses on the perspective of the environmental impact of production activities. In this definition, the environmental efficiency is measured in two ways. First, without considering the efficiency of input, it is measured by the ratio of economic value (GDP) to the impact of environmental pollution, which is the reciprocal of the pollution intensity (Schaltegger and Sturm, 1990; Wang, 2011). The second method considers the efficiencies of both input and output, and it is called comprehensive environmental efficiency or environmental total factor efficiency (Wang et al., 2010; Xu, 2012) or environmental productivity. Obviously, these two definitions of environmental efficiency do not consider the affordability of consumers when pollution is emitted. For example, in densely populated cities, the air pollution emissions impose different environmental impacts than those in the sparsely populated suburbs.

In the measurement of environmental efficiency, Stochastic Frontier Analysis (SFA) (Thijssen, 1999; Tan et al., 2013), Multi-Criteria Decision-Making method (MCDM) (Montanari, 2004), Data Envelopment Analysis (DEA) and other research methods have all been used. Among them, non-parametric methods (such as DEA, etc.) can reduce the subjectivity of the measurement results as there is no need to construct the production function in advance. Therefore, compared with parametric methods (such as SFA), non-parametric methods are more widely used, The DEA method has proven to be a very effective tool to measure the efficiencies and productivities of similar decision-making units (DMUs) and is therefore widely used in industrial, urban, regional, and global productivity and efficiency evaluations. Many scholars have used the DEA model to measure environmental efficiency. Faere et al. (1989) was the first to propose the DEA model for environmental efficiency evaluation. Bevilacqua and Braglia (2002) used the data of seven oil refineries in Italy from 1993 to 1996, selected six indices such as CO, CO_2, SO_2 and petroleum processing output, and evaluated the environmental efficiency using the CCR model. Aldanondo et al. (2014) used the DEA model to quantitatively analyze environmental efficiencies of organic agriculture and traditional agriculture in Spain, and concluded that the organic agriculture is more efficient than the traditional one under the same environmental impact. Many scholars have also used DEA to measure the environmental efficiency in China (Chen, 2008; Reinhard et al., 2000; Tone, 2002). Wang et al. (2009) established a DEA efficiency evaluation model, selected data from 28 provinces in China from 2001 to 2005, and measured environmental efficiency from the perspective of environmental regulation. The results show that areas with better environmental efficiencies account for 10% to 20%. Wu and Ma (2016) used the DEA method to calculate the ecological efficiency of 31 provinces in China from 2009 to 2013, and then used the Tobit model to analyze the factors affecting ecological efficiency. The results show that the per capita GDP and the geographical position of the east have positive impacts on ecological efficiency, while the industrial structure and population density have negative impacts. It can be seen that the DEA method has been widely used to evaluate environmental efficiency. The weight can be determined according to the principle of optimality to calculate the relative efficiency of each DMU, and then the efficiency values and improvement directions of all DMUs can be obtained. However, the radial problem existing in the traditional DEA models affects the accuracy of efficiency evaluation (the technical efficiency of the DMU is 1), and the complete ordering between the evaluated units cannot be addressed. What is more, these models only focus on a single perspective (input or output perspective), which do not fully reflect the actual situation in the excessive investment and production. In order to solve the radial problem in the traditional DEA models, scholars have applied the SBM model,

http://www.aloki.hu ● ISSN 1589 1623 (Print) ● ISSN 1785 0037 (Online)
DOI: http://dx.doi.org/10.15666/aeer/1704_89859005

the super-efficiency DEA model and a combination of the two to measure the efficiency of various industries. For instance, Yan and Hou (2018) used the super-efficiency SBM model to measure the urban ecological efficiency in China. Zhang and Ma (2018) constructed an efficiency evaluation index system for the urban energy saving and environmental protection industry, based on the principle of the super-efficiency SBM model.

However, most applications of the relevant non-radial model often overlook the environmental efficiency problems that exist in the production process, including environmental pollution.

This paper conducts a comparative study on the measurement of environmental efficiency from the perspective of "environmental impacts of producers' economic activities". It proposes that environmental efficiency is actually the economic efficiency after the environmental factors are taken into account, that is, the economic level achieved at the expense of certain environmental loss. The following innovative research is conducted on this definition: First, this paper uses the entropy weight method to combine undesired outputs (waste gas, wastewater, solid waste) into an indicator to reflect the overall environmental pollution status. Second, this paper fully considers the role of the environmental pollution variable (pollutants) in environmental efficiency, and uses the super-efficiency SBM model to effectively solve the radial problem and the incomplete ordering of units in the traditional model. As a result, the status quo can be more objectively and truly reflected.

The rest of this paper is organized as follows. Section 2 briefly introduces the development of the DEA model, and describes the super-efficiency SBM model used in this paper. Section 3 constructs the input-output index system and comprehensively evaluates environmental pollution indices. Section 4 uses the super-efficiency SBM model to measure the environmental efficiencies of different regions in China, compares them with the measurement results of the BCC model, and analyzes the redundancy rate of input and output. Finally, the conclusions are presented in section 5.

Materials and methods

Data Envelopment Analysis (DEA) is a non-parametric frontier efficiency analysis method. It was proposed by American operation researchers Chames and Copper in 1978. Their first basic model of DEA is the CCR model, established on the relative efficiency evaluation. After the introduction of this model, many different DEA models emerged. Regarding the concept of "return to scale" in economics research, Banker proposed a BCC model based on variable-scale returns by adding constraints. After many years of development, now the DEA model can be divided into two major categories: radial models and non-radial models. CCR and BCC are radial models (i.e., maintaining quantitative output or input so that inputs or outputs are proportionally reduced or increased). This feature of the radial model makes the result very different from the actual situation. Later, some scholars began to study non-radial models and proposed additive DEA and SBM models. In terms of model improvement, many scholars have made a lot of contributions in enriching relevant theories and practices of DEA.

The basic principle of the DEA model is to treat each individual as a single DMU for evaluation. Many DMUs within a system can be regarded as an evaluation group, and then the overall input-output ratio can be measured. The weight of each input or output

http://www.aloki.hu ● ISSN 1589 1623 (Print) ● ISSN 1785 0037 (Online)
DOI: http://dx.doi.org/10.15666/aeer/1704_89859005

of a DMU is taken as a variable in the evaluation, so as to determine the efficient production frontier. In the efficiency evaluation, DEA can spontaneously include all data points in the efficiency frontier according to the structural characteristics of the source data, thus saving the prior work like determining the specific function form and improving the process and research efficiency. The relative efficiency (i.e. 1) of all the points on the efficiency frontier represents the highest level, and the relative efficiencies of the remaining points are distributed between 0 and 1. The calculation results can be obtained according to the efficiency frontier ratio, which is obtained from previous calculation.

Model framework

CCR model

The model assumes that there are n DMUs, each of which has m input indices and s output indices, which are similar to the input and output indices in economics. We denote DMU_j as DMU j, x_{ij} as the ith input of DMU j, where $x_{ij} > 0$; y_{rj} as the rth output of DMU j, where $y_{rj} > 0$; v_i as a measure of the ith input, which is also called the weight; u_r as a measure of the rth output, i = 1, 2, 3, …, m; j = 1, 2, 3, …, n; r = 1, 2, 3,…, s. For the sake of convenience, let $X_j = (x_{1j}, x_{2j}, x_{3j}, \ldots x_{mj})$, j = 1, 2, 3, …, n; $Y_j = (y_{1j}, y_{2j}, y_{3j}, \ldots y_{sj})$, j = 1, 2, 3, …, n; $v = (v_1, v_2, \ldots v_m)$; and $u = (u_1, u_2, \ldots u_r)$. Now let us analyze the efficiency evaluation problem of the decision-making unit DMU_j. The fractional model of the CCR model is shown in *Equation 1:*

$$\max \frac{u_r y_0}{v_m x_0} \qquad \text{(Eq.1)}$$
$$s.t. \frac{u_r y_{rj}}{v_m x_{mj}} \le 1, j = 1,2,...n$$
$$u \ge 0, v \ge 0$$

Convert the above fractional model to an equivalent linear model *Equation 2:*

$$\max u_r y_{r0} \qquad \text{(Eq.2)}$$
$$s.t. v_m x_{i0} - u_r x_{r0} \ge 0, j = 1,2,...n$$
$$v_m x_{i0} = 1, v \ge 0, u \ge 0$$

The dual programming expression for the above linear programming is shown in *Equation 3:*

$$\min \theta - \varepsilon \left(\sum_{i=1}^{m} s_i^- + \sum_{r=1}^{s} s_r^+ \right) \qquad \text{(Eq.3)}$$
$$s.t. \sum x_i \lambda_i + s^- \le \theta x_0, i = 1,2,...m$$
$$\sum y_j \lambda_j - s^+ \ge y_0, j = 1,2,...n$$
$$\lambda_j, s^+, s^- \ge 0$$

http://www.aloki.hu ● ISSN 1589 1623 (Print) ● ISSN 1785 0037 (Online)
DOI: http://dx.doi.org/10.15666/aeer/1704_89859005

If the optimal solution to *Equation 3* is (λ^*, θ*, s^+*, s^-*), then the following results can be obtained: 1) If θ* < 1, the obtained DMU is DEA inefficient; 2) If θ* = 1, and s^-* or s^+* is not equal to 0, then the DMU obtained is DEA weakly efficient; 3) If θ* = 1, and, s^-* and s^+* are equal to 0, then the DMU obtained is DEA efficient. The above is based on the DEA model with the same input, and the results will be opposite for the output-oriented DEA, which studies the problem of constant input and maximum output.

The premise for the CCR model is that the return to scale is constant, that is, when a DMU is DEA efficient, it is also efficient in technology and scale. Being efficient in technology means that the production is at its best, and the system can use the existing input to get the best output. Being efficient in scale means that production is in a state of constant scale and efficiency. Under this state, if the input is expanded by N times, the output will also be expanded by N times.

BCC model

The BCC model based on the variable-scale premise is expressed in *Equation 4* (the following BCC model is input-oriented):

$$\max \frac{u_r y_{r0} - u_0}{v_m x_0} \quad \text{(Eq.4)}$$
$$s.t. v_m x_j - u_r y_j + u_0 \geq 0, j = 1,2,...n$$
$$v_m x_0 = 1, v \geq 0, u \geq 0$$

Its dual model expression is *Equation 5:*

$$\min \theta - \varepsilon \left(\sum_{i=1}^{m} s_i^- + \sum_{r=1}^{s} s_r^+\right) \quad \text{(Eq.5)}$$
$$s.t. \sum x_i \lambda_i + s^- \leq \theta x_0, i = 1,2,...m$$
$$\sum y_j \lambda_j - s^+ \geq y_0, j = 1,2,...n$$
$$\sum \lambda_j = 1$$
$$\lambda_j \geq 0, j = 1,2,...n$$

The BCC model is based on the assumption of variable return to scale (VRS), that is, the impact of scale compensation on efficiency is taken into account in the evaluation of DMUs, so this model can be used to obtain the scale benefits of the DMU, helping decision makers adjust their scale and increase their relative efficiency. Based on this, the input-oriented BCC model is selected to calculate the environmental efficiency. Similar to the CCR model, in this model we can also judge whether the DMU is efficient according to the optimal solution of the model and the value of the slack variable. The specific analysis is as follows: If the optimal solution of *Equation 5* is (λ^*, θ*, s^+*, s^-*), then the following results can be obtained: (1) If θ* < *1*, the obtained DMU is DEA inefficient; (2) If θ* = 1, and *s*-* or s^+* is not equal to 0, the DMU

http://www.aloki.hu ● ISSN 1589 1623 (Print) ● ISSN 1785 0037 (Online)
DOI: http://dx.doi.org/10.15666/aeer/1704_89859005

obtained is DEA weakly efficient; (3) If $\theta^* = 1$, and, s^{-*} and s^{+*} are equal to 0, then the DMU obtained is DEA efficient.

SBM model

The SBM model (Tone, 2001) solves the efficiency evaluation problem that the units of input or output variables are inconsistent; in other words, this model is units invariant.

$$\min\rho = \frac{1 - \frac{1}{\mathrm{m}}\sum_{i=1}^{m}\frac{s_i^-}{x_{i0}}}{1 + \frac{1}{\mathrm{s}}\sum_{r=1}^{s}\frac{s_r^+}{y_{r0}}} \quad \text{(Eq.6)}$$

$$\text{s.t.}\sum_{j=1}^{n}\lambda_j x_{ij} + s_i^- = x_{i0},, \mathrm{i} = 1,2,...,\mathrm{m}$$

$$\sum_{j=1}^{n}\lambda_j y_{rj} - s_{\mathrm{r}}^+ = y_{r0}, \mathrm{r} = 1,2,...,\mathrm{s}$$

$$\lambda_j, s_i^-, s_r^+ \geq 0, \mathrm{j} = 1,2,...,\mathrm{n}$$

The model in *Equation 6* is a fractional programming, which can be transformed into the following linear programming form:

$$\min\tau = \mathrm{t} - \frac{1}{\mathrm{m}}\sum_{i=1}^{m}\frac{\bar{s}_i^-}{x_{i0}} \quad \text{(Eq.7)}$$

$$\text{s.t.}t + \frac{1}{\mathrm{s}}\sum_{r=1}^{s}\frac{\bar{s}_r^+}{y_{r0}} = 1$$

$$\sum_{j=1}^{n}\bar{\lambda}_j x_{ij} + \bar{s}_i^- = tx_{i0}, \mathrm{i} = 1,2,...,\mathrm{m}$$

$$\sum_{j=1}^{n}\bar{\lambda}_j y_{rj} - \bar{s}_i^+ = ty_{r0}, \mathrm{r} = 1,2,...,\mathrm{s}$$

$$\bar{\lambda}_j, \bar{s}_i^-, \bar{s}_r^+ \geq 0, \mathrm{j} = 1,2,...,\mathrm{n}$$

The optimal solution to linear programming *Equation 7* is τ^*, t^*, $\bar{\lambda}^*\bar{s}^{-*}$, $\bar{s}^{+*}$. The necessary and sufficient condition for the decision-making unit *DMU* to be SBM efficient is: $\tau^* = 1$. The value of the objective function is equal to 1, which means that all slack variables have a value of 0; in other words, there is no excessive input or insufficient output in the evaluated DMU. Similarly, under the assumption of VRS, you only need to add $\sum\lambda_j = 1$ in the constraints of the model.

Super-efficiency DEA model

Andersen and Petersen proposed the super-efficiency DEA model to compare the efficiency values of efficient DMUs. This model makes up for the shortcoming of traditional DEA models that efficient DMUs cannot be compared. The super-efficiency

http://www.aloki.hu ● ISSN 1589 1623 (Print) ● ISSN 1785 0037 (Online)
DOI: http://dx.doi.org/10.15666/aeer/1704_89859005

DEA model obtains the DEA efficiency of each DMU by analyzing the data of input and output indices, and points out the reasons why other DMUs are not DEA efficient and also the direction and extent of optimization.

The evaluation diagrams of the traditional DEA model and the super-efficiency DEA model are shown in *Figures 1* and *2*.

Figure 1 is the traditional DEA model, where the DMUs that satisfy the DEA are A, B, C, and D, which constitute the production frontier. Point E is the DEA inefficient DMU. Take the two DMUs B and E for example. The intersection of the connection between the two points and point O and the production frontier are respectively B_1 and E_1. The efficiency value of point B is E_B: $OB_1/OB = 1$, and that of point E is EE: $OE_1/OE < 1$. Similarly, the efficiency values of the three points A, C and D are also 1, and the DMU is DEA efficient here. For DEA inefficient DMUs, the efficiency value is less than 1. *Figure 2* is the super-efficiency DEA model. It is assumed that ACD constitutes the production frontier. At this time, the efficiency value of point B is $EB = OB_1/OB > 1$. Similarly, assuming that ABD constitutes the production frontier, there will also be $EC > 1$. Here comes the problem. As points ABCD are all DEA efficient, they still constitute the production frontier, and the efficiency value of the originally inefficient DMU E is still less than 1.

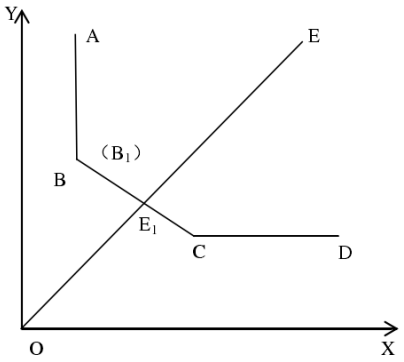

Figure 1. *Traditional DEA model*

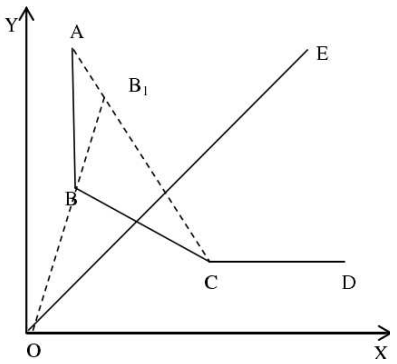

Figure 2. *Super efficiency DEA model*

Super-efficiency SBM model

Considering that a DEA efficient DMU will have an efficiency value of 1 in the SBM model, it is impossible to compare multiple efficient DMUs. This is actually a

http://www.aloki.hu ● ISSN 1589 1623 (Print) ● ISSN 1785 0037 (Online)
DOI: http://dx.doi.org/10.15666/aeer/1704_89859005

sorting problem. The super-efficiency SBM model makes the measurement results closer to reality. It optimizes the slack variable as the objective function (solving the radial problem of the model) and gives the DMU a more reasonable direction for input and output improvement, and in addition, it can be used for sorting the efficiency values of multiple efficient DMUs. The model combines the super-efficiency DEA model and the SBM model. As the input or output orientation will affect the slack of input or output, here the non-oriented model is selected to ensure the rationality of the calculation results.

Under the condition of variable return to scale, the super-efficiency SBM model is as follows:

$$\rho = \min \frac{\frac{1}{m}\sum_{i=1}^{m} \overline{x_i} / x_{ik}}{\frac{1}{s}\sum_{r=1}^{s} \overline{y_r} / y_{rk}} \quad \text{(Eq.8)}$$

$$\text{s.t.} \sum_{\substack{j=1 \\ j \neq k}}^{n} \lambda_j x_j \leq \overline{x}; \sum_{\substack{j=1 \\ j \neq k}}^{n} \lambda_j y_j \leq \overline{y}$$

$$x_{ik} = \sum_{i=1}^{n} x_{ij}\lambda_j + s_i^-, y_{rk} = \sum_{i=1}^{n} y_{rj}\lambda_j - s_r^+$$

$$\overline{x} \geq x_k, \overline{y} \leq y_k$$

$$\sum_{\substack{j=1 \\ j \neq k}}^{n} \lambda_j = 1, \overline{y} \geq 0, \lambda \geq 0$$

In *Equation 8:* ρ is the efficiency value, ($\overline{x}$, $\overline{y}$) the reference point of the decision variable, s^- the slack variable of the input, s^+ the desired output slack variable, the subscript k of the variable in the model the kth DMU being evaluated, and λ the weight vector. When $\rho < 1$, it indicates that the DMU is inefficient. When $\rho > 1$, the DMU is in an active state.

This paper uses the superior improved DEA model - the super-efficiency SBM model to evaluate the environmental emission efficiencies of different regions in China to solve the radial problem. The super-efficiency SBM model can also sort the efficient DMUs.

Data collection and processing

Data description

Selection of indices: input indices for measuring environmental efficiency include the number of employees at the end of the year, investment in fixed assets, energy consumption and industrial pollution discharge (including wastewater, solid waste and waste gas), etc.; the output index is the total GDP of each province or city. In this paper, three industrial wastes are used as the environmental pollution variable.

This paper selects the data of 30 provinces in China from 2010 to 2015 as samples. Tibet is not included here because its data are unavailable. In addition, the wastewater discharge in 2010 is replaced by industrial wastewater discharge. The original data are extracted from the China Statistical Yearbook, the China Environmental Statistics Yearbook, and the China Energy Statistics Yearbook. The model selected has multiple

http://www.aloki.hu ● ISSN 1589 1623 (Print) ● ISSN 1785 0037 (Online)
DOI: http://dx.doi.org/10.15666/aeer/1704_89859005

inputs and multiple outputs, with labour, fixed asset investment and energy consumption as the inputs, three wastes (wastewater, industrial waste gas, industrial solid waste) as the environmental pollution variable, and provincial GDP as the desired output. Specific indices selected are elaborated as follows:

(1) Labour input

Labour is an indispensable input factor in economic activities. In environmental efficiency research, labour input should be considered comprehensively in terms of both quantity and quality. Now in the statistical yearbook, most of the labour input is reflected in the quantity, and the labour flow is frequent, which does not reflect labour efficiency. By referring to the existing literatures, this paper uses the number of employed people at the end of each year as the index of labour input.

(2) Energy input

Energy is an essential factor in production activities. In the related research on environmental efficiency, a large number of researchers have gradually considered energy as an input factor into the index system (Mutani et al., 2018; Vand et al., 2018). The rapid economic growth is inseparable from the massive consumption of energy, but the latter is also accompanied by the generation of a large number of pollutants. Therefore, this paper also incorporates energy consumption as an input index into the model to measure environmental efficiency. Here the specific index is the total energy consumption of each province.

(3) Capital input

In some studies, the capital input variable is the capital stock calculated by the perpetual inventory method. There are methods to determine the base capital stock and depreciation, and different methods will result in different results. Therefore, this paper uses capital investment as the capital input. Fixed assets investment plays a vital role in the system, because it can reflect the country's financial policy support. In order to make the data comparable, the capital input data are all converted according to the fixed assets investment index of each province or city into equivalent data in 2010, with the unit being 100 million RMB.

(4) Pollution discharge

Due to the external effects of production, pollutant discharge is inevitable in production activities. Here, this paper refers to Chen (2009) approach: environmental pollution is taken as an input factor. Considering the incomplete data of pollutants in the yearbooks, and the problem that industrial pollutant discharge occupies a large share, this paper comprehensively evaluates the basic data of "three wastes", and uses an entropy weight method to synthesize a comprehensive environmental pollution index as an input variable in the DEA model reflecting the overall pollution status. This is included in the framework of environmental efficiency measurement.

(5) Desired output

The regional GDP reflects the output of production activities in a region during a certain period. This paper follows the traditional practice and uses the GDP of each province as an important index to reflect output. Taking into account the real output results, the nominal GDP of each province and city will be reduced by 2010 and converted into the real GDP reflecting the actual output of the region. Here the GDP data and indices of each province are from *China Statistical Yearbook* of each year.

The selected input-output indices are explained in *Table 1*.

http://www.aloki.hu ● ISSN 1589 1623 (Print) ● ISSN 1785 0037 (Online)
DOI: http://dx.doi.org/10.15666/aeer/1704_89859005

Table 1. *Selection of input and output indices*

Index	Variable	Variable declaration
Factor input	Labor input	Number of working population at the end of the year in the region
	Capital input	investment in the fixed assets
	Energy consumption	Regional total energy consumption
Pollution emission	Industrial pollutant	Environmental pollution composite index
Expected output	Regional economic output	Regional GDP

Evaluation of the comprehensive environmental pollution index

In order to reflect the pollutant discharges of provinces and municipalities, according to the records of the pollutant indices in the statistical yearbooks and based on the principles of scienticity, rationality and availability, the index system consists of three indices (industrial waste gas emissions, wastewater discharge and industrial solid waste production) to measure the discharge of pollutants nationwide. The environmental pollution index results are a principal part of the environmental efficiency assessment.

First, considering the dimensionality of the three indices, the normalization method is used to normalize the differences between the indices, with the formula expressed as follows *Equation 9:*

$$x'_{ij} = \frac{x_{ij} - \min x_j}{\max x_j - \min x_j} \quad \text{(Eq.9)}$$

where i denotes each province and j denotes a pollutant index.

Second, obtain the information entropy of each index *Equation 10:*

$$e_j = -\ln(n)^{-1} \sum_{i=1}^{n} p_{ij} \ln p_{ij} \quad \text{(Eq.10)}$$

$$p_{ij} = \frac{x'_{ij}}{\sum_{i=1}^{n} x'_{ij}}$$

If $p_{ij} = 0$, then $p_{ij} \ln p_{ij} = 0$.

Third, with the information entropy e_j of each index obtained in step 2, the weight of each index is obtained as follows (*Eq.11*):

$$w_j = \frac{1 - e_j}{k - \sum e_j} \quad \text{(Eq.11)}$$

Fourth, the comprehensive environmental pollution index is *Equation 12:*

$$E = \sum w_j p_{ij} \quad \text{(Eq.12)}$$

http://www.aloki.hu ● ISSN 1589 1623 (Print) ● ISSN 1785 0037 (Online)
DOI: http://dx.doi.org/10.15666/aeer/1704_89859005

Through the above calculations, the results of the comprehensive environmental pollution indices of provinces and municipalities in China in all years are obtained, as shown in *Table 2*.

Table 2. *Comprehensive environmental pollution indices of various provinces and municipalities nationwide from 2010 to 2015*

Region	2010	2011	2012	2013	2014	2015
Beijing	0.0912	0.0734	0.0617	0.0532	0.0569	0.0562
Tianjin	0.0748	0.0590	0.0680	0.0528	0.0621	0.0618
Hebei	0.7464	0.7742	0.7740	0.7834	0.7742	0.7753
Shanxi	0.4168	0.4225	0.4384	0.4496	0.4519	0.4959
Nei Monggol	0.3499	0.3364	0.3425	0.3097	0.3773	0.4387
Liaoning	0.4193	0.4405	0.4417	0.4061	0.4767	0.5466
Jilin	0.1327	0.1176	0.1130	0.0975	0.1059	0.1228
Heilongjiang	0.1526	0.1373	0.1448	0.1270	0.1397	0.1540
Shanghai	0.2071	0.1483	0.1476	0.1338	0.1316	0.1320
Jiangsu	0.5396	0.5145	0.5257	0.5078	0.5532	0.5534
Zhejiang	0.3452	0.2987	0.2973	0.2773	0.2887	0.2940
Anhui	0.2683	0.3000	0.3131	0.2949	0.3094	0.3412
Fujian	0.2580	0.2150	0.2146	0.2122	0.1952	0.1939
Jiangxi	0.2168	0.2233	0.2196	0.2132	0.2170	0.2408
Shandong	0.6123	0.5323	0.5282	0.5159	0.5620	0.6200
Henan	0.4054	0.4255	0.4260	0.4274	0.4453	0.4377
Hubei	0.2705	0.2611	0.2486	0.2396	0.2531	0.2700
Hunan	0.2621	0.2393	0.2431	0.2300	0.2228	0.2301
Guangdong	0.5572	0.4984	0.5002	0.4811	0.4954	0.4992
Guangxi	0.2907	0.2548	0.2673	0.2145	0.2091	0.1993
Hainan	0.0078	0.0064	0.0064	0.0100	0.0062	0.0058
Chongqing	0.1348	0.1013	0.0968	0.0946	0.0975	0.1026
Sichuan	0.3412	0.2990	0.3019	0.2907	0.3129	0.2989
Guizhou	0.1507	0.1199	0.1437	0.1801	0.1816	0.1661
Yunnan	0.1847	0.2577	0.2405	0.2312	0.2348	0.2505
Shaanxi	0.1841	0.1539	0.1564	0.1544	0.1781	0.2063
Gansu	0.0782	0.1104	0.1203	0.0998	0.1072	0.1161
Qinghai	0.0299	0.1105	0.1132	0.1043	0.1222	0.1615
Ningxia	0.1101	0.0642	0.0600	0.0520	0.0679	0.0601
Xinjiang	0.1134	0.1063	0.1518	0.1659	0.1774	0.1707

As can be seen from *Table 2*, the heavily polluted areas are concentrated in Hebei, Shanxi, Liaoning, Jiangsu, Shandong and Guangdong, etc. In contrast, Beijing, Tianjin, Hainan and Ningxia, etc. have smaller pollution emissions The comprehensive environmental pollution index is incorporated into the framework of the environmental efficiency assessment, which can fully reflect economic output and environmental pollution.

http://www.aloki.hu ● ISSN 1589 1623 (Print) ● ISSN 1785 0037 (Online)
DOI: http://dx.doi.org/10.15666/aeer/1704_89859005

Results and discussion

Estimation of environmental efficiency in various provinces and municipalities

Traditional DEA models tend to ignore the undesired output indices such as pollutants, when considering the accuracy of evaluation. This imposes certain constraints on the selection and evaluation of indices in environmental efficiency evaluation. In order to visually reflect the impact of pollutant emission indices on environmental efficiency results, both the traditional BCC model and the super-efficiency SBM model are used here for comparison. The BCC model excludes the environmental pollution index, but other input and output indices remain unchanged. Through calculation, the environmental efficiency values of various provinces and municipalities in China from 2010 to 2015 (the data in Tibet are not available) are obtained, as shown in *Table 3*.

Table 3. *Environmental efficiency values of various provinces and municipalities in China from 2010 to 2015*

Region	2010		2011		2012	
	BCC	SE-SBM	BCC	SE-SBM	BCC	SE-SBM
Beijing	1.000	1.2697	1.000	1.226	1.000	1.299
Tianjin	1.000	1.0060	1.000	1.024	1.000	1.020
Hebei	0.467	0.4095	0.484	0.385	0.490	0.378
Shanxi	0.452	0.3480	0.403	0.321	0.404	0.305
Nei Monggol	0.657	0.4445	0.697	0.432	0.716	0.428
Liaoning	0.610	0.4959	0.669	0.467	0.663	0.460
Jilin	0.515	0.4604	0.498	0.475	0.517	0.464
Heilongjiang	0.523	0.4672	0.506	0.460	0.466	0.423
Shanghai	1.000	1.1548	1.000	1.184	1.000	1.200
Jiangsu	1.000	1.0187	1.000	1.026	1.000	1.033
Zhejiang	0.956	0.8494	0.938	0.839	0.939	0.811
Anhui	0.627	0.3895	0.608	0.373	0.605	0.358
Fujian	0.749	0.5808	0.730	0.565	0.744	0.553
Jiangxi	0.737	0.4299	0.704	0.417	0.713	0.411
Shandong	0.822	0.6821	0.829	0.687	0.829	0.685
Henan	0.586	0.5076	0.582	0.495	0.595	0.489
Hubei	0.563	0.4794	0.529	0.468	0.531	0.466
Hunan	0.589	0.4897	0.547	0.477	0.555	0.472
Guangdong	1.000	1.2451	1.000	1.260	1.000	1.278
Guangxi	0.595	0.3920	0.574	0.382	0.571	0.371
Hainan	1.000	2.0915	1.000	3.711	1.000	3.535
Chongqing	0.497	0.4267	0.482	0.445	0.515	0.445
Sichuan	0.496	0.4239	0.494	0.442	0.511	0.447
Guizhou	0.489	0.3378	0.353	0.301	0.316	0.263
Yunnan	0.459	0.3385	0.437	0.307	0.411	0.297
Shaanxi	0.562	0.4401	0.542	0.436	0.535	0.420
Gansu	0.447	0.3720	0.392	0.313	0.360	0.287
Qinghai	1.000	1.1678	1.000	1.101	1.000	1.098
Ningxia	0.887	0.6952	0.881	1.027	0.890	1.038
Xinjiang	0.511	0.4586	0.407	0.389	0.406	0.332

http://www.aloki.hu ● ISSN 1589 1623 (Print) ● ISSN 1785 0037 (Online)
DOI: http://dx.doi.org/10.15666/aeer/1704_89859005

Table 3. cont. *Environmental efficiency values of various provinces and municipalities in China from 2010 to 2015*

Region	2013		2014		2015	
	BCC	SE-SBM	BCC	SE-SBM	BCC	SE-SBM
Beijing	1.000	1.316	1.000	1.289	1.000	1.298
Tianjin	1.000	1.027	1.000	1.026	1.000	1.031
Hebei	0.479	0.382	0.479	0.377	0.470	0.377
Shanxi	0.398	0.299	0.388	0.282	0.367	0.272
Nei Monggol	0.717	0.423	0.728	0.391	0.726	0.429
Liaoning	0.660	0.485	0.667	0.467	0.625	0.484
Jilin	0.536	0.475	0.546	0.460	0.562	0.448
Heilongjiang	0.460	0.417	0.494	0.428	0.501	0.432
Shanghai	1.000	1.152	1.000	1.149	1.000	1.165
Jiangsu	1.000	1.045	1.000	1.052	1.000	1.055
Zhejiang	0.901	0.796	0.908	0.790	0.892	0.796
Anhui	0.564	0.343	0.568	0.336	0.568	0.335
Fujian	0.739	0.546	0.734	0.552	0.745	0.561
Jiangxi	0.651	0.390	0.637	0.380	0.622	0.371
Shandong	0.823	0.706	0.826	0.705	0.822	0.685
Henan	0.624	0.487	0.625	0.484	0.631	0.486
Hubei	0.580	0.477	0.587	0.478	0.601	0.483
Hunan	0.607	0.486	0.620	0.497	0.629	0.501
Guangdong	1.000	1.273	1.000	1.266	1.000	1.249
Guangxi	0.550	0.367	0.541	0.360	0.535	0.358
Hainan	1.000	2.506	1.000	3.922	1.000	3.810
Chongqing	0.556	0.454	0.564	0.448	0.565	0.454
Sichuan	0.534	0.454	0.536	0.450	0.545	0.462
Guizhou	0.316	0.245	0.294	0.237	0.288	0.239
Yunnan	0.399	0.291	0.387	0.281	0.399	0.280
Shaanxi	0.517	0.408	0.517	0.394	0.506	0.391
Gansu	0.326	0.271	0.301	0.256	0.306	0.254
Qinghai	1.000	1.110	1.000	1.108	1.000	1.114
Ningxia	0.859	1.053	0.866	1.045	0.852	1.077
Xinjiang	0.402	0.308	0.410	0.279	0.405	0.276

It can be seen from the above table that the environmental efficiency was not balanced in China, and during the investigation period, the extreme difference in environmental efficiency was expanding year by year. The provinces (municipalities) with an efficiency of greater than 1 during the investigation period are Beijing, Tianjin, Qinghai, Shanghai, Guangdong, Hainan and Jiangsu, where the economic environment is relatively stable, and most of which are eastern provinces, with high investments in pollution control; the provinces ranking last in terms of environmental efficiency are Guizhou, Gansu, Shanxi, Yunnan and Xinjiang. This paper analyzes the differences between economic efficiency and environmental efficiency, and the comparison results are shown in the above table. It should be noted that when the relative efficiency evaluation value of the DEA is 1, the DMU is DEA efficient; and when the relative

http://www.aloki.hu ● ISSN 1589 1623 (Print) ● ISSN 1785 0037 (Online)
DOI: http://dx.doi.org/10.15666/aeer/1704_89859005

efficiency is less than 1, the DMU is DEA inefficient. Through comparative analysis, the following two conclusions are obtained:

First, the BCC model does not contain any undesired output. Among the evaluation results, 7 DMUs have an economic efficiency of 1, which cannot be further compared, while the super-efficiency SBM model takes the environmental pollution variable into account. It can be seen that there are 7 DMUs that achieve an efficiency value of greater than 1, thus they can be further compared.

Second, after the environmental pollution index is taken into account, except for 6 areas like Hainan, Qinghai, Shanghai and Jiangsu whose environmental efficiencies are all greater than 1, the other 24 DEA inefficient areas see significant declines in the efficiency values: the annual average interval of the BCC model for environmental pollution variable is [0.590, 0.617], and the annual average interval for the super-efficiency SBM model with the environmental pollution variable is [0.440, 0.497]. *Figure 3* compares the calculation results of the two models in 2015. It can be clearly seen that the evaluation efficiencies in the super-efficiency SBM model are all lower than those in the BCC model, except those of the DEA efficient DMUs. If Beijing, Shanghai, Hainan and other provinces in the efficiency frontier are used as benchmarks, there will be a lot to improve in Shanxi, Guizhou and Yunnan with the same input and output. This shows that there are significant gaps in environmental efficiency among provinces, and the lower the efficiency value, the greater the potential for improvement.

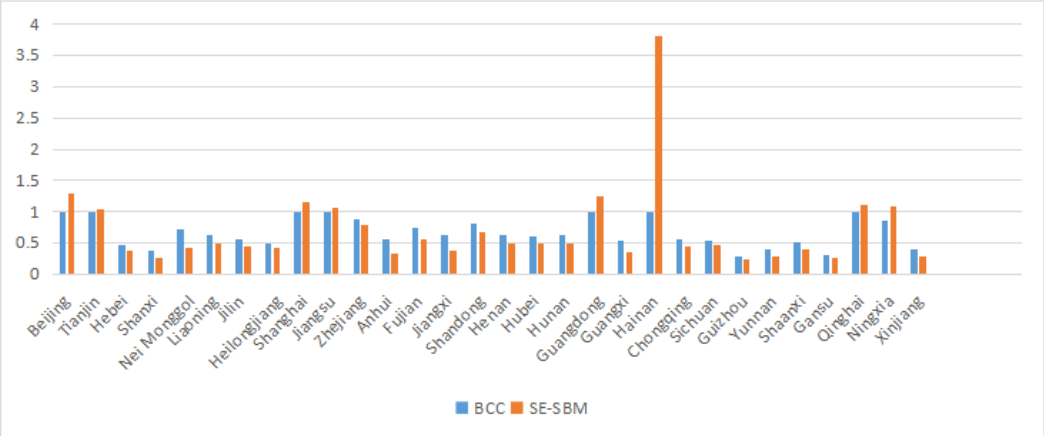

Figure 3. *Overview of environmental efficiency in provinces and municipalities of China in 2015*

To a certain extent, the above results reflect the actual differences in the transformation of the production capacity into environmental efficiency by various provinces and municipalities in China. On the whole, the environmental efficiency performance of the provinces and municipalities in China is generally not good, except for a few regions, which have achieved relatively high environmental efficiencies thanks to the long-term economic accumulation. China has a vast territory, where the regional location and factor endowments vary greatly among provinces and municipalities, so the gaps between environmental efficiency are inevitable and also reasonable. Under the new concept of economic development, it is necessary to improve the regional economy and reduce the damages to the environment. In addition to the above reasons, low-efficiency areas blindly pursue high output without considering the

http://www.aloki.hu ● ISSN 1589 1623 (Print) ● ISSN 1785 0037 (Online)
DOI: http://dx.doi.org/10.15666/aeer/1704_89859005

environmental tolerance, which also cause environmental inefficiency. Therefore, China still has a long way to go in terms of environmental efficiency improvement.

Considering that there are a few large extremum values in the super-efficiency SBM model, the provinces and municipalities with efficiency values greater than or equal to 1 during the investigation period are excluded, and only the differences in the efficiency of economic output and the efficiency of environmental pollution variable are taken into account. From *Table 4,* it can be seen that the efficiency value in the super-efficiency model sees a significant reduction, indicating that the addition of the environmental pollution index has great negative impact on the efficiency value. Nevertheless, the reduction in efficiency shows a decreasing trend year by year, indicating that the national economic level is improving. At the same time, the environmental quality is also showing a good trend, and the environmental efficiency value considering the environmental pollution variable is getting closer to that without considering the environmental pollution variable. The gaps are being gradually narrowed because during 2011-2015, i.e. the 12th five-year period, China put more emphasis on the ecological civilization construction and developed and implemented strict emission reduction measures and regulations in the production activities under the 12th Five-Year Plan, which greatly improved the awareness of environmental protection in this country.

Table 4. *Comparison of the results of the BCC model and the super-efficiency SBM model*

Year	2010	2011	2012	2013	2014	2015
BCC	0.5998	0.5777	0.5775	0.5738	0.5749	0.5723
SE-SBM	0.4747	0.4489	0.4348	0.4323	0.4241	0.4261
D-value	0.1251	0.1288	0.1427	0.1415	0.1508	0.1462

Differences in efficiency levels among the four regions

Due to geographical reasons, there are large differences in environmental efficiency between regions. According to the regional data from the National Bureau of Statistics, this paper divides the provinces and municipalities in China into four regions, namely the eastern region, including Beijing, Fujian, Guangdong, Hebei, Jiangsu, Shandong, Shanghai, Tianjin, Hainan and Zhejiang; the central region, including Anhui, Henan, Hunan, Jiangxi, Hubei and Shanxi; the western region, including Gansu, Guangxi, Guizhou, Inner Mongolia, Ningxia, Qinghai, Shaanxi, Chongqing, Sichuan, Xinjiang, Tibet and Yunnan; the northeastern region, including Heilongjiang, Jilin, and Liaoning. In this paper, Tibet is not included due to lack of data. The average environmental efficiencies of the four major regions in the major years are compared with the national level, as shown in *Table 5*.

Table 5. *Environmental efficiency mean values of major years in four major regions*

Region \ Year	2010	2011	2012	2013	2014	2015
Eastern	1.0308	1.1906	1.1792	1.075	1.2128	1.2026
Northeastern	0.4745	0.4673	0.4491	0.4589	0.4513	0.4548
Central	0.4407	0.4253	0.4169	0.4136	0.4096	0.4079
Western	0.4997	0.5067	0.4934	0.4895	0.4771	0.485
Nationwide	0.6624	0.7144	0.7023	0.6664	0.7062	0.7058

http://www.aloki.hu ● ISSN 1589 1623 (Print) ● ISSN 1785 0037 (Online)
DOI: http://dx.doi.org/10.15666/aeer/1704_89859005

Table 6 shows that the environmental efficiencies of the above several regions in China are quite different - the efficiency value in the eastern region is [1.03, 1.22], the central region [0.40, 0.45], the western region [0.47, 0.51], the northeast region [0.44, 0.48] and the national level [0.66, 0.72]. Despite a few inefficient provinces, the efficiency value in the eastern region is much higher than those in the other three regions and the national average; on the other hand, the environmental efficiencies of the western region, the northeast region and the central region are all lower than the national average.

Table 6. *Analysis of input and output redundancy of environmental efficiency in provinces and municipalities of China in 2015*

DMU	Reference set	Number of employees	Energy consumption	Fixed asset investment	Environmental pollution index	Regional GDP
Beijing	Tianjin, Shanghai, Hainan	-28.546	2749.201	0	0.044	0
Tianjin	Beijing, Shanghai, Ningxia	110.811	-1461	-4984.455	0	0
Hebei	Shanghai, Guangdong	-2195.15	-15475.072	-19300.051	-0.594	0
Shanxi	Beijing	-687	-12531	-6230.685	-0.44	6816.804
Nei Monggol	Beijing	-278	-12074	-5844	-0.382	1474.195
Liaoning	Shanghai, Guangdong	-801.312	-9327.276	-9806.287	-0.396	0
Jilin	Beijing	-295	-1289	-5073.682	-0.067	6754.161
Heilongjiang	Beijing	-849	-5273	-2302.637	-0.098	4858.581
Shanghai	Beijing, Guangdong	266.56	-2485.894	2850.598	-0.037	0
Jiangsu	Shanghai, Guangdong	1052.741	-1662.856	-18937.337	-0.085	0
Zhejiang	Beijing, Guangdong	-412.985	-2876.456	-10217.698	-0.05	0
Anhui	Beijing, Guangdong	-3124.258	-5332.103	-15624.926	-0.282	0
Fujian	Beijing, Guangdong	-1147.921	-3318.144	-11283.023	-0.099	0
Jiangxi	Beijing	-1430	-1587	-9145.104	-0.185	4746.947
Shandong	Beijing, Guangdong	-1218.132	-11521.409	-21100.034	-0.192	0
Henan	Beijing, Guangdong	-3774.24	-8552.825	-19667.714	-0.234	0
Hubei	Beijing, Guangdong	-1823.084	-6547.908	-14263.017	-0.157	0
Hunan	Beijing, Guangdong	-2172.16	-5738.215	-12524.51	-0.119	0
Guangdong	Jiangsu	-1460	90	17120.606	0.054	-3738.185
Guangxi	Beijing	-1634	-2908	-7936.452	-0.143	4838.593

http://www.aloki.hu ● ISSN 1589 1623 (Print) ● ISSN 1785 0037 (Online)
DOI: http://dx.doi.org/10.15666/aeer/1704_89859005

Hainan	Beijing, Ningxia	-168.807	3511.272	192.264	0.054	0
Chongqing	Beijing	-521	-2081	-6270.042	-0.046	5811.257
Sichuan	Beijing, Guangdong	-2800.317	-9051.883	-13611.917	-0.167	0
Guizhou	Beijing	-761	-3095	-3012.665	-0.11	12002.69
Yunnan	Beijing	-1756	-3504	-5398.654	-0.194	8072.753
Shaanxi	Beijing	-885	-4863	-9605.846	-0.15	3194.829
Gansu	Beijing	-350	-670	-1160.211	-0.06	13490.221
Qinghai	Hainan, Ningxia	112.12	0	315.671	-0.121	648.559
Ningxia	Hainan, Qinghai	112.115	-2701.808	-166.791	0	193.215
Xinjiang	Beijing	-9	-8798	-2948.25	-0.114	11237.835

Redundancy analysis of input and output

If the efficiency of a DMU is less than 1, then it is DEA inefficient. The reasons why it is different from the DMUs in the frontier include excessive input, excessive undesired output and insufficient desired output. The super-efficiency SBM model adds slack variables to the objective function to provide information on the input and output redundancy of each DMU, and clearly points out the direction for efficiency improvement. Input redundancy includes fixed asset investment, labour force population, total energy consumption and environmental pollution index. The desired output redundancy is expressed in GDP. Section 3 of this paper uses the super-efficiency SBM model to measure the environmental efficiency values of 30 provinces in China from 2010 to 2015. This section takes the redundancy of input and output of environmental efficiency in various provinces and municipalities in China in 2015 for example.

In *Table 6*, we list the improvement goals for each province (negative data indicate the required reductions). From this table, it can be seen that the provinces and municipalities with lower efficiencies have the problems like excessive investment, insufficient output, unreasonable input of factors, insufficient control of environmental pollution and less-than-desired output. Those with high environmental efficiencies also require efficiency improvement. For example, Jiangsu has met the requirement in terms of economic output, so there is no need for improvement in this area, but compared with Shanghai and Guangdong, it still needs to reduce energy consumption, fixed asset investment and control of environmental pollution (by respectively 1662.856, 18937.337 and 0.085). So with Shanghai and Guangdong as the frontiers, Jiangsu needs to impose reasonable control over the input factors to achieve the optimal level of efficiency.

This paper also conducts more detailed and in-depth analysis of the input and output redundancy of each region. In terms of labour, Tianjin, Shanghai, Jiangsu, Qinghai, and Ningxia need to increase their input, and the remaining provinces and municipalities need to reduce it. Excessive labour input will hinder regional economic growth and also put pressure on the environment. In reality, it is not feasible to reduce the population of labour force, so this requires more rational allocation of labour resources. It is important to improve the quality of the labour force and implement the people-oriented social

http://www.aloki.hu ● ISSN 1589 1623 (Print) ● ISSN 1785 0037 (Online)
DOI: http://dx.doi.org/10.15666/aeer/1704_89859005

development concept. In terms of energy consumption, except the four regions - Beijing, Guangdong, Hainan and Qinghai, all provinces and municipalities need reductions. Energy consumption is accompanied by the generation of large amounts of pollutants, so controlling energy consumption is an important way to improve environmental efficiency. As the "fuel" to the social and economic development, energy is essential to the economic growth. Under the current severe energy consumption situation, a lot of effort needs to be made in the energy structure adjustment so as to better control energy consumption and reduce emissions. In terms of fixed assets investment, Qinghai, Hainan, Guangdong and Shanghai need moderate increases, while the other provinces have excessive investment in fixed assets. This shows that the capital investment does not conform to its own actual development in many provinces of China, manifested in unreasonable investment and utilization. Similarly, in terms of the environmental pollution index, most provinces do not have good performances – they all need to reduce the pollution index and control the pollutant emissions. In terms of the desired output, 50% of the provinces do not need to increase GDP, and the total GDP of these regions rank high.

Conclusion

This paper firstly introduces the concept of environmental efficiency, selects the input and output indices of environmental efficiency, and then uses the super-efficiency SBM model considering environmental pollution to measure the environmental efficiency of 30 provinces and municipalities in China from 2010 to 2015.

It can be concluded that the addition of the environmental pollution variable results in significant declines in the efficiencies of DEA inefficient provinces. The overall environmental efficiency in China is low, and the environmental efficiencies of the four regions vary significantly. The areas with high environmental efficiencies fall into two categories: the first are the economically developed provinces in the eastern coastal region, which all have solid economic bases; the second are remote provinces, such as Qinghai and Ningxia in the western region, with small economic aggregate and low environmental pollution. The economic advantage obviously plays a greater role in the evaluation of environmental efficiency, and it is scattered nationwide - Beijing-Tianjin region, Yangtze River Delta region, and Pearl River region, which are consistent with the urban agglomerations in the developed regions of China. The areas with good natural environment and low economic levels represented by Qinghai and Ningxia are examples of high environmental efficiency. These areas focus on the coordinated development of the economic environment. Those that need to improve environmental efficiency include: provinces with regional economic characteristics, such as Fujian and Shandong; and the central and western provinces with obvious industrial characteristics and serious environmental pollution. From the above analysis, it can be seen that the environmental efficiencies of the provinces and municipalities vary greatly, and judging from the data every year, the gaps are gradually increasing.

Through comparative analysis of the four regions, it is found that the environmental efficiency in the eastern region is much higher than those of the other three regions. The overall economic level in the eastern region is high and the pollution control is also better than that in the others. The northeastern and central regions have similarly low environmental efficiencies. Due to the vast territory of the western region, the environmental efficiencies of the provinces there vary greatly, but the overall

http://www.aloki.hu ● ISSN 1589 1623 (Print) ● ISSN 1785 0037 (Online)
DOI: http://dx.doi.org/10.15666/aeer/1704_89859005

environmental efficiency level is better than that in the northeastern and central regions. In terms of environmental efficiency gaps, the difference in the eastern region has been large for many years, those in the northeastern and central regions are maintained at a low level, and that in the western region is increasing year by year, indicating that the gaps are generally expanding in China, which is a bad signal for the coordination between the economy and the environment.

Improper behaviours in production activities should be cut off from the source, rather than be remedied afterwards. The government should play the positive role of economic resources, rationally plan the utilization of investments in environmental protection, and guide enterprises to carry out energy conservation and pollution reduction. Judging from the current situation, the policy environment in China has not yet reached the desired level, and thus it is necessary to build an intellectual property protection system and a fair competition system. At present, the economic development is not balanced among different regions of China. Each region should rationally adjust the proportions of the three major industries in light of its own situation. The central and western regions rely mainly on the secondary industry, which hinders the development of new economic growth points. In order to improve the economic environment and make the regional industries more competitive, enterprises with "high energy consumption and low production" should be restricted and green and low-carbon recycling industries with high added value should be vigorously developed.

In the follow-up study, further exploration and research are needed in the following aspects. (1) The research on the region can further deepen to the prefecture-level city and county level, and expand the research perspective on environmental efficiency measurement. (2) With the continuous improvement of statistical data, the consumer's tolerance for pollution emissions should be included in the research field to further enrich the content of environmental efficiency measurement. (3) This paper considers the macro level more. The follow-up research can analyze the environmental efficiency from a smaller micro level, such as the corporate governance structure and enterprise property rights arrangement.

Acknowledgements. This paper is supported by the Philosophy Social Science Foundation of Zhejiang Province (19NDJC198YB), Natural Science Foundation of China (71403247; 71673250), First Class Discipline of Zhejiang-A (Zhejiang Gongshang University-Statistics), Zhejiang province advantage subject (Zhejiang Gongshang University-Statistics), Zhejiang Statistical Science Project, and the graduate innovation project of Zhejiang Gongshang University.

REFERENCES

[1] Aldanondo-Ochoa, A. M., Casasnovas-Oliva, V. L., Arandia-Miura, A. (2014): Environmental efficiency and the impact of regulation in dryland organic vine production. – Land Use Policy 36: 275-284.

[2] Beukes, P. C., Gregorini, P., Romera, A. J., Levy, G., Waghorn, G. C. (2010): Improving production efficiency as a strategy to mitigate greenhouse gas emissions on pastoral dairy farms in New Zealand. – Agriculture Ecosystems & Environment 136(3): 358-365.

[3] Bevilacqua, M., Braglia, M. (2002): Environmental efficiency analysis for Eni oil refineries. – Journal of Cleaner Production 10(1): 85-92.

[4] Chen, A. (2008): Evaluation of China's regional ecological efficiency and its influencing factors: a case study of interprovincial data from 2000 to 2006. – Chinese Journal of Management Science S1: 566-570.

http://www.aloki.hu ● ISSN 1589 1623 (Print) ● ISSN 1785 0037 (Online)
DOI: http://dx.doi.org/10.15666/aeer/1704_89859005

[5] Chen, S. Y. (2009): Energy consumption, carbon dioxide emissions and sustainable development of China's industry. – Economic Research Journal (4): 41-55.
[6] Faere, R., Grosskopf, S., Lovell, C. A. K., Pasurka, C. (1989): Multilateral productivity comparisons when some outputs are undesirable: a nonparametric approach. – The Review of Economics and Statistics 71(1): 90.
[7] Halkos, G. E., Tzeremes, N. G. (2013): A conditional directional distance function approach for measuring regional environmental efficiency: evidence from UK regions. – European Journal of Operational Research 227(1): 182-189.
[8] Montanari, R. (2004): Environmental efficiency analysis for Enel thermo-power plants. – Journal of Cleaner Production 12(4): 403-414.
[9] Mutani, G., Fontanive, M., Arboit, M. E. (2018): Energy-use modelling for residential buildings in the metropolitan area of Gran Mendoza (AR). – Tecnica Italiana - Italian Journal of Engineering Science 61+1(2): 74-82.
[10] Reinhard, S., Lovell, C. A. K., Thijssen, G. J. (2000): Environmental efficiency with multiple environmentally detrimental variables; estimated with SFA and DEA. – European Journal of Operational Research 121(2): 287-303.
[11] Schaltegger, S., Sturm, A. (1990): Environmental rationality. – Die Unternehmung 4: 117-131.
[12] Tan, X., Cao, Y. Q., Shi, L., Zheng, S. Y., Ma, Z. (2013): Comparative study on environmental efficiency in the three northeastern provinces: 1991-2010. – Productivity Research 4: 109-112.
[13] Thijssen, G. (1999): Econometric estimation of technical and environmental efficiency: an application to Dutch dairy farms. – American Journal of Agricultural Economics 81(1): 44-60.
[14] Tone, K. (2001): A slacks-based measure of efficiency in data envelopment analysis. – European Journal of Operational Research 130(3): 498-509.
[15] Tone, K. (2002): A slacks-based measure of super-efficiency in data envelopment analysis. – European Journal of Operational Research 143(1): 32-41.
[16] Vand, A. Z., Mirzaei, M., Ahmadi, M. H., Lorenzini, G., Kumar, R., Jilte, R. (2018): Technical and economical optimization of CHP systems by using gas turbine and energy recovery system. – Mathematical Modelling of Engineering Problems 5(4): 286-292.
[17] Wang, B., Wu, Y., Yan, P. (2010): Environmental efficiency and environmental total factor productivity growth in China's regional economies. – Economic Research Journal 45(5): 95-109.
[18] Wang, D. P., Zhu, Y. C. (2011): Dynamic evaluation of water environmental efficiency in China's seven river basins. – China Population, Resources and Environment 21: 9.
[19] Wang, Q., Gu, X. W., Wang, J., Ding, Y. (2007): Research on environmental load and environmental efficiency in China. – Journal of Northeastern University 28(4): 589-591.
[20] Wang, Q. W., Zhou, D. Q., Chen, H. T. (2009): Technological progress and energy efficiency: an analysis based on the ARDL method. – Journal of Applied Statistics and Management 28(5): 913-920.
[21] Wu, M. R., Ma, J. (2016): Analysis of China's regional ecological efficiency measurement and its influencing factors—based on the DEA-Tobit two-step method. – Technology Economics 35(3): 75-80.
[22] Xu, Y. J. (2012): Research on environmental efficiency and environmental total factor productivity of China's industrial sector. – Journal of Renmin University of China in Chinese 20-67.
[23] Yan, J. Y., Hou, M. Y. (2018): Study on the technical efficiency and time-space distribution of China's mineral resources industry chain. – China Mining Magazine (2): 65-69.
[24] Zhang, J. L. (2008): Research on eco-economic efficiency evaluation of production enterprises. – Central South University: phd thesis.

http://www.aloki.hu ● ISSN 1589 1623 (Print) ● ISSN 1785 0037 (Online)
DOI: http://dx.doi.org/10.15666/aeer/1704_89859005

[25] Zhang, X. M., Ma, P. Q. (2018): Research on efficiency evaluation and comparison of urban energy saving and environmental protection industry based on super-efficiency SBM model: a case study of Lanzhou City. – Science and Technology Management Research 38: 268-274.

http://www.aloki.hu ● ISSN 1589 1623 (Print) ● ISSN 1785 0037 (Online)
DOI: http://dx.doi.org/10.15666/aeer/1704_89859005

GEOCHEMICAL FEATURES, ISOTOPE COMPOSITIONS AND ENVIRONMENTAL IMPACTS OF HOT SPRINGS IN KEJIE FAULT AND CHANGNING-MENGLIAN STRUCTURAL BELT

BA, J. J. – LYU, Y.* – PAN, M. – ZHANG, Q. Y. – LIANG, B.

Institute of Karst Geology, CAGS/Key Laboratory of Karst Dynamics, MNR&GZAR
Guilin 541004, China

**Corresponding author*
e-mail: lvy@karst.ac.cn

(Received 18th Mar 2019; accepted 17th May 2019)

Abstract. To disclose the exact geochemical features of the hot springs in western Yunnan, China, this paper reviews the geological settings of Changning County, western Yunnan, and analyzes the geochemical features of local hot springs, which are controlled by Kejie Fault and Changning-Menglian (C-M) Structural Belt. On this basis, the author explored the isotopes of H, O, C, recharge source, recharge elevation circulation path and formation age of the geothermal flow, examined the main chemical process in the geothermal flow movement, especially in the mixing process, and determined the geochemical formation model and geological settings of the fault-controlled geothermal field in the research area. The results show that the hot springs are typical fault-controlled geothermal resources; the meteoric water is the main supply source of the hot springs; the hot springs are neither volcanic nor magmatic; despite the slight difference in activities and formation causes, the hot springs in both western and eastern parts of the research area were recharged by paleo-precipitation recharge before Late Pleistocene.
Keywords: *hot springs, isotopes, formation model, geothermal resources, western Yunnan, China*

Introduction

The world boasts huge reserves of geothermal energy, which promises efficient, stable power generation. If properly utilized, geothermal energy could promote energy conservation, reduce carbon emissions and mitigate global warming (Ahmadi et al., 2018; Ba et al., 2018; Mawarni et al., 2018). China is the second largest holder of geothermal reserves, most of which exist in tectonically active belts and large sedimentary basins (Wang et al., 2000; Guo, 2012). In general, there are abundant low-temeprature geothermal resouces in the uplift and subsidence areas of the continental crust, and some high-temperature ones across Yunnan and Tibet in southwestern China (Guo et al., 2013).

In the border areas between Tibet and Yunnan, the heat state of lithosphere has been shaped by the tectonically extrusion of the southeastern edge of Qinghai-Tibet Plateau since the Cenozoic era. The heat flow in this region far exceeds 70 mW/m^2, and peaks at 120.5 mW/m^2 in Tengchong, western Yunan Province, twice the global mean value (61.6 mW/m^2) (Du et al., 2005), revealing the typical geothermal features of a modern tectonically active area. The regional distribution of heat flow, especially that of abnormally high geo-temperature, is highly consistent with the pattern of deep faults.

The deep faults control the regional structure framework, affecting the formation and distribution of secondary structural belts. For example, the fault-controlled geothermal resources in western Yunnan possess the following features: large scale, shallow burial and high temperature (Mongillo, 2010; Ba et al., 2018). These faults also create a good

http://www.aloki.hu ● ISSN 1589 1623 (Print) ● ISSN 1785 0037 (Online)
DOI: http://dx.doi.org/10.15666/aeer/1704_90079024

condition for magma intrusion and convection (Edmunds, 2004; Olivier et al., 2011) and a passageway to the heat sources deep in the mantle, providing favorable paths for hot springs (Brown et al., 2003; Lachenbruch et al., 2013; Awaleh et al., 2015). In the said region, there are 139 hot springs with temperatures above 150°C, including 49 (35.3%) in western Yunnan. Many of them correspond with the hydrothermally active spots along the Kejie Fault and its secondary faults.

Over the years, some scholars have explored the distribution features, heat control mechanism and conformation model of Keijie Fault and the nearby Changning-Menglian (C-M) Structural Belt in western Yunnan (Wang et al., 2000; Guo, 2012; Ba et al., 2018). However, none of them has explained the exact geochemical features of the hot springs in this region, not to mention creating a conformation model of the local geothermal field.

To fill in these gaps, this paper reviews the geological settings of Changning County, western Yunnan, analyzes the chemical features of local hot springs, namely, hydro-chemical type, phase equilibrium, water-rock interaction, flow runoff and isotope features, and discusses about the isotopes of H, O, C, recharge source, supply elevation circulation path and formation age of the geothermal flow. In addition, the author examined the main chemical process in the geothermal flow movement, especially in the mixing process, and finally determined the geochemical formation model and geological settings of the fault-controlled geothermal field in the research area.

Materials and methods

Geological background

Located in Changning County, western Yunnan, the research area is high in the north and low in the south, with mountains and river valleys spanning in the north-south direction. In the west of the research area lies a U-shaped basin (elevation: 840~2,525 m) along the Kejie Fault, where the annual mean temperature is 19.5°C and the annual precipitation is 960 mm. In the eastern part, there is the Changning Basin (elevation: 1,562~2,525 m), where the climate is moderate and humid, the annual mean temperature is 14.9°C and the annual precipitation is 1,253.1 mm.

From the perspective of tectonics, the research area belongs to Baoshan Block, a part of the Yunnan-Burma-Thailand-Malaysia microplate, and falls between the C-M Structural Belt and the Yangtze Block (*Figure 1a*). The C-M Structural Belt is formed through the collision between two microcontinents within the remnant Paleo-Tethys Ocean realm. Despite the complex tectonics, the internal structure of the structural belt can be clearly identified (Xu et al., 2016).

Geological settings of Kejie Fault

Kejie Fault is an important fault in western Yunnan, controlling the sedimentation, metamorphism and magmatic activities since the Early Paleozoic era. The control effect is particularly prominent in Late Paleozoic Era. During the Lancang Orogeny, the fault appeared in the junction between Baoshan Block and C-M Structural Belt, and controlled the stratigraphic sedimentation for a longtime before the Permian era.

Kejie Fault consists of a primary fault and two secondary faults. The north-south primary fault spans 1,000 m in 20° east of north from Kejie Town to Kasi Town, and dips steeply towards the east by 60°~90°. The two secondary faults extend from north to

http://www.aloki.hu ● ISSN 1589 1623 (Print) ● ISSN 1785 0037 (Online)
DOI: http://dx.doi.org/10.15666/aeer/1704_90079024

northwest, and intersect the primary fault at acute angles. Numerous hot springs (S1~S7) are exposed along the two secondary faults (*Figure 1b*).

There is a 200~500 m wide breccia fracture zone within the Kejie Fault, as well as a north-south fold deformation zone in the northwest part. The metamorphic rocks are 90° ∠40° on the eastside, which intersects the fault at an acute angle. The Yanshanian acidic intrusive rocks are also deformed, becoming schistous and partly mylonitic. Many places of the fault are hidden under the Quaternary sediments, forming continuous gullies and beaded Cenozoic sedimentary basins with obvious neo-tectonic features.

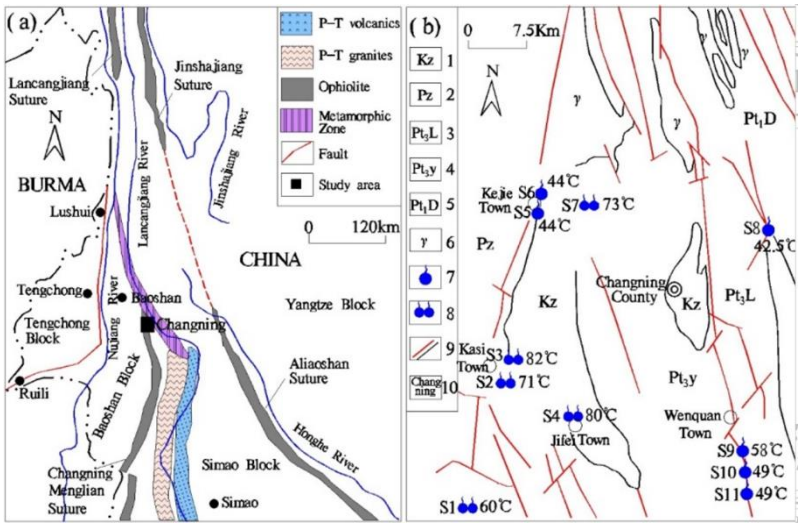

Figure 1. *(a) Geological sketch map of western Yunnan; (b) Hot springs*
Note: 1-Cenozoic Erathem; 2-Paleozoic Erathem; 3- Proterozoic Lancang Formation; 4-Proterozoic Yungou Formation; 5- Proterozoic Damenglong Formation ; 6-Granite; 7-Hot spring; 8-Group of hot springs; 9-Boundary of Fault and stratigraphic boundaries; 10-Changning County; S1: Kasihe Hot Spring Group; S2: Liangyuan Hot Spring Group; S3: Ganlanhe Hot Spring Group; S4: Jifei Hot Spring Group; S5: Dadi Hot Spring; S6: Suanxi Hot Spring; S7: Yudili Hot Spring Group; S8: Xiazhai Hot Spring; S9 Qingyunge Hot Spring; S10: Xiaoqiao Hot Spring; S11: chenjia Hot Spring

Geological settings of C-M Structural Belt

The 10~60 km-wide C-M Structural Belt runs through the research area from the northwest to the south. The belt has been shaped like a narrow wedge in the northwest, adjacent to Xiqianjie Fault and Baoshan- Zhenkang Block in the west, and bordered by Lancangjiang Fault and Yangtze Block in the east. Many hot springs are exposed along the belt in Wenquan Town, southern Changning County.

As a remnant of the C-M ocean basin, the belt mainly consists of Carboniferous metabasites, volcanic rocks, altered diabases and a few low-grade metamorphic siltstones. The rock stratum includes Proterozoic Damenglong Formation, Neoproterozoic Lancang Formation, Devonian Wenquan Formation, Devonian Pingzhang Formation, Devonian- Carboniferous Nanduan Formation and Permian Laba Formation. There are also a few acidic volcanic rocks of Triassic Huaimang Formation, molasses deposit of Triassic Sanchahe Formation, and clastic deposits in continental basins of Pliocene Mangbang Formation.

http://www.aloki.hu ● ISSN 1589 1623 (Print) ● ISSN 1785 0037 (Online)
DOI: http://dx.doi.org/10.15666/aeer/1704_90079024

Sample analysis

A total of 19 geothermal water samples were acquired from the research area, including 4 samples collected by delta δD, 4 by delta $\delta^{18}O$, 4 by $\delta^{3}H$, 2 by $\delta^{14}C$ and 5 by $\delta^{13}C$. All water samples were stored in low-density polyethylene bottles without any special pretreatment. Among them, $\delta^{3}H$, $\delta^{18}O$ and $\delta^{14}C$ samples were measured on a MAT253 isotope ratio mass spectrometer, and $\delta^{13}C$ samples on a stable isotope ratio mass spectrometer (SIRMS), with the aid of acid hydrolysis.

For hydro-chemical analysis of ions, the 50 mL polyethylene sampling bottles were filled up with $\delta^{3}H_{H2O}$ and $\delta^{18}O_{H2O}$ samples, to prevent the formation of bubbles. The cations (Ca^{2+}, Mg^{2+}, Na^{+}, and K^{+}) were analyzed on an AA-100 atomic absorption spectrometer, after super pure HNO_3 (1:1) had been added to the samples until the pH value fell below 2. The HCO_3^- was titrated by an alkalimeter with precision of 0.1 mmol/L, the pH of the water was determined by a WTW Multi3430 multiparameter meter with precision of 0.01. The anions (SO_4^{2-}, Cl^-, and NO_3^-) were measured through high-performance liquid chromatography.

All water samples were analyzed at the Institute of Karst Geology, Chinese Academy of Geological Sciences.

Results

The geothermal resources in the research area mainly exist in the fault zone amidst fold mountains. Most of them are of medium to low temperature. As shown in *Figure 1b*, the research area can be divided into Kejie Town area in the west (the western part) and Wenquan Town area in the east (the eastern part).

Geothermal control area in Kejie Fault

Geochemical features and formation conditions of the hot springs in Kejie Town area

As mentioned in Section 2, the geothermal sources in Kejie Fault are controlled by the primary and secondary faults. At the intersections between the faults, the clastic sediments in the Cenozoic depression provide a good thermal cover for the geothermal reservoirs. Several hot springs are exposed in the western part of the research area. Seven of them were selected for investigation. As shown in *Table 1*, the temperature of every spring is above 40°C (the temperature of the hottest spring: 90°C) and the total flow rate of these springs reaches 11.56 L/s (the flow rate of the fastest flowing spring: 3.42 L/s).

Table 1. *Flow rates and temperatures of the hot springs in the western part*

Area	Tepid hot springs				High temperature hot springs		Medium-high temperature hot springs		Low temperature hot springs	
	Spots	Flow rate (L/s)	High temperature (°C)	Low temperature (°C)	Spots	Flow rate (L/s)	Spots	Flow rate (L/s)	Spots	Flow rate (L/s)
Kejie Town	7	11.56	90	44	1	1.47	6	10.09	-	-
Wenquan Town	3	13.90	58	23	-	-	2	6.54	1	7.36

http://www.aloki.hu ● ISSN 1589 1623 (Print) ● ISSN 1785 0037 (Online)
DOI: http://dx.doi.org/10.15666/aeer/1704_90079024

Most of the water samples appear at the bottom of the Piper trilinear diagram of hydro-chemical ions (*Figure 2*). Obviously, the main cations in the water samples are Na^+, Ca^{2+} and K^+, and their contents differ from spring to spring. The water in S5 belongs to the Ca-Na type, with a high content of Ca^{2+}; the water in S3 belongs to the Na-K type, with greater-than-90% contents of Na^+ and K^+; the water in the other springs belongs to the Na-Ca type. The high content of Ca^{2+} in these hot springs can be attributed to the geothermal interaction between water and rock.

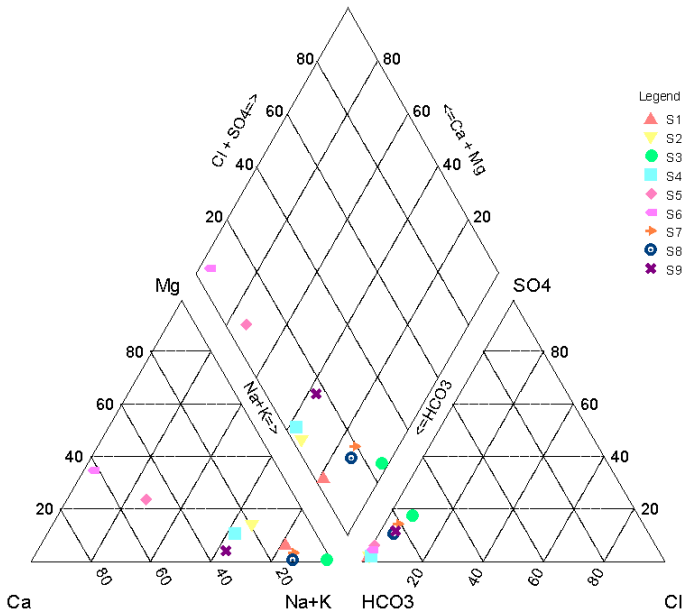

Figure 2. *The Piper trilinear diagram of hydro-chemical ions of the hot springs in the western part*

Since all samples appear at the bottom left of the Piper diagram on anions, HCO_3^- is the dominant anion in all the water samples. In particular, the HCO_3^- contents in S2 and S5 are over 90%, while those of Cl^- and SO_4^{2-} are below 10%. Of course, the springs differ in the exact content of HCO_3^-, due to the varied degrees of carbonate decomposition.

Below is a brief analysis of the ion contents in four of the seven hot springs: S2, S3, S4 and S7.

S2: This group of hot springs is located on the Kejie Fault, with a complete generation-reservoir-cover system. The reservoir stratum is the footwall in the west of the fault, which consists of broken quartz sandstone, siltstone of Xiangyangsi Formation, Lower Devonian Series (D_{1x}), while the cover stratum is the hanging wall of semi-consolidated conglomerate and argillaceous siltstone of Mangbang Formation Pliocene Series (N_2m). As shown in *Table 2*, HCO_3^- (973.75 mg/L) is the dominant anion in S2, accounting for 97.7% of anions in the spring water; other anions like Cl^- and SO_4^{2-} have a very low presence. Na^+ and K^+ are the main cations, taking up 74.84% of all cations in the spring water, while the Ca^{2+} content stands at 17.53%. Meanwhile, the total dissolved solid (TDS) is as high as 938.12 mg/L.

S3: On the north of Ganlahe valley, this group of 10 hot springs belongs to the Yungou Formation, Neoproterozoic Nanhua Series. This formation mainly consists of

http://www.aloki.hu ● ISSN 1589 1623 (Print) ● ISSN 1785 0037 (Online)
DOI: http://dx.doi.org/10.15666/aeer/1704_90079024

regional low-grade metamorphic rocks like sericite-phyllite. Under the intrusion of Cretaceous biotite adamellite, the rocks have partially evolved into thermal metamorphic hornfels. The formation is well developed, with a secondary joint parallel to the north-northwest fault. The total flow rate of S3 stands at 8.0 L/s (the flow rate of the fastest-flowing spring is 2.5 L/s), and the temperature at the spring mouths reaches 82°C (*Table 2*). The spring water is colorless and transparent, and belongs to the hydro-chemical type of HCO_3-Na+K, owing to the few travertines at the spring mouths.

Table 2(a). *Common hydro-chemical features of the hot springs in the western part*

Sample (No.)	T (°C)	Common Cation (mg/L)				
		K^+	Na^+	Ca^{2+}	Mg^{2+}	NH_4^+
Kasihe (S1)	60.0	28.1	254.0	35.8	11.7	1.10
Liangyuan (S2)	71.0	65.0	219.8	66.7	28.0	1.05
Ganlanhe (S3)	82.0	1.5	89.1	1.5	0.2	0.03
Jifei (S4)	90.0	20.3	162.4	65.6	14.9	2.65
Dadi (S5)	44.0	6.0	69.7	121.8	34.6	<0.02
Suanxi (S6)	44.0	1.4	4.1	75.4	25.4	<0.02
Yudili (S7)	73.0	9.1	111.6	13.4	2.2	3.23
Xiazhai (S8)	42.5	1.0	47.8	6.4	0.1	0.29
Qingyunge (S9)	58.0	11.0	129.2	63.0	4.4	1.94

Table 2(b). *Common hydro-chemical features of the hot springs in the western part*

Sample (No.)	T (°C)	Common anions (mg/L)						
		Cl^-	SO_4^{2-}	HCO_3^-	CO_3^{2-}	F^-	NO_3^-	NO_2^-
Kasihe (S1)	60.0	6.04	11.86	843.18	0	1.88	1.31	0.006
Liangyuan (S2)	71.0	9.13	11.17	973.75	0	0.86	1.27	0.034
Ganlanhe (S3)	82.0	5.55	16.15	91.24	25	20.73	1.09	0.010
Jifei (S4)	90.0	8.28	8.55	706.32	0	3.58	1.06	<0.002
Dadi (S5)	44.0	2.80	31.57	654.41	0	1.46	1.09	<0.002
Suanxi (S6)	44.0	1.49	11.97	335.07	0	0.73	2.22	<0.002
Yudili (S7)	73.0	9.75	37.23	270.57	0	12.80	1.06	<0.002
Xiazhai (S8)	42.5	2.30	5.89	62.92	31	3.94	1.07	<0.002
Qingyunge (S9)	58.0	16.62	50.11	471.93	0	5.55	1.06	<0.002

S4: This group of 18 springs is exposed in the valley and restricted by the northwestern fault, featuring a complete generation-reservoir-cover system. The reservoir stratum is mainly made up of volcanic rocks (dacite liparite) in the Triassic Manghuai Formation, while the cover stratum is semi-consolidated conglomerate and argillaceous siltstone of Pliocene Mangbang Formation (N_2m). The temperature of spring water falls between 42 and 80°C, and that of the hottest spring mouth reaches 90°C (higher than the local boiling point of water (*Table 2*).

S7: The geothermal resource in this group of springs is deep circulating and low in temperature, due to the well-developed, complex fault nearby. The stratum belongs to Yungou Formation, Neoproterozoic Nanhua Series, which encompasses regional low-

http://www.aloki.hu ● ISSN 1589 1623 (Print) ● ISSN 1785 0037 (Online)
DOI: http://dx.doi.org/10.15666/aeer/1704_90079024

grade metamorphic rocks like sericite-phyllite and mic schist. The spring group is exposed in the east-west secondary fracture, which is perpendicular to the main fault. The flow rate and temperature of S7 are respectively 3.42L/s and 73°C (*Table 2*). The spring water belongs to the hydro-chemical type of HCO_3-Na (*Table 2*), due to the thick travertines around the spring mouths. The TDS is 0.47 g/L, consisting of F, SiO_2, As, Mn, HPO_4, etc. Both H_2S and SiO_2 exist in the spring water, in which the SiO_2 content (124.52 mg/L) far exceeds the standard for mineral water.

According to the hydro-chemical features, the Schoeller plots of the hot springs in the western part were drawn on AquaChem (*Figures 3 and 4*). These plots show that the different ions have similar trend in content in the water samples of different hot springs. This means these springs are recharged by the same reservoir source and formed under the same conditions, forming similar fault-controlled geothermal resources.

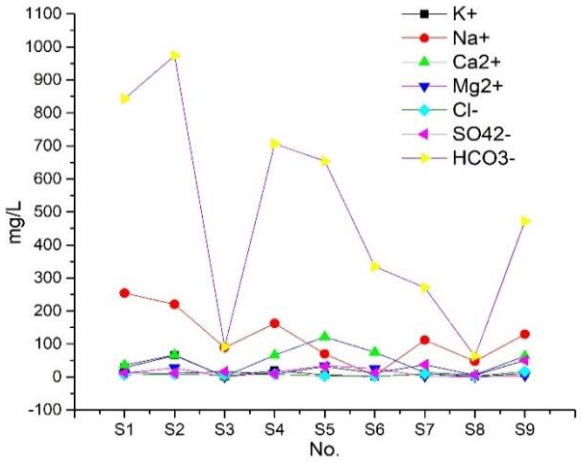

Figure 3. *Main ion contents of the hot springs in the western part*

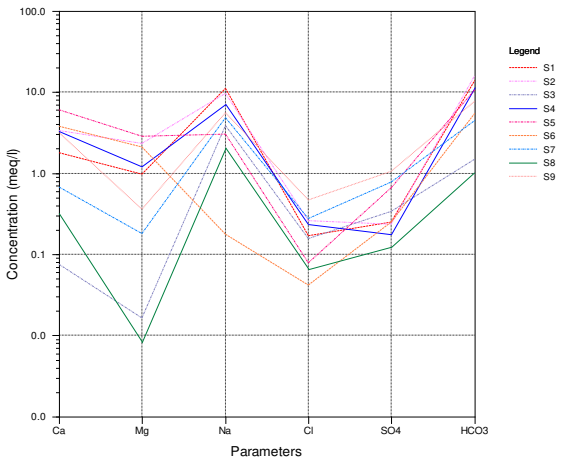

Figure 4. *Schoeller plots of the hot springs in the western part*

In addition, F^- anions were observed in the water of the hot springs in the western part. These anions are produced through the weathering of tourmaline, mica and apatite

http://www.aloki.hu ● ISSN 1589 1623 (Print) ● ISSN 1785 0037 (Online)
DOI: http://dx.doi.org/10.15666/aeer/1704_90079024

in geothermal reservoirs. The content of F^- in the spring water has many to do with the groundwater type, lithological features of surrounding rocks, degree of water-rock interaction and environmental temperature. The pH and flow temperature are the leading influencing factors of the content. As shown in *Figure 5*, the F^- content is positively correlated with the temperature of the exposed hot springs.

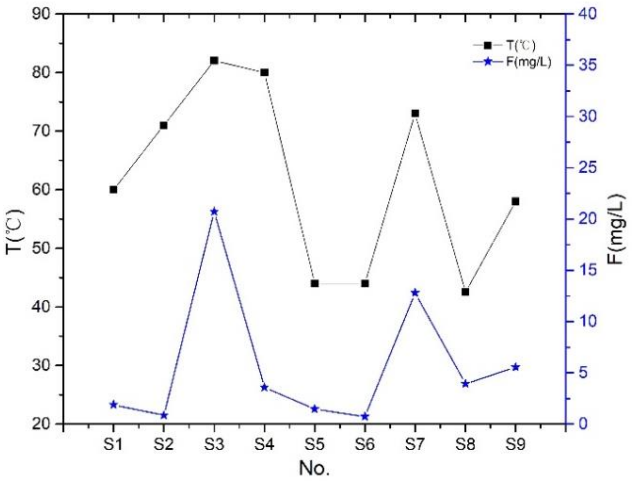

Figure 5. *Relationship between temperature and F− content of the hot springs in the western part*

Potential environmental impacts of the hot springs in the western part

The heavy metal contents of these hot springs were measured. The results show that the spring water enjoys an overall good quality, and can be exploited as geothermal resources. The contents of trace elements in the spring water are listed in *Table 3* below.

Table 3(a). *Trace elements of the hot springs in the western part*

Sample (No.)	Trace elements (mg/L)					
	Zn	Co	Mn	As	Hg	TFe
Kasihe (S1)	<0.002	<0.002	0.056	<0.002	<0.0001	0.014
Liangyuan (S2)	<0.002	<0.002	0.082	0.007	<0.0001	0.220
Ganlanhe (S3)	<0.002	<0.002	0.0022	<0.002	<0.0001	0.015
Jifei (S4)	<0.002	<0.002	0.046	<0.002	<0.0001	0.007
Dadi (S5)	<0.002	<0.002	0.011	0.014	<0.0001	0.110
Suanxi (S6)	<0.002	<0.002	<0.001	<0.002	<0.0001	0.005
Yudili (S7)	<0.002	<0.002	0.049	<0.002	<0.0001	0.016
Xiazhai (S8)	<0.002	<0.002	<0.001	<0.002	<0.0001	0.004
Qingyunge (S9)	<0.002	<0.002	0.026	0.004	<0.0001	0.120

It can be seen that the spring water has high contents of As, Mn, and Hg (2.0~14.0 μg/L, 11.0~82.0 μg/L and 0.1 μg/L, respectively). The As content in S5 (14.00 μg/L) hot springs is much higher than that (2.0~7.0 ug/L) in any other spring. This may be the result of the leaching after water-rock interaction.

http://www.aloki.hu ● ISSN 1589 1623 (Print) ● ISSN 1785 0037 (Online)
DOI: http://dx.doi.org/10.15666/aeer/1704_90079024

Table 3(b). *Trace elements of the hot springs in the western part*

Sample (No.)	Special Projects (mg/L)					
	SiO_2	Free CO_2	PO_4^{3-}	Hydrochemical types	Water hardness	pH
Kasihe (S1)	92.09	5.62	<0.02	HCO_3-Na·Ca	137.72	7.61
Liangyuan (S2)	48.26	7.49	0.07	HCO_3-Na·Ca	281.80	6.99
Ganlanhe (S3)	73.58	0.00	<0.02	HCO_3-Na	4.40	8.95
Jifei (S4)	70.37	9.37	<0.02	HCO_3-Na·Ca	224.95	6.67
Dadi (S5)	30.33	9.37	0.03	HCO_3- Ca·Na	446.70	6.64
Suanxi (S6)	16.02	5.62	<0.02	HCO_3-Ca	292.96	7.43
Yudili (S7)	117.22	3.75	<0.02	HCO_3-Na	42.49	7.70
Xiazhai (S8)	42.65	0.00	<0.02	HCO_3-Na	16.11	9.17
Qingyunge (S9)	89.97	5.62	<0.02	HCO_3·Cl -Na·Ca	175.41	7.31

Geochemical-chronological features of carbon, hydrogen and oxygen isotopes of the hot springs in the western part

The hot springs S2~S5 and S7 were subjected to isotopic analysis on $\delta D_{(V\text{-}SMOW)}$, $\delta^{18}O_{(V\text{-}SMOW)}$, $^3H_{(TU)}$, dissolved inorganic carbon $\delta^{13}C_{DIC(V\text{-}PDB)}$‰, particulate organic carbon $\delta^{13}C_{POC(V\text{-}PDB)}$‰ and dissolved organic carbon $\delta^{13}C_{DOC(V\text{-}PDB)}$‰. The results in *Tables 4 and 5* show that δD, $\delta^{18}O$ and ^3H fall in the ranges of −79.1~−84.2, −10.66~−11.76 and <2, respectively; the $\delta^{13}C_{DIC}$, $\delta^{13}C_{POC}$ and $\delta^{13}C_{DOC}$ fall in the ranges of −1.37~−4.24, −15.88~−27.08 and −24.62~−31.16, respectively; The $\delta D_{(V\text{-}SMOW)}$, $\delta^{18}O_{(V\text{-}SMOW)}$, $\delta^{13}C_{DIC(V\text{-}PDB)}$‰ and $\delta^{13}C_{POC(V\text{-}PDB)}$‰ average at −81.62, −2.32, −2.04 and −22.84, respectively. In addition, only S2 has a positive value of $\delta^{13}C_{DIC}$, as shown in *Figure 6*.

Table 4. *Isotopic test results on $\delta D_{(V\text{-}SMOW)}$, $\delta^{18}O_{(V\text{-}SMOW)}$ and $^3H_{(TU)}$ of the hot springs in the western part*

Name (No.)	$\delta D_{(V\text{-}SMOW)}$‰	$\delta^{18}O_{(V\text{-}SMOW)}$‰	^3H(TU)
Liangyuan (S2)	−82.1	−11.34	＜2
Ganlanhe (S3)	−82.5	−11.58	＜2
Jifei (S4)	−84.2	−11.26	＜2
Dadi (S5)	−79.1	−10.66	＜2

Table 5. *Isotopic test results on $\delta^{13}C_{DIC(V\text{-}PDB)}$‰, $\delta^{13}C_{POC(V\text{-}PDB)}$‰ and $\delta^{13}C_{DOC(V\text{-}PDB)}$‰ of the hot springs in the western part*

Name (No.)	Sample Type	$\delta^{13}C_{DIC(V\text{-}PDB)}$‰	$\delta^{13}C_{POC(V\text{-}PDB)}$‰	$\delta^{13}C_{DOC(V\text{-}PDB)}$‰
Liangyuan (S2)	water sample	1.37	−27.08	−24.62
Ganlanhe (S3)	water sample	−4.24	−15.88	−31.16
Jifei (S4)	water sample	−1.82	−26.69	-
Dadi (S5)	water sample	−3.45	−25.28	-
Yudili（S7）	water sample	−2.04	−19.27	−29.58

It can also be seen that the pH values of these hot springs range between 6.64 and 8.95 (*Table 3*); the dissolved inorganic carbon exists as HCO_3^-, such that the $\delta^{13}C_{DIC}$ value is basically the same as $\delta^{13}C_{HCO3^-}$.

http://www.aloki.hu ● ISSN 1589 1623 (Print) ● ISSN 1785 0037 (Online)
DOI: http://dx.doi.org/10.15666/aeer/1704_90079024

Furthermore, the S4 hot spring received ^{14}C isotopic dating (half-life period: 5,730 a), which puts its age at 16,510±1,600a. The result indicates that S4 received paleo-precipitation recharge before Late Pleistocene. The temperature of S4 can reach 90°C, an evidence of good geothermal property and a closed supply condition.

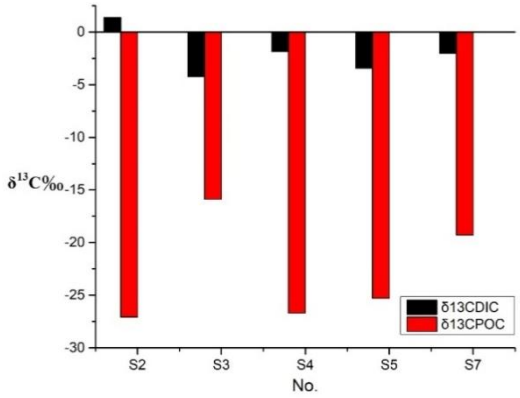

Figure 6. *$\delta^{13}C_{DIC}$ of the hot springs in the western part*

Geothermal control area in C-M Structural Belt

Geochemical features of hot springs in the eastern part

In the eastern part of the research area, the distribution of hot springs is mainly controlled by the C-M structural belt. The typical hot springs in this area are S8~S10. Here, S10 is selected as an example to analyze the geochemical features of hot springs in the eastern part of the research area.

The S10 spring group is exposed on the west side of the valley. The stratum mainly consists of sericite and marble in Pingzhang Formation, Carboniferous system (C_1pz). In terms of nappe structure, the stratum thrusts itself up the intermontane conglomerate and interbedded sandstone and mudstone of Triassic Sanchahe Formation (T_3sc). Thus, the underground geothermal water encounters the T_3sc layer and becomes exposed on the ground (*Figure 7*).

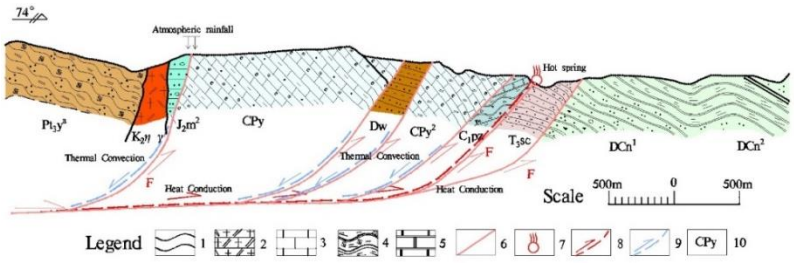

Figure 7. *Hydrothermal circulation of S10*
Note: 1-Schist; 2-Adamellite; 3-Limestone; 4-Slate; 5-Marble; 6-Fault; 7-Hot springs; 8-Geothermal water migration path; 9-Recharge water migration path; 10-Stratigraphic age

For the four-mouth spring group, the total flow rate stands at 11.9 L/s (the flow rate of the fastest flowing mouth is 2.3 L/s), and the temperature falls between 23 and 65°C. With pale yellow sulfur deposits and obvious H_2S gas around some mouths, the spring

http://www.aloki.hu ● ISSN 1589 1623 (Print) ● ISSN 1785 0037 (Online)
DOI: http://dx.doi.org/10.15666/aeer/1704_90079024

group belongs to the hydro-chemical type of HCO_3-Na·Ca, the TDS is 0.57 g/L. The contents of F^- and SiO_2 are 5 mg/L and 88.7 mg/L, respectively. In summary, the spring water of S10 fits in with the definition of mineral water.

Geochemical-chronological features of carbon, hydrogen and oxygen isotopes of the hot springs in the eastern part

The hot springs S8~S10 were subjected to isotopic analysis on $\delta D_{(V\text{-}SMOW)}$, $\delta^{18}O_{(V\text{-}SMOW)}$, $^3H_{(TU)}$, $\delta^{13}C_{DIC(V\text{-}PDB)}$‰, $\delta^{13}C_{POC(V\text{-}PDB)}$‰ and $\delta^{13}C_{DOC(V\text{-}PDB)}$‰. The results in *Tables 6 and 7* show that $\delta D_{(V\text{-}SMOW)}$, $\delta^{18}O_{(V\text{-}SMOW)}$ and $^3H_{(TU)}$ fall in the ranges of −78.1~−85.8, −10.76~−11.81 and < 2, respectively. The $\delta^{13}C_{DIC(V\text{-}PDB)}$‰, $\delta^{13}C_{POC(V\text{-}PDB)}$ ‰ and $\delta^{13}C_{DOC(V\text{-}PDB)}$‰ amount to −0.90~−9.26, −23.54 and −25.66~−28.90, respectively. These results are similar with those of the hot springs in the wester part, except for the smaller fraction of biogenic water. This means geothermal water in the eastern part circulates deeper than that in the western part.

Table 6. *Isotopic test results on $\delta D_{(V\text{-}SMOW)}$, $\delta^{18}O_{(V\text{-}SMOW)}$ and $^3H_{(TU)}$ of the hot springs in the eastern part*

Name (No.)	$\delta D_{(V\text{-}SMOW)}$‰	$\delta^{18}O_{(V\text{-}SMOW)}$‰	^3H(TU)
Xiazhai (S8)	−85.8	−11.81	＜2
Qingyunge (S9)	−78.1	−10.76	＜2

Table 7. *Isotopic test results on $\delta^{13}C_{DIC(V\text{-}PDB)}$‰, $\delta^{13}C_{POC(V\text{-}PDB)}$‰ and $\delta^{13}C_{DOC(V\text{-}PDB)}$‰ of the hot springs in the eastern part*

Name (No.)	$\delta^{13}C_{DIC(V\text{-}PDB)}$‰	$\delta^{13}C_{POC(V\text{-}PDB)}$‰	$\delta^{13}C_{DOC(V\text{-}PDB)}$‰
Xiazhai (S8)	−9.26	−23.54	−28.90
Qingyunge (S9)	−0.90	-	−25.66

In addition, the hot springs in the eastern part received ^{14}C isotopic dating (half-life period: 5,730 a), which puts their ages at 17,220±550a. The result indicates that the hot springs received paleo-precipitation supply before Late Pleistocene. The geothermal water circulated slowly and formed the springs before S4.

Discussion

Mixing features of hot water and cold water

The geothermal water is inevitably mixed with cold water as it rises to the surface. The fractions of cold water in S3, S4, S7 and S10 were computed, and recorded in *Figure 8*, where the ordinate value of the intersection between curves *X*t and *X*si stands for the theoretical fraction of cold water.

As shown in the figure, the cold-water fractions of S3, S4, S7 and S10 are 66%, 67%, 77% and 70%, respectively. Meanwhile, the temperatures of S3, S4, S7 and S10 are 175°C, 176°C, 250°C and 200°C, respectively. Hence, the cold-water fraction is positively correlated to temperature. Similarly, the cold-water fraction and temperature of S2 were computed as 53% and 130°C, respectively.

http://www.aloki.hu ● ISSN 1589 1623 (Print) ● ISSN 1785 0037 (Online)
DOI: http://dx.doi.org/10.15666/aeer/1704_90079024

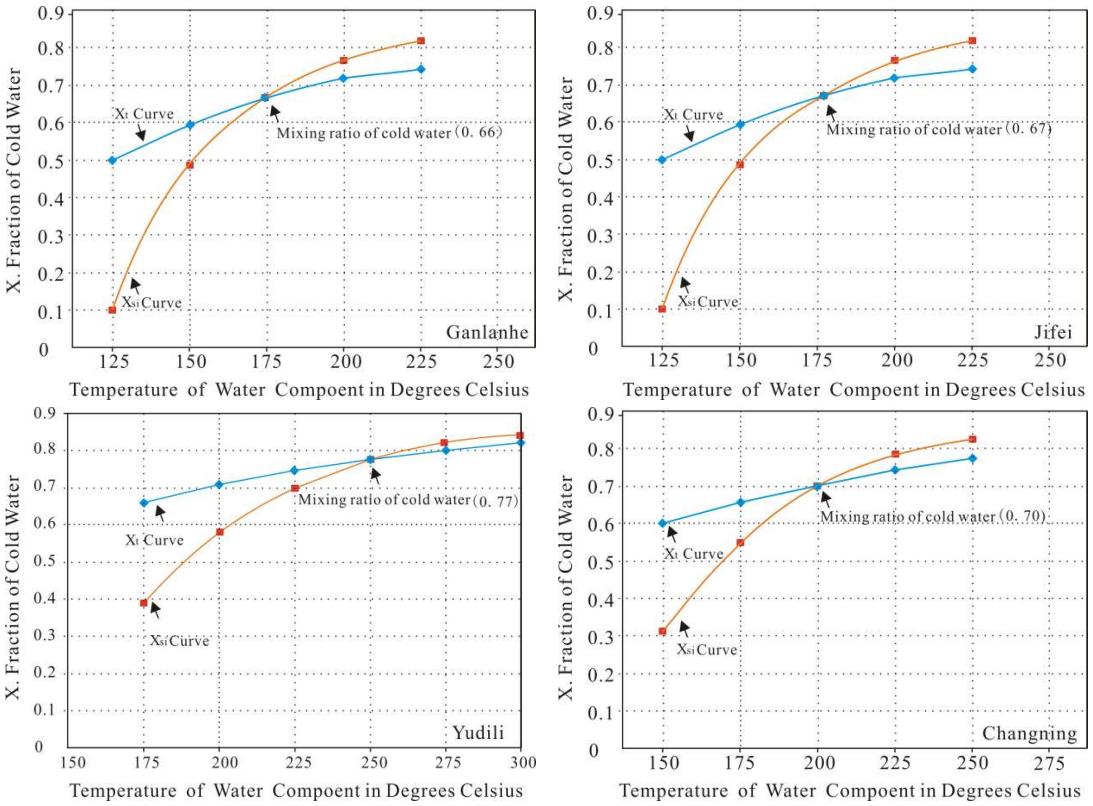

Figure 8. *The fractions of cold water in the hot springs (Transverse axis-°C; Vertical axis-%)*

Geochemical features of the hot springs

Oxygen isotope shift and water-rock interaction

The supply source of hot springs is generally determined through the comparison of global/local meteoric water line and H-O isotopes in the spring water (White et al., 2005; Dotsika et al., 2006; Han et al., 2015). The elevation effect of H–O isotopes can be used to calculate the recharge elevation of the hot springs, laying the basis for formation modelling of geothermal fields (Kose, 2007; Yamanaka et al., 2010).

Considering the conditions of the research area, δD and $\delta^{18}O$ can be adopted for the computation of the supply elevation. For high-temperature geothermal fields, the recharge sources are usually in remote or mountainous areas. Thus, the δD and $\delta^{18}O$ values of such fields are often lower than those of surface water and shallow groundwater (Zhou et al., 2009; Dotsika et al., 2010; Ba et al., 2018).

In view of the shift in $\delta^{18}O$ value (*Figure 9*) between the spring water and meteoric water line (*Table 1*), the author used *d*-excess = $\delta D - 8\delta^{18}O$ to calculate the exchange degree of $\delta^{18}O$. The *d*-excess of the hot springs in the research area is shown in *Figure 10*, where the line of *d*-excess = 10‰ is the global meteoric water line proposed by Craig in 1961 (Kim et al., 1997; Zuo et al., 2014; Ingvar, 2016). It can be seen that the *d* values of the hot springs mostly fall between the *d* = 0‰ line and the *d* = 10‰ line, and stay close to the latter line as compared to the former line.

The difference between the hot springs in the $\delta^{18}O$ shift can be explained by their difference in vaporization and the mixing features of hot water and cold water.

http://www.aloki.hu ● ISSN 1589 1623 (Print) ● ISSN 1785 0037 (Online)
DOI: http://dx.doi.org/10.15666/aeer/1704_90079024

The above results show that the $\delta^{18}O$ in the spring water equals that of meteoric water before shifting by 0.5~1.0%. Thus, the hot springs are recharged by meteoric water with $\delta^{18}O$ shifting, and the water-rock interaction conditions of the geothermal reservoir is relative closed. The significant isotope exchange in the hot springs can be attributed to the high temperature of geothermal reservoir and the long circulation distance (Fournier, 1977; Edmunds, 2004; Chandrajith et al., 2013).

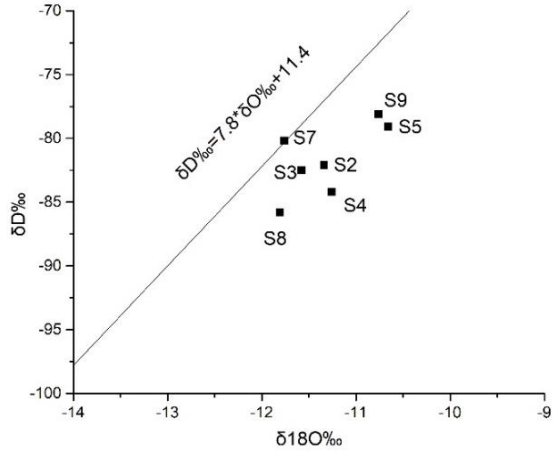

Figure 9. *The δD and $\delta^{18}O$ compositions of the hot springs*

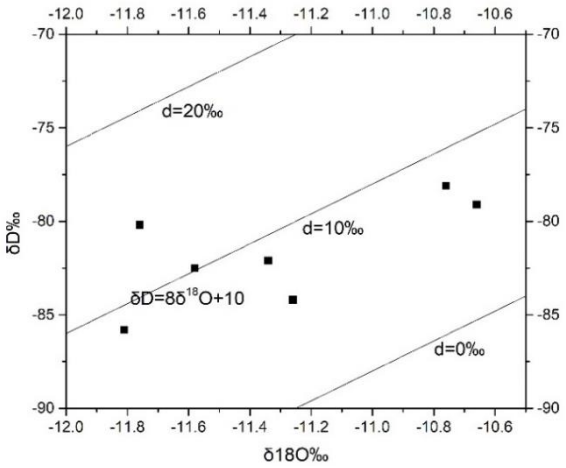

Figure 10. *The δD-$\delta^{18}O$ values of the hot springs*

According to the isotopic analysis, the δD and $\delta^{18}O$ values are close to meteoric water line. This means the hot springs agree with meteoric water in δD and $\delta^{18}O$ features. Besides, the lack of positive shift of $\delta^{18}O$ reflects a relatively low temperature of deep geothermal reservoir. Therefore, the hot springs are neither volcanic nor magmatic (Portugal et al., 2005; Chandrajith et al., 2013).

Considering the elevation effect of δD and $\delta^{18}O$, the groundwater elevation H (i.e. the height above sea level) can be defined as *Eq.1*:

$$H = (\delta_G - \delta_P) / k + h \quad \text{(Eq.1)}$$

http://www.aloki.hu ● ISSN 1589 1623 (Print) ● ISSN 1785 0037 (Online)
DOI: http://dx.doi.org/10.15666/aeer/1704_90079024

where h is the elevation of sampling point; δ_G is the $\delta^{18}O$ (δD) in the groundwater; δ_P is the $\delta^{18}O$ (δD) in the meteoric water around the sampling point; k is the elevation gradient of $\delta^{18}O$ (or δD) in the meteoric water (‰/100m). Using *Equation (1)*, the H values of hot springs in the research area were computed with K=−2.6‰/100m and δD =−63.5‰ (Xu et al., 2016).

The calculated results in *Table 8* show that the meteoric water is the main recharge source of the hot springs; the recharge elevation lies between 1,549 and 2,403 m (mean value: 1,921 m); the supply elevation is positively correlated with the elevation of the spring mouth; the values of $\delta^{18}O$ and δD are linearly correlated. To sum up, the exposed hot springs are a mixture of low-temperature shallow groundwater and high-temperature deep groundwater. This conclusion echoes with the results of the hydro-chemical analysis.

Table 8. *Elevation features of isotopic recharge area of groundwater in the research area*

Hot Spring No.	δD‰	$\delta^{18}O$‰	Spring Mouth Elevation	H (m)
S2	−82.1	−11.34	943	1658.38
S3	−82.5	−11.58	1096	1826.76
S4	−84.2	−11.26	1020	1816.15
S5	−79.1	−10.66	949	1549.00
S7	−80.2	−11.76	1311	1953.30
S8	−85.8	−11.81	1546	2403.69
S9	−78.1	−10.76	1683	2244.53

Temperature of geothermal reservoir

The temperature of geothermal reservoir can be measured by "geochemical thermometers", i.e. chemical contents and isotopes like SiO_2, Na-K, Na-K-Ca and $\delta^{18}O$ in sulphate (Zhang et al., 2008; Zhou et al., 2009).

Here, the Na-K-Mg triangular diagram is employed to judge if cationic geochemical thermometers are suitable for the hot springs (Giggenbach, 1988). As shown in *Figure 11*, all the water samples throng the corner of $Mg^{0.5}$, reflecting the high Mg^{2+} content in the samples and its impacts on the calculation of geochemical thermometers. Thus, SiO_2 geochemical thermometers are the best choice to calculate the temperature of our geothermal reservoirs.

In this way, it is learned that the geothermal reservoir temperatures of S2 and S5 are 100.1 and 79.8°C, respectively; the mean annual temperature in the research area is 19.5°C, with a geothermal gradient of 20 m/°C. Setting the annual constant temperature to 30 m, the SiO_2 geochemical thermometer without vapor loss T_1 and the chalcedony geochemical thermometer T_2 can be respectively calculated as *Eq.2* and *Eq.3*:

$$T_1 = 1309 / (5.19 - LgC_{SiO2}) - 273.15 \quad \text{(Eq.2)}$$

$$T_2 = 1032 / (4.69 - LgC_{SiO2}) - 273.15 \quad \text{(Eq.3)}$$

where T is the temperature of geothermal reservoir; C_{SiO2} is the mass concentration of SiO_2 (mg/L). According to the calculated results in *Table 9*, the temperatures of our

http://www.aloki.hu ● ISSN 1589 1623 (Print) ● ISSN 1785 0037 (Online)
DOI: http://dx.doi.org/10.15666/aeer/1704_90079024

geothermal reservoirs belong to the interval of 80~146°C, with the mean value of 111.8°C. Thus, there is a great potential for exploitation of geothermal resources in the research area.

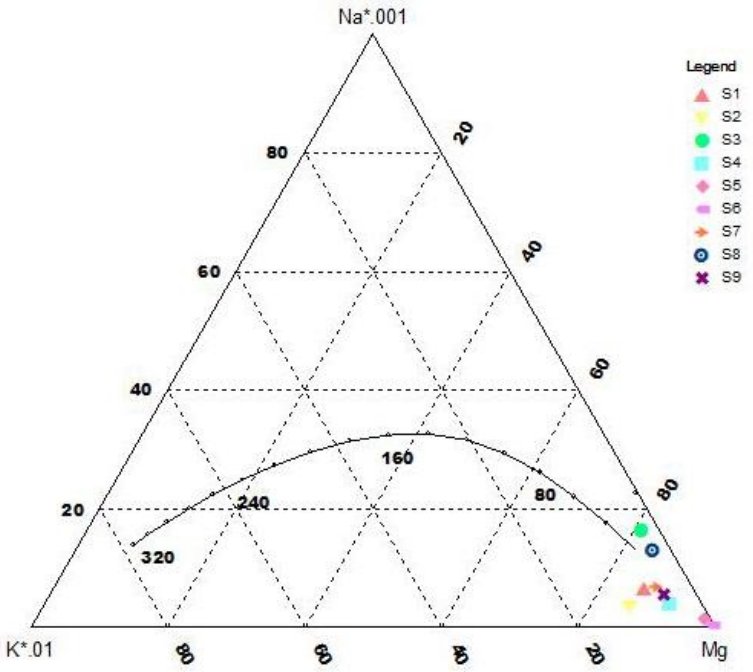

Figure 11. *Na-K-Mg triangular diagram of the hot springs*

Table 9. *Calculation results of geothermal reservoir temperature (°C)*

Sample	SiO_2 (mg/L)	Equation (2)	Equation (3)	Temperature
S2	48.26	100.16	70.11	71.0
S3	73.58	120.74	92.38	82.0
S4	70.37	118.45	89.89	80.0
S5	30.33	79.86	48.53	44.0
S7	117.22	146.26	120.59	73.0
S8	42.65	94.54	64.10	42.5
S9	89.97	131.37	104.06	58.0

Conclusions

The geothermal fields in the research area are controlled by the primary and secondary faults. At the intersections between the faults, the clastic sediments in the Cenozoic depression provide a good thermal cover for the geothermal reservoirs. The Kejie Fault controls the sedimentation, metamorphism and magmatic activities since the Early Paleozoic era. The control effect is particularly prominent in Late Paleozoic era. The C-M Structural Belt controls the distribution of geothermal resources in the eastern part of the research area.

The temperature of the hot springs in the research area can reach 90°C. The water of all the hot springs has good quality, belongs to the hydro-chemical type of HCO_3-Na,

http://www.aloki.hu ● ISSN 1589 1623 (Print) ● ISSN 1785 0037 (Online)
DOI: http://dx.doi.org/10.15666/aeer/1704_90079024

and shares the same recharge source and stable formation conditions. These hot springs provide typical fault-controlled geothermal resources.

The meteoric water is the main supply source of the hot springs; the recharge elevation lies between 1,549 and 2,403 m (mean value: 1,921 m); the recharge elevation is positively correlated with the elevation of the spring mouth; The cold-water fractions in S3, S4, S7 and S1 fall in the range of 66%~77%; the temperatures of our geothermal reservoirs belong to the interval of 80~146°C, with the mean value of 111.8°C, which are controlled by Kejie Fault and C-M Structural Belt.

In the hot springs, the dissolved inorganic carbon exists as HCO_3^-, and the $\delta^{13}C_{DIC}$ value is similar to the value of $\delta^{13}C_{HCO3}$−; the δD and $\delta^{18}O$ features are the same as those of meteoric water; the lack of positive shift of $\delta^{18}O$ reflects a relatively low temperature of deep geothermal reservoir, meaning that the hot springs are neither volcanic nor magmatic; the significant isotope exchange in the hot springs can be attributed to the high temperature of geothermal reservoir and the long circulation distance.

The ^{14}C isotopic dating shows that the hot springs in the eastern part and S4 are respectively aged 17,220±550a and 16,510±1,600a. The C-M Structural Belt has a longer groundwater circulation path than Kejie Fault. Despite the slight difference in activities and formation causes, the hot springs in both western and eastern parts of the research area were recharged by paleo-precipitation recharge before Late Pleistocene.

The geothermal resources have great potential for development in the study area. It is necessary to conduct deep drilling, evaluation and scientific research to identify the potential of resources and provide scientific basis for development and utilization planning.

The potential assessment of geothermal resources in the study area is still in a stable state. It is necessary to strengthen exploration, research and monitoring, accelerate the development and utilization of geothermal energy in deep fault zone, promote the release of energy in fault zone and reduce the risk of earthquake occurrence.

Acknowledgements. This research was supported by the National Key Research and Development Program of China (No. 2018YFC0604301), the Guangxi Natural Science Foundation (No.2018GXNSFAA294046, NO.2017GXNSFAA198208), the National key Research and Development Program of China (No.2017YFC0406104) and the Geological survey project of China (No. DD20190562).

REFERENCES

[1] Ahmadi, M. H., Ramezanizadeh, M., Nazari, M. A., Lorenzini, G., Kumar, R., Jilte, R. (2018): Applications of nanofluids in geothermal: A review. – Mathematical Modelling of Engineering Problems 5(4): 281-285.

[2] Awaleh, M. O., Hoch, F. B., Boschetti, T., Soubaneh, Y. D., Egueh, N. M., Elmi, S. A. (2015): The geothermal resources of the republic of djibouti – ii: geochemical study of the lake abhe geothermal field. – Journal of Geochemical Exploration 159(6): 129-147.

[3] Ba, J. J., Su, C. T., Li, Y. Q. (2018): Characteristics of heat flow and geothermal fields in Ruidian, Western Yunnan Province, China. – International Journal of Heat and Technology 36(4): 1203-1211.

[4] Ba, J. J., Su, C. T., Li, Y. Q. (2018): A case study on heat source mechanism of high-temperature geothermal field. – Annales de Chimie Science des Matériaux 42(1): 129-147.

http://www.aloki.hu ● ISSN 1589 1623 (Print) ● ISSN 1785 0037 (Online)
DOI: http://dx.doi.org/10.15666/aeer/1704_90079024

[5] Brown, K. L., Simmons, S. F. (2003): Precious metals in high-temperature geothermal systems in New Zealand. – Geothermics 32(4): 619-625.
[6] Chandrajith, R., Barth, J. A. C., Subasinghe, N. D., Merten, D., Dissanayake, C. B. (2013): Geochemical and isotope characterization of geothermal spring waters in sri lanka: evidence for steeper than expected geothermal gradients. – Journal of Hydrology (Amsterdam) 476(7): 360-369.
[7] Dotsika, E., Leontiadis, I., Poutoukis, D. (2006): Fluid geochemistry of the Chios geothermal area, Chios Island, Greece. – Journal of Volcanology and Geothermal Research 154(3-4): 237-250.
[8] Dotsika, E., Poutoukis, D., Raco, B. (2010): Fluid geochemistry of the methana peninsula and loutraki geothermal area, greece. – Journal of Geochemical Exploration 104(3): 97-104.
[9] Du, J., Liu, C., Fu, B. (2005): Variations of geothermometry and chemical–isotopic compositions of hot spring fluids in the Rehai geothermal field, southwestern China. – Journal of Volcanology & Geothermal Research 142: 243-261.
[10] Edmunds, W. M. (2004): Bath thermal waters: 400 years in the history of geochemistry and hydrology. – 200 Years of British Hydrogeology 225(1): 193-199.
[11] Fournier, R. O. (1977): Chemical geothermometers and mixing models for geothermal systems. – Geothermics 5: 41-50.
[12] Giggenbach, W. F. (1988): Geothermal solute equilibria. Derivation of Na-K-Mg-Ca bioindicators. – Geochimica et Cosmochimica Acta 52(12): 2749-2765.
[13] Guo, Q. H. (2012): Hydrogeochemistry of high–temperature geothermal systems in China: A review. – Applied Geochemistry 27(10): 1887-1898.
[14] Guo, S. Y., Li, X. J. (2013): Reservoir stratum characteristics and geothermal resources potential of Rongcheng uplift geothermal field in Baoding, Hebei. – Chinese Journal of Geology 48(3): 922-931.
[15] Han, K., Gan, F. P., Chen, Y. L. (2015): The structure characteristics and geological significance in the northern segment of Kejie Fault. – Progress in Geophysics (in Chinese) 30(1): 70-76.
[16] Ingvar, B. F. (2016): Geothermal energy for the benefit of the people. – Renewable and Sustainable Energy Reviews 3: 299-312.
[17] Kim, S. T., O'Neil, J. R. (1997): Equilibrium and nonequilibrium oxygen isotope effects in synthetic carbonates. – Geochimica Et Cosmochimica Acta 61(16): 3461-3475.
[18] Kose, R. (2007): Geothermal energy potential for power generation in Turkey: A case study in Simav, Kutahya. – Renewable and Sustainable Energy Reviews 11(3): 497-511.
[19] Lachenbruch, A. H., Sass, J. H. (2013): The stress heat-flow paradox and thermal results from Cajon Pass. – Geophysical Research Letters 15(9): 981-984.
[20] Mawarni, L. W., Maryanto, S., Nadhir, A. (2018): Magnetic method used in geothermal reservoirs identification in Kasinan-Songgoriti, East Java, Indonesia. – Environmental and Earth Sciences Research Journal 5(4): 87-93.
[21] Mongillo, M. A. (2010): Preface to geothermics special issue on sustainable geothermal utilization. – Geothermics 39(4): 279-282.
[22] Olivier, J., Venter, J., Jonker, C. S. (2011): Thermal and chemical characteristics of hot water springs in the northern part of the Limpopo province, South Africa. – Water SA 37(4): 427-436.
[23] Portugal, E., Sandoval, F., Barragan, R. M. (2005): Isotopic (δ18O,δD) patterns in Los Azufres (Mexico) geothermal fluids related to reservoir exploitation. – Geothermics 34(4): 527-547.
[24] Wang, G. L., Zhang, F. W., Liu, Z. M. (2000): An analysis of present situation and prospects of geothermal energy development and utilization in the world. – Acta Geoscientia Sinica 2: 134-139.
[25] White, P. A., Hunt, T. M. (2005): Simple modelling of the effects of exploitation on hot springs, Geyser Valley, Wairakei, New Zealand. – Geothermics 34(2): 184-204.

http://www.aloki.hu ● ISSN 1589 1623 (Print) ● ISSN 1785 0037 (Online)
DOI: http://dx.doi.org/10.15666/aeer/1704_90079024

[26] Xu, S. G., Ba, J. J., Chen, X. F. (2016): Predicting Strata Temperature Distribution from Drilling Fluid Temperature. – International Journal of Heat and Technology 34(2): 345-350.
[27] Yamanaka, T., Shimada, J., Hamada, Y. (2010): Hydrogen and oxygen isotopes in precipitation in the northern part of the North China Plain: climatology and inter-storm variability. – Hydrological Processes 18(12): 2211-2222.
[28] Zhang, G. P., Liu, C. Q., Liu, H. (2008): Geochemistry of the Rehai and Ruidian geothermal waters, Yunnan Province, China. – Geothermics 37(1): 73-83.
[29] Zhou, X., Fang, B., Zhou, H. Y. (2009): Isotopes of deuterium and oxygen–18 in thermal groundwater in China. – Environmental Geology 57(8): 1807-1814.
[30] Zuo, Y. H., Qiu, N. S., Hao, Q. Q. (2014): Present Geothermal Fields of the Dongpu Sag in the Bohai Bay Basin. – Acta Geologica Sinica (English Edition) 3: 915-930.

http://www.aloki.hu ● ISSN 1589 1623 (Print) ● ISSN 1785 0037 (Online)
DOI: http://dx.doi.org/10.15666/aeer/1704_90079024

HEAVY METAL POLLUTION CONTROL METHOD BASED ON CHEMICAL SOLIDIFICATION TECHNOLOGY

JIA, Q.

North China University of Water Resources and Electric Power, Zhengzhou 450000, China

Henan Engineering Research Center of Water Pollution and Soil Damage Remediation Zhengzhou 450000, China

Henan Key Laboratory of Water Environment Simulation and Treatment Zhengzhou 450000, China
(e-mail: jiamoney@126.com; phone: +86-1760-371-6888)

(Received 18th Mar 2019; accepted 17th May 2019)

Abstract. In view of the harm caused by sludge in the ecological environment, this paper adopts the solidification treatment technology based on the principle of environmental ecological effect to analyze the heavy metal pollution sources in sludge. With the aid of the solidification technology and considering the physical and chemical blocking effects of heavy metals, it analyzes the effect of the solidification technology in treatment of heavy metals at different ratios. The results show that the smaller the particle size, the better the leaching of heavy metals in the sludge; and that the leaching rate is higher under the acidic condition than under the alkaline one. Through research it is found that the impact of heavy metals in the sludge on the environment is influenced by two factors - the controlled distance and the time, so a model can be constructed to predict the migration parameters of heavy metals in the sludge according to the influencing predictors. Then based on the migration parameters, this paper introduces the inverse problem of pollution source control and the control method to optimize the problem. Through the above discussion, it proposes an environmental-effect-oriented heavy metal pollution control method, that is, optimizing the solidified materials by converting the source control problem to the inverse problem of capacity control. In this way, the concentrations of heavy metals in the sludge after solidification treatment can be effectively controlled to meet the requirements of environmental effects.
Keywords: *heavy metal pollution, ecological effect principle, heavy metal migration parameters, source control method, model prediction*

Introduction

Sludge is an inevitable product of sewage treatment and has a great impact on the environmental and ecological balance (Crivello, 2002; Zhang et al., 2018). The heavy metals, microorganisms and organic impurities attached to the forming process make the sludge treatment extremely complicated. According to statistics (Shukla et al., 2004), the amount of sludge accounts for about 2%-7% of the total treatment volume of sewage, and the annual investment and operating costs of sludge treatment account for 25%-30% and 25-40% of the sewage treatment costs, it takes a large part of the investment, for this reason, many scholars at home and abroad have carried out a lot of research on it, and have proposed the treatment methods and research ideas for the comprehensive utilization of sludge from different degrees. The research of many scholars has carried out meticulous research on it from the perspectives of reduction, stabilization, harmlessness and resource utilization, however, research on the comprehensive impact of heavy metals in sludge on environmental and ecological effects is still rare (Hong et al., 2014; Lee et al., 2014; Maati et al., 2018; Wang et al., 2018). Based on the principle of environmental ecological effects, Alvarez et al. (2002)

http://www.aloki.hu ● ISSN 1589 1623 (Print) ● ISSN 1785 0037 (Online)
DOI: http://dx.doi.org/10.15666/aeer/1704_90259034

started from an environmental perspective, applied the solidification technology to convert it into a process of non-flowability or solid formation, regardless of whether chemical bonding occurs between the waste and the curing agent, through the separation effect of this technology, they achieved the objective to control the harm of heavy metal to environmental pollution (Olier and Cosgrove, 2004), and improved the quality of the ecological environment.

Solidification technology uses cement to solidify the waste and cement the particles in the waste through the product of the cement hydration reaction (Yan et al., 2011; Zheng and Zhang, 2018). After solidification, the sludge forms denser blocks that have lower water permeability, so that the heavy metals existing in the form of oxides, hydroxides, insoluble salts, etc. in the sludge are continuously extracted and filtered out by adjusting the pH and Eh values of the sludge during the water treatment process. In this way, the harm of sludge is reduced (Nishioka et al., 2000). Based on the above theories, this paper adopts solidification technology to ensure the solidification conditions of heavy metal by changing the chemical and physical conditions of the solidified body, and based on this, it controls the heavy metal pollution control methods by discussing the control mechanism of heavy metals. This paper mainly discusses the control methods of two heavy metal elements Cu and Zn under the ecological effect conditions. The experimental study in this paper can effectively remove heavy metals in sludge and optimize sludge solidification effects and methods.

Materials and methods

During water treatment process, 50%-80% of the heavy metals in the sewage is concentrated in the sludge (Whanger, 2002; Georgieva, 2017). The solidification treatment technology is used to improve the properties of the sludge, making it a useful soil engineering material. The solidification technology mainly treats heavy metals in sludge, reduces the risk of metal leaching and its environmental hazard by reducing the water permeability of solidified sludge (Ying and Fang, 2006). Solidification technology reduces the impact of heavy metals on the environment through physical and chemical effects, the following passages will verify the solidification technology for the treatment of heavy metals in sludge by analyzing the principles and methods based on physical and chemical mechanisms.

Results

Physical blocking effect of solidification methods on heavy metals

This experiment took samples from typical sections from the upstream and midstream reaches of the Tianjin Beitang Sewage River and the Dagu Sewage River. In order to ensure the continuity and representativeness of the samples, the sampling was conducted respectively in the wet season, the normal season, and the dry season; and a total of 36 sets of samples had been taken. Then, the *Soil Physical and Chemical Analysis Method* was adopted to classify and test the collected samples, and the classified samples were subject to solidification process. The solidified sludge is dried and then crushed to different particle sizes, and sieved for classification. Then, X-ray diffraction (Japan Spv019) is used to analyze whether it will cause the destruction of the integrity of the organic matters in the solidified sludge, that is, whether there is a

http://www.aloki.hu ● ISSN 1589 1623 (Print) ● ISSN 1785 0037 (Online)
DOI: http://dx.doi.org/10.15666/aeer/1704_90259034

possibility of failure using physical method to treat the samples. Experimental method adopts the heavy metal leaching method: cement, sludge and water are arranged in a ratio of 1:2:5 and 2:2:5, respectively. For the heavy metal leaching experiment, at a soil-water ratio of 1:10, the samples with different particle sizes are mixed with the leaching solution, stirred, and shaken at different frequencies, then stand for more than 30 minutes, vacuum filtered, and use spectrophotometer (Beijing Ruili WFX130) to determine the concentration of Cu and Zn. The experimental results and data are shown in *Table 1*.

Table 1. *Relationship between solidified sludge particles and heavy metal leaching*

Particle(mm)	Cu leaching rate(%)		Zn leaching rate(%)	
0.06	18.8	16.8	27.8	25.8
0.09	17.2	14.9	24.2	22.9
0.52	13.8	12.7	18.8	16.7
0.65	10.7	9.6	15.7	14.6
0.82	8.5	7.3	10.5	9.3
2.5	5.2	3.8	8.2	7.8
3.8	3.1	2.2	6.8	6.2
7.2	1.5	0.7	5.2	0.7

Chemical blocking effect of solidification methods on heavy metals

The previous study shows that, the stabilizing effect of solidified sludge heavy metals is due to the pH of the solidified sludge itself, it produces an incompatible or complexing effect on heavy metals to enhance their stability. The chemical blocking experiment is mainly to clarify the buffering effect of the sludge on the environmental changes after solidification. It changes the influence of its own chemical properties on heavy metal leaching by setting the external acid-base environment. By setting the leaching solution with different PH value and Eh value, the leaching solution of this paper is prepared by using hydrochloric acid and sodium hydroxide solutions, and the designed experiment is carried out according to the experimental ratio method of the physical effect, and the final experimental data is shown in *Table 2* and *Figures 1-2*.

Table 2. *Leaching rate of heavy metals under different pH values*

PH	Cu leaching rate(%)			Zn leaching rate(%)		
1	73	45	25	82	45	38
2	46	32	15	67	32.8	28.8
3	32	19	11	45	28.7	23.9
4	28	13	8.7	31	21.8	18.7
5	16	7.6	7.7	22	17.5	17.8
6	8	6.2	6.2	13	13.4	12.9
7	6	5.6	5.5	8.7	11.7	11.8
8	5.6	4.8	4.7	6.3	8.9	7.9
9	5.2	3.2	2.8	4.7	5.3	4.2
10	4.6	2.8	2.7	7.8	7.2	7.1
11	3.8	2.4	2.2	10.2	9.8	10.3
12	2.2	1.9	1.7	12.4	12.3	12.4
13	1.8	1.4	1.5	14.5	13.7	13.9

http://www.aloki.hu ● ISSN 1589 1623 (Print) ● ISSN 1785 0037 (Online)
DOI: http://dx.doi.org/10.15666/aeer/1704_90259034

Through the study of solidification and leaching treatment of heavy metals by physical effects and chemical effects, the experimental results show that different particle sizes have different effects on solidification and leaching of heavy metals. The trend in *Figures 3-4* shows that, the leaching rate of particle size at different pH values first decreases and then increases, with the increase of particle size, the ratio of leached heavy metals shows a decreasing trend. The existing form of heavy metals largely determines the pH value, the trend in *Figures 1-2* shows that the chemical route for solidifying heavy metals is to change the external chemical conditions, and the leaching rate is higher when it is acidic.

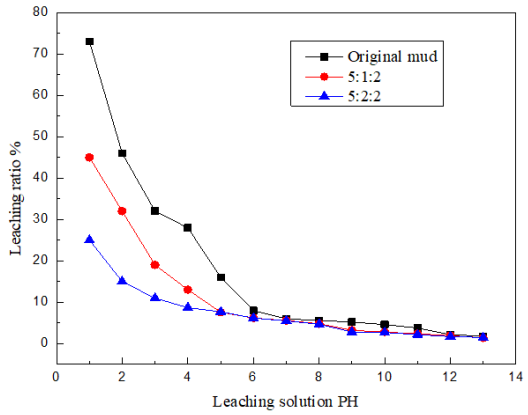

Figure 1. *Leaching rate of Cu under different PH solidified sludge*

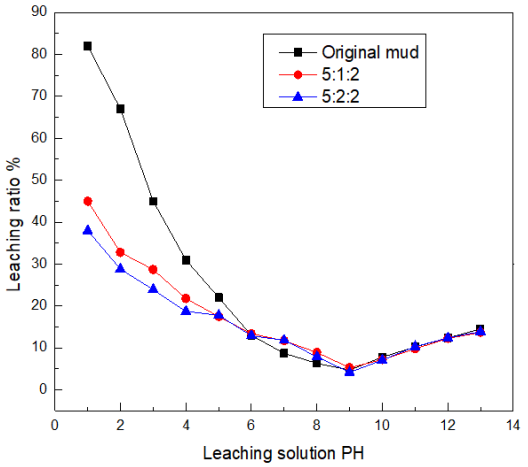

Figure 2. *Leaching rate of Zn under different PH solidified sludge*

Discussion

Prediction of heavy metal pollution in sludge

Assume after solidification, all the indicators of the sludge meet the standards of conventional soils (Xi-Shen et al., 2002), the model diagram of simulating the solidified sludge as the fill soil is as follows:

The mathematical formula of the above physical model is:

http://www.aloki.hu ● ISSN 1589 1623 (Print) ● ISSN 1785 0037 (Online)
DOI: http://dx.doi.org/10.15666/aeer/1704_90259034

$$Rd\frac{\partial C}{\partial t} = D_L\frac{\partial^2 C}{\partial x^2} + DT\frac{\partial^2 C}{\partial y^2} - Vx\frac{\partial C}{\partial x} - Vy\frac{\partial C}{\partial y} \quad \text{(Eq.1)}$$

where, C is the concentration of the substance, DL and DT are the vertical and horizontal dispersion coefficients, Vx and Vy are the flow rates in the X and Y directions, respectively. Using the above model and numerical method, the conditions of heavy metal sludge at different solidification levels are predicted (Philip et al., 2006), the prediction results are:

$$D_T = a_T\frac{V^2{}_x}{V} + a_L\frac{V^2{}_y}{V} \quad \text{(Eq.2)}$$

$$D_T = a_T\frac{V^2{}_x}{V} + a_L\frac{V^2{}_y}{V} \quad \text{(Eq.3)}$$

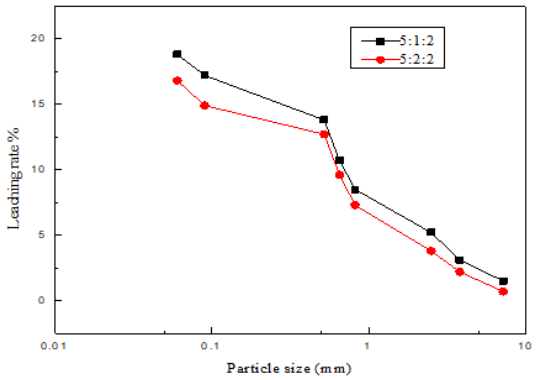

Figure 3. *Leaching rate of Cu under different particle size solidified sludge*

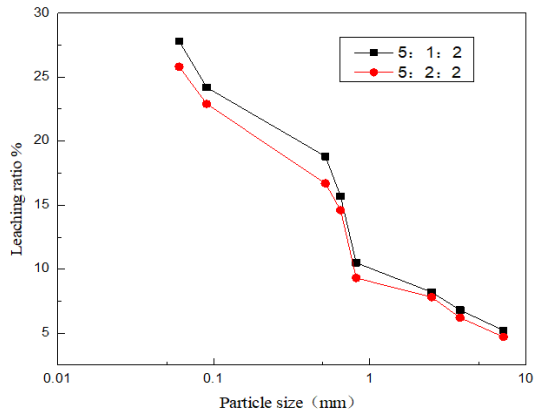

Figure 4. *Leaching rate of Zn under different particle size solidified sludge*

According to *Eq. (1) – (3)*, calculate and analyze the parameters of the experimental materials listed in *Table 3*, and conduct experimental data simulation and calculation for 10 to 200 iterations, the final calculation results are shown in *Table 4*.

http://www.aloki.hu ● ISSN 1589 1623 (Print) ● ISSN 1785 0037 (Online)
DOI: http://dx.doi.org/10.15666/aeer/1704_90259034

Table 3. *Experimental material parameters*

Material parameters	Slime	5:1:1	5:1:2	5:2:3	Surrounding medium
Permeability coefficient K(cm/s)	1.25×10^{-6}	7.23×10^{-7}	8.27×10^{-6}	3.58×10^{-6}	5.25×10^{-6}
Vertical dispersion a_l(cm)	0.031	0.065	0.081	0.105	87
Block coefficient R_d	8.92	11.5	12.6	14.1	6.9
Initial concentration C(mg/l)	5.314	4.365	4.187	3.789	0
Effective porosity n_e	0.356	0.423	0.463	0.321	0.75

Table 4. *Prediction of experimental data and results*

	Slime	5:1:1	5:1:2	5:2:3
10	4.25	4.16	2.89	2.72
20	4.11	3.91	2.69	2.45
30	3.89	3.79	2.22	1.89
40	3.65	3.35	1.78	1.37
50	3.25	3.05	1.58	1.09
60	3.12	2.82	1.07	0.89
70	3.08	2.48	0.75	0.68
80	2.98	1.98	0.48	0.51
90	2.76	1.74	0.32	0.31
100	2.12	1.32	0.15	0.12
110	1.78	1.18	0.06	0.03
120	1.43	1.03	0.04	0.01
130	1.22	0.92	0.02	-
140	0.89	0.69	-	-
150	0.74	0.34	-	-
160	0.42	0.12	-	-
170	0.31	0.031	-	-
180	0.14	0.014	-	-
190	0.08	0.008	-	-
200	0.02	0.002	-	-

Using above theoretical model and numerical method, the diffusion coefficient of the sludge to the environment was calculated by *Eq. (1), Eq. (2) and (3)* respectively measure the pollution degree of different coordinate directions, and predict the heavy metal pollution of solidified sludge of different solidification levels, and the prediction was conducted based on principle of heavy metal migration parameters. This paper took the variation characteristics of Zn as an example to investigate the pollution law of heavy metals to the environment. *Table 3* shows the parameters of the experimental materials.

According to the data in *Tables 3 and 4* and the prediction analysis schemes, it can be known that: (1) The influence of heavy metals in the sludge on environmental pollution gradually increases with time, and the untreated sludge has a much larger groundwater pollution range than the sludge after solidification treatment, and the concentration is higher than the concentration of the sample after solidification; (2) The release rate of heavy metals in the solidified sludge is much smaller than that of untreated sludge, and the released heavy metals will also be diluted by groundwater to reduce the harm to the environment; (3) With the improvement of the solidification level, the pollution of heavy metals to the environment is gradually reduced, and the pollution of heavy metals can be controlled by increasing the solidification level.

http://www.aloki.hu ● ISSN 1589 1623 (Print) ● ISSN 1785 0037 (Online)
DOI: http://dx.doi.org/10.15666/aeer/1704_90259034

Heavy metal migration parameters

Based on the prediction method and control mechanism (Weng et al., 2001; Dragana et al., 2016), the permeability curve of heavy metals in solidified sludge was measured by a flexible permeation meter to obtain the diffusion degree and permeation structure coefficient of two heavy metal elements of Cu and Zn. The test ratios are designed by changing the incorporation amount of cement and sludge, 5 ratios are set to perform the test, respectively are: 5:1:1, 5:1:3, 5:2:2, 5:3:2. According to the prediction results, the heavy metal concentration change values collected in different time periods are classified, and the maximum concentration value is taken as the initial concentration of heavy metals in the solidified sludge, and the calculated actual value of concentration is shown in *Table 5*.

The data in *Table 5* and the trends of *Figures 5-6* show that, the parameter results obtained based on the prediction are close the trend of heavy metals in the solidified sludge of the actual calculation result, so this test method can characterize the demand of the special pollutant parameters.

Table 5. *Concentration of heavy metals in different days under different cement / sludge ratios*

days	Zn migration concentration				Cu migration concentration			
	5:1:1	5:1:3	5:2:2	5:2:3	5:1:1	5:1:3	5:2:2	5:2:3
1	4.8	3.7	3.6	3.2	0.46	0.36	0.39	0.34
2	3.1	3.3	3.2	3.1	0.33	0.32	0.33	0.31
3	0.9	2.8	2.7	2.8	0.12	0.18	0.26	0.25
4	0.2	1.5	2.2	2.7	0.08	0.14	0.18	0.24
5	0.02	0.6	1.9	2.4	0.03	0.09	0.12	0.19
6	-	0.3	0.8	2.1	-	0.05	0.08	0.16
7	-	0.15	0.25	1.7	-	0.03	0.06	0.11
8	-	0.05	0.17	1.6	-	0.02	0.06	0.09
9	-	-	-	1.3	-	0.01	0.02	0.06
10	-	-	-	0.9	-	-	-	0.06
15	-	-	-	0.3	-	-	-	0.03
20	-	-	-	0.05	-	-	-	0.01

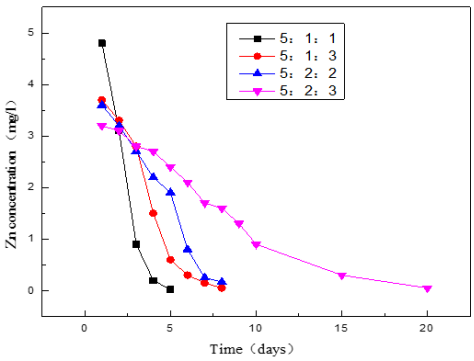

Figure 5. *Concentration migration of heavy metal Zn under different proportions and days*

According to Yao. et al. (2015) and the trend of *Figure 6* we can know that, the pollution intensity of solidified sludge to the environment is mainly determined by the

http://www.aloki.hu ● ISSN 1589 1623 (Print) ● ISSN 1785 0037 (Online)
DOI: http://dx.doi.org/10.15666/aeer/1704_90259034

migration rate of the metal. The migration rate of the metal is determined by the ratio of cement and sludge, the dispersion degree of the sludge, the retardation coefficient of the metal, and the flow rate, etc. The concentration of heavy metals changes significantly with the migration time. The migration trend of different ratios shows that the concentration migration of heavy metals is most closely related to the number of days in the initial experiment. The migration ability of heavy metals is concentrated in the first 1-2 days. After 5 days, it tends to be balanced or cannot be detected anymore. Different ratios indicate that the migration rate is greater than the diffusion degree. Therefore, when the heavy metal control method is involved, the retardation coefficient of the migration medium should be emphasized.

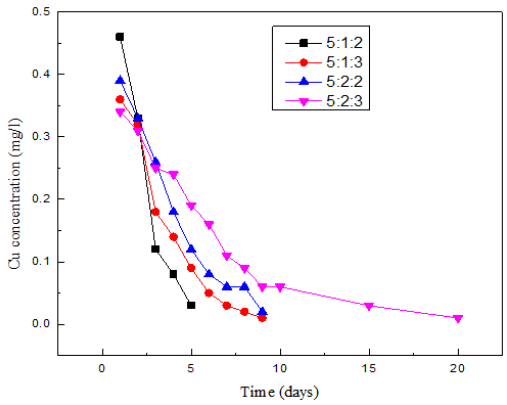

Figure 6. *Concentration migration of heavy metal Zn under different proportions and days*

Heavy metal pollution control method

It can be seen from the discussion that the pollutants contained in the sludge will inevitably enter the surrounding environment by penetrating into groundwater or surface runoff during the formation process, and the heavy metals is a potential danger source to the pollution of groundwater. The existing forms of heavy metals are mostly in a soluble state, and there are many hidden dangers of heavy metal pollution to the environment. According to the principle of environmental ecological effect, the theory of pollution source control reverse problem is used to investigate the concentration of metal in solidified sludge. (Yi et al., 2010) further discussed and optimized the solidified materials, and converted the problem of metal pollution control to the inverse and optimization problem of pollution source control.

To solve the inverse problem of the source item, we must first establish its mathematical model of the reverse source control (Plaia and Bondi, 2006), that is, select a calculation area, and use the solidified sludge as the filling material in the area, establish the model according to the prediction results of section 3.1, try to control the release of heavy metal concentration in the solidified sludge within the environmental tolerance range to meet the environmental capacity requirements.

In order to verify the above model, the solidified sludge sample is subjected to vacuum saturation treatment, and the concentration of heavy metals in the solidified sludge was determined by centrifugal separation method. After solidifying, vacuuming, and twice centrifugal separating, the concentration of heavy metals in pore water is detected, the results of repeated tests are tested for significance using regression

http://www.aloki.hu ● ISSN 1589 1623 (Print) ● ISSN 1785 0037 (Online)
DOI: http://dx.doi.org/10.15666/aeer/1704_90259034

equations, and the significant test results are consistent with predicted trends, therefore, the control method discussed above can control the pollution of heavy metals to the environment.

Conclusions

(1) The pollution control problem of heavy metals in solidified sludge can be transformed into source item control inverse problem and solidified material optimization problem. By quantifying the requirements of environmental capacity, we can limit the concentration of heavy metals in the solidified sludge. Through optimizing the solidification conditions and material parameters, we could obtain the pollution control scheme.

(2) Based on the principle of ecological environment effect, the sludge solidification treatment technology can measure the occurrence regularity of heavy metals by physical and chemical environment, and it can improve the leaching rate of heavy metals in the sludge, thereby improving the utilization effect of the sludge after solidification, so that it can meet the requirements of geomaterials.

(3) The control of heavy metal pollution is essentially a problem of source control, through centrifugation, separation and solidification technologies, we can control the pollution of heavy metals to the environment. The research results and methods of this paper can quantitatively reduce metal pollution by solidification technology and separation method.

Acknowledgements. Henan Science and Technology Project “Study on Biological Toxicity of Water Quality in Henan Province” (No.152102310343). Research Start up Fund of North China university of Water Resources and Electric Power (No:201621).

REFERENCES

[1] Alvarez, E. A., Mochón, M. C., Jiménez Sánchez, J. C., Ternero Rodríguez, M. (2002): Heavy metal extractable forms in sludge from wastewater treatment plants. – Chemosphere 47(7): 765-775.

[2] Crivello, J. V. (2002): Advanced curing technologies using photo-and electron beam induced cationic polymerization. – Radiation Physics & Chemistry 63(1): 21-27.

[3] Georgieva, V. (2017): Generalized net model of mechanical wastewater pre-treatment. – International Journal Bioautomation 21(1): 133-144.

[4] Hong, S., Khim, J. S., Ryu, J., Kang, S. G., Shim, W. J. (2014): Environmental and ecological effects and recoveries after five years of the hebei spirit oil spill, taean, korea. – Ocean & Coastal Management 102(275): 522-532.

[5] Lee, C. H., Lee, B. Y., Chang, W. K., Hong, S., Song, S. J., Park, J. (2014): Environmental and ecological effects of lake shihwa reclamation project in south korea: a review. – Ocean & Coastal Management 102: 545-558.

[6] Maati, A., Ouakdi, E. H., Tabourot, L., Balland, P., Demouche, M. (2018): Modelling of the thermomechanical behaviour of FCC metals under various conditions. – Annales de Chimie - Science des Matériaux 42(1): 115-127.

[7] Nishioka, M., Yanagisawa, K., Yamasaki, N. (2000): Solidification of sludge ash by hydrothermal hot-pressing. – Research Journal of the Water Pollution Control Federation 62(7): 926-932.

http://www.aloki.hu ● ISSN 1589 1623 (Print) ● ISSN 1785 0037 (Online)
DOI: http://dx.doi.org/10.15666/aeer/1704_90259034

[8] Oliver, B. G., Cosgrove, E. G. (2004): The efficiency of heavy metal removal by a conventional activated sludge treatment plant. – Water Research 8(11): 869-874.
[9] Philip, L., Lyengar, L., Venkobachar, C. (2006): Immobilised microbial reactor for heavy metal pollution control. – International Journal of Environment & Pollution 6(2-3): 277-284.
[10] Plaia, A., Bondi, A. L. (2006): Single imputation method of missing values in environmental pollution data sets. – Atmospheric Environment 40(38): 7316-7330.
[11] Shukla, V., Bajpai, M., Singh, D. K., Singh, M., Shukla, R. (2004): Review of basic chemistry of uv-curing technology. – Pigment & Resin Technology 33(5): 272-279.
[12] Wang, W., Zhang, K. F., Zhou, X. L., Wang, C. L., Huo, Z. K., Ye, P. F., Meng, X. Q. (2018): Deep reduction recovery of iron from copper slag. – Revue des Composites et des Matériaux Avancés 28(4): 539-549.
[13] Weng, L., Temminghoff, E. J., Riemsdijk, W. H. V. (2001): Contribution of individual sorbents to the control of heavy metal activity in sandy soil. – Environ.sci.technol. 35(22): 4436-4443.
[14] Whanger, P. D. (2002): Selenium in the treatment of heavy metal poisoning and chemical carcinogenesis. – Journal of Trace Elements & Electrolytes in Health & Disease 6(4): 209.
[15] Xi-Shen, Z., An-Huai, L. U., Xiang, G., Jin, Z., De-Sheng, Z. (2002): Contamination of heavy metals in soil present situation and method. – Soil & Environmental Sciences 11(1): 79-84.
[16] Yan, J., Fanyong, S., Nanwen, Z., Tingting, G. (2011): Experiments on solidification of sewage sludge with different solidifying agents. – Environmental Pollution & Control 33(2): 74-78.
[17] Yi, C., Li-Jiang, X., Xiao-Yong, Y. U. (2010): Identification method of rural environmental pollution and its application. – Journal of Agro-Environment Science 29(11): 2221-2227.
[18] Ying, X., Fang, Z. (2006): Experimental research on heavy metal wastewater treatment with dipropyl dithiophosphate. – Journal of Hazardous Materials 137(3): 1636-1642.
[19] Zhang, J. X., Sun, W. G., Niu, F. S., Wang, L., Zhao, Y. W., Han, M. M. (2018): Atmospheric sulfuric acid leaching thermodynamics from metallurgical zinc-bearing dust sludge. – International Journal of Heat and Technology 36(1): 229-236.
[20] Zheng, L., Xia, Z., Zhang, X. Y. (2018): Comparison between geopolymer reaction and cement hydration in solidification of fly ash generated in municipal solid waste incineration. – Revue des Composites et des Matériaux Avancés 28(3): 395-403.

http://www.aloki.hu ● ISSN 1589 1623 (Print) ● ISSN 1785 0037 (Online)
DOI: http://dx.doi.org/10.15666/aeer/1704_90259034

ENVIRONMENTAL EFFICIENCY ASSESSMENT AND DIFFERENCE ANALYSIS OF INDUSTRIAL CLUSTER DISTRICTS IN CHINA

LI, X.[1,2,3] – CAI, Q.[2] – YANG, X. Y.[2*]

[1]*Post-Doctoral Mobile Station of Theoretical Economics, Yunnan University, Kunming 650091, China*

[2]*Guizhou University of Finances and Economics, Huaxi University Town, Guiyang 550025, China*

[3]*Research Center for Technological Innovation, Tsinghua University, Beijing 100084, China*

**Corresponding author*
e-mail: 116993312@qq.com; phone: +86-187-9882-7991; fax: +86-0851-8851-0477

(Received 18th Mar 2019; accepted 17th May 2019)

Abstract. We used the Slacks-based Model (SBM) to calculate the environmental efficiency value of industrial cluster districts in China based on the panel data of 30 regions from 2007 to 2014, at the same time, in order to make a comparative analysis with the economic efficiency values not considering carbon emissions, the model presented by Banker, Charnes and Cooper (BCC) for estimating technical and scale inefficiencies in data envelopment analysis was used to calculate the environmental efficiency not considering the desirable output of carbon emissions, and we also analyzed the regional differences in China's environmental efficiency. The results showed that the environmental efficiency value of industrial cluster districts in China ranged between 0.83 and 0.94 not considering carbon emission, and it had a certain degree of reduction when considering the effect of undesirable output, maintaining values between 0.74 and 0.84, and which showed that there was much room for improving the environmental condition of the industrial cluster districts in China. Carbon emission had a great impact on the environment of China's industrial cluster, which resulted in a greater degree of efficiency loss. And it showed that the carbon emissions showed a great difference to the sensitivity degree of influence on regional environmental efficiency.
Keywords: *desirable output, undesirable output, carbon emissions, SBM model, economic efficiency*

Introduction

In recent years, several industrial clusters were built in China. Industrial cluster has made great contribution to the development of regional economy as a unique form of industrial organization. However, because of the large-scale converging of industry in the area, it has a greater impact on the regional resources, energy and ecological system, and this way of economic development with high resource consumption and high pollution emissions will directly lead to the high carbon emission. Under the background of low carbon economy and green development, the high carbon emissions seriously restrict the sustainable development of regional ecosystem, so it requires us to carry out theoretical and practical research on the environmental impact owning to the converging of industry. As a comprehensive index to evaluate the development of economy and environment, environmental efficiency is helpful to the decision makers to find out the problems in the process of the development of regional economic, and then put forward the effective measures through assessing the environment efficiency (Cheng et al., 2014). Therefore, it has important practical significance how to promote the low-carbon

http://www.aloki.hu ● ISSN 1589 1623 (Print) ● ISSN 1785 0037 (Online)
DOI: http://dx.doi.org/10.15666/aeer/1704_90359049

development of China's industrial cluster districts and improve its environmental efficiency under the background of low-carbon and green development.

In recent years, the domestic and foreign scholars have also made positive progress in the research of environmental efficiency, the research mainly focuses on four aspects: the concept of environmental efficiency, the measuring method of environmental efficiency, the regional difference of environmental benefits, and the influencing factors of environmental benefits. The domestic and foreign scholars have different views on the definition of environmental efficiency. Although there is no uniform definition of environmental efficiency, the formulation also has the difference between environmental efficiency and ecological efficiency, and the definition of the environmental efficiency by WBCSD is widely recognized and accepted. At present, the domestic and foreign scholars mainly use the methods of life cycle method, multi-criteria decision making method, stochastic frontier analysis, distance function method and data envelopment analysis (DEA). For example, Maxime et al. (2006) constructed an evaluation model of environmental efficiency by using the method of JWDEA and the directed distance function. Liu et al. (2011) applied the method of super efficiency DEA to assess the ecological efficiency and the regional ecological efficiency in China. Deng Bo used the model of two stages DEA to make an empirical research on the regional ecological efficiency of China. Wang and Wu (2011) used the data development analysis model to analyze and evaluate the environmental efficiency of China's provinces and cities, and analyzed the influence factors of industrial ecological efficiency by using the Tobit regression model. Wang et al. (2011) built an environmental efficiency measurement model of different process efficiency from the perspective of system integration. About the research of regional differences of environmental benefits, the domestic and foreign scholars have studied the industrial economic development of various districts in China from many aspects and angles. For example, Li (2012) used the SBM model to analyze the environmental efficiency of the Eastern region, central region and Western region in China. Wang et al. (2011) established the energy environment measurement model by using data envelopment analysis and directed distance function and used this model to study the environmental efficiency of China's provinces. Yang and Song (2011) studied the impact of environmental efficiency from three factors of system, regional and economic operating. Qi (2012) used the DEA Max model to study the environmental efficiency of the industry in Guangxi province. The influencing factors of environmental efficiency mainly focused on the international trade and foreign direct investment (FDI) in the early research. However, the speed of economic and social development is so fast that the factors which affect the environmental efficiency are also increasing. Charmondusit and Keartpakpraek evaluated the ecological efficiency from three indicators of material consumption, water use and hazardous waste. Yang et al. (2012) believed that the GDP, FDI, structural factors and the public's environmental awareness have different levels of impact on the environmental efficiency. Tan et al. (2013) used stochastic frontier analysis and beyond logarithmic production function model to assess the environmental efficiency of three provinces in Northeast China from 1991 to 2010. Fu et al. (2013) constructed the evaluation model of coal enterprise ecological efficiency by using the DEA method. Zhang (2013) evaluated and analysed the eco-efficiency based on panel data of Western China's Provinces 2000-2010. Gao (2014) used the Tobit model to analyze the influence factors and the degree of environmental efficiency of Guangdong province and the four major regions from 2000 to 2012. Rong (2015) evaluated the environment of Western in China and analyzed the influence factors of

http://www.aloki.hu ● ISSN 1589 1623 (Print) ● ISSN 1785 0037 (Online)
DOI: http://dx.doi.org/10.15666/aeer/1704_90359049

environmental efficiency under the carbon emission constraints. Li et al. (2017) analyzed the evolution of environmental regulation strategy among local governments and its impact on regional ecological efficiency in china.

In summary, the researches of environmental efficiency by domestic and foreign scholars have a theoretical summary and exploration of methods, especially the research field of its concept and evaluation, and they offered a certain foundation for our further research. However, from the research point of view, the research on the industrial level and regional level is few, and the research on the regional environmental efficiency of China's industrial cluster is still in a blank stage, at the same time, the research literature about the measurement of environmental efficiency under the constraint of carbon emission is relatively few. From the aspects of the research method, most of the literatures used the data envelopment analysis model, which leads to the distortion of efficiency evaluation. Therefore, we attempted to compensate the lack of the study above, and we used the panel data from 2010 to 2015 and estimated the environmental efficiency under the constraints of carbon emission by using the SBM model to find out the differences of the regional environmental benefits of industrial clusters.

Materials and methods

Research method and establishment of model

It can be seen from the above research, most scholars in previous studies took the environmental pollution as an input or a negative output, and used the DEA model to calculate the efficiency value which including environmental pollution, but it did not take into account the relaxation problem of input-output fully, and it distorted the efficiency of the evaluation object. So Cooper et al. (2007) put forward the SBM model of data envelopment analysis with non radial and non angle (Slacks-based Model), the model considered the slack problem of the input output caused by angle and radial selection as far as possible, it could not only overcome the shortcomings of the traditional model, but also it could effectively deal with the problem of excessive input and output, it reflected the essence of efficiency evaluation more compared with other models. At present, the domestic scholars have already begun to use the SBM model to calculate the environmental benefits in China, for example, Pan and Ying (2013) used the SBM model with non radial, non angle to calculate the agricultural ecological efficiency of China's 30 provinces, and gave the way to improve the efficiency of agricultural ecology. Tian et al. (2014) calculated the China's agricultural environmental efficiency for the 2002-2012 based on the SBM model. Rong (2015) used the SBM model to calculate and analyze the static environmental efficiency of the western region under the constraints of carbon emission in the western region in China from 2000 to 2012. Gao (2014) calculated the economic efficiency values of non-expected output factors without considering the constraints of carbon emission and environmental efficiency values of non-expected output factors with considering the constraints of carbon emission of four major regions in Guangdong province by using the BCC model and SBM-V model. Huang and Shi (2015) built a SBM model including R&D investment and calculated the environmental efficiency and the growth rate of the total factor of environment in China, and the influence factors of total factor productivity of regional environmental factors were analyzed by Tobit model based on the theory of R&D. Guo et al. (2015) used the non expected SBM model system evaluated the total factor energy efficiency of 28 provinces in China, and the spatial convergence of the

http://www.aloki.hu ● ISSN 1589 1623 (Print) ● ISSN 1785 0037 (Online)
DOI: http://dx.doi.org/10.15666/aeer/1704_90359049

provincial total factor energy efficiency was studied by using the spatial econometric model based on the economic geography distance weight. Therefore, the theoretical and empirical researches showed that it was feasible to use the SBM model to evaluate the regional environmental efficiency based on the non-expected output. Based on this, according to the actual situation of industrial cluster district in China, we also use the SBM model with non-expected value to calculate the environmental efficiency of China's industrial clusters region under the constraints of carbon emission.

Due to the SBM model is introduced by the literature above, so we introduce the model of this paper according to the research of Gao (2014) and Rong (2015). The SBM model assumes that there are *n* decision making units, each of which has input (which is expressed by m), expected output (which is expressed by s_1) and non-expected output (which is expressed by s_2), and the three vectors are expressed as $x \in R^m$, $y^g \in R^{s_1}$ and $y^b \in R^{s_2}$, so we can define the following matrix:

$$\begin{aligned} X &= [x_1, x_2, \ldots, x_n] \in R^{m \times n} \\ Y^g &= [y_1^g, y_2^g, \ldots, y_n^g] \in R^{s_1 \times n} \\ Y^b &= [y_1^b, y_2^b, \ldots, y_n^b] \in R^{s_2 \times n} \\ X > 0, Y^g &> 0, Y^b > 0 \end{aligned} \quad \text{(Eq.1)}$$

The production possibility set *p* of constant returns to scale can be defined as follows:

$$P = \left\{(x, y^g, y^b \mid x \geq \lambda X, y^g \leq \lambda Y^g, y^b \geq \lambda Y^b, \lambda \geq 0)\right\},\ \lambda \in R^n \quad \text{(Eq.2)}$$

The above set satisfies the following three assumptions:

(1) Undesirable output of environmental efficiency has the feature of weakly disposal: if $(y, b) \in P(x), 0 \leq \theta \leq 1$, so $(\theta y, \theta b) \in P(x)$ is satisfied, and this condition means that if you want to reduce the desirable output, it is necessary to reduce the desirable output.

(2) Desirable output has the feature of disposing freedom: if $(y, b) \in P(x)$ and $y^* \leq y$, so $(y^*, b) \in P(x)$ is satisfied. This condition means that expected output can be freely controlled, but the desirable output remains the same. In generally, it is not possible for the operational efficiency of the enterprise to achieve a reduction in desirable output without a corresponding reduction in output if sustained input.

(3) Desirable output and undesirable output have zero Union: if $(y, b) \in P(x)$ and b = 0, so y = 0 is satisfied. This condition means that there is undesirable output without the desirable output.

According to the above, the SBM model based on the undesirable output can be expressed as follows:

$$\rho^* = \min \frac{1 - \frac{1}{m}\sum_{i=1}^{m} \frac{s_i^-}{x_{i0}}}{1 + \frac{1}{s_1 + s_2}\left(\sum_{r=1}^{s_1} \frac{s_r^g}{y_{r0}^g} + \sum_{r=1}^{s_2} \frac{s_r^b}{y_{r0}^b}\right)} \quad \text{(Eq.3)}$$

http://www.aloki.hu ● ISSN 1589 1623 (Print) ● ISSN 1785 0037 (Online)
DOI: http://dx.doi.org/10.15666/aeer/1704_90359049

$$s.t.\begin{cases} x_0 = \lambda X + s^- \\ y_0^g = \lambda Y^g - s^g \\ y_0^b = \lambda Y^b + s^b \\ s^- \geq 0, s^g \geq 0, s^b \geq 0, \lambda \geq 0 \end{cases} \quad \text{(Eq.4)}$$

In the above formula, s is the slack variable of input and output, s^- and s^b represent the redundant of the input and the output, s^g expresses the deficiency of expected output, λ is the weight vector. The objective function ρ^* strictly monotone decreasing function of s^- and s^b, and $\rho^* \in (0,1)$. According to the research of Cooper et al. (2007), the loss of environmental efficiency can be decomposed into:

(1) Input redundancy

$$IE_x = \frac{1}{m}\sum_{i=1}^{m}\frac{s_i^-}{x_{i0}} \quad \text{(Eq.5)}$$

It means reduced proportion of input elements.

(2) Desirable output deficiency

$$IE_y = \frac{1}{s_1 + s_2}\sum_{r=1}^{s_1}\frac{s_r^g}{y_{r0}^g} \quad \text{(Eq.6)}$$

It means the expansion ratio of expected output.

(3) Undesirable output redundancy

$$IE_u = \frac{1}{s_1 + s_2}\sum_{r=1}^{s_2}\frac{s_r^b}{y_{r0}^b} \quad \text{(Eq.7)}$$

Selection of the research indexes and data sources

Owning to the environmental efficiency reflects the development of coordination status of resource conservation, environmental protection and regional economic growth. Therefore, we mainly consider the three factors during selecting the rating index of the environmental efficiency. The domestic and foreign scholars have conducted a lot of research about evaluation index of environmental efficiency at the current, based on the existing research on the input indicators and output indicators, and combining with the actual research object, the index selection and calculation methods in this paper are as follows:

(1) Input index

Energy input: It shows that how much energy is used in the process of development in the industrial clusters region. Because the total energy consumption statistics is not appeared yet in all provinces in China over the years, therefore, according to the research result of Guo et al. (2015) as well as the physical consumption of the main energy sources in each province and the conversion coefficient, the calculation method is as follows:

http://www.aloki.hu ● ISSN 1589 1623 (Print) ● ISSN 1785 0037 (Online)
DOI: http://dx.doi.org/10.15666/aeer/1704_90359049

$$E_{i,t} = \sum_{j=1}^{n} e_{i,t,j} \bullet c_j \quad \text{(Eq.8)}$$

Among them, $E_{i,t}$ represents the total energy consumption of the industrial cluster region i in t year, $e_{i,t,j}$ represents the energy j consumption of the industrial cluster region i in t year, c_j represents the conversion coefficient of energy j.

Capital input: In recent years, a large number of literatures have tried to estimate the stock of capital in China, and the different methods used by different scholars. Some scholars used the method of perpetual inventory, while some scholars used the annual average balance of net fixed assets as capital stock. Here, according to the research result of Rong (2015) and Zhang et al. (2004), we use the method of perpetual inventory to estimate capital stock. The basic formula is as follows:

$$K_t = I_t + (1-\delta)K_{t-1} \quad \text{(Eq.9)}$$

Among them, K_t represents the capital stock at time t, and K_{t-1} represents the capital stock at time $t-1$. I_t represents the amount of investment at time t, δ represents the depreciation rate. We take 2007 year for the initial years of the calculation, and take the total amount of fixed capital formation divided by 10% as the initial capital stock of provinces and municipalities in 2005 year, the formation total of annual fixed capital as the amount of investment, and we calculate the capital stock with of the depreciation rate (which is 9.6%).

Labor factor input: We take the annual average number of employees in the enterprises in the industrial cluster region as the labor input.

Land input: At present, different scholars have different represent ways, some scholars used the built area, some scholars used the area of crop planting and aquaculture, and some scholars used the area of cultivated land and construction land. Here, we use the built area as the evaluation index.

(2) Desirable output

We use the GDP of every industrial clusters region to show the expected output. And the GDP deflator is converted to the constant price GDP in 2007 as the base year.

(3) Undesirable output

In this paper, owning to we study the environmental efficiency under the constraint of carbon emission. Therefore, we choose the index of co_2 emission as the non-expected output. Because the statistics of carbon emissions of monitoring the various provinces and cities in China is not exist, therefore, according to the studies of Rong (2015), and the estimation method of IPCC national greenhouse gas emission inventory guide in the 2006, we take the sum of eight main sources of the product of energy consumption and the respective carbon dioxide emission factors to calculate the co_2 emission. Specific calculation formula is as follows:

$$m_{co_2} = \sum_{i=1}^{8} m_i \times QDW_i \times E_i \quad \text{(Eq.10)}$$

Among them, m_{co_2} represents the emission of co_2 (10000 t), m_i represents the energy consumption by end (10000 t, 100 million m^3), QDW_i represents low calorific value of

http://www.aloki.hu ● ISSN 1589 1623 (Print) ● ISSN 1785 0037 (Online)
DOI: http://dx.doi.org/10.15666/aeer/1704_90359049

various types of energy (KJ/Kg, KJ/m^3), E_i represents co_2 emission factors of various types of co_2 (Kg/TJ).

(4) Control variables

The regional energy efficiency is not only affected by the factors such as capital, labor and energy inputs, but also is related to the technological progress, regional industrial structure and other variables. According to the research of Guo et al. (2015), we select three control variables in this paper:

Investment of R&D: It is expressed by the value of the ratio of R&D investment to regional GDP in industrial cluster region. It represents the scientific and technological innovation of the regional enterprises and the technical progress of the industry, and the improvement of the production efficiency, and thus improving the overall environmental efficiency of the region.

Industrial structure: It is expressed by the value of the ratio of the second industry in the industrial clusters region to the GDP. Industry is the largest energy consumption in the three major industries, and the efficiency of the industry is relatively low, the greater the proportion may lead to the low efficiency of overall.

System variable: It is expressed by the value of the ratio of fiscal expenditure to GDP in industrial clusters region. The index reflects the government's interference extent to the regional economy, and it affects the regional environmental efficiency to a certain extent.

Data source description

The input-output data are derived from the years of "China Statistical Yearbook", "China Environmental Yearbook", "China Environmental Statistics Yearbook", "Chinese Energy Statistics Yearbook", "China Statistical Yearbook of science and technology", "China land and resources Yearbook", "IPCC national greenhouse gas emission inventory in 2006", and provincial Environmental Statistics Bulletin, and the composition of 2007-2014 in 30 provinces, autonomous regions and municipalities. Taking into account the consistency and availability of data, the panel data set of Tibet and Taiwan, Hongkong, and Macao are not included in the study. In addition, we still divide China into four regions of eastern, central, western and and northeast according to the traditional division method, which includes 11 provinces in the eastern region, 8 provinces in central region and including 11 provinces in western (Except Tibet) when we analyze the environmental efficiency of industrial cluster region.

Results and discussion

Overall environmental efficiency evaluation

We use the SBM model to calculate the value of China's industrial clusters region from 2007 to 2014, and in order to compare the efficiency environment with the situation which does not consider the carbon emissions, we use the BCC model to calculate the efficiency environment which not consider the carbon emissions. We use Matlab7.0 to calculate the economic efficiency and environmental efficiency. The value of environmental efficiency and economic efficiency of China's industrial cluster region from 2007 to 2014 in two cases are shown in *Table 1* and *Figure 1*. As we can see from *Table 1* and *Figure 1,* the environmental efficiency value of industrial cluster districts in China ranged between 0.83 and 0.94 not considering the carbon emissions and other

http://www.aloki.hu ● ISSN 1589 1623 (Print) ● ISSN 1785 0037 (Online)
DOI: http://dx.doi.org/10.15666/aeer/1704_90359049

undesirable output if we use the BCC model to evaluate the efficiency of economic growth of industrial cluster districts in China. But the efficiency of China's industrial cluster districts has a certain degree of reduction compared with before when we consider the effect of undesirable output, and the value ranged between 0.74 and 0.84, and they are not up to 1, it shows that there is much room to improve the environmental condition of the industrial cluster districts in China.

Table 1. *The value of environmental efficiency and economic efficiency from 2007 to 2014*

Year	Environmental efficiency value	Year	Economic efficiency value
2007	0.81	2007	0.94
2008	0.79	2008	0.90
2009	0.76	2007	0.86
2010	0.78	2010	0.87
2011	0.80	2011	0.91
2012	0.74	2012	0.83
2013	0.77	2013	0.85
2014	0.84	2014	0.9

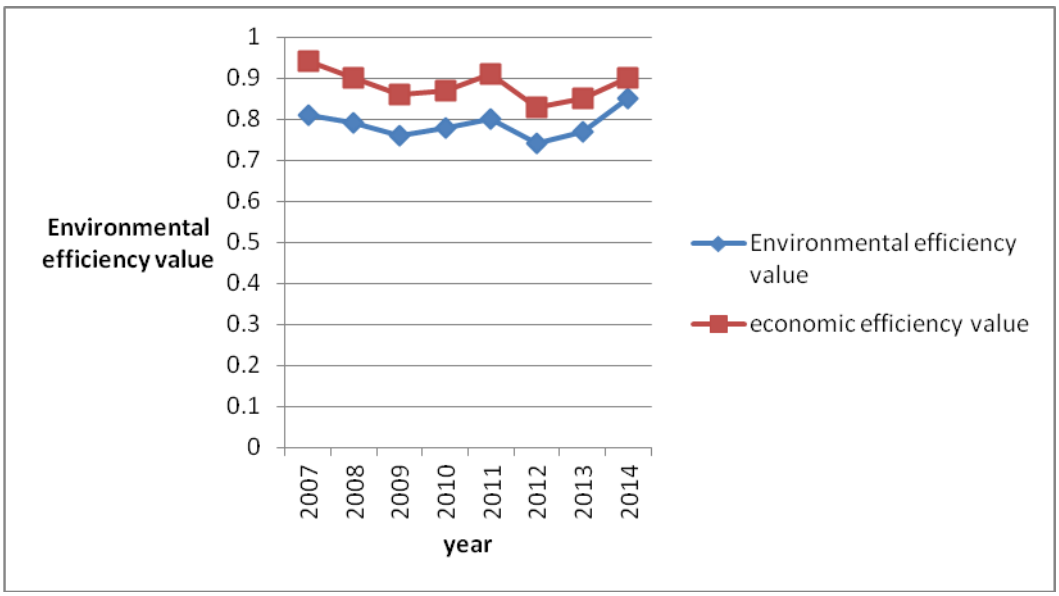

Figure 1. *Environmental efficiency value of carbon emission and not considering carbon emission from 2007 to 2014 years*

The result shows that the carbon emission has a great impact on the environment of China's industrial cluster, and it results in a greater degree of efficiency loss, so the carbon emission has become a problem that cannot be ignored in the environmental governance. It means that the efficiency evaluation is distorted in the case of non-expected output without taking into account the pollution discharge, and it also proves that using the SBM model to evaluate the efficiency of carbon emission is suitable, and this model improves the accuracy and credibility of the environmental efficiency evaluation in the presence. At the same time, from the perspective of the time

http://www.aloki.hu ● ISSN 1589 1623 (Print) ● ISSN 1785 0037 (Online)
DOI: http://dx.doi.org/10.15666/aeer/1704_90359049

dimension, the environmental efficiency value of China's industrial cluster region displays the style of "W" under the constraint of carbon emission in the sample range, and the change is relatively large. But they continue to narrow the gap, the main reason is that the government in China implemented the energy-saving emission reduction measures, and put forward the concept of ecological civilization construction, people's awareness of environmental protection had been enhanced.

Analysis on the difference of regional environmental efficiency

According to the general method of regional division, we take the four regions of the Eastern, Central, Western and Northeastern as the research unit in this paper. Also, we use the BCC model to calculate the economic efficiency value for the China's industrial clusters in Eastern region, Central region, Western region and Northeast region from 2007 to 2014 not considering the carbon emissions, and then we use the SBM model to calculate the economic efficiency value for the China's industrial cluster districts in Eastern, Central, Western and Northeast from 2007 to 2014 with considering the carbon emissions, and explore the difference and change features. Owning to the limited space and combine with the characteristics of the stage of China's regional economic development, we only show the results in 2008, 2010, 2012 and 2014 in *Tables 2* and *3*.

(1) Environmental efficiency of various regions of China's industrial cluster not considering carbon emissions. As we can see from *Table 2* and *Figure 2,* the average value of environmental efficiency of the Eastern region, the Central region, the Northeast region and the Western region from 2007 to 2014 is 0.806, 0.686, 0.959 and 0.571 from the perspective of regional, and the result is consistent with the conclusions of the existing literatures, and it means that the eastern region has achieved some results after transforming to the intensive economic growth mode with low consumption, low pollution and high efficiency. At the same time, it reflects a good phenomenon that the environment quality of traditional industry in underdeveloped areas will not be better than the development area, the economy of the eastern region in China is not only better than the central region, the northeast region and the western region, but also the environmental pollution control and to keep less pollution obviously are still better than less developed areas. In addition, the difference of environmental efficiency between the central region and the eastern region decreases with time, and the difference of environmental efficiency among the western region, the northeast region and the central region tends to increase, this result means that the west is in a very unfavorable situation in terms of environmental efficiency. In addition, the annual average value of the environmental efficiency of the eastern region changes relatively stable, while the annual average value of the central region, the northeast region and the western region change greatly from the change trend from 2007 to 2014.

From the level of provincial, the environmental efficiency of the developed areas in the eastern region such as Tianjin, Beijing, Jiangsu, Shanghai, Guangdong, Zhejiang, Shandong has been in the forefront in the above 8 years. The reason is that the modern industrial system which takes the modern service industry as the leading industry in the developed area of eastern region has been built to mature, and the energy consumption continues to decline, and the formulation and implementation of energy-saving emission reduction measures is also ahead of other regions. So it can be seen that changing the mode of economic development and promoting the optimization and upgrading of the industrial structure is very important to improve the efficiency of the regional environment. The lowest efficiency value is Shanxi Province where the coal industry as

http://www.aloki.hu ● ISSN 1589 1623 (Print) ● ISSN 1785 0037 (Online)
DOI: http://dx.doi.org/10.15666/aeer/1704_90359049

the core of the in the central region, and because the province ignored the development of technology in the process of industrial, so it results in inefficient use of resources and negative influence on environment efficiency. The environmental efficiency of under-developed areas in the western region such as Ningxia, Qinghai, Guizhou have been in the lag in the above 8 years, and it shows that the economic growth mode of the western region is still mainly extensive, and the economic development is relatively backward.

In summary, the environmental efficiency of China's industrial cluster regional is decreasing from coastal areas to inland and from east to west, and the differences of regional environmental efficiency presents the features of marginalization.

Table 2. *The environmental efficiency (not considered the carbon emissions)*

Province	2008	2010	2012	2014	Mean value
Beijing	1	1	1	1	1
Tianjin	1	1	1	1	1
Hebei	0.90	0.84	1	0.94	0.92
Hainan	0.96	0.93	0.91	0.97	0.935
Shanghai	1	1	1	1	1
Jiangsu	0.95	0.92	0.90	0.97	0.925
Zhejiang	0.96	0.91	0.90	0.98	0.928
Fujian	0.94	0.93	0.90	0.96	0.923
Shandong	0.93	0.91	0.88	0.95	0.91
Guangdong	1	1	1	1	1
Eastern average	0.964	0.944	0.949	0.979	0.959
Liaoning	0.75	0.70	0.65	0.80	0.675
Jilin	0.69	0.64	0.60	0.78	0.628
Heilongjiang	0.65	0.61	0.56	0.74	0.59
Northeast average	0.717	0.65	0.603	0.773	0.686
Shanxi	0.46	0.48	0.43	0.5	0.468
Anhui	0.9	0.92	0.94	0.95	0.926
Jiangxi	0.92	0.88	0.96	0.97	0.933
Henan	0.72	0.68	0.76	0.8	0.74
Hubei	0.86	0.88	0.90	0.91	0.886
Hunan	0.88	0.9	0.92	0.94	0.91
Central average	0.79	0.79	0.818	0.845	0.806
Inner Mongolia	0.56	0.58	0.53	0.6	0.568
Guangxi	0.65	0.7	0.74	0.8	0.723
Chongqing	0.99	0.96	0.98	0.95	0.97
Sichuan	0.71	0.75	0.79	0.84	0.773
Guizhou	0.32	0.36	0.31	0.37	0.34
Yunnan	0.58	0.60	0.64	0.68	0.625
Shanxi	0.57	0.59	0.62	0.65	0.608
Gansu	0.52	0.5	0.54	0.57	0.53
Qinghai	0.44	0.43	0.47	0.5	0.46
Ningxia	0.42	0.41	0.38	0.36	0.393
Xinjiang	0.43	0.4	0.41	0.45	0.423
Western average	0.563	0.571	0.535	0.615	0.571

http://www.aloki.hu ● ISSN 1589 1623 (Print) ● ISSN 1785 0037 (Online)
DOI: http://dx.doi.org/10.15666/aeer/1704_90359049

Table 3. *The environmental efficiency from 2007 to 2014 years (considering the carbon emissions)*

Province	2008	2010	2012	2014	Mean value
Beijing	1	1	0.96	1	0.978
Tianjin	1	0.94	0.95	1	0.956
Hebei	0.78	0.8	0.92	0.88	0.845
Hainan	0.92	0.87	0.84	0.88	0.878
Shanghai	1	0.95	0.94	1	0.953
Jiangsu	0.90	0.86	0.82	0.95	0.856
Zhejiang	0.90	0.87	0.84	0.98	0.873
Fujian	0.89	0.87	0.83	0.95	0.86
Shandong	0.88	0.83	0.82	0.94	0.843
Guangdong	1	0.94	0.96	1	0.956
Eastern average	0.927	0.893	0.888	0.958	0.917
Liaoning	0.68	0.6	0.55	0.7	0.583
Jilin	0.59	0.54	0.50	0.65	0.528
Heilongjiang	0.54	0.51	0.46	0.6	0.488
Northeast average	0.603	0.55	0.503	0.65	0.577
Shanxi	0.4	0.41	0.37	0.39	0.393
Anhui	0.8	0.82	0.84	0.85	0.828
Jiangxi	0.82	0.78	0.86	0.87	0.833
Henan	0.62	0.58	0.66	0.71	0.643
Hubei	0.76	0.79	0.80	0.82	0.793
Hunan	0.81	0.84	0.85	0.87	0.84
Central average	0.702	0.703	0.73	0.752	0.722
Inner Mongolia	0.46	0.48	0.43	0.5	0.468
Guangxi	0.55	0.6	0.64	0.7	0.623
Chongqing	0.88	0.86	0.89	0.9	0.883
Sichuan	0.61	0.65	0.69	0.74	0.673
Guizhou	0.22	0.26	0.21	0.27	0.24
Yunnan	0.48	0.50	0.54	0.58	0.525
Shanxi	0.47	0.49	0.52	0.55	0.508
Gansu	0.42	0.4	0.44	0.47	0.433
Qinghai	0.34	0.33	0.37	0.4	0.36
Ningxia	0.32	0.31	0.28	0.26	0.293
Xinjiang	0.33	0.3	0.31	0.35	0.323
Western average	0.462	0.471	0.484	0.52	0.484

It can be seen from *Figure 3* that the gap of the environmental efficiency value among the four major regions is still large. Compared *Figure 2* with *Figure 3,* we can know that the environmental efficiency value has a certain degree of reduction compared with not considering the carbon emissions. From the perspective of regional, carbon emission has a great impact on the differences degree of regional environmental efficiency. In the consideration of carbon emissions, we found that the environmental efficiency of the eastern region declined, but the change extent is slightly, however, the environmental efficiency value of the central region, the eastern region and the western

http://www.aloki.hu ● ISSN 1589 1623 (Print) ● ISSN 1785 0037 (Online)
DOI: http://dx.doi.org/10.15666/aeer/1704_90359049

region decreased significantly, and it also shows that the difference of sensitivity degree of the influence of carbon emissions on the regional environmental efficiency.

(2) The environmental efficiency of various regions of China's industrial clusters with considering the carbon emissions. In the case of considering carbon emissions, the trends of environmental efficiency in the four regions are shown in *Table 3* and in *Figure 3*.

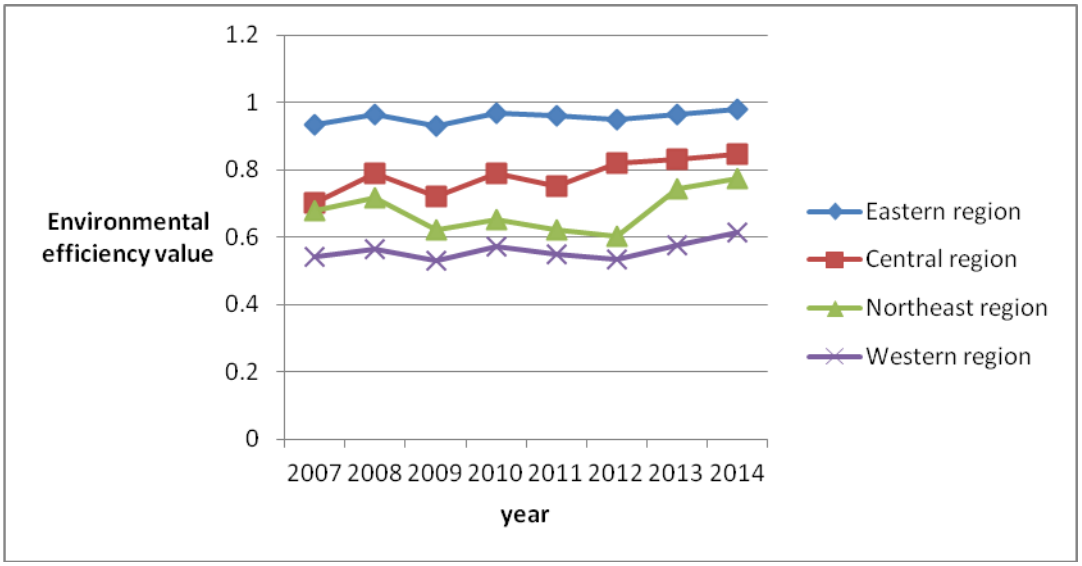

Figure 2. *Change trend of regional environmental efficiency not considering the carbon emissions*

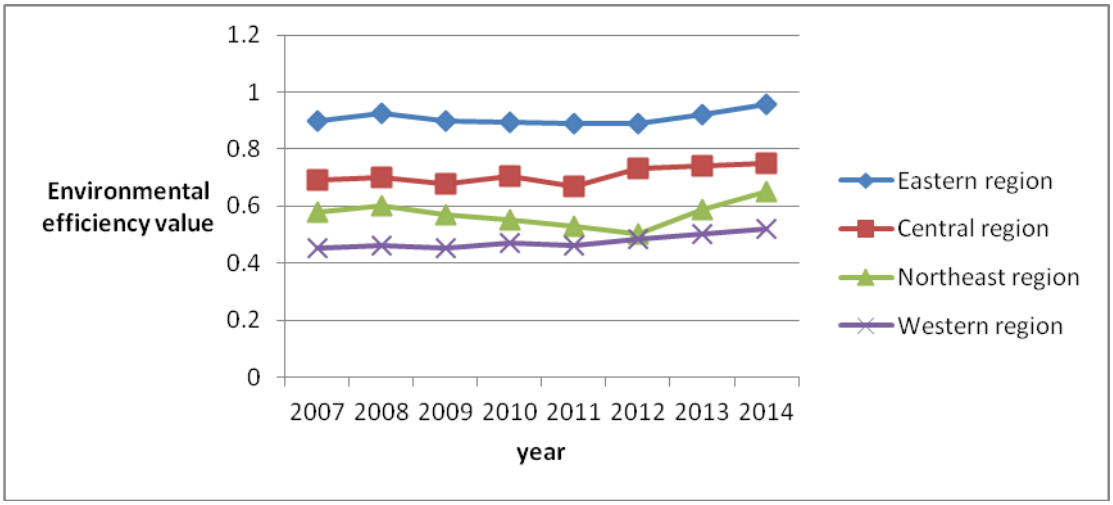

Figure 3. *Change trend of regional environmental efficiency with considering carbon emissions*

Conclusions

According to the above research, we get the main conclusions are as follows:

(1) The environmental efficiency value of industrial clusters region in China ranged between 0.83 and 0.94 without considering the carbon emissions and other undesirable output if we use the BCC model to evaluate the efficiency of economic growth of

http://www.aloki.hu ● ISSN 1589 1623 (Print) ● ISSN 1785 0037 (Online)
DOI: http://dx.doi.org/10.15666/aeer/1704_90359049

industrial cluster districts in China. But the efficiency of China's industrial clusters region has a certain degree of reduction compared with before when we consider the effect of undesirable output, and the value ranged between 0.74 and 0.84, and they are not up to 1, it shows that there is much room to improve the environmental condition of the industrial cluster districts in China.

(2) The environmental efficiency value of China's industrial cluster region display the style of "W" under the constraint of carbon emission in the sample range, and the change is relatively large. But the gap is becoming narrow continuously, the main reason is that the government in China implemented the energy-saving emission reduction measures, and put forward the concept of ecological civilization construction, people's awareness of environmental protection had been enhanced, but there exits occasional rebound phenomenon.

(3) The carbon emission has a great impact on the environment of China's industrial cluster, and it results in a greater degree of efficiency loss, and it also proves that the SBM model is suitable to evaluate the efficiency of carbon emission, and it improves the accuracy and credibility of the environmental efficiency evaluation.

(4) The results proved that the highest environmental efficiency is the eastern region, the worst environmental efficiency is the western region. In addition, the annual average value of the environmental efficiency of the eastern region changes relatively stable, while the annual average value of the central region, the northeast region and the western region change greatly. That is to say, the environmental efficiency of China's industrial cluster regional is decreasing from coastal areas to inland and from east to west, and the differences of regional environmental efficiency presents of marginalization.

(5) In the case of considering the carbon emissions, the gap among the eastern region, the central region, the northeast region and the western region is still relatively large, and compared with not considering the carbon emissions, the environmental efficiency value has a certain degree of reduction. From the perspective of regional, carbon emission has a great impact on the differences degree of regional environmental efficiency. In the consideration of carbon emissions, we found that the environmental efficiency of the eastern region declined, but the change extent is slightly, however, the environmental efficiency value of the central region, the eastern region and the western region decreased significantly.

Environmental efficiency evaluation is a relatively new issue. However, there are still some problems and shortcomings. Many work needs to be further studied and improved in the future.

(1) We can analyze the mechanism of location selection and product structure on environmental efficiency from the perspective of industry and enterprise.

(2) We can compare China's environmental efficiency with other countries in the world, and find out the gap between China and other countries.

(3) We can evaluate the total factor environmental efficiency under taking into account a variety of pollutants (such as CO_2, SO_2, COD), so we can better find the environment problems.

Acknowledgements. This article is funded by the National Social Science Fund Project (14CJY002), joint fund project of Ministry of Commerce and Guizhou University of finance and economics (2017SWBZD19).

http://www.aloki.hu ● ISSN 1589 1623 (Print) ● ISSN 1785 0037 (Online)
DOI: http://dx.doi.org/10.15666/aeer/1704_90359049

REFERENCES

[1] Cheng, J. H., Sun, Q., Guo, M. J., Xu, W. Y. (2014): Study on regional differences and dynamic evolution of China's ecological efficiency. – China Population, Resources and Environment 24(1): 47-53.
[2] Cooper, W. W., Seiford, L. M., Tone, K. (2007): Data Envelopment Analysis. Second Ed. – Kluwer Academic Publishers, Boston.
[3] Fu, L. N., Chen, X. H., Leng, Z. H. (2013): Urban agglomerations eco-efficiency analysis based on super efficiency DEA model: case study of Chang-Zhu-Tan "3+5" urban agglomeration. – China Population, Resources and Environment 23(4): 169-175.
[4] Gao, W. (2014): Study on the regional differences and influencing factors of industrial environmental efficiency in Guangdong province. – East China University of Science and Technology 4: 22-28.
[5] Guo, W., Sun, T., Zhou, P. (2015): Evaluation of regional total factor energy efficiency and its spatial convergence in China: based on an improved non-expected SBM model. – Systems Engineering 33(5): 70-74.
[6] Huang, Y. C., Shi, Q. P. (2015): Research on the regional environmental efficiency and environmental factors in China: analysis of the SBM model based on including R & D investment. – China Population, Resources and Environment 25(12): 25-29.
[7] Li, J. (2012): Study on Differences and Regulations of Environmental Efficiency in China. – Social Sciences Academic Press, Beijing.
[8] Li, X., Wang, Y., Li, C. L. (2017): Evolution of environmental regulation strategy among local governments and its impact on regional ecological efficiency in China. – Environmental Engineering & Management Journal 16(10): 2425-2433.
[9] Liu, B. Q., Li, L. M., Song, J. K. (2011): China Regional eco-efficiency measurement and difference analysis. – Techno-Economics and Management Research 10: 3-6.
[10] Maxime, D., Marcotte, M., Arcand, Y. (2006): Development of eco-efficiency indicators for the Canadian food and beverage industry. – Journal of Cleaner Production 14(6-7): 636-648.
[11] Pan, D., Ying, R. Y. (2013): Agricultural eco-efficiency evaluation in China based on SBM model. – Acta Ecologica Sinica 33(12): 3837-3845.
[12] Qi, H. Y. (2012): Study on Industrial Environmental Efficiency and Its Influencing Factors in Guangxi Province. – School of Economics and Management, Guangxi Normal University.
[13] Rong, J. B. (2015): Evaluation of environmental efficiency in China's western region under the constraint of carbon emission. – Zhejiang University 3: 18-29.
[14] Tan, X., Cao, Y. Q., Shi, L. (2013): A comparative study of environmental efficiency in three northeastern provinces: 1991-2010. – Productivity Study 4: 109-112.
[15] Tian, W., Yang, L. J., Jiang, J. (2014): Measurement and analysis of China's agricultural environmental efficiency under the perspective of low carbon: Based on the SBM model of the non-expected output. – The Observation of China's Rural 5: 59-62.
[16] Wang, E. X., Wu, C. Y. (2011): Study on the differences of spatial temporal for inter provincial ecological efficiency in China based on super efficiency DEA model. – Journal of Management Science 8(3): 443-447.
[17] Wang, K. L., Yang, B. C., Yang. L. (2011): Environmental efficiency measurement model and empirical study of interprovincial energy utilization in China. – Systems Engineering 29(1): 8-14.
[18] Yang, J., Song, M. L. (2011): Research on regional environmental efficiency of China under the vision of sustainable development: Based on the Super-SBM and panel data model. – Business Economics and Management 9: 57-62.
[19] Yao, Y. L., Jia, K. L., Wang, J. F., Feng, S. (2012): Space analysis on regional eco-efficiency based on DEA model: a case study for Ningxia Hui autonomous region. – Journal of Xinyang Normal University: Natural Science Edition 25(3): 324-328.

http://www.aloki.hu ● ISSN 1589 1623 (Print) ● ISSN 1785 0037 (Online)
DOI: http://dx.doi.org/10.15666/aeer/1704_90359049

[20] Zhang, J., Wu, G., Zhang, J. (2004): China's provincial material capital stock estimate of 1952-2000. – Economic Research Journal 10: 35-44.
[21] Zhang, X. M. (2013): The Evaluation and dynamic analysis of eco-efficiency: based on panel data of western China's provinces 2000-2010. – Economic Theory and Business Management 2: 78-85.

http://www.aloki.hu ● ISSN 1589 1623 (Print) ● ISSN 1785 0037 (Online)
DOI: http://dx.doi.org/10.15666/aeer/1704_90359049

PREVENTING SPONTANEOUS COMBUSTION OF COAL FROM DAMAGING ECOLOGICAL ENVIRONMENT BASED ON THERMOGRAVIMETRIC ANALYSIS

GUO, J.[1,2] – YAN, H.[1] – LIU, Y.[1,2*] – LI, S. S.[1]

[1]*School of Safety Science and Engineering, Xi'an University of Science and Technology Xi'an 710054, China*

[2]*Key Laboratory of Western Mine and Hazard Prevention, Ministry of Education of China Xi'an 710054, China*

[*]*Corresponding author*
e-mail: 18120089021@stu.xust.edu.cn

(Received 18th Mar 2019; accepted 17th May 2019)

Abstract. As a global disaster, spontaneous combustion of coal leads to a series of problems, like atmospheric pollution and geological damage, which seriously affects the ecological environment. Therefore, protecting the environment through the prevention of the spontaneous combustion of coal is necessary and worthy of further study. The spontaneous combustion of coal could be characterized by thermogravimetric (TG) characteristics. Thus, the TG test was performed to study the characteristics of non-caking coal during spontaneous combustion. The results show that the combustion process of coal mainly includes loss of water and weight, oxidation, thermal decomposition, combustion and burnout. Both heating rate and oxygen concentration can affect the combustion reaction process of coal. Heating rate is positively correlated with the combustion reaction time, characteristic temperature and oxidation reaction rate of coal. The higher the oxygen concentration, the shorter the combustion reaction time, the lower the characteristic temperature, the higher the oxidation reaction rate. The research results can provide certain theoretical basis for preventing coal spontaneous combustion, and be helpful for the protection of atmospheric environment.
Keywords: *environmental protection, coal fire, disaster prevention, non-caking coal, spontaneous combustion, TG-DSC synchronous analysis*

Introduction

Coal fire disasters spread all over the world. As a global disaster, spontaneous combustion of coal has caused huge environmental pollution and resource loss, seriously threatening the natural environment and safety production of coalmine (Tomescu et al., 2017). As a large coal country, China's coal resources still occupy a major position in the energy industry (Guo et al., 2018; Guo et al., 2019). However, in the process of resource utilization, a series of damages have been caused to the environment, coal fire disasters are often accompanied by secondary disasters, such as induction of gas explosion and dust explosion, and as a result, large amount of poisonous harmful gas and dust is released, causing pollution to atmosphere environment, endangering human health (Toropov et al., 2018; Benmenine and Bentebbiceh, 2018; Habib et al., 2019). Heavy metals produced by combustion will cause pollution to surface water and shallow groundwater, changes water quality and worsens water environment (Wei and Yu, 2017). In addition, coal fire disasters will cause a series of geological effects, leading to changes in geological structure and degradation of surface soil quality (Zeng et al., 2018), and seriously affecting ecological balance.

http://www.aloki.hu ● ISSN 1589 1623 (Print) ● ISSN 1785 0037 (Online)
DOI: http://dx.doi.org/10.15666/aeer/1704_90519064

By studying the mechanism of spontaneous combustion of coal, a lot of scholars have given a relatively clear explanation of the mechanism of spontaneous combustion of coal (Deng et al., 2016; Wen et al., 2017; Kong et al., 2017; Lu et al., 2018; Wang et al., 2018). Under the condition of high temperature and low oxygen concentration, the coal sample can continue to react and release a lot of heat to maintain the development of the fire area. During the development and evolution of the fire area, the heating rate of coal samples will decrease due to water evaporation and other reasons, but the overall trend is increasing (Jin et al., 2015). Studies have shown that TG and DTG curves of coal combustion reaction under low oxygen concentration are close to the high temperature zone, the ignition temperature is basically unchanged, the burnout temperature increases, and the combustion rate decreases (Wang et al., 2010). Ash, volatiles, moisture and other factors can affect the minimum ignition temperature of coal, and the minimum ignition temperature of coal with different degrees of metamorphism is different (Deng et al., 2014). Yi et al. (2014) compared the combustion characteristics of coal samples under the atmosphere of O_2/N_2 and O_2/CO_2 by using the TG analysis method, and found that the combustion performance of coal samples under the atmosphere of O_2/CO_2 was better. The higher the volatile content of coal, the more obvious the fluctuation of combustion parameters.

Research on the control of coalfire in the coal field and the mine have had a breakthrough, and effectively reduce the environmental pollution caused by spontaneous combustion of coal. However, factors affecting the spontaneous combustion process of coal are very complex, including external factors are and intrinsic factors (Liu et al., 2014). Under the action of different factors, the changing rules of characteristic parameters of the spontaneous combustion of coal appear different. Therefore, there are still many problems to be solved to prevent the spontaneous combustion of coal.

By using TG experiment method, the combustion characteristic of non-caking coal was studied under the conditions of different oxygen concentration and heating rate in this paper, to reveal the influence laws of the above dual factors on spontaneous combustion of coal. This study is helpful to the prevention and control of spontaneous combustion of non-caking coal, and is of great significance to reduce environmental pollution by saving fossil resources.

Materials and Methods

Selection and preparation of samples

In the experiments, the non-caking coal was selected from Shigetai Coal Mine. The central part of raw coal was taken out under the condition of nitrogen protection, and crushed to a particle size of 0.09-0.106 mm. Then, sealed and stored.

Experimental facility and principle

STA 449 F3 synchronous thermal analyser was adopted in the experiment, which mainly consists of sample holder, temperature programmable furnace, water bath and electronic computer.

According to the experimental principle, coal structure and environmental factors can directly impact the combustion process of pulverized coal. The TG-DSC synchronous thermal analysis experiment is to control the temperature and reaction atmosphere

http://www.aloki.hu ● ISSN 1589 1623 (Print) ● ISSN 1785 0037 (Online)
DOI: http://dx.doi.org/10.15666/aeer/1704_90519064

conditions by computer; as the temperature in the reaction atmosphere increases according to a certain gradient, the mass change of the pulverized coal can be obtained in real time; as the pulverized coal reaches the set temperature, the relationship between pulverized coal quality and temperature is obtained, i.e., the TG curve. The first-order differentiation of the TG curve can obtain the relationship between the change rate of the pulverized coal mass and the temperature, i.e., the DTG curve.

In the experimental method, the tested coal sample was placed on the top of the sample holder through a ceramic crucible, and directly connected to a precision thermo-balance. The precision thermo-balance can simultaneously measure the mass change of the sample and finally obtain the TG curve. The sample crucible and the reference crucible were placed on the top of the sample holder separately, and the thermocouple wire connected on both sides of the crucible can measure the temperature signals in real time. Then it was converted into the heat signal by temperature signal synchronization to finally obtain the DSC curve.

Experimental conditions

The experiments were conducted in the conductions: the STA 449 F3 synchronous thermal analyser used; the coal sample dosage of 10 mg; the temperature range between 30 -1000°C; the total gas flow rate controlled by software to 100 ml/min; the heating rates of 5, 10, 15°C/min respectively; the pulverized coal in the air atmosphere (21%, 13%, and 5% oxygen concentration).

Results

Thermal weight loss characteristics

TG/DTG curve characteristics

Figures 1-3 show the TG/DTG curves of non-caking coal powder at different oxygen concentrations and heating rates. It can be seen from *Figures 1-3* that the oxidative combustion process of pulverized coal can be divided into five stages, namely, the water and weight loss stage, the weight gain oxidation stage, the thermal decomposition stage, the combustion stage and the burnout stage.

(1) Loss of water and weight stage (30 -180°C)

As the temperature rises, in the initial stage of the pulverized coal, the gas trapped in the non-caking coal clearance is driven to escape from the powder. At the same time, the moisture of the powder also begins to evaporate by heat, which in turn leads to an increase in weight loss. In contrast, with the evolution of the combustion oxidation process of pulverized coal, the coal-oxygen combination gradually begins, making the powder quality increase with the decrease of water loss, and offsetting the initial water loss quality of pulverized coal. As the temperature increases continuously, this offsetting effect works more significantly until the pulverized coal quality reaches a minimum for the first time, indicating that the initial weight loss stage is terminated.

(2) Weight gain oxidation stage (180 -300°C)

Along with the continuous temperature increase, the active group of the pulverized coal powder released from heat is gradually increased, and then the consumption of oxygen is also increased. Most of the oxygen molecules participate in the coal-oxygen complex reaction (Ma et al., 2014), while those not participating in the oxidation reaction adhere to the surface of the pulverized coal molecules, which restricts the

http://www.aloki.hu ● ISSN 1589 1623 (Print) ● ISSN 1785 0037 (Online)
DOI: http://dx.doi.org/10.15666/aeer/1704_90519064

smooth release of the gas in the combustion products, and increasing the quality of the pulverized coal in a short time.

(3) Thermal decomposition stage (300 -410°C)

At this stage, the quality of pulverized coal is macroscopically expressed as weight loss again. The reactive functional groups in the pulverized coal molecules are released, in which the aromatic ring nucleus and other groups are largely broken. Then, the active structure that has not participated in the oxidation reaction in the previous stage also begins to bind oxygen molecules to produce CO, CO_2, and H_2O (g) etc. Besides, the pulverized coal itself desorbs due to the temperature increase and produce volatiles, resulting in a more decrease in the quality of the pulverized coal.

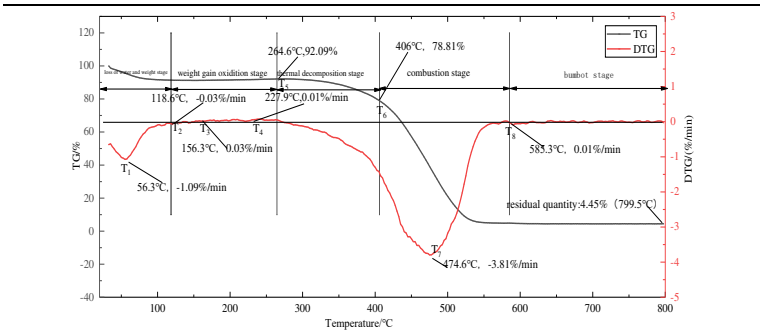

(a) At heating rate of 5°C/min

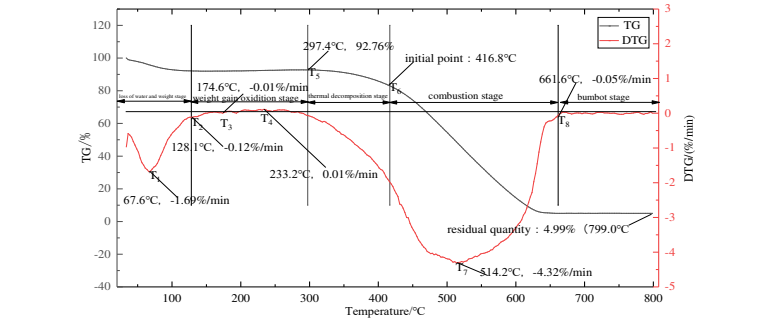

(b) At heating rate of 10°C/min

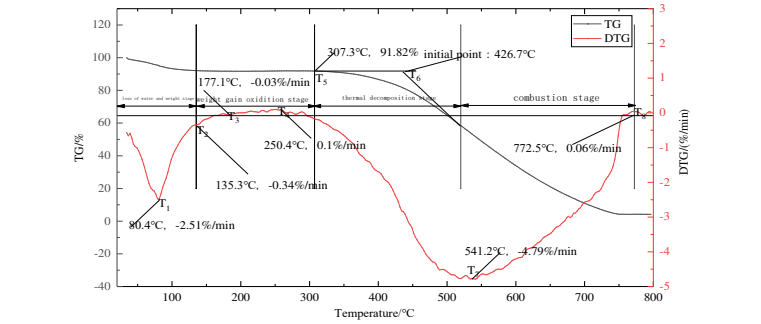

(c) At heating rate of 15°C/min

Figure 1. *Oxygen concentration of 5%, TG/DTG curve results at different heating rates*

(4) Combustion stage (410 -550°C)

When the temperature reaches the ignition temperature, the pulverized coal begins to react, the powder quality decreases rapidly, and a violent combustion reaction occurs

http://www.aloki.hu ● ISSN 1589 1623 (Print) ● ISSN 1785 0037 (Online)
DOI: http://dx.doi.org/10.15666/aeer/1704_90519064

inside the pulverized coal molecules, which release a large amount of heat, and simultaneously generate many gaseous products such as CO, CO_2, and water vapour, etc. until the combustibles of pulverized coal burn completely and the quality no longer changes.

(5) Burnout stage (550 -800°C)

In this stage, the quality of pulverized coal remains basically the same, and the ash content in the pulverized coal directly determines the percentage of the residue remaining after the burnout of pulverized coal.

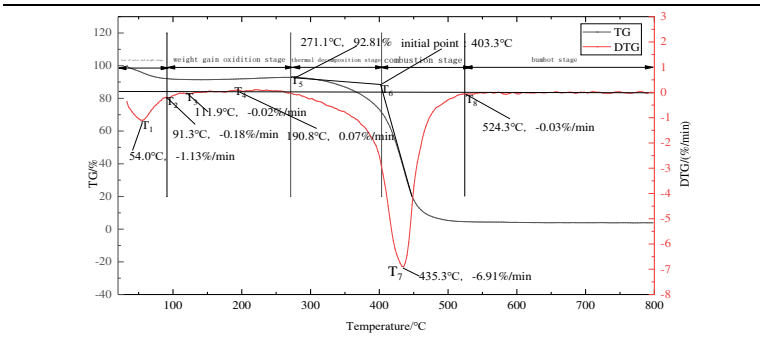

(a) At heating rate of 5°C/min

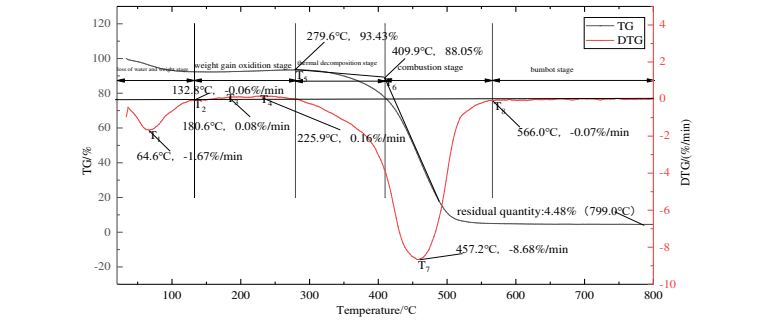

(b) At heating rate of 10°C/min

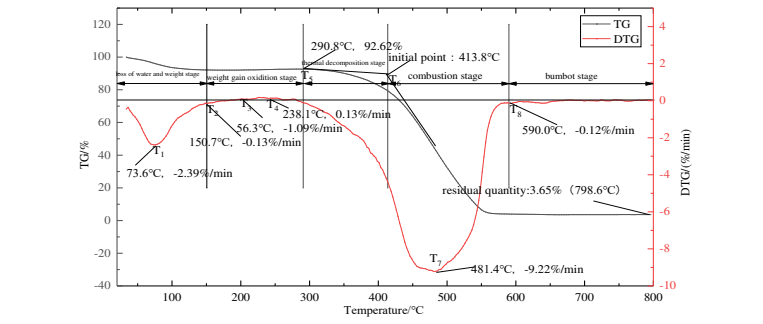

(c) At heating rate of 15°C/min

Figure 2. *Oxygen concentration of 13%, TG/DTG curve results at different heating rates*

Characteristic temperature

In the oxidative combustion process of coal sample, the characteristic temperature point of coal can be obtained by analysing the experimental TG data (Zhang et al., 2011), which mainly includes the critical temperature (T_1) with the highest weight loss rate during the early-stage water evaporation and index gas escape, the dry cracking

http://www.aloki.hu ● ISSN 1589 1623 (Print) ● ISSN 1785 0037 (Online)
DOI: http://dx.doi.org/10.15666/aeer/1704_90519064

temperature at the lowest weight loss point (T_2), the active temperature of the initial weight gain (T_3), the increasing temperature (T_4), the thermal decomposition temperature (T_5) at the maximum quality of coal sample before combustion, the oxygen absorption weight of the coal sample and the ignition temperature (T_6) at which the reaction consumption reaches equilibrium, the maximum weight loss rate temperature (T_7) corresponding to the maximum trough of the DTG curve, and the burnout temperature (T_8) when the pulverized coal is completely burned and the mass is not changed.

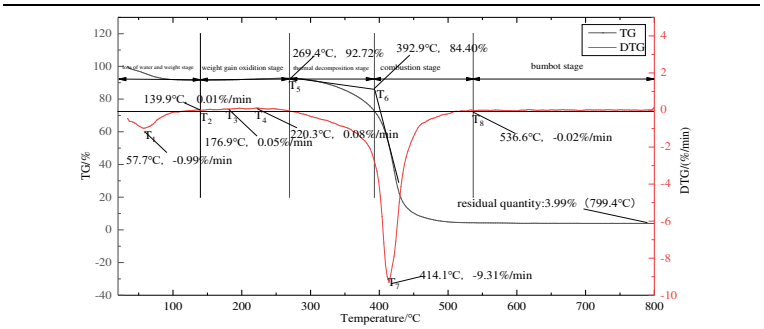

(a) At heating rate of 5°C/min

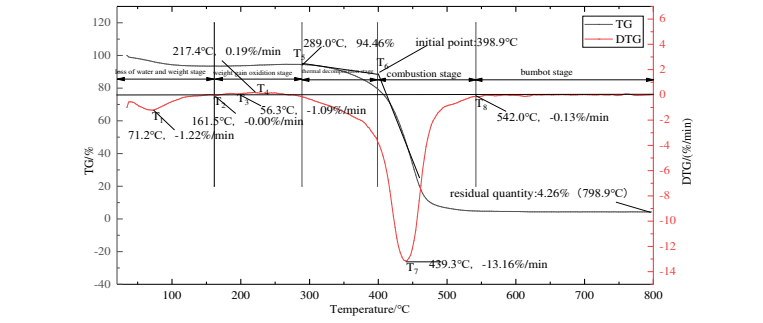

(b) At heating rate of 10°C/min

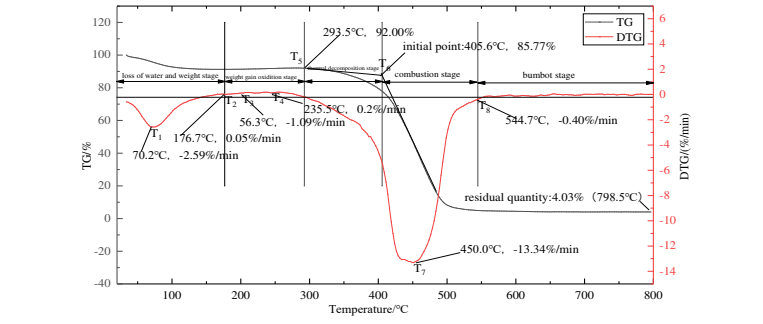

(c) At heating rate of 15°C/min

Figure 3. *Oxygen concentration of 21 %, TG/DTG curve results at different heating rates*

Change law of characteristic temperature in combustion process of pulverized coal

The characteristic temperature during the combustion of pulverized coal is shown in *Table 1*. In *Table 1*, the characteristic temperature under different oxygen concentration and different heating rate conditions was compared and analysed. It's found that the characteristic temperature changes significantly from the starting temperature point to

http://www.aloki.hu ● ISSN 1589 1623 (Print) ● ISSN 1785 0037 (Online)
DOI: http://dx.doi.org/10.15666/aeer/1704_90519064

the ignition temperature range. Therefore, in order to study the combustion process of pulverized coal under the condition of different heating rates and oxygen concentration, the critical temperature T_1, the dry cracking temperature T_2, and the ignition temperature T_6 were selected. *Figure 4* shows the characteristic temperature changes of non-caking coal powder at the same oxygen concentration and different heating rate.

Table 1. *Characteristic temperature table of coal sample*

Oxygen concentration /%	Heating rate/ °C /min	Critical temperature T_1/°C	Dry cracking temperature T_2/℃	Active temperature T_3/°C	Growth temperature T_4/°C	Thermal decomposition temperature T_5/°C	Ignition temperature T_6/°C	Maximum combustion rate temperature T_7/°C	Burnout temperature T_8/°C
5	5	56.3	118.6	156.3	227.9	264.6	410.0	474.5	585.3
5	10	67.6	128.1	174.5	233.2	297.4	416.8	514.2	661.6
5	15	80.4	135.3	177.1	250.4	307.3	426.7	541.1	772.5
13	5	54.0	91.3	111.3	190.8	271.1	403.3	435.7	524.3
13	10	64.6	132.8	180.6	225.9	279.6	409.9	457.2	566.0
13	15	73.6	150.7	201.3	238.1	290.8	413.8	481.4	590.0
21	5	57.7	139.9	176.9	220.3	269.4	392.9	414.1	536.6
21	10	71.2	161.5	188.5	217.4	289.0	398.9	439.3	542.0
21	15	70.2	176.7	198.4	235.5	292.5	405.6	450.0	544.7

Figure 4(a),(b), and (c) depict the changes of characteristic temperature (critical temperature T_1, dry cracking temperature T_2, and ignition temperature T_6) at the oxygen concentration of 5%, 13%, and 21% under different heating rates of the non-caking coal.

For non-caking coal, with the oxygen concentration constant, the overall trend of the characteristic temperature for the coal sample increases with the increase of the heating rate. Taking the oxygen concentration of 5% as an example, for the coal samples at the heating rate of 5°C/min, the critical temperature was 56.3°C, the dry cracking temperature was 118.6°C, and the ignition temperature was 410.0°C; at the heating rate of 10°C/min, the critical temperature was 67.6°C, the cracking temperature was 128.1°C, and the ignition temperature was 416.8°C; at the heating rate of 15°C/min, the critical temperature was increased to 80.4°C, the dry cracking temperature was 135.3°C, and the ignition temperature was 426.7°C.

By comparing *(a), (b), and (c)* in *Figure 4* it can be clearly seen that when the oxygen concentration is constant, the heating rate affects the characteristic temperature during the combustion of the coal sample in different degrees: dry cracking temperature>critical temperature>ignition temperature. The reason may be that the dry cracking temperature is the temperature point at which the weight loss of the coal sample reaches the maximum before combustion; before this temperature point, the coal powder makes the adsorption/desorption and thermal decomposition reaction internally, and these reactions are more affected by the heating rate. Therefore, the heating rate can directly affect the temperature of the cracking temperature. Besides, the heating rate has little effect on the ignition temperature of the coal sample, because a series of reactions by coal ignition shall cause more volatiles and indicator gases from the coal powder., but the heating rate cannot effectively extend the time and progress of these volatiles and gases reacting with oxygen.

http://www.aloki.hu ● ISSN 1589 1623 (Print) ● ISSN 1785 0037 (Online)
DOI: http://dx.doi.org/10.15666/aeer/1704_90519064

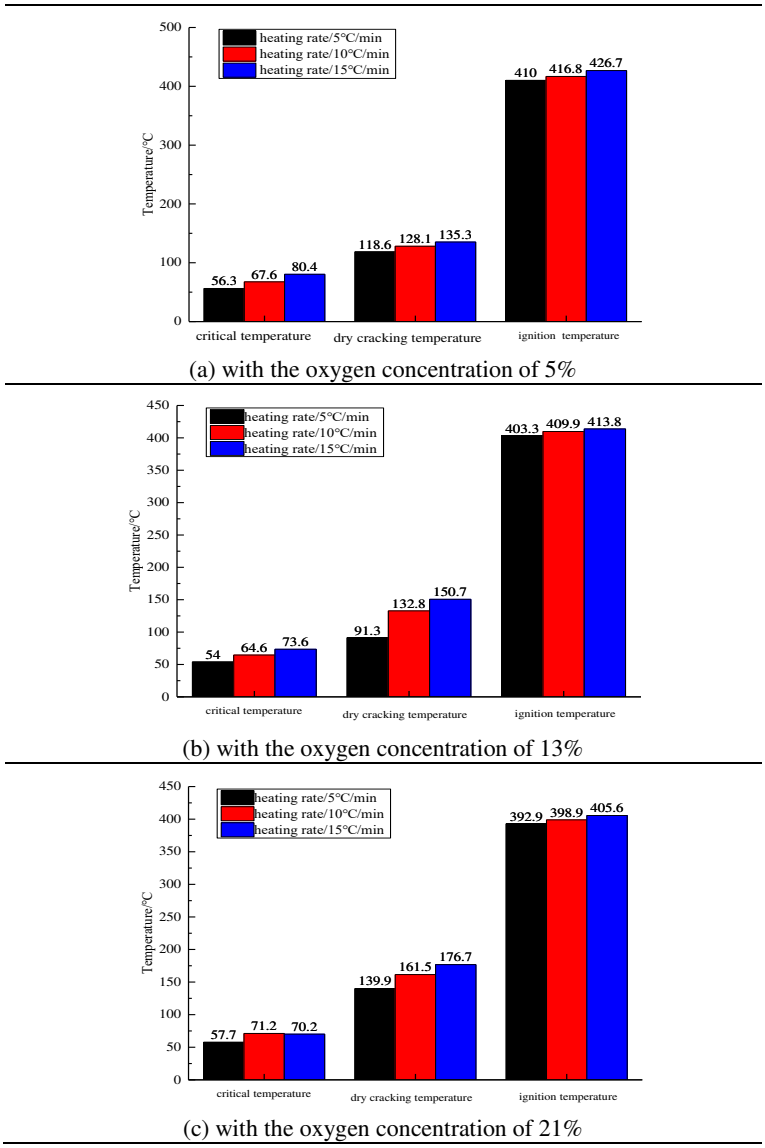

Figure 4. *Characteristic temperature of non-caking coal at the same oxygen concentration and different heating rate*

Figure 5 shows the characteristic temperature changes of non-caking coal powder at the same heating rate and different oxygen concentration. *Figure 5(a),(b), and (c)* show the characteristic temperatures changes of the non-caking coal powder with different oxygen concentrations at the heating rate of 5, 10, and 15°C/min (critical temperature T_1, dry cracking temperature T_2, and ignition point T_6).

Taking the heating rate of 15°C/min as an example, with the oxygen concentration of 5%, the critical temperature of the coal sample was 80.4°C, the dry cracking temperature was 135.3°C, and the ignition temperature was 426.7°C; with the oxygen concentration of 13%, the critical temperature was 73.6°C, the dry cracking temperature was150.7°C, and the ignition temperature was 413.8°C; with the oxygen concentration of 21%, the critical temperature of the coal sample was reduced to 70.2°C, the dry cracking temperature was increased to 176.7°C, and the ignition temperature was lowered to 405.6°C.

http://www.aloki.hu ● ISSN 1589 1623 (Print) ● ISSN 1785 0037 (Online)
DOI: http://dx.doi.org/10.15666/aeer/1704_90519064

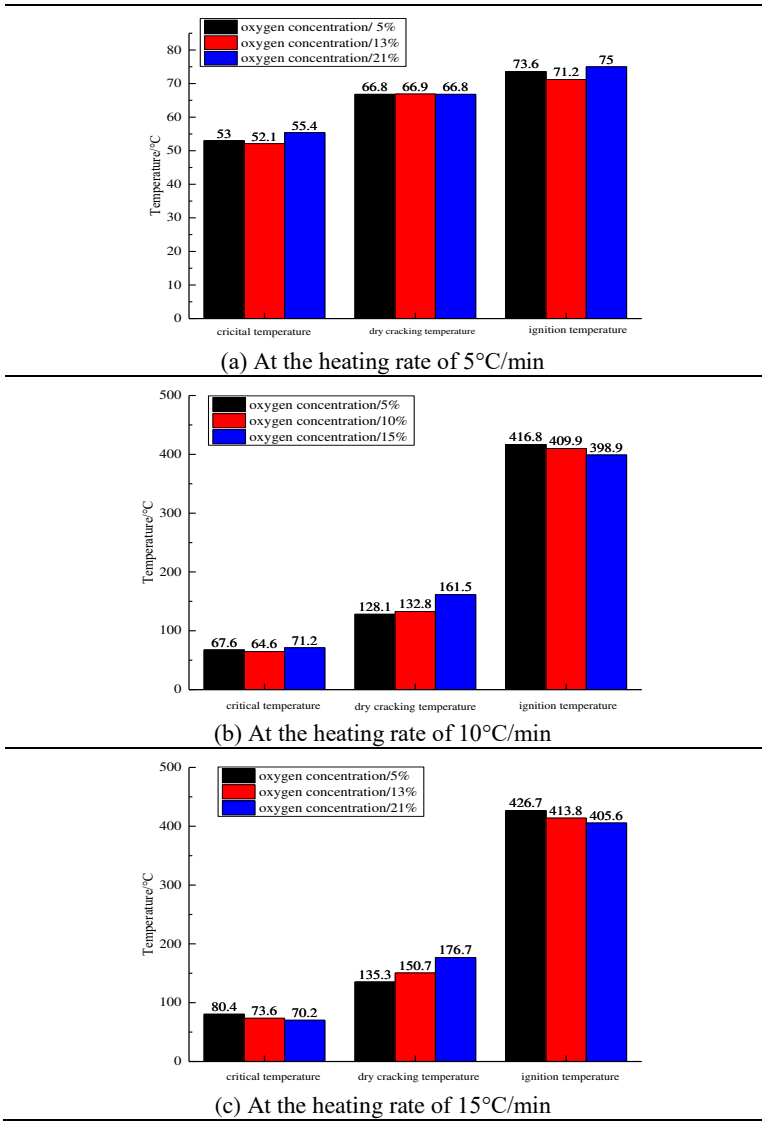

Figure 5. *The characteristic temperature of coal sample in the same heating rate and different oxygen concentration*

By comparing *(a), (b), and (c)* in *Figure 5*, it can be clearly seen that when the heating rate is constant, the oxygen concentration is positively correlated with the dry cracking temperature of the coal sample combustion process, and negatively correlated with the critical temperature and the ignition temperature (Wang et al., 2014). The effect of oxygen concentration on characteristic temperature is: critical temperature<ignition temperature<dry cracking temperature. During the combustion of coal powder before the critical temperature, less of oxygen is required for the counter-reaction is less, so the oxygen concentration has unobvious effects on the change trend of the pulverized coal critical temperature. But the pulverized coal needs to consume a large amount of oxygen for combustion before reaching the ignition temperature, and the oxygen concentration in the environment directly determines the rate of the oxidation reaction, thus, the changes of oxygen concentration have greater effects on the ignition temperature than on heating rate.

http://www.aloki.hu ● ISSN 1589 1623 (Print) ● ISSN 1785 0037 (Online)
DOI: http://dx.doi.org/10.15666/aeer/1704_90519064

Effect of heating rate and oxygen concentration on combustion process of pulverized coal

Effect of heating rate on combustion process of pulverized coal

Under the condition of a certain oxygen concentration, the effect of heating rate on the combustion process of pulverized coal was analysed. Taking the non-caking coal powder under the experimental conditions of 13% oxygen concentration as an example, the TG, DTG and DSC curves at the heating rates of 5, 10, 15°C/min were obtained (*Figure 6*).

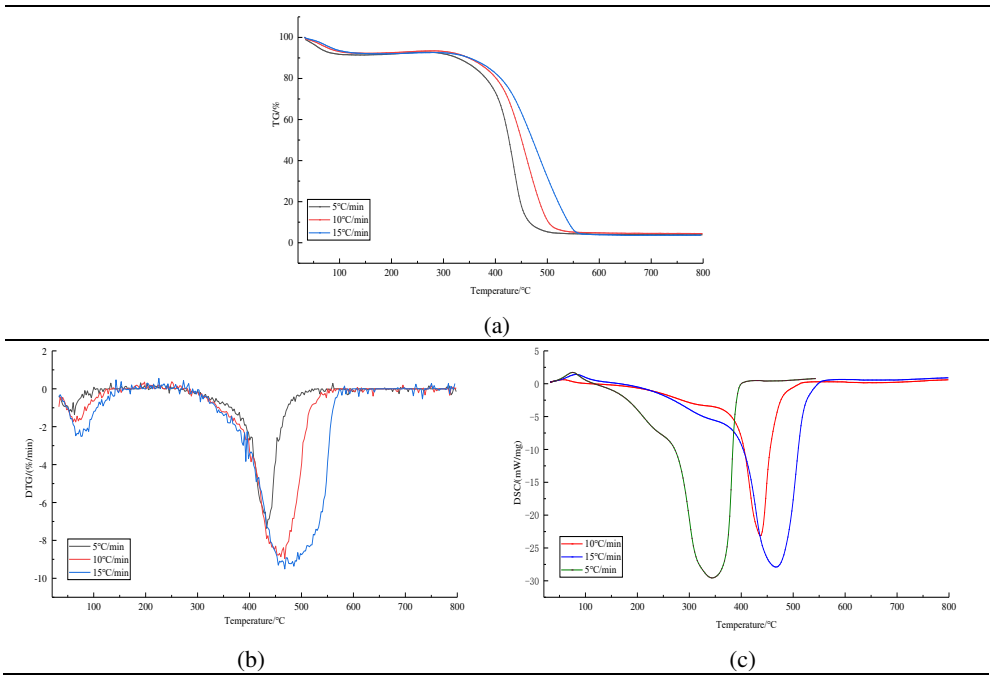

Figure 6. *TG, DTG and DSC curves with oxygen concentration of 13%, heating rate 5, 10 and 15°C/min*

It can be seen from *Figure 6* that under the same oxygen concentration, the heating rate increases continuously, which results in the hysteresis phenomenon of the TG curve. The heating rate can directly determine the temperature of the pulverized coal. However, under the condition of a certain oxygen concentration, the functional groups in the pulverized coal and the structure involved in the pulverized coal combustion reaction cannot all involved in the reaction, and there further occurs the high temperature side shift on the characteristic temperature point of the pulverized coal (Xiao et al., 2007).

It can be seen from the DTG curve that the critical point of the weight loss rate is the ignition point. Before the critical point, the heating rate has little effect on the weight loss rate of coal powder; after the critical point, the effect is more significant. The reason is that the heating rate can prolong or shorten the time of coal and oxygen recombination, and the faster heating rate can cause the non-heterogeneous phase ignition of coal powder, resulting in a longer reaction process. This is expressed as hysteresis in the DTG image.

http://www.aloki.hu ● ISSN 1589 1623 (Print) ● ISSN 1785 0037 (Online)
DOI: http://dx.doi.org/10.15666/aeer/1704_90519064

The DSC curve shows that the heating rate is positively correlated with the temperature required to reach the maximum exothermic value, which is consistent with the trend of the TG/DTG curve.

Effect of oxygen concentration on combustion process of pulverized coal

Under the condition of constant heating rate, the effect of oxygen concentration on the combustion process of pulverized coal was analysed. Taking the non-caking coal powder under the experimental conditions of heating rate 10°C/min as an example, the TG, DTG and DSC curves with the oxygen concentration of 5, 13, and 21% respectively were obtained (*Figure 7*).

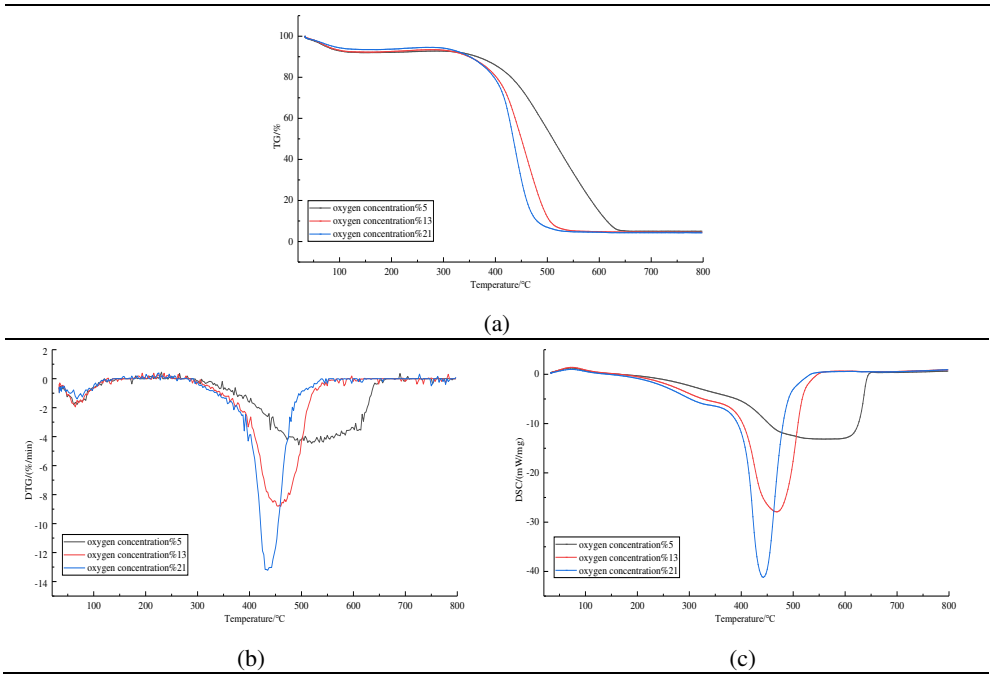

Figure 7. *The results of TG, DTG and DSC curves at the heating rate of 10°C/min, oxygen concentration 5, 13, and 21%*

It can be seen from *Figure 7* that with the heating rate constant, when the oxygen concentration decreases from 21% to 13% and then to 5%, TG, DTG and DSC all show a phenomenon of shifting to high temperature. This is because the oxygen concentration can directly determine the amount of oxygen molecules in the oxidation reaction of coal powder. The greater the oxygen concentration, the more oxygen molecular weight involved in the oxygen reaction of coal powder, which shortens the time required to burn coal samples of the same quality, resulting in a lower reaction temperature.

Discussion

Under the condition of the same oxygen concentration and different heating rate, the characteristic temperature point of non-caking coal samples is shifted to the high temperature point, which is shown as the TG curves will show hysteresis phenomenon with the increase of heating rate. The weight loss rate of coal samples takes the ignition point as the critical point. Before the critical point, the heating rate has little influence on

http://www.aloki.hu ● ISSN 1589 1623 (Print) ● ISSN 1785 0037 (Online)
DOI: http://dx.doi.org/10.15666/aeer/1704_90519064

the weight loss rate of coal powder, and after the critical point, the effect is significant. In addition, the heating rate has a promoting effect on the weight loss rate of coal samples, and the maximum exothermic strength increases, which shows the same characteristics as the DSC curves. The higher the heating rate is, the longer the reaction process of the coal sample is, indicating that the higher heating rate leads to the heterogeneous combustion of pulverized coal, which to some extent increases the reaction time.

Under certain heating rate, with the reduction of oxygen concentration of coal sample weight loss rate, the maximum heat strength is reduced, this is due to the decreasing concentration of oxygen in oxidation reaction of oxygen reduction, oxidation of coal sample strength decreased. Moreover, the critical point of coal sample weightlessness with low oxygen concentration move to higher temperature, is largely due to reduced oxygen concentration, lead to slow reaction process.

Heating rate and oxygen concentration will affect the combustion reaction of coal samples. When the oxygen concentration is constant, the key to control the ignition of coal is to reduce the heating rate. Similarly, when the heating rate is constant, the key is to reduce the oxygen concentration for inhibit the development of combustion. Based on the TG experiments with different heating rates and oxygen concentrations, the characteristics of combustion of non-caking coal under two-factor conditions were analysed, so as to control the occurrence of coal combustion, and to reduce the waste of resources and the generation of pollutants.

Conclusions

The combustion process of non-caking coal powder mainly includes the water and weight loss stage of coal, the weight gain oxidation stage, the thermal decomposition stage, the combustion stage and the burnout stage. In the oxidative combustion process of coal samples, the characteristic temperature points of coal samples can be obtained by analysing the TG experimental data, including critical temperature (T_1), dry cracking temperature (T_2), active temperature (T_3), and increasing temperature (T_4), thermal decomposition temperature (T_5), ignition temperature (T_6), DTG maximum weight loss rate temperature (T_7), and burnout temperature (T_8).

The heating rate is positively correlated with the combustion reaction time, characteristic temperature and oxidation reaction rate of pulverized coal. The higher the oxygen concentration, then the shorter the combustion time of the coal sample, the lower its characteristic temperature, and the higher the oxidation reaction rate.

The influence of oxygen concentration on combustion characteristic is more obvious than that of heating rate. Under the condition of high heating rate and oxygen concentration, the maximum exothermic strength of coal sample is the highest, the weight loss is the fastest, and the ignition of the coal is easier.

Due to the diversity of coal types, the TG characteristics of different ranks of coal need to be tested and analysed in future research, so as to reduce resource waste and environmental pollutions, and to prevent spontaneous combustion of coal from damaging ecological environment.

Acknowledgements. This research was supported by the National Key R&D Program of China (grant number 2018YFC0808201); China Postdoctoral Science Foundation (grant number 2017M623209); Natural Science Basic Research Program of Shaanxi (grant number 2018JQ5080; 2018JM5009); Special scientific research project of Shaanxi Provincial Education Department (grant number 17JK0495).

http://www.aloki.hu ● ISSN 1589 1623 (Print) ● ISSN 1785 0037 (Online)
DOI: http://dx.doi.org/10.15666/aeer/1704_90519064

REFERENCES

[1] Benmenine, D., Bentebbiceh, A. (2018): Influence of air preheat temperature and excess air in a reverse flow combustor. – Instrumentation Mesure Métrologie 17(1): 93-111.
[2] Deng, J., Qu, J., Wang, Q. H. (2014): Experimental study on minimum ignition temperature of bituminous coal dust cloud. – Mining Safety and Environmental Protection 41(6): 13-18.
[3] Deng, J., Zhao, J. Y., Zhang, Y. N., Wang, C. P. (2016): Micro-characteristics of spontaneous combustion of second oxidation with different rank coals. – Journal of China Coal Society 41(5): 1164-1172.
[4] Guo, J., Liu, Y., Cheng, X. J., Yan, H., Xu, Y. Q. (2018): A novel prediction model for the degree of rescue safety in mine thermal dynamic disasters based on fuzzy analytical hierarchy process and extreme learning machine. – International Journal of Heat and Technology 36(4): 1336-1342.
[5] Guo, J., Wen, H., Zheng, X. Z., Liu, Y., Cheng, X. J. (2019): A method for evaluating the spontaneous combustion of coal by monitoring various gases. – Process Safety and Environmental Protection 126: 223-231.
[6] Habib, M. A., Basuki, T., Miyashita, S. (2019): Assessment of natural radioactivity in coals and coal combustion residues from a coal-based thermoelectric plant in Bangladesh: implications for radiological health hazards. – Environmental Monitoring and Assessment 191(1): 27.
[7] Jin, Y. F., Guo, J., Wen, H. (2015): Experimental study on combustion characteristic parameters of high temperature and poor oxygen oxide in coal spontaneous combustion. – Journal of China Coal Society 40(3): 596-602.
[8] Kong, B., Li, Z. H., Yang, Y. L. (2017): A review on the mechanism, risk evaluation, and prevention of coal spontaneous combustion in China. – Environmental Science and Pollution Research 24(30): 23453-23470.
[9] Liu, W., Qin, Y. P.,Yang, X. B. (2014): Experimental study for impact of volatile matter on spontaneous combustion characteristics of coal. – Journal of China Coal Society 39(5): 891-896.
[10] Lu, X. X., Zhao, H. R., Zhu, H. Q., Han, Y., Xue, X. (2018): Characteristic rule of spontaneous combustion tendency of oxidized coal at recrudescence stage. – Journal of China Coal Society 43(10): 2809-2816.
[11] Ma, L., Deng, J., Wang, W. F. (2014): Effect of CO_2 on low temperature oxidation reaction process of coal. – Journal of Xi' an University of Science and Technology 34(4): 379-383.
[12] Tomescu, C., Prodan, M., Vatavu, N. (2017): Monitoring the work environment using thermal imaging cameras in order to prevent the self-ignition of coal. – Environmental Engineering and Management Journal 16(6): 1389-1393.
[13] Toropov, E. V., Osintsev, K. V., Aliukov, S. V. (2018): Analysis of the calculated and experimental dependencies of the combustion of coal dust on the basis of a new methodological base of theoretical studies of heat exchange processes. – International Journal of Heat and Technology 36(4): 1240-1248.
[14] Wang, C. A., Liu, Y. H., Che, D. F. (2010): Experimental investigation on combustion characteristics of coals in low oxygen concentration with thermogravimetry. – Journal of Engineering Thermorphysics 31(10): 1785-1788.
[15] Wang, F. S., Yang, S. Q., Li, Z. B. (2014): Study on heating rate law of low temperature oxidation process of coal samples with different particle sizes. – Coal Science and Technology (5): 62-64.
[16] Wang, K., Zhai, X. W., Deng, J., Liu, X. R., Zhang, Y. N. (2018): Application of liquid CO_2 conveying technology for fire control in goaf. – International Journal of Heat and Technology 36(2): 657-662.

http://www.aloki.hu ● ISSN 1589 1623 (Print) ● ISSN 1785 0037 (Online)
DOI: http://dx.doi.org/10.15666/aeer/1704_90519064

[17] Wei, B., Yu, J. (2017): An investigation of the health effects caused by exposure to arsenic from drinking water and coal combustion: arsenic exposure and metabolism. – Environ Sci Pollut Res Int 24(6): 1-8.
[18] Wen, H., Guo, J., Jin, Y. F., Wang, K., Zhang, Y. T., Zheng, X. Z. (2017): Experimental study on the influence of different oxygen concentrations on coal spontaneous combustion characteristic parameters. – International Journal of Oil, Gas and Coal Technology 16(2): 187-202.
[19] Xiao, Y., Ma, L., Wang, Z. P. (2007): Study the characteristic temperature of coal spontaneous combustion process by thermogravimetric analysis. – Coal Science and Technology 35(5): 73-76.
[20] Yi, B. J., Zhang, L. Q., Mao, Z. H. (2014): Effect of the particle size on combustion characteristics of pulverized coal in an O_2/CO_2 atmosphere. – Fuel Process Technology 128(10): 17-27.
[21] Zeng, Q., Zhao, L. H. (2018): Investigation of the potential risk of coal fire to local environment: A case study of Daquanhu coal fire, Xinjiang region. – China Science of the Total Environment 640-641: 1478-1488.
[22] Zhang, Y. N., Deng, J., Wen, H. (2011): TG/DTG experiment on characteristic temperature of spontaneous combustion of huating coal. – Journal of Xi'an University of Science and Technology 31(6): 659-662,667.

http://www.aloki.hu ● ISSN 1589 1623 (Print) ● ISSN 1785 0037 (Online)
DOI: http://dx.doi.org/10.15666/aeer/1704_90519064

CARBON MONOXIDE DIFFUSION AND VENTILATION IN UNDERGROUND GARAGE

PENG, S. B.[1*] – CHEN, Q. K.[1] – GUO, B. Y.[2] – PEI, G. H.[3]

[1]*School of Civil Engineering & Architecture, Southwest Petroleum University, Chengdu 610500, China*

[2]*Petroleum Engineering School, Southwest Petroleum University, Chengdu 610500, China*

[3]*School of Architectural Economics & Business Administration, Hubei Business College, Wuhan 430079, China*

**Corresponding author*
e-mail: shanbipeng@swpu.edu.cn; phone: +86-135-5039-6539

(Received 18th Mar 2019; accepted 17th May 2019)

Abstract. In this paper, the numerical simulation method of computational fluid dynamics (CFD) was combined with field experiment to explore the carbon monoxide (CO) diffusion and ventilation in an underground garage. Firstly, a finite-element model was set up for the garage, and used to simulate the CO concentration and air velocity. Then, the simulated results were proved valid against the data of field experiment. After that, a ventilation plan was designed with one fan running for 20 min, three times a day in the rush hours. The simulation results show that this plan could not lower the CO concentration below the required level (30mg/m^3). Thus, the running time of the fan was extended to 30 min per time. It is found that the new ventilation plan could effectively control the CO concentration. Next, the third ventilation plan was developed with two fans running together for 10 min, three times a day in the rush hours, and was proved as valid through simulation. Due to its advantage in power consumption, the third plan was identified as the optimal ventilation plan for the garage. The three-fan or four-fan ventilation plans were not considered because they must be noisier and costlier than the two-fan ventilation plan. Although the structure of underground garages (such as height, area, etc.) is different, most of them are common in high tightness and structural independence. The method mentioned in this study that using the necessary air parameters of measuring points in underground garage to simulate the status of airflow and CO concentration is effective.
Keywords: *underground garage, airflow, pollution diffusion, air quality, numerical simulation*

Introduction

Recent years has seen a growing concern about the air quality in underground garage. In such a highly closed space, it is difficult for the air inside the underground garage to exchange with ground air. The toxic gases emitted by cars in the garage may over-accumulate, such as carbon monoxide (CO), nitrogen oxides (NO_x) and hydrocarbons. Large quantities of harmful gases will reduce the air quality and human body comfort even lead disease or death. And among them, produced CO is more toxic and concentrated than the other harmful gases in process of vehicles cold starting and idle speeding (Chen, 2001). Hence, this paper attempts to control CO concentration by ventilation in order to solve the problem of air quality.

To control CO concentration, the key lies in the relationship between air flow and pollutant distribution, as the air quality in underground garage may vary with the ventilation conditions. So far, this relationship has been mainly explored through field experiment and numerical simulation. The typical field experiments are reviewed as follows.

Xu (2015) investigated the flow field in underground space by tracer gas method, revealing that different ventilation states lead to different distribution of tracer gas. Kierat et

http://www.aloki.hu ● ISSN 1589 1623 (Print) ● ISSN 1785 0037 (Online)
DOI: http://dx.doi.org/10.15666/aeer/1704_90659081

al. (2018) applied the same method to assess the exposure of indoor breathing air, and found that the exposure of indoor air pollution is affected by the air flow interaction in the breathing zone. With the aid of federal equivalent method, Zhao et al. (2017) studied the seasonal concentrations of PM 2.5 and other pollutants in underground garage, concluding that natural ventilation alone cannot dilute particles effectively in the residential garage. Targeting a wavy air-water interface, Buckley and Verson (2017) measured the airflow through laser induced fluorescence (LIF) flow visualization and particle image velocimetry (PIV). Zhang et al. (2008) adopted the hydroxybenzene reagent method to capture the concentration of formaldehyde, and discovered that the air quality is severely affected by the emission of materials in the compartments of many compact cars sold in China.

The numerical simulation has been increasingly employed recently, thanks to its low consumption of manpower and materials. The fluid state is usually simulated by the computational fluid dynamics (CFD). For instance, Liu et al. (2019a, 2018, 2016a, b), Yong et al. (2017) studied flow characteristics of gas in a pipe and analyzed the formation mechanism of trailing oil. Kurnia et al. (2014) numerically simulated the methane dispersion in an underground mine. Wang et al. (2016) explored the storage temperature field in a non-ventilated underground granary using the CFD. Choi et al. (2013) relied on the CFD to investigate the hydrogen leakage of cars in underground garage. Papakonstantinou et al. (2003) examined the air quality and CO dispersion of underground garage through the numerical method and experiment. Xue and Ho (2000) set up a model of underground garage and simulated CO diffusion and heat conduction. Wang et al. (2009) simulated the diffusion of dust at underground power house. Widiatmojo et al. (2013) evaluated the gas diffusion of turbulent flow in mine ventilation system by numerical simulation. Hong et al. (2010) studied the influence of branch tunnels on CO diffusion at underground power house. Bai et al. (2016) probed into the flow field of a train running to the rescue station through both experiment and simulation. Wang et al. (2017) simulated and calculated how forced ventilation affects the water spray and dust suppression on the work face of coal mine. Wang and Ren (2013) carried out a CFD analysis on the behavior of dust flow and air flow above an underground bin. Bascompta et al. (2016) and Liu et al. (2019b) tackled the impacts of ventilation layout on the environment using the geographical information system (GIS).

Concerning pollutant distribution and flow field in closed space, the existing studies either resort to CFD simulation or rely on field experiment. There are relatively few studies that combine these two approaches. To make up for this gap, the CFD simulation and field experiment are combined in this paper to discuss the CO concentration at an underground garage. The experimental data help determine parameters of boundary conditions, and verify the availability of the modelling, thus ensuring the simulation accuracy.

Generally, the structure of underground garages is different due to various requirements, however they are common in their special characteristics such as high air tightness and structural independence. Although the results of this real case may not apply to all cases, the proposed method in this paper that combines the CFD and field experiment is proved available. The ventilation analysis of different underground garages only needs to adjust the geometry model and the relevant environmental parameters.

Methodology

Research object

http://www.aloki.hu ● ISSN 1589 1623 (Print) ● ISSN 1785 0037 (Online)
DOI: http://dx.doi.org/10.15666/aeer/1704_90659081

This paper tackles a real problem in an underground garage within a university of southwestern China's Sichuan Province. The photos and model of the garage are presented in *Figure 1*. The cars in the garage were defined as pollution sources.

As shown in *Figure 1*, the 48 m × 45 m × 3 m (L×W×H) garage has about 200 parking spaces, 3 aisles (b~d) and one secure channel (f). Under pressure difference, a limited amount of fresh air can enter the garage through ventilation shafts (e). The airflow in the garage is driven by the thermal and wind pressures from the natural ventilation system, and the mechanical force of fans.

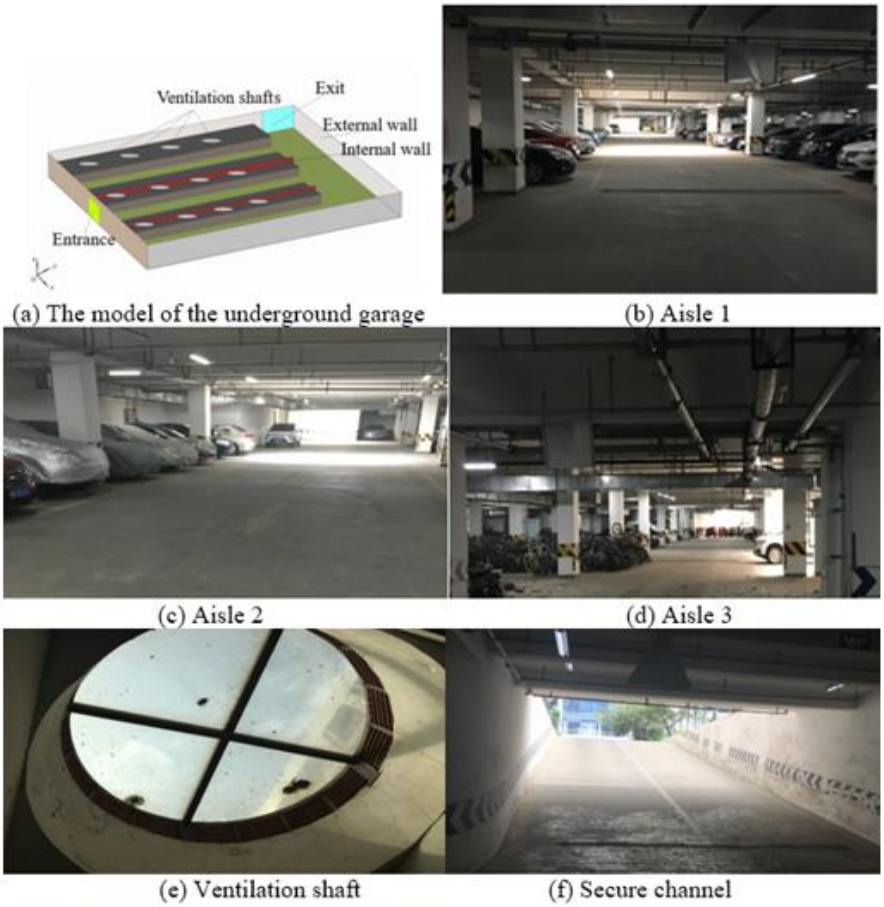

Figure 1. *The model (a) and photos (b~g) of the underground garage*

The measured pressure is positive at each ventilation shaft, and negative at the entrance. This means the fresh air flows into the garage from the entrance and leaves from the shafts. The flowing process is illustrated in *Figure 2*.

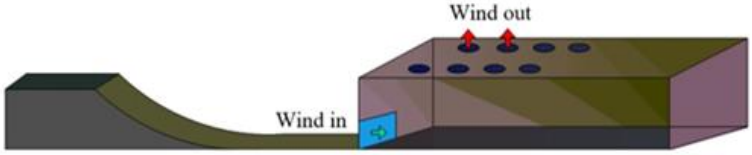

Figure 2. *The flowing process in the underground garage*

http://www.aloki.hu ● ISSN 1589 1623 (Print) ● ISSN 1785 0037 (Online)
DOI: http://dx.doi.org/10.15666/aeer/1704_90659081

The space of underground garage is divided into three areas by two internal walls with four exhaust fans located in different positions (*Fig. 3*). Each fan runs at 500~750 rpm, propelling 32,000~42,000 m^3 fresh air per hour.

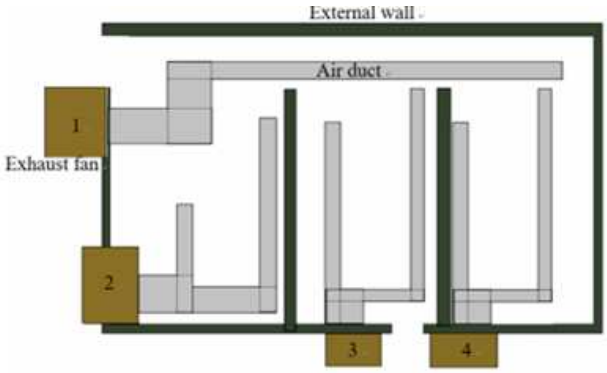

Figure 3. *The layout plan of the underground garage*

In this research, several ventilation conditions were simulated by the CFD, and verified by the experimental data. On this basis, the most cost-effective control plan for CO concentration was selected as the optimal solution.

Field experiment

The underground garage was divided into four areas for measurement, namely, the parking lots (D), secure channel (A), aisles (B), plus the entrance and exit (C) (*Fig. 4*). The CO concentration was measured in rush hours (i.e. 8am, 12pm and 2pm) as well as at 10am and 4pm. The data collected at two hours later were taken as control data.

Figure 4. *The measuring points in the underground garage*

The air velocity and CO concentration were respectively measured by a hot-wire anemometer (error: ± 0.03; range: 0.15~30 m/s) and a Z500XP CO sensor (error: ± 0.05; range: 0~300 ppm) (*Fig. 5*). Before measuring the air velocity, the probe of the hot-wire anemometer should be set perpendicularly to the wind direction. During the measurement, the CO sensor should be turned on and placed at the measuring point for a few minutes.

http://www.aloki.hu ● ISSN 1589 1623 (Print) ● ISSN 1785 0037 (Online)
DOI: http://dx.doi.org/10.15666/aeer/1704_90659081

(a) Hot-wire anemometer (b) CO sensor

Figure 5. *Measuring instruments*

The CO concentration of the aisles must be strictly controlled to protect the health of pedestrians. The three aisles in the underground garage were numbered as aisle 1, aisle 2 and aisle 3. Five measuring points were arranged in the middle of each aisle at an equal interval from the entrance to the exist (*Fig. 6*).

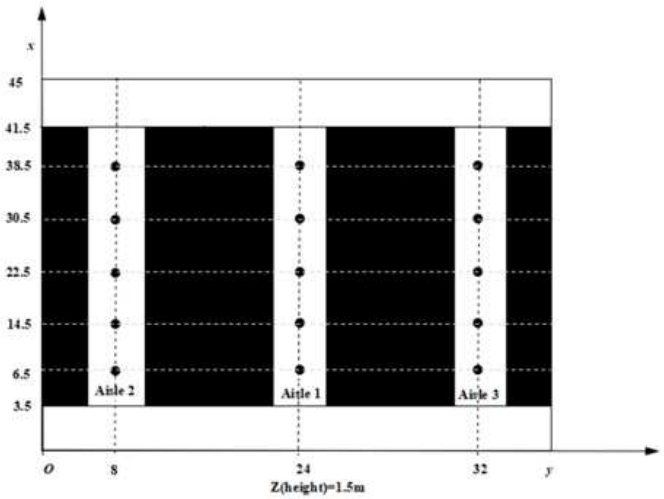

Figure 6. *The aisles and measuring points*

To investigate whether the outside environment will affect the airflow and CO diffusion in the underground garage, air velocity and CO concentration are measured respectively at each measuring point and outdoor for several times in one week. The mean of the five results was taken as the final value, when record the CO concentration, the unit "ppm" was converted into "mg/m^3":

$$\frac{mg}{m^3} = \frac{M}{22.4} \times \text{pp}m \times \frac{273}{273+T} \times \frac{P}{101325} \quad \text{(Eq.1)}$$

where T is the measured temperature; P is the measured pressure (Bar); M is the molecular mass of the measured gas.

The measured data are recorded in *Tables 1* and *2*. The results from *Tables 1* and *2* directly show the CO concentration and air velocity of each measuring point and outdoor. It can be found in *Table 1* that the CO concentration various from 1.8 mg/m^3 to

http://www.aloki.hu ● ISSN 1589 1623 (Print) ● ISSN 1785 0037 (Online)
DOI: http://dx.doi.org/10.15666/aeer/1704_90659081

2.6 mg/m^3 but the CO concentration of underground garage is much higher. It proofs that CO concentration of underground garage is mainly affected by the parking vehicles, low CO concentration of outdoor cannot greatly affect that of underground garage.

Table 1. *The CO concentration in different areas (mg/m^3)*

Outdoor		Point 1	Point 2	Point 3	Point 4	Point 5
2.6	Aisle 1	34	33	43	32	25
	Aisle 2	11	21	27	23	16
	Aisle 3	13	18	31	23	21
2.1	Aisle 1	33	30	41	31	25
	Aisle 2	13	22	29	25	20
	Aisle 3	14	18	30	25	18
1.8	Aisle 1	35	33	42	29	23
	Aisle 2	15	20	31	25	17
	Aisle 3	17	20	31	24	19
2.0	Aisle 1	34	32	38	31	26
	Aisle 2	12	21	32	26	19
	Aisle 3	15	19	29	27	21
2.1	Aisle 1	37	34	37	28	24
	Aisle 2	14	19	30	27	18
	Aisle 3	16	23	29	24	20
1.8	Aisle 1	36	35	39	30	25
	Aisle 2	12	20	33	24	19
	Aisle 3	16	20	32	27	22
1.9	Aisle 1	35	34	40	29	27
	Aisle 2	14	17	28	25	17
	Aisle 3	14	22	29	25	19

Table 2. *The air velocity in different areas (m/s)*

Outdoor		Point 1	Point 2	Point 3	Point 4	Point 5
2.5 m/s	Aisle 1	0.39	0.22	0.19	0.16	0.15
	Aisle 2	0.09	0.1	0.1	0.16	0.14
	Aisle 3	0.05	0.07	0.18	0.21	0.11
3.5 m/s	Aisle 1	0.41	0.21	0.21	0.17	0.17
	Aisle 2	0.08	0.12	0.11	0.15	0.15
	Aisle 3	0.07	0.05	0.17	0.21	0.12
2.7 m/s	Aisle 1	0.38	0.23	0.2	0.15	0.15
	Aisle 2	0.08	0.12	0.11	0.13	0.16
	Aisle 3	0.06	0.08	0.2	0.2	0.14
5 m/s	Aisle 1	0.4	0.2	0.22	0.16	0.14
	Aisle 2	0.09	0.11	0.13	0.19	0.15
	Aisle 3	0.04	0.1	0.19	0.18	0.13
4.7 m/s	Aisle 1	0.37	0.21	0.17	0.18	0.13
	Aisle 2	0.07	0.09	0.09	0.15	0.18
	Aisle 3	0.05	0.06	0.18	0.19	0.12
3.2 m/s	Aisle 1	0.41	0.22	0.19	0.16	0.15
	Aisle 2	0.1	0.11	0.12	0.17	0.17
	Aisle 3	0.07	0.07	0.17	0.21	0.14
5.6 m/s	Aisle 1	0.4	0.24	0.2	0.17	0.16
	Aisle 2	0.07	0.12	0.11	0.16	0.17
	Aisle 3	0.06	0.06	0.19	0.22	0.12

http://www.aloki.hu ● ISSN 1589 1623 (Print) ● ISSN 1785 0037 (Online)
DOI: http://dx.doi.org/10.15666/aeer/1704_90659081

With air velocity ranging from 2.5 to 5.6 m/s, the air flow of each measuring point is stable within 0.5 m/s. This fully demonstrated that the underground garage is a greatly sealed space. Although the environmental factor of outdoor has impact on airflow of underground garage, it affects the entrance and exit which are set as boundary in simulation more. Hence, it is just need change the parameter of boundary condition when simulate the air status of underground garage.

CFD numerical simulation

(1) Governing equations

The governing equations include the conservations of mass and momentum (Dokos, 2017; Su et al., 2019):

Conservation of mass:

$$\frac{\partial P}{\partial \mathrm{t}}+\frac{\partial(\rho \mu_x)}{\partial x}+\frac{\partial(\rho \mu_y)}{\partial y}+\frac{\partial(\rho \mu_z)}{\partial z}=0 \quad \text{(Eq.2)}$$

Conservation of momentum:

$$U_j=\frac{\partial U_i}{x_j}=-\frac{1}{\rho}\frac{\partial \rho}{x_i}+\frac{\partial}{\partial x_i}(vt\frac{\partial U_i}{x_j}-U_iU_j) \quad \text{(Eq.3)}$$

(2) Model selection

There are many CFD models with different functions and applicable scopes.

There are some models can be selected in CFD, the function of each model is different and can be used in various industries. In terms of function, the models were summarized by Varga et al. (2017) standard K-epsilon (k-ε), Re-Normalisation Group (RNG) k-ε, and realizable k-ε. Among them, the standard k-ε model is chosen in our research. The two basic transport equations and the component transport equation of this model can be respectively expressed as:

$$U_j\frac{\partial U_i}{\partial x_j}=\frac{\partial}{\partial x_j}(\frac{vt}{\sigma_k}\frac{\partial k}{\partial x_j})+vt(\frac{\partial U_i}{\partial x_j}+\frac{\partial U_j}{\partial x_i})\frac{\partial U_i}{\partial x_j}-\varepsilon \quad \text{(Eq.4)}$$

$$U_j\frac{\partial \varepsilon}{\partial x_j}=-\frac{\partial}{\partial x_j}(\frac{vt}{\sigma_k}\frac{\partial k}{\partial x_j})+\frac{\varepsilon}{k}\left[C_{\varepsilon 1}vt(\frac{\partial U_i}{\partial x_j}+\frac{\partial U_j}{\partial x_i})\frac{\partial U_i}{\partial x_j}-C_{\varepsilon 2}\varepsilon\right] \quad \text{(Eq.5)}$$

$$\frac{\partial \mu_j}{\partial x_j}=\frac{\partial}{\partial x_j}D\frac{\partial C_i}{\partial x_j}-C_{\varepsilon 2}\varepsilon \quad \text{(Eq.6)}$$

where μ_x, μ_y and μ_z are the velocity component in the x, y and z directions, respectively (m/s); t is the time(s); ρ is the density (kg/m^3); i and j are the serial number of the three directions and the 3D coordinates (i = 1, 2, 3; j = 1, 2, 3); U_j is the mean velocity of the three directions; μ_i and μ_j are the pulsating velocity components of different directions; V_t is turbulence viscosity coefficient; C_i is the per-unit CO concentration; S_i is the pollution source; D is the diffusion coefficient (m/s).

http://www.aloki.hu ● ISSN 1589 1623 (Print) ● ISSN 1785 0037 (Online)
DOI: http://dx.doi.org/10.15666/aeer/1704_90659081

(3) Computational domain and meshing

Since its birth in 1953, numerical simulation has been steadily improved. In 1973, Bruce and Peaceman simulated the 1D unsteady and radial flow of the gas phase. With the rapid development of computer science, the CFD has proliferated rapidly to various industries. Considering its complex structure, the underground garage was simplified into a collection of regular geometric figures. The parking spaces and internal walls were treated as equal size rectangles, while the ventilation shafts were considered as equal size circles. The entire garage was meshed into 224,094 tetrahedral grids (*Fig. 7*).

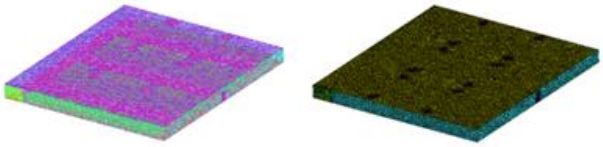

Figure 7. *The grid model of the underground garage*

(4) Boundary conditions and gas components

The entrance, the exit and the ventilation shafts were considered as velocity boundaries. The air velocity measured at such boundaries was 1 m/s in the experiment. The rectangles in the grid model, which represent the parking spaces, are set as pollution sources. The standard wall function was adopted.

The parameter of fluid (i.e. the gas components in underground garage) are necessary, owing to the use of the component transport equation in the simulation. The gas components be added were determined as CO, CO_2, N_2, O_2 and water vapor. The parameter of each gas component was set to be same as the air, except CO and CO_2, which is a source of pollution. The mass diffusivity of CO was obtained from the test: 1.0368 m^2/h.

After defining the boundary conditions, the CO concentration and air velocity were simulated under natural ventilation. Since the breathing height of a person is about 1.5 m, the plane of "axis z = 1.5 m" was selected to output the simulation results.

Results and discussion

Validation and analysis

The simulation results were verified against the data of field experiment, aiming to verify that they are not outliers.

(1) Validation of air velocity

Figure 8 shows the contour of the simulated air velocities and *Figure 9* presents the simulated air velocities of each aisle. Obviously, aisle 1, which is the closest to the entrance, had the fastest air velocity among all aisles. Besides, the air velocity decreased with the growth in the distance to the entrance. In aisles 2 and 3, the air velocities were stabilized between 0 m/s and 0.5 m/s.

http://www.aloki.hu ● ISSN 1589 1623 (Print) ● ISSN 1785 0037 (Online)
DOI: http://dx.doi.org/10.15666/aeer/1704_90659081

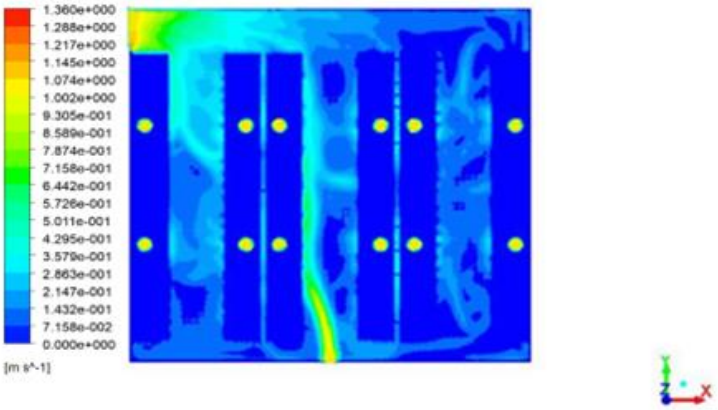

Figure 8. *Contour of air velocity (m/s)*

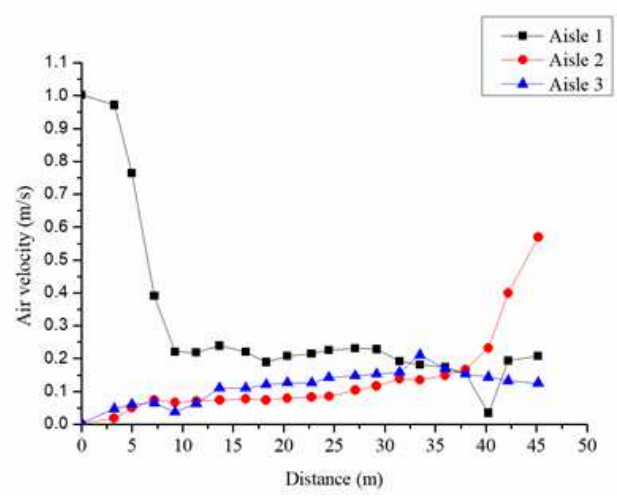

Figure 9. *Simulated air velocity of each aisle (m/s)*

Figure 10 compares the simulated data and experimental data on the air velocity at each measuring point of each aisle. During the experiment, the air velocity of each aisle was measured at 12 points, which were arranged at an equal interval from the entrance to the exit. Distance on the transverse axis of the figures below is the distance between measuring point and wall of where secure channel located. Each experimental value was taken from the mean of five repeated measurements. As shown in *Figure 10*, the simulation error is obviously acceptable.

(2) Validation of CO concentration

The CO concentration of the underground garage was simulated under natural ventilation. The simulated results are shown in *Figures 11* and *12*.

During the field experiment, the CO concentration at each of the five measuring points of each aisle was measured at the five time points of 8 am, 10 am, 12 pm, 2 pm and 4 pm, and compared with the corresponding simulated value. The measured CO concentrations of each area and the rush hour CO concentrations at each measuring point are listed in *Tables 3* and *4*, respectively.

http://www.aloki.hu ● ISSN 1589 1623 (Print) ● ISSN 1785 0037 (Online)
DOI: http://dx.doi.org/10.15666/aeer/1704_90659081

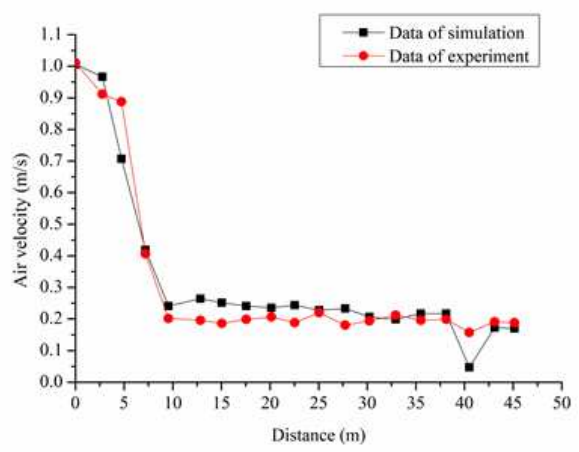

Figure 10. *Simulated air velocities vs. experimental air velocities*

Figure 11. *Contour of simulated CO concentration (mg/m^3)*

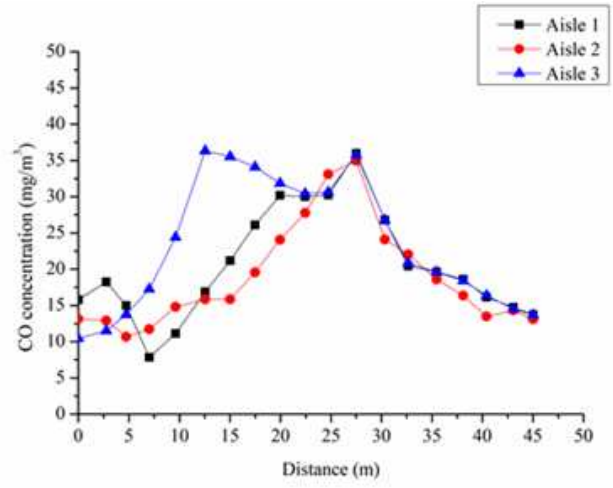

Figure 12. *Simulated CO concentration of each aisle (mg/m^3)*

In rush hour 8 am, 12 am, and 2 pm, the CO concentration in B and D increased obviously, but in A and C, the CO concentration changed slightly. This is because the

http://www.aloki.hu ● ISSN 1589 1623 (Print) ● ISSN 1785 0037 (Online)
DOI: http://dx.doi.org/10.15666/aeer/1704_90659081

area A and C is close to the outside and is easier to obtain the gas exchange. Area B is the pollution source and the CO concentration in area B that consists of three aisles is major object in the analysis. By comparing the data from *Tables 3* and *4*, it is obtained that in the underground garage, the CO concentration of measuring points will be affected by the inlet and outlet. Hence, the CO is mainly distributed in center underground garage which means the max CO concentration appears in this area.

Table 3. *The CO concentration in different areas (mg/m^3)*

Areas	8am	10am	12pm	2pm	4pm
A	17	15	20	16	21
B	42	32	40	44	31
C	14	13	15	14	12
D	40	32	38	42	33

Table 4. *The rush hour CO concentration at each measuring point (mg/m^3)*

Areas	Point 1	Point 2	Point 3	Point 4	Point 5
Aisle 1	35	33	40	30	25
Aisle 2	13	20	30	25	18
Aisle 3	15	20	30	25	20

As can be seen in *Table 4*, the CO concentration was higher in aisle 1 than in the other two aisles. The CO level in aisle 1 was above the required level of 30 mg/m³, indicating that more fresh air should be introduced to this aisle. The simulated and experimental data of the three aisles are compared in *Figures 13–15*.

The above figures show that the simulated data of each aisle deviated from the experimental data by only 5~20%, far lower than the allowable error (20%) for engineering application. Thus, the simulation results are proved as valid.

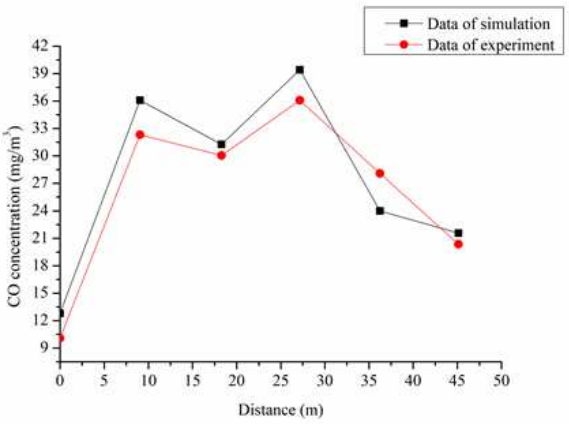

Figure 13. *Simulated CO concentrations vs. experimental CO concentrations in aisle 1*

http://www.aloki.hu ● ISSN 1589 1623 (Print) ● ISSN 1785 0037 (Online)
DOI: http://dx.doi.org/10.15666/aeer/1704_90659081

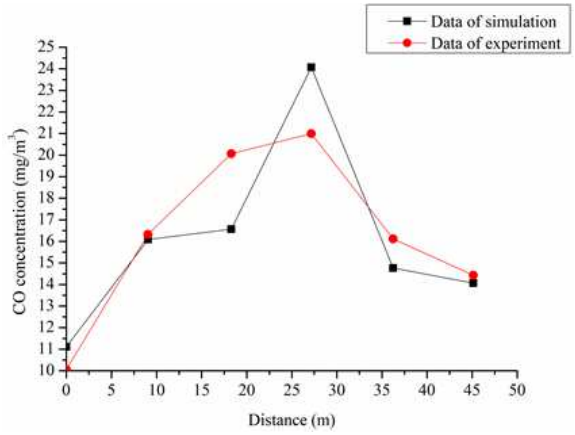

Figure 14. *Simulated CO concentrations vs. experimental CO concentrations in aisle 2*

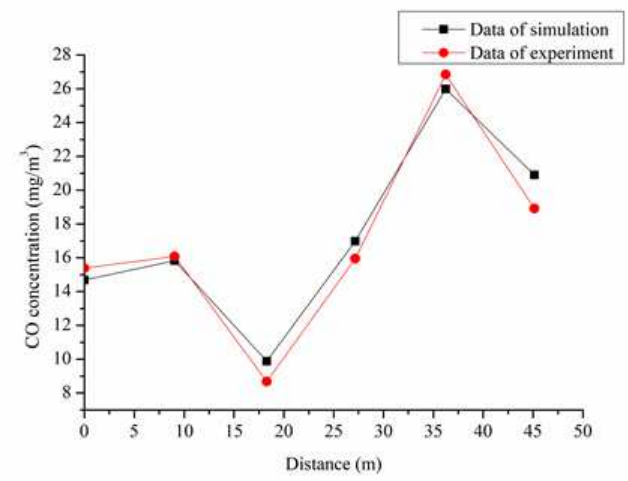

Figure 15. *Simulated CO concentrations vs. experimental CO concentrations in aisle 3*

Discussion of the ventilation plan

The key to mechanical ventilation lies in the wind volume, which is positively correlated with the running time of the fan. If the fan works continuously for the entire day, the pollutants can absolutely be emptied, leading to a better air quality. However, the prolonged operation of the fan will produce lots of noises and consumes much energy and money. Thus, it is very important to determine the running time of the fan.

The simulated data show that the CO concentration in most areas of the garage was below the required level of 30 mg/m^3, except the central part. Besides, aisle 1 had a higher CO concentration than the other aisles. Therefore, the next step is to simulate the operation of fan 3#, which is responsible for ventilating aisle 1. The running time of the fan was determined by the air volume needed to maintain the air quality in the garage:

$$G = \frac{3600M}{C_2 - C_1} \quad \text{(Eq.7)}$$

where M is the CO volume; C_2 is the maximum CO concentration; C_1 is the minimum CO concentration. M can be calculated as:

http://www.aloki.hu ● ISSN 1589 1623 (Print) ● ISSN 1785 0037 (Online)
DOI: http://dx.doi.org/10.15666/aeer/1704_90659081

$$M = n \times r \times q \times t \quad \text{(Eq.8)}$$

where n is the number of cars; r is the frequency of cars entering the garage; q is the CO volume released per car; t is the operating time of each car in the garage. The value of M was calculated as 5,304 g and the air volume needed to maintain the air quality in the garage was determined as 53,040 m^3.

The running time was set empirically to 20 min, three times per day in the rush hours, for the following reasons: the CO concentration under natural ventilation is only slightly above the required level; it is unknown how long the fan must run before the CO concentration falls below the required level. Moreover, the outlet of the fan was set as the velocity boundary with the velocity of 6 m/s. Under these conditions, the author performed a simulation on the mechanical ventilation and analyzed whether the CO concentration can meet the required level in rush hours. The simulated CO concentrations are illustrated in *Figures 16* and *17*.

As shown in the figures above, when the fan ran for 20 min, the CO concentration of the whole garage was controlled effectively, except for some points in aisle 1 (> 30 mg/m^3). Thus, the running time of the fan was extended to 30 min each time for another simulation. The simulated CO concentrations are displayed in *Figures 18* and *19*.

The above figures show that, when the fan ran for 30 min, the CO concentration of each aisle was controlled below the required level. The airflow of one fan in operation is different from that of several fans operating together. However, it is unnecessary to turn on all the fans in the garage at the same time, because the CO concentration is only slightly above the required level. Considering that aisle 3 had denser CO than aisle 2, the author continued to simulate the CO concentration in the garages with fan 3# (aisle 1) and fan 4# (aisle 3) running for 10 min, three times a day in the rush hours. The simulated CO concentrations are displayed in *Figures 20* and *21*.

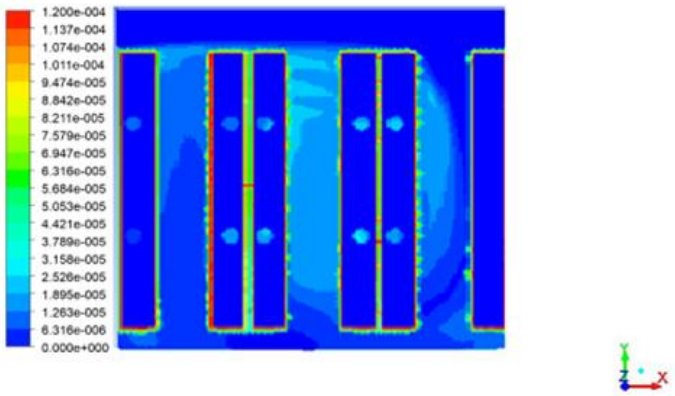

Figure 16. *The contour of CO concentration (20 min; 1 fan)*

http://www.aloki.hu ● ISSN 1589 1623 (Print) ● ISSN 1785 0037 (Online)
DOI: http://dx.doi.org/10.15666/aeer/1704_90659081

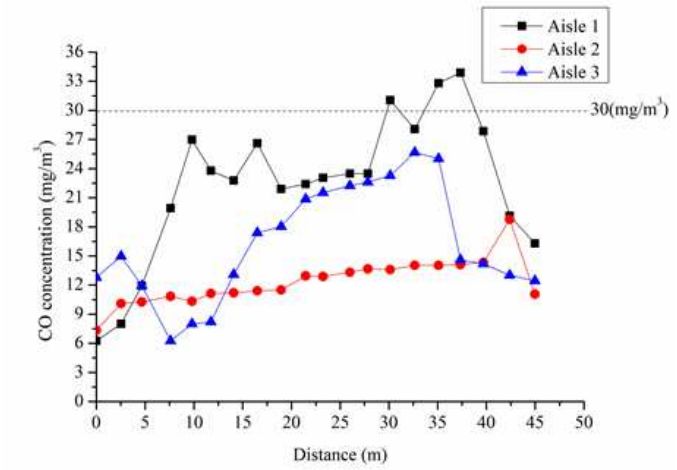

Figure 17. *The CO concentration of each aisle (20 min; 1 fan)*

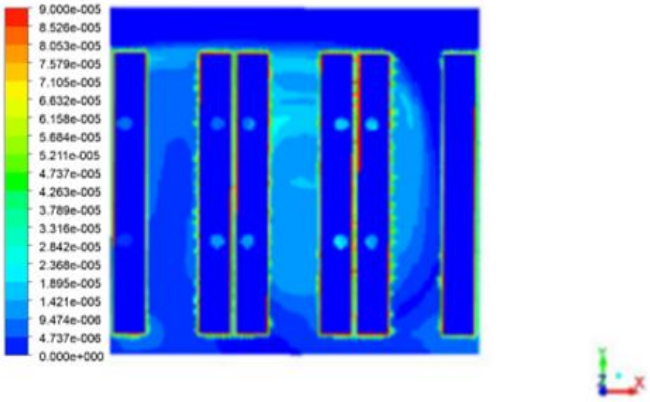

Figure 18. *The contour of CO concentration (20 min; 1 fan)*

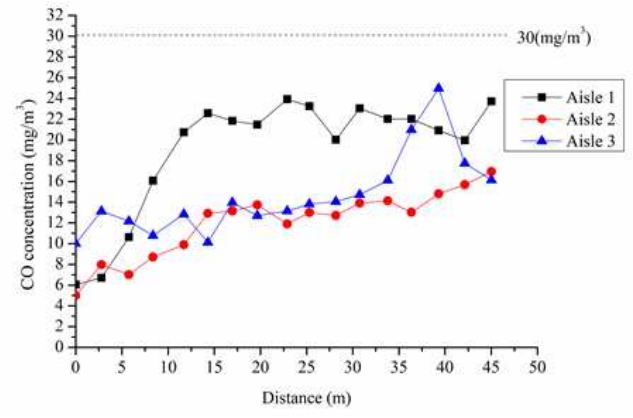

Figure 19. *The CO concentration of each aisle (30 min; 1 fan)*

http://www.aloki.hu ● ISSN 1589 1623 (Print) ● ISSN 1785 0037 (Online)
DOI: http://dx.doi.org/10.15666/aeer/1704_90659081

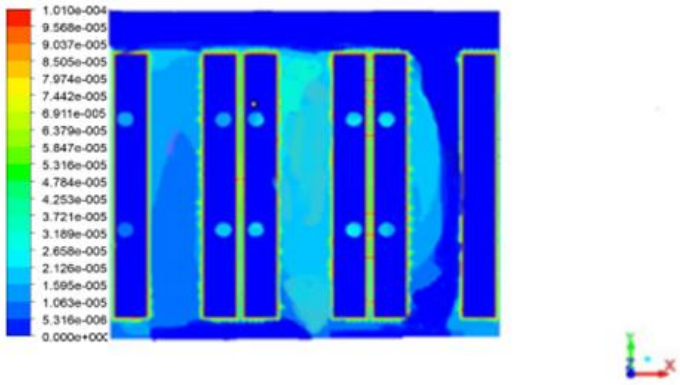

Figure 20. *The contour of CO concentration (10 min; 2 fan)*

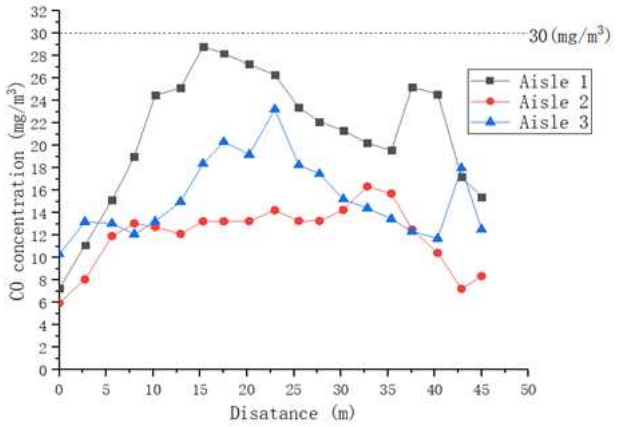

Figure 21. *The CO concentration of each aisle (10 min; 2 fan)*

As can be seen from the above figures, when the two fans ran 10 min together, the CO concentration of each aisle was below the required level, indicating the two-fan ventilation plan is satisfactory. The same ventilation effect can also be achieved through the simultaneous operation of 3 or 4 fans for a shorter time. The three-fan or four-fan ventilation plans were not considered because they must be noisier and costlier than the two-fan ventilation plan. Moreover, according to the nameplate of the fans, the power of each fan is about 24 kw, it means that this ventilation scheme can save about 1.44×10^4 kJ electricity power comparing with another scheme.

Compared with other studies about ventilation in underground garage, the method used in this paper that combining field experiment and simulation is more convenient and effective. In practical cases, more measurements make the analysis more accurate. However, measuring at the necessary area and using the measuring data into the simulation, then carrying out analysis with the finite element method is simpler and effective. Although error of numerical simulation cannot be avoided, confine it in a low range by optimizing the grid and choosing an appropriate algorithm can solve this problem.

http://www.aloki.hu ● ISSN 1589 1623 (Print) ● ISSN 1785 0037 (Online)
DOI: http://dx.doi.org/10.15666/aeer/1704_90659081

Conclusions

This paper combines numerical simulation with field experiment to study the pollutant diffusion and ventilation of an underground garage. Firstly, a numerical model was established to explore the diffusion features of pollutants under natural ventilation, and several ventilation plans were designed. After that, the flow field of the garage was investigated with the entrance, exit and ventilation shafts being considered as velocity boundaries, the air in the garage as an incompressible fluid, and the state of air flow as a turbulent flow. The simulated results show that the CO concentration of the garage was slightly above the required level (30 mg/m^3).

Considering the rated capacity of each exhaust fan, the first ventilation plan was designed to let one fan run for 20 min, three times a day in the rush hours. This plan was found to lower the CO concentration, but not below the required level. Thus, the second plan was designed to increase the running time to 30 min per time. The simulation results show that the second plan reduced the CO concentration in each aisle below the required level, indicating that this plan is satisfactory. Similarly, the third plan was simulated with two fans running together for 10 min per time, and proved satisfactory as well. This plan is enough for the ventilation of the garage because the three-fan or four-fan ventilation plans must be even noisier and costlier. The second and third ventilation plans were further compared. The third plan, i.e. the two-fan plan, was selected as the optimal ventilation plan, because it consumed 33% fewer power.

Acknowledgements. This research is supported by Applied Basic Research Program of Sichuan Province (Grant No.: 2019YJ0352).

REFERENCES

[1] Bai, Y., Zeng, Y., Zhang, X., Yan, X., Ruan, L., Zhou, X. (2016): Numerical and experimental study on the flow field induced by a train urgently speeding to the rescue station. – Tunnelling & Underground Space Technology 58: 74-81.

[2] Bascompta, M., Castanon, A. M., Sanmiquel, L. (2016): A GIS-based approach: influence of the ventilation layout to the environmental conditions in an underground mine. – Journal of Environmental Management 182: 525-530.

[3] Buckley, M. P., Veron, F. (2017): Airflow measurements at a wavy air–water interface using PIV and LIF. – Experiments in Fluids 58(11): 161.

[4] Chen, G. (2001): Determination and control of ventilation at underground garage. – Heating, Ventilating & Air Conditioning 32(1): 62-63.

[5] Choi, J., Hur, N., Kang, S., Lee, E. D., Lee, K. B. (2013): A CFD simulation of hydrogen dispersion for the hydrogen leakage from a fuel cell vehicle in an underground parking garage. – International Journal of Hydrogen Energy 38(19): 8084-8091.

[6] Dokos, S. (2017): Fluid Mechanics. Modelling Organs, Tissues, Cells and Devices. – Springer, Berlin.

[7] Hong, K., Wang, X., Zhou, Z., Zhou, S. (2010): Influence of branch tunnels on CO diffusion simulation of main underground powerhouse construction ventilation. – International Conference on Biomedical Engineering and Informatics 7: 2654-2657.

[8] Kierat, W., Bivolarova, M., Zavrl, E., Popiolek, Z., Melikov, A. (2018): Accurate assessment of exposure using tracer gas measurements. – Building & Environment 131: 163-173.

http://www.aloki.hu ● ISSN 1589 1623 (Print) ● ISSN 1785 0037 (Online)
DOI: http://dx.doi.org/10.15666/aeer/1704_90659081

[9] Kurnia, J. C., Sasmito, A. P., Mujumdar, A. S. (2014): CFD simulation of methane dispersion and innovative methane management in underground mining faces. – Applied Mathematical Modelling 38(14): 3467-3484.
[10] Liu, E., Li, W., Cai, H., Peng, S. (2019a): Formation Mechanism of Trailing Oil in Product Oil Pipeline. – Processes 7: 7.
[11] Liu, E., Lv, L., Ma, Q., Kuang, J., Zhang, L. (2019b): Steady-state optimization operation of the West-East Gas Pipeline. – Advances in Mechanical Engineering 11(8): 1-14.
[12] Liu, E. B., Yan, S. K., Peng, S. B. (2016a): Noise silencing technology for manifold flow noise based on ANSYS fluent. – Journal of Natural Gas Science and Engineering 29(2): 322-328.
[13] Liu, E. B., Yan, S. K., Peng, S. B. (2016b): Large eddy simulation and FW-H acoustic analogy of flow-induced noise in elbow pipe. – Journal of Computational and Theoretical Nanoscience 12(9): 2866-2873.
[14] Liu, E. B., Peng, S. B., Yang, T. W. (2018): Noise silencing technology for upright venting pipe jet noise. – Advances in Mechanical Engineering 10(8): 1-15.
[15] Papakonstantinou, K., Chaloulakou, A., Duci, A., Vlachakis, N., Markatos, N. (2003): Air quality in an underground garage: computational and experimental investigation of ventilation effectiveness. – Energy & Buildings 35(9): 933-940.
[16] Su, Z. Liu, E., Xu, Y. (2019): Flow field and noise characteristics of manifold in natural gas transportation station. – Oil & Gas Science and Technology-Revue d'IFP Energies Nouvelles 74: 1-12.
[17] Varga, S., Soares, J., Lima, R., Oliveira, A. C. (2017): On the selection of a turbulence model for the simulation of steam ejectors using CFD. – International Journal of Low-Carbon Technologies 12(3): 233-243.
[18] Wang, H., Wang, C., Wang, D. (2017): The influence of forced ventilation airflow on water spray for dust suppression on heading face in underground coal mine. – Powder Technology 320: 498-510.
[19] Wang, X. L., Zhang, Z. Q., Li, T., Liu, X. P. (2009): Dust diffusion simulation in the third layer construction of underground powerhouse. – School of Environmental Science and Engineering Tianjin University (English version) 15(2): 135-139.
[20] Wang, Z., Ren, T. (2013): Investigation of airflow and respirable dust flow behaviour above an underground bin. – Powder Technology 250(12): 103-114.
[21] Wang, Z. Q., Peng, Y., Zheng, J. H. (2016): Computational fluid dynamics simulation of storage temperature field in a non-ventilated underground granary. – Modern Food Science & Technology 32(1): 170-174.
[22] Widiatmojo, A., Sasaki, K., Widodo, N. P., Sugai, Y., Sinaga, J., Yusuf, H. (2013): Numerical simulation to evaluate gas diffusion of turbulent flow in mine ventilation system. – International Journal of Mining Science and Technology 23(3): 349-355.
[23] Xu, G. (2015): Remote characterization of ventilation systems using tracer gas and CFD in an underground mine. – Safety Science 74:140-149.
[24] Xue, H., Ho, J. C. (2000): Modelling of heat and carbon monoxide emitted from moving cars in an underground car park. – Tunnelling and Underground Space Technology incorporating Trenchless Technology Research 15(1): 101-115.
[25] Yong, C., Xu, P., Hao, Y. (2017): Mechanical performance experiments on rock and cement, casing residual stress evaluation in the thermal recovery well based on thermal-structure coupling. – Energy Exploration & Exploitation 35: 591-608.
[26] Zhang, G. S., Li, T. T., Luo, M., Liu, J. F., Liu, Z. R., Bai, Y. H. (2008): Air pollution in the microenvironment of parked new cars. – Building & Environment 43(3): 315-319.
[27] Zhao, Y., Song, X., Wang, Y., Zhao, J., Zhu, K. (2017): Seasonal patterns of pm10, pm2.5, and pm1.0 concentrations in a naturally ventilated residential underground garage. – Building & Environment 124: 294-314.

http://www.aloki.hu ● ISSN 1589 1623 (Print) ● ISSN 1785 0037 (Online)
DOI: http://dx.doi.org/10.15666/aeer/1704_90659081

A NEW BP NEURAL NETWORK FUSION ALGORITHM FOR MULTI-SOURCE REMOTE SENSING DATA ON GROUNDWATER

ZHANG, F.[1,2*] – XUE, H. F.[2] – ZHANG, Y. H.[1]

[1]*Yulin University of School of Information Engineering of Shannxi Province, Yulin 719000, China*

[2]*China Aerospace Academy of Systems Science and Engineering, Beijing 100048, China*

**Corresponding author*
e-mail: tfnew21@sina.com; phone: +86-136-4922-0169; fax: +86-091-2389-1364

(Received 18th Mar 2019; accepted 17th May 2019)

Abstract. This paper aims to enhance the accuracy and reduce the cost of the fusion of multi-source remote sensing data. For this purpose, the existing multi-source remote sensing data fusion methods were reviewed in detail. Then, a new back propagation (BP) neural network (BPNN) fusion algorithm for the groundwater was put forward based on hybrid soft computing. Using the function approximation ability of BP neural network, it was combined with the Kalman filter to form an optimization method. The BP neural network was coupled with the particle swarm optimization (PSO) algorithm into the PSO-BPNN-EKF data fusion algorithm. On this basis, the least squares support vector machine (LSSVM) was introduced to create the LSSVM-PSO data fusion algorithm. Through simulation experiments, it is learned that the proposed algorithm can effectively fuse the multi-source remote sensing data on groundwater, especially in the case of big data. The research findings shed a new light on the fusion of remote sensing data collected by multiple sensors.
Keywords: *groundwater, Kalman filter, data fusion, particle swarm optimization, hybrid soft computing*

Introduction

Back propagation (BP) neural networks (BPNNs) are neural network models based on the cross section of machine learning and neural networks. BP neural networks are computing systems vaguely inspired by the biological neural networks that constitute animal brains (Costantiti et al., 1997). A BPNN is based on a collection of connected units or nodes called artificial neurons which loosely model the neurons in a biological brain. Each connection, like the synapses in a biological brain, can transmit a signal from one artificial neuron to another. For any remote sensing platform, it is impossible to fully reflect the features of the ground target through the remote sensing data acquired by a single sensor. Facing multi-source spatial data, the geographic information system (GIS) data acquisition has become a popular choice. However, the resulting data resources differ in coordinate system, scale standard and storage format, making it difficult for data integration and sharing. The traditional data fusion algorithm requires a more accurate mathematical model of the object, which is not suitable for complex models, by using BP neural network algorithm to realize multi-sensor data fusion, the prior requirement of object is not high, and it has strong adaptive ability (Pohl and Van Genderen, 1998). Against this backdrop, the researchers on remote sensing have paid much attention to the removal of redundancy in data acquired by multiple sensors and improve data fusion and sharing. In light of this, this paper attempts to develop an effective multi-source remote sensing data fusion technology based on BP neural network, using BP neural network to fuse sensor data can improve the stability and accuracy of sensors.

http://www.aloki.hu ● ISSN 1589 1623 (Print) ● ISSN 1785 0037 (Online)
DOI: http://dx.doi.org/10.15666/aeer/1704_90839095

Traditional neural network training algorithm is slow in convergence and easy to fall into local optimum. In recent years, swarm intelligence optimization algorithms such as particle swarm optimization (algorithm) have better global convergence performance and can be used to train neural network parameters and structures. This model mechanistically reflects the natural process but fails to reflect the interaction between man and nature. To solve the problem, the data fusion technology, a desirable tool for estimation and identification, can be introduced to the model, allowing the timely and reliable acquisition of multi-format information from multiple sources like experts and the multimedia. Currently, the key data fusion technologies include the estimation technique, fuzzy set theory, clustering analysis, template method, human-computer interaction, expert system, multimedia technology, neural network method, distributed database technology and parallel processing technology (Li et al., 2018; Neelapu et al., 2018; Bhoi, 2017; Li, 2017; Liu and Xu, 2017; Hu et al., 2017; Zhang et al., 2010). Coupled with geophysical and geological databases, these technologies can increase the constraint recognition of in remote sensing applications, allowing them to describe the spatial geometry of the target from different aspects.

For efficient and accurate multi-source remote sensing data on groundwater, this paper creates a BP neural network fusion algorithm. Specifically, the extended Kalman filter (EKF) was adopted to sample the prior information and coupled with the particle swarm optimization (PSO) model and BP neural network (BPNN) into the PSO-BPNN-EKF data fusion algorithm. On this basis, the least squares support vector machine (LSSVM) was introduced to create the LSSVM-PSO data fusion algorithms.

Materials and methods

Neutral network data fusion methods

Neural network model

The typical three-layer neural network model is given in *Figure 1,* BPNN is a multi-layer feedforward network trained according to error back propagation algorithm. This algorithm can learn and store a great deal of mapping relations of input-output model, without the need to disclose in advance the mathematical equation that describes these mapping relations. The learning rule is to adopt the steepest descent method in which the back propagation is used to regulate the weight value and threshold value of the network to achieve the minimum error sum of square (Li et al., 2018). The structures of the BP neural networks are relatively mature in both network theory and performance. The distinctive advantage is that it has a strong nonlinear mapping capability and flexible network structure. In this paper, the BPNN is optimized using the PSO to speed up the convergence and avoid the local minimum trap.

Optimization of neural network parameters

The error correction algorithm is often used in the training process of feedforward neural networks. The most typical error correction algorithm is BP algorithm. The algorithm first generates a set of weights randomly, and then calculates the weight correction by gradient descent method until the training error reaches the target precision range. But the most obvious defect of this algorithm is slow convergence and sometimes even no convergence.

http://www.aloki.hu ● ISSN 1589 1623 (Print) ● ISSN 1785 0037 (Online)
DOI: http://dx.doi.org/10.15666/aeer/1704_90839095

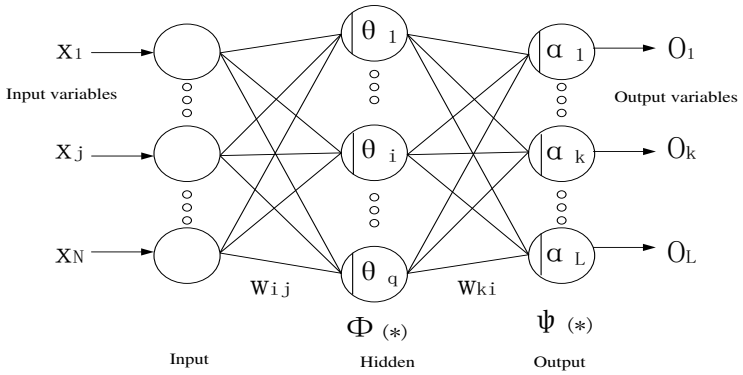

Figure 1. *Structure diagram of three-layer neural network model*

This paper used the optimization of neural network parameters translation method to build the training dataset. Using BP neural network's function approximation ability, BP neural network and Kalman filter are combined to form an estimator, which can make full use of sensor information from different noise pollution, improve estimation performance while maintaining estimation. The filtered computational structure is as simple as possible. Before network training, we must first normalize the data to ensure that the output of the network layer is not too small. What the initial value of the center vector p_i is determined by training samples, and where the $p_i = (p_{i1}, p_{i2}, p_{i3}, p_{i4},)$. If it belongs to the training sample set of the first kind of data change, It is represented as $\{S_1, S_2,\ldots, S_m\}$, and the initial value of each element in the centre vector p_1 is the average value of each element in the input vector of these samples. Firstly, take the logarithm of the sensor information from different noise pollution data which is denoted as is shown in *Figure 2*.

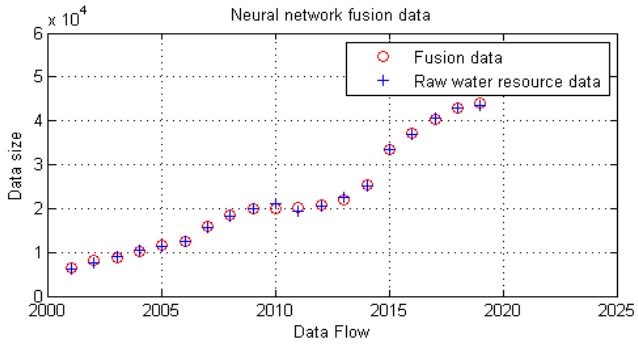

Figure 2. *Neural network fusion data*

KF data fusion

The traditional filtering algorithms mainly target the state variables of the system to be processed. Their performance depends on the system model, the input signal and the measured signal (Ryu and Huber, 2007). For these algorithms, form transformation is required to get the estimates of model parameters. In other words, the state equation and output equation need to be transformed from the standard form via bit filtering, with unknown parameters as the state variables. The transformation equation can be expressed as *Equation 1:*

http://www.aloki.hu ● ISSN 1589 1623 (Print) ● ISSN 1785 0037 (Online)
DOI: http://dx.doi.org/10.15666/aeer/1704_90839095

$$\begin{cases} x = ax + 1 \\ y = z \end{cases} \Rightarrow \begin{cases} \begin{bmatrix} x \\ a \end{bmatrix} = \begin{bmatrix} ax \\ 0 \end{bmatrix} + \begin{bmatrix} 1 \\ 0 \end{bmatrix} \\ y = \begin{bmatrix} 1 & 0 \end{bmatrix} \begin{bmatrix} z \\ a \end{bmatrix} \end{cases} \quad \text{(Eq.1)}$$

In a dynamic environment, the Kalman filter is often employed thanks to its real-time integration of data. The filter can describe linear differential equations of a discrete-time system. Let $x \in R^n$ be the state variables. Then, the state equation can be expressed as *Equation 2:*

$$x_k = f_k(x_{k-1}, \mu_{k-1}, \omega_{k-1}) + a_{k-1} \quad \text{(Eq.2)}$$

The measured variables $z \in R^m$ can be obtained as *Equation 3:*

$$z_k = h_k(x_k, \nu_k) + \beta_k \quad \text{(Eq.3)}$$

In the above equations, a_{k-1} is the system noise at time *k–1*; β_k is the measured noise; ω_k and v_k are two random variables representing the excited noise and the observed noise, respectively; μ_k and ω_k are the noises of the driving function and zero-mean normalization, respectively; x_k and z_k are the nonlinear functions of the state variables and measured variables, respectively.

The EKF is an extension of the Kalman filter. The basic idea of the EKF is to convert nonlinear vector function *f*(.) and nonlinear system model *f*(.) into linear filter values. Following this train of thoughts, *Equations 2* and *3* can be expanded into a Taylor series (*Eq. 4*) to obtain the linear model of the system. Then, the basic equations of the Kalman filter can be applied to solve the nonlinear filtering problem.

$$\begin{cases} x_k = f_k(x_{k-1}, \mu_{k-1}, \omega_{k-1}) + \dfrac{\partial f(x)}{\partial x} \Big| x = x_{k-1} + \alpha_{k-1} \\ z_k = h_1(x_k) + \dfrac{\partial f(x)}{\partial x} \Big| x = x_k + \beta_k \end{cases} \quad \text{(Eq.4)}$$

Particle swarm optimization algorithm

The PSO is a computational method that optimizes a problem by iteratively trying to improve a candidate solution with regard to a given measure of quality. It solves a problem by having a population of candidate solutions, here dubbed particles, and moving these particles around in the search-space according to simple mathematical formulae over the particle's position and velocity. Each particle's movement is influenced by its local best-known position but is also guided toward the best-known positions in the search-space, which are updated as better positions are found by other particles. This is expected to move the swarm toward the best solutions (Quiroga et al., 2013). Below is a brief description of the standard PSO algorithm.

Suppose there are a *d*-dimensional search space and a population containing N_p particles. Let $x_i^t = (x_{i1}^t, x_{i2}^t, \ldots, x_{id}^t)$ be a *d*-dimensional vector representing the initial position of particle *i* of the *t*-th generation, let the vector $v_i^t = (v_{i1}^t, v_{i2}^t, \ldots, v_{id}^t)$ be the velocity of particle *i*, i.e., the rate of change in the position, and let

http://www.aloki.hu ● ISSN 1589 1623 (Print) ● ISSN 1785 0037 (Online)
DOI: http://dx.doi.org/10.15666/aeer/1704_90839095

$p_i^t = (p_{i1}^t, p_{i2}^t, \ldots, p_{id}^t)$ be the best known position of particle i of the t-th generation. Then, the velocity and position of particle i can be obtained by updating *Equations 5* and *6* below.

$$v_{ij}(t+1) = \omega \cdot v_{ij}(t) + c_1 \cdot rand1_{ij} \cdot (pbest_{ij}(t) - x_{ij}(t) + c_2 \cdot (gbest_j(t) - x_{ij}(t) \quad \text{(Eq.5)}$$

$$x_{ij}(t+1) = x_{xj}(t) + v_{ij}(t+1) \quad \text{(Eq.6)}$$

where t is the iteration number; ω is the inertia coefficient; c_1 and c_2 are acceleration coefficients; $rand_1$ and $rand_2$ two uniformly-distributed random independent numbers in [0, 1]. The values of ω, c_1 and c_2 value should be determined according to the specific problem.

The performance of the PSO can be greatly enhanced if ω decreases linearly with the increase in the number of iterations as *Equation 7:*

$$\omega = \omega_{\min} + (iter_{\max} - iter) \times (\omega_{\max} - \omega_{\min}) / iter_{\max} \quad \text{(Eq.7)}$$

where ω_{min} and ω_{max} are the maximum and minimum weighting factors, respectively; $iter$ is the current iteration number; $iter_{max}$ is the maximum number of iterations. The flight speed v_i falls between the maximum and minimum weighting factors. This constraint condition ensures the convergence to the optimal solutions and improves the global search ability of the PSO.

LSSVM data fusion methods

The SVM (Jalalkamali et al., 2011) is a supervised learning model with associated learning algorithms that analyze data used for classification and regression analysis. It is known for its excellent generalization in the case of small samples. The SVM learning has been commonly used for the analysis on spatial data (Babaoğlu et al., 2010; Awan et al., 2013). The traditional SVM aims to solve convex quadratic optimization problems. However, the kernel matrix of the SVM has to occupy a large storage capacity, and the solution becomes less efficient when the sample size is excessively large. For this reason, the LSSVM (Zhang, 2011; Üstün et al., 2005) has been developed to improve the optimization effect. The new model replaces the traditional inequality constraints with an equality equation in the construction of the optimal objective function. Thus, the optimization process is transformed into the solution of a set of linear equations. In this way, the LSSVM achieves twice the efficiency of the traditional SVM. Despite the reduced cost, the LSSVM faces the loss of sparsity of the traditional method, owing to the use of ε - insensitive loss function.

Suppose there is a sample containing n training sets $\{(x_1,y_1),(x_2,y_2),\ldots,(x_N,y_N)\}$, where $x_k \in R^p$ the k-th input vector is. Assuming that the dataset is linearly separable, there must exist a linear classifier $y(x) = \omega^T \varphi(x) + b$ in the input space. If an optimization problem is nonlinear and separable, a nonlinear function φ(.) can be adopted to map the

http://www.aloki.hu ● ISSN 1589 1623 (Print) ● ISSN 1785 0037 (Online)
DOI: http://dx.doi.org/10.15666/aeer/1704_90839095

raw data space into a high-dimensional feature space, before looking for the classification surface-dimensional feature space $y(x) = \omega^T\varphi(x) + b$.

To obtain the optimal high-dimensional plane, the inequality equation needs to be introduced to the traditional SVM as *Equation 8:*

$$\begin{aligned} &\min_{w,b,\gamma} \quad -\gamma \\ &s.t \qquad y_i(<w,x_i>+b) \geq \gamma, i=1,...,\xi \\ &\|w\|^2 = 1 \end{aligned} \tag{Eq.8}$$

where γ is the spacer; ξ is the number of training samples; x_i is the vector of the i-th training sample; w is the weight vector; b is the threshold; y_i are the marked samples ($y_i = \begin{cases} 1 & x_i \in \omega_1 \\ -1 & x_i \in \omega_2 \end{cases}$); ω_i is the class of the i-th sample.

Then, the Lagrange function can be established as *Equation 9:*

$$\begin{aligned} L(w,b,\gamma,a,\lambda) = \\ -\gamma - \sum_{i=1}^{\xi} a_i[y_i(\langle w,x_i\rangle + b) - \gamma] \\ +\lambda(\|w\|^2 - 1) \end{aligned} \tag{Eq.9}$$

Unlike the traditional SVM, the LSSVM is built with equality constraint instead of the inequality constraint. Hence, the optimization problem can be expressed as *Equation 10:*

$$\begin{aligned} &\min_{w,b,\xi} J(w,b,\xi) = \frac{1}{2}w^T w + \frac{\gamma}{2}\sum_{i=1}^{N}\xi_i^2 \\ &s.t \quad y_i[w^T\varphi(x_i) + b] = 1 - \xi_i, i = 1,2...,N \end{aligned} \tag{Eq.10}$$

Then, the structure of the Lagrangian dual problem can be expressed as *Equation 11:*

$$L = J - \sum_{j=1}^{N} a_k\{y_k[w^T\varphi(x_k) + b] + \xi_i - 1\} \tag{Eq.11}$$

According to the optimization conditions, the partial derivatives of w, b, ξ and a can be obtained as *Equation 12* and set to zero.

$$\begin{cases} w = \sum_{i=1}^{N} a_i y_i \varphi(x_i) \\ \sum_{i=1}^{N} a_i y_i = 0 \\ a_i = \gamma\xi_i \\ y_i[w^T\varphi(x_i) + b] - 1 + \xi_i = 0 \end{cases} \tag{Eq.12}$$

http://www.aloki.hu ● ISSN 1589 1623 (Print) ● ISSN 1785 0037 (Online)
DOI: http://dx.doi.org/10.15666/aeer/1704_90839095

Under the above conditions, the kernel function can be defined as $k(x_i,y_i) = \psi(x_i)\psi(y_i)$. Then, the optimization problem can be transformed into solving the linear equations as *Equation 13*.

$$\begin{bmatrix} 0 & 1 & ... & 1 \\ 1 & k(x_1,x_1) & \dots & k(x_1,x_N) \\ \vdots & \vdots & \vdots & \vdots \\ 1 & k(x_N,x_1) & \cdots & k(x_N,x_N)+1/c \end{bmatrix} \begin{bmatrix} b \\ a_1 \\ \vdots \\ a_N \end{bmatrix} = \begin{bmatrix} 0 \\ y_1 \\ \vdots \\ y_N \end{bmatrix} \quad \text{(Eq.13)}$$

The above linear equations can be solved by the LSSVM classifier as *Equation 14:*

$$f(x) = sign(\sum_{i=1}^{N} a_i y_i K(x,x_i) + b) \quad \text{(Eq.14)}$$

The radial-basis function (RBF) can be selected as the kernel function, as *Equation 15:*

$$k(x_i, y_i) = \exp(\frac{-1\|x_i - y_i\|^2}{2\sigma^2}) \quad \text{(Eq.15)}$$

Based on these parameters, the penalty factor C and kernel function parameters σ can be obtained through the common optimization procedure.

BP neural network data fusion model

Soft computing was proposed by Prof. Zadein in the 1990s to solve uncertainty problems through fuzzy and intelligent technologies. The method is capable of tackling one or more complex datasets in realistic environment. Unlike traditional hard computing, soft computing does not pursue the exact solution, considering the inaccuracies in real-world problems and the high cost of the traditional method (Zhang et al., 2013). Instead, it pursues the next best solution when it is impossible or extremely difficult to obtain the optimal solution.

So far, soft computing has been extensively applied to data fusion and classification. This technology can combine the member attributes of fusions sequence into different logic structures (i.e. series structure, mosaic structure and parallel structure), depending on the specific data. Here, the parallel structure is adopted for fusing the remote sensing data on groundwater.

PSO-BPNN-EKF

In this paper, the PSO-BPNN-EKF optimization algorithm is proposed by optimizing the EKF state equation with the PSO, the algorithm uses PSO instead of the parameters in BPNN training algorithm and optimizes BP parameters. Each particle is a vector representing a set of parameters. The process of finding the global optimum is the process of obtaining the optimal parameters. Before the optimization, the particle set converges to the high likelihood area, which is far away from the true state. This

http://www.aloki.hu ● ISSN 1589 1623 (Print) ● ISSN 1785 0037 (Online)
DOI: http://dx.doi.org/10.15666/aeer/1704_90839095

problem is solved by the optimization, together with particle degeneration and in accuracy prediction. The PSO-EKF algorithm consists of the following steps:

(1) Initialization

Let N be the number of particles, and $p(x_0)$ be the initial population. Set the initial values of parameters as $\Delta x_0 = 0$, $p_0 = C_{x0}$ and $C_{x0} = 1.5$.

(2) Importance sampling

Adjust the velocity and position of each particle $v_k^i = \omega v_{k-1}^i + \gamma rand_i(p_{k-1}^g - x_{k-1}^i)$, and update the state of the particle according to the EKF algorithm. In other words, estimate the state of the particle $\hat{x}_k^i = x_k^i + \Delta x_k^i + v_k^i$ at time k according to the EKF importance sampling algorithm. Find the mean x_k^{-i} and variance P_{xk}^i of the particle set $\{\hat{x}_k^i\}_{i=1}^N$. Update the weight of the particles in the set x_k^i according to the importance of the density function $\left(x_k^i | x_{k-1}^i, \omega_k\right) = N(\hat{x}_k^i, x_k^{-1}, P_{xk}^i)$.

(3) Recompiling

Estimate the posterior probability of the target state at time k $x_k = \sum_{i=1}^N x_k^i \omega_k^i$, and find the current global optimal solution p_k^g. For $k = k + 1$, return to Step (2) and estimate the posterior probability of the target state at the next time.

PSO-based LSSVM parameter optimization

The LSSVM parameters γ and σ directly impact the prediction accuracy. Normally, the parameter space is search exhaustively to optimize these two parameters. However, it is difficult to determine the reasonable range of each parameter. To solve the difficulty, the LSSVM parameters were optimized by the PSO through the following steps (Yu et al., 2012; Anand et al., 2013).

(1) Initialize the PSO parameters, including population size, learning factor, maximum number of iterations, and the initial velocity and position of the particles.

(2) Predict the particle vector of each LSSVM learning sample, and obtain the current position, prediction error and fitness of each particle. Then, compare the current fitness of each particle with the best-known fitness. If the former is better, it should be selected as the optimal position of the particle.

(3) Compare the optimal position of each particle with the best known global position. If the former is better, it should be selected as the optimal global position.

(4) Calculate the inertia weight according to *Equation 7* and update the particle velocity and position according to *Equations 5* and *6,* respectively.

(5) Terminate the search process if the termination condition is satisfied; otherwise, return to Step (2) and start a new round of search.

Results

The study area is Yulin Prefecture in northern China's Shaanxi Province. There are 12 river basins in the prefecture, with a perennial mean runoff of 1.9446 billion m^3. Under the reliabilities of 50%, 75% and 95%, the annual runoff is 1.847, 1.504 and

http://www.aloki.hu ● ISSN 1589 1623 (Print) ● ISSN 1785 0037 (Online)
DOI: http://dx.doi.org/10.15666/aeer/1704_90839095

1.136 billion m^3. Specifically, the perennial mean runoff of the 10 outflow basins stands at 1.8099 billion m^3. Under the reliabilities of 50%, 75% and 95%, the annual runoff is 1.7194, 1.4034 and 1.0660 billion m^3. The perennial mean runoff of the other 2 inflow basins amounts to 0.1347 billion m^3. Under the reliabilities of 50%, 75% and 95%, the annual runoff is 0.1277, 0.1001 and 0.0699 billion m^3. The central districts, including Shenmu County, Fugu County, Yuyang District and Hengshan County, have a perennial mean runoff of about 1.557 billion m^3. Under the reliabilities of 50%, 75% and 95%, the annual runoff is 1.477, 1.201 and 0.907 billion m^3. The peripheral districts like Jingbian County have a perennial mean runoff of about 0.388 billion m^3. Under the reliabilities of 50%, 75% and 95%, the annual runoff is 0.370, 0.303 and 0.327 billion m^3. The annual runoffs are recorded in *Table 1*. The water quality of major rivers is given in *Table 2*.

Table 1. *Annual runoffs in Yulin Prefecture*

River basin	Basin area (km^2)	Average annual runoff (million m^3)	Average runoff depth (mm)	Different frequencies annual runoff (million m^3)		
				50%	75%	95%
Huangfuchuan	2 827	1. 546	54. 69	1.326	0.868	0.498
Shimizu River	321	0. 183	57. 01	0.160	0.111	0.067
Sichuan Gushan	261	0. 195	74. 71	0.171	0.112	0.064
Kuye River	4 629	3. 096	66. 88	2.876	2.146	1.409
Wudinghe River	9 396	4. 260	45. 34	4.133	3.478	2.708
Total	17434	9.28	298.63	8.666	6.715	4.746

Table 2. *Groundwater quality in the study area*

River	PH value	Dissolved oxygen (mg/L)	Oxygen consumption (mg/L)	Total hardness (Germany degrees)	Salinity (g/L)
Lu River (Hengshan)	7.6	2.3	5.4	14.0	0.92
Wudinghe River (Xiangshui)	7.6	3.7	2.4	10.1	0.77
Wudinghe River (Baijia Chuan)	8.2	6.3	1.4	12.1	0.53
Tuweihe (upstream)	7.4	4.3	2.1	8.26	0.23
Tuweihe (downstream)	7.9	3.2	2.9	8.27	0.20
Kuye River (upstream)	7.4	3.1	3.3	9.81	0.28
Kuye River (midstream)	7.9	6.1	4.1	11.36	0.32
Kuye River (downstream)	7.4	5.1	4.5	9.53	0.26
Jia Lu River	7.9	4.2	3.1	6.7	0.22
Bali River	7.3	5.5	3.2	8.8	0.25

To validate the proposed PSO-BPNN-EKF algorithm, the performance of the PSO-BPNN-EKF and PSO-SVM were contrasted with that of the KF, the EKF, the PSO-KF, the LSSVM-PSO and the BP- PSO-BPNN-EKF through 100 Monte-Carlo simulations with $\delta = 2$ at the number of particles of 50, 100 and 150. The results of different algorithms are shown in *Table 3*.

http://www.aloki.hu ● ISSN 1589 1623 (Print) ● ISSN 1785 0037 (Online)
DOI: http://dx.doi.org/10.15666/aeer/1704_90839095

Table 3. *Results of contrastive algorithms*

Filter	PF	EPF	PSO-EPF	PSO-SVM	PSO-BPNN-EKF
N = 60 Variance	4.199	3.823	2.310	2.121	2.112
N = 100 Variance	3.523	3.123	2.132	2.092	2.093
N = 160 Variance	3.223	3.121	2.622	2.122	2.031
N = 260 Variance	2.133	1.987	1.232	1.154	1.131

Considering the good nonlinear fitting effect of the RBF, the function was adopted as an improved kernel for the LSSVM. The selection of parameters is essential to the performance of the LSSVM model. In this paper, the parameters are determined by the improved PSO as: number of particles $N = 25$, the maximum number of iterations $G_{max} = 100$, the learning factors $c_1 = 1.5$ and $c_2 = 1.5$, the inertia weight = 0.9. Then, the LSSVM-PSO model was simulated on the Matlab. The particle position was updated constantly until the termination condition was satisfied. In this way, the optimal RBF parameters σ was determined as 0.5, and the normalization parameter c was identified as 60. Next, the optimal parameters were adopted for the fusion of groundwater data by the LSSVM-PSO model. The results are presented in *Figure 3*. And then we compare the experimental results of data fusion between LSSVM-PSO and PSO-BPNN-EKF algorithm, as shown in *Figure 4*. In order to more clearly observe the change of the value of the sum of squares of errors, *Figure 5* has trained the variation of the sum of error squared sum of the PSO-BPNN-EKF algorithm.

Discussion

According to lab analysis, the groundwater quality in the central districts is as follows: the pH ranges in 7.6~8.3, the total hardness falls in 10.1~17.3 (°D), the salinity belongs to 0.33~0.92 g/L, and the poisonous contents like mercury, arsenic and chromium VI are minimal or non-detectable. Overall, the quality of the groundwater meets the *Standards for Drinking Water Quality* (GB5749-2006) and *Standards for Irrigation Water Quality* (GB 5084-2005). In the peripheral district, the groundwater in a few areas is not suitable for drinking or irrigation, as its hardness and salinity are higher than the specified ranges.

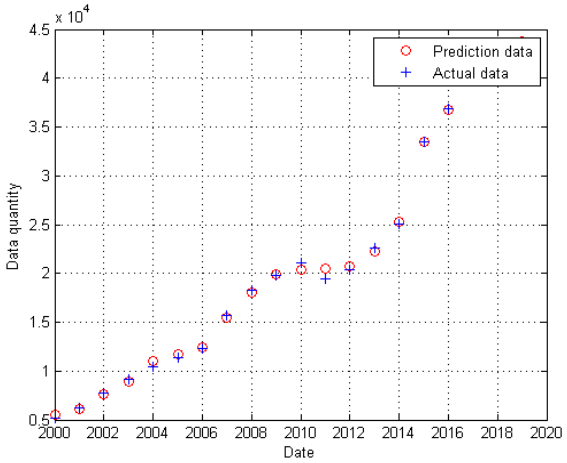

Figure 3. *Comparison of neural network water resources data volume learning and testing*

http://www.aloki.hu ● ISSN 1589 1623 (Print) ● ISSN 1785 0037 (Online)
DOI: http://dx.doi.org/10.15666/aeer/1704_90839095

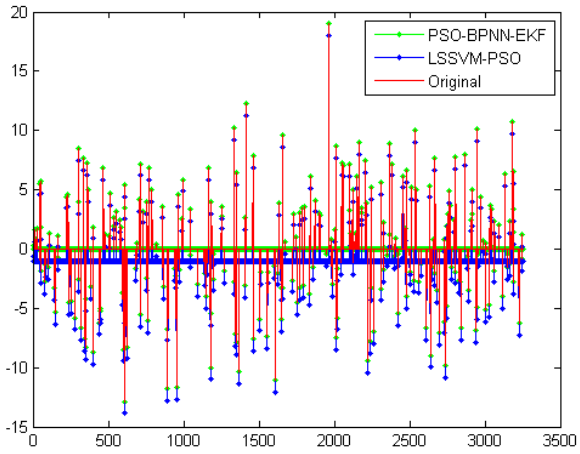

Figure 4. *Comparison of data prediction results between LSSVM-PSO and PSO-BPNN-EKF algorithm*

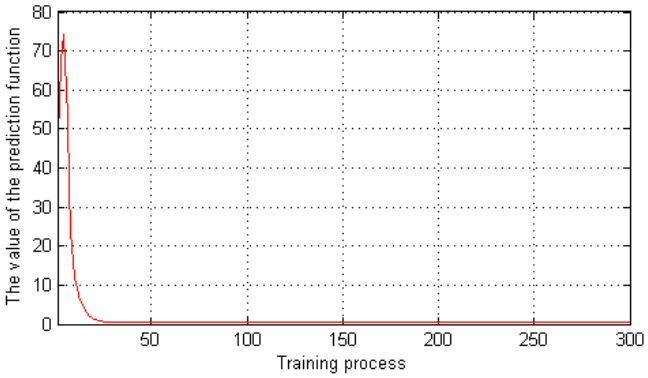

Figure 5. *Variation of square sum of errors in training neural network*

As shown in *Table 2,* the groundwater in the study area has simple chemical compositions. In the loess area, the groundwater is of the HCO_3-CaMg type with a salinity below 0.5 g/L; in the plain areas, the groundwater mainly belongs to the $ClSO_4$-N_8 type with a salinity between 1.0 g/L and 18.46 g/L.

As shown in *Table 3,* when the number of particles $N = 100$, the PSO-SVM achieved a much better performance than the other algorithms, as evidenced by the extremely low error. This means the PSO optimization of EKF state equations increases the particle diversity and enhances the filtering accuracy. Overall, the proposed PSO-BPNN-EKF and PSO-SVM boasted the best performance, followed by the PSO-BPNN-EKF, the EKF and the LSSVM. The ranking demonstrates the effectiveness of the proposed algorithm.

Conclusions

Real-time monitoring of groundwater resources with multiple sensors is a difficult dynamic control problem, due to the large scale and heterogeneity of multi-source data. The existing models cannot satisfactorily reduce the dimensions of the monitoring data. Therefore, this paper attempts to create an innovative approach for dynamic monitoring

http://www.aloki.hu ● ISSN 1589 1623 (Print) ● ISSN 1785 0037 (Online)
DOI: http://dx.doi.org/10.15666/aeer/1704_90839095

of groundwater based on large data. For this purpose, a new data fusion algorithm was proposed, aiming to reduce the data size and energy consumption in the fusion process. Inspired by the superiority of artificial neural networks, the rough set theory and the PSO were employed to reduce the complexity of the proposed algorithm. Through several simulations, it is proved that the proposed algorithm can process data more efficiently than the BPNN and the PSO, two popular data processing methods. The excellent performance is attributable to the reduction of data table in the case of big data. The research findings shed new light on the fusion of remote sensing data collected by multiple sensors. Further studies are expected to understand the connotation of the problem of big data fusion, in the era of big data, the analysis and mining for the multi-source remote sensing data is a research field and which attracts much attention. To effectively learn the characteristics of massive, low-quality, heterogeneous, high-dimensional and fast-changing big data, there are still a series of problems and challenges. Our study provides a corresponding multi-source remote sensing data fusion algorithm for the incompleteness of multimodal data, real-time processing and multi-source data fusion.

Acknowledgements. This work is partially supported by the National Natural Science Foundation of China (Grant No. U1501253, No. 51651901); Natural Science Basic Research Plan in Shaanxi Province of China (2017NY-134, 2016KJXX-62, 2016NY141, 2017NY132); Funding Project for Department of Yulin University (16GK24) and Thanks for the help.

REFERENCES

[1] Anand, A, Galelli, S, Lakshminarayanan, S, Sundaramoorthy, S. (2013): Coordinating multiple model predictive controllers for the management of large-scale water systems. – Journal of Hydroinformatics 15(2): 293-305.

[2] Awan, U. K., Tischbein, B., Martius, C. (2013): Combining hydrological modeling and GIS approaches to determine the spatial distribution of groundwater recharge in an arid irrigation scheme. – Irrigation Science 31(4): 793-806.

[3] Babaoğlu, İ., Findik, O., Ülker, E. (2010): A comparison of feature selection models utilizing binary particle swarm optimization and genetic algorithm in determining coronary artery disease using support vector machine. – Expert Systems with Applications 37(4): 3177-3183.

[4] Bhoi, A. K. (2017): Classification and clustering of Parkinson's and healthy control gait dynamics using LDA and K-means. – International Journal Bioautomation 21(1): 19-30.

[5] Costantiti, M., Farina, A., Zirilli, F. (1997): The fusion of different resolution SAR images. – Proceedings of the IEEE 85(1): 139-146.

[6] Hu, T., Lv, J., Xie, Q. S., Sun, H., Yuan, Q. N. (2017): A novel human behaviour information coding method based on eye-tracking technology. – Traitement du Signal 34(3-4): 153-173.

[7] Jalalkamali, A., Sedghi, H., Manshouri, M. (2011): Monthly groundwater level prediction using ANN and neuro-fuzzy models: a case study on Kerman plain, Iran. – Journal of Hydroinformatics 13(4): 867-876.

[8] Li, B., Zhang, C., Han, C., Bai, B. X. (2018): Fingertip data fusion of Kinect v2 and leap motion in unity. – Ingénierie des Systèmes d'Information 23(6): 143-159.

[9] Li, M. X., Liao, R. Q., Dong, Y. (2018): A new BP neural network model for the prediction problem of equally spaced time sequences and its application. – NeuroQuantology 16(6): 28-32.

http://www.aloki.hu ● ISSN 1589 1623 (Print) ● ISSN 1785 0037 (Online)
DOI: http://dx.doi.org/10.15666/aeer/1704_90839095

[10] Li, Z. J. (2017): Application of neural network technology in machining error recovery. – Academic Journal of Manufacturing Engineering 15(3): 6-11.
[11] Liu, B. L., Xu, X. W. (2017): A power system active power network loss based calculation method on partial priority clustering algorithm. – Review of Computer Engineering Studies 4(1): 17-21.
[12] Neelapu, R., Devi, G. L., Rao, K. S. (2018): Deep learning based conventional neural network architecture for medical image classification. – Traitement du Signal 35(2): 169-182.
[13] Pohl, C., Van Genderen, J. L. (1998): Multisensor image fusion in remote sensing: concepts, methods and applications. – International Journal of Remote Sensing 19(5): 823-854.
[14] Quiroga, V. M., Popescu, I., Solomatine, D. P., Bociort, L. (2013): Cloud and cluster computing in uncertainty analysis of integrated flood models. – Journal of Hydroinformatics 15(1): 55-70.
[15] Ryu, H. R., Huber, M. (2007): A particle filter approach fro multi-target tracking. – IEEE/RSJ International Conference on Intelligent Robots and Systems, October 29 - November 2, 2007, San Diego, CA.
[16] Üstün, B., Melssen, W. J., Oudenhuijzen, M., Buydens, L. M. C. (2005): Determination of optimal support vector regression parameters by genetic algorithms and simplex optimization. – Analytical Chimica Acta 544(1): 292-305.
[17] Yu, F., Lu, W., Li, P., Xin, X., Li, J. (2012): Dynamic optimal control for groundwater optimization management with covariates. – Journal of Hydroinformatics 14(2): 386-394.
[18] Zhang, F. (2011): Research on water-saving irrigation automatic control system based on internet of things. – Proceedings of ICEICE 2011: 2541-2544.
[19] Zhang, F., Xue, H. F., Xu, D. S., Zhang, Y. H., You, F. (2013): Big data cleaning algorithms in cloud computing. – International Journal of Online Engineering 9(3): 77-81.
[20] Zhang, K., Huang, H. P., Yang, H. T., Xie, Q. (2010): A transformer fault diagnosis method integrating improved genetic algorithm with least square support vector machine. – Power System Technology 34(2): 164-168.

http://www.aloki.hu ● ISSN 1589 1623 (Print) ● ISSN 1785 0037 (Online)
DOI: http://dx.doi.org/10.15666/aeer/1704_90839095

SOCIAL STABILITY RISK EVALUATION OF MAJOR WATER CONSERVANCY PROJECTS IN FRAGILE ECO-ENVIRONMENT REGIONS

WU, Q.[1,2] – WANG, L.[2*] – JIN, N.[3] – LI, N.[2] – HU, X.[2]

[1]*College of Management, Xi'an University of Architecture & Technology*
Yanta Rd. 13, Beilin District, Xi'an 710055, China

[2]*School of Civil Engineering, Xi'an University of Architecture & Technology*
Yanta Rd. 13, Beilin District, Xi'an 710055, China

[3]*Shaanxi Province Institute of Water Resource and Electric Power Investigation & Design*
East St. 57, Beilin District, Xi'an 710001, China

[*]*Corresponding author*
e-mail: wllucky2019@163.com

(Received 18th Mar 2019; accepted 17th May 2019)

Abstract. Considering the importance of social stability risk evaluation for major water conservancy projects (MWCPs), this paper creates a feasible evaluation index system for such projects in fragile eco-environment regions (FEER) through literature review, questionnaire surveys and data analysis. Then, a risk evaluation model was construction based on the set pair analysis (SPA) and the principal component analysis (PCA). The proposed model was applied to a MWCP in Shaanxi Province, China, revealing that the project has a low level of social stability risk. The evaluation result agrees with the actual situation, confirming the reliability and rationality of the proposed model. On this basis, several suggestions were proposed to further mitigate the social stability risks of the MWCPs in the FEER. The research findings provide a valuable reference for similar projects in FEER.
Keywords: *social risk, index system, set pair analysis (SPA), suggestions, China, case study*

Introduction

Water conservancy projects bring many benefits to regional and national development, such as controlling flood, protecting the eco-environment, rationalizing the use of water resources, and promoting economic development. In recent years, water conservancy projects are springing up across China, in response to the surging demand for industrial and domestic water (Qu, 2017). A total of RMB 713.24 billion yuan was spent on water conservancy projects in 2017, and another 100 billion was added in the following year. In Shaanxi Province alone, 172 major water conservancy projects (MWCPs) were kicked off in 2018.

The water conservancy projects that have a huge construction scale and involve numerous factors are defined as MWCPs. In China, such projects need to be approved by the central and provincial governments. Unlike the general projects, an MWCP features a long construction period, a high investment and a large demand for land resources. In addition, such projects construction is faced with various health, ecological and economic issues (Wang et al., 2015). For example, the project party needs to consider house demolition, resettlement and compensation for reservoir immigrants. If not solved properly, these problems may lead to social instability in the project area, especially in fragile eco-environment regions (FEER).

http://www.aloki.hu ● ISSN 1589 1623 (Print) ● ISSN 1785 0037 (Online)
DOI: http://dx.doi.org/10.15666/aeer/1704_90979111

For MWCPs, the social stability risks mainly refer to the negative social impacts of the project construction and operation on the residents in the project area. The residents may file petitions, resort to violence or take part in mass unexpected incidents, if their interests are undermined by the project. The social stability risks of MWCPs are not uncommon. Among the 527 MWCPs funded by the World Bank, only 30 has not caused social instability, and 27 has destabilized the local society. The mean yield of the 30 project stands at 18.3%, while that of the 27 projects lingers at 8.6%. In 2017, the Chinese government pledged to take heavy measures against major risks of MWCPs, with the aim to improve prevention mechanisms and resolve social tensions. Over the years, the management of social stability risks has become an important aspect in the evaluation of MWCPs. Therefore, it is imperative to develop a realistic index system to rationally quantify the social stability risks of MWCPs.

The contents shape the outcomes of the evaluation of social stability risks, and the countermeasures against such risks. Without proper contents, it would be impossible to achieve the goals of project investment (SGJ, 2012; Shi et al., 2015; Yang and Lv, 2017).

Some scholars argued that a complete evaluation of social stability risks in MWCPs should cover social impacts, social suitability and social risks, and tackle such factors as the stakeholders, local population, production activities, social organizations and cultural acceptability (Becker, 2001; Eskesen et al., 2004). However, Zhang et al. (2013) suggested including social impacts, economic impacts and environmental impacts into the social stability risk evaluation of MWCPs. To achieve scientific and democratic social stability risk evaluation, Liao (2018) advised to clarify the status and duties of citizens, the government and third parties in the evaluation through "confrontational debates", fully assess the public participation and opinions of project construction, identify the project impacts on poverty, gender, immigration and ethnic minorities, and monitor the various aspects (e.g. life, resettlement and social development) of the project in a timely manner. Meanwhile, the Chinese Ministry of Water Resources stipulated that the social stability risks of MWCPs should be evaluated from the perspectives of legality, rationality, feasibility and controllability. However, this provision has not been well implemented in the existing practices.

In the evaluation of social stability risks, the index system should reflect all key attributes of the target MWCP, and contain indices that are properly correlated with each other. A suitable index system is the first step in reducing the social stability risks and the early prevention of social instability.

In 1984, the World Bank requested all construction projects to include social risk evaluation in the feasibility study (Dani, 2003). Many scholars understood the social risks of construction projects as those arising from the different responses of stakeholders to specific issues and from the conflict between policymakers and the stakeholders (Hu et al., 2013). Following this train of thought, Wang and Zhang (2012) design an evaluation index system for social stability risks, which contains such indices as institutional role, behavior, stakeholder and social risk. In 2001, the former Chinese Ministry of Railways required all railway projects to assess their social stability risks from both macro and micro angles, against indices like social impacts and the degree of integration with the local environment. He et al. (2018) explore the relationship between stakeholders and risk factors and identifies the key indices of social stability risks by social network analysis.

On MWCPs, the existing studies generally set up the evaluation index system of social stability risks from the following aspects: policy, economy, society, environment,

http://www.aloki.hu ● ISSN 1589 1623 (Print) ● ISSN 1785 0037 (Online)
DOI: http://dx.doi.org/10.15666/aeer/1704_90979111

behavior and governance (Sun, 2011; Peng et al., 2013; Xiao et al., 2016; Zhu et al., 2016; Hu, 2016). Using engineering analysis method, Huang et al. (2013) discussed the social stability risks of MWCPs in three dimensions, namely, social risk exposure, social sensitivity, and coping capacity. Some scholars include the public perception of risk in the index system for evaluation of social stability risks (Guo, 2012; Hu and Wang, 2014; Zhu et al., 2014; Yin et al., 2018; Zhang and Zhu, 2018; Fan, 2018). Inspired by social combustion theory and social vulnerability theory, Yang (2012) and Feng et al. (2017) measured social stability risks against such four indices as conflict diffuseness, conflict severity, conflict persistence and the total amount of conflicts. Liu et al. (2016) classified the risk factors into procedural risks, cognitive risks and friction risks. Targeting MWCPs, Teng et al. (2014) set up an index system for social stability risk evaluation, including but not limited to individual, family, political structure, social structure, direct impacts, public resources, eco-environment, social adaptability, and community. Chen and Wang (2018) identified the risk factors of public-private partnership (PPP) project against the indices of the government, social capital, public and environment, and summed up the risk formation mechanism. Liu and Wang (2017), and Yu et al. (2016) probed into the evaluation index system of social stability risks in urban transit projects and major river projects, but did not come up with a unified index system.

MWCPs involve numerous influencing factors, making it difficult to use a unified evaluation method. The evaluation method should properly quantify the degree and probability of each social stability risk.

From the angle of stakeholders, Jiao et al. (2015) evaluated the social stability risks of MWCPs by the fuzzy weighting method. Song (1995) assessed the social stability risks of MWCPs using the state-response mechanism. Cao et al. (2013) carried out a questionnaire survey on engineers and social evaluation experts, asked them to rate each social stability risk, and determined the weight of each risk based on the ratings. Chen et al. (2013) adopted the analytic hierarchy process (AHP) to assess the social stability risks of MWCPs. Sturk et al. (1996) suggested that the fault tree analysis (FTA) and the hazard and operability study (HAZOP) are applicable to risk evaluation, and successfully employed the FTA to evaluate the social stability risks of an actual project. Clark and Borst (2002) relied on the risk index method to assess various risks on the underground transit line in Seattle. Based on the entropy-weight and matter-element extension model, Dong et al. (2018) proposed a social stability risk evaluation method for highway projects, which computes the classical domain and the correlation function of each index, takes the entropy as the weight of the index, calculates the comprehensive correlation and then grades the social stability risks of the project.

In summary, the following methods have been frequently adopted to evaluate the social stability risks of MWCPs: the AHP, fuzzy comprehensive evaluation (FCE), grey comprehensive evaluation, principle of Maximum Entropy (Li et al., 2009), group decision AHP (GAHP) (Kong et al., 2015), hierarchal holographic modeling (HHM), fuzzy variable theory (Xiao, 2017) and evaluation models combining various mathematical methods (He and Yang, 2014; Wu et al., 2016; Ma, 2017; Wang, 2017; Ge et al., 2018). These methods share some common defects. For example, the evaluation indices are too rigid to evaluate ambiguous, random and uncertain phenomena, the risk levels are determined rather subjectively, and the computing is so complex as to produce errors.

http://www.aloki.hu ● ISSN 1589 1623 (Print) ● ISSN 1785 0037 (Online)
DOI: http://dx.doi.org/10.15666/aeer/1704_90979111

Materials and Methods

Evaluation index system

Preliminary selection

As required by the Chinese Ministry of Water Resources, legality, rationality, feasibility and controllability were the contents of our evaluation of social stability risks in MWCPs. On this basis, the indices of each content were selected preliminarily, forming a hierarchy structure. Next, the preliminary evaluation index system was set up in light of the indices in actual cases, those in similar projects and the features of the target project.

Index screening

The indices are qualitative variables that measure the subjective feelings of the respondents. Here, each index was rated against a 5-point Likert scale (1: Very unimportant; 2: Unimportant; 3: Neither important nor unimportant; 4: Important; 5: Very important). Before issuing the formal questionnaire, all items were subjected to several tests (*Table 1*). The unqualified terms were deleted in view of the experts' opinions.

(1) Correlation test

The correlation test aims to determine the Pearson product moment coefficient, i.e. the correlation between an item's scores and the total test scores, of each item. The test results show that three indices, including decision-making power $u_{11,}$ institutional construction u_{12} and acquisition and demolition scale $u_{13,}$ were not significant or slightly significant ($p<0.4$). Thus, these descriptive items are not highly correlated with the scale.

The Chinese Ministry of Water Resources specified that the evaluation entity of social stability risks should be designated by the people's government in the project area or its subordinate departments, have clear management organization and relevant rules and regulations, and maintain no direct interest-relationship with the project; the social stability risk evaluation report should be signed by the people's government in the project area. Therefore, the decision-making power and institutional construction of government departments are not inducers of social stability risks.

In addition, the rationality of acquisition and demolition scale depends on the quality of planning, design and related measures. This item is not a direct cause of social risk events. To sum up, the decision-making power, institutional construction and acquisition and demolition scale were deleted from our index system.

(2) Validity test

Before the factor analysis, the remaining 21 items received the validity test. The results show that the Kaiser-Meyer-Olkin (KMO) value was 0.679, above the 0.6 threshold; the p value of Bartlett's test of sphericity was 0.000, which is significant at the level of 0.05. This means the proposed scale is suitable for factor analysis.

From the factor analysis, the minimum common value u_{43} was determined as 0.510, and all items were above 0.2, indicating that the factor acceptable. Besides, the factor load was greater than 0.5 and the cumulative contribution rate of the four factors reached 70.189%, above the required rate of 70%. Therefore, the 21 items can be retained for subsequent analysis and the scale is of good validity.

(3) Reliability test

The Cronbach's alpha of the total scale (0.931) was greater than 0.9, signifying the good overall reliability of the scale. Generally, when the total correlation of the

http://www.aloki.hu ● ISSN 1589 1623 (Print) ● ISSN 1785 0037 (Online)
DOI: http://dx.doi.org/10.15666/aeer/1704_90979111

correction item is below 0.4, an item should be deleted if the Cronbach's alpha after deletion is greater than or equal to that of the total scale. Among the 21 items, the resettlement plan u_{29} had a Cronbach's alpha lower than 0.4, and the Cronbach's alpha after deleting this item equaled that of the total scale. After consulting experts, it is confirmed that this term is a trigger of mass unexpected incidents in similar projects, and thus not deleted. The other items all passed the reliability test. The Cronbach's alphas of the subscales also passed the test, indicating that the scale reliability will not increase after removal of any item. As a result, all 21 items can be retained for subsequent analysis and the scale is of high reliability.

Table 1. *The results of the reliability test (Wu, 2010)*

Item	Correlation coefficient between the item and the total score		Homogeneity test					Remarks
	Pearson Correlation	Significant (bilateral)	Corrected item total relevance	alpha value after the item is deleted	Subscale alpha value	Commo-nality	Factor load	
u_{11}	0.044	0.807						Deleted
u_{12}	0.34	0.053						Deleted
u_{13}	0.582	0	0.498	0.927	0.717	0.742	0.779	Reserved
u_{14}	0.455	0.008	0.4	0.93		0.51	0.517	Reserved
u_{15}	0.774	0	0.726	0.924		0.89	0.783	Reserved
u_{21}	0.678	0	0.677	0.924		0.689	0.722	Reserved
u_{22}	0.723	0	0.719	0.923		0.8	0.659	Reserved
u_{23}	0.822	0	0.812	0.922		0.805	0.629	Reserved
u_{24}	0.757	0	0.71	0.923		0.729	0.545	Reserved
u_{25}	0.745	0	0.761	0.922	0.875	0.799	0.777	Reserved
u_{26}	0.448	0.009	0.403	0.929		0.781	0.802	Reserved
u_{27}	0.679	0	0.646	0.925		0.659	0.729	Reserved
u_{28}	0.733	0	0.687	0.924		0.698	0.701	Reserved
u_{29}	0.408	0.019	0.325	0.931		0.827	0.882	Reserved
u_{31}	0.551	0.001	0.477	0.928		0.694	0.749	Reserved
u_{32}	0.659	0	0.613	0.925		0.68	0.688	Reserved
u_{33}	0.486	0.004	0.381	0.93	0.717	0.526	0.622	Reserved
u_{34}	0.349	0.046						Deleted
u_{35}	0.813	0	0.78	0.923		0.68	0.582	Reserved
u_{41}	0.682	0	0.651	0.925		0.813	0.681	Reserved
u_{42}	0.664	0	0.668	0.925		0.639	0.579	Reserved
u_{43}	0.516	0.002	0.493	0.928	0.815	0.449	0.587	Reserved
u_{44}	0.649	0	0.574	0.926		0.696	0.787	Reserved
u_{45}	0.652	0	0.646	0.925		0.634	0.737	Reserved
Discrimi-nant criterion	≥0.400	p<0.05	≥0.400	≤aggregate alpha coefficient 0.931	≥0.7	≥0.2	≥0.5	

Construction of index system

The expression of the indices was further refined and renumbered, forming a reliable and valid index system containing 21 indices (*Table 2*).

http://www.aloki.hu ● ISSN 1589 1623 (Print) ● ISSN 1785 0037 (Online)
DOI: http://dx.doi.org/10.15666/aeer/1704_90979111

Table 2. *The evaluation index system for social stability risks of MWCPs*

Aim	Criteria layer	Assessment factor	Indicator layer	Influence level	Indicator interpretation
Social Stability Risk Assessment system for Large Hydraulic Engineering Projects	Legality U_1	Decision making procedure	Project approval process u_{11}	0.0533	Whether the design report related to the project project and its approval documents are complete.
			Information disclosure and mass participation u_{12}	0.047	Whether the project information related to the masses is public.
		Decision content	Project site selection u_{13}	0.0895	Whether it is consistent with comprehensive planning, regional development planning, and special planning
	Rationality U_2	Decision motivation	Most people's interests u_{21}	0.0317	Whether it meets the interests of the majority.
		Interest adjustment	The production and living standards of the land-expropriated people u_{22}	0.066	Is it possible to ensure that the production and living standards after the relocation of immigrants meet or exceed the original level?
			Economic burden of the land-expropriated people u_{23}	0.0595	Whether to bring excessive economic burden to the masses.
			Mass gain u_{24}	0.0455	Whether to make the immigrants satisfied.
			Compensation standard for land acquisition and house demolition u_{25}	0.0328	Whether the state and the locality have gaps in the compensation standards for land and housing, and the inconsistency of policies.
		Acceptance	Compensation funds for land acquisition and house demolition u_{26}	0.0438	Whether the compensation fund management system is established and improved, whether there is a possibility of breeding corruption, misappropriation, and delay in issuance.
			The acceptance of income changes by the masses u_{27}	0.0478	Changes in immigration work after relocation can cause income changes to be accepted.
		Implementing measures	Planning design u_{28}	0.045	Is it recognized by the government and other relevant departments?
			Resettlement plan u_{29}	0.0443	Can it be accepted by most people?
	Feasibility U_3	Policy convergence	Policy continuity, stability and coordination with relevant policies u_{31}	0.0625	Can it ensure policy continuity, stability and coordination with relevant policies?
		Support	Safeguards u_{32}	0.0298	Whether the has a specific security plan.
			Ecological environment risk u_{33}	0.0673	Whether measures have been taken for risks such as sudden water pollution accidents and invasion of alien species.
		Easy to operate	Related supporting measures u_{34}	0.0506	Have you been cautiously argued?
	Controllability U_4	Potential negative effect	Social security hazard u_{41}	0.0328	Influx of outsiders during construction period, improper management, whether it is possible to conflict with local residents.
			Negative paradox u_{42}	0.0378	Whether it has a negative impact.
		Degree of opposition	Public safety u_{43}	0.0324	Occurrence possibility.
		Prevention and resolution measures	Prevention and emergency measures u_{44}	0.0499	Are there preventive and coping measures?
			Public opinion and guidance u_{45}	0.0305	Is the preparation sufficient?

http://www.aloki.hu ● ISSN 1589 1623 (Print) ● ISSN 1785 0037 (Online)
DOI: http://dx.doi.org/10.15666/aeer/1704_90979111

Evaluation Model

Set pair analysis (SPA)

The SPA (Zhao, 2000) is an effective way to quantify random, ambiguous and uncertain problems. It enjoys great advantages in quantifying the uncertainty between multiple factors. Taking the target problem as a system, the certain features are considered as the same or opposite to each other, the uncertain features are deemed as different, and the target system is analyzed from the same, different, and opposite aspects. The set pair is a pair of two sets with a certain correlation.

Let H=(X,Y) be a pair set, and N be the total number of features in the set. It is assumed that the set contains S same features, P opposite features and F different features, that is, N=S+F+P. Then, the correlation degree of the system can be described as (Wang et al., 2009; Yang et al., 2014):

$$\mu = \mathbf{a} + bi + cj = \frac{S}{N} + \frac{F}{N}i + \frac{P}{N}j \quad \text{(Eq.1)}$$

where $i \in [-1,1]$ is the difference coefficient for uncertain features; j=-1 is the oppositeness coefficient for certain features. The key to the SPA lies in the determination of the correlation degree μ and the difference coefficient i.

Evaluation model

(1) Grading of risk probability

The risk probability refers to the possibility of occurrence of the risk index. In this paper, the subjective probability estimation is employed, which infers the risk probability based on estimators, expert experience, and similar events. The risk probability was empirically divided into five levels: very high, high, medium, low and very low. The five qualitative levels were respectively converted into quantitative figures like zero, the three quartering points of [0, 1] and one (*Table 3*).

Table 3. *Risk probability criterion*

Risk level	Quantitative standard	Level description
Very high(k=1)	(0.8,1]	Almost certain
Higher(K=2)	(0.6,0.8]	Very likely to happen
Medium(K=3)	(0.4,0.6]	May happen
Lower(K=4)	(0.2,0.4]	Less likely to occur
Very low(K=5)	[0,0.2]	The possibility of occurrence is small, almost impossible

(2) Determination of correlation degree

The correlation degree quantifies the proximity of the two sets in the set pair, and reveals the complex relationship between the two sets. Inspired by the SPA theory, the correlation degree μ_{nk} was constructed between the value xn of each index in the index system and the five risk probability levels k. The relationship between each index and each level can be calculated as (Li et al., 2019):

http://www.aloki.hu ● ISSN 1589 1623 (Print) ● ISSN 1785 0037 (Online)
DOI: http://dx.doi.org/10.15666/aeer/1704_90979111

$$\mu_{n1}=\begin{cases}1 & s_0 \le x_n \lhd s_1\\ 1-2\dfrac{x_n-s_1}{s_2-s_1} & s_1 \le x_n \lhd s_2\\ -1 & x_n \ge s_2\end{cases} \quad \text{(Eq.2)}$$

$$\mu_{n2}=\begin{cases}1-2\dfrac{s_1-x_n}{s_1-s_0} & s_0 \le x_n \lhd s_1\\ 1 & s_1 \le x_n \lhd s_2\\ 1-2\dfrac{x_n-s_1}{s_2-s_1} & s_2 \le x_n \lhd s_3\\ -1 & x_n \ge s_3\end{cases} \quad \text{(Eq.3)}$$

$$\mu_{n3}=\begin{cases}-1 & s_0 \le x_n \lhd s_1\\ 1-2\dfrac{s_2-x_n}{s_2-s_1} & s_1 \le x_n \lhd s_2\\ 1 & s_2 \le x_n \lhd s_3\\ 1-2\dfrac{x_n-s_3}{s_4-s_3} & s_3 \le x_n \lhd s_4\\ -1 & s_4 \le x_n \lhd s_5\end{cases} \quad \text{(Eq.4)}$$

$$\mu_{n4}=\begin{cases}-1 & x_n \lhd s_2\\ 1-2\dfrac{s_3-x_n}{s_1-s_0} & s_2 \le x_n \lhd s_3\\ 1 & s_3 \le x_n \lhd s_4\\ 1-2\dfrac{x_n-s_4}{s_5-s_4} & s_4 \le x_n \lhd s_5\end{cases} \quad \text{(Eq.5)}$$

$$\mu_{n5}=\begin{cases}-1 & x_n \le s_3\\ 1-2\dfrac{s_4-x_n}{s_4-s_3} & s_3 \le x_n \lhd s_4\\ 1 & s_4 \le x_n \lhd s_5\end{cases} \quad \text{(Eq.6)}$$

where s_0~s_5 are the critical values of the indices.

(3) Determination of degree of impact

The degree of impact of each risk index was assessed by the synthetic evaluation based on the principal component analysis (PCA). The PCA mainly determines the degree of impact based on expert scores and simplified linear relationships (Han et al., 2012). The PCA-based synthetic evaluation is implemented in four steps:

Step 1: Normalize the sample matrix $X=(x_{ij})_{n\times p}$ into Z, and compute the correlation coefficient matrix R.

Step 2: Calculate the eigenvalue λ_k of the correlation matrix R, and determine the number (m) of principal components F_j. Here, more than 85% of the principal components are selected, and the remaining components are neglected.

Step 3: Determine the degree of impact of each risk index using the following model:

$$F_j = u_{1j}\omega_1 + u_{2j}\omega_2 + \cdots u_{nj}\omega_n \quad \text{(Eq.7)}$$

where $u_{ij}=\dfrac{f_{ij}}{\sqrt{\lambda_j}}$ is decision matrix coefficient; f_{ij} is the initial factor load.

http://www.aloki.hu ● ISSN 1589 1623 (Print) ● ISSN 1785 0037 (Online)
DOI: http://dx.doi.org/10.15666/aeer/1704_90979111

Step 4: Construct a comprehensive evaluation function F_z; obtain the comprehensive value of the risk index score from the expert score x_{ij}:

$$V_{Zi} = \sum_{j=1}^{n} a_j x_{ij} \quad \text{(Eq.8)}$$

The degree of impact of each risk factor:

$$\omega_i = \frac{V_{Zi}}{\sum_{i=1}^{h} V_{Zi}} \quad \text{(Eq.9)}$$

In this way, the model on the degree of impact of each risk index can be obtained as:

$$F_z = \sum_{j=1}^{m} \left(\lambda_j / k \right) F_j = a_{1m}\omega_1 + a_{2m}\omega_2 + \ldots a_{nm}\omega_n \quad \text{(Eq.10)}$$

where $a_1, \cdots, a_n$ are the overall importance of indices in the principal component.

Using the SPSS 20.0 and the above method, the initial degree of impact of each index can be computed as:

$$\begin{cases} F_1 = 0.1080\omega_1 + 0.0866\omega_2 + \ldots + 0.1322\omega_{21} \\ F_2 = -0.0064\omega_1 - 0.0321\omega_2 + \ldots - 0.0106\omega_{21} \\ \ldots \\ F_5 = -0.0228\omega_1 + 0.0298\omega_2 + \ldots - 0.0069\omega_{21} \end{cases}$$

The secondary model was obtained from the above results and the expert score sheet as: $F_z = 0.1335\omega_1 + 0.1259\omega_2 + \ldots + 0.0905\omega_{21}$. The degree of impact of each of 21 risk indices was $\omega = (\omega_1, \omega_1, \cdots, \omega_{21})$=(0.0533, 0.0470, ..., 0.0305).

(4) Calculation of comprehensive correlation

The comprehensive correlation between index n and the risk probability level k can be determined as:

$$V_{ik} = \sum_{i=1}^{n} \omega_i \mu_{ik} \quad \text{(Eq.11)}$$

(5) Determining the evaluation scores

According to the basic principle of the SPA, the score of the risk probability is the level corresponding to the maximum value of the comprehensive correlation:

$$U = \max_{j=1}^{k} \{v_{ik}\} \quad \text{(Eq.12)}$$

Results

Basic information

The research target is an MWCP in the FEER of northwestern China's Shaanxi Province. With a total investment of RMB 20 billion yuan, the project covers an area of

http://www.aloki.hu ● ISSN 1589 1623 (Print) ● ISSN 1785 0037 (Online)
DOI: http://dx.doi.org/10.15666/aeer/1704_90979111

14,00 km^2. To prevent the occurrence of mass unexpected incidents, the author carried out an evaluation of the social stability risks of the project.

Prior to the evaluation, a questionnaire survey was carried out in 35 administrative villages of 10 districts and counties. The questionnaire covers the attitude to the project, the impacts on local environment, the impacts on production and life, the compensation for losses, public participation, and so on. In total, 1,200 questionnaires were released, 86% of which were recovered. Meanwhile, a few questionnaires were issued to test the authenticity, credibility and perfection of the survey. The results indicate that the survey contents lay a solid basis for risk evaluation.

The questionnaire data show that 1,028 villagers were not against the project, including 951 supporters, 77 unconcerned and 3 opponents. The support rate is as high as 99.7%. Only 57 villagers worried about the risk of social instability, while 974 did not have the worry. Most villagers learned about the project from a simple information source. Specifically, 992 villagers heard of the project from the bulletin board of the local cooperative, and 8 never heard of the project. In addition, 10 villagers were included in the resettlement plan. Most respondents (1,124) were concerned about the compensation standards for land acquisition and house demolition, such as the compensation time. In general, land acquisition, relocation and resettlement and the temporary shutdown of the irrigation facilities are the main aspects of the project that may affect the local production and life. Besides, conflicts may arise between the construction team and the villagers.

According to the actual situation of the project area, a social stability risk evaluation report was prepared, and several risk mitigation measures were proposed, together with an emergency response plan.

Risk evaluation

Based on the survey data, the social risks of the project were evaluated by the proposed method. The expert scores on each index was averaged as the final score (*Table 4*). The correlation degrees of each index and the evaluation levels were computed by *Equations (2) and (6)* (*Table 5*).

Table 4. *Mean expert score on each index*

Index	Experts rating average	Own interval	Risk level	Index	Experts rating average	Own interval	Risk level
u_{11}	0.76	(0.6,0.8]	Higher	u_{29}	0.44	(0.4,0.6]	Medium
u_{12}	0.6	(0.4,0.6]	Medium	u_{31}	0.5	(0.4,0.6]	Medium
u_{13}	0.7	(0.6,0.8]	Higher	u_{32}	0.56	(0.4,0.6]	Medium
u_{21}	0.72	(0.6,0.8]	Higher	u_{25}	0.46	(0.4,0.6]	Medium
u_{22}	0.6	(0.4,0.6]	Medium	u_{26}	0.6	(0.4,0.6]	Medium
u_{23}	0.8	(0.6,0.8]	Higher	u_{27}	0.84	(0.6,0.8]	Higher
u_{24}	0.62	(0.6,0.8]	Higher	u_{28}	0.7	(0.6,0.8]	Higher
u_{25}	0.62	(0.6,0.8]	Higher	u_{29}	0.6	(0.4,0.6]	Medium
u_{26}	0.66	(0.6,0.8]	Higher	u_{31}	0.72	(0.6,0.8]	Higher
u_{27}	0.6	(0.4,0.6]	Medium	u_{32}	0.8	(0.6,0.8]	Higher
u_{28}	0.6	(0.4,0.6]	Medium				

http://www.aloki.hu ● ISSN 1589 1623 (Print) ● ISSN 1785 0037 (Online)
DOI: http://dx.doi.org/10.15666/aeer/1704_90979111

Table 5. *The correlation degrees of each index and the evaluation levels*

Index	Degree of contact for different evaluation levels					Index	Degree of contact for different evaluation levels				
	Very high	**Higher**	**Medium**	**Lower**	**Very low**		**Very high**	**Higher**	**Medium**	**Lower**	**Very low**
	(0.8,1]	**(0.6,0.8]**	**(0.4,0.6]**	**(0.2,0.4]**	**[0,0.2]**		**(0.8,1]**	**(0.6,0.8]**	**(0.4,0.6]**	**(0.2,0.4]**	**[0,0.2]**
u_{11}	-1	-1	-0.6	1	0.8	u_{29}	-1	0.6	1	-0.6	-1
u_{12}	-1	-1	1	1	-1	u_{31}	-1	-1	1	0	-1
u_{13}	-1	-1	0	1	0	u_{32}	-1	-0.6	1	0.6	-1
u_{21}	-1	-1	-0.2	1	0.2	u_{33}	-1	0.4	1	-0.4	-1
u_{22}	-1	-1	1	1	-1	u_{34}	-1	-1	1	1	-1
u_{23}	-1	-1	-1	1	1	u_{41}	-1	-1	-1	0.6	1
u_{24}	-1	-1	0.8	1	-0.8	u_{42}	-1	-1	0	1	0
u_{25}	-1	-1	0.8	1	-0.8	u_{43}	-1	-1	1	1	-1
u_{26}	-1	-1	0.4	1	0.3	u_{44}	-1	-1	-0.2	1	0.2
u_{27}	-1	-1	1	1	-1	u_{45}	-1	-1	-1	1	1
u_{28}	-1	-1	1	1	-1						

Based on the correlation degrees of each index and the evaluation levels, the weight of each index was determined according to *Equation (11)*. The comprehensive correlation degree of each index can be calculated as:

$$v=(-0.9998, -0.82278, 0.40176, 0.74716, -0.36044)^T$$

By *Equation (12)*, the maximum connection degree was obtained as 0.74716, and the corresponding interval of evaluation level was (0.2, 0.4). The results show that the social stability risk of the major water conservancy project in the fragile eco-environment region is lower than the actual situation after implementing the mitigation measures. This is consistent with the actual situation.

Discussion

The existing studies on MWCPs evaluation mainly concentrate on economic benefits and environmental impacts, failing to tackle the social stability risks. What is worse, there is a severe lacking of the social stability risk evaluation of the MWCPs in the FEER, which is essential to the protection of project safety and sustainability.

To make up for this gap, this paper creates a feasible evaluation index system for social stability risks of the MWCPs in FEER through literature review, questionnaire survey and data analysis. Then, a risk evaluation model was construction based on the SPA and PCA. The proposed model was applied to a MWCP in Shaanxi Province, China, revealing that the project has a low level of social stability risk. The evaluation result agrees with the actual situation, confirming the reliability and rationality of the proposed model.

The research findings provide a valuable reference for similar projects in FEER. The risk evaluation provides a reference for the design of measures to reduce the risk of the project. Based on the actual situation of the study area and the existing studies, the author puts forward several suggestions on social risk mitigation to further mitigate the social stability risks of the WMCPs in the FEER.

(1) Address the concerns and protect the vital interests of the locals.

http://www.aloki.hu ● ISSN 1589 1623 (Print) ● ISSN 1785 0037 (Online)
DOI: http://dx.doi.org/10.15666/aeer/1704_90979111

The compensation policies and resettlement measures should be publicized in the project area. To formulate a feasible compensation plan, the construction team must fully understand the local conditions, solicitate the opinions of the affected, and obey the relevant regulations. Moreover, the resettlement site and supporting facilities should be selected rationally and developed rapidly. The local governments need to step up the resolution of disputes over compensation allocation and pay the compensation in time.

(2) Enhance eco-environment protection and reduce the environmental impact.

The project party must strictly abide by regulations on environmental protection, adopt practical engineering and biological measures, and strengthen environmental monitoring and management. The construction plan should be optimized to prevent water pollution, curb ecological deterioration, and avoid geological disasters. Ultimately, the negative environmental impact should be reduced to the acceptable level.

(3) Improve safety awareness and strengthen risk monitoring and response.

The project safety should be prioritized through project construction and operation. During the construction, the project party should actively learn from best practices and achieve civilized construction, the local government should implement strict supervision, and the villagers should engage in safety monitoring and report. After the project enters operation, the risk monitoring should be implemented consistently through site visits, field surveys and regular patrols.

(4) Establish and improve the risk management linkage mechanism for social stability.

The project party should establish and improve a robust mechanism of social stability and work safety. For example, the construction procedures should be followed strictly, and the applications for pre-approval be filed timely; effective working forms and response plans should be formulated as per the project features and requirements; the social risk sources should be avoided throughout the project. In addition, efforts should be paid to enhance the awareness of risk, emergency, conflict and crisis management.

(5) Cooperate with the local government to coordinate and solve problems.

The project party should actively cooperate with the local government in problem coordination and solution. Specifically, the party needs to maintain an effective communication channel with the locals, and share the information smoothly with the local government. In the event of social stability risks, the project party and the local government should work together to prevent and resolve such risks.

(6) Actively explore new measures to prevent and resolve social stability risks.

The relevant parties need to further investigates the issues on social stability risks, and actively explore new measures to prevent and eliminate such risks. The new measures should be prepared based on the opinions and problems raised by the most affected residents and the local government, with the aim to nip the problems in the bud.

Conclusions

The social stability risks are highly dynamic, and the interaction between risk factors may trigger new risk factors in unsteady areas. Due to the geographical and project characteristics, there are some limitations in the selection of evaluation indicators. It can further adjust and improve the indicator system according to the actual needs of the project. Although the target project has a low social stability risk, the occurrence of individual conflicts cannot be ruled out. This calls for a more detailed risk mitigation strategy, which will be discussed in future research.

http://www.aloki.hu ● ISSN 1589 1623 (Print) ● ISSN 1785 0037 (Online)
DOI: http://dx.doi.org/10.15666/aeer/1704_90979111

Acknowledgements. This work is supported by the National Natural Science Foundation of China (grant no. 51678479), the Shaanxi Provincial Science and Technology Department Natural Science Basic Research Plan (grant no. 2018JM5129), and the Shaanxi Provincial Department of Education special scientific research project (grant no. 18JK0417).

REFERENCES

[1] Becker, H. A. (2001): Social impact assessment. – European Journal of Operational Research 128(2): 311-321.
[2] Cao, F., Shao, D. K., Wang, Z. S. (2013): Social Stability Risk Assessment and Social Support Analysis of Major Engineering Projects-A Questionnaire Survey Based on a Major Natural Gas Pipeline Project. – Journal of Chinese Academy of Governance (6): 91-95.
[3] Chen, X. Z., Hu, X. M. (2013): A Study on Social Risk Assessment of Major Projects: from the Perspective of Social Expectation. – Journal of Beijing University of Aeronautics and Astronautics (Social Sciences Edition) 26(2): 15-18.
[4] Chen, Z. D., Wang, Y. (2018): Fault Tree Analysis of Social Risk of PPP Projects. – Journal of Engineering Studies 10(02): 159-167.
[5] Clark, G. T., Borst, A. (2002): Addressing risk in Seattle's underground. – PB Network (1): 34-37.
[6] Dani, A. A. (2003): Social analysis sourcebook: incorporating social dimensions into bank-supported projects.
[7] Dong, Z., Wang, H., Dong, X. L. (2018): Evaluation Method for Highway Project Social Stability Risk Based on Entropy Weight Extension Matter-element Model. – China Journal of Highway and Transport 31(09): 191-198.
[8] Eskesen, S. D., Tengborg, P., Kampmann, J., Veicherts, T. H. (2004): Guidelines for tunnelling risk management: international tunnelling association, working group no. 2. – Tunnelling & Underground Space Technology 19(3): 217-237.
[9] Fan, X. (2018): Review of Social Stability Risk Assessment System for Large Construction Projects. – Journal of Engineering Studies 10(1): 98-106.
[10] Feng, Z. Z., Zhang, Y. (2017): The causes and classification of social stability risk of large projects. – Adm. Forum 1: 97-101.
[11] Ge, W., Li, Z. K., Li, J. J. (2018): Improved Set Pair Analysis and its application to Social Impact Assessment of Dam-break. – Journal of Yangtze River Scientific Research Institute: 1-7.
[12] Guo, X. (2012): The Management and Control on the Social Stability Risk of the Major Project. – Chongqing Social Sciences (7): 14-18.
[13] Han, X. H., Zhang, Y. H., Sun, F. J. (2012): The method of determining index weights based on the principal component analysis. – Journal of Ordnance Equipment Engineering 33(10): 124-126.
[14] He, G. M., Yang, Y. (2014): Social Stability Risk Assessment of Jianli-Jiangling Highway Project - Based on Fuzzy Analytic Hierarchy Process. – Applied Mechanics & Materials 584-586: 2193-2198.
[15] He, Z., Huang, D. C., Zhang, C. Z., Fang, J. (2018): Toward a Stakeholder Perspective on Social Stability Risk of Large Hydraulic Engineering Projects in China: A Social Network Analysis. – Sustainability 10(4): 1223.
[16] Hu, Y., Chan, A. P. C., Le, Y., Jin, R. (2013): From construction megaproject management to complex project management: bibliographic analysis. – Journal of Management in Engineering 31(4): 04014052.
[17] Hu, X., Wang, F. (2014): A New Social Stability Risk Assessment Analysis Framework: Risk Perception Perspective. – Chinese Public Administration (4): 102-108.

http://www.aloki.hu ● ISSN 1589 1623 (Print) ● ISSN 1785 0037 (Online)
DOI: http://dx.doi.org/10.15666/aeer/1704_90979111

[18] Hu, X. M. (2016): Social Stability Risk Events of Sensitive Project—Process Model and Participat Action Logic. – China Natl. School Adm 2: 58-62.
[19] Huang, D., Zhang, C., Upmanu, L., Xu, M. (2013): Study on the Social Stability Risk of Large Hydraulic Project. – China Population Resources and Environment 23(04): 89-95.
[20] Jiao, X. P., Guo, X. P., Li, A. P. (2015): Study on social stability risk assessment of large-scale engineering projects -- from the perspective of stakeholders. – Chinese Engineering Consulting (8): 28-30.
[21] Kong, Y., Gao, S., Wu, X. (2015): Social Stability Risk Assessment of Seawall Construction Project Based on Group Analytic Hierarchy Process. – Journal of China Three Gorges University (Natural Sciences) 37(5): 30-33.
[22] Li, A. H., Liu, H., Geng, L. H., (2009): Review of risk analysis of hydraulic engineering system. – Advances in Water Science 20(3): 453-459.
[23] Li, Z. K., Li, W., Ge, W. (2019): Dam Breach Environmental Impact Evaluation Based on Set Pair Analysis-Variable Fuzzy Set Coupling Model. – Journal of Tianjin University (Science and Technology) 52(3): 269-276.
[24] Liao, X. (2018): The Construction of A Risk Assessment Model for the "Confrontation Style" of Large Administrative Decision-making. – Journal of Chinese Public Administration 1: 58-63.
[25] Liu, Z., Zhu, Z., Wang, H. (2016): Handling social risks in government-driven mega project: An empirical case study from West China. – International Journal of Project Management 34(2): 202-218.
[26] Liu, X. H., Wang, Z. N. (2017): Urban Rail Transit Social Stability Risk Assessment. – Construction Technology 46(S2): 1480-1482.
[27] Ma, C. G. (2017): The research on risk assessment of social stability of hydraulic engineering based on FAHP and entropy weight. – North China University of Water Resource and Electric Power.
[28] Peng, Z., Cao, F., Li, H., Shao, D. (2013): A New Indicator System for Chinese Social Stability Risk Assessment: Based on Governance of the Social Ecology System. – China Public Administration Review (2).
[29] Qu, X. E. (2017): Comprehensive evaluation of water resources carrying capacity in Shaanxi Province. – Journal of Arid Land Resources and Environment 31(2): 91-97.
[30] SGJ (2012): The Circular of the Ministry of Water Resources on Printing and Distributing the “Interim Measures for Social Stability Risk Assessment of Major Water Conservancy Projects”. – (SGJ [2012] No. 474).
[31] Shi, Q., Liu, Y., Zuo, J., Pan, N., Ma, G. (2015): On the management of social risks of hydraulic infrastructure projects in china: a case study. – International Journal of Project Management 33(3): 483-496.
[32] Song, L. H. (1995): Social Risk Index System and Social Volatility Mechanism. – SOCIOLOGICAL RESEARCH (6): 90-95.
[33] Sturk, R., Olsson, L., Johansson, J. (1996): Risk and decision analysis for large underground projects as applied to the Stockholm Ring Road Tunnels. – Tunneling and Underground Space Technology 11(2): 157-164.
[34] Sun, Y. (2011): Analysis on Large Social Problems in the Three Gorges Reservoir Area in Post -migration Period: Their Causes and the Suggestions for Their Solution. – China Soft Science (6): 24-33.
[35] Teng, M. M., Han, C. F., Liu, X. H. (2014): Index System for Social Impact Assessment of Large-Scale Infrastructure Projects in China. – China Population Resources and Environment 24(9): 170-176.
[36] Wang, W. S., Jin, J. L., Ding, J. (2009): A new approach to water resources system assessment: Set pair analysis method. – Science in China (Series E: Technological Sciences) 52(10): 3017-3023.

http://www.aloki.hu ● ISSN 1589 1623 (Print) ● ISSN 1785 0037 (Online)
DOI: http://dx.doi.org/10.15666/aeer/1704_90979111

[37] Wang, D., Zhang, Y. (2012): Operational Framework and Policy Suggestions for Social Stability Risk Assessment System of Large Engineering Projects. – Journal of Chinese Public Administration 12.
[38] Wang, B., Huang, D., Hua, J., Zhang, C. (2015): Research on the Social Stability Risk Assessment and Empirical Analysis of Hydraulic Engineering Construction. – China Population Resources and Environment 25(4): 149-154.
[39] Wang, J. L. (2017): The major project AHP-FCE method based on social stability risk assessment. – Social Scientist 2: 67-73.
[40] Wu, M. L. (2010): Questionnaire Statistical Analysis Practice-SPSS Operation and Application. – Chongqing: Chongqing University Press. 192-292.
[41] Wu, S. W., Qin, P., Gao, J. (2016): Application of Entropy Weight and Set Pair Analysis Theory to Risk Assessment of Dam Operation. – Journal of Yangtze River Scientific Research Institute 33(6): 36-40.
[42] Xiao, Q., Zhu, Z., Liu, H. (2016): Study on Non-intervention Online Assessment Model for Social Stability Risks of Large Engineering Projects. – Journal of Public Administration 9(1): 86-109,184.
[43] Xiao, Y. (2017): Social stability risk assessment of river engineering based on fuzzy variable theory. – Jiangsu Water Resources (10): 48-52.
[44] Yang, F. Y. (2012): On the Application of Social Combustion Theory in "Large Engineering Projects" - The Theoretical Foundation and Method Model of Social Stability Risk Assessment of Large Engineering Projects. – Journal of Zhejiang Provincial Party School 4.
[45] Yang, F. G., Liang, Y., Vijau, P. S. (2014): Debris flow hazard assessment using set pair analysis models: Take beichuan county as an example. – Journal of Mountain Science 11(4): 1015-1022.
[46] Yang, Y., Lv, X. (2017): Study on the Construction of Quantitative Index Mechanism of Social Stability Risk Assessment and Its Systematic System. – Industrial & Science Tribune 16(21): 202-204.
[47] Yin, H., Jiang, R., Lin, P. (2018): Research on Social Stability Risk of PX Project. – Journal of Engineering Studies 10(3): 276-287.
[48] Yu, W. X., Sun, B., Zhou, Y. (2016): Social Stability Risk Assessment and Control of LargeScale River Course Projects: Taking Huai River RH Project as an Example. – Journal of Hohai University (Philosophy and Social Sciences) 18(4): 71-76, 91-92.
[49] Zhang, C. Z., Huang, D. C., Hua, J. (2013): Social Stability Risk Assessment for Large Hydraulic Projects. – Tsinghua University Press.
[50] Zhang, Y., Zhu, D. (2018): The Stakeholder Participation of Major Policy Social Stability Risk Assessment: Action Logic and Pattern Construction. – The Journal of Shanghai Administration Institute 19(5): 70-81.
[51] Zhao, K. Q. (2000): Set Pair Analysis and Its Preliminary Application. – Hangzhou: Zhejiang Science and Technology Press.
[52] Zhu, Z., Li, Z. X. (2014): Research on the Affectomg Factors of Public Participation Willingness in Social Stability Risk Evaluation. – Journal of Xi'an Jiaotong University (Social Sciences) 34(2): 49-55.
[53] Zhu, Z., Wang, Q., Guo, X. (2016): Research on Social Stability Risk Evaluation of Engineering Projects-Factor Analysis based on the Public "Risk - Benefit" Perception Perspective. – Journal of Xi'an Jiaotong University (Social Sciences) 36(3): 61-68.

http://www.aloki.hu ● ISSN 1589 1623 (Print) ● ISSN 1785 0037 (Online)
DOI: http://dx.doi.org/10.15666/aeer/1704_90979111

DEGRADATION OF SULFAMETHAZINE BY SE-FENTON METHOD

DING, S. M.[1,2*] – LI, M.[1]

[1]*College of Chemistry and Chemical Engineering, Southwest University, Chongqing 400715, China*

[2]*Chongqing Multiple-Source Technology Engineering Research Center for Ecological Environment Monitoring, Yangtze Normal University, Chongqing 408100, China*

**Corresponding author*
e-mail: ding717@126.com; phone: + 86-133-8329-3867

(Received 18th Mar 2019; accepted 17th May 2019)

Abstract. Photodegradation is one of the important methods of antibiotic treatment in water environment. This paper studies the treatment effect of sulfamethazine by solar electric-Fenton (SE-Fenton) technology, observes the contribution of OH concentration to degradation, and involves the effect of pH value, voltage and Fe^{2+} concentration on the treatment effect. The experiment shows that the degradation rate of sulfamethazine can be effectively improved by the solar-powered Fenton system. The optimum conditions for the degradation system are pH 3.0, 25 mg/L Fe^{2+} concentration, and the applied voltage of 3 V. This study provides a basis for the removal of sulfonamide antibiotic contamination in water environment.
Keywords: *sulfanilamide, solar electric-Fenton, antibiotics, photolysis, advanced oxidation technology*

Introduction

The sulfonamide antibiotics are synthetic broad-spectrum antibiotics, with the structure of aminobenzene sulfonamide, and have been used in clinical medicine for 50 years. Because of its stable nature, convenient use and high safety, it is widely used in medicine. On the other hand, the absorption capacity of human beings or organisms is weak, and more than 80% of it is released into the environment in the original form, so it is often detected in the environment, with the detection rate ranking top among all kinds of drugs (Kolpin et al., 2002; Kemper, 2008). Because of its long-standing existence in the environment such as water and soil, it affects the original microbial population in the environment, gives birth to bacteria with extensive drug resistance, or induces gene mutations, thyroid hyperplasia or tumors in rodents (Martinez et al., 2008; Littlefieldna et al., 1989).

Due to the above reasons, the treatment technology of antibiotic pollution in the environment is getting more and more attention. Advanced oxidation technology is a water treatment technology developed in recent years, characterized by the generation of hydroxyl radicals (OH) with strong oxidizing ability, and is a method of oxidizing macromolecule refractory organics into low toxic or non-toxic small molecule substance under the reaction conditions of high temperature and high pressure, electricity, sound, light, catalyst and the like (Oller et al., 2011). Fenton technology is often used for the treatment of refractory organics. With good treatment efficiency of Fenton method and high mineralization rate of organic pollutants, it is simple and practical, and its application range is increasing continuously. In recent years, solar-Fenton (S-Fenton), electric-Fenton (E-Fenton), ultrasonic-Fenton and other advanced

http://www.aloki.hu ● ISSN 1589 1623 (Print) ● ISSN 1785 0037 (Online)
DOI: http://dx.doi.org/10.15666/aeer/1704_91139120

oxidation technologies have been derived (Serna-Galvis et al., 2016). The Fenton technology forms hydroxyl radicals mainly by reaction, with the main reaction steps as follows (Christopher et al., 2007).

$$Fe^{2+} + H_2O_2 \rightarrow Fe^{3+} + OH^- + HO\cdot \quad \text{(Eq.1)}$$

$$Fe^{3+} + H_2O_2 \rightarrow H^+ + Fe(HO_2)^{2+} \quad \text{(Eq.2)}$$

$$Fe(HO_2)^{2+} \rightarrow Fe^{2+} + HO_2\cdot \quad \text{(Eq.3)}$$

$$FeOH^{2+} + H_2O_2 \rightarrow Fe(OH)(HO_2)^+ + H^+ \quad \text{(Eq.4)}$$

$$Fe(OH)(HO_2)^+ \rightarrow Fe^{2+} + HO_2\cdot + OH^- \quad \text{(Eq.5)}$$

$$OH + Organics \rightarrow H_2O + Degradation\ products \rightarrow CO^{2+}\ H_2O \quad \text{(Eq.6)}$$

On the basis of Fenton method and the application of light, the content of Fe^{2+} in Fenton reagent can be reduced, the reaction rate of H_2O_2 and the production rate of OH can be increased, so that the mineralization of organicsr can be more thorough (Elmolla and Chaudhuri, 2009, 2011). The E-Fenton method produces Fe^{2+} and H_2O_2 by electrochemical process. The E-Fenton method mainly involves the cathode E-Fenton method, the basic principle of which is to spray oxygen on the cathode of the electrolytic cell and reduce it to H_2O_2 at the cathode as shown in *Equation 7*. Then, H_2O_2 reacts with the added Fe^{2+} to produce ·OH and thus reacts with the organics (Brillas et al., 2009; Yahya et al., 2016).

$$O_2 + 2H^+ + 2e^- \rightarrow H_2O_2 \quad \text{(Eq.7)}$$

Compared with the S-Fenton method, the E-Fenton method has the mechanism of generating H_2O_2 automatically, and higher utilization rate of H_2O_2. The disadvantage is low current efficiency. If the amount of processing is very large, the amount of electricity input is increased and the cost will also be high, which limit its wide application. The photoelectric Fenton method, which combines the advantages of S-Fenton and E-Fenton, has attracted much attention in recent years. Compared with artificial light source, the low cost of sunlight makes it the research hotspot of S-Fenton method. The SE-Fenton technology simultaneously utilizes the characteristics of automatically generating H_2O_2 by the E-Fenton method and the advantage of circulating Fe^{2+}/Fe^{3+} by S-Fenton to increase the concentration of ·OH, and save costs with sunlight. At present, the research is mainly applied to the treatment of refractory organics such as dyes and antibiotics (Valero et al., 2010; Mahmoodi et al., 2011; Almeida et al., 2015; Pérez et al., 2015, 2017). Casado and Fornaguera (2006) uses this method to treat organic acids such as p-benzoic acid, 2,4-dichlorophenoxyacetic acid and oxalic acid, and completely mineralize the organic acids for about 1 h. Flox et al. (2007) also studied the degradation of phenol-containing wastewater and 4-chloro-o-phenoxypropionic acid by SE-Fenton technology, with good results.

Sulfamethazine (SMT) is a kind of sulfonamides, which is mainly used to treat avian cholera, avian typhoid and chicken coccidiosis. More attempts have been made to treat sulfonamides with advanced oxidation technology (Alam et al., 2009; Batista and

http://www.aloki.hu ● ISSN 1589 1623 (Print) ● ISSN 1785 0037 (Online)
DOI: http://dx.doi.org/10.15666/aeer/1704_91139120

Nogueira, 2012; Sopaj et al., 2016). Because of its stability in the environment, the degradation effect needs to be further improved. In this paper, the SE-Fenton technology is used to treat SMT, which provides basic data for the treatment of antibiotic wastewater.

Materials and methods

Drugs

Sulfamethazine (SMT, purity is equal to or more than 99%, SINOPHARM), methanol (chromatographic purity, Chengdu Kelong Chemical Reagent Factory), and acetonitrile (chromatographic purity, Tianjin Damao Chemical Reagent Factory). Ferrous sulfate (analytical purity), potassium dihydrogen phosphate (analytical purity), dipotassium hydrogen phosphate (analytical purity), sodium hydroxide and sulfuric acid are analytical purities. The experimental water is ultrapure water.

Main instruments

High Performance Liquid Chromatography (LC-2010A HT, Shimadzu, Japan); Circulating Water Vacuum Pump (Gongyi Yuhua Instrument Co., Ltd.), pH Meter (Shanghai LIDA Instrument Factory), TASI-8731 Digital Illuminometer (Suzhou TASI Electronics Co., Ltd.)

Experimental device

Experimental device of SE-Fenton is as *Figure 1*.

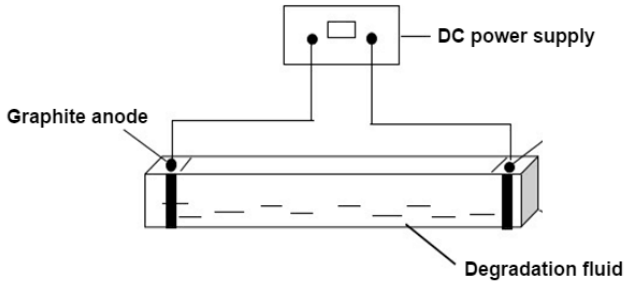

Figure 1. *Experimental device*

Experimental method

Determination of SMT

SMT in water is determined by HPLC with SHIMADZU VP-ODS-C18 column (25 cm × 4.6 mm, 5 μm). The detection wavelength is 270 nm. Mobile phase: 0.017 mol/L phosphate: Acetonitrile (80: 20) buffer solution; flow rate is 1 mL/min, sample volume is 20 μL, column temperature is 30 °C.

Control experiment

In the electrolyzing cell, 1 L of 10 mg/L SMT standard working fluid is added, and 1 mL of 25 mg/mL ammonium ferrous sulfate solution is added. The pH of NaOH

http://www.aloki.hu ● ISSN 1589 1623 (Print) ● ISSN 1785 0037 (Online)
DOI: http://dx.doi.org/10.15666/aeer/1704_91139120

solution and H_2SO_4 solution is adjusted to be 3.0. Under different conditions, S-Fenton degradation, E-Fenton degradation (applied voltage 3 V) and SE-Fenton degradation reaction were carried out. Take 1 mL of the reaction solution in the sampling bottle at different time intervals to determine the SMT concentration.

Degradation of SMT under solar photovoltaic conditions

In the electrolyzing cell, 1 L 10 mg/L SMT standard working fluid is added, 25 mg/mL ammonium ferrous sulfate solution is added. The pH of the solution is adjusted with NaOH solution and H_2SO_4 solution. Graphite electrodes are inserted on both sides of the electrolyzing cell, DC power supply is connected and applied voltage is regulated. The oxygen for manufacturing H_2O_2 is supplied to the degradation system with an aerator at the cathode.

For sunshine conditions, select the sunny days from July to August in Chongqing, from 11: 00 a.m. noon to 14: 00 p.m. The light intensity (600 00~780 00 LUX) empowers the degradation system to the degradation reaction under sunlight, and samples are taken at different time periods. The SMT concentration of the system is measured by high performance liquid chromatograph at different sampling time.

Determination of ·OH in the process of degradation

Because benzene reacts with ·OH to form phenol with good selectivity and few by-products, benzene is often used as ·OH trapping agent to produce phenol, and its concentration represents the concentration of OH in solution. In preparing the degradation solution, add benzene, make the concentration of benzene in the degradation solution be 7000 $\mu mol \cdot L^{-1}$, adjust to the desired pH value, carry out the degradation reaction, sample 1 mL at different time intervals as required, and determine phenol concentration in solution by high performance liquid chromatography. The determination conditions are as follows: SHIMADZU VP-ODS-C18 column (25 cm × 4.6 mm, 5 μm), column temperature of 30 °C, UV detector wavelength of 270 nm, the mobile phase of methanol (V): Water (V) = 60: 40, the flow rate of 1.0 $mL \cdot min^{-1}$, the injection volume of 20 μL, and the retention time of phenol as 3.01 min.

Results and discussion

Degradation of SMT by different Fenton systems

Add 1 mL of 25 mg/mL ammonium ferrous sulfate solution to 1 L of 10 mg/L of SMT degradation solution, adjust the pH of the solution to be 3.0, and use E-Fenton, S-Fenton and SE-Fenton systems to degrade SMT, respectively. The degradation rate of SMT by different systems is shown in *Figure 2a.* From the figure, it can be seen that the degradation rate of three different Fenton systems increases with the increase of the reaction time. The OH produced during the degradation of three different systems is determined and the results are shown in *Figure 2b.* It is obvious that the degradation rate of SMT in different systems is positively related to the concentration of ·OH produced in the system. At the same time, the degradation rate of SMT is the highest by the SE-Fenton system, followed by the S-Fenton system and the lowest by the E-Fenton system. These results indicate that all three systems can promote the degradation of SMT, in which S-Fenton and E-Fenton technology can produce synergetic effect and enhance the degradation ability. However, the degradation effect of S-Fenton is better

http://www.aloki.hu ● ISSN 1589 1623 (Print) ● ISSN 1785 0037 (Online)
DOI: http://dx.doi.org/10.15666/aeer/1704_91139120

than that of E-Fenton, mainly because of the synergistic effect of ultraviolet light and Fe^{2+} on the catalytic decomposition of H_2O_2 produced in the system.

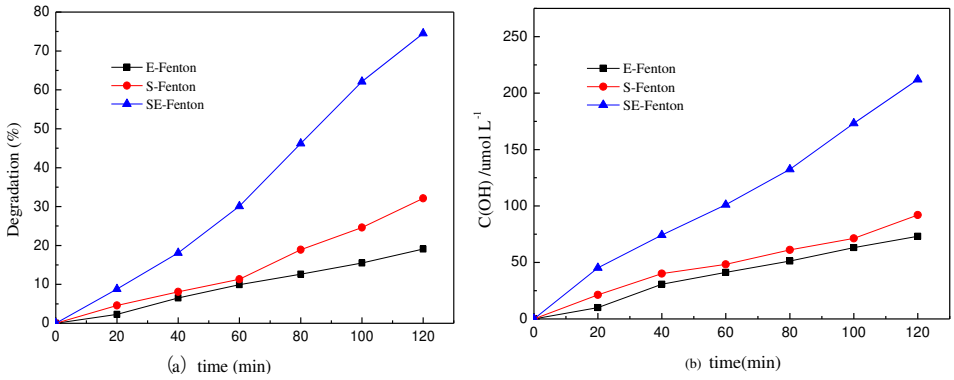

Figure 2. *Degradation effect of SMT by different Fenton systems and the corresponding OH concentration of the system. SMT 10 mg/L, pH = 3.0, sunlight intensity (65000~78000 LUX)*

Effect of pH on SE-Fenton degradation of SMT

Many studies have shown that Fenton systems usually have better ability to degrade organics under acidic conditions (Alam et al., 2009), so this experiment is carried out at pH 1.0, 3.0, 5.0, and 7.0. It can be seen from *Figure 3* that in the reaction time of the first 30 min, the degradation efficiency of SMT does not differ greatly under the conditions of pH 1.0, 3.0 and 5.0, and after 30 min, the system with pH 3.0 has the best effect on SMT degradation. When pH is higher than 3.0, ranging from 3.0 to 7.0, the degradation efficiency of SMT becomes smaller and smaller. In the system with pH 7, the degradation rate of SMT in 120 min is only about 10%. When the pH is lower than 3.0, the degradation rate of SMT is also greatly reduced. Some studies have shown that when pH is less than 3.0, the ferric ion concentration in the Fenton system decreases, thus inhibiting the formation of OH. When pH is higher than 4.0, $Fe(OH)_3$ precipitates will occur in the solution. The higher the pH is, the more precipitates will be formed, which will prevent the circulation of Fe^{2+} and Fe^{3+} in Fenton system and is unfavorable to the formation of·OH. Therefore, the optimum pH for SE-Fenton degradation of SMT is 3.0, and the pH of the system is 3.0 in the following experiments.

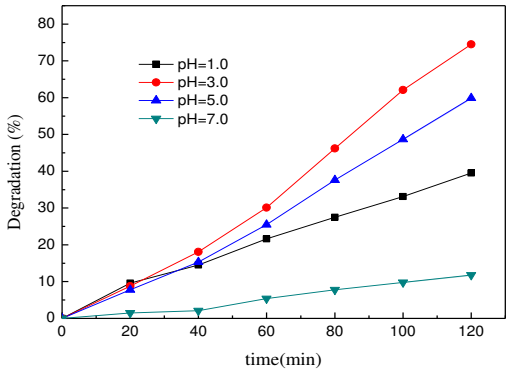

Figure 3. *Effect of pH on SE-Fenton degradation of SMT. 1L 10 mg/L SMT degradation solution; E = 3V; Fe^{2+} concentration of 25 mg/L; light intensity: pH = 1.0(65500~72000 LUX); pH = 3.0(68000~72000 LUX); pH = 5.0(64000~735 00 LUX); pH = 7.0(61300~723 00 LUX)*

http://www.aloki.hu ● ISSN 1589 1623 (Print) ● ISSN 1785 0037 (Online)
DOI: http://dx.doi.org/10.15666/aeer/1704_91139120

Effect of applied voltage on SE-Fenton degradation of SMT

The degradation efficiency of the SMT increases as the applied voltage increases, as shown in *Figure 4*. This is due to an increase in the applied voltage of the electrolytic cell, which accelerates the generation of the cathode H_2O_2, resulting in an increase in the concentration of·OH. The difference among the voltages 3 V, 5 V and 7 V used in the experiments is not too large, so the degradation efficiency of SMT is not improved significantly. The influence of the applied voltage of 3 V and 7 V on SMT degradation is very small. In view of saving cost and energy, under this experimental condition, when the applied voltage is 3 V, the degradation effect of SMT is the best.

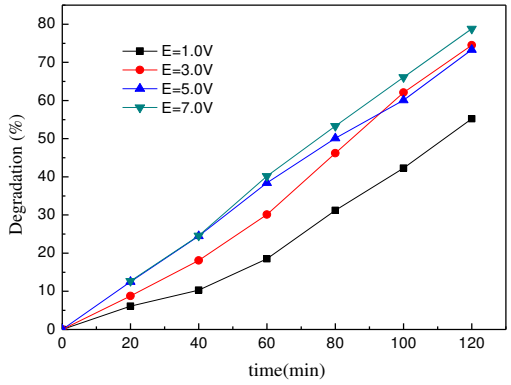

Figure 4. *Effect of applied voltage on SE-Fenton degradation of SMT. 1L 10 mg/L SMT degradation solution; pH = 3; Fe^{2+} concentration of 25 mg/L; Light intensity: E = 1.0 V (65000~76000 LUX); E = 3.0 V (65000~78000 LUX); E = 5.0 V (55000~70000 LUX); E = 7.0 V (56700~69700 LUX)*

Effect of Fe^{2+} dosage

The results of *Figure 5* show that in the range of concentration given in the experiment, when the concentration of Fe^{2+} is 25 mg/L, the degradation effect of SMT is the best.

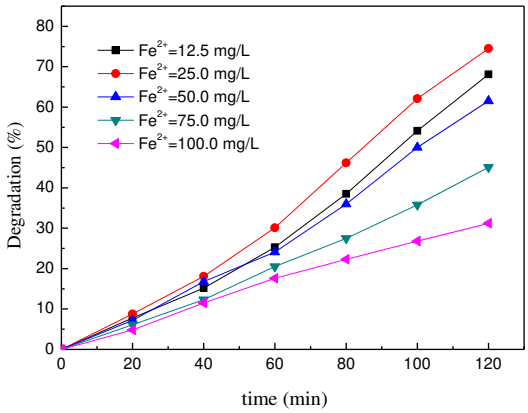

Figure 5. *Effect of Fe^{2+} dosage. E = 3V; pH = 3; 10 mg/L SMT Degradation solution; Light intensity: Fe^{2+} = 12.5 mg/L (64000—70000 LUX); Fe^{2+} = 25 mg/L (65000—78000 LUX); Fe^{2+} = 50 mg/L (63000~75000 LUX); Fe^{2+} = 75 mg/L (63000~75700 LUX); Fe^{2+} = 100 mg/L (64200~76000 LUX)*

http://www.aloki.hu ● ISSN 1589 1623 (Print) ● ISSN 1785 0037 (Online)
DOI: http://dx.doi.org/10.15666/aeer/1704_91139120

When Fe^{2+} concentration is lower than this value, the degradation rate decreases. When the concentration of Fe^{2+} is higher than this value, the higher the concentration is, and the lower the degradation effect of SMT is. This is because a suitable concentration of Fe^{2+} will improve the utilization efficiency of H_2O_2, too low Fe^{2+} is not sufficient to decompose H_2O_2, and less ·OH produced is not conducive to degradation. Some studies have shown that excessively high concentration of Fe^{2+} will decompose H_2O_2, which is unfavorable to the formation of ·OH, resulting in the decrease of the degradation effect of SMT (Sire's et al., 2007).

Conclusions

(1) Under the same conditions, the degradation rate of sulfamethazine is 32.1%, 19.1% and 74.5% respectively by S-Fenton, E-Fenton and SE-Fenton systems separately. The degradation rate of sulfamethazine is greatly improved by SE-Fenton technology, and the advantages of the combined technologies are demonstrated by comparison with those of S-Fenton and E-Fenton.

(2) The results show that OH produced by SE-Fenton system is positively related to the degradation rate of SMT. Under the same conditions, the concentration of ·OH produced in the degradation process of S-Fenton, E-Fenton and SE-Fenton in 120 min is 92 $\mu mol \cdot L^{-1}$, 73.2 $\mu mol \cdot L^{-1}$ and 212 $\mu mol \cdot L^{-1}$ respectively, which indicates that the synergistic mechanism of photo-electric interaction in SE-Fenton system promotes the production of ·OH.

(3) In this experimental system, the optimum conditions for degradation of 1 L 10 mg/L SMT by SE-Fenton technology are as follows: pH is 3.0, concentration of Fe^{2+} is 25 mg/L, and the applied voltage is E = 3 V, which has the best degradation effect.

(4) Solar photoelectric Fenton technology has good degradation efficiency for sulfonamide, but because of the unstable sunlight and pH = 3 as the optimum degradation condition, the application of solar photoelectric Fenton technology is limited. Further research and development of sulfonamide degradation technology and methods in near-neutral water are needed.

Acknowledgements. This work was financially supported by Natural Science and Technology Project of Chongqing Municipal Education Commission (No. KJ111311).

REFERENCES

[1] Alam Trovo, G., Raquel Nogueira, F. P., Ana, A., Amadeo, R. (2009): Degradation of sulfamethoxazole in water by solar S-Fenton. Chemical and toxicological evaluation. – Water Research 43: 3922-3931.

[2] Almeida, L. C., Silva, B. F., Zamomi, M. V. (2015): Photoelectrocatalytic/photo E-Fenton coupling system using a nanostructured photoanode for the oxidation of a textile dye: kinetics study and oxidation pathway. – Chemosphere 136: 63-71.

[3] Batista, A. P., Nogueira, R. P. (2012): Parameters affecting sulfonamide S-Fenton degradation - iron complexation and substituent group. – Journal of Photochemistry and Photobiology A: Chemistry 232: 8-13.

[4] Brillas, E., Sirés, I., Oturan, M. A. (2009): E-Fenton technology and related electrochemical technologies based on Fenton's reaction chemistry. – Chemical Reviews 109(12): 6570-631.

http://www.aloki.hu ● ISSN 1589 1623 (Print) ● ISSN 1785 0037 (Online)
DOI: http://dx.doi.org/10.15666/aeer/1704_91139120

[5] Casado, J., Fornaguera, J. (2006): Pilot scale mineralization of organic acids by E-Fenton process plus sunlight exposure. – Water Research 40: 2511-2516.
[6] Christopher, K., Duesterberg, T., David, W. (2007): Kinetic modeling of the oxidation of p-hydroxybenxoic acid by Fenton's reagent: implications of the role of quinones in the redox cycling of iron. – Environ. Sci. Technol 41: 4103-4110.
[7] Elmolla, E. S., Chaudhuri, M. (2009): Degradation of the antibiotics amoxicillin, ampicillin and cloxacillin in aqueous solution by the S-Fenton technology. – Journal of Hazardous Materials 172(2-3): 1476-1481.
[8] Elmolla, E. S., Chaudhuri, M. (2011): Combined S-Fenton-SBR process for antibiotic wastewater treatment. – Journal of Hazardous Materials 192(3): 1418-1426.
[9] Flox, C., Pere-Llus, C., Centellas, F. et al. (2007): Solar photo E-Fenton degradation of cresols using a flow reactor with a boron-doped diamond anode. – Applied Catalysis B: Environmental 75: 17-28.
[10] Kemper, N. (2008): Veterinary antibiotics in the aquatic and terrestrial environment. – Ecol. Indic. 8: 1-13.
[11] Kolpin, D. W., Furlong, E. T., Meyer, M. T. E., Zaugg, S. D., Barber, L. B., Buxton, H. T. (2002): Pharmaceuticals, hormones, and other organic wastewater contaminants in U.S. streams, 1999-2000: A national reconnaissance. – Environmental Science and Technology 36(6): 1202-1211.
[12] Littlefieldna, N. A., Gaylor, D. W., Blackwell, B. N., Allen, R. R. (1989): Chronic toxicity/carcinogenicity studies of sulpha meth azine in B6C3F1 mice. – Food Chem Toxicol 27(7): 455-463.
[13] Mahmoodi, N. M., Salchi, R., Arami, M. (2011): Binary system dye removal from colored textile wastewater using activated carbon: kinetic and isotherm studies. – Desalination 272(1/2/3): 187-195.
[14] Martinez, J. L., Baquero, F., Canton, R. (2008): Antibiotics and antibiotic resistance in water environments. – Current Opinion in Biotechnology 19(3): 260-265.
[15] Oller, I., Malato, S., Sanchez-Perez, J. A. (2011): Combination of advanced oxidation processes and biological treatments for wastewater decontamination—a review. – Science of the Total Environment 409(20): 4141-4166.
[16] Pérez, T., Garcia-Segura, S., El-Ghenymy, A. (2015): Solar photoE-Fenton degradation of the antibiotic metronidazole using a flow plant with a Pt/air-diffusion cell and a CPC photoreactor. – Electrochimica Acta 165(9): 173-181.
[17] Pérez, T., Sirés, I., Brillas, E., Nava, J. L. (2017): Solar photoE-Fenton flow plant modeling for the degradation of the antibiotic erythromycin in sulfate medium. – Electrochimica Acta 228: 45-56.
[18] Serna-Galvis, E. A., Silva-Agredo, J., Giraldo, A. L., Florez, O. A., Torrespalma, R. A. (2016): Comparison of route, mechanism and extent of treatment for the degradation of a β-lactam antibiotic by TiO2, photocatalysis, sonochemistry, electrochemistry and the S-Fenton system. – Chemical Engineering Journal 284: 953-962.
[19] Sire's, I., Gamrrido, J. A., Mari'a, R. (2007): Catalytic behavior of the Fe3+/Fe2+ system in the E-Fenton degradation of the antimicrobial chlorophene. – Applied Catalysis B: Environmental 72: 382-394.
[20] Sopaj, F., Oturan, N., Pinson, J., Oturan, M. A. (2016): Effect of the anode materials on the efficiency of the E-Fenton technology for the mineralization of the antibiotic sulfamethazine. – Applied Catalysis B Environmental 199: 331-341.
[21] Valero, D., Ortiz, J. M., Expósito, E., Montiel, V., Aldaz, A. (2010): Electrochemical wastewater treatment directly powered by photovoltaic panels: electrooxidation of a dye-containing wastewater. – Environmental Science & Technology 44(13): 5182-5187.
[22] Yahya, M. S., El, K. M., Oturan, N., Ei Kacemi, K., Oturan, M. A. (2016): Mineralization of the antibiotic levofloxacin in aqueous medium by E-Fenton technology: Kinetics and intermediates products analysis. – Environmental Technology 37(10): 1276-1287.

http://www.aloki.hu ● ISSN 1589 1623 (Print) ● ISSN 1785 0037 (Online)
DOI: http://dx.doi.org/10.15666/aeer/1704_91139120

URBAN PLANNING DESIGN AND SUSTAINABLE DEVELOPMENT OF FOREST BASED ON HEAT ISLAND EFFECT

WANG, X. H.[1] – WU, Y.[2*] – GONG, J.[3] – LI, B.[4] – ZHAO, J. J.[4]

[1]*College of Landscape Architecture and Arts, Northwest A & F University, Yangling 712100, China*

[2]*School of Architecture, Chang'an University, Xi'an 710061, China*

[3]*Jiangxi Urban and Rural Planning & Design General Institute, Nanchang 330000, China*

[4]*Xi'an Urban Planning & Design Institute, Xi'an 710082, China*

**Corresponding author*
e-mail: wxhxbdx@sina.com; phone: +86-180-3219-7955

(Received 18th Mar 2019; accepted 17th May 2019)

Abstract. Under the background of rapid development of urbanization, how to make rational use of land resources is the main content of urban planning design. The unreasonable distribution of urban land intensifies the influence range and intensity of urban heat island effect, and the cooling and humidification of urban vegetation can effectively alleviate the surface temperature of cities and towns. Under this trend, based on the study of urban heat island effect and in view of the ecological benefit of forest cities, this paper makes systematic planning for the green space pattern of Shijiazhuang City, and puts forward the optimization strategy to realize the sustainable development of the urban ecological environment. The results show that the urban heat island effect increases with the increase of the urban planning forest coverage, and the urban forest has a certain threshold to alleviate the urban heat island effect, so the patch arrangement of the forest should be controlled. The forest planning pattern in urban planning can be adjusted and optimized to increase the urban forest patch shape index, thereby increasing the coupling degree between forest vegetation and environment, and maximizing the reduction of heat island effect. This study provides a theoretical basis for minimizing the heat island effect in the process of urban planning.

Keywords: *urban planning, forest, ecological benefits, heat island effect, planning pattern, environmental coupling*

Introduction

Urbanization continues to develop rapidly, which aggravates the change in urban land use types and causes urban climate change such as temperature rise and humidity decrease in urban areas, particularly, the heat island effect in urban environmental problems (Ahmed et al., 2015). In the layout of urban planning, the effective measures to alleviate the heat island effect include urban forest, green land and water body, among which forests as the "dispatcher" of the nature exist in a large amount in the city, with flexibility in activity (Li et al., 2018). All trees in parks, residential areas, blocks and around roads are part of the urban forest. In order to maintain and improve the ecological environment, the necessity and importance of building forest cities are becoming increasingly apparent in urban planning (Wang et al., 2015; Kamruzzaman et al., 2018). The planning design of urban forests not only increases urban green coverage, but also plays an important role in protecting natural ecology and improving human living environment (Hyoungsub et al., 2018).

http://www.aloki.hu ● ISSN 1589 1623 (Print) ● ISSN 1785 0037 (Online)
DOI: http://dx.doi.org/10.15666/aeer/1704_91219129

The design and planning of urban forests has high social benefits, which promote the development of cultural education, enhance urban landscape leisure and improve the urban ecological environment (Gago et al., 2013). The systematic planning and arrangement urban forests can form a comprehensive environment for coordinated development with the cities, thereby better improving the urban ecology and living environment (Senanayake et al., 2013). The planning and design state of urban forests is mainly distributed in point, strip, ring and wedge shape, all of which input fresh air to the cities, improving urban climate, environment and ventilation conditions (Wonorahardjo, 2012). Urban forest plays a good role in regulating urban heat island effect. The surface temperature can be reduced by more than 15 °C in urban forest-covered areas, and the body temperature under shade can be reduced by 3–5 °C (Weilin et al., 2017). However, due to the scarcity of available land resources in cities, it is difficult to improve the heat island effect in urban forest planning design. Therefore, it is an important research direction to optimize the urban forest design pattern and focus on the sustainable development of urban forests (Krüger and Emmanuel, 2013). Based on the study of urban heat island effect, this paper aims at the ecological benefit of forest cities, systematically plans the green space pattern of Shijiazhuang City, Hebei Province, China and puts forward the optimization strategies to realize the sustainable development of urban planning.

Materials and methods

The effective planning design of urban forests can improve the urban landscape. The ecological layout of urban forests should be combined with the natural topographic features of each urban area. The service radius of urban forests is the focus of urban planning design and also relates to the sustainable development of urban ecology (Jay and Schraml, 2013). GIS is a quantitative technical analysis method, and provides a more accurate technical method for the study of heat island effect and urban forest pattern planning in Shijiazhuang City.

There are many measures to alleviate the heat island effect through urban planning, such as greening, energy saving, water permeability, increasing the urban forest space, and strengthening the road forest penetration rate, all of which have the effect of cooling the cities. The overall layout of urban forests is based on local conditions, balanced, systematic, ecological and people-oriented (Madanian and Cost, 2017). *Table 1* is the relevant indicators of the national forest city standard system, which requires the forest coverage rate of the built-up area not less than 17%, the urban road forest penetration rate not less than 60%, the extension rate of the shaded parking lots not less than 60%, and the intensity of urban heat island effect less than 3 °C.

Results

Analysis of forest planning pattern in central urban area of Shijiazhuang City

With the development of satellite remote sensing technology, the method of retrieving surface temperature is constantly updated, and the surface temperature is greatly influenced by forest vegetation index (VI). VI and the surface temperature are calculated as shown in *Equations 1* and *2,* respectively:

http://www.aloki.hu ● ISSN 1589 1623 (Print) ● ISSN 1785 0037 (Online)
DOI: http://dx.doi.org/10.15666/aeer/1704_91219129

$$VI = \frac{\rho_{NIR} - \rho_{Red}}{\rho_{NIR} + \rho_{Red}} \quad \text{(Eq.1)}$$

$$LST = \frac{T}{1+(\lambda * \frac{T}{\rho}) * \ln \varepsilon} - 273.15 \quad \text{(Eq.2)}$$

where ρNIR represents the reflectance of the near infrared band, ρRed represents the reflectance of the infrared band, λ represents the central wavelength with a value of 11.80 μm, ρ = 1.438 × 10-2 K, ε represents the emissivity value, when VI >, take value of 1 + 0.027ln (VI), when VI ≤ 0, take value of 0.99925.

Table 1. *National forest city standard system related indicators*

Index	National forest city standard	
	Basic item	**Promotion item**
Built-up area forest coverage rate	≥ 17%	≥ 20%
Built-up areas green coverage rate	≥ 35%	≥ 38%
Urban road forest penetration rate	≥ 60%	≥ 70%
Urban road green space compliance rate	≥ 80%	≥ 80%
Promotion rate of shade parking lot	≥ 60%	≥ 70%
Ecological and landscape restoration rate of damaged abandoned land	≥ 75%	≥ 80%
Urban heat island effect intensity	≥ 3 °C	≥ 2.5 °C

Figure 1 shows the classification results of remote sensing images in Shijiazhuang City. The forest coverage area is 14%. In recent year, Shijiazhuang City has persisted in planning and adjusting the layout of urban forests to increase urban vegetation coverage. *Figure 2* is the relevant statistics of vegetation in the central urban area of Shijiazhuang City, and *Figure 2a* is the per capita public green area in the urban areas. It can be seen that the per capita public green area does not increase linearly, but from 2012 to 2018, the per capita public green area in urban areas increased from 9.2 m^2 to 10.4 m^2; *Figure 2b* shows there is a trend of annual increase in trees at the end of the year, but the growth area has been flat in the past two years, increasing to 15.88 million trees in 2018 from 13.22 million in 2012; *Figure 2c* indicates that the number of vegetation trees on both sides of the sidewalks increased from 243,000 to 288,000. Although the area of per capita public green area and the vegetation and trees on both sides of sidewalks in each year do not show the trend of increasing year by year, the urban vegetation planning area increases greatly as a whole, which serves the purpose of alleviating the urban heat island effect. *Figure 3* shows the forest coverage rate of some counties in Shijiazhuang City. Among the ten districts and counties in Shijiazhuang City, the forest coverage rate in 7 districts and counties exceeds 30%, and is less than 30% in 3 districts and counties.

Analysis on the benefits of urban forest cooling

Figure 4 is a graph of superimposing urban forest distribution and surface temperature. In the figure, green is urban forest area. It is found that there is almost no heat island effect in green land location by GIS observation and the heat island effect still exists in areas without vegetation coverage. *Figure 5* shows the trend of intensity change of heat island effect in some urban areas of Shijiazhuang City. It can be seen that the intensity of

http://www.aloki.hu ● ISSN 1589 1623 (Print) ● ISSN 1785 0037 (Online)
DOI: http://dx.doi.org/10.15666/aeer/1704_91219129

heat island effect in Xinhua, Zhengding, Wuji, Chang'an and Lingshou counties increased by 1.44 °C, 1.65 °C, 1.2 °C, 0.98 °C and 1.0 °C from 2004 to 2018, respectively. The comparison of forest coverage rate and heat island intensity in some counties of Shijiazhuang City shows that the higher the urban forest coverage rate is, the smaller the increase value of urban heat island intensity is and the buffering effect of urban forests on ground cooling. However, due to the influence of urban planning distribution structure and vegetation coverage area, the heat island effect is obvious in areas far from urban forests. Therefore, in order to alleviate the urban heat island effect effectively, it is necessary to optimize the urban forest space construction in the process of urban planning, and improve the thermal effect space by changing the urban forest pattern.

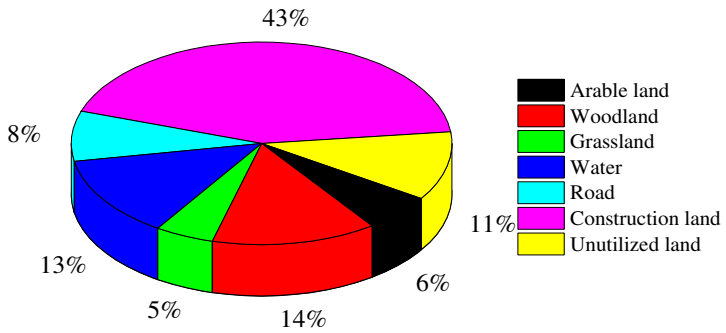

Figure 1. *Statistics on classification results of remote sensing images in Shijiazhuang City*

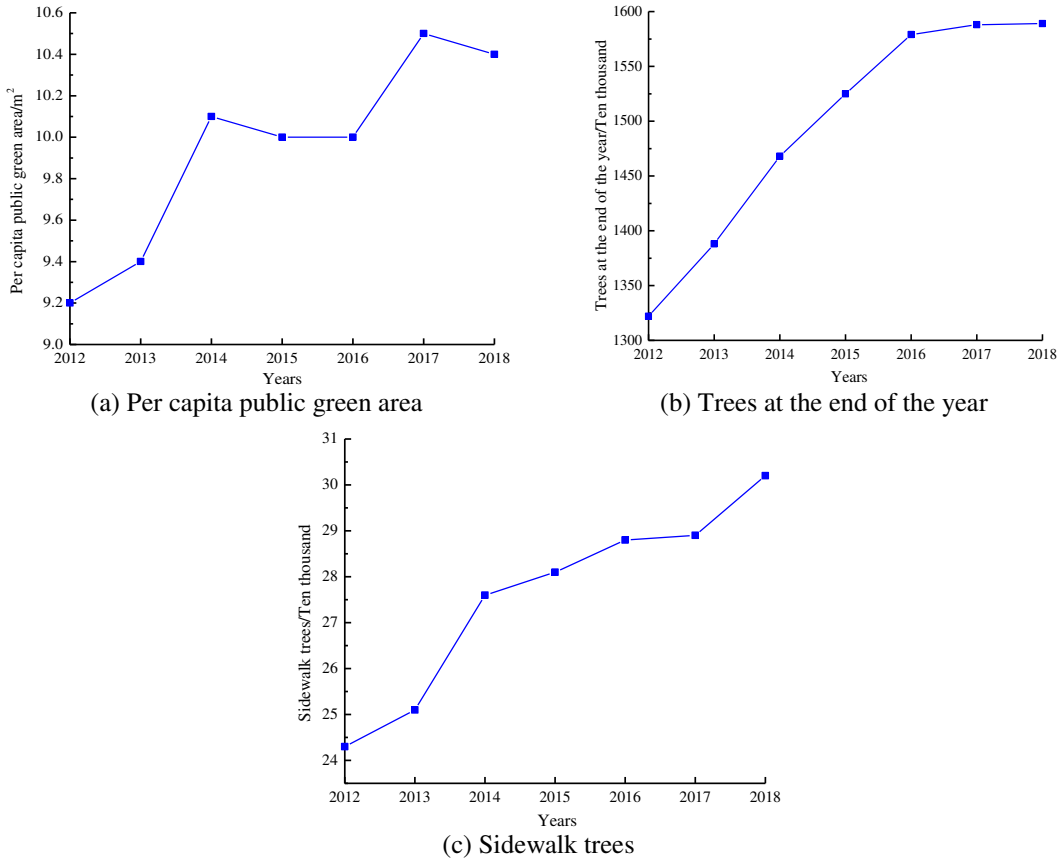

(a) Per capita public green area

(b) Trees at the end of the year

(c) Sidewalk trees

Figure 2. *Vegetation related statistics in the central area of Shijiazhuang City*

APPLIED ECOLOGY AND ENVIRONMENTAL RESEARCH 17(4):9121-9129.
http://www.aloki.hu ● ISSN 1589 1623 (Print) ● ISSN 1785 0037 (Online)
DOI: http://dx.doi.org/10.15666/aeer/1704_91219129

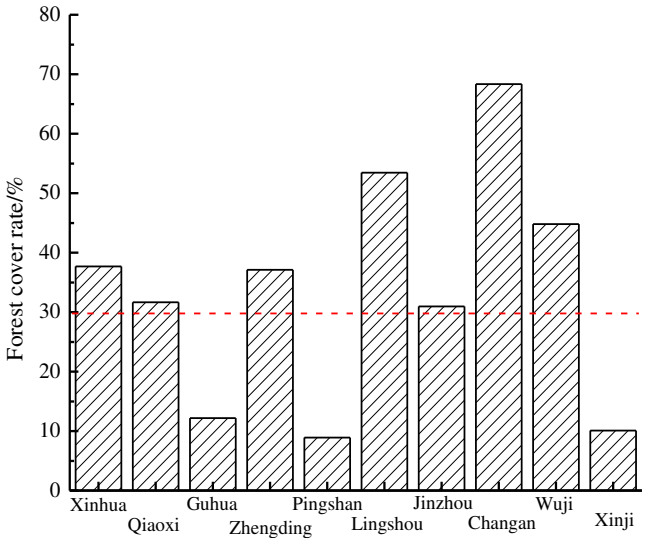

Figure 3. *Forest coverage rate in some counties of Shijiazhuang City*

Figure 4. *Urban forest distribution status and surface temperature overlay*

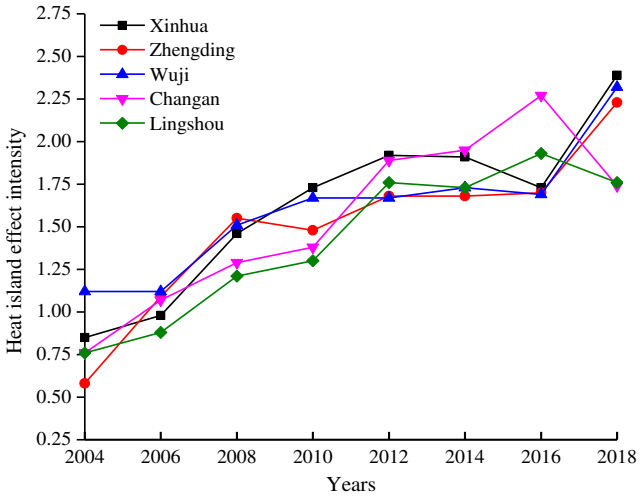

Figure 5. *Trend map of heat island effect intensity in some urban areas of Shijiazhuang City*

http://www.aloki.hu ● ISSN 1589 1623 (Print) ● ISSN 1785 0037 (Online)
DOI: http://dx.doi.org/10.15666/aeer/1704_91219129

Discussion

Optimization measures of forest urban planning pattern in Shijiazhuang City

The total amount and area of forests in urban planning design are constant, but the planning pattern can be adjusted and optimized. The spatial pattern of urban forests affects the type structure of urban forests and the intensity of urban heat island. *Table 2* shows the type structure of urban forests in Shijiazhuang City. According to the type structure of urban forests, the proportion of park vegetation is the largest, accounting for 38.93% of the total vegetation area, followed by road vegetation and protective vegetation, while the vegetation area of residential areas is very small. However, the area of residential areas is the largest, which is the important reason for the uneven distribution of heat island effect. The planning area of vegetation in residential areas needs to be further improved in the process of urban planning.

Table 2. *Type structure of urban forest in Shijiazhuang City*

Urban forest type	Area/hectare	Proportion/%
Park vegetation	1263.76	38.93
Unit affiliated vegetation	119.46	3.68
Residential areas vegetation	190.55	5.87
Road vegetation	864.15	26.62
Protective cover vegetation	768.06	23.66
Production vegetation	40.25	1.24
Total	3246.23	100%

Figure 6 is the statistics of relevant data of forest cultivation in Shijiazhuang City in recent years, the area of forest cultivation and the number of forest cultivation fields all show a trend of decreasing. The urban forest has a certain threshold to alleviate the urban heat island effect, and the patch arrangement of the forest should be controlled. *Figure 7* is a schematic diagram of the cooling efficiency of centralized and dispersed urban forests. Large area of urban forests breaking into parts can expand the scope of cooling and urban forests are evenly distributed with better benefits. The distance and quantity of urban forest patches should also be reasonably distributed, and the ideal distribution area is to maximize the influence range of the respective forest patches. However, the urban development should consider the layout of buildings, water bodies, roads, and others and it is not possible to arrange according to the ideal distribution. In order to maximize the benefits of urban forests, it is necessary to design the patch shape of the planning areas reasonably, increase the urban forest patch shape index, thus enhancing the coupling degree of forest vegetation and environment, and maximizing the reduction of heat island effect.

Optimization measures for improving heat island effect of urban forests

It is found that the urban heat island effect increases with the increase of urban forest coverage, so it is feasible to increase urban forest coverage. *Figure 8* is a structural diagram of the urban planning and construction of Shijiazhuang, which is combining different urban forest landscape elements according to their own characteristics so as to build a characteristic forest city and improve the diversity of the urban ecosystem.

http://www.aloki.hu ● ISSN 1589 1623 (Print) ● ISSN 1785 0037 (Online)
DOI: http://dx.doi.org/10.15666/aeer/1704_91219129

Table 3 is the planning of artificial afforestation in Shijiazhuang City. In the future, the urban forest area will be expanded through the projects of mountain afforestation, conversion of farmland to forests, reforestation and afforestation subsidy.

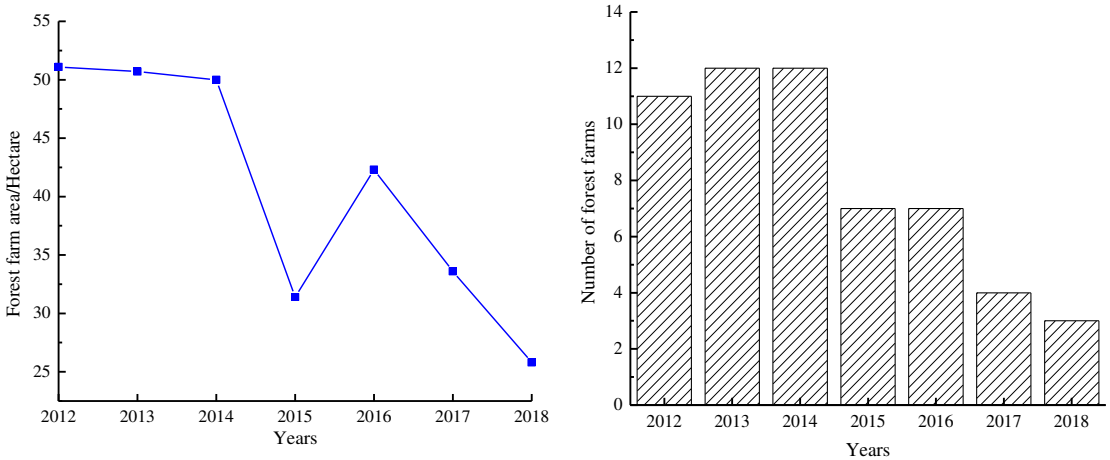

(a) Afforestation area (b) Forest farms number

Figure 6. *Statistics of related data on afforestation in Shijiazhuang City in recent years*

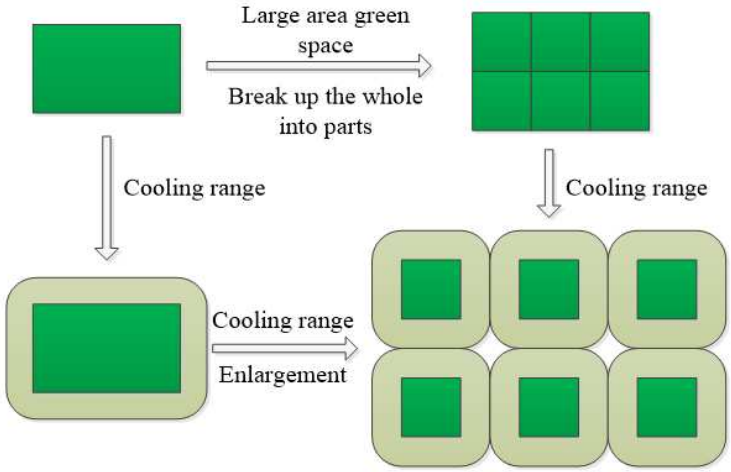

Figure 7. *Schematic diagram of cooling and decentralized urban forest cooling benefits*

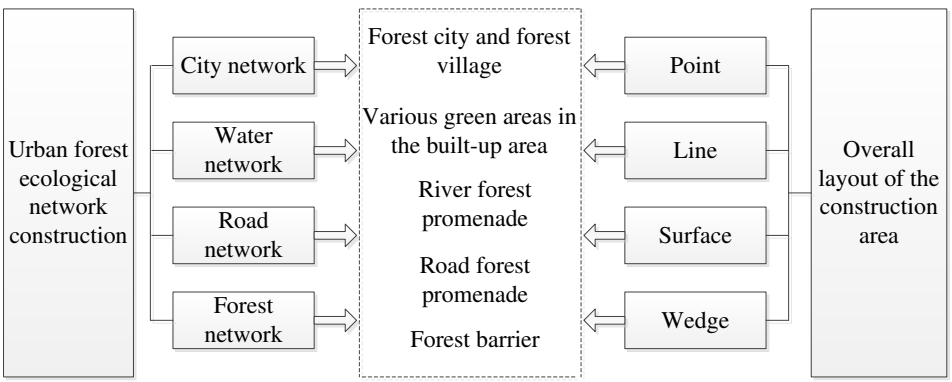

Figure 8. *Shijiazhuang City urban planning construction structure*

http://www.aloki.hu ● ISSN 1589 1623 (Print) ● ISSN 1785 0037 (Online)
DOI: http://dx.doi.org/10.15666/aeer/1704_91219129

Table 3. *Shijiazhuang City afforestation planning*

Project Name	2019-2021	2022-2024	2025-2027	2028-2030
Mountain afforestation	980.42	300	286	250
Returning farmland to forest	260	100	100	100
Forest afforestation	433.08	150	140	120
Afforestation subsidy project afforestation	400	100	96	80
Total	2073.5	650	622	550

order to increase the urban forest coverage area and the cooling area of urban forest patches, it is necessary to make full use of the urban gray space to improve the urban forest coverage rate, occupy a large number of urban land space to plan and construct forest patches, and expand the development direction of urban greening. In addition, in order to compound greening, different land types, community structure and tree species composition will produce different environmental effects, so it is essential to rationally select vegetation species of different levels, utilize limited patch space, increase space greening amount, and improve surface cooling effect. Suitable vegetation types should be selected, with trees or ornamental plants with the ability of cooling and humidification for residential vegetation and roadside vegetation. The government departments should also set a reasonable indicator of urban vegetation coverage rate, and the vegetation coverage rate should be faster than the growth rate of urban buildings and population; optimize the management and control requirements of vegetation planning, and in addition to retaining the original vegetation and green space planning, strengthen the vegetation of each land to meet the standards. The government can also expand the planning area of urban forests, reduce the intensity of heat island effect, and realize the sustainable development of urban ecological environment by implementing the mechanism of green subsidy and reward, optimizing urban laws and regulations, and expanding the way of green publicity.

Conclusions

Based on the study of urban heat island effect, this paper systematically plans the green space pattern of Shijiazhuang City and puts forward the optimization strategies in the view of the ecological benefits of urban forests. The concrete conclusions are as follows:

(1) The urban forests can buffer the ground cooling, but the heat island effect is obvious in the area far away from the urban forests due to the influence of the urban planning distribution structure and the vegetation coverage area, and the thermal effect space can be improved by changing the urban forest pattern.

(2) In order to maximize the benefits of urban forests, it is necessary to design the patch shape of the planning area reasonably, and increase the urban forest patch shape index, thereby increasing the coupling degree of forest vegetation and environment, and maximizing the reduction of heat island effect.

(3) It is feasible to increase urban forest coverage rate and reduce heat island effect. It is necessary to increase forest area from urban planning, optimization of vegetation type and community structure and government level so as to realize sustainable development of urban ecological environment.

http://www.aloki.hu ● ISSN 1589 1623 (Print) ● ISSN 1785 0037 (Online)
DOI: http://dx.doi.org/10.15666/aeer/1704_91219129

(4) The planning and design of forest cities is a long-term work. At present, there is no relevant data and theoretical research is not mature, so the remote sensing can be used to retrieve surface temperature to analyze the heat island effect of forest cities in the future.

REFERENCES

[1] Ahmed, A. Q., Ossen, D. R., Jamei, E., Manaf, N. A., Said, I., Ahmad, M. H. (2015): Urban surface temperature behaviour and heat island effect in a tropical planned city. – Theoretical and Applied Climatology 119(3-4): 493-514.
[2] Gago, E. J., Roldan, J., Pacheco-Torres, R., Ordóez, J. (2013): The city and urban heat islands: a review of strategies to mitigate adverse effects. – Renewable and Sustainable Energy Reviews 25: 749-758.
[3] Hyoungsub, K., Donghwan, G., Yong, K. H. (2018): Effects of urban heat island mitigation in various climate zones in the United States. – Sustainable Cities and Society 41(8): 841-852.
[4] Jay, M., Schraml, U. (2013): Managing city forests for or in spite of recreation? perspectives of forest managers. – European Journal of Forest Research 132(1): 93-105.
[5] Kamruzzaman, M., Deilami, K., Yigitcanlar, T. (2018): Investigating the urban heat island effect of transit oriented development in Brisbane. – Journal of Transport Geography 66: 116-124.
[6] Krüger, E., Emmanuel, R. (2013): Accounting for atmospheric stability conditions in urban heat island studies: the case of Glasgow, UK. – Landscape and Urban Planning 117: 112-121.
[7] Li, G., Zhang, X., Mirzaei, P. A., Zhang, J., Zhao, Z. (2018): Urban heat island effect of a typical valley city in china: responds to the global warming and rapid urbanization. – Sustainable Cities and Society 38(4): 736-745.
[8] Madanian, S., Costa, C. S. (2017): A model for evaluating a greenbelt planning in the city of Qazvin (Iran) using Micmac method. – Modeling Earth Systems & Environment 3(4): 1503-1513.
[9] Senanayake, I. P., Welivitiya, W. D. D. P., Nadeeka, P. M. (2013): Remote sensing based analysis of urban heat islands with vegetation cover in Colombo City, Sri Lanka using Landsat-7 ETM+ data. – Urban Climate 5: 19-35.
[10] Wang, Y., Berardi, U., Akbari, H. (2015): Comparing the effects of urban heat island mitigation strategies for Toronto, Canada. – Energy and Buildings 114: 2-19.
[11] Weilin, L., Xiaoping, L., Dagang, W., Yanling, S. (2017): The impact of energy consumption on the surface urban heat island in China's 32 major cities. – Remote Sensing 9(3): 250.
[12] Wonorahardjo, S. (2012): New concepts in districts planning, based on heat island investigation. – Procedia Social and Behavioral Sciences 36: 235-242.

http://www.aloki.hu ● ISSN 1589 1623 (Print) ● ISSN 1785 0037 (Online)
DOI: http://dx.doi.org/10.15666/aeer/1704_91219129

TOMATO YELLOW LEAF CURL VIRUS (TYLCV) STRAINS AND EPIDEMIOLOGICAL ROLE OF *BEMISIA TABACI* (HEMIPTERA: ALEYRODIDAE) BIOTYPES ON TOMATO AGROECOLOGY IN TURKEY

FIDAN, H.[1*] – KARACAOGLU, M.[2] – KOC, G.[3] – CAGLAR, B. K.[4]

[1]*Plant Protection Department, Faculty of Agriculture, Akdeniz University, Antalya, Turkey*

[2]*Plant Protection Department, Faculty of Agriculture, Malatya Turgut Ozal University, Malatya, Turkey*

[3]*Subtropical Fruits Research and Experimental Center, Çukurova University, Adana, Turkey*

[4]*Department of Plant Protection, Faculty of Agriculture, Cukurova University, Adana, Turkey*

**Corresponding author*
e-mail: hakanfidantr@hotmail.com.tr

(Received 18th Mar 2019; accepted 3rd May 2019)

Abstract. The aim of this study was to determine the strains of tomato yellow leaf curl virus (TYLCV) on the tomato plants growing intensively in Adana, Mersin and Antalya provinces and also investigate the transmissibility of virus by the vector *B. tabaci* biotypes in 2015 and 2017. For this purpose, unperiodical field observations were paid in different districts of those provinces. The TYLCV infected tomato plants and whiteflies on these plants were collected from different greenhouses and fields. The 747 samples of tomato infected with TYLCV were tested by PCR techniques. It was determined that the strains TYLCV-Israel, TYLCV-Sicilia, TYLCV-Sardinia and TYLCV-Mild were found to be infected via strain specific primers. PCR study also indicated that the same strains of TYLCV were also found on the whitefly samples collected from the infected tomato plants. DNA analyses by using specific primer Bem 23-F and R in an individual single whitefly, due to clarification of *B. tabaci* biotypes, has clearly showed that biotype B is a common vector of TYLCV in Turkey. Molecular techniques identified that Israel, Sardinia, Sicilia and Mild strain of TYLCV were present in three tomato cultivation areas in Mediterranean Region. *B. tabaci* biotype *B* (formerly *B. argentifolii*) was detected as a vector of those of strains. It was observed that (%92) *B. tabaci* Biotype B and (%8) Biotype Q others were responsible for transmission as vector of TYLC respectively. Individual viruliferous Biotype B samples examined in PCR showed that the most determined TYLCV strain as Israel was the most common among the strains, what were identified.
Keywords: *TYLCV strains' molecular epidemiology, Bemisia tabaci biotypes, impact on agroecology, Turkey*

Introduction

Tomato yellow leaf curl virus (TYLCV) is a member of *Begomovirus* genus in Geminiviridae family causes severe crop losses in tomato cultivars up to 100% (Czosnek and Laterrot, 1997). It has a broad host range with various plant families such as *Solanaceae* (tomato, peppers, various nightshade weeds, and ornamental plants), *Malvaceae* (cheeseweed) and *Fabaceae* (beans). TYLCV causes yellow leaf edges, upward leaf curling, leaf mottling, small leaf, and flower drop. The infected plants in early stages do not bear fruit and stunting, depend on seasonal conditions and cvs. susceptibility, is observed on plants. TYLCV genome consists of circular, single-stranded DNA (ssDNA) approximately 2.7 kb long (Gronenborn, 2007). Long-distance

http://www.aloki.hu ● ISSN 1589 1623 (Print) ● ISSN 1785 0037 (Online)
DOI: http://dx.doi.org/10.15666/aeer/1704_91319144

spread of TYLCV occurs primarily by movement of infected plant material or by wind dispersal of whiteflies, acquisited the virus (Torre et al., 2018). The virus, was first discovered in 1939 in Israel and Jordan (Avidov, 1944), was officially named *Tomato yellow leaf curl virus* (TYLCV) and consists of different strains; *Tomato yellow leaf curl* Israel (TYLCSV-Is), *Tomato yellow leaf curl virus*-Mild (TYLCV-Mld), Sardinia (TYLCV-Sa), *Tomato yellow leaf curl* Sicily (TYLCSV-Sic), *Tomato yellow leaf curl virus*-Morocco (TYLCV-Mo), *Tomato yellow leaf curl* Malaga (TYLCV-Mal) *Tomato yellow leaf curl* Axarquia (TYLCV-Ax), *Tomato yellow leaf curl* China (*TYLCV-Ch)* and *Tomato yellow leaf curl* Thailand *(TYLCV-Th.)* (Fauquet et al., 2008; Abhary et al., 2006).

Since, the disease has spread rapidly to the Middle East and the Mediterranean coast, Asia, Africa, Europe, the United States, Australia, Italy and many other countries (Accotto et al., 2000; Boulton, 2003; Moriones and Navas-Castillo, 2000). In Turkey, TYLCV was first discovered in Mediterranean region by Yılmaz (1978). And then it was reported as the most devastating virus disease at tomato both in greenhouses and the field in Turkey by Abak et al. (1991). On the other hand, presence of whiteflies was known well in Cukurova region due to its severe damage to cotton production (Karut et al., 2015; Satar and Ulusoy, 2016)

Whiteflies are insects belonging to family *Aleyrodidae* which cause direct by phloem-feeding and indirect damage by transmission of viruses including begomoviruses (Brown and Czosnek, 2002; Jones, 2003; Navas-Castillo et al., 2011). The transmission of TYLCV by whiteflies is circulative semi-persistent manner. There are several reports of whitefly presence and economic damage in Turkey (Ulusoy et al., 2012; Bayhan et al., 2006). Morphological discrimination of whitefly biotypes is difficult. But it is possible by using molecular methods (Papayiannis et al., 2009). Most common whitefly biotypes in Turkey are biotype B and Q (Karut et al., 2012; Satar and Ulusoy, 2016) similar with various reports around the world (Konjevic et al., 2018; Li et al., 2017)

The aim of this work was to investigate of TYLCV strains epidemiology and its strict vector *Bemisia tabaci* biotypes on agroecology by reliable technique such as Polymerase Chain Reaction (PCR) in southern coast of Turkey. In fact, that there is not any verification.

Materials and methods

Surveys were conducted in Adana and Mersin provinces having typical Mediterranean climate in Turkey. Leaf samples from symptomatic tomato plants that showing typical TYLCV symptoms (upward leaf curling, yellowing, distortion and stunting) asymptomatic leaf samples as negative control and whiteflies were collected from 245 different greenhouses which were located in several areas in south of Turkey (Adana, Mersin, Antalya) (*Fig. 1*).

Total RNA isolation, polymerase chain reaction (PCR) and phylogenetic analysis

Total DNA was extracted from leaf tissues according to Scientific GeneJET Plant Genomic DNA Purification Mini Kit. Strain-specific primers identified by Anfoka et al. (2005, 2008) were used to determine TYLCV strains (*Tables 1* and *2*).

DNA extraction from an individual whitefly: Total DNA was isolated from individual whiteflies as described by Zeidan and Czosnek (1991). In the modified

http://www.aloki.hu ● ISSN 1589 1623 (Print) ● ISSN 1785 0037 (Online)
DOI: http://dx.doi.org/10.15666/aeer/1704_91319144

simple procedure, individual whiteflies were ground 40 µl of DNA extraction buffer (50 mM Thris. HCl (pH8.0), 0.5% Tween 20, 0.025 mg/ml Proteinase K) and incubated at 65 °C for 2 h. After incubation, 20 µl 5 M potassium acetate was added and placed on ice 5-15 min. Centrifuged 10 min and placed 50 µl of supernatant into a 1.5 ml micro centrifuge tube. Added 30 µl cold isopropanol, mix, and hold on ice about 5 min centrifuged 10 min, draw off and discarded most of the supernatant, added 75 µl of cold 70% ethanol, mix gently, and centrifuge 2 min, Remove and discard nearly all of the supernatant being careful to not remove the pellets. Let pellets dry for about 10 min then add 40 µl of sterile distilled water. These DNAs were used to identify white fly biotypes with the codominant SCAR markers Bem-23 (Bel-Kadhi, 2008) (*Table 1*). The PCR of TYLCV strains were obtained with DreamTaq Green PCR Master Mix (2X) (K1081Thermo Scientific, Germany) according to the manufacturer's instructions. PCR cycle parameters were as follows: one cycle at 95 °C for 3 min; 36 cycles at 95 °C for 45 s, I, Primer Set 52, II. Primer set 62° and Whitefly primer 55 °C for 45 s, and 72 °C for 45 s, followed by one cycle at 72 °C for 7 min and lastly storing at 4 °C until electrophoresis.

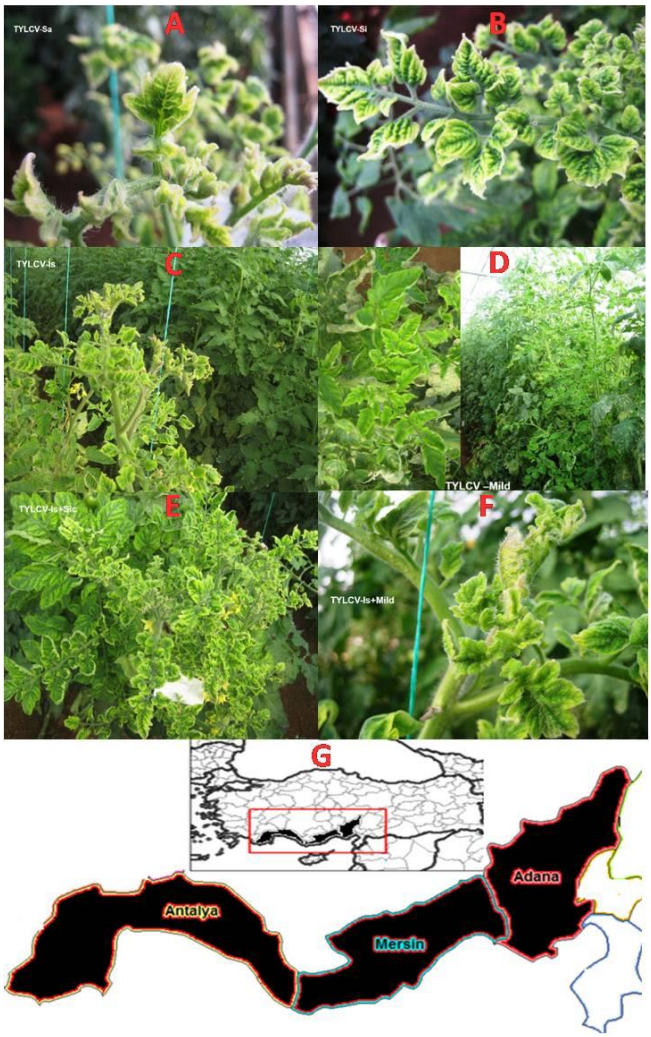

Figure 1. *TYLVC symptoms of different strains from Turkey. A: TYLCV-Sar.; B: TYLCV-Sic; C: TYLCV-Is; D: TYLCV-Mil.; E: TYLCV-Is + Sic.; F: TYLCV-Is + Mild; G: Surveying map of Mediterranean area of Turkey*

http://www.aloki.hu ● ISSN 1589 1623 (Print) ● ISSN 1785 0037 (Online)
DOI: http://dx.doi.org/10.15666/aeer/1704_91319144

Table 1. *Strain -specific primer codes and sequences (5'-3') used in identification of TYLCV strains*

Primer codes for TYLCV	Sequences
TYLCV1	5'-TTTTATTTGTTGGTGTTTGTAGTTGAAG-3'
TYLCV2	5'-ATATTGATGGTTTTTTCAAAACTTAGAAG-3'
TYLCV3	5'-ACGTAGGTCTTGACATCTGTTGAGCTC-3'
TYLCV4	5'-AAGTGGGTCCCACATATTGCAAGAC-3'
TYLCV5	5'-ATTGACCAAGATTTTTACACTTATCCC-3'
TYLCV6	5'-ATACTTGGACACCTAATGGCTATTTGG-3'
TYLCV7	5'-TGCCTTGGACA(A/G)TGGGG(A/G)CAGCAG-3'
TYLCV8	5'-TGGAAAGTACCCCATTCAAGAACATC-3'
Primer codes for *B. tabaci* biotypes	**Sequences**
Bem-23-F	5'-CGGAGCTTGCGCCTTAGTC-3' B Biotype 220 bp
Bem-23-R	5'-CGGCTTTATCATAGCTCTCGT-3' Q Biotype 410 bp

Table 2. *Strain -specific primer pairs for PCR and the expected PCR product sizes*

Strain-specific primer pairs for different TYLCV strains	Primer codes	Expected product size
Multiplex PCR: I primer combination		
Tomato yellow leaf curl virus (TYLCV-Is)	TYLCV6, TYLCV7	543 bp
Tomato yellow leaf curl virus-Sicilia (TYLCV-Sic)	TYLCV8, TYLCV6	946 bp
Tomato yellow leaf curl virus-Mild (TYLCV-Mld)	TYLCV5, TYLCV4	316 bp
Multiplex PCR II. primer combination		
Tomato yellow leaf curl virus-Israel (TYLCV-Is)	TYLCV3, TYLCV4	634 bp
Tomato yellow leaf curl virus Sardinia (TYLCSV-Sa)	TYLCV1, TYLCV2	433 bp
Tomato yellow leaf curl virus-Mild (TYLCV-Mld)	TYLCV5, TYLCV4	316 bp

Analysis of PCR products

PCR reaction mixture (Ten microlitres) was combined with gel loading buffer and analyzed on a 1.5% agarose gel containing 0.5 mg/ml of ethidium bromide and photographed (Sambrook et al., 1989). 100 bp DNA ladder (Thermo) or Bio Marker^{TM} Low (Bio Ventures, Inc.) were used on each gel to determine the length of the amplified product. PCR-amplicons run at 100 V for 70 to 80 min, and the gel was stained with ethidium bromide.

Sequence analysis

Expected PCR products from TYLCV strains were re-amplified by using Finnzymes' Phusion® High-Fidelity DNA Polymerase enzyme and 10 µl of PCR products were checked. Remaining PCR products were sent to Sentobiolab commercial firm and nucleotide sequence of amplified regions were determined. Nucleotide sequences were checked and edited by using Bioedit then checked for protein synthesis to determine the sequences are significant or not by ExPASy programme. Valid sequences were compared with strains of TYLCV gen bank (NCBI, National Center for Biotechnology Information).

http://www.aloki.hu ● ISSN 1589 1623 (Print) ● ISSN 1785 0037 (Online)
DOI: http://dx.doi.org/10.15666/aeer/1704_91319144

Results

Surveys are conducted for collecting whiteflies and young tomato leaf samples from symptomatic plants that are related with suspicion of TYLCV infection from Adana, Antalya and Mersin between 2015 and 2017 (*Table 3*). Virus symptoms differ due to various factors such as climate, plant variety and infection period. It is common using indicator plants to identify the viral agent meanwhile for TYLCV, there is no practical identification method than molecular characterization of strains due to not transmitted by mechanic transmission. On the other hand, no symptomatic differences between TYLCV strains were observed up to date.

Table 3. *Collected virus isolate numbers and locations according to province and districts*

	Province	**Samples**			**Province**	**Samples**			**Province**	**Samples**		
	Adana	I	II	III	**Antalya**	I	II	III	**Mersin**	I	II	III
	Tuzla	11	12	8	Alanya	13	17	14	Tarsus	9	8	11
	Karataş	9	11	12	Manavgat	14	12	11	Mezitli	14	17	10
	Yüreğir	13	10	20	Serik	24	19	9	Kocahasanlı	19	9	11
Districts	Seyhan	12	11	16	Merkez	27	14	13	Erdemli	19	10	11
	Misis	8	11	7	Kemer	7	6	1	Silifke	18	13	10
	Ceyhan	10	10	9	Kumluca	7	8	6	Kazanlı	10	8	14
	Yumurtalık	10	14	10	Finike	8	8	8	Aydıncık	7	11	8
					Kaş	6	2	1	Anamur	5	4	2
Province totals		**234**				**255**				**258**		
Regional total samples						**747**						

I: year 2015, II: year 2016, III: year 2017

PCR

Simultaneously, there are no apparent macroscopic biotype differences between white-fly species. In autumn season, TYLCV can be monitored in every greenhouse. Predisposition for TYLCV such as low-quality greenhouse structures, openings for whiteflies, causes high infection rates (*Table 3*).

Considering the observations, 747(234: Adana, 255: Antalya, 258: Mersin) infected plants and 852 whiteflies (274: Antalya, 216: Mersin, 362: Adana) from different locations of the provinces were collected. Also, 91 plant samples were among them collected from open fields in Adana (*Table 4*).

Determination of TYLC strains by multiplex PCR: I. Multiplex primer pairs for TYLCV-Is, TYLCV-Sic and TYLCV-Mild; II. Multiplex primer pairs for TYLCV-Is, TYLCV-Sar (ES) and TYLCV-Mld. These multiplex sets differentiated the strains as expected. Same multiplex sets also used for detecting TYLCV and its strains within whiteflies. Leaf samples were studied with 25 µl PCR mixture by using 96 well plates. For whitefly samples, 15 µl PCR mixture was used due to low concentration of DNA.

The TYLCV strain specific PCR results realized that the most common infection was occurred by 100%. Consequently, detected as mixed between 86% TYLCV Israel + Mild strains (*Tables 4*, *5, 6* and *7*). Following this, 10% TYLCV-Is + TYLCV-

http://www.aloki.hu ● ISSN 1589 1623 (Print) ● ISSN 1785 0037 (Online)
DOI: http://dx.doi.org/10.15666/aeer/1704_91319144

Sic, TYLCV Sic + TYLCV- Sar. 4.5% mixed infection rate was approximately 20% in Antalya, Mersin and Adana.

The sequence analysis and multiple sequence alignment were carried out using Chromas (Technelsium DNA Sequencing Software Australia) and CodonCode Corporation (Florida) software. The TYLCV strain specific PCR sequences were analyzed in National Center for Biotechnology Information (NCBI) using nucleotide BLAST. The agarose gel electrophoresis TYLCV multiplex PCR amplifications is shown in *Figures 2A, B* and *3*.

Table 4. *Approximate number of collected plant and whitefly samples from greenhouses from provinces*

Province	Total samples	TYLCV Is	TYLCV Mld	TYLCV Sic	TYLCV Sar	Total whiteflies	B biotype	Q biotype
Adana	234	234	204	5	8	362	329	33
Antalya	255	255	215	57	27	274	257	17
Mersin	258	258	225	16	14	216	201	15
Total	**747**	**100%**	**86%**	**10%**	**6.5%**	**852**	**92%**	**8%**

Table 5. *TYLCV strains and whitefly biotypes in Adana*

Adana	Total	TYLCV Is		TYLCV Mild		TYLCV Sic		TYLCV Sa		Total	*B tabaci* B biotype		*B tabaci* Q biotype	
		+	%	+	%	+	%	+	%		+	%	+	%
Tuzla	41	41	100	32	78	-	0	-	0	51	46	91	5	9
Karataş	42	42	100	35	83	1	2	2	5	54	49	90	5	10
Yüreğir	33	33	100	30	91	2	6	3	9	57	53	94	4	6
Seyhan	29	29	100	27	93	2	7	3	10	53	48	90	5	10
Misis	26	26	100	24	92	-	0	-	0	44	40	93	4	7
Ceyhan	29	29	100	26	91	-	0	-	0	57	51	91	6	9
Yumurtalık	34	34	100	30	89	-	0	-	0	46	42	92	4	8
Total	**234**	**234**	**100**	**204**	**87**	**5**	**2**	**8**	**3.4**	**362**	**329**	**90**	**33**	**10**

Table 6. *TYLCV strains and whitefly biotypes in Antalya*

Antalya	Total	TYLCV Is		TYLCV Mild		TYLCV Sic		TYLCV Sar		Total	*B tabaci* B biotype		*B tabaci* Q biotype	
		+	%	+	%	+	%	+	%		+	%	+	%
Alanya	44	44	100	39	88	2	4.5	2	4.5	58	54	94	4	6
Manavgat	37	37	100	30	82	3	8	3	8	39	36	93	3	7
Serik	52	52	100	49	94	4	7.6	6	11.5	59	54	93	5	7
Merkez	54	54	100	41	76	11	20	6	11	35	34	98	1	2
Kemer	14	14	100	10	76	9	64	-	0	11	10	96	1	4
Kumluca	21	21	100	18	89	14	66	5	24	49	48	99	1	1
Finike	24	24	100	20	83	11	45	3	12.5	13	12	98	1	2
Kaş	9	9	100	8	90	3	33	2	22	10	9	96	1	4
Total	**255**	**255**	**100**	**215**	**84**	**57**	**22**	**27**	**10.5**	**274**	**257**	**93.7**	**17**	**6.3**

http://www.aloki.hu ● ISSN 1589 1623 (Print) ● ISSN 1785 0037 (Online)
DOI: http://dx.doi.org/10.15666/aeer/1704_91319144

Table 7. *TYLCV strains and whitefly biotypes in Mersin*

Mersin	Total	TYLCV Is		TYLCV Mild		TYLCV Sic		TYLCV Sar		Total	*B tabaci* Biotype B		*B tabaci* Biotype Q	
		+	%	+	%	+	%	+	%		+	%	+	%
Tarsus	28	28	100	25	89	1	3.5	1	3.5	28	26	95	2	5
Mezitli	41	41	100	34	83	-	0	2	5	35	34	98	1	2
Kocahasanlı	39	39	100	34	87	4	10	3	7	32	30	94	2	6
Erdemli	40	40	100	36	90	5	12	4	10	31	28	91	3	9
Silifke	41	41	100	37	91	3	7	2	5	30	27	92	3	8
Kazanlı	32	32	100	28	89	-	0	2	6	26	25	99	1	1
Aydıncık	26	26	100	22	88	3	11.5	-	0	24	22	93	2	7
Anamur	11	11	100	9	90	-	0	-	0	10	9	92	1	8
Total	**258**	**258**	**100**	**225**	**87**	**16**	**6.2**	**14**	**5.4**	**216**	**201**	**93**	**15**	**7**

Positive controls (biotype B and biotype Q) for white-fly population experiments were provided from Israel. (Dr. A. Rami Horowitz Agricultural Research Organization, Gilat Research Center, Institute of Plant Protection, Department of Entomology, Israel). B biotype white-flies in *Figure 4*. were determined by codominant SCAR markers Bem-23-F and Bem-23-R which was developed by Bel-Kadhi (2008).

The results show that *B. tabaci* biotype B (92%) is prevalent in the majority of the surveyed sites, whereas biotype Q was only found in 8%. In each three provinces where surveyed, *Bemisia tabaci* biotype B was the most common and effective vector for TYLCV.

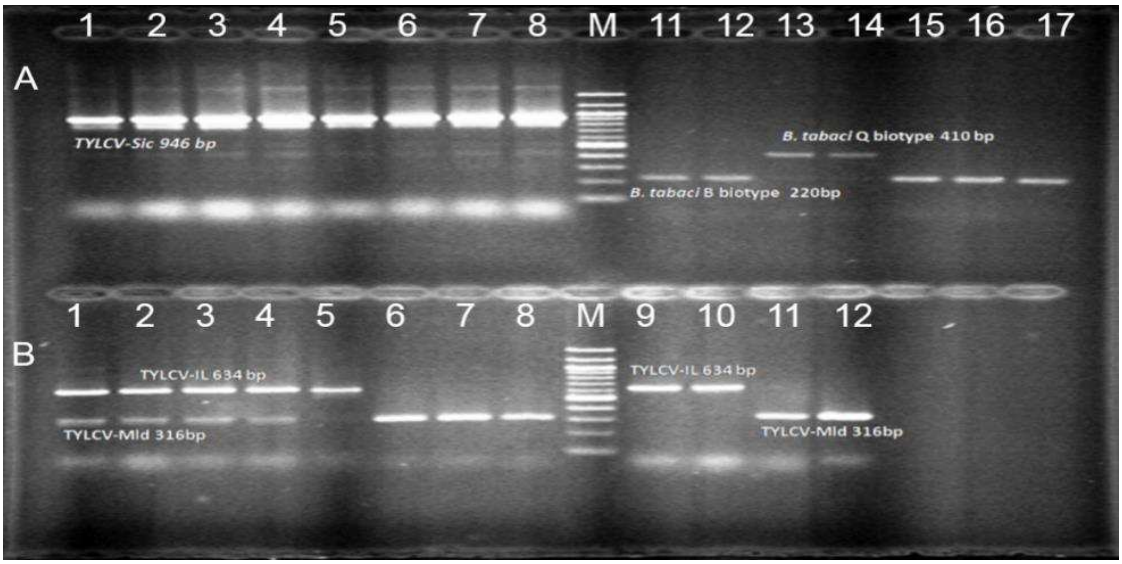

Figure 2. A *Strain specific PCR results for TYLCV. Left side: 1-2 From a single whitefly TYLCV-Sic 946 bp 3-8 From infected plant TYLCV-Sic 946 bp M 100 plus bp standard DNA ladder; 11-12 B. tabaci biotype B 220 bp;13-14 B. tabaci biotype Q (410 bp); 15-17 B. tabaci biotype B by codominant SCAR markers Bem-23-F and Bem-23-R products with 220 bp.* ***B*** *Strain specific PCR results f or TYLCV. Left side: Using Multiplex PCR set II 1-4 mix infection of TYLCV-Is (634 bp) and TYLCV-Mld (316 bp); Strain specific PCR 5-8 TYLCV-Mld single infection; M 100 plus bp standard DNA ladder; 9-10 TYLCV-Is (634 bp); 11-12 TYLCV-Mld single infection*

http://www.aloki.hu ● ISSN 1589 1623 (Print) ● ISSN 1785 0037 (Online)
DOI: http://dx.doi.org/10.15666/aeer/1704_91319144

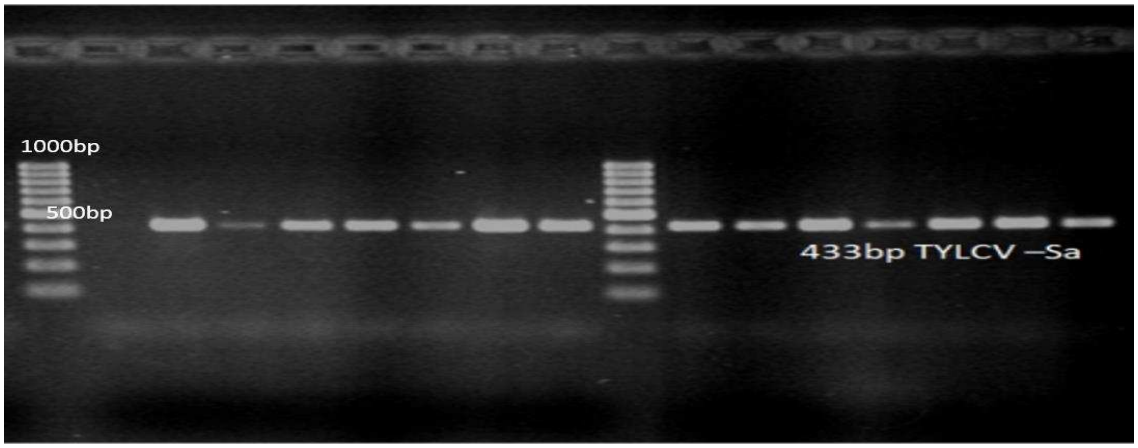

Figure 3. *Strain specific PCR results for tomato yellow leaf curl Sardinia virus (TYLCSV-Sa) 433 bp*

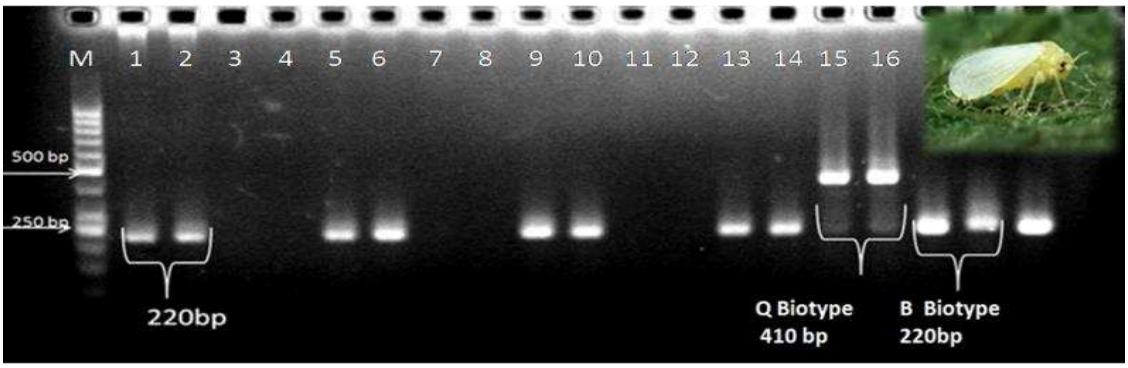

Figure 4. *Gel image of one white-fly biotyping M; Thermo Scientific GeneRuler 50 bp DNA Ladder. Line 1,2,5,6,9,10,13,14,17,18,19 B. tabaci Biotype B (220 bp), Line 15,16 Btabaci biotype Q (410 bp) Line 3,4 Aphis gossypii DNA samples Line 7,8; Frankliniella occidentalis DNA; 11,12; Ceratitis capitata DNA samples*

Phylogenetic analysis

In sequence comparisons (NCBI Query ID lcl|29009), TYLCV Israel isolate showed 97-98% similarity with Lebanon, Israel and Morocco isolates, Mild isolates showed 96-99% similarity with Lebanon, Spain, Italy and USA isolates. Sardinia and Sicily isolates were 94-97% similar with Italy, Spain and Morocco isolates (|EU143755.1, AF260331.1, FJ012359.1, EU719081.1) (*Fig. 5*).

Haplotype analysis was evaluated at "dnasp5.exe" programmed. When isolates from three provinces compared, TYLCV-Mld isolates were belonged a haplotype, on the other hand, each TYLCV-Sic isolates had different haplotypes. TYLCV-Is and TYLCV-Sa had two haplotypes as Adana and Antalya, both Mersin and Adana isolates haplotypes were detected identical

The sequences were compared and verified in the NCBI Blast system. Verified Sequences TYLCV-Is (MH367503, MK536596) to the NCBI system; TYLCV-Mld (MK536597); TYLCV-Sar (MK536600,) and TYLCV-Sic (MK536601, MK536602) are registered as isolates.

http://www.aloki.hu ● ISSN 1589 1623 (Print) ● ISSN 1785 0037 (Online)
DOI: http://dx.doi.org/10.15666/aeer/1704_91319144

The phylogenetic analysis utilizes that the tree is separated into two main groups (Group I and Group II) and Group I divides to 3 subgroups. TYLCV-Mild isolate from Turkey has a unique haplotype which is clustered in Subgroup 1C despite of showing approximately 93-98% similarity with other isolates around the world. TYLCV Mild isolates from Malaga, Lebanon, and Jordan are clustered in Group 1A alongside with TYLCV-Is isolate. TYLCV-Sar and TYLCV-Sic isolates are clustered in Group 1B with other Jordan, Italy and Spain isolates which shows that these isolates are related in the terms of phylogenetic.

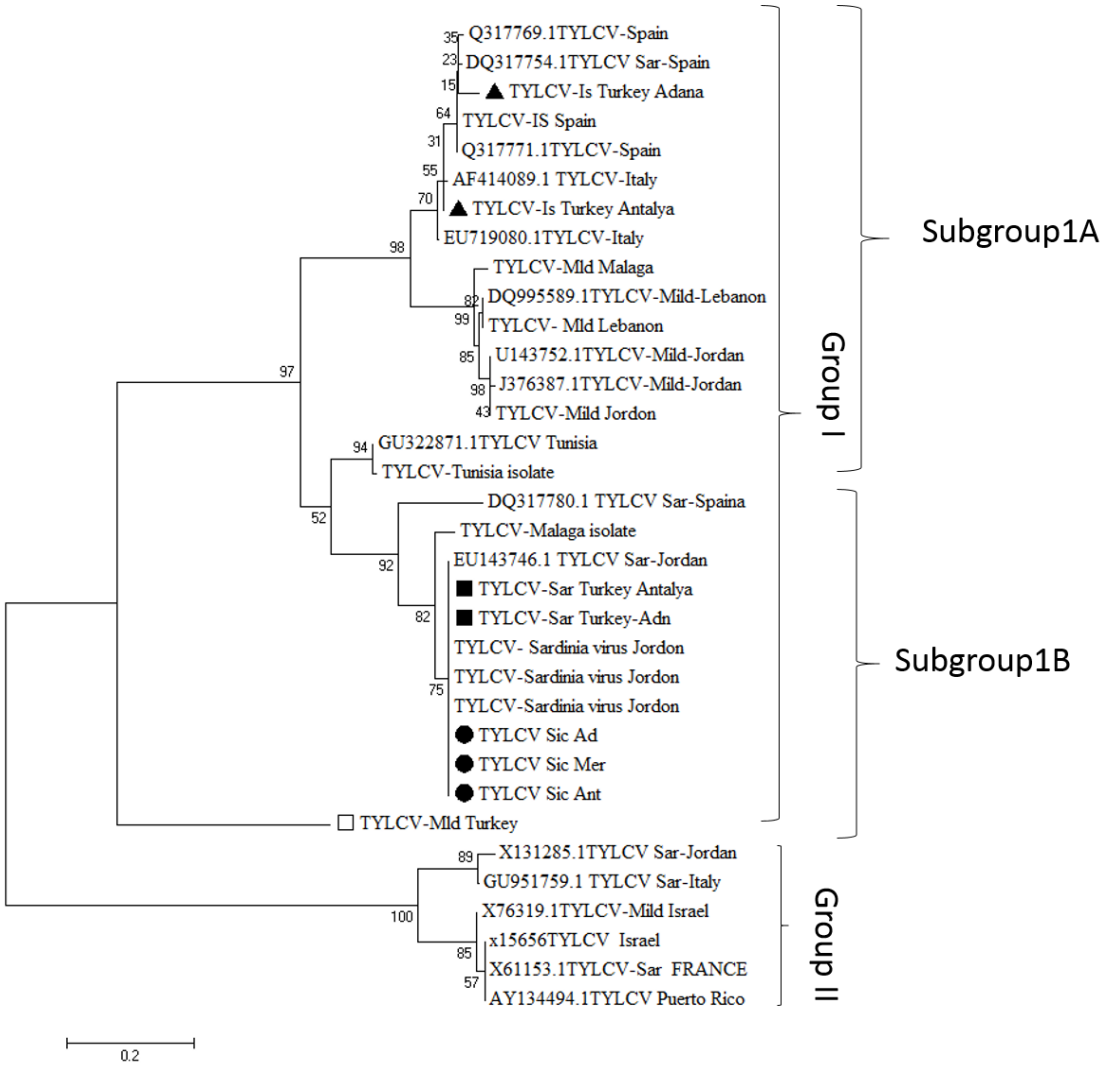

Figure 5. *After haplotype analysis, phylogenetic trees were constructed with MEGA 7 programme. Related 24 isolates were selected by using BLAST analysis in NCBI database and Neighbour-joining method was used TYLCV isolates from three provinces in Turkey*

Discussion

With this study, TYLCV strains and whitefly biotypes were determined which are two of the major problems of greenhouse tomato cultivation. TYLCV was observed in almost every greenhouse especially in autumn season. Temperature changes effect directly whitefly migration to greenhouses feeding behavior therefore TYLCV infection

http://www.aloki.hu ● ISSN 1589 1623 (Print) ● ISSN 1785 0037 (Online)
DOI: http://dx.doi.org/10.15666/aeer/1704_91319144

rate in greenhouses increases significantly as well its transmission. Although chemical management starts at threshold white-fly adult population. Nevertheless, observations showed that insecticides have not suppressed whitefly population even by rotating insecticides with different mode of action. In addition to these, insufficient knowledge of growers, presence of primitive greenhouse and growing conditions, no precautions for whiteflies such as many cavities around the greenhouses are making TYLCV infection spreading rapidly. Widespread infection causes virus to evolve more rapidly.

The most common observed strain was TYLCV-Is and TYLCV-Mld mixed infection in south coastal region of Turkey where the Mediterranean climate is dominant. On the other hand, this is the first report of TYLCV Sic. and Sar strains Mediterranean region of Turkey. Until the present study they have not been characterized and confirmed yet with reliable molecular methods such a PCR analyses at Turkey. There were TYLCV-Sic. strain infection found with general average 10% ratios where infections ratios were 6.2% Mersin, 2% Adana and 22% Antalya provinces respectively. Furthermore, there were TYLCV-Sar infections obtained general infection rate was 6.5% where infection ratios were 3,4% Adana, 10,5% Antalya and 5,4% Mersin respectively. Similar results have also determined from an individual whitefly's genomic structures had revealed TYLCV-Sic and TYLCV-Sar strains in PCR analysis.

Greenhouse studies for whiteflies showed that biotype B was the most common with aprox.92% average in all three provinces. Other studies about the biotypes of whiteflies at vegetables in Turkey also support this result. Ulusoy et al. (2012) reported that for vegetables biotype B and for cotton biotype Q are common whitefly populations. Therefore, this supports the results about detecting 10% biotype Q in Adana province (Karatas, Yuregir counties) where the production of cotton is widely done and after cotton harvest, whiteflies are rushing to higher temperature such as greenhouse tomato production areas. TYLCV transmission can be done by both B and Q biotypes however biotype B is more effective than Q biotype (Ajlan et al., 2007; Bel-Kadhi et al., 2008; Czosnek, 2008; Haider et al., 2017).

For detection, Multiplex PCR primer pairs and codominant SCAR markers was used considering the expenses, time wasting and more method steps (like RLFP) was the issue of the given methods in EPPO bulletin. This study proved that there are cheap, fast methods which have less error rates. Also there are no TYLCV Far East Asia and Africa strains in Turkey (Ohnishi et al., 2016). At least low incidence rate of Sardinia and Sicily which were South European strains (Italy, Spain, Morocco, Tunisia isolates) could be considered as positive finding of the study. Due to the fact that It is important to further exacerbate the damage caused by the existing strains. Furthermore, it is thought that there will be less chance of impact on the formation of undesired recombination between strains or isolates in the ecosystem both in and around the production area.

Conclusion

There are many ways to control TYLCV infection (Czosnek et al., 2017). Chemical control of whitefly is not the absolute solution therefore resistance to TYLCV through genetic means such as TY-1 and TY-3 genes (Zamir et al., 1994), TY-1 (Ji et al., 2007; Torre et al., 2018) or Co dominant Sequence Characterized Amplified Regions (SCAR) still are better options. Presence of many strains and multi gene controlled resistance decreased efficiency of TY1 gene. For this purpose, to overcome like breeding

http://www.aloki.hu ● ISSN 1589 1623 (Print) ● ISSN 1785 0037 (Online)
DOI: http://dx.doi.org/10.15666/aeer/1704_91319144

problems TY3 gene based codominant SCAR markers were developed, are supply Marker Assisted Selection for heterozygotes resistance and also homozygote susceptibility against to all Mediterranean isolates. Although there should be more studies to determine which strains involve in cultivation areas due its tendency to evolve or recombination. The strain identification has a solid importance, gives more effective directions for breeding supplied by well-characterized TYLCV strains. This study showed that there are at least four strains in Turkey and their contribution throughout Mediterranean coast. Focusing on resistant cultivars and their capacity to control the virus in Turkey as well as limiting its transmission by whiteflies could minimize damage caused by TYLCV.

The Mediterranean line has important agricultural trade areas and all kind of commercial products have been imported. This revealed contribution the natural distribution and occurrence of TYLCV in areas located. Our results pointed out the vector types with molecular techniques and sanitary conditions for TYLCV, present in tomato fields, are transmitted by white flies. The management of these vectors are so hard due to high reproductive ability, having broad range of hosts and ability to form insecticides durable species or types. In addition, the presence of vector whiteflies in the greenhouse and outside, the absence of biological and chemical control agents, takes to higher the infection. TYLCV has been spread more and more by vectors from different weeds to tomato are cultivated in greenhouse.

But nevertheless, TYLCV has a lower impact on production as it can be well controlled by molecular resistance breeding in soon.

This manuscript may also indicate sources of local TYLCV strains in tomato produced provinces. Uncontrolled distribution of *B. tabaci* types could be vectors of TYLCV strains; if whiteflies migration by air-ways or plant transportations could commence TYLCV infections at Mediterranean Countries.

The PCR technique, was standardized and successfully applied for TYLCV and *B. tabaci* biotypes, put forwarded relations between virus strain and vector bio types by Molecular assays. Therefore, Epidemiological role and feeding behaviors of *Bemisia tabaci* (Hemiptera: Aleyrodidae) Biotypes' for TYLCV strains on Tomato Agro Ecology in Turkey, has been become well understandable as agricultural host reservoir. Novel management strategies for disease vector complexities will be devised upon these studies to protect sanitized and resistance plants, often depends on the activation of vectors and pathogen (Razukas et al., 2007). Therefore, transmissibility of TYLCV (specially mixed infections) could be prevented.

Detailed project has planned for unknown epidemiological features of the virus vector relations (Islam et al., 2016). The determining the virus ecology and molecular origin were another outcome of results. High successful control of TYLCV spread relies upon easy discovery of these infections in stock planting material. All positive samples which were detected in this study have been eradicated.

This report is unique signature step for initiating researches on impact of whitefly vectors to the agro ecology. It is important because different virus isolates or their strains are caused disease in different host species during whitefly migration. It is possible that new isolates can result virus diseases in host plants even mixed or different isolates in whiteflies will cause possible recombination. This is not possible to estimate the adverse effects and epidemiology of the recombinants in the agricultural ecology and in the natural ecology without observing or living.

http://www.aloki.hu ● ISSN 1589 1623 (Print) ● ISSN 1785 0037 (Online)
DOI: http://dx.doi.org/10.15666/aeer/1704_91319144

Acknowledgments. Thanks to: Republic of Turkey Ministry of Agriculture and Forestry General Directorate of Agricultural Research and Polices Project Number TAGEM–BS–10/10–01 /02-08

Conflict of interests. The authors declare that they have no conflict of interests.

Ethical approval. This article does not contain any studies with human participants or animals performed by any of the authors.

REFERENCES

[1] Abak K., Yılmaz M. A., Kesici S. (1991): Problème de TYLCV en Turquie et moyen sutilisés pour diminuer son effet. – Proceeding of Seminar on Resistance to TYLCV, Avignon 1991, pp. 28-30.
[2] Abhary, M. K., Anfoka, G. H., Nakhla, M. K., Maxwell, D. P. (2006): Post-transcriptional gene silencing in controlling viruses of the tomato yellow leaf curl virus complex. – Archives of Virology 151: 2349-2363.
[3] Accotto, G. P., Navas-Castillo, J., Noris, E., Moriones, E., Louro, D. (2000): Typing of tomato yellow leaf curl viruses in Europe. – Eur. J. Plant Pathol. 106: 179-186.
[4] Ajlan, A., MGhanem, G. A. M., Abdulsalam, K. S. (2007): Tomato yellow leaf curl virus (TYLCV) in Saudi Arabia: identification, partial characterization and virus-vector relationship. – Arab J. Biotech. 10(1): 179-192.
[5] Anfoka, G. H., Abhary, M., Nakhla, M. K. (2005): Molecular identification of species of the Tomato yellow leaf curl virus complex in Jordan. – J. Plant Pathol. 87: 61-66.
[6] Anfoka, G., Abhary M., Haj Ahmad, A. F., Hussein, A., Rezk, F., Akad, Y., Abou-Jawdah, M. et al. (2008): Survey of tomato yellow leaf curl disease-associated viruses in the eastern Mediterranean basin. – Journal of Plant Pathology 90(2): 311-320.
[7] Avidov, H. Z. (1944): Tobacco Whitefly in Israel. – Hassadeh, Tel Aviv, pp. 1-33 (in Hebrew).
[8] Bayhan, E., Ulusoy, M. R., Brown, J. K. (2006): Host species, distribution, and natural enemies of *Bemisia tabaci* "B biotype" (Homoptera: Aleyrodidae) in Turkey. – J. Pestic. Sci. 79: 233-240.
[9] Bel-Kadhi, M. S., Onillon, J. C., Cenis, J. L. (2008): Molecular characterization of *Bemisia tabaci* biotypes in Southern Tunisia. – Tunisian Journal of Plant Protection 3: 79-85.
[10] Boulton, M. I. (2003): Geminiviruses: major threats to world agriculture. – Ann. Appl. Biol. 142: 143.
[11] Brown, J. K., Czosnek, H. (2002): Whitefly Transmitted Viruses. – Academic Press, New York, pp. 65-100.
[12] Czosnek, H. (2008): Tomato Yellow Leaf Curl Virus. – In: Mahy, B. W. J., Van Regenmortel, M. H. V. (eds.) Encyclopedia of Virology. Elsevier, Oxford, pp. 138-145.
[13] Czosnek, H., Laterrot, H. (1997): A worldwide survey of tomato yellow leaf curl viruses. Arch. Bemisia tabaci. – J. Gen. Virol. 72: 2607-2614.
[14] Czosnek, H., Shalev, A. H., Sobol, H., Gorovits, R., Ghanim, M. (2017): The incredible journey of Begomo viruses in their whitefly vector. – Viruses 9: 273. DOI: 10.3390/v9100273.
[15] Fauquet, C. M., Briddon, R. W., Brown, J. K., Moriones, E., Stanley, J., Zerbini, M., Zhou, X. (2008): Geminivirus strain demarcation and nomenclature. – Arch Virol 153: 783-821.
[16] Gronenborn, B. (2007): The Tomato Yellow Leaf Curl Virus Genome and Function of Its Proteins. – In: Czosnek, H. (ed.) Tomato Yellow Leaf Curl Virus Disease: Management, Molecular Biology, Breeding for Resistance. Springer, Dordrecht, pp. 67-84.
[17] Haider, S., Khan, M. A., Jahanzaib, M. (2017): Characterization of epidemiologicalfactorsforthewhitefly (*Bemisiatabaci* Genn.) population and tomato leaf

http://www.aloki.hu ● ISSN 1589 1623 (Print) ● ISSN 1785 0037 (Online)
DOI: http://dx.doi.org/10.15666/aeer/1704_91319144

curl virus disease (TLCVD) incidence on tomato genotypes in Faisalabad. – Pakistan Journal of Entomology and Zoology Studies 5(4): 747-752.

[18] Islam, W., Zhang, J., Adnan, M., Noman, A., Zaynab, M., Wu, Z. (2016): Plant virus ecology: a glimpse of recent accomplishments. – Applied Ecology and Environmental Research 15(1): 691-705.

[19] Isler, N., Ozgur A. F. (1992): The effect of planting time and row spacing on population development of whitefly (*Bemisia tabaci*) and plant phenology and yield. – Turk. Entomol. Dergisi 16: 87-98.

[20] Ji, Y., Schuster, D. J., Scott, J. W. (2007): Ty-3, a begomovirus resistance locus near the Tomato yellow leaf curl virus resistance locus Ty-1 on chromosome 6 of tomato. – Mol Breeding 20: 271-284.

[21] Jones, D. R. (2003): Plant viruses transmitted by whiteflies. – Eur. J. Plant Pathol. 109: 195-219.

[22] Karut, K., Malik, A. A. Y., Kazak, C., Kamberoğlu, M. A., Ulusoy, M. R. (2012): Determination of biotypes of bemisia tabaci (Gennadius 1889) (Hemiptera: Aleyrodidae) on different host plant in Adana (Balcali) by using two different molecular methods. – Turkiye Entomoloji Dergisi - Turkish Journal of Entomology 36: 93-100.

[23] Karut, K., Kaydan, M. B., Tok, B., Döker, İ., Kazak, C. (2015): A new record for (Gennadius) (Hemiptera species complex of Turkey. – Journal of Applied Entomology 139: 158-160.

[24] Konjevic, A., Milovac, Z., Kontsedalov, S., Kanakala, S., Ghanim, M. (2018): First interception of Bemisiatabaci Mediterranean (Q biotype) in Serbia. – J. Appl. Entomol. 142: 627-631.

[25] Li, J., Ding, T. B., Chi, H., Chu, D. (2017): Effects of tomato chlorosis virus on the performance of its key vector, Bemisiatabaci, in China. – J. Appl. Entomol. 142(3): 296-304.

[26] Moriones, E., Navas-Castillo, J. (2000): Tomato yellow leaf curl virus, an emerging virus complex causing epidemics worldwide. – Virus Res. 71: 123-134.

[27] Navas-Castillo, J., Fiallo-Olivé, E., Sánchez-Campos, S. (2011): Emerging virus diseases transmitted by whiteflies. – Ann Rev Phytopathol. 49: 219-248.

[28] Ohnishi, J., Yamaguchi, H., Saito, A. (2016): Analysis of the mild strain of tomato yellow leaf curl virus, which overcomes Ty-2 gene-mediated resistance in tomato line H24. – Arch. Virol. 161(8): 2207-17. DOI: 10.1007/s00705-016-2898-4.

[29] Papayiannis, L. C., Katis, N. I., Idris, A. M., Brown, J. K. (2011): Identification of weed hosts of *Tomato yellow leaf curl virus* in Cyprus. – Plant Dis. 95: 120-125.

[30] Razukas, A., Jundulas, J., Asakavıcıute, R. (2007): Potato cultivars susceptibility to potato late blight (Phytopthtora infestans). – Applied Ecology and Environmental Research 6(1): 95-106.

[31] Sambrook, J., Fritschi, E. F., Maniatis, T. (1989): Molecular Cloning: A Laboratory Manual. – Cold Spring Harbor Laboratory Press, New York.

[32] Satar, G., Ulusoy, M. R. (2016): Biotype detection of Bemisia tabaci (Gennadius) (Hemiptera: Aleyrodidae) populations collected from Mediterranean Region Türk. – Entomol. bült. 6(3): 205-212.

[33] Torre, C., Donaire, L., Gómez-Aix, C., Juárez, M., Peterschmitt, M., Urbino, C., Hernando, Y., Agüero, J., Aranda, M. A. (2018): Characterization of begomoviruses sampled during severe epidemics in tomato cultivars carrying the *Ty-1* Gene. – Int. J. Mol. Sci. 19: 2614.

[34] Ulusoy M. R., Karut K., Çalişkan A. F. (2012): Faunistic studies on Aleyrodidae species of Aegen Region. – Türkiye Entomoloji Bülteni 2: 251-267.

[35] Yilmaz, M. A. (1978): Domateslerde Domates Sarı Yaprak Kıvırcıklık Virüsü. – Doğa 2: 248-250.

http://www.aloki.hu ● ISSN 1589 1623 (Print) ● ISSN 1785 0037 (Online)
DOI: http://dx.doi.org/10.15666/aeer/1704_91319144

[36] Zamir, D., Ekstein Michelson, I., Zakay, Y., Navot, N., Zeidan, M., Sarfatti, M., Eshed, Y., Harel, E., Pleban, T., van Oss, H. (1994): Mapping and introgression of a tomato yellow leaf curl virus tolerance gene, Ty-1. – Theor Appl Genet 88:141-146.
[37] Zeidan, M., Czosnek, H. (1991): Acquisition of tomato yellow leaf curl virus by the whitefly *Bemisia tabaci*. – Journal of General Virology 72: 2607-2614.

http://www.aloki.hu ● ISSN 1589 1623 (Print) ● ISSN 1785 0037 (Online)
DOI: http://dx.doi.org/10.15666/aeer/1704_91319144

ISOLATION AND MOLECULAR CHARACTERIZATION OF PHOSPHATE SOLUBILIZING FILAMENTOUS FUNGI FROM SUBTROPICAL SOILS IN OKINAWA

ISLAM, M. K.[1,2,3] – SANO, A.[1,2] – MAJUMDER, M. S. I.[1,2] – HOSSAIN, M. A.[1,2*] – SAKAGAMI, J.-I.[1,4]

[1]*The United Graduate School of Agricultural Sciences, Kagoshima University, Kagoshima, Japan*

[2]*Faculty of Agriculture, University of the Ryukyus, Okinawa 903-0213, Japan*

[3]*Department of Soil Science, Faculty of Agriculture, Patuakhali Science and Technology University, Patuakhali, Bangladesh*

[4]*Faculty of Agriculture, Kagoshima University, Kagoshima, Japan*

**Corresponding author*
e-mail: amzad@agr.u-ryukyu.ac.jp; phone: +81-98-895-8824; fax: +81-98-895-8741

(Received 19th Mar 2019; accepted 24th May 2019)

Abstract. Phosphorus (P) is an essential nutrient element required for plant growth and development. Low phosphorus availability in soil is one of the major constrains for crop production. Phosphate solubilizing fungi enhance available phosphorous released from soils and contribute to fulfill the plants phosphorous requirement. This study aimed to isolate and identify potential phosphate solubilizing fungi from subtropical soils for environment friendly biofertilizer development. Sixteen fungal strains were isolated and identified as *Aspergillus* spp., *Penicillium* spp. and *Talaromyces* spp. from subtropical dark red soil, red soil and grey soil based on phosphate solubilization index, morphological studies and the sequences of β-tubulin and/or Calmodulin. Subsequently, fungal isolates having excellent phosphate solubilization efficiency were selected by their potential in broth containing insoluble $Ca_3(PO_4)_2$, $AlPO_4$ and $FePO_4$. Interestingly, *Aspergillus niger* isolates (strain SI-10URAgr, SI-11URAgr and SI-12URAgr) have marked phosphate solubilization ability regardless of the substrates followed by *Panicillium oxalicum* and *Talaromyces pinophilus.* In addition, there was inverse proportion between the pH and phosphate solubilizing capacities. These excellent properties of strains suggested that they have a great potential for agricultural utilization as environmentally sound biofertilizer. In this study, phosphate solubilization by filamentous fungi is reported for the first-time in subtropical Okinawa.
Keywords: *phosphorous, Aspergillus niger, biofertilizer, eco-friendly nutrient management, subtropical soil*

Introduction

Phosphorus (P) is one of the major nutrients for crop production (Reena et al., 2013). This nutrient play important physiological and bio chemical activities of plants, like, photosynthesis, energy and sugar production, nucleic acid synthesis, and promotes nitrogen fixation in legume plants (Saber et al., 2005). Phosphorus promotes the strength of grain crop straw, flower initiation and fruit settings, root development and seed formation (Sharma et al., 2013) and disease resistance capacity of plants (Richardson et al., 2007). In soils, only 0.1% of the total P exists in a soluble form available for plant uptake because of its fixation into an unavailable form (Zhou et al., 1992; Khan et al., 2010). In order to provide this nutrient, farmers use chemical fertilizers. The most widely used fertilizers are obtained from the acidification of rock phosphates with strong acids which not only represent a major cost of agricultural

http://www.aloki.hu ● ISSN 1589 1623 (Print) ● ISSN 1785 0037 (Online)
DOI: http://dx.doi.org/10.15666/aeer/1704_91459157

production but also impose adverse environmental impacts on overall soil health, terrestrial, freshwater and marine resources (Sing et al., 2011; Tilman et al., 2001).

The major soils in sub-tropical Okinawa are, red soil, dark-red soil and grey soil which are phosphorous deficient (Oshiro et al., 2016). The red soil and dark red soil have low pH value (5.4 and 6.6 respectively), one the other hand grey soil has high pH value (8.4). Large amount of soluble P fertilizers is widely used in order to increase agricultural production world widely (Bo et al., 2011). Moreover, the efficiency of applied P fertilizers in chemical form rarely exceeds 30% due to its fixation, either in the form of iron/aluminium phosphate in acidic soils or in the form of calcium phosphate in neutral to alkaline soils (Norish et al., 1983; Lindsay et al., 1989). According to the latest estimates, the global reserve of P could become depleted within 50-100 years (Heppel et al., 2016). Besides the efficient use of P reserves, it is also important to reduce the current wastage of P fertilizers and to recover applied P. The realization of all these potential problems associated with chemical P fertilizers has led to the search for environmentally compatible and economically feasible alternative strategies for improving crop production in low or P-deficient soils (Zaidi et al., 2009).

The microbial inoculants (biofertilisers) function as key player in sustainable agriculture by improving soil fertility and crop productivity (Deepak et al., 2014). Especially, fungi are able to penetrate in to deep underground and show good attachment to insolubilized P particles as results of its hyphal structure compared to bacteria and actinomycetes. Furthermore, fungi are good acid producer and consequently show greater phosphate solubilization activity than bacteria (Deepak et al., 2014; Jose et al., 2010). Among these, *Aspergillus* spp., *Penicilium* spp., *Talaromyces* spp. and *Eupenicilium* spp. are considered “key organisms” in the P cycle (Jose et al., 2010). However most of the fungal species solubilize inorganic calcium phosphate and have a limited capacity to solubilize aluminium or iron phosphate. There are few in vitro studies concerning the solubilization of other phosphates by fungal species. To address this limitation, the present study aims to isolate and identify new isolates of indigenous phosphate solubilizing filamentous fungi which could be potential to solubilize both tricalcium phosphate, aluminium phosphate and iron phosphate.

Materials and methods

Isolation

The study was carried out in the Mycology Laboratory, Faculty of Agriculture, University of the Ryukyus, Okinawa, Japan during August 2017–November 2018 under a class II biohazard cabinet (BHC-1306IIA/3B, AIRTECH, Tokyo, Japan) followed to the biosafety classification by National Institute of Infectious Disease of Japan, because of possibilities of including toxic fungal species treated as BSL2 during the isolation.

The sampling area located at 26.5000°N and 128.0000°E (*Fig. 1*). Its climate is subtropical, temperatures range from 10 to 32 °C. Low temperature (10 to 26 °C) exists in winter season and higher temperature (27 to 32 °C) exists in summer with a humidity level near 100%. The major soil types are dark red soil, red soil and grey soil in this area.

Zero to fifty cm depth soil samples were collected from ten different locations of three type soils using sterile auger. One-hundred-gram soil was taken from each sampling point and it makes a total of 500 g composite sample (five points from each location make one composite sample). The samples were transferred to laboratory in

http://www.aloki.hu ● ISSN 1589 1623 (Print) ● ISSN 1785 0037 (Online)
DOI: http://dx.doi.org/10.15666/aeer/1704_91459157

sterile sealed polythene bag under aseptic condition and stored at room temperature. Then microbiological study was done as early as possible.

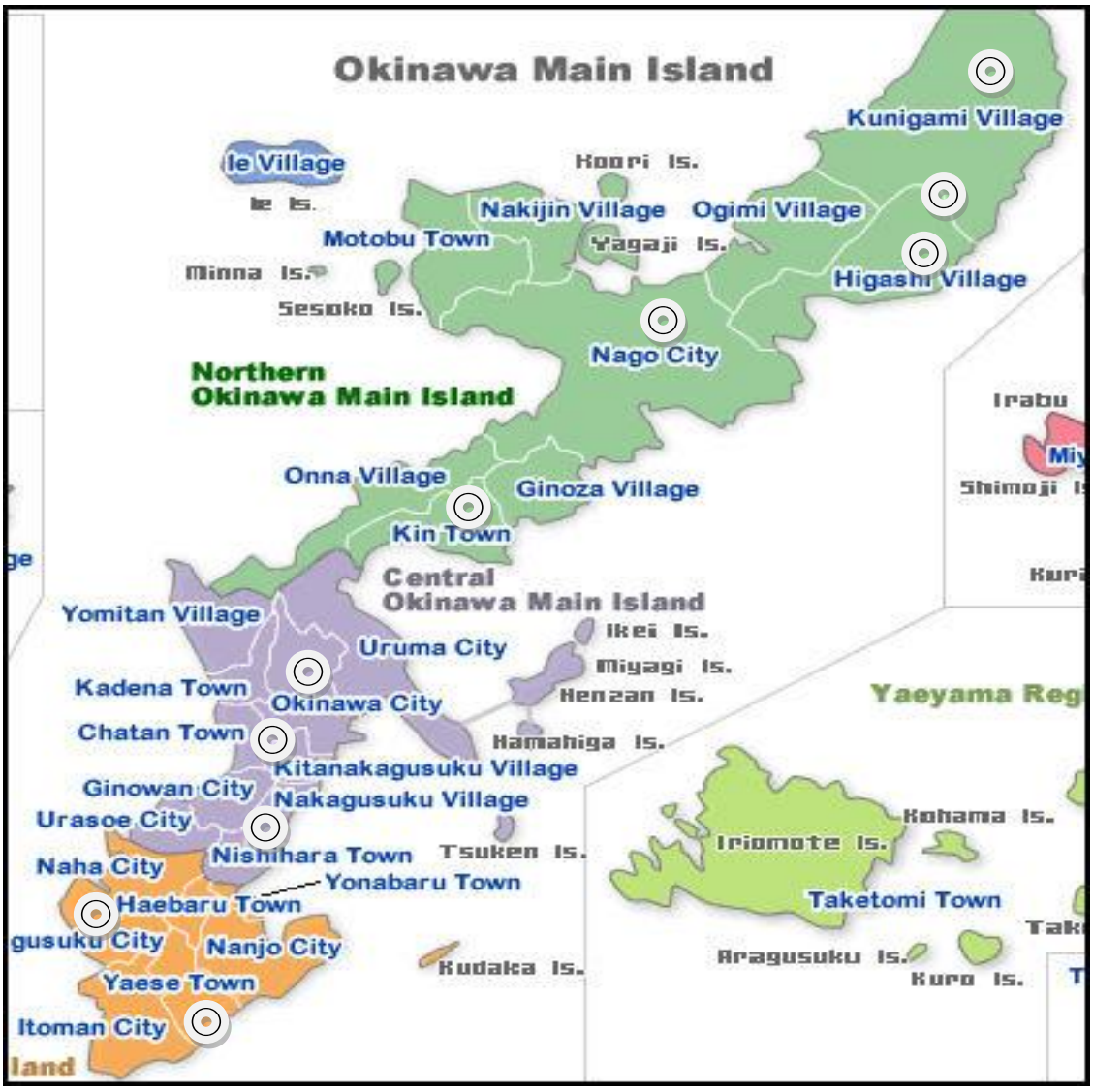

Figure 1. *Geographical map of the study area indicated sampling location*

For isolating phosphate solubilizing fungi Pikoveskaya's (PKV) agar medium was used. Pikoveskaya's (PKV) agar medium consisted of 10.0 g glucose, 5.0 g $Ca_3(PO_4)_2$, 0.5 g $(NH_4)_2SO_4$, 0.1 g $MgSO_4 .7H_2O$, 0.02 g NaCl, 0.02 g KCl, 0.003 g $FeSO_4 .7H_2O$, 0.003 g $MnSO_4 \cdot H_2O$ 0.5 g yeast extract, 15.0 g agar and 1000 mL distilled water (Rao, 1982). In this medium $Ca_3 (PO_4)_2$ was used as a source of insoluble phosphate. The medium was autoclaved at 121 °C for 15 min. About 20 ml of the sterilized medium poured into each petri dish and allowed to solidify before inoculation. Chloramphenicol was also used to avoid bacterial growth.

Isolation of phosphate solubilizing fungi using serial dilution plate technique. Five-gram soil sample was diluted in to 50 ml of sterile water. It was vigorously shaken until to get homogenous suspension and serially diluted to 10^{-1}, 10^{-2}, 10^{-3} and 10^{-4}. From each dilution, 200 µL was plated on Pikovskaya's agar. The phosphate solubilizing

http://www.aloki.hu ● ISSN 1589 1623 (Print) ● ISSN 1785 0037 (Online)
DOI: http://dx.doi.org/10.15666/aeer/1704_91459157

fungi were identified by the presence of a clear halo around the colonies after 7 days incubation at 25 °C (Rao, 1982). The experiment was performed in triplicate. Phosphate solubilizing fungi of the soil samples were isolated and purified by transferring into new plates. The pure cultures were preserved on potato dextrose agar slants at 4 °C for further study. Phosphate solubilisation index was measured using the following formula (Birhanu et al., 2017):

$$SI = [\text{Colony diameter} + \text{Halo zone diameter}] / \text{colony diameter}$$

Identification of phosphate solubilizing fungi

The genera of phosphate solubilizing fungal isolates were identified based on the taxonomic keys based on morphologies (Watanabe, 2010). The keys were the color and tint in colony overs and revers, presence of aerial hyphae, colony surface texture, colony margin and pattern of pigment exudations. Wet mounts prepared from micro culture were mounted in lacto phenol and lacto phenol cotton blue. Microscopic examination and photomicrography were performed with an OLYMPUS BX50 microscopy equipped with image Analysis system (Olympus Corporation, Tokyo, Japan).

DNA was extracted from one piece of fungal mycelia from a culture incubated at 25 °C for 48 h on Sabrouraud medium containing 2% glucose and 1% peptone using a DEXPAT kit (TaKaRa, Japan) to identify the isolates at genetic level (Yamaguchi et al., 2014). Beta- tubulin gene sequences amplified with primers bt2a and bt2b and calmodulin genes amplified with primers CMD5 and CMD6 were determined (Samson et al., 2014). Sequences were analyzed by the NCBI BLAST tool to classify and identify closely related fungal sequences. We identified the isolates to the certain species if the BLAST results showed similarity values of 98% or higher.

Preparation of spore suspension

Sporulated pure fungal cultures slants were selected for preparation of spore suspension by using standard procedure. A total volume of 5 ml sterile water with twin 80 was added in culture slants and the fungal colony surface was lightly scraped by sterile bamboo stick. The cultures were passing through a syringe with staff cotton. Spore count was done by a hemocytometer and the suspension was adjusted to approximately10^6 spores mL^{-1}.

Quantitative estimation of phosphate solubilization

It was carried out using Erlenmeyer flask containing 40 ml Pikoveskaya's (PKV) broth medium supplemented with 0.5% tricalcium phosphate [$Ca_3 (PO_4)_2$], aluminium phosphate ($AlPO_4$) and iron phosphate ($FePO_4$). After sterilization, the medium of each flask was inoculated with the 5% (v/v) spore suspension of a particular fungal isolate containing 10^6 spores mL^{-1}. Sterile distilled water inoculated flaks was treated as control. Three replicates were maintained for each test isolate and mean value was recorded. Incubation was done at 25 °C in an incubator shaker at 120 rpm up to 9 days. The samples were autoclaved and centrifuged at 5000 rpm for 25 min to remove any suspended solids and mycelial parts. Then the cultures were filtered through 0.45 µm pore size syringe filter unit (Advantech, japan). The filtrates were used for analysis of soluble phosphate and pH value. The pH value of the culture supernatants was

http://www.aloki.hu ● ISSN 1589 1623 (Print) ● ISSN 1785 0037 (Online)
DOI: http://dx.doi.org/10.15666/aeer/1704_91459157

determined by a pH meter (Horiba, Japan) equipped with a glass electrode. The amount of soluble phosphorus in culture supernatants was measured by molybdenum blue method and expressed as mg/L (Morphy and Riley, 1962). Samples cultured for 3, 6 and 9 days were compared. After calculation of mean phosphate degradation ability from 16 isolates of each day, we selected the adequate period for the comparison depending on the substrate.

Effect temperature on the growth and survival of isolates

The isolates were cultured on PDA slants in triplicate and incubated at temperature at 35, 37 and 42 °C for 7 days to evaluate the growth of mycelia. Growth of isolates at 25 °C (room temperature) treated as positive control.

Statistical analysis

All experiments were conducted in triplicate and data were analyzed using Microsoft Excel program. The mean values were compared by Fisher test and significant differences were detected at $p < 0.05$ level. Correlation between solubilized phosphate and pH of the medium was determined by using Pearson correlation studies.

Results

Screening and identification of phosphate solubilizing fungi

A total of 16 fungal isolates showed phosphate solubilizing activities. The isolates were 6 *Aspergillus* spp., 6 *Penicillium* spp. and 2 *Taleromyces* spp. identified based on colony morphology, microscopic observation and Beta-tubulin and/or calmodulin sequences (*Table 1*).

Table 1. *List of fungal strains with gene bank accession number isolated from dark red, red and grey soils of subtropical environment*

Isolates	Strain in gene bank	Soil types	Sampling places	Organisms	Accession number	
					Beta tubulin gene	Calmodulin gene
1	SI-1URAgr	Dark red soil	Nishihara, Okinawa	*Penicillium sp.*	LC425316	Not done
2	SI-2URAgr	Dark red soil	Nishihara, Okinawa	*Aspergillus floccosus*	LC425317	Not done
3	SI-3URAgr	Dark red soil	Nishihara, Okinawa	*Aspergillus niveus*	LC425318	LC425334
4	SI-4URAgr	Grey soil	Nishihara, Okinawa	*Talaromyces pinophilus*	LC425319	LC425335
5	SI-5URAgr	Grey soil	Nishihara, Okinawa	*Aspergillus niveus*	LC425320	LC425336
6	SI-6URAgr	Grey soil	Nishihara, Okinawa	*Penicillium oxalicum*	LC425321	Not done
7	SI-7URAgr	Red soils	Kunigami, Okinawa	*Penicillium sp.*	LC425322	Not done
8	SI-8URAgr	Red soils	Kunigami, Okinawa	*Penicillium sp.*	LC425323	Not done
9	SI-9URAgr	Red soils	Kunigami, Okinawa	*Penicillium sp.*	LC425324	Not done
10	SI-10URAgr	Red soils	Kunigami, Okinawa	*Aspergillus niger*	LC425325	LC425337
11	SI-11URAgr	Red soils	Yanbaru forest, Okinawa	*Aspergillus niger*	LC425326	LC425338
12	SI-12URAgr	Red soils	Yanbaru forest, Okinawa	*Aspergillus niger*	LC425327	LC425339
13	SI-13URAgr	Dark red soil	Nishihara, Okinawa	*Penicillium sp.*	LC425328	LC425340
14	SI-14URAgr	Dark red soil	Nishihara, Okinawa	*Aspergillus floccosus*	LC425329	Not done
15	SI-15URAgr	Grey soil	Nishihara, Okinawa	*Talaromyces pinophilus*	LC425330	Not done
16	SI-16URAgr	Dark red soil	Nishihara, Okinawa	*Penicillium oxalicum*	LC425331	Not done

http://www.aloki.hu ● ISSN 1589 1623 (Print) ● ISSN 1785 0037 (Online)
DOI: http://dx.doi.org/10.15666/aeer/1704_91459157

Qualitative phosphate solubilization

Sixteen fungal isolates showed significant phosphate solubilization in Pikovskaya agar medium using tricalcium phosphate as the substrate. The phosphate solubilization index (PSI) ranged from 1.42 to 2.24 (*Table 2*). Isolate SI-16URAgr (*Penicillium oxalicum*) produced highest PSI; 2.24 (*Fig. 2*), whereas; the smallest PSI of 1.42 was achieved from SI-3URAgr (*Aspergillus nevius*)

Table 2. *In vitro phosphate solubilization in solid medium by 16 fungal strains*

Sl. No.	Fungal strain	Type of fungi	PSI
1	SI-1URAgr	*Penicillium sp.*	1.6 ± 0.03^{d}
2	SI-2URAgr	*Aspergillus floccosus*	1.67 ± 0.08^{d}
3	SI-3URAgr	*Aspergillus niveus*	1.42 ± 0.02^{e}
4	SI-4URAgr	*Talaromyces pinophilus*	1.8 ± 0.04^{c}
5	SI-5URAgr	*Aspergillus niveus*	1.67 ± 0.05^{d}
6	SI-6URAgr	*Penicillium oxalicum*	1.78 ± 0.03^{c}
7	SI-7URAgr	*Penicillium sp.*	1.5 ± 0.05^{d}
8	SI-8URAgr	*Penicillium sp.*	1.56 ± 0.08^{d}
9	SI-9URAgr	*Penicillium sp.*	1.42 ± 0.04^{e}
10	SI-10URAgr	*Aspergillus niger*	1.91 ± 0.03^{b}
11	SI-11URAgr	*Aspergillus niger*	1.66 ± 0.04^{d}
12	SI-12URAgr	*Aspergillus niger*	1.64 ± 0.04^{d}
13	SI-13URAgr	*Penicillium sp.*	2.02 ± 0.24^{b}
14	SI-14URAgr	*Aspergillus floccosus*	1.62 ± 0.09^{d}
15	SI-15URAgr	*Talaromyces pinophilus*	1.72 ± 0.04^{d}
16	SI-16URAgr	*Penicillium oxalicum*	2.25 ± 0.06^{a}

PSI: Phosphate solubilization index
Values given are the mean ± standard deviation of three independent replicates
Same letter in the column are not significantly different at $p < 0.05$ by Fisher's test

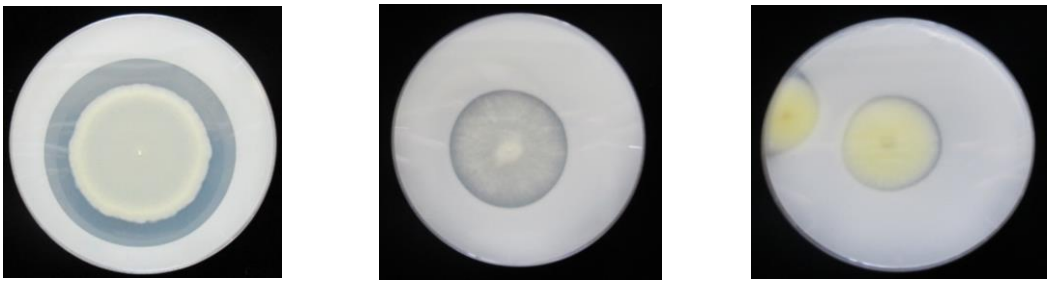

A B C

Figure 2. *Clear halo formation by representative fungal isolates in Pikovskaya agar plates (A: Penicillium oxalicum, B: Aspergillus niger and C: Talaromyces pinophilus)*

Quantitative phosphate solubilization

Phosphate solubilizations by the isolated fungi were analyzed in Pikovskaya broth medium using three substrates of recalcitrant phosphate compounds: tricalcium phosphate [$Ca_3(PO_4)_2$], aluminium phosphate ($AlPO_4$) and iron phosphate ($FePO_4$). The

http://www.aloki.hu ● ISSN 1589 1623 (Print) ● ISSN 1785 0037 (Online)
DOI: http://dx.doi.org/10.15666/aeer/1704_91459157

P-solubilizing ability of fungal isolates varied with incubation period and substrates. The best period of observation was selected considering their mean P solubilization, which 9 days for $Ca_3(PO4)_2$ and 6 days for both $AlPO_4$ and $FePO_4$ (*Table 3*).

Table 3. *Selection for the best period of phosphate solubilization by fungal strains*

Solubilized phosphate (mg/L)								
Tricalcium phosphate (TCP)			**Aluminium phosphate (Al-P)**			**Iron phosphate (Fe-P)**		
3 days	**6 days**	**9 days***	**3 days**	**6 days8***	**9 days**	**3 days**	**6 days***	**9 days**
192.2±106.2	245.4±101.5	303.4±216.3	81.4±31.6	236.0±167.6	194.2±192.5	93.6±93.7	173.4±212.0	156.5±171.7

Values given are the mean ± standard deviation of P solubilized by 16 fungal isolates
An asterisk (*) indicated the highest solubilization day

The strongest phosphate (P) solubilization effect was found in the medium containing $Ca_3(PO_4)_2$ followed by $AlPO_4$ and $FePO_4$ (*Table 4*). The solubilized P ranged between 73.2-759.4 mg/L, 85.6-599.6 mg/L and 36.6-663.8 mg/L from $Ca_3(PO_4)_2$, $AlPO_4$ and $FePO_4$ respectively. Among the isolates the highest amount of P was solubilized by *Aspergillus niger* followed by *Penicillium oxalicum* and *Talaromyces pinophillus.* Finally, *Aspergillus niger* strain SI-10URAgr, SI-11URAgr and SI-12URAgr were considered as outstanding isolates because solubilized P was higher than sum of the mean and standard deviation of P solubilized by 16 isolates. The amount of solubilized P from $Ca_3(PO_4)_2$ was 759.5, 647.8 and 670.5 mg/L; from $AlPO_4$ was 388.0, 558.3 and 599.7 mg/L and from $FePO_4$ was 663.8, 555.9 and 517.0 mg/L respectively (*Table 4*). SI-10URAgr showed outstanding performance in both $Ca_3(PO_4)_2$ and $FePO_4$ solubilization but in case of $AlPO_4$, it was very close to the outstanding.

Table 4. *Comparison of phosphate solubilization from different substrate by phosphate solubilizing fungal strains*

Sl. No.	***Fungal strain***	***Type of fungi***	***Solubilized phosphate (mg/L)***		
			TCP	**Al-P**	**Fe-P**
1	SI-1URAgr	*Penicillium sp.*	295.5	166.7	176.0
2	SI-2URAgr	*Aspergillus floccosus*	83.5	190.3	42.4
3	SI-3URAgr	*Aspergillus niveus*	73.3	96.3	41.4
4	SI-4URAgr	*Talaromyces pinophilus*	175.9	194.9	36.1
5	SI-5URAgr	*Aspergillus niveus*	126.1	102.6	39.4
6	SI-6URAgr	*Penicillium oxalicum*	240.5	370.0	41.9
7	SI-7URAgr	*Penicillium sp.*	157.9	108.0	40.5
8	SI-8URAgr	*Penicillium sp.*	84.2	256.7	38.4
9	SI-9URAgr	*Penicillium sp.*	207.7	90.6	37.4
10	SI-10URAgr	*Aspergillus niger*	759.5*	388.0	663.8*
11	SI-11URAgr	*Aspergillus niger*	647.8*	558.3*	555.9*
12	SI-12URAgr	*Aspergillus niger*	670.5*	599.7*	517.0*
13	SI-13URAgr	*Penicillium sp.*	305.4	101.8	86.9
14	SI-14URAgr	*Aspergillus floccosus*	321.9	333.2	227.5
15	SI-15URAgr	*Talaromyces pinophilus*	308.0	134.8	48.0
16	SI-16URAgr	*Penicillium oxalicum*	397.2	85.7	182.9
		Mean±Sd	303.4 ± 216.3	236.0 ± 167.6	173.4 ± 212.0

TCP: tricalcium phosphate; Al-P: aluminium phosphate and Fe-P: iron phosphate
An asterisk (*) indicated outstanding values of solubilized phosphate. It was higher than sum of mean and standard deviation of P solubilized by 16 fungal isolates
Values given are the mean ± standard deviation of P solubilized by 16 fungal isolates

http://www.aloki.hu ● ISSN 1589 1623 (Print) ● ISSN 1785 0037 (Online)
DOI: http://dx.doi.org/10.15666/aeer/1704_91459157

pH value of the culture medium

pH of the culture medium exhibited the opposite changes. It decreased with the increased amount of soluble P in the medium. Correlation studies showed a significant inverse relationship between soluble P and pH of the culture medium (*Fig. 3*). The strongest negative correlation was observed in all fermented broth culture and correlation coefficient (r) was -0.88, -0.74 and -0.84 in TCP, Al-P and Fe-P respectively.

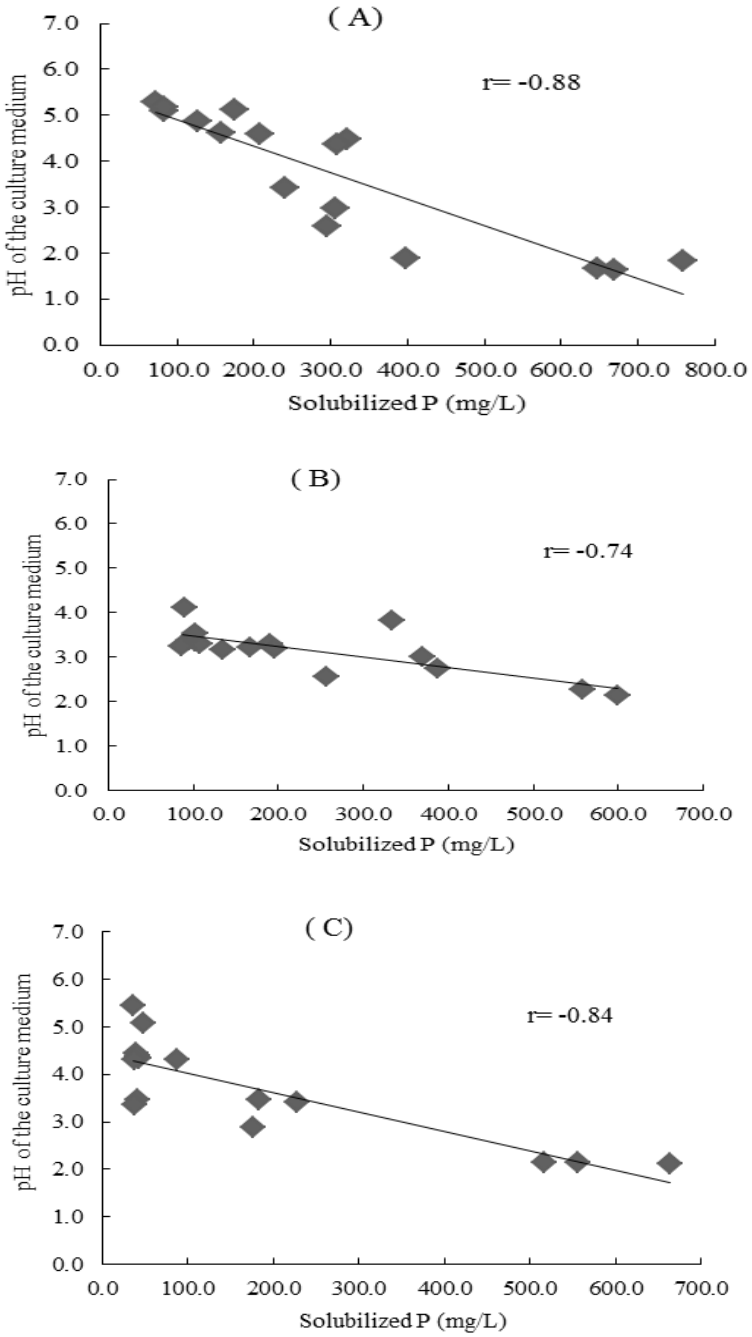

Figure 3. *Pearson's correlation between soluble phosphate and pH of the culture medium supplemented with [$Ca_3(PO_4)_2$] (A), $AlPO_4$ (B) and $FePO_4$ (C); inoculated by 16 fungal strains*

http://www.aloki.hu ● ISSN 1589 1623 (Print) ● ISSN 1785 0037 (Online)
DOI: http://dx.doi.org/10.15666/aeer/1704_91459157

Temperature effects on isolates

Survival of the isolates at different temperature was tested (*Table 5*). SI-7URAgr, SI-8URAgr and SI-9URAgr could grow and survived up to 35 °C while SI-1URAgr and SI-13URAgr survived up to 37 °C and other isolates were capable to grow at 42 °C.

Table 5. *The growth and survival of isolated phosphate solubilizing fungal strains at different temperature*

Sl. No.	*Fungal strains*	*Name of the fungi*	*Growth temperature*			
			Positive control 25 °C	**35** °C	**37** °C	**42** °C
1	SI-1URAgr	*Penicillium sp.*	+	+	+	-
2	SI-2URAgr	*Aspergillus floccosus*	+	+	+	+
3	SI-3URAgr	*Aspergillus niveus*	+	+	+	+
4	SI-4URAgr	*Talaromyces pinophilus*	+	+	+	+
5	SI-5URAgr	*Aspergillus niveus*	+	+	+	+
6	SI-6URAgr	*Penicillium oxalicum*	+	+	+	-
7	SI-7URAgr	*Penicillium sp.*	+	+	-	-
8	SI-8URAgr	*Penicillium sp.*	+	+	-	-
9	SI-9URAgr	*Penicillium sp.*	+	+	-	-
10	SI-10URAgr	*Aspergillus niger*	+	+	+	+
11	SI-11URAgr	*Aspergillus niger*	+	+	+	+
12	SI-12URAgr	*Aspergillus niger*	+	+	+	+
13	SI-13URAgr	*Penicillium sp.*	+	+	+	-
14	SI-14URAgr	*Aspergillus floccosus*	+	+	+	+
15	SI-15URAgr	*Talaromyces pinophilus*	+	+	+	+
16	SI-16URAgr	*Penicillium oxalicum*	+	+	+	-

(+) indicated growth of fungi, (-) indicated no growth

Discussion

The sixteen P solubilizing fungal strains were isolated from the dark red, red and grey soils of subtropical Okinawa. The isolates were belonging to the genera of *Aspergillus, Penicilium* and *Talaromyces*.

According to Zang et al. (2018), Mendes et al. (2014) and Ruangsanka (2014), there were diversities on the isolation rate of phosphate solubilizing fungi depending on area. They reported that the most dominant genera of P solubilizing filamentous fungi are *Aspergillus, Penicilium* and *Talaromyces*, however, there were large variations in phosphate solubilizing abilities among fungal species (Barrooso et al., 2006; Surange et al., 1985). At the present studies, strains SI-10URAgr, SI-11URAgr and SI-12URAgr identified as *A. niger*, showed excellent P solubilizing abilities regardless of the phosphate substrates. It suggested that phosphate solubilizing abilities in *A. niger* is an universal property.

Among the filamentous fungi *Aspergillus* spp. are widely used for the production of fermented foods, organic acids and enzymes (Wongwicharn et al., 1999). Especially, *A. niger* has a long history of industrial usage, which means many strains already have a GRAS ("generally regarded as safe") status (Wongwicharn et al., 1999). It has been used for commercial production of many enzymes, e.g. pectinase, glucose oxidase,

http://www.aloki.hu ● ISSN 1589 1623 (Print) ● ISSN 1785 0037 (Online)
DOI: http://dx.doi.org/10.15666/aeer/1704_91459157

glucoamylase, hemicellulase, glucanases, acid proteinase, catalase (Aguilar and Huitron, 1993; Liu et al., 1999; Garhartz, 1990) and citric acid (Friedrich et al., 1989; Gokhale et al., 1991; Lee et al., 1989).

Interestingly, beside *A. niger* species, *P. oxalicum* (SI-14URAgr) also showed an excellent phosphate degradation ability on halo assay. According to Jain et al. (2014), Johri et al. (1999), Alam et al. (2002), Elias et al. (2016) and Jain et al. (2017) solid medium using agar plates performed better phosphate degradation ability than those in liquid media. Thus, it is impossible to ignore the *P. oxalicum* isolate SI-16URAgr. *Penicillium* spp. is important in the natural environment as well as food and drug production. Some members of the genus produce penicillin, a molecule that is used as an antibiotic, which kills or stops the growth of certain bacteria spp. Other species are used in cheese industries (https://en.wikipedia.org/wiki/*Penicillium*). *Penicillium oxalicum* produces secalonic acid D, chitinase and oxalic acid (https://en.wikipidia.org/wiki/Penicillium_oxalicum).

The solubilization of $Ca_3(PO_4)_2$ was the highest, followed by $AlPO_4$ and $FePO_4$ because $AlPO_4$ and $FePO_4$ have complex structure than $Ca_3(PO_4)_2$. Zang et al. (2018) and Son et al. (2006) reported that fungi exhibited low P solubilizing ability in media containing $AlPO_4$ and $FePO_4$. The mechanisms of phosphate solubilization by microorganisms are very complex and are not completely known yet (Bo et al., 2011). The very common mechanisms are acidification, chelation and exchange reactions (Bo et al., 2011). Organic acids play an important role in phosphate solubilization processes, which can help the release of P by providing protons and complexing anions, or ligand exchange reactions or complexion of metal ions release to solution. Zang et al. (2018) and Scervino et al. (2013) reported that organic acids production depends on the interaction of P source and fungi.

In this study, *A. niger* showed the highest efficiency in P solubilization by decreasing pH of the culture medium, which indicated higher amount of organic acid production. Silva et al. (2014), Li et al. (2016) and Barroso et al. (2006) reported that *A. niger* produce higher amount of organic acids and enhance phosphate solubilization. Zang et al. (2018) reported that solubilization of the different P sources mostly depended on the amount of organic acids production by fungi. Tricarboxylic acids such as citric acid, oxalic acid and other lower molecular weight organic acids are considered to be the main contributors to phosphate solubilization and a decrease in pH of the medium (Bo et al., 2011).

It was observed that phosphate solubilization was negatively correlated with pH of the medium. There are several reports where such correlation was documented (Pandey et al., 2008; Jain et al., 2012; Xio et al., 2015). The activities in lower pH indicated that the increase of organic acids in the medium (Pradhan and Sukla, 2005; Saxena et al., 2013). However, soluble P was increased without changing pH in some occasion because of other mechanism (Jain et al., 2012 and 2017), such as chelation and exchange reactions (Bo et al., 2011).

Conclusions

Isolates *A. niger* strain SI-10URAgr, SI-11URAgr and SI-12URAgr have unique capabilities to solubilized three insoluble phosphate compounds and may become an important bio resource for soil fertility management as well as sustainable crop production and pollution free environment.

http://www.aloki.hu ● ISSN 1589 1623 (Print) ● ISSN 1785 0037 (Online)
DOI: http://dx.doi.org/10.15666/aeer/1704_91459157

Acknowledgements. This manuscript has been considered as the requirement of doctoral degree for the first author.

REFERENCES

[1] Aguilar, G., Huitron, C. (1993): Conidial and mycelial-bound exo-pectinase of *Aspergillus* sp. FEMS. – Microbiol. Lett. 108: 127-132.
[2] Alam, S., Khalil, S., Ayub, N. Rashid, M. (2002): In vitro solubilization of inorganic phosphate by phosphate solubilizing microorganisms (PSM) from maize rhizosphere. – Int J Agric Biol 4: 454-458.
[3] Barroso, C. B., Pereira, G. T., Nahas, E. (2006): Solubilization of CaHPO4 and AlPO4 by *Aspergillus niger* in culture media with different carbon and nitrogen sources. – Braz J Microbiol. 37: 434-438.
[4] Birhanu, G., Zerihun, T., Genene, T., Endegena, A., Misganaw, W., Endeshaw, A. (2017): Phosphate solubilizing fungi isolated and characterized from teff rhizosphere soil collected from North Showa and Go jam, Ethiopia. – A. J. of Microbiology Research 11(17): 687-696.
[5] Bo, C., Yan, W., Pengming, L., Biao, L. Meiying, G. (2011): Isolation and phosphate solubilizing ability of a fungus, *Penicillium* sp. from soil of alum mine. – JBM 51: 5-14.
[6] Deepak, B., Mohammad, W. A., Ranjan, K. S., Narendra, T. (2014): Biofertilisers function as key player in sustainable agriculture by improving soil fertility, plant tolerance and crop productivity. – Microbial Cell Factories 13: 66.
[7] Elias, F., Woyessa, D., Muleta, D. (2016): Phosphate solubilization potential of rhizospere fungi isolated from plants in Jimma zone, Southwest Ethiopia. – Inter J Microbiol. DOI: 10.1155/2016/5472601.
[8] Friedrich, J., Cimerman, A., Steiner, W. (1989): Submerged production of pectolytic enzymes by Aspergillus niger: Effect of different aeration/agitation regimes. – Applied Microbiology and Biotechnology 31: 490-494.
[9] Gerhartz, W. (1990): Industrial Uses of Enzymes. – In: Gerhartz, W. (ed.) Enzyme in Industry Production and Application. VCH publishers, Germany, pp. 77-92.
[10] Gokhale, D. V., Patil, S. G., Bastawde, K. B. (1991): Optimization of cellulase production by Aspergillus niger NCIM 1207. – Applied Biochemistry and Biotechnology 30: 99-109.
[11] Heppell, J., Payvandi, S., Talboys, P., Zygalakis, K. C., Fliege, J., Langton, D. (2016): Modeling the optimal phosphate fertilizer and soil management strategy for crops. – Plant Soil 401(1-2): 135-149.
[12] Jain, R., Saxena, J., Sharma, V. (2012): Solubilization of inorganic phosphates by Aspergillus awamori S19 isolated from agricultural soil of semi-arid region. – Annals Microbiol. 62: 725- 735.
[13] Jain, R., Saxena, J., Sharma, V. (2014): Differential effects of immobilized and free forms of phosphate solubilizing fungal strains on the growth and P uptake of mungbean plants. – Annals Microbiol. 64: 1523-1534.
[14] Jain, R., Saxena, J., Sharma, V. (2017): The ability of two fungi to dissolve hardly soluble phosphates in solution. – Mycology 8(2): 104-110.
[15] Johri, J. K., Surange, S., Nautiyal, C. S. (1999): Occurrence of salt, pH and temperature tolerant phosphate solubilizing bacteria in alkaline soils. – Curr Microbiol. 39: 89-93.
[16] Jose, M. S., Milton, P. M., Ivana, D. M., Marina, R., Nubia, S. M., Alicia, G. (2010): Soil fungal isolates produce different organic acid patterns involved in phosphate salts solubilization. – Biol Fertil Soils 46: 755-763.
[17] Khan, M. S., Zaidi, A., Ahemad, M., Oves, M., Wani, P. A. (2010): Plant growth promotion by phosphate solubilizing fungi–current perspective. – Archives of Agronomy and Soil Science 56(1): 73-98.

http://www.aloki.hu ● ISSN 1589 1623 (Print) ● ISSN 1785 0037 (Online)
DOI: http://dx.doi.org/10.15666/aeer/1704_91459157

[18] Lee, Y. H., Lee, C. W., Chang, H. N. (1989): Citric acid production by *Aspergillus niger* immobilized on polyurethane foam. – Applied Microbiology and Biotechnology 30: 141-143.
[19] Li, Z. et al. (2016): A study of organic acid production in contrast between two phosphate solubilizing fungi: *Penicillium oxalicum* and *Aspergillu niger.* – Sci. Rep. 6: 25313.
[20] Lindsay, W. L., Vlek, P. L. G., Chien, S. H. (1989): Phosphate Minerals. – In: Dixon J. B., Weed, S. B. (eds.) Minerals in Soil Environment. Soil Science Society of America, Madison, WI, pp. 1089-1130.
[21] Liu, J. Z., Yang, H. Y., Weng, L. P., Ji, L. N. (1999): Synthesis of glucose oxidase and catalase by A. niger in resting cell culture system. – Lett. Appl. Microbiol. 29: 337-341. 20.
[22] Mendes, G. D. O., Freitas, A. L. M., Pereira, O. L., Silva, I. R., Vassilev, N. B., Costa, M. D. (2014) Mechanism of phosphate solubilization by fungal isolates when exposed to different P sources. – Ann. Microbiol. 64(1): 239-249.
[23] Murphy, J. Riley, H. P. (1962): A modified single solution method for the determination of phosphate in natural waters. – Anal Chim Acta. 27: 31-36.
[24] Norrish, K., Rosser, H. (1983): Mineral Phosphate. – In: CSIRO, Division of Soils (ed.) Soils: An Australian Viewpoint. Academic Press, London, pp. 335-361.
[25] Oshiro, M., Hossain, M. A., Nakamura, I., Akamine, H., Tamaki, M., Bhowmic, P. C., Nose, A. (2016): Effects of soil types and fertilizers on growth, yield, and quality of edible Amaranthus tricolor lines in Okinawa, Japan. – Plant Production Science 19(1): 61-72.
[26] Pandey, A., Das, N., Kumar, B., Rinu, K., Trivedi, P. (2008): Phosphate solubilization by Penicillium spp. isolated from soil samples of Indian Himalayan region. – World J Microbiol Biotechnol. 24: 97-102.
[27] Pradhan, N. Sukla, L. B. (2005): Solubilization of inorganic phosphate by fungi isolated from agricultural soil. – African J Biotechnol. 5: 850-854.
[28] Rao, N. S. S. (1982): Phosphate Solubilization by Soil Microorganisms. – In: Subba Rao, N. S. (ed.) Advances in Agricultural Microbiology. Butterworth-Heinemann, Oxford.
[29] Reena, T. Dhanya, H. Deepthi, M. S., Pravita, D. (2013): Isolation of phosphate solubilizing bacteria and fungi from rhizosphere soil from banana plants and its effect on the growth of *Amaranthu cruentus* L. – IOSR-JPBS 5(3): 6-11.
[30] Richardson, A. E. (2007): Making Microorganisms Mobilize Soil Phosphorus. – In: Velázquez, E., Rodríguez-Barrueco, C. (eds.) First International Meeting on Microbial Phosphorus Solubilization, Springer, Dordrecht, pp. 85-90.
[31] Ruangsanka, S. (2014): Identification of phosphate solubilizing fungi from the asparagus rhizosphere as antagonists of the root and crown root pathogen Fusarium oxysporum. – Science Asia 40: 16-20.
[32] Saber, K. L., Nahla, A. D., Chedly, A. (2005): Effect of p on nodule formation and nitrogen fixation in bean. – Agron. Sustain. Dev. 25: 389-393.
[33] Samson, R. A., Visagie, C. M., Houbraken, J., Hong, S. B., Hubka, V., Klaassen, C. H. W., Perrone, G., Seifert, K. A., Suska, A.,. Tanney, J. B., Kocsube, S., Szigeti, G., Yaguchi, T., Frisvad, J. C. (2014): Phylogeny, identification and nomenclature of the genus *Aspergillus.* – Studies in Mycology 78: 141-173.
[34] Saxena, J., Basu, P., Jaligam, V., Chandra, S. (2013): Phosphate solubilization by a few fungal strains belonging to the genera *Aspergillus* and *Penicillium.* – Afr J Microbiological Res. 7: 4862-4869.
[35] Scervino, J. M., Mesa, M. P., Mónica, I. D., Recchi, M., Moreno, S., Godeas, A. (2013): Soil fungal isolates produce different organic acid patterns involved in phosphate salts solubilization. – Biol Fertil Soils 49(6): 779-779.
[36] Sharma, S., Sayyed, R., Trivedi, M., Gobi, T. (2013): Phosphate solubilizing microbes: sustainable approach for managing phosphorus deficiency in agricultural soils. – Springer Plus 2: 587.

http://www.aloki.hu ● ISSN 1589 1623 (Print) ● ISSN 1785 0037 (Online)
DOI: http://dx.doi.org/10.15666/aeer/1704_91459157

[37] Silva, U. d. C., Mendes, G. D. O., Silva, N. M. R. M., Duarty, J. L., Silva, I. R. (2014): Fluoride-tolerant mutants of *Aspergillus niger* Show enhanced phosphate solubilization capacity. – PLoS One 9(10): e110246. DOI: 10.1371/journal.pone.0110246.
[38] Singh, H., Reddy, S. M. (2011): Effect of inoculation with phosphate solubilizing fungus on growth and nutrient uptake of wheat and maize plants fertilized with rock phosphate in alkaline soils. – Eur J Soil Biol. 47: 30-34.
[39] Son, H. J., Park, G. T., Cha, M. S., Heo, M. S. (2006): Solubilization of insoluble inorganic phosphates by a novel salt- and pH-tolerant *Pantoea agglomerans* R-42 isolated from soybean rhizosphere. – Bioresource Technol. 97(2): 204-210.
[40] Surange, S. (1985): Comparative phosphate solubilizing capacity of some soil fungi. – Curr. Sci. 54: 1134-1135.
[41] Tilman, D., Fargione, J., Wolff, B. D., Antonio, C., Dobson, A., Howarth, R., Schindler, D., Schlesinger, W. H., Simberloff, D., Wackhamer, D. (2001): Forecasting agriculturally driven global environmental change. – Science 292: 281-284.
[42] Watanabe, T. (2010): Pictorial Atlas of Soil and Seed Fungi Morphologies of Cultured Fungi and Key to Species. 3rd. Ed. – CRC Press, Florida.
[43] Wongwicharn, A., McNeil, B., Harvey, L. M. (1999): Effect of oxygen 507 enrichment on morphology, growth, and heterologous protein 508 production in chemostat cultures of Aspergillus niger B1-D. 509. – Biotechnol Bioeng 65: 416-424.
[44] Xiao, C. Q., Fang, Y. J., Chi, R. A. (2015): Phosphate solubilization *in vitro* by isolated *Aspergillus niger* and *Aspergillus carbonarius.* – Res Chem Intermed 41: 2867-2878.
[45] Yamaguchi, S., Sano, A., Hiruw, A. M., Murata, M., Kaneshima, T., Murata, Y., Takahashi, H., Takahashi, S., Takahashi, Y., Chibana, H., Touyama, H., Nguyen, H. T. T., Nakazato, Y., Uhera, Y., Hirakawa, M., Imura, Y., Tereshima, Y., Kawamoto, Y., Takahashi, K., Sugiyama, K., Hiruma, M., Murakami, M., Hosokawa. A., Uezata, H. (2014): Isolation of dermatophytes and domestic fowl (*Gallus domesticus*). – Mycopathologia 178: 135-143.
[46] Zaidi, A., Khan, M. S., Ahemad, M., Oves, M., Wani, P. A. (2009): Recent Advances in Plant Growth Promotion by Phosphate-Solubilizing Microbes. Microbial Strategies for Crop Improvement. – Springer-Verlag, Berlin Heidelberg, pp. 23-50.
[47] Zhang, Y., Chen, F-S., Wu, X-Q., Luan, F-G., Zang, L-P., Fang, X-M., Wan, S-Z., hu, X-F., Ye, J-R. (2018): Isolation and characterization of two phosphate solubilizing fungi from rhizosphere soils of moso bamboo and their functional capacities when exposed to different phosphorus sources and pH environment. – PloS One 13(7): e0199625.
[48] Zhou, K., Binkley, D., Doxtader, K. G. (1992): A new method for estimating gross phosphorus mineralization and immobilization rates in soils. – Plant Soil 147: 243-250.

http://www.aloki.hu ● ISSN 1589 1623 (Print) ● ISSN 1785 0037 (Online)
DOI: http://dx.doi.org/10.15666/aeer/1704_91459157

RESEARCH ON THE CONSTRUCTION OF ZHAOQING URBAN ECOLOGICAL INFRASTRUCTURE BASED ON ECOLOGICAL SECURITY

ZHANG, H.

College of Life Sciences, Zhaoqing University, Guangdong, China
(e-mail: zhang-hongg@163.com)

(Received 19th Mar 2019; accepted 22nd May 2019)

Abstract. In the process of urbanization, the region faces environmental problems such as destruction of ecological corridors, fragmentation of biological habitats, and soil erosion, which pose potential risks to the regional ecological environment. Therefore, it is of great significance to identify lands with ecological conflict, establish core ecological protection zones and ecological corridors, and build an ecological security pattern for regional sustainable development. The research subject of this paper is Zhaoqing area. From the perspective of landscape ecological security pattern, it identifies the green land in Zhaoqing City, hydrological system, local culture, natural ecological protection, and the chance of geological disasters, and combines RS (Remote Sensing) and GIS (Geographic Information System) technology to evaluate green land and identify environmental core protection. Urban ecological infrastructure patterns are built in district, ecological corridors and ecological buffer zones and land with ecological conflict is curbed form expansion. The study found that it is necessary to carry out controlled development of ecological conflict zones such as the Xijiang River Basin, the Beiling Mountain Forest Land, and the Gaoyao Plain to ensure the safety of the fundamental ecological facilities in Zhaoqing.
Keywords: *core ecological protection zone, ecological assessment, ecological source, ecological buffer zone, control development*

Introduction

At present, China's rapid economic development promotes urban construction, but it is accompanied by an ecological environmental crisis that threatens the national ecological security. The expansion rate of urban construction land in China is significantly higher than the population growth rate. In the past 34 years, China's urban construction land has increased by 6.44 times, with an average annual growth rate of 6.27%. The per capita construction area of Chinese cities is 129.57 m^2, which significantly exceeds the national standards, and is also significantly higher than the average of 84.4 m^2 per capita in developed countries and 83.3 m^2 per capita in other developing countries (The 13th Five-Year Ecological Protection Plan of the Ministry of Environmental Protection of China, 2016). This trend extends from the eastern coastal areas to the inland, and from the central towns rural areas, forming a situation of "city in green retreat", destroying the original ecological balance, causing regional ecological, environmental crisis and seriously affecting regional ecological security. For the sustainable development of the city, the fundamental green land of the city must be protected and the urban ecosystem must be perfected. Protection of green land is the most critical task at the moment. To improve the urban ecosystem, it is necessary to discriminate the urban environmental protection area, rationally plan the urban spatial structure and urban development direction, optimize the urban functional structure, and reduce the contradiction between urban expansion and ecological land use.

In order to solve the contradiction between urban expansion and ecological land use, Chinese and foreign scholars have made a series of explorations and achieved specific

http://www.aloki.hu ● ISSN 1589 1623 (Print) ● ISSN 1785 0037 (Online)
DOI: http://dx.doi.org/10.15666/aeer/1704_91599169

results. For example, the savvy growth theory proposed by American scholar Doyle focuses on the balance between urban expansion and ecological protection. The ecological planning theory put forward by domestic scholar Yu Kongjian and others put emphasis on the priority of green land protection and the control of the integrity of the ecological structure. In recent years, Chen Yimin and Peng Jiajie have used the landscape ecological index and landscape ecological risk assessment methods to construct a spatial conflict measurement model to assess the spatial conflict level under rapid urbanization. These theories emphasize the balanced relationship between environmental protection and urban development and have been widely recognized by the urban planning industry. Based on the GIS spatial analysis model, this paper simulates and analyzes the spatial conflicts and ecological security risks of urban ecological land in Zhaoqing City, and provides a scientific basis for urban development and protection.

Ecological infrastructure concept

The concept of ecological infrastructure was first proposed in the 1984 UNESCO Man and Biosphere Programme (MAB). The ecological infrastructure is a natural system, which is essential for the survival of urban and rural residents and their inhabitants. It provides residents with fresh air, food, sports, recreation, safe haven, aesthetics and education. With the deepening of research, the idea of ecological infrastructure is reflected in the emphasis from simple "protection" to the use of EI (ecological infrastructure) to guide the development of the city, thus achieving the "EI-oriented urban development" approach (Yu et al., 2005).

In the process of urbanization in China, we face the problem of urbanization and ecological environmental protection. Unreasonable urban development and construction have damaged the regional ecosystem structure, resulting in weakened ecosystem service functions, seriously threatening residents' production and life, and affecting sustainable environmental development. It is crucial for the government, especially urban planning administrators, to find out methods that benefit the balance between urban development pressure and ecological environment protection, the restoration of the natural system of the city, and sustainable urban development. Urban safety development depends on the basic maintenance of ecosystem services.

Landscape ecological security pattern theory

There are some potential spatial patterns in urban landscapes, which are composed of vital ecological nodes, corridors and location relationships. This pattern plays a crucial role in maintaining and controlling an ecological process called landscape ecology (Yu, 1999). Safety pattern: Landscape ecological security pattern is based on landscape ecology theory and method in the late 1990s. Based on the relationship between landscape processes and patterns, it is critical to distinguish the health and safety of these processes through the analysis and simulation of landscape processes. Landscape pattern: The landscape ecological security approach takes the landscape process (including regional hydrological cycle, species space movement, disaster process diffusion and urban sprawl expansion) as a process of achieving landscape control and coverage by overcoming spatial resistance. To achieve effective control and coverage, strategically important landscapes must be captured. Elements, spatial locations, and

http://www.aloki.hu ● ISSN 1589 1623 (Print) ● ISSN 1785 0037 (Online)
DOI: http://dx.doi.org/10.15666/aeer/1704_91599169

connections: The pattern formed by such vital elements, strategic locations and connections is the landscape ecological security pattern, which is essential for maintaining and controlling ecological processes or other horizontal processes (Yu, 1999).

At present, the relatively mature method for identifying the landscape ecological security pattern is to realize landscape control by constructing the Minimum Cumulative Resistance (MCR) of the ecological process. The MCR model is based on the GIS spatial analysis module to analyze the degree of separation of landscape patches and serve as the basis for landscape pattern optimization. The landscape pattern optimization MCR model is mainly realized in the GIS by relying on the minimum cost distance (Cost Distance) model. By using the landscape resistance surface characteristics to distinguish the landscape ecological strategic points, it extends to the discrimination of the landscape ecological security pattern. The equation for calculating the MCR model can be expressed as follows:

$$MCR = \sum_{j=n}^{i=m} (D_{ji} \times R_i) \quad \text{(Eq.1)}$$

where f is an unknown positive function, reflecting the positive correlation between the minimum resistance of any point in space and the spatial distance of the base i of a landscape that it traverses and the characteristics of the landscape base. D_{ij} is the spatial distance of the base i of a landscape from the source j to a point in space; R_i is the resistance of landscape i to the movement of a species. Although the function f is unknown, the $(D_{ij} \times R_i)$ value can be regarded as a relative measure of the path of a species from a source to a point in space, where the maximum value of resistance from all sources to that point is used. Measuring the accessibility of this point, the constructed resistance surface can reflect the potential possibilities and trends of species movement (Ahern, 1995; Yu, 1996). The landscape ecological security pattern theory as a dynamic spatial structure model is a method of constructing ecological infrastructure. It regards the horizontal landscape process as a process of overcoming spatial resistance to achieve landscape control and coverage, and requires corresponding constraints and discriminant parameters, theoretical and technical support in hydrology and ecology.

Construction of ecological infrastructure in Zhaoqing urban area

By analyzing ecological services and ecological process functions, American landscape ecology experts Ahern and Ndubisi categorized ecological infrastructure into three types: Biotic, Abiotic, and Culture (Ndubisi, 2002). This comprehensive and inclusive model based on landscape ecology recognizes the interaction between biotic and abiotic systems and humans (Gan et al., 2007). It is also known as the ABC model and is widely used in the planning and construction of ecological infrastructure in the application in United States (Xiao et al., 2017). As a result of ecological security pattern of different types of landscapes, ecological infrastructure reflects the realization of ecological functions and the integrity of ecological processes. The completion of ecological processes requires the support of ecological space, and the ecological infrastructure is the guarantee of ecological functions.

This paper analyzes the non-construction land structure of Zhaoqing City, draws on the ecological infrastructure concept, and uses the ABC model as a framework to

http://www.aloki.hu ● ISSN 1589 1623 (Print) ● ISSN 1785 0037 (Online)
DOI: http://dx.doi.org/10.15666/aeer/1704_91599169

identify the landscape ecological security pattern. Through the computational composition and spatial superposition of the Zhaoqing urban ecological infrastructure network, the geological, biological, hydrological and the landscape ecological security pattern of local culture forms the ecological infrastructure for the healthy development of Zhaoqing.

Research scope and data source

Zhaoqing City is located in the central and western part of Guangdong Province, northwest of the Pearl River Delta. The city has jurisdiction over Dinghu District, Duanzhou District, Gaoyao District, Zhaoqing High-tech Zone (Dawang), Zhaoqing New District, and other five districts. The total area of the city is 2990 km^2. The overall planning of Zhaoqing City is characterized by high terrain in the northwest and south, and flat terrain in the northeast to southwest. The low-mountain landforms in the northwest and the south are mainly distributed in the main mountain bodies such as Beiling Mountain, Dinghu Mountain and Rouge Mountain. The main urban construction land is distributed in the northeast to southwest plain. The basic pattern of Zhaoqing City from south to north is "river, city, lake, mountain, forest", the spatial pattern of the strip city, and the city forms a trend of developing eastward with the end state as the center. With the difficulty and timing of data acquisition being considered, this investigation selects the remote sensing image of LANDSAT (Tursing Landsat System) TM series as the main data source, and combines Zhaoqing urban topographic map, land use status map and land use change table, processing and analysis.

Zhaoqing City hydrological system security pattern

Floods are inevitable as part of the river's natural processes, but floods can be minimized through ecological planning. From the perspective of spatial planning, by studying the distribution pattern of floodplain, provides a basis for planning land use decision-making, and planning flood-prone areas as wetlands and open spaces is an effective way to reduce flood disasters and their effects (Xiao et al., 2017). The flood safety pattern of Zhaoqing City should be started from different scales of watersheds. By establishing a coordinated flood control system, corresponding flood control, measures should be in accordance with the risk level.

Since this investigation is based on GIS simulations, it is necessary to calculate the flood level of different safety levels or the adjustable flood flow and the flow that can be safely discharged and the adjustable flood storage. Therefore, it is necessary to obtain historical hydrological and monitored storm runoff data to calculate the flood level. The reasonable height and the area where the flood spreads is reduced. At the same time, by collecting the flooding range of historic floods, the different ranges of floodplain, flood detention zone and flood protection zone are analyzed. Moreover, the scale, pattern and river channel buffer width of different flood risks are determined, and the star lake and east channel are established. Different levels of safety concerning Honghu, Poyang Lake and other ecological wetlands, rivers and rivers coordinated flood control dynamic system are determined according to different risk levels.

The hydrological analysis module in GIS is a means to effectively analyze and simulate hydrological processes, which can simulate the regional runoff process and identify potential wetlands. The hydrological analysis module generally requires digital elevation data (DEM) to simulate the runoff process, and then establishes a flood

http://www.aloki.hu ● ISSN 1589 1623 (Print) ● ISSN 1785 0037 (Online)
DOI: http://dx.doi.org/10.15666/aeer/1704_91599169

surface based on the flood level at different safety levels to obtain the flood submerged range. The Zhaoqing City is mainly composed of the Xijiang River Basin and the Xinghu Wetland, the Jiukeng River Reservoir (Kowloon Lake) Wetland Core Area and the New Area Wetland Core Area. The hydrological analysis module in GIS comprehensively evaluates the ecological and social benefits of the Xijiang River Basin and its wetlands, and follows the protection of its ecosystem health. The spatial and spatial pattern of wetland resources is planned for the connectivity between the corridors and wetlands, the stability of large wetland patches, and the ecological channels provided for urban groups.

It is selected as a concrete case to discuss the flood control safety pattern based on flood volume. Firstly, the CAD contour data of Zhaoqing New District is converted into DEM data as the basic data of runoff process simulation. Through GIS simulation of the runoff process, the location and extent of potential wetlands can be obtained by encountering stagnation points in low-lying areas, mainly distributed in the wet areas of the Xijiang River Basin. Based on the Arc GIS, the flood surface elevation raster data is established based on the flood water level, and the simulated water level of each point in the area is obtained (Yu, 1999). Subsequently, we calculate the difference between the elevation of the flood surface and the terrain elevation to obtain the flood inundation range of different return periods. The main flood control area in Zhaoqing is along the Xijiang River and some rivers (*Fig. 1*).

Zhaoqing City geological hazard safety pattern

Through the sensitivity analysis of regional geological disasters in Zhaoqing City, we summarized the distribution of geological disaster safety patterns. First, we determined the source of geological hazards by superimposing the spatial distribution of various geological hazards such as mountain collapse, landslide, slip, ground subsidence and ground fissure on the Zhaoqing regional GIS map. Subsequently, through the analysis of the types of local disasters and the analysis of land use patterns in disaster-prone areas, the regional and spatial linkages that play a vital role in the protection of geological disasters were determined. The extent of the buffer zone is affected by factors such as the type of geological hazard, development intensity, distribution, the frequency of occurrence, topographic and geological conditions, precipitation conditions and intensity of human activities (Russell and Wang, 1997). Finally, based on the spatial superposition of the spatial distribution of various disaster sources, the safety pattern of geological disasters with different safety levels was obtained.

The geological disaster factors of Zhaoqing City mainly include various geological disaster factors such as mountain collapse, landslide, slippage, land subsidence and ground fissure. Based on GIS, the elevation and slope are graded to obtain the sensitivity distribution of geological disasters. The spatial distribution of geological disaster sources is identified by superimposing various geological disaster factors (*Table 1; Fig. 2*).

Zhaoqing City biosafety security pattern

The biosafety safety pattern is mainly to construct the minimum resistance model (*Eq. 1*) to simulate the minimum resistance value that the species needs to overcome in space motion, and then to identify the landscape safety pattern by analyzing the resistance surface outside the core habitat (source). The safe pattern of biological processes

http://www.aloki.hu ● ISSN 1589 1623 (Print) ● ISSN 1785 0037 (Online)
DOI: http://dx.doi.org/10.15666/aeer/1704_91599169

generally consists of sources (core habitats), buffer zones (low-resistance areas around the source), corridors and radiant channels (low-resistance channels connecting multiple sources), and strategic points (critical to biological processes), which constitute elements of the landscape (Yu et al., 2005). This method of identifying the landscape safety pattern can select the model to analyze, so as to achieve the identification of the "matrix-corridor-plaque" model in landscape ecology. It is best to select migratory birds as indicator species, which is conducive to the communication between elements. Sexuality reflects the strategy of the overall biological safety of the region.

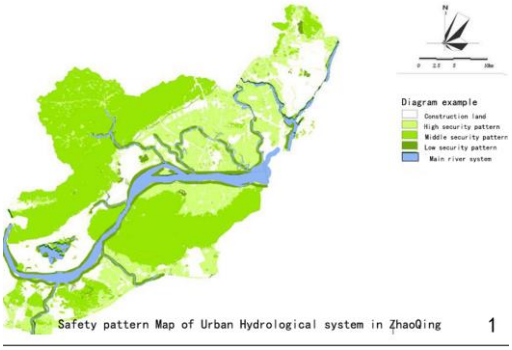

Figure 1. *Zhaoqing urban hydrological security map*

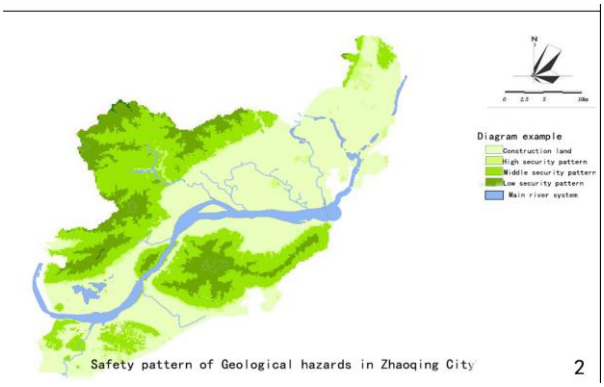

Figure 2. *Zhaoqing urban geological security map*

Table 1. *Identification of geological disaster sources in Zhaoqing City*

Level of safety Risk source	Debris flow, landslide, collapse	Fracture zone	Ground setting
Low safety level	Elevation > 1000 m, slope > 30 degree, collapse center	100 m around the fault zone	Surface subsidence center zone, cumulative settlement > 2.0 m
Medium safety level	The height is 500 m, the slope is 15-30°, the center of collapse is 300 m	300 m around the fault zone	150 m around the land subsidence center, cumulative settlement > 1.5 m
High safety level	Collapse center 500 m	500 m around the fracture zone	The circumference of the center of the heart is 300 m, and the cumulative subsidence is 0.3 cu 1.0 m

http://www.aloki.hu ● ISSN 1589 1623 (Print) ● ISSN 1785 0037 (Online)
DOI: http://dx.doi.org/10.15666/aeer/1704_91599169

Wetland and forest land with an area larger than 25 hm^2 in the Zhaoqing City area are selected as the habitat of protected species. The spatial resistance coefficient of different land cover types is set by using the spatial resistance coefficient of different land cover types (*Table 2*). Superimposed, the resistance surface of the space movement of the protected species and the ecological corridor with the least space resistance of the species movement are obtained, and the bio-protection safety pattern of Zhaoqing City based on the analysis of the horizontal ecological process is formed. According to the calculation, the three ecological green nucleuses of Dinghushan, Rougekeshan and Sihui12 are formed. The three ecological corridors of Xijiang River, Minjiang River and Beijiang River are beneficial to the protection of biodiversity (*Fig. 3*).

Table 2. *Spatial resistance coefficient of minimum cost distance model analysis*

Attributes	Coefficient of drag	Attributes	Coefficient of drag
Water system river	150	High density construction land	10000
Forest land	275	Highway	600
Open forest land	50	Tidal flat	150
Shrub forest	40	Natural conservation land	-5
Base pond	100	Farmland	325
Meadow	30		
Dry farm	300		
Low density construction land	1000		

Zhaoqing City's local cultural security pattern

It is necessary to study the current landscape from the historical perspective as a result of past natural processes and human interference (Costanza, 2008). From the perspective of ecosystem service functions, it is critical to integrate the natural environment characteristics and local cultural characteristics into the local landscape and cultural heritage resources. They have many functions such as cultural diversity, spiritual and religious values, educational values, social connections, aesthetics and enlightenment, cultural heritage values, recreation and ecotourism. The introduction of the concept of ecosystem service function makes people's understanding of the local cultural landscape not only stay in the cultural sense, but the dual carrier of culture and natural function (Jongman, 1995).

The study of the local cultural landscape safety pattern is the "source" of the local cultural landscape elements in the region, and regards people's recreation activities as a process of horizontal expansion. Through the establishment of spatial resistance surface, the safety pattern of the local cultural landscape is constructed. As the birthplace of Guangfu culture, Zhaoqing selects the cultural landscape protection units such as the Zhaoqing Fucheng historical and cultural district and the typical Guangfu village and the Gaojiu area, the Sangji fish pond agricultural culture demonstration area as the source of the local cultural security pattern. The land cover type sets different spatial resistance coefficients, and the minimum cumulative resistance surface is established by the distance model to obtain the safety landscape of the local culture landscape with different safety levels (*Fig. 4*).

http://www.aloki.hu ● ISSN 1589 1623 (Print) ● ISSN 1785 0037 (Online)
DOI: http://dx.doi.org/10.15666/aeer/1704_91599169

Zhaoqing comprehensive ecological infrastructure

Based on the above-mentioned hydrological system safety pattern, geological disaster safety pattern, biological protection safety pattern and local cultural security pattern, spatial computing and superposition based on GIS, and the comprehensive ecological infrastructure of Zhaoqing City with different security levels are determined (*Fig. 3; Table 3*).

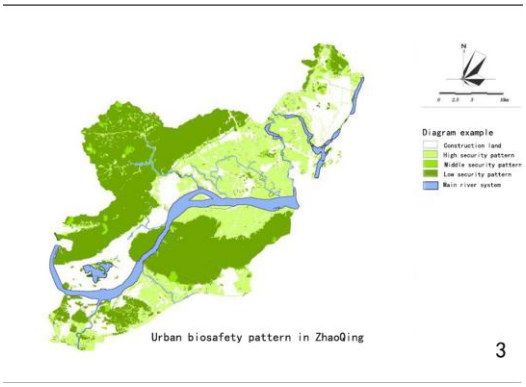

Figure 3. *Zhaoqing City biosafety map*

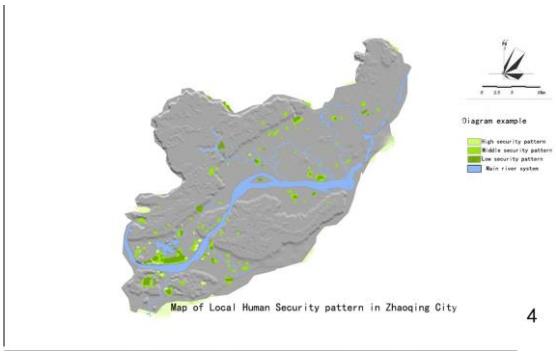

Figure 4. *Zhaoqing City humanities security map*

Table 3. *Area and proportion of ecological infrastructure at different safety levels in Zhaoqing City*

Ecological security level	Ecological infrastructure occupation		Construction land	
	Area/km^2	Scale/%	Area/km^2	Scale/%
Low safety level	1072	35.86	1918	64.14
Medium safety level	1829	61.18	1161	38.82
High safety level	2321	77.64	669	22.36

The comprehensive ecological infrastructure of Zhaoqing City is divided into three different security levels: EI with high security level is the ideal state to realize the functions of various ecosystems in the region. The security scope can be moderately opened according to local conditions. The medium-safety level EI is an appropriate scale to maintain a complete ecosystem of the region, and can be constructed within

http://www.aloki.hu ● ISSN 1589 1623 (Print) ● ISSN 1785 0037 (Online)
DOI: http://dx.doi.org/10.15666/aeer/1704_91599169

certain limits. The low-safety level EI is the threshold for ensuring urban ecological security, and is an insurmountable red line in urban and rural development and construction. Zhaoqing's current development is at a high level of safety, but it is still prudent to develop in some highly ecologically sensitive areas.

Zhaoqing City ecological conflict space recognition

The identification of the ecological conflict space in Zhaoqing City depends on the map layer map superposition method. By superimposing the GIS map of the medium security level in Zhaoqing City on the spatial distribution map of the current construction land, it can be found that the ecological conflict space of Zhaoqing City is concentrated in the edge belt of the existing built-up area, such as the Beiling High Ridge Area of Zhaoqing and Zhaoqing High-tech Zone (large Wang) in the north and the periphery of Dinghu Mountain in Zhaoqing New District. In addition, the ecological infrastructure of the low (bottom line) safety level in Duanzhou District and Dinghu District is affected by the embedded construction land, and the ecological conflict area is distributed along the mainstream of the Xijiang River, which has a great impact on the ecological environment. The ecological conflict area in Duanzhou District is dotted, although the area is small, because it is the red line of regional ecological security, the impact on regional ecological processes and ecological functions is more prominent (*Fig. 5*). Thus, it should be controlled. In addition, it is necessary to control development in the vicinity of Jiukenghe Reservoir and Dinghu Mountain in ecologically sensitive areas should be controlled for development.

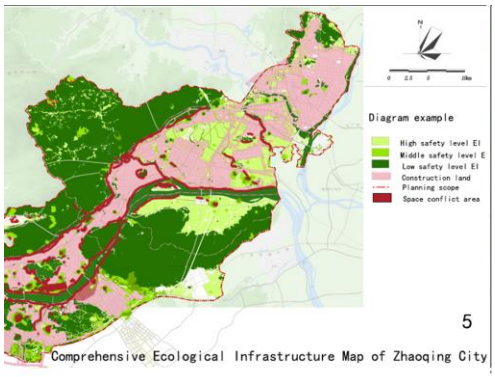

Figure 5. *Zhaoqing City ecological conflict zone map*

Conclusions

With Zhaoqing urban area as the research object, this investigation quantitatively evaluates hydrological systems, biological protection and local culture services, and the chance of geological disasters. From the perspective of natural land evolution, the investigation is based on landscape ecological security pattern theory and MCR model, utilizing RS and GIS space. With the aid of analytical techniques, through the spatialization of spatial data and spatial model calculations, the non-biological-biological-cultural analysis framework was used to identify the geological disasters, hydrological systems, biological protection and local cultural security patterns in Zhaoqing City. Superimposing a single ecological security pattern to achieve an

http://www.aloki.hu ● ISSN 1589 1623 (Print) ● ISSN 1785 0037 (Online)
DOI: http://dx.doi.org/10.15666/aeer/1704_91599169

integrated ecological infrastructure with different levels of security (*Fig. 6*). The results show that ecological land covers an area of 657.8 km^2, accounting for 22% of the research land, of which the ecological land with an area larger than 10 km^2 is used as the source, about 568.1 km^2, accounting for 19% of the research land, mainly the North Ridge Forest. The composition concerns land, lake and wetland.

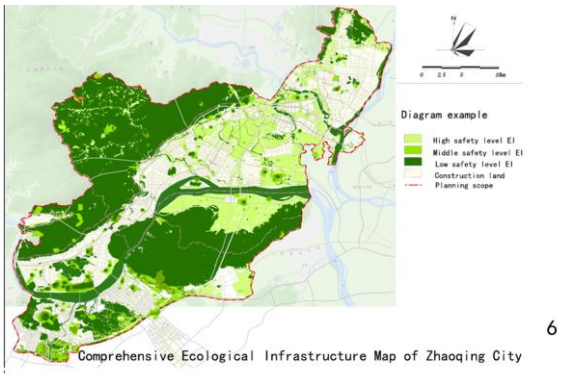

Figure 6. *Zhaoqing City comprehensive infrastructure map*

Besides, ecological buffer zone accounted for 55.64%, while development and construction zone and 22.36%, respectively. The ecological buffer zone as the ecological source of the protection wall should be limited development, but the proportion should not be less than 30%;

In addition, the potential ecological corridors are mainly composed of waters, forests and cultivated land. The Xijiang River, the Beijiang River and the lakes and the surrounding cultivated land and forest land together constitute an ecological corridor, which plays a role in connectivity.

Moreover, ecological source areas, ecological corridors and ecological buffers together constitute the ecological security pattern of Zhaoqing City. In short, the ecological pattern of Zhaoqing City has formed a spatial pattern of "one area, two corridors and three cores" relying on natural local conditions.

By superimposing construction land on ecological infrastructures with different safety levels, it can be seen that the ecological conflict space in Zhaoqing City is mainly concentrated along the Beiling Mountains and the Xijiang River Basin and Xinghu Lake. Drawing on the optimal landscape pattern of "segregation between clusters", according to the characteristics of the Zhaoqing area and the actual land use pattern, the "matrix-corridor-plaque" model has become the regional ecological security and the urban and rural non-construction land structure. Inevitably, the "Mountain-Reservoir-Farmland-City-Xijiang River" model is a concrete manifestation of the research paradigm of landscape pattern of landscapes. As the ecological bottom line of landscape ecological security pattern, urban and rural non-construction land must protect these bottom lines as ecological infrastructure, in order to realize the basic pattern of Zhaoqing livable city, which has far-reaching strategic significance for scientific planning urban development and expansion.

The study proposes to increase the ecological protection of Zhaoqing ecological source, strengthen the construction of ecological protection measures, find and control the source of ecological safety hidden dangers, and inhibit the development of bad trends. It helps to actively regulate the ecological buffer zone for ecological security

http://www.aloki.hu ● ISSN 1589 1623 (Print) ● ISSN 1785 0037 (Online)
DOI: http://dx.doi.org/10.15666/aeer/1704_91599169

deterioration in the region, and achieve positive effect on urban ecological security management and monitoring. It is suggested that in the process of building a specific ecological security infrastructure, it is necessary to cooperate with relevant government departments, take into account the development goals of the city, and conduct in-depth research in actual operations.

REFERENCES

[1] Ahern, J. (1995): Greenways as a planning strategy. – Landscape and Urban Planning 33(1-3): 131-155.
[2] Costanza, R. (2008): Ecosystem services: multiple classification systems are needed. – Biological Conservation 141(2): 350-352.
[3] Gan, H. X, Deng, J. H., Zheng, B. (2007): Calculation of inundation range based on GIS. – People's Pearl River 6: 98-100.
[4] Jongman, R. H. G. (1995): Nature conservation planning in Europe: developing ecological networks. – Landscape and Urban Planning 32: 169-183.
[5] Ndubisi, F. (2002): Ecological Planning: A Historical and Comparative Synthesis. – Johns Hopkins University Press, Baltimore.
[6] Russell, H, Wang, J, B. (1997): People and the Land through Time: Linking Ecology and History. – Yale University Press, New Haven.
[7] Tony, H., Wang, J. B. (2014): Ecological landscape, water sensitive urban design and green infrastructure. – Chinese Garden 4: 20-24.
[8] Xiao, H. B., Sheng, S, Liu, J. (2017): Study on construction of ecological infrastructure in Foshan City based on landscape ecological security pattern evaluation. – Chinese Garden 33(11): 118-122.
[9] Yu, K. J. (1996): Security patterns and surface model in landscape planning. – Landscape and Urban Planning 36(5): 1-17.
[10] Yu, K. J. (1999): Landscape ecological security pattern of biological protection. – Journal of Ecology 19(1): 8-15.
[11] Yu, K. J, Li, D. H., Liu, H. L. (2005): The "Counter-Planning" Approach. – China Construction Industry Press, Beijing.

http://www.aloki.hu ● ISSN 1589 1623 (Print) ● ISSN 1785 0037 (Online)
DOI: http://dx.doi.org/10.15666/aeer/1704_91599169

RELATIONSHIP BETWEEN STAND TYPES AND HABITAT SELECTIONS FOR BIG WILD MAMMAL SPECIES

ÖZKAZANÇ, N. K.

Department of Forest Engineering, Faculty of Forestry, Bartın University
Bartın 74100, Turkey
e-mail: nozkazanc@bartin.edu.tr; fax: +90-(378)-2233-51-60; GSM +90-560-611-8089
ORCID ID: 0000-0001-7098-447X

(Received 20th Mar 2019; accepted 24th May 2019)

Abstract. Forests are among the most important wild life areas that provide shelter for various wild animals within different living areas they have. Shortly, selection of habitat which is defined as living area, by the wild animals is effected by variables such as stand types, altitude, flora, sloping direction, and soil composition. Among these factors stand type which forms the forest structure is one of the most important factors in the habitat selection. This study has been conducted on Bartin-Soku Wild Life Development Area with the aim to determine the impact of wild animals on habitat selection. For this purpose for determining the habitat selection of big mammals photo traps are placed at 78 points. The total working time of each photo traps is determined 3800 days. Although 12 pieces of big wild mammals were determined on the area, only 9 of them were considered for evaluation. As a result of study it has been determined that mixed stands were preferred more when compared with pure stands, mixed stands of fir and beech were preferred more when compared with other mixed stands, and healthy and old stands were preferred more when compared with the disrupted ones.
Keywords: *stand, wildlife, forest, roe deer, wild board, bear*

Introduction

Wild animals are an important and fundamental particular of ecosystem where they exist. However, just like all other ecosystem features, wild animals are also under the threat of mainly human originating dangers. As a result of this, different wild animal species have been influenced on local or global scale and while populations of certain species got reduced, some species were faced with the danger of getting extinct (Marrison et al., 2007).

The situation is the same in Turkey which has got a rich fauna both due to its geographical location and due to different ecosystem features it bears. According to different sources, in Turkey mammals were determined to as 418 pieces of birds, 120 reptiles, 22 amphibians (URL1), 161 pieces of mammals, 460 pieces of birds, 141 pieces of reptiles (Çagatay et al., 2012), 104 pieces of mammals, 418 pieces of birds (Çanakçıoglu and Mol, 1996), 160 pieces of mammals (Bora, 2001), 169 pieces of mammals (Özkazanç, 2012) as being the species observed. According to the recent data in Turkey there are species of 482 pieces of birds (URL2), 172 pieces of mammals (URL3), 157 pieces of amphibians and reptiles (Baran et al., 2012).

No matter what wild animal species is concerned, one of the most important factors influencing their lives is surely the habitats they are using. Protection of wild animals in natural living environments and their sustainability is based on knowing their habitat preferences well. According to Oğurlu (2001) habitat is the environment where a population exists, provides shelter, develops, reproduces, and continues its generation to exist. Wild animals can use different habitats for various purposes such as getting nourishment, reproducing, and nesting. Even if purposes of usage can be different, as wild

http://www.aloki.hu ● ISSN 1589 1623 (Print) ● ISSN 1785 0037 (Online)
DOI: http://dx.doi.org/10.15666/aeer/1704_91719184

animals make preferences of habitats, they consider all habitat components. For this reason, the structure of habitat components with many variables and the influence of each factor in the components should be considered (Oğurlu and Yavuz, 1999). Habitat is an integrity being composed of plants, soil structure, location, altitude of an area as well as components such as other wild animals that use that area. However in the habitat preferences of wild animals, most important one among these elements is mainly the plants.

Plants have direct and indirect influences on habitat preferences of wild animals (Suel et al., 2013). In habitat selection of wild animals, in addition to existence of plant varieties, their distribution is also very important. Because factors relating with raising environment in an area has influence on distribution of plant varieties and distribution of plants has direct impact on distribution of wild animals making use of various functions and opportunities such as sheltering, hiding and getting nourishment as being provided by these plants (Oğurlu and Aksan, 2013).

Analyzing the habitat distribution, finding correlation between habitat variables and distribution of wild animal species and their habitat preferences, are important in revealing ecology of wild animals and in managing wild life. Because information such as existence, abundance, distribution, and nourishment of animals on an area are predicted as being based on habitat situation and quality (Aksan et al., 2014). In this way, influence of changes occurring in the habitat, on the species or population of species and influence in species or population of species on the habitat can be predicted. This is effective in planning wild life.

Majority of big wild mammals are dependent on forests for survival. Because food, water, and land areas which they need for surviving exist in the forests. Besides forests also bear different wild life areas within themselves.

Besides the fact that migration routes that are used by wild animals have the richest habitat features, high sloping areas have got varieties of species. Furthermore, increase in habitat heterogeneity also increase varieties of species (Liu et al., 2017).

Stands which are defined as forest structure is described as forest section which differentiates itself from its environment with respect to at least one of the forest establishment features such as production material, age, tree species, components of tree species, layering, closeness, frequency, and specific bonitet differences and which covers an area of at least one hectare (Genç et al., 2012).

Bartin-Soku Wild Life Protection Area, which forms the study area, has been registered as per the decision of Council of Ministers being dated 13.09.2006 with no 2006/10966. Target species on this area of 17.000 hectares are specified as red deer and roe deer.

This study was conducted to determine the habitat preferences of large mammal wild animals living in the research area. Thus, in the forestry applications to be made in the field, wildlife requests can be evaluated. The destruction of wildlife areas will can be prevented with forestry practices.

Material and Method

Material

Main materials in the study are wild mammals and stand types they are using. Photo traps have been used for gathering data and for obtaining coordinates of photo trap points GPS has been used. The photo traps were used in the bushnell brand, 3264 x 2448 photo

http://www.aloki.hu ● ISSN 1589 1623 (Print) ● ISSN 1785 0037 (Online)
DOI: http://dx.doi.org/10.15666/aeer/1704_91719184

resolution and 1920 x 1080 video resolution. The study area is Bartin-Soku Wild Life Protection Area, which is the most important wildlife areas of the western Black Sea in Turkey. The center of research area is 20 km away from the nearest settlement. Kızıllar, Uluköy, Konak and Kırıklar villages are most near. Kızıllar, Uluköy, Konak and Kırıklar villages are most near settlement to research area. But there are very low human popülations in here. Although the working area has different types of stands, its water presence, surface structure and living cover characteristics are very similar.

Method

With photo traps that are placed in appropriate places on special living areas of wild animals such as their passage points, nourishment areas and resting areas, wild animals preferring that area could be determined. This study was conducted between July 2015 and September 2016. However, it was impossible to reach the area due to snow in winter and the works were slowed during this period. While the photo traps were placed on the site, attention was paid to the habitat types and different habitats of the species targeted. By considering criteria such as season, land structure and stand type, photo traps were controlled between 15 and 30 days and the images being obtained were transferred to computer. All images taken from photo traps were examined in detail and the species were determined and each detected species was processed on the stand map. During the period of study, at 78 different points with numbers of 3800 photo trap days, 4.940 pieces of photos and video records were obtained. As a result of the study in line with the data being obtained by determining density areas of each wild mammal species, stand types of these areas were specified and analysis were made on habitat selections of species. The coordinates of the photo traps are given in *Table 1* and the distributions in the field are given in *Figure 1*.

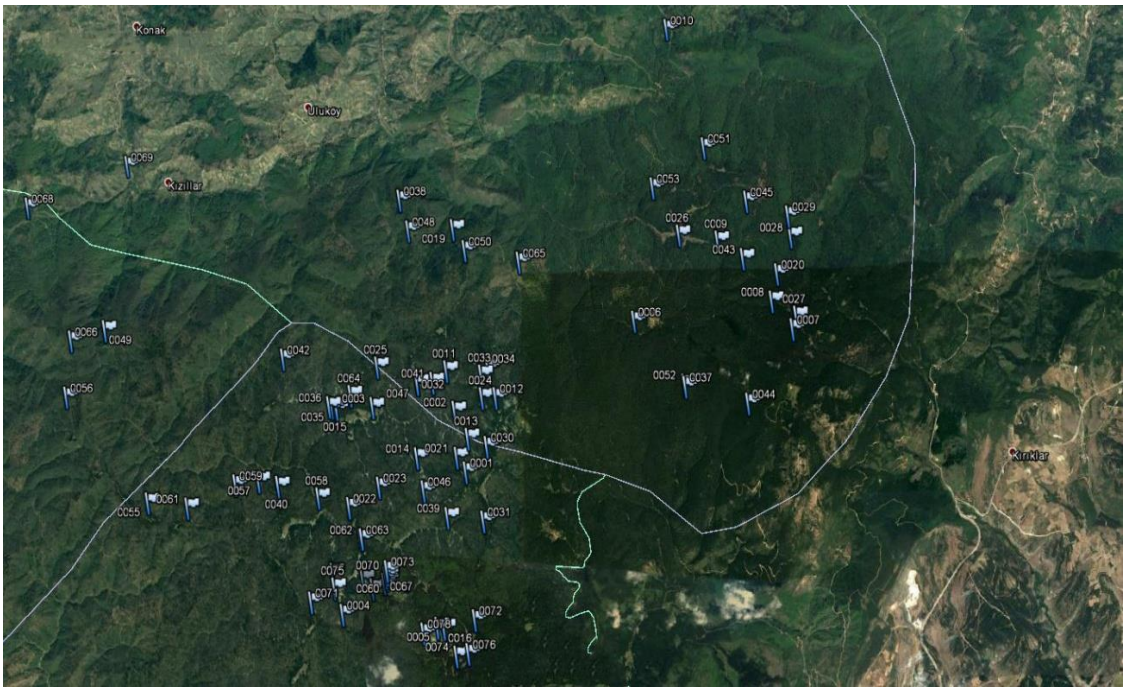

Figure 1. *Distribution map of photo traps in the field*

http://www.aloki.hu ● ISSN 1589 1623 (Print) ● ISSN 1785 0037 (Online)
DOI: http://dx.doi.org/10.15666/aeer/1704_91719184

Table 1. *The coordinates of the photo traps*

No.	East (E)	North (N)	Height (m)	Direction	No.	East (E)	North (N)	Height (m)	Direction
1	464745.15	4577116.77	1641.2	150.99°	**40**	460690.89	4576838.31	1452.2	222.44°
2	464494.43	4579266.72	1461.7	140.59°	**41**	464029.15	4578823.45	1536.1	141.10°
3	462726.39	4578344.98	1405.5	203.82°	**42**	460794.1	4579288.86	1350.7	260.57°
4	462093.41	4574394.73	1538.2	192.85°	**43**	470710.4	4581179.05	1378.7	78.35°
5	464108.28	4574123.14	1486.4	171.78°	**44**	470760.8	4578397.48	1644.6	99.63°
6	468362.18	4579984.48	1281.1	86.44°	**45**	470788.87	4582286.71	1392.8	70.56°
7	471705.63	4579810.34	1685.8	88.93°	**46**	463835.22	4576753.11	1588.9	170.00°
8	471292.94	4580347.74	1511.5	85.04°	**47**	463697.43	4578795.12	1452.9	157.62°
9	470183.21	4581530.14	1260.9	74.73°	**48**	463468.28	4581771.63	1169	3.48°
10	469147.31	4585785.11	814.3	43,40°	**49**	456860.78	4579861.21	1236.3	271.16°
11	464327.68	4579044.01	1499.9	122.95°	**50**	464701.16	4581378.6	1253.5	38.87°
12	465385.59	4578529.85	1590.6	119.31°	**51**	469881.24	4583329.13	1353.2	60.70°
13	764780.85	4577749.97	1490.4	143.05°	**52**	469410.73	4578767.31	1559.6	98.40°
14	463682.97	4577378.25	1455.7	171.09°	**53**	468776.23	4582560.34	1360.4	61.97°
15	461943.1	4578318.85	1398.8	224.92°	**54**	457846.84	4576521.44	1332.5	239.64°
16	464252.15	4574105.11	1500.3	170.36°	**55**	456046.04	4578572.7	1215.8	260.94°
17	461856.49	4575164.67	1402.5	197.74°	**56**	460240.98	4576926.24	1307.2	227.83°
18	462716.35	4574861.45	1441.8	186.96°	**57**	461531.61	4576600.1	1313.9	209.87°
19	464432.98	4581800.8	1105.9	27.35°	**58**	459779.58	4576873.83	1476.4	231.23°
20	471409.32	4580870.62	1552.5	81.44°	**59**	463031.77	4575053.9	1533	183.40°
21	464552.16	4577396.82	1641	151.76°	**60**	458715.65	4576422.63	1397.6	234.36°
22	462202.96	4576415.5	1356.6	198.69°	**61**	462450.92	4575808.49	1384	192.47°
23	462870.58	4576820.71	1473.8	188.81°	**62**	462479.65	4575812.89	1361	192.08°
24	465090.46	4578529.05	1548.8	123.29°	**63**	462258.15	4578578.77	1402.8	233.54°
25	462837.22	4579124.44	1380.7	220.51°	**64**	465872.56	4581148.5	1230.4	59.97°
26	469347.08	4581652.53	1234.5	71.70°	**65**	456112.88	4579665.42	1190.2	269.46°
27	471796.14	4580050.89	1504.1	87.32°	**66**	463009.23	4575098.42	1529.8	183.72°
28	471718.94	4581589.37	1483.6	77.00°	**67**	454884.5	4582340.39	680.3	287.09°
29	471665.97	4581985.25	1418.2	74.36°	**68**	456995.89	4583205.39	1357.7	298.69°
30	465193.07	4577599.1	1612.1	138.12°	**69**	463034.26	4575149.95	1572	183.45°
31	465113.36	4576176.54	1625.2	152.86°	**70**	461424.28	4574637.95	1556.1	200.37°
32	463697.43	4578795.12	1452.9	157.62°	**71**	464914.37	4574272.85	1514.3	163.44°
33	465078.58	4578960.64	1595.3	112.56°	**72**	463035.46	4575220.3	1581.5	183.49°
34	465219.94	4579099.96	1598.3	107.25°	**73**	464516.66	4573575.81	1500	168.75°
35	461837.41	4578344.28	1386.4	227.55°	**74**	461894.83	4574897.48	1431	196.32°
36	461785.48	4578364.54	1389.7	228.95°	**75**	464773.79	4573623.96	1499.1	166.35°
37	469434.29	4578720.92	1574.8	98.80°	**76**	462972.7	4574976.04	1498.3	184.06°
38	463280.28	4582373.87	1179	358.61°	**77**	463811.81	4574023.03	1546.5	174.87
39	464331.9	4576227.53	1443.1	163.63°	**78**	462499.48	4575035.53	1352.7	189.83°

http://www.aloki.hu ● ISSN 1589 1623 (Print) ● ISSN 1785 0037 (Online)
DOI: http://dx.doi.org/10.15666/aeer/1704_91719184

Findings

As a result of studies, on the area 12 different wild mammal species were determined. But since among these species, Eurasian otter (*Lutra lutra* L. 1758), golden jackal (*Canis aureus* L. 1758) and European hare (*Lepus europaeus* L. 1758) were determined at a single point, habitat selection of remaining 9 species of wild mammals were evaluated as per stand types. The some informations of wild animals identified in the study area was provide in *Table 2*.

These species were determined at 12 different stand types having different sizes and densities on the area of study (*Table 3*).

Table 2. *Information relating with the species being determined*

Species	Number of observation points	Number of views
Brown bear (*Ursus arctos* L., 1758)	35	147
Roe deer (*Capreolus capreolus* L., 1758)	61	683
Red deer (*Cervus elaphus* L., 1758)	7	18
Red fox (*Vulpes vulpes* L., 1758)	44	411
Grey wolf (*Canis lupus* L., 1758)	14	59
European badger (*Meles meles* L., 1758)	9	29
Stone marten (*Martes foina* (Erxleben, 1777))	30	96
Wild boar (*Sus scrofa* L., 1758)	41	542
Wild cat (*Felis silvestris* Schreber, 1777)	21	59

Table 3. *Types of stands and their features, in area*

BKn	Broken (B) beech (Kn) stand. It could not be mentioned about any kind of closeness.
GA	Pure fir (G) selection forest. (A: Stand having more number of individuals with thick diameter stages when compared with optimal; Old selected stands)
GÇsKnD	Stand of fir (G)-scots pine (Çs)-beech (Kn) mixture with dominance of firs. (D: Stand being other than A, B and C classes or being composed of mixture; actual selection stand).
GKnA	Stand of fir (G) -beech (Kn) mixture with dominance of firs. (A: Stand having more number of individuals with thick diameter stages when compared with optimal; Old selected stands)
GKnD	Stand of fir (G) - beech (Kn) mixture with dominance of firs. (D: Stand being other than A, B and C classes or being composed of mixture; actual selection stand).
KnÇsA	Stand of beech (Kn) -scots pine (Çs) mixture with dominance of beeches. (A: Stand having more number of individuals with thick diameter stages when compared with optimal; Old selected stands).
KnÇsGD	Stand of beech (Kn)-scots pine (Çs)-fir (D) mixture with dominance of beeches (D: Stand being other than A, B and C classes or being composed of mixture; actual selection stand).
KnD	Pure beech (Kn) selection stand (D: Stand being other than A, B and C classes or being composed of mixture; actual selection stand).
KnDybc	Beech (Kn) and other leafed (Dy) mixed stand. “b (There are individuals from b:Trellis-Pole age (8-19.9 cm)) and c (c: Thin woody age (20-35.9 cm))”, Those from “b” age are in majority numbers.
KnGA	Mixed stand of beech (Kn) and firs (G) with dominance of beech. (A: Stand having more number of individuals with thick diameter stages when compared with optimal; Old selected stands).
KnGD	Mixed stand of beech (Kn) and firs (G) with dominance of beech. (Stand being other than A, B and C classes or being composed of mixture; actual selection stand).
OT	Treeless forest soil

When stand features are considered it is seen that beech and firs which are dominant tree types on the area, are present both as mixed with each other and other varieties and on certain areas there are pure cultures. In line with the data being obtained, stand preferences of wild animals on the area are given numerically in *Table 4* and total number

http://www.aloki.hu ● ISSN 1589 1623 (Print) ● ISSN 1785 0037 (Online)
DOI: http://dx.doi.org/10.15666/aeer/1704_91719184

of individuals being determined in different stand types have been submitted in the form of a graphic in *Figure 2*.

It is observed that on the area there are changes in habitat preferences of wild animals as per the stands. Species have mainly preferred mixed stands and secondarily they have preferred pure stands. Mixed stand types of fir and beech were preferred more when compared with other stands. Among all stand types while GKnA has been the most preferred one, KnGA has been preferred secondarily. Other mixed stands were preferred in the order of KnGD, GÇsKnD, KnÇsA, KnDybc, and KnÇsGD. In the ranking of GA, KnD, BKn pure stands were less preferred by wild animals. Nude areas (OT) have been the habitats on the area that were least preferred.

Table 4. *Number of large mammal wild animals detected compared to the stand types in the area*

Stand Types	Brown bear	Roe deer	Red deer	Red fox	Grey wolf	European badger	Stone marten	Wild boar	Wild cat	Total
BKn	1	17	8	0	0	1	3	0	1	31
GA	6	31	0	10	1	0	4	2	6	60
GÇsKnD	2	69	0	23	8	0	7	8	5	122
GKnA	48	284	2	197	22	22	27	244	14	860
GKnD	16	8	0	2	0	1	1	4	0	32
KnÇsA	16	1	0	0	2	0	0	31	4	54
KnÇsGD	1	11	0	4	0	0	5	6	6	33
KnD	2	1	0	4	2	0	17	13	1	40
KnDybc	32	0	0	0	0	0	1	0	1	34
KnGA	23	154	4	86	17	1	15	183	20	503
KnGD	0	104	4	84	7	4	16	41	1	261
OT	0	3	0	1	0	0	0	10	0	14

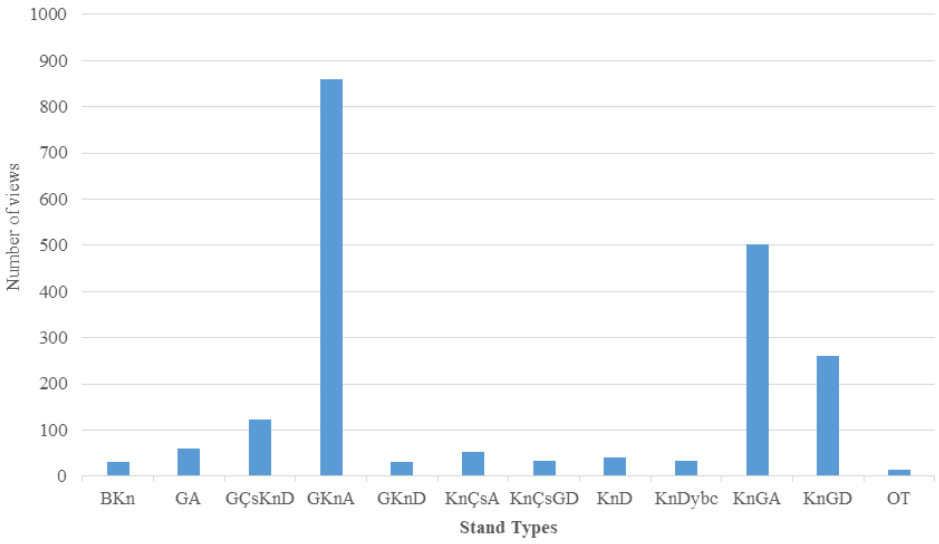

Figure 2. *Number of views to big mammals in stand types*

In habitat preferences of wild animals on the area as depending on stands, other variables that were effective have been A and D. In the stands where there are same tree mixtures, it is seen that A class of stands were significantly more preferred when

http://www.aloki.hu ● ISSN 1589 1623 (Print) ● ISSN 1785 0037 (Online)
DOI: http://dx.doi.org/10.15666/aeer/1704_91719184

compared with D class of stands. Hence while in GKn stand type with A class of mixtures, 860 individuals were observed, in D class of same mixture only 32 individuals were observed. Similar situation also attracts attention with KnG mixture. In this type of mixture while 503 individuals were observed in A class, 262 individuals were observed in D class. This situation reveals that regarding habitat selection of wild animals as per the stands, besides mixed type of stands, they preferred aged selection forests with more number of individuals having thick diameter stages more.

Stand preferences of wild animals on the area show parallelism with each other. However differences are observed in certain varieties. Wild boar, which is one of the dominant species on the area has preferred KnGA more when compared with other species. Again, wild boar and brown bear were seen more at KnÇsA when compared with other wild animals. A situation that is contrary to general preferences is seen with brown bear. KnDybc, which is not preferred by almost any wild animal species, has been preferred by brown bear as secondary stand type (*Figure 3*). The habitat preferences and distributions of each species is shown in *Figure 4*.

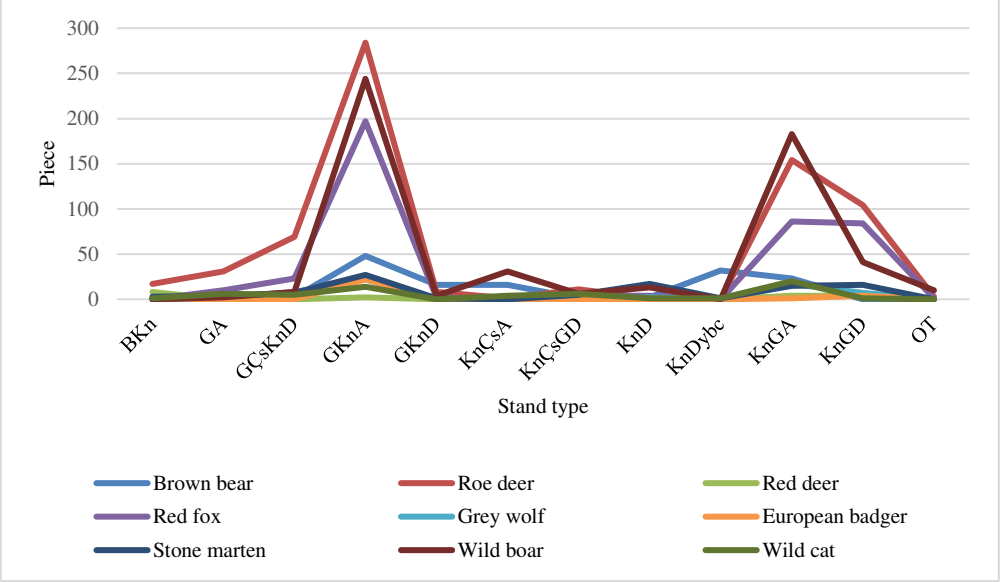

Figure 3. *Stand preferences of big mammals on the area of study*

Conclusion and Discussion

With respect to regional landscapes and sustainability of biological varieties, forest areas bear significant importance (Finch and Ruggiero, 1993). Forests are not only areas which are covered with forest trees but they are an integrity together with all ecosystem components. Among the living segments forming the forest, wild mammal species constitute one of the most important groups. Stand types are influential in different ways in habitat selection of wild mammal species. In line with the results we obtained, mixed and healthy stands are preferred more by wild animals when compared with pure and corrupt stands. Furthermore it is seen that besides stand mixture, stand class was also effective in habitat selection. Hence, A class of mixed stands have been preferred more by wild animals when compared with D class of same mixture.

In the study they conducted at Bolu Seven Lakes Natural Park, Nabioglu and Keten (2016) have stated that oak forests were quite densely used by wild animals.

http://www.aloki.hu ● ISSN 1589 1623 (Print) ● ISSN 1785 0037 (Online)
DOI: http://dx.doi.org/10.15666/aeer/1704_91719184

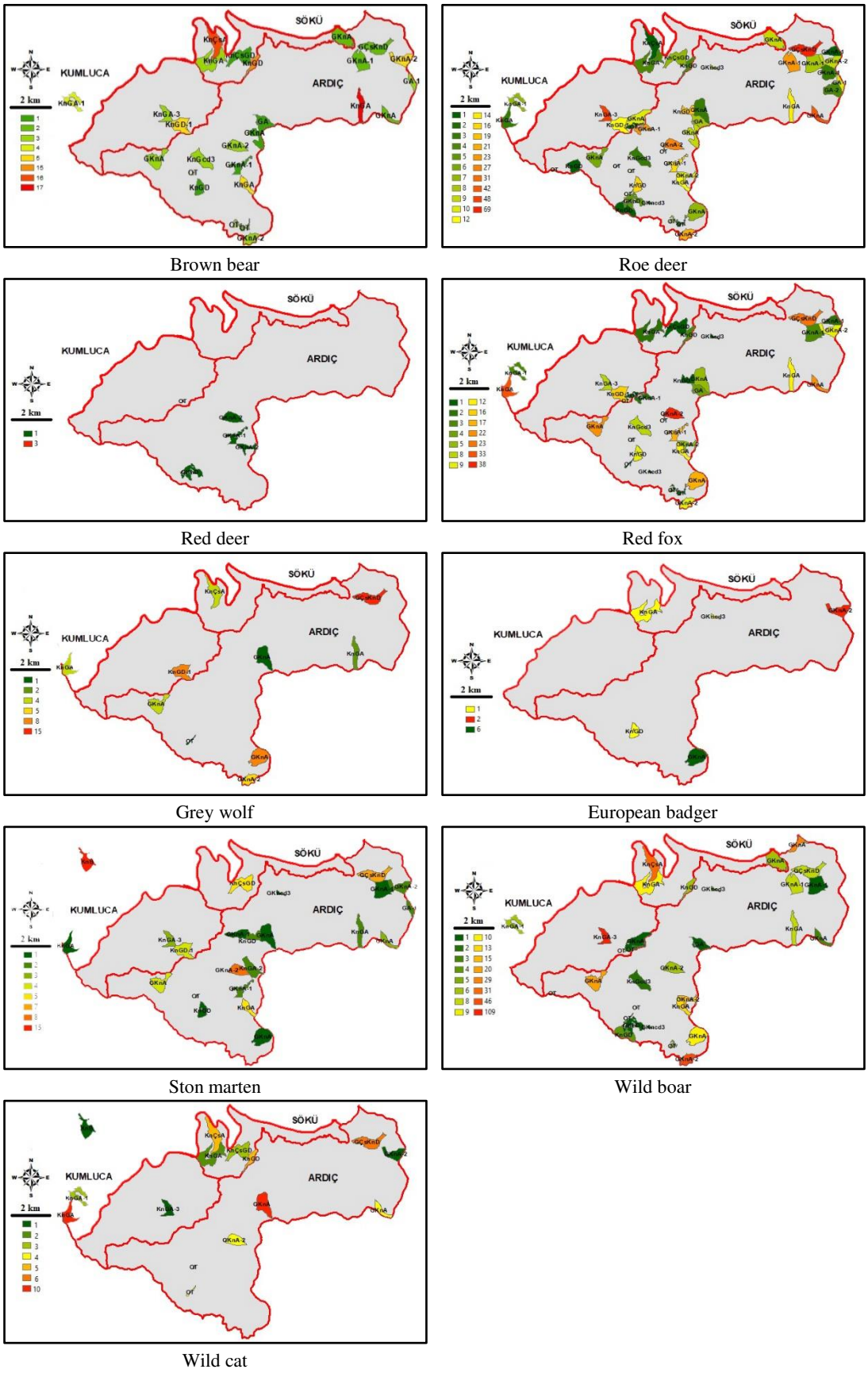

Figure 4. *Stand preferences and spatial distribution of large mammals in area*

http://www.aloki.hu ● ISSN 1589 1623 (Print) ● ISSN 1785 0037 (Online)
DOI: http://dx.doi.org/10.15666/aeer/1704_91719184

They have stated that as the area and near environment were suitable for wild life and as the area had protection status for the development of wild animals, these factors have been influential in this particular. At this point, with respect to habitat selection of wild animals, besides convenience of area, it is clearly revealed that area needs to be effectively protected either naturally or with human impact.

Areas where woody type of varieties are highly present, are seen as the sign of existence of wild animals. The more the woody type of varieties are, the more living areas the wild animals can find for their activities such as sheltering, hiding, having nourishment and resting and these will be areas which will be preferred more by the wild animals (Oğurlu and Aksan, 2013). Both the varieties and quantities of woody types are plenty on our study area and this is one of the most important reasons that increase richness of wild life on this area.

All of the 9 big wild mammals on the study area have mostly preferred stand type of GknA and they have secondarily preferred stand type of KnGA. All of the species have preferred mixed stand types more when compared with the pure ones. However it attracts attention that mixtures where fir is dominant are preferred more when compared with mixtures where beech is dominant.

Habitat selection of brown bears that make up the biggest specie on the area, are influenced from many variables including humans as not being solely effected by stand types (Frackowiak et al., 2014; Rigg, 2005). Brown bears that mainly prefer high altitudes keep away from settlement places (Rigg, 2005).

Even though they are seen in all stand types in our study, brown bears mostly prefer stand type of GKnA. However, as being different from other species it is seen that the stand type which they prefer secondarily has been KnDybc. This stand type is almost not preferred by other species. It is possible for brown bears that walk long distances during the day, to use different types of stands. We have frequently observed the foot prints and stools of brown bears on the forest roads which support this theory.

In Seven Lakes National Park, Beşkardeş (2016) have observed brown bears more at coniferous and other leafed mixtures where oak is seen to be dense, when compared with coniferous and other types of mixtures where beech is seen to be dense. Besides on this area closed stands are preferred more by brown bears when compared with sparse ones.

Roe deer which is the dominant specie on the area prefer closed fir and beech forests where human pressure is less but they don't want to have frequent sub-vegetation (Keten, 2017). On the research area as complying with Keten (2017), roe deers have mostly preferred stand types of GKn and KnG. However, in his study Keten (2017) has determined that roe deers used pure forests of fir, beech, oak and scots pine with similar ratios to the mixed forests. On the contrary in our study pure stands were preferred less by roe deers when compared with other mixed stands.

Mancinelli et al. (2015) have stated that roe deers went to places with dense shadow areas in order to hide from the heat in summer time and that they preferred young ash tree and hazelnut stands for this reason. Furthermore in this study it was mentioned that plant cover phenology was influential in the habitat selection of roe deers and that gemmiferous bushes, new leaves and fruits and newly growing grass were effective in habitat selection. Again it was determined that this specie preferred forests with scote pine and pyrenean oak more in Spain and that they got nourishment at places where there were blackberries, roses, shrubs and kochia in the lower flora structure (Virgos and Telleria, 2011).

Both of these studies support our study on the basis. Even if the types of trees are different, it is seen that roe deers preferred mixed stands more. Similarly, sub-flora which

http://www.aloki.hu ● ISSN 1589 1623 (Print) ● ISSN 1785 0037 (Online)
DOI: http://dx.doi.org/10.15666/aeer/1704_91719184

roe deers prefer for getting nourishment completely matches with sub-flora structures of GKnA and KnGA where roe deers have been mostly observed.

Red deers which are one of the target species on the area prefer forest areas which are calm and dense and where there are open areas and meadows in surrounding places. Besides preferring leafy and mixed forests, they can also prefer pure cultures. An important factor is that sub-layer is rich and it is situated close to water resources (Kumbasli, 2006). However, habitat preferences of red deers also change as depending on seasons (Zang et al., 2013).

Red deers which are among rare species prefer beech and especially pure beech stands more when compared with other species. Although they get nourishment at the small open areas within dense forests, beech forests which are on the study area provide more nourishment environment for this specie.

Red fox, which is another dominant specie has been observed densely at the stands of GKnA and KnGA as being similar to other species. But it attracts attention that red fox prefers KnGD stand as much as KnGA.

Cagnacci et al. (2004) state that habitat selections of red fox living on mountain areas could vary depending on the seasons. Red foxes prefer forest habitats more than open areas according to Etten et al. (2007). Similarly in our study it is seen that red foxes preferred mixed stands mainly having firs more when compared with other stand types. While red foxes were observed 222 times at the stands where firs were dominant, they were observed 179 times at the stands where beeches were dominating and where there were also firs.

Gresy wolf which is the most important predatory specie on our study area show harmonization with preference of general stands as being similar to other species. Another particular which attracts attention in this harmonization is that grey wolf prefers the same habitats as roe deers, being their most important hunt, with similar density ratios. For example the most preferred type GKnA is preferred by roe deer with a ratio of 41.5%, whereas it is preferred by grey wolf with a ratio of 37%, while they prefer the type of KnGA with ratios of 41.5% and 37%, respectively.

One of the best models determining the distribution of grey wolves on an area is the forest cover (Jedrzejewski et al., 2015). Wolves which generally prefer coniferous and mixed forests, do not like forests which are young and which drop leaves (Koskela et al., 2013).

European badger, which is one of the most rare species on the area mostly prefer open areas in the forests (Unal, 2011), and they are seen more on the regions where plant cover is more frequent and where human activities are rare (Özen and Uluçay, 2010). Soil's being suitable for digging is another important factor in the habitat selection of badger (Suel et al., 2013). Oğurlu and Aksan (2013) have stated that since planting areas could easily be digged and as the trunk branches of cedar tree were close to the ground and as their bottom parts provided sheltering, it was suitable for European badger to nest at these places. On the other hand since trees were dense on black pine areas and as the live cover below was weak due to their falling parts, and as the soil was tight and solid, they were not considered to be appropriate to meet the needs of European badger for hiding, finding shelter and nesting.

According the the data we have obtained, European badgers were observed more on GKnA type of stands when compared with other types of stands. This type of stand was preferred by badgers both due to its mixture and soil features. European badgers don't prefer stands with pure beech or mixtures being mainly composed of beech and it is

http://www.aloki.hu ● ISSN 1589 1623 (Print) ● ISSN 1785 0037 (Online)
DOI: http://dx.doi.org/10.15666/aeer/1704_91719184

thought that the reason for this is because sub-layer of this type of stands is coated with dense live or dead covers. This causes European badgers not to be able to dig the soil easily.

Stone marten which realizes less daily migrations when compared with other species prefers GknA mostly and it prefers KnD secondarily. Virgos et al. (2010) have stated that although stone marten was a predatory trees played an important role in their habitat selections. It is possible to observe marten at bushes and trees and at places where there are herbaceous plants (Suel et al., 2013). Stone marten, which we mostly observe at forest sections, sub-layers of which have developed, are not seen at open forest soils. It is found out that when stone martens left their nests inside dead tree blocks or wood blocks fallen on ground, they would hunt in the near environment and that they were returning back to their nests. Hence Bull et al. (2005) have stated that stone marten mostly preferred fir and spruce forests where there were dead trees and blocks. In the same study it was emphasized that martens rapidly left the areas where trees were cut.

Wild boar, which preferred juicy fruits in summer and dry fruits and seedy plants rich with fats in the winter season (Oğurlu and Aksan, 2013), which move around the living areas and which pile under dense plant covers and which get their nourishment on areas where there are tuber plants (Suel et al., 2013) have preferred stands having beeches as dominant tree types as they contained more water sources and as they met their food requirements better. Aksan et al. (2014) have stated that ideal places for wild boars were forest areas where soil type had characteristics of sandstone and that they did not prefer bushes and step areas. Wild boars do not use habitats randomly and mostly they act selectively among existing biotopes and in their habitat selections there are variations as per the seasons (Santos et al., 2004). In habitat selections of wild boars nourishment richness, level of hiding, sloping are the determinant factors (Xu, 2011).

In a study being conducted in Poland it was stated that wild boars preferred beech and horn beam forests and that they kept away from fir forests and that beech-horn beam forests were very important for wild animals (Fonsenca, 2008). In another study being conducted in Poland by Gorecki et al. (2009) it was determined that wild boars were mostly present within scote pines in fresh mixed wild leafed forest habitats.

In the studies we conducted it was seen that as being different from other species wild boars preferred stand types such as KnGA and KnÇsA where wide leafed trees were dominant. These stands meet the most convenient features for wild boars. As sub-flora of beech was more dense when compared with fir on the study area, a better environment was present for wild boars to rest and to hide. Again wild boar has been the only specie being observed on bare forest soil. Bare forest soils that were on the study area contained plenty of tuber plants which wild boars especially preferred as food. This situation caused for this specie to get nourishment here.

Wild cat which was the only cat specie being observed on the area was seen on all types of stands but with arc ratios. Just like other species wild cat was observed mostly at the stands of GKnA and KnGA. Wild animals being present on the area are active during the day time and they sometimes go to far distances away from their nests. Sarmento et al. (2006) have found out that for habitat usage wild cats preferred local and mainly forest areas. However besides forests shrubberies are also preferred by wild cats and even at certain places agricultural areas are also being used (Lozana, 2010).

http://www.aloki.hu ● ISSN 1589 1623 (Print) ● ISSN 1785 0037 (Online)
DOI: http://dx.doi.org/10.15666/aeer/1704_91719184

Recommendations

For long years forest activities and wild life activities have contradicted with each other. Especially after cuttings at wide areas, big or very small open areas have formed in the forests. As the study area is a very important production field for regional forestry, this situation has significant impact on wild life on the area. Similarly forest fires and pesticides that are used against harmful forest insects form threats for many wild animal species. However by using appropriate forest management techniques, while forest planning is made, wild life can be improved.

Formation of mixed stands, mixed types of trees, existence of individuals with different ages bear significant impact on improving varieties of types in forest ecosystem. However regarding the types to be used for afforestation, attention should be paid in preferring local types and for them to comply with local conditions. At this point while making new afforestation works, it bears significant importance to avoid pure cultures in forest administration and to establish mixed cultures and to plant fruit trees that are effective in the nourishment of wild animals. Planting apple and pear trees for brown bears and trees of bushes having grape-like fruits or berries at local points for roe deers and red deers are important for development and sustainability of wild life.

It is significantly important to realize cutting activities as being required for forestry, by paying attention not to ruin stand types and classes, not to change closeness and densities in a significant way and most importantly to realize these activities in periods other than reproduction and breeding periods of wild animals.

Mainly afforestation and production activities that will be realized by considering the requests of wild animals and all forestry applications bear significant importance for the sustainability of wild animals.

Acknowledgements. This study was produced from 2014-FEN-A05 project supported by BAP Coordinator of Bartın University. We would like to express our appreciation to the Bartın University Scientific Research Project Commission, for their support.

REFERENCES

[1] Aksan, Ş., Özdemir, İ., Oğurlu, İ. (2014): Modeling the distributions of some wild mammalian species in Gölcük Natural Park/Turkey. – Biological Diversity and Conservation ISSN 1308-8084 Online; ISSN 1308-5301 7(1): 1-15.

[2] Baran, İ., Ilgaz, Ç., Avcı, A., Kumlutaş, Y., Olgun, K. (2012): Amphibians and Reptiles of Turkey. – TÜBİTAK Popular Science Books 207. ISBN 978-975-403-703-6.

[3] Beşkardeş, V. (2016): Large-bodied mammals and their habitat preferences in autumn in Yedigöller Wildlife Reserve. – Journal of Forestry 12(1): 137-144.

[4] Bora, M. E. (2001): Basic Education Book for Sustainable Hunting. – T.C. Ministry of Forest General Directorate of National Parks and Hunting Wildlife. Education.

[5] Bull, E. L., Heater, T. W., Shepherd, J. F. (2005): Habitat selection by the American marten in northeastern oregon. – Northwest Science 79(1): 37-43.

[6] Cagnacci, F., Alberto, M., Lovari, S. (2004): Habitat selection by the red fox "Vulpes vulpes" (L. 1758) in an Alpine area. – Ethology Ecology and Evolution: 103-116. DOI: 10.1080/08927014.2004.9522640.

[7] Çağatay, A., Terzioğlu, E., Ekmen, Z. İ., Erdoğan, E. (2012): Biological Diversity Monitoring and Evaluation Report. – ISBN: 978-605-4610-23-5. Ministry of Culture Publisher Certificate Number: 15108.

http://www.aloki.hu ● ISSN 1589 1623 (Print) ● ISSN 1785 0037 (Online)
DOI: http://dx.doi.org/10.15666/aeer/1704_91719184

[8] Çanakçıoğlu, H., Mol, T. (1996): Wildlife Knowledge. – İstanbul University Edition No: 3948, Faculty Edition No: 440 ISBN: 975-404-424-4 İstanbul.
[9] Etten, K. W., Wilson, K. R., Crabtree, R. L. (2007): Habitat use of red foxes ın Yellowstone National Park based on snow tracking and telemetry. – Journal of Mammalogy 88(6): 1498-1507.
[10] Finch, D. M., Ruggiero, L. F. (1993): Wildlife habitats and biological diversity in the Rocky Mountains and Northern Great Plains. – Natural Areas Journal 13(3): 191-203.
[11] Fonseca, C. (2008): Winter habitat selection by wild boar Sus scrofa in southeastern Poland. – Eur J Wildl Res 54: 361-366. DOI 10.1007/s10344-007-0144-9.
[12] Frackowiak, W., Theuerkauf, J., Pirga, B., Gula, R. (2014): Brown bear habitat selection in relation to anthropogenic structures in the Bieszczady Mountains, Poland. – Biologia 69/7: 926-930. Section Zoology DOI: 10.2478/s11756-014-0386-4.
[13] Genç, M., Kasarcı, E., Kaya, C. (2012): A Silvicultural evaluation on the researches of stand structure. – Artvin Çoruh University Journal of Forestry Faculty 13(2): 291-303.
[14] Gorecki, G., Labudzki, L., Skubis, J., Wlazelko, M. (2009): Habitat selection of wild boar (Sus scrofa) in the Zielonka Game Investigatory Centre – Radio Telemetry Research. – Acta Sci. Pol. Silv. Colendar. Rat. Ind. Lignar. 8(3): 15-27.
[15] Jedrzejewski, W., Niedzialkowska, M., Mysiajek, R. W., Nowak, S., Jedrzejewska, B. (2005): Habitat selection by wolves Canis lupus in the uplands and mountains of southern Poland. – Acta Theriologica 50(3): 417-428.
[16] Keten, A. (2017): Distribution and habitat preference of roe deer (Capreolus capreolus L.) in Düzce province of Turkey. – İstanbul University, Journal of the Forestry Faculty 67(1): 22-28. DOI: 10.17099/jffiu.89577.
[17] Koskela, A., Kaartinen, S., Aspi, J., Kojola, I., Helle, P., Rytkönen, S. (2013): Does grey wolf presence affect habitat selection of wolverines? – Ann. Zool. Fennici 50: 216-224. ISSN 0003-455X (print), ISSN 1797-2450 (online) Finnish Zoological and Botanical Publishing Board.
[18] Kumbaşlı, M. (2006): The Field assessment of deer density. – İstanbul University, Journal of the Forestry Faculty B Serial 56(2): 123-133.
[19] Liu, X., Wu, P., Shao, X., Songer, M., Cai, Q., He, X., Zhu, Y. (2017): Diversity and activity patterns of sympatric animals among four types of forest habitat in Guanyinshan Nature Reserve in the Qinling Mountains, China. – Environ Sci Pollut Res 24: 16465-16477. DOI 10.1007/s11356-017-9232-x.
[20] Lozana, J. (2010): Habitat use by European wildcats (Felis silvestris) in central Spain: What is the relative importance of forest variables? – Animal Biodiversity and Conservation 33.2: 143-150. ISSN: 1578–665X.
[21] Mancinelli, S., Petersa, W., Boitani, L., Hebblewhite, M., Cagnacci, F. (2015): Roe deer summer habitat selection at multiple spatio-temporal scales in an Alpine environment. – Hystrix, the Italian Journal of Mammalogy ISSN 1825-5272 30th November Associazione Teriologica Italiana doi:10.4404/hystrix-26.2-1122.
[22] Morrison, J. C., Sechrest, W., Dinerstein, E., Wilcove, D. S., Lamoreux, J. F. (2007): Persistence of large mammal faunas as indicators of global human impacts. – Journal of Mammalogy 88(6): 1363-1380.
[23] Nabioğlu, M., Keten, A. (2016): Mammals determined by wildlife camera trap in pure oak stand in Bolu-Yedigöller Wildlife Reserve. – Journal of Forestry Research 1(3): 62-68.
[24] Oğurlu, İ., Yavuz, H. (1999): A computer programme for determining habitat preference based on dung frequencies of some herbivore mammals. – Tr. J. of Zoology (23): 241-249.
[25] Oğurlu, İ. (2001): Wild Life Ecology. – Süleyman Demirel University Edition No: 19, Isparta, 975-7929-37-9, 296 s.
[26] Oğurlu, İ., Aksan, Ş. (2013): Determination of indicator woody plant species for potential habitats of some wild mammalian species. – SDU Journal of Forestry Faculty 14: 81-87.

http://www.aloki.hu ● ISSN 1589 1623 (Print) ● ISSN 1785 0037 (Online)
DOI: http://dx.doi.org/10.15666/aeer/1704_91719184

[27] Özen, A. S., Uluçay, İ. (2010): Ecologıcal, biological and taxonomical characterıstıcs of Meles meles Linnaeus, 1758 (Mammalia: Carnivora) in Kütahya. – Dumlupınar University Journal of the Institute of Science and Technology 21: 9-20.
[28] Özkazanç, N. K. (2012): Mammal animals were determınated in Bartın-Sökü Wildlife Protection Area. – Bartın Faculty of Forestry Journal 14(21): 92-99.
[29] Rigg, R. (2015): A review of studies on brown bear (Ursus arctos) ecology in relation to home range, habitat selection, activity patterns, social organisation, life histories and population dynamics. – Oecologia Montana 14: 47-59.
[30] Santos, P., Almeıda, L. M., Fonseca, F. P. (2014): Habitat selection by wild boar Sus scrofa L. in Alentejo, Portugal. – Galemys 16 (nº especial): 167-184. ISSN: 1137-8700.
[31] Sarmento, P., Cruz, J., Tarroso, P., Fonseca, C. (2006): Space and Habitat Selection by Female European Wild Cats (Felis silvestris silvestris). – Wildl. Biol. Pract. 2(2): 79-89. DOI:10.2461/wbp.2006.2.10.
[32] Süel, H., Ertuğrul, E. T., Aksan, Ş., Ünal, Y., Akdemir, D., Cengiz, G., Bayrak, H., Ersin, M. Ö., Oğurlu, İ., Ozkan, K., Özdemir, İ. (2013): Indicator species of habitat preferences to wildlife animals in Köprüçay District. – 3rd International Geography Symposium GEOMED 553-565.
[33] URL1: http://web.deu.edu.tr/famer/canlilar_dunyasi.htm.
[34] URL2: http://www.trakus.org.
[35] URL3: http://www.tramem.org.
[36] Ünal, Y. (2011): Game & Wildlife inventory in Isparta - Yazılıkaya. – Süleyman Demirel University Graduate School of Natural and Applied Sciences.
[37] Virgos, E., Tellería, J. L. (1998): Roe deer habitat selection in Spain: Constraints on the distribution of a species. – Canadian Journal of Zoology 76: 1294-1299. DOI: 10.1139/z98-065.
[38] Virgos, E., Cabezas-Diaz, S., Mangas, J. G., Lozano, J. (2010): Spatial distribution models in a frugivorous carnivore, the stone marten (Martes foina): is the Freshy-Fruit availability a useful predictor? – Animal Biology 60(4): 423-436.
[39] Xu, T. F., Cai, C. J., Ju, Y. Y., Zhao, L. (2011): Autumn habitat selection of wild boar in the Fenghuangshan Nature Reserve, Heilongjiang Province. – Beijing Linye Daxue Xuebao/Journal of Beijing Forestry University 33(3): 86-91.
[40] Zhang, M., Liu, Z., Teng, L. (2013): Seasonal habitat selection of the red deer (Cervus elaphus alxaicus) in the Helan Mountains, China. – Zoologia 30(1): 24-34. http://dx.doi.org/10.1590/S1984-46702013000100003.

http://www.aloki.hu ● ISSN 1589 1623 (Print) ● ISSN 1785 0037 (Online)
DOI: http://dx.doi.org/10.15666/aeer/1704_91719184

LIFE CYCLE OF CEDAR PROCESSIONARY MOTH (*THAUMETOPOEA ISPARTAENSIS* DOĞANLAR & AVCI) IN TURKEY (LEPIDOPTERA: NOTODONTIDAE)

KÜÇÜKOSMANOĞLU, A.

Faculty of Forestry, İstanbul University-Cerrahpaşa, Sarıyer, Istanbul, Turkey
(e-mail: aliko@istanbul.edu.tr)

(Received 20th Mar 2019; accepted 24th May 2019)

Abstract. *Thaumetopoea ispartaensis* Doğanlar and Avcı (Lepidoptera: Notodontidae) (cedar processionary moth: CPM) is one of the most dangerous pests of *Cedrus libani* A. Rich. living in abundance in forests of the Isparta region and some forests of Taurus Mountain in Southern Turkey. The present study was conducted to study the biology of *T. ispartaensis* which was recorded and defined first time in Turkey and its damage on cedar needles. The study was conducted in Isparta-Senirkent Kapıdağ Forests (between 1250 and 1650 m; 38° 06' N, 30° 45' E) where the pest caused most damage. It was determined that *T. ispartaensis* was a monophagous species of *C. libani*. The flight period of the pest lasted from mid-August to mid-September. Females laid eggs underside of twigs (mean 3.5 mm diameter) on the lower part of trees. Eggs were covered by scales which were colored similar to the bark of shoot. Egg numbers of egg batches varied between 39 and 245 (mean 121). The caterpillars started to hatch in the second half of April, and it had five instars. The caterpillar hatching rate from eggs was found as 87.5%. The caterpillars which built the nests on stems and shoots fed at nights and stayed in their nests in the daytime. Mature larvae started to pass into the soil for pupating from the beginning of July. The pupation was determined in the first half of July, in a depth of 5-15 cm of soil, in the sun-exposed places in cedar woods along the sides of the roads. *T. ispartaensis* was determined as univoltine species.
Keywords: *cedar pest, needle, moth, biology, Turkey*

Introduction

Taurus cedar (*Cedrus libani* A. Rich.) is one of four cedar species distributed across the world. The Taurus cedar, which is naturally found in Turkey, Lebanon, and Syria, is distributed across approximately 482.391 hectares (ha) in Turkey. The broadest natural distribution of Taurus cedar, one of the most important forest trees of Turkey, is in the Taurus Mountains of Turkey. Cedar is significant from the historical, cultural, aesthetic, scientific and economic perspectives (Aksoy and Özalp, 1990; Anonymous, 2015). It grows in Mediterranean Mountain climates and has distinct ring boundaries. Its growth age is said to reach up to 500 years. Cedar generally occurs between 800 and 2100 m elevations (Evcimen, 1963).

The species of the genus *Thaumetopoea* (Lepidoptera, Notodontidae, Thaumetopoeinae) has an important place in forest fauna and human health as they are defoliators of trees and they release urticating hairs at the larval stage that are a source of allergy. Within the genus, there are two groups associated with conifers which are characterized by larval feeding in winter or spring-summer, so the groups are called 'winter' and 'summer' processionary moths (Basso et al., 2016).

Three species of processionary moths (Notodontidae: Thaumetopoeinae) can be found in cedar (*Cedrus* spp.) including *Thaumetopoea bonjeani* (Powell) in *C. atlantica* Man. in North Africa (Tunisia, Morocco, and Algeria), *T. libanotica* Kiriakoff & Talhouk in Lebanon and *T. ispartaensis* in *C. libani* in Turkey (Battisti et al., 2015). These species are close to *T. pinivora* living on pines in Europe and belong to the group

http://www.aloki.hu ● ISSN 1589 1623 (Print) ● ISSN 1785 0037 (Online)
DOI: http://dx.doi.org/10.15666/aeer/1704_91859190

of the "summer processionary caterpillars." All have their larval development from the beginning of spring until the beginning of summer (Demolin, 1988; El Yousfi, 1989; Kiriakoff and Talhouk, 1975; Mouna and Fabre, 2005).

T. ispartaensis has been identified as a new species from Turkey in the Isparta region of Asia Minor located in the Lakes District area in 2001. *T. ispartaensis* is one of the most important insects of Taurus cedar forests in the Isparta region and in some forests of Taurus Mountain in Southern Turkey. The only determined host species of *T. ispartaensis* is *C. libani*. The wingspan of the males and females is 26-29 mm and 34-37 mm, respectively. The larvae feed on the needless of cedar trees and produce tiny hairs containing and urticating substance, which causes contact dermatitis (Doğanlar and Avcı, 2001).

Materials and methods

The studies of the biology of the insect were carried out at Isparta/Senirkent Kapıdağ cedar forest where the insect was first detected. Field studies were conducted between 2012 and 2016 to determine the biology of the pest in natural conditions. Most of the egg clusters and larvae various stages were collected in the forest during study period. Eggs collected from the field were brought to the laboratory and measurements and counts were performed.

The study area was located in the Western Mediterranean of Turkey. It was about 65 km from Isparta city (*Fig. 1*). The study area is located at 38°06'N., 30°45'E., average slope 23°, predominately north facing aspect, about 1365 m altitudes, and about 1223 ha in size. The study area is found on calcareous formations of Eocene age. The soil varies from shallow to medium and medium-deep and is generally stony. The soil is varies from shallow, medium, medium-deep, and are generally stony. However, many cracks between limestone blocks contain fine soil and create a physiologically deep soil (Evcimen, 1963). This region is in the transitional zone between the Mediterranean climate and the continental climate with colder winters and hotter summers.

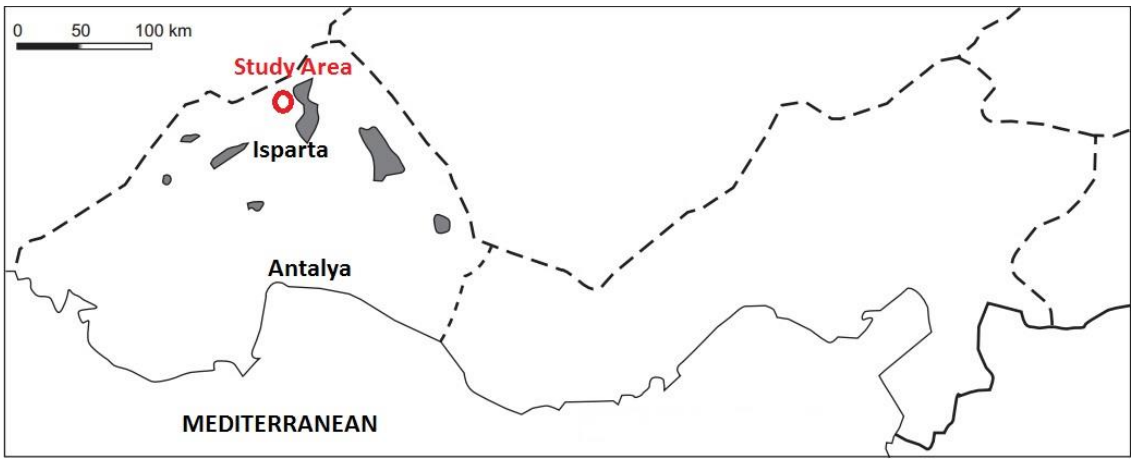

Figure 1. *The study area in Isparta City, south-western Anatolia, Turkey*

The egg-batches were collected in October-December 2013 and 2014. All egg-batches were taken from underside of twigs of *C. libani*. Ninety-five egg-batches,

http://www.aloki.hu ● ISSN 1589 1623 (Print) ● ISSN 1785 0037 (Online)
DOI: http://dx.doi.org/10.15666/aeer/1704_91859190

oviposited over two annual generations, were studied. After collection, the batches were put singly in test tubes with cotton stoppers and placed in the laboratory at 21-24 °C, where further investigations were also performed. The scales covering the egg-batches were removed, counted and measured.

The biology of the pest has been tracked in field conditions. For this purpose, observations were made with periods of 2-3 weeks within the fields, in areas where the spread of the insect was determined. In the egg period, following the hatched of larvae up to pupa period studies were carried out within certain trees. In order to determine some morphological features of *T. ispartaensis*, several measurements and observations were made in larvae and pupae collected from field. Measurements were performed on 20 individuals for each period. Field observations were recorded on a regular basis and the biology of the insect in natural conditions was determined. Also, mature larvae and pupae brought to the laboratory were monitored until the adult outgrowth, within the plastic containers that have soil in their lower part.

Results

Thaumetopoea ispartaensis (described as *Traumatocampa ispartaensis* by Doğanlar and Avcı in 2001) is one of the most dangerous pests living in the *Cedrus libani* forests in the Isparta region and on the Taurus Mountains in Southern Turkey. The pest is distributed between 1250 and 1650 m. The caterpillars feed on the needles of cedar trees and have urticating hairs that cause contact dermatitis especially after the third instar.

The study was conducted in Isparta/Senirkent Kapıdağ Cedar Forest where the most massive damage occurred. It was determined that *T. ispartaensis* is a monophagous species and feed on only *C. libani*. *T. ispartaensis* belongs to the group of the summer processionary moths, just like *T. pinivora*, and adapts to high elevation.

Adults appear from the mid-August to the end of September, depending on the temperature and altitude (earlier at a lower elevation). Egg-laying started soon after emergence and copulation, as in other Notodontidae species. Copulation started a few hours after the adults had emerged and then egg deposition took place during the same night. Females oviposit on the underside of *C. libani* twigs. Egg batches are covered by grayish brown scales, similar to the color of the bark, and therefore the batches are indistinguishable. Only one egg-batch was laid by one female during its very short life. Oviposition by the moth in all cases was found to occur from the tip to base of the twigs. This observation was made based on the position of scales which covered the eggs. The eggs were deposited below the surface of the twigs were 2-5 mm diameter (average 3.5 mm). The color of the eggs was white. The length of the egg-batches varied from 7 to 36 mm (average 17 mm). A one cm egg-row contained a mean number of 10.5 (10.1-10.9) eggs (*Fig. 2*).

The number of eggs per egg batch varies between 39 and 245 (mean 121). The eggs hibernate and this period continues for approximately seven months. The larvae hatched in the last week of March and the first half of April of the following year and started to cause damage by feeding needles. It was observed that the larvae fed in nights and stayed in nests during day time.

The larvae live together in silky grayish nests until the 5th instar which is the last instar. They build their loose nests on the trunk or branch of host trees and nests become thicker (but it is still quite loose in comparison to pine processionary moth nests) as larvae feed during 2.5 months, generally between the late April and mid-July. In spring,

http://www.aloki.hu ● ISSN 1589 1623 (Print) ● ISSN 1785 0037 (Online)
DOI: http://dx.doi.org/10.15666/aeer/1704_91859190

larvae resume feeding on the needles, reaching up to 3.0-3.5 cm in length by summer. The mature larvae are the most destructive ones and may cause severe infestation resulting in the complete defoliation of large surfaces of cedar forests. The nests become clear in May and grow large at the end of this month. They spin cotton like webs when they are active. The mature larvae of *T. ispartaensis* live in aggregations in silky nests (*Fig. 2*). Damaged parts of the tree with dead agglutinated needles remain long after the feeding period.

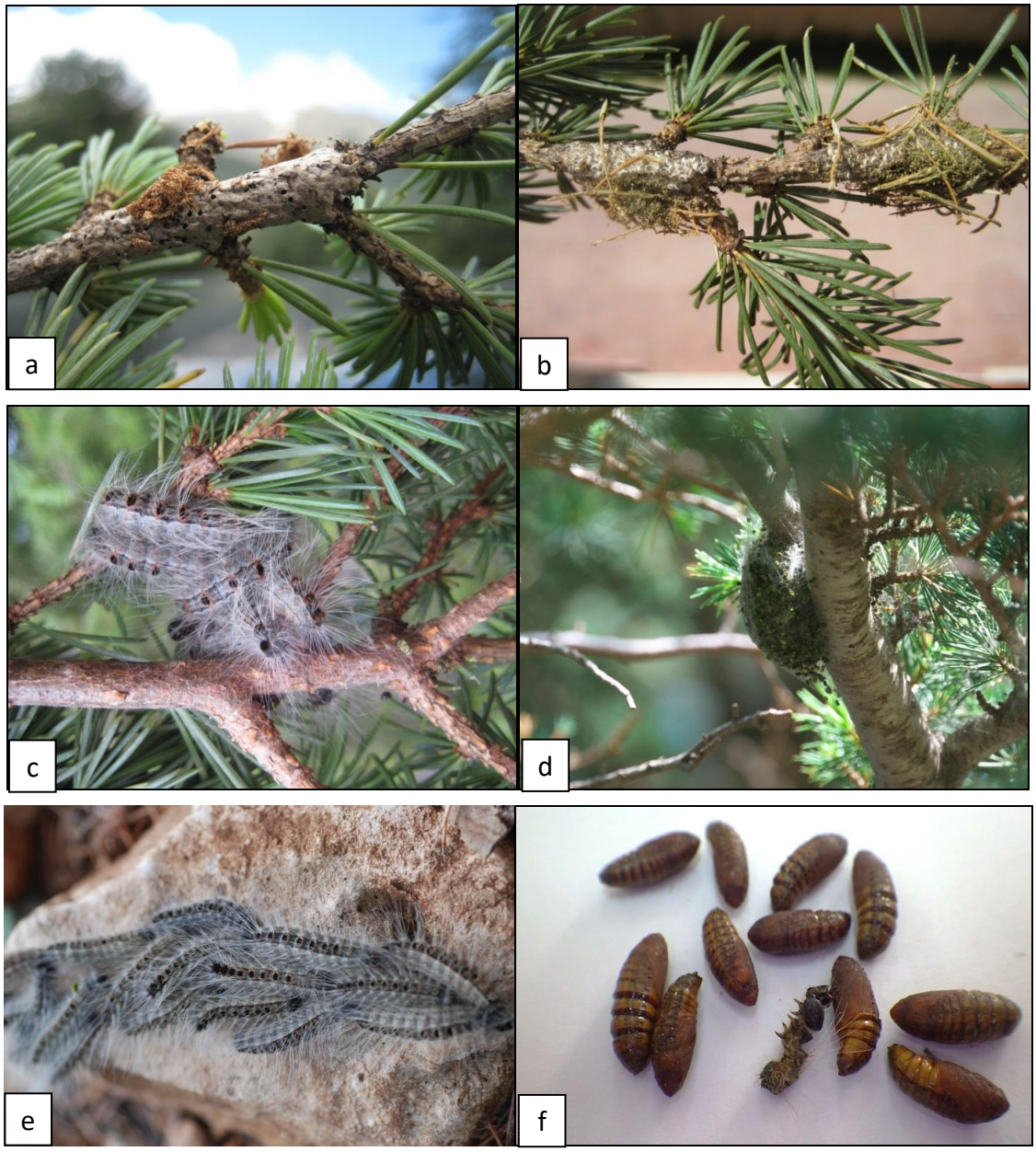

Figure 2. *Thaumetopoea ispartaensis a) egg batches b) damage that young larvae cause c) mature larvae d) nest of larvae e) larvae on soil for pupation f) pupae*

The pupation takes places at the beginning of July in lower elevations, and it takes places in the second half of this month in higher altitudes, in a depth of 5-15 cm of soil,

http://www.aloki.hu ● ISSN 1589 1623 (Print) ● ISSN 1785 0037 (Online)
DOI: http://dx.doi.org/10.15666/aeer/1704_91859190

in sunlit cedar forest floors, especially along roadsides. In mid-June, fully grown larvae of *T. ispartaensis* drop to the forest floor and pupate in the surface litter and soil. There follows a short pre-pupal stage, after which the pupae remain in the litter until adult emergence. The pupa develops in a cocoon which is gray-brown (*Fig. 2*). There is no observation about the capacity of the pupae to prolong the diapause.

The adult appears in the middle of August, and adult hatchings become the highest level in the last period of this month. Flying period continues in September decreasingly. It was determined that *T. ispartaensis* has one generation and the mean lengths of egg, larva, and pupa periods are 228, 98 and 36 days, respectively (*Fig. 3*).

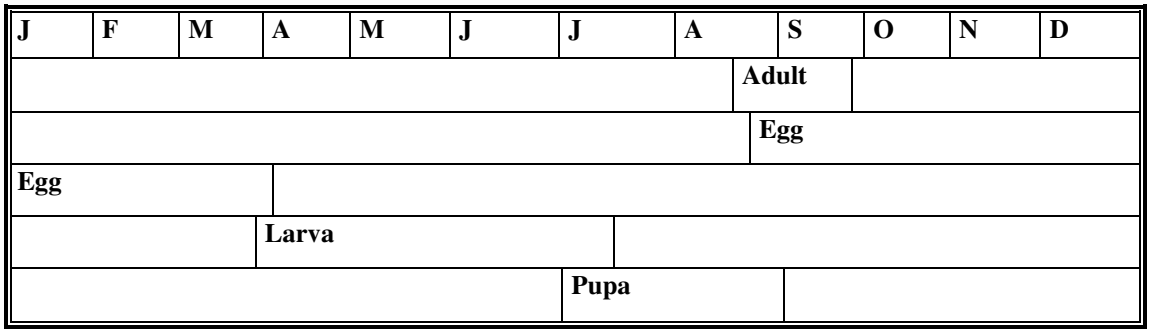

Figure 3. *Life history of Traumatocampa ispartaensis Doğanlar & Avcı in Turkey*

Discussion

T. ispartaensis display similar phenology as *T. bonjeani* in the C. *atlantica* forest in the Atlas Mt. in North Africa. Oviposition of *T. bonjeani* takes place in August-September on small twigs, and the eggs are also covered with scales. The eggs hibernate and hatch in the spring during March-April of the following year (Demolin, 1988).

At the same time, the biology of *T. ispartaensis,* shows great resemblance with the biology of *T. libanotica* that located in the forests of Bsharry, Tannourine and Shouf in Lebanon. *T. libanotica* lives in these regions between 1400-2000 m above sea level and its adult period is remarked as August-October (Kiriakoff and Talhouk, 1975; Nemer et al., 2018).

The egg rows of *T. ispartaensis* were not generally tidy, more random than the egg rows of *T. pityocampa*, *T. wilkinsoni* or *T. solitaria*. The eggs of *T. solitaria* are white above, grayish-yellow below, hexagonal and deposited in a flat, one layered, symmetrical, hexagonal cluster. The eggs of *T. pityocampa* and *T. wilkinsoni* are deposited around one or more pine needles or small twigs. They are deposited in one-layered cylindrical clusters. T*r. ispartaensis* eggs were observed to be white in contrast to the eggs of *T. pityocampa.*

Cedar processionary moth significantly damages *Cedrus libani*. In the spring of 1998, a notodontid moth, an outbreak of the cedar processionary moth *T. ispartaensis,* began about 400 ha in 75-year-old Lebanon cedar trees in Isparta. From 1999 to 2003, CPM larvae were present in the same stands and again caused defoliation. We identified regional outbreaks of CPM by synchronous and sustained growth periods of the trees. Growth functions were defined as the cumulative sum of radial increment. Tree ring evidence suggests that a large scale outbreak occurred in 1954 (from 1954 to 1961) and small outbreaks occurred in 1947 (1947-1951), in 1985 (1985-1988), and 1998 (1998-2003) in the study area. The average diameter growth reductions for around 1947, 1954, 1985, and 1998 were 40%, 28% 17%, and 10% of potential, respectively.

http://www.aloki.hu ● ISSN 1589 1623 (Print) ● ISSN 1785 0037 (Online)
DOI: http://dx.doi.org/10.15666/aeer/1704_91859190

T. ispartaensis population in Isparta has been observed since 1999, and an outbreak was recorded only between 1998 and 2003 (Avcı and Carus, 2005), whereas it was impossible to see even a single nest in some years such as 2012. Further studies are indeed required to understand the population dynamics of the species.

The conifers of the genus *Cedrus* seem to be associated with the summer *Thaumetopoea*, although further studies are needed to clarify the evolutionary history of the group (Basso et al., 2016).

Thaumetopoea ispartaensis belongs to the *Thaumetopoea* genus, of which four other species are wide spread in Turkey, namely *wilkinsoni*, *pityocampa*, *solitaria* and *processionea* attacking various types of plants and trees. A detailed study of the biology of the cedar processionary moth in the all stages has been presented in this study.

REFERENCES

[1] Aksoy, H., Özalp, G. (1990): Forest communities of cedar in Turkey. – Proceedings of International Cedar Symposium, 22–27 October 1990, Antalya, pp. 93-102 (in Turkish).

[2] Anonymous (2015): Turkey Forests Assets. – Republic of Turkey, Ministry of Forestry and Water Affairs, General Directorate of Forestry, Ankara, Turkey (in Turkish).

[3] Avcı, M., Carus, S. (2005): The impact of cedar processionary moth [*Traumatocampa ispartaensis* (Doğanlar & Avcı) (Lepidoptera: Notodontidae)] outbreaks on radial growth of Lebanon cedar (*Cedrus libani* A. Rich.) trees, Turkey. – J. Pest Sci. 78: 91-98.

[4] Basso, A., Simonato, M., Cerretti, P., Paolucci, P., Battisti, A. (2016): A review of the "summer" *Thaumetopoea* spp. (Lepidoptera: Notodontidae, Thaumetopoeinae) associated with *Cedrus* and *Pinus*. – Turkish Journal of Forestry 17(Special Issue): 31-39.

[5] Battisti, A., Avcı, M., Avtzis, D. N., Ben Jamaa, M. L., Berardi, L., Berretima, W., Branco, M., Chakali, G. et al. (2015): Natural History of the Processionary Moths (*Thaumetopoea* spp.): New Insights in Relation to Climate Change. – In: Roques, A. (ed.) Processionary Moths and Climate Change: An Update, Chapter 2. Springer, Dordrecht, pp. 15-79.

[6] Demolin, G. (1988): La processionaire du cedre: Thaumetopoea bonjeani (Powell), Rapport Scientifique et Rapport Iconographique-Intensification de la Protection Phytosanitaria des Forēsts, Algeria 1986-1987. – FAO-Report. FAO, Rome.

[7] Doğanlar, M., Avcı, M. (2001): A new species of *Traumatocampa* Wallengren (Lepidoptera: Thaumetopoeidae) feeding on cedar from Isparta (Turkey). – Tr. J. of Ent. 25(1): 19-22.

[8] El Yousfi, M. (1989): La processionaria del cedro, *Thaumetopoea bonjeani* (Powell). – Bol. Sanidad. Veg. Plagas. 15: 43-46.

[9] Evcimen, B. S. (1963): The yield, economic important and management basis of the Lebanon cedar forests. – OGM Publ. no: 355/16. Ankara, Turkey (in Turkish with English summary).

[10] Kiriakoff, G., Talhouk, A. S. (1975): *Thaumetopoea libanotica* spec. nov. (Lepidoptera: Thaumetopoeidae). – Opusc. Zool. (Munich) 137: 1-5.

[11] Mouna, M., Fabre, J. P. (2005): Pests Insects of Cedars: *Cedrus atlantica* Manetti, *C. libani* A. Richard and *C. brevifolia* Henry in the Mediterranean Area. – In: Lieutier F., Ghaioule, D. (eds.) Entomological Research in Mediterranean Forest Ecosystems. INRA Editions, Paris, pp. 89-104.

[12] Nemer, N., Najem, M., Ezzedine, S., Frerot, B. (2018): Insights on the *Thaumetopoea* species in Lebanon and identification of *Thaumetopoea libanotica* sexual pheromone. – First Meeting Working Group (Processionary moth), 05-08 December, Hammamet, Tunisia.

http://www.aloki.hu ● ISSN 1589 1623 (Print) ● ISSN 1785 0037 (Online)
DOI: http://dx.doi.org/10.15666/aeer/1704_91859190

LEACHING TREATMENT METHOD OF PETROLEUM HYDROCARBON POLLUTION IN FARMING LAND FOR ECOLOGICAL PROTECTION IN CHINA

SHANG, Z. X.[1,2] – ZHENG, X. L.[1*] – MA, Y. F.[2]

[1]*College of Environmental Science and Engineering, Ocean University of China*
Qingdao, Shandong Province, China

[2]*School of Resources and Environmental Engineering, Shandong University of Technology*
Zibo, Shandong Province, China
(phone: +86-13964398213)

[*]*Corresponding author*
e-mail: Understand27@163.com

(Received 21st Mar 2019; accepted 24th May 2019)

Abstract. Ectopic elution is a commonly used method for remediation of petroleum hydrocarbon contaminated soil. In the work, surfactant was used to wash petroleum hydrocarbon contaminated soil. Then, we investigated the effects of different surfactant combination ratio and concentration, the auxiliary concentration and temperature on the removal efficiency of petroleum hydrocarbon pollutants. The results showed that the oil solubilization capacity of Tw-80 was higher than that of SDS (Sodium dodecyl sulphate, SDS), and the removal rate of oil was the highest when the compound ratio of SDS/Tw-80 was 50-60. With the increase of surfactant concentration and temperature, the oil removal rate increased. The increase of alkaline solution was in favour of heavy oil separation and removal of tricyclic aromatic compounds. Sodium chloride, calcium chloride and magnesium chloride reduced the removal rate of oil, while sodium sulfate, sodium bicarbonate, sodium bicarbonate, sodium silicate and sodium phosphate increased the removal rate of oil.
Keywords: *ecological protection, petroleum hydrocarbon contaminated soil, surfactant, elution treatment, oil removal rate*

Introduction

During the drilling, exploitation and transportation process of petroleum, the pollutants are released into the surrounding soil environment due to dropping and leaking, which changes the physical and chemical properties of soil. It is difficult to grow for Crops and surface vegetation, causing significant damage to the ecological environment. In particular, aromatic substances, which are more toxic to petroleum, can accumulate in crops and threaten human through the food chain (Kim et al., 2017). At present, soil excavation, soil steam extraction, extraction, bioremediation and elution are the main removal methods of petroleum hydrocarbons in soil (Åslund et al., 2013; Dong et al., 2015; Kim et al., 2017). Soil excavation is to excavate the contaminated soil and then cover with fresh, unpolluted soil. It is suitable for the small-scale polluted areas as well as the subsequent treatment of excavated soil. As people usually use incineration method, the cost of pollution treatment is very high. Soil steam extraction has a good effect on high vapor pressure compounds (e.g., hydrocarbons), rather than on non-volatile organic compounds such as polyaromatic hydrocarbons and polychlorinated biphenyls (PCBs) (Mota et al., 2015; Mauko et al., 2018).

Bioremediation is more challenging when petroleum is mixed with water. The easy-to-degrade substance has good treatment effect, but the effect is not significant for the

http://www.aloki.hu ● ISSN 1589 1623 (Print) ● ISSN 1785 0037 (Online)
DOI: http://dx.doi.org/10.15666/aeer/1704_91919204

organic matter that is not easy to be biodegraded by oxygen. The leaching method includes the traditional pump extraction and the surface active agent solution leaching developed in recent years. Due to the low solubility of petroleum pollutants in water, the ideal effect cannot be achieved by the traditional pump leaching method with clean water.

In comparison, the heterotopic elution of surfactant has advantages, such as low energy consumption, small equipment investment, simple process, wide application range, fast speed and waste reduction. It has been widely studied in Europe, America and Japan, applied to remediation of organic matter, heavy metals and radioactive contaminated soil (Arauzo et al., 2015). However, the methods of surface active agent heterotopic elution for remediation of petroleum-contaminated soil are limited to laboratory research, large-scale and flexible soil elution equipment.

The work used an anionic-Nonionic surfactant to elute oil-contaminated soil, and investigated the effects of various operating conditions on the removal rate of petroleum as well as the mechanism of action. Some technical supports were provided for the remediation of petroleum contaminated soil with surfactant elution. This investigation, concerning the effect of solubilizing petroleum with single surfactant and compound surfactant, was to determine the necessary operating conditions of surfactant elution experiment by single factor experiment. Besides, we studied the influence factors of complex surfactant elution on remediation of petroleum contaminated soil, the samples before and after leaching by three-dimensional fluorescence spectroscopy, and the changes of petroleum components in the soil before and after treatment.

Mechanism of action

Mechanism of synergism of surfactants

Subheading

Surfactant (surface active agents) refers to a class of substances that can significantly reduce solvent surface tension and liquid-liquid interfacial tension. It has certain structure, hydrophilic and oil-friendly properties and special adsorption (Arauzo et al., 2015). When the concentration of surfactant in water is low, it exists in the form of monomer in water and adsorbs at the water-gas interface. The increase of its concentration in water leads to the increased adsorption of surfactant at the water-gas interface. As a result, the interfacial tension between water and gas decreases. The hydrophobic part of the surfactant molecule interacts with each other to form the association in the solution, namely the concentration of micelle (micelle). Surfactant forms a micelle in water, which is the CMC (critical micelle concentration). CMC is an important index to measure the properties of surfactants. In CMC, surfactant solutions have the lowest interfacial tension and can dissolve insoluble petroleum pollutants (Arauzo et al., 2015) (See *Fig. 1*).

At present, most researchers believe that surfactants remove petroleum pollutants from soil through the following mechanisms (Elazhari-Ali et al., 2013; Akinlua et al., 2015; Gao et al., 2016; Brown et al., 2017), curling (rollup) and solubilizing (solubilization). Generally, surfactants below or above CMC can improve the removal of petroleum pollutants in soil. Therefore, the mechanism of shrinkage and solubilization functions.

http://www.aloki.hu ● ISSN 1589 1623 (Print) ● ISSN 1785 0037 (Online)
DOI: http://dx.doi.org/10.15666/aeer/1704_91919204

Surfactant solubilization mechanism

Solubilization refers to the situation that the insoluble petroleum pollutants adsorbed by the soil are desorbed from the soil under the action of surfactants and distributed to the water phase. It depends on the formation of the insoluble organic pollutants in the micellar phase of the aqueous solution by the surfactants. Solubilization usually occurs above the critical micelle concentration due to a large number of surfactant micelles formed in aqueous solution (Jha et al., 2018).

There are lots of studies about the solubilisation of PAH (polycyclic aromatic hydrocarbon, PAH) and other insoluble organic pollutants by surfactants (Li et al., 2014; Yang et al., 2015; Janajreh et al., 2018). Edwards et al. focused on the solubilization of PAHs by Brij30, Igepal CA-720, Tergitol NP-10 and Triton X-100 (Mortazavi et al., 2013; Fallah et al., 2015). The concept of molar solubilization ratio (Molar Solubilization Ratio, MSR) is proposed to describe the solubilization of surfactant solution quantitatively, as shown in *Eq.(1)*.

$$MSR = (S - S_{cmc})P(C_s - C_{mcm}) \quad \text{(Eq.1)}$$

where C_s and C_{cmc} are the concentrations of surfactant solution greater than/equal to CMC, respectively; S and S_{cmc} in CMC are the apparent solubilities of organic matter when the surfactant concentrations are C_s and C_{cmc}.

Another quantitative description of solubilization of surfactants is the partition coefficient (K_{mc}) of micelle phase P-water phase, as shown in *Eq.(2)*.

$$K_{mc} = X_{mc}PX_a \quad \text{(Eq.2)}$$

where X_{mc} is the molar fraction of organic matter in the micellar phase, which can be calculated by using *Eq.(3)*.

$$X_{mc} = (S - S_{cmc})P(C_s - C_{cmc} + S - S_{cmc}) \quad \text{(Eq.3)}$$

Parameter X_a is the molar fraction of organic matter in the aqueous phase. In dilute solution, V_w is the molar volume of water (0.101805 L/mol), so we can obtain *Eq.(4)*.

$$K_{mc} = 5514\,MSRP[S_{cmc}(1 + MSR)] \quad \text{(Eq.4)}$$

Experiment

Experimental materials

According to the situation of China's Tarim oil and gas field and its surrounding areas, we considered the complex composition of drilling mud and the uneven distribution properties of surrounding desert sand, to make sure the representativeness of the collected mud and surrounding desert sand samples. In the 1 m^2 sample plot the sample was evenly distributed and the water-based mud of 10 wells in the 1 m^2 plot and the sand layer of 0-20 cm in the surrounding 10 m area were collected. A total of 12 water-based mud samples and sand analysis samples were collected. Mud samples were stored in cold storage until analysis, and confined storage reduced the volatilization and interference from the surrounding environment. The soil samples were processed within

http://www.aloki.hu ● ISSN 1589 1623 (Print) ● ISSN 1785 0037 (Online)
DOI: http://dx.doi.org/10.15666/aeer/1704_91919204

14 days of pre-treatment, and the extract analysis was completed within 40 days. After mixing the soils, dry naturally at room temperature, and remove the residual roots, plastics and other debris. Then, grind with a mortar, and sift over 100 meshes. Finally, store it in a brown wide-mouth bottle. Some physical and chemical properties of the soil are determined (See *Table 1*).

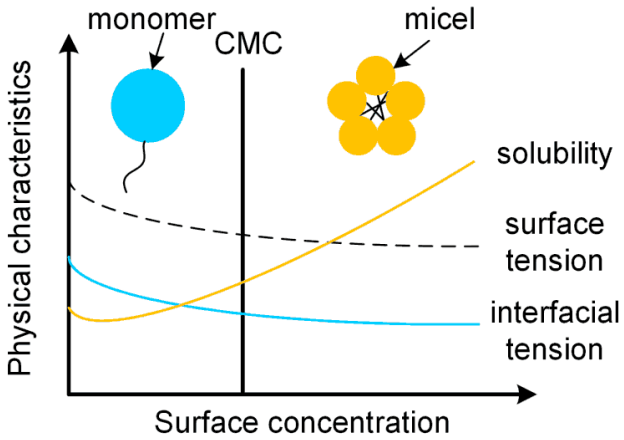

Figure 1. *Surface tension, Interfacial tension and Pollutant Solubility changes with Surfactant concentration*

Table 1. *Physical and chemical parameters of soils used (TOC is the total organic carbon, and TPH is the total petroleum hydrocarbons in soil)*

pH	Rate of water content (%)	Salt content (%)	TOC (g/kg)	TPH (%)
7.41	1.09	0.43	3.21	0.05

Experimental content

Preparation of petroleum-contaminated soil samples

At first, some crude oil was taken and dissolved by dichloromethane. Then, some spare soil was put into the beaker. The solid-liquid mixture was stirred by a glass rod. Finally, the solvent of the mixture was evaporated in the ventilating cabinet and simulated soil sample was obtained.

Method for determination of petroleum in soil

The concentration of petroleum in the solution was determined by ultraviolet spectrophotometry. Crude oil was used to prepare 1.0 g/L standard solution with dichloromethane as solvent. The standard solution was diluted by UV spectrophotometer (HACH-DR6000), and scanned in the wavelength range of 200-400 nm.

Weigh 0.1 g of petroleum in a beaker, and dissolve it in dichloro-A hospital. Then, transfer it to 100 mL volume bottle and set volume. The standard oil storage solution concentration is 1,000 mg/L. The solution was taken from 5 mL volume bottle to 25 mL volume bottle with the fixed volume. The oil concentration was 200 mg/L; 0. 4, 0.8, 1.2, 1.6, 2 and 10 mL colorimetric tubes were removed, and the volume was fixed to the

http://www.aloki.hu ● ISSN 1589 1623 (Print) ● ISSN 1785 0037 (Online)
DOI: http://dx.doi.org/10.15666/aeer/1704_91919204

mark line. The standard solutions for this series of concentrations were 8,16,24,32 and 40 mg/L.

The oil contents of the eluted soil and the original soil were used to calculate the removal rate, as given by *Eq.(5)*.

$$R = \left[1 - \frac{(A-B)*N*25*100}{K*1000*1000*2w}\right]*100\% = \left[1 - \frac{(A-B)*N}{800Kw}\right]*100\% \quad \text{(Eq.5)}$$

where R is the removal rate; A the absorbance; $A=K\times B$ is the standard curve; N the dilution multiple; w the oil content of the oily soil sample.

Solubilization test

Mix the 0.1 g petroleum and 50 mL surfactant solution with different concentration and its compound solution (50:1) into a 100 mL plug cone bottle and oscillate at a constant temperature oscillator at 25°C for 5 h at a speed of 150 r/min. After the solution was quiesced in the funnel for 2 h, the lower part of the solution was removed for 10 mL. Dichloromethyl chloride was used to extract, with ultraviolet spectrophotometry used to determine the concentration of petroleum in the solution. The solubilization effect is calculated by *Eqs.(1), (2), (3) and (4)*.

Influencing factors of leaching repair

a. Complex proportion

2.5 g oily soil sample containing 5% oil was put into a 100 mL plug conical bottle. The compound ratios (SDS: Tw-80) of 4 g/L were10: 1, 20: 1, 30: 1, 40: 1, 50: 1, 60: 1.70: 1.80: 1.90: 1 and 100: 1 for 50 mL. The sample was placed on the constant temperature oscillator at 25°C for 1 hour at the rate of 150 r/min. After stilling for 10 min, the supernatant was discarded, and the soil was set at 105°C for 1 h. After cooling, 2.0 g was added to 20 mL dichloromethane, and then put into an ultrasonic cleaner. The temperature was adjusted to 30°C, with extraction for 15 min. The extractive was poured into 50 mL centrifugation tube, and the supernatant was collected at 4,000 r/min rotating speed for 5 min. The volume of the supernatant was fixed, with the measured absorbance and the calculated oil removal rate.

b. Surfactant concentration

The concentration of surfactant solution was 0, 1, 2, 3, 4, 5 and 6 g/L, respectively. Other operating conditions were referred to *Eq.(1)*.

c. Leaching temperature

Run the constant temperature oscillator, and adjust the temperature to 10, 20, 25, 30, 40, 50 and 60°C. Other operating conditions refer to *Eq.(1)*.

d. PH value of the solution

The soil sample containing 5% oil was put into 100 mL plug conical bottle, added with surfactant solution. The pH value of the solution was adjusted to 3, 5, 7, 9 and 11 with sodium hydroxide and hydrochloric acid solution, respectively. Other operating conditions were referred to *Eq.(1)*.

e. Effect of adding inorganic salts

Add different concentrations of sodium chloride, calcium chloride, magnesium chloride, sodium sulfate, sodium bicarbonate, sodium silicate and sodium phosphate surfactant solutions. Other operating conditions refer to *Eq.(1)*.

http://www.aloki.hu ● ISSN 1589 1623 (Print) ● ISSN 1785 0037 (Online)
DOI: http://dx.doi.org/10.15666/aeer/1704_91919204

Results and discussions

Method for determination of petroleum in soil

The UV spectrophotometer was used to select the standard solution of 254 nm in the wavelength range of 200-400 nm. The standard curve for the experiment is given in *Figure 2*. The oil removal rate was calculated by *Eq.(5)*. In *Figure 3*, 284/336 nm is the excitation/emission peak corresponding to light oil, and 256/360 nm heavy oil corresponding excitation/emission peak.

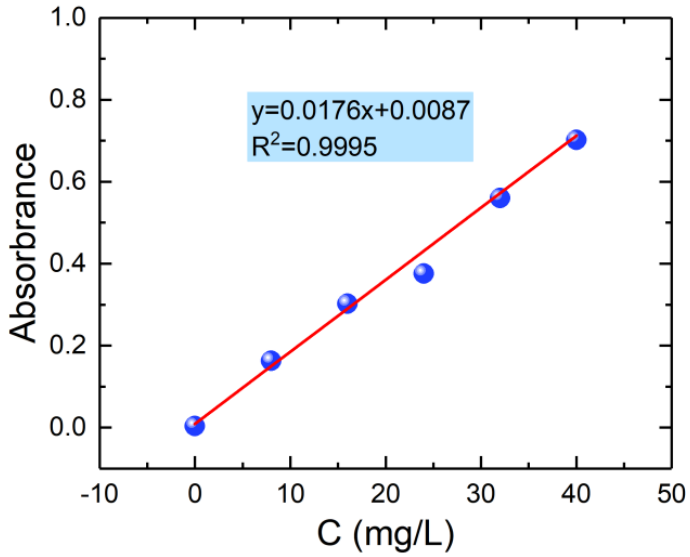

Figure 2. *Standard curves for experiments*

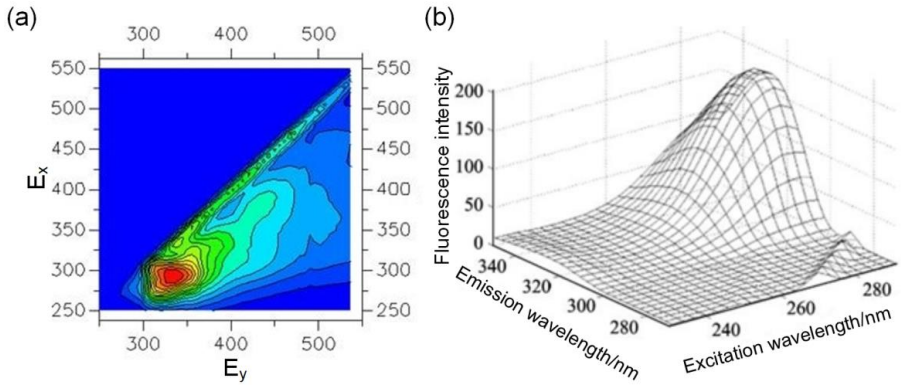

Figure 3. *Three-dimensional fluorescence analysis of crude oil*

The emission wavelength of 325 nm is equivalent to a ring, a binary aromatic compound (abbreviated as one, two rings), a 350 nm equivalent to a binary ring, a tricyclic aromatic light compound (hereinafter referred to as Bicyclic), and a tricyclic aromatic compound (tricyclic) of 375 nm, that equals to the tricyclic aromatic compound (tricyclic) (Lu et al., 2014; Meshram et al., 2017).

The content of heavy oil in crude oil was higher than that of light oil, and the content of tricyclic aromatic hydrocarbon in aromatic hydrocarbon was the highest. Compared

http://www.aloki.hu ● ISSN 1589 1623 (Print) ● ISSN 1785 0037 (Online)
DOI: http://dx.doi.org/10.15666/aeer/1704_91919204

with crude oil, the light intensity of light oil and aromatics under tricyclic ring decreased significantly in undried soil samples. In the preparation of soil samples, the light oil and aromatic hydrocarbon components under tricyclic ring migrated to the atmosphere due to their natural volatilization. The components of light oil were volatile in the preparation of samples, but the components of heavy oil were not easy to volatilize. Compared with the undried soil samples, the fluorescence intensity of light oil components of contaminated soil samples decreased slightly after drying, while the light burst intensity of heavy oil components decreased obviously. The possible reason was that the light intensity of the heavy oil group was lower than that of non-dried soil samples. Components were converted into volatile substances when dried at high temperatures.

Solubilization test

Figure 4 shows the solubilization effect of the mixture of two surfactants on petroleum in the selected mass concentration range. According to the literature, the solubilization capacity of Tw-80 is higher than that of SDS, and the solubilization effect of the compound surfactant is close to that of SDS (Shi et al., 2013; Enright et al., 2017).

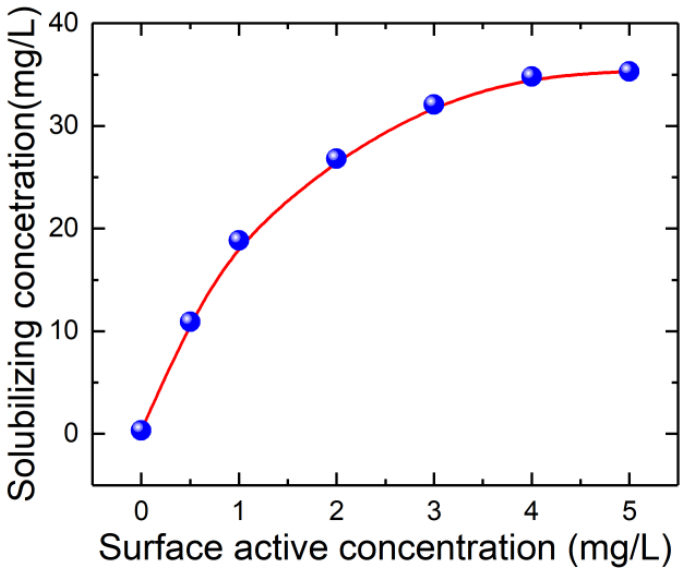

Figure 4. *Solubilization curve of SDS/Tw-80 after blending*

However, the amount of SDS used is reduced by one time, indicating that the complex surfactant can improve the solubilization of the surfactant to solubilize petroleum. Therefore, the compound surfactant is used to carry on the petroleum elution experiment.

Factors affecting leaching repair

Compound proportion

Figure 5 shows the effect of complex ratio on the removal of petroleum from surfactant solution. It is evident that as the ratio of SDS and Tw-80 increases, the effect of the ratio of the compound on the oil removal rate increases first and then becomes

http://www.aloki.hu ● ISSN 1589 1623 (Print) ● ISSN 1785 0037 (Online)
DOI: http://dx.doi.org/10.15666/aeer/1704_91919204

smaller. This is because the interaction between the two compounds can be found when the ratio is around 50, and the effect of the compound ratio on the decreasing rate is the highest. According to *Figure 6*, when the ratio of SDS and Tw-80 is 50-60, the oil removal rate reaches the maximum. The anion surfactant SDS is electronegative in the solution, not easy to be adsorbed by the soil. While the Nonionic surfactant Tw-80 is not ionized in the solution, it is electro neutral, easy to be adsorbed by the soil with negative charge.

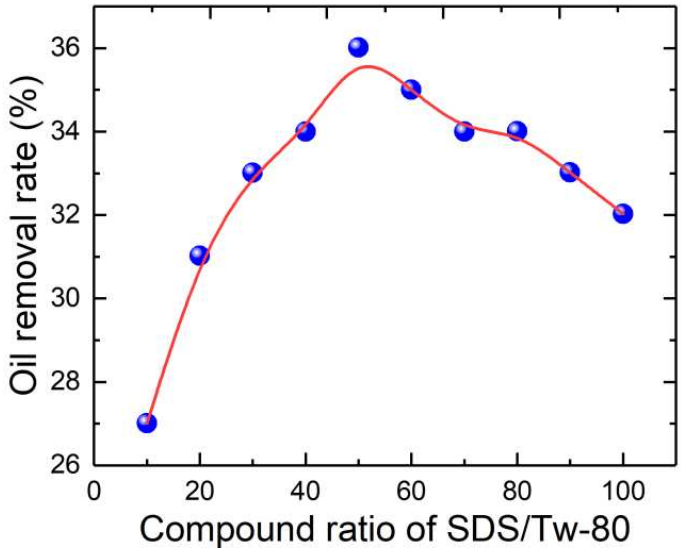

Figure 5. *Effect of compound proportion on oil Removal rate*

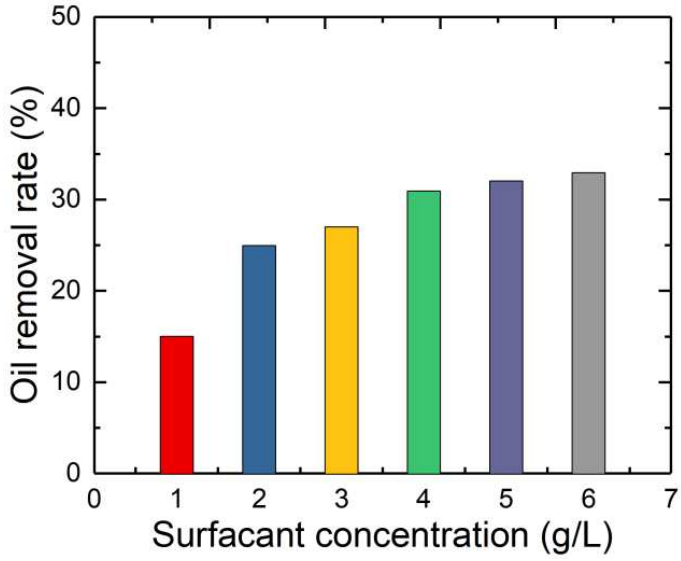

Figure 6. *Effect of surfactant concentration on oil Removal rate*

With the SDS, the weak intermolecular interaction of Tw-80 is replaced by the interaction between hydrophilic ion dipoles to form mixed micelles (Carbone et al., 2013), which can reduce the soil adsorption, ensure the effective mass concentration

http://www.aloki.hu ● ISSN 1589 1623 (Print) ● ISSN 1785 0037 (Online)
DOI: http://dx.doi.org/10.15666/aeer/1704_91919204

and improve the oil removal rate. Besides, for nonionic surface activity in complex surfactants, the larger proportion of the surfactant means the smaller CMC and the higher removal rate (Elazhari-Ali et al., 2013). Moreover, the CMC (2.5 g/L) of SDS is much larger than that of Tw-80 (0.013 g/L). The increased ratio of SDS to surfactant increases the critical micelle concentration of surfactant, which leads to the decrease of oil removal rate inthe same concentration. The compound ratio of SDS/Tw-80 selected in the experiment was 50:1.

Surfactant concentration

Figure 6 shows the effect of surfactant concentration on oil removal by elution. With the increased surfactant concentration, the oil removal rate increases. When the removal rate is larger than 4 g/L, the removal rate of the easily desorbed oil component in the soil will be washed down, and the removal rate will no longer increase (Gros et al., 2014). Excessive use can lead to a waste of chemicals and secondary soil pollution. Therefore, the optimum concentration of surfactant for remediation of contaminated soil should be considered based on the economy and environmental protection. The concentration selected in the experiment was 4 g/L.

Leaching temperature

Based on *Figure 7*, we speculate that the temperature has a significant effect on the oil removal rate and the removal rate increases with the increase of temperature. High temperature has following advantages: enhancing the fluidity of oil, weakening the adhesion force of soil, providing the energy needed for desorption, and promoting desorption of oil.

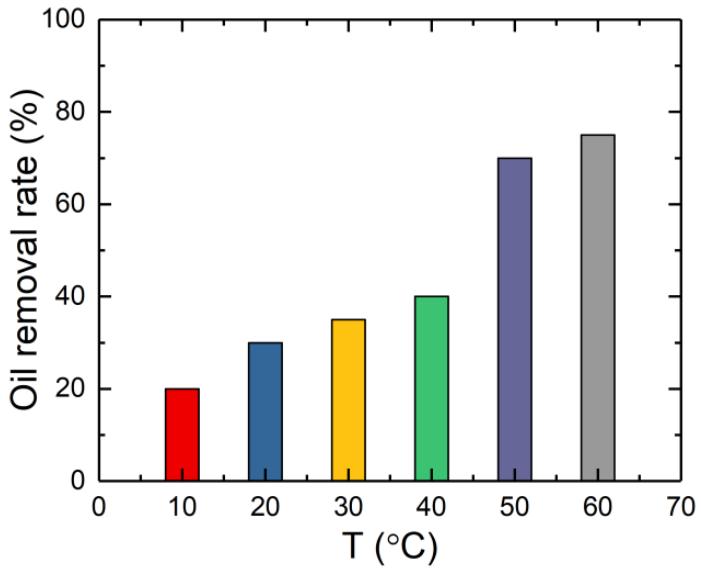

Figure 7. *Effect of leaching temperature on oil Removal rate*

The increase of temperature prevents the adsorption of Tw-80, and the increased solubility of SDS by soil is beneficial to the formation of micelles. However, if the temperature is too high, the surface activity and solubility of nonionic surfactants will

http://www.aloki.hu ● ISSN 1589 1623 (Print) ● ISSN 1785 0037 (Online)
DOI: http://dx.doi.org/10.15666/aeer/1704_91919204

be decreased, with the reduced oil removal rate. With the high temperature, the energy consumption increases, so the appropriate temperature should be chosen according to the repair concrete condition. The work studied the remediation of petroleum contaminated soil by surfactant at room temperature, with the experimental temperature of 25°C.

Solution pH

Figure 8 shows the effect of pH value on the removal of petroleum by surfactant solution leaching. The removal rate of petroleum increases with the increased pH value. The increase of the alkalinity of solution leads to the increased negative charge of the soil particles, the increased repulsion between surfactant molecules and the soil, and the decreased adsorption of the soil. In addition, the alkaline substance in surfactant solution can react with the acid substance in petroleum to form salts, which increases the water solubility of petroleum. Some components have certain surface activity, which can improve the removal rate of petroleum. Furthermore, the increase of pH in surfactant solution reduces the interfacial tension.

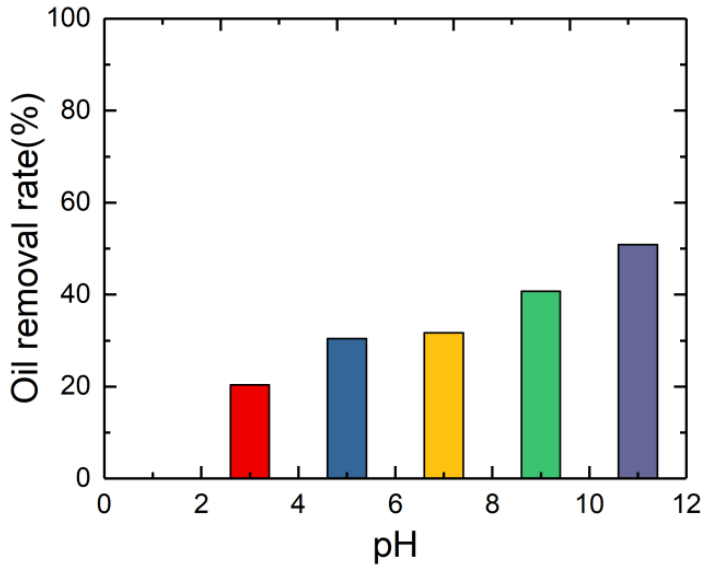

Figure 8. *Effect of PH value of solution on oil deoiling rate(PH is hydrogen ion concentration)*

Effect of adding inorganic salts

Figures 9 and *10* indicate the effect of inorganic salts on the removal of petroleum from surfactant solution. *Figure 9* shows that with the increase of concentration, sodium chloride, Korea chloride (In the field of inorganic chemistry, it is a salt compound formed by the combination of a negatively charged chloride ion and a positively charged cation of another element.) and magnesium chloride reduce the oil removal rate. *Figure 10* shows the oil removal rate is increased by sodium sulfate, sodium bicarbonate, sodium cinnamate and sodium phosphate.

SDS ionizes in the water can produce CI2H25O-SO3-, energy and Ca^{2+}, Mg^{2+} and form precipitation. Sodium ion produced by sodium chloride ionization can increase the diffusion double layer of the ionic micelle and improve the activity of surfactant. However, it exchanges calcium ion from the soil, reducing the effective active

http://www.aloki.hu ● ISSN 1589 1623 (Print) ● ISSN 1785 0037 (Online)
DOI: http://dx.doi.org/10.15666/aeer/1704_91919204

substances of SDS and destroying the compound system. The addition of calcium chloride and magnesium chloride not only leads to the formation of precipitation of SDS directly, but also interacts with soil, block the void of soil and hinder the transfer of oil to surfactant solution. Although sodium sulfate brings a large number of sodium ions, but sulfate provides a lot of negative charges, and reduces the adsorption of surfactant, surface tension of surfactant solution and interfacial tension between oil and water.

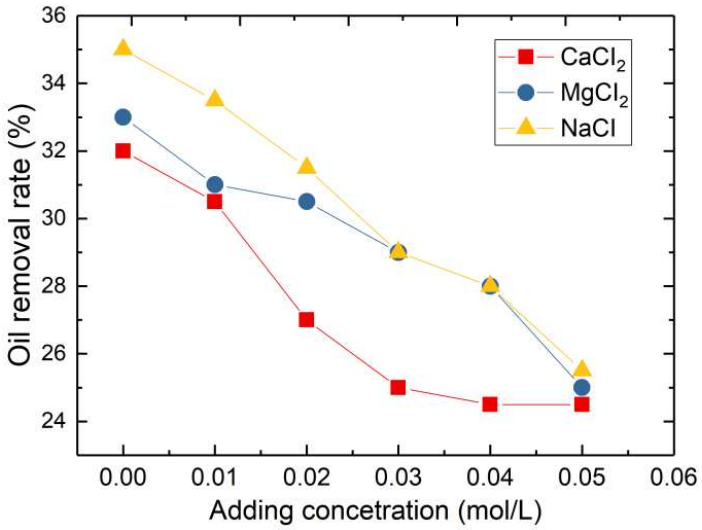

Figure 9. *Effect of adding inorganic salts such as sodium chloride, calcium chloride and magnesium chloride on oil deoiling rate*

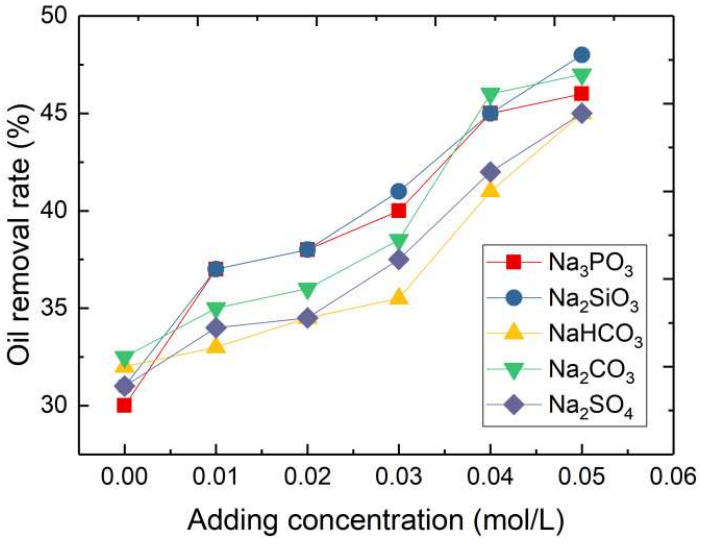

Figure 10. *Effect of adding inorganic salts such as sodium sulfate, sodium bicarbonate, sodium silicate and sodium phosphate on oil deoiling rate*

Finally, the solubilization of surfactants is improved. Sodium carbonate, sodium bicarbonate, sodium WaaS and sodium phosphate are all strong alkali and weak acid

http://www.aloki.hu ● ISSN 1589 1623 (Print) ● ISSN 1785 0037 (Online)
DOI: http://dx.doi.org/10.15666/aeer/1704_91919204

salts. Hydrolysis makes surfactant solution alkaline, which is beneficial to the removal rate of petroleum. The cation produced by ionization of three inorganic salts can precipitate with the continuous ion in the solution and reduce the negative effect of the hardness ion. In addition, sodium silicate and its hydrolysate can be adsorbed on the surface of soil particles to form a protective film, thus preventing the desorbed oil from being adsorbed again by the soil. Although the above inorganic salts can bring about the precipitation effect of sodium ions, the positive effects of these inorganic salts on the improvement of removal rate are more evident than these adverse effects. On the whole, these inorganic salts play an essential role in promoting oil elution.

According to the above figures, the results of the solidified oil-containing soil and the directly solidified product leachate are quite different. A series of surfactants and composite surfactants were used to determine the oil solubilisation and single factor experiments to determine the surfactant elution. The results showed that the anionic-nonionic surfactant was used to elute oil-contaminated soil. The method is better than the previous method and has superior performance. It can provide some technical support for surfactant elution and oil-contaminated soil.

Conclusions

Based on the ecological protection, the work discussed the method of petroleum hydrocarbon pollution leaching in farming land, and used the ex-situ leaching for soil remediation. In terms of the solubilization, a series of comparative experiments were established to analyse the effects of concentration and ratio of surfactant concentration as well as the addition of additives on the leaching. The following conclusions are obtained.

a. The oil solubilization of Tw-80 was higher than that of SDS. The removal rate of SDS/Tw-80 complex surfactant solution increased first and then decreased with the increase of SDS ratio. The maximum value was obtained when the compound ratio ranged from 50 to 60. From the oil elution effect, economy and benefit to experiment, 1h was selected as the oscillation time.
b. The higher the surfactant concentration was, the higher the oil removal rate was. When the surfactant concentration was higher than 4 g/L, the oil removal rate increased slowly. In the range of 10 to 60°C, the temperature had a significant effect on the removal rate of petroleum in contaminated soil. The removal rate increased with the increase of temperature. The high temperature was beneficial to the removal of polycyclic aromatic hydrocarbons (PAHs). Alkaline environment was good for the removal of petroleum, heavy oil components and tricyclic aromatic compounds.
c. The addition of inorganic salts affected the oil elution with surfactants. Sodium chloride, calcium chloride and magnesium chloride reduced the removal rate of oil, while sodium sulfate and sodium bicarbonate reduced the removal efficiency of oil eluted by sodium chloride, calcium chloride and magnesium chloride. Sodium silicate and sodium phosphate increased the removal rate of oil eluted.
d. According to experimental results, it can be concluded that the anion-nonionic surfactant proposed in this paper is better than the previous method, and can provide better technical support for surfactant elution and oil-contaminated soil.

http://www.aloki.hu ● ISSN 1589 1623 (Print) ● ISSN 1785 0037 (Online)
DOI: http://dx.doi.org/10.15666/aeer/1704_91919204

REFERENCES

[1] Akinlua, A., Jochmann, M. A., Schmidt, T. C. (2015): Ionic Liquid as Green Solvent for Leaching of Polycyclic Aromatic Hydrocarbons from Petroleum Source Rock. – Industrial & Engineering Chemistry Research 54(51): 12960-12965.

[2] Arauzo, M., Martínez-Bastida, J. J. (2015): Environmental factors affecting diffuse nitrate pollution in the major aquifers of central Spain: groundwater vulnerability vs. groundwater pollution. – Environmental Earth Sciences 73(12): 1-16.

[3] Arauzo, M., Valladolid, M. (2015): Drainage and N-leaching in alluvial soils under agricultural land uses: Implications for the implementation of the EU Nitrates Directive. – Agriculture Ecosystems & Environment 179(5): 94-107.

[4] Åslund, M. W., Stephenson, G. L. (2013): Comparison of earthworm responses to petroleum hydrocarbon exposure in aged field contaminated soil using traditional ecotoxicity endpoints and (1) H NMR-based metabolomics. – Environmental Pollution 182: 263-268.

[5] Brown, D. M., Okoro, S., Van, G. J. (2017): Comparison of landfarming amendments to improve bioremediation of petroleum hydrocarbons in Niger Delta soils. – Science of the Total Environment 596-597: 284-292.

[6] Carbone, C., Dinelli, E., Marescotti, P. (2013): The role of AMD secondary minerals in controlling environmental pollution: Indications from bulk leaching tests. – Journal of Geochemical Exploration 132(3): 188-200.

[7] Dong, W., Lin, X., Du, S. (2015): Risk assessment of organic contamination in shallow groundwater around a leaching landfill site in Kaifeng, China. – Environmental Earth Sciences 74(3): 2749-2756.

[8] Elazhari-Ali, A., Singh, A. K., Davenport, R. J. (2013): Biofuel components change the ecology of bacterial volatile petroleum hydrocarbon degradation in aerobic sandy soil. – Environmental Pollution 173(1): 125-132.

[9] Enright, E. F., Joyce, S. A., Gahan, C. G. M. (2017): Impact of Gut Microbiota-Mediated Bile Acid Metabolism on the Solubilization Capacity of Bile Salt Micelles and Drug Solubility. – Mol Pharm 14(4): 1251-1263.

[10] Fallah, M., Shabanpor, M., Ebrahimi, S. (2015): Evaluation of petroleum impacts on some properties of loamy sand soil with the main focus on hydraulic properties. – Environmental Earth Sciences 74(6): 4751-4762.

[11] Gao, S. S., Xu, P., Zhou, F. (2016): Quantifying nitrogen leaching response to fertilizer additions in China's cropland. – Environmental Pollution 211(211): 241-251.

[12] Gros, J., Reddy, C. M., Aeppli, C. (2014): Resolving biodegradation patterns of persistent saturated hydrocarbons in weathered oil samples from the Deepwater Horizon disaster. – Environmental Science & Technology 48(3): 1628-1637.

[13] Janajreh, I., Alshehi, A. (2018): Anaerobic co-digestion of petroleum hydrocarbon waste and wastewater treatment sludge. – International Journal of Hydrogen Energy: 1-12.

[14] Jha, S. K., Ahmad, Z., Crowley, D. E. (2018): Fuzzy-genetic approaches for estimation of microbial rock phosphate solubilization in sandy clay loam textured soil. – Computers & Electronics in Agriculture 150: 125-133.

[15] Kim, J., Lee, A. H., Chang, W. (2017): Enhanced bioremediation of nutrient-amended, petroleum hydrocarbon-contaminated soils over a cold-climate winter: The rate and extent of hydrocarbon biodegradation and microbial response in a pilot-scale biopile subjected to natural seasonal freeze-thaw temperatures. – Science of the Total Environment 612: 903-910.

[16] Li, X., Wang, X., Zhang, Y. (2014): Extended petroleum hydrocarbon bioremediation in saline soil using Pt-free multianodes microbial fuel cells. – Rsc Advances 4(104): 59803-59808.

[17] Li, J., Jia, C., Ying, L. (2015): Multivariate analysis of heavy metal leaching from urban soils following simulated acid rain. – Microchemical Journal 122(9): 89-95.

http://www.aloki.hu ● ISSN 1589 1623 (Print) ● ISSN 1785 0037 (Online)
DOI: http://dx.doi.org/10.15666/aeer/1704_91919204

[18] Lu, L., Huggins, T., Jin, S. (2014): Microbial metabolism and community structure in response to bioelectrochemically enhanced remediation of petroleum hydrocarbon-contaminated soil. – Environmental Science & Technology48(7): 4021-4026.
[19] Ma, J., Deng, Y., Yuan, T., Zhou, J., Alvarez, P. J. J. (2015): Succession of microbial functional communities in response to a pilot-scale ethanol-blended fuel release throughout the plume life cycle. – Environmental Pollution 198: 154-160.
[20] Mauko, A. P., Oprčkal, P., Mladenovič, A. (2018): Comparative Life Cycle Assessment of possible methods for the treatment of contaminated soil at an environmentally degraded site. – Journal of Environmental Management 218: 497-508.
[21] Meshram, P., Pandey, B. D., Mankhand, T. R. (2014): Extraction of lithium from primary and secondary sources by pre-treatment, leaching and separation: A comprehensive review. – Hydrometallurgy 150: 192-208.
[22] Mortazavi, B., Horel, A., Beazley, M. J. (2013): Intrinsic rates of petroleum hydrocarbon biodegradation in Gulf of Mexico intertidal sandy sediments and its enhancement by organic substrates. – Journal of Hazardous Materials 244-245(2): 537-544.
[23] Mota, I. D. O. D., Castro, J. A. D., Rui, D. G. C. (2015): Study of electroflotation method for treatment of wastewater from washing soil contaminated by heavy metals. – Journal of Materials Research & Technology 4(2): 109-113.
[24] Shi, Z., Chen, J., Yin, X. (2013): Effect of anionic-nonionic-mixed surfactant micelles on solubilization of PAHs. – J Air Waste Manag Assoc 63(6): 694-701.
[25] Yang, X., Yuan, X., Zhang, A. (2015): Spatial distribution and sources of heavy metals and petroleum hydrocarbon in the sand flats of Shuangtaizi Estuary, Bohai Sea of China. – Marine Pollution Bulletin 95(1): 503-512.

http://www.aloki.hu ● ISSN 1589 1623 (Print) ● ISSN 1785 0037 (Online)
DOI: http://dx.doi.org/10.15666/aeer/1704_91919204

BIOSYNTHESIS AND CHARACTERIZATION OF SILVER NANOPARTICLES USING KING OYSTER (*PLEUROTUS ERYNGII*) EXTRACT: EFFECT ON SOME MICROORGANISMS

ACAY, H.[1*] – BARAN, M. F.[2]

[1]*Department of Nutrition and Dietetic, School of Health, Mardin Artuklu University, Mardin, Turkey*

[2]*Medical Laboratory Techniques, Vocational Higher School of Healthcare Studies, Mardin Artuklu University, 47200 Mardin, Turkey*

**Corresponding author*
e-mail: hilalacay@gmail.com

(Received 21st Mar 2019; accepted 24th May 2019)

Abstract. The integration of the principles of green chemistry into nanotechnology has become one of the key issues in nanotechnology research. Metal nanoparticle production, which does not contain toxic chemicals and does not harm the environment, needs to be developed to avoid adverse effects on medical applications. In this study, *Pleurotus eryngii* (PE) extract was used for preparation of silver nanoparticles (AgNPs). The presence of AgNP was understood that after adding 1 mM silver nitrate (AgNO3) to the fungus extract, the reaction turned from the open yellow to reddish brown. The analysis of samples taken at different times with the UV-Visible Spectrophotometer (UV-Vis) confirms the formation of PE-AgNPs. The Scanning electron microscopy-Energy Dispersive X-Ray Spectrum (SEM-EDX) analysis showed that spherical nanoparticles were formed. X-ray crystallography (XRD), analysis is calculated from Debye-Sherers inequality, in which PE-AgNP synthesized in the study was 18.45 nm in size. It has been demonstrated by using the minimum Inhibitory Concentration (MIC) method in which AgNPs have strong antimicrobial activity.
Keywords: *antimicrobial activity, XRD, SEM, TGA-DTA, AgNPs, Pleurotus eryngii*

Introduction

Nanoparticles (NPs) are particles having a size of 100 nm or less. Because they have a large surface area that allows them to be used in new applications, they tend to react differently from large substances containing the same composition particles (Abou El-Nour et al., 2010). The new features that NP has gained make them versatile in many research areas such as biomedical applications, drug exploration, luminescence, cosmetics and renewable energy technologies (Chaudhuri and Paria, 2012; Tran et al., 2013; Rauwel et al., 2015). Therefore many researchers have studied the synthesis of NP using various physical and chemical methods (Remya, et al., 2017). However, it is stated that the synthesis of nanoparticles with green chemistry approaches using biological entities such as plants, fungi, bacteria, algae and actinomycetes provides additional advantages over other methods because it is simple, cost-effective, reliable, and environment-friendly. For this purpose, the use of biological synthesis approaches for many researchers is increasingly important (Kumar and Yadav, 2009).

The fact that microbial infection is a serious problem in the agriculture and healthcare sector has made it mandatory to develop new antimicrobial agents with highly versatile properties such as antimicrobial effect strength, harmonious and low toxicity. In this context, the electrostatic attraction between the positively charged NPs and the negatively charged microbial cells has received worldwide attention due to the

http://www.aloki.hu ● ISSN 1589 1623 (Print) ● ISSN 1785 0037 (Online)
DOI: http://dx.doi.org/10.15666/aeer/1704_92059214

large surface/volume ratio resulting in improved physicochemical properties of NPs and increased antimicrobial activity (Lakshmeesha et al., 2014; Kavyashree et al., 2015). Antimicrobial properties of NP's, including Antibacterial and antifungal activities, have recently been reported extensively (Mallmann et al., 2015; Salem et al., 2015; Elgorban et al., 2016).

As reported, silver antimicrobial plays a unique role in catalytic and biological systems (Nadagouda et al., 2009). The synthesis of silver nanoparticles, compared to other metals, has become more important as an antimicrobial agent against the ever-increasing threats posed by antibiotic resistant microbes (Panaek, et al., 2006; Parashar et al., 2009).

Edible fungi, flavonoids, phenolic acids, tannins and oxidized polyphenols due to numerous reducing biomolecules has attracted great attention in NP synthesis (Philip, 2009; Palacios et al., 2011). In addition, mushroom extract has a high protein content and the carbonyl group of amino acids has the ability to prevent the aggregation of NP's and thus stabilize them in aqueous solution (Al-Batal et al., 2013). Numerous reducing biomolecules, micelles that offer a large surface area for interaction, because of the enzymes they secrete is thought to increase the effect of the functional groups of the nanoparticles and make the mushrooms advantageous compared to other organic sources.

In the literature, it is stated that mushroom extracts such as Volvariella volvacea, Pleurotus sajor Caju, Pleurotus Florida, Ganoderma lucidum, Agaricus bisporus, Inonotus Obliquius were used successfully in AgNP synthesis (Nagajyothi et al., 2014). However, there was no evidence that the *Pleurotus eryngii* extract was used. In the light of the above information, it is aimed to determine AgNP synthesis, characterization and antimicrobial activity of the obtained PE-AgNP's using Pleurotus eryngii which contains many active ingredients.

Materials and methods

Macrofungus

Pleurotus eryngii used in the study was obtained from Hakkari/Turkey in April-May 2018. Diagnostic macroscopic investigations were carried out using field study on ecological structural features and 500 g samples stored in the Microbiology-Biochemistry Research Laboratory of Mardin Artuklu University.

Microorganisms

For testing antimicrobial activity; *Escherichia coli* ATCC 25922, Staphylococcus *aureus* ATCC 25923, *Streptococcus pyogenes* ATCC 19615 *Pseudomonas* aeruginosa ATCC 27853, standard bacterial strains with *Candida albicans* ATCC 10231 strains are available in the Microbiology-Biochemistry Research Laboratory of Mardin Artuklu University.

Preparation of mushroom extract

Pleurotus eryngii extract was used to prepare AgNP synthesis. The mushrooms collected from the field work, after washing with tap water, it was finally washed with distilled water. 200 g fresh sample, divided into small pieces, was boiled in 90 °C in distilled water 1000 ml. It was then cooled at room temperature and used in the AgNPs synthesis after filtration with Whatman No. 1 Filter paper (Acay et al., 2019).

http://www.aloki.hu ● ISSN 1589 1623 (Print) ● ISSN 1785 0037 (Online)
DOI: http://dx.doi.org/10.15666/aeer/1704_92059214

Synthesis of PE- AgNPs

Generally, the color change in the synthesis of AgNPs is determined by time-dependent UV-vis spectrophotometry measurements (Pugazhendhi et al., 2018). Therefore 1 mM AgNO3 solution is prepared. The Extract and solution were mixed at the rate of 1:5 and the colour change at room temperature was expected to occur. Reduction of the silver ions was observed to change the white colored solution to dark brown. The resulting dark-colored solution is centrifuged 5 min at 10000 rpm to remove the upper liquid phase and wash with distilled water until the remaining solid was clear. The obtained AgNPs were left to dry in the oven at 65 °C for 48 h and then allowed to dry and stored for characterization.

Characterization of silver nanoparticles

The characterization of silver nanoparticles was carried out as follows according to the methods described earlier (Baran, 2018). The UV-Vis Spectrophotometer was used which very useful technique for the primary characterization of prepared PE-AgNPs. In the study, the formation of silver nanoparticles was observed with measurements made at one hour intervals using the SHIMADZU UV-3600 Model UV-Vis Spectrophotometer in the reduction of Ag+ ions to Ago form in the solution. The AgilentCary 360 model FTIR device was used for the evaluation of the functional groups involved and responsible for the reduction. The X-ray refractivity pattern of the Obtained nanoparticles was done with the Crystal Dimension analysis RadB-DMAX II computer-controlled X-rays diffraction difractometry. The appearance of the nanoparticles and the silver element composition were analyzed by the EVO 40 LEQ Model device. In order to determine at what temperature the Nanoparticles were deteriorate, the AgNP was used to measure the flow rate of 20 mL/min in the N2 (g) atmosphere with a heating rate of 10 °C/min and the Shimadzu TGA-60 H Model device for TGA and DTA results at 25-900 °C.

Determination of antimicrobial effect

In the study, Antimicrobial activity *Escherichia coli* ATCC 25922, *Staphylococcus aureus* ATCC 25923, *Streptococcus pyogenes* ATCC 19615 *Pseudomonas aeruginosa* ATCC 27853, standard bacterial strains and *Candida albicans* ATCC 10231 strains were determined by using microdilusion method on the Minimum Inhibiting Concentration (MIC) In the study, microplate wells were left to incubate at 37 °C with the appropriate amounts of Mueller Hinton broth, Mc Farland 0.5 concentration adjusted microorganism solutions and PE-AgNP solution. The lowest concentration in the absence of reproduction after incubation was determined as the MIC value (Wang et al., 2017; Elshikh et al., 2016). Commercial antibiotics were used as control for Gram (+) (vancomycin), Gram (-) (colistin) bacteria and fungus (fluconazole). In addition, the effect of $AgNO^3$ solution was investigated. The study was performed with 3 repetitions and the mean values were determined as MIC value.

Results and discussion

AgNPs have free electrons that lead to surface plasmon resonance (SPR) absorption band due to the combined vibrations of the electrons of the metal nanoparticles with the light wave in the resonance (Nath et al., 2007). When the Mushroom extract was added

http://www.aloki.hu ● ISSN 1589 1623 (Print) ● ISSN 1785 0037 (Online)
DOI: http://dx.doi.org/10.15666/aeer/1704_92059214

to an aqueous silver nitrate solvent, the surface of the metal nanoparticles resulted in a colour change from yellow to dark orange (*Fig. 1*) in 5 days due to stimulation of plasmon vibrations. In the analysis of UV-vis spectroscopy, the formation of silver nanoparticles was observed with samples taken at one hour intervals. As shown in *Figure 1,* the absorption spectrum values of the samples taken without mixing for one hour at room temperature were measured and gave significant plasmon resonance at a maximum of 461 nm. Ramy and Hashem (2014) in their study using Pleurotus ostreatus extract obtained a maximum value of 450 Nm, while Ahmad et al. (2003) reported that the solution prepared using mushroom extract gave a maximum plasmon resonance of 436 Nm. Our results are consistent with previous studies (Huang et al., 2007; Verma et al., 2010).

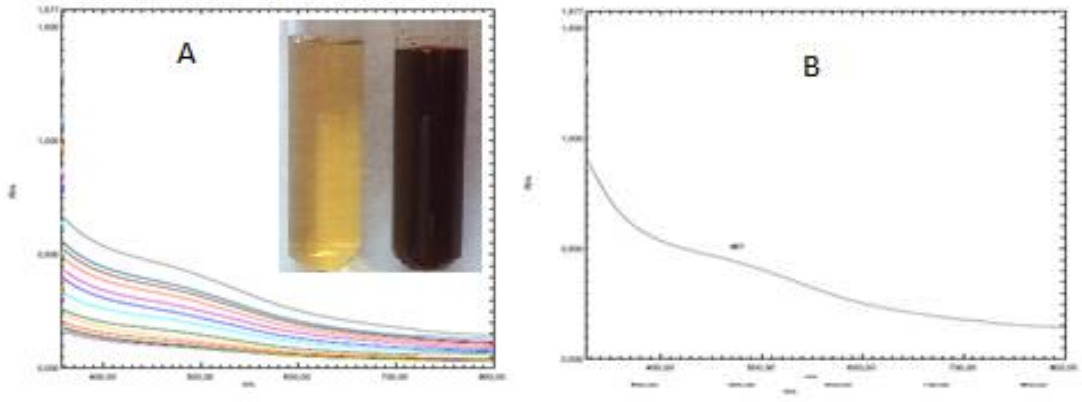

Figure 1. *A) Time dependent of PEAgNPs in UV visible spectroscopy. B) Synthesis of PEAgNP at UV spectrophotometry maximum absorbance value*

The XRD technique is a non-destructive technique and is used to describe the crystalline phase of nanoparticles. The X-ray diffraction pattern obtained for the PE-AgNP sample is shown in *Figure 2*. The PE-AgNP structure synthesized in the resulting diffraction pattern was obtained from the 111, 200, 220 and 311 characteristic pics ($2\theta = 32.41°$, 46.33°, 64.90° and 77.75° values). The crystal particle size of the obtained globally structured PE-AgNPs used Debye-Scherrer's inequality; the size of the synthesized nanoparticles was calculated to be 18.45 nm.

From Debye-Scherrer's equation (Baran, 2019):

$$D = K\lambda / (\beta \cos\theta) \qquad \text{(Eq.1)}$$

Inequality (*Eq. 1*): D = Particle size (nm), K = Fixed (0.90), λ = Wavelength X-ray (1.5406 °A), β = half of the highest peak value is specified in radians (FWHM), θ = fracture angle.

Owait and Ibraheem (2017) reported that mushroom metal-NP's are generally spherical and their size varies between 0.4 nm and $\geq$ 300 nm, but most are less than 75 nm. Considering the particle size, especially for biological applications, it is stated that the particle sizes between 30 and 150 nm are measurable, and a key used in the study of biological properties (Thorek and Tsourkas, 2008). The fact that the crystal grain size of the obtained global structure *PE*-AgNP is 18.45 nm suggests a new assessment.

http://www.aloki.hu ● ISSN 1589 1623 (Print) ● ISSN 1785 0037 (Online)
DOI: http://dx.doi.org/10.15666/aeer/1704_92059214

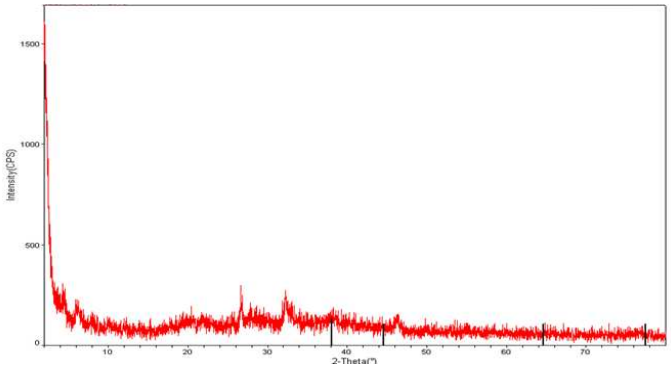

Figure 2. *XRD measurements of AgNPs confirming the spherical crystalline structure of PE-AgNPs*

FT-IR identifies functional groups connected to the surface of metal nanoparticles, since identical absorption patterns are different from those corresponding to free groups, and gives information about the surface chemistry of nanoparticles.

As shown in *Figure 3,* the results of P. eryngy extract and PE-AgNPs were compared as a result of the FT-IR. It is thought that; the peak at 3529 cm^{-1} stems from NH; the peak at 3270 cm^{-1} stems from OH conjugated to free water, alcohol, and phenol groups; the shift at 1672-1635 cm^{-1} stems from carbonyl or primary amide band; and the reason for the peak at 2114 cm^{-1} is C≡C alkyne or C-N group. These functional groups play a role in the reduction (*Fig. 3*). Mandal et al. (2005) stated that proteins in P. ostreatus fungi could bind to nanoparticles by free amine or cysteine groups in proteins and thus stabilize AgNPs.

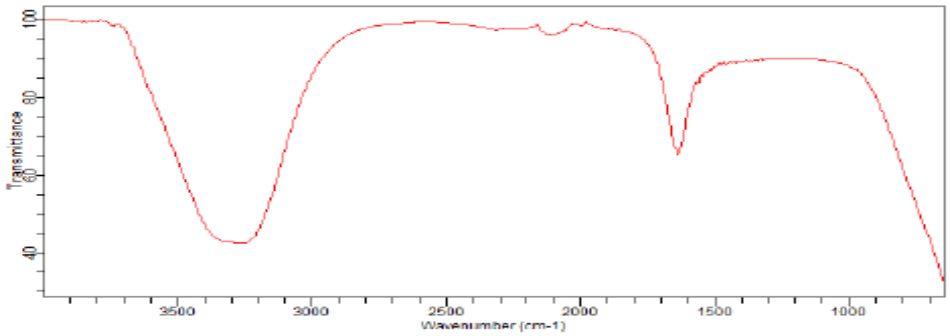

A

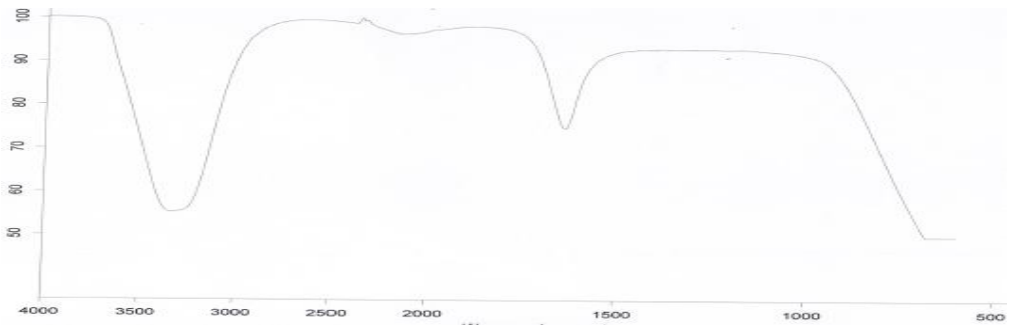

B

Figure 3. *A. FT-IR spectrum of P eryngii extract spectrum. B. FT-IR spectrum of synthesised PE-AgNPs*

http://www.aloki.hu ● ISSN 1589 1623 (Print) ● ISSN 1785 0037 (Online)
DOI: http://dx.doi.org/10.15666/aeer/1704_92059214

Scanning Electron Microscope (SEM) is a tool that scans the surface of the sample and records the return of the beam. Since metal nanoparticles are electrically conductive, they are easy to scan with SEM. SEM analyses of spherical PE-AgNP obtained in 18.45 NM size are shown in *Figure 4*. So far, the researchers have identified a wide range of shapes, such as spherical, diamond, rod-like, and cube, whose diameters are smaller than 1 to 100 nm, as shown in their characterization patterns (Banerjee and Rai, 2017).

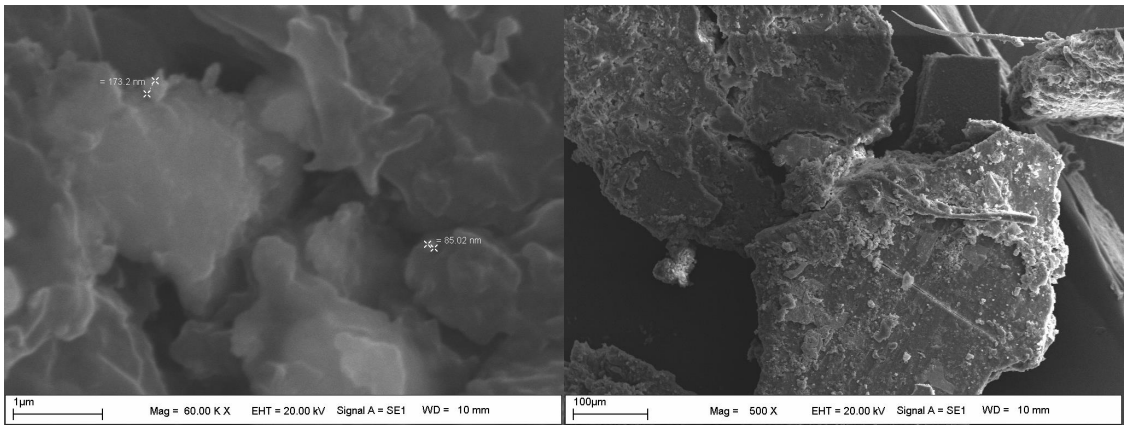

Figure 4. *Images of synthesised PE-AgNP of SEM analyses*

In addition, it was observed that the particles that were synthesized by EDX analysis were in elemental form (*Fig. 5*).

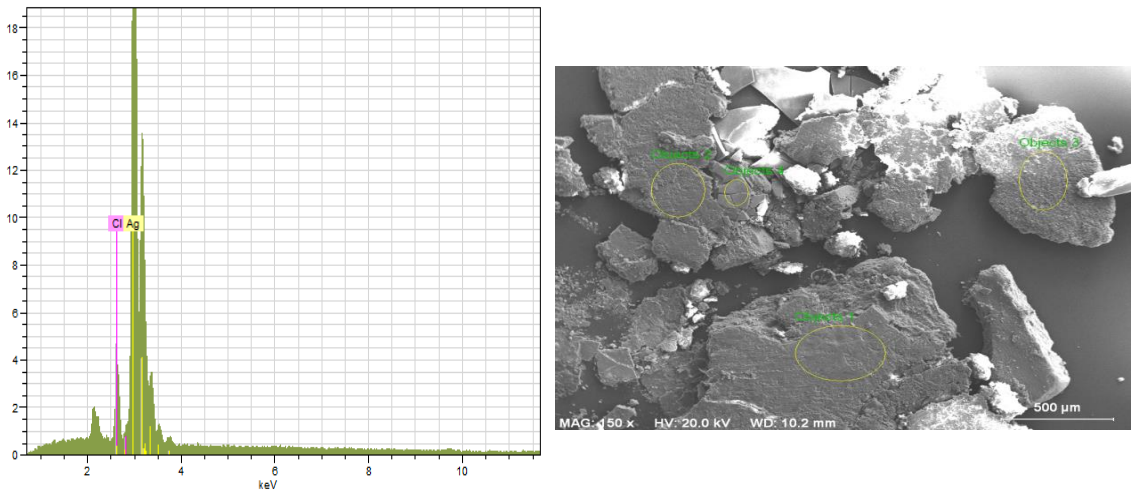

Figure 5. *EDX profile of PE-AgNPs showing its elemental composition*

Nanoparticles prepared with mushroom extract (PE-AgNPs) between 30-900 °C TGA and DTA data were analyzed at a flow rate of 20 mL min^{-1} in N2 (g) atmosphere with a heating rate of 10 °C min^{-1}. The TGA curve shows a loss of sample mass due to thermal degradation and the DTA curve indicates the maximum temperature of decomposition at each stage of the degradation (Baran, 2019, 2018). It is thought that

http://www.aloki.hu ● ISSN 1589 1623 (Print) ● ISSN 1785 0037 (Online)
DOI: http://dx.doi.org/10.15666/aeer/1704_92059214

the 3% mass loss of the synthesized nanoparticule at 11-102 °C is due to moisture, 2.5% loss of the 102-179 °C is due to H2O formation of OH groups side by side, 33.5% loss of the 179-390 °C is due to phenolicity or ring groups, and the 27% loss of the 390-881 °C is due to the degradation of the substance. In this study, PE-AgNPs synthesized up to 881 °C were also shown in *Figure 6*. Although TGA-DTA analysis of plant-derived AgNPs was performed in the literature, no relevant TGA-DTA data on mushroom-based AgNP were found.

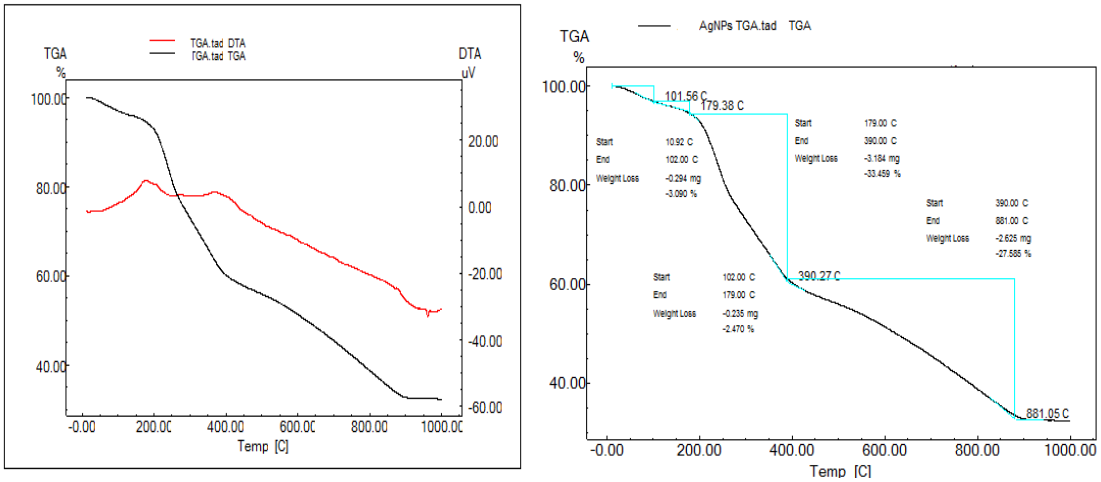

Figure 6. *TGA-DTA analysis result of synthesised PE-AgNPs*

It is widely known that resistance to antibiotics in microbes is a global problem that worsens at an alarming rate. It has become a major problem in many infectious diseases such as multiple antibiotic resistant bacteria and tuberculosis. Some studies in the past have shown that biologically synthesized metal nanoparticles have more biological activity than physically and chemically synthesized nanoparticles (Antony et al. 2011; Manikprabhu et al., 2013). Gopinath et al. (2015) reported that AgNPs synthesized from Fusarium oxysporum and antibiotics showed antimicrobial activity both individually and in combination against these bacteria the results of the same study confirmed that all resistant bacteria that are normally resistant to antibiotics are sensitive to the presence of AgNPs. In another study, Haq et al. (2015) showed that AgNPs synthesized from five fungal species (*Agaricus bisporus, Helvella lacunosa, Ganoderma applanatum, Pleurotus florida and Fomes fomentarius*) showed antimicrobial activity against methicillin-resistant *S. aureus*. However, AgNPs synthesized from *Agaricus bisporus* have been reported to be more powerful than the other four AgNPs. The antimicrobial activity of PE-AgNPs used in the study against *E. coli, S. aureus, S. pyogenes and P. aeruginosa* with standard bacterial strains and *C. albicans* strain is shown in *Table 1*. MIC values of PE-AgNP and silver nitrate were examined and compared. The study was performed with 3 repetitions and the mean values were determined as MIC value.

The MIC values of *S. aureus, S. pyogenes, E. coli, P. aeruginosa* and *C. albicans,* respectively, 0.07, 0035, 0.018, 0035 and 0.07 mg L^{-1} results were obtained (*Table 1*). Compared with Silver nitrates and antibiotics, AgNP can be used as an alternative to existing antibiotics as a result.

http://www.aloki.hu ● ISSN 1589 1623 (Print) ● ISSN 1785 0037 (Online)
DOI: http://dx.doi.org/10.15666/aeer/1704_92059214

Table 1. *MIC values of synthesized PE-AgNPs (mg l^{-1})*

Microorganisms	AgNPs	Silver nitrat	Antibiotic
S. aureus ATCC 25923	0.07	2.65	1
S. pyogenes ATCC 19615	0.035	1.32	1
E. coli ATCC25922	0.018	0.66	2
P. aeruginosa ATCC 27853	0.035	0.66	2
C. albicans ATCC 10231	0.07	0.66	

Conclusions

It is clear that *P. eryngii,* a renewable fungus, can be effectively used to synthesize bioactive nanoparticles using cheap substances in an environmentally friendly and non-toxic environment. The synthesis of PE-AgNPs was carried out at room temperature for 5 days by adding the fungus extract to an aqueous silver nitrate solvent. It was observed that PE-AgNPs with a crystal size of 18.45 nm and a spherical appearance showed a strong antimicrobial activity against human pathogen microorganisms. In this study, we believe that synthesized PE-AgNPs can contribute greatly to the search for antimicrobial agents. At the same time, these biosynthesized AgNPs can be used as effective growth inhibitors in various microorganisms; this makes them applicable to various medical devices, industrial, food, agricultural, biotechnological and environmental applications.

REFERENCES

[1] Abou El-Nour, M. M., Eftaiha, A., Al-Warthan, A., Ammar, R. A. A. (2010): Synthesis and application of silver nanoparticles. – Arab J Chem 3: 135-140.

[2] Acay, H., Baran, M. F., Eren, A. (2019): Investigating antimicrobial activity of silver nanoparticles produced through green synthesis using leaf extract of common grape (Vitis vinifera). – Applied Ecology and Environmental Research 17(2): 4539-46.

[3] Ahmad, A., Mukherjee, P., Senapati, S., Mandal, D., Khan, M. I., Kumar, R., Sastry, M. (2003): Extracellular biosynthesis of silver nanoparticles using the fungus Fusarium oxysporum. – Colloids Surf B Biointerfaces 28(4): 313-318.

[4] Antony, J. J., Sivalingam, P., Siva, D., Kamalakkannan, S., Anbarasu, K., Sukirtha, R. et al. (2011): Comparative evaluation of antibacterial activity of silver nanoparticles synthesized using Rhizophora apiculata and glucose. – Colloids Surf B Biointerfaces 88(1): 134_40.

[5] Banerjee, K., Rai, V. R. (2017): A review on mycosynthesis, mechanism, and characterization of silver and gold nanoparticles. – Bio NanoSci 8(1): 17-31. https://doi.org/10.1007/s12668-017-0437-8.

[6] Baran, M. F. (2018): Green synthesis of silver nanoparticles (Agnps) using Pistacia terebinthus leaf extract: antimicrobial effect and characterization. – EJONS International Journal on Mathematic, Engineering and Natural Sciences (5)67-75.

http://www.aloki.hu ● ISSN 1589 1623 (Print) ● ISSN 1785 0037 (Online)
DOI: http://dx.doi.org/10.15666/aeer/1704_92059214

[7] Baran, M. F. (2019): Synthesis, characterization and investigation of antimicrobial activity of silver nanoparticles from Cydonia oblonga leaf. – Applied Ecology and Environmental Research 17(2): 2583-2592.
[8] Chaudhuri, R. G., Paria, S. (2012): A novel method for the templated synthesis of Ag2S hollow nanospheres in aqueous surfactant media. – J Colloid Interf Science 369: 117-122.
[9] El-Batal, A. I., Hashem, A. A., Abdelbaky, N. M. (2013): Gamma radiation mediated green synthesis of gold nanoparticles using fermented soybean-garlic aqueous extract and their antimicrobial activity. – Springer Plus 2: 129-139.
[10] Elgorban, A. M., El-Samawaty, A. M., Yassin, M. A., Sayed, S. R., Adil, S. F., Elhindi, K. M., Bakri, M., Khan, M. (2016): Antifungal silver nanoparticles: synthesis, characterization and biological evaluation. – Agric. Environ. Biotechnol. 30: 56-62.
[11] Elshikh, M., Ahmed, S., Funston, S., Dunlop, P., McGaw, M., Marchant, R., Banat, I. M. (2016): Resazurin-based 96-well plate microdilution method for the determination of minimum inhibitory concentration of biosurfactants, Biotechnol. – Lett. 38: 1015-1019.
[12] Gopinath, P. M., Narchonai, G., Dhanasekaran, D., Ranjani, A., Thajuddin, N. (2015): Mycosynthesis, characterization and antibacterial properties of AgNPs against multidrug resistant (MDR) bacterial pathogens of female infertility cases. – Asian J Pharma Sci 10: 138-45.
[13] Haq, M., Rathod, V., Singh, D., Singh, A. K., Ninganagouda, S., Hiremath, J. (2015): Dried mushroom Agaricus bisporus mediated synthesis of silver nanoparticles from Bandipora District (Jammu and Kashmir) and their efficacy against Methicillin resistant Staphylococcus aureus (MRSA) strains. – Nanosci Nanotechnol Int J 5(1): 1_8.
[14] Huang, J. L., Li, Q. B., Sun, D. H., Lu, Y. H., Su, Y. B., Yang, X., Wang, H. X., Wang, Y. P., Shao, W. Y., He, N., Hong, J. Q., Chen, C. X. (2007): Biosynthesis of silver and gold nanoparticles by novel sundried Cinnamomum camphora leaf. – Nanotechnology 18: 1-11.
[15] Kavyashree, D., AnandaKumari, R., Nagabhushana, H., Sharma, S. C., Vidya, Y. S., Anantharaju, K. S., Daruka Prasad, B., Prashantha, S. C., Lingaraju, K., Rajanaik, H. (2015): Orange red emitting Eu3 + doped zinc oxide nanophosphor material prepared using Guizotia abyssinica seed extract: structural and pho-toluminescence studies. – J. Lumin. 167: 91-100.
[16] Kumar, V., Yadav, S. K. (2009): Plant-mediated synthesis of silver and gold nanoparticles and their applications. – J. Chem. Technol. Biotechnol. 84(2): 151-157.
[17] Lakshmeesha, T. R., Sateesh, M. K., Daruka, P. B., Sharma, S. C., Kavyashree, D., Chandrashekar, M., Nagabhushana, H. (2014): Reactivity of crystalline ZnO superstructures against fungi and bacterial pathogens: synthesized using Nerium oleander leaf extract. – Cryst. Growth Des. 14: 4068-4079.
[18] Mallmann, E. J. J., Cunha, F. A., Castro, B. N. M. F., Maciel, A. M., Menezes, E. A., Fechine, P. B. A. (2015): Antifungal activity of silver nanoparticles obtained by green synthesis. – Rev. Inst. Med. Trop. Sao Paulo 57: 165-167.
[19] Mandal, S., Phadtre, S., Sastry, M. (2005): Interfacing biology with nanoparticles. – Curr Appl Phys 5: 118-127.
[20] Manikprabhu, D., Lingappa, K. (2013): Microwave assisted rapid and green synthesis of silver nanoparticles using a pigment produced by Streptomyces coelicolor klmp33. – Bioinorg Chem Appl. http://dx.doi.org/10.1155/2013/341798.
[21] Nadagouda, M. N., Hoag, G., Collins, J., Varma, R. S. (2009): Green synthesis of Aunanostructures at room temperature using biodegradable plant surfactants. – Cryst. Growth Des. 9: 4979-4983.
[22] Nagajyothi, P. C., Sreekanth, T. V. M., Lee, J. L., Lee, K. D. (2014): Mycosynthesis: Antibacterial, antioxidant and antiproliferative activities of silver nanoparticles synthesized from *Inonotus obliquus* (Chaga mushroom) extract. – J Photochem Photobiol B Biol 130: 299-304.

http://www.aloki.hu ● ISSN 1589 1623 (Print) ● ISSN 1785 0037 (Online)
DOI: http://dx.doi.org/10.15666/aeer/1704_92059214

[23] Nath, S. S., Chakdar, D., Gope, G. (2007): Synthesis of CdS and ZnS quantum dots and their applications in electronics. – Nanotrends J. Nanotechnol. Appl. 02(03).
[24] Owaid, M. N., Ibraheem, I. J. (2017): Mycosynthesis of nanoparticles using edible and medicinal mushrooms. – Eur. J. Nanomed. 9(1): 5-23.
[25] Palacios, I., Lozano, M., Moro, C., D'arrigo, M., Rostagno, M., Martínez, J., García-Lafuente, A., Guillamón, E., Villares, A. (2011): Antioxidant properties of phenolic compounds occurring in edible mush- rooms. – Food Chem. 128: 674-678.
[26] Panaek, A., Kvitek, L., Prucek, R., Kolar, M., Veerova, R., Pizurova, N., Sharma, V. K., Nevena, T., Zboril, R. (2006): Silver colloid nanoparticles: synthesis, characterization, and their antibacterial activity. – J. Phys. Chem. B 110: 16248.
[27] Parashar, V., Parashar, R., Sharma, B., Pandey, A. C. (2009): Parthenium leaf extract mediated synthesis of silver nanoparticles: a novel approach towards weed utilization. – Dig. J. Nanomater Bios. 4: 45-50.
[28] Philip, D. (2009): Biosynthesis of Au, Ag and Au-Ag nanoparticles using edible mushroom extract. – Spectrochim. Acta Mol. Biomol. Spectrosc. 73: 374-381.
[29] Pugazhendhi, A., Prabakar, D., Jacob, J. M., Karuppusamy, I., Saratale, R. G. (2017): Synthesis and characterization of silver nanoparticles using Gelidium amansii and its antimicrobial property against various pathogenic bacteria. – Microbial Pathogenesis S0882-4010(17)31356-6.
[30] Ramy, S. Y., Hashem, A. S. (2014): Biosynthesis and characterization of silver nanoparticles produced by Pleurotus ostreatus and their anticandidal and anticancer activities. – World J Microbiol Biotechnol 30: 2797-2803.
[31] Rauwel, P., Rauwel, E., Ferdov, S., Singh, M. P. (2015): Silver nanoparticles: synthesis, properties, and applications. – Adv. Mater. Sci. Eng. 624394.
[32] Remya, V. R., Abitha, V. K., Rajput, P. S., Rane, A. V., Dutta, A. (2017): Silver nanoparticles green synthesis: a mini review. – Chem. Int. 3(2) 165-171.
[33] Salem, W., Leitner, D. R., Zingl, F. G., Schratter, G., Prassl, R., Goessler, W., Reidl, J., Schild, S. (2015): Antibacterial activity of silver and zinc nanoparticles against Vibrio cholerae and enterotoxic Escherichia coli. – Int. J. Med. Microbiol. 305: 85-95.
[34] Thorek, D. L., Tsourkas, A. (2008): Size, charge and concentration dependent uptake of iron oxide particles by non-phagocytic cells. – Biomaterials 29(26): 3583-3590.
[35] Tran, Q. H., Nguyen, V. Q., Le, A. T. (2013): Silver nanoparticles: synthesis, properties, toxicology, applications and perspectives. – Adv. Nat. Sci. Nanosci. Nanotechnol. 4: 033001.
[36] Verma, V. C., Kharwar, R. N., Gange, A. C. (2010): Biosynthesis of antimicrobial silver nanoparticles by the endophytic fungus Aspergillus clavatus. – Nanomedicine (Lond) 5: 33-40.
[37] Wang, L., Hu, C.., Shao, L. (2017): The antimicrobial activity of nanoparticles: present situation and prospects for the future. – Int J Nanomedicine 12: 1227-1249.

http://www.aloki.hu ● ISSN 1589 1623 (Print) ● ISSN 1785 0037 (Online)
DOI: http://dx.doi.org/10.15666/aeer/1704_92059214

INFLUENCE OF N SPLIT APPLICATION ON NH_3 VOLATILIZATION LOSSES AND N RECOVERY EFFICIENCY FROM PLASTIC MULCHING MAIZE IN LOESS PLATEAU, CHINA

WANG, S. J.[1] – LUO, S. S.[2] – GAO, Q.[1*] – LI, S. Q.[3*]

[1]*College of Resource and Environment, Key Laboratory of Soil Resource Sustainable Utilization for Jilin Province Commodity Grain Bases, Jilin Agricultural University, Changchun 130118, China*

[2]*Key Laboratory of Mollisols Agroecology, Northeast Institute of Geography and Agroecology, Chinese Academy of Sciences, Changchun 130102, China*

[3]*State Key Laboratory of Soil Erosion and Dryland Farming on the Loess Plateau, Chinese Academy of Sciences and Ministry of Water Resource, Yangling 712100, China*

**Corresponding authors*
e-mail: gyt199962@163.com; sqli@ms.iswc.ac.cn

(Received 29th Mar 2019; accepted 24th May 2019)

Abstract. Ammonia (NH_3) volatilization is one of the main reasons of applied-N loss from agricultural cropping systems. Adjusting the application timing of N fertilizer to improve temporal synchronicity between crop-N demand and soil-N availability could result in higher nitrogen (N) recovery efficiency (NRE) and lower N losses. A two-year experiment was conducted to investigate the effect of split fertilizer N application on NH_3 volatilization, grain yield, and NRE. Four treatments were included according to the N application ratio: (i) a single application of total N fertilizer at sowing (N1), (ii) N applied with two splits at a ratio of 4:6 (N2), (iii) N applied with three splits at a ratio of 4:3:3 (N3), and (iv) no N applied as a control (N0). The results show that NH_3 fluxes peaked at 3-5 days after fertilization and then dropped sharply within the next week. NH_3 fluxes increased significantly with N application rate and were significantly and positively correlated with soil NH_4^+-N content. Slight precipitation (< 10 mm) promoted NH_3 volatilization, while heavy precipitation (> 10 mm) restrained it. Applying N with two or three splits significantly increased the grain yield, total N uptake, and NRE of maize and significantly reduced NH_3 volatilization losses.
Keywords: *Dräger-tube method, N application time, N application rate, N loss, grain yield*

Introduction

Ammonia (NH_3) volatilization is a major pathway of nitrogen (N) losses in agricultural systems worldwide, which results in low fertilizer N recovery efficiency (NRE) and many other environmental issues, such as soil acidification and surface water eutrophication through N deposition (Behera et al., 2013). In addition, NH_3 is considered a dominant air pollution source, accounting for 25-60% of the total PM2.5 mass (Sutton et al., 2013), and could become a secondary source of N_2O (Sutton et al., 2008). Agricultural activities reportedly contribute up to 90% of the total NH_3 emissions to the atmosphere (Boyer et al., 2002), with the majority originating from livestock production and approximately 12% resulting from N fertilizer application (Ferm, 1998). An average of 18% of applied synthetic fertilizer N is estimated to be lost as NH_3 globally (Pan et al., 2016). China is the world's largest NH_3 emitter with annual emissions that are 2.7 and 3.0 times higher than those of the European Union and the

http://www.aloki.hu ● ISSN 1589 1623 (Print) ● ISSN 1785 0037 (Online)
DOI: http://dx.doi.org/10.15666/aeer/1704_92159227

United States, respectively (Paulot et al., 2014). The total NH_3 emission of China was estimated to be 3.55 Tg N in 2005, with an estimated 13.2% of N from fertilizer NH_3 volatilizing (Zhang et al., 2011). The factors influencing NH_3 volatilization include environmental parameters, such as soil pH, moisture, and temperature as well as precipitation (Ma et al., 2010; Yang et al., 2015; Pan et al., 2016) and N fertilizer management practices, such as the use of different types of N fertilizer, N rate and application methods (Liu et al., 2015; Yang et al., 2019).

Urea is one of the most widely used N fertilizers worldwide because of its high N concentration, and its hydrolysis is known as a key process in inducing NH_3 volatilization by producing highly concentrated NH_4^+-N with sharply increased pH (Black et al., 1987). NH_3 volatilization from urea accounts for approximately 10-35% of the N applied in field crop planting (Soares et al., 2012). Due to the different demand of plants for N at different growth stages, surplus nitrogen is a great environmental risk in that it can leach into groundwater or be lost to the atmosphere through NH_3 volatilization and denitrification. Thus, adjusting the application timing of N fertilizer and improving temporal synchronicity between crop-N demand and soil-N availability are key strategies for improving the NRE (Ribaudo et al., 2011). Field experimental data have shown that grain yields, plant N uptake, and NRE increase with increases in topdressed N fertilizer (López-Bellido et al., 2005; Cui et al., 2008). Scharf et al. (2002) found that crop yields were still responsive to N application until the silking (R1) stage but that the potential yields were not achieved when N applications were delayed until that stage. Applying N with three splits could produce higher grain yields and higher cumulative N_2O emissions than a single application of N (Wang et al., 2016). Previous studies have shown that high rates of N lead to much higher NH_3 losses, and the emissions response to increasing N input is exponential rather than linear (Ma et al., 2010). Therefore, we hypothesize that maintaining a low rate of N application by using a split application should reduce NH_3 volatilization losses.

Plastic mulching is used worldwide in vegetable and grain production, especially in arid, semiarid and subhumid areas (Chen et al., 2014), due to its ability to increase soil temperature and moisture, reduce water evaporation, and improve soil nutrient availability (Li et al., 2004). In addition, as a physical barrier, plastic mulching restricts gas exchange between the soil and atmosphere, thus affecting NH_3 volatilization. However, there is little information concerning NH_3 volatilization losses from maize under plastic mulching. The objective of this study was to quantify the effect of N split application on NH_3 volatilization, crop yields, and NRE in a plastic mulching maize cropping system on the Loess Plateau of China.

Materials and methods

Site description

The field experiment was conducted at Changwu Agricultural and Ecological Experimental Station of Chinese Academy of Sciences (35.28°N, 107.88°E, 1200 m altitude) in 2014 and 2015, which has a semiarid climate on the Loess Plateau of China. From 2009 to 2013, the mean annual air temperature is 9.7 °C, and the average annual precipitation is 555 mm, 73% of this falls during the maize growth season (MS), whereas the average potential evaporation is 1560 mm. Total precipitation during MS was 375 mm in 2014, and 361 mm in 2015, respectively. The main cropping system in this area includes harvesting one crop of maize or wheat per year. The soil at the

http://www.aloki.hu ● ISSN 1589 1623 (Print) ● ISSN 1785 0037 (Online)
DOI: http://dx.doi.org/10.15666/aeer/1704_92159227

experiment site is classified as Cumuli-Ustic Isohumosols according to the Chinese Soil Taxonomy (Gong et al., 2007). The soil properties at the top 20 cm were: bulk density 1.3 g cm^{-3}, pH 8.3, organic C 8.1 g kg^{-1}, total N 1.0 g kg^{-1}, available phosphorus (Olsen-P) 21.5 mg kg^{-1}, and available potassium (NH_4OAc-K) 135.2 mg kg^{-1}, and mineral N (NO_3^--N + NH_4^+-N) 28.3 mg kg^{-1}.

Experimental design

The experimental design consisted of a completely randomized block with three replicates and an area of 5 m × 6 m for each plot. The split application of N at the same rate of 225 kg ha^{-1} was the major factor that was investigated. The four treatments were (i) no N as a control (N0), (ii) 100% N applied at sowing (N1), (iii) N applied at the sowing and jointing (V8) stages in a ratio of 4:6 (N2), and (iv) N applied at the sowing, V8 and R1 stages in a ratio of 4:3:3 (N3). Half-film mulching was performed for all of the plots; the width of the plastic film and the interval of two films were both 0.5 m, and maize was seeded on both sides of the film, with a row spacing of 0.5 m. For basal N, N fertilizer in the form of urea (N 46%) was manually distributed over the soil surface prior to sowing and then mixed with the soil of the 0-15 cm layer; for topdressed N, N fertilizer was applied in a band in the middle of the no-film rows at a depth of 5 cm. Each plot was supplied with 40 kg P ha^{-1} (calcium superphosphate, P_2O_5, 12%) and 80 kg K ha^{-1} (potassium sulfate, K_2O, 45%) at sowing with the base N fertilizer. A high-yielding maize hybrid (Pioneer 335) was used in this study; the plant density was 65,000 plants ha^{-1}.

NH_3 volatilization measurements

The calibrated Dräger-Tube method (DTM) was used to quantify NH_3 volatilization (Pacholski et al., 2006) as this method has been shown to be well suited for NH_3 measurements in multiplot field trials (Ni et al., 2014; Wolf et al., 2014). During the measurement, four stainless steel rings were installed in the upper soil of one plot for each treatment directly after fertilization, 2 on the edge of the mulch, and 2 on the bare land, then they were connected to an NH_3 indicator tube and an automatic pump to ensure a defined flow rate. Air was simultaneously sucked through four connected chambers and led through a NH_3 tube (*Fig. 1*). Damaged tubes were exchanged by new tubing. Using Drägertubes for different NH_3 concentration ranges allowed measurements of NH_3 concentrations ranging from 0.1 to 70 ppm. In conjunction with all NH_3 measurements, wind speeds at heights of 2.0 m and 0.2 m were recorded every 10 min for the duration of every measuring period (approximately 10-14 days after N fertilizer application until NH_3 volatilization losses were no longer detected), which were used for calculating the calibrated NH_3 fluxes.

Soil property measurements

Soil samples at a 20 cm depth were taken from each plot for the moisture and NH_4^+-N determinations, while NH_3 volatilization was measured using a 4-cm-diameter gauge auger. Each sample was a composite of two subsamples, of which one was taken from the no-mulch bands and the other was taken from film mulched bands, to represent the aggregate condition. The samples were oven-dried at 105 °C for 24 h to a consistent weight to determine the gravimetric soil water content, and the soil water-filled pore space (WFPS) was subsequently calculated using *Equation 1*. To determine the soil

http://www.aloki.hu ● ISSN 1589 1623 (Print) ● ISSN 1785 0037 (Online)
DOI: http://dx.doi.org/10.15666/aeer/1704_92159227

NH_4^+-N content, representative fresh subsamples (5 g) were extracted using 50 ml of a 1 mol L^{-1} KCl solution, and the extracts were analyzed using an automated flow injection analyzer (FLOWSYS, Italy). The soil temperatures at the surface and at a depth of 10 cm were measured using portable digital thermometers (JM624, Jinming Instrument Ltd., Tianjin, China). Precipitation data were obtained from an automatic weather station near the experimental site.

$$WFPS = \frac{\text{Soil water content}(\%) \times \text{Soil bulk density}}{1 - \frac{\text{Soil bulk density}}{2.65}} \times 100\% \quad \text{(Eq.1)}$$

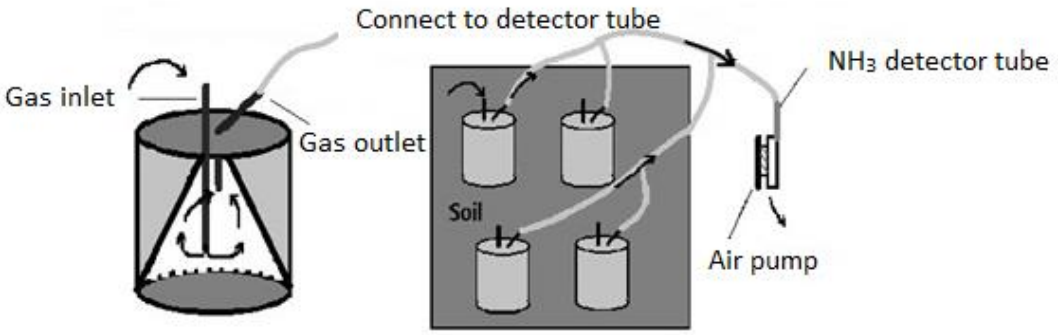

Figure 1. *Schematic diagram of NH_3 volatilization measurements*

Grain yield and N recovery efficiency

At harvest, 8 m^2 (4 rows each 4 m long) in the middle of each plot was manually harvested to determine the grain yield, and the grain yield was expressed at 15.5% moisture.

N recovery efficiency (NRE) was calculated by difference method using *Equation 2*.

$$NRE\ (\%) = \frac{\text{N uptake in fertilized plot}\ (\text{kg hm}^{-2}) - \text{N uptake in unfertilized plot}\ (\text{kg hm}^{-2})}{\text{N application rates}\ (\text{kg hm}^{-2})} \quad \text{(Eq.2)}$$

Statistical analysis

Statistical analysis was conducted using the SPSS 20.0 software package for one-way analysis of variance (ANOVA); the statistically significant differences between different treatments were tested by the least significant difference (LSD) at the 5% level. The Pearson correlation analysis was performed to investigate the correlations between the NH_3 volatilization flux and soil variables.

Results

Soil WFPS, temperature and NH_4^+-N content

The soil WFPS and temperature during NH_3 volatilization measurements over two years are shown in *Figure 2*. The mean soil temperature during the application of basal N, topdressed N at the V8 stage (T_{V8}-N) and topdressed N at the R1 stage (T_{R1}-N) were 15.5 °C, 21.3 °C and 21.7 °C, respectively, in 2014 and were 15.6 °C, 18.3 °C and 18.4 °C, respectively, in 2015. Soil WFPS fluctuated with precipitation events, varying

http://www.aloki.hu ● ISSN 1589 1623 (Print) ● ISSN 1785 0037 (Online)
DOI: http://dx.doi.org/10.15666/aeer/1704_92159227

from 20.6 to 59.4% in 2014 and from 36.7 to 64.4% in 2015, and there was no difference among the four treatments.

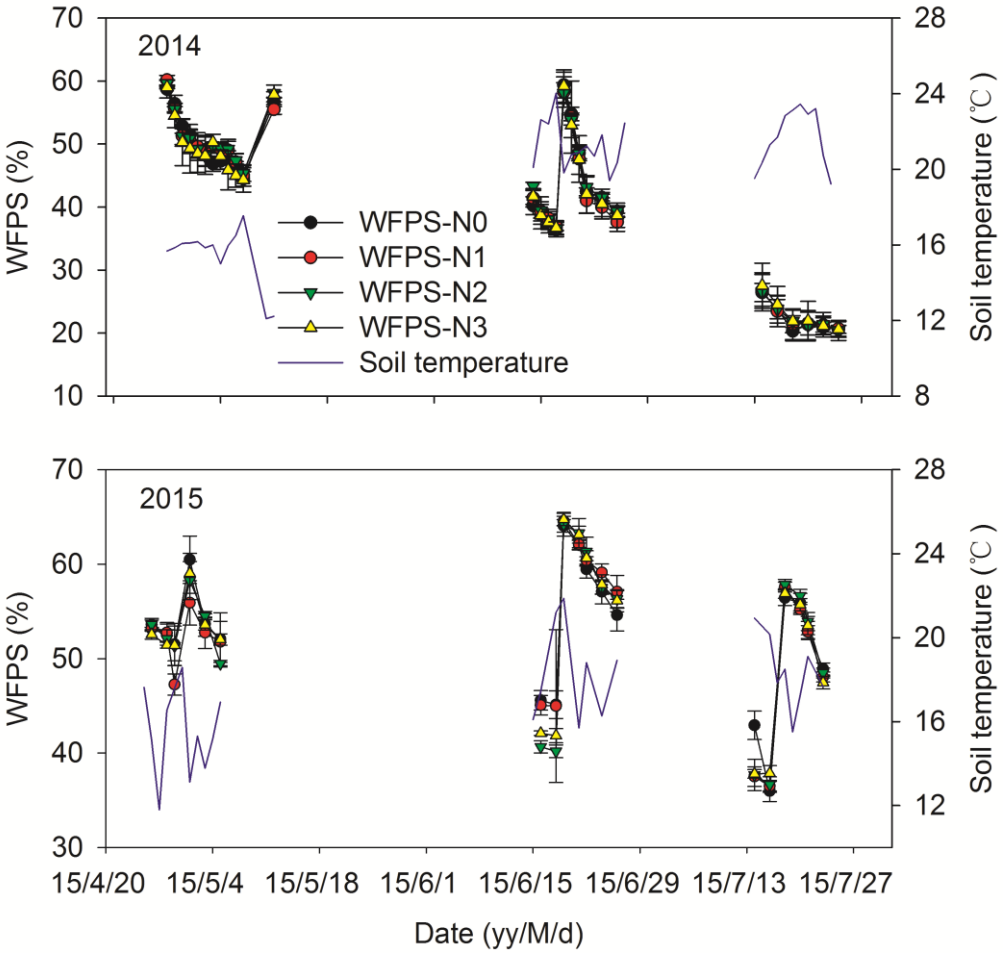

Figure 2. *Soil moisture and temperature dynamics during NH_3 volatilization measurements in 2014 and 2015*

The soil NH_4^+-N content increased sharply after the application of N fertilizer and then returned to normal within approximately one week (*Fig. 3*). The mean soil NH_4^+-N content during the basal N application in the N1 treatment was 66.1 mg kg^{-1}, which was significantly higher than that in the N2 (20.7 mg kg^{-1}) and N3 (17.9 mg kg^{-1}) treatments in 2014. Relatively low soil NH_4^+-N content was measured during basal N application in 2015, with mean values of 21.6, 5.1 and 4.2 mg kg^{-1} in the N1, N2 and N3 treatments, respectively. After the T_{V8}-N application, the mean soil NH_4^+-N content was 55.9 mg kg^{-1} and 26.1 mg kg^{-1} in treatments N2 and N3, respectively, in 2014 and 163.1 mg kg^{-1} and 77.7 mg kg^{-1}, respectively, in 2015, respectively. After the T_{R1}-N application in the N3 treatment, the mean soil NH_4^+-N content reached 33.2 mg kg^{-1} and 59.1 mg kg^{-1} in 2014 and 2015, respectively. Overall, the mean soil NH_4^+-N contents across the whole growth period were 4.2, 28.5, 30.3 and 24.6 mg kg^{-1} in the N0, N1, N2 and N3 treatments, respectively, in 2014 and were 1.5, 7.4, 59.1 and 49.1 mg kg^{-1}, respectively, in 2015.

http://www.aloki.hu ● ISSN 1589 1623 (Print) ● ISSN 1785 0037 (Online)
DOI: http://dx.doi.org/10.15666/aeer/1704_92159227

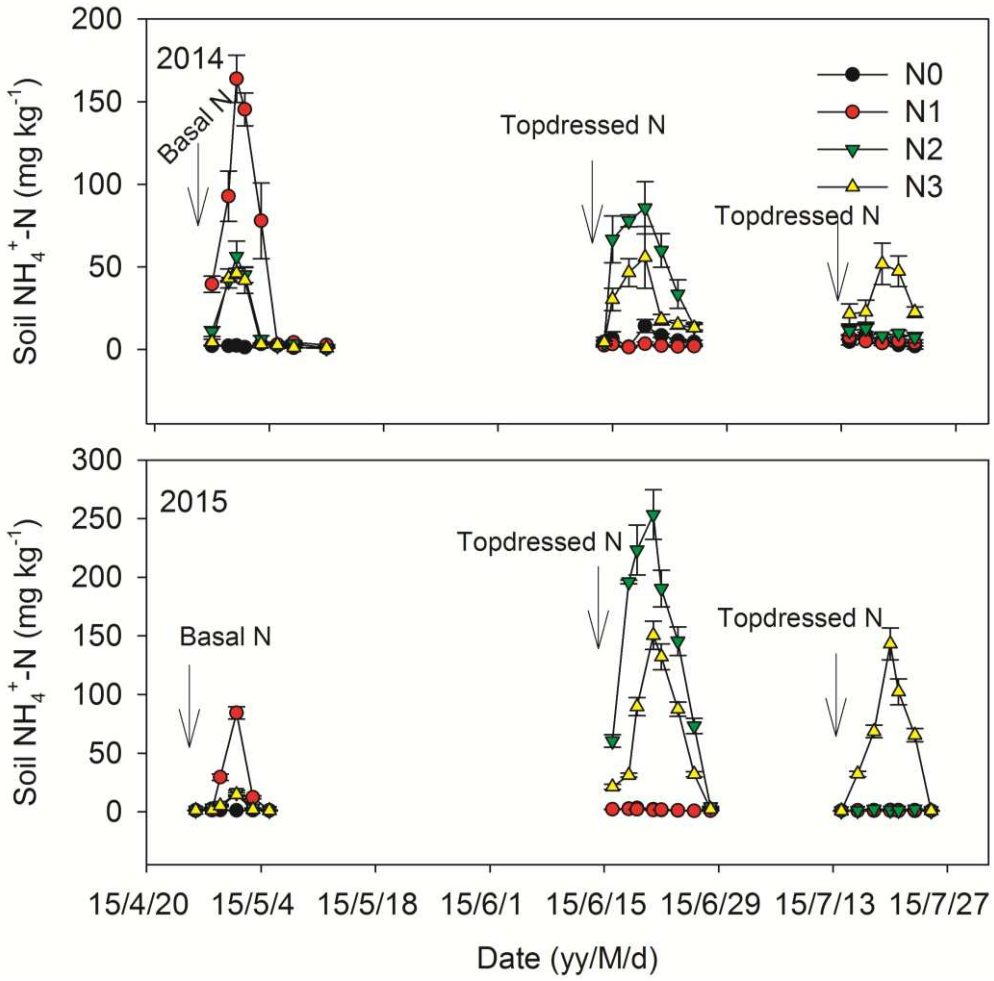

Figure 3. *Soil NH_4^+-N dynamics after the application of basal and topdressed N in 2014 and 2015. Bars denote standard deviations of soil NH_4^+-N content on three replicate plots*

NH_3 volatilization flux

The dynamics of NH_3 volatilization fluxes with different N split applications are shown in *Figure 4*. Since NH_3 volatilization mainly occurred after fertilization, it was only determined within two weeks after fertilization in this study. Under different N application periods, the rate of NH_3 volatilization usually peaked at 3-5 days after fertilization and then dropped sharply within the next week. After the basal N application, the mean NH_3 volatilization rate in the two years was 71 g ha^{-1} h^{-1} in the N1 treatment, which was significantly higher than the 5, 24, 27 g ha^{-1} h^{-1} in the N0, N2 and N3 treatments, respectively, due to its higher N application rate. The highest volatilization rates from N1 were 193 and 234 g ha^{-1} h^{-1} after the basal N applications in 2014 and 2015, respectively, while only 100-130 g ha^{-1} h^{-1} were observed in the N2 and N3 treatments. After the T_{V8}-N application, the mean rates of NH_3 volatilization from the N2 treatment were 18.8 and 26.5 g ha^{-1} h^{-1} in 2014 and 2015, respectively, which were significantly higher than those from the N3 treatment (10.4 g ha^{-1} h^{-1} in 2014 and 11.8 g ha^{-1} h^{-1} in 2015). A small emissions peak emerged in the N3 treatment when T_{R1}-N was applied, with the highest volatilization rates of 37.5 g ha^{-1} h^{-1} in 2014 and 77.5 g ha^{-1} h^{-1} in 2015.

http://www.aloki.hu ● ISSN 1589 1623 (Print) ● ISSN 1785 0037 (Online)
DOI: http://dx.doi.org/10.15666/aeer/1704_92159227

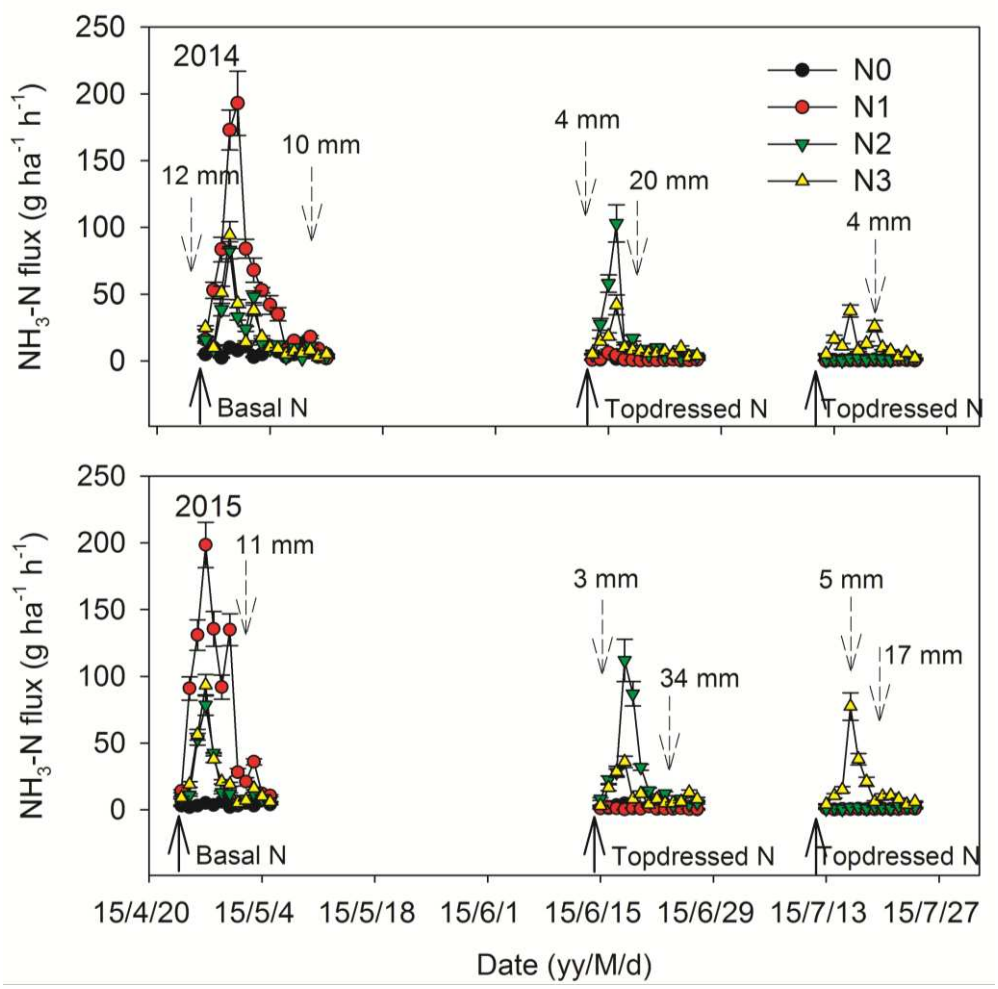

Figure 4. *NH_3 volatilization fluxes after the application of basal and topdressed N in 2014 and 2015. Bars denote standard deviations of NH_3 fluxes on three replicate plots*

The total NH_3 volatilization and fertilizer-induced emission (FIE) are shown in *Table 1*. The total NH_3 volatilizations under different N split applications were 13.5-20.4 kg ha^{-1} and 14.2-21.5 kg ha^{-1} in 2014 and 2015, respectively, accounting for 6.0%-9.1% and 6.3%-9.6% of the total N application rates, respectively. The amount of NH_3 volatilization increased with increasing N levels applied after the basal or topdressed N applications. Compared to the single N application (N1), N applications with two or three splits significantly reduced the NH_3 volatilization losses by 30.5%. The FIE of NH_3 from basal N was 7.6% (averaged over two years), which was significantly higher than that from topdressed N (5.2%) in the N2 treatment. For the N3 treatment, a higher FIE of NH_3 was measured from basal N (8.4%) than from topdressed N (5.7%).

The NH_3 volatilization flux was significantly and positively correlated with the soil NH_4^+-N content, while no significant correlation was observed among the NH_3 volatilization flux, soil WFPS and temperature (*Table 2*).

Grain yield and N recovery efficiency

Compared with the N0 treatment, the N fertilizer application treatments significantly increased the grain yield of maize, varying from 12.4 to 13.3 t ha^{-1} under different N

http://www.aloki.hu ● ISSN 1589 1623 (Print) ● ISSN 1785 0037 (Online)
DOI: http://dx.doi.org/10.15666/aeer/1704_92159227

split applications over two years. The mean yields in the two years were 13.2 and 13.4 t ha^{-1} in the N2 and N3 treatments, respectively, which were significantly higher than that of in the treatment N1 of 12.4 t ha^{-1}. The total N uptake varied from 193.9 to 238.5 kg ha^{-1} in the fertilized treatments, and split N application significantly increased the total N uptake. The average NRE across two years was 47.3%, 58.8% and 67.1% in the N1, N2 and N3 treatments, respectively. In comparison to N1, applying N with two or three splits increased the NRE significantly.

Table 1. *Accumulated NH_3 volatilization and fertilizer induced emission (FIE) from basal and topdressed N fertilizer*

Treatments		N rate (kg ha^{-1})	Total NH_3 volatilization (kg ha^{-1})		Fertilizer-induced emission (%)	
			2014	2015	2014	2015
N1		225	20.4 aA	21.5 aA	9.1 aA	9.6 aA
N2	B	90	7.1 b	6.5 b	7.9 a	7.2 b
	T_{V8}	135	6.4 b	7.7 b	4.7 b	5.7 c
	Total	225	13.5 B	14.2 B	6.0 B	6.3 B
N3	B	90	7.8 b	7.3 b	8.6 a	8.1 b
	T_{V8}	67.5	3.4 c	3.5 c	5.0 b	5.2 c
	T_{R1}	67.5	3.6 c	4.9 c	5.4 b	7.3 b
	Total	225	14.8 B	15.7 B	6.6 B	7.0 B

Different lowercase letters within a column indicate significant differences ($p < 0.05$). Different capital letters within a column indicate significant differences ($p < 0.05$). B denotes basal N; T_{V8} and T_{R1} denote topdressed N at the eight-leaf stage and the silking stage, respectively

Table 2. *The relationship between NH_3 volatilization flux and soil properties*

	Soil NH_4^+-N	WFPS	Soil temperature
NH_3 flux	0.288**	0.021	-0.089

**Correlation is significant at the 0.01 level

Discussion

Urea applied to soil will be rapidly hydrolyzed into ammonium nitrogen at appropriate temperature and humidity and then easily converted into NH_3 volatilization loss (Li et al., 2018). The total cumulative NH_3 loss under different N split applications ranged from 6.2 to 9.4% of the applied N in this study (*Table 1*), which were slightly lower than the emissions factor of 10% of applied N advocated by the IPCC (2007). A lower FIE of less than 2.5% has also been reported by another study on the Loess Plateau in rain-fed winter wheat field (Yang et al., 2015). Cai et al. (2002) found that the NH_3 volatilization losses range from 11 to 48% of the applied N to maize. The lower NH_3 losses in the present study than in Cai et al. (2002) may be attributed to the application method of N fertilizer. In this study, basal N was broadcast on the surface and then was mixed into soil; for topdressed N, N fertilizer was applied in a band in the middle of the no-film rows at a depth of 5 cm. NH_3 volatilization losses of N fertilizer are closely related to the application technique and N rate (Sommer et al., 2003; Zhao et al., 2009). In comparison to surface application, deep placement of N fertilizer could

http://www.aloki.hu ● ISSN 1589 1623 (Print) ● ISSN 1785 0037 (Online)
DOI: http://dx.doi.org/10.15666/aeer/1704_92159227

reduce NH_3 losses substantially (Zeng et al., 2016). Rochette et al. (2013) reported that NH_3 volatilization losses were 50% of applied N when urea was banded at the surface and incorporation of the band decreased emissions by an average of 7% cm^{-1}. Pan et al. (2016) also found that in comparison to surface application, deep placement significantly decreased NH_3 volatilization through the incorporation of fertilizer at 54.7%.

A previous study reported that a split applications of N fertilizer did not affect NH_3 volatilization, regardless of splitting frequency (Pan et al., 2016). In our study, applying N with two or three splits significantly decreased NH_3 volatilization by 30.5% over two years, and the FIE from topdressed N was significantly lower than that from basal N (*Table 1*). One possible reason for this discrepancy is the different application method with basal and topdressed N, as described above. Basal N was broadcast on the surface and then mixed with the 0-15 cm soil; however, some of the N fertilizer was still exposed on the soil surface, increasing the risk of NH_3 losses compared to that with topdressed N. In addition, N losses through NH_3 volatilization increase with an increasing rate of N application in soils (Tian et al., 2001; Zhao et al., 2009), and previous studies have shown that the NH_3 emissions response to increasing N input is exponential rather than linear (Ma et al., 2010). In the present study, all N fertilizer was applied as basal dressing in treatment N1, which led to large amounts of NH_3 volatilization.

NH_3 volatilization is a physical process that is mainly influenced by the concentration of NH_4^+-N in the soil solution and by the resistance to NH_3 movement from the soil matrix (Sommer et al., 2004). Rochette et al. (2013) found cumulative losses increased exponentially with increasing maximum NH_4^+-N measured in the surface soil during the experiment. Consistent with previous reports, significant and positive correlations were observed between NH_3 volatilization flux and soil NH_4^+-N contents in this study (*Table 2*). Soil temperature and moisture are two other important factors affecting NH_3 volatilization. Fan et al. (2011) reported that the cumulative NH_3 volatilization loss increased by 1.6 fold in sandy soil when the temperature increased from 20 to 30 °C. A study in the wheat growing season showed that soil temperature has positive effects on NH_3 fluxes during Oct-Dec but has negative effects during Feb.-May (Yang et al., 2015). However, no significant correlations were observed between NH_3 flux and soil temperature in the present study. This difference could be explained by the influence of precipitation events on the soil temperature and NH_3 volatilization flux. In some cases, high NH_3 emissions occurred following precipitation events when the soil temperature was relatively low. Soil moisture had significant positive effects on NH_3 fluxes, which could explain 7.3-19.7% of the variation in the NH_3 fluxes (Yang et al., 2015). Bosch-Serra et al. (2014) found that NH_3 volatilization was significantly reduced when the WFPS in the 0-30 cm soil layer was less than 56%. In this study, no significant correlations were observed between the NH_3 flux and soil WFPS. This result may be attributed to the different effects of precipitation amount on NH_3 fluxes. Previous studies have reported that the magnitude of NH_3 losses was largely influenced by small temporal differences in the weather and initial soil moisture content (Engel et al., 2011; Turner et al., 2012). The largest losses (30-44% of applied N) occurred after urea was applied to high-water content soil surfaces, followed by a period of slow drying with little or no precipitation (Engel et al., 2011). Light precipitation and high soil moisture would increase NH_3 volatilization risk by promoting urea hydrolysis, while heavy precipitation may effectively mitigate NH_3 losses by leaching

http://www.aloki.hu ● ISSN 1589 1623 (Print) ● ISSN 1785 0037 (Online)
DOI: http://dx.doi.org/10.15666/aeer/1704_92159227

unhydrolyzed urea into the soil profile (Holcomb et al., 2011). In this study, the NH_3 flux increased sharply following slight precipitation events of 3 mm and 5 mm after topdressed N was applied at the V8 and R1 stages, respectively, in 2015. We also observed that the NH_3 flux was restrained rapidly by heavy precipitation of 20 mm after the application of topdressed N at the V8 stage in 2014 (*Fig. 4*).

Adjusting the application timing of N fertilizer and improving temporal synchronicity between crop-N demand and soil-N availability is a key strategy for improving the NRE (Ribaudo et al., 2011). In the present study, higher grain yields, total N uptake, and NRE were observed from the plots under N split applications than in the other plots (*Table 3*). Similar to our results, Shi et al. (2012) also found that the grain yield and NRE increased significantly when N fertilizer application was divided into an appropriate ratio of basal and topdressed N. Yi et al. (2008) reported that the NRE increased by more than 2 fold when N was applied with splits of 1:1 compared with a split of 2:1 of basal to topdressed N. This result may be attributed to the lower N demand in the early growth stage of maize and the increased risk of leaching from a large amount of N fertilizer input. Kettering et al. (2013) indicated that applying fertilizer N with 3-4 splits according to a plant's N needs could reduce N leaching and increase the NRE.

Table 3. *Grain yield, total N uptake and N recovery efficiency*

Treatments	Grain Yield (t ha^{-1})		Total N uptake (kg ha^{-1})		NRE (%)	
	2014	2015	2014	2015	2014	2015
N0	8.6 c	3.6 c	125.2 d	50.1 d		
N1	12.7 b	12.1 b	218.7 c	169.1 c	41.6 c	52.9 c
N2	13.3 a	13.0 a	242.8 b	197.0 b	52.3 b	65.3 b
N3	13.5 a	13.2 a	255.0 a	221.9 a	57.7 a	76.4 a

Different lowercase letters within a column indicate significant differences ($p < 0.05$)

Conclusions

NH_3 flux was positively correlated with soil NH_4^+-N content and was greatly affected by precipitation events. Applying N with two or three splits significantly increased the grain yield, total N uptake, and NRE of maize and significantly reduced NH_3 volatilization losses. The coupling effect of N fertilizer application and precipitation on NH_3 volatilization should be further investigated in the future.

Acknowledgements. This research was financially supported by the Ministry of Science and Technology of China (2015CB150402), National Key Research and Development Plan (2017YFD0200100, 2017YFD0201807), National Natural Science Foundation of China (41601308, 41601310).

REFERENCES

[1] Behera, S. N., Sharma, M., Aneja, V. P., Balasubramanian, R. (2013): Ammonia in the atmosphere: a review on emission sources, atmospheric chemistry and deposition on terrestrial bodies. – Environmental Science and Pollution Research 20(11): 8092-8131.

[2] Black, A., Sherlock, R., Smith, N. (1987): Effect of urea granule size on ammonia volatilization from surface-applied urea. – Fertilizer Research 11(1): 87-96.

http://www.aloki.hu ● ISSN 1589 1623 (Print) ● ISSN 1785 0037 (Online)
DOI: http://dx.doi.org/10.15666/aeer/1704_92159227

[3] Bosch-Serra, À. D., Yagüe, M. R., Teira-Esmatges, M. R. (2014): Ammonia emissions from different fertilizing strategies in Mediterranean rainfed winter cereals. – Atmospheric Environment 84: 204-212.
[4] Boyer, E. W., Goodale, C. L., Jaworski, N. A., Howarth, R. W. (2002): Anthropogenic Nitrogen Sources and Relationships to Riverine Nitrogen Export in the Northeastern U.S.A. – In: Boyer, E. W., Howarth, R. W. (eds.) The Nitrogen Cycle at Regional to Global Scales. Springer, Dordrecht, pp. 137-169.
[5] Cai, G. X., Chen, D. L., Ding, H., Pacholski, A., Fan, X. H., Zhu, Z. L. (2002): Nitrogen losses from fertilizers applied to maize, wheat and rice in the North China Plain. – Nutrient Cycling in Agroecosystems 63(2): 187-195.
[6] Chen, X., Cui, Z., Fan, M., Vitousek, P., Zhao, M., Ma, W., Wang, Z., Zhang, W., Yan, X., Yang, J., Deng, X., Gao, Q., Zhang, Q., Guo, S., Ren, J., Li, S., Ye, Y., Wang, Z., Huang, J., Tang, Q., Sun, Y., Peng, X., Zhang, J., He, M., Zhu, Y., Xue, J., Wang, G., Wu, L., An, N., Wu, L., Ma, L., Zhang, W., Zhang, F. (2014): Producing more grain with lower environmental costs. – Nature 514(7523): 486-489.
[7] Cui, Z. L., Zhang, F. S., Chen, X. P., Miao, Y. X., Li, J. L., Shi, L. W., Xu, J. F., Youliang, Y. L., Liu, C. S., Yang, Z. P., Qiang, Z., Huang, S. M., Bao, D. J. (2008): On-farm evaluation of an in-season nitrogen management strategy based on soil N-min test. – Field Crops Research 105(1-2): 48-55.
[8] Engel, R., Jones, C., Wallander, R. (2011): Ammonia volatilization from urea and mitigation by NBPT following surface application to cold soils. – Soil Science Society of America Journal 75: 2348-2357.
[9] Fan, X. H., Li, Y. C., Alva, A. K. (2011): Effects of temperature and soil type on ammonia volatilization from slow-release nitrogen fertilizers. – Communications in Soil Science and Plant Analysis 42(10): 1111-1122.
[10] Ferm, M. (1998): Atmospheric ammonia and ammonium transport in Europe and critical loads: a review. – Nutrient Cycling in Agroecosystems 51(1): 5-17.
[11] Gong, Z., Zhang, G., Chen, Z. (2007): Pedogenesis and Soil Taxonomy (in Chinese). – Science Press Publishing, Beijing.
[12] Holcomb, J. C., Sullivan, D. M., Horneck, D. A., Clough, G. H. (2011): Effect of Irrigation Rate on Ammonia Volatilization. – Soil Science Society of America Journal 75: 2341-2347.
[13] Kettering, J., Ruidisch, M., Gaviria, C., Ok, Y. S., Kuzyakov, Y. (2013): Fate of fertilizer ^{15}N in intensive ridge cultivation with plastic mulching under a monsoon climate. – Nutrient Cycling in Agroecosystems 95(1): 57-72.
[14] López-Bellido, L., López-Bellido, R. J., Redondo, R. (2005): Nitrogen efficiency in wheat under rainfed Mediterranean conditions as affected by split nitrogen application. – Field Crops Research 94(1): 86-97.
[15] Li, F.-M., Wang, J., Xu, J.-Z., Xu, H.-L. (2004): Productivity and soil response to plastic film mulching durations for spring wheat on entisols in the semiarid Loess Plateau of China. – Soil and Tillage Research 78(1): 9-20.
[16] Li, M., Wang, Y., Adeli, A., Yan, H. (2018): Effects of application methods and urea rates on ammonia volatilization, yields and fine root biomass of alfalfa. – Field Crops Research 218: 115-125.
[17] Liu, T. Q., Fan, D. J., Zhang, X. X., Chen, J., Li, C. F., Cao, C. G. (2015): Deep placement of nitrogen fertilizers reduces ammonia volatilization and increases nitrogen utilization efficiency in no-tillage paddy fields in central China. – Field Crops Research 184: 80-90.
[18] Ma, B. L., Wu, T. Y., Tremblay, N., Deen, W., McLaughlin, N. B., Morrison, M. J., Stewart, G. (2010): On-farm assessment of the amount and timing of nitrogen fertilizer on ammonia volatilization. – Agronomy Journal 102: 134-144.

http://www.aloki.hu ● ISSN 1589 1623 (Print) ● ISSN 1785 0037 (Online)
DOI: http://dx.doi.org/10.15666/aeer/1704_92159227

[19] Ni, K., Pacholski, A., Kage, H. (2014): Ammonia volatilization after application of urea to winter wheat over 3 years affected by novel urease and nitrification inhibitors. – Agriculture, Ecosystems & Environment 197: 184-194.
[20] Pacholski, A., Cai, G., Nieder, R., Richter, J., Fan, X., Zhu, Z., Roelcke, M. (2006): Calibration of a simple method for determining ammonia volatilization in the field - comparative measurements in Henan Province, China. – Nutrient Cycling in Agroecosystems 74(3): 259-273.
[21] Pan, B., Lam, S. K., Mosier, A., Luo, Y., Chen, D. (2016): Ammonia volatilization from synthetic fertilizers and its mitigation strategies: a global synthesis. – Agriculture, Ecosystems & Environment 232: 283-289.
[22] Paulot, F., Jacob, D. J., Pinder, R. W., Bash, J. O., Travis, K., Henze, D. K. (2014): Ammonia emissions in the United States, European Union, and China derived by high-resolution inversion of ammonium wet deposition data: interpretation with a new agricultural emissions inventory (MASAGE_NH_3). – Journal of Geophysical Research: Atmospheres 119(7): 4343-4364.
[23] Ribaudo, M., Hansen, L., Livingston, M., Mosheim, R., Williamson, J., Delgado, J. (2011): Nitrogen in agricultural systems: Implications for conservation policy. – USDA-ERS Economic Research Report Number 127, Washington, DC.
[24] Rochette, P., Angers, D. A., Chantigny, M. H., Gasser, M.-O., MacDonald, J. D., Pelster, D. E., Bertrand, N. (2013): Ammonia volatilization and nitrogen retention: how deep to incorporate urea? – Journal of Environmental Quality 42: 1635-1642.
[25] Scharf, P. C., Wiebold, W. J., Lory, J. A. (2002): Corn Yield Response to Nitrogen Fertilizer Timing and Deficiency Level. – Agronomy Journal 94(3): 435-441.
[26] Shi, Z., Jing, Q., Cai, J., Jiang, D., Cao, W., Dai, T. (2012): The fates of 15N fertilizer in relation to root distributions of winter wheat under different N splits. – European Journal of Agronomy 40: 86-93.
[27] Soares, J. R., Cantarella, H., Menegale, M. L. d. C. (2012): Ammonia volatilization losses from surface-applied urea with urease and nitrification inhibitors. – Soil Biology and Biochemistry 52: 82-89.
[28] Sommer, S. G., Génermont, S., Cellier, P., Hutchings, N., Olesen, J. E., Morvan, T. (2003): Processes controlling ammonia emission from livestock slurry in the field. – European Journal of Agronomy 19(4): 465-486.
[29] Sommer, S. G., Schjoerring, J. K., Denmead, O. T. (2004): Ammonia emission from mineral fertilizers and fertilized crops. – Advances in Agronomy 82: 557-622.
[30] Sutton, M. A., Erisman, J. W., Dentener, F., Möller, D. (2008): Ammonia in the environment: From ancient times to the present. – Environmental Pollution 156(3): 583-604.
[31] Sutton, M. A., Reis, S., Riddick Stuart, N., Dragosits, U., Nemitz, E., Theobald Mark, R., Tang, Y. S., Braban Christine, F., Vieno, M., Dore Anthony, J., Mitchell Robert, F., Wanless, S., Daunt, F., Fowler, D., Blackall Trevor, D., Milford, C., Flechard Chris, R., Loubet, B., Massad, R., Cellier, P., Personne, E., Coheur Pierre, F., Clarisse, L., Van Damme, M., Ngadi, Y., Clerbaux, C., Skjøth Carsten, A., Geels, C., Hertel, O., Wichink Kruit Roy, J., Pinder Robert, W., Bash Jesse, O., Walker John, T., Simpson, D., Horváth, L., Misselbrook Tom, H., Bleeker, A., Dentener, F., de Vries, W. (2013): Towards a climate-dependent paradigm of ammonia emission and deposition. – Philosophical Transactions of the Royal Society B: Biological Sciences 368(1621): 20130166.
[32] Tian, G., Cai, Z., Cao, J., Li, X. (2001): Factors affecting ammonia volatilisation from a rice–wheat rotation system. – Chemosphere 42(2): 123-129.
[33] Turner, D. A., Edis, R. E., Chen, D., Freney, J. R., Denmead, O. T. (2012): Ammonia volatilization from nitrogen fertilizers applied to cereals in two cropping areas of southern Australia. – Nutrient Cycling in Agroecosystems 93(2): 113-126.

http://www.aloki.hu ● ISSN 1589 1623 (Print) ● ISSN 1785 0037 (Online)
DOI: http://dx.doi.org/10.15666/aeer/1704_92159227

[34] Wang, S., Luo, S., Li, X., Yue, S., Shen, Y., Li, S. (2016): Effect of split application of nitrogen on nitrous oxide emissions from plastic mulching maize in the semiarid Loess Plateau. – Agriculture, Ecosystems & Environment 220: 21-27.
[35] Wolf, U., Fuß, R., Höppner, F., Flessa, H. (2014): Contribution of N_2O and NH_3 to total greenhouse gas emission from fertilization: results from a sandy soil fertilized with nitrate and biogas digestate with and without nitrification inhibitor. – Nutrient Cycling in Agroecosystems 100(1): 121-134.
[36] Yang, Q., Liu, P., Dong, S., Zhang, J., Zhao, B. (2019): Effects of fertilizer type and rate on summer maize grain yield and ammonia volatilization loss in northern China. – Journal of Soils and Sediments 19(5): 2200-2211.
[37] Yang, Y., Zhou, C., Li, N., Han, K., Meng, Y., Tian, X., Wang, L. (2015): Effects of conservation tillage practices on ammonia emissions from Loess Plateau rain-fed winter wheat fields. – Atmospheric Environment 104: 59-68.
[38] Yi, Z., Wang, P., Hong, B., Lu, L., Yu, G. (2008): Effect of base N to dress N ratio on water and nitrogen utilization, growth of summer maize in North China Plain. II. Nitrogen accumulation and translocation of summer maize and dynamics of soil inorganic N. – Chinese Journal of Eco-Agriculture 16(1): 86-90.
[39] Zeng, J., Liu, X., Song, L., Lin, X., Zhang, H., Shen, C., Chu, H. (2016): Nitrogen fertilization directly affects soil bacterial diversity and indirectly affects bacterial community composition. – Soil Biology and Biochemistry 92: 41-49.
[40] Zhang, Y., Luan, S., Chen, L., Shao, M. (2011): Estimating the volatilization of ammonia from synthetic nitrogenous fertilizers used in China. – Journal of Environmental Management 92(3): 480-493.
[41] Zhao, X., Xie, Y. X., Xiong, Z. Q., Yan, X. Y., Xing, G. X., Zhu, Z. L. (2009): Nitrogen fate and environmental consequence in paddy soil under rice-wheat rotation in the Taihu Lake region, China. – Plant and Soil 319(1-2): 225-234.

http://www.aloki.hu ● ISSN 1589 1623 (Print) ● ISSN 1785 0037 (Online)
DOI: http://dx.doi.org/10.15666/aeer/1704_92159227

MULTI-FEATURE SPARSE CONSTRAIN MODEL FOR CROP DISEASE RECOGNITION

WU, Y. R.[1] – LI, J. H.[2*]

[1]*Zhongkai Science and Technology Development Company, Zhongkai University of Agriculture and Engineering, Guangzhou 510225, China*

[2]*The Laboratory of Language Engineering and Computing, Guangdong University of Foreign Studies, Guangzhou 510006, China*

**Corresponding author*
e-mail: lijianhonghappy@163.com

(Received 1st Apr 2019; accepted 17th May 2019)

Abstract. Disease recognition based on crop leaf image is considerably important and significant, which is a challenging project due to the complicated nature of disease leaf image itself and the unavoidable degradations sourced from external imaging environment. In the recognition process, these traditional approaches generally stack one or more different modalities of features extracted from disease leaf images to be discriminated or trained, but do not deeply explore the relationships between features. For conquering this problem, we proposed a new crop disease recognition approach based on multi-feature sparse constrain model, which includes three steps: lesion segmentation, feature extraction and disease recognition. During the phase of disease recognition, the characteristic of our proposed is that the introduced multi-task joint sparse representation model can promote these sparse representation vectors corresponding to the different modalities of features to share similar structures to some extent with the specific styles of features extracted from the same training set. The proposed approach not only improve the efficiency significantly but also make the decision more robust. We verify the proposed approach with images of diseased cucumber, and the experiments demonstrate that our proposed method is remarkable superior to the state of the art algorithms and the correct recognition rate of our approach is 88.05%, which is higher 11.3% percentage than the benchmark of SVM method.
Keywords: *crop disease identification, multi-task learning, joint sparse representation, accelerated proximal gradient, lesion segmentation, feature extraction*

Introduction

Crop diseases have long been considered as one of the primary threats to reduce crop yield and quality. According to recent reports, the global plant yield has reduced by at least 10% each year due to the crop diseases (Mutka and Bart, 2015). It can be seen that whether crop diseases can be discovered in time is significantly important for increasing the production and quality of agricultural products. However, the identification of crop diseases to date has remained on the basis of artificial judgment, which is inefficient and subjective. In China, due to the lack of professional agricultural technicians, farmers usually are forced to judge the type and evaluate its degree of diseases according to their past experience. The wrong diagnosis and the resulting pesticide abuse are extremely common as expected. Therefore, it is urgently to find a timely, accurate and low-cost approach to alleviate the present condition

Due to the huge driving force of the potential market and the rapid development of computer vision and machine learning technology, in recent years, crop disease identification has received widespread attention by researchers, and a large number of related algorithms have been proposed. Generally speaking, the common disease

http://www.aloki.hu ● ISSN 1589 1623 (Print) ● ISSN 1785 0037 (Online)
DOI: http://dx.doi.org/10.15666/aeer/1704_92299245

identification algorithms mainly include 4 steps (Iqbal et al., 2018; Golhani et al., 2018; Dhingra et al., 2019; Zhang et al., 2017b, 2018; Zhang and Wang, 2016), followed by disease image pre-processing, disease lesion segmentation, disease feature extraction, and disease species identification. In the pre-processing step, image enhancement operations, such as median filtering (Unay et al., 2011; Sun et al., 2018), histogram equalization (Khirade and Patil, 2015), etc., are usually adopted to avoid interference of notorious noise and uneven illumination in the sample image. Lesion segmentation refers to the localization process to find the lesion areas with pixel level in the leaf images. The commonly used algorithms include K-means algorithm (Zhang et al., 2018, 2017a; Ghosh and Dubey, 2013; Prajapati et al., 2016), OTSU algorithm (Zhang and Wang, 2016; Dey et al., 2016), and super pixel clustering (Zhang and Zhu, 2017). When the lesion area is separated, it is necessary to extract some modality features such as color, shape, texture or other attributes of the lesion. Whether the extracted features are appropriate or not directly determines the effectiveness of the disease identification algorithm. Common feature extraction methods include: Principle Component Analysis (PCA) (Zhang and Wu, 2017), wavelet analysis (Kleynen et al., 2005; Shaik et al., 2018), PSO (Muthukannan and Latha, 2015), gray level co-occurrence matrix (Iqbal et al., 2018) and so on. In general, the identification of a particular disease can use only one modality feature, however when distinguishing many kinds of diseases, mining the complementary information between the different modality features will obtain higher accuracy rate than just one. Disease identification is the final step of the approach which refers to taking advantage of the pattern recognition technology to classify the extracted features to achieve the purpose of identification. Commonly used disease classification algorithms include artificial neural networks (Bashish et al., 2011), support vector machine (Rumpf et al., 2010; Arivazhagan et al., 2013), K-nearest neighbor algorithms (Zhang et al., 2015), and sparse representation (Zhang and Wu, 2017), so on. Meanwhile, we also found that with the rise of deep learning, this technology has also been applied in the field of crop diseases identification.

In theory, deep learning not only avoids lesion segmentation and feature extraction steps, thus brings great convenience into the designing algorithm process, but also improves the correct recognition rate significantly (Ma et al., 2018; Grinblat et al., 2016; Zhang et al., 2019; Sladojevic et al., 2016; Lu et al., 2017). However, it is coexisting that deep learning technology is extremely demanding on the quantity and quality of samples. Accurate identification of any kind of disease requires massive standard sample images, complex parameter debugging and abnormal time-consuming model training. In the process of training the deep learning model, even an additional hardware device - Graphic Process Unit (GPU) is necessary. Obviously, subjecting to these factors such as geography, season and cost, the harsh conditions almost impossible to achieve.

In response to the above-mentioned problems, we are committed to developing a new crop disease identification approach, which can accurately and swiftly determine the type of disease according to the appearance of leaf diseases image. At the same time, this approach is not limited to the quantity and quality of training samples to save the cost of collecting samples. We summarize the main contributions of our algorithm proposed in this paper as follows:

1. Based on the sparse theory, we propose a new crop disease identification algorithm. The algorithm uses the multi-feature sparse constrain to describe the proposed prior, constructs the cost function, and successfully optimizes the cost function with the algorithm of accelerated proximal gradient. By comparing the

http://www.aloki.hu ● ISSN 1589 1623 (Print) ● ISSN 1785 0037 (Online)
DOI: http://dx.doi.org/10.15666/aeer/1704_92299245

recognition efficiency of cucumber leaf disease, the recognition efficiency of the algorithm is obviously better than other state of the art algorithms.

2. Inspired by the idea of multi-task learning, we find a new prior, which points out that the different modalities of disease features can be represent with the corresponding features extracted from the training set. The structure of the sparse coefficient vectors should be similar. This proposed multi-feature sparse constrain model has a more realistic constraint effect, and the resulting sparse coefficient is more accurate, robust, and close to the actual situation.
3. Because there is no complicated training process and cumbersome parameter setting step in this paper, the principle of our algorithm is well comprehensible, thus its calculation process is simple and easy to operate. More unexpected is that the performance of our approach is still extraordinary excellent in the case of insufficient training samples. This characteristic can help us conquer the difficulty of the dependence on a large number of samples, which are susceptible to various factors for obtaining.

In the first section, we summarized the significance and status quo of automatic disease identification. Some related work to our algorithm will be introduced in the second part. The first will elaborate the proposed algorithm, including 4 steps: pre-processing, detection feature extraction and recognition. In the fourth part, we will give the comparison results of the proposed algorithm and other state of the art algorithms, and further analyze the performance of the algorithm. The last section is the conclusion and prospect of the paper, and it points out the unresolved problems in the fields of automatic disease identification and puts forward our working plan in the future.

Related work

At the beginning of this century, neuroscientists found in their research that for images entering in the human eye, the human visual system uses sparse representation to represent it with the help of as little as possible base feature (Rao et al., 2002). Inspired by this phenomenon, sparse representation has been widely used and deeply researched in machine learning and computer vision (Wright et al., 2009; Yang et al., 2010; Mei and Ling, 2011). The equation it needs to solve can be expressed as

$$\underset{w}{arg\,min}\frac{1}{2}\|y - D\omega\|_2^2 + \lambda\|\omega\|_0 \quad \text{(Eq.1)}$$

where y is a certain form of feature vector extracted from the input image, D is an over-complete dictionary composed of numerous base vectors, and the base vector in the dictionary is called “atom”. In general, a dictionary can be constructed by extracting features of a corresponding form from a collection of sample images. w is a sparse coefficient vector that needs to be solved and can sparsely represent the feature y. $\|w\|_0$ is L_0 norm represents the number of non-zero elements in the vector. However, *Equation 1* is non-convex, and the solution is very difficult to find. It is usually necessary to relax the constraint and replace the L_0 norm in *Equation 1* with the L_1 norm, thus to solve it with Lasso algorithm (Wright et al., 2009; Yang et al., 2010; Mei and Ling, 2011).

Image classification based on sparse representations shows great potential for crop disease identification (Zhang and Wu, 2017). It does not require a large number of

http://www.aloki.hu ● ISSN 1589 1623 (Print) ● ISSN 1785 0037 (Online)
DOI: http://dx.doi.org/10.15666/aeer/1704_92299245

training samples, and can accurately identify the types of diseases for most "regular" diseased leaves. However, in the process of optimizing the cost function, the Lasso algorithm usually selects atoms in the disease "dictionary" by an approximately random way to fit the disease features to be tested. The robustness of the recognition algorithm makes the judgment unstable. At the same time, in the optimal computing process, it is possible to wrongly make some discriminative 'atom' participate in the computing thus lead to the recognition accuracy rate reducing. In addition, in the case of recognition disease by multi-modality of features, the image classification technique based on sparse representation just stacks features such as color, shape, texture or spatial distribution of the same sample indiscriminately into one vector in the process of feature extraction, without considering the correlation between different kinds of features. This is essentially equivalent to constrain the sparse coefficients of these different forms of features to be identical. Obviously, if the judgments with these different forms of features are separately, some ambiguous conclusions may be drawn; and these identical sparse vectors corresponding to that different modality features are separately contrary to the real situation, which will introduce new errors and affect the judgment.

In fact, if considering the disease recognition with some modality feature as a task, a large number of researches have shown that (Zhang et al., 2018, 2017a; Zhang and Wang, 2016; Unay et al., 2011; Sun et al., 2018; Khirade and Patil, 2015) when there are some commonalities among these being learned tasks, improving the recognition efficiency by mining the relative information is feasible (Ozawa et al., 2009; Argyriou et al., 2008; Bickel et al., 2008; Caruana, 1997), which is called multi-task learning or transfer learning (Caruana, 1997). In the field of machine learning and computer vision, when the related tasks are affected by some common factors, the ability of multi task learning or transfer learning to improve the generalization ability is significant by mining relationship among tasks especially in the case of insufficient training samples. The basic idea of this paper is that when we use sparse representation to describe a testing feature with K modalities, and the dictionary is constructed by the corresponding K modalities of features extracted from the same training set, thus for each modality, we can consider it as a task. The fact is that when the reconstruction error is smallest, the smallest number of 'atoms' from one class can linearly represent the multi-feature, which can be considered as the final classifying result.

Materials and methods

Lesion segmentation and feature extraction

Assuming that there are J kinds of disease images in data set X, and n_j samples in disease j, the total number of samples in disease set is $\sum_{j=1}^{J} n_j = N$. For each disease image, we extract K different kinds of features such as color, shape, texture, etc. The training set can be expressed as

$$X = \begin{bmatrix} X_1^1 & X_2^1 & \cdots & X_J^1 \\ X_1^2 & X_2^2 & \cdots & X_J^2 \\ \vdots & \vdots & \cdots & \vdots \\ X_1^K & X_2^K & \cdots & X_J^K \end{bmatrix}_{M \times N} \quad \text{(Eq.2)}$$

http://www.aloki.hu ● ISSN 1589 1623 (Print) ● ISSN 1785 0037 (Online)
DOI: http://dx.doi.org/10.15666/aeer/1704_92299245

where $X_j^k \in R^{m_k \times n_j}$ represents the *k-th* class feature of the *j-th* type of disease image, and each column in X_j^k is a feature vector with dimension m_k. $X^k = [X_1^k, X_2^k \cdots, X_j^k]$ is a matrix of $m_k \times N$ representing the *k-th* class feature of the disease set. $X_j = \left[(X_j^1)^T, (X_j^2)^T, \cdots, (X_j^K)^T, \right]^T$ is a matrix of $M \times n_j$ representing the disease features of n_j samples in the *j-th* disease, and the dimension of each disease feature vector is $\sum_{k=1}^{K} m_k = M$. For a diseased leaf image to be tested, we extract its *K*-modalities features $y^k \in R^{m_k}$, (*k = 1, 2, ..., K*), and the feature vector of the diseased leaf image to be tested can be expressed as $Y = [(y^1)^T, (y^2)^T, \cdots, (y^K)^T]^T, Y \in R^M$. For the feature vector Y, we hope that each y^k can be sparsely represented by the corresponding feature X^k in the training set, and the obtained *K* sets of coefficients should have similar spare structure. The mathematical representation of this idea can be described in *Equation 3*.

$$arg\ \min_w \frac{1}{2}\sum_{k=1}^{K}\left\|y^k \sum_{j=1}^{J} X_j^k W_j^k\right\|_2^2 + \lambda \left\|\left(\|W_1\|_F, \|W_2\|_F, \cdots, \|W_J\|_F\right)\right\|_0 \quad \text{(Eq.3)}$$

where $W_j^k \in R^{n_j}$ represents the coefficient vector corresponding to the feature in the *k*-th form of the *j*-th disease image set, and the matrix $W_j = [W_j^1, W_j^2, \cdots, W_j^k], W_j \in R^{n_j \times k}$, vector $W^k = \left[(W_1^k)^T, (W_2^k)^T, \cdots, (W_j^k)^T\right]^T$, $W^k \in R^n$, $\|W\|_{1,2} = \sum_{i=1}^{n} \|R_i(W)\|_2$, and R_i are responsible for extracting the *i*-th row of the coefficient matrix *W*. The concrete expression of the coefficient matrix is

$$W = \begin{bmatrix} W_1^1 & W_1^2 & \cdots & W_1^K \\ W_2^1 & W_2^2 & \cdots & W_2^K \\ \vdots & \vdots & \cdots & \vdots \\ W_J^1 & W_J^2 & \cdots & W_J^K \end{bmatrix}_{n \times k} \quad \text{(Eq.4)}$$

where $\|W_j\|_F$ refers to the Frobenius norm of the matrix W_j, and $\|x\|_0$ refers to the L_0 norm of the vector x, that is the number of non-zero elements in the vector x. However, the L_0 norm in *Equation 3* makes the cost function non-convex, and to find the solution is very difficult. In order to solve the problem, we relax the cost function to *Equation 5*

$$arg\ \min_w \frac{1}{2}\sum_{k=1}^{K}\|y^k - X^k W^k\|_2^2 + \lambda \sum_{j=1}^{J}\|W_j\|_F \quad \text{(Eq.5)}$$

We call *Equation 5* a multi-feature sparse constrain model. Its solution is simple to solve. We use the accelerated proximal gradient method to solve the problem. For detailed solution steps, please refer to *Algorithm 2* in this paper.

Multi-feature sparse constrain

The accurate detection of the lesion area and extracting appropriate features play an important role in the disease identification process. The *K*-means clustering algorithm is one of the classic algorithms for image segmentation. It divides all the pixels of the input image into *K* classes according to the feature of each pixel. Since the content of the disease image is relatively fixed, it can generally be regarded as consisting of a healthy area, a diseased area, and a transitional area between the two. Therefore, the

http://www.aloki.hu ● ISSN 1589 1623 (Print) ● ISSN 1785 0037 (Online)
DOI: http://dx.doi.org/10.15666/aeer/1704_92299245

determination of *K* and the selection of cluster centers are relatively easy. In this paper, we use the *K*-means clustering algorithm to segment disease images. The RGB value of each pixel is taken as its feature vector. The core idea of the k-means algorithm is to divide *n* RGB vectors into *k* clusters, so that the sum of the squares of the distance between the RGB vector in each cluster and the cluster center is the smallest. The algorithm flow is as shown in *Algorithm 1*.

Algorithm 1. *K-means algorithm segmentation*

1. Select *K* Pixels as the initial cluster centers randomly;
2. Calculate the distance between the remaining samples and each cluster center, classify the sample into this class with the nearest distance;
3. Re-compute the average value of each class and update the clustering center of each class with the criterion function

$$\mathrm{E} = \sum_{i=1}^{C} \sum_{x \in C_i} \left\| x - x_{C_i} \right\|^2$$

4. When the criterion function no longer converges, the clustering result is output, otherwise it is repeated Step2~Step4.

The *K*-means algorithm divides all pixels in the disease image into *K* categories. Next, you need to find the class of the pixel in the disease area accurately in this *k*-type pixel. In fact, because the characteristics of different diseases on the leaves are different, it is very difficult to find out the common characteristics of various diseases and directly locate the class of the diseased pixels. However, the characteristics of the healthy area of the leaf are easy to find and stable from the perspective of color and texture. To this end, we find the pixels of the healthy area from the *K*-type of pixels, and the remaining pixels are considered to be the pixels of the diseased area. This method will judge some of the transitional pixels between the healthy area and the diseased area as the disease content, so that some initial characteristics of the disease can be reflected from the information provided by the disease area, on the one hand, the early symptoms can be reflected in the extracted features, and on the other hand, the efficiency of recognition of the overall disease is also improved. *Figure 1* shows the segmentation results of four disease images. It can be seen from the results given that the pixels of most disease areas can be correctly found by the *K*-means algorithm. After locating the disease region, we will extract feature for the disease areas. 4- Unicom disease region is first determined region area, and further select intermediate 4- Unicom disease region to extract features. In this paper, we consider the three aspects of color, shape and texture to extract the feature of the diseased area. In order to avoid the affection of scale and direction, we try to select some features that will not disturbed by the scaling and rotation factors. We have selected a total of 28 features, including 4 color features, 6 shape features, and 18 texture features. The specific feature name and the corresponding feature can be found in the *Appendix*. After normalizing the different types of feature vectors, they connected each other to construct the feature vector we need to use.

Disease identification

The process of disease classification is relatively simple. For each type of disease *j*, *Equation 6* is used to calculate the reconstruction error between the testing feature and its fitting result, and select *j** corresponding to the smallest error as the decision.

http://www.aloki.hu ● ISSN 1589 1623 (Print) ● ISSN 1785 0037 (Online)
DOI: http://dx.doi.org/10.15666/aeer/1704_92299245

$$j^* = arg\ \min_j \sum_{k=1}^{K} \theta^k \left\| y^k - X_j^k W_j^k \right\|_2^2, \mathrm{j} = 1,2,\cdots,\mathrm{J} \quad \text{(Eq.6)}$$

where $\{\theta^k\}_{k=1}^K$ are the weights of the different feature forms in the recognition process. According to the definition, we will elaborate weight parameter $\{\theta^k\}_{k=1}^K$ in the experimental part. Further, the disease category j^* which minimizes the error of the reconstructed test disease feature is selected as the final recognition result. The pseudo code of the process is shown in *Algorithm 2*.

Algorithm 2. *Multi-task joint sparse representation*

Input: disease feature set X, label k, y
Output: the disease category number j^*
1. Initialization: $v^0 = 0, \alpha_0 = 1$
2. For $t = 1: T$
3. Compute W^{t+1}

$$W_j^{(t+1)} = \left[1 - \frac{\lambda\eta}{\left\|[V^t - \eta\nabla f(V^t)]_j\right\|_2}\right]_+ [V^t - \eta\nabla f(V^t)]_j$$

4. Compute V^{t+1}

$$V^{(t+1)} = W^{(t+1)} + \frac{\alpha_{(t+1)(1-\alpha_t)}}{\alpha_t}(W^{(t+1)} - W^t)$$

5. $\alpha_t = 2/(t+3)$
6. $t = t + 1$;
7. End
8. $j^* = arg\ \min_j \sum_{k=1}^{K} \theta^k \left\| y^k - X_j^k W_j^k \right\|_2^2$
9. Return j^*

Experiment and analysis

In order to verify the effectiveness of the proposed algorithm, we conducted extensive experiments on cucumber leaf diseases image and do comparisons with state of the art results published in recent years. These state of the art algorithms include SR (Zhang and Wu, 2017), SVM (Rumpf et al., 2010), ANN (Bashish et al., 2011), TF (Arivazhagan et al., 2013), and KNN (Zhang et al., 2015). All experiments were performed on a computer with 1.8 GHz CPU and 2 GB cache and a 64bit Windows 2K operating system was installed in it. All the algorithms including ours proposed in this paper were coded and implemented on MATLAB2015b platform. The results of the participating comparison algorithm are basically consistent with the results given in the experimental part of the corresponding paper.

Parameter settings

The cucumber leaf disease image used in this paper are collected in the farm of Zhongkai University of Agricultural and Engineering. All the disease leaves are obtained by agronomy students under the guidance of professional teachers through digital cameras or smart phones, and the corresponding disease types are labeled by agriculture experts. In the process of obtaining examples, in order to avoid the interference of uneven illumination, atmospheric turbulence and other factors, our

http://www.aloki.hu ● ISSN 1589 1623 (Print) ● ISSN 1785 0037 (Online)
DOI: http://dx.doi.org/10.15666/aeer/1704_92299245

image acquisition process is completed indoors, and set the same shooting environment for each image. All captured images are set to 800 × 800 pixels by cutting or zooming, etc. All images are three-channel color images and saved as "jpg" format. A partial images selected form the data set is shown in *Figure 2*. The data set contained 1,120 images with seven common diseases, i.e., downy mildew, bacterial angular, Corynespora cassiicola, scab, gray mold, anthracnose, powdery mildew. Each disease contained 160 samples and for each disease, we selected 100 samples randomly for training in our model, and the remaining 60 examples were used for testing. Considering that there may still exist noise or uneven illumination introduced during the shooting process, we perform smoothing and histogram equalization before starting the diseased region segmentation step. Next, extract the features of each disease image according to the explanation in Section 3.2, and add labels for each example to construct a training data set. Further, the sparse coefficient W is obtained by the *Equation 5,* and the type of the disease is judged by the *Equation 6*. The feature weight parameters in *Equation 6* are set to: color weight $\theta^1 = 0.5$, shape weight $\theta^2 = 0.3$, texture weight $\theta^3 = 0.2$, and the settings will be explained in next sub-section.

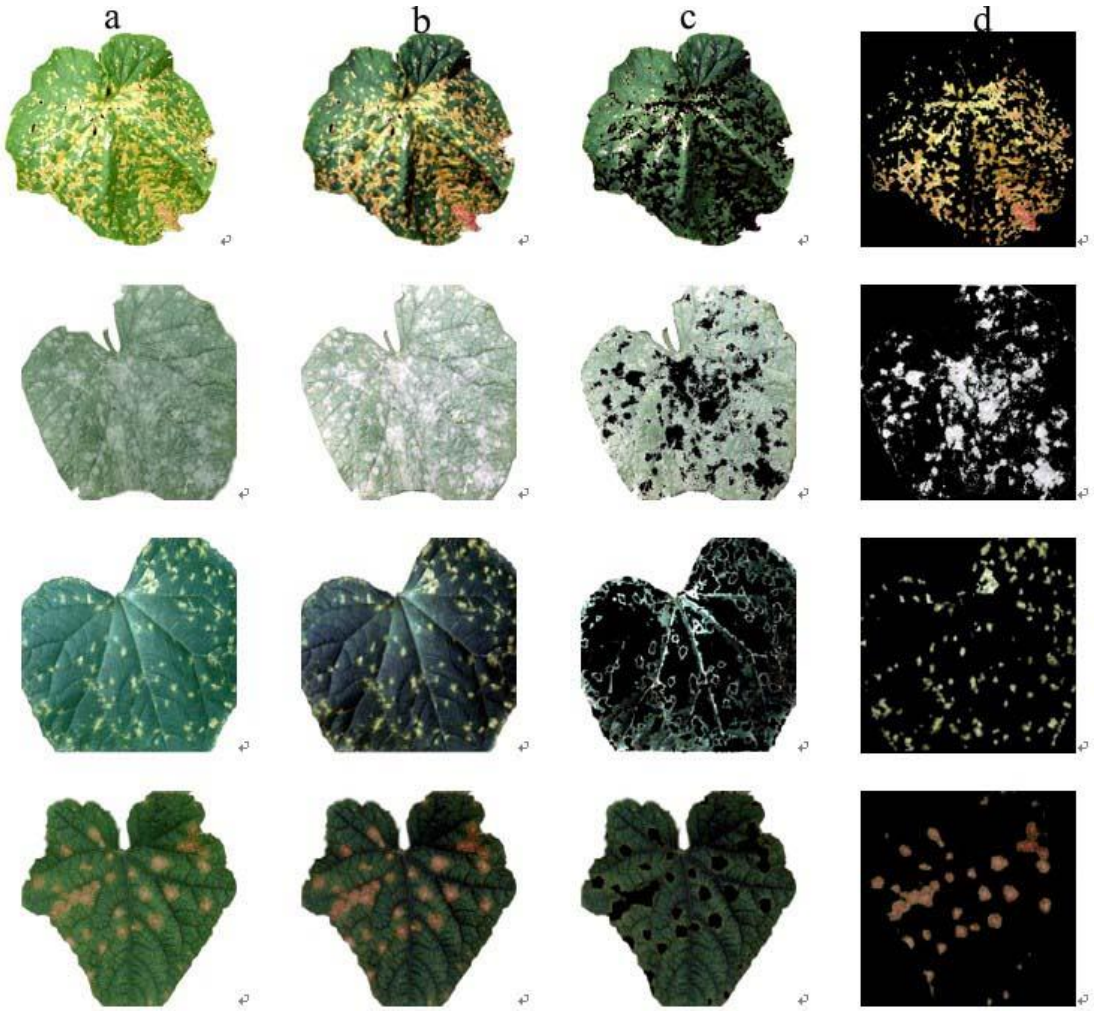

Figure 1. *The results of healthy region and legion region with K-means segmentation (the disease names from the top line to the final line are bacterial angular, powdery mildew, Corynespora cassiicola and anthracnose separately). (a) Disease leaf images; (b) Enhancement leaf image; (c) Healthy region; (d) Legion region algorithm*

http://www.aloki.hu ● ISSN 1589 1623 (Print) ● ISSN 1785 0037 (Online)
DOI: http://dx.doi.org/10.15666/aeer/1704_92299245

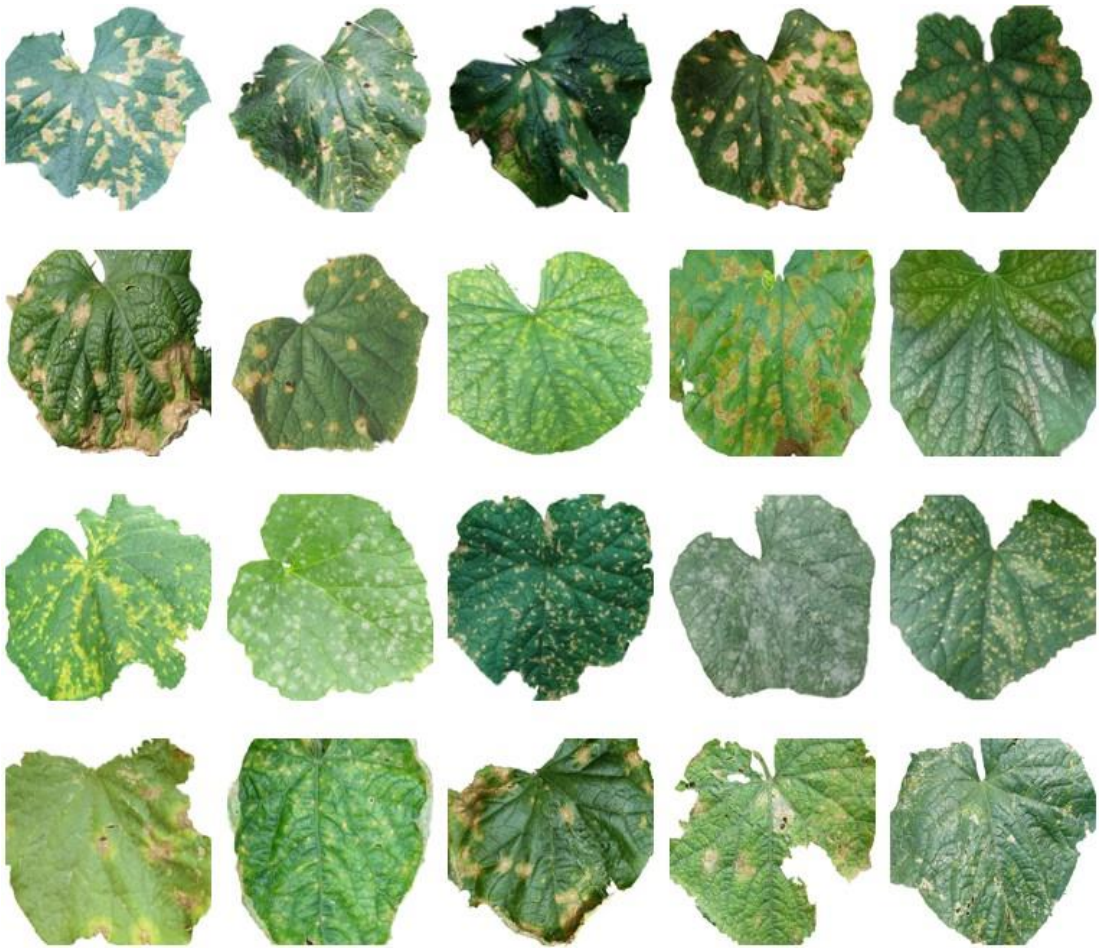

Figure 2. *Partial cucumber disease leaf examples*

According to *Figure 3,* we can conclude that the accuracy of our method is obviously better than the sparse representation with a single feature and better than other state of the art algorithms without considering the relationship between features such as the algorithm of (Zhang and Wu, 2017).

Experimental results

After obtaining the training and testing data, we randomly selected a certain number of samples in each type of disease image as "atoms" to construct a dictionary to identify the disease of testing example. The results are shown in *Figure 3*. In the case of considering only one feature, the method degenerates into a sparse representation recognition algorithm. Since only one feature form is considered, its recognition efficiency is low. The solution of sparse coefficient is similar to SR algorithm, but due to the single feature form, its recognition efficiency is lower than the SR algorithm. The SR algorithm uses sparse representation classification theory for disease identification, which just stacks color features, shape features and texture features indiscriminately. In the process of solving sparse coefficients, the SR algorithm randomly select as few as possible "atoms" to approximately fit the testing example which is unstable. However, our method comprehensively considers the sparse coefficient vectors of the

http://www.aloki.hu ● ISSN 1589 1623 (Print) ● ISSN 1785 0037 (Online)
DOI: http://dx.doi.org/10.15666/aeer/1704_92299245

corresponding different modalities features as similar as possible, which is a stronger constraint and makes the recognition results more accurate.

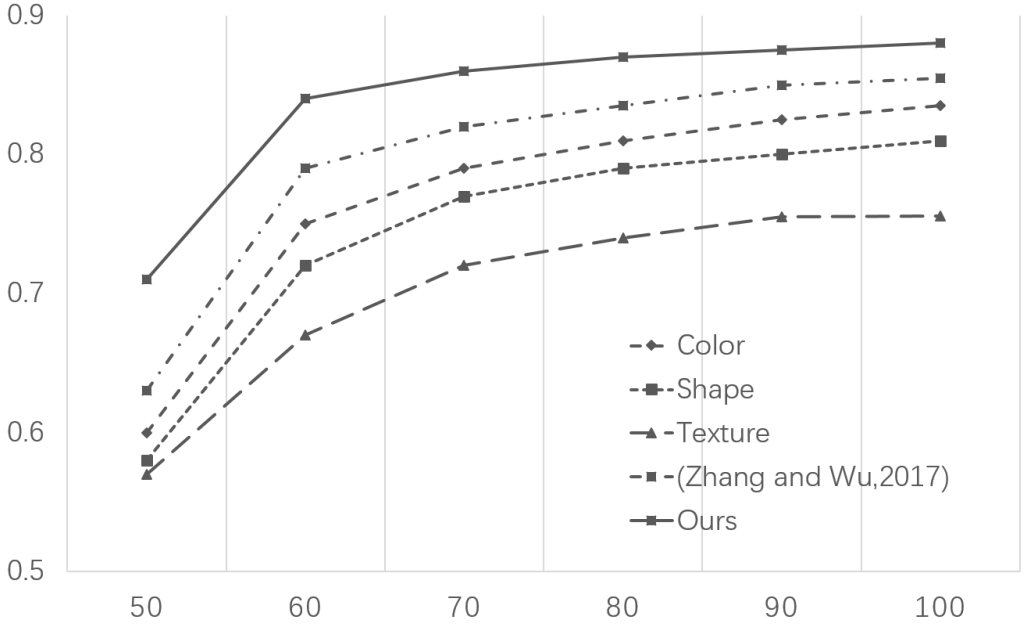

Figure 3. *The accuracy curve of cucumber disease identification*

At the same time, we can notice that our algorithm has increased the recognition efficiency as the number of training samples increases, and it is always higher than other methods.

Observing the experimental results given in *Figure 3*, we can see that when the three features of color, shape and texture are processed separately, the efficiency of each is not the same. In order to quantify the proportional relationship between them and determine the parameters $\{\theta^k\}$, we set the color and shape characteristics in the range of, and quantize, and the step size is set to 0.1. After the color feature weight and the shape feature weight are determined, the texture feature weight may not be displayed. However, for each set of weight values, a disease identification test was conducted to obtain an average accuracy rate, and the results are shown in *Figure 4*. It can be seen from *Figure 4* that when $\theta^1 = 0.5$, $\theta^2 = 0.3$, $\theta^3 = 0.2$, the recognition rate reaches the maximum value, so other experiments in this paper are performed according to this setting.

Furthermore, according to the conclusion of *Figure 4*, we set the number of atoms in the dictionary to 700, (that means that 100 samples for each type of disease to participate in the training), and test the correct recognition rate and average consumption of the disease with the selected state of the art algorithms. The comparison results of the correct recognition rate of the disease are shown in *Table 1*, and the average time consumed by these algorithms is shown in *Table 2*. By observing the experimental data exhibited in *Tables 1* and *2*, it is not difficult to find that our algorithm has the highest accuracy and the minimum average time to identify the results of the identification of these seven diseases.

http://www.aloki.hu ● ISSN 1589 1623 (Print) ● ISSN 1785 0037 (Online)
DOI: http://dx.doi.org/10.15666/aeer/1704_92299245

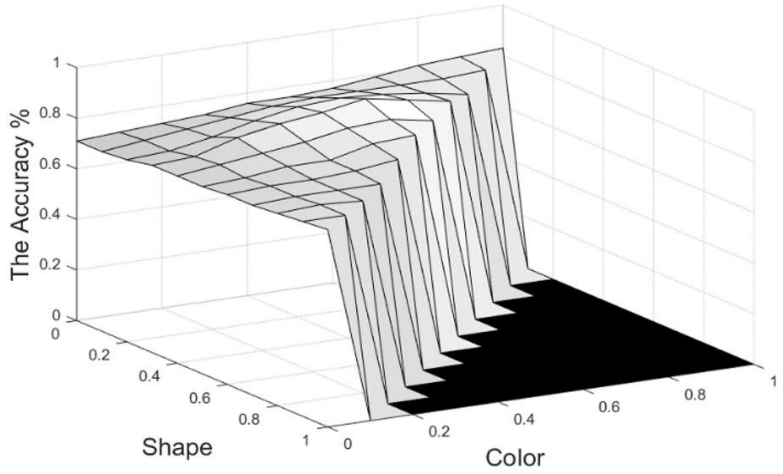

Figure 4. *The varying surface of recognition accuracy rate with the feature weights*

Table 1. *The comparisons of precision rate between ours and the state of the art*

Disease name	SVM (Rumpf et al., 2010)	ANN (Bashish et al., 2011)	TF (Arivazhagan et al., 2013)	KNN (Zhang et al., 2015)	SR (Zhang and Wu, 2017)	Ours
Downy mildew	81.30	82.17	81.18	82.56	88.48	89.53
Bacterial angular	70.38	71.38	79.34	79.36	82.40	83.04
Corynespora cassiicola	71.86	72.20	76.49	77.68	84.18	86.41
Scab	73.19	70.88	73.65	73.10	83.15	84.37
Gray mold	85.35	87.35	85.20	86.41	91.29	93.53
Anthracnose	78.25	74.06	89.24	81.78	84.38	90.86
Powdery mildew	77.41	77.66	74.59	83.25	86.28	88.58
Average	76.82	76.53	79.96	80.59	85.74	88.05

Table 2. *The comparison of average consuming time between the state of the art algorithms and ours*

	SVM	ANN	TF	KNN	SR	Ours
Average consuming time	22.6	10.8	12.5	36.7	11.8	7.3

Discussion

From the above experiments, we can find that in the cucumber diseases identification, our algorithm shows significant advantage in the correct recognition rate and the consuming time comparison. Next, we analyze the reasons about the above conclusion. First, the artificial neural network algorithm uses the training samples as input data to adjust the weight coefficients of the neural nodes, and uses these coefficients to fit the test sample to achieve classification. Such algorithms have higher self-adaptive and generalization ability. However, these algorithms are strongly dependent on training samples and sensitive to initial weight coefficients of neural node. In the process of calculation, they are easy to converge the local minima, thus causing misclassification.

http://www.aloki.hu ● ISSN 1589 1623 (Print) ● ISSN 1785 0037 (Online)
DOI: http://dx.doi.org/10.15666/aeer/1704_92299245

The SVM algorithm is a classic two-classification algorithm. It has a good generalization ability for the two-class problem in small sample environments. However, the large-scale multi-classification problem is not ideal, and the SVM algorithm needs to be solved by means of quadratic programming. The support vector will involve the calculation of the *N*-order matrix (*N* is the number of samples). When *N* is large, it will take up more memory and consume a longer time. Similarly, the KNN algorithm is simple in principle and suitable for nonlinear multi-classification problems. Such algorithms are heavily dependent on data and sensitive to noise. In high-dimensional data, the distance and similarity between two data points are not always. It is directly proportional, and these will affect its accuracy. At the same time, such algorithms need to calculate the distance between the test sample and each training sample, and it takes a lot of time to calculate. The SR algorithm uses the features of the sample set to sparsely represent the test features, and uses the class with the lowest reconstruction error as the classification result. This method is more accurate than other methods, but in the process of solving the sparse coefficient, the feature vector in the approximate random sample is used to fit the sparse coefficient, so that the judgment result is unstable and the recognition efficiency has room for further improvement.

All of the above algorithms use three different modality features of color, shape and texture, and all three different forms of features are simply stacked and calculated as a unified feature vector without considering these three different form features. It is against this problem that this paper designs a multi-task joint sparse representation algorithm, which requires different forms of features under the same sample set, and the sparse coefficients should have similar structures. *Figure 5-A* shows the sparse coefficients of the randomly extracted samples in the multi-task connection sparse representation, and *Figure 5-B* shows the reconstruction errors obtained by the sparse coefficients for the different disease features. In addition, the time complexity of the accelerated near-end gradient method used is O (*N*), where *N* is the number of samples, which means that the algorithm can complete the calculation quickly.

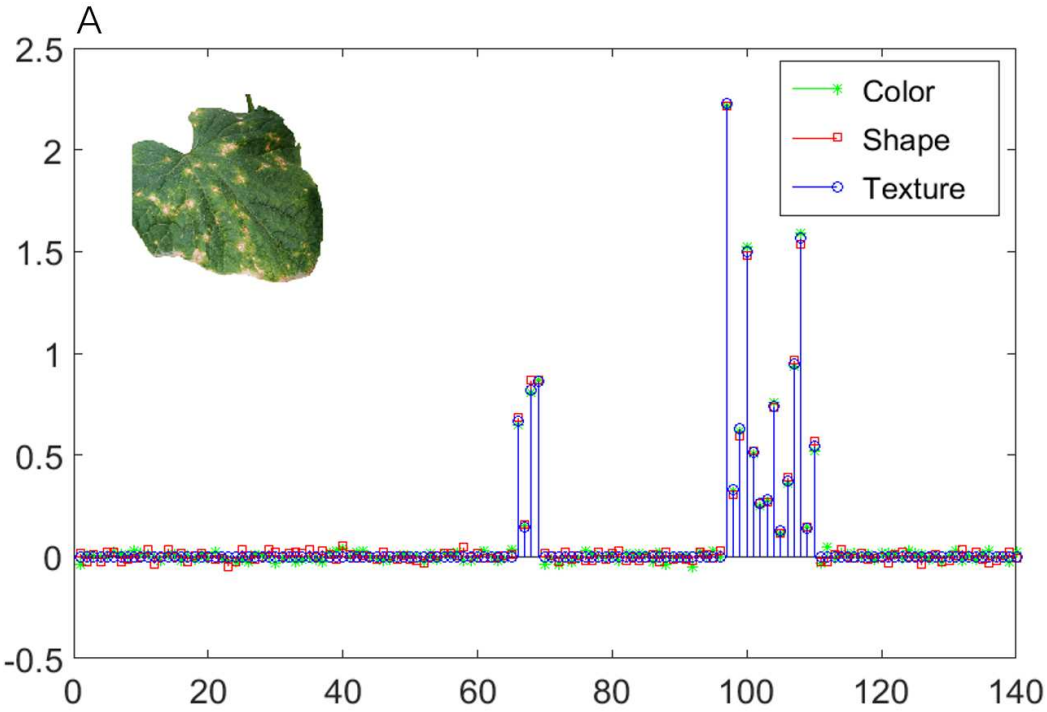

http://www.aloki.hu ● ISSN 1589 1623 (Print) ● ISSN 1785 0037 (Online)
DOI: http://dx.doi.org/10.15666/aeer/1704_92299245

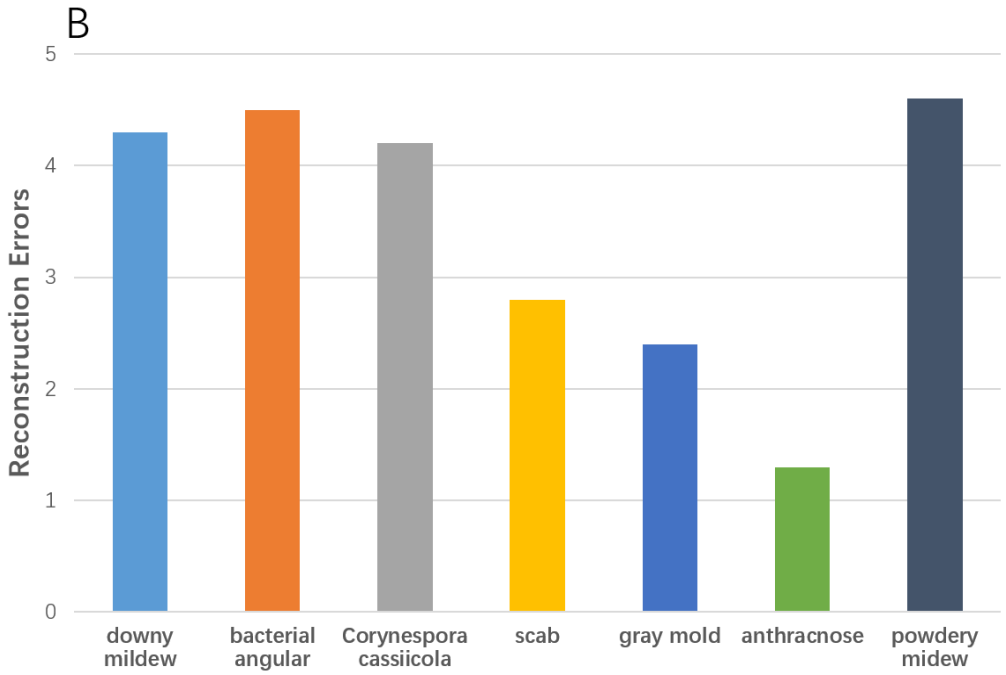

Figure 5. *Multi-task joint sparse coefficient and the reconstruction error visualization of anthracnose example. A: Multi-task sparse coefficients display B: the reconstructed errors of input feature generated from different tasks with sparse coefficients*

As shown in *Figure 5A,* the sparse features of color, shape and texture of multi-task sparse representation are approximately zero in most diseases and significantly non-zero in a small number of positions, and they have similar structures. The minimum value in B represents the minimum reconstruction error, that is, the classification of diseases of input samples.

Conclusion

Inspired by the idea of multi-task learning, we extracted many different types of disease features from multiple disease leaf samples for disease identification, and introduced multi-task joint sparse representation to model the data, with the commonality of different forms of disease features. Improve recognition efficiency and enhance the robustness of recognition. This algorithm is applied to the identification of cucumber diseases. Experiments show that this algorithm is superior to the disease identification algorithm based on sparse representation and other frontier algorithms that are involved in comparison in recognition rate and robustness. The recognition accuracy reaches 88.05%. It can be found from the experimental part of this paper that although the approach proposed in this paper has greatly reduced the algorithm's dependence on samples, sample collection is still an indispensable step of the algorithm. At the same time, we found that the extraction of disease feature for the accurate identification also played a vital role. In the following research, we hope to obtain a wider range of leaf disease image through the unmanned aircraft system, and then extract some special features from these pictures or video to avoid the time-consuming and inefficient leaf collection step.

http://www.aloki.hu ● ISSN 1589 1623 (Print) ● ISSN 1785 0037 (Online)
DOI: http://dx.doi.org/10.15666/aeer/1704_92299245

Acknowledgements. This work is supported by the national natural science foundation of China (No. 61877013), the natural science foundation of Guangdong province (No. 2017A030310618) , the Key Platform and Research Project of Guangdong Province(2017GXJK073), the science and technology program of Guangdong province (No. 2016A020210131).

REFERENCES

[1] Argyriou, A., Evgeniou, T., Pontil, M. (2008): Convex multi-task feature learning. – Mach. Learn 73(3): 243-272.
[2] Arivazhagan, S., Shebiah, R. N., Ananthi, S., Varthini, S. V. (2013): Detection of unhealthy region of plant leaves and classification of plant leaf diseases using texture features. – Agricultural Engineering International: CIGR Journal 15(1): 211-217.
[3] Bashish, A. D., Braik, M., Bani-Ahmad, S. Detection and classification of leaf diseases using K-means-based segmentation and neural-networks based classification. – Information Technology Journal 10(2): 267-275.
[4] Bickel, S., Bogojeska, J., Lengauers, T., Scheffer, T. (2008): Multi-task learning for HIV therapy screening. – Mach Learn 23: 56-63.
[5] Caruana, R. (1997): Multi-task learning. – Mach Learn 28(1): 41-75.
[6] Dey, A. K., Sharma, M., Meshram, M. R. (2016): Image processing based leaf rot disease, detection of betel vine (Piper betle L.) – Procedia Computer Science 85: 748-754.
[7] Dhingra, G., Kumar, V., Joshi, H. D. (2019): A novel computer vision based neutrosophic approach for leaf disease identification and classification. – Measurement 135: 782-794.
[8] Ghosh, S., Dubey, S. K. (2013): Comparative analysis of k-means and fuzzy c-means algorithms. – International Journal of Advanced Computer Science and Applications 4(4): 35-39.
[9] Golhani, K., Balasundram, S. K., Vadamalai, G., Pradhan, B. (2018): A review of neural networks in plant disease detection using hyperspectral data. – Information Processing in Agriculture 5: 354-371.
[10] Grinblat, G. L., Uzal, L. C., Larese, M. G., Granitto, P. M. (2016): Deep learning for plant identification using vein morphological patterns. – Computers and Electronics in Agriculture 127: 418-424.
[11] Iqbal, Z., Khan, M. A., Sharif, M. (2018): An automated detection and classification of citrus plant diseases using image processing techniques: a review. – Computers and Electronics in Agriculture 153: 12-32.
[12] Khirade, S. D., Patil, A. B. (2015): Plant disease detection using image processing. – International Conference on Computing Communication Control & Automation, IEEE Computer Society 153: 26-27.
[13] Kleynen, O., Leemans, V., Destain, M. F. (2005): Development of a multi-spectral vision system for the detection of defects on apples. – Journal of Food Engineering 69(1): 41-49.
[14] Lu, Y., Yi, S. J., Zeng, N. Y., Liu, Y. R., Zhang, Y. (2017): Identification of rice diseases using deep convolutional neural networks. – Neurocomputing 267: 378-384.
[15] Ma, J. C., Du, K. M., Zheng, F. X., Zhang, L. X., Gong, Z. H., Sun, Z. F. (2018): A recognition method for cucumber diseases using leaf symptom images based on deep convolutional neural network. – Computers and Electronics in Agriculture 154: 18-24.
[16] Mei, X., Ling, H. (2011): Robust visual tracking and vehicle classification via sparse representation. – IEEE Transactions on Pattern Analysis and Machine Intelligence 33(11): 2259-2272.
[17] Muthukannan, K., Latha, P. (2015): A PSO model for disease pattern detection on leaf surfaces. – Image Analysis & Stereology 34(3): 209-216.

http://www.aloki.hu ● ISSN 1589 1623 (Print) ● ISSN 1785 0037 (Online)
DOI: http://dx.doi.org/10.15666/aeer/1704_92299245

[18] Mutka, A. M., Bart, R. S. (2015): Image-based phenotyping of plant disease symptoms. – Frontiers in Plant Science 5: 734.
[19] Ozawa, S., Roy, A., Roussinov, D. (2009): A multitask learning model for online pattern recognition. – IEEE Trans Neural Netw 20(3): 430-445.
[20] Prajapati, B. S., Dabhi, V. K., Prajapati, H. B. (2016): A survey on detection and classification of cotton leaf diseases. – Electrical, Electronics, and Optimization Techniques (ICEEOT), International Conference, IEEE 2016: 2499-2506.
[21] Rao, R. P. N., Olshausen, B. A., Lewicki, M. S. (2002): Probabilistic models of the brain: Perception and neural function. MIT press. – Massachusetts Institute of Technology 220: 334.
[22] Rumpf, T., Mahlein, A. K., Steiner, U., Oerke, E. C., Dehne, H. W., Plümer, L. (2010): Early detection and classification of plant diseases with support vector machines based on hyperspectral reflectance. – Computers and Electronics in Agriculture 74(1): 91-99.
[23] Shaik, D. A., Akshay, G. G., Prashant, A. C., Parmeshwar, L. K. (2016): Intelligent autonomous farming robot with plant disease detection using image processing. – International Journal of Advanced Research in Computer and Communication Engineering 5(4): 1012-1016.
[24] Sladojevic, S., Arsenovic, M., Anderla, A., Culibrk, D., Stefanovic, D. (2016): Deep neural networks based recognition of plant diseases by leaf image classification. – Computational Intelligence and Neuroscience 2016: 3289801.
[25] Sun, G. L., Jia, X. L., Geng, T. Y. (2018): Plant diseases recognition based on image processing technology. – Journal of Electrical and Computer Engineering 2018: 1-7.
[26] Unay D, Gosselin B, Kleynen O, Leemans, V., Destainc, M., Debeir, O. (2011): Automatic grading of Bi-colored apples by multispectral machine vision. – Computers and Electronics in Agriculture 75(1): 204-212.
[27] Wright, J., Yang, A. Y., Ganesh, A., Sastry, S. S., Ma, Y. (2009): Robust face recognition via sparse representation. – IEEE Transactions on Pattern Analysis and Machine Intelligence 31(2): 210-227.
[28] Yang, J. C., Wright, J., Huang, T. S., Ma, Y. (2010): Image super-resolution via sparse representation. – IEEE Transactions on Image Processing 19(11): 2861-2873.
[29] Zhang, S., Wang, Z. (2016): Cucumber disease recognition based on Global-Local Singular value decomposition. – Neurocomputing 205: 341-348.
[30] Zhang, S., Huang, W., Zhang, C. (2019): Three-channel convolutional neural networks for vegetable leaf disease recognition. – Cognitive Systems Research 53: 31-41.
[31] Zhang, S. W., Shang, Y. J., Wang, L. (2015): Plant disease recognition based on plant leaf image. – Journal of Animal & Plant Sciences 25(3): 42-45.
[32] Zhang, S. W., Wu, X. W., You, Z. H., Zhang, L. Q. (2017a): Leaf image based cucumber disease recognition using sparse representation classification. – Computers and Electronics in Agriculture 134: 135-141.
[33] Zhang, S. W., Zhu, Y. H., You, Z. H., Wu, X. W. (2017b): Fusion of super-pixel, expectation maximization and PHOG for recognizing cucumber diseases. – Computers and Electronics in Agriculture 140: 338-347.
[34] Zhang, S. W., Wang, H. X., Huang, W. Z., You, Z. H. (2018): Plant diseased leaf segmentation and recognition by fusion of superpixel, K-means and PHOG. – Optik-International Journal for Light and Electron Optics 157: 866-872.

http://www.aloki.hu ● ISSN 1589 1623 (Print) ● ISSN 1785 0037 (Online)
DOI: http://dx.doi.org/10.15666/aeer/1704_92299245

APPENDIX

Feature list

Type	Index	Name	Formula
Color	C_1	Mean	$\mu_L = \sum_b bp(b)$
	C_2	Variance	$\sigma_L^2 = \sum_b (b - C_1)^2 p(b)$
	C_3	Energy	$E_L = \sum_n (p(b))^2$
	C_4	Standard Color Histogram	$h_{C_I} = p(p \in I_{C_I}) = \frac{H_{C_I}(I)}{A}$
$p(b)$: the probability of the level b			
Shape	S_1	Rectangularity	$S_1 = A/S_{MBR}$
	S_2	Compactness	$S_2 = 4\pi A/P^2$
	S_3	Elongation	$S_3 = \frac{MRB'S\ width}{MRB'S\ length}$
	S_4	Circularity	$S_4 = (4AMRB'S\ length)/\pi$
	S_5	Sphericity	$S_5 = \frac{Inscribed\ Radius}{Circumscibed\ Radius}$
	S_6	Lobation	$S_6 = R_1/M$
A: the area of diseased region; S_{MBR} : the areas of minimum bounding rectangles; P: Lesion length; MRB: minimum bounding rectangles; M: The shortest distance from the center of mass of a region to the boundary			
Texture	T_1	Contrast	$T_1 = \sum_{i,j} (i-j)^2 p(i,j,d,\theta)$
	T_2	Angular Second Moment	$T_2 = \sum_{i,j} p(i,j,d,\theta)^2$
	T_3	Entropy	$T_3 = -\sum_{i,j} p(i,j,d,\theta) \ln p(i,j,d,\theta)$
	T_4	Correlation	$T_4 = \frac{(\sum_{i,j}((iy)p(i,j,d,\theta) - \mu_x\mu_y))}{\sigma_x\sigma_y}$
	T_5	Homogeneity	$T_5 = \sum_{i,j} \frac{p(i,j,d,\theta)}{1+(i-j)^2}$
	T_6	Dissimilarity	$T_6 = \sum_{i,j} p(i,j,d,\theta)\lvert i-j\rvert$
	T_7	Mean_X	$T_7 = \sum_i i \sum_j p(i,j,d,\theta)$
	T_8	Mean_Y	$T_8 = \sum_j j \sum_i p(i,j,d,\theta)$

http://www.aloki.hu ● ISSN 1589 1623 (Print) ● ISSN 1785 0037 (Online)
DOI: http://dx.doi.org/10.15666/aeer/1704_92299245

	T_9	Variance_X	$T_9 = \sum_i (j - T_7)^2 \sum_j p(i,j,d,\theta)$
	T_{10}	Variance_Y	$T_{10} = \sum_i (j - T_8)^2 \sum_j p(i,j,d,\theta)$
	T_{12}	Inverse Difference	$T_{12} = \sum_{i,j} \frac{p(i,j,d,\theta)}{1 + \lvert i - j \rvert}$
	T_{13}	Inverse Different Moment Normalized	$T_{13} = \sum_{i,j} \frac{p(i,j,d,\theta)N^2}{N^2 + (i-j)^2}$
	T_{14}	Sum Average	$T_{13} = \sum_{i=0}^{2(N-1)} iP_{x+y}(i)$
	T_{15}	Sum Entropy	$T_{15} = -\sum_{i=0}^{2(N-1)} iP_{x+y}(i)\log(P_{x+y}(t))$
	T_{16}	Sum Variance	$T_{16} = -\sum_{i=0}^{2(N-1)} (i - SENT)^2 P_{x+y}(i)$
	T_{17}	Difference Entropy	$T_{17} = \sum_{i=0}^{N-1} P_{x-y}(t)\log(P_{x-y}(i))$
	T_{18}	Maximum Probability	$T_{18} = \sum_{i,j} \max\,(p(i,j,d,\theta))$
N: gray levels			

http://www.aloki.hu ● ISSN 1589 1623 (Print) ● ISSN 1785 0037 (Online)
DOI: http://dx.doi.org/10.15666/aeer/1704_92299245

IMPACTS OF BIOTURBATION FROM TUBIFICIDAE ON THE ELECTROCHEMICAL PERFORMANCE AND MICROBIAL COMMUNITY OF SEDIMENT MICROBIAL FUEL CELLS

XU, P.[1] – WANG, H. P.[1] – WANG, X.[1*] – YANG, W. L.[2] – YU, E. H.[3] – YAN, X. J.[1]

[1]*School of Resource and Environmental Sciences, Hubei International Scientific and Technological Cooperation Base of Sustainable Resource and Energy, Wuhan University, Wuhan 430079, China*

[2]*Department of Civil and Environmental Engineering, The Pennsylvania State University, University Park, PA 16802, USA*

[3]*School of Engineering, Newcastle University, Newcastle upon Tyne, NE1 7RU, UK*

**Corresponding author*
e-mail: xu.wang@whu.edu.cn; phone: +86-27-6877-5637

(Received 3rd Apr 2019; accepted 17th May 2019)

Abstract. Sediment microbial fuel cells (SMFCs) have been examined extensively for bioremediation, but the impact of organisms that live in the sediment has not been previously investigated. In this study, the impacts from the bioturbation of Tubificidae on the electrochemical performance and microbial community of SMFCs were investigated using lake water and sediment. It was observed that Tubificidae were burrowing in the sediment and eventually dwelled on the anode of SMFCs. Although the voltage output of the SMFC in the presence of Tubificidae experienced a dramatic decline at the beginning of operation, it outperformed that of the SMFC in the absence of Tubificidae after operating for 30 days. The polarization curves of the SMFC anode and Shannon diversity index suggested that the anodic biofilm was devoured by Tubificidae. However, the cathode performance was improved due to more chemical oxygen demand (COD) and ammonia-nitrogen (NH_3-N) released from the sediment. After 90 days of operation, a high loss on ignition (LOI) removal efficiency of 24.5 ± 3% was achieved by combining the anodic oxidation of SMFC and the ingestion of Tubificidae. This study shows that SMFCs can alleviate the impact of Tubificidae on pollutants transfer to overlying water and still remove organic matters from the sediment effectively.
Keywords: *bioturbation, ingestion, organic matters removal, sediment microbial fuel cells, Tubificidae*

Introduction

Freshwater bodies (e.g., lakes, rivers and reservoirs) are crucial resources for drinking water supply, agricultural irrigation and industrial activities. However, water contamination has posed a severe challenge to the sustainability of freshwater resources and is arousing worldwide concerns (Li and Yu, 2015). Sediment is the natural sink of pollutants in the aquatic environment (Peng et al., 2009; Kanzari et al., 2014; Payne et al., 2013). Previous studies have revealed that various pollutants released from the sediment can lead to water contamination when the external input of pollutants (e.g., agricultural runoffs, effluents from wastewater treatment plants and factories, etc.) is low (Qin, 2002). Therefore, it is of great importance to take measures to alleviate pollutant transfer from the sediment to the aquatic environment.

Sediment microbial fuel cells (SMFCs) have attracted increasing attention for their environmental remediation of freshwater bodies (Wang et al., 2016; Chen et al., 2012; Franco et al., 2018; Yan et al., 2012; Xia et al., 2015; Zhao et al., 2016; Shiriny and

http://www.aloki.hu ● ISSN 1589 1623 (Print) ● ISSN 1785 0037 (Online)
DOI: http://dx.doi.org/10.15666/aeer/1704_92479261

Bayareh, 2018; Sajana et al., 2014). In most SMFCs, anodes are buried beneath the anaerobic sediment and cathodes are placed in the aerobic overlying water. Exoelectrogenic microorganisms on the anode degrade organic matter and release electrons to the anode and then through the external circuit to the cathode. Finally, dissolved oxygen (DO) and protons in water combine with electrons to produce water and electricity (Li and Yu, 2015). Compared to other techniques, such as dredging, ozonation and intruding bio-agents, SMFCs using bacteria from environment therefore has least impact on natural environment, and also it is self-sustained by generating electricity (Aloisio et al., 2018; Franco et al., 2018; Li and Yu, 2015; Li et al., 2017; Payne et al., 2013; Sherafatmand and Ng, 2015; Xia et al., 2015). For example, SMFC can increase the redox potential of sediment by oxidizing the organic matters and thus the methane (greenhouse gas) production can be inhibited (Hong et al., 2008b). Polycyclic aromatic hydrocarbons (PAHs) is a class of contaminations from the incomplete combustion of fossil fuels. These compounds are of major public concern due to their toxicity to organisms in carcinogenic and mutagenic potential. SMFCs were used for the removal of PAHs under anaerobic or aerobic conditions (Sherafatmand and Ng, 2015), and with good removal rates of naphthalene (76.9%), acenaphthene and phenanthrene under anaerobic conditions, while producing a power density of 3.63 ± 0.37 mW•m^{-2}. Beside PAHs, cyanobaterial bloom biomass and total petroleum hydrocarbon (TPH) can be effectively degraded by microorganisms on the bioanode of SMFCs (Morris and Jin, 2012; Zhou et al., 2015). The biocathode of SMFCs can be used for in-situ denitrification (Wang et al., 2016; Zhang and Angelidaki, 2012). The results suggested that the SMFC with a small external resistance was more effective for the in-situ denitrification. In addition, the acclimated SMFC biocathode contained mixed microbial communities which could facilitate denitrification, oxygen reduction and ammonia oxidation reactions (Wang et al., 2016). Recently, an SMFC with a novel tubular air cathode was proposed for facilitating air transfer to the cathode (Yuan et al., 2010), which greatly improved biodegradation efficiencies. Additionally, phosphorous flux from overlying water to sediment can be enhanced by employing SMFCs which can oxidize Fe^{2+} to Fe^{3+} and store phosphorous substances in sediment in stable forms (Yang et al., 2016). There are numerous reports in improving the performance of SMFCs. Abazarian et al. revealed that SMFC voltage increased when cells connected in series (Abazarian et al., 2016). However, voltage reversal occurred in this case which causes the total voltage to be less than the sum of individual cell voltages in the channel (Abazarian et al., 2016). Placing sheet iron out of the circuit can improve the iron reduction microbial activity. Within the circuit, it produces a large number of electrons from the electrochemical corrosion yielding higher power production (Zhang et al., 2015). An algae assisted cathode was also proposed for SMFCs and the performance was 2.4 fold higher than that of the SMFC with bare cathode (Wang et al., 2014).

While significant progress of SMFCs for bioremediation has been made, there are still many unclear effects from real aquatic environment on the electrochemical performance and microbial community structure of SMFCs. *Oligochaetes* include the *tubificids*, pot worms and ice worms (*Enchytraeidae*), blackworms (*Lumbriculidae*) and several interstitial marine worms. They are bottom invertebrates frequently used for evaluating the quality of freshwater habitats under their trophic conditions (Krodkiewska and Michalik-Kucharz, 2009). They can be widely distributed in natural water bodies, and they are considered as one of the major bioturbation sources (e.g., feeding, burrowing and locomotory activities) in sediments (Fisher et al., 1980).

http://www.aloki.hu ● ISSN 1589 1623 (Print) ● ISSN 1785 0037 (Online)
DOI: http://dx.doi.org/10.15666/aeer/1704_92479261

Bioturbation can not only cause significant mixing of freshwater bodies with sediment, but it also changes the physical and chemical properties of the sediment. In this work, SMFCs were constructed with carbon felt which is a cheap, stable and biocompatible material (Christwardana et al., 2018; Huong Le et al., 2017). *Oligochaetes* community was first analyzed, and then they were introduced to SMFCs (1.0 L beakers). During 90 days of operation, bioturbation by *Oligochaetes* was monitored, and their impacts on the overlying water, electrochemical performance of whole cell and each electrode were investigated. 16S rDNA pyrosequencing was conducted to analyze the anodic microbial communities of the SMFCs.

Materials and methods

Sampling and analysis

Surface sediments (0 to ~10 cm) were collected using a grab sampler (2.0 L) from Xinghu Lake (114.366037°E, 30.533637°N) near Wuhan University, China. Sediment samples were sieved through a 1.0 mm sieve to remove large debris and then mechanically homogenized. The freshwater was collected from the same location and used throughout the experiment without further treatment. All samples were stored in a refrigerator at 4.0 °C. The LOI of sediment samples was determined using the procedure described previously at a temperature of 550 °C for 2 h (Hong et al., 2008a). Chemical oxygen demand (COD) and NH_3-N of the freshwater were analyzed according to APHA Standard Methods. pH and conductivity of the overlying water were measured by an electrode probe (Shanghai INESA Scientific Instrument Co., Ltd., China). The DO in the overlying water was monitored everyday using a portable multimeter (HQ30D, Hach, USA) and the DO in the sediment was measured five times to avoid severe oxygen penetration to SMFC anodes. All measurements were taken at least 3 times.

Oligochaetes were provided by the Institute of Hydrobiology, Chinese Academy of Sciences. They were examined under an Olympus BX60 microscope equipped with a DP12 digital camera and AnaliSIS 3.2 (Soft Imaging System) software. *Limnodrilus* (with smaller sizes) have no caudal gills and can be further divided into *Limnodrilus hoffmeisteri* and *Limnodrilus claparedeianus* according to their mature sexual organs; *Branchiura* (which are mainly *Branchiura sowerbyi*) are bigger than *Limnodrilu* and have conspicuous gills in their tails. The tails of *Branchiura* often cross the sediment and swing in water to breathe oxygen. Overall, *Tubificidae* was identified as the predominant species (*Fig. 1*).

SMFC construction and operation

Graphite felt 5.0 mm in thickness (Zhongxin Co. Ltd., China) was washed thoroughly with ethanol and DI water before use. Then, it was cut into circular wafers 7.5 cm in diameter (~44.2 cm^2) for use as the SMFC electrodes. The distance between the anode and the cathode was fixed at 7.0 cm. The SMFC was placed into a 1.0 L beaker and the anode was buried 3.0 cm below the sediment-water interface. Afterwards, the beaker was transferred to a larger container (10 L) which contained 3.0 L of freshwater, and a flow rate of 1.0 $L \cdot h^{-1}$ was maintained in the SMFC reactor using a peristaltic pump (*Fig. 2*). The purpose of this reactor design was to constrain *Oligochaetes* in a small area and also maintain the DO in the reactor at a relatively high level (due to the larger area) for inoculating the biocathode of the SMFC. An external

http://www.aloki.hu ● ISSN 1589 1623 (Print) ● ISSN 1785 0037 (Online)
DOI: http://dx.doi.org/10.15666/aeer/1704_92479261

resistance of 500 Ω was used to connect the electrodes using titanium wires. After start-up for approximately 35 days, the SMFC was transferred to a beaker with fresh sediment. Then, *Oligochaetes* (with a density of about 2000 ind. 0.1 m^{-2}) were added into a beaker (denoted as TUB-1). For comparison, the reactors only containing sediment, only containing *Tubificidae* and only containing SMFC were assembled (denoted as Control-S, Control-T and TUB-0). All reactors were kept in incubators at 25 °C for 90 days. The reactors were routinely replenished with DI water to maintain a constant water level.

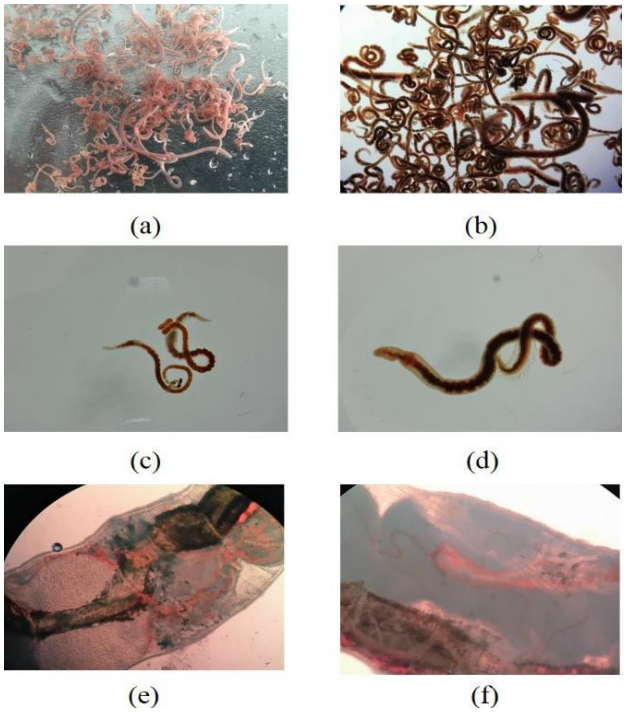

Figure 1. *Optical images of sub-species:* ***a*** *and* ***b*** *Tubificidae under microscope;* ***c*** *Limnodrilus;* ***d*** *Branchiura Sowerbyi;* ***e*** *The penis sheath of Limnodrilus Hoffmeisteri;* ***f*** *The penis sheath of Limnodrilus Claparedeianus*

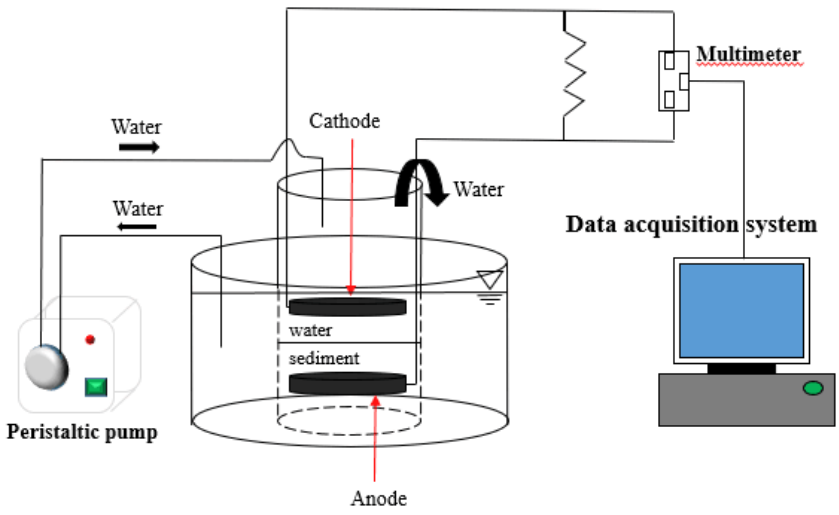

Figure 2. *Schematic diagram of experimental setup*

http://www.aloki.hu ● ISSN 1589 1623 (Print) ● ISSN 1785 0037 (Online)
DOI: http://dx.doi.org/10.15666/aeer/1704_92479261

Electrochemical characterization

The voltage of external resistance was recorded at 10 min intervals using a data acquisition system (Model 2700, Keithley Instrument, USA). Polarization curves were obtained at a scan rate of 0.1 $mV \bullet s^{-1}$ using a potentiostat (CHI 604E, Chenhua instrument Co., Ltd., China). Electrode potential were recorded and reported versus Ag/AgCl (3.0 M KCl, saturated AgCl). The power density can be calculated by the obtained voltage using *Equation 1:*

$$P = I \times U \quad \text{(Eq.1)}$$

where P is the power density ($mW \bullet m^{-2}$), I is the current density ($mA \bullet m^{-2}$) and U is the voltage output (V).

Microbial community analysis

For high-throughput MiSeq Illumina sequencing of the 16S rDNA, biofilms on the anode of SMFC were sampled after 90 days by repeatedly scraping the cross-section of the graphite felt electrode using a sterile blade. The DNA extraction kit (MOBIO Laboratories, CA, USA) was used for extracting 250 mg DNA from the sample. The purity and concentration of DNA were checked through running samples on 1.0% agarose gels. DNA was amplified following the protocol described previously (Wang et al., 2016). PCR amplifications were conducted in triplicate with the primer set 515F (5'-GTGCCAGCMGCCGCGGTAA-3') and 926R (5'-CCGTCAATTCMTTTGAGTTT-3') that amplifies the V4-V5 region of the 16S rDNA.

Sequencing was determined on an Illumina MiSeq platform. The 16S rDNA gene sequences generated were analyzed using the bioinformatic software package Mothur using the MiSeq SOP Pipeline to analyze a multiplexed set of samples on a single run. The paired reads were assembled using make.contigs that extract the sequences and quality score data from the fastq files, which creates the reverse complement of the reverse read. Then, the paired end reads were assembled into a contig. Screen.seqs which was used to remove low quality reads by the following filtering parameters, maxambig=0, minlength=200 and maxlength=580, maxhomop=8. The remained sequences were simplified using the unique.seqs command to generate a unique set of sequences, and they were aligned with the SILVA databases (version 119). The filter.seqs was used to remove empty columns from our alignment, which provided short length of filtered alignment. Further de-noise sequences were pre-clustered using the pre.cluster command (http://www.mothur.org/wiki/Pre.cluster) for up to 4 differences between sequences. All reads were checked for chimeras using UCHIME algorithm and the chimeric sequences were removed by the chimera.uchime command with default parameters. Silva 119 reference sequence files were used to classify (classify.seqs) our sequences, then the Wang method was used with a confidence threshold of 80%. No-bacteria sequences were deleted. The distance matrix between the aligned sequences was generated by the dist.seqs command. At last, these sequences were clustered to OTUs (operational taxonomic units) at 97% sequence identity (furthest neighbor method). A majority consensus taxonomy for each OTU was obtained by the classify.otu command with default parameters.

http://www.aloki.hu ● ISSN 1589 1623 (Print) ● ISSN 1785 0037 (Online)
DOI: http://dx.doi.org/10.15666/aeer/1704_92479261

Results and discussion

Impacts of Tubificidae on the water quality and loss on ignition (LOI) in the sediment with and without SMFC

The bioturbation of *Tubificidae* and SMFC both have profound impact on the sediment and overlying water. COD, NH_3-N and organic matter are important indicators of contaminations in natural water bodies and they are also the food for bacteria on SMFCs.

The chemical oxygen demand (COD) and NH_3-N concentrations in all reactors except Control-T declined rapidly during the initial 25 days, their degradation rates were sluggish after 25 days (*Fig. 3a* and *b*). The removal rate of NH_3-N was accelerated after 15 days because high COD concentration inhibits ammonia oxidation (*Fig. 3b*) (Hanaki et al., 1990). For Control-T, the final COD and NH_3-N were highest (20.0 ± 0.15 mg•L-1 and 0.98 ± 0.04 mg•L-1), which suggested the bioturbation from Tubificidae can accelerates the release rate of pollutants from the lake sediment (Fisher et al., 1980). The final COD (9.8 ± 0.5 mg•L-1) and NH_3-N (0.56 ± 0.02 mg•L-1) were much lower in TUB-1. Previous reports revealed that the biocathode of SMFCs can digest COD as carbon/food sources for bacterial metabolism (Sajana et al., 2014). It is worth of noting that the NH_3-N was significantly removed in Control-S, which is similar to that in TUB-0. However, the final CODs in TUB-0 (8.5 ± 0.13 mg•L-1) was around 6 mg•L^{-1} lower than that in Control-S. It is well-known in wastewater treatment that COD is much easier to be oxidized than NH_3-N (Hanaki et al., 1990). All parameters can also be found in *Table 1*.

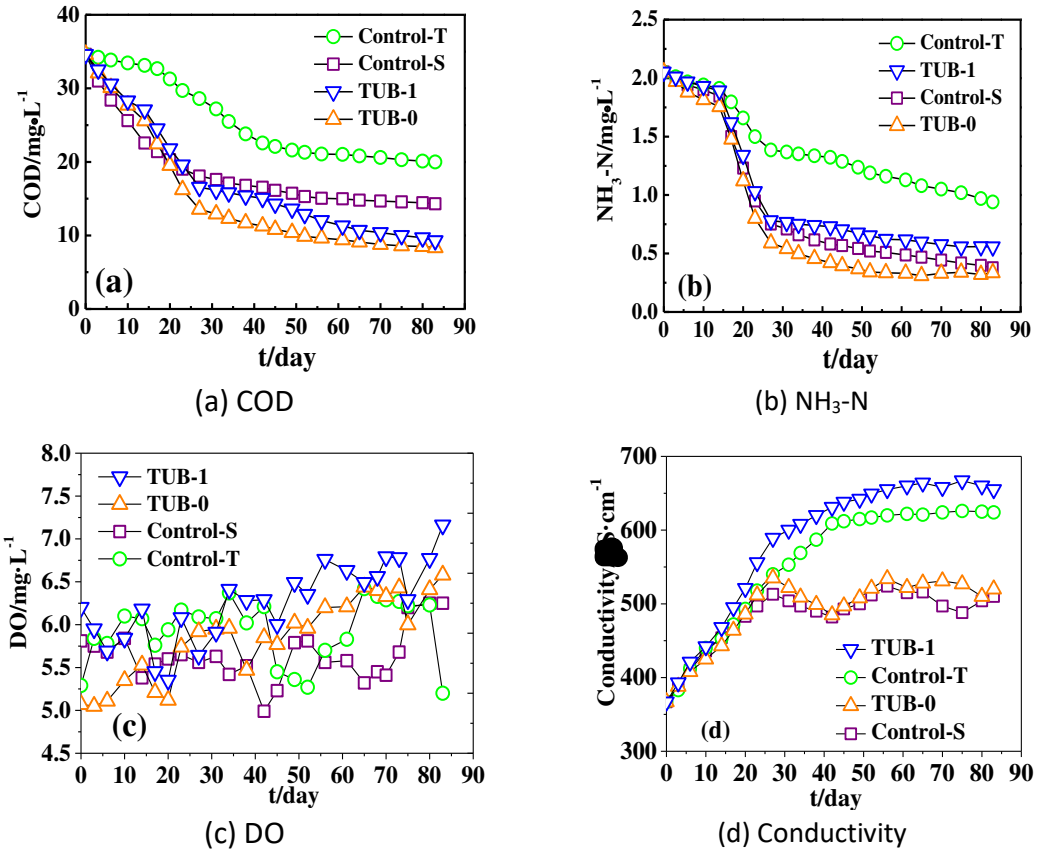

Figure 3. *Water quality of the overlying water in different reactors*

http://www.aloki.hu ● ISSN 1589 1623 (Print) ● ISSN 1785 0037 (Online)
DOI: http://dx.doi.org/10.15666/aeer/1704_92479261

The DO in the overlying water in different reactors ranged from 5.0 to 7.0 mg•L^{-1} (*Fig. 3c*). The conductivity of the overlying water in all reactors started increase, then it reached a plateau after around 25 days of operation. The conductivities in TUB-1 (660 ± 5.0 μS•cm^{-1}) and Control-T (624 ± 2.0 μS•cm^{-1}) after 25 days of operation were higher than that in TUB-0 (519 ± 8.0 μS•cm^{-1}) and Control-S (500 ± 11.0 μS•cm^{-1}) (*Fig. 3d*). During these measurements, it was observed that *Tubificidae* was burrowing in the sediment and formed tunnels that can increase the releasing rate of soluble chemical compounds (e.g. soluble COD, NH_4^+ and sulfates) (*Fig. 4*) (Mccaffrey et al., 1980; Florian and Lemoine, 2010). SMFCs enhanced the degradation of COD and NH_3-N in the overlying water using bio-cathodes, which is consistent with previous reports (Wang et al., 2016; Li et al., 2017). In addition, the DO inside the sediment of Control-T and TUB-1 was also measured and the results were low in two reactors even when the sediment became more porous (*Table 1*). This is due to the strong respiration effect from *Tubificidae* and they consumes the most of DO in the sediment (Lou et al., 2013).

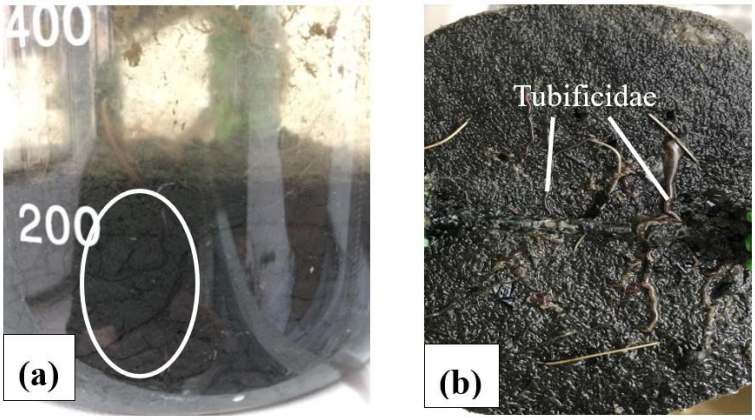

Figure 4. *Optical image of* ***a*** *tunnels from Tubificidae burrowing and* ***b*** *the SMFC anode in TUB-1*

Table 1. *pH and pollutant concentration in the overlying water and DO in the sediment*

Samples	Control-S	Control-T	TUB-0	TUB-1
pH	8.10 ± 0.16	7.98 ± 0.12	7.96 ± 0.17	8.12 ± 0.12
DO (mg/L)	0.48 ± 0.06	0.21 ± 0.01	0.17 ± 0.03	0.14 ± 0.04
Initial COD concentration(mg/L)	34.6 ± 0.01	34.6 ± 0.01	34.6 ± 0.01	34.6 ± 0.01
Final COD concentration (mg/L)	14.5 ± 0.16	20.0 ± 0.15	8.5 ± 0.13	9.8 ± 0.5
COD removal efficiency	58.1%	42.2%	76.0%	71.7%
Initial NH_3-N concentration (mg/L)	2.05 ± 0.01	2.05 ± 0.01	2.05 ± 0.01	2.05 ± 0.01
Final NH_3-N concentration (mg/L)	0.38 ± 0.01	0.98 ± 0.04	0.33 ± 0.01	0.56 ± 0.02
NH_3-N removal efficiency	81.6%	54.2%	83.6%	72.8%

The largest decrease ($24.5 \pm 3\%$) of LOI in the sediment was obtained using the SMFC in TUB-1 (*Fig. 5*). Numerous investigations reported that *Tubificidae* ingest organic matters effectively and thus be used for sludge minimization (Lou et al., 2013; Wei et al., 2003). The SMFC in TUB-0 exhibited a LOI removal efficiency of $16 \pm 1.5\%$ which was similar to that in Control-T ($16.3 \pm 1.5\%$) while it was only

http://www.aloki.hu ● ISSN 1589 1623 (Print) ● ISSN 1785 0037 (Online)
DOI: http://dx.doi.org/10.15666/aeer/1704_92479261

2.2 ± 1% in Control-S. A LOI removal efficiency of ~22% after 6 months of operation was reported in the field test using the SMFC under a closed-circuit condition (Hong et al., 2008a, b). The higher electrochemical performance of SMFCs and the bioturbation of *Tubificidae* were attributed to the high LOI removal efficiency (24.5 ± 3%) in this work.

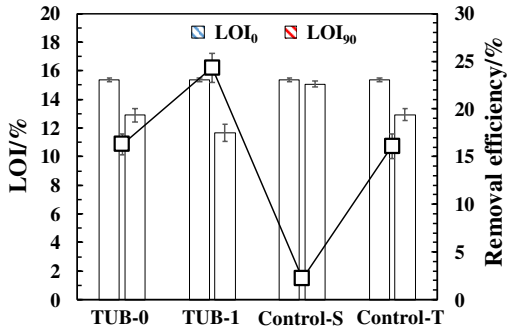

Figure 5. *LOI changes in the sediment. LOI0 and LOI90 represent the initial and final values of LOI in the sediment. Error bars indicate range of duplicate results*

Electrochemical performance of SMFCs in the presence and absence of Tubificidae

Tubificidae does not just redistributed the pollutants, they also inter-reacted with the electrodes of SMFCs. After 9 days of *Tubificidae* addition, the voltage output of SMFC started to decline steeply from around 300 mV to 130 mV (*Fig. 6*). Meanwhile, there was no visual on *Tubificidae* burrowing in the sediment after 10 days since the SMFC was transferred to the container of TUB-1. At the end of 90 day's operation, electrodes were removed from containers and it was found that *Tubificidae* dwelled in the porous graphite felt electrodes (*Fig. 4*). Previous studies revealed that *Oligochaetes* spent their life in the root zone of aquatic plants and other organic matter enriched areas (e.g. plant debris, bacteria) for food (Rota and De Jong, 2015; Vanamala Naidu et al., 1981). They can assimilate organic detritus and bacteria (Kemp, 1987). In this study, the SMFC anode acted as the root zone of aquatic plants and the biofilm on the electrode could be ingested by bioturbators, which caused the loss of the electrochemical performance.

However, it was found that the cell voltage in TUB-1 increased and it exceeded the initial value and the voltage of the SMFC in TUB-0 at day 30. To further examine the potential changes of electrodes, linear sweep voltammetry (LSV) was conducted in a three-electrode system (*Fig. 7a*). Before *Tubificidae* addition, the reaction rate on the cathode (upper figure) was slow and it was the limiting step of whole cell reaction compared to the anode. Once the SMFC was transferred to the *Tubificidae* containing sediment, the anode performance decreased in terms of open circuit potential (OCP) and limiting current. After ~30 days of operation, the anode performance partially recovered except for OCP. It was reported that the low concentration of DO significantly reduced the respiration rate of *Tubificidae* (Van Hoven, 1975), hence the anodic biofilm of the SMFC in TUB-1 could be recovered to some extent. On the other hand, the electrochemical performance of whole cell SMFCs (data not shown) and electrodes in the absence of *Tubificidae* decreased slightly after 50 days (*Fig. 8*). Although the increase of DO in the sediment was claimed by previous reports to be responsible for the performance drop due to the bacteria on SMFC anode are anaerobic, DO results in the sediment were not monitored or reported (Zhao et al., 2016). In this study, DO

http://www.aloki.hu ● ISSN 1589 1623 (Print) ● ISSN 1785 0037 (Online)
DOI: http://dx.doi.org/10.15666/aeer/1704_92479261

beneath the sediment remains low during operation in TUB-0 and TUB-1. Thus, the performance loss of the SMFC anode in TUB-1 was attributed by the ingestion of worms rather than the increase of DO in the sediment. The cathode performance of the SMFC in TUB-1 was improved significantly after *Tubificidae* addition for about 30 days. This is because of more COD and NH_3-N released from the sediment to the overlying water (*Fig. 3a* and *b*). More COD in the overlying water provided more food for the biofilm growth on the cathode. Overall, the SMFC performance in TUB-1 was improved from 70 mW•m^{-2} to 93 mW•m^{-2} (*Fig. 7b*).

Microbial community analysis

The microbial community of the pristine sediment, overlying water, anode biofilms of SMFCs in TUB-0 and TUB-1 were analyzed to reveal the enrichment of genera with potential exoelectrogenic capability using 16S rDNA pyrosequencing. The diversity index (5.27) of pristine sediment was highest, which is consistent with previous reports (Zhao et al., 2016; Lu et al., 2014). The diversity index of the anodic biofilm in TUB-0 (4.75) was higher than that of the SMFC in TUB-1 (4.50) (*Table 2*). The result further confirmed the anodic biofilm was consumed by *Tubificidae* and led a lower diversity index (*Fig. 6*).

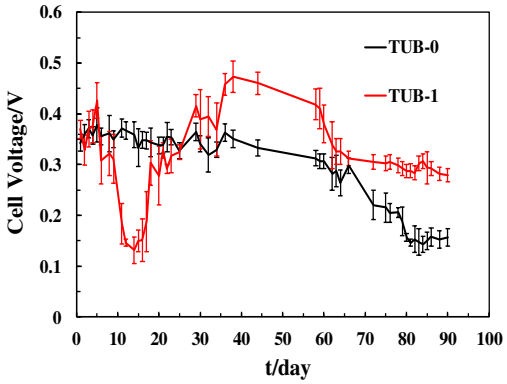

Figure 6. *Voltage output of SMFCs with and without Tubificidae. Error bars indicate range of duplicate results*

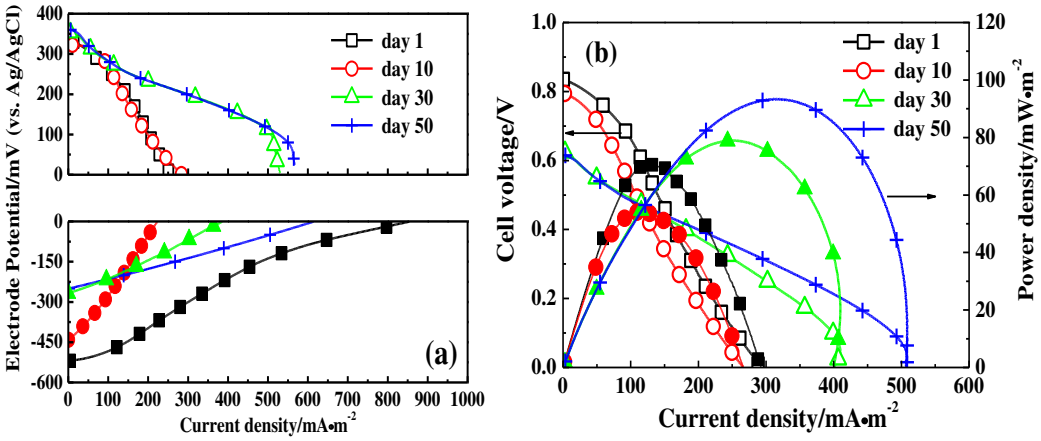

Figure 7. a *LSV curves of the SMFC anode and cathode.* ***b*** *Polarization curves of the SMFC in TUB-1 after Tubificidae addition*

http://www.aloki.hu ● ISSN 1589 1623 (Print) ● ISSN 1785 0037 (Online)
DOI: http://dx.doi.org/10.15666/aeer/1704_92479261

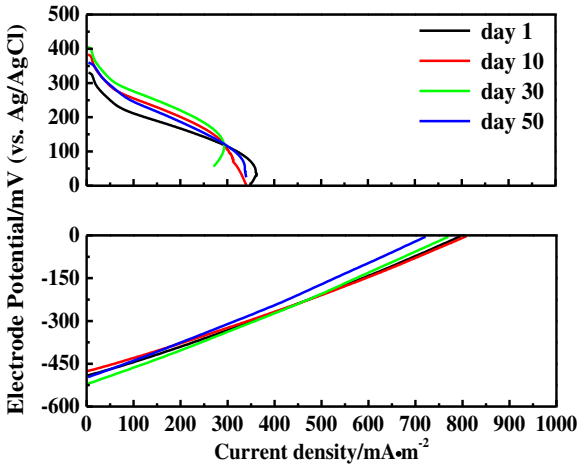

Figure 8. *LSV curves of the SMFC anode and cathode in TUB-0*

Table 2. *Shannon diversity indexes of different samples*

Samples	Shannon index
Pristine sediment	5.27
Overlying water	4.0
TUB-0	4.75
TUB-1	4.51

The taxonomic analysis of bacterial DNA sequences shows that the microbial community of the anodic biofilm of the SMFC with *Tubificidae* was altered, compared to that of the SMFC without *Tubificidae*. Specifically, *Proteobacteria* was the dominant phylum in all samples (*Fig. 9*) and previous studies reported the same finding (Yan et al., 2015; Logan and Rabaey, 2012).

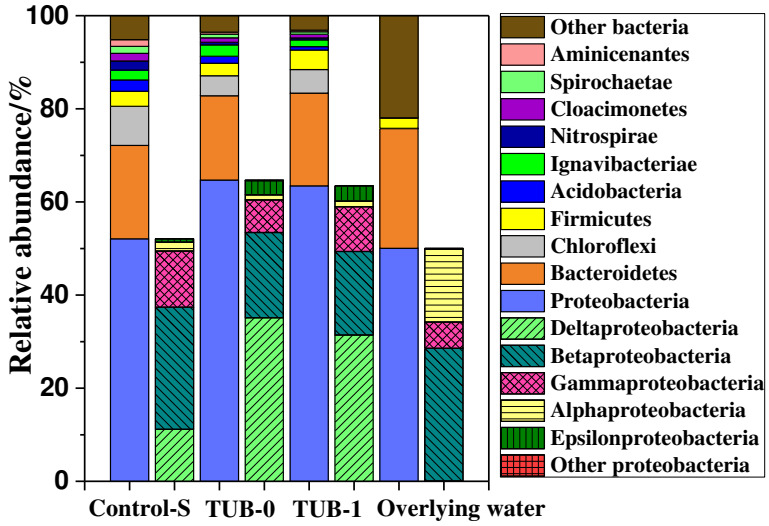

Figure 9. *Taxonomic classification of bacterial DNA sequences from the communities of different samples at the phylum level and the most dominant phylum of Proteobacteria at the class level*

http://www.aloki.hu ● ISSN 1589 1623 (Print) ● ISSN 1785 0037 (Online)
DOI: http://dx.doi.org/10.15666/aeer/1704_92479261

From the class level, *Deltaproteobacteria* in the anodic biofilm were increased compared to that in the pristine sediment. *Desulfobulbus* (11.7%) and *Geobacter* (10.3%) were the dominant genera at genus level in the anodic biofilm of the SMFC in TUB-0 (*Fig. 10a* and *b*).

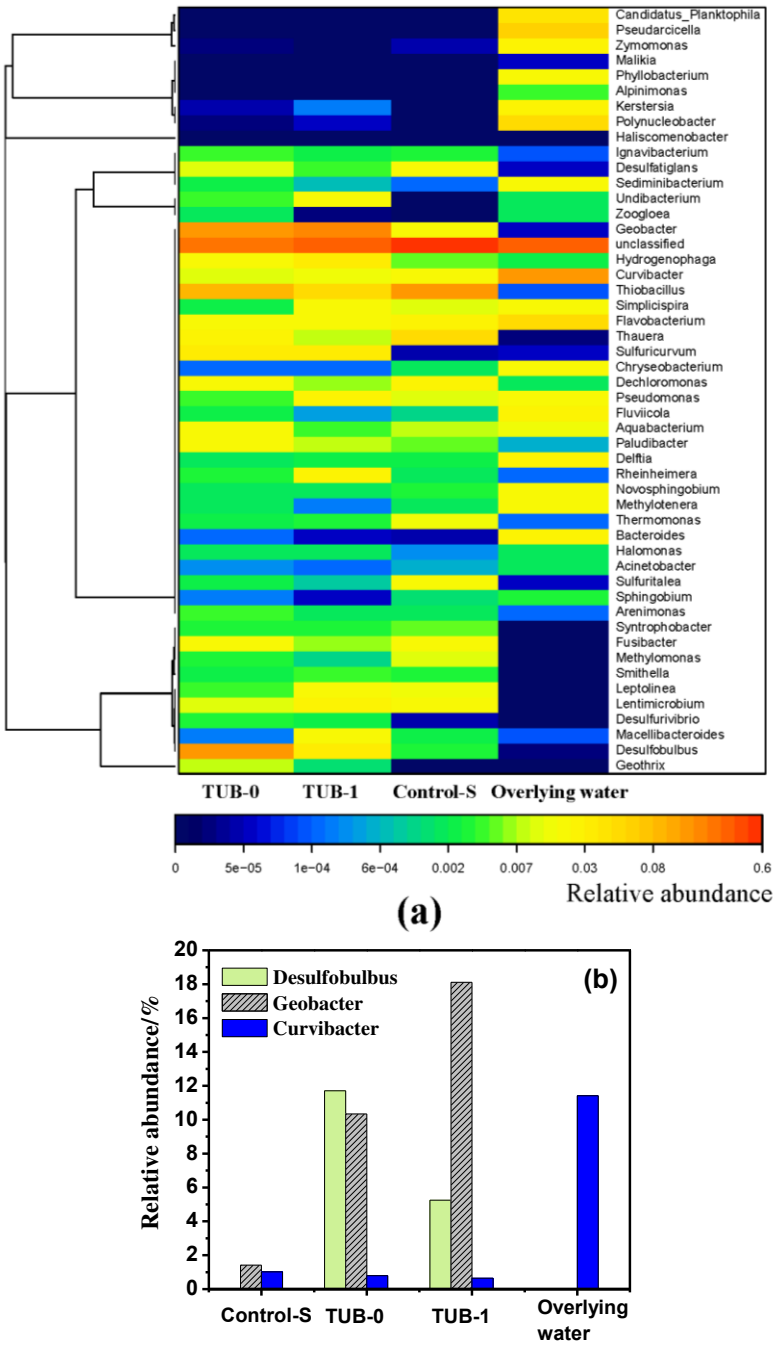

Figure 10. a *Heatmap of all samples at the genus level.* ***b*** *The relative abundances of Desulfobulbus, Geobacter and Curvibacter in different samples*

Geobacter is well-known bacteria that can directly digest acetic acid or other small organic molecules (e.g. Ethanol) to produce electricity (Logan and Rabaey, 2012).

http://www.aloki.hu ● ISSN 1589 1623 (Print) ● ISSN 1785 0037 (Online)
DOI: http://dx.doi.org/10.15666/aeer/1704_92479261

Desulfobulbus are also proved to be exoelectrogenic micro-organisms that can oxidize S^0 in sediments. Their abundance increased and identified as one of predominant genera in the anodic biofilm of SMFCs as previously reported (Yan et al., 2015; Lu et al., 2015; Ryckelynck et al., 2005). In TUB-1, the predominant genus in the SMFC anode was *Geobacter* (18.1%) alone while the relative abundance of *Desulfobulbus* was only 5.25%. *Oligochaetes* are the host of several sulfur oxidizing bacteria and these bacteria can compete with *Desulfobulbus* for the S^0 source in the vicinity of bioanodes (Bergin et al., 2018; Blazejak et al., 2005). Hence, the microbial activity of *Desulfobulbus* was suppressed due to the strong bioturbation of *Tubificidae* in this study. A similar completion also exists between *Geobacter* on the anode of SMFC and methanogens on organic matters in sediments for the same substrate. Therefore, the use of SMFC can inhibits methane production from sediment. *Thiobacillus*, a strain of genera was reported with the ability of using sulfur as energy sources (Boden, 2017), were 9.1%, 7.7% and 5% in Control-S, TUB-0 and TUB-1. This result also confirms the competing mechanism described above. *Curvibacter* was the predominant genus (11.4%) in the overlying water and it is a well-established aerobic bacterium. The higher abundance of aerobic bacteria (*Polynucleobacter*, *Kerstersi, phyllobacterium, fluviicola*) in overlying water was found in most of water bodies (Chen et al., 2017; Halkjær et al., 2009). The low relative abundances of *Curvibacter* in the sediment of Control-S (1.0%), the SMFC anode of TUB-0 (0.8%) and TUB-1 (0.64%) confirmed that the DO beneath the sediment in all reactors remained low during operation.

The protein contents in SMFC electrodes were also examined. However, it was impossible for us to separate worms from the SMFC anode in TUB-1 since they dwelled inside the anode. After 90 days of operation, the protein contents of the SMFC cathode in TUB-1 and TUB-0 were 0.379 $g \bullet m^{-2}$ and 0.269 $g \bullet m^{-2}$. The higher protein content of the SMFC cathode in TUB-1 suggested that more bacteria enriched on the electrode and resulted in better electrochemical performance (*Fig. 7a*).

Conclusions

The present study demonstrated that the organic matter removal and electrochemical performance of SMFCs were enhanced by the bioturbation of *Tubificidae*. For the first time, it was found that *Tubificidae* dwelled on the carbon felt anode of SMFCs and devoured the biofilm. After 90 days of operation, a high LOI removal efficiency of $24.5 \pm 3\%$ was achieved in TUB-1. The SMFC performance in the presence of *Tubificidae* increased from 70 $mW \bullet m^{-2}$ to 93 $mW \bullet m^{-2}$. The bioturbation of *Tubificidae* suppressed the acclimation of *Desulfobulbus* on the bioanode of SMFCs. The sediment beneath the water-sediment interface remained anaerobic in the presence of *Tubificidae*.

Acknowledgements. The authors would like to thank Prof. Bruce E. Logan from Penn state University for editing the manuscript and Dr. Yongjing Zhao from the Institute of Hydrobiology, Chinese Academy of Sciences, for providing Oligochaetes samples. This work is financially supported by the national major project of water pollution control and treatment (Grant No. 2017ZX07204004-01), National Natural Science Foundation of China (Grant No.21406171 and No. 51778265) and the Fundamental Research Funds for the Central Universities (Grant No. 2042018kf0244).

http://www.aloki.hu ● ISSN 1589 1623 (Print) ● ISSN 1785 0037 (Online)
DOI: http://dx.doi.org/10.15666/aeer/1704_92479261

REFERENCES

[1] Abazarian, E., Gheshlaghi, R., Mahdavi, M. A. (2016): The effect of number and configuration of sediment microbial fuel cells on their performance in an open channel architecture. – Journal of Power Sources 325: 739-744.
[2] Aloisio, D., Ferraro, M., Brunaccini, G., Sergi, F., Randazzo, N., Dispenza, G., Antonucci, V. (2018): Modeling, realization and test on field of a fuel cell-Na/NiCl2 battery hybrid system as a base transceiver station power supply. – Instrumentation Mesure Métrologie 17(3): 423-442.
[3] Bergin, C., Wentrup, C., Brewig, N., Blazejak, A., Erséus, C., Giere, O., Schmid, M., De Wit, P., Dubilier, N. (2018): Acquisition of a novel sulfur oxidizing symbiont in the gutless marine worm Inanidrilus exumae. – Applied and Environmental Microbiology 84(7): e02267-17.
[4] Blazejak, A., Erséus, C., Amann, R., Dubilier, N. (2005): Coexistence of bacterial sulfide oxidizers, sulfate reducers, and spirochetes in a gutless worm (Oligochaeta) from the Peru Margin. – Applied and Environmental Microbiology 71(3): 1553-1561.
[5] Boden, R. (2017): Editorial: 115 years of sulfur microbiology. – FEMS Microbiology Letters 364(6).
[6] Chen, J., Zhang, L., Hu, Y., Huang, W., Niu, Z., Sun, J. (2017): Bacterial community shift and incurred performance in response to in situ microbial self assembly graphene and polarity reversion in microbial fuel cell. – Bioresource Technology 241: 220-227.
[7] Chen, Z., Huang, Y. C., Liang, J. H., Zhao, F., Zhu, Y. G. (2012): A novel sediment microbial fuel cell with a biocathode in the rice rhizosphere. – Bioresource Technology 108: 55-59.
[8] Christwardana, M., Frattini, D., Accardo, G., Yoon, S. P., Kwon, Y. (2018): Early stage performance evaluation of flowing microbial fuel cells using chemically treated carbon felt and yeast biocatalyst. – Applied Energy 222: 369-382.
[9] Fisher, J. B., Lick, W. J., McCall, P. L., Robbins, J. A. (1980): Vertical mixing of lake sediments by tubificid oligochaetes. – Journal of Geophysical Research: Oceans 85(C7): 3997-4006.
[10] Florian, M. B., Lemoine, D. G. (2010): Ecosystem engineering by tubificid worms stimulates macrophyte growth in poorly oxygenated wetland sediments. – Functional Ecology 24(2): 444-453.
[11] Franco, F. D., Burgio, G., Santamaria, M. (2018): Chitosan-Heteropolyacid membranes for direct methanol fuel cells. – Revue des Composites et des Matériaux Avancés 28(2): 141-147.
[12] Halkjær, N. P., Caroline, K., J., S. R., Lund, N. J. (2009): Identity and ecophysiology of filamentous bacteria in activated sludge. – FEMS Microbiology Reviews 33(6): 969-998.
[13] Hanaki, K., Wantawin, C., Ohgaki, S. (1990): Effects of the activity of heterotrophs on nitrification in a suspended growth reactor. – Water Research 24(3): 289-296.
[14] Hong, S. W., Chang, I. S., Choi, Y. S., Kim, B. H., Chung, T. H. (2008a): Responses from freshwater sediment during electricity generation using microbial fuel cells. – Bioprocess and Biosystems Engineering 32(3): 389-395.
[15] Hong, S. W., Kim, J., Yong, S. C., Tai, H. C. (2008b): Field experiments on bioelectricity production from lake sediment using microbial fuel cell technology. – Bulletin Korean Chemical Society 29(11): 2189-2194.
[16] Huong Le, T. X., Bechelany, M., Cretin, M. (2017): Carbon felt based electrodes for energy and environmental applications: A review. – Carbon 122: 564-591.
[17] Kanzari, F., Syakti, A. D., Asia, L., Malleret, L., Piram, A., Mille, G., Doumenq, P. (2014): Distributions and sources of persistent organic pollutants (aliphatic hydrocarbons, PAHs, PCBs and pesticides) in surface sediments of an industrialized urban river (Huveaune), France. – Science of the Total Environment 478: 141-151.

http://www.aloki.hu ● ISSN 1589 1623 (Print) ● ISSN 1785 0037 (Online)
DOI: http://dx.doi.org/10.15666/aeer/1704_92479261

[18] Kemp, P. F. (1987): Potential impact on bacteria of grazing by a macrofaunal deposit feeder, and the fate of bacterial production. – Marine Ecology Progress Series 36(2): 151-161.
[19] Krodkiewska, M., Michalik Kucharz, A. (2009): The bottom Oligochaeta communities in sand pits of different trophic status in Upper Silesia (Southern Poland). – Aquatic Ecology 43(2): 437-444.
[20] Li, H., Tian, Y., Qu, Y., Qiu, Y., Liu, J., Feng, Y. (2017): A Pilot scale benthic microbial electrochemical system (BMES) for enhanced organic removal in sediment restoration. – Scientific Reports 7: 39802.
[21] Li, W. W., Yu, H. Q. (2015): Stimulating sediment bioremediation with benthic microbial fuel cells. – Biotechnology Advances 33(1): 1-12.
[22] Logan, B. E., Rabaey, K. (2012): Conversion of wastes into bioelectricity and chemicals by using microbial electrochemical technologies. – Science 337(6095): 686-690.
[23] Lou, J., Cao, Y., Sun, P., Zheng, P. (2013): The effects of operational conditions on the respiration rate of tubificidae. – PLoS ONE 8(12): e81219.
[24] Lu, L., Huggins, T., Jin, S., Zuo, Y., Ren, Z. J. (2014): Microbial metabolism and community structure in response to bioelectrochemically enhanced remediation of petroleum hydrocarbon contaminated soil. – Environmental Science & Technology 48(7): 4021-4029.
[25] Lu, L., Xing, D., Ren, Z. J. (2015): Microbial community structure accompanied with electricity production in a constructed wetland plant microbial fuel cell. – Bioresource Technology 195: 115-121.
[26] Mccaffrey, R. J., Myers, A. C., Davey, E., Morrison, G., Bender, M., Luedtke, N., Cullen, D., Froelich, P., Klinkhammer, G. (1980): The relation between pore water chemistry and benthic fluxes of nutrients and manganese in Narragansett Bay, Rhode Island. – Limnology and Oceanography 25(1): 31-44.
[27] Morris, J. M., Jin, S. (2012): Enhanced biodegradation of hydrocarbon contaminated sediments using microbial fuel cells. – Journal of Hazardous Materials 213-214: 474-477.
[28] Payne, R. B., Fagervold, S. K., May, H. D., Sowers, K. R. (2013): Remediation of polychlorinated biphenyl impacted sediment by concurrent bioaugmentation with anaerobic halorespiring and aerobic degrading bacteria. – Environmental Science & Technology 47(8): 3807-3815.
[29] Peng, J. F., Song, Y. H., Yuan, P., Cui, X. Y., Qiu, G. L. (2009): The remediation of heavy metals contaminated sediment. – Journal of Hazardous Materials 161(2-3): 633-640.
[30] Qin, B. (2002): Approaches to mechanisms and control of eutrophication of shallow lakes in the middle and lower reaches of the Yangze River. – Journal of Lake Sciences 14(3): 193-202.
[31] Rota, E., de Jong, Y. (2015): Fauna Europaea: annelida terrestrial oligochaeta (Enchytraeidae and Megadrili), aphanoneura and polychaeta. – Biodiversity Data Journal (3): e5737.
[32] Ryckelynck, N., Stecher, H. A., Reimers, C. E. (2005): Understanding the anodic mechanism of a seafloor fuel cell: interactions between geochemistry and microbial activity. – Biogeochemistry 76(1): 113-139.
[33] Sajana, T. K., Ghangrekar, M. M., Mitra, A. (2014): Effect of operating parameters on the performance of sediment microbial fuel cell treating aquaculture water. – Aquacultural Engineering 61: 17-26.
[34] Sherafatmand, M., Ng, H. Y. (2015): Using sediment microbial fuel cells (SMFCs) for bioremediation of polycyclic aromatic hydrocarbons (PAHs). – Bioresource Technology 195: 122-130.
[35] Shiriny, A., Bayareh, M. (2018): Numerical study of heat transfer and pressure drop in a fuel cell with porous material. – Annales de Chimie - Science des Matériaux 42(3): 323-334.

http://www.aloki.hu ● ISSN 1589 1623 (Print) ● ISSN 1785 0037 (Online)
DOI: http://dx.doi.org/10.15666/aeer/1704_92479261

[36] Van Hoven, W. (1975): Aspects of the respiratory physiology and oxygen preferences of four aquatic oligochaetes (Annelida). – Zoologica Africana 10(1): 29-44.
[37] Vanamala Naidu, K., Kalpana, K. (1981): Suresh Kumar, K., Aquatic oligochaeta from among the roots of eicHhornia crassipes Solms. – Hydrobiologia 76(1): 103-112.
[38] Wang, D. B., Song, T. S., Guo, T., Zeng, Q., Xie, J. (2014): Electricity generation from sediment microbial fuel cells with algae assisted cathodes. – International Journal of Hydrogen Energy 39(25): 13224-13230.
[39] Wang, Y., Hu, J., Wang, L., Shan, D., Wang, X., Zhang, Y., Mao, X., Xing, L., Wang, D. (2016): Acclimated sediment microbial fuel cells from a eutrophic lake for the in situ denitrification process. – RSC Advances 6(83): 80079-80085.
[40] Wei, Y., Van Houten, R. T., Borger, A. R., Eikelboom, D. H., Fan, Y. (2003): Minimization of excess sludge production for biological wastewater treatment. – Water Research 37(18): 4453-4467.
[41] Xia, C., Xu, M., Liu, J., Guo, J., Yang, Y. (2015): Sediment microbial fuel cell prefers to degrade organic chemicals with higher polarity. – Bioresource Technology 190: 420-423.
[42] Yan, Z., Song, N., Cai, H., Tay, J. H., Jiang, H. (2012): Enhanced degradation of phenanthrene and pyrene in freshwater sediments by combined employment of sediment microbial fuel cell and amorphous ferric hydroxide. – Journal of Hazardous Materials 199-200: 217-225.
[43] Yan, Z., Jiang, H., Cai, H., Zhou, Y., Krumholz, L. R. (2015): Complex interactions between the macrophyte Acorus calamus and microbial fuel cells during pyrene and benzo[a]pyrene degradation in sediments. – Scientific Reports 5: 10709.
[44] Yang, Q., Zhao, H., Zhao, N., Ni, J., Gu, X. (2016): Enhanced phosphorus flux from overlying water to sediment in a bioelectrochemical system. – Bioresource Technology 216: 182-187.
[45] Yuan, Y., Zhou, S., Zhuang, L. (2010): A new approach to in situ sediment remediation based on air cathode microbial fuel cells. – Journal of Soils and Sediments 10(7): 1427-1433.
[46] Zhang, H., Zhu, D., Song, T. S., Ouyang, P., Xie, J. (2015): Effects of the presence of sheet iron in freshwater sediment on the performance of a sediment microbial fuel cell. – International Journal of Hydrogen Energy 40(46): 16566-16571.
[47] Zhang, Y., Angelidaki, I. (2012): Bioelectrode based approach for enhancing nitrate and nitrite removal and electricity generation from eutrophic lakes. – Water Research 46(19): 6445-6453.
[48] Zhao, Q., Li, R., Ji, M., Ren, Z. J. (2016): Organic content influences sediment microbial fuel cell performance and community structure. – Bioresource Technology 220: 549-556.
[49] Zhou, Y. L., Jiang, H. L., Cai, H. Y. (2015): To prevent the occurrence of black water agglomerate through delaying decomposition of cyanobacterial bloom biomass by sediment microbial fuel cell. – Journal of Hazardous Materials 287: 7-15.

http://www.aloki.hu ● ISSN 1589 1623 (Print) ● ISSN 1785 0037 (Online)
DOI: http://dx.doi.org/10.15666/aeer/1704_92479261

ENVIRONMENTAL REGULATION, DIRECTED TECHNOLOGICAL CHANGE, AND ECONOMIC GROWTH: FROM THE PERSPECTIVE OF GREEN GROWTH

ZHOU, J. M.[1,2] – ZHAO, Y. Z.[2*] – KUANG, H. B.[2]

[1]*Business School, Dalian University of Foreign Languages, Dalian 116044, China*

[2]*Collaborative Innovation Center for Transport Studies, Dalian Maritime University Dalian 116026, China*

[*]*Corresponding author*
e-mail: zhaoyuzhe@126.com; phone: +86-18-698-606-670; fax: +86-411-8472-8856

(Received 3rd Apr 2019; accepted 17th May 2019)

Abstract. For the problem concerning how the implementation of environmental regulations should be performed, one must examine their impacts on the selection of directed technological innovations to achieve green growth. A nonlinear control model was created in which the constraint is to constantly improve the quality of the environment and ensure a consistent and balanced growth rate with the objective function being the goal of using green growth to maximize social welfare. Using optimal control theory and the maximum principle, we separately obtained the qualitative expression of capital allocation and optimal consumption growth. The model simulation results illustrate the following points: although brown capital is superior in production flexibility in the process of capital accumulation, green capital is still an important pillar of support for maintaining the economic growth of a society as a whole; although brown capital is able to bring about a greater consumption growth rate, the implementation of environmental regulations is sufficient to promote capital allocation to shift towards green technological innovation. In addition, greater emphasis in this aspect shall be more useful for the usage of green capital and play a more effective role in the use of green technological innovation to achieve green growth.
Keywords: *environmental governance, capital allocation, green technological innovation, brown technological innovation, optimal control model, capital accumulation, environmental quality*

Introduction

The key variables for explaining economic growth using traditional neoclassical economic growth theories are mainly capital, labor (including human resource capital), technology, and regulations. The standard for measuring economic growth is gross domestic product (GDP) and per capita income. However, amid the growth of contemporary society, GDP and per capita income are not the only yardsticks for reflecting social progress. Regardless of whether the ecosystem has a positive or negative impact, it has a direct impact on people's quality of life. Therefore, to reflect the goal of sustainable social growth, we must discard the original "GDP-oriented economic growth theory" and include resource usage and environmental impacts in mainstream economic growth theories to construct a "green growth theory", which we use as a new perspective of current mainstream economic research. With regard to green growth (OECD, 2011), technological innovation is the most important factor (Caselli, 2005) for maintaining economic growth. The implementation of some environmental regulations may affect the costs and earnings from technological innovation and change its direction of technological innovation. This effect may lead to "brown technological innovation that relies mainly on pollution-oriented inputs" and "green technological innovation (Demirel and Kesidou, 2011; Zhang and Zhu, 2012; Li et al., 2018) that

http://www.aloki.hu ● ISSN 1589 1623 (Print) ● ISSN 1785 0037 (Online)
DOI: http://dx.doi.org/10.15666/aeer/1704_92639278

attempts to reduce resource utilization and environmental impacts", both of which are problems related to direction-orientated technological innovation. Currently, research into these problems heavily focuses on the dominant factors (Gerlagh, 2011; Gans, 2011) that affect the selection of directed technological innovation. However, we need a further breakthrough to determine how the implementation of environmental regulations will affect the selection of directed technological innovations and what impact this implementation will have on the economic growth of society as a whole.

Currently, there are mainly two perspectives in relevant literature on the impact of the implementation of environmental regulations on technological innovation. The first viewpoint is the "Porter Hypothesis", which argues that the implementation of environmental policies can drive technological innovation and that these innovative technologies often originate from activities such as "learning by doing" and adapting to the local environment. Hart (2004) argues that if the next generation of products is cleaner than the previous generation of products, then the introduction of pollution taxes can reduce the inventory ratios of old products, which may in turn accelerate the elimination of obsolete production capacity and encourage the research and development of new technologies. Ghisetti and Pontoni (2015) prove that if companies or private departments are required to provide compensated protection of eco-service systems, then the implementation of environmental regulations can still improve technological standards. Jaffe et al. (2002), Hamamoto (2006), Zhang et al. (2011), Nick et al. (2012) and Rubashkina et al. (2015) support the "Porter Hypothesis" from the perspective of companies and society as a whole. These studies indicate that we not only view technological innovation from the internal perspective of companies. There is another perspective that opposes the "Porter Hypothesis". Stokey (1998) argues that when the implementation of environmental regulations requires a reduction in the mining of certain fossil fuels, this requirement will not only reduce the marginal output of capital but also reduce innovation in that particular field. "Learning by doing" is restricted, and the accumulation of knowledge capital is also reduced. In addition, the reduction of capital returns also further reduces the extent of technological inputs by companies. Arduini and Cesaroni (2001) use European chemical industrial data, Nakano (2003) uses data from the Japanese paper-making industry, and Barbera and McConnel (1990) use empirical study results of US industrial data to prove that the implementation of environmental regulations does not play a significant catalytic role in technological advancement and efficiency improvement.

The above-mentioned research debates the impact of the implementation of environmental regulations on technological innovation from two opposing perspectives. However, these existing studies have not taken into account the differentiation of directed technological innovation and dynamic changes in environmental regulatory strength. First, the crux of whether the implementation of environmental regulations can be a driver of green growth lies in the correct selection of environmental regulatory strength (Li and Tao, 2012). Only by selecting the environmental regulatory strength that corresponds with the level of economic growth will the long-term implementation of environmental regulations not obstruct the green growth of society as a whole. Zhang et al. (2011) construct a model to illustrate the impact of environmental regulatory strength on technological innovation and use empirical data to demonstrate the U-shaped relationship between environmental regulatory strength and technological innovation. Shen (2012) argues that the level of economic growth determines the impact of environmental regulations on technological innovation. In China, such regulations

http://www.aloki.hu ● ISSN 1589 1623 (Print) ● ISSN 1785 0037 (Online)
DOI: http://dx.doi.org/10.15666/aeer/1704_92639278

have a significant catalytic effect on the highly economically developed eastern regions of China but have a suppressive effect on the central and western regions of China. Second, not all technological innovations can be effective in protecting the environment while maintaining economic growth. The differentiation of directed technological innovation is one of the core contents regarding the study of green growth drivers. Targeting the impact of the implementation of environmental regulations, Smulders and Werf (2005) differentiate technological innovations into brown technological innovations and green technological innovations. Goulder (2004) and Smulders and Nooij (2003) argue that when it is relatively difficult for capital inputs to replace resource factor inputs, investments in green technology are necessary to maintain long-term economic growth. In their model analysis, during the implementation of environmental regulations, only green technological innovations are faster than brown technology innovations, and the negative impact of the reduction in resource utilization shall be effectively offset by green technological innovations. However, in the event of market failure, there is no guarantee that technological innovation can guarantee that the expected trajectory can be achieved even while underpinned by environmental regulations. Maria and Werf (2008) demonstrate that when intellectual property cannot be protected, green technological innovation drivers may be reduced, which may cause technological innovation to shift towards brown technology. The organic direction-oriented technological innovation model constructed by Bondarev et al. (2014) further proves that with adequate guidance from environmental regulations, green technological innovation activities will be more active and boost the overall production rate and levels of economic growth.

After studying the above-mentioned literature concerning environmental regulatory strength and directed technological innovation to explore methods of how to achieve green growth, it can be observed that few academics are able to establish a quantitative model to explain these two important factors and the objective of green growth. Rauscher (2009) constructs an organic growth model based on environmental economics to quantitatively illustrate brown technological innovation investment and green technological innovation investment. Furthermore, Moser et al. (2013) use composite functions to produce a quantitative expression of green growth targets based on the model built by Rauscher (2009) and use a partial equilibrium model to analyze the directed effects of environmental regulations of different strengths on brown technological innovation and green technological innovation. The above-mentioned models are verifiable quantitative models concerning the strength of environmental regulations and directed technological innovations that verify the importance of technological innovations in realizing green growth, but they generally ignore the fact that technological innovation is a driving factor of green growth despite not being final objective. Green growth has a guiding and binding effect (Zhang and Zhu, 2012) on the direction of technological innovation. On the other hand, the utility functions concerning green growth in the model constructed by Moser et al. (2013). only takes into account a special situation in which the relative risk aversion coefficient is 1 but not general scenarios.

Therefore, the present research, which is based on the model constructed by Rauscher (2009) and Moser et al. (2013), also includes brown technological innovation and green technological innovation in the capital accumulation analytical framework. *Figure 1* shows that there is an assumption that the effect of economies of scale is unchanged and that there is perfect competition in the market, taking into account

http://www.aloki.hu ● ISSN 1589 1623 (Print) ● ISSN 1785 0037 (Online)
DOI: http://dx.doi.org/10.15666/aeer/1704_92639278

pollution control efforts and environmental governance costs under different environmental regulatory strengths. This has led to the creation of a non-linear optimal control model in which the objective function is the green growth target of maximizing social welfare and the constraints are ensuring sustained growth with a balanced growth rate and sustained improvement in environmental quality.

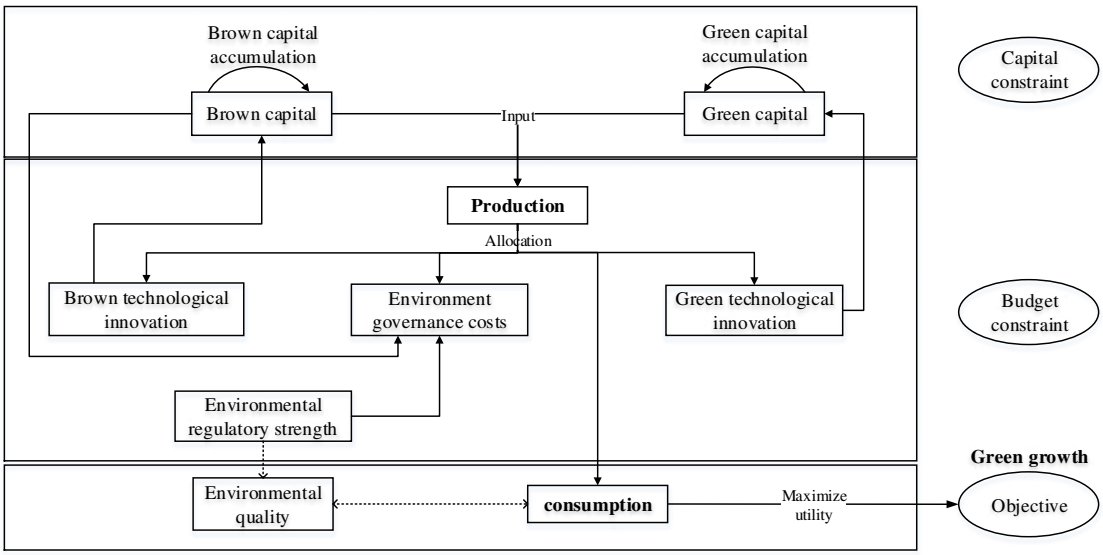

Figure 1. *Structure of the theoretical model on the impact of the environmental regulatory strength on directed technological innovation*

The second section involves hypothetical conditions concerning the impact of environmental regulatory strength on directed technological innovation, which leads to the creation of a more applicable non-linear optimal control model. The third section seeks an analytical solution to the model in a balanced situation. The fourth section uses parameter values to perform a value simulation of the model created and the analytical solution sought. Finally, we derives a research conclusion.

Materials and methods

Objective function

Regarding the utility function *U(C(t), E(t))* of the green objective, the Cobb-Douglas function format is used, and consumption *C(t)* and environmental quality *E(t)* are used as the independent variables of the utility function. For the random variables *x(t)* and $\dot{x}(t) = dx / dt$, the expression can be simplified by omitting the time variable *t* as follows:

$$U(C,E) = \begin{cases} \dfrac{(CE^{\eta})^{1-\theta}}{1-\theta}, & \theta \neq 1, 0 \leq \eta < 1, \\ \ln C + \eta \ln E, & \theta = 1, 0 \leq \eta < 1. \end{cases} \quad \text{(Eq.1)}$$

In *Eq.1*, the objective of maximizing social welfare concerns the maximizing of the total discounted value of the instantaneous utility of consumers, i.e. $\max \int_0^{\infty} U(C,E)e^{-\rho t}dt$,

http://www.aloki.hu ● ISSN 1589 1623 (Print) ● ISSN 1785 0037 (Online)
DOI: http://dx.doi.org/10.15666/aeer/1704_92639278

where the ρ variable is the discount rate of the consumers' subjective time, $\theta>0$ is the relative risk aversion coefficient, and the weighted parameter $\eta>0$ is the environmental quality utility index.

Constraints

(1) Assuming the effects of economies of scale remain unchanged, all production uses a standardized technology to produce similar products. The Cobb-Douglas function format is adopted for the production of the product, with the production factors being differentiated into brown capital and green capital, which can be displayed as $Y=bK^{\alpha}G^{1-\alpha}$, where b is the size parameter for the production function, K is the brown capital stock, G is the green capital stock, and $\alpha\in(0,1)$ is the production flexibility of brown capital during the production process (also referred to as productive capital flexibility).

(2) Assuming the effects of economies of scale remain unchanged, we adopt the Cobb-Douglas function format for capital accumulation. The production factors are mainly composed of the capital stock and different technological innovation investment inputs, which means that the brown capital and green capital accumulation process has the form,

$$\dot{K} = dK^{\delta} R_K^{1-\delta} - \phi K \quad \text{(Eq.2)}$$

$$\dot{G} = eG^{\sigma} R_G^{1-\sigma} - \psi G \quad \text{(Eq.3)}$$

In *Eq.2* and *Eq.3*, R_K is the brown technological innovation investment and R_G is the green technological innovation investment. d is the brown capital accumulation size parameter, e is the green capital accumulation size parameter, δ, $\sigma\in(0,1)$ are production flexibilities during the accumulation of brown capital and green capital, Φ is the depreciation ratio of brown capital, and Ψ is the depreciation ratio of green capital. Assuming that the positive impact of capital stock inputs on capital accumulation is smaller than the technological innovation investment inputs, the production flexibility of capital stock amid capital accumulation should be smaller than the technological innovation investments. In other words, δ, $\sigma\in(0,0.5)$. In addition, compared to green capital, capital accumulation (Bondarev et al., 2014) is easier for brown capital. In that case, the production flexibility of green capital amid capital accumulation should not be larger than brown capital. In other words, $\sigma\leq\delta$.

(3) Assuming there is perfect competition in the market, for the products produced that can be used for consumption, brown technological innovation investments, green technological innovation investments, and environmental pollution governance, the budget constraints can be expressed as follows: $Y(K,G)-C-w(R_K+R_G)-X(E)K=0$. Here, w refers to the inorganic opportunity costs of technological innovation investments, $X(E)$ refers to the environmental regulatory strength, and $X(E)K$ refers to the environment governance costs. Among these, there is a positive relationship between environmental regulatory strengths $X(E)$ and environmental quality E. Assuming $X(E)$ concerns the monotonically increasing function of E, it can be displayed as $X(E)=aE^{\beta}$, where $a>0$ is referred to as the fixed proportional coefficient for eliminating costs and $\beta>1$ is the index for eliminating costs.

http://www.aloki.hu ● ISSN 1589 1623 (Print) ● ISSN 1785 0037 (Online)
DOI: http://dx.doi.org/10.15666/aeer/1704_92639278

Non-linear optimal control model

To summarize the above, the utility function *U(C,E)* adopting a logarithmic form is a strongly convex function, satisfying the conditions for establishing an optimal control model. Taking into account the changes in the brown capital stock *K*, green capital stock *G*, brown technological innovation investment R_K, green technological innovation investment R_G and environmental governance costs *X(E)K*, we give the following non-linear optimal control model,

$$\max_{C,E} W = \max_{C,E} \int_0^{\infty} U(C,E) \cdot e^{-\rho t} dt \tag{Eq.4}$$

s.t. *Eq.1~Eq.3*.

$$Y = bK^{\alpha} G^{1-\alpha} \tag{Eq.5}$$

$$bK^{\alpha} G^{1-\alpha} - C - w(R_K + R_G) - aE^{\beta} \cdot K = 0 \tag{Eq.6}$$

$$K(0) = K_0 > 0\,,\ G(0) = G_0 > 0 \tag{Eq.7}$$

where R_K and R_G are the control variables and *K*, *G*, and *C* are the state variables.

To find the optimal solution, taking λ_K and λ_G to be the common-mode variables of brown capital stock *K* and green capital stock *G* (shadow prices with different capital stock), the Hamiltonian in *Eq.8* is formed as follow,

$$H(\cdot) = \frac{(CE^{\eta})^{1-\theta}}{1-\theta} + \lambda_K \left(dK^{\delta} R_K^{1-\delta} - \phi K \right) + \lambda_G \left[eG^{\sigma} R_G^{1-\sigma} - \psi G \right] \tag{Eq.8}$$

We apply standard Pontryagin maximum principle to find a control optimal in problem of *Eq.1~Eq.7*, the maximization conditions should satisfy

$$\frac{\partial H}{\partial R_K} = 0 \tag{Eq.9}$$

$$\frac{\partial H}{\partial R_G} = 0 \tag{Eq.10}$$

This maximization leads to the Euler equation,

$$\dot{\lambda}_K = -\frac{\partial H}{\partial K} + \rho \lambda_K \tag{Eq.11}$$

$$\dot{\lambda}_G = -\frac{\partial H}{\partial G} + \rho \lambda_G \tag{Eq.12}$$

http://www.aloki.hu ● ISSN 1589 1623 (Print) ● ISSN 1785 0037 (Online)
DOI: http://dx.doi.org/10.15666/aeer/1704_92639278

Under the requirement that the following set of transversality conditions,

$$\lim_{t\to\infty} e^{-\rho t}\lambda_K K = 0 \tag{Eq.13}$$

$$\lim_{t\to\infty} e^{-\rho t}\lambda_G G = 0 \tag{Eq.14}$$

From *Eq.9~Eq.12*, it then follows that the costate variable associated to brown capital stock *K* and green capital stock *G*,

$$\lambda_K = \frac{wC^{-\theta}E^{\eta(1-\theta)}}{d(1-\delta)K^{\delta}R_K^{-\delta}} > 0 \tag{Eq.15}$$

$$\lambda_G = \frac{wC^{-\theta}E^{\eta(1-\theta)}}{e(1-\sigma)G^{\sigma}R_G^{-\sigma}} > 0 \tag{Eq.16}$$

In *Eq.15~Eq.16*, both λ_K and λ_G are positive values. Therefore, the Hession matrix of the Hamiltonian is as follows,

$$\begin{aligned} \mathrm{H} &= \begin{pmatrix} \dfrac{\partial^2 H}{\partial R_K^2} & \dfrac{\partial^2 H}{\partial R_K \partial R_G} \\ \dfrac{\partial^2 H}{\partial R_K \partial R_G} & \dfrac{\partial^2 H}{\partial R_G^2} \end{pmatrix} \\ &= \begin{pmatrix} -w^2\theta C^{-\theta-1}E^{\eta(1-\theta)} - \lambda_K d\delta(1-\delta)K^{\delta}R_K^{-\delta-1} & -w^2\theta C^{-\theta-1}E^{\eta(1-\theta)} \\ -w^2\theta C^{-\theta-1}E^{\eta(1-\theta)} & -w^2\theta C^{-\theta-1}E^{\eta(1-\theta)} - \lambda_G e\sigma(1-\sigma)\mathrm{G}^{\sigma}R_G^{-\sigma-1} \end{pmatrix} \end{aligned} \tag{Eq.17}$$

The *Eq.17* is negative definite, which means that current-value of the Hamiltonian is a strongly convex function which has a maximum value.

Results

From *Eq.6*, we can obtain consumption *C*, which is the function of variables *K*, *G*, R_K, and R_G, which is as follows:

$$C(K,G,R_K,R_G) = bK^{\alpha}G^{1-\alpha} - w(R_K + R_G) - aE^{\beta}K \tag{Eq.18}$$

The problem of *Eq.1~Eq.7* can be simplified to a problem with only four variables, i.e., *K*, *G*, R_K, and R_G, where *Eq.8* is the objective function, *Eq.2*, *Eq.3*, *Eq.9~Eq.14* and *Eq.18* are the constraints, R_K and R_G are the control variables, and *K* and *G* are the state variables.

From *Eq.9*, we can obtain the equation

$$\frac{\dot{\lambda}_K}{\lambda_K} = -\theta\frac{\dot{C}}{C} - \delta\frac{\dot{K}}{K} + \delta\frac{\dot{R}_K}{R_K} \tag{Eq.19}$$

http://www.aloki.hu ● ISSN 1589 1623 (Print) ● ISSN 1785 0037 (Online)
DOI: http://dx.doi.org/10.15666/aeer/1704_92639278

combining *Eq.11*, we can obtain the equation

$$\frac{\dot{\lambda}_K}{\lambda_K} = \rho + \phi - d\delta\left(\frac{R_K}{K}\right)^{1-\delta} - \frac{d(1-\delta)}{w}\left(\frac{R_K}{K}\right)^{-\delta}\left[\alpha b\left(\frac{G}{K}\right)^{1-\alpha} - aE^{\beta}\right] \quad \text{(Eq.20)}$$

Similarly, from *Eq.10*, we can obtain the equation

$$\frac{\dot{\lambda}_G}{\lambda_G} = -\theta\frac{\dot{C}}{C} - \sigma\frac{\dot{G}}{G} + \sigma\frac{\dot{R}_G}{R_G} \quad \text{(Eq.21)}$$

combining *Eq.12*, we can obtain the equation

$$\frac{\dot{\lambda}_G}{\lambda_G} = \rho + \psi - e\sigma\left(\frac{R_G}{G}\right)^{1-\sigma} - \frac{e(1-\sigma)}{w}\left(\frac{R_G}{G}\right)^{-\delta}(1-\alpha)b\left(\frac{G}{K}\right)^{-\alpha} \quad \text{(Eq.22)}$$

To achieve green growth, we set K and G to be constants, which means $\dot{R}=\dot{G}=0$. Combining *Eq.2* and *Eq.3*, we can obtain the equations

$$\frac{R_K}{K} = \left(\frac{\phi}{d}\right)^{1/(1-\delta)} \quad \text{(Eq.23)}$$

$$\frac{R_G}{G} = \left(\frac{\psi}{e}\right)^{1/(1-\sigma)} \quad \text{(Eq.24)}$$

Combining *Eq.19~Eq.24*, the optimal capital allocation G/K, and the optimal growth rate of investment for different technological innovations $\dot{R}/R$, and the optimal consumption growth rate $\dot{C}/C$ can be obtained as *Eq.25~Eq.28*

$$\frac{G}{K} = \frac{e(1-\alpha)(1-\sigma)}{\alpha d(1-\delta)}\left(\frac{\psi}{e}\right)^{\sigma/(\sigma-1)}\left(\frac{d}{\phi}\right)^{\delta/(\delta-1)}\frac{\rho+\phi+\theta g-\delta\phi+\frac{ad(1-\delta)}{w}\left(\frac{\phi}{d}\right)^{\delta/(\delta-1)}E^{\beta}}{\rho+\psi+\theta g-\sigma\psi} \quad \text{(Eq.25)}$$

$$\frac{\dot{R}_K}{R_K} = \frac{\rho+\phi+\theta g_C}{\delta} - \phi - \frac{d(1-\delta)}{w\delta}\left(\frac{\phi}{d}\right)^{\delta/(\delta-1)}\left[\alpha b\left(\frac{G}{K}\right)^{1-\alpha} - aE^{\beta}\right] \quad \text{(Eq.26)}$$

$$\frac{\dot{R}_G}{R_G} = \frac{\rho+\psi+\theta g_C}{\sigma} - \psi - \frac{e(1-\sigma)}{w\sigma}\left(\frac{\psi}{e}\right)^{\sigma/(\sigma-1)}(1-\alpha)b\left(\frac{G}{K}\right)^{-\alpha} \quad \text{(Eq.27)}$$

$$\frac{\dot{C}}{C} = \rho + \psi - \sigma\psi - \frac{e(1-\sigma)}{w}\left(\frac{\psi}{e}\right)^{-\frac{\delta}{1-\delta}}(1-\alpha)b\left(\frac{G^*}{K}\right)^{-\alpha} \quad \text{(Eq.28)}$$

http://www.aloki.hu ● ISSN 1589 1623 (Print) ● ISSN 1785 0037 (Online)
DOI: http://dx.doi.org/10.15666/aeer/1704_92639278

Discussion

Data source

The empirical value of different parameters in nonlinear optimal control model of existing research is shown as *Table 1*.

Refer to *Figure 1* for the "experience points" of different parameters for the models being researched. We perform a data simulation of the relationship between environmental regulatory strength *E*, capital allocation *G/K*, and the growth rate of investment for different technological innovations $\dot{R}/R$.

Table 1. *Key parameter values*

Parameter	Value	Definition	Reference Source
a	1	Fixed Proportional Coefficient for eliminating costs	Rauscher, 2009
α	0.6	Productive Capital Flexibility	Roseta-Palma et al., 2010
b	1	Size Parameter of Production Function	Antoci et al., 2012
d	1	Size Parameter of Brown Capital Accumulation	Antoci et al., 2012
e	1	Size Parameter of Green Capital Accumulation	Feenstra et al., 2001
ρ	0.05	Discount Rate	Chu and Lai, 2013
θ	2-2.5	Relative Risk Aversion Coefficient	Antoci et al., 2012
w	0.1	Inorganic Opportunity Costs Of Technological Innovation Investments	Antoci et al., 2012
β	2	Index for Eliminating Costs	Antoci et al., 2012
η	0.4	Environmental Quality Utility Index	Antoci et al., 2012
δ	0.4	Production Flexibility Where Brown Capital Is Being Accumulated	Feenstra et al., 2001
σ	0.3	Production Flexibility Where Green Capital Is Being Accumulated	Rauscher, 2009
φ	0.01	Brown Capital Depreciation Rate	Bilancini and D'Alessandro, 2012
ψ	0.01	Green Capital Depreciation Rate	Bovenberg and Smulders, 1996
a	1	Fixed Proportional Coefficient For Eliminating Costs	Rauscher, 2009

Analysis of the impact of environmental quality E on capital allocation G/K

We perform a data simulation of the impact of different environmental quality *E* on the capital allocation *G/K*, with the balanced growth rate as $g=0.0235$, the discount rate as $\rho=0.05$, productive capital flexibility as $\alpha=0.6$, and the inorganic opportunity costs of technological innovation investment as $w=0.1$, and the other parameters are fixed. *Figure 2* indicates that the capital allocation *G/K* concerns the strongly monotonically increasing concave function of the environmental regulatory strength *E*. With an increase in *E*, the environmental quality, the green capital ratio *G/(K+G)* increases and accelerates faster. When $E=0$, which represents the absence of environmental regulations, brown capital can be accumulated (Bondarev et al., 2014) relatively easily compared to green capital, which will cause brown capital to be used as much as possible during production. However, using brown capital can further pollute the environment. In addition, environmental regulations strength *X(E)* and environmental quality *E* are positively correlated, which thus results in an increase in expenditure on environmental governance costs *X(E)K*. Once the environmental quality *E* increases, the green capital ratio *G/(K+G)* presents a growth trend because the use of green capital can replace brown capital to reduce environmental pollution. At this point, brown capital is no longer considered to be critical capital for production, which causes capital

http://www.aloki.hu ● ISSN 1589 1623 (Print) ● ISSN 1785 0037 (Online)
DOI: http://dx.doi.org/10.15666/aeer/1704_92639278

allocation to switch towards green technological innovation. In addition, this trend becomes more significant as environmental quality E increases to $E=1$, which refers to stricter environmental regulations.

To more clearly explain the impact of environmental quality E on capital allocation G/K, we perform a data simulation of the impact of different environmental qualities E on the capital allocation G/K, with the balanced growth rate as $g=\{0,0.0135,0.0235, 0.0535\}$ and the other parameters being fixed. *Figure 2* shows that the balanced growth rate g and capital allocation G/K are negatively correlated. However, this finding does not change the impact of environmental quality E on capital allocation G/K. When the environmental quality is $E = 0.7$, the different balanced growth rates g corresponding to capital allocation ratio G/K are P_0, $P_{0.0135}$, $P_{0.0235}$, and $P_{0.0535}$, with $P_0 > P_{0.0135} > P_{0.0235} > P_{0.0535}$, respectively. The implication is that in the same environmental quality E, when the balanced growth rate g is higher, the green capital ratio $G/(K+G)$ is lower, which illustrates the production flexibility of brown capital in capital accumulation. This finding signifies the easing of the fall of capital accumulation, in which brown capital is being used as much as possible.

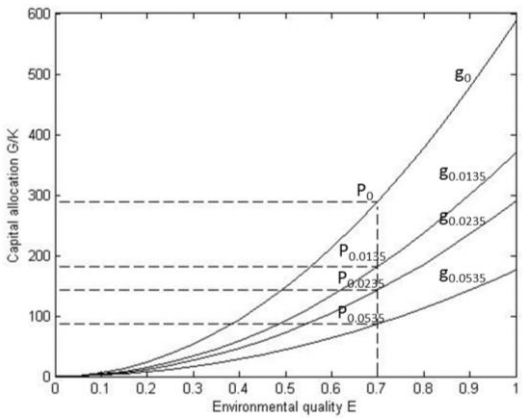

Figure 2. *Impact of balanced growth rate g on capital allocation G/K*

Furthermore, we perform a data simulation of the impact of different environmental qualities E on the capital allocation G/K where the discount rate is $\rho=\{0.001,0.01,0.015, 0.05\}$, production capital flexibility is $\alpha=\{0.8,0.7,0.6,0.5\}$, the inorganic opportunity costs of technological innovation investment are $w=\{0.05,0.1,0.15,0.2\}$, and the other parameters are fixed. *Figure 3* and *Figure 4* show that the green capital ratio $G/(K+G)$ will exhibit a growing trend when the same environmental quality E declines, the discount rate ρ declines, or production capital flexibility α declines. The implication is that when brown capital is producing, which negatively affects consumption and environmental pollution governance, the utilization of brown capital will be reduced. This reduction will stagnate the economic growth of society as a whole. Given this situation, it is possible to simulate a recovery in economic growth by simply raising green capital utilization efforts, which proves that green capital is an important pillar for maintaining the economic growth of society as a whole. On the other hand, there is a negative correlation between the inorganic opportunity costs of technological innovation investment w and the green capital ratio $G/(K+G)$. For details, refer to *Figure 5*. Assuming that environmental quality E does not change, the increase in the inorganic opportunity costs of technological innovation investment w means that similar

http://www.aloki.hu ● ISSN 1589 1623 (Print) ● ISSN 1785 0037 (Online)
DOI: http://dx.doi.org/10.15666/aeer/1704_92639278

subsidies are given whether the technological innovation is green or brown. The implication is that provided that the requirements under environmental qualities *E* are satisfied, priority is given to the utilization of brown capital. Thus, brown capital shall enjoy greater production flexibility in capital accumulation.

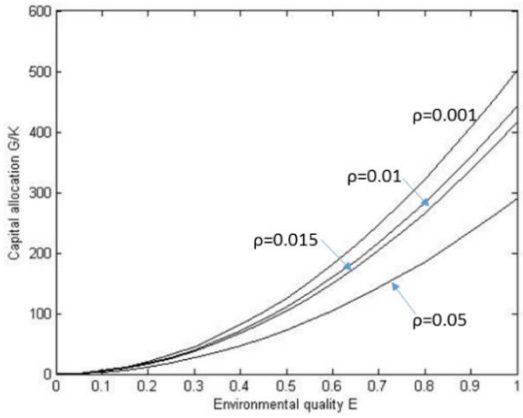

Figure 3. *Impact of discount rate ρ on capital allocation G/K*

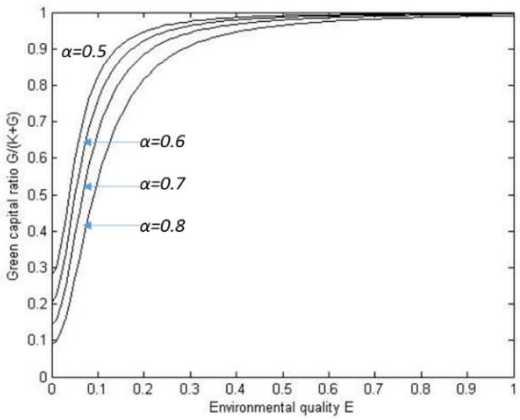

Figure 4. *Impact of production capital flexibility α on capital allocation G/K*

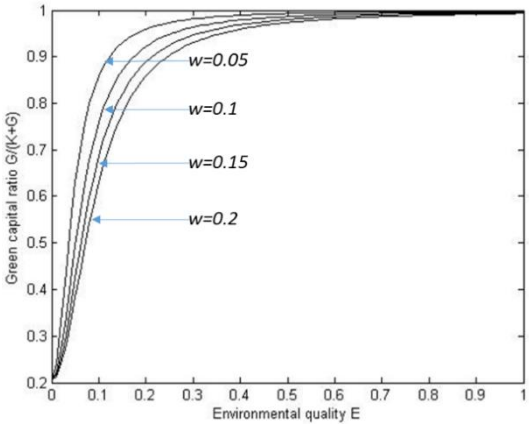

Figure 5. *Impact of technological innovation investment inorganic opportunity costs w on capital allocation G/K*

http://www.aloki.hu ● ISSN 1589 1623 (Print) ● ISSN 1785 0037 (Online)
DOI: http://dx.doi.org/10.15666/aeer/1704_92639278

Impact of capital allocation G/K on the optimal consumption growth rate Ċ/C

Incorporating *Eq.25* in *Eq.26* and *Eq.27*, the growth rate of investment for different technological innovations $\dot{R}/R$ reconstructs the partial derivatives of capital allocation G/K

$$\frac{\partial \dot{R}_K / R_K}{\partial G / K} = -\frac{\alpha b d (1-\delta)(1-\alpha)}{w\delta}\left(\frac{g_K + \phi}{d}\right)^{\delta/(\delta-1)}\left(\frac{G}{K}\right)^{-\alpha} < 0 \qquad \text{(Eq.29)}$$

$$\frac{\partial \dot{R}_G / R_G}{\partial G / K} = \frac{\alpha b e (1-\alpha)(1-\sigma)}{w\sigma}\left(\frac{g_G + \psi}{e}\right)^{\sigma/(\sigma-1)}\left(\frac{G}{K}\right)^{-1-\alpha} > 0 \qquad \text{(Eq.30)}$$

From *Eq.29* and *Eq.30*, it is observed that the obtainable investment ratio of brown technological innovation $\dot{R}_K/R_K$ is related to the monotonous decreasing function of capital allocation G/K. In addition, the investment rate of green technological innovation $\dot{R}_G/R_G$ is related to the monotonous increasing function of capital allocation G/K. We perform a data simulation of the impact of different capital allocation G/K on the investment rate of technological innovation $\dot{R}/R$ with $g=0.0135$ and the other parameters being fixed. *Figure 6* shows that the investment rate of both brown technological innovation $\dot{R}_K/R_K$ and the investment rate of green technological innovation $\dot{R}_G/R_G$ converge to a certain fixed value; however, the convergence value of the investment rate of green technological innovation $\dot{R}_G/R_G$ is higher than the investment rate of brown technological innovation $\dot{R}_K/R_K$. Once, which means that the investments rates of technological innovation have reached equilibrium, the capital allocation $(G/K)^*$ reaches the optimal balanced capital allocation ratio $(G/K)^*=0.5$. The implication is that green technological innovation investments relative to brown technological innovation investments can bring about a greater value of economic growth.

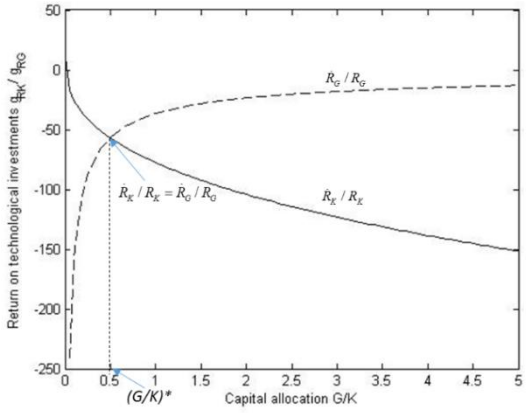

Figure 6. *Impact of capital allocation G/K on the rate of technological investments Ṙ/R*

To further clarify the impact of capital allocation G/K on the optimal consumption growth rate $\dot{C}/C$, we perform a simulation on the impact of different capital allocation G/K on the optimal consumption growth rate $\dot{C}/C$, where the capital allocation ratio is $G/K=\{0.2,0.5,1\}$ and the other parameters are fixed. *Figure 7* shows that for different

http://www.aloki.hu ● ISSN 1589 1623 (Print) ● ISSN 1785 0037 (Online)
DOI: http://dx.doi.org/10.15666/aeer/1704_92639278

capital allocation ratios *G/K*, the trajectory of the optimal consumption growth rate is different. Only when *G/K=0.5* is the optimal consumption growth rate the highest. In addition, with an increase in environmental regulations, there is a monotonic increase in the optimal consumption growth rate. Regarding two other situations in which *G/K<0.5* and *G/K>0.5*, the optimal consumption growth rate must be lower than *G/K=0.5*. Simultaneously, from the analysis in *Figure 6*, we know that *G/K=0.5* is also the equilibrium point of the investment rate of technological innovation.

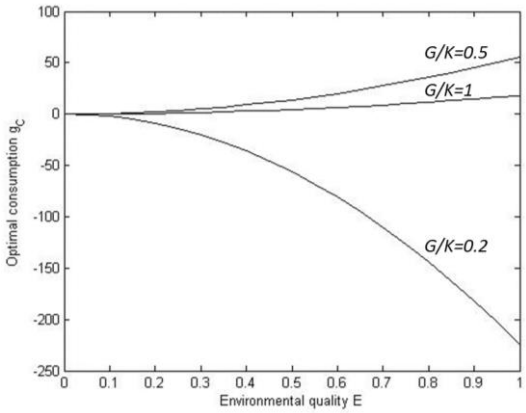

Figure 7. *Impact of capital allocation G/K on optimal consumption growth rate Ċ/C*

Because it is not necessary to consider a negative impact on the environment due to the lower research and development costs of brown technological innovation, the products that were put into production will have greater profits and market potential. Therefore, brown capital stock will increase by a greater extent along with capital accumulation. However, this increase may easily spark a new vicious cycle of economic growth that over-relies on brown technological innovation. By analyzing the optimal consumption growth rate, we can determine that it is mainly driven by brown capital and that the impact of green capital on the optimal consumption growth rate must be lower than that of brown capital. In addition, other than consumption per se, environmental improvements would benefit the social welfare that people eventually seek. Therefore, from another perspective, as environmental regulations increase, even if green capital does not result in a rapid growth in consumption, improvements in the environment will compensate for this shortcoming, which not only proves that the implementation of environmental regulations can help increase the drivers of green technological innovation but also further proves that green technological innovation can boost the economic growth of society as a whole. The reason is the social value that it brings is much greater. In particular, it can also effectively ease the negative impact on the environment.

Conclusion

From the perspective of green growth theory, the present research takes into account the impact of the implementation of environmental regulations on directed technological innovations and incorporates the following into the framework for the analysis of capital accumulation:

http://www.aloki.hu ● ISSN 1589 1623 (Print) ● ISSN 1785 0037 (Online)
DOI: http://dx.doi.org/10.15666/aeer/1704_92639278

(1) Brown technological innovation that involves environmental regulations and environmental governance costs;

(2) Green technological innovations that can effectively protect the environment.

Assuming the effect of the economies of scale remains unchanged and that there is perfect competition in the market, we draw reference from the method of quantitative expression of green growth targets by Moser et al. (2013) and the method of brown technological innovation investment and green technological innovation investments by Rauscher (2009). In doing so, we construct a non-linear optimal control model in which the relative risk aversion coefficient >0, the green growth target of maximizing social welfare is the objective function, and the constraint is the ensuring of the constant growth of the balanced growth rate and the constant improvement in environmental quality. Using optimal control theory and the maximum principle, we separately obtain the quantitative expression for the investment rate of brown technological innovation $\dot{R}_K/R_K$, the investment rate of green technological innovation $\dot{R}_G/R_G$, and capital allocation G/K. Finally, we perform a data simulation of the problem regarding the impact of environmental regulatory strength on the selection of directed technological innovation to drive the economic growth of society as a whole. The simulation results are as follows:

(1) Environmental regulatory strength E has a positive impact on the green capital ratio $G/(K+G)$, which means that the implementation of environmental regulations can subdue the increase in environmental pollution and achieve the shift of capital allocation towards green technological innovation fields.

(2) The balanced growth rate g, the discount ratio ρ, productive capital flexibility α, and the inorganic opportunity costs of technological innovation investment w have a negative impact on the green capital ratio $G/(K+G)$, which proves that brown capital has superior production flexibility in capital accumulation. Although this finding means that brown capital can ease the fall in capital accumulation, it also proves that green capital is necessary for the economic growth of society as a whole.

(3) The green capital ratio $G/(K+G)$ has a negative impact on the investment rate of brown technological innovation $\dot{R}_K/R_K$ and a positive impact on the investment rate of green technological innovation $\dot{R}_G/R_G$. However, green technological innovation, relative to brown technological innovation, can create a greater value of economic growth.

(4) The environmental quality E has a positive impact on the investment rate of technological innovation $\dot{R}_K/R_K = \dot{R}_G/R_G$ and the corresponding green capital ratio $G/(K+G)$ when in a balanced state. This result not only reconfirms that the stronger the implementation of environmental regulations is, the more it benefits the utilization of green capital, but it also further affirms that the implementation of environmental regulations will direct capital allocation towards the new field of green technological innovations. The reason is the utilization of green technological innovations shall play a more effective role than brown technological innovations in achieving green growth (a rise in economic growth and improvement in environmental quality).

The above-mentioned simulation results can provide government decision makers with proven management guidance in formulating suitable environmental regulations with the aim of directing capital allocation towards green technological innovation fields and further achieving green growth. However, the present research also takes into account relatively ideal external factors such as the effects of economies of scale remaining unchanged, the operating status of the market economy, the relationship

http://www.aloki.hu ● ISSN 1589 1623 (Print) ● ISSN 1785 0037 (Online)
DOI: http://dx.doi.org/10.15666/aeer/1704_92639278

between pollution governance efforts and environmental regulatory strength, the capital allocation, and production technological conditions under different types of capital. Therefore, our next research direction will involve taking into account more realistic factors or problems with green growth after adequately broadening the scope of the above-mentioned assumptions.

Acknowledgements. We are grateful for financial support to the first author from the International Cooperation and Exchanges NSFC of China (71320107006) and Program for Innovative Research Team in University of Ministry of Education of China (IRT_17R13); and to the second and corresponding author from the NSFC of China (71831002, 71403035), Foundation for Humanities and Social Sciences of Ministry of Education of China (18YJC630261) and Key R&D Program for Soft Science Project of Liaoning Province of China (2018401030).

REFERENCES

[1] Antoci, A., Russu, P., Ticci, E. (2012): Environmental externalities and immiserizing structural changes in an economy with heterogeneous agents. – Ecological Economics 81(3): 80-91.
[2] Arduini, R., Cesaroni, F. (2002): Environmental technologies in the European chemical industry. – Lem working papers series, Sant'Anna School of Advanced Studies, Pisa, Italy.
[3] Barbera, A. J., Mcconnell, V. D. (1990): The impact of environmental regulations on industry productivity: direct and indirect effects. – Journal of Environmental Economics & Management 18(1): 50-65.
[4] Bilancini, E., D'Alessandro, S. (2011): Long-run welfare under externalities in consumption, leisure, and production: a case for happy degrowth vs. Unhappy growth. – Ecological Economics 84(6): 194-205.
[5] Bondarev, A., Clemens, C., Greiner, A. (2014): Climate change and technical progress: impact of informational constraints. – In: Dynamic Optimization in Environmental Economics. Dynamic Modeling and Econometrics in Economics and Finance 15. Berlin, Heidelberg: Springer.
[6] Bovenberg, A. L., Smulders, S. A. (1996): Transitional impacts of environmental policy in an endogenous growth model. – International Economic Review 37(4): 861-893.
[7] Caselli, F. (2005): Accounting for cross-country income differences. – Lse Research Online Documents on Economics 1(5): 679-741.
[8] Chu, H., Lai, C. C. (2013): Abatement R&D, market imperfections, and environmental policy in an endogenous growth model. – Journal of Economic Dynamics & Control 41(1): 20-37.
[9] Demirel, P., Kesidou, E. (2011): Stimulating different types of eco-innovation in the UK: government policies and firm motivations. – Ecological Economics 70(8): 1546-1557.
[10] Feenstra, T., Kort, P. M., Zeeuw, A. D. (2001): Environmental policy instruments in an international duopoly with feedback investment strategies. – Journal of Economic Dynamics & Control 25(10): 1665-1687.
[11] Gans, J. S. (2009): Innovation and climate change policy. – American Economic Journal Economic Policy 4(4): 125-145.
[12] Gerlagh, R. (2011): Too much oil. – CESifo Economic Studies 57(1): 79-102.
[13] Ghisetti, C., Pontoni, F. (2015): Investigating policy and R&D effects on environmental innovation: a meta-analysis. – Ecological Economics 118(5): 57-66.
[14] Goulder, L. H. (2004): Induced technological change and climate policy. – Pew Center on Global Climate Change, Arlington, VA.

http://www.aloki.hu ● ISSN 1589 1623 (Print) ● ISSN 1785 0037 (Online)
DOI: http://dx.doi.org/10.15666/aeer/1704_92639278

[15] Hamamoto, M. (2006): Environmental regulation and the productivity of japanese manufacturing industries. – Resource & Energy Economics 28(4): 299-312.
[16] Hart, R. (2004): Growth, environment and innovation - a model with production vintages and environmentally oriented research. – Journal of Environmental Economics & Management 48(3): 1078-1098.
[17] Jaffe, A. B., Newell, R. G., Stavins, R. N. (2002): Technological change and the environment. – Social Science Electronic Publishing 1(3): 461-516.
[18] Johnstone, N., Hascic, I., Poirier, J., Hemar, M., Michel, C. (2012): Environmental policy stringency and technological innovation: evidence from survey data and patent counts. – Applied Economics 44(17): 2157-2170.
[19] Li, L., Tao, F. (2012): Selection of the optimal environmental regulatory strength in China's manufacturing sector: A perspective based on green total factor productivity. – Industrial Economics of China 5(5): 70-82.
[20] Li, J. W., Guan, Q., Yang, H. (2018): Winter energy consumption in reading space of green library in cold regions. – International Journal of Heat and Technology 36(4): 1256-1261.
[21] Maria, C. D., Werf, E. V. D. (2008): Carbon leakage revisited: unilateral climate policy with directed technical change. – Environmental and Resource Economics 39(2): 55-74.
[22] Moser, E., Prskawetz, A., Tragler, G. (2013): Environmental regulations, abatement and economic growth. – In: Green Growth and Sustainable Development. Dynamic Modeling and Econometrics in Economics and Finance 14. Berlin, Heidelberg: Springer.
[23] Nakano, M. (2003): Can environmental regulation improve technology and efficiency: an empirical analysis using the Malmquist productivity Index. – Eaere 6: 28-30.
[24] OECD. (2011): Towards green growth. – OECD Meeting of the Council (16): 8-37.
[25] Rauscher, M. (2009): Green r&d versus end-of-pipe emission abatement: a model of directed technical change. – Working paper No. 106, Thuenen-Series of Applied Economic Theory, Institute of Economics, University of Rostock, Rostock.
[26] Roseta-Palma, C., Ferreira-Lopes, A., Sequeira, T. N. (2010): Externalities in an endogenous growth model with social and natural capital. – Ecological Economics 69(3): 603-612.
[27] Rubashkina, Y., Galeotti, M., Verdolini, E. (2015): Environmental regulation and competitiveness: empirical evidence on the porter hypothesis from european manufacturing sectors. – Ssrn Electronic Journal 83(35): 288-300.
[28] Shen, N. (2012): Threshold effect of the impact of environmental regulations on regional technological innovation. – China's population, resources, and environment 22: 12-16.
[29] Smulders, S., Nooij, M. D. (2003): The impact of energy conservation on technology and economic growth. – Resource & Energy Economics 25(1): 59-79.
[30] Smulders, S., Werf, E. V. D. (2008): Climate policy and the optimal extraction of high- and low-carbon fossil fuels. – Canadian Journal of Economics/Revue canadienne d'économique 41(4): 1421-1444.
[31] Stokey, N. L. (1998): Are there limits to growth. – International Economic Review 39(1): 1-31.
[32] Zhang, C., Lu, Y., Guo, L. (2011): Environmental regulatory strength and advancement in production technology. – Economic research 2: 113-124.
[33] Zhang, J. L., Zhu, L. (2012): Research on industrial enterprise technological innovation effectiveness based on green growth in different parts of China. – Technological economic research in quantitative economics 2: 113-125.

http://www.aloki.hu ● ISSN 1589 1623 (Print) ● ISSN 1785 0037 (Online)
DOI: http://dx.doi.org/10.15666/aeer/1704_92639278

UNDESIRABLE OUTPUT IN EFFICIENCY: EVIDENCE FROM WASTEWATER TREATMENT PLANTS IN CHINA

FENG, Y.[1,2] – FENG, J. K.[1*] – LEE, J. H.[3] – LU, C. C.[3] – CHIU, Y. H.[3]

[1]*School of Economics & Management of Northwest University, Xi'an 710122, China*

[2]*Business College of Northwest University of Political Science and Law, Xi'an 710122, China*

[3]*Department of Economics, Soochow University, Taipei 10048, Taiwan, R.O.C.*

[*]*Corresponding author*
e-mail: 778970455@qq.com; phone: +86-029-8818-2575

(Received 3rd Apr 2019; accepted 17th May 2019)

Abstract. This study focuses on sewage sludge treatment and applies the Bad Output model to deal with desirable and undesirable outputs independently. This approach provides an objective way to assess the technical efficiency of wastewater treatment plants in eastern China and provides a reference for the development of the Midwest. The efficiency score results of 518 plants show some volatility - the average efficiency score is 0.29; 27 plants' efficiency scores are close to 1; 146 plants have an efficiency score of between 1 and the average efficiency score. The higher efficiency score regions are Hainan, Guangdong, Fujian, and Beijing, while by contrast, Hebei, Shanghai, and Tianjin have average efficiency scores lower than the other regions. The results of the adjustment ratio in wastewater treatment or sewage sludge water contents illustrate that most regions exhibit efficiency volatility, and some regions can no longer can support wastewater treatment or sewage sludge water contents.
Keywords: *data envelopment analysis (DEA), undesirable outputs mode, wastewater treatment efficiency, sewage sludge water contents*

Introduction

Ever since the initiation of market reforms and opening up in China, its economy has developed very rapidly. In 2014, China's GDP hit US$ 10.36 trillion, accounting for 13.3% of the world's total GDP. At the same time, energy consumption has also grown rapidly with economic growth, accounting for 21.09% of global energy consumption in 2014 (National Bureau of Statistics, 2015). It has also brought about serious environmental pollution, in order to promote economic development China has proposed the binding target of "energy conservation and emission reduction" during the "11th Five-Year Plan". For the "12th Five-Year Plan", the target is to cut the country's energy consumption per unit of GDP by 18.4%. China's State Council's "Thirteenth Five Energy-saving Emission Reduction Comprehensive Work Plan" stated that by 2020, energy consumed should only be 15% of China's GDP level in 2015.

The sewage treatment process requires a lot of energy, and thus the sewage treatment industry is also an "energy saving" binding indicator for the integrated source of pollution in the area of intensive treatment. Under the increase of industrialization and an improvement in people's environmental awareness, the wastewater treatment industry in China has developed quite strongly. At the end of 2014, China had a total of 3362 urban wastewater treatment plants (WWTPs) with a total capacity of 160 million tons / day and a total wastewater treatment volume of 47.6 billion tons. Due to the continuous improvement of effluent quality requirements of WWTPs, the energy consumption cost of these plants accounts for 40%-80% of its operation and

http://www.aloki.hu ● ISSN 1589 1623 (Print) ●ISSN1785 0037 (Online)
DOI: http://dx.doi.org/10.15666/aeer/1704_92799290

maintenance costs, with the power consumption of wastewater treatment increasing to 0.3 kwh/m^3. Moreover, at least 83% of WWTPs consume more energy than found in the data, which is more than 0.45 kwh/m^3. Compared to other developed countries, the difference is significant (Pan, 2014). Wastewater treatment costs are now averaging at US$ 0.8/m^3, and high energy problems have become major urban wastewater treatment operating efficiency constraints.

Due to the high operating costs of sewage treatment plants, low load rates, and other issues, some municipal wastewater treatments plants cannot operate normally, or even operate inefficiently for a long time, or even are left unused, thus resulting in the failure of WWTPs to play the role of water protection and also causinga waste of huge investment capital. Studies on the efficiency of WWTPs may help to significantly reduce costs, improve environmental improvements, and also maintain the sustainability of WWTPs (Guerrini et al., 2013; Georgieva, 2017).

The operation of a wastewater treatment plant is accompanied by a large amount of sludge. With the improvement of wastewater treatment capacity and improvement of effluent quality in China, the amount of sludge is increasing at an annual rate of 15%. Sludge disposal has therefore become an increasingly prominent environmental problem in the country. Sludge treatment also affects the entire wastewater treatment plant operation results. While a reasonable and safe disposal of sludge is an important part of the municipal wastewater treatment process, unfortunately, for the reasons of a lack of capital in China, insufficient knowledge, and limited technology and policy, the disposal of sludge has not been paid enough attention. The existence of the hidden danger of secondary pollution caused by the sludge problem greatly reduces the environmental benefits produced by WWTPs and has caught the nation's concern (Dai, 2012). Assessing the efficiency of WWTPs but ignoring the sludge indicator will produce an unbiased result and also departs from the actual problem of these plants in China. However, traditional efficiency measures of WWTPs focus only on the desirable outputs and fail to consider environmentally undesirable by-products of the production processes.

Within the extensive literature on data envelopment analysis (DEA), comparatively little research has focused on the relationship between desirable and undesirable output. Some studies that have include Yang and Pollitt (2009), Emrouznejad et al. (2010), Sueyoshi and Goto (2011), Wang et al. (2012), and Chiu et al. (2016). This literature provides a good research perspective and analysis approach for our own study to bring the sludge indicator in as an undesirable output.

In view of the problems mentioned above, the purpose of this study focuses on analyzing the efficiency of WWTPs by incorporating the results in Tone (2001) who advocate an undesirable output in the variable-returns-to- scale envelopment models. After its market reforms and opening up, economic growth in eastern China has always been higher than in the central and western regions. By the end of 2014, the eastern region's GDP accounted for 55.34% of the national total, far exceeding the total from the central and western regions. Economic development has been accompanied by resource consumption and environmental pollution, so that at the end of 2014, the eastern region's industrial wastewater emissions and urban domestic sewage emissions accounted for 53.24% and 52.46% of the country's total, respectively. At the same time, the eastern region's industrial wastewater treatment investment is also far higher than that in the central and western regions, accounting for over 55% of the national total. Therefore, analyzing wastewater treatment in the eastern region is of great significance

http://www.aloki.hu ● ISSN 1589 1623 (Print) ●ISSN1785 0037 (Online)
DOI: http://dx.doi.org/10.15666/aeer/1704_92799290

for China to achieve its goal of "energy conservation and emission reduction" and to build a resource-saving and environment-friendly society. This can also be a reference for the development of the Midwest.

The remainder of this study is the following. Section 2 is the literature review. Section 3 is the research method. Section 4 is the empirical results. Section 5 is the conclusions.

The performance measurement of WWTPs in the past has focused on improving the technical indicators to obtain good effluent quality (Wen et al., 2009; Bolong et al., 2009; Santos et al., 2011; Zanetti et al., 2012; Luo et al., 2014; Zhang et al., 2016). As the research has deepened in this field along with the development of analysis methods, scholars have proposed integrated performance indicators that are technical, economic, and environmental in quantitative analysis (Yang, 2017).

Stochastic frontier analysis (SFA) and Data Envelopment Analysis (DEA) are two main approaches for efficiency assessment - namely, parametric and non-parametric methods (Tiedemann et al., 2010; Ferro et al., 2014). Both of these two methods have been widely used to estimate the efficiency of water utilities (Guerrini et al., 2011; Portela et al., 2011; Guerrini et al., 2013; Carvalho and Marques, 2014; Lannier and Porcher, 2014).

Many studies document the usefulness of the efficiency assessment of WWTPs and measure the so-called efficiency in order to save operational cost and improve sustainability (Hernández-Sancho et al., 2011; Sala-Garrido et al., 2012; Molinos-Senante et al., 2014, 2015b; Chen et al., 2015; Guerrini et al., 2015). Yang (2017) adopts the DEA-SBM model to measure the TFE of wastewater control in 39 industrial sectors in China from 2003 to 2014. However, these studies above only set positive inputs and outputs, and most scholars focus on sludge treatment like sludge stabilization with various physical, chemical, and biological technologies (Zhang et al., 2007; Kelessidis and Stasinakis, 2012; Yu et al., 2013; Yang et al., 2015; He et al., 2018;) and sludge disposal methods such as sanitary landfill, incineration, land application, and building materials (Cai et al., 2007; Hale et al., 2012; Wang et al., 2012). Few studies in the literature look at sludge efficiency in an economic way. Sewage sludge as an inevitable by-product of the wastewater treatment process, which may result in secondary pollution, presents a number of environmental concerns, but no study adopts a sewage sludge indicator as an undesirable output to comprehensively assess the efficiency of WWTPs.

Various approaches recently have enabled DEA to deal with undesirable outputs. They can be summarized into four types as follows (Gomes and Lins, 2007; Chiu et al., 2016). The first method uses a reciprocal of undesirable output to evaluate the efficiency (Golany and Roll, 1989; Lovell et al., 1995; Scheel, 2001). The second method considers the undesirable outputs as inputs (Hailu and Veeman, 2001). The third one is the data transformation function approach (Seiford and Zhu, 2002, 2005). The last type is the directional distance function approach (Chung et al., 1997). Alternatively, Tone (2001) proposes a slacks-based measure of efficiency, which is non-radial and non-oriented, and deals with input/output slacks directly. Following this is Sharp et al. (2007), who modify the slacks-based measure to overcome the lack of translation invariance by drawing on the ideas from the range directional model.

These articles have been recently extended to energy and environment studies, but do not evaluate the efficiency of WWTPs. Evaluating the efficiency of WWTPs without considering the sludge problem, which may cause secondary pollution, will be biased.

http://www.aloki.hu ● ISSN 1589 1623 (Print) ●ISSN1785 0037 (Online)
DOI: http://dx.doi.org/10.15666/aeer/1704_92799290

The reasonable and safe disposal of sludge has especially become an important bottleneck, actually restricting the healthy and benign development of WWTPs in China. Therefore, our study comprehensively considers the economic and environmental benefits of WWTPs and constructs a DEA model with sludge disposal as an undesirable output in order to objectively evaluate the efficiency.

Because of the different economic development levels, urbanization process, and natural geographical conditions in the different regions and provinces of China, there are some obviously differences about wastewater treatment, such as wastewater emissions and the total volume of disposal wastewater and utilization rate of WWTPs between eastern and western cities. Since the eastern region is the most developed area of China, it contributes more than 50% to economic volume. Thus, the development of WWTPs in eastern China is also in the leading position along with serious sludge treatment, and hence our study focus on the eastern region to evaluate the efficiency of WWTPs and uses anundesirable output DEA model. The results provide effective suggestions for China.

Materials and methods

DEA method

Data Envelopment Analysis (DEA) is a method for measuring the relative efficiency of a set of Decision Making Units (DMUs), which apply multiple inputs to produce multiple outputs over a period of time. DEA was originally developed by Charnes et al. (1978) under the assumption of constant returns to scale (CCR model). Banker et al. (1984) extend the CCR model to include variable returns to scale and develop the BCC model.

In the Banker et al. (1984) model, we denote the set of DMUs as J, where each DMU j ∈J. Let us define the following variables: Y_j is the output of the DMU, X_i is the input of the DMU, Z_i is the weight of DMU, and s_j^- and s_j^+ are the input slacks and the output slacks, respectively. Here, θ_i is the score of the DMU. We set up the input-oriented BCC method used to calculate technical efficiency as:

$$\max: \theta$$

$$\text{s.t.} \sum_{j=1}^{n} z_j x_j + s^- = x_0$$

$$\sum_{j=1}^{n} z_j y_j - s^+ = \theta y_0$$

$$\sum_{j=1}^{n} z_j = 1$$

$$z_j \geq 0, j = 1, \cdots, n$$

Though CCR and BCC mainly focus on desirable output or input, in the real world the production process or the content of output may not be a desirable output. In an actual production process, unwanted by-products may appear during input and output conversion, such as wastewater, exhaust gas, and carbon dioxide. In the traditional DEA

http://www.aloki.hu ● ISSN 1589 1623 (Print) ●ISSN1785 0037 (Online)
DOI: http://dx.doi.org/10.15666/aeer/1704_92799290

model, if the relative inefficient DMUs have desirable (good) and undesirable (bad) inputs/outputs to adjust, then they increase or decrease simultaneously, because they cannot just increase the desirable output yet not decrease the undesirable output.

To address the above problem, Tone (2001) applies the undesirable DEA model, which classifies output items into desirable and undesirable outputs. Both kinds of outputs have no inter-relationship, which isdifferent from the undesirable output model where a reduction of bad outputs inevitably reduces desirable outputs. Hence, this situation can be improved.

Undesirable outputs model

In light of the environmental protection consciousness in modern society, undesirable outputs of production and social activities, e.g., hazardous wastes and air pollutants have been strongly recognized as societal maladies. Thus, the development of technologies with less undesirable outputs is the main subject in every area of production. DEA usually assumes that producing more outputs relative to less input resources illustrates a standard of efficiency. In the presence of undesirable outputs, nevertheless, technologies with more desirable outputs and less undesirable outputs relative to less input resources should be recognized as being efficient.

This model deals with the same problem by applying a slacks-based measure of efficiency (SBM). SBM is non-radial and non-oriented and utilizes input and output slacks directly in producing an efficiency measure. This paper applies the Bad Output model to deal with desirable and undesirable outputs independently. We decompose the output matrix Y into (Y^g, Y^b), where Y^g and Y^b denote desirable and undesirable output matrices, respectively. For a DMU (x_o, y_o), the decomposition is denoted as (x_o, y_o^g, y_o^b).

We conceptualize the production possibility set defined as *Eq.1*:

$$P = \left\{ \left((x, y^g, y^b) \middle| x \geq X\lambda, y^g \leq Y^g\lambda, y^b \geq Y^b\lambda, L \leq e\lambda \leq U, \lambda \geq 0 \right) \right\} \quad \text{(Eq.1)}$$

Here, λ is the intensity vector, and L and U are the lower and upper bounds of the intensity vector, respectively. We define the efficiency status in this framework as follows.

A DMU (x_o, y_o^g, y_o^b) is efficient in the presence of bad outputs, if there is no vector $(x_o, y^g, y^b) \in P$ such that $x_o \geq x, y_o^g \leq y^g, y_o^b \geq y^b$with at least one stringent inequality.

According to the definition, SBM runs as *Eq.2*:

$$\theta^* = \min \frac{1 - \frac{1}{m}\sum_{i=1}^{m} \frac{\bar{s_{io}}}{x_{io}}}{1 + \frac{1}{s}\left(\sum_{r=1}^{s_1} \frac{s_r^g}{y_{ro}^g} + \sum_{r=1}^{s_2} \frac{s_r^b}{y_{ro}^b} \right)}$$

subject to

$$x_o = X\lambda + s^-$$
$$y_o^g = Y\lambda - s^g$$
$$y_o^b = Y\lambda + s^b \quad \text{(Eq.2)}$$
$$L \leq e\lambda \leq U$$
$$s^-, s^g, s^b, \lambda \geq 0$$

http://www.aloki.hu ● ISSN 1589 1623 (Print) ●ISSN1785 0037 (Online)
DOI: http://dx.doi.org/10.15666/aeer/1704_92799290

The vectors s^- and s^b correspond to excesses in inputs and undesirable outputs, respectively, while s^g expresses shortages in desirable outputs. Here, s_1 and s_2 denote the number of elements in s^b and s^g, and $s = s_1 + s_2$. Let an optimal solution of the above program be $(\theta^*, s^{-^*}, s^{g^*}, s^{b^*})$. We can then illustrate that the DMU (x_o, y_o^g, y_o^b) is efficient in the presence of undesirable outputs if and only if $\theta^* = 1, \text{i.e.}, s^{-^*} = 0, s^{g^*} = 0, s^{b^*} = 0$. If the DMU is inefficient, i.e., $\theta^* < 1$, then it can be improved and become efficient by deleting the excesses in inputs and undesirable outputs and increasing the shortfalls in desirable outputs by the following projection *Eq.3*.

$$x_o \Leftarrow x_o - s^{-^*} \qquad y_o^g \Leftarrow y_o^g + s^{g^*} \; y_o^b \Leftarrow y_o^b - s^{b^*} \tag{Eq.3}$$

In the Undesirable (Bad) Output model, we set weights upon undesirable and desirable outputs through the keyboard before running the model. If we supply $w_1 (\geq 0)$ and w_2 (≥ 0) as the weights to desirable and undesirable outputs, respectively, then the model calculates the relative weights as $W_1 = sw_1/(w_1 + w_2)$ and $W_2 = sw_2/(w_1 + w_2)$, W2 =sw2(w1 +w2), and the objective function is then modified to *Eq.4*:

$$\theta^* = \min \frac{1 - \frac{1}{m} \sum_{i=1}^{m} \frac{\bar{s_{io}}}{x_{io}}}{1 + \frac{1}{s} \left(w_1 \sum_{r=1}^{s_1} \frac{s_r^g}{y_{ro}^g} + w_2 \sum_{r=1}^{s_2} \frac{s_r^b}{y_{ro}^b} \right)} \tag{Eq.4}$$

The defaults in *Eq.4* are w_1 =1 and w_2 =1. In accordance with the degree of stress on undesirable outputs evaluation, you can put a large w_2 against w_1, and vice versa.

Results

The research samples cover the 518 WWTPs in eastern China according to the China Energy Statistical Yearbook dataset in 2015. We use ten regions and five variables here, as shown in *Table 1*: the regions are Shanghai, Shandong, Guangdong, Tianjin, Beijing, Jiangsu, Liaoning, Hebei, Hainan, and Fujian. The five variables include two as output variables and three as input variables. The output variables are wastewater treatment and the undesirable output of sewage sludge water contents; the input variables are equipment investment, electricity usage, and employees. This study concludes with implications for theoretical research. These variables may lead to a better understanding and merging with input variables and output variables of recent studies. The input variables and output variables are shown to be significantly related.

In order to clarify the influence of the regions, we conduct an analysis of Shandong, Guangdong, and the other regions, with *Table 2* presenting the descriptive statistics of the input and output variable data for them as follows.

(1) Wastewater treatment: The wastewater treatment average of all plants is 18.335 million m^3, where Shandong is 18.171 million m^3, and Guangdong is 25.257 million m^3. The max wastewater treatment plant is 328.5 million m^3 from Beijing, while the lowest wastewater treatment plant is 10.95 million m^3 from Shandong.

(2) Sewage sludge water contents: In general, for the water content of sewage sludge, a lower value is better. The average sewage sludge water contents from the 518 plants

http://www.aloki.hu ● ISSN 1589 1623 (Print) ●ISSN1785 0037 (Online)
DOI: http://dx.doi.org/10.15666/aeer/1704_92799290

are 76.36%. Shandong is 77.65%, Guangdong is 75.71%, and the other regions are 76.14%. The average sewage sludge water content is higher by 1.28% at Shandong versus Guangdong is lower 0.65%, other regions lower 0.23%. The lowest sewage sludge water content plant is 0.8% from Jiangsu, while the highest sewage sludge water content plant is 99% from Liaoning. In general, a lower sewage sludge water content is better. Guangdong and other regions have lower sewage sludge water contents than Shandong in 2014 -that is, Shandong must improve versus the other regions in terms of controlling sewage sludge water content.

(3) Equipment investment: Equipment investment increased at an average rise of CNY 16.417 million. The highest equipment investment is CNY 6.818 billion in Jiangsu, with the lowest equipment investment at CNY 0.156 in Guangdong.

(4) Electricity usage: The average electricity usage of all plants is 4,487,008.87 kwh, where Shandong is 4,749,826.54 kwh, and Guangdong is 5,364,878.92 kwh. The highest electricity usage plant is at 96,054,400 kwh in Guangdong, while the lowest electricity usage plant is at 47.46 kwh in Hainan.

(5) Employees: The average number of employees of all plants is 62.64 persons, where Shandong is 71.56 persons and Guangdong is 78.75 persons. The plant with the most employees is in Shandong at 575 persons, while Fujian, Guangdong, and Liaoning have 6 persons in their plants, representing the least number of employees.

Table 1. *Regions and input and output variables*

Region	Output Variable	Input Variable
1. Shanghai 2. Shandong 3. Guangdong 4. Tianjin 5. Beijing 6. Jiangsu7.Liaoning8. Hebei 9.Hainan10.Fujian	1. wastewater treatment 2. sewage sludge water contents	1. equipment investment 2. electricity usage 3. employees

Table 2. *Descriptive statistics*

Region		Output Variable		Input Variable		
		Wastewater Treatment	Sewage Sludge Water Content	Equipment Investment	Electricity Usage	Employee
Shandong	Region	117	117	117	117	117
	Max	11059.50	85.00	8225.00	23806880.	574.72
	Min	10.95	40.00	3.75	72.00	8.18
	Average	1817.10	77.65	503.54	4749826.54	71.56
	Stdev	1629.22	6.30	1276.24	4724107.43	77.87
Guang-dong	Region	142	142	142	142	142
	Max	22861.26	86.00	4523.00	96054400.00	553.01
	Min	16.26	20.00	0.02	35310.00	5.82
	Average	2525.75	75.71	198.96	5364878.92	78.75
	Stdev	3094.67	8.34	502.68	10424243.63	90.84
Others	Region	259	259	259	259	259
	Max	32850.00	280.00	681822.00	75712596.00	468.30
	Min	14.60	8.00	0.40	47.46	5.58
	Average	1461.42	76.14	2946.89	3886981.02	49.77
	Stdev	2635.92	16.39	42362.80	6234240.36	63.07
10Regions	Region	518	518	518	518	518
	Max	32850.00	280.00	681822.00	96054400.00	574.72
	Min	10.95	8.00	0.02	47.46	5.58
	Average	1833.52	76.36	1641.72	4487008.87	62.64
	Stdev	2619.64	12.73	29933.05	7371638.54	75.88

Data source: Authors' Collection

http://www.aloki.hu ● ISSN 1589 1623 (Print) ●ISSN1785 0037 (Online)
DOI: http://dx.doi.org/10.15666/aeer/1704_92799290

Discussion

The wastewater treatment of China was 71.617 billion m^3 in 2014, with 37.727 billion m^3 from the eastern region. By contrast, this area value GDP, water resources and wastewater treatment highly with other area.

We use DEA-Solver software to evaluate the 518 WWTPs' efficiency and analyze each plant's ranking. From the undesirable model, we find that 27 plants have efficiencies equal to 1. More plants from Guangdong have an efficiency score equal to 1.

Table 3 shows the differences between the average efficiency score and the higher/lower average efficiency score of each region. The average efficiency score is 0.29 for the 518 plants, and the higher efficiency score regions are Hainan, Guangdong, Fujian, and Beijing. Hainan and Beijing have a greater percentage of efficiency scores close to 1 versus the other regions. The plants' average efficiency score between 1 and average efficiency score was 146 plants in 2014 and the major regions were form Guangdong, Fujian and Shandong. In some regions, the average efficiency score is lower, because, they no longer are able to support wastewater treatment or sewage sludge water contents. For example, Hebei, Shanghai, and Tianjin, their average efficiency scores are lower than the other regions.

Table 3. *Efficiency score results of each region*

Region	Over all of the Efficiency Score					Between 1 and Average Efficiency Score		
	Total	Average	Score=1	Percentages of the score=1	Higher Average Percentage	Total	Average	Percentages
Guangdong	142	0.37	13	9.15%	52.11%	61	0.41	42.96%
Shandong	117	0.26	5	4.27%	50.00%	20	0.46	17.09%
Hebei	81	0.24	1	1.23%	50.00%	16	0.38	19.75%
Jiangsu	62	0.24	1	1.61%	30.77%	14	0.37	22.58%
Fujian	50	0.35	3	6.00%	25.00%	22	0.40	44.00%
Liaoning	39	0.28	1	2.56%	24.19%	11	0.39	28.21%
Shanghai	11	0.14		0.00%	21.37%			0.00%
Hainan	8	0.43	2	25.00%	20.99%	2	0.35	25.00%
Tianjin	4	0.12		0.00%	0.00%			0.00%
Beijing	4	0.33	1	25.00%	0.00%			0.00%
total	518	0.29	27	5.21%	33.40%	146	0.41	28.19%

Data source: Authors' Collection

Table 4 lists the ten regions' efficiency score and improvement by the undesirable model. We note that there are several issues between regions and their efficiency score. For example, in Fujian, Guangdong, Liaoning, and Hainan, their average efficiency scores are higher than the other regions. In other words, each region has too much investment into the input variables; Jiangsu by CNY 699,193; Shandong by CNY 56.59 million; and Guangdong by CNY 23.35 million on equipment investment. Guangdong exceeds electricity usage by 405,729,807 kwh; Shandong by 394,761,772 kwh; and Jiangsu by 178,827,079 kwh. By contrast, the output variables should be increased in each region. Jiangsu should increase 4,973 thousand m^3, Jiangsu should be increase 2,137 thousand m^3 and Jiangsu should be increase 2,061 thousand m^3 in the wastewater treatment, and the sewage sludge water contents should be decrease 602 percentages in Guangdong, 355 percentages in Jiangsu and 336 percentages in Fujian.

http://www.aloki.hu ● ISSN 1589 1623 (Print) ●ISSN1785 0037 (Online)
DOI: http://dx.doi.org/10.15666/aeer/1704_92799290

Table 4. *Inefficiency scores and improvement of each region*

Region	Total	Avg. Score	Slack Excess			Slack Shortage	
			Equipment Investment	Electricity Usage	Employee	Wastewater Treatment	Sewage Sludge Water Contents
Guangdong	129	0.30	23,354	405,729,807	7,328	1,757	602
Shandong	112	0.23	56,590	394,761,772	6,438	119	243
Hebei	80	0.23	19,826	167,187,348	2,536	2,137	297
Jiangsu	61	0.22	699,193	178,827,079	2,637	4,973	355
Fujian	47	0.31	8,319	46,420,398	1,128	2,061	336
Liaoning	38	0.26	2,574	108,908,648	1,308	-	62
Shanghai	11	0.14	6,814	58,625,773	1,161	-	76
Hainan	6	0.25	11,985	15,853,913	297	-	10
Tianjin	4	0.12	3,248	13,232,191	200	1,924	-
Beijing	3	0.10	6,686	35,327,785	301	356	18
Total	491	0.25	838,588	1,424,874,714	23,334	13,326	1,997

Data source: Authors' Collection

Conclusion

The GDP of China is US$ 10.36 trillion, making upto 13.3% of global GDP and 21.09% of global energy consumption. Environmental topics in recent years have become more popular in the world, but few scholars have discussed wastewater treatment efficiency and the effects of sewage sludge water contents. Some regions in China have spent a lot of resources into increasing wastewater treatment or reducing sewage sludge water contents, while some regions have lower efficiency scores versus others. Some regions' efficiency score has fallen in order to control electricity usage or equipment investment.

This research reports the efficiency scoresof regions in China by the Tone (2001) undesirable DEA Model. After evaluating ten regions and data on 518 plants in eastern China, we provide the following conclusions below.

(1) The efficiency scores from the 518 plants exhibit some volatility: 27 plants have efficiency scores close to 1; 146 plants have efficiency scores between 1 and 0.

(2) The average efficiency score is 0.29 from the 518 plants, with higher efficiency scores coming from Hainan, Guangdong, Fujian, and Beijing. By contrast, Hebei, Shanghai, and Tianjin have average efficiency scores that are lower than the other regions.

(3) There are 491 inefficient plants, whose average efficiency score is 0.25. The inputs including equimpment investment, electricity usage and employee of WWTPs performed invest too much, which need to be decreased by different level. The equimpment investment excess the optimum level of CNY 838,588, the exctricity usage with the excess consumption of 1,424,874,714 kwh, and the employee with the excess of 23,334 persons.The wastewater treatment volume need to be increase 13,326 thousand m^3 and sewage sludge water contents will be decrease 1,997 percentages.

The efficiency results of wasteter treatment assessment will be different while considersing the sludge problem or not. As a by-product, sludge in WWTPs is harmful to the environment, which is urgent to strenthen the treatment and disposal. At present, 90% WWTPs in China have realized sludge dewatering and reduction treatment, but the proportion of WWTPs that have achieved sludge biological stabilization treatment is

http://www.aloki.hu ● ISSN 1589 1623 (Print) ●ISSN1785 0037 (Online)
DOI: http://dx.doi.org/10.15666/aeer/1704_92799290

less than 3%. Most of the sludge has not been stabilized and landfill directly, and less than 20% sludge has been safely treated and disposed (Kan Liao et al., 2019). The efficiency of WWTPs can be evaluated comprehensively and objectively by building the index system with sludge indicator in. In order to impove the efficiency of WWTPs, it is necessary to regularly maintain the machineryandequipmentand improve its utilization efficiency, also control the electricity consompution to reduce electricity charges, and reasonably allocate the staff to control labor costs.

Acknowledgements. We acknowledge the financial support from the "Young Academic Innovation Team of Northwest University of Political Science and Law", Special Scientific Research Projects of Shaanxi Education Department in 2019 "Study on audit evaluation of government environmental performance: a case study of water pollution prevention and control in Shaanxi province" (016166523), the Improvement of Legal System of PPP model of Urban Sewage Treatment Industry in China(17BFX042), Study on Cost Structure, Appropriate Scale and Service Efficiency of Urban Sewage Treatment(17YJA790062), Study on Efficiency Evaluation and Promotion Path of Urban Water Pollution Control in Shaanxi Province(2015D064).

REFERENCES

[1] Bolong, N., Ismail, A. F., Salim, M. R., Matsuura, T. (2009): A review of the effects of emerging contaminants in wastewater and options for their removal. – Desalination 238(1): 229-246.
[2] Cai, Q. Y., Mo, C. H., Wu, Q. T., Zeng, Q. Y., Katsoyiannis, A. (2007): Occurrence of organic contaminants in sewage sludges from eleven WWTPs, China. – Chemosphere 68(9): 1751-1762.
[3] Carvalho, P., Marques, R. C. (2014): Computing economies of vertical integration, economies of scope and economies of scale using partial frontier nonparametric methods. – Eur J Oper Res 234(1): 292-307.
[4] Chen, Z., Zayed, T., Qasem, A. (2015): An efficiency-centred hierarchical method to assess performance of WWTPs. – International Journal of Environmental Research 9(1): 1-8.
[5] Chiu, Y. H., Shyu, M. K., Lu, C. C. (2016): Undesirable output in efficiency and productivity: Example of the G20 countries. Energy Source. – Part B: Economics, Planning, and Policy 11(3): 237-243.
[6] Chung, Y. H., Fare, R., Grosskopf, S. (1997): Productivity and undesirable outputs: A directional distance function approach. – J. Environ. Manage 51: 229-240.
[7] Dai, X. H. (2012): Current situation and consideration of municipal sludge treatment and disposal in China. – Water supply and drainage 2(38): 1-5.
[8] Emrouznejad, A., LatefAnouze, A., Thanassoulis, E. (2010): A semi-oriented radial measure for measuring the efficiency of decision making units with negative data, using DEA. – Eur. J. Oper. Res 200: 297-304.
[9] Ferro, G., Lentini, E. J., Mercadier, A. C., Romero, C. A. (2014): Efficiency in Brazil's water and sanitation sector and its relationship with regional provision, property and the independence of operators. – Utility Policy 28: 42-51.
[10] Georgieva, V. (2017): Generalized net model of mechanical wastewater pre-treatment. – International Journal Bioautomation 21(1): 133-144.
[11] Golany, B., Roll, Y. (1989): An Application Procedure for DEA. – Omega 17: 237-250.
[12] Gomes, E. G., Lins, M. P. E. (2007): Modelling undesirable outputs with zero sum gains data envelopment analysismodels. – Journal of the Operational Research Society 2: 1-8.
[13] Guerrini, A., Romano, G., Campedelli, B. (2011): Factors affecting the performance of water utility companies. – Int J Public Sector Manag 4(6): 543-566.

http://www.aloki.hu ● ISSN 1589 1623 (Print) ●ISSN1785 0037 (Online)
DOI: http://dx.doi.org/10.15666/aeer/1704_92799290

[14] Guerrini, A., Romano, G., Campedelli, B. (2013): Economies of scale, scope, and density in the Italian water sector: a two-stage data envelopment analysis approach. – Water Resour Manag 27(13): 4559-4578.
[15] Guerrini, A., Romano, G., Leardini, C., Martini, M. (2015): Measuring the efficiency of wastewater services through data envelopment analysis. – Water Science and Technology 71(12): 1845-1851.
[16] Hailu, A., Veeman, T. S. (2001): Non-parametric productivity analysis with undesirable outputs: An application to the Canadian pulp and paper industry. – Am. J. Agr. Econ 83: 605-616.
[17] Hale, R. C., Guardia, L. M. J., Harvey, E., Chen, D., Mainor, T. M., Luellen, D. R. (2012): Polybrominated diphenyl ethers in US sewage sludges and biosolids: temporal and geographical trends and uptake by corn following land application. – Environ. Sci. Technol 46(4): 2055-2063.
[18] He, F., Wang, J., Chen, W. (2018): Numerical simulation and analysis of the effect of baffle distance and depth on solid-liquid two-phase flow in circular secondary clarifier. – International Journal of Heat and Technology 36(1): 111-117.
[19] Hernández-Sancho, F., Molinos-Senante, M., Sala-Garrido, R. (2011): Energy efficiency in Spanish WWTPs: A non-radial DEA approach. – Science of the Total Environment 409(14): 2693-2699.
[20] Kelessidis, A., Stasinakis, A. S. (2012): Comparative study of the methods used for treatment and final disposal of sewage sludge in European countries. – Waste Manag 32(6): 1186-1195.
[21] Lannier, A. L., Porcher, S. (2014): Efficiency in the public and private French water utilities: prospects for benchmarking. – Apply Economic 46(5): 556-572.
[22] Liao, K., Yang, H. W., Wang, H. (2019): Brief Analysis and Suggestions on the Present Situation of Treatment and Disposal of Municipal Sludge in Guangdong Province. – Guangdong Chemical Industry 46(4): 126-127+129.
[23] Lovell, C. A. K., Pastor, J. T., Turner, J. A. (1995): Measuring macroeconomic performance in the OECD: A comparison of European and non-European countries. – Eur J Opl Res 87: 507-518.
[24] Luo, W. F. I., Hai, W. E. (2014): High retentionmembrane bioreactors: challenges and opportunities. – Bioresource Technology 167: 539-546.
[25] Molinos-Senante, M., Hernandez-Sancho, F., Sala-Garrido, R. (2014): Benchmarking in WWTPs: A tool to save operational costs. – Clean Technologies and Environmental Policy 16(1): 149-161.
[26] Molinos-Senante, M., Hernández-Sancho, F., Sala-Garrido, R. (2015b): Comparing the dynamic performance of wastewater treatment systems: A metafrontier Malmquist productivity index approach. – Journal of Environmental Management 161: 309-316.
[27] National Bureau of Statistics. (2015): China Statistical Yearbook [R/OL]. – http://www.stats.gov.cn/tjsj/ndsj/.
[28] Pan, R. S. (2014): To achieve of energy saving and emission reduction in sewage treatment plant. – Science and technology and enterprise 1: 77.
[29] Portela, M. C. A. S., Thanassoulis, E., Horncastle, A., Maugg, T. (2011): Productivity change in the water industry in England and Wales: application of the meta-Malmquist index. – J Oper Res Soc 62(12): 2173-2188.
[30] Sala-Garrido, R., Molinos-Senante, M., Hernández-Sancho, F. (2012): How does seasonality affect water reuse possibilities? An efficiency and cost analysis. – Resources, Conservation and Recycling 58: 125-131.
[31] Santos, A., Ma, W., Judd, S. J. (2011): Membrane bioreactors: two decades of research and implementation. – Desalination 273(1): 148-154.
[32] Scheel, H. (2001): Undesirable Outputs in Efficiency Valuations. – European Journal of Operational Research 132: 400-410.

http://www.aloki.hu ● ISSN 1589 1623 (Print) ●ISSN1785 0037 (Online)
DOI: http://dx.doi.org/10.15666/aeer/1704_92799290

[33] Seiford, L. M., Zhu, J. (2002): Modeling undesirable factor in efficiency evaluation. – Eur. J. Oper. Res 142: 16-20.
[34] Seiford, L. M., Zhu, J. (2005): A response to comments on modeling undesirable factors in efficiency evaluation. – Eur. J. Oper. Res 161: 579-581.
[35] Sharp, J. A., Meng, W., Liu, W. (2007): A modified slacks-based measure model for data envelopment analysis with "natural" negative outputs and inputs. – J. Oper. Res. Soc 58: 1672-1677.
[36] Sueyoshi, T., Goto, M., (2011): DEA approach for unified efficiency measurement: Assessment of Japanese fossil fuel power generation. – Energ. Econ 33: 292-303.
[37] Tiedemann, T., Francksen, T., Latacz-Lohmann, U. (2010): Assessing the performance of German Bundesliga football players: a nonparametric metafrontier approach. – CEJOR 19(4): 571-587.
[38] Tone, K. (2001): A slacks-based measure of efficiency in data envelopment analysis. – Eur. J. Oper. Res 130: 498-509.
[39] Wang, J., Zhang, Z. J., Chi, L. N. (2012): Character and model of anaerobic granular sludge formation in the sanitary landfill. – Adv. Mater. Res 455: 1297-1302.
[40] Wang, Q., Zhou, P., Zhou, D. (2012): Efficiency measurement with carbon dioxide emissions: The case of China. – Appl. Energ 90: 161-166.
[41] Wen, Q., Tutuka, C., Keegan, A., Jin, B. (2009): Fate of pathogenic microorganisms and indicators in secondary activated sludge WWTPs. – J. Environ. Manag 90: 1442-1447.
[42] Yang, H., Pollitt, M. (2009): Incorporating both undesirable outputs and uncontrollable variables into DEA: The performance of Chinese coal-fired power plants. – Eur. J. Oper. Res 197: 1095-1105.
[43] Yang, G., Zhang, G. M., Wang, H. C. (2015): Current state of sludge production, management, treatment and disposal in China. – Water Research 78: 60-73.
[44] Yang, W. X., Li, L. G. (2017): Efficiency Evaluation and Policy Analysis of Industrial Wastewater Control in China. – Energies 10: 1-18.
[45] Yu, S., Zhang, G., Li, J., Zhao, Z., Kang, X. (2013): Effect of endogenous hydrolytic enzymes pretreatment on the anaerobic digestion of sludge. Bioresour. – Technol 146: 758-761.
[46] Zanetti, L., Frison, N., Nota, E., Tomizioli, M., Bolzonella, D., Fatone, F. (2012): Progress in real-time control applied to biological nitrogen removal from wastewater. A short-review. – Desalination 286: 1-7.
[47] Zhang, P., Zhang, G., Wang, W. (2007): Ultrasonic treatment of biological sludge: floc disintegration, cell lysis and inactivation. Bioresour. – Technol 98(1): 207-210.
[48] Zhang, Q., Hu, J., Lee, D. J. (2016): Aerobic granular processes: current research trends. – Bioresource Technology 210: 74-80.

http://www.aloki.hu ● ISSN 1589 1623 (Print) ●ISSN1785 0037 (Online)
DOI: http://dx.doi.org/10.15666/aeer/1704_92799290

AN ECONOMICAL LOGISTICS PRICING SYSTEM FOR URBAN SOLID WASTES BASED ON BENEFITS AND PERFORMANCE ANALYSIS

CHEN, J. H. – CAI, Y.*

Changzhou College of Information Technology, Changzhou 213164, China

**Corresponding author*
e-mail: cychjh_2005@aliyun.com

(Received 3rd Apr 2019; accepted 17th May 2019)

Abstract. With complex composition and wide distribution, the urban solid wastes increase with the intensity and range of human activities. After analyzing benefits and performance, this paper sets up a benefit-performance model for urban solid wastes, and discusses the logistics pricing system for solid wastes in the municipal districts of south eastern China's Hangzhou. The research results show that: the logistics pricing system for urban solid wastes contains transport pricing and disposal pricing; the "reverse logistics" of solid wastes can produce economic benefits, and the most economic way to dispose of solid wastes is to transport them to the terminal station for treatment; the dual variable reflects the relationship between the disposal amount and logistics pricing of solid wastes; there is an optimal daily disposal volume for solid wastes in the transfer stations of each municipal district in Hangzhou; if the daily disposal volume is below or above the allowable range computed by the decision variable in the objective function, then the logistics pricing will increase. The research findings lay the theoretical basis for the design of the logistics pricing system for urban solid wastes that combines environmental and economic benefits.
Keywords: *solid waste, benefit-performance, logistics pricing, reverse logistics, economic benefits*

Introduction

Recent years has seen the proliferation of environmental problems from developed countries to developing countries. For example, the environment in China is now threatened by the growth in resource demand and urban population, which is fueled by the booming economy. In urban areas, the greatest threat to environment lies in the treatment of solid wastes (Garchitorena et al., 2017; Marino et al., 2017; Gattringer, 2018; Zheng et al., 2018). The various kinds of solid wastes produced by urban citizens are both uncertain and risky to process and difficult to manage. According to incomplete statistics, each urban citizen generates 0.60~1.40 kg/day of solid wastes, half of which is catering waste (Gendron, 2014). In addition, there are many problems in the management of urban solid wastes. With significant regional differences, the logistics dispatch of such wastes mainly depends on fiscal appropriation and economic benefits (Frank et al., 2016).

Currently, urban solid wastes are being treated through landfill, incineration, composting or comprehensive method, aiming to turn them into harmless substances (Lan et al., 2012; Mangone, 2016). Some scholars have created a logistics pricing model for solid wastes based on cost-effectiveness, which minimizes the disposal cost of urban solid wastes, achieves complete non-hazardous treatment and realizes multi-objective optimization of logistics pricing system (Ostberg et al., 2012; Lan, 2018). Some scholars found that it is much costlier to mitigate the environmental pollution of solid wastes than transport such wastes, and suggested to analyze the logistics cost-

http://www.aloki.hu ● ISSN 1589 1623 (Print) ● ISSN 1785 0037 (Online)
DOI: http://dx.doi.org/10.15666/aeer/1704_92919300

effectiveness of solid wastes based on logistics pricing system before solving the environmental and economic problems caused by solid wastes (Zhang et al., 2011).

From the perspective of marketization, this paper analyzes the benefits and performance of the logistics pricing system for solid wastes in the municipal districts of southeastern China's Hangzhou, with the aim to develop an economical logistics pricing system.

Materials and Methods

Logistics cover the entire process of transport, facility operation and management. Similarly, logistics pricing involves such aspects as transport, facilities and management (Ambrogi and Mineo, 2016; Feng et al., 2017; Lalami et al., 2017; Li et al., 2017; Duan, 2018; Tan et al., 2018). The logistics of solid wastes can be divided into "forward" logistics and "reverse logistics". The latter refers to the recycling and reuse of solid wastes. In this paper, the logistics of solid wastes refers to the economic cost of the collection, classification, handling or storage of solid wastes (Mulligan and Lombardo, 2016). There is no "reverse logistics" in traditional solid waste logistics systems (Ayodele et al., 2018). With the growing awareness of eco-environmental protection, more and more people now favor the green treatment of solid waste, giving birth to the "resource-product-waste-renewable resource" economic model. In this way, the logistics cost of solid wastes has plunged over the years. *Figure 1* illustrates the logistics network for urban solid wastes.

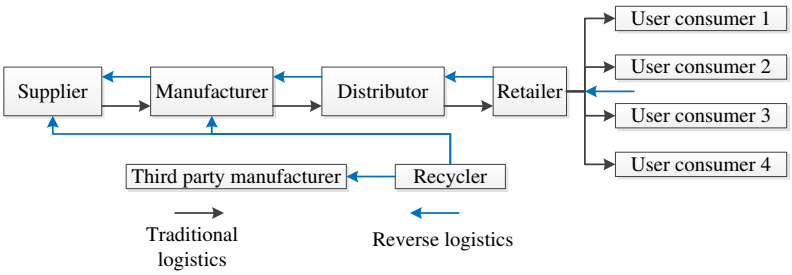

Figure 1. *Logistics network for urban solid wastes*

The logistics system for urban solid wastes is reversible, inactive, complex and uncertain (Gafurov et al., 2014). In urban areas, the disposal of solid wastes is driven by multiple factors, such as legal mandates, economic benefits, environmental protection and social wellness (Zhu et al., 2018). *Table 1* lists the total and per-capita daily production of urban solid wastes in many countries. It can be seen that urban Chinese generates a relatively low amount of solid wastes on average. Due to the huge population, however, China is now the largest producer of solid wastes. The total production of solid wastes in China is 1.014 times that of the US, 5.775 times that of France, 5.920 times that of the UK, 4.211 times that of Japan and 10.241 times that of South Korea. *Figure 2* shows the average composition of solid wastes in Chinese cities. Obviously, the catering waste takes up an increasingly large portion in solid wastes year by year, reaching 70% in recent years, while the proportions of dust and construction wastes are gradually declining. The other solid wastes like plastics, metal and tree branches are relatively few and stable over the years.

http://www.aloki.hu ● ISSN 1589 1623 (Print) ● ISSN 1785 0037 (Online)
DOI: http://dx.doi.org/10.15666/aeer/1704_92919300

Table 1. *Total and per-capita daily production of urban solid wastes in many countries*

Country	Urban solid waste production/×10^4t	Urban solid waste production rate (kg/day/People)
America	21020.6	2
France	3690.5	1.53
Britain	3600.3	1.53
Japan	5061.1	1.04
Korea	2081.2	1.09
China	21313.5	0.85

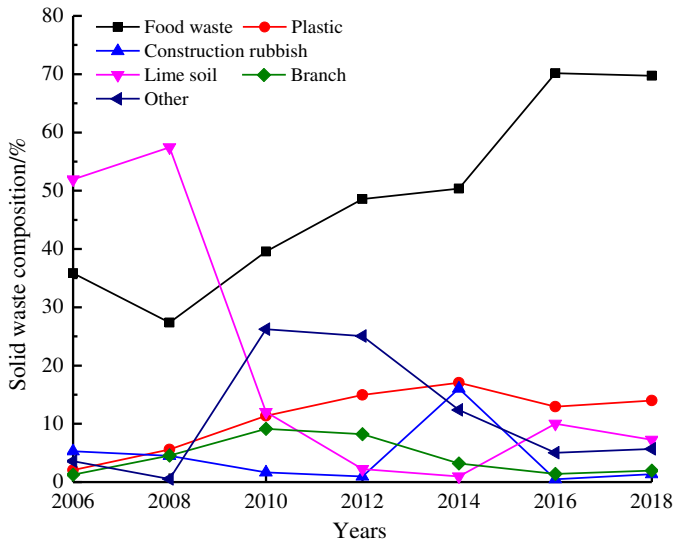

Figure 2. *The average composition of solid wastes in Chinese cities*

Results and Discussion

Benefit model for logistics pricing of urban solid wastes

The logistics pricing system for urban solid wastes covers issues of economy, environment and society, requiring scientific and rational resource allocation. Taking solid wastes as a commodity, the environmental pollution caused by the commodity should be controlled through analysis on both benefits and performance. The logistics transport cost of solid wastes should be compared with the monetary income in reverse logistics. The composition of solid wastes in downtown Hangzhou is explained in *Figure 3*. As shown in the figure, 62.5% of the solid wastes are catering waste, 11.5% are paper, 12% are plastics, 3% are glass, and 1% are metal. The catering waste is not recyclable and cannot produce any benefit. By contrast, the other wastes can bring benefits through recycling. Hence, the benefit function of logistics pricing R_1 can be constructed as:

$$R_1 = \sum_{i=1}^{n} Q_i r_i p_i \quad (i = 1,2,3,\ldots,n) \qquad \text{(Eq.1)}$$

where Q_i is the reverse flow amount of each kind of urban solid waste (ton); r_i is the proportion of each kind of recyclable urban solid waste (%); p is the recycling price of each kind of urban solid waste (RMB yuan/ton).

http://www.aloki.hu ● ISSN 1589 1623 (Print) ● ISSN 1785 0037 (Online)
DOI: http://dx.doi.org/10.15666/aeer/1704_92919300

Besides the benefit of direct recycling, urban solid wastes can produce composting benefit R_2, power generation benefit R_3 and landfill gas benefit R_4. Among them, the power generation benefit R_3 can be expressed as:

$$R_3 = \sum_{j=1}^{n} Q_j \varphi p \quad (j = 1,2,3,\dots,n) \qquad \text{(Eq.2)}$$

where Q_j is the total amount of solid wastes used for power generation (ton); φ is the energy conversion efficiency of solid wastes (kWh/ton); p is the price of each kWh of electricity (RMB yuan).

Then, the total benefit function can be expressed as:

$$R = R_1 + R_2 + R_3 + R_4 \qquad \text{(Eq.3)}$$

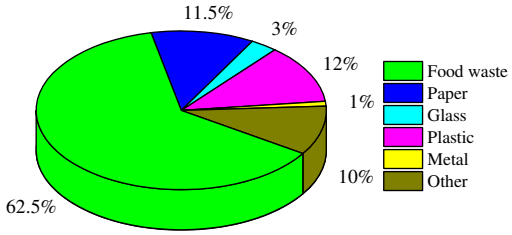

Figure 3. *The composition of solid wastes in downtown Hangzhou*

Performance model for logistics pricing of urban solid wastes

Through the economic analysis, it is learned that the logistics pricing system for urban solid wastes contains transport pricing and disposal pricing. The former is further split into transport machine pricing and labor pricing, and the latter covers the full-lifecycle pricing of the machine. In Hangzhou, the solid waste transport performance is RMB 2.2 yuan/km/ton, and the closest transfer station of solid waste lies 12 km away from the terminal station. The solid wastes are loaded into trucks at the transfer stations, and transported to the terminal for classification and disposal. *Table 2* compares the disposal costs of urban solid wastes in Hangzhou. It can be seen that the disposal at the transfer stations is the cheapest method.

Table 2. *Comparison of disposal costs of urban solid wastes (RMB yuna/ton)*

Urban solid waste treatment measures	Unit disposal cost
Transfer station	28.4
Composting field	218.6
Incineration plant	253.6
Sanitary landfill	73.4
Integrated treatment plant	98.8

The performance function C can be expressed as:

$$C = \sum_{i=1}^{n} (t_i d_i + D_i) X_i \quad (i = 1,2,3,\dots,n) \qquad \text{(Eq.4)}$$

http://www.aloki.hu ● ISSN 1589 1623 (Print) ● ISSN 1785 0037 (Online)
DOI: http://dx.doi.org/10.15666/aeer/1704_92919300

where t_i and d_i are respectively the unit transport cost and unit transport distance of solid wastes, respectively; D_i and X_i are the unit disposal performance and unit logistics volume of municipal solid wastes, respectively.

Empirical analysis

This subsection mainly explores the economic and environmental benefits of urban solid waste treatment. To minimize the volume and harm of solid wastes, the optimal solution must have the lowest logistics pricing. Logistics pricing is a linear planning problem. The logistics pricing at the terminal varies with the transport distances. There are ten municipal districts in Hangzhou. The transfer-terminal distance differs from district to district. Thus, each transfer station should have a unique objective function and constraints. The general mathematical model can be expressed as:

$$Z = F(X) = \begin{cases} \max(\min) f_1(X) \\ \max(min) f_2(X) \\ \cdots \\ \max(min) f_n(X) \end{cases} \quad \text{(Eq.5)}$$

$$S.t.\, \varphi(X) = \begin{Bmatrix} \emptyset_1(X) \\ \emptyset_2(X) \\ \cdots \\ \emptyset_n(X) \end{Bmatrix} \leq G = \begin{Bmatrix} g_1 \\ g_2 \\ \cdots \\ g_n \end{Bmatrix} \quad \text{(Eq.6)}$$

where $X=[x_1, x_2, x_3,\ldots, x_n]^T$ is the decision variable.

The annual outputs of catering and industrial solid wastes in Hangzhou are presented in *Figure 4*. It can be seen that Hangzhou produces fewer and fewer industrial solid waste over the years, but more and more catering solid waste. In 2018, the output of catering solid waste was 19 times that of industrial solid waste.

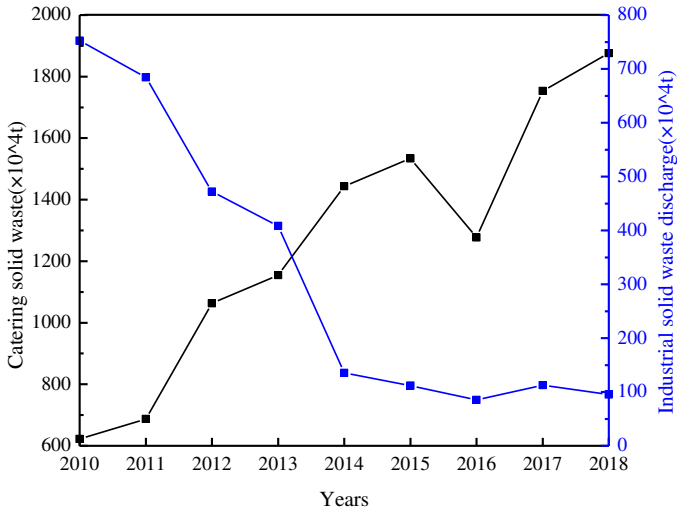

Figure 4. *The annual outputs of catering and industrial solid wastes in Hangzhou*

The total investment of Hangzhou in solid waste treatment is shown in *Figure 5*. It can be observed that the investment increased first and then declined. The highest

http://www.aloki.hu ● ISSN 1589 1623 (Print) ● ISSN 1785 0037 (Online)
DOI: http://dx.doi.org/10.15666/aeer/1704_92919300

investment appeared in 2016. This trend is attributable to the implementation of "reverse logistics" in recent years, as the city started to highlight the relationship between economy and environment. The terminal stations have began creating benefits from urban solid wastes. Then, the benefit-performance optimization model can be set up based on an interactive linear and general optimization solver:

Logistics pricing function:

$$C=n_1\times x_1+n_2\times x_2+n_3\times x_3+\ldots\ldots+n_i\times x_i \quad \text{(Eq.7)}$$

where n_i is the unit pricing (RMB yuna/ton); x_i is the proportion of solid wastes received by each terminal station to the total solid wastes received by all terminal stations in the municipal districts (%).

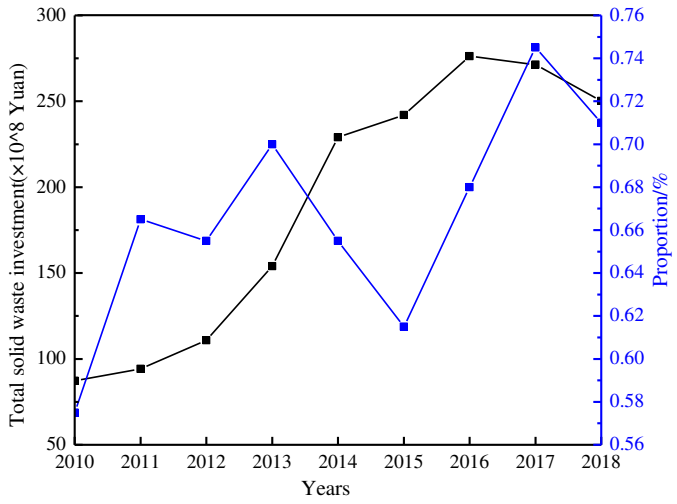

Figure 5. *The total investment of Hangzhou in solid waste treatment*

Recycling benefit function:

$$R1=194.69\times(w1+w2+w3+\ldots\ldots+wi) \quad \text{(Eq.8)}$$

Compositing benefit function:

$$R2=\lambda1\times w1+\lambda2\times w2+\lambda3\times w3+\ldots\ldots+\lambda i\times wi \quad \text{(Eq.9)}$$

Incineration benefit function:

$$R3=\omega1\times w1+\omega2\times w2+\omega3\times w3+\ldots\ldots+\omega i\times wi \quad \text{(Eq.10)}$$

Landfilling benefit function:

$$R_4=\gamma_1\times w_1+\gamma_2\times w_2+\gamma_3\times w_3+\ldots\ldots+\gamma_i\times w_i \quad \text{(Eq.11)}$$

where w_i is the composition of solid wastes; λ_i, ω_i and γ_i are the unit benefit of composting, incineration and landfilling of solid wastes, respectively.

http://www.aloki.hu ● ISSN 1589 1623 (Print) ● ISSN 1785 0037 (Online)
DOI: http://dx.doi.org/10.15666/aeer/1704_92919300

Improvement strategies

The ten municipal districts, denoted as 1~10 respectively, in Hangzhou are listed in *Table 3*. The daily disposal amount and dual variable of solid wastes in each municipal district are illustrated in *Figure 6*. If the dual variable is positive, then the disposal amount is negatively correlated with the logistics pricing, that is, the pricing decreases with the growth in disposal amount. The inverse is also true.

Table 3. *List of municipal districts in Hangzhou*

Number	Municipal district	Number	Municipal district
1	Shangcheng area	6	Binjiang area
2	Xiacheng area	7	Xiaoshan area
3	Xihu area	8	Yuhang area
4	Jianggan area	9	Linan area
5	Gongshu area	10	Fuyang area

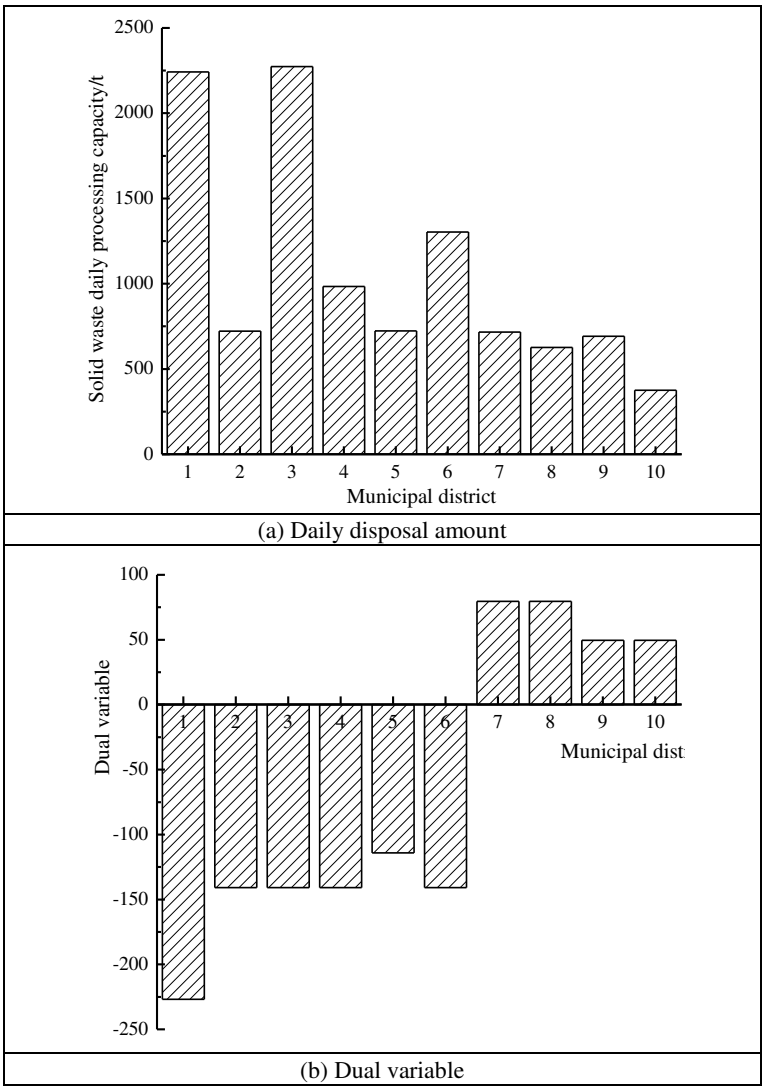

Figure 6. *The daily disposal amount and dual variable of solid wastes in each municipal district*

http://www.aloki.hu ● ISSN 1589 1623 (Print) ● ISSN 1785 0037 (Online)
DOI: http://dx.doi.org/10.15666/aeer/1704_92919300

The optimal daily disposal volume of solid wastes in each municipal district was obtained according to the decision variable in the objective function. *Figure 7* gives the allowable change of solid wastes in each municipal district under a constant optimal base.

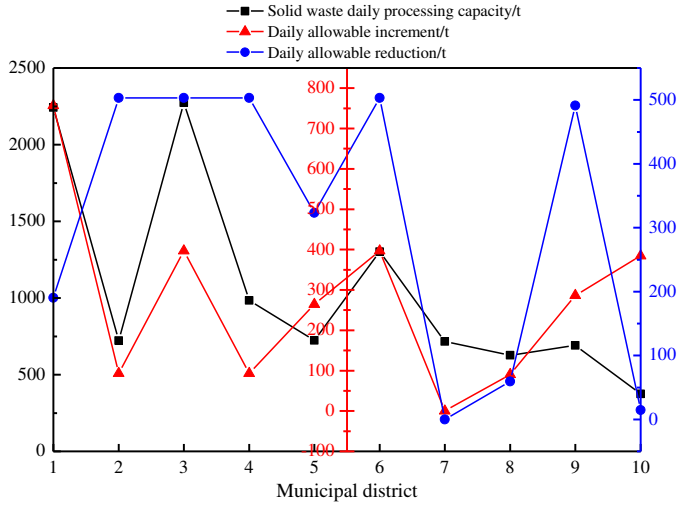

Figure 7. *The allowable change of solid wastes in each municipal district under a constant optimal base*

If the daily disposal volume is below or above the allowable range, then the logistics pricing will increase. With the improvement of living standards, more and more solid wastes are being generated year by year. To reduce the generate of solid wastes, the government should step up its promotion of the solid waste disposal system that combines environmental and economic effects, and encourage waste classification at the source. Furthermore, the solid waste disposal ability of each transfer or terminal station should be controlled according to the benefit-performance theory and the disposal capacity of the existing facilities.

Conclusions

From the perspective of marketization, this paper analyzes the benefits and performance of the logistics pricing system for solid wastes in the municipal districts of Hangzhou, with the aim to develop an economical logistics pricing system. The main conclusions are as follows:

(1) The catering waste takes up an increasingly large portion in solid wastes year by year, reaching 70% in recent years, while the proportions of dust and construction wastes are gradually declining. The other solid wastes like plastics, metal and tree branches are relatively few and stable over the years.

(2) The logistics pricing system for urban solid wastes covers issues of economy, environment and society, requiring scientific and rational resource allocation. Taking solid wastes as a commodity, the environmental pollution caused by the commodity should be controlled through analysis on both benefits and performance. Logistics pricing is a linear planning problem. The logistics pricing at the terminal varies with the transport distances.

http://www.aloki.hu ● ISSN 1589 1623 (Print) ● ISSN 1785 0037 (Online)
DOI: http://dx.doi.org/10.15666/aeer/1704_92919300

(3) The dual variable reflects the relationship between the disposal amount and logistics pricing of solid wastes. If the daily disposal volume is below or above the allowable range, then the logistics pricing will increase.

(4) There are many assumptions in the application of benefit-performance theory. The cost calculation in this paper is not comprehensive and neglects the environmental damage caused by the generation, stacking and disposal of solid wastes. Future research should seek to try to solve problems in a smaller range.

Acknowledgements. This research was supported by Jiangsu University Philosophy and social science key construction Base project "Manufacturing industry and Internet integration Innovation Development Research base" (2018ZDJD-B017); Changzhou Institute of Information Technology Key research base of humanities and social sciences "Manufacturing and amp; Internet fusion Innovation Development Research Base".

REFERENCES

[1] Ambrogi, V., Mineo, T. C. (2016): Benefits of comprehensive rehabilitation therapy in thymectomy for myasthenia gravis: a propensity score matching analysis. – American Journal of Physical Medicine and Rehabilitation 96(2): 77-83.

[2] Ayodele, T. R., Alao, M. A., Ogunjuyigbe, A. S. O. (2018): Recyclable resources from municipal solid waste: assessment of its energy, economic and environmental benefits in Nigeria. – Resources, Conservation and Recycling 134: 165-173.

[3] Duan, L. M. (2018): Path planning for batch picking of warehousing and logistics robots based on modified a* algorithm. – Academic Journal of Manufacturing Engineering 16(2): 99-106.

[4] Feng, Y., Xu, C. R., Wang, Y. S. (2017): Evaluation on site selection of mobilization logistics center based on principal component analysis. – Academic Journal of Manufacturing Engineering 15(4): 55-60.

[5] Frank, W., Drechsler, M., Johst, K., Mewes, M., Sturm, A. (2016): A novel, spatiotemporally explicit ecological-economic modeling procedure for the design of cost-effective agri-environment schemes to conserve biodiversity. – American Journal of Agricultural Economics 98(2): 489-512.

[6] Gafurov, I., Panasyuk, M., Pudovik, E. (2014): Interregional logistic center as the growth point of regional economics. – Procedia Economics and Finance 15: 474-480.

[7] Garchitorena, A., Sokolow, S. H., Roche, B., Ngonghala, C. N., Jocque, M., Lund, A. (2017): Disease ecology, health and the environment: a framework to account for ecological and socio-economic drivers in the control of neglected tropical diseases. – Philosophical Transactions of the Royal Society B: Biological Sciences 372(1722): 20160128.

[8] Gattringer, C. W. (2018): A revisited conceptualization of plastic pollution accumulation in marine environments: insights from a social ecological economics perspective. – Marine Policy 96: 221-226.

[9] Gendron, C. (2014): Beyond environmental and ecological economics: proposal for an economic sociology of the environment. – Ecological Economics 105: 240-253.

[10] Lalami, I., Frein, Y., Gayon, J. P. (2017): Demand variability and value of information sharing in the supply chain. A case study in the automotive industry. – Journal Européen des Systèmes Automatisés 50(1-2): 157-186.

[11] Lan, Y., Cui, B., Zhang, Y., Han, Z., Gao, N., Wang, T. (2012): Influence of raised fields on ecological environment and economic benefits in baiyangdian lake, China. – Procedia Environmental Sciences 13: 680-686.

http://www.aloki.hu ● ISSN 1589 1623 (Print) ● ISSN 1785 0037 (Online)
DOI: http://dx.doi.org/10.15666/aeer/1704_92919300

[12] Lan, C. F. (2018): Coordination of vendor managed inventory supply chain with price-sensitive demand under consumer balking behaviour. – Journal Européen des Systèmes Automatisés 51(1-3): 125-140.
[13] Li, M. Y., Wang, X. F., Zhang, X., Li, X. L. (2018): Optimization design of multi-echelon recycling networks for third-party reverse logistics provider in the context of binary path selection. – Academic Journal of Manufacturing Engineering 16(1): 97-105.
[14] Mangone, G. (2016): Constructing hybrid infrastructure: exploring the potential ecological, social, and economic benefits of integrating municipal infrastructure into constructed environments. – Cities 55: 165-179.
[15] Marino, C., Nucara, A., Nucera, G., Pietrafesa, M. (2017): Economic, energetic and environmental analysis of the waste management system of Reggio Calabria. – International Journal of Heat and Technology 35(S1): S108-S116.
[16] Mulligan, R. F., Lombardo, G. A. (2016): Panama canal expansion: fuel economy and logistical risk. – WMU Journal of Maritime Affairs 15(1): 5-15.
[17] Östberg, K., Hasselström, L., Håkansson, C. (2012): Non-market valuation of the coastal environment – uniting political aims, ecological and economic knowledge. – Journal of Environmental Management 110: 166-178.
[18] Tan, J., Wang, Z. G., Jiang, G. Q. (2018): Modelling and simulation of the balance of supply chain ecosystem. – Journal Européen des Systèmes Automatisés 51(4-6): 273-281.
[19] Zhang, J. W., Zhu, M. J., Zhang, L. W. (2011): Research on system constitution of the logistics ecological environment. – Procedia Engineering 15: 375-380.
[20] Zheng, L., Xia, Z., Zhang, X. Y. (2018): Comparison between geopolymer reaction and cement hydration in solidification of fly ash generated in municipal solid waste incineration. – Revue des Composites et des Matériaux Avancés 28(3): 395-403.
[21] Zhu, H. Q., Qiu, Y., Jiang, T. H. (2018): Strategies for adopting unified object identifiers in logistics resource integration environments. – Journal of Discrete Mathematical Sciences and Cryptography 21(4): 991-1003.

http://www.aloki.hu ● ISSN 1589 1623 (Print) ● ISSN 1785 0037 (Online)
DOI: http://dx.doi.org/10.15666/aeer/1704_92919300

THE RISK MEASUREMENT OF CHINA'S CARBON FINANCIAL MARKET: BASED ON GARCH AND VAR MODEL

WANG, L.[1*] – TANG, L.[2] – QIU, X. M.[1] – ZHANG, X. X.[2] – MA, R. H.[1]

[1]*Economic and Trade College, University of Electronic Science and Technology of China Zhongshan Institute, Zhongshan 528499, China*

[2]*Management College, University of Electronic Science and Technology of China Zhongshan Institute, Zhongshan 528499, China*

[*]*Corresponding author*
e-mail: 838241358@qq.com; phone: +86-1591-7293-187

(Received 3rd Apr 2019; accepted 17th May 2019)

Abstract. By studying five carbon emission exchanges (Beijing, Shanghai, Shenzhen, Guangdong, and Hubei) within China, this study uses the GARCH model to explore the price volatility characteristics of regional carbon trading markets and measures the trading market risks based on VaR model. The results show that the adopted GARCH (1,1) risk model fits well with the characteristics of returns. Besides, fluctuation shock varies among different exchanges, and the volatility of carbon price is influenced more by the heterogeneity of the external environment of the carbon market than the role of internal market mechanisms. The value-at-risk varies between exchanges. These findings pose more challenges to the risk monitoring of carbon finance markets. Therefore, the current work attempts to recommend the establishment of a unified national carbon trading market to control risks and maintain stable market development.
Keywords: *carbon finance, VaR, GARCH, ARCH-LM test, Kupiec failure frequency test*

Introduction

Carbon dioxide is the main factor causing the greenhouse effect. With the advances of economic development, China's carbon dioxide emission have become one of the highest in the world. As a result, while China is facing huge pressure for emissions reduction, it has also generated the conditions and foundations for building a carbon market. The market mechanism is an effective method to save energy and reduce emissions. Since the enforcement of the Kyoto Protocol, western developed countries have established carbon trading markets that target carbon dioxide emission producers. The largest and most developed is the European Union Emission Trading Scheme (EUETS), established in 2005. Additionally, the development of international carbon finance market has proven that the emissions trading theory in economics is indeed effective in combating climate change. As one of the largest global carbon resource holders, China is also one of the largest carbon emission suppliers in the carbon market. Since November of 2013, China has successively established eight pilot carbon exchanges, in Shenzhen, Beijing, Shanghai, Hubei, Tianjin, Guangdong, Chongqing, and Fujian. Their total trading volume has already reached 14,000 tons, calculated from the commencement of carbon emission trading, by April 2018, and the total turnover exceeded 2.5 billion CNY. With the expansion of trade scale and the continuous improvement of trading operation mechanisms, these trading markets could play a more significant role in China's energy conservation and emission reduction tasks.

http://www.aloki.hu ● ISSN 1589 1623 (Print) ● ISSN 1785 0037 (Online)
DOI: http://dx.doi.org/10.15666/aeer/1704_93019315

Carbon finance refers to the transformation of carbon emission rights into a commodity that meets international certification standards via market-oriented tools and means for trading. The research on carbon finance risks started by focusing mainly on the classification and influencing factors of carbon trading risks. Regarding the classification and definition of carbon trading risks, Larson and Parks (1999) clarified that the trading risk of carbon finance exists in many aspects such as project preparation, implementation, evaluation, approval, secondary market, and target market. They analyzed the types of trading risks, and classified them into three types: performance risk, price risk, and policy risk. When qualitatively analyzing carbon emission reduction projects, Laurikka and Springer (2003) classified the ones into six categories, of which, the price risk, cost risk, and quantity risk were the primary risks. Dutschke et al. (2004) categorized the clean development mechanism (CDM) risks into three types: baseline estimation risk, commercial risk, and institutional risk. Regarding the research on the impact of carbon trading risk, Mansanet-Bataller et al. (2010) adopted a multivariate approach to analyze the risks from the perspective of carbon price fluctuations. Their results show that the carbon price was significantly influenced by energy prices and extreme weather. Carmona et al. (2010) found that the long-term and short-term emission reduction projects affected the price volatility of carbon emission allocations in varying ways, and that the energy price trends and the factors influencing carbon emissions (e.g. weather, power plant interruption accidents, etc.) were also closely related to the volatility of carbon prices. Additionally, scholars including Alberola et al. (2008), Kijima et al. (2010), Ibrahim and Kalaitzoglou (2006), and Labatt and White (2011) have also conducted related research.

In China, the carbon trading markets, compared to the western countries, was established much later. Wang and Song (2009) classified the carbon finance risks into three categories, namely the operational risks of carbon financial derivatives, the political risks of carbon finance, and the economic risks of macro-economy. According to Sun (2015), the risk structure of carbon finance market is constituted primarily by uncertain policy risks, liquidity risks, and political risks, while the major causes of these included inadequate supporting policies and laws, uncertain future international situation, insufficient knowledge of entities, lack of professionals, and imperfect service system of carbon finance organizations.

In general, despite the differing classifications of carbon trading risks by domestic and foreign experts, scholars, and organizations, all the risk types are encompassed within two major categories of non-systematic risks and systemic risks. In terms of risk-inducing influences, including weather, energy prices, project emission reduction cycles, macro factors, trading systems, etc. The remainder of this study is organized as follows: Section 2 describes the model setup; Section 3 presents the data description and validation; Section 4 is the empirical analysis and the last Section provides conclusions.

Materials and Methods

Methods

There are two major market risks faced by carbon finance trading entities in the market. One is the change in market size and the other is the fluctuation of carbon emission rights price. In addition, these two are mutually dependent. The change in market size can cause price fluctuations, and its risk is ultimately reflected in the price

http://www.aloki.hu ● ISSN 1589 1623 (Print) ● ISSN 1785 0037 (Online)
DOI: http://dx.doi.org/10.15666/aeer/1704_93019315

volatility risk. This study assesses the risk of carbon finance market by measuring the price volatility risk.

Market risk and VaR model

The portfolio theory proposed by Markowitz (1952) in 1952 marks beginning of market risk quantification in the risk research, in which, he measured the risk level of a financial product using the mean of returns divided by the variance. With the increasing maturity of risk research in recent years, the value at risk (VaR) measure has been the primary choice for academia in researching risk management. VaR refers to the maximum possible loss of a financial asset during the holding period at a certain confidence level under normal market fluctuations. Its value represents the level of market risk quite concisely. According to its definition, VaR is expressed as:

$$\mathrm{Prov}(\Delta P > \mathrm{VaR}) = 1 - \alpha \quad \text{(Eq.1)}$$

where, ΔP denotes the loss of a financial asset within the holding period Δt; VaR denotes the value at risk under confidence level of 1-α. Suppose that the initial price of a financial asset is P_0, and the rate of return is R, then the ending price is $P = P_0 \times (1+R)$. When expected value and volatility of the return R are μ and e, respectively, then the minimum value of the financial asset at a given confidence level is $P^* = P_0 \times (1+R^*)$. Hence:

$$\mathrm{VaR} = \mathrm{E}(P) - P^* = E(P_0 \times (1+R)] - P_0(1+R^*) = -P_0 \times (R^* - \mu) \quad \text{(Eq.2)}$$

Calculation of VaR on this basis is equivalent to determining the minimum value P* or the minimum rate of return R^*.

The above process describes a general approach to calculating VaR. In practice, the VaR solutions are classified into historical standard deviation methods, Risk Metrics, ARCH methods, etc., depending on how the market factor volatility is estimated. It is more reasonable to use the GARCH model from the ARCH family for financial time series with high peak and heavy tail characteristics.

GARCH model and EGARCH

Engle (1982) proposed an ARCH (autoregressive conditional heteroskedasticity) model to avoid the influences of conditional heteroskedasticity in time series on empirical results. The canonical form of the ARCH(q) model is as follows:

$$\sigma_t^2 = \alpha_0 + \sum_{i=1}^{q} \alpha_i \varepsilon_{t-i}^2 \quad \text{(Eq.3)}$$

where, $\sigma_t^2 = Var(\varepsilon_t | \Omega_{t-1})$ presents all information of conditional variance Ω_{t-1} at and before time t−1. In accordance with the ARCH model, the conditional variance of random error u_t depends on its previous value of u_{t-1}.

However, in practical application the ARCH model tends to require a higher lag order, which leads to increased number of parameters under estimation, thereby affecting the accuracy of estimations. To address this problem, Bollerslev et al. (1986) proposed the GARCH (generalized autoregressive conditional heteroskedasticity) model based on the research conducted by Engle, which is as follows:

http://www.aloki.hu ● ISSN 1589 1623 (Print) ● ISSN 1785 0037 (Online)
DOI: http://dx.doi.org/10.15666/aeer/1704_93019315

$$R_t = \mu_t + \varepsilon_t \quad t = 1,2,\dots,T \tag{Eq.4}$$

$$\sigma_t^2 = \alpha_0 + \sum_{i=1}^{q} \alpha_i \varepsilon_{t-i}^2 + \sum_{j=1}^{p} \beta_j \sigma_{t-j}^2 \tag{Eq.5}$$

Among the above formulas, the mean equation presented in *Eq. 4* is an exogenous function with an error term. The establishment of this equation can directly eliminate linear correlation between the antecedent and consequent terms of the series. *Eq. 5* is a conditional variance equation, where ε_{t-i}^2 denotes the square of lag random error in the mean equation. It is the volatility information in the initial measurement period, which is also considered as the ARCH term. σ_{t-j}^2 denotes the forecast variance of the previous period, i.e. the GARCH term. σ_t^2 can be considered as a positive weighted average of the previous residuals, which is consistent with the volatility clustering. To be specific, large volatility may lead to greater changes; conversely, small volatility may cause small changes. The GARCH(1,1) model is the most typically used in practical application.

However, the disadvantages of GARCH model are that it strictly restricts the non-negativity of coefficient parameters, and fails to reflect the leverage effect of financial market, thus easily leading to deviations when applied in the financial market. The EGARCH (exponential GARCH) model overcomes the above deficiencies effectively and thus it is more widely used in present financial research. The expression for the conditional variance of EGARCH model is:

$$\ln\sigma_t^2 = \alpha_0 + \sum_{i=1}^{p} \alpha_i \left| \frac{\varepsilon_{t-1}}{\sigma_{t-1}} - E\left(\frac{\varepsilon_{t-1}}{\sigma_{t-1}}\right) \right| + \sum_{k=1}^{r} \gamma \frac{\varepsilon_{t-k}}{\sigma_{t-k}} \tag{Eq.6}$$

Using natural logarithm as the conditional variance, the EGARCH model illustrates that the expressive form of leverage effect is exponential. The model also introduces a parameter γ. If γ=0, it indicates that the volatilities produced by the price rising and falling symmetrically are identical. If γ>0, it indicates that the volatility by price rising is greater than that by price falling, and vice versa if γ<0.

A key issue in ARCH family models is the choice of error term distribution. In research, normal distribution is usually taken as an assumption. However, in practice, the tail of unconditional distribution for financial time series is often wider than the normal distribution. Therefore, normal distribution is incapable of accurately reflecting the tail characteristics of residual distribution, while the t distribution and the GED (generalized error distribution) can preferably capture the heavy tailed phenomenon. In the following, we separately obtain the log-likelihood functions of the standard normal distribution, GED, and t distribution by denoting the parameter vector by θ as follows:

(1) The log-likelihood function of the GARCH (1,1) model whose residuals follow normal distributed is:

$$\ln L(\theta) = -\frac{T}{2}\ln(2\pi) - \frac{1}{2}\sum_{t=1}^{T} ln\sigma_t^2 - \frac{1}{2}\sum_{t=1}^{T} \varepsilon_t^2 \Big/ \sigma_t^2 \tag{Eq.7}$$

The variable σ_t^2 is the conditional variance of u_t.

(2) The log-likelihood function of the GARCH (1,1) model whose residuals follow GED is:

http://www.aloki.hu ● ISSN 1589 1623 (Print) ● ISSN 1785 0037 (Online)
DOI: http://dx.doi.org/10.15666/aeer/1704_93019315

$$\ln L(\theta) = -\frac{T}{2}\ln\left(\frac{\Gamma(\frac{1}{r})^3}{\Gamma(\frac{3}{r})(\frac{r}{2})^2}\right) - \frac{1}{2}\sum_{t=1}^{T} ln\sigma_t^2 - \frac{1}{2}\sum_{t=1}^{T}\left(\frac{\Gamma(3/r)(\varepsilon_t^2)^2}{\sigma_t^2\Gamma(1/r)}\right)^{r/2} \quad \text{(Eq.8)}$$

where, Γ (·) is a Gamma function. When the parameter r= 2, the GED becomes a normal distribution; when r< 2, the GED has a heavier tail than the normal distribution; when r>2, the GED has a lighter tail than the normal distribution.

(3) The log-likelihood function of the GARCH (1,1) model whose residuals follow student's t distribution is:

$$\ln L(\theta) = -\frac{T}{2}\ln\left(\frac{\pi(k-2)\Gamma(k/2)^2}{\Gamma[(k+1)/2]^2}\right) - \frac{1}{2}\sum_{t=1}^{T} ln\sigma_t^2 - \frac{k+1}{2}\sum_{t=1}^{T}\ln\left(1+\frac{\varepsilon_t^2}{\sigma_t^2(k-2)}\right) \quad \text{(Eq.9)}$$

The parameter estimation in *Eq. 9* is in actual the problem of maximizing the log-likelihood function under a degree of freedom k> 2 constraint. When k→∞, the t distribution approaches a normal distribution.

Materials

Selection of sample data

Currently, spot market enjoys the largest trading volume in China's carbon finance market based on the data consisting mainly of the trading volumes and turnovers of eight pilot carbon emission exchanges. The analysis of these data allows us to understand the risk profile of the carbon finance market. In view of the differing establishment time of China's carbon finance pilots, the daily trading volume and turnover data from January 2016 to April 2018 (totaling 563 trading days) are selected in the proposed study. Since the data from pilot sites in Chongqing, Fujian, and Tianjin are comparatively smaller and lacks statistical significance, modeling analysis is not performed herein for these three regions. The data used in the current study comes from the Chinese carbon trading website.

Statistical characteristics of return series for various exchanges

(1)Trend analysis of return time series

Establishment of a return index for the carbon finance market is attempted by utilizing the daily data from the above carbon emission exchanges. The average transaction price P_t of sample data is represented by the ratio of the current day's turnover to the current day's volume. Considering the stability of data, the rate of return R_t is represented by the logarithmic form as follows:

$$R_t = \ln P_t - \ln P_{t-1} \quad \text{(Eq.10)}$$

The EVIEWS 10.0 software is employed to plot the time series graph of returns (*Figure 1*). Obviously, the logarithmic returns for the five pilot exchanges all fluctuate around zero. When the fluctuations are large, the changes in successive periods are larger; when the fluctuations are small, the changes in successive periods are smaller, exhibiting a distinct "volatility clustering" effect.

(2) Normality test

The Jurque-Bera statistic is a commonly used method for testing normal distribution and its calculation formula is as follows:

http://www.aloki.hu ● ISSN 1589 1623 (Print) ● ISSN 1785 0037 (Online)
DOI: http://dx.doi.org/10.15666/aeer/1704_93019315

$$JB = \frac{n}{6}[S^2 + \frac{(K-3)^2}{4}] \quad \text{(Eq.11)}$$

where, n is the sample size, S is the skewness, and K is the kurtosis. Under the normality assumption, JB obeys $\chi^2(2)$ distribution, with a critical value of 5.99147 at a 5% significance level. If the JB statistic exceeds its critical value, the null hypothesis of normal distribution will be rejected. *Table 1* lists the JB statistics (*Eq. 11*) calculated by EVIEWS 10.0. As the JB statistics for the five pilot exchanges are all considerably above the critical values, the returns of the exchanges all show obvious non-normality. *Table 1* shows that the kurtoses of the five pilot sites are all greater than 3 and the skewness are different from 0. Therefore, the return curves present a "sharp peak and heavy tail" distribution features.

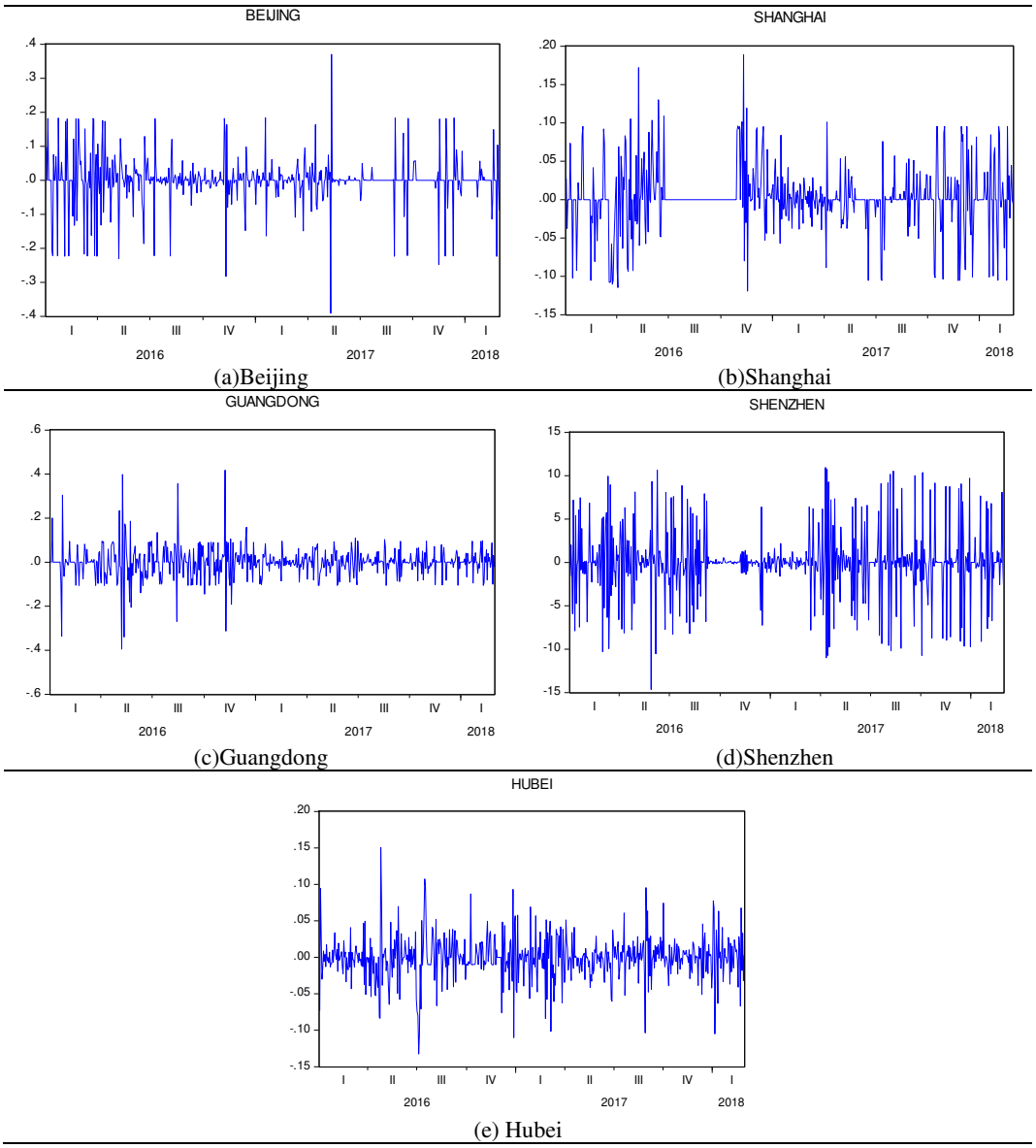

(a)Beijing (b)Shanghai

(c)Guangdong (d)Shenzhen

(e) Hubei

Figure 1. *Rate of return trend in carbon trading market*

http://www.aloki.hu ● ISSN 1589 1623 (Print) ● ISSN 1785 0037 (Online)
DOI: http://dx.doi.org/10.15666/aeer/1704_93019315

(3) Stationary test for logarithmic returns of various carbon exchanges

The stationarity test results with augmented Dickey-Fuller (ADF) test are shown in *Table 2*, showing that return series of the five pilot sites all reject the null hypothesis that "there exists at least one unit root" at the 1% significance level, suggesting that the logarithmic returns of the five pilot sites are stationary series.

(4) Heteroscedasticity test

A Lagrange Multiplier (LM) is then used to perform the lag ARCH test on the residuals of mean equations for the five carbon trading exchanges, and the results are shown in *Table 3*. The p values of the F statistic and the Obs*R-squared statistic are all close to zero, and the results all reject the null hypothesis, indicating the presence of heteroskedasticity in the returns of various pilot sites. The heteroskedasticity can reflect the extreme price fluctuations and extreme risks of carbon exchanges in various regions. This suggests that China's carbon finance market may be at risk, which necessitates its risk analysis.

Obviously, the p-value is zero after the squared residuals of returns, for various exchanges lag a certain order; therefore, the null hypothesis is rejected. The ARCH effect is considered to exist in the residual series of each exchange's regression model.

Table 1. *Normality test*

Item	Beijing	Shanghai	Guangdong	Shenzhen	Hubei
JB statistic	1061.912	169.4251	1944.742	68.7976	223.5930
skewness	-0.6903	0.1561	0.0706	-0.0769	-0.0699
kurtosis	9.585	5.6693	0.1198	4.7056	6.0841

Table 2. *ADF Test at the 1% significance level*

Item	Beijing	Shanghai	Guangdong	Shenzhen	Hubei
ADF test statistic	-23.9183	-21.7936	-21.6165	-16.4819	-26.5245
Test critical values	-3.441777	-3.441757	-3.441777	-3.441840	-3.441757
Prob.*	0.0000	0.0000	0.0000	0.0000	0.0000

Table 3. *ARCH-LM Test*

Exchange	Lag Rank	F statistic	p-value	T×R2 statistic	p-values
Beijing	1	39.03165	0.0000	36.61471	0.0000
Shanghai	7	48.21587	0.0000	44.54611	0.0000
Guangdong	3	63.60045	0.0000	57.30778	0.0000
Shenzhen	2	9.513342	0.0001	18.49639	0.0001
Hubei	1	207.5346	0.0000	151.8873	0.0000

Results

In the current study, the lag order of ARCH(p) and calculation of the AC and PAC for the residuals sum of squared of regression models coefficients were used in the Eviews10.0 software. The results show that the AC and PAC are significantly non-zero, while the Q statistics are highly significant. Therefore, the research method of this paper is identified as GARCH(1,1).

http://www.aloki.hu ● ISSN 1589 1623 (Print) ● ISSN 1785 0037 (Online)
DOI: http://dx.doi.org/10.15666/aeer/1704_93019315

Parameter estimations by GARCH and EGARCH models

The GARCH(1,1) (*Eq. 5*) under standard normal distribution (*Eq. 7*), GED (*Eq. 8*), and t-distribution (*Eq. 9*) are used separately herein to perform parameter estimation on the five carbon trading exchanges' returns. *Table 4* displays the most suitable method. It is found that the GED is most appropriate for residuals distribution of the four exchanges except for Guangdong, where the adjustment of tail bias with normal distribution is needed.

According to the estimations in *Table 4*, the mean value is the greatest for Beijing, and the least for Shanghai. The reason may be that Beijing has a large market volume and faces great risks. By contrast, the trading volume in Shanghai has been quite low in the past two years, so it is at a smaller risk. In addition, Shanghai exchange's return shock decays the slowest, followed by Hubei.

Table 4. *Parameter estimations at GARCH(1,1) and EGARCH(1,1) models*

Parameter	Beijing	Shanghai	Guangdong	Shenzhen	Hubei
Mean equation					
AR(1)	-0.418418 (0.0000)	-0.009039 (0.0000)	-0.271687 (0.0000)	-0.201236 (0.0000)	-0.172881 (0.0000)
AR(2)	-0.321769 (0.0000)		-0.142413 (0.0044)		
Variance equation					
α	0.000848 (0.0042)	8.98*10-14 (0.0000)	0.000834 (0.0000)	0.046786 (0.0000)	0.000264 (0.0000)
α_i	0.128381 (0.0154)	0.320059 (0.0000)	0.565035 (0.0000)	0.698226 (0.0727)	0.616326 (0.0003)
β	0.367891 (0.0280)	0.485901 (0.0000)	0.395047 (0.0000)	-0.041038 (0.3810)	0.189103 (0.0688)
ν	0.017480 (0.0000)	0.284511 (0.0000)	0#	0.614986 (0.0000)	1.051873 (0.0000)
γ	0.102220 (0.0026)	-0.033219 (0.1139)	0.090221 (0.0091)	-0.204153 (0.0471)	-0.026748 (0.7711)
AIC	-17.09388	-8.639286	-2.774323	-0.471930	-4.552960
SC	-17.04757	-8.600750	-2.735734	-0.433394	-4.514424

Note: # indicates that the residual series uses a normal distribution to adjust the tail bias

Concerning the variance models, all α and β values are significant at a significance level of 10% aside from the insignificant β value for Shenzhen, indicating that these models can well depict the volatility clustering feature of the returns in various carbon trading markets. The α value represents the impact of the external market environmental factors on the rate of return, while the β value represents the impact of return volatility on itself. Greater β value indicates longer effect of the return volatility on itself, i.e. the presence of long-term memory effect. Based on *Table 4*, it can be seen that Shanghai has the largest β value of 0.485901, indicating that the 48.5901% of the variance impact in the current period will continue to exist in the next period. This suggests that the decay of the impact is the slowest for Shanghai, followed by Beijing and Guangdong. The risks faced by the three exchanges in Guangdong, Shenzhen, and Hubei are mainly from the impact of external shocks (α_i>β), indicating that the heterogeneity of the external environments for these three markets is more influential to the carbon price volatility than the role of internal market mechanism. For Beijing, on the contrary, the risks mainly come from internal market mechanism. The α values of the five exchanges are significantly less than 1, with αi+β <1. This indicates that the fluctuation of return

http://www.aloki.hu ● ISSN 1589 1623 (Print) ● ISSN 1785 0037 (Online)
DOI: http://dx.doi.org/10.15666/aeer/1704_93019315

attenuates gradually in response to externalities, and that both external factors and internal impact have slow disappearing influences on the rate of return. Shanghai exhibits the largest β value, followed by Guangdong and Beijing. This shows that the return volatilities of these three exchanges have a long-term impact on themselves, which possess a certain memory effect. The γ coefficients are significantly non-zero for all exchanges other than Hubei, where the value is insignificant. Beijing, Shanghai, and Guangdong exhibit positive γ coefficients, indicating that the impact of positive rate of return for carbon finance is greater than the negative shock of the same degree, whereas, an opposite trend is observed for Shenzhen.

Daily VaR values for various exchanges

The daily VaR values at a 95% confidence level are calculated using the conditional variance of the above models, and the statistical results are presented in *Table 5*.

Table 5. *The calculation results at the VaR model*

Exchange	Min.	Max.	Mean	Standard deviation	Failed days	Failed rate	LR statistic	LR critical value*
Beijing	-1.199	-0.0879	-0.3	0.13918	3	0.535%	0.6413	6.635
Shanghai	-0.314	-9×10^{-7}	-0.0629	0.05752	8	1.424%	0.3908	6.635
Guangdong	-1.857	-0.1508	-0.2834	0.17172	2	0.357%	1.354	6.635
Shenzhen	-6.385	-0.1692	-1.8937	0.31346	5	0.89%	0.0312	6.635
Hubei	-1.919	-1.3664	-1.6794	0.10021	0	0%	—	6.635

*: at a 1% significant level

We can determine the market volatility of exchanges based on the standard deviations of daily VaR values. The greater the standard deviation, the higher the volatility of market. As shown in *Table 5*, Shenzhen has the highest volatility, whereas Shanghai is the lowest. The exchanges can be arranged in a descending order of volatility as Shenzhen> Guangdong> Beijing> Hubei> Shanghai. Shenzhen's trading volume and turnover are second only to Hubei among the five pilot sites, and its mean VaR is the largest. This is mainly attributed to the abnormally large standard deviations resulting from the large fluctuations of individual average transaction prices.

Results of Kupiec failure frequency test

Kupiec (1995) proposed a failure frequency test to posteriorly testify and evaluate VaR efficiency. Its procedure is as follows: Assuming that the significant level is α, and the actual loss is $\triangle P=P_t-P_{t-1}$, failure is considered when $\triangle P>$ VaR. The number of inspection days is denoted by T, the number of failed days is denoted by N, and the frequency of failure is denoted by P= N/T. At a significance level of α, the expected failure probability is E(P)= P*=1-α. The "likelihood ratio test" is adopted for failure detection, whose mathematical expression is

$$LR = -2\log\left[(1-p^*)^{(T-N)}(p^*)^N\right] + 2\log\left[\left(1-\frac{N}{T}\right)^{(T-N)}\left(\frac{N}{T}\right)^N\right] \quad \text{(Eq.12)}$$

where, the LR statistic follows χ2(1), with a critical value of 6.635 at a 1% significant level. If the LR value is greater than 6.635, the VaR model is considered invalid. Smaller LR value indicates a more effective model, which can more easily pass the test.

http://www.aloki.hu ● ISSN 1589 1623 (Print) ● ISSN 1785 0037 (Online)
DOI: http://dx.doi.org/10.15666/aeer/1704_93019315

Table 5 shows the calculations by *Eq. 12*. At a 99% confidence level, the results of Kupiec failure frequency test for the five exchanges do not reject the null hypothesis, so the model is valid. Thus, the GARCH-VaR risk model used in this paper can well fit the characteristics of returns.

Discussion

The carbon trading market currently consists of the allocation market (primary market), the spot market (secondary market), and the derivatives market. Among them, the allocation market is responsible for the total amount setting and the initial allocation of allowances, whose chief function is to create carbon allowances. The spot market is a place for spot trading of allowances, which plays the role of basic price discovery and resource circulation. The derivatives market is a place for trading carbon futures, carbon options and other carbon financial derivatives, whose role is to further deepen price discovery, hedging and to avoid risks. Different levels of markets face varying risks, which need to be analyzed separately.

Allocation market risks

The function of allocation market is to create products and provide a basis of trading. Its risks mainly exist in the following aspects:

Total carbon allowance setting risk

Total carbon allowance setting risk refers to the risk brought by drastic fluctuations of carbon allowance price due to the unreasonable total allowance setting by the government. Unreasonable total allowance setting includes both excessive and over-tight setting. Excessive allowance setting will lead to weakened incentive mechanism for emission reduction, so that businesses do not have enough incentive to reduce emissions. Over-tight allowance setting, on the other hand, will lead businesses to bear excessively high cost, thus affecting their competitiveness. In its first stage, EUETS caused carbon price slump due to the excessive allowance issuance, where the price was close to zero. Thus, how to determine the issuing amount will affect the price of carbon market.

Carbon allowance allocation risk

Carbon allowance allocation, which is closely related to the total amount setting, refers to the government's allocation of allowances to businesses by ways like free distribution and paid auctions. The allowance allocation risk is the risk brought about by the unfair distribution of allowances, which is attributable mainly to the defects in the allowance approval procedure. Currently, the common approval methods in the carbon trading market are the Grandfather clauses and the Industry baseline, which have respective advantages and disadvantages. The advantage of the grandfather clauses is that it considers the historical fairness, but its disadvantage is that the reliability of future prediction using historical data is not high. Meanwhile, the Industry baseline often determines a benchmark based on industry-leading levels, and the portion that is superior to the benchmark is eligible for free allowances, while the portion inferior to the benchmark requires purchase of allowances. The advantages of this method are that it encourages technological improvement and the promotion and popularization of

http://www.aloki.hu ● ISSN 1589 1623 (Print) ● ISSN 1785 0037 (Online)
DOI: http://dx.doi.org/10.15666/aeer/1704_93019315

advanced technologies. Its disadvantage is the complicated and costly process of determining the baseline.

Carbon leakage risk

Carbon leakage refers to a situation in which the businesses in countries with strict environmental policies shift to countries without strict environmental policies to trigger rising carbon emissions in the migrant countries. The occurrence of carbon leakage stems mainly from concerns about production cost increase. The carbon leakage problem is inevitable as long as the environmental policies of various countries are inconsistent. Due to the territorial feature of the carbon emission system, environmental policies often have an effect only on domestic companies, but are powerless to foreign companies. Therefore, domestic companies have a strong incentive to transfer production to other countries that are not strictly implementing environmental policies for cost reduction purposes, thereby resulting in the carbon leakage.

Spot market risks

Spot market, also known as the secondary market, is an important part of the carbon trading market. The risks in the spot market mainly include: performance risk and illegal operation risk.

Performance risk

Performance risk refers to the possibility of loss to the one trading party who has fulfilled the transactional obligation after conclusion of a carbon allowance transaction (trading) caused by the failure of the other party to perform the payment obligation in accordance with the transaction contract. Aside from involving qualifications and integrity of both parties, the performance risk sources may also cover the entire trading system. This necessitates checking the transaction system of carbon trading market in an all-round way, including whether the allowance allocation is too loose or too tight; whether the carbon emission monitoring, reporting and verification system is sound; whether the market operation is effective, etc.

Illegal operation risk

Illegal operation risks can generally be classified into the following categories: The first category is serious crimes using the carbon market as a tool, such as fraud, money laundering, and terrorist financing. The most famous events were the phishing involving carbon emissions rights across Europe, Japan and New Zealand that was uncovered in Germany in February 2010, and a VAT carousel fraud took place in the UK in June 2012. The second category is financial market violations, including market manipulation, insider dealing, etc.

Derivatives market risks

Derivatives market, also known as the tertiary market, faces many risks due to the complexity of trading derivatives such as futures and options. Based on the early development experience of global carbon trading market, these risks mainly include: liquidity risk, credit risk and investor risk.

http://www.aloki.hu ● ISSN 1589 1623 (Print) ● ISSN 1785 0037 (Online)
DOI: http://dx.doi.org/10.15666/aeer/1704_93019315

Liquidity risk

Liquidity risk is classified into the market liquidity risk and the financial liquidity risk. The former is mainly reflected in the insufficient market trading volume or inactive market transactions, whose essential cause is the inadequate market depth and breadth. The financial liquidity risk refers to the possibility that the investor is unable to fulfill the payment obligation upon contract expiration due to lack of current funds, or meet margin calls in accordance with the contract at the time of settlement. Rather than existing in isolation, liquidity risk is often accompanied by other risks. Sometimes, however, it may also mean that the trading mechanism itself is flawed.

Credit risk

Credit risk, also known as default risk, refers to the possibility of loss to one trading party caused by refusal of the other party to perform the agreed terms. The emergence of credit risk is often related to the immature carbon trading market and the imperfect relevant systems.

Investor risk

Investor risk is mainly reflected in the influences of unreasonable structure and poor quality of investors on the operation of carbon trading market. Investors are classified into the institutional investors and the individual investors. In mature markets, institutional investors should account for a larger proportion. In the current stage, investor risk is mainly concentrated in the derivatives market. This necessitates setting reasonable thresholds and conditions for investors participating in the carbon derivatives trading, so as to ensure the effective linkage and functioning of the carbon trading markets at various levels.

Policy suggestions

The successive establishment of carbon trading markets in China is of milestone significance to the development of China's carbon finance market, which shows that China has begun to seek the dynamic balance between low-carbon economic development, corporate growth, and eco-environmental protection via market and price mechanisms. Ensuring the orderly fluctuations in China's carbon trading prices guarantees the effective monitoring and control of carbon finance market risks and promotes the stable development of the carbon finance market. We put forward the following suggestions:

Firstly, it is necessary to enhance the rationality of policies, thus gradually integrating the carbon market. Since China's eight major pilot sites for carbon emission trading have taken the lead in accumulating experience, the industries covered by all or most of these sites, such as the power and cement industries, should be the first to be considered for integration. In the meanwhile, a unified quota system should be implemented for the emission control firms of these industries. On the basis of vigorously advancing the pilot sites for carbon emission trading, a unified national control over total quantity should be practiced. Furthermore, quota should be allocated based on factors like regional GDP and carbon emission demands, and a carbon quota trading mechanism should be established to foster a fair and active carbon trading market.

http://www.aloki.hu ● ISSN 1589 1623 (Print) ● ISSN 1785 0037 (Online)
DOI: http://dx.doi.org/10.15666/aeer/1704_93019315

Secondly, it is necessary to improve the level of risk management as well to monitor and control risks: 1. Perfecting the legal framework, and standardizing the carbon trading market system. The regulatory issues involving the carbon finance market must be addressed by legal means. Regulations related to the construction of carbon trading markets should be legislated to enable the stable and orderly development of the carbon finance market. The strong policy dependence of carbon finance itself determines that it is necessary to legally clarify the institutional arrangements for the carbon trading markets, and to incorporate risk issues into the legal context in order to adjust interest relationships, regulate carbon markets, and control risks. 2. The close monitoring of carbon price fluctuations and establishment of a risk measurement system. The GARCH-VaR model established in this paper has certain referential significance in measuring market risk. The supervisory authorities should thus establish a risk measurement system, and set a daily VaR monitoring value for each market to serve as a "risk pre-warning line", so as to improve the early warning capability against risks.

Finally, construction of carbon trading market infrastructures should be strengthened. Respecting the construction of primary carbon trading market (carbon allowance approval, issuance, etc.), the development of greenhouse gas inventory and the construction of statistical accounting systems should be accelerated. It is necessary to prioritize the establishment of greenhouse gas reporting systems for key industries, and establish a sound auction procedure to ensure the smooth delivery of carbon emission rights. Concerning the secondary carbon trading market (spot trading), the role of the carbon emission rights registration system should be played to enhance the market liquidity and improve the trading efficiency. As for the carbon futures market, formulation of carbon futures trading rules covering market participants, delivery system, and price formation mechanism is necessary by learning from the useful international experiences about design of carbon futures contracts, product pricing, trading rules, risk control mechanisms, investor eligibility management, etc.

Eventually, a unified carbon emission trading system with Chinese characteristics should be built, forming a triopoly with the EUETS and the Chicago Climate Exchange (CCX), thus promoting the green and sustainable development on a global scale.

Conclusions

In this study, the GARCH(1,1) and EGARCH(1,1) models are used to estimate the price volatilities for different exchanges based on the data features of daily returns, and the VaR model is used to calculate the risks in China's carbon trading market. The main results as follows:

(1) The daily returns of China's carbon finance present a sharp peak and heavy tail pattern, which do not follow the normal distribution. The GARCH(1,1) model can well characterize the sharp peak and heavy tail of daily return series for China's carbon finance.

(2) The volatility of returns at different pilot sites measured with the GARCH(1,1) model finds that the volatility shock decays to varying degrees among different sites. For Shanghai, Guangzhou, and Beijing, the intrinsic shock exerts a prolonged impact on the return volatility.

(3) The α values are all greater than the β values for the pilot sites except for Beijing, proving that the carbon price volatility is more likely to be affected by the heterogeneity

http://www.aloki.hu ● ISSN 1589 1623 (Print) ● ISSN 1785 0037 (Online)
DOI: http://dx.doi.org/10.15666/aeer/1704_93019315

of the external environment for carbon finance market than the role of internal market mechanism.

(4) The VaR model is used to test the market risk of the five exchanges, the result shows that the level of market risk varies among the exchanges in different regions, which are ranked into Shenzhen, Guangdong, Beijing, Hubei, and Shanghai in a descending order of volatility.

(5) The GARCH-VaR risk measurement model is ideal upon validation through the Kupiec failure frequency test.

The paper measures the risks in China's Carbon Financial Market based on GARCH-VaR model. Though periodical achievements have been obtained, the following few questions still request further research. Firstly, the risk measurement model should incorporate other social and policy factors, such as GDP variation, industry structure, etc. Secondly, the general formula employed by the paper in VaR measurement does not distinguish rise risk and fall risk, but measures the general VaR value instead. Therefore, it needs to respectively measure rise risk and fall risk in following sections.

Acknowledgements. The authors are grateful for the financial support provided by the University of Electronic Science and Technology of China, Zhongshan Institute Scientific Research Starting fund for PHD (26-415YKQ12), Zhongshan science and Technology Bureau (2016B2154) and the humanities and social sciences fund of the Ministry of Education (14YJC790172).

REFERENCES

[1] Alberola, E., Chevallier, J., Chèze, B. (2008): Price drivers and structural breaks in European carbon prices 2005-2007. – Energy Policy 36(2): 787-797.
[2] Bollerslev, T. (1986): Generalized autoregressive conditional heteroskedasticity. - Journal of Econometrics 31(3): 307-327.
[3] Carmona, R., Fehr, M., Hinz, J. (2010): Optimal stochastic control and carbon price formation. – Society for Industrial and Applied Mathematics.
[4] Dutschke, M., Schlamadinger, B., Wong, J. L. P. (2004): Value and risks of expiring carbon credits from CDM afforestation and reforestation. – Social Science Electronic Publishing 5.
[5] Engle, R. F. (1982): Autoregressive Conditional Heteroscedasticity with Estimates of the Variance of United Kingdom Inflation. – Econometrica 50(4): 987-1007.
[6] Ibrahim, B. M., Kalaitzoglou, I. A. (2006): Why do carbon prices and price volatility change? – Journal of Banking & Finance 63: 76-94.
[7] Kijima, M., Maeda, A., Nishide, K. (2010): Equilibrium pricing of contingent claims in tradable permit markets. – Journal of Futures Markets 30(6): 559-589.
[8] Kupiec, P. (1995): Techniques for Verifying the Accuracy of Risk Measurement Models. - Social Science Electronic Publishing 3(2): 73-84.
[9] Labatt, S., White, R. R. (2011): Carbon finance: the financial implications of climate change. – John Wiley & Sons.
[10] Larson, D. F., Parks, P. (1999): Risks, Lessons Learned, and Secondary Markets for Greenhouse Gas Reductions. – Policy Research Working Paper.
[11] Laurikka, H., Springer, U. (2003): Risk and return of project-based climate change mitigation: a portfolio approach. – Global Environmental Change 13(3): 207-217.
[12] Mansanet-Bataller, M., Pardo, A., Valor, E. (2006): CO_2 Prices, Energy and Weather. – Energy Journal 28(3): 73-92.
[13] Markowitz, H. (1952): Portfolio selection. – The Journal of Finance 7(1): 77-91.
[14] Sun, Z. D. (2015): Risk of Trading Market in Carbon Finance.

http://www.aloki.hu ● ISSN 1589 1623 (Print) ● ISSN 1785 0037 (Online)
DOI: http://dx.doi.org/10.15666/aeer/1704_93019315

[15] Wang, L., Song, Y. (2009): Study on financial innovation and risk prevention of carbon trading in China. – Modern Finance & Economics 2009(6): 30-34.

http://www.aloki.hu ● ISSN 1589 1623 (Print) ● ISSN 1785 0037 (Online)
DOI: http://dx.doi.org/10.15666/aeer/1704_93019315

ENVIRONMENTAL REGULATION, PUBLIC PARTICIPATION AND HAPPINESS: EMPIRICAL RESEARCH BASED ON CHINESE GENERAL SOCIAL SURVEY OF 2015

ZHENG, Y.[1,2] – YANG, R.Y.[3*]

[1]*School of Humanities, Economics, and Laws, Northwestern Polytechnical University Xi'an 710072, China*

[2]*Education Center of MPA, Northwestern Polytechnical University, Xi'an 710072, China*

[3]*College of Management and Economics, Tianjin University, Tianjin 300072, China*

[*]*Corresponding author*
e-mail: yangruoyu1993abc@163.com; phone: +86-155-1086-6322

(Received 3rd Apr 2019; accepted 17th May 2019)

Abstract. From the dual perspectives of "performance model" and "expectation model", this paper studies the influences of government regulation and public participation on satisfaction with environmental governance and individuals' happiness based on the data from the Chinese General Social Survey in 2015 (CGSS2015). By constructing the structure-equation model (SEM), it was found that: (1) both environmental regulation and public participation can significantly promote individuals' happiness, and the significance of the former is higher than that of the latter; (2) the improvement of satisfaction with environmental governance can effectively enhance individuals' happiness, and it plays an intermediary role in the relationship between environmental regulation, public participation and individuals' happiness. (3) individual characteristics also affect happiness. The economic and social status of the individuals play a positive moderating role in the relationship between environmental regulation and public participation and happiness. Therefore, we should strengthen government regulation and at the same time ensure public participation and change the "process orientation" to "problem orientation" and "result orientation" to truly improve environmental governance performance and public satisfaction. Meanwhile, the government should also pay attention to the environmental demands and living needs of the vulnerable group to realize social justice and improve individuals' happiness.
Keywords: *environmental regulation, public participation, performance model, expectation model happiness*

Introduction

According to previous studies, even though micro-factors such as individual characteristics (income, employment, education, marriage and so on) can explain many variations of citizens' happiness, there still remain variations that are unexplained. Happiness also can be affected by some external macro-factors, including social environment and natural environment which heavily rely on government intervention (Ott, 2010). Utilitarians point out that governments should try their best to create the greatest happiness for the greatest number of people (Veenhoven, 2010). Although many scholars are still debating on whether it should be used as the basic principle and aim for laws and public policies and questioning its feasibility and risks, the concept that individuals' happiness is an important part of value orientation has been generally recognized (Duncan, 2010; Frey and Gallus, 2013). Bhutan has already used the Gross National Happiness Index since 1972 to evaluate the performance of the government. Besides, many other countries have also promoted the application of the happiness

http://www.aloki.hu ● ISSN 1589 1623 (Print) ● ISSN 1785 0037 (Online)
DOI: http://dx.doi.org/10.15666/aeer/1704_93179332

index in the government management practices, such as France, the United States and China.

In recent years, environmental pollution has become a global issue, seriously affecting the health and living quality of the people around the world and decreasing their happiness. Juncal et al. studied the relationship between air pollution, climate and individuals' happiness in Spain, and found that air pollution can have various impacts on people's happiness in different aspects (Cuñado and Gracia, 2013). By utilizing the panel data of the happiness survey carried out in ten countries, Welsch provided cross-border evidence for the negative relationship between air pollution and subjective sense of happiness (Welsch, 2006); Mackerron found that the respondents will feel a strong sense of happiness when they are in a beautiful natural environment rather than a more common external environment (Mackerron and Mourato, 2013).

In this context, the influence of government environmental regulation on national happiness has become an important topic that is widely concerned by both the academic circle and the government departments. In 2016, the Chinese government announced that China has entered the "13th Five-Year Plan" period, and would pay high attention to environmental regulation. On 4th January, 2016, the Central Environmental Protection Supervision Group was formally established and began to carry out environmental protection supervision in all provinces. In October 2017, President Xi of the People's Republic of China clearly pointed out that China would "construct an environmental management system led by the government, dominated by enterprises, and in which social organizations and the public are to participate (Wang and Li, 2018)", and pay more attention to the effective role of public participation in the environmental governance. In the previous environmental regulations, many parties have been involved, including government administration bodies and also a diversity of social organizations and people. The enhancement of the environmental governance performance in China, to a large extent, can be attributed to both the institutionalized regulatory policies and non-institutionalized public participation. Various social subjects, such as environment protection organizations, third-party agents and citizens, are all playing important roles (Dungumaro and Madulu, 2003). Among them, the most extensive participants are undoubtedly individual citizens, and the most common and direct way is participating in the environmental governance process by filing petition letters and reports and protecting their own rights through the judicial way. When a pollution incident breaks out, the direct participation of the public often plays a crucial role. Therefore, this paper intends to perform an empirical analysis of the relationships between government regulation, public participation, satisfaction with environmental governance and individuals' happiness using the data of CGSS2015.

Literature Review and Hypotheses

Improving public satisfaction and individuals' happiness has become an important goal for the government. Overall speaking, the influential factors to public service satisfaction can be divided into three categories - macro-factors, including government management and public service, meso-factors, including social organization development and public participation, and micro-factors, including personal development and personal expectation. Currently, there are few literatures focusing on the study of the influential mechanism for satisfaction with environmental governance, not to say the related empirical studies. With the improvement of people's living

http://www.aloki.hu ● ISSN 1589 1623 (Print) ● ISSN 1785 0037 (Online)
DOI: http://dx.doi.org/10.15666/aeer/1704_93179332

standards and the prominence of environmental pollution issues, both government departments and the public have increasing demands for environmental governance. However, satisfaction with environmental governance is a kind of subjective feeling of an individual, so it is necessary to study the micro-factors to personal perception. In the previous literatures, it can be found that the explanation models about satisfaction mainly consist of two perspectives, with one being the performance model perspective, and the other, the expectation model perspective. From the perspective of the latter, the public evaluation of government is a function of various government performances. Public satisfaction mainly depends on the performance that the government demonstrates in various aspects (Swindell and Kelly, 2000). From the perspective of the expectation model, the public evaluation of service is based on the comparison between the service quality they have truly received/felt and the one they expect. The most famous model is the service quality model (Parasuraman et al., 1988). This theory believes that satisfaction measures the gap between the performance perceived and the one expected by the public. That is to say, there is a significant positive correlation between performance and satisfaction if expectation remains unchanged (Parasuraman et al., 1991). To some extent, the improvement of satisfaction will also promote the improvement of individuals' happiness. Therefore, the government's environmental regulation and the satisfaction of public expectation will not only help improve satisfaction, but also lead to the improvement of happiness. This paper builds a new theoretical model by incorporating environmental regulation and public participation into the analytical framework and conduct in-depth research on the influencing mechanism for satisfaction with environmental governance and individuals' happiness based on these two perspectives.

Environmental governance and individuals' happiness

Environmental economists and happiness economists are all very concerned about environmental pollution problems, and they believe that in order to guarantee the happy life for the current generation and the welfare of the people in the future, it is necessary to reduce pollution and protect the natural environment (Menz, 2011). The studies carried out by previous scholars show that the environmental pollution has a negative relationship with the individuals' happiness. Welsch first analyzed air quality by measuring the pollutants such as sulfur dioxide and nitrogen dioxide, and studied the relationship between air pollution and individuals' subjective happiness using cross-sectional data from 54 countries. The results show that air pollution can significantly reduce individuals' happiness (Welsch, 2002). It affects individuals' happiness through the following ways: first, air pollution, water pollution and other common environmental pollution would affect individuals' health, furthermore reducing their subjective happiness (Yang and Liao, 2017); second, environmental pollution causes inconvenience to individuals' life, thus affecting their happiness. Environmental regulation can promote economic transformation and achieve green development to a certain extent (Chen and Yang, 2018). Therefore, this paper proposes the first hypothesis:

H1: Environmental regulation has a positive impact on happiness

Public participation and individuals' happiness

In the process of environmental regulation, government regulation is indispensable, but the public is also an important force and plays an important role in environmental

http://www.aloki.hu ● ISSN 1589 1623 (Print) ● ISSN 1785 0037 (Online)
DOI: http://dx.doi.org/10.15666/aeer/1704_93179332

protection. Public participation makes the decisions more rational and efficient and the whole society can be mobilized to protect the environment, which is the fundamental solution to the environment protection (Yang and Chen, 2019). Public participation enables people to better express their demands and intentions and exercise their environmental rights. Therefore, in the modern society, the role of public participation is becoming increasingly prominent. In the process of environmental regulation, we often face the double troubles of "market failure" and "government failure". In this case, public participation is undoubtedly the only way to eliminate environmental pollution. In this process, the expectations of stakeholders will be better satisfied and thus the sense of happiness will be enhanced. Therefore, this paper proposes the second hypothesis:

H2: Public participation has a positive impact on happiness.

Environmental regulation and satisfaction with government governance

From the perspective of the performance model, previous scholars generally believe that how the government performs determines the results of public evaluation and satisfaction (Kelly and Swindell, 2002). In a country like China, environmental protection and environmental accountability are the two most effective regulation methods. Increasing the weight of environmental protection assessment in performance assessment indices and adopting various forms of environmental accountability systems from the central government to the local government have both produced obvious effects and improved public satisfaction with environmental governance. In 2015, the Chinese government issued an outline for building a law-based government, which points out that the achievements in legal construction will also be incorporated into the index system. In recent years, the legalization of Chinese environmental regulation has been improving continually. Strengthening the legalization of environmental governance is not only beneficial to dealing with more serious environmental problems, but also conducive to the reconstruction of ecological responsibilities and the protection and realization of citizens' environmental rights. Therefore, the level of legalization of environmental governance has an influence over public's satisfaction. When the environmental governance tends to be more legalized, and the law systems more standardized, the quality of governmental regulation and service will be significantly improved, the environmental governance will enter a virtuous circle, and the public's satisfaction with environmental governance will be greatly improved (Kim and Kim, 2012). Based on this, this paper measures the degree of environmental governance by two indices - "environmental accountability" and "environmental governance legalization level", and proposes the hypothesis below:

H3: Environmental regulation has a positive impact on the satisfaction with government governance.

Public participation and satisfaction with government governance

From the prospective of the expectation model, the public satisfaction is a relative concept, which can be reflected by the gap between the actual performance and the expected one. Based on this model, previous scholars think that when the expectation is effectively satisfied, public satisfaction will be obviously improved (Parasuraman et al., 2002). In fact, public expectation is subjective and difficult to quantify. With the transformation of the government functions and the reform of administrative systems, public participation has become an effective method to express the demands and

http://www.aloki.hu ● ISSN 1589 1623 (Print) ● ISSN 1785 0037 (Online)
DOI: http://dx.doi.org/10.15666/aeer/1704_93179332

expectations of the public. The higher the public participation, the more easily the expectation can be satisfied. Therefore, this paper uses the effectiveness of public participation to reflect the satisfaction degree of public expectation, which consists of two dimensions: the effectiveness of the process and that of the result. The former provides the public with more channels and ways to report their environmental problems, which realizes “procedural justice”. The effectiveness of the result means that the problems reported by the public can be truly solved, and that the environmental demands can be really satisfied. Ensuring the result effectiveness of public participation can help quickly solve environmental problems that have not been discovered by the government departments and cannot be solved by the market mechanism, so this realizes "outcome justice". In the real life, as a kind of political participation, petition has increasingly become an important means for citizens to interact with government departments and solve environmental problems (Tang, 2000). The process and result effectiveness of petition not only truly meets public’s expectation, but also improves their satisfaction towards environmental governance. Based on this, this paper proposes the hypothesis below:

H4: Public participation has a positive impact on satisfaction with government governance.

Satisfaction with government governance and individual’s satisfaction

The government has an important influence on individuals’ happiness with its resources and policies. The difference in government performance is one of the most important reasons for the differences in individuals’ happiness in different countries (Ott, 2011). Ott (2015) thinks that a good government protects human rights and judicial justice, alleviates social injustice and provides a good living environment and social environment for the public, thus improving individuals’ happiness. The government has the power to control the system execution, make policies and allocate resources, which can have direct impacts on the market, the society and even each individual, so a standardized and effective government has positive impacts on individuals’ happiness and accordingly, the improvement of the satisfaction with government governance will promote the individuals’ happiness (Coggburn and Schneider, 2003). Based on this, this paper proposes the fifth hypothesis:

H5: Satisfaction with government governance has a positive impact on individuals’ happiness.

Intermediary role of satisfaction with government governance

According to the above analysis, environmental regulation and public participation can help improve the satisfaction with government governance; and the satisfaction with government governance can further promote the improvement of individuals’ happiness. There is a high correlation between the quality of government public service and the public's satisfaction with public service. The latter can directly reflect the former (Swindell and Kelly, 2000). The level of government public service quality also directly influences individuals’ happiness. After comparing the impacts of government governance quality between the developed countries and the developing countries using the citizen satisfaction index in the world values survey (WVS), Helliwell found that in developing countries, the satisfaction with government public services has a greater impact on national happiness (Helliwell and Huang, 2008). Therefore, the satisfaction

http://www.aloki.hu ● ISSN 1589 1623 (Print) ● ISSN 1785 0037 (Online)
DOI: http://dx.doi.org/10.15666/aeer/1704_93179332

with government governance can be regarded as an intermediary variable. Based on this, this paper proposes the sixth hypothesis and sub-hypothesis.

H6: Satisfaction with government governance plays an intermediary role in the relationship between environmental regulation, public participation and individuals' happiness.

H6a: Satisfaction with government governance plays an intermediary role in the relationship between environmental regulation and individuals' happiness.

H6b: Satisfaction with government governance plays an intermediary role in the relationship between public participation and individuals' happiness.

Moderating role of individual characteristics (economic and social status)

Some individual characteristics, such as gender, age, education and income, would affect citizens' expectation, thus affecting the satisfaction with environmental governance and individuals' happiness. According to previous studies, income can reflect a person's economic status, and there is a certain positive correlation between income and subjective happiness (Shields et al., 2009). Higher education background can increase individual's independence and help form good interpersonal relations, and promote public participation and improvement of happiness (Chen, 2012). Besides, based on the "profit-cost" allocation, the group with higher economic status enjoys more profits generated at the expense of environment, but they use their economics advantages to pass on the environmental consequences and environmental governance accountability to the relatively more vulnerable groups. However, the poor are less able to migrate than the rich and less able to avoid environmental pollution. Generally speaking, the group with higher income and education background has more ways to express their claims and participate in the public. Therefore, this paper uses economic income and education level to measure the economic and social status of individual characteristics, and puts forward the following hypotheses:

H7: The higher the economic and social status, the more significant the positive impact of environmental regulation on individuals' happiness.

H8: The higher the economic and social status, the more significant the positive impact of public participation on individuals' happiness.

Above all, this paper mainly studies the impacts of environmental regulation and public participation on individuals' happiness. During the process, satisfaction with government governance is an intermediate variable, while individual income and education level are moderating variables. The theoretical model constructed according to the research hypothesis is shown in *Figure 1*. Since the age and gender of individuals also have impacts on happiness (Cai et al., 2018), this paper takes these two factors as control variables for analysis in the data processing process.

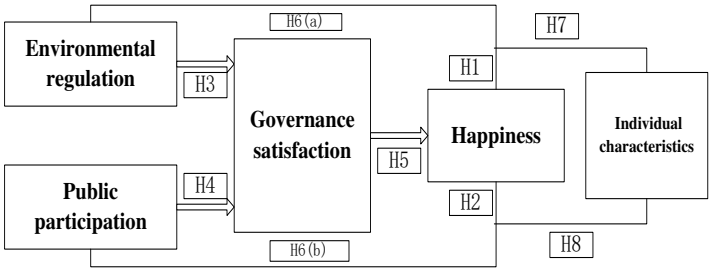

Figure 1. *Variable models in this paper*

http://www.aloki.hu ● ISSN 1589 1623 (Print) ● ISSN 1785 0037 (Online)
DOI: http://dx.doi.org/10.15666/aeer/1704_93179332

Materials and Methods

Materials

In this paper, environmental accountability and the environmental regulation legalization level are used to measure the government environment regulation. In the CSSS survey, there are six modules-A, B, C, D, E and F, in which F is the "legal module", consisting of questions on government accountability and regulatory compliance, with environmental regulation sub-questions. The corresponding original questions are "Will the government be held accountable when the government leaders blindly pursue output value and neglect the supervision on enterprise pollution discharge, resulting in environment deterioration?" and "How is the government's compliance with laws when it is handling environmental pollution?". The higher the score, the stronger the government's environmental regulation and the higher the level of legalization.

In terms of public participation, when an individual is facing environmental pollution issues, the common way to safeguard his or her rights is to file a petition letter. With the gradual improvement of the environmental protection petition system in China, petition now plays an increasingly important role in environmental regulation. In the real life, there are two requirements to be met if environmental pollution problems can be solved by petition: first, the public's petition rights have been safeguarded; second, the environmental problems reported by the public have been effectively solved. This paper measures public participation from the two dimensions: first, "will the petition be blocked" (process effectiveness), second, "can the petition solve your problem" (result effectiveness). In the CGSS survey module F, the questions related to petition have been set. The original questions are respectively "Do you agree with the following: petition will not be blocked" and "Do you agree with the following: petition can solve the problem". The higher score is, the higher degree of public participation there will be.

The satisfaction with government governance is covered by question B15 in the module B of the CGSS questionnaire. The original question is "Are you satisfied with the government's performance in environmental protection?" This paper determines the satisfaction degree of environmental governance based on this. In the original questionnaire, the corresponding ratings are "very satisfied--satisfied--neutral--dissatisfied--very dissatisfied", with a score from 1 to 5. This paper uses the negative numbers, so that the higher the score is, the higher the satisfaction degree will be.

Concerning the happiness and individual's economic social status, there are relative questions in module A of the CGSS questionnaire. The question about happiness is "Generally speaking, are you happy?" In the choices, 1 represents "very unhappy", and 5 "very happy". The higher the score is, the happier the respondent is. The income in individual characteristics refers to the actual income of the respondent. The education background is divided into 13 grades, with 1 representing "illiterate", 13 "Postgraduate and above". The higher the score is, the higher the education level is. In control variables, age is 2018 minus the year of birth. Men are assigned with a value of 1, while women, 2.

Study samples and data sources

The related variable data in this paper are mainly from the survey results of Chinese General Social Survey in 2015 (CGSS2015), which is the first national, comprehensive, continual and large-scale social investigation program in China. The purpose is to

http://www.aloki.hu ● ISSN 1589 1623 (Print) ● ISSN 1785 0037 (Online)
DOI: http://dx.doi.org/10.15666/aeer/1704_93179332

regularly and systematically collect data of Chinese people and various aspects of Chinese society, summarize the long-term trends of social changes, explore social issues of great theoretical and practical significance, promote the openness and sharing of domestic social science research and provide data for government decision-making and international comparative research. Since 2003, it has carried out sample surveys among 10,000 families in 31 provinces in China annually. The lasted survey was carried out in 2015 with the data released in January 2018. The survey comprehensively measures the living and development status of urban and rural residents, public's satisfaction with social governance, and individual's perception of the government's legal construction. The samples are large in size and widely distributed in China, which is suitable for the correlation analysis in this study. In the specific analysis process, some data have been processed, and the choices "unable to answer", "refuse to answer", "don't know" and "not applicable" are regarded as missing values. Variable measurement and data processing are shown in *Table 1*.

Table 1. *Variable measurement and data processing*

Category	Variable	Survey Item	Illustrate
Independent variable	Environmental regulation	1: Will the government be asked to take the responsibility when the government leaders exclusively pursue output value and neglect the supervision for the enterprise pollution discharge which resulted in the environment deterioration? 2: How is the government's level of handling environmental pollution in accordance with law	The higher the score is, the stronger the government's environmental regulation and the higher the level of legalization will be.
	Public participation	1: Will be the petition blocked 2: Can the petition solve your problem	The higher score means the higher degree of public participation.
Moderating variable	Individual features	1: Annual gross income	The bigger the value, the higher the income.
		2: Educational level.	The higher the value, the higher the degree
Intermediary variable	Satisfaction	Are you satisfied with the government's performance in environmental protection?	The higher the value is, the higher the satisfaction degree is.
Control variable	Gender	Gender	Male is 1, female is 2
	Age	Date of birth	2018 minus date of birth
Dependent variable	Happiness	Generally speaking, are you happy	The higher the value, the higher the degree.

In the specific survey process, module A is the core, and module B is the "ten-year review" module, in which all questions are mandatory to the respondents. The samples for dependent variables and control variables in this paper cover more than 10,000 families. However, module F module only conducted a sampling survey among more than 3,000 households. After data sorting, it was found that only 3,777 people were required to complete this section. Considering there are missing values, the effective sample size would be even less than 3,777. Therefore, only more than 3,000 samples are used for the independent variables in this paper.

http://www.aloki.hu ● ISSN 1589 1623 (Print) ● ISSN 1785 0037 (Online)
DOI: http://dx.doi.org/10.15666/aeer/1704_93179332

Results

Reliability test and single-dimension analysis

This study adopts the software SPSS 21.0 and AMOSS 21.0, respectively, to test the reliability and validity structures of the choices for measurement, and uses the CITC and reliability analysis methods to analyze the reliability of the choices, with CITC>0.3 and Cronbach's α>0.7 as the criteria. The survey choices in the table correspond to those in the questionnaire. The analysis results show that all the CITC values are greater than 3, and that the overall Cronbach's α parameters are all greater than 0.7, which meet the reliability requirements, and thus the choices can be applicable to future analysis.

Before analyzing the factors, it is necessary to confirm whether there are common factors in the data. Bartlett sphere test is used to test whether the related matrix is the unit matrix or not, which indicates the suitability of the factor model. The KMO (Kaiser-Meyer-Olkin) value indicates whether the selected samples are suitable or not and also whether the information is suitable for factor analysis. The KMO value ranges from 0 to 1. It is generally believed that a value above 0.9 means the sample is very suitable, that 0.8-0.9, the sample is quite suitable, that 0.7-0.8, the sample is suitable, and that a value below 0.5, the sample is not suitable. The probability P-value of the Bartlett sphere test should be less or equal to the significance level. *Table 2* shows that the KMO values of all the variables are greater than 0.7 in this study, which is suitable for future study.

Table 2. *Results of KMO and Bartlett's test*

Variable	Dimension	KMO	Bartlett's Test			Suitability
			Chi-square	Freedom	P	
Independent variable	Environmental regulation	.789	570.197	6	.000	Fit
	Public participation	.779	519.290	6	.000	Fit
Intermediary	Satisfaction	.886	1065.282	15	.000	Very fit
Moderating1	Income	.715	299.969	6	.000	Fit
Moderating2	Educational level	.723	308.471	6	.000	Fit

In order to further guarantee the validity of the scale, this study carries out exploratory factor analysis (EFA) to understand whether the number and content of levels in the scale are consistent with those of the operational definition. The results show that the load values of the two factors extracted from the independent variables meet the analysis requirements and the overall validity is acceptable.

Descriptive statistical analysis

Table 3 is the descriptive statistical analysis results of the data after being processed. Since there are only 3,777 respondents for module F, this paper carries out two descriptive statistical analysis based on the related variables, including the overall sample statistical analysis, and the subsample statistical analysis for the answers only in module F. Among the variables, the value of the environmental governance legalization is greater than that of environmental accountability, which shows that the respondents generally believe that the level of legalization in environmental governance is higher than the level of accountability. But both values are lower than 3, which shows that neither factor is at a high level.

http://www.aloki.hu ● ISSN 1589 1623 (Print) ● ISSN 1785 0037 (Online)
DOI: http://dx.doi.org/10.15666/aeer/1704_93179332

Table 3. *Results of descriptive statistic analysis*

Measurement Item (Variable Code)	N	Min	Max	Average	Standard Deviation
Environmental Accountability (EC)	3236	1	5	2.63	1.12
Governance Legalization (EL)	3641	1	5	2.95	0.88
Petition can't be Blocked (P1)	3337	1	5	2.61	1.06
Petition can Solve Problem (P2)	3341	1	5	2.73	1.06
The Whole Sample					
Personal Annual Gross Income (I1)	10363	0	9999990	32805.33	205840.55
Education Level (ED1)	10939	1	13	4.87	3.11
Government Governance Satisfaction (S1)	10820	-1	-5	-2.7	0.92
Gender(G1)	10968	1	2	1.53	0.50
Age (A1)	10968	21	98	53.4	16.90
Individuals' happiness (H1)	10953	1	5	3.87	0.821
Sub-sample					
Personal Annual Gross Income (I2)	3578	0	2000000	27792.19	59698.21
Education Level (ED2)	3767	1	13	4.82	3.07
Government Governance Satisfaction (S2)	3739	-1	-5	-2.7	0.91
Gender (G2)	3777	1	2	1.53	0.50
Age (A2)	3777	21	98	53.22	17.07
Individuals' happiness (H2)	3735	1	5	3.81	0.81

In the whole samples, the value of the variable individuals' happiness is 3.87, and 59.97% of the respondents are in the "relatively happy" status. The maximum score for the satisfaction with government environmental governance is -1, the minimum value -5, and the average -2.7. The choice with a score of -2 is "satisfied", and 42.0% of the respondents chose it. The choice with a score of -3 is "neutral", which 32.7% of the respondents chose. It can be clearly seen that the majority citizens are satisfied with the government's environmental governance work, but the average value of happiness is greater than that of satisfaction. Concerning the individual characteristics, the average amount of annual income per capita was 32805.33 RMB, and the standard deviation was as high as 205840.55 RMB, which shows the respondents have great income disparities. According to the official data from the national bureau of statistics, the per capita disposable income of Chinese residents in 2014 was 20167 RMB. So overall, the income level of the respondents is higher than the national average. In terms of education, the average score is 4.87. In the original questionnaire, a score of 5 corresponds to vocational high school, so the average score means that the education level of the respondents is between junior and senior high school, which is consistent with the actual situation - nine-year compulsory education - in China. However, the education level of the urban and rural residents as a whole still remains to be improved compared with that in western developed countries.

The extreme, average and standard deviation of the mediating variables and dependent variables in the sub-samples are generally consistent with those in the overall samples. The gender distribution in the system variable is consistent with that in the overall samples, and the male-female ratio is relatively balanced. The maximum personal annual income in the moderating variable is 2 million RMB, the average and the standard deviation are respectively 27792.19 RMB and 59698.21 RMB which are both lower than the results in the overall samples. This shows that the individual income disparity of the sub-samples is relatively small, which is consistent with the actual situation. The highest education level in the moderating variable is basically consistent with the overall situation in the overall samples. This indicates that the sub-samples are highly representative and suitable for further analysis.

http://www.aloki.hu ● ISSN 1589 1623 (Print) ● ISSN 1785 0037 (Online)
DOI: http://dx.doi.org/10.15666/aeer/1704_93179332

Hypothesis verification results

Table 4 shows the results of multiple regression analysis involving environment regulation, public participation, satisfaction with government governance as well as individuals' happiness and other variables.

Table 4. *Results of multiple regression analysis*

Variable (Code)	Governance satisfaction		Individuals' happiness								
Variable (Code)	**Model1**	**Model2**	**Model3**	**Model4**	**Model5**	**Model6**	**Model7**	**Model8**	**Model9**	**Model10**	**Model11**
Gender (G2)	-0.038	-.034	-.033	-.039	-.038	-.038	-.035	-.038	-.038	-.038	-.037
Age (A2)	0.002*	0.002*	0.002*	0.002*	0.002*	0.002*	0.002*	0.002*	0.002*	0.002*	0.002*
Environmental regulation (ER)	0.192***		0.203**			0.179*		0.215***		0.207***	
Public participation (PP)		0.083**		0.091**			.087*		0.145***		0.104***
S2					1.018**	1.003**	1.009*				
ER*I2								.162***			
PP*I2									0.104**		
ER*ED2										.151***	
PP*ED2											0.101**
F	28.809**	29.756***	30.524***	31.535***	31.783***	32.094***	32.656***	33.821***	33.804***	33.719***	33.699***
R^2	.14	0.16	0.15	.14	.16	0.14	0.15	.19	.19	.18	.18

Note: ***, ** and * are significant at the statistical levels of 0.01, 0.05, and 0.1 respectively

Model 1 and model 2 respectively focus on the impacts of environmental regulation and public participation on satisfaction with government governance. Among the control variables, gender has no significant impact on satisfaction with government environmental governance, but age is positively correlated with satisfaction with government environmental governance, indicating that young people are less satisfied compared with elder people. Both environmental regulation and public participation can positively promote the improvement of satisfaction with government governance, which verifies hypothesis 3 and hypothesis 4, and the significance of government regulation is higher than that of public participation. Model 3 and model 4 show that gender has no significant impact on individuals' happiness, and age is positively correlated with happiness, indicating that compared with young people, elder people are happier. Both environmental regulation and public participation have significant positive impacts on individuals' happiness, which verifies hypothesis 1 and hypothesis 2, and the coefficient of government regulation is higher than that of public participation. Model 5 reflects that satisfaction with government governance has a positive impact on happiness, which verifies hypothesis 5.

Model 6 shows that the impact of the independent variable environment regulation on individuals' happiness is obviously reduced after the satisfaction with government governance is added, which reflects that there is a significant partial mediating effect between environmental regulation and individuals' happiness; model 7 also shows that the impact of the independent variable public participation on individuals' happiness is obviously reduced after the satisfaction with government governance is added, which reflects that there is a significant partial mediating effect between public participation and individuals' happiness. Based on the above analysis, hypothesis 6a and

http://www.aloki.hu ● ISSN 1589 1623 (Print) ● ISSN 1785 0037 (Online)
DOI: http://dx.doi.org/10.15666/aeer/1704_93179332

hypothesis 6b are also verified. Model 8 shows the impact of the mutual interaction between environmental regulation and personal income on individuals' happiness, and compared with that in model 3, the significance of environmental regulation is improved. Module 9 shows the impact of the interaction between public participation and personal income on individuals' happiness, and the significance of public participation is improved when compared with that in, module 4, which verifies hypothesis 7. Model 10 shows the impact of environmental regulation and education interaction on individuals' happiness. Compared with that in model 3, the impact of environmental regulation is significantly enhanced. Model 11 shows the impact of the interaction between public participation and education on individuals' happiness. Compared with that in model 4, the impact of public participation is significantly enhanced. Therefore, education level also has a positive moderating effect, proving Hypothesis 8.

Robustness test

In fact, there are many forms of public participation in environmental governance and right relief. Besides petition, judicial litigation is undoubtedly a relatively common way. In order to verify the reliability of the results in *Table 4*, this paper replaces the two questions used in the above questionnaire to measure the "effectiveness of public participation" and replaces the questions related to petition with those related to environmental lawsuit. In module F in the CGSS2015 questionnaire, questions F10 and F11 cover the timeliness and the enforcement effort of the court when the public participates in environmental governance through litigation, which could be used to measure the process and result effectiveness of public participation. The original question F10 is "If there is an enterprise nearby discharging waste gas or sewage in violation of regulations, which results in serious harm to the health of the residents, how soon do you think the court will make a decision if you file a lawsuit, asking the above enterprise to compensate for loss?" The higher the score is for the question, the stronger the process effectiveness of public participation will be. The original question for F11 is "If the court's ruling is in favor of the residents, but the enterprise doesn't execute the ruling and the resident applies for compulsory execution, how do you think the execution will go?" The higher the score is for the question, the stronger the process effectiveness of public participation will be. Therefore, this paper covers the two dimensions of the variable "public participation effectiveness" with the above two questions to test its robustness. Overall, the results are generally consistent with *Table 4*. Therefore, the models in this paper have strong robustness.

Discussion

Improving the government environmental governance and the effectiveness of public participation is both beneficial to improving satisfaction and happiness

The study in this paper indicates that guaranteeing the effectiveness of environmental accountability and expanding the ways of public participation can effectively solve the environmental pollution issues, and improve the satisfaction with government environmental governance and individuals' happiness. Therefore, we should further improve the mechanism of public participation in environmental governance and formulate the legal system at the macro level to protect the right of the public to report

http://www.aloki.hu ● ISSN 1589 1623 (Print) ● ISSN 1785 0037 (Online)
DOI: http://dx.doi.org/10.15666/aeer/1704_93179332

problems and claim for compensation, encourage the development of environmental protection organization and take social organizations as the bridge between the government and the public to effectively carry out environmental regulation at the meso level, and set up hotlines and email boxes for reporting of environmental protection problems at the micro level so that individuals can more actively participate in the environmental regulation process.

Satisfaction with government governance plays an intermediary role between environmental regulation, public participation and individuals' happiness

Besides strengthening government regulation and expanding the ways for public participation, we should also make effort to improve effectiveness and truly solve environmental problems. We should shift the focus from "process orientation" and "input orientation" to "problem orientation" and "result orientation". After receiving reports and feedbacks from the public, practical implementation plans should be put forward to truly solve environmental problems. Only when the public's requirements are fully met, can we promote the improvement of the environmental governance system and realize "process justice" and "outcome justice", so as to ensure environmental protection development and improve individuals' happiness.

Individual's economic and social status plays a positive moderating role in the relationship among environmental regulation, and public participation and individuals' happiness

Overall, people with higher income and education level have more ways to express their own demands, higher awareness of safeguarding their environment rights, as well as more ways for public participation. The higher the income is, the more significant the impact of environmental regulation and public participation will be on individuals' happiness. This requires the government to apply various methods to improve individuals' happiness according to the real situations, pay attention to the environmental demands and living requirements of the group with lower income and education background. The group with higher economic status enjoys more profits generated at the expense of the environment, but they can utilize their economics advantages to pass on the environmental consequences and environmental governance accountability to the relatively more vulnerable groups. Therefore, the government should adjust public finance in the second distribution and allocate more public expenditures to the vulnerable groups so as to meet their demands, promote social justice and further improve individuals' happiness.

Conclusions

The results of the empirical study show that both reinforcing government accountability and improving the environmental governance legalization level can effectively improve the satisfaction with environmental governance and individuals' happiness. We should make full use of environmental accountability in the future, and increase the number and weights of environmental performance indices in the government management performance system, intensify accountability and implement environmental regulatory policies. At the same time, we should make environmental governance more legalized and standardized, set up specific laws and regulations on

http://www.aloki.hu ● ISSN 1589 1623 (Print) ● ISSN 1785 0037 (Online)
DOI: http://dx.doi.org/10.15666/aeer/1704_93179332

environment regulation, punishment and safeguarding of rights, improve relevant systems and mechanisms and establish a sound environment regulation system.

Overall, the score of satisfaction with government environmental governance is lower than the average score of individuals' happiness. The satisfaction with government environmental governance has positive impacts on individuals' happiness, and plays an intermediary role between environmental regulation, public participation and individuals' happiness. It acts on individuals' happiness in both objective and subjective ways. Environmental governance can solve environmental pollution issues and enhance the public's satisfaction towards public service, thus improving individuals' happiness. Therefore, we should focus on improving the efficiency of government environmental governance, meeting public needs, and improving environmental governance satisfaction.

Individual's economic and social status plays a positive moderating role in the relationships between environmental regulation, public participation and individuals' happiness. It is clear that the higher the income is, the greater the effect of the independent variable will be on individual's happiness, education level also has a positive moderating effect. Therefore, the government should also pay attention to taking different measures according to the needs of different groups of people in the process of environmental governance.

This study has certain limitations due to limited time and space. The questionnaire is only issued in China and only reflects the situation in the year of 2015. We can issue questionnaires on a larger scale in the future, Conducting cross-country research and multinational comparison. It is also possible to conduct follow-up surveys and collect data for many years, analyze and study years of panel data. Research the influences of government regulation and public participation on satisfaction with environmental governance and individuals' happiness in different countries at different times.

Acknowledgements. This research was funded by "Humanities and Social Science Foundation of Ministry of Education of China" (grant number 19YJCZH267) and supported by "the Fundamental Research Funds for the Central Universities" (grant number 31020170QD107), and by Major theoretical and practical research projects in the social sciences of Shaanxi Province (grant number 2019C152).

REFERENCES

[1] Cai, J., Zhang, L., Zhao, Y., Coyte, P. C. (2018): Psychological mechanisms linking county-level income inequality to happiness in China. – International Journal of Environmental Research and Public Health 15: 2667.

[2] Chen, W. (2012): How education enhances happiness: comparison of mediating factors in four east asian countries. – Social Indicators Research 106(1): 117-131.

[3] Chen, W., Yang, R. (2018): Evolving temporal-spatial trends, spatial association, and influencing factors of carbon emissions in mainland China: Empirical analysis based on provincial panel data from 2006 to 2015. – Sustainability 10(8): 2809.

[4] Coggburn, J. D., Schneider, S. K. (2003): The relationship between state government performance and state quality of life. – International Journal of Public Administration 26(12): 1337-1354.

[5] Cuñado, J., Gracia, F. (2013): Environment and happiness: New evidence for Spain. – Social Indicators Research 112(3): 549-567.

[6] Duncan, G. (2010): Should happiness-maximization be the goal of government. – Journal of Happiness Studies 11(2): 163-178.

http://www.aloki.hu ● ISSN 1589 1623 (Print) ● ISSN 1785 0037 (Online)
DOI: http://dx.doi.org/10.15666/aeer/1704_93179332

[7] Dungumaro, E. W., Madulu, N. F. (2003): Public participation in integrated water resources management: The case of Tanzania. – Physics & Chemistry of the Earth Parts A/b/c 28(20): 1009-1014.
[8] Frey, B. S., Gallus, J. (2013): Political economy of happiness. – Applied Economics 45(30): 4205-4211.
[9] Helliwell, J. F., Huang, H. (2008): How's your government? International evidence linking good government and well-being. – British Journal of Political Science 38(04): 85-108.
[10] Kelly, J. M., Swindell, D. (2002): A multiple–indicator approach to municipal service evaluation: correlating performance measurement and citizen satisfaction across jurisdictions. – Public Administration Review 62(5): 610-621.
[11] Kim, S., Kim, D. (2012): Does government make people happy: Exploring new research directions for government's roles in happiness. – Journal of Happiness Studies 13(5): 875-899.
[12] Mackerron, G., Mourato, S. (2013): Happiness is greater in natural environments. – Global Environmental Change 23(5): 992-1000.
[13] Menz, T. (2011): Do people habituate to air pollution? Evidence from international life satisfaction data. – Ecological Economics 71: 211-219.
[14] Ott, J. (2010): Greater Happiness for a greater number: Some non-controversial options for governments. – Journal of Happiness Studies 11(5): 631-647.
[15] Ott, J. C. (2011): Government and happiness in 130 nations: good governance fosters higher level and more equality of happiness. – Social Indicators Research 102(1): 3-22.
[16] Ott, J. (2015): Impact of size and quality of governments on happiness: Financial Insecurity as a key-problem in market-democracies. – Journal of Happiness Studies 16(6): 1639-1647.
[17] Parasuraman, A., Zeithaml, V. A., Berry, L. L. (1988): SERVQUAL: A multiple-item scale for measuring consumer perceptions of service quality. – Journal of Retailing 64(1): 12-40.
[18] Parasuraman, A., Berry, L. L., Zeithaml, V. A. (1991): Refinement and reassessment of the SERVQUAL scale. – Journal of Retailing 67(8): 1463-1467.
[19] Parasuraman, A., Berry, L. L., Zeithaml, V. A. (2002): Refinement and reassessment of the SERVQUAL scale. – Journal of retailing 67(4): 114.
[20] Shields, M. A., Price, S. W., Wooden, M. (2009): Life satisfaction and the economic and social characteristics of neighborhoods. – Journal of Population Economics 22(2): 421-443.
[21] Swindell, D., Kelly, J. M. (2000): Linking citizen satisfaction data to performance measures. – Public Performance & Management Review 24(1): 30-52.
[22] Tang, X. (2010): Reforms in the petition letter and visit system of China and construction of a harmonious society. – Frontiers of Law in China 5(1): 77-90.
[23] Veenhoven, R. (2010): Greater happiness for a greater number. – Journal of Happiness Studies 11(5): 605-629.
[24] Wang, M., Li, S. (2018): Understanding social governance model and a better life value from the report of 19th national congress of the communist party of China. – Chinese Public Administration (3): 60-63.
[25] Welsch, H. (2002): Preferences over prosperity and pollution: Environmental valuation based on happiness surveys. – Kyklos 55(4): 473-494.
[26] Welsch, H. (2006): Environment and happiness: Valuation of air pollution using life satisfaction data. – Ecological Economics 58(4): 801-813.
[27] Yang, R., Liao, Z. (2017): PM2.5 with five pollutants, environmental management, and tuberculosis evidence from four Chinese municipalities. – Boletín de Malariologíay Salud Ambiental 57(2): 58-70.

http://www.aloki.hu ● ISSN 1589 1623 (Print) ● ISSN 1785 0037 (Online)
DOI: http://dx.doi.org/10.15666/aeer/1704_93179332

[28] Yang, R., Chen, W. (2019): Spatial Correlation, Influencing Factors and Environmental Supervision on Mechanism Construction of Atmospheric Pollution: An Empirical Study on SO_2 Emissions in China. – Sustainability 11(6): 1742.

http://www.aloki.hu ● ISSN 1589 1623 (Print) ● ISSN 1785 0037 (Online)
DOI: http://dx.doi.org/10.15666/aeer/1704_93179332

A GREEN SUPPLY CHAIN COORDINATION CONTRACT CONSIDERING LOSS AVERSION AND CARBON EMISSIONS

LAN, C. F.

School of Economics, Fuyang Normal University, Fuyang 236037, China

Anhui Provincial Key Laboratory of Regional Logistics Planning and Modern Logistics Engineering, Fuyang 236037, China
(e-mail: lchfym@sina.com)

(Received 3rd Apr 2019; accepted 17th May 2019)

Abstract. Focusing on a two-echelon green supply chain in the context of carbon emissions, this paper sets up a Stackelberg game model of a loss-averse retailer and a risk-neutral manufacturer according to the prospect theory, solves the equilibrium ordering and green emission reduction strategies under decentralized decision-making by inverse induction, and then puts forward a cost sharing-revenue sharing contract to coordinate the supply chain. The results show that the positive/negative correlation between the retailer's optimal order quantity and the loss aversion coefficient depends on the distribution of random demand and the scale of unit shortage penalty cost; the green supply chain with loss aversion and carbon emissions can be coordinated if the retailer shares some of the manufacturer's green emission reduction cost and enjoys part of the manufacturer's profit; the parameters of the coordinate contract are constrained by the wholesale price of the manufacturer, but proper parameter values can ensure the Pareto optimization of the profits of both parties. Finally, numerical analysis shows that the proposed coordination contract can coordinate the target supply chain.
Keywords: *loss-averse, cap and trade, green emission reduction, cost sharing, revenue sharing*

Introduction

Since it was proposed by Michigan State University in 1996, green supply chain management has been emphasized and enforced by more and more governments and enterprises (Handfield et al., 1996). In China, many laws and regulations have been launched to encourage enterprises to develop clean energy and produce green products, enabling them to overcome green trade barriers in multilateral trade (Zhang, Zheng and Hu, 2019). For example, the Chinese State Council released the "Made in China 2025" strategy in May 2015, raising the concept of "green manufacturing". In March 2016, the National Development and Reform Commission issued the *Guiding Opinions on Promoting Green Consumption*, calling enterprises to promote the construction of green supply chains. Nowadays, people are increasingly aware of the importance of resources and the environment, and holding a favorable attitude towards green and low-carbon concepts. With the continued expansion of green consumers, modern enterprises are obliged to enhance the positive externalities of their products, and introduce greener products to the market. Against this backdrop, the green supply chain becomes a new hotspot in the research of supply chains.

The green supply chain has been studied extensively from multiple angles at home and abroad. For instance, Zhang and Liu (2013) created three coordination mechanisms to discuss the coordination of three-echelon green supply chain system. Xie (2015) introduced government subsidy into the analysis on the greenness and price of green supply chain products, and coordinated the supply chain with wholesale price contract and revenue sharing contract. Sheu and Chen (2012) suggested that the government should

http://www.aloki.hu ● ISSN 1589 1623 (Print) ● ISSN 1785 0037 (Online)
DOI: http://dx.doi.org/10.15666/aeer/1704_93339346

take incentives to coordinate the green supply chain. Basiri and Heydari (2017) relied on a mathematical programming model to examine the channel coordination of two-echelon green supply chains. Zhang et al. (2018) established four green supply chain game models considering the participants' fairness preference, product greenness and government subsidy, and set up a coordination model based on cost and revenue sharing contract.

With the dawn of the low-carbon era, consumers are more willing to buy green products with carbon labels (Shuai and Zhang, 2013). Meanwhile, the carbon emission trading market has been unified by the government, allowing enterprises to buy or sell emission permits in a free manner. The trading mechanism encourages the enterprises to reduce carbon emission and improve product greenness (Jing et al., 2018). As a result, more and more scholars have turned their attention to supply chain problems in the context of carbon emission. For example, Hua et al. (2011) investigated the order quantity and inventory management of enterprises under the carbon cap and trading policy. Jaber et al. (2013) looked for the optimal inventory strategy under the same conditions. Du et al. (2013) analyzed the effect of carbon cap on the coordination of a two-echelon supply chain, in which the upstream manufacturer emits carbon in the production process. Zhang, Dong and Zhang (2019) discussed the selection of supply chain strategies under such factors as carbon quota and trading mechanism, emission reduction technology and the low-carbon preference of consumers.

To sum up, there are not many reports on green supply chain in the context of carbon emissions. Most of the existing studies assume that the decision-maker is purely rational, which goes against the reality. The actual market is full of uncertainties. Hence, the members of a supply chain face various risks of loss. If the supply chain is small, the participants are often loss-averse (Li et al., 2013). The loss aversion behavior was first discussed in the prospect theory (Kahneman and Tversky, 2013). Since then, many scholars have integrated the behavior with operation management. For example, He and Zhou (2011) studied the impact of loss aversion on the portfolio model. Liu and Shum (2013) explored the effect of loss-averse consumers on enterprise pricing. Liu and Fan (2017) probed into the coordination of two-echelon supply chain considering product quality and loss aversion. Du et al. (2018) investigated the effect of loss aversion behavior on the two-echelon supply chain with random supply and demand. Samatli-Pac et al. (2018) discussed the impact of consumer loss aversion on repurchase strategies and supply chain coordination.

Obviously, the previous research has not tackled the decision-making and coordination of green supply chain that consider loss aversion behavior. To make up for this gap, this paper attempts to coordinate the green supply chain in the context of loss aversion and carbon emissions. Firstly, a Stackelberg game model was established based on the prospect theory, covering a loss-averse retailer and a risk-neutral manufacturer. Then, the equilibrium ordering and green emission reduction strategies were solved under the decentralized decision-making mode, and the effect of the retailer's loss aversion behavior on the optimal order quantity was analyzed in detail. Finally, a cost sharing-revenue sharing contract was designed to coordinate the said supply chain.

Materials and methods

Problem description

This paper targets a two-echelon green supply chain consisting of a risk-neutral manufacturer and a loss-averse retailer. The manufacturer is assumed as the leader in

http://www.aloki.hu ● ISSN 1589 1623 (Print) ● ISSN 1785 0037 (Online)
DOI: http://dx.doi.org/10.15666/aeer/1704_93339346

the market and the retailer, a follower. The two parties are in a Stackelberg game of complete information. The manufacturer first determines the green emission reduction level θ of a product, and then the retailer decides on the order quantity q of the product. Let w and c be the unit wholesale price and the unit production cost of the manufacturer, respectively, and p, v and g be the unit retail price, unit salvage value and unit shortage cost of the retailer, respectively. Here, it is assumed that $p > w > c > v$.

Hypothesis 1: The manufacturer, as the subject of carbon emissions, receives a free carbon quota E from the government. Under the carbon cap and trading policy, the enterprise needs to purchase emission permit in the carbon trading market if it emits more carbon than the quota; otherwise, the enterprise can sell the surplus permit. The unit transaction price p_t is exogenous. Without emission reduction technology, i.e. $\theta = 0$, the amount of carbon emitted by the manufacturer is denoted as e; after adopting the technology, that amount is reduced to $(1-\theta)e$. Here, θ $(0 \leq \theta < 1)$ refers to the emission reduction efficiency of the manufacturer.

Hypothesis 2: In commodity trading, the greenness of a product is often described by the energy rating label, the carbon label, the content of harmful substances, and the recyclability of the parts. Thus, the product greenness can be observed and calculated. To make its products greener, the manufacturer should step up its R&D investment on green emission reduction. Inspired by the investment cost model, this paper depicts the emission reduction cost with the quadratic cost function: $H(\theta) = 0.5\alpha\theta^2$, where α is the green emission reduction cost.

Hypothesis 3: The market demand of a product is stochastic and depends on product greenness. The market demand function of a product is assumed as *Equation 1*.

$$D(\theta) = A + B\theta + \varepsilon = y(\theta) + \varepsilon \quad \text{(Eq.1)}$$

where A is the market demand, B is the green preference of consumers, and ε is a continuous random variable in the interval $[M, N]$. The cumulative distribution function and probability density function of the variable are denoted as $F(\varepsilon)$ and $f(\varepsilon)$, respectively.

Under the above hypotheses, the retailer's and manufacturer's profit functions for fulfilling any demand x can be respectively expressed as *Equations 2* and *3*.

$$\pi_r(q) = pmin(q, D) + v(q-D)^+ - g(D-q)^+ - wq = \begin{cases} (p-v)x + (v-w)q, & x < q \\ (p-w+g)q - gx, & x \geq q \end{cases} \quad \text{(Eq.2)}$$

$$\pi_m(\theta) = (w-c)q + p_t[E - (1-\theta)e] - \frac{1}{2}\alpha\theta^2 \quad \text{(Eq.3)}$$

Decision-making model based on loss aversion

Considering the loss aversion of the retailer, the simple piecewise linear function was introduced to describe the decision-maker (Kahneman and Tversky, 2013). Let π be the profit of the decision-maker. Then, the utility function of the decision-maker can be defined as *Equation 4*.

$$U(\pi) = \begin{cases} \pi, & \pi \geq 0, \\ \lambda\pi, & \pi < 0. \end{cases} \quad \text{(Eq.4)}$$

http://www.aloki.hu ● ISSN 1589 1623 (Print) ● ISSN 1785 0037 (Online)
DOI: http://dx.doi.org/10.15666/aeer/1704_93339346

The retailer's expected utility was discussed under two conditions.

Lemma 1 (i) If $x < q$ and $\pi_1 = (p-v)x + (v-w)q = 0$ is the retailer's profit function, then the breakeven point of the demand is $x_1 = \frac{(w-v)q}{p-v}$, i.e. the retailer makes no profit when the demand $x = \frac{(w-v)q}{p-v}$, makes profit when $x > \frac{(w-v)q}{p-v}$, and suffers losses when $x < \frac{(w-v)q}{p-v}$. In this case, the retailer's expected utility is $E[U(\pi_1)] = \lambda \int_M^{x_1-y(\theta)} \pi_1 f(\varepsilon)\, d\varepsilon + \int_{x_1-y(\theta)}^{q-y(\theta)} \pi_1 f(\varepsilon)\, d\varepsilon$.

(ii) If $x \geq q$ and $\pi_2 = (p-w+g)q - gx = 0$ is the retailer's profit function, then the breakeven point of the demand is $x_2 = \frac{(p-w+g)q}{g}$, i.e. the retailer makes no profit when the demand $x = \frac{(p-w+g)q}{g}$, makes profit when $x > \frac{(p-w+g)q}{g}$, and suffers losses when $x < \frac{(p-w+g)q}{g}$. In this case, the retailer's expected utility is $E[U(\pi_2)] = \int_{q-y(\theta)}^{x_2-y(\theta)} \pi_2 f(\varepsilon)\, d\varepsilon + \lambda \int_{x_2-y(\theta)}^{N} \pi_2 f(\varepsilon)\, d\varepsilon$.

According to Lemma 1, the retailer's expected utility can be described as *Equation 5*.

$$E\left[U\left(\pi_r(q)\right)\right] = E\left[U\left(\pi_1\right)\right] + E\left[U\left(\pi_2\right)\right] = \lambda \int_M^{x_1-y(\theta)} \pi_1 f(\varepsilon) d\varepsilon + \int_{x_1-y(\theta)}^{q-y(\theta)} \pi_1 f(\varepsilon) d\varepsilon + \int_{q-y(\theta)}^{x_2-y(\theta)} \pi_2 f(\varepsilon) d\varepsilon + \lambda \int_{x_2-y(\theta)}^{N} \pi_2 f(\varepsilon) d\varepsilon = E\left(\pi_r(q)\right) + (\lambda - 1)\left[\int_M^{x_1-y(\theta)} \pi_1 f(\varepsilon) d\varepsilon + \int_{x_{2-y(\theta)}}^{N} \pi_2 f(\varepsilon) d\varepsilon\right] \quad \text{(Eq.5)}$$

where $E(\pi_r(q)) = \int_M^{q-y(\theta)} \pi_1 f(\varepsilon)\, d\varepsilon + \int_{q-y(\theta)}^{N} \pi_2 f(\varepsilon)\, d\varepsilon$ is the expected utility of risk-neutral retailer.

Equation 5 means the expected utility of loss-averse retailer equals the expected profit plus the total expected underage and overage losses, biased by a factor of $\lambda - 1$. Note that $\lambda - 1$ is the loss aversion factor. In particular, when $\lambda = 1$, the second term on the right side of the equation disappears. In this case, the retailer's expected utility equals the expected profit, that is, the retailer is risk-neutral.

The decision-making problem of a loss-averse retailer and a risk-neutral manufacturer can be respectively expressed as *Equations 6* and *7*.

$$max_{q>0}\, E\left[U(\pi_r(q))\right] \quad \text{(Eq.6)}$$

$$max_{0\leq\theta<1}\, \pi_m(\theta) \quad \text{(Eq.7)}$$

Optimal strategy in decentralized mode

Under decentralized decision-making, the manufacturer and the retailer only consider their own profits (utilities) and make decisions independently. As the leader of the Stackelberg game, the manufacturer first determines the green emission reduction level

http://www.aloki.hu ● ISSN 1589 1623 (Print) ● ISSN 1785 0037 (Online)
DOI: http://dx.doi.org/10.15666/aeer/1704_93339346

θ of a product, and then the retailer, as the follower, decides on the order quantity q of the product. By inverse induction, the author calculated the optimal order quantity q_λ^* of the loss-averse retailer before deriving the optimal green input level θ^* of the manufacturer.

Theorem 1: $E\left[U\left(\pi_r(q)\right)\right]$ is a strict concave function with respect to q, and $\max_{q>0} E\left[U\left(\pi_r(q)\right)\right]$ has a unique optimal solution q_λ^* that satisfies *Equation 8*.

$$\int_{\frac{(w-v)q}{p-v}-y(\theta)}^{q-y(\theta)}(v-w)f(\varepsilon)d\varepsilon+\int_{q-y(\theta)}^{\frac{(p-w+g)q}{g}-y(\theta)}(p-w+g)f(\varepsilon)d\varepsilon+$$
$$\lambda\left[\int_{M}^{\frac{(w-v)q}{p-v}-y(\theta)}(v-w)f(\varepsilon)d\varepsilon+\int_{\frac{(p-w+g)q}{g}-y(\theta)}^{N}(p-w+g)f(\varepsilon)d\varepsilon\right]=0 \quad \text{(Eq.8)}$$

Proof: Substituting π_1, π_2, x_1 and x_2 into *Equation 5*, we have:

$$E\left[U\left(\pi_r(q)\right)\right]=\lambda\int_{M}^{\frac{(w-v)q}{p-v}-y(\theta)}\left\{(p-v)\left[y(\theta)+\varepsilon\right]+(v-w)q\right\}f(\varepsilon)d\varepsilon+$$
$$\int_{\frac{(w-v)q}{p-v}-y(\theta)}^{q-y(\theta)}\left\{(p-v)\left[y(\theta)+\varepsilon\right]+(v-w)q\right\}f(\varepsilon)d\varepsilon+$$
$$\int_{q-y(\theta)}^{\frac{(p-w+g)q}{g}-y(\theta)}\left\{(p-w+g)q-g\left[y(\theta)+\varepsilon\right]\right\}f(\varepsilon)d\varepsilon+ \quad \text{(Eq.9)}$$
$$\lambda\int_{\frac{(p-w+g)q}{g}-y(\theta)}^{N}\left\{(p-w+g)q-g\left[y(\theta)+\varepsilon\right]\right\}f(\varepsilon)d\varepsilon$$

Then, the first- and second-order derivatives of *Equation 9* relative to q can be obtained as *Equations 10* and *11*.

$$\frac{dE\left[U(\pi_r(q))\right]}{dq}=\int_{\frac{(w-v)q}{p-v}-y(\theta)}^{q-y(\theta)}(v-w)f(\varepsilon)\,d\varepsilon+\int_{q-y(\theta)}^{\frac{(p-w+g)q}{g}-y(\theta)}(p-w+g)f(\varepsilon)\,d\varepsilon+$$
$$\lambda\left[\int_{M}^{\frac{(w-v)q}{p-v}-y(\theta)}(v-w)f(\varepsilon)\,d\varepsilon+\int_{\frac{(p-w+g)q}{g}-y(\theta)}^{N}(p-w+g)f(\varepsilon)\,d\varepsilon\right] \quad \text{(Eq.10)}$$
$$\frac{d^2E[U(\pi_r)]}{dq^2}=-(p-v+g)f\left(q-y(\theta)\right)-\frac{\lambda-1}{(p-v)g}$$

$$\left[g(w-v)^2f\left(\frac{(w-v)q}{p-v}-y(\theta)\right)+(p-v)(p-w+g)^2f\left(\frac{(p-w+g)q}{g}-y(\theta)\right)\right] \quad \text{(Eq.11)}$$

http://www.aloki.hu ● ISSN 1589 1623 (Print) ● ISSN 1785 0037 (Online)
DOI: http://dx.doi.org/10.15666/aeer/1704_93339346

Since $p > v$ and $\lambda \geq 1$, we have $\frac{d^2E[U(\pi_r)]}{dq^2} < 0$, indicating that $E\left[U\left(\pi_r(q)\right)\right]$ is a strict concave function with respect to q. Considering the first-order condition $\frac{dE\left[U\left(\pi_r(q)\right)\right]}{dq} = 0$, it can be seen that the unique optimal solution q_λ^* of loss-averse retailer satisfies *Equation 8*.

If the retailer is risk-neutral, i.e. $\lambda = 1$, then *Equation 8* can be rewritten as *Equation 12*.

$$\int_M^{q-y(\theta)} f(\varepsilon)\, d\varepsilon = \frac{p-w+g}{p-v+g} \tag{Eq.12}$$

Therefore, the optimal order quantity of risk-neutral retailer $q_1^* = F^{-1}\left(\frac{p-w+g}{p-v+g}\right) + y(\theta)$.

The effect of loss aversion of the retailer on the optimal order quantity can be summed up as Property 1 below.

Property 1: If $(w-v)F\left(x_1 - y(\theta)\right) + (p-w+g)F\left(x_2 - y(\theta)\right) < (p-w+g)$, then $\frac{dq_\lambda^*}{d\lambda} > 0$; if $(w-v)F\left(x_1 - y(\theta)\right) + (p-w+g)F\left(x_2 - y(\theta)\right) = (p-w+g)$, then $\frac{dq_\lambda^*}{d\lambda} = 0$; if $(w-v)F\left(x_1 - y(\theta)\right) + (p-w+g)F\left(x_2 - y(\theta)\right) > (p-w+g)$, then $\frac{dq_\lambda^*}{d\lambda} < 0$.

Proof: The following *Equation 13* can be derived from the implicit function theorem:

$$\frac{dq_\lambda^*}{d\lambda} = \frac{\frac{\partial^2 E[U(\pi_r)]}{\partial q \partial \lambda}}{\frac{\partial^2 E[U(\pi_r)]}{\partial q^2}} = \frac{(p-w+g) - (w-v)F\left(x_1 - y(\theta)\right) - (p-w+g)F\left(x_2 - y(\theta)\right)}{\frac{\partial^2 E[U(\pi_r)]}{\partial q^2}} \tag{Eq.13}$$

Besides, *Equation 11* shows that $\frac{\partial^2 E[U(\pi_r)]}{\partial q^2} < 0$. Thus, the sign of $\frac{dq_\lambda^*}{d\lambda}$ is opposite to the positivity/negativity of $(p-w+g) - (w-v)F\left(x_1 - y(\theta)\right) - (p-w+g)F\left(x_2 - y(\theta)\right)$. Q.E.D.

Property 1 indicates that the optimal order quantity of loss-averse retailer is closely related to the demand distribution and the unit shortage cost. Without considering shortage cost, i.e. $g = 0$, we have $x_2 - y(\theta) \to +\infty$. Thus, the condition $(w-v)F\left(x_1 - y(\theta)\right) + (p-w)F\left(x_2 - y(\theta)\right) > (p-w)$ is always valid. Under this condition, the retailer's order quantity decreases with the growth of the loss aversion coefficient λ and has nothing to do with the random distribution of the market demand. If shortage cost is considered, any of the three conditions of Property 1 is possible, depending on the distribution of the random market demand. In this case, the relationship between the optimal order quantity of the retailer and the loss aversion coefficient λ is determined by the distribution of the random market demand.

Consider the manufacturer's optimal green emission reduction strategy, the manufacturer's expected profit function can be derived from *Equation 3:*

$$E[\pi_m(\theta)] = (w-c)q + p_t[E - (1-\theta)e] - \frac{1}{2}\alpha\theta^2 \tag{Eq.14}$$

http://www.aloki.hu ● ISSN 1589 1623 (Print) ● ISSN 1785 0037 (Online)
DOI: http://dx.doi.org/10.15666/aeer/1704_93339346

Since $\frac{d^2E[\pi_m(\theta)]}{d\theta^2} = -\alpha < 0$, the optimal green emission reduction level of risk-neutral manufacturer can be obtained by finding the first-order derivative of *Equation 14* relative to θ:

$$\theta^* = \frac{p_t e}{\alpha} \quad \text{(Eq.15)}$$

It can be seen from *Equation 15* that, under decentralized decision-making, the optimal green emission reduction level of the manufacturer is positively correlated with the unit carbon transaction price in the market and the carbon emission of product, negatively correlated with the green cost coefficient of the product, but not related to the retailer's order quantity.

Optimal strategy in centralized mode

Under centralized decision-making, the overall profit of the supply chain can be expressed as *Equation 16*.

$$\pi_{mr}(q,\theta) = pmin(q,D) + v(q-D)^+ - g(D-q)^+ - cq + p_t\left[E-(1-\theta)e\right] - \frac{1}{2}\alpha\theta^2 = \begin{cases} (p-v)x + (v-c)q + p_t\left[E-(1-\theta)e\right] - \frac{1}{2}\alpha\theta^2, & x < q \\ (p-c+g)q - gx + p_t\left[E-(1-\theta)e\right] - \frac{1}{2}\alpha\theta^2, & x \geq q \end{cases} \quad \text{(Eq.16)}$$

The mathematical expectation of the above equation can be obtained as *Equation 17*.

$$E[\pi_{mr}(q,\theta)] = \int_M^{q-y(\theta)} \left\{(p-v)[y(\theta)+\varepsilon] + (v-c)q + p_t[E-(1-\theta)e] - \frac{1}{2}\alpha\theta^2\right\} f(\varepsilon)\,d\varepsilon + \int_{q-y(\theta)}^{N} \left\{(p-c+g)q - g[y(\theta)+\varepsilon] + p_t[E-(1-\theta)e] - \frac{1}{2}\alpha\theta^2\right\} f(\varepsilon)d\varepsilon = (p-v+g)\int_M^{q-y(\theta)}[y(\theta)+\varepsilon]f(\varepsilon)\,d\varepsilon - (p-v+g)qF(q-y(\theta)) + (p-c+g)q - g[y(\theta)+\mu] + p_t [E-(1-\theta)e] - \frac{1}{2}\alpha\theta^2 \quad \text{(Eq.17)}$$

The partial derivatives of *Equation 17* can be computed as *Equations 18–20*.

$$\frac{\partial^2 E[\pi_{mr}(q,\theta)]}{\partial q^2} = -(p-v+g)f(q-y(\theta)) \quad \text{(Eq.18)}$$

$$\frac{\partial^2 E[\pi_{mr}(q,\theta)]}{\partial q\partial\theta} = (p-v+g)Bf(q-y(\theta)) \quad \text{(Eq.19)}$$

$$\frac{\partial^2 E[\pi_{mr}(q,\theta)]}{\partial \theta^2} = -B^2(p-v+g)f(q-y(\theta)) - \alpha \quad \text{(Eq.20)}$$

http://www.aloki.hu ● ISSN 1589 1623 (Print) ● ISSN 1785 0037 (Online)
DOI: http://dx.doi.org/10.15666/aeer/1704_93339346

Combining *Equations 18–20*, the determinant of the Hessian matrix for the expected profit of the supply chain in the centralized mode can be obtained as *Equation 21*.

$$\begin{vmatrix} \frac{\partial^2 E[\pi_{mr}(q,\theta)]}{\partial q^2} & \frac{\partial^2 E[\pi_{mr}(q,\theta)]}{\partial q \partial \theta} \\ \frac{\partial^2 E[\pi_{mr}(q,\theta)]}{\partial \theta \partial q} & \frac{\partial^2 E[\pi_{mr}(q,\theta)]}{\partial \theta^2} \end{vmatrix} = \alpha(p-v+g)f\big(q-y(\theta)\big) > 0 \qquad \text{(Eq.21)}$$

whereas $\frac{\partial^2 E[\pi_{mr}(q,\theta)]}{\partial q^2} < 0$, $E[\pi_{mr}(q,\theta)]$ is a concave relative to both q and θ. Hence, there exists a unique optimal combination of solutions (q^0,θ^0), such that the overall profit of the supply chain reaches the maximum. Let $\frac{\partial E[\pi_{mr}(q,\theta)]}{\partial q} = 0$ and $\frac{\partial E[\pi_{mr}(q,\theta)]}{\partial \theta} = 0$. The optimal solutions of the supply chain can be obtained as *Equation 22*.

$$\begin{cases} q^0 = F^{-1}\left(\frac{p-c+g}{p-v+g}\right) + y(\theta) \\ \theta^0 = \frac{(p-c)B+p_t e}{\alpha} \end{cases} \qquad \text{(Eq.22)}$$

Equation 22 shows that $\theta^0 = \frac{(p-c)B+p_t e}{\alpha} > 0$. Since (q^0,θ^0) is the unique optimal combination of solutions to the entire supply chain, we have $E[\pi_{mr}(q^0,\theta^0)] > E[\pi_{mr}(q^0,0)]$.

Therefore, it can be concluded that the supply chain profit can be improved by increasing the product greenness under centralized decision-making, as the carbon quota is laid down by the government and the environmental awareness is growing among consumers. In other words, green products can bring more profits.

Under decentralized decision-making, the manufacturer and the retailer are actually implementing the wholesale price contract. Comparing *Equation 8*, *Equation 15* and *Equation 22*, it can be seen that the green supply chain considering carbon emissions and loss aversion cannot be coordinated under this contract. This calls for a rational and effective contract that ensures the coordination of the supply chain.

Results and discussion

Coordination contract

The previous analysis shows that the green supply chain considering carbon emissions and loss aversion cannot be coordinated under the wholesale price contract. The main reason lies in the fact, under the decentralized decision-making, the manufacturer needs to bear all the cost of green emission reduction but only receives part of the supply chain profit, while the retailer needs to bear all the inventory cost of the entire supply chain induced by oversupply. As a result, the manufacturer is reluctant to improve product greenness, and the retailer is conservative about the order quantity, aiming to reduce the risk. To improve product quality, reduce oversupply risk and achieve supply chain coordination, this paper modifies the traditional revenue sharing contract into a cost sharing-revenue sharing contract $\{k, \varphi\}$, in which the retailer bears (1- k) ($0 < k < 1$) of the manufacturer's green emission reduction cost and receives

http://www.aloki.hu ● ISSN 1589 1623 (Print) ● ISSN 1785 0037 (Online)
DOI: http://dx.doi.org/10.15666/aeer/1704_93339346

$\varphi(0 < \varphi < 1)$ of the sales profit. Under this contract, the expected profits of the retailer and the manufacturer can be respectively expressed as *Equations 23* and *24*.

$$\pi_r(q,\theta,k,\varphi) = \varphi\left[pmin(q,D) + v(q-D)^+ - g(D-q)^+\right] - wq - \frac{1}{2}\alpha(1-k)\theta^2 \quad \text{(Eq.23)}$$

$$\begin{aligned}\pi_m(q,\theta,k,\varphi) &= (1-\varphi)\left[pmin(q,D) + v(q-D)^+ - g(D-q)^+\right] \\ &+ (w-c)q + p_t\left[E-(1-\theta)e\right] - \frac{1}{2}\alpha k\theta^2\end{aligned} \quad \text{(Eq.24)}$$

According to *Equations 23* and *24*, the contract $\{k, \varphi\}$ only includes transfer payment within the supply chain. The total profit of the two parties is still equal to the result of *Equation 16*.

Similar to the proof of Theorem 1, the following result can be derived from *Equation 23*.

Theorem 2. Under the cost-and-revenue sharing contract, for any $0 \le \theta < 1$, the expected utility of the loss-averse retailer $E\left[U\left(\pi_r(q,\theta,k,\varphi)\right)\right]$ is a concave function relative to q, and $max_{q>0}\, E\left[U\left(\pi_r(q,\theta,k,\varphi)\right)\right]$ has a unique optimal solution q^{λ} that satisfies *Equation 25*.

$$\begin{aligned}&\int_{x_3-y(\theta)}^{q-y(\theta)} (\varphi v - w) f(\varepsilon) d\varepsilon + \int_{q-y(\theta)}^{x_4-y(\theta)} (\varphi p - w + \varphi g) f(\varepsilon) d\varepsilon + \\ &\lambda\left[\int_{M}^{x_3-y(\theta)} (\varphi v - w) f(\varepsilon) d\varepsilon + \int_{x_4-y(\theta)}^{N} (\varphi p - w + \varphi g) f(\varepsilon) d\varepsilon\right] = 0\end{aligned} \quad \text{(Eq.25)}$$

where $x_3 = \frac{wq - \varphi vq - \frac{1}{2}\alpha(1-k)\theta^2}{\varphi(p-v)}$ and $x_4 = \frac{\varphi(p+g)q - wq - \frac{1}{2}\alpha(1-k)\theta^2}{\varphi g}$.

Finding the expectation of *Equation 24*, the expected profit function of the manufacturer can be obtained as *Equation 26*.

$$\begin{aligned}&E\left[\pi_m(q,\theta,k,\varphi)\right] = (1-\varphi)(p-v+g)\int_{M}^{q-y(\theta)} \left[y(\theta)+\varepsilon\right] f(\varepsilon) d\varepsilon - \\ &(1-\varphi)(p-v+g)qF\left(q-y(\theta)\right) + \left[(1-\varphi)(p+g) + w - c\right]q - \\ &(1-\varphi)g\left[y(\theta)+\mu\right] + p_t\left[E-(1-\theta)e\right] - \frac{1}{2}\alpha k\theta^2\end{aligned} \quad \text{(Eq.26)}$$

The above equation shows that, for any $q > 0$, $max_{0\le\theta<1}\, E[\pi_m(q,\theta,k,\varphi)]$ has a unique optimal solution θ^{λ} that satisfies *Equation 27*.

$$\theta = \frac{B(1-\varphi)(p-v+g)F\left(q-y(\theta)\right) - (1-\varphi)Bg + p_t e}{\alpha k} \quad \text{(Eq.27)}$$

http://www.aloki.hu ● ISSN 1589 1623 (Print) ● ISSN 1785 0037 (Online)
DOI: http://dx.doi.org/10.15666/aeer/1704_93339346

Next, the author analyzed how the cost-and-revenue sharing contract coordinates the green supply chain considering carbon emission and loss aversion. Firstly, the manufacturer, as the leader of the Stacklberg game, can set proper parameter values $\{k, \varphi\}$ according to the known loss aversion level λ of the retailer, forcing the retailer to choose the optimal ordering strategy $q^{\lambda} = q^{0} = F^{-1}\left(\frac{p-c+g}{p-v+g}\right) + y(\theta)$, i.e. $q^{\lambda} = q^{0}$ satisfying *Equation 25*. Then, it can be seen that $\theta = \frac{(1-\varphi)(p-c)B+p_t e}{\alpha k}$ by substituting $q = q^{0}$ into *Equation 27*. Compared with *Equation 22*, it is learned that the value of *k* must equal $\frac{(1-\varphi)(p-c)B+p_t e}{(p-c)B+p_t e}$ under the coordination contract.

Note that the manufacturer's profit must not fall below the profit in decentralized decision-making. Otherwise, it will not actively participate in the cost-and-revenue sharing contract. In other words, the wholesale price per unit of product *w* must satisfy the following set of *Equation 28*.

$$\begin{cases} \frac{\partial E[U(\pi_r(q,\theta,k,\varphi))]}{\partial q}\Big|_{q^{\lambda}=q^{0},\theta^{\lambda}=\theta^{0}} = 0 \\ \frac{\partial E[\pi_m(q,\theta,k,\varphi)]}{\partial \theta}\Big|_{q^{\lambda}=q^{0},\theta^{\lambda}=\theta^{0}} = 0 \\ E[\pi_m(q,\theta,k,\varphi)]\big|_{q^{\lambda}=q^{0},\theta^{\lambda}=\theta^{0}} = \delta \end{cases} \quad \text{(Eq.28)}$$

where δ is any constant that is no smaller than $E[\pi_m(\theta^*)]$. The overall profit of the supply chain can be allocated elastically between the retailer and the manufacturer by adjusting the value of δ. The allocation depends on the bargaining power of the two parties. Moreover, there should also be an upper limit to the wholesale price. Otherwise, there will be no solution to the contract parameters, making the contract meaningless. In particular, when δ satisfies $0 < \delta - E[\pi_m(\theta^*)] < E[\pi_{mr}(q^0,\theta^0)] - E[\pi_r(q^*)]$, the overall profit of the supply chain is optimized, and both the manufacturer and the retailer are expected to receive more profit than the decentralized decision-making. Thus, the two parties can receive Pareto optimal profits under certain conditions, using the proposed cost-revenue sharing contract.

Considering the different decision-making goals between loss aversion and risk neutrality, the above cost-revenue sharing contract fulfills three conditions: maximizing the overall profit of the supply chain; maximizing the expected utility of the loss-averse party (retailer); ensuring that the expected profit of the risk-neutral party (manufacturer) is no less than its retained profit. Through reasonable parameter design, both members of the supply chain will be encouraged to actively participate in this cost-revenue sharing contract.

Numerical examples

The above model was subjected to numerical experiments on the Matlab. Firstly, the loss-averse retailer and the risk-neutral manufacturer were compared in terms of the decision variables and expected profits (utilities) under different decision-making modes, aiming to verify the effectiveness of the proposed coordination contract. After that, the author carried out a sensitivity analysis on the parameters of the decentralized model, e.g. loss aversion coefficient and wholesale price, to see their impacts on the optimal order quantity of the retailer. The market demand was assumed as

http://www.aloki.hu ● ISSN 1589 1623 (Print) ● ISSN 1785 0037 (Online)
DOI: http://dx.doi.org/10.15666/aeer/1704_93339346

$D(\theta) = 50 + 4\theta + \varepsilon$, with $\varepsilon \sim U[-50,50]$ and $H(\theta) = 0.5 \times 200\theta^2$. The other parameters are listed in *Table 1*.

Table 1. *Parameter settings*

Parameter	p	w	c	g	v	p_t	e	E	λ	k	φ	μ
Value	45	20	15	5	10	5	10	8	1.2	0.37	0.89	841

The above model was adopted to calculate the optimal decision variables and the expected profits (utilities) of the retailer, the manufacturer and the supply chain under three conditions, namely, centralized decision-making, decentralized decision-making and the cost-and-revenue-sharing contract. The calculated results are shown in *Table 2*.

Table 2. *Comparison of optimal decision variables and expected profits (utilities) under different decision-making modes*

Decision-making mode	q	θ	$\pi_r(q)$	$E[U(\pi_r)]$	π_m	π_{mr}
Centralized decision-making	91	0.85	—	—	—	1584
Decentralized decision-making	74	0.25	686	572	366	1052
Coordination contract	91	0.85	743	604	841	1584

As shown in *Table 2*, the retailer's order quantity was 18.7% smaller under decentralized decision-making than under centralized decision-making, owing to the double marginalization effect. After introducing the cost-and-revenue sharing contract, the expected profit of the entire supply chain reached that under the centralized decision-making, the manufacturer saw its green emission reduction level increasing from 0.25 (decentralized decision-making) to 0.85 (centralized decision-making) and expected profit growing by nearly 1.3 times, and the retailer witnessed a 5.6% increase in expected utility and an 8.3% growth in expected profit from the levels under centralized decision-making. Therefore, the proposed coordination contract both improves the expected profit of the entire supply chain and achieves the Pareto optimization of the profits (utilities) of the manufacturer and the retailer. Both parties of the supply chain will be incentivized to conclude such a contract.

Next, the loss aversion behavior and purchase price were subjected to sensitivity analysis, aiming to disclose their impacts on the retailer's optimal order quantity. Relevant numerical experiments were carried out with the loss aversion coefficient λ and the wholesale price w as variables. The experimental results are presented in *Figures 1* and *2*.

As shown in *Figure 1,* the retailer's optimal order quantity decreased with the increase of the loss aversion coefficient. It can be seen from Property 1 that the third condition is always satisfied under the uniform distribution of the random market demand. In this case, the retailer's order quantity is negatively correlated with the loss aversion coefficient, and the overage cost is greater than the shortage cost. To avoid losses, the loss-averse retailer will cut down the order quantity.

As shown in *Figure 2,* the retailer's optimal order quantity dropped almost linearly with the rising purchase price. This trend can be attributed to the following reasons. When the retail price is exogenous, the retailer will receive less profit per unit of

http://www.aloki.hu ● ISSN 1589 1623 (Print) ● ISSN 1785 0037 (Online)
DOI: http://dx.doi.org/10.15666/aeer/1704_93339346

product with the growth in the unit product wholesale price; the rising purchase cost will indirectly push up the overage capacity cost. To minimize its loss, the loss-averse retailer cannot but reduce the order quantity.

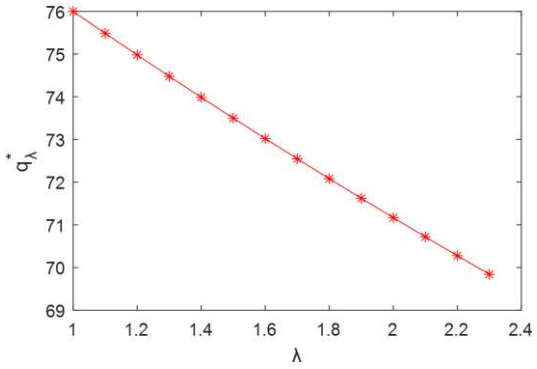

Figure 1. *Effect of loss aversion level on optimal order quantity*

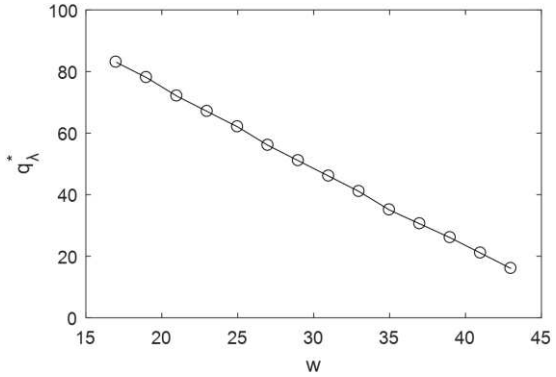

Figure 2. *Effect of wholesale price on optimal order quantity*

Conclusions

This paper explores the coordination of a two-echelon green supply chain, consisting of a loss-averse retailer and a risk-neutral manufacturer, in the context of carbon emissions. Considering the loss aversion of the retailer, the objective function was set up by the prospect theory. On this basis, a Stackelberg game model was constructed under decentralized decision-making, and the manufacturer's optimal green emission reduction decision and the retailer's optimal order quantity were solved by inverse induction. The results were compared with those under the optimal decision of the supply chain under centralized decision-making. Then, a cost-and-revenue sharing coordination contract was designed to ensure the Pareto optimization of the profits (utilities) of both parties under the loss-averse decision goal.

The above conclusions were drawn based on the revenue sharing contract. The future research will extend the research problem to discuss other coordination mechanisms (e.g. flexible quantity contract, buy-back contract and price discount contract). To make our model more realistic, the loss aversion of the manufacturer will be added, and multiple manufacturers and retailers will be considered.

http://www.aloki.hu ● ISSN 1589 1623 (Print) ● ISSN 1785 0037 (Online)
DOI: http://dx.doi.org/10.15666/aeer/1704_93339346

Acknowledgements. The author gratefully acknowledges financial support from the Key Project of Humanities and Social Science Research in Colleges and Universities in Anhui Province (SK2018A0274) and the General Project of Foreign Visits and Training of Outstanding Young and Cadre Talents in Colleges and Universities (gxgwfx2018060) and the Key project of the Youth Talent Funds of Fuyang Normal University (rcxm201708).

REFERENCES

[1] Basiri, Z., Heydari, J. (2017): A mathematical model for green supply chain coordination with substitutable products. – Journal of Cleaner Production 145: 232-249.
[2] Du, S., Zhu, L., Liang, L., Ma, F. (2013): Emission-dependent supply chain and environment-policy-making in the 'cap-and-trade' system. – Energy Policy 57: 61-67.
[3] Du, S., Zhu, Y., Nie, T., Yu, H. (2018): Loss-averse preferences in a two-echelon supply chain with yield risk and demand uncertainty. – Operational Research 18(2): 361-388.
[4] Handfield, R. B., Walton, S. V., Melnyk, S. A. (1996): Green supply chain: best practices from the furniture industry. – Proceedings, Annual Meeting of the Decision Science Institute USA 3: 1295-1297.
[5] He, X. D., Zhou, X. Y. (2011): Portfolio choice under cumulative prospect theory: An analytical treatment. – Management Science 57(2): 315-331.
[6] Hua, G., Cheng, T. C. E., Wang, S. (2011): Managing carbon footprints in inventory management. – International Journal of Production Economics 132(2): 178-185.
[7] Jaber, M. Y., Glock, C. H., El Saadany, A. M. A. (2013): Supply chain coordination with emissions reduction incentives. – International Journal of Production Research 51(1): 69-82.
[8] Jing, Y., Meng, Y., Qin, K. (2018): Research on coordination contract for green supply chain with carbon emission under stochastic demand. – Science & Technology and Economics 31(6): 106-110.
[9] Kahneman, D., Tversky, A. (2013): Prospect Theory: An Analysis of Decision under Risk. – In: Maclean, L. C., Ziemba, W. T. (eds.) Handbook of the Fundamentals of Financial Decision Making, Part I. World Scientific, New Jersey, pp. 99-127.
[10] Li, J., Zhou, Y., Xiao, D., Zhong, Y. (2013): Revenue-sharing contract in supply chains with single supplier and multiple loss-averse retailers. – Journal of Management Sciences in China 16(2): 71-82.
[11] Liu, Q., Shum, S. (2013): Pricing and capacity rationing with customer disappointment aversion. – Production and Operations Management 22(5): 1269-1286.
[12] Liu, Y., Fan, Z. (2017): Supply chain coordination contract model considering loss aversion and quality level. – Chinese Journal of Management Science 25(1): 65-77.
[13] Samatli-Pac, G., Shen, W., Hu, X. (2018): The Impact of consumer loss aversion on returns policies and supply chain coordination. – International Journal of Operations Research and Information Systems 9(4): 1-20.
[14] Sheu, J. B., Chen, Y. J. (2012): Impact of government financial intervention on competition among green supply chains. – International Journal of Production Economics 138(1): 201-213.
[15] Shuai, C., Zhang, Y. (2013): Variance analysis of consumers' willingness to pay for low-carbon products in China based on scenario experiment with carbon labeling. – China Soft Science 7: 61-70.
[16] Xie, G. (2015): Modeling decision processes of a green supply chain with regulation on energy saving level. – Computers & Operations Research 54: 266-273.
[17] Zhang, C., Zheng, B., Hu, C. (2019): Research on quantitative analysis and coordination of green supply chain management. – Logistics Engineering and Management 41(2): 1-4.

http://www.aloki.hu ● ISSN 1589 1623 (Print) ● ISSN 1785 0037 (Online)
DOI: http://dx.doi.org/10.15666/aeer/1704_93339346

[18] Zhang, C. T., Liu, L. P. (2013): Research on coordination mechanism in three-level green supply chain under non-cooperative game. – Applied Mathematical Modelling 37(5): 3369-3379.
[19] Zhang, H., Huang, J., Cui, Y. (2018): Game models and contract of green supply chain considering fairness preference and government subsidies. – Journal of Industrial Technological and Economics 37(1): 111-12.
[20] Zhang, L., Dong, K., Zhang, R. (2019): Supply chain coordinated ordering and pricing model based on carbon cap-and-trade. – Chinese Journal of Management Science 27(1): 63-72.

http://www.aloki.hu ● ISSN 1589 1623 (Print) ● ISSN 1785 0037 (Online)
DOI: http://dx.doi.org/10.15666/aeer/1704_93339346

IMPACTS OF TOURISM DEVELOPMENT AND TOURIST ACTIVITIES ON ENVIRONMENT IN SCENIC ECOTOURISM SPOTS

LIU, L.[1,2] – KONG, L.[3,4] – FENG, Y. X.[1,2*] – QIN, D. D.[1] – MAO, N.[1]

[1]*School of Art and Design of Zheng Zhou University of Light Industry Zhengzhou 450002, China*

[2]*Henan cultural industry development research base, Zhengzhou 450002, China*

[3]*International Education College of Zheng Zhou University of Light Industry Zhengzhou 450002, China*

[4]*Business School, Edinburgh Napier University, Edinburgh EH14 1DJ, UK*

[*]*Corresponding author*
e-mail: 2505000065@qq.com

(Received 3rd Apr 2019; accepted 17th May 2019)

Abstract. Scenic ecotourism spots, as major attractors of tourists, boast great economic values and development potentials. Many local governments have developed a series of tourism resources with the aim to fully utilize resources and promote regional economy. However, the tourism development has exerted negative environmental impacts on scenic ecotourism spots. Targeting Xixi Wetland Park, Hangzhou, southeastern China's Zhejiang Province, this paper explores the effects of tourism development and tourist activities on the soil and water environments in scenic ecotourism spots, and draws the following conclusions: The environment in the ecotourism scenic spot is influenced in varied degrees by both tourism development and tourist activities; soil porosity can characterize how tourism development and tourist activities affect the environment of scenic ecotourism spots; the impacts of tourism development or tourist activities on scenic ecotourism spots can be demonstrated by the pH, chemical oxygen demand (COD), total ammonia nitrogen (TAN) and turbidity of water bodies.
Keywords: *ecotourism scenic spots, tourist resources, tourist activities, tourist development, environmental impact*

Introduction

The ecological environment should be fully protected, because it is the common wealth of all humans (Movono et al., 2018). In China, the rapid development of tourism has brought many problems to resource, environment and management. Many local governments have developed a series of tourism resources with the aim to fully utilize resources and promote regional economy. However, the tourism development has exerted negative impacts on ecological environment, especially in scenic spots (Olafsdóttir and Runnstrom, 2009; Anctil and Blanc, 2016). According to incomplete statistics, more than one-fourths of scenic ecotourism spots in China have been damaged by tourism development, causing degradation of tourism resources and weakening of ecological functions (Aryal et al., 2018). Tourism development has a long-lasting impact on ecological environment. In fact, the ecological impact of a development project persists throughout the construction process. The full-lifecycle impact has been observed in many scenic ecotourism spots (Iliev and Dejan, 2018).

http://www.aloki.hu ● ISSN 1589 1623 (Print) ● ISSN 1785 0037 (Online)
DOI: http://dx.doi.org/10.15666/aeer/1704_93479355

The ecological impacts of tourism development and tourist activities can be divided into environmental impacts and non-polluting ecological impacts (Wu and Tsai, 2016). Focusing on scenic ecotourism spots, the existing studies have mainly explored the ecological impacts of tourism development from soil erosion degree, biodiversity index, vegetation cover change rate, biomass loss, habitat function and water environment quality, revealing that the continuous tourism development and tourist activities have led to changes in ecological function (Ke, 2012; Lyon et al., 2017). In environmental ecology, the environmental impact in scenic ecotourism spots is relative to the ecological impact of tourism pollution, and the environment of scenic ecotourism spots should be dominated by natural landscape, supplemented by artificial tourism construction and development (Ingelmo and Abedin, 2013). Targeting the Xixi Wetland Park in Hangzhou, southeastern China's Zhejiang Province, this paper investigates how tourism development and tourist activities affect the soil and water environment in scenic ecotourism spots, and analyzes the factors affecting the environment of the ecotourism scenic spot.

Methodology

Tourism development and tourist activities have concentrated impacts on the ecotourism environment. The impacts can accumulate over time but the intensity is on a gradual decline (Mbaiwa, 2011). For a species in the ecological environment, it will actively adapt to the changes in its habitat induced by tourism development or tourist activities; otherwise, the species will be naturally eliminated. If the species can survive and reproduce in the new habitat, the original ecosystem will be changed substantially (Sigurðardóttir and Steinthorsson, 2018).

For tourism development and tourist activities, the impacts on scenic ecotourism spots have three dimensions: intensity, frequency and duration. The ecological species will not be severely damaged if all three dimensions are controlled within a reasonable range (Saarinen and Lenao, 2014). The development of an ecological community is dynamic, rather than instantaneous. The general process includes such four phases as non-interference, co-interference, sharing and evolution. Any organism failing to adapt to co-interference will be eliminated (Dillimono and Dickinson, 2015). The factors in the ecosystem are mutually constrained, and a complete ecosystem must be open and balanced.

To attract more tourists, the Xixi Wetland Park has developed many tourism projects and conducted various tourist activities, which are bound to influence the environment of the scenic spot. The park environment is dominated by water, soil and vegetation. For simplicity, this paper attempts to disclose how tourism development and tourist activities affect the soil environment and water environment, and identify the factors affecting the environment of the ecotourism scenic spot. To test the soil environment, several soil samples were collected from a sample plot and subjected to measurements of pH, water content, porosity and heavy metal content. A total of ten sampling points was arranged, and divided into mixed points and control points. Note that each pair of mixed point and control point were from similar areas. To test the water environment, several water samples were collected from ten sampling points, and subjected to measurements of pH, chemical oxygen demand (COD), total ammonia nitrogen (TAN) and turbidity. The test methods for Soil and water index test methods are listed in *Table 1*.

http://www.aloki.hu ● ISSN 1589 1623 (Print) ● ISSN 1785 0037 (Online)
DOI: http://dx.doi.org/10.15666/aeer/1704_93479355

Table 1. *Test methods for soil and water indices*

Soil testing indicators	Method	Water testing indicators	Method
PH	Potential method	PH	Glass electrode method
Water content	Drying method	Chemical oxygen demand	Dichromate method
Porosity	Paraffin process	Ammonia-nitrogen value	Spectrophotometry
Heavy metal content	Spectrophotometry	Turbidity	Spectrophotometry

Test Results

Impacts of tourism development and tourist activities on soil environment

The soil environment provides the species of scenic ecotourism spots with the venue to exchange materials. The impacts of tourism development and tourist activities on the soil environment is directly reflected by the the variation in the physical state of the soil and the change of the species. The development intensity or activity scale is positively correlated with the soil aggregation and compaction. On the development intensity/activity scale of tourism, the ten sampling points can be ranked as No. 7 > No. 8 > No. 2 > No. 1 > No. 4 > No. 6 > No. 5 > No. 10 > No. 9 > No. 3.

Figure 1 shows the change of water content of mixed samples and control samples at different sampling points. It can be seen that the two types of samples had the same trend of water content, but the trend was not consistent with the variation in development intensity/activity scale. Thus, the water content variation cannot mirror the environmental impacts of tourism development or tourist activities.

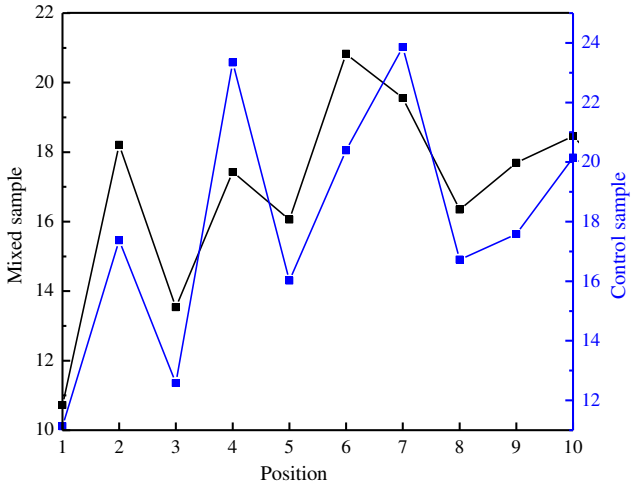

Figure 1. *The change of water content of mixed samples and control samples at different sampling points*

Figure 2 depicts the porosity changes of mixed samples and control samples at different sampling points. Obviously, the soil is less compacted at a high porosity. The results of porosity analysis show that the soil porosity followed the same trend with development intensity/activity scale. In other words, the environmental impacts of tourism development or tourist activities can be measured by soil porosity. In the ecotourism scenic spot, the heavy metals in soil mainly come from the dusts discharged from nearby factories, the solid wastes carried by tourists and the development of

http://www.aloki.hu ● ISSN 1589 1623 (Print) ● ISSN 1785 0037 (Online)
DOI: http://dx.doi.org/10.15666/aeer/1704_93479355

tourism facilities. *Figure 3* presents the comprehensive pollution index (CPI) of heavy metals at different sampling points. Except a few points, the heavy metal CPI exhibited the same trend with soil porosity, indicating that tourism development and activities will push up the heavy metal CPI in soil.

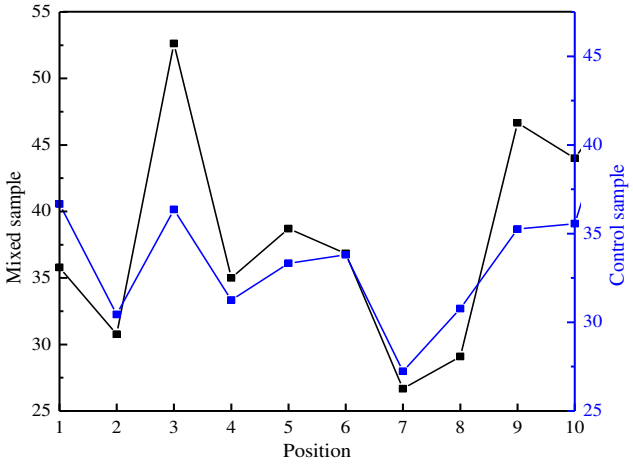

Figure 2. *The change of soil porosity of mixed samples and control samples at different sampling points*

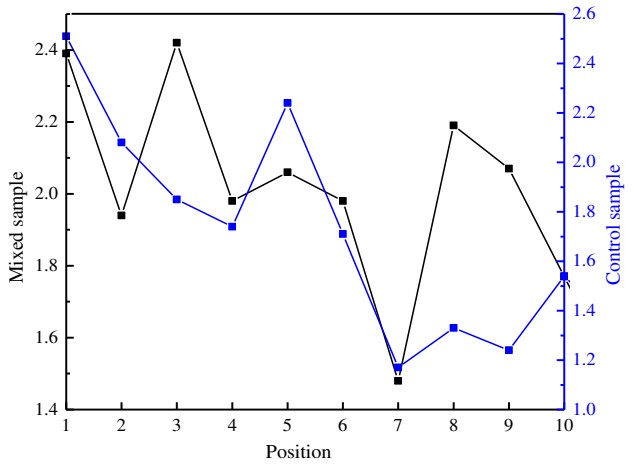

Figure 3. *The heavy metal CPIs at different sampling points*

Impacts of tourism development and tourist activities on water environment

By observing the artificial lakes in Xixi Wetland Park, the water environment in the park is found to be dead water, with no river channel to the external water bodies. The water bodies in the park are mainly polluted by tourist toilets, catering, animal foods, surface garbage, etc. On the development intensity/activity scale of tourism, the ten sampling points can be ranked as No. 7 > No. 8 > No. 2 > No. 1 > No. 4 > No. 6 > No. 5 > No. 10 > No. 9 > No. 3.

The pH, COD, TAN and turbidity measured at the different sampling points are respectively displayed in *Figures 4-7*. As shown in these figures, the pH in lake water remained basically the same across the park. The peak pH was measured at No. 10

http://www.aloki.hu ● ISSN 1589 1623 (Print) ● ISSN 1785 0037 (Online)
DOI: http://dx.doi.org/10.15666/aeer/1704_93479355

sampling point, which has the most intense tourist activities. This is attributable to the alkaline wastes left by tourists. The pH at No. 4 sampling point was not consistent with the development intensity/activity scale, which is probably the result of the acidic substances discharged by surrounding enterprises or residential areas. Thus, the pH of the water samples can reflect the degree of environmental impacts of tourism development and tourist activities on the ecotourism scenic spot. Besides, the COD and TAN variations could partially demonstrate how tourism development and tourist activities affect the ecotourism scenic spot. However, the two indices may also change due to non-tourism issues like animal wastes. In addition, the turbidity, an indicator of sediments of water bodies, basically agreed with the development intensity/activity scale in change law. To sum up, the impacts of tourism development or tourist activities on scenic ecotourism spots can be demonstrated by the pH, COD, TAN and turbidity of water bodies.

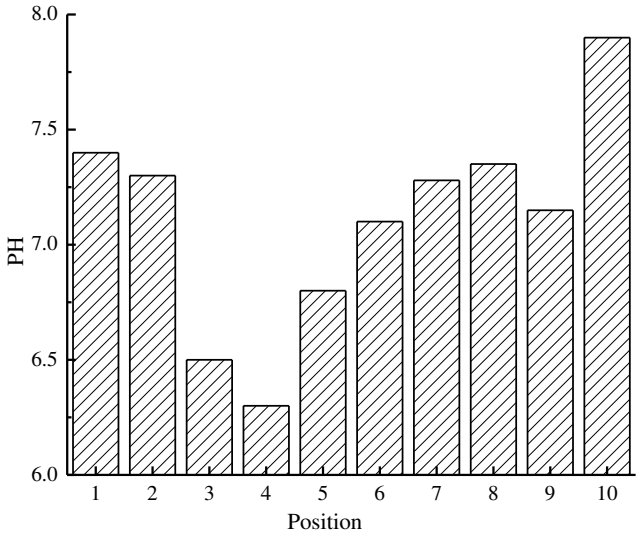

Figure 4. *The change of pH at different sampling points*

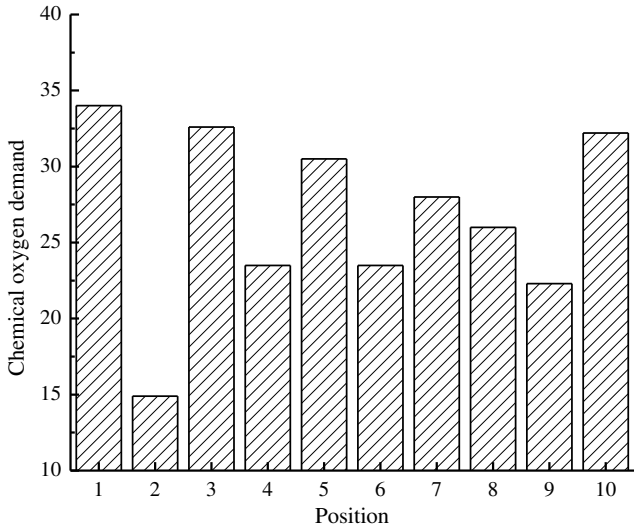

Figure 5. *The change of COD at different sampling points*

http://www.aloki.hu ● ISSN 1589 1623 (Print) ● ISSN 1785 0037 (Online)
DOI: http://dx.doi.org/10.15666/aeer/1704_93479355

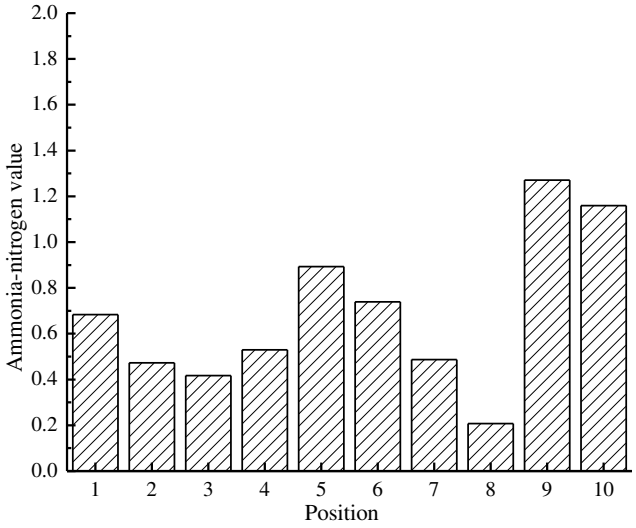

Figure 6. *The change of TAN at different sampling points*

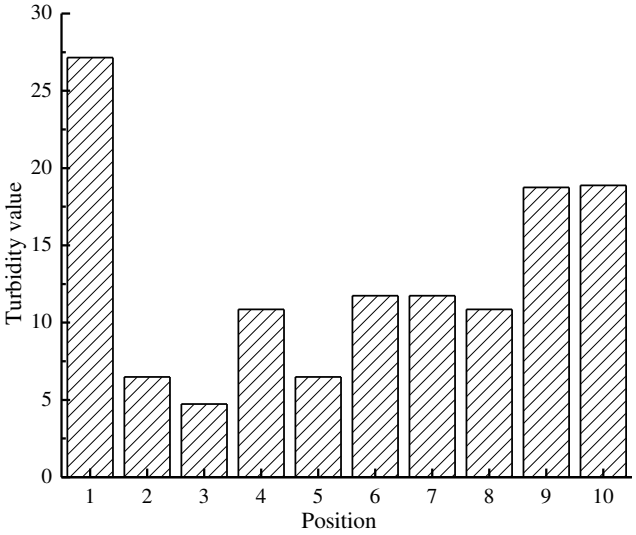

Figure 7. *The change of turbidity at different sampling points*

Discussion

Influencing factors of the environment in scenic ecotourism spots

The change curve of tourist market in Xixi Wetland Park (*Figure 8*) shows that the number of tourists to the park increases year by year, and peaks from May to August each year. In this section, the author analyzed the tourism development and tourist activities affect the soil and water conditions in the park, and discovered that the environment in the ecotourism scenic spot is influenced in varied degrees by both tourism development and tourist activities. Owing to tourism development and tourist activities, the soil becomes less porous and more compacted. The soil hardness is mostly affected by tourist activities and tourism construction projects. The changing soil environment will suppress the animal diversity in the soil, and directly affect the plant metabolism.

http://www.aloki.hu ● ISSN 1589 1623 (Print) ● ISSN 1785 0037 (Online)
DOI: http://dx.doi.org/10.15666/aeer/1704_93479355

The water environment has a great regulatory effect on the park. The turbidity increase and pH change of the water bodies are the combined effect of the garbage left by tourists, the distributions from tour boats and the discharge of various organic matters and minerals. *Figure 9* depicts the impacts of travel distance on the relative coverage and the relative number of species. With the growth in travel distance, the relative coverage of species increased annually at a decreasing rate, while the relative number increased first and then decreased.

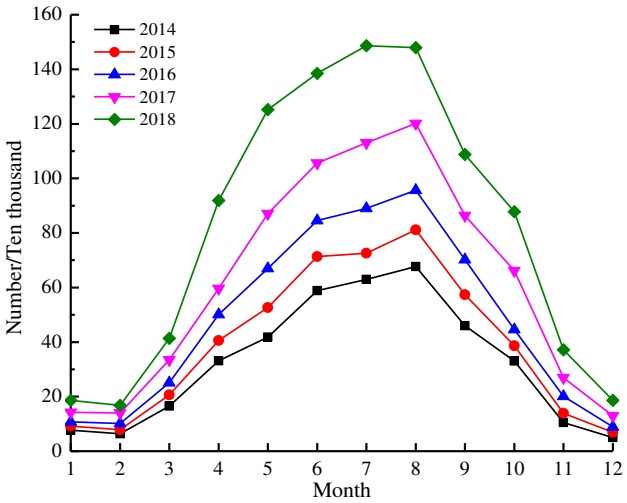

Figure 8. *The change of tourist market in Xixi Wetland Park*

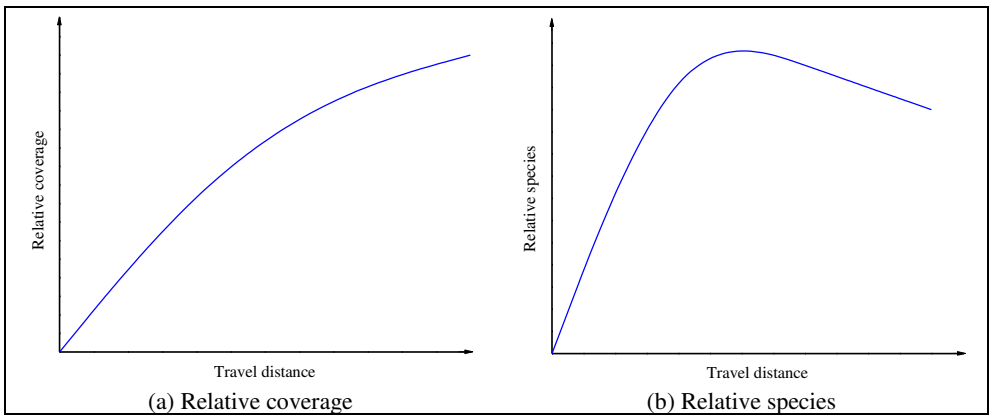

Figure 9. *Impacts of travel distance on relative coverage and relative number of species*

Measures and suggestions on enhancing environmental protection

China has not issued any law on ecotourism. In fact, tourism development should be regulated by effective legal means, so should the tourists in tourist activities. Any unit or individual should abide by the planning of scenic ecotourism spots. None should develop tourism projects arbitrarily in violation of regulations. Every ecotourism scenic spot should establish a sound environmental monitoring system. As shown in *Figure 10*, an effective environmental monitoring system for scenic ecotourism spots should cover four aspects, including ecological environment (air, hydrology, soil and vegetation),

http://www.aloki.hu ● ISSN 1589 1623 (Print) ● ISSN 1785 0037 (Online)
DOI: http://dx.doi.org/10.15666/aeer/1704_93479355

tourist, rare species and forest resources. The monitor or monitoring department should put forward relevant protection measures after rational evaluation and analysis. Currently, the eco-tourism scenic spots should strengthen the monitoring and control of the tourist activity environment, reasonably control the tourist inflow into the scenic environment, and prevent the eco-tourism scenic spots from overloading and the resulting impacts.

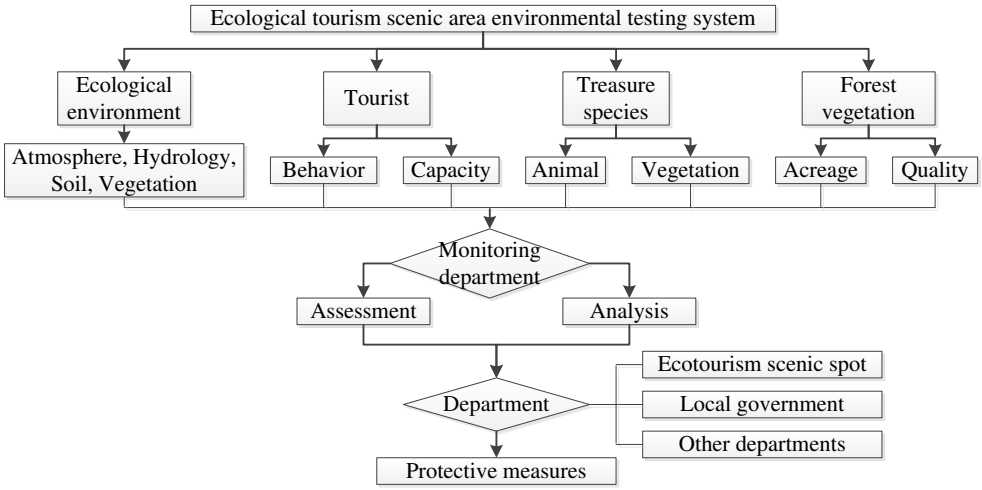

Figure 10. *An effective environmental monitoring system for ecological tourism scenic spots*

Conclusions

Taking Xixi Wetland Park for example, this paper explores the effects of tourism development and tourist activities on the soil and water environments in scenic ecotourism spots. The main conclusions are as follows:

(1) The soil is less compacted at a high porosity. Soil porosity is the best indicator of how tourism development and tourist activities affect the environment of scenic ecotourism spots, followed by the heavy metal CPI. By contrast, the water content variation in soil cannot demonstrate the impacts well.

(2) The impacts of tourism development or tourist activities on scenic ecotourism spots can be demonstrated by the pH, COD, TAN and turbidity of water bodies.

(3) The environment in the ecotourism scenic spot is influenced in varied degrees by both tourism development and tourist activities. With the growth in travel distance, the relative coverage of species increased annually at a decreasing rate, while the relative number increased first and then decreased.

(4) At present, there are few studies on ecological impact evaluation and impact source evaluation of tourism development and activities on eco-tourism scenic spots, and the qualitative and quantitative relationship between them is not clear, with the evaluation indexes involved with each other. The mechanism between ecological impact evaluation indicators and impact sources should be further studied.

Acknowledgements. (1) Henan provincial department of science and technology key research and development and promotion special project (tackling key problems in science and technology): research on the analysis and reconstruction technology of parametric spatial texture characteristics in the development of traditional villages in central China (182102310963), 2018/01-2019/12, presided over

http://www.aloki.hu ● ISSN 1589 1623 (Print) ● ISSN 1785 0037 (Online)
DOI: http://dx.doi.org/10.15666/aeer/1704_93479355

and under research. (2) Research project of Henan science and technology think tank in 2018: research on regional feature extraction and activation path of traditional villages in central China under the background of rural revitalization (hnkjzk-2019-54b), 2019/01-2019/12, presided over and under research. (3) 2016 Zheng Zhou Institute of Light Industry doctoral research fund funded project: research on the restoration and activation strategy of traditional village texture in the area with remnants and debris-taking Henan province as an example (2016BSJJ061), 2017/01-2019/12, presided over and under research.

REFERENCES

[1] Anctil, A., Blanc, D. L. (2016): An educational simulation tool for integrated coastal tourism development in developing countries. – Journal of Sustainable Tourism 24(5): 783-798.
[2] Aryal, S., Cockfield, G., Maraseni, T. N. (2018): Globalisation and traditional social-ecological systems: understanding impacts of tourism and labour migration to the transhumance systems in the himalayas. – Environmental Development 25: 73-84.
[3] Dillimono, H. D., Dickinson, J. E. (2015): Travel, tourism, climate change, and behavioral change: travelers' perspectives from a developing country, nigeria. – Journal of Sustainable Tourism 23(3): 437-454.
[4] Iliev, D. (2018): Regional inequalities and contemporary problems in regional tourism development: a case of macedonia. – Anatolia 29(3): 368-378.
[5] Ingelmo, I. A. (2013): Design and development of a sustainable tourism indicator based on human activities analysis in inle lake, myanmar. – Procedia-Social and Behavioral Sciences 103: 262-272.
[6] Ke, L. (2012): New development direction on worse ecological system resource of china eco-tourism. – Energy Procedia 14: 445-450.
[7] Lyon, A., Hunter-Jones, P., Warnaby, G. (2017): Are we any closer to sustainable development? listening to active stakeholder discourses of tourism development in the waterberg biosphere reserve, south africa. – Tourism Management 61: 234-247.
[8] Mbaiwa, J. E. (2011): Changes on traditional livelihood activities and lifestyles caused by tourism development in the okavango delta, botswana. – Tourism Management 32(5): 1050-1060.
[9] Movono, A., Dahles, H., Becken, S. (2018): Fijian culture and the environment: a focus on the ecological and social interconnectedness of tourism development. – Journal of Sustainable Tourism 26(3): 451-469.
[10] Olafsdóttir, R., Runnstrom, M. C. (2009): A gis approach to evaluating ecological sensitivity for tourism development in fragile environments. a case study from SE iceland. – Scandinavian Journal of Hospitality and Tourism 9(1): 22-38.
[11] Saarinen, J., Lenao, M. (2014): Integrating tourism to rural development and planning in the developing world. – Development Southern Africa 31(3): 363-372.
[12] Sigurðardóttir, I., Steinthorsson, R. S. (2018): Development of micro-clusters in tourism: a case of equestrian tourism in northwest iceland. – Scandinavian Journal of Hospitality and Tourism 18(3): 261-277.
[13] Wu, C. C., Tsai, H. M. (2016): Capacity building for tourism development in a nested social–ecological system—a case study of the south penghu archipelago marine national park, taiwan. – Ocean & Coastal Management 123: 66-73.

http://www.aloki.hu ● ISSN 1589 1623 (Print) ● ISSN 1785 0037 (Online)
DOI: http://dx.doi.org/10.15666/aeer/1704_93479355

THE EFFECTS OF WATERSHED FLOOD PEAKS ON THE HYDROLOGY AND WATER RESOURCES BASED ON THE LOGNORMAL DISTRIBUTION MODEL

WANG, Y.[1,2] – FENG, M. Q.[1*] – ZHANG, J.[1]

[1]*State Key Laboratory Base of Eco-Hydraulic Engineering in Arid Area, Xi'an University of Technology, Xi'an 710048, China*

[2]*Hydrology and Water Resources Survey Bureau of Shanxi Province, Taiyuan 030001, China*

**Corresponding author*
e-mail: mqfeng@xaut.edu.cn

(Received 3rd Apr 2019; accepted 17th May 2019)

Abstract. Flood is one of the most frequent natural disasters in the world; therefore, it is the focus of hydrologic research to reveal the effects of such factors as precipitation and peak discharge on the hydrological and water environments. Taking the Jialingjiang Watershed as an example, this paper collects the peak discharge data and historical data in the watershed and then studies the effects of watershed flood peaks on the hydrology and water resources and water environment in the Jialingjiang Watershed using the method combining data statistics and theoretical analysis based on the lognormal distribution model, and predicts the peak discharge in this area using the three-parameter lognormal distribution model. According to the research results, the parameter values are obtained for the Jialingjiang Watershed in the three-parameter lognormal distribution model; the three-parameter lognormal distribution model can reasonably reveal the scale effect law of the confluence area in the watershed peak discharge distribution; and the flood discharge distribution in a small watershed is significantly steeper than that in a large watershed. This study lays a theoretical foundation for the evaluation and prediction of the basic situation of hydrology and water resources in different watersheds.
Keywords: *watershed flood peak, hydrology and water resources, lognormal distribution model, runoff, confluence area*

Introduction

With the rapid economic and technological development, human activities are bringing significant impacts on the global natural environment (Del Giudice et al., 2014; Kuntiyawichai et al., 2014), resulting in changes in the runoff and hydrological cycle paths in the basin and ultimately leading to changes in the characteristics of hydrology and water resources (Al-Rawas and Valeo, 2010; Burton et al., 1997; Cannistraro et al., 2017; Sanjeev, 2017; Zhang et al., 2014). Studies have found that changes in the hydrology and water resources in the watershed can also cause errors in the hydrological analysis data, which will result in differences between the research results and the actual regional hydrological conditions and laws and consequently adversely affect the development and effective utilization of water resources (Ademila and Saloko, 2018; Olang and Fürst, 2011; Guo et al., 2016).

Runoff is formed throughout the process from precipitation to water flowing out of the area interface. Poorly developed runoff is one of the causes to flood (Chinnasamy et al., 2017; Hoseini et al., 2016). As one of the major natural disasters in the world, flood is always a threat to people's lives and properties and land resources (Te et al., 2010). In recent years, due to the over-exploitation of vegetation resources and reckless development of land resources, the ecological environment has been gradually

http://www.aloki.hu ● ISSN 1589 1623 (Print) ● ISSN 1785 0037 (Online)
DOI: http://dx.doi.org/10.15666/aeer/1704_93579366

deteriorating, and floods have occurred frequently, causing serious losses to residents near the waters (Enzel et al., 1993; Drake, 2014; Koutroulis and Tsanis, 2010). Therefore, studying the occurrence rule and formation mechanism of flood is of significant social significance to preventing and predicting flood.

The lognormal distribution model is a data analysis method used in cases where there are random variables (Martinezgoytre et al., 1994; Xin and Venkataramana, 2012; Zhang et al., 2001). In the analysis of the formation and development of watershed flood peaks and their effects on the regional hydrological conditions, there are a series of random variables such as peak discharge and confluence area. For some of them, the distribution can be reasonably analyzed and the relationships between them determined with the lognormal analysis model.

Based on the lognormal distribution model, this paper analyzes the variation law of flood by analyzing the changes in rainfall discharge and flood characteristics in the watershed, and then analyzes the regional variation characteristics of watershed flood peaks and explores the effects of flood peak flow on the hydrology and water resources in a certain area, with a view to providing certain support for the development of water resources in watersheds and the summarization of the development patterns of hydrology and water resources.

Materials and methods

In recent years, in order to characterize the relationship between the confluence area and the peak discharge and their influences in the distribution of the annual maximum peak flow, some scholars have proposed different distribution models for different variable distribution forms (Gupta et al., 1994; Lanfredi et al., 1998). Studies have shown that the lognormal distribution model can organically relate the flood peaks of the watershed to its confluence area. Therefore, this paper uses the lognormal distribution model to analyze the influences of the flood peaks in the Jialingjiang Watershed on the hydrology and water resources.

Lognormal distribution function

The lognormal distribution is a continuous probability distribution function that can be used to characterize the right-skewed distribution. After transformation of the lognormal distribution function, if y obeys the lognormal distribution, then lny obeys the normal distribution, and the lognormal distribution probability density function is shown in *Equation 1,* where μ_x is the mean of the parameter x; and σ_x is the dispersion of the parameter x, and it is always greater than zero. From this, it can be seen that the curve of the logarithmic distribution function is determined by the corresponding mean and the dispersion parameter. According to the graph of the lognormal distribution probability density function as shown in *Figure 1,* when the logarithmic mean μ_{lny} is constant, the peak position of the probability density function graph is determined by the logarithmic dispersion σ_{lny}. The greater the logarithmic dispersion, the wider the convex part of the probability density function graph, and the more blunt the peak; and conversely, the sharper the peak. When the logarithmic dispersion is constant, the peak position of the probability density function graph is determined by the logarithmic mean μ_{lny}. The smaller the logarithmic mean is, the more left the peak of the graph will go to,

http://www.aloki.hu ● ISSN 1589 1623 (Print) ● ISSN 1785 0037 (Online)
DOI: http://dx.doi.org/10.15666/aeer/1704_93579366

i.e. the smaller the x-coordinate of the peak will be; and conversely, the more right it will go to and the greater its x-coordinate will be.

$$p(y)=\frac{1}{\sigma_{\ln y} y\sqrt{2\pi}} e^{\frac{(\ln y-\mu_{\ln y})}{2\sigma_{\ln y}^2}}, \quad (0<y<+\infty) \tag{Eq.1}$$

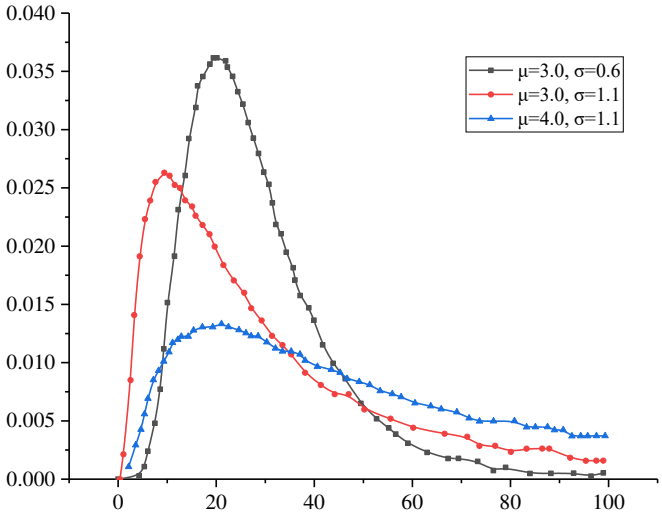

Figure 1. *Lognormal distribution*

The distribution characteristics of the above lognormal distribution function can be determined by two parameters, logarithmic mean and logarithmic dispersion. However, studies have shown that the shape of the lognormal distribution is generally asymmetrical, so the degree of skew the curve distribution is also essential. In the probabilistic statistical analysis, the coefficient of skewness Cs of the data distribution is defined in *Equation 2,* where μ^3 is the third-order center distance of y, and σ is the mean square error of y. When the coefficient of skewness is 0, the lognormal distribution is symmetric; when it is less than 0, the lognormal distribution is left-skewed; and when it is greater than 0, the lognormal distribution is right-skewed.

$$C_s=\frac{\mu^3}{\sigma^3} \tag{Eq.2}$$

Two-parameter lognormal distribution model

The two-parameter lognormal distribution model is a distribution model proposed by Prof. Smith, in which a random variable y is set to satisfy the two-parameter lognormal distribution LN(y: μ, σ^2), where μ is the mean of the random variable lny; and σ^2 is the variance of lny. If x is a random variable obeying the standard normal distribution, the random variable y can be expressed by *Equation 3*. Both μ *and* σ^2 have a linear relationship with the confluence area S in the watershed analysis, then they can be expressed by *Equations 4* and *5,* respectively.

$$y = exp(\mu + \sigma x) \tag{Eq.3}$$

http://www.aloki.hu ● ISSN 1589 1623 (Print) ● ISSN 1785 0037 (Online)
DOI: http://dx.doi.org/10.15666/aeer/1704_93579366

$$\mu = n_1 + n_2 lnS \quad \text{(Eq.4)}$$

$$\sigma^2 = m_1 - m_2 lnS \quad \text{(Eq.5)}$$

Combine the above equations, and we obtain *Equation 6* can be obtained. If the coefficient m_1 is much greater than m_2, then *Equation 6* can be approximated to *Equation 7,* $f(z) = exp(n_1 + m_1 x)$ and $\theta(z) = n_2 - 0.5 m_2 x$. Therefore, when μ *and* σ^2 are in linear relationships with the confluence area of the watershed, the relationship between the flow Q of the watershed flood peak and the confluence area S is a power function.

$$y = exp(n_1 + n_2 lnS + \sqrt{}(m_1 - m_2 lnS)x) \quad \text{(Eq.6)}$$

$$Q = exp[n_1 + n_2 lnS + (m_1 - 0.5 m_2 lnS)x] = f(z)S^{\theta z} \quad \text{(Eq.7)}$$

Three-parameter lognormal distribution model

Experts and scholars have improved the two-parameter lognormal distribution model and proposed a three-parameter lognormal distribution model to more accurately analyze the inherent law of hydrology and water resources. In this model, it is considered that the random variable y obeys the three-parameter lognormal distribution, that is, LN(y: μ, σ^2, a). The random variable x obeys the standard normal distribution, so the random variable y is expressed in *Equation 8,* and the mean of y is shown in *Equation 9*. The mean μ and variance σ^2 of the random variable lny are still expressed by *Equations 4* and *5,* while the parameter a is shown in *Equation 10*. The meaning of each parameter is the same as above. Based on the above descriptions, the three-parameter lognormal distribution model can be determined by six parameters - s_1, s_2, n_1, n_2, m_1, m_2, and then the parameters related to the flood peak discharge distribution in each confluence area S in the watershed can be obtained to determine the distribution pattern of watershed flood peaks. At last, the regional analysis of the flood and the estimation of the peak discharge in the watershed are conducted.

$$y = exp(\mu + \sigma x) + a \quad \text{(Eq.8)}$$

$$E(y) = exp(\mu + 0.5\sigma^2) + b \quad \text{(Eq.9)}$$

$$b = E(y) - exp(\mu + 0.5\sigma^2) = e^{s_1} A^{s_2} - e^{n_1 + m_1/2} A^{n_2 - m_2/2} \quad \text{(Eq.10)}$$

Flood peak data of Jialingjiang Watershed

This paper selects the annual flood peak data acquired at 31 hydrological stations in Jialingjiang Watershed (as shown in *Fig. 2*) for study. The confluence area of each station is controlled within 50–150,000 km^2. The maximum peak discharge data of each station in different years is shown in *Table 1*.

Results

Analysis of annual watershed flood peaks

According to the data in the *Table 1*, a double logarithmic relationship graph between the controlled confluence area *S* at each station and the mean of the maximum

http://www.aloki.hu ● ISSN 1589 1623 (Print) ● ISSN 1785 0037 (Online)
DOI: http://dx.doi.org/10.15666/aeer/1704_93579366

peak values Q is drawn. $f = 0.01$, 0.1 and 0.4 are shown in *Figures 3, 4* and *5,* respectively. It can be seen that the relationship between log$Q(S)$ and log$S$ is approximately linear, indicating that the peak discharge Q is scale invariant with the confluence area. At different frequencies f, the slope of the line is different, which represents the scale index. In other words, as the confluence area S changes, the mean Q of the maximum peak values satisfies the multi-scale form.

Calculate the 1^{st}-7^{th} moment $M = E[Q^h(S)]$ of each station, and plot the double logarithmic relationships between the watershed area and the 2^{nd} order matrix and the 4^{th} order matrix, as shown in *Figures 6* and *7*. Similarly, the relationship between log$M(S)$ and log$S$ (see *Fig. 8*) is approximately linear, indicating that the peak discharge Q is scale invariant with the watershed area changing. Calculate the scale value θ at different frequencies f through linear regression analysis, as shown in *Table 2*. It can be seen that the scale index increases with the increase of frequency, indicating that the peak discharge of a large flood in the low return period grows more slowly than that of a small flood in the high return period. In other words, the peak discharge values of a small watershed are more steeply distributed, which is in line with the actual conditions.

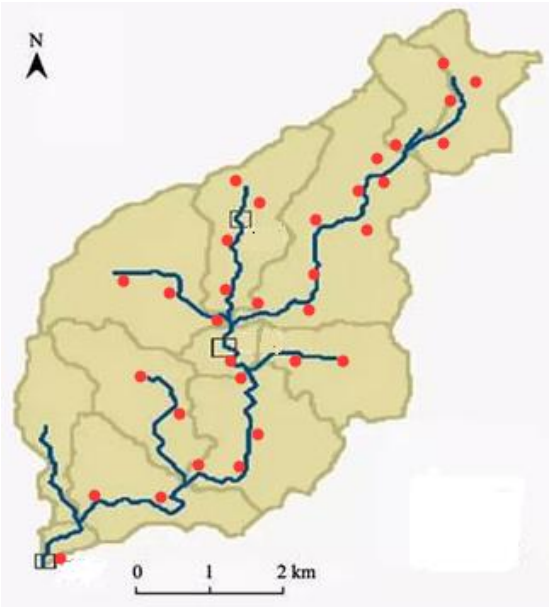

Figure 2. *Map of the Jialingjiang Watershed*

Table 1. *Flood data at different stations in the watershed*

No.	Confluence area (km^2)	Mean value of flood peak discharge (m^3/s)	Years (up to 2018)
1	254	235	21
2	5187	5068	30
3	91	86	25
4	90546	90428	24
5	8874	9857	18
6	632	649	38
7	14812	15065	29
…	…	…	…
31	6857	6843	42

http://www.aloki.hu ● ISSN 1589 1623 (Print) ● ISSN 1785 0037 (Online)
DOI: http://dx.doi.org/10.15666/aeer/1704_93579366

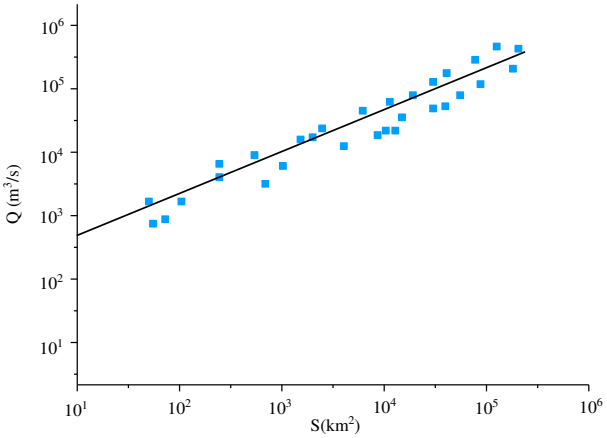

Figure 3. *Double logarithmic relationship between peak discharge and confluence area (f = 0.02)*

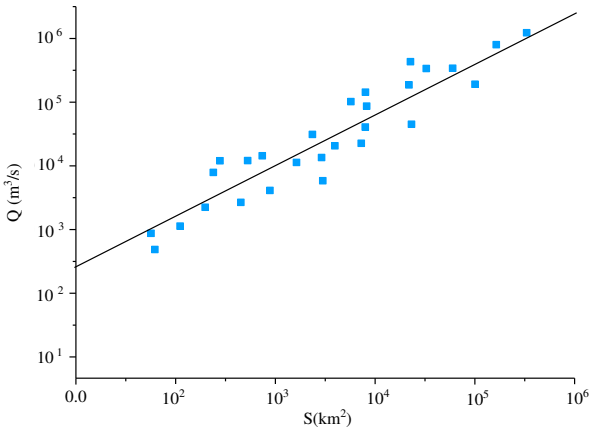

Figure 4. *Double logarithmic relationship between peak discharge and confluence area (f = 0.1)*

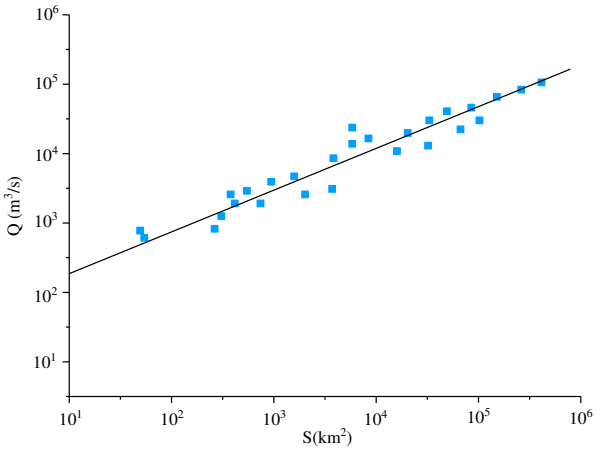

Figure 5. *Double logarithmic relationship between peak discharge and confluence area (f = 0.31)*

http://www.aloki.hu ● ISSN 1589 1623 (Print) ● ISSN 1785 0037 (Online)
DOI: http://dx.doi.org/10.15666/aeer/1704_93579366

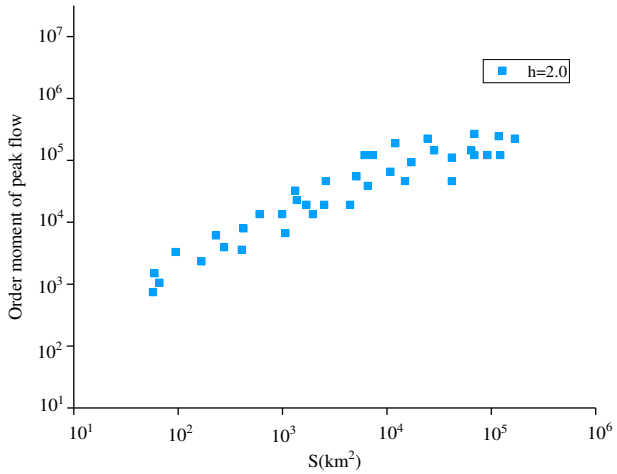

Figure 6. *Relationship between second-order moment and watershed area*

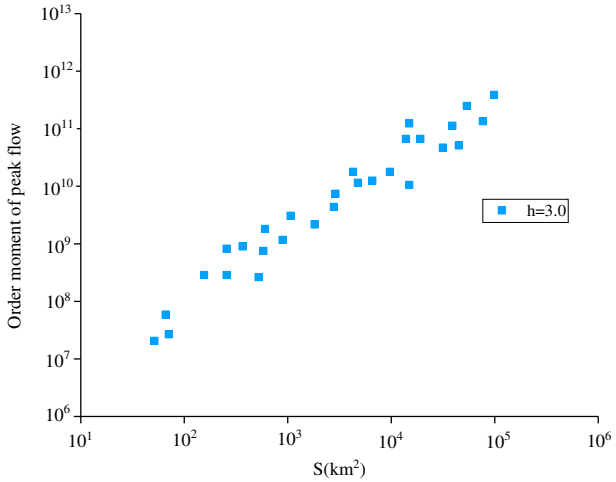

Figure 7. *Relationship between third-order moment and watershed area*

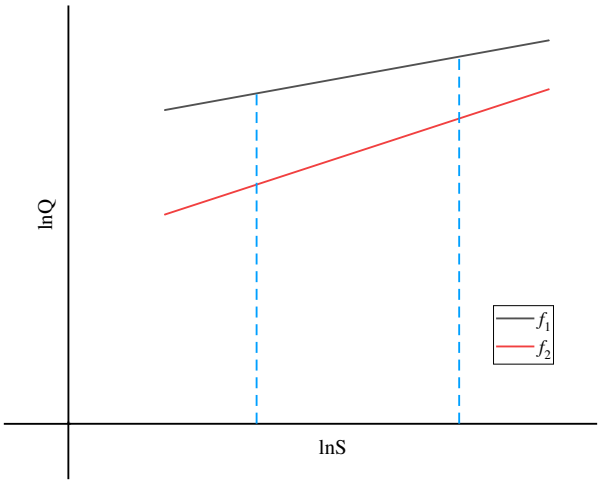

Figure 8. *Relationship between peak discharge and confluence area*

http://www.aloki.hu ● ISSN 1589 1623 (Print) ● ISSN 1785 0037 (Online)
DOI: http://dx.doi.org/10.15666/aeer/1704_93579366

Table 2. *Scaling index of peak discharge at different frequencies*

P	0.1%	0.2%	0.5%	1%	2%	10%	15%	20%	31%
θ(f)	0.538	0.542	0.547	0.552	0.578	0.609	0.657	0.673	0.701

Analysis on the application of the lognormal distribution model

According to the scale invariance feature, the peak discharge of the area where the no existing data is available can be calculated based on the annual peak discharge of the area where it is available. In this way, the probability distribution of the former can also be obtained.

Take the hydrological station in the Jialingjiang Watershed as an example. The flow control area of the hydrological station is 82,391 km^2. According to the 35-year maximum flow probability distribution map, the distribution of the flow data matches *f*-3. Suppose another hydrological station, with a control area of 725 km^2, has no data available. Then, according to the scale index θ found in *Table 2*, the peak discharge probability value of the area with no data can be obtained based on the existing data of the area with data. *Table 3* shows the calculated peak discharge values and the true ones, which are almost consistent.

Table 3. *Calculations for the application example*

P(%)	Q(Aref)(m^2/s)	Q(A)(m^2/s)	
		True value	Calculated value
0.1%	52264	4562	4412
0.2%	42142	3244	3135
0.5%	38263	2806	2709
1%	36021	2623	2645
2%	35682	2453	2346
10%	30347	2074	2012
15%	27803	1678	1789
20%	23649	1241	1231
31%	16323	954	924

Discussion

According to the three-parameter lognormal distribution model, the six parameters (n_1, n_2, m_1, m_2, s_1 and s_2) are used to determine the three parameters μ, σ^2 and b of the lognormal distribution, and thus the distribution of the watershed flood peaks with different confluence area *S* in the Jialing River Basin. Finally, the design peak discharge in the area with no data can be estimated based on the existing hydrologic data of the area with data.

According to the model, relevant data from 31 hydrological stations in the Jialingjiang Watershed are selected, and the six parameters are all obtained: $s_1 = 2.341$, $s_2 = 0.573$; $n_1 = 2.453$, $n_2 = 0.756$; and $m_1 = 0.273$, $m_2 = 0.026$. Based on this, the mean μ, the dispersionσ^2 and the parameter b in the three-parameter lognormal distribution model are determined. Then the distribution of the flood peaks in the Jialingjiang Watershed is obtained according to the analysis in Section 3 above, and the effects of

http://www.aloki.hu ● ISSN 1589 1623 (Print) ● ISSN 1785 0037 (Online)
DOI: http://dx.doi.org/10.15666/aeer/1704_93579366

flood peaks on the hydrology and water resources in the watershed are determined, together with preliminary evaluation on the water environment. The results also show that the lognormal distribution model selected in this paper can reasonably predict the impact of the flood peaks in the Jialingjiang Watershed on the conditions of hydrology and water resources in this region.

Conclusion

Taking the Jialingjiang Watershed as an example, this paper collects the peak discharge data and historical data in the watershed and then studies the effects of watershed flood peaks on the hydrology and water resources and water environment in the Jialingjiang Watershed using three-parameter lognormal distribution model. The main conclusions are as follows:

(1) The three-parameter lognormal distribution model is more applicable to the analysis and evaluation of hydrologic conditions in river watersheds than the two-parameter one. The former can reasonably characterize the scale effect law of the confluence area in the watershed peak discharge distribution.

(2) The peak discharge in the Jialingjiang Watershed changes with the confluence area in a scale-invariant way; the values of the 6 parameters in the lognormal distribution model can be determined according to the confluence area S, and then based on this, the distribution of watershed flood peaks can be determined.

(3) The study on the effects of peak discharge in Jialingjiang Watershed on the hydrological and water environments in this area further deepens our understanding of the development patterns of and influencing factors to the hydrological conditions in this area and provides technical materials and theoretical support for the rational development of hydrology and water resources in this area in the next steps.

Acknowledgements. The authors would like to thank all of the researchers who participated in the project. The authors would also like to thank the Research and Extension of Water Conservancy Science and Technology in Shanxi Province (201625) for financial support. Furthermore, the authors would like to thank the anonymous reviewers for their helpful and constructive comments.

REFERENCES

[1] Ademila, O., Saloko, B. (2018): Hydrogeoelectrical evaluation of groundwater flow pattern in a basement complex terrain, Southwest Nigeria. – Environmental and Earth Sciences Research Journal 5(1): 7-14.

[2] Al-Rawas, G. A., Valeo, C. (2010): Relationship between wadi drainage characteristics and peak-flood flows in arid northern Oman. – Hydrological Sciences Journal 55(3): 377-393.

[3] Burton, T. A. (1997): Effects of basin-scale timber harvest on water yield and peak streamflow1. – JAWRA Journal of the American Water Resources Association 33(6): 10.

[4] Cannistraro, G., Cannistraro, M., Trovato, G. (2017): Islands "Smart Energy" for eco-sustainable energy a case study "Favignana Island". – International Journal of Heat and Technology 35(S1): S87-S95.

[5] Chinnasamy, P., Muthuwatta, L., Eriyagama, N., Pavelic, P., Lagudu, S. (2017): Modeling the potential for floodwater recharge to offset groundwater depletion: a case study from the Ramganga basin, India. – Sustainable Water Resources Management 4(2): 331-344.

http://www.aloki.hu ● ISSN 1589 1623 (Print) ● ISSN 1785 0037 (Online)
DOI: http://dx.doi.org/10.15666/aeer/1704_93579366

[6] Del Giudice, G., Rasulo, G., Siciliano, D., Padulano, R. (2014): Combined effects of parallel and series detention basins for flood peak reduction. – Water Resources Management 28(10): 3193-3205.
[7] Drake, C. W. (2014): Assessment of flood mitigation strategies for reducing peak discharges in the Upper Cedar River watershed. – Master of Science Thesis, University of Iowa. DOI: 10.17077/etd.yu3t0xjm.
[8] Enzel, Y., Ely, L. L., House, P. K., Baker, V. R., Webb, R. H. (1993): Paleoflood evidence for a natural upper bound to flood magnitudes in the Colorado river basin. – Water Resources Research 29(7): 2287-2297.
[9] Guo, Y., Chang Huang, C., Pang, J., Zhou, Y., Zha, X., Mao, P. (2016): Reconstruction palaeoflood hydrology using slackwater flow depth method in the Yanhe River valley, middle Yellow River basin, China. – Journal of Hydrology 2016: 156-171. DOI: 10.1016/j.jhydrol.2016.11.017.
[10] Gupta, V. K., Mesa, O. J., Dawdy, D. R. (1994). Multiscaling theory of filood peaks: regional quantile analysis. – Water Resource 30(12): 3405-3421.
[11] Hoseini, Y., Azari, A., Pilpayeh, A. (2016): Flood modeling using WMS model for determining peak flood discharge in southwest Iran case study: simili basin in Khuzestan province. – Applied Water Science 7(6): 3355-3363.
[12] Koutroulis, A. G., Tsanis, I. K. (2010): A method for estimating flash flood peak discharge in a poorly gauged basin: case study for the 13-14 January 1994 flood, Giofiros basin, Crete, Greece. – Journal of Hydrology (Amsterdam) 385(1-4): 150-164.
[13] Kuntiyawichai, K., Sri-Amporn, W., Pruthong, C. (2014): Quantifying consequences of land use and rainfall changes on maximum flood peak in the lower Nam Phong river basin. – Advanced Materials Research 931-932: 791-796.
[14] Lanfredi, M., Macchiato, M., Ragosta, M., Serio, C. (1998). Time correlation structure in hourly concentration time series of CO, NOx, and O3 in urban areas. – Fractals 6(2): 151-158.
[15] Martinezgoytre, J., House, P. K., Baker, V. R. (1994): Spatial variability of small-basin paleoflood magnitudes for a southeastern Arizona mountain range. – Water Resources Research 30(5): 1491-1501.
[16] Olang, L. O., Fürst, J. (2011): Effects of land cover change on flood peak discharges and runoff volumes: model estimates for the Nyando river basin, Kenya. – Hydrological Processes 25(1): 80-89.
[17] Sanjeev, R. (2017): Geophysical resistivity survey (VES) for selection of appropriate artificial recharge (Ar) structures for augmentation of groundwater resources in Gwalior, MP, India. – Environmental and Earth Sciences Research Journal 4(1): 7-11.
[18] Te, L. A. H., Aerts, J. C. J. H., Bakker, A. M. R., Kwadijk, J. C. J. (2010): Simulating low-probability peak discharges for the Rhine basin using resampled climate modeling data. – Water Resources Research 46(46): 135-146.
[19] Xin, J., Venkataramana, S. (2012) Impacts of climate change on hydrology and water resources in the Boise and Spokane River Basins. – JAWRA Journal of the American Water Resources Association 48(2): 197-220.
[20] Zhang, Q., Gu, X., Singh, V. P., Xiao, M., Xu, C. Y. (2014): Stationarity of annual flood peaks during 1951-2010 in the pearl river basin, China. – Journal of Hydrology 519: 3263-3274.
[21] Zhang, Y., Smith, J. A., Baeck, M. L. (2001): The hydrology and hydrometeorology of extreme floods in the great plains of eastern nebraska. – Advances in Water Resources 24(9): 1037-1049.

http://www.aloki.hu ● ISSN 1589 1623 (Print) ● ISSN 1785 0037 (Online)
DOI: http://dx.doi.org/10.15666/aeer/1704_93579366

URBAN AIR QUALITY ASSESSMENT METHOD BASED ON GIS TECHNOLOGY

JIA, Q.

North China University of Water Resources and Electric Power, Zhengzhou 450000, China

Henan Engineering Research Center of Water Pollution and Soil Damage Remediation, Zhengzhou 450000, China

Henan Key Laboratory of Water Environment Simulation and Treatment, Zhengzhou 450000, China
e-mail: jiamoney@126.com; phone: +86-176-0371-6888

(Received 3rd Apr 2019; accepted 17th May 2019)

Abstract. The environmental impact of air pollutants emitted by energy consumption is becoming more and more serious. Air quality monitoring and evaluation is an important method to study the formation characteristics of regional air pollution, as well as an important means of comprehensive control and measurement of regional air pollution. In this paper, the emission list of Volatile Organic Compounds (VOCs) pollutants is established based on GIS technology, and the atmospheric diffusion of VOCs pollutants with five concerns in Shijiazhuang City is simulated by using AERMOD system model. The results show that the main industrial emission sources of VOCs come from steel, casting and cement industries, the flowing sources mainly come from diesel motor vehicles, and the surface sources come from vegetation and building ornaments. The AERMOD model has good applicability to the simulation of VOCs emissions. This paper gives full play to the spatial analysis ability of GIS technology and makes visual analysis of the evaluation results so as to provide decision-making basis for air quality prediction.
Keywords: *environment, air quality, atmospheric pollution, GIS technology, VOCs, AERMOD model*

Introduction

In recent years, with the rapid development of economy, the large-scale emergence of chemical enterprises results in the rapid increase in the types and mass concentration of pollutants in the atmospheric environment, and environmental quality has become a key issue for urban sustainable development that must be addressed as soon as possible (Mujtaba et al., 2016). According to the forecast data provided by the environmental management department, emergency measures may be taken to deal with heavy air pollution, such as strict control of motor vehicle exhaust emission, chemical enterprise discharge and construction dust emission (Pope and Wu, 2014; Merbitz et al., 2012). In addition, the technical support role of environmental prediction and analysis in environmental management is brought into full play to improve the quality of the atmospheric environment (Chattopadiay et al., 2010). The air quality prediction and evaluation model is an important technical method for atmospheric environmental quality detection. By establishing mathematical models of environmental pollutants under various topographical and meteorological conditions, it is possible to learn the physical and chemical mechanisms of transportation, diffusion, transformation and removal of pollutants in the atmospheric environment (Superczynski and Christopher, 2011; Zhan et al., 2018).

At present, the research of air quality evaluation model develops with the development of industrial society, and goes through the process of continuous improvement and development (Kumar et al., 2016; Vlachostas et al., 2010). In the air

http://www.aloki.hu ● ISSN 1589 1623 (Print) ● ISSN 1785 0037 (Online)
DOI: http://dx.doi.org/10.15666/aeer/1704_93679375

quality evaluation model, the atmospheric pollutant diffusion model is established by applying the meteorological principle to forecast the diffusion of environmental pollutants by means of computer technology in combination with the atmospheric dynamics principle, the atmospheric physics and the atmospheric chemistry application foundation (Elbir et al., 2010). The air quality assessment model is classified into local scale, urban scale and regional scale by simulation scale. In general, the urban scale is used for environmental quality prediction and evaluation (Barrile et al., 2018; Steve et al., 2008; Wang et al., 2015). Geographic information system (GIS) can manage spatial data by spatial location and study the interrelationship among various spatial entities. The GIS technology can visualize the air quality forecast data (Righini et al., 2014; Tirmizi and Tirmizi, 2018). In this paper, GIS technology is applied to the detection and evaluation of urban air quality and the spatial analysis ability of GIS technology is brought into full play to visually analyze the evaluation results so as to provide decision-making basis for air quality prediction.

Materials and methods

Industrial sources, flow sources, and surface sources

The establishment of an urban air pollution emission list is an effective tool for assessing urban air quality, which should specifically include emission source spatial location, emission data and emission parameters (Borrego et al., 2016; Siliello et al., 2014). There are three types of air pollution sources in urban areas: industrial, flow and surface sources (Carbajal-Hernández et al., 2012). *Table 1* shows the source identification of the pollution sources. Except for the industrial sources where O3 comes from, the common atmospheric pollutants will be generated from the three major pollution sources. Relying on GIS technology, each pollution space is located by using longitude and latitude coordinate positioning method (Borbet et al., 2018). The industrial source estimation method includes the actual monitoring method, the emission factor method and the material balance method. The VOCs emission factor is generally determined with reference to the Atmospheric Volatile Organic Matter Source Emission Inventory issued by the State. The flow sources are mainly motor vehicle emissions, and the main emissions are VOCs and NO_2. Surface sources include dust emission and combustion of domestic fuels, and surface sources of pollutant VOCs include vegetation, landfill sites and hospitals.

Table 1. *Source identification of pollution sources*

Classification	Contaminant category						
	$PM_{2.5}$	PM_{10}	SO_2	NO_2	CO	VOCs	O_3
Industrial source	√	√	√	√	√	√	√
Flow source	√	√	√	√	√	√	
Surface source	√	√	√	√	√	√	

Uncertainty analysis of pollution sources

Air quality is related not only to the spatial location and emission of emission sources, but also to meteorological conditions, including wind speed and wind direction.

http://www.aloki.hu ● ISSN 1589 1623 (Print) ● ISSN 1785 0037 (Online)
DOI: http://dx.doi.org/10.15666/aeer/1704_93679375

Figure 1 shows the monthly average wind speed monitored in Shijiazhuang City. It can be seen that Shijiazhuang City has the maximum average wind speed in March and the minimum average wind speed in October. *Figure 2* shows the air pollution emission in downtown Shijiazhuang City. It can be seen that the surface source is the largest source of VOCs, with a sharing rate of over 63%, and the industrial source is the primary source of PM_{10}, SO_2, NO_x, CO and O_3. According to incomplete statistics, the total emission amount of VOCs in the central urban area of Shijiazhuang reached 31,101.36 t in 2017. *Figure 3* shows the composition of urban atmospheric pollutant VOCs emission sources, vegetation, industrial and architectural ornaments are the three major sources of VOCs, accounting for 36.57%, 33.25% and 14.05% respectively. The quantitative estimation of VOCs pollutant emission source inventory is calculated by selecting representative emission factors and activity level data, which with greater uncertainties due to the instrument measurement, the representativeness of source test and random error.

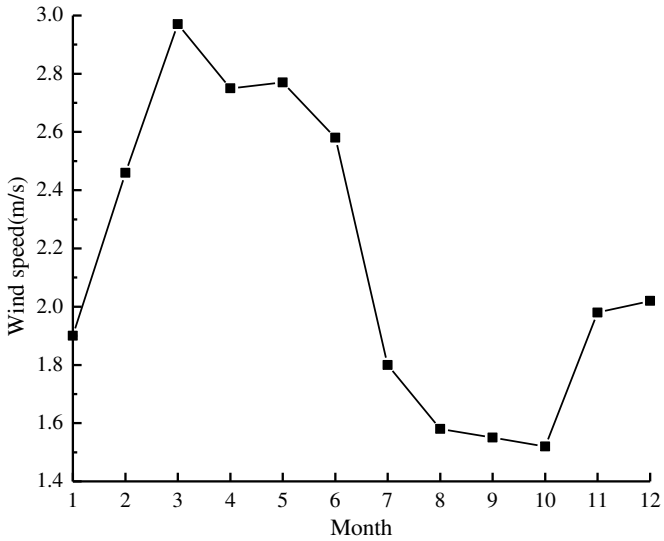

Figure 1. *Shijiazhuang City monitors monthly average wind speed*

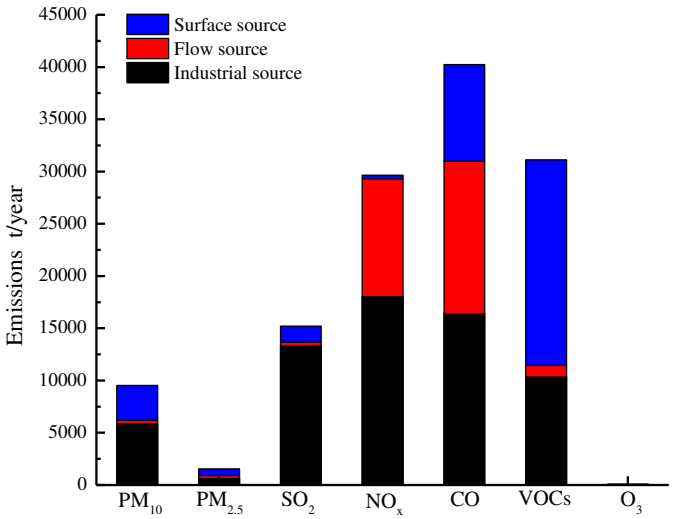

Figure 2. *Air pollution emissions in downtown Shijiazhuang*

http://www.aloki.hu ● ISSN 1589 1623 (Print) ● ISSN 1785 0037 (Online)
DOI: http://dx.doi.org/10.15666/aeer/1704_93679375

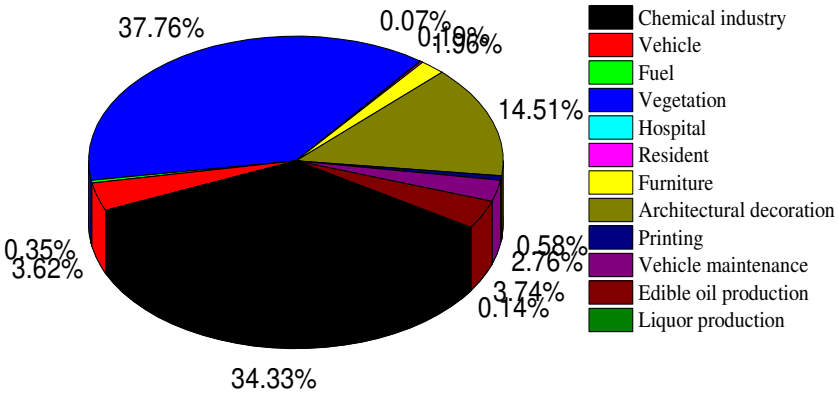

Figure 3. *Urban air pollutant VOCs emission source composition*

Results

Basic data required for the model operation

AERMOD model is used to calculate the atmospheric pollutant concentration. When simulating the horizontal diffusion of industrial source plume pollutants, the mass concentration of grid coordinate point (x, y, z) is assumed to be c (x, y, z) without considering the influence of topography. Considering the influence of the topography conditions, the total mass concentration of the grid point c (x, y, z) is shown in *Equation 1:*

$$C_r(x,y,z) = \lambda c(x,y,z) + (1 - \theta)c(x,y,z) \quad \text{(Eq.1)}$$

where, θ represents the decomposition streamline height; λ and θ represent the weight functions for horizontal and vertical point source diffusion states, respectively, as shown in *Equations 2* and *3:*

$$\lambda = 0.5(1 + \xi) \quad \text{(Eq.2)}$$

$$\xi = \frac{\int_0^H C(x,y,z)dz}{\int_0^\infty c(x,y,z)dz} \quad \text{(Eq.3)}$$

The basic data required for the model operation include pollution source parameters, meteorological data parameters, predicted point source coordinates, ground and high-altitude meteorological data. For industrial chimneys, the point source parameters include the height of the chimney, outlet inner diameter, discharge velocity and emission rate, while the surface source parameters include height, direction angle, length and emission rate.

Model verification method

For the convenience of simulation, the simulation results of atmospheric diffusion model are verified by using the developed AERMOD system, and necessary corrections are made to the model. The AERMOD model has been used by some scholars to verify the simulation results of SO_2. The results show that the correlation coefficient between the monitored value and the simulated value of SO_2 is 0.67, which indicates that the

http://www.aloki.hu ● ISSN 1589 1623 (Print) ● ISSN 1785 0037 (Online)
DOI: http://dx.doi.org/10.15666/aeer/1704_93679375

AERMOD model has good applicability to the simulation of SO_2 emissions. In addition, some researchers have applied the AERMOD model to the industrial point source pollutant emission area, which proved that the AERMOD model has good practicability in simulating pollution diffusion in the small and medium scale research area, and provides effective prediction data for air quality evaluation.

Discussion

Model validation

Table 2 is the emission list of pollution sources in downtown Shijiazhuang City. In selecting data of AERMOD model, it is necessary to add pollutants according to the factors of pollutants, and predict and simulate the residential areas, cultural areas and industrial areas in downtown Shijiazhuang City, with the secondary ambient air quality standard. The topographical parameters input in the AERMOD model include longitude and latitude coordinates and elevation, and the ground meteorological data include wind speed, wind direction, total cloud volume and dry-bulb temperature, where the wind direction, wind speed and dry-bulb temperature are the average value of observation data 24 times a day, and the total cloud volume is the average of 5 observations per day. *Table 3* shows the location of project concerns for prediction. According to the requirements of environmental air quality monitoring and monitoring location, five representative concerns are set up in this study and the model is simulated for a total of 20 days.

Table 2. *List of pollution sources in downtown Shijiazhuang*

Classification	Contaminant category						
	$PM_{2.5}$	PM_{10}	SO_2	NO_2	CO	VOCs	O_3
Industrial source	5853.37	608.2	13309	18014.2	16372.20	10334.1	75.8
Flow source	323.88	292.0	377.86	11268.01	14612.88	1089.8	
Surface source	3330.04	630.15	1507.73	320.15	9204.15	19665.36	
Total	9507.29	1530.35	15194.59	29602.36	43189.23	31089.26	75.8

Table 3. *Forecast project focus location*

Concern point	Position (m)		
	X	Y	Altitude
Mine monitoring station	6918.81	-9254.65	65.91
City No. 1 Middle School	11038.22	4099.08	64.83
Monitoring station	11428.7	3151.55	67.03
Daying Street monitoring station	6773.08	1044.0	62.02
Stylistic center monitoring station	10975.48	754.73	67.45

Forecast results and analysis

Figure 4 is a comparison between predicted results and monitoring results of VOCs of five concerns It can be seen that the predicted concentration values of VOCs in Shijiazhuang No. 1 High School are relatively high, while the predicted concentration

http://www.aloki.hu ● ISSN 1589 1623 (Print) ● ISSN 1785 0037 (Online)
DOI: http://dx.doi.org/10.15666/aeer/1704_93679375

values of monitoring station are relatively low, which is mainly because the selected monitoring station is located in the suburb of Shijiazhuang, and related to the coal or biomass fuel of the surrounding residents, the predicted values and monitoring values of the other three stations have the same trend. *Table 4* is the predicted results of VOCs of five concerns, and *Table 5* is the daily average predicted results of VOCs. The annual concentration of VOCs in Shijiazhuang City is predicted with the concern where the daily average concentration of VOCs is the highest among five concerns as the monitoring point. The concentration of VOCs predicted by AERMOD model is 0.1668 mg/m^3, accounting for more than 110% of the standard rate, and appears in October in Shijiazhuang City, which is the month with the lowest wind speed.

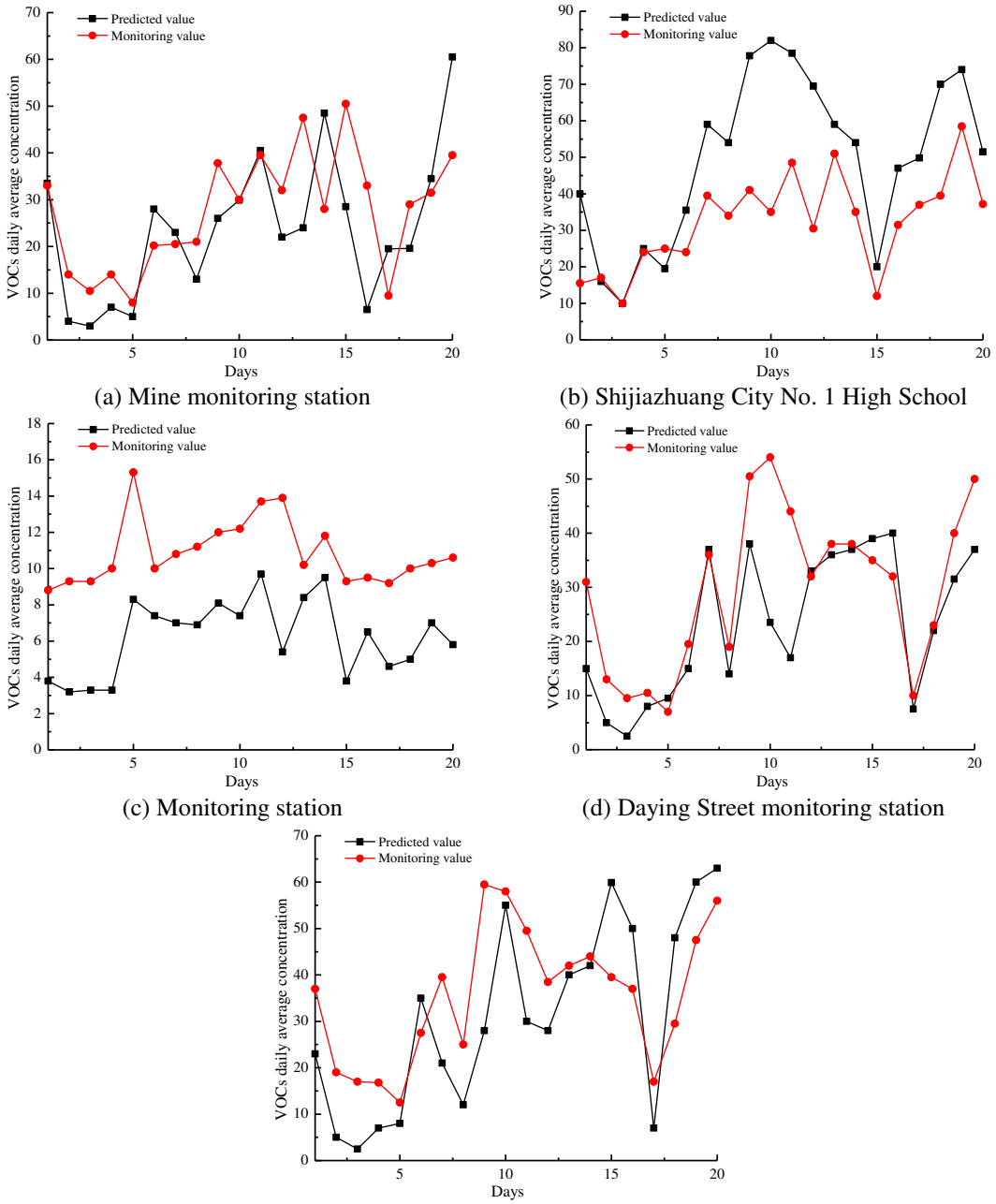

(a) Mine monitoring station

(b) Shijiazhuang City No. 1 High School

(c) Monitoring station

(d) Daying Street monitoring station

(e) Stylistic center monitoring station

Figure 4. *Comparison of VOCs prediction results and monitoring results of five concerns*

http://www.aloki.hu ● ISSN 1589 1623 (Print) ● ISSN 1785 0037 (Online)
DOI: http://dx.doi.org/10.15666/aeer/1704_93679375

Table 4. *Five concerns VOCs prediction results (μg/m³)*

Monitoring site location	VOCs		
	Predictive value	Monitoring value	Ratio
Mine monitoring station	37.38	28.85	1.296
City No. 1 Middle School	25.14	26.23	0.9586
Monitoring station	6.07	11.03	0.5506
Daying Street monitoring station	30.24	31.38	0.964
Stylistic center monitoring station	33.33	36.12	0.923
Average	26.432	26.722	0.990

Table 5. *Daily average forecast results of VOCs*

Focus point	Position (m)			Predictive value	Standard value	Occupancy rate (%)
	X	Y	Altitude			
Mine monitoring station	6918.81	-9254.65	65.91	0.171	0.152	112.5
City No. 1 Middle School	11038.22	4099.08	64.83	0.011	0.152	7.24
Monitoring station	11428.7	3151.55	67.03	0.079	0.152	51.97
Daying Street monitoring station	6773.08	1044.0	62.02	0.015	0.152	9.87
Stylistic center monitoring station	10975.48	754.73	67.45	0.143	0.152	94.08

Conclusions

In this paper, GIS technology is applied to the detection and evaluation of urban air quality, and the spatial analysis ability of GIS technology is brought into full play to visually analyze the evaluation results. The concrete conclusions are as follows:

(1) The surface source is the largest source of VOCs, with a sharing rate of over 63%, and vegetation, industrial and architectural ornaments are the three major sources of VOCs, accounting for 36.57%, 33.25% and 14.05% respectively.

(2) The basic data required for the AERMOD model operation include pollution source parameters, meteorological data parameters, predicted point source coordinates, ground and high-altitude meteorological data. The research indicates that the AERMOD model has good applicability to the simulation of SO2 emissions.

(3) The comparison between predicted results and monitoring results of VOCs of five concerns in Shijiazhuang City shows that the predicted concentration values of VOCs in Shijiazhuang No. 1 High School are relatively high, while the predicted concentration values of monitoring station are relatively low, and the predicted values and monitoring values of the other three stations have the same trend.

(4) Here only considers the impact of multiple point sources on the concentration of VOCs in Shijiazhuang City. The follow-up study can be made with additional pollution sources such as linear and surface sources to more roundly evaluate urban air quality.

http://www.aloki.hu ● ISSN 1589 1623 (Print) ● ISSN 1785 0037 (Online)
DOI: http://dx.doi.org/10.15666/aeer/1704_93679375

Acknowledgements. Henan Science and Technology Project "Study on Biological Toxicity of Water Quality in Henan Province" (No. 152102310343). Research Start up Fund of North China university of Water Resources and Electric Power (No: 201621).

REFERENCES

[1] Barrile, V., Fotia, A., Bilotta, G. (2018): Geodatabase for the assessment of energetic potential of territory. – Ingénierie des Systèmes d'Information 23(6): 7-17.
[2] Borbet, T. C., Gladson, L. A., Cromar, K. R. (2018): Assessing air quality index awareness and use in Mexico City. – BMC Public Health 18(1): 538.
[3] Borrego, C., Costa, A. M., Ginja, J., Amorim, M., Coutinho, M., Karatzas, K. D., Sioumis, T., Katsifarakis, N., Konstantinidis, K., Vito, S. D., Esposito, E., Smith, P. D., André, N., Gérard, P., Francis, L. A., Castell, N., Schneider, P., Viana, M., Minguillón, M. C., Reimringer, W., Otjes, R., Sicard, V. O., Pohle, R., Elen, B., Suriano, D., Pfister, V., Prato, M., Dipinto, S., Penza, M. (2016): Assessment of air quality microsensors versus reference methods: the Eunetair joint exercise. – Atmospheric Environment 147: 246-263.
[4] Carbajal-Hernández, J. J., Sánchez-Fernández, L. P., Carrasco-Ochoa, J. A., Martínez-Trinidad, J. F. (2012): Assessment and prediction of air quality using fuzzy logic and autoregressive models. – Atmospheric Environment 60(6): 37-50.
[5] Chattopadhyay, S., Gupta, S., Saha, R. N. (2010): Spatial and temporal variation of urban air quality: a GIS approach. – Journal of Environmental Protection 1(3): 264-277.
[6] Cinderby, S., Snell, C., Forrester, J. (2008): Participatory GIS and its application in governance: the example of air quality and the implications for noise pollution. – Local Environment 13(4): 309-320.
[7] Elbir, T., Mangir, N., Kara, M., Simsir, S., Eren, T., Ozdemir, S. (2010): Development of a GIS-based decision support system for urban air quality management in the city of istanbul. – Atmospheric Environment 44(4): 441-454.
[8] Kumar, A., Gupta, I., Brandt, J., Kumar, R., Dikshit, A. K., Patil, R. S. (2016): Air quality mapping using GIS and economic evaluation of health impact for Mumbai city, India. – Journal of the Air & Waste Management Association 66(5): 470-481.
[9] Merbitz, H., Buttstädt, M., Michael, S., Dott, W., Schneider, C. (2012): GIS-based identification of spatial variables enhancing heat and poor air quality in urban areas. – Applied Geography 33(1): 94-106.
[10] Mujtaba, S. M., Husain, T., Alharbi, B. (2016): Optimization of air quality monitoring network using GIS based interpolation techniques. – Journal of Environmental Protection 7(6): 895-911.
[11] Pope, R., Wu, J. (2014): A multi-objective assessment of an air quality monitoring network using environmental, economic, and social indicators and GIS-based models. – Journal of the Air & Waste Management Association 64(6): 721-737.
[12] Righini, G., Cappelletti, A., Ciucci, A., Cremona, G., Piersanti, A., Vitali, L. (2014): GIS based assessment of the spatial representativeness of air quality monitoring stations using pollutant emissions data. – Atmospheric Environment 97: 121-129.
[13] Silibello, C., Bolignano, A., Sozzi, R., Gariazzo, C. (2014): Application of a chemical transport model and optimized data assimilation methods to improve air quality assessment. – Air Quality Atmosphere & Health 7(3): 283-296.
[14] Superczynski, S. D., Christopher, S. A. (2011): Exploring land use and land cover effects on air quality in central Alabama using GIS and remote sensing. – Remote Sensing 3(12): 2552-2567.
[15] Tirmizi, S. T., Tirmizi, S. R. U. H. (2018): GIS based risk assessment of oil spill and gas leakage vulnerable zones in Pakistan. – Mathematical Modelling of Engineering Problems 5(3): 190-196.

http://www.aloki.hu ● ISSN 1589 1623 (Print) ● ISSN 1785 0037 (Online)
DOI: http://dx.doi.org/10.15666/aeer/1704_93679375

[16] Vlachokostas, C., Nastis, S. A., Achillas, C., Kalogeropoulos, K., Karmiris, I., Moussiopoulos, N. (2010): Economic damages of ozone air pollution to crops using combined air quality and GIS modelling. – Atmospheric Environment 44(28): 3352-3361.
[17] Wang, W., Ying, Y., Wu, Q., Zhang, H., Ma, D., Xiao, W. (2015): A GIS-based spatial correlation analysis for ambient air pollution and AECOPD hospitalizations in Jinan, China. – Respiratory Medicine 109(3): 372-378.
[18] Zhan, N. Y., Gao, Z., Deng, Y. F. (2018): Diffusion of vehicle exhaust pollutants in typical street canyons. – International Journal of Heat and Technology 36(3): 835-839.

http://www.aloki.hu ● ISSN 1589 1623 (Print) ● ISSN 1785 0037 (Online)
DOI: http://dx.doi.org/10.15666/aeer/1704_93679375

EFFECTS OF LAND USE FEATURES IN BLOCKS ON THE SELECTION OF LOW-CARBON TRAVEL BY URBAN RESIDENTS

LI, L.[1] – ZHANG, X.[2] – ZHANG, X. Q.[1] – HOU, Q. H.[1*] – LUO, X. Q.[1]

[1]*School of Architecture, Chang'an University, Shanxi 710061, China*

[2]*Pomegranate Group, Fengtai District, Beijing 10071, China*

**Corresponding author*
e-mail: houquanhua@chd.edu.cn

(Received 3rd Apr 2019; accepted 17th May 2019)

Abstract. This paper attempts to disclose the effects of land use pattern on the selection of low-carbon travel by urban residents. Targeting 19 blocks in north western China's Xi'an, the author collected data from various sources, including phone signals, app records and field surveys, and divided the blocks into two groups based on the difference in land use pattern. The multi-source data ensures the objectivity and accuracy of the analysis. Then, the relationship models between block land use features and residents' travel methods were established based on the Logit model, and the effects of six land use features on the selection of low-carbon travel were discussed in detail. The research results show a strong correlation between land use pattern and travel mode of the residents in the 19 blocks; the six land use features have different impacts on the travel mode; the residents in the two types of blocks prefer different low-carbon travel methods. This research lays a scientific basis for the optimization of urban space and land use.
Keywords: *green and low-carbon, travel methods, Logit model, land use characteristics, city blocks*

Introduction

The travel frequency and range of urban residents are affected by the land use pattern. In fact, the residents mainly consider two factors when choosing between different travel methods, namely, their own needs (e.g. work, shopping and entertainment) and the land use features (e.g. form, intensity and function). To encourage low-carbon travel, it is necessary to disclose the effects of land use features on travel mode and identify the control indices of intensive land use in blocks, which are the basic units of the urban area. In this way, more residents will choose low-carbon travel, reducing the carbon emissions in transport and protecting the environment (Tu and Ma, 2018).

The studies on land use pattern generally hold that dense grids and small roads are conducive to low-carbon travel among residents (Friedman and Cammalleri, 1994; Liu and Qing, 2011; Susan, 1996; Newman and Kenworthy; 1996; Hou et al., 2018; Zhang et al., 2018; Pan, 2010). Some scholars compared the effects of different block types on residents' low-carbon travel, including traditional hutongs, dense square grids, neighborhood units, and superblocks, and concluded that the residents are more likely to adopt low-carbon travel in traditional hutongs and dense square grids (Qin and Tian, 2013; Huang et al., 2013; Chai et al., 2011). However, there is not yet an agreement on the spacing in the road network. Atash (1994) suggested that most residents prefer walking over driving if the destination is 400 m away or within 5 min drive, while Xiao (2011) claimed that most people are willing to walk to a destination within 150 m.

http://www.aloki.hu ● ISSN 1589 1623 (Print) ● ISSN 1785 0037 (Online)
DOI: http://dx.doi.org/10.15666/aeer/1704_93779389

On land use intensity, many scholars have found that high residential density suppresses car usage, travel frequency and commuting distance, while promoting non-motorized travel (Hou and Wang, 2016; Forsyth et al., 2007; Handy, 1992; Giuliaono. and Naravan, 2003; Levinson and Kumar, 1997). Compared to rural areas, the urban area has a large population and a high plot ratio. Thus, the travel demand of urban residents is more sensitive to the changes in land use than that of rural residents. Facing the mixture of various types of land use, the urban residents often choose to travel on foot or bike within a small range (Zhou and Yang, 2005). Some scholars noted that the plot ratio has a positive impact on traffic flow intensity, and thus promotes public transport among urban residents (Caldera et al., 2017; Mao et al., 2004, 2005, 2002).

On land use function, the degree of mixed land use is positively correlated with the ratio of public transport and walking (Frank and Pivo, 1994; Friedman et al., 1994; Kockelman, 1997; Ewing and Fanag, 2008; Greenwald and Boarnet, 2002), and that of walking and biking (Zhou and Qian, 2014; Wang and Chai, 2009; Pan et al., 2009; Ma et al., 2013, 2011). In addition, it is often believed that the urban residents' choice between travel methods depends heavier on the degree of mixed land use in the workplace than that in residential areas (Ewing et al., 2003; Maat and Timmermans, 2009). However, some scholars argued that the degree of mixed land use has little effect on the choice of travel methods (Liu et al., 2010; Cervero, 1995). Moreover, many scholars held that the balance between working function and residential function of land use will shorten the commuting time and increase the ratio of walking and biking (Cervero, 1989; Long et al., 2012; Tana et al., 2015). The travel features of residents can be judged more clearly with land use function data from multiple sources (Long et al., 2012; Hou et al., 2018, 2017).

In view of the above, this paper attempts to disclose the relationship between low-carbon travel and block land use using multi-source data on various transport modes, and clarify the influence mechanism of land use on low-carbon travel through qualitative and quantitative analyses. With the aid of big data technology, the spatiotemporal features of low-carbon travel were discussed in the context of land use, and determined in an objective and scientific manner. The research findings shed new light on the optimization of block structure, enrich theories and methods of block land use, and promote low-carbon travel among urban residents.

Methodology

Background

(1) Research object

The existing studies have shown that the urban residents' selection of travel methods, and their carbon emissions in travel, are greatly affected by the intensity, form and function of land use. Thus, the three land use indices of blocks must be arranged in a scientific manner. Based on the geographic information system (GIS), this paper selects 19 blocks from Xi'an, the seat of northwestern China's Shaanxi Province, and divides them into two groups by land use function. As shown in *Figure 1,* the blocks *a*, *b*, *e*, *h*, *l*, *n*, *o*, *q* and *r* were categorized as housing-oriented blocks, because more than half of the land in each of them is used for residential purpose; the blocks *c*, *d*, *f*, *g*, *i*, *j*, *k*, *m*, *p* and *s* were classified as job-oriented blocks, because more than half of the land in each of them is used for working purpose.

http://www.aloki.hu ● ISSN 1589 1623 (Print) ● ISSN 1785 0037 (Online)
DOI: http://dx.doi.org/10.15666/aeer/1704_93779389

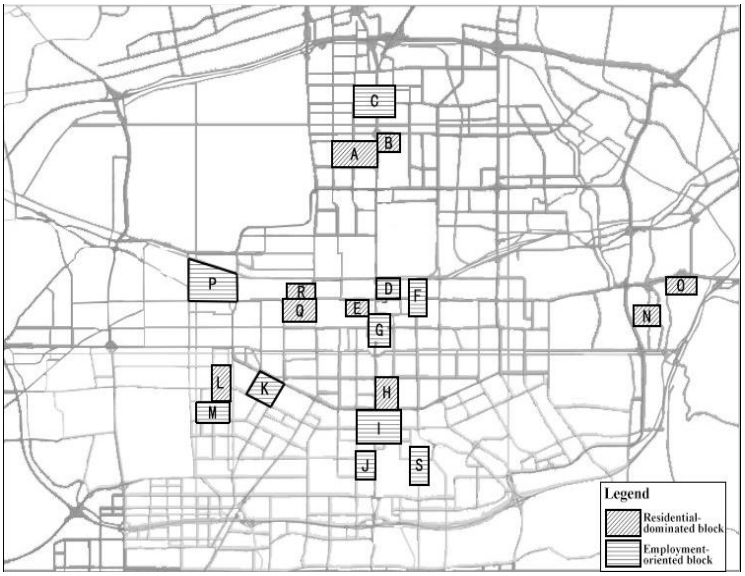

Figure 1. *Classification of the target blocks*

(2) Data on residents' travel

The data on residents' travel data (e.g. distance, frequency, trajectory and mode) were extracted from phone signals, app records and field surveys in the two weeks from Nov. 5~18, 2018. Specifically, the phone signals were acquired from China Unicom, the service provider to 17.07% of all phone users in Shaanxi; the app records were obtained from the GPS data in the bike sharing app Mobike; the field surveys were carried out in the 18 blocks to verify the results of phone signals and app records, collecting 1,900 data entries.

(3) Data on land use

The data on land use were obtained from digital maps, satellite images and phone signals. The digital maps were adopted to determine the nature of land use in each block, and verified against the remote-sensing satellite images. The residential and working situation were evaluated using the phone signals.

Index preparation

In this paper, the land use indices that greatly affect low-carbon travel are determined in three steps: quantifying the land use features, selecting the features related to travel mode through Pearson correlation analysis, and evaluating the relationship between feature indices and low-carbon travel by the Logit model. The specific process is explained as follows.

(1) Feature indices of land use

Inspired by the existing studies, six feature indices about land use function, intensity and form were found to be highly relevant to how urban residents choose between travel methods. The six indices are the degree of mixed land use, the job-housing ratio, building density, plot ratio, road density and the ratio of open space.

The degree of mixed land use M can be calculated as:

http://www.aloki.hu ● ISSN 1589 1623 (Print) ● ISSN 1785 0037 (Online)
DOI: http://dx.doi.org/10.15666/aeer/1704_93779389

$$M = -\sum_i \left[\left(\frac{b_i}{a} \right) \ln \left(\frac{b_i}{a} \right) \right] \quad \text{(Eq.1)}$$

where a is the total area of all types of buildings in a block (m^2); b is the area of type i buildings in the block (m^2).

The job-housing ratio JHR can be calculated as:

$$JHR = \frac{J_i}{H_i} \quad \text{(Eq.2)}$$

where JHR_i is the job-housing ratio of block i; J_i is the number of jobs in block i; H_i is the resident population in block i.

The building density B can be calculated as:

$$B = \frac{S_f}{L} \quad \text{(Eq.3)}$$

where S_f is the floor area of all buildings in a block (m^2); L is total land area in the block (m^2).

The plot ratio P can be calculated as:

$$P = \frac{S_a}{L} \quad \text{(Eq.4)}$$

where S_a is the total building area of a block (m^2); L is total land area in the block (m^2).

The road density ρ can be calculated as:

$$\rho = \left(\sum_i l_i \right) \Big/ L \quad \text{(Eq.5)}$$

where L_i is the length of road i in a block; L is total land area in the block (m^2).

The ratio of open space O can be calculated as:

$$o = \frac{S_g}{L} \quad \text{(Eq.6)}$$

where S_g is the area of public green space in a block (m^2); L is total land area in the block (m^2).

(2) Pearson correlation analysis

The Pearson correlation analysis was performed on SPSS, aiming to clarify how different land use features are correlated to each other and select the features that are relevant to low-carbon travel.

http://www.aloki.hu ● ISSN 1589 1623 (Print) ● ISSN 1785 0037 (Online)
DOI: http://dx.doi.org/10.15666/aeer/1704_93779389

(3) Logit model analysis

Taking the total population of each block as the behavioral decision unit, the optimal travel mode will be selected by the block residents from a set of independent alternatives. Hence, the Logit model was selected to determine the relationship between typical land use features and low-carbon travel.

Let U_{in} be the utility of choosing travel mode i from the set of alternatives C_n in block n, that is, the effect of land use features on the travel mode selection of the residents in the block. When two alternatives i and j are available ($i, j \in C_n$ and $i \neq j$), the residents of block n will select travel mode i only if U_{in} is greater than U_{jn}. According to the random utility theory, U_{in} can be expressed as:

$$U_{in} = V_{in} + \varepsilon_{in} \quad \text{(Eq.7)}$$

where V_{in} is utility constant when travel mode i is selected for block n; ε_{in} is the change in utility probability resulted from the implicit preference unique to the block residents.

If ε_{in} and V_{in} are independent of each other and ε_{in} obeys the Gumbel distribution, then the probability that the block residents choose travel mode i can be described as:

$$P_{in} = \frac{\exp(\lambda V_{in})}{\sum_{j \in c_n - i} \exp(\lambda V_{in})} \quad \text{(Eq.8)}$$

Next, the utility constant when travel mode i is selected for block n (V_{in}) can be described by the following linear function:

$$V_{in} = \sum_k \beta_{kin} \chi_{kin} \quad \text{(Eq.9)}$$

where x_{kin} is the k-th land use index when selected travel mode i is selected for block n; β_{kin} is the undetermined coefficient of x_{kin}. The value of β_{kin} can be calibrated by survey data. Taking the logarithm on both sides of *Equation 9,* the contribution rates of six different travel methods P_{in} (i.e. walking, bike, e-bike, motorcycle, bus, metro, car) can be expressed as:

$$\ln(P_{in}) = \lambda \sum_k \beta_{kin} \chi_{kin} - \ln\left[\sum_{j \in c_n - i} \exp\left(\lambda \sum_k \beta_{kjn} \chi_{kjn} \right) \right] \quad \text{(Eq.10)}$$

where the terms on the right side are the utility functions of the six travel methods. Based on the features of the research data, a multiple linear regression model can be established to describe the impacts of land use features on residents' travel mode:

$$y_{in} = \ln(p_{in}) = \beta_{oin} + \sum_k \beta_{kin} \chi_{kin} + \in_{in} \quad \text{(Eq.11)}$$

where y_{in} is the logarithm of the current sharing rate of the six travel methods; x_{in} is an explanatory variable with the same meaning above; β_{0in} and β_{kin} are regression

http://www.aloki.hu ● ISSN 1589 1623 (Print) ● ISSN 1785 0037 (Online)
DOI: http://dx.doi.org/10.15666/aeer/1704_93779389

coefficients; $\in_{in}$ is a random parameter. Obviously, the regression coefficient β_{0in} satisfies:

$$\beta_{oin} = -\ln\left[\sum_{j\in c_n\text{-}i} \exp\left(\lambda \sum_{k} \beta_{kjn}\chi_{kjn}\right)\right] \quad \text{(Eq.12)}$$

The equation is clearly workable.

Results

Features of residents' travel mode and land use

As mentioned before, the blocks *a*, *b*, *e*, *h*, *l*, *n*, *o*, *q* and *r* were categorized as housing-oriented blocks, and the blocks *c*, *d*, *f*, *g*, *i*, *j*, *k*, *m*, *p* and *s* were classified as job-oriented blocks.

(1) Low-carbon travel features of residents

The research data show that the residents in the 19 blocks mainly travel by walking, bike, e-bike, motorcycle, bus, metro and car.

The traffic flow in the housing-oriented blocks is relatively low, and dominated by walking and bike. By contrast, the job-oriented blocks have a high traffic flow, most of which occurs on bus and subway.

The residents in blocks *a*, *b*, *e*, *n*, *o*, *l* and *m* often engage in short-distance travels (< 1.5 km), those in blocks *d*, *f*, *g*, *h*, *i*, *j*, *k*, *l*, *m*, *n*, *q*, *r* and *s* are frequently involved in mid-distance travels (1.5~3 km), and those in blocks *m* and *p* mainly travel over long distances (3~21 km). The residents in block *c* have equal probability to embark on short-, mid- and long-distance travels.

The ratio of each low-carbon travel mode is listed in *Table 1*.

Table 1. *The ratio of each low-carbon travel mode*

Block name	Travel mode					
	Pedestrian	Bicycle	Electric bicycle or motorcycle	Conventional public transportation	Metro	Car
A	6.84%	4.94%	5.19%	16.42%	17.19%	49.41%
B	18.53%	7.13%	8.62%	15.35%	15.34%	35.02%
C	17.10%	16.51%	11.93%	15.52%	13.12%	25.82%
D	15.24%	5.65%	7.69%	15.76%	37.33%	18.33%
E	37.75%	15.35%	25.20%	9.47%	5.18%	7.06%
F	15.04%	27.45%	25.26%	9.80%	13.42%	9.03%
G	22.43%	3.63%	5.49%	19.94%	33.32%	15.19%
H	12.21%	2.67%	6.80%	17.40%	39.08%	21.84%
I	4.75%	1.68%	3.26%	16.30%	55.34%	18.67%
J	29.80%	36.20%	11.93%	2.53%	12.62%	6.93%
K	10.04%	14.75%	20.25%	8.70%	15.02%	31.24%
L	21.85%	13.38%	10.50%	8.61%	10.13%	35.53%
M	13.13%	8.94%	22.52%	25.48%	9.19%	20.74%
N	31.16%	9.40%	16.38%	16.38%	11.13%	15.56%
O	27.43%	22.01%	8.85%	14.51%	11.62%	15.58%

http://www.aloki.hu ● ISSN 1589 1623 (Print) ● ISSN 1785 0037 (Online)
DOI: http://dx.doi.org/10.15666/aeer/1704_93779389

P	22.63%	12.61%	21.55%	10.02%	12.31%	20.87%
Q	20.14%	22.62%	12.02%	13.26%	13.55%	18.41%
R	16.96%	27.33%	16.20%	8.65%	11.27%	19.58%
S	6.67%	1.22%	3.47%	30.82%	19.28%	38.55%

(2) Land use features of the blocks

Based on the six feature indices (*Eqs. 1–6*), the land use features of the 19 blocks were obtained in the aspects of function, intensity and form. The results are displayed in *Table 2*.

Table 2. *The land use features of the blocks*

Block name	Land area (ha)	Building area (10^4 m^2)	Building density (%)	Floor area ratio	Building mixing degree	Density of road network (km/km^2)	Open space proportion (%)	Employment-housing ratio
A	35.99	77.54	26.07	2.15	1.38	6.791	8.2	0.254
B	21.99	14.97	21.45	0.68	0.69	8.844	4.02	0.597
C	161.52	121.77	13.99	0.75	1.86	6.165	24.43	0.518
D	26.83	49.99	34.97	1.86	1.45	10.324	8.72	0.647
E	10.28	21.55	62.58	2.1	0.91	16.476	0	0.312
F	56.38	131.62	39.53	2.33	1.54	14.056	6.72	1.22
G	55.19	122.31	42.17	2.22	1.96	11.732	6.62	1.3
H	77.36	252.47	31.83	3.26	0.69	7.466	0.65	0.592
I	53.29	103.02	30.92	1.93	1.73	7.492	4.79	0.79
J	42.24	80.63	35.62	1.91	1.58	7.838	5.42	0.36
K	47.07	112.3	27.44	2.39	1.22	12.344	13.26	1.579
L	79.63	133.21	18.43	1.67	0.82	7.946	3.91	0.322
M	77.48	70.08	25.39	0.9	0.97	6.899	3.85	0.456
N	33.2	32.9	37.85	0.99	1.49	4.939	2.26	0.348
O	36.22	54.14	23	1.49	0.8	5.794	10.49	0.218
P	252.46	400	33.91	1.58	1.55	4.241	2.37	0.217
Q	79.83	176.34	33.26	2.21	1.32	6.848	5.16	0.425
R	38	60.41	34.17	1.59	1.25	10.358	17.17	0.672
S	63.88	83.1	29.65	1.3	1.79	11.679	30.93	0.863

Correlation analysis

(1) Correlation between travel methods and land use features

The correlation analysis between travel methods and land use features was carried out and the results were presented in the form of a matrix (*Table 3*). As shown in *Table 3*, the building density has a positive impact on the ratio of walking (significance < 0.05) and a negative impact on the ratio of car travel (significance < 0.01). The metro travel enjoys a significant positive correlation with plot ratio and degree of mixed land use (0.05 < significance < 0.1). In addition, the six travel methods have unobvious correlations with job-housing ratio, road density and ratio of open space.

http://www.aloki.hu ● ISSN 1589 1623 (Print) ● ISSN 1785 0037 (Online)
DOI: http://dx.doi.org/10.15666/aeer/1704_93779389

Table 3. *Correlation matrix between travel methods and land use features*

		Building mixing degree	Employment-housing ratio	Building density	Floor area ratio	Road network density	Open space proportion
Pedestrian	Pearson correlation	-.187	-.426	.479*	-.142	.042	-.404
	Significant (two-tailed)	.442	.069	.038	.563	.863	.086
Bicycle	Pearson correlation	.072	-.112	.102	.017	.068	.002
	Significant (two-tailed)	.770	.648	.677	.944	.782	.992
Electric bicycle or motorcycle	Pearson correlation	-.211	.033	.388	-.050	.278	-.268
	Significant (two-tailed)	.385	.893	.101	.839	.248	.268
Conventional public transportation	Pearson correlation	-.046	.101	-.190	-.270	-.079	.366
	Significant (two-tailed)	.852	.680	.436	.264	.749	.123
Subway	Pearson correlation	.391	.318	.004	.395	-.026	-.077
	Significant (two-tailed)	.098	.184	.987	.094	.916	.753
Car	Pearson correlation	-.203	-.011	-.616**	-.171	-.199	.369
	Significant (two-tailed)	.404	.966	.005	.483	.414	.120

*At the 0.05 level (dual side), the correlation is significant
**At the 0.01 level (both sides), the correlation is significant

(2) Correlation between land use features

The correlation analysis shows no correlation between the three land use features that are significantly correlated to the selection of travel mode (*Table 4*).

Table 4. *Correlation matrix between land use features*

		Building mixing degree	Building density	Floor area ratio
Building mixing degree	Pearson correlation	1	.127	.022
	Significant (two-tailed)		.603	.929
Building density	Pearson correlation	.127	1	.408
	Significant (two-tailed)	.603		.083
Floor area ratio	Pearson correlation	.022	.408	1
	Significant (two-tailed)	.929	.083	

**At the 0.01 level (two-tailed), the correlation is significant

http://www.aloki.hu ● ISSN 1589 1623 (Print) ● ISSN 1785 0037 (Online)
DOI: http://dx.doi.org/10.15666/aeer/1704_93779389

Relationship models between land use features and low-carbon travel

The logit model (*Eqs. 7–12*) can be used to calculate the correlation between land use characteristics and low-carbon travel characteristics in different types of blocks.

(1) The relationship model for housing-oriented blocks

Based on the results of regression analysis the relationship models between land use features and low-carbon travel in housing-oriented blocks can be constructed as:

$$y_{11} = -0.894 + 0.00592z_1 - 0.0677z_2 + 0.00192z_3 + 0.0352z_4 - 0.00296z_5 + 0.00867z_6 \quad \text{(Eq.13)}$$

$$y_{12} = -0.98 - 0.0233z_1 + 0.0444z_2 - 0.0171z_4 - 0.001z_5 - 0.0125z_6 \quad \text{(Eq.14)}$$

$$y_{13} = -1.158 + 0.0062z_1 + 0.0122z_2 - 0.0269z_4 + 0.0136z_5 - 0.016z_6 \quad \text{(Eq.15)}$$

$$z_1 = \frac{x_1^2}{100}, z_2 = \frac{x_2^3}{10000}, z_3 = \frac{x_3^3}{10000}, z_4 = \frac{x_4^3}{10000}, z_5 = \frac{x_5^2}{100}, z_6 = x_6 \quad \text{(Eq.16)}$$

where y_{in} is the probability logarithm of block i to choose travel mode n ($i = 1$ for housing-oriented blocks; $i = 2$ for job-oriented blocks; $n = 1$ for zero-carbon travel methods like walking and bike; $n = 2$ for high-carbon travel methods like e-bike, motorcycle and car; $n = 3$ for low-carbon travel methods like bus and metro); x_j is the standardized value of land use index j ($j = 1$ for building density; $j = 2$ for plot ratio; $j = 3$ for the degree of mixed land use; $j = 4$ for road density; $j = 5$ for the ratio of open space; $j = 6$ for job-housing ratio).

(2) The relationship model for job-oriented blocks

Based on the results of regression analysis, the relationship models between land use features and low-carbon travel in job-oriented blocks can be constructed as:

$$y_{21} = -0.262 - 0.149z_1 - 0.253z_2 + 0.0383z_3 + 0.091z_4 - 0.0231z_5 + 0.0426z_6 \quad \text{(Eq.17)}$$

$$y_{22} = -1.339 + 0.336z_2 - 0.0604z_3 - 0.111z_4 + 0.0221z_5 - 0.0525z_6 \quad \text{(Eq.18)}$$

$$y_{23} = -2.201 - 0.0083z_1 + 0.0543z_2 + 0.0422z_3 + 0.0474z_4 + 0.00071z_5 - 0.0149z_6 \quad \text{(Eq.19)}$$

where the symbols have the same meanings as above.

Discussion

The traffic flow is essential to the research on the travel features of urban residents. The phone signals can accurately reflect the traffic flows of travel methods like car, bus and metro. However, it is difficult to obtain the complete traffic flows of walking and bike from phone signals, due to the long intervals between two collections. Thus, the

http://www.aloki.hu ● ISSN 1589 1623 (Print) ● ISSN 1785 0037 (Online)
DOI: http://dx.doi.org/10.15666/aeer/1704_93779389

records of Mobike and field survey data were necessary for correction of the data acquired from phone signals.

The nature of land use has a great impact on the traffic flow and ratio of each travel mode. For instance, the residential-oriented blocks have a far smaller traffic flow than the job-oriented ones. In general, the residential-oriented blocks are dominated by non-motorized travel while the job-oriented blocks are dominated by motorized travel.

In residential-oriented blocks (*Eqs. 13–16*), building density promotes the ratio of zero- and low-carbon travel methods and inhibits that of high-carbon travel methods; the plot ratio suppresses the ratio of zero-carbon travel methods, but promotes that of high- and low-carbon travel methods; the degree of mixed land use improves the ratio of zero-carbon travel methods, with no significant impact on high- and low-carbon travel methods; road density has a positive impact on the ratio of zero-carbon travel methods, and a negative impact on low- and high-carbon travel methods; the ratio of open space reduces the ratio of zero- and high-carbon travel methods, yet increases the ratio of low-carbon travel methods; the job-housing ratio enhances the ratio of zero-carbon travel methods, and lowers the ratio of high- and low-carbon travel methods.

In job-oriented blocks (*Eqs. 17–19*), building density has an unobvious effect on the ratio of high-carbon travel methods; the plot ratio promotes the ratio of high- and low-carbon travel methods; the degree of mixed land use and road density both elevate the ratio of zero- and low-carbon travel methods, and reduce that of high-carbon travel methods; the ratio of open space inhibits the ratio of zero-carbon travel methods, but promotes the ratio of low- and high-carbon travel methods; the job-housing ratio has a positive effect on the ratio of zero-carbon travel methods and an inhibiting effect on the ratio of high- and low-carbon travel methods.

Conclusions

The previous studies on the effect of land use pattern on residents' travel mode are highly subjective due to the difficulty in data acquisition, failing to verify their theoretical hypotheses. This paper objectively demonstrates how land use features affect the low-carbon travel among urban residents. The research data were collected from various sources, including phone signals, app records and field surveys, making it possible to analyze and verify the effects in an objective manner. Two models were established to depict the relationship between block land use features and residents' travel methods, and the effects of six land use features on the selection low-carbon travel were discussed in details. The main conclusions are as follows.

The nature of land use has a great impact on the traffic flow and ratio of each travel mode. In other words, the land use pattern is a significant determinant of the travel features of urban residents.

The residential-oriented blocks feature high building density, low plot ratio, high degree of mixed land use, low ratio of open space and high job-housing ratio. The residents in these blocks prefer non-motorized, low-carbon travel methods. By contrast, the job-oriented blocks have low building density, high plot ratio, high degree of mixed land use, medium road density, high ratio of open space and low job-housing ratio. The residents in these blocks are used to public travel methods.

The future research will further eliminate the errors in feature extraction, widen the scope of research area, and simplify the index system.

http://www.aloki.hu ● ISSN 1589 1623 (Print) ● ISSN 1785 0037 (Online)
DOI: http://dx.doi.org/10.15666/aeer/1704_93779389

Acknowledgements. The research of this paper was funded by Shaanxi natural science basic research project (No.2017jm5124) and Shaanxi science and technology plan project (No.2017jm5124) "soft science research plan" general project (No.2017jm5124). Research project on major theoretical and practical issues in social science of Shaanxi province in 2018 (No.2018z026, 2018Z026), The Soft Science Program of the Ministry of Housing and urban-rural Development (No. 2016-k2-020), special fund for basic research operating expenses of central universities (No.310841172001, 300102418101).

REFERENCES

[1] Atash, F. (1994): Redesigning suburbia for walking and transit: emerging concepts. – Urban Planning and Development 120(1): 48-57.
[2] Caldera, M., Puglisi, G., Zanghirella, F., Margiotta, F., Ungaro, P., Talucci, V., Cammarata, G. (2017): Proposal of a survey-based methodology for the determination of the energy consumption in the residential sector. – International Journal of Heat and Technology 35(S1): S152-S158.
[3] Cervero, R. (1989): Jobs-housing balancing and regional mobility. – Journal of the American Planning Association 55(2): 136-150.
[4] Cervero, R. (1995): Planned communities, self-containment and commuting: a cross-national perspective. – Urban Studies 32(7): 1135-1161.
[5] Chai, Y. W., Xiao, Z. P., Liu, Z. L. (2011): Comparative analysis on CO2 emission per household in daily travel based on spatial behavior constraints. – Scientia Geographica Sinica 31(7): 843-849.
[6] Ewing, R., Fang, R. (2008): The impact of urban form on U.S. residential energy use. – Housing Policy Debate 19(1): 1-30.
[7] Ewing, R., Pendall, R., Chen, D. (2003): Measuring sprawl and its transportation impacts. – Transportation Research Record: Journal of the Transportation Research Board 1831(1): 175-183.
[8] Forsyth, A., Oakes, J. M., Schmitz, K. H. (2007): Does residential density increase walking and other physical activity. – Urban Studies 44(4): 679-697.
[9] Frank, L. D., Pivo, G. (1994): Impacts of mixed use and density on utilization of three modes of travel: single-occupant vehicle, transit and walking. – Transportation Research Record 1466: 44-52.
[10] Friedman, A., Cammalleri, V. (1994): Reducing energy, resources and construction waste through effective residential unit design. – Building Research and Information 22(2): 103-108.
[11] Friedman, B., Gordon, S. P., Peers, J. B. (1994): The effect of neo-traditional neighborhood design on travel characteristics. – Transportation Research Record 1400: 63-70.
[12] Giuliaono, G., Naravan, D. (2003): Another look at travel patterns and urban form the US and Great Britain. – Urban Studies 40(11): 2295-2312.
[13] Greenwald, M. J., Boarnet, M. G. (2002): The built environment as a determinant of walking behavior: analyzing non-work pedestrian travel in Portland, Oregon. – Transportation Research Record 1780: 33-42.
[14] Handy, S. (1992): How Land-Use Pattern Affect Travel Patterns: A Bibliography. CPL Bibliography. – Council of Planning Librarians, Chicago.
[15] Hou, Q. H., Wang, W. H. (2016): Interactive control of land use intensity for hierarchical regulatory plan. – Journal of Computational and Theoretical Nanoscience 13(2): 1283-1290.
[16] Hou, Q. H., Yang, S. L., Fang, Y. N., Zhang, L. D. (2017): Research on the application of AVC theory in data analysis of urban affairs and planning method. – Cluster Compute 6: 1-14.

http://www.aloki.hu ● ISSN 1589 1623 (Print) ● ISSN 1785 0037 (Online)
DOI: http://dx.doi.org/10.15666/aeer/1704_93779389

[17] Hou, Q. H., Zhang, X., Li, B., Zhang, X. Q., Wang, W. H. (2018): Identification of low-carbon travel block based on GIS hotspot analysis using spatial distribution learning algorithm. – Neural Computing and Applications 3: 1-11.
[18] Huang, J. N., Du, N. R., Liu, P. (2013): An exploration of land use mix around residence and family commuting caused carbon emission: a case study of Wuhan City in China. – International Urban Planning 28(2): 25-30.
[19] Kockelman, K. M. (1997): Travel behavior as a function of accessibility, land-use mixing, and land-use balance: evidence from the San Francisco Bay area. – Transportation Research Record 1607: 116-125.
[20] Levinson, D. M., Kumar, A. (1997): Density and the journey to work. – Growth and Change 28(2): 147-172.
[21] Liu, C., Qing, S. (2011): An empirical analysis of the influence of urban form on household travel and energy consumption. – Computers Environment and Urban Systems 35(5): 317-357.
[22] Liu, J. J., Wang, W., Cheng, L. (2010): Effect of land-use on resident travel mode in compact single center city. – Journal of Transport Information and Safety 28(2): 74-78.
[23] Long, W., Zhang, Y., Cui, C. Y. (2012): Identifying commuting pattern of Beijing using bus smart card data. – Acta Geographica Sinica 67(10): 1339-1352.
[24] Ma, J., Chai, Y. W., Liu, Z. L. (2011): The mechanism of CO_2 emissions from urban transport based on individuals' travel behavior in Beijing. – Acta Geographica Sinica 66(8): 2023-1032.
[25] Ma, J., Liu, Z. L., Chai, Y. W. (2013): Urban form and carbon emissions from urban transport: based on the analysis of individual behavior. – Urban Planning International 28(2): 19-24.
[26] Maat, K., Timmermans, H. (2009): Influence of the residential and work environment on car use in dual- earner households. – Transportation Research Part A: Policy and Practice 43(7): 654-664.
[27] Mao, J. X., Yan, X. P. (2002): The mutual relationship between urban transport system and land use in China. – Urban Planning Forum (4): 34-37.
[28] Mao, J. X., Yan, X. P. (2005): Impacts of urban transport system on urban land use—Case Study of Guangzhou City. – Scientia Geographica Sinica 28(3): 3353-3360.
[29] Mao, J. X., Yan, X. P., Wang, F. (2004): The influence of high-density land development on traffic system—with Guangzhou as an example. – Planners 30(12): 99-104.
[30] Newman, P. W. G., Kenworthy, J. R. (1996): The land use-transport connection: an overview. – Land Use Policy 13(1): 1-22.
[31] Pan, H. X. (2010): Urban spatial structure towards low carbon new urban transport and land use model. – Urban Development Studies 17(1): 40-45.
[32] Pan, H. X., Shen, Q., Zhang, M. (2009): Influence of urban form on travel behavior in four neighborhoods of Shanghai. – Urban Studies 44(2): 274-294.
[33] Qin, B., Tian, H. (2013): The impact of community spatial form on residents' carbon emissions. – China Urban Planning Society: Urban Age, Collaborative Planning. Proceedings of 2013 China Urban Planning Annual Conference, pp. 613-623.
[34] Susan, H. (1996): Urban form and pedestrian choices: study of Austin neighborhoods. – Transportation Research Record: Journal of the Transportation Research Board 1552: 135-144.
[35] Tana., Chai, Y. W., Guan, M. B. (2015): The relationship between the built environment and car travel distance on weekdays in Beijing. – Acta Geographica Sinica 75(10): 1675-1685.
[36] Tu, J. Z., Ma, D. L. (2018): A spatial economics perspective on convergence research of carbon emissions performance in China. – International Journal of Heat and Technology 36(3): 962-972.

http://www.aloki.hu ● ISSN 1589 1623 (Print) ● ISSN 1785 0037 (Online)
DOI: http://dx.doi.org/10.15666/aeer/1704_93779389

[37] Wang, D. G., Chai, Y. V. (2009): The jobs-housing relationship and commuting in Beijing, China: the legacy of Danwei. – Journal of Transportation. Geography 17(1): 30-38.
[38] Xiao, Y. (2011): Preliminary Study on Urban Block Planning under Green Scale. – Huazhong University of Science and Technology, Wuhan.
[39] Zhang, X., Liu, Y., Hou, Q. H. (2018): Characteristics of built environment in low-carbon travel block based on GIS hotspot technology. – Journal of Chang'an University Natural Edition 38(1): 89-97.
[40] Zhou, Y., Qian, C. Y. (2014): Neighborhood functions and layout for low carbon transportation. – Planners 30(9): 82-87.
[41] Zhou, S. H., Yang, L. J. (2005): The influence of urban land use intensity on urban traffic. – Urban Planning Forum (2): 75-80.

http://www.aloki.hu ● ISSN 1589 1623 (Print) ● ISSN 1785 0037 (Online)
DOI: http://dx.doi.org/10.15666/aeer/1704_93779389

WEATHER THREAT ASSESSMENT BASED ON DYNAMIC BAYESIAN NETWORK

MIAO, Y. F.[1] – WANG, L.[1] – ZHANG, G. A.[1] – SU, Q. H[2*] – LI, X. L.[1]

[1]*Department of Radio Navigation, Air Force Communication NCO Academy*
Dalian 116600, China

[2]*School of Information and Mathematics, Yangtze University*
Jingzhou 434023, China

**Corresponding author*
e-mail: suqhdd@126.com

(Received 3rd Apr 2019; accepted 17th May 2019)

Abstract. This paper aims to ascertain the variation in weather threat over time. To this end, the author established an assessment model of weather threat based on the Dynamic Bayesian Networks (DBN). Then, the Hidden Markov Model (HMM) was introduced to assess the level of weather threat. To validate the proposed method, a simulation was carried out on an Unmanned Aerial Vehicle (UAV), considering all five key weather factors affecting UAV safety. The results show that the DBN-based model is much more effective than the ordinary Bayesian Network (BN) in handling fuzzy information and complex weather conditions. The research findings shed new light on the accurate rout planning of an UAV.
Keywords: *UAV, DBN, HMM inference, forward-backward algorithm, conditional probability*

Introduction

Weather is a non-negligible factor in the rout planning of an UAV. Changeable weather poses a major threat to UAVs safety during reconnaissance missions. To minimize weather-induced loss and identify a safe route for UAVs, it is an urgent task to accurately quantify weather threat. Weather threat is too ambiguous, uncertain and time-dependent to be quantified by classical methods like function method (Paris and Erdogan, 1963). For instance, Tan and Du (2009) and Kilby and Hosseini (2004) reported that neither manned aircraft weather assessment nor engineering mathematic model can yield desirable results on weather threat on UAVs. Zhang et al. (2014) suggested that Gaussian approximation may lead to adverse weather.

Many researches have been done on weather threat quantification. Ramli et al. (2014) solved the weather threat on airport security by fuzzy logic. Adiwijaya (2013) created a prediction model based on weather data, and enhanced its forecast accuracy by the hybrid fuzzy-genetic algorithm. Zhu et al. (2011) identified eight weather factors that affect flight safety, and assessed the level of weather threat by the backpropagation (BP) neural network. Based on neural network and fuzzy logic, Al-Matarneh et al. (2014) developed different weather prediction models for different regions. Sannakki et al. (2013) adopted feed forward neural network to predict disease outbreaks in grapes induced by weather. The static BN (Zhu et al., 2015; Luo and Chen, 2008) was also applied to the quantitative assessment of weather threat.

In general, the above studies overlooked the time-dependence, failing to ascertain the variation in weather threat over time. The problem can be solved by DBN, a modelling and inference tool of dynamic and uncertain events. The DBN has been extensively applied in such fields as speech recognition (Zweig and Russell, 1998), threat

http://www.aloki.hu ● ISSN 1589 1623 (Print) ● ISSN 1785 0037 (Online)
DOI: http://dx.doi.org/10.15666/aeer/1704_93919400

assessment (Tang et al., 2007; Zhang et al., 2005), and bio-sequence analysis (Tian and Lu, 2004; Hou et al., 2010).

In view of the above, this paper sets up an assessment model of weather threat, and proposes the DBN-based synthetic fuzzy assessment method for the level of weather threat. The goal is to obtain a logical level of weather threat in consideration of various factors. Specifically, the simple weight mathematical assessment was improved to evaluate the threat index under the combined effect of various weather factors. The proposed method can significantly enhance the validity, feasibility and accuracy of weather threat assessment.

The remainder of this paper is organized as follows: Section 2 introduces the Static Bayesian Network (SBN), the DBN, and Forward-Backward (FB) algorithm; Section 3 establishes a weather threat model; Section 4 assesses weather threat through simulations and experiments; Section 5 wraps up this paper with some meaningful conclusions.

Materials and methods

Bayesian networks

Bayesian networks are invented to handle vague and uncertain issues in the field of artificial intelligence. As an important tool of uncertainty inference, the networks apply probability and statistics in complex domains. The SNB is a Directed Acyclic Graph (DAG), a finite directed graph with no directed cycles. In the DAG, each node represents a variable, and the edge between two nodes reflects the direct dependence between the two corresponding variables.

In general, the SBN consists of a structure diagram and a Conditional Probability Table (CPT). The CPT is a set of random variables to demonstrate marginal probability of a single variable with respect to the others. If a SBN provides sufficient conditional probabilities to derive any joint probability with given variables, then the network is considered calculable or inferential.

If $X = X_1, X_2, \ldots, X_n$ is the set of variables, then the joint probability distribution can be expressed as *Equation 1:*

$$P(X_1,...,X_N) = P(X_1)P(X_2 \mid X_1)...P(X_N \mid X_1,...,X_{N-1}) = \prod_{i=1}^{N} P(X_i \mid X_{1...i-1}) = \prod_{i=1}^{N} P(X_i \mid P_{arent}(X_i)) \quad \text{(Eq.1)}$$

where $P_{arent}(X_i)$ are the parent nodes of X_i.

The SBN takes no account of the time elements of variables. Considering these elements, the network will change along the timeline, forming a DBN (Murphy, 2002). The DBN estimates the model state at each moment or a given moment based on multiple time observations, and deduces the final result through comprehensive consideration of the observations. The same features observed at different periods can supplement each other. Thus, the DBN overcomes the limit of single evidence inference, and acquires a strong inference power.

Figure 1 depicts the extension of the DBN along the timeline. It is clear that the DBN contains an initial network B_0 and a transfer network $B_{\rightarrow}$. The initial network represents the initial state of the network. The probability distribution of variables in the initial state is denoted as p(b[0]). The transfer network $B_{\rightarrow}$ describes the dependencies

http://www.aloki.hu ● ISSN 1589 1623 (Print) ● ISSN 1785 0037 (Online)
DOI: http://dx.doi.org/10.15666/aeer/1704_93919400

between adjacent time slices in the network. The state transition probability between time t and time t + 1 is denoted as as p(x[t + 1]|x[t]). To sum up, the DBN can disclose the causal relationships between variables, and identify the evolutionary state of variables on time series, making it an ideal tool for simulating and inferring dynamic events.

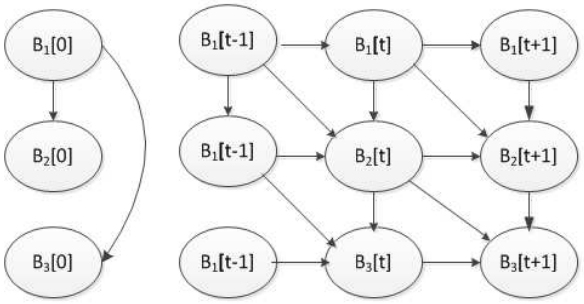

Figure 1. *Initial network and transfer network structure of DBN*

FB algorithm

Aiming to derive the probable values of hidden variables from numerous observed variables, the DBN is inextricably linked with the standard HMM. The network topologies of the two are interconvertible. The HMM inference is highly time-dependent if there are only a few DBN nodes (Xiao, 2006).

There are two main algorithms for HMM inference: the FB algorithm and Viterbi decoding algorithm. Considering the research content, the author adopted the FB algorithm to assess the level of weather threat. For the given model $\mu = (A,B,\pi)$ and observation sequence Y, the FB algorithm was introduced to infer occurrence probability of the sequence $P(Y|\lambda)$. The FB algorithm relies on recursion operation to reduce the computing complexity in probability-solving problem.

(1) Forward algorithm

The forward variable is defined as: $\alpha_t(i) = P(y_1, y_2, \ldots, y_t, x_t = i|\lambda)$.

Initialization (*Eq. 2*):

$$\alpha_1(i) = \pi_i b_i(y_1), 1 \le i \le n \tag{Eq.2}$$

Recursion (*Eq. 3*):

$$\alpha_{t+1}(j) = \left[\sum_{i=1}^{n} \alpha_t(i) a_{ij}\right] b_j(y_{t+1}) \quad t = 1,2,...,T-1 \tag{Eq.3}$$

Result (*Eq. 4*):

$$P(Y_T \mid \lambda) = \sum_{i=1}^{n} \alpha_T(i) \tag{Eq.4}$$

http://www.aloki.hu ● ISSN 1589 1623 (Print) ● ISSN 1785 0037 (Online)
DOI: http://dx.doi.org/10.15666/aeer/1704_93919400

(2) Backward algorithm

The backward variable is defined as: $\beta_t(i) = P(y_{(t+1)}, y_{(t+2)}, \ldots, y_T, x_t = i|\lambda)$.
Initialization (*Eq. 5*):

$$\beta_T(i) = 1, 1 \le i \le n \tag{Eq.5}$$

Recursion (*Eq. 6*):

$$\beta_t(i) = \left[\sum_{j=1}^{n} a_{ij} b_j(y_{t+1})\right] \beta_{t+1}(j) \quad t = 1, 2, ..., T-1 \tag{Eq.6}$$

Result (*Eq. 7*):

$$P(Y_T \mid \lambda) = \sum_{i=1}^{n} \pi_i \beta_1(i) \tag{Eq.7}$$

The forward and backward algorithms are combined as the FB algorithm which is shown in *Equation 8:*

$$P(Y_T \mid \lambda) = \sum_{i=1}^{n} \alpha_t(i) \beta_t(i) \, 1 \le t \le T \tag{Eq.8}$$

The DBN-based weather threat assessment model for UAVs was set up in the following steps: First, determine the weather factors that affect the UAVs safety; second, carry out quantitative analysis on each factor; third, determine the CPT and Transition Probability Table (TPT).

Weather factors affecting UAVs safety

The accuracy inference of weather threat level relies on the determination of typical weather factors. In light of the features of DBN, four factors were selected out of the various weather factors that affect the UAVs safety.

Threat Level (TL): As the parent node, the TL assesses the threat condition probability of UAVs flight at a certain point under various weather factors. In the US, EU and China, the weather TLs are depicted by four colours: blue (common), yellow (serious), orange (severe) and red (dangerous).

Weather Type (WT): Each type of weather has its unique impact on UAVs flight. For simplicity, the weather conditions were divided into 3 levels: mild (breeze, drizzle, sunny, etc.), common (moderate rain, fresh breeze, etc.) and dangerous (thunderstorm, tornado, etc.). The division clarifies the threat levels and reflects the features of DBN.

Intensity of effect (IOE): The intensity of effect varies with weather types. It is quantitatively classified in this paper.

Relative Location (RL): Both the effect range of weather and UAVs location are constantly changing. Therefore, the distance from the UAVs to the effect centre of the weather changes all the time. The variation in the relative location has a significant impact on the level of weather threat.

http://www.aloki.hu ● ISSN 1589 1623 (Print) ● ISSN 1785 0037 (Online)
DOI: http://dx.doi.org/10.15666/aeer/1704_93919400

Flight Type (FT): The UAVs flies at different altitudes depending on the specific conditions. The maneuver operations include steep climb, dive, quick turn, and gentle turn. Under the same condition, the damage probability of the UAVs changes with time. It is assumed that the sudden flight operations (e.g. steep climb, dive, quick turn) are much more likely to be threatened than smooth flight operations (e.g. gentle turn).

The above factors were taken as the key to the flight analysis of the UAVs. Considering the factor of time, the authors created a weather threat assessment model as shown in *Figure 2*.

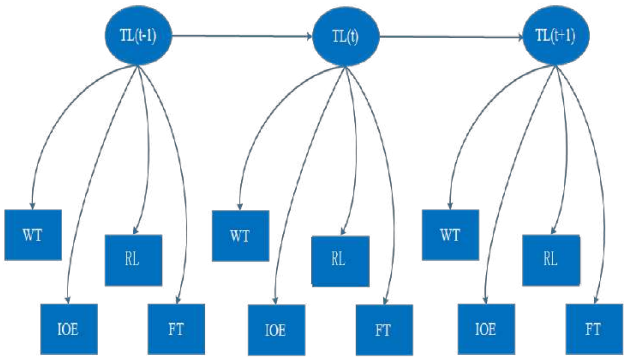

Figure 2. *DBN model of weather threat*

Quantification of each factor

Let S be the set of states of each node in the model. The factors were distinguished by the following subscripts:

S_{WT} = {dangerous, common, gentle};
S_{IOE} = {powerful, strong, middle, weak};
S_{RL} = {far, medium, near};
S_{FT} = {sudden flight, smooth flight}.

As mentioned before, the weather conditions were divided into 3 levels. The levels were ranked as dangerous weather, common weather and mild weather in descending order of the threat level to the UAVs.

Four-level quantification was employed to identify the exact IOE of each weather type. The distance from the UAVs to the energy centre was also taken into account in the quantification process. Its effect on threat level was ascertained by three-level quantification.

Furthermore, the flight attitudes of UAVs were classified into two categories. The sudden flight operations pose a great threat to UAVs, while the smooth flight operations have a limited threat. For convenience, the flight attitudes were partitioned according to the possible directions.

Determination of the CPT

The CPT was adopted to depict the casual relationship between the threat level in the DBN and the relevant factors. The table reflects the expert knowledge, including the experience and priori knowledge. Owing to subjectivity, there is a certain deviation between the expert knowledge and the actual results. If conditions permit, the CPT

http://www.aloki.hu ● ISSN 1589 1623 (Print) ● ISSN 1785 0037 (Online)
DOI: http://dx.doi.org/10.15666/aeer/1704_93919400

should be modified to a certain extent. *Table 1* shows the CPT of the factors in the weather threat assessment model.

Table 1. *Conditional probability table of weather factors*

Threat level	P(WT|TL) [dangerous, common, gentle]	P(IOE|TL) [powerful, strong; middle, weak]	P(RL|TL) [far, medium, near]	P(FT|TL) [sudden flight, smooth flight]
Low	0.15 0.25 0.60	0.15 0.15 0.20 0.50	0.10 0.40 0.50	0.20 0.80
Middle	0.20 0.45 0.35	0.35 0.45 0.10 0.10	0.20 0.60 0.20	0.30 0.70
High	0.80 0.15 0.05	0.80 0.10 0.05 0.05	0.70 0.20 0.10	0.80 0.20

In *Table 1*, the first column lists the conditional probabilities of the three weather types ($P(WT|TL)$), which are respectively 15%, 25% and 60% at low TL, 20%, 45% and 3 at medium TL, and 80%, 15% and 5% at high TL. The conditional probabilities of the other factors can be understood in a similar way.

Determination of the TPT

As shown in *Table 2*, the random probability refers to the state transition probability between two time slices when the network changes along the timeline.

Table 2. *Transition probability table of DBN*

TL(t) \ TL(t + 1)	Low	Middle	High
Low	0.7	0.2	0.1
Middle	0.15	0.65	0.2
High	0.1	0.2	0.7

Results and discussion

The proposed DBN-based weather threat assessment model was applied to a simulation, aiming to infer the probabilities of different weather threat levels. Then, the weather threat levels were derived accurately, laying the basis for scientific route planning of UAVs.

Without any observational evidence, the high threat level (P_{TL}^{H}), the medium threat level (P_{TL}^{M})) and the low threat level (P_{TL}^{L})) were assumed as 0.3, 0.4 and 0.3, respectively. Suppose the nodes are mutually independent. Then, the author began to collect the data on each node. Assuming that a UAVs was on a mission, the weather conditions were monitoring at ten different moments of the flight, and the factors related to the threat of the target UAVs were described in real time.

Based on the observational evidence, ten observed values of the target were recorded (*Table 3*). The weather threat levels were figured out by comparing the data on the target UAVs at different moments. Next, the weather threat was assessed by the DBN and the ordinary Bayesian network (BN), respectively. The assessment results are presented in *Table 4* and *Figure 3*. When the data were normal, both the DBN and the BN inferred the right results, despite a slight difference.

http://www.aloki.hu ● ISSN 1589 1623 (Print) ● ISSN 1785 0037 (Online)
DOI: http://dx.doi.org/10.15666/aeer/1704_93919400

Table 3. *Observation evidence table of UAVs at different time*

Time	WT (dangerous, common, gentle)	IoE (powerful, strong, middle, weak)	RL (far, medium, near)	FT (sudden flight, smooth flight)
1	(0.2, 0.3, 0.5)	(0.1, 0.15, 0.2, 0.55)	(0.1, 0.2, 0.7)	(0.3, 0.7)
2	(0.3, 0.5, 0.2)	(0.1, 0.2, 0.2, 0.5)	(0.1, 0.2, 0.7)	(0.4, 0.6)
3	(0.3, 0.5, 0.2)	(0.2, 0.2, 0.5, 0.1)	(0.1, 0.3, 0.6)	(0.35, 0.65)
4	(0.25, 0.55, 0.2)	(0.05, 0.65, 0.25, 0.05)	(0.3, 0.5, 0.2)	(0.3, 0.7)
5	(0.3, 0.6, 0.1)	(0.3, 0.5, 0.1, 0.1)	(0.2, 0.6, 0.2)	(0.7, 0.3)
6	(0.7, 0.2, 0.1)	(0.1, 0.6, 0.2, 0.1)	(0.2, 0.7, 0.1)	(0.4, 0.6)
7	(0.6, 0.3, 0.1)	(0.6, 0.2, 0.15, 0.05)	(0.25, 0.55, 0.3)	(0.45, 0.55)
8	(0.7, 0.2, 0.1)	(0.7, 0.1, 0.1, 0.1)	(0.6, 0.3, 0.1)	(0.75, 0.25)
9	(0.3, 0.6, 0.1)	(0.1, 0.1, 0.7, 0.1)	(0.6, 0.2, 0.2)	(0.4, 0.6)
10	(0.2, 0.5, 0.3)	(0.65, 0.05, 0.15, 0.15)	(0.7, 0.2, 0.1)	(0.65, 0.35)

Table 4. *Simulation results of weather threat when data is normal*

Time	Assessment results of weather threat by DBN			Assessment results of weather threat by BN		
	High	Middle	Low	High	Middle	Low
1	0.0003	0.0075	0.9923	0.0012	0.0154	0.9834
2	0.0010	0.0685	0.9304	0.0093	0.1564	0.8343
3	0.0159	0.5164	0.4677	0.0296	0.6391	0.3314
4	0.2264	0.7018	0.0718	0.2500	0.6750	0.0750
5	0.4868	0.5110	0.0022	0.3855	0.6072	0.0072
6	0.7548	0.2421	0.0031	0.5517	0.4565	0.0217
7	0.9373	0.0618	0.0009	0.7317	0.2561	0.0122
8	0.9941	0.0059	0.0000	0.9480	0.0516	0.0004
9	0.9782	0.0206	0.0012	0.7485	0.2156	0.0359
10	0.9580	0.0415	0.0005	0.8540	0.1435	0.0026

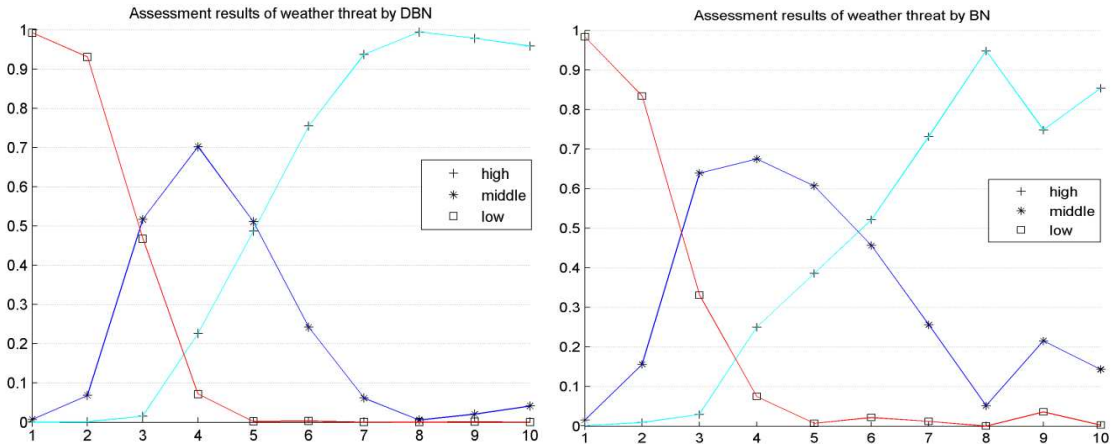

Figure 3. *Assessment results of weather threat using DBN and BN*

http://www.aloki.hu ● ISSN 1589 1623 (Print) ● ISSN 1785 0037 (Online)
DOI: http://dx.doi.org/10.15666/aeer/1704_93919400

Sometimes, the data became abnormal due to measuring error or other reasons. Here, $P_{IoE}^{9} = (0.7,0.1,0.1,0.1)$ was changed to $P_{IoE}^{9} = (0.1,0.1,0.7,0.1)$, where P_{IoE}^{t} is the observation probability of the IoE at time t. In this case, the assessment results are given in *Table 5* and *Figure 4*.

Table 5. *Simulation results of weather threat using DBN and BN when abnormal data occurred*

Time	Assessment results of weather threat by DBN			Assessment results of weather threat by BN		
	High	Middle	Low	High	Middle	Low
1	0.0003	0.0075	0.9923	0.0012	0.0154	0.9834
2	0.0010	0.0685	0.9304	0.0093	0.1564	0.8343
3	0.0158	0.5166	0.4676	0.0296	0.6391	0.3314
4	0.2257	0.7024	0.0718	0.2500	0.6750	0.0750
5	0.4850	0.5127	0.0022	0.3855	0.6072	0.0072
6	0.7514	0.2455	0.0031	0.5517	0.4565	0.0217
7	0.9315	0.0676	0.0010	0.7317	0.2561	0.0122
8	0.9806	0.0193	0.0000	0.9480	0.0516	0.0004
9	0.7551	0.2386	0.0063	0.1773	0.7660	0.0567
10	0.8874	0.1115	0.0010	0.8540	0.1435	0.0026

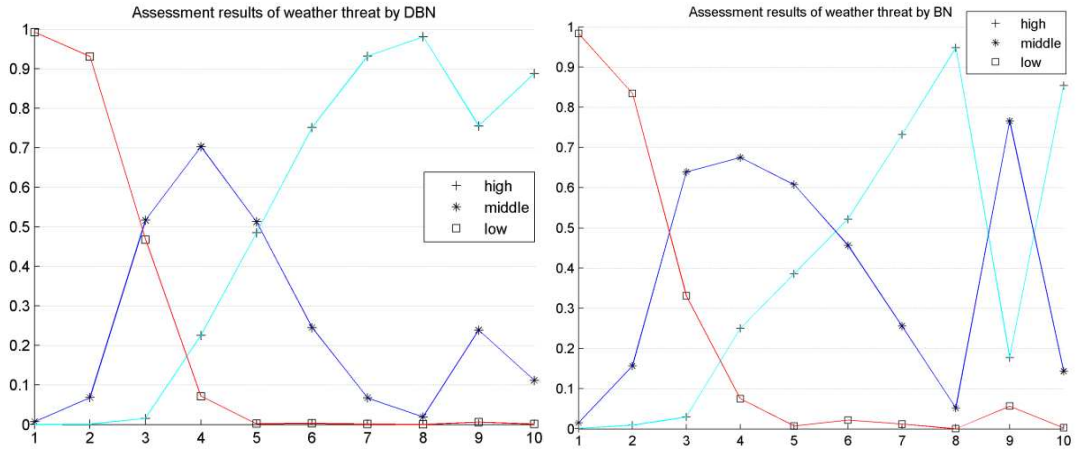

Figure 4. *Assessment results of weather threat when abnormal data occurred*

As shown in *Figure 4,* the DBN managed to infer the weather threat correctly before and after the abnormal data occurred at time 9, although the states of weather factors changed over time and the threat levels were unclear according to the reference tables. By contrast, the BN only derived the right results based on the current data. Therefore, the DBN is much more accurate than the BN in the inference of weather threat level, in spite of the alteration or missing of the feature values.

Conclusions

This paper puts forward a weather treat assessment model based on the DBN, and determines the probability distribution of weather threat level by the HMM inference

http://www.aloki.hu ● ISSN 1589 1623 (Print) ● ISSN 1785 0037 (Online)
DOI: http://dx.doi.org/10.15666/aeer/1704_93919400

method. The model considers all the key factors affecting the weather threat level, including some continuous observed data. Through the numerical simulation of UAVs flight, it is concluded that the DBN-based model is effective and feasible. The model has a great potential of application in fields like battlefield situation assessment, target recognition, etc. In the next step, it is proposed to automatically construct a meteorological threat assessment model through Bayesian learning method, which makes the constructed model more reasonable and accurate, and applies the weather threat assessment results to multi-UAV multi-target mission planning.

REFERENCES

[1] Adiwijaya, N. F. (2013): A rainfall forecasting using fuzzy system based on genetic algorithm. – 2013 International Conference of Information and Communication Technology, pp. 111-115. DOI: 10.1109/ICoICT.2013.6574557.

[2] Al-Matarneh, L., Sheta, A., Bani-Ahmad, S., Alshaer, J., Al-Oqily, I. (2014): Development of temperature-based weather forecasting models using neural networks and fuzzy logic. – International Journal of Multimedia and Ubiquitous Engineering 9(12): 343-36.

[3] Hou, Y. Y., Guo, W. Q., Zhu, Z. (2010): Threat assessment based on variable parameter dynamic Bayesian network. – Proceedings of the 29th Chinese Control Conference, 29-31 July, Beijing, pp. 1230-1235.

[4] Kilby, J., Hosseini, G. (2004): Wavelet analysis of surface electromyography signals. – The 26th Annual International Conference of the IEEE Engineering in Medicine and Biology Society 1: 384-387.

[5] Luo, Y. Z., Chen, J. (2008): Modeling and assessment of weather threat based on Bayesian networks. – Computer Simulation 25(11): 52-55.

[6] Murphy, K. P. (2002): Dynamic Bayesian networks: representation, inference and learning. – Doctoral Dissertation of California University, pp. 14-15.

[7] Paris, P., Erdogan, C. (1963): A critical analysis of crack propagation laws. – Journal of Basic Engineering 85(4): 528-534.

[8] Ramli, A. A., Islam, M. R., Farhan, M., Salamat, M. A., Kasim, S. (2014): A practical weather forecasting for air traffic control system using fuzzy hierarchical technique. – Advances in Intelligent Systems and Computing 287: 99-109.

[9] Sannakki, S., Rajpurohit, V. S., Sumira, F., Venkatesh, H. (2013): A neural network approach for disease forecasting in grapes using weather parameters. – 4th International Conference on Computing, Communications and Networking Technologies, 4-6 July, Tiruchengode, India, pp. 1-5. DOI: 10.1109/ICCCNT.2013.6726613.

[10] Tan, Y. F., Du, L. (2009): Study on wavelet transform in the processing for ECG signals. – 2009 WRI World Congress on Software Engineering, 19-21 May, Xiamen, China, pp. 515-519.

[11] Tang, Z., Gao, X. G., Zhang, Y. (2007): Overview of research on assessment model of radiant threat rank based on dynamic Bayesian network. – Proceedings of the IEEE International Conference on Automation and Logistics, 18-21 Aug, Jinan, China, pp. 1067-1071.

[12] Tian, F. Z., Lu, Y. C. (2004): A DBN inference algorithm using junction tree. – Fifth World Congress on Intelligent Control and Automation, 15-19 June, Hangzhou, China, pp. 4236-4240.

[13] Xiao, Q. K. (2006): Study on in intelligent autonomous optimization mechanisms based-on dynamic Bayesian networks. – Doctoral Dissertation of Northwestern Polytechnical University, pp. 32-33.

http://www.aloki.hu ● ISSN 1589 1623 (Print) ● ISSN 1785 0037 (Online)
DOI: http://dx.doi.org/10.15666/aeer/1704_93919400

[14] Zhang, B., Tang, L., Roemer, M. (2014): Probabilistic weather forecasting analysis for unmanned aerial vehicle path planning. – Journal of Guidance, Control, and Dynamics 37(1): 309-312.
[15] Zhang, L., Dimitris, S., Alia-Klein, N., Volkow, N. D., Goldstein, R. Z. (2005): Modeling neuronal interactivity using dynamic Bayesian networks. – Advances in Neural Information Processing Systems 18: 1593-1600.
[16] Zhu, G, Zhou, S., Ye, S., Wang, M., Wang, Y. (2011): Weather threat modeling and assessment based on BP neural networks. – Electronics Optics &Control 18(3): 69-73.
[17] Zhu, G. T., Zhou, S. D., Ye, S., Wang, Y., Wu, J. (2015): Weather threat modeling and assessment for UAV based on BN. – Computer Measurement & Control 19(9): 233-238.
[18] Zweig, G., Russell, S. (1998): Speech recognition with dynamic Bayesian networks. – Doctoral Dissertation, University of California, Berkeley, pp. 173-180.

http://www.aloki.hu ● ISSN 1589 1623 (Print) ● ISSN 1785 0037 (Online)
DOI: http://dx.doi.org/10.15666/aeer/1704_93919400

THE MASTER PLANNING AND CONSTRUCTION PLAN OF FOREST CITIES BASED ON LOW CARBON EFFECT

SHAO, F.* – XIE, X. D.

College of Architecture and Urban Planning, Qingdao University of Technology, Qingdao 266033, China

**Corresponding author*
e-mail: shaofengwid5545@126.com; phone: +86-180-3219-7955

(Received 3rd Apr 2019; accepted 17th May 2019)

Abstract. With the growth of population and the rapid development of economic level, the emission of greenhouse gases increases greatly, and the form, degree and structure of resource utilization tend to be diversified. Based on the diversity of ecological environment, the utilization of resources shows the diversity of utilization functions. However, the unreasonable carbon emission leads to the decrease of the resource carrying capacity, and its prominent impact on the ecological environment is reflected in the population growth, the inharmonious development of the energy consumption and the urban greening construction. The results of this study show that economic development and forest city construction mutually promote each other. Expanding forest area and improving urban forest accessibility are the most direct effective way to achieve direct emission reduction and forest city target requirements. Based on the four major categories including basis, ecology, economy and industry, and culture covering 12 small indicators proposed by SWOT analysis, technical supports should be provided to the specific forest city planning and construction. This study provides a theoretical basis for the sustainable development of low-carbon environment.
Keywords: *low-carbon effect, resource carrying capacity, SWOT analysis, evaluation indicators, forest cities*

Introduction

With the rapid development of urbanization and the sharp convergence of population in cities and towns, the urban industrialization represented by high energy, high consumption and high emissions has brought unprecedented opportunities to the development of cities. But at the same time its massive greenhouse gas emissions poses irreparable impact on the urban ecological environment and climate change (Huang et al., 2018; Gotovsky et al., 2018; Lodi et al., 2017; Marino et al., 2017; Oguzie et al., 2010; Han, 2011). A series of environmental problems resulting therefrom bring greater negative factors to the development of the cities (Wang and Watson, 2010). Currently, the greenhouse gas is an important contributor to global warming (Koo et al., 2014). High-energy carbon consumption is key to the production of greenhouse gases (Chuai et al., 2015). In view of the importance of a good ecological environment and a sustainable natural environment to urban development, many scholars have paid more and more important attention to the research on how to solve urban high emissions and realize the development of ecological balance (Duane et al., 2012). A great deal of research on eco-cities focus on how to realize the development mode of low-carbon circular economy and the application method of low-carbon effect to the sustainable development of ecological environment (Hosseini and Rezaei, 2013; Scully-Russ, 2012). The theory of low-carbon city put forward is suitable for the urban development in China at present, so the theory of urban planning and construction based on low-carbon effect is of great significance.

http://www.aloki.hu ● ISSN 1589 1623 (Print) ● ISSN 1785 0037 (Online)
DOI: http://dx.doi.org/10.15666/aeer/1704_94019410

Population, resources, environment and development constitute the sub-system of regional economic development, which is the main problem that affects the economic development of a region. To solve this problem from the root, a large number of scholars and urban development practice have given the direction – low-carbon circular economy development model, the low-carbon model of resources development and utilization is designed to promote regional economic development, and a region's carbon consumption and environmental capacity is proportional (Chen, 2012). However, high energy carbon emissions are bound to cause damage to ecosystems (Liu et al., 2017; Yang and Kong, 2012). If human beings want to survive and develop, they must consume resources. If they want to develop sustainably, they must develop and utilize resources according to local conditions on the basis of not destroying the ecological environment. The carrying capacity of resources in a region is limited. Under the action of ecological drive, the carrying capacity of regional resources is gradually decreasing. At present, the comprehensive evaluation indicator of resource utilization efficiency and economic development is ecological footprint. The study of ecological footprint is based on the complex system of "ecology-economy-sustainability". The forest city is an effective way to alleviate the warming of atmospheric environment and solve the greenhouse gas emission. The environmental capacity and forest greening rate of a region are the key indexes to measure the construction of forest cities. Based on the action of low-carbon effect, this study discusses the master planning and construction plan of forest cities, establishes the urban economic development model of low-carbon effect, and realizes the sustainable development of urban regional economy.

Materials and methods

The ecological sensitivity of forest cities is the key index to judge the carrying capacity of forest cities based on the principle of low-carbon consumption, and the ecological environment state is evaluated according to the concept and method of ecology and sustainable development to balance the specific population. The amount of green resources that people need to offset the hazardous substances released for the development of production and consumption of human is the basis for planning the plot ratio of forest cities (Mcintosh et al., 2015; Burrows and Appold, 2015). The calculation of the ecological rate is as shown in *Equation 1,* and the evaluation index is shown in *Table 1:*

$$EF = N \times ef = N\sum_{i=1}^{n}(ai) = N\sum_{i=1}^{n}(C_i / P_i)(i = 1.2.3...n) \quad \text{(Eq.1)}$$

EF is the total index of ecological sensitivity; N is the number of urban carbon consumption items; ef is the equivalent value of carbon consumption per capita in the city; N is the population; i is the type and attribute of consumer goods; ai is the biological production area occupied by each person of the i-th substance; C_i is the average oxygen released by the i-th greening species; P_i is the average production capacity of the i-th substance.

Ecological environmental carrying capacity refers to the ratio of released greenhouse waste to waste absorbed by photosynthesis of green plants. The value of the carrying capacity required for forest city development is expressed as (Schebitz et al., 2014):

http://www.aloki.hu ● ISSN 1589 1623 (Print) ● ISSN 1785 0037 (Online)
DOI: http://dx.doi.org/10.15666/aeer/1704_94019410

$$FR = (PW + DW) \times (1 - \delta) \quad \text{(Eq.2)}$$

where PW represent the carbon value of the production emission; DW indicates the scale of forest greening; δ represents the carbon consumption rate.

Table 1. *Evaluation factors and their classification of the ecological sensitivity*

Ecological factors	Insensitivity	Slight sensitive	Moderately sensitive	Highly sensitive	Extremely sensitive
Vegetation	<0.33	0.33~0.52	0.53~0.64	0.65~0.72	≥ 0.73
Slope	<4	4-9.2	9.3-14.6	14.7~31.2	≥ 33
Altitude	<145	146-287	288~476	478~792	≥ 793
Hierarchical assignment	1	3	5	7	9

Results

SWOT analysis of establishing low-carbon effect forest cities

The SWOT analysis will examine the strengths, weaknesses, opportunities, and challenges of the subjects studied. Through detailed investigation and analysis, the influencing factors are sequenced according to the importance and the correlation analysis is arranged in matrix mode. Then, the relationship among the various factors is analyzed with system analysis under the principle of mutual matching. In order to construct a forest city with low carbon effect, SWOT analysis should be carried out on the construction of the city according to the results of statistical investigation, and the construction strategy of SWOT analysis strategy for forest city construction is shown in *Table 2.*

Table 2. *The construction of national forest SWOT strategy analysis matrix*

Classification	Category	Analysis process			
Internal conditions	Strength	Government Attention	Abundant resources	Urban priority development zone	Experience and reference
	Weakness	Potential hazards of soil and water resources	Forestry development guarantee	Land used for building	
External conditions	Opportunities	Opportunity	Strategy	Policy	Upsurge
	Threats	Development	Compete	Ecological function	Capital

In accordance with the analysis model of *Table 1,* with reference to the data of Yearbook of the National Bureau of Statistics in 2018, the low-carbon construction effect and the total investment ratio of forest construction of major green forest cities are analyzed according to the ecological sensitivity and carrying capacity calculation scheme, providing practical support for the feasibility analysis, with the results shown in *Figure 1.*

Figure 1 shows that the SWOT analysis indexes analyzed in this study are positively correlated with the construction planning effect of the forest cities. In light of the fact that the primary task of the master planning of forest cities based on the low-carbon effect is to carry out the SWOT analysis on a statistical basis, and according to the

http://www.aloki.hu ● ISSN 1589 1623 (Print) ● ISSN 1785 0037 (Online)
DOI: http://dx.doi.org/10.15666/aeer/1704_94019410

above analysis plan and the examples of the construction of individual cities, it is confirmed that the construction of forest-oriented cities should be analyzed from the following three aspects. First, the SWOT analysis on the construction of the city as a forest city shall be thoroughly carried out to clearly recognize that the city in the construction process needs what experience data and absorb what ways and methods for improvement. Second, we should formulate a strategy for the development of low-carbon economy for modernization, so that the economic development of cities should be coordinated with the construction of ecological environment and the construction of national forests. Third, we should actively respond to the challenges brought by the acceleration of the green urbanization process, analyze the national policies and local environmental characteristics, dare to expose the problems, turn the disadvantages into advantages for the development, and strengthen the situation and determination of realizing the low-carbon forest cities. From the above three aspects, the changing trend of the greening rate of the main greening cities in different years is shown in *Figure 2*.

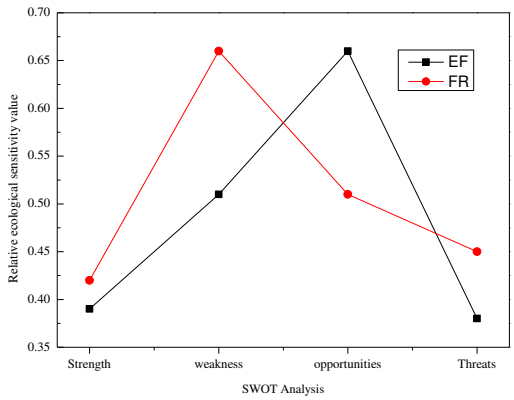

Figure 1. *Statistical analysis of different evaluation indicators based on SWOT*

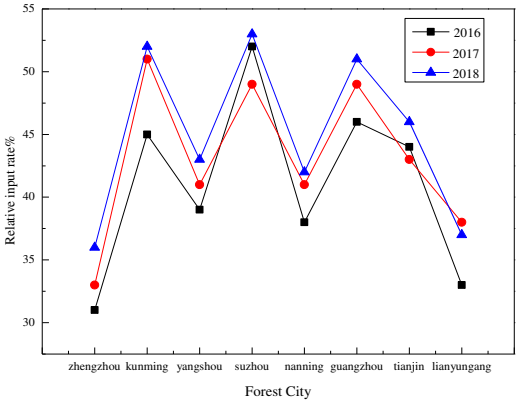

Figure 2. *Statistical value of greening rate of green city in different years*

Construction of forest city evaluation indexes based on low-carbon requirements

After the SWOT analysis on the construction of low-carbon forest cities, it is necessary to establish quantifiable evaluation indexes to measure the specific targets and strategies of forest urban planning and construction. In this study, forest city

http://www.aloki.hu ● ISSN 1589 1623 (Print) ● ISSN 1785 0037 (Online)
DOI: http://dx.doi.org/10.15666/aeer/1704_94019410

sensitivity and low-carbon effect bearing capacity are used to measure the result of the comprehensive action of human and natural environment, and the balance of ecological environment causes the changes in regional material flow, energy flow and information flow, so as to construct the evaluation indexes and provide technical support for the construction of forest cities with low-carbon effect as the target. According to the four factors of basic index, ecological index, economic and industrial index and cultural index, this study evaluates the order and feasibility criterion of construction index. Refer to *Table 3* for comprehensive evaluation index and its reference value.

Table 3. *Establishing evaluation index of green forest city*

Index system	Evaluation content	Quantitative indicators	Low carbon significance
Basic index	Forest coverage	≥ 35%	Carbon absorption
	Urban green coverage rate	≥ 40%	
	Per capita park green space	More than 11 m^2	Fixed carbon emission reduction
	Greening of important water sources	≥ 55%	
	Road greening	≥ 70%	
Ecological indicators	Suburban forest naturalness	Naturality below 0.5	Improving forest quality
	Bio-diversity	Species diversity	
	Forest soil protection	Reducing soil and water loss	
Economic and industrial indicators	Forest tending and forest management	Close to nature	Developing low carbon economy
	Ecotourism	Ecotourism construction	
	Forest production base	Forest related income	
	Forest nursery	Self-sufficiency rate ≥ 70%	
Cultural indicators	Popular science sites	Number of popular science places	Improving forest carbon sequestration
	Voluntary tree planting	Compulsory tree planting rate for all	

Table 3 summarizes and analyzes the master planning and evaluation indexes for the construction of low-carbon cities. To build low-carbon forest cities, it is first to combine the index requirements of national forest cities and to compare the current situation of the city with the actual data according to a large number of investigations. In accordance with the evaluation result, the corresponding strategies are adopted. The overall construction idea of forest cities at the present stage is to increase the forest coverage rate, the green area, the green belt area, and the green rate, adopt the appropriate forest seedling cultivation method and expand popular science places to improve the forest city construction planning based on the low-carbon effect.

Discussion

Sustainable low carbon forest city planning

The evaluation index of constructing low-carbon forest cities provides the basis and direction for the master planning of constructing low-carbon forest cities. How to realize the sustainable, reduced and economical low-carbon city construction needs to

http://www.aloki.hu ● ISSN 1589 1623 (Print) ● ISSN 1785 0037 (Online)
DOI: http://dx.doi.org/10.15666/aeer/1704_94019410

have clear planning idea and construction outline in the planning. Based on the literature review and the results of forest city construction, this study puts forward the process and method of low-carbon city construction. The definition of low-carbon cities mainly includes low-carbon city, low-carbon city life, low-carbon city economy, low-carbon urban transportation and low-carbon urban culture. The low-carbon urban forests include low-carbon urban forest construction and urban forest conservation. The low - carbon city life explores the code of conduct for low-carbon cities. The low-carbon urban transportation only considers the urban overrunning road. The low-carbon city culture focuses on the publicity and education of the concepts related to the low carbon and urban forests and forest cities. See *Figure 3* for the constituent elements of the low-carbon forest city construction.

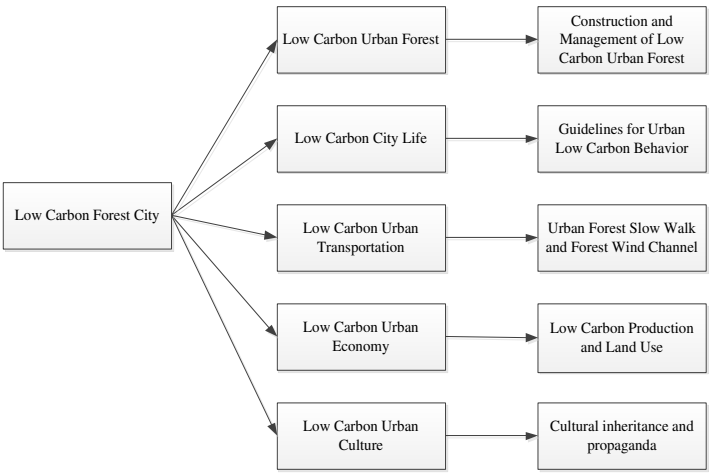

Figure 3. *Low-carbon forest city form the element –level analysis*

Feasibility method of forest city construction with low-carbon effect

In order to control the steady state of forest ecological carrying capacity, it is necessary to control the relationship among population scale, economic development and resource carrying capacity. *Figure 4* is a two-way optimization model of forest environmental carrying capacity and population scale. It can be seen that with the continuous improvement of the economic level, the population scale will correspondingly increase, and when the population scale increases to a certain amount, the economic level will show relatively rapid growth. Carbon emissions are proportional to population scale. People's production and living activities will result in greater carbon emissions. That is to say, the moderate population scale related to living standards will increase with the increase of carbon emissions and the improvement of economic level. Therefore, the development is on the rise or in the developed cities, the analysis of the population structure and industrial structure can show that the urban construction based on low-carbon effect is imminent and suitable for carbon emission evaluation so as to put forward the feasibility of the construction planning plan purposefully.

Based on the feasibility plan for urban forest construction, it is necessary to make clear the main contents of the low carbon for forest cities and deduce the design scheme that satisfies the evaluation method through function analysis. The main functions of the scheme are as follows: first, direct emission reduction; second, indirect emission

http://www.aloki.hu ● ISSN 1589 1623 (Print) ● ISSN 1785 0037 (Online)
DOI: http://dx.doi.org/10.15666/aeer/1704_94019410

reduction; third, increase in the ecological capacity. On the one hand, urban forest can directly reduce the carbon dioxide content by absorbing carbon dioxide, which is a direct effective way to realize low-carbon content of cities. On the other hand, the rational distribution of urban forest can completely change the pattern of urban land use, make the urban green land more reasonable, and reduce the concentration distribution of urban carbon emissions to a certain extent. Secondly, the vertical gas exchange is increased by the transpiration of the forests, so the heat island effect is alleviated, and the gas emission and accumulation of the greenhouse can be effectively reduced. Therefore, the direct low-carbon measures of low-carbon forest cities are to build urban forests vigorously. Its main function is shown in *Figure 5*.

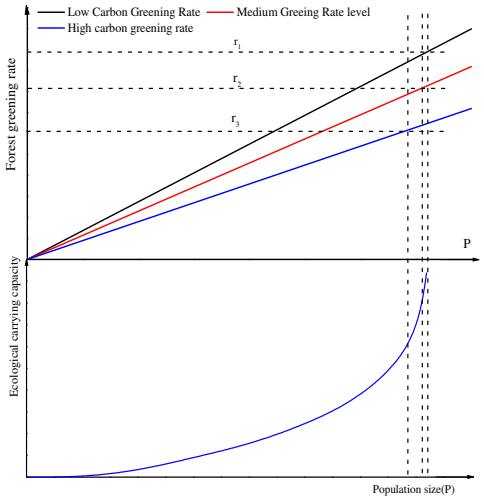

Figure 4. *Two-way optimization model of ecological equilibrium capacity and population size*

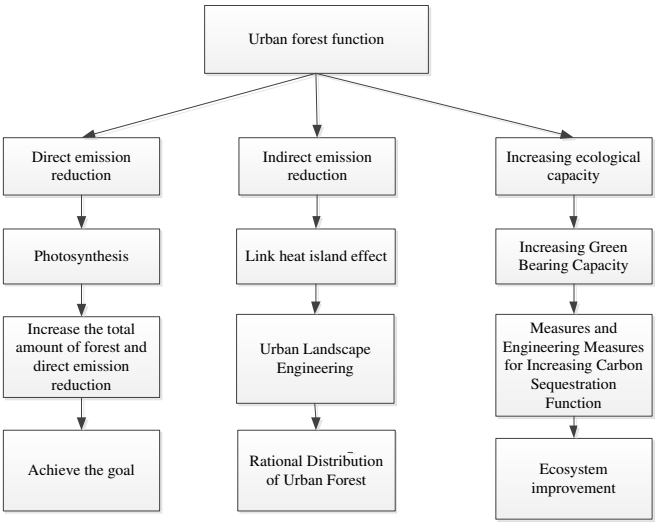

Figure 5. *Low-carbon effect analysis diagram of the urban forest*

Through the judgment of the evaluation indicators for the construction of forest cities with low-carbon effect and the understanding of the feasibility construction steps of the construction plan and their significance, the conceptual and leading guidance is

http://www.aloki.hu ● ISSN 1589 1623 (Print) ● ISSN 1785 0037 (Online)
DOI: http://dx.doi.org/10.15666/aeer/1704_94019410

provided for the master planning, but the overall construction plan of forest cities is based on the statistical mathematics, probability mathematics, analysis and checking computations. Therefore, in order to have a clearer working step for the overall construction plan, it is necessary to clarify the thought of study on the accessibility of urban forest construction. By referring to *Figure 6* and through accessibility analysis, it is possible to identify the weak points of greening construction and the points to be strengthened, so as to carry out targeted and planned implementation of block division units for forest city construction.

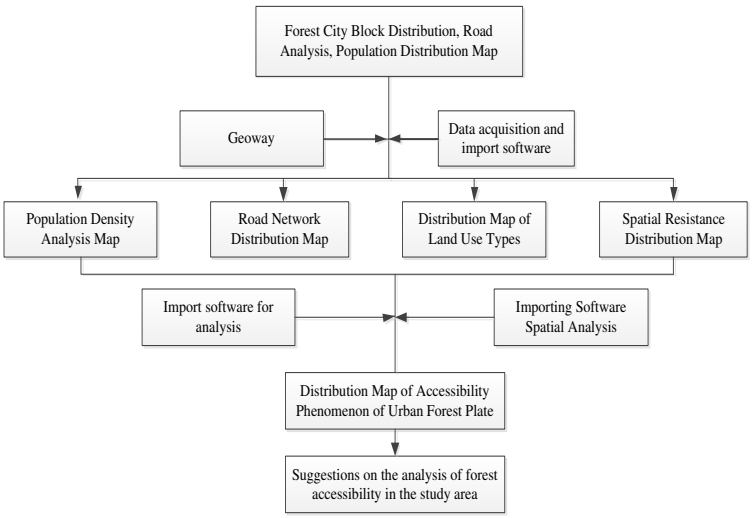

Figure 6. *The research route of achieving standards in forest cities*

Conclusions

Based on the principle of low-carbon effect, this study makes qualitative and quantitative analysis on the master planning and construction steps of forest cities, and thus provides the basis for sustainable and low-carbon forest city construction. The concrete conclusions are as follows:

(1) The driving factors of the change in the low-carbon environmental carrying capacity include natural factors and human factors, the growth of population and the construction of urbanization industry can promote the construction of forest cities to a certain extent, expanding the forest area and improving urban forest accessibility is the most direct and effective way to achieve the direct emission reduction and forest city target;

(2) This study introduces SWOT analysis and puts forward the evaluation indexes of forest const ruction covering 4 major categories and 12 small categories, providing data support for the hypothesis on the master planning;

(3) The construction of low-carbon forest cities has the sustainable development significance to the development of cities. The construction of low-carbon forest city in the future is the supporting construction project of industrialization development. The study provides the qualitative analysis index for the overall construction and planning of forest cities and also offers the basis and scheme for the basic research on the construction of forest cities.

http://www.aloki.hu ● ISSN 1589 1623 (Print) ● ISSN 1785 0037 (Online)
DOI: http://dx.doi.org/10.15666/aeer/1704_94019410

REFERENCES

[1] Burrows, C. R., Appold, M. S. (2015): Hydrology of the forest city basin, mid-continent, USA: implications for CO_2 sequestration in the St. Peter Sandstone. – Environmental Earth Sciences 73(4): 1409-1425.
[2] Chen, H. (2012): Establishment of national forest city based on the construction of ecological civilization in china. – Fish Physiology & Biochemistry 38(4): 1099-106.
[3] Chuai, X., Huang, X., Wang, W., Zhao, R., Zhang, M., Wu, C. (2015): Land use, total carbon emissions change and low carbon land management in coastal Jiangsu, China. – Journal of Cleaner Production 103: 77-86.
[4] Duane, B., Hyland, J., Rowan, J. S., Archibald, B. (2012): Taking a bite out of Scotland's dental carbon emissions in the transition to a low carbon future. – Public Health 126(9): 770-777.
[5] Gotovsky, M., Gotovsky, A., Mikhailov, V., Kolpakov, S., Lychakov, V., Sukhorukov, Y. (2018): Formic acid cycle as partial alternative to Allam cycle less expensive and simpler. – Tecnica Italiana - Italian Journal of Engineering Science 61+1(2): 49-54.
[6] Han, Y., Shi, J., Xu, L., Cao, W. Q., Dong, H. (2011): Tic precipitation induced effect on microstructure and mechanical properties in low carbon medium manganese steel. – Materials Science & Engineering A 530: 643-651.
[7] Hosseini, S. M., Rezaei, A. (2013): Developing an information system for sustainable natural resource management in Alborz watershed, northern Iran. – Systemic Practice and Action Research 26(2): 131-152.
[8] Huang, K., Yang, X., Lu, Y., Mi, C. C., Kondlapudi, P. (2018): Ecological driving system for connected/automated vehicles using a two-stage control hierarchy. – IEEE Transactions on Intelligent Transportation Systems 19(7): 2373-2384.
[9] Koo, C., Kim, H., Hong, T. (2014): Framework for the analysis of the low-carbon scenario 2020 to achieve the national carbon emissions reduction target: focused on educational facilities. – Energy Policy 73: 356-367.
[10] Liu, Y., Tian, Y., Chen, M. (2017): Research on the prediction of carbon emission based on the chaos theory and neural network. – International Journal Bioautomation 21(S4): 339-348.
[11] Lodi, C., Malaguti, V., Contini, F. M., Sala, L., Muscio, A., Tartarini, P. (2017): University energy planning for reducing energy consumption and GHG emissions: the case study of a university campus in Italy. – International Journal of Heat and Technology 35(S1): S27-S32.
[12] Marino, C., Nucara, A., Nucera, G., Pietrafesa, M. (2017): Economic, energetic and environmental analysis of the waste management system of Reggio Calabria. – International Journal of Heat and Technology 35(S1): S108-S116.
[13] Mcintosh, J., Martini, A., Petsch, S., Huang, R., Nüsslein, K. (2015): Biogeochemistry of the forest city basin coalbed methane play. – International Journal of Coal Geology 76(1): 111-118.
[14] Oguzie, E. E., Enenebeaku, C. K., Akalezi, C. O., Okoro, S. C., Ayuk, A. A., Ejike, E. N. (2010): Adsorption and corrosion-inhibiting effect of *Dacryodis edulis* extract on low-carbon-steel corrosion in acidic media. – Journal of Colloid and Interface Science 349(1): 283-292.
[15] Schebitz, N., Brockmann, M., Schie, L. C., Kuck, D., Staubach, M., Fricke, N. (2014): Information modalities and timing of ecological driving support advices. – IET Intelligent Transport Systems 8(6): 534-542.
[16] Scully-Russ, E. (2012): Human resource development and sustainability: beyond sustainable organizations. – Human Resource Development International 15(4): 399-415.
[17] Wang, T., Watson, J. (2010): Scenario analysis of China's emissions pathways in the 21st century for low carbon transition. – Energy Policy 38(7): 3537-3546.

http://www.aloki.hu ● ISSN 1589 1623 (Print) ● ISSN 1785 0037 (Online)
DOI: http://dx.doi.org/10.15666/aeer/1704_94019410

[18] Yang, S., Kong, D. (2012): Expansion of construction land and its effect on forest based on road network character: a case study of Shenzhen city. – Ecology & Environmental Sciences 21(2): 286-292.

http://www.aloki.hu ● ISSN 1589 1623 (Print) ● ISSN 1785 0037 (Online)
DOI: http://dx.doi.org/10.15666/aeer/1704_94019410

WAVELET ANALYSIS ON EFFECTS OF CLIMATE CHANGE ON HYDROLOGY AND WATER RESOURCES

ZHANG, J.[1,2] – FENG, M. Q.[1*] – WANG, Y.[1]

[1]*State Key Laboratory Base of Eco-Hydraulic Engineering in Arid Area, Xi'an University of Technology, Xi'an 710048, China*

[2]*Shanxi Conservancy Technical College, Yuncheng 044004, China*

**Corresponding author*
e-mail: mqfeng@xaut.edu.cn

(Received 3rd Apr 2019; accepted 17th May 2019)

Abstract. The global warming has triggered climate change, which has a certain impact on the redistribution of hydrology and water resources, and may even tilts the ecological balance. This paper sums up the trends of some climate and hydrological indices in several Chinese rivers, namely, temperature, precipitation and runoff, and examines how these indices vary with the time. Then, the wavelet analysis was introduced to disclose the hidden features of temperature, precipitation and runoff time series, revealing certain correlations between these series. As a result, the effect of temperature on precipitation was explored through correlation analysis, so was that of temperature and precipitation on runoff. Finally, the ecological water demands in the upstream, midstream and downstream of the target river were computed, and found to change in a similar way to temperature and precipitation. The research findings shed new light on the maintenance of hydrology and water resources in rivers and the handling of relevant problems.
Keywords: *temperature, precipitation, runoff, water resources, ecology, ecological balance*

Introduction

The rapid development of global economy and industry has pushed up the emission of carbon dioxide, inducing climate warming around the world (Bertuzzo and Mari, 2017; Quilty and Adamowski, 2018). The rising temperature melts ice in polar regions, elevates the sea level and triggers various environmental problems (Liu et al., 2018; Jódar et al., 2017; Rad et al., 2017). For example, the temperature variation may cause changes in water evaporation and precipitation, exerting certain impacts on terrestrial hydrology and water resources (Ademila and Saloko, 2018; Baker, 2017; Mcknight, 2017; Moungar et al., 2018; Na et al., 2017). The redistribution of water resources in turn increases the chance of floods and droughts, tilts the ecological balance, and even endangers the survival of humans and other living things on Earth (Seiller et al., 2017; Dile et al., 2018; Zhao et al., 2017).

To solve these problems, this paper analyzes how climate conditions affect hydrology and examines the necessary hydrological conditions for ecological balance. Much research has been done on the hydrological impacts of climate conditions at home and abroad. However, there is not yet a unified understanding about how the climate affects the hydrology (Hutton et al., 2017; Blöschl, 2017; Ouyang et al., 2017). On ecology and hydrology, the study of the ecological demand for hydrology and water resources started early, yielding fruitful results. In the beginning, the water resources needed for ecology were investigated with the goal of satisfying the water demand for living organisms in river areas. Later, some scholars held that simply fulfilling this demand cannot ensure the relative stability of the ecology; the water resources should

http://www.aloki.hu ● ISSN 1589 1623 (Print) ● ISSN 1785 0037 (Online)
DOI: http://dx.doi.org/10.15666/aeer/1704_94119423

be sufficient to maintain a certain degree of liquidity, i.e. the ability to purify itself (Mccurley and Jawitz, 2017). Most mature ecological and hydrological models are created in developed countries in Europe and North America. European countries have developed more such models than anywhere else. *Table 1* lists the applications of typical ecological and hydrological models since the 1980s.

Table 1. *Typical ecological and hydrological models*

Decade	Reference	Region	Application
1980s	Sharpley and Williams (1990)	North America	Evaluation of land and water management
1990s	Krysanova et al. (1998)	Europe	Hydrological simulation of vegetation growth
2000s	Ek et al. (2000)	Europe	Development of modules containing biotic and abiotic information for geological information system (GIS) and ecological protection/evaluation system
2000s	Arabi et al. (2007)	North America	Hyrological prediction of water quality
2010s	Acreman and Holden (2013)	Europe	Evaluation of climate impact on hydrology

As shown in *Table 1*, most of the existing studies consider ecological issue separately from the hydrological issue. There is no report on the relationship between the two issues. However, the relationship must be studied in order to disclose the effect of hydrological conditions on ecological balance.

To sum up, there are a series of problems to be solved, despite some research results on how climate affects hydrological conditions and how hydrology impacts ecology. Hence, this paper attempts to solve the problems concerning the relevant influence mechanisms, and shed new light on ecological protection in the context of global warming.

Materials and methods

Basic information

In this paper, Jinghe River in China is taken as the research object and denoted as river A. The mainstream was divided into three sections: the upstream (A1), the midstream (A2) and the downstream (A3). There are three water sources of river A, namely, Laohe River (B), Nanhe River (C) and Qinhe River (D). Among them, rivers B and C have richer water resources than river D. The position distribution of the hydrological station is shown in *Figure 1.* In *Table 2*, the research data were collected from six hydrological stations, which are respectively located on A1, A2, A3, B, C, D.

Table 2. *The basic information on the rivers*

River	Watershed area (km^2)	Annual mean runoff (100 million m^3)
A	52,977	55.61
B	30,251	23.64
C	19,321	19.76
D	10,231	7.98

http://www.aloki.hu ● ISSN 1589 1623 (Print) ● ISSN 1785 0037 (Online)
DOI: http://dx.doi.org/10.15666/aeer/1704_94119423

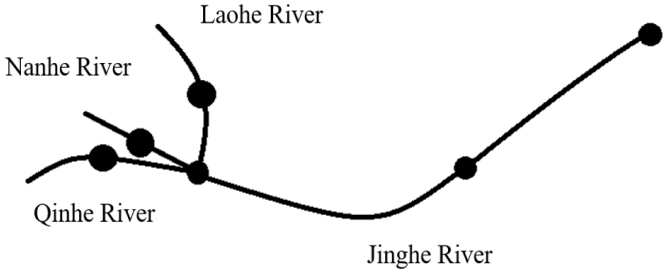

Figure 1. *Hydrological station location*

The statistical data in 2017 show that the watershed of Jinghe River generally enjoys abundant grassland and forestland resources. However, there are some sections with inadequate water resources, sparse vegetation and fragile ecology. The vegetation information in the upstream, midstream and downstream of Jinghe River (A1~A3) and in Laohe River, Nanhe River and Qinhe River (B~C) is provided in *Table 3*.

Table 3. *The vegetation information in the watersheds of the rivers*

Watershed		Forest land (Million acres)	Grassland (Million acres)	Total area (Million acres)
A	A1	899.3	115	1,014.3
	A2	497.8	500.9	998.7
	A3	100.9	232.9	332.8
B		1,000.6	1,098.3	2,098.9
C		438.6	760.1	1,198.7
D		329.7	547.2	876.9

Climate conditions

This paper mainly targets the meteorological data of the watershed of Jinghe River in the past 50 years (1969~2018).

Temperature

The annual mean temperature trend from 1969 to 2018 was plotted as *Figure 1*. The temperature trend can be linearly fitted by the *Equation 1:*

$$y = 0.03081x - 50.83708 \quad \text{(Eq.1)}$$

The coefficient of determination of the fitting formula reached 0.61097, an evidence of good linear fitting effect. As shown in *Figure 2,* the temperature increased with the elapse of time, which agrees with the trend of global warming in recent decades. The rising temperature in Jinghe River watershed manifests the global warming phenomenon. Of course, *Figure 2* also shows that the temperature growth was not always at the same rate in the fifty years. The rising speed was much faster in the latest 20~30 years.

The decadal temperature change in *Figure 3* reflects that the temperatures in 1989~1998 and 1999~2008 were much higher than those in 1969~1978 and 1979~1988,

http://www.aloki.hu ● ISSN 1589 1623 (Print) ● ISSN 1785 0037 (Online)
DOI: http://dx.doi.org/10.15666/aeer/1704_94119423

and slightly higher than that in 2009~2018. In general, the temperature underwent an obvious increase, followed by a slight decline.

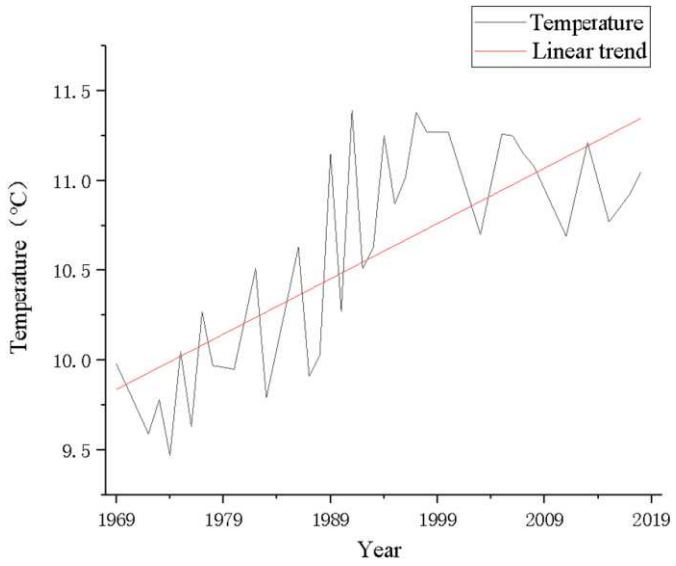

Figure 2. *Interannual temperature change*

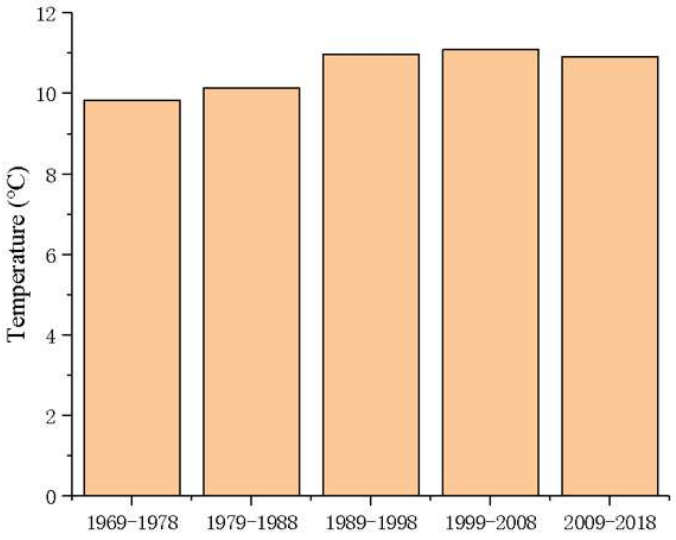

Figure 3. *Decadal temperature change*

Precipitation

The variation in the annual mean precipitation from 1969 to 2018 is illustrated in *Figure 4*. The precipitation trend can be linearly fitted by the *Equation 2:*

$$y = 0.94536x - 1798.87651 \quad \text{(Eq.2)}$$

The coefficient of determination of the fitting formula reached 0.61097, revealing a good linear fitting effect. As shown in *Figure 4*, the precipitation showed an obvious growth over time.

http://www.aloki.hu ● ISSN 1589 1623 (Print) ● ISSN 1785 0037 (Online)
DOI: http://dx.doi.org/10.15666/aeer/1704_94119423

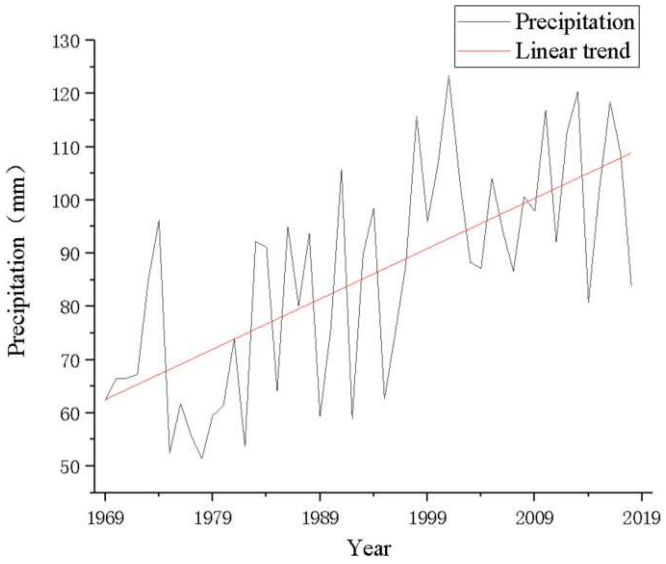

Figure 4. *Interannual precipitation change*

The decadal precipitation change in *Figure 5* shows that the precipitation continued to rise, but at a slower speed in 2009~2018.

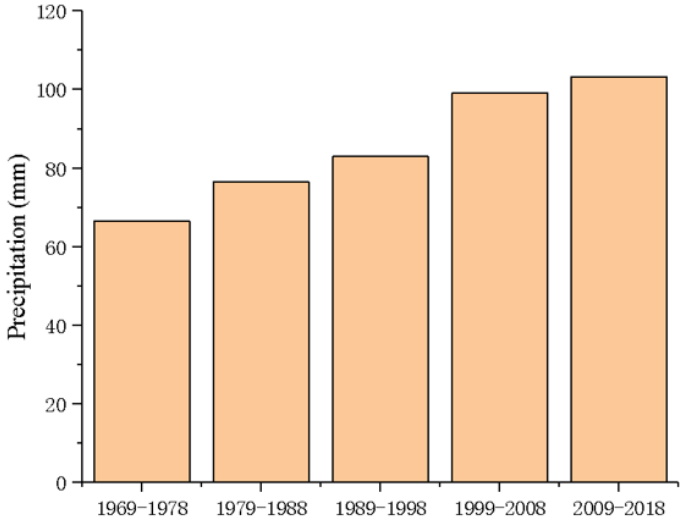

Figure 5. *Decadal precipitation change*

Runoff features

The redistribution of water resources is an important consequence of global warming. In this paper, the research data are collected from different hydrological stations, including the runoffs of rivers B, C and D and the three sections of Jinghe River.

The interannual runoff changes of rivers B, C and D were linearly fitted by the *Equations 3–5*.

$$y = 0.48481x - 929.22809 \quad \text{(Eq.3)}$$

http://www.aloki.hu ● ISSN 1589 1623 (Print) ● ISSN 1785 0037 (Online)
DOI: http://dx.doi.org/10.15666/aeer/1704_94119423

$$y = 0.51626x - 979.6944 \quad \text{(Eq.4)}$$

$$y = 0.32655x - 594.53929 \quad \text{(Eq.5)}$$

The coefficient of determinations of the above fitting formulas were respectively 0.32811, 0.11164 and 0.05515. The slopes of *Equations 3* and *4* were significantly different from 0, but the slope of *Equation 5* is not. As shown in *Figures 6–8,* the runoffs of rivers B, C and D exhibited a growing trend over time.

The interannual runoff changes of the upstream A1, midstream A2 and downstream A3 of Jinghe River were linearly fitted by the *Equations 6–8*.

$$y = -0.3567x + 770.62988 \quad \text{(Eq.6)}$$

$$y = -0.26977x + 580.15361 \quad \text{(Eq.7)}$$

$$y = -0.42499x + 873.68232 \quad \text{(Eq.8)}$$

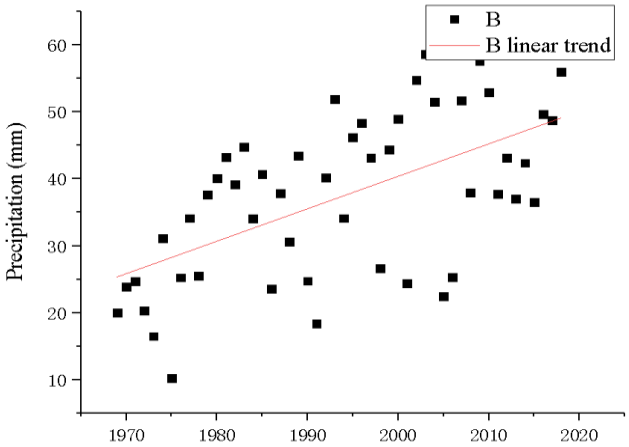

Figure 6. *Interannual runoff change in River B*

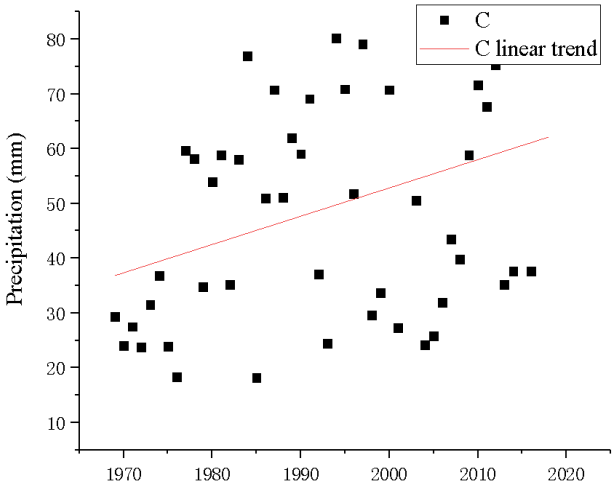

Figure 7. *Interannual runoff change in River C*

http://www.aloki.hu ● ISSN 1589 1623 (Print) ● ISSN 1785 0037 (Online)
DOI: http://dx.doi.org/10.15666/aeer/1704_94119423

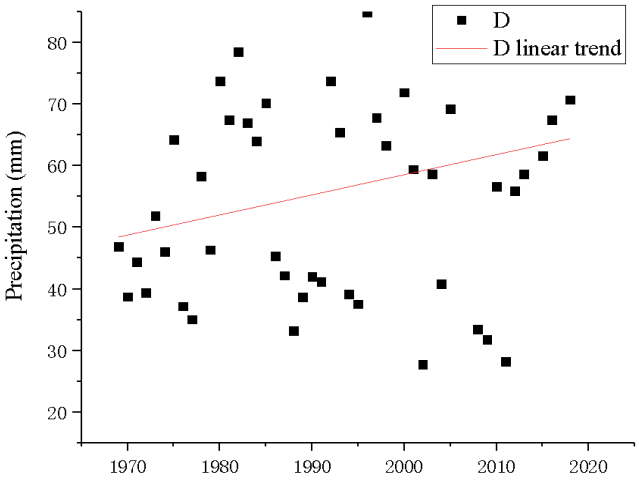

Figure 8. *Interannual runoff change in River D*

The coefficient of determinations of the above fitting formulas were, respectively, 0.08028, 0.05 and 0.13372. The slopes of *Equations 6* and *8* were significantly different from 0, but the slope of *Equation 7* is not. As shown in *Figures 9–11,* the runoff of river A showed a certain decline in the research period, indicating the possible overuse of the water resources in the river. The excess water consumption for industry and agriculture may increase the water evaporation, reduce the vegetation area, and thus tilt the ecological balance.

Analysis process

Figure 12 shows our analysis process. In this paper, two important indices of climate, temperature and precipitation, are subjected to feature analysis, and then investigated to disclose how each of them affects the runoff. The index features were examined through wavelet analysis, and the runoff impacts of each index were studied by correlation analysis.

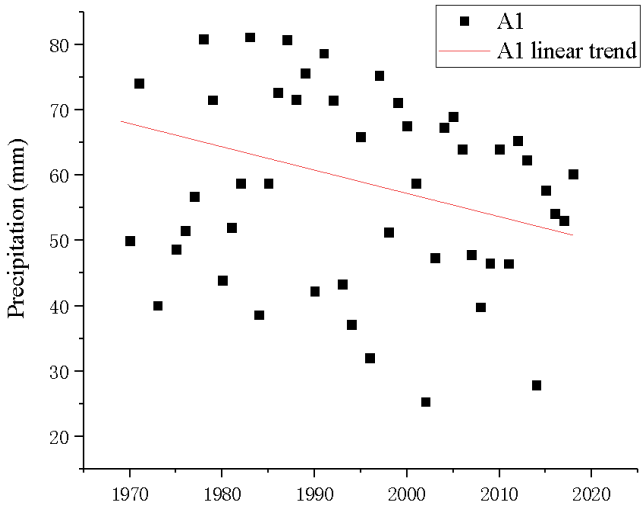

Figure 9. *Interannual runoff change in A1*

http://www.aloki.hu ● ISSN 1589 1623 (Print) ● ISSN 1785 0037 (Online)
DOI: http://dx.doi.org/10.15666/aeer/1704_94119423

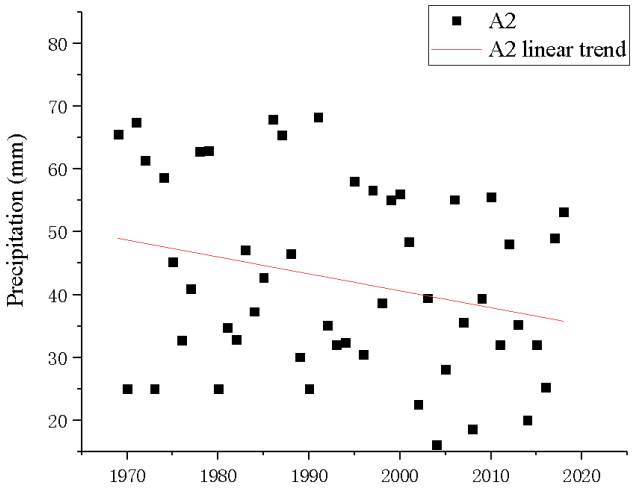

Figure 10. *Interannual runoff change in A2*

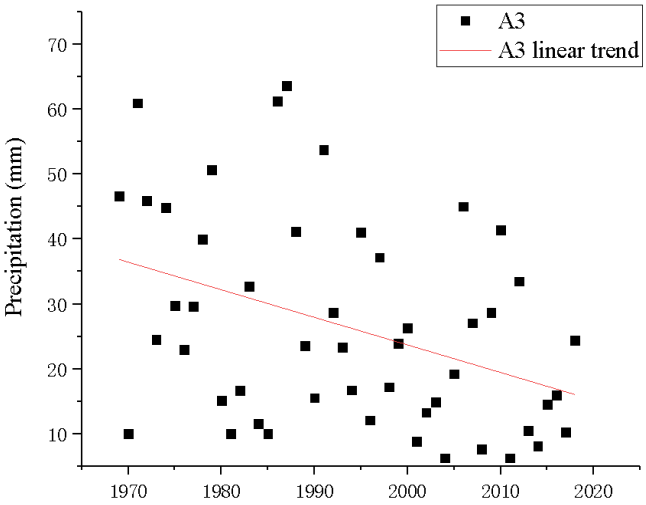

Figure 11. *Interannual runoff change in A3*

Results

Analysis of index features

Wavelet analysis is an approach for multi-resolution statistical analysis. Compared with the traditional time series analysis, this approach does well in mining out hidden information from the research data, and enjoys great value in reference and application. In this paper, wavelet analysis is adopted to explore the data periodicity, which cannot be achieved by traditional statistical methods. The results of our wavelet analysis are listed below.

(1) The temperature time series was periodic on multiple scales, especially on the scales of 15~30, 7~22 and 2~9. The periodicity was obvious through the research period on the first two scales, and only in part of the research period on the last scale. The most obvious periodicity was observed on 15~30.

http://www.aloki.hu ● ISSN 1589 1623 (Print) ● ISSN 1785 0037 (Online)
DOI: http://dx.doi.org/10.15666/aeer/1704_94119423

(2) Similar to the temperature time series, the precipitation time series also exhibited periodicity on multiple scales, especially on the scales of 15~29, 6~21 and 2~7. The periodicity was obvious through the research period on the first two scales, and only in part of the research period on the last scale. The most obvious periodicity was observed on 15~29.

(3) On the runoff time series, the runoff of Laohe River had the same strong period performance with the regional temperature, the runoff of Nanhe River had the same strong period performance with the regional precipitation, and the runoff of Qinhe River had the same strong period performance with the regional precipitation; For Jinghe River, the upstream, midstream and downstream agreed with the regional temperature in the strong period performance.

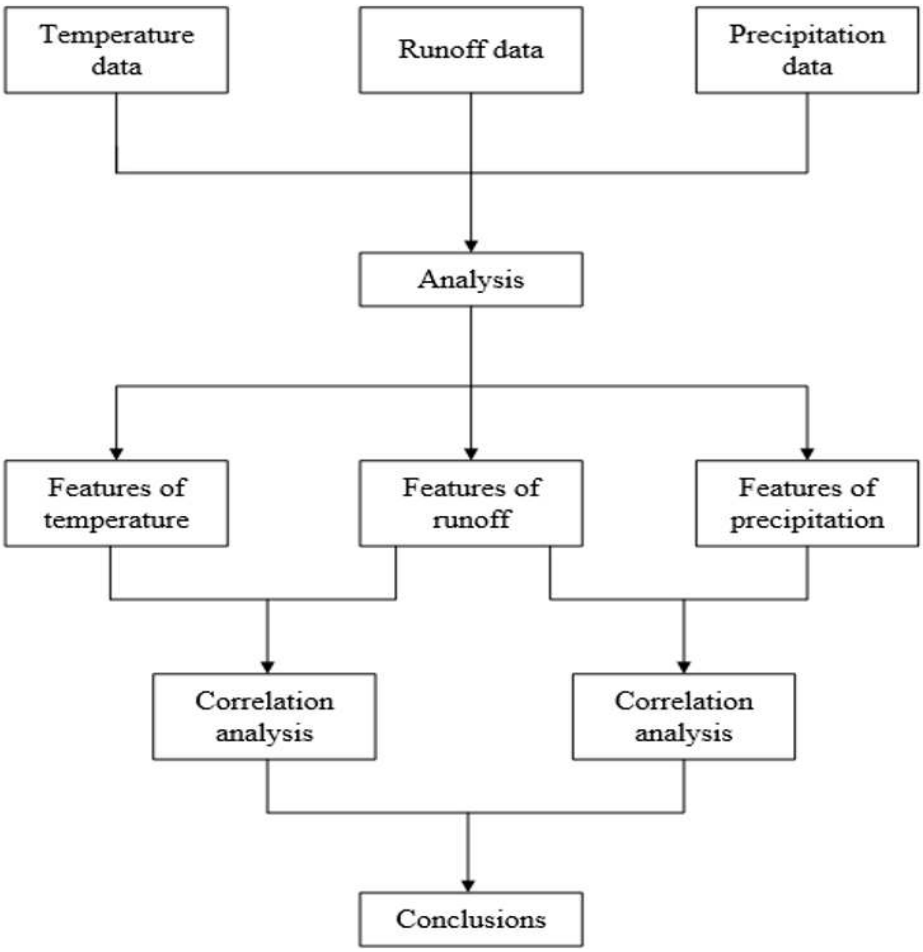

Figure 12. *Analysis process*

Correlation analysis

Through the analysis on index features, it is learned that the river runoffs were consistent with temperature and precipitation in strong period performance. In this subsection, the effects of temperature and precipitation are further discussed through correlation analysis. The results are shown in *Table 4*, where T is temperature, P is precipitation, and AR~DR are the runoffs of Jinghe River, Laohe River, Nanhe River and Qinhe River (A~D), respectively.

http://www.aloki.hu ● ISSN 1589 1623 (Print) ● ISSN 1785 0037 (Online)
DOI: http://dx.doi.org/10.15666/aeer/1704_94119423

Table 4. *Results of correlation analysis*

	T	P	AR	BR	CR	DR
T	1**	0.560**	0.393**	0.402**	0.286**	0.285**
P	0.560**	1**	0.378**	0.322**	0.244**	0.284**

**The corresponding statistic is significant on the level of 0.01. The correlation analysis reveals significant correlations between temperature, precipitation and the runoffs of Jinghe River, Laohe River, Nanhe River and Qinhe River

Ecological water demand

To disclose the impacts of climate change on ecological balance, one of the keys is to check if the runoff satisfies the ecological water demand. The data on the area of different types of vegetation in Jinghe River watershed were incomplete. The only available data were recorded in 1975, 1995, 2000, 2010, 2014 and 2017. Therefore, the data on the area and density of different types of vegetation, as well as on the water demand for the normal growth of each plant, were extracted from these years, and used to compute the ecological water demands. The results are shown in *Figure 13*.

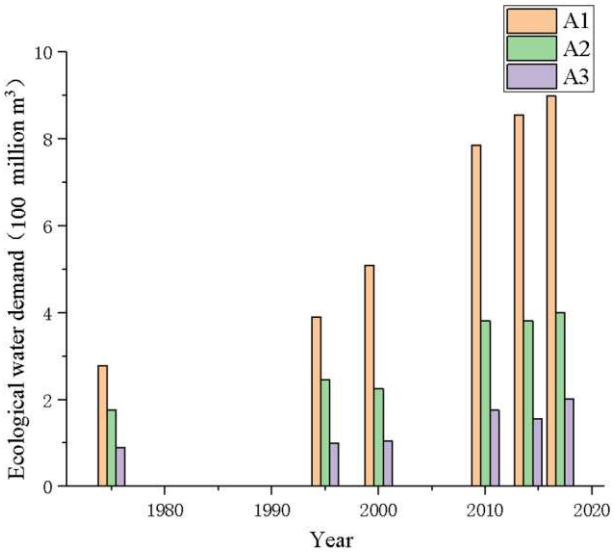

Figure 13. *Ecological water demand*

It can be seen from *Figure 13* that the ecological water demands in the upstream, midstream and downstream of Jinghe River were all on the rise. The trend is similar to that of temperature and precipitation.

Discussion

Our research shows that both the temperature and precipitation in Jinghe River basin were on the rise in the reesarch period, which is similar to most regions across the globe (Bertuzzo and Mari, 2017). One of the more striking features of Jinghe River basin is that: the precipitation increased slightly in 2009~2018, despite the lack of obvious growth in temperature. Considering the regional vegetation area, the phenonmenon can

http://www.aloki.hu ● ISSN 1589 1623 (Print) ● ISSN 1785 0037 (Online)
DOI: http://dx.doi.org/10.15666/aeer/1704_94119423

be attributed to the significant growth in vegetation coverage and the further increase in evaporation in the river basis during 2009~2018.

The wavelet analysis and correlation analysis agree that temperature, precipitation and climate conditions have certain correlations with river runoff, which echoes the conclusions of the previous studies (Na et al., 2017). As shown in *Table 4*, the temperature has a significant impact on precipitation and the two indices are positively correlated, that is, the precipitation increases with temperature. This relationship may be the result of the intense evaporation of surface water under high temperature. Meanwhile, the river runoffs are positively correlated with both temperature and precipitation, but the correlation coefficients are only 0.402 at the highest. This value is lower than that of the other studies (Bertuzzo and Mari, 2017). Hence, there must be other major water sources in the watersheds, such as glacial water and groundwater, that weakens the impact of climate indices on runoffs.

The analysis on ecological water demand indicates that the ecological water demands in the upstream, midstream and downstream of Jinghe River were all on the rise, exhibiting a similar trend to that of temperature and precipitation. This trend is consistent with the previous conclusions (Blöschl, 2017; Ouyang et al., 2017). The possible reasons are as follows. With the growth in temperature, more water is evaporated, leading to an increase in precipitation. In this situation, the vegetation area continues to expand. That is why the ecological water demand is on the rise.

Currently, the river runoff basically satisfies the ecological water demand, indicating that the ecological balance in the river shed has not been severely damaged. Of course, it should be aware that the growing vegetation coverage may reduce the amount of precipitation flowing into the river. Considering the recent runoff decline in river A (*Figs. 9–11*), more attention should be paid to prevent the overuse of water resources and the ensuing ecological damages.

Conclusions

(1) The trend analysis on climate indices shows that both temperature and precipitation in the research area showed an interannual growth, which echoes the trend of global warming. After analyzing the runoffs, it is noted that the upstream, midstream and downstream runoffs in Jinghe River showed a decline interannually, a signal for the possible waste of water resources in Jinghe River watershed. The waste threatens the ecological balance in the watershed.

(2) The wavelet analysis was performed to analyze the features of temperature, precipitation and runoff time series, revealing the consistency between the three indices in periodicity over time.

(3) After the correlation analysis of temperature, precipitation and runoffs, the author discovered the significant impact of temperature on precipitation, and the limited effects of temperature and precipitation on runoffs. The small correlation coefficients between runoffs and temperature/precipitation may be the result of the composition of runoff sources in the study area.

Acknowledgements. The authors would like to thank all of the researchers who participated in the project. The authors would also like to thank the Research and Extension of Water Conservancy Science and Technology in Shanxi Province (201625) for financial support. Furthermore, the authors would like to thank the anonymous reviewers for their helpful and constructive comments.

http://www.aloki.hu ● ISSN 1589 1623 (Print) ● ISSN 1785 0037 (Online)
DOI: http://dx.doi.org/10.15666/aeer/1704_94119423

REFERENCES

[1] Acreman, M., Holden, J. (2013): How wetlands affect floods. – Wetlands 33(5): 773-786.
[2] Ademila, O., Saloko, B. (2018): Hydrogeoelectrical evaluation of groundwater flow pattern in a Basement Complex terrain, Southwest Nigeria. – Environmental and Earth Sciences Research Journal 5(1): 7-14.
[3] Arabi, M., Rao, S. G., Hantush, M. M. (2007): A probabilistic approach for analysis of uncertainty in the evaluation of watershed management practices. – Journal of Hydrology 333(2): 459-471.
[4] Baker, V. R. (2017): Debates-hypothesis testing in hydrology: pursuing certainty versus pursuing uberty. – Water Resources Research 53(3): 1770-1778.
[5] Bertuzzo, E., Mari, L. (2017): Hydrology, water resources and the epidemiology of water-related diseases. – Advances in Water Resources 108: 329-331.
[6] Blöschl, G. (2017): Debates-hypothesis testing in hydrology: introduction. – Water Resources Research 53(3): 1767-1769.
[7] Dile, Y. T., Tekleab, S., Kaba, E. A., Gebrehiwot, S. G., Worqlul, A. W., Bayabil, H. K. (2018): Advances in water resources research in the upper Blue Nile basin and the way forward: a review. – Journal of Hydrology 560: 407-423.
[8] Ek, R. V., Witte, J. P. M., Runhaar, H., Klijn, F., Zalewski, M. (2000): Ecological effects of water management in the Netherlands: the model Demnat. – Ecological Engineering 16(1): 127-141.
[9] Hutton, C., Wagener, T., Freer, J., Han, D., Duffy, C., Arheimer, B. (2017): Reply to comment by Melsen et al. on "most computational hydrology is not reproducible, so is it really science?" – Water Resources Research 53(3): 2570-2571.
[10] Jódar, J., Carpintero, E., Martos-Rosillo, S., Ruiz-Constán, A., Marín-Lechado, C., Cabrera-Arrabal, J. A. (2017): Combination of lumped hydrological and remote-sensing models to evaluate water resources in a semi-arid high altitude ungauged watershed of Sierra Nevada (southern Spain). – Science of the Total Environment 625: 285.
[11] Krysanova, V., Müller-Wohlfeil, D. I., Becker, A. (1998): Development and test of a spatially distributed hydrological/water quality model for mesoscale watersheds. – Ecological Modelling 106(2-3): 261-289.
[12] Liu, D., Guo, S., Shao, Q., Pan, L., Xiong, L., Le, W. (2018): Assessing the effects of adaptation measures on optimal water resources allocation under varied water availability conditions. – Journal of Hydrology 556: 759-774.
[13] Mccurley, K. L., Jawitz, J. W. (2017): Hyphenated hydrology: interdisciplinary evolution of water resource science. – Water Resources Research 53(4): 2972-2982.
[14] Mcknight, D. M. (2017): Debates—hypothesis testing in hydrology: a view from the field: the value of hydrologic hypotheses in designing field studies and interpreting the results to advance hydrology. – Water Resources Research 53(3): 1779-1783.
[15] Moungar, H., Azzi, A., Sahli, Y., Haida, A. (2018): Monthly fresh water yield analysis of three solar desalination units a comparative study in the south Algeria climatic condition. – International Journal of Heat and Technology 36(4): 1330-1335.
[16] Na, Y., Ke, Z., Yang, H., Zhao, Q., Qin, H., Yinshan, X. U. (2017): Evaluation of the trmm multisatellite precipitation analysis and its applicability in supporting reservoir operation and water resources management in Hanjiang basin, China. – Journal of Hydrology 549: 313-325.
[17] Ouyang, W., Gao, X., Hao, Z., Liu, H., Shi, Y., Hao, F. (2017): Farmland shift due to climate warming and impacts on temporal-spatial distributions of water resources in a middle-high latitude agricultural watershed. – Journal of Hydrology 547: 156-167.
[18] Quilty, J., Adamowski, J. (2018): Addressing the incorrect usage of wavelet-based hydrological and water resources forecasting models for real-world applications with best practices and a new forecasting framework. – Journal of Hydrology 563: 336-353.

http://www.aloki.hu ● ISSN 1589 1623 (Print) ● ISSN 1785 0037 (Online)
DOI: http://dx.doi.org/10.15666/aeer/1704_94119423

[19] Rad, A. M., Ghahraman, B., Khalili, D., Ghahremani, Z., Ardakani, S. A. (2017): Integrated meteorological and hydrological drought model: a management tool for proactive water resources planning of semi-arid regions. – Advances in Water Resources 107: 336-353.
[20] Seiller, G., Roy, R., Anctil, F. (2017): Influence of three common calibration metrics on the diagnosis of climate change impacts on water resources. – Journal of Hydrology 547: 280-295.
[21] Sharpley, A. N., Williams, J. R. (1990): Epic-erosion/productivity impact calculator: 2. user manual. – Technical Bulletin – United States Department of Agriculture 4(4): 206-207.
[22] Zhao, C. S., Yuan, Z., Yang, S. T., Hua, X., Ying, S., Yang, Z. Y. (2018): Quantifying effects of hydrological and water quality disturbances on fish with food-web modeling. – Journal of Hydrology 560: 1-10.

http://www.aloki.hu ● ISSN 1589 1623 (Print) ● ISSN 1785 0037 (Online)
DOI: http://dx.doi.org/10.15666/aeer/1704_94119423

THERMAL DECOMPOSITION KINETICS OF POTATO POWDER

LI, P. H. – LIN, Q.* – LIN, L. – LIU, H. – ZHANG, Z.

Xichang University, Xichang 61500, China

**Corresponding author*
e-mail: 13778672269@qq.com; phone: +86-137-7867-2269

(Received 3rd Apr 2019; accepted 17th May 2019)

Abstract. This paper studies the thermal decomposition kinetics of potato powder under static air atmosphere using a DTG-60 differential thermal-thermogravimetric analyzer, with an aim of exploring the thermal stability of potato powder under high temperature. The authors conducted condition experiments on the samples, optimized various parameters that affect thermal analysis and determined the appropriate test conditions. Then, the mechanism function that for the thermal decomposition kinetics study of potato powder was explored, and the powder's thermal decomposition kinetic parameters were calculated along with the kinetic equation using the Coats-Redfern method. The results show that the suitable test conditions for thermal decomposition of potato powder include a heating rate β of 15 °C/min and a sample mass of 2.695 mg. The temperature is 559.18 K (286.03 °C) when the decomposition starts at the initial stage of reaction; the activation energy value is E = 339.810 kJ/mol and the pre-exponential factor A = $e^{75.32}$. The kinetic equation is $\frac{d\alpha}{dt} = e^{75.32-\frac{339810}{8.314T}}(1-\alpha)$.

Keywords: *potato powder, thermal decomposition, differential thermal-thermogravimetric analysis, kinetics, thermal stability, the Coats-Redfern method*

Abbreviations: *E:* activation energy, KJ•mol^{-1}; *G(α):* kinetics mode function; *TGA curve:* thermogravimetric analysis curve; *DTA curve:* differential thermal analysis curve; *K:* thermokinetic temperature, unit in K (Kelvin); *α:* solid sample mass conversion rate; *T:* temperature, K; *β:* differential thermal analysis heating rate °C/min; *f(α):* reaction mechanism function; *R:* ideal gas constant, 8.314 KJ•mol^{-1}; *Exp:* natural logarithm; E_0: activation energy calculated by the FWO method, KJ•mol^{-1}; E_s: activation energy calculated by the Stava-Sestak method, KJ•mol^{-1}; *t:* time, unit: second

Introduction

Potato is one of the most common vegetables in our daily life. Not only does it have protein that is similar to animal protein (better than soy protein), but it also contains some macro and trace elements that are not found in some vegetables and fruits (Alonso et al., 2001; Zeng et al., 2015). Thanks to its rich nutrition, nice flavor and low price, potato has been very popular among the majority of families. In order to alleviate the current food shortage in China, research has been carried out actively in various places on potato as staple food (Bao et al., 2013; Kim et al., 2013), and a series of potato products have been developed, including potato cakes, noodles and buns (Chen, 2009; Zhang et al., 2013), which are very popular among consumers. Sichuan is a major potato producing province, with the total potato planting area ranking the fourth in China, and the total output ranking the first. In this province, Liangshan Prefecture is one of the main producing areas due to the great variety, excellent flavor and aftertaste of potatoes there (Huang et al., 2018). Liangshan Yi Autonomous Prefecture has now established standardized potato production bases, with four indicators - planting area, output, commodity volume and economic benefit ranking the first in the province, thus providing a good platform for potato research (Xie, 2014).

http://www.aloki.hu ● ISSN 1589 1623 (Print) ● ISSN 1785 0037 (Online)
DOI: http://dx.doi.org/10.15666/aeer/1704_94259436

The differential thermal analysis method is a test method that consumes only a small amount of samples, requires only simple operations and produces images which are easy to understand and analyze (Ike, 2018; Stenseng et al., 2001). It has been widely applied in the chemical industry to explore a series of physical, chemical or physicochemical changes in the heating process of samples (Zhao, 2005), such as weight loss, crystal structure changes, oxidation and thermal decomposition, etc., which has further promoted the development of the chemical industry. In recent years, through continuous improvement and correction by many researchers, the differential thermal analysis method has been gradually applied to other fields, showing its advantages such as short test time, simple operation and accurate results (Liu et al., 2013). If a sample and a reference material are heated at the same time, when the sample exhibits physical, chemical or physicochemical changes, the thermal effect will also change, resulting in a certain temperature difference between the sample and the reference material. This method, which determines the correlation between the sample-reference temperature difference and the time or temperature under the programmed temperature, is what we call the differential thermal analysis method.

The thermal decomposition kinetics study of potato powder by the differential thermal analysis method can help manufacturers better understand the thermodynamic properties of potato powder so that they can better utilize it during processing to increase its added value, improve the economic benefits of potatoes and thus drive the prosperous development of the potato industry in Liangshan and make relevant industries more standardized and internationalized (Fan et al., 2015).

Materials and methods

Test materials

The fresh potatoes were acquired from a produce market in Anning Town, Xichang City, Liangshan Prefecture, Sichuan Province.

Instruments and conditions

DTG-60 differential thermal-thermogravimetric analyzer (*Fig. 1*), produced by Shimadzu. The atmosphere condition for the test was static air; the reference material was an empty ceramic crucible; and the temperature rise range was 25~600 °C.

Figure 1. *DTG-60 differential thermal-thermogravimetric analyzer*

Test methods

In this test, according to the differential thermal analysis method, the atmospheric condition was set to be static air in the program, then the test conditions were changed

http://www.aloki.hu ● ISSN 1589 1623 (Print) ● ISSN 1785 0037 (Online)
DOI: http://dx.doi.org/10.15666/aeer/1704_94259436

by changing the heating rate or sample mass. In this way, different differential thermal analysis maps were obtained. Then the DTA curves obtained were analyzed and compared to determine the optimal test conditions for the potato powder thermal analysis. Under the optimal test conditions, the sample potato powder was subjected to thermal analysis and an image obtained, and then the image was subjected to thermogravimetric and differential thermal analysis. After analysis, calculation and collation of data, the activation energy value E and the pre-exponential factor value A of the thermal decomposition reaction of potato powder were calculated using the Coats-Redfern integration method.

(1) Preparation of materials

The process flow is as follows:
Sampling→pre-treatment→pulping→filtering→drying→grinding→sieving (80 meshes)

The moisture content of the dried potato sample was controlled to 13.5% or less. The determination of the moisture content was carried out by reference to GB 5009.3-2016.

(2) Condition experiments

The compatibility and thermal stability of the energetic materials can be reflected directly by the characteristic quantities in the thermal analysis such as the heat change ΔH, the initial temperature T_0, the final temperature T_e, the peak temperature T_p and the weight loss M_l, etc. or the kinetic parameters further obtained from these quantities (Song and Wu, 2016). The heating rate β and the sample size m may both have some effects on these characteristic quantities, which adds a lot of uncertainty to the experiment. Therefore, it is necessary to analyze the DTA curve, including the peak time, shape and smoothness, so as to obtain the optimal thermal analysis conditions for potato powder. In this experiment, two groups of single-factor tests were designed, to measure the effects of different masses (6 different masses) and of different heating rates (4 different heating rates) on the DTA curve of potato powder.

(3) Determination of the kinetic equation

Obtain a complete and smooth thermogram of the peak through the single-factor test. Measure the weight loss rate under each temperature range through the thermogravimetric curve, and then select the appropriate mechanism function $G(\alpha)$. Based on the straight line relationship of $\ln\left[\frac{G(\alpha)}{T^2}\right]$ with $\frac{1}{T}$, find the linear regression equation of the curve with a good linearity (R^2 is the closest to 1), and then calculate the activation energy E and the pre-exponential factor A which are closest to the true values using the slope and intercept of the linear regression equation (Ghaly et al., 2005).

Results and discussion

Effects of different thermal analysis conditions on the thermal decomposition of potato powder

The results obtained by differential thermal analysis are usually affected by the physical and chemical properties of the material being tested, the precision of the instrument, the samples used and the test conditions, among which, the conditions for thermal analysis have significant effects on the obtained thermogram. In this

http://www.aloki.hu ● ISSN 1589 1623 (Print) ● ISSN 1785 0037 (Online)
DOI: http://dx.doi.org/10.15666/aeer/1704_94259436

experiment, two groups of single-factor tests were carried out in the static air atmosphere, aiming to explore the effects of different sample masses and heating rates on the peak of the thermogram.

(1) Effects of sample mass on the thermal decomposition process of potato powder

For some energetic materials, the mass of a sample has little or no effect on the characteristic quantities of thermal decomposition temperature, but for others, it does on certain characteristic quantities. To investigate the effect of sample mass on the thermal decomposition image of potato powder, 6 tests were performed, with the sample mass changing in a gradient manner, as shown in *Figure 2*.

It can be seen from *Figure 2* that there are two distinct endothermic peaks in the thermographic curves of potato powder with different masses. Under some heating rates, a small endothermic peak can be seen before the main reaction zone. The peaks generally show the same trend, indicative of the common thermal characteristics of potato powder. It is not hard to conclude that when the sample mass increases, the peak area will become larger and the error will increase due to the longer reaction time recorded by the instrument. It can be seen that when the mass of the test sample was 2.695 mg, the peak shown was better separated from those in the cases of other masses, and was sharp with a great intensity and a small area. Since DTG-60 is a highly sensitive instrument, if the sample size is too large, it will exceed the measuring range and contaminate the instrument. Therefore, the minimal sample mass that can be identified by DTG-60 should be used as long as it can ensure good separation effect, peak intensity and peak shape (Chen et al., 2001).

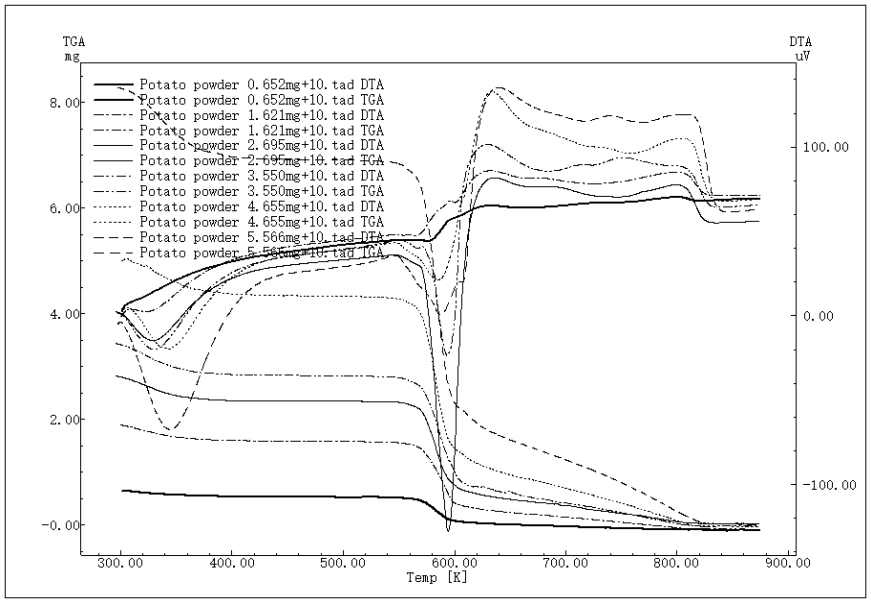

Figure 2. *Differential thermal-thermogravimetric curve of potato powder with different masses*

(2) Effects of temperature rise rate on the thermal decomposition process of potato powder

The effects of the heating rate β on the characteristic quantities of thermal analysis are not only reflected in the changes in the peak area, but also in the position of the peak

http://www.aloki.hu ● ISSN 1589 1623 (Print) ● ISSN 1785 0037 (Online)
DOI: http://dx.doi.org/10.15666/aeer/1704_94259436

temperature. So the adoption of different heating rates β can help understand and analyze the thermal behaviours of materials. This experiment designed four different heating rates β, namely 20 °C/min, 15 °C/min, 10 °C/min and 5 °C/min, respectively, so that the DTA curves of the potato powder under the four different heating rates were obtained as follows.

As can be seen from *Figure 3,* there is a large endothermic peak in all the thermographic curves of the potato powder, and all the peaks have basically the same characteristics. The differential thermal scan of each sample showed good reproducibility, indicative of the common thermal characteristics of potato powder. The faster the heating rate β is, the shorter the reaction time of the sample will be recorded by the instrument DTG-60, the sharper the peak will become and the greater the distance will be between the decomposition and equilibrium conditions of the sample particles (Chakraborty, 2015), thus resulting in a baseline drift and making the two adjacent peaks overlapping. This will reduce the resolution and make the instrument less sensitive. On the contrary, the slower the heating rate β is, the smaller the drift of the baseline will be, and the closer the system will get to the equilibrium conditions. In this way, the peak will be shallower and wider and can be better separated with the adjacent one, thus improving the resolution of the thermogram. However, it will take a longer time to determine the sample. In summary, the optimal heating rate obtained for this experiment is 15 °C/min.

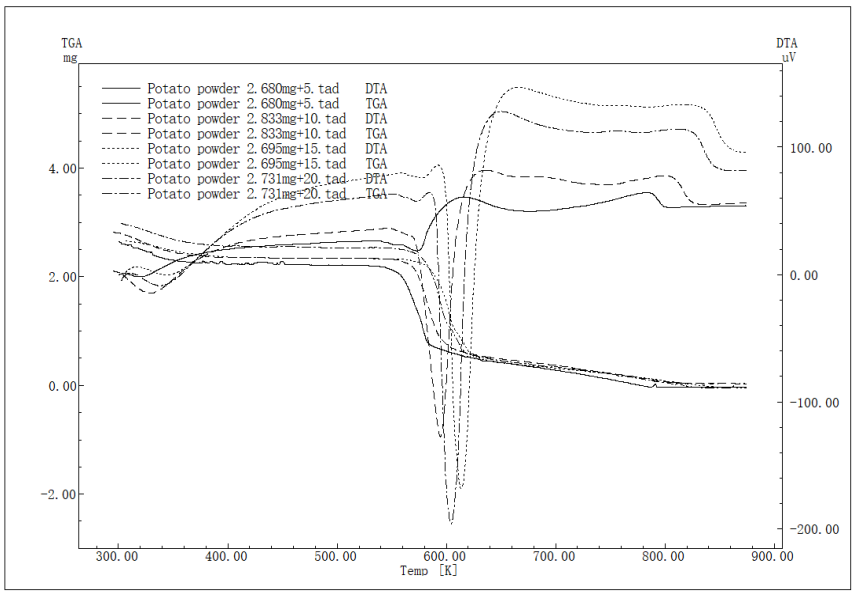

Figure 3. *Differential thermal-thermogravimetric curve of potato powder under different heating rates*

Through analysis the characteristic quantities in the thermogram, such as peak time, shape and smoothness, it can be concluded that the peak shape was the best when the sample mass was 2.695 mg and the heating rate 15 °C/min. The main peak was also sharp and smooth when the heating rate was 20 °C/min, but the instrument was less sensitive as the heating rate was fast (Xu et al., 2017). In summary, when the sample mass was 2.695 mg and the heating rate 15 °C/min, the thermogram will be easier and more effective for thermal analysis.

http://www.aloki.hu ● ISSN 1589 1623 (Print) ● ISSN 1785 0037 (Online)
DOI: http://dx.doi.org/10.15666/aeer/1704_94259436

Analysis of the thermal decomposition process of potato powder

Through the above condition tests, it is found that the thermogram obtained was the best for thermal analysis when the sample mass was 2.695 mg and the heating rate 15 °C/min. This thermogram (*Fig. 4*) was then used in this research to investigate the thermal decomposition process of potato powder, calculate the kinetic parameters and determine the kinetic equation.

As can be seen from *Figure 4,* the thermal decomposition process of potato powder consists of four stages and produces a small amount of residual ash.

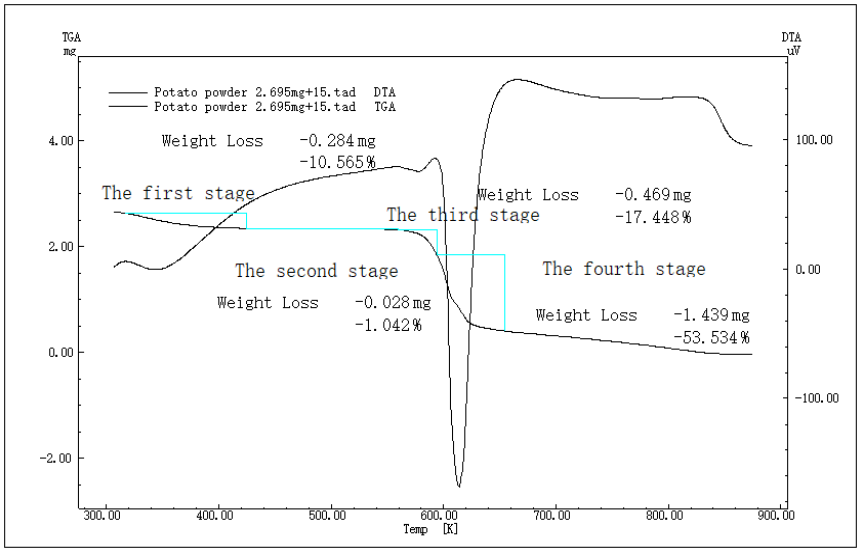

Figure 4. *Optimal thermal analysis map*

Stage 1 is 316.68~425.11 K (43.53~151.96 °C). It is generally considered that the part before 400 K (128.55 °C) is the water loss process, so Stage 1 is mainly the weight loss process (Wu et al., 2002).

Stage 2 is 425.11~559.18 K (151.96~286.03 °C). It is the transition stage of the thermal decomposition of potato powder, where the potato powder has stable properties, so it is the safe temperature range for food processing.

Stage 3 is 559.18~593.90 K (286.13~320.75 °C). Part of the small molecule substances begin to undergo the thermal decomposition reaction, so it is the initial stage of the whole reaction.

Stage 4 is 593.90~654.02 K (320.75~380.87 °C). It is the main reaction stage of thermal decomposition. It is generally believed that the test sample is internally restructured in this temperature range, producing mainly small molecule compounds and vaporizable macromolecules that exhibit significant weight losses. The relevant data are shown in *Table 1*.

Table 1. *Related data of potato powder during thermal decomposition*

Material	First weight loss		Second weight loss		Third weight loss		Residual ash /mg
	TG loss of weight /%	DTG peak temperature/K	TG loss of weight /%	DTG peak temperature /K	TG loss of weight /%	DTG peak temperature /K	
Potato powder	10.565	343.430	17.448	577.890	53.534	613.760	0.143

http://www.aloki.hu ● ISSN 1589 1623 (Print) ● ISSN 1785 0037 (Online)
DOI: http://dx.doi.org/10.15666/aeer/1704_94259436

Determination of the thermal decomposition kinetic mechanism function

The Coats-Redfern integration method has been widely used in thermal decomposition kinetics studies, as it can well reflect the mechanism of the thermal decomposition reaction. In the kinetic data processing, this paper also adopted this method to calculate the kinetic parameters and the kinetic equation for the thermal decomposition process of potato powder. The equation is derived as follows using the Coats-Redfern integration method (under non-isothermal conditions):

According to the mass equation, the reaction rate equation can be expressed as *Equation 1:*

$$\frac{d\alpha}{dT} = kf(\alpha) \quad \text{(Eq.1)}$$

where α is the conversion percentage, $\alpha = \frac{m_0 - m}{m_0 - m_f}$, also called the conversion rate; m is the sample mass, m_0 the initial reaction mass and m_f the final reaction mass; T is the temperature; k is the constant of reaction rate; f(α) is the differential form of the kinetic mechanism function.

The Arrhenius equation is *Equation 2:*

$$K = A\exp(-\frac{E}{RT}) \quad \text{(Eq.2)}$$

where A is the pre-exponential factor; E the activation energy, J/mol; R the molar gas constant, 8.314 J/ (K·mol); and T the thermodynamic temperature.

Substitute *Equation 2* into *Equation 1,* and we have *Equation 3:*

$$\frac{d\alpha}{dT} = \frac{A}{\beta}\exp\ (-\frac{E}{RT})f(\alpha) \quad \text{(Eq.3)}$$

where β is the heating rate.

Separate the variable, and we have *Equation 4:*

$$\frac{d\alpha}{f(\alpha)} = \frac{A}{\beta}exp(-\frac{E}{RT})dT \quad \text{(Eq.4)}$$

Integrate the two sides of the equation (*Eq. 5*):

$$\int_0^\alpha \frac{d\alpha}{f(\alpha)} = \int_0^T \frac{A}{\beta}Aexp(-\frac{E}{RT})dT \quad \text{(Eq.5)}$$

Rearrange the integral *Equation 5,* and we have the coast-Redfield integral equation (*Eq. 6*)*:*

$$\ln\left[\frac{G(\alpha)}{T^2}\right] = \ln\frac{AR}{\beta E} - \frac{E}{RT} \quad \text{(Eq.6)}$$

Plot a graph with $\ln\left[\frac{G(\alpha)}{T^2}\right]$ as the x-axis and $\frac{1}{T}$ as the y-axis, and we can obtain a straight line, with a slope of $-\frac{E}{R}$ (if the n value is correct), and an intercept of $\ln\frac{AR}{\beta E}$. And then the E and A values can be calculated through the equation.

http://www.aloki.hu ● ISSN 1589 1623 (Print) ● ISSN 1785 0037 (Online)
DOI: http://dx.doi.org/10.15666/aeer/1704_94259436

In order to calculate the activation energy E and the pre-exponential factor A of the potato powder more accurately, the experimental data of four mechanism functions commonly used for the calculation of starch activation energy were listed below and compared to find out the linear regression equation with the best linear fit (*Eqs. 7–10*):

$$-\ln(1-\alpha) = G(\alpha) \quad \text{(Eq.7)}$$

$$[-\ln(1-\alpha)]^{\frac{2}{3}} = G(\alpha) \quad \text{(Eq.8)}$$

$$[-\ln(1-\alpha)]^{\frac{1}{2}} = G(\alpha) \quad \text{(Eq.9)}$$

$$[-\ln(1-\alpha)]^{\frac{1}{3}} = G(\alpha) \quad \text{(Eq.10)}$$

(1) Kinetic analysis on the major stages of thermal decomposition of potato powder

The main stage of the thermal decomposition of potato powder is the main reaction stage as most of the changes in the material occur in this temperature range. Relevant kinetic data in the main stage of the thermal decomposition are listed in *Table 2* (Yue et al., 2012).

Draw the scatter plot of $\ln\left[\frac{G(\alpha)}{T^2}\right]$ and $\frac{1}{T}$, as shown in *Figure 5.*

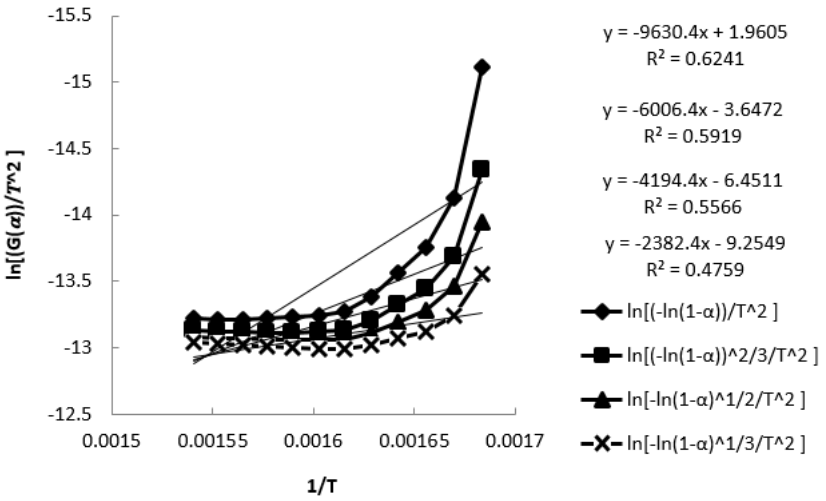

Figure 5. *Scatter plot of* $ln\left[\frac{G(\alpha)}{T^2}\right]$ *and* $\frac{1}{T}$ *in the main reaction stage*

From the above four mechanism functions and the scatter plot of $\frac{1}{T}$, it can be seen that the linear regression equation has a low linear fit, so the main reaction stage does not conform to the first-order kinetic equation, which requires further discussion.

(2) Kinetic analysis on the initial thermal decomposition stage of potato powder

The initial stage of the thermal decomposition of potato powder, where the internal small-molecule substances of the potato begin to undergo thermal decomposition, marks

http://www.aloki.hu ● ISSN 1589 1623 (Print) ● ISSN 1785 0037 (Online)
DOI: http://dx.doi.org/10.15666/aeer/1704_94259436

the change of potato powder properties. The kinetic data of the thermal decomposition of potato powder at the initial stage are listed in *Table 3*.

Draw the scatter plot of $\ln\left[\frac{G(\alpha)}{T^2}\right]$ and $\frac{1}{T}$, as shown in *Figure 6.*

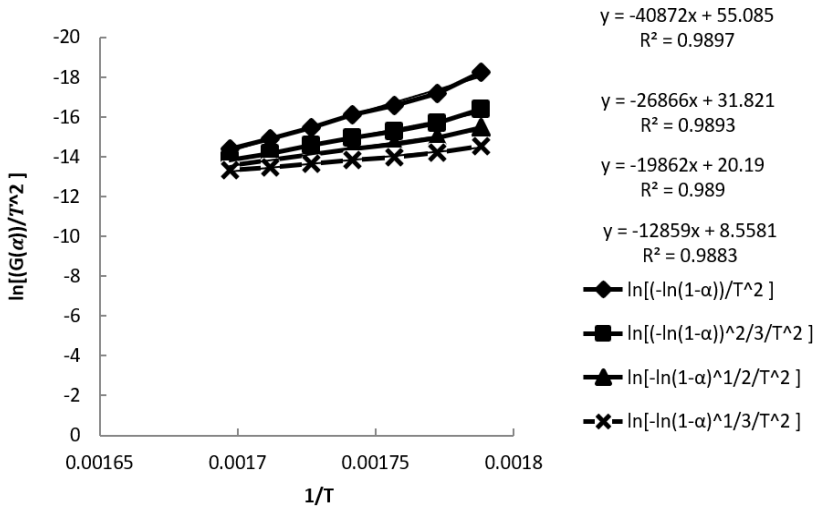

Figure 6. *Scatter plot of* $ln\left[\frac{G(\alpha)}{T^2}\right]$ *and* $\frac{1}{T}$ *in the initial reaction stage*

From the above four mechanism functions and the scatter plot of $\frac{1}{T}$, it can be seen that, when $G(\alpha) = -\ln(1-\alpha)$, the correlation coefficient is 0.9897; when $G(\alpha) = [-\ln(1-\alpha)]^{\frac{2}{3}}$, it is 0.9893; when $G(\alpha) = [-\ln(1-\alpha)]^{\frac{1}{2}}$, it is 0.989; when $G(\alpha) = [-\ln(1-\alpha)]^{\frac{1}{3}}$, it is 0.9883. So the linear regression equations obtained based on the above four mechanism functions all have a good linear fit and conform to the first-order kinetic equation. And when $G(\alpha) = -\ln(1-\alpha)$, the linear fit is the best; in other words, if $G(\alpha) = -\ln(1-\alpha)$ is adopted, the activation energy value E and the pre-exponential factor value A calculated will be closer to the true values.

Table 2. *Kinetic data of the main thermal decomposition stage of potato powder*

Sample	**T/K**	α/%	$\ln\left[\frac{G(\alpha)}{T^2}\right]$			
			Equation 7	***Equation* 8**	***Equation* 9**	***Equation* 10**
Potato powder	594.02	9.19	-15.1132	-14.3334	-13.9435	-13.5536
	599.02	23.03	-14.1310	-13.6842	-13.4608	-13.2374
	604.02	32.11	-13.7560	-13.4397	-13.2816	-13.1235
	609.02	37.91	-13.5648	-13.3178	-13.1943	-13.0707
	614.02	44.05	-13.3836	-13.2024	-13.1118	-13.0212
	619.02	48.33	-13.2715	-13.1331	-13.0639	-12.9947
	624.02	49.96	-13.2399	-13.1174	-13.0562	-12.9949
	629.02	50.97	-13.2271	-13.1141	-13.0577	-13.0012
	634.02	51.75	-13.2206	-13.1151	-13.0624	-13.0096
	639.02	52.46	-13.2163	-13.1175	-13.0681	-13.0187
	644.02	53.05	-13.2150	-13.1218	-13.0752	-13.0286
	649.02	53.53	-13.2169	-13.1283	-13.0839	-13.0396

http://www.aloki.hu ● ISSN 1589 1623 (Print) ● ISSN 1785 0037 (Online)
DOI: http://dx.doi.org/10.15666/aeer/1704_94259436

Table 3. *Kinetic data of the initial thermal decomposition stage of potato powder*

Sample	T/K	α/%	$\ln\left[\frac{G(\alpha)}{T^2}\right]$			
			Equation 7	***Equation* 8**	***Equation* 9**	***Equation* 10**
Potato powder	559.18	0.37	-18.2451	-16.3811	-15.4490	-14.5170
	564.18	1.08	-17.1945	-15.6866	-14.9326	-14.1787
	569.18	2.01	-16.5858	-15.2867	-14.6370	-13.9875
	574.18	3.31	-16.0970	-14.9666	-14.4015	-13.8363
	579.18	6.25	-15.4637	-14.5502	-14.0934	-13.6367
	584.18	11.16	-14.8746	-14.1632	-13.8075	-13.4518
	589.18	17.86	-14.3835	-13.8415	-13.5705	-13.2995

Determination of the thermal decomposition kinetic parameters and calculation of the kinetic equation

Since the main reaction stage does not conform to the first-order kinetic equation, the following section only analyzes the initial stage of the entire reaction.

Since the main reaction stage does not conform to the first-order kinetic equation, the following section only analyzes the initial stage of the entire reaction.

Through the linear relation analysis of $\ln\left[\frac{-\ln(1-\alpha)}{T^2}\right]$ and $\frac{1}{T}$, it can be seen that the linear regression equation is y = -40872x + 55.085. By the Coats-Redfern integral method, it can be found that the slope is $-40872 = -\frac{E}{R}$ and that the intercept $55.085 = \ln\frac{AR}{\beta E}$. From $-\frac{E}{R} = -40872$, it can be concluded that the activation energy E = 339.810 kJ/mol, and from $\ln\frac{AR}{\beta E} = 55.085$, the pre-exponential factor can be obtained, which is A = $e^{75.32}$.

From $G(\alpha) = -\ln(1-\alpha) = \int \frac{d\alpha}{f(\alpha)}$, it can be deduced that $f(\alpha) = 1-\alpha$, so the kinetic equation for potato powder is: $\frac{d\alpha}{dt} = e^{75.32-\frac{339810}{8.314T}}(1-\alpha)$.

Conclusions

(1) Under different sample masses and heating rates, the areas and time of the peaks in the thermograms of the potato powder are significantly different. Through condition tests, it is found that the optimal test conditions for the thermal decomposition of potato powder include a heating rate β of 15 °C/min and a sample mass of 2.695 mg.

(2) Through the analysis of the thermal decomposition process of potato powder, it can be concluded that the weight loss of potato powder occurred in the temperature range of 316.68~425.11 K (43.53~151.96 °C). When the temperature exceeded 559.18 K (286.03 °C), the potato powder started to experience thermal decomposition.

(3) Through the above analysis, it can be seen that, when $G(\alpha) = -\ln(1-\alpha)$, i.e. when the Coats-Redfern integral equation is $\ln\left[\frac{-\ln(1-\alpha)}{T^2}\right] = \ln\frac{AR}{\beta E} - \frac{E}{RT}$, the activation energy value E and the pre-exponential factor value A obtained are the closest to reality. Through the above calculations, it can be found that the thermal decomposition kinetic parameters of potato powder are as follows: the activation energy E = 339809.81 J/mol

http://www.aloki.hu ● ISSN 1589 1623 (Print) ● ISSN 1785 0037 (Online)
DOI: http://dx.doi.org/10.15666/aeer/1704_94259436

(339.81 KJ/mol) and the pre-exponential factor $A = e^{75.32}$, and that the thermal decomposition kinetic equation $\frac{d\alpha}{dt} = e^{75.32-\frac{339810}{8.314T}}(1-\alpha)$.

(4) In this paper, only differential thermal analysis method was used to study the pyrolysis kinetics of potato powder, but potato powder was also affected by many other factors in the processing process, so it can be further explored from the aspects of environmental humidity and PH of processing in the future.

Acknowledgements. Breeding and Promotion of New Specialized Potato Varieties for Staple Food in Panxi Area (Project No. 2016NYZ0032-4), National Modern Agricultural Industry Technology System Sichuan Potato Innovation Team (Sichuan Provincial Finance Education [2019] No. 59). Research on Key Brewing Techniques of Potato Liquor by Solid Fermentation, Academic Leader and Technology Leader Training Fund Project of Liangshan Prefecture, 2017. Key Brewing Technology of Potato Liquor by Solid Fermentation, Project of Sichuan Education Department, 17ZA0351. Research on Microbial Community During the Brewing Process of Potato Fermented Products: Taking Potato-Fermented Tartary Buckwheat Wine as an Example, Project of Sichuan Science and Technology Department, 2018JY0396.

REFERENCES

[1] Alonso, M., Borrego, A. G., Alvarez, D., Menéndez, R. (2001): A reactivity study of chars obtained at different temperatures in relation to their petrographic characteristics. – Fuel Processing Technology 69(3): 257-272.

[2] Bao, H. H., Zhou, R., Liu, Y. L., Cao, L. K., Yang, Z. H. (2013): Development of green tea flavored potato whole powder cookies. – Academic Periodical of Farm Products Processing 9: 23-25.

[3] Chakraborty, S. (2015): Effect of potato powder supplementation and spices addition on physical and sensory properties of cookies. – International Journal of Research in Engineering and Technology 3(4): 408-416.

[4] Chen, L. T., Dong, Z. R., Huang, T. S. (2001): Application of differential thermal analysis in physical and chemical experiments. – Laboratory Research and Exploration 20(2): 96-98.

[5] Chen, Z. C. (2009): Development of potato whole flour bread. – Grain Science and Technology and Economy 3: 50-51.

[6] Fan, S. Q., Chen, S., Tang, X. Y., Xiao, Z. Y., Deng, P., Yao, P. N., Sun, Z. P., Zhang, Y., Chen, C. Y. (2015): Kinetic model of continuous ethanol fermentation in closed-circulating process with pervaporation membrane bioreactor by Saccharomyces cerevisiae. – Bioresource Technology 117(2): 169-175.

[7] Ghaly, A. E., Kamal, M., Correia, L. R. (2005): Kinetic modelling of continuous submerged fermentation of cheese whey for single cell protein production. – Bioresource Technology 96(10): 1143-1152.

[8] Huang, H. Y., Li, J. L., Liu, H. (2018): Thermal analysis kinetics of Tartary buckwheat flour. – International Journal of Heat and Technology 36(4): 1414-1422.

[9] Ike, C. C. (2018): Exponential fourier integral transform method for stress analysis of boundary load on soil. – Mathematical Modelling of Engineering Problems 5(1): 33-39.

[10] Kim, D., Ahn, S., Moon, C., Choi, G., Kim, T., Sung, Y. (2013): Effect of blending ratio on combustion performance in blends of biomass and coals of different ranks. – Experimental Thermal and Fluid Science (47): 232-240.

[11] Liu, Z., Wu, Z., Li, R., Fan, X. (2013): Two-stage foam separation technology for recovering potato protein from potato processing wastewater using the column with the spiral internal component. – Journal of Food Engineering 114(02): 192-198.

http://www.aloki.hu ● ISSN 1589 1623 (Print) ● ISSN 1785 0037 (Online)
DOI: http://dx.doi.org/10.15666/aeer/1704_94259436

[12] Song, S. S., Wu, T. X. (2016): Study on degradation kinetics of Pitaya pigment. – Storage and Process 169(5): 74-79.
[13] Stenseng, M., Jensen, A., Dam-Johansen, K. (2001): Investigation of biomass pyrolysis by thermogravimetric analysis and differential scanning calorimetry. – Journal of Analytical and Applied Pyrolysis 58(1): 765-780.
[14] Wu, P., Zhu, H., Zhang, W., Zhao, F. Q., Yuan, C., Yin, C. M., Qiu, G. (2002): TG Characteristics of GAP Fuel-Rich Propellant and its Ingredients. – Energetic Materials 10(1): 18-20.
[15] Xie, Y. G. (2014): Accelerate the development of Liangshan Prefecture's characteristics and superior quality agricultural industry. – Resource Development & Market (11): 1366-1370.
[16] Xu, Z., Wang, S. N., Zhao, D., Yang, P. (2017): Advances in preparation, properties and main food processing of potato whole flour. – Science and Technology of Food Industry 38(19): 322-326.
[17] Yue, J., Zhu, Z. C., Cao, H. (2012): Study on the basic characteristics of different varieties of potato powder. – Feed Research (10): 81-83.
[18] Zeng, D. Y., Xu, D., Liu, G. (2015): Potato nutrition review. – Chinese Potato Journal 29(4): 233-243.
[19] Zhang, K., Zhang, K., Cao, Y., Pan, W. (2013): Co-combustion characteristics and blending optimization of tobacco stem and high-sulfur bituminous coal based o-n thermogravimetric and mass spectrometry analyses. – BioresourcesTechnology 131: 325-332.
[20] Zhao, J. W. (2005): Modern Food Testing Technology. – China Light Industry Press, Beijing.

http://www.aloki.hu ● ISSN 1589 1623 (Print) ● ISSN 1785 0037 (Online)
DOI: http://dx.doi.org/10.15666/aeer/1704_94259436

PATH OPTIMIZATION OF COLD CHAIN DISTRIBUTION WITH MULTIPLE DISTRIBUTION CENTERS CONSIDERING CARBON EMISSIONS

REN, X. Y.[1] – CHEN, C. F.[1] – XIAO, Y. L.[1,2*] – DU, S. C.[1]

[1]*School of Management Engineering and Business, Hebei University of Engineering, Handan 056038, China*

[2]*Faculty of Business, Economics and Accountancy, University Malaysia Sabah, Kota Kinabalu 88400, Malaysia*

**Corresponding author*
e-mail: 12357414@qq.com

(Received 3rd Apr 2019; accepted 17th May 2019)

Abstract. With the growing awareness of green logistics, the carbon emissions must be considered in the cold chain distribution (CCD). Whereas the traditional regional distribution mode cannot deliver multiple small batches to designated regions right on time, this paper establishes a mathematical model for the minimal distribution cost of fresh food based on the resource/information sharing between multiple distribution centers (multi-DC) and the soft time window constraint, aiming to satisfy the new demands on logistics distribution (e.g. high timeliness, low cost, greenness and resource/information sharing). The total cost refers to the sum of vehicle dispatch cost, transport cost, time penalty cost, cargo loss cost and carbon emissions cost. Next, the proposed model was solved by the hybrid algorithm of artificial fish-swarm algorithm (AFSA) and ACA (AFSA-ACA hybrid algorithm). The simulation examples show that the multi-DC CCD mode can effectively reduce the total distribution cost and carbon emission cost compared to the traditional regional CCD mode.
Keywords: *green logistic, low carbo distribution, semi-open cold chain distribution (CCD), artificial fish-swarm algorithm (AFSA), ant colony algorithm (ACA)*

Introduction

Facing the growing demand for fresh food, cold chain distribution (CCD) enterprises are constantly increasing the number of vehicles and distribution centers (DCs), aiming to deliver multiple small batches to designated regions right on time. The semi-open multi-DC joint CCD fully uses the existing vehicles and lowers the distribution cost. This distribution mode overcomes the defects of the traditional regional distribution mode, such as insufficient distribution capacity, the lack of resources, the inability to share information, and the regional limitation. Therefore, it is very important to explore the path optimization of semi-open multi-DC CCD.

In recent years, fruitful results have been achieved on CCD path optimization, which is a type of vehicle routing problem (VRP) (Dantzig and Ramser, 1959). For example, Lan et al. (2013) classified CCD modes, helped enterprises choose the suitable collaborative distribution model, and reduced the cost of enterprise distribution. For the minimal distribution cost, Wang et al. (2018) established and solved an optimization model for multi-temperature cold-storage CCD under stochastic demand.

Considering the limitation of the standard algorithms, some scholars have introduced improved algorithms or the time window constraint to explore the CCD path optimization. For instance, Wang and Luo (2017) optimized the CCD path with time window using the improved intelligent water drops algorithm. To coordinate the time

http://www.aloki.hu ● ISSN 1589 1623 (Print) ● ISSN 1785 0037 (Online)
DOI: http://dx.doi.org/10.15666/aeer/1704_94379453

window of consumer demand with the temperature control of fresh food, Wang et al. (2019) constructed an optimization model that minimizes the distribution cost and value loss of fresh food, and solved the model using a hybrid algorithm between the genetic algorithm (GA) and the tabu search (TS) (hybrid GA-TS). Liang et al. (2016) included the fuzzy time window into the CCD, set up a multi-objective optimization model for the minimal cost and maximum consumer satisfaction, and solved the model by the improved GA.

With the boom of third-party logistics, the traditional regional single-DC distribution mode can no longer fulfil the demand of distribution enterprises, and is being replaced by the open and semi-open multi-DC distribution modes. On open multi-DC distribution, Yang et al. (2016), Yu and Xie (2011) and Baldacci et al. (2013) all assumed that any vehicle must leave from a virtual DC to the actual DCs, before implementing the distribution tasks, and the trip between the virtual and actual DCs incurs no cost. Considering the diversity and mutual exclusion of products, the various types of vehicles and the matching between products and vehicles, Liu and Guo (2016) put forward the open-loop multi-DC path optimization problem with time window constraint, set up the corresponding mathematical model, and solved the model with hybrid GA and the adaptive GA, respectively. Ge et al. (2016) proposed the multi-DC distribution mechanism with open vehicle parking strategy, and created and solved a mathematical model for the minimal fuel consumption. Liu et al. (2010) employed the two-stage heuristic algorithm to solve the multi-yard distribution VRP under the constraint of vehicle load.

On semi-open multi-DC CCD, Fan et al. (2018) presented a semi-open multi-DC distribution mode, constructed a mathematical model for the minimum cost under time window constraint, and solved the fresh food CCD by the ant colony algorithm (ACA). Ho et al. (2007), Adelzadeh et al. (2014) and Liu (2013) respectively solved the multi-yard VRP under time window constraint with the hybrid GA, simulated annealing (SA) algorithm and the adaptive GA based on artificial bee colony (ABC) algorithm.

The carbon emissions should be considered in the path optimization of CCD (Chaabane et al., 2012), as required by the government's policies on carbon emissions reduction, the concept of green logistics development, and the coordination between CCD and ecological environment. Gac (1996) examined the relationship between CCD development and greenhouse effect, and put forward measures to curb the CCD impacts on greenhouse effect. Vanek and Sun (2008) investigated the relationship between the maintenance of food shelf life, energy consumption and environmental pollution, built a relevant energy consumption model, and proposed the strategy for selection of transport modes. James et al. (2010) studied how climate change and temperature rise influence food quality, and designed measures to improve the energy efficiency in each link of the CCD. Considering carbon emissions, Kang et al. (2019) and Fan et al. (2017) both constructed CCD path optimization models for the minimal total cost under time window constraint, and solved the simulation examples by the ACA improved by the 2-opt local search mechanism and the improved GA, respectively. Palmer (2007) established a path optimization model with time window, with the aim to optimize distance, time and carbon emissions, and verified the CO_2 emissions reduction effect of speed through the analysis on the variation in CO_2 emissions under different congestion conditions. Bao and Zhang (2018) introduced the carbon emissions into the path optimization model of semi-open multi-DC CCD, and solved the model by the improved GA.

http://www.aloki.hu ● ISSN 1589 1623 (Print) ● ISSN 1785 0037 (Online)
DOI: http://dx.doi.org/10.15666/aeer/1704_94379453

The research results on CCD both bring economic benefits to enterprises and promote the greenness of the CCD. However, the existing studies on semi-open multi-DC CCD fail to fully consider the cost incurred in the distribution process, or the insufficiency of self-owned vehicles (some vehicles are rented from third parties). To overcome the defects of these studies, this paper designs a global network covering all consumers, assuming that the enterprise has multiple DCs and sufficient vehicles, and establishes a comprehensive semi-open multi-DC CCD model constrained by soft time window. The model attempts to minimize the sum of vehicle dispatch cost, transport cost, time penalty cost, cargo loss cost and carbon emissions cost. In addition, the proposed model was solved by the hybrid algorithm of artificial fish-swarm algorithm (AFSA) and ACA (AFSA-ACA hybrid algorithm). The simulation examples show that the multi-DC CCD mode is better than the traditional regional CCD mode.

Materials and methods

Problem description

This paper mainly studies the "many-to-many" semi-open multi-DC CCD mode. In this cross-regional network distribution mechanism, "many" DCs serve "many" consumers, and share with each other the consumer information, resources and vehicles. Considering carbon emissions, a semi-open multi-DC CCD path optimization model was established to deliver multiple small batches to designated regions. Below is a description of our research problem.

It is assumed that a distribution enterprise serves N consumers with M DCs and K vehicles. During the distribution, each DC should be open to all vehicles, and play the role of the final destination or stopover point. After completing the distribution task, a vehicle does not need to return to the original DC, but to any of the nearby DCs. The consumers only receive distribution services and do not allow the stopover of vehicles. The vehicles are sufficient to satisfy the distribution demand. However, the route, distance and stopover DCs vary with vehicles and trips, due to the limitations of the load, speed and distance of the vehicles. The distance between each DC and each consumer is known, so is the distance between consumers. This paper designs a penalty function based on time window, because late distribution will damage the quality of fresh food and cause dissatisfaction among consumers. The carbon emissions from the CCD are mainly from energy consumption and refrigeration.

Based on the above, this paper constructs a mathematical model to minimize the total cost, which covers vehicle dispatch cost, transport cost, time penalty cost, cargo loss cost and carbon emissions cost. Besides, the improved GA was designed to solve the model and optimize the delivery path. The optimal path can minimize the path length, increase vehicle utilization, lower carbon emissions and reduce the total cost of the distribution service. *Figure 1* illustrates the semi-open multi-DC CCD mode.

Model hypotheses

(1) The vehicles are of the same model and the same specifications. The maximum load, fuel consumption and refrigeration performance are known in advance.

(2) There are enough vehicles to satisfy the demand of all consumers.

(3) The order quantity completed by each vehicle should not surpass the maximum load.

http://www.aloki.hu ● ISSN 1589 1623 (Print) ● ISSN 1785 0037 (Online)
DOI: http://dx.doi.org/10.15666/aeer/1704_94379453

(4) The demand of each consumer can only be fulfilled by one vehicle through one service.

(5) Each consumer sets out a time window on the delivery time, and will not accept the service before the earliest acceptable time or after the latest acceptable time.

(6) The position of each DC and each consumer is known in advance. Every DC boasts sufficient cargoes and the ability to serve the consumer demand.

(7) All vehicles must start from a DC. After completing the distribution task, a vehicle does not need to return to the original DC, but to any of the nearby DCs.

(8) Two drivers are arranged for each vehicle, so that they can take turns to rest. The labor cost and vehicle operation cost are both included in the dispatch cost.

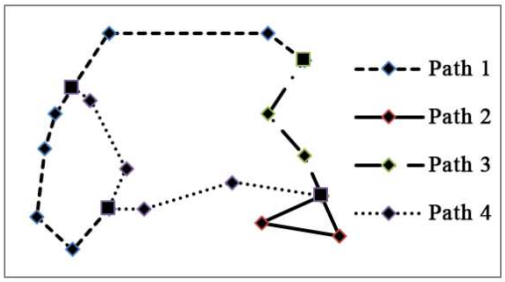

Figure 1. *Sketch map of the semi-open multi-DC CCD mode*

Model construction

Symbols

M: The set of DCs, $M\{m|m = 1,2,\ldots|M|\}$;

N: The set of consumers, $N\{n|n = 1,2,\ldots|N|\}$;

K: The set of vehicles, $K\{k|k = 1,2,\ldots|K|\}$;

K_{n1}: The set of consumers served by vehicle k on the l-th distribution trip, $N_{k1} \in N, 0 \le 1 \le num$, $num = |N|$, where num is the number of elements in N;

Q: The maximum load of each vehicle;

q_j: The demand of consumer j, $q_j>0$;

d_{ij}: The distance between consumer i and consumer j;

i and j: The serial number of nodes, $\forall i, j \in M \cup N$;

X_{ij}^k: The vehicle movement variable; if vehicle k moves from consumer i to consumer j, then $X_{ij}^k = 1$, otherwise, $X_{ij}^k = 0$;

S_k: The time that vehicle k leaves from DC for the last trip;

v: The vehicle speed;

C_1: The dispatch cost per trip of a vehicle;

C_2: The transport cost per unit distance of a vehicle;

C_3: The unit time penalty cost for early arrival or late delivery of a vehicle;

C_4: The cargo loss cost of a vehicle;

P: The unit value of fresh food;

θ_1: The proportion of cargo loss en route;

θ_2: The proportion of cargo loss in loading/unloading;

T_j^k: The time vehicle k arrives at consumer j;

http://www.aloki.hu ● ISSN 1589 1623 (Print) ● ISSN 1785 0037 (Online)
DOI: http://dx.doi.org/10.15666/aeer/1704_94379453

t_i: The time vehicle k serves at consumer i;
C_0: The unit carbon emissions cost.

Mathematical model

(1) Time penalty cost. To ensure the temperature and humidity of fresh food and satisfy the consumer's time requirement, the distributor must deliver the cargoes within the agreed time period. However, the cargoes may not be delivered within the agreed period for various reasons in actual distribution. Hence, the concept of soft time window emerged: the distributor can deliver the cargoes beyond the agreed time period but within the maximum tolerable period of the consumer, while bearing a certain time penalty cost (Dai and Liang, 2017). In this paper, a penalty function is designed according to the time window of the consumers. Specifically, no penalty cost will be incurred if the cargoes are delivered within the period $[E_j, L_j]$ agreed by consumer j and the distributor; the consumer will not accept any service beyond the period $[ET_j, LT_j]$, where ET_j and LT_j are respectively the earliest and latest delivery times the consumer can tolerate; a certain penalty cost will be incurred according to the arrival time of the vehicle if the cargoes are delivered between $[ET_j, E_j]$ and $[L_j, LT_j]$. The time windows of consumer j are described as *Figure 2*.

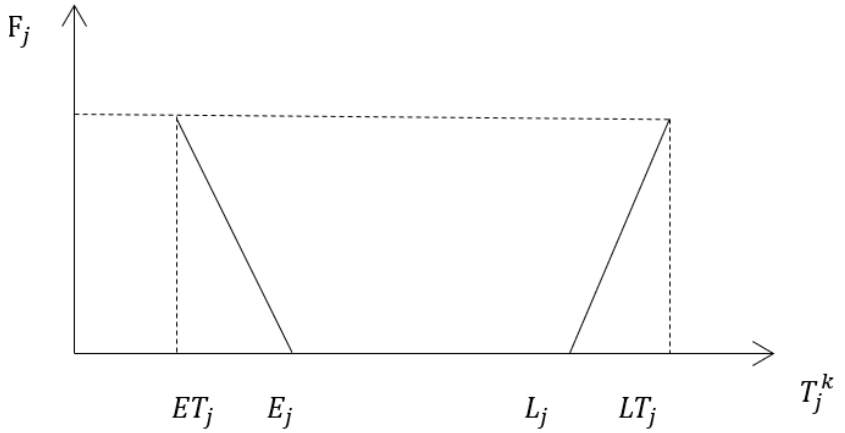

Figure 2. *Sketch map of the time windows of consumer j*

The time penalty cost can be expressed as *Equation 1:*

$$F_j\left(T_j^k\right) = \begin{cases} C_3\left(E_j - T_j^k\right), & ET_j \le T_j^k \le E_j \\ 0, & E_j \le T_j^k \le L_j \\ C_3\left(T_j^k - L_j\right), & L_j \le T_j^k \le LT_j \end{cases}; \quad \text{(Eq.1)}$$

(2) Cargo loss cost. The CCD of fresh food must meet the requirements on temperature and humidity. The fresh food may suffer from a certain loss during the long-distance transport and loading/unloading (Fan et al., 2017). Considering the effects of transport and loading/unloading on the quality and value of fresh food, this paper assumes that the temperature remains constant in the vehicle during distribution, and

http://www.aloki.hu ● ISSN 1589 1623 (Print) ● ISSN 1785 0037 (Online)
DOI: http://dx.doi.org/10.15666/aeer/1704_94379453

excludes the impacts from other factors. In other words, the cargo loss of fresh food is assumed to be correlated with the distribution distance and the door opening in loading/unloading. Hence, the cargo loss cost was calculated based on the two issues. Let $P(\theta_1 d_{ij} + \theta_2 q_j)$ be the cargo loss cost incurred as vehicle j moves from consumer i to consumer j and completes the delivery to consumer j. Then, the total cargo loss cost through the distribution process can be calculated as *Equation 2:*

$$C_4 = P \sum_{i \in M \cup N} \sum_{j \in K \cup N} \sum_{k \in K} x_{ij}^k (\theta_1 d_{ij} + \theta_2 q_j) \quad \text{(Eq.2)}$$

(3) Carbon emissions cost. The CCD releases more CO_2 than the distribution of ordinary cargoes. The carbon emissions in the CCD mainly comes from fuel combustion, which depends on the transport distance is and the cargo load (Xiao et al., 2012; Duro, 2013). The fuel consumption per unit distance μ can be regarded as a linear function of the cargo load q: $\mu(q) = a(Q_0 + q) + b$ where Q_0 is the dead load of the vehicle, and a and b are linear function coefficients. When a vehicle is under fully load, the fuel consumption per unit distance $\mu^* = a(Q_0 + Q) + b$; when a vehicle is under zero load, the fuel consumption per unit distance $\mu_0 = aQ_0 + b$. To sum up, the fuel consumption can be expressed as: $\mu(q) = \mu_0 + \left(\frac{(\mu^* - \mu_0)}{Q} q \right)$. Let Q_{ij} be the load of vehicle k moving from consumer i to consumer j, and $\mu(Q_{ij})$ be the fuel consumption of vehicle k per unit of distance. Then, the carbon emissions cost can be expressed as $C(Q_{ij}) = C_0 d_{ij} e_0 \mu(Q_{ij})$.

Based on the above description and hypotheses, the path optimization model for the minimal total distribution cost can be established as *Equation 3:*

$$\begin{aligned} MinC = {} & C_1 \sum_{i \in M \bigcup N} \sum_{j \in M \cup N} \sum_{k \in K} x_{ij}^k + C_2 \sum_{i \in M \cup N} \sum_{j \in M \cup N} \sum_{k \cup K} x_{ij}^k d_{ij} \\ & + \sum_{j \in M \cup N} \sum_{k \cup K} F_j(T_j^k) + P \sum_{i \in M \cup N} \sum_{j \in M \cup N} \sum_{k \cup K} x_{ij}^k (\theta_1 d_{ij} + \theta_2 q_j) \\ & + C_0 e_0 \sum_{i \in M \cup N} \sum_{j \in M \cup N} \sum_{k \in K} d_{ij} \mu(Q_{ij}) x_{ij}^k \end{aligned} \quad \text{(Eq.3)}$$

s.t.

$$\sum_{j \in N} x_{ij}^k q_j \le Q, \forall i \in M \quad \text{(Eq.4)}$$

$$\sum_{i \in M \cup N} \sum_{k \in K} x_{ij}^k = 1, \forall j \in N \quad \text{(Eq.5)}$$

$$\sum_{j \in M \cup N} \sum_{k \in K} x_{ij}^k = 1, \forall i \in N \quad \text{(Eq.6)}$$

http://www.aloki.hu ● ISSN 1589 1623 (Print) ● ISSN 1785 0037 (Online)
DOI: http://dx.doi.org/10.15666/aeer/1704_94379453

$$\sum_{i \in M} \sum_{j \in M} x_{ij}^{k} = 0, \forall k \in K \quad \text{(Eq.7)}$$

$$\sum_{i \in M} \sum_{j \in N} x_{ij}^{k} = \sum_{i \in N} \sum_{j \in M} x_{ij}^{k}, \forall k \in K \quad \text{(Eq.8)}$$

$$\sum_{i \in N_{kl}} \sum_{j \in N_{kl}} x_{ij}^{k} \leq \left| N_{kl} \right| - 1, \forall k \in K, \forall N_{kl} \subseteq N, 0 \leq l \leq num \quad \text{(Eq.9)}$$

$$x_{ij}^{k} \left(T_{j}^{k} - T_{i}^{k} \right) \geq 0 \quad \text{(Eq.10)}$$

$$T_{j}^{k} = \sum_{i \in M \cup N} \left(T_{i}^{k} + \frac{d_{ij}}{v} + t_{i} \right) x_{ij}^{k}, k \in K, j \in M \cup N \quad \text{(Eq.11)}$$

$$x_{ij}^{k} = \{0,1\}, \forall i, j \in M \cup N, \forall k \in K \quad \text{(Eq.12)}$$

where *Equation 3* is the objective function about the minimal total cost of distribution, including the vehicle dispatch cost, transport cost, time penalty cost, cargo loss cost and carbon emissions cost; *Equations 4–12* are the constraints of the model, which respectively specifies the vehicle load cannot surpass the maximum load, that each consumer can only be served once, that a vehicle must leave the consumer after completing the task, that a vehicle cannot move from a DC directly to another DC, that a vehicle can return to any DC after completing the task, that the branch constraint is removed, that each vehicle must deliver cargoes in strict accordance with the sequence of consumers, that the time vehicle k arrives at customer j, and that $x_{ij}^{k} = 1$ if vehicle k moves from consumer i to consumer j ($x_{ij}^{k} = 0$ if otherwise).

Algorithm design

Assuming the existence of a virtual DC, this paper attempts to solve the semi-open multi-DC CCD path optimization problem as the AFSA-ACA hybrid algorithm. The hybrid algorithm was proposed by introducing the crowding factor of the AFSA to the ACA. This factor can adjust the pheromone concentration left by the ants on the search paths, and thus control the aggregation behavior of the ant colony, leading to the optimal solution. In this way, the AFSA-ACA hybrid algorithm manages to avoid the local optimal trap. The original ACA often falls into this trap due to the following reasons: In the ACA, the path selection of the ant colony is easily affected by the pheromone concentration. Thus, the suboptimal solution often appears in advance, and the pheromones continue to accumulate on the suboptimal paths.

ACA

The ACA was first proposed by the Italian scholar Dorigo and Gambardella (1997). For an ant k in path selection, the probability that the ant moves from node i to node j at time t can be calculated from the pheromone concentration and heuristic information on the path between the two nodes, as shown in *Equation 13:*

http://www.aloki.hu ● ISSN 1589 1623 (Print) ● ISSN 1785 0037 (Online)
DOI: http://dx.doi.org/10.15666/aeer/1704_94379453

$$P_{ij}^{k}(t) = \begin{cases} [\tau_{ij}]^{\alpha}[\eta_{ij}]^{\beta} \Big/ \sum_{j \in J_k(i)} [\tau_{ij}]^{\alpha}[\eta_{ij}]^{\beta}, & j \in J_k(i); \\ 0, & otherwise \end{cases} \quad \text{(Eq.13)}$$

where: τ_{ij} is the residual pheromone concentration on the path between node i and node j; $\eta_{ij} = 1/d_{ij}$ is a heuristic function about the expectation of ant k to move from node i to node j (the smaller d_{ij}, the greater η_{ij} and the higher $P_{ij}^{k}(t)$; $J_k(i) = \{1,2,\ldots,n\} - tabu_k$ is the set of cities that ant k is allowed to choose from, with $tabu_k$ being the tabu list of ant k (the nodes that the ant has served); α is the relative importance of pheromone concentration; β is the importance of the heuristic function, i.e. the importance the ant attaches to the heuristic information.

After one cycle, the global pheromone of the distribution optimization plan involving all ants should be updated. Following the ant-cycle update strategy, the pheromone concentration on each path can be updated by *Equations 14–16:*

$$\tau_{ij}(t+n) = (1-\rho)\tau_{ij}(t) + \Delta\tau_{ij} \quad \text{(Eq.14)}$$

$$\Delta\tau_{ij} = \sum_{k=1}^{K} \Delta\tau_{ij}^{k} \quad \text{(Eq.15)}$$

$$\Delta\tau_{ij}^{k} = \begin{cases} \frac{Z}{L_k}, & if\ ant\ k\ passes\ through\ path\ e(i,j)\ in\ the\ current\ cycle; \\ 0, & if\ otherwise. \end{cases} \quad \text{(Eq.16)}$$

where ρ is the pheromone evaporation rate $0 < \rho \leq 1$;$1-\rho$ is the persistence coefficient of the pheromone); $\Delta\tau_{ij}^{k}$ is the pheromone increment on the path $e(i,j)$ in this iteration; $\Delta\tau_{ij}^{k}$ is the amount of pheromone released by ant k on the path $e(i,j)$ in this iteration; Z is a constant; L_k is the path length covered by ant k in this iteration; $e(i,j)$ is the path from node i to node j.

AFSA

Proposed by Li et al. (2002), the AFSA divides the behaviors of fish swarm into foraging, clustering, tailgating and random behaviors by mimicking the activites of actual fish. During foraging and tailgating, the fish swarm will cluster in the area rich in food, which is similar to the search for the optimal solution. To prevent premature convergence, the crowding factor δ is introduced to control the aggregation concentration of the fish swarm, thus avoiding the local optimal trap.

Let $\delta(t)$ be the crowding factor at time t, X_i be the current state of an artificial fish (AF) and Y_i be the food concentration. Then, the AF searches for the number n_f of its partners and the center position X_c of the current neighborhood. During clustering,

http://www.aloki.hu ● ISSN 1589 1623 (Print) ● ISSN 1785 0037 (Online)
DOI: http://dx.doi.org/10.15666/aeer/1704_94379453

if $Y_c/n_f > \delta(t)Y_i$, then the fish swarm will move one step toward the center position of the partners; otherwise, the fish swarm will start foraging.

During tailgating, if $Y_j/n_f > \delta Y_i$, then the fish swarm will move one step toward the direction of the partner with the best state X_j in the search space; otherwise, the fish swarm will start foraging. Here, X_i, n_f and Y_j have the same meanings as above.

AFSA-ACA hybrid algorithm

In our AFSA-ACA hybrid algorithm, the crowding factor $\delta(N_c)$in the *Nc*-th iteration can be expressed as *Equation 17:*

$$\delta(N_c) = \gamma e^{-cn} \quad \text{(Eq.17)}$$

where γ is the closeness to the extreme value; c is the coefficient of variation.

Following the ant-cycle update rule, the crowding factor $\varepsilon_{ij}(N_c)$ of the phenomenon on the transfer target path in the *Nc*-th iteration acquired by the ACA can be expressed as *Equations 18:*

$$\varepsilon_{ij}(N_c) = 1 - \tau_{ij}(N_c) \Big/ \sum_{i \neq j} \tau_{ij} \quad \text{(Eq.18)}$$

In each iteration, our AFSA-ACA hybrid algorithm first uses the ACA and the roulette strategy to compute the transfer probability of ants between the consumers that satisfy all constraints conditions (e.g. time window and maximum load) and exist outside the tabu list, to select the next consumer to be served, and determine the transfer target path. Then, the AFSA is called to compute the pheromone crowdedness on that path, to see if the path is selectable. If $\varepsilon_{ij}(N_c) > \delta(N_c)$, the path will be selected; otherwise, the ant will stopover at a nearby actual DC, remove the vehicle information and finally return to the virtual DC. If the ant can go on with distribution, it should replenish the cargoes at the actual DC it visited before returning to the virtual DC. Assuming that no cost is incurred and no time is consumed in the replenishment, the actual DC will be added to the current solution. Then, the transfer probabilities will be recalculated and the consumer will be selected again.

The specific flow of the AFSA-ACA hybrid algorithm is illustrated in *Figure 3*.

Simulation and discussion

Calculation example

There is no universal set of examples for semi-open multi-DC CCD, for the distribution mode is subjected to multiple constraints. This paper carries out simulation using the data (Fan et al., 2018). The calculation example is shown in *Table 1*.

It is assumed that a fresh food logistics enterprise W owns one virtual DC and 4 actual DCs, and serves 48 main consumers. The enterprise operates sufficient refrigerated vehicles, which have the same specifications. The maximum load Q is 10 t, the mean speed is $60km/h$, the vehicle dispatch cost C_1 is RMB 600 yuan, and the

http://www.aloki.hu ● ISSN 1589 1623 (Print) ● ISSN 1785 0037 (Online)
DOI: http://dx.doi.org/10.15666/aeer/1704_94379453

transport cost per unit of distance C_2 is RMB 10 yuan. The enterprise and each consumer agree to deliver the fresh food within the time window $[E_j, L_j]$, where E_j is between 6 and 9 and L_j is between 9 and 17. The earliest tolerable delivery time ET_j is 2 h before the E_j, and the latest tolerable delivery time LT_j is 2 h after the L_j. The time penalty cost C_3 is RMB 50 yuan/h if the fresh food is delivered earlier than E_j or later than L_j. The value of the fresh food is RMB 5,000 yuan/t. The proportion of cargo loss en route θ_1 is 0.1%, and that in loading/unloading θ_2 is 0.2%. The CO_2 emissions coefficient e_0 is 2.61 kg/L, and the unit cost of carbon emissions C_0 is RMB 0.1 yuan/kg. For a fully-loaded vehicle, the fuel consumption per unit distance μ_0 is 1 L/km; for a zero-loaded vehicle, the fuel consumption per unit distance μ^* is 2 L/km. The paths between different nodes are considered as straight lines. The distance between consumers and that between consumer and DC are computed by $d_{ij} = \sqrt{(x_i - x_j)^2 + (y_i - y_j)^2}$.

Distribution modes

Inspired by the decomposition method, the traditional distribution mode firstly sorts the 48 consumers through k-means clustering, and allocates them to 4 DCs. Then, the distribution plan was prepared to minimize the total distribution cost. In this plan, each DC is responsible for the distribution to the consumers in the specified region; each vehicle must return to the original DC after completing the tasks in the responsible region.

The proposed distribution mode considers the 48 consumers as a whole and makes uniform planning of the distribution plan. In this mode, each vehicle can stopover or replenish its cargoes after serving a batch of consumers, until completing all distribution tasks.

In this section, both distribution modes are solved by the AFSA-ACA hybrid algorithm. Through repeated simulations on the example, the basic parameters of the hybrid algorithm were set as: $N_{cmax} = 1000$, $Ant\_num = 50$, $\alpha = 1$, $\beta = 3$, and $\rho = 0.5$. The τ_{ij} was initialized as 1. The crowding factors were computed as $\gamma = 0.9$ and $c = 0.0002$. The simulations were run on Matlab2014b and the optimal paths of the two distribution modes were subjected to comparative analysis.

Figure 4 shows the optimal path of enterprise M obtained for the traditional mode. A total of 7 vehicles are needed to serve the 48 consumers, which were allocated to the 4 DCs by k-means clustering. The consumers and paths of each vehicle are listed in *Table 2*.

Figure 5 shows the optimal path of enterprise M obtained for the proposed mode. In this mode, the 48 consumers are viewed as a whole and the 4 DCs share resources with each other. After completing the tasks of the original DC, each vehicle can stopover or replenish its cargoes at a nearby DC; then, the vehicle can continue with distribution until completing all consumer orders in the whole network. A total of 5 vehicles are needed to serve all consumers in this mode. The consumers and paths of each vehicle are listed in *Table 3*.

http://www.aloki.hu ● ISSN 1589 1623 (Print) ● ISSN 1785 0037 (Online)
DOI: http://dx.doi.org/10.15666/aeer/1704_94379453

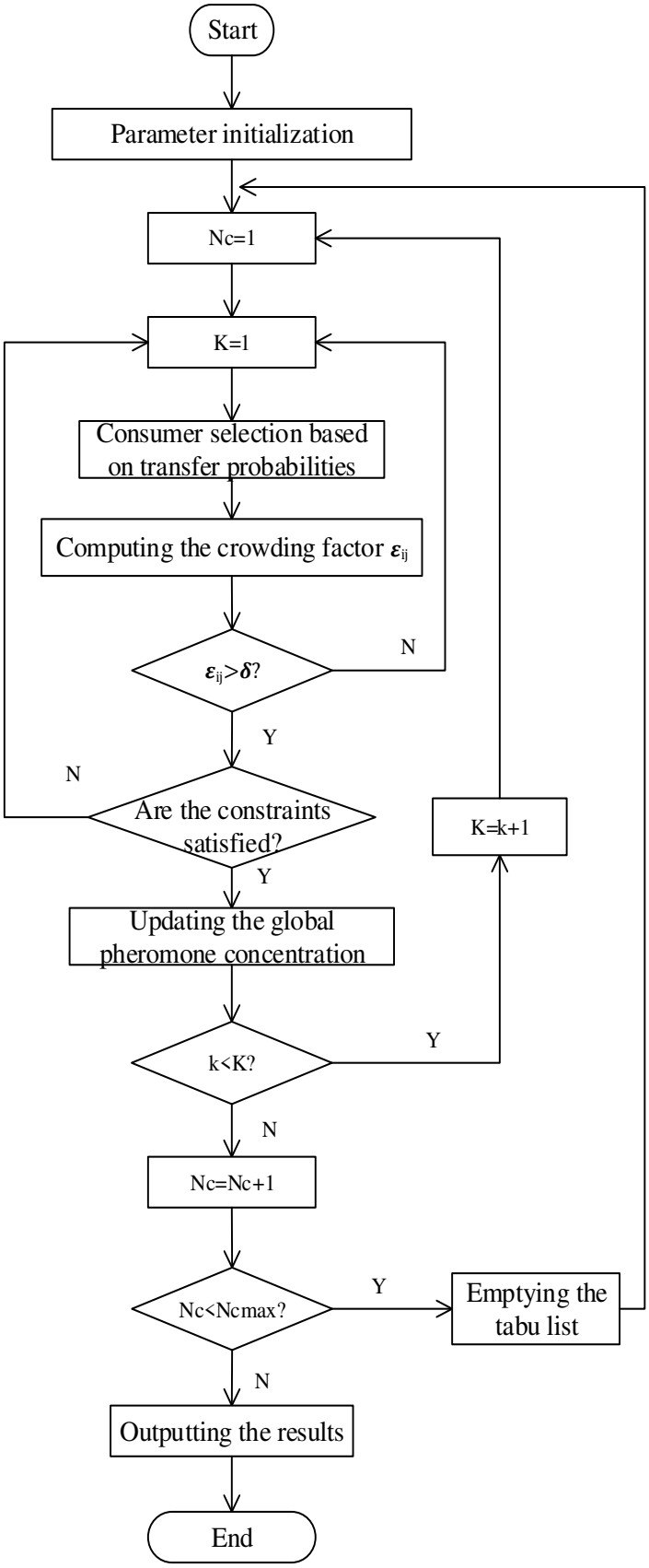

Figure 3. *The workflow of the AFSA-ACA hybrid algorithm*

http://www.aloki.hu ● ISSN 1589 1623 (Print) ● ISSN 1785 0037 (Online)
DOI: http://dx.doi.org/10.15666/aeer/1704_94379453

Table 1. *Information on the multi-DC calculation example*

No.	Node	Position coordinates		Requirement	Operation time	Time windows			
		x	y			ET_j	E_j	L_j	LT_j
1	Virtual Distribution Center	-	-	-	-	-	-	-	-
2	Distribution Center A	4.16	13.56	0	0		6	19	
3	Distribution Center B	21.39	17.11	0	0		6	19	
4	Distribution Center C	-36.12	49.10	0	0		6	19	
5	Distribution Center D	-31.20	0.24	0	0		6	19	
6	Customer Point 1	-29.73	64.14	1.2	0.40	4.5	6.5	10.0	12.0
7	Customer Point 2	-30.66	5.46	0.8	0.27	5.5	7.5	16.5	18.5
8	Customer Point 3	51.64	5.47	1.6	0.53	6.5	8.5	15.5	17.5
9	Customer Point 4	-13.17	69.34	0.5	0.17	5.5	7.5	16.5	18.5
10	Customer Point 5	-67.41	68.32	1.2	0.40	6.5	8.5	13.5	15.5
11	Customer Point 6	48.91	6.27	0.5	0.17	5.5	7.5	16.5	18.5
12	Customer Point 7	5.24	22.26	1.3	0.43	4.5	6.5	9.5	11.5
13	Customer Point 8	-65.00	77.23	2.0	0.67	6.5	8.5	13.5	15.5
14	Customer Point 9	-4.18	-1.57	1.3	0.43	4.5	6.5	10.0	12.0
15	Customer Point 10	23.03	11.64	1.8	0.60	5.5	7.5	16.5	18.5
16	Customer Point 11	25.48	6.29	0.7	0.23	6.5	8.5	13.5	15.5
17	Customer Point 12	-42.62	-26.39	0.6	0.20	5.5	7.5	16.5	18.5
18	Customer Point 13	-76.67	99.34	0.9	0.30	5.5	7.5	15.5	17.5
19	Customer Point 14	-20.67	57.89	0.9	0.30	4.5	6.5	10.5	12.5
20	Customer Point 15	-52.04	6.57	0.4	0.13	4.5	6.5	9.5	11.5
21	Customer Point 16	-41.38	50.82	2.5	0.83	5.5	7.5	16.5	18.5
22	Customer Point 17	-91.94	27.59	0.5	0.17	5.5	7.5	15.5	17.5
23	Customer Point 18	-65.12	30.21	1.7	0.57	4.5	6.5	9.5	11.5
24	Customer Point 19	18.60	96.72	0.3	0.10	5.5	7.5	16.5	18.5
25	Customer Point 20	-40.94	83.21	1.6	0.53	4.5	6.5	12.0	14.0
26	Customer Point 21	-37.76	-33.33	2.5	0.83	5.5	7.5	12.0	14.0
27	Customer Point 22	23.77	29.08	2.1	0.70	5.5	7.5	16.5	18.5
28	Customer Point 23	-43.03	20.45	1.4	0.47	5.5	7.5	16.5	18.5
29	Customer Point 24	-35.30	-24.90	1.9	0.63	4.5	6.5	16.5	18.5
30	Customer Point 25	-54.76	14.37	1.4	0.47	6.5	8.5	13.5	15.5
31	Customer Point 26	-49.33	33.37	0.6	0.20	4.5	6.5	12.0	14.0
32	Customer Point 27	57.40	23.82	1.6	0.53	5.5	7.5	16.5	18.5
33	Customer Point 28	-22.75	55.41	0.9	0.30	5.5	7.5	13.5	15.5
34	Customer Point 29	-56.62	73.34	2.0	0.67	5.5	7.5	16.5	18.5
35	Customer Point 30	-38.56	-3.70	1.3	0.43	4.5	6.5	12.0	14.0
36	Customer Point 31	-16.78	19.54	1.0	0.33	5.5	7.5	15.5	17.5
37	Customer Point 32	-11.56	11.62	1.6	0.53	4.5	6.5	10.5	12.5
38	Customer Point 33	-46.55	97.97	1.9	0.63	4.5	6.5	9.5	11.5
39	Customer Point 34	16.23	9.32	2.2	0.73	5.5	7.5	12.0	14.0
40	Customer Point 35	1.29	7.35	1.4	0.47	5.5	7.5	16.5	18.5
41	Customer Point 36	-26.40	29.53	1.0	0.33	6.5	8.5	14.0	16.0
42	Customer Point 37	4.35	14.69	1.1	0.37	5.5	7.5	15.5	17.5
43	Customer Point 38	-50.67	-23.13	1.5	0.50	5.5	7.5	16.5	18.5
44	Customer Point 39	-22.83	-9.81	1.3	0.43	4.5	6.5	12.0	14.0
45	Customer Point 40	-71.10	-18.62	1.5	0.50	5.5	7.5	16.5	18.5
46	Customer Point 41	-7.85	32.07	0.8	0.27	5.5	7.5	16.5	18.5
47	Customer Point 42	11.88	-24.93	2.2	0.73	5.5	7.5	11.5	13.5
48	Customer Point 43	-18.93	-23.73	2.4	0.80	5.5	7.5	16.5	18.5
49	Customer Point 44	-11.92	11.76	0.3	0.10	5.5	7.5	16.5	18.5
50	Customer Point 45	29.84	11.63	2.5	0.83	5.5	7.5	11.5	13.5
51	Customer Point 46	12.27	-55.81	1.9	0.63	4.5	6.5	13.5	15.5
52	Customer Point 47	-37.93	-21.61	2.1	0.70	5.5	7.5	12.0	14.0
53	Customer Point 48	42.88	-2.97	1.0	0.33	5.5	7.5	16.5	18.5

http://www.aloki.hu ● ISSN 1589 1623 (Print) ● ISSN 1785 0037 (Online)
DOI: http://dx.doi.org/10.15666/aeer/1704_94379453

Table 2. *Optimal distribution path of each vehicle in the traditional mode*

Vehicle	Customers	Route and arrival time
1	6	C-20-33-13-8-5-29-C 6-6.53-7.36-8.49-9.21-10.03-10.63-11.83
2	8	C-15-17-18-25-23-26-1-16-C 6-6.76-7.64-8.26-9.15-9.84-10.55-11.36-12.05-12.97
3	11	C-19-41-4-14-28-36-32-44-39-31-2-C 6-7.21-8.47-9.37-9.77-10.12-10.86-11.58-12.12-12.62-13.55-14.21-15.21
4	6	D-30-40-38-12-47-21-D 6-6.14-7.17-8.02-8.66-8.97-9.87-11.27
5	6	A-46-35-9-43-24-37-A 6-7.16-8.86-9.5-10.37-11.44-13-13.39
6	5	B-7-42-34-11-22-B 6-6.28-7.5-8.81-9.7-10.31-11.21
7	6	B-27-45-6-3-48-10-B 6-6.61-7.64-8.8-9.02-9.75-10.49-11.19

Table 3. *Optimal distribution path of each vehicle in the proposed mode*

Vehicle	Customers	Route and arrival time
1	12	A-46-42-48-11-34-10-B-45-6-3-27-22-37-A 6-7.16-8.3-9.66-10.32-10.71-11.56-12.26-12.43-13.59-13.81-14.66-15.76-16.86-17.25
2	13	C-33-20-1-14-28-32-41-4-19-B-31-44-35-43-D 6-6.83-7.72-8.62-9.2-9.55-10.6-11.48-12.38-13.25-14.68-15.32-15.8-16.13-17.22-18.47
3	13	B-7-9-39-24-47-30-D-21-12-38-40-17-23-2-D 6-6.28-7.14-7.91-8.67-9.37-10.37-10.94-11.51-12.48-12.82-13.67-15.01-16-16.79-16.75
4	5	D-15-18-26-25-36-C 6-6.36-6.94-7.78-8.31-9.32-10.01
5	5	C-13-8-5-29-16-C 6-7.08-7.8-8.62-9.22-10.34-11.26

Comparative analysis

Table 4 compares the optimal distribution plans of the two distribution modes. Under the traditional mode, the total travel distance was 1,393.45 km, and the total distribution cost was RMB 25,920.97 yuan, including RMB 577.36 yuan of carbon emissions cost. Under the proposed mode, the total travel distance was 1,337.27 km, and the total distribution cost was RMB 23,699.18 yuan, including RMB 501.73 yuan of carbon emissions cost.

As shown in *Figure 4*, the consumers in the traditional mode were served by region, and each vehicle must return to the original DC after completing the tasks in the responsible region. As shown in *Figure 5*, the proposed mode realized transregional distribution: after completing the current task, each vehicle can stopover or replenish its cargoes at a nearby DC; then, the vehicle can continue with distribution until completing all consumer orders in the whole network. Compared with the traditional mode, the proposed mode can distribute fresh food efficiently with a few vehicles, a

http://www.aloki.hu ● ISSN 1589 1623 (Print) ● ISSN 1785 0037 (Online)
DOI: http://dx.doi.org/10.15666/aeer/1704_94379453

short distance and a low cost, and saves resources in the return trips of vehicles. Besides, the proposed mode can effectively reduce the carbon emissions cost, which is in line with the green development of the enterprise.

Table 4. *Distribution index comparison between the two distribution modes*

Distribution mode	Distribution distance	Total distribution cost	Dispatch cost	Transportation cost	Time penalty cost	Cost of goods damage	Cost of carbon emissions
District distribution	1393.45	25920.97	4200.0	13934.50	257.50	6951.61	577.36
Joint distribution	1337.27	23699.18	3000.0	13372.70	253.50	6571.25	501.73

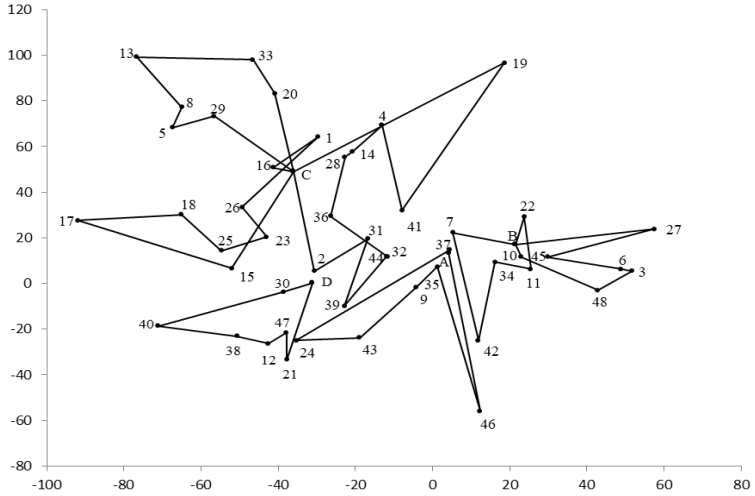

Figure 4. *The optimal path for the traditional mode*

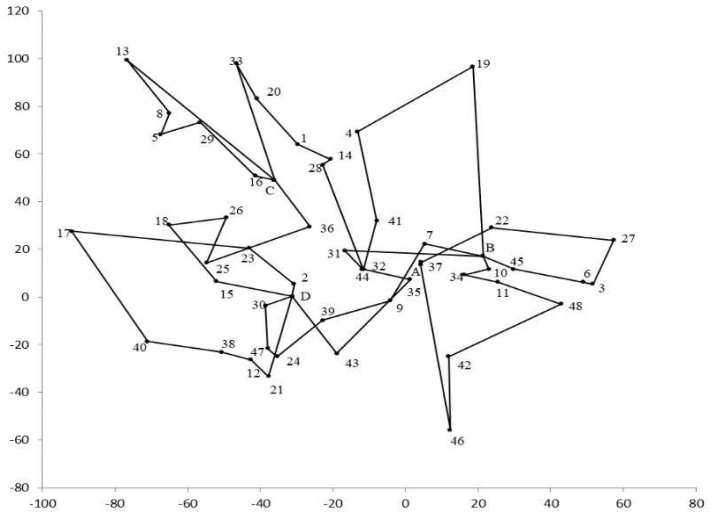

Figure 5. *The optimal path for the proposed mode*

http://www.aloki.hu ● ISSN 1589 1623 (Print) ● ISSN 1785 0037 (Online)
DOI: http://dx.doi.org/10.15666/aeer/1704_94379453

Conclusions

Targeting the fresh food distribution, this paper puts forward a semi-open multi-DC CCD model based on multi-DC resource sharing and time window constraint. The proposed model was solved by the AFSA-ACA hybrid algorithm. The semi-open multi-DC distribution mode was proved to have smaller total travel distance and total cost than the traditional regional distribution mode, and, in particular, a much lower carbon emissions cost. The semi-open multi-DC distribution mode provides enterprises an important tool to save resources, realize multi-DC resource sharing, maximize economic and environmental benefits. The research findings lay a solid theoretical basis for the distribution of fresh food.

Although the content of this paper provides some reference value for fresh product distribution enterprises in planning low-carbon distribution routes, the model built in this paper is based on certain assumptions and constraints. So the research is still incomplete. This paper assumes that the same type of vehicle, the same temperature and uniform speed are constraints for distribution. Multi-type vehicle, multi-temperature joint distribution and the variable speed can be considered in the study of path optimization CCD with multi-DC considering carbon emissions in future researches.

Acknowledgements. The research of this paper is supported by Social Science Foundation of Hebei Province (HB17GL022), Research Projects of Innovative Talents Training Fund of Hebei Province (A2016001120), Project of Scientific Research Project of Hebei Provincial Education Department (SD181012, SD161009).

REFERENCES

[1] Adelzadeh, M., Asl, V. M., Koosha, M. (2014): A mathematical model and a solving procedure for multi-depot vehicle routing problem with fuzzy time window and heterogeneous vehicle. – The International Journal of Advanced Manufacturing Technology 75(5-8): 793-802.

[2] Baldacci, R., Mingozzi, A., Roberti, R., Calvo, R. W. (2013): An exact algorithm for the two-echelon capacitated vehicle routing problem. – Operations Research 61(2): 298-314.

[3] Bao, C. L., Zhang, S. B. (2018): Route optimization of cold chain logistics in joint distribution: with consideration of carbon emission. – Industrial Engineering and Management 23(5): 95-100, 107.

[4] Chaabane, A., Ramudhin, A., Paquet, M. (2012): Design of sustainable supply chains under the emission trading scheme. – International Journal of Production Economics 135(1): 37-49.

[5] Dai, X. J., Liang, C. J. (2017): Cold storage type of multi-temperature distribution problem with the soft time windows. – Journal of Chongqing Normal University (Natural Science Edition) 34(5): 18-25.

[6] Dantzig, G. B., Ramser, J. H. (1959): The truck dispatching problem. – Management Science 6(1): 80-91.

[7] Dorigo, M., Gambardella, L. M. (1997): Ant colony system: a cooperative learning approach to the traveling salesman problem. – IEEE Transactions on Evolutionary Computation 1(1): 53-56.

[8] Duro, J. (2013): International mobility in carbon dioxide emissions. – Energy Policy 55: 208-216.

http://www.aloki.hu ● ISSN 1589 1623 (Print) ● ISSN 1785 0037 (Online)
DOI: http://dx.doi.org/10.15666/aeer/1704_94379453

[9] Fan, H. M., Yang, X., Li, D., L. Y., Liu, P. C., Wu, J. X. (2018): Half-open multi-depot vehicle routing problem based on joint distribution mode of fresh food. – Computer Integrated Manufacturing System 25(1): 1-15.
[10] Fan, L. N., Dong, D. Y., Li, J. Y., Liu, C., Ding, Y. (2017): Route optimization of cold chain logistics based on fresh agricultural products. – Journal of Shenyang University (Natural Science Edition) 29(2): 125-131.
[11] Fan, S. Q., Lou, D., Sun, Y. (2017): Optimization study on vehicle distribution routing of cold-chain logistics for fresh agricultural products. – Storage and Process 17(6): 106-111.
[12] Gac, A. (1996): The cold chain and the greenhouse effect. – Comptes Rendus de l'Academie d'Agriculture de France 82(6): 119-133.
[13] Ge, X. L., Xu, M. Z., Wang, W. X. (2016): Route optimization of urban logistics in joint distribution. – Control and Decision-Making 31(3): 503-512.
[14] Ho, W., Ho, G. T. S., Ji, P., Lau, H. (2007): A hybrid genetic algorithm for the multi-depot vehicle routing problem. – Engineering Applications of Artificial Intelligence 21(4): 548-557.
[15] James, S. J., James, C., Sant'Ana, A. D. S. (2010): The food cold-chain and climate change. – Food Research International 43(7): 1944-1956.
[16] Kang, K., Han, J., Pu, W., Ma, Y. F. (2019): Optimization research on cold chain distribution routes considering carbon emissions for fresh agricultural products. – Computer Engineering and Application 55(2): 259-265.
[17] Lan, H. J., Xue, H. L., Tian, Y. B. (2013): Classification and application on food cold chain collaborative distribution models. – LISS 2012: 123-128.
[18] Li, X. L., Shao, Z. J., Qian, J. X. (2002): An optimizing method based on autonomous animals fish-swarm algorithm. – System Engineering Theory and Practice 22(11): 32-38.
[19] Liang, C. J., Huang, T., Xu, D. H., Ding, Y. (2016): A solution for cold chain distribution with fuzzy time window based on improved genetic algorithm. – Journal of Guangxi University (Natural Science Edition) 41(3): 826-835.
[20] Liu, C. Y. (2013): An improved adaptive genetic algorithm for the multi-depot vehicle routing problem with time window. – Journal of Networks 8(5): 1035.
[21] Liu, J. L., Guo, X. P. (2016): Multi-depot open vehicle routing problem with exclusive products and heterogeneous vehicles. – Journal of Systems Management 25(1): 129-138.
[22] Liu, R., Jiang, Z., Fung, R. Y. K., Chen, F., Liu, X. (2010): Two-phase heuristic algorithms for full truckloads multi-depot capacitated vehicle routing problem in carrier collaboration. – Computers & Operations Research 37(5): 950-959.
[23] Palmer, A. (2007): The development of an integrated routing and carbon dioxide emissions model for goods vehicles. – PhD Thesis, School of Management, Cranfield University.
[24] Vanek, F., Sun, Y. (2008): Transportation versus perishability in life cycle energy consumption: a case study of the temperature-controlled food product supply chain. – Transportation Research Part D Transport & Environment 13(6): 383-391.
[25] Wang, S. Y., Sun, H., Mou, J. J. (2018): Optimization of cold-storage multi-temperature joint distribution based on stochastic demands. – Systems Engineering-Theory Methodology Application 27(4): 712-721.
[26] Wang, Y., Zhang, J., Liu, Y., Xu, M. Z. (2019): Optimization method study of fresh good logistics distribution based on time window and temperature control. – Control and Decision-Making. DOI: 10.13195/j.kzyjc.2018.1662.
[27] Xiao, Y., Zhao, Q., Kaku, I, Xu, Y. C. (2012): Development of a fuel consumption optimization model for the capacitated vehicle routing problem. – Computers & Operations Research 39(7): 1419-1431.
[28] Yang, X., Fan, H. M., Zhang, X. N., Li, Y. (2016): Optimization of multi-deport open vehicle routing problem with fuzzy time window. – Computer Integrated Manufacturing System 22(7): 1768-1778.

http://www.aloki.hu ● ISSN 1589 1623 (Print) ● ISSN 1785 0037 (Online)
DOI: http://dx.doi.org/10.15666/aeer/1704_94379453

[29] Yu, B., Xie, Y. X. (2011): A parallel improved ant colony optimization for multi-depot vehicle routing problem. – The Journal of the Operational Research Society 62(1): 183-188.

http://www.aloki.hu ● ISSN 1589 1623 (Print) ● ISSN 1785 0037 (Online)
DOI: http://dx.doi.org/10.15666/aeer/1704_94379453

EVALUATION OF THE INTERACTION EFFICIENCY BETWEEN ECO-ENVIRONMENT AND ECONOMIC DEVELOPMENT IN CHINA

CAO, L.[1,2] – MA, Z. X.[3] – MUREN[4,5*] – CUI, W.[4] – SIQIN[1]

[1]*School of Mathematics Science, Inner Mongolia University, Hohhot 010021, China*

[2]*College of Computer and Information, Inner Mongolia Medical University, Hohhot 010110, China*

[3]*School of Economics and Management, Inner Mongolia University, Hohhot 010021, China*

[4]*Inner Mongolia University of Technology, Hohhot 010051, China*

[5]*Key Laboratory of Rail Transit, Beijing Jiaotong University, Beijing 100044, China*

**Corresponding author*
e-mail: muren@imut.edu.cn; phone:+86-185-8601-0847

(Received 3rd Apr 2019; accepted 17th May 2019)

Abstract. The protection of eco-environment is the basis of economic development. It is the interaction between eco-environment and economic development that promotes the development of human society. Therefore, it is important to obtain relevant data and select an appropriate evaluation method to find out how these two are interacting with each other. In this paper, a new data envelopment analysis (DEA) model based on generalized DEA method and the multi-level index synthesis method is proposed for the first time to evaluate the interaction efficiency between eco-environment and economic development in Chinese provinces. Through correlation analysis of the indices, a scientific index system is established. After index synthesis, the new order of efficient provinces is established, and the improvement information for inefficient provinces has also been obtained. In addition, more scientific suggestions are put forward for the protection of eco-environment and economic development in China.
Keywords: *multi-objective decision making, efficiency, generalized DEA, index synthesis, partial ordered relation*

Introduction

No economic activity of mankind can be carried out without using nature resources, such as land, trees, water and so on (Brown, 2000). A well-protected eco-environment can provide continuous, high-quality and large amounts of resources for the sustainable economic development (Gaspar et al., 2017); on the other hand, a poorly-protected eco-environment will affect the stability and speed of economic development. Therefore, protection of eco-environment is the foundation of economic development. At the same time, economic development plays a decisive role in the virtuous cycle of eco-environment. No doubt, the economic development can cause damages to the eco-environment, especially the high-consumption, high-pollution and low-output production modes, which result in soil erosion, serious desertification and water and air pollution. However, the rapid economic development can also provide financial support for the protection and improvement of eco-environment, so as to maintain its healthy development.

http://www.aloki.hu ● ISSN 1589 1623 (Print) ● ISSN 1785 0037 (Online)
DOI: http://dx.doi.org/10.15666/aeer/1704_94559471

Many developed countries used to promote the rapid economic development at the expense of the environment (Mittler and Knirsch, 2007). China also had a similar experience. As a developing country, it has maintained its economic growth rate above 8%, and even achieved a growth of 14% from 2000 to 2012, as shown in *Figure 1*, but this has been at the cost of environment to varying degrees. The smog in Beijing, the desertification in Inner Mongolia and the floods in the South are all clear evidence.

At present, the Chinese government has realized the importance of eco-environment protection (Zhou, 2015). It no longer blindly pursues rapid economic growth, but pays more attention to the sustainable development of both the environment and the economy. As a result, the GDP growth rate in China began to decline from 2013 to 2017, and the magnitude was the highest among the top five economies of the world. From the perspective of GDP, GDP and per capita GDP have been rising steadily on the whole, as shown in *Figure 2*.

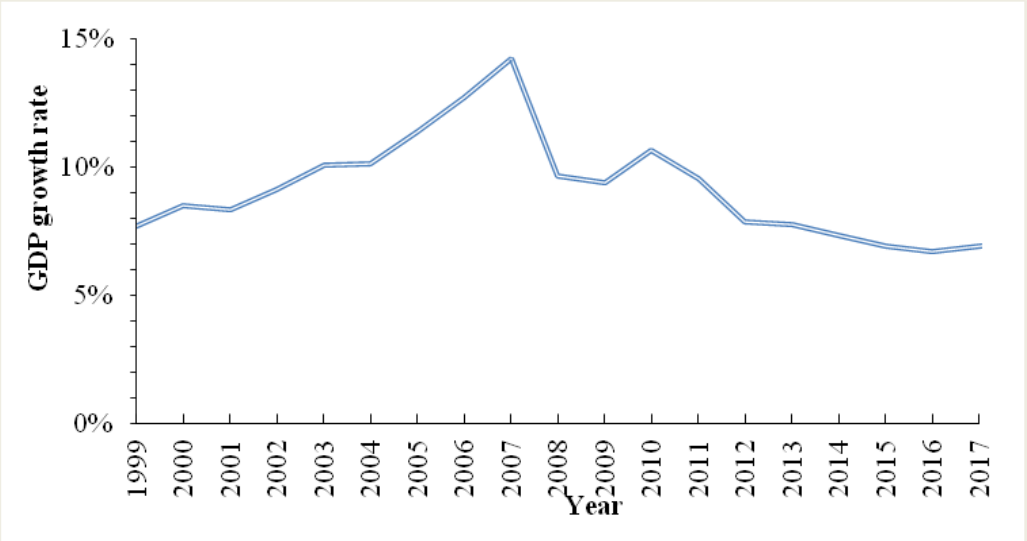

Figure 1. *GDP growth rate from 1999 to 2017 in China*

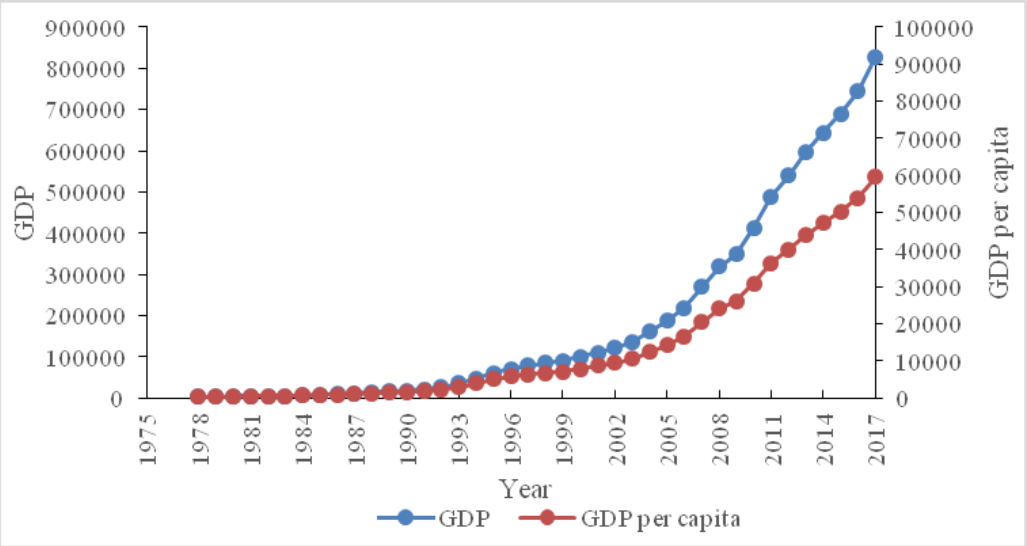

Figure 2. *GDP and GDP per capita from 1978 to 2017 in China*

http://www.aloki.hu ● ISSN 1589 1623 (Print) ● ISSN 1785 0037 (Online)
DOI: http://dx.doi.org/10.15666/aeer/1704_94559471

We can see that the shares of the primary and secondary industries, i.e., agriculture and manufacturing, in the national economy continue to decrease, whereas that of the tertiary industry continues to expand, as shown in *Figure 3*. In 2017, for example, the services industry accounted for 52.2 percent of China's GDP, up by 0.3 percent, while agriculture accounted for 7.1 percent and manufacturing 40.7 percent in China. Although the share of the secondary industry has declined, it still accounts for 40.7%. Without strict protection of the eco-environment, it will cause great damages. Take Inner Mongolia for example, the share of the primary industry declined significantly, that of the secondary industry rose first and then declined, and that of the tertiary industry was relatively stable on the whole, but it rose after 2011, as shown in *Figure 4*. It can be said that the environment of Inner Mongolia was greatly affected by the industrial structure until after 2011.

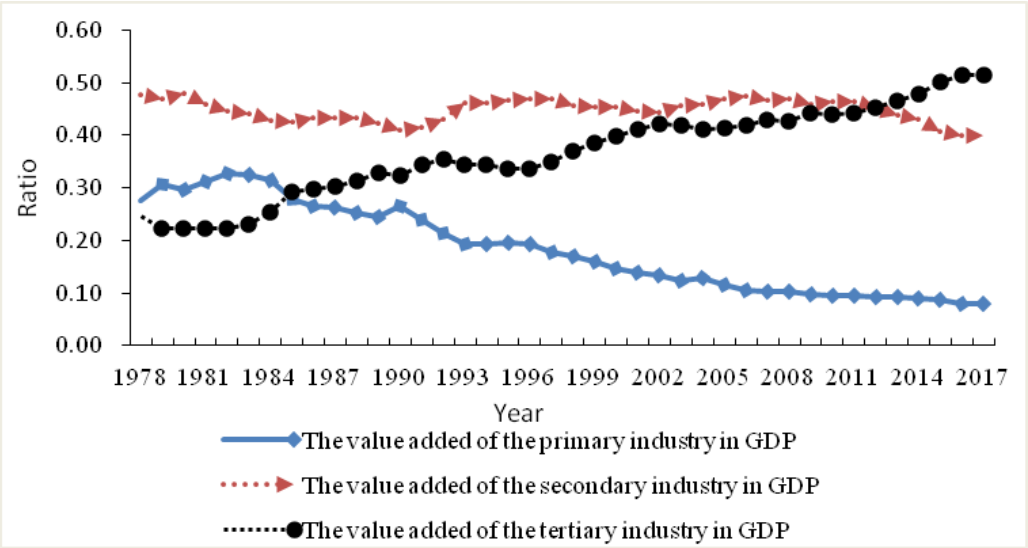

Figure 3. *Primary, secondary and tertiary industries in GDP from 1978 to 2017 in China*

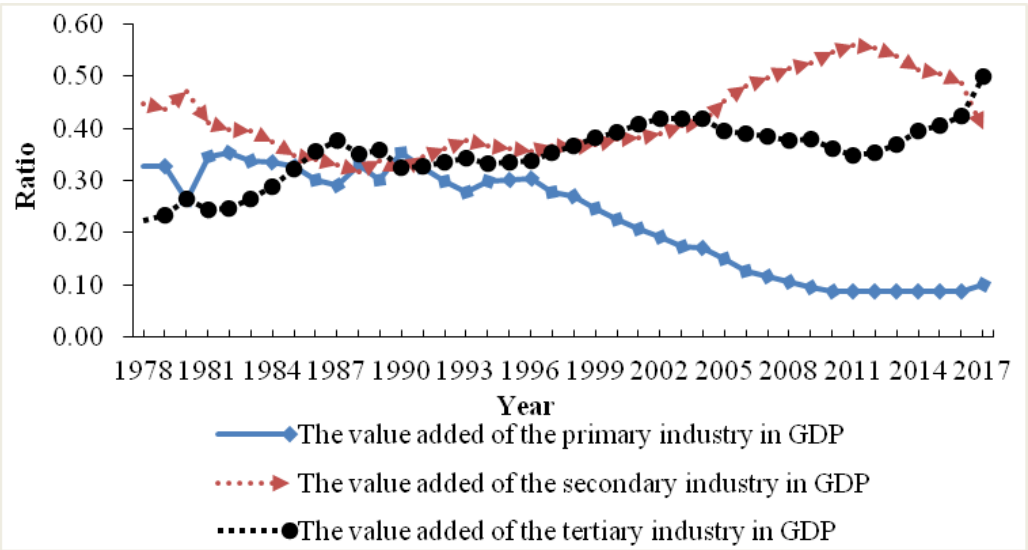

Figure 4. *Primary, secondary and tertiary industries in GDP from 1978 to 2017 in Inner Mongolia*

http://www.aloki.hu ● ISSN 1589 1623 (Print) ● ISSN 1785 0037 (Online)
DOI: http://dx.doi.org/10.15666/aeer/1704_94559471

As discussed above, China has gone through the process of developing economy at the expense of environment. Although in recent years, China has made great achievements in eco-environmental protection and at the same time successfully accomplished the targets set in the 13th five-year plan (2016-2020), as reported at the Second Session of the 13th National People's Congress, there is still much work to do due to the seriousness of the previous damages.

The interaction between eco-environment and economic development promotes the development of human society (Diao et al., 2009). So finding out how these two are interacting with each other using relevant data and appropriate methods has become a hot research topic. Most of the existing studies discussed how to maximize economic development with the minimum eco-environment damage based on the input-output efficiency. This idea is consistent with the theory of the data envelopment analysis (DEA) method (Banker et al., 1984; Charnes et al., 1978; Färe and Frosskopf, 1985; Seiford and Thrall, 1990). So the DEA method has been widely used in the eco-environment and economic efficiency analysis in recent years. For example, Moutinho et al. (2017) analyzed the economic and environmental efficiency assessment in EU cross-country based on DEA and the quantile regression approach. Mavi et al. (2018) applied a two-stage network DEA method based on goal programming to analyze the joint effects of eco-environment and eco-innovation on the countries in the Organization for Economic Co-operation and Development (OECD). Halkos et al. (2018) estimated the efficiency of the power generation sector in the USA by using window DEA (W-DEA) to model the relationships between environmental efficiency and economic growth. Moutinho et al. (2018) analyzed the performances of a number of German and French cities using the DEA technique. Song et al. (2018) conducted DEA to evaluate the environmental efficiency of Chinese regions. It should be emphasized that there have been many studies on the efficiency evaluation of the eco-environment and economic development in China in recent years. These studies can be summarized as follows: (1) The traditional DEA model is directly used for evaluation, and for example, Jia and Liu used the input-oriented BCC-type DEA models to calculate energy and environment efficiency of 30 provinces in China (2012), and some papers discussed environment efficiency based on the DEA-SBM model (Chang et al., 2014; Ma et al., 2017; Yang et al., 2012); (2) the traditional DEA method is combined with other methods (Lee et al., 2013); and (3) the traditional DEA model is improved, and for example, Liu et al. (2018) brought forward an ideal point cross efficiency (IPCE) model to avoid the disadvantage of the 'self-evaluation' method and analyzed the carbon emissions efficiency of 10 typical urban agglomerations from 2008 to 2015 in China, and Wang and Wu (2014) proposed a new two-stage multiplier DEA approach to evaluate the environmental and economic performance of 30 provinces and municipalities in China.

Since the eco-environment system and economic system are complex systems, many indices in the eco-environment system are likely to affect economic development. How many indices are selected in the research will bring different efficiency evaluation results. At present, most of the studies use only a small number of indices to evaluate the eco-environment and economic development efficiency. But that does not mean the number of selected indices can be excessively large, because in that case, the majority of DMUs will be regarded as efficient when the DEA method is applied to the evaluation, which is useless to the decision makers.

http://www.aloki.hu ● ISSN 1589 1623 (Print) ● ISSN 1785 0037 (Online)
DOI: http://dx.doi.org/10.15666/aeer/1704_94559471

DEA is particularly applicable to the analysis of complex systems such aseco-environment and economy systems. However, the DEA method also has some disadvantages that cannot be overcome because of the complexity of the systems. Firstly, the evaluation result may over-emphasize the role of secondary indices. Secondly, it often appears that most DMUs are efficient. Thirdly, it has high requirements on projection. Fourthly, it cannot determine how to improve the original indices after the synthetic of indices.

In order to solve the above problems, this paper applies the generalized DEA method and the multi-level index synthesis technique for the first time to evaluate the interaction efficiency between eco-environment and economic development. The generalized DEA proposed is based on sample evaluation (Ma et al., 2002, 2003, 2012, 2018). The evaluation reference set is not limited to the optimal criteria. For example, the admission line for college entrance examination reflects the average level, and the bottom line in wind risk analysis reflects the minimum evaluation criteria. Of course, sometimes the evaluation criteria may be specific units, such as selected templates, standards or certain objects. Such problems cannot be solved by the traditional DEA. The multi-level index synthesis technique can not only obtain the ranking of DMUs, but also solve the ranking problem that most DMUs are efficient, and obtain the improved information of the original index (Muren et al., 2013).

Materials and methods

Multi-level index synthesis method

Suppose that there are n DMU*s*. $x_{ij}^{(l)}$ denotes the value of the lth lower index of the ith input index of the jth DMU, $y_{rj}^{(t)}$ denotes the value of the tth lower index of the rth input index of the jth DMU, and $x_{ij}^{(l)}$ and $y_{rj}^{(t)}$ are both positive. Suppose there is another $\bar{n}$ sample DMUs as the reference sample for evaluation. $\bar{x}_{ij}^{(l)}$ denotes the value of the lth lower index of the ith input index of the jth sample DMU, $\bar{y}_{rj}^{(t)}$ denotes the value of the tth lower index of the rth input index of the jth sample DMU, and $\bar{x}_{ij}^{(l)}$ and $\bar{y}_{rj}^{(t)}$ are both positive. The input-oriented synthesis model based on generalized DEA is represented as follows when the pth DMU is evaluated, where $1 \le p \le n$.

$$
(IGDEA)\begin{cases}
\min \theta - \varepsilon(\sum_{i=1}^{m}\sum_{l=1}^{L_i} a_i^l s_i^{l-} + \sum_{r=1}^{s}\sum_{t=1}^{T_r} b_r^t s_r^{t+}) \\
\text{s.t.} \quad \sum_{j=1}^{\bar{n}} \bar{x}_{ij}^{(l)} \lambda_j + s_i^{l-} = \theta x_{ip}^{(l)}, \quad l = 1,2,\cdots,L_i, \quad i = 1,2,\cdots,m \\
\quad \sum_{j=1}^{\bar{n}} \bar{y}_{rj}^{(t)} \lambda_j - s_r^{t+} = y_{rp}^{(t)}, \quad t = 1,2,\cdots,T_r \ \ r = 1,2,\cdots,s \\
\quad \delta_1(\sum_{j=1}^{\bar{n}} \lambda_j - \delta_2(-1)^{\delta_3} \lambda_{\bar{n}+1}) = \delta_1 \\
\quad \sum_{l=1}^{L_i} a_i^l s_i^{l-} \ge 0, i = 1,2,\cdots,m, \\
\quad \sum_{t=1}^{T_r} b_r^t s_r^{t+} \ge 0, \quad r = 1,2,\cdots,s \\
\quad \lambda_j \ge 0, \quad j = 1,2,\cdots,\bar{n}+1
\end{cases}
\qquad \text{(Eq.1)}
$$

http://www.aloki.hu ● ISSN 1589 1623 (Print) ● ISSN 1785 0037 (Online)
DOI: http://dx.doi.org/10.15666/aeer/1704_94559471

where:

$\lambda = (\lambda_1, \lambda_2, \cdots, \lambda_n)$,

$S^- = (s_1^{1-}, \cdots, s_1^{L_1-}, \cdots, s_m^{1-}, \cdots, s_m^{L_m-})$ $S^{(l)-} = (s_1^{1-}, \cdots, s_1^{L_1-}, \cdots, s_m^{L_1-})$,

$S^+ = (s_1^{1+}, \cdots, s_1^{T_1+}, \cdots, s_S^{1+}, \cdots, s_s^{T_s+})$.

Definition 1 Assuming that $\theta^0, \lambda, \lambda_{n+1}^0, S^{-0}, S^{+0}$ is the optimal solution of model *Equation 1,* we can call DMU*p* is IG-DEA efficient if it meets one of the following conditions,

(1) $\theta^0 = 1, \sum_{l=1}^{L_i} a_i^l s_i^{l-0} = 0, i = 1, 2, \cdots, m,$ and $\sum_{t=1}^{T_r} b_r^t s_r^{t+0} = 0, r = 1, 2, \cdots s$;

(2) $\theta^0 > 1$;

(3) Model (1) has no feasible solution.

Definition 2 Assuming that $\theta^0, \lambda, \lambda_{n+1}^0, S^{-0}, S^{+0}$ is the optimal solution of model *Equation 1,* let $\hat{x}_{ip}^{(l)} = \theta^0 x_{ip}^{(l)} - s_i^{l-0}$, $\hat{y}_{rp}^{(t)} = y_{rp}^{(t)} + s_r^{t+0}, l = 1, 2, \cdots, L_i, i = 1, 2, \cdots, m, t = 1, 2, \cdots, T_r$, $r = 1, 2, \cdots, s$ and the projection of DMU*p* on the effective surface of the sample is expressed as $((\tilde{x}_{1p}^{(1)}, ..., \tilde{x}_{1p}^{(L_1)}, ..., \tilde{x}_{mp}^{(1)}, ..., \tilde{x}_{mp}^{(L_m)}), (\tilde{y}_{1p}^{(1)}, ..., \tilde{y}_{1p}^{(T_1)}, ..., \tilde{y}_{sp}^{(1)}, ..., \tilde{y}_{sp}^{(T_s)}))$.

However, in many practical evaluation problems, input is often constant. In this case, the DMU can only be improved by increasing the output. Therefore, the study on the output-oriented efficiency evaluation model is equally important. The output-oriented synthesis model based on generalized DEA is represented in model *Equation 2*.

$$(OGDEA)\begin{cases} \max \varphi + \varepsilon(\sum_{i=1}^{m}\sum_{l=1}^{L_i} a_i^l s_i^{l-} + \sum_{r=1}^{s}\sum_{t=1}^{T_r} b_r^t s_r^{t+}) \\ \text{s.t.} \quad \sum_{j=1}^{n} \bar{x}_{ij}^{(l)} \lambda_j + s_i^{l-} = x_{ij_0}^{(l)}, \quad l = 1, 2, \cdots, L_i, \quad i = 1, 2, \cdots, m \\ \sum_{j=1}^{n} \bar{y}_{rj}^{(t)} \lambda_j - s_r^{t+} = \varphi y_{rj_0}^{(t)}, \quad t = 1, 2, \cdots, T_r \ r = 1, 2, \cdots, s \\ \delta_1(\sum_{j=1}^{n} \lambda_j - \delta_2(-1)^{\delta_3} \lambda_{n+1}) = \delta_1 \\ \sum_{l=1}^{L_i} a_i^l s_i^{l-} \geq 0, i = 1, 2, \cdots, m \\ \sum_{t=1}^{T_r} b_r^t s_r^{t+} \geq 0, \quad r = 1, 2, \cdots, s \\ \lambda_j \geq 0, \quad j = 1, 2, \cdots, n+1 \end{cases} \quad \text{(Eq.2)}$$

Definition 3 Assuming that $\varphi^0, \lambda^0, \lambda_{n+1}^0, S^{-0}, S^{+0}$ is the optimal solution of model *Equation 2* and $\varphi^0 = 1$ $\sum_{l=1}^{L_i} a_i^l s_i^{l-0} = 0, i = 1, 2, \cdots, m,$ $\sum_{t=1}^{T_r} b_r^t s_r^{t+0} = 0,$ $r = 1, 2, \cdots, s,$ and DMU*p* is call OG-DEA efficient. The efficiency of DMU*p* is expressed as $\frac{1}{\varphi^0}$.

Definition4 Assuming that $\varphi^0, \lambda^0, \lambda_{n+1}^0, S^{-0}, S^{+0}$ is the optimal solution of model *Equation 2,* let $\hat{x}_{ij0}^{(l)} = x_{ij0}^{(l)} - s_i^{l-0}, \hat{y}_{rj0}^{(t)} = \varphi^0 y_{rj0}^{(t)} + s_r^{t+0}, l = 1, 2, \cdots, L_i, i = 1, 2, \cdots, m, t = 1, 2, \cdots, T_r, r = 1, 2, \cdots, s$

http://www.aloki.hu ● ISSN 1589 1623 (Print) ● ISSN 1785 0037 (Online)
DOI: http://dx.doi.org/10.15666/aeer/1704_94559471

and the projection of DMU_{j0} on the effective surface of the sample is expressed as $((\tilde{x}_{1j_0}^{(1)},...,\tilde{x}_{1j_0}^{(L_1)},...,\tilde{x}_{mj_0}^{(1)},...,\tilde{x}_{mj_0}^{(L_m)}),(\tilde{y}_{1j_0}^{(1)},...,\tilde{y}_{1j_0}^{(T_1)},...,\tilde{y}_{sj_0}^{(1)},...,\tilde{y}_{sj_0}^{(T_s)}))$.

Selection of environmental and economic indices

There are many indices to evaluate the degree of eco-environment damages and the level of pollution. In the Statistical Yearbook of China, there are 21 sub-indices under the index of resource and environment, and there are further sub-indices under each sub-index. Taking the index of 'Collection, Transport and Disposal of Urban Consumption Wastes' for example, there are 16 sub-indices under it. The sub-indices under the resource and environment index are not only numerous, but also have complex relations among them, including certain degree of correlation.

Through review of relevant documents, it is found that the main pollutants in waste water and the main pollutants in waste gas are mainly selected by researchers in the evaluation on the environments of various provinces in China. In fact, for a country with a high urbanization level, municipal solid waste (MSW) has also become an important index to the environment. Therefore, this paper decides to adopt the above three environmental indices to evaluate the environmental status and analyze the impact on the economy of every province in China.

In order to reflect these environmental indices more accurately, this paper digs into the sub-indices of the above three indices. The results show that there are strong correlations between these indices. If all the sub-indices are selected as input indices, it will be difficult to distinguish the main differences in environmental status among the provinces by the DEA method because of the data correlation. Therefore, scientific selection and combination of these indices is an important prerequisite for better evaluation of environmental status.

For the 14 sub-indices under the index 'Discharge of Main Pollutants in Waste Water', this paper removes the indices with relatively small discharges and low correlation with the main index, and then selects the typical indices with high correlations. Finally, the sub-indices selected are 'Total Waste Water Discharged', 'Petroleum Discharge in Waste Water', and 'Plumbum Discharge in Waste Water'.

For the 3 sub-indices under the index 'Emission of Main Pollutants in Waste Gas', the correlation between them is between 0.7 and 0.8, and the difference between the data is not obvious, so three sub-indices are all selected, namely 'Sulphur Dioxide Emission in Waste Gas', 'Nitrogen Oxides Emission in Waste Gas' and 'Smoke and Dust Emission in Waste Gas'.

For the 11 sub-indices under the index 'Collection, Transport and Disposal of Urban Consumption Wastes', only two sub-indices are selected, namely 'Volume of Garbage Disposal' and 'Treatment Rate of Consumption Wastes', because there is no significant correlation between them, but strong correlation between the other indices and the index of 'Volume of Garbage Disposal'.

Many economic and social activities have had significant impacts on the eco-environment. Some of the most important economic indices are selected, which are 'Gross Regional Product', 'Local Government's Expenditure', 'Local Government's Revenue', and 'Income and Consumption Expenditure by Nationwide, Urban and Rural Households'.

For the 14 sub-indices under the index 'Regional Gross Product', the correlation between the 2 sub-indices 'Gross Regional Product' and 'Per Capita Gross Regional

http://www.aloki.hu ● ISSN 1589 1623 (Print) ● ISSN 1785 0037 (Online)
DOI: http://dx.doi.org/10.15666/aeer/1704_94559471

Product' is weak, but all other sub-indices have strong correlations with 'Gross Regional Product'. Therefore, only the two sub-indices 'Gross Regional Product' and 'Per Capita Gross Regional Product' are selected.

For the 22 sub-indices under the index 'Local Governments Revenue', since all sub-indices are counted in big numbers, some smaller sub-indices are eliminated. There are strong correlations between all the remaining sub-indices and the sub-index 'Local Governments General Budgetary Revenue', so the latter is selected. For the 21 indices under 'Local Governments Expenditure', only the 'Local Governments General Budgetary Expenditure' index is selected.

For the 6 sub-indices under the index 'Income and Consumption Expenditure by Nationwide, Urban and Rural Households (new caliber)', all have strong correlations with 'Per Capita Disposable Income Nationwide', so only the latter is selected.

Evaluation index system

Through the above-mentioned index selection, the following index system is established to evaluate the eco-environmental situation in the provinces of China, as shown in *Figure 5*.

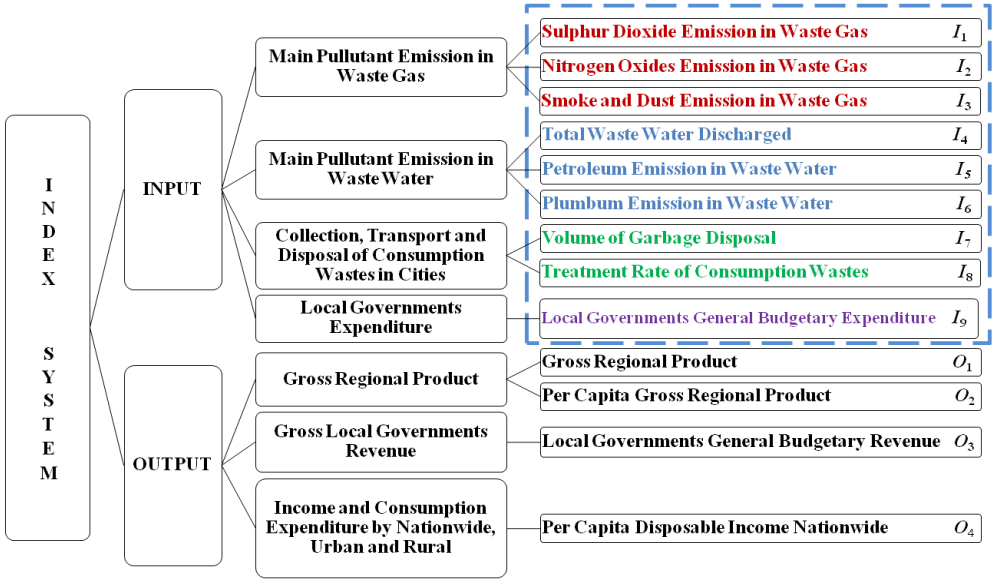

Figure 5. *Index system structure*

Results and discussion

Environment-economy interaction efficiency of Chinese provinces in 2017

There are some differences in the dimensions of data, which can easily lead to errors in the calculation results. Therefore, this paper puts all the input-output indices between 0.1 and 1 through the following normalization formulas.

$$x_{ij} = 0.1 + \frac{0.9(x_{ij} - \min\limits_{1\le j\le n} x_{ij})}{\max\limits_{1\le j\le n} x_{ij} - \min\limits_{1\le j\le n} x_{ij}} \quad i = 1,2,\cdots,9,\ j = 1,2,\cdots,31 \qquad \text{(Eq.3)}$$

http://www.aloki.hu ● ISSN 1589 1623 (Print) ● ISSN 1785 0037 (Online)
DOI: http://dx.doi.org/10.15666/aeer/1704_94559471

$$y_{kj} = 0.1 + \frac{0.9(y_{kj} - \min\limits_{1\le j\le n} y_{kj})}{\max\limits_{1\le j\le n} y_{kj} - \min\limits_{1\le j\le n} y_{kj}} \quad k = 1,2,3,4,\ j = 1,2,\cdots,31 \qquad \text{(Eq.4)}$$

After normalization, the efficiency values of 31 provinces in the CCR model and the BCC model are calculated using the software MATLAB. The results are shown in *Table 1*.

From *Table 1*, it can be seen that 16 provinces are efficient and 15 other provinces are inefficient in the BCC model before index synthesis. The order is as follows: Beijing, Fujian, Guangdong, Hainan, Heilongjiang, Jiangsu, Jilin, Ningxia, Qinghai, Shaanxi, Shandong, Shanghai, Tianjin, Tibet, Yunnan, Zhejiang > Liaoning > Chongqing > Henan > Guangxi > Shanxi > Hebei > Xinjiang > Hubei > Sichuan > Jiangxi > Inner Mongolia > Guizhou > Hunan > Anhui > Gansu. After index synthesis, the results obtained by the BCC model show that 13 provinces are efficient and 18 provinces are inefficient. The order of efficiency is as follows: Beijing, Fujian, Guangdong, Hainan, Heilongjiang, Jiangsu, Jilin, Ningxia, Qinghai, Shanghai, Tianjin, Tibet, Zhejiang > Shandong > Shanxi > Henan > Xinjiang > Chongqing > Hebei > Shaanxi > Guizhou > Hunan > Sichuan > Guangxi > Liaoning > Anhui > Inner Mongolia > Jiangxi > Gansu > Yunnan, in which a new order for Shaanxi, Shandong and Yunnan is obtained.

Table 1. *Results of eco-environmental evaluation in China in 2017*

Province	CCR		BCC		Province	CCR		BCC	
	Original index	Synthesized index	Original index	Synthesized index		Original index	Synthesized index	Original index	Synthesized index
Beijing	1.0000	1.0000	1.0000	1.0000	Hubei	0.8810	0.7715	0.8982	0.8419
Tianjin	1.0000	1.0000	1.0000	1.0000	Hunan	0.8814	0.7378	0.8817	0.8148
Hebei	0.9297	0.7243	0.9315	0.8452	Guangdong	1.0000	1.0000	1.0000	1.0000
Shanxi	0.7951	0.7927	0.9513	0.9089	Guangxi	0.8768	0.6180	0.9521	0.8014
Inner Mongolia	0.8521	0.6343	0.8865	0.7390	Hainan	1.0000	1.0000	1.0000	1.0000
Liaoning	0.7677	0.7535	0.9853	0.7864	Chongqing	0.8391	0.7900	0.9670	0.8587
Jilin	1.0000	1.0000	1.0000	1.0000	Sichuan	0.8267	0.6634	0.8951	0.8065
Heilongjiang	0.7368	0.6891	1.0000	1.0000	Guizhou	0.7917	0.6065	0.8846	0.8199
Shanghai	1.0000	1.0000	1.0000	1.0000	Yunnan	0.9267	0.5541	1.0000	0.6608
Jiangsu	1.0000	1.0000	1.0000	1.0000	Tibet	0.8140	0.7021	1.0000	1.0000
Zhejiang	1.0000	1.0000	1.0000	1.0000	Shaanxi	1.0000	0.7067	1.0000	0.8414
Anhui	0.8533	0.6759	0.8557	0.7843	Gansu	0.7009	0.5639	0.8484	0.7233
Fujian	1.0000	0.9987	1.0000	1.0000	Qinghai	0.8117	0.8068	1.0000	1.0000
Jiangxi	0.8576	0.6769	0.8888	0.7328	Ningxia	0.9689	0.9689	1.0000	1.0000
Shandong	1.0000	0.9843	1.0000	0.9862	Xinjiang	0.6992	0.5700	0.9252	0.8706
Henan	0.9337	0.7948	0.9636	0.8903					

It is known from *Table 1* that the efficiency values of some provinces have changed significantly after index synthesis. Some of the efficient provinces have become inefficient, such as Shandong, whose efficiency drops to 0.9843 in the CCR model and 0.9862 in the BCC model in 2017, and Yunnan, whose efficiency drops to 0.6608 in the BCC model in 2017 and so on. In the BCC model, the number of efficient provinces decreases from 16 to 13 after index synthesis. To some extent, it shows that the environmental status of these provinces is below the desired level, and only by enlargement of their advantages, can they become efficient. In fact, the evaluation

http://www.aloki.hu ● ISSN 1589 1623 (Print) ● ISSN 1785 0037 (Online)
DOI: http://dx.doi.org/10.15666/aeer/1704_94559471

results after index synthesis are more reasonable, because they have considered the environmental indices of each province comprehensively.

The projection information of the DMUs on the production frontier will become the projection information of the composite indices after index synthesis. Thus, the improvement of the original input indices of each province and the results of the total improvement ranking are given in *Table 2* by using the relevant theories proposed in the section of Materials and Methods**.** The input-oriented projection improvement information of Chinese provinces in the BCC model under the assumption of variable returns to scale (VRS) is shown in *Table 2*.

From *Table 2*, the following conclusions can be drawn. First, the table shows how the all original indices are improved and the total improvement of each province. There are three provinces with total improvement being more than 75%, which are Hebei, Inner Mongolia and Liaoning. Second, there are three provinces which become inefficient after index synthesis, namely Shandong, Yunnan and Shaanxi. It can be seen that they still have shortcomings. For example, Shandong has a total improvement of 38.22%, with the sulphur dioxide emission, nitrogen oxides emission and smoke and dust emission in waste gas being more than 9% redundant. Other indices also have a small amount of redundancy. Finally, the calculation results in *Table 2* show that the model can not only identify high system efficiency, but also discover more inefficient information in systems and provide the improvement of all the indices.

Table 2. *Input-oriented projection improvement information of the provinces in the BCC model under the assumption of VRS*

	I1	**I2**	**I3**	**I4**	**I5**	**I6**	**I7**	**I8**	**I9**	**Total improvement**
Liaoning	12.53%	12.23%	15.81%	4.02%	1.27%	8.67%	4.09%	10.37%	7.07%	76.06%
Inner Mongolia	17.36%	10.88%	15.86%	1.74%	3.27%	3.12%	2.76%	12.80%	8.04%	75.83%
Hebei	16.10%	17.75%	19.33%	1.82%	0.71%	2.75%	2.52%	7.69%	6.92%	75.59%
Jiangxi	4.82%	4.82%	5.47%	4.67%	15.01%	6.36%	3.21%	12.34%	9.25%	65.95%
Yunnan	7.43%	3.81%	4.54%	3.56%	12.58%	2.18%	3.83%	13.01%	13.09%	64.03%
Shanxi	18.77%	11.58%	13.71%	0.70%	0.33%	0.93%	1.14%	3.81%	2.34%	53.31%
Xinjiang	12.90%	8.19%	14.00%	0.85%	0.59%	1.85%	1.38%	4.12%	7.96%	51.84%
Guizhou	17.11%	6.63%	5.75%	1.28%	0.75%	2.39%	1.76%	7.62%	5.64%	48.93%
Hunan	2.21%	2.26%	2.02%	4.87%	5.44%	8.54%	3.23%	9.20%	8.56%	46.33%
Anhui	3.97%	4.83%	4.24%	2.40%	1.26%	3.64%	3.19%	10.75%	9.02%	43.30%
Sichuan	3.69%	2.84%	2.23%	3.00%	1.69%	2.56%	4.13%	9.21%	13.41%	42.76%
Gansu	4.72%	2.81%	3.35%	1.47%	4.62%	2.21%	2.38%	13.13%	6.29%	40.98%
Shandong	12.76%	12.76%	9.10%	0.41%	0.15%	0.39%	0.70%	1.10%	0.85%	38.22%
Shaanxi	4.68%	3.71%	3.85%	1.45%	1.03%	1.97%	1.71%	7.68%	5.20%	31.28%
Guangxi	2.07%	2.33%	2.18%	1.96%	1.75%	1.48%	2.34%	9.90%	6.61%	30.62%
Hubei	1.92%	1.98%	1.61%	1.97%	1.43%	2.12%	3.15%	7.88%	7.23%	29.29%
Chongqing	3.87%	2.28%	1.78%	1.41%	0.50%	1.48%	1.89%	6.93%	4.17%	24.31%
Henan	1.63%	2.21%	1.26%	1.88%	0.56%	1.53%	2.33%	5.43%	6.04%	22.87%

Environment-economy interaction efficiency of Chinese provinces from 2013 to 2017

Due to the fluctuation and differences of economic development and environmental status in different provinces in different years, it is not enough to use only one year's

http://www.aloki.hu ● ISSN 1589 1623 (Print) ● ISSN 1785 0037 (Online)
DOI: http://dx.doi.org/10.15666/aeer/1704_94559471

data to evaluate the overall situation of each province. To this end, this paper uses the input-output data of Chinese provinces from 2013 to 2017.

Based on the average input and output data of Chinese provinces from 2013 to 2017, the sample DMUs of each province are provided. Then the environmental evaluation results of each province are proposed, as shown in *Table 3*.

From *Table 3*, the following conclusions can be drawn. First, there are 16 provinces are efficient and 15 other provinces are inefficient in the BCC model before index synthesis. The order is as follows: Beijing, Tianjin, Liaoning, Jilin, Heilongjiang, Shanghai, Jiangsu, Zhejiang, Fujian, Shandong, Guangdong, Hainan, Tibet, Gansu, Qinghai, Ningxia > Chongqing > Xinjiang > Hebei > Inner Mongolia > Guizhou > Shanxi > Hubei > Hunan > Henan > Jiangxi > Sichuan > Anhui > Yunnan > Guangxi > Shaanxi. Second, after index synthesis, it is not difficult to find that the efficiency values of some provinces have changed significantly. Some of these efficient provinces have become inefficient, such as Liaoning, whose efficiency drops to 0.8365 in the BCC model. The new order of these provinces is obtained as follows: Beijing, Tianjin, Jilin, Heilongjiang, Shanghai, Jiangsu, Zhejiang, Fujian, Shandong, Guangdong, Hainan, Tibet, Gansu, Qinghai, Ningxia > Hebei > Liaoning > Shanxi > Hunan > Xinjiang > Henan > Chongqing > Sichuan > Guangxi > Guizhou > Jiangxi > Inner Mongolia > Shaanxi > Anhui > Yunnan. From this, it can be seen that the most of the provinces with high efficiency are located in the east region, and the average efficiency of the east region is the highest. The average efficiency of the central region is similar to that of the western region, but the most of the provinces with low efficiency are located in the west region.

Table 3. *Results of environment-economy interaction efficiency in Chinese provinces from 2013 to 2017 based on the generalized DEA method*

Province	CCR		BCC		Province	CCR		BCC	
	Original index	Synthesized index	Original index	Synthesized index		Original index	Synthesized index	Original index	Synthesized index
Beijing	1.0000	1.0000	1.0000	1.0000	Hubei	0.8468	0.7731	0.9133	0.8722
Tianjin	1.0000	1.0000	1.0000	1.0000	Hunan	0.8754	0.7512	0.8863	0.8304
Hebei	0.8991	0.7977	0.9739	0.8695	Guangdong	1.0000	1.0000	1.0000	1.0000
Shanxi	0.7622	0.7605	0.9218	0.8344	Guangxi	0.7992	0.6857	0.8352	0.7990
Inner Mongolia	0.9473	0.7124	0.9508	0.7861	Hainan	1.0000	1.0000	1.0000	1.0000
Liaoning	0.8397	0.7955	1.0000	0.8365	Chongqing	0.7965	0.7762	0.9794	0.8152
Jilin	1.0000	0.8849	1.0000	1.0000	Sichuan	0.8218	0.6871	0.8656	0.8002
Heilongjiang	0.9827	0.8719	1.0000	1.0000	Guizhou	0.6954	0.5925	0.9233	0.7952
Shanghai	1.0000	1.0000	1.0000	1.0000	Yunnan	0.7132	0.5673	0.8414	0.7277
Jiangsu	1.0000	1.0000	1.0000	1.0000	Tibet	0.7407	0.7106	1.0000	1.0000
Zhejiang	1.0000	1.0000	1.0000	1.0000	Shaanxi	0.8161	0.7058	0.8341	0.7843
Anhui	0.8208	0.6781	0.8414	0.7552	Gansu	0.7641	0.6791	1.0000	1.0000
Fujian	1.0000	1.0000	1.0000	1.0000	Qinghai	0.7981	0.7724	1.0000	1.0000
Jiangxi	0.8268	0.6903	0.8796	0.7877	Ningxia	1.0000	1.0000	1.0000	1.0000
Shandong	1.0000	1.0000	1.0000	1.0000	Xinjiang	0.7037	0.5896	0.9762	0.8273
Henan	0.8470	0.7608	0.8854	0.8212					

Then the results of the improved input indices of each province and the total improvement ranking from 2013 to 2017 in the input-oriented model are obtained using similar method to that for 2017. The relevant results are shown in *Table 4*.

http://www.aloki.hu ● ISSN 1589 1623 (Print) ● ISSN 1785 0037 (Online)
DOI: http://dx.doi.org/10.15666/aeer/1704_94559471

The projection improvement of the efficient provinces are all zero, so the relevant results of these provinces are not given in *Table 4*.

From the results of *Table 2* and *4*, it can be found that there is a certain difference between the results of the overall improvement in 2017 and from 2013 to 2017, which indicates that the pollution process in the eco-environment of each province was changing. Liaoning saw the biggest change, and Inner Mongolia and Hebei Province had the greatest difficulty in eco-environment management.

In order to more visually reflect the projection improvement difficulty coefficients of the comprehensive evaluation on the environment in different provinces, the relevant hotspot distribution map is drawn according to the size of the projection improvement quantity of the provinces in *Figure 6*. The darker the colour, the worse the comprehensive evaluation effect of the environment, and the higher the difficulty coefficient of projection improvement.

From *Figure 6*, it is easy to find that the provinces with the highest comprehensive efficiency of eco-environment from 2013 to 2017 based on the generalized DEA are located in the economically developed coastal areas, and that the most economically backward four regions also have high efficiency. The efficiency of environmental status management in northern and central provinces is relatively low, and the difficulty coefficients are relatively large. Inner Mongolia, Shanxi and Xinjiang take coal and other energy as the main driving force for development, while Hebei Province mainly relies on iron and steel for development. Their efficiency is poor and it may be difficult to complete rapid projection improvement within a short time.

Table 4. *Projection improvement information of Chinese provinces in CCR for the average input-output data from 2013 to 2017 based on the generalized input-oriented DEA method*

Province	I1	I2	I3	I4	I5	I6	I7	I8	I9	Total improvement
Inner Mongolia	16.63%	15.02%	13.27%	4.10%	7.79%	13.81%	3.18%	13.53%	10.57%	97.90%
Shanxi	19.25%	16.13%	19.14%	4.17%	1.97%	10.98%	3.13%	10.13%	7.08%	91.98%
Xinjiang	14.22%	13.30%	13.47%	3.68%	2.16%	11.57%	4.74%	11.76%	13.52%	88.42%
Hebei	13.58%	16.58%	17.47%	5.14%	1.58%	9.67%	3.46%	8.63%	9.60%	85.71%
Yunnan	9.55%	6.96%	5.95%	4.67%	8.23%	5.17%	5.06%	17.00%	18.17%	80.76%
Jiangxi	6.06%	6.12%	5.69%	6.39%	11.63%	11.49%	3.54%	13.52%	11.59%	76.03%
Guizhou	15.69%	8.26%	6.40%	2.86%	1.58%	5.03%	4.00%	17.31%	13.78%	74.91%
Hunan	3.45%	3.21%	2.72%	7.37%	16.30%	9.79%	4.29%	12.24%	12.38%	71.75%
Anhui	5.23%	7.27%	5.53%	4.63%	2.17%	7.63%	4.61%	15.95%	14.59%	67.61%
Liaoning	11.65%	11.03%	12.02%	3.23%	1.01%	5.81%	4.57%	8.70%	8.99%	67.01%
Sichuan	5.58%	4.36%	3.27%	4.54%	2.11%	5.01%	6.52%	14.54%	20.32%	66.25%
Shaanxi	8.21%	7.37%	6.88%	3.31%	2.20%	7.79%	4.05%	13.89%	10.97%	64.67%
Henan	5.12%	6.42%	3.82%	6.51%	2.55%	8.96%	5.19%	10.86%	14.16%	63.59%
Gansu	8.73%	6.41%	5.67%	3.53%	9.33%	7.96%	3.03%	4.59%	9.52%	58.77%
Hubei	2.98%	2.97%	2.47%	4.95%	3.37%	8.71%	4.63%	9.54%	11.22%	50.84%
Guangxi	3.42%	3.43%	3.13%	3.24%	2.99%	2.88%	3.65%	15.01%	10.95%	48.70%
Heilongjiang	8.05%	9.88%	10.52%	1.33%	0.56%	1.64%	1.94%	2.11%	8.87%	44.90%
Chongqing	4.21%	2.84%	2.17%	2.34%	0.94%	2.97%	2.89%	11.01%	7.23%	36.60%
Jilin	4.86%	5.75%	5.14%	2.82%	1.49%	5.50%	1.63%	2.09%	4.72%	34.00%
Tibet	0.96%	0.96%	0.96%	0.96%	0.97%	0.96%	2.23%	17.88%	3.44%	29.32%
Qinghai	1.44%	1.07%	1.66%	1.78%	2.16%	4.21%	1.33%	8.52%	2.89%	25.06%

http://www.aloki.hu ● ISSN 1589 1623 (Print) ● ISSN 1785 0037 (Online)
DOI: http://dx.doi.org/10.15666/aeer/1704_94559471

Figure 6. *Hotspot map of difficulty coefficient for projection improvement of environmental status in China from 2013 to 2017*

Improvement, projection and importance information before and after the synthesis of various indices

Although the improvement of eco-environmental inputs in each province from 2013 to 2017 is proposed above, it is unrealistic to make the improvement according to this model. Managers need more learning to complete the gradual improvement. Muren et al. (2013) provided a DEA method based on the partial ordered set theory, which can give the complex partial ordered relations among DMUs and provide information for DMUs, such as improvement, projection and importance.

The partial ordered relations among Chinese provinces are shown in *Figures 7* and *8*. It is easy to find that the original status which involves less partial ordered relations among provinces has turned into one with more partial ordered relation after index synthesis.

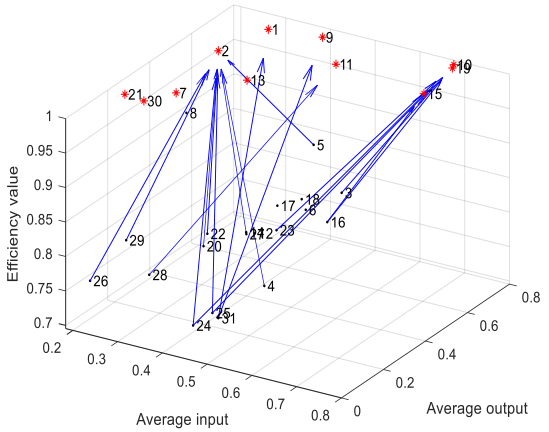

Figure 7. *Partial ordered relations among the provinces in the CCR model before index synthesis*

http://www.aloki.hu ● ISSN 1589 1623 (Print) ● ISSN 1785 0037 (Online)
DOI: http://dx.doi.org/10.15666/aeer/1704_94559471

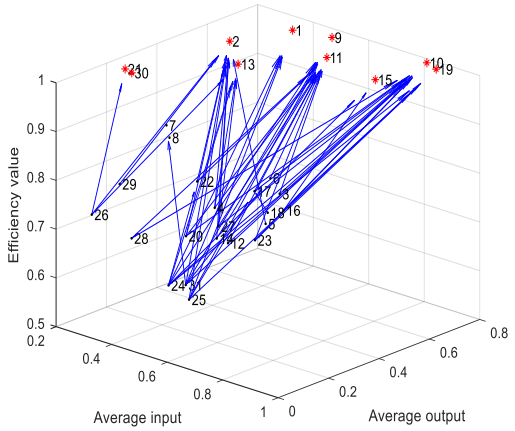

Figure 8. *Partial ordered relations among the provinces in the CCR model after index synthesis*

In *Table 5*, we proposed the ways of improvements and projections and the importance of learning for different provinces in the CCR model. The inefficient provinces can improve their input data according to the partial ordered relations between efficient provinces. For example, Inner Mongolia can improve its efficiency by learning from Tianjin.

Table 5. *Improvement and projection methods and learning importance of different provinces in the CCR model*

		Original indices in the CCR model			Synthesized Indices in the CCR model		
Number	**Provinces**	**Improved benchmark**	**Projection benchmark**	**Learning importance**	**Improved benchmark**	**Projection benchmark**	**Learning importance**
1	Beijing	---	---	1	---	---	3
2	Tianjin	---	---	9	---	---	11
3	Hebei	---	10	0	---	1,11	0
4	Shanxi	---	2	0	---	2,11,13	0
5	Inner Mongolia	---	2	0	---	2	0
6	Liaoning	---	---	0	---	11	1
7	Jilin	---	---	0	---	---	1
8	Heilongjiang	---	---	0	---	---	0
9	Shanghai	---	---	1	---	---	3
10	Jiangsu	---	---	5	---	---	12
11	Zhejiang	---	---	1	---	---	15
12	Anhui	---	---	0	---	1,11	0
13	Fujian	---	---	0	---	---	5
14	Jiangxi	---	---	0	---	2,11	0
15	Shandong	---	---	1	---	---	2
16	Henan	---	10,15	0	---	1,15,19	0
17	Hubei	---	---	0	---	1,11	2
18	Hunan	---	---	0	17	1,11	0
19	Guangdong	---	---	0	---	---	4
20	Guangxi	---	2	0	---	2,1,11,13	0
21	Hainan	---	---	0	---	---	1
22	Chongqing	---	2	0	---	2,11	1
23	Sichuan	---	10	0	---	1,11,19	0
24	Guizhou	---	2,10	0	22	1,2,9,1,11,13,15,19	0
25	Yunnan	---	2,10	0	17	1,2,9,1,11,19	0
26	Tibet	---	2	0	---	2,13,21	0
27	Shaanxi	---	2	0	---	2,1,11,13	0
28	Gansu	---	11	0	---	1,11	0
29	Qinghai	---	2	0	---	2	0
30	Ningxia	---	---	0	---	---	0
31	Xinjiang	---	1,9	0	6,7	1,2,9,1,11	0

http://www.aloki.hu ● ISSN 1589 1623 (Print) ● ISSN 1785 0037 (Online)
DOI: http://dx.doi.org/10.15666/aeer/1704_94559471

With the relevant information provided in *Figure 8* and *Table 5*, each province can determine its own improvement benchmark and projection benchmark. At the same time, the state should give certain rewards to those provinces with higher performance, and impose corresponding punishments on those that perform poorly so that they will take scientific and sustainable eco-environmental governance strategies as soon as possible

Conclusions

The synthesis and projection theory of input-output indices of DMUs based on generalized DEA provides a new basis for ranking and improvement of DMUs. The improved method is highly applicable in the horizontal and vertical evaluation and improvement of enterprises or government departments with time series data. In this paper, taking the evaluation on the interaction between eco-environment and economy among Chinese provinces as an example, through reasonable index selection and processing, an evaluation index system with strong logical relationships is constructed, and the evaluation of provinces is carried out with the generalized DEA model. Relevant data analysis results show that the synthesis of the input-output indices of each province can help further discover the efficiency gaps between the provinces, and also provide the improvement scale and direction of the main pollution sources in the eco-environment of each province. Finally, the combination of the index synthesis theory and the partial ordered set theory provides a new basis for the mutual learning among provinces. These basic models and methods further enrich and improve the scientific evaluation on eco-environment, and provide detailed quantitative indices for the protection and governance of eco-environment.

The rationality of index synthesis and projection of DMU is worthy of further study. It will also be of great significance to evaluate the interaction efficiency between eco-environment and economic development in China from the time series data of industrial structure of each province. At the same time, these theories and methods proposed in this paper can be extended to the assessment the interaction efficiency between eco-environment and economic development in other countries, which will help to formulate rational environmental protection programmes, better protect the earth and safeguard the global climate, and it lay theoretical and practical foundation for the comprehensive, balanced and sustainable development of eco-environment and economy.

Acknowledgements. The authors would like to thank the anonymous reviewers for the useful comments on this work, and the support from, National Natural Science Funds of China (No. 71661025, 71401084), Inner Mongolia Natural Science Foundation (No. 2017JQ02, 2017MS072, 2016MS0705), Inner Mongolia Grassland Talent Project (No. 12000-12102012), China Post-doctoral Fund (No. 2018M631323), and Project of Inner Mongolia Institute of Data Science and Big Data (No. BDY18007).

REFERENCES

[1] Banker, R. D., Charnes, A., Cooper, W. W. (1984): Some models for estimating technical and scale inefficiencies in data envelopment analysis. – Management Science 30(9): 1078-1092.

http://www.aloki.hu ● ISSN 1589 1623 (Print) ● ISSN 1785 0037 (Online)
DOI: http://dx.doi.org/10.15666/aeer/1704_94559471

[2] Brown, G. M. (2000): Renewable natural resource management and use without markets. – Journal of Economic Literature 38(4): 875-914.
[3] Chang, Y. T., Park, H. S., Jeong, J. B., Lee, J. W. (2014): Evaluating economic and environmental efficiency of global airlines: a SBM-DEA approach. – Transportation Research Part D Transport & Environment 27(1): 46-50.
[4] Charnes, A., Cooper, W. W., Rhodes, E. (1978): Measuring the efficiency of decision making units. – European Journal of Operational Research 6(2): 429-444.
[5] Diao, X. D., Zeng, S. X., Tam, C. M., Tam, V. W. Y. (2009): EKC analysis for studying economic growth and environmental quality: a case study in China. – Journal of Cleaner Production 17(5): 541-548.
[6] Färe, R., Grosskopf, S. (1985): A nonparametric cost approach to scale efficiency. – Scandinavian Journal of Economics 87(4): 594-604.
[7] Gaspar, J. D. S., Marques, A. C., Fuinhas, J. A. (2017): The traditional energy-growth nexus: A comparison between sustainable development and economic growth approaches. – Ecological Indicators 75: 286-296.
[8] Halkos, G. E., Polemis, M. L. (2018): The impact of economic growth on environmental efficiency of the electricity sector: A hybrid window DEA methodology for the USA. – Journal of Environmental Management 211: 334-346.
[9] Jia, Y. P., Liu, R. Z. (2012): Study of the energy and environmental efficiency of the Chinese economy based on a DEA model. – Procedia Environmental Sciences 13(10): 2256-2263.
[10] Lee, S. K., Mogi, G., Hui, K. S. (2013): A fuzzy analytic hierarchy process (AHP)/data envelopment analysis (DEA); hybrid model for efficiently allocating energy R&D resources: In the case of energy technologies against high oil prices. – Renewable & Sustainable Energy Reviews 21: 347-355.
[11] Liu, B. Q., Tian, C., Li, Y. Q., Song, H. H., Ma, Z. X. (2018): Research on the effects of urbanization on carbon emissions efficiency of urban agglomerations in China. – Journal of Cleaner Production 197(1): 1374-1381.
[12] Ma, X., Raheel, M., Xue, T. T., Wang, J. D. (2017): Measurement of China's regional eco-economy input efficiency and its temporal-spatial evolution. – China Population Resources and Environment 11: 13-23.
[13] Ma, Z. X. (2002): Frontier that formed by some sample units and its applying. – Journal of Inner Mongolia University (Natural Science Edition) 33: 606-610.
[14] Ma, Z. X. (2003): Frontier that formed by some sample units and its applying. – Systems Engineering-Theory and Practice 23: 32-27.
[15] Ma, Z. X. (2012): DEA model with generalized reference set and its properties. – Systems Engineering and Electronics 34: 709-714.
[16] Ma, Z. X., Cao, L., Bao, S. Q. G. W. (2018): A resource optimized allocation method of multi-level complex system. – Systems Engineering-Theory & Practice 38(7): 1802-1818.
[17] Mavi, R. K., Saen, R. F., Goh, M. (2018): Joint analysis of eco-efficiency and eco-innovation with common weights in two-stage network DEA: a big data approach. – Technological Forecasting and Social Change 144: 553-562.
[18] Mittler, D., Knirsch, J. (2007): Improved market access at the expense of the environment? The environmental risks of the NAMA negotiations at the WTO. – Environmental Politics 16(1): 113-123.
[19] Moutinho, V., Madaleno, M., Robaina, M. (2017): The economic and environmental efficiency assessment in EU cross-country: Evidence from DEA and quantile regression approach. – Ecological Indicators 78: 85-97.
[20] Moutinho, V., Madaleno, M., Robaina, M., Villar, J. (2018): Advanced scoring method of eco-efficiency in European cities. – Environmental Science and Pollution Research 25(2): 1637-1654.

http://www.aloki.hu ● ISSN 1589 1623 (Print) ● ISSN 1785 0037 (Online)
DOI: http://dx.doi.org/10.15666/aeer/1704_94559471

[21] Muren, Ma, Z. X., Wei, C. (2013): Data envelopment analysis based on partial ordered set theory. – Systems Engineering and Electronic Technology 35(2): 350-356.
[22] Seiford, L. M., Thrall, R. M. (1990): Recent development in DEA. The mathematical programming approach to frontier analysis. – Journal of Economics 46(1-2): 7-38.
[23] Song, M., Peng, J., Wang, J., Zhao, J. (2018): Environmental efficiency and economic growth of China: a ray slack-based model analysis. – European Journal of Operational Research 269(1): 51-63.
[24] Wang, P., Wu, J. (2014): Environment and economic performance evaluation of 30 provinces and municipalities in China based on a two-stage multiplier DEA approach. – International Journal of Information & Decision Sciences 6(2): 182-192.
[25] Yang, Q. S., Zhang, Y., Li, Y. J. (2012): Research on environmental efficiency evaluation of urban agglomerations in northeast China based on DEA model. – Economic Geography 32(9): 51-60.
[26] Zhou, Y. (2015): State power and environmental initiatives in China: analyzing China's green building program through an ecological modernization perspective. – Geoforum 61: 1-12.

http://www.aloki.hu ● ISSN 1589 1623 (Print) ● ISSN 1785 0037 (Online)
DOI: http://dx.doi.org/10.15666/aeer/1704_94559471

EFFECTS OF ENVIRONMENTAL PARAMETERS ON THE ULTRAVIOLET DEGRADATION OF METHYLPHOSPHONATE

ZHANG, C. – JI, H. B.*

School of Energy & Environmental Engineering, University of Science and Technology Beijing Beijing 100083, China

**Corresponding author*
e-mail: ji.hongbing@hotmail.com; phone: +86-183-1131-2619

(Received 3rd Apr 2019; accepted 17th May 2019)

Abstract. Considering the heavy presence of methylphosphonate (MPn) and its derivatives in nature and their potential hazard to human health, this paper attempts to clarify the ultraviolet (UV) degradation kinetics of the MPn under different environmental parameters. Several tests were carried out to measure UV degradation efficiency of the MPn with different combinations of the following factors: radiation time, light intensity, pH and initial concentration. The analysis on the test results show that the MPn can hardly degrade under the UV intensity of 400 W but degraded gradually under the UV intensity of 1,200 W, peaking at the rate of 94.5% within 58 h. The degradation kinetics can be described by the first-order reaction model, and the degradation rate constant was calculated as 0.032 h^{-1}. The MPn degradation efficiency varied with the pH values. The different pH media could be ranked as pH 10 > pH 13> pH 2 > pH 7 in descending order of the efficiency, indicating that the MPn degradation is more efficiency under alkaline condition. In addition, the MPn degradation became less efficient with the growth in initial concentration, as the intermediate products compete with the reactive oxygen species (ROS). The above results provide a valuable reference for environmental protection and pollution control.
Keywords: *methylphosphonate (MPn), degradation efficiency, photo-oxidation, phosphonate*

Introduction

Phosphonates are an important component of organophosphorus compounds and have the general formula $RP(=O)(OR')_2$. With a relatively stable C-P covalent bond, this component is difficult to degrade and easy to reside in nature. The heavy presence of phosphonate compounds in the environment poses a potential hazard to human health.

Methylphosphonate (MPn) is a relatively simple phosphonate. It is the degradation product of neurotoxic agents like Sarin and Soman and flame retardants like methylphosphinate. The MPn serves as a key reactant in the synthesis of metal phosphonate compounds. Such compounds are novel materials for molecular sieves, ion exchange columns and magnetic motion conductors (Maeda et al., 1995; Edgar et al., 2002; Langley et al., 2008; Bauer et al., 2010). The MPn and its derivatives also act as reaction intermediates for the production of fungicides, insecticides and petroleum additives. When these chemicals are produced and utilized, the MPn is carried by wastewater into the environment, and then absorbed in soil particles and chelated with heavy metal ions. All these lead to the wide existence of the MPn exists in soil and water (Shao et al., 2015). Recent studies have considered the MPn as a potential source of methane in the ocean (Karl et al., 2008; Metcalf et al., 2012; Born et al., 2017; Yu et al., 2018). Oceanic methane accounts for about 4% of global methane budget, making up a key link in the global methane cycle (Sandy et al., 2013). As a well-known greenhouse gas, methane has recently been proved as a cause of the greenhouse effect on the Earth surface. Therefore, the degradation and cycling of MPn have a great significance to greenhouse effect and global climate change.

http://www.aloki.hu ● ISSN 1589 1623 (Print) ● ISSN 1785 0037 (Online)
DOI: http://dx.doi.org/10.15666/aeer/1704_94739482

In general, phosphonates can be decomposed through biodegradation, photodegradation, chemical oxidation. The natural photodegradation of organic pollutants mainly occurs under ultraviolet (UV) radiation, which takes up about 5% of the total solar radiation reaching the Earth, and other factors like the atmospheric oxygen (Deanin et al., 1970). For phosphonates, UV degradation exists as one possible pathway of decomposition. The decomposition is thorough and irreversible, bringing fundamental changes to the pollution status in water environment (Lu et al., 2018; Acero et al., 2019; Gao et al., 2019). Therefore, photodegradation promises a bright future for the removal of phosphonate pollutants.

The existing studies on MPn decomposition in nature have focused on the microbial degradation pathway (Matys et al., 2001, 2004), failing to explore the pathway and kinetics of the UV degradation pathway. In fact, the efficiency of phosphonate degradation may be affected by various environmental parameters, such as pH, concentration and light intensity. To promote the MPn removal in water, it is necessary to explore the UV degradation of pollutants under different environmental parameters.

Taking the MPn as a typical phosphonate pollutant, this paper examines the UV degradation kinetics of the MPn under different environmental parameters, including radiation time, light intensity, pH and initial concentration.

Methodology

Materials

All chemicals in this research were purchased from Sigma-Aldrich. Among them, the MPn reaches the purity ≥99.9%, and the other chemicals are of the analytical grade. The UV source is an Ace Glass 7900 photo-oxidation apparatus with a 1,200 W lamp. The chemical structure of the MPn is shown in *Figure 1* below.

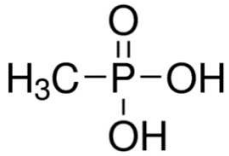

Figure 1. *Chemical structure of the MPn*

Test procedure

Test on the effect of light intensity

To begin with, 12 mL of 10 mM MPn solution (pH≈2) was respectively transferred to two quartz tubes, and separately placed in two photochemical reactors for illumination. One of the reactors has a 400 W mercury lamp and the other, a 1,200 W mercury lamp. The UV emitted from both lamps are consistent with natural UV in composition: primarily UVA (315~400 nm) and UVB (280~315 nm), with a small amount of UVC. The test temperature was controlled below 40°C by a circulating-water air-cooling system. Meanwhile, a control test was carried out to verify whether the MPn can be hydrolyzed by thermolysis in aqueous solution without UV radiation. Specifically, 12 mL of MPn aqueous solution was added to a quartz tube and wrapped in aluminum foil, before being placed in a dark environment. During the reaction,

http://www.aloki.hu ● ISSN 1589 1623 (Print) ● ISSN 1785 0037 (Online)
DOI: http://dx.doi.org/10.15666/aeer/1704_94739482

0.1 mL of sample was taken every 4 h, and diluted 10 times with deionized water, such that the phosphate concentration fell below 1 mM. Next, the phosphate concentration was measured by colorimetric analysis according to the phospho-molybdate blue assay (Murphy and Riley, 1962). All the degradation experiments were run in triplicates.

Test on the effect of pH

The pH of 10 mM MPn solution was respectively adjusted from ~2 to 2, 7, 10 and 13 with 1 M and 5 M NaOH. Then, 12 mL of MPn solution of each pH was transferred to a quartz tube and placed into the photochemical reactor for UV radiation. The UV light was emitted from a 1,200 W mercury lamp. During the radiation, 0.1 mL of sample was taken every 12 h and diluted 10 times for phosphate concentration measurement.

Test on the effect of initial concentration

The MPn aqueous solutions were dispensed separately at the concentrations of 2.5 mM, 5 mM and 10 mM. After shaking, 10 mL of the solution at each concentration was transferred to a quartz tube and relocated to a photochemical reactor for UV radiation. The UV light was emitted from a 1,200 W mercury lamp. During the radiation, 0.1 mL of sample was taken every 12 h and diluted 10 times for phosphate concentration measurement.

Analysis procedure

One of the final products of the MPn is orthophosphate. The formation of orthophosphate can represent the MPn degradation rate, owing to the simple molecular structure of the MPn. In our research, the MPn degradation efficiency is computed by (Yuan et al., 2014):

$$\eta = (C_t / C_0) \times 100\% \quad \text{(Eq.1)}$$

where η is the UV degradation efficiency of MPn; C_t is residual concentration of MPn after t-hour radiation; C_0 is the initial concentration of the MPn in the aqueous solution.

The degradation kinetics of the MPn over time was analyzed by the first-order reaction kinetics model below:

$$\ln (C_t / C_0) = - kt \quad \text{(Eq.2)}$$

where k is the degradation rate constant of the first-order reaction kinetics, h^{-1}; t is the reaction time.

Figures and linear fitting analysis were done by OriginPro 2016 software.

Results and Discussion

Effect of radiation time

Figure 2 presents the relationship between radiation time and UV degradation rate of the MPn under the Light intensity of 1,200 W, the initial MPn concentration of 10 mM, the pH of 2 and the temperature below 40°C. It can be seen that the MPn degradation rate increased significantly with the elapse of the radiation time. As the radiation time grew from 0 to 58 h, the MPn degradation rate soared from 0 to 94.5%. In the control

http://www.aloki.hu ● ISSN 1589 1623 (Print) ● ISSN 1785 0037 (Online)
DOI: http://dx.doi.org/10.15666/aeer/1704_94739482

test, no thermolysis degradation was observed during the reaction period, indicating that the MPn will not hydrolyze spontaneously without UV light. Hence, the MPn degradation is attributable to UV radiation.

Much research has been done on the UV degradation mechanism of organic compounds (Chen et al., 2007; Rao and Chu, 2010). Since orthophosphate is a final product of the MPn, the C-P bond dissociation must take place in order to completely decompose the MPn. According to the previous results on UV degradation mechanism, the C-P bond dissociation under UV photolysis can be ascribed to the nucleophilic substitution of the reactive oxygen species (ROS) in the aqueous environment, which are generated by the electronic excitation of the MPn. The UV degradation mechanism of the MPn is detailed below.

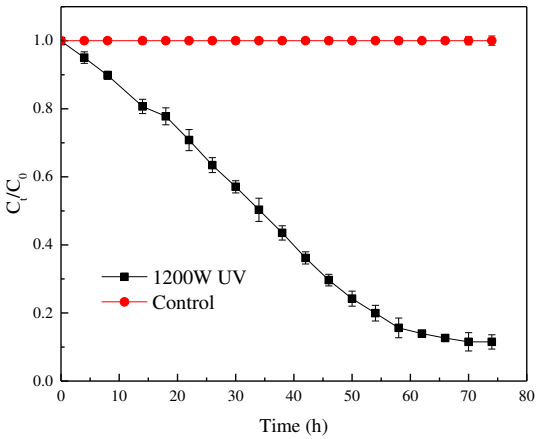

Figure 2. *Effect of radiation time on UV degradation efficiency of the MPn*

The MPn molecular contains functional groups that can absorb the UV. The absorbed energy will elevate the molecular from the stable ground state to an unstable excitation state (Deanin et al., 1970). The relatively reactive species can transfer electrons to acceptors in the aqueous solution, creating free radicals. In the presence of dissolved oxygen, the free radicals are recombined or hydrolyzed into groups, which then form peroxy radicals through the reaction with oxygen (Bustos et al., 2019). After further photolysis, the peroxy radicals will be converted to hydrogen peroxides (Chen and Liu, 2007), and finally decomposed into hydroxyl radicals that attack the methyl groups in the MPn.

Effect of light intensity

The effective removal of pollutants from wastewater hinges on the optimal UV light intensity for MPn degradation. In this research, the effect of light intensity on MPn degradation is investigated under the UV lights emitted from a 400 W mercury lamp and a 1,200 W mercury lamp. *Figure 3* depicts the relationship between light intensity and MPn degradation rate under the UV intensities of 400 W and 1,200 W, the initial MPn concentration of 10 mM, the pH of 2 and the temperature below 40ºC.

As shown in *Figure 3*, the MPn degradation rate was much slower under 400 W UV radiation than 1,200 W. Under the 400 W UV source, only ~3% of MPn were decomposed after an 80 h exposure. The degradation rate was greatly accelerated under

http://www.aloki.hu ● ISSN 1589 1623 (Print) ● ISSN 1785 0037 (Online)
DOI: http://dx.doi.org/10.15666/aeer/1704_94739482

the 1,200 W UV source: the MPn degradation was very fast and then gradually slowed down in the first 58 h, peaking at 94.5%.

As mentioned above, the ROS produced in the aqueous solution is the cause to MPn degradation. Under the 400 W mercury lamp, the amount of ROS generated per unit time was very limited. Coupled with the intense energy required to cleavage the C-P bond, the limited amount of ROS makes it slow for the MPn to be degraded under the 400 W UV source.

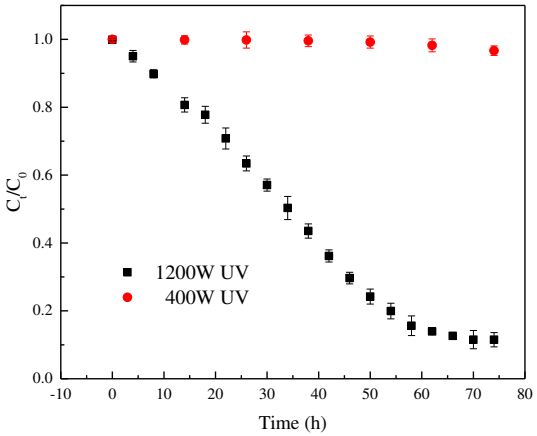

Figure 3. *Effect of light intensity on the UV degradation efficiency of the MPn*

The MPn degradation reflects the typical degradation kinetics of organic compounds: the degradation proceeds rapidly at the beginning, and gradually slows down near the peak rate. Here, the degradation kinetics of the MPn under different UV intensities are described by the first-order reaction equation (*Eq.2*) and the results are shown in *Figure 4*. Obviously, the first-order reaction equation described the reaction process well (R^2=0.97).

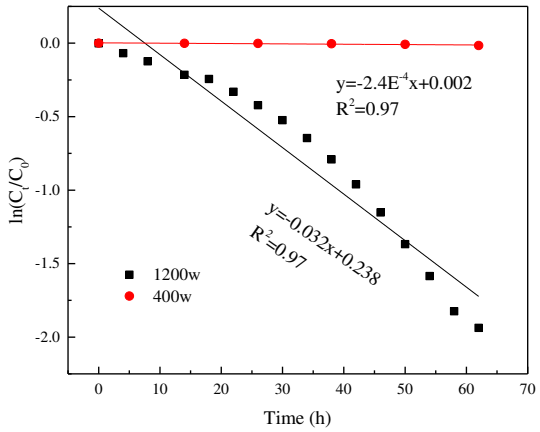

Figure 4. *UV degradation kinetics of the MPn under different UV intensities*

The calculated kinetics parameters are listed in *Table 1*. It can be seen that the degradation rate constant (k) of the MPn was only $2.4E^{-4}$ h^{-1} under 400 W UV radiation. During the radiation, only 3% of the MPn was decomposed. By contrast, under 1,200 W

http://www.aloki.hu ● ISSN 1589 1623 (Print) ● ISSN 1785 0037 (Online)
DOI: http://dx.doi.org/10.15666/aeer/1704_94739482

UV radiation, the degradation rate constant increased 133 times to 0.031 h^{-1}, and the photolysis half-life reduced to 21.66 h. It can be concluded that the UV intensity plays a significant positive role in the MPn removal in wastewater treatment.

Table 1. *Kinetics parameters of UV degradation of the MPn under different light intensities (C_0=10mM)*

Light Sources	Photolysis Equation	Rate Constant *k* (h^{-1})	Photolysis Half-Life $t_{1/2}$ (h)	Coefficient of Determination (R^2)
1,200W Mercury Lamp	$\ln(C_t/C_0) = -0.032\ t$	0.032	21.66	0.97
400W Mercury Lamp	$\ln(C_t/C_0) = -2.4E^{-4}\ t$	$2.4E^{-4}$	2,888.11	0.97

Effect of pH

In nature, the pH value differs from one aquatic environment to another. The pH is essential to the degradation of the organic pollutants, as it can affect the photochemical reaction kinetics in pollutant treatment. Under different pH values, the organic pollutants have different molecular forms, and thus exhibit varied physicochemical properties and toxicities.

Figure 5 displays the relationship between pH and MPn degradation rate under the UV intensity of 1,200 W, the initial MPn concentration of 10 mM, the pH of 2, 7, 10 and 13 and the temperature below 40ºC. As can be seen from the figure, the different pH values could be ranked as pH 10 > pH 13> pH 2 > pH 7 in descending order of MPn degradation efficiency. The degradation efficiency increased in acidic and alkaline solutions. Within 50 h exposure to UV radiation, 96% of the MPn in acidic and alkaline media were decomposed, while only 84% were degraded in the neutral solution.

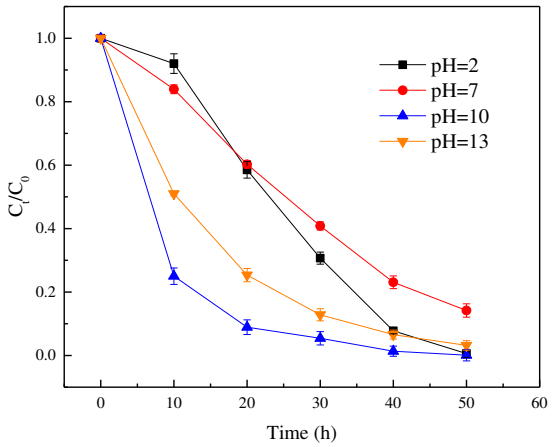

Figure 5. *Effect of pH on the UV degradation efficiency of the MPn*

Many scholars (Wei et al., 2000; Santos-Beneit, 2015) agree that organophosphorus compounds are more easily to photolyze in acidic and alkaline solutions than in neutral medium. In aqueous solutions, the molecular forms of organophosphorus compounds depend on the pH value. For instance, Li et al. (2016) studied the effect of pH on the photolysis of sulfamethazine (SMZ), concluding that the SMZ photolysis efficiency

http://www.aloki.hu ● ISSN 1589 1623 (Print) ● ISSN 1785 0037 (Online)
DOI: http://dx.doi.org/10.15666/aeer/1704_94739482

varies greatly with pH values: the SMZ degrades much faster in strong alkaline and acidic conditions than in neutral and alkalescent condition. This is because the SMZ mainly ionizes in the form of SMZ^- and SMZ^+ in alkaline and acidic conditions, respectively, but exists in the stable molecular state in neutral condition. The ionization of the SMZ in different pH media affects its photolysis kinetics.

As an organic acid, the MPn ionizes in the form of $CH_3PO(OH_2)_2^{2+}$ and $CH_3PO(OH)(OH_2)^+$ in acidic condition. When the pH is adjusted to alkaline condition by NaOH solution, the MPn mainly exists as $CH_3PO(OH)O^-$ and $CH_3POO_2^{2-}$. The ionization weakens the molecular bond energy, pushing up the speed of photolysis reaction.

The first-order reaction model (*Eq.2*) was used to describe the UV degradation kinetics of the MPn at different pH values. The linear fitting results of ln (C_t/C_0) to time t are shown in *Table 2*. It is observed that the UV degradation of the MPn was well described by the first-order reaction model ($R^2 \geq 0.97$). The kinetics parameters were calculated and listed in *Table 2*. As shown in the table, the photolysis half-life of MPn in the solution was 17.32 h, 23.1 h, 10.05 h and 7.07 h respectively at the pH of 2, 7, 10 and 13. The degradation rate constants *k* at the four pH levels were 0.04, 0.03, 0.069 and 0.098, respectively. The MPn degradation rate at the pH of 10 was 3.3 times that at the pH of 7 and 2.5 times that at the pH of 2.

Table 2. *Kinetic parameters of UV degradation of the MPn at different pH values (C_0=10mM)*

pH	Photolysis Equation	Rate Constant *k* (h^{-1})	Photolysis Half-Life $t_{1/2}$ (h)	Coefficient of Determination (R^2)
2	$\ln(Ct/C_0)=-0.040t$	0.04	17.32	0.97
7	$\ln(Ct/C_0)=-0.030t$	0.03	23.10	0.98
10	$\ln(Ct/C_0)=-0.098t$	0.098	7.07	0.99
13	$\ln(Ct/C_0)=-0.069t$	0.069	10.05	0.97

The formation of hydroxyl radicals (HO·) in aqueous solution is the key to the UV degradation of organophosphorus compounds (Evgenidou et al., 2006; Manassero et al., 2010). In alkaline medium, the abundance of hydroxyl groups (OH^-) in solution may boost the formation of hydroxyl radicals, thus speeding up the degradation reaction. To sum up, the pH condition is very important for UV degradation of the MPn and the alkaline medium is preferred for MPn wastewater treatment.

Effect of initial concentration

Figure 6 illustrates the relationship between initial concentration and the UV degradation rate of MPn under the UV intensity of 1,200 W, the initial MPn concentration of 2.5, 5 and 10 mM, the pH of 2 and the temperature below 40ºC. As shown in the figure, the three initial concentrations could be ranked in descending order as 2.5 mM > 5 mM > 10 mM by the degradation efficiency. It took about 20 h, 30 h and 50 h for the 2.5, 5 and 10 mM MPn solutions to reach the peak efficiency, respectively. In general, the lower the initial concentration, the more efficiency the MPn degradation.

The above results echo that of Yuan (2007) on photolysis kinetics of paclobutrazol at different initial concentrations: the photolysis efficiency is negatively correlated with the initial concentration. This correlation can be explained as follows. Under the same UV intensity, the amount of ROS produced in solution is fixed at a certain volume and

http://www.aloki.hu ● ISSN 1589 1623 (Print) ● ISSN 1785 0037 (Online)
DOI: http://dx.doi.org/10.15666/aeer/1704_94739482

time. With the increase in MPn concentration, the ratio of ROS to the MPn continues to fall, leading to the decline in degradation efficiency. In addition, the intermediate products of MPn degradation compete with the ROS, thus reducing the degradation rate. The denser the MPn, the greater the number of intermediate products.

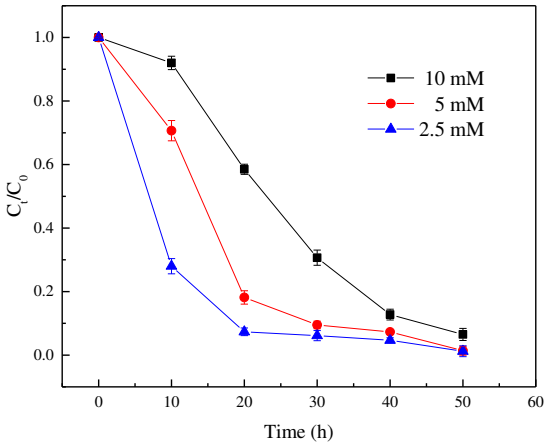

Figure 6. *Effect of initial concentration on the UV degradation efficiency of MPn*

Conclusions

The environmental parameters are key factors for UV degradation of the MPn. The MPn can be easily degraded under the UV intensity of 1,200 W, and exhibit typical degradation features of organic compounds over time. However, the MPn is difficult to degrade under a low UV intensity (400 W). The optimal pH for UV degradation of the MPn is the pH of 10. The MPn can be degraded more efficiently under a low initial concentration. These conclusions provide a valuable reference for the MPn removal in wastewater treatment.

REFERENCES

[1] Acero, J. L., Real, F. J., Benitez, J. F., Matamoros, E. (2019): Degradation of neonicotinoids by UV irradiation: Kinetics and effect of real water constituents. – Separation and Purification Technology 211: 218-226.

[2] Bauer, E. M., Bellitto, C., Imperatori, P., Righini, G., Colapietro, M., Portalone, G., Gómez-García, C. J. (2010): A Novel 1D-AF Hybrid Organic−Inorganic Chromium(II) Methyl Phosphonate Dihydrate: Synthesis, X-Ray Crystal and Molecular Structure, and Magnetic Properties. – Inorganic Chemistry 49(16): 7472-7477.

[3] Born, D. A., Ulrich, E. C., Ju, K. S., Peck, S. C., Van der Donk, W. A., Drennan, C. L. (2017): Structural basis for methylphosphonate biosynthesis. – Science 358(6368): 1336.

[4] Bustos, N., Cruz-Alcalde, A., Iriel, A., Cirelli, F. A., Sans, C. (2019): Sunlight and UVC-254 irradiation induced photodegradation of organophosphorus pesticide dichlorvos in aqueous matrices. – Sci Total Environ 649: 592-600.

[5] Chen, S., Liu, Y. (2007): Study on the photocatalytic degradation of glyphosate by TiO(2) photocatalyst. – Chemosphere 67(5): 1010-1017.

[6] Chen, Y., Wu, F., Lin, Y., Deng, N., Bazhin, N., Glebov, E. (2007): Photodegradation of glyphosate in the ferrioxalate system. – J Hazard Mater 148(1-2): 360-365.

http://www.aloki.hu ● ISSN 1589 1623 (Print) ● ISSN 1785 0037 (Online)
DOI: http://dx.doi.org/10.15666/aeer/1704_94739482

[7] Deanin, R. D., Orroth, S. A., Eliasen, R. W., Greer, T. N. (1970): Mechanism of ultraviolet degradation and stabilization in plastics. – Polymer Engineering & Science 10(4): 228-234.
[8] Edgar, M., Carter, V. J., Tunstall, D. P., Grewal, P., Favre-Nicolin, V., Cox, P. A., Wright, P. A. (2002): Structure solution of a novel aluminium methylphosphonate using a new simulated annealing program and powder X-ray diffraction data. – Chemical Communications 8: 808-809.
[9] Evgenidou, E., Konstantinou, I., Fytianos, K., Albanis, T. (2006): Study of the removal of dichlorvos and dimethoate in a titanium dioxide mediated photocatalytic process through the examination of intermediates and the reaction mechanism. – Journal of Hazardous Materials 137(2): 1056-1064.
[10] Gao, Z. C., Lin, Y. L., Xu, B., Xia, Y., Hu, C. Y., Zhang, T. Y., Gao, N. Y. (2019): Effect of UV wavelength on humic acid degradation and disinfection by-product formation during the UV/chlorine process. – Water Research 154: 199-209.
[11] Karl, D. M., Beversdorf, L., Björkman, K. M., Church, M. J., Martinez, A., Delong, E. F. (2008): Aerobic production of methane in the sea. – Nature Geoscience 1(7): 473-478.
[12] Langley, S., Helliwell, M., Sessoli, R., Teat, S. J., Winpenny, R. E. P. (2008): Synthesis and Structural and Magnetic Characterization of Cobalt(II) Phosphonate Cage Compounds. – Inorganic Chemistry 47(2): 497-507.
[13] Li, R., Jia, X., Jia, Q., Wang, C. (2016): Effect of pH and Dissolved Oxygen in Water on the Photolysis of Sulfamethazine. – Environmental Science & Technology 39.
[14] Lu, T., Solis-Ramos, E., Yi, Y., Kumosa, M. (2018): UV degradation model for polymers and polymer matrix composites. – Polymer Degradation and Stability 154: 203-210.
[15] Maeda, K., Akimoto, J., Kiyozumi, Y., Mizukami, F. (1995): AlMepO-α: A novel open-framework aluminum methylphosphonate with organo-lined unidimensional channels. – Angewandte Chemie International Edition in English 34(11): 1199-1201.
[16] Manassero, A., Passalia, C., Negro, A. C., Cassano, A. E., Zalazar, C. S. (2010): Glyphosate degradation in water employing the H2O2/UVC process. – Water Research 44: 3875-3882.
[17] Matys, S. V., Laurinavichius, K. S., Krupyanko, V. I., Nesmeyanova, M. A. (2001): Optimization of degradation of methylphosphonate - analogue of toxic pollutants with direct C-P bond by Escherichia coli. – Process Biochemistry 36(8–9): 821-827.
[18] Matys, S. V., Kuzmina, N. M., Laurinavichius, K. S., Nesmeyanova, M. A. (2004): Effect of environmental factors on degradation of the C-P bond of methylphosphonate by Escherichia coli cells. – Process Biochemistry 39(9): 1063-1071.
[19] Metcalf, W. W., Griffin, B. M., Cicchillo, R. M., Gao, J., Janga, S. C., Cooke, H. A., Van der Donk, W. A. (2012): Synthesis of Methylphosphonic Acid by Marine Microbes: A Source for Methane in the Aerobic Ocean. – Science 337(6098): 1104.
[20] Murphy, J., Riley, J. P. (1962): A modified single solution method for the determination of phosphate in natural waters. – Analytica Chimica Acta 27: 31-36.
[21] Rao, Y. F., Chu, W. (2010): Degradation of linuron by UV, ozonation, and UV/O(3) processes--effect of anions and reaction mechanism. – J Hazard Mater 180(1-3): 514-523.
[22] Sandy, E. H., Blake, R. E., Chang, S. J., Jun, Y., Yu, C. (2013): Oxygen isotope signature of UV degradation of glyphosate and phosphonoacetate: Tracing sources and cycling of phosphonates. – Journal of Hazardous Materials 260: 947-954.
[23] Santos-Beneit, F. (2015): The Pho regulon: a huge regulatory network in bacteria. – Front Microbiol 6: 402.
[24] Shao, X., Ge, H., Li, Z., Ren, C., Wang, J. (2015): Solubility of methylphosphonic acid in selected organic solvents. – Fluid Phase Equilibria 390: 7-13.
[25] Wei, J., Furrer, G., Schulin, R. (2000): Kinetics of carbosulfan degradation in the aqueous phase in the presence of a cosolvent. – Journal of Environmental Quality 29(5): 1481-1487.

http://www.aloki.hu ● ISSN 1589 1623 (Print) ● ISSN 1785 0037 (Online)
DOI: http://dx.doi.org/10.15666/aeer/1704_94739482

[26] Yu, C., Wang, F., Chang, S. J., Yao, J., Blake, R. E. (2018): Phosphate oxygen isotope evidence for methylphosphonate sources of methane and dissolved inorganic phosphate. - Sci Total Environ 644: 747-753.
[27] Yuan, F. (2007): Research on the Photochemical Degradation of Paclobutrazol in Aquesous Solution. - (Master), Hunan Agricultural University.
[28] Yuan, Z., Yao, J., Liu, H., Han, J., Trebse, P. (2014): Photodegradation of organophosphorus pesticides in honey medium. - Ecotoxicol Environ Saf 108: 84-88.

http://www.aloki.hu ● ISSN 1589 1623 (Print) ● ISSN 1785 0037 (Online)
DOI: http://dx.doi.org/10.15666/aeer/1704_94739482

ENVIRONMENTAL IMPACT OF TOURISM ACTIVITIES ON ECOLOGICAL NATURE RESERVES

HAN, F. L.[1*] – LI, C. T.[2]

[1]*Suihua University, Heilongjiang 152061, China*

[2]*Harbin Normal University, Heilongjiang 150025, China*

[*]*Corresponding author*
e-mail: h200168106@163.com

(Received 3rd Apr 2019; accepted 17th May 2019)

Abstract. With the rapid development of tourism, tourism activities have a certain impact on the environment of ecological nature reserves. Taking Wuyishan National Nature Reserve as the research object, this paper explores the impact of tourism activities on the environmental carrying capacity, vegetation landscape and atmospheric environment of natural ecological protection areas, and seeks measures for the coordinated development of tourism activities and ecological natural protection. The results show that the results of different tourism carrying capacity components vary greatly, and the number of tourists in Wuyishan National Nature Reserve has exceeded the value of tourism environmental carrying capacity. The influence of tourism activities on vegetation landscape is great and 6 out of the 20 samples tested are moderate interference. The closer the samples are to the travel path, the greater the interference degree on vegetation landscape is, the greater the interference by tourism activities is, and the smaller the ecological benefit value of the sample is. This study provides a theoretical and experimental basis for the sustainable development of tourism activities and ecological nature reserves.

Keywords: *tourist activities, ecological nature reserve, environmental science, ecological benefits, sustainable development*

Introduction

With the development of economy and the change of people's thought, tourism is called the gold medal industry in the 21st century. Tourism activities have the functions of increasing knowledge, cultivating sentiment, raising quality, promoting civilization and strengthening physique. It is also a symbol of the ever-increasing economic and cultural life of people (Jurigová and Zuzana, 2016; Movono et al., 2018). However, tourism activities are carried out with the complex activities of human beings, and the consumption of resources caused by tourism activities is increasing, which brings a plenty of environmental pressure on the ecological environment, including soil pollution, solid waste discharge, noise pollution and predatory development of lands in reserves (Mirela and Butnaru, 2015). The ecological nature reserves are the areas divided by the State and the region in order to maintain species diversity. They are of great significance to maintain the ecological balance, protect the natural and historical heritage and promote the development of scientific research and tourism. We should be pay attention to the protection and restoration of diversity of animal and plant species in ecological nature reserves, as well as protection and development of regional characteristics and natural landscape (Popp, 2014; Giddy and Webb, 2015). The tourism activities in ecological nature reserves can drive local economic development, bring considerable economic benefits to the local area, and bring natural landscapes to tourists, but the construction of tourism infrastructure in nature reserves and the trampling of

http://www.aloki.hu ● ISSN 1589 1623 (Print) ● ISSN 1785 0037 (Online)
DOI: http://dx.doi.org/10.15666/aeer/1704_94839492

tourists cause damage to the reserves (Hjalager and Johansen, 2013). In recent years, the ecological protection and restoration of eco-tourism areas are lagging behind due to the destruction of tourism activities. People gradually realize that tourism activities are a "double-edged sword", and eco-tourism has gradually developed into a favored way in the tourism market, with a focus on conservation of the natural environment and the natural landscape (Buswell and Buswell, 2011; Tikkanen et al., 2017). The national ecological nature reserves are the main carriers for tourism activities, with a limited capacity to withstand people's interference and destruction, and tourism activities will be destroyed to varying degrees and may cause species degradation in serious cases (Krupczek and Micha, 2016). Taking Wuyishan National Nature Reserve as the research object, this paper explores the impact of tourism activities on the environmental carrying capacity, vegetation landscape and atmospheric environment of natural ecological protection areas, and seeks measures for the coordinated development of tourism activities and ecological natural protection.

Materials and Methods

The environmental carrying capacity of national ecological nature reserves is an important index to limit the excessive tourism intensity, and represents the threshold for the capacity to support human socio-economic activities in certain period, under certain conditions and specific regional conditions (Nyahunzvi and Kennedy, 2015). The environmental carrying capacity not only refers to macroscopic natural environment, but also includes social environment, spiritual environment and management environment. It has objectivity, comprehensiveness, variability, feedback and finitude (Hayward and Kuwahara, 2013). Taking Wuyishan National Nature Reserve as an example, the indexes of its environmental carrying capacity includes resource space carrying capacity, ecological environment, economic environment and social environment carrying capacity (Ritter, 2009).

Table 1 shows the distribution of tourist sources in Wuyishan National Nature Reserve and the main domestic tourists come from Jiangxi, Fujian and Guangdong.

Table 1. *Distribution of tourist sources in Wuyishan National Nature Reserve*

Province	Passenger origin	Province	Passenger origin
Jiangxi	15.52%	Hunan	7.89%
Fujian	17.63%	Hubei	6.23%
Jiangsu	9.3%	Shandong	2.65%
Zhejiang	6.8%	Beijing	2.11%
Guangdong	13.65%	Sichuan	1.99%
Anhui	5.5%	Other	10.73%

Figure 1 shows the annual tourists in Wuyishan National Nature Reserve and the annual tourists increase year by year, up by 2.44 times from more than 6.4 million tourists in 2010 to more than 15.62 million in 2018. According to the official statistics of Wuyishan National Nature Reserve, the total number of tourists received exceeded 15 million for the first time in 2018, nearly 2.8 million more than in 2017, which is the biggest growth year.

http://www.aloki.hu ● ISSN 1589 1623 (Print) ● ISSN 1785 0037 (Online)
DOI: http://dx.doi.org/10.15666/aeer/1704_94839492

This paper mainly analyses the carrying capacity of ecological environment and social economy, among which the carrying capacity of ecological environment includes the carrying capacity of atmospheric environment (gaseous pollutants and suspended particles), water environmental carrying capacity (chemical oxygen content and ammonia nitrogen content index), and socio-economic carrying capacity includes psychological and spatial capacity (Hanna et al., 2015). *Figure 2* is the environmental bearing capacity value of Wuyishan National Nature Reserve. It can be seen that the environmental bearing capacity value of each index is different greatly, and the ecological environment bearing capacity is the largest, which is calculated according to the current bearing capacity value. At present, the total amount of tourists received in Wuyi Mountain exceeds the carrying capacity of water resources and environment.

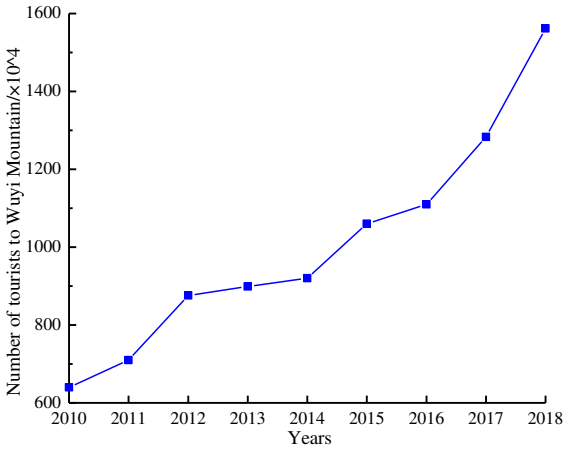

Figure 1. *Annual reception volume of tourists in Wuyishan National Nature Reserve*

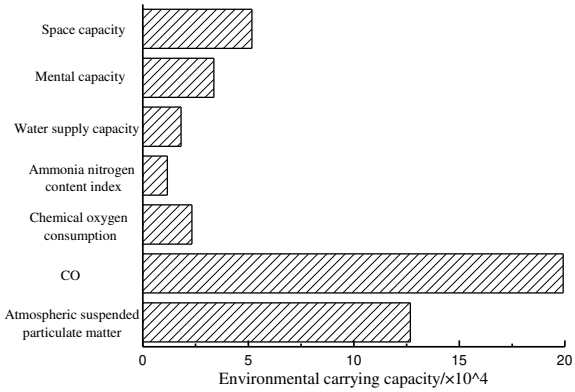

Figure 2. *Environmental carrying capacity of Wuyishan Ecological Nature Reserve*

Results

Ecological response of vegetation landscape to the interference of tourism activities

The vegetation landscape is the main component of Wuyishan National Nature Reserve, which is the most susceptible to the influence of tourism activities. The destruction of the vegetation landscape by tourism activities is divided into systematic destruction and local destruction. *Table 2* shows the purposes of visiting Wuyi

http://www.aloki.hu ● ISSN 1589 1623 (Print) ● ISSN 1785 0037 (Online)
DOI: http://dx.doi.org/10.15666/aeer/1704_94839492

Mountain. According to the questionnaire, tourists come to Wuyi Mountain mainly to enjoy the scenery and relax and the diversity of vegetation species provides a rich experience to tourists. According to the investigation results, the trees in Wuyishan National Nature Reserve contain 14 families, 18 genera, and 24 species, 32 species in shrub layer, 41 species in herbaceous layer, while the vegetation is rich in species.

Table 2. *Tourists visit Wuyishan for the purpose of travel*

Tourism purpose	Enjoy the scenery	Exercise	Relax	Delicious snack	Other
Proportion/%	57.61%	9.23%	26.59%	3.13%	3.44%

Figure 3 shows a vegetation landscape ecological effect evaluation system, which includes four parts such as vegetation importance, species diversity, community structure ratio and plant dominance. Wuyi Mountain is divided in 20 10 m × 10 m sample squares, and the species, height, coverage and cluster of species in the samples are recorded. The evaluation index TD of Wuyi Mountain vegetation landscape is as follows:

$$TD = 1 - \frac{S/S_{max}+H/H_{max}+C/C_{max}+L/L_{max}}{4} + A \quad \text{(Eq.1)}$$

where S, H, C and L represent the number of actual species, average height of species, vegetation coverage and vertical structure of vegetation in the samples, S_{max}, H_{max}, C_{max} and L_{max} represent the maximum value of the data measured in the samples, and A represents the ecological dominance value.

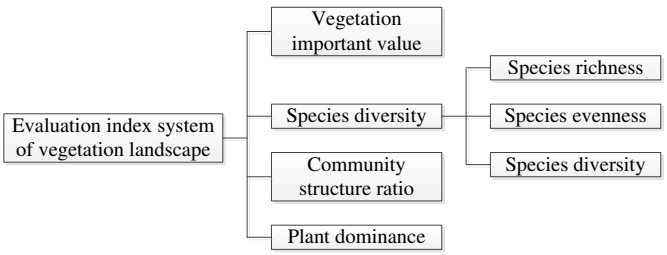

Figure 3. *Vegetation landscape ecological effect evaluation system*

Figure 4 shows the influence of tourism activities on the number of vegetation species and vegetation coverage, and the larger the number of vegetation species and vegetation coverage value are, the greater the species richness is.

Figure 5 shows the impact of tourism activities on the average height and vertical structure of vegetation. The higher the average height and the vertical structure of vegetation are, the more vegetation the tree layer has. *Figure 6* shows the ecological benefit value of the vegetation landscape of Wuyi Mountain. The larger the interference by the tourism activity is, the smaller the ecological benefit value of the samples is, and the quality of the vegetation landscape is deteriorated due to the tourism activity. *Table 3* is the calculation of the interference degree of the selected samples. It can be seen that the interference degree of samples 5-10 is severe, and that of other samples is mild.

http://www.aloki.hu ● ISSN 1589 1623 (Print) ● ISSN 1785 0037 (Online)
DOI: http://dx.doi.org/10.15666/aeer/1704_94839492

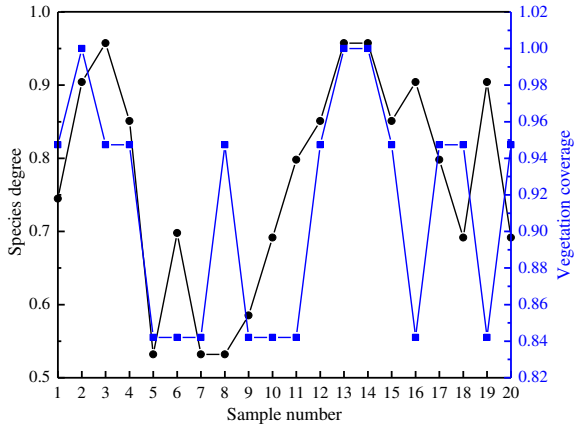

Figure 4. *Effects of tourism activities on the number of vegetation species and vegetation coverage*

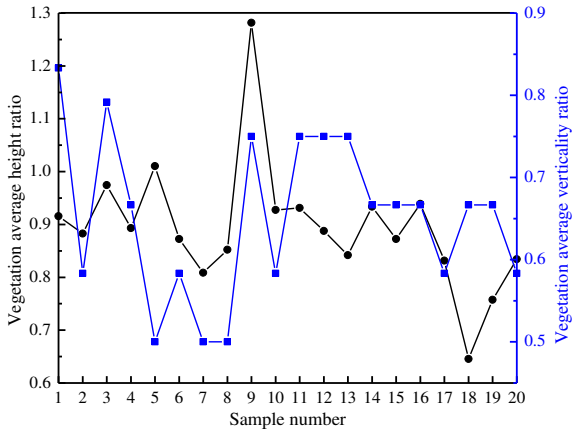

Figure 5. *Effects of tourism activities on the average height of vegetation and the vertical structure of vegetation*

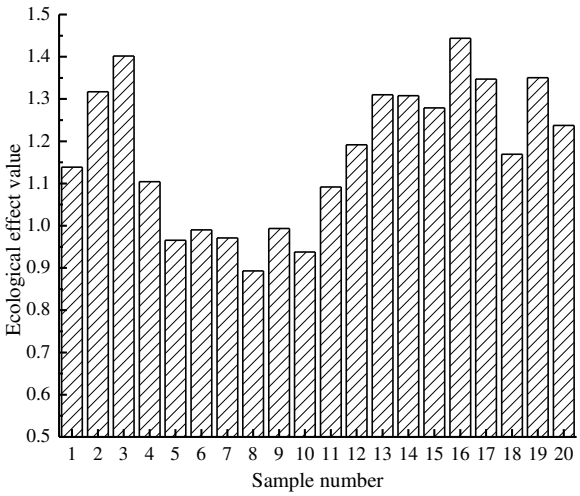

Figure 6. *Ecological benefit value of vegetation landscape in Wuyi Mountain*

http://www.aloki.hu ● ISSN 1589 1623 (Print) ● ISSN 1785 0037 (Online)
DOI: http://dx.doi.org/10.15666/aeer/1704_94839492

Table 3. *Calculation of the degree of interference of the selected sample*

NO.	Interference degree	NO.	Interference degree	NO.	Interference degree
1	Mild interference	8	Moderate interference	15	Mild interference
2	Mild interference	9	Moderate interference	16	Mild interference
3	Mild interference	10	Moderate interference	17	Mild interference
4	Mild interference	11	Mild interference	18	Mild interference
5	Moderate interference	12	Mild interference	19	Mild interference
6	Moderate interference	13	Mild interference	20	Mild interference
7	Moderate interference	14	Mild interference		

Analysis of the impact of tourism distance on vegetation landscape

The overall impact of tourism activities on the vegetation landscape is minimal, but greater on the local areas, which is manifested in the trampling and picking of the vegetation by tourists, resulting in the inhibition of the growth and development of the vegetation and the change of the vegetation coverage. Water and soil pollution caused by tourism activities will also affect the growth and development of vegetation.

In this experiment, the vegetation coverage and species diversity are taken as evaluation index. With 10 sample plots in total, each sample plot comprises four samples, with a size of 1 m × 1 m, and the distances of the four samples to the tourism path are 0 m, 5 m, 10 m and 15 m, respectively. Taking relative coverage as the research object, the richness index of species is as follows:

$$R = (S - 1)/lnN \quad \text{(Eq.2)}$$

where, S represents the total number of species in a single sample and N represents the sum of species importance values in all test samples.

Figure 7 shows the relative coverage of the vegetation and the change of the species number in the samples with different travel distance.

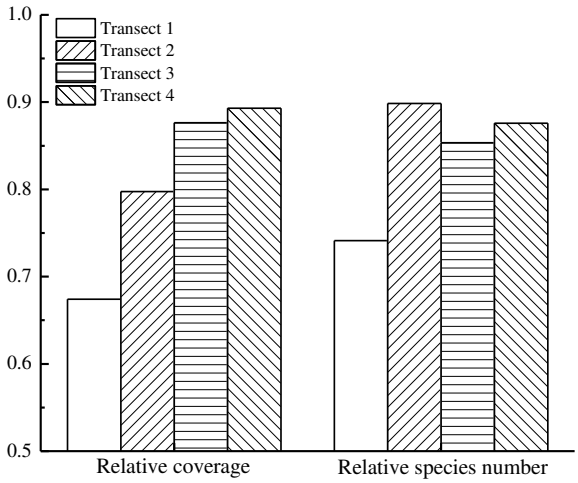

Figure 7. *Changes in relative coverage and species of vegetation distance from different tourism activities*

http://www.aloki.hu ● ISSN 1589 1623 (Print) ● ISSN 1785 0037 (Online)
DOI: http://dx.doi.org/10.15666/aeer/1704_94839492

It can be clearly seen that the relative coverage of the vegetation and the change of the species number show different changing law. The further the tourist path is, the larger the relative coverage of the vegetation is. The number of species in the sample with the distance of 0 m to tourist path is the least, the number of species in the sample with the distance of 5 m is the largest, and the number of species in the samples 3 and 4 is less than that of the sample 2, that's, the vegetation diversity increases not far from the distance from the tourist path, which may be related to the "moderate interference hypothesis". *Figure 8* shows the degree of tourism interference in different tourism distance zones and the coverage ratio, the height relative ratio and the vertical structure of the vegetation show the same trend, and the smaller the travel distance is, the larger the coverage ratio, the height relative ratio and the vertical structure value of the vegetation are, which is opposite to the changing law of the interference degrees, and the interference degree decreases with the increase of the travel distance, which conforms to the natural law.

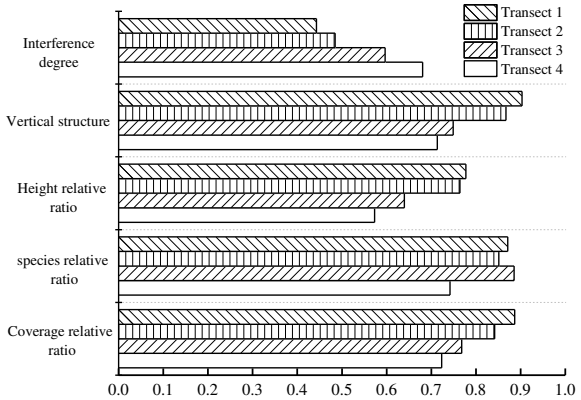

Figure 8. *Different tourist distances with tourist interference*

Discussion

Ecological response of environmental quality to the interference of tourism activities

Environmental quality is also an important index to measure the environment of ecological nature reserves. Air pollution, water pollution and noise pollution will all affect the soil, vegetation and animals in the nature reserves. In this paper, three indexes of atmospheric pollutants such as CO, ammonia nitrogen and total suspended particulate matter are tested. *Table 4* shows the monitoring results of the main atmospheric pollutants in Wuyishan National Nature Reserve.

Table 4. *Monitoring results of major atmospheric pollutants in Wuyishan National Nature Reserve*

Project	CO	Ammonia nitrogen content	Suspended particulate matter
Jiu Quxi	0.015	0.016	0.124
Da Zangfeng	0.014	0.010	0.099
Fu Rongtan	0.015	0.006	0.089
Wo Longfeng	0.014	0.008	0.065
Mean	0.0145	0.010	0.0943
National standard	0.05	0.05	0.12

http://www.aloki.hu ● ISSN 1589 1623 (Print) ● ISSN 1785 0037 (Online)
DOI: http://dx.doi.org/10.15666/aeer/1704_94839492

Compared with the national natural standards, the overall environmental quality of Wuyishan National Nature Reserve is the first-class standard, but the total suspended particulate matter content of Jiuqu River is higher than the first-class standard. *Figure 9* shows the changing value of total suspended particulate matter concentration in different places. The fluctuation of total suspended particulate matter concentration in Jiuqu River is the most obvious, with the highest concentration value at 16 pm, mainly because passengers returning from other scenic spots successively view Jiuqu River, and the vehicles pass frequently, causing a gradual increase in the concentration value.

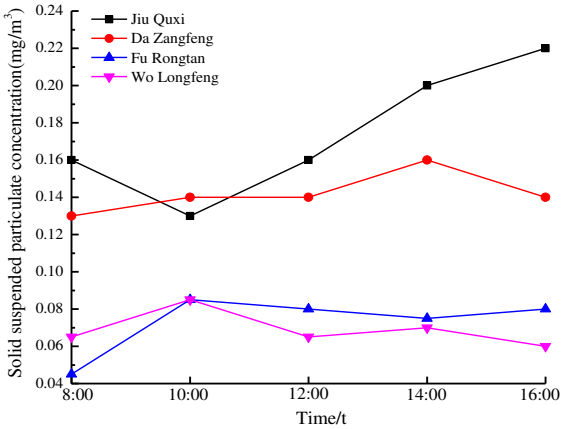

Figure 9. *Increasing values of total suspended particulate matter at different locations*

Measures for coordinated development of tourism activities and ecological nature protection

The impact of tourism activities on the environment of ecological nature reserves is inevitable. If tourism planning and management work is in place, the sustainable development of tourism activities and environmental protection can be realized. At present, the laws and regulations on tourism management in Wuyishan National Nature Reserve are not sound, the natural resources are seriously destroyed, and there is no necessary supervision and management system. In order to achieve ecological sustainability, we should strengthen the management of managers, operators and tourists. Tourists are the direct participants of tourism activities, so this paper will focus on the relevant management measures for tourists. First of all, tourists should manage and restrict their own behavior and put an end to uncivilized behaviors such as picking up, littering and painting in the reserves. Third, we should standardize tourism behavior, strengthen the popularization and education of ecological science in tourism activities, and ensure the harmony and unity of tourism activities and ecological environment. Finally, we should have meaningful tourism activities, implementing the eco-environmental protection and sustainable development throughout the tourism activities.

Conclusions

Taking Wuyishan National Nature Reserve as the research object, this paper explores the impact of tourism activities on environmental carrying capacity, vegetation landscape and atmospheric environment of natural ecological reserve. The specific conclusions are as follows:

http://www.aloki.hu ● ISSN 1589 1623 (Print) ● ISSN 1785 0037 (Online)
DOI: http://dx.doi.org/10.15666/aeer/1704_94839492

The environmental carrying capacity of each index of Wuyishan National Nature Reserve is different greatly, and the carrying capacity of ecological environment is the largest. According to the current carrying capacity value, the total amount of tourists received in Wuyi Mountain exceeds the environmental carrying capacity of water resources.

The number of species in the sample with the distance of 0 m to tourist path is the least, and the number of species in the sample with the distance of 5 m is the largest. The coverage ratio, height relative ratio and vertical structure of vegetation show the same changing law, that's, the smaller the tourist path distance is, the larger the coverage ratio, height relative ratio and vertical structure value of vegetation are, which is opposite to the changing law of interference degree value. The interference decreases with the increase of the tourist path distance.

The larger the interference of tourism activities is, the smaller the ecological benefit value of the tested sample is. The result of testing the atmospheric pollutants shows that the impact of tourism activities on the atmospheric environment is small.

At present, the calculation of environmental carrying capacity is based on the intensity of tourist source activities. No quantitative analysis was made on whether tourism will affect the atmospheric environment and water environment of Wuyishan Ecological Nature Reserve, and the degree of the impact, so the scientific quantitative research and analysis can be carried out in the future.

Acknowledgements. Heilongjiang Natural Science Foundation (QC2017086); Heilongjiang Youth Innovative Talents Project (UNPYSCT-2017174); Suihua University of Cold Black Soil and Culture Research Project (H201701002); Suihua University of Applied Research Project (Y201701002); Suihua University of Scientific Research and Innovation Team (SIT04B003).

REFERENCES

[1] Buswell, R. J. (2011): Mallorca and tourism: History, economy and environment.
[2] Giddy, J. K., Webb, N. L. (2015): The influence of the environment on motivations to participate in adventure tourism: the case of the tsitsikamma. – South African Geographical Journal 98(2): 351-366.
[3] Hanna, P., Johnson, K., Stenner, P., Adams, M. (2015): Foucault, sustainable tourism, and relationships with the environment (human and nonhuman). – GeoJournal 80(2): 301-314.
[4] Hayward, P., Kuwahara, S. (2013): Divergent trajectories: environment, heritage and tourism in tanegashima, mageshima and yakushima. – Journal of Marine and Island Cultures 2(1): 29-38.
[5] Hjalager, A. M., Johansen, P. H. (2013): Food tourism in protected areas sustainability for producers, the environment and tourism. – Journal of Sustainable Tourism 21(3): 417-433.
[6] Jurigová, Z. (2016): Tourism: new destination of global business environment. – International Advances in Economic Research 22(3): 351-352.
[7] Kennedy Nyahunzvi, D. (2015): Negotiating livelihoods among chivi curio traders in a depressed zimbabwe tourism trading environment. – Anatolia 26(3): 397-407.
[8] Kruczek, Z., Michał, K. (2016): Post-industrial tourism as a means to revitalize the environment of the former oil basin in the Polish Carpathian mountains. – Polish Journal of Environmental Studies 25(2): 895-902.

http://www.aloki.hu ● ISSN 1589 1623 (Print) ● ISSN 1785 0037 (Online)
DOI: http://dx.doi.org/10.15666/aeer/1704_94839492

[9] Mirela, S., Butnaru, G. I. (2015): Research on tourists' perception of the relationship between tourism and environment. – Procedia Economics and Finance 20: 595-600.
[10] Movono, A., Dahles, H., Becken, S. (2018): Fijian culture and the environment: a focus on the ecological and social interconnectedness of tourism development. – Journal of Sustainable Tourism 26(3): 451-469.
[11] Popp, P. K. (2014): Vacationland: tourism and environment in the colorado high country. – Journal of American History 101(1): 350-351.
[12] Ritter, F. (2009): The encyclopedia of tourism and recreation in marine environments. – Annals of Tourism Research 36(3): 538-539.
[13] Tikkanen, J., Hokajärvi, R., Hujala, T., Kurttila, M. (2017): Ex ante evaluation of a pes system: safeguarding recreational environments for nature-based tourism. – Journal of Rural Studies 52: 42-55.

http://www.aloki.hu ● ISSN 1589 1623 (Print) ● ISSN 1785 0037 (Online)
DOI: http://dx.doi.org/10.15666/aeer/1704_94839492

ESTIMATION OF CARBON EMISSION AND IDENTIFICATION OF DRIVING FACTORS IN THE CIRCUM-CHANGSHA-ZHUZHOU-XIANGTAN URBAN AGGLOMERATION OF CHINA

DENG, Q. Z. – TIAN, Y. C.*

School of Business, Hunan University of Science and Technology, Xiangtan 411201, China

**Corresponding author*
e-mail: 819326168@qq.com

(Received 3rd Apr 2019; accepted 17th May 2019)

Abstract. Based on panel statistics on Circum-Changsha-Zhuzhou-Xiangtan urban agglomeration of China in 2008-2016, the area's carbon emissions originate from three distinct sources: agriculture, industry and transportation in a "bottom-up" way for estimation. The Logarithmic Mean Divisia Index (LMDI) model is used to identify the driving factors that influence carbon emission in this urban agglomeration. Finally, the interaction between carbon emission and economic development was scientifically evaluated based on decoupling elasticity index. The results show: (1) the carbon emission of Circum-Changsha-Zhuzhou-Xiangtan urban agglomeration increased in 2008-2011, and slightly fluctuated in 2011-2016. According to the Environmental Kuznets Curve (EKC), there is an obvious "inverted-U" curve between carbon emission and per capita Gross Domestic Product (GDP), means the carbon emission will be effectively controlled as the economic development reaches a certain level; (2) LMDI decomposition shows the economic growth and human capital played a positive role in promoting the growth and change of carbon emissions of the whole urban agglomeration, while the energy intensity and industrial structure had a negative effect; (3) the decoupling level of Circum-Changsha-Zhuzhou-Xiangtan urban agglomeration as a whole tends to be slightly higher than the growth rate of carbon emission, among which the core region has a weak decoupling trend while Hengyang and Changde of China repeatedly appear to be in strong decoupling state.
Keywords: *green development, EKC curve, LMDI model, decoupling index, emission-reduction*

Introduction

The increasing greenhouse effect drew international attention towards problems concerning the ecological environment. At the Copenhagen meeting, China promised to "reduce the carbon dioxide emission per unit GDP by 40-45% by 2020 compared to 2005." Subsequently, the State Council listed low carbon level as one of the important development goals in the Plan for Ecological Environment Protection during the Thirteenth Five-year Plan Period. In the process of accelerating the development of urbanization, the rapid concentration of industry and population makes cities become the key areas of energy conservation and emission reduction. Therefore, China has successively issued many plans for building low-carbon cities. Located in the middle reaches of the Yangtze River Economic Belt of China, the Circum-Changsha-Zhuzhou-Xiangtan urban agglomeration is responsible for the rise of the central region. Under the two development strategies of the Belt and Road and Circum-Changsha-Zhuzhou-Xiangtan Integration, the Circum-Changsha-Zhuzhou-Xiangtan urban agglomeration should set up a model among the urban agglomerations in the middle reaches of the Yangtze River as well as bear more responsibilities in national and regional development and environmental governance. In this context, scholars have produced researches on CO_2 which mainly include the following aspects: (1) Carbon emissions estimates. Most scholars calculate the carbon emission based on the carbon emission

http://www.aloki.hu ● ISSN 1589 1623 (Print) ● ISSN 1785 0037 (Online)
DOI: http://dx.doi.org/10.15666/aeer/1704_94939504

coefficient method (Ning and Zhang, 2014; Gong, 2015), and some scholars estimate the carbon emission amount through the indirect calculation method. The input-output method is mostly used for the calculation of implied carbon dioxide (He, 2012; Zhao et al., 2019). Due to the input-output method's lack of accuracy, the life cycle method is also favored by many scholars (Xia et al., 2010; Cao et al., 2011). (2) Identification of driving factors. With the help of LMDI decomposition method, many scholars can calculate the driving direction and contribution value of each factor (Li and Zhang, 2016; Sun and Zhou, 2017), and some scholars use Stochastic Impacts by Regression on Population, Affluence, and Technology (STIRPAT) model to conduct regression analysis and calculate the regression coefficient of driving factors. The direction and magnitude are judged by the positive and negative values of the coefficients (Feng et al., 2019). In addition, some scholars use the Kaya identity to analyze (Pan and Hu, 2019; Wang and He, 2018). (3) Study on the potential of reducing carbon emission. There are many theoretical analyses on the potential of carbon emission reduction (Tian and Ding, 2018; Zhang et al., 2015). Some scholars use the model to quantify the potential of carbon emission reduction, such as using decoupling index to quantify the potential of carbon emission reduction into elasticity index (Wang and Zhu, 2018; He and Cai, 2016), or different carbon emission scenarios are respectively set to predict the value based on the regression coefficients and the difference between each prediction result is calculated (Li et al., 2018; Gu et al., 2013). In view of the existing research, the research methods on carbon emission have been more comprehensive, but most of the research objects are based on the national or provincial panel data, while the literature on urban agglomerations for the early stage is less. Therefore, the carbon emission of Circum-Changsha-Zhuzhou-Xiangtan urban agglomeration is estimated from three perspectives such as agriculture, industry and transportation in a "bottom-up" way. At the same time, the relationship between carbon emission and GDP per capita is fitted, and the factors that drive the change of urban carbon emission are decomposed through LMDI model. Finally, the decoupling elasticity is established to analyze the dependence between urban carbon emission and economic development, so as to find a more suitable emission reduction path for the development of Circum-Changsha-Zhuzhou-Xiangtan urban agglomeration, and provide more scientific policy suggestions for its green, coordinated and sustainable development.

Materials and methods

Method for estimating carbon emissions

In this paper, the "bottom-up" method is used to calculate the emissions of CO_2 in the primary industry (agriculture), the secondary industry (industry) and the tertiary industry (transportation (the main carbon source)) and summarize to obtain the emissions of CO_2 in the Circum-Changsha-Zhuzhou-Xiangtan urban agglomeration of China. The detailed calculation ideas are as follows:

$$C_{\mathrm{tj}} = C_{Atj} + C_{Itj} + C_{Ttj} \quad \text{(Eq.1)}$$

where C_{tj} indicates the emission of the j city in the t year, C_{Atj}, C_{Itj} and C_{Ttj} indicate the emissions of CO_2 in the j city in the t year from agriculture, industry and

http://www.aloki.hu ● ISSN 1589 1623 (Print) ● ISSN 1785 0037 (Online)
DOI: http://dx.doi.org/10.15666/aeer/1704_94939504

transportation. The calculation formula for carbon emissions in different industries is broken down as follows:

(1) Carbon emission from urban agriculture. The sources of carbon emission in agriculture mainly come from agricultural cultivation and fertilization. Therefore, four factors such as agricultural machinery, effective irrigation area, chemical fertilizer and rural electricity are selected to calculate the urban agricultural carbon emission. The formula is as follows:

$$C_{Atj}=\sum_{t} F_{ti} \cdot \rho_i \quad \text{(Eq.2)}$$

where C_{Atj} indicates the carbon emission of the j city in the t year, F_{ti} indicates the total consumption of the i agricultural element in the t year, and ρ_i indicates the corresponding carbon emission factor of the i element. According to the calculation of agricultural carbon emissions in Jiangxi Province (Cao and Cao, 2016), the carbon emission coefficients of agricultural machinery, effective irrigation area, fertilizer and rural electricity consumption are selected respectively as 1.8 t/103 kw·h, 20.476 t/103 km^3, 0.8956 t/t, 9.26 t/104 kw·h.

(2) Carbon emission from urban industry. Considering the availability and representativeness of the data, this paper selects the total amount of energy used by the large industrial enterprises after being converted into standard coal to calculate the urban industrial carbon emission. The calculation formula is as follows:

$$C_{Itj}=\sum_{t} F_{ti} \cdot \rho_i \quad \text{(Eq.3)}$$

where C_{Itj} indicates the industrial carbon emission of the j city in the t year, F_{ti} indicates the consumption of the i energy in the t year, and ρ_i indicates the corresponding carbon emission factor of the i energy. The carbon emission coefficient of standard coal is 2.493 t/t, taken based on the IPCC China Greenhouse Gas Emission List.

(3) Carbon emission from urban transportation. According to the method of calculating the carbon emission in transportation and the applicability of the data in existing literature, this paper selects the emission of CO_2 from passenger and freight vehicles C_{Tptj} and residential vehicles C_{Tutj} to replace the carbon emission of urban transportation. The calculation formula is as follows:

$$C_{Ttj}=C_{Tptj}+C_{Tutj} \quad \text{(Eq.4)}$$

The carbon emissions of passenger and freight vehicles are calculated by using the calculation method of the United Nations World Tourism Organization (UNWTO), and the carbon emission of each traffic mode is estimated by the product of the turnover of each traffic mode and the corresponding carbon emission coefficient. The formula is as follows:

$$C_{Tptj}=\sum_{t} F_{pti} \cdot \rho_i \quad \text{(Eq.5)}$$

http://www.aloki.hu ● ISSN 1589 1623 (Print) ● ISSN 1785 0037 (Online)
DOI: http://dx.doi.org/10.15666/aeer/1704_94939504

where, C_{Tptj} indicates the emission of CO_2 from passenger and freight vehicles, F_{pti} indicates the turnover of the i traffic mode in the t year, and ρ_i indicates the corresponding carbon emission factor of different turnover modes. In view of China's lack of authoritative turnover carbon emission data, this paper determines passenger vehicle carbon emission coefficient (He, 2010; Paul and Ghislain, 2010), which is converted to a freight carbon emission factor according to the unit cargo turnover provided by Greenhouse Gas Protocol and European Chemical Industry Association. The transport modes of passenger transport and freight transport statistics are railway, highway, waterway and aviation, and the emission coefficients of passenger transport turnover are respectively 27 g/p·km and 133 g/p·km, the emission coefficients of freight transport turnover are respectively 28 g/ton·km, 327 g/ton·km, 53 g/ton·km and 1,961 g/ton·km.

$$C_{Tutj} = \sum_t G_{uti} \times S_{uti} \times Q_{uti} \times J_{uti} \quad \text{(Eq.6)}$$

where, C_{Tutj} indicates the emission of CO_2 from residential vehicles in the j city in the t year, G_{uti} indicates the fuel consumption of 100 km of the i transportation mean, S_{uti} indicates the annual mileage of the i transportation mean, and J_{uti} indicates the carbon emission factor of the i transportation mean. Due to the difficulty in obtaining the corresponding data on the energy consumption and mileage of residential vehicles, according to the calculation of the carbon emissions in transportation of Wuhan (Gong, 2015) and Zhengzhou (Ning, 2014) and in combination with the per capita GDP difference of different provinces, this paper estimates the average annual mileage of different residential vehicles in the cities of the the Circum-Changsha-Zhuzhou-Xiangtan urban agglomeration proportionally. The fuel consumption of private cars for 100 km is mainly 93#, taking 0.1 L/km and the motorcycles mainly 125 motorcycles taking 0.22 L/km.

Drive factor decomposition model

The LMDI decomposition method overcomes the problem that the traditional decomposition method has the residual term. Therefore, according to the analysis framework (Albrecht et al., 2002), the carbon emission of Circum-Changsha-Zhuzhou-Xiangtan urban agglomeration of China is decomposed as follows:

$$C = \sum_i \left(\frac{C_i}{E_i} \times \frac{E_i}{E} \times \frac{E}{Y} \times \frac{Y}{P} \times P \right) \quad \text{(Eq.7)}$$

where, C indicates the total carbon emission of Circum-Changsha-Zhuzhou-Xiangtan urban agglomeration, C_i indicates the total carbon emission of the i industry, E_i indicates the energy consumption of the i industry, E indicates the total energy consumption of urban agglomerations, Y indicates the GDP of urban agglomeration and P indicates employees in the urban agglomeration. In order to facilitate that decomposition, it is expanded to the follow form:

$$A_i = \frac{C_i}{E_i}, \quad B_i = \frac{E_i}{E}, \quad D = \frac{E}{Y}, \quad I = \frac{Y}{P}, \quad K = P \quad \text{(Eq.8)}$$

http://www.aloki.hu ● ISSN 1589 1623 (Print) ● ISSN 1785 0037 (Online)
DOI: http://dx.doi.org/10.15666/aeer/1704_94939504

Ai, Bi, D, I and K respectively indicate carbon emission coefficient effect, industrial structure effect, energy intensity effect, economic development effect and human capital effect.

If the total carbon emission of urban agglomerations in the basic period is set as C^0, after T period, the change in the total carbon emission of urban agglomeration can be expressed as:

$$\begin{aligned}\Delta C &= C^T - C^O \\ &= \Delta C_{Ai} + \Delta C_{Bi} + \Delta C_D + \Delta C_I + \Delta C_K\end{aligned} \quad \text{(Eq.9)}$$

Considering that the energy carbon emission coefficient is constant, ΔC_{Ai} is not considered in actual calculation. According to the study (Ang et al., 1998), the expression of contribution value of each element can be further expressed as

$$\begin{aligned}&\Delta C_{Bi}=\sum_i\left(\frac{C_i^T-C_i^0}{\ln C_i^T-\ln C_i^0}\right)\times\ln\left(\frac{B_i^T}{B_i^0}\right);\ \Delta C_D=\sum_i\left(\frac{C_i^T-C_i^0}{\ln C_i^T-\ln C_i^0}\right)\times\ln\left(\frac{D^T}{D^0}\right)\\ &\Delta C_I=\sum_i\left(\frac{C_i^T-C_i^0}{\ln C_i^T-\ln C_i^0}\right)\times\ln\left(\frac{I^T}{I^0}\right);\ \Delta C_K=\sum_i\left(\frac{C_i^T-C_i^0}{\ln C_i^T-\ln C_i^0}\right)\times\ln\left(\frac{K^T}{K^0}\right)\end{aligned} \quad \text{(Eq.10)}$$

Decoupling elasticity coefficient

According to the explanation of the decoupling analysis elasticity (Tapio, 2005), the decoupling elasticity coefficient can be expressed as:

$$e_j=\frac{\Delta C_j / C_j}{\Delta GDP_j / GDP_j} \quad \text{(Eq.11)}$$

where, e_j indicates the decoupling elasticity coefficient of the j city, and C_j indicates the total carbon emission of the j city. The different elasticity magnitudes represent different decoupling states, and the specific corresponding relationship is shown in *Table 1*.

Table 1. *Type of Tapio decoupling elasticity*

Status		Environmental pressure	Economic growth	Elasticity
Negative decoupling	Weak negative decoupling	＜0	＜0	0 ≤ t ＜0.8
	Strong negative decoupling	＞0	＜0	t ＜0
	Expansion negative decoupling	＞0	＞0	t ＞1.2
Decoupling	Decline decoupling	＜0	＜0	t ＞1.2
	Strong decoupling	＜0	＞0	t ＜0
	Weak decoupling	＞0	＞0	0 ≤ t ＜0.8
Connection	Decay connection	＜0	＜0	0.8 ≤ t ≤ 1.2
	Expansion connection	＞0	＞0	0.8 ≤ t ≤ 1.2

http://www.aloki.hu ● ISSN 1589 1623 (Print) ● ISSN 1785 0037 (Online)
DOI: http://dx.doi.org/10.15666/aeer/1704_94939504

Data sources

This paper chooses Circum-Changsha-Zhuzhou-Xiangtan urban agglomeration of China as the research object, which includes the core area (Changsha, Zhuzhou, and Xiangtan); and radiation area (Hengyang, Yueyang, Changde, Yiyang and Loudi). The time span of data collection is from 2008 to 2016. The relevant data are mainly from the Statistical Yearbook of Hunan Province, the Statistical Yearbook of Chinese Cities and the Statistical Annual Report published by the statistical offices of each city from 2009 to 2017.

Results and discussion

Estimation results of carbon emission from Circum-Changsha-Zhuzhou-Xiangtan urban agglomeration of China

Carbon emission and carbon emission intensity of Circum-Changsha-Zhuzhou-Xiangtan urban agglomeration of China from 2008 to 2016 are shown in *Table 2*. As can be seen in *Figure 1*, the carbon emission of the Circum-Changsha-Zhuzhou-Xiangtan urban agglomeration from 2008 to 2016 can be divided into two phases. The first phase, 2008-2011, shows a steady upward trend in total carbon emissions at a relatively high growth rate, with the highest growth rate (15.18%) in 2011, increasing from 26.21×10^7 tons in 2010 to 30.19×10^7 tons in 2011, and the carbon emissions of the three major industries also increased rapidly in this period. In the second phase, 2011-2016, the total carbon emissions fluctuated slightly, with positive and negative growth alternately. The industrial carbon emission fell several times at this phase. Except for a sharp rise of the carbon emission due to the large amount of fertilizer used for the flood in 2013, it showed a slow growth in all other times. The carbon emission in transportation industry after 2011 had a lower growth rate.

Table 2. *Carbon emissions of Circum-Changsha-Zhuzhou-Xiangtan urban agglomeration in 2008-2016*

Year	Carbon emissions of the Changsha, Zhuzhou and Xiangtan urban agglomerations (10,000 tons)				Carbon intensity (ton/10,000 yuan)
	Agricultural carbon emissions	Industrial carbon emissions	Transportation carbon emissions	Total carbon emissions	
2008	670	19093	1681	21444	2.45
2009	765	20899	2196	23860	2.31
2010	795	22569	2849	26213	2.09
2011	877	25805	3509	30191	1.95
2012	880	24658	4548	30086	1.70
2013	1326	25322	5214	31862	1.62
2014	986	23932	5594	30512	1.41
2015	981	23006	6022	30009	1.28
2016	1000	22956	6479	30435	1.19

http://www.aloki.hu ● ISSN 1589 1623 (Print) ● ISSN 1785 0037 (Online)
DOI: http://dx.doi.org/10.15666/aeer/1704_94939504

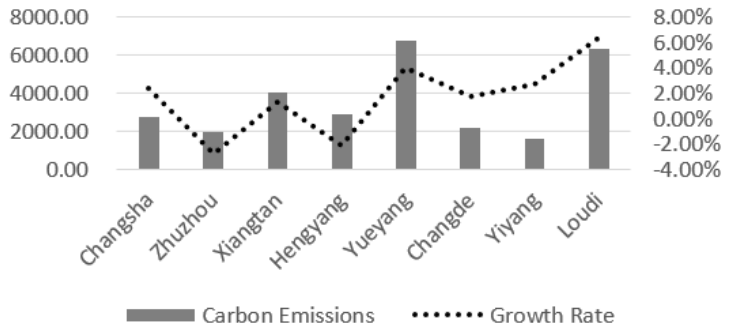

Figure 1. *Carbon emissions and growth rate of Circum-Changsha-Zhuzhou-Xiangtan urban agglomeration in 2008-2016*

The EKC curve (Grossman and Krueger, 1995) is used to further explore the relationship between economic development and environmental pollution. Based on the data of carbon emissions and GDP per capita from 2008 to 2016 in the Circum-Changsha-Zhuzhou-Xiangtan urban agglomeration, a EKC curve regression model for the urban carbon emission including primary, secondary and tertiary terms is established:

$$Y = \alpha_0 + \alpha_1 X + \alpha_2 X^2 + \alpha_3 X^3 + \varepsilon \quad \text{(Eq.12)}$$

where Y and X respectively indicate the carbon emission and per capita GDP of the urban agglomeration, and α0, α1, α2, α3 and ε indicate the parameters to be estimated and the random error term. The regression analysis and test are carried out by using the software of E-Views (9.0). It is found that the quadratic function fitting curve is the best, with the fitting degree of 0.971, the F value is 101.75, and the P values all pass the significance test. The metrology model is shown in *Figure 2*, the carbon emission and per capita GDP of Circum-Changsha-Zhuzhou-Xiangtan urban agglomeration shows an obvious "inverted-U" curve.

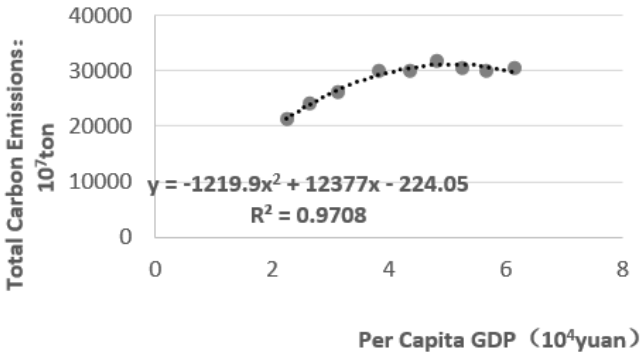

Figure 2. *Curve of carbon emissions and per capita GDP Circum-Changsha-Zhuzhou-Xiangtan urban agglomeration in 2008-2016*

According to the derivation of the fitting curve, the stagnation point is 5.073, that is, when the per capita GDP exceeds 5.073, the carbon emission is likely to fall, which

http://www.aloki.hu ● ISSN 1589 1623 (Print) ● ISSN 1785 0037 (Online)
DOI: http://dx.doi.org/10.15666/aeer/1704_94939504

may be due to complicated reasons: for example, the vigorous development of heavy industry in the early period of the economic downturn to rapidly improve the economic level has led to increased pollution. As the environment deteriorates and resource scarcity increases, the public has paid more attention to energy conservation and emission reduction and accelerated the research and development of high-tech and environmentally-friendly technology products, so the urban carbon emission has in turn been controlled.

Driving factor decomposition results

The LMDI decomposition results are shown in *Table 3*, as can be seen in conjunction with the judgement matrix (*Table 4*). During 2008-2016, the carbon emission in the Circum-Changsha-Zhuzhou-Xiangtan urban agglomeration of China increased 5 times and decreased 3 times, industrial structure and energy intensity suppressed the carbon emission of the urban agglomeration, and the economic development and human capital played an important role. Among them, the economic effect is the most remarkable, and its annual contribution to the growth of the carbon emission in the Circum-Changsha-Zhuzhou-Xiangtan urban agglomeration was 87%, so the increase of carbon emission in the urban agglomeration mainly depended on the driving value of economic development. The negative driving effect of industrial structure was obvious from 2009 to 2012, but the driving effect of energy intensity from 2012 to 2016 was obviously higher than that of industrial structure, and the contribution value increased rapidly. The growth in carbon emission in the urban agglomeration slowed down after 2013.

Table 3. *Driving factors decomposition of carbon emissions of Circum-Changsha-Zhuzhou-Xiangtan urban agglomeration in 2008-2016*

Year	ΔC	ΔC_{Bi}	ΔC_D	ΔC_I	ΔC_K
2009	5.58	-19.43	-9.62	28.94	5.69
2010	22.37	-37.08	-23.88	72.57	10.76
2011	63.57	-62.61	-23.08	129.64	19.61
2012	49.13	-74.66	-63.86	164.11	23.55
2013	57.09	-81.65	-84.97	195.47	28.25
2014	36.23	-83.85	-122.35	212.82	29.61
2015	34.09	-75.60	-153.83	228.54	34.98
2016	41.86	-73.85	-174.31	249.76	40.27

Table 4. *Driver factors judgment matrix of Circum-Changsha-Zhuzhou-Xiangtan urban agglomeration in 2008-2016*

Period	ΔC	ΔC_{Bi}	ΔC_D	ΔC_I	ΔC_K
2008-2011	↑	-	-	+	+
2011-2012	↓	-	-	+	+
2012-2013	↑	-	-	+	+
2013-2015	↓	-	-	+	+
2015-2016	↑	-	-	+	+
		Not obvious	Obvious	Obvious	Not obvious

http://www.aloki.hu ● ISSN 1589 1623 (Print) ● ISSN 1785 0037 (Online)
DOI: http://dx.doi.org/10.15666/aeer/1704_94939504

From the time series, the contribution value of each factor is increasing year by year. Besides the negative growth of industrial structure after 2014, there is still room for adjustment. The growth rate of the contribution of the four driving factors to the urban carbon emission has gradually slowed down, but the growth rate gap is relatively obvious, of which the energy intensity contribution value has the fastest growth, with an average annual growth rate of 62.52%. Therefore, in 2013, its contribution value quickly exceeded the industrial structure and gradually had a gap, effectively suppressing the increase of carbon emissions of the urban agglomeration, which indicates that giving enough attention to energy consumption can effectively promote the process of green development.

Decoupling analysis

From *Table 5*, the overall results show that the decoupling elasticity of the Circum-Changsha-Zhuzhou-Xiangtan urban agglomeration of China was mainly declining, with strong decoupling in 2011-2012, 2013-2014 and 2014-2015, that is, the carbon emission is decreasing with the economic growth, but weak decoupling in the rest of the years, which indicates that the overall economic growth rate is slightly higher than the carbon emission growth rate, and there is a strong decoupling trend.

Table 5. *Decoupling status of Circum-Changsha-Zhuzhou-Xiangtan urban agglomeration in 2008-2016*

City	E/S	2008-2009	2009-2010	2010-2011	2011-2012	2012-2013	2013-2014	2014-2015	2015-2016
Chang	E	0.6048	0.4357	0.5588	0.1536	0.6658	-0.3655	0.2734	1.4824
Sha	S	W.D	W.D	W.D	W.D	W.D	S.D	W.D	E.N.D
Zhu	E	0.3767	0.6397	0.0470	0.0796	0.4271	-1.1267	-1.3301	0.5989
Zhou	S	W.D	W.D	W.D	W.D	W.D	S.D	S.D	W.D
Xiang	E	1.7249	0.0253	0.5722	-0.4813	0.0212	-0.6897	-1.3624	-0.0452
Tan	S	E.N.D	W.D	W.D	S.D	W.D	S.D	S.D	S.D
Heng	E	1.0532	0.6965	0.7723	-0.9595	0.1059	-1.2691	-1.0552	-0.1453
Yang	S	E.C	W.D	W.D	S.D	W.D	S.D	S.D	S.D
Yue	E	-0.1865	0.3940	1.0166	0.5749	0.6323	-1.0038	0.6645	0.1260
Yang	S	S.D	W.D	E.C	W.D	W.D	S.D	W.D	W.D
Chang	E	0.7776	0.9752	0.6518	-0.4805	0.9637	-0.4340	-0.2543	-1.0754
De	S	W.D	E.C	W.D	S.D	E.C	S.D	S.D	S.D
Yi	E	0.9668	0.6350	0.7119	-0.4823	0.9568	-0.0705	0.2528	0.3337
Yang	S	E.C	W.D	W.D	S.D	E.C	S.D	W.D	W.D
Lou	E	1.7686	0.6999	0.6472	0.0717	0.7693	0.4934	-0.3180	0.0324
Di	S	E.N.D	W.D	W.D	W.D	W.D	W.D	S.D	W.D
Total	E	0.6217	0.4618	0.6515	-0.02482	0.52295	-0.42865	-0.1989	0.15586
	S	W.D	W.D	W.D	S.D	W.D	S.D	S.D	W.D

"E"stands for Elasticity; "S" stands for Status; "W.D"stands for Weak negative decoupling; "S.D"stands for Strong decoupling; "E.N.D"stands for Expansion negative decoupling; "E.C"stands for Expansion connection

By cities of the Circum-Changsha-Zhuzhou-Xiangtan urban agglomeration of China, there have been four strong decoupling phenomena in Changde and Hengyang, in which Hengyang was in the state of expansion connection during 2008-2009, that is, its carbon emission increased faster than the economic growth. It has been in a strong decoupling state since 2013. Changsha, Zhuzhou and Xiangtan, as the core regions of the Circum-

http://www.aloki.hu ● ISSN 1589 1623 (Print) ● ISSN 1785 0037 (Online)
DOI: http://dx.doi.org/10.15666/aeer/1704_94939504

Changsha-Zhuzhou-Xiangtan urban agglomeration, are not in an ideal state of decoupling, and Changsha's carbon emission increased rapidly, with a negative decoupling of expansion between 2015 and 2016, that is, the growth rate of carbon emissions was far faster than the economic growth rate. In the later development, we should pay attention to the environmental governance. After 2013, Zhuzhou and Xiangtan mainly show a strong decoupling trend, that is, the correlation between economic development and carbon emission will gradually weaken, which is more conducive to energy conservation and emission reduction. The decoupling in Yiyang and Loudi was not satisfactory. The economic growth rate was slightly higher than the carbon emission growth rate, but lower than the average level of the urban agglomeration. According to the "inverted-U" curve between carbon emission and per capita GDP in *Figure 2*, Yiyang and Loudi are still in the increasing stage of "inverted-U" curve, so the two cities should first focus on promoting the economy, only after the economic development to a certain level, is there enough funds and foundation to effectively promote energy-saving and emission reduction.

Conclusions and suggestions

In this paper, the carbon emission of the Circum-Changsha-Zhuzhou-Xiangtan urban agglomeration of China is decomposed into three parts: agriculture, industry, and transportation. At the same time, based on the panel data from 2008 to 2016, this paper uses LMDI decomposition method to calculate the direction and contribution value of the different factors that drive the carbon emission change of the urban agglomeration. Finally, the decoupling elasticity index is used to calculate the decoupling elasticity of each city and the urban agglomeration as a whole, and the following conclusions are drawn:

First of all, the annual growth rate of carbon emission of the Circum-Changsha-Zhuzhou-Xiangtan urban agglomeration is decreasing gradually though its carbon emission is rising and the fluctuation of industrial carbon emission is the most obvious. Therefore, the carbon emission of the whole city has an alternatively positive and negative growth trend after 2011. According to the results of the EKC curve, it is found that the carbon emission and the per capita GDP have a relatively obvious "inverted-U" curve, that is, when the per capita GDP reaches the stagnation point of 5.073 of the curve, with the increase of per capita GDP, the carbon emission shows a downward trend instead. Second, from the driving factors, industrial structure and energy intensity have the restraining effect on the total carbon emission, while economic development and population scale have driven the growth of the carbon emission, of which the driving role of economic development is the most significant and is the main reason for the increase in the carbon emission. The restraining effect of energy intensity gradually shows up in the later period and exceeds the negative driving effect of industrial structure, as the main factor that promotes the decrease in the carbon emission intensity. Finally, the overall decoupling of the Circum-Changsha-Zhuzhou-Xiangtan urban agglomeration is good and its carbon emission growth is always weaker than economic growth in the research period. The elasticity decoupling result in Hengyang and Changde is better, and their economic development and carbon emission both show strong decoupling trend but still have great room in Loudi and Yiyang. However, in Changsha, Zhuzhou and Xiangtan, as the core region of the urban agglomeration, the effect of decoupling is not obvious though the level of the economic development is

http://www.aloki.hu ● ISSN 1589 1623 (Print) ● ISSN 1785 0037 (Online)
DOI: http://dx.doi.org/10.15666/aeer/1704_94939504

relatively high, and the economic development is only slightly faster than the growth of carbon emission. In the later development, more emphasis should be placed on energy conservation and emission reduction

In the future research, there is still something worthy of further exploration. First of all, for the research objectives, this paper only studies the Circum-Changsha-Zhuzhou-Xiangtan urban agglomeration, which includes eight cities, the results are not universal; the range of the research objectives can be expended in the future. And then, due to the lack of some data, the calculation of carbon emissions is not comprehensive, for example, date of agricultural film and pesticides have not found. Finally, for the driving factors of carbon emissions, this paper only chooses the most significant four factors according to the research of a large amount of literatures, which can be extended for more measurement. Under such circumstances, this paper can only be regarded as a rough evaluation and preliminary study on the carbon emissions of the Circum-Changsha-Zhuzhou-Xiangtan urban agglomeration. As for the more in-depth content and more precise conclusions, it needs to be enriched in the future research. At the same time, I also hope that the research in this paper can be used as a reference for the research work of other scholars, and can provide useful thinking for the green development and practical work of urban agglomerations.

Acknowledgements. The authors would like to thank the referee for his helpful advice and comments. This is a project supported by Hunan Provincial Association of Social Sciences think tank project (ZK2019031) and Scientific Research Fund of Hunan Provincial Education Department (16A079).

REFERENCES

[1] Albrecht, J., François, D., Schoors, K. (2002): A Shapley decomposition of carbon emissions without residuals. – Energy Policy 30(9): 727-736.
[2] Cao, H. J., Song, S. L., Du, Y. B., Chen, P. (2011): Evaluation method and application for carbon emissions of machine tool based on life cycle assessment. – Computer Integrated Manufacturing Systems 17(11): 2432-243.
[3] Cao, J. W., Cao, L. J. (2016): Research on measurement and effecting factors of agricultural carbon emission in Jiangxi province. – Ecological Economy 32(7): 66-68+167.
[4] Feng, J., Zhang, S., Wang, T. (2019): Analysis of China's interprovincial land use carbon emissions and its influencing factors. – Statistics and Decision 35(5): 141-145.
[5] Gong, Y. Y. (2015): Carbon emission calculation and influential factor decomposition of the transportation sector in Wuhan city. – China Population, Resources and Environment 25(S1): 470-474.
[6] Grossman, G. M., Krueger, A. B. (1995): Economic growth and environment. – The Quarterly Journal of Economic 110(2): 353-377.
[7] Gu, B. H., Tan, X. C., Chi, H., Wang, Y. Y. (2013): A carbon dioxide reduction potential model for chemical industry. – Chinese Journal of Management Science 21(5): 141-148.
[8] He, J. C., Li, Y. Z. (2016): Estimation of CO_2 emission of locomotives in China during 1975-2005. – Advances in Climate Change Research 6(1): 35-39.
[9] He, Y., Cai, M. T. (2016): Decoupling relationship between economic growth and resource environment in Beijing-Tianjin-Hebei region. – Journal of Beijing Institute of Technology (Social Sciences) 18(5): 33-41.
[10] He, Y. Q. (2012): The measurement and application of industry complete carbon emissions. – Statistical Research 29(3): 67-72.

http://www.aloki.hu ● ISSN 1589 1623 (Print) ● ISSN 1785 0037 (Online)
DOI: http://dx.doi.org/10.15666/aeer/1704_94939504

[11] Li, J., Guo, J., Yuan, Q. M. (2018): Forecast of energy demand and policy impact under the background of the coordinated development in Beijing-Tianjin-Hebei Region. – Journal of Arid Land Resources & Environment 32(5): 5-11.
[12] Li, Y. M., Zhang, Y. G. (2016): Spatial decomposition analysis of factors affecting China's carbon emissions. – Journal of China University of Geosciences (Social Science) 16(3): 73-85.
[13] Ning, X. J., Zhang, J. P. (2014): Spatial and temporal characteristics of carbon emissions from urban resident travel in Zhengzhou. – Resource Science 36(5): 1021-1028.
[14] Pan, W., Hu, C. (2019): Study on carbon emissions decomposition of energy consumption in different industries in China. – Statistics and Decision 35(4): 141-145.
[15] Peeters, P., Dubois, G. (2010): Tourism travel under climate change mitigation constraints. – Journal of Transport Geography 18(3): 447-457.
[16] Sun, Y. F., Zhou, M. (2017): Decoupling and driving factors analysis between the energy carbon emissions and economic growth in China. – Review of Economy and Management 33(6): 21-30.
[17] Tapio, P. (2005): Towards a theory of decoupling: degrees of decoupling in the EU and the case of road traffic in Finland between 1970 and 2001. – Transport Policy 12(2): 137-151.
[18] Tian, H., Ding, C. A. (2018): The spatial and temporal differences of carbon emissions in regional Tourism—a case study of Shandong province. – Journal of Beijing Institute of Technology (Social Science) 20(6): 45-54.
[19] Wang, J., Zhu, C. Z. (2018): international comparison of decomposition factors and decoupling effects of agricultural carbon emissions. – Statistics and Decision 34(11): 104-108.
[20] Wang, Y. B., He, Y. P. (2018): Study on greenhouse gas emission from urban waste disposal and influence mechanism. – Journal of Xi'an Jiaotong University (Social Sciences) 38(1): 60-70.
[21] Xia, D. J., Ren, Y. L., Shi, L. F. (2010): Measurement of life-cycle carbon equivalent emissions of coal-energy chain. – Statistical Research 27(8): 82-89.
[22] Zhang, Y., Xiong, X. P., Kang, Y. B. (2015): Study on influencing factors and carbon emission reduction pathway for transportation sector of China. – Environmental Protection 43(11): 54-57.
[23] Zhao, Y. W., Zuo, H. B., She, X. F., Wang, G., Xue, Q. G., Wang, J. S. (2019): Case study on calculation method of carbon dioxide emission in iron and steel industry. – Nonferrous Metals Science and Engineering 10(1): 34-40.

http://www.aloki.hu ● ISSN 1589 1623 (Print) ● ISSN 1785 0037 (Online)
DOI: http://dx.doi.org/10.15666/aeer/1704_94939504

THE EFFECT OF METEOROLOGICAL FACTORS ON ROAD TRAFFIC INJURIES IN BEIJING

SONG, X.[1#] – ZHAO, X.[2#] – ZHANG, Y.[2] – LI, Y.[3] – YIN, C.[2] – CHEN, J.[4*]

[1]*School of Management, Lanzhou University, Lanzhou City, China*

[2]*Department of Neurology, The General Hospital of the People's Liberation Army, Beijing, China*

[3]*Department of Neurology, The First Affiliated Hospital of Zhengzhou University, Zhengzhou, China*

[4]*Health Bureau, Logistics Support Department of the Central Military Commission, Beijing, China*

[#]*These authors have contributed equally to this research and should be considered as co-first authors.*

**Corresponding author*
e-mail: gafm71@163.com

(Received 16th Apr 2019; accepted 22nd May 2019)

Abstract. The goal of this study is to establish the relationship between RTI and the meteorological factors, and make a precise prediction of the occurrence of RTI in China. The statistical data was collected from four tertiary hospitals in Beijing from 2008 to 2012. The association was analyzed using a backward propagation-artificial neural network model (BP–ANN) regression model (built by Matlab) which has three layers (including one hidden layer). Based on the SPSS 20.0 platform, regression analysis was used to evaluate the effect of meteorological factors on RTI. The results show that the most significant factors are atmospheric pressure, temperature, precipitation and sunshine duration, whereas wind speed is less significant. The combination of long sunshine duration, high temperature, low pressure and high humidity is the high-risk condition that leads to RTI. The coefficient ($r = 0.7199$) obtained by the PB neural network is much higher than the coefficient ($r = 0.427$) obtained by the Stepwise Regression Model. Meteorological factors have a certain effect on traffic injury severity. And the BP–ANN model is a quite precise prediction model for RTI, and this research can provide technical support for the improvement of forecasting and early warning of RTI, in further.
Keywords: *risk factors, traffic accident, regression analysis, artificial neural network model, risk warning*

Introduction

Road traffic injuries (RTI) are a major global public security issue (Toroyan, 2009). According to a recent report of the World Health Organization (WHO) in May 2015, 1.24 million people are killed by RTIs annually all over the world. This is the leading cause of death in the 15-29 age group. About 91% of the deaths occur in the low and middle-income countries, while these countries only occupy half of vehicles in the world. It is estimated that RTI will cause 1.9 million deaths from fatal accidents in 2020, and RTI will become the fifth leading cause of death in 2030 (World Health Organization, 2015). For China, the largest developing country in the world, the annual number of deaths caused by RTI increased from about 50,000 in the mid-1980s to more than 100,000 at present (Zhang, et al., 2007; Dong and Peng, 2012). The mortality of

http://www.aloki.hu ● ISSN 1589 1623 (Print) ● ISSN 1785 0037 (Online)
DOI: http://dx.doi.org/10.15666/aeer/1704_95059514

China is very moderate compared to the average value of world. However, China has the largest population in the world, which makes the death toll huge and result in heavy disease burden and enormous medical expenditure. RTI have become one of the leading causes of unintentional death in China (Gao et al., 2013). Beijing, as the capital of China, has the largest number of vehicles in the country, so, the research about RTI is indispensable.

Thus far, research on RTI focused primarily on human factors, mechanical factors, and road facilities (Evans, 2001; Bendak, 2005; Nakahar et al., 2005; Javouhey et al., 2006; Morgan and Mannering, 2011). However, meteorological factors have received little attention. Nevertheless, the occurrence of RTI is the combined result of human factors, mechanical factors, road facilities and meteorological factors. The change of meteorological factor will have an effect on the other three, leading to the occurrence of RTI. Meteorological factors can cause RTI by affecting mental and psychological state, reaction time, vision, vehicle flow and speed, as well as road conditions (Majdzadeh et al., 2008; Abe et al., 2008; Naci et al., 2009; Gill and Goldacre, 2009; Cools and Moons, 2010; Akin et al., 2011; Kim et al., 2012; Kashani et al., 2012; Grjibovski et al., 2013). For example, precipitation can make road slippery, reduce the friction between vehicles and roads, and increase the difficulty of operating vehicles. Rainfall can reduce the clarity of the windshield of the vehicle. Rainy days will also cause poor visibility of the surrounding environment, affecting both drivers' and pedestrians' vision. Therefore, it is necessary to study the influence of meteorological factors on RTI for effective prevention of traffic injury.

Based on statistical data collected from four tertiary[1] hospitals in Haidian District, Beijing from 2008 to 2012, the effect of gender, age, date and the effect of meteorological factors were studied using regression analysis in order to determine the main influencing factors on RTI. These factors were used as the predictors in the construction of a backward propagation-artificial neural network model (BP–ANN) with Matlab. BP-ANN is one of the most successful algorithms for the machine learning study which is originally inspired by modeling biological neural systems (more details in the "Model structure" section). Stephan (Stephan et al., 2003) used BP-ANN to create the risk evaluation to prostate cancer. In the study it was found that the ANN technique can be applied to the problems which cannot be solved by any other effective way, and it is particularly suited to evaluate the risk of cancer. In fact, the BP-ANN model can not only used to evaluate the disease, but also to some other significant field. Therefore, we introduced BP-ANN here to make a precise prediction of the occurrence of RTI and provide technical support for decreasing RTI and reducing economic loss.

Resources and methods

Resources

In this study, statistical data of 1825 groups from Jan 1st, 2008 to Dec 31st, 2012 were collected from four tertiary hospitals in Haidian District, Beijing. The data of each group consist of the number of RTI, pressure, humidity, temperature, sunshine duration, rainfall and wind speed in Haidian District. Those meteorological data mentioned above

[1]Tertiary hospital is the highest level of Chinese hospital grade, with more than 501 beds, and provides high-level specialist medical services, performs higher education and scientific research tasks in several regions.

http://www.aloki.hu ● ISSN 1589 1623 (Print) ● ISSN 1785 0037 (Online)
DOI: http://dx.doi.org/10.15666/aeer/1704_95059514

were provided by the National Scientific Data Sharing Platform for Population and Health. All the collected data were divided and analyzed according to three dimensions: the age and gender of each injured person, weekly number of RTI, and the value of the corresponding meteorological data (average values for each week).

Regression analysis

Based on the SPSS 20.0 platform, regression analysis was used to evaluate the effect of meteorological factors on RTI. Major influencing factors were determined through the comparison of the Pearson correlation coefficient (r) and its statistical significance (p) between meteorological factors and RTI. Moreover, the correlation between RTI and the different meteorological factors (such as temperature, relative humidity, pressure, precipitation, sunshine time and wind speed, respectively) were analyzed to determine the main influencing factors.

Construction of the BP-ANN model

Data set

All the data were used to construct the BP–ANN model with Matlab. 195 randomly selected groups were used as the training data set and the other 65 groups were used as the test data to evaluate the performance of the optimal BP–ANN model. The large difference between the dimension and the data values of the meteorological factors might affect the forecasting performance of the BP–ANN model. Therefore, the meteorological factors were employed as the independent variables, including atmospheric pressure, atmospheric temperature, precipitation and sunshine duration. And the gaps of each level of these independent variables in the model were 5 hPa, 5 °C, 2 mm and 2 h respectively. Meteorological parameters are input variables as while as the weekly RTI are output variables.

Model structure

Three parts mainly composed of BP-ANN model: an input layer, a hidden layer and an output layer. There are several nodes in each layer mapping the input vector (in the input layer) to the output vector (in the output layer) by a continuingly updating weight vector (in hidden layer). The weight is updated by each iteration error (the difference between the output value and the real value). The model iterates until the prediction matches the real scenario. BP-ANN is a data-based research method. It uses real world data as the input training set to predict output values in the future without any human experiences.

In our study, the data in the input layer (4~5 neurons) were selected from those meteorological factors which directly or indirectly affect RTI, based on the regression analysis. A suitable number of hidden neurons should be determined during model construction. The number of RTI was chosen as the output layer in the BP model.

The tansig and purelin were selected as transfer functions in the hidden layer and output layer, respectively. The traingdx, an adaptive training function with momentum, was used for network training. This algorithm is able to adjust the learning rate and the incidental momentum automatically, avoiding local minima. Moreover, it accelerates the convergence rate considerably (Shi et al., 2009).

http://www.aloki.hu ● ISSN 1589 1623 (Print) ● ISSN 1785 0037 (Online)
DOI: http://dx.doi.org/10.15666/aeer/1704_95059514

Evaluation of model performance

We used the mean squared error (MSE), one of the most widely used evaluation indices of model performance between the monitored and predicted values, to test the prediction accuracy of our BP–ANN model: smaller values of the MSE represent better performance of the model. Another common evaluation index is the correlation coefficient (r), a measure of the relationship between monitored and predicted values. A higher r indicates better performance of the BP–ANN model.

Results and discussion

Influence of different factors on RTI

Influence of gender and age on RTI

Summary statistics of the age and gender distribution of outpatients from 2008 to 2012 (1,827 days) are shown in *Table 1*. In total, 6,295 hospital admissions for RTI were recorded, and the value was the statistical description of daily value of the patient demographics.

Table 1. *Summary statistics of the age and gender distribution of outpatients*

Term		Mean	SD	Min	Median	Max	IQR
Gender	Male	2.10	1.48	0	2	10	2
	Female	1.35	1.28	0	1	20	2
Age	1-17	0.29	0.15	0	1	4	1
	18-40	1.68	0.97	0	3	10	5
	41-65	1.25	0.83	0	3	13	4
	>65	0.22	0.12	0	1	11	2

SD: standard deviation, IQR: inter quartile range

It is seen that there were approximately 4 RTI per day, on average. The number of male traffic injury patients (2.10 cases per day) was larger than that of female (1.35 cases per day). The ratio of male to female is 1.56:1. In the 1-17 age group, 0.29 cases of traffic injury occurred, on average, every day. In the 18-40, 41-65 and 65 or over age groups, the daily traffic injury cases were, on average, 1.68, 1.25 and 0.22, respectively. The maximum mean value of the youth group is 1.35 times that of the adult group, 5.79 times that of the adolescent group and 7.64 times that of the aged group. The result is similar to what was reported by Yu and Wang et al. (2004), who discovered that young male adults, as the primary labor force, are more exposed to traffic injury. The relationship between these meteorological factors and RTI will be analyzed in next.

Influence of the days of the week and of mental state

The variation of the number of RTI is indicated in *Table 2*. From 2008 to 2011, the number of outpatients was rising and the growth rate was 9.73%, 9.20% and 4.40%, respectively. Comparing with the figures corresponding to the periods 2008-2009 and 2009-2010, during the period 2010-2011 RTI decreased sharply. Until 2012, the number of outpatients had fallen to 1125 cases and the decline rate was 27.38%. The reason

http://www.aloki.hu ● ISSN 1589 1623 (Print) ● ISSN 1785 0037 (Online)
DOI: http://dx.doi.org/10.15666/aeer/1704_95059514

might be that the "vehicle purchase restriction policy" introduced in Beijing in 2011, which greatly reduced the private car purchases. On Monday, Wednesday, Saturday and Sunday, the average total number of outpatient visits is similar: 182, 186, 179, 183 cases respectively. The number of RTI patients is 2.5% higher on Sunday than that of Saturday, however, the chi-square test showed that the difference is statistical meaningless. In contrast, it reached a peak (202 cases) on Friday and a valley (163 cases) on Tuesday. The data above were divided into 2 parts. One was from Monday to Thursday and the other was from Friday to Sunday. The corresponding averages were 173.6 and 188.2, respectively. This is similar to the result of "a week working rhythm", by D. S. Moskowitz. The research concluded that people tend to be more energetic at the beginning of the week and then gradually get fatigued. Especially on Tuesday, people are more controlled, efficient and concentrated on work. In contrast, they are more reckless on Friday. It is reported that on Friday, drivers hasten to participate in entertainment activities and alcohol consumption is higher. This leads to a 13% higher occurrence rate of RTI.

Table 2. *Comparison of RTI on different days in one week*

Year	Mon	Tue	Wed	Thu	Fri	Sat	Sun	Total
2008	167	147	171	157	184	145	152	1123
2009	155	135	197	187	201	184	185	1244
2010	202	205	187	158	227	194	197	1370
2011	216	176	213	178	236	209	205	1433
2012	169	150	160	142	164	162	178	1125
Average	181.8	162.6	185.6	164.4	202.4	178.8	183.4	1259

The influence of drinking and medicine should be considered in this study. But according to the information gathered from the emergency doctors who collected the data, the RTI caused by drunk driving only occupies the proportion very few. Meanwhile, Saha et al. (2016) pointed out that the odds of risk factors (alcohol, drug involvement and so on) were low, among these fatalities associated with adverse weather conditions. So it can be considered that the effect of drinking and medicine are minimal.

Determination of critical meteorological factors

To study the effect of meteorological factors on RTI in Beijing, the Spearman Correlative Analysis Method was employed. It was found that performance was superior when weekly data was used. Comparing to daily data (level of meteorological factor), it was able to eliminate strong "Weekly Effect" of RTI. The correlation among RTI, pressure, temperature, relative humidity, precipitation, sunshine duration and wind speed, on weekly basis, is shown in *Table 3*.

It was shown that RTI have a strong positive correlation with temperature, precipitation and sunshine duration and were negatively correlated with pressure. No correlation of statistical significance with wind speed was obtained.

According to Hani et al. (2009), as temperature increases, the sensitivity of body decreases, the heart rate increases and the driving and physical capacity decrease. Moreover, temperature increase could cause debility and that could seriously affect

http://www.aloki.hu ● ISSN 1589 1623 (Print) ● ISSN 1785 0037 (Online)
DOI: http://dx.doi.org/10.15666/aeer/1704_95059514

drivers (Cool and Moons, 2010; Keay and Simmonds, 2005). As reported previously (Brijs et al., 2006; Bossche and Wets, 2005), temperature is positively correlated with vehicle flow and speed, which are the important factors in RTI. This research showed that RTI are positively correlated with sunshine duration, as in Brijs et al. (2006). A longer sunshine duration will lead to the increases of air temperature. On the one hand, high atmospheric temperature will induce drivers' persistent excitability of nervous system; they will get tired more easily than usual. On the other hand, the longer sunshine show that the daytime is longer than night time, people prefer to drive on the daytime. Therefore, RTI increase accordingly.

Table 3. *Spearman correlations between RTI and meteorological factors*

	RTI	**Temperature (°C)**	**Relative humidity (%)**	**Pressure (hPa)**	**Precipitation (mm)**	**Sunshine time (h)**	**Wind speed (m/s)**
RTI	1.000						
Temperature (°C)	0.103**	1.000					
Relative humidity (%)	0.033**	0.394**	1.000				
Pressure (hPa)	-0.079**	-0.872**	-0.375 **	1.000			
Precipitation (mm)	0.043**	0.199**	0.471**	-0.258**	1.000		
Sunshine time (h)	0.084**	0.175**	-0.561**	-0.084**	-0.363**	1.000	
Wind speed (m/s)	0.036	-0.026*	-0.477**	0.013	0.025*	0.265**	1.000

*$P < 0.05$; **$P < 0.01$

In this study, it is shown that there is a positive correlation between the precipitation and RTI (OR = 0.148, $p < 0.05$). Precipitation can reduce the friction coefficient, the visibility of the surroundings and the sharpness of the windshield (Qiu and Nixon, 2008). Moreover, it may influence the judgment of drivers and pedestrians (Andrey, 2010). Wang et al. (2014) pointed out that rain and snow are the two leading causes of traffic accidents in Gansu province, China. They account for 97.58% of the traffic accidents caused by meteorological causes. Some studies have confirmed that precipitation is an important risk factor (Bendak, 2005; Zhang et al., 2000; Warrell and Univ, 2012), whereas others assert that rain may in fact reduce the risk of car accidents, as drivers are forced to drive at lower speeds (Hani et al., 2009; Zhang et al., 2000). This may be attributed to regional differences.

In this study, it is shown that the number of outpatients is negatively correlated with pressure. Warrell and others found that the emotions of people and animals could be affected by low pressure, with symptoms such as chest distress, shortness of breath and irritability (Warrell and Univ, 2012; Franka and Rupprecht, 2011; Alice et al., 2011). The combination of high temperature, low pressure, and high humidity has a negative effect on physical capacity; therefore drivers should be particularly attentive to the pedestrians.

In any event, atmospheric pressure, temperature, precipitation and sunshine duration may be considered as the major meteorological factors that influence RTI in Beijing.

Prediction of RTI using a BP–ANN model

An increase of the number of hidden neurons can improve prediction accuracy. However, this leads to a longer learning process and reduced ability for generalization (May and Sivakumar, 2009; Sadrzadeh et al., 2009). In contrast, a decrease in the number of hidden neurons will result in smaller fault tolerance and capacity to identify

http://www.aloki.hu ● ISSN 1589 1623 (Print) ● ISSN 1785 0037 (Online)
DOI: http://dx.doi.org/10.15666/aeer/1704_95059514

the new data that will be imported (Maier and Jain, 2010). Thus, the number of hidden neurons should be suitably chosen in order to enhance the prediction accuracy of the BP–ANN model. In this paper, a comparison of the value of the MSEs of the true value and the forecasting value of the test data with different number of hidden neurons (3~12) in the hidden layer was made, in order to obtain the optimal performance of the BP–ANN model. The result is shown as *Figure 1*. When the number of neurons was 6 in the hidden layer, the minimum MSE (which was obtained after 30 parallel calculations) of the true and the forecasting value was 0.48. This signified optimal performance of the BP–ANN model.

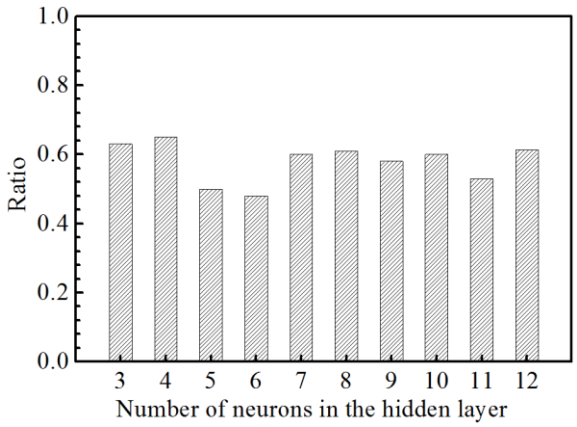

Figure 1. *Ratio of MSEs of the true value to forecasting value vs. different number of neurons in the hidden layer*

Figure 2a and *b* show the relationship between the true value and the forecasting value of the test data with optimal performance of the BP–ANN model. Since our investigation of the RTI was conducted in Beijing, a relatively high coefficient ($r = 0.7199$) was obtained. This is much higher than the coefficient ($r = 0.427$) obtained using the Stepwise Regression Model (Ji, 2015). Thus, the BN-ANN model constructed in this work was capable of making an effective prediction of the RTI when using the average pressure, temperature, rain and sunshine duration as the input data.

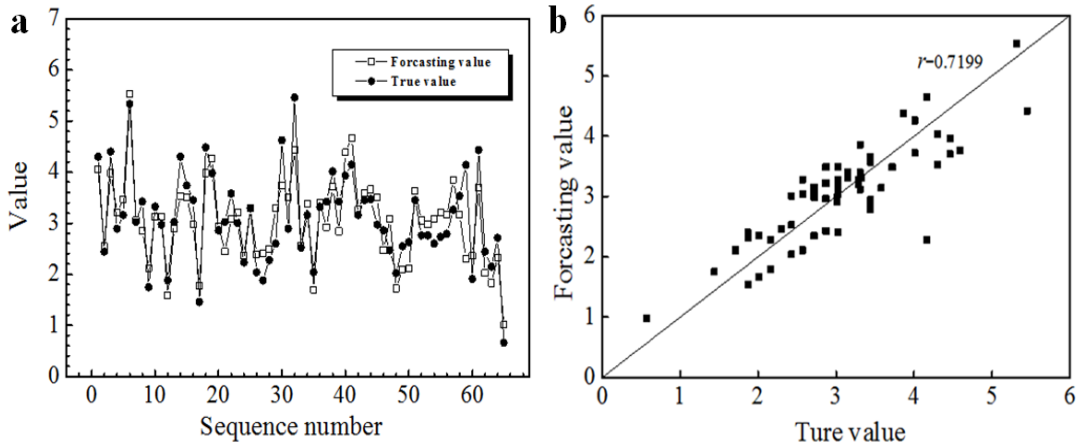

Figure 2. *Regression plots (a) and comparison (b) of the true and forecasting values of the test data of RTI*

http://www.aloki.hu ● ISSN 1589 1623 (Print) ● ISSN 1785 0037 (Online)
DOI: http://dx.doi.org/10.15666/aeer/1704_95059514

Moreover, the model performed better when it was used for the prediction of RTI in the interval between 2 to 4. This is probably due to the relatively limited data set and the small interval used for the construction of the BP–ANN model. Therefore, effort should be made to supply more data to the prediction model.

Conclusions

In this study, A BP–ANN regression model is investigated to analyze the relationship between the meteorological factors and RTI. The main conclusions can be summarized as below:

1) Young males (18 to 40 years old) own the highest probability of occurrence of RTI; and Friday is day with highest frequency of RTI in a week.

2) Furthermore, meteorological factors have a certain effect on traffic injury severity. The most significant factors are atmospheric pressure, temperature, precipitation and sunshine duration, whereas wind speed is less significant. The combination of long sunshine duration, high temperature, low pressure and high humidity is the high-risk condition that leads to RTI.

3) It can be concluded that the BP–ANN model is a quite precise prediction model for RTI, Furthermore, this research can provide technical support for the improvement of forecasting and early warning of RTI, in further.

Acknowledgements. This research is supported by the National Key R&D Program of China (2017YFC1307700).

REFERENCES

[1] Abe, T., Tokuda, Y., Ohde, S., Ishimatsu, S., Nakamura, T., Birrer, R. B. (2008): The influence of meteorological factors on the occurrence of trauma and motor vehicle collisions in Tokyo. – Emergency Medicine Journal 25(11): 769-772.

[2] Akin, D., Sisiopiku, V. P., Skabardonis, A. (2011): Impact of weather on traffic flow characteristics of urban freeways in Istanbul. – Procedia - Social and Behavioral Sciences 16: 89-99.

[3] Alice, L., Green, L., Dunn, J. R. (2011): Rabies epidemiology, risk assessment, and pre- and post exposure vaccination. – The Veterinary Clinics of North America. Exotic Animal Practice 14(3): 507-518.

[4] Andrey, J. (2010): Long-term trends in weather-related crash risk. – Journal of Transport Geography 18: 247-258.

[5] Bendak, S. (2005): Seat belt utilization in Saudi Arabia and its impact on road accident injuries. – Accident Analysis & Prevention 37: 367-371.

[6] Bossche, F., Wets, G. (2005): Role of exposure in analysis of accidents: a Belgian case study. – Journal of the Transportation Research Board 1908: 96-103.

[7] Brijs, T., Offermans, C., Hermans, E. (2006): Impact of weather conditions on road board safety investigated on hourly basis. – Transportation Research Board 85th Annual Meeting, Washington, DC.

[8] Cools, M., Moons, E. (2010): Assessing the impact of weather on traffic intensity. – Weather Clim Soc 2: 60-68.

[9] Dong, X. M., Peng, L. (2012): The development of intervention on traffic accident injury. – Chinese Journal of Public Health 28: 569-571.

http://www.aloki.hu ● ISSN 1589 1623 (Print) ● ISSN 1785 0037 (Online)
DOI: http://dx.doi.org/10.15666/aeer/1704_95059514

[10] Evans, L. (2001): Female compared with male fatality risk from similar physical impacts. – The Journal of Trauma 50: 281-288.
[11] Franka, R., Rupprecht, C. E. (2011): Treatment of rabies in the 21st century: curing the incurable. – Future Microbiol 6(10): 1135-1140.
[12] Gao, J. H., Zhu, Y., Li, L. P. (2013): The association between meteorological factors and traffic injury sufferers admitted to a tertiary hospital in Shantou City. – Inj Med 2: 26-31.
[13] Gill, M., Goldacre, M. J. (2009): Seasonal variation in hospital admission for road traffic injuries in England: analysis of hospital statistics. – Injury Prevention 15(6): 374-378.
[14] Grjibovski, A. M., Kosbayeva. A., Menne, B. (2013): The effect of ambient air temperature and precipitation on monthly counts of salmonellosis in four regions of Kazakhstan, Central Asia, in 2000-2010. – Epidemiology and Infection 2(3): 1-8.
[15] Hani, S., Dong, J., Jiwon, K. (2009): Incorporating Weather Impacts in Traffic Estimation and predication system. – U.S. Department of Transportation, Research and Innovative Technology Administration, Washington, DC.
[16] Javouhey, E., Guerin, A. C., Chiron, M. (2006): Incidence and risk factors of severe traumatic brain injury resulting from road accidents: a population-based study. – Accident Analysis & Prevention 38(2); 225-233.
[17] Ji, C. H. (2015): Analysis of trauma incidence characteristics in Beijing and its relationship with meteorological conditions. – Lanzhou University 6.
[18] Kashani, A. T., Shariat-Mohaymany, A., Ranjbari, A. (2012): Analysis of factors associated with traffic injury severity on rural roads in Iran. – Journal of Injury & Violence Research 4(1): 36.
[19] Keay, K., Simmonds, I. (2005): The association of rainfall and other weather variables with road traffic volume in Melbourne, Australia. – Accident Analysis & Prevention 37(1): 109-124.
[20] Kim, Y., Kim, H., Shin, S. D., Hong, Y. C. (2012): Different influence of outdoor temperature on traumatic and non-traumatic injuries. – Journal of Trauma and Acute Care Surgery 73(4): 944-949.
[21] Maier, H. R., Jain, A. G. (2010): Methods used for the development of neural networks for the prediction of water resource variables in river systems: current status and future directions. – Environmental Modelling and Software 25: 891-909.
[22] Majdzadeh, R., Khalagi, K., Naraghi, K., Motevalian, A., Eshraghian, M. R. (2008): Determinants of traffic injuries in drivers and motorcyclists involved in an accident. – Accident Analysis & Prevention 40: 17-23.
[23] May, D. B., Sivakumar, M. (2009): Prediction of urban storm water quality using artificial neural networks. – Environmental Modelling and Software 24(2): 296-302.
[24] Morgan, A., Mannering, F. L. (2011): The effects of road-surface conditions, age, and gender on driver-injury severities. – Accident Analysis & Prevention 43: 1852-1863.
[25] Naci, H., Chisholm, D., Baker. TD. (2009): Distribution of road traffic deaths by road user group: a global comparison. – Injury Prevention 15(1): 55-59.
[26] Nakahar, S., Chadbunchachai, W., Ichikawa, M., Tipsuntornsak, N., Wakai, S. (2005): Temporal distribution of motorcyclist injuries and risk of fatalitiesin relation to age, helmet use, and riding while intoxicated in KhonKaen, Thailand. – Accident Analysis & Prevention 37: 833-842.
[27] Qiu, L., Nixon, W. A. (2008): Effects of adverse weather on traffic crashes: systematic review and meta-analysis. – Transportation Research Record Journal of the Transportation Research Board 2055: 139-146.
[28] Sadrzadeh, M., Mohammadi, T. J., Ivakpour, J., Kasiri, N. (2009): Neural network modeling of Pb2+ removal from wastewater using electrodialysis. – Chemical Engineering and Processing 48(8): 1371-1381.
[29] Saha, S., Schramm, P., Nolan, A., Hess, J. (2016): Adverse weather conditions and fatal motor vehicle crashes in the United States, 1994-2012. – Environmental Health 15(1): 104.

http://www.aloki.hu ● ISSN 1589 1623 (Print) ● ISSN 1785 0037 (Online)
DOI: http://dx.doi.org/10.15666/aeer/1704_95059514

[30] Shi, Y., Zhao, X. T., Zhang, Y. M., Ren, N. Q. (2009): Back propagation neural network (BPNN) prediction model and control strategies of methanogen phase reactor treating traditional Chinese medicine wastewater (TCMW). – Journal of Biotechnology 144(1): 70-74.
[31] Stephan, C., Vogel, B., Cammann, H., Lein, M., Klevecka, V., Sinha, P., Kristiansen, G., Schnorr, D., Jung, K., Loening, S. A. (2003): An artificial neural network as a tool in risk evaluation of prostate cancer. Indication for biopsy with the PSA range of 2–20 microg/l. – Der Urologe Ausg A 42(9): 1221-1229.
[32] Toroyan, T. (2009): Global status report on road safety: time for action. – Inj Prev 15(4): 286.
[33] Wang, Y. S., Pu, S., Meng, L. X., Chen, C., Fang, Y. M. (2014): Analysis of meteorological effect of highway traffic accidents in Gansu. – Gansu Science and Technology 44(21): 25-28.
[34] Warrell, M. J., Univ, O. (2012): Current rabies vaccines and prophylaxis schedules: Preventing rabies before and after exposure. – Travel Medicine and Infectious Disease 10(1): 1.
[35] World Health Organization (2015): The 358th live report of WHO. – World Health Organization, Geneva.
[36] Yu, J. M., Wang, Y. C. (2004): Retrospective Study on Road Related Injury. – Journal of Tong Ji University 12: 513-516.
[37] Zhang, J., Lindsay, J., Clarke, K., Robbins, G., Mao, Y. (2000): Factors affecting the severity of motor vehicle traffic crashes involving elderly drivers in Ontario. – Accident Analysis and Prevention 32(1): 117-125.
[38] Zhang, X. J., Chen, Z. D., Hao, Y. C., Gao, S. X., Chen, Y. Q. (2007): Analysis of road traffic accident injury from 1951~2014 in China. – Chinese Journal of Public Health 23(10): 1214-1215.

http://www.aloki.hu ● ISSN 1589 1623 (Print) ● ISSN 1785 0037 (Online)
DOI: http://dx.doi.org/10.15666/aeer/1704_95059514

EFFECT OF METEOROLOGICAL FACTORS ON RESPIRATORY SYSTEM DISEASES IN FUNAN, CHINA

ZHAO, X. Y.[1] – ZHANG, Y.[1] – FAN, G. C.[2] – LI, Y. P.[3] – YIN, CH. Y.[1] – CHEN, J. Y.[4*]

[1]Department of Neurology, the General Hospital of the People's Liberation Army Beijing, China

[2]News Office of Lanzhou Public Security Bureau Lanzhou, China

[3]Department of Neurology, the First Affiliated Hospital of Zhengzhou University Zhengzhou, China

[4]Health Bureau, Logistics Support Department of the Central Military Commission Beijing, China

[*]Corresponding author
e-mail: kkn2oa@163.com

(Received 19th Apr 2019; accepted 17th May 2019)

Abstract. To explore meteorological and environmental impacts on human health, a distributed lag non-linear model and a generalized additive model were employed to study the exposure-response relationship between meteorological factors and respiratory system diseases from 2013 to 2016 in Funan, China. The results showed that the decline in patient numbers occurs in the high temperature seasons. At a short time lag, high temperature is a risk factor, but high temperature reduces the number of patients with respiratory system disease at long time lags. Low relative humidity (RH) increases the risk of respiratory system diseases, and largescale 48-hour temperature changes (ΔT48) increase the risk of disease for a whole range of lags. There is a remarkable correlation between morbidity and meteorological factors, with temperature minima corresponding to peaks in the number of patients. For low RH, the lag effect is obvious for the first 4 days; for higher RH, the effect is weak. A back-propagation artificial neural network model constructed in this study was capable of effectively predicting respiratory system disease, using average temperature, ΔT48, RH, and maximum wind speed as inputs.
Keywords: *temperature, relative humidity, respiratory system diseases, generalized addictive model, distributed lag nonlinear models*

Introduction

Due to their high morbidity and difficulty of prevention, respiratory system diseases are currently the fourth leading cause of death in Chinese cities (13.1%), and the third leading cause of death in villages (16.1%) (Chakraborty et al., 2014). Prevention of respiratory system diseases is still unsolved. From the perspective of disease prevention, meteorological factors are uncontrollable. There is no doubt, however, that predictable meteorological conditions affect the risk rate (RR) and criticality of respiratory system diseases to some degree, although the relevant research is quite limited (Winkelstein et al., 1968; Kim et al., 1996).

Respiratory system diseases are common and frequently occurring diseases that have been studied for a long time. In the international classification of diseases ICD-10 (a coding of diseases and signs, symptoms, abnormal findings, complaints, social circumstances, and external causes of injury or disease), beside diseases of the full

http://www.aloki.hu ● ISSN 1589 1623 (Print) ● ISSN 1785 0037 (Online)
DOI: http://dx.doi.org/10.15666/aeer/1704_95159528

respiratory system (J00-J99), there are two other subclasses, upper respiratory tract infections (URI) and lower respiratory tract infections (LRI) (Miyamoto et al., 2008; D'amato and Cecchi, 2008). Bull and Quayle (1982) argued that respiratory system diseases are affected by many factors, including but not limited to nutrition intake, climatic variation, and air quality. Ricciardolo et al. (2004) pointed out that the correlation between air contaminants (such as nitric oxide) and respiratory system diseases is strong, but that climate change is certain to affect air contamination even though no relevant research exists. Barreca (2012) found that extremely humid conditions increase the morbidity of respiratory system diseases; however, compare with extreme climate conditions, the study of changing trend of regular climate is more useful. Even though, the effects of meteorological factors on respiratory diseases are still unclear. And current knowledge which provided by experimental studies on the relationship is not sufficient (Kunst et al., 1993). Although the aforementioned studies have not fully clarified the relationship between meteorological elements and respiratory system diseases, fortunately, the most influential factors (such as the temperature and relatively humidity) are clearly known. Thus, quantitative research on the relationship between meteorological elements and respiratory system diseases is necessary.

In order to make such research meaningful, a representative sample is necessary. Funan county, situated in southeast China, is about 500 kilometers from the Yellow Sea. Funan has a standard temperate continental monsoon climate (Liu and Ding, 2010), with four distinct seasons. As this village has never been studied before, no urban heat island effect as well as over use of air conditioner, the influence of meteorological factors is more obvious, and differently from a city, the minimal size of the transient population reinforces the connection between patients and meteorological factors. Thus patient data concerning respiratory system diseases in Funan constitute a representative sample.

In this study, to aid in establishing and perfecting the health early-warning system, the relationship between meteorological elements and respiratory system diseases was systematically evaluated. A generalized additive model (GAM, widely applied inthe meteorological, environmental, and health fields) and a distributed lag nonlinear model (DLNM, used to describe the lagged effect of meteorological elements on health) were employed to quantitatively analyze the effects of several meteorological elements. The relative risk (RR) was used to represent the impact of a set of meteorological factors (Holcomb et al., 2001; Hoek et al., 2013; Liang, 2015; Song et al., 2018). Temperature, relative humidity (RH) and heat index (HI) were the primary meteorological factors analyzed. This study hopes to study the temperature and other meteorological elements affect the respiratory system to improve the meteorological factors on he health early-warning system. The results have far-reaching implications for respiratory system disease prevention, not only for Funan County, but also for other regions with similar climate conditions.

Materials and Methods

Data concerning diseases and meteorological elements

Funan (Anhui Province, China) has a population of 1.697 million, including 884,000 males and 813,000 females, with a sex ratio of 1.087:1. Statistical data from respiratory disease patients were collected from Jan 1, 2013 to Dec 31, 2016. The data were 391185 cases which included the date of inpatient visits, age, sex, primary diagnosis

http://www.aloki.hu ● ISSN 1589 1623 (Print) ● ISSN 1785 0037 (Online)
DOI: http://dx.doi.org/10.15666/aeer/1704_95159528

and address. Respiratory disease (ICD-10: J00-J99), upper respiratory disease (J00-J06, J30-J39), and lower respiratory disease (J20-J22, J40-J47) were classified according to the 10th revision of International Classification of Diseases. A total of 50 680 people were hospitalized for respiratory diseases, of which 31267 were hospitalized for upper infections and 6942 for respiratory infections.

The meteorological data mentioned above were provided by the China meteorological data sharing service system (http://cdc.nmic.cn/home.do). The data contained daily mean temperature, daily minimum temperature, daily maximum temperature, and relative humidity, were obtained and other variables from the China. The relationship between these meteorological elements and the status of the patients was systematically examined in this study.

Analysis methods

To quantitatively analyze the effects of different meteorological elements, a generalized additive model (GAM) and a distributed lag non-linear model (DLNM) were used.

A GAM assumes that linear variables and non-linear variables can be combined in the form of a sum, in which the effects of the non-linear variables can be represented by nonlinear function terms (Barnett et al., 2012; Gasparrini et al., 2015; Barr and Zacks, 2017). There are no restrictions concerning dependence relationships between the causal variables, so the flexibility of a GAM is high. A GAM uses a link function to describe the relationship between the mean of the response variable and a smooth function of each explanatory variable (Yee and Mitchell, 1991). The advantage of a GAM is the ability of this type of model to deal with highly non-linear and non-monotonic relationships between the response and the explanatory variables. In this study, smooth functions (thin-plate spline, natural spline, B-spline) were used for fitting the independent variables. The Akaike information criterion (AIC) was used to test the goodness of fit for the time series data. The model can be written as:

$$log(n) = s(Temp) + s(med\_age) + s(gender\_ratio) + \\ +s(\Delta T48, df = 7) + s(RH) + s(Wind\_max, df = 6) + dow + \alpha \quad \text{(Eq.1)}$$

where n is the number of patients; log is used as a link function; s() denotes the thin-plate spline functions for nonlinear variables; Temp, med_age, sex_ratio, ΔT48, RH and wind_max represent the temperature, median age, sex ratio, temperature difference during 48 hours (ΔT48), RH, maximum wind speed, respectively; dow (representing the effect of weekday) is a dummy variable, and αrepresents the residuals of the GAM.

The DLNM has long been used to describe the lagged effect of meteorological elements on health outcomes (Gasparrini et al., 2010; Wu et al., 2013; Gasparrini et al., 2014). It uses a cross-basis function to describe a two-dimensional relationship along the dimensions of meteorological element and lag. The choice of cross-basis functions for the meteorological element and lag are independent, so spline or linear functions can be used, while polynomial functions can be used for the lag. The resulting estimates can be plotted using a three-dimensional graph to show the relative risks for both meteorological elements and lags (MacDonald, 2015). Cross-basis functions for the meteorological elements (daily average temperature, HI, RH and so on) were established in this study. These effects were estimated using nonlinear smoothing functions for both dimensions,

http://www.aloki.hu ● ISSN 1589 1623 (Print) ● ISSN 1785 0037 (Online)
DOI: http://dx.doi.org/10.15666/aeer/1704_95159528

in which a natural cubic spline was used for each meteorological element and a polynomial spline for the lag effect. To avoid singularity of the model, it is necessary to avoid having too many nonlinear terms. In this study, therefore, we examined only one variable for each model (the temperature in model I and HI in model II). Step-wise backwards selection was employed in the models. Also, because the HI is computed from RH and temperature, when we included HI in the model, we excluded the other two variables. Thus, the final model can be written as follows:

For temperature:

$$log(n) = cb(Temp) + s(med\_age) + s(gender\_ratio) + \\ +s(\Delta T48, df = 7) + s(RH) + s(Wind\_max, df = 6) + dow + \alpha \quad \text{(Eq.2)}$$

For HI:

$$log(n) = cb(HI) + s(med\_age) + s(gender\_ratio) + \\ +s(\Delta T48, df = 7) + s(Wind\_max, df = 6) + dow + \alpha \quad \text{(Eq.3)}$$

where *cb* denotes the cross-basis functions for nonlinear variables, and the other terms are defined as in *Equation 1*.

We also introduce the risk ratio (RR), defined as the ratio of the probability of disease development in a group exposed to a specified environment to the probability in a non-exposed control group. The RR (representing the risk of casualties caused by a unit change of environmental conditions), which can be calculated using the GAM, was used to quantify the impact of meteorological factors on the respiratory patients. The range of RR is (0, ∞); RR = 1 means no connection between exposure to an environmental condition and disease; RR < 1 means that that exposure results in a reduction of the incidence of the disease (i.e. exposure is a protective factor); and RR > 1 means the opposite (Wong et al., 1999). The corresponding 95% confidence interval was calculated using the equation:

$$95\%CI = \exp[(\beta \pm 1.96SE) \times dt] \quad \text{(Eq.4)}$$

The analyses were performed using the R-3.3.2 software environment. The "mgcv" program package was used for the GAM, and the "dlnm" program package was used for the DLNM.

Additionally, artificial neural network models trained by back-propagation (BP-ANN), originally inspired by biological neural systems, have been among the most successful algorithms for machine learning. In the disease field, BP has been used widely as a method and also a benchmark for predicting disease incidence. It can be superior to other methods because of its highly flexible ability to model nonlinearities.

BP-ANN model is mainly composed of three parts: an input layer, a hidden layer and an output layer. There are several nodes in each layer mapping the input vector (in the input layer) to the output vector (in the output layer) by a continuingly updating weight vector (in hidden layer). The weight is updated by the each iteration error (the difference between the output value and the real value). In our study, the data in the input layer (4~5 neurons) were selected from those meteorological factors which directly or indirectly

http://www.aloki.hu ● ISSN 1589 1623 (Print) ● ISSN 1785 0037 (Online)
DOI: http://dx.doi.org/10.15666/aeer/1704_95159528

affect respiratory system diseases determined during model construction. The number of respiratory system diseases was chosen as the output layer in the BP model.

The tansig and purelin were selected as transfer functions in the hidden layer and output layer, respectively. An adaptive training function with momentum was used for network training. This algorithm is able to adjust the learning rate and the incidental momentum automatically to avoid the local minima. Moreover, it accelerates the convergence rate considerably. Therefore, we introduce a BP-ANN model here with the goal of making precise predictions of respiratory system diseases and thereby providing technical support for decreasing diseases and reducing economic loss.

Results

Summary statistics for respiratory diseases are shown in *Table 1*. During the period of 4 years covered by this study, the average number of patients with respiratory system disease was about 38 per day (male: 24 per day, female: 14 per day). The number of patients with URI was much less than the number with LRI.

Table 1. *Composition ratio of different diseases in respiratory system*

Sequence of diseases	Name of disease	Number	Constituent ratio
1	Tracheitis	14167	27.95
2	Bronchitis	12442	24.55
3	Chronic obstructive pulmonary diseases	9413	18.57
4	Asthma	7669	15.13
5	Pulmonary heart disease	4671	9.22

The *Table 2* shows the composition ratio of different diseases in respiratory system. The top five diseases in respiratory system composition ratio are: tracheitis (27.95%), bronchitis (24.55%), chronic obstructive pulmonary diseases (18.57%), asthma (15.13%), pulmonary heart disease (9.22%). The *Table 2* shows the incidence of respiratory diseases was negatively correlated with daily mean temperature, daily mean air pressure and relative humidity, the correlation coefficients are -0.343, -0.032 and -0.122 ($p<0.01$), and positively correlated with 48-hour temperature change and wind speed, the correlation coefficients are 0.080 and 0.076 ($p<0.01$), respectively.

Table 2. *Spearman correlations between respiratory system disease and meteorological factors*

	Patients	Temperature	ΔT48	Pressure	Wide	RH
Patients	1.000					
Temperature	-0.343**	1.000				
ΔT48	0.080**	0.178**	1.000			
Pressure	-0.032**	0.121**	-0.173**	1.000		
Wide	0.076**	-0.072**	-0.159**	0.262**	1.000	
RH	-0.122**	0.269**	-0.164**	0.579**	0.060**	1.000

Note: *$p<0.01$, **$p<0.01$

http://www.aloki.hu ● ISSN 1589 1623 (Print) ● ISSN 1785 0037 (Online)
DOI: http://dx.doi.org/10.15666/aeer/1704_95159528

Age and sex distribution of respiratory system disease

For respiratory system diseases, as shown in *Fig. 1*, the morbidity for male patients was higher than that for female patients ($p<0.0001$). The median number of male and female patients were 21 and 12 per day, respectively.

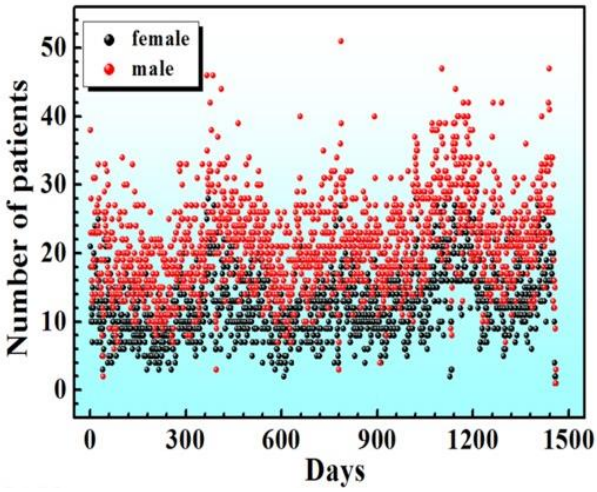

Figure 1. *Incidence of respiratory diseases per day, split by sex*

The morbidities for different age groups showed marked differences ($p<0.0001$), as shown in *Fig. 2*. For LRI, URI and total respiratory diseases, the peak morbidity appeared for newborns. The number of URI patients decreased as age increased. The trends for LRI and total respiratory disease were very similar, except that a secondary peak occurred for the age range 65-75. During the 5 years studied, the numbers of patients with respiratory system disease were relatively stable; however, the day-to-day variability was remarkable.

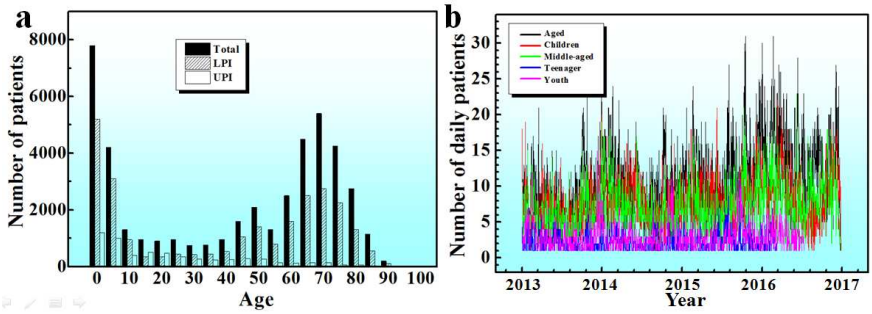

Figure 2. *Age distributions and incidences. (a) Histogram showing incidence of upper respiratory tract infections (URI), lower respiratory tract infections (LRI), and total respiratory disease, for each 10-year age group; (b) Number of patients in each age group, for each day*

For LRI and total respiratory disease, the occurrence of two peaks can be accounted for as follows: First, infants have lower resistance, their clinical symptoms are more obvious, and they make a larger number of hospital visits than adults. Second, resistance is progressively reduced as people move into old age, while the rate of visits will decrease

http://www.aloki.hu ● ISSN 1589 1623 (Print) ● ISSN 1785 0037 (Online)
DOI: http://dx.doi.org/10.15666/aeer/1704_95159528

if the patient is too old (more than 75). In other words, the total number of elderly patients is much less than the numbers of young and middle-aged patients. The trend for URI is different, however, because the number of URI patients (compared with LRI or total respiratory disease) is very small, and the accuracy of the statistical data is inadequate. Consequently, in the following sections, the URI is negligible.

Relationship between meteorological elements and respiratory system disease

Based on the results of the GAM, there was a remarkable correlation between morbidity and meteorological factors such as wind max and ΔT48. The relationships between the number of patients each day and various meteorological factors (temperature, HI, RH) are shown in *Fig. 3*.

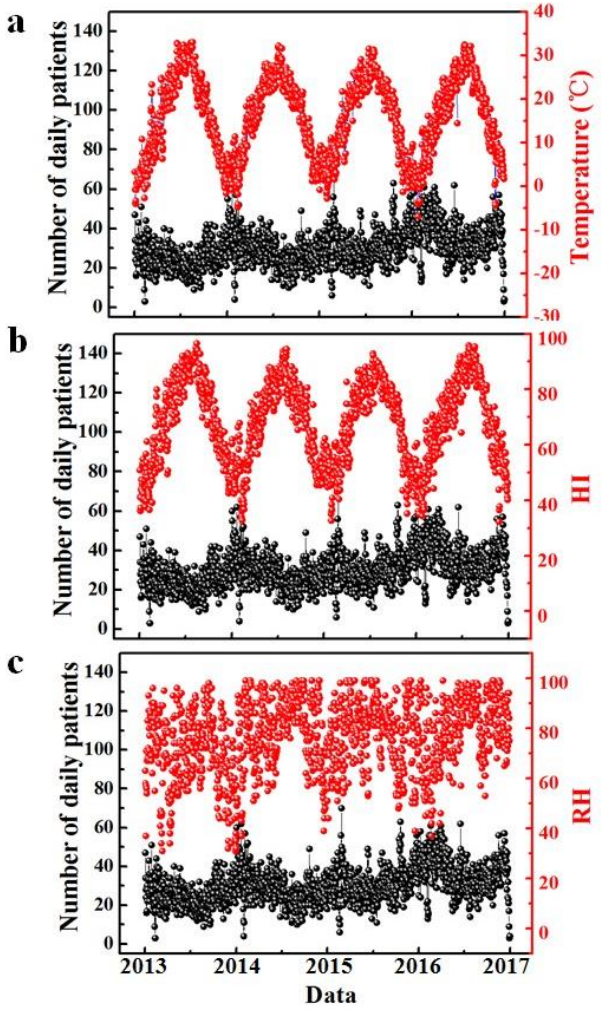

Figure 3. *Variations in three meteorological factors, and their relationships with the number of patients. (a) Plot of temperature and number of patients, by day (b) Plot of heat index (HI) and number of patients, by day. (c) Plot of relative humidity and number of patients, by day*

The patient number showed a yearly rhythm city, but the amplitude was not very high, with a difference between maximum and minimum of about 20. Meanwhile, because of the continental monsoon climate, the variations of temperature showed a similar

http://www.aloki.hu ● ISSN 1589 1623 (Print) ● ISSN 1785 0037 (Online)
DOI: http://dx.doi.org/10.15666/aeer/1704_95159528

sinusoidal variation. Minima in temperature corresponded to peaks in patient numbers. A similar relationship was observed between HI and number of patient. For RH, on the other hand, neither early periodicity nor any relationships with the number of patients were obvious.

The relationships between daily patient numbers and season (or month) are presented in *Fig. 4*. For total respiratory disease, the daily patient numbers for spring and winter were higher, and the number of patients in summer was lowest; the difference between the winter (maximum) and the summer (minimum) was about 30. The 3 months showing the smallest numbers were July, August, and September, corresponding to the summer season. The peak month was January. The distribution as a whole showed a "V" shape. For URI, due to the absence of significance in the statistical data, no systematic results can be stated.

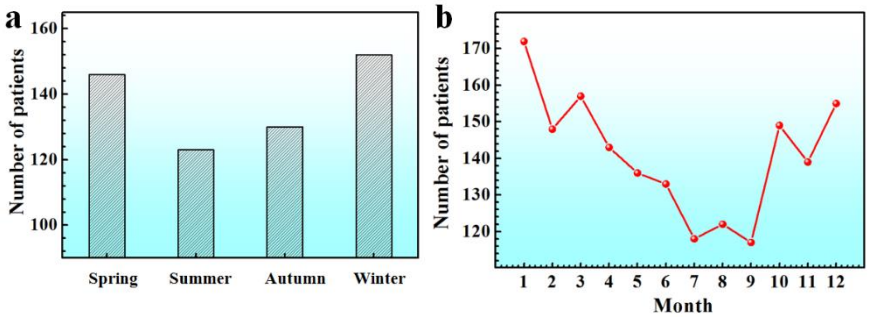

Figure 4. *Changes in number of patients as a function of time of year. (**a**) Histogram showing number of patients for each season. (**b**) Plot of number of patients for each month of the year*

Relationship between meteorological factors and number of patients

For the DLNM, the effects of sex, age, ΔT48 and wind_max were analyzed using the model shown in *Equation 2*. The maximum of lag employed was 10 days in this study, which was considered sufficient for the current study.

Fig. 5(a) shows a three-dimensional plot of the calculated RR versus temperature and time lag. The maximum RR, corresponding to lags of 0 and 7 days, was 1.05; the minimum RR was 0.92. Examining the contour plot in *Fig. 5(b)* and the curves in *Fig. 5(c)*, it can be seen that the lag effect of high temperature reached a maximum value at about 4 days; and for low temperature, at about 7 days. An interesting phenomenon can be seen here: low temperature results in the number of patients increasing typically 5 to 9 days after onset, while having protective effects in the first 4 days; whereas for high temperature, the pattern is the opposite, with protective effects for the sixth to ninth days, but harmful effects on the first to sixth days. The analysis also demonstrates a strong protective effect (high RR) of high temperatures on the first day. For a lag of 3 days, high temperature is a risk factor, but for lag of 7 days, low temperature is a risk. By 10 days, almost all temperature effects disappeared. Meanwhile, based on the previous study (*Fig. 3*), in fact, the relationship among the lag days, patient number and HI is very similar to the relationship, as revealed in *Fig. 5*. Although, the models for temperature and HI are not identical, the variation is the same.

Fig. 6(a) and *Fig. 6(b)* show three-dimensional and contour plots of RR as a function of RH and lag. For a lag of 3 days, low RH increases the risk of respiratory system disease. The minimum located at the lower left of the *Fig. 6(b)* indicates that for the first day, low

http://www.aloki.hu ● ISSN 1589 1623 (Print) ● ISSN 1785 0037 (Online)
DOI: http://dx.doi.org/10.15666/aeer/1704_95159528

RH shows a strong protective effect. For the lower values of RH (<50), the lag effect is obvious, attenuating after 4 days; for higher RH (>55), the effect of RH on respiratory system diseases is weak (RR≈1). The effect of ΔT48 is shown in *Fig. 6(c)* and *Fig. 6(d)*. It can be seen that high ΔT48 increases the risk of disease for the entire range of lags; lower ΔT48 plays a protective role for the first day and for lags of 5-9 days. For values of ΔT48 lower than zero, however, no cumulative effect can be observed.

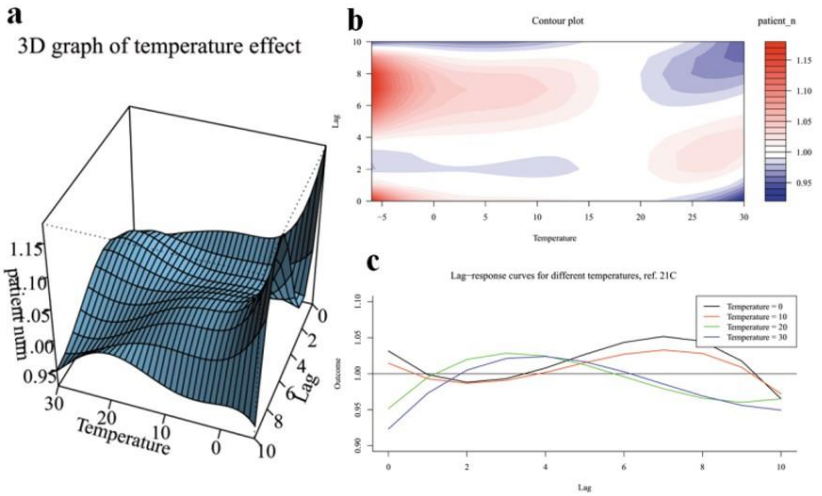

Figure 5. *Relative risk (RR) as a function of temperature, for time lags ranging from 0 to 10 days. (a) 3D plot of RR as a function of temperature and lag. (b) Contour map of the same data shown in panel a. (c) Lag-response curves for four different temperatures*

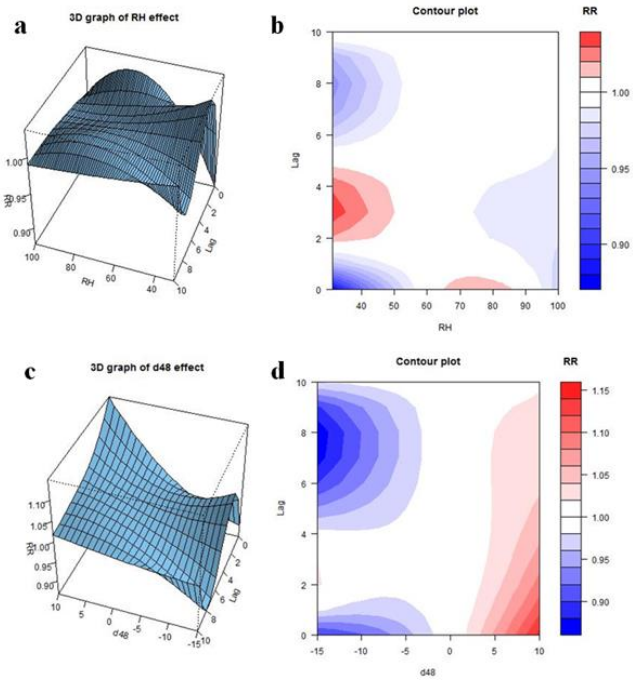

Figure 6. *Effects of relative humidity (RH) and 48-hour time difference (ΔT48) on relative risk (RR), for time lags ranging from 0 to 10 days. (a) 3D plot of RR as a function of RH and lag. (b) Contour plot of the same data shown in panel a. (c) 3D plot of RR as a function of ΔT48 and lag. (d) Contour plot of the same data shown in panel c*

http://www.aloki.hu ● ISSN 1589 1623 (Print) ● ISSN 1785 0037 (Online)
DOI: http://dx.doi.org/10.15666/aeer/1704_95159528

Discussion

This study investigated the effects of weather on the age and sex distribution of respiratory system disease. Based on the analyses above, it can be concluded that there are strong connections between several meteorological elements and respiratory system disease. When the most important elements, such as temperature, RH, ΔT48 and wind-max, are incorporated into a model (all the selected elements are exhibited in *Equations (1) to (3)*, it can be seen that there is a negative correlation between the number of patients and the daily mean temperature (as shown in *Fig. 4*).

Because the coldest month is January, with the temperature often near or below zero for lengthy periods, the cumulative effect of temperature on respiratory system diseases s strong; thus it is not difficult to understand why the peak patient numbers appear in January. The main groups at high risk for respiratory system disease in cold temperatures are infants and the elderly. For the elderly, the older they are, the weaker their regulating ability; whereas for infants, their sensitivity is due to underdevelopment. The atmospheric pressure in winter, higher than in summer, can cause labored breathing due to the smaller pressure difference between the human body and the atmosphere. The dynamics of the respiratory system also imply that the exchange of gases inside and outside of the lungs is reduced. Also, cold air and the resulting high pressure and low humidity can combine in irritating the respiratory system. Furthermore, in winter, people spend much more time indoors, thereby increasing the probability of cross infection.

The temperature of February was colder than in March, but the number of patients was smaller. This may be attributable to the spring festival of China, the most important traditional festival, occurring in February. During the spring festival, people do not want to seek medical help except in an emergency, while at the same time the number of available medical workers is reduced. From January to March, the value of ΔT48 is positive, which also increases the risk of disease. In summer, the daily high temperature is usually above 30°C. Although, the cumulative effect can be found in the *Fig. 5(c)* from the 4~7 lag days. The most important consequence of such temperatures is a protective effect at long lags. The effects of high RH are not particularly strong. For the Funan area, where traditional agriculture is the backbone of the economy, summer is the busiest season for many people; this factor may also reduce the number of patients requesting treatment.

The coldest winter in several years came at the end of 2016 (*Fig. 3(a)*). At that time, a sudden cold wave struck most of China, including the Funan area, and the number of patients with respiratory system diseases also peaked. This phenomenon is an additional indication that extended cold temperatures are a risk factor.

To further demonstrate the effects of high or low temperatures on respiratory system diseases, the plots in *Fig. 7* can be used to examine the RR resulting from heat waves and cold spells, using different temperature thresholds. The threshold for temperature was set at different percentiles of the daily mean temperature range, and durations ranging from 1 consecutive day to 4 consecutive days were analyzed. In *Fig. 7(a)* and *Fig.7(b)*, the effects of a heat wave on respiratory disease incidence at 0 lag days and 4 lag days are very similar. As the temperature threshold increases, the RR increases, but all the values of RR are less than 1, indicating that heat waves had a consistent protective effect. For cold spells, however, the lag effect is obvious. In *Fig. 7(c)*, at a lag of 7 days, when the threshold temperature percentile is 4%, the RR is 1.58. The colder the air, the higher the risk ratios, but the RR is always higher than 1. The relationship between RR and ΔT48 threshold percentile is shown in *Fig.7(d)*. The RR was basically unchanged after 1 (or 3

http://www.aloki.hu ● ISSN 1589 1623 (Print) ● ISSN 1785 0037 (Online)
DOI: http://dx.doi.org/10.15666/aeer/1704_95159528

or 4) consecutive days below a given temperature percentile threshold; but for 2 consecutive days, there is an obvious downtrend of RR.

To distribute medical resources efficiently and provide suitable medical care, the prediction of respiratory system disease is indispensable. In fact, a number of prediction methods have been proposed. For example, Liu and Ding (2010) used a multi-principal component regression model to predict the death rate caused by respiratory system disease, yielding a correlation of r=0.755. In this study, a BP–ANN was used to predict the disease; the results are shown in *Fig. 8*.

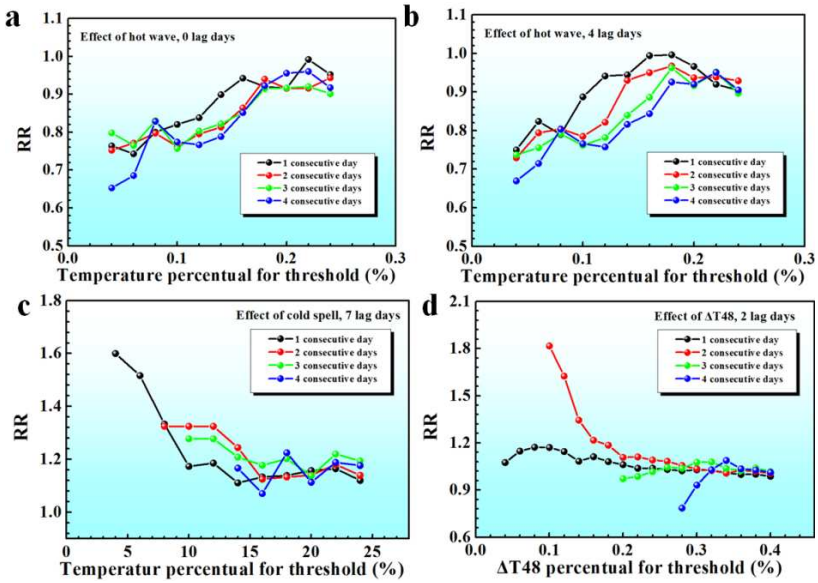

Figure 7. *Effects of heat waves and cold spells on relative risk (RR), using different temperature percentiles as thresholds. (a) Effects of heat waves of varying durations, at a lag of 0 days; (b) Effects of heat waves of varying durations, at a lag of 4 days; (c) Effects of cold spells of varying durations, at a lag of 7 days; (d) Effects of sustained temperature changes of varying durations, at a lag of 2 days*

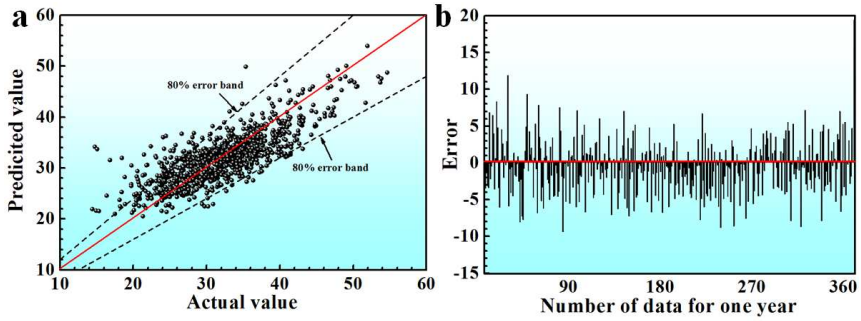

Figure 8. *Prediction accuracy of a back-propagation artificial neural network model. (a) Scatter-plot of predicted values versus actual values of numbers of patients; (b) Day-by-day errors over the course of 1 year*

Because our investigation of the respiratory system disease was conducted in Funan, a relatively high correlation was obtained. As shown in *Fig. 8(a)*, most of the predicted values are located within the 80% error band, and the number of positive errors is less

http://www.aloki.hu ● ISSN 1589 1623 (Print) ● ISSN 1785 0037 (Online)
DOI: http://dx.doi.org/10.15666/aeer/1704_95159528

than that of negative errors. The errors of February and March are slightly higher; this can be attributed to the complex influence factors for those months.

Thus, the BP-ANN model constructed in this work was capable of effectively predicting respiratory system disease, using the average temperature, ΔT48, RH and wind_max as input data.

Conclusions

In this study, the distributed lag non-linear model and generalized additive model were investigated to analyze the influence of meteorological factors on respiratory system diseases in Funan, China from 2013 to 2016. Furthermore, a BP-ANN based prediction method for respiratory system diseases has been developed. The main conclusions can be summarized as follows.

During the 4 years, the average number of daily patients of respiratory system disease is about 30; the morbidity of male patients is a little higher than that of female patients, and infants were the highest risk group. There is a remarkable correlation between morbidity and meteorological factors, with temperature minima corresponding to peaks in the number of patients. This may be attributed to a reduction in outdoor activities in winter as well as the influence of cross-infection. For low RH, a lag effect is obvious for the first 4 days; for higher RH, the effect is weak. Air with low RH and low temperature can lead to an increase in the number of patients with respiratory diseases, the weather conditions will dries the mucosa of the respiratory tract and damage sepithelial cells, increasing the susceptibility of the population. High ΔT48 increases the risk of disease at all time lags, while low ΔT48 decreases the risk at lags of 5-9 days. The BP-ANN model constructed in this work was capable of making an effective prediction of the respiratory system disease, with the main input variables selected being average temperature, ΔT48, RH and wind_max. A relatively high correlation was obtained for this prediction method. These developments have conducive to the distribution of medical resources and provision of appropriate medical care, not only in the Funan area, but for the entire monsoon region. In the next step of research, the pathogenic mechanism of meteorological factors on the respiratory effect should by studied, and it will reach a more accurate prediction of the target.

Conflicts of Interests. The authors declare no conflict of interests.

Acknowledgements. This research is supported by the National Key R&D Program of China (2017YFC1307700).

REFERENCES

[1] Barnett, A. G., Hajat, S., Gasparrini, A. (2012): Cold and heat waves in the United States. – Environmental Research 112: 218-224.

[2] Barr, J. R., Zacks, S. (2017): GLiM: Generalized linear models. – Encyclopedia with Semantic Computing and Robotic Intelligence 1(1): 1630016.

[3] Barreca, A. I. (2012): Climate change, humidity, and mortality in the United States. – Journal of Environmental Economics and Management 63(1): 19-34.

http://www.aloki.hu ● ISSN 1589 1623 (Print) ● ISSN 1785 0037 (Online)
DOI: http://dx.doi.org/10.15666/aeer/1704_95159528

[4] Bull, A. T., Quayle, J. R. (1982): New Dimensions in Microbiology: An Introduction. – Philosophical Transactions of the Royal Society B: Biological Sciences 297(1088): 447-457.
[5] Chakraborty, S., Kumar, A., Tiwari, R., Rahal, A., Malik, Y., Dhama, K., Pal, A., Prasad, M. (2015): Advances in Diagnosis of Respiratory Diseases of Small Ruminants. – Veterinary Medicine International 2014: 508304.
[6] D'amato, G., Cecchi, L. (2008): Effects of climate change on environmental factors in respiratory allergic diseases. – Clinical & Experimental Allergy 38: 1264-1274.
[7] Gasparrini, A., Armstrong, B., Kenward, M. G. (2010): Distributed lag non-linear models. – Statistics in Medicine 29(21): 2224-2234.
[8] Gasparrini, A. (2014): Modeling exposure-lag-response associations with distributed lag non-linear models. – Statistics in Medicine 33(5): 881-899.
[9] Gasparrini, A., Guo, Y., Hashizume, M. (2015): Mortality risk attributable to high and low ambient temperature: a multicounty observational study. – The Lancet 386(9991): 369-375.
[10] Hoek, G., Krishnan, R. M., Beelen, R., Peters, A., Ostro, B., Brunekreef, B., Kaufman, J. D. (2013): Long-term air pollution exposure and cardio- respiratory mortality: a review. – Environmental Health: A Global Access Science Source 12(1): 43.
[11] Holcomb, J. W. L., Chaiworapongsa, T., Luke, D. A., Burgdorf, K. D. (2001): An odd measure of risk: use and misuse of the odds ratio. – Obstetrics & Gynecology 98(4): 685-688.
[12] Kim, P. E., Musher, D. M., Glezen, W. P., Rodriguez-Barradas, M. C., Nahm, W. K., Wright, C. E. (1996): Association of invasive pneumococcal disease with season, atmospheric conditions, air pollution, and the isolation of respiratory viruses. – Clinical Infectious Diseases 22(1): 100-106.
[13] Kunst, A. E., Looman, C. W. N., Mackenbach, J. P. (1993): Outdoor air temperature and mortality in the Netherlands: a time-series analysis. – American Journal of Epidemiology 137(3): 331-341.
[14] Liang, S., Saxena, M., Finfer, S., Myburgh, J. (2015): Impact of high temperature on long-term outcomes in patients with traumatic brain injury: A systematic review of observational studies. – Australian Critical Care 28: 42-43.
[15] Liu, W. J., Ding, G. X. (2010): Climate Characteristics of Subtropical High in Western Pacific. – Journal of Anhui Agricultural Sciences 38(16): 8533-8535.
[16] MacDonald, G. (2015): Elements of Time Series Econometrics: An Applied Approach. – In: Kočenda, E., Černý, A. (eds.) Economic Record 91(293): 269-270. 2nd edition (Karolinum Press, Prague, 2014).
[17] Miyamoto, T., Kitayama, T., Kumagai, S., Mori, K., Kitamura, S., Shindo, S. (2008): An energy trading system with consideration of CO2 emissions. – Electrical Engineering in Japan 162: 54-63.
[18] Ricciardolo, F. L. M., Sterk, P. J., Gaston, B., Folkerts, G. (2004): Nitric oxide in health and disease of the respiratory system. – Physiological Reviews 84(3): 731-765.
[19] Song, X. P., Wang, S. G., Li, T. S., Tian, J. H., Ding, G. W., Wang, J. X., Wang, J. X., Shang, K. Z. (2018): The impact of heat waves and cold spells on respiratory emergency department visits in Beijing, China. – Science of The Total Environment 615: 1499-1505.
[20] Winkelstein, J. W., Kantor, S., Davis, E. W., Maneri, C. S., Mosher, W. E. (1968): The relationship of air pollution and economic status to total mortality and selected respiratory system mortality in men: I. Suspended particulates. – Archives of Environmental Health An International Journal 16(3): 401-405.
[21] Wong, T. W., Lau, T. S., Yu, T. S., Neller, A., Wong, S. L., Tam, W., Pang, S. W. (1999): Air pollution and hospital admissions for respiratory and cardiovascular diseases in Hong Kong. – Occupational and environmental medicine 56(10): 679-683.

http://www.aloki.hu ● ISSN 1589 1623 (Print) ● ISSN 1785 0037 (Online)
DOI: http://dx.doi.org/10.15666/aeer/1704_95159528

[22] Wu, W., Xiao, Y., Li, G., Zeng, W., Lin, H., Rutherford, S., Xu, Y., Luo, Y., Xu, X., Chu, C., Ma, W. (2013): Temperature–mortality relationship in four subtropical Chinese cities: a time-series study using a distributed lag non-linear model. – Science of the Total Environment 449: 355-362.
[23] Yee, T. W., Mitchell, N. D. (1991): Generalized additive models in plant ecology. – Journal of Vegetation Science 2(5): 587-602.

http://www.aloki.hu ● ISSN 1589 1623 (Print) ● ISSN 1785 0037 (Online)
DOI: http://dx.doi.org/10.15666/aeer/1704_95159528

INFLUENCE OF COLLECTION TIME ON THE DETERMINATION OF ROOT EXUDATES IN *FRAXINUS MANDSHURICA* BY THE METABOLOMICS METHOD

LI, L. Y.[1,2] – FENG, C. X.[1] – ZHANG, Y. D.[1*]

[1]*College of Forestry, Northeast Forestry University*
Harbin 150040, Heilongjiang, People's Republic of China

[2]*Heilongjiang BaYi Agricultural University*
Daqing 163319, Heilongjiang, People's Republic of China

**Corresponding author*
e-mail: zhyd63@163.com

(Received 18th Apr 2019; accepted 10th Jun 2019)

Abstract. Root exudates play an important role in the control of soil ecology because they are major sources of organic carbon and energy for plants, and they drive the carbon cycle of forest ecosystems. However, qualitative and quantitative methods for analysis of root exudates are poorly developed. In this study, *Fraxinus mandshurica* was used as research material for studying the influence of different collection times on the chemical composition of root exudate. The study employed qualitative and metabolomic analyses of root exudates with gas chromatography-mass spectrometry, and quantitatively analyzed root exudates of *F. mandshurica* with ultrahigh performance liquid chromatography (UPLC) and high performance ion chromatography (HPIC) methods. Root exudates were collected after harvest for 24 h at 6 h-intervals, and then analyzed. The types of sugars, amino acids, and organic acids in the root exudates were not significantly different among the four exudate samples. The results indicated that collection time strongly influenced the level of organic compounds in root exudates from *F. mandshurica*, with an optimal collection time of 12 h. In addition, quantitative analysis of root exudates using UPLC and HPIC had greater advantage, when compared with conventional analytical methods.
Keywords: *Fraxinus mandshurica, exudate, qualitative analysis, quantitative analysis, GC-MS, UPLC, HPIC*

Introduction

Root exudates refer to organic compounds actively or passively released from plant roots to the surrounding rhizosphere under specific conditions. Exudates include some low molecular weight compounds such as organic acids, sugars, phenols, and amino acids (Malandrino et al., 2011). Some high molecular weight organic compounds such as proteins and mucus are also present in exudates (Dijkstra and Cheng, 2007). Studies have shown that root exudates influence soil material cycling by changing the physical and chemical properties of soil (Materechera et al., 1992; Oades, 2010). Root exudates are affected by plant nutrient uptake (Li et al., 2007; Dinkelaker et al., 2010). They are involved plant signal transduction (Peters et al., 1986; Akiyama et al., 2005), and they interact with rhizospheric microorganisms (Bardgett et al., 2005; Singh and Mukerji, 2006). Root exudates significantly change the abundance and activity of soil microorganisms, thereby profoundly affecting organic matter decomposition and nutrient metabolism in the rhizosphere (Phillips et al., 2009; Yin et al., 2013). Root exudates play important roles in the regulation of soil nutrient transformation. These

http://www.aloki.hu ● ISSN 1589 1623 (Print) ● ISSN 1785 0037 (Online)
DOI: http://dx.doi.org/10.15666/aeer/1704_95299545

findings were based on analysis of the composition of root exudates. Thus, analysis of composition of root exudates is of great significance.

Research related to identification of the compositions of root exudates have focused mainly on sugars, amino acids and organic acids (Kuo et al., 1982; Zhen et al., 2004; Sandnes et al., 2005; Kerdchoechuen, 2005; Chang et al., 2008; García et al., 2010; Carvalhais et al., 2011). Thus, there is dearth of information on other components of exudates. There is need for a comprehensive analysis of the composition and trends of root exudates because they vary in types and amounts under different treatment conditions. In addition, many factors influence the composition of root exudates. These include forest type, tree species, environmental conditions, and soil nutrient availability (Zhang et al., 2007; Fransson and Johansson, 2010; Shi et al., 2011). Water culture collection method has been widely used for the collection of root exudates because it is simple to implement, and it reflects changes in certain root secretions to a certain extent, while eliminating interference from soil microorganisms (Phillips et al., 2006). However, the influence of collection time on water culture collection method for the analysis of root exudates has not been investigated. Recent studies have employed collection times of 6, 12, 18, and 24 h (Li et al., 2014; Liu et al., 2016). The compositions of root exudates have also been shown to change as a function of collection time (Bowsher et al., 2015). This is so because plants and the environment change over time in ways that affect the results of compositional analysis of root exudates. However, no studies have so far been carried out on the trends of changes in compositions of root exudates over time. Currently, studies on root exudates have concentrated mostly on qualitative analysis, with only few reports on quantitative studies. Qualitative analysis usually involves the use of various solvents to extract root exudates, and carrying out analysis using gas chromatography (GC) or gas chromatography-mass spectrometer (GC-MS). However, these methods may seriously affect the accuracy of the analysis. Quantitative analysis often involves the use of amino acid analyzer (for amino acids), high performance liquid chromatography (for organic acids), and anthrone reagent and phenol-sulfuric acid colorimetric assays (for sugars) (Xiao et al., 2015; Zhang et al., 2016; Wang et al., 2016). The accuracy and limits of detection of these methods are poor, and they lack specificity. Thus, the quantitative results are not reliable and credible. In recent years, GC-MS, ultra-performance liquid chromatography (UPLC), high performance ion chromatography (HPIC), metabolomics, and other related hi-tech methods have been widely used. These methods have the advantages of high accuracy and precision, and low detection limits, and they provide rapid analysis within relatively wide linear ranges (Rissanen et al., 2006; Kajos et al., 2015; Dietrich et al., 2016; Gargallogarriga et al., 2017). However, few studies and applications exist based on these methods for the analysis of root exudates. Therefore, it is necessary to use these methods for the analysis of root exudates.

Previous studies related to root exudates have mainly concentrated on short-growing-period plants such as crops and vegetables (Venkatasubbarao and NoriharuAe, 1997; Paynel et al., 2001; Luo et al., 2014), while similar studies on perennial forest species are rare. *Fraxinus mandshurica* (*F. mandshurica*), an important afforestation tree species with high ecological and economic value in Northeast China, has roots with well-developed branching structure (Mei et al., 2006; Ren et al., 2010). It is suitable for the study of root biology, especially in the determination and analysis of root exudates, and it has a certain level of practical significance. Therefore, in this study, the root exudates of *F. mandshurica* in the cold forests of northeastern China were qualitatively analyzed

http://www.aloki.hu ● ISSN 1589 1623 (Print) ● ISSN 1785 0037 (Online)
DOI: http://dx.doi.org/10.15666/aeer/1704_95299545

using GC-MS technology, and the metabolomic differences at different collection times were determined. Based on qualitative analysis, the amino acids and organic acids were analyzed using targeted UPLC method, while the sugars were analyzed with targeted HPIC method. The trend of changes in the composition and contents of components of root exudates of *F. mandshurica* at different collection times were analyzed to determine the best collection time. The goal of the present study was to establish efficient qualitative and quantitative methods for analyzing root exudates, and to provide a theoretical reference for this process.

Materials and Methods

Plant materials and culture methods

One-year-old *F. mandshurica* saplings with uniform size and robustness were selected to ensure as much consistency as possible between individual saplings. These saplings were grown in the nursery of Forestry and Environmental Sciences, Northeast Forestry University of China. The saplings were pre-cultured for 7 days using deionized water, and then cultured using a nutrient solution. The nutrient solution was replaced every 3 days during culture. The pH of the nutrient solution was adjusted to 5.5 with 0.1 M NaOH or 0.1 M HCl, and 24 h ventilation was maintained constantly. After 15 days of continuous culture, the root exudates were collected. At that time, the *F. mandshurica* saplings had vigorous root growth.

Collection of roof exudates

Prior to analysis, the roots of each *F. mandshurica* sapling were removed from the nutrient solution, washed 3–5 times with deionized water, and placed inside a 100-mL beaker which was shaded with black rubberized fabric. Then, the root exudates were collected after 6, 12, 18, and 24 h. Finally, the root exudates were dried using a vacuum freeze-drying machine (Shanghai Yuming Instrument Co., Ltd., Shanghai, China). At least, six replicate samples were used for each group of experiments.

The GC-MS analysis preprocessing methods

Next, qualitative and metabolite analyses of the root exudates were carried out using GC-MS analysis in accordance with the method of Suzuki et al. (2009), with a slight modification. First, freeze-dried root exudates were added to a cold methanol: water = 4:1 solution (1 mL). This was blown to dryness with nitrogen. Then, 20 μL of internal standard (L-2-chlorobenzene alanine, 0.3 mg/mL, configuration of methanol) was added. This was then mixed with 600 μL methanol-acetonitrile (2:1) and stirred for 30 sec. The root exudates were extracted after 10 min in an ice water bath with an ultrasonic cleaning machine (Ji Ning SIONBEST Biology Machinery Co., Ltd., Shandong, China). Next, samples were centrifuged for 15 min at 13000 rpm and at temperature of 4°C. Then, 500 μL supernatant was loaded into a glass derivative bottle, and the samples were dried with a centrifuge drying apparatus (Labconco Corporation, Kansas, Missouri, USA). Thereafter, 80 μL of 15 g/L methoxyamine hydrochloride pyridine was added and allowed to react for 90 min, with oscillation of the reaction mixture at 37°C. Next, 80 μL bis(trimethylsilyl)trifluoroacetamide (1% trimethylchlorosilane) was added and allowed to react with the oxime reaction for 60 min at 70°C, accompanied with

http://www.aloki.hu ● ISSN 1589 1623 (Print) ● ISSN 1785 0037 (Online)
DOI: http://dx.doi.org/10.15666/aeer/1704_95299545

oscillation (Young et al., 2010). Finally, the samples were filtered into GC sample bottles using a filter membrane (Pall Corporation., New York, USA) (0.45 μm), and used in the metabolomic analysis with GC-MS.

Chromatographic conditions for GC-MS analysis

A GC-MS analyzer 7890A-5975C (Agilent, Santa Clara, CA, USA) and an HP-5MS capillary chromatographic column (30 m × 0.25 mm × 0.25 μm, Agilent J&W Scientific, Folsom, CA, USA) were used for GC analysis. The initial temperature of the chromatographic column was 60°C, and it was ramped up to 310°C at the rate of 8°C/min, and held for 6 min. Sample volume was 1 μL, inlet temperature was 260°C, and high purity helium was used as carrier gas at a flow rate of 1.0 mL/min. Electric impact was used as ion (EI) and the ion source temperature was 230°C. Quadrupole temperature was 150°C, and the electron energy was 70 eV. The scanning square was full scan mode (SCAN), and the quality scanning range was 50–600 m/z. Continuous sample analysis was carried out in random order to avoid the influence caused by fluctuation in the instrument signal.

Metabolite identification and integration of data matrix

The original data of GC/MS (D format) was converted to general format (CDF format) through Chem Station analysis software (Version E.02.02.1431, Agilent, USA), and the data pre-processing used Chroma TOF software (Version 4.34, LECO, St Joseph, MI, USA). It included peak extraction, noise elimination and deconvolution, and used the standards of the US National Institute of Standards and Technology and the Fiehn database to identify metabolites. Finally, peak alignment was performed, and 3D data matrix (original data matrix) in CSV format was derived.

Methods used for metabolite data analysis

The metabolite content was used as X variable. Then, a matrix was established and imported into SIMCA-P 14.1 (Umea, Sweden) software for multivariate statistical analysis. The clustering was analyzed using PCA (principal component analysis, PCA). Then, a reliable statistical analysis model was established using partial least-squares discriminant analysis (PLS-DA) which searched for significant differences between samples taken at different time points, and identified which biomarkers were useful for classification. The reliability of the model was evaluated using the explanatory power of model to variables (R2) and predictive ability (Q2), while the fit of the model was assessed using overfitting evaluation index R2- and Q2-intercepts. Significant differences between metabolites was determined using loading plot of PLS-DA and the Variable Importance for the Projection (VIP). The biomarker was VIP>1.

Analysis of amino acid content

The amino acid content was analyzed with UPLC. The amino acids were derivatized using o-phthaldialdehyde and fluorenylmethyl chloroformate, and qualitative analysis was carried out through the retention times of chromatographic peaks, while quantitative analysis was done using external standard method. Freeze-dried root exudates were used for analysis of amino acid targets, with addition of deionized water (1 mL) under

http://www.aloki.hu ● ISSN 1589 1623 (Print) ● ISSN 1785 0037 (Online)
DOI: http://dx.doi.org/10.15666/aeer/1704_95299545

ultrasonic conditions. After centrifugation for 10 min at 12000 rpm, it was filtered through a 20 μm filter membrane.

Preparation amino acid standard samples

Amino acid standard (1 mL, 1000 pmol/μL) was divided into ten parts (100 μL). The standard contained aspartic acid (Asp), glutamic acid (Glu), asparagine (Asn), serine (Ser), glutamine (Gln), histidine (His), glycine (Gly), threonine (Thr), arginine (Arg), alanine (Ala), tyrosine (Tyr), valine (Val), methionine (Met), tryptophan (Trp), phenylalanine (Phe), isoleucine (Ile), leucine (Leu), lysine (Lys), and proline (Pro). Amino acid supplement solution I was prepared by weighing Asn (237.8 mg), hydroxyproline (236 mg), Glu (263.08 mg) and Trp (367.8 mg) into a measuring flask (100 mL), and adding 0.1 M hydrochloric acid (50 mL). The amino acids were dissolved under ultrasonic conditions, and then diluted to scale with deionized water. Amino acid supplement solution II was prepared by dissolving norvaline (234.32 mg) in 100 mL of 0.1 M HCL in a 200 mL measuring flask, under ultrasonic conditions and then diluting to scale with deionized water. This solution was used as an internal standard solution. The mixed standard solution was prepared by mixing amino acid supplement solutions I and II (10 μL of each). The mixture was vortexed using a vortex vibration instrument (Shanghai Jingke Industrial Co., Ltd., Shanghai, China). The mixed standard solution was diluted to 1:1000, 5:1000, 10:1000, 100:1000, 200:1000, 500:1000, and 1000:1000 to generate gradient concentrations of each amino acid standard i.e. 1 nmol/mL, 5 nmol/mL, 10 nmol/mL, 100 nmol/mL, 200 nmol/mL, 500 nmol/mL, and 1000 nmol/mL, respectively.

UPLC detection method

Model U3000 DGLC UPLC analyzer (Thermo Fisher Scientific, Waltham, MA, USA) and Advance Bio AAA C18 chromatographic column (4.6×100 mm, 2.7 μm, Agilent J&W Scientific, Folsom, CA, USA) were used for amino acid analysis. The automatic sampler program involved valve switch to bypass 6 sec after sample injection. The sample (1.0 μL) and borate buffer (2.5 μL) were mixed five times at the cleaning mouth (3.5 μL), and after 12 sec, o-phthaldialdehyde (0.5 μL) was added, and mixed ten times at cleaning mouth (4.0 μL). Next, fluorenylmethyl chloroformate (0.4 μL) was added and mixed ten times at cleaning mouth (4.4 μL), followed with addition of double-distilled water (ddH_2O) (15.6 μL) and mixing eight times at cleaning mouth (20 μL). Finally, the sample was injected into the chromatographic column. The chromatographic conditions were: column temperature of 40°C and flow rate of 1.5 ml/min. Mobile phase A was 10 mM sodium hydrogen phosphate and 10 mM sodium borate solution, with pH adjusted to 8.2 with hydrochloric acid. Mobile phase B was methanol: acetonitrile: water at volume ratio of 45: 45: 10. The gradient program used was 2% B for 0-13.4 min, 57% B for 13.4-13.5 min, 100% B for 13.5-15.7 min, and 2% B for 15.7-18.0 min. The study was carried out at 338 nm (bandwidth 10 nm, reference 390 nm, bandwidth 20 nm, first class amino acids); and 262 nm (bandwidth 16 nm; reference 324 nm, bandwidth 8 nm, level two amino acids). The wavelength was switched after lysine peaks (the experiment was set to switch from 338 nm to 262 nm in 10 min). Chameleon software ver. 7.2 (Thermo Fisher Scientific, Leipzig, Germany) was used for data analysis and final data collation.

http://www.aloki.hu ● ISSN 1589 1623 (Print) ● ISSN 1785 0037 (Online)
DOI: http://dx.doi.org/10.15666/aeer/1704_95299545

Target analysis method for sugars

Sugars were analyzed using HPIC. First, the sugars were separated in an anion exchange column and detected with a pulse integral amperometric detector (Thermo Fisher). The retention time of chromatographic peaks were determined, and quantitative analysis were carried out using the external standard method. Freeze-dried root exudates were used for sugar target analysis, which involved adding deionized water (1 mL) under ultrasonic conditions, centrifugation for 10 min at 12,000 rpm, and filtration through a 20-μm filter membrane.

Preparation of standard sugar solutions

First, 100 mg of each sugar was dissolved in 10 mL of deionized water, and the solution was diluted 100 times. The sugar standards used were fucose (fuc), arabinose (ara), galactose (gal), glucose (glc), xylose (xyl), mannose (man), fructose (fru), ribose (rib), galacturonic acid (gal-AC), and glucuronic acid (glc-AC). The concentration of the standard solution was 100 μg/mL. Each mixed standard solution was diluted at ratios of 1:100, 5:100, 10:100, 20:100, 30:100, 40:100, 50:100, and 60:100, so that the concentration of each sugar standard after dilution was 1 μg/mL, 5 μg/mL, 10 μg/mL, 20 μg/mL, 30 μg/mL, 40 μg/mL, and 60 μg/mL, respectively.

HPIC detection method

An ICS5000 HPIC analyzer (Thermo Fisher) and Dionex™ CarboPac™ PA20 (3.0×150 mm, Thermo Fisher) were used for the analysis of sugars, along with an electrochemical detector at a flow rate of 0.5 ml/min. Mobile phase A was double distilled ddH_2O, while mobile phase B was 200 mM NaOH, and mobile phase C was 200 mM NaOH:500 mM NaAC. The gradient program was 97.5% A + 2.5% B for 0–25 min; 77.5% A + 2.5% B + 20% C for 25.0–40 min; 100% C for 40.0–50 min; and 97.5% A + 2.5% B for 50.0–60 min. Chameleon software (7.2) was used for data analysis and final data collation.

Organic acid analysis method

Organic acid contents were determined using HPIC. The organic acids were separated with AS11 HC. Qualitative analysis was done by measuring the retention time of chromatographic peaks, while quantitative analysis was done using external standard method. Freeze-dried root exudates were used for organic acid target analysis after addition of deionized water (1 mL) under ultrasonic conditions, centrifugation for 10 min at 12,000 rpm, and filtration through a 20-μm filter membrane.

Preparation of standard solutions of organic acids

Standard solutions were prepared for lactic, acetic, propionic, formic, isobutyric, butyrate, isovalerate, valerate, isohexadecanoic, hexadecanoic, palmitic, succinic, tartaric, and oxalic acids by dissolving 100 mg of each organic acid in 10 mL of deionized water and diluting the resultant solution 100 times. The concentration of each standard solution was 100 μg/mL. Serial dilutions of each standard solution were prepared at ratios of 1:100, 5:100, 10:100, 20;100, 30;100, 40;100, 50;100, and 60;00 to yield organic acid standard concentrations of 1 μg/mL, 5 μg/mL, 10 μg/mL, 20 μg/mL, 30 μg/mL, 40 μg/mL, and 60 μg/mL, respectively.

http://www.aloki.hu ● ISSN 1589 1623 (Print) ● ISSN 1785 0037 (Online)
DOI: http://dx.doi.org/10.15666/aeer/1704_95299545

HPIC detection method

An ICS5000 HPIC analyzer (Thermo Fisher), an AS11 HC Dionex™ (4.0×250 mm, Thermo Fisher), and an AS11 HC Guard (4.0×50 mm, Thermo Fisher) were used for organic acid analysis with an electrochemical detector, flow rate of 1.0 ml/min, and column temperature of 30°C. Mobile phase A was ddH_2O (18.2MΩ Pall, USA), while mobile phase B was 100 mM KOH (HPLC, Sigma, USA). The gradient elution program was 2.0% B for 0-15 min; 15% B for 15-30 min; 40% B for 30-40 min; 50% B for 40-45 min; and 2.0% B for 45-53 min. Chameleon software (7.2) was used for data analysis and collation of final data.

Statistical analysis

Data are presented as mean ± standard deviation (n=6). Statistical analyses were performed with SAS statistical program. Statistical significance of differences amongst the groups were analyzed with one-way analysis of variance (ANOVA), followed by Duncan's test. Statistical significance was assumed at $p < 0.05$.

Results and Discussion

Results of root exudate metabolite analysis using GC-MS

The qualitative analysis of the root exudates of *F. mandshurica* was carried out using GC-MS. Two hundred and nineteen compounds were found in the root exudates of *F. mandshurica*. The root exudates contained lactic, acetic, oxalic, tartaric, succinic, and other small molecular organic acids such as aspartic acid, asparagine, glycine, alanine, valine, isoleucine, and leucine, amongst others. The other compounds included amino acids, xylose, fructose, glucose and other sugars. Erythronolactone, hydroxylamine, monostearin, nicotinic acid, ribitol, methylhydantoin, phytosphingosine, linoleic acid, hexadecane, sedoheptulose, and other small molecular metabolites were also present. The result agrees with those obtained in previous studies which reported the presence of many compounds in the root exudate (Luo et al., 2014; Han et al., 2015). Luo found 62 compounds in Sedum alfredi, including organic acids, amino acids, sugars and other small molecular metabolites. Over 100 compounds were identified in *Capsicum chinense* Jacquin, including organic acids, amino acids, sugars and other small molecular weight metabolites (alkane, lipids, acids, alcohols, phenols, aldehydes, oxime, pyrrolidone, amide, amine and naphthalene compounds) (Han et al., 2015). The type of compound present in plant exudates is determined by factors such as species of plant, period of growth, nutrient level and environmental pressure (Carvalhais et al., 2011; Selvakumar and Panneerselvam, 2012). The present study also found that the compounds in root exudates of *F. mandshurica* varied at different collection times. Therefore, a metabolomics analysis was carried out on the original data of GC/MS (CDF format), so as to identify the differences in levels of metabolites of root exudates of F. mandshurica as a function of time of collection. Plots of PCA scores (*Fig. 1-a*) showed that samples at different collection times had a preliminary clustering trend, meaning that metabolites in samples collected at different times were different. In addition, quality control samples were clustered and distributed in the score map, indicating an improvement in the stability of the detection platform. The results of the PLS-DA score plots (*Fig. 1-b*) showed that the samples collected at different times were completely clustered and separated, and

http://www.aloki.hu ● ISSN 1589 1623 (Print) ● ISSN 1785 0037 (Online)
DOI: http://dx.doi.org/10.15666/aeer/1704_95299545

sample distribution for samples collected from 6 h to 24 h showed a gradual and progressive relationship.

Through model verification analysis (*Fig. 2*), this study found that the interpretations of the model for X and Y variables were R^2X=0.441 and R^2Y=0.907, respectively, and the prediction of the variable Q^2Y was 0.622, which showed that the model was of good quality. After 999 permutation tests, R^2-interposition was 0.593, Q^2-interposition was −0.450, and all random permutations produced R^2Y and Q^2 values smaller than the original R^2Y, Q^2 values, indicating that the PLS-DA model was robust.

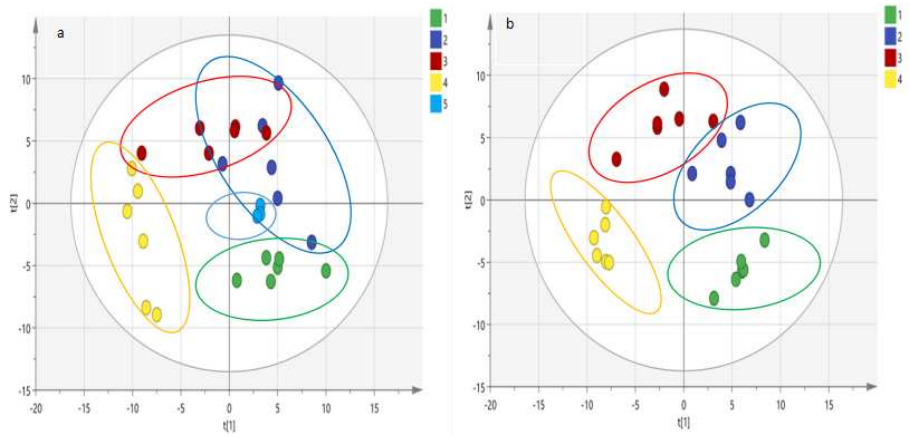

Figure 1. *(a) Principal component analysis (PCA) and (b) partial least-squares discriminant analysis (PLS-DA) score plots of root exudates of the F. mandshurica. Collection times were at (1) 6 h, (2) 12 h, (3) 18 h and (4) 24 h. (5): quality control sample*

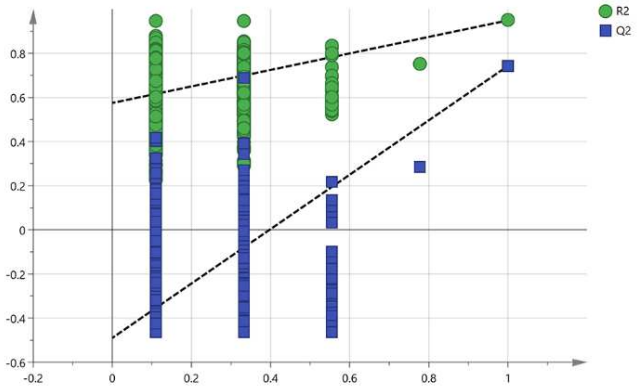

Figure 2. *Verification analysis of partial least-squares discriminant analysis model. The explanatory of models R^2 and the predicted performances of models Q^2 were 0.593 and 0.450 respectively. Overfitting of the model was discriminated using R^2- intercepts and Q^2-intercepts*

Results of the loading plot of the PLS-DA model (*Fig. 3*) showed that the samples from different collection times differed significantly, and the differential metabolites were identified using VIP analysis. These included glycolic acid, acetophenone, glucose-1-phosphate, 15-keto-prostaglandin, dithioerythritol, dehydroabietic acid, thioctamide, synephrine, hippuric acid, quinic acid, sedoheptulose, nicotinamide, 2-hydroxybiphenyl, 2-deoxyuridine, 2-furoic acid, maleamate, 6-hydroxy caproic acid trimer, beta-

http://www.aloki.hu ● ISSN 1589 1623 (Print) ● ISSN 1785 0037 (Online)
DOI: http://dx.doi.org/10.15666/aeer/1704_95299545

hydroxypyruvate, halostachine, and other metabolites, totaling 88 compounds (VIP>1). The results showed that the secondary metabolites accounted for a larger proportion of the metabolites that differed significantly at different collection times, while the sugars, amino acids, and small molecular organic acids were not significantly different amongst root exudates of *F. mandshurica* collected at different times. The results are in agreement with the findings of previous studies, which were mainly focused on sugars, amino acids, and organic acids (Huang et al., 1996; Maqsood et al., 2011; Carvalhais et al., 2011). Therefore, the present study quantitatively analyzed the sugar, amino acid, and organic acid compounds in the root exudate of *F. mandshurica*, and investigated how these compounds varied at different collection times. This was with a view to determining the optimal collection time of the root exudate.

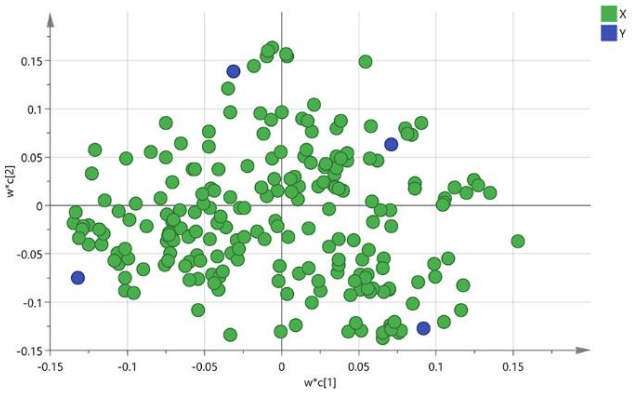

Figure 3. *Loading plot of partial least-squares discriminant analysis model for root exudates of F. mandshurica: (X) root exudate variable, (Y) group (collection time) variable*

Results of amino acid analysis of root exudates using UPLC

Qualitative analysis was done using the retention time of chromatographic peaks (*Fig. 4*), while quantitative analysis was carried out using the external standard method. Results of amino acid analysis of root exudates from *F. mandshurica* (*Table 1*) showed that the primary amino acids were Asp, Asn, Gly, Ala, Val, Ile, and Leu. There was a wide variation in amino acids between the results obtained from UPLC analysis and results from GC-MS analysis. There were fewer amino acids in UPLC analysis results than in GC-MS analysis results. This variation was probably due to the fact that the detection limit of GC-MS is lower than that of UPLC. Thus, when the amino acid content is low, it may be below the lower limit for UPLC detection, resulting in inability of the UPLC method to detect some amino acids. It was also found that the varieties and the contents of amino acids varied significantly at different collection times. The amount and varieties of amino acids found initially showed significantly increasing trend as the collection time increased (0-12 h), but decreased significantly after 12 h. Indeed, only Gly was present in the root exudates at 18 h and 24 h. This occurred because the amino acids from root exudates were used as nitrogen substrates by *F. mandshurica*. Thus, with continuous use, the amino acids were close to depletion at 18-24 h. Therefore, the best time to collect the root exudates for the determination of amino acid content is 12 h. The content of Gly was the highest among the various amino acids of root exudates. The contents of Leu, Val, and Ile were also high. However, the contents of Ala, Asp, and Asn

http://www.aloki.hu ● ISSN 1589 1623 (Print) ● ISSN 1785 0037 (Online)
DOI: http://dx.doi.org/10.15666/aeer/1704_95299545

were the lowest at 12 h, based on analysis of variance. Therefore, in the present study, UPLC had a lower detection limit for amino acids, relative to previous studies that used amino acid analyzer (Dong et al., 2015; Pan et al., 2016). Thus, the UPLC method employed here can be used for the determination of low levels of amino acids in root exudates.

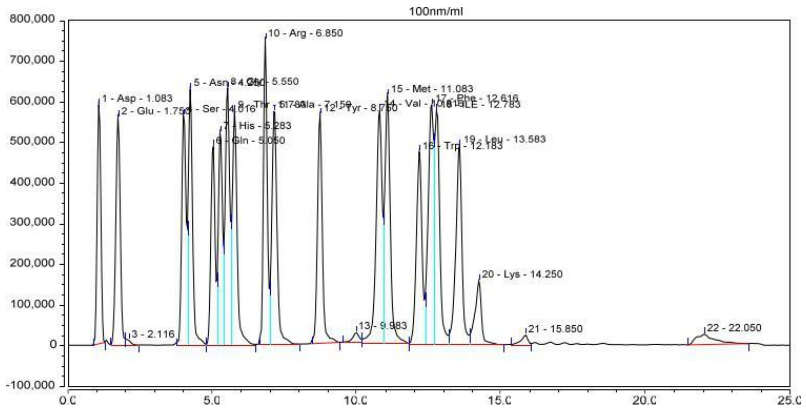

Figure 4. *Ultra-high performance liquid chromatography (UPLC) chromatogram of amino acid standards at concentration of 100 nmol/mL. Retention times of amino acids for: peak 1, arginine (Arg), 1.083 min; peak 2, glutamic acid (Glu), 1.750 min; peak 4, serine (Ser), 4.016 min; peak 5, asparagine (Asn), 4.250 min; peak 6, glutamine (Gln), 5.050 min; peak 7, histidine (His), 5.283 min; peak 8, glycine (Gly, 5.550 min; peak 9, threonine (Thr), 5.783 min; peak 10, argnine (Arg), 6.850 min; peak 11, alanine (Ala), 7.150 min; peak 12, tyrosine (Tyr), 8.750 min; peak 14, valine (Val), 10.816 min; peak 15, methionine (Met), 11.083 min; peak 16, tryptophan (Trp), 12.183 min; peak 17, phenylalanine (Phe), 12.616 min; peak 18, isoleucine (Ile), 12.783 min; peak 19, leucine (Leu), 13.583 min; peak 20, lysine (Lys), 14.250 min. Peaks 3, 13, 21, and 22 were solvent peaks*

Table 1. *Amino acid contents of root exudates of F. mandshurica as determined using UPLC. (There were 4 treatments based on collection times of 6 h, 12 h, 18 h and 24 h)*

Time of collection	Amino acid content (nmol/mL)						
	Asp	Asn	Gly	Ala	Val	Ile	Leu
6 h	n.a.	$0.66\pm0.08^{a, D}$	$7.02\pm0.15^{b, A}$	n.a.	$1.07\pm0.07^{b, C}$	n.a.	$3.51\pm0.21^{b, B}$
12 h	1.30 ± 0.04^{F}	$0.22\pm0.03^{b, G}$	$20.66\pm0.51^{a, A}$	3.05 ± 0.11^{E}	$7.93\pm0.26^{a, B, C}$	7.39 ± 0.17^{D}	$8.15\pm0.44^{a, B}$
18 h	n.a.	n.a.	4.59 ± 0.14^{c}	n.a.	n.a.	n.a.	n.a.
24 h	n.a.	n.a.	3.01 ± 0.27^{d}	n.a.	n.a.	n.a.	n.a.

Lower case letters a-d indicate intra-group differences ($p<0.05$), while uppercase letters A-G indicate inter-group differences ($p<0.05$)

Analysis of sugars in root exudates by HPIC

Quantitative analysis of sugars in root exudates was done with HPIC using retention times of chromatographic peaks (*Fig. 5*), while quantitative analysis was done using the external standard method. The results of the analysis of sugars in root exudates of *F. mandshurica* (*Table 2*) showed that the major sugars were Fuc, Ara, Gal, Glc, Xyl, Man, Fru, and Glc-AC. The types of sugars identified varied greatly between the results for HPIC and GC-MS

http://www.aloki.hu ● ISSN 1589 1623 (Print) ● ISSN 1785 0037 (Online)
DOI: http://dx.doi.org/10.15666/aeer/1704_95299545

analyses, with HPIC showing much smaller amounts and fewer types of sugars than GC-MS. This occurred probably because GC-MS detected smaller amounts of sugars than HPIC. Other sugars were present in low levels in the root exudates, but the amounts were lower than the HPIC detection limit. It was also found that the type and amounts of sugars differed significantly at different collection times. The amounts and varieties of sugars tended to increase significantly as the collection time increased (0-12 h).

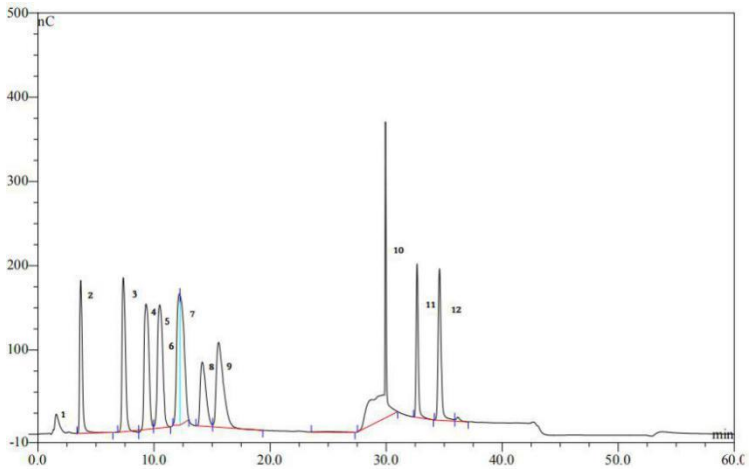

Figure 5. *High performance ion chromatography (HPIC) chromatogram of sugar standards at concentration of 30 ug/mL. the retention times were: peak 2, fucose (Fuc), 3.67 min; peak 3, arabinose (Ara), 7.35 min; peak 4, galactose (Gal), 10.48 min; peak 5, glucose (Glc), 12.17 min; peak 6, mannose (Man), 12.98 min; peak 7, xylose (Xyl), 14.15 min; peak 8, fructose (Fru), 15.12 min; peak 9, ribose (Rib), 15.62 min; peak 11, galacturonic acid (Gal-AC), 32.67 min, and peak 12, glucuronic acid (Glc-AC), 34.60 min. Peaks 1 and 10 were solvent peaks*

Table 2. *Sugar content of root exudates of F. mandshurica, as determined using high performance ion chromatography. (There were 4 treatments based on collection times of 6 h, 12 h, 18 h and 24 h)*

Time of collection	Sugar content (μg/mL)							
	Fuc	Ara	Gal	Glc	Xyl	Man	Fru	Glc-AC
6 h	$2.62\pm0.01^{a, D}$	$7.14\pm0.24^{b, B}$	$7.03\pm0.34^{b, B}$	$20.21\pm0.52^{b,A}$	n.a.	$4.47\pm0.28^{b,C}$	n.a.	n.a.
12 h	$2.59\pm0.02^{a, F}$	$51.08\pm1.26^{a,B}$	$9.91\pm0.64^{a, D}$	136.93 ± 2.37^{aA}	$11.27\pm0.62^{a,C}$	$8.72\pm0.57^{a,E}$	12.59 ± 0.62^{C}	$12.05\pm0.71^{a,C}$
18 h	n.a.	$4.88\pm0.03^{c, D}$	$6.28\pm0.11^{c, C}$	$12.78\pm0.84^{c,A}$	$10.81\pm0.14^{a,B}$	n.a.	n.a.	$0.65\pm0.08^{b, E}$
24 h	n.a.	$4.33\pm0.03^{d, D}$	$5.72\pm0.06^{d, B}$	$4.98\pm0.22^{d, C}$	$11.49\pm0.37^{a,A}$	n.a.	n.a.	$0.54\pm0.11^{b, E}$

Lower case letters (a-d) indicate intra-group differences ($p<0.05$), while uppercase letters (A-G) indicate inter-group difference ($p<0.05$)

However, the amount and varieties of sugars decreased significantly after 12 h. This occurred because *F. mandshurica* utilized the sugars from the root exudates as carbon substrates. Thus, the amount of sugar left decreased with time, and was almost exhausted at 24 h. Interestingly, the content of xylose did not vary significantly after 12 h, probably because the coefficient of xylose by plants and microorganisms is low (Jeffries, 1983). Therefore, the best time to collect in root exudates for the determination of sugar content

http://www.aloki.hu ● ISSN 1589 1623 (Print) ● ISSN 1785 0037 (Online)
DOI: http://dx.doi.org/10.15666/aeer/1704_95299545

of *F. mandshurica* was 12 h. The content of Glc was the highest among the sugars in the root exudates, while the contents of Ara, Gal, Xyl, Man, Fru, Glc-AC were higher, with Fuc being the lowest in quantity at 12 h, based on analysis of variance. Therefore, in the present study, HPIC had a lower limit of detection, relative to previous studies which used the anthrone and phenol-sulfuric acid colorimetric assay methods (Zhang et al., 2016; Jiang et al., 2018). Thus, the HPIC method used here can be used for the determination of low levels of sugars in root exudates.

Analysis of organic acids in root exudates using HPIC

The quantitative analysis of organic acids in root exudates was done with HPIC using external standard method, while qualitative analysis was done using the retention time of chromatographic peaks (*Fig. 6*). The results of the analysis of organic acids in root exudates of *F. mandshurica* (*Table 3*) showed that the major organic acids were propionic, valeric, lactic, succinic, tartaric, and oxalic acids.

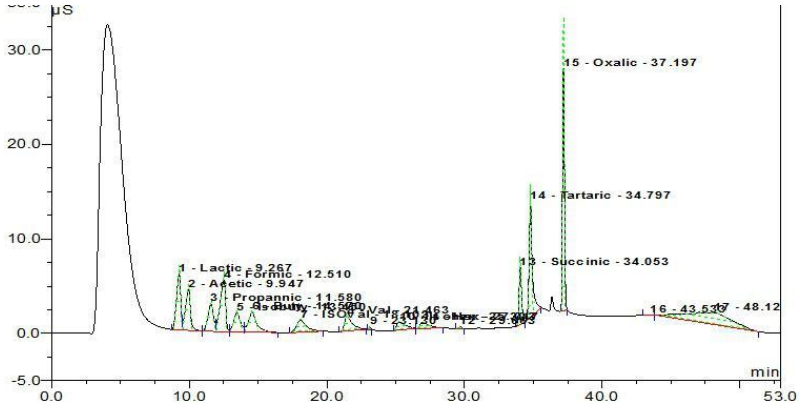

Figure 6. *High performance ion chromatography (HPIC) chromatogram of organic acid standards at concentration of 40 µg/mL. Retention times were: peak 1, lactic acid, 9.27 min; peak 2, acetic acid, 9.95 min; peak 3, propionic acid, 11.58 min; peak 4, formic acid, 12.51 min; peak 5, isobutyric acid, 13.45 min; peak 6, butyrate acid, 14.57 min; peak 7, isovalerate acid, 18.10 min; peak 8, valerate acid, 21.46 min; peak 10, isohexadecanoic acid, 25.30 min; peak 11, hexadecanoic acid, 27.02 min; peak 13, succinic acid, 34.05 min; peak 14, tartaric acid, 34.80 min, and peak 15, oxalic acid, 37.20 min. Peaks 9, 12, 16, and 17 were solvent peaks*

Table 3. *Organic acid analysis of root exudates in F. mandshurica using high performance ion chromatography. This study had four treatments based on collection times of 6 h, 12 h, 18 h, and 24 h*

Time of collection	The organic acid content (µg/mL)					
	Propionic	Valeric	Lactic	Succinic	Tartaric	Oxalic
6 h	$6.37\pm0.22^{d, B}$	n.a	n.a.	$2.69\pm0.19^{b, C}$	$9.29\pm0.38^{d, A}$	$1.86\pm0.12^{c, D}$
12 h	$13.78\pm0.73^{a, B}$	$0.47\pm0.26^{a, F}$	$0.84\pm0.19^{a, E}$	$6.61\pm0.53^{a, D}$	$22.91\pm0.87^{a, A}$	$7.34\pm0.53^{a, C}$
18 h	$11.48\pm0.37^{b, B}$	n.a	$0.13\pm0.08^{b, D}$	$6.79\pm0.46^{a, C}$	$23.86\pm0.66^{b, A}$	$6.78\pm0.44^{a, C}$
24 h	$10.55\pm0.42^{c, B}$	n.a	n.a.	$6.41\pm0.33^{a, C}$	$21.61\pm0.59^{c, A}$	$4.88\pm0.32^{b, D}$

The lower case letters a-d indicate intra-group difference ($p<0.05$) and the uppercase letters of A-G indicate inter-group difference ($p<0.05$)

http://www.aloki.hu ● ISSN 1589 1623 (Print) ● ISSN 1785 0037 (Online)
DOI: http://dx.doi.org/10.15666/aeer/1704_95299545

These results are similar to those reported by other workers (Niu et al., 2017; Wu et al., 2018). The types of organic acids varied greatly between results from HPIC and GC-MS analyses, with HPIC being less sensitive in the detection of organic acids than GC-MS. This is due to the fact that GC-MS is more sensitive than HPIC, and so can detect smaller amounts of organic acids. Other organic acids were present in low levels in the root exudate, but the amounts were lower than the detection limit of HPIC. It was also found that the types and amounts of organic acids varied significantly at different collection times. The types and varieties of organic acids present tended to increase over time (0-12 h), with slight declines after 12 h. Again, this trend is most likely due to the fact that *F. mandshurica* used the organic acids as carbon substrates, leading to their decline in concentration with time. Therefore, the best collection time for the determination of organic acid content of root exudates of *F. mandshurica* is 12 h after collection of the roots. Tartaric acid was found in the highest amount among the organic acids of root exudates, while higher levels of propionic, succinic, and oxalic acids were present at 12 h.

Conclusion

The results obtained in this study indicate that time of collection has a strong influence on the varieties and concentrations of organic compounds in the root exudate of *F. mandshurica* obtained using water culture collection method. The collection time for qualitative analysis of sugars, amino acids, and organic acids with GC-MS can be arbitrary chosen within 24 h, theoretically. However, the use of GC-MS in the present study has shown the presence of 219 compounds in the root exudates of *F. mandshurica,* with the highest contents at collection time of 12 h. Over 200 compounds have been identified in the root exudates of several economic forest trees using GC-MS at collection time of 12 h (Sun et al., 2003). Forty compounds were found in the root exudates of *Gymnorrhiza* seedling using GC-MS at the collection time of 6 h (Liu et al., 2011). However, only 17 compounds were found in the root exudates of *Rubber* seedling using GC-MS, at the collection time of 6 h (Wang et al., 2010). In another study, over 100 compounds were identified in the root exudates of *Capsicum chinense* Jacquin at collection time of 120 h (Han et al., 2015). The use of GS-MS also resulted in the identification of 55 organic compounds in the root exudates of *Fritillaria pallidiflora* Schvek seedlings at collection time of 72 h (Wang et al., 2009). Sometimes, the results may not be accurate because of the low concentration of root exudate available at the beginning of the collection, apart from the findings that root exudates are affected by plants and microorganisms after 12 h (Fransson and Johansson, 2010; Shi et al., 2011).

In the present study, the optimal collection time for quantitative analysis of sugars, amino acids, and organic acids using UPLC and HPIC target analysis methods was 12 h. The HPIC detection limit for sugar content and organic acid content was 0.1 μg/mL. However, the HPLC detection limit of sugar content in root exudates was 3 μg/mL (Gao et al., 2017), while the detection limit using anthrone and phenol-sulfuric acid colorimetric assay was 10 μg/mL (Zhang et al., 2016). In another study, the HPLC detection limit of organic acid content in root exudates was 12.5 μg/mL (Gao et al., 2018). Thus, the UPLC and HPIC target analysis methods have low detection limits and relatively wider linear ranges than the current methods. Therefore, the UPLC, HPIC target analysis methods provide a good quantitative analytical method for identification and measurement root exudates. We believe that these methods should be popularized and

http://www.aloki.hu ● ISSN 1589 1623 (Print) ● ISSN 1785 0037 (Online)
DOI: http://dx.doi.org/10.15666/aeer/1704_95299545

widely used. Forest researchers will need to consider the collection time when gathering root exudates so as to maximize the accuracy of results from qualitative and quantitative analyses of root exudates. In addition, the water culture system used to collect root exudates in this study is free from external interferences. However, there are many microorganisms in the actual rhizosphere. These microorganisms use the exudates to carry out their own metabolic activities, thereby affecting the results of measurements. Therefore, more studies are needed on methods of determination of root exudates in rhizosphere environment, the dynamic changes in root exudates, changes in root exudates under different external influences, and mechanisms involved in plant-soil-microbe interactions mediated by root exudates.

Acknowledgements. We thank Letpub Editing (https://www.letpub.com.cn/) for editing this manuscript. We thank the National Key R & D Program of China (2017YFD0600605) for funding support.

Conflicts of Interests. The authors declare no conflict of interests.

REFERENCES

[1] Akiyama, K., Matsuzaki, K., Hayashi, H. (2005): Plant sesquiterpenes induce hyphal branching in arbuscular mycorrhizal fungi. – Nature 435(7043): 824-827.
[2] Bardgett, R. D., Yeates, G. W., Anderson, J. M. (2005): Patterns and determinants of soil biological diversity. – Biological Diversity & Function in Soils 22: 100-118.
[3] Bowsher, A. W., Ali, R., Harding, S. A., Tsai, C. J., Donovan, L. A. (2015): Analysis of wild sunflower (Helianthus annuus L.) root exudates using gas chromatography-mass spectrometry. – Journal of Plant Nutrition and Soil Science 178(5): 776-786.
[4] Carvalhais, L. C., Dennis, P. G., Fedoseyenko, D., Borriss, R., vonWiren, N. (2011): Root exudates of sugars, amino acids, and organic acids by maize as affected by nitrogen, phosphorus, potassium, and iron deficiency. – Journal of Plant Nutrition and Soil Science 174(1): 3-11.
[5] Chang, E. H., Zhang, S. F., Wang, Z. Q., Wang, X. M., Zhang, J. H. (2008): Effect of Nitrogen and Phosphorus on the Amino Acids in Root Exudates and Grains of Rice During Grain Filling. – Acta Agronomica Sinica 34(4): 612-618.
[6] Dietrich, S., Floegel, A., Troll, M., Kühn, T., Rathmann, W., Peters, A., Sookthai, D., von Bergen, M., Kaaks, R., Adamski, J., Prehn, C., Boeing, H., Schulze, M. B., Illig, T., Pischon, T., Knüppel, S., Wang-Sattler, R., Drogan, D. (2016): Random Survival Forest in practice: a method for modelling complex metabolomics data in time to event analysis. – International Journal of Epidemiology 45(5): 1406-1420.
[7] Dijkstra, F. A., Cheng, W. (2007): Moisture modulates rhizosphere effects on C decomposition in two different soil types. – Soil Biology & Biochemistry 39(9): 2264-2274.
[8] Dinkelaker, B., Römheld, V., Marschner, H. (2010): Citric acid excretion and precipitation of calcium citrate in the rhizosphere of white lupin (*Lupinus albus* L.). – Plant, Cell & Environment 12(3): 285-292.
[9] Dong, Y., Dong, K., Tang, L., Zheng, Y., Li, X. R., Hu, G. B., Liu, Y. M. (2015): Relationship of free amino acids in root exudates with wilt disease (FUSARIUM OXYSPORUM) of faba bean. – Acta pedologica sinica 52(4): 919-925.
[10] Fransson, P. M., Johansson, E. M. (2010): Elevated CO and nitrogen influence exudates of soluble organic compounds by ectomycorrhizal root systems. – FEMS Microbiology Ecology 71(2): 186-196.

http://www.aloki.hu ● ISSN 1589 1623 (Print) ● ISSN 1785 0037 (Online)
DOI: http://dx.doi.org/10.15666/aeer/1704_95299545

[11] Gao, Q., Han, Z. T. (2017): Determination of soluble sugars in forest biomass raw materials by high performance liquid chromatography-differential refractive index detector. – Chinese Journal of Analysis Laboratory 36(12): 1406-1410.
[12] Gao, Y. Y., Peng, Z. F., Yang, C., Chang, M. Y., Zhu, M. L. (2018): Determination of the Effect of Organic Acids in Ricinus Communis L. Roots under Copper Stress by HPLC. – Guangdong Chemical Industry 45(21): 10-14.
[13] García, J. A. L., Barbas, C., Probanza, A., Barrientos, M. L., Gutierrez Mañero, F. J. (2010): Low molecular weight organic acids and fatty acids in root exudates of two Lupinus cultivars at flowering and fruiting stages. – Phytochemical Analysis Pca 12(5): 305-311.
[14] Gargallogarriga, A., Wright, S. J., Sardans, J., Pérez-Trujillo, M., Oravec, M., Večeřová, K., Urban, O., Fernández-Martínez, M., Parella, T., Peñuelas, J. (2017): Long-term fertilization determines different metabolomic profiles and responses in saplings of three rainforest tree species with different adult canopy position. – Plos One 12(5): 177030.
[15] Han, X., Yang, Y., Sun, J. H., Liu, Z. H., Niu, Y., Cao, Z. M. (2015): Identification of chemical components of root exudates of sand-cultured capsicum Chinese Jacquin. – Chinese Journal of Tropical Agricultural 35(12): 73-79.
[16] Huang, C., Webb, M. J., Graham, R. D. (1996): Pot size affects expression of Mn efficiency in barley. – Plant and Soil 178(2): 205.
[17] Jeffries, T. W. (1983): Utilization of xylose by bacteria, yeasts, and fungi. – Advances in Biochemical Engineering / Biotechnology 27(27): 1-32.
[18] Jiang, Z., Xiao, X. J., Zhang, Z. L., Qiao, M. F., He, W., Liu, Q., Yin, H. J. (2018): Effects of night-time warming on the rates and main chemical components of root exudates produced by Picea asperata seedlings in subalpine coniferous forests. – Acta ecologica sinica 38(9): 308-309.
[19] Kajos, M. K., Rantala, P., Hill, M., Hellén, H., Aalto, J., Patokoski, J., Taipale, R., Hoerger, C. C., Reimann, S., Ruuskanen, T. M., Rinne, J., Petäjä, T. (2015): Ambient measurements of aromatic and oxidized VOCs by PTR-MS and GC-MS: intercomparison between four instruments in a boreal forest in Finland. – Atmospheric Measurement Techniques 8(4): 3753-3802.
[20] Kerdchoechuen, O. (2005): Methane emission in four rice varieties as related to sugars and organic acids of roots and root exudates and biomass yield. – Agriculture Ecosystems & Environment 108(2): 155-163.
[21] Kuo, Y. H., Lambein, F., Ikegami, F., Van Parijs, R. (1982): Isoxazolin-5-ones and Amino Acids in Root Exudates of Pea and Sweet Pea Seedlings. – Plant Physiology 70(5): 1283-1289.
[22] Li, L., Li, S. M., Sun, J. H., Zhou, L. L., Bao, X. G., Zhang, H. G., Zhang, F. S. (2007): Diversity enhances agricultural productivity via rhizosphere phosphorus facilitation on phosphorus-deficient soils. – Proceedings of the National Academy of Sciences of the United States of America 104(27): 11192-11196.
[23] Li, J., Jiang, X. M., Yin, H. J., Yin, C. Y., Wei, Y. H., Liu, Q. (2014): Root exudates and soil microbes in three Picea asperata plantations with different stand ages. – Ying Yong Sheng Tai Xue Bao 25(2): 325-332.
[24] Liu, X. Y., Chen, X., Wu, L., Chen, M., Zhou, K. B. (2016): GC-MS Analysis of Root Exudates of Gymnorrhiza Seedings. – Chinese Journal of Tropical Crops 37(4): 835-843.
[25] Luo, Q., Sun, L. N., Hu, X. M. (2014): The variation of root exudates from the hyperaccumulator Sedum alfredii under cadmium stress: metabonomics analysis. – Plos One 9(12): 115581.
[26] Malandrino, M., Abollino, O., Buoso, S., Giacomino, A., La Gioia, C., Mentasti, E. (2011): Accumulation of heavy metals from contaminated soil to plants and evaluation of soil remediation by vermiculite. – Chemosphere 82(2): 169-178.
[27] Maqsood, M. A., Hussain, S., Aziz, T., Ashraf, M. (2011): Wheat-Exuded Organic Acids Influence Zinc Release from Calcareous Soils. – Pedosphere 21(5): 657-665.

http://www.aloki.hu ● ISSN 1589 1623 (Print) ● ISSN 1785 0037 (Online)
DOI: http://dx.doi.org/10.15666/aeer/1704_95299545

[28] Materechera, S. A., Dexter, A. R., Alston, A. M. (1992): Formation of aggregates by plant roots in homogenised soils. – Plant & Soil 142(1): 69-79.
[29] Mei, L., Wang, Z., Han, Y., Gu, J., Wang, X., Cheng, Y., Zhang, X. J. (2006): Distribution patterns of Fraxinus mandshurica root biomass, specific root length and root length density. – Chinese Journal of Applied Ecology 17(1): 1-4.
[30] Niu, F. H., Li, Z. H., Chen, S. X. (2017): Effect of Phosphorus Levels on Organic Acids in Eucalyptus duhhii Root Exudates. – Eucalypts Science & Technology 34(1): 1-8.
[31] Oades, J. M. (2010): Mucilages at the root surface. – European Journal of Soil Science 29(1): 1-16.
[32] Pan, S. W., Yuan, X., Liu, C., Li, Y. L., Yang, T., Tang, H. Y., Huang, F. Y. (2016): Effects of Pyrene on Low Molecule Weight Organic Compounds in the Root Exudates of Five Species of Festuca. – Environmental Science 37(6): 2368-2375.
[33] Paynel, F., Murray, P. J., Cliquet, J. B. (2001): Root exudates: A pathway for short-term N transfer from clover and ryegrass. – Plant & Soil 229(2): 235-243.
[34] Peters, N. K., Frost, J. W., Long, S. R. (1986): A plant flavone, luteolin, induces expression of Rhizobium meliloti nodulation genes. – Science 233(4767): 977-980.
[35] Phillips, R. P., Fahey, T. J. (2006): Tree Species and Mycorrhizal Associations Influence the Magnitude of Rhizosphere Effects. – Ecology 87(5): 1302-1313.
[36] Phillips, R. P., Bernhardt, E. S., Schlesinger, W. H. (2009): Elevated CO_2 increases root exudates from loblolly pine (Pinus taeda) seedlings as an N-mediated response. – Tree Physiology 29(12): 1513-1523.
[37] Ren, J., Xu, C. Y., Wei, Y. B., Lin, Y. M., Duan, Y. H. (2010): Seasonal dynamics and influence factor of root respiration of Fraxinus mandushurica in the Changbai Mountain. – Scientia Silvae Sinicae 46(5): 77-83.
[38] Rissanen, T., Hyötyläinen, T., Kallio, M., Kronholm, J., Kulmala, M., Riekkola, M. L. (2006): Characterization of organic compounds in aerosol particles from a coniferous forest by GC-MS. – Chemosphere 64(7): 1185-1195.
[39] Sandnes, A., Eldhuset, T. D., Wollebaek, G. (2005): Organic acids in root exudates and soil solution of Norway spruce and silver birch. – Soil Biology & Biochemistry 37(2): 259-269.
[40] Selvakumar, G., Panneerselvam, P. (2012): Bacterial Mediated Alleviation of Abiotic Stress in Crops. Bacteria in Agrobiology: Stress Management. – Springer Berlin Heidelberg 34(2): 205-224.
[41] Shi, S., Condron, L., Larsen, S., Richardson, A. E., Jones, E. E., Jiao, J., O'Callaghan, M., Stewart, A. (2011): In situ sampling of low molecular weight organic anions from rhizosphere of radiata pine (Pinus radiata) grown in a rhizotron system. – Environmental & Experimental Botany 70(2): 131-142.
[42] Singh, G., Mukerji, K. G. (2006): Root Exudates as Determinant of Rhizospheric Microbial Biodiversity. – Soil Biology 7: 39-53.
[43] Sun, H. Y., Wang, Y. Z., Yang, L. (2003): Analysis of the major components of root exudates released from several economic forest tree using GC-MS. – Journal of Forestry Research 14(2): 127-129.
[44] Suzuki, K., OkazakiI, K., Tawaraya, K., Osaki, M., Shinano, T. (2009): Gas chromatography–mass spectrometry associated global analysis of rice root exudates under aseptical conditions. – Soil Science & Plant Nutrition 55(4): 505-513.
[45] Venkatasubbarao, G., NoriharuAe, T. (1997): Genotypic variation in iron-, and aluminum-phosphate solubilizing activity of pigeonpea root exudates under P deficient conditions. – Soil Science & Plant Nutrition 43(2): 295-305.
[46] Wang, Y., Kaisar, S., Li, J., Zhu, G. Q., Song, T. S., Liu, L. (2009): Analysis of Components in Root Exudates of Fritillaria pallidiflora Schvek Seedlings at Different Ages by Gas Chromatography-mass Spectrometry. – Acta Botanica Boreali-Occidentalia Sinica 29(2): 384-389.

http://www.aloki.hu ● ISSN 1589 1623 (Print) ● ISSN 1785 0037 (Online)
DOI: http://dx.doi.org/10.15666/aeer/1704_95299545

[47] Wang, W. B., Wu, X. P., Yin, Y. L., Guo, H. C., Luo, X. H. (2010): GC-MS Analysis of Rubber Seedling Root Exudates with Nutrient Solution Cultivation. – Chinese Journal of Tropical Crops 31(12): 2281-2286.
[48] Wang, J. X., Zhan, F. D., Li, Y., Zu, Y. Q., Qin, L., He, Y. M. (2016): Effects of Arabisalpina L. var. parviflora Franch and Zea mays L. intercropping system on root-exudated organic acids under lead stress. – Chinese Journal of Eco-Agriculture 24(3): 365-372.
[49] Wu, C. C., Liu, J., Zhang, X. D. (2018): Determination of organic acids in the root exudates of Cr-hyperaccumulator Leersia hexandra Swartz using high performance liquid chromatography. – Chinese Journal of Chromatography 36(2): 167-172.
[50] Xiao, J. X., Zheng, Y., Tang, L., Dong, Y. (2015): Effect of Wheat and Faba Bean Intercropping on Sugar and Amino Acid Exuded by Roots. – Ecology and Environmental Sciences 24(11): 1825-1830.
[51] Yin, H., Li, Y., Xiao, J., Xu, Z., Cheng, X., Liu, Q. (2013): Enhanced root exudates stimulates soil nitrogen transformations in a subalpine coniferous forest under experimental warming. – Global Change Biology 19(7): 2158-2167.
[52] Young, R. F., Coy, D. L., Fedorak, P. M. (2010): Evaluating MTBSTFA derivatization reagents for measuring naphthenic acids by gas chromatography-mass spectrometry. – Analytical Methods 2(6): 765-770.
[53] Zhang, X. Z., Li, T. X., Wang, Y. D. (2007): Relationship between growth environment and root exudates of plants: A review. – Chinese Journal of Soil Science 38(4): 785-789.
[54] Zhang, A. H., An, N. B., Lei, F. J., Ma, W. L., Chi, K., Zhang, L. X. (2016): Chemotaxis response of Erwinia carotovora on sugars and amino acids of root exudates of Panax ginseng. – China Journal of Chinese Materia Medica 41(21): 3937-3941.
[55] Zhen, W., Wang, X., Cao, K., Jin, Z. J. (2004): Study on determination and allelopathy of amino acids in strawberry root exudates and decomposing products. – Journal of Agricultural University of Hebei 27(2): 76-80.

http://www.aloki.hu ● ISSN 1589 1623 (Print) ● ISSN 1785 0037 (Online)
DOI: http://dx.doi.org/10.15666/aeer/1704_95299545

TRACE METAL ENVIRONMENTAL CONTAMINATION RECORDS IN CORE SEDIMENTS OF GORGAN BAY IN THE SOUTHEAST OF THE CASPIAN SEA

BAGHERI, H. – MAHMUDY GHARAIE, M. H. * – MOUSSAVI HARAMI, R. – KHANEHBAD, M.

Department of Geology, Faculty of Sciences, Ferdowsi University of Mashhad, Mashhad, Iran

**Corresponding author*
e-mail: mhmgharaie@um.ac.ir

(Received 4th Nov 2018; accepted 22nd May 2019)

Abstract. In this study five sedimentary cores were collected from Gorgan Bay (southeastern part of the Caspian Sea). Concentrations of elements were measured to determine depositional trends and geo-statistical assessment of toxic elements was carried out. Al, Fe, K, Mg, Na and S content increased in all 5 cores, from the bottom to near the top layer, with maximum concentrations at 15–45 cm depths. However, for the toxic elements, maximum concentration of As, Cr, Cu, Pb, Zn, Co and Ni varied in different depth of 5-15 cm and 80-120 cm. Enrichment factors (EFs) and pollution load index (PLI) were calculated to assess the enrichment and pollution of heavy elements in the bay sediments. Except for Ca and S, all studied elements showed positive and significant correlations with Fe and Al, which indicate the same source (human or natural). Principal component analysis (PCA) indicated that sediments were influenced by both geologic and anthropogenic impacts. According to the EFs, most toxic elements showed no significant enrichment and no pollution in the core sediments. Based on PLI average value in all cores, the southeast coast of the Caspian Sea (Gorgan Bay) should be classified as not metal polluted, but in recent decades there has been a dramatic increase of toxic elements that needs more attention and also monitoring.
Keywords: *heavy metals, sedimentary cores, geochemistry, source*

Introduction

The study of core sediments is very useful to detect different natural process such as paleoclimate changes, or anthropogenic activities on sedimentary environments (Harikumar and Nasir, 2010) by examining the geochemical and geo-statistical data (Karbassi et al., 2005; Mohamed et al., 2005; Sun et al., 2012; Vallius, 2014; Veerasingam et al., 2015). The coastal zones with their variable physical and chemical properties are suitable environment for the assessment of pollutant accumulations in aquatic ecosystems, where the bottom sediments are affected by both dissolved heavy elements or on surface absorbed particles transported from land to the basin (Harbison, 1986; Szefer et al., 1995). Heavy metal concentrations from natural and anthropogenic sources in coastal area can be increased through high input after intense rock-minerals weathering in the land or due to urbanization (Harikumar and Nasir, 2010). Anthropogenic pollutions in aquatic environments have direct influence on coastal ecosystems (Alessandro et al., 2006). In fact, core sediments obtained from the coastal areas provide a good chronological record of contamination (Morelli et al., 2012). Understanding trace metal emissions in coastal environments is an important task for researcher sand policy planners, and regulatory actions can be implemented to reduce health risks potential.

http://www.aloki.hu ● ISSN 1589 1623 (Print) ● ISSN 1785 0037 (Online)
DOI: http://dx.doi.org/10.15666/aeer/1704_95479559

Study area

Gorgan Bay (Southeastern part of the Caspian Sea) is a unique brackish water body, semi-confined triangular-shaped having about 500 km^2 area, maximum depth of 4 m and average depth 1.5 m, high ecological value and hydromorphological properties such as depth variation, freshwater flow and wave exposure. It is located at the south-east of the Caspian Sea in both Golestan and Mazandaran provinces (*Fig. 1*). Gorgan Bay was formed during the late Holocene period by a coastal barrier system (sandy spit) which is named Miankaleh spite (Kakroudi et al., 2012). There are no tides in the Gorgan Bay like in other parts of the Caspian Sea. It is connected to the Caspian Sea through Ashoradeh-Bandar Torkaman mouth, (Approximately; width of 400 m, 3 km long) with strong currents in the area affected by storm surge. Water balance in the Gorgan Bay is influenced by water evaporation, precipitation, intrusion from the Caspian Sea, and to a lesser extent by fresh river water (Sharbaty, 2011, 2012). It receives freshwater from a number of rivers and small streams, Gorgan-rud River from the north of the inlet and Qarehsu river enters from the east.

Several works on distributions of heavy metals and other pollutants have been carried out in this area (Kasymov., 1989; Tait et al., 2004; Parr et al., 2007; Karbassi et al., 2008; Bastami et al., 2012; Nasrolahi et al., 2017), but no studies have focused on the trends of metals on different core sediments in this area. The aims of the current study are: (1) to describe the vertical variation of elements from east to west of Gorgan Bay; (2) to estimate the geochemical sources of major and trace metals in sediments using coefficient correlation and principal component analysis (PCA); and (3) to assess enrichment and possible contamination of trace metals in sediments, using enrichment factors (EFs) and pollution load index (PLI).

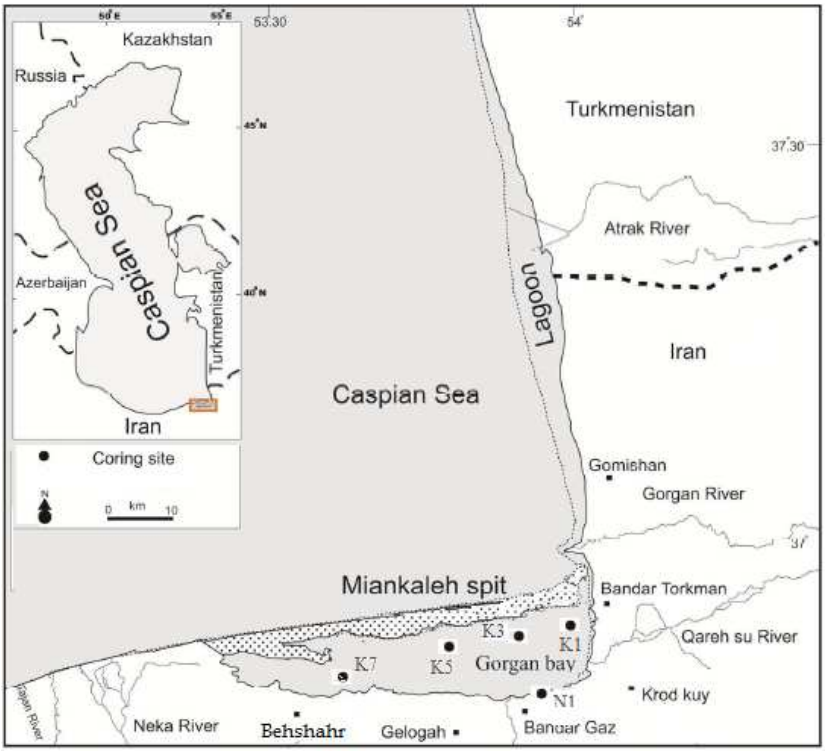

Figure 1. *The locations of the core sampling sites*

http://www.aloki.hu ● ISSN 1589 1623 (Print) ● ISSN 1785 0037 (Online)
DOI: http://dx.doi.org/10.15666/aeer/1704_95479559

Materials and methods

Five sedimentary cores with different length were collected using a gravity corer on August 2016 (*Table 1*). Samples were packed and carried in ice-boxes to the laboratory and stored at 4 °C until analysis. After opening the cores, about 25 subsamples picked from each core (each 5 cm 1 subsample and totally 120 subsamples). Subsamples were dried in an oven and then powdered by using a mortar then screened with a 0.5 mm sieve to remove large particles. Sediment samples (1 g) were digested using a mixed solution of 1:3 nitric acid : hydrochloric acid for 3 h. The solution was cooled, filtered through Whatman-42 and diluted to 50 ml volume using distilled water (APHA et al., 2005). Concentrations of major elements (Al, Ca, Fe, K, Mg, Na, and S) and trace metals (As, Co, Cr, Cu, Ni, Pb, and Zn) were measured by using inductively coupled plasma-optical emission spectrometry (ICP-OES; Varian 735 ES series), Arsenic (As) analysis was carried out by using atomic absorption spectrometry (model SOLAAR, M5) Data recoveries of the analysed element areas are the followings: Al (100%–101%), Ca (97.6%–97.8%), Fe (100%–101%), K (103%–104%), Mg (95.1%–95.3%), Na (102%–103%), S (98.7%–100%), As (112%–113%), Co (105%–111%), Cr (88.5%–88.7%), Cu (98.3%–98.8%), Ni (97.5%–98.7%), Pb (118%–121%), and Zn (93.2%–93.5%).

Table 1. *Geographic position, length and depth of each core in Gorgan Bay*

Core name	Water depth (m)	Core length (m)	Longitude	Latitude
K1	2.6	1.78	54° 0’ 42.34	36° 51’ 49.9
K3	3.24	1.67	53° 54’ 38.86	36° 50’ 33.5
K5	2.8	1.34	53° 48’ 43.5	36° 50’ 21.35
K7	0.4	1.3	53° 36’ 18.87	36° 48’ 26.31
N1	0.1	0.98	53° 54’ 62.5	36° 47’ 6.19

Grain size analysis was performed using laser particle size analyzer (HORIBA-LA950, France & Japan) in Iranian National Institute for Oceanography laboratory. Before analysis, about 4 g samples were cremated in an oven at 550 °C for 4 h and then at 950 °C for 1 h to remove organic matter and biogenic carbonate, respectively.

Pearson correlation analysis and PCA were conducted to specify geochemical associations and certainly the factors controlling the geochemical origin in coastal sediments (Bastami etal, 2014). A two-tailed Pearson correlation coefficient was used in correlation analysis. PCA was performed on a correlation matrix; N80% of the total variance was computed for principal components. Pearson correlation coefficients and PCA were accomplished using the SPSS 20.0 software. Enrichment factor (EF) as an appropriate index was calculated to determine anthropogenic or geogenic source of the toxic elements by normalizing their concentrations according to the sediment texture properties (Morillo et al., 2004; Selvaraj et al., 2004; Adamo et al., 2005; Vald’es et al., 2005; Shi et al., 2010; Morelli et al.2012; Zhang et al., 2013). To calculate the EF, Al is widely used in the equation as aluminum silicate, it is predominant at the coastal areas. Enrichment Factor is determined as follows (Huang and Lin, 2003; Woitke et al., 2003):

$$\text{Enrichment Factor} = (H / Al)_{\text{sample}} / (H / Al)_{\text{background}} \quad \text{(Eq.1)}$$

http://www.aloki.hu ● ISSN 1589 1623 (Print) ● ISSN 1785 0037 (Online)
DOI: http://dx.doi.org/10.15666/aeer/1704_95479559

where (H / Al) $_{sample}$ and $H / Al)_{background}$ are heavy metal concentrations in sample and background reference, respectively. In this study, we used background concentrations of heavy metals in K5 sediment core at the depth of 85 cm which are 2.96, 11.50, 53.01, 14.33, 27.43, 11.80 ppm and 41.60 for As, Co, Cr, Cu, Ni, Pb, and Zn, respectively (De Mora et al., 2004).

Results and discussion

Vertical distributions of selected elements in cores K1, K3, K5, K7 and N1 are presented in *Figure 2*. A lot of runoff and eroded sediments from several sources such as human activities and river systems (Bagheri et al., 2012) enters terrigenous materials into the Gorgan Bay. Generally concentration of Al, Fe, K, Mg, Na and S increased from the bottom to the top layers in the cores, and the maximum concentrations of these major elements were observed at depths of 15–45 cm in all cores, while the toxic elements have different trends. In core K1, the highest concentrations of Cr (75.95 ppm), Ni (83.22 ppm) and Zn (83.22 ppm) were determined at 5 cm depth, As (9.39 ppm) at 10 cm, Cu (36.64 ppm) at 15 cm, Co (21.79 ppm) at 30 cm and Pb (22.01 ppm) at 35 cm depth.

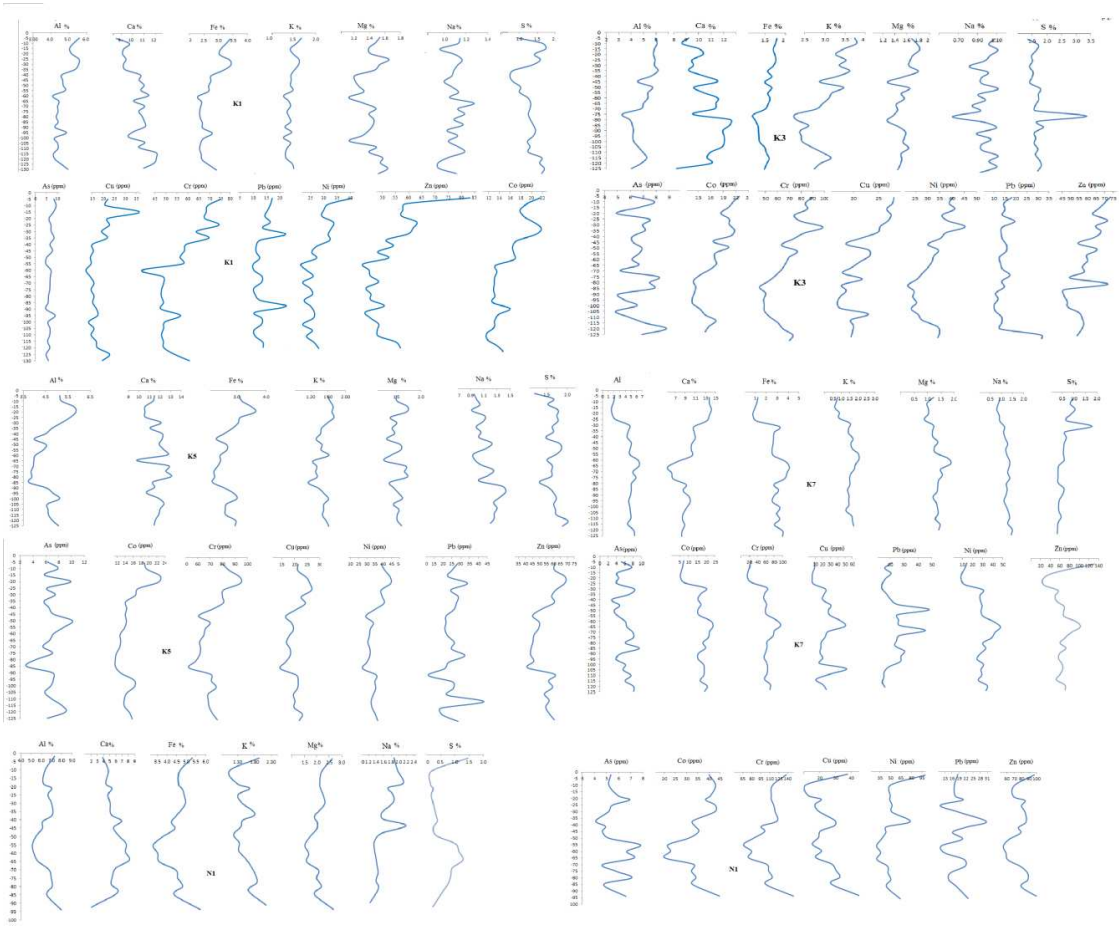

Figure 2. *Vertical distributions of major and trace metals in cores*

http://www.aloki.hu ● ISSN 1589 1623 (Print) ● ISSN 1785 0037 (Online)
DOI: http://dx.doi.org/10.15666/aeer/1704_95479559

In core K3, the highest concentration of Cu (28.04 ppm), Co (22.04 ppm) and Zn (73.45 ppm) were observed at 5 cm depth, for Cr (98.44) and Ni (45.26 ppm) at 10 cm depth, and for As (8.81 ppm) and Pb (31.38 ppm) at 120 cm depth.

In core K5 maximum concentrations of all heavy metals were observed at a depth of 15-20 cm, expect for As (10.15) at 50 and Pb (43.08) at 110 cm. opposite of this trend in west and south of Gorgan bay in the K7, N1 cores, the highest value of trace elements reported in different depths as As (9.55, 7.80 mg/g) at 85, 55 cm; Co (23.79, 44.79 mg/g); Cr (95.11, 149.4 mg/g) at 65, 94 cm; Ni (47.37, 105.4 mg/g) at 65,5; Cu (52.05, 45.20 mg/g) at 105,94 cm; Pb (48.13, 30.6 mg/g) at 50, 37cm and Zn (131.6, 106.7 mg/g) at 5, 94 cm depth (*Fig. 2*).

Heavy metals show some information about source and migration of sediments. For example, high correlations between heavy metals probably mean these elements reflect similar origin or share analogous transformation and immigration processes in the certain situation. The major factors affecting spatial variation of trace elements in the sediments are organic matter and the grain size (Aloupi and Angelidis, 2001; Huang and Lin, 2003; Liaghati et al., 2004). The fine grains, have high surface/volume ratio and cation absorption potential, and are more effective adsorbents of contaminated organic and inorganic materials (McCave, 1984; Horowitz and Elrick, 1987). Fine-grained sediments, which contain lots of organic matter are more contaminated than coarse-grained sediments (DeMora et al., 2004). However, some studies have reported an inverse relationship between particle size and metal content (Bastami et al., 2014). In our study, in most cores, all elements showed positive and significant correlation (except for Ca and S) with Fe and Al indicating the same origin or input source of these elements (human or natural) into the Gorgan Bay. Also, there was a positive and significant correlation between As, Fe, Zn, Cr, Ni, Cu and K, indicating that these elements have the same origin and the same behavior in the studied area. Sulfur and calcium had a negative correlation with most of the heavy metals which indicates different origin or behavior of these elements in the environment. Also, in core N1, arsenic had a negative correlation with most metals while it was positively correlated with calcium and showed negative correlation with iron and aluminum, which probably indicates the biological origin of this metalloid.

Three principal components (PC) were extracted from the core K1 sediments, which accounted for about 81.74% of the total variance. The first component (PC1) accounted for 58.21%, the second component (PC2) accounted for 14.26% and the third component (PC3) accounted for 8.22% of the total variance (*Fig. 3*). In PC1 high loadings of major elements (Al, Fe, K and Ca) and heavy metals (Co, Cr, Ni, As, Cu, Pb and Zn) were observed (from 0.617 to 0.958). The elements Al, Fe and K mainly represent lithogenic origin after weathering and erosion of rocks and soil parent materials, PC1 described the lithogenic source bound in aluminosilicate minerals. The second component (PC2) also showed Mg and S with moderate to high loadings (0.791-0.901) and Na with high loading counted in the third component (PC3).

In core K3, we extracted 3 PCs, which accounted for about 82.43% of the total variance (*Fig. 4*). Based on the loading distribution of the variable elements, Al, Ca, Fe, K, Mg, Cr, Ni, Cu, Co and Zn constituted a firmly related group (PC1) with 55.81% of the total variance. While another group was composed of Na and S (PC2) with 14.24% of the total variance. The third component (PC3) accounted for 12.37% and had high loadings on As and Pb. These results may indicate the different origins or controlling factors of the heavy metal distributions in the Gorgan Bay sediments. In this area, the

http://www.aloki.hu ● ISSN 1589 1623 (Print) ● ISSN 1785 0037 (Online)
DOI: http://dx.doi.org/10.15666/aeer/1704_95479559

lithogenic source acted as the main factor accounting for PC1, while PC2 and PC3 may be derived from the urban source.

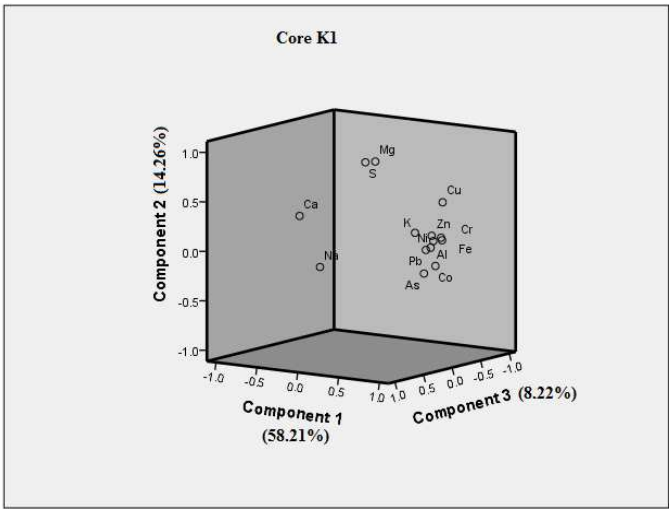

Figure 3. *PCA plot of elements in core K1*

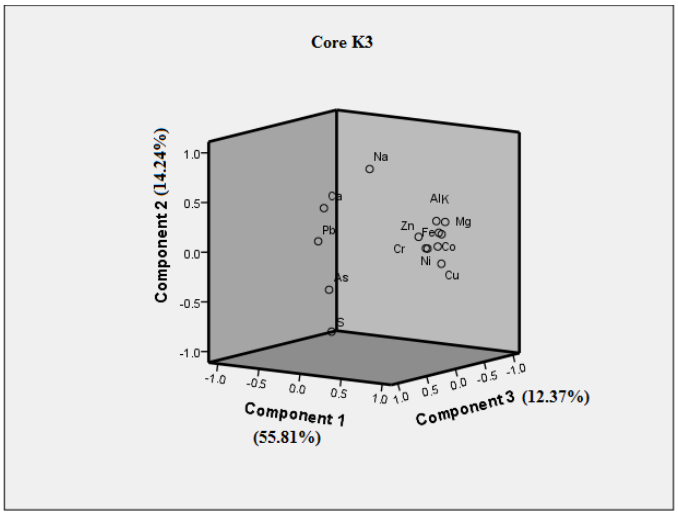

Figure 4. *PCA plot of elements in core K3*

In core K5, we extracted 3 PCs, which accounted for about 80.26% of the total variance (*Fig. 5*). The first component (PC1) accounted for 55.30% of the total variance and included all variable element except for Na, S, Pb and As, while the second component (PC2) accounted for 14.37% with high loading on Na, S and As (0.61-.82) and the PC3 accounted for 10.58% with high loading on Pb.

In core K7 (*Fig. 6*) that was obtained from west of the Gorgan Bay, 3 PCs were extracted and total variance was 86.55% (*Fig. 5*). In this core unlike in the other 4 cores Na and S with other elements (Al, Ca Fe, K, Mg, Cr, Ni, Cu, and Co), Zn with high loading on PC2, and Pb and As show loading on PC3, which accounted 65.11%, 11.79% and 9.65% respectively. In the studied area PCA showed anthropogenic input of Pb and Zn from the industrial activities (anthropogenic source), which are widely used

http://www.aloki.hu ● ISSN 1589 1623 (Print) ● ISSN 1785 0037 (Online)
DOI: http://dx.doi.org/10.15666/aeer/1704_95479559

as the main components in several industrial processes. In fact, those elements were partially derived from the anthropogenic source.

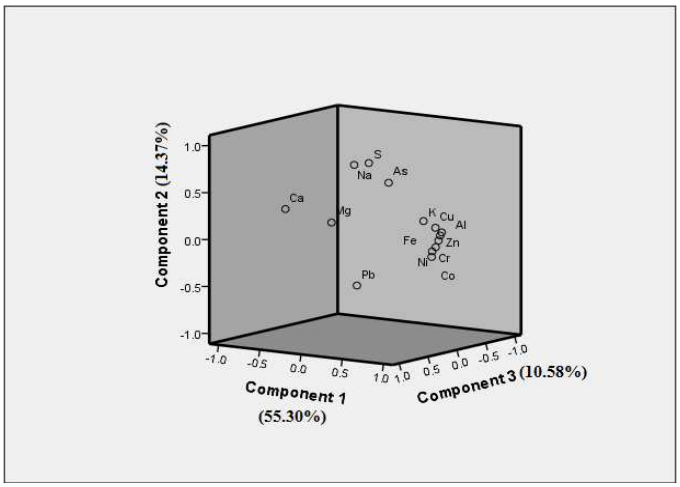

Figure 5. *PCA plot of elements in core K5*

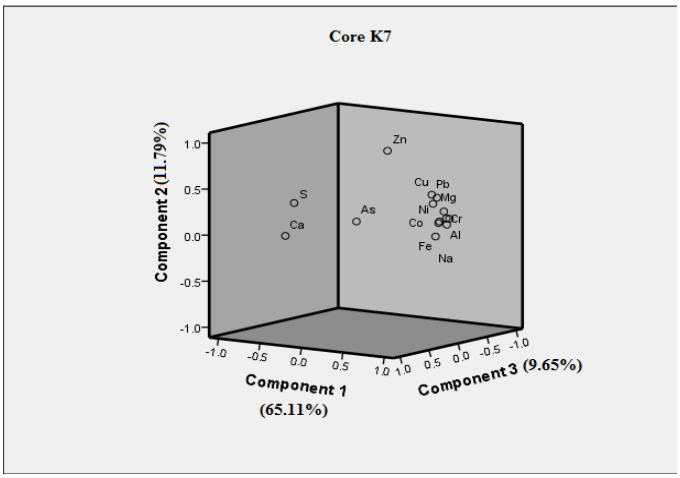

Figure 6. *PCA plot of elements in core K7*

Finally in core N1 (*Fig. 7*), 3 extracted PCs accounted for about 86.89% of the total variance. The PC1, PC2 and PC3 were 54.31%, 20.15% and 12.42% of the total variance, respectively (*Fig. 5*). The first principal component (PC1) included all elements expect for Na and S (that are considered as PC2) and As, Pb (that are considered as PC3) were lithogenic source. The PC2 also showed that Cu, Co, Pb and Zn had loadings on (0.16–0.63), indicating that these elements were partially derived from the anthropogenic source. Overall, all metals in the Gorgan bay sediments were mostly derived from the geologic origin (geogenic), except for western part of the bay, where the toxic elements were mainly derived from terrestrial discharge of industrial activities (anthropogenic).

Enrichment factor is a useful index to assess the heavy metals contamination in the soil and sediments (Feng et al., 2004; Reddy et al., 2004; Han et al., 2006; Chen, 2007; Çevik et al., 2009; Bastami et al., 2012). EF values are interpreted as; EF < 1, no

http://www.aloki.hu ● ISSN 1589 1623 (Print) ● ISSN 1785 0037 (Online)
DOI: http://dx.doi.org/10.15666/aeer/1704_95479559

enrichment; EF 1 to 3, minor enrichment; EF 3 to 5, moderate enrichment; EF 5 to 10, moderately severe enrichment; EF 10 to 25, severe enrichment; EF 25 to 50, very severe enrichment and EF > 50 extremely severe enrichment (Grant and Middleton, 1990; Loska et al., 1997; Abrahim and Parker, 2008). In this study, EF values in all core samples ranged in no-enrichment (EF < 1) to minor enrichment (EF 1 to 3) suggesting no anthropogenic enrichment of the toxic elements, except for Pb and Zn in core7, which show moderate enrichment of these elements (EF 3-5) and indicate that anthropogenic source of Zn and Pb were significantly polluted the sediments of core 7 (*Fig. 8*).

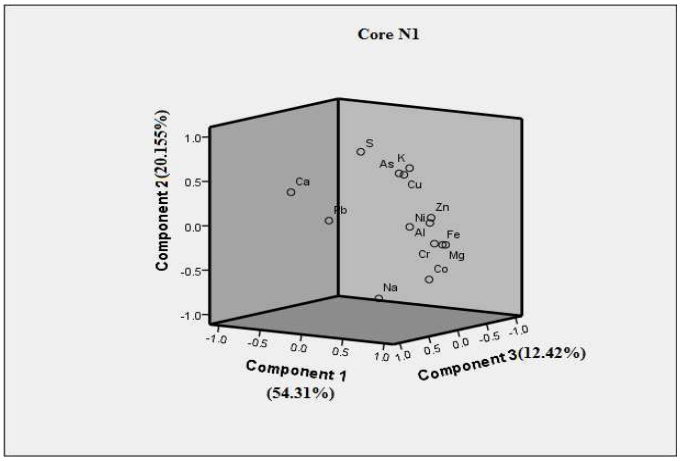

Figure 7. *PCA plot of elements in core N1*

To assess the sediment environmental quality, an integrated pollution load index (PLI) of seven toxic elements was calculated as suggested by Suresh et al. (2011).

$$PLI = (CF1 \times CF2 \times CF3 \times \ldots\ldots CFn)\ 1/n \qquad \text{(Eq.2)}$$

An area with PLI value > 1 is polluted whereas PLI value < 1 indicates no contamination (Chakravarty and Patgiri, 2009; Seshan et al., 2010). Concentrations of the elements in shale (sedimentary rock), which refer to the average concentration of the earth crust (Turekian and Wedepohl, 1961), were used as the reference baselines in this study. The PLI was calculated for all five studied cores and based on seven toxic elements of As, Pb, Co, Cr, Ni, Cu, and Zn (*Table 2*). The maximum and the minimum calculated PLI were 1.07 and 0.26, respectively (*Table 2*).

Table 2. *Comparison of toxic metals in each cores (ppm) with base value and PLI*

Metals	K1			K3			K5			K7			N1		
	Ave±Std	Max	Min	Ave±Std	Max	Min	Ave±Std	Max	Min	Ave±Std	Max	Min	Ave±Std	Max	Min
As	6.65±1.28	9.39	4.70	6.60±1.03	8.81	4.84	6.93±1.60	10.15	2.96	6.11±1.79	9.55	2.89	5.76±1.06	7.80	4.12
Co	15.63±3.16	21.79	11.68	16.78±3.53	22.81	11.68	15.19±3.01	22.81	11.50	16.20±5.34	23.79	5.37	34.63±7.40	44.79	20.24
Cr	56.38±9.68	75.08	38.89	67.41±14.4	98.44	44.88	71.76±10.3	94.24	53.01	57.43±20.92	95.11	15.32	106.35±21.14	149.60	65.89
Cu	17.96±4.99	36.64	12.14	21.72±3.65	28.04	16.80	20.44±3.05	26.63	14.33	22.80±12.23	52.04	6.01	24.09±8.98	45.20	11.31
Ni	27.26±4.44	40.49	21.26	32.07±6.28	45.26	21.99	35.15±4.4	44.58	27.43	28.15±9.92	47.37	8.78	50.32±17.78	105.40	30.01
Pb	13.41±3.31	22.46	9.88	15.43±5.24	31.38	10.16	25.15±5.8	43.08	11.80	22.93±8.60	48.13	14.33	18.34±4.73	30.60	10.95
Zn	52.33±8.72	83.22	42.66	59.36±8.24	73.45	46.09	54.50±7.8	68.37	41.60	66.32±22.01	131.60	23.86	78.14±13.45	106.70	55.45
PLI	0.57			0.63			0.63			0.71			0.83		

http://www.aloki.hu ● ISSN 1589 1623 (Print) ● ISSN 1785 0037 (Online)
DOI: http://dx.doi.org/10.15666/aeer/1704_95479559

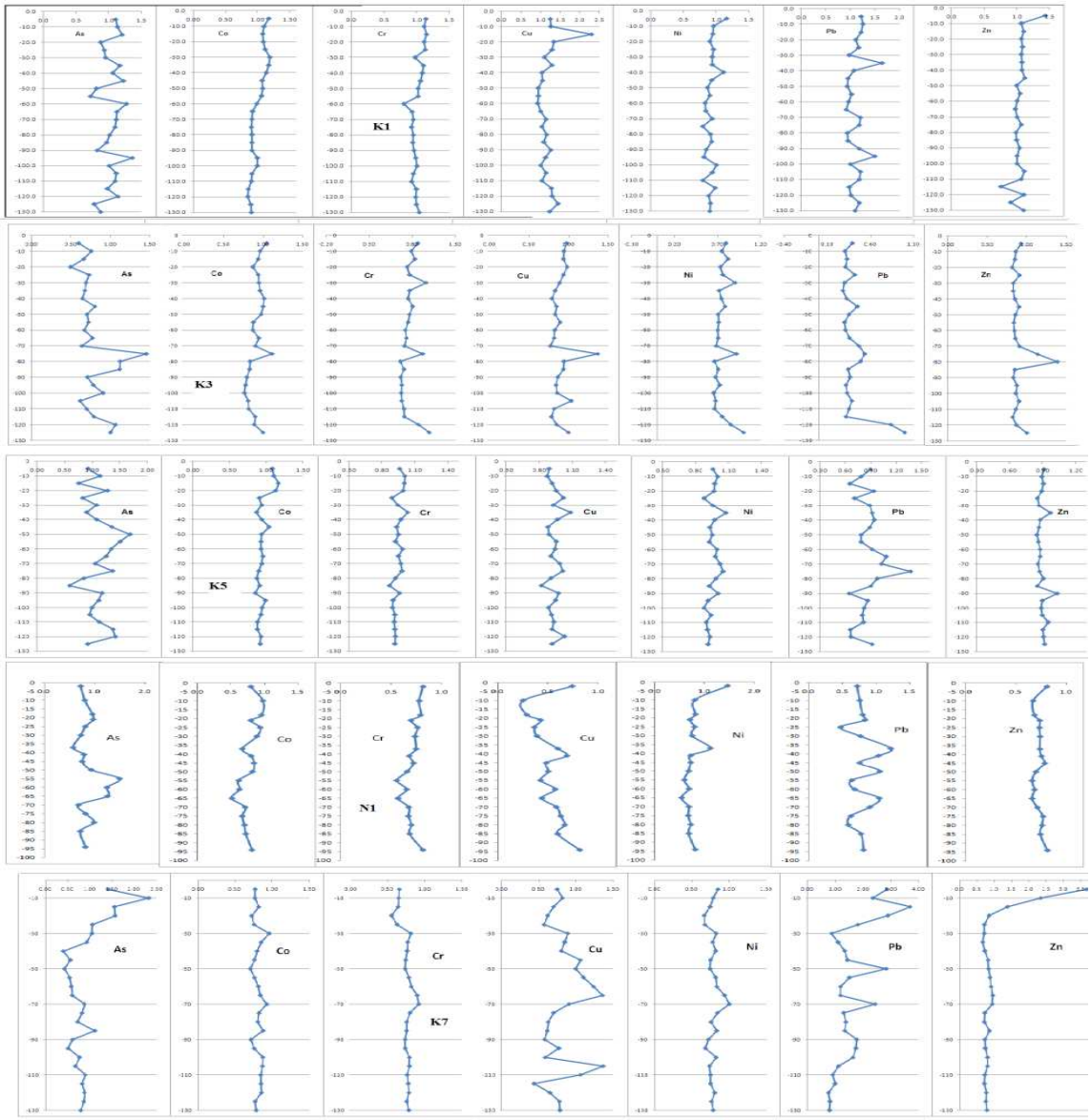

Figure 8. *Enrichment factor trend of heavy metals in cores*

Results showed that the PLI value of the elements in average sediment was lower than that in surface sediment in cores K1, K3, K5, K7 and N1, which can be attributed to direct discharges from urban area and fisheries boats carrying toxic elements, contaminants in study areas, especially in core N1 area. Based on average of PLI value in all cores, southeast coast of the Caspian Sea (Gorgan Bay) should be classified as no toxic pollution (*Table 3*), but in recent decades there has been a dramatic increase that needs more attention and consideration. Finally, comparison of toxic elements with the quality guidelines (NOAA, ISQG) showed the range between the two guideline (level of some elements as As, Ni, Cu, Pb was higher than ERL and lower than ERM). However, because of ecosystem condition, tourism and aquatic resources, this area, must be prevented, managed and monitored properly before they constitute a serious threat to the health of the environment and the organisms.

http://www.aloki.hu ● ISSN 1589 1623 (Print) ● ISSN 1785 0037 (Online)
DOI: http://dx.doi.org/10.15666/aeer/1704_95479559

Table 3. *Comparison of this study with other studies and quality guidelines*

Region	Pb (ppm)	Cu (ppm)	Zn (ppm)	As (ppm)	Ni(ppm)	Co(ppm)	Cr(ppm)	Reference
Gorgan Bay	9.88-43.8	6.01-45.2	23.8-106.18	2.89-10.15	8.78-105.4	5.37-44.8	15.3-149.6	This study
Southeast coast of the Caspian Sea	13.00±3.14 (9-16)	9.09±3.16 (5-14)	28.00±5.71 (22.33-36.33)	4.11±1.27 (2.36-5.16)	17.42±3.78 (16.33-24)	-	-	Bastami et al. (2014)
Caspian Sea (Iran)	18.0±4.17 (11.3-24.6)	34.7±11.9 (13.2-50.9)	85.3±17.9 (55.9-146)	12.5±3.04 (6.97-20.1)	51.6±11.8 (29.4-67-8)	15.9±4 (6.9-24.2)	85.2±15.3 (59.6-128)	De Mora et al. (2004)
Jurujuba sound (Brazil)	61±35 (5–123)	51±40 (5–213)	158±97 (15–337)	-	48±19 (15-79)	-	89±19 (15-79)	Baptista Neto et al. (2001)
Black Sea	19.44±12.48 (2.1-43.5)	30.67±18.76 (4.61-75.72)	69.00±57.03 (1-174)	-	49.8±34.81 (1-117)	20.76±18.55 (1.57-71.59)	57.2±41.85 (1-120)	Secrierus and Secrierus (2002)
Mediterranean Sea	23.81±12.80 (8-54)	85.87±65.63 (10-208)	115.75±62.75 (38-227)	9.43±4.80 (5-24)	16.31±5.85 (8-29)	-	17.43±5.83 (10-26)	Moreno et al. (2009)
ERL	46.7	34	150	8.2	21	-	81	Long et al. (1995)
ERM	218	270	410	70	52	-	370	Long et al. (1995)
ISQG	30.2	18.7	124	7.24	-	-	52.3	ISQG
PEL	112	108	271	41.6	-	-	160	ISQG

ERL = Effect range low (NOAA); ERM = Effect range medium (NOAA); ISQG = Interim sediment quality guideline (Environment Canada); PEL = Probable effects level (Environment Canada)

Conclusion

In this study concentrations and geochemical trends of some major elements (Al, Fe, K, Mg, Na and S) and heavy metals (As, Cu, Ni, Co, Pb, Cr, Zn), in 5 cores from Gorgan Bay were determined. in all K1, K3, K5, K7, N1 cores major element concentrations increased from the bottom to the top layer, and the maximum concentrations of these major elements in cores were observed at depths of 15–45 cm. All elements showed a positive and significant correlation (except Ca and S) with Fe and Al and represent the same input source (human or natural), also there was a positive and significant correlation between arsenic, Fe, Zn, Cr, Co, Ni, Cu and K, indicating that these metals have the same origin and the same behaviour in this area. Sulfur and calcium had a negative correlation with most of the heavy metals which indicates different behaviour and origin of these elements in the environment. PCA represent all metals were mostly derived from the geological origin in sediments of the Gorgan Bay, except for western part which was mainly derived from terrestrial discharge of industrial activities. EF values in all cores ranged no enrichment (EF < 1) to minor enrichment (EF 1 to 3) suggesting no anthropogenic enrichment, expect Pb and Zn in core 7 showed moderate enrichment (EF 3-5) which indicated that anthropogenic Zn and Pb enriched and polluted significantly sediment core 7. Based on the average of PLI values for these 5 cores and 7 trace metals (As, Co, Cr, Cu, Ni, Pb, and Zn), the southeast coast of the Caspian Sea (Gorgan Bay) should be classified as no metal pollution but in recent decades there has been a dramatic increase specially in the coastal area of K7, that needs more attention and consideration.

Acknowledgements. This study has been supported by Ferdowsi University of Mashhad-international Campus. The study was conducted as PhD thesis (#3/41676) contribution of the first author (H. B.). We

http://www.aloki.hu ● ISSN 1589 1623 (Print) ● ISSN 1785 0037 (Online)
DOI: http://dx.doi.org/10.15666/aeer/1704_95479559

are grateful to Mr. Nyestani, Shimiyar Analytical Laboratories Ltd. in Tehran, for providing information on the methods and standard specifications which helped in the completion of this paper.

REFERENCES

[1] Abrahim, G. M. S., Parker, R. J. (2008): Assessment of heavy metal enrichment factors and the degree of contamination in marine sediments from Tamaki Estuary, Auckland, New Zealand. – Estuarine, Coastal and Shelf Science 136: 227-238.

[2] Adamo, P., Arienzo, M., Imperato, M., Naimo, D., Nardi, G., Stanzione, D. (2005): Distribution and partition of heavy metals in surface and sub-surface sediments of Naples city port. – Chemosphere 61: 800-809.

[3] Alessandro, B., Giovanni, B., Nicola, C. (2006): Heavy metals in marine sediments of Taranto Gulf (Ionian Sea, southern Italy). – Mar. Chem. 99: 227-235.

[4] Aloupi, M., Angelidis, M. O. (2001): Geochemistry of natural and anthropogenic metals in the coastal sediments of the island of Lesvos, Aegean Sea. – Journal of Environmental Pollution 113: 211-219.

[5] APHA, AWWA, WEF (2005): Standard Methods for Examination of Water and Wastewater. – APHA, AWWA, WEF, Washington, DC.

[6] Baptista Neto, J. A., Smith, B. J., McAllister, J. J. (2001): Heavy metal concentrations in surface sediments in a near shore environment, Jurujuba Sound, Southeast Brazil. – Environmental Pollution 109: 1-9.

[7] Bagheri, H., Lahijani, H., Kakroodi, A. (2012): Mineralogy of Late Quaternary Sediments in Miankalehspite. – Iranian National Institute for Oceanography and Atmospheric Science, Tehran (Persian report).

[8] Bastami, K., Bagheri, H., Haghparast, S., Soltani, F., Hamzehpoor, A., Bastami, M. D. (2012): Geochemical and geo-statistical assessment of selected heavy metals in the surface sediments of the Gorgan Bay, Iran. – Marine Pollution Bulletin 64: 2877-2884.

[9] Bastami, K., Bagheri, H., Kheirabadi, V., GhorbanzadehZaferani, G., Teymori, M. B., Hamzehpoor, A., Soltani, F., Haghparast, S., MoussaviHarami, S. R., FarzanehGhorghani, N., Ganji, S. (2014): Distribution and ecological risk assessment of heavy metals in surface sediments along southeast coast of the Caspian Sea. – Marine Pollution Bulletin 81(1): 262-267.

[10] Çevik, F., Göksu, M. Z. L., Derici, O. B., Fındık, Ö. (2009): An assessment of metal pollution in surface sediments of Seyhan dam by using enrichment factor, geoaccumulation index and statistical analyses. – Environmental Monitoring and Assessment 152: 309-317.

[11] Chakravarty, M., Patgiri, A. D. (2009): Metal pollution assessment in sediments of the Dikrong River, NE India. – Journal Human Ecology 27(1): 63-67.

[12] Chen, W. Q. (2007): Heavy metal contamination in western Xiamen Bay sediments and its vicinity, China. – Marine Pollution Bulletin 54: 974-982.

[13] De Mora, S., Sheikholeslami, M., Wyse, E., Azemard, S., Cassi, R. (2004): An assessment of metal contamination in coastal sediments of the Caspian Sea. – Marine Pollution Bulletin 48(1-2): 61-77.

[14] Feng, H., Han, X., Zhang, W., Yu, L. (2004): A preliminary study of heavy metal contamination in Yangtze River intertidal zone due to urbanization. – Marine Pollution Bulletin 49(11-12): 910-915.

[15] Grant, A., Middleton, R. (1990): An assessment of metal contamination of sediments in the Humber Estuary. – Estuarine, Coastal and Shelf Science 31: 71-85.

[16] Han, Y., Du, P., Cao, J., Eric, S. P. (2006): Multivariate analysis of heavy metal contamination in urban dusts of Xi'an Cent, China. – The Science of the Total Environment 355: 176-186.

http://www.aloki.hu ● ISSN 1589 1623 (Print) ● ISSN 1785 0037 (Online)
DOI: http://dx.doi.org/10.15666/aeer/1704_95479559

[17] Harbison, P. (1986): Mangrove muds: a sink and a source for trace metals. – Mar. Pollut. Bull. 17(6): 246-250.
[18] Harikumar, P. S., Nasir, U. P. (2010): Ecotoxicological impact assessment of heavy metals in core sediments of a tropical estuary. – Ecotoxicol. Environ. Saf. 73: 1742-1747.
[19] Horowitz, A. J., Elrick, K. A. (1987): The relation of stream sediment surface area, grain size and composition to trace element chemistry. – Applied Geochemistry 2: 437-451.
[20] Huang, K. M., Lin, S. (2003): Consequences and implication of heavy metal spatial variations in sediments of the Keelung River drainage basin, Taiwan. – Chemosphere 53: 1113-1121.
[21] Huang, J. X., Yin, Y., Xu, J., Zhu, X. B. (2007): Spatial accumulation features and environment efficiency of heavy metals in intra-tidal surface sediments of Guanhe estuary, Northern Jiangsu. – Mar. Geol. Quat. Geol. 27(5): 23-32.
[22] Kakroodi, A, A., Kroonenberg, S., Hoogendoorn, R. (2012): Rapid Holocene sea-level changes along the Iranian Caspian coast. – Quaternary International 263: 93-103.
[23] Karbassi, A. R., Nabi-Bidhendi, G. R., Bayati, I. (2005): Environmental geochemistry of heavy metals in a sediment core of Bushehr, Persian Gulf, Iran. – J. Environ. Health Sci. Eng. 2(4): 255-260.
[24] Karbassi, A. R., Nouri, J., Mehrdadi, N., Ayaz, G. O. (2008): Flocculation of heavy metals during mixing of freshwater with Caspian Sea water. – Environ. Geol. 53: 1811-1816.
[25] Kasymov, A. G. (1989): Abundance of zooplankton and zoobenthos in Baku Bay, Caspian Sea. – Oceanology 28(4): 524.
[26] Liaghati, T., Preda, M., Cox, M. (2004): Heavy metal distribution and controlling factors within coastal plain sediments, Bells Creek catchment, southeast Queensland, Australia. – Environment International 29: 935-948.
[27] Long, E. R., Mac Donald, D. D., Smith, S. L., Calder, F. D. (1995): Incidence of adverse biological effects within ranges of chemical concentrations in marine and estuarine sediments. – Environmental Management 19: 18-97.
[28] Loska, K., Cebula, J., Pelczar, J., Wiechuła, D., Kwapulinski, J. (1997): Use of enrichment and contamination factors together with geo accumulation indexes to evaluate the content of Cd, Cu, and Ni in the Rybnik water Reservoir in Poland. – Water, Air, and Soil Pollution 93: 347-365.
[29] McCave, I. N. (1984): Size spectra and aggregation of suspended particles in the deep ocean. – Deep Sea Research 31(4): 329-352.
[30] Mohamed, A. W. (2005): Geochemistry and sedimentology of core sediments and the influence of human activities, Qusier, Safaga and Hasighada Harbors, Red sea coast Egypt. – Egypt. J. Aquat. Res. 31(1): 92-103.
[31] Moreno, M., Albertelli, G., Fabiano, M. (2009): Nematode response to metal, PAHs and organic enrichment in tourist marinas of the Mediterranean Sea. – Marine Pollution Bulletin 58: 1192-1201.
[32] Morelli, G., Gasparon, M., Fierro, D., Hu, W. P., Zawadzki, A. (2012): Historical trends in tracemetal and sediment accumulation in intertidal sediments of Moreton Bay, southeast Queensland, Australia. – Chem. Geol. 300-301: 152-164.
[33] Morillo, J., Usero, J., Gracia, I. (2004): Heavy metal distribution in marine sediments from the southwest coast of Spain. – Chemosphere 55: 431-442.
[34] Nasrolahi, A., Smith, B. D., Ehsanpour, M.; Afkhami, M., Rainbow, P. S. (2017): Biomonitoring of trace metal bioavailability in the barnacle along the Iranian coast of the Caspian Sea. – Iranian Journal of Fisheries Sciences 16(1)1-25.
[35] Parr, T. D., Tait, R. D., Maxon, C. L., Newton, F. C., Hardin, J. L. (2007): A descriptive account of benthic macrofauna and sediment from an area of planned petroleum exploration in the southern Caspian Sea. – Estuarine, Coastal and Shelf Science 71: 170-180.

http://www.aloki.hu ● ISSN 1589 1623 (Print) ● ISSN 1785 0037 (Online)
DOI: http://dx.doi.org/10.15666/aeer/1704_95479559

[36] Reddy, M. S., Basha, S., Kumar, V. G. S., Joshi, H. V., Ramachandraiah, G. (2004): Distribution, enrichment and accumulation of heavy metals in coastal sediments of Alange Sosiya ship scrapping yard, India. – Marine Pollution Bulletin 48: 1055-1059.
[37] Secrierus, D., Secrierus, A. (2002): Heavy metal enrichment of man-made origin of superficial sediment on the continental shelf of the north-western Black Sea. – Estuarine Coastal Shelf Science 54: 513-526.
[38] Selvaraj, K., Ram Mohan, V., Szefer, P. (2004): Evaluation of metal contamination in coastal sediments of the Bay of Bengal, India: Geochemical and statistical approaches. – Marine Pollution Bulletin 49: 174-185.
[39] Seshan, B. R. R., Natesan, U., Deepthi, K. (2010): Geochemical and statistical approach for evaluation of heavy metal pollution in core sediments in southeast coast of India. – International Journal Environment Science Technology 7(2): 291-306.
[40] Sharbaty, S. (2011): Two dimensional simulation of flow pattern in Gorgan Bay by using Mike21 software. – Journal of Water and Soil Conservation 18(4): 241-246.
[41] Sharbaty, S. (2012): 3-D simulation flow pattern in the Gorgan Bay in during summer. – International Journal of Engineering Research and Applications (IJERA) 2(3)700-707.
[42] Shi, G., Chen, Z., Xu, S., Zhang, J., Wang, L., Bi, C. Teng, J. (2008): Potentially toxic metal contamination of urban soils and roadside dust in Shanghai, China. – Environ. Pollut. 156: 251-260.
[43] Sun, Q. L., Liu, D. Y., Liu, T., Di, B. P., Wu, F. (2012): Temporal and spatial distribution of trace metals in sediments from the northern Yellow Sea coast, China: implications for regional anthropogenic processes. – Environ. Earth Sci. 66: 697-705.
[44] Suresh, G., Ramasamy, V., Meenakshisundaram, V., Venkatachalapathy, R., Ponnusamy, V. (2011): Influence of mineralogical and heavy metal composition on natural radionuclide contents in the river sediments. – Applied Radiation and Isotopes 69: 1466-1474.
[45] Szefer, P., Glassby, P., Pempkowiak, J., Kaliszan, R. (1995): Extraction studies of heavy metalpollution in surfacial sediments from the southern Baltic Sea off Poland. – Chem. Geol.120: 111-126.
[46] Tait, R. D., Maxonm, C. L., Parr, T. D., Newton, F. C., Hardin, J. L. (2004): Impact assessment and benthic recruitment following exploration drilling in the south Caspian Sea. – 7th SPE international Conference on Health, Safety, and Environment in oil and Gas Exploration, Calgary, Canada, Mar 29-31.
[47] Turekian, K. K., Wedepohl, K. H. (1961): Distribution of the elements in some major units of the earth crust. – Geol. Soc. Am. Bull. 72: 175-192.
[48] Vallius, H. (2014): Heavy metal concentrations in sediment cores from the northern BalticSea: declines over the last two decades. – Mar. Pollut. Bull. 79: 359-364.
[49] Vald'es, J., Vargas, G., Sifeddine, A., Ortlieb, L., Guinez, M. (2005): Distribution and enrichment evaluation of heavy metals in Mejillones Bay Northern Chile: geochemical and statistical approach. – Marine Pollution Bulletin 50: 1558-1568.
[50] Veerasingam, S., Vethamony, P., Mani, M. R., Fernandes, B. (2015): Depositional record of trace metals and degree of contamination in core sediments from the Mandovi estuarine mangrove ecosystem, west coast of India. – Mar. Pollut. Bull. 91: 362-367.
[51] Woitke, P., Wellmitz, J., Helm, D., Kube, P., Lepom, P., Litheraty, P. (2003): Analysis and assessment of heavy metal pollution in suspended solids and sediments of the river Danube. – Chemosphere 51: 633-642.
[52] Zhang, R., Zhang, F., Ding, Y. J., Gao, J. R., Chen, J., Zhou, L. (2013): Historical trends in the anthropogenic heavy metal levels in the tidal flat sediments of Lianyungang, China. – J. Environ. Sci. (China) 25(7): 1458-1468.

http://www.aloki.hu ● ISSN 1589 1623 (Print) ● ISSN 1785 0037 (Online)
DOI: http://dx.doi.org/10.15666/aeer/1704_95479559

PREDICTION OF ANNUAL RUNOFF AT THE DANJIANGKOU RESERVOIR, CHINA BASED ON FORECAST DOMAIN

YANG, M. X.[1*] – ZHANG, Y.[2*] – WANG, H.[1] – JIANG, Y. Z.[1] – XU, Z.[3] – LEI, X. H.[1]

[1]*State Key Laboratory of Simulation and Regulation of Water Cycle in River Basin, China Institute of Water Resources and Hydropower Research, Beijing 100038, China*

[2]*School of Software, Nanchang Hangkong University, Nanchang 330063, China*

[3]*China Water Rights Exchange Company Limited, Beijing 100053, China*

**Corresponding authors*
e-mail: yangmx@iwhr.com; phone:+86-18-046-555-306
e-mail: zyan_iwhr@163.com; phone: +86-13-651-210-838

(Received 27th Nov 2018; accepted 1st May 2019)

Abstract. As the water resource management progresses rapidly in recent years, middle and long-term runoff forecast has become increasingly important. Conventional multi-category runoff prediction usually utilizes manually specified threshold values to categorize runoff categories. However, this approach is arguably subjective, and it neglects fuzziness and peculiarity of hydrometeorological time series. To address this issue, a new concept, forecast domain, is proposed in this study. Cluster analysis of runoff time series was carried out with the Gaussian Mixture Model, and Support Vector Classification was then used to establish the nonlinear relationships between forecast domain and various potential predictors. The current study focuses on the Danjiangkou Reservoir, the source of the Central Route of the South-North Water Transfer Project in China. We use the 25-year data (1981-2005) for model training, and the Danjiangkou runoff data during last 11 years (2006-2016) are used for model validation. It is shown that the runoff forecast domain obtained from the unsupervised clustering is reasonable and appropriate for categorizing runoff categories. Further forecast experiments reveal that this model may shed some light on the prediction of annual mean runoff at the Danjiangkou Reservoir.
Keywords: *middle and long-term runoff forecast, category runoff prediction, Gaussian Mixture Model, cluster analysis, Support Vector Classification*

Introduction

Middle and long-term runoff forecast refers to the quantitative or qualitative prediction of runoff of various water bodies, e.g., rivers, reservoirs, and lakes, over the time horizon from more than three days up to one year. Runoff forecast is usually based on the past and present hydrological and meteorological information, as well as fundamental principles and methodologies based on several related disciplines including hydrology, meteorology, hydrodynamics, and statistics (Fan, 1999). As the water resource management progresses rapidly in recent years, middle and long-term runoff forecast has become increasingly more important and pressing.

Recent studies have made effort to address this issue. Yang et al. (2005) constructed a long-term runoff forecast system during the dry season by combining the continuous rainfall-runoff model and the long-term weather outlook. Their model was found to perform reasonably well. Hong et al. (2016) applied the genetic algorithm to improve the phase-space reconstruction method, and developed a new nonlinear model for monthly mean runoff. Their model was tested in four types of experiments using data from six hydrological stations along the Yellow River and the Yangtze River. Forecast experiments

http://www.aloki.hu ● ISSN 1589 1623 (Print) ● ISSN 1785 0037 (Online)
DOI: http://dx.doi.org/10.15666/aeer/1704_95619575

show that the medium- and long-term runoff forecast is satisfactory at these stations. A number of other recent studies further applied recently developed machine learning and artificial intelligence techniques to extended range runoff forecasts. Coulibaly et al. (2015) investigated the impact of climate trends on the forecast accuracy using a recurrent neural network (RNN), which was trained using time series of runoff to eight large hydropower systems in Quebec and Labrador and several selected climate indices. Results from the forecast experiments indicate that the use of BWA, PNA and ENSO indices leads to better forecast skill than the SLP or NAO indices alone. Maslova et al. (2016) constructed a model by combing wavelet decomposition and Bayesian machine learning regression techniques. The authors compared their model with that of the wavelet and artificial neural networks-based model and evaluated the effects of different wavelet boundary rules with synthetic and real runoff data collected from the Yellowstone River in the Uinta Basin in Utah. It is shown that their model accuracy can be improved by using a new wavelet boundary rule introduced in that study. Yang et al. (2017) applied three machine learning techniques to runoff forecast: Random Forest (RF), Artificial Neural Network (ANN) and Support Vector Regression (SVR). They compared the performance for forecasting one-month-lead reservoir runoff for two headwater reservoirs in USA and China, respectively. It is shown that RF yields the best statistical performances among the three. Tan et al. (2018) made an attempt to improve the decomposition-ensemble framework and proposed an adaptive model for medium and long-term runoff forecast in both the dry and flood seasons. The authors recommended to use SAR (1) model in the dry season and AEEMD-ANN model in the flood season to forecast the monthly runoff in Yangtze River Basin.

Formation of runoff is a result of complex interaction among a range of physical processes, including precipitation, evaporation, and confluence, and human activities. The category of complexity dictates that runoff forecast is inherently stochastic and highly uncertain. Therefore, it is challenging to predict the accurate value of future runoff based on qualitative analysis of physical processes. Besides, one may predict runoff categories instead of single values. The extension of prediction from single values to the runoff categories may help improve forecast reliability and enhance practical values of runoff forecast for the development and utilization of water resources. Indeed, past experience suggests that predicting runoff categories is more reliable and informative compared to single value prediction, as it improves the precision of the forecast e.g. Kasiviswanathan et al. (2013) and Ye et al. (2014). Quan et al. (2014) developed a method to construct prediction rainfall runoff categories with an artificial neural network (ANN) model. The model was calibrated by generating ensemble predictions, and tested in a real-world case study of rainfall-runoff data. The authors showed that the peak flows are predicted with improved accuracy with this method compared to traditional single point forecasts by ANNs. Li et al. (2017) calibrated and validated the different distribution types of Bayesian forecasting system for the observed 52 floods during 2004-2014 at the ZheXi basin. They showed that the Log Weibull and empirical Bayesian probabilistic model perform the best on average compared with the other distribution models. However, one limitation in these studies is that these methods require manually specifying the prediction categories. Because of the fuzziness of runoff, it may be argued that these conventional methods neglect peculiarity of hydrometeorological time series.

One method to objectively classify runoff categories is to apply sequence clustering analysis, which takes full consideration of fuzziness in runoff time series and provides faithful representation of the physical laws governing runoff. For example, Hou et al. (2016) combined three methods: sequenced sample clustering, set pair analysis (SPA), and Markov

http://www.aloki.hu ● ISSN 1589 1623 (Print) ● ISSN 1785 0037 (Online)
DOI: http://dx.doi.org/10.15666/aeer/1704_95619575

chains; this approach leads to multiple improvements compared to the conventional weighted Markov chains. Based on these methods, the authors constructed a prediction model for annual mean precipitation. The results show that the improvements lead to better classification of precipitation, sharper forecast probability distribution, and improved forecast precision. Zhao et al. (2017) proposed to use cluster analysis to examine anomaly correlation, a performance measure of raw general circulation model forecasts in the three-dimensional space of latitude, longitude, and initialization forecast time. Totz et al. (2017) developed a new cluster-based empirical model to forecast winter precipitation anomalies. They compared this model with dynamic forecast models and a canonical correlation analysis-based prediction model. The results indicated that this new prediction method performs better regarding timing and pattern correlation in the Mediterranean and European regions. Another widely used clustering method is the Gaussian Mixture Model (GMM), which is a parametric model based on Gaussian distribution and trained with the Expectation Maximization algorithm. The GMM can objectively classify runoff without human intervention, hence better suitable for classifying runoff categories for prediction.

Motivated by these efforts and considerations, we proposed the concept of forecast domain. Cluster analysis was conducted on the multiple year runoff data using the GMM, and resultant clusters are then used to construct forecast domain. Finally, Support Vector Classification (SVC) is adopted to predict the forecast domain. We apply this model to the forecast runoff at the Danjiangkou Reservoir, which is the primary water source of the Central Route of the South-North Water Transfer Project.

This paper make two main contributions. On the one hand it applied sequence clustering analysis which takes full consideration of fuzziness in runoff time series and provides faithful representation of the physical laws governing runoff. On the other hand it proposed a concept of forecast domain to expand the prediction results from specific values to the range, and the characteristics of the runoff change interval state were more evident.

Materials and Methods

Overview of the geography and climate of the Danjiangkou Reservoir area

The Danjiangkou (DJK) Reservoir (110 °E - 112°E，32°N-33°N, abbreviated as DJK hereafter) is the largest artificial fresh water lake in Asia (Li and Zhang, 2014). DJK is located at the boundary between the Danjiangkou city, Hubei Province and Zhechuan County, Hunan Province. DJK is the confluence of Han River and Danjiang River, with a drainage area of 17,916 km^2. The terrain of DJK is characterized by great elevation differences, steep slopes, and deeply dissected topography. The highest altitude reaches 1,798.9 m, with relative relief 1,711.9 m. The topography of the DJK area is overall higher to the northwest, and lower in the southeast, with steep terrain in the north and gentle slopes in the south, and alternating basins and canyons along the Han River (Bao, 2013). Situated in the transition zone to humid and warm climate within northern subtropical climate belt, DJK has a semi-humid continental climate, with four distinct seasons and precipitation is abundant in the wet season. Primary soil types in the DJK area include mountain yellow-brown earth soil, cinnamon soil, mountain brown soil, purple soil etc. The main forest and vegetation types are coniferous forests, broad-leaved forest, bamboo forest, shrub, and shrub meadow (Liao, 2011).

As the water source of the Central Route of the South-North Water Transfer Project, DJK has a storage capacity of 17.64 billion m^3, with averaged incoming runoff 39.35 billion

http://www.aloki.hu ● ISSN 1589 1623 (Print) ● ISSN 1785 0037 (Online)
DOI: http://dx.doi.org/10.15666/aeer/1704_95619575

m^3. Incoming runoff occurs mainly during the wet season (July – October) with an estimation of more than 60% of the annual total in this season (Li et al., 2008, 2009; Yang et al., 2012). The catchment area of the reservoir area is formed by the convergence of the Han River and the Dan River. Its main tributaries include the Qianyou River, Jinqian River, Si River etc. The largest tributaries of the Dan River include the Qi River and Laoguan River. Hydraulic constructions built on the upstream of the DJK, many large reservoirs along the Han River, as shown in *Figure. 1*.

Figure 1. *The geography in the upstream of DJK and the distribution of hydrometeorological stations*

The Central Route of the South-North Water Transfer Project provides water supplies to more than 20 medium and large cities in Henan province, and Hebei province, including Tianjin and Beijing. Annual water transfer is estimated to reach ~9.5 billion m^3 by the end of the first phase project, and will reach ~13.0 billion m^3 in the medium and long term. The Central Route of the South_North Water Transfer Project is expected to significantly relieve the water shortage crisis in many regions of northern China (Chen et al., 2015).

Data sources

The climate indices dataset from CMA Climate Center (http://cmdp.ncc-cma.net/cn/monitoring.htm) includes 130 indices for atmosphere and ocean circulations. Correlation analysis (Keane and Adrian, 1993) is conducted between the annual mean runoff at DJK and individual climate indices at the previous year. In addition to these climate indices, accumulated precipitation at the previous year is also considered in our model as a predictor, because precipitation is one of the primary factors contributing to runoff.

http://www.aloki.hu ● ISSN 1589 1623 (Print) ● ISSN 1785 0037 (Online)
DOI: http://dx.doi.org/10.15666/aeer/1704_95619575

Gaussian Mixed Model (GMM)

GMM was developed based on Hidden Markov Model (HMM) (Eddy, 1996), and it belongs to a broad class of the unsupervised clustering methods (Reynolds, 2009). In essence, GMM is a multidimensional probability distribution function. Gaussian distributions are linearly weighted to characterize statistical distributions of the samples fully. Characteristic parameters spanning the space determine the model parameters (Mcnicholas and Murphy, 2008). In this paper, the actual runoff value of DJK from 1981 to 2016 was selected for clustering steps for clustering analysis in GMM may be summarized as follows:

(1) Suppose samples follow k mixed Gaussian distribution. Initialize μ_j , Σ_j , $j \in \{1,\cdots,k\}$ for each GMM.

(2) For each sample x^i , where $i \in \{1,\cdots,m\}$, compute the probability w_j^i that x^i follows GMM as following:

$$w_j^i = p\left(x^i \mid z^i = j\right) = \frac{1}{(2\pi)^{\frac{n}{2}} \left|\sum\right|^{\frac{1}{2}}} e^{\frac{1}{2}(x^i-\mu_j)\Sigma^{-1}(x^i-\mu_j)^T} \quad \text{(Eq.1)}$$

where z^i is the category of x^i .

(3) Update parameters of each Gaussian distribution:

$$\mu_j = \frac{\sum_{i=1}^m w_j^i x^i}{\sum_{i=1}^m w_j^i} \quad \text{(Eq.2)}$$

$$\sum_j = \frac{\sum_{i=1}^m w_j^i (x^i-\mu_j)(x^i-\mu_j)^T}{\sum_{i=1}^m w_j^i} \quad \text{(Eq.3)}$$

(4) Iterate steps (2) and (3) until the Gaussian parameters μ_j and $\sum_j$ converge.

(5) With the known Gaussian parameters μ_j and $\sum_j$ from the above step, iterate throughout all the samples and classify the samples according to the maximum probability.

Support Vector Classification (SVC)

The Support Vector Machines (SVM) is a type of the supervised classification methods developed from convex optimization (Vapnik, 1999; Hsu, 2010). SVC has been applied to classification and regression prediction problems. For classification, SVC can be grouped in two types: linear SVC and nonlinear SVC (Brereton and Lloyd, 2010). Linear SVC method solves the following optimization problem to identify the optimal classification interface:

$$\max_a L = \sum_{i=1}^N a_i - \frac{1}{2}\sum_{i,j=1}^N a_i y_i a_j y_j (x_i \cdot x_j) \quad \text{(Eq.4)}$$

http://www.aloki.hu ● ISSN 1589 1623 (Print) ● ISSN 1785 0037 (Online)
DOI: http://dx.doi.org/10.15666/aeer/1704_95619575

where the objective function is subject to the following constrains:

$$\sum_{i=1}^{N} a_i y_i = 0, a_i \in [0, C], i = 1, \cdots, N \quad \text{(Eq.5)}$$

where a and a_i are Laplacian multipliers, c is the penalty factor.

Nonlinear SVC makes use of kernel functions and the optimal problem can be expressed as:

$$\max_{a} L = \sum_{i=1}^{N} a_i - \frac{1}{2} \sum_{i,j=1}^{N} a_i y_i a_j y_j K(x_i \cdot x_j) \quad \text{(Eq.6)}$$

The classifiers in linear and nonlinear SVC may be expressed as:

$$f(x) = sign\left(\sum_{i=1}^{N} a_i^* y_i (x \cdot x_i) + b^* \right) \quad \text{(Eq.7)}$$

$$f(x) = sign\left(\sum_{i=1}^{N} a_i^* y_i K(x \cdot x_i) + b^* \right) \quad \text{(Eq.8)}$$

where a_i^* is from the coupled optimal solution, and b^* is the offset coefficient. Commonly used kernel functions include: linear kernels, $K(x, x') = x\ x'$; polynomial kernels, $K(x, x') = [(x\ x') + 1]^d$; Gaussian radial basis function (RBF) kernel, $K(x, x') = \exp(-\left\| x - x' \right\|^2 / 2\sigma^2)$; where x, x' are vectors, and d is the degree of the polynomials, and σ is the bandwidth of the Gaussian kernel.

Results and Discussion

Figure 2 shows the annual mean incoming runoff at DJK from 1981 to 2016. It is evident that the annual runoff varies over a wide range. Therefore, it is difficult to accurately predict future values based on qualitative analysis of physical factors. This study develops a new model based on runoff classification and forecast domain to categorize annual runoff at DJK in the past 36 years, conduct forecast experiments, and perform validation of this forecast model.

Classification of runoff

Several methods have been used to classify runoff categories in the past: aggregate standard deviation, mean deviation, and percent deviation. Here we use the percent deviation method that calculated the distance percentage between the annual runoff value and the average of the 36 years (1981-2016) runoff to classify the DJK runoff data into two categories. If the percent deviation is negative, the year of runoff category is designated as 1; if it is positive, the category is designated as 2. *Table 1* lists the classification of runoff based on percent deviation into two categories derived from this method.

http://www.aloki.hu ● ISSN 1589 1623 (Print) ● ISSN 1785 0037 (Online)
DOI: http://dx.doi.org/10.15666/aeer/1704_95619575

Similarly, we further classify this DJK runoff data into 5 categories: Category 1 for percent deviation less than –20% , the percent deviation falls between –20% and –10%is Category 2 , Category 3 for percent deviation between 10% and –10%,. The percent deviation between 10% and 20% is Category 4 and greater than 20% is Category 5. Result from this percent deviation classification of the 36-year data is listed in *Table 2*.

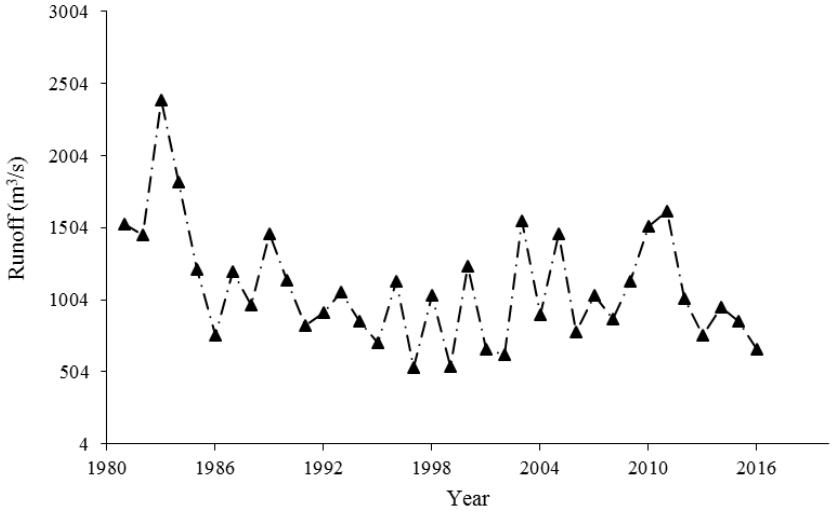

Figure 2. *Annual average runoff trend of DJK in 1981-2016*

Table 1. *Classification of runoff into two domains*

Year	Distance to average(%)	Domain	Years	Distance to average(%)	Domain
1981	40.51	2	1999	-50.16	1
1982	33.98	2	2000	13.56	2
1983	119.95	2	2001	-39.40	1
1984	67.72	2	2002	-42.53	1
1985	11.36	2	2003	42.89	2
1986	-30.57	1	2004	-17.15	1
1987	10.25	2	2005	34.16	2
1988	-10.80	1	2006	-28.09	1
1989	34.62	2	2007	-4.92	1
1990	4.83	2	2008	-20.18	1
1991	-24.32	1	2009	4.09	2
1992	-16.14	1	2010	39.40	2
1993	-2.99	1	2011	48.69	2
1994	-21.66	1	2012	-7.13	1
1995	-34.99	1	2013	-30.39	1
1996	4.18	2	2014	-12.74	1
1997	-50.80	1	2015	-21.10	1
1998	-4.75	1	2016	-39.40	1

Classification of forecast domain

Considering the distribution characteristics of the runoff sequence, the intrinsic distribution rule of the runoff sequence can be more effectively described, and the divided

http://www.aloki.hu ● ISSN 1589 1623 (Print) ● ISSN 1785 0037 (Online)
DOI: http://dx.doi.org/10.15666/aeer/1704_95619575

runoff interval is more reasonable. Based on this assumption, we proposed a new method called forecast domain. With this method, the GMM is used to cluster the annual mean runoff. Gaussian probability distribution is then linearly weighted to fit the full statistical distribution, which reduces sampling noise and helps achieve better classification. The number of the iteration steps is set as 100, and the number of the clusters is 2. Forecast domain was constructed based on the results of the above cluster analysis. *Table 3* lists the results of the classification of forecast domain derived from this method.

Table 2. *Classification of runoff into five domains*

Year	Distance to average(%)	Domain	Year	Distance to average(%)	Domain
1981	40.51	5	1999	-50.16	1
1982	33.98	5	2000	13.56	4
1983	119.95	5	2001	-39.40	1
1984	67.72	5	2002	-42.53	1
1985	11.36	4	2003	42.89	5
1986	-30.57	1	2004	-17.15	2
1987	10.25	4	2005	34.16	5
1988	-10.80	2	2006	-28.09	1
1989	34.62	5	2007	-4.92	3
1990	4.83	3	2008	-20.18	1
1991	-24.32	1	2009	4.09	3
1992	-16.14	2	2010	39.40	5
1993	-2.99	3	2011	48.69	5
1994	-21.66	1	2012	-7.13	3
1995	-34.99	1	2013	-30.39	1
1996	4.18	3	2014	-12.74	2
1997	-50.80	1	2015	-21.10	1
1998	-4.74	3	2016	-39.40	1

Table 3. *Classification of forecast domain into two categories*

Year	Forecast domain	Year	Forecast domain	Year	Forecast domain
1981	2	1993	1	2005	2
1982	2	1994	1	2006	1
1983	2	1995	1	2007	1
1984	2	1996	1	2008	1
1985	1	1997	1	2009	1
1986	1	1998	1	2010	2
1987	1	1999	1	2011	2
1988	1	2000	2	2012	1
1989	2	2001	1	2013	1
1990	1	2002	1	2014	1
1991	1	2003	2	2015	1
1992	1	2004	1	2016	1

Similarly, GMM clustering of DJK annual runoff classifies the forecast domain into five categories. The number of the iteration steps is 100, and the number of the clusters is 5. *Table 4* lists the five forecast domains derived from this method.

http://www.aloki.hu ● ISSN 1589 1623 (Print) ● ISSN 1785 0037 (Online)
DOI: http://dx.doi.org/10.15666/aeer/1704_95619575

Table 4. *Classification of forecast domain into five categories*

Years	Forecast domain	Year	Forecast domain	Year	Forecast domain
1981	3	1993	2	2005	3
1982	3	1994	1	2006	1
1983	5	1995	1	2007	2
1984	4	1996	2	2008	1
1985	2	1997	1	2009	2
1986	1	1998	2	2010	3
1987	2	1999	1	2011	3
1988	2	2000	2	2012	2
1989	3	2001	1	2013	1
1990	2	2002	1	2014	2
1991	1	2003	3	2015	1
1992	2	2004	1	2016	1

Result Analysis

The CMA climate indices database is preprocessed in the following two steps. First, for a small number of missing values in this dataset, linear interpolation is used to fill these missing values. Second, a linear correlation is computed between the annual mean runoff at DJK and the climate indices at the previous year. Twenty climate indices that have the highest correlation with the DJK annual runoff are selected based on this lead correlation analysis. We use the 25-year data (1981-2005) for model training, and the DJK runoff data during last 11 years (2006-2016) are used for model validation. DJK has an Asian subtropical monsoon climate. Its precipitation mainly comes from two meteorological moisture sources: warm and humid moisture transport from the southeast and southwest (Guo and Jin, 1997). In addition, sea surface temperature at the Pacific Ocean and the Indian Ocean also play essential roles in the eastern Asia climate. Considering these factors, the following prediction factors are selected in *Table 5*: sea surface temperature anomalies at the NINO W region (September of the previous year), latitudinal position index of polar vortex center in Northern Hemisphere (May of the previous year), area index of warm pool in Western Pacific (July of the previous year), number of cold air (November of the previous year), location the subtropical high in South China Sea (December of the previous year), intensity of eastern Asian trough in June, and accumulated precipitation of DJK in the previous year. These variables are entered intothe SVC model. Prediction is then conducted for the conventional classification categories derived from the percent deviation method and forecast domain derived from the GMM classification method.

Table 5. *Correlation coefficients between the predictors and annual mean runoff*

No.	Factors	Correlation coefficient
1	Sea surface temperature departure index of NINO W district in September of the previous year	0.46
2	The latitude index of the polar vortex in the Northern Hemisphere in May of the previous year	0.46
3	Western Pacific warm pool area index in July of the previous year	0.43
4	The number of cold air in November of the previous year	0.42
5	The position index of the South China Sea subtropical high ridge in December of the previous year	0.42
6	East Asia trough intensity index in June of the previous year	0.40

http://www.aloki.hu ● ISSN 1589 1623 (Print) ● ISSN 1785 0037 (Online)
DOI: http://dx.doi.org/10.15666/aeer/1704_95619575

Forecast and validation of runoff categories classification

To eliminate untended influence of the dimensions of various indices, the Min-Max Normalization method is utilized to normalize each index. *Figure 3* shows the forecast validation of the two classification categories from SVC. *Figure 4* shows the SVC forecast results of five classification categories. If the predicted results of a certain sample coincide with the real results, it indicates that the prediction is correct and the opposite is wrong. It is evident that ifthe classification of runoff into two categories, only the year 2009 and the year 2011 are predicted to be wrong, and the accuracy is 82%. However, if the classification of runoff is classified into five categories, the accuracy dropped to 45%.

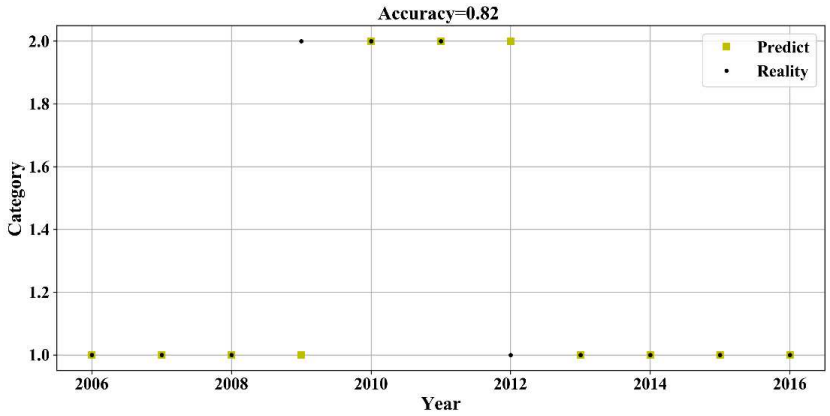

Figure 3. *SVC forecast based on two classification categories of runoff*

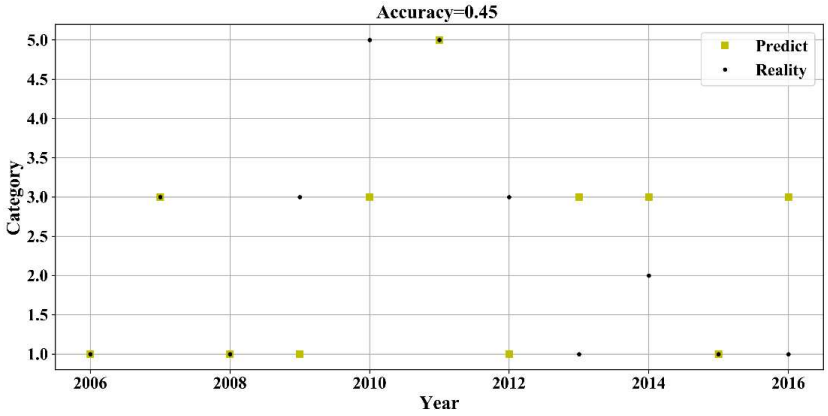

Figure 4. *SVC forecast based on five classification categories of runoff*

Forecast and validation of forecast domain

The similar forecast experiments are conducted. The forecast results based on SVC model by two and five classification categories of forecast domain are shown in *Figure 5* and *Figure 6*. The validation set represents the DJK runoff data during last 11 years (2006-2016) and the category means the classification of forecast domain. Compared with last section, when the classification of forecast domain into two categories, SVC forecast based on forecast domain performed better, and the accuracy

http://www.aloki.hu ● ISSN 1589 1623 (Print) ● ISSN 1785 0037 (Online)
DOI: http://dx.doi.org/10.15666/aeer/1704_95619575

up to 91%. However, when the classification of forecast domain into five categories, the accuracy also declined. We can conclude that whether it is two categories or five categories, the accuracy based on forecast domain is higher than the original classification.

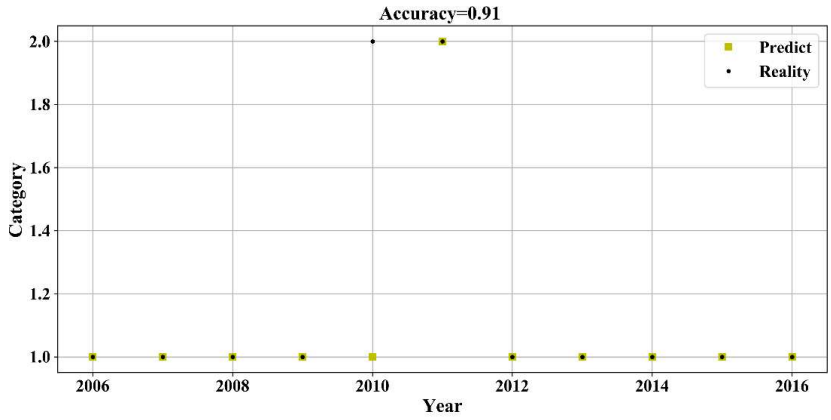

Figure 5. *SVC forecast based on two classification categories of forecast domain*

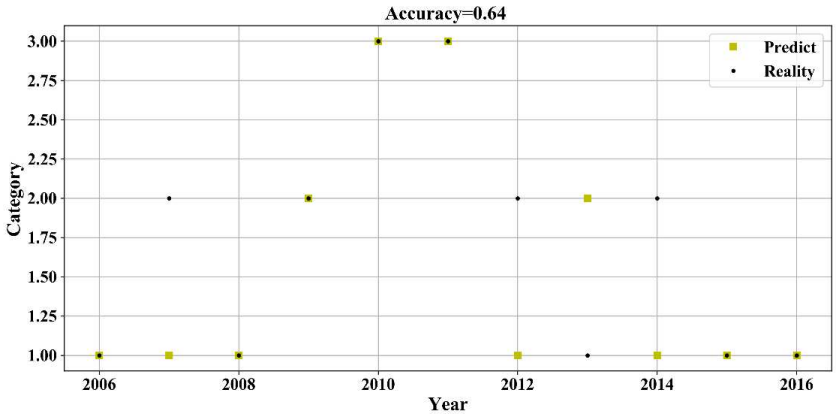

Figure 6. *SVC forecast based on five classification categories of forecast domain*

Table 6 summarizes the accuracy of SVC forecast based on theclassification methods by conventional percent deviation and forecast domain.

Table 6. *Comparisons of the SVC forecast by conventional percent deviation and forecast domain*

Accuracy	Two runoff categories	Two forecast domains	Five runoff categories	Five forecast domains
SVC	82%	91%	45%	64%

Reliability and performance of our prediction model are assessed with three forecast skill metrics: precision, recall rate (Buckland and Gey, 1994) and the F1 measure (Lipton et al., 2014). Precision indicates among the predicted results how many positive predictions are true positive. Precision is defined as:

http://www.aloki.hu ● ISSN 1589 1623 (Print) ● ISSN 1785 0037 (Online)
DOI: http://dx.doi.org/10.15666/aeer/1704_95619575

$$Precision = \frac{number\ of\ true\ positives}{number\ of\ positives} \quad \text{(Eq.9)}$$

Recall measures among the relevant samples how many are correctly predicted, defined as:

$$Recall = \frac{correctly\ predicted\ number\ of\ true\ positives}{total\ number\ of\ relevant\ levels} \quad \text{(Eq.10)}$$

F1 is defined as the harmonic mean of precision and recall:

$$F1 = \frac{2}{\frac{1}{Precision} + \frac{1}{Recall}} \quad \text{(Eq.11)}$$

These three skill metrics from these prediction experiments for the conventional classification categories and forecast domain are summarized in *Figure 7*.

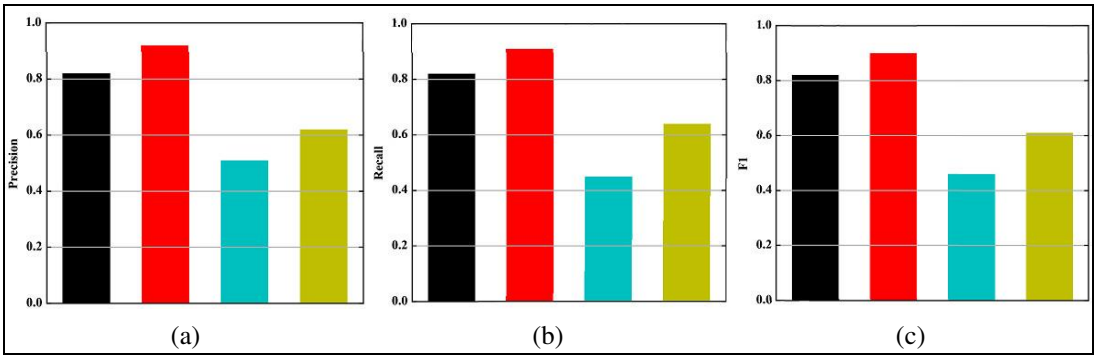

Figure 7. *Precision, recall, and F1 measures from the SVC forecast based on conventional percent deviation and forecast domain*

According to *Figure 3* and *Figure 4*, SVC prediction performs well for the two runoff categories derived from the percent deviation method, and the precision is 82%. However, the precision decreases to 45% by adopting the five runoff categories. In contrast, precision reaches 91% by using the two classification categories of forecast domain derived from the GMM clustering, and it remains 65% based on five classification categories of forecast domain.It is suggested that forecast domain method is more flexible and reliable. *Figure 7* further shows that regardless of the number of runoff categories, for all three metrics, SVC prediction based on forecast domain perform better than that based on conventional classification categories. Therefore, we conclude that the GMM clustering derived forecast domain is better suitable for the prediction of annual runoff at the DJK.

Model comparison

In order to better reflect the feasibility of this model, chooses Naive Bayes to compare with. The result is shown below.

http://www.aloki.hu ● ISSN 1589 1623 (Print) ● ISSN 1785 0037 (Online)
DOI: http://dx.doi.org/10.15666/aeer/1704_95619575

It can be seen from *Figure 8* and *Figure 9* that when two runoff categories performed, Naïve Bayes has a poor recall rate and is unstable compared with the SVC; when performing the five runoff categories, the accuracy of the two methods both are low and the effect is average. In summary, SVC has higher accuracy and stability.

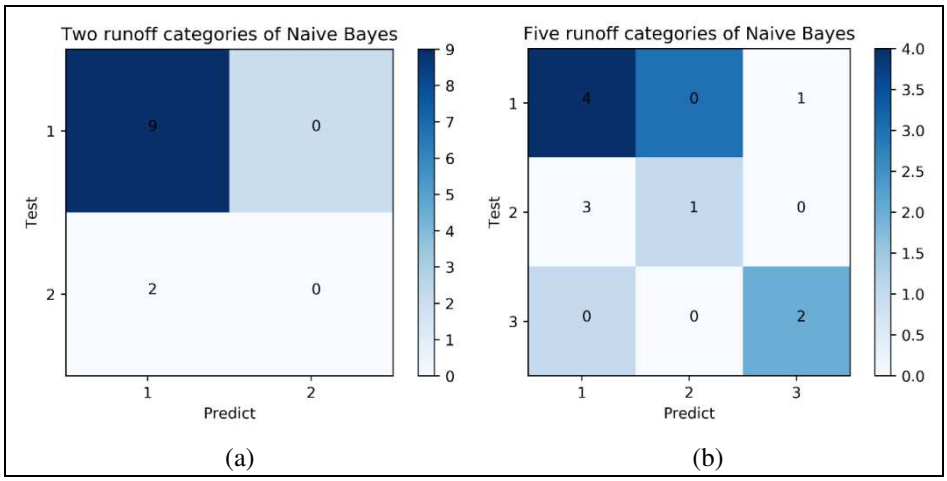

Figure 8. *Naive Bayes evaluation results*

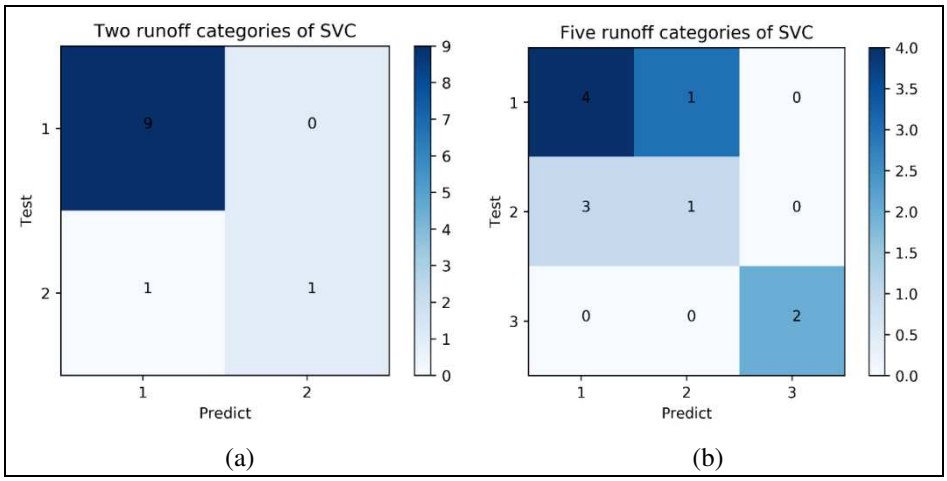

Figure 9. *SVC evaluation results*

Conclusion

The current study focuses on the DJK, the main water source of the Central Route of the South-North Water Transfer Project. We have developed a prediction model for annual mean runoff based on forecast domain instead of conventional classification method of runoff. Gaussian Mixed Model is utilized to cluster the 36-year annual runoff at DJK. Forecast domain was further derived following the GMM clustering and fed to the Support Vector Classification model. Forecast experiments based on forecast domain and conventional classification categories are conducted and compared. The results can be summarized as follows:

http://www.aloki.hu ● ISSN 1589 1623 (Print) ● ISSN 1785 0037 (Online)
DOI: http://dx.doi.org/10.15666/aeer/1704_95619575

(1) Extending the prediction of single value to prediction of multiple forecast domain help better characterize and quantify the variability of runoff. This development bears important practical values to the water resource management and utilization.

(2) Application of sequence clustering analysis to classification takes consideration of the full distribution of runoff, which in turn helps better characterize the statistical distribution of runoff, and further justify objective classification of the runoff categories.

(3) Precipitation is one of the primary factors contributing to runoff. As a result, accumulated precipitation at the previous year should be included as a predictor.

Our results highlight that it is feasible to predict annual runoff based on forecast domain. This results may pave the way for the operational forecast of the annual runoff at the DJK. Our future research endeavors will be devoted to further improving the model in the following aspects:

(1) Using different feature selection method to characterize and understand potential nonlinear relationships among the predictors to achieve further forecast improvement.

(2) For the forecast domain developed in this study, we will apply the k-nearest neighbor's algorithm to predict future annual incoming runoff within a time range of interests at the DJK.

Acknowledgements. This paper was supported by National Key Research and Development Project (2016YFC0402201); National Science Foundation for Young Scientists of China (Grant No.51709271); Young Elite Scientists Sponsorship Program by CAST (2017QNRC001).

REFERENCES

[1] Bao, H. (2013): Analysis of the impact of the middle route project of south-to-north water diversion on the biodiversity of Danjiangkou reservoir area. – Northeast Forestry University, Harbin.

[2] Brereton, R. G., Lloyd, G. R. (2010): Support vector machines for classification and regression. – Analyst 135(2): 230-67. DOI:10.1039/b918972f.

[3] Buckland, M., Gey, F. (1994): The relationship between Recall and Precision. – Journal of the Association for Information Science & Technology 45(1): 12-19.

[4] Chen, P., Li, L., Zhang, H. B. (2015): Spatio-Temporal Variations and Source Apportionment of Water Pollution in Danjiangkou Reservoir Basin, Central China. – Water 7(6): 2591-2611.

[5] Coulibaly, P., Anctil, F., Rasmussen, P., Bobée, B. (2015): A recurrent neural networks approach using indices of low-frequency climatic variability to forecast regional annual runoff. – Hydrological Processes 14(15): 2755-2777.

[6] Eddy, S. R. (1996): Hidden Markov models. – Curr. Opin. Struct. Biol. 6: 361-365.

[7] Fan, Z. (1999): Medium and long-term hydrological forecast. – Hohai University Press, Nanjing.

[8] Guo, H. J., Jin, R. L. (1997): Status Quo and Change Trend of Water Resources in the Upper Reaches of Danjiangkou Reservoir. – Resources Science 24(1): 28-34.

[9] Hou, Z. Y., Lu, W. X., Song, W. B., Li, M. N., Chen, M. (2016): An annual rainfall forecast model based on ordered sample clustering for weighted Markov chains. – Systems Engineering Theory & Practice 36(4): 1066-1071.

[10] Hsu, C. W. (2010): A practical guide to support vector classification 67(5).

[11] Kasiviswanathan, K. S., Cibin, R., Sudheer, K. P., Chaubey, I. (2013): Constructing prediction interval for artificial neural network rainfall runoff models based on ensemble simulations. – J.Hydrol. 499(499): 275-288.

http://www.aloki.hu ● ISSN 1589 1623 (Print) ● ISSN 1785 0037 (Online)
DOI: http://dx.doi.org/10.15666/aeer/1704_95619575

[12] Keane, R. D., Adrian, R. J. (1993): Theory of cross-correlation analysis of PIV images. – Springer Netherlands 1-25.
[13] Li, S. Y., Gu, S., Liu, W. Z., Han, H. Y., Zhang, Q. F. (2008): Water quality in relation to land use and land cover in the upper Han River Basin, China. – Catena 75(2): 216-222.
[14] Li, S. Y., Cheng, X. L., Xu, Z. F., Han, H. Y., Zhang, Q. F. (2009): Spatial and temporal patterns of the water quality in the Danjiangkou Reservoir, China. – International Association of Scientific Hydrology Bulletin 54(1): 124-134.
[15] Li, S. Y., Zhang, Q. F. (2014): Partial pressure of CO2 and CO2 emission in a monsoon-driven hydroelectric reservoir (Danjiangkou Reservoir), China. – Ecol. Eng. 71(71): 401-414.
[16] Li, W., Zhou, J., Sun, H., Feng, K., Zhang, H., Tayyab, M. (2017): Impact of Distribution Type in Bayes Probability Flood Forecasting. – Water Resour. Manage. 31(3): 1-17.
[17] Liao, W. (2011): Research on Land Use Changes and Ecological Security Control in Danjiangkou Reservoir Area. – Central China Normal University, Wuhan.
[18] Lipton, Z., Elkan, C., Naryanaswamy, B. (2014): Optimal Thresholding of Classifiers to Maximize F1 Measure. – Springer Berlin Heidelberg 225-239 pp.
[19] Maslova, I., Ticlavilca, A. M., Mckee, M. (2016): Adjusting wavelet-based multiresolution analysis boundary conditions for long-term streamflow forecasting. – Hydrological Processes 30(1): 57-74.
[20] McNicholas, P. D., Murphy, T. B. (2008): Parsimonious Gaussian mixture models. – Statistics & Computing 18(3): 285-296.
[21] Quan, H., Srinivasan, D., Khosravi, A. (2014): Particle swarm optimization for construction of neural network-based prediction intervals. – Neurocomputing 127(6): 172-180.
[22] Reynolds, D. (2009): Gaussian Mixture Models. – Springer US, 93-105 pp.
[23] Tan, Q. F., Lei, X. H., Wang, X., Wang, H., Wen, X., Ji, Y., Kang, A. Q. (2018): An adaptive middle and long-term runoff forecast model using EEMD-ANN hybrid approach. – Journal of Hydrology 567: 767-780.
[24] Totz, S., Tziperman, E., Coumou, D., Pfeiffer, K., Cohen, J. (2017): Winter Precipitation Forecast in the European and Mediterranean Regions Using Cluster Analysis. – Geophys. Res. Lett. 44(24).
[25] Vapnik, V. N. (1999): An overview of statistical learning theory. – IEEE Trans. Neural Networks 10(5): 988-99.
[26] Yang, T. C., Yu, P. S., Chen, C. C. (2005): Long-term runoff forecasting by combining hydrological models and meteorological records. – Hydrological Processes 19(10): 1967-1981.
[27] Yang, Q., Xie, P., Shen, H., Xu, J., Wang, P., Zhang, B. (2012): A novel flushing strategy for diatom bloom prevention in the lower-middle Hanjiang River. – Water Res. 46(8): 2525-2534.
[28] Yang, T. T., Asanjan, A. A., Welles, E., Gao, X. G., Sorooshian, S., Liu, X. (2017): Developing reservoir monthly inflow forecasts using artificial intelligence and climate phenomenon information. – Water Resources Research 53(4): 2786-2812.
[29] Ye, L., Zhou, J. Z., Zeng, X. F., Guo, J., Zhang, X. X. (2014): Multi-objective optimization for construction of prediction interval of hydrological models based on ensemble simulations. – Journal of Hydrology 519: 925-933.
[30] Zhao, T. T. G., Liu, P., Zhang, Y. Y., Ruan, C. Q. (2017): Relating anomaly correlation to lead time: Clustering analysis of CFSv2 forecasts of summer precipitation in China. – Journal of Geophysical Research Atmospheres 122(17): 9094-9106.

http://www.aloki.hu ● ISSN 1589 1623 (Print) ● ISSN 1785 0037 (Online)
DOI: http://dx.doi.org/10.15666/aeer/1704_95619575

EFFECTS OF THE ENVIRONMENT AND SPATIAL FACTORS ON THE REGENERATION OF *ARAUCARIA* FOREST FRAGMENTS, SOUTHERN BRAZIL

DUARTE, S. W.[1*] – HOFFMANN, L. T.[1] – MAÇANEIRO, J. P.[2] – FENILLI, T. A. B.[1] – SCHORN, L. A.[1]

[1]*Departamento de Engenharia Florestal, Universidade Regional de Blumenau Box. 89030-000 Blumenau, Brazil*

[2]*Departamento de Engenharia Florestal, Universidade Federal do Paraná Box. 80210-170 Curitiba, Brazil*

[*]*Corresponding author*
e-mail: swduarte0@gmail.com; phone: +55-47-3221-6043

(Received 30th Nov 2018; accepted 27th Feb 2019)

Abstract. The floristic patterns of the Atlantic Forest can be explained by different environmental factors. However, recent studies have pointed to the influence of spatial factors on the structure of forest communities. In this study, we evaluated whether environmental and spatial variables influence the distribution of regenerative species in the *Araucaria* forest in Southern Brazil. We analyzed the vegetation in 20 circular plots with 2.5 m radius each. The environmental variables open-canopy and Ca/K content of soil were the most important predictors of floristic variations in the study area, explaining 9% of the species distribution, while the pure spatial structure explained 7% of the community structure. Although much of the floristic variation remained unexplained (75%), the results indicated the complex effect of environmental and spatial variables on the regeneration patterns of the Araucaria Forest in Southern Brazil.
Keywords: *spatial structure, environmental factors, subtropical rainforest, soil-vegetation, RDA*

Introduction

The Atlantic Forest domain is a global hotspot for the conservation of biodiversity and covers approximately 1,300,000 km² of the Brazilian territory. These forests are characterized by different forest types/subdomains, being distributed along the Brazilian coast and occurring more pronounced in the Southeast and South regions (Rocha and Silva, 2013). These forests have a high species richness and a high value of endemism when compared to other Brazilian domains, however, due to a historical process of deforestation and human occupation, the Atlantic Forest is currently fragmented, presenting only 11.7% of its original coverage (Ribeiro et al., 2011). In the State of Santa Catarina, Southern of Brazil, the Atlantic Forest involves different forest types, of which the *Araucaria* forest stands out, with the Brazilian pine (*Araucaria angustifolia)* as the characteristic element (Bertol.) Kuntze), with emphasis on other species of the families Lauraceae and Meliaceae (Kersten et al., 2015). In general, the distribution of this forest type is associated with intrinsic soil, geomorphological and climatic conditions, as well as being influenced by extreme environmental factors (i.e., storms, frost, fires) (IBGE, 2012; Higuchi et al., 2016; Souza et al., 2017).

In recent years, the *Araucaria* forest regeneration has been the subject of several ecological studies, and the analysis of vegetation related to environmental factors has helped answer some questions about the distribution of tree species in environmental

http://www.aloki.hu ● ISSN 1589 1623 (Print) ● ISSN 1785 0037 (Online)
DOI: http://dx.doi.org/10.15666/aeer/1704_95779589

gradients (Higuchi et al., 2016). Among the environmental factors that affect the distribution of the regeneration of the *Araucaria* Forest, we highlight luminosity, open-canopy, elevation, pedological and geomorphological characteristics, among others (Higuchi et al., 2015). Although environmental factors are widely known as promoters of the Atlantic Forest distribution, little attention has been paid to spatial factors, which are important and may influence the distribution of plant species in subtropical forests (Maçaneiro et al., 2016a).

The spatial factors can be connected to biotic/stochastic processes, such as dispersion, pollination and competition (Diniz-Filho et al., 2012; Peña-Claros et al., 2012; Lewis et al., 2014). Due to the difficulty in measuring these data, spatial factors are generally neglected in vegetation studies, however, the inclusion of the spatial structure is fundamental, because it assists in the identification of important environmental processes, the variability of species in different locations, environmental heterogeneity and the effect of abiotic processes (Lewis et al., 2014). For example, environmental factors such as luminosity affect the dynamics and establishment of forest regeneration (Peixoto et al., 2012; Horn et al., 2015), while soil and topography are related to the distribution of species in environmental gradients (Dubuis et al., 2012; Baldeck et al., 2013; Mélo et al., 2013; Maçaneiro et al., 2016a). On the other hand, the spatial structure of the community directly influences the colonization and evolution of the species, becoming a fundamental mechanism in the distribution of vegetation in subtropical forests (Urbanetz et al., 2003; Baldeck et al., 2013; Neuschulz et al., 2016).

Thus, the development of studies related to natural regeneration as a function of the analysis of environmental and spatial variables becomes essential to explain the processes that control the establishment and distribution of regenerating species in the *Araucaria* Forest of Southern Brazil. In this sense, in the present study we analyze two main questions: (1) Which environmental factors influence the distribution patterns of regenerative species? We expect to find a great effect of soil and canopy opening in determining floristic composition, because these are well known to be the main factors conditioning changes in the composition of vegetation in the Atlantic Rainforest at local scales (Higuchi et al., 2015, 2016; Souza et al., 2017; Maçaneiro et al., 2019). (2) Is the spatial structure of the community related to regenerative species and environmental factors? We expect to find a significant effect of space, because recent studies have indicated that inclusion of the spatial component in the analysis of vegetation patterns helps in the identification of ecological processes (Maçaneiro et al., 2016a; Loebens et al., 2018). Thus, the spatial component may be important to determine the distribution of species regeneration in Atlantic Rainforest in Southern Brazil.

Material and Methods

Study area

The present study was carried out in forest fragments of the company *Florestal Gateados*, located in the municipality of Campo Belo do Sul, State of Santa Catarina, Southern Brazil (*Figure 1*). The property is located in the Pelotas river basin and in the *Campos de Lages* region. It is part of the *RPPN Emílio Einsfeld Filho*, which has a total area of 6,328.60 ha and elevation varying from 620 to 980 meters a.s.l. (27°55' and 28°05' S – 50°55' and 50°45' W).

The climate of the study region, according to the Köppen classification, is of the type Cfb – humid mesothermic temperate climate with mild summer, and with average

http://www.aloki.hu ● ISSN 1589 1623 (Print) ● ISSN 1785 0037 (Online)
DOI: http://dx.doi.org/10.15666/aeer/1704_95779589

annual temperature ranging from 12 to 16°C, average annual total rainfall of 1,600 to 1,900 mm and relative humidity of 78 to 80% (Alvares et al., 2013). The geology of the region is formed by the *São Bento* Group, which is composed of the *Serra Geral* Formation, which is constituted mainly by intrusions of basalts, diabase and acid lavas (Santa Catarina, 1986). The predominant soils formed by these types of rocks in the study area are Litholic Neosol, Haplic Cambisol and Nitosols (Santos et al., 2018).

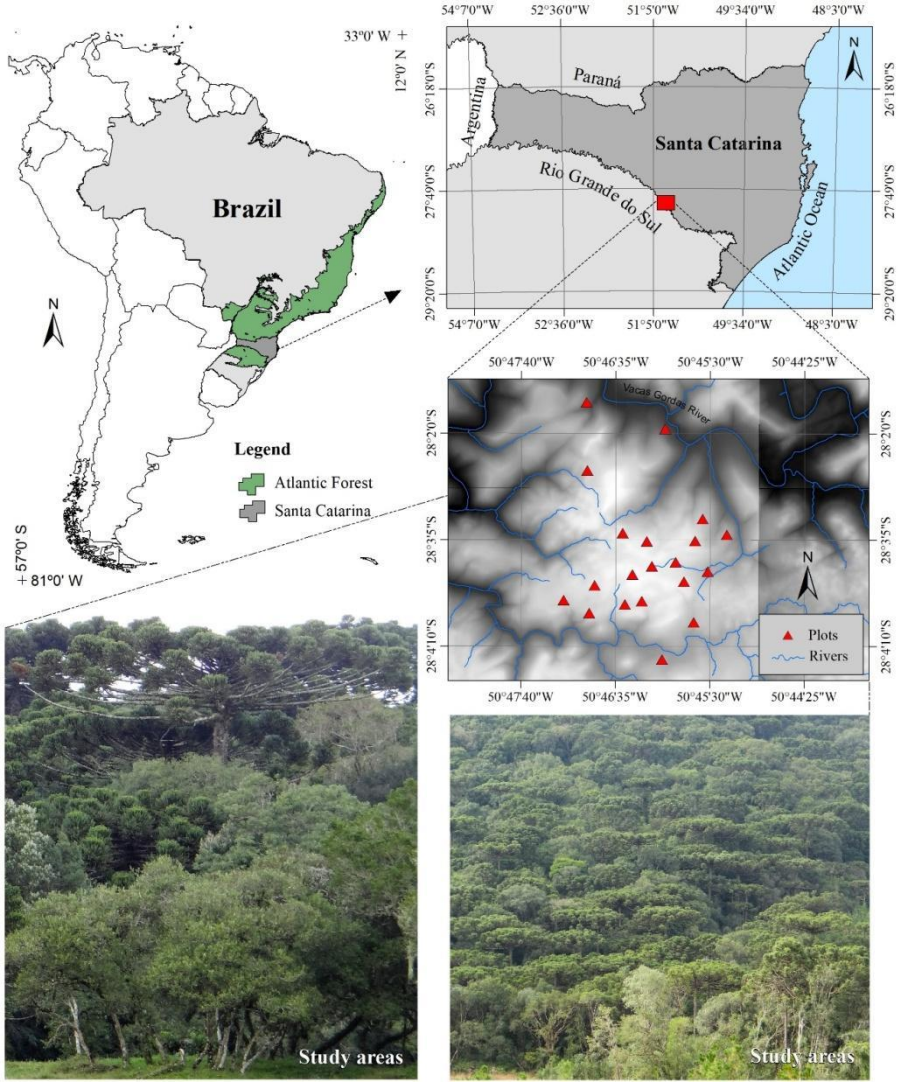

Figure 1. *Studied area at RPPN Emílio Einsfeld Filho, Santa Catarina State, Southern Brazil, and the distribution of the sample plots*

The vegetation of the studied area is constituted by the *Araucaria* Forest (Mixed Needle-Broadleaved Forest – Oliveira-Filho, 2015). This vegetation is characterized by the presence of dense clusters formed by *Araucaria angustifolia* and associated with several tree and shrub species of the Myrtaceae and Lauraceae families (Kersten et al., 2015). Currently, the vegetation in the study area is in advanced stage of regeneration, with about 35 years without anthropic exploration (Maçaneiro et al., 2018).

http://www.aloki.hu ● ISSN 1589 1623 (Print) ● ISSN 1785 0037 (Online)
DOI: http://dx.doi.org/10.15666/aeer/1704_95779589

Data collection

For data collection we installed 20 plots of 2.5 meters radius, in which we sampled all regenerating individuals with diameter at breast height (DBH) < 15 cm and with a minimum height of 50 cm. We collected the data between December/2015 and April/2016. We identified the collected botanical material by comparison with exsicates deposited in the Herbarium Dr. Roberto Miguel Klein and by consulting the taxonomic literature and the specialists of the *Universidade Regional de Blumenau* (FURB) and the *Universidade do Estado de Santa Catarina* (UDESC). We used the species classification system proposed by APG IV (2016) and PPG I (2016).

To obtain the chemical properties of the soil, in each plot we collected soil samples in the depth of 0-20 cm. Then, we stored the samples in plastic bags and sent to the Laboratory of Soil Analysis of EPAGRI (*Empresa de Pesquisa Agropecuária e Extensão Rural de Santa Catarina*) to obtain the chemical variables: clay content (%), phosphorus (P), potassium (K), organic matter (%), aluminum (Al), calcium (Ca), magnesium (Mg) and cation exchange (CTC), aluminum saturation (m%) and base saturation (V%) and pH (Santos et al., 2018).

To obtain the physical properties of the soil, we collected samples with volumetric rings of the Kopecky type of known volume, *i.e.* we collected two points per plot. After these collections, we stored and weighed the samples for later drying in a drying kiln (105°C). The moisture parameters (%) of these samples were determined by the volumetric method and soil density ($g.cm^{-3}$) according to Teixeira et al. (2017). Then, to verify the influence of the canopy opening and the luminous intensity on the natural regeneration, for each site, six hemispherical photographs were taken 10 m apart (see Pinagé et al., 2013). We use a Nikon D3100 digital SLR camera and Nikon Fish-eye Nikkor 10.5 mm lens (*Figure 2*). The photos were analyzed in the software CAN_EYE v6.3.8 to obtain the values of canopy opening and leaf area (Weiss and Baret, 2010). We measured the luminosity index with the aid of a digital *luxímetro*, in the center of each subplot and in the open field (Suganuma et al., 2008).

Figure 2. *Hemispherical photography captured inside regeneration plots of the Araucaria Forest with high (A) and low (B) canopy opening, Southern Brazil*

Data analysis

We analyzed the influence of environmental and spatial variables on regenerating vegetation through canonical analysis of RDA (Borcard et al., 2011; Legendre and Legendre, 2012). We removed collinear environmental variables through principal component analysis (PCA) in PC-ORD 6.0 (McCune and Mefford, 2011). After this procedure, the environmental variables that remained in the analysis were elevation, soil humidity (%), canopy opening (%), leaf area (m^2), luminosity (%), pH-H_2O, SMP

http://www.aloki.hu ● ISSN 1589 1623 (Print) ● ISSN 1785 0037 (Online)
DOI: http://dx.doi.org/10.15666/aeer/1704_95779589

index, base saturation (V%), sum of bases (S), clay content (%), potassium (K), aluminum (Al), calcium (Ca), magnesium (Mg), potential acidity (H+Al), CTC at pH 7.0, Na at CTC and Ca/K and Mg/K ratios in soil.

In the abundance matrix of individuals, we removed the species that presented only one individual in the sample, since these contribute little to the data set and may hinder vegetation analysis (Legendre and Legendre, 2012). After this procedure, we applied the 'standardized score' transformation in the environmental variables, to correct the differences between the units of measure. We used the geographical coordinates (latitude and longitude) of the plots to create spatial variables called MEMs (*Moran's Eigenvector Maps*) in the R Environment using the "spacemakeR" package, as recommended by Borcard et al. (2011). We made the selection of the significant MEMs by means of the "forward" method and we also selected the environmental variables by another RDA. Finally, we processed the last RDA in PC-ORD 6.0 (McCune and Mefford, 2011), using abundance matrices with environmental (standardized) and spatial variables (MEMs) selected to verify the effect of these variables on species composition in the area of study. We verified the statistical significance of the ordering axes of the RDAs through 999 Monte Carlo permutations (Legendre and Legendre, 2012).

Then, we effected the partitioning of the variance into the data set in order to separate the fractions relative to the environment [a], the spatially structured environment [b], only the space [c] and the undetermined variables [d]. In this analysis, we used the "vegan", "packfor", "spacemakeR" and "spdep" packages in the R Environment.

Results

In the study area we sampled 466 individuals (11,867 ind.ha^{-1}) belonging to 60 species and 24 botanical families (*Table 1*). The species in the regenerative stratum with the highest density and frequency were *Allophylus edulis* (A. St.-Hil.) Radlk., *Myrsine umbellata* Mart., *Casearia decandra* Jacq. and *Matayba elaeagnoides* Radlk. (*DR*=39.1% and *FR*=26.3%).

Table 1. *List of the 15 species with the highest density and frequency values in the natural regeneration of the Araucaria forest in Southern Brazil*

Species	Abbreviation	*DA*	*DR*	*FA*	*FR*
Allophylus edulis (A.St.-Hil. et al.) Hieron. ex Niederl	*All edu*	1,732	14.6	65.0	7.6
Myrsine umbellata Mart.	*Myr umb*	1,197	10.1	55.0	6.4
Casearia decandra Jacq.	*Cas dec*	917	7.7	45.0	5.3
Matayba elaeagnoides Radlk.	*Mat ela*	789	6.7	60.0	7.0
Eugenia sp.	*Eug sp.*	738	6.2	40.0	4.7
Sebastiania brasiliensis Spreng.	*Seb bra*	688	5.8	25.0	2.9
Allophylus guaraniticus (A. St.-Hil.) Radlk.	*All gua*	637	5.4	40.0	4.7
Miconia cinerascens Miq.	*Mic cin*	509	4.3	10.0	1.2
Annona emarginata (Schltdl.) H.Rainer	*Ann ema*	484	4.1	25.0	2.9
Cinnamodendron dinisii Schwacke	*Cin din*	382	3.2	35.0	4.1
Rudgea parquioides (Cham.) Müll.Arg	*Rud par*	357	3.0	30.0	3.5
Araucaria angustifolia (Bertol.) Kuntze	*Ara ang*	331	2.8	35.0	4.1
Eugenia uniflora L.	*Eug uni*	306	2.6	30.0	3.5
Styrax leprosus Hook. *et* Arn.	*Sty lep*	255	2.1	25.0	2.9
Brunfelsia pilosa Plowman	*Bru pil*	229	1.9	20.0	2.3
Other species	-	2,317	19.5	315.0	36.8

DA = absolute density (ind.ha^{-1}), DR = relative density (%), FA = absolute frequency (%), FR = relative frequency (%)

http://www.aloki.hu ● ISSN 1589 1623 (Print) ● ISSN 1785 0037 (Online)
DOI: http://dx.doi.org/10.15666/aeer/1704_95779589

In the redundancy analysis (RDA), the plots differed according to the variation in environmental and spatial variables. The eigenvalues of the first two ordering axes explained 36.1% of the data variance (axis 1 = 23.4%, axis 2 = 12.7%) and presented significance by the Monte Carlo test ($p \leq 0.05$). The environmental and spatial variables that correlated with axis 1 were Ca/K, MEM 3 and MEM 17, while for axis 2 only the degree of canopy opening (*Figure 3*, *Table 2*).

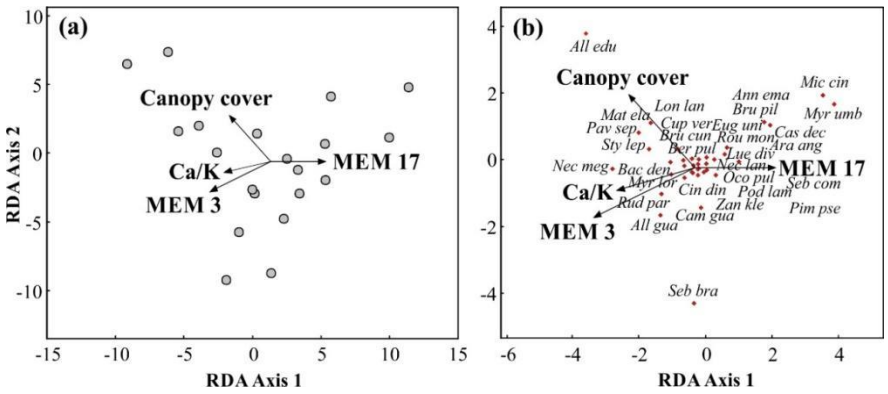

Figure 3. *Redundancy analyzes (RDA) produced by plots, species and environmental and spatial variables for the Araucaria forest regeneration in Southern Brazil*

Table 2. *Environmental and spatial variables produced by the RDA for Araucaria forest regeneration in southern Brazil. R^2 adjusted, F and p were obtained by ANOVA after partitioning of the variance*

Predictor	Average value	R^2 adjusted (%)	*F* (ANOVA)	*p* (ANOVA)
MEM 3	-	11.0	3.4	0.001
Ca/K	13.7	10.4	3.3	0.009
Canopy opening	17.9	7.6	2.6	0.01
MEM 17	-	4.4	1.9	0.03

In the ordination diagram of the plots, we verified that the first two axes had a strong relation between canopy opening and the spatial variable MEM 17 (*Table 2*). The axes formed two groups of plots, the first one being related to light intensity in the environment and the second, to the spatial structure of the community. In addition, we observed the formation of a short gradient related to the Ca/K content (*Figure 3a*).

In the diagram of species ordination, we verified a strong association with the canopy opening and the density of regenerating individuals of *Allophylus edulis, Matayba elaeagnoides, Muellera campestris, Cupania vernalis, Brunfelsia cuneifolia, Pavonia sepium* (*Figure 3b*), while in closed canopy sites (generally located below the broad canopies of *Araucaria angustifolia*) we found other predominant species (e.g., *Campomanesia guaviroba, Zanthoxylum kleinii, Cinnamodendron dinisii* and *Sebastiania brasiliensis*). Also, we observed in *Figure 1b* an association between variables MEM 17 and Ca/K. In this case, certain species occurred in soils with high index of Ca/K (e.g., *Nectandra megapotamica, Baccharis dentata*, *Rudgea parquioides* and *Allophylus guaraniticus*). On the other hand, species like *Casearia decandra, Araucaria angustifolia* and *Ocotea pulchra* are usually associated to soils with less Calcium and Potassium index, but they are positively influenced by spatial component MEM 17.

http://www.aloki.hu ● ISSN 1589 1623 (Print) ● ISSN 1785 0037 (Online)
DOI: http://dx.doi.org/10.15666/aeer/1704_95779589

Partitioning of variance revealed that fractions [a] "pure" environment (F = 2.071, p=0.008) and [c] "pure" space (F = 1.773, p = 0.02) were significant (*Figure 4*). The fraction [b], related to space + environment, indicated that part of the analyzed environmental variables (9%) is structured in space, while the [a] "pure" environment (9%) and [c] "pure" space (7%) stood out among fractions. However, the fraction [d] relative to the undetermined variables explained most of the vegetation variation in the study area (75%).

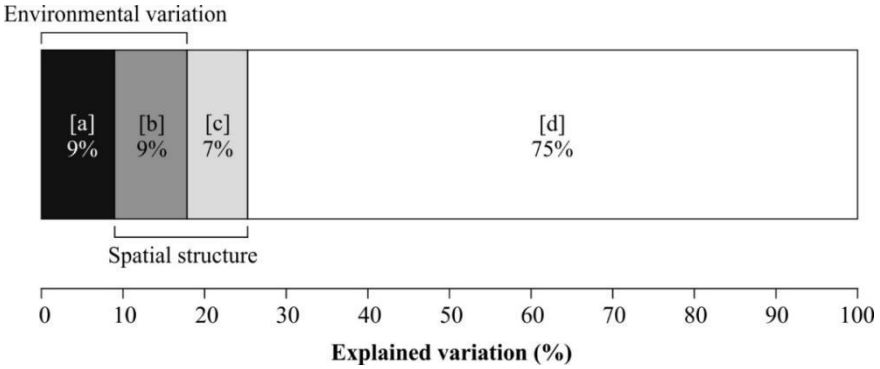

Figure 4. *Partition of the variance by the redundancy analysis to determine the fractions "pure" environment [a], space + environment [b], "pure" space [c] and undetermined variables [d] for the Araucaria forest regeneration in Southern Brazil*

Discussion

Our results indicate that some of the quantified environmental variables influence the distribution of the regenerating species of the *Araucaria* Forest in the South of Brazil. They also indicate that the spatial structure, generally neglected in studies on subtropical forest regeneration, plays an important role in forest regeneration. The spatial structure is less relevant to environmental variables but influences the distribution of some species. Among the factors that influenced the distribution of regenerating species the most in the *Araucaria* Forest is the variation related to the canopy opening. Studies related to the distribution of species have shown that the luminosity variation within the forest influences the species distribution (Duarte et al., 2002; Higuchi et al., 2015). The canopy opening and the variation of luminosity are related to climatic events (e.g., storm) that occurred prior to the development of the present study, and may be influencing the distribution of the species. Biotic/stochastic events may alter light input into the forest, affecting the dynamics of regeneration within tropical forests (Peixoto et al., 2012; Horn et al., 2015; Kersten et al., 2015).

We verified high density of regenerating individuals of *Allophylus edulis* in plots with greater canopy opening, indicating that this species frequently occurs in open areas such as forest edges or natural clearings (Maçaneiro et al., 2016b). The luminosity is one of the main factors that affect the establishment and growth of plants, being fundamental in the structure of the forests (Duarte et al., 2002). In our study, we verified different levels of luminosity within the forest, associated to stochastic factors and/or possibly to successional processes. These conditions reflect in the existence of different environments within the forest, which are explored by groups of species with different survival abilities (Baldeck et al., 2013). Thus, the differences in floristic composition

http://www.aloki.hu ● ISSN 1589 1623 (Print) ● ISSN 1785 0037 (Online)
DOI: http://dx.doi.org/10.15666/aeer/1704_95779589

and density of the species correspond mainly to the intensity of the canopy opening within the forest.

Considering the influence of environmental variables on forest regeneration, we observed that the soil Ca/K content positively influences the distribution of some species (e.g., *Nectandra megapotamica*, *Rudgea parquioides*). Soil fertility, for example, is usually associated with some chemical element present in a greater or lesser quantity, varying in relation to local soil characteristics, depth and texture, among others. Studies have shown a strong relationship between soil characteristics and floristic composition, generally associated with pH, texture and moisture content (Dubuis et al., 2012; Mélo et al., 2013), differently from what we observed in this study. The presence of Ca/K in the soil may influence the distribution process of the species because they are elements associated with germination, growth and resistance at low temperatures. In our study, the environmental variables (represented by the canopy opening and the presence of Ca/K) were not the only processes that explained the species distribution.

The spatial component may be associated with biotic/stochastic processes (e.g., dispersion, facilitation, competition, pollination and predation) (Lewis et al., 2014), which in this study revealed a significant fraction of the floristic patterns. Among the stochastic processes that can influence the spatial distribution, dispersion plays a fundamental role in the colonization of regenerating species and is influenced by several external components (e.g., animals, wind) (Wang and Smith 2002; Urbanetz et al., 2003; Neuschulz et al., 2016). The facilitacion and competition processes can also influence the spatial distribution of species, but these processes do not depend on the physical factors of the environment and may occur in different climatic conditions (Mélo et al., 2013). In this case, we observed that climatic events and stochastic process may be influencing the species distribution and are playing a role in the colonization of certain species in regeneration. Environments that present adversities can act like an ecological filter, in order to affect the performance of some species (Temperton and Hobbs, 2004; Gotelli, 2007). Likewise, the maintenance and establishment of regeneration in the study area may be occurring through the processes of pollination and seed predation (Wang and Smith, 2002). Therefore, to determine these ecological patterns it is necessary to replicate the study to create forest patterns (Scipioni et al., 2009).

In the present study, the partitioning of the data set variance indicated that the highest percentage of factors that interfered in distribution patterns is related to unknown fractions (75%). According to Lewis et al. (2014), variation of species composition along the plots and heterogeneity are factors that increase the unknown fractions. In addition, the environmental variables used are not necessarily the predictors that best explain the species distribution variations (Soininen, 2014). Another reason is the weakening of environmental responses when using the variance partition (Angeler et al., 2013). Likewise, it revealed that “pure” environment factors (9%) and “pure” space (7%) were statistically significant, being important predictors to explain the distribution of regenerating species in the *Araucaria* Forest in Southern Brazil. In this way, it is crucial to carry out new studies, which aim to include observations on dispersion, pollination and competition patterns, among others, to respond unknown factors (Diniz-Filho et al., 2012; Peña-Claros et al., 2012).

http://www.aloki.hu ● ISSN 1589 1623 (Print) ● ISSN 1785 0037 (Online)
DOI: http://dx.doi.org/10.15666/aeer/1704_95779589

Conclusion

Although much floristic variation remained unexplained, the results indicated the complex effect of environmental and spatial variables on the regeneration patterns of the *Araucaria* Forest in Southern Brazil. The environmental variable with the greatest influence on the distribution of the natural regeneration of the *Araucaria* Forest was the opening of the canopy. This variable affected certain species of the regenerating component. In addition to this variable, the soil Ca/K content influenced certain species, but it was not as fundamental as the canopy opening. Despite the environmental influence on the species distribution, it is important to emphasize the importance of the spatial structure on the forest regeneration, being this one of the variables that influenced the vegetation the most. In the same sense, the spatial components generally neglected in ecological studies have shown great influence in the distribution and must be taken into consideration to analyze forest environments.

Considering that the study was developed at a local scale, other works should be developed to determine the floristic pattern for the *Araucaria* Forest. It is important to investigate further the association between species and environmental standards and to analyze the influence of different spatial variables such as competition, dispersion, microclimate, among other variables not presented in this study, since the addition of these variables may increase the predictive power of floristic patterns in subtropical forests.

Acknowledgements. The authors are grateful to *Coordenação de Aperfeiçoamento de Pessoal de Nível Superior* (CAPES) and *Conselho Nacional de Desenvolvimento Científico e Tecnológico* (CNPq) for their research fellowship grant (141232/2018-8). We also thank Marta Helena Cúrio de Caetano from FURB Idiomas for English review.

REFERENCES

[1] Alvares, C. A., Stape, J. L., Sentelhas, P. C., Gonçalves, J. L. M., Sparovek, G. (2013): Köppen's climate classification map for Brazil. – Meteorologische Zeitschrift 22(6): 711-728.

[2] Angeler, D. G., Göthe, E., Johnson, R. K. (2013): Hierarchical dynamics of ecological communities: do scales of space and time match? – PLoS One 8(7): e69174.

[3] APG IV. (2016): An update of the Angiosperm Phylogeny Group classification for the orders and families of flowering plants: APG IV. – Botanical Journal of the Linnean Society 181(1): 1-20.

[4] Baldeck, C. A., Harms, K. E., Yavitt, J. B., John, R., Turner, B. L., Valencia, R., Navarrete, H., Davies, S. J., Chuyong, G. B., Kenfack, D., Thomas, D. W., Madawala, S., Gunatilleke, N., Gunatilleke, S., Bunyavejchewin, S., Kiratiprayoon, S., Yaacob, A., Supardi, M. N., Dalling, J. W. (2013): Soil resources and topography shape local tree community structure in tropical forests. – Proceedings of the Royal Society B: Biological Sciences 280(1753): 2012-2532.

[5] Borcard, D., Gillet, F., Legendre, P. (2011): Numerical Ecology with R. – Dordrecht London Heidelberg, New York.

[6] Diniz-Filho, J. A. F., Siqueira, T., Padial, A. A., Rangel, T. F., Landeira, V. L., Bini, L. M. (2012): Spatial autocorrelation analysis allows disentangling the balance between neutral and niche processes in metacommunities. – Oikos 121(2): 201-210.

http://www.aloki.hu ● ISSN 1589 1623 (Print) ● ISSN 1785 0037 (Online)
DOI: http://dx.doi.org/10.15666/aeer/1704_95779589

[7] Duarte, L., Dillenburg, L. R., Rosa, L. M. G. (2002): Assessing the role of light availability in the regeneration of Araucaria angustifolia (Araucariaceae). – Australian Journal of Botany 50: 741-751.
[8] Dubuis, A., Giovanettina, S., Pellissier, L., Pottier, J., Vittoz, P., Guisan, A. (2012): Improving the prediction of plant species distribution and community composition by adding edaphic to topo-climatic variables. – Journal of Vegetation Science 24(4): 593-606.
[9] Gotelli, N. J. (2007): Sucessão. – In: Gotelli, N. J. (ed.) Ecologia. Editora Planta, Londrina, Brasil, 328p.
[10] Higuchi, P., Silva, A. C., Buzzi Junior, F., Negrinii, M., Ferreira, T. S., Souza, S. T., Santos, K. F., Vefago, M. B. (2015): Determinant factors on natural regeneration in a fragment of araucaria forest on Santa Catarina State plateau. – Scientia Forestalis 43(106): 251-259.
[11] Higuchi, P., Silva, A. C., Ferreira, T. S., de Souza, S. T., Gomes, J. P., da Silva, K. M. (2016): Floristic and structure of the tree component and relation with environmental variables in a forest remnant in Campos Novos–SC. – Ciência Florestal 26(1): 35-46.
[12] Horn, J., Becher, M. A., Kennedy, P. J., Osborne, J. L., Grimm, V. (2015): Multiple stressors: using the honeybee model BEEHAVE to explore how spatial and temporal forage stress affects colony resilience. – Oikos 125(7): 1001-1016.
[13] IBGE. (2012): Manual Técnico da Vegetação Brasileira. – Rio de Janeiro, Instituto Brasileiro de Geografia e Estatística, Brazil.
[14] Kersten, R. A., Borgo, M., Galvão, F. (2015): Floresta Ombrófila Mista: aspectos fitogeográficos, ecológicos e métodos de estudo. – In: Eisenlohr, P. V., Felfili, J. M., Melo, M. M. R. F., Andrade, L. A., Meira Neto, J. A. A. (eds.) Fitossociologia no Brasil: métodos e estudos de casos. UFV, Viçosa, Brasil.
[15] Legendre, P., Legendre, L. (2012): Numerical ecology. – Elsevier, Amsterdam, Netherlands.
[16] Lewis, R. J., Pakeman, R. J., Marrs, R. H. (2014): Identifying the multi-scale spatial structure of plant community determinants of an important national resource. – Journal of Vegetation Science 25(1): 184-197.
[17] Loebens, R., da Silva, A. C., Higuchi, P., Mafra, A. L., da Silva, J. O., Gonçalves, D. A., Souza, K., Cruz, A. P., Rodrigues Jr., L. C., Dalla Rosa, A.., Lima, C. L., Buzzi Jr., F. (2018): Partitioning of floristic-structural variation of the tree component in an alluvial Araucaria Forest in Southern Brazil. – Ciência Florestal 28(2): 554-566.
[18] Maçaneiro, J. P., Oliveira, L. Z., Seubert, R. C., Eisenlohr, P. V., Schorn, L. A. (2016a): More than environmental control at local scales: do spatial processes play an important role on floristic variations in Subtropical Forests? – Acta Botanica Brasilica 30(2): 183-192.
[19] Maçaneiro, J. P., Seubert, R. C., Heilmann, A., Schorn, L. A. (2016b): Regeneration of a Mixed Ombrophilous Forest on the Santa Catarina Plateau. – Biotemas 29(4): 31-42.
[20] Maçaneiro, J. P., Gasper, A. L., Galvão, F., Schorn, L. A. (2018): Dispersion and aggregation patterns of tree species in Araucaria Forest, Southern Brazil. – Anais da Academia Brasileira de Ciências 90(2 Suppl. 1): 2397-2408.
[21] Maçaneiro, J. P., Liebsch, D., Gasper, A. L., Galvão, F., Schorn, L. A. (2019): Structural and floristic variations in an Atlantic Subtropical Rainforest in Southern Brazil. – Floresta e Ambiente 26(1): e20160101.
[22] McCune, B., Mefford, M. J. (2011): PC-ORD: Multivariate analysis of ecological data, Version 6. – MjM Software Design. Gleneden Beach, Oregon.
[23] Mélo, M. A., Budke, J. C., Henke-Oliveira, C. (2013): Relationships between structure of the tree component and environmental variables in a subtropical seasonal forest in the upper Uruguay River valley, Brazil. – Acta Botanica Brasilica 27(4): 751-760.

http://www.aloki.hu ● ISSN 1589 1623 (Print) ● ISSN 1785 0037 (Online)
DOI: http://dx.doi.org/10.15666/aeer/1704_95779589

[24] Neuschulz, E. L., Mueller, T., Schleuning, M., Böhning-Gaese, K. (2016): Pollination and seed dispersal are the most threatened processes of plant regeneration. – Scientific Reports 6(29839): 1-6.
[25] Oliveira-Filho, A. T. (2015): Um sistema de classificação fisionômico-ecológico da vegetação neotropical: segunda aproximação. – In: Eisenlohr, P. V., Felfili, J. M., Melo, M. M. F., Andrade, L. A., Meira-Neto, J. A. A. (eds.) Fitossociologia no Brasil: métodos e estudos de caso. Viçosa: Editora UFV.
[26] Peixoto, K. S., Sanchez, M., Pedroni, F., Ribeiro, M. N., Facure, K. G., Klein, V. L. G. (2012): Dinâmica da comunidade arbórea em uma floresta estacional semidecidual sob queimadas recorrentes. – Acta Botanica Brasílica 26(3): 697-708.
[27] Peña-Claros, M., Poorter, L., Alarcon, A., Blate, G., Choque, U., Fredericksen, T. S., Justiniano, M. J., Leano, C., Licona, J. C., Pariona, W., Putz, F. E., Quevedo, L., Toledo, M. (2012): Soil effects on forest structure and diversity in a moist and a dry Tropical Forest. – Biotropica 44(3): 276-283.
[28] Pinagé, E. R., Gomes, A. R, Osako, L. S., Matricardi, E. A. T., Guimarães, U. S., Santos, A. H. H. (2013): Estimativa da fração de cobertura florestal em áreas de manejo florestal com a utilização do analisador ótico LAI-2000 e fotografias hemisféricas. – In: XVI Simpósio brasileiro de Sensoriamento Remoto, pp. 2944-2951.
[29] PPG I. (2016): A community-derived classification for extant lycophytes and ferns. – Journal of Systematics and Evolution 54(6): 563-603.
[30] Ribeiro, M. C., Martensen, A. C., Metzger, J. P., Tabarelli, M., Scarano, F., Fortin, M. J. (2011): The Brazilian Atlantic forest: a shrinking biodiversity hotspot. – In: Zachos, F. E., Habel, J. C. (eds.) Biodiversity hotspots. Springer, Heidelberg.
[31] Rocha, R. P., Silva, M. B. (2013): História Biogeográfica da Mata Atlântica: Opiliões (Arachnida) como modelo para sua inferência. – In: Carvalho, C. J. B., Almeida, E. A. B. (eds.) Biogeografia da América do Sul: Padrões e processos. Roca, São Paulo, Brasil.
[32] Santa Catarina. (1986): Atlas de Santa Catarina. – GAPLAN/SUEGI, Florianópolis.
[33] Santos, H. G., Jacomine, P. K. T., Anjos, L. H. C., Oliveira, V. A. V., Lumbreras, J. F., Coelho, M. R., Almeida, J. A., Cunha, T. J. F., Oliveira, J. B. (2018): Sistema Brasileiro de Classificação de Solos. – Embrapa, Distrito Federal.
[34] Scipioni, M. C., Longhi, S. J., Araújo, M. M., Reinert, D. J. (2009): Regeneração natural de um fragmento da Floresta Estacional Decidual na Reserva Biológica do Ibicuí-Mirim (RS). – Floresta 39(1): 675-690.
[35] Soininen, J. A. (2014): A quantitative analysis of species sorting across organisms and ecosystems. – Ecology 95(12): 3284-3292.
[36] Souza, C. C., Higuchi, P., Silva, A. C., Souza, K., Rosa, A. D., Rech, C. C. C., Rodrigues Júnior, L. C., Walter, F. F. (2017): Floristic-structural variation of natural regeneration along different topographic positions of an ecotonal forest in Santa Catarina, Brazil. – Revista Árvore 41(3): e410305.
[37] Suganuma, S. M., Torezan, J. M. D., Cavalheiro, A. L., Vanzela, A. L. L., Benato, T. (2008): Comparando metodologias para avaliar a cobertura do dossel e a luminosidade no sub-bosque de um reflorestamento e uma floresta madura. – Revista Árvore 32(2): 377-385.
[38] Teixeira, P. C., Donagemma, G. K., Fontana, A., Teixeira, W. G. (2017): Manual de métodos de análise de solo. – Embrapa, Brasília.
[39] Temperton, V. M., Hobbs, R. J. (2004): The search for ecological assembly rules and its relevance to restoration ecology. – In: Temperton, V. M., Hobbs, R. J., Nuttle, T., Halle, S. (eds.) Assembly rules and restoration ecology: brindging the gap between theory and practice. Island Press, New York.
[40] Urbanetz, C., Oliveira, V. M., Raimundo, R. L. G. (2003): Padrão espacial, escala e síndromes de dispersão. – Relatório Unicamp.
[41] Wang, B. C., Smith, T. B. (2002): Closing the seed dispersal loop. – Trends in Ecology and Evolution 17(8): 379-386.

http://www.aloki.hu ● ISSN 1589 1623 (Print) ● ISSN 1785 0037 (Online)
DOI: http://dx.doi.org/10.15666/aeer/1704_95779589

[42] Weiss, M., Baret, F. (2010): Venμs biophysical variable products algorithm theoretical basis document. – EMMAH, INRA.

APPENDIX

Appendix 1. *Floristic field data for the Araucaria forest regeneration in Southern Brazil*

Family	Species	n	*DA*	*DR*	*FA*	*FR*
Annonaceae	*Annona emarginata* (Schltdl.) H.Rainer	19	484	4.1	25.0	2,9
Araucariaceae	*Araucaria angustifolia* (Bertol.) Kuntze	13	331	2.8	35.0	4,1
Asteraceae	*Baccharis dentata* (Vell.) G.M.Barroso	3	76	0.6	5.0	0,6
	Piptocarpha angustifolia Dusén ex Malme	1	25	0.2	5.0	0,6
Canellaceae	*Cinnamodendron dinisii* Schwacke	15	382	3.2	35.0	4,1
Celastraceae	*Schaefferia argentinensis* Speg.	1	25	0.2	5.0	0,6
Euphorbiaceae	*Bernardia pulchella* (Baill.) Müll.Arg.	2	51	0.4	5.0	0,6
	Sebastiania brasiliensis Spreng.	27	688	5.8	25.0	2,9
	Gymnanthes klotzschiana Müll.Arg.	3	76	0.6	15.0	1,8
Fabaceae	*Muellera campestris* (Mart. ex Benth.) M.J. Silva & A.M.G. Azevedo	2	51	0.4	5.0	0,6
Lauraceae	*Cinnamomum amoenum* (Nees & Mart.) Kosterm.	1	25	0.2	5.0	0,6
	Nectandra lanceolata Nees	2	51	0.4	5.0	0,6
	Nectandra megapotamica (Spreng.) Mez	6	153	1.3	20.0	2,3
	Ocotea puberula (Rich.) Nees	1	25	0.2	5.0	0,6
	Ocotea pulchella (Nees & Mart.) Mez	1	25	0.2	5.0	0,6
	Ocotea pulchra Vattimo-Gil	4	102	0.9	15.0	1,8
	Ocotea sp. Aubl.	2	51	0.4	10.0	1,2
Loganiaceae	*Strychnos brasiliensis* Mart.	1	25	0.2	5.0	0,6
Malvaceae	*Luehea divaricata* Mart. & Zucc.	3	76	0.6	15.0	1,8
	Pavonia sepium A.St.-Hil.	6	153	1.3	10.0	1,2
Melastomataceae	*Miconia cinerascens* Miq.	20	509	4.3	10.0	1,2
Meliaceae	*Trichilia elegans* A.Juss.	1	25	0.2	5.0	0,6
Myrtaceae	*Campomanesia guaviroba* (DC.) Kiaersk.	4	102	0.9	10.0	1,2
	Eugenia rostrifolia D.Legrand	1	25	0.2	5.0	0,6
	Eugenia sp. L.	29	738	6.2	40.0	4,7
	Eugenia uniflora L.	12	306	2.6	30.0	3,5
	Myrceugenia mesomischa (Burret) D.Legrand & Kausel	1	25	0.2	5.0	0,6
	Myrcia glabra (O.Berg) D.Legrand	1	25	0.2	5.0	0,6
	Myrcia hartwegiana (O.Berg) Kiaersk.	1	25	0.2	5.0	0,6
	Pimenta pseudocaryophyllus (Gomes) Landrum	2	51	0.4	5.0	0,6
Oleaceae	***Ligustrum lucidum* W.T.Aiton	1	25	0.2	5.0	0,6
Podocarpaceae	*Podocarpus lambertii* Klotzsch ex Endl.	4	102	0.9	10.0	1,2
Primulaceae	*Myrsine coriacea* (Sw.) R.Br. ex Roem. & Schult.	1	25	0.2	5.0	0,6
	Myrsine parvula (Mez) Otegui	2	51	0.4	5.0	0,6
	Myrsine umbellata Mart.	47	1197	10.1	55.0	6,4
Proteaceae	*Roupala montana* Aubl.	2	51	0.4	10.0	1,2
Rubiaceae	*Rudgea parquioides* (Cham.) Müll.Arg.	14	357	3.0	30.0	3,5
Rutaceae	*Zanthoxylum kleinii* (R.S.Cowan) P.G.Waterman	3	76	0.6	10.0	1,2
	Zanthoxylum rhoifolium Lam.	1	25	0.2	5.0	0,6
Salicaceae	*Casearia decandra* Jacq.	36	917	7.7	45.0	5,3
	Casearia obliqua Spreng.	1	25	0.2	5.0	0,6
Sapindaceae	*Allophylus edulis* (A.St.-Hil. et al.) Hieron. ex Niederl.	68	1732	14.6	65.0	7,6
	Allophylus guaraniticus (A. St.-Hil.) Radlk.	25	637	5.4	40.0	4,7
	Cupania vernalis Cambess.	3	76	0.6	10.0	1,2
	Matayba elaeagnoides Radlk.	31	789	6.7	60.0	7,0
Solanaceae	*Brunfelsia cuneifolia* J.A.Schmidt	3	76	0.6	10.0	1,2
	Brunfelsia pilosa Plowman	9	229	1.9	20.0	2,3
Styracaceae	*Styrax leprosus* Hook. & Arn.	10	255	2.1	25.0	2,9
Thymelaeaceae	*Daphnopsis racemosa* Griseb.	1	25	0.2	5.0	0,6
Winteraceae	*Drimys brasiliensis* Miers	1	25	0.2	5.0	0,6

http://www.aloki.hu ● ISSN 1589 1623 (Print) ● ISSN 1785 0037 (Online)
DOI: http://dx.doi.org/10.15666/aeer/1704_95779589

-	NI 01	3	76	0.6	10.0	1,2
-	NI 02	4	102	0.9	10.0	1,2
-	NI 03	2	51	0.4	5.0	0,6
-	NI 04	1	25	0.2	5.0	0,6
-	NI 05	1	25	0.2	5.0	0,6
-	NI 06	3	76	0.6	5.0	0,6
-	NI 07	1	25	0.2	5.0	0,6
-	NI 08	2	51	0.4	5.0	0,6
-	NI 09	1	25	0.2	5.0	0,6
Total		466	11,867	100,00	855.00	100.00

** = alien species, DA = absolute density (ind.ha^{-1}), DR = relative density (%), FA = absolute frequency (%), FR = relative frequency (%)

Appendix 2. *Environmental average field data for the Araucaria forest regeneration in Southern Brazil*

Environmental data	Average (n=20)	Variance	SD
Elevation (m)	897	3712	61
Clay (%)	36.95	81.00	9.00
pH	4.37	0.43	0.66
SMP (%)	4.89	0.52	0.72
K (mg/dm³)	151.00	3,242.32	56.94
Al (cmolc/d)	2.64	3.74	1.93
Ca (cmolc/d)	6.01	41.56	6.45
Mg (cmolc/dm)	1.50	3.10	1.76
H+Al (cmolc/dm³)	20.17	136.20	11.67
CTCpH (cmolc/dm²)	28.06	59.96	7.74
Na CTC-Al (%)	37.40	781.20	27.95
Sat CTC-V (%)	31.13	942.13	30.69
Sum of bases (%)	7.89	64.65	8.04
Ca/K	13.68	147.97	12.16
Mg/K	3.58	16.44	4.06
Humidity (%)	49.0	329.30	18.15
Canopy opening (%)	17.9	34.76	5.90
Leaf area (m²)	5.00	0.47	0.69
Luminosity (%)	0.86	0.002	0.04

http://www.aloki.hu ● ISSN 1589 1623 (Print) ● ISSN 1785 0037 (Online)
DOI: http://dx.doi.org/10.15666/aeer/1704_95779589

SELECTIVE LOGGING INTENSITY ALTERS THE POPULATION STAND STRUCTURE OF *CULLENIA-MESUA-PALAQUIUM* DOMINATED TROPICAL WET EVERGREEN FOREST OF THE WESTERN GHATS, SOUTH INDIA

RAMACHANDRAN, V. S.[1#] – MOHANDASS, D.[2#] – CAMPBELL, M. J.[3] – MAMMIDES, C.[4] – SHAO, S-C.[5*]

[1]*Centre for Environmental Studies, Amrita Vishwa Vidyapeetham (University) Amrita Nagar, Ettimadai, Coimbatore – 641112, Tamil Nadu, India*

[2]*Ecological Field Station, Edhkwehlynawd Botanical Refuge (EBR) Amaggal Forest, Doddacombai – 643 219, Nilgiris, India*

[3]*Centre for Tropical Environmental and Sustainability Science (T.E.S.S.) School of Marine and Tropical Biology, James Cook University, Cairns, Queensland, Australia*

[4]*Guangxi Key Laboratory of Forest Ecology and Conservation, College of Forestry Guangxi University, Daxuedonglu 100, Nanning 530004, P.R. China*

[5]*Gardening and Horticulture Department, Xishuangbanna Tropical Botanical Garden Chinese Academy of Sciences, Yunnan 666303, P.R. China*

[#]*These authors equally contributed to this paper.*

[*]*Corresponding author*
e-mail: shaoshicheng@xtbg.org.cn; phone: +86-189-8819-6796

(Received 12th Jan 2019; accepted 24th May 2019)

Abstract. The present study was conducted in a population structure of selectively logged tropical wet evergreen forest, *Cullenia-Mesua-Palaquium* (CMP) forest series in the tropical wet evergreen forests of the Nelliampathy Hills, Western Ghats. The study was aimed to focus on how selectively logged treatment influences the density and basal area of CMP forest series stand structure. We sampled the number of individual trees (≥ 1 cm dbh, diameter at breast height) of CMP at 30 sites (20 × 50 m quadrat size), covering an area of 30.8 hectare (ha) in total. A total of 5936 tree individuals sampled had a mean density of 246 ha^{-1} and basal area of 20.73 metre square (m^2) ha^{-1} from an area of 0.1 to 2.5 ha. Tree density per hectare and basal area differed significantly among plots with different logging treatments. Tree density and basal area were significantly lower in highly logged plots as compared to moderately logged and unlogged plots. The density of smaller trees was significantly higher in moderately logged plots. We suggest that heavy logging treatments might be a serious threat to the CMP forest series and may possibly alter its population structure and that the moderately logged treatments showed positive impacts on CMP stand structure and regeneration.
Keywords: *basal area, disturbance, forest management, large trees, tree extraction*

Introduction

Globally, more than 400 million hectares of tropical forest are in the logging estates (Blaser et al., 2011; Senior et al., 2017; Silva et al., 2018) and the world's tropical forests have been affected by intensive commercial logging for at least several decades (Johns and Skorupa, 1987; Chapman and Chapman, 1997; Gardner et al., 2009; Putz et al., 2012; Poudyal et al., 2018). Logging is a major threat in reducing the native forest

http://www.aloki.hu ● ISSN 1589 1623 (Print) ● ISSN 1785 0037 (Online)
DOI: http://dx.doi.org/10.15666/aeer/1704_95919607

area (Gatti et al., 2015) and potentially results in species extinction (Pimm and Raven, 2000). In addition to clear cut logging, selective logging is also an important driver of forest alteration across the tropics with ~20% of all tropical forests selectively logged between 2000 and 2005 (Asner et al., 2009; Ansell et al., 2011; Magrach et al., 2016). Selective logging can negatively alter the ecological interaction of the remnant tree diversity and population structure leading to a negative impact on forest structure (Okuda et al., 2003; Yamada et al., 2013; Gatti et al., 2015). As a result of the alteration of ecological interactions in the forest due to selective logging (Schleuning et al., 2011; Magrach et al., 2016), many endemic and rare species could possibly decline at a rapid pace (Laurance et al., 1999; Zhu et al., 2004). Therefore, logging activity poses a serious threat to the long-term sustainability of the population of certain tree species in the tropical forest ecosystem.

In this study, silviculture practices is defined as the process by which the trees established in large area of forest would be removed and replaced by new tree regeneration, resulting in the production of distinctive forms of woods (Troup, 1966). It is also demarcated as "the art and science of producing and tending forests by manipulating their species establishment, species composition, structure and dynamics to fulfil the tropical forest management purposes" (ITTO, 2002). Therefore, tropical silviculture practices may play a major role in the present and future to ensure forest sustainability and sustainable production of forest products (Peña-Claros et al., 2008; Villegas et al., 2009). However, silviculture systems emphasizes the method of raising forest products by the influence of timber extraction (Ramachandran, 2008). Previous studies also demonstrates that silviculture was carried out by clearcutting (Hoffman, 1924; Isaac, 1956), partial cutting or selective logging (Kirkland and Brandstrom, 1936).

Selective logging activity may also decrease the forest area (McDonald et al., 2006) and remove the larger trees in a tropical forest (Osazuwa-Peters et al., 2015). Both forest area and the large tree presence are crucial in determining the capacity of the tropical forest to sequester carbon (Slik et al., 2013). Therefore, examination of selective logging impacts on selected tropical forests is important to determine the impact of human interventions on the population structure of plant communities. Some studies suggests that efficient management of selective logging could bring a number of trials that are related to the enhancement of forest products (Rist et al., 2012; d'Annunzio et al., 2015) and aid in preventing carbon emissions, including reduction of the available terrestrial biodiversity among tropical forests (Leadley et al., 2014; Köhl et al., 2015; Pearson et al., 2017). However, several studies also report that the real selective logging negatively impacts on forest community, which leads to forest degradation and reduction of forest products supplements (Irland, 2011; Hethcoat et al., 2018), in turn diminishing the volume of carbon stock perspective and the value of wildlife habitat (Martin et al., 2015).

In the Western Ghats of southern India, there is a number of designated series of forest types encompassing a rich endemic and endangered tree flora (Pascal, 2004; Ramesh et al., 2009). Of these, the *Cullenia-Mesua-Palaquium* forest series (hereafter referred to as "CMP forest") found in the mid-elevation (700-1400 m) regions of the Western Ghats is considered a unique (Pascal, 2004) and important tropical wet evergreen climax forest type (Ramesh et al., 2009). In some parts of the Western Ghats, human disturbance of CMP forests has resulted in the loss and heavy fragmentation of this forest type along with thicket formations within some human maintained savannas

http://www.aloki.hu ● ISSN 1589 1623 (Print) ● ISSN 1785 0037 (Online)
DOI: http://dx.doi.org/10.15666/aeer/1704_95919607

(Pascal, 2004). The current study was conducted in mid-elevation (700-1400 m) regions of the tropical wet evergreen forest of the Nelliampathy Hills, southern Western Ghats. Logging began in this region during the 1950s and continued into the 1980s in order to increase forest trees as a method of silviculture solely for timber extraction. As a result, several of the forest series including CMP forest have experienced significant disturbance and fragmentation. In this study, we examined the residual influence of previously selected logging treatments nearly 20 years after the intensive selective logging ceased. Examinations include a comparison of the recovery of stand structure and tree density of the CMP forest series, which have been logged at different intensities post-logging. Prior to this research, there was no reliable information available on the impact of logging treatments on any of the regional forest series nor the population structure of the trees in these areas of the Western Ghats. Therefore, this study is the first attempt to examine the impact of selective logging treatments on the tree population structure of CMP forest. The study addresses the following hypotheses: 1) the total density and basal area of CMP forest series would increase in response to different intensities of selective logging; 2) the small (> 1 cm diameter at breast height (dbh) and large (> 30 cm dbh) tree density and basal area of CMP forest series would increase in response to different intensities of selective logging; 3) logging treatment would have a significant influence on tree density and basal area of CMP series along with different elevational gradients.

Materials and Methods

Study area

The study was conducted in the tropical evergreen wet evergreen forest of the Nelliampathy Hills of the Western Ghats in South India (*Figure 1A*). The elevation ranges from 780 to 1633 m asl. Nelliampathy hills run south from the edge of the Palghat Gap and the junction of Anamalai and Parambikulam Hills (*Figure 1A*).

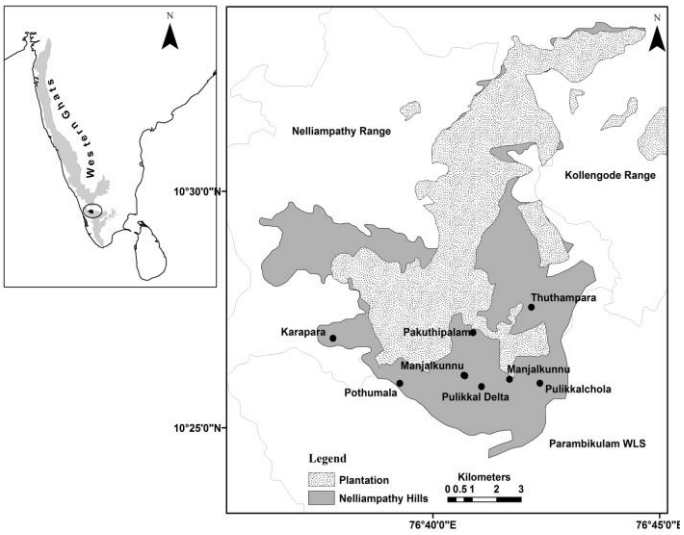

Figure 1A. *Map shows that locations of the major study areas in the Nelliampathy hill ranges, namely (i) Karapara, (ii) Manjalkunnu (iii) Pakuthipalam (iv) Pothumala (v) Pulikkalchola (iv) Thuthampara, including the 30 sampled sites (see Appendix 1) examined in the tropical evergreen forests of the Western Ghats, southern India*

http://www.aloki.hu ● ISSN 1589 1623 (Print) ● ISSN 1785 0037 (Online)
DOI: http://dx.doi.org/10.15666/aeer/1704_95919607

The rock formation of Nelliampathy is composed of Cambrian cover and entirely reconfirmed as faults and metamorphism (Mani, 1974; Krishnan, 1974). The Pre-Cambrian crystalline rocks contain Khondalite series of Gneiss and Charnockite series of granite intrusions (Nair, 1988). The soil of the study area is generally red, sandy loam, porous with a pH ranging from 4.5 to 7.5 though the soil in the flat areas along the hills contain loam mixed with high levels of clay (Chandrasekaran et al., 1977). The tropical evergreen forest of the study site has been classified as medium elevation type of the *Cullenia exarillata-Mesua ferrea-Palaquium ellipticum* forest composition (Pascal, 1988; Ramachandran and Swarupanandan, 2013). As mentioned, large areas of these forests were selectively logged during the period 1950-1986 (Matthew, 2001); however, areas of old-growth unlogged forests still exist.

The study was carried out in the Pulikkalchola forests located at 10° 47' N and 76° 70' E. The climate is humid with the mean annual rainfall of the study area over a 10-year period from 1995-2004 of 2457 mm. Rainfall in this region is characterized as monsoonal peaks from June to August while a distinct dry season runs from December to March. The minimal and maximal rainfall reported from 1994-2004 was 626-2028 mm and 1441-4278 mm, respectively. The number of rainy days varied from 127−144 a^{-1}. The annual average temperature of the study area ranged from 5°C to 30°C (Ramachandran and Swarupanandan, 2013, 2018). During the comparatively dry period of December to March, the mean monthly temperatures ranged 20.4–25.2°C (Ramachandran and Swarupanandan, 2013; IMD, 2018). Rainfall increased > 79% in study areas during the year 2018 (IMD, 2018).

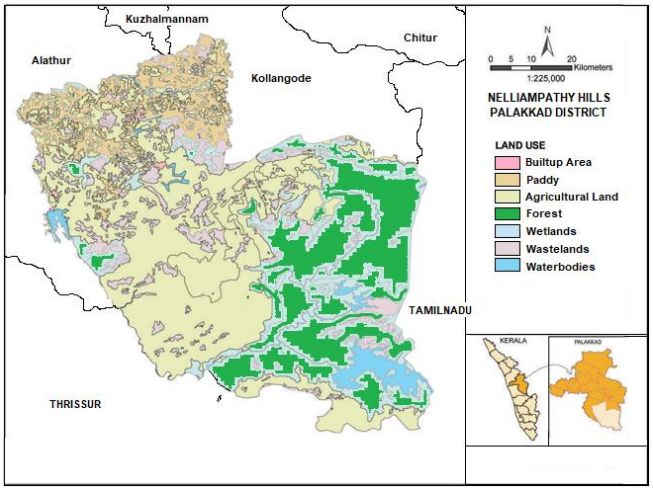

Figure 1B. *Map showing that land use changes which displayed the builtup area, paddy field, agricultural land, forest area, wetland, wastelands and waterbodies in the of Nelliampathi Hills, Palakkad district of the Western Ghats, India*

The dominant vegetation series of the study region are *Cullenia exillarita* A. Robyns (Malvaceae), *Mesua ferrea* L. (Calophyllaceae) and *Palaquium ellipticum* (Dalzell) Baill. (Sapotaceae). These species are tall trees with heights ranging between 30 and 40 m and are commonly located in the interior of the continuous forest patches of the tropical wet evergreen forests of the Nelliampathy Hills. The trees generally do not branch out until they reach a certain height (approximately 10 m). The dominant tree

http://www.aloki.hu ● ISSN 1589 1623 (Print) ● ISSN 1785 0037 (Online)
DOI: http://dx.doi.org/10.15666/aeer/1704_95919607

species in *Cullenia-Mesua-Palaquium* (CMP) forest series is of a unique structure at a particular elevation ranging 550–700 m altitude in the Western Ghats (Pascal, 2004). The forests produce large fleshy fruits which serve as useful food resources for the resident birds and mammals. Moreover, the area is the primary habitat for the endangered lion-tailed macaque (Pascal, 1988; Ganesh and Davidar, 1999). These forest series species are an important resource for wild animals despite the fact that they display a narrow geographical distribution in the Western Ghats.

Description of selective logging treatments

Selective logging was considered only as a silvicultural system implemented in the natural forests of Kerala (FAO, 1984, 1985; Chundamannil, 1993). It started as early as 1885 (Nair, 1988). In the study area, a part of the growing stock in the form of mature trees was removed during the 1950s, 1960s, 1970s and 1980s, encompassing a large area each year, either at the same time or at an interval of 15-30 years (Baur, 1964; FAO, 1989; Lamprecht, 1993). This selective logging system practiced in India is actually a Quasi-Selection System or Selection Felling (Troup, 1916; Seth, 1960) or the Selective Felling/Logging (Lal, 1961; Srivastava, 1983). In the early 1950s, forest administration used a method of treatment for the vast extent of the forest using a limitedly trained staff with poor silvicultural knowledge. They chose selective felling as the only method available to make use of the stock of mature and over-mature trees of marketable species (Troup, 1916, 1921). In this method, mature trees of selected species with a minimum girth limit (> 30 cm to 80 cm girth) were logged under a definite felling cycle, leaving only the seed bearers where natural regeneration is deficient. In India, this is the most widely practiced system applicable to the evergreen, moist deciduous and dry deciduous forests (FAO, 1989). Selective logging was applied and aimed to increase the regeneration of species by improving the light conditions of the forest floor (Stracey, 1959; FAO, 1984; Kadambi, 1986). In the studied plots, selective logging was implemented to extract CMP species suitable for railway sleepers, ship masts and electric poles (Nair, 1961; FAO, 1989).

In the present study, selective logging treatments were categorized into high, moderate and unlogged treatments. The plots are defined where the trees were selectively extracted and removed to serve as timber during 1950-1985. We categorized the treatment of selective logging based on the removal of a number of trees per hectare as: (1) High-logging: where the CMP trees were removed based on fixed minimum diameter limit that varied from 30−60 cm dbh with a felling cycle of 15-30 years. The area studied included the number of trees that were removed from an area of 10−20 ha^{-1} and the minimum distance between two trees marked for felling fixed at 20 m. (2) Moderate-logging: The technique was similar to high-logging, however, the trees were removed from 2−6 ha^{-1} area keeping the same distance of 20 m between the tree removed. (3) Unlogged: No logging work was undertaken over a century. The above information was collected from forest department records.

Field sampling

During the year 2004-2006, we surveyed and sampled the tree population of CMP species using quadrat methods. We laid randomly 20 × 50 m quadrats and subdivided the plot into 10 × 10 m subplots for sampling in 30 sites (*Appendix 1*). The total

http://www.aloki.hu ● ISSN 1589 1623 (Print) ● ISSN 1785 0037 (Online)
DOI: http://dx.doi.org/10.15666/aeer/1704_95919607

sampled area was 30.8 ha. All the individuals encountered with a minimum dbh of ≥ 1 cm (diameter at breast height) were measured at 1.3 m from above ground level (Dallmeier et al., 1992), excluding the buttresses. All individuals were marked and numbered sequentially using aluminum tags (Ramachandran and Swarupanandan, 2013). Species specimen was collected, identified and deposited in the herbarium of Kerala Botanical Herbarium Center.

Data analysis

All individuals of the studied CMP species were counted from sample plots. They were converted into per hectare and later log-transformed for data analysis. The basal area of each individual was calculated using the formula $(DBH)^2 \times \pi/4$ (Mohandass and Davidar, 2009) and then converted into log-transformed among logging treatments. The mean and standard error of tree numbers and basal area of CMP was compared among logging treatments (such as high, moderate and unlogged). We categorized trees with a dbh of < 50 cm as smaller trees and the trees with a dbh of > 50 cm as larger trees (Persha and Blomley, 2009). The mean tree density and basal area of smaller stem dbh class (≤ 49.9 cm dbh) and larger stem dbh class (≥ 50 cm dbh) were calculated and log-transformed for analysis to compare among logging treatments. Analysis of variance (ANOVA) was used to test for differences in the mean number of tree individuals and basal area of CMP among logging treatments. We also used ANOVA to test for differences in the mean number of smaller trees and larger trees among logging treatments. F-statistic is the ratio of one-way ANOVA where F = variation between vegetation parameter means / variation within the vegetation parameters. Number of treatments (N) and degree of freedom (DF) were included in F-statistics. The P-value is the probability of given statistical model where the null hypothesis is true and the values greater than or equal to the actual observed values are indicated as significant differences (Wasserstein et al., 2016).

We used the Tukey's pairwise comparison to check for significant differences in tree density and basal area of CMP between and within the logging treatments (high, moderate and unlogged). Repeated measures of ANOVA was used to test the effect of post-logging recovery of CMP tree density and the basal area between high and moderate logging as compared to unlogged sites. We estimated mean value of post-logging age class of CMP tree density and basal area that included smaller and larger tree density and the basal area of CMP among different logging treatments. In addition, we also tested CMP forest recovery in order to compare the mean value of tree density and basal area of those vegetation parameters by ANOVA. Analysis of covariance (ANCOVA) was used to test the effect of logging treatment on tree density and basal area. All statistical analysis was performed using the software MedCalc. (version 12.2.1.0).

Results

A total of 5936 tree individuals with density ranging 17.3 to 1250 per hectare and average basal area of 20.73 m^2 ha^{-1} (≥ 1 cm dbh) were recorded from various logged treatments for the three species that were under study - *Cullenia exallirata, Mesua ferrea and Palaquium ellipticum*. The tree individuals ranging from 19–155 were enumerated in highly logged plots, 200–697 from moderately logged plots and 83–334 stems from unlogged plots. The basal area of the studied species ranged from 1.3–19.5

http://www.aloki.hu ● ISSN 1589 1623 (Print) ● ISSN 1785 0037 (Online)
DOI: http://dx.doi.org/10.15666/aeer/1704_95919607

m^2 ha^{-1} in highly logged plots, 13.3–79.4 m^2 ha^{-1} in moderately logged plots and 6.9–56.1 m^2 ha^{-1} in unlogged plots.

Treatment of logging on CMP tree density

In highly logged plots, the mean number of trees accounted for 111.8 ± 13.89 (std. error), while it was 402.58 ± 67.2 and 180.12 ± 30.62 in moderately and unlogged plots. It shows that the density of CMP series differed significantly (ANOVA $F_{3,29}$=12.69, P = 0.0001) among different logging treatments. Moreover, Tukey's HSD comparison shows that mean tree density was significantly higher in moderately logged plots compared to high (Tukey's HSD = 6.88, P = 0.0002) and unlogged plots (Tukey's HSD = 4.11, P = 0.019). However, no significant difference was found in the mean density of trees between high and unlogged plots (Tukey's HSD = 2.76, P = 0.1431; *Figure 2a*).

Treatment of logging on CMP basal area

The mean basal area of trees in highly logged plots was 10.94 ± 1.5 (m^2 ha^{-1}; std. error), 39.92 ± 8.91 (m^2 ha^{-1}) in moderately logged plots and 22.3 ± 5.5 (m^2 ha^{-1}) in unlogged plots. The basal area of three tree species differed significantly (ANOVA $F_{3,29}$=8.36, P = 0.0012) among various sites with different logging treatments. Mean basal area of moderately logged plots was significantly higher (Tukey's HSD = 5.42, P = 0.002). In contrast, there was no significant difference found between moderately logged and unlogged plots (Tukey's HSD = 2.42, P = 0.22) or between highly logged and unlogged plots (Tukey's HSD = 3.0, P = 0.104; *Figure 2b*).

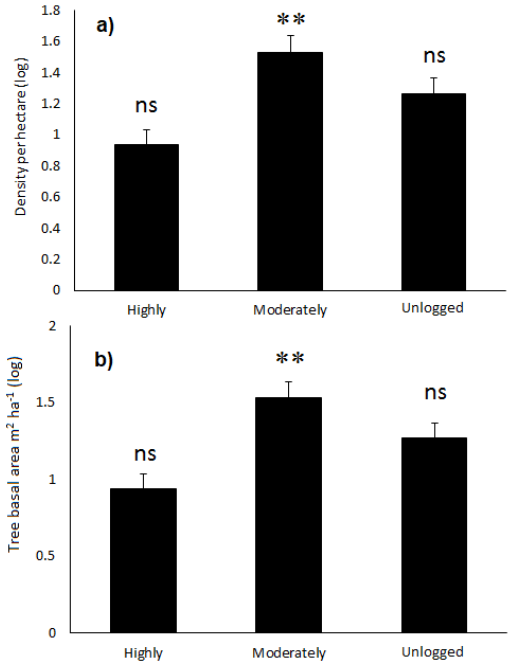

Figure 2. *Treatments of different logging on (a) CMP mean tree density and (b) mean basal area (m^2ha^{-1}) of the tropical mid-elevation wet evergreen forests of the Nelliampathy Hills, Western Ghats, southern India (Significant level: **p < 0.001; ns = not significant)*

http://www.aloki.hu ● ISSN 1589 1623 (Print) ● ISSN 1785 0037 (Online)
DOI: http://dx.doi.org/10.15666/aeer/1704_95919607

Treatment of logging on smaller and larger tree density and basal area

The density of smaller trees (≤ 49.9 cm dbh) and larger trees (≥ 50 cm dbh) differed significantly among different logging treatments (Small trees: $F_{3, 29} = 29.87$, P = 0.0001; Large trees: $F_{3, 29} = 3.22$, P = 0.05). Density of smaller trees was significantly higher in moderately and unlogged plots compared to highly logged plots (*Figure 3a*). Similarly, the density of larger trees was significantly higher in moderately logged plots than the highly logged plots ($F_{3, 29} = 8.13$, P = 0.002). However, no significant difference was found between moderate and unlogged plots (Tukey HSD = 2.63, P = 0.169; *Figure 3b*).

Similarly, the basal area of smaller and larger trees also differed significantly ($F_{3,29}$=17.2, P = 0.0001; $F_{3, 29} = 7.192$, P = 0.003, respectively) among various logging treatments. Basal area of smaller trees were significantly higher in moderately logged plots than the highly logged and unlogged plots (Tukey's HSD = 7.88, P = 0.0001; Tukey's HSD = 6.79, P = 0.0003); however, there was no significant difference found between highly logged and unlogged plots (Tukey's HSD = 1.09, P = 0.724; *Figure 3c*). For large trees, the basal area was significantly higher in moderately logged plots (Tukey's HSD = 4.9, P = 0.005) than the highly logged and unlogged plots. Similarly, there was no significant difference found between highly logged and unlogged plots (Tukey's HSD = 3.137, P = 0.08; *Figure 3d*).

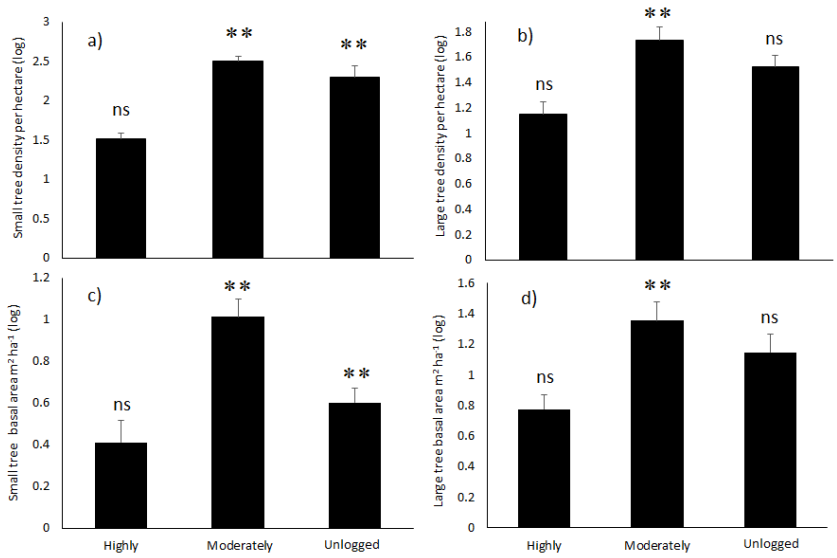

Figure 3. *Treatment of logging on CMP smaller and larger tree density and basal area (log transformed) in the tropical mid-elevation wet evergreen forests of the Nelliampathy hills, Western Ghats, southern India (a) small mean tree density and (b) large tree density in response to different logging treatments (c) small mean tree basal area and (d) large mean basal area in response to different logging treatments (Significant level: **p < 0.001; ns = not significant)*

CMP recovery after logging years

Tree density and basal area differed significantly among various sites due to logging treatment influencing CMP recovery (F = 4.01, P = 0.001 and F = 5.1, P = 0.002),(*Table 1*). All recovery periods (15-24, 25-34 and 35-45 after logging years) from highly logged sites influenced lower stem density and basal area compared to moderately

http://www.aloki.hu ● ISSN 1589 1623 (Print) ● ISSN 1785 0037 (Online)
DOI: http://dx.doi.org/10.15666/aeer/1704_95919607

logged sites (*Table 2*). Small and large tree density and basal area of highly logged sites were lower than that of the moderately logged sites, indicating that the moderately logged sites may have influenced the high number of trees as compared to highly logged sites through CMP forest series recovery by the effect of selective logging (*Table 2*).

Table 1. *Repeated measures of ANOVA was used to test post-logging recovery and interacting between and within the variable factors of stem density and basal area of highly logged and moderately logged plots compared to unlogged sites in the CMP forest series of the Western Ghats, southern India*

Source of variation	Sum of squares	df	Mean squares	F-ratio	P-value
Tree density	379909.6	4	94977.4	4.4	0.008
Residual	539508.0	25	21580.3		
Tree density × Post-logging effects	103544.6	8	12943.1	4.01	0.001
Residual	161457.1	50	3229.1		
Basal area	5388.9	4	1347.2	4.6	0.006
Residual	7321.4	25	292.9		
Basal area × Post-logging effects	1541.6	8	192.8	5.1	0.001
Residual	1887.6	50	37.8		

Table 2. *Post-logging on all tree density (ha^{-1}) and basal area (m^2 ha^{-1}) of CMP series, smaller stem density, larger stem density and basal area of CMP series along logging treatment in the Western Ghats, southern India*

	Density ha^{-1}		**Basal area m^2 ha^{-1}**	
Post-logging years	Highly	Moderate	Highly	Moderate
18-24	107.5 ± 49.5	438.5 ± 122.5	12.98 ± 4.22	43.27 ± 17.24
25-34	118.1 ± 16.90	253.5 ± 13.71	11.67 ± 1.80	27.01 ± 13.71
35-45	93.67 ± 37.56	478 ± 122.34	7.17 ± 3.87	46.28 ± 17.71
	Smaller tree density ha^{-1}		**Smaller tree basal area m^2 ha^{-1}**	
Post-logging years	Highly	Moderate	Highly	Moderate
18-24	86 ± 44	367 ± 89	3.7 ± 1.2	16.1 ± 4.1
25-34	98.7 ± 14.42	215.5 ± 37.5	3.51 ± 0.52	5.5 ± 0.2
35-45	81 ± 32.56	401.67 ± 93.74	2.27 ± 0.921	12.43 ± 2.44
	Larger tree density ha^{-1}		**Larger tree basal area m^2 ha^{-1}**	
Post-logging years	Highly	Moderate	Highly	Moderate
18-24	21.5 ± 5.5	71.5 ± 33.5	9.25 ± 3.05	27.15 ± 13.15
25-34	19.4 ± 3.45	38 ± 16	8.16 ± 1.39	21.5 ± 13.5
35-45	12.67 ± 7.75	76.33 ± 28.60	4.9 ± 3.066	33.83 ± 15.42

Discussion

Our results suggest that moderate logging treatment increased the tree density and basal area of *Cullenia exillarita*, *Mesua ferrea* and *Palaquium ellipticum,* causing a positive impact on the population structure of these forest layers type in the mid-elevation evergreen forests of the Western Ghats. Besides, the study also showed that the tree density and basal area varied significantly, suggesting that the moderate logging influenced a higher number of smaller and larger trees. The basal area in the moderately logged plots was also higher than that of unlogged and highly logged plots. The total basal area of trees from the highly logged plots was found to be significantly lower than

http://www.aloki.hu ● ISSN 1589 1623 (Print) ● ISSN 1785 0037 (Online)
DOI: http://dx.doi.org/10.15666/aeer/1704_95919607

that of the moderately logged plots and unlogged plots. Post-logging recovery influenced stem density and basal area of CMP trees compared to unlogged sites; however, there was no significant difference found between highly logged and moderately logged plots during the post-logging periods. In addition, we found that the treatment of logging significantly affected the tree density and basal area with an increase in the altitude of 750 m to 1250 m. Therefore, the treatment of logging changed the population structure of *Cullenia-Mesua-Palaquium* forest series significantly in the mid-elevation evergreen forests of the Western Ghats.

Logging treatment on tree density of CMP forest series

Previous studies showed logging to be a kind of disturbance that impacts tree diversity, species composition and forest structure (Ferry et al., 2002; Lima et al., 2002; Rutten et al., 2015; Katovai et al., 2016). According to our results, high logging sites showed a considerably low density of CMP species, due to the formation of more gaps which resulted in reduced tree regeneration. The increased light levels in the forest understorey after highly selective logging may result in sudden occurrence of many herbaceous and woody pioneer species (Woods, 1989; Nykvist, 1996; Pinard et al., 1996, 2000; Cochrane and Schultze, 1999; Fredericksen and Mostacedo, 2000; Ferry et al., 2002). This may inhibit the growth of CMP forest species regeneration and would cause a decline in the density and basal area of CMP species in the highly logged sites.

In the tropical forests of the Western Ghats, shade tolerance is an important factor which supports tree regeneration (Mohandass et al., 2016). Generally, in tropical forests, large forest trees provide more shade which would facilitate tree regeneration. Due to logging of large trees, if the shade is not sparse it may inhibit the regeneration of CMP species. Moreover, high logging pressure also resulted in increased human intervention, particularly in the highly logged plots, which disrupted tree regeneration (Rivett et al., 2016) and eventually resulted in a low number of small trees and large trees of CMP species. Therefore, it has been observed that high logging treatment may cause negative impacts on CMP series of tree recruitment and regeneration. This would be one of the major factors in changing the population structure of CMP canopy forest layer in the studied forest sites. The moderate treatment of logging influences relatively a low number of trees that are cut and results in maintaining a high number of CMP tree individuals. This results in a significantly high number of CMP trees as compared to high logging. Moreover, moderate logging treatment provided sufficient shade and light due to gap formation that facilitated a high number of tree recruitment and regeneration. Furthermore, our results showed that the small tree size numbers (≤ 50 cm dbh) increased significantly due to moderate logging. For some unknown reasons, the large trees were not harvested in some of the moderately logged plots in the study area (Ramachandran, 2008). Moderately logged plots had a large number of trees than the unlogged plots. Eventually, the large number of trees were higher as compared to unlogged plots; however, no significant difference was found on large trees (≥ 50 cm dbh) between highly logged and unlogged plots. In the highly logged and unlogged plots, large trees were not regularly removed and perhaps this might be the reason for not showing any significant differences. Though unlogged treatment showed a significantly high number in the density of smaller trees of CMP as compared to highly logged plots, there was no significant difference in the density of CMP trees between moderately logged and unlogged plots. It suggests that unlogged plots had regular tree recruitment and regeneration with less intensive disturbance by human logging, which

http://www.aloki.hu ● ISSN 1589 1623 (Print) ● ISSN 1785 0037 (Online)
DOI: http://dx.doi.org/10.15666/aeer/1704_95919607

could have influenced a neutral response in regeneration of small trees and a tendency to maintain large trees.

Logging treatment on a basal area of CMP forest layer

Estimating the basal area of CMP forest layer could be an important measure on forest stand structure of CMP forest layer among logged treatment plots. In the highly logged plots, basal area of CMP trees was consistently lower as compared to moderate and unlogged plots. Due to high logging treatments, smaller and large trees are lesser in number as they are harvested constantly leading to the low value of the basal area, affecting the CMP layer of forest structure. Human activity of high logging affects smaller trees as well as larger trees in numbers that may reduce the rate of tree size. Similar to density, the basal area also showed a significantly negative impact on the CMP forest layer due to high logging treatment in the studied sites. However, CMP forest layer showed significantly higher value in the basal area due to a high number of smaller trees and larger trees between moderately logged and unlogged plots. Interestingly, large tree density did not show a significant difference between the different logging methods, whereas the basal area of moderately logged plots showed a significant difference compared to high and unlogged plots. This shows that the moderately logged plots maintained large tree growth structure. Moreover, smaller trees basal area was significantly low in unlogged plots compared to moderately logged plots and the unlogged plots had a high number of large trees compared to moderately logged plots. In terms of basal area, large numbers of small trees are accumulated in moderately logged plots that exhibit a basal area significantly higher compared to highly logged and unlogged plots and shows a positive response to CMP forest layer by moderate logging treatment. Therefore, the differences in smaller and larger tree density and basal area of CMP forest layer between forest sites strongly depend on logging treatments (Bonnell et al., 2011) in the studied regions.

Post-logging recovery on tree density and the basal area along logging treatments

Several studies demonstrated that post-logging recovery and age influence species composition, density, basal area or biomass of tropical forests (Ferry et al., 2002; McDonald et al., 2008; Osazuwa-Peters et al., 2015; Darrigo et al., 2016; Arevalo et al., 2016; Katovai et al., 2016). We found that post-logging recovery on CMP tree density and the basal area was significantly higher in logged sites as compared to unlogged sites. This indicates that the logging treatments exhibit a positive response on CMP forest series in the studied sites. However, the study suggests that the moderately logged treatment type would be more effective for the regeneration and maintenance of the CMP tree densities. Removal of more trees (10-20 year per hectare) would be less effective for regeneration of CMP forest trees. Our results showed that tree numbers and basal area of moderately logged plots were higher than the highly logged sites. In addition, it was also observed that 25-35 and 35-45 post-logging recovery showed a significant difference in stem density and basal area. These indicate that the recovery of high tree density could be slow regeneration processes in the studied forests.

Logging treatment on tree density and the basal area along elevation gradients

It has been shown by our study that at all elevation gradients, the logging treatments significantly changed the population structure of CMP forest layer in the studied plots.

http://www.aloki.hu ● ISSN 1589 1623 (Print) ● ISSN 1785 0037 (Online)
DOI: http://dx.doi.org/10.15666/aeer/1704_95919607

High logging activity tend to alter the forest structure of CMP series by removing the best mature stems in all elevation gradients. Obviously, tree species require high light incidence at the seedling stage for survival and growth (Kleinschroth et al., 2013). Canopy opening might be increased for seedling recruitment through consistent amount of light availability. These seedlings may be that of a large amount of herbaceous and pioneer species that may inhibit the growth or regeneration of CMP species in all elevation gradients. Direct light intensity may influence a significant amount of temperature which may decline seedling recruitment of CMP species in all logged plots and elevations. Therefore, logging affects all elevation gradients and possibly influences similar consequences on tree density and basal area of CMP forest series. Therefore, enrichment planting should be considered in heavily degraded or logged areas (Kleinschroth et al., 2013) along the gradients.

Conclusion

Our results support that the logging treatments produces a significant impact on the population structure of *Cullenia-Mesua-Palaquium* forest series in the studied plots. Our study concludes that the moderately logged treatment resulted in a significant increase in the number of small and large trees. Highly logged plots showed a significant decline in the number of small trees as compared to moderately logged and unlogged plots. These support the fact that the heavy logging method might be a serious threat to the population structure of *Cullenia-Mesua-Palaquium* forest series. Moreover, *C. exallilata* and *P. ellipticum* are endemic species. Hence, it is very important to preserve this population in the mid-elevation layer of the Western Ghats. It is imperative to avoid heavy logging treatment to facilitate regeneration and to create dense population structure of the CMP forest series. The Forestry management strategy to understand how selective logging supports natural regeneration of CMP forest series due to canopy openness is crucial. Therefore future research is required to examine the natural regeneration process to understand fully the seedling dynamics of CMP forest series. In addition, further experimental study needs to be undertaken to understand the impact of logging treatment on habitat species – specifically in relation to endemism and climate change.

Acknowledgements. We are grateful to K. Swarupanandan, Forest Ecology and Biodiversity Conservation Division, Kerala Forest Research Institute, for his inordinate support during field work and thesis submission. We thank the two anonymous reviewers whose comments have greatly improved this manuscript. We thank Ms. Nisha Gopalakrishnan who helped us edit the manuscript. We are grateful to the Ministry of Environment and Forests, Government of India for the financial support, which made this study possible. Dr. J.K. Sharma and Dr. K.V. Sankaran, the former Directors of the Kerala Forest Research Institute are acknowledged for rendering the institutional facilities. We are thankful to Kerala Plantation Development Corporation for providing rainfall data; Mr. K. Sunil Kumar, Mr. Balu and Mr. Devendran for assisting us during the field study. The first author would like to thank Dr. Abhayamrita Chaitanya, Pro-Chancellor, AVVU, for providing an opportunity to work at his institutional facilities and for his support.

http://www.aloki.hu ● ISSN 1589 1623 (Print) ● ISSN 1785 0037 (Online)
DOI: http://dx.doi.org/10.15666/aeer/1704_95919607

REFERENCES

[1] Arevalo, B., Valladarez, J., Muschamp, S., Kay, E., Finkral, A., Roopsind, A., Putz, F. E. (2016): Effects of reduced-impact selective logging on palm regeneration in Belize. – Forest Ecology and Management 369: 155-160.
[2] Balasubramanyan, K. (1987): Impact of selection felling in a forest ecosystem in Kerala. – KFRI Research Report no. S3. Kerala Forest Research Institute, Thrissur, Kerala, India.
[3] Baur, G. N. (1964): The ecological basis of rain forest management. – Forestry Commission of New South Wales, Sydney, Australia.
[4] Bonnell, T. R., Reyna-Hurtado, R., Chapman, C. A. (2011): Post-logging recovery time is longer than expected in an East African tropical forest. – Forest Ecology and Management 261: 855-864.
[5] Chandrasekharan, K. P., Muhammed Moosa, M., Ananthasubramonian, A. S. (1977): The first working plan for the Nemmara Forest Division: 1969-70 to 1983-84. – Government of Kerala, Trivandrum, 96 pp.
[6] Chandrashekara, U. M. (1991): Studies on the gap phase dynamics of a humid tropical forest. – Ph. D. Thesis. Jawaharlal Nehru University, New Delhi, India.
[7] Chapman, C. A., Chapman, L. J. (1997): Forest regeneration in logged and unlogged forests of Kibale National Park, Uganda. – Biotropica 29: 396-412.
[8] Chundamannil, M. (1993): History of forest management in Kerala. KFRI Research Report No.89. – Kerala Forest Research Institute, Thrissur, Kerala, India.
[9] d'Annunzio, R., Sandker, M., Finegold, Y., Min, Z. (2015): Projecting global forest area towards 2030. – Forest Ecology and Management 352: 124-133.
[10] Dallmeier, F., Kabel, M., Rice, R. (1992): Methods for long-term biodiversity inventory plots in protected tropical forests. – In: Dallmeier, F. (ed.) Long-term monitoring of biological diversity in tropical forest areas: Methods for establishment and inventory of permanent plots. MAB Digest 11. UNESCO, Paris.
[11] Darrigo, M. R., Venticinque, E. M., Santos, F. A. M (2016): Effects of reduced impact logging on the forest regeneration in the central Amazonia. – Forest Ecology and Management 360: 52-59.
[12] FAO. (1984): Intensive multiple-use forest management systems in Kerala (India). – FAO forestry Paper 53. FAO of UN, Rome.
[13] FAO. (1985): Intensive multiple-use forest management systems in the tropics. – FAO forestry Paper 55. FAO of UN, Rome.
[14] FAO. (1989): Review of forest management systems of Tropical Asia. – FAO forestry paper 89. FAO of UN, Rome, 228 pp.
[15] Ganesh, T., Davidar, P. (1999): Fruit Biomass and Relative Abundance of Frugivores in a Rain Forest of Southern Western Ghats, India. – Journal of Tropical Ecology 15: 399-413.
[16] Gardner, T. A., Barlow, J., Chazdon, R., Ewers, R. M., Harvey, C. A., Peres, C. A., Sodhi, N. S. (2009): Prospects for tropical forest biodiversity in a human-modified world. – Ecology Letters 12: 561-582.
[17] Gatti, R. C., Castaldi, S., Lindsell, J. A., Coomes, D. A., Marchetti, M., Maesano, M., Paola, A. D., Paprella, F., Valentini, R. (2015): The impact of selective logging and clear cutting on forest structure, tree diversity and above-ground biomass of African tropical forests. – Ecological Research 30: 119-132.
[18] Hethcoat, M. G., Edwards, D. P., Carreiras, J. M. B., Bryant, R. G., França, F. M., Quegan, S. (2018): A machine learning approach to map tropical selective logging. – Remote Sensing of Environment: https://doi.org/10.1101/451856.
[19] IMD. (2018): Report: Rainfall over kerala during monsoon season – 2018 and forecast for next 5 days. – Earth System Science Organization, Government of India.
[20] Irland, L. C. (2011): Timber productivity research gaps for extensive forest management. – Small-scale Forestry 10: 389-400.

http://www.aloki.hu ● ISSN 1589 1623 (Print) ● ISSN 1785 0037 (Online)
DOI: http://dx.doi.org/10.15666/aeer/1704_95919607

[21] Johns, A. D., Skorupa, J. P. (1987): Responses of rainforest primates to habitat disturbance: A review. – International Journal of Primatology 8: 157-191.
[22] Kadambi, K. (1986): Methods of increasing growth and obtaining regeneration of tropical rainforest. – In: Haig, I. T., Huberman, M. A., Din, V. A. (eds.) Tropical Silviculture. Vol. 2, FAO Forest and Forest Product Studies No.13, Periodical Experts Book Agency, Delhi. Pages: 67-78.
[23] Katovai, E., Sirikolo, M., Srinivasan, U., Edwards, W., Laurance, W. F. (2016): Factors influencing tree diversity and compositional change across logged forests in the Solomon Islands. – Forest Ecology and Management 372: 53-63.
[24] Kleinschroth, F., Schöning, C., Kungu, J. B., Kowarik, I., Cierjacks, A. (2013): Regeneration of the East African timber tree *Ocotea usambarensis* in relation to historical logging. – Forest Ecology and Management 291: 396-403.
[25] Köhl, M., Lasco, R., Cifuentes, M., Jonsson, Ö., Korhonen, K. T., Mundhenk, P., de Jesus Navar, J., Stinson, G. (2015): Changes in forest production, biomass and carbon: Results from the 2015 UN FAO Global Forest Resource Assessment. – Forest Ecology and Management 352: 21-34.
[26] Krishnan, M. S. (1974): Geology. – In: Mani, M. S. (ed.) Ecology and biogeography in India. Dr.W.B. Junk, b.v.Publishers, the Hague, 773 pp. Pages: 60-98.
[27] Lal, A. B. (1961): Silvicultural systems and forest management. – Jugal Kishore and Co., Dehra Dun, India.
[28] Lamprecht, H. (1993): Silviculture in the tropical natural forests. – In: Pancel, L. (ed.) Tropical forestry hand book. Vol.1, Springer-Verlag, New York. Pages: 728-810.
[29] Leadley, P. W., Krug, C. B., Alkemade, R., Pereira, H. M., Sumaila, U. R., Walpole, M., Marques, A., Newbold, T., Teh, L. S. L., van Kolck, J., Bellard, C., Januchowski-Hartley, S. R., Mumby, P. J. (2014): Progress towards the Aichi Biodiversity Targets: An Assessment of Biodiversity Trends, Policy Scenarios and Key Actions. – Secretariat of the Convention on Biological Diversity, Montreal, Canada. viewed 20/09/2017, <https://www.cbd.int/doc/publications/cbd-ts-78-en.pdf.
[30] Lima, A. P., de Lima, O. P., Magnusson, W. E., Higuchi, N., Reis, F. Q. (2002): Regneration of five commercially-valuable tree species after experimental logging in an Amazonian forest. – R. Árvore, Viçosa-MG 26: 567-571.
[31] Mani, M. S. (1974): Physical features. – In: Mani, M. S. (ed.) Ecology and biogeography in India. Dr.W.B. Junk, b.v. Publishers, The Netherlands. Pages: 11-59.
[32] Martin, P. A., Newton, A. C., Pfeifer, M., Khoo, M., Bullock, J. M., (2015): Impacts of tropical selective logging on carbon storage and tree species richness: a meta-analysis. – Forest Ecology and Management 356: 224-233.
[33] McDonald, R. I., Motzkin, G., Bank, M., Kittredge, D. B., Burk, J., Foster. D. (2006): Forest harvesting and land-use conversion over two decades in Massachusetts. – Forest Ecology and Management 227: 31-41.
[34] Mohandass, D., Davidar, P. (2009): Floristic structure and diversity of a tropical montane evergreen forest (shola) of the Nilgiri Mountains, southern India. – Tropical Ecology 50: 219-229.
[35] Mohandass, D., Chhabra, T., Pannu, R. S., Beng, K. C. (2016): Recruitment of saplings in active tea plantations of the Nilgiri Mountains: Implications for restoration ecology. – Tropical Ecology 57: 101-118.
[36] Nair, S. S. C. (1998): Long-term conservation potential of natural forests in the Southern Western Ghats of Kerala. – MAB Report, Dept. of Environment, Government of India, 324 pp.
[37] Okuda, T., Suzuki, M., Adachi, N., Quah, E. S., Hussein, N. A., Manokaran, N. (2003): Effect of selective logging on canopy and stand structure and tree species composition in a lowland dipterocarp forest in peninsular Malaysia. – Forest Ecology and Management 175: 297-320.

http://www.aloki.hu ● ISSN 1589 1623 (Print) ● ISSN 1785 0037 (Online)
DOI: http://dx.doi.org/10.15666/aeer/1704_95919607

[38] Osazuwa-Peters, O. L., Chapman, C. A., Zanne, A. E. (2015): Selective logging: does the imprint remain on tree structure and composition after 45 years? – Conservation Physiology 3: doi:10.1093/conphys/cov012.
[39] Pascal, J. P. (1988): Wet evergreen forests of the Western Ghats of India: ecology, structure, floristic composition and succession. – Institut Francais de Pondichery, India.
[40] Pascal, J. P., Ramesh, B. R., De Francheschi, D. (2004): Wet evergreen forest types of the southern Western Ghats, India. – Tropical Ecology 45: 281-292.
[41] Pearson, T. R., Brown, S., Murray, L., Sidman, G. (2017): Greenhouse gas emissions from tropical forest degradation: an underestimated source. – Carbon Balance Management 12: 1-11.
[42] Persha, L., Blomley, T. (2009): Management decentralization and montane forest conditions in Tanzania. – Conservation Biology 23(6): 1485-1496.
[43] Pimm, S. L., Raven, P. (2000): Biodiversity extinction by numbers. – Nature 403: 843-845.
[44] Poudyal, B. H., Maraseni, T., Cockfield, G. (2018): Evolutionary dynamics of selective logging in the tropics: A systematic review of impact studies and their effectiveness in sustainable forest management. – Forest Ecology and Management 430: 166-175.
[45] Putz, F. E., Zuidema, P. A., Synnott, T., Pena-claros, M., Pinard, M. A., Sheil, D., Vanclay, J. K., Sist, P., Gourlet-Fleury, S., Griscom, B., Palmer, J., Zagt, R. (2012): Sustaining conservation values in selectively logged tropical forests: the attained and the attainable. – Conservation Letters 5: 296-303.
[46] Ramachandran, V. S., Swarupanadan, K. (2013): Structure and floristic composition of old growth (unlogged) wet evergreen forests of Nelliampathy hills, southern Western Ghats. – Journal of Forestry Research 24: 37-46.
[47] Ramachandran, V. S., Swarupanandan, K. (2018): Ecological status of *Palaquium ravii,* an Endangered Endemic Tree, in the Nelliampathy Hills of the Western Ghats, India. – The Indian Forester 144: 164-168.
[48] Ramesh, B. R., Swaminath, M. H., Patil, S., Aravajy, S., Elouard, C. (2009): Assessment and Conservation of Forest Biodiversity in the Western Ghats of Karnataka, India. – Assessment of Tree Biodiversity, Logging Impact and General Discussion. Institut Francais de Pondichery. p 65-121.
[49] Rivett, S. L., Bicknell, J. E., Davies, Z. (2016): Effect of reduced-impact logging on seedling recruitment in a Neotropical forest. – Forest Ecology and Management 367: 71-79.
[50] Rutten, G., Ensslin, A., Hemp, A., Fischer, M. (2015): Forest structure and composition of previously selectively logged and non-logged montane forests at Mt. Kilimanjaro. – Forest Ecology and Management 337: 61-66.
[51] Senior, R. A., Hill, J. K., Benedick, S., Edwards, D. P. (2017): Tropical forests are thermally buffered despite intensive selective logging. – Global Change Biology: 1267-1278.
[52] Seth, S. K. (1960): Soils of the tropical moist evergreen forests of India. – Proceedings of Tropical Moist Evergreen Forest Symposium, Forest Research Institute, DehraDun, India.
[53] Silk, J. W. F., Veryburg, R. W., Kebler, P. J. A. (2002): Effects of fire and selective logging on the tree species composition of lowland dipterocarp forest in East Kalimantan, Indonesia. – Biodiversity and Conservation 11: 85-98.
[54] Silva, P. H., Gomide, L. R., Figueiredo, E. O., Carvalho, L. M. T., Ferraz Filho, A. C. (2018): Optimal selective logging regime and log landing location models: a case study in the Amazon forest. – Acta Amazonica 48: 18-27.
[55] Srivastava, T. N. (1983): A bridged glossary of technical terms. – FRI and Colleges, Dehra Dun, India.
[56] Stracey, P. D. (1959): The silviculture and management of tropical rain forest in India. – Indian Forester 85: 385-409.

http://www.aloki.hu ● ISSN 1589 1623 (Print) ● ISSN 1785 0037 (Online)
DOI: http://dx.doi.org/10.15666/aeer/1704_95919607

[57] Troup, R. S. (1916): A note on some European silvicultural systems, with suggestions for improvements in Indian forest management. – Superintendent of printing, Calcutta, India.
[58] Wasserstein, R. L., Lazar, N. A. (2016): The ASA's Statement on p-Values: Context, Process, and Purpose. – The American Statiscian 70: 129-133.
[59] Yamada, T., Hosaka, T., Okuda, T., Kassim, A. R. (2013): Effects of 50 years of selective logging on demography of trees in a Malaysian lowland forest. – Forest Ecology and Management 310: 531-538.

http://www.aloki.hu ● ISSN 1589 1623 (Print) ● ISSN 1785 0037 (Online)
DOI: http://dx.doi.org/10.15666/aeer/1704_95919607

APPENDIX

Appendix 1. *Site code, sampled area (ha), number of total trees, basal area (m^2 ha^{-1}), number of smaller trees and basal area (m^2 ha^{-1}), number of larger trees and basal area (m^2 ha^{-1}) and logging treatment of the tropical mid-elevation wet evergreen forests of the Western Ghats, southern India*

Site Code	Altitude (m)	Sampled area (ha)	Number of trees	Basal area m^2 ha^{-1}	Number of smaller trees	Basal area of smaller trees	Number of larger trees	Basal area of large trees	Logging treatments
SLKP1	950-980	2.3	697	79.36	570	16.1	127	63.2	Moderately
SLKP2	950	1.1	19	1.30	16	0.5	3	0.8	Highly
SLMK1ha	780	1	27	1.45	25	0.2	2	1.3	Highly
SLMKD1	780-950	0.6	190	14.88	168	5.9	22	9.0	Highly
SLMKD2	850-900	0.3	81	6.74	73	3.1	8	3.6	Highly
SLMKInd	850-900	0.6	173	16.65	145	4.7	28	11.9	Highly
SLMKIV	780-800	0.6	138	14.47	110	3.6	28	10.9	Highly
SLMKIX	750-760	1	307	40.72	253	5.7	54	35.0	Moderately
SLMKIX1ha	780	1	150	19.49	116	5.2	34	14.3	Highly
SLMKVII	780	0.2	45	7.66	30	2.0	15	5.7	Highly
SLMKXIV	780-920	1	200	13.30	178	5.3	22	8.0	Moderately
SLPC	750-800	2.3	274	18.75	246	7.8	28	11.0	Moderately
SLPC1ha	780	2	124	5.75	117	2.7	7	3.0	Highly
SLPD1	750-800	2.3	463	40.74	389	13.4	74	27.3	Moderately
SLPD2	780	0.6	128	10.21	111	4.1	17	6.1	Highly
SLPD3	760-780	0.5	155	17.06	120	3.5	35	13.6	Highly
SLPM05ha	1095	0.5	117	14.22	95	3.5	22	10.7	Highly
SLPO	1096-1250	0.5	157	17.20	130	4.9	27	12.3	Highly
SLPP	780-1050	2.5	561	60.51	456	20.2	105	40.3	Moderately
SLTP	750-800	2.4	316	26.03	278	12.0	38	14.0	Moderately
SLTP05ha	800	0.5	58	8.75	42	2.5	16	6.2	Highly
SLTPJK1ha	800	1	115	8.34	104	2.9	11	5.4	Highly
ULKPA1ha	1150	1	116	10.07	98	2.7	18	7.4	Unlogged
ULKPB1ha	1250	1	83	21.27	47	2.4	36	18.9	Unlogged
ULMK	950-1050	0.5	217	31.39	164	4.3	53	27.1	Unlogged
ULMM	850	0.6	262	21.06	226	5.0	36	16.1	Unlogged
ULPC	780	0.8	188	16.77	156	4.5	32	12.3	Unlogged
ULPC1ha	780	1	116	6.86	103	3.1	13	3.7	Unlogged
ULPM	1050-1150	1	334	56.09	238	10.0	96	46.1	Unlogged
ULPM05ha	1100	0.1	125	14.76	96	3.5	29.00	11.3	Unlogged

http://www.aloki.hu ● ISSN 1589 1623 (Print) ● ISSN 1785 0037 (Online)
DOI: http://dx.doi.org/10.15666/aeer/1704_95919607

PHYTOREMEDIATION CAPABILITY OF WATER CLOVER (*MARSILEA CRENATA* (L). PRESL.) IN SYNTHETIC PB SOLUTION

RACHMADIARTI, F.* – TRIMULYONO, G.

Faculty of Mathematics and Sciences, Universitas Negeri Surabaya, Jalan Ketintang, Surabaya 60123, East Java, Indonesia

**Corresponding author*
e-mail: fidarachmadiarti@unesa.ac.id; phone/fax: +62-31-8296427

(Received 19th Sep 2018; accepted 13th Jun 2019)

Abstract. The effect of lead (Pb) pollution on water clover resistance was determined by the Pb distribution and the percentage of free amino acids in plant tissues. Water clover plant from Surabaya, Indonesia was collected and plants of equal size were grown hydroponically. They were exposed into 0, 1, 5, 10 mgL^{-1} of Pb concentration for 10, 20, and 30 days. The experiment was a randomized completely block design with 3 replications. The Pb concentration was measured by inductively coupled plasma (ICP) and the free amino acid was analyzed by HPLC (High-Pressure Liquid Chromatography). The Pb concentration in plant organs and its free amino acids content indicated that water clover plant was resistance on Pb accumulation and affected their growth which potential for phytoremediation. The highest concentration of Pb was found in root tissue, followed by stem and leaf tissues. These findings indicated the respond of water clover plants resist on Pb that determined by the increased percentage of free amino acids and phytochelatins such as glutamic acid, cysteine, glycine, and proline.
Keywords: *free amino acid, phytoremediation, Pb, water clover*

Introduction

Contamination of heavy metals is increasingly widespread as a result of different activities such as lead (Pb) pollution. Pb is a heavy metal that causes poisoning in humans (Jaishankar et al., 2014). High Pb concentration can be found in industrial waste, in household detergents, other laundry products, and in cigarettes (Nakata et al., 2017). Pb is known as teratogenic and toxicity (Duruibe et al., 2007), such as inhibits the haemoglobin synthesis, causes kidney malfunction, affects reproductive systems and cardiovascular system, causes acute and chronic damage to the central nervous system and peripheral nervous system (Ghosh and Singh, 2005).

In plants, Pb causes a decrease of chlorophyll synthesis, inhibits photosynthesis, inhibits mineral collection, water imbalance and changes in the structure and permeability of the cell membrane, as well as other effects (Seregin and Ivanove, 1998).

In addition, Pb triggers the establishment of reactive oxygen species (ROS) and induces oxidative stress that causes the protein trafficking in plants (Yun et al., 2001; John et al., 2008; Stoyanova and Doncheva, 2002).

Nitrogen metabolism is central to plants response against heavy metals. It due to plants synthesize with a variety of metabolites when exposed to heavy metals and accumulate to the concentrations in the millimolar range, especially specific amino acids (Sharma and Dietz, 2006). Glycine and glutamic acid are involved in glutathione synthesis and phytochelatins, which plays a role in the binding of heavy metals. Arginine acts as a molecular marker and antioxidants in the polyamine synthesis (Sharma and Dietz, 2006; Khawas, 2011). Proteinogenic prolific amino acid as a radical

http://www.aloki.hu ● ISSN 1589 1623 (Print) ● ISSN 1785 0037 (Online)
DOI: http://dx.doi.org/10.15666/aeer/1704_96099619

scavenger, electron sink, macromolecules stabilizer, cell wall components (Matysik et al., 2002), osmoregulation and in metal binding (Sharma and Dietz, 2006). These amino acids are considered as important plant mechanisms against heavy metal stress.

Reduction of heavy metals concentration is urgently needed in the environment. Many methods have been developed to clean up the pollutant from water, but it seems that the plant is the cheapest and easiest method. "Phytoremediation" has been used widely, to remediate either contaminated soils or polluted water (Göthberg et al., 2004). The success of phytoremediation depends on growth rate and the plant ability to uptake the metals from the growth medium. Plants must produce sufficient biomass and able to accumulate a high concentration of heavy metals in their tissue.

The water clover is a hydrophyte plant with thin cuticle, constantly open stomata, has air bladder, and thin roots. A previous study of clover plants (*Marsilea crenata* Presl.) at wetlands of Wiyung, Ketintang, and Kendung in Surabaya city, Indonesia showed the plant ability to absorb Pb. The clover plant is commonly used as a vegetable by Surabaya city communities and the surrounding area. It indicates that the plant contains a concentration > 0.05 mg Pb kg^{-1}. This exceeds the quality standards provided by WHO (1996). Surprisingly, the plant growth is not affected by the heavy metal, as the plant was still growing with the average plant height of 13.9–19.4 cm. Wiadnya (2004) also observed Pb absorption by water clover in the limited volume media experiment. Previous research conducted by Nurhayati et al. (2015) which observe the stunted growth of water clover after treated in Pb media; the higher the Pb concentration, the slower the growth. Novi and Abdillah (2017) observed the ability of water clover and hydrilla to decrease the Pb concentration in paper liquid waste after 5, 10, and 15 days. Another plant in the same division, *Salvine minima*, also has the ability to accumulate Pb up to 0.1243 mgm^2 per day (Iha and Bianchini, 2015). These findings indicated the tolerance of water clover to heavy metal and the possibility to be categorized as an "accumulator or hyperaccumulator" plant.

Pb pollution does not seem to be declining in the future because Pb pollution sources are an unavoidable aspect in modern human life (Yang et al., 2000). Therefore, it is necessary to investigate the different of Pb concentration and exposure duration on plant tissue growth, and the percentage of free amino acids in clover plants that grow on Hogland solution. This research aim is to evaluate the capability of water clover as an agent for phytoremediation to heavy metal particularly the lead (Pb) based on its growth and the accumulation of Pb capacity.

Materials and methods

The water clover plant was grown in medium containing Pb solution to investigate the resistance and free amino acid. The medium was added with Pb solution (depend on the experimental treatments), i.e: (1) 0 Pb as the control; (2) 1.0 mgL^{-1} of $Pb(NO_3)_2$ solution; (3) 5.0 mgL^{-1} of $Pb(NO_3)_2$ solution; and (4) 10.0 mgL^{-1} of $Pb(NO_3)_2$ solution. The Pb concentration was based on the previous study (Herawati, 2008; Rachmadiati et al., 2012). These treatments were conducted in a split-plot design with 3 replications.

Water clover was collected from wetlands at Kendung (Surabaya, East Java, Indonesia). Initially, the plants were grown in a plastic chamber containing 20 L of Hoagland's media in a glass house over 5 days. This was done to reduce environmental contamination and adapt the plants to glasshouse conditions. Subsequently, plants of water clover were selected with 90 g biomass. Each plant was grown for 10 days in a

http://www.aloki.hu ● ISSN 1589 1623 (Print) ● ISSN 1785 0037 (Online)
DOI: http://dx.doi.org/10.15666/aeer/1704_96099619

plastic chamber containing 20 L distillation water and Hoagland's solution (Göthberg et al., 2004).

These acclimated plants were used for further study. Water clover plants were selected with stems length of 20-25 cm and roots length of 8-10 cm. The plants were cleaned with distilled water and placed in glass aquarium of 40 cm length, 30 cm width, and 35 cm depth which consist of 5 L distilled water and Hoagland's solution. Every aquarium was filled with 100 g of the acclimated water clover. The variety pH of the medium was applied from 5.4 – 6.9 at the beginning of the experiment, and 6.5 – 7.0 at the end of the experiment. The plants were illuminated sunlight 12:12 h at light-dark cycle with photon flux density at 389 candles. All of the plant samples (destructive sampling) from each glass aquarium were harvested at 10, 20, and 30 days. Then, the biomass yield and metal content were measured (*Fig. 1*).

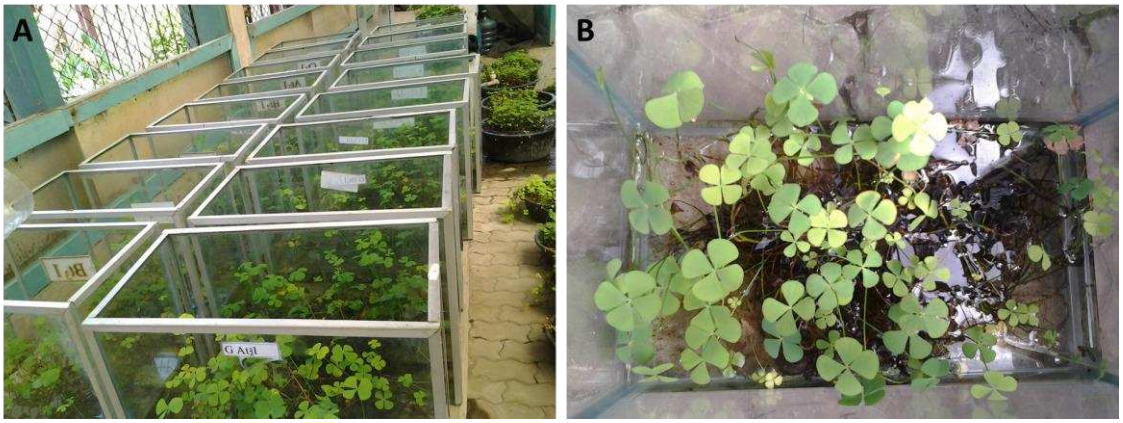

Figure 1. *Water clover (Marsillea crenata) plant in the glass aquarium experiment. A. General view. B. Overhead view*

Harvested plants were divided into three parts: roots, stem, and leaves. Each part of the plant was placed at the dried oven at 80 °C for 48 h and weighed to determine its dry weight. To further analysis, 5 g of each plant was taken and dried plant tissues with a mill. Then, 0.5 g of powdered sample was diluted with 5 ml of HNO_3 and 50 ml of deionized double distilled water. Pb analysis was performed by using the extraction method (Gothberg et al., 2004). Then, the digested samples and 50 ml of media samples were analyzed by inductively coupled plasma (Teledyne Leeman Labs) to determine the Pb concentration. The total accumulation and partitioning of the metals by the plants were calculated. Plant biomass yield was measured on dry weight basis.

Several different steps were performed in order to identify free amino acids. Initially, the reagent kit was prepared, followed by solvent preparation and sample preparation of HPLC (High-Pressure liquid Chromatography) with hydrolysis processes and derivatization (Waters, 2017).

Preparation of reagent kit

Reagent kit was prepared by heating at 55 °C. The vial 24 (AcrQ fluo reagent powder) was heated 2-3 min. Then, 1 ml of AccQ fluorine reagent diluent was inserted into vial 2A followed by heating and mixing until the powder spread evenly.

http://www.aloki.hu ● ISSN 1589 1623 (Print) ● ISSN 1785 0037 (Online)
DOI: http://dx.doi.org/10.15666/aeer/1704_96099619

Solvent preparation

Solvent solutions were prepared by mixing 19 g Sodium Acetate and 2.27 g TEA into 1 L of water. Then, 40% of phosphoric acid (+ 6 mL or more) was added until pH 5.1 followed by adding 5 mL ACN (ACETONITRILE) and water (Waters, 2017).

Hydrolysis

Hydrolysis was performed with 100 mg of the sample that accurately weighed. The sample was placed into tube and mixed with 5 ml 6N HCL. Drying sample was performed by using Nitrogen or Argon; each tube was closed and placed into an oven at 112 °C for 22 h and the sample was filtered by using 0.45 pm of filter paper. Then, 100 ml of filtered sample was diluted with 5 ml of MiliQ water (Waters, 2017).

Derivatization

The 50 pL of diluted sample was mixed with 350 pL AccQ derivatization buffer and 100 pL AccQ fluor reagent to derivatize. The mixed solution was shaken briefly and placed into the water that has been heated at 55 °C for 10 min. Then, the sample can be injected into the HPLC (Waters, 2017).

Data analysis

Experimental design

The research was a completely randomized design with three replicates for each treatment. The first treatment was the heavy metal concentration containing K1: 0 mgL^{-1}; K2: 1 mgL^{-1}; K3: 5 mgL^{-1}; and K4: 10 mgL^{-1} of Pb. The second treatment was the variety time of observation, 10^{th}, 20^{th}, and 30^{th} day respectively.

Variables

The observed variables were: (1) the plant's biomass; (2) Pb content in roots, stems, and leaves; (3) the Pb removal percentage; and (4) the produced free amino acid percentage in the root.

Statistical analysis

The observation data was analyzed by ANOVA and followed by Tukey *ad hoc* test with a 95% confidence level using Genstat 15 edition resources statistical program. Then, the free amino acid was analyzed descriptively based on the percentage and total protein.

Results

The growth of water clover at various medium conditions is presented in *Table 1*. There was a positive growth of water clover at 10, 20, and 30 days observation. It seems that water clover was easily adapted to the new environment. Therefore, water clover was not to require adaptation periods. The growth of water clover at various Pb concentrations was significantly different ($p < 0.05$). It indicated that the higher Pb concentration, the slower the growth of the water clover (*Table 1*). This is due to the more Pb is absorbed water clover plants and affects the metabolism. Although the

http://www.aloki.hu ● ISSN 1589 1623 (Print) ● ISSN 1785 0037 (Online)
DOI: http://dx.doi.org/10.15666/aeer/1704_96099619

growth tended to slow, the ability of plants to absorb Pb remains "high", which can be seen in *Table 2*. Interestingly, there were no visible poisoning symptoms beside the slowed growth after morphological observation (data not shown).

Table 1. *The growth of water clover at different Pb concentrations*

Pb concentration (mg L^{-1})	Dried biomass at (g/plant)		
	10 days	20 days	30 days
0	15.470^{dA}	16.555^{dB}	17.384^{dC}
1	14.525^{cA}	15.547^{cB}	16.366^{cC}
5	13.510^{bA}	14.308^{bB}	14.770^{bC}
10	12.810^{aA}	13.475^{aB}	3.895^{aC}

Means followed by the same letters, in the same column are not significantly different (p = 0.05), small letter for concentration and capital letter for detention time

As shown in *Table 1*, it demonstrated that the water clover grows well in lead-polluted solution. However, compared to early observation, the growth of water clover was much slower. The capability of water clover to remove Pb from solution was shown in *Table 2*. There was significantly different from the removal by water clover.

Table 2. *Percentage removal Pb by water clover*

Pb concentration (mg L^{-1})	Percentage removal Pb by plants		
	10 days	20 days	30 days
1	100 ± 0.04^{aA}	98.00 ± 0.04^{aA}	100 ± 0.04^{aA}
5	100 ± 0.04^{aA}	99.90 ± 0.04^{aA}	99.40 ± 0.04^{aA}
10	100 ± 0.04^{aA}	99.90 ± 0.04^{aA}	99.65 ± 0.04^{aA}

Means followed by the same letters, in the same column are not significantly different (p = 0.05)

The water clover plants were able to absorb Pb concentration in the organs, although their growth was considerably slower as shown in *Table 1*. It is important noted that water clover plants are able to remove Pb from the solution. Then, the highest Pb concentration of water clover was found in root tissues (*Table 3*).

The presence of Pb in root tissues of water clover was relatively constant with the plant of age, except for 10 days after treatment. Pb concentration in roots tissues of water clover was not differences. As shown in *Table 4*, Pb concentration in stem tissues indicated significant differences compared to leave tissues.

Table 3. *Pb concentration in various plant tissues*

Day	1 mg L^{-1} Pb (mg kg^{-1})			5 mg L^{-1} Pb (mg kg^{-1})			10 mg L^{-1} Pb (mg kg^{-1})		
	Roots	Stems	Leaves	Roots	Stems	Leaves	Roots	Stems	Leaves
10	0.8 ± 0.15^{bA}	0.40 ± 0.03^{bA}	0.18 ± 0.00^{aA}	1.93 ± 0.05^{bA}	2.29 ± 0.05^{bA}	0.58 ± 0.05^{bA}	3.80 ± 0.05^{bA}	2.65 ± 0.05^{bA}	0.82 ± 0.05^{bA}
20	1.2 ± 0.05^{bB}	0.09 ± 0.05^{bB}	0.13 ± 0.01^{aB}	7.88 ± 0.05^{bB}	5.01 ± 0.05^{bB}	0.01 ± 0.05^{bB}	9.74 ± 0.05^{bB}	6.79 ± 0.05^{bB}	0.01 ± 0.05^{bB}
30	1.3 ± 0.05^{bB}	0.20 ± 0.01^{bB}	0.12 ± 0.01^{aB}	9.10 ± 0.05^{bB}	0.58 ± 0.05^{bB}	0.02 ± 0.05^{bB}	13.12 ± 0.05^{bB}	0.72 ± 0.05^{bB}	0.02 ± 0.05^{bB}

Means followed by the same letters for the same time of measurements, in the same column (small letters) and rows (capital letters) are not significantly different (p = 0.05)

http://www.aloki.hu ● ISSN 1589 1623 (Print) ● ISSN 1785 0037 (Online)
DOI: http://dx.doi.org/10.15666/aeer/1704_96099619

The amino acid content was found to see the plants response against heavy metal stress. A significant difference in the percentage of each amino acid produced by the clover water plants were recognized (*Table 4*).

As presented in *Table 4,* there were 17 types of amino acids. The percentage of amino acids decreased and had low value (0.000) except for cysteine after 20 days of Pb exposed. In addition, lysine and isoleucine also indicated a low value (0.000) on the concentration of 5 mg L^{-1} after 20 days of Pb exposed.

Table 4. *Free amino acids (%) of water clover exposed to lead at 20 days (n = 3)*

Amino acid	Concentration of Pb (mg L^{-1}) at … days		
	1	5	10
	20	20	20
Aspartic acid	0.086±0.006^{a}	0.269±0.030^{a}	0.126±0.104^{a}
Serine	0.290±0.014^{a}	0.286±0.006^{b}	0.107±0.042^{c}
Glutamic acid	0.137±0.006^{a}	0.136±0.001^{a}	0.126±0.015^{a}
Glycine	0.155±0.001^{a}	0.135±0.006^{a}	0.100±0.050^{a}
Histidine	0.182±0.045^{a}	0.133±0.039^{a}	0.051±0.023^{a}
Agrinine	0.266±0.051^{a}	0.199±0.129^{a}	0.076±0.035^{a}
Threonine	0.318±0.053^{a}	0.205±0.121^{a}	0.086±0.042^{a}
Alanin	0.353±0.033^{a}	0.269±0.086^{ab}	0.094±0.050^{b}
Proline	0.372±0.201^{a}	0.116±0.164^{a}	0.095±0.057^{a}
Cystine	0.230±0.014^{a}	0.014±0.020^{b}	0.000±0.000^{b}
Tyrosine	0.159±0.153^{a}	0.050±0.013^{a}	0.041±0.021^{a}
Valine	0.246±0.105^{a}	0.247±0.132^{a}	0.090±0.042^{a}
Metheonine	0.036±0.036^{a}	0.013±0.018^{a}	0.012±0.007^{a}
Lysine	0.135±0.191^{a}	0.440±0.269^{a}	0.425±0.057^{a}
Isoleucine	0.110±0.156^{a}	0.188±0.103^{a}	0.072±0.028^{a}
Leucine	0.231±0.141^{a}	0.281±0.140^{a}	0.730±0.823^{a}
Phenylalanine	0.339±0.013^{a}	0.163±0.066^{ab}	0.059±0.028^{b}

Means followed by the same letters in the same rows are not significantly different (p = 0.05)

Discussion

The water clover showed stunted growth after exposed with Pb even though there was no morphological alteration. It indicated that water clover plants are able to accumulate with Pb in the long period based on the growth of biomass after observed in 20th and 30th day. These findings suggested the potency of water clover as a biological agent for phytoremediation due to the ability to accumulate heavy metal in

its tissues. Similar research was conducted using the *Salvinea culcullata* water plant by Phetshombat et al. (2006), which can accumulate Pb until 16.36 mgKg^{-1} under 40 mgL^{-1} but showed chlorosis in its leaf after long exposure.

The Pb exposure eventually affects the metabolism of the plant (Gomez et al., 2009). Similar to Cd exposure, Pb was found to slow the growth in several aquatic plants, such as *Lymnochasris flava* species and *Ipomoea aquatica* (Rachmadiarti et al., 2012). Pb interferes the tissue permeability (Fahr, 2013), increases the bound pectin to middle lamella of cell walls which inhibit the cell expansion (Krzeslowska, 2011), and affects the growth hormones, auxin metabolism, and its carrier. Pb also trigger the disorder in

http://www.aloki.hu ● ISSN 1589 1623 (Print) ● ISSN 1785 0037 (Online)
DOI: http://dx.doi.org/10.15666/aeer/1704_96099619

some plant metabolism such as photosynthetic pathway and peroxidase induction that plays a role in indole acetic acid degradation for growth and cell multiplication (Hoffman et al., 1985; McComb et al., 2012).

The mechanism behind the higher Pb concentration in the roots may include the binding of the positively charged toxic metals ion to negative charges in the cell walls (Matysik et al., 2002). In most plants, a larger proportion of the metal was retained in the roots and thereby prevented from interfering with the sensitive metabolic reaction in the shoot. It due to an internal mechanism to avoid toxic metal concentration in the shoot (Fahr et al., 2013).

The root has the tendency to accumulate a high concentration of Pb compared to in shoot (Gothberg et al., 2004). About 95% roots of Pb accumulated in a number species of brassica family other plants were in the roots (Kumar et al., 1995). However, concentration Pb in leaves are lower than in the stems because the leaves of water clover are very thin and Pb can lose through leaves transpiration. The stem accumulated high concentration of Pb compared to in leaves. It due to the possibility of the stem in the water (growing media). In addition, water clover as ferns (*Pteridophyta*) that has a vascular cylinder on the rod shape of concentric systems amphichiral in the xylem. The starch content and the veins size in the xylem have a larger size than the phloem. In addition, Mitel Lamela connected between the xylem cells.

In contrast, there was no significant difference in Pb content in leaves of clover water. It may occur due to the concentration of treatment. At low concentration of Pb until it reaches 0 in the leaves. It can be caused by water clover has a small, thin, and wide structure of leaves. Therefore, the absorption of the nutrients including Pb trigger small translocate into the leaves. In addition, Pb has been concentrated in the roots and accumulated in the stem. It due to the epidermal tissue on water clover leaves consists of a layer. Thus, the accumulation of Pb is less than the stem. The Cu metal content presented on other types of clover plants (*Marsilea quadrifolia*) is lower than *Echornia crassipes* and *Vallisneria spiralis.* Although the content of Pb on clover leaves is lower than on the stem, but the content of Pb in the roots of the clover is higher than in shoot (stem + leaves).

The content of Pb in the leaves indicated that the dosage of Pb concentration at the bellow limit allowed for foodstuffs (0.5 mg/kg^{-1}) unless the treatment of 10 mgL^{-1} at 10 days of observation (WHO, 1996). It suggested that clover water have been used to remediate Pb synthetic solution at a concentration of up to 10 mgL^{-1} with 20 days and it can be consumed based on the food security terms.

Generally, only a small portion of metal is brought up by the roots and transported to the shoot. It has been reported that the exclusion of metal from networks above the ground is a tolerance strategy against metals (Taylor and Crowder, 1983). The root has a higher tolerance than the shoot. In addition, it has a tendency to decrease translocation by increasing metal concentrations in the roots and included the general characteristics of various type of metals and plants. The binding of toxic metal through the positive ions to negative ions in the cell walls of the root, the formation of *metal phytate*, and khelasi on the phytochelatin followed by an accumulation in vacuoles are the mechanism by reducing transport and improving metal tolerance (Gothberg et al., 2004).

Kamel (2008) reported the adaptability of plants to extract metals from the water and the aptitude of plants to transfer metals from plant root to shoot. The concentration free amino acid in roots of water clover at some concentrations up to 30 days as shown in

http://www.aloki.hu ● ISSN 1589 1623 (Print) ● ISSN 1785 0037 (Online)
DOI: http://dx.doi.org/10.15666/aeer/1704_96099619

Table 4. The percentage of these amino acids was decreased. It due to the adaptation to heavy metal exposure which relatively high from 5 to10 ppm from amino acids. There are 6 amino acids (arginine, proline, leucine, valine, serine and glycine) and has acts an important role in the regulation of osmotic plant (Mansour, 2000). Arginine is involved in the synthesis of polyamines and acts as a molecular marker and antioxidant (Sharma and Dietz, 2006).

In the present study, the presence of proline showed its role moving between tissue and protect plants against stress. It due to its role as a major compound for carbon and nitrogen source, protect of cytoplasmic enzymes, and maintenance of cellular structures. High sensitivity in the metabolism of proline synthesis and its degradation has advantageous to control the adverse metabolic processes (Kamel, 2008). Proline serves as a radical scavenger, electron sink, stabilizer of macromolecules, cell wall components (Matysik et al., 2002), as well as osmoregulator and metal binding (Sharma and Dietz, 2006). Proline has been found at *Helianthus annuus* which accumulate with Pb, Cd, Cu, and Zn (Kastori et al., 1992). The existence of Ni in *Alyssum lesbiacum* plant was found to increase histidine in the xylem (Kramer et al., 1997). Hyperaccumulation of Ni triggers by histidine that translocates Ni from roots to shoot (Kerkeb and Kramer, 2003).

The percentage of amino acids in plants growing on Pb treatment has been investigated. The continued increase of amino acids occurred on plant exposed with Pb from 10 days up to 20 days. In contrast, reduced amino acid occurred on day 30, followed by the slow growth of plants. The increase of these amino acids in accordance with the Pb concentration which is absorbed by the roots did not a difference between 20 and 30 days (*Table 4*). Syam et al. (2010) reported that the biosynthetic pathway of *Salvinia minima* triggers Pb^{2+} detoxification. It has been indicated for other organisms, as part of the mechanism to cope with this metal in roots and leaves.

The root of water clover plant contains the amino acid, glutamic acid, and cysteine. They are dimeric amino acid formed by the oxidation of two cysteine residues that make a disulfide bond covalently. This organosulfur compound has the formula $(SCH_2CH(NH_2)CO_2H)_2$) and glycine. It is related to the multitude of amino acid protein from contaminated locations through the biosynthesis of phytochelatin and metallothioneins. The synthesis of phytochelatins and metallothioneins are the response of plants to trigger several metals or metalloid. Because of the similarity with metallothioneins, the phytochelatins have been known as class III of metallothioneins. Phytochelatins have a major function as detoxification. Meanwhile, metallothioneins has function in assisting the translocation of some metals. A gene family encodes metallothioneins, while phytochelatins produced enzymatically (Christopher and Peter, 2002). Plants also develop detoxification by inducing the protein synthesis due to the stress of phytochelatins and metallothioneins and high intensity in mango and apricot (Khawas, 2011).

Conclusion

The water clover growth, the concentration of Pb and free amino acid in plant organs indicated that water clover plants were survived and continued their growth. The highest concentration of Pb was found in root tissue followed by stem and leaf tissues. The phytochelatin production by clover plant as a resistance respond. In addition, it was followed by an increased percentage of free amino acids and the presence of

http://www.aloki.hu ● ISSN 1589 1623 (Print) ● ISSN 1785 0037 (Online)
DOI: http://dx.doi.org/10.15666/aeer/1704_96099619

phytochelatins such as glutamic acid, cysteine, glycine and proline. Based on this study result, it is imperative to investigate further the phytoremediation capability of water clover by increasing the Pb concentration and in the smaller time frame.

Acknowledgements. This work was supported by Fundamental Research, Directorat Research and Community Services, the Ministry of Research and Technology, Indonesia.

Conflict of interests. The authors declare that there is no conflict of interests.

REFERENCES

[1] Celebi, S., Kendir, S. (2002): Toxicity assessment of a dye industry treatment sludge. – Waste Management and Research 20: 541-545.
[2] Christopher, C., Peter, G. (2002): Phytochelatins and metallothioneins: Roles in heavy metal detoxification and homeostasis. – Annual Review of Plant Biology 53: 159-182.
[3] Duruibe, J. O., Ogwuebu, M. O. C., Egwurugwu, J. N. (2007): Heavy metal pollution and human biotoxic effects. – International Journal of Physical Sciences 2: 112-118.
[4] Fahr, M., Laplaze, L., Bendaou, N., Hocher, V., Mzibri, M. E., Bogusz, D., Smouni, A. (2013): Effect of lead on root growth. – Frontiers in Plant Science 4.
[5] Ghosh, M., Singh. (2005): A review on phytoremediation of heavy metals and utilization of it's by products. – Applied Ecology and Environmental Research 3: 1-18.
[6] Göthberg, A., Greger, M., Holm, K., Bengtsson, B. E. (2004): Influence of nutrient levels on uptake and effect of mercury, cadmium, and lead in water spinach. – Journal of Environmental Quality 33: 1247-1255.
[7] Grill, E., Löeffler, S., Winnacker, E. L., Zenk, M. H. (1989): Phytochelatin, the heavy metal binding peptides of plants, are synthesized from glutathione by a specific gamma–glutamylcysteine dipeptidyl transpeptidase (phytochelatin synthase). – Proceedings of the National Academy of Sciences of the United States of America 86: 6838-6842.
[8] Herawati, E. Y. (2008): Lamun (Cymodocea rotundata), Thalassia hemprichii, dan Enhalus acoroides sebagai Bioindikator Logam Berat Timbal (Pb) di Perairan Pesisir Jawa Timur. – PhD Thesis, Disertasi Brawijaya University, Indonesia.
[9] Iha, D. S., Bianchin., I. (2015): Phytoremediation Of Cd, Ni, Pb, and Zn By *Salvinia minima*. – International Journal of Phytoremediation 17: 929-935.
[10] Jaishankar, M., Tseten, T., Anbalagan, N., Mathew, B. B., Beeregowda, K. N. (2014): Toxicity, mechanism and health effects of some heavy metals. – Interdisciplinary Toxicology 7: 60-72.
[11] John, R., Ahmad, P., Gadjil, K., Sharma, S. (2008): Effect of cadmium and lead on growth, biochemical parameters and uptake in *Lemna polyrhizal*. – Plant, Soil and Environment 54: 262-270.
[12] Kamel, H. A. (2008): Lead accumulation and its effect on photosynthesis and free amino acids in *Vicia faba* grown hydroponically. – Australian Journal of Basic and Applied Sciences 2: 438-446.
[13] Kastori, R., Petrovic, M., Petrovic, N. (1992): Effect of excess lead, cadmium, copper and zinc on water relations in sunflower. – Journal of Plant Nutrition 15: 2427-2439.
[14] Kerkeb, L., Krämer, U. (2003): The role of free histidine in xylem loading of nickel in *Alyssum lesbiacum* and *Brassica juncea*. – Plant Physiology 131: 716-724.
[15] Khawas, S. A. (2011): Certain medicinal plants as biomonitors to roadside automotive pollution. – Journal of Food, Agriculture & Environment 9: 593-598.
[16] Kozhevnikova, A. D., Seregin, I. V., Bystrova, E. I., Belyaeva, A. I., Kataeva, M. N., Ivanov, V. B. (2009): The effects of lead, nickel, and strontium nitrates on cell division and elongation in maize roots. – Russian Journal of Plant Physiology 56: 242-250.

http://www.aloki.hu ● ISSN 1589 1623 (Print) ● ISSN 1785 0037 (Online)
DOI: http://dx.doi.org/10.15666/aeer/1704_96099619

[17] Krämer, U., Grime, G. W., Smith, J. A. C., Hawes, C. R., Baker, A. J. M. (1997): Micro-PIXE as a technique for studying nickel localization in leaves of the hyperaccumulator *Alyssum lesbiacum*. – Nuclear Instruments and Methods in Physics Research Section B: Bearn Interactions with Materials and Atoms 130: 346-350.
[18] Kumar, P. N., Dushenkov, V., Motto, H., Raskin, I. (1995): Phytoextraction: the use of plants to remove heavy metals from soils. – Environmental Science and Technology 29: 1232-1238.
[19] Loeffler, S., Hochberger, A., Grill, E., Winnacker, E. L., Zenk, M. H. (1989): Termination of the phytochelatin synthase reaction through sequestration of heavy metals by the reaction product. – FEBS Letters 258: 42-46.
[20] Mansour, M. M. F. (2000): Nitrogen containing compounds and adaptation of plants to salinity stress. – Biologia Plantarum 43: 491-500.
[21] Matysik, J., Alia, Bhalu, B., Mohanty, P. (2002): Molecular mechanisms of quenching of reactive oxygen species by proline under stress in plants. – Current Science 82: 525-532.
[22] McComb, J., Hentz, S., Gloria, S. Miller, G. S., Begonia, M., Begonia, G. (2012): Effects of lead on plant growth, lead accumulation and phytochelatin contents of hydroponically-grown Sesbania Exaltata. – World Environment 2: 38-43.
[23] Mohamed, S. B. (2005): Phytotoxicity of lead (Pb) to SDS-PAGE protein profile in root nodules of faba bean (*Vicia faba* L.) plants. – Pakistan Journal of Biological Sciences 8: 687-690.
[24] Nakata, N., Nakayama, S. S. M., Oroszlany, B., Ikenaka, Y., Mizukawa, H., Tanaka, K., Harunari, T., Tanikawa, T., Darwish, W. H., Yohannes, Y. B., Saengtienchai, A., Ishizuka, M. (2017): Monitoring lead (Pb) pollution and identifying Pb pollution sources in Japan using stable Pb isotope analysis with kidneys of wild rats. – International Journal of Environmental Research and Public Health 14(1): 56. DOI: 10.3390/ijerph14010056.
[25] Novi., C., Abdilah., N., A. (2017): Fitoremediasi logam timbal (Pb) dari limbah cair industri kertas dengan pemanfaatan *Marsilea crenata* dan *Hydrilla verticillata*. – Journal of Science Pharmacy 3: 29-33.
[26] Nurhayati, A., Hariadi. Y. C., Lestari, P. (2015): Early detection of lead stress on Marsilea crenata L. – Procedia Environmental Science 28: 57-66.
[27] Parameswaran, A., Majeti, N. V. P. (2005): Modulation of cadmium-induced oxidative stress in *Ceratophyllum demersum* by zinc involves ascorbate-glutathione cycle and glutathione metabolism. – Plant Physiology and Biochemistry 43: 107-116.
[28] Rachmadiarti, F., Soehono, L. A., Utomo, W. H., Yanuwiyadi, B., Fallowfield, H. 2012. Resistance of yellow velvetleaf (Limnocharis flava (L.) Buch.) exposed to lead. – Journal of Applied Environmental and Biological Sciences 2: 210-215.
[29] Seregin, I. V., Ivanove, V. B. (1998): The transport of cadmium and lead ions through root tissues. – Russian Journal of Plant Physiology 45: 780-785.
[30] Sharma, S. S., Dietz, K. J. (2006): The significance of amino acids and amino acid-derived molecules in plant responses and adaptation to heavy metal stress. – Journal of Experimental Botany 57: 711-726.
[31] Stoyanova, Z., Doncheva, S. (2002): The effect of zinc supply and succinate treatment on plant growth and mineral uptake in pea plant. – Brazilian Journal of Plant Physiology 14: 111-116.
[32] Syam, S. A., Rupali, D., Dibyendu, S., Konstantinos, C. M., Conor, P. M., Shivendra, V. S., Stephan, B. H. B. (2010): Synthesis of phytochelatins in vetiver grass upon lead exposure in the presence of phosphorus. – Plant and Soil 326: 171-185.
[33] Taylor, G. T., Crowder, A. (1983): Use of DCB technique for extraction of hydrous iron oxides from roots of wetland plant. – America Journal of Botany 70: 1254-1257.
[34] Waters. (2017): AccQ•Tag Amino Acid Analysis Column. – Waters Corporation, Milford, MA. www.waters.com.
[35] WHO (1996): Trace Elements in Human Nutrition and Health. – World Health Organization (WHO), Geneva.

http://www.aloki.hu ● ISSN 1589 1623 (Print) ● ISSN 1785 0037 (Online)
DOI: http://dx.doi.org/10.15666/aeer/1704_96099619

[36] Yang, Y. Y., Jung, J. I. Y., Song, W. Y., Suh, H. S., Lee, Y. (2000): Identification of rice varieties with high tolerance or sensitivity to lead and characterisation of the mechanism of tolerance. – Plant Physiology 124: 1019-1026.
[37] Yun, Y. S., Park, D., Park, J. M., Volesky, B. (2001): Biosorption of trivalent chromium on the brown seaweed biomass. – Environmental Science & Technology 35: 4353-4358.
[38] Zitka, O., Krystofova, O., Sobrova, P., Adama, V., Zehnalek, J., Beklova, M., Kizek, R. (2011): Phytochelatin synthase activity as a marker of metal pollution. – Journal of Hazardous Materials 192: 794-800.

http://www.aloki.hu ● ISSN 1589 1623 (Print) ● ISSN 1785 0037 (Online)
DOI: http://dx.doi.org/10.15666/aeer/1704_96099619

DIVERSITY AND DISTRIBUTION OF FLORA IN MURREE-KOTLI SATTIAN-KAHUTA NATIONAL PARK, PAKISTAN

AHMED, W.[1] – QURESHI, R.[1*] – MUNAZIR, M.[2] – RAHIM, B. Z.[3] – MUNIR, M.[4] – KOUSAR, R.[1] – MAQSOOD, M.[1] – ABBAS, Q.[5] – QASEEM, M. F.[1] – KHAN, A. M[1] – IQBAL, M.[6] – BHATTI, M. I.[7]

[1]*Department of Botany, Pir Mehr Ali Shah Arid Agriculture University, Murree Road, Shamsabad, 46300 Rawalpindi, Punjab, Pakistan*

[2]*Department of Botany, Government College, Women University, 51040 Sialkot, Punjab, Pakistan*

[3]*Department of Botany, Baluchistan University, 87500 Quetta, Baluchistan, Pakistan*

[4]*Department of Botany, University of Animal & Plant Sciences, Ravi Campus, Pattoki, Punjab, Pakistan*

[5]*Department of Biological Sciences, Karakorum International University, Gilgit-Baltistan, Gilgit, Pakistan*

[6]*Department of Entomology, Pir Mehr Ali Shah Arid Agriculture University, Murree Road, Shamsabad, 46300 Rawalpindi, Punjab, Pakistan*

[7]*Department of Plant Pathology, Sindh Agriculture University, Sub-Campus Umarkot, Sindh, Pakistan*

**Corresponding author*
e-mail: rahmatullahq@yahoo.com

(Received 9th Feb 2019; accepted 24th May 2019)

Abstract. Present endeavor was aimed at recording the flora of Murree-Kotli Sattian-Kahuta National Park (MKSKNP), Pakistan. The whole project area was surveyed thoroughly from March, 2013 till October, 2015 and 624 plant species belonging to 361 genera and 106 families were recorded. Of them, 24 ferns, four gymnosperms and 596, angiosperms (144 monocots and 452 dicots) were recorded from the park area. Poaceae was the largest family (80 spp., 12.82%), followed by Fabaceae (60 spp., 9.62%) and Asteraceae (55 spp., 8.81%). Most of the studied area was inhabited by native species (528 spp., 84.62%), followed by weeds (48 spp., 7.69%), cultivated species (21 spp., 3.37%) and naturalized (18 spp., 2.88%). Two species viz., *Aristolochia punjabensis* and *Buxus papillosa* were found endemic to Pakistan. This national park is composed of three localities (viz., Murree Kotli Sattian and Kahuta) and the pair-wise comparison revealed maximum similarity between Murree and Kotli Sattian pair due to their adjacency and similar climatic conditions. Similarly, the other pair (i.e. Kotli Sattian and Kahuta) was also closely located towards southern part and had similar floristic elements. This study serves as a platform for the detailed floristic and ecological studies to be carried out by the researchers.
Keywords: *ecological studies, endemic, floristic elements, maximum similarity, sustainable utilization*

Introduction

The flora is the compilation of all plants confined to the particular territory or region (Hooker, 1897). The correctly identified plants are very important since they are the key to the literature. Various types of flora exist like native flora, agricultural flora/garden flora, weed flora, etc. Since plants of the world are extremely variable, therefore a wide

http://www.aloki.hu ● ISSN 1589 1623 (Print) ● ISSN 1785 0037 (Online)
DOI: http://dx.doi.org/10.15666/aeer/1704_96219650

range of Floras are available ranging from concise or field Flora to research Flora normally, the flora is assisted with the keys and description (Ali, 2008).

The floristic checklists may serve as a platform for more detailed study from the particular area and in many cases; this may be the only source of botanical information (Kent, 2011). Because of their conciseness, the listing of species is easy approach in vegetation study because it can be done in a relatively small timeframe, easy to handle and provide fundamental information for understanding the biodiversity issues (Ilyas et al., 2012). The floristic study provide baseline for further future taxonomic, ecological, ethnobotanical, conservation and forest management projects (Khan et al., 2015).

Pakistan has moderate diversity in terms of the flora and approximately 5,700 species of vascular plants have been reported (Stewart, 1972). Many floristic studies have been conducted from various parts of Pakistan and reported checklists (Chaudhri and Chuttar, 1966; Bhatti et al., 1999, 2001; Qureshi and Bhatti, 2005; Parveen and Hussain, 2007; Hussain et al., 2008; Qureshi, 2008a, 2012; Qureshi et al., 2011a, b, 2014; Shaheen et al., 2014a; Wariss et al., 2014; Ilyas et al., 2018; Khan et al., 2018). From Rawalpindi and adjoining area, an outdated account has been previously reported (Ahmad, 1964; Stewart, 1967; Shaheen et al., 2014b). Some of other studies include Sher and Khan (2007), Djaha et al. (2008), Saima et al. (2009), Qureshi and Bhatti (2010), Haq et al. (2010), Nazir et al. (2014), Khan et al. (2015) and Badshah et al. (2016). Because of diverse topographic and microhabitat variation along with very high elevational differences, the study area harbors rich plant biodiversity, which needs to be protected and conserved as soon as possible. The present study was aimed to enlist existing floristic diversity as an effort to highlight the rich phytodiversity of the area which will provide a baseline for planning conservation effort and further ecological investigation.

Materials and methods

Study area

Murree-Kotli Sattian-Kahuta National Park (MKSKNP) is composed of three distinct localities (i.e. Murree, Kotli Sattian, Kahuta) of district Rawalpindi, Pakistan. It lies at 33° 21’ to 34° 01’ N latitudes and 73° 11’ to 73° 38’ E longitude in the district Rawalpindi, Pakistan with an area of 934 km^2 (*Fig. 1*). Climatically, the study area is subtropical to temperate owing to elevational changes varying from 500 to 2270 m. The study area is located on the lateral spur of the Sub-Himalayan Mountains bounded by river Jhelum in the east, Islamabad in west, Khyber Pakhtunkhwa in the north and Gujar Khan in the south. The topography of the study area at higher altitude is mainly composed of rugged terrain with narrow valleys and relatively flat at the lower elevations. The hilly area contains valleys created by fast flowing running water of streams and rivers. The water courses are gradually made deeper by the fast flow of water which erodes the soil and carries valuable mineral to low lying downstream areas, resulting in alluvial deposits making these areas more fertile then hilly areas for cultivation (Khan et al., 2011).

Floristic enumeration

Plant specimens were collected from 246 sampling sites in the study area from August, 2013 to September, 2016. For this purpose, the whole study area was thoroughly visited covering all seasonal variations by walking method (Nazar et al.,

http://www.aloki.hu ● ISSN 1589 1623 (Print) ● ISSN 1785 0037 (Online)
DOI: http://dx.doi.org/10.15666/aeer/1704_96219650

2008). Plant specimens were collected in triplicate, pressed, dried and mounted on standard herbarium sheets. Gymnosperm and Angiosperm were identified with the help of *Flora of Pakistan* (Stewart, 1972; Nasir and Ali, 1970-1989; Ali and Nasir, 1989-1991; Ali and Qaiser, 1993-2009); while, the Cryptogamic Flora of Pakistan (Nakaike and Malik, 1992) was used to identify the Pteridophytes. Nomenclature of the taxa was validated from The Plant List (TPL, 2013). Voucher specimens were deposited in the herbarium of Pir Mehr Ali Shah (PMAS), Arid Agriculture University Rawalpindi, Pakistan.

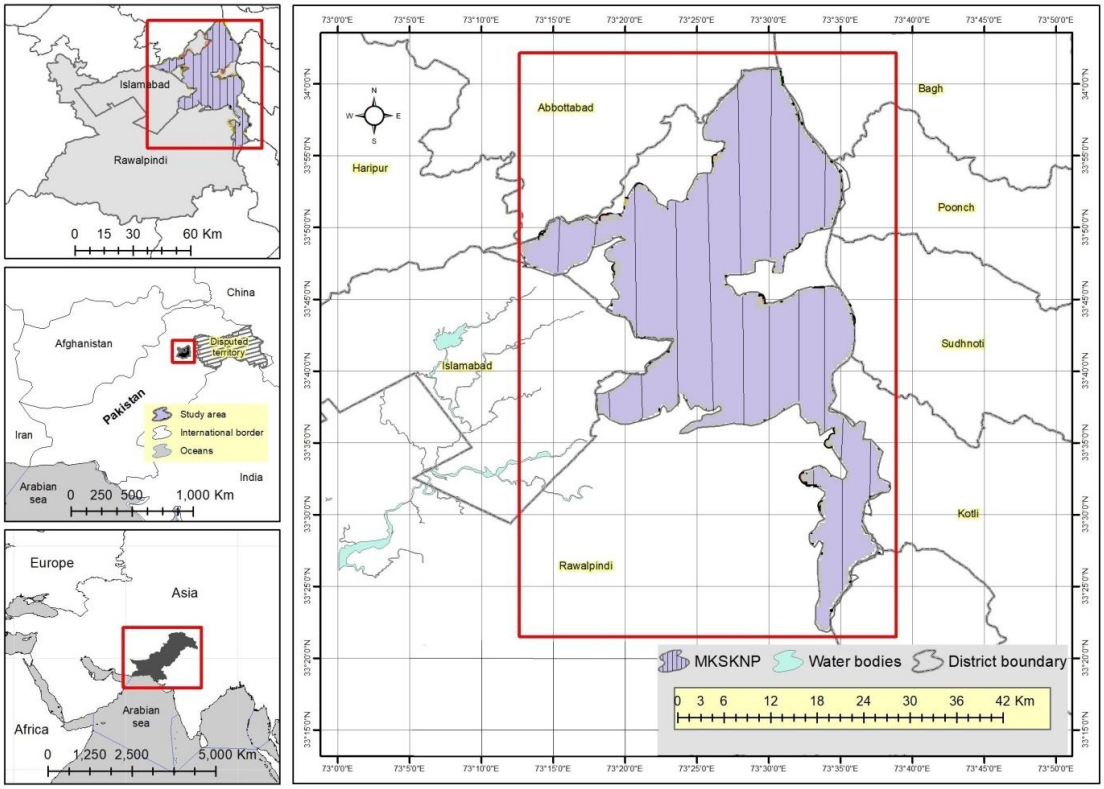

Figure 1. *Location map of the study area*

Family importance index (FII) and genera importance index (GII)

In order to calculate sharing of each family and genus, family importance index (FII) and genera importance index (GII) were calculated by using following formulae:

$$FII = \frac{\text{No. of species of a family}}{\text{Total No. of species recorded}} \times 100 \quad \text{(Eq.1)}$$

$$GII = \frac{\text{No. of species of a genus}}{\text{Total No. of species recorded}} \times 100 \quad \text{(Eq.2)}$$

Diversity index (SI)

The similarity index (SI) between localities was calculated after Kent (2011) by using following formula:

http://www.aloki.hu ● ISSN 1589 1623 (Print) ● ISSN 1785 0037 (Online)
DOI: http://dx.doi.org/10.15666/aeer/1704_96219650

$$Ss = \frac{2a}{2a+b+c} \quad \text{(Eq.3)}$$

where “a” is the number of species common to both habitats, while “b” is the number of species in habitat 1 and “c” is the number of species in habitat 2.

Results

Floristic diversity

The vascular flora of Murree-Kotli Sattian-Kahuta National Park (MKSNP) is comprised of 624 plant species belonging to 361 genera and 106 families (*Appendix*). Two species such as *Aristolochia punjabensis* and *Buxus papillosa* were found endemic to Pakistan. There was diversity of elevational ranges recorded from sampling sites right from Beor (500 m) to Patriata (2155 m). The detail of sampling sites along with coordinates and altitude is provided in *Table 1*. The census of the flora indicates that it includes 24 ferns, 4 gymnosperms and 596 angiosperms (i.e. 144 monocotyledon and 452 dicotyledons). Geographically, the park area shared 0.12% of the whole area of country but contains significantly higher flora diversity (10.79%) than the flora of Pakistan (*Table 2*). Compared to the vascular plants of the country, the project area was found rich in pteridophytes (18.75%) and gymnosperms (17.39%), followed by monocotyledons (12.63%) and dicotyledons (10.06%) as indicated in *Table 2*.

Table 1. *Location of sampling sites of Murree-Kotli Sattian-Kahuta National Park*

Sample No.	Locality	Latitude	Longitude	Altitude
S1	Lehtrar	33°45'03.09"N	73°29'23.01"E	1098
S2	Baroa	33°49'35.02"N	73°14'05.00"E	1181
S3	Baroa	33°49'25.01"N	73°14'04.00"E	1128
S4	Baroa	33°49'32.01"N	73°14'17.09"E	1098
S5	Baroa	33°49'20.07"N	73°14'17.01"E	1051
S6	Lehtrar	33°44'22.07"N	73°28'44.02"E	1028
S7	Kror	33°43'08.49"N	73°25'41.03"E	1006
S8	Danoi	33°44'59.00"N	73°29'25.02"E	1125
S9	Bagga Reserve Forest	33°44'07.44"N	73°25'44.01"E	1049
S10	Angori	33°48'04.03"N	73°20'22.03"E	1088
S11	Deral Reserve Forest	33°59'37.15"N	73°29'48.45"E	1017
S12	Lehtrar	33°42'03.01"N	73°26'08.40"E	1049
S13	Kohati Reserve Forest	33°56'17.03"N	73°31'33.08"E	1064
S14	Kohati Reserve Forest	33°55'49.06"N	73°31'15.01"E	1088
S15	Kohati Reserve Forest	33°55'37.00"N	73°31'05.09"E	1107
S16	Kohati Reserve Forest	33°55'22.24"N	73°31'07.48"E	1127
S17	Agori	33°48'07.08"N	73°20'43.49"E	1130
S18	Sain	33°48'38.06"N	73°22'54.02"E	1075
S19	Agori	33°48'06.04"N	73°20'29.06"E	1077
S20	Agori	33°48'05.08"N	73°20'33.05"E	1081
S21	Pastal	33°50'37.05"N	73°20'06.07"E	1168
S22	Pastal	33°50'37.07"N	73°20'06.03"E	1168
S23	Pastal	33°50'36.04"N	73°20'18.07"E	1150
S24	Pastal	33°50'18.05"N	73°20'09.03"E	1020
S25	Lehtrar Uper	33°41'37.00"N	73°26'24.08"E	1060

http://www.aloki.hu ● ISSN 1589 1623 (Print) ● ISSN 1785 0037 (Online)
DOI: http://dx.doi.org/10.15666/aeer/1704_96219650

Sample No.	Locality	Latitude	Longitude	Altitude
S26	Lehtrar Uper	33°41'56.00"N	73°26'21.12"E	1189
S27	Lehtrar Uper	33°41'39.01"N	73°26'41.07"E	1130
S28	Bhangal Reserve Forest	33°44'05.00"N	73°26'56.04"E	1026
S29	Danoi	33°44'50.09"N	73°29'24.06"E	1196
S30	Parinola Reserve Forest	33°44'33.01"N	73°30'59.09"E	1069
S31	Kamra Reserve Forest	33°45'47.02"N	73°33'30.04"E	1095
S32	Paija Kamra	33°44'52.03"N	73°32'16.01"E	1024
S33	Paija Kamra	33°45'08.54"N	73°32'32.23"E	1100
S34	Gehl	33°48'39.33"N	73°23'01.58"E	1024
S35	Sain	33°48'48.44"N	73°23'30.26"E	1119
S36	Gehl	33°48'58.54"N	73°23'27.21"E	1144
S37	Salgran	33°48'04.23"N	73°20'02.30"E	1011
S38	Salgran	33°48'11.05"N	73°20'25.01"E	1081
S39	Angori	33°48'28.03"N	73°21'58.08"E	1081
S40	Angori	33°48'27.03"N	73°22'09.05"E	1055
S41	Angori	33°48'21.07"N	73°22'22.02"E	1029
S42	Angori	33°48'21.08"N	73°22'21.01"E	1027
S43	Sain	33°48'33.04"N	73°22'55.04"E	1059
S44	Trait	33°49'58.38"N	73°18'04.26"E	1145
S45	Sain	33°48'45.03"N	73°23'09.02"E	1121
S46	Angori	33°48'43.01"N	73°23'22.04"E	1142
S47	Phaphreel	33°49'53.01"N	73°23'08.09"E	1115
S48	Angori Villge	33°48'12.07"N	73°20'17.04"E	1045
S49	Angori Villge	33°48'32.01"N	73°22'08.09"E	1099
S50	Patriata	33°51'32.03"N	73°28'54.01"E	2020
S51	Patriata	33°50'50.03"N	73°28'57.01"E	2143
S52	Patriata	33°50'47.07"N	73°29'06.01"E	2108
S53	Patriata	33°50'37.08"N	73°29'09.09"E	2026
S54	Patriata	33°51'09.03"N	73°28'42.05"E	2068
S55	Loer Topa	33°53'06.00"N	73°26'06.03"E	2102
S56	Loer Topa	33°53'06.08"N	73°26'10.07"E	2101
S57	Patriata	33°51'03.03"N	73°28'57.07"E	2155
S58	Patriata	33°51'15.03"N	73°28'51.04"E	2153
S59	Patriata	33°51'07.45"N	73°28'48.44"E	2010
S60	Bhurban	33°56'22.09"N	73°26'47.07"E	2091
S61	Bhurban	33°56'26.03"N	73°26'48.06"E	2030
S62	Bhurban	33°56'28.08"N	73°26'53.01"E	2029
S63	Loer Topa	33°53'06.08"N	73°26'02.08"E	2027
S64	Deerkot Reserve Forest	33°50'41.08"N	73°29'34.05"E	1829
S65	New Murree	33°52'29.09"N	73°27'46.00"E	1830
S66	Deerkot Reserve Forest	33°50'28.01"N	73°29'22.07"E	1955
S67	Deerkot Reserve Forest	33°51'40.04"N	73°29'38.07"E	1845
S68	Deerkot Reserve Forest	33°50'00.06"N	73°29'05.02"E	1829
S69	Kasairi Reserve Forest	33°54'19.07"N	73°26'38.01"E	1827
S70	Kasairi Reserve Forest	33°54'18.07"N	73°26'40.01"E	1855
S71	Kasairi Reserve Forest	33°50'40.06"N	73°29'23.04"E	1944
S72	Patriata	33°49'53.01"N	73°28'56.02"E	1853
S73	Patriata	33°51'56.44"N	73°28'59.41"E	1830
S74	Patriata	33°51'51.26"N	73°28'53.43"E	1820

http://www.aloki.hu ● ISSN 1589 1623 (Print) ● ISSN 1785 0037 (Online)
DOI: http://dx.doi.org/10.15666/aeer/1704_96219650

Sample No.	Locality	Latitude	Longitude	Altitude
S75	Patriata	33°51'57.13"N	73°29'15.42"E	1913
S76	Patriata	33°52'18.02"N	73°29'34.06"E	1826
S77	Loer Topa	33°53'19.03"N	73°25'57.02"E	1925
S78	New Muree	33°52'33.08"N	73°26'08.09"E	1819
S79	New Muree	33°52'46.08"N	73°26'11.06"E	1859
S80	Bhurban Reserve Forest	33°56'34.05"N	73°26'52.00"E	1951
S81	Bhurban Reserve Forest	33°56'35.04"N	73°26'50.03"E	1969
S82	Bhurban Reserve Forest	33°57'06.00"N	73°27'13.02"E	1916
S83	Kasairi Forest	33°55'24.3"N	73°27'20.3"E	1811
S84	Kasairi Forest	33°55'13.08"N	73°27'00.03"E	1812
S85	Kasairi Forest	33°54'37.02"N	73°26'21.02"E	1945
S86	Kasairi Forest	33°54'25.05"N	73°26'24.01"E	1944
S87	Bhurban Reserve Forest	33°56'48.09"N	73°26'27.04"E	1864
S88	Bhurban Reserve Forest	33°56'39.07"N	73°26'36.08"E	1909
S89	Bhurban Reserve Forest	33°56'38.10"N	73°26'45.54"E	1927
S90	Bhurban Reserve Forest	33°56'38.52"N	73°26'38.59"E	1917
S91	Bhurban Reserve Forest	33°56'34.12"N	73°26'43.06"E	1933
S92	Bhurban Reserve Forest	33°56'45.07"N	73°26'54.24"E	1851
S93	Bhurban Reserve Forest	33°56'49.13"N	73°26'27.67"E	1852
S94	Kasairi Forest	33°54'47.07"N	73°26'18.01"E	1920
S95	Bhurban Reserve Forest	33°56'46.07"N	73°26'48.05"E	1802
S96	Deerkot Reserve Forest	33°50'34.39"N	73°29'19.09"E	1976
S97	New Murree	33°52'29.09"N	73°27'46.00"E	1830
S98	Patriata	33°52'26.28"N	73°29'42.53"E	1798
S99	Patriata	33°52'43.08"N	73°29'49.06"E	1825
S100	Deerkot	33°52'49.00"N	73°29'58.02"E	1798
S101	Deerkot	33°52'27.00"N	73°30'18.09"E	1810
S102	Deerkot	33°52'36.02"N	73°30'7.08"E	1791
S103	Deerkot	33°52'09.02"N	73°29'25.06"E	1802
S104	Patriata	33°52'48.09"N	73°26'28.07"E	1794
S105	Patriata	33°50'23.09"N	73°28'06.01"E	1777
S106	Patriata	33°49'48.02"N	73°28'01.04"E	1761
S107	Balawra	33°48'51.06"N	73°30'07.04"E	1628
S108	New Muree	33°52'44.07"N	73°26'49.43"E	1748
S109	New Muree	33°52'15.07"N	73°27'47.43"E	1707
S110	Gora Gali	33°52'40.03"N	73°20'56.01"E	1673
S111	Mohra Shareef	33°56'55.06"N	73°26'05.06"E	1759
S112	Mohra Shareef	33°56'56.07"N	73°26'10.06"E	1617
S113	Chajana	33°53'26.58"N	73°30'01.63"E	1620
S114	Kohati	33°53'29.05"N	73°30'06.01"N	1632
S115	Chajana	33°53'41.13"N	73°30'45.86"E	1700
S116	Chajana	33°53'31.04"N	73°31'04.55"E	1691
S117	Bhurban Reserve Forest	33°56'51.07"N	73°26'27.03"E	1791
S118	Bhurban Reserve Forest	33°56'55.06"N	73°26'25.01"E	1774
S119	Bhurban Reserve Forest	33°56'55.00"N	73°26'30.08"E	1738
S120	Bun Karor	33°49'01.06"N	73°27'29.05"E	1724
S121	Bun Karor	33°48'54.05"N	73°27'12.08"E	1718
S122	Bun Karor	33°48'51.07"N	73°27'09.06"E	1737
S123	Lehtrar	33°43'01.07"N	73°26'52.01"E	1658

http://www.aloki.hu ● ISSN 1589 1623 (Print) ● ISSN 1785 0037 (Online)
DOI: http://dx.doi.org/10.15666/aeer/1704_96219650

Sample No.	Locality	Latitude	Longitude	Altitude
S124	Aliot	33°56'57.59"N	73°28'20.42"E	1604
S125	Aliot	33°56'47.08"N	73°27'53.03"E	1734
S126	Bara Hoter Reserve Forest	33°52'52.07"N	73°25'18.09"E	1668
S127	Bhurban Reserve Forest	33°56'49.00"N	73°26'46.09"E	1742
S128	Trait	33°51'36.06"N	73°20'05.08"E	1611
S129	Trait	33°51'36.01"N	73°20'14.08"E	1646
S130	Ghora Gali	33°52'48.05"N	73°20'59.09"E	1647
S131	Lehtrar	33°43'00.04"N	73°29'55.01"E	1420
S132	Lehtrar	33°43'31.09"N	73°30'23.03"E	1511
S133	Lehtrar	33°43'30.05"N	73°30'16.01"E	1518
S134	Lehtrar	33°43'46.05"N	73°30'20.06"E	1592
S135	Lehtrar	33°43'46.05"N	73°30'11.09"E	1512
S136	Danoi	33°44'03.03"N	73°29'32.08"E	1456
S137	Parinola Reserve Forest	33°43'52.05"N	73°29'52.04"E	1487
S138	Nar	33°43'06.03"N	73°30'01.06"E	1486
S139	Balawra	33°48'59.03"N	73°30'59.09"E	1459
S140	Balawra	33°49'00.09"N	73°31'18.05"E	1480
S141	Balawra	33°48'57.06"N	73°31'01.05"E	1460
S142	Balawra	33°48'47.08"N	73°31'08.03"E	1444
S143	Kotli Sattian	33°48'49.01"N	73°31'34.05"E	1457
S144	Kotli Sattian	33°48'50.06"N	73°31'51.09"E	1520
S145	Chajana	33°53'41.23"N	73°30'58.22"E	1577
S146	Chajana	33°53'40.08"N	73°31'17.56"E	1519
S147	Garian Reserve Forest	33°51'00.59"N	73°25'25.54"E	1402
S148	Garian Reserve Forest	33°51'28.48"N	73°25'54.40"E	1408
S149	Kala Basand Reserve Forest	33°45'36.09"N	73°25'03.05"E	1426
S150	Ban Karoor	33°47'21.47"N	73°25'47.08"E	1481
S151	Aliot	33°56'59.44"N	73°28'13.47"E	1594
S152	Ocha	33°58'00.00"N	73°26'42.06"E	1409
S153	Ocha	33°57'55.03"N	73°26'38.06"E	1443
S154	Ocha	33°57'54.02"N	73°26'32.01"E	1442
S155	Gora Gali	33°51'47.05"N	73°20'01.05"E	1517
S156	Gora Gali	33°51'39.08"N	73°20'03.08"E	1524
S157	Gora Gali	33°51'47.02"N	73°19'56.02"E	1465
S158	Samli	33°50'41.07"N	73°18'55.09"E	1210
S159	Parinola	33°44'11.02"N	73°29'35.08"E	1357
S160	Kotli Sattian	33°46'42.03"N	73°30'28.09"E	1295
S161	Danoi	33°44'29.07"N	73°29'02.08"E	1305
S162	Patriata Reserve Forest	33°52'33.80"N	73°31'05.50"E	1341
S163	Dewal Reserve Forest	33°59'25.04"N	73°29'03.05"E	1230
S164	Dewal Reserve Forest	33°59'12.05"N	73°29'15.09"E	1341
S165	Gehl Tanda	33°52'30.31"N	73°31'14.05"E	1320
S166	Gehl Tanda	33°52'23.42"N	73°31'22.11"E	1350
S167	Nankot Reserve Forest	33°50'37.06"N	73°19'29.02"E	1257
S168	Sang Reserve Forest	33°41'20.06"N	73°26'45.00"E	1258
S169	Parinola Reserve Forest	33°44'07.03"N	73°29'43.04"E	1286
S170	Parinola Reserve Forest	33°44'22.05"N	73°29'50.08"E	1217
S171	Lower Danoi	33°44'43.07"N	73°29'27.08"E	1290
S172	Glehragali	33°49'59.15"N	73°24'16.36"E	1331

http://www.aloki.hu ● ISSN 1589 1623 (Print) ● ISSN 1785 0037 (Online)
DOI: http://dx.doi.org/10.15666/aeer/1704_96219650

Sample No.	Locality	Latitude	Longitude	Altitude
S173	Parinola Reserve Forest	33°44'15.01"N	73°30'03.01"E	1188
S174	Parinola Reserve Forest	33°05'33.03"N	73°18'56.06"E	1221
S175	Nankot Reserve Forest	33°50'30.05"N	73°19'04.03"E	1306
S176	Phaphreel	33°49'03.07"N	73°23'36.05"E	1208
S177	Phaphreel	33°49'51.01"N	73°24'27.02"E	1332
S178	Kohati	33°53'51.49"N	73°29'35.14"E	1336
S179	Kohati	33°53'54.09"N	73°29'42.09"E	1341
S180	Kohati Rod	33°54'36.00"N	73°30'24.17"E	1330
S181	Ambani	33°42'36.02"N	73°21'08.53"E	898
S182	Ambani	33°42'39.04"N	73°21'08.11"E	939
S183	Kalla Basand Reserve Forest	33°44'03.02"N	73°22'17.07"E	856
S184	Simli Dam	33°43'09.34"N	73°22'39.01"E	832
S185	Lehtrar	33°43'02.07"N	73°26'53.03"E	922
S186	Bagga Reserve Forest	33°44'01.01"N	73°25'34.04"E	949
S187	Bagga Reserve Forest	33°43'06.36"N	73°25'44.06"E	983
S188	Bagga Reserve Forest	33°43'15.05"N	73°25'38.07"E	960
S189	Kror	33°42'27.06"N	73°25'16.09"E	957
S190	Kror	33°42'26.06"N	73°25'03.09"E	925
S191	Dewal Reserve Forest	33°59'57.22"N	73°30'26.31"E	812
S192	Kohati Reserve Forest	33°56'43.05"N	73°31'57.09"E	920
S193	Kohati Reserve Forest	33°57'37.19"N	73°31'45.42"E	843
S194	Kohati Reserve Forest	33°56'07.56"N	73°32'20.20"E	851
S195	Kohati Reserve Forest	33°56'19.03"N	73°31'33.44"E	1034
S196	Kohati Reserve Forest	33°56'46.04"N	73°31'43.02"E	976
S197	Phangal Reserve Forest	33°43'12.02"N	73°26'29.07"E	961
S198	Angori Reserve Forest	33°48'58.59"N	73°22'36.17"E	935
S199	Angori Reserve Forest	33°43'26.01"N	73°26'27.08"E	939
S200	Mangal Forest	33°47'05.01"N	73°19'41.09"E	950
S201	Mangal Forest	33°47'07.01"N	73°20'18.05"E	891
S202	Mangal Forest	33°46'49.03"N	73°20'37.02"E	903
S203	Mangal Forest	33°45'50.02"N	73°20'58.08"E	878
S204	Mangal Forest	33°46'30.56"N	73°20'36.53"E	882
S205	Mangal Forest	33°46'37.25"N	73°19'32.13"E	905
S206	Angori	33°47'11.07"N	73°19'22.06"E	952
S207	Nakka	33°48'34.03"N	73°22'06.06"E	951
S208	Nakka	33°49'24.08"N	73°16'52.01"E	839
S209	Salgaran	33°49'25.01"N	73°16'55.01"E	854
S210	Pail	33°49'47.08"N	73°17'01.01"E	826
S211	Trail	33°49'47.21"N	73°17'28.08"E	834
S212	Nandkot Reserve Forest	33°49'47.07"N	73°19'49.09"E	924
S213	Nandkot Reserve Forest	33°49'47.02"N	73°19'36.04"E	971
S214	Nandkot Reserve Forest	33°49'49.03"N	73°19'57.01"E	972
S215	Lehtrar	33°41'05.32"N	73°24'57.59"E	854
S216	Ambani Reserve Forest	33°42'47.07"N	73°21'12.04"E	788
S217	Ambani Reserve Forest	33°43'11.04"N	73°21'05.57"E	788
S218	Simli	33°43'37.03"N	73°21'19.03"E	770
S219	Gianthal	34°00'36.07"N	73°30'43.42"E	665
S220	Gianthal	34°00'11.29"N	73°30'40.32"E	757
S221	Nara	33°30'32.56"N	73°33'45.44"E	640

http://www.aloki.hu ● ISSN 1589 1623 (Print) ● ISSN 1785 0037 (Online)
DOI: http://dx.doi.org/10.15666/aeer/1704_96219650

Sample No.	Locality	Latitude	Longitude	Altitude
S222	Nara	33°30'25.44"N	73°33'50.10"E	622
S223	Nara	33°30'38.49"N	73°33'43.24"E	649
S224	Nara	33°32'22.44"N	73°33'15.01"E	653
S225	Nara	33°32'22.08"N	73°32'58.09"E	634
S226	Nara	33°32'14.50"N	73°33'17.55"E	684
S227	Nara	33°32'21.34"N	73°32'51.56"E	608
S228	Nara	33°32'27.54"N	73°32'32.44"E	640
S229	Gura Reserve Forest	33°35'35.09"N	73°34'53.08"E	650
S230	Gura Reserve Forest	33°35'57.58"N	73°34'47.13"E	701
S231	Karoot	33°35'20.44"N	73°34'28.44"E	635
S232	Nara	33°32'37.42"N	73°32'25.59"E	641
S233	Karot	33°35'41.01"N	73°35'04.01"E	599
S234	Karot	33°35'43.01"N	73°36'22.08"E	514
S235	Karot	33°35'57.09"N	73°35'03.06"E	591
S236	Karot	33°35'43.01"N	73°34'56.04"E	585
S237	Karot	33°30'17.44"N	73°34'14.14"E	573
S238	Karot	33°35'33.03"N	73°35'03.01"E	525
S239	Karot	33°35'36.02"N	73°35'39.01"E	512
S240	Azad Pattan	33°43'46.44"N	73°36'12.32"E	501
S241	Azad Pattan	33°43'41.07"N	73°36'15.08"E	503
S242	Azad Pattan	33°40'21.05"N	73°33'21.05"E	510
S243	Nara	33°32'17.44"N	73°32'46.48"E	582
S244	Karot	33°35'44.48"N	73°35'52.24"E	551
S245	Beor	33°34'57.59"N	73°34'09.27"E	576
S246	Beor	33°29'35.44"N	73°36'07.19"E	500

Table 2. *Comparison of the flora of the project area with the flora of Pakistan*

Plant group	Number of species		Percentage
	National Park (area: 934 km^2)	Pakistan (area: 796095 km^2) (Stewart, 1967)	
Ferns	24	128	18.75
Gymnosperms	4	23	17.39
Monocotyledons	144	1140	12.63
Dicotyledons	452	4492	10.06
Total	624	5783	10.79

Family importance index (FII) and genera importance index (GII)

By using *Equation 1,* the contribution of each family was calculated and according to it, Poaceae was the largest family that shared 80 species (12.82%), followed by Fabaceae (60 spp., 9.62%), Asteraceae (55 spp., 8.81%), Cyperaceae (30 spp., 4.81%) and Lamiaceae (27 spp., 4.33%). Other dominant families with 10 or more species were Rosaceae (19 spp., 3.04%), Apiaceae, Brassicaceae and Euphorbiaceae (12 spp., 1.92% each), Convolvulaceae and Ranunculaceae (11 spp., 1.76% each), Acanthaceae, Amaranthaceae and Polygonaceae (10 spp., 1.60% each); whereas, the remaining families were represented by less than 10 species (*Fig. 2*).

http://www.aloki.hu ● ISSN 1589 1623 (Print) ● ISSN 1785 0037 (Online)
DOI: http://dx.doi.org/10.15666/aeer/1704_96219650

The genera importance index (GII) as calculated through *Equation 2* indicated that the largest genus was *Euphorbia* that contributed 10 species (2.67%), followed by *Carex* (9 spp., 2.4%), *Cyperus* (8 spp., 2.13%), *Eragrostis, Poa, Ficus*, *Medicago*, *Rubus* and *Swertia* (6 spp., 1.6% each), while rest of genera shared less than five plant species (*Fig.* 3).

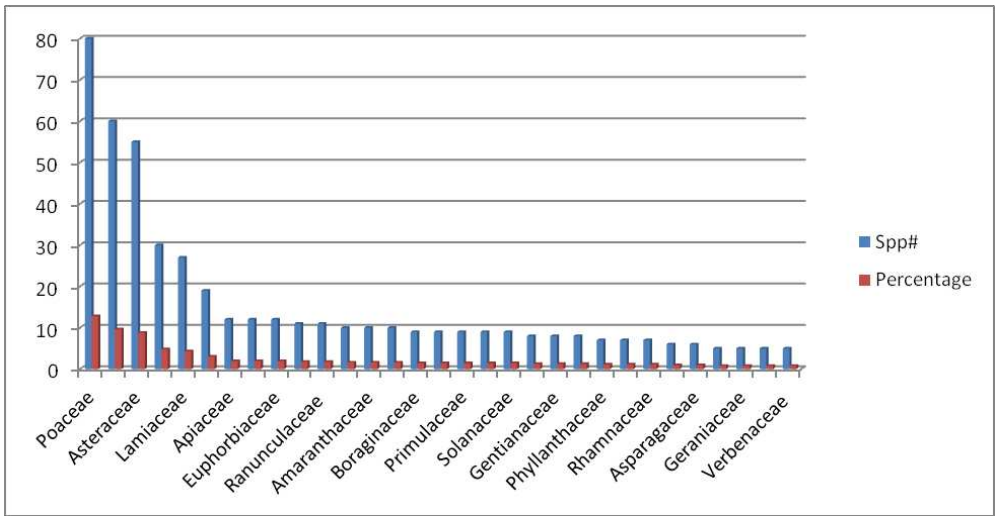

Figure 2. *Family importance index (FII) of the flora of Murree-Kotli Sattian-Kahuta National Park, Pakistan*

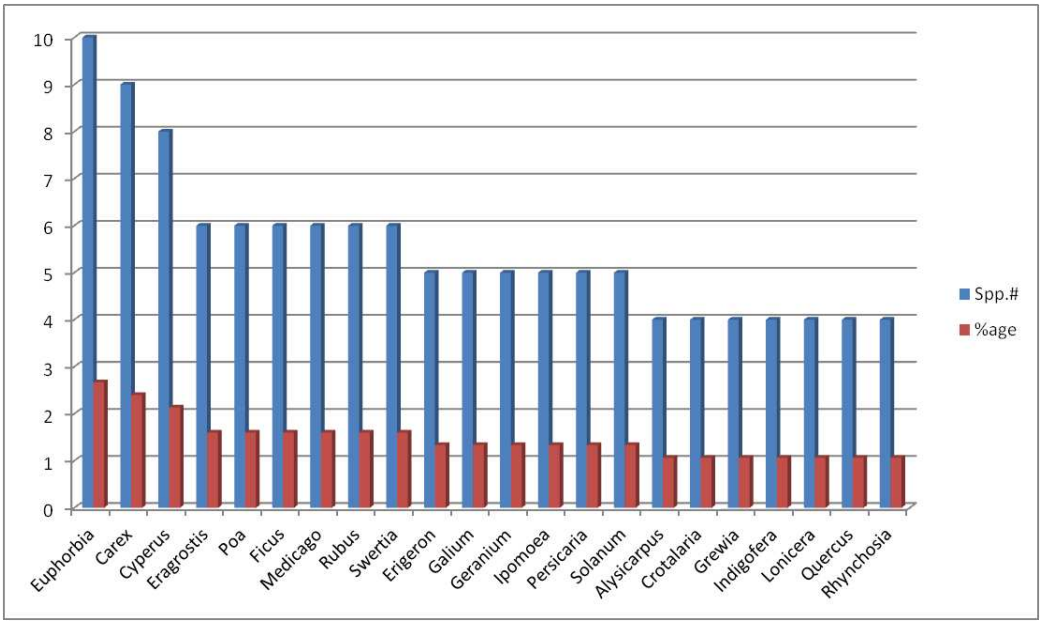

Figure 3. *Genera importance index (GII) of the flora of Murree-Kotli Sattian-Kahuta National Park, Pakistan*

Taxonomic status and diversity

Comparing with related floras, most of the project area was inhabited by native species (528 spp., 84.62%), followed weeds (48 spp., 7.69%), cultivated species

http://www.aloki.hu ● ISSN 1589 1623 (Print) ● ISSN 1785 0037 (Online)
DOI: http://dx.doi.org/10.15666/aeer/1704_96219650

(21spp., 3.37%), naturalized (18 spp., 2.88%), invasive (4 spp., 0.64%), introduced (3 spp., 0.48%), while two species such as *Aristolochia punjabensis* and *Buxus papillosa* were found endemic to Pakistan as shown in *Figure 4*.

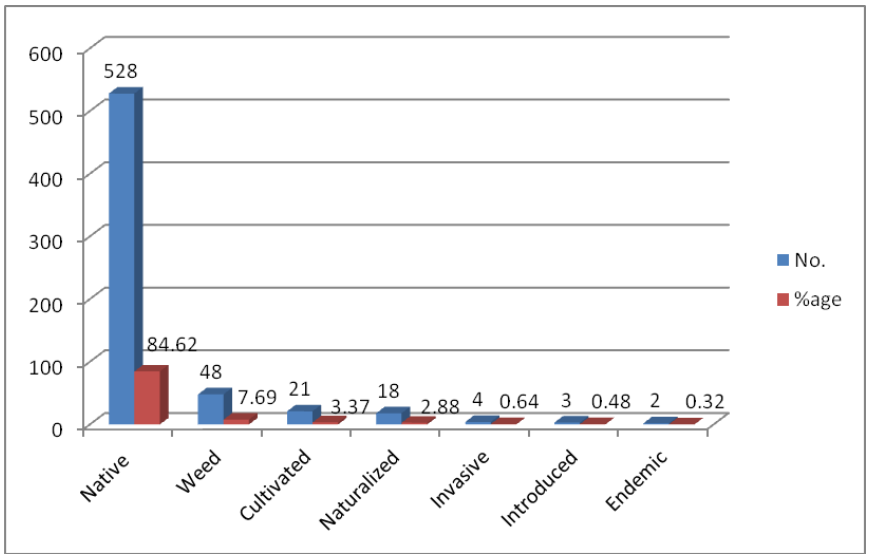

Figure 4. *Status of the flora of Murree-Kotli Sattian-Kahuta National Park*

Diversity index (DI)

The park area is composed of three localities viz., Murree Kotli Sattian and Kahuta. By using *Equation 3,* the pair-wise comparison revealed maximum similarity between Murree and Kotli Sattian sharing maximum species (518) with 89 distinct taxa and 47.94% similarity (*Table 3*). This similarity may be attributed due to their adjacency and similar climatic conditions. Likewise, the other pair viz., Kotli Sattian and Kahuta was also closely situated at the foothills towards southern part and ranked 2nd in terms of sharing species (416 spp.) with 131 distinct species and 46.27%. On the contrary, the 3rd pair comprising Murree and Kahuta was farther from each other and had least similarity in terms of species composition (i.e. 405 spp.). Since, Murree and Kotli Sattian regions are located in northeastern part of park where Himalayan floristic elements are dominant characteristically. On the other hand, The Kahuta is located at low elevation and towards southwest, therefore represented mostly by scrub forest.

Table 3. *Similarity index between pairs of localities from Murree-Kotli Sattian-Kahuta National Park*

Attribute	Murree vs. Kotli Sattian	Murree vs. Kahuta	Kotli Sattian vs. Kahuta
Shared species	518	405	416
Distinct species	89	215	131
Similarity %	47.94	44.14	46.27

Life forms

Eight life forms of the flora were determined from the Murree-Kotli Sattian-Kahuta National Park in which perennial herbs were dominating the area with 241 species

http://www.aloki.hu ● ISSN 1589 1623 (Print) ● ISSN 1785 0037 (Online)
DOI: http://dx.doi.org/10.15666/aeer/1704_96219650

having proportion of 38.62% of the total flora. It was followed by annual herbs (199 species, 31.89%), deciduous shrubs (62 spp., 9.94%), deciduous trees (46 spp., 7.37%), climbers (26 spp., 4.17%), evergreen shrubs and evergreen trees (23 spp., 3.69% each), while parasites were only 4 (*Fig. 5*).

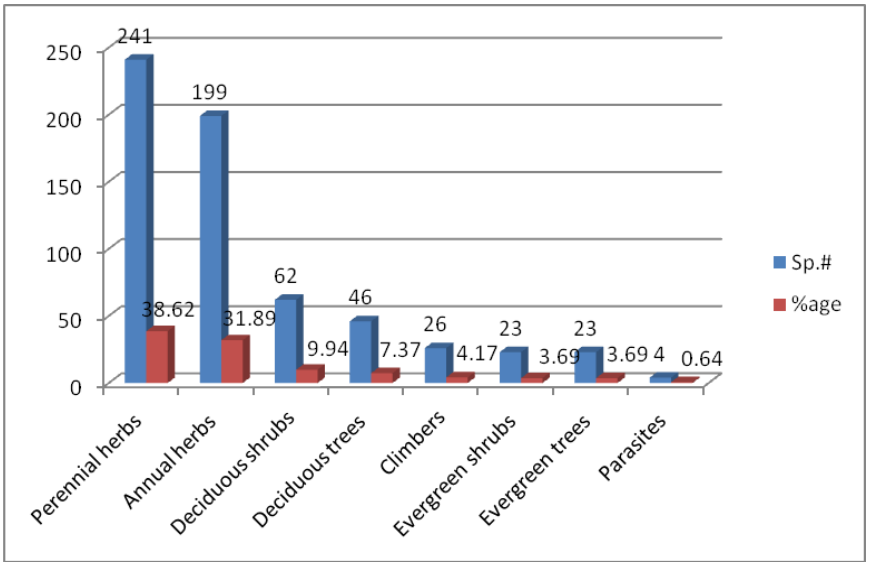

Figure 5. *Life form of the flora of Murree-Kotli Sattian-Kahuta National Park*

Locality-wise diversity

Murree-Kotli Sattian-Kahuta National Park (MKSNP) is located in the lateral spur of Himalayan Mountain in district Rawalpindi and contributed by three Tehsils such as Murree, Kotli Sattian and Kahuta. The detailed inventory is compiled and provided in *Appendix.* Localities-wise species diversity recorded as follows:

1. Murree hills

From the Murree hills, in all 592 vascular plants are documented (*Appendix*). This zone had the highest plant diversity compared to the rest of the localities. Besides, 74 species such as *Abies pindrow, Achillea millefolium, Aconitum laeve, Aegopodium burttii, Agrostis gigantea, Alisma plantago-aquatica, Anaphalis adnata, A. busua, A. margaritacea, Andrachne cordifolia, Anemone tetrasepala, A. vitifolia, Aquilegia pubiflora, Aralia cachemirica, Aristolochia punjabensis, Aster flaccidus, A. himalaicus, Buxus papillosa, Calanthe tricarinata, Carex schlagintweitiana, Carpesium abrotanoides, Cedrus deodara, Cephalanthera longifolia, Cornus macrophulla, C. oblonga, Corydalis murreeana, Daphne papyracea, Dryopteris stewartii, Elaeagnus angustifolia, Eleocharis uniglumis, Epipactis gigantea, E. helleborine, E. persica, Equisetum hyemale, Eryngium caeruleum, Gentiana argentea, G. olivieri, Habenaria furcifera, Heracleum cachemiricum, H. candicans, Hypericum dyeri, Ilex dipyrena, Impatiens bicolor, I. brachycentra, I. edgeworthii, Kyllinga squamulata, Lepidium didymium, Leucanthemum vulgare, Machilus duthiei, Malaxis muscifera, Mimosa himalayana, Myrsine semiserrata, Neolitsea pallens, Oxytropis mollis, Polystichum aculeatum, Primula denticulata, Prunella vulgaris, Quercus dilatata, Reinwardtia indica, Rhododendron arboretum, Sarcococca saligna, Solena amplexicaulis, Spiraea*

http://www.aloki.hu ● ISSN 1589 1623 (Print) ● ISSN 1785 0037 (Online)
DOI: http://dx.doi.org/10.15666/aeer/1704_96219650

canescens, Spiranthes sinensis, Swertia ciliata, S. cordata, S. paniculata, S. tetragona, Trifolium pretense, Tulipa clusiana, Valeriana hardwickii, Viburnum cotinifolium, V. grandiflorum and *V. mullaha* reported as distinct and unique species only recorded from this locality.

2. Kotli Sattian

This is the second most diverse locality containing 533 vascular plants (*Appendix*). Fifteen plant species were found unique to this locality which include *Cheilanthes argentea, Crotalaria prostrata, C. retusa, Eranthemum pulchellum, Hylodesmum podocarpum, Hypodematium crenatum, Pupalia lappacea, Rhynchosia capitata, R. himalensis, Scandix pecten-veneris, Scurrula pulverulenta, Trianthema portulacastrum, Uraria picta, Vincetoxicum canescens* and *V. hirundinaria*.

3. Kahuta

This locality is found mostly in low to medium elevation and found least diverse in terms of the flora. There are only 433 plant species documented from this area (*Appendix*). With reference to unique flora, 17 species are recorded as an indicator species such as *Alysicarpus bupleurifolius, A. monilifer, A. ovalifolius, A. rugosus, Atylosia mollis, A. platycarpa, A. scarabaeoides, Crotalaria calycina, Curculigo orchioides, Dregea volubilis, Hydrilla verticillata, Kydia calycina, Potamogeton perfoliatus, Pueraria tuberosa, Tephrosia strigosa, Veronica anagallis-aquatica* and *Viola pilosa*.

Discussion

The present study investigated the flora of Murree-Kotli Sattian-Kahuta National Park (MKSNP) and documented 624 vascular plants distributed across 361 genera and 106 families (*Appendix*). This work serves as checklist of the species and such kind of research is the main source for the botanical information which may serve as a benchmark for more detailed study (Kent, 2011; Reddy et al., 2011). Besides, it provides baseline for further taxonomic, ecological, ethnobotanical, conservation and forest management projects (Khan et al., 2015). The park area geographically represents only 0.12% of the land area of the country but harbors rich floristic diversity (10.79%) (*Table 3*) which can be attributed to diverse microhabitat variations because of considerable variation in elevation, topographic, edaphic factors and indeed anthropogenic effect had a major influence in controlling the vegetation (Gunatilleke and Gunatilleke, 1985). With reference to the families contribution, Poaceae was recorded as the largest family by contributing 80 species, followed by Fabaceae (60 spp.), Asteraceae (55 spp.), Cyperaceae (30 spp.) and Lamiaceae (27 spp.) as shown in *Figure 3*. Some of the studies such as Qureshi (2008a,b), Qureshi et al. (2011a, b, 2014), Shaheen et al. (2014a), Wariss et al. (2014), Ilyas et al. (2018) and Khan et al. (2018) had reported domination of Poaceae that may be indicator of subtropical forest vegetation and degradation of forest habitats.

Amongst the life forms, the flora was dominated by perennial to annual herbs in the whole project area (*Fig. 4*). This kind of assemblage of herbs is indicating a typical tropical to subtropical plant life in the park area revealing a response to the climate coupled with availability of plentiful moisture in the form of rainfall (Qureshi, 2008b,

http://www.aloki.hu ● ISSN 1589 1623 (Print) ● ISSN 1785 0037 (Online)
DOI: http://dx.doi.org/10.15666/aeer/1704_96219650

2009; Qureshi et al., 2014; Wasim et al., 2019). The inhabitation of herbal coverage from lower to upper elevation has been reported from other temperate regions of Himalaya (Ren et al., 2006; Zhang et al., 2009; Khan, 2012; Ilyas, 2015; Ilyas et al., 2015). With respect to woody vegetation, shrubs were more dominated in the area that is in agreement of other studies from Himalaya regions (Gairola et al., 2010; Qureshi et al., 2011a b, 2014; Chawla et al., 2012).

The flora of this park area is very rapidly deteriorating due to manmade activity. The people of the area are intentionally removing shrubs and providing opportunity for grasses and other herbs to flourish which they collect as winter fodder. Similar trend has been observed from other regions of Himalaya (Consiglio et al., 2006; Irwin and Narasimhan, 2011; Ilyas et al., 2012, 2013, 2015).

The floristic list of the study area might provide a little insight in understanding the ecosystem dynamics, along with physiological and reproductive aspect of vegetation. The floristic list of the study area could be the potential source for ethno-pharmacological studies, because many of the plant species reported in this study are medicinal one (Saqib et al., 2014). The floristic list of the study area could be the potential source for ethno-pharmacological studies (Ilys et al., 2013; Saqib et al., 2014). The park area is comprised on three localities (viz., Murree Kotli Sattian and Kahuta) and their comparison revealed that maximum similarity between Murree and Kotli Sattian is because adjacency and similar climatic condition (*Table 3*). Similarly, the other pair viz., Kotli Sattian and Kahuta was also closely located towards southwest and had similar floristic elements. Contrary, Murree and Kahuta were farther from one another and had variation in climatic conditions that resulted in least similarity in vegetation composition.

Conclusion

This is a comprehensive study not previously reported on the flora of Murree-Kotli Sattian-Kahuta National Park. It reflected the detail of their biology and plant life of the area. The detail of richness, diversity and similarity between various habitat types/localities are also discussed and highlighted. Locality-wise unique, rare and endemic species are highlighted in order to give insight for the rehabilitation and conservation efforts by the park manager for their sustainable use and availability for future generation. Therefore, this study serves as a platform for the detailed floristic and ecological studies to be carried out by the researchers. This study will be helpful for foresters/managers, plant biologist and ecologist for further detailed work. On the other hand, this ecosystem is under continuous and ever increasing human pressure in the form of deforestation, overgrazing and human settlement construction, which resulted in sever degradation the natural vegetation of the study area. Efforts are required to rehabilitate of certain eroded area and protection of key habitat indicator species.

REFERENCES

[1] Ahmed, I. (1964): Vegetation of the salt range. – Pakistan Journal of Forestry 14: 36-62.
[2] Ali, S. I. (2008): Significance of flora with special reference to Pakistan. – Pakistan Journal of Botany 40: 967-971.
[3] Ali, S. I., Nasir, Y. J. (1989-1991): Flora of Pakistan (Fascicle series). – Islamabad, Karachi.

http://www.aloki.hu ● ISSN 1589 1623 (Print) ● ISSN 1785 0037 (Online)
DOI: http://dx.doi.org/10.15666/aeer/1704_96219650

[4] Ali, S. I., Qaiser, M. (1993-1995, 2000-2009): Flora of Pakistan (Fascicle series). – Islamabad, Karachi.
[5] Ali, S. I., Nasir, E., Qaiser, M. (1972-2009): Flora of Pakistan. – Pakistan Agricultural Research Council and the University of California, USA.
[6] Al-Sheikh, A. E. M., Ghanim. A. (2004): Biodiversity of plant communities in the Jal Az-Zor National Park, Kuwait. – Kuwait Journal of Science and Engineering 31: 77-105.
[7] Badshah, L., Hussain, F., Sher, Z. (2016): Floristic inventory, ecological characteristics and biological spectrum of plants of Parachinar, Kurram agency, Pakistan. – Pakistan Journal of Botany 48: 1547-1558.
[8] Barakat, N., El-Gawad, A., Laudadio, V., Kabiel, H., Tufarelli, V., Cazzato, E. (2014): A contribution to the ecology and floristic markers of plant associations in different habitats of Sinai Peninsula, Egypt. – Rendiconti Lincei 25: 479-490.
[9] Batalha, M. A., Martins, F. R. (2004): Floristic, frequency and vegetation life-form spectra of a Cerrado site. – Brazlian Journal of Biology 64: 203-209.
[10] Bhatti, G. R., Qureshi, R., Remon, R. A. (1999): Flora of Rohri Hills. – Ancient Sindh 5: 7-22.
[11] Bhatti, G. R., Muqarrab, S., Qureshi, R. (2001): Floristic study of Arid Zone (Desert Nara Region), Sindh, Pakistan. – Final Technical Report, Pakistan Science Foundation Project No. (45).
[12] Chawla, A., Parkash, O., Sharma, V., Rajkumar, S., Gopichand, B. L., Sing, R. D., Thukral, A. K. (2012): Vascular plants of Kinnuar, Himachal Pradesh, India. – Check List 8: 321-348.
[13] Consiglio, T., Schatz, G. E., Mcpherson, G., Lowry, P. P., Rabenantoandro, J., Rogers, Z. S., Gairola, S., Sharma, C. M., Rana, C. S., Ghildiyal, S. K., Suyal, S. (2010): Phytodiversity (Angiosperms and Gymnosperms) in Mandal-Choptaforest of Garhwal Himalaya, Uttarakhand, India. – Nature and Science 8: 1-17.
[14] Gunatilleke, C., Gunatilleke, I. (1985): Phytosociology of Sinharaja, a contribution to rain forest conservation in Sri Lanka. – Biological Conservation 31: 21-40.
[15] Haq, F. U. (2011): Conservation status of the critically endangered and endangered species in the nandiar khuwar catchment district Battagram, Pakistan. – International Journal of Biodiversity and Conservation 3: 27-35.
[16] Hooker, J. D. (1883-1897): Flora of British India. Vol. I-VII. – Reev and Company, London.
[17] Hussain, K., Shahzad, A., Hussnain, S. Z. (2008): An ethnobotanical survey of important wild medicinal plants of Hattar District Haripur, Pakistan. – Ethnobotany Leaflets 12: 29-35.
[18] Ilyas, M. (2015): Phytosociology and ethnobotanical appraisal of Kabal valley Swat with especial reference to plant biodiversity conservation. – (Unpublished) PhD Thesis, Department of Botany, PMAS Arid Argiculture University Rawalpindi.
[19] Ilyas, M., Shinwari, Z. K., Qureshi, R. (2012): Vegetation composition and threats to the Montane temperate forest ecosystem of Qalagai hills, Swat, Khyber Pakhtunkhwa, Pakistan. – Pakistan Journal of Botany44: 113-122.
[20] Ilyas, M., Qureshi, R., Shinwari, Z. K., Muhammad, A., Mirza, S. N. (2013): Some ethnoecological aspects of the plants of Qalagai hills, Kabal valley, Swat, Pakistan. – International Journal of Agriculture and Biology 15: 801-810.
[21] Ilyas, M., Qureshi, R., Akhtar, N., Munir, M., Haq, Z. (2015): Vegetation analysis of Kabal valley, district Swat, Pakistan using multivariate approach. – Pakistan Journal of Botany 47: 77-86.
[22] Ilyas, M., Qureshi, R., Akhtar, N., Haq, Z. Khan, A. M. (2018): Floristic diversity and vegetation structure of the remnant subtropical broad leaved forests from Kabal Valley, Swat, Pakistan. – Pakistan Journal of Botany 50: 217-230.
[23] Irwin, S. J., Narasimhan, D. (2011): Endemic genera of angiosperms in India: a review. – Rheedea 21: 87-105.

http://www.aloki.hu ● ISSN 1589 1623 (Print) ● ISSN 1785 0037 (Online)
DOI: http://dx.doi.org/10.15666/aeer/1704_96219650

[24] Kent, M. (2011): Vegetation Description and Data Analysis: A Practical Approach. – John Wiley & Sons, Chichester.
[25] Khan, A. M., Qureshi, R., Qaseem, M. F., Munir, M., Ilyas, M., Saqib, Z. (2015): Floristic checklist of district Kotli, Azad Jammu &Kashmir. – Pakistan Journal of Botany 47: 1957-1968.
[26] Khan, A. M., Qureshi, R., Arshad, M., Mirza, S. N. (2018): Climatic and flowering phenological relationships of western Himalayan flora of Muzaffarabad District, Azad Jammu And Kashmir, Pakistan. – Pakistan Journal of Botany 50: 1093-1112.
[27] Khan, A. N., Collins, A. E., Qazi, F. (2011): Causes and extent of environmental impacts of landslide hazard in the Himalayan region: a case study of Murree, Pakistan. – Natural Hazards 57: 413-434.
[28] Khan, S. M., Page, S. H., Ahmad, H., Shaheen, H., Harper, D. M. (2012): Vegetation dynamics in the Western Himalayas, diversity indices and climate change. – Science Technology and Devlopment 31: 232-243.
[29] Khan, S. M., Page, S., Ahmad, H., Ullah, Z., Shaheen, H., Ahmad, M., Harper, D. (2013): Phyto-climatic gradient of vegetation and habitat specificity in the high elevation western Himalayas. – Pakistan Journal of Botany 45: 223-230.
[30] Nakaike T, Malik, S. (1992-1993): Cryptogrammic flora of Pakistan. – National Science Museum, Tokyo.
[31] Nasir, E., Ali, S. I. (1970-1989): Flora of Pakistan. – Pakistan Agricultural Research Council, The University of California, USA.
[32] Nazar, R., Begum, S., Naz, A., Qureshi, A., Memon, R. A., Chaudhry, A. K., Akram, Z. (2008): Weed flora of Pir Mehr Ali Shah Agriculture University Rawalpindi: winter aspect. – Pakistan Journal of Weed Science and Research 14: 55-72.
[33] Nazir, A., Malik, R. N., Shaheen, H. (2014): Floristic composition, life form and leaf spectra of plant communities recorded at Sarsawa hills district Kotli, Azad Kashmir. – African Journal of Soil Sciences 2: 77-78.
[34] Parveen, A. Hussain, M. I. (2007): Plant biodiversity and phytosociological attributes of Gorakh hill. – Pakistan Journal of Botany 38: 691-698.
[35] Qureshi, R. (2008a): Preliminary floristic list of Chotiari Wetland Complex, Nawab Shah, Sindh, Pakistan. – Pakistan Journal of Botany 40: 2281-2288.
[36] Qureshi, R. (2008b): Vegetation assessment of Sawan Wari of Nara desert, Pakistan. – Pakistan Journal of Botany 40: 1885-1896.
[37] Qureshi, R. (2012): The Flora of Nara Desert, Pakistan. – Nova Science Publishers, New York.
[38] Qureshi, R., Bhatti, G. R. (2005): Nara Desert, Pakistan: Part 1: soils, climate and vegetation. – Rangeland 27: 27-31.
[39] Qureshi, R., Bhatti, G. R. (2010): Floristic inventory of Pai Forest, Nawab shah, Sindh, Pakistan. – Pakistan Journal of Botany 42: 2215-2224.
[40] Qureshi, R., Bhatti, G. R., Shabbir, G. (2011a): Floristic inventory of Pir Mehr Ali Shah Arid Agriculture University Research Farm at Koont and its surrounding areas. – Pakistan Journal of Botany 43: 1679-1684.
[41] Qureshi, R., Khan, W. A., Bhatti, G. R., Khan, B., Iqbal, S., Ahmad, M. S., Abid, M. (2011b): First report on the biodiversity of Khunjerab National Park, Pakistan. – Pakistan Journal of Botany 43: 849-861.
[42] Qureshi, R., Shaheen, H., Ilyas, M., Wasim, A., Munir, M. (2014): Phytodiversity and plant life of Khanpur dam, Khyber Pakhtunkhwa. – Pakistan Journal of Botany 46: 841-849.
[43] Reddy, C. S., Babar, S., Amarnath, G., Pattanaik, C. (2011): Structure and floristic composition of tree stand in tropical forest in the Eastern Ghats of northern Andhra Pradesh, India. – Journal of Forestry Research 22: 491-500.

http://www.aloki.hu ● ISSN 1589 1623 (Print) ● ISSN 1785 0037 (Online)
DOI: http://dx.doi.org/10.15666/aeer/1704_96219650

[44] Ren, H. B., Niu, S. K., Zhang, L. Y., Ma., K. P. (2006): Distribution of vascular plant species richness along an elevational gradient in the Dongling mountains, Beijing, China. – Journal of Integrative Plant Biology 48: 153-160.
[45] Saqib, Z., Mahmood, A., Malik, R. N., Mahmood, A., Syed, J. H., Ahmad, T. (2014): Indigenous knowledge of medicinal plants in Kotli Sattian, Rawalpindi district, Pakistan. – Journal of Ethnopharmacol 151: 820-828.
[46] Shaheen, H., Qureshi, R., Akram, A., Gulfraz, M., Potter, D. (2014a): A preliminary floristic checklist of Thal Desert Punjab, Pakistan. – Pakistan Journal of Botany 46: 13-18.
[47] Shaheen, H., Qureshi, R., Zahra, I., Munir, M., Ilyas, M (2014b): Floristic diversity of Santh Saroola, Kotli Sattian, Rawalpindi, Pakistan. – Pakistan Journal of Botany 46: 1945-1954.
[48] Sher, Z., Khan, Z. U. (2007): Floristic composition, life form and leaf spectra of the vegetation of Chagharzai Valley, District Buner. – Pakistan Journal of Plant Science 13: 57-66.
[49] Stewart, R. R. (1967): Checklist of the plants of Swat state, Northwest Pakistan. – Pakistan Journal of Forestery 1: 457-528.
[50] Stewart, R. R. (1972): An Annotated Catalogue to Vascular Plants of West-Pakistan and Kashmir. – In: Nasir E., Ali S. I. (eds.) Flora of West Pakistan. Fakhri, Karachi.
[51] TPL (2013): Onward (continuously updated). The Plant List. Version 1.1. – http//www.theplantlist.org (accessed 10/5/16).
[52] Wariss, H. M., Pirzada, S. A., Alam, K., Anjum, S., Qureshi, R. (2014): Flora of Lal Suhanra National Park, Bahawalpur, Punjab, Pakistan. – Pakistan Journal of Botany 46: 1331-1341.
[53] Wasim, A., Qureshi, R., Arshad, M. (2019): Floristic, frequency and vegetatio-biological spectra of Murree-Kotli Sattian-Kkahuta national park, Pakistan. – Pakistan Journal of Botany 51: DOI: 10.30848/PJB2019-2(20).
[54] Zhang, D. C., Zhang, Y. H., Boufford, D. E., Sun, H. (2009): Elevational patterns of species richness and endemism for some important taxa in the Hengduan Mountains, southwestern China. – Biodiversity and Conservation18: 699-716.

APPENDIX

The floristic checklist of Murree-Kotli Sattian-Kahuta National Park Pakistan

Group/family	Sr#		Habit	Status	Murree	K. Sattian	Kahuta
Pteridophytes							
1. Adiantaceae	1	*Adiantum capillus-veneris* L. (WA-251)	PH	Native	√	√	√
	2	*A. caudatum* L. (WA-95)	PH	Native	√	√	√
	3	*A. incisum* Forssk. (WA-252)	PH	Native	√	√	√
	4	*A. venustum* D. Don. (WA-253)	PH	Native	√	√	√
	5	*Onychium contiguum* Wall. ex C. Hope (WA-96)	PH	Native	√	√	—
2. Aspleniaceae	6	*Asplenium adiantum-nigrum* L. (WA-254)	PH	Native	√	√	—
	7	*A. trichomanes* L. (WA-256)	PH	Native	√	√	√
	8	*A. dalhousiae* Hook. (WA-255)	PH	Native	√	√	—
3. Dennstaedtiaceae	9	*Pteridium aquilinum* (L.) Kuhn (WA-381)	PH	Native	√	√	√
4. Dryopteridaceae	10	*Dryopteris filix-mas* (L.) Schott (WA-382)	PH	Native	√	√	—
	11	*D. ramosa* (C. Hope) C. Chr. (WA-241)	PH	Native	√	√	—
	12	*D. stewartii* Fraser-Jenk. (WA-190)	PH	Native	√	—	—
	13	*Polystichum aculeatum* (L.) Roth ex Mert. (WA-383)	PH	Native	√	—	—
5. Equisetaceae	14	*Equisetum arvense* L. (WA-615)	PH	Native	√	√	√

http://www.aloki.hu ● ISSN 1589 1623 (Print) ● ISSN 1785 0037 (Online)
DOI: http://dx.doi.org/10.15666/aeer/1704_96219650

Group/family	Sr#		Habit	Status	Murree	K. Sattian	Kahuta
	15	*E. hyemale* L. (WA-224)	PH	Native	√	—	—
	16	*E. ramosissimum* (Desf.) (WA-384)	PH	Native	√	√	√
	17	*Hippochaete debilis* (Roxb. ex Vaucher) Ching (WA-385)	PH	Native	√	√	√
6. Pteridaceae	18	*Allantodia squamigera* (Mett.) Ching (WA-586)	PH	Native	√	√	√
	19	*Cheilanthes argentea* (S.G. Gmel.) Kunze (WA-387)	PH	Native	—	√	√
	20	*Cheilanthes farinosa* (Forssk.) Kaulf. (WA-585)	PH	Native	√	√	√
	21	*Coniogramme rosthornii* Hieron. (WA-386)	PH	Native	√	√	—
	22	*Pteris cretica* L. (WA-189)	PH	Native	√	√	√
	23	*P. vittata* L. (WA-257)	PH	Native	√	√	√
7. Hypodematiaceae	24	*Hypodematium crenatum* (Forssk.) Kuhn (WA-591)	PH	Native	—	√	—
Gymnosperms							
8. Pinaceae	25	*Abies pindrow* (Royle ex D.Don) Royle (WA-258)	ET	Native	√	—	—
	26	*Cedrus deodara* (Roxb. ex D. Don) G. Don (WA-172)	ET	Native	√	—	—
	27	*Pinus roxburghii* Sarg. (WA-203)	ET	Native	√	√	√
	28	*P. wallichiana* A.B. Jacks. (WA-99)	ET	Native	√	√	√
Monocotyledons							
9. Alismataceae	29	*Alisma plantago-aquatica* L. (WA-617)	PH	Native	√	—	—
10. Amaryllidaceae	30	*Allium cepa* L. (WA-225)	PH	Cultivated	√	√	√
	31	*A. sativum* L. (WA-100)	AH	Cultivated	√	√	√
11. Araceae	32	*Aralia cachemirica* Decne. (WA-388)	PH	Native	√	—	—
	33	*Arisaema flavum* (Forssk.) Schott (WA-259)	PH	Native	√	√	—
	34	*A. jacquemontii* Blume (WA-97)	PH	Native	√	√	—
	35	*Sauromatum venosum* (Dryand. ex Aiton) Kunth (WA-226)	PH	Native	√	√	√
12. Asparagaceae	36	*Agave americana* L. (WA-227)	PH	Cultivated	√	√	√
	37	*Asparagus adscenden* Roxb. (WA-378)	PH	Native	√	√	—
	38	*A. capitatus* Baker (WA-379)	PH	Native	√	√	√
	39	*A. filicinus* Buch.-Ham. ex D.Don (WA-380)	PH	Native	√	√	√
	40	*A. racemosus* Willd. (WA-98)	PH	Native	√	√	—
	41	*Ophiopogon intermedius* D. Don (WA-377)	PH	Native	√	√	—
13. Commelinaceae	42	*Commelina paludosa* Blume (WA-103)	PH	Native	√	√	√
14. Convallariaceae	43	*Polygonatum verticillatum* (L.) All. (WA-260)	PH	Native	√	√	—
	44	*P. multiflorum* (L.) All. (WA-261)	PH	Native	√	√	—
15. Cyperaceae	45	*Bolboschoenus maritimus* subsp. affinis (Roth) T. Koyama (WA-101)	PH	Native	√	√	√
	46	*Carex canescens* L. (WA-182)	PH	Native	√	√	√
	47	*C. cardiolepis* Nees (WA-262)	PH	Native	√	√	√
	48	*C. cuprina* (Sándor ex Heuff.) Nendtv. ex A.Kern. (WA-609)	PH	Native	√	√	√
	49	*C. fedia* Nees (WA-183)	PH	Native	√	√	—
	50	*C. filicina* Nees (WA-104)	PH	Native	√	√	—
	51	*C. hebecarpa* C.A. Mey. (WA-181)	PH	Native	√	√	—
	52	*C. schlagintweitiana* Boeck. (WA-180)	PH	Native	√	—	—
	53	*C. foliosa* D. Don (WA-263)	PH	Native	√	√	√
	54	*C. psychrophila* Nees (WA-264)	PH	Native	√	√	√
	62	*C. alopecuroides* Rottb. (WA-391)	PH	Native	√	√	√
	55	*Cyperus compressus* L. (WA-102)	AH	Native	√	√	√
	56	*C. difformis* L. (WA-376)	AH	Native	√	√	√
	57	*C. iria* L. (WA-265)	AH	Weed	√	√	—
	58	*C. laevigatus* L. (WA-375)	PH	Native	√	√	—

http://www.aloki.hu ● ISSN 1589 1623 (Print) ● ISSN 1785 0037 (Online)
DOI: http://dx.doi.org/10.15666/aeer/1704_96219650

Group/family	Sr#		Habit	Status	Murree	K. Sattian	Kahuta
	59	*C. niveus* Retz. (WA-389)	PH	Native	√	√	√
	60	*C. rotundus* L. (WA-431)	PH	Weed	√	√	√
	61	*C. squarrosus* L. (WA-390)	AH	Native	√	√	√
	63	*Eleocharis uniglumis* (Link) Schult. (WA-432)	PH	Native	√	—	—
	64	*Eriophorum comosum* (Wall.) Nees (WA-392)	PH	Native	√	√	—
	65	*Fimbristylis dichotoma* (L.) Vahl (WA-266)	PH	Native	√	√	√
	66	*F. rigidula* Nees (WA-267)	PH	Native	√	√	√
	67	*F. schoenoides* (Retz.) Vahl (WA-393)	PH	Native	√	√	√
	68	*F. squarrosa* Vahl (WA-607)	AH	Native	√	√	√
	69	*Kobresia laxa* Nees (WA-599)	PH	Native	√	√	—
	70	*Kobresia sanguinea* (Boott) Raymond (WA-370)	PH	Native	√	√	√
	71	*Kyllinga squamulata* Vahl (WA-371)	PH	Native	√	—	—
	72	*Pycreus pumilus* (L.) Nees (WA-374)	AH	Native	√	√	—
	73	*P. flavidus* (Retz.) T. Koyama (WA-373)	AH	Native	√	√	√
	74	*Schoenoplectus litoralis* (Schrad.) Palla (WA-372)	PH	Native	√	√	—
16. Hypoxidaceae	75	*Curculigo orchioides* Gaertn. (WA-229)	PH	Native	—	—	√
17. Hydrocharitaceae	76	*Hydrilla verticillata* (L.f.) Royle (WA-228)	PH	Native	—	—	√
18. Juncaceae	77	*Juncus articulatus* L. (WA-394)	PH	Native	√	√	—
	78	*J. inflexus* L. (WA-268)	PH	Native	√	√	—
	79	*J. maritimus* Lam. (WA-608)	PH	Native	√	√	—
19. Liliaceae	80	*Tulipa clusiana* DC. (WA-230)	PH	Native	√	—	—
20. Orchidaceae	81	*Calanthe tricarinata* Lindl. (WA-604)	PH	Native	√	—	—
	82	*Cephalanthera longifolia* (L.) Fritsch (WA-395)	PH	Native	√	—	—
	83	*Epipactis gigantea* Douglas ex Hook.	PH	Native	√	—	—
	84	*E. helleborine* (L.) Crantz (WA-270)	PH	Native	√	—	—
	85	*E. persica* (Soó) Hausskn. ex Nannf. (WA-272)	PH	Native	√	—	—
	86	*Habenaria furcifera* Lindl. (WA-587)	PH	Native	√	—	—
	87	*Malaxis muscifera* (Lindl.) Kuntze (WA-588)	PH	Native	√	—	—
	88	*Spiranthes sinensis* (Pers.) Ames (WA-271)	PH	Native	√	—	—
21. Poaceae	89	*Agrostis gigantea* Roth (WA-396)	PH	Native	√	—	—
	90	*A. stolonifera* L. (WA-398)	PH	Native	√	√	√
	91	*Apluda mutica* L. (WA-397)	PH	Native	√	√	√
	92	*Aristida cyanantha* Steud. (WA-231)	PH	Native	√	√	√
	93	*Arthraxon lancifolius* (Trin.) Hochst. (WA-369)	PH	Native	√	√	√
	94	*A. prionodes* (Steud.) Dandy (WA-367)	PH	Native	√	√	√
	95	*Arundinella nepalensis* Trin. (WA-368)	PH	Native	√	√	√
	96	*Arundo donax* L. (WA-453)	PH	Naturalized	√	√	√
	97	*Avena fatua* L. (WA-364)	PH	Weed	√	√	√
	98	*Bothriochloa bladhii* (Retz.) S.T. Blake (WA-365)	PH	Native	√	√	√
	99	*Brachiaria eruciformis* (Sm.) Griseb. (WA-366)	AH	Native	√	√	√
	100	*B. ramosa* (L.) Stapf (WA-597)	AH	Native	√	√	√
	101	*B. reptans* (L.) C.A. Gardner & C.E. Hubb. (WA-200)	AH	Weed	√	√	√
	102	*Bromus hordeaceus* L. (WA-399)	PH	Native	√	√	√
	103	*B. pectinatus* Thunb. (WA-361)	AH	Native	√	√	√
	104	*B. catharticus* Vahl (WA-362)	PH	Naturalized	√	√	√
	105	*B. ramosus* Huds. (WA-363)	PH	Native	√	√	√
	106	*Brachypodium sylvaticum* (Huds.) P. Beauv. (WA-598)	AH	Native	√	√	—
	107	*Capillipedium parviflorum* (R.Br.) Stapf (WA-400)	PH	Native	√	√	—
	108	*Cenchrus ciliaris* L. (WA-133)	PH	Native	√	√	√
	109	*C. pennisetiformis* Steud. (WA-356)	PH	Native	√	√	√
	110	*C. setiger* Vahl (WA-357)	PH	Native	√	√	√

http://www.aloki.hu ● ISSN 1589 1623 (Print) ● ISSN 1785 0037 (Online)
DOI: http://dx.doi.org/10.15666/aeer/1704_96219650

Group/family	Sr#		Habit	Status	Murree	K. Sattian	Kahuta
	111	*Chrysopogon aucheri* (Boiss.) Stapf. (WA-354)	PH	Native	√	√	√
	112	*C. serrulatus* Trin. (WA-355)	PH	Native	√	√	√
	113	*C. gryllus* (L.) Trin. (WA-401)	PH	Native	√	√	√
	114	*Cymbopogon martini* (Roxb.) Will. Watson (WA-433)	PH	Native	√	√	√
	115	*Cynodon dactylon* (Linn.) Pers. (WA-353)	PH	Native	√	√	√
	116	*Dactylis glomerata* L. (WA-434)	PH	Native	√	√	√
	117	*Dactyloctenium aegyptium* (L.) Willd. (WA-402)	PH	Weed	√	√	√
	118	*Desmostachya bipinnata* (L.) Stapf (WA-360)	PH	Native	√	√	√
	119	*Dichanthium annulatum* (Forssk.) Stapf (WA-232)	PH	Native	√	√	√
	120	*D. foveolatum* (Delile) Roberty (WA-107)	PH	Native	√	√	√
	121	*Digitaria sanguinalis* (L.) Scop. (WA-352)	AH	Native	√	√	√
	122	*Echinochloa crus-galli* (L.) P. Beauv.(WA-403)	AH	Weed	√	√	√
	123	*Eragrostis curvula* (Schrad.) Nees (WA-358)	AH	Native	√	√	√
	124	*E. amabilis* (L.) Wight & Arn.(WA-350)	AH	Native	√	√	√
	125	*E. cilianensis* (All.) Janch. (WA-596)	AH	Native	√	√	√
	126	*E. minor* Host. (WA-359)	AH	Native	√	√	√
	127	*E. papposa* (Desf. ex Roem. & Schult.) Steud. (WA-351)	PH	Native	√	√	√
	128	*E. pilosa* (L.) P. Beauv. (WA-105)	AH	Native	√	√	√
	129	*Eulaliopsis binata* (Retz.) C. E. Hubb. (WA-404)	PH	Native	√	√	√
	130	*Festuca gigantea* (L.) Vill. (WA-600)	PH	Native	√	√	√
	131	*Festuca kashmiriana* Stapf (WA-610)	PH	Native	√	√	√
	132	*Heteropogon contortus* (Linn.) P. Beauv. ex Roem. & Schult. (WA-454)	PH	Native	√	√	√
	133	*Imperata cylindrica* (L.) Raeuschel (WA-405)	PH	Native	√	√	√
	134	*Lolium perenne* L. (WA-187)	PH	Native	√	√	√
	135	*L. persicum* Boiss. & Hohen. (WA-108)	AH	Native	√	√	√
	136	*L. temulentum* L. (WA-188)	AH	Weed	√	√	√
	137	*Oplismenus compositus* (L.) P. Beauv. (WA-191)	PH	Native	√	√	√
	138	*Panicum antidotale* Retz (WA-595)	PH	Naturalized	√	√	√
	139	*Paspalidium flavidum* (Retz.) A. Camus (WA-427)	PH	Naturalized	√	√	√
	140	*Paspalum dilatatum* Poir. (WA-457)	PH	Naturalized	√	√	√
	141	*P. distichum* L. (WA-544)	PH	Native	√	√	√
	142	*Pennisetum glaucum* (L.) R. Br. (WA-455)	AH	Cultivated	√	√	√
	143	*P. orientale* Rich. (WA-503)	PH	Native	√	√	√
	144	*Phalaris minor* Retz. (WA-106)	AH	Native	√	√	√
	145	*Piptatherum aequiglume* (Duthie ex Hook. f.) Roshev. (WA-406)	PH	Native	√	√	√
	146	*P. hilariae* Pazij (WA-435)	PH	Native	√	√	√
	147	*P. gracile* Mez (WA-602)	PH	Native	√	√	√
	148	*Poa alpina* L. (WA-273)	PH	Native	√	√	√
	149	*P. annua* L. (WA-274)	AH	Weed	√	√	√
	150	*P. nemoralis* L. (WA-603)	PH	Native	√	√	√
	151	*P. polycolea* Stapf (WA-533)	PH	Native	√	√	√
	152	*P. pratensis* L. (WA-533)	PH	Native	√	√	√
	153	*P. infirma* Kunth (WA-275)	AH	Weed	√	√	√
	154	*Polypogon fugax* Nees ex Steud. (WA-436)	AH	Weed	√	√	√
	155	*P. monspeliensis* (Linn.) Desf. (WA-408)	AH	Weed	√	√	√
	156	*P. viridis* (Gouan) Breistr. (WA-601)	PH	Native	√	√	√
	157	*Rostraria cristata* (L.) Tzvelev (WA-545)	AH	Weed	√	√	√
	158	*Saccharum bengalense* Retz. (WA-409)	PH	Native	√	√	√
	159	*S. ravennae* (L.) L. (WA-411)	PH	Native	√	√	√

http://www.aloki.hu ● ISSN 1589 1623 (Print) ● ISSN 1785 0037 (Online)
DOI: http://dx.doi.org/10.15666/aeer/1704_96219650

Group/family	Sr#		Habit	Status	Murree	K. Sattian	Kahuta
	160	*S. spontaneum* L. (WA-527)	PH	Native	√	√	√
	161	*Setaria pumila* (Poir.) Roem. & Schult. (WA-276)	AH	Weed	√	√	√
	162	*S. verticillata* (L.) P. Beauv. (WA-412)	AH	Invasive	√	√	√
	163	*S. viridis* (L.) P. Beauv. (WA-234)	AH	Weed	√	√	√
	164	*Sorghum bicolo*r (Linn.) Moench. (WA-413)	AH	Cultivated	√	√	√
	165	*S. halepense* (L.) Pers.(WA-235)	PH	Native	√	√	√
	166	*Tetrapogon villosus* Desf. (WA-414)	PH	Native	√	√	√
	167	*Themeda anathera* (Nees ex Steud.) Hack. (WA-201)	PH	Native	√	√	√
	168	Zea mays L. (WA-277)	AH	Cultivated	√	√	√
22. Potamogetonaceae	169	*Potamogeton perfoliatus* L. (WA-592)	PH	Native	—	—	√
23. Smilacaceae	170	*Smilax aspera* L. (WA-111)	C	Native	√	√	—
	171	*S. glaucophylla* Klotzsch (WA-112)	C	Native	√	√	—
24. Xanthorrhoeaceae	172	*Asphodelus tenuifolius* Cav. (WA-543)	AH	Native	√	√	√
Dicotyledons							
25. Acanthaceae	173	*Barleria cristata* L. (WA-236)	DS	Native	√	√	√
	174	*B. acanthoides* Vahl. (WA-109)	DS	Native	√	√	√
	175	*Dicliptera bupleuroides* Nees (WA-415)	PH	Native	√	√	√
	176	*Eranthemum pulchellum* Andrews (WA-605)	ES	Native	—	√	—
	177	*Justicia adhatoda* L. (WA-237)	ES	Native	√	√	√
	178	*J. japonica* Thunb. (WA-349)	ES	Weed	√	√	√
	179	*J. quinqueangularis* K. D. Koenig ex Roxb. (WA-346)	PH	Native	√	√	√
	180	*Strobilanthes dalhousieanus* (Nees) C. B. Clarke (WA-177)	DS	Native	√	√	—
	181	*S. urticifolia* Wall. ex Kuntze (WA-110)	DS	Native	√	√	—
	182	*S. glutinosa* J. Graham (WA-345)	DS	Native	√	√	—
26. Adoxaceae	183	*Viburnum cotinifolium* D. Don (WA-205)	ES	Native	√	—	—
	184	*V. grandiflorum* Wall. ex DC. (WA-278)	ES	Native	√	—	—
	185	*V. mullaha* Buch.-Ham. ex D. Don (WA-344)	ES	Native	√	—	—
27. Aizoaceae	186	*Trianthema portulacastrum* L. (WA-343)	AH	Weed	—	√	√
28. Amaranthaceae	187	*Achyranthes aspera* L. (WA-114)	PH	Weed	√	√	√
	188	*A. bidentata* Blume (WA-238)	PH	Weed	√	√	√
	189	*Aerva javanica* (Burm. f.) Juss. ex Schult. (WA-115)	PH	Native	√	√	√
	190	*Alternanthera pungens* Kunth (WA-341)	PH	Naturalized	√	√	√
	191	*Amaranthus spinosus* L. (WA-340)	AH	Native	√	√	√
	192	*A. viridis* L. (WA-437)	AH	Native	√	√	√
	193	*Chenopodium album* L. (WA-314)	AH	Native	√	√	√
	194	*Digera muricata* (L.) Mart. (WA-342)	AH	Weed	√	√	√
	195	*Dysphania ambrosioides* (L.) Mosyakin & Clemants (WA-546)	AH	Naturalized	√	√	—
	196	*Pupalia lappacea* (L.) Juss. (WA-542)	PH	Weed	—	√	√
29. Anacardiaceae	197	*Cotinus coggygria* Scop. (WA-279)	DS	Native	√	√	—
	198	*Lannea coromandelica* (Houtt.) Merr. (WA-339)	DS	Native	√	√	√
	199	*Pistacia chinensis* Bunge (WA-239)	DT	Native	√	√	√
	200	*Pistacia integerrima* J. L. Stewart ex Brandis (WA-240)	DT	Native	√	√	√
30. Apiaceae	201	*Aegopodium burttii* Nasir (WA-416)	PH	Native	√	—	—
	202	*Bupleurum marginatum* Wall. ex DC. (WA-418)	PH	Native	√	√	√
	203	*Carissa opaca* Stapf ex. Haines (WA-199)	ES	Native	√	√	√
	204	*Centella asiatica* (L.) Urb. (WA-336)	PH	Native	√	√	—
	205	*Coriandrum sativum* L. (WA-505)	AH	Cultivated	√	√	√
	206	*Eryngium caeruleum* M. Bieb. (WA-299)	AH	Native	√	—	—

http://www.aloki.hu ● ISSN 1589 1623 (Print) ● ISSN 1785 0037 (Online)
DOI: http://dx.doi.org/10.15666/aeer/1704_96219650

Group/family	Sr#		Habit	Status	Murree	K. Sattian	Kahuta
	207	*Foeniculum vulgare* Miller. (WA-337)	PH	Cultivated	√	√	√
	208	*Heracleum. cachemiricum* C. B. Clarke (WA-338)	PH	Native	√	—	—
	209	*Heracleum candicans* Wall. ex DC. (WA-280)	PH	Native	√	—	—
	210	*Psammogeton biternatum* Edgew. (WA-547)	PH	Native	√	√	√
	211	*Scandix pecten-veneris* L. (WA-223)	AH	Weed	—	√	√
	212	*Torilis japonica* (Houtt.) DC. (WA-623)	AH	Weed	√	√	—
31. Apocynaceae	213	*Dregea volubilis* (L. f.) Benth. ex Hook. f. (WA-119)	C	Native	—	—	√
	214	*Nerium oleander* L. (WA-335)	ES	Native	√	√	√
	215	*Tylophora hirsuta* Wight (WA-594)	C	Native	√	√	√
32. Aquifoliaceae	216	*Ilex dipyrena* Wall. (WA-117)	ET	Native	√	—	—
33. Araliaceae	217	*Hedera nepallensis* K. Koch (WA-116)	C	Native	√	√	√
34. Aristolochiaceae	218	*Aristolochia punjabensis* Lace (WA-532)	C	Native	√	—	—
35. Asclepiadaceae	219	*Calotropis procera* (Aiton) Dryand. (WA-333)	ES	Native	√	√	√
	220	*Periploca aphylla* Decne. (WA-334)	ES	Native	√	√	√
	221	*Vincetoxicum canescens* (Willd.) Decne. (WA-118)	PH	Native	—	√	√
	222	*V. hirundinaria* Medik. (WA-565)	PH	Native	—	√	√
36. Asteraceae	223	*Achillea millefolium* L. (WA-523)	PH	Native	√	—	—
	224	*Adenostemma lavenia* (L.) Kuntze (WA-573)	AH	Native	√	√	√
	225	*Ageratum conyzoides* (L.) L. (WA-550)	AH	Native	√	√	√
	226	*Ainsliaea latifolia* (D. Don) Sch. Bip. (WA-548)	PH	Native	√	√	—
	227	*Anaphalis adnata* DC. (WA-120)	AH	Native	√	—	—
	228	*A. busua* (Buch.-Ham.) DC. (WA-570)	AH	Native	√	—	—
	229	*A. margaritacea* (L.) Benth. & Hook. f. (WA-281)	AH	Native	√	—	—
	230	*Artemisia dubia* Wall. ex Besser (WA-529)	AH	Native	√	√	—
	231	*A. scoparia* Waldst. & Kitam. (WA-551)	DS	Native	√	√	√
	232	*A. vulgaris* L. (WA-552)	PH	Native	√	√	√
	233	*Aster flaccidus* Bunge (WA-124)	PH	Native	√	—	—
	234	*A. aitchisonii* Boiss. (WA-282)	PH	Native	√	√	√
	235	*A. himalaicus* C. B. Clarke (WA-549)	PH	Native	√	—	—
	236	*Bidens biternata* (Lour.) Merr. & Sherff (WA-298)	AH	Native	√	√	√
	237	*Calendula officinalis* L. (WA-553)	AH	Native	√	√	—
	238	*Carpesium abrotanoides* L. (WA-530)	AH	Native	√	—	—
	239	*C. cernuum* L.(WA-572)	AH	Weed	√	√	√
	240	*Carthamus oxycantha* M. Bieb (WA-554)	AH	Weed	√	√	√
	241	*Cichorium intybus* L. (WA-614)	PH	Weed	√	√	√
	242	*Cirsium arvense* (L.) Scope. (WA-555)	PH	Native	√	√	√
	243	*Conium maculatum* L. (WA-606)	PH	Native	√	√	√
	244	*Conyza canadensis* (L.) Cronq. (WA-122)	AH	Native	√	√	√
	245	*Cousinia thomsonii* C. B. Clarke (WA-283)	PH	Native	√	√	—
	246	*Crepis multicaulis* Ledeb. (WA-534)	PH	Native	√	√	—
	247	*Eclipta prostrata* (L.) L. (WA-439)	AH	Native	√	√	√
	248	*Erigeron canadensis* L. (WA-556)	AH	Native	√	√	√
	249	*E. multiradiatus* (Lindl. ex DC.) Benth. ex C. B. Clarke (WA-536)	PH	Native	√	√	√
	250	*E. aegyptiacus* L. (WA-123)	AH	Native	√	√	√
	251	*E. bonariensis* L. (WA-440)	AH	Native	√	√	√
	252	*E. trilobus* (Decne.) Boiss. (WA-125)	AH	Native	√	√	√
	253	*Gerbera gossypina* (Royle) Beauverd (WA-284)	PH	Native	√	√	—
	254	*Inula cappa* (Buch.-Ham. ex D. Don) DC. (WA-575)	DS	Native	√	√	—
	255	*Lactuca serriola* L. (WA-577)	AH	Native	√	√	√

http://www.aloki.hu ● ISSN 1589 1623 (Print) ● ISSN 1785 0037 (Online)
DOI: http://dx.doi.org/10.15666/aeer/1704_96219650

Group/family	Sr#		Habit	Status	Murree	K. Sattian	Kahuta
	256	*L. brunoniana* (DC.) Wall. ex C.B. Clarke (WA-178)	AH	Native	√	√	√
	257	*L. dissecta* D. Don (WA-285)	PH	Native	√	√	√
	258	*L. secunda* (C. B. Clarke) Hook. f. (WA-426)	PH	Native	√	√	—
	259	*Launaea procumbens* (Roxb.) Ram. & Rajgo. (WA-574)	PH	Native	√	√	√
	260	*Leucanthemum vulgare* (Vaill.) Lam (WA-580)	PH	Native	√	—	—
	261	*Myriactis nepalensis* Less. (WA-287)	PH	Native	√	√	√
	262	*M. wightii* DC. (WA-286)	AH	Native	√	√	√
	263	*Parthenium hysterophorus* L. (WA-537)	AH	Invasive	√	√	√
	264	*Saussurea heteromalla* (D. Don) Hand.-Mazz. (WA-441)	AH	Invasive	√	√	√
	265	*S. atkinsonii* C. B. Clarke (WA-417)	AH	Native	√	√	√
	266	*Senecio nudicaulis* Buch.-Ham. ex D. Don (WA-578)	AH	Native	√	√	—
	267	*Siegesbeckia orientalis* L. (WA-442)	AH	Native	√	√	—
	268	*Silybum marianum* (L.) Gaertin (WA-443)	PH	Native	√	√	√
	269	*Sonchus arvensis* L. (WA-526)	AH	Native	√	√	√
	270	*S. asper* (L.) Hill (WA-571)	AH	Native	√	√	√
	271	*S. oleraceus* L. (WA-569)	AH	Native	√	√	√
	272	*Tagetes minuta* L. (WA-425)	AH	Invasive	√	√	√
	273	*Taraxacum campylodes* G. E. Haglund	PH	Native	√	√	√
	274	*T. wallichii* DC. (WA-70)	PH	Native	√	√	√
	275	*Tridax procumbens* (L.) L. (WA-242)	PH	Native	√	√	√
	276	*Xanthium strumarium* L. (WA-581)	AH	Native	√	√	√
	277	*Youngia japonica* (L.) DC. (WA-583)	AH	Native	√	√	√
37. Balsaminaceae	278	*Impatiens* bicolor Royle (WA-290)	AH	Native	√	—	—
	279	*I. brachycentra* Kar. & Kir (WA-288)	AH	Native	√	—	—
	280	*I. edgeworthii* Hook. f. (WA-289)	AH	Native	√	—	—
	281	*Sinopodophyllum hexandrum* (Royle) T.S. Ying (WA-144)	PH	Native	√	√	—
38. Berberidaceae	282	*Berberis lycium* Royle. (WA-174)	DS	Native	√	√	√
	283	*B. parkeriana* C. K. Schneid. (WA-291)	DS	Native	√	√	—
39. Boraginaceae	284	*Buglossoides tenuiflora* (L. f.) I. M. Johnst. (WA-291)	AH	Native	√	√	√
	285	*Cynoglossum glochidiatum* Wall. ex Benth. (WA-444)	AH	Native	√	√	√
	286	*C. lanceolatum* Forssk. (WA-445)	AH	Native	√	√	√
	287	*Ehretia acuminata* R. Br. (WA-563)	DT	Native	√	√	√
	288	*E. obtusifolia* Hochst. ex A. DC. (WA-528)	DS	Native	√	√	√
	289	*Heliotropium strigosum* Willd. (WA-566)	AH	Native	√	√	√
	290	*H. crispum* Desf. (WA-447)	AH	Native	√	√	√
	291	*H. europaeum* L. (WA-524)	AH	Native	√	√	√
	292	*Trichodesma indicum* (L.) Lehm. (WA-446)	PH	Native	√	√	√
40. Brassicaceae	293	*Alliaria petiolata* (M.Bieb.) Cavara & Grande (WA-510)	AH	Native	√	√	√
	294	*Arabis amplexicaulis* Edgew. (WA-557)	PH	Native	√	√	√
	295	*A. nova* Vill. (WA-616)	AH	Native	√	√	√
	296	*Brassica napus* L. (WA-522)	AH	Cultivated	√	√	√
	297	*Capsella bursa-pastoris* (L.) Medik (WA-576)	AH	Weed	√	√	√
	298	*Cardamine impatiens* L. (WA-562)	AH	Weed	√	√	√
	299	*Crucihimalaya himalaica* (Edgew.) Al-Shehbaz, O'Kane & R. A. Price (WA-521)	AH	Native	√	√	√
	300	*Lepidium sativum* L. (WA-448)	AH	Cultivated	√	√	√
	301	*L. didymum* L. (WA-558)	AH	Native	√	—	—

http://www.aloki.hu ● ISSN 1589 1623 (Print) ● ISSN 1785 0037 (Online)
DOI: http://dx.doi.org/10.15666/aeer/1704_96219650

Group/family	Sr#		Habit	Status	Murree	K. Sattian	Kahuta
	302	*Nasturtium officinale* R. Br. (WA-559)	PH	Native	√	√	√
	303	*Raphanus sativus* L. (WA-568)	AH	Cultivated	√	√	√
	304	*Sisymbrium irio* L. (WA-449)	AH	Native	√	√	√
41. Buxaceae	305	*Buxus papillosa* C.K. Schneid. (WA-564)	ES	Endemic to the Pakistan	√	—	—
	306	*Sarcococca saligna* (D. Don) Muell.-Arg. (WA-292)	ES	Native	√	—	—
42. Cactaceae	307	*Opuntia monacantha* (Willd.) Haw. (WA-561)	ES	Native	√	√	√
43. Campanulaceae	308	*Campanula pallida* Wall (WA-438)	AH	Native	√	√	√
44. Cannabaceae	309	*Cannabis sativa* L. (WA-331)	AH	Native	√	√	√
45. Caprifoliaceae	310	*Lonicera hispida* Pall. ex Schult. (WA-612)	ES	Native	√	√	—
	311	*L. myrtillus* Hook. f. & Thomson (WA-560)	ES	Native	√	√	—
	312	*L. quinquelocularis* Hard. (WA-206)	DS	Native	√	√	—
	313	*L. webbiana* Wall. ex DC. (WA-520)	DS	Native	√	√	—
46. Caryophyllaceae	314	*Cerastium glomeratum* Thuill. (WA-567)	AH	Native	√	√	√
	315	*Silene conoidea* L. (WA-525)	AH	Weed	√	√	√
	316	*Stellaria media* (L.) Vill. (WA-579)	PH	Weed	√	√	√
	317	*Vaccaria hispanica* (Mill.) Rauschert (WA-471)	AH	Native	√	√	√
47. Celastraceae	318	*Cassine glauca* (Rottb.) Kuntze (WA-519)	DT	Native	√	√	√
	319	*Euonymus fimbriatus* Wall. (WA-10)	DT	Native	√	√	√
	320	*E. hamiltonianus* Wall. (WA-330)	DS	Native	√	√	√
	321	*Maytenus royleanus* (Wall. ex Lawson) Cufodontis (WA-329)	ES	Native	√	√	√
48. Convolvulaceae	322	*Convolvulus arvensis* L. (WA-500)	C	Native	√	√	√
	323	*C. prostratus* Forssk. (WA-499)	C	Native	√	√	√
	324	*Cuscuta. reflexa* Roxb. (WA-94)	P	Native	√	√	√
	325	*C. gigantea* Griff. (WA-328)	P	Native	√	√	—
	326	*Evolvulus alsinoides* (L.) L. (WA-327)	AH	Native	√	√	√
	327	*Ipomoea carnea* Jacq. (WA-293)	C	Native	√	√	√
	328	*I. eriocarpa* R. Br. (WA-496)	C	Native	√	√	√
	329	*I. hederacea* (L.) Jacq. (WA-497)	C	Native	√	√	√
	330	*I. nil* (L.) Roth (WA-294)	C	Naturalized	√	√	√
	331	*I. purpurea* (L.) Roth (WA-517)	C	Native	√	√	√
49. Cornaceae	332	*Cornus macrophulla* Wall. (WA-295)	ET	Native	√	—	—
	333	*Cornus oblonga* Wall (WA-265)		Native	√	—	—
50. Cucurbitaceae	334	*Solena amplexicaulis* (Lam.) Gandhi (WA-296)	C	Native	√	—	—
51. Dioscoreaceae	335	*Dioscorea belophylla* (Prain) Voigt ex Haines (WA-494)	C	Native	√	√	—
	336	*D. bulbifera* L. (WA-518)	C	Native	√	√	—
	337	*D. deltoidea* Wall. ex Griseb. (WA-495)	C	Native	√	√	√
52. Ebenaceae	338	*Diospyros lotus* L. (WA-493)	ET	Cultivated	√	√	—
53. Elaeagnaceae	339	*Elaeagnus angustifolia* L. (WA-489)	ET	Native	√	—	—
54. Ericaceae	340	*Rhododendron arboreum* Sm. (WA-490)	ET	Native	√	—	—
55. Euphorbiaceae	341	*Euphorbia clarkeana* Hook. f. (WA-492)	AH	Native	√	√	√
	342	*E. granulata* Forssk. (WA-540)	AH	Weed	√	√	√
	343	*E. helioscopia* L. (WA-491)	AH	Weed	√	√	√
	344	*E. heterophylla* L. (WA-620)	AH	Native	√	√	—
	345	*E. hirta* L. (WA-515)	AH	Native	√	√	√
	346	*E. indica* Lam. (WA-539)	AH	Native	√	√	√
	347	*E. prolifera* Buch.-Ham. ex D. Don (WA-621)	AH	Native	√	√	√
	348	*E. prostrata* Aiton (WA-516)	AH	Weed	√	√	√
	349	*E. royleana* Boiss (WA-618)	AH	Native	√	√	√
	350	*E. wallichii* Hook. f. (WA-619)	AH	Native	√	√	√

http://www.aloki.hu ● ISSN 1589 1623 (Print) ● ISSN 1785 0037 (Online)
DOI: http://dx.doi.org/10.15666/aeer/1704_96219650

Group/family	Sr#		Habit	Status	Murree	K. Sattian	Kahuta
	351	*Mallotus philippensis* (Lam.) Müll. Arg. (WA-210)	DS	Native	√	√	√
	352	*Ricinus communis* L. (WA-211)	ES	Native	√	√	√
56. Fabaceae	353	*Acacia catechu* (Linn. f.) Willd (WA-501)	DS	Native	√	√	√
	354	*A. modesta* Wall. (WA-197)	DS	Native	√	√	√
	355	*A. nilotica* (L.) Delile (WA-196)	DS	Native	√	√	√
	356	*Albizzia lebbeck* Benth.	DS	Native	√	√	√
	357	*Alysicarpus bupleurifolius* (L.) DC.	AH	Native	—	—	√
	358	*A. rugosus* (Willd.) DC. (WA-93)	AH	Native	—	—	√
	359	*A. monilifer* (L.) DC. (WA-218)	AH	Native	—	—	√
	360	*A. ovalifolius* (Schum.) Leonard (WA-511)	AH	Native	—	—	√
	361	*Argyrolobium roseum* (Cambess.) Jaub. & Spach (WA-512)	AH	Native	√	√	√
	362	*Astragalus leucocephalus* Bunge (WA-92)	PH	Native	√	√	—
	363	*Atylosia mollis* "Benth., p.p.A" (WA-250)	AH	Native	—	—	√
	364	*A. platycarpa* Benth. (WA-249)	AH	Native	—	—	√
	365	*A. scarabaeoides* (L.) Benth. (WA-217)	AH	Native	—	—	√
	366	*Bauhinia variegata* L. (WA-243)	DT	Native	√	√	√
	367	*Butea monosperma* (Lam.) Taub. (WA-514)	DT	Native	√	√	√
	368	*Cassia fistula* L. (WA-216)	DT	Native	√	√	√
	369	*Crotalaria prostrata* Willd. (WA-91)	PH	Native	—	√	√
	370	*C. retusa* L. (WA-213)	PH	Native	—	√	√
	371	*C. calycina* Schrank (WA-214)	PH	Native	—	—	√
	372	*C. medicaginea* Lam. (WA-215)	PH	Native	√	√	√
	373	*Dalbergia sissoo* DC. (WA-209)	DT	Cultivated	√	√	√
	374	*Desmodium elegans* DC (WA-89)	DS	Native	√	√	—
	375	*D. gangeticum* (L.) DC. (WA-297)	DS	Native	√	√	—
	376	*D. laxiflorum* DC. (WA-508)	DS	Native	√	√	—
	377	*Hylodesmum podocarpum* (DC.) H. Ohashi & R. R. Mill (WA-57)	DS	Native	—	√	—
	379	*Indegofera cordifolia* Roth (WA-219)	AH	Native	√	√	√
	380	*I. hebepetala* Baker (WA-509)	AH	Native	√	√	√
	381	*I. heterantha* Brandis (WA-506)	DS	Native	√	√	—
	378	*Indigofera linifolia* (L. f.) Retz. (WA-538)	AH	Native	√	√	√
	382	*Lathyrus aphaca* L. (WA-507)	AH	Weed	√	√	√
	383	*Lathyrus sphaericus* Retz. (WA-590)	AH	Native	√	√	√
	384	*Lespedeza juncea* (L. f.) Pers. (WA-87)	PH	Native	√	√	√
	385	*Leucaena leucocephala* (Lam.) de Wit	ET	Cultivated	√	√	√
	386	*Lotus corniculatus* L. (WA-504)	PH	Native	√	√	√
	387	*Medicago edgeworthii* Sirj. (WA-221)	AH	Native	√	√	√
	388	*M. lupulina* L. (WA-2)	AH	Native	√	√	√
	389	*M. laciniata* (L.) Mill. (WA-483)	AH	Native	√	√	√
	390	*M. orbicularis* (L.) Bartal. (WA-220)	AH	Native	√	√	√
	391	*M. polymorpha* L. (WA-481)	AH	Weed	√	√	√
	392	*M. sativa* L. (WA-482)	AH	Native	√	√	√
	393	*Melilotus indicus* (L.) All. (WA-88)	AH	Native	√	√	√
	394	*Mimosa himalayana* Gamble (WA-488)	DT	Native	√	—	—
	395	*Oxytropis mollis* Benth. (WA-313)	PH	Native	√	—	—
	396	*Pongamia pinnata* (L.) Pierre (WA-502)	ET	Native	√	√	√
	397	*Pueraria tuberosa* (Willd.) DC. (WA-479)	C	Native	—	—	√
	398	*Rhynchosia capitata* (Roth) DC. (WA-476)	C	Native	—	√	√
	399	*R. himalensis* Baker (WA-477)	C	Native	—	√	√
	400	*R. minima* (L.) DC (WA-480)	PH	Native	√	√	√
	401	*R. pseudo-cajan* Cambess (WA-486)	DS	Native	√	√	√

http://www.aloki.hu ● ISSN 1589 1623 (Print) ● ISSN 1785 0037 (Online)
DOI: http://dx.doi.org/10.15666/aeer/1704_96219650

Group/family	Sr#		Habit	Status	Murree	K. Sattian	Kahuta
	402	*Robinia pseudoacacia* L. (WA-3)	DT	Naturalized	√	√	—
	403	*Taverniera cuneifolia* (Roth) Ali (WA-487)	DT	Native	√	√	√
	404	*Tephrosia strigosa* (Dalzell) Santapau & Maheshw. (WA-584)	AH	Native	—	—	√
	405	*Trifolium dubium* Sibth. (WA-301)	PH	Introduced	√	√	—
	406	*T. repens* L. (WA-300)	PH	Native	√	√	—
	407	*T. pratense* L. (WA-478)	PH	Native	√	—	—
	408	*Trigonella emodi* Benth. (WA-171)	AH	Native	√	√	√
	409	*T. gracilis* Benth. (WA-170)	AH	Native	√	√	√
	410	*Uraria picta* (Jacq.) DC. (WA-611)	AH	Native	—	√	√
	411	*Vicia sativa* L. (WA-128)	AH	Weed	√	√	√
	412	*V. monantha* Retz. (WA-129)	AH	Native	√	√	√
57. Fagaceae	413	*Quercus dilatata* Royle (WA-126)	ET	Native	√	—	—
	414	*Q. glauca* Thunb. (WA-173)	ET	Native	√	√	—
	415	*Q. incana* Bartram (WA-86)	ET	Native	√	√	—
58. Gentianaceae	416	*Gentiana argentea* (Royle ex D. Don) Royle ex D. Don (WA-83)	AH	Native	√	—	—
	417	*G. olivieri* Griseb. (WA-302)	PH	Native	√	—	—
	418	*Swertia alata* C. B. Clarke (WA-4)	AH	Native	√	√	—
	419	*S. angustifolia* Buch.-Ham. ex D. Don (WA-131)	AH	Native	√	√	—
	420	*S. ciliata* (D. Don ex G. Don) B. L. Burtt (WA-85)	AH	Native	√	—	—
	421	*S. cordata* (Wall. ex G. Don) C. B. Clarke (WA-132)	AH	Native	√	—	—
	422	*S. paniculata* Wall. (WA-84)	AH	Native	√	—	—
	423	*S. tetragona* R.H. Miao (WA-130)	AH	Native	√	—	—
59. Geraniaceae	424	*Geranium lucidum* L. (WA-1)	AH	Native	√	√	—
	425	*G. mascatense* Boiss. (WA-138)	AH	Native	√	√	—
	426	*G. nepalense* Sweet (WA-303)	AH	Native	√	√	—
	427	*G. rotundifolium* L. (WA-137)	AH	Native	√	√	√
	428	*G. wallichianum* D. Don ex Sweet (WA-136)	AH	Native	√	√	√
60. Grossulariaceae	429	*Ribes alpestre* Wall. ex Decne. (WA-589)	DS	Native	√	√	—
61. Hamamelidaceae	430	*Parrotiopsis jacquemontiana* (Decne.) Rehder (WA-5)	DS	Native	√	√	—
62. Hypericaceae	431	*Hypericum dyeri* Rehder (WA-347)	DS	Native	√	—	—
	432	*H. oblongifolium* Choisy (WA-135)	DS	Native	√	√	—
	433	*H. perforatum* L. (WA-134)	PH	Native	√	√	—
63. Juglandaceae	434	*Juglans regia* L. (WA-169)	ET	Naturalized	√	√	—
64. Lamiaceae	435	*Ajuga bracteosa* Wall. ex Benth. (WA-165)	PH	Native	√	√	√
	436	*A. parviflora* Benth. (WA-166)	AH	Native	√	√	√
	437	*Anisomeles indica* (L.) Kuntze (WA-222)	PH	Native	√	√	√
	438	*Callicarpa macrophylla* Vahl (WA-32)	DS	Native	√	√	—
	439	*Clinopodium umbrosum* (M. Bieb.) Kuntze (WA-474)	PH	Native	√	√	√
	440	*Colebrookea oppositifolia* Sm. (WA-49)	DS	Native	√	√	√
	441	*Isodon coetsa* (Buch.-Ham. ex D. Don) Kudô (WA-473)	PH	Native	√	√	√
	442	*I. lophanthoides* (Buch.-Ham. ex D. Don) H. Hara (WA-475)	AH	Native	√	√	√
	443	*I. rugosus* (Wall. ex Benth.) Codd (WA-304)	DS	Native	√	√	√
	444	*Lamium album* L. (WA-168)	PH	Native	√	√	√
	445	*L. cephalotes* (Roth) Spreng. (WA-246)	AH	Native	√	√	√
	446	*Leucas lanata* Baker (WA-167)	PH	Native	√	√	√
	447	*L. decemdentata* (Willd.) Sm (WA-245)	PH	Native	√	√	√
	448	*L. nutans* (Roth) Spreng. (WA-50)	PH	Native	√	√	√

http://www.aloki.hu ● ISSN 1589 1623 (Print) ● ISSN 1785 0037 (Online)
DOI: http://dx.doi.org/10.15666/aeer/1704_96219650

Group/family	Sr#		Habit	Status	Murree	K. Sattian	Kahuta
	449	*Mentha longifolia* (L.) L. (WA-44)	PH	Native	√	√	√
	450	*M. royleana* Wall. ex Bth. (WA-43)	PH	Native	√	√	√
	451	*Micromeria biflora* (Buch.-Ham. ex D. Don) Benth. (WA-244)	PH	Native	√	√	√
	452	*Origanum vulgare* L. (WA-305)	PH	Native	√	√	—
	453	*Phlomoides spectabilis* (Falc. ex Benth.) Kamelin & Makhm. (WA-624)		Native	√	√	—
	454	*Prunella vulgaris* L (WA-6)	PH	Native	√	—	—
	455	*Pseudocaryopteris bicolor* (Roxb. ex Hardw.) P.D. Cantino (WA-531)	DS	Native	√	√	—
	456	*Pseudocaryopteris foetida* (D. Don) P.D. Cantino (WA-582)	DS	Native	√	√	√
	457	*Rydingia limbata* (Benth.) Scheen & V.A. Albert (WA-31)	DS	Native	√	√	√
	458	*Salvia moorcroftiana* Wall. ex Benth. (WA-26)	PH	Native	√	√	√
	459	*S. plebeia* R. Br. (WA-46)	PH	Weed	√	√	√
	460	*Teucrium quadrifarium* Buch.-Ham. (WA-622)	PH	Native	√	√	√
	461	*T. royleanum* Wall. ex Benth. (WA-40)	PH	Native	√	√	√
	462	*Vitex negundo* L. (WA-472)	DS	Native	√	√	√
65. Lauraceae	463	*Neolitsea pallens* (D. Don) Momiy. & H. Hara (WA-139)	ET	Native	√	—	—
	464	*Machilus duthiei* King (WA-140)	ET	Native	√	—	—
66. Linaceae	465	*Reinwardtia indica* Dumort. (WA-29)	DS	Native	√	—	—
67. Loranthaceae	466	*Scurrula pulverulenta* (Wall.) G. Don (WA-45)	P	Native	—	√	—
68. Lythraceae	467	*Woodfordia fruticosa* (L.) Kurz (WA-7)	DS	Native	√	√	√
69. Malvaceae	468	*Abutilon bidentatum* Hochst. ex Rich. (WA-47)	DT	Native	√	√	√
	469	*Bombax ceiba* L. (WA-30)	DT	Cultivated	√	√	√
	470	*Corchorus aestuans* L. (WA-430)	DS	Native	√	√	√
	471	*Kydia calycina* Roxb. (WA-48)	DT	Native	—	—	√
	472	*Malva neglecta* Waller. (WA-28)	AH	Weed	√	√	√
	473	*Malvastrum aboriginum* B.L. Rob. (WA-202)	AH	Native	√	√	√
	474	*Sida cordifolia* L. (WA-207)	AH	Native	√	√	√
	475	*S. cordata* (Burm. f.) Borss. Waalk. (WA-51)	AH	Native	√	√	√
70. Mazaceae	476	*Mazus alpinus* Masam. (WA-458)	AH	Native	√	√	√
71. Meliaceae	477	*Melia azedarach L.*	DT	Native	√	√	√
72. Menispermaceae	478	*Cissampelos pareira* L. (WA-247)	C	Native	√	√	√
73. Molluginaceae	479	*Mollugo nudicaulis* Lam. (WA-27)	AH	Native	√	√	√
74. Moraceae	480	*Broussonetia papyrifera* (L.) L'Hér. ex Vent. (WA-429)	DT	Naturalized	√	√	√
	481	*Ficus auriculata* Lour. (WA-428)	DT	Native	√	√	√
	482	*F. benghalensis* L. (WA-248)	ET	Native	√	√	√
	483	*F. carica* L. (WA-8)	DT	Cultivated	√	√	√
	484	*F. palmata* Forssk. (WA-306)	DT	Native	√	√	√
	485	*F. religiosa* L. (WA-141)	ET	Native	√	√	√
	486	*F. sarmentosa* Buch.-Ham. ex Sm. (WA-33)	C	Native	√	√	—
	487	*Morus alba* L. (WA-142)	DT	Native	√	√	√
	488	*M. nigra* L. (WA-143)	DT	Native	√	√	√
75. Myrtaceae	489	*Eucalyptus camaldulensis* Dehnh. (WA-456)	DT	Introduced	√	√	√
76. Nitrariaceae	490	*Peganum harmala* L. (WA-39)	AH	Native	√	√	√
77. Nyctaginaceae	491	*Boerhavia procumbens* Banks ex Roxb. (WA-9)	PH	Native	√	√	√
	492	*Mirabilis jalapa* L. (WA-233)	AH	Naturalized	√	√	√
78. Oleaceae	493	*Jasminum humile* L. (WA-307)	DS	Native	√	√	—
	494	*J. officinale* L. (WA-470)	DS	Native	√	√	—
	495	*Olea ferruginea* Royle (WA-195)	ET	Native	√	√	√

http://www.aloki.hu ● ISSN 1589 1623 (Print) ● ISSN 1785 0037 (Online)
DOI: http://dx.doi.org/10.15666/aeer/1704_96219650

Group/family	Sr#		Habit	Status	Murree	K. Sattian	Kahuta
79. Orobanchaceae	496	*Oenothera rosea* L'Hér. ex Aiton (WA-34)	PH	Native	√	√	—
80. Oxalidaceae	497	*Oxalis corniculata* L. (WA-192)	AH	Native	√	√	√
	498	*O. pes-caprae* L. (WA-208)	PH	Native	√	√	√
81. Papaveraceae	499	*Corydalis murreeana* Jafri (WA-41)	AH	Native	√	—	—
	500	*Fumaria indica* (Hausskn.) Pugsley (WA-450)	AH	Native	√	√	√
82. Phyllanthaceae	501	*Andrachne cordifolia* (Decne.) Müll. Arg. (WA-176)	DS	Native	√	—	—
	502	*Bridelia verrucosa* Haines (WA-52)	*DS*	Native	√	√	√
	503	*Glochidion heyneanum* (Wight & Arn.) Wight (WA-25)	*ET*	Native	√	√	—
	504	*Phyllanthus emblica* L. (WA-38)	*DT*	Native	√	√	√
	505	*P. niruri* L. (WA-451)	*AH*	Native	√	√	√
	506	*P. urinaria* L. (WA-53)	*AH*	Native	√	√	√
	507	*P. virgatus* G. Forst. (WA-24)	*AH*	Native	√	√	√
83. Plantaginaceae	508	*Bacopa monnieri* (L.) Wettst. (WA-35)	AH	Native	√	√	√
	509	*Nanorrhinum ramosissimum* (Wall.) Betsche (WA-54)	AH	Native	√	√	√
	510	*Plantago lanceolata* L. (WA-452)	PH	Weed	√	√	√
	511	*P. major* L. (WA-185)	PH	Native	√	√	—
	512	*P. ovata* Forssk. (WA-184)	PH	Native	√	√	√
	513	*Veronica anagallis-aquatica* L. (WA-460)	PH	Native	—	—	√
	514	*V. arvensis* L (WA-308)	AH	Native	√	√	√
84. Polygalaceae	515	*Polygala abyssinica* R. Br. ex Fresen (WA-81)	PH	Native	√	√	—
	516	*P. arvensis* Willd. (WA-459)	PH	Native	√	√	—
	517	*P. erioptera* DC. (WA-55)	PH	Native	√	√	—
85. Polygonaceae	518	*Persicaria amplexicaulis* (D. Don) Ronse Decr. (WA-80)	PH	Native	√	√	—
	519	*P. barbata* (L.) H. Hara (WA-309)	AH	Native	√	√	—
	520	*P. hydropiper* (L.) Delarbre (WA-79)	AH	Native	√	√	—
	521	*P. mitis* (Schrank) Holub (WA-11)	AH	Native	√	√	√
	522	*P. nepalensis* (Meisn.) Miyabe (WA-56)	AH	Native	√	√	√
	523	*Polygonum aviculare* L. (WA-310)	AH	Native	√	√	√
	524	*P. plebeium* R. Br. (WA-37)	AH	Native	√	√	√
	525	*Rumex dentatus* L. (WA-61)	AH	Weed	√	√	√
	526	*R. hastatus* D. Don (WA-82)	PH	Native	√	√	√
	527	*R. nepalensis* Spreng. (WA-36)	PH	Native	√	√	—
86. Primulaceae	528	*Anagallis arvensis* L. (WA-78)	AH	Weed	√	√	√
	529	*Androsace foliosa* Duby (WA-158)	PH	Native	√	√	√
	530	*A. rotundifolia* Hardw. (WA-75)	PH	Native	√	√	√
	531	*A. umbellata* (Lour.) Merr. (WA-60)	AH	Native	√	√	√
	532	*Embelia robusta* Roxb. (WA-23)	DS	Native	√	√	√
	533	*Lysimachia pyramidalis* Wall. (WA-62)	AH	Native	√	√	√
	534	*Myrsine africana* L (WA-194)	ES	Native	√	√	√
	535	*M. semiserrata* Wall. (WA-12)	DS	Native	√	—	—
	536	*Primula denticulata* Sm. (WA-145)	PH	Native	√	—	—
87. Punicaceae	537	*Punica granatum* L. (WA-64)	DS	Native	√	√	√
88. Ranunculaceae	538	*Aconitum laeve* Royle (WA-59)	PH	Native	√	—	—
	539	*Anemone tetrasepala* Royle (WA-146)	PH	Native	√	—	—
	540	*A. vitifolia* Buch.-Ham. ex DC. (WA-76)	PH	Native	√	—	—
	541	*Aquilegia pubiflora* Wall. ex Royle (WA-63)	PH	Native	√	—	—
	542	*Clematis barbellata* Edgew. (WA-311)	C	Native	√	√	√
	543	*C. grata* Wall. (WA-147)	C	Native	√	√	—
	544	*C. montana* Buch.-Ham. ex DC. (WA-58)	C	Native	√	√	√

http://www.aloki.hu ● ISSN 1589 1623 (Print) ● ISSN 1785 0037 (Online)
DOI: http://dx.doi.org/10.15666/aeer/1704_96219650

Group/family	Sr#		Habit	Status	Murree	K. Sattian	Kahuta
	545	*Ranunculus arvensis* L. (WA-312)	AH	Weed	√	√	√
	546	*R. laetus* Wall. ex Hook. f. & J.W. Thomson (WA-157)	PH	Native	√	√	√
	547	*R. muricatus* L. (WA-148)	AH	Weed	√	√	√
	548	*R. sceleratus* L. (WA-149)	AH	Native	√	√	√
89. Rhamnaceae	549	*Rhamnus purpurea* Edgew. (WA-77)	DT	Native	√	√	—
	550	*R. triquetra* (Wall.) Brandis (WA-22)	DT	Native	√	√	—
	551	*R. virgata* Roxb. (WA-13)	DT	Native	√	√	—
	552	*Sageretia thea* (Osbeck) M.C. Johnston (WA-461)	DS	Native	√	√	√
	553	*Ziziphus jujuba* Mill. (WA-462)	DT	Cultivated	√	√	√
	554	*Z. mauritiana* Lam. (WA-155)	DT	Native	√	√	√
	555	*Z. oxyphylla* Edgew. (WA-156)	DS	Native	√	√	√
90. Rosaceae	556	*Agrimonia eupatoria* L. (WA-463)	AH	Native	√	√	√
	557	*Cotoneaster affinis* Lindl. (WA-464)	DS	Native	√	√	√
	558	*Duchesnea indica* (Jacks.) Focke (WA-186)	PH	Native	√	√	√
	559	*Fragaria nubicola* (Hook. f.) Lindl. ex Lacaita (WA-465)	PH	Native	√	√	√
	560	*Malus domestica* Borkh. (WA-466)	DT	Cultivated	√	√	√
	561	*Potentilla reptans* L. (WA-320)	PH	Native	√	√	√
	562	*Prunus armeniaca* L. (WA-113)	DT	Cultivated	√	√	√
	563	*P. domestica* L. (WA-315)	DT	Cultivated	√	√	√
	564	*P. persica* (L.) Batsch (WA-121)	DT	Cultivated	√	√	√
	565	*Pyrus pashia* Buch.-Ham. ex D. Don (WA-204)	DT	Native	√	√	√
	566	*Rosa moschata* Herrm. (WA-316)	DS	Native	√	√	—
	567	*R. multiflora* Thunb. (WA-513)	DS	Native	√	√	—
	568	*Rubus ellipticus* Sm. (WA-469)	DS	Native	√	√	√
	569	*R. anatolicus* Focke (WA-593)	DS	Native	√	√	—
	570	*R. fruticosus* L. (WA-14)	DS	Native	√	√	—
	571	*R. niveus* Thunb. (WA-179)	DS	Native	√	√	—
	572	*R. sanctus* Schreb. (WA-317)	DS	Native	√	√	—
	573	*R. ulmifolius* Schott (WA-410)	DS	Native	√	√	—
	574	*Spiraea canescens* D. Don (WA-21)	DS	Native	√	—	—
91. Rubiaceae	575	*Galium acutum* Edgew. (WA-159)	AH	Native	√	√	√
	576	*G. aparine* L. (WA-424)	AH	Native	√	√	√
	577	*G. asperifolium* Wall. (WA-161)	AH	Native	√	√	√
	578	*G. elegans* Wall. ex Roxb. (WA-160)	PH	Native	√	√	√
	579	*G. rotundifolium* L. (WA-193)	PH	Native	√	√	√
	580	*Himalrandia tetrasperma* (Wall. ex Roxb.) T. Yamaz. (WA-423)	DS	Native	√	√	√
	581	*Pavetta tomentosa* Roxb. ex Sm. (WA-318)	DS	Native	√	√	√
	582	*Rubia cordifolia* L. (WA-162)	C	Native	√	√	√
	583	*Wendlandia heynei* (Schult.) Santapau & Merchant (WA-20)	DT	Native	√	√	√
92. Rutaceae	584	*Zanthoxylum armatum* DC. (WA-422)	DS	Native	√	√	√
93. Salicaceae	585	*Flacourtia indica* (Burm. f.) Merr. (WA-152)	DT	Native	√	√	√
	586	*Populus deltoides* Marshall (WA-421)	DT	Naturalized	√	√	√
	587	*Salix acmophylla* Boiss. (WA-15)	DT	Native	√	√	√
	588	*S. tetrasperma* Roxb. (WA-485)	DT	Naturalized	√	√	—
	589	*Xylosma longifolia* Clos (WA-150)	DT	Native	√	√	—
94. Sapindaceae	590	*Aesculus indica* (Wall. ex Cambess.) Hook. (WA-468)	DT	Native	√	√	—
	591	*Cardiospermum halicacabum* L. (WA-151)	AH	Native	√	√	√
	592	*Dodonaea viscosa* (L.) Jacq. (WA-198)	ES	Native	√	√	√
95. Saxifragaceae	593	*Bergenia ciliata* (Haw.) Sternb. (WA-19)	PH	Native	√	√	—

http://www.aloki.hu ● ISSN 1589 1623 (Print) ● ISSN 1785 0037 (Online)
DOI: http://dx.doi.org/10.15666/aeer/1704_96219650

Group/family	Sr#		Habit	Status	Murree	K. Sattian	Kahuta
96. Scrophulariaceae	594	*Verbascum thapsus* L. (WA-319)	PH	Native	√	√	√
97. Simaroubaceae	595	*Ailanthus altissima* (Mill.) Swingle (WA-16)	DT	Naturalized	√	√	√
98. Solanaceae	596	*Datura innoxia* Mill. (WA-17)	AH	Naturalized	√	√	√
	597	*D. stramonium* L. (WA-68)	AH	Native	√	√	√
	598	*Physalis divaricata* D. Don (WA-326)	AH	Weed	√	√	√
	599	*Solanum americanum* Mill. (WA-163)	AH	Weed	√	√	√
	600	*S. erianthum* D. Don (WA-325)	AH	Native	√	√	—
	601	*S. incanum* L. (WA-324)	AH	Weed	√	√	√
	602	*S. surattense* Burm. f (WA-67)	AH	Native	√	√	√
	603	*S. villosum* Mill. (WA-164)	AH	Weed	√	√	√
	604	*Withania somnifera* (L.) Dunal. (WA-74)	PH	Native	√	√	√
99. Thymelaeaceae	605	*Daphne pappyracea* Wall. ex G. Don. (WA-175)	ES	Native	√	—	—
100. Tiliaceae	606	*Grewia asiatica* L. (WA-69)	DT	Native	√	√	√
	607	*G. eriocarpa* Juss. (WA-613)	DT	Native	√	√	√
	608	*G. optiva* J.R. Drumm. ex Burret (WA-153)	DT	Native	√	√	√
	609	*G. tenax* (Forssk.) Fiori (WA-71)	DT	Native	√	√	√
101. Ulmaceae	610	*Celtis australis subsp. caucasica* (Willd.) C.C. Towns. (WA-154)	ET	Native	√	√	√
102. Urticaceae	611	*Debregeasia saeneb* (Forssk.) Hepper & J.R.I. Wood (WA-72)	ES	Native	√	√	√
	612	*Urtica dioica* L. (WA-18)	PH	Native	√	√	—
	613	*U. pilulifera* L. (WA-73)	PH	Native	√	√	√
103. Valerianaceae	614	*Valeriana hardwickii* Wall. (WA-420)	PH	Native	√	—	—
	615	*V. jatamansi* Jones (WA-348)	PH	Native	√	√	—
104. Verbenaceae	616	*Glandularia aristigera* (S. Moore) Tronc. (WA-332)	AH	Introduced	√	√	√
	617	*Lantana camara* L. (WA-323)	ES	Naturalized	√	√	√
	618	*L. indica* Roxb. (WA-322)	ES	Naturalized	√	√	√
	619	*Phyla nodiflora* (L.) Greene (WA-419)	AH	Native	√	√	√
	620	*Verbena officinalis* L. (WA-321)	AH	Weed	√	√	√
105. Violaceae	621	*Viola cancescens* Wall. (WA-467)	PH	Native	√	√	√
	622	*V. pilosa* Blume (WA-66)	PH	Native	√	√	—
	623	*V. stochsii Boiss.*(WA-212)	PH	Native	—	—	√
106. Zygophyllaceae	624	*Tribulus terrestris* L. (WA-65)	AH	Weed	√	√	√
				Total	**592**	**533**	**433**

http://www.aloki.hu ● ISSN 1589 1623 (Print) ● ISSN 1785 0037 (Online)
DOI: http://dx.doi.org/10.15666/aeer/1704_96219650

AN EXAMINATION OF LAND USE IN THE AMASYA DEVELOPMENT PLAN THROUGH CLUSTER ANALYSIS

ERGEN, M.[1*] – ERGEN, Y. B.[2]

[1]*Department of Architecture, Faculty of Fine Arts and Design, Siirt University, Siirt, Turkey*

[2]*Department of Urban and Regional Planning, Faculty of Fine Arts and Design, Siirt University, Siirt, Turkey*

**Corresponding author*
e-mail: mustafaergen2002@yahoo.com; phone: +90-537-911-4234

(Received 26th Feb 2019; accepted 1st Jul 2019)

Abstract. In this study, existing and future land use patterns were examined in the development plan for Amasya using hierarchical cluster analysis. To this end, the area encompassed by the Amasya development plan was partitioned into grids to examine their proximities and similarities to each other in terms of land use. In addition, linkages among the grids were investigated with respect to the land use patterns. Linkages among land use functions were determined in this research through cluster analysis. After exposing the similarities among the grids, the shortcomings with regard to the necessary social infrastructure within the grids were identified, and the requirements of similar urban development approaches to grids with similar characteristics were described. This paper emphasizes the need for healthy, sustainable development and a planned and balanced distribution of social infrastructure in urban development plans.
Keywords: *land use patterns, grids, hierarchical cluster analysis, social infrastructure, similar characteristics*

Introduction

The way in which land is used can provide essential resources and is one of the most central factors that affect urban development (Foley et al., 2005; Niedertscheider and Erb, 2014). This important factor reveals that city planning must use sustainable approaches that satisfy human needs. For this to be successful, it is imperative to fully understand how land is categorized in city development plans. Numerous land use factors, such as green space and housing space, shape how urban areas should be developed. For example, housing space shapes urban development by providing living quarters for current and future populations, and this basic necessity can be constructed when urban development is correctly planned.

In Turkey, land use issues in urban areas cannot be resolved using only ad-hoc solutions. There exists a significant deficit of knowledge regarding land use factors in cities as well as how land is used (Niedertscheider and Erb, 2014). As a precondition in preparing for future land use modifications, land use decisions to changes in previous underlying development must be analyzed (Dearing et al., 2010; Niedertscheider and Erb, 2014). Hierarchical analysis is regarded as one of the most powerful instruments (R Core Team, 2015; Manjunath et al., 2018) by which to understand future development options that affect current land use. Many studies on land use changes are highly limited mainly because of the lack of data sets on land systems and dynamics as well as the underlying factors that affect these changes (Singh et al., 2013; Niedertscheider and Erb, 2014).

http://www.aloki.hu ● ISSN 1589 1623 (Print) ● ISSN 1785 0037 (Online)
DOI: http://dx.doi.org/10.15666/aeer/1704_96519668

Results of studies on urban development plans in Turkey are conducted to work in concert with planning requirements, a balanced distribution of social and technical infrastructure, and in accordance with standards and needs. For example, in Turkey's development plans, the distribution of and need for green areas per person or the distance to neighborhood schools are important for healthy urbanization. A 10 m^2 green area/capita should be included in all urban development plans. When we analyzed the urban structure of Amasya, we found that a linear urban structure is formed between the Yeşilırmak River and two mountain ranges. This situation creates problems for physical expansion of the city, because the topography in Amasya is not flat enough to accommodate sufficient residential and development areas. Because of this topography, a balanced distribution of social infrastructure in urban development is indispensable for a healthy urban structure.

Balanced distribution means that the population living within any city grid has equal access to all social facilities, and that all social facilities appeal equally to everyone, or that the population is distributed evenly within each grid. In short, balanced distribution describes how urban development within each grid is self-sufficient and does not need external intervention**.** The grids contain urban land use forms which are created by Municipality for the future urban development in Amasya. Types of land uses come from legal Municipality creation into the grids. It is proved that the form of land uses is the main research data for analysing grids and current Amasya city development condition.

Cluster analysis is a suitable method by which to identify analogous groups of objects called "clusters" (Mooi and Sarstedt, 2011). A central feature of this analysis is its ability to refer directly to either understanding development options or to land use relationships in this study (Alvarenga et al., 2013; Niedertscheider and Erb, 2014). The core area of urban usage is the transition zone between land use similarities and differences (Bo, et al., 2011). The approaches to the similarities and differences in this cluster analysis provided us with ideas about land use distribution, which supported our deductions related to recent land use and the social infrastructure. In addition, cluster analysis is a highly useful method by which to understand the trends in urban development for future perspectives.

Land use change is defined as a transformation of one land use into another format, or a complete change from an old land use to a new land use (Liu et al., 2014). There are many studies related to land use change (McHarg, 1992; Erickson, 1995; Milesia et al., 2003; Nuissl et al., 2009; Song, et al., 2013; Cinelli, et al., 2014; Liu et al., 2014; Krekel, et al., 2016; Lu and Ke, 2018). It is important to study land use development because it has a profound impact on options for future city development (Liu et al., 2014). This paper brings together, in a systematic way, the results of many recent studies on urban form, especially on land use (Ozus et al., 2012).

In their 2014 research, Grecchi, et al. investigated changes in land use using raster data from different dates. Another 2014 study by Kline et al. analyzed land use plans within different governing regimes. Likewise, Sharifi et al. (2014) investigated the regulation and control over master plans for urban growth using monitoring, and Liu et al., 2014 conducted a compatibility analysis for land use, which identified compatibility analysis criteria, such as topography, geology, and socioeconomics. The monitoring method is most prevalent in land use analyses. In their study, Ozus et al. (2012) used cluster analysis to examine how travel demand shaped the spatial structure of Istanbul; however, land use that does not involve transportation is also important. We use a

http://www.aloki.hu ● ISSN 1589 1623 (Print) ● ISSN 1785 0037 (Online)
DOI: http://dx.doi.org/10.15666/aeer/1704_96519668

cluster analysis of land use patterns to demonstrate a more effective use of this method in planning. This study also presents the urban social infrastructure issues, such as easy access to primary schools and enough green areas per person, using an agglomerative hierarchical cluster analysis. This identifies the social infrastructure problems in urban development and is a departure from other studies because it emphasizes the need for an innovative and comprehensible approach to land use. In this context, an innovative approach refers to identifying the current distribution of the social infrastructure and the necessary strategies for the future by looking at existing land use within the city.

In addition, the methods used in the present study to analyze land use suitability first emerged in 1992 with Ian McHarg's *Design with Nature* and are still used today in many studies. In 200 the results of a study by Randolph showed that land use suitability analysis provided information about lands suitable for settlement or about the most suitable settlement areas for land use and their development based on specific criteria. This study was not to determine the most suitable areas for settlement but to determine the distribution of social service areas within the city and designated in the development plans that the municipalities are supposed to follow and to choose the areas of social infrastructure in urban areas and determine the similarities among them in the city grids. The similarities among these areas reveal an analysis of the current situation, such as whether development has been homogeneous, and can generate prospective inferences. Our analysis is based on the current situation for land use in urban areas and does not consider settlement or suitability for future development.

From this study, the best planning approaches used for urban planning are presented to help facilitate effective and more resolution-oriented decisions to enable an understanding of land use areas. For example, it is necessary to determine where within the city there is a lack of social facilities and to decide within which areas these facilities will be designed. It is also important to create suitable designs for this area, to fill the need for urban social facilities within the city, and to resolve the deficiencies in urban design and urban planning within the city's existing development.

The aim of this study was to explore the direction that future social infrastructure development within Amasya will take by analyzing its land use using the cluster analysis method. Land use is the most important dimension of urban development within cities, and its intensity has become an important indicator of the relationship between current and future urban development (Hubacek and van den Bergh, 2006; Shi and Yu, 2014). Moreover, in the study, the distribution of spaces in terms of their land use similarities and differences will be investigated to make recommendations for future urban development. This new methodological approach will provide a new perspective to development plans in Turkey. These similarities and differences will be useful for illustrating the imbalances of social infrastructures in land use and identifying whether the Amasya can provide sufficient infrastructure within every region and every area to accommodate its citizens. Accordingly, this paper will focus on the necessity of reanalyzing the city's approach to creating social infrastructure that is incorporated into urban development plans.

This study presents a land use analysis that is used to assess development options in Amasya. The hierarchical analysis helps to analyze urban development by providing a good assessment of land use development while revealing the similarities and dissimilarities among the various urban spaces. Our main research questions are as follows: how well is the social infrastructure, such as green areas, schools, and hospitals, throughout an urbanized area distributed as it is intended (e.g., primary

http://www.aloki.hu ● ISSN 1589 1623 (Print) ● ISSN 1785 0037 (Online)
DOI: http://dx.doi.org/10.15666/aeer/1704_96519668

schools within a perimeter of 500-m of settlements, or green areas should be 10 m^2/person) and is it balanced? If there is an unbalanced distribution of social infrastructure, what do we need to do to balance the distribution of that infrastructure in future urban development plans? The second question will be important when discussing how the social infrastructure will be planned in future urban development and how the lack of social infrastructure within the city will be alleviated. Using an agglomerative hierarchical cluster analysis, this research investigated the sufficiency of urban social infrastructure and whether urban areas have been developed in a healthy manner.

The role of cluster analysis in planning practices

There is a wide variety of planning practices with different purposes in Turkey's land planning system. Among Turkey's planning stages, cluster analysis is most useful for land use plans, one category of plans. We conducted our analysis at this planning stage because land use plans provide the existing land use patterns during the decision-making process. Although this method was chosen specifically for Turkey's planning system, it can be used for any country and on any land use plan because it increased information on the quality of life within the regions studied. With this method, existing land use can be accurately determined, and a planning process can be created accordingly. The following text explains this more clearly by providing a hierarchical scheme of the plans in Turkey's planning system (*Fig. 1*) with additional social infrastructure within the new developments.

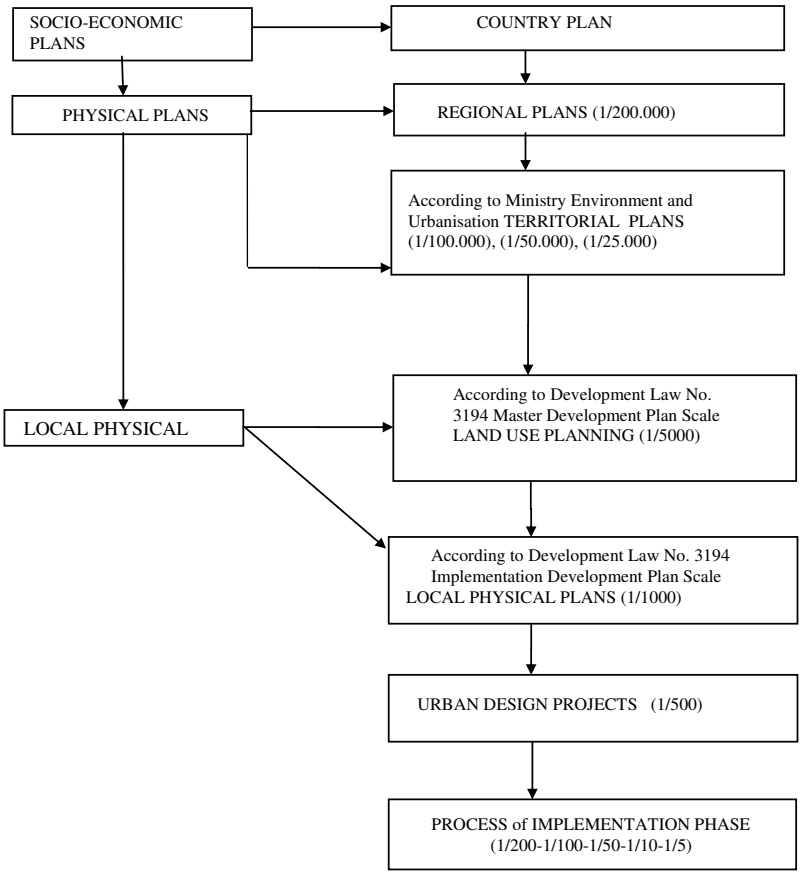

Figure 1. *Turkish planning system. (Source: Türk, 2002)*

http://www.aloki.hu ● ISSN 1589 1623 (Print) ● ISSN 1785 0037 (Online)
DOI: http://dx.doi.org/10.15666/aeer/1704_96519668

The area studied was divided into grids. The characteristic feature of each grid is to be a homogeneous distribution of mixed land use and have the ability to describe the necessary services, such as hospitals, schools, and recreational areas (social infrastructure), that are included in land use and urban development. The square grids are used to investigate the distribution of social infrastructure within ~500 m of the center of the city, which also helped understand which social infrastructure is accessible in each grid. The fact that the grids offer the opportunity to develop a planning approach that is a sounder, sustainable, and provides accessible social infrastructure and has a command of the entire city reveals the most significant feature of this arrangement—the location of these social infrastructures. The need for social services within the grid areas that do not have them is not emphasized, and the study does not suggest that the needs be satisfied. Thus, the results provide information on how social infrastructure is distributed within the grids and how the transportation issues and other recommendations were resolved.

The grids included all areas within the borders of the municipal adjacent areas. If each social service and the population within the grids were to be discussed presumptively and evenly, there would be equal and balanced distribution within the city. We recognize that this approach is similar to developing an imaginary ideal city, and the aim here is not to disperse the population accordingly, but to understand and explain how urban areas would be developed in such cases. Keeping the same populations within each grid is an imaginary approach, and dispersing a population according to ideal land use is impossible and meaningless. The population of Amasya is 113.932 (Turkstat, 2018), and a balanced plan should propose a balanced distribution of the city's population. If we can employ approximately 3.452 people within each grid, we can have a balanced distribution of housing as well. The acceptable size of housing per person is between 12 and 24 m^2 in Turkey's planning system and, accordingly, the maximum area of housing within the grid is 82.848 m^2. According to legislation, land use planning administrators in Turkey are obligated to designate 10 m^2 of green area/person in a development plan; therefore, 34.520 m^2 within each grid must be designated as green areas. Moreover, hospital building floor space must be 0.11 m^2/person, which means that 379.5 m^2 of building floorspace must be designated as hospital building floorspace within each grid. The total area for healthcare services includes other facilities, such as 0.05 m^2/person (172.6 m^2) for dispensaries and 0.15 m^2/person (517.8 m^2) for other facilities; therefore, total healthcare space within each grid would be 1069.9 m^2. However, it is highly likely that the existing land use situation is not similar to this, in which case, it is necessary to take measures to correct the situation with additional social infrastructure within the new developments.

Materials and methods

Area of study

Figure 2 shows the boundaries of the center of Amasya and the area analyzed for this research. Amasya is located in the Black Sea Region of Turkey and is surrounded by Tokat on the east, Tokat and Yozgat on the south, and Samsun on the north (Turkstat, 2012). Amasya's average altitude is 1150 m, with the altitude in the center of the city being only 411 m. The city is located between the east longitudes of 34°57′06″–36°31′53″ and the north latitudes of 41°04′54″–40°16′16″ (Turkstat, 2012).

http://www.aloki.hu ● ISSN 1589 1623 (Print) ● ISSN 1785 0037 (Online)
DOI: http://dx.doi.org/10.15666/aeer/1704_96519668

Archaeological excavations have revealed that the city dates back 7500 years, making it one of the most important cities in history (Governorship of Amasya, 2017).

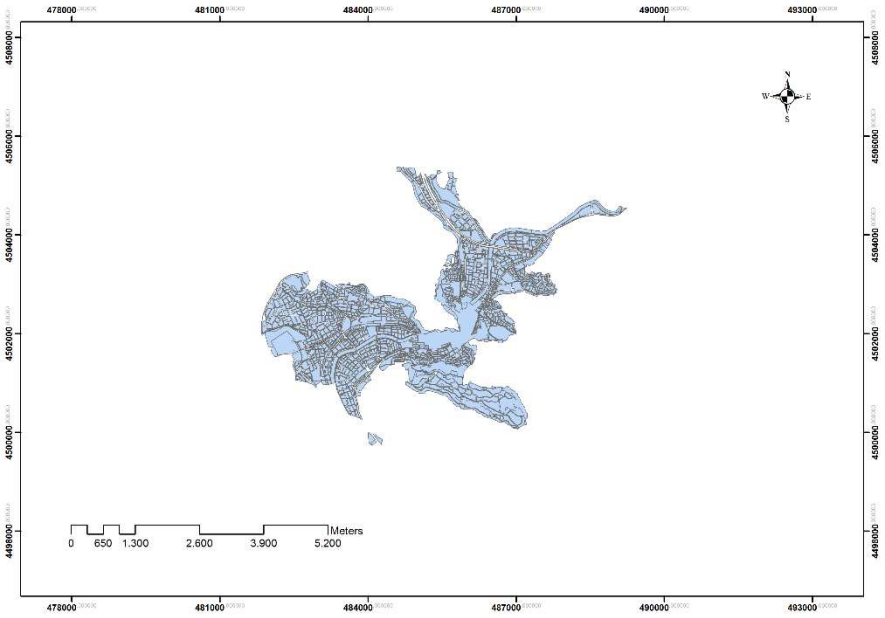

Figure 2. *The analysis area of Amasya, Turkey. (Source: The map was obtained from Amasya Municipality with NetCAD program. The map was converted to ArcGIS and prepared by the authors for description of analyzing areas in Amasya)*

The methods used are based on a case study of Amasya. It was evident from the findings that Amasya was most likely a city in which traditional urban planning practices would have been the norm. In Turkey, such practices always lack adequate social infrastructure; therefore, in this article, analyses are conducted on how the urban development plans should be constructed, using Amasya as an example.

Materials

Urban development plans can be obtained from municipal authorities in Turkey in which the administrators are obligated to prepare development plans for each municipality. A development plan is a periodic study that is required to ensure healthy urban development. Moreover, development plans are prepared using up-to-date information on land use; therefore, in our research, the analyses use development plans that were prepared by the Amasya Municipality. The data for this research were obtained from these urban development plans and analyzed using cluster analysis. Thirty-three grids were produced using the urban development plans with the help of ArcGIS based on the land use data (*Fig. 3*). To explain the methods, we used the Lance–Williams algorithm, which was formulated in 1967 by Lance and Williams as follows (*Eq. 1*):

$$d(i + j,k) = a_i\, d(i,k) + a_j\, d(j,k) + b,d(i,j) + c \left| d(i,k) - d(j,k) \right| \qquad \text{(Eq.1)}$$

http://www.aloki.hu ● ISSN 1589 1623 (Print) ● ISSN 1785 0037 (Online)
DOI: http://dx.doi.org/10.15666/aeer/1704_96519668

The formula displays the distance between clusters k and i + j. This study addresses the similarities and dissimilarities between data using single linkage, average linkage, and complete linkage cluster analyses, which are part of the agglomerative hierarchical analysis.

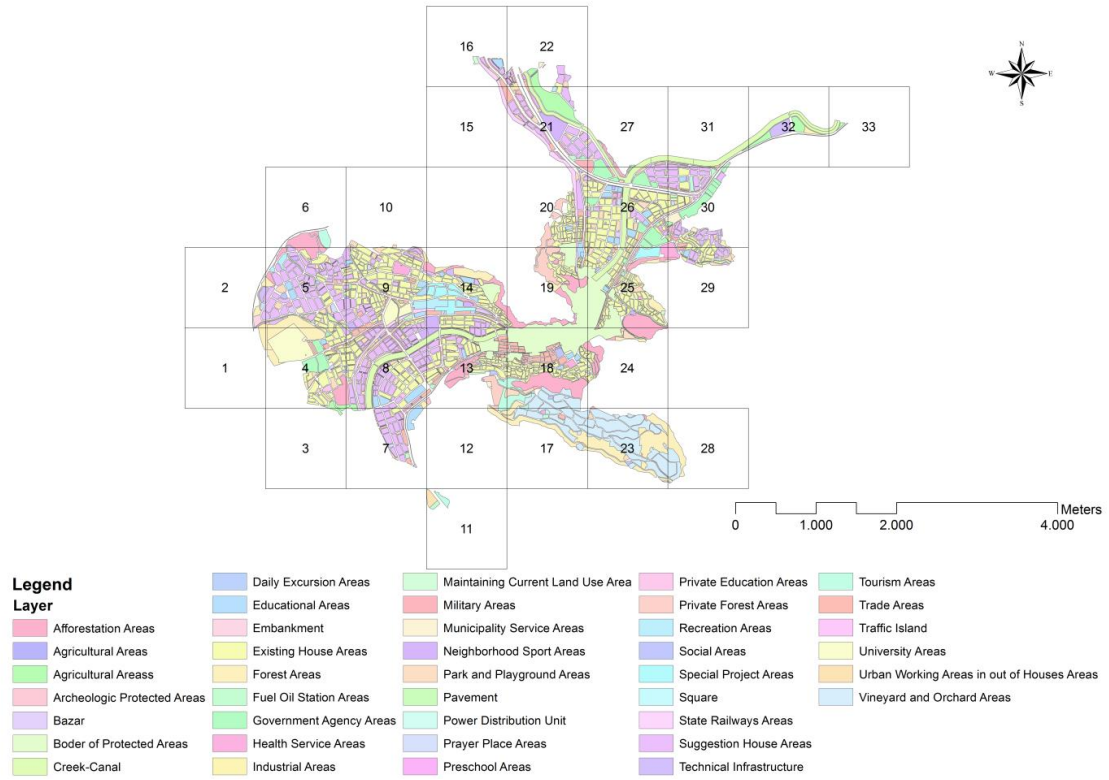

Figure 3. *Land Use and Grids of Study Area. (Source: The map was obtained from Amasya Municipality in a GIS format. The map was converted to ArcGIS and prepared by the authors for analyzing land uses in Amasya)*

The data on the land use map were first transformed from the NetCAD format to the ArcGIS format. To make them suitable for analysis, georeferences were created in ArcGIS WGS 1984 Universal Transverse Mercator (UTM) Zone. Grids were produced within ArcGIS, and data were obtained for each grid. The raw data obtained were normalized using Matedit to make them analyzable. We began by normalization the analysis to eliminate redundant variables in the database. Then, we conducted an agglomerative hierarchical analysis using Minitab. The results obtained from this analysis revealed the urban development approaches for similar and different grids. Hawth's analysis tools in ArcGIS automatically generated the grids. Using the UTM zone, these tools generated equal 1- by 1-km squares. By doing so, we were able to analyze the included land uses and the values of the social infrastructure within the land uses. Using this program, analyses conducted for future land development will shed light on future advances. Each grid allowed for meaningful analyses that could be conducted based on Hawth's analysis tools. We determined that conducting these analyses using smaller or larger grids would not be feasible.

http://www.aloki.hu ● ISSN 1589 1623 (Print) ● ISSN 1785 0037 (Online)
DOI: http://dx.doi.org/10.15666/aeer/1704_96519668

Cluster analysis is used in many research studies, including the wastewater treatment study byBayo and Castellanos (2016), who matched the similarities in the cluster analysis to principal factors to attain results, and the research conducted by Ozus et al. (2012), who used a hierarchical cluster analysis to identify similar transportation behaviors among districts within Istanbul. As mentioned, agglomerative hierarchical cluster analysis is a widely used method, and unlike those used in other studies, this method is used in our research to identify how urban land use is distributed and determine the distribution of social infrastructure areas within the city grids.

Agglomerative hierarchical cluster analysis was chosen to study land use patterns using data obtained on decisions from the city's urban land use plan. In this sense, cluster analysis can be used as a tool to analyze only land use development, and allows us to examine the required healthcare, housing, and green spaces for 100 ha of land and to make better planning decisions. After selecting the best cluster analysis, the information necessary to plan similar and different places within that grid is provided.

Methodology

All grids were created using the same method with GEOSTAT, which comprises all of the urban areas in Europe and divides them into grids. The GEOSTAT grid size of 1 km^2 is based on a population density of at least 5000 people within an area of 300 km^2 (Paffi et al., 2016). The grids created in this study were applied to the entire city. The aim was to ensure that the populations living within each region of the city were equally represented and had equal accessibility to the city's social facilities; therefore, this study sought to research and identify how much of the population living within each city grid actually realized that goal.

One of the key rules in this method is that grids be a particular uniform size. In these grids of a predetermined size, it was not necessary to have either all or part of the land use plan. The number of grids, which is determined by applying an area of particular size in the land use plan, is used as the basis. Thus, it is important to divide the selected area into grids rather than to divide the area of the plan into grids. As a result of the analyses, 33 grids were created using Hawth's analysis tool. Each equal grid provides a way by which to analyze the land use of the entire area. In some of the emerging grids, there was very little area available for land use, the most important reason for which is that land use divided into equal grids decreases at the edges of the city and intensifies at the focal points of urbanization; however, our tools offered the opportunity to analyze both the farthest point and the most intensely urbanized area within the equal grid areas.

Agglomerative hierarchical analysis

Cluster analysis is a form of statistical analysis used for examining multivariate data with the objective being to uncover or discover groups or clusters that are similar to and different from each other (Everitt, 2005; Ozus, et al., 2012). Cluster analysis is linked to a correlation matrix; however, it can generally conduct analyses in different forms (Robinson, 1998).

In our study, cluster analyses were performed using the linkage method. Through these analyses, grids with the highest proximity and those with the most linkages were identified. Using the linkage method, proximities among the grids were calculated on the basis of the correlations among them. As stated, three types of linkage methods were used in our study.

http://www.aloki.hu ● ISSN 1589 1623 (Print) ● ISSN 1785 0037 (Online)
DOI: http://dx.doi.org/10.15666/aeer/1704_96519668

At the analysis stage, the cophenetic correlation method was used to find the best approach to agglomerative hierarchical cluster analysis and to be able to conduct the related analyses. This is the best method by which to understand the phenomenon of future urban development. Accordingly, the current situation in urban development sheds light on future approaches to development.

Identifying the best cluster approach

Clusters were validated using the cophenetic correlation, a commonly used measurement in hierarchical clustering (Ozus et al., 2012). The Matlab code given below was used for this analysis (Anonymous, 2018):

$$c = \text{cophenet}(Z,Y)$$
$$[c,d] = \text{cophenet}(Z,Y)$$

In the cophenetic correlation coefficient values, the best cluster analysis linkage method is identified when the value of r approaches 1. Conversely, if the value approaches the linkage method should not be chosen. As the *Table 1* illustrates, all linkage methods in the cophenetic correlation coefficient analysis could be used for this analysis. It also shows that average linkage was the best approach, although all were similar. Accordingly, groupings of clusters on the map, which were created using average linkage, are described here and shown in *Figure 4*.

In addition, grids and land uses were correlated to better understand the linkages among them, and the findings were evaluated. Data on the current state, obtained using the average linkage method, will influence planning decisions.

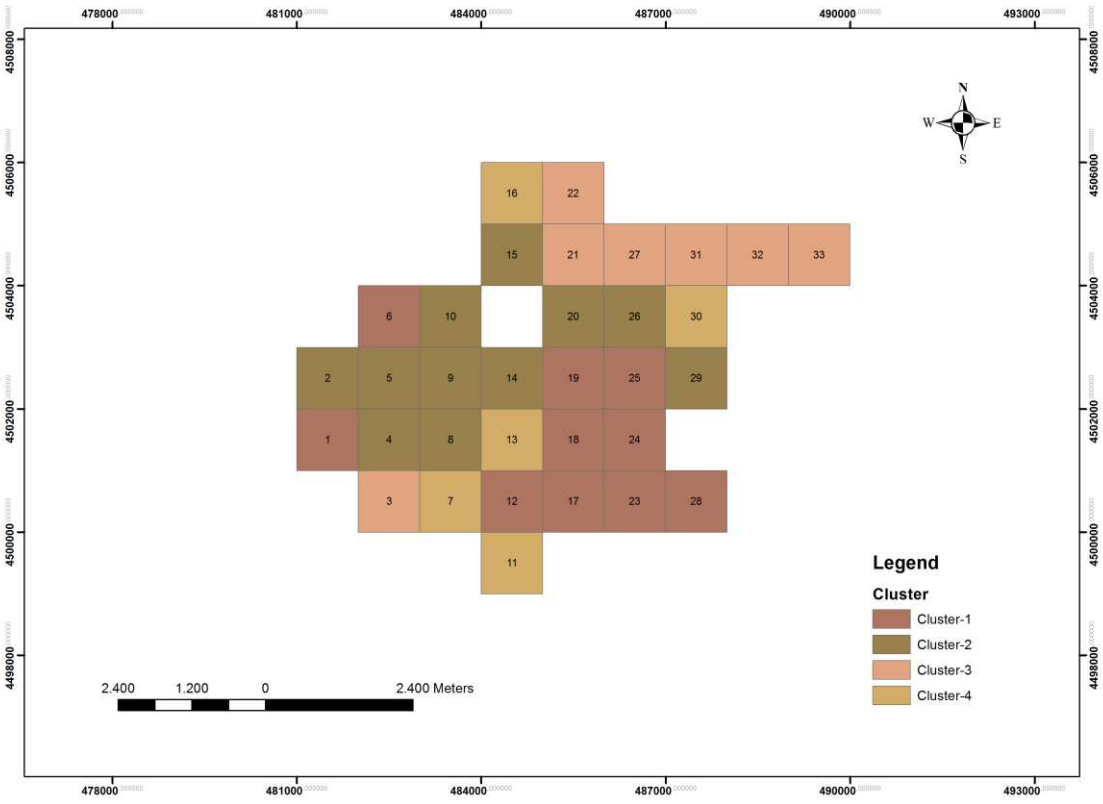

Figure 4. *Clustering analysis map created using grids and average linkage*

http://www.aloki.hu ● ISSN 1589 1623 (Print) ● ISSN 1785 0037 (Online)
DOI: http://dx.doi.org/10.15666/aeer/1704_96519668

Table 1. *The cophenetic correlation coefficient values*

Linkage method	Cophenetic correlation coefficient
Single linkage	r = 0.8211
Complete linkage	r = 0.8043
Average linkage	r = 0.8285

Results

Average linkage cluster

In average linkage analysis, the average distance between two clusters is considered. Average linkage was formulated by the Lance–Williams algorithm created in 1967 by considering the average distances between the clusters of $i + j$ and k.

$$d\,(Ci, Cj) = \frac{1}{nj+ni} \sum_{a \in Ci, a \in cj} d(a, b) \qquad \text{(Eq.2)}$$

In the analyses performed using Minitab, the following average linkage results were obtained (*Fig. 5*).

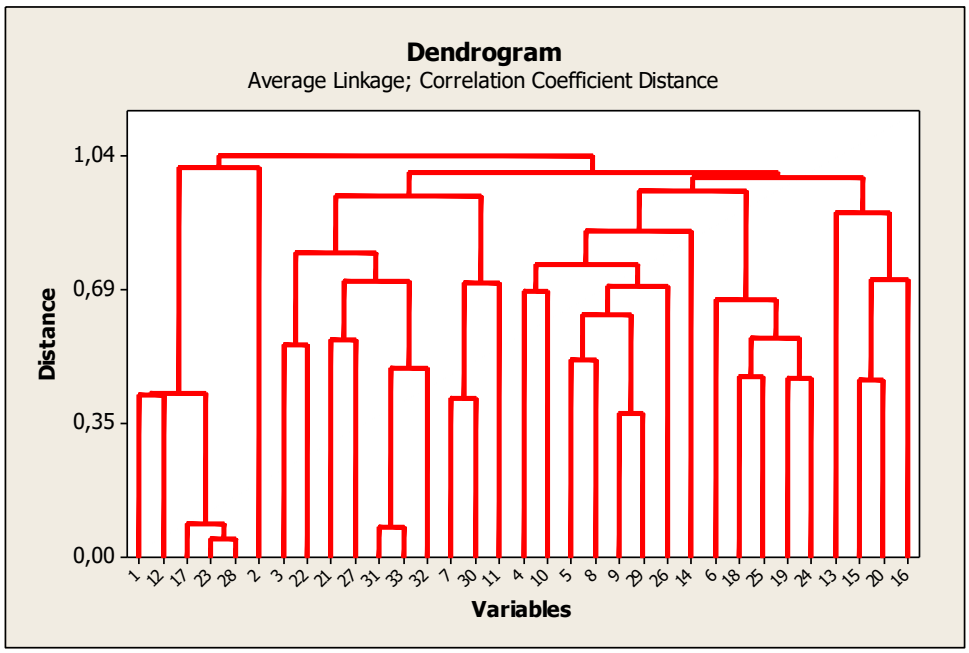

Figure 5. *Dendrogram for average linkage analysis*

The similarity between the 23rd and the 28th grids is striking (*Table 2*). It can be seen from *Table 2* that the similarity level, 9.642 and distance, 0.0471 stand out. The 1st and 3rd grids are those that are the most distant from each other. While the similarity level is 48.023 the distance level is 1.03953.

Here are the clusters that result; ***Cluster-1:*** Grid- Grid-1 Grid-1 Grid-2 Grid-2 Grid-Grid-1 Grid-2 Grid-1 Grid-2 ***Cluster-2:*** Grid- Grid- Grid-2 Grid-1 Grid-1 Grid-2 Grid-Grid-1 Grid- Grid- Grid-26 ***Cluster-3:*** Grid- Grid-2 Grid-2 Grid-2 Grid-3 Grid-3 Grid-3 ***Cluster-4:*** Grid- Grid-3 Grid-1 Grid-1 Grid-16.

http://www.aloki.hu ● ISSN 1589 1623 (Print) ● ISSN 1785 0037 (Online)
DOI: http://dx.doi.org/10.15666/aeer/1704_96519668

Table 2. *Correlation coefficient distance, average linkage amalgamation steps*

Step	Number of clusters	Similarity level	Distance level	Clusters joined		New clusters	Number of observation in new cluster
1	32	97.6422	0.04716	23	28	23	2
2	31	96.1314	0.07737	31	33	31	2
3	30	95.7281	0.08544	17	23	17	3
4	29	81.2948	0.37410	9	29	9	2
5	28	79.4171	0.41166	7	30	7	2
6	27	79.0926	0.41815	1	12	1	2
7	26	78.8213	0.42357	1	17	1	5
8	25	77.0723	0.45855	15	20	15	2
9	24	76.8737	0.46253	19	24	19	2
10	23	76.6006	0.46799	18	25	18	2
11	22	75.4615	0.49077	31	32	31	3
12	21	74.5501	0.50900	5	8	5	2
13	20	72.6308	0.54738	3	22	3	2
14	19	71.9760	0.56048	21	27	21	2
15	18	71.7084	0.56583	18	19	18	4
16	17	68.6349	0.62730	5	9	5	4
17	16	66.6087	0.66783	6	18	6	5
18	15	65.6034	0.68793	4	10	4	2
19	14	64.8900	0.70220	5	26	5	5
20	13	64.5707	0.70859	7	11	7	3
21	12	64.3221	0.71356	21	31	21	5
22	11	64.0159	0.71968	15	16	15	3
23	10	62.1014	0.75797	4	5	4	7
24	9	60.7311	0.78538	3	21	3	7
25	8	57.7172	0.84566	4	14	4	8
26	7	55.3648	0.89270	13	15	13	4
27	6	53.1801	0.93640	3	7	3	10
28	5	52.6014	0.94797	4	6	4	13
29	4	50.9603	0.98079	4	13	4	17
30	3	50.2563	0.99487	3	4	3	27
31	2	49.6676	1.00665	1	2	1	6
32	1	48.0233	1.03953	1	3	1	33

A landuse development model can be created based on decisions made from data obtained using the average linkage method. To understand the balanced distribution of land use with respect to accessibility to the services (such as schools, hospitals etc.), information on land use must be gathered and the lack of efficient social infrastructure must be identified. Efficient use of the land helps create sustainable and habitable cities by ensuring a sufficiently balanced hospital accessibility, green areas per person in square meters (or other ratio), or other infrastructure in urban development. In this sense, average linkage, which is obtained using the cophenetic coefficient correlation

http://www.aloki.hu ● ISSN 1589 1623 (Print) ● ISSN 1785 0037 (Online)
DOI: http://dx.doi.org/10.15666/aeer/1704_96519668

method in agglomerative hierarchical cluster analysis is the best approach. Thus, our findings in this study were evaluated using this type of analysis.

The results from our cluster analyses illustrated land use within each grid. With specific regard to how social infrastructure is distributed by identifying similar and different land uses within each grid and which precautions we should take in urban development plans based on these results, this study was able to obtain results that would help guide future planning. The results of the similar and different grids are provided below.

In the average linkage analysis, the 23rd and 28th grids emerged as the most similar; therefore, land use in these grids was examined in more detail. The 23rdgrid comprised 0.43% social areas, 1.56% park and playground areas, 36.80% forest areas, 0.52% afforestation areas, and 60.69% vineyard and orchard areas. On the other hand, the 28th grid comprised 50.52% forest areas and 49.48% vineyard and orchard areas. We observed that these grids are mostly composed of green spaces, although we also observed that urban development is slowly emerging within the 23rd grid. The observation that these two grids are near each other suggests that urban development within the 23rd grid will pose a threat to the green spaces within the 28th grid.

Using average linkage, we observed that the 1st and 3rd grids are most distant from each other. Murtagh and Legendre (2011) reported that the study conducted using the Lance–Williams (1967) used controlled dissimilarity of object distance for cluster analysis. In the present study, the differences among the grids were analyzed using cluster analysis, which found the most distance between the 1st and 3rd grids. In addition, the program that was used statistically analyzed the differences among the grids; therefore, we can consider that the 1st and 3rd grids are different from each other. Grid1 comprises3.6% traffic islands and 96.4% forest areas, whereas 100% of grid3 is composed of agricultural areas. The fact that, in particular, grid1 contains traffic islands implies that this space will threaten forest areas in the future; however, it can be argued that the same urban development approach should not be recommended for these spaces because the grids are highly dissimilar and that grid which consists of forest areas, does not have traffic islands.

Grids 5 and 9 emerged as not entirely the same but also not too distant from each other. These grids are located nearly in the middle in all three linkage methods. Grid5 comprises university areas (0.64%), tourism areas (0.14%), power distribution areas (0.14%), existing house areas (10.95%), technical infrastructure areas (0.28%), trade areas (0.71%), social areas (0.71%), neighborhood sport areas (0.71%), health service areas (0.36%), recreational areas (1.92%), median strips (0.21%), trade areas (0.85%), park and playground areas (7.32%), private education areas (0.36%), educational areas (2.56%), forest areas (9.31%), suggested house areas (51.10%), municipality service areas (0.85%), a creek–canal (3.20%), afforestation areas (6.68%), and places of worship (1%). On the other hand, grid9 comprises a university area (7.06%), existing house areas (45.36%), technical infrastructure (0.07%), trade areas (5.69%), social areas (0.52%), neighborhood sport areas (0.78%), health service areas (3.46%), government agency areas (0.59%), recreation areas (1.96%), median strips (0.13%), park and playground areas (8.24%), private education areas (0.13%), educational areas (3.40%), forest areas (0.46%), suggested housing areas (16.99%), a creek–canal (0.78%), afforestation areas (0.78), places of worship (0.65%), state railway areas (2.09%), and fuel areas (0.59%). Although both grids have significant empty space for proposed housing, we observed that the social infrastructure support that would be necessary after

http://www.aloki.hu ● ISSN 1589 1623 (Print) ● ISSN 1785 0037 (Online)
DOI: http://dx.doi.org/10.15666/aeer/1704_96519668

urban development, such as green spaces and healthcare units, is not adequate, and that no scenario to meet this need has been proposed. As stated, each grid covers an area of 1 km^2; therefore, there is an apparent need for additional space to support the social infrastructure within the grid.

This research methods helps to determine the adequacy of land use distribution and demonstrates how creating these grids can guide urban development administrators in their decisions for future development. Similarities and differences found in cluster analysis help us determine the extent to which the existing members of a good urban infrastructure are sufficient as well as what is still needed. By presenting an alternative approach, this method helps to revise urban development plans and develop better approaches to future development.

In our study, using the grid approach allowed us to reveal any insufficiency in the social infrastructure within the city. The need to overcome these insufficiencies in social infrastructure in future urban development is highlighted. The results of the analysis show that green areas and other social services mentioned in planning practices are not evenly distributed among close, far, and neither close nor far grids. For example, grid1 has a green area ratio of 96.4%—a large amount of green areas. The fact that urban pressure on green areas and that some social service areas in urban development encroach on green areas indicates that, in the future, urban areas will be developed in these areas. Thus, the municipality's development proposals should protect green areas within administrative limits. In addition, this clearly shows that urbanization has yet to begin in grid 1; therefore, green area standards are very high while social infrastructure, such as healthcare and education, is insufficient in this grid according to Turkey's planning standards, such as that requiring that a primary school should be within 500 m from residential areas. As mentioned, to balance this distribution through planning, we can calculate the balance of the distribution of green areas and other services within these grids, which are either higher or lower than the standards. For example, when we calculate green areas without distinguishing between passive and active green areas, only grid3 displays a problem, while grids 2 and 28appear to have achieved the standards. On the contrary, grids 2 and 28are insufficient in terms of land available for healthcare services, while grids 5 and 9 have sufficient land designated for healthcare. Land use planning in these areas was unbalanced with respect to healthcare services. To better understand land use patterns in the next stage of our study, we examined the correlations among the grids.

Using a correlation analysis, the relationships among grids can be understood more clearly. Analyses of land use in urban development helped us to determine the interplay among the grids as well as to identify the variables that shape the future direction of development. The correlation analysis revealed the development pattern of the city's land. The analysis shows that insufficient social infrastructure (such as healthcare facilities) in grids 2 and 28 are among the city's biggest problems. Considering the tourism factor that is characteristic of the city, which was revealed using correlation analysis, this problem should be considered a priority and must be addressed in any new developments.

When examining the social infrastructural units in detail within the grids, grids 1 1 1 2 2 3 and 29 attracted our attention. In the cluster analysis, we found that healthcare services came together in clusters 1 and 2. Access to healthcare services was within ~2–3 km between the grids. In grid one state-owned hospital provides full healthcare services. When we assessed the distribution of the existing residential areas, we

http://www.aloki.hu ● ISSN 1589 1623 (Print) ● ISSN 1785 0037 (Online)
DOI: http://dx.doi.org/10.15666/aeer/1704_96519668

observed that grids 1 22.2 and 30 were within 6–7 km of the hospital, which is relatively far in emergencies. Even if there is no space for healthcare within a reasonable distance, our analysis showed that roadways to hospitals from more distant grids and providing alternative transportation options are suitable alternatives.

To investigate the relationship among grids in cluster analysis in more detail, a correlation analysis was conducted on land use. A strong correlation of 0.99 was found among the grids and among daily travel areas. Moreover, there is a noteworthy correlation of 0.95 between daily travel areas and archeologically protected areas. The same correlation was observed between technical infrastructure areas and industrial areas. Because the transportation network in Amasya is central, a strong correlation among the grids and the archeologically protected areas and daily travel shows the strength of the city's tourism potential. In addition, we can prove a dependency for the development of industrial areas on technical infrastructure areas through the correlations found in terms of land use.

Discussion

Cluster analysis was used to statistically explain where similar land use areas were concentrated. Cluster analysis is an important method by which to identify similar planning approaches in areas with the same land use characteristics and urban development, for determining any existing deficiencies in social facilities, and for gaining an understanding of social transport distances. In addition, this analysis serves to determine which clusters yield positive or negative results on a region-by-region basis.

Agglomerative hierarchical cluster analysis yielded very important findings for Amasya, including how land use is distributed and how land use should be planned. Mcharg (1992) is credited with having developed a land suitability model to ensure a healthy and balanced land use structure; however, our study failed to discern an approach to identify the social facilities in the current planned area or to provide development based on such an approach.

A development plan that identifies areas lacking social facilities and how to eliminate these deficiencies is important because it helps to make our cities healthier and more livable. Land structure and transport are significant factors that affect development planning; therefore, despite the improvements we have achieved, the issue of the lack of social facilities within the city must be resolved to the greatest extent possible. Although the situation that emerged when we examined the grids in terms of transport distances appeared to be positive, particularly for the healthcare sector, the same could not be said about access to a full-service hospital.

It is found that spatial land use arrangement and development is the main planning approach for the healthy future development of the cities. Cortinovis et al. (2019) were also examined urban spatial development and were emphasized the spatial arrangement of land uses as a crucial issue in their research. The healthy distribution of social infrastructure is one of the key point to prove sustainable urban development in the cities.

We were able to examine both the existence and the lack of social infrastructure areas within the grids in this research. It is worth noting here that the results from the analysis demonstrated that the distribution of the social infrastructure was neither satisfactory nor within the boundaries that delineated accessibility. In making these

http://www.aloki.hu ● ISSN 1589 1623 (Print) ● ISSN 1785 0037 (Online)
DOI: http://dx.doi.org/10.15666/aeer/1704_96519668

determinations, the social infrastructure facilities that were within ~500 m of the center of the grids, in terms of accessibility, were taken into consideration.

A particularly remarkable finding was that the healthcare facilities were generally concentrated in clusters1 and while the educational facilities were largely concentrated in clusters and 4. Given that clusters1 and 2 were mostly within the city's center, the social facilities within these clusters were more accessible and numerous. Although the lay of the land appears to have negatively affected the social infrastructure balance in areas outside the city's center, grids19 and 24 within the city's center appeared to also experience the same negative impact because of the topography of its land.

In addition, not all of the educational institutions were at the same level of accessibility; that is, when we made the distinction among primary schools, we observed that not all educational facilities were within the 500 m-perimeter accessibility boundary. According to the results of the analysis of the land use map, planning decisions dictating that the planning areas within clusters be included as part of the planning activity are important for ensuring that the same planning perspectives can be established. Cluster analysis enabled us to define the areas in which a similar planning approach should be conducted. Grid analysis, which helps to evaluate accessibility and similarity, sheds light on how urban planning should be pursued.

The methods used in this research are proposed important approaches to helping to implement plans for healthy urban development. The similarities and differences identified within the grids through hierarchical cluster analysis provide important clues oriented toward urban development decisions. In addition, they help identify the shortcomings in urban social infrastructure, which is a key component of urban development, and help to make recommendations accordingly.

The grid system is an analytical tool that is frequently used with raster data and infrequently used for urban social services. The grids were developed to generate information about how urban areas are developed. This study used grids to enable a more detailed examination using vector data for the first time to analyze urban social services. Grids were formed using GIS and the Hawth's analysis tool, which is frequently used by ecologists and biologists, to create an essential guide to how urban areas are developed. The cluster analyses conducted from grids using Minitab, the most appropriate was average linkage analysis. Differences among the grids were examined, and the social service areas in the grids were analyzed. The results of the analyses generated important clues about whether social services were or were not in each grid and where they should have been located.

The analyses of the grids revealed the inadequacy of educational space, healthcare space, and space for parks and gardens. In this respect, authorities should take such social infrastructural spaces into consideration when making decisions about areas of urban development. The methods used in this study offer a new understanding and approach to urban development plans in Turkey.

Into summarize, this study analyzed whether the uses of space for social infrastructural, green area, tourism, commercial enterprises, educational facilities, and similar other social services are adequate and balanced in Amasya's land use plans. In the analyses, the Amasya urban development plan was partitioned into 33 grids, each of which covering 100 Ha. Accordingly, analyses were performed within the grids that were categorized as follows:

- Grids that comprise a planned space between ~90% and 100%,
- Grids that comprise a planned space of ~50%, and

http://www.aloki.hu ● ISSN 1589 1623 (Print) ● ISSN 1785 0037 (Online)
DOI: http://dx.doi.org/10.15666/aeer/1704_96519668

- Grids that comprise a planned space between ~10% and 25%.

We concluded based on these analyses that the City of Amasya Urban Development Plan was inadequate in its green area designations, and that it includes a faulty planning decision because it prescribes green spaces to be located at the extreme edges of urban space.

Our findings show the importance of a social infrastructure for a healthy urban environment. This fact, which this study makes apparent, is one of the most important elements to be discussed in approaches to urban development. A development plan's balanced distribution of social infrastructure in urban areas is important for a city's inhabitants. This study claims that urban land use is also significant for the development of social infrastructure.

Conclusion

The conclusion of this study found that a method by which to analyze an urban development plan can be balanced based on land use grids using cluster analysis. It also identified relationships between land use types using correlation analysis. There are several studies on land use; however, the focus of many is restricted to how land use has changed over the years. Unlike other studies, our study emphasizes the short comings in land use in terms of urban planning and identifies the deficiencies in the social infrastructural aspects of urban planning. The findings of this paper demonstrate that social infrastructure is insufficient in urban development and is not being distributed in a balanced way. In this sense, the focus is on the distribution of land use values in urban development, rather than on the changing values of land use in urban development. For example, a high density of green areas in one place and a lack of them in other places appears as an indication of whether that city is developing in a healthy and balanced way; therefore, this study brings a new perspective for future research. If we consider the findings of this study, we get a better understanding of the importance of social infrastructure in urban development.

In conclusion, the methods used in this study offer a new dimension to general land use and to the improvement of urban development plans in Turkey. These methods can be further improved in future studies because they provide a basis through which a new methodological approach can be used in other fields.

REFERENCES

[1] Alvarenga, R. A. F., Dewulf, J., Langenhove, H. V., Huijbregts, M. A. J. (2013): Exergy-based accounting for land as a natural resource in life cycle assessment. – The International Journal of Life Cycle Assessment 1(9): 939–947.

[2] Anonymous (2018): COPHENET. – https://www.mathworks.com/help/stats/cophenet.html (accessed 15.09.2018).

[3] Bayo, J., Castellanos, J. L. (2016): Principal factor and hierarchical analyses for the performance assessment of an urban wastewater treatment plant in the southeast of Spain. – Journal of Chemosphere 152-162.

[4] Bo, H., Shu, L., Shu-hua, L. (2011): Ecological landscape planning and design of an urban landscape fringe area: a case study of Yang' an District of Jiande City. 2011

http://www.aloki.hu ● ISSN 1589 1623 (Print) ● ISSN 1785 0037 (Online)
DOI: http://dx.doi.org/10.15666/aeer/1704_96519668

International Conference on Green Building and Sustainable Cities. – Procedia Engineering 21: 414-420.

[5] Cinelli, M., Coles, S. R., Kirwan, K. (2014): Analysis of the potentials of multi criteria decision analysis methods to conduct sustainability assessment. – Journal of Ecological Indicators 46: 138-148.

[6] Cortinovis, C., Haase, D., Zanon, B., Geneletti, D. (2019): Is urban spatial development on the right track? Comparing strategies and trends in the European Union. – Journal of Landscape and Urban Planning 18: 22-37.

[7] Dearing, J. A., Ademola, K. B., Anette, R., Billie, L. T., Sander, van der L. (2010): Complex land systems: the need for long time perspective to assess their future. – Ecology and Society 15(4): 21: 1-19.

[8] Erickson, D. (1995): Rural land use and land cover change. – Journal of Land Use Policy 1(3): 223-236.

[9] Everitt, B. S. (2005): An R and S-PLUS ® Companion to Multivariate Analysis. – Springer, London.

[10] Foley, J. A., Defries, R, Asner, G. P., Barford, C., Bonan, G., Carpenter, S. R., Chapin, F. S., Coe, M. T., Daily, G. C., Gibbs, H. K., Helkowski, J. H., Holloway, T., Howard, E. A., Kucharik, C. J., Monfreda, C., Patz, J. A., Prentice, I. C., Ramankutty, N., Snyder, P. K. (2005): Global consequences of land use. – Journal of Science 309(5734): 570-574.

[11] Governorship of Amasya (2017): City Guide of Amasya. – Publication Number 38. www.amasyakulturturizm.gov.tr/Eklenti/706rehber-tr-mailpdf.pdf?0 (accessed 25.09.2017).

[12] Grecchi, C. R., Gwyn, Q. H. J., Bénié, G. B., Formaggio, A. R., Fahl, F. C. (2014): Land use and land cover changes in the Brazilian Cerrado: a multidisciplinary approach to assess the impacts of agricultural expansion. – Journal of Applied Geography 55: 300-312.

[13] Hubacek, K., van den Bergh, J. C. J. M. (2006): Changing concepts of 'land' in economic theory: from single to multi-disciplinary approaches. – Journal of Ecological Economics 56: 5-27.

[14] Kline, J. D., Thiers, P., Ozawac, C. P., Yeakley, J. A., Gordone, S. N. (2014): How well has land-use planning worked under different governance regimes? A case study in the Portland, OR-Vancouver, WA Metropolitan Area, USA. – Journal of Landscape and Urban Planning 131: 51-63.

[15] Krekel, C., Kolbe, J., Wüstemann, H. (2016): The greener, the happier? The effect of urban land use on residential well-being. – Journal of Ecological Economics 121: 117-127.

[16] Lance, G., N., Williams, T. (1967): A general theory of classificatory sorting strategies 1. Hierarchical system. – The Computer Journal: 373-380.

[17] Liu, Y., Yang, R., Long, H., Gao, J., Wang, J. (2014): Implications of land-use change in rural China: a case study of Yucheng, Shandong Province. – Journal of Land Use Policy 40: 111-118.

[18] Lu, X., Ke, S. (2018): Evaluating the effectiveness of sustainable urban land use in China from the perspective of sustainable urbanization. – Journal of Habitat International 7: 90-98.

[19] Manjunath, M., Zhang, Y., Kim, Y., Yeo, S. H., Sobh, O., Russell, N., Followell, C., Bushell, C., Ravaioli, U., Song J. S. (2018): ClusterEnG: an interactive educational web resource for clustering and visualizing high-dimensional data. – Peer J Comput. Sci. 4: e155. DOI: 10.7717/peerj-cs.15.

[20] McHarg, I. L. (1992): Design with Nature, 25th Anniversary. – John Wiley and Sons Inc., Hoboken, NJ, pp.1-198.

[21] Milesia, C., Elvidgeb, C. D., Nemania, R. R., Running, S. W. (2003): Assessing the impact of urban land development on net primary productivity in the southeastern United States. – Journal of Remote Sensing of Environment 86: 401-410.

http://www.aloki.hu ● ISSN 1589 1623 (Print) ● ISSN 1785 0037 (Online)
DOI: http://dx.doi.org/10.15666/aeer/1704_96519668

[22] Mooi, E., Sarstedt, M. (2011): A Concise Guide to Market Research. The Process, Data, and Methods Using IBM SPSS Statistics. – Springer, Berlin.
[23] Murtagh, F., Legendre, P. (2011): Ward's hierarchical clustering method: clustering criterion and agglomerative algorithm. – arXiv:1111.6285.
[24] Niedertscheider, M., Erb, K. (2014): Land system change in Italy from 1884 to 2007: analysing the north-south divergence on the basis of an integrated indicator framework. – Journal of Land Use Policy 39: 366-375.
[25] Nuissl, H., Haase, D., Lanzendorf, M., Wittmer, H. (2009): Environmental impact assessment of urban land use transitions. A context-sensitive approach. – Journal of Land Use Policy 26: 414-424.
[26] Ozus, E., Akın, D., Çiftçi, M. (2012): Hieararchical cluster analysis of multicenter development and travel patterns in İstanbul. – Journal of Urban Planning and Development 138: 303-318.
[27] Paffi, M., Siragusa, A., Ferri, S., Halkia, M. (2016): Measuring the accessibility of urban green areas. – JRC Technical Reports, Publications Office of the European Union. http://publications.jrc.ec.europa.eu/repository/bitstream/JRC102525/190916_siragusa_%20jrc_techrep_accessibility_online.pdf (accessed 19.01.2018).
[28] Randolph, J. (2004): Environmental Land Use Planning and Management. – Island Press, Washington, DC.
[29] R Core Team (2015): R: A Language and Environment for Statistical Computing. – R Foundation for Statistical Computing, Vienna. http://www.R-project.org/ (accessed on 3 March 2017).
[30] Robinson, M. G. (1998): Methods and Techniques in Human Geography. – John Wiley and Sons Ltd., Chichester.
[31] Sharifi, A., Chiba, Y., Okamoto, K., Yokoyama, S., Murayama, A. (2014): Can master planning control and regulate urban growth in Vientiane, Laos? – Journal of Landscape and Urban Planning 131: 1-13.
[32] Shi, P., Yu, D. (2014): Assessing urban environmental resources and services of Shenzen China: a landscape-based approach for urban planning and sustainability. – Journal of Landscape and Urban Planning 125: 290-297.
[33] Singh, S. J., Haberl, H., Chertow, M., Mirtl, M., Schmid, M. (2013): Long-Term Socio-Ecological Research. Studies in Society: Nature Interactions Across Spatial and Temporal Scales. – Springer, New York, pp. 1-561.
[34] Song, Y., Merlin, L., Rodriguez, D. (2013): Comparing measures of urban land use mix. – Journal of Computers, Environment and Urban Systems 42: 1-13.
[35] Turkstat (Turkey Statistical Institute) (2012): Chosen Indicators of Amasya. – Publication Number 408. www.tuik.gov.tr/ilGostergeleri/iller/AMASYA.pdf (accessed 10.08.2014).
[36] Turkstat (Turkey Statistical Institute) (2018): Population Report of Amasya, Central Dissemination System. – https://biruni.tuik.gov.tr/medas/?kn=95&locale=en (accessed 31.03.2019).
[37] Türk, S., S. (2002): Land development and realization of local physical plans in urban areas in Turkey: a model. – FIG XXII International Congress, Washington DC. https://www.fig.net/resources/proceedings/fig_proceedings/fig_2002/Ts8-1/TS8_1_turk.pdf (accessed 20.06.2016).

http://www.aloki.hu ● ISSN 1589 1623 (Print) ● ISSN 1785 0037 (Online)
DOI: http://dx.doi.org/10.15666/aeer/1704_96519668

ASSESSMENT OF HEAVY METAL AND TOXIC ELEMENT CONTENT IN BARLEY (*HORDEUM VULGARE* L.) AND SOIL

BENGISU, G.

Department of Field Crops, Faculty of Agriculture, Harran University, Şanlıurfa-Mardin Karayolu Üzeri 18.Km, Harran, Sanliurfa, Turkey
(e-mail: gbengisu@hotmail.com; phone: +90-414-318-3000; fax: +90-414-318-3190)

(Received 13th Mar 2019; accepted 13th Jun 2019)

Abstract. One of the largest problems threatening human and animal health is environmental pollution, which has increased in parallel with industrialization and population growth. Because of environmental pollution, pollution in agricultural soils and plant products has approached dangerous levels. Barley, which is commonly used in animal nutrition and the food industry, is one of the plants that is affected by such pollution. In these plants, it is very important to determine the level of pollution present for the sake of both human and animal health. In accordance with this purpose, we measured the levels of Cd, Cu, Fe, Mn, Ni, Pb, and Znin barley plants and soil samples collected from three locations in Southeastern Anatolia, where barley production is common in Turkey. Results show that the concentrations of mineral elements except Fe in the soil samples are below critical limits. Instead of high Fe concentration in soils, all mineral elements in plant samples collected from all locations are below critical limits. The concentrations measured in soil and barley samples from the Kiziltepe location were the lowest.
Keywords: *barley, cadmium, copper, iron, manganese, nickel, lead, zinc*

Introduction

Irregular urbanization, the proximity of agricultural land to city centers, increased household and industrial wastes, heavy metals emitted from chimneys and exhaust fumes cause heavy metal accumulation in plants and, subsequently, changes in their physiological and genetic structures. While heavy metals such as copper (Cu), zinc (Zn), cobalt (Co), manganese (Mn), nickel (Ni) and molybdenum (Mo) are absolutely necessary for plant growth, lead (Pb), vanadium (V), aluminum (Al), arsenic (As), mercury (Hg), cadmium (Cd) and selenium (Se) have toxic effects. If the heavy metal content in plants is above the prescribed limit, serious health problems can develop in the humans and other animals that eat these plants (Okturen and Sonmez, 2006; Caglairmak and Hepcimen, 2010; Nagajyoti et al., 2010).

For example, cadmium has toxic effects on all organ systems in animals. In cases of cadmium poisoning, a decrease in feed consumption, reduced growth, infertility, a decreased number of pups, liver and kidney damage, anemia and death are observed (Bernhoft, 2013). In cattle with acute copper poisoning, gastrointestinal inflammation, swelling, diarrhea and the rapid loss of fluid-electrolyte are observed, and in other animals, loss of appetite and severe depression are observed. If acute poisoning is not treated, death may occur within three days (Scott et al., 2011). The most common effects of the Nickel poisoning are lung cancer, kidney edema, allergic reactions, a decreased number of sperm and sperm abnormalities (Kawanishi et al., 2001). Nausea, vomiting, epigastric pain, lethargy, and fatigue occur with extremely high levels of zinc intake (Fosmire, 1990). Manganese toxicity tends to lead to neurological symptoms, including headaches, muscle cramps, fatigue and aggressiveness (Aschner et al., 2009). Excess lead accumulates in the bones and destroys the kidney, brain and nervous system (Kahvecioglu et al., 2004). Excessive amounts of iron can damage to various organs and

http://www.aloki.hu ● ISSN 1589 1623 (Print) ● ISSN 1785 0037 (Online)
DOI: http://dx.doi.org/10.15666/aeer/1704_96699677

systems, especially the liver, pancreas and other endocrine organs, as well as the heart (Aydin, 2008).

Barley (*Hordeum vulgare* L.), which we have investigated in this study, is widely used in human nutrition and animal feeding. Barley is used as feed crop and the beer industry's main raw material in Turkey, and it is the second most produced cereal, with wheat being the first. Heavy metals are difficult to remove from the environment. They also cannot be chemically or biologically degraded (Chaney et al., 1997). Barley is among the best performing grass species in terms of extracting some toxic metals from the soil (Ebbs and Kochian, 1998).

In this study, we aimed to measure mineral element content (Cd, Cu, Fe, Mn, Ni, Pb and Zn) in barley plants and soil collected from various locations.

Material and methods

Sampling

The study was carried out in the Southeastern Anatolia region of Turkey in 2016. A total of thirty barley and soil samples were collected from three locations in this region from the Çınar District of Diyarbakir (Latitude: 37° 43' 27" N, Longitude: 40° 24' 54" E), the Siverek District of Şanlıurfa (Latitude: 37° 45' 7" N, Longitude: 39° 19' 55" E), and the Kızıltepe District of Mardin (Latitude: 37° 11' 23" N Longitude: 40° 34' 47" E) (*Fig. 1*).

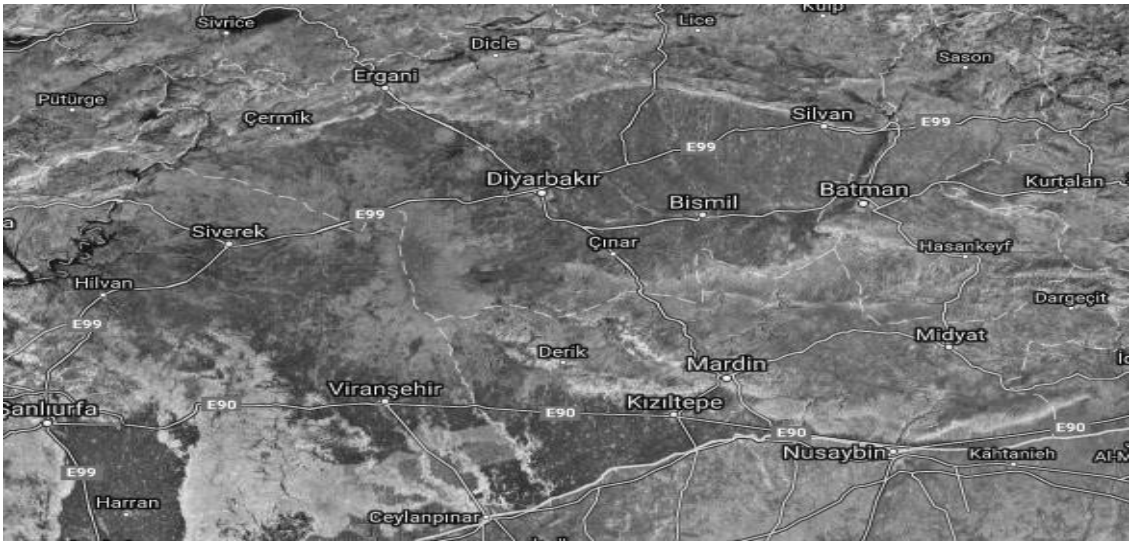

Figure 1. *Sampling locations (Çinar, Kiziltepe and Siverek)*

When the data for the soil and barley specimens were analyzed, ten samples from each station were analyzed separately, and the arithmetic average of the values obtained was found. All barley samples were commercially available. In order to preserve the original quality of the barley, the samples were stored at an ambient temperature in sealed plastic bags prior to any conditioning. Distilled water was further purified with a Milli-Q™ system (Millipore Corporation, USA) and used throughout the experiments. The hydrogen peroxide (H_2O_2, 30%) and nitric acid (HNO3, 65%) used for the digestion were of analytical grade (E. Merck, Darmstadt, Germany).

http://www.aloki.hu ● ISSN 1589 1623 (Print) ● ISSN 1785 0037 (Online)
DOI: http://dx.doi.org/10.15666/aeer/1704_96699677

Digestion procedure

A Berghof MWS-3 model microwave digestion system (Berghof, USA) was used for the digestion of the barley samples. Microwave (MW) digestion was carried out as follows: half-gram barley samples and a solid reference material were weighed and transferred into pressure-resistant PTFE vessels, and 9.0 mL of the acid mixture (HNO_3–H_2O_2, 2:1) was added to each sample. The vessels were closed, and a total of six samples were evenly spaced on the microwave oven carousel. The program of the MW digestion is provided below (*Table 1*).

Table 1. *Operating conditions for two-stage digestion by microwave oven (Tuzun and Yakut, 2009)*

Step 1	**1**	**2**	**3**	**Step 2**	**1**	**2**
T (0C)	140	160	190	T (0C)	160	100
Ta [min]a	5	3	5	Ta [min]a	3	1
Time [min]b	5	10	20	Time [min]b	15	15

The power applied was 800 W. After the digestion procedure, the reaction mixture was evaporated in order to remove the acids. Then, the residue was dissolved in approximately 25 mL of Milli-Q™ water (Millipore Corporation, USA). Then, ICP-OES measurements of Cd, Cu, Fe, Mn, Ni, Pband Zn were performed for the diluted solutions (Celik et al., 2014).

Instrumentation

An Optima™ 2100 DV (dual view) inductively coupled plasma optical emission spectrometer (Perkin Elmer, Inc., Shelton, CT, USA) was used for the determination of Cu, Fe, Mn, Ni, Pb and Zn in the barley and soil in the diluted solutions. The instrumental operating parameters are listed in *Table 2*. All of the procedures, from sampling to analysis, were also applied to blanks in order to evaluate any metal contamination during the analytical procedure. A blank was simultaneously prepared, and all procedures were applied before the measurements. The selection of the instrumental parameters and optical wavelengths was based on obtaining good sensitivity, ensuring reasonable detection limits and eliminating interferences (Duz et al., 2012). All samples were digested and analyzed in triplicate. The analytical wavelengths and average detection limits calculated for all measurements are listed below (*Table 2*).

Analytical procedure

The limits of detection (LOD) and limits of quantification (LOQ) for each metal were determined as follows: ten independent analyses of a blank solution spiked with the metal at a lower level concentration on the analytical curve were performed. The LOD and LOQ were calculated using the standard deviation (σ) of these determinations (LOD = 3 x σ, and LOQ = 10 x σ) (Bora et al., 2015). The analytical wavelengths and average detection limits calculated for all measurements, as well as the minimum, maximum and average concentrations of the elements in the samples, are listed below (*Table 3*).

http://www.aloki.hu ● ISSN 1589 1623 (Print) ● ISSN 1785 0037 (Online)
DOI: http://dx.doi.org/10.15666/aeer/1704_96699677

Table 2. *Operating conditions of the ICP-OES (Perkin Elmer Optima 2100 DV)*

Parameter	
RF power (W)	1450
Plasma gas flow rate (L min−1)	15
Auxiliary gas flow rate (L min−1)	0.2
Nebulizer gas flow rate (L min−1)	0.8
Sample flow rate (L min−1)	1.5
View mode	Axial
Read	Peak Area
Source equilibration time (s)	15
Read delay (s)	30
Replicates	3
Background correction	2-point (manual correction)
Spray chamber	Scott type
Nebuliser	Cross-Flow GemTip
Detector	CCD
Purge gas	Nitrogen
Shear gas	Air
Gas	Agron
Wavelength (nm)	Ni: 231.604, Se: 196.090

Table 3. *Linear range, regression, correlation coefficient (R), LOD and LOQ of the proposed method*

Element	Linear range (µg kg-1)	Regression	R	LOD (µg kg^{-1})	LOQ (µg kg^{-1})
Cd	0-100	y = 0.0354 x + 0.0180	0.9954	0.0132	0.0396
Cu	0-100	y = 2.2233 x + 1.8768	0.9997	0.3597	1.1978
Fe	0-100	y = 1.1027 x + 1.0178	0.9877	0.1287	0.4286
Mn	0-100	y = 0.3952x + 0.0158	0.9996	0.1768	0.5887
Ni	0-100	y = 0.7425 x + 0.2422	0.9999	0.4377	1.4575
Pb	0-100	y = 0.0879 x + 0.1034	0.9998	0.0832	0.2771
Zn	0-100	y = 0.2204 x + 0.4320	0.9997	1.2320	4.1025

Accuracy and precision of the method

As a certified standard reference material (CRM 1573a), tomato leaves (National Institute of Standards and Technology, NIST, Gaithersburg, MD, USA) were used to assess the accuracy and precision of the method. The accuracy of the entire proposed method was confirmed via a standard reference material analysis. As can be seen below (*Table 4*), the method was validated through the analysis of the CRM, NIST 1573a, with good recoveries.

Results and discussion

The average mineral element values for the soil samples taken from the three locations are provided in *Table 5*.

http://www.aloki.hu ● ISSN 1589 1623 (Print) ● ISSN 1785 0037 (Online)
DOI: http://dx.doi.org/10.15666/aeer/1704_96699677

Table 4. *Certified and determined values of metals in the CRM (NIST 1573a), tomato leaves*

Element	Certified value (mg/kg)	Found value (mg/kg)	Recovery
Cd	1.52 ± 0.04	1.50 ± 0.02	98.68
Cu	4.70 ± 0.14	4.68 ± 0.08	99.57
Fe	368 ± 7	364 ± 1	98.91
Mn	246 ± 8	249 ± 2	101.22
Ni	1.59 ± 0.07	1.62 ± 0.03	101.89
Pb	30.9 ± 0.7	32.1 ± 0.2	103.89
Zn	1.52 ± 0.04	1.50 ± 0.02	98.68

Table 5. *Average mineral element values for soil samples taken from three locations (mean ± standard deviation)*

Soil	Cd (mg/kg)	Cu (mg/kg)	Fe (%)	Mn mg/kg	Ni (mg/kg)	Pb (mg/kg)	Zn (mg/kg)
Cinar	1.02 ± 0.08	34.23 ± 2.43	1.67	24.5 ± 6	18.37 ± 0.89	3.59. ± 0.46	66.74 ± 2.13
Kiziltepe	0.94. ± 0.05	25.78 ± 1.65	1.28	10.2 ± 4	15.52 ± 0.13	2.44 ± 0.14	59.14. ± 0.94
Siverek	0.96 ± 0.07	29.05 ± 1.21	2.56	17.6 ± 4	19.24 ± 0.25	2.98 ± 0.24	67.37 ± 3.28

As shown in *Table 5*, the heavy metal contents of the soil samples were determined to be 0.94-1.02 mg/kg for Cd, 25.78-34.23 mg/kg for Cu, 1.28-2.56% for Fe, 10.2-24.5 mg/kg for Mn, 15.52-19.24 mg/kg for Ni, 2.44-3.59 mg/kg for Pb and 59.14-67.37 mg/kg for Zn. The highest values for Cd (1.02 mg/kg), Cu (34.23 mg/kg), Mn (24.5 mg/kg) and Pb (3.59 mg/kg) were obtained from the Çınar location. The highest values for Fe (2.56%), Ni (19.24 mg/kg), and Zn (67.37 mg/kg) were found in the Siverek location's soil. The Kızıltepe location's soil had the lowest values for all elements. The data obtained from the Fe measurements are expressed as percentages because the measured values are too high in soils. The averages of mineral element values of barley samples taken from three locations are given below (*Table 6*).

Table 6. *Average mineral element values for barley samples taken from three locations (mean ± standard deviation)*

Barley	Cd mg/kg	Cu (mg/kg)	Fe (mg/kg)	Mn mg/kg	Ni (mg/kg)	Pb (mg/kg)	Zn (mg/kg)
Cinar	N.D.	4.14 ± 0.21	67.14 ± 1.27	19.13 ± 0.45	1.71 ± 0.15	0.65 ± 0.03	18.89 ± 0.85
Kiziltepe	N.D.	2.57 ± 0.14	47.54 ± 0.82	9.48 ± 0.12	1.44 ± 0.63	N.D.	15.69 ± 0.64
Siverek	N.D.	3.42 ± 0.50	96.94 ± 4.28	15.14 ± 0.89	2.12 ± 0.28	0.54 ± 0.05	20.56 ± 1.43

N.D.: undeterminable

As shown in *Table 6*, the heavy metal content of the barley samples was 2.57-4.14 mg/kg for Cu, 47.54-96.94 mg/kg for Fe, 9.48-19.13 mg/kg for Mn, 1.44-2.12 mg/kg for Ni, 0.54-0.65 mg/kg for Pb and 15.69-20.56 mg/kg for Zn. The amount of Cd in the barley plants was undeterminable (N.D.) for all locations. Lead measurements were also undeterminable (N.D.) in barley samples taken from Kızıltepe location. While the highest mean values of Cu (4.14 mg/kg), Mn (19.13 mg/kg) and Pb

http://www.aloki.hu ● ISSN 1589 1623 (Print) ● ISSN 1785 0037 (Online)
DOI: http://dx.doi.org/10.15666/aeer/1704_96699677

(0.65 mg/kg) were obtained for the Çınar location, the highest Fe (96.94 mg/kg), Ni (2.12 mg/kg) and Zn (20.56 mg/kg) values were obtained from the Siverek location. The Kızıltepe location had the lowest average values for all elements.

When we consider the soil and plant samples analyzed, we see that the Kızıltepe location has less Cd, Cu, Fe, Mn, Ni, Pb and Zn content than the Çınar and Siverek locations. The presence of Cd in plant samples taken from all three locations and Pb in samples taken from the Kiziltepe location could not be determined.

The heavy metal limit for European countries, according to the Republic of Turkey's Ministry of Environment and Urban Soil Pollution Control Regulations limit values for heavy metals in soil and the WHO/FAO values for plants, are provided in *Tables 7, 8* and *9*.

Table 7. *The heavy metal limit values for European Countries, mg/kg (Ozturk, 2017)*

Country	Quality standard	Cd	Cu	Ni	Pb	Zn
Austria	Regulation on Biowaste Class A	1	150	60	120	500
Belgium	Ministry of Agriculture	1.5	90	20	120	300
Denmark	Ministry of Agriculture	0.4	1000	30	120	4000
Germany	Regulation on Biowaste Type II	1.5	100	50	150	400
Ireland	Draft	1.5	100	50	150	350
Luxembourg	Ministry of Environment	1.5	100	50	150	400
Netherland	Second Class Compost	1	60	20	100	200
Spain	Class A	2	100	60	150	400
Sweden	Quality Assurance Organization	1	100	50	100	300
England	TCA Quality Label	1.5	200	50	150	400

Table 8. *The heavy metal limit values for soil in Turkey (Anonymous, 2005)*

Elements	pH 5-6 (mg/kg)	pH > 6 (mg/kg)
Cd	1	3
Cu	50	140
Fe	4.5	4.5
Mn	70	70
Ni	30	75
Pb	50	300
Zn	150	300

Table 9. *The heavy metal limit values allowed by the WHO/FAO for plants (FAO/WHO, 2003)*

Elements	Limit values (mg/kg)
Cd	0.5
Cu	5
Fe	30
Ni	5
Pb	2
Zn	50

http://www.aloki.hu ● ISSN 1589 1623 (Print) ● ISSN 1785 0037 (Online)
DOI: http://dx.doi.org/10.15666/aeer/1704_96699677

Comparing *Tables 7, 8* and *9*, we can see that the amounts of mineral elements in the plant and soil samples are generally within the permissible limits. However, the Fe in both the soil and plant samples is well above the limit values for all three locations. The Fe is twice the allowed amount in the Çınar location and three times that in the Siverek location. Excess Fe element in the soil causes excess Fe in plant samples. In all three locations, the increased Fe, both in the soil and in the vegetation, is due to the fact that the soils and rocks of the region are rich in Fe. Özkan (2017) notes that as the distance from the highways decreases, the heavy metal levels in the plant and soil decrease in proportion to the distance. Our study suggests, no heavy metal pollution in the soil and in the plants growing in the study locations. In addition, he reports that in this soil, Fe levels are slightly above but the limit value but do not constitute a problem for plants (Ozkan, 2017). Karataş et al. (2007) investigated the concentrations of Cu, Cr, Ni and Pb in agricultural soils and wheat and reported that the heavy metal concentration in wheat did not reach the level of toxicity (Karatas et al., 2007).

Similar studies of mineral substances have been conducted. In a study conducted in the province of Elazığ, Cu, Ni and Mn content were reported to be 1595, 489 and 1406 ppm, and these values were several times higher than those found in uncontaminated soils (Sasmaz and Yaman, 2008). In the soil of the Gediz basin, the following values have been reported: Pd 5.98-15.5 μg/g, Cd 1.5-3.2 μg/g, Ni 16.9-39.17 μg/g, Cu 26.04-65.9 μg/g, Fe 11.69-30.0 μg/g and Zn 38.33-106.6 μg/g (Oner and Celik, 2011). Copper, Zn, Fe, Ni, and Mn were found to be in the range of 20-50, 77-1443, 26 353-66 815, 20-61 and 152-1320 ppm in soil samples investigated in Niğde Province, respectively (Turan et al., 2006). In China, the heavy metal content of sediments was found to be as follows: Zn 59.85 mg/kg, Cu 24.81 mg/kg, Pb 18.31 mg/kg, Ni 9.24 mg/kg, Cd 0.34 mg/kg (Wu et al., 2015). In Polonia, the following values were found: Cd 1.1-2.1 mg/kg, Ni 6.3-15.1 mg/kg, Cu 3.8-73.1 mg/kg, Pb 30.5-94.1 mg/kg, Zn 43.0-189.7 mg/kg, Mn 34.3-225.5 mg/kg and Fe 1853.3-21198.5 mg/kg (Mazur et al., 2013).

Correlation analysis between investigated traits

Correlation coefficients were calculated with the JMP statistical program (software of the SAS program) to identify the relationships between the investigated parameters (Kalayci, 2005). The correlation analysis of the six heavy metals is shown in *Table 10*. It can be seen from *Table 10* that strong positive correlations were observed for Fe-Ni, Fe-Zn, Fe-Pb, Ni-Zn, Cu-Pb, Cu-Mn, Zn-Pb and Pb-Mn, indicating the existence of a common origin for these metals.

Table 10. *Correlation analysis of heavy metal concentrations for barley in the study area*

	Fe	**Ni**	**Cu**	**Zn**	**Pb**	**Mn**
Fe	1.00	0.89**	0.46	0.95**	0.69*	0.50
Ni		1.00	0.22	0.91**	0.55	0.33
Cu			1.00	0.54	0.91**	0.94**
Zn				1.00	0.81**	0.63
Pb					1.00	0.96**
Mn						1.00

** and * correlations are significant at the 0.01 and 0.05 level, respectively

http://www.aloki.hu ● ISSN 1589 1623 (Print) ● ISSN 1785 0037 (Online)
DOI: http://dx.doi.org/10.15666/aeer/1704_96699677

The greatest correlation coefficient (r = 0.96) was observed between Pb and Mn, and the lowest correlation coefficient (r = 0.22) was identified between Ni and Cu. There isa very important positive relationship between Fe with Ni and Zn, between Ni and Zn, between Cu and both Pb and Mn, between Zn and Pb, between Pb and Mn, and between Pb and Fe.

Conclusions

In areas where industrial wastes are released into the environment without being subjected to any filtering treatment, heavy metal levels are well above the values allowed in the soil. These heavy metals accumulating in the soil have passed through underground water resources and vegetation and threatened human and animal health. As seen in this study, heavy metal pollution in rural areas is typically within prescribed limits without Fe content. This situation is desirable. However, the repetition of similar studies at specific time intervals is important for in continuing this positive situation.

REFERENCES

[1] Anonymous (2005): Official newspaper. – Regulation of Control of Soil Pollution. No: 25831: Date: 31.05.2005.
[2] Aschner, M., Erikson, K. M., Herrero Hernández, E., Tjalkens, R. (2009): Manganese and its role in Parkinson's disease: from transport to neuropathology. – Neuromolecular Med 11: 252-267.
[3] Aydin, I. (2008): Comparison of dry, wet and microwave digestion procedures for the determination of chemical elements in wool samples in Turkey using ICP-OES technique. – Microchem. J. 90: 82-87.
[4] Bernhoft, R. A. (2013): Cadmium toxicity and treatment. – The Scientific World Journal. Article ID 394652.
[5] Bora, T., Aksoy, C., Tunay, Z., Aydın, F. (2015): Determination of trace elements in illicit spice samples by using ICP-MS. – Microchemical Journal 123: 179-184.
[6] Caglairmak, N., Hepcimen, A. Z. (2010): Effect of heavy metal soil pollution on food chain and human health. – Academic Food J. 8: 31-35.
[7] Celik, K. S., Aydin, F., Duz, M. Z., Aydin, I., Erdogan, S., Akbag, O., Hamamci, C. (2014): Simultaneous determination of transition metals in hazelnuts (Corylusavellana L.) by ICP-OES. – Atomic Spectroscopy 35: 200-204.
[8] Chaney, R. L., Malik, M., Li, Y. M., Brown, S. L., Brewer, E. P., Angle, J. S., Baker, A. J. M. (1997): Phytoremediation of soil metal. – Curr Opin Biotechnol 8: 279-284.
[9] Duz, M. Z., Celik, K. S., Aydin, I., Erdogan, S., Aydin, F., Hamamci, C. (2012): Microwave digestion followed by ICP-OES for the determination of Al, Cd, Cr, Cu, Fe, Ni, Pb, and Sn in maize. – Atomic Spectroscopy 33: 78-82.
[10] Ebbs, S. D., Kochian, L. V. (1998): Phytoextraction of zinc by oat (Avena sativa), barley (Hordeum vulgare), and Indian mustard (Brassica juncea). – Environmental Science & Technology 32(6): 802-806.
[11] FAO/WHO (2003): Codex Alimentarius International Food Standards Codex Stan - 179: 2003. – Codex Alimentarius Commission, Rome.
[12] Fosmire, G. J. (1990): Zinc toxicity. – Am J ClinNutr 51: 225-227.
[13] Kahvecioglu, O., Kartal, G., Guven, A., Timur, S. (2004): Environmental effects of metals-III. – Metalurjij. 138: 64-71.
[14] Kalayci, M. (2005): Use JUMP with Examples and Anova Models for Agricultural Research. – Anatolia Agricultural Research Institute Directorate Publications No: 21.

http://www.aloki.hu ● ISSN 1589 1623 (Print) ● ISSN 1785 0037 (Online)
DOI: http://dx.doi.org/10.15666/aeer/1704_96699677

[15] Karatas, M., Guler, E., Dursun, S., Ozdemir, C., Argun, M. E. (2007): Determination of Cu, Cr, Ni and Pb concentrations in wheat and agricultural soils collected from Cengilli site of Konya main wastewater system. – S Ü Fen Ed Fak Fen Derg 29: 91-99.
[16] Kawanishi, S., Inoue, S., Oikawa, S., Yamashita, N., Toyokuni, S., Kawanishi, M., Nishino, K. (2001): Oxidative DNA damage in cultured cells and rat lungs by carcinogenic nickel compounds. – Free Radic Biol Med 31: 108-16.
[17] Mazur, Z., Radziemska, M., Maczuga, O., Makuch, A. (2013): Heavy metal concentrations in soil and moss (Pleuroziumschreberi) near railroad lines in Olsztyn (Poland). – Fresenius Environmental Bulletin 22(4): 957-963.
[18] Nagajyoti, P. C., Lee, K. D., Sreekanth, T. V. M. (2010): Heavy metals, occurrence and toxicity for plants: a review. – Environmental Chemistry Letters 8: 199-216.
[19] Okturen, A., Sonmez, F. (2006): The effect of heavy metal toxicity on plant metabolism. – Derim 23(2): 36-45.
[20] Oner, O., Celik, A. (2011): Investigation of some pollution parameters in water and sediment samples collected from the lower Gediz River Basin. – Ekoloji 20(78): 48-52.
[21] Ozkan, A. (2017): Heavy metal pollution in agricultural lands and plants around Antakya-Cilvegözü highway. – Çukurova University Journal of the Faculty of Engineering and Architecture 32(3): 9-18.
[22] Ozturk, M. (2017): Compost Production from Animal Behavior and Wastes. – Ministry of Environment and Urbanization, Ankara.
[23] Sasmaz, A., Yaman, M. (2008): Determination of Different Metal Levels in Soil, Plant and Water Samples in the vicinity of Maden (Elazığ) Copper Bed. – The Scientific and Technological Research Council of Turkey, Project Number: 105Y051.
[24] Scott, P. R., Penny, C. D., Macrae, A. I. (2011): Cattle Medicine. – Manson Publishing Ltd., London.
[25] Turan, H., Ozdemir, Z., Zorlu, S. (2006): Investigation of biogeochemical anomalies for Cu, Zn, Fe, Mn and Ni in the Çiftehan (Ulukışla-Niğde) area. – İstanbul Üniv. Müh. Fak. Yerbilimleri Dergisi 19(2): 131-140.
[26] Tuzun, Y., Yakut, M. (2009): Iron metabolism and hereditary hemochromatosis. – Current Gastroenterology 13: 94-100.
[27] Wu, Z., Geng, J., Huang, L. (2015): Heavy metal contamination in sediments and mangroves from Maowei Gulf, South China. – Fresenius Environmental Bulletin 24(3b): 1091-1097.

http://www.aloki.hu ● ISSN 1589 1623 (Print) ● ISSN 1785 0037 (Online)
DOI: http://dx.doi.org/10.15666/aeer/1704_96699677

NATURAL HERBICIDAL POTENTIAL OF SELECTED PLANTS ON GERMINATION AND SEEDLING GROWTH OF WEEDS

ANWAR, T.[1*] – ILYAS, N.[1] – QURESHI, R.[1] – QURESHI, H.[1] – KHAN, S.[2] – KHAN, S. A.[3] – FATIMAH, H.[4] – WASEEM, M.[4]

[1]*Department of Botany, Pir Mehr Ali Shah Arid Agriculture University, Murree Road, Shamsabad, Rawalpindi, 46300 Punjab, Pakistan*

[2]*Department of Environmental Science, Gomal University, Dera Ismail Khan, 29050 Khyber Pakhtunkhwa, Pakistan*

[3]*Department of Earth and Environmental Science, Bahria University, Islamabad Campus Shangrilla Road, Sector E-8, Islamabad 44000, Pakistan*

[4]*Department of Biology, Allama Iqbal Open University, H-8, Islamabad 44000, Pakistan.*

**Corresponding author*
e-mail: drtauseefanwar@yahoo.com; phone: +92-333-686-0562

(Received 14th Mar 2019; accepted 1st May 2019)

Abstract. Use of synthetic herbicides is increasing globally. Application of heavy doses of herbicides is directly / indirectly causing negative impact on crop quality, human health and environment. Allelopathic weeds have wide application prospects in increasing crop production, plant protection and biological control. Current study was conducted to evaluate allelopathic activity of aqueous extracts of *Carica papaya, Lantana camara, Rhazya stricta* and *Pinus roxburghii* against selected weeds viz. *Phalaris minor*, *Avena fatua*, *Chenopodium album*, *Euphorbia helioscopia* and *Rumex dentatus* on filter paper, soil and agar at 100%, 75%, 50% and 0% concentration. Germination percentage (%), radicle length (cm) and plumule length (cm) were parameters to assess allelopathic potential. The STATISTIX 9 software was used to analyse data. Based on results, it was concluded that aqueous extract of *R. stricta, P. roxburghii, C. papaya* and *L. camara* possess potential inhibitory effects amongst which *L. camara* showed most prominant inhibitory effects towrads weeds. The germination and growth inhibition effects were found in order *L. camara*>*P. roxburghii*>*R. stricta*>*C. papaya*. Detailed field study is recommended to establish allelopathic potential of these species.
Keywords: *food security, allelopathic potential, weed management, growth retardation, aqueous extract, natural herbicides*

Introduction

Food production must increase by 70% to feed world population that is expected to reach 9.6 billion by 2050. This challenge is even greater, when we take into account the scarcity of new arable land, the effects of climate change on agricultural production and the societal demand for decreasing the environmental impact of agriculture. Weed management will be of crucial importance, given that crop yield losses caused by weeds (about 32%) are higher than those caused by either pathogens (15%) or pests (18%) (Van Evert et al., 2016). Several studies have reported significant yield losses in corn due to weed competition. Edalat et al. (2011) estimated a global 10% loss of agricultural production due to competitive effect of weeds.

Wheat (*Triticum aestivum* L.) is one of the most important cereal crop of the world. Its role is quite important in provision of human nutrition. Its contents comprise starch (59-89%), protein (10-15.4%), fats (1.4-2.1%), inorganic ions (1.3-2.2%), vitamin E, and vitamin B-complex. Wheat provides about 73% of caloric portion of a person's average diet (Rueda-Ayala

http://www.aloki.hu ● ISSN 1589 1623 (Print) ● ISSN 1785 0037 (Online)
DOI: http://dx.doi.org/10.15666/aeer/1704_96799689

et al., 2011). The average annual production of wheat is quite low in Pakistan compared to other agricultural economies. There are two ways for increasing wheat production; (1): by increasing cultivation area (2): by increasing yield per hectare. The first option is not practicable due to limited availability of land and irrigation water. Therefore, wheat production in Pakistan can only be increased by getting higher yield per hectare. There are many factors, which cause dcrease wheat production e.g., delayed sowing, less amount of fertilizers and weed interference. Weed infestation is serious threat to wheat production (Khan et al., 2016). In Pakistan, weeds cause about 45% loss in wheat production. Grain produce in Pakistan can be increased up to 41% if weeds are managed properly (Anwar et al., 2019). If weed management strategies are not devised, greater production losses in wheat yield can take place.

Traditional methods of weed control are time consuming and laborious. Although chemical control may enhance crop production, but concurrently effect the environment and human health. In addition, heading up of synthetic herbicide resistant weeds is another area of concern (Arafat et al., 2015). Herbicide remnants in crops, soil and underground water, cause evolution of resistant weed biotypes and are linked to health threats. Due to negative effect of synthetic chemicals, we are in demand of new classes of chemicals, especially, biodegradable products such as those originating from plants, which have the potential of being developed as herbicides (Aryakia et al., 2015). Allelopathy is a natural and eco-friendly technique. This strategy might be one of the very efficient tools for weed management and thereby increasing crop production (Kamran et al., 2017). Allelochemicals could be obtained from different tissues (flower, roots, stem and leaves) of plants (Zhou et al., 2004). These chemicals have capacity of producing wide array of biological effects and are quite useful for weed control processes (Ahmed et al., 2014). Natural herbicides obtained from allelopathic plants can help in reducing usage of synthetic herbicides. Natural herbicides will cause less pollution as well as alleviate human health concerns. The most commonly available allelochemicals are cinnamic and benzoic acids, alkaloids, flavonoids, phenolics, glucosionates and terpenes (Khan et al., 2014).

Keeping all this in view, present study conducted to evaluate *Rhazya stricta* Decne, *Lantana camara* L., *Carica papaya* L. and *Pinus roxburghii* Sarg. for allelopathic activity against major weeds of wheat crop viz. *Phalaris minor*, *Avena fatua*, *Chenopodium album*, *Euphorbia helioscopia* and *Rumex dentatus*. Selection of the plants was baseed on available literature about allelopathy of these plants (Qureshi et al., 2014; Sharma et al., 2016; Garima and Devi, 2017; Alqarawi et al., 2018).

Materials and methods

Allelopathic potential of leaves of selected plants viz., *R. stricta, P. roxburgii, C. papaya, L. camara* was evaluated. Fresh leaves for each species were collected, washed under running tap water and dried at 30°C in laboratory. Dried leaves were crushed using heavy duty blender to make fine powder (mesh size 2 mm) and preserved in air tight plastic zip lock bags. Seeds of test weeds viz. *Phalaris minor, Avena fatua, Chenopodium album, Euphorbia helioscopia* and *Rumex dentatus* were procured from the Barani Agricultural Research Institute (BARI), Pakistan. Seeds were surface sterilized by 2% solution of Sodium hypochlorite (Biljana and Kragujevac, 2015).

Dried leaf powder of each plant species (10 gm) was soaked in 100 ml distilled water and agitated for 24 hours on orbital shaker (25ºC;160 rpm). The filtrate was obtained through Whatman filter paper No. 1. The final volume of filtrate was adjusted to 100 ml that gave 10% water extract as stock solution. Three concentrations i.e. T_1 (0%), T_2 (50%), T_3 (75%) while T_4 (100%) were further prepared. Bioassays were carried out using soil and filter paper as medium.

http://www.aloki.hu ● ISSN 1589 1623 (Print) ● ISSN 1785 0037 (Online)
DOI: http://dx.doi.org/10.15666/aeer/1704_96799689

An aliquot (15 ml) of extract for each of three concentrations was added on 25 g soil per petri dish while 5 ml extract on filter paper per petri dish. Ten seeds of weed test species were used per petri dish. Each treatment was replicated three times. The petri dishes were wrapped with aluminium foil and incubated in growth chamber (NTS Model MI-25S set at 28°C) for 15 days (Anwar et al., 2017). The germination percentage (%), lengths of radicle and plumule (cm) was calculated by comparing to control (Maharjan et al., 2007). The statistical analysis was carried out using STATISTIX 9 and means were separated by Fisher's protected LSD test (Nekonam et al., 2014).

Results and Discussion

Allelopathic potential of R. stricta

The results showed that *R. stricta* aqueous extract inhibited seed germination of *C. album* (35%) followed by *R. dentatus* (32%) and *P. minor* (31%) on filter paper, whereas, there was non-significant effect on germination percentage of *A. fatua* and *E. helioscopia*. Similarly, *R. stricta* aqueous extract on soil inhibited seed germination of *R. dentatus* (40%), *C. album* (39%) and *P. minor* (37%). Maximum (96%) seed germination was observed for *A. fatua* and *E. helioscopia* while minimum seed germination was noted for *C. album* (65%) and *R. dentatus* (60%) on filter paper and soil, respectively. It indicated inhibitory compounds in leaves of *R. stricta*. The results agree with Chon et al. (2005) who proposed growth reduction in test species by toxic compounds in *R. stricta* leaf aqueous extract. Maximum radicle length inhibition was shown by *R. dentatus* (44%) and *A. fatua* (40%) by *R. stricta* aqueous extract on filter paper. Likewise, extract on soil caused radicle length reduction of *R. dentatus* (48%) followed by *A. fatua (*45%). Radicle length of *C. album*, *P. minor* and *E. helioscopia* remained unaffected. The minimum radicle length was observed for *R. dentatus* (56% and 52% on filter paper and soil, respectively) while maximum radicle length (97%) was noted for *C. album*, *P. minor* and *E. helioscopia*. Aqueous extract of *R. stricta* significantly inhibited the plumule length of *A. fatua* (27%) and *R. dentatus* (25%) on filter paper. Interestingly, there was no inhibitory effect on plumule of *P. minor*, *E. helioscopia* and *C. album*. *R. stricta* aqueous extract inhibited plumule length of *A. fatua* (33%) and *R. dentatus* (28%) in soil. Minimum plumule length was noted for *T. aestivum* (49%) on filter paper and soil (45%) while maximum plumule length was noted for *P. minor*, *E. helioscopia* and *C. album* (96% for all) (*Fig. 1*). Wardle et al. (1992) noted that seed germination, radicle and plumule growth for grass weeds were significantly reduced by *R. stricta* extract. Similar results were reported by Assaeed and Al-Doss (1997) who reported inhibitory effect on germination rate and percentage of test species along morphological irregularities in radicle and plumule of test species (*Farsetia aegyptia, Pennisetum divisum, Haloxylon salicornicum*, *Lasiurus scindicus*) by leaves of *R. stricta*. Growth was significantly affected by allelopathic interaction on soil in contrast to filter paper as described by Hegazy and Fadl-Allah (1995) and El-Khatib (2000). While exploring possible mechanism of action, Alqarawi et al. (2018) reported growth and metabolism disfunctioning in *S. villosa* by *R. stricta* leaf aqueous extracts by hampering membrane functioning and photosynthetic capacity. El-khawas and Shehata (2005) reported change in enzyme activities, which affect the transport of storage substances in seed during growth. Furthermore, toxic compounds in *R. stricta* extract affect osmotic factors (Assaeed and Al-Doss, 1997).

http://www.aloki.hu ● ISSN 1589 1623 (Print) ● ISSN 1785 0037 (Online)
DOI: http://dx.doi.org/10.15666/aeer/1704_96799689

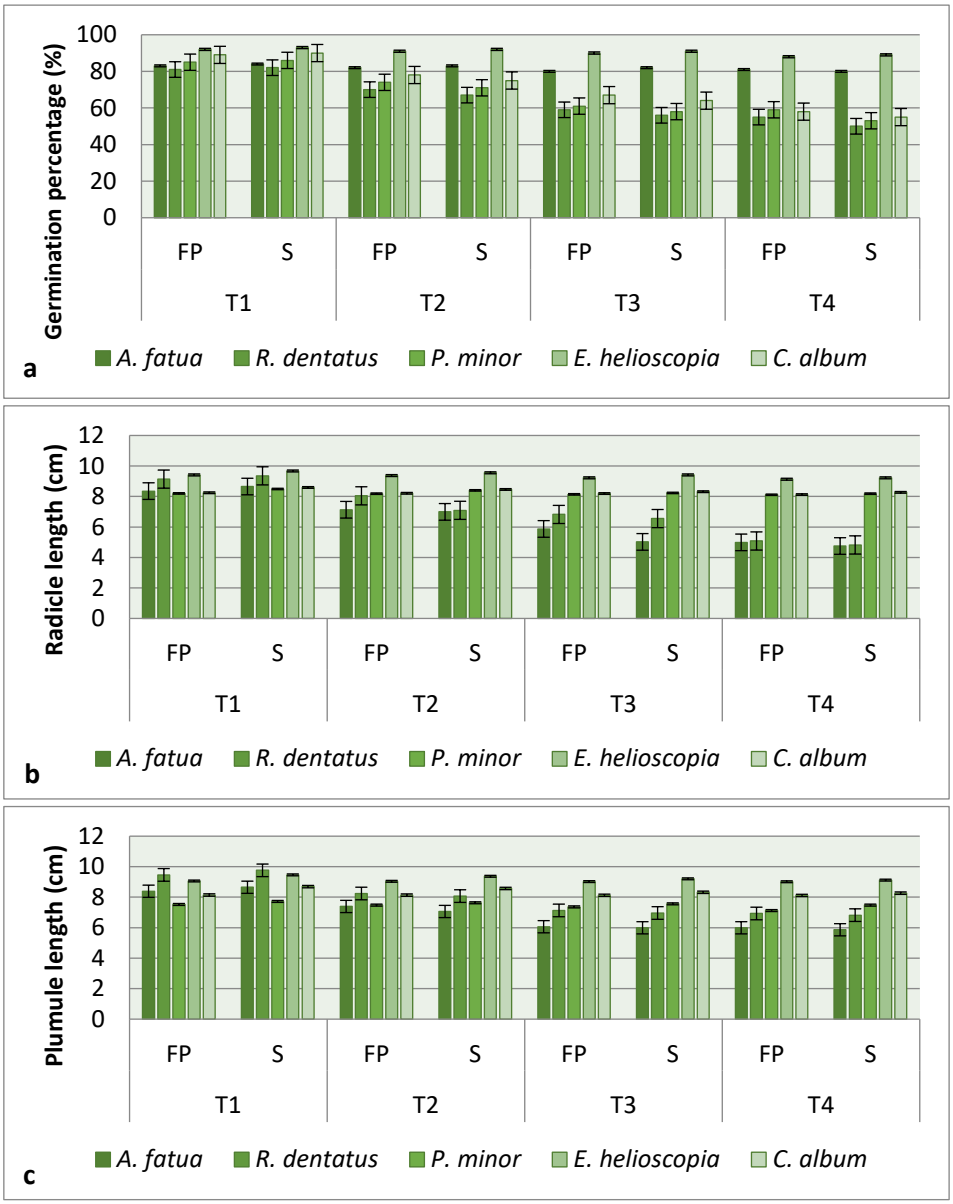

Figure 1. *Allelopathic potential of R. stricta aqueous extract on (a): germination percentage, (b): radicle length (c): plumule length against test species on filter paper (FP) and soil (S) where; T_1 (control), T_2 (50%), T_3 (75%) and T_4 (100%)*

Allelopathic potential of L. camara

L. camara aqueous extract inhibited seed germination of *R. dentatus* (58%) followed by *E. helioscopia* (57%), *A. fatua* (56%) and *P. minor* (55%) on filter paper and *E. helioscopia* (65%) followed by *P. minor* (63%), *R. dentatus* (61%), *A. fatua* (60%) on soil. Maximum (96%) germination was observed for *C. album* while minimum for *A. fatua* (42%) and *E. helioscopia* (35%) on filter paper and soil, respectively. Jabeen and Ahmed (2009) found germination and growth inhibition in *Cucurbita pepo* by allelopathic action of *L. camara* leaf aqueous extract. Highest radicle length inhibition was exhibited by *A. fatua* (52%), *P. minor* (51%) and *C. album* (50%) on filter paper, while on soil extract caused significant radicle length reduction of *A. fatua* (54%),

http://www.aloki.hu ● ISSN 1589 1623 (Print) ● ISSN 1785 0037 (Online)
DOI: http://dx.doi.org/10.15666/aeer/1704_96799689

P. minor (53%) and *C. album* (52%). Minimum radicle length was noted for *A. fatua* i.e. 48% and 46% on filter paper and soil, respectively. Maximum radicle length was noted for *R. dentatus* and *E. helioscopia* (97% for each). Aqueous extract of *L. camara* inhibited plumule length of *E. helioscopia* (52%), *A. fatua* (51%), *R. dentatus* (50%) and *C. album* (50%) on filter paper. There was no significant effect on plumule elongation of *P. minor*. Likewise, *L. camara* aqueous extract inhibited plumule length of *E. helioscopia* (56%), *C. album* (55%), *R. dentatus* (53%) and *A. fatua* (53%) on soil. Minimum plumule length was noted for *E. helioscopia* i.e. 48% and 44% on filter paper and soil, respectively. Maximum plumule length (96%) was noted for *P. minor* (*Fig. 2*).

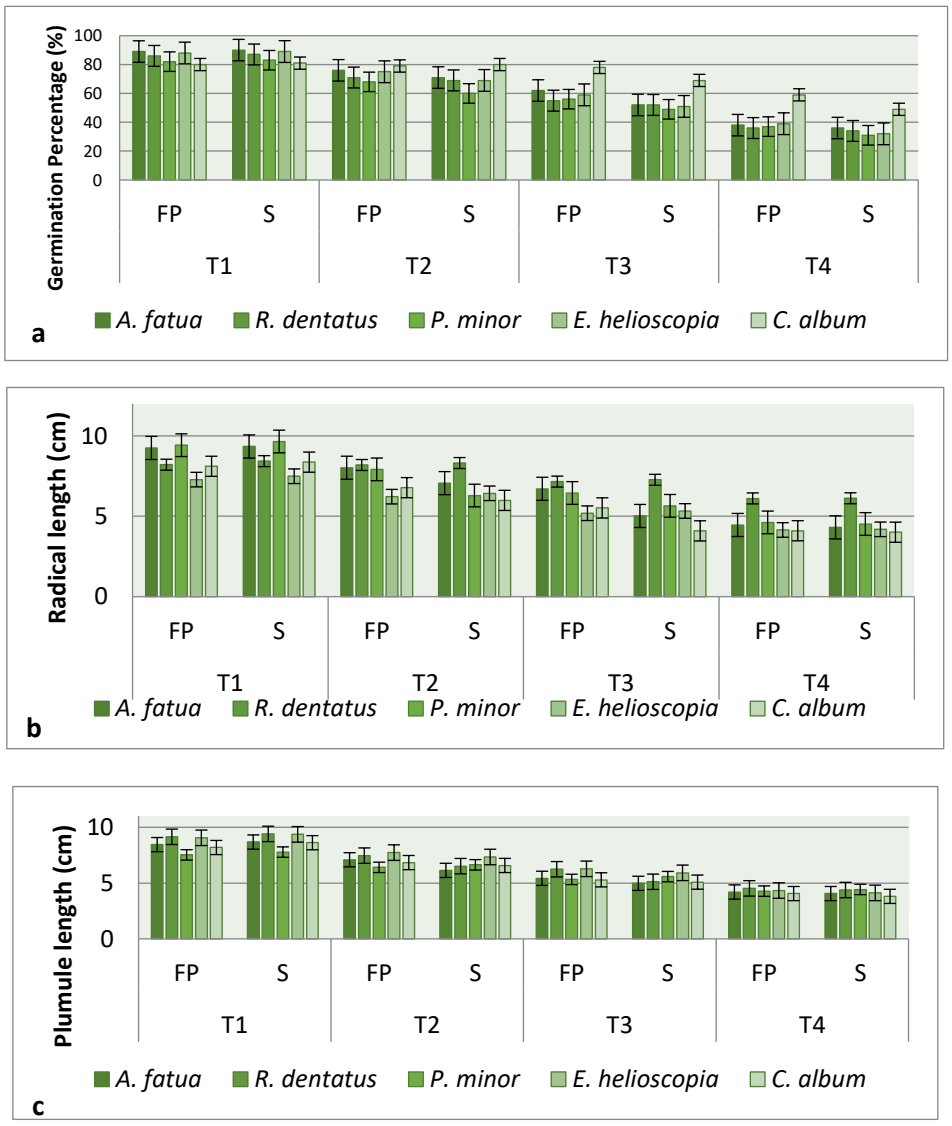

Figure 2. *Allelopathic potential of L. camara aqueous extract on (a): germination percentage, (b): radicle length (c): plumule length against test species on filter paper (FP) and soil (S) where; T_1 (control), T_2 (50%), T_3 (75%) and T_4 (100%)*

Tadele (2014) described concentration dependent and species-specific allelopathic potential of leaf aqueous extract of *L. camara* on root and shoot elongation. The aqueous

http://www.aloki.hu ● ISSN 1589 1623 (Print) ● ISSN 1785 0037 (Online)
DOI: http://dx.doi.org/10.15666/aeer/1704_96799689

extract of *L. camara* suppressed seed germination and growth of different agricultural crops (Sharma et al., 2005; Ahmed et al., 2007). These results were in accordance to Hussain et al. (2011) and Iramus et al. (2011) who noted retardation in root length of *Vigna radiata* due to inhibitory potential of *L. camara* leaf extract. Enyew and Raja (2015) observed significant retardation in root elongation by *L. camara* leaf aqueous extract in *Zea mays*. Aqueous extracts from *L. camara* leaves caused tissues decay, damages, and subsequent retarded growth of *Eichhornia crassipes* (Saxena, 2000).

Allelopathic potential of C. papaya

C. papaya aqueous extract inhibited germination percentage of *E. helioscopia* (35%) followed by *P. minor* (33%) and *A. fatua* (32%) on filter paper. Similarly, on soil, seed germination of *P. minor* (40%) was inhibited followed by *A. fatua* (39%) and *E. helioscopia* (38%). Maximum (96%) germination was observed for *R. dentatus* and *C. album*. Minimum germination was noted for *E. helioscopia* (65%) and *P. minor* (60%) on filter paper and soil, respectively. Highest radicle length inhibition was exhibited by *P. minor* (36%) and *R. dentatus* (35%) in *C. papaya* aqueous extract on filter paper. Likewise, extract on soil caused significant radicle length reduction of *P. minor* (43%) and *R. dentatus* (40%). Radicle length of *C. album, A. fatua* and *E. helioscopia* remained unaffected. Maximum radicle length (97%) was noted for *C. album, A. fatua* and *E. helioscopia*. The aqueous extract of *C. papaya* inhibited plumule length of *P. minor* (34%) and *C. album* (33%) on filter paper. *C. papaya* aqueous extract significantly inhibited plumule length of *C. album* (43%) and *P. minor* (42%) on soil. Minimum plumule length was noted for *P. minor* (66%) and *C. album* (57%) on filter paper and soil. Maximum plumule length (96%) was noted for *A. fatua*, *R. dentatus and E. helioscopia* (*Fig. 3*). Wabo et al. (2011) studied root and shoot elongation inhibition along germination of *Lactuca sativa* seedling that was significantly checked by *C. papaya* aqueous extract. Beneficial secondary metabolites such as chlorogenic acid, quercetin, kaempferol, caffeic acid, p-coumaric acid and protocatechuic acid had reported from *C. papaya* that might be responsible for its phytotoxic/allelopathic potential (Canini et al., 2007). Many of those phenolics have been described as allelochemicals (Miean et al., 2001).

Allelopathic potential of P. roxburghii

Aqueous extract of *P. roxburghii* needles inhibited germination percentage of *C. album* and *A. fatua* by 54%, 48% and 43%, respectively on filter paper. Similarly, *P. roxburghii* aqueous extract on soil inhibited seed germination of *C. album* and *A. fatua* by 50% and 44%, respectively. Maximum (98%) germination was observed for *R. dentatus*, *P. minor* and *E. helioscopia*. The aqueous extract of *P. roxburghii* exhibited radicle length inhibition of *C. album* (40%) followed by *R. dentatus* (39%) on filter paper, whereas, no significant effect was noted for *P. minor, E. helioscopia* and *A. fatua*. Similarly, application of extract to soil suppressed radicle length of *C. album* and *R. dentatus* by 46% and 41%, respectively. Maximum (98%) radicle length was observed for *P. minor, E. helioscopia* and *A. fatua*. Minimum radicle length was noted for *C. album* i.e. 60% and 54% on filter paper and soil, respectively. The aqueous extract of *P. roxburghii* inhibited the plumule length of *A. fatua* (38%) and *R. dentatus* (34%) on filter paper.

http://www.aloki.hu ● ISSN 1589 1623 (Print) ● ISSN 1785 0037 (Online)
DOI: http://dx.doi.org/10.15666/aeer/1704_96799689

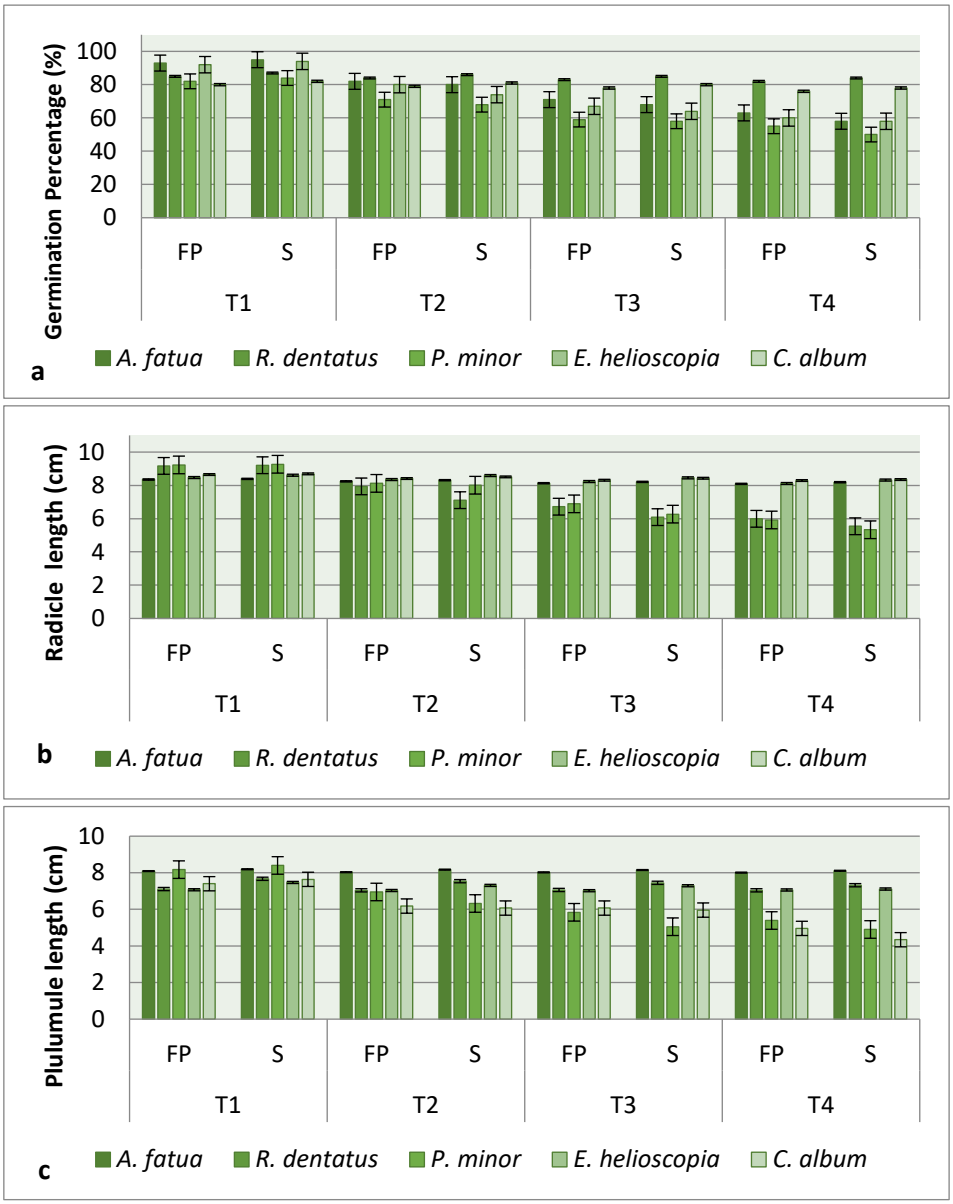

Figure 3. *Allelopathic potential of C. papaya aqueous extract on (a): germination percentage, (b): radicle length (c): plumule length against test species on filter paper (FP) and soil (S) where; T_1 (control), T_2 (50%), T_3 (75%) and T_4 (100%)*

Likewise, *P. roxburghii* aqueous extract inhibited plumule length of *A. fatua* (40%) and *R. dentatus* (39%) in soil. Maximum plumule length (98%) was noted for *P. minor, E. helioscopia* and *C. album* while minimum plumule length was noted for *A. fatua* showing 62% and 60% on filter paper and soil, respectively (*Fig. 4*). Maximum germination was observed for *R. dentatus*, *P. minor* and *E. helioscopia*. Maximum radicle length was observed for *P. minor, E. helioscopia* and *A. fatua.* Minimum radicle length was noted for *C. album*. Maximum plumule length was noted for *P. minor, E. helioscopia* and *C. album*. Minimum plumule length was noted for *A. fatua*. Aqueous extract of *P. roxburghii* needles suppressed growth of mustard and wheat seedlings while that of *P. brutia* needles suppressed growth of *Lolium multiflorum* and *Poa pratensis* seedlings

http://www.aloki.hu ● ISSN 1589 1623 (Print) ● ISSN 1785 0037 (Online)
DOI: http://dx.doi.org/10.15666/aeer/1704_96799689

(Baroniya and Baroniya, 2014). Current study is in accordance with Singh et al. (2001) who determined seedling growth and seed germination of *Capsicum annuum, Pisum sativum* and *Oryza sativa* was retarded by *Pinus* needles. Likewise, results were explained by Madgil and Kapil (1990) for *Amaranthus paniculatus* and *Trifolium pratense* seeds treated with leaf extract of *P. roxburghii*. Kil and Yim (1983) observed that toxic compounds produced by *P. densiflora* checked seed germination and growth of species. The phenolic composites of *P. rigida* exhibited retardation effect on *Cassia mimosoides*. Fresh, senesced, and decaying needles from *P. halepensis* exhibit potent inhibitory potential on *Festuca arundinacea*, *Cyanodon dactylon*, *Avena sativa* and *Lemna minor* (Nektarios et al., 2005).

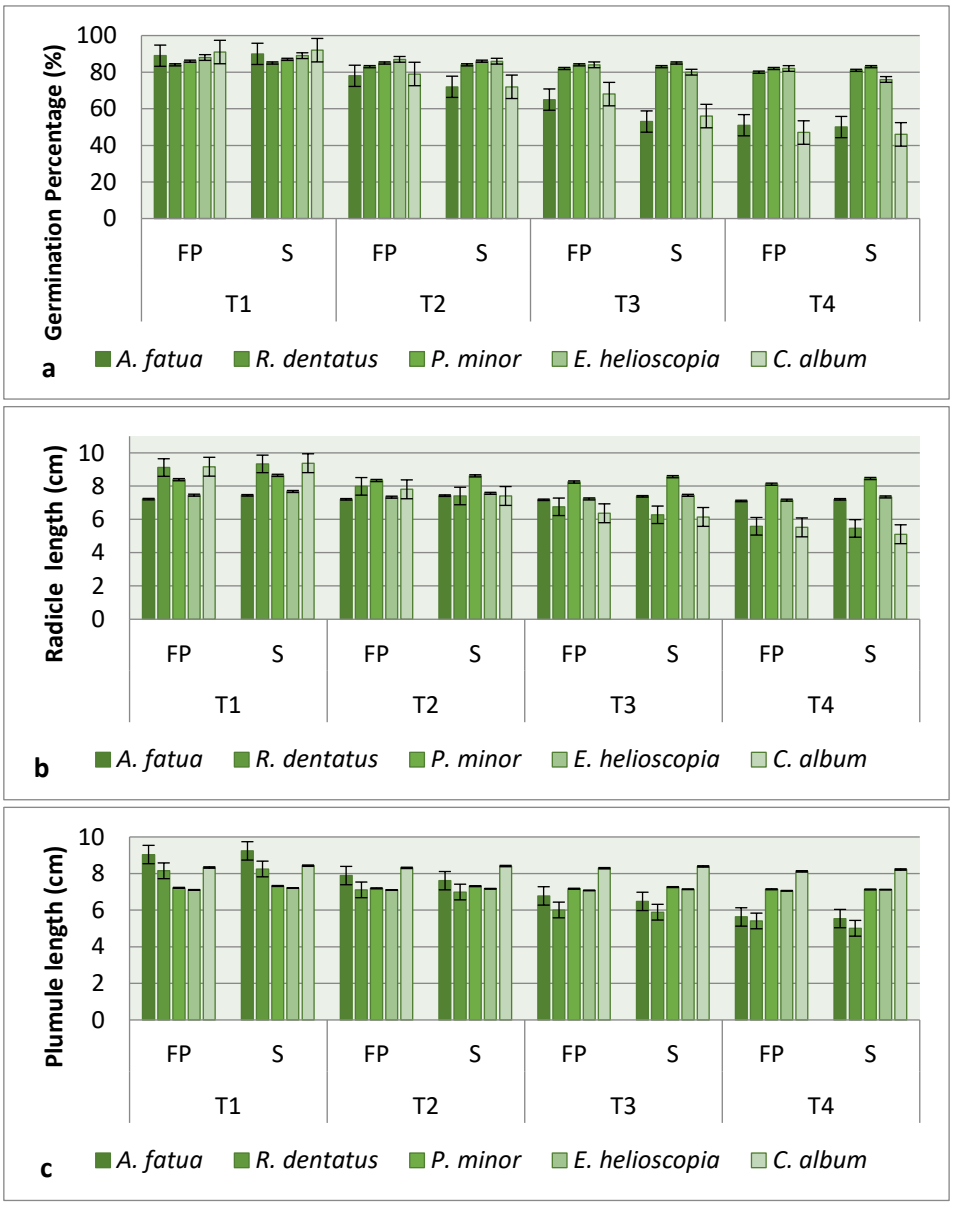

Figure 4. *Allelopathic potential of L. camara aqueous extract on (a): germination percentage, (b): radicle length (c): plumule length against test species on filter paper (FP) and soil (S) where; T_1 (control), T_2 (50%), T_3 (75%) and T_4 (100%)*

http://www.aloki.hu ● ISSN 1589 1623 (Print) ● ISSN 1785 0037 (Online)
DOI: http://dx.doi.org/10.15666/aeer/1704_96799689

The germination and growth inhibition effects were found in order *L. camara*>*P. roxburghii*>*R. stricta*>*C. papaya*. Relatively greater (but statistically non-significant) values for germination and growth inhibition were recorded on soil medium compared to filter paper.

Conclusions

Present results indicated that aqueous extract of selected plants at higher concentrations reduce the seed germination, radicle and plumule length of weeds associated with the wheat crop. Results provide evidence about herbicidal potential of test species viz. *L. camara*, *P. roxburghhii, C. Papaya* and *R. stricta* against weeds of wheat crop (*Avena fatua, Phalaris minor, Chenopodium album* and *Rumex dentatus*). Further work is needed to appraise the potential inhibitory effects of allelochemicals from these plants.

REFERENCES

[1] Ahmed, R., Uddin, M. B., Khan, M. A., Mukul, S. A., Hossain, M. K. (2007): Allelopathic effects of *Lantana camara* on germination and growth behavior of some agricultural crops in Bangladesh. – J. For. Res. 18: 301-304.

[2] Ahmed, S. A., El-Rokiek, K. G., El-Masry, R. R., Messiha, N. K. (2014): The efficiency of allelochemicals in the seed powder of *Eruca sativa* in controlling weeds in *Pisum sativum*. – Middle East Journal of Agricultural Research 3: 757-762.

[3] Alqarawi, A. A., Hashem, A., Kumar, A., Al-Arjani, A. F., Abd-Allah, E. F., Dar, B. A., Wirth, S., Davranov, K., Egamberdieva, D. (2018): Allelopathic effects of the aqueous extract of *Rhazya stricta* on growth and metabolism of *Salsola villosa*. – Plant Biosystems 152: 1263-1273.

[4] Anwar, T., Ilyas, N., Qureshi, R., Qureshi, H., Gilani, N., Khan, S., Khan, S. A., Fatimah, H., Waseem, M., Mahmood, R. T., Maqsood, M. (2019): comparative allelopathic activity of *Rhazya stricta, Pinus roxburghii, Carica papaya* and *Lantana camara* against noxious weeds. – Appl. Ecol. Env. Sci. 17: 7175-7187.

[5] Anwar, T., Khalid, S., Mazhar, R., Qureshi, H., Rashid, M. (2017): Herbicidal potential of selected species to overcome weed infestation in *Triticum aestivum*, *Zea mays* and *Helianthus annuus*. – Pak. J. Weed Sci. Res. 23: 49-63.

[6] Arafat, Y., Khalid, S., Lin, W., Fang, C., Sadia, S., Ali, N., Azeem, S. J. (2015): Allelopathic evaluation of selected plants extract against broad and narrow leaves weeds and their associated crops. – Academic J. Agric. Res. 3: 226-234.

[7] Aryakia, E., Naghavi, M. R., Farahmand, Z., Fazeli, S. A. S. (2015): Evaluating allelopathic effects of some plant species in tissue culture media as an accurate method for selection of tolerant plant and screening of bioherbicides. – J. Agric. Sci. Technol. 17: 1011-1023.

[8] Assaeed, A. M., Al-Doss, A. A. (1997): Allelopathic effects of Rhazya stricta on seed germination of some range plant species. – Annals Agric. Sci. 42: 159-167.

[9] Baroniya, S. S., Baroniya, M. B. (2014): Germination and early seedling growth of mustard and wheat as affected by allelopathic activity of Pinus needle extracts. – Int. Res. J. Environ. Sci. 3: 27-34.

[10] Biljana, M. B., Kragujevac, D. Z. J. (2015): Allelopathic relations of selected cereal and vegetable species during seed germination and seedling growth. – J. Sci. 37: 135-142.

[11] Canini, A., Alesiani, D., Arcangelo, G., Tagliatesta, P. (2007): Gas Chromatography-Mass Spectrometry analysis of phenolic compounds from *Carica papaya* L. leaf. – J. Food Compos. Anal. 20: 584-590.

http://www.aloki.hu ● ISSN 1589 1623 (Print) ● ISSN 1785 0037 (Online)
DOI: http://dx.doi.org/10.15666/aeer/1704_96799689

[12] Chon, S. U., Jang, H. G., Kim, D. K., Kim, Y. M., Boo, H. O., Kim, Y. J. (2005): Allelopathic potential in lettuce *(Lectuca sativa* L.). – Plant Science and Horticulture 206: 309-317.
[13] Edalat, M., Ghadiri, H., Hamzehzarghani, H., Kazemeini, S. A. (2011): Prediction of corn yield loss due to different redroot pigweed density and irrigation level using empirical models. – Australian J. Crop Sci. 5(2): 187-196.
[14] El-Khatib, A. A. (2000): The ecological significance of allelopathy in the community organization of allhagrae- corum. – Biological Plantarum 43: 42-431.
[15] El-Khawas, S. A., Shehata, M. M. (2005): The allelopathic potentialities of *Acacia nilotica* and *Eucalyptus rostrata* on monocot (*Zea mays* L.) and Dicot (*Phaseolus vulgarise* L.). – Plant Biotechnol. 4: 23-34.
[16] Enyew, A., Raja, N. (2015): Allelopathic effect of *Lantana camara* L. leaf powder on germination and growth behavior of maize, Linn. and wheat, *Triticum turgidum* Linn. cultivars. – Asian J. Agric. Res. 7: 4-10.
[17] Garima, Devi, M. (2017): Allelopathy in agroforestry: A review. – J. Pharmacognos. Phytochem. 6(3): 686-688.
[18] Hegazy, A. K., Fadl-Allah, E. M. (1995): Inhibition of seed germination and seedling growth by *Cleome droserifolia* and allelopathic effect on fungi. – Egypt. J. Arid Environ. 29: 3-13.
[19] Hussain, M. I., González, L., Reigosa, M. J. (2011): Allelopathic potential of *Acacia melanoxylon* on the germination and root growth of native species. – Weed Biol. Manag. 11: 18-28.
[20] Iramus, S., Moinuddin, A., Syed, T. A. (2011): Allelopathic effect of scarlet pimpernel (*Anagallis arvensis*) on seed germination and radicle elongation of mung bean and pearl millet. – Pak. J. Bot. 43: 351-355.
[21] Jabeen, N., Ahmed, M. (2009): Possible allelopathic effect of three different weeds on germination and growth of maize (*Zea mays*) cultivars. – Pak. J. Bot. 41: 1677-1683.
[22] Kamran, M., Raza, A., Ali, Q., Ali, H. H., Chattha, M. S. (2017): Investigating the influence of fertilizer and allelopathic water extracts on maize and associated weeds. – Pak. J. Weed Sci. Res. 23: 361-378.
[23] Khan, I., Ali, Z., Khan, M. I., Hussain, Z., Khan, I. A., Waqas, M., Khan, R., Khan, S. (2014): Allelopathic effects of some weeds on chickpea crop. – Pak. J. Weed Sci. Res. 20: 207-211.
[24] Khan, R., Khan, M. A., Shah, S., Uddin, S., Ali, S., Ilyas, M. (2016): Bioherbicidal potential of plant extracts against weeds of wheat crop under agro-climatic conditions of Peshawar-Pakistan. – Pak. J. Weed Sci. Res. 22: 285-294.
[25] Kil, S. B., Yim, Y. J. (1983): Allelopathic effects of *Pinus densiflora* on undergrowth of red pine forest. – J. Chem. Ecol. 9: 1135-1151.
[26] Madgil, D., Kapil, M. (1990). Allelopathic activity of *Pinus roxburghii* Sarg. and *Rhododendron arboreum* Sm. leaves. – Indian Forest 116: 512-514.
[27] Maharjan, S., Shrestha, B. B., Jha, P. K. (2007): Allelopathic effects of aqueous extract of *Parthenium hysterophorus* L. on seed germination and seedling growth of some cultivated and wild herbaceous species. – Sci. World 5: 35-39.
[28] Miean, K., Mohamed, H., Flavanoid, S. (2001): Myricetin, Quercetin, Kaempferol, Luteolin, and Apigenin: Content of edible tropical plants. – J. Agric. Food Chem. 49: 3106-3112.
[29] Nekonam, M. S., Kraimmojeni, H., Sharifnabi, B., Razmjoo, J., Amini, H., Bahrami, F. (2014): Assessment of some medicinal plants for their allelopathic potential against redroot pigweed (*Amaranthus retroflexus*). – J. Plant Prot. Res. 54: 90-95.
[30] Nektarios, P. A., Economou, G., Avgoulas, C. (2005): Allelopathic effects of *Pinus halepensis* needles on turfgrasses and biosensor plants. – Hortscience 40: 246-250.

http://www.aloki.hu ● ISSN 1589 1623 (Print) ● ISSN 1785 0037 (Online)
DOI: http://dx.doi.org/10.15666/aeer/1704_96799689

[31] Qureshi, H., Arshad, M., Bibi, Y. (2014): Toxicity assessment and phytochemical analysis of *Broussonetia papyrifera* and *Lantana camara*: Two notorious invasive plant species. – J. Biodivers. Environ. Sci. 5(2): 508-517.
[32] Rueda-Ayala, V. P., Rasmussen, J., Gerhards, R., Fournaise, N. E. (2011): The influence of post-emergence weed harrowing on selectivity, crop recovery and crop yield in different growth stages of winter wheat. – Weed Res. 51: 478-488.
[33] Saxena, M. K. (2000): Aqueous leachate of *Lantana camara* kills water hyacinth. – J. Chem. Ecol. 26: 2435-2447.
[34] Sharma, G. P., Raghubanshi, A. S., Sing, J. S. (2005): *Lantana* invasion: an overview. – Weed Biol. Manag. 5: 157-167.
[35] Sharma, N. K., Batish, D. R., Singh, H. P., Kohli, R. K. (2016): Allelopathic effect of *Pinus roxburghii* on an understorey plant *Bidens pilosa*. – Annals Plant Sci. 5(10): 1446-1450.
[36] Singh, H. P., Kohli, R. K., Batish, D. R. (2001): Allelopathic interference of *Populus deltoids* with some winter season crops. – Agronomy 21: 139-146.
[37] Tadele, D. (2014): Allelopathic Effects of Lantana (*Lantana camara* L.) leaf extracts on germination and early growth of three agricultural crops in Ethiopia. – Momona Ethiopian J. Sci. 6: 111-119.
[38] Van Evert, F. K., Fountas, S., Jakovetic, D., Crnojevic, V., Travlos, I., Kempenaar, C. (2016): Big data for weed control and crop protection. – Weed Res. https://doi.org/10.1111/wre.12255.
[39] Wabo, P. J., Ngankam, N. J. D., Bilong, B. C. F., Mpoame, M. (2011): A comparative study of the ovicidal and larvicidal activities of aqueous and ethanolic extracts of pawpaw seeds *Carica Papaya* (Caricaceae) on *Heligmosomoides Bakeri*. – Asian Pac. J. Trop. Med. 24: 447-450.
[40] Wardle, D. A., Nicholson, K. S., Ahmed, M. (1992): Comparison of osmotic and allelopathic effects of grass leaf extracts on grass seed germination and radicle elongation. – Plant and Soil 140: 315-319.
[41] Zhou, Y. H., Yu, J. Q., Huang, L. F., Nogues, S. (2004): The relationship between CO_2 assimilation, photosynthetic electron transport, and water-water cycle in chill-exposed cucumber leaves under low light and subsequent recovery. – Plant Cell Environ. 27: 1503-1514.

http://www.aloki.hu ● ISSN 1589 1623 (Print) ● ISSN 1785 0037 (Online)
DOI: http://dx.doi.org/10.15666/aeer/1704_96799689

PERFORMANCE OF VAPOUR PRESSURE MODELS IN THE COMPUTATION OF VAPOUR PRESSURE AND EVAPOTRANSPIRATION IN ABHA, ASIR REGION, SAUDI ARABIA

ISLAM, S.[1*] – ABDULLAH, R. A. B.[1] – ALGAHTANI, A.[2,3] – IRSHAD, K.[4] – HIROL, H.[1]

[1]*Department of Civil Engineering, University Teknologi Malaysia P.O. Box 81310 Johor Bahru, Johor, Malaysia*

[2]*Mechanical Engineering Department, College of Engineering, King Khalid University, Abha 61413 Asir, Kingdom of Saudi Arabia*

[3]*Research Centre for Advanced Materials Science (RCAMS), King Khalid University, PO Box 9004, Abha-61413, Asir, Kingdom of Saudi Arabia*

[4] *Center of Research Excellence in Renewable Energy (CoRERE), King Fahd University of Petroleum &Minerals, Dhahran, Saudi Arabia*

[*]*Corresponding author*
e-mail: isaiful2@graduate.utm.my; phone:+966-59-521-9933.; fax: +966-17-241-8816

(Received 14th Mar 2019; accepted 22nd May 2019)

Abstract. The FAO-56 Penman-Monteith model is recognized as the standard method for estimating reference evapotranspiration (ETo) which requires daily meteorological data as inputs. Among all input data, vapour pressure deficit (VPD) is one of the critical parameter that drives evapotranspiration (ETo), and is of fundamental importance in crop models. In this study effort has been made to compare six vapour pressure models during four seasons. Three vapour pressure models (Models 1–3) selected as mentioned in Irrigation and Drainage Paper-56 of the Food and Agriculture Organization (FAO-56) and Models 4-6 has been selected from literature survey. Model 1, which uses daily maximum and minimum temperature, relative humidity (RH), is the preferred method to estimate actual air pressure (AE) hence it is used as standard for comparing other models. The effectiveness of vapour pressure models were measured by statistical tools and ranked according to Global Performance Indicator (GPI) where higher value of GPI represent best model. The ranking order using GPI shows that Model 5 resulted in best estimation capability with a GPI of 2.77. Moreover, the effect of variation in wind speed on the performance of the vapour pressure models in ETo estimation is also assessed.
Keywords: *agriculture, cropping period, global performance index, vapour pressure deficit, water deficit*

Introduction

The Kingdom of Saudi Arabia (KSA) like Semi-Arid Asir region Abha suffers large water deficit which is due to climate change during past decades. Climate change is crucial part for well-planned water resource management in semi-arid region, Saudi Arabia (Tarawneh and Chowdhury, 2018). Therefore, it is important to understand relation of climatic parameter with environment in order to reduce vulnerability caused by growing new crops in climate change environment and for efficient water management system (DeNicola et al., 2015). Earlier studies have stated an increase of agricultural water demand by 5–15% during 2050, due to increased evapotranspiration rate. According to Chowdhury and Al-Zahrani (2013), rise of temperature by 1 °C would

http://www.aloki.hu ● ISSN 1589 1623 (Print) ● ISSN 1785 0037 (Online)
DOI: http://dx.doi.org/10.15666/aeer/1704_96919715

likely to change the thermal limits of a crop by 10–30%, which will affect crop yields (Lelieveld, 2012). Apart from this, rise in temperature by 1 °C would likely to increase the capacity of air to hold water vapour by 7%, which in turn reduces precipitation rate (Trenberth, 2011). Hence, the water resources system and soil–water balance system will affect further (Kang et al., 2009).

The water consumption by agricultural field is estimated to be 88% of the annual water use (Multsch et al., 2017). The water shortage in Saudi Arabia indicates highest index as compared to other countries (Baig and Straquadine, 2014). Al-Zahrani (2019) stated that the KSA is portrayed among few countries where withdrawal of water exceeds 33.33% of the total available water supply. The irrigation of agricultural field requires knowledge of when to irrigate and the amount of water to apply. This depends on local atmospheric conditions, where precipitation and evapotranspiration (ETo) play a key role (Kumar et al., 2012). Hence knowledge of ETo is essential in water resources management, for both natural and agricultural ecosystems, particularly for irrigation (Allen et al., 1998).

The Direct method of estimating evapotranspiration is lysimeter which provides high accuracy (Liu et al., 2017; Hirschi et al., 2017). However, it is very costly and requires many highly expensive and sophisticated equipment for measurement. To overcome this problem the frequently used method for obtaining reference evapotranspiration presented in the Food and Agricultural Organization of the United Nations (FAO) Irrigation and Drainage Paper 56 depends only on meteorological observations and crop coefficients estimated based on surface conditions (Allen et al., 1998). The application of FAO56-PM is limited due to an insufficient network of the meteorological observatory and proper maintenance (Pandey et al., 2016). Alternatively, numerous studies in different climatic conditions evaluated the applicability of less data-demanding empirical ETo methods using sophisticated and straightforward techniques against FAO56- PM (Pandey and Pandey, 2018; Cadro et al., 2017). However, the FAO-56 Penman–Monteith Model which bears high correlation with lysimeter measurement for estimated of evapotranspiration (Nolz et al., 2016). The reference crop evapotranspiration (ETo) estimations using the FAO Penman-Monteith equation (PM-ETo) require a set of weather data including maximum and minimum air temperatures (Tmax, Tmin), actual vapour pressure, solar radiation, and wind speed. Among all weather parameter, vapour pressure deficit is an important factor in the estimation of ETo. It is defined as difference between saturated vapour pressure and actual vapour pressure (Seager et al., 2015). Various models are available to estimate vapour pressure. However, use of different models in determining actual vapour pressure will result in different values of actual vapour pressure and thus different values of ETo will be estimated. In some earlier studies (Burman et al., 1987; Weiss, 1977), it was observed that ETo can be determined with good accuracy regardless of the model used for the vapour pressure estimation. However, a few studies (Saxton, 1975; Sadler and Evans, 1989; Yoder et al., 2005), which were carried out to analyse the sensitivity of ETo to the vapour pressure deficit (VPD), suggested a considerable change in estimated ETo values when the value of VPD changed. Howell (1995) evaluated some methods that calculate VPD for Bushland (Texas). Weather data containing maximum-minimum temperature along with mean dewpoint temperature were found to provide the most accurate calculations of VPD in the study area. Ojha et al. (2010) compared the performance of the three FAO-56 models (for ea estimation) in the estimation of open water evapouration in a semiarid region (Udaipur, India). Their results showed that Model 1 performed better than the other two models in estimating open water evapouration using the Penman combination approach.

http://www.aloki.hu ● ISSN 1589 1623 (Print) ● ISSN 1785 0037 (Online)
DOI: http://dx.doi.org/10.15666/aeer/1704_96919715

The past studies in the study region were basically on assessing different ETo models against theFAO-56 Penman Monteith model based on Central and Eastern region of Saudi Arabia (Salih and Sendil, 1984; Al-Omran et al., 2004; Elnesr et al., 2010; Al-Ghobari, 2000; Madugundu et al., 2017). However, no such studies recorded so far about the vapour pressure model from the literature in Kingdom of Saudi Arabia. In order to fill this void, an effort was made to estimate six vapour pressure model based on availability of meteorological data for the period from 1988-2018 and by recognizing the best suitable method by computing global performance index as an alternative to model 1 which is taken as standard in this study. The finding of the research work can be helpful in reducing the error during evapotranspiration computation, Moreover the best evaluated model equation for evapotranspiration could assist in computing evapotranspiration in future in the field of crop water management system, climate change studies, irrigation and water resource planning.

Study area

Site description

The research work deals with Abha mountainous region of Asir province, Kingdom of Saudi Arabia having an area of 370 km^2 located between the latitude of 18°10′12.39″N and 18°23′33.05″N and longitude of 42°21′41.58″E and 42°39′36.09″E as shown in *Figure 1*. The zone is prone to heavy rainfall as compared to other parts of Saudi Arabia. The elevation varies from 1951 to 2991 m (msl) with average precipitation of 355 mm which mainly occurs between June and October. According to the topographical features of the investigation region, it is found to have weak geology because of the precipitation and slope nature during the past few years (Mallick et al., 2018).

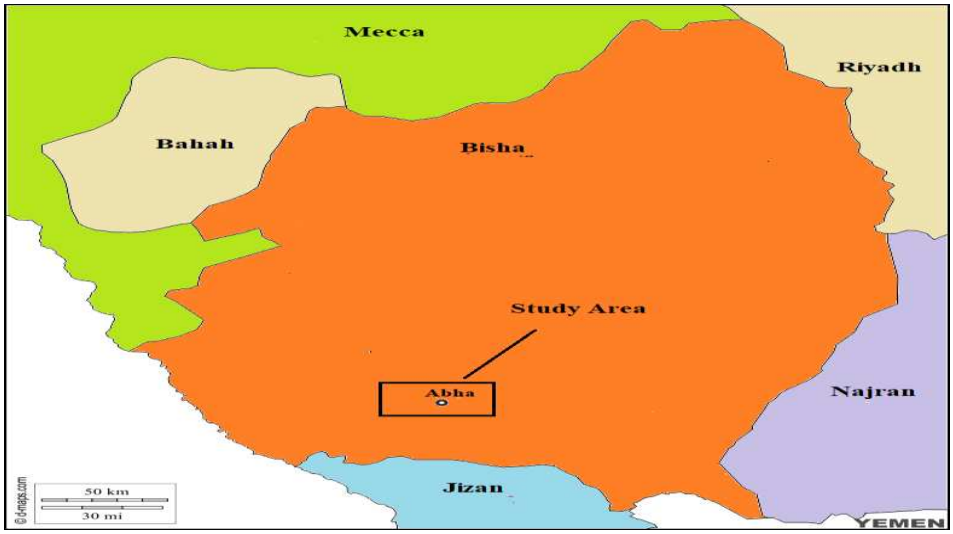

Figure 1. *Location map of Abha Asir region, Kingdom of Saudi Arabia*

Data availability

In this research work, weather parameters were collected from Abha meteorological weather station for the period between 1988–2018 which includes wind velocity, maximum and minimum temperature, mean temperature, mean relative humidity and

http://www.aloki.hu ● ISSN 1589 1623 (Print) ● ISSN 1785 0037 (Online)
DOI: http://dx.doi.org/10.15666/aeer/1704_96919715

solar radiation as well. The data collected were checked by (Allen, 1996). The variation of minimum, maximum and mean temperature along with standard deviation is shown in *Figure 2a-c,* while the mean, minimum and maximum relative humidity along with standard deviation is shown in *Figure 2d-f.*

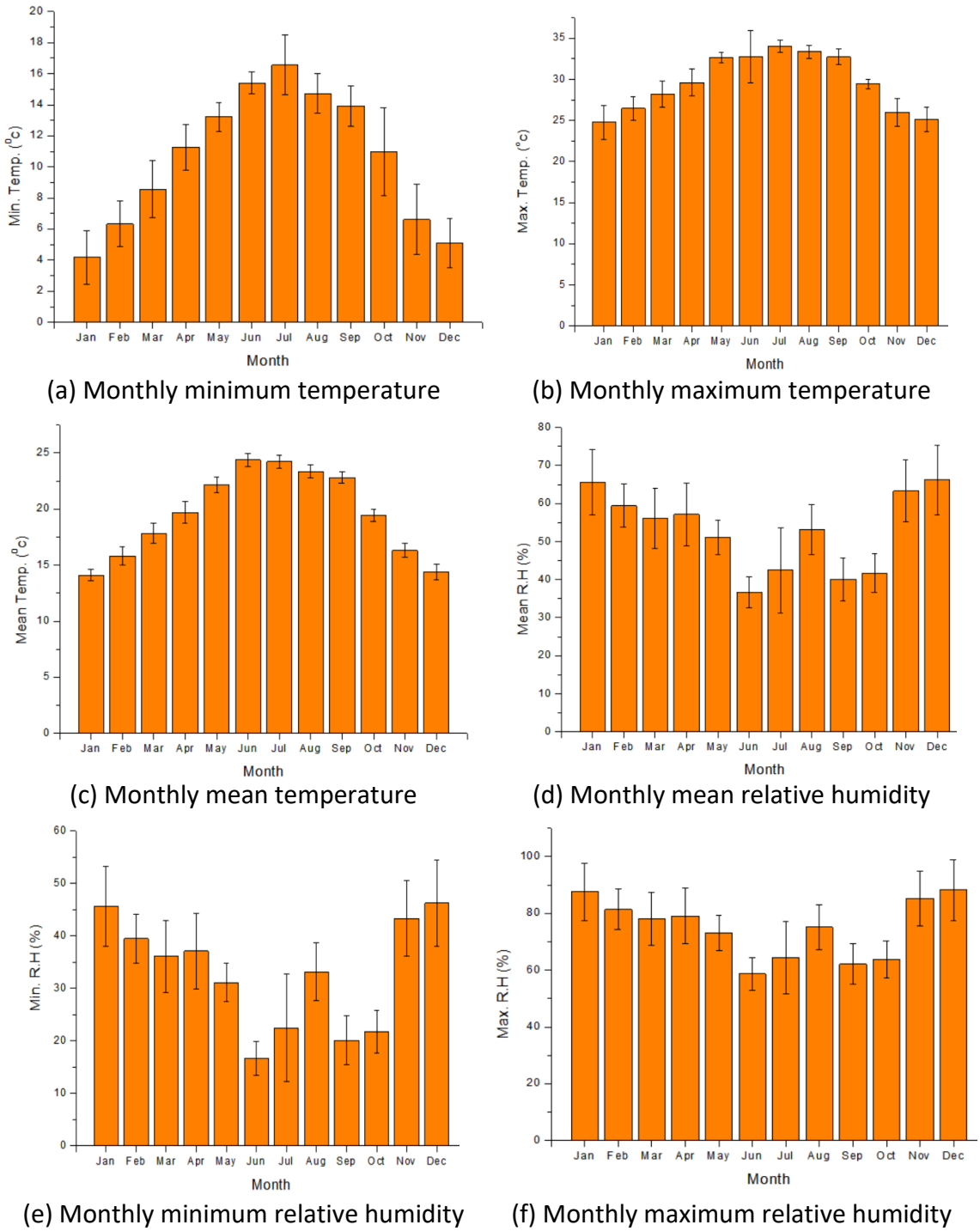

Figure 2. *Average monthly climatic data value for the period between 1988 and 2018*

http://www.aloki.hu ● ISSN 1589 1623 (Print) ● ISSN 1785 0037 (Online)
DOI: http://dx.doi.org/10.15666/aeer/1704_96919715

Methodology

Various vapour pressure model taking into account in this study are based on available literature. In this research work vapour pressure model were estimated by six model based on available climatic data. The values estimated from different model were compared with the value obtained from standard model 1 for four seasons as shown in *Table 1,* where each of the four cropping seasons is divided into four crop growth stages as per the guidelines provided in Allen et al. (1998). The four crop growth stages are (I) initial stage, (II) development stage, (III) midseason stage, and (IV) end season stage. The crop growth stages are used as periods to compare the actual vapour pressure and ETo values determined by using the six VP models. The performance of vapour pressure models was computed based on overall effect of evaluation criteria called as Global performance index. The ranking was done in order to get most promising model which can be used alternative to model 1. The flowchart as shown in *Figure 3* described the stepwise procedure to compute most promising model among five model (excluding model 1) to be used as alternate of model 1.

Table 1. *Details of the cropping periods*

Season	Duration		Crop growing stage				Total days
	From	To	I	II	III	IV	
Winter	21-Dec	20-Mar	10	20	40	20	90
Spring	21-Mar	20-Jun	10	20	40	22	92
Summer	21-Jun	22-Sep	10	20	40	23	93
Autumn	23-Sep	20-Dec	10	20	40	20	90

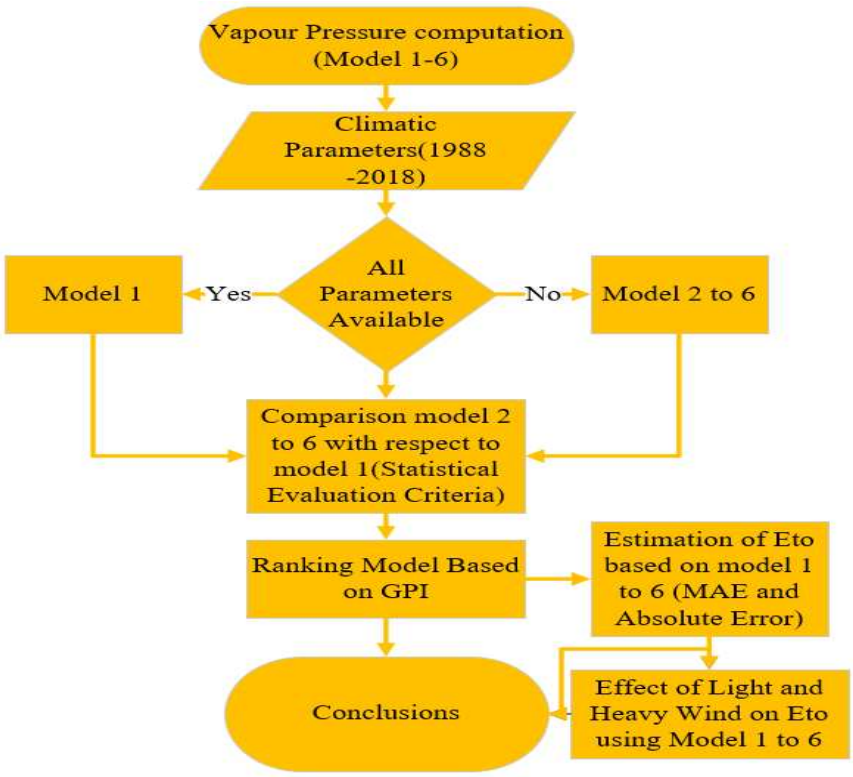

Figure 3. *Flowchart for methodology*

http://www.aloki.hu ● ISSN 1589 1623 (Print) ● ISSN 1785 0037 (Online)
DOI: http://dx.doi.org/10.15666/aeer/1704_96919715

Reference evapotranspiration and vapour pressure model

This study work aims to analyse various vapour pressure models which is one of the most critical component of reference evapotranspiration computation by the standard FAO56-PM model in the Abha Asir region, Kingdom of Saudi Arabia. The selection of methods was based on their wide acceptance, simple calculation procedure and applicability in present conditions. The models are shown by *Equations 2-8*. If all the required variables are available, it is advisable to use Model 1. Model 2 is used when the credibility of minimum RH (RHmin) data is in doubt, whereas Model 3 is used when only mean RH (RHmean) data are available. Details about the calculation of actual vapour pressure using RH and temperature data can also be found in Allen et al. (2011). The use of different models in determining actual vapour pressure will result in different values of actual vapour pressure and thus different values of ETo will be estimated.

The FAO Penman-Monteith equation for estimating ETo values recommended by Food and Agriculture Organisation, Irrigation and Drainage Paper-56 (FAO-56) (and is given as *Eq. 1*) and moreover equation for vapour pressure (Models 1-3) also suggested in FAO-56 documentation (Allen et al., 1998):

$$\mathrm{ETo} = \frac{0.408\times\Delta\times(\mathrm{Rn}-\mathrm{G})+\gamma\times\left(\frac{900}{\mathrm{T}+273}\right)\times u_2\times(e_s-e_a)}{\Delta+\gamma\times(1+0.34u_2)} \quad \text{(Eq.1)}$$

$$\text{Model 1 } e_a = \frac{\left[\left\{e_s(T_{min})\times\frac{RH_{max}}{100}\right\}+\left\{e_s(T_{max})\times\frac{RH_{min}}{100}\right\}\right]}{2} \quad \text{(Eq.2)}$$

$$\text{Model 2 } e_a = e_s(T_{min}) \times \frac{RH_{max}}{100} \quad \text{(Eq.3)}$$

$$\text{Model 3 } e_a = \frac{RH_{mean}}{100} \times \left[\frac{\{e_s(T_{max})+e_s(T_{min})\}}{2}\right] \quad \text{(Eq.4)}$$

A VP model (referred here as Model 4), which uses RHmean and Tmean for calculation of actual vapour pressure was reported by Irmak et al. (2005) represented by *Equation 5:*

$$\text{Model 4 } e_a = \frac{RH_{mean} \times e_s(T_{mean})}{100} \quad \text{(Eq.5)}$$

Upreti and Ojha (2017) suggested that by using the Lawrence Tdew–RH relationship (*Eq. 6*), fairly accurate estimates of dewpoint temperature can be obtained, which in turn can be used for the calculation of actual vapour pressure values:

$$T_{dew} \perp = T_{mean} - (20 - 0.2RH_{mean})(\frac{T_{K-mean}}{300})^2 - 0.00135(RH_{mean} - 84)^2 + 0.35 \quad \text{(Eq.6)}$$

where Tdew ⊥ = dew point temperature value in °C obtained using the Tdew–RH relationship proposed by Lawrence (2005); Tmean (°C) and RHmean (%) are the daily mean values of temperature and RH, respectively; TK mean is the daily mean temperature in kelvin.

http://www.aloki.hu ● ISSN 1589 1623 (Print) ● ISSN 1785 0037 (Online)
DOI: http://dx.doi.org/10.15666/aeer/1704_96919715

Values of Tdew ⊥ (determined by using *Equation 6*) are then used to calculate the daily actual vapour pressure values using *Equation 7*. This proposed approach is mentioned here as Model 5:

$$\text{Model 5 } e_a(T) = 0.6108exp\left[\frac{17.27T_{dew}\perp}{T_{dew\perp}+237.3}\right] \quad \text{(Eq.7)}$$

As per FAO-56 document (Allen et al., 1998), daily values of actual vapour pressure can be estimated by using *Equation 8* assuming daily minimum temperature (Tmin) near the dewpoint temperature (T_{dew}):

$$\text{Model 6 } e_a(T) = 0.6108exp\left[\frac{17.27T_{min}}{T_{min}+237.3}\right] \quad \text{(Eq.8)}$$

$$e_s = 0.6108exp\left[\frac{17.27T_{mean}}{T_{mean}+237.3}\right] \quad \text{(Eq.9)}$$

$$e_s = \frac{\{e_s(T_{max})+e_s(T_{min})\}}{2} \quad \text{(Eq.10)}$$

Note: ETo = reference evapotranspiration (mm day−1); Rn = net radiation at the crop surface (MJm^{-2} day^{-1}); G = soil heat flux density (MJm^{-2} day^{-1})) that is taken as zero for daily ETo estimation; T = temperature at 2 m height (°C); u_2 = wind speed at 2 m height (m s^{-1}); e_s = saturation vapour pressure (kPa); e_a = actual vapour pressure (kPa); (e_s–e_a) = vapour pressure deficit (kPa); Δ = slope of vapour pressure curve (kPa °C^{-1}); and γ = psychrometric constant (kPa °C^{-1}); T_{max} = Maximum Temperature (°C); T_{min} = Minimum Temperature (°C); T_{mean} = Mean Temperature (°C); RH_{mean} = Mean Relative Humidity (%); RH_{max} = Maximum Relative Humidity (%); RH_{min} = Minimum Relative Humidity (%); $T_{dew}\perp$=dew point temperature value in °C; $T_{K\text{-}mean}$ is the daily mean temperature in kelvin.

Evaluation criteria and global performance index (GPI)

The GPI is computed by using ten statistical measure such as Mean Absolute Error (MAE), Root Mean Square Error (RMSE), Mean Absolute Relative Error (MARE), Uncertainty at 95% (U95), Root mean squared relative error (RMSRE), Relative Root Mean Square Error (RRMSE), Mean Bias Error (MBE), Coefficient of determination (R^2), Maximum Absolute Relative Error (erMax) and t-statistics (Ali and Jamil, 2019). For Coefficient of determination (R^2), 1 is taken as ideal value, while for all other statistical zero is taken as ideal value. Despotovic et al. (2015) proposed the GPI by scaling the values of statistical tools in between 0 and 1. Further by subtracting the scaled values of error indicators from the corresponding medians and adding up the differences so obtained using the weight factors. Mathematically, for the i^{th} model:

$$GPI_i = \sum_{j=1}^{10}\alpha_j(\tilde{y}_j - \tilde{y}_{ij}) \quad \text{(Eq.11)}$$

where α_j have a value of + 1 for statistical errors having a recommended value of 0 and a value of -1 for statistical errors that have a recommended high value of 1 (e.g. R^2). $\tilde{y}_j$ and $\tilde{y}_{ij}$ are the median and scaled values, respectively.

http://www.aloki.hu ● ISSN 1589 1623 (Print) ● ISSN 1785 0037 (Online)
DOI: http://dx.doi.org/10.15666/aeer/1704_96919715

Willmott and Matsuura (2005) used MAE as statistical measure as shown by *Equation 12*:

$$MAE = \frac{1}{n}\sum_{i=1}^{n}\left|e_{a,Mi} - e_{a,M1}\right| \quad \text{(Eq.12)}$$

$$RMSE = \left[\frac{1}{n}\sum_{i=1}^{n}\left(e_{a,Mi} - e_{a,M1}\right)^2\right]^{\frac{1}{2}} \quad \text{(Eq.13)}$$

$$MARE = \frac{1}{n}\sum_{i=1}^{n}\left|\frac{e_{a,Mi} - e_{a,M1}}{e_{a,Mi}}\right| \quad \text{(Eq.14)}$$

Behar et al. (2015) and Gueymard (2014) applied U_{95} in modelling of solar radiation as given by *Equation 15:*

$$U_{95} = 1.96(SD^2 + RMSE^2)^{\frac{1}{2}} \quad \text{(Eq.15)}$$

$$RMSRE = \sqrt{\frac{1}{n}\sum_{i=1}^{n}\left(\frac{e_{a,Mi} - e_{a,M1}}{e_{a,Mi}}\right)^2} \quad \text{(Eq.16)}$$

Li et al. (2013) applied RRMSE as a statistical performance measure in the modelling of global solar radiation as given by *Equation 17:*

$$RRMSE = 100 \times \frac{\sqrt{\frac{1}{n}\sum_{i=1}^{n}\left(e_{a,Mi} - e_{a,M1}\right)^2}}{\sum_{i=1}^{n} e_{a,Mi}} \quad \text{(Eq.17)}$$

$$MBE = \frac{1}{n}\sum_{i=1}^{n}\left(e_{a,Mi} - e_{a,M1}\right) \quad \text{(Eq.18)}$$

$$R^2 = 1 - \frac{\sum_{i=1}^{n}\left(e_{a,Mi} - e_{a,M1}\right)^2}{\sum_{i=1}^{n}\left(e_{a,Mi} - e_{a,Mi_{av}}\right)^2} \quad \text{(Eq.19)}$$

$$erMAX = max\left(\left|\frac{e_{a,Mi} - e_{a,M1}}{e_{a,Mi}}\right|\right) \quad \text{(Eq.20)}$$

$$t = \left[\frac{(n-1)MBE^2}{RMSE^2 - MBE^2}\right]^{\frac{1}{2}} \quad \text{(Eq.21)}$$

Results

Comparison of the actual vapour pressure values

In this study work six vapour pressure models are used for the computation of daily actual vapour pressure values which is one of the important parameter for estimating

http://www.aloki.hu ● ISSN 1589 1623 (Print) ● ISSN 1785 0037 (Online)
DOI: http://dx.doi.org/10.15666/aeer/1704_96919715

daily ETo values. *Table 2* shows the average of daily values of actual vapour pressure for the crop growth stages of the four seasons (winter, spring, summer, autumn). Each of the four cropping seasons is divided into four crop growth stages as per the guidelines provided in Allen et al. (1998). The four crop growth stages are (I) initial stage, (II) development stage, (III) midseason stage, and (IV) end season stage. The crop growth stages are used as periods to compare the actual vapour pressure and ETo values determined by using the six VP models.

Table 2. *Average of daily ea(kPa) for the crop growth stages of the four seasons*

Stages	Model 1	Model 2	Model 3	Model 4	Model 5	Model 6
Winter						
Initial	1.07	1.00	1.33	1.09	1.04	1.25
Development	1.06	0.95	1.21	1.09	1.04	1.22
Mid season	1.07	0.97	1.19	1.10	1.05	1.25
Late season	1.17	1.07	1.27	1.20	1.14	1.32
Overall	1.09	1.00	1.25	1.12	1.07	1.26
Spring						
Initial	1.11	1.02	1.24	1.15	1.09	1.25
Development	1.22	1.12	1.37	1.26	1.19	1.40
Mid season	1.26	1.16	1.41	1.29	1.24	1.45
Late season	1.09	1.01	1.16	1.12	1.11	1.32
Overall	1.17	1.08	1.30	1.20	1.16	1.35
Summer						
Initial	1.08	1.00	1.15	1.11	1.11	1.32
Development	1.24	1.15	1.38	1.28	1.23	1.44
Mid season	1.38	1.28	1.55	1.41	1.36	1.57
Late season	0.99	0.92	1.04	1.01	1.00	1.21
Overall	1.17	1.09	1.28	1.20	1.18	1.39
Autumn						
Initial	1.09	1.02	1.18	1.12	1.10	1.31
Development	0.88	0.83	0.96	0.90	0.87	1.08
Mid season	1.05	0.98	1.14	1.07	1.02	1.23
Late season	1.05	0.98	1.14	1.07	1.02	1.23
Overall	1.02	0.95	1.11	1.04	1.00	1.21

The estimated actual vapour pressure values depends on the air temperature and amount of humidity in the air. The daily values of actual vapour pressure calculated using the six VP models is shown in *Figure 4*. Among six VP models, Model 1 which uses daily maximum and minimum values of temperature and RH, is considered the most reliable model for determining the values of actual vapour pressure and is recommended if all the meteorological variables required are available.

Models 2 and 3 should be used only if any of the data required for Model 1 are either unavailable or doubtful (Allen et al.,1998; Ojha et al., 2010). Therefore, the daily values of actual vapour pressure calculated using Models 2–6 are compared with the daily values of actual vapour pressure obtained by using Model 1 in order to find which VP model should be used if all meteorological variables required for Model 1 are not available. The daily percentage errors of Models 2–6 averaged for 12-day intervals in the determination of actual vapour pressure values are shown in *Figure 5*.

http://www.aloki.hu ● ISSN 1589 1623 (Print) ● ISSN 1785 0037 (Online)
DOI: http://dx.doi.org/10.15666/aeer/1704_96919715

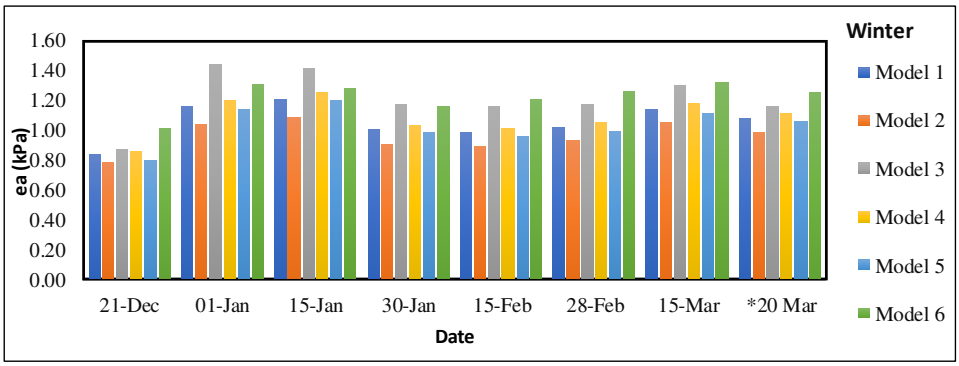

(a)

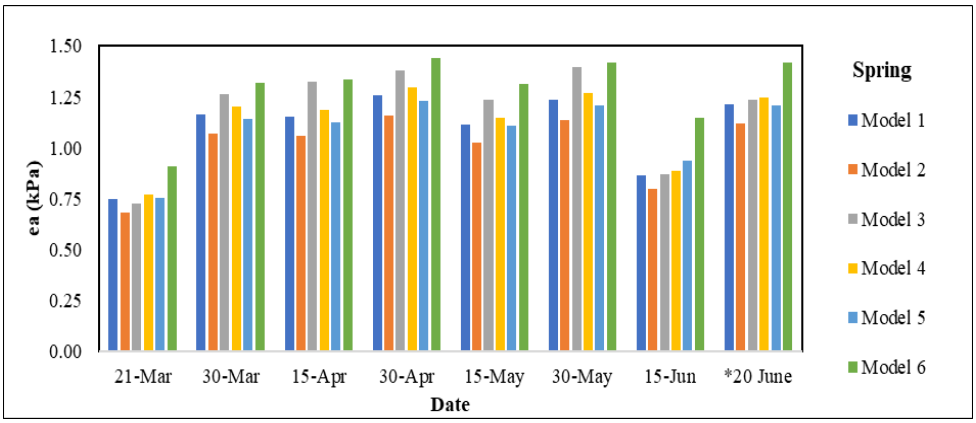

(b)

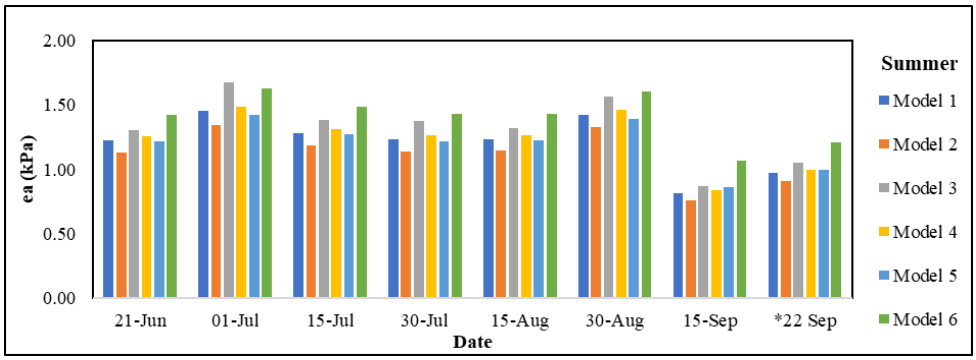

(c)

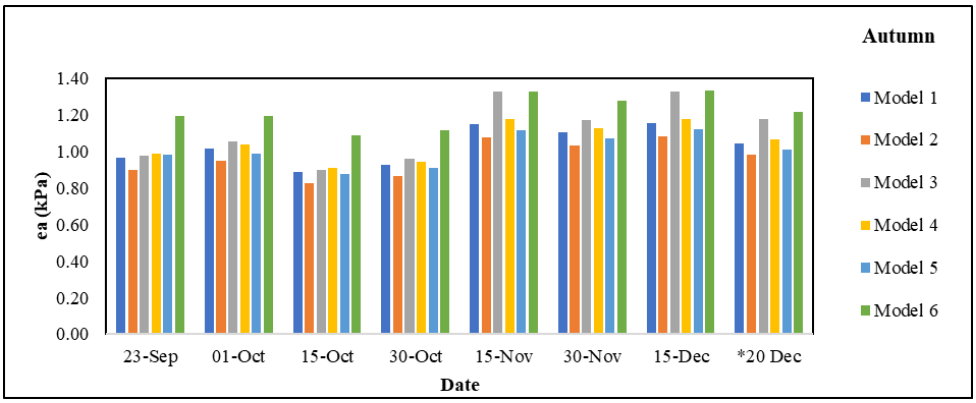

(d)

Figure 4. *Comparison of daily values of actual vapour pressure calculated using the six vapour pressure models for the cropping periods*

http://www.aloki.hu ● ISSN 1589 1623 (Print) ● ISSN 1785 0037 (Online)
DOI: http://dx.doi.org/10.15666/aeer/1704_96919715

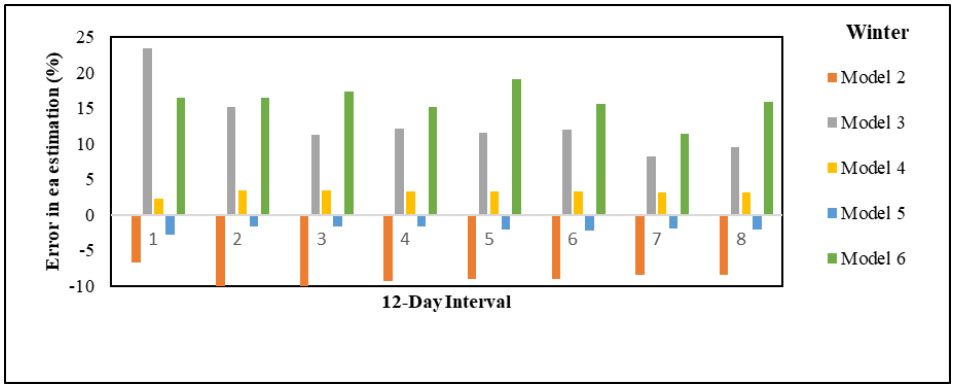

(a)

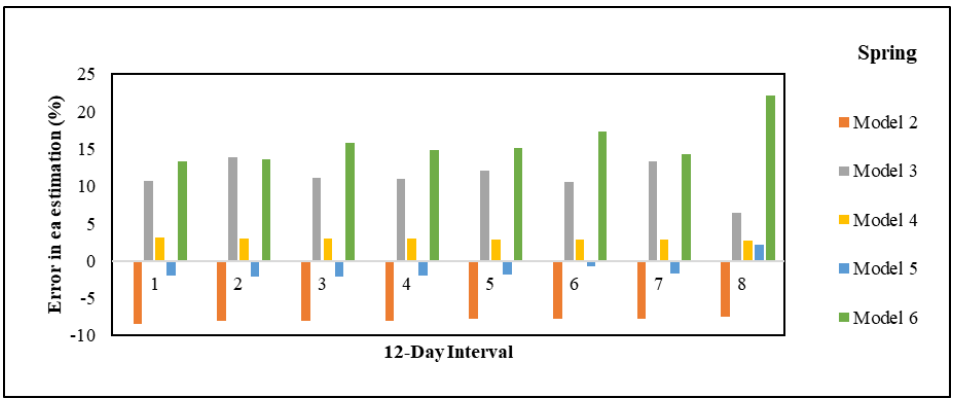

(b)

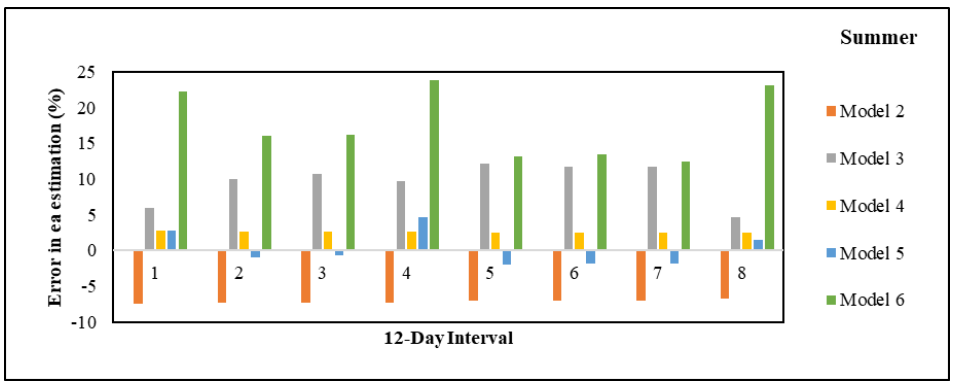

(c)

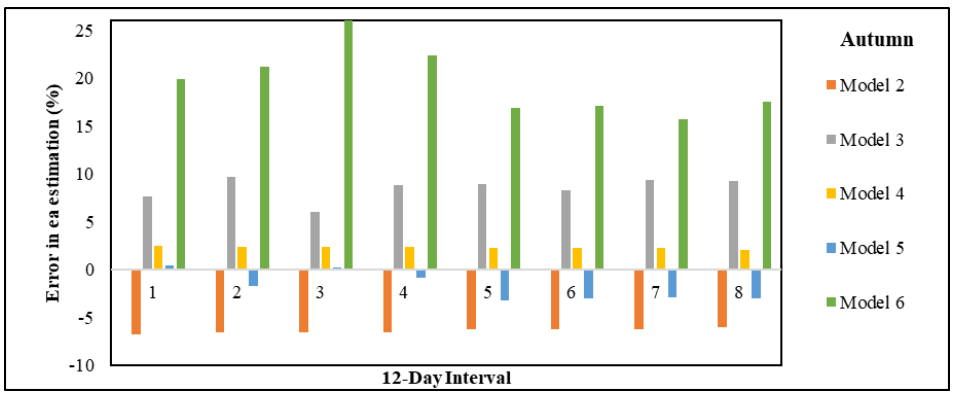

(d)

Figure 5. *Comparison of mean error (w.r.t. Model 1) in estimation of actual vapour pressure values for 12-day intervals*

http://www.aloki.hu ● ISSN 1589 1623 (Print) ● ISSN 1785 0037 (Online)
DOI: http://dx.doi.org/10.15666/aeer/1704_96919715

However, on the basis of *Figure 5,* the relative accuracy of the VP models to determine daily actual vapour pressure values cannot be evaluated because they are the error values averaged for 12-day intervals, and negative and positive errors can cancel out each other to an extent. A better evaluation of the accuracy of the VP models is performed by comparing the absolute errors of the models in actual vapour pressure estimation. These daily absolute errors averaged for 12-day intervals (MAE) are shown in *Figure 6*. The Mean absolute error (MAE) values (w.r.t. Model 1) in the estimation of actual vapour pressure for 12-day intervals over the four seasons are shown in *Table 3.*

Table 3. *Mean absolute error (MAE) values (w.r.t. Model 1) in the estimation of actual vapour pressure for 12-day intervals over the four seasons*

Models	Model 2	Model 3	Model 4	Model 5	Model 6
Maximum MAE (%)	12.00	26.49	4.91	7.49	28.66
Minimum MAE (%)	8.00	8.84	3.54	1.94	13.95
Average MAE (%)	9.57	13.74	4.24	3.21	19.73

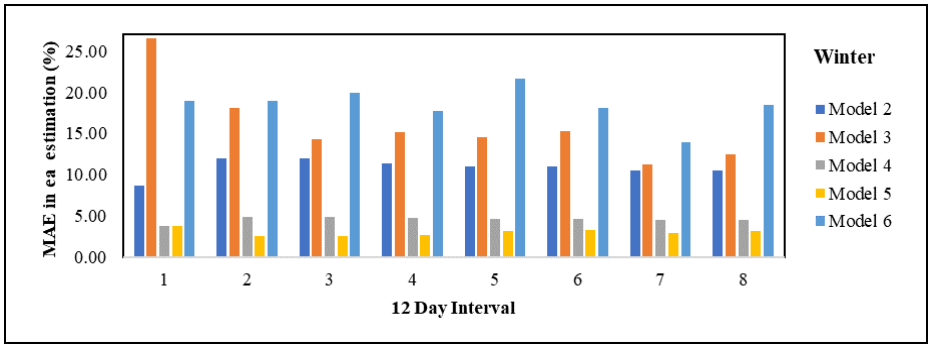

(a)

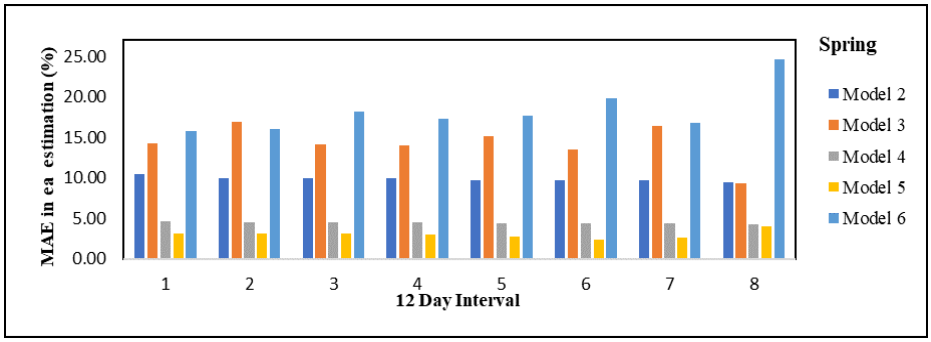

(b)

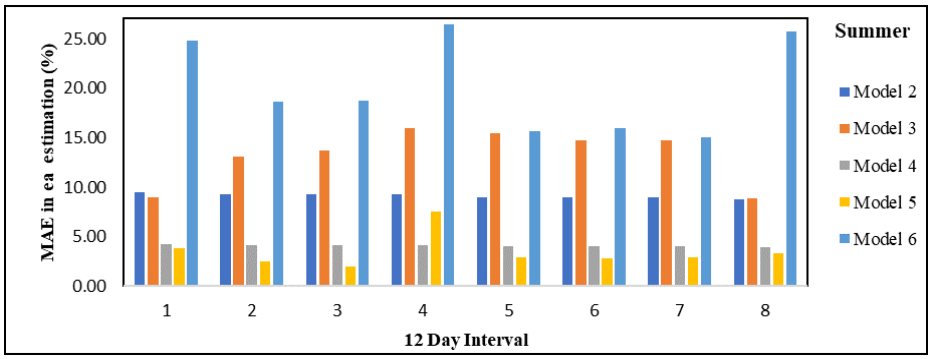

(c)

http://www.aloki.hu ● ISSN 1589 1623 (Print) ● ISSN 1785 0037 (Online)
DOI: http://dx.doi.org/10.15666/aeer/1704_96919715

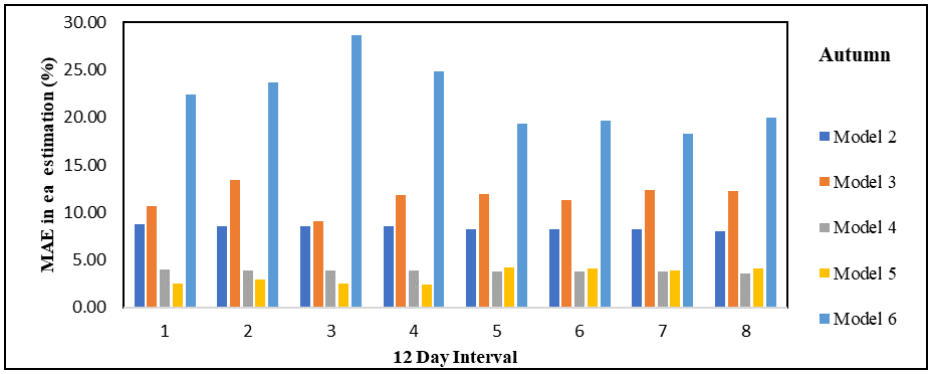

(d)

Figure 6. *Comparison of mean absolute error (w.r.t. Model 1) in estimation of actual vapour pressure values for 12-day intervals*

Comparative study of ETo estimates using six vapour pressure models

Vapour-pressure deficit (VPD) is an important parameter that is computed in evapotranspiration (ETo) models. Hence daily values of actual vapour pressure estimated by Models 1–6 were used to determine the reference (ETo) as required by FAO Penman-Monteith equation. The seasonal crop stage–wise sums of these daily ETo values for the four cropping seasons are tabulated in *Table 4*.

Table 4. *Comparison of ETo (mm/day) values estimated using the six vapour pressure models*

		ETo(M1)	ETo(M2)	ETo(M3)	ETo(M4)	ETo(M5)	ETo(M6)
Winter	Initial	23.76	24.86	19.13	11.94	24.31	20.76
	Development	16.81	12.02	23.36	23.32	16.11	23.71
	Midseason	81.12	86.67	75.03	66.36	82.34	72.85
	Late season	46.33	50.67	41.81	39.02	47.37	39.35
	Overall season	168.02	174.22	159.33	140.64	170.12	156.67
Spring	Initial	28.83	30.79	26.26	23.79	29.30	25.90
	Development	48.75	51.92	43.61	40.85	49.58	43.06
	Midseason	105.03	110.42	97.06	95.31	106.17	94.69
	Late season	75.22	77.40	73.34	67.67	74.79	69.20
	Overall season	257.83	270.54	240.27	227.62	259.84	232.86
Summer	Initial	38.65	39.72	37.62	34.67	38.32	35.56
	Development	68.31	70.46	65.23	56.20	68.32	63.17
	Midseason	133.23	138.20	124.97	106.16	134.26	123.48
	Late season	86.68	88.68	85.02	70.87	86.41	80.26
	Overall season	326.87	337.06	312.84	267.90	327.31	302.47
Autumn	Initial	37.21	38.13	36.09	27.80	37.29	34.36
	Development	75.12	76.81	72.67	51.06	75.31	69.09
	Midseason	99.79	103.90	94.27	60.37	101.64	88.81
	Late season	40.54	42.72	36.94	23.06	41.61	34.44
	Overall season	252.67	261.56	239.97	162.28	255.85	226.71

http://www.aloki.hu ● ISSN 1589 1623 (Print) ● ISSN 1785 0037 (Online)
DOI: http://dx.doi.org/10.15666/aeer/1704_96919715

It is evident from the reference evapotranspiration computation that all the models performs well enough if total value of ETo for the whole cropping season is taken into consideration. The close values of reference evapotranspiration ETo in *Table 4* as estimated based on six vapour pressure model show that the total value of ETo of a cropping season is not much affected by the choice of the VP model that is used to determine the daily actual vapour pressure values for the study area. The error in ETo estimation is highest for Model 4 (*Figure 7*), which shows the daily error averaged for 12-day intervals. From *Figure 7* it is evident that Model 2 most of the time overpredicts ETo, the reason being underprediction of actual vapour pressure values by model 2. Models 3–6 underpredict ETo as these overpredicted actual vapour pressure values. *Figure 8* shows the 12-day averages of daily absolute errors in ETo estimation. It is clearly observed in *Figure 8* that the performance of Model 5 is best among all VP models as the MAE values are the least for all the intervals for model 5. In *Figure 8,* both the maximum and minimum MAE values for a 12-day interval can be seen corresponding to Model 6, which further highlights the erratic estimation of actual vapour pressure and thus ETo by Model 6. *Table 5* shows the maximum, minimum, and average of the MAE values for all 12-day intervals across the four cropping seasons. It can be verified from *Table 5* that in data-constrained conditions, Model 5 is the most accurate VP model among the five models, followed by Model 3. Model 4, which uses only Tmean data (other models use Tmax and Tmin data) has the highest overall MAE of the five models. Though daily Tmean data are observed to be enough for the accurate estimation of daily values of actual vapour pressure, it results in relatively higher errors in ETo estimation as compared to the other models, which use both Tmax and Tmin. This is because the values of saturated vapour pressure are underestimated when only daily Tmean values are used (as in Model 4). However, there is significant variation in the estimated values of actual vapour pressure using the VP models; the choice of VP model does not affect the seasonal value of ETo considerably in this study.

Table 5. *Mean absolute error (MAE) values (w.r.t. Model 1) in the estimation of reference evapotranspiration for 12-day intervals over the four seasons*

Models	Model 2	Model 3	Model 4	Model 5	Model 6
Maximum MAE (%)	12.27	13.69	10.13	5.67	15.71
Minimum MAE (%)	1.72	3.15	3.09	1.46	8.32
Average MAE (%)	6.19	7.63	5.35	2.78	10.78

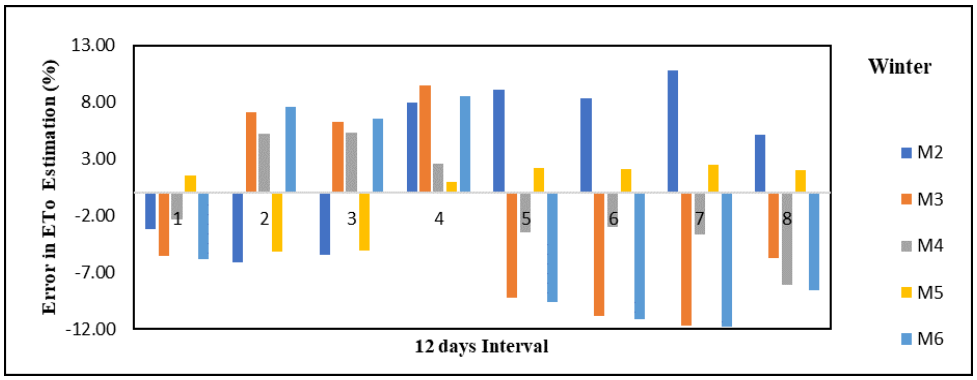

(a)

http://www.aloki.hu ● ISSN 1589 1623 (Print) ● ISSN 1785 0037 (Online)
DOI: http://dx.doi.org/10.15666/aeer/1704_96919715

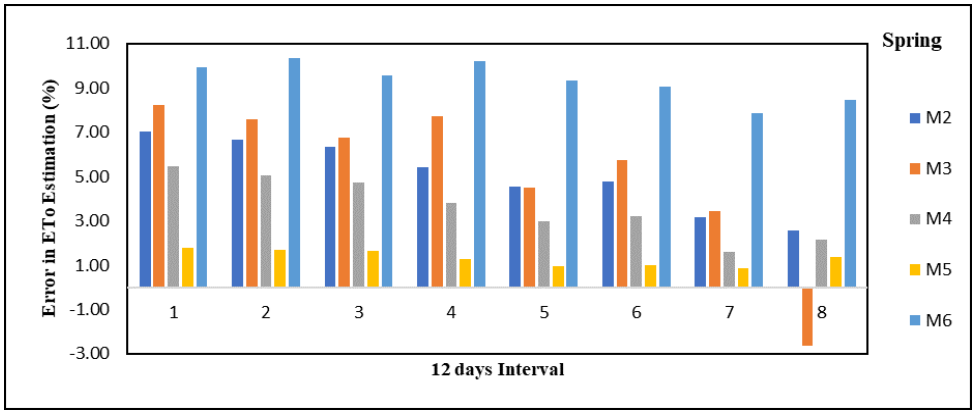

(b)

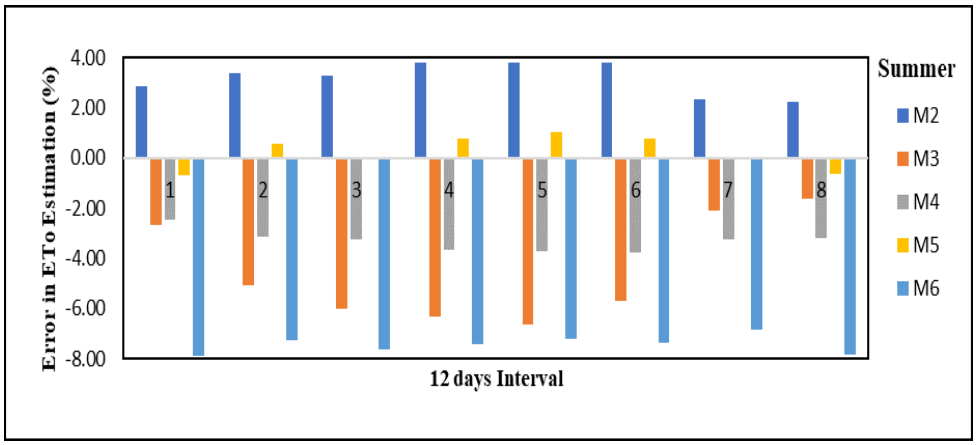

(c)

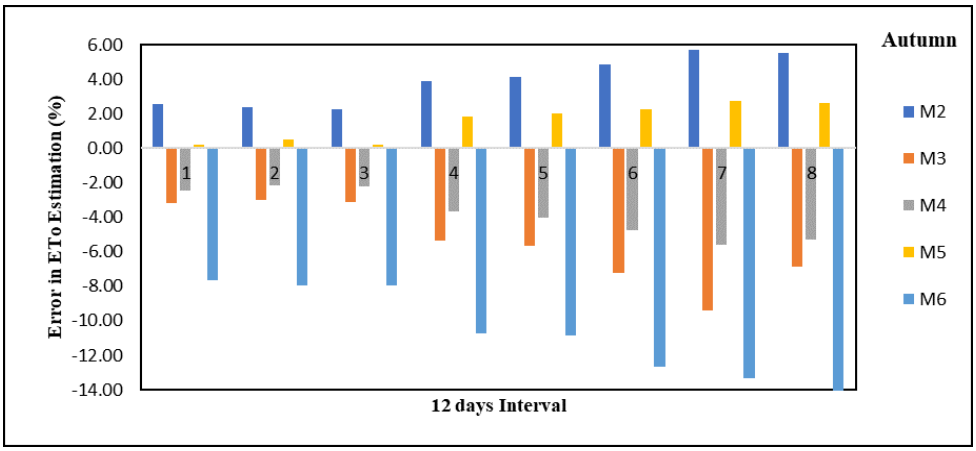

(d)

Figure 7. *Comparison of mean error (w.r.t. Model 1) in ETo estimation for 12-day intervals.*

Table 6. *Maximum and minimum wind speed for the four seasons*

Season	Max. wind velocity	Range	Min. wind velocity	Range
Winter	5.24	Gentle to moderate	1.5	Light to slight
Spring	2.99		1.12	
Summer	2.62		0.75	
Autumn	3.37		1.2	

http://www.aloki.hu ● ISSN 1589 1623 (Print) ● ISSN 1785 0037 (Online)
DOI: http://dx.doi.org/10.15666/aeer/1704_96919715

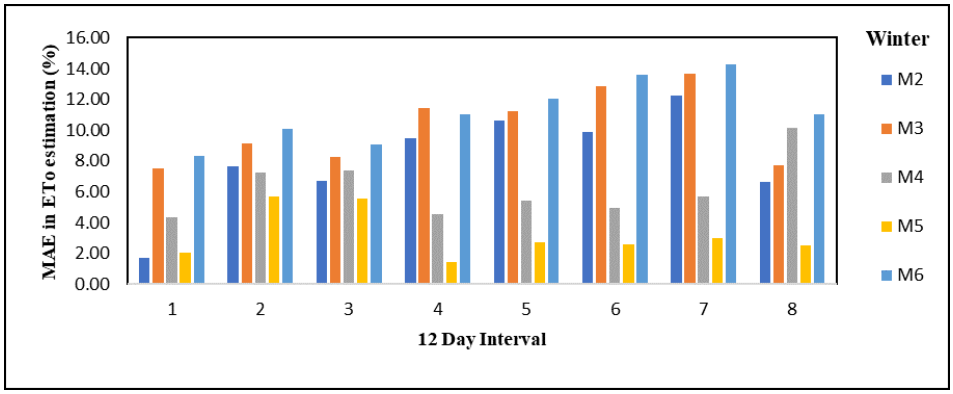

(a)

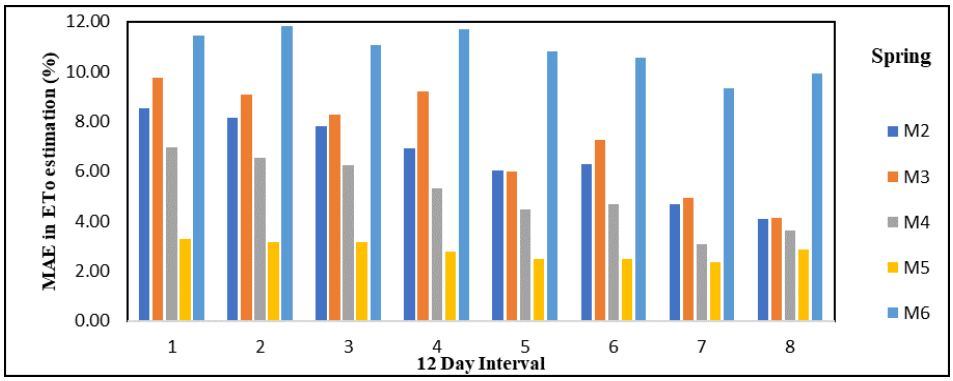

(b)

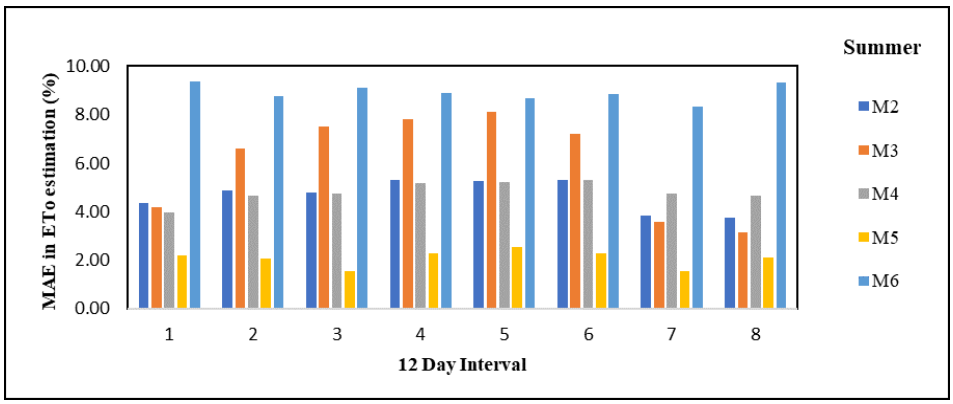

(c)

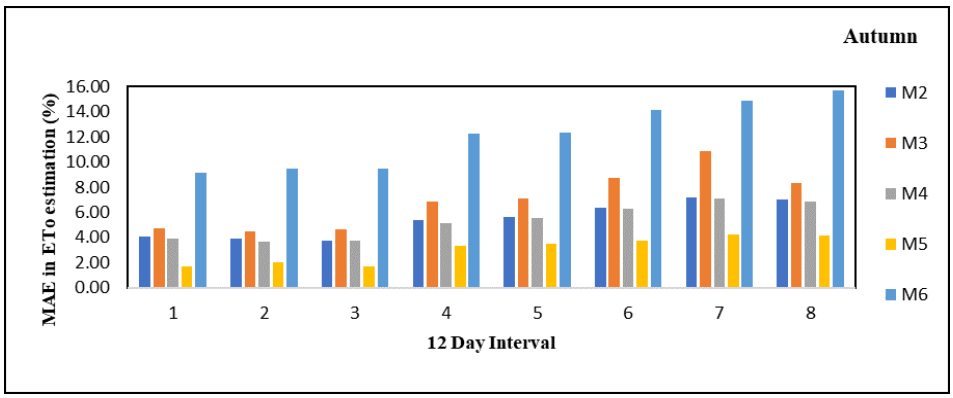

(d)

Figure 8. *Comparison of mean absolute error (w.r.t. Model 1) in ETo estimation for 12-day intervals*

http://www.aloki.hu ● ISSN 1589 1623 (Print) ● ISSN 1785 0037 (Online)
DOI: http://dx.doi.org/10.15666/aeer/1704_96919715

Performance of the vapour pressure models with variation of wind velocity

From the study, the performance of the five vapour pressure models (Models 2–6) is found to provide very reasonable result in ETo estimation for the four seasons for Abha region when compared to that of Model 1. The ETo values estimated provides satisfactory output even though there were relatively higher errors in the estimation of actual vapour pressure values. The reason may be due to the lower values of wind speed in the study area. As the ETo estimated from standard FAO Penman-Monteith method based on the product of wind speed (u_2) and vapour pressure deficit. The average wind speed data at 2 m height used in this study for ETo calculation by the FAO Penman-Monteith method are tabulated in *Table 6.*

According to Allen et al. (1998), the maximum wind speed values are in the category of gentle to moderate winds (2.62-5.24 m/s) while the minimum wind speed values falls under the category of light to slight winds (0.75-1.5 m/s). Therefore, in order to observe the effect of differences of result between higher wind speed values and lower wind speed values in the performance of VP models for ETo estimation. Taking all the parameters as before and wind speed data as shown in *Table 6* are used to determine the ETo. For all models (Models 2–6), the error in ETo estimation increased when higher values of wind speeds were used. This clearly shows that with the increase in wind speed, the error in the estimation of ETo values due to the error in the values of e_a or VPD values will increase. The performance of Model 5 is found satisfactory, followed by Model 3. All the other models have an average value of mean absolute error (*Figure 9*). Therefore, the accurate estimation of actual vapour pressure or VPD plays a key role in estimating ETo values accurately, although for light winds, this effect is much less and becomes pronounced when the wind speed is higher. Similar findings were observed by (Upreti and Ojha, 2018).

Ranking of vapour pressure model in global performance index

The statistical analysis was performed by considering ten parameters in order to judge the reliability of five vapour pressure model as compared to standard actual vapour pressure model 1 as shown in *Table 7*. The scaled values of statistical errors between 0 and 1 as described in *Table 8* and the GPI values for five models are shown in *Table 9*. In addition, the variation of GPI is also shown by *Figure 10*. The GPI value ranges from -4 to 2.771. Among 5 models, 2 models shows positive GPI value while 3 models have negative GPI as shown in *Figure 10*. The highest value of GPI is shown by Model 5. Hence it can be seen that GPI has simplified the statistical outcomes to identify the performance of models. *Table 9* shows the ranking of the models on the basis of their GPI values sorted in descending order, since the highest GPI value represent the best performing model.

Table 7. *Estimated value of statistical indicator*

	MAE	RMSE	MARE	U95	RMSRE	RRMSE	MBE	R^2	ERMAX	TTEST
Model2	0.0854	0.0875	0.0754	0.1754	0.0763	0.0215	0.0854	0.9953	0.1000	85.8353
Model3	0.122	0.159	0.105	0.373	0.138	0.039	-0.121	0.855	1.319	22.000
Model 4	0.031	0.032	0.027	0.064	0.028	0.008	-0.031	0.990	0.034	84.176
Model 5	0.024	0.028	0.023	0.073	0.037	0.007	0.015	0.986	0.522	11.669
Model 6	0.189	0.193	0.175	0.387	0.189	0.047	-0.189	0.956	1.023	88.591

http://www.aloki.hu ● ISSN 1589 1623 (Print) ● ISSN 1785 0037 (Online)
DOI: http://dx.doi.org/10.15666/aeer/1704_96919715

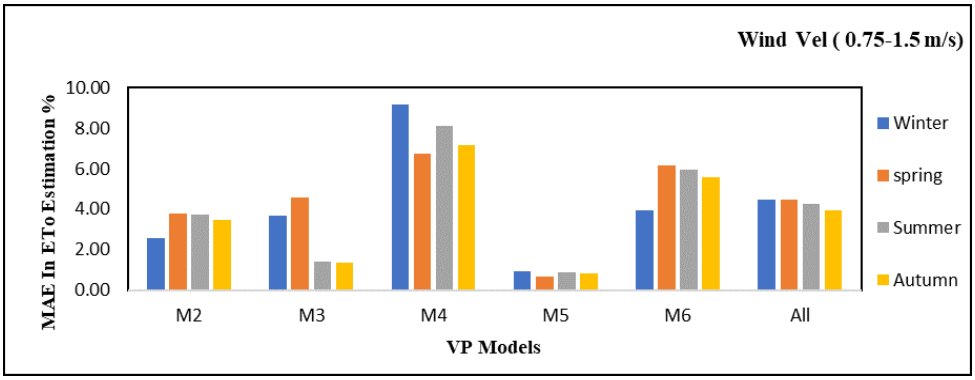

(a)

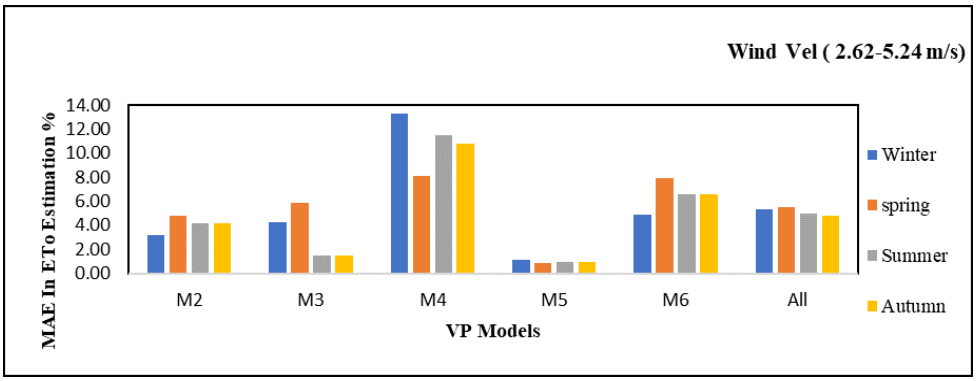

(b)

Figure 9. *Comparison of mean absolute error (w.r.t. Model 1) in daily ETo estimation for different wind speed ranges*

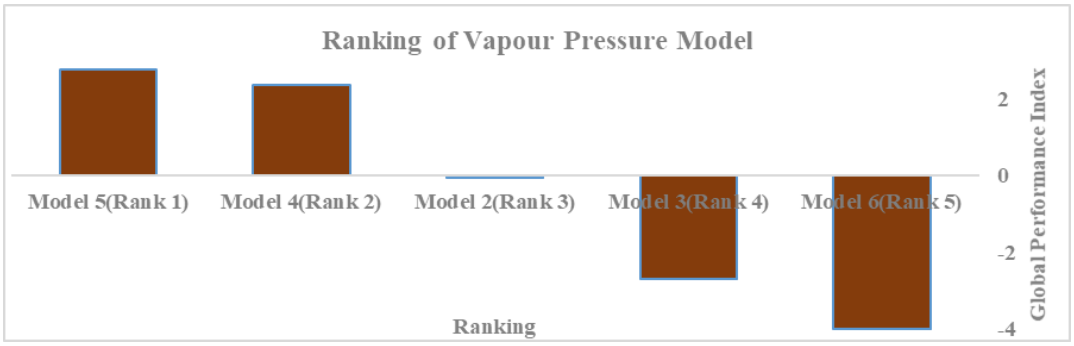

Figure 10. *Ranking of vapour pressure model*

Table 8. *Scaled (0-1) value of statistical indicator*

	Scaled									
Model	MAE	RMSE	MARE	U95	RMSRE	RRMSE	MBE	R^2	ERMAX	TTEST
Model2	0.373	0.359	0.346	0.346	0.302	0.359	1.000	1.000	0.051	0.964
Model3	0.596	0.795	0.543	0.958	0.681	0.795	0.248	0.000	1.000	0.134
Model 4	0.043	0.020	0.031	0.000	0.000	0.020	0.576	0.962	0.000	0.943
Model 5	0.000	0.000	0.000	0.030	0.059	0.000	0.743	0.934	0.380	0.000
Model 6	1.000	1.000	1.000	1.000	1.000	1.000	0.000	0.720	0.769	1.000

http://www.aloki.hu ● ISSN 1589 1623 (Print) ● ISSN 1785 0037 (Online)
DOI: http://dx.doi.org/10.15666/aeer/1704_96919715

Table 9. *Global performance index and rank of five models*

Model	MAE	RMSE	MARE	U95	RMSRE	RRMSE	MBE	R^2	ERMAX	TTEST	GPI	Rank
Model 5	0.373	0.359	0.346	0.316	0.243	0.359	-0.167	0.000	0.000	0.943	2.771	1
Model 4	0.331	0.339	0.316	0.346	0.302	0.339	0.000	-0.029	0.380	0.000	2.381	2
Model 2	0.000	0.000	0.000	0.000	0.000	0.000	-0.424	-0.066	0.328	-0.022	-0.051	3
Model 3	-0.222	-0.436	-0.197	-0.612	-0.379	-0.436	0.328	0.934	-0.620	0.808	-2.701	4
Model 6	-0.627	-0.641	-0.654	-0.654	-0.698	-0.641	0.576	0.214	-0.390	-0.057	-4.000	5

Discussion

This study investigated performance of vapour pressure models using weather data for Abha meteorological weather station in the computation of vapour pressure and evapotranspiration in Abha, Asir Region, Saudi Arabia. Effort has been made to compare six vapour pressure model during four seasons and ranking has been done using global performance index. The values estimated from different actual vapour pressure model were compared with the value obtained from standard model 1 which uses daily maximum and minimum values of temperature and RH, and is considered the most reliable model for determining the values of actual vapour pressure for four seasons (Allen et al., 1998). The daily percentage errors for actual vapour pressure were estimated for Models 2–6 averaged for 12-day intervals in the determination of actual vapour pressure. Based on error it was found that Model 2 generally underpredicts actual vapour pressure value. Models 3, 4, and 5 overpredicted the actual vapour pressure value. Model 6, which uses daily minimum temperature, has the most erratic behavior in estimating the actual vapour pressure value. The relative accuracy of the VP models to determine daily actual vapour pressure values cannot be evaluated because they are the error values averaged for 12-day intervals, and negative and positive errors can cancel out each other to an extent. A better evaluation of the accuracy of the VP models is performed by comparing the absolute errors of the models in actual vapour pressure estimation. The MAE for each of cropping season is much less for Models 4 and 5 as compared to the MAE values for Models 2, 3, and 6. Both Models 4 and 5 use daily RHmean and Tmean data for the estimation of actual vapour pressure values. Overall, the performance of Model 6 in the determination of actual vapour pressure values is the poorest among the five models. The lower MAE values for Models 4 and 5 indicate that these may be used for the determination of daily actual vapour pressure values in Abha regions with similar climates instead of Models 2 and 3, both of which the FAO-56 paper advised for use if all variables required for Model 1 were not available. Further daily values of actual vapour pressure estimated by Models 1–6 were used to determine the reference (ETo) as required by FAO Penman- Monteith equation. The seasonal crop stage–wise sums of these daily ETo values were used for the four cropping seasons. The error in ETo estimation is highest for Model 4, which shows the daily error averaged for 12-day intervals. Clearly, for all intervals, the maximum error in ETo estimation is for Model 4, even though the same model (along with Model 5) estimated the actual vapour pressure values most accurately. This can be attributed to the inaccurate determination of saturated vapour pressure values because the saturated vapour pressure value for Model 4 is determined differently from the other models. The better performance of Model 5 in ETo estimation also verifies this because both Models 4 and 5 determined actual vapour pressure values with similar accuracy. Therefore, the determination of daily saturated vapour pressure value should be done by equation of

http://www.aloki.hu ● ISSN 1589 1623 (Print) ● ISSN 1785 0037 (Online)
DOI: http://dx.doi.org/10.15666/aeer/1704_96919715

saturated vapour pressure which uses both daily Tmax and Tmin instead of using equation in which only the daily Tmean value is used. It is evident that Model 2 most of the time overpredicts ETo, the reason being underprediction of actual vapour pressure values by model 2. Models 3–6 underpredict ETo as these overpredicted actual vapour pressure values. The performance of Model 5 is best among all VP models as the MAE values are the least for all the intervals for model 5. Both the maximum and minimum MAE values for a 12-day interval can be seen corresponding to Model 6, which further highlights the erratic estimation of actual vapour pressure and thus ETo by Model 6. Model 5 is the most accurate VP model among the five models, followed by Model 3. Model 4, which uses only Tmean data (other models use Tmax and Tmin data) has the highest overall MAE of the five models. Though daily Tmean data are observed to be enough for the accurate estimation of daily values of actual vapour pressure, it results in relatively higher errors in ETo estimation as compared to the other models, which use both Tmax and Tmin. This is because the values of saturated vapour pressure are underestimated when only daily Tmean values are used (as in Model 4). However, there is significant variation in the estimated values of actual vapour pressure using the VP models; the choice of VP model does not affect the seasonal value of ETo considerably in this study. The ETo values estimated provides satisfactory output even though there were relatively higher errors in the estimation of actual vapour pressure values. The reason may be due to the lower values of wind speed in the study area. As the ETo estimated from standard FAO Penman-Monteith method based on the product of wind speed (u2) and Vapour Pressure Deficit. For all models (Models 2–6), the error in ETo estimation increased when higher values of wind speeds were used. This clearly shows that with the increase in wind speed, the error in the estimation of ETo values due to the error in the values of ea or VPD values will increase. The performance of Model 5 is found satisfactory, followed by Model 3. All the other models have an average value of mean absolute error. Therefore, the accurate estimation of actual vapour pressure or VPD plays a key role in estimating ETo values accurately, although for light winds, this effect is much less and becomes pronounced when the wind speed is higher. Similar findings were observed by (Upreti and Ojha, 2018).

The performance of vapour pressure models was computed based on overall effect of evaluation criteria called as global performance index. The ranking was done in order to get most promising model which can be used alternative to model 1. From analysis it was evident that Model 5 provides best performance and model 6 worst.

Hence it is evident that actual vapour pressure is important parameter which is used for vapour pressure deficit which in turn used in reference evapotranspiration equation. VPD is an integrated variable for atmospheric water demand that depends on both air temperature and humidity, VPD will increase with ongoing climate warming, which suggests that atmospheric water demand or drought will also increase under such a scenario (Zhang et al., 2017). Therefore, it is necessary to investigate the relationship between increased VPD and crop yields on the regional or global scale. Lobell et al. (2013) indicated that increases in VPD contribute to water stress and affect crop growth and yield in two ways. First, the crops increase their demand for soil water to maintain carbon assimilation at a given rate; and second, the crops reduce the supply of soil water through elevated transpiration rates. Therefore, maize yield declined with increased VPD (Lobell et al., 2013). Shuai et al. (2013) found that VPD affected yield variability through its effects on water stress. Crops that were negatively related to VPD were usually located in areas where the mean VPD during the crop growing period was

http://www.aloki.hu ● ISSN 1589 1623 (Print) ● ISSN 1785 0037 (Online)
DOI: http://dx.doi.org/10.15666/aeer/1704_96919715

higher. The changes in the sensitivity of crop yields to VPD can be attributed to changes in VPD itself, cultivars and agronomic management practices; for example, increasing crop sowing densities could increase crop sensitivity to VPD (Lobell et al., 2014). Adopting drought-tolerant cultivars and technologies, as well as increasing irrigation areas, might decrease the sensitivity of crop yields to VPD. The decline in reliability of water resources necessitates careful planning for water demand satisfaction under the highly variable demand characteristics in Saudi Arabia (Tarawneh and Chowdhury, 2018).

This study tries to explain the six-vapour pressure model in semi-arid region in Saudi Arabia. However, different regions show different behavior with respect to seasonal variability of rainfall, temperature change, agricultural activities, soil types and crop types. Future study must understand the overall implications of climate change in Saudi Arabia and investigate the possibility of scheduling and/or shifting crop producing periods.

Conclusions

The present research work deals with six vapour pressure models in order to determine six sets of daily values of actual vapour pressure for four seasons. The six sets of daily computed actual vapour pressure from six models were then used to compute ETo by standard FAO56 Penman-Monteith equation. The performance evaluation of the five models (Models 2–6) was analyzed by comparing the values of the estimates of actual vapour pressure and ETo with those of Model 1, which is recommended in the literature to determine daily actual vapour pressure values if all meteorological variables required are available using global performance index. From the research work it can be concluded that:

1. From global performance index, Models 5 and 4 have higher accuracy in the estimation of daily actual vapour pressure values with GPI Value of 2.77 and 2.38 respectively as compared to Models 2, 3 (vapour pressure models mentioned in FAO-56), and 6 with GPI value of -0.051,-2.7 and -4 respectively.
2. Daily Tmean values (Model 4) are found to be not good enough for the estimation of vapour pressure deficit because this underestimate the daily saturation vapour pressure, which results in underestimation of ETo. This highlights the importance of the requirement of daily Tmax–Tmin data for accurate estimation of daily ETo
3. The result obtained from global performance index shows that the performance of the Model 5, which is based on the Lawrence Tdew–RH relationship is closest to Model 1 in ETo estimation when compared to the other models. On the basis of this study, it is recommended to use Model 5 for estimation of actual vapour pressure and ETo when only daily RHmean data are available
4. The result with wind speed shows that error in actual vapour pressure with light winds do not affect ETo estimation much. However, the effect of actual vapour pressure values becomes significantly high on ETo estimation for higher wind speed ranges.
5. The results of this study could be used by water management system, crop cultivators, crop advisors, researchers and students from universities and

http://www.aloki.hu ● ISSN 1589 1623 (Print) ● ISSN 1785 0037 (Online)
DOI: http://dx.doi.org/10.15666/aeer/1704_96919715

research centre. Moreover it can be benefitted by makers of decision and in the vast field of agriculture, hydrology and environment.

6. The present results demonstrated that atmospheric VPD played significant roles in modulating water movement along the soil-plant-atmospheric continuum, and these findings can be applied to greenhouse production. VPD regulation efficiently moderated plant water stress and maintained water balance by reducing the atmospheric driving force

Acknowledgements. The authors would like to acknowledge the Deanship of Scientific Research (King Khalid University, Ministry of Education, Kingdom of Saudi Arabia) for providing administrative and financial support (award number R.G.P.1./74/40). The authors of current work wish to thank Universiti Tecknologi Malaysia, Johor Bahru for their facilities and Lab support. We would also like to thank general authority of the meteorological department, Abha, Asir region, Saudi Arabia for providing the weather data.

Conflict of interests. The authors declare no conflict of interests**.**

REFERENCES

[1] Al-Ghobari, H. M. (2000): Estimation of reference evapotranspiration for southern region of Saudi Arabia. – Irrigation Science 19(2): 81-86.

[2] Al-Mostafa, Z. A., Maghrabi, A. H., Al-Shehri, S. M. (2014): Sunshine-based global radiation models: a review and case study. – Energy Conversion and Management 84: 209-216.

[3] Al-Omran, A. M., Al-Ghobari, H. M., Alazba, A. A. (2004): Determination of evapotranspiration of tomato and squash using lysimeters in central Saudi Arabia. – International Agricultural Engineering Journal 13(142): 27-36.

[4] Al-Zahrani, K. H., Baig, M. B., Straquadine, G. S. (2019): Food Waste in the Kingdom of Saudi Arabia: Implications for Extension Education. – In: Behnassi, M. et al. (eds.) Climate Change, Food Security and Natural Resource Management. Springer, Cham, pp. 73-101.

[5] Ali, M., Jamil, B. (2019): Estimating diffuse solar radiation in India: performance characterization of generalized single-input empirical models. – Urban Climate 27: 314-350.

[6] Allen, R. G. (1996): Assessing integrity of weather data for reference evapotranspiration estimation. – Journal of Irrigation and Drainage Engineering 122(2): 97-106.

[7] Allen, R. G., Pereira, L. S., Raes, D., Smith, M. (1998): Crop evapotranspiration-guidelines for computing crop water requirements. – FAO irrigation and drainage paper 56. Fao, Rome 300(9): D05109.

[8] Allen, R. G., Pereira, L. S., Howell, T. A., Jensen, M. E. (2011): Evapotranspiration information reporting: II. Recommended documentation. – Agricultural Water Management 98(6): 921-929.

[9] Baig, M. B., Straquadine, G. S. (2014): Sustainable Agriculture and Rural Development in the Kingdom of Saudi Arabia: Implications for Agricultural Extension and Education. – In: Behnassi, M. et al. (eds.) Vulnerability of Agriculture, Water and Fisheries to Climate Change. Springer, Dordrecht, pp. 101-116.

[10] Behar, O., Khellaf, A., Mohammedi, K. (2015): Comparison of solar radiation models and their validation under Algerian climate. The case of direct irradiance. – Energy Conversion and Management 98: 236-251.

http://www.aloki.hu ● ISSN 1589 1623 (Print) ● ISSN 1785 0037 (Online)
DOI: http://dx.doi.org/10.15666/aeer/1704_96919715

[11] Burman, R. D., Jensen, M., Allen, R. G. (1987): Thermodynamic factors in Evapotranspiration. – In: James, L. G., English, M. J. (eds.) Irrigation Systems for the 21st Century. – ASCE, New York, pp. 140-148.
[12] Čadro, S., Uzunović, M., Žurovec, J., Žurovec, O. (2017): Validation and calibration of various reference evapotranspiration alternative methods under the climate conditions of Bosnia and Herzegovina. – International Soil and Water Conservation Research 5(4): 309-324.
[13] Chowdhury, S., Al-Zahrani, M. (2013): Implications of climate change on water resources in Saudi Arabia. – Arabian Journal for Science and Engineering 38(8): 1959-1971.
[14] DeNicola, E., Aburizaiza, O. S., Siddique, A., Khwaja, H., Carpenter, D. O. (2015): Climate change and water scarcity: the case of Saudi Arabia. – Annals of Global Health 81(3): 342-353.
[15] Despotovic, M., Nedic, V., Despotovic, D., Cvetanovic, S. (2015): Review and statistical analysis of different global solar radiation sunshine models. – Renewable and Sustainable Energy Reviews 52: 1869-1880.
[16] ElNesr, M., Alazba, A., Abu-Zreig, M. (2010): Spatio-temporal variability of evapotranspiration over the Kingdom of Saudi Arabia. – Applied Engineering in Agriculture 26(5): 833-842.
[17] Gueymard, C. A. (2014): A review of validation methodologies and statistical performance indicators for modeled solar radiation data: towards a better bankability of solar projects. – Renewable and Sustainable Energy Reviews 39: 1024-1034.
[18] Hirschi, M., Michel, D., Lehner, I., Seneviratne, S. I. (2017): A site-level comparison of lysimeter and eddy covariance flux measurements of evapotranspiration. – Hydrology and Earth System Sciences 21(3): 1809-1825.
[19] Howell, T. A., Dusek, D. A. (1995): Comparison of vapour-pressure-deficit calculation methods—southern high plains. – Journal of Irrigation and Drainage Engineering 121(2): 191-198.
[20] Irmak, S., Howell, T. A., Allen, R. G., Payero, J. O., Martin, D. L. (2005): Standardized ASCE Penman-Monteith: impact of sum-of-hourly vs. 24-hour timestep computations at reference weather station sites. – Transactions of the ASAE 48(3): 1063-1077.
[21] Kang, Y., Khan, S., Ma, X. (2009): Climate change impacts on crop yield, crop water productivity and food security. A review. – Progress in Natural Science 19(12): 1665-1674.
[22] Kumar, R., Jat, M. K., Shankar, V. (2012): Methods to estimate irrigated reference crop evapotranspiration. A review. – Water Science and Technology 66(3): 525-535.
[23] Lelieveld, J., Hadjinicolaou, P., Kostopoulou, E., Chenoweth, J., El Maayar, M., Giannakopoulos, C., Xoplaki, E. (2012): Climate change and impacts in the Eastern Mediterranean and the Middle East. – Climatic Change 114(3-4): 667-687.
[24] Li, M. F., Tang, X. P., Wu, W., Liu, H. B. (2013): General models for estimating daily global solar radiation for different solar radiation zones in mainland China. – Energy Conversion and Management 70: 139-148.
[25] Liu, X., Xu, C., Zhong, X., Li, Y., Yuan, X., Cao, J. (2017): Comparison of 16 models for reference crop evapotranspiration against weighing lysimeter measurement. – Agricultural Water Management 184: 145-155.
[26] Lobell, D. B., Hammer, G. L., McLean, G., Messina, C., Roberts, M. J., Schlenker, W. (2013): The critical role of extreme heat for maize production in the United States. – Nature Climate Change 3(5): 497.
[27] Lobell, D. B., Roberts, M. J., Schlenker, W., Braun, N., Little, B. B., Rejesus, R. M., Hammer, G. L. (2014): Greater sensitivity to drought accompanies maize yield increase in the US Midwest. – Science 344(6183): 516-519.
[28] Madugundu, R., Al-Gaadi, K. A., Tola, E., Hassaballa, A. A., Patil, V. C. (2017): Performance of the metric model in estimating evapotranspiration fluxes over an irrigated

http://www.aloki.hu ● ISSN 1589 1623 (Print) ● ISSN 1785 0037 (Online)
DOI: http://dx.doi.org/10.15666/aeer/1704_96919715

field in Saudi Arabia using Landsat-8 images. – Hydrology and Earth System Sciences 21(12): 6135-6151.

[29] Mallick, J., Hang, H. T., Islam, S., Khan, R. A. (2017): Geospatial Approach on Landslide Susceptibility Zonation and Geo-design in Semi-arid Mountainous Watershed, Saudi Arabia. – In: Kallel, A. et al. (eds.) Proceedings of Euro-Mediterranean Conference for Environmental Integration, Tunisia. Springer, Cham, pp. 1833-1835.

[30] Multsch, S., Alquwaizany, A. S., Alharbi, O. A., Pahlow, M., Frede, H. G., Breuer, L. (2017): Water-saving strategies for irrigation agriculture in Saudi Arabia. – International Journal of Water Resources Development 33(2): 292-309.

[31] Nolz, R., Cepuder, P., Eitzinger, J. (2016): Comparison of lysimeter based and calculated ASCE reference evapotranspiration in a subhumid climate. – Theoretical and Applied Climatology 124(1-2): 315-324.

[32] Ojha, C. S. P., Khobragade, S. D., Adeloye, A. J. (2010): Estimating air vapour pressure in a semiarid region using FAO-56 methodology. – Journal of Irrigation and Drainage Engineering 137(8): 491-500.

[33] Pandey, P. K., Dabral, P. P., Pandey, V. (2016): Evaluation of reference evapotranspiration methods for the northeastern region of India. – International Soil and Water Conservation Research 4(1): 52-63.

[34] Pandey, V., Pandey, P. K. (2018): Calibration and ranking of Valiantzas reference evapotranspiration equations under the humid climate of northeast India. – Journal of Water and Climate Change. DOI: 10.2166/wcc.2018.305.

[35] Sadler, E. J., Evans, D. E. (1989): Vapour pressure deficit calculations and their effect on the combination equation. – Agricultural and Forest Meteorology 49(1): 55-80.

[36] Salih, A. M., Sendil, U. (1984): Evapotranspiration under extremely arid climates. – Journal of Irrigation and Drainage Engineering 110(3): 289-303.

[37] Saxton, K. E. (1975): Sensitivity analyses of the combination evapotranspiration equation. – Agricultural Meteorology 15(3): 343-353.

[38] Seager, R., Hooks, A., Williams, A. P., Cook, B., Nakamura, J., Henderson, N. (2015): Climatology, variability, and trends in the US vapour pressure deficit, an important fire-related meteorological quantity. – Journal of Applied Meteorology and Climatology 54(6): 1121-1141.

[39] Shuai, J., Zhang, Z., Liu, X., Chen, Y., Wang, P., Shi, P. (2013): Increasing concentrations of aerosols offset the benefits of climate warming on rice yields during 1980–2008 in Jiangsu Province, China. – Regional Environmental Change 13(2): 287-297.

[40] Stone, R. J. (1993): Improved statistical procedure for the evaluation of solar radiation estimation models. – Solar Energy 51(4): 289-291.

[41] Tarawneh, Q., Chowdhury, S. (2018): Trends of climate change in Saudi Arabia: implications on water resources. – Climate 6(1): 8.

[42] Trenberth, K. E. (2011): Changes in precipitation with climate change. – Climate Research 47(1-2): 123-138.

[43] Upreti, H., Ojha, C. S. P. (2017): Estimation of relative humidity and dew point temperature using limited meteorological data. – Journal of Irrigation and Drainage Engineering 143(9): 05017005.

[44] Upreti, H., Ojha, C. S. P. (2018): Evaluation of the vapour pressure models in the estimation of actual vapour pressure and evapotranspiration. – Journal of Irrigation and Drainage Engineering 144(11): 05018007.

[45] Weiss, A. (1977): Algorithms for the calculation of moist air properties on a hand calculator. – Transactions of the ASAE 20(6): 1133-1136.

[46] Willmott, C. J., Matsuura, K. (2005): Advantages of the mean absolute error (MAE) over the root mean square error (RMSE) in assessing average model performance. – Climate Research 30(1): 79-82.

http://www.aloki.hu ● ISSN 1589 1623 (Print) ● ISSN 1785 0037 (Online)
DOI: http://dx.doi.org/10.15666/aeer/1704_96919715

[47] Yoder, R. E., Odhiambo, L. O., Wright, W. C. (2005): Effects of vapour-pressure deficit and net-irradiance calculation methods on accuracy of standardized Penman-Monteith equation in a humid climate. – Journal of Irrigation and Drainage Engineering 131(3): 228-237.

[48] Zhang, S., Tao, F., Zhang, Z. (2017): Spatial and temporal changes in vapour pressure deficit and their impacts on crop yields in China during 1980–2008. – Journal of Meteorological Research 31(4): 800-808.

http://www.aloki.hu ● ISSN 1589 1623 (Print) ● ISSN 1785 0037 (Online)
DOI: http://dx.doi.org/10.15666/aeer/1704_96919715

COMBINING ABILITIES AND HETEROSIS OF BODY WEIGHT IN A DIALLEL CROSS FROM THREE SOUTH AFRICAN INDIGENOUS CHICKEN GENOTYPES

TYASI, T. L.[1*] – NORRIS, D.[1] – NG'AMBI, J. W.[1] – MABELEBELE, M.[2]

[1]*Department of Agricultural Economics and Animal Production, University of Limpopo, Private Bag X1106, Sovenga, Polokwane, South Africa*

[2]*Department of Agriculture and Animal Health, College of Agriculture and Environmental Sciences, University of South Africa, Pretoria, South Africa*

**Corresponding author*
e-mail: louis.tyasi@ul.ac.za

(Received 18th Mar 2019; accepted 24th May 2019)

Abstract. This study was conducted to estimate heterosis effects, specific and general combining abilities existing within growth traits. A 3 x 3 diallel mating system involved three indigenous chicken genotypes namely Potchefstroom Koekoek (P), Venda (V) and Ovambo (O) was used to produce three purebreds (P x P, V x V, O x O), three crossbreds (P x O, P x V, O x V) and three reciprocals (O x P, V x P, V x O). The body masses of 225 chicks recorded at ages 0, 4, 8 and 10 weeks, were used to make an estimation of heterosis, specific combining ability (SCA) and general combining ability (GCA). Results indicated that the crossbreed between P sires and O dams provided the uppermost heterosis for growth traits (30.07%). GCA and SCA showed the importance ($P \leq 0.05$) for body weight from hatch up to 10 weeks of age. P genotype gave the positive effects of GCA and P x V crossbreed resulted in positive effects of SCA. It thus, be concluded that Potchefstroom Koekoek genotype might be used in the crossbreeding with other indigenous chicken genotypes to improve growth traits.
Keywords: *Potchefstroom Koekoek, Venda, Ovambo, crossbred, purebred*

Introduction

Indigenous chickens comprise about 80% of the national poultry flocks in Africa (Darre, 2012). Despite their importance, indigenous chickens have slow growth rates and relatively low mature weight (Norris and Ng'ambi, 2007). There are several indigenous chicken genotypes in South Africa (Malatji et al., 2016) including Potchefstroom Koekoek, Venda and Ovambo chicken genotypes. Potchefstroom Koekoek chicken genotype is a composite chicken genotype which was developed from three European poultry breeds namely White Leghorn, Black Australorp and Bared Plymouth Rock. This genotype is black and white speckled colour pattern, and was bred for both egg and meat production (Mutibvu et al., 2019). Ovambo chicken genotype is originated from Namibia and predominantly dark coloured that reach sexual maturity at 2.2 kg body weight for males and 1.5 kg for females at about 140 days old (Motsepe et al., 2016). Venda chicken genotype was first discovered in Venda region of Limpopo province, South Africa and is dual purpose, moderately large and multi-coloured predominated with white, black and red colours (Mphaphathi et al., 2016).

To date, in South Africa there is limited scientific information on crossbreeding of local chicken genotypes to improve growth traits. The aims of the study were to discover and underline the general combining abilities, heterotic effects and specific combining abilities for body weight in a three-way cross between Potchefstroom

http://www.aloki.hu ● ISSN 1589 1623 (Print) ● ISSN 1785 0037 (Online)
DOI: http://dx.doi.org/10.15666/aeer/1704_97179723

Koekoek, Ovambo and Venda chicken genotypes. According to Musa et al. (2015), crossing indigenous chicken genotypes has led to the improvement in growth rates and body weight. This study will help chicken farmers to determine the perfect combination of indigenous chicken genotypes during breeding program to improve body weight.

Materials and methods

Study site

The study was conducted at the same site described by Brown and Ng'ambi (2019). However, the current study was conducted between November 2012 and February 2013.

House preparation

Water disinfected with Jeyes fluid bought from a company in Polokwane called NTK was applied in hatchery and experimental houses. After, both hatchery and experimental houses were left to dry for 7 days to break the life cycle of possible disease caused by the organisms that were not killed by the disinfectant the houses were left empty for one week after cleaning. All the equipment such as feeders, wire separators and drinkers as well as the incubator were cleaned thoroughly and disinfected. New disinfectant was added daily and the footbath was thoroughly cleaned.

Data collection

Individual body weights of 180 chicks from a diallel cross of three indigenous chicken genotypes, namely Potchefstroom Venda (V), Koekoek (P) and Ovambo (O) were noted at the end of a week period from hatch up to 10 weeks of age. 10 hens from each genotype were allocated casually to be bred with two roosters of each genotype. Their eggs were gathered and noted down daily according to breeds and crossbreds. The eggs were weighed up and hatched independently according to breeds and crossbreds. Nine genetic groups of P x P, V x V, O x O, P x V, P x N, V x P, V x O, O x P, and O x V chicks were obtained, accordingly. The hatched chicks were wing banded until 8 weeks of age followed by leg banding to keep their breed and crossbred group identity'. The chickens were reserved as a unit on a litter floor, in a semi-open house that has been separated according to their breeds and crossbreds. They were medicated equally and were subjected to the same climatic conditions managerial and hygienic. During the process of rearing periods and brooding, all chicks were fed *ad-libitum* using standard commercial starter (21% crude, 3,000 kcal and protein (CP) metabolize capable energy (ME)/kg) from the time they hatched till they were four weeks, trailed by a cultivator diet (2,900 kcal ME/kg and 18% CP) to 62 days old. Water was provided *ad-libitum*. Artificial heat was provided at (32 °C) using continuous light program and ultraviolet lights were provided. Ventilation was controlled through curtain rails.

Statistical analysis

The effect of genetic group on body weight was tested using the general linear model (GLM) procedure of Statistical Analysis System software program (SAS, 2008). Duncan's multiple range test was used for significant means at $P<0.05$. The following model was used:

$$Y_{ij}=\mu+G_i+e_{ij} \quad \text{(Eq.1)}$$

http://www.aloki.hu ● ISSN 1589 1623 (Print) ● ISSN 1785 0037 (Online)
DOI: http://dx.doi.org/10.15666/aeer/1704_97179723

where Y_{ij} = body weight of bird in i^{th} genetic group, μ = overall mean, G_i = fixed effect of the i^{th} genetic group and e_{ij} = random error.

Heterosis was calculated according to Fairfull (1990) and the following formula was applied:

$$H\% = \left[\frac{AB(0.5AA+0.5BB)}{(0.5AA+0.5BB)}\right] x100 \quad \text{(Eq.2)}$$

where H% = percentage heterosis, AB = crossbred genotype, AA and BB = sire and dam genotypes. General and specific combining abilities were calculated in the form of means (Falconer, 1988). The following formulas were used:

$$\text{Specific combining ability (SCA)} = \frac{AB+BA}{2} \quad \text{(Eq.3)}$$

$$\text{General combining ability (GCA)} = \frac{A+GCA(B)}{2} \quad \text{(Eq.4)}$$

where AB = cross between genotype A and B, and BA = its reciprocal.

Results

Body weight at different weeks of age

The results showed body weights at different weeks of age differed significantly ($P<0.05$) among the nine genetic groups (*Table 1*). Least square means showed that Potchefstroom Koekoek (P) and Ovambo (O) had higher hatch weight (30 g) followed by P x V and V x O with 29.60 g, and O x V (28.80 g), respectively. Nonetheless, there was no substantial variance ($P > 0.05$) between P x O, O x V and V X P at hatch, with body weights of 27.60, 28.80 and 28 g. Results also indicated that Venda chickens performed better in body weight when crossed with Ovambo in comparison with other crosses during the hatch period. For purebreds, Ovambo and Potchefstroom Koekoek were heavier (30 g) than the Venda chickens (20 g) at hatch. For crosses, the P x V was heavier (29.60 g) when compared to O x V and P x O which their body weight was 27.60 g also 28.80 g, respectively. For purebreds, Potchefstroom Koekoek had a heavier body weight (256 g) as compared to other purebreds in the fourth week. There were no differences in the fourth week, ($P > 0.05$) among the Ovambo purebred, V x P and O x V. With respect to crosses, P x O had a higher body weight (256 g) in compared to the O x V and P x V which their weights were of 255.92 and 232 g, respectively. Among the reciprocals, O x P body weighed higher (276 g) in comparison with the V x O and V x P which weighed 232 g and 244 g, respectively.

Heterosis

Heterosis results (*Fig. 1*) with respect to crosses showed that O x V had affirmative heterosis in all different ages. P x O had positive heterosis from hatching to 4 weeks of age only and afterwards had negative heterosis while P x V had positive heterosis at all different ages apart from 10 weeks of age, respectively. With deference to reciprocals, the V x P had positive heterosis at all ages whereas the O x P exhibited negative heterosis at all ages of measurement except 4 weeks of age, respectively. V x O showed

http://www.aloki.hu ● ISSN 1589 1623 (Print) ● ISSN 1785 0037 (Online)
DOI: http://dx.doi.org/10.15666/aeer/1704_97179723

positive heterosis at hatching and four weeks of age and indicated negative heterosis at 8 weeks and 10 weeks of age.

Table 1. *Least squares means for body weight (g) from hatch up to 10 weeks during different age intervals for purebreds, reciprocals and crosses*

Genetic groups	Number of chicks	Age (week)			
		Hatch	BW4	BW8	BW10
Purebreds					
P x P	25	30.00[a]	256.00[b]	800.00[d]	1366.67[b]
O x O	25	30.00[a]	232.00[e]	1000.00[a]	1233.33[d]
V x V	25	20.00[d]	204.00[f]	630.00[g]	1000.00[h]
Crosses					
P x O	25	27.60[b]	256.00[b]	800.00[d]	1280.00[c]
P x V	25	29.60[a]	255.92[c]	770.00[e]	1133.33[f]
O x V	25	28.80[ab]	232.00[e]	830.00[c]	1133.33[f]
Reciprocals					
O x P	25	21.60[c]	276.00[a]	800.00[d]	1166.67[e]
V x P	25	28.00[b]	232.00[e]	930.00[b]	1433.33[a]
V x O	25	29.60[a]	244.00[d]	700.00[f]	1033.33[g]

[a-g]Least square means in the same column with different superscripts differ significantly ($P < 0.05$)
P = Potchefstroom Koekoek, V = Venda and O = Ovambo.

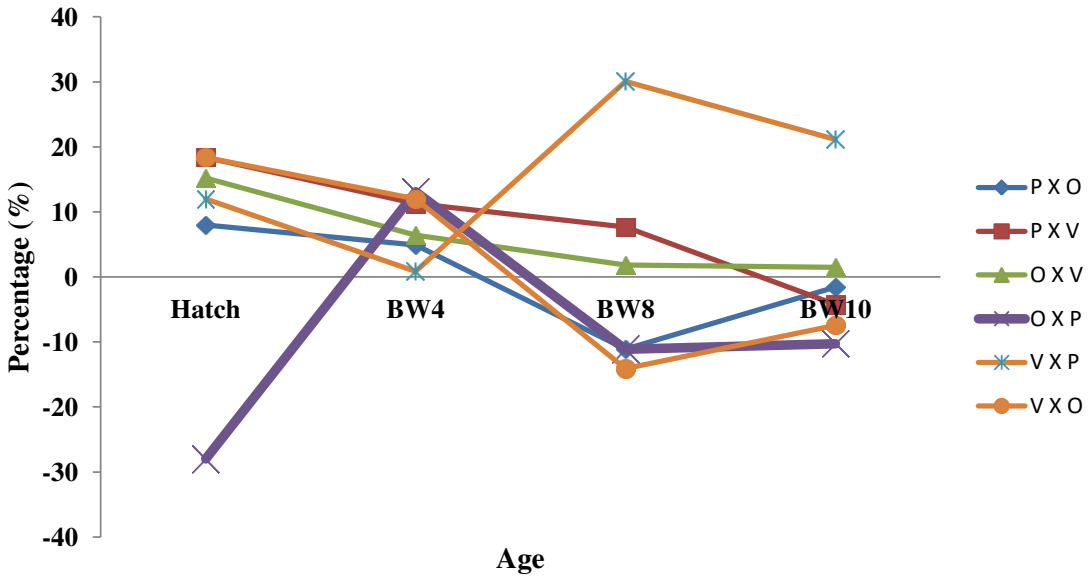

Figure 1. *Heterosis percentages for body weight at different ages. P X O, P X V and O X V are the crosses between Potchefstroom Koekoek sire and Ovambo dam, Potchefstroom Koekoek sire and Venda dam, and Ovambo sire and Venda dam, respectively. O X P, V X P and V X O are the reciprocals between Ovambo sire and Potchefstroom Koekoek dam, Potchefstroom Koekoek dam and Venda sire, and Ovambo dam and Venda sire. X indicates the cross between genotypes. Hatch is the body weight after hatching, BW4 is body weight at four weeks, BW8 is body weight at eight weeks and BW10 is a body weight at ten weeks of age.*

http://www.aloki.hu ● ISSN 1589 1623 (Print) ● ISSN 1785 0037 (Online)
DOI: http://dx.doi.org/10.15666/aeer/1704_97179723

Combining abilities

SCA effects and estimates of GCA are presented in *Table 2*. GCA showed that the P breed had positive effects during the studied periods. However, O genotype had a positive effect during the studied ages, except at 10 weeks of age. The Venda genotype had the lowest negative estimates at all stages of growth. SCA showed that the P x O crossbred had negative effect at hatch, 8 weeks and 10 weeks of age, and a positive effect at 4 weeks of age in comparison among crossbreds. P x V crossbred gave positive effects at all different ages. O x V crossbred had positive effects at hatch and at 4 weeks of age; however, it showed negative effects at 8 weeks and 10 weeks, respectively.

Table 2. *Crossbreeding genetic parameters for body weight at different ages of measurement*

Parameters	Hatch	4 weeks	8 weeks	10 weeks
General combining abilities				
$_{g}^{P}$	0.56	12.22	10.00	93.34
$_{g}^{O}$	0.69	2.23	48.33	-17.78
$_{g}^{V}$	-1.24	-14.45	-58.33	-75.56
Specific combining abilities				
$_{s}^{PO}$	-3.89	8.45	-65.00	-50.00
$_{s}^{PV}$	2.24	3.09	91.67	67.78
$_{S}^{OV}$	2.51	7.12	-31.67	-21.11

g = general combining ability, s = specific combining ability.

Discussion

This study was directed to investigate heterosis, specific combining abilities and general combining abilities for body weight traits after crossing three South African indigenous chicken genotypes; namely Potchefstroom Koekoek, Venda and Ovambo. Our results based on cross for heterosis, the effects for body weights were mostly positive and ranged from -14.11 to 30.07% during different age intervals up to 10 weeks of age. However, Musa et al. (2015) reported that heterosis for body weight ranged from -9.44 to 13.48% after crossing three genotypes of Nigerian indigenous chickens. Results of the current study revealed that the P x V cross had encouraging heterosis at all different ages of measurement except at 10 weeks of age when compared to its reciprocal V x P, that had positive heterosis at all ages and highest 10 weeks of age. The O x V had positive low heterosis for body weight at the different weeks of age when compared to its reciprocal V x O which had negative heterosis for body weight at all weeks of measurement except at hatch and 4 weeks of age. These findings indicate that Potchefstroom Koekoek sires and Ovambo dams as well as Venda and Venda sires gave the highest heterosis for growth traits. Furthermost reviewed studies showed that body weights of crossbred chickens at different ages were related with negative and positive heterosis effects for growth traits (Sutherland et al., 2018; Musa et al., 2015; Siwendu et al., 2012). However, Nwenya et al. (2017) reported a positive heterosis for body weight after crossing Naked neck and Frizzled feather chickens. Our heterosis results might stand as an encouraging element for the poultry breeders in South Africa to cross these two breeds (Venda female and Potchefstroom Koekoek male) and (Ovambo female and Venda male) to get hybrid vigour in growth traits. Furthermore, we also estimated the general combining abilities and specific combining abilities among purebreds and

http://www.aloki.hu ● ISSN 1589 1623 (Print) ● ISSN 1785 0037 (Online)
DOI: http://dx.doi.org/10.15666/aeer/1704_97179723

crosses of South African indigenous chicken genotypes. General combining ability (SCA) was a significant source of variability among purebred groups on body weights at different growth stages. This importance showed the importance of preservative components. These results are similar with the work of Musa et al. (2015), who found general combining ability estimations more significant and of higher in three genotypes of Nigerian indigenous chickens. Adebambo et al. (2010) reported the significant of GCA for body weight using three chicken genotypes. Our findings recognized that Potchefstroom Koekoek chicken genotype had the uppermost (best) encouraging effect of general combining ability at all ages of measurement excluding at hatch and 8 weeks of age while the Venda breed had negative effect at all ages. Specific combining ability results point out that P x V provided positive estimates for body weight throughout the different weeks of measurement. This cross could be recommended for the future. In addition, P x O had high negative estimates for body weight at all the ages of measurement except for 4 weeks of age.

Conclusion

Diallel cross mating system was performed in three South African indigenous chicken genotypes to estimate crossbreeding parameters. Heterosis estimations indicate that crosses between the Venda dams and Potchefstroom Koekoek sires as well as between the Ovambo dams and Venda sires provided the highest heterosis effect for body weight. It might be significant to contemplate developing a composite chicken genotype based on the estimations of heterosis, specific combining ability and general combining ability. The current study has shown the significance of bearing in mind the estimates of heterosis effects, general combining ability and specific combining ability effect before planning any crossbreeding program.

REFERENCES

[1] Adebambo, A. O., Ikeobi, C. O. N., Ozoje, M. O., Oduguwa, O. O., Adebambo, O. A. (2010): Combining abilities of growth traits among pure and crossbred meat type chickens. – Architecture Zoo Technology 60: 953-963.

[2] Brown, D., Ng'ambi, J. W. (2019): Effects of dietary vachelia karrooleaf meal inclusion on meat quality and histological parameters in Pedi bucks fed a setaria verticillatahay-based diet. – Applied Ecology and Environmental Research 17(2): 2893-2909.

[3] Darre, M. J. (2012): The Importance of Poultry in Our Lives. – Department of Animal Sciences, University of Connecticut, Storrs, CT.

[4] Fairfull, R. W. (1990): Heterosis. – In: Crawford, R. D. (ed.) Poultry Breeding and Genetics. Elsevier, Amsterdam, pp. 913-933.

[5] Falconer, D. S. (1988): Introduction to Quantitative Genetics. – John Wiley and Sons, New York.

[6] Malatji, D. P., Tsotetsi, A. M., van Marle-Koster, E., Muchadeyi, F. C. (2016): A description of village chicken production systems and prevalence of gastrointestinal parasites: Case studies in Limpopo and KwaZulu-Natal provinces of South Africa. – Onderstepoort Journal of Veterinary Research 83(1): 1-8.

[7] Motsepe, R., Mabelebele, M., Norris, D., Brown, D., Ngambi, J., Ginindza, M. (2016): Carcass and meat quality characteristics of South African indigenous chickens. – Biological and Biotechnological Sciences 50(4): 580-587.

http://www.aloki.hu ● ISSN 1589 1623 (Print) ● ISSN 1785 0037 (Online)
DOI: http://dx.doi.org/10.15666/aeer/1704_97179723

[8] Mphaphathi, M. L., Seshoka, M. M., Luseba, D., Sutherland, B., Nedambale, T. L. (2016): The characterization and cryopreservation of Venda chicken semen. – Asian Pacific Journal of Reproduction 5(2): 132-139.
[9] Musa, A. A., Orunmuyi, M., Akpa, G. N., Olutunmogun, A. K., Muhammad, H., Adedibu, I. I. (2015): Diallel analysis for body weight involving three genotypes of Nigerian indigenous chickens. – South African Journal of Animal Science 45(2): 188-197.
[10] Mutibvu, T., Chimonyo, M., Halimani T. E. (2019): Effect of strain, sex and rearing system on carcass and fat yield of Naked Neck, Ovambo and Potchefstroom Koekoek chickens. – Indian Journal of Animal Research. DOI: 10.18805/ijar.B-944.
[11] Norris, D., Ng'ambi, J. W. (2007): Genetic parameter estimates for body weight in local Venda chickens. – Tropical Animal Health Production 38: 7-8.
[12] Nwenya, J. M., Nwakpu, E. P., Nwose, N. R., Ogbuagu, P. K. (2017): Performance and heterosis of indigenous chicken crossbreed (Naked Neck x Frizzled Feather) in the humid tropics. – Journal of Poultry Research 14(2): 07-11.
[13] SAS (2008): User Guide: Statistics Release 9.2. – Statistical Analysis System Institute, Inc., Cary, North Caroline.
[14] Siwendu, N. A., Norris, D., Ng'ambi, J. W., Shimelis, H. A., Benyi, K. (2012): Heterosis and combining ability for body weight in a diallel cross of three chicken genotypes. – Tropical Animal Health Production 20: 23-25.
[15] Sutherland, D. A. T., Honaker, C. F., Dorshort, B., Anderson, L., Siegel, P. B. (2018): Asymmetries, heterosis and phenotypic profiles of red junglefowl, White Plymouth Rocks, and F_1 and F_2 reciprocal crosses. – Journal of Applied Genetics 59(2): 193-201.

http://www.aloki.hu ● ISSN 1589 1623 (Print) ● ISSN 1785 0037 (Online)
DOI: http://dx.doi.org/10.15666/aeer/1704_97179723

ANALYSIS ON THE WIND-BLOWN SAND ENTERING THE RESERVOIR OF SANSHENGGONG WATER CONTROL PROJECT

LI, Z. Q.[1,2] – LI, Q. Y.[3*] – WANG, Y. M.[1] – LIU, L. H.[4]

[1]*School of Water Resources and Hydropower, Xi'an University of Technology, Xi'an 710048, China*

[2]*Huangzangsi Project Construction & Management Bureau, HRB, Lanzhou 730030, China*

[3]*Henan Vocational College of Water Conservancy and Environment, Zhengzhou 462000, China*

[4]*North China University of Water Resources and Electric Power, Zhengzhou 450045, China*

**Corresponding author*
e-mail: 46189156@qq.com

(Received 18th Mar 2019; accepted 17th May 2019)

Abstract. Considering the potential threats of wind-blown sand to the reservoir capacity of Sanshenggong Water Control Project (SWCP), this paper calculates the amount of wind-blown sand in the reservoir based on the change of reservoir capacity, using sand balance method and cross-section method. Then, the calculated amount was compared with the amount of wind-blown sand measured through field monitoring. Synthesizing the calculation results of the three methods, it is considered that the amount of wind-blown sand into the reservoir is about 0.7~1 million tons per year. The research findings provide a good reference for silt prevention.
Keywords: *sand balance method, sand flow, the yellow river, cross-section method, field monitoring*

Introduction

Located near the Yellow River, the Ulan Buh Desert is widely known for limited rainfall, high evaporation rate and frequent gales (Chen et al., 2016). Each year, a lot of sand is blown from the desert into the Yellow River, making the desert a major source of sediment in the river. Wind erosion in this area has attracted much attention from the academia, yielding successful researches on the hazards and control of wind erosion, the law of sand dune movement and the physical features of sand. However, there is no quantitative analysis on these movements and features (Chen et al., 2015; Yin et al., 2017).

The sand from the desert has many negative impacts on Sanshenggong Water Control Project (SWCP), a local water conservancy project on the main stream of the Yellow River in Daokou, Bayannur, Inner Mongolia. The main function of the project is diversion and irrigation, which relies heavily on reservoir capacity. The silt in the SWCP reservoir mainly come from the sediment of upstream water and the wind-blown sand from Ulan Buh Desert.

Considering the features of reservoir deposition, this paper calculates the amount of wind-blown sand in the reservoir based on the change of reservoir capacity, using sand balance method and cross-section method. Then, the calculated amount was compared with the amount of wind-blown sand measured through field monitoring (Youssef et al., 2012).

http://www.aloki.hu ● ISSN 1589 1623 (Print) ● ISSN 1785 0037 (Online)
DOI: http://dx.doi.org/10.15666/aeer/1704_97259733

Materials and methods

Study area

With an elevation of 1,052 m, the SWCP (40°18'42"N, 107°01'39"E) controls a 314,000 km^2 basin area. It is a low-head diversion project with irrigation as its main function. The other functions include navigation, transport, power generation and industrial water supply. The project was constructed between 1959 and 1961 (Mao, 2013). The storage capacity was designed as 0.8 billion m^3 (Liu et al., 2016), and stands at 0.952 billion m^3 under the normal storage level of 1,055.0 m.

Located at the entry of the SWCP reservoir, the Dangkou Hydrological Station marks the start of the backwater area, which extends 53.8km before reaching the end at the dam site of the SWCP. The SWCP reservoir is a plain river reservoir with an average width of 2,000 m, half of which belongs to the main channel. The project area has a continental monsoon climate in the middle temperate zone. The left and right banks of the project area are a flat beach of sediment and an Ordos terrace, respectively.

The SWCP provides an important guarantee for irrigation in the Hetao region in the upper reaches of the Yellow River, which used to suffer from frequently droughts and floods, and greatly lowered the amount of sand in the diversion canal. Statistics show that the amount of sand in the main channel of the Yellow River in the Hetao section has been reduced by 60% since the completion of the SWCP (Mao, 2013). The decline in sedimentation saves lots of irrigation cost.

Data collection

The research data were extracted from the Validated Data Compilation (1961~2000) of the SWCP in Inner Mongolia Reaches of the Yellow River, the hydrological data (1962~2014) of Dangkou Hydrological Station, the Sediment Source and Siltation Change in Ningxia–Inner Mongolia (NIM) Reaches of the Yellow River and the Feasibility Study Report on Phase 2 Flood Control Project in Inner Mongolia Reaches of the Yellow River. Meanwhile, the amount of wind-blown sand into the SWCP reservoir was calculated from the field measured data.

The amount of wind-blown sand into the SWCP reservoir was calculated three times, respectively through the combination of sand balance method and cross-section method, the storage capacity method and field observation.

Sediment balance method and cross-section method

Sediment balance method and cross-section method (a.k.a. the topographic method) are two popular ways to compute the amount of sand in a river section.

Sediment balance method

By this method, the amount of sand in the river section ΔW_s is calculated from to the amount of sand entering and leaving the river section, as shown in *Equation 1:*

$$\Delta W_S = W_j + W_h - W_c - W_y \quad \text{(Eq.1)}$$

where W_j is the amount of sand entering the reservoir at the entrance; W_h is the amount of sand entering the reservoir from the tributaries; W_c is the amount of sand leaving the river section at the exit; W_y is the amount of sand diverted away from the reservoir.

http://www.aloki.hu ● ISSN 1589 1623 (Print) ● ISSN 1785 0037 (Online)
DOI: http://dx.doi.org/10.15666/aeer/1704_97259733

In the SWCP reservoir, there is no tributary that transports sand into the river section. Rather, lots of sand are blown by wind from the banks into the Yellow River. Hence, the above formula should be revised by replacing the W_h with the amount of wind-blown sand W_{fs}, as shown in *Equation 2:*

$$\Delta W_S = W_j + W_{fs} - W_c - W_y \quad \text{(Eq.2)}$$

Cross-section method

The cross-section method is implemented in the following steps: selecting several cross-sections from the river section, measuring the topography of each cross-section before and after a time period, obtaining the silting area of each cross-section in that period (Thomas, 2011), calculating the sand amount of the river channel between these cross-sections, and deriving the total amount of sand in the entire river section in that period. The cross-section method can be divided into several categories, as shown in *Equations 3* and *4*.

(1) Trapezoidal method

$$\sum_{i=1}^{n} V_i = \sum_{i=1}^{n-1} \frac{1}{2}(\Delta A_i + \Delta A_{i+1}) \times \Delta L_i \quad \text{(Eq.3)}$$

where V_i and ΔA_i are the sand amount and silting area of the i-th cross-section, respectively; ΔA_{i+1} is the silting area of the i + 1-th cross-section; L_i is the distance between the first and i + 1-th cross-sections; N is the number of cross-sections. In this method, the river section between two adjacent cross-sections is viewed as a trapezoid for sand amount computation.

(2) Cone method

$$\sum_{i=1}^{n} V_i = \sum_{i=1}^{n-1} \frac{1}{3}(\Delta A_i + \Delta A_{i+1} + \sqrt{\Delta A_i \times \Delta A_{i+1}}) \times \Delta L_i \quad \text{(Eq.4)}$$

The parameters are the same as those in *Equation 3* above.

Comparison between the two methods

The sand balance method and cross-section method have their respective merits and defects. The sand balance method is suitable for calculating the sand amount in different periods, especially in short periods. However, some systematic errors may occur in the computation, and the calculated amount may deviate from the actual amount if there are any uncontrolled areas. As for the cross-section method, the calculation accuracy is affected by the sparse layout of cross-sections and the limited number of measuring points. The error of this method will be magnified by a low amount of sand. Through repeated comparison, most researchers agree that the two methods have basically the same computing accuracy.

In this paper, the two methods are adopted to calculate the amount of wind-blown sand into the SWCP reservoir. Firstly, the sand amount of the reservoir was computed by the cross-section method. The result is the sand amount in the river section ΔW_s, which contains the wind-blown sand. Since the cross-section method cannot determine

http://www.aloki.hu ● ISSN 1589 1623 (Print) ● ISSN 1785 0037 (Online)
DOI: http://dx.doi.org/10.15666/aeer/1704_97259733

the specific amount of wind-blown sand, the sand balance method was introduced to calculate the amount of sand leaving the river section at the Daokou Hydrological Station W_c and the amount of sand diverted away from the reservoir W_y. Then, the amount of wind-blown sand was computed by subtracting the amount of sand entering the reservoir at the entrance W_j from the total amount of sand leaving the reservoir W_c and W_y.

Storage capacity method

Based on the features of water and sand flows, the storage capacity method computes the annual mean runoff and the sand transport in each period of the past years, and determines the amount of wind-blown sand into the study area according to the siltation of the reservoir section (Chattopadhyay, 2011). The calculation formula is shown in *Equation 5:*

$$S_{win} = \frac{r \times H \times L \times B \times R_c}{R} \quad \text{(Eq.5)}$$

where S_{win} is the amount of wind-blown sand entering the Yellow River (103 kg); γ is the volume of the wind-blown sand (1.4 × 103 kg/m^3); H is the sedimentary thickness (m); L is the length of the river section affected by the sand blown from the desert (m); B is the width of the river section (m); R_c is the proportion of wind-blown sand in the total amount of sand in the river section (61%); R is the proportion of wind-blown sand that deposited in the river section in the total amount of wind-blown sand (70.74%).

Field observation

Established in 2011, Ulan Buh Desert Wind and Sand Comprehensive Observation Base monitors eleven types of land uses, including the mobile, semi-mobile, fixed and semi-fixed sand dunes in the study area. The observation plots cover typical areas with similar topography. The volume of wind-blown sand was recorded by the wind-sand collector, and then the transport rates of wind-blown sand were computed for different kinds of sand dunes, eliminating the volume in invalid wind directions (Kisi, 2014).

In 2014, several 10 m-tall wind-blown sand flux towers were set up along the Yellow River to observe the settlement of suspended particles in the wind-blown sand. These towers were arranged in a straight line pointing toward the northwest direction. The observation lasted from May 26, 2014 to May 26, 2015. The annual sand flow at the height of 1~10 m were observed on the left and right banks. The amount of Suspended sand entering the Yellow River S_{sus} (t/yr) can be calculated as shown in *Equation 6:*

$$S_{sus} = \left(S_l - S_r\right) \times L \quad \text{(Eq.6)}$$

where, S_i and S_r are the amounts of sand entering the river from the left bank and the right bank, respectively (kg/m/yr); L is the length of the river section affected by the sand blown from the desert (km)

http://www.aloki.hu ● ISSN 1589 1623 (Print) ● ISSN 1785 0037 (Online)
DOI: http://dx.doi.org/10.15666/aeer/1704_97259733

Results

Features of wind-blown sand into the reservoir

The water and sand in the SWCP reservoir can be traced to different sources. About 99% of water and 44% of sand in this river section come from the reaches above Lanzhou. Due to the completion of several water conservancy projects in the upper reaches (Longyangxia Reservoir and Liujiaxia Reservoir), the amount of water entering the SWCP reservoir has been decreasing year by year.

In the SWCP reservoir, the perennial mean water inflow of the reservoir has dropped from 30.312 billion m^3 before 1981 to 30.094 billion m^3 in 1981~1990, 21.277 billion m^3 in 1991~2000, and 193.69 billion m^3 in 2001~2010, despite a slight increase to 26.489 billion m^3 after 2011. Overall, the water inflow in 1991~2000 is 29.30% lower than that in 1981~1990. The minimum water inflow appeared in 1997, which is only 16.4 billion m^3. The reduction in water inflow is accompanied by the stabilization of inflow and water volume. In 2012, the main stream in the upper reaches saw the biggest flood since 1989. In the Ningxia-Inner Mongolia reaches of the Yellow River, the water flow remained above 2,000 m^3/s for 48 consecutive days, pushing up the annual total water flow to 32.907 billion m^3, the highest level since 1989.

The sand inflow into the SWCP reservoir peaked in the 1960s, and decreased continuously ever since. Despite the slight recovery of water inflow after 2010, the sand inflow into the reservoir remained at a very low level. In 2011~2014, the sand inflow was merely 0.28 billion tons, about 16.57% of the sand inflow in the 1960s. Even if a major flood occurred in 2012, the sand inflow was only 0.48 billion tons in that year, which is lower than that in other years with smaller water flow. The sand inflow was further suppressed in 2014, due to the completion of the Haibowan Water Conservancy Project. In that year, the annual sand inflow at Dangkou Hydrological Station reached the lowest point (105 million tons) since the 1960s.

The water and sand inflow features of the SWCP reservoir in each period are presented in *Table 1*. Judging characteristic by the perennial variation in water and sand inflows, the water and sand conditions of the SWCP reservoir are favorable for long-term maintenance of the storage capacity.

Table 1. *Features of water and sand inflows to the SWCP reservoir*

Time slot	Average annual runoff ($10^8 m^3$)	Average annual sediment transport (10^8 t)
1962-1970	317.62	1.69
1971-1980	288.61	0.9
1981-1990	300.94	0.99
1991-2000	212.77	0.95
2001-2010	193.69	0.53
2011-2014	264.89	0.28

Reservoir siltation

Since the SWCP entered service, the sand amount in the reservoir is mainly affected by the inflow of the upstream water. Generally, a large inflow brings about scouring and a small inflow leads to silting. So far, the SWCP reservoir has mainly suffered from

http://www.aloki.hu ● ISSN 1589 1623 (Print) ● ISSN 1785 0037 (Online)
DOI: http://dx.doi.org/10.15666/aeer/1704_97259733

silting. As shown in *Figure 1,* the storage capacity of the reservoir has changed since its completion. The siltation of the reservoir can be divided into the following phases.

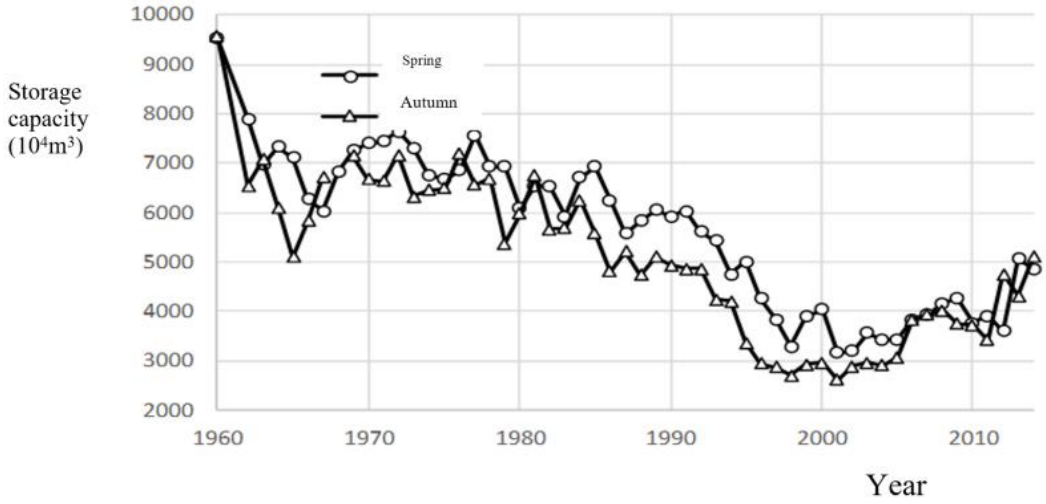

Figure 1. *Variation of storage capacity in the SWCP reservoir*

(1) Spring 1961~spring 1965

In the years right after the completion of the SWCP, the water flow rate and the sand-carrying ability both decreased across the reservoir, causing serious siltation of the reservoir. From May 1961 to August 1962, the cross-sectional flow reached 32 million m^3, about 40% of the designed storage capacity. Shoals and sandbars appeared and developed rapidly under the upper and lower sluice gates. In this period, the storage capacity was reduced from 952.5 million m^3 to 712 million m^3. The storage capacity shrank by 124.5 million m^3 in four years at an annual decreasing rate of 6.01 million m^3.

(2) Spring 1965~spring 1981

Over these 16 years, the reservoir capacity was reduced by 5.7 million m^3 from 71.2 million m^3 to 65.4 million m^3. The annual mean loss of reservoir capacity was 360,000 m^3, which is relatively small.

(3) Spring 1981~spring 1990

From 1981 to 1990, the siltation situation worsened in the reservoir, as the reservoir capacity dropped by 683 million m^3 per year. The loss rate was slightly higher than that in the previous phase. From 654.4 million m^3 to 599.9 million m^3, the total loss of reservoir capacity was 6.15 million m^3.

(4) Spring 1990~spring 2000

This period, the Yellow River Basin witnessed continuous dry years. Under the combined effects of Longyangxia Reservoir and Liujiaxia Reservoir, the reservoir capacity was reduced from 59.29 million m^3 to 40.49 million m^3. The total and annual mean loss of reservoir capacity were respectively 18.8 million m^3 and 1.88 million m^3. From spring 1961 to spring 2000, a total of 54.7 million m^3 sand deposited in the reservoir (Zhao, 2004), averaging at 1.565 million m^3 per year.

http://www.aloki.hu ● ISSN 1589 1623 (Print) ● ISSN 1785 0037 (Online)
DOI: http://dx.doi.org/10.15666/aeer/1704_97259733

(5) Spring 2000~spring 2014

In this period, the sand amount in the reservoir was smaller than that in any of the previous periods. The reservoir capacity rebounded under the slight scouring. The storage capacity increased at an annual mean rate of 0.579 million m^3 from 40.49 million m^3 in spring 2000 to 48.59 million m^3 in spring 2014. Throughout the five phases, the sand amount deposited in the reservoir totaled 466.6 million m^3, putting the perennial mean deposition at 0.88 million^3.

Calculated amount of wind-blown sand into the reservoir

As mentioned before, the amount of wind-blown sand into the SWCP reservoir was computed through the combination of sand balance method and cross-section method, the storage capacity method and field observation.

Results of the combined method

The amount of wind-blown sand into the reservoir was computed by the sand balance method and cross-section method according to the sand outflow in 1963~2012 measured in several hydrological stations and the sand diversion data in the reservoir. The results are illustrated in *Figure 2*.

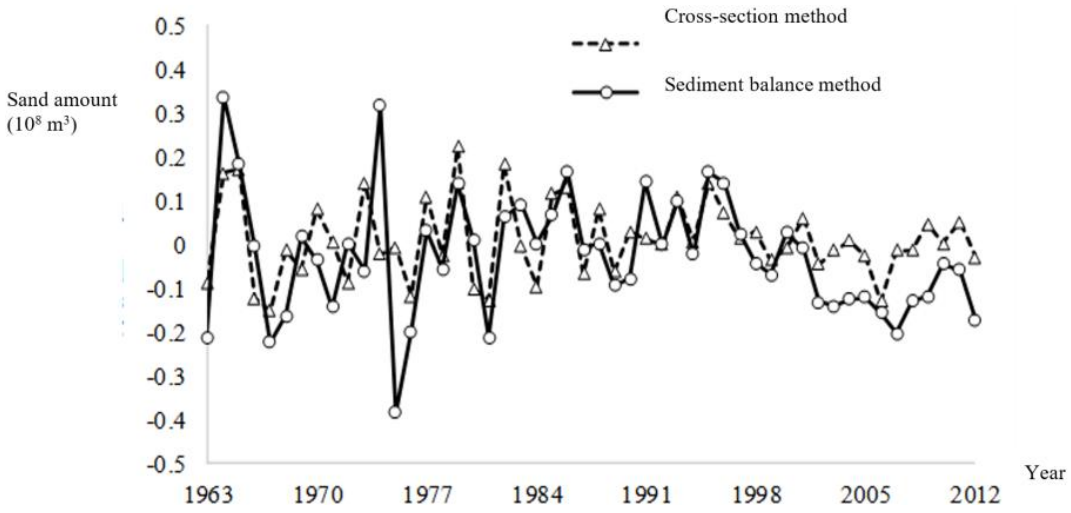

Figure 2. *The annual amount of wind-blown sand into the reservoir*

The results of the two methods are compared in *Table 2*. It can be seen that the sand amounts derived by the two methods differed by 0.345 billion tons in 50 years, i.e. 704,000 tons per year. Hence, the annual amount of wind-blown sand into the reservoir was about 704,000 tons.

Table 2. *Comparison between the results of the cross-section method and the sand balance method in 1963~2012 (ton)*

Method	Trapezoidal method	Cone method	Wind-sand siltation weight
Annual average	0.0109	0.0152	0.0043
Total	0.505	0.850	0.345

http://www.aloki.hu ● ISSN 1589 1623 (Print) ● ISSN 1785 0037 (Online)
DOI: http://dx.doi.org/10.15666/aeer/1704_97259733

Results of the storage capacity method

From 1961 to 2014, the storage capacity of SWCP reservoir was reduced from 955.5 million m^3 to 485.9 million m^3; meanwhile, a total of 466.6 million m^3 of sand was deposited, averaging at 123.25 million tons per year (volume weight: 1,400 kg/m). The variation of storage capacity through the five phases is illustrated in *Table 3*. The analysis on the metal element content in the river shows that the wind-blown sand was about 61% of all deposition in the river channel, accounting for 70.74% of the total amount of wind-blown sand entering the Yellow River. The annual amount of wind-blown sand into the Yellow River in the SWCP reservoir was about 106.28 million tons.

Table 3. *Variation of storage capacity in the SWCP reservoir in 1961~2014*

Period	Storage capacity change (10,000 m^3)	Storage capacity change (10,000 tons)	Average annual change (10,000 tons)
1961-1970	-2119	-2966.6	-329.62
1970-1980	-1323	-1852.2	-185.22
1980-1990	-154	-215.6	-21.56
1990-2000	-1880	-2632	-263.2
2000-2010	-278	-389.2	-38.92
2010-2014	1088	1523.2	380.8

Results of field observation

According to the current classification of land use types, the lengths of mobile and semi-fixed sand dunes near the river section are 22.3 km and 3.1 km, respectively. Through field observation, it is learned that the 22.3 km-long mobile sand dunes released 783,900 tons, 481,100 tons, 316,600 tons and 301,900 tons of sand into the river section, respectively, in 2013, 2014, 2015 and 2016.

Discussion

To sum up, the annual mean amount of wind-blown sand into the river section obtained by the combined method was 704,000 tons (1963~2012), acquired by the storage capacity method was 106,280,000 tons (1961~2014), while observed in the field was 783,900 tons, 481,000 tons, 316,000 tons and 301,900 tons, respectively, in 2013, 2014, 2015 and 2016.

Each of the three methods have their own features. The combined method inherits the test errors, the storage capacity method faithfully reflects the long-term variation and siltation of reservoir capacity, while the field observation is limited to the period from 2013 to 2016. Synthesizing the calculation results of the three methods, it is considered that the amount of wind-blown sand into the reservoir is about 0.7~1 million tons per year.

Conclusions

Considering the potential threats of wind-blown sand to the reservoir capacity of Sanshenggong Water Control Project (SWCP), this paper calculates the amount of

http://www.aloki.hu ● ISSN 1589 1623 (Print) ● ISSN 1785 0037 (Online)
DOI: http://dx.doi.org/10.15666/aeer/1704_97259733

wind-blown sand in the reservoir based on the change of reservoir capacity, using sand balance method and cross-section method. Then, the calculated amount was compared with the amount of wind-blown sand measured through field monitoring. Synthesizing the calculation results of the three methods, it is considered that the amount of wind-blown sand into the reservoir is about 0.7~1 million tons per year. The research findings provide technical product for siltation prevention and reduction. The field observation of Aeolian sand is a long-term process. It is suggested that the field monitoring of Aeolian sand should be continued in the next step, and the observation types, density and frequency should be further improved to provide a solid data support platform for desert control and the development and utilization of Sanshenggong Water Control Project.

Acknowledgements. This work was supported by the National Key Research and Development Project(2018YFC0407401).

REFERENCES

[1] Chattopadhyay, S. J. D. C. G. (2011): Univariate modelling of monthly maximum temperature time series over Mann–Kendall trend analysis of tropospheric ozone using ARIMA northeast India: neural network versus Yule-Walker equation based approach. – Meteorological Applications 18: 70-82.

[2] Chen, X. C., Guo, J. Y., Dong, Z., Li, H. L., Li, J. R., Wang, H. Y. (2015): Characteristics of heavy metal distribution and grain size in surface sediments of barchans dunes of the Wuhai section in Ulan Buh Desert. – Journal of Soil and Water Conservation 29(3): 47-51.

[3] Chen, X. C., Guo, J. Y., Dong, Z., Li, H. L., Li, J. R., Wang, H. Y. (2016): Grain size characteristics of dust fall in the Ulan Buh Desert. – Journal of Desert Research 36(2): 295-301.

[4] Kisi, O., Ay, M. (2014): Comparison of Mann–Kendall and innovative trend method for water quality parameters of the Kizilirmak River, Turkey. – Journal of Hydrology 513: 362-375.

[5] Liu, R., Chen, G. Y. (2016): Analysis of variation of sediment inflow and storage capacity of Sanshenggong water control project. – Inner Mongolia Water Resources 2: 10.

[6] Mao, C. Y. (2013): Review of water and sediment dispatching in the initial stage of Sanshenggong hydraulic construction project of the Yellow River. – Inner Mongolia Water Resources 5: 22-23.

[7] Thomas, D. S. G. (2011): Process, Form and Change in Drylands. – John Wiley & Sons, Chichester.

[8] Yin, R. P., Guo, J. Y., Dong, Z., He, J. L., Li, J. R., Tian, S. M., Dai, Y. J. (2017): Wind velocity and sand flow transport characteristics of different height typical dunes in Ulan Buh Desert along the Yellow River. – Research of Soil and Water Conservation 24(5): 157-161.

[9] Youssef, F., Visser, S., Karssenberg, D. (2012): Calibration of RWEQ in a patchy landscape; a first step towards a regional scale wind erosion model. – Aeolian Research (4): 467-476.

[10] Zhao, W. B. (2004): Understanding and analysis of sediment treatment in Sanshenggong water control project of the Yellow River. – Inner Mongolia Water Resources (2): 56-58.

http://www.aloki.hu ● ISSN 1589 1623 (Print) ● ISSN 1785 0037 (Online)
DOI: http://dx.doi.org/10.15666/aeer/1704_97259733

ESTIMATION OF SOME GENETIC PARAMETERS USING LINE×TESTER ANALYSIS OF COMMON WHEAT (*TRITICUM AESTIVUM* L.)

HAMA-AMIN, T. N.* – TOWFIQ, S. I.

Crop Science Department, College of Agricultural Sciences, University of Sulaimani Sulaimani, Iraq

**Corresponding author*
e-mail: taban.najmaddin@univsul.edu.iq, tabantaby@yahoo.com

(Received 19th Mar 2019; accepted 13th Jun 2019)

Abstract. Seven common wheat (*Triticum aestivum* L.) cultivars were crossed in a line×tester matting design. The 12 F_1 and their parents were evaluated using a Completely Randomized Block Design (CRBD) replicated three times in Kurdistan Reign-Iraq at two different locations, first Kanipanka in Sharazoor Valley, and the second was Qlyasan Agricultural Research Station, University of Sulaimani, during the winter season of 2017-2018. The Least Significant Differences Test (LSD) at ($P \leq 0.05$) was carried out to compare the means of the characters. The results confirmed that sufficient genetic variability was included with all traits studied. The cross Aras×Iba-95 at Kanipanka location and Klal×Cham-6 at Qlyasan location had better grain yield/plant mean than their parents. The cross Aras×Iba-95 and Klal×Cham-6 at both locations exhibited maximum positive heterosis for grain yield/plant and most of their components. Line parents Aras and Klal are good general combiners for grain yield/plant and most its components at both locations respectively. The cross Aras×Iba-95 is the better specific combiner to increase grain yield/plant at both sites. The superiority of non-additive type of gene actions in controlling the inheritance of these characters was confirmed.
Keywords: *heterosis, combining ability, heritability, gene action*

Introduction

Bread wheat (*Triticum aestivum* L.) is the most important crop being one-fifth of the total calories for the population of the world (Sehgal et al., 2015). Wheat cultivation represents approximately 19% of global main cereal crop production (Todorovska et al., 2009). Considerable cultivated species of wheat include: *Triticum aestivum*, which is a hexaploid species and is widely seeded in the world (Moon, 2008). It has been imposed that the world population would increase to over 9 billion by the year 2050 (United Nations, Population Division, 2015). The population growth will increase the request for wheat crop by 60% compared with current years. To meet this demand, global annual yield increases have to rise from the current level of 1% per year to 1.6% per year until 2050 (Wheat, 2014). For this cause, the breeders have to share demanding need to increase yield potential of wheat by creating new wheat varieties with likable genetic makeup (Erkul et al., 2010). This could be reached by searching maximum genetic potential from available wheat germplasm (Khan et al., 2007). Common wheat is one of the earliest domesticated crops. It is a prime staple food for around 40% of the world's population (Kuzmanovic et al., 2014). Wheat provides about 20% of the calorific input for the world population and, for cereal crops has the third highest global production after maize and rice (FAO, 2014). Wheat is widely cultivated in various regions of the world, being well suited for growth in area between latitudes of 30° and 60° N and 27° and 40° S (Curtis, 2002). 349 million

http://www.aloki.hu ● ISSN 1589 1623 (Print) ● ISSN 1785 0037 (Online)
DOI: http://dx.doi.org/10.15666/aeer/1704_97359752

tons of this crop was harvested in 2016, and more than 220 million hectare of the world was cultivated by wheat. Due to the raising of the world population, wheat plays a main role in the national economy of developing countries. Read wheat is one of the major food grain crops in the world, as it provides 20% of the total energy and protein in the human diet (FAO, 2016). Most of wheat planted areas are located in arid or semi-arid regions where a biotic stresses, especially drought stress, are a main constraint for wheat production (Tahmasebi et al., 2014). Current wheat production does not meet global demand due to the declining arable land area, increasing global population, and the effects of climate condition change on the environment (Tester and Langridge, 2010; Altieri and Nicholls, 2017). To meet the need for population growth, the country's wheat requirement by 2030 has been estimated at 100 million metric tons and to reach this goal, wheat productivity has to be increased at the rate of <1per annum and this can be fulfilled through horizontal approach i.e. by rising area under cultivation or through varietal/hybrid improvement, which is one of the substantial tool to take a volume jump in production and productivity under various agro- climatic conditions (Rahul, 2017). Developing hybrid wheat varieties with desirable traits require a thorough knowledge about the existing genetic variability (Maniee et al., 2009; Kahrizi et al., 2010a,b). The more the genetic diverse parents, the greater the chances of obtaining higher heterotic expression in F_1s and broad spectrum of variability in segregating population (Shekhawat et al., 2001). The line × tester analysis method proposed by Kempthorne (1957) is one of the powerful tools available to evaluate the combining ability effects and aids in selecting desirable parents and crosses for exploitation in pedigree breeding (Basbag, 2007; Jain and Sastry, 2012; Rashid et al., 2013). Performances itself do not necessarily reveal which parents are best or weak combiners. To get up this difficulty, it is necessary to collect information on the nature of gene effects. General combining ability is assigned to additive type of gene effects, while specific combining ability is attributed to non-additive of gene works. Non-additive gene type of actions is not reliably fixable whereas additive type of gene effects or complementary type epistatic gene interactions is reliably fixable (Xiang and Li, 2001; Yan and Hunt, 2002; Iqbal et al., 2007). The objectives of this study are to estimate the combining ability, to estimate the nature and magnitude of gene actions, to evaluate heterosis and heritability for yield and yield related traits in a line × tester method in bread wheat.

Materials and methods

This study was carried out at two different locations, in Kurdistan Region-Iraq. First Kanipanka Nursery Station (Lat 35° 22′; N, Long 45° 43′; E, 550 masl) in Sharazoor Valley 35 km East of Sulaimani City, and second was at Qlyasan Agricultural Research Station, College of Agricultural Sciences-University of Sulaimani located (Lat 35° 34′ 307″; N, Long 45° 21′ 992″; E, 765 masl) 2 km North West of Sulaimani City, during 2017-2018. The experimental material comprises seven bread wheat (*Triticum aestivum* L.) genotypes. Four genotypes (Aras, Hasad, Kauz and Klal) were used as females, hereafter designated as lines, and three genotypes (Iba-95, Cham-6 and Saber beg) were used as males, fixed as testers. The seven parents were crossed to produce 12 F_1 crosses according to the line×tester mating design developed by Kempthorne (1957). F_1 seeds were sown in the field, along with their parents, in Complete Randomize Block Design (CRBD) with three replication. Each plot comprised one row of 2 m length with space

http://www.aloki.hu ● ISSN 1589 1623 (Print) ● ISSN 1785 0037 (Online)
DOI: http://dx.doi.org/10.15666/aeer/1704_97359752

of 40 cm between rows and seeds were placed 15 cm apart. Five competitive plants (excluding border plants) were chosen and data were recorded for:

1-Evaluated traits:

Number of spikes/plant, Weight of spikes/plant (g), Average spike weight (g), Spike length (cm), Number of grains/spike, Weight of grains/spike (g), 1000-grain weight (g), Biological yield/plant, Grain yield/plant and Harvest index.

2-Genetic parameters:

General Combining Ability (gca) and effects, Specific Combining Ability (sca) and effects, Heterosis percentage as the F_1s deviation from average parental values, Heritability in Broad Sense, Heritability in Narrow Sense, Average Degree of Dominance (ā).

3-Association analysis and path coefficient analysis.

The collected data were submitted to analysis of variance as proposed by Steel and Torrie (1980) to estimate significant differences among genotypes. Combining ability effects are very important genetic parameters in determining the next phase of breeding programs. They were computed according to the line×tester method (Singh and Chaudhary, 1985).

Climate conditions of Sulaimani region

The climate of Sulaimani governorate is semi-arid environment: wet and cold in winter dry and hot in summer; During July and August, the average temperature is between 39-43ºC, and overwhelmingly amount to nearly 50ºC. Autumn means high temperatures are 20-30ºC in October, cooling slightly in November. Precipitation is limited to winter and spring months, and the overall average annual rainfall of 550-700 mm was at Sulaimani city. An overview of experimental conditions is given in *Table 1*.

Table 1. *The meteorological data of the two locations*

Month	Kanipanka location				Qlyasan location			
	Min Temp.(C°)	Max Temp.(C°)	Avg. Temp.(C°)	Rainfall (mm)	Min Temp.(C°)	Max Temp.(C°)	Avg. Temp.(C°)	Rainfall (mm)
October	22.6	30.0	15.1	-	10.4	33.1	21.2	10.0
November	14.4	20.0	8.8	71	7.6	23.9	14.2	114.6
December	10.2	16.1	4.4	18.5	-2.5	17.8	7.0	22.2
January	7.8	12.5	3.1	60	1.4	15.6	7.8	72.4
February	10.3	14.9	6.1	281	-2.3	20.9	8.7	323.0
March	14.7	21.3	8.1	19	1.0	24.4	13.0	44.6
April	17.1	24	10.5	90.5	2.2	31.6	17.4	98.6
May	22.2	29.5	15.0	68	13.0	38.1	24.7	70.4
Total rainfall				608				755.8

Soil analysis

The soil samples for both locations were taken from both sites in Sulaimani governorate in Kurdistan region, Iraq. It was obtain from surface (0-30 cm), and air dried which ground to pass through a 2-mm sieve prior to analysis, shown in *Table 2*.

http://www.aloki.hu ● ISSN 1589 1623 (Print) ● ISSN 1785 0037 (Online)
DOI: http://dx.doi.org/10.15666/aeer/1704_97359752

Table 2. *Some physicochemical properties of the soil samples for locations of the experiment*

Location	Physical properties of the studied soil / Particle size distribution (PSD) g/kg						
	Sand		Silt	Clay	Texture class		
Kanipanka	214.00		540.00	246.00	Salty loam		
Qlyasan	90.40		508.40	401.20	salty clay		
	Chemical properties of the studied soil						
	pH dS m^{-1}	EC_e g kg^{-1}	OM $Cmol_c$ kg^{-1}	CEC mg kg^{-1}	Available P	$CaCO_3$ equivalent g kg^{-1}	
						Total	Active
Kanipanka	8.05	0.16	22.03	22.10	7.44	195.00	100.00
Qlyasan	7.80	0.38	16.06	29.76	9.61	230.00	117.00
	Soluble ions mmol L^{-1}						
	Ca^{2+}	Mg^{2+}	Na^{+}	K^{+}	HCO_3^{-}	Cl^{-}	SO_4^{2-}
Kanipanka	1.20	1.05	0.19	0.05	3.20	0.90	0.91
Qlyasan	2.20	1.80	0.10	0.13	2.34	0.80	0.88
	Available micronutrients mg kg^{-1}						
	Zn		Cu		Fe		
Kanipanka	1.563		5.07		5.15		
Qlyasan	0.450		4.96		3.23		

Results

The analysis of variance ratified highly significant genotype effect for all characters studied. This confirmed the presence of enough genetic variability among genotypes at both locations. The mean squares for parents was highly significant for number of spikes/plant, average spike weight, biological yield/plant and harvest index, but it was significant for spike length, number of grains/spike, weight of grains/spike and 1000-grain weight, while for other characters it was not significant at the first location. At the second location the mean squares for parents was highly significant for all characters except biological yield/plant, grain yield/plant and harvest index which was not significant. The mean squares due to crosses were highly significant for all characters at both locations with the exception of number of spikes/plant and average spike weight which was significant at the second location (*Table 3*).

The mean performance of parents and F_1s crosses for all characters were represented in *Table 4*. At the first location the cross Aras×Iba-95 recorded the highest value for grain yield/plant 53.827 g, and some of its components such as number of spikes/plant, weight of spikes/plant and biological yield/plant with 30.176, 68.915 g and 157.762, respectively. The cross Kauz×Iba-95 exhibited maximum value for average spike weight, weight of grains/spike and harvest index 4.941 g, 3.695 g and 0.438, respectively. Regards to the parental performance at the same location the line parent Hasad produced the highest value for average spike weight, 1000-grain weight and harvest index 4.463 g, 53.468 g and 0.466, respectively, but the tester parent Saber beg produced the maximum weight for grain yield/plant 34.493 g and most its components such as number of spikes/plant, weight of spikes/plant, spike length and biological yield/plant 26.167, 53.748 g, 12.420 cm and 162.153 g, respectively. At the second location the cross Klal×Cham-6 produced the highest value for grain yield/plant and number of spikes/plant reached 23.422 g and 9.333 spikes, respectively. The cross Hasad×Iba-95 produced the highest amount for average spike weight, weight of grains/spike and harvest index reached 4.540 g, 3.439 g and 0.541, respectively. The

http://www.aloki.hu ● ISSN 1589 1623 (Print) ● ISSN 1785 0037 (Online)
DOI: http://dx.doi.org/10.15666/aeer/1704_97359752

line parent Hasad showed maximum value for weight of spikes/plant, average spike weight, weight of grains/spike, 1000-grain weight and biological yield/plant with 34.018, 4.783, 3.627, 58.691 and 125.960 g, respectively. Maximum grain yield/plant recorded by the tester parent Cham-6 with 21.185 g.

Table 3. *ANOVA table for the studied characters (1st location upper value and 2nd location lower value)*

S.O.V	d.f	M.S									
		No. of spikes/plant	Weight of spikes/plant (g)	Average spike weight(g)	Spike length(cm)	No. of grains/spike	Weight of grains/spike (g)	1000-grain weight (g)	Biological yield/plant	Grain yield/plant	Harvest index
blocks	2	0.070 0.189	10.306 61.171	0.215 0.128	0.345 1.009	127.753 31.498	0.128 0.087	2.240 2.520	307.184 1214.901	63.330 6.308	0.005 0.003
Genotypes	18	93.041** 7.504**	464.387** 61.797**	1.408** 0.834**	1.753** 2.544**	334.113** 199.325**	0.973** 0.614**	76.626** 198.271**	3192.694** 2232.995**	246.838** 21.414**	0.019** 0.038**
Parents	6	91.123** 14.540**	277.571n.s 61.770**	0.842** 1.132**	0.9593* 1.371**	234.524* 278.275**	0.655* 0.760**	66.086* 188.862**	3462.575** 842.537n.s	48.537n.s 3.422n.s	0.030** 0.002n.s
P*C	1	1.320n.s 4.035n.s	298.983n.s 22.784n.s	0.238n.s 0.017n.s	2.461** 1.264n.s	0.5411n.s 22.060n.s	0.255n.s 0.080n.s	123.451* 5.125n.s	622.038n.s 11351.405**	111.556n.s 16.808*	0.002n.s 0.159**
Crosses	11	102.426** 3.982*	581.323** 65.358**	1.822** 0.746*	2.121** 3.300**	418.760** 172.377**	1.212** 0.583**	78.119** 220.962**	3279.183** 2162.480**	367.301** 31.646**	0.015** 0.047**
Lines	3	146.488** 0.546n.s	1530.861** 56.173n.s	2.121* 0.125n.s	4.120** 3.701**	690.911* 288.908*	1.160* 0.035n.s	137.449* 229.919*	10083.346** 2297.184n.s	994.871** 34.161*	0.006n.s 0.024n.s
Testers	2	67.000* 9.215*	197.865n.s 80.703*	4.721** 1.834*	1.749* 2.724*	711.784* 26.134n.s	3.510** 1.438*	110.988n.s 440.316*	42.918n.s 3039.766n.s	280.862n.s 35.245*	0.032* 0.085**
L*T	6	92.204** 3.956*	234.373n.s 64.835**	0.707* 0.694*	1.246** 3.291**	185.010n.s 162.859*	0.472n.s 0.571**	37.497n.s 143.365*	955.856n.s 1802.699*	82.330n.s 29.189**	0.013** 0.046**
Error	36	10.857 1.508	157.351 13.375	0.229 0.278	0.301 0.331	90.950 51.654	0.202 0.147	22.494 44.161	797.276 673.454	72.233 3.901	0.003 0.004

Data in *Table 5* illustrate the estimation of heterosis values determined as the percentage of F1s deviation from mid parental value. The cross Aras×Iba-95 showed maximum positive heterosis values for grain yield/plant 129.087% and some its components such as number of spikes/plant, weight of spikes/plant and biological yield/plant reached 129.114, 126.554 and 119.050% respectively, while the cross Kauz×Saber beg showed maximum negative heterosis value for grain yield/plant -54.917% and most its components such as weight of spikes/plant, average spike weight, spike length, number of grains/spike, weight of grains/spike and biological yield/plant reached -59.244, -35.415, -10.034, -44.598, -38.727 and -53.409% respectively at the first location, while at the second location maximum positive heterosis for grain yield/plant was 18.137% recorded by the cross Klal×Cham-6, but the cross Aras×Saber beg produced maximum positive heterosis for average spike weight, number of grains/spike and weight of grains/spike reached 19.432, 39.719 and 24.923%, respectively. The cross Hasad×Saber beg produced maximum negative value for grain yield/plant -41.316% and some its components such as weight of spikes/plant, average spike weight, weight of grains/spike and 1000-grain weight reached -51.048, -30.277, -34.955 and -23.423%, respectively.

http://www.aloki.hu ● ISSN 1589 1623 (Print) ● ISSN 1785 0037 (Online)
DOI: http://dx.doi.org/10.15666/aeer/1704_97359752

Table 4. *Averages of studied characters for parents and their F_1 crosses (1^{st} location upper value and 2^{nd} location lower value)*

Crosses and Parents	No. of spikes/plant	Weight of spikes/plant (g)	Average spike weight(g)	Spike length(cm)	No. of grains/spike	Weight of grains/spike (g)	1000-grain weight (g)	Biological yield/plant(g)	Grain yield/plant(g)	Harvest index
1 x 5	30.167	68.915	4.545	12.433	67.867	3.378	49.851	157.762	53.827	0.362
	8.000	31.132	3.747	8.400	64.200	2.989	46.566	42.358	20.407	0.489
1 x 6	14.667	48.114	4.465	12.300	68.267	3.252	48.912	146.752	40.226	0.277
	9.000	26.958	3.405	9.367	50.533	2.584	51.102	79.728	15.782	0.202
1 x 7	15.000	44.165	4.011	13.100	68.867	2.886	41.912	121.195	33.655	0.312
	8.833	22.960	3.591	11.367	69.533	2.720	39.540	67.511	17.510	0.274
2 x 5	15.500	45.955	4.714	13.261	63.167	3.345	53.710	100.730	33.517	0.331
	6.833	19.775	4.540	9.367	59.867	3.439	57.385	48.059	16.983	0.541
2 x 6	15.500	54.517	4.789	13.200	59.000	3.547	61.422	116.190	41.957	0.358
	9.167	28.958	4.333	10.267	51.600	3.354	66.413	61.356	20.737	0.339
2 x 7	23.167	49.395	3.453	12.000	49.733	2.321	47.470	124.278	33.105	0.278
	8.167	15.612	2.667	10.400	49.400	1.818	36.963	67.733	12.207	0.198
3 x 5	10.167	31.282	4.941	12.200	67.800	3.695	54.415	56.940	24.360	0.438
	6.000	17.997	3.729	10.133	53.200	2.778	52.581	43.049	16.231	0.385
3 x 6	12.833	37.498	4.331	12.367	57.333	3.312	58.090	73.510	25.387	0.357
	9.333	24.983	3.980	10.933	64.867	3.056	47.225	116.105	22.735	0.196
3 x 7	11.167	17.980	2.537	10.700	32.133	1.727	53.629	65.773	14.285	0.217
	9.167	26.847	3.148	11.667	53.867	2.388	44.900	43.736	20.818	0.483
4 x 5	17.333	27.690	3.353	11.067	52.000	2.493	48.914	97.763	23.667	0.247
	9.000	26.582	3.648	11.633	68.267	2.592	38.076	115.053	20.943	0.230
4 x 6	12.167	29.710	3.542	12.033	51.067	2.511	49.971	61.643	23.797	0.372
	9.333	27.860	3.923	11.500	66.867	3.027	45.269	100.662	23.422	0.243
4 x 7	9.833	32.382	3.009	11.113	40.800	2.095	51.066	95.213	18.985	0.207
	6.833	22.897	3.538	9.833	65.333	2.593	41.114	67.688	18.512	0.273
Line 1	15.500	29.352	3.100	11.033	41.133	2.117	52.338	59.797	22.222	0.414
	8.500	22.738	3.148	10.100	47.600	2.392	50.764	97.788	20.060	0.210
Line 2	10.833	34.978	4.463	11.367	60.267	3.218	53.468	87.040	28.780	0.466
	8.167	34.018	4.783	10.900	62.200	3.627	58.691	125.960	20.572	0.175
Line 3	10.833	34.483	4.453	11.367	61.067	3.317	51.508	120.190	28.878	0.252
	6.000	21.937	3.461	9.767	51.533	2.613	50.665	82.145	18.703	0.248
Line 4	17.333	24.616	3.677	12.400	58.267	2.555	43.873	115.332	25.085	0.223
	9.000	22.447	3.706	11.167	64.867	2.778	42.848	77.243	18.467	0.243
Tester 5	10.833	31.486	4.165	11.367	69.533	3.088	44.944	84.245	24.771	0.293
	8.500	25.257	3.923	11.667	75.400	2.778	36.563	111.882	19.863	0.184
Tester 6	15.667	42.536	3.618	12.067	51.733	2.576	51.624	129.536	29.417	0.230
	8.500	23.673	3.675	11.100	56.000	2.753	49.100	104.700	21.185	0.202
Tester 7	26.167	53.748	3.404	12.420	54.933	2.319	42.182	162.153	34.493	0.218
	13.333	29.765	2.866	10.300	51.933	1.963	37.847	102.673	21.030	0.218
LSD ($p \leq 0.05$)	5.456	20.772	0.792	0.909	15.792	0.744	7.854	46.757	14.074	0.093
	6.056	0.874	0.953	11.901	0.634	11.004	42.973	3.270	0.105	2.034

http://www.aloki.hu ● ISSN 1589 1623 (Print) ● ISSN 1785 0037 (Online)
DOI: http://dx.doi.org/10.15666/aeer/1704_97359752

Table 5. *% Heterosis values for F1 crosses (1st location upper value and 2nd location lower value)*

Crosses	No. of spikes/plant	Weight of spikes/plant (g)	Average spike weight(g)	Spike length(cm)	No. of grains/spike	Weight of grains/spike (g)	1000-grain weight (g)	Biological yield/plant	Grain yield/plant	Harvest index
1 x 5	129.114	126.554	25.124	11.012	22.651	29.790	2.488	119.050	129.087	2.499
	-5.882	29.729	5.997	-22.818	4.390	15.616	6.648	-59.595	2.229	148.223
1 x 6	-5.882	33.859	32.917	6.494	47.021	38.580	-5.905	55.020	55.799	-13.886
	5.882	16.171	-0.195	-11.635	-2.445	0.454	2.343	-21.251	-23.474	-1.859
1 x 7	-28.000	6.294	23.350	11.711	43.373	30.117	-11.317	9.209	18.681	-1.108
	-19.084	-12.539	19.432	11.438	39.719	24.923	-10.756	-32.644	-14.772	28.093
2 x 5	43.077	38.285	9.256	16.666	-2.671	6.094	9.153	17.617	25.177	-12.868
	-18.000	-33.277	4.296	-16.987	-12.984	7.390	20.489	-59.587	-15.997	201.578
2 x 6	16.981	40.663	18.528	12.660	5.357	22.441	16.891	7.297	44.189	2.972
	10.000	0.390	2.467	-6.667	-12.690	5.141	23.226	-46.800	-0.679	79.505
2 x 7	25.225	11.342	-12.228	0.897	-13.657	-16.176	-0.743	-0.256	4.641	-18.771
	-24.031	-51.048	-30.277	-1.887	-13.435	-34.955	-23.423	-40.749	-41.316	0.508
3 x 5	-6.154	-5.163	14.650	7.331	3.828	15.362	12.833	-44.295	-9.187	60.636
	-17.241	-23.729	1.011	-5.443	-16.176	3.054	20.562	-55.626	-15.831	78.378
3 x 6	-3.145	-2.627	7.310	5.548	1.655	12.398	12.651	-41.127	-12.903	48.374
	28.736	9.552	11.547	4.792	20.645	13.902	-5.328	24.279	13.993	-13.037
3 x 7	-39.640	-59.244	-35.415	-10.034	-44.598	-38.727	14.482	-53.409	-54.917	-7.660
	-5.172	3.852	-0.495	16.279	4.124	4.371	1.456	-52.671	4.790	107.439
4 x 5	23.077	-1.287	-14.481	-6.872	-18.623	-11.626	10.146	-2.029	-5.059	-4.393
	2.857	11.446	-4.361	1.898	-2.662	-6.695	-4.103	21.669	9.279	7.656
4 x 6	-26.263	-11.514	-2.892	-1.635	-7.152	-2.131	4.653	-49.652	-12.675	64.480
	6.667	20.815	6.296	3.293	10.645	9.474	-1.534	10.652	18.137	9.064
4 x 7	-46.847	-24.017	-20.504	-6.558	-34.440	-22.515	17.224	-22.716	-35.931	-19.035
	-37.405	-16.772	4.233	-10.470	2.618	9.408	10.507	-36.904	-9.464	35.543
S.E	13.844	13.677	6.152	2.771	7.986	7.080	3.357	14.339	14.425	9.266
	5.534	7.036	3.443	3.447	4.722	4.445	4.131	12.584	5.307	25.955

Table 6 clarified the general combining ability effect of parents. Combining ability plays important role in the estimation of inbred in terms of their breeding values, and this will help to decide efficient breeding method to be applied in segregating generation. Data in the same table revealed that the line parent Aras recorded significant and positive gca effect for grain yield and most its components viz. number of spikes/plant, weight of spikes/plant, number of grains/spike and biological yield/plant, while the tester parent Iba-95 gave significant and positive gca effect for average spike weight, weight of grains/spike and harvest index. Most negative gca effect values for the characters recorded by line parent Kauz and tester parent Saber beg at the first location. At the second location the highest positive and significant gca effect values for grain yield/plant and some its components such as spike length, number of grains/spike and biological yield/plant recorded by the line parent Klal, but the tester parent Cham-6 exhibited the highest positive and significant gca values for number of spikes/plant,

http://www.aloki.hu ● ISSN 1589 1623 (Print) ● ISSN 1785 0037 (Online)
DOI: http://dx.doi.org/10.15666/aeer/1704_97359752

weight of spikes/plant and weight of grains/spike. Maximum negative gca effect values for most characters recorded by the line parent Hasad and the tester parent Saber beg.

Table 6. *Estimation of gca effect for the parents (1st location upper value and 2nd location lower value)*

Parents	No. of spikes/plant	Weight of spikes/plant	Average spike weight	Spike length	No. of grains/spike	Weight of grains/spike	1000-grain weight	Biological yield/plant	Grain yield/plant	Harvest index
1	4.319	13.098	0.366	0.463	11.831	0.292	-4.722	40.424	12.005	0.004
	0.306	2.637	-0.106	-0.694	1.628	-0.014	-1.525	-7.887	-0.958	0.001
2	2.431	9.322	0.344	0.672	0.797	0.191	2.587	12.254	5.629	0.009
	-0.250	-2.932	0.159	-0.394	-6.172	0.092	6.326	-12.037	-2.215	0.038
3	-4.236	-11.714	-0.038	-0.392	-4.081	0.031	3.765	-36.071	-9.220	0.024
	-0.139	-1.104	-0.068	0.506	-2.483	-0.038	0.974	-3.456	1.071	0.034
4	-2.514	-10.706	-0.673	-0.743	-8.547	-0.514	-1.630	-16.606	-8.414	-0.038
	0.083	1.399	0.015	0.583	7.028	-0.041	-5.775	23.381	2.102	-0.073
S.E lines	1.098	4.181	0.159	0.183	3.179	0.150	1.581	9.412	2.833	0.019
	0.409	1.219	0.176	0.192	2.396	0.128	2.215	8.650	0.658	0.021
5	2.667	2.827	0.414	0.092	6.206	0.348	0.109	1.820	3.279	0.031
	-0.847	-0.509	0.229	-0.522	1.589	0.171	1.391	-8.957	-0.216	0.090
6	-1.833	1.826	0.308	0.327	2.414	0.275	2.985	-1.955	2.278	0.028
	0.903	2.810	0.223	0.111	-1.328	0.227	5.241	18.376	1.812	-0.076
7	-0.833	-4.653	-0.722	-0.420	-8.619	-0.623	-3.094	0.136	-5.556	-0.060
	-0.056	-2.301	-0.451	0.411	-0.261	-0.398	-6.632	-9.419	-1.595	-0.014
S.E testers	0.951	3.621	0.138	0.158	2.753	0.130	1.369	8.151	2.453	0.016
	0.354	1.056	0.152	0.166	2.075	0.111	1.918	7.491	0.570	0.018

Data represent in *Table 7* explain the sca effect of the F_1 crosses at both locations, sca is mainly a function of dominance variance, it helps in the identification of superior cross combination of heterosis. At the first location the cross Aras×Iba-95 was the best specific combiner for number of spikes/plant, weight of spikes/plant, biological yield/plant and grain yield/plant, while the cross Kauz×Iba-95 was the better specific combiner for average spike weight, number of grains/spike, weight of grains/spike and harvest index. At the second location the cross Aras×Iba-95 was the best specific combiner for grain yield/plant, while the cross Hasad×Iba-95 was the best specific combiner for average spike weight, weight of grains/spike and harvest index. The cross Kauz×Cham-6 was the best specific combiner for number of grains/spike and biological yield/plant.

Some genetic parameters present in *Table 8* for both locations. At the first location the variance of sca effect was greater than those of gca effect for all characters except biological yield/plant and grain yield/plant, indicating to the importance of non additive gene effect in the inheritance of these characters, but for biological yield/plant and grain yield/plant the additive gene effect is more important in the inheritance of both. At the second location it was indicated that the magnitude of sca variance is larger than those of gca effect for all characters, confirming the importance of non additive gene effect in the inheritance of these characters. The average degree of dominance values are more than one for most characters at both locations.

http://www.aloki.hu ● ISSN 1589 1623 (Print) ● ISSN 1785 0037 (Online)
DOI: http://dx.doi.org/10.15666/aeer/1704_97359752

Table 7. *Estimation of sca effect for the F1 crosses (1st location upper value and 2nd location lower value)*

Crosses	No. of spikes/plant	Weight of spikes/plant	Average spike weight	Spike length	No. of grains/spike	Weight of grains/spike	1000-grain weight	Biological yield/plant	Grain yield/plant	Harvest index
1 x 5	7.556	12.357	-0.209	-0.270	-6.672	-0.142	2.850	14.039	7.979	0.014
	0.236	4.624	-0.063	-0.789	1.189	0.053	-0.561	-11.884	2.723	0.077
1 x 6	-3.444	-7.444	-0.183	-0.638	-2.481	-0.195	-0.965	6.804	-4.621	-0.068
	-0.514	-2.868	-0.399	-0.456	-9.561	-0.407	0.125	-1.847	-3.929	-0.043
1 x 7	-4.111	-4.913	0.393	0.908	9.153	0.337	-1.886	-20.844	-3.358	0.055
	0.278	-1.755	0.462	1.244	8.372	0.354	0.436	13.731	1.206	-0.034
2 x 5	-5.222	-6.827	-0.019	0.348	-0.339	-0.074	-0.600	-14.822	-5.955	-0.023
	-0.375	-1.165	0.465	-0.122	4.656	0.398	2.407	-2.034	0.557	0.092
2 x 6	-0.722	2.735	0.163	0.053	-0.714	0.201	4.236	4.413	3.486	0.008
	0.208	4.700	0.264	0.144	-0.694	0.256	7.585	-16.070	2.283	0.056
2 x 7	5.944	4.093	-0.144	-0.401	1.053	-0.127	-3.636	10.410	2.469	0.015
	0.167	-3.535	-0.729	-0.022	-3.961	-0.654	-9.992	18.103	-2.840	-0.148
3 x 5	-3.889	-0.465	0.590	0.352	9.172	0.436	-1.072	-10.287	-0.263	0.069
	-1.319	-4.770	-0.119	-0.256	-5.700	-0.134	2.955	-15.624	-3.481	-0.060
3 x 6	3.278	6.752	0.087	0.284	2.497	0.126	-0.273	10.058	1.765	-0.008
	0.264	-1.102	0.138	-0.089	8.883	0.088	-6.252	30.099	0.995	-0.083
3 x 7	0.611	-6.287	-0.677	-0.636	-11.669	-0.561	1.345	0.230	-1.503	-0.061
	1.056	5.872	-0.020	0.344	-3.183	0.046	3.297	-14.474	2.486	0.143
4 x 5	1.556	-5.064	-0.362	-0.430	-2.161	-0.221	-1.178	11.070	-1.761	-0.060
	1.458	1.311	-0.284	1.167	-0.144	-0.317	-4.801	29.542	0.201	-0.109
4 x 6	0.889	-2.043	-0.067	0.302	0.697	-0.131	-2.998	-21.275	-0.630	0.069
	0.042	-0.729	-0.003	0.400	1.372	0.063	-1.459	-12.182	0.651	0.071
4 x 7	-2.444	7.108	0.429	0.128	1.464	0.352	4.177	10.204	2.392	-0.009
	-1.500	-0.581	0.287	-1.567	-1.228	0.254	6.260	-17.360	-0.852	0.038
S.E	1.902	7.242	0.276	0.317	5.506	0.259	2.738	16.302	4.907	0.032
	0.709	2.111	0.305	0.332	4.149	0.221	3.837	14.983	1.140	0.036

The simple correlation coefficient among studied characters represent in *Table 9* at both locations. At the first location the character number of spikes/plant recorded positive and highly significant correlation with weight of spikes/plant, biological yield/plant and grain yield/plant 0.721, 0.709 and 0.681, respectively. Weight of spikes/plant recorded positive and highly significant correlation with spike length, biological yield/plant and grain yield/plant 0.644, 0.760 and 0.939, respectively. Spike length exhibited positive and highly significant correlation with grain yield/plant 0.652, but it recorded positive and significant correlation with number of grains/spike and weight of grains/spike 0.597 and 0.549, respectively. Positive and highly significant correlation was recorded between number of grains/spike and each of grain weight/spike and grain yield/plant 0.849 and 0.609, respectively. Positive and significant correlation was recorded between weight of grains/spike and each of harvest index and grain yield/plant with 0.531 and 0.551, respectively. Positive and highly significant correlation was recorded between biological yield/plant and grain yield/plant

http://www.aloki.hu ● ISSN 1589 1623 (Print) ● ISSN 1785 0037 (Online)
DOI: http://dx.doi.org/10.15666/aeer/1704_97359752

0.755. At the second location the character number of spikes/plant correlated positively and significantly with weight of spikes/plant 0.492, while weight of spikes/plant recorded positive and highly significant correlation with grain yield/plant 0.677. Positive and significant correlation recorded between spike length and biological yield/plant 0.487. Positive and highly significant correlation was recorded between weight of grains/spike and 1000-grain weight 0.691.

Table 8. *Estimation of some genetic parameters (1st location upper value and 2nd location lower value)*

Parameters	No. of spikes/plant	Weight of spikes/plant	Average spike weight	Spike length	No. of grains/spike	Weight of grains/spike	1000-grain weight	Biological yield/plant	Grain yield/plant	Harvest index
$\sigma^2 e$	10.857	157.351	0.229	0.301	90.950	0.202	22.494	797.261	72.233	0.003
	1.508	13.375	0.278	0.331	51.654	0.147	44.161	673.454	3.901	0.004
σ^2gca	0.441	14.966	0.048	0.038	10.083	0.032	1.752	100.222	12.293	0.00007
	0.001	0.023	0.002	0.0004	0.411	0.0005	3.347	15.520	0.106	0.00005
σ^2sca =σ^2D	27.115	25.674	0.159	0.315	31.353	0.090	5.001	52.860	3.366	0.003
	0.816	17.153	0.139	0.987	37.068	0.142	33.068	376.415	8.429	0.014
σ^2gca /σ^2sca	0.016	0.583	0.302	0.120	0.322	0.354	0.350	1.896	3.653	0.023
	0.001	0.001	0.016	0.0004	0.011	0.003	0.101	0.041	0.013	0.003
σ^2A	0.882	29.933	0.096	0.076	20.167	0.064	3.505	200.444	24.586	0.0001
	0.002	0.045	0.004	0.001	0.821	0.001	6.695	31.040	0.212	0.0001
ā	7.842	1.310	1.820	2.888	1.763	1.680	1.689	0.726	0.523	6.593
	26.816	27.576	7.870	51.017	9.502	16.988	3.143	4.925	8.918	16.989
h²b.s	0.721	0.261	0.528	0.564	0.362	0.433	0.274	0.241	0.279	0.520
	0.352	0.563	0.339	0.749	0.423	0.493	0.474	0.377	0.689	0.778
h²n.s	0.023	0.141	0.199	0.109	0.142	0.179	0.113	0.191	0.245	0.023
	0.001	0.001	0.011	0.001	0.009	0.003	0.080	0.029	0.017	0.005

Table 9. *The simple correlation coefficient among all pairs of traits at both locations (1st location upper value and 2nd location lower value)*

Characters	No. of spikes/plant	Weight of spikes/plant (g)	Spike length(cm)	No. of grains/spike	Weight of grains/spike(g)	1000-grain weight (g)	Biological yield/plant(g)	Harvest index	Grain yield/plant(g)
No. of spikes/plant	1.000								
Weight of spikes/plant (g)	0.721	1.000							
	0.492								
Spike length(cm)	0.345	0.644	1.000						
	0.312	0.047							
No. of grains/spike	0.120	0.467	0.597	1.000					
	-0.015	0.215	0.416						
Weight of grains/spike(g)	-0.071	0.424	0.550	0.850	1.000				
	-0.313	0.381	-0.061	0.372					
1000-grain weight (g)	-0.354	-0.020	0.008	-0.184	0.349	1.000			
	-0.311	0.203	-0.365	-0.401	0.691				
Biological yield/plant(g)	0.709	0.760	0.431	0.356	0.127	-0.415	1.000		
	0.384	0.358	0.487	0.278	0.052	-0.182			
Harvest index	-0.142	0.107	0.168	0.323	0.531	0.442	-0.431	1.000	
	-0.299	-0.061	-0.399	-0.067	0.261	0.300	-0.819		
Grain yield/plant(g)	0.681	0.939	0.652	0.609	0.551	-0.031	0.756	0.179	1.000
	0.400	0.677	0.351	0.335	0.357	0.097	0.479	-0.073	

http://www.aloki.hu ● ISSN 1589 1623 (Print) ● ISSN 1785 0037 (Online)
DOI: http://dx.doi.org/10.15666/aeer/1704_97359752

Data represent in *Table 10* illustrate the path coefficient analysis, indicating to the direct and indirect effects on grain yield. At first location the highest positive direct effect was recorded by number of grains/spike reached 0.947 and followed by 1000-grain weight with 0.589, while the highest negative direct effect recorded by weight of grains/spike reached -0.735. The highest positive indirect effect was 0.805 recorded by number of grains/spike via weight of grains/spike and followed by number of grains/spike via spike length. The highest negative indirect effect in grain yield was -0.624 recorded by weight of grains/spike via number of grains/spike and followed by -0.403 for weight of grains/spike via spike length. At second location the highest positive direct effect in grain yield recorded by 1000-grain weight reached 1.425 and followed by number of grains/spike with 1.072, whilst only weight of grains/spike recorded negative direct effect reached -1.387. Maximum positive indirect effect was 0.984 recorded by 1000-grain weight via weight of grains/spike and the highest negative indirect effect was -0.958 recorded by weight of grains/spike via 1000-grain weight.

Table 10. *Path coefficient analysis Illustrates direct effect (diagonal values) and indirect effect of studied characters in grain yield at both locations (1st location upper value and 2nd location lower value)*

Characters	No. of spikes/plant	Weight of spikes/plant (g)	Spike length(cm)	No. of grains/spike	Weight of grains/spike(g)	1000-grain weight (g)	Biological yield/plant(g)	Harvest index
No. of spikes/plant	0.205	0.201	-0.006	0.113	0.052	-0.206	0.356	-0.031
	0.081	0.171	0.051	-0.017	0.434	-0.443	0.366	-0.244
Weight of spikes/plant (g)	0.148	0.279	-0.012	0.442	-0.311	-0.011	0.382	0.024
	0.040	0.349	0.008	0.230	-0.528	0.290	0.338	-0.050
Spike length(cm)	0.071	0.180	-0.018	0.565	-0.404	0.005	0.216	0.037
	0.025	0.016	0.164	0.446	0.085	-0.520	0.461	-0.327
No. of grains/spike	0.025	0.130	-0.011	0.947	-0.624	-0.108	0.179	0.071
	-0.001	0.075	0.068	1.072	-0.516	-0.571	0.263	-0.055
Weight of grains/spike(g)	-0.014	0.118	-0.010	0.805	-0.735	0.206	0.064	0.117
	-0.025	0.133	-0.010	0.399	-1.387	0.984	0.049	0.214
1000-grain weight (g)	-0.073	-0.005	-0.0001	-0.174	-0.256	0.589	-0.208	0.098
	-0.025	0.071	-0.060	-0.430	-0.958	1.425	-0.172	0.246
Biological yield/plant(g)	0.145	0.212	-0.008	0.337	-0.093	-0.245	0.502	-0.095
	0.031	0.125	0.080	0.298	-0.072	-0.259	0.947	-0.671
Harvest index	-0.029	0.030	-0.003	0.306	-0.390	0.260	-0.216	0.221
	-0.024	-0.021	-0.066	-0.072	-0.362	0.428	-0.776	0.818

Discussion

The results confirmed that the data for all characters under the study can be analyzed further to estimate general and specific combining ability effects. Similar results confirmed that both gca and sca variances were significant for most of the characters indicating importance of both additive as well as non additive components of genetic variance in the control of these traits (Kumar et al., 2011; Singh et al., 2013; Rahul, 2017). Also similar results reported by Burungale et al. (2011), Mandal et al. (2016), and Nataša et al. (2017). Highly significant differences among genotypes were recorded for all characters, also significant differences were recorded among the mean performance of F_1s crosses (Fellahi et al., 2013; Kalhoro et al., 2015). Significant positive and negative heterosis for all characters were recorded, also significant positive

http://www.aloki.hu ● ISSN 1589 1623 (Print) ● ISSN 1785 0037 (Online)
DOI: http://dx.doi.org/10.15666/aeer/1704_97359752

relative heterosis for grain yield recorded previously by Ajmal et al. (2004), Akram et al. (2004), Akbar et al. (2009), Ashadusjman et al. (2012), Devi et al. (2013), Anonymous (2015), and Rahul (2017). The gca effect is primarily function of additive genetic variance, which helps in the selection of suitable good general combiner parent for hybridization (Rahul, 2017). These results are in confirmation with Kumar et al. (2011), Kapoor et al. (2011), Singh et al. (2013), Raj and Kandalkar (2013), Aslam et al. (2014), Ismail (2015), Kalhoro et al. (2015), and Kandil et al. (2016). According to Kenga et al. (2004) cross-combinations with high means, appropriate sca estimates and involving at least one of the parents with high gca would likely enhance the concentration of desirable genes to improve target traits. Present findings are in confirmation with Kumar et al. (2011), Kapoor et al. (2011), Singh et al. (2013), Raj and Kandalkar (2013), Aslam et al. (2014), Kalhoro et al. (2015), and Kandil et al. (2016). The average degree of dominance values are more than one for most characters at both locations. Previous reports confirmed the importance of over dominance in the inheritance of the grain weight/ spike of wheat which was pointed out by Petrović et al. (2012) and Adel and Ali (2013). Obverse to these results, the importances of partial dominance in the inheritance of this trait were reported by Kohan and Heidari (2014). However, the selection in early generations for the trait grain weight/spike would be difficult due to over-dominance type of gene action which indicates that the selection for this trait in advanced segregating generations would be more efficient (Nazir et al., 2014; Yao et al., 2014; Shehzad et al., 2015). While, partial dominance effect was observed in the inheritance of this trait reported by Farooq et al. (2011) and Rashid et al. (2013). Similar results, which indicated the importance of the dominant component in the genetic variance and over-dominant inheritance of the grain weight/ spike, have been also pointed out by El-Hosary et al. (2015). Converse to these results, the high value of the additive component and partial dominance responsible for the inheritance of grain weight/spike was observed by Minhas (2012) and Kohan and Heidari (2014). Heterosis estimates, for different morphological and yield related characters, are attributed to both additive and non additive gene actions. Heritability gives information about genetic variation; it is important for predicting the response to selection in the superseding generations. Heritability is dependent upon the type of gene action (Swati and Ramesh, 2004; Hasnain et al., 2006; Chowdhary et al., 2007). At the first location heritability in broad sense was high for number of spikes/plant, average spike weight, spike length and harvest index, while for the other characters it was low to moderate. At the second location it was high for spike weight/plant, spike length, grain yield/plant and harvest index, but for the rest it was low to moderate. Heritability in narrow sense was found to be low for almost all character at both locations. High heritability accompanied with high genetic advance shows that the heritability is due to additive genetic control and selection may be effective in early generations for these traits (Jamil et al., 2017). Heritability estimates varied from 54.48 to 80.91%. Highest heritability 80.91% was observed for the cross combination Fareed 06×9242, While the lowest value of heritability 54.48% was estimated in cross combination Fareed 06×9317 (Waqas et al., 2014). Heritability for grain yield/plant was 0.68 in Kaleemullah et al. (2015), who said that this traits is greatly under genetic controlled and less influenced by environment. The estimates of heritability in narrow sense were medium to high reported by Yadav et al. (2011). Significant and positive correlation was recorded between grain yield and most its components. These results are harmony with those reported by Tofiq (2004), Hama-Ali (2006), Hama-Ameen (2008), Mohsin et al. (2009)

http://www.aloki.hu ● ISSN 1589 1623 (Print) ● ISSN 1785 0037 (Online)
DOI: http://dx.doi.org/10.15666/aeer/1704_97359752

and Fellahi et al. (2013). Estimation of the correlation between yield and its components alone is not enough to tell as the importance of each one of these components in determining the grain yield (Bhutta et al., 2005; Bhutto et al., 2005; Anwar et al., 2009; Ali and Shakor, 2012). Similar results are agreement with a positive correlation of grain yield with number of grains/spike and 1000-grain weight, with support the present studies (Belay et al., 1993; Aycecik and Yildirim, 2006). Positive and highly significant correlations recorded between grain yield/plant and harvest index reported by Tawfiq et al. (2016). The path analysis is used to find the direct or indirect effects of some yield components on grain yield in relation to yield with other components. Many researchers have been done on wheat breeding in which both correlation and path analysis methods were simultaneously used. Positive and significant correlation between plant height and grain yield were reported in many studies (Khayatnezhad et al., 2010; Zakizadeh et al., 2010; Amri et al., 2011). It was shown that seed numbers/spike has a positive effect on grain yield (Taleei and Bahram-Nejad, 2003; Foroozanfar et al., 2011). Path analysis conducted by a large number of researchers, it has been observed that 1000-grain weight has a positive effect on yield, followed by spike length, while grains/spike had a negative direct effect on grain yield associated a positive direct effect and negative indirect effect on grain yield via harvest index, while biological yield had the highest direct effect on grain yield refers to followed by weight of main spike, they show that the biological yield and weight of main spike can be used as criteria for selection to improve the yield of wheat grain (Mohammadi et al., 2007; Mollasadeghi et al., 2011; Iftikhar et al., 2012; Ayer et al., 2017).

Conclusion

Line parent Aras and tester parent Iba-95 was found to be a good general combiner for grain yield/plant at the first location, which produced a best specific combiner for this character, while at the second location the line parent Aras and the tester parent Iba-95 were poor general combiner for grain yield/plant, whilst they produced the best specific combiner for this character. Low ratio of σ^2gca/σ^2sca for most characters at the first location and for all characters at the second location and low estimates of heritability in narrow sense confirmed involvement of both additive and non additive gene effects with preponderance of non additive type of gene actions. The preponderance of non additive type of gene actions clearly indicated that selection of superior plants should be postponed to later generations.

Good general combine line parents like Aras and Klal for yield and most related components at both locations could be used in the development of high yielding varieties through selection for promising segregating cross generations. The crosses Aras×Iba-95 and Klal×Cham-6 was found high yielding which were very desirable for further breeding program.

REFERENCES

[1] Adel, A. A., Ali, E. A. (2013): Gene action and combining ability in a six parent diallel cross of wheat. – Asian J. Crop Sci. 5(1): 14-23.

[2] Ajmal, S., Asif, M., Munir, M. (2004): Implication of combining ability: Analysis of some characteristics of spring wheat. – Quarterly Sci Vision 9(1-2): 1-5.

http://www.aloki.hu ● ISSN 1589 1623 (Print) ● ISSN 1785 0037 (Online)
DOI: http://dx.doi.org/10.15666/aeer/1704_97359752

[3] Akbar, M., Anwar, J., Hussain, M., Qureshi, M. H., Khan, S. (2009): Line × tester Analysis in bread wheat (Triticum aestivum L.). – J Agric Res 47(1): 411.
[4] Akram, Z., Ajmal, S. U., Khan, K. S., Qureshi, R., Zubair, R. (2004): Combining ability estimates of some yield and quality related traits in spring wheat (Triticum aestivum L.). – Pak J Bot 43(1): 221-231.
[5] Ali, I., Shakor, E. (2012): Heritability, variability, genetic correlation and path analysis for quantitative traits in durum and bread wheat under dry farming conditions. – Mesopotamia Journal of Agriculture 40(4): 27-39.
[6] Altieri, M. A., Nicholls, C. I. (2017): The adaptation and mitigation of traditional agriculture in a changing climate. – Climatic Change 140: 33-45.
[7] Amri, M., Kazemi-Arbat, H., Rustaei, M. (2011): Relation Ships of some morphologic and physiologic traits with grain yield and its components in wheat (Triticum aestivum L.). – The 1th national conference of new concepts in agriculture. Islamic Azad University. Savah branch.
[8] Anonymous (2015): Progress Report of All India Coordinated Wheat and Barley Improvement Project, 2014-2015. – IIW and BR, India, pp. 1: 1.
[9] Anwar, J., Ali, M., Hussain, M., Sabir, W., Khan, M., Zulkiffal, M., Abdullah, M. (2009): Assessment of yield criteria in bread wheat through correlation and path analysis. – Journal of Animal and Plant Sciences 19(4): 185-188.
[10] Ashadusjman, M., Shamsuddoha, M., Alam, M. J., Begum, M. O. (2012): Combining ability and gene action for different root characters in spiring wheat. – J Env Sci and natural resources 5(2): 73-76.
[11] Aslam, R., Munawar, M., Salam, A. (2014): Genetic architecture of yield components accessed through line×tester analysis in wheat (Triticum aestivum L.). – Universal J PL Sci 2(5): 93-96.
[12] Aycecik, M., Yildirim, T. (2006): Path coefficient analysis of yield and yield components in bread wheat (Triticum aestivum L.) genotypes. – Pak J. Bot. 38(2): 417-424.
[13] Ayer, D. K., Shama, A., Ojha, B. R., Paudel, A., Dhakal, K. (2017): Correlation and path coefficient analysis in advanced wheat genotypes. – SAARC. J. Agri. 15(1): 1-12.
[14] Basbag, S., Ekinci, R., Gencer, O. (2007): Combining ability and heterosis for earliness characters in line x tester population of Gossypium hirsutum L. – Hereditas 144(5): 185-190.
[15] Belay, S., Struik, P. C., Nachit, M. M., Peacock, J. M. (1993): Ontogenic analysis of yield components and yield stability of durum wheat in water- limited environments. – Euphytica 71(3): 211-219.
[16] Bhutta, W. M., Akhtar, J., Anwar-ul-Haq, M., Ibrahim, M. (2005): Cause and effect relations of yield components in spring wheat (Triticum aestivum L.) under normal conditions. – Caderno de Pesquisa Sér. Bio., Santa Cruz do Sul. 17(1): 7-12.
[17] Bhutto, L. A., Soomro, Z. A., Ansari, B. A., Jarwar, A. R., Jalbani, B. H. (2005): Estimation of phenotypic correlation between grain yield and Its main components in Brassica species. – Indus J. of P Sci. 3(4): 327-331.
[18] Burungale, S. V., Chauhan, R. M., Gami, R. A., Thakor, D. M., Patel, P. T. (2011): Combining ability analysis for grain and quality traits in bread Wheat (Triticum aestivum L.). – Trends in Bio Science 4(1): 120-122.
[19] Chowdhary, M. A., Sajad, M., Ashraf, M. I. (2007): Analysis on combining ability of metric traits in bread wheat (Triticum aestivum L.). – Journal of Agricultural Research 45(1): 11-17.
[20] Curtis, B. (2002): Wheat in the world. – In: Curtis, B., Rajaram, S., Macpherson, H. (eds.) Bread wheat improvement and production. Food and Agricultural Organization of the United Nations, Rome.
[21] Devi, L., Swati, G. P., Singh, M., Jaiswal, J. P. (2013): Heterosis studies for yield and yield contributing traits in bread wheat (Triticum aestivum L.). – The Bioscan 8(3): 905-909.

http://www.aloki.hu ● ISSN 1589 1623 (Print) ● ISSN 1785 0037 (Online)
DOI: http://dx.doi.org/10.15666/aeer/1704_97359752

[22] El-Hosary, A. A., Gehan, A., El-Deen, N. (2015): Genetic analysis in the F1 and F2 wheat generations of dilllel crosses. – Egypt. J. Plant Breed. 19(2): 355-373.
[23] Erkul, A., Unay, A., Konak, C. (2010): Inheritance of yield and yield components in bread wheat (Triticum aestivum L.) cross. – Turk. J. Field Crops 15(2): 137-140.
[24] FAO (2014): Statistical year book (2014). – Asia and the pacific food and agricultural.
[25] FAO (2016): Statistical yearbook (2016). – Area and production.
[26] Farooq, J., Khaliq, I., Kashif, M., Ali, Q., Mahpara, S. (2011): Genetic analysis of relative cell injury percentage and some yield contributing traits in wheat under normal and heat stress conditions. – Chil. J. Agr. Res. 71: 511-520.
[27] Fellahi, Z. E. A., Hannachi, A., Bouzerzour, H., Boutekrabt, A. (2013): Line × Tester Mating Design Analysis for Grain Yield and Yield Related Traits in Bread Wheat (Triticum aestivum L.). – Hindawi Publishing Corporation International Journal of Agronomy Volume 2013, Article ID 201851, 9 pages http://dx.doi.org/ 10.1155/2013/201851.
[28] Fellahi, Z., Hannachi, A., Bouzerzour, H., Boutekrabt, A. (2013): Correlation between traits and path analysis coefficient for grain yield and other quantitative traits in bread wheat under semi arid conditions. – Journal of Agriculture and Sustainability 3(1): 16-26.
[29] Foroozanfar, M., Bihamta, M. R., Peyghambary, A., Zeynali, H. (2011): Evaluation of Bread Wheat Genotypes Under Normal and Water Stress Conditions SNPS for Agronomic Traits. – The Science of Sustainable Agriculture Journal 21: 33-46.
[30] Hama-Ali, E. O. (2006): Estimation of Heterosis and Heritability in Half Diallel Crossing in some Local Common Wheat (Triticum aestivum L.). – M.Sc. Thesis. College of Agriculture University of Sulaimani.
[31] Hama-Ameen, T. N. (2008): Full Diallel Crosses in Durum Wheat (Triticum durum). – M.Sc. Thesis. College of Agriculture University of Sulaimani.
[32] Hasnain, Z., Abbas, G., Saeed, A., Shakeel, A., Muhammad, A., Rahim, M. A. (2006): Combining ability for plant height and yield related traits in wheat (Triticum aestivum L.). – Journal of Agricultural Research 44: 167-175.
[33] Iftikhar, R., Khaliq, I., Kashif, M., Ahmad, M., Ullah, S. (2012): Study of morphological traits affecting grain yield in wheat (Triticum aestivum L.) under field stress condition. – Middle-East Journal of Scientific Research 11: 19-23.
[34] Iqbal, M., Navabi, A., Salmon, D. F., Yang, R. C., Murdoch, B. M., Moore, S. S., Spaner, D. (2007): Genetic analysis of flowering and maturity time in high latitude spring wheat: genetic analysis of earliness in spring wheat. – Euphytica 154(1-2): 207-218.
[35] Ismail, K. A. S. (2015): Heterosis and combining ability analysis for yield and its Components in Bread Wheat (Triticum aestivum L.). – Int J Curr Microbiol App Sci 4(8): 1-9.
[36] Jain, S. K., Sastry, E. V. D. (2012): Heterosis and combining ability for grain yield and its contributing traits in bread wheat (Triticum aestivum L.). – RRJAAS 1: 17-22.
[37] Jamil, A., Khan, Sh., Sayal, O. U., Waqas, M., Ullah, Q., Ali, S. (2017): Genetic variability, broad sense heritability and genetic advance studies in bread wheat (Triticum aestivum L.) germplasm. – Pure Appl. Biol. 6(2): 538-543.
[38] Kahrizi, D., Cheghamirza, K., Kakaei, M., Mohammadi, R., Ebadi, A. (2010a): Heritability and genetic gain of some morpho-physiological variables of Durum wheat (Triticum turgidum var. durum). – Afr. J. Biotechnol. 9(30): 4687-4691.
[39] Kahrizi, D., Maniee, M., Mohammadi, R., Cheghamirza, K. (2010b): Estimation of genetic parameters related to morpho-agronomic traits of Durum wheat (Triticum turgidum var. durum). – Biharean Biologist 4(2): 93-97.
[40] Kaleemullah, I., Khalil, H., Subhan, F., Rabi, F., Bostan, N., Qureshi, S., Ahmad, W. (2015): Heritability, selection response and correlation for yield and yield components in irrigated wheat. – ARPN J. Agric. & Biosci. 10(6): 217-225.
[41] Kalhoro, F. A., Rajpar, A. A., Kalhoro, Sh. A., Mahar, A., Ali, A., Otho, S. A., Soomro, R. N., Ali, F., Baloch, Z. A. (2015): Heterosis and Combing Ability in F1 Population of

http://www.aloki.hu ● ISSN 1589 1623 (Print) ● ISSN 1785 0037 (Online)
DOI: http://dx.doi.org/10.15666/aeer/1704_97359752

Hexaploid Wheat (Triticum Aestivum L.). – American Journal of Plant Sciences 6(7): 1011-1026.

[42] Kandil, A. A., Sharief, A. E., Gomaa, H. S. M. (2016): Estimation of general and specific combining ability in bread wheat (Triticum aestivum L.). – Int J Agri R 8(2): 37-44.

[43] Kapoor, E., Mondal, S., Dey, T. (2011): Combining ability analysis for yield and yield contributing traits in winter and spring wheat combinations. – J Wheat Res 3(1): 52-58.

[44] Kempthorne, O. (1957): An Introduction to Genetic Statistics. – John Wiley & Sons, New York, NY, USA.

[45] Kenga, R., Alabi, S. O., Gupta, S. C. (2004): Combining ability studies in tropical sorghum (Sorghum bicolor (L.) Moench). – Field Crops Research 88(2-3): 251-260.

[46] Khan, M. A., Ahmad, N., Akbar, M., Rehman, A., Iqbal, M. M. (2007): Combining ability analysis in wheat. – Pak. J. Agri. Sci. 44(1): 1-5.

[47] Khayatnezhad, M., Zaefizadeh, M., Gholamin, R., Jamaati-e-Somarin, Sh. (2010): Study of Genetic Diversity and Path Analysis for Yield in Durum Wheat Genotypes under Water and Dry Condition. – World Applied Sciences Journal 9(6): 655-665.

[48] Kohan, M. Z., Heidari, B. (2014): Diallel cross study for estimating genetic components underlying wheat grain yield. – J. Biol. Environ. Sci. 8(22): 37-51.

[49] Kumar, A., Mishra, V. K., Vyas, R. P., Singh, V. (2011): Heterosis and combining ability analysis in bread wheat (Triticum aestivum L.). – J PL Breeding and Crop Sci 3(10): 209-217.

[50] Kuzmanovic, L., Gennaro, A., Benedettelli, S., Dodd, I. C., Quarrie, S. A., Ceoloni, C. (2014): Structural-functional dissection and characterization of yield-contributing traits originating from a group 7 chromosome of the wheatgrass species Thinopyrum ponticum after transfer into durum wheat. – Journal of Experimental Botany 65: 509-525.

[51] Ljubičić, N., Petrović, S., Kostic, M., Dimitrijević, M., Hristov, N., Kondic-Spika, A., Jevtic, R. (2017): Diallel analysis of some important grain yield traits in bread wheat crosses. – Tukish Journal of Field Crops 22(1): 1-7.

[52] Mandal, A. B., Madhuri, G. (2016): Combining ability analysis for morphological and yield traits in wheat (Triticum aestivum L.). – J. Plant Sci. Res. 3(2): 157.

[53] Maniee, M., Kahrizi, D., Mohammadi, R. (2009): Genetic variability of some morpho-physiological traits in Durum wheat (Triticum turgidum var. durum). – J. Appl. Sci. 9(7): 1383-1387.

[54] Minhas, N. M. (2012): Genetic Analysis for Grain Yield, Quality and Biochemical Traits in Wheat. – Ph.D. Dissertation, University of Rawalpindi, Pakistan.

[55] Mohammadi, A., Majidi, E., Bihamta, M. R. (2007): Heidari Sharifabad S. Evaluation of drought stress on agro - morphological characteristics in some wheat cultivars. – Pajouhesh & Sazandegi 73: 184-192.

[56] Mohsin, T., Khan, N., Naqvi, F. N. (2009): Heritability, phenotypic correlation and path coefficient studies for some agronomic characters in synthetic elite lines of wheat. – J. Food Agric. Environ 7(3-4): 278-282.

[57] Mollasadeghi, V., Imani, A. A., Shahryari, R., Khayatnezhad, M. (2011): Correlation and path analysis of morphological traits in different wheat genotypes under end drought stress condition. – Middle-East Journal of Scientific Research 7(2): 221-224.

[58] Moon, D. (2008): In the Russian Steppes: The Introduction of Russian Wheat on the Great Plains of the United States of America. – Journal of Global History 3: 203-225. http://dx.doi.org/10.1017/S1740022808002611.

[59] Nazir, A., Khaliq, I., Farooq, J., Mahmood, K., Mahmood, A., Hussain, M. M., Shahid, M. (2014): Pattern of inheritance in some yield related parameters in spring wheat (Triticum aestivum L.). – Am. J. Biol. and Life Sci. 2(6): 180-186.

[60] Petrović, S., Dimitrijević, M., Ljubičić, N., Banjac, B. (2012): Diallel analysis of quantitative traits in wheat crosses. – In: Proceedings of the 47th Croatian and 7th International Symposium on Agriculture, Publisher University of Zagreb Faculty of Agriculture, Croatia, pp. 313-317.

http://www.aloki.hu ● ISSN 1589 1623 (Print) ● ISSN 1785 0037 (Online)
DOI: http://dx.doi.org/10.15666/aeer/1704_97359752

[61] Rahul, S. R. (2017): Combining Ability and Heterosis for Morpho-Physiological Characters on Bread Wheat (Triticum aestivum L.). – Agricultural Research & Technology Open Access Journal. ISSN: 2471-6774.
[62] Raj, P., Kandalkar, V. S. (2013): Combining ability and heterosis analysis for grain yield and its components in wheat. – J Wheat Res 5(1): 45-49.
[63] Rashid, M. A. R., Khan, A. S., Iftikhar, R. (2013): Genetic studies for yield and yield related parameters in bread wheat. – Am. Eurasian J. Agric. Environ. Sci. 12(12): 1579-1583.
[64] Sehgal, D., Vikram, P., Sansaloni, C. P., Ortiz, C., Pierre, C. S., Payne, T., Ellis, M., Amri, A., Petroli, C. D., Wenzl, P., Singh, S. (2015): Exploring and mobilizing the gene bank biodiversity for wheat improvement. – PLoS ONE 10(7): e0132112. doi: 10.1371/journal.pone.0132112.
[65] Shehzad, M., Hussain, S. B., Qureshi, M. K., Akbar, M., Javed, M., Imran, H. M., Manzoor, S. A. (2015): Diallel cross analysis of plesiomorphic traits in Triticum aestivum L. genotypes. – Genet. Mol. Res. 14(4): 13485-13495.
[66] Shekhawat, U. S., Vijay, P., Singhania, D. L. (2001): Genetic divergence in barley (Hordeum vulgare L.). – Indian J. Agric. Res. 35(2): 121-123.
[67] Singh, R. K., Chaudhary, B. D. (1985): Biometrical Methods in Quantitative Genetic Analysis. – Kalyani, New Delhi, India.
[68] Singh, K., Singh, U. B., Sharma, S. N. (2013): Combining ability analysis for yield and its components in bread wheat (Triticum aestivum L.). – J Wheat Res 5(1): 63-67.
[69] Steel, R. G. D., Torrie, J. H. (1980): Principles and Procedures of Statistics: A Biometrical Approach. – McGraw Hill, New York, NY, USA.
[70] Swati, P. G., Ramesh, B. R. (2004): The nature and divergence in relation to yield traits in rice germplasm. – Annals of Agricultural Research 25: 598-602.
[71] Tahmasebi, S., Heidari, B., Pakniyat, H., Kamali, J., Reza, M. (2014): Independent and combined effects of heat and drought stress in the Seri M82× Babax bread wheat population. – Plant Breeding 133: 702-711.
[72] Taleei, A., Bahram-Nejad, B. (2003): A Study of Relationship Between Yield and Its Components in Landrace Populations of Wheat from Western Parts of Iran Using Multivariate Analysis. – Iranian Journal of Crop Sciences. Sci. 34(4): 949-959.
[73] Tawfiq, S. I., Haseeb, S., Abdulkhaleq, D. A., Hama, S. J. (2016): The Simple Correlation and Path Coefficient Analysis for Yield and Some Yield Components of Durum Wheat in Two Seasons in Iraqi Kurdistan. – Journal of Zankoy Sulaimani 18(3): 323-332.
[74] Tester, M., Langridge, P. (2010): Breeding technologies to increase crop production in a changing world. – Science 327: 818-822.
[75] Todorovska, E., Christov, N., Slavov, S., Christova, P., Vassilev, D. (2009): Biotic stress resistance in wheat breeding and genomic selection implications. – Biotechnol Biotec Eq. 23(4): 1417-1426.
[76] Tofiq, Sh. I. (2004): Partial Diallel Crossing in Common and Durum Wheat. – Ph.D. Dissertation Submitted to College of Agricultural University of Sulaimani.
[77] United Nations, Department of Economic and Social Affairs, Population Division, (2015): World Population Prospects: The 2015 Revision, Key Findings and Advance Tables. – Working Paper No. ESA/P/WP.241.
[78] Waqas, M., Faheem, M., Khan, A. S., Shazad, M., Ansari, M. A. A. (2014): Estimation of heritability and genetic advance for some yield traits in eight F2 populations of wheat (Triticum aestivum L.). – Sci. Lett. 2(2): 43-47.
[79] Wheat (2014): Wheat: Vital grain of civilization and food security. – In: 2013 Annual Report, CGIAR Research Program on Wheat. CGIAR Research Program on Wheat (Wheat), Mexico, D.F.
[80] Xiang, B., Li, B. (2001): A new mixed analytical method for genetic analysis of diallel data. – The Canadian Journal of Forest Research 31(12): 2252-2259.

http://www.aloki.hu ● ISSN 1589 1623 (Print) ● ISSN 1785 0037 (Online)
DOI: http://dx.doi.org/10.15666/aeer/1704_97359752

[81] Yadav, A. K., Maan, R. K., Kumar, S., Kumar, P. (2011): Variability, heritability and genetic advance for quantitative characters in hexaploid wheat (Triticum aestivum L.). – Electronic Journal of Plant Breeding 2: 405-408.
[82] Yan, W., Hunt, L. A. (2002): Biplot analysis of diallel data. – Crop Science 42(1): 21-30.
[83] Yao, J., Ma, H., Yang, X., Yao, G., Zhou, M. (2014): Inheritance of grain yield and its correlation with yield components in bread wheat (Triticum aestivum L.). – Afr. J. Agric. Res. 13(12): 1379-1385.
[84] Zakizadeh, M., Esmaeilzadeh, M., Kahrizi, D. (2010): Study on genetic variation and relationship between plant characteristics and grain yield in long spike bread wheat (Triticum aestivum L.) genotypes-using multivariate analysis. – Iranian Journal of Crop Sciences (in Persian) 12(2): 18-30.

http://www.aloki.hu ● ISSN 1589 1623 (Print) ● ISSN 1785 0037 (Online)
DOI: http://dx.doi.org/10.15666/aeer/1704_97359752

SYMBIOTIC MYCORRHIZAL FUNGI ISOLATED VIA EX SITU SEED BAITING INDUCE SEED GERMINATION OF *DENDROBIUM CATENATUM* LINDL. (ORCHIDACEAE)

SHAO, S.-C. – XI, H.-P. – MOHANDASS, D.*

Gardening and Horticulture Department, Xishuangbanna Tropical Botanical Garden, Chinese Academy of Sciences, Mengla County, Yunnan 666303, P. R. China

**Corresponding author*
e-mail: dmohandass997@yahoo.com

(Received 20th Mar 2019; accepted 24th May 2019)

Abstract. The epiphytic orchid species *Dendrobium catenatum* is extensively used as a traditional medicine in China. Overexploitation has led to endangerment and rarity of the species in the wild, and conservation measures are immediately needed. As in many orchid species, mycorrhizal symbiotic seed germination is recognized as a powerful tool for orchid seedling propagation, reintroduction, and species conservation. Obtaining efficient and specific fungi for enhancing seed germination, protocorm formation, and further seedling development is a prerequisite. In this study, eight purified fungal strains were isolated from host orchid protocorms via an ex situ baiting technique. Phylogenetic analysis using ITS-rDNA placed the eight fungal strains into the taxa Tulasnellaceae, Ceratobasidiaceae, and Sebacinales, the typical orchid mycorrhizal symbionts. The fungi induced seed germination and also increased growth during protocorm formation, seedling formation, and seedling development. One strain in particular (SSCDO-5) exhibited significant benefits under 12/12 h light/dark conditions between 20 and 90 days after sowing. Our results suggest that inoculation with the fungus SSCDO-5 might assist in the propagation of *D. catenatum* and could be employed ex situ and in situ for conservation purposes.
Keywords: *conservation effort, photoperiod, reintroduction, seedling development, Tulasnellaceae*

Introduction

Symbiotic fungi play an important role in the orchid life cycle, from seed germination, through protocorm formation to seedling development, and even into adulthood when they provide nutrition supplemental to photosynthesis (Selosse and Roy, 2009). Mycorrhizal studies are essential and necessary to ensure success in propagation from seeds and to benefit integrated orchid conservation. Highly compatible symbiotic fungi can play a major role in the initiation of seed germination and recruitment of Orchidaceae (Park and Lee, 2013; Rasmussen et al., 2015; Khamchatra et al., 2016; Huang et al., 2018). The isolation, identification, and culture of germination-enhancing fungi are prerequisites for symbiotic seed germination and seedling growth.

Most studies have focused on screening fungi effective in promoting seed germination, mainly using different strains acquired from roots (Johnson et al., 2007; Stewart and Kane, 2007; Chutima et al., 2011; Wu et al., 2012; Fracchia et al., 2016). Among these, 14 fungi isolates from the roots of 10 species were assessed in terms of germination percentage of *Cynorkis purpurea* seeds, which displayed low specificity for germination in vitro (Rafter et al., 2016). However, only a few studies have examined epiphytic orchids using in situ baiting techniques applied to seed germination in association with symbiotic mycorrhizal fungi (Wang et al., 2011; Zi et al., 2014; Zhou and Gao, 2016). Herrera et al. (2016) found that 13 mycorrhizal isolates from 7 hosts

http://www.aloki.hu ● ISSN 1589 1623 (Print) ● ISSN 1785 0037 (Online)
DOI: http://dx.doi.org/10.15666/aeer/1704_97539771

had the ability to induce seed germination with various efficiencies and low specificity in vitro. Wu et al. (2012) inoculated seeds of *Dendrobium catenatum* with four symbiotic fungi in vitro (strains C20 from *D. catenatum* and L12, L24b, and L28 from *D. loddigesii*) and found that strains L24b and L28 had significantly higher germination rates, but the seeds did not form seedlings. Two *Tulasnella* strains isolated from roots of an endangered species, *D. nobile*, differed in their ability to facilitate germination and subsequent development in *D. officinale* (= *D. catenatum*) in vitro (Tan et al., 2014). Swangmaneecharern et al. (2012) found that four out of five fungal strains from other genera could form pelotons in *Dendrobium* spp.

Although it is more convenient to isolate symbiotic fungi from roots to screen for effective species in vitro, this approach is biased toward specificity under experimental conditions and not necessarily those pertaining in the field where the ecological conditions are more specific (Masuhara and Katsuya, 1994; Steinfort et al., 2010). Masuhara and Katsuya also found that most *Rhizoctonia* spp. not associated with the in situ germination of *Spiranthes sinensis* var. *amoena* induced seed germination in vitro, demonstrating differences in seed specificity according to conditions (Masuhara and Katsuya, 1994). Based on this characteristic, Rasmussen et al., (2015) suggested that non-compatible fungi may stimulate germination per se, but are not necessary to support subsequent seedling development. Other authors have also agreed that the orchid–fungus relationship is not the same in in situ and in vitro conditions (Zi et al., 2014; Cruz-Higareda et al., 2015). The use of germination-promoting fungi isolated from protocorms in situ/ex situ of the same species can ensure high compatibility and adaptation between orchid species and fungal partners and thus support restoration efforts and orchid conservation (Zi et al., 2014; Shao et al., 2017; Huang et al., 2018).

However, it is difficult to gather protocorms in the wild because they are very small and sparsely distributed. The use of in situ and ex situ baiting methods has been proposed to overcome such problems and ensure effective protocorm sampling (Rasmussen and Whigham, 1993; Brundrett et al., 2003). The ex situ baiting method allows close observation of the germination process, and provides time for choosing the optimum stage for mycorrhizal fungus isolation. Xu and Guo (1989) isolated an effective symbiotic fungus, *Mycena osmundicola*, from protocorms of *Gastrodia elata* by ex situ baiting; subsequently, the fungus was successfully applied in the industrial propagation and plantation of *G. elata* in China. Using ex situ seed baiting techniques, Sheng et al. (2012) obtained one mycorrhizal fungus from *Cymbidium mannii*, an epiphytic orchid species, which proved to be effective for seed germination, and protocorm and seedling development.

D. catenatum Lindley is a perennial, epiphytic orchid from China having medicinal properties. It is used in the treatment of diabetes and improvement of the immune system, as well as an ornamental plant. There has been a drastic reduction in wild populations of *D. catenatum* that has driven the species to the verge of extinction, mainly caused by overexploitation and habitat degradation in recent decades. The low fertility rate and inherently slow growth of the species have also contributed to its current scarcity in the wild. Asymbiotic, sterile, vegetative tissue culture of *D. catenatum* has been successfully developed, but the survival rate of sterile plants and the seedling growth rate are low, meaning this technique is unlikely to contribute to preserving the genetic diversity of this species. In vitro symbiotic seed germination assays of *D. catenatum* using fungal isolates obtained from mature orchid plants have been considered and performed to screen for the presence of effective fungal strains

http://www.aloki.hu ● ISSN 1589 1623 (Print) ● ISSN 1785 0037 (Online)
DOI: http://dx.doi.org/10.15666/aeer/1704_97539771

(Wu et al., 2012). It was found that the seeds of *D. catenatum* could form a symbiotic relationship with *Epulorhiza* spp. and *Alternaria* spp. with low specificity in vitro, but the germination rate was significantly low. Wang et al., (2011) conducted in vitro symbiotic seed germination of *D. catenatum* using fungal strains obtained from protocorms of *D. chrysanthum* via in situ baiting methods, and one fungus (SHH53) successfully improved seed germination and seedling development to stage 5. Other researchers have reported the use of two *Tulasnella* strains (JC-02 and JC-05) isolated from the roots of *D. nobile* for the symbiotic seed germination of *D. catenatum* (Wang et al., 2011; Tan et al., 2014). These results demonstrated that the two different strains of *Tulasnella* varied in their ability to facilitate germination/development of *D. catenatum* seeds in vitro. To the best of our knowledge, no fungal strains isolated from host protocorms have been reported to date. This study addresses the following hypotheses: (1) different fungal strains isolated from the same host protocorm would enhance seed germination; (2) the fungal strains that influence seed germination and seedling development would be from closely related taxa; (3) different fungal strains would influence seed germination at different times after sowing; and (4) the photoperiod would influence seed germination differently under different fungal strains.

Materials and methods

Plant species

The study species, *D. catenatum*, is a lithophyte or epiphyte growing in moderately humid mountains at an elevation of ca. 1600 m. It is widely distributed in central and south China, including Anhui, Fujian, Guangxi, Sichuan, Taiwan, Yunnan, and Zhejiang provinces (*Fig. 1*). It flowers from March to June with 10%-17% fruit set, and seeds become mature during December (Liu et al., 2011).

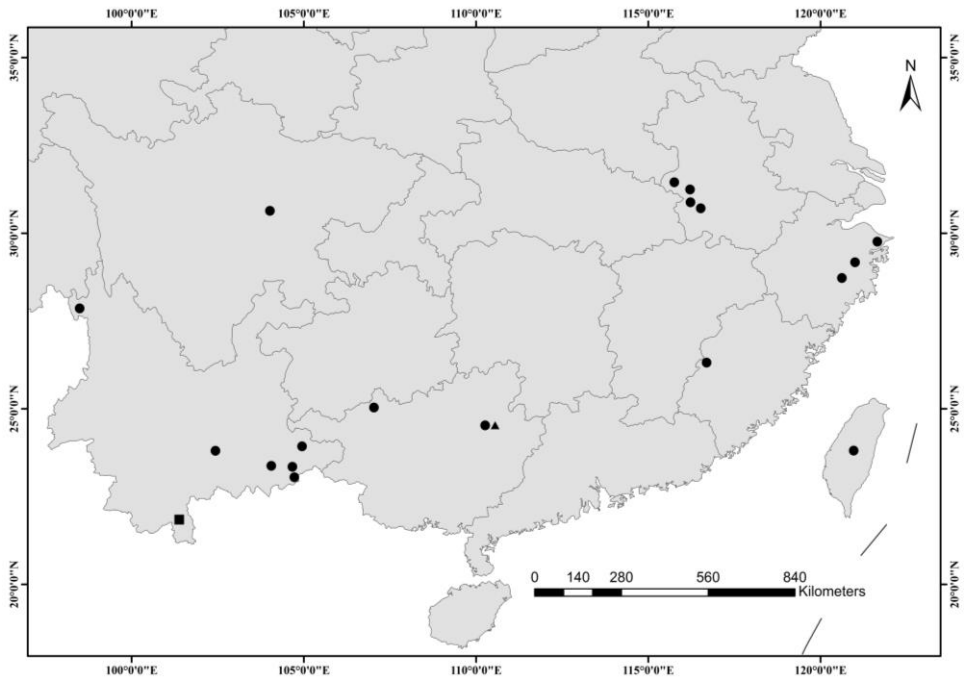

Figure 1. *Sketch map of distribution sites of the species D. catenatum by closed circles; sampling sites by closed triangle; and study site by closed squares*

http://www.aloki.hu ● ISSN 1589 1623 (Print) ● ISSN 1785 0037 (Online)
DOI: http://dx.doi.org/10.15666/aeer/1704_97539771

Study sites

Nearly dehisced fruits set by natural pollination, and substrates for ex situ baiting, were collected from wild populations of *D. catenatum* in Shuangjiang town, Lipu county, Guangxi Zhuang Autonomous Region, China (*Fig. 1*). Ex situ baiting to induce protocorm formation and screening for germination-enhancing fungi were performed in Xishuangbanna Tropical Botanical Garden (XTBG; 21°45′N, 101°02′E; altitude, 580 m), Yunnan Province (*Fig. 1*).

Seed collection and storage

The capsules were surface-sterilized using 75% ethanol, rinsed three times in sterile distilled water, and opened with a sterile scalpel under laminar flow. The seeds were transferred to airtight glass containers with anhydrous calcium chloride. After 4 days, the seeds were stored in a glass vial at 4 °C for short-term preservation and at −20 °C for long-term storage. Seed viability was 89.85% based on an assessment of approximately 480 seeds using the triphenyl tetrazolium chloride test.

Protocorm induction by ex situ baiting of D. catenatum seeds

The substrates, consisting of bark, moss, litter, and humus, were collected within 20 cm of the maternal plants and brought back to the laboratory within 48 h of harvest. The ex situ baiting mixture was saturated with sterile water, homogenized with a blender, and dispensed into petri dishes (9.0 cm in diameter). A designated number of seeds were resuspended in 0.1% sterilized agar solution and the drops were spread on a nylon mesh (ca. 2 × 3 cm) with 45 μm pores. Each mesh contained 120 seeds and each petri dish had 4 meshes. All the dishes were incubated in a plant growth chamber (MGC-450HP, Shanghai Yiheng Instruments Co., Ltd, Shanghai, China) at 25 ± 1 °C with 12/12 h light/dark (L/D) photoperiod at 1600 lux light intensity. Germination was monitored every 2 weeks, and protocorms that had reached stage 2 and seedlings that had reached stage 3 were then used to extract endophytic fungi.

Isolation of symbiotic fungus from protocorms

Symbiotic fungus isolation was performed according to the method proposed by Zi et al. (2014) with slight modifications. Developing protocorms at stage 2 or 3 were gathered and surface-sterilized using sodium hypochlorite solution containing 1% available chlorine for 3–5 min, and then washed 3–4 times with sterile distilled water. The protocorms were then cut into two parts using a sterilized blade, plated onto petri dishes containing fresh potato dextrose agar (PDA), and then incubated at 25.0 ± 1.0 °C in the dark. One complete protocorm was also grown to test the sterilization of the blade. After 3–5 days, once fungal hyphae had emerged from the edge of the broken protocorms, the hyphae tips were sub-cultured from the medium and transferred to new plates with PDA and incubated under the same conditions. The fungal isolates were purified 3–4 times by excising the hyphal tips onto fresh PDA petri dishes.

Molecular identification of fungal isolates and phylogenetic analysis

Using conventional CTAB method, we extracted DNA from fungi cultured in potato dextrose broth for 5 days. The primers ITS1 and ITS4 (White et al., 1990) were used to amplify nuclear ribosomal internal transcribed spacer (nrITS) using a Biometra gradient

http://www.aloki.hu ● ISSN 1589 1623 (Print) ● ISSN 1785 0037 (Online)
DOI: http://dx.doi.org/10.15666/aeer/1704_97539771

thermal cycler (070-801, Göttingen). Polymerase chain reaction products were purified using Sangon's purification kit, and sequencing was performed by Sangon Company (Sangon Biotech Co., Ltd, Shanghai, China). The ITS-rDNA sequences obtained from each isolate were compared to those deposited in the GenBank database by BLAST, providing the identification of isolates to the genus or species level when the ITS sequence similarity exceeded 97% or 99%, respectively (Zi et al., 2014).

Twelve related representative sequences of ITS-rDNA of orchid mycorrhizal fungi from NCBI (https://www.ncbi.nlm.nih.gov/) and eight newly generated sequences were used for phylogenetic analysis. *Armillaria sinapina* was set as the outgroup, following similar studies (Tan et al., 2014). Alignment of nucleotide sequences was performed by Clustal X version 1.81 (Thompson et al., 1997). Phylogenetic analysis was conducted in MEGA 6.0 (Tamura et al., 2013) with the Maximum Likelihood method based on the best model Kimura 2-parameter + Gamma model (BIC = 8533.566, AIC = 8265.917, lnL = −4095.821), with Bootstrap Replications = 1000, Rates among Sites = uniform rates. Initial tree(s) for the heuristic search was obtained by applying the Nearest-Neighbor-Interchange method. The tree with the highest log likelihood is shown. The percentage of trees in which the associated taxa clustered together is shown next to the branches.

Testing fungal capacity to promote seed germination

Seeds of *D. catenatum* were removed from storage at −20 °C and kept at ambient temperature overnight. According to the sterilization method of *Paphiopedilum spicerianum* seeds by Chen et al. (2015), seeds of *D. catenatum* in syringes fitted with 3×3 cm nylon cloth plot with 45 μm pores were first sterilized by washing with sterile distilled water for 5–10 min and then with sodium hypochlorite solution containing 1% available chlorine, and finally washed with sterile distilled water three to four times. Subsequently, the seeds were transferred to 0.1% sterile agar solution and ca. 80 seeds were resuspended in 1.0 mL of agar solution using a pipette and transferred to petri dishes containing 25 mL of sterile oat meal agar medium (OMA, 4 g/L). Once the seed suspension was completed, each dish was inoculated with one 0.5-cm^3 piece of fungal inoculum placed in the center of the petri dish, and a sterile PDA plot without fungus was also placed as a control referring to Zi et al. (2014). Fungus-inoculated petri dishes were randomly assigned to either a continuous dark treatment (0/24 h, L/D) or a 12-h photo period (12/12 h, L/D) with 1800 lux white fluorescent light at 25.0 ± 1.0 °C. All petri dishes were assessed under a dissecting microscope (Shanghai Bimu Bearing Co Ltd, Shanghai, China), and the exact number of seeds at various stages was recorded for each petri dish after 20, 50, and 90 days. Each experiment was replicated four times and petri dishes were placed in the same growth chamber. The percentages of protocorm (stage 2), seedling (stage 3), and seedling development (stage 4) were recorded for each dish, with contaminated dishes being excluded from the assessment.

Statistical analysis of germination and seedling development

Germination and seedling development were divided into five stages (*Table 1*) as described by Arditti (1967) with slight modification (both rupture of testa and appearance of protomeristem were regarded as stage 2). Seeds were considered germinated once they reached stage 2 to rule out the possibility that embryo swelling because of imbibed water was counted as germination (Rafter et al., 2016). The number

http://www.aloki.hu ● ISSN 1589 1623 (Print) ● ISSN 1785 0037 (Online)
DOI: http://dx.doi.org/10.15666/aeer/1704_97539771

of protocorms (P), seedling formation (S), and seedling development (L) were calculated as a percentage of the total number of seeds (t): P = number/t × 100. Generalized linear model was applied on the effect of treatments. Different day intervals and photoperiod conditions were considered as fixed factors. Protocorm formation, seedling formation, and seedling development were considered as dependent variables. All the data were arcsine transformed to obtain normal distributions. Analysis of variance was applied to find differences in seed germination by the effect of treatments and different days separately. Tukey's multiple range test was applied and the significant differences between treatments were analyzed ($P \leq 0.05$). All the statistical analyses were performed using SPSS version 20.0 software (SPSS Inc., Chicago, USA).

Table 1. *Developmental stages and features of symbiotic seed germination of D. catenatum (modified on the basis of Arditti, 1967)*

Seed germination stage	Description
0	No germination
1	Imbibed seed, swollen and still covered by testa
2	Protocorm formation and development (rupture of testa, appearance of protomeristem = germination)
3	Seedling formation (emergence of first leaf in early stage)
4	Seedling development (Emergence of second leaf and continue development)

Results

Seed baiting to induce protocorms

After 45 days, 25 out of 88 petri dishes were found with seeds germinated to stage 2 and 3, but no seedlings with two leaves (stage 4) were found. From these 25 dishes, 32 developed protocorms with promeristem and 12 seedlings with one leaf (stage 3) were harvested.

Molecular identification of endophytic fungi

Seven fungal strains (labeled SSCDO-1, SSCDO-3 to SSCDO-8) were successfully isolated from the protocorms and seedlings. All sequences of ITS-rDNA were submitted to GenBank with accession number MH348611-MH348617. Using Blast searches in NCBI, seven of the strains were attributed to the three most common orchid mycorrhizal taxa: the sequences of strains SSCDO-1, SSCDO-3, and SSCDO-4 had 98% similarity to uncultured Tulasnellaceae clone PM13 (GQ241803.1); SSCDO-5 was similar to the uncultured Tulasnellaceae clone (KX387600.1) with 99% identity (confirming the allocation of associated fungi in Guangxi by fungal isolation and molecular detection reported by Downing et al. (2017); SSCDO-6 was similar to uncultured Sebacinales (FJ788824.1); SSCDO-7 was close to uncultured Tulasnellaceae clone PM1 (GQ241802.1) and SSCDO-8 matched uncultured *Thanatephorus* (AB712285.1) (*Fig. 2*). Phylogenetic analysis of ITS-rDNA demonstrated that the strains SSCDO-1, SSCDO-3, SSCDO-4, SSCDO-5, and SSCDO-7 formed a clade (clade I; BP = 89; Tulasnellaceae); SSCDO-8 and uncultured *Thanatephorus* AB712285.1 formed a second clade (clade II; BP = 55; *Thanatephorus*); and SSCDO-6 and uncultured Sebacinales FJ788824.1 a third (clade III; BP = 97; *Sebacinales*) (*Fig. 2*). Clades II and III are sister clades, paraphyletic to clade I.

http://www.aloki.hu ● ISSN 1589 1623 (Print) ● ISSN 1785 0037 (Online)
DOI: http://dx.doi.org/10.15666/aeer/1704_97539771

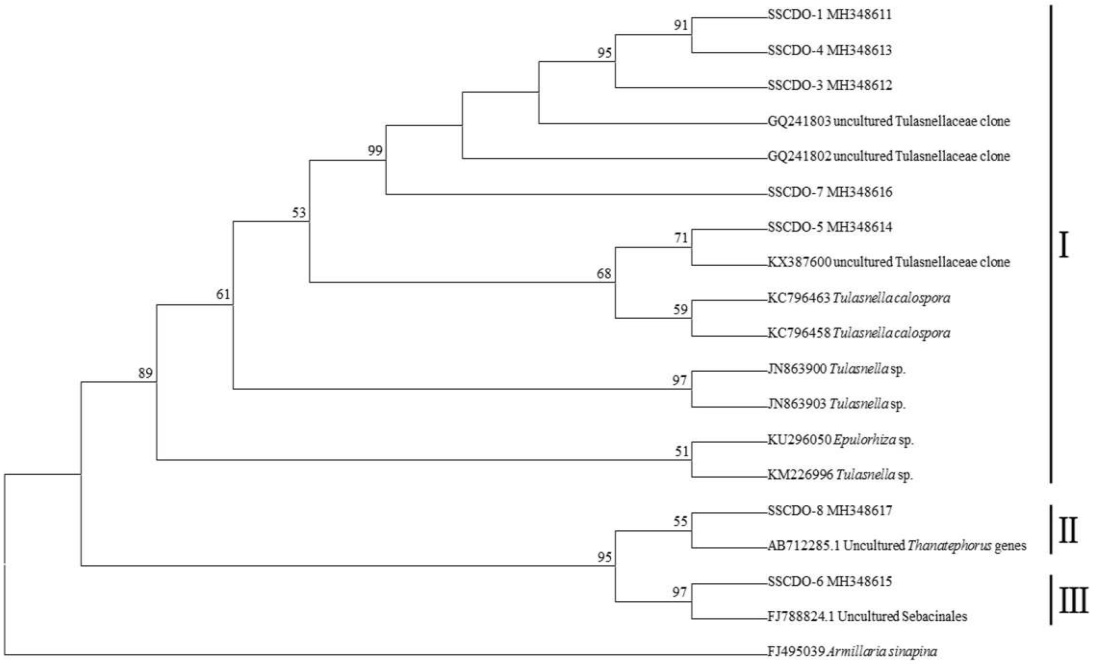

Figure 2. *Consensus tree by neighbor-joining of ITS-rDNA sequences of fungi from protocorms of D. catenatum, related sequences, and FJ495039 (Armillaria sinapina) as the outgroup. Bootstrap values ≥ 50% are shown above the branches. Clades I, II, and II are shown by vertical bars at the right-hand side*

Effect of fungal isolates and photoperiod on D. catenatum germination

Stage 2 − Protocorm formation and development

Different fungal inoculation treatments significantly influenced protocorm formation ($F_{8, 191} = 27.60$; $p < 0.0001$). Protocorm formation was not influenced by time (20, 50, and 90 days) after seed sowing, but it was significantly influenced by photoperiod ($F_{1, 191} = 52.59$; $p < 0.0001$). The interactions treatment × days and photoperiod × days had no significant influence on protocorm formation ($F_{16, 191} = 1.22$; $p = 0.259$); in contrast, the interaction treatment × photoperiod showed a significant variation on protocorm formation ($F_{8, 191} = 3.04$; $p < 0.01$). However, the interaction treatment × days × photoperiod showed no influence on protocorm formation.

Fungal inoculations SSCDO-5 and SSCDO-8 significantly influenced protocorm formation, followed by SSCDO-6 and SSCDO-7 (Tukey's HSD test). The mean protocorm formation after sowing was 44.56 ± 3.08% at 20 days, 42.33 ± 2.85% at 50 days, and 44.56 ± 2.42% at 90 days, with no significant differences between different days ($F_{2, 191} = 0.215$; $p = 0.807$). After 20 days, different treatments showed significant differences in protocorm formation ($F_{8, 57} = 8.052$; $p < 0.0001$), with SSCDO-5 having the most influence followed by SSCDO-1, SSCDO-8, and SSCDO-2. In addition, treatments showed significant differences on protocorm formation after 50 days ($F_{8, 62} = 5.44$; $P < 0.0001$) and after 90 days ($F_{8, 70} = 9.699$; $p < 0.0001$). In particular, treatments SSCDO-8 and SSCDO-5 highly influenced the protocorm formation after 50 and 90 days. Protocorm formation was always improved with 12/12 L/D conditions versus 0/24 L/D conditions (*Fig. 3a*), significantly for most treatments, but not for SSCDO-5 and SSCDO-8 (*Table 3*).

http://www.aloki.hu ● ISSN 1589 1623 (Print) ● ISSN 1785 0037 (Online)
DOI: http://dx.doi.org/10.15666/aeer/1704_97539771

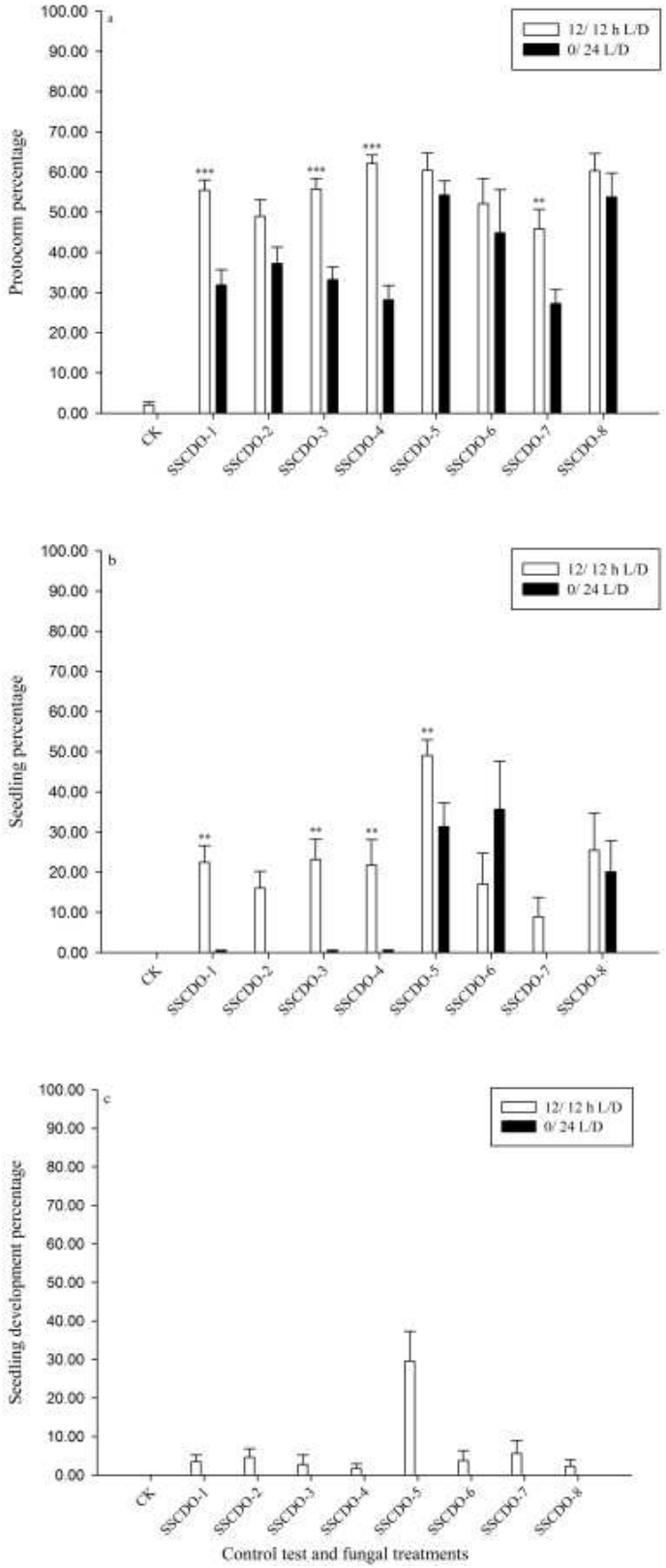

Figure 3. *The effects of fungal treatments on each seed germination stage after 90 days of inoculation.* ***a*** *Protocorm formation (%);* ***b*** *Seedling formation (%);* ***c*** *Seedling development (%). Asterisks denote statistically significant differences between light/dark treatments with the same fungus (**P < 0.01; ***P < 0.0001)*

http://www.aloki.hu ● ISSN 1589 1623 (Print) ● ISSN 1785 0037 (Online)
DOI: http://dx.doi.org/10.15666/aeer/1704_97539771

Stage 3 − Seedling formation

Fungal inoculation treatments significantly influenced seedling formation ($F_{8, 191} = 13.19$; $p < 0.0001$), as did days and photoperiod ($F_{1, 191} = 16.82$; $p < 0.0001$ and $F_{1, 191} = 17.86$; $p < 0.0001$, respectively). The interaction treatment × days did not influence the growth of seedling formation ($F_{16, 191} = 1.59$; $p = 0.08$), whereas the interaction treatment × photoperiod significantly influenced seedling formation ($F_{8, 191} = 3.46$; $p < 0.001$), as did the interaction days × photoperiod. However, the interaction treatment × days × photoperiod had no influence on seedling formation ($F_{16, 191} = 1.32$; $p = 0.192$).

Treatment with SSCDO-5 significantly increased seedling formation compared with control and other treatments, followed by SSCDO-6 and SSCDO-8 (Tukey's HSD multiple range test; *Table 2*).

Table 2. *Generalized linear model shows that the effect of treatments (eight fungal strains and control test), different days after seed sowing (20, 50 and 90 days) and photoperiod (0/24 h L/D, 12/12 h L/D) on protocorm formation, seedlings formation and seedlings development of D. catenatum*

Source	Dependent variable	Df	Mean square	F-test
Treatment	ProtocormF	8, 191	5279.7	27.60***
	SeedlingF	8, 191	2939.5	13.19***
	SeedlingD	8, 191	337.8	10.59***
Days	ProtocormF	2, 191	240.1	1.26^{ns}
	SeedlingF	2, 191	3747.5	16.82***
	SeedlingD	2, 191	731.8	22.95***
Photoperiod	ProtocormF	1, 191	10060.8	52.59***
	SeedlingF	1, 191	3980.1	17.86***
	SeedlingD	1, 191	1245.0	39.04***
Treatment × days	ProtocormF	16, 191	233.7	1.22^{ns}
	SeedlingF	16, 191	353.3	1.59^{ns}
	SeedlingD	16, 191	115.9	3.63***
Treatment × light	ProtocormF	8, 191	582.4	3.04**
	SeedlingF	8, 191	772.0	3.46**
	SeedlingD	8, 191	337.8	10.59***
Days × light	ProtocormF	2, 191	127.4	0.67^{ns}
	SeedlingF	2, 191	1946.4	8.73***
	SeedlingD	2, 191	731.8	22.95***
Fungi × days × light	ProtocormF	16, 191	167.4	0.88^{ns}
	SeedlingF	16, 191	294.7	1.32^{ns}
	SeedlingD	16, 191	115.9	3.63***
Error	ProtocormF	138, 191	191.3	
	SeedlingF	138, 191	222.8	
	SeedlingD	138, 191	31.9	

Suffix F = formation; suffix D = development; ***indicates significance level $P < 0.0001$; **indicates significance level $P < 0.001$; ns = not significant. DF values showing number of variables in correspondence to the total number of replicates of the each factor

http://www.aloki.hu ● ISSN 1589 1623 (Print) ● ISSN 1785 0037 (Online)
DOI: http://dx.doi.org/10.15666/aeer/1704_97539771

Mean seedling formation was 5.01 ± 1.74% at 20 days, 17.36 ± 2.77% at 50 days, and 23.92 ± 2.85% at 90 days after sowing with no significant differences on the production of seedlings in response to different days. In addition, different fungal strains showed significant differences on seedling formation at 20 days ($F_{8, 57} = 43.15$; $p < 0.0001$), at 50 days ($F_{8, 62} = 4.18$; $p < 0.001$), and at 90 days after seed sowing ($F_{8, 70} = 2.098$; $p < 0.0001$). In general, light (12/12 L/D conditions) significantly influenced seedling growth compared with darkness (e.g., for SSCDO-1, SSCDO-3, SSCDO-4, and SSCDO-5), whereas seedling growth was not significantly different for SSCDO-8 (*Table 2*; *Fig. 3b*).

Stage 4 − Seedling development

The fungal strains significantly influenced seedling development ($F_{8, 191} = 10.59$; $p < 0.0001$), and this varied significantly at different times after seed sowing ($F_{2, 191} = 22.95$; $p < 0.0001$). In addition, the photoperiod significantly influenced seedling development ($F_{1, 191} = 39.04$; $p < 0.0001$). Interestingly, the interaction fungal inoculation treatment × days also showed a significant variation on seedling development ($F_{16, 191} = 3.63$; $p < 0.0001$), as did the dual interaction treatment × photoperiod ($F_{8, 191} = 10.59$; $p < 0.0001$). Moreover, the dual interaction days × photoperiod showed significant differences on seedling development and the interaction treatment × days × photoperiod also showed significant differences ($F_{16, 191} = 3.63$; $p < 0.0001$).

In particular, the fungal strain SSCDO-5 significantly influenced seedling development compared with control and other treatments (Tukey's HSD test; *Table 3*). There was no seedling development 20 days after seed sowing, although seedling development was found at 50 days (1.57 ± 0.86%) and 90 days (7.76 ± 1.77%), with significant differences in seedling development at different days after sowing by the effect of all treatments ($F_{2, 191} = 11.45$; $p < 0.0001$). In addition, different fungal strains exhibited significant differences in seedling development at 50 days ($F_{8, 62} = 4.98$; $p < 0.0001$) and at 90 days ($F_{8, 70} = 3.804$; $p < 0.001$) (*Table 2*). Among these, SSCDO-5 significantly increased the seedling development at 50 and 90 days (*Table 3*). Seedling development only occurred under light conditions (12/12 L/D) with the different treatments (*Fig. 3c*); there was no seedling development in darkness.

Discussion

Ex situ baiting isolation

The present study in *D. catenatum* showed that the ex situ baiting technique resulted in the successful isolation of specific symbiotic mycorrhizal fungal strains that effectively induced seed protocorm formation. In our study, after 1.5 months, protocorms and seedlings with one leaf were successfully induced in 0.42% of seeds by ex situ baiting, and compatible and adaptive fungal strains were obtained successfully from host protocorms. This method could be considered for broader application to induce protocorm formation and to isolate mycorrhizal symbionts in other epiphytic orchids.

Phylogeny of symbiotic fungi

The fungi isolated from the protocorms in the present study belong to the families Tulasnellaceae, Ceratobasidiaceae, and Sebacinales. All the fungal isolates belonging to the clades of Tulasnellaceae, Sebacinales, and Thanatephorus had high similarity to fungi from the roots of *D. catenatum* (Xing et al., 2013). Taxa in Tulasnellaceae have often

http://www.aloki.hu ● ISSN 1589 1623 (Print) ● ISSN 1785 0037 (Online)
DOI: http://dx.doi.org/10.15666/aeer/1704_97539771

been found in association with tropical epiphytic and terrestrial orchids (Sathiyadash et al., 2014; Zi et al., 2014; Zhou and Gao, 2016). This study is the first report on symbiotic seed germination in the species *D. catenatum* induced by fungi from the host protocorm origin induced using ex situ baiting techniques but not from roots.

Table 3. *The effect of different days and treatments on differences in mean percentage growth of protocorms formation, seedlings formation and seedlings development on D. catenatum*

Seeds after sowing	Treatment	Protocorm formation	Seedling formation	Seedling development
		Mean	Mean	Mean
20 days	SSCDO-1	56.3 ± 5.3bc	0.9 ± 0.5a	0
	SSCDO-2	51.1 ± 5.1bc	0.0 ± 0.0a	0
	SSCDO-3	49.3 ± 6.6bc	2.0 ± 1.1a	0
	SSCDO-4	45.7 ± 9.5bc	0.5 ± 0.5a	0
	SSCDO-5	65.6 ± 5.2c	41.0 ± 5.7b	0
	SSCDO-6	45.9 ± 11.0bc	3.1 ± 3.1a	0
	SSCDO-7	29.6 ± 7.5ab	0.0 ± 0.0a	0
	SSCDO-8	53.8 ± 5.2bc	0.9 ± 0.6a	0
	CK	0.7 ± 0.5a	0.0 ± 0.0a	0
	ANOVA (F), N = 8, DF = 57	8.05***	43.15***	-
50 days	SSCDO-1	45.0 ± 5.6b	17.6 ± 4.8abc	0.0 ± 0.0a
	SSCDO-2	44.5 ± 5.1b	9.7 ± 3.8abc	0.0 ± 0.0a
	SSCDO-3	45.5 ± 5.8b	16.7 ± 7.0abc	0.0 ± 0.0a
	SSCDO-4	47.5 ± 9.1b	9.3 ± 6.7ab	0.0 ± 0.0a
	SSCDO-5	50.3 ± 3.3b	41.7 ± 2.4c	14.1 ± 6.3b
	SSCDO-6	53.3 ± 12.2b	36.2 ± 14.6bc	0.0 ± 0.0a
	SSCDO-7	33.6 ± 6.8b	0.0 ± 0.0a	0.0 ± 0.0a
	SSCDO-8	56.4 ± 8.7b	25.0 ± 12.0abc	0.0 ± 0.0a
	CK	0.0 ± 0.0a	0.0 ± 0.0a	0.0 ± 0.0a
	ANOVA (F), N = 8, DF = 62	5.44***	4.18**	4.98***
90 days	SSCDO-1	43.0 ± 4.3b	24.2 ± 6.8	6.4 ± 2.6a
	SSCDO-2	39.6 ± 5.9b	18.1 ± 6.5ab	7.7 ± 3.4a
	SSCDO-3	43.5 ± 4.7b	21.5 ± 7.8ab	4.8 ± 4.1a
	SSCDO-4	51.5 ± 5.2b	25.7 ± 8.2ab	2.6 ± 1.7a
	SSCDO-5	58.2 ± 5.0b	40.5 ± 10.3b	32.4 ± 11.7b
	SSCDO-6	47.8 ± 8.4b	30.1 ± 10.6ab	5.2 ± 3.5a
	SSCDO-7	47.7 ± 2.6b	13.4 ± 6.8ab	8.3 ± 4.9a
	SSCDO-8	61.2 ± 4.3b	38.3 ± 9.4b	3.5 ± 2.4a
	CK	0.0 ± 0.0a	0.0 ± 0.0a	0.0 ± 0.0a
	ANOVA (F), N = 8, DF = 70	9.699***	2.098***	3.804**

CK = Control. Values are provided as mean ± S.E. In a column, values followed by a different lowercase letter(s) are significantly different at the 5% level according to Tukey's HSD multiple range test. ***Significance level $P < 0.0001$. **Significance level $P < 0.001$

http://www.aloki.hu ● ISSN 1589 1623 (Print) ● ISSN 1785 0037 (Online)
DOI: http://dx.doi.org/10.15666/aeer/1704_97539771

In vitro symbiotic seed germination

Fungal treatment

It has been suggested that in theory any fungal strain isolated from the protocorms of one species may promote seed germination and protocorm formation in that species, and this has been proved experimentally on *D. catenatum* in the present study. The strains SSCDO-1, SSCDO-2, SSCDO-3, SSCDO-4, and SSCDO-7 showed similar effects on protocorm formation and development (*Table 4*; *Fig. 4b*) represented by the fungus SSCDO-4. The percentage of seedlings with one leaf was higher with SSCDO-1, SSCDO-3, and SSCDO-4 than with SSCDO-2 and SSCDO-7, but no significant differences were found with the other fungal strains. Steinfort et al. (2010) found a similar tendency in the germination of *Bipinnula fimbriata* at stage 2, with the fungal strain P2VT-03 showing a significantly higher germination rate than the strains F2VT-02 and F2VT-03, although all of them belonged to the same species, *Tulasnella calospora*; the strain F6VT-02 showed a stronger effect on seed germination at stage 2 than strain F3VC-02 of the same species. Xu et al. (2017) found that a strain of *T. calospora*, Tco2, showed more effective promotion of seed germination and protocorm differentiation in *Epidendrum secundum* than another strain of the same species. Results from the present study also suggested that fungal strains of the same species (Tulasnellaceae) vary in their influence on germination and growth of seeds.

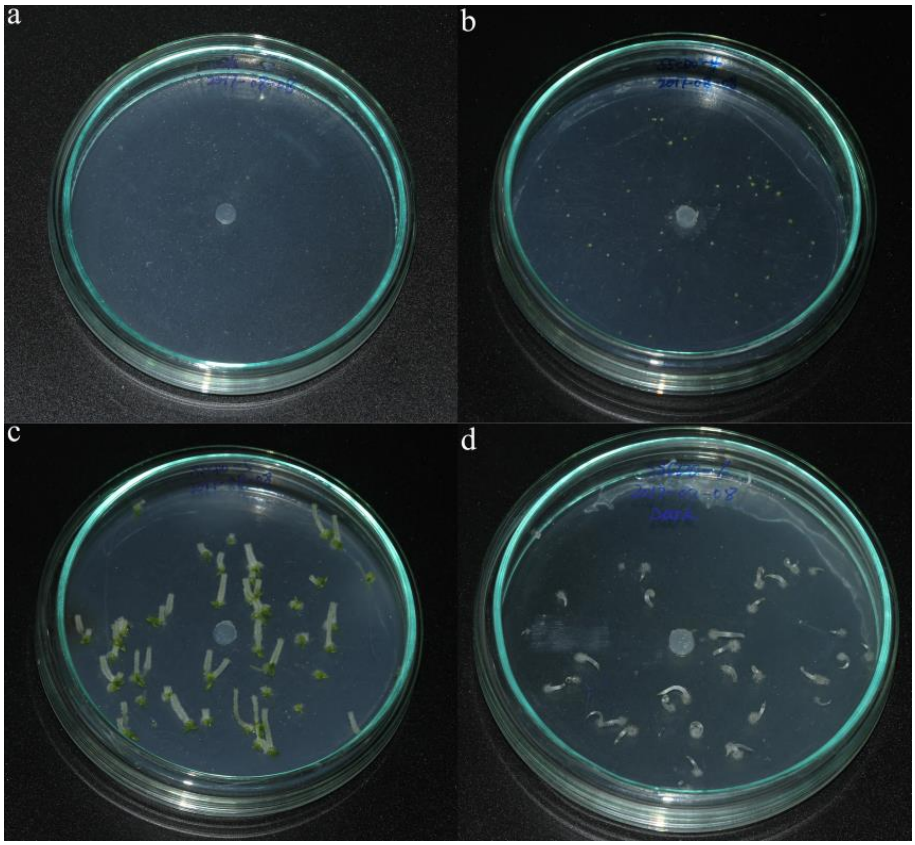

Figure 4. *Symbiotic seed germination of D. catenatum 90 days after sowing.* ***a*** *Control test.* ***b*** *Protocorm formation and seedling formation following inoculation with varying fungal treatments (represented by SSCDO-4) under light conditions.* ***c*** *Seedling development (with SSCDO-5 inoculation) in light conditions.* ***d*** *Abnormal seedlings in dark conditions (represented by SSCDO-6)*

http://www.aloki.hu ● ISSN 1589 1623 (Print) ● ISSN 1785 0037 (Online)
DOI: http://dx.doi.org/10.15666/aeer/1704_97539771

After 90 days with the control treatment, protocorms had still not formed (*Fig. 4a*); however, after only 20 days of treatment with the fungal strains, protocorms had formed, indicating that fungal inoculation plays a significant role in germination. The fungal strains SSCDO-5, SSCDO-6, and SSCDO-8 significantly influenced the growth of protocorms and seedling formation (one-leaf seedlings) measured at different times after sowing. In particular, SSCDO-5 significantly influenced protocorm formation and seedling development in *D. catenatum* (more so than other fungal strains), promoting the best seedling development and maximum number of seedlings with two leaves and long roots (*Table 4*; *Fig. 4c*). Potentially, then, SSCDO-5 might be of use in efficiently initiating seed germination and promoting further seedling development, and this could be potential for mass seedling propagation in a conservation program.

Table 4. *Effect of fungal inoculation treatment on protocorm formation (%), seedling formation (%), and seedling development (%) on the species D. catenatum under in vitro conditions*

Treatments	Protocorm formation (%)	Seedling formation (%)	Seedling Development (%)
	Mean ± S.E	Mean ± S.E	Mean ± S.E
SSCDO-1	47.6 ± 3.0bc	15.1 ± 3.4abc	2.4 ± 1.1a
SSCDO-2	44.6 ± 3.2bc	10.0 ± 3.1abc	2.9 ± 1.4a
SSCDO-3	46.1 ± 3.2bc	13.4 ± 3.8abc	1.6 ± 1.4a
SSCDO-4	48.6 ± 4.2bc	13.2 ± 4.4abc	1.0 ± 0.7a
SSCDO-5	57.7 ± 2.8c	41.1 ± 3.9d	16.3 ± 5.3b
SSCDO-6	49.1 ± 5.7bc	24.9 ± 6.9cd	2.2 ± 1.5a
SSCDO-7	37.4 ± 3.6b	4.9 ± 2.7ab	3.0 ± 1.9a
SSCDO-8	57.5 ± 3.5c	23.2 ± 6.1bcd	1.3 ± 1.0a
CK	0.2 ± 0.2a	0.0 ± 0.0a	0.0 ± 0.0a
ANOVA (F), N = 8, DF = 191	21.0***	7.96***	5.26***

CK = control. Values are given as mean ± S.E. In a column, values followed by a different lowercase letter(s) are significantly different at the 5% level according to Tukey's HSD multiple range test. ***Significance level $P < 0.0001$. The row in SSCDO-5 boldface indicates the significantly higher value on different growth formation as compared to other treatments)

The present results also support the hypothesis that mycorrhizal fungi isolated from protocorms would produce seed germination and advance development to a higher stage, with high compatibility and adaptivity (Sharma et al., 2003). Several previous studies have put forward a similar hypothesis for various terrestrial and epiphytic orchids (Sharma et al., 2003; Sathiyadash et al., 2014; Zi et al., 2014; Wang et al., 2016; Shao et al., 2017).

Days

The different observation days after sowing time play a significant role for the percentage of seed germination, with protocorm formation being higher at 20 and 90 days. Subsequently, the percentage of seedling formation was higher at 50 and 90 days, and while there was no seedling development (two-leaf seedlings) at 20 days, two-leaf seedlings were found at 50 and 90 days after sowing following fungal inoculation

http://www.aloki.hu ● ISSN 1589 1623 (Print) ● ISSN 1785 0037 (Online)
DOI: http://dx.doi.org/10.15666/aeer/1704_97539771

treatment. In addition, protocorm formation had increased at 20 days (mean = 49.63%), at 90 days (mean = 48.07%), and at 50 days (mean = 46.79%) with all treatments. Seedling formation increased only gradually over time, and developed seedlings (two-leaf stage) were only found at 90 days (none at 20 or 50 days), in line with a previous study (Huang et al., 2018). Another study in *D. catenatum* reported seedling development (stage 5) after 12 weeks (84 days) under optimal conditions under the influence of fungal strains (Wang et al., 2011), similar to the findings of the present study, and Tan et al. (2014) also reported that seed germination was higher at stage 3 and lower at stages 4 and 5 under the influence of an effective fungal strain JC-05. Overall, in the present study, while periods of 20 and 50 days after sowing were significant for the formation of protocorm and seedlings during the earlier stages of seed germination, seedling development significantly increased by 90 days under the influence of fungal inoculation treatments.

Photoperiod

In the present study, the response of photoperiod is positive for seed germination and seedling development. There was a significant variability in germination rate under the light photoperiod (12/12 h L/D) with all fungal strains when considering seedlings with two leaves, indicating different degrees of compatibility between seeds and fungal strains. No seedlings were formed in the dark conditions, indicating that light is likely a key ecological factor for protocorm development and seedling formation. Interestingly, a small number of seedlings with one leaf were found under dark conditions, but the seedling development that did occur was not via leaves but via roots (*Fig. 4d*), reflecting results reported in previous studies (Tan et al., 2014; Cui et al., 2012).

Conclusion

Dendrobium catenatum, an epiphytic orchid, is now rare and endangered in China, its population having been reduced by over exploitation for traditional medicine. Consequently, it has become necessary to develop a standard protocol for efficient plant reproduction in situ. This study confirms that symbiotic mycorrhizal fungi (the strains SSCDO-5) support protocorm formation, seedling formation, and sapling development under light conditions as observed at 20-90 days after sowing. Fungal strains of the same species (*Tulasnellaceae spp*.) isolated from protocorms might be more compatible and specific. Performance of strain SSCDO-5 should be tested in the wild when considering direct sowing for reintroduction and conservation. Ex situ baiting techniques for symbiotic seed germination might prove valuable for the conservation of *D. catenatum*, helping in future orchid production, reintroduction in both in situ and ex situ conservation efforts, and under in vitro experimental conditions. We believe that direct sowing of *D. catenatum* seeds inoculated with specific symbiotic fungi might prove successful for reintroduction or orchid plant production, and would encourage sustainable management for traditional medicinal practices.

Acknowledgements. The authors thank Ms. Xiu-Qing Xie for her kind assistance in preparatory laboratory work and symbiotic seed germination in vitro and Dr. Zhi-Yong Liao for his advice on data analysis.

http://www.aloki.hu ● ISSN 1589 1623 (Print) ● ISSN 1785 0037 (Online)
DOI: http://dx.doi.org/10.15666/aeer/1704_97539771

REFERENCES

[1] Arditti, J. (1967): Factors affecting the germination of orchid seeds. – The Botanical Review 33: 1-97.

[2] Brundrett, M. C., Scade, A., Batty, A. L., Dixon, K. W., Sivasithamparam, K., (2003): Development of in situ and ex situ seed baiting techniques to detect mycorrhizal fungi from terrestrial orchid habitats. – Mycological Research 107: 1210-1220.

[3] Chen, Y., Goodale, U. M., Fan, X. L., Gao, J. Y. (2015): Asymbiotic seed germination and in vitro seedling development of Paphiopedilum spicerianum: an orchid with an extremely small population in China. – Global Ecology and Conservation 3: 367-378.

[4] Chutima, R., Dell, B., Lumyong, S. (2011): Effects of mycorrhizal fungi on symbiotic seed germination of *Pecteilis susannae* (L.) Rafin (Orchidaceae), a terrestrial orchid in Thailand. – Symbiosis 53: 149-156.

[5] Cruz-Higareda, J. B., Luna-Rosales, B. S., Barba-Alvarez, A. (2015): A novel seed baiting technique for the epiphytic orchid *Rhynchostele cervantesii*, a means to acquire mycorrhizal fungi from protocorms. – Lankesterlana 15: 67-76.

[6] Cui, Q. H., Sun, Y. Y., Li, K., Duan, M. L. (2012): Seed preservation and germination process of morphological development of *Dendrobium devonianum* Paxt. – Acta Agriculturae Universitatis Jiangxiensis 34: 0533-0536 (in Chinese with English Abstract).

[7] Downing, J. L., Liu, H., Shao, S. C., Wang, X. L., McCormick, M., Deng, R. Y., Gao, J. Y. (2017): Contrasting changes in biotic interactions of orchid populations subject to conservation introduction vs. conventional translocation in tropical China. – Biological Conservation 212: 29-38.

[8] Fracchia, S., Aranda-Rickert, A., Rothen, C., Sede, S. (2016): Associated fungi, symbiotic germination and in vitro seedling development of the rare Andean terrestrial orchid *Chloraea riojana*. – Flora 224: 106-111.

[9] Herrera, H., Valadares, R., Contreras, D., Bashan, Y., Arriagada, C. (2016): Mycorrhizal compatibility and symbiotic seed germination of orchids from the coastal range and Andes in south central Chile. – Mycorrhiza 27: 175-188.

[10] Huang, H., Zi, X. M., Lin, H., Gao, J. Y. (2018): Host-specificity of symbiotic mycorrhizal fungi for enhancing seed germination, protocorm formation and seedling development of over-collected medicinal orchid, *Dendrobium devonianum*. – Journal of Microbiology 56: 42-48.

[11] Johnson, T. R., Stewart, S. L., Dutra, D., Kane, M. E., Richardson, L. (2007): Asymbiotic and symbiotic seed germination of *Eulophia alta* (Orchidaceae) - preliminary evidence for the symbiotic culture advantage. – Plant Cell Tissue Organ 90: 313-323.

[12] Khamchatra, N., Dixon, K. W., Tantiwiwat, S., Piapukiew, J. (2016): Symbiotic seed germination of an endangered epiphytic slipper orchid, *Paphiopedilum villosum* (Lindl.) Stein. from Thailand. – South African Journal of Botany 104: 76-81.

[13] Liu, Z. J., Zhang, Y. T., Wang, Y., Huang, Q. H., Chen, S. C., Chen, L. J. (2011): Recent developments in the study of rapid propagation of *Dendrobium catenatum* Lindl. with a discussion on its scientific and Chinese names. – Plant Science Journal 29: 763-772 (in Chinese with English Abstract).

[14] Masuhara, G., Katsuya, K. (1994): In situ and in vitro specificity between *Rhizoctonia* spp. and *Spiranthes sinensis* (Persoon) Ames. var. *amoena* (*M. bieberstein*) Hara (Orchidaceae). – New Phytologist 127: 711-718.

[15] Park, E. J., Lee, W. Y. (2013): In vitro symbiotic germination of myco-heterotrophic *Gastrodia elata* by *Mycena* species. – Plant Biotechnology Reports 7: 185-191.

[16] Rafter, M., Yokoya, K., Schofield, E. J., Zettler, L. W., Sarasan, V. (2016): Non-specific symbiotic germination of *Cynorkis purpurea* (Thouars) Kraezl., a habitat-specific terrestrial orchid from the central highlands of Madagascar. – Mycorrhiza 26: 541-552.

http://www.aloki.hu ● ISSN 1589 1623 (Print) ● ISSN 1785 0037 (Online)
DOI: http://dx.doi.org/10.15666/aeer/1704_97539771

[17] Rasmussen, H. N., Whigham, D. F. (1993): Seed ecology of dust seeds in situ: A new study technique and its application in terrestrial orchids. – American Journal of Botany 80: 1374-1378.
[18] Rasmussen, H. N., Dixon, K. W., Jersakova, J., Tesitelova, T. (2015): Germination and seedling establishment in orchids: a complex of requirements. – Annals of Botany 116: 391-402.
[19] Sathiyadash, K., Muthukumar, T., Murugan, S. B., Sathishkumar, R., Pandey, R. R. (2014): In vitro symbiotic seed germination of South Indian endemic orchid *Coelogyne nervosa*. – Mycoscience 55: 183-189.
[20] Selosse, M-A., Roy, M. (2009): Green plants that feed on fungi: facts and questions about mixotrophy. – Trends in Plant Science 14: 64-70.
[21] Shao, S. C., Burgess, K. S., Cruse-Sanders, J. M., Liu, Q., Fan, X. L., Huang, H., Gao, J. Y. (2017): Using in situ symbiotic seed germination to restore over-collected medicinal orchids in southwest China. – Frontiers in Plant Science 8: 888.
[22] Sharma, J., Zettler, L. W., Van Sambeek, J. W., Ellerieck, M. R., Starbuck, C. J., (2003): Symbiotic seed germination and mycorrhizae of the federally threatened *Platanthera praeclara* (Orchidaceae). – The American Midland Naturalist 149: 104-120.
[23] Sheng, C. L., Li, Y. I., Gao, J. Y. (2012): Ex situ symbiotic seed germination, isolation and identification of effective symbiotic fungus in *Cymbidium mannii* (Orchidaceae). – Chinese Journal of Plant Ecology 36: 859-869 (in Chinese with English Abstract).
[24] Steinfort, U., Verdugo, G., Besoain, X., Cisternas, M. A. (2010): Mycorrhizal association and symbiotic germination of the terrestrial orchid *Bipinnula fimbriata* (Poepp.) Johnst (Orchidaceae). – Flora 205: 811-817.
[25] Stewart, S. L., Kane, M. E., (2007): Symbiotic seed germination and evidence for in vitro mycobiont specificity in *Spiranthes brevilabris* (Orchidaceae) and its implications for species-level conservation. – In Vitro Cellular & Developmental Biology - Plant 43: 178-186.
[26] Swangmaneecharern, P., Serivichyaswat, P., Nontachaiyapoom, S. (2012): Promoting effect of orchid mycorrhizal fungi *Epulorhiza* isolates on seed germination of *Dendrobium* orchids. – Scientia Horticulturae 148: 55-58.
[27] Tamura, K., Stecher, G., Peterson, D., Filipski, A., Kumar, S. (2013): MEGA6: molecular evolutionary genetics analysis version 6.0. – Molecular Biology and Evolution 30: 2725-2729.
[28] Tan, X. M., Wang, C. L., Chen, X. M., Zhou, Y. Q., Wang, Y. Q., Luo, A. X., Liu, Z. H., Guo, S. X. (2014): In vitro seed germination and seedling growth of an endangered epiphytic orchid, *Dendrobium officinale*, endemic to China using mycorrhizal fungi (*Tulasnella* sp.). – Scientia Horticulturae 165: 62-68.
[29] Thompson, J. D., Gibson, T. J., Plewniak, F., Jeanmougin, F., Higgins, D. G., (1997): The CLUSTAL_X windows interface: flexible strategies for multiple sequence alignment aided by quality analysis tools. – Nuclear Acid Research 25: 4876-4882.
[30] Wang, H., Fang, H. Y., Wang, Y. Q., Duan, L. S., Guo, S. X. (2011): In situ seed baiting techniques in *Dendrobium officinale* Kimuraet migo and *Dendrobium nobile* Lindl.: The endangered Chinese endemic *Dendrobium* (Orchidaceae). – World Journal of Microbial Biotechnology 27: 2051-2059.
[31] White, T. J. B., Bruns, T., Lee, S., Taylor, J. (1990): Amplification and Direct Sequencing of Fungal Ribosomal RNA Genes for Phylogenetics. – In: Inis M. A., Gelfand, D. H., Sninsky, J. J., White, T. J. (ed.) PCR Protocols: A Guide to Methods and Applications. Academic Press, San Diego.
[32] Wu, H. F., Song, X. Q., Liu, H. X. (2012): Ex-situ symbiotic seed germination of *Dendrobium catenatum*. – Acta Ecologica Sinica 32: 2491-2497 (in Chinese with English Abstract).

http://www.aloki.hu ● ISSN 1589 1623 (Print) ● ISSN 1785 0037 (Online)
DOI: http://dx.doi.org/10.15666/aeer/1704_97539771

[33] Xing, X. K., Ma, X. T., Deng, Z. H., Chen, J., Wu, F. Z., Guo, S. X. (2013): Specificity and preference of mycorrhizal associations in two species of the genus *Dendrobium* (Orchidaceae). – Mycorrhiza 23: 317-324.
[34] Xu, J. T., Guo, S. X. (1989): Fungus associated with nutrition of seed germination of *Gastrodia elata*: *Mycena osmundicola* Lange. – Acta Mycologica Sinica 8: 221-226.
[35] Xu, L., Tian, J. N., Wang, T., Li, L. B. (2017): Symbiosis established between orchid and *Tulasnella* spp. fungi. – Journal of Nuclear Agricultural Sciences 31: 876-883.
[36] Zhou, X., Gao, J. Y. (2016): Highly compatible Epa-01 strain promotes seed germination and protocorm development of *Papilionanthe teres* (Orchidaceae). – Plant Cell, Tissue and Organ Culture 125: 479-493.
[37] Zi, X. M., Sheng, C. L., Goodale, U. M., Shao, S. C., Gao, J. Y. (2014): In situ seed baiting to isolate germination-enhancing fungi for an epiphytic orchid, *Dendrobium aphyllum* (Orchidaceae). – Mycorrhiza 24: 487-499.

APPENDIX

Table A1. *Effect of treatments, different days after seed sowing (20, 50 and 90 days) and photoperiod (0/24 h L/D, 12/12 h L/D) on protocorm formation (PF), seedling formation (SF) and seedling development (SD) of D. catenatum was analysis by the Generalized Linear Model (GLM)*

Tests of between-subjects effects							
Source	**Dependent variable**	**Type III sum of squares**	**df**	**Mean square**	**F**	**Sig.**	**Partial ETA squared**
Corrected model	PF	66251.216[a]	53	1250.023	6.534	.000	.715
	SF	61084.418[b]	53	1152.536	5.172	.000	.665
	SD	16249.261[c]	53	306.590	9.613	.000	.787
Intercept	PF	315286.495	1	315286.495	1648.148	.000	.923
	SF	36025.433	1	36025.433	161.658	.000	.539
	SD	1244.975	1	1244.975	39.037	.000	.221
Fungi	PF	42237.221	8	5279.653	27.599	.000	.615
	SF	23516.125	8	2939.516	13.191	.000	.433
	SD	2702.134	8	337.767	10.591	.000	.380
Days	PF	480.116	2	240.058	1.255	.288	.018
	SF	7494.928	2	3747.464	16.816	.000	.196
	SD	1463.664	2	731.832	22.947	.000	.250
Light	PF	10060.827	1	10060.827	52.593	.000	.276
	SF	3980.068	1	3980.068	17.860	.000	.115
	SD	1244.975	1	1244.975	39.037	.000	.221
Fungi * days	PF	3738.838	16	233.677	1.222	.259	.124
	SF	5652.889	16	353.306	1.585	.080	.155
	SD	1854.342	16	115.896	3.634	.000	.296
Fungi * light	PF	4659.075	8	582.384	3.044	.003	.150
	SF	6176.256	8	772.032	3.464	.001	.167
	SD	2702.134	8	337.767	10.591	.000	.380
Days * light	PF	254.811	2	127.406	.666	.515	.010
	SF	3892.707	2	1946.354	8.734	.000	.112
	SD	1463.664	2	731.832	22.947	.000	.250

http://www.aloki.hu ● ISSN 1589 1623 (Print) ● ISSN 1785 0037 (Online)
DOI: http://dx.doi.org/10.15666/aeer/1704_97539771

Fungi * days * light	PF	2678.830	16	167.427	.875	.599	.092
	SF	4715.129	16	294.696	1.322	.192	.133
	SD	1854.342	16	115.896	3.634	.000	.296
Error	PF	26399.054	138	191.297			
	SF	30753.224	138	222.849			
	SD	4401.073	138	31.892			
Total	PF	461498.129	192				
	SF	141339.060	192				
	SD	22848.824	192				
Corrected total	PF	92650.270	191				
	SF	91837.642	191				
	SD	20650.334	191				

[a]R Squared = .715 (Adjusted R Squared = .606)
[b]R Squared = .665 (Adjusted R Squared = .537)
[c]R Squared = .787 (Adjusted R Squared = .705)

Table A2. *Effects of days after seed sowing (20 days) on protocorm formation, seedling formation and seedling development of D. catenatum*

ANOVA

		Sum of squares	**df**	**Mean square**	**F**	**Sig.**
PF	Between groups	17862.897	8	2232.862	8.053	.000
	Within groups	13586.390	49	277.273		
	Total	31449.288	57			
SF	Between groups	8735.217	8	1091.902	43.151	.000
	Within groups	1239.895	49	25.304		
	Total	9975.113	57			
SD	Between groups	.000	8	.000	.	.
	Within groups	.000	49	.000		
	Total	.000	57			

Table A3. *Effects of days after seed sowing (50 days) on protocorm formation, seedling formation and seedling development of D. catenatum*

ANOVA

		Sum of squares	**df**	**Mean square**	**F**	**Sig.**
PF	Between groups	14183.535	8	1772.942	5.443	.000
	Within groups	17588.268	54	325.709		
	Total	31771.803	62			
SF	Between groups	11474.560	8	1434.320	4.176	.001
	Within groups	18545.377	54	343.433		
	Total	30019.936	62			
SD	Between groups	1239.046	8	154.881	4.984	.000
	Within groups	1678.045	54	31.075		
	Total	2917.091	62			

http://www.aloki.hu ● ISSN 1589 1623 (Print) ● ISSN 1785 0037 (Online)
DOI: http://dx.doi.org/10.15666/aeer/1704_97539771

Table A4. *Effects of days after seed sowing (90 days) on protocorm formation, seedling formation and seedling development of D. catenatum*

ANOVA						
		Sum of squares	**df**	**Mean square**	**F**	**Sig.**
PF	Between groups	16241.252	8	2030.157	9.699	.000
	Within groups	12977.528	62	209.315		
	Total	29218.781	70			
SF	Between groups	8578.690	8	1072.336	2.098	.049
	Within groups	31687.926	62	511.096		
	Total	40266.616	70			
SD	Between groups	5104.227	8	638.028	3.804	.001
	Within groups	10397.796	62	167.706		
	Total	15502.023	70			

Table A5. *Effect of fungal inoculation treatments on the growth formation of protocorm, seedling and seedling development of the species D. catenatum under in vitro conditions*

ANOVA						
		Sum of squares	**df**	**Mean square**	**F**	**Sig.**
PF	Between groups	44342.513	8	5542.814	20.997	.000
	Within groups	48307.757	183	263.977		
	Total	92650.270	191			
SF	Between groups	23707.942	8	2963.493	7.960	.000
	Within groups	68129.700	183	372.293		
	Total	91837.642	191			
SD	Between groups	3860.007	8	482.501	5.259	.000
	Within groups	16790.327	183	91.750		
	Total	20650.334	191			

http://www.aloki.hu ● ISSN 1589 1623 (Print) ● ISSN 1785 0037 (Online)
DOI: http://dx.doi.org/10.15666/aeer/1704_97539771

IMPACT OF RESISTANCE INDUCERS ON BIOCHEMICAL ATTRIBUTES OF ONION LEAVES AGAINST PURPLE BLOTCH (*ALTERNARIA PORRI*)

MANSHA, M. Z.[1*] – HABIB, A.[2] – ASHRAF, W.[3] – SHAKEEL, Q.[3] – RAHEEL, M.[3] – ZAMAN, Q.[4] – AATIF, H. M.[1] – TAHIR, M.[5]

[1]*College of Agriculture, Bahauddin Zakariya University, Bahadur Sub Campus, Layyah, Pakistan*

[2]*Department of Plant Pathology, University of Agriculture, Faisalabad, Pakistan*

[3]*Discipline of Plant Pathology, University College of Agriculture and Environmental Sciences The Islamia University of Bahawalpur, Pakistan*

[4]*Department of Environmental Sciences, The University of Lahore, Lahore, Pakistan*

[5]*Department of Entomology, University College of Agriculture and Environmental Sciences The Islamia University of Bahawalpur, Pakistan*

[*]*Corresponding author*
e-mail: mianzeeshan121@gmail.com; phone: +92-333-252-7711

(Received 22nd Mar 2019; accepted 13th Jun 2019)

Abstract. In this study, we investigated the induced defense response and protective effects of onion against *Alternaria porri* by application of salicylic acid (SA) and benzothiadiazole (Bion®) through foliar application and seedling root dipping method in onion for two years under greenhouse conditions. Completely randomized design (CRD) under factorial arrangement was performed with three replicates. Reduction in the disease severity was observed in plants treated with Bion® and SA. Bion® and SA inoculated with the pathogen showed significantly higher PAL, PO, PPO activity, and phenolic contents than inoculated water-treated plants 2 days after the treatment during both years. Increasing trend was observed in disease severity and biochemical contents during the second year. In conclusion, the results of this study provide evidence that application of simple non-toxic chemical solutions like SA and Bion® can control purple blotch of onion by the modification of biochemical attributes.
Keywords: *Bion, salicylic acid, enzymatic activity, foliar application, seedling root dipping*

Introduction

Onion is among the five most valuable vegetable crops in the world (Cramer, 2000). It adds excellent taste to dishes and also has a number of therapeutic properties such as antibacterial, antifungal, anti-inflammatory, antiseptic and antispasmodic effects (Griffiths et al., 2002). Over the world it occupies an area of 4033.93 thousand hectares and production 78.5 million tons (FAO, 2012). In Pakistan, it occupies an area of 135.1 thousand ha, with production of 1763 thousand tons and contribute to the economy of the country (Govt. of Pakistan, 2014-15). Among the onion producing countries China stood first and India second in area and production in the world. Pakistan is on seventh number for production of onion (Aloch et al., 2014).

Overall onion is attacked by sixty six diseases in the world, in which thirty eight are of fungal diseases, ten bacterial, six nematode, three viral and one phytoplasmal disease.

http://www.aloki.hu ● ISSN 1589 1623 (Print) ● ISSN 1785 0037 (Online)
DOI: http://dx.doi.org/10.15666/aeer/1704_97739784

Purple blotch is most destructive one among fungal diseases and cause paramount losses to onion crop (Yadav et al., 2013).

Control of this disease by using disease free seeds, resistant cultivars and fungicidal sprays are successful but have their disadvantages, such as the brief commercial life of resistant cultivars or occurrence of fungicide resistance (Hayes and Johnston, 1971; Leadbeater et al., 1997). Due to these disadvantages, there is a continuous requirement for inducing resistance to plants against the disease. Induced resistance (1R) is a new technology for crop protection that assumed to be much more environmentally sound than traditional practices (Sonnemann et al., 2002).

Several chemicals like 2,6-dichloroisonicotinic acid (INA), Beta-amino butyric acid (BABA), potassium salts, benzothiadiazole and salicylic acid (SA) were documented in induction of SAR in variety of plants against several pathogens of plants (Oostendorp et al., 2001).

The first indication that SA may be associated with plant resistance was given by White (1979), who observed that application of SA in tobacco leaves improved protection from consequent infection by tobacco mosaic virus. Initially, Van Loon (1983) reported the possibility of association between salicylic acid and systemic acquired resistance. Benzothiadiazole (S-methylbenzo-1,2,3-thiadiazole-7-carbothiate, BTH) form a class of chemicals which induce the mechanism of defense in plant (Kunz et al., 1997). Their mode of action include stimulation of systemic acquired resistance downstream of salicylic acid.

Schonbeck et al. (1980) reported that resistance inducers enhance the biochemical that serve as a marker of ISR. This include deposition of lignin, assimilation of phytoalexins, cell wall polymers reinforcement (Thangavelu et al., 2003) and enhancement of enzymes like PPO and PAL (He et al., 2002). Peroxidase involved in papillae formation, hypersensitive response and lignin polymerization (Nicholson and Hammerschmidt, 1992; Bestwick et al., 1998).

So keeping in view the importance of resistance inducers the experiment was planned to assess the impact of Bion® and SA in resistance induction in onion against purple blotch to observe the mechanisms of resistance including enzyme related to resistance, under controlled environment.

Materials and Methods

Enhancement of resistance against the disease

Experiment was conducted during 2015-16 in green house of Department of Plant Pathology, University of Agriculture, Faisalabad, Pakistan. Seeds of Red Imposta (High yield cultivar) were sown, 23rd October and 25th October during 2015-16 respectively, in trays and in green house with temperature kept at 20 ± 2ºC during the day and 18 ± 2ºC at night and transplanted after fifty six days in thirty centimeter pots. *Alternaria porri* culture (*Fig. 1*) was made by isolating it from diseased onion leaves and incubated at 25 ± 1ºC for 15 days. Bion® (125 ppm) and salicylic acid (2 mM) were applied through seedling root dipping method and foliar application against purple blotch of onion. Ten ml of sterile distilled water was then added to each plate and colonies were scraped with a sterile needle. The resulting conidial suspension was diluted to 5×10^4 conidia per ml and inoculated onto leaves and seed-stalks of 110-day-old onion plants using an atomizer. Distilled water was used for Bion® and salicylic acid dissolving regarding desired concentrations (125 ppm and 2 mM)

http://www.aloki.hu ● ISSN 1589 1623 (Print) ● ISSN 1785 0037 (Online)
DOI: http://dx.doi.org/10.15666/aeer/1704_97739784

respectively, and then sprayed on entire plants through foliar application (50 ml per seedling) while seedlings were dipped in inducers solution before transplanting in case of seedling root dipping method, two days before inoculation with the pathogen. Plants were kept in a greenhouse after the application of treatments. For controls, the plants were inoculated or un inoculated but sprayed with water. The experiment was repeated twice under greenhouse conditions in 2015 and 2016. Autoclaved pots (20 cm in diameter) were filled with autoclaved clay soil and each pot planted with two seedlings. Three replicates were used, and each replicate consisted of four pots. Disease severity data was collected by following the 0-5 rating scale (Sharma, 1986). Biochemical contents of treated and untreated plants were analyzed after 0, 2, 4, 6, 8 and 10 days by using following procedure.

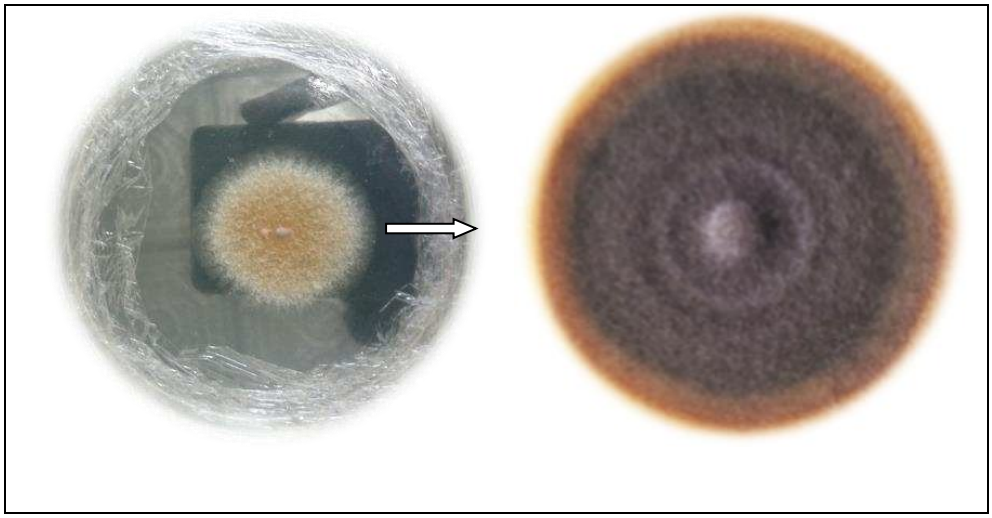

Figure 1. *Pure culture of Alternaria porri*

Data collection

Sample preparation for biochemical analysis

"Samples of leaf tissue (1 g fresh weight) for enzyme extraction were harvested at 0, 2, 4, 6, 8, and 10 days after application for each treatment, weighed and immersed in liquid nitrogen. The frozen leaf segments for each sample were homogenized (1:5 w/v) in an ice-cold mortar using 50 mM potassium phosphate buffer (pH 7.0) containing 1 M NaCl, 1% polyvinylpyrrolidone, 1 mM EDTA and 10 m M β-mercaptoethanol. The homogenates were centrifuged at 17,000 g for 20 min at 4°C. The supernatant (crude enzyme extract) was collected and divided into 1.5 ml portions. Protein concentrations were determined using bovine serum albumin as a standard according to Bradford (1976)".

Activity of peroxidase (PO) was analyzed by following the protocol of Urbanek et al. (1991), polyphenol oxidase (PPO) was measured according to the Gauillard et al. (1993) method. In case of phenylalanine ammonia-lyase (PAL) activity was assessed by using the Nagarathna et al. (1993) technique and Malick and Singh (1980) method was used for phenolic contents in the onion leaves.

http://www.aloki.hu ● ISSN 1589 1623 (Print) ● ISSN 1785 0037 (Online)
DOI: http://dx.doi.org/10.15666/aeer/1704_97739784

Statistical analysis

"Data collected from each experiment were analyzed using Statistix 8.1 software. Least significant difference (LSD) test at 5% probability level was applied to compare the treatment means".

Results

Effect of resistance inducers on disease severity (%) of onion leaf

Resistance inducers *i.e.* Bion and salicylic acid (Ch) applied through seedling root dipping and foliar application methods (M) significantly ($p \leq 0.05$) minimized the severity (%) of disease in onion plants during both years. During first year reduction in disease severity was up to 24.53% and 25.92% during 2nd year. In comparison for days (D) at 5th and 15th day minimum reduction in disease severity (37.24%, 40.12%) was observed during both years. During 2015, maximum reduction in severity of disease was observed in case of foliar application as compared to seedling root dipping. Bion showed maximum reduction in disease severity (21.55%) while salicylic acid showed (28.26%) as compared to control which exhibited (44.94%) disease severity. In case of interaction between Ch × D × M a non-significant behavior was observed with respect to disease severity, whereas, D ×M, Ch × D and Ch × M showed their significant impact in reduction of purple blotch severity (%) during both years (*Table 1*).

Table 1. *Impact of Bion and Salicylic acid applied through foliar and seedling root dipping methods on severity (%) of disease at different days*

Factors	Disease Severity (%)	
Days (D)	**2015**	**2016**
5	24.53 C	25.92 C
10	32.97 B	34.62 B
15	37.24 A	40.12 A
Method (M)		
Foliar Application	30.26 B	32.52 B
Seedling root dipping	32.90 A	33.85 A
Chemicals (Ch)		
Control	44.94 A	45.98 A
BION	21.55 C	23.25 C
Salicylic acid	28.26 B	30.39 B
LSD (D) ($p \leq 0.05$)	1.09	1.16
LSD (M) ($p \leq 0.05$)	0.91	0.98
LSD (Ch) ($p \leq 0.05$)	1.11	1.20
D × M ($p \leq 0.05$)	*	*
Ch × D ($p \leq 0.05$)	**	**
Ch × M ($p \leq 0.05$)	**	**
Ch × D × M ($p \leq 0.05$)	NS	NS

Any two means within a column followed by same letters are not significant at $p \leq 0.05$. * = Significant at $p \leq 0.05$; ** = Significant at $p \leq 0.01$; NS = Non-significant

Impact of inducers application through towards peroxidase (PO) activity (change in absorbance/min/mg of protein)

Peroxidase activity was significantly ($p \leq 0.05$) increased after the application of Bion and salicylic acid through seedling root dipping and foliar application during 2015-16. Peroxidase activity was maximum at day 10 (3.16) and minimum (0.69) when

http://www.aloki.hu ● ISSN 1589 1623 (Print) ● ISSN 1785 0037 (Online)
DOI: http://dx.doi.org/10.15666/aeer/1704_97739784

resistance inducers applied (0 day). Foliar application of resistance inducers increased the activity of peroxidase (1.96) over seedling root dipping (1.84). Peroxidase activity in inoculated plants was higher over plants without inoculation. Maximum peroxidase activity was found in plants on which Bion + *A. porri* (2.11) was applied as compare to plants where salicylic acid + *A. porri* (1.95) was applied. High peroxidase activity (2.02) was observed where Bion was applied followed by salicylic acid treated plants (1.86). Control plants showed minimum peroxidase activity (1.68). In 2016, similar but increase in peroxidase activity was observed (*Table 2*).

Table 2. *Impact of Bion and Salicylic acid applied through various methods on biochemical at different days*

Factors	PAL		PH		PO		PPO	
Days (D)	**2015**	**2016**	**2015**	**2016**	**2015**	**2016**	**2015**	**2016**
0	2.42 F	2.48 F	8.39 F	8.42 F	0.69 F	0.70 F	0.39 F	0.41 F
2	6.11 E	6.89 E	18.15 E	19.85 E	1.18 E	1.22 E	0.64 E	0.67 E
4	11.55 D	12.21 D	23.13 D	24.62 D	1.45 D	1.48 D	0.92 D	0.96 D
6	13.67 C	14.97 C	33.72 C	35.43 C	2.13 C	2.19 C	1.06 C	1.14 C
8	16.59 B	18.22 B	45.18 B	46.36 B	2.80 B	2.88 B	1.23 B	1.32 B
10	19.24 A	21.28 A	55.54 A	56.13 A	3.16 A	3.23 A	1.34 A	1.41 A
Method (M)								
Foliar Application	12.59 A	14.06 A	33.78 A	34.76 A	1.96 A	2.01 A	0.98 A	1.03 A
Seedling root dipping	10.60 B	11.29 B	27.59 B	28.84 B	1.84 B	1.89 B	0.88 B	0.94 B
Treatments (T)								
Control	8.98 F	8.17 F	26.13 F	17.50 F	1.68 F	1.75 F	0.74 F	0.79 F
Control + *A. porri*	10.03 E	9.91 E	29.72 E	21.85 E	1.79 E	1.83 E	0.83 E	0.88 E
BION	15.29 B	15.59 B	40.31 B	41.50 B	2.02 B	2.07 B	1.03 B	1.09 B
Salicylic acid	12.01 D	11.44 D	31.42 D	27.35 D	1.86 D	1.90 D	0.90 D	0.95 D
Bion + *A. porri*	16.93 A	17.50 A	47.14 A	48.21 A	2.11 A	2.16 A	1.09 A	1.16 A
Salicylic acid + *A. porri*	13.92 C	13.43 C	33.26 C	34.38 C	1.95 C	1.98 C	0.98 C	1.03 C
LSD (D) ($p \leq 0.05$)	1.03	0.73	2.01	1.17	0.02	0.01	0.01	0.01
LSD (M) ($p \leq 0.05$)	0.61	0.42	0.69	0.67	0.01	0.02	0.008	0.006
LSD (Ch) ($p \leq 0.05$)	1.05	0.73	1.19	1.17	0.02	0.01	0.01	0.01
D × M ($p \leq 0.05$)	NS	**	**	**	NS	**	NS	*
Ch × D ($p \leq 0.05$)	**	**	**	**	**	**	**	**
Ch × M ($p \leq 0.05$)	NS	NS	*	NS	NS	NS	NS	NS
Ch × D × M ($p \leq 0.05$)	NS	NS	*	**	**	NS	NS	NS

PAL = Phenylalanine ammonia lyase; PH = Phenolics; PO = Peroxidase; PPO = Polyphenol oxidase. Any two means within a column followed by same letters are not significant at $p \leq 0.05$. * = Significant at $p \leq 0.05$; ** = Significant at $p \leq 0.01$; NS = Non-significant

During 2015, interaction between Ch × D × M expressed significant increase in peroxidase activity (*Fig. 2*), whereas, interaction between these three factors was non-significant during the year 2016. Interaction between Ch × D showed significant increase in peroxidase activity during both years, whereas, D × M interaction was non-significant with respect to peroxidase activity but this interaction was significantly impacted during 2016.

Impact of inducers application through towards polyphenol oxidase (PPO) activity (change in absorbance/min/mg of protein)

Polyphenol oxidase activity was significantly ($p \leq 0.05$) increased after the application of Bion and salicylic acid through seedling root dipping and foliar

http://www.aloki.hu ● ISSN 1589 1623 (Print) ● ISSN 1785 0037 (Online)
DOI: http://dx.doi.org/10.15666/aeer/1704_97739784

application during 2015-16. Polyphenol oxidase was maximum at day 10 (1.34) and minimum (0.39) when resistance inducers applied (0 day). Foliar application of resistance inducers increased the activity of Polyphenol oxidase (0.98) over seedling root dipping (0.88). Polyphenol oxidase activity in inoculated plants was higher over plants without inoculation. Maximum polyphenol oxidase activity was assessed in plants on which Bion + *A. porri* (1.09) was applied as compare to plants where salicylic acid + *A. porri* (0.98) was applied. High polyphenol oxidase activity (1.03) was observed where Bion was applied followed by salicylic acid treated plants (0.90). Control plants showed minimum polyphenol oxidase activity (0.74). In 2016, similar but increase in polyphenol oxidase activity was observed. Interactive effect of Ch × D × M exhibited non-significant behavior with respect to polyphenol oxidase activity during both years, whereas, Ch × D showed significant increase in polyphenol oxidase activity during 2015-16. During 2016, D × M interaction significantly increased the polyphenol oxidase activity but this interaction was non-significant during 2015 (*Table 2*).

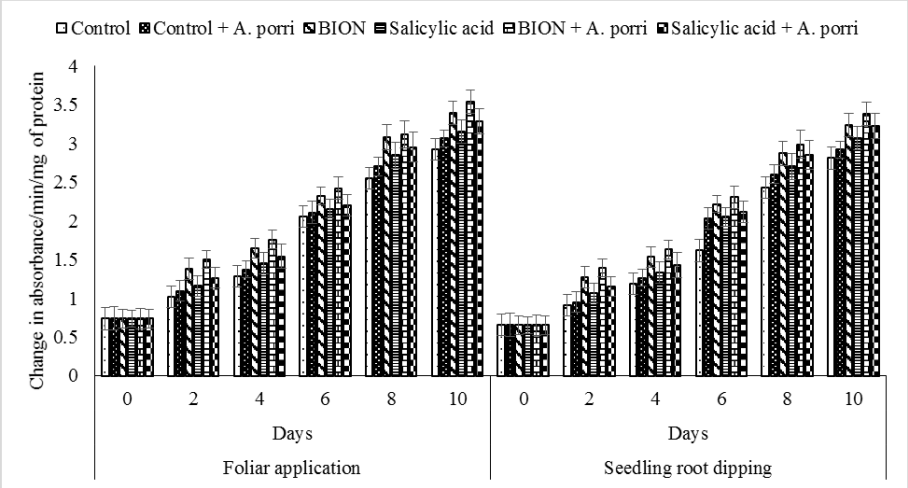

Figure 2. *Interaction between chemicals, days and application method on peroxidase activity as influenced by the various resistance inducers treated through different methods*

Impact of inducers application through towards phenylalanine ammonia lyase (PAL) activity (µmol of cinnamic acid/min/mg of protein)

Phenylalanine ammonia lyase activity was significantly ($p \leq 0.05$) increased after the application of Bion and salicylic acid through seedling root dipping and foliar application during 2015-16. Phenylalanine ammonia lyase was maximum at day 10 (19.24) and minimum (2.42) when resistance inducers applied (0 day). Foliar application of resistance inducers increased the activity of phenylalanine ammonia lyase (12.59) over seedling root dipping (10.60). Phenylalanine ammonia lyase activity in inoculated plants was higher over plants without inoculation. Maximum phenylalanine ammonia lyase activity was found in plants on which Bion + *A. porri* (16.93) was applied as compare to plants where salicylic acid + *A. porri* (13.92) was applied. High Phenylalanine ammonia lyase activity (15.29) was observed where Bion was applied followed by salicylic acid treated plants (12.01). Control plants showed minimum phenylalanine ammonia lyase activity (8.98). In 2016, similar but increase in phenylalanine ammonia lyase activity was observed (*Table 2*). Phenylalanine ammonia

http://www.aloki.hu ● ISSN 1589 1623 (Print) ● ISSN 1785 0037 (Online)
DOI: http://dx.doi.org/10.15666/aeer/1704_97739784

lyase activity was increased significantly in case of interaction between D × M during 2016, whereas, non-significant behavior of mentioned interaction was observed during 2015. Ch × D interaction impacted positively in increasing of phenylalanine ammonia lyase activity during both years, whereas, non-significant behavior was observed in case of Ch × M. Combined interactive impact of all three factors was non-significant during both years (*Table 2*).

Impact of inducers application through towards total phenolics (µm/g of plant tissues)

Phenolic contents were significantly ($p \leq 0.05$) increased after the application of Bion and salicylic acid through seedling root dipping and foliar application during 2015-16. Phenolic contents were maximum at day 10 (55.54) and minimum (8.39) when resistance inducers applied (0 day). Foliar application of resistance inducers increased the phenolic contents (33.78) over seedling root dipping (27.59). Phenolic contents in inoculated plants were higher over plants without inoculation. Maximum phenolic contents were observed in plants on which Bion + *A. porri* (47.14) was applied as compare to plants where salicylic acid + *A. porri* (33.26) was applied. High phenolic contents (40.31) were observed where Bion was applied followed by salicylic acid treated plants (31.42). Control plants showed minimum phenolic contents (26.13). In 2016, similar but increase in phenolic contents were observed (*Table 2*). Interaction of all three factors (Ch × D × M) positively increased the phenolic contents during both years (*Fig. 3*). In the same way D × M and Ch × D showed significant enhancement of phenolic contents in both years, whereas, these contents were significantly impacted during 2015 in case of interaction between Ch × M and non-significant in the year 2016.

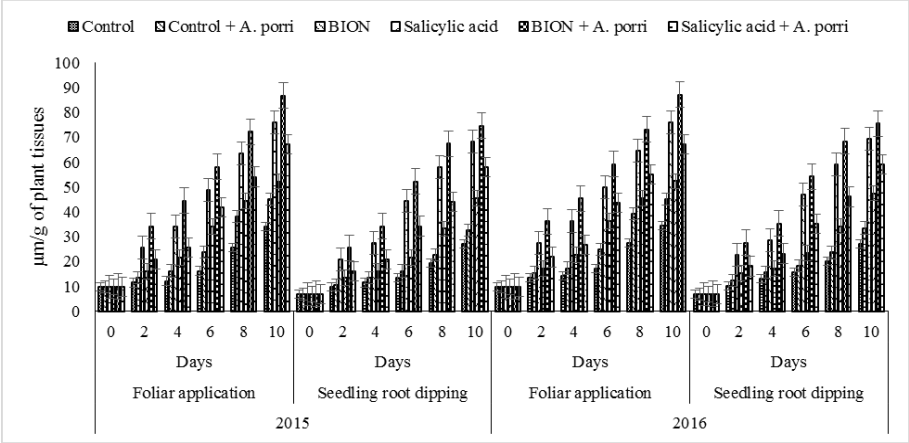

Figure 3. *Interaction between chemicals, days and application method on total phenolics as influenced by the various resistance inducers treated through different methods*

Discussion

Present study showed that Bion® and Salicylic acid application minimized the purple blotch severity in onion plants up to 10 days after plants that were inoculated with *A. porri* (*Table 1*). Several reports have been documented regarding the efficiency of Bion® and Salicylic acid against fungal and bacterial diseases (Ishii et al., 1999; Baysal et al., 2005). These results are consistent with the findings of Abo-Elyousr et al. (2009)

http://www.aloki.hu ● ISSN 1589 1623 (Print) ● ISSN 1785 0037 (Online)
DOI: http://dx.doi.org/10.15666/aeer/1704_97739784

who observed the reduction in severity of stemphylium blight in onion after application of salicylic acid. Abo-Elyousr et al. (2008) observed the same results in case of Bion®. Achuo et al. (2004) found that rustication of *Botrytis cinerea* infection on tomato was achieved after Bion® treatment, and those of the findings of Elmer (2006), who observed the suppression of Fusarium wilt of cyclamen in greenhouse. Mosa (2002) reported that SA at the rate of 1 mM reduce the severity of rice blast.

From the literature it was obvious that presence of Polyphenoloxidase (PPO), Phenylalanine ammonia-lyase (PAL), Peroxidase and total Phenolic contents is necessary because their role in systemic acquired resistance in different plants (He et al., 2002).

Foliar application of Bion® and SA significantly enhanced the PO, PPO, PAL and total Phenolics at all sampling times as compared to seedling root dipping, the highest level at ten days after application (*Table 2, Fig. 2 and Fig. 3*). These results are in line with Abo-Elyousr et al. (2009) who observed the increase in PO activity when onion plants were inoculated with *Stemphylium vesicarium* two days after application of SA. Abo-Elyousr et al. (2008) observed similar results in case of Bion® in onion. Schneider and Ullrich (1994) found increase in PO activity in cucumber and tobacco leaves after treatment with SA. Mcghie et al. (1997) also observed increased in activity of PO in sugarcane cells treated with an elicitor derived from *Pachymetra chaunorhiza*. Significant increase in the activity of PO helped to achieve enhanced resistance against *Clavibacter michiganensis* in tomato plants treated with acibenzolar-S-methyl (ASM) (Baysal et al., 2003). PO activity increased as systemic resistance enhanced in plants against a variety of pathogen (Baysal et al., 2005) which induced the numerous mechanisms of defense in plants like biosynthesis of lignin, cell walls oxidative cross linkage and generation of reactive oxygen species (Bestwick et al., 1998). Enhancement in activity of PO was found in soybean plants sprayed with benzothiadiazole (Nafie and Mazen, 2008). Karthikeyan et al. (2009) reported increased PO activity in black gram exogenously applied SA (100 ppm) and BTH (100 ppm) providing resistance against urdbean leaf crinkle virus. Farouk and Osman (2012) also observed enhanced PO activity in beans species treated with SA and methyl ester of jasmonic acid.

Abo-Elyousr et al. (2009) observed the increase in PPO activity when onion plants were inoculated with *Stemphylium vesicarium* two days after application of SA. Abo-Elyousr et al. (2008) also observed similar results in case of Bion® in onion. Last step of lignin and oxidative phenols was catalyzed by PPO (Baysal et al., 2005). "Polyphenol oxidase (PPOs) catalyzing the oxygen dependent oxidation of phenols to quinines are ubiquitous among angiosperms and assumed to be involved in plant defense against pests and pathogens (Yedidia et al., 2003)".

PAL is the first enzyme of the phenylpropanoid pathway, which synthesizes various phenolic compounds (Tower and Wat, 1979). PAL activity is associated with biosynthesis of various compounds including SA in the defense system of plant (Mauch-Mani and Slusarenko, 1996). These results are in line with Abo-Elyousr et al. (2009) who assessed the enhanced activity of PAL when onion plants were inoculated with *Stemphylium vesicarium* two days after application of SA. Abo-Elyousr et al. (2008) observed similar results in case of Bion® in onion. Chakraborty et al. (1993) observed increased PAL activity in *B. napus* after 12 hrs of *Leptosphaeria maculans* inoculation. Nighat et al. (2001) also observed increased PAL activity in chickpea cultivars inoculated with *Ascochyta rabiei*. Tian et al. (2006) observed that elicitors significantly enhanced the activity of PAL and minimized the incidence of *A. alternata*

http://www.aloki.hu ● ISSN 1589 1623 (Print) ● ISSN 1785 0037 (Online)
DOI: http://dx.doi.org/10.15666/aeer/1704_97739784

in *Pyrus pyrifolia*. Raju et al. (2008) observed increased PAL activity in shoots of resistant cultivar of chickpea (*Cicer arietinum* L.) than susceptible cultivar when treated with SA and Spermine against *Fusarium oxysporum*. Jayalakshmi et al. (2009) reported increased PAL activity in the roots of chickpea inoculated with biocontrol agent, *Trichoderma harzianum*. Rajab et al. (2009) observed increased PAL activity in *Sesamum prostratum* calli challenged with *Fusarium oxysporum*. Abdel-Monaim et al. (2011) observed that soybean seeds treated with Benzothiadiazole + humic acid enhanced the PAL activity providing resistance against Fusarium wilt disease. Mandavia et al. (2012) studied the effect of foliar spray of brassinolide (10 and 15 ppm) and SA (300 and 500 ppm) on groundnut and observed that 500 ppm SA was most effective in induction of PAL activity.

Phenolic contents enhanced in case of Bion + *A. porri*, up to 10 days, applied through foliar application (*Table 2, Figure 2*). Increased activity showed that strong correlation may exist between resistance level and phenolic contents (Hahlbrock and Scheel, 1989). Results of this study consistent with Abo-Elyousr et al. (2009) who observed the increase in total Phenolics when onion plants were inoculated with *Stemphylium vesicarium* two days after application of SA. Abo-Elyousr et al. (2008) observed similar results in case of Bion® in onion. Stadnik and Buchenauer (2000) observed the enhancement of PAL activity and accumulation of cell wall-bound phenolic compounds in BTH treated wheat plants. Anttonen et al. (2003) observed increased level of two flavanols, i.e., quercetin and kaempferol in BTH treated berries under field conditions. Katoch (2005) observed increased o-dihydroxy phenol content in pea plants sprayed with 5 mM SA compared to control plants. Karthikeyan et al. (2009) reported a 2-fold increase in the accumulation of total phenol content in black gram plants treated with SA (100 ppm) and BTH (100 ppm). “By summing up the finding of the research the application of Bion is very helpful in reducing the disease severity in the onion as compared to the SA. However, improvement in the defense related attributes by the modulation of enzymatic activities was noticed in case of Bion + *A. porri* applied through foliar feeding as compared to the seedling root dipping method during both years”.

Conclusion

Results of present study showed that Bion could be non-hazardous towards environment and low cost approach towards mentioned malady controlling programs. Foliar application of Bion + *A. porri* enhanced the resistance through increased biochemical attributes than seedling root dipping against *A. porri* during study period but still further investigation is required under field condition for the endorsement of application strategies of resistance inducers for achieving the productive success in onion crop.

REFERENCES

[1] Abdel-Monaim, M. F., Ismail, M. E., Morsy, K. M. (2011): Induction of systemic resistance in soybean plants against Fusarium wilt disease by seed treatment with benzothiadiazole and humic acid. – Notulae Scientia Biologicae 3: 80-89.

[2] Abo-Elyousr, A. M. K., Hussein, M. A. M., Allam, A. D. A., Hassan, A. H. M. (2008): Enhanced onion resistance against stemphylium leaf blight disease, caused by

http://www.aloki.hu ● ISSN 1589 1623 (Print) ● ISSN 1785 0037 (Online)
DOI: http://dx.doi.org/10.15666/aeer/1704_97739784

Stemphylium vesicarium, by Di-potassium phosphate and Benzothiadiazole treatments. – The Plant Pathology Journal 24: 171-177.

[3] Abo-Elyousr, A. M. K., Hussein, M. A. M., Allam, A. D. A., Hassan, A. H. M. (2009): Salicylic acid induced systemic resistance on onion plants against *Stemphylium vesicarium*. – Archives of Phytopathology and Plant Protection 42: 1042-1050.

[4] Achuo, E. A., Audenaert, K., Meziane, H., Hofte, M. (2004): The salicylic acid-dependent defence pathway is effective against different pathogens in tomato and tobacco. – Plant Pathology 53: 65-72.

[5] Alam, S. S., Ahmad, M., Alam, S., Usman, A., Ahmad, M. I., Naveedullah, M. (2007): Variation in garlic varieties for reaction to natural infection of *Puccinia porri wint* and *Alternaria porri clif* at swabi, NWFP. – Sarhad Journal of Agriculture 23(1).

[6] Aloch, R. A., Baloch, S. U., Baloch, S. K., Baloch, H. N., Badini, S. A., Bashir, W., Baloch, A. B., Baloch, J. (2014): Economic analysis of onion (*Allium cepa* L.) production and marketing in District Awaran, Balochistan. – Journal of Economics and Sustainable Development 5: 192.

[7] Anttonen, M., Hukkanen, A., Tillikkala, K., Karjalainen, R., Hicklenton, P., Mass, J. (2003): Benzothiadiazole induces defense response in berry crops. – Acta Horticulturae 626: 177-82.

[8] Baysal, O., Soylu, E. M., Soylu, S. (2003): Induction of defence-related enzymes and resistance by the plant activator acibenzolar-S-methyl in tomato seedlings against bacterial canker caused by *Clavibacter michiganensis* sp. *michiganensis*. – Plant Pathology 52: 747-53.

[9] Baysal, O., Ziya, Y. G., Ornek, H., Ahmet, D. (2005): Induction of oxidants in tomato leaves treated with D1-B-Amino butyric acid (BABA) and infected with *Clivabacter michiganensis* spp. *michiganensis*. – European Journal of Plant Pathology 112: 361-369.

[10] Bestwick, C. S., Brown, I. R., Mansfield, J. W. (1998): Localized changes in peroxidase activity accompany hydrogen peroxide generation during the development of a non host hypersensitive reaction in lettuce. – Plant Physiology 118: 1067-1078.

[11] Bradford, M. (1976): A rapid and sensitive methods for the quantization of microgram quantities of protein utilizing the principle of protein dye binding. – Analytical Biochemistry 72: 248-250.

[12] Chakraborty, U., Chakraborty, B. N., Kapoor, M. (1993): Changes in the levels of peroxidase and phenylalanine ammonia lyase in *Brassica napus* cultivars showing variable resistance to *Leptoshaeria maculans*. – Folia Microbiologica 38: 491-96.

[13] Cramer, C. S. (2000): Breeding and genetics of Fusarium basal rot resistance in onion. – Euphytica 115: 159-66.

[14] Elmer, W. H. (2006): Effects of acibenzolar-S-methyl on the suppression of Fusarium wilt of cyclamen. – Crop Protection 25: 671-676.

[15] FAO (2012): Food and Agricultural Organization of United Nations. – Rome, Italy.

[16] Farouk, S., Osman, M. A. (2012): Alleviation of oxidative stress induced by spider mite invasion through application of elicitors in bean plants. – Egyptian Journal of Biology 14: 1-13.

[17] Gauillard, F., Richard-Forget, F., Nicolas, J. (1993): New spec-trophotometric assay for polyphenol oxidase activity. – Analytical Biochemistry 215: 59-65.

[18] Govt. of Pakistan (2014-15): Economic survey of Pakistan ministry of food, agriculture and livestock. – Federal bureau of statistics.

[19] Griffiths, G., Trueman, L., Crowther, T., Thomas, B., Smith, B. (2002): Onions a global benefit to health. – Phytotherapy Research 16: 603-15.

[20] Hahlbrock, K., Scheel, D. (1989): Physiology and molecular biology of phenyl propanoid metabolism. – Annual Review of Plant Physiology and Molecular Biology 40: 347-69.

[21] Hayes, J. D., Johnston, T. D. (1971): Breeding for disease resistance. – In: Western, J. H. 62-68.

http://www.aloki.hu ● ISSN 1589 1623 (Print) ● ISSN 1785 0037 (Online)
DOI: http://dx.doi.org/10.15666/aeer/1704_97739784

[22] He, C. Y., Hsiang, T., Wolyn, D. J. (2002): Induction of systemic disease resistance and pathogen defence responses in Asparagus officinalis with nonpathogenic strains of *Fusarium oxysporum*. – Plant Pathology 51: 225-230.
[23] Ishii, H., Tomita, Y., Horio, T., Narusaka, Y., Nakazawa, Y., Nishimura, K., Iwamoto, S. (1999): Induced resistance of acibenzolar-S-methyl (CGA 245704) to cucumber and Japanese peardiseases. – European Journal of Plant Pathology 105: 77-85.
[24] Jayalakshmi, S. K., Raju, S., Usha, R. S., Benagi, V., Sreeramulu, K. (2009): *Trichoderma harzianum* L1 as a potential source for lytic enzymes and elicitor of defense responses in chickpea (*Cicer arietinum* L.) against wilt disease caused by *Fusarium oxysporum* f. sp. *ciceri*. – Australian Journal of Crop Science 3: 44-52.
[25] Karthikeyan, G., Doraisamy, S., Rabindran, R. (2009): Induction of systemic resistance in black gram (*Vigna mungo*) against urdbean leaf crinkle virus by chemicals. – Archives of Phytopathology and Plant Protection 42: 1-15.
[26] Katoch, R. (2005): Effect of elicitors and *E. polygoni* inoculation on the activity of phenol metabolizing enzymes in garden pea (*Pisum sativum* L.). – Indian Journal of Agricultural Biochemistry 18: 87-91.
[27] Kunz, W., Schurter, R., Maetzke, T. (1997): The chemistry of benzothiadiazole plant activators. – Pesticide Science 50: 275-82.
[28] Leadbeater, J. D., Oostendrop, M., Ruess, W. (1997): Optimiziting the use of inducers of host resistance. Optimizing cereal inputs: its scientific basis. Part-2. Crop protection and Systems. – Aspects of Applied Biology 50: 171-278.
[29] Malick, C. P., Singh, M. B. (1980): Phenolics. – In: Plant enzymology and histoenzymology. Kalyani Publishers, New Delhi.
[30] Mandavia, M. K., Raval, L., Mandavia, C., Karkar, C. (2012): Effect of brassinolide and salicylic acid on biochemical parameters and yield of groundnut. – Indian Journal of Agricultural Biochemistry 25: 20-24.
[31] Mauch-Mani, B., Slusarenko, A. J. (1996): Production of salicylic acid precursors is a major function of phenylalanine ammonia-lyase in the resistance of Arabidopsis to *Peronospora parasitica*. – The Plant Cell 8: 203-12.
[32] Mcghie, T. K., Mase, N. P., Maclean, D., Croft, B. J., Smith, G. R. (1997): Biochemical responses of suspension-cultured sugarcane cells to an elicitor derived from the root pathogen *Pachymetra chaunorhiza*. – Australian Journal of Plant Physiology 24: 143-49.
[33] Mosa, A. A. (2002): Management of sugar beet powdery mildew by foliar spraying of potassium phosphate salts. Arab Univ. – Journal of Agricultural Research 10: 1043-1057.
[34] Nafie, E., Mazen, M. M. (2008): Chemical-induced resistance against brown stem rot in soybean: The effect of benzothiadiazole. – Journal of Applied Science Research 4: 2046-2064.
[35] Nagarathna, K. C., Shetty, S. A., Shetty, H. S. (1993): Phenylalanine ammonia lyase activity in pearl millet seedlings and its relation to downy mildew disease resistance. – Journal of Experimental Botany 265: 1291-1296.
[36] Nicholson, R. L., Hammerschmidt, R. (1992): Phenolic compounds and their role in disease resistance. – Annual Review of Phytopathology 30: 369-389.
[37] Nighat, S., Jamil, F. F., Riffat, P. (2001): Accumulation of phytoalexins and PAL in chickpea after inoculation with *Ascochyta rabiei* and their role in defense mechanism. – Pakistan Journal of Botany 33: 373-382.
[38] Oostendorp, M., Kunz, W., Dietrich, B., Staub, T. (2001): Induced disease resistance in plants by chemicals. – European Journal of Plant Pathology 107: 19-28.
[39] Rajab, R., Rajan, S. S., Satheesh, L. S., Harish, S. R., Sunukumar, S. S., Sandeep, B. S., Mohan, T. C. K., Murugan, K. (2009): Hypersensitive response of *Sesamum prostratum* Retz. elicited by *Fusarium oxysporum* f. *sesame* (Schelt) Jacz Butler. – Indian Journal of Experimental Biology 47: 834-38.
[40] Raju, S., Jayalakshmi, S. K., Sreeramulu, K. (2008): Comparative study on the induction of defense related enzymes in two different cultivars of chickpea (*Cicer arietinum* L.)

http://www.aloki.hu ● ISSN 1589 1623 (Print) ● ISSN 1785 0037 (Online)
DOI: http://dx.doi.org/10.15666/aeer/1704_97739784

genotypes by salicylic acid, spermine and *Fusarium oxysporum* f. sp. *ciceri*. – Australian Journal of Crop Science 2: 121-40.

[41] Schneider, S., Ullrich, W. R. (1994): Differential induction of resistance and enhanced enzyme activities in cucumber and tobacco caused by treatment with various abiotic and biotic inducers. – Physiology and Molecular Plant Pathology 45: 291-304.

[42] Schonbeck, F., Dehne, H. W., Beicht, W. (1980): Activation of unspecific resistance mechanisms in plants. – Journal of Plant Disease Protection 87: 654-666.

[43] Sharma, S. R. (1986): Effect of fungicidal on purple blotch and bulb yield of onion. – Indian Phytopathology 39: 78-82.

[44] Sonnemann, I., Finkhaeuser, K., Wolters, V. (2002): Does induced resistance in plants effects the below ground community? – Applied Soil Ecology 21: 179-185.

[45] Stadnik, M. J., Buchenauer, H. (2000): Inhibition of phenylalanine ammonia-lyase suppresses the resistance induced by benzothiadiazole in wheat to *Blumeria graminis* f. sp. *tritici*. – Physiology and Molecular Plant Pathology 57: 25-34.

[46] Thangavelu, R., Palaniswami, A., Doraiswamy, S., Velazhahan, R. (2003): The effect of *Pseudomonas fluorescens* and *Fusarium oxysporum* f. sp. *cubense* on induction of defense enzymes and phenolics in banana. – Biologia Plantarum 46: 107-112.

[47] Tian, S., Yakun, W., Qin, G., Xu, Y. (2006): Induction of defense responses against Alternaria rot by different elicitors in harvested pear fruit. – Applied Microbiology and Biotechnology 70: 729-734.

[48] Tower, G. N., Wat, C. K. (1979): Phenylpropanoid metabolism. – Planta Medica 37: 97-114.

[49] Urbanek, H., Kuzniak-Gebarowska, E., Herka, H. (1991): Elicitation of defence responses in bean leaves by *Botrytis cinerea polygalacturonase*. – Acta Physiologiae Plantarum 13: 43-50.

[50] Van Loon, L. C. (1983): The induction of pathogenesis related protein by pathogens and specific chemicals. – Netherlands Journal of Plant Pathology 89: 265-273.

[51] White, R. F. (1979): Acetyl salicylic acid (aspirin) induces resistance to tobacco mosaic virus in tobacco. – Virology 99: 410-422.

[52] Yadav, P. M., Rakholiya, K. B., Pawar, D. M. (2013): Evaluation of bioagents for management of the onion purple blotch and bulb yield loss assessment under field conditions. – An international Journal of Life Sciences 8: 1295-1298.

[53] Yedidia, I., Shoresh, M., Kerem, Z., Benhamou, N., Kapulnik, Y., Chet, I. (2003): Concomitant induction of systemic resistance to *Pseudomonas syringae* pv. *lachrymans* in cucumber by *Trichoderma asperellum* (T-203) and the accumulation of phytoalexins. – Applied and Environmental Microbiology 69: 7343-7353.

http://www.aloki.hu ● ISSN 1589 1623 (Print) ● ISSN 1785 0037 (Online)
DOI: http://dx.doi.org/10.15666/aeer/1704_97739784

SSR ANALYSIS OF SOME SYNONYMS AND HOMONYMS OF GRAPE CULTIVARS (*VITIS VINIFERA* L.) GROWING IN SOUTHEASTERN TURKEY

KARATAŞ, H.

Dicle University, Agriculture Faculty, Horticulture Department, 21280 Diyarbakır, Turkey (e-mail: hkaratas@dicle.edu.tr; phone: +90-412-248-8509)

(Received 26th Mar 2019; accepted 13th Jun 2019)

Abstract. The goal of this study was to analyze the genetic diversity of grape cultivars growing in Diyarbakır and Şanlıurfa by performing SSR molecular identification of the synonymous and homonymous genotypes of 21 cultivars growing in these two regions to investigate the homonyms (*Vitis vinifera* L. cvs.). Microsatellite analysis was performed using a minimal standard SSR marker set involving 7 highly polymorphic loci (VVS2, VVMD5, VVMD7, VVMD27, VrZAG47, VrZAG62, and VrZAG62). Mean number of alleles per locus was 7.14 (range, 7-9), with the highest number of alleles detected in VVS2 and the lowest in VVMD7, VVMD27. The expected and observed heterozygosity were 0.70 and 0.69, respectively. The dendrogram indicated 3 distinct groups, each of which involved several subgroups. A total of 5 synonyms and 10 homonyms were identified for the 21 genotypes.
Keywords: *Vitis vinifera L., grape cultivars, DNA extraction, synonym, homonym, dendrogram*

Introduction

Diyarbakır and Şanlıurfa provinces are located in Southeastern Turkey where viticulture is widely performed. Grapevine is a well-known perennial garden plant well adapted to these regions. Some preliminary surveys and genomic studies have revealed more than 70 grape cultivars growing in these two regions. Moreover, these two regions not only are well-known for viticulture but also are among the regions with the highest grape production in Turkey. Nevertheless, there is little or no information regarding the exact cultivar-based vineyard capacity of these regions.

The use of different regional names for grape cultivars results in major problems and confusion regarding the correspondence between these names and those used in studies and those used in each phase of production. However, these problems and confusion can be eliminated by the administration of molecular markers of polymorphism.

The aim of this study was to analyze the genetic diversity of grape cultivars growing in Diyarbakır and Şanlıurfa by performing molecular identification of the genotypes of cultivars growing in these two regions and to investigate the homonyms used for the 21 distinct cultivars (*Vitis vinifera* L. cvs.) previously identified in these regions using the SSR technique. Simple Sequence Repeats (SSR) is a well-known molecular marker which has been commonly used for the identification of cultivars and the determination of synonyms and homonyms of grape genotypes (Thomas and Scott, 1993; Bowers et al., 1996; Meredith et al., 1996; Sefc et al., 1997, 1999; Meredith, 2001; Riaz et al., 2002; Fatahi et al., 2003; Grando et al., 2003; Hvarleva et al., 2004; Riaz et al., 2004; Adam-Blondon et al., 2004; Zulini et al., 2005; Costantini et al., 2005; Di Vecchi Staraz et al., 2006, 2009; Şelli et al., 2007; Bodor et al., 2010; Cipriani et al., 2010; Ocete et al., 2011; De Andres et al., 2011; Garcia-Munoz et al., 2012; Emanuelli et al., 2013; Alifragkis et al., 2015; Maletic et al., 2015; Biagini et al., 2016; Li et al., 2017; Zequim Maia et al., 2018; Van Heerden et al., 2018).

http://www.aloki.hu ● ISSN 1589 1623 (Print) ● ISSN 1785 0037 (Online)
DOI: http://dx.doi.org/10.15666/aeer/1704_97859793

Materials

Molecular analysis was conducted on 21 grapevine genotypes including 9 cultivars collected from Diyarbakir Province and its districts (D), 8 cultivars collected from Şanlıurfa Province and its districts (Ş) and 4 genotype samples of the cultivars that had been previously transplanted to the Tekirdağ National Germplasm Repository Vineyard (TD, TŞ) (*Figure 1*).

Figure 1. *Provinces where the grapevine genotypes collected from Turkey*

One-year-old seedlings with 3-5 buds were collected from each genotype and were planted in polyethylene tubes filled with a 2:2:1 mixture of perlite, turf, and powder and then germinated in greenhouse conditions until the buds were rooted. DNA extraction was performed with the fresh leaves of these buds, as described by (Lodhi et al., 1994).

Methods

In order to allow a comparison among internationally grown homonymous varieties, a minimal standard SSR marker set was employed (This et al., 2004), which includes 7 highly polymorphic loci as follows: VVS2, VVMD5, VVMD7, VVMD27, VrZAG47, VrZAG62, VrZAG79 (*Table 1*).

DNA amplification was carried out using GeneAmp PCR System 9700 with EU-Applied Biossystems, followed by PCR optimization for each cultivar. PCR amplification was achieved using a reaction volume of 20 µl containing 5 µl of DNA (10 ng/µl), 2 µl of 10X Buffer (Qiagen), 1.2 µl of Mg Cl2 (Qiagen), 0.6 µl of dNTP (10mM), 1 µl of primer (25 µM) 1,1 µl of primer 2 (25 µM), 0.2 µl of GoldTaq (0.5 U), and 9 of µl distilled water. Touchdown PCR was carried out using the following cycling conditions: 95°C for 10 min, 94°C for 30 s, and 52°C for VVS2, VVMD5, and VVMD7, 58°C for VVMD27, 55°C for VrZAG47, and 62°C for VrZAG62 and VrZAG79 for 30 s each, based on the rate of primer annealing, with a decrease of 0.2°C/cycle. After completing 25 cycles, additional 15 cycles were administered with a reduction of 5°C from the primer annealing temperature, finally followed by holding at 72°C for 40 min.

To understand whether amplification occurs for each fragment in each locus, at least 10 fragments typifying each locus were placed on agarose gel. After viewing the amplification, the amplified fragments were subjected to sequencing using ABI Prism

http://www.aloki.hu ● ISSN 1589 1623 (Print) ● ISSN 1785 0037 (Online)
DOI: http://dx.doi.org/10.15666/aeer/1704_97859793

3730 automated DNA sequencer with GeneScan™ 500 LIZ™ dye Size Standard. The outcomes were analyzed, visualized, and processed using GeneMapper v 3.7 software. The number of alleles in each locus was calculated based on the peak levels.

Table 1. *Primers used for the study*

Primer	5´-3´	Base sequences of primers		Reference
VVS2	F	VIC-CAG CCC GTA AAT GTA TCC ATC	Vic	Thomas and Scott (1993)
	R	AAA TTC AAA ATT CTA ATT CAA CTG G		
VVMD5	F	6-FAM-CTA GAG CTA CGC CAA TCC AA	Fam	Bowers et al. (1996, 1999)
	R	TAT ACC AAA AAT CAT ATT CCT AAA		
VVMD7	F	NED-AGA GTT GCG GAG AAC AGG AT	Ned	
	R	CGA ACC TTC ACA CGC TTG AT		
VVMD27	F	NED-GTA CCA GAT CTG AAT ACA TCC GTA AGT	Ned	
	R	ACG GGT ATA GAG CAA ACG GTG T		
VrZAG47	F	VIC-GGTCTGAATACATCCGTAAGTATAT	Vic	Sefc et al. (1999)
	R	ACGGTGTGCTCTCATTGTCATTGAC		
VrZAG62	F	6-FAM-GGT GAA ATG GGC ACC GAA CAC ACG C	Fam	
	R	CCA TGT CTC TCC TCA GCT TCT CAG C		
VrZAG79	F	6-FAM-AGA TTG TGG AGG AGG GAA CAA ACC G	Fam	
	R	TGC CCC CAT TTT CAA ACT CCC TTC C		

Genetic similarity between the 21 genotype samples characterized by 7 loci was analyzing using the Microsat software (Minch et al., 1995) and the genetic parameters (number of alleles per locus, allele frequency, expected heterozygosity, observed heterozygosity, parentage, null allele frequency, and probability of identity) were analyzed using the IDENTITY 1.0 software (Wagner and Sefc, 1999). The dendrograms were formed and viewed using the NTSys software (version 2.02g, Exeter Software, Setauket, NY). Clustering analysis was carried out using the UPGMA method (Unweighted Pair-Group Method using Arithmetic means).

Result and Discussion

Data regarding the molecular analysis of the 21 genotype samples characterized by 7 loci were presented in *Table 2* in the form of peak levels and the number of alleles and basepair per locus.

The SSR analysis indicated a total of 50 alleles for the 21 genotype samples obtained from Diyarbakır, Şanlıurfa, and the Tekirdağ National Germplasm Repository Vineyard. *Table 3* presents the number of alleles and the expected and observed heterozygosity for these genotypes. Mean number of alleles per locus was 7.14, which was reported to be 9.6, by Borrego et al. (2001) who analyzed 406 accessions characterized by 8 microsatellite markers, 11.4 by Fatahi et al. (2003) who analyzed 62 genotypes characterized by 9 microsatellite markers, 8.1 by Hvarleva et al. (2004) who analyzed 74 accessions characterized by 9 microsatellite markers, 9.1 by Akkak et al. (2005) who analyzed 60 local cultivars characterized by 12 microsatellite markers, 11.9 by Vouillamoz et al. (2006), who analyzed 116 accessions characterized by 12 microsatellite markers. Of these studies, the ones that identified higher mean numbers of alleles compared to that of our study were carried out with higher numbers of genotypes that also showed greater variation compared to those in our study. However, the studies conducted by Crespan and Milani (2001), Dangl et al. (2001), Hvarleva et al. (2004) and Costantini

http://www.aloki.hu ● ISSN 1589 1623 (Print) ● ISSN 1785 0037 (Online)
DOI: http://dx.doi.org/10.15666/aeer/1704_97859793

et al. (2005) were carried out with lower numbers of genotypes and therefore detected lower mean numbers of alleles compared to that of our study (*Table 3*). On the contrary, although Fatahi et al. (2003) and Akkak et al. (2005) analyzed a smaller variety of genotype samples, the two studies identified greater mean numbers of alleles compared to that of our study.

Table 2. *Allele sizes of the genotypes characterized by 7 microsatellite loci*

No	Genotype	VVS2		VVMD5		VVMD7		VVMD27		VrZAG47		VrZAG62		VrZAG79	
1	*D* Abderi	131	133	230	232	240	244	181	181	159	159	186	190	246	246
2	*TD*Abderi	131	133	230	232	240	244	181	181	159	159	186	190	246	246
3	*Ş* Avderi	139	149	228	234	244	244	191	191	169	169	190	202	254	254
4	*D* Hatunparmağı beyaz	139	143	232	242	236	244	191	191	169	169	186	202	244	248
5	*D* Hatunparmağı siyah	121	121	232	242	236	252	185	191	163	169	202	202	244	246
6	*Ş* Hatunparmağı siyah	131	149	230	232	230	244	191	191	169	169	194	202	244	254
7	*Ş* Hatunparmağı beyaz	131	133	222	230	244	246	191	191	169	169	190	202	240	248
8	*D* Kızılbanki	131	141	232	236	240	246	181	191	159	169	188	188	244	246
9	*Ş* Kızılbanki	131	141	222	232	240	246	181	191	159	169	188	188	244	254
10	*D* Şire mazrumi	131	131	232	232	244	246	191	191	155	169	198	202	244	246
11	*D* Şire şirelik	131	131	232	232	244	246	177	191	155	169	198	202	244	244
12	*Ş* Şire	133	139	222	234	244	246	177	191	155	169	194	198	246	256
13	*D* Tahannebi	131	131	232	232	244	246	177	191	155	169	198	202	244	246
14	*TD* Tahannebi	131	155	230	234	244	244	191	191	169	169	190	202	254	254
15	*Ş* Tahannebi	131	155	230	234	244	244	191	191	169	169	190	202	254	254
16	*TD* Siyahüzüm	133	155	222	232	244	246	181	191	159	169	190	198	244	246
17	*Ş* Siyahüzüm	133	139	222	234	244	246	191	191	155	169	194	198	246	246
18	*D* Şarabi	149	155	232	234	244	246	183	191	161	169	190	198	248	256
19	*Ş* Şarabi	141	149	230	242	230	246	175	191	153	169	202	202	240	244
20	*D* Zerik	133	153	230	232	244	244	191	191	157	169	190	198	248	254
21	*TŞ* Zerik	131	143	228	228	244	246	191	191	155	155	190	202	246	248

D: Diyarbakır Province; *T:* Tekirdag Province (National Germplasm Repository Vineyard); *Ş:* Sanlıurfa Province; *TD:* Tekirdag National Germplasm Repository (studied cultivars from Diyarbakır); *TŞ:* National Germplasm Repository (studied cultivars from Sanliurfa)

Microsatellite markers used in our study, the most polymorphic marker was VVS2 (9 alleles) and the lowest were VVMD7 and VVMD27 (7 alleles) (*Table 3*). Similarly, previous studies also indicated that VVS2 the most polymorphic marker, followed by VVMD5 and VVMD27 (9 alleles), and VVMD7, VrZAG62, and VrZAG79 (7 alleles) (López et al., 1999; Borrego et al., 2001; Lefort and Roubelakis-Angelakis, 2001; Fatahi et al., 2003; Martín et al., 2003; Núñez et al., 2004). In our study, the expected heterozygosity per locus ranged from 0.47 and 0.80, with lowest expected heterozygosity detected in VVMD27 and the highest in VVS2. However, no significant difference was found between these two values, implicating that the cultivars analyzed in our study were highly heterozygous. In contrast, the observed heterozygosity detected in our study was lower than those reported in the literature (Sefc et al., 2000; Dangl et al., 2001; Fatahi et al., 2003; Aradhya et al., 2003; Costantini et al., 2005; Vouillamoz et al., 2006).

Clustering analysis was performed based on the proportion of shared alleles between the cultivars collected from Diyarbakır and Şanlıurfa. The dendrogram indicated 3

http://www.aloki.hu ● ISSN 1589 1623 (Print) ● ISSN 1785 0037 (Online)
DOI: http://dx.doi.org/10.15666/aeer/1704_97859793

distinct groups, each of which involved several subgroups. The dendrogram demonstrated that the genotypes of the cultivars obtained from these two regions were not completely dissimilar but showed close relationship with each other (*Figure 2*).

Table 3. *Number of alleles per locus, He, Ho, and PI*

Marker	Number of alleles	He	Ho	PI
VVS2	9	0.80	0.82	0.78
VVMD5	7	0.78	0.82	0.75
VVMD7	6	0.64	0.82	0.59
VVMD27	6	0.47	0.41	0.44
VrZAG47	8	0.65	0.55	0.61
VrZAG62	7	0.79	0.77	0.77
VrZAG79	7	0.79	0.64	0.76
Mean	**7.14**	**0.70**	**0.69**	**0.67**

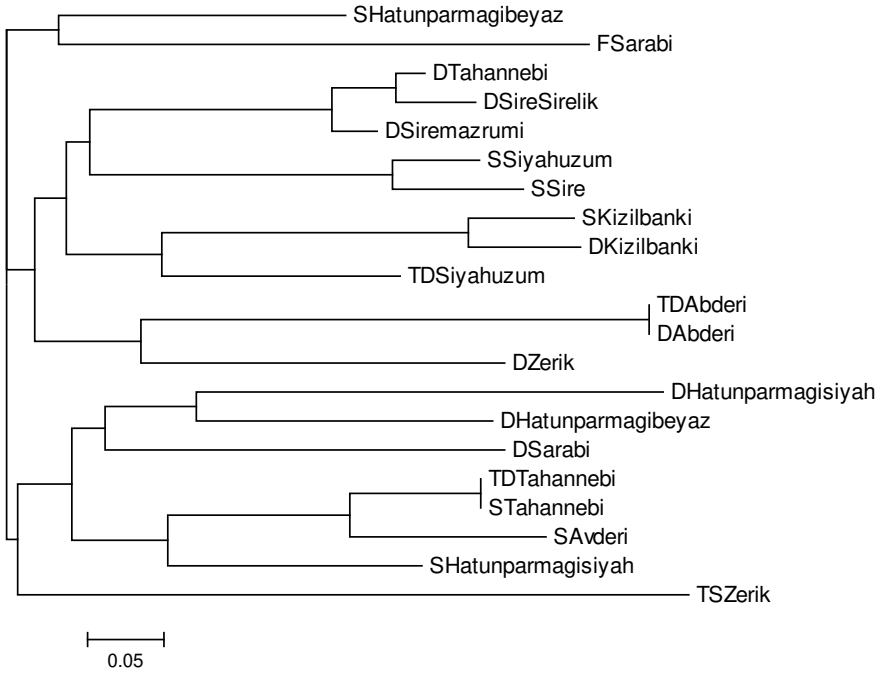

Figure 2. *Dendogram of 21 grape cultivars (Diyarbakır-Şanlıurfa) based on similarity index from SSR data*

The dendrogram indicated that only 6 out of the 17 cultivars sampled from Diyarbakır and Şanlıurfa were classified as homonyms or as cultivars with highly similar names (i.e. clustered in the same group on the dendrogram). However, 2 out of the 4 cultivars sampled from the Tekirdağ National Germplasm Repository Vineyard were found to have dissimilar names (i.e. not clustered in the same group on the dendrogram). The dendrogram also revealed that some of the cultivars with the same name were genetically not identical, which suggests that some of the grape cultivars growing in these regions might develop different genetic traits over time due to the different ecological conditions they grow in. Accordingly, the overwhelming presence of homonyms used for grape

http://www.aloki.hu ● ISSN 1589 1623 (Print) ● ISSN 1785 0037 (Online)
DOI: http://dx.doi.org/10.15666/aeer/1704_97859793

genotypes is a major problem for the viticulture in Turkey. The extent of this problem is well elucidated in the present study.

The molecular analysis indicated that 5 synonyms and 10 homonyms were identified for the 21 genotypes analyzed with 7 microsatellite markers based on the proportion of shared alleles among the genotypes (*Table 3*). Nevertheless, no clear information was available as to which homonym represented the real name of each genotype.

Table 4. *Synonyms and homonyms identified for the genotype samples obtained from Diyarbakır and Şanlıurfa*

Synonyms
D Tahannebi, *D* Şire şirelik
Ş Siyahüzüm, *Ş* Şire
D Hatunparmağı siyah, *D* Hatunparmağı beyaz
Homonyms
Ş Hatunparmağı beyaz, *Ş* Hatunparmağı beyaz (*D* Hatunparmağı siyah-*D* Hatunparmağı beyaz)
D Şire mazrumi, *Ş* Şire, *D* Şire şirelik
Ş Avderi (*D* Abderi- *TD* Abderi)
D Tahannebi (*TD* Tahannebi-*Ş* Tahannebi)
D Şarabi, *Ş* Şarabi
TD Siyahüzüm, *Ş* Siyahüzüm
D Zerik, *TŞ* Zerik

The microsatellite analysis revealed a total of 13 distinct cultivars for the 21 genotype samples. This finding implicates that the gene sources of the cultivars growing in these two regions should be protected. Moreover, it was also revealed that the 7 loci used in our study were highly appropriate for genetic analysis of grape cultivars and the identification of synonyms and homonyms.

Conclusion

A high level of allelic polymorphism was found between the cultivars that were expected to have dissimilar names and between the cultivars that were expected to have similar names. In our study it was observed that the level of detected polymorphism is highly can be influenced by the source materials. This differentiation of nomenclature could be attributed to several conditions. First, the cultivars with the same names might have been initially genetically identical but later grown in different ecological conditions for long years and thus might have become genetically dissimilar and this differentiation might have been further intensified through the use of different names for the cultivars transplanted to the Tekirdağ National Germplasm Repository Vineyard. Secondly, this differentiation could be associated with the production of these cultivars for constant vegetative propagation and the somatic mutations induced by environmental factors. Turkey is home to numerous grape cultivars with the same or different names as a result of a long-standing viticulture tradition in Anatolia dating back to 7,000-8,000 years ago. To protect this genetic potential, devising a rational nomenclature and identifying the relationships among these cultivars by using DNA-based markers is highly essential.

http://www.aloki.hu ● ISSN 1589 1623 (Print) ● ISSN 1785 0037 (Online)
DOI: http://dx.doi.org/10.15666/aeer/1704_97859793

REFERENCES

[1] Adam-Blondon, A. F., Roux, C., Claux, D., Butterlin, G., Merdinoglu, D., This, P. (2004): Mapping 245 SSR markers on the Vitis vinifera genome: a tool for grape genetics. – Theoretical and Applied Genetics 109(5): 1017-1027.

[2] Akkak, A., Boccacci, P., Lacombe, T., Botta, R. (2005): Relationships and genetic diversity of grapevine (Vitis vinifera L.) grown in Algeria and in Mediterranean basin. – Electronic Forum on Biotechnology in Food and Agriculture, Conference 13. International Workshop, 5- March 2005, Turin, Italy. (Poster).

[3] Alifragkis, A., Cunha. J., Pereira. J., Fevereiro, P., Eiras Dias, J. (2015): Identity, synonymies and homonymies of minor grapevine cultivars maintained in the Portuguese ampelographic collection. – Ciência Téc Vitic 30: 43-52.

[4] Aradhya, M. K., Dangl, G. S., Prins, B. H., Boursiquot, J. M., Walker, M. A., Meredith, C. P., Simon, C. J. (2003): Genetic structure and differentiation in cultivated grape, Vitis vinifera L. – Genet. Res. Camb. 81: 179-192.

[5] Biagini, B., Imazio, S., Scienza, A., Failla, O., De Lorenzis, G. (2016): Renewal of wild grapevine (Vitis vinifera L. subsp. sylvestris (Gmelin) Hegi) populations through sexual pathway: Some Italian case studies. – Flora 219: 85-93.

[6] Bodor, P., Höhn, M., Pedryc, A., Deák, T., Dücső, I., Uzun, I., Cseke, K., Böhm, É. I., Bisztray, G. D. (2010): Conservation value of the native Hungarian wild grape (Vitis silvestris Gmel.) evaluated by microsatellite markers. – Vitis 49(1): 23-27.

[7] Borrego, J., Rodriguez, I., Andrés, M. T., Martin, J., Chavez, J., Cabello, F., Ibáñez, J. (2001): Characterization of the most important Spanish grape varieties through isoenzyme and microsatellite analysis. – Proc. Int. Symp. on Molecular Markers. Acta Hort. 546: 371-375.

[8] Bowers, J. E., Dangl, G. S., Vignani, R., Meredith, C. P. (1996): Isolation and characterization of new polymorphic simple sequence repeat loci in grape (Vitis vinifera L.). – Genome 39: 628-633.

[9] Bowers, J. E., Dangl, G. S., Meredith, C. P. (1999): Development and characterization of additional microsatellite DNA markers for grape. – Am. J. Enol. Vitic. 50(3): 243-246.

[10] Cipriani, G., Spadotto, A., Jurman, I., Di Gaspero, G., Crespan, M., Meneghetti, S., Frare, E., Vignani, R., Cresti, M., Morgante, M., Pezzotti, M., Pe, E., Policriti, A., Testolin, R. (2010): The SSR-based molecular profile of 1005 grapevine (Vitis vinifera L.) accessions uncovers new synonymy and parentages, and reveals a large admixture amongst varieties of different geographic origin. – Theor Appl Genet 121: 1569-1585.

[11] Costantini, L., Monaco, A., Vouillamoz, J. F., Forlani, M., Grando, M. S. (2005): Genetic relationships among local Vitis vinifera cultivars from Campania (Italy). – Vitis 44(1): 25-34.

[12] Crespan, M., Milani, N. (2001): The Muscats: A molecular analysis of synonyms, homonyms and genetic relationship within a large family of grapevine cultivars. – Vitis 40(1): 23-30.

[13] Dangl, G. S., Mendum, M. L., Prins, B. H., Walker, A. M., Meredith, C. P., Simon, C. J. (2001): Simple sequence repeat analysis of a clonally propagated species: A tool for managing a grape germplasm collection. – Genome 44: 432-438.

[14] De Andrés, M. T., Benito, A., Pérez-Rivera, G. (2012): Genetic diversity of wild grapevine populations in Spain and their genetic relationships with cultivated grapevines. – Molecular Ecology 21: 800-816.

[15] Di-Vecchi Staraz, M., Laucou, V., Bruno, G., Lacombe, T., Gerber, S., Bourse,T., Boselli, M., This, P. (2009): Low Level of Polen-Mediated Gene Flow from Cultivated to Wild Grapevine: Consequences fort he Evolution of the Endangered Subspecies Vitis vinifera L. subsp. silvestris. – Journal of Heredity 100(1): 66-75.

[16] Emanuelli, F., Lorenzi, S., Grzeskowiak, L., Catalano, V., Stefanini, M., Troggio, M., Myles, S., Martinez-Zapater, J. M., Zyprian, E., Moreira, F. M., Grando, M. S. (2013):

http://www.aloki.hu ● ISSN 1589 1623 (Print) ● ISSN 1785 0037 (Online)
DOI: http://dx.doi.org/10.15666/aeer/1704_97859793

Genetic diversity and population structure assessed by SSR and SNP markers in a large germplasm collection of grape. – BMC Plant Biol. 13: 39. DOI: 10.1186/1471-2229-13-39.

[17] Fatahi, R., Ebadi, A., Bassil, N., Mehlenbacher, S. A., Zamani, Z. (2003): Characterization of Iranian grapevine cultivars using microsatellite markers. – Vitis 42(4): 185-192.

[18] Grando, M. S., Bellin, D., Edwards, K. J., Pozzi, C., Stefanini, M., Velasco, R. (2003): Molecular linkage maps of Vitis vinifera L. and Vitis riparia Mchx. – Theoretical and applied genetics 106(7): 1213-1224.

[19] Hvarleva, T., Rusanov, K., Lefort, F., Tsvetkov, I., Atanassov, A., Atanassov, I. (2004): Genotyping of Bulgarian Vitis vinifera L. cultivars by microsatellite analysis. – Vitis 43(1): 27-34.

[20] Lefort, F., Roubelakis-Angelakis, K. A. (2001): Genetic comparison of Greek cultivars of Vitis vinifera L. by nuclear microsatellite profiling. – American Journal of Enology&Viticulture 52(2): 101-108.

[21] Li, B., Jianfu, J., Xiucai, F., Ying, Z., Haisheng, S., Guohai, Z., Chonghuai, L. (2017): Molecular characterization of Chinese grape landraces (*Vitis* L.) using microsatellite DNA markers. – Hort Science 52: 533-540.

[22] Lodhi, M. A., Daly, M. J., Ye, G. N., Weeden, N. F., Reisch, B. I. (1994): A simple and efficient method for DNA extraction from grapevine cultivars and Vitis species. – Plant Mol. Biol. 12(1): 6-13.

[23] Lópes, M. S., Sefc, K. M., Dias, E. E., Steinkellner, H., Machado, M. L. D., Machado, A. D. (1999): The use of microsatellites for germplasm management in a Portuguese grapevine collection. – Theor. Appl. Genet. 99(3-4): 733-739.

[24] Maletıć, E., Pejıć, I., Karogla Kontıć, J., Zdunıć, G., Preıner, D., Simon, S., Andabaka, Z., ZuljMihaljevic, M., Bubola, M., Markovic, Z., Stupic, D., Mucalo, A. (2015): Ampelographic and genetic characterization of Croatian grapevine varieties. – Vitis 54(Special Issue): 93-98.

[25] Martin, J. P., Borrego, J., Cabello, F., Ortiz, J. M. (2003): Characterization of the Spanish diversity grapevine cultivars using sequence-tagged microsatellite site markers. – Genome 46: 1-9.

[26] Martinez, L. E., Cavagnaro, P. F., Masuelli, R. W., Zuniga, M. (2006): SSR-based assessment of genetic diversity in Sout American Vitis vinifera varieties. – Plant Science 170: 1036-1044.

[27] Meredith, C., Dangl, G. S., Bowers, J. E. (1996): Clarifying the identitiy of some California winegrapes by DNA profilling. – Riv. Vitic. Enol. 49(1): 65-68.

[28] Meredith, C. (2001): Grapevine genetics: probing the past and facing the future. – Agriculturae Conspectus Sientificus 66: 21-25.

[29] Minch, E., Ruiz-Linares, A., Goldstein, D. B., Feldman, M., Cavalli-Sforza, L. L. (1995): Microsat (version 1.4d): a computer program for calculating various statistics on microsatellite allele data. – Stanford. California, University of Stanford.

[30] Nuñez, Y., Fresno, J., Torres, V., Ponz, F., Gallego, F. J. (2004): Practical use of microsatellite markers to manage Vitis vinifera germplasm: Molecular identification of grapevine samples collected blindly in D.O. "El Bierzo" (Spain). – Journal of Horticultural Science & Biotechnology 79(3): 437-440.

[31] Ocete, R., Arroya-Garcia, R., Morales, M. L., Cantos, M., Gallardo, A., Perez, M. A., Gomez, I., Lopez, M. A. (2011): Characterization of Vitis vinifera L. subspecies sylvestris (Gmelin) Hegi in the Ebro river Basin (Spain). – Vitis 50(1): 11-16.

[32] Riaz, S., Garrison, K. E., Dangl, G. S. (2002): Genetic divergence and chimerism within ancient asexually propagated winegrape cultivars. – Journal of the American Society for Horticultural Science 127(4): 508-514.

[33] Riaz, S., Dangl, G. S., Edwards, K. J., Meredith, C. P. (2004): A microsatellite marker based framework linkage map of Vitis vinifera L. – Theor. Appl. Genet. 108: 864-872.

http://www.aloki.hu ● ISSN 1589 1623 (Print) ● ISSN 1785 0037 (Online)
DOI: http://dx.doi.org/10.15666/aeer/1704_97859793

[34] Sefc, K. M., Steinkellner, H., Wagner, H. W., Glössl, J., Regner, F. (1997): Application of microsatellite markers to parentage studies in grapevine. – Vitis 36(4): 179-183.
[35] Sefc, K. M., Steinkellner, H., Glössl, J., Kampfer, S., Regner, F. (1998): Reconstruction of a grapevine pedigree by microsatellite analysis. – Theoretical and Applied Genetics 97(1-2): 227-231.
[36] Sefc, K. M., Regner, F., Turetschek, E., Glössl, J., Steinkellner, H. (1999): Identification of microsatellite sequences in Vitis riparia and their applicability for genotyping of different Vitis species. – Genome 42: 367-373.
[37] Sefc, K. M., Lopes, M. S., Lefort, F., Botta, R., Roubelakis-Angelakis, K. A., Ibañez, J., Pejic, I., Wegner, H. W., Glössl, J., Steinkellner, H. (2000): Microsatellite variability in grapevine cultivars from different European regions and evaluation of assignment testing to assess the geographic origin of cultivars. – Theor. Appl. Genet. 100: 498-505.
[38] Şelli, F., Bakır, M., İnan, G., Aygün, H., Boz, Y., Yaşasın, A. S., Özer, C., Akman, B., Söylemezoğlu, G., Kazan, K., Ergül, A. (2007): Simple sequence repeat-based assessment of genetic diversity in Dimrit and Gemre grapevine accessions from Turkey. – Vitis 46(4): 182-187.
[39] This, P., Jung, A., Boccacci, P., Borrego, J., Botta, R., Constantini, L., Crespan, M., Dangl, G. S., Eisenheld, C., Ferreria-Montteiro, F., Grando, S., Ibáñez, J., Lacombe, T., Laucou, V., Magalhães, R., Meredith, C. P., Milani, N., Peterlunger, E., Regner, F., Zulini, L., Maul, E. (2004): Development of a standard set of microsatellite reference alleles for identification of grape cultivars. – Theor. Appl. Genet. 109: 1448-1458.
[40] Thomas, M. R., Scott, N. S. (1993): Microsatellite repeats in grapevine reveal DNA polymorphisms when analyzed as sequence-tagged sites (STSs). – Theoretical and Applied Genetics.
[41] Van Heerden, C. J., Burger, P., Prins, R. (2018): Microsatellite-based DNA fingerprinting of selected grapevine cultivars. – S. Afr. J. Enol. Vitic. 39(1): 58-66.
[42] Vouillamoz, J. F., McGovern, P., Ergül, A., Soylemezoglu, G., Tevzadze, G., Meredith, C. P., Grando, M. S. (2006): Genetic characterization and relationships of traditional grape cultivars from Transcaucasia and Anatolia. – Plant Genetic Resources 4(2): 144-158.
[43] Wagner, H. W., Sefc, K. M. (1999): IDENTITY 1.0. Centre for Applied Genetics. – University of Agricultural Science, Vienna.
[44] Zequim Maia, S. H., Aparecida de Oliveira-Collet, S., Mangolin, C. A., Maria de Fátima, P. S. M. (2018): Differential genetic stability in vineyards of the cultivar 'Italy' (*Vitis vinifera* L.) cultivated in different regions of Southern and Southwestern Brazil. – Ciência Téc. Vitiv. 33(1): 66-77.
[45] Zullini, L., Fabro, E., Peterlunger, E. (2005): Characterisation of the grapevine cultivar Picolit by means of morphological descriptors and molecular markers. – Vitis 44(1): 35-38.

http://www.aloki.hu ● ISSN 1589 1623 (Print) ● ISSN 1785 0037 (Online)
DOI: http://dx.doi.org/10.15666/aeer/1704_97859793

ANALYSIS OF PLANT SPECIES USED IN URBAN OPEN SPACES: THE TRABZON CASE

TARAKCI EREN, E.

Department of Landscape Architecture, Karadeniz Technical University, Trabzon, Turkey
(e-mail: eminem_tarakci@hotmail.com; phone: +90-543-818-4642)

(Received 26th Mar 2019; accepted 13th Jun 2019)

Abstract. The implementation phase of the present study was conducted in 3 stages. In the first stage, the plant material used in the open green spaces in the urban center of Trabzon province was analyzed and plant inventory was investigated in these spaces to determine the species, characteristics and intended use of the plants. Thus, it was determined that 129 plant taxa were used in Trabzon public open green spaces. Forty-two taxa were indigenous to Turkey and 87 were exotic. It was identified that 34 were in the gymnosperm plant group and 95 were in angiosperm plant group. It was identified that 21 taxa were highly prevalent (5) in urban open green areas, 24 taxa were very prevalent (4), 35 taxa were moderately prevalent (3), 22 taxa were less prevalent (2), and 27 taxa were not prevalent (1). In the second stage, the objectives of planting and planting designs were investigated. It was determined that the plants were used for both aesthetic and functional purposes in these areas, but their aesthetic use was more common. In the third stage, the occupant satisfaction levels for the planting designs in these urban open green spaces were determined using a survey conducted with the occupants.
Keywords: *plant taxa, planting design, plant use, aesthetic and functional plant design, Trabzon, Turkey*

Introduction

Turkey is one of the richest countries in indigenous vegetation. The presence of Mediterranean, Iranian-Turanian and European-Siberian floristic regions in Anatolia and their fusion in certain areas are the main reasons for this wealth (Davis, 1965-1988). Furthermore, diverse climate, and topographic, geological and geomorphological diversity, the presence of various aquatic environments such as seas, lakes and streams may be the other factors that affect herbaceous and woody plant diversity in Turkey (Turkmen, 1987; Özer et al., 2009). The most important factor is the presence of several topographic and geological structures in the country. Turkey, with around 9,000 plant species and 3000 endemic plants, is among the countries with the richest flora in its climate zone.

The abundant plant diversity in Turkey expands the choices in plant use. Plants are used for a wide variety of aesthetic and functional purposes (Tarakci Eren and Var, 2016). Esthetically they have the potential of creating positive perceptions about the location due to their properties such as the fruits, flowers and color, their two or three-dimensional views due to planting design aspects such as lighting, shadows and reflections, providing color, texture and form aesthetics due to seasonal changes, providing aesthetics images with branches and barks, harmonic and contrast views created with other landscape elements, creating focus on one element, and the potential of decorative features due to the beauty of structural and vegetal properties (Tarakci Eren et. al., 2016; Tarakci Eren et. al., 2017).

Functionally, they are used to create spaces, hierarchy in space, to emphasize structure in landscapes, to relate and connect various objects and spaces, to strengthen the topographic structure, to soften structural landscape, to create perceptual effects, for example, to make the space look more spacious, to create vistas, to provide inter-spatial

http://www.aloki.hu ● ISSN 1589 1623 (Print) ● ISSN 1785 0037 (Online)
DOI: http://dx.doi.org/10.15666/aeer/1704_97959811

transition, to create attraction, to create a signal effect, to orient, to emphasize, to create focus, to allow the space to acquire character, to symbolize, to limit and create a border, to screen, to provide privacy and a habitat for the fauna and flora, to prevent erosion, avalanche and landslides, to reduce dust in the air and prevent noise, to balance the moisture and temperature, and to reduce the intensity of light in urban areas (Tarakci Eren et. al., 2018). Furthermore, objectives such as improvement of landfills, providing a comfortable and safe journey on highways etc. could be listed (Lorenz, 1975; Cepel, 1988; Ürgenç, 1990; Walker, 1991; Walker, 1991; Braun and Fluckiger, 1998; Beckett et al., 1998; Novak et al., 2000; Tarakci Eren et. al., 2017).

With the transformation of urban open green spaces into built areas, unplanned or uncontrolled changes have led to the destruction and fragmentation of natural urban spaces. This forced the inhabitants to live under adverse environmental conditions and experience psychological, recreational and social problems. Today, natural and cultural green spaces are replaced by masses of buildings. The decrease in open green species, especially in the cities, leads to the deterioration of the urban ecological balance (Akpınar et al., 1992). In order to eliminate these problems, environmental planning is prioritized in urban spaces. Especially, the plants are very important in the design of relevant open-green spaces (Erenberk, 1992). Plants attract individuals and animals with their flowers, leaves, trunks, fruits and fragrances (Sakıcı, 2009). Plants undertake the tasks of enclosure, bordering, creating personal spaces, softening, revitalizing, filtering the sun, cleaning the air, providing a habitat for birds and introducing the nature to human life (Tyson, 1998). The potential benefits of living in contact with nature were explored by scholars in environmental psychology, and it has been widely accepted in environmental literature that association with nature has positive effects on human psychology. It was reported that individuals benefit from the direct interaction with the nature (active contact) and watching the flowers in a park or trees through a window or by just viewing it (passive contact), and even knowing that these areas exist nearby please the individuals and provide psychological benefits (Ulrich and Parson, 1992). Plants used in urban environment have functional benefits for the ecosystem such as saving energy, humidification (Beckett et al., 2000; Akbari et al., 2001) noise reduction (Çepel, 1988; Walker, 1991; Bayramoğlu et al., 2014), reduction of the effects of wind, dust and greenhouse effects (Novak et al., 2000; Akbari, 2001; Novak and Crane, 2002) preventing light reflections (Heisler, 1986; Walker, 1991; Heisler and Grant, 2000). Furthermore, plants are also quite important to remind the time to individuals due to seasonal characteristics such as early flowering, late coloration and long flowering (Sakıcı, 2009).

Plant properties such as fragrance, edible fruits, seeds, color changes, as well as shading, visual buffer and wind chamber formation, especially creating wildlife habitat for birds and butterflies should be considered in plant selection. Non-stability of plants reminds us life. Birth, growth, death and re-existence, which are part of the life cycle, are events that we recognize by seasonal changes (Sakıcı, 2009). The growth and maturation of the flowers and the falling leaves in autumn remind individuals that the days pass quickly (Mcdowell, 1997). Plants also have several positive psychological effects. Plants play an important role in self-respect. In open green spaces, the planting design improves the value of the space, prevents monotony, allows for recreational activities and socialization. Urban open green spaces play a calming, relaxing role (Smardon, 1990). Landscape architects should design the landscape with knowledge on plant properties and their contribution to the space and should make decisions about

http://www.aloki.hu ● ISSN 1589 1623 (Print) ● ISSN 1785 0037 (Online)
DOI: http://dx.doi.org/10.15666/aeer/1704_97959811

plant locations and plant species in the beginning of the design when conducting spatial arrangements. Unfortunately, several mistakes are made in plant design in current environmental arrangements. This also significantly affects the occupancy of the space. In the present study, the properties of the plant species preferred in the public open green spaces in Trabzon and their intended use were investigated, the occupant satisfaction levels were determined, and plant designs were analyzed.

Materials and methods

The study was conducted in the most heavily occupied green space in the province of Trabzon. Trabzon province is located in the Eastern Black Sea region. Trabzon is surrounded by Giresun province on the west, Gümüshane province on the south, Rize province on the east, and the Black Sea on the north. Trabzon province is between north 0° 33' and 41° 07' latitudes and east 39° 07' and 40° 30' longitudes. Surface area of the province is 4685 km², the population is 786,326 based on 2017 data. Beach Park (1), Ganita Beach Park (2), Zağnos Recreation Area (3), Square Park (4), and Turkish-Japanese Friendship Park (5) were included in the study area. These areas are marked in the Trabzon urban center map presented in *Figure 1*.

Figure 1. *Analyzed open and green spaces in Trabzon*

On-site observation, examination, analysis, survey and evaluation methods were used in the study. Materials utilized in the first stage included five open green spaces in Trabzon urban center and the plant taxa used in these spaces. The methods included on-site observation, examination, analysis, and evaluation. Plant species in open and green areas in the study area were identified and their intended use were discussed. After identification of the plants, the frequencies of the species used in each open green space were determined (1: very low prevalence, 2 low prevalence, 3 moderate prevalence, 4 high prevalence, 5 very high prevalence) and the most preferred plant species were determined in Trabzon urban center. The materials used in the second stage included 5 open green spaces in Trabzon and planting designs utilizded in these areas. The methodology included observation, examination, analysis and evaluation, similar to the first stage. The intended use of planting designs was analyzed based on both aesthetic (12 criteria) and functional criteria (14 criteria). The material used in the third stage included the open green spaces and their occupants. The survey methodology was used. Thus, the satisfaction levels of the occupants of these spaces were determined. In the present study, which was conducted in three stages, the data obtained in each stage were analyzed together. Furthermore, inadequate planting designs were examined, and solutions were recommended.

http://www.aloki.hu ● ISSN 1589 1623 (Print) ● ISSN 1785 0037 (Online)
DOI: http://dx.doi.org/10.15666/aeer/1704_97959811

Findings

First stage findings

In the 5 urban open and green spaces determined as the study area, 116 species in 83 genera and 129 subspecies of the above-mentioned species were identified. 34 were in Gymnosperm plant group and 95 were in Angiosperm plant group. The taxa identified in all five parks out of the total 129 taxa were as follows: *Berberis thunbergii* 'Atropurpurea', *Buxus sempervirens, Cedrus deodara, Cedrus libani, Cercis siliquastrum, Euonymus japonica, Eouymus japonia* 'Aureus', *Euonymus japonica* 'Aureo- variegutus', *Hibiscus syriacus, Laurus nobilis*, *Laurocerasus officinalis Morus alba* 'Pendula', *Picea pungens* 'Glauca', *Pittosporum tobira* 'Nana', *Platanus orientalis*, *Prunus cerasifera* 'Atropurpurea', *Rosmarinus officinalis, Syringa vulgaris, Tilia platyphllos, Yucca filemantosa*. These included a total of 21 taxa. The taxa identified in 4 of the 5 parks were as follows: *Acer palmatum Betula pendula*, *Campsis radicans, Cupressus arizonica* 'Glauca Multiponpon', *Cupressus macrocarpa* 'Goldcrest', *Gingko biloba, Hydrangea macrophylla, Juniperus pfitzeriana, Lagerstroemia indica, Ligustrum japonicum, Ligustrum japonicum* 'Variegatum', *Magnolia grandiflora, Nerium oleander, Philadelphus coranarius, Pinus pinea, Pittosporum tobira, Pittosporum tobira* 'Variegatum', *Platycladus orientalis, Rosa sp., Spirea x vanhoutteii, Taxus baccata, Thujo occidentalis, Thujo plicata, Viburnum opulus, Wisteria sinensis*. These included a total of 24 taxa. The taxa identified in 3 of the 5 parks were as follows: *Abies nordmanniana, Acer buergerianum, Aesculus hipocastanum, Albizia julibrissin, Azalea japonica, Citrus lemon, Cotoneaster frigidus* 'Cornubia', *Crataegus oxyacantha, Cryptomeria japonica* var. Elegance, *Cupressus sempervirens* 'Pyramidalis', *Cupressocyparis leylandii*, *Fagus orientalis, Hedera helix, Juniperus communis, Juniperus chinensis* 'Pfitzeriana Glauca', *Liquidambar orientalis, Liriodendron tuliphifera, Magnolia soulengeana, Parthenocissus tricuspidata* 'Vetchii', *Paulownia tomentosa, Phoenix canariensis, Photina fraseri, Phus typhina, Picea orientalis, Prunus serrulata* 'Kanzan', *Punica granatum, Pyracantha coccinea* 'Lalendei', *Quercus pontica, Rhododendron ponticum, Salix babylonica*, *Sparteum junceum, Trachycarpus fortuneii, Viburnum tinus, Washingtonia filifera, Wisteria floribunda.* These included a total of 35 taxa. The taxa identified in 2 of the 5 parks were as follows: *Acer pseudoplatanus, Catalpa bignonioides, Citrus reticulata, Citrus sinensis, Cotoneaster franchetti, Cryptomeria japonica, Eribotria japonica, Eounymus alatus* 'Compactus', *Forsythia x intermedia, Fraxinus excelsior, Hedera helix* 'Eleganttissima', *Jasminum fruticans, Juniperus chinensis, Koelreuteria paniculata, Melia azaderach, Phyllostachys pubescens, Picea pungens, Pyracantha coccinea Robinia pseudoacacia, Robinia pseudoacacia* 'Umbraculifera', *Rubus sp., Viburnum plicatum'*dur. These included a total of 22 taxa. The taxa identified in only 1 park were as follows: *Acacia cynophylla, Acer negundo, Acer platonoides, Acer rubrum, Alnus orientalis, Alnus glutinosa, Camelia japonica, Chamaecyparis lawsoniana* 'Ellwoodii', *Chamaecyparis pisifera, Chamaecyparis nootkatensis* 'Pendula', *Cotoneaster dammeri, Crataegus leevigata* 'Pauls Scarlet', Cupressoparis leylandii 'Multiponpon', *Eucalyptus camaldulensis, Jasminum officinale,, Juniperus virginniana, Nandina domestica, Olea europaea, Pinus mugo, Pinus nigra, Pinus nigra pallasiana var. Pyramidalis, Pinus pinaster, Prunus avium, Quercus cerris, Sequoia sempervirens, Sequoiadendron giganteum, Vitis vinifera*. These included a total of 27 taxa (*Table 1*).

http://www.aloki.hu ● ISSN 1589 1623 (Print) ● ISSN 1785 0037 (Online)
DOI: http://dx.doi.org/10.15666/aeer/1704_97959811

Table 1. *The number of taxa identified in each urban open space based on genera, species, sub-species and plant groups*

	Open green space code				
	1	**2**	**3**	**4**	**5**
Genus	77	70	56	37	46
Species	99	81	67	45	60
Subspecies	110	92	73	50	64
Gymnosperm	28	18	19	13	18
Angiosperm	82	74	54	37	46

As seen in *Figure 2,* it was determined that 21 out of 129 taxa were highly prevalent (5), i.e., these taxa were found in all five urban open green spaces, 24 taxa were prevalent (4), i.e., these taxa were found in four urban open green spaces, 35 taxa were moderately prevalent (3), i.e., these taxa were found in three urban open green spaces, 22 taxa were less prevalent (2), i.e., these taxa were found in two urban open green spaces, and 27 taxa were not prevalent (1), i.e., these taxa were found in only one urban open green space (*Tables 2* and *3*).

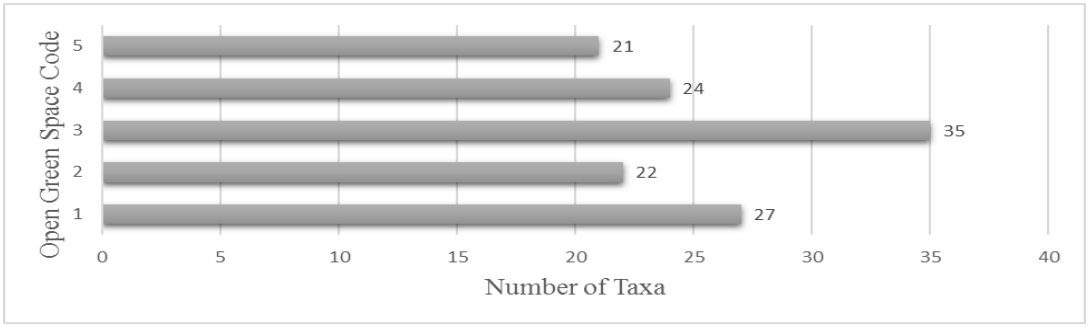

Figure 2. *Distribution of 129 taxa identified in all urban green spaces based on the green space*

Second stage findings

The reasons for the use of these taxa in plant designs in urban open and green spaces are summarized in *Table 4*. In this respect, aesthetic purposes were addressed in 12 headings and functional purposes were examined under 14 headings.

Initially, the purposes such as creating spatial subdivisions, changing scale and Vista were not taken into consideration when considering the aesthetic purposes at the Beach Park. In other words, aesthetical purposes (100%) and functional purposes (78%, 57) were mainly considered in this park. In Ganita Beach Park, 75% of aesthetic purposes and 57.14% of functional purposes were taken into consideration. In the Zağnos Recreation Area, 100% of the aesthetic purposes and 85.71% of the functional purposes were taken into consideration. 91% of the aesthetic purposes were taken into consideration in the Square Park, while 100% of the functional purposes were taken into consideration. In the Turkish-Japanese Friendship Park, 100% of the aesthetic and functional purposes were taken into consideration. All aesthetic purposes were taken into account in at least four of five urban open green spaces. Functional purposes were considered in at least two urban open green spaces (*Table 5*).

http://www.aloki.hu ● ISSN 1589 1623 (Print) ● ISSN 1785 0037 (Online)
DOI: http://dx.doi.org/10.15666/aeer/1704_97959811

Table 2. *The study area and properties*

Beach Park	**1** 	The beach park is a 9 km long and on average 250 m wide Trabzon coastal arrangement between the Ganita park and Beşirli district. Beach Park, is built on the reclaimed land to improve the reduced coastal areas in the city and it has several functions. Some include children's playgrounds, food and beverage areas, hiking and biking paths. Trabzon Beach Park included 99 species and 110 subspecies in 77 genera. 28 species were in Gymnosperm plant group and 82 were in Angiosperm plant group. It was found that the species were used for both functional and aesthetic purposes
Ganita Beach Park	**2** 	It is a coastal park on the coastal road next to the Black Sea in the İskenderpaşa neighborhood in Ortahisar district. The park includes viewing areas, tea garden, restaurant, wildlife, hiking areas, children's playground, boating facilities, boat tours, fishing areas, sports areas.81 species and 92 subspecies in 70 genera were determined. 18 were in Gymnosperm plant group and 74 were in Angiosperm plant group. Species were used for both functional and aesthetic purposes. However, it was determined that they were mainly used for aesthetic purposes
Zağnos Recreation Area	**3** 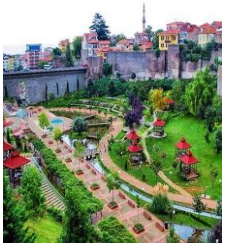	Trabzon Zağnos Valley includes an area of approximately 96,000 square meters and about 700 m long to the South, between 100 and 150 meters wide, limited by Maras Street on the north. Zağnos Valley is located on Yavuz Sultan Selim Boulevard within the boundaries of Gülbahar Hatun neighborhood in Ortahisar District. The area includes an amphitheater, pond, viweing areas, water games, exhibition venues, wildlife, restaurant, tea house, waterfall, and hiking paths. In total, 67 species and 73 subspecies in 56 genera were determined. 19 were in Gymnosperm plant group, and 54 were in Angiosperm plant group. Species were used for both functional and aesthetic purposes. However, it was determined that they were mainly used for aesthetic purposes
Square Park	**4** 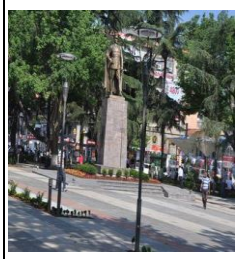	It is located in İskenderpaşa neighborhood in the central Ortahisar district in Trabzon on Uzun Street, between the Gazipaşa and Taksim ramps and covers an area of 15,000 square meters. It is bordered by Kemerkaya Street to the north, Çömlekçi Street to the east, Maraş Street to the west and Taksim park to the south. Since it is both a square and a park, it was coined as the Square Park. 37 different genera, 45 species in these genera and 50 varieties in these species with different forms and features were determined. 13 taxa were in Gymnosperm plant group and 37 were in Angiosperm plant group. Species were used for both functional and aesthetic purposes. However, it was determined that they were mainly used for aesthetic purposes
Turkish-Japanese Friendship Park	**5** 	Turkish-Japanese Friendship Park is located in Ortahisar District, Kalkınma neighborhood, Coastal Road area in Trabzon. Built on an area of 30,000 m2, it is surrounded by the Black Sea on the north, Forum shopping mall on the south, 100th Year park on the east, and Değirmendere industrial site on the west. The area includes spaces that reclect the cultures of the two countries. It includes plants specific to Japanese gardens, dry stone gardens, ponds, tea houses, cascade ponds, plants, pergolas, etc. A total of 46 genera and 60 plant species and 64 subspecies in these genera were determined. 18 were in Gymnosperm plant group and 46 were in Angiosperm plant group. Species were used for both functional and aesthetic purposes in this park. However, two purposes were considered equally in planting designs

http://www.aloki.hu ● ISSN 1589 1623 (Print) ● ISSN 1785 0037 (Online)
DOI: http://dx.doi.org/10.15666/aeer/1704_97959811

Table 3. *Plant taxa identified in the study area*

Code	Plant taxa
1	*Acer buergerianum Acer negundo, Acer palmate, Acer pseudoplatanus, Aesculus hipocastanum, Albizia julibrissin, Alnus orientalis Azalea japonica, Berberis thunbergii* 'Atropurpurea'*, Betula pendula, Buxus semmpervirens, Camelia japonica, Campsis radicans, Catalpa bignonioides, Cedrus deodara, Cedrus libani, Cercis siliquastrum, Chamaecyparis lawsoniana* 'Ellwoodii'*, Chamaecyparis pisifera, Chamaecyparis nootkatensis* 'Pendula'*, Cotoneaster franchetti, Cotoneaster frigidus* 'Cornubia'*, Crataegus oxyacantha, Cryptomeria japonica, Cryptomeria japonica* var Elagance*, Cupressus arizonica 'Glauca Multiponpon', Cupressus macrocarpa* 'Goldcrest*', Cupressus sempervirens* 'Pyramidalis'*, Cupressoparis leylandii, Cupressoparis leylandii* 'Multiponpon'*, Eribotria japonica, Eounymus alatus* 'Compactus'*, Euonymus japonica, Eouymus japonia* 'Aureus*', Euonymus japonicus* 'Aureo-variegutus'*, Fagus orientalis, Forsythia x intermedia, Fraxinus excelsior, Gingko biloba, Hedera helix, Hibiscus syriacus, Hydrangea macrophylla, Jasminum fruticans, Juniperus communis, Juniperus pfitzeriana, Juniperus chinensis, Juniperus chinensis* 'Pfitzeriana Glauca'*, Juniperus virginniana, Koelreuteria paniculata, Lagerstroemia indica, Laurus nobilis, Laurocerasus officinalis, Ligustrum japonicum, Ligustrum japonicum* Variegatum, *Liquidambar orientalis, Liriodendron tuliphifera, Magnolia grandiflora, Magnolia soulengeana, Melia azaderach, Morus alba* 'Pendula'*, Nerium oleander, Parthenocissus tricuspidata* 'Vetchii'*, Paulownia tomentosa, Philadelphus coranarius, Phoenix canariensis, Photina fraseri, Phus typhina, Phyllostachys pubescens, Picea pungens, Picea pungens* 'Glauca'*, Picea orientalis, Pinus pinea, Pinus pinaster, Pittosporum tobira, Pittosporum tobira* 'Nana'*, Pittosporum tobira* 'Variegatum'*, Platanus orientalis, Platycladus orientalis, Prunus avium, Prunus cerasifera* 'Atropurpurea'*, Prunus serrulata* 'Kanzan'*, Punica granatum, Pyracantha coccinea, Pyracantha coccinea* 'Lalendei'*, Quercus pontica, Rhododendron ponticum, Robinia pseudoacacia, Robinia pseudoacacia* 'Umbraculifera'*, Rosa sp., Rosmarinus officinalis, Rubus sp., Salix babylonica, Sequoia sempervirens, Sequoiadendron giganteum, Sparteum junceum, Spirea x vanhouttei, Syringa vulgaris, Taxus baccata, Thujo occidentalis, Thujo plicata , Tilia platyphyllos, Trachycarpus fortuneii, Viburnum opulus, Viburnum plicatum, Viburnum tinus, Vitis vinifera, Washingtonia filifera, Wisteria floribunda, Wisteria sinensis, Yucca filementosa*
2	*Abies nordmanniana, Acacia cynophylla, Acer buergerianum, Acer negundo, Acer pseudoplatanus, Aesculus hipocastanum, Albizia julibrissin, Alnus glutinosa, Azalea japonica, Berberis thunbergii* 'Atropurpurea'*, Betula pendula, Buxus semmpervirens, Campsis radicans, Catalpa bignonioides, Cedrus deodora, Cedrus libani, Cercis siliquastrum, Citrus limon, Citrus reticulata, Cotoneaster franchetti, Cotoneaster frigidus* 'Cornubia'*, Crataegus oxyacantha, Cryptomeria japonica, Cryptomeria japonica* var Elagance*, Cupressus macrocarpa* 'Goldcrest'*, Cupressus sempervirens* 'Pyramidalis'*, Cupressoparis leylandii, Eucalyptus camaldulensis, Euonymus japonica, Eouymus japonia* 'Aureus'*, Euonymus japonicus* 'Aureo- Variegutus'*, Fagus orientalis, Forsythia x intermedia, Fraxinus excelsior, Hedera helix* 'Eleganttissima'*, Hedera helix, Hibiscus syriacus, Hydrangea macrophylla, Jasminum fruticans, Juniperus pfitzeriana, Juniperus chinensis, Juniperus chinensis* 'Pfitzeriana Glauca'*, Koelreuteria paniculata, Lagerstroemia indica, Laurus nobilis, Laurocerasus officinalis, Ligustrum japonicum, Ligustrum japonicaum* Variegatum, *Liquidambar orientalis, Liriodendron tuliphifera, Magnolia grandiflora, Magnolia soulengeana, Melia azaderach, Morus alba* 'Pendula'*, Nerium oleander, Parthenocissus tricuspidata* 'Vetchii'*, Paulownia tomentosa, Philadelphus coranarius, Phoenix canariensis, Phus typhina, Picea pungens, Picea pungens* 'Glauca'*, Picea orientalis, Pinus pinea, Pinus pinaster, Pittosporum tobira, Pittosporum tobira* 'Nana'*, Pittosporum tobira* 'Variegatum'*, Platanus orientalis, Platycladus orientalis, Prunus cerasifera* 'Atropurpurea'*, Punica granatum, Pyracantha coccinea, Pyracantha coccinea* 'Lalendei'*, Quercus pontica, Robinia pseudoacacia, Robinia pseudoacacia* 'Umbraculifera'*, Rosa sp., Rosmarinus officinalis, Rubus sp., Salix babylonica, Sparteum junceum, Spirea x vanhouttei, Syringa vulgaris, Thujo occidentalis, Tilia platyphyllos, Trachycarpus fortuneii, Viburnum opulus, Viburnum tinus, Washingtonia filifera, Wisteria sinensis, Yucca filementosa*

http://www.aloki.hu ● ISSN 1589 1623 (Print) ● ISSN 1785 0037 (Online)
DOI: http://dx.doi.org/10.15666/aeer/1704_97959811

3	*Acer buergerianum Acer negundo, Acer palmatum, Acer pseudoplatanus, Aesculus hipocastanum, Albizia julibrissin, Alnus orientalis, Azalea japonica, Berberis thunbergii 'Atropurpurea', Betula pendula, Buxus semmpervirens, Camelia japonica, Campsis radicans, Catalpa bignonioides, Cedrus deodara, Cedrus libani, Cercis siliquastrum, Chamaecyparis lawsoniana 'Ellwoodii', Chamaecyparis pisifera, Chamaecyparis nootkatensis 'Pendula', Cotoneaster franchetti, Cotoneaster frigidus 'Cornubia', Crataegus oxyacantha, Cryptomeria japonica, Cryptomeria japonica* var Elagance*, Cupressus arizonica 'Glauca* Multiponpon', *Cupressus macrocarpa 'Goldcrest', Cupressus sempervirens 'Pyramidalis', Cupressoparis leylandii, Cupressoparis leylandii 'Multiponpon', Eribotria japonica, Eounymus alatus 'Compactus', Euonymus japonica, Eouymus japonia 'Aureus', Euonymus japonicus 'Aureo-Variegutus', Fagus orientalis, Forsythia x intermedia, Fraxinus excelsior, Gingko biloba, Hedera helix, Hibiscus syriacus, Hydrangea macrophylla, Jasminum fruticans, Juniperus communis, Juniperus pfitzeriana, Juniperus chinensis, Juniperus chinensis 'Pfitzeriana Glauca', Juniperus virginniana, Koelreuteria paniculata, Lagerstroemia indica, Laurus nobilis, Laurocerasus officinalis, Ligustrum japonicum, Ligustrum japonicum variegatum, Liquidambar orientalis, Liriodendron tuliphifera, Magnolia grandiflora, Magnolia soulengeana, Melia azaderach, Morus alba 'Pendula', Nerium oleander, Parthenocissus tricuspidata 'Vetchii', Paulownia tomentosa, Philadelphus coranarius, Phoenix canariensis, Photina fraseri, Phus typhina, Phyllostachys pubescens, Picea pungens, Picea pungens glauca, Picea orientalis, Pinus pinea, Pinus pinaster, Pittosporum tobira, Pittosporum tobira 'Nana', Pittosporum tobira 'Variegatum', Platanus orientalis, Platycladus orientalis, Prunus avium, Prunus cerasifera 'Atropurpurea', Prunus serrulata 'Kanzan', Punica granatum, Pyracantha coccinea, Pyracantha coccinea 'Lalendei', Quercus pontica, Rhododendron ponticum, Robinia pseudoacacia, Robinia pseudoacacia 'Umbraculifera', Rosa sp., Rosmarinus officinalis, Rubus sp., Salix babylonica, Sequoia sempervirens, Sequoiadendron giganteum, Sparteum junceum, Spirea x vanhouttei, Syringa vulgaris, Taxus baccata, Thujo occidentalis, Thujo plicata, Tilia platyphyllos, Trachycarpus fortuneii, Viburnum opulus, Viburnum plicatum, Viburnum tinus, Vitis vinifera, Washingtonia filifera, Wisteria floribunda, Wisteria sinensis, Yucca filementosa*
4	*Abies nordmanniana, Acer buergerianum, Acer palmatum, Aesculus hipocastanum, Albizia julibrissin, Berberis thunbergii 'Atropurpurea', Betula pendula, Buxus semmpervirens, Cedrus deodara, Cedrus libani, Cercis siliquastrum, Citrus limon, Citrus reticulata, Citrus sinensis, Cupressus arizonica 'Glauca* Multiponpon', *Cupressus macrocarpa* 'Goldcrest', *Euonymus japonica, Eouymus japonia 'Aureus', Euonymus japonicus* 'Aureo- Variegutus', *Gingko biloba, Hibiscus syriacus, Hydrangea macrophylla, Juniperus pfitzeriana, Laurus nobilis, Laurocerasus officinalis, Ligustrum japonicum, Ligustrum japonicum 'Variegatum', Liquidambar orientalis, Liriodendron tuliphifera, Morus alba* 'Pendula', *Nerium oleander, Paulownia tomentosa, Photina fraseri, Picea pungens 'Glauca', Picea orientalis, Pittosporum tobira, Pittosporum tobira 'Nana', Pittosporum tobira* 'Variegatum', *Platanus orientalis, Platycladus orientalis, Prunus cerasifera 'Atropurpurea', Prunus serrulata 'Kanzan', Rhododendron ponticum, Rosmarinus officinalis, Syringa vulgaris, Taxus baccata, Thujo occidentalis, Thujo plicata, Tilia platyphyllos, Yucca filementosa*
5	*Acer palmatum, Acer platonoides, Acer rubrum, Azalea japonica, Berberis thunbergii 'Atropurpurea', Betula pendula, Buxus semmpervirens, Camelia japonica, Campsis radicans, Cedrus deodara, Cedrus libani, Cercis siliquastrum, Cotoneaster dammeri, Crataegus leevigata* 'Pauls Scarlet', *Cupressus arizonica 'Glauca* Multiponpon', *Cupressus macrocarpa 'Goldcrest', Cupressus sempervirens* 'Pyramidalis', *Cupressoparis leylandii, Cupressoparis leylandii 'Multiponpon', Eounymus alatus* 'Compactus', *Euonymus japonica, Eouymus japonia 'Aureus', Euonymus japonicus 'Aureo- variegutus', Fagus orientalis, Gingko biloba, Hibiscus syriacus, Juniperus communis, Juniperus pfitzeriana, Juniperus chinensis, Lagerstroemia indica, Laurus nobilis, Laurocerasus officinalis, Magnolia grandiflora, Morus alba 'Pendula', Nandina domestica, Philadelphus coranarius, Phus typhina, Phyllostachys pubescens, Picea pungens 'Glauca', Pinus mugo, Pinus nigra, Pinus nigra pallasiana var. 'Pyramidalis', Pinus pinea, Pittosporum tobira 'Nana', Platanus orientalis, Prunus cerasifera 'Atropurpurea', Prunus serrulata 'Kanzan', Quercus cerris, Quercus pontica, Rhododendron ponticum, Rosa sp., Rosmarinus officinalis, Salix babylonica, Sequoiadendron giganteum, Spirea x vanhouttei, Syringa vulgaris, Taxus baccata, Thujo occidentalis, Thujo plicata, Tilia platyphyllos, Viburnum opulus, Wisteria floribunda, Wisteria sinensis, Yucca filementosa*

http://www.aloki.hu ● ISSN 1589 1623 (Print) ● ISSN 1785 0037 (Online)
DOI: http://dx.doi.org/10.15666/aeer/1704_97959811

Table 4. *Intended use for the plants in Trabzon urban open green spaces*

	Urban open green spaces	Code	1	2	3	4	5
Aesthetic	Positive and negative perception capability of the plants	**E1**	**V**		**V**	**V**	**V**
	Two and three dimensionality	**E2**	**V**		**V**	**V**	**V**
	Seasonal changes	**E3**	**V**	**V**	**V**	**V**	**V**
	Creating color aesthetics with components such as leaves, flowers, fruits, etc.	**E4**	**V**	**V**	**V**	**V**	**V**
	Branching, bark and linearity	**E5**	**V**	**V**	**V**	**V**	**V**
	Creating contrast with other landscaping elements, form, texture and color effects	**E6**	**V**	**V**	**V**	**V**	**V**
	Attracting attention and focus as a solitary element	**E7**	**V**	**V**	**V**	**V**	**V**
	Creating impressive traces on the ground	**E8**	**V**		**V**	**V**	**V**
	Reflective element (mirror effect)	**E9**	**V**	**V**	**V**	**V**	**V**
	Light-shadow element	**E10**	**V**	**V**	**V**		**V**
	Audiovisual effects created by the wind	**E11**	**V**	**V**	**V**	**V**	**V**
	Decorative element or plastic object	**E12**	**V**	**V**	**V**	**V**	**V**
Functional	Creating spatial organizations	**F1**	**V**		**V**	**V**	**V**
	Creating spatial subsections	F2			**V**	**V**	**V**
	Definition and association of the design	**F3**	**V**	**V**	**V**	**V**	**V**
	Supporting or strengthening an existing design	**F4**	**V**	**V**	**V**	**V**	**V**
	Orientation	**F5**	**V**	**V**	**V**	**V**	**V**
	Scale diversification and creating an illusion	F6				**V**	**V**
	Creating spatial depth through layering	**F7**	**V**		**V**	**V**	**V**
	Creating vista or visual enclosure	F8				**V**	**V**
	Creating a background	**F9**	**V**	**V**	**V**	**V**	**V**
	Invitation	**F10**	**V**	**V**	**V**	**V**	**V**
	Distinguishing, emphasizing and creating a focus on the space	**F11**	**V**		**V**	**V**	**V**
	Creating a character for the space, defining or symbolizing the space	**F12**	**V**		**V**	**V**	**V**
	Bordering	**F13**	**V**	**V**	**V**	**V**	**V**
	Creating privacy (privacy control)	**F14**	**V**		**V**	**V**	**V**

Table 5. *Consideration of aesthetic and functional purposes in Trabzon urban green spaces*

	1	**2**	**3**	**4**	**5**
Aesthetic purposes (%)	100	75	100	91.6	100
Functional purposes (%)	78.57	57.14	85.71	100	100

When each aesthetic purpose was examined separately in five urban open green spaces, it was observed that the 'positive and negative perceptions created by plants' coded as E1, 'two and three dimensionality' coded as E2, and 'creating impressive traces on the ground' coded as 'E8' were not considered at the Ganita Beach Park. The 'light-shadow element' coded as E10 was not taken into consideration only in the Square Park (*Fig. 3*).

http://www.aloki.hu ● ISSN 1589 1623 (Print) ● ISSN 1785 0037 (Online)
DOI: http://dx.doi.org/10.15666/aeer/1704_97959811

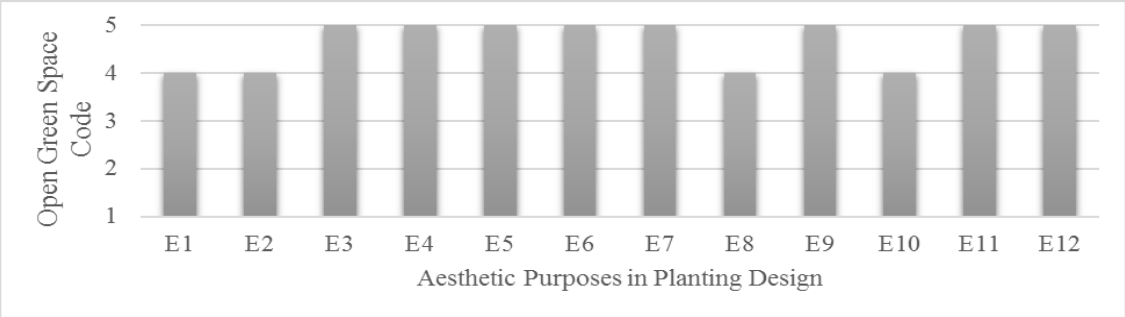

Figure 3. *The number of urban open green spaces where aesthetic purposes were considered in plant design*

When each functional purpose was examined in the five open green fields, it was determined that 'creating spatial organizations' coded as F1 was not considered in Ganita Beach Park, F2 was not considered in Coast and Ganita parks, F6 was not considered in Coast, Ganita and Zagnos open green spaces, F7 was not considered in Ganita Beach Park, F8 was not considered in Ganita and Zagnos open green spaces, F11, F12 and F14 was not considered in Ganita Beach Park (*Fig. 4*).

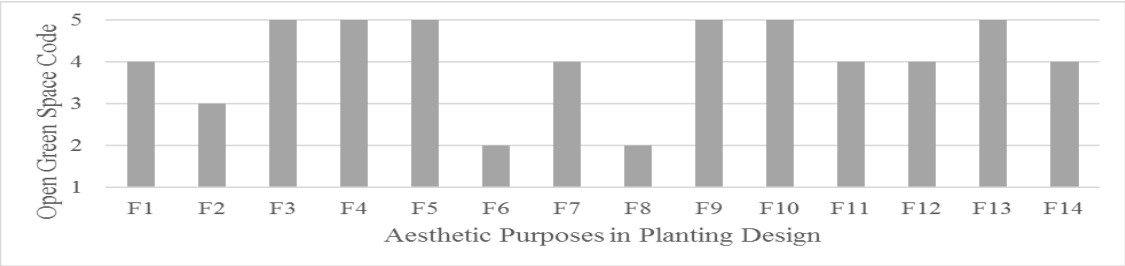

Figure 4. *The number of urban open green spaces where functional purposes were considered in plant design*

Aesthetic and functional planting was the aim in the Beach Park as observed in the planting design samples provided in four photographs in *Table 6*.

Table 6. *Planting design samples in Beach Park*

Beach Park			
			
A. purpose	F. purpose	A. purpose	A. purpose
Forsythia x intermedia *Cotaneaster frigida* 'Cornubia' *Prunus cerasifera* 'Atropurpurea'	*Cotaneaster frigida* 'Cornubia' *Prunus cerasifera* 'Atropurpurea'	*Spirea x vanhoutteii* *Morus alba* 'Pendula' *Washingtonia filifera*	*Washingtonia filifera* *Laurocerasus officinalis*

http://www.aloki.hu ● ISSN 1589 1623 (Print) ● ISSN 1785 0037 (Online)
DOI: http://dx.doi.org/10.15666/aeer/1704_97959811

Mostly aesthetic planting was the aim in Turkish-Japanese Friendship Park as observed in the planting design samples provided in *Table 7*.

Table 7. *Planting design samples in Turkish-Japanese Friendship park*

Turkish-Japanese Friendship Park			
			
A. and F. purpose	A. purpose	A. purpose	A. purpose
Prunus ceracifera 'Atropurpurea'	*Acer rumbum* *Eounymus japonica* 'Aureus' *Buxus sempervirens*	*Camelia j.*	*Viburnum plicatum* *Pinus mugo*

Mostly aesthetic planting was the aim in the Square Park as observed in the planting design samples provided in *Table 8*.

Table 8. *Planting design samples in Square Park*

Square Park		
		
Aesthetic purpose	Aesthetic purpose	Aesthetic and functional purpose
Prunus ceracifera 'Atropurpurea'	*Betula pendula*	*Cedrus libani* *Hydrangea macrophyll*a

Plant design samples and the plant taxa used in these designs are presented in *Table 9*.

Third stage findings

The determination of occupant satisfaction level of the occupants of open green spaces in Trabzon city was conducted with a scale where the values of 1 and 2 reflected dissatisfaction, 3 represented neither satisfaction nor dissatisfaction and 4 and 5 reflected satisfaction with the space. The Cronbach Alpha reliability test was used to determine the reliability of the scale and it was determined that the scale was reliable. The mean occupant satisfaction scores were calculated for the five urban open green spaces and the difference between these values was determined by one-way analysis of variance (*Tables 10* and *11*).

http://www.aloki.hu ● ISSN 1589 1623 (Print) ● ISSN 1785 0037 (Online)
DOI: http://dx.doi.org/10.15666/aeer/1704_97959811

Table 9. *Planting design samples*

Zağnos Valley recreation area		
		
Aesthetic purpose	Aesthetic and functional purpose	Aesthetic and functional purpose
Euonymus japonica 'Aurea variageta'	*Trachycarpus fortuneii* *Olea europa* *Prunus cerasifera* 'Atropurpurea'	*Wisteria sinensis*

Table 10. *The occupants' satisfaction with planting designs in each urban open green space*

	Urban open green space code					
	1	**2**	**3**	**4**	**5**	
Satisfied (mean)	3.40	3.10	3.55	3.04	3.53	F: 6.811
Satisfied (sd)	1.167	1.111	.996	1.261	1.238	Sig: .000

Table 11. *Analysis of variance*

	Sum of squares	**df**	**Mean square**	**F**	**Sig.**
Between groups	36.562	4	9.141	6.811	.000
Within groups	1066.937	795	1.342		
Total	1103.500	799			

In *Table 12,* the asterisk in the mean difference column indicates that there was a difference between the satisfaction levels for planting designs in urban open green spaces. There was a significant difference at 0.05 level between the satisfaction levels of planting designs in urban open green areas when denoted with an asterisk. Thus, the difference between the satisfaction level of the occupants for the Beach Park planting design and the Square Park (.356) was below the significance level of 0.05. In other words, satisfaction level for the Beach Park was higher than the satisfaction level for Square Park. Similarly, there were differences between the satisfaction levels for Ganita Park and the Zağnos Recreation Area and of Turkish Japanese Friendship Park planting designs.

Discussion and conclusion

The plants preferred in open green spaces designed in urban areas exhibit a dynamic structure and constantly change urban aesthetics and ecology. Especially when the selections are right and planted at the right location based on the aesthetic and functional purposes, planting design makes significant contributions to not only the urban aesthetics but also the value of the real estate in the city (Tyruainen, 1997). In

http://www.aloki.hu ● ISSN 1589 1623 (Print) ● ISSN 1785 0037 (Online)
DOI: http://dx.doi.org/10.15666/aeer/1704_97959811

recent years, extensive research was conducted on plant material in urban open green areas and urban ecology (Düzenli et al., 2018; Potgieter et al., 2019; Schebella et al., 2019; Yan et al., 2019; Rumble et al., 2019; Yılmaz et al., 2018).

Table 12. *Multiple correlation*

	UOGA	UOGA	Mean difference (İ-J)	Standart error	Sig.
	I	J			
TUKEY HSD	1	2	.300	.130	.141
		3	-.150	.130	.775
		4	.356*	.130	.048
		5	-.131	.130	.849
	2	1	-.300	.130	.141
		3	-.450*	.130	.005
		4	.056	.130	.993
		5	-.431*	.130	.008
	3	1	.150	.130	.775
		2	.450*	.130	.005
		4	.506*	.130	.001
		5	.019	.130	1.000
	4	1	-.356*	.130	.048
		2	-.056	.130	.993
		3	-.506*	.130	.001
		5	-.487*	.130	.002
	5	1	.131	.130	.849
		2	.431*	.130	.008
		3	-.019	.130	1.000
		4	.487*	.130	.002

UOGA: urban open green spaces code

The open green space planning in urban areas often emphasizes the improvement of the quality of life of individuals (Fainstein and Campell, 1996; Salon, 2002; Mumcu et al., 2013), in this respect, it aims to ensure the use of indigenous plant species and to maintain sustainability of other areas of ecological concern (Forman, 2008).

Thanks to plant taxa used in urban open and green areas, the areas with a form and design acquire an anatomy as well. As the plants change, they occupy a place in the function of the urban ecosystem. Thus, functional objectives that planting designs should emphasize emerge.

Urban open green spaces that transform urban spaces into natural areas thanks to the plants, albeit partially, are usually under intensive human management or occupancy (Kurdoğlu et al., 2018). Transportation of plant taxa indigenous to rural areas to urban areas and their utilization in plant designs would lead to natural vegetation patterns. In contrast, the opposite would lead to a contradiction between indigenous and non-indigenous plant species in urban open green spaces.

In the present study, 10 of the 21 most prevalent plant taxa used in the open green areas in Trabzon city were selected from indigenous and 11 were selected from exotic

http://www.aloki.hu ● ISSN 1589 1623 (Print) ● ISSN 1785 0037 (Online)
DOI: http://dx.doi.org/10.15666/aeer/1704_97959811

plants. Of the 129 taxa identified, only 42 were indigenous to Turkey. Although the diversity of plant species was sufficient, the selection of indigenous plant species was not sufficient. Plant species that reflect the characteristic of the region should be preferred. One of the study areas was rich in exotic species diversity when compared to the other areas due to the fact that its concept was Turkish-Japanese friendship.

Aesthetically positive plants are those that the designers want to be noticed or emphasized in a space, while negative plants are not to be noticed. The plants used in the open green areas in the city of Trabzon fulfilled this purpose with distinct aesthetic characters such as leaves, fruits, flowers and color effects, trunks or forms. Another aesthetic aim is the shadows and reflections provided by plants due to natural and artificial lighting elements. In the five urban open green areas reviewed in the present study, the plants exhibited two- or three-dimensional properties. In addition to the evergreen plants used, varieties that change with seasons were also preferred, thus creating impressive landscapes. Deciduous plants formed aesthetic values in winter with their trunks and branching calligraphy. They added an interesting character to the design with their extraordinary shoots and bark patterns. They created harmony or contrast with the pavements and other structural landscaping elements in study areas. In the five parks where the study was conducted in Trabzon, certain taxa were used as solitary plants (*Platanus orientalis, Acer rubrum, Gingko biloba, Salix babylonica* vb) or to attract the attention to certain sections. In order to make the monotonous pavements that are monotonous both horizontally and vertically entertaining, the plants were used as pavements or cover elements. Due to the wind speed and direction, especially the tress in the Beach Park and trees at Ganita Beach Park achieved movement and sound. In all the study areas, fine-delicate, drooping plants such as *Betula pendula* and *Salix babylonica* created an elegant appearance by swinging lightly with the wind.

It is known that plants are a design material in landscape design, and they are used when creating spaces just like other material. The crowns of plants are considered as the cover and trunks are considered as walls of the space. Thus, the plants are used in solitary or in groups to create spaces and sub-spaces in study areas. Also, linear, radial, clustered and grid type designs were adopted in the plant compositions in study areas. In study areas, primary, secondary and tertiary spaces were created based on the field composition and the hierarchical properties of the area. For this purpose, the color, size, linearity, or organization of the plant are considered in hierarchical orders (Yildizci, 1988). It is possible to clarify an existing or planned design with plant compositions, and to associate the objects and spaces in the design. Thus, the plant compositions in study areas aimed to support and to strengthen the design and to provide an integral visual perception.

Planting could associate the objects and spaces. Plants undertake separative and integrative functions in adjacent spaces structurally, create a determinative, rhythmic and emphasizing effects, and provide connections especially in rural and urban landscapes. Furthermore, planting design could be conducted to obtain effects such as strengthening or hiding the topographic structure. In the present study, it mostly strengthened the lines of design since these areas were urban areas without any slopes. The selected *Platanus orientalis* species at the Beach Park was planted in higher intervals from its crown, leading to an open and spacious perception. In contrast, *Ligustrum japonicum* species was planted in frequent intervals and adjacent to each other, creating a border effect and leading to closed perception. When the study areas are examined, it was observed that vistas were created with plant design in only two

http://www.aloki.hu ● ISSN 1589 1623 (Print) ● ISSN 1785 0037 (Online)
DOI: http://dx.doi.org/10.15666/aeer/1704_97959811

urban open green areas. The creation of vista in the design of the study areas were mostly created with structural landscaping elements, with the only exceptions of the Square Park and Turkish-Japanese Friendship Park.

After the findings obtained by the researcher, it was determined that the occupant satisfaction was the highest in the planting designs at Zağnos Recreation Area. This was followed by the Turkish-Japanese Friendship Park, Beach Park, Ganita and the Square Park, respectively. Occupant evaluations demonstrated there were differences between the satisfaction levels of the occupants about the planting designs. The reason for this difference was the utilized plant taxa used as determined in the previous stages.

The three urban open green areas (Beach Park, Zağnos Recreation Area, Turkish-Japanese Friendship Park) investigated in the present study were built very recently. The other two areas were urban renewal projects and recently renovated areas. Therefore, the study findings demonstrated that there have been developments in the design of urban green open spaces and these were designed by expert teams, and the resulting plating designs were appreciated by the occupants.

According to these results, the following points should be considered in the selection of plant species in urban light green areas and in the implementation of planting designs;

In the first place, the designer should create a list of plants which can be used by considering ecological, edaphic and climatic data in the region. The designer should also take into account the structural and visual characteristics of the plants while creating these plant lists, such as the habitats of plants, body trunk bark, branches, shoots, bud, leaves, flowers, seeds and cones should be well aware. because the structural characteristics of the plants also form their visual characteristics. A planting design should be designed by taking one or more of the principles of harmony, contrast, repetition, rhythm, scale, ratio, emphasis, domination, balance and unity. the functions of these planting designs should be functional as well as aesthetic. In other words, except for the beautiful views that the aesthetic views of the plants offer, space creation, supporting the existing structural design, providing inter-space transition, creating emphasis and focus, limiting or creating a border, making screens, providing privacy privacy.

REFERENCES

[1] Akbari, H. (2001): Shade trees reduce building energy use and CO_2 emissions from power plants. – Environmental Pollution 116(1): 119-126.

[2] Akbari, H., Pomerantz, M., Taha, H. (2001): Cool surfaces and shape trees to reduce energy use and improve air quality in urban areas. – Solar Energy 70(3): 295-310.

[3] Akpınar, N., Karadeniz, N., Talay, İ. (1992): Ülkemizde çim tohumlarının durumu ve geleceği. – Peyzaj Mimarlığı 92(2): 25-26.

[4] Bayramoğlu, E., Özdemir, B., Demirel, Ö. (2014): Gürültü Kirliliğinin Kent Parklarina Etkisi Ve Çözüm Önerileri: Trabzon Kenti Örneği. – İnönü Üniversitesi Sanat Ve Tasarım Dergisi 4(9): 35-42.

[5] Beckett, K. P., Freer-Smith, P. H., Taylor, G. (1998): Urban woodlands; their role in reducing the effects of particulate pollution. – Environmental Pollution 99: 347-360.

[6] Beckett, K. P., Freer-Smith, P. H., Taylor, G. (2000): Particulate pollution capture by urban trees; effects of species and windspeed. – Global Change Biology 6(3): 995-1003.

[7] Braun, S., Fluckiger, W. (1998): Soil amendments for plantings of urban trees. – Soil and Tillage Research 49(3): 201-209.

http://www.aloki.hu ● ISSN 1589 1623 (Print) ● ISSN 1785 0037 (Online)
DOI: http://dx.doi.org/10.15666/aeer/1704_97959811

[8] Cepel, N. (1988): Peyzaj Ekolojisi. – İstanbul Universitesi Orman Fak., Yayyn No: 3510, İstanbul.
[9] Davis, P. H. (1965-1985) Flora of Turkey and East Aegean Islands. – Edinburgh Univ. Press, Edinburgh.
[10] Düzenli, T., Tarakci Eren, E., Baltacı, H., and Aktürk, E. (2018): Bitkisel Peyzaj Tasarımında Renk Tercihleri: Ktü Kanuni Kampüsü Örneği. – Journal of International Social Research 11(55).
[11] Ekim, T., Koyuncu, M., Erik, S., İlarsan, R. (1989): Türkiyenin tehlike altındaki nadir ve endemik bitki türleri. – Türkiye tabiatını koruma derneği yayın no: 18, Ankara.
[12] Erenberk, H. (1992): Büyük Ağaçların Söküm ve Dikimi. – Peyzaj Mimarlığı 92(2): 33-36.
[13] Fainstein, S. S., Campbell, S. (2002): Readings in Urban Theory. – Wiley-Blackwell, London.
[14] Forman, R. T. T. (2008): Urban Regions, Ecology and Planning Beyond City. – Cambridge University Press, Cambridge.
[15] Heisler, G. M. (1986): Effects of individual trees on the solar radiation climate of small buildings. – Urban Ecology 9(3): 337-359.
[16] Heisler, G. M., Grant, R. H. (2000): Ultraviolet radiation in urban ecosystems with consideration of effects on human healthy. – Urban Ecosystems 4(3): 193-229.
[17] Leszczynski, N. A. (1999): Planting the Landscape. – John Wiley and Sons, Inc, London.
[18] Lorenz, E. N. (1975): Climatic Predictability. – In: Bolin, B. et al. (eds.) The Physical Basis of Climate and Climate Modelling (Vol. 16). GARP Publication Series, Geneva, pp. 132-136.
[19] Kelkit, A. (2002): Çanakkale kenti açık-yeşil alanlarda kullanılan bitki materyali üzerine bir araştırma. – Ekoloji 10(43): 17-21.
[20] Kurdoğlu, B. Ç., Yeniçirak, P. Ö., Bayramoğlu, E. (2018): Ekolojik Duyarlilik Analizi: Kaçkar Dağlari Milli Parki Örneği. – Journal of International Social Research 11(61).
[21] McDowell, M. J. (1997): The role and application of horticultural therapy with ınstitutionalized older people. – Master Thesis, Mcgill University, Montreal.
[22] Mumcu, S., Yılmaz, S., Özbilen, A. (2013): Ekolojik yaklaşımlar doğrultusunda çevresel tercih modeli. – Türkiye Ormancılık Dergisi 14(2): 143-151.
[23] Novak, D. J., Civerolo, K. L., Rao, S. T., Sistla, G., Luley, C. J., Crane, D. E. (2000): A modeling study of the impact of urban trees on ozone. – Atmospheric Environment 34(10): 1601-1613.
[24] Novak, D. J., Crane, D. E. (2002): Carbon storage and sequestration by urban trees in the USA. – Environmental Pollution 116(3): 381-389.
[25] Potgieter, L. J., Gaertner, M., O'Farrell, P. J., Richardson, D. M. (2019): Perceptions of impact: invasive alien plants in the urban environment. – Journal of Environmental Management 229: 76-87.
[26] Rumble, H., Angeoletto, F., Connop, S., Goddard, M. A., Nash, C. (2019): Understanding and Applying Ecological Principles in Cities. – In: Lemes de Oliveira, F., Mell, I. (eds.) Planning Cities with Nature. Springer, Cham, pp. 217-234.
[27] Sakıcı, Ç. (2009): Ruh ve sinir hastalıkları hastanelerinde açık alan terapi ünitelerinin peyzaj tasarımı: Ataköy (Trabzon) ruh sağlığı ve hastalıkları hastanesi örneği. – Doktora Tezi, K. T. Ü. Fen Bilimleri Enstitüsü, Trabzon.
[28] Schebella, M. F., Weber, D., Schultz, L., Weinstein, P. (2019): The wellbeing benefits associated with perceived and measured biodiversity in Australian urban green spaces. – Sustainability 11(3): 802.
[29] Smardon, R. C. (1990): Perception and aesthetics of the urban environment: review of the role of vegetation. – Landscape and Urban Planning 15(1-2): 85-106.
[30] Urgenc S (1990): Genel Plantasyon ve Adaclandyrma Teknidi. – İstanbul Univ. Yayın No: 3644, İstanbul.

http://www.aloki.hu ● ISSN 1589 1623 (Print) ● ISSN 1785 0037 (Online)
DOI: http://dx.doi.org/10.15666/aeer/1704_97959811

[31] Ulrich, R. S. (2001): Effects of healthcare environmental design on medical outcomes. – In: Design and Health: Proceedings of the Second International Conference on Health and Design. Svensk Byggtjanst, Stockholm, pp. 49-59.
[32] Uslu, O., Türkmen, A. (1987): Su kirliligi ve kontrolü. – TC Basbakanlik Çevre Gen Müd Yay Egt Dizisi, 1.
[33] Tarakci Eren, E., Var, M. (2016): Parkların bitkisel tasarımında kullanılan taksonlar: Trabzon Kent Merkezi Örneği. – Artvin Çoruh Üniversitesi Orman Fakültesi Dergisi 17(2): 200-213.
[34] Tarakci Eren, E., Alpak, E. M., Düzenli, T. (2016): Mevsimsel Bitki Görünümlerinin Tercih Ve Algisal Farkliliklarinin Belirlenmesi. – Uluslararası Bilimsel Araştırmalar Dergisi (Ibad): 3(1): 145-154.
[35] Tarakci Eren, E., Düzenli, T., Alpak, E. M. (2018): Sınır elemanı olarak kullanılan bitkiler ve kullanım işlevleri; KTÜ kampüsü. – Kastamonu Üniversitesi Orman Fakültesi Dergisi 18(2): 108-120.
[36] Tarakci Eren, E., Yılmaz, S., Düzenli, T. (2017): Drawing a Planting Plan in the Process of the Environmental Design Project. – In: Salman, S. (ed.) Academic Researches in Architecture, Engineering Planning and Design. Gece Kitapligi, Ankara.
[37] Turkmen, N. (1987): Cukurova Universitesi Kampus Alanının Dogal Bitkileri, Hayat Formları ve Habitatları. – Doctoral Dissertation, Msc Thesis, Cukurova Universitesi, Adana.
[38] Tyson, M. M. (1998): The Healing Landscape: Therapeutic Outdoor Environments. – McGraw-Hill, New York.
[39] Tyruainen, L. (1997): The amenity value of the urban forest an application of the hedonic pricing method. – Landscape and Urban Planning 37: 211-222.
[40] Walker, T. D. (1991): Planting Design. – Van Nostrand Reinhold, New York.
[41] Yan, Z., Teng, M., He, W., Liu, A., Li, Y., Wang, P. (2019): Impervious surface area is a key predictor for urban plant diversity in a city undergone rapid urbanization. – Science of the Total Environment 650: 335-342.
[42] Yılmaz, H. (1995): Erzurum kenti okul bahcelerinin peyzaj mimarlydy ilkeleri yonunden incelenmesi. – Ataturk Univ. Zir. Fak. Derg. 26(4): 537-547.
[43] Yılmaz, S., Özgüner, H., Mumcu, S. (2018): An aesthetic approach to planting design in urban parks and greenspaces. – Landscape Research 43(7): 965-983.
[44] Yıldızcı, A. C. (1982): Concept of open space, urban texture and green texture- urban landscape planning. – PhD Thesis. Istanbul Technical University, Istanbul (in Turkish).

http://www.aloki.hu ● ISSN 1589 1623 (Print) ● ISSN 1785 0037 (Online)
DOI: http://dx.doi.org/10.15666/aeer/1704_97959811

THE HYDRAULIC CONDUCTIVITY OF MODEL SOIL-BENTONITE CUT-OFF WALL BACKFILLS UNDER CALCIUM CHLORIDE SOLUTION

WANG, R.[1,2,3] – XU, H. Q.[1,3*] – ZHOU, A. Z.[3] – JIANG, P. M.[1,3] – LIU, S. Q.[3] – SONG, M. M.[3]

[1]*Joint Technology Transfer Center of Yancheng Polytechnic College, 224005 Yancheng, P. R. China*

[2]*Shandong Academy of Building Research, 250000 Jinan, P. R. China*

[3]*School of Architecture and Civil Engineering, Jiangsu University of Science and Technology, 212003 Zhenjiang, P. R. China*

[*]*Corresponding author*
e-mail: hankinxu@163.com; phone: +86-157-5177-8209; fax: +86-0515-8858-3900

(Received 28th Mar 2019; accepted 22nd May 2019)

Abstract. In landfill, cut-off walls have been widely used as in situ barriers to isolate contaminants and control the migration of contaminated groundwater. How the permeability of the wall changes as exposed to pollutants is unclear. In view of this issue, Fujian standard sand was used to simulate the stratum, and four clay were used as the mixed material. After mixing, pouring and consolidation, the hydraulic conductivity and water characteristic curve were measured. The results showed that when the permeation of the sand-clay mixtures was stabilized by a 0.2 mol/L calcium chloride solution under the additive amount of 10% clay, the hydraulic conductivity increased to different degrees compared with that permeated with tap water, but did not increase more than tenfold. Moreover, the porosity didn't change significantly after the stabilization of the permeation of the calcium chloride solution in the four kinds of sand-clay mixtures but decreased slightly. The experimental results showed that the replacement between calcium ions and univalent cations on the surface of clay mineral particles decreases the thickness of the diffused double layer and the content of bound water; thus, the effective porosity increases, which may be the main reason for the increase of the permeability.
Keywords: *regional soil and water contamination, landfills, engineering barriers, leachate, permeability*

Introduction

With the rapid economic development and the improvement of urbanization in China, the output of garbage is increasing, as is the number of landfills. In 2008, the environmental protection special inspection campaign of eight ministries and commissions of the State Council carried out a diagnostic investigation of the scale of landfill sites, anti-seepage measures, and the operation of leachate treatment facilities throughout the country. The results showed that there are 935 open and closed refuse landfills in China, 34% of which do not take anti-seepage measures. These simple landfills without strict designs and construction, especially those without a bottom seepage control system, have become a major environmental hazard. In the future, the number of pollution control projects needed for this kind of landfills will increase gradually. It is very difficult and costly to rebuild horizontal seepage control systems in the bottom of exhausted landfills. Therefore, constructing a closed vertical cut-off wall has been widely applied. Soil-bentonite cut-off walls are also used to prevent pollutants from leaking into the groundwater and soil at the Rocky Mountain Arsenal site (Patton et

http://www.aloki.hu ● ISSN 1589 1623 (Print) ● ISSN 1785 0037 (Online)
DOI: http://dx.doi.org/10.15666/aeer/1704_98139826

al., 2007), which is a chemical weapons and pesticide production wasteland in the United States. It is also common to make up for the loss or failure of horizontal anti-seepage systems by using a vertical cut-off wall. There are few reports of concrete examples of vertical cut-off wall construction in existing refuse landfills in China, but vertical anti-seepage control systems have also been used in the construction of new landfills. During the 4th phase construction of the Shanghai Laogang Municipal Solid Waste Landfill built on the intertidal zone, a vertical cut-off wall of cement-bentonite was applied to the new landfill (Fei et al., 2005). In summing up the technology of vertical cut-off walls, Yao and Bao mentioned that the plain-type landfills of the Shanghai Laogang 4th Phase, Central Tangshan, Gangyang, and Taizhou all adopted anti-seepage control methods combining the horizontal and vertical methods (Yao and Bao, 2008). The horizontal-vertical anti-seepage system was also used in the expansion of the Landfill in Qizi Mountain, Suzhou.

Concerning the aspects of the material, design and construction of vertical cut-off walls, in summing up the vertical cut-off technology of landfills in our country, Jing et al. thought that because of a late start, the methods of water conservancy, geology and civil engineering of the anti-seepage material and construction technology were borrowed, especially grouting anti-seepage technology (Jing et al., 2006). In addition, theoretical or technical methods for anti-seepage of landfills have not been developed yet. However, cut-off walls of soil-clay material have good engineering characteristics, and the anti-seepage and anti-fouling properties have received much attention. The construction procedure of clay-based vertical cut-off walls is to excavate the trench first and adopt 4% ~ 6% mud counterfort at the same time, mix the excavated stratum and clay proportionally, and then mix the produced mixture fully with the mud in the trench (Rumer and Ryan, 1995). Then, the sand-clay mixture is backfilled with a collapsing slump of 100 ~ 150 mm, and a vertical cut-off barrier with a hydraulic conductivity of less than 10^{-7} cm/s is formed. Devlin and Parker have studied the anti-fouling performance of soil-bentonite cut-off walls (Devlin and Parker, 1996). Through theoretical calculations, it was concluded that when the thickness of the cut-off wall is 1 m and the hydraulic conductivity is less than 5×10^{-8} cm/s, the hydraulic transportation of pollutants can be effectively controlled, and the escape of pollutants mainly occurs through the slow molecular diffusion process. Thus, how to make the hydraulic conductivity of the clay and stratum less than 5×10^{-8} cm/s has become an important problem in engineering.

The chemical compatibility between the backfill material of cut-off wall and the contaminants in the leachate is very important for clay-based cut-off walls. For example, the hydraulic conductivity of the backfill material of soil-bentonite cut-off walls, geosynthetic clay liners (GCL) and compacted sand-bentonite mixtures may increase due to the interaction between the backfill material and inorganic cations (Jo et al., 2005; Katsumi et al., 2008). Grube found that when sodium hydroxide solution permeated soil-bentonite backfill material, the impermeability decreased by 5 ~ 10 times (Grube, 1992). The increase of the concentration of organic solutions and electrolyte solutions or the effect of strong acid solution will change the structure of clay, especially bentonite, and lead to an increase by orders of magnitude in the hydraulic conductivity. Lee et al. found that the liquid limit, settling volume and expansion index create a critical threshold for the increase of the hydraulic conductivity through permeability testing and settlement testing (Lee et al., 2005). Fan et al. mixed lead nitrate solution of different concentrations with kaolin-bentonite to simulate cut-off wall contamination by lead (Fan et al., 2013). They carried out consolidation tests and settlement tests. The hydraulic conductivity of

http://www.aloki.hu ● ISSN 1589 1623 (Print) ● ISSN 1785 0037 (Online)
DOI: http://dx.doi.org/10.15666/aeer/1704_98139826

the mixture increased 2 ~ 15 times with the increase of the lead concentration. This was attributed to the compression of the double layer and the change of the surface charge of the soil particles.

The above research reveals that the change of the electrochemical environment in soil has a key effect on the hydraulic conductivity, but it can also be seen that the change rule of the hydraulic conductivity is not uniform in terms of quantity because of the different types of clay used. It is obvious that the chemical substances not only change the viscosity of the permeant fluid but also block the movement of water, and changes of the electrochemical environment in the soil and changes of the bound water around the clay particles result in the change of the micro-pore structure. This may be the main reason why the effects of chemical solutions are different from those of water permeation. Thus, it is necessary to study the influence of chemical solutions on the hydraulic conductivity when using different clay minerals. In this research, four kinds of clay are used to carry out laboratory experiments.

Materials and Methods

Materials

Because the stratum varies according to the site conditions, considering the adverse conditions of the soil layer properties in the simulated site, Fujian standard sand (commercial) is selected to simulate the stratum and is hereinafter referred to as FSS,. The basic physical properties are shown in *Table 1* (Hu and Yang, 2012).

Table 1. *Physical properties of the model stratum*

G_s	C_u	ρ_{dmax}(g/cm^3)	ρ_{dmin}(g/cm^3)	e_{max}	e_{min}
2.64	5.99	1.74	1.43	0.85	0.52

Table 2. *Geotechnical properties of the four clays*

Type	G_s	w_L (%)	w_p (%)	Swell index (mL/(2g))
Clay-K	2.68	39	23	2.6
Clay-J	2.72	48	24	3.1
Clay-A	2.72	53	27	4.1
Bent-A	2.70	301	56	38.5

The four kinds of natural clay (powdery) are as follows. Clay-K is produced in Lingshou County, Shijiazhuang, Hebei Province, and the main clay mineral is kaolinite; Clay-J is produced in Jiangning District, Nanjing, Jiangsu Province, and the main clay mineral is illite; Clay-A is produced in the Inner Mongolia Autonomous Region, and the main clay mineral is palygorskite; and Bent-A is produced in Anji, Huzhou, Zhejiang, and the main clay mineral is montmorillonite. The basic physical properties of the above four kinds of clay are obtained according to the Standard for Soil Test Method (GB/T

http://www.aloki.hu ● ISSN 1589 1623 (Print) ● ISSN 1785 0037 (Online)
DOI: http://dx.doi.org/10.15666/aeer/1704_98139826

50123-1999) and Bentonite (GB/T 20973-2007), as shown in *Table 2*. The clay and standard sand are dried at 105°C for 24h ~ 48h.

Permeability tests of permeant fluids are carried out using tap water and $CaCl_2$ solution, respectively. The properties of these fluids are shown in *Table 3*. The reason why we choose $CaCl_2$ solution is because of the widespread use of $CaCl_2$ to evaluate the effects of multivalent cations on hydraulic conductivity in previous experimental studies (Shackelford et al., 2000). Although various multivalent cations may be contained in the leachate of the actual landfill, the influence of these cations on the chemical compatibility of the clay barriers will not be very different. For example, the experiments of Jo et al. and Kolstad et al. show that the types of the divalent cations (Cu^{2+}, Mg^{2+}, Zn^{2+} and Ca^{2+}) have no significant effect on the free expansion and hydraulic conductivity of GCL at a given concentration (Jo et al., 2001; Kolstad et al., 2004).

Table 3. *Basic properties of the permeant fluids used*

Permeant fluid	$CaCl_2$ concentration (mol/L)	Ca^{2+} concentration (mg/L)	Electrical conductivity (ms/m)
Tap water	--	15.8	95
$CaCl_2$ solution	0.2	5120.4	8230

The particle size distribution curves of Fujian standard sand and the four types of clay are shown in *Fig. 1*. It can be seen from the figure that apart from the relatively large particle size of bentonite, the particle size distribution, clay content and fine granule content of the other 3 types of clay are similar.

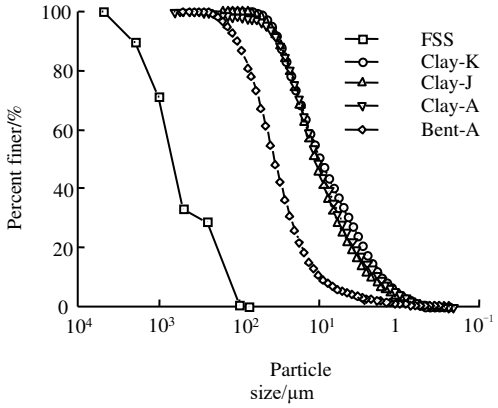

Figure 1. *Particle size distributions of the five soils in this study*

Sample preparation

The standard sand is mixed uniformly with a certain amount of clay, and then mixed with the prepared 5% mud (Rumer and Ryan, 1995) to form a pouring sample similar to concrete mortar. To simulate the backfill mixture used in actual construction, the slump of the permeable sample is controlled within the range of 100 ~ 150 mm. In the

http://www.aloki.hu ● ISSN 1589 1623 (Print) ● ISSN 1785 0037 (Online)
DOI: http://dx.doi.org/10.15666/aeer/1704_98139826

experiment, the additive amount of clay of 10% (percentage of the clay dry mass to the standard sand dry mass) is used.

Improved flexible wall permeability test

The RST-1 flexible wall permeameter developed by Nanjing Soil Instruments is modified due to the weak self-standing property of the samples. Referring to the improvement idea for a triaxial apparatus by Min et al., a cutting ring with many holes of 3 mm in diameter is added to the periphery of the sample (Min et al., 2019). In this way, the sample can be self-standing, and the confining pressure can be applied to the sidewall of the sample (see *Fig. 2*). Compared with the rigid wall permeameter, this setup can effectively prevent the influence of sidewall seepage. At the same time, the stress state of the cut-off wall in the actual project can be simulated in a relatively real way by applying the confining pressure of 100 kPa and then conducting the permeability test. The osmotic pressure difference is 70 kPa, the diameter of the sample is 7 cm, and the height is 4 cm. The test method of flexible wall permeability refers to ASTM D5084 (ASTM, 2010). During the experiment, the sample is permeated at 25℃ room temperature.

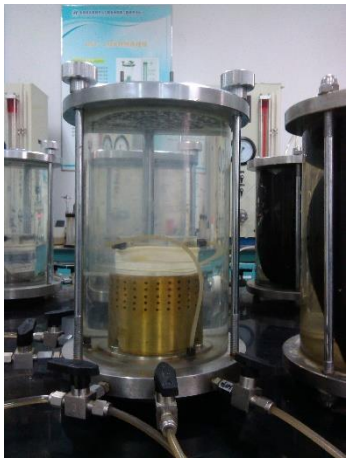

Figure 2. *An improved flexible wall permeameter*

Bound water matric suction test

To understand the changes of the binding state of water in the soil after adding clay, the centrifugal moisture metre is used to measure the bound water content (mass percentage of bound water and pore water) of the sample after completion of the test. The centrifugal moisture metre is based on the principle that the centrifugal force generated by high-speed rotation can separate water with low potential energy. The amounts of water retained in the sample at different speeds are measured, and then the separating potential energy is calculated according to the rotating speed. Finally, the relation between the potential energy and water is obtained. This experiment uses the Himac high-speed freezing centrifuge manufactured by HITACHI (see *Fig. 3*), and the detailed operation is shown in the literature (Zhu et al., 2007).

http://www.aloki.hu ● ISSN 1589 1623 (Print) ● ISSN 1785 0037 (Online)
DOI: http://dx.doi.org/10.15666/aeer/1704_98139826

Figure 3. *The centrifuge used in the test*

Results

Effect of $CaCl_2$ solution on the hydraulic conductivity of the sand-clay mixture

At the same addition rate of 10%, the changes over time of the obtained hydraulic conductivity of 0.2 mol/L $CaCl_2$ solution in the four sand-clay mixtures are collected, and *Fig. 4* is obtained. Fig. 4(a), 4(b), 4(c), and 4(d) show the curves of hydraulic conductivity variable against time for the sand-Clay-K, sand-Clay-J, sand-Clay-A and sand-Bent-A mixtures. It can be seen from the figure that the hydraulic conductivity of sand-Clay-K, sand-Clay-A and sand-Bent-A increases to varying degrees, except for the hydraulic conductivity of the sand-Clay-J mixture, which decreases slightly, and the hydraulic conductivity of sand-Clay-K, sand-Clay-A and sand-Bent-A increases to some extent. The hydraulic conductivity of sand-Clay-K and sand-Clay-A fluctuates by one order of magnitude, but the hydraulic conductivity of sand-Bent-A mixture varies greatly. During the process, the maximum hydraulic conductivities of sand-Clay-K, sand-Clay-J, sand-Clay-A and sand-Bent-A are 3.517×10^{-5} cm/s, 3.018×10^{-5} cm/s, 3.278×10^{-5} cm/s, 3.129×10^{-5} cm/s, respectively.

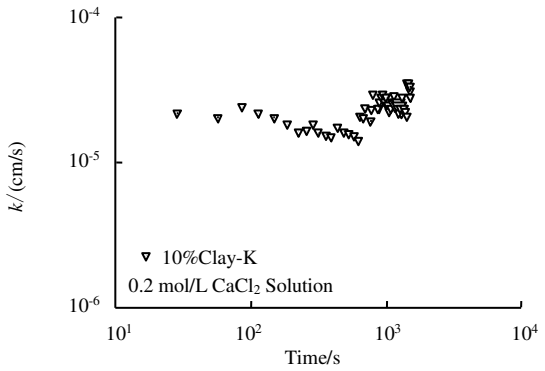

(a) adding 10% Clay-K

http://www.aloki.hu ● ISSN 1589 1623 (Print) ● ISSN 1785 0037 (Online)
DOI: http://dx.doi.org/10.15666/aeer/1704_98139826

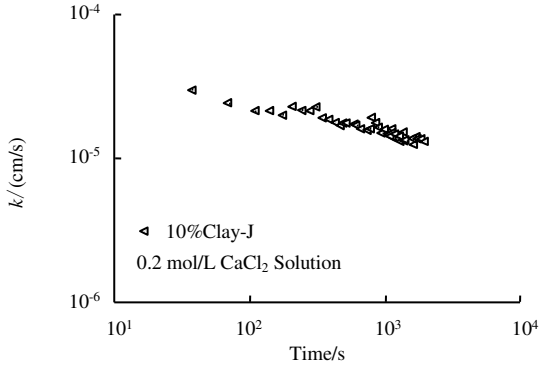

(b) adding 10% Clay-J

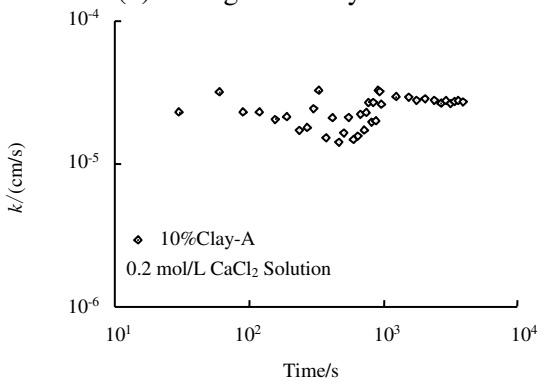

(c) adding 10% Clay-A

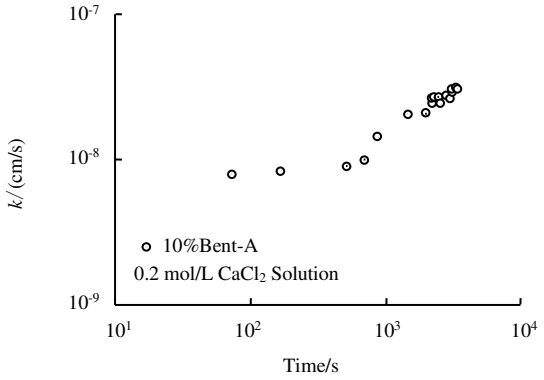

(d) adding 10% Bent-A

Figure 4. *Changes of the hydraulic conductivity of the sand-clay mixtures with time*

Table 4. *Hydraulic conductivity k with the permeant fluid of tap water or $CaCl_2$ solution*

Permeant **fluid**	***k*/(cm/s)**			
	sand-Clay-K	**sand-Clay-J**	**sand-Clay-A**	**sand-Bent-A**
Tap water	1.064×10^{-5}	3.222×10^{-6}	3.979×10^{-6}	3.169×10^{-9}
$CaCl_2$ solution	3.238×10^{-5}	1.470×10^{-5}	2.758×10^{-5}	2.811×10^{-8}

http://www.aloki.hu ● ISSN 1589 1623 (Print) ● ISSN 1785 0037 (Online)
DOI: http://dx.doi.org/10.15666/aeer/1704_98139826

In addition, the stabilized hydraulic conductivities of tap water and $CaCl_2$ solution are compared and analysed in four kinds of sand-clay mixtures with 10% content, as shown in *Table 4* and *Fig. 5*.

In contrast, the final hydraulic conductivity ratios of $CaCl_2$ solution and tap water in sand-Clay-K and sand-Clay-J are less than 5, but the hydraulic conductivity ratio of $CaCl_2$ solution and tap water in sand-Clay-A and sand-Bent-A is between 5 and 10.

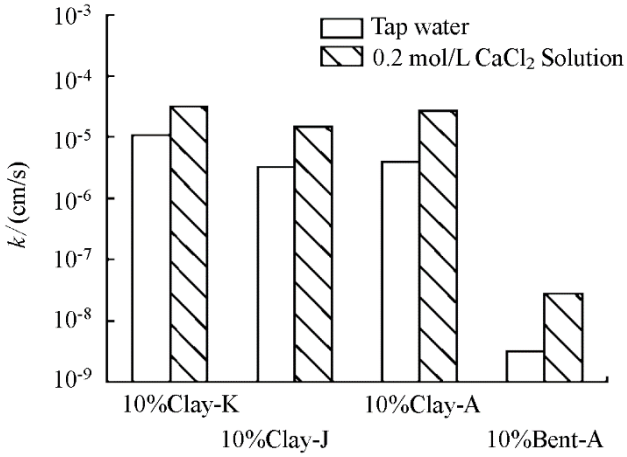

Figure 5. *Hydraulic conductivity of the mixture permeated by tap water or $CaCl_2$ solution*

Effect of $CaCl_2$ solution on the porosity of the sand-clay mixture

Previous studies have analysed the changes of hydraulic conductivity on the basis of changes in the porosity. The porosity *n* of the samples after permeation by tap water and $CaCl_2$ solution are also measured and calculated in the four sand-clay mixtures, respectively. The comparison of porosity between tap water and $CaCl_2$ solution is obtained, which is shown in *Fig. 6* and *Table 5*.

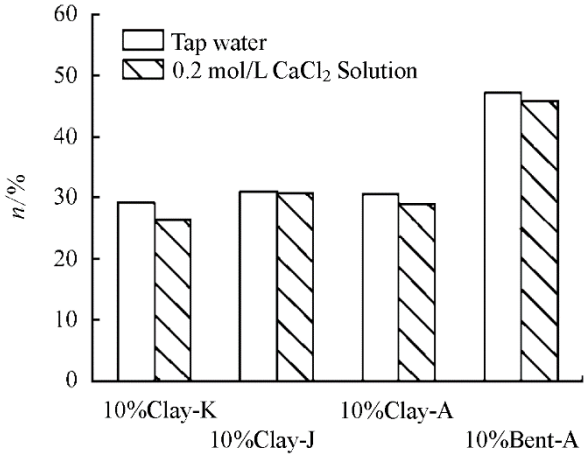

Figure 6. *The porosities of sand-clay mixtures permeated by tap water or $CaCl_2$ solution*

Overall, the porosity of tap water and $CaCl_2$ solution in the four sand-clay mixtures after permeation do not change significantly but generally decrease, because the chemical

http://www.aloki.hu ● ISSN 1589 1623 (Print) ● ISSN 1785 0037 (Online)
DOI: http://dx.doi.org/10.15666/aeer/1704_98139826

reaction between $CaCl_2$ and the clay minerals forms a small number of new compounds (Yanful et al., 1995), which clog the internal water-conducting pore channels in the mixture, resulting in the reduction of porosity. Thus, for a sand-clay mixture, the hydraulic conductivity of the mixture changes over time during the whole process of permeation by $CaCl_2$ solution.

Table 5. *The porosity n of the sand-clay mixtures permeated by tap water or $CaCl_2$ solution*

Permeant fluid	*n*/%			
	sand-Clay-K	sand-Clay-J	sand-Clay-A	sand-Bent-A
Tap water	29.26	31.05	30.72	47.07
$CaCl_2$ solution	26.24	30.63	28.82	45.57

Effect of $CaCl_2$ solution on the bound water content of the sand-clay mixture

The permeability of soil has a certain relationship with the pore size, and it may also have a certain relationship with the form of water in the pores. When researching the micro electric field effect of the seepage of tiny-particle clay, Liang et al. found that the bonding of soil particle surfaces will affect the permeability of the soil under the interaction of a clay-water-electrolyte system (Liang et al., 2010). Based on the consideration of whether the bound water has an effect on the permeability of the mixture, moisture centrifugal dehydration is carried out on the mixtures to determine the *pF* value of the binding potential energy of the pore water in each sample (logarithm of the centimetre height of the water column of the water suction in the soil), which is shown in *Fig. 7*. Referring to the research result of Lebedev, the *pF* value of 3.8 is used to distinguish bound water from free water (Lebedev, 1936). The bound water content in mixture can be obtained from the intercept of the moisture content with the *pF* value of more than 3.8 from the water characteristic curve. *Fig. 8* and *Table 6* show the comparison of the content of bound water between the effects of tap water and $CaCl_2$ solution after permeation in the four kinds of sand-clay mixtures.

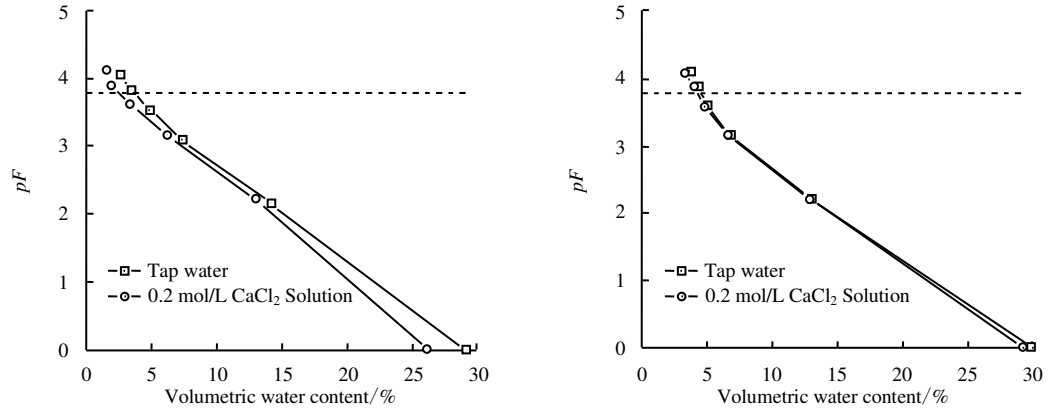

(a) adding 10% Clay-K (b) adding 10% Clay-J

http://www.aloki.hu ● ISSN 1589 1623 (Print) ● ISSN 1785 0037 (Online)
DOI: http://dx.doi.org/10.15666/aeer/1704_98139826

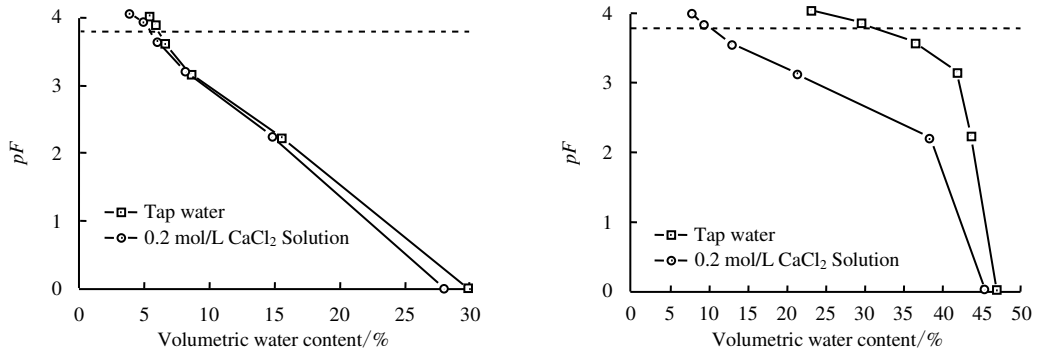

(c) adding 10% Clay-A (d) adding 10% Bent-A

Figure 7. *Soil-water characteristic curves of mixtures permeated by tap water or $CaCl_2$ solution*

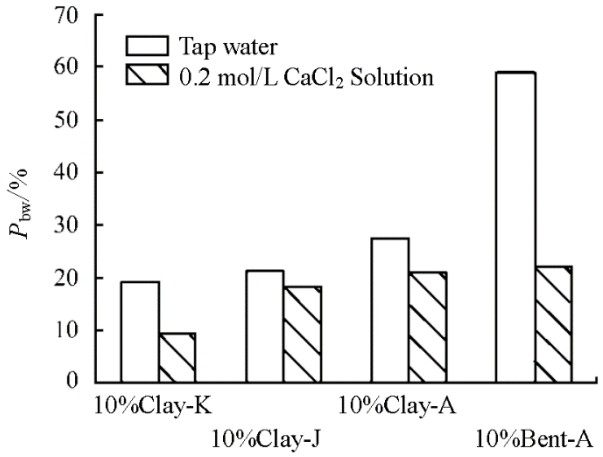

Figure 8. *Bound water percentages P_{bw} of sand-clay permeated by tap water or $CaCl_2$ solution*

Table 6. *Bound water percentages with the permeant liquid of tap water or $CaCl_2$ solution*

Permeant **fluid**	**Bound water percentage P_{bw}/%**			
	sand-Clay-K	**sand-Clay-J**	**sand-Clay-A**	**sand-Bent-A**
Tap water	19.15	21.16	27.41	59.03
$CaCl_2$ solution	9.31	18.18	20.91	22.15

Compared with those using tap water, the bound water content of the samples using $CaCl_2$ solution in sand-Clay-K, sand-Clay-J, sand-Clay-A and sand-Bent-A mixtures after permeation decrease to some extent. In addition, the change of the bound water content of the sand-Bent-A mixture is the largest.

http://www.aloki.hu ● ISSN 1589 1623 (Print) ● ISSN 1785 0037 (Online)
DOI: http://dx.doi.org/10.15666/aeer/1704_98139826

Discussion

By combining *Fig. 5* and *Fig. 6*, it can be seen that the hydraulic conductivity of $CaCl_2$ solution in the four kinds of sand-clay mixture after permeation increases to varying degrees and that the corresponding porosity does not increase but decreases slightly. This is different from the common phenomenon in which the porosity of clay minerals decreases and the hydraulic conductivity decreases (Mesri and Olson, 1971). Thus, It is speculated that in the process of permeation of the sand-clay mixture, the water with a certain degree of binding ability to clay particles in the pore water is relatively stagnant. It may be an abnormal liquid with mechanical properties between those of a solid and a liquid (Sridharan et al., 1986) and showing viscosity, that is, there is a water film with a large binding potential energy to soil particles around the clay particles. This is the inner layer-Stern layer of the diffused double layer (stern layer) (Yuan, 2012), as shown in *Fig. 9*.

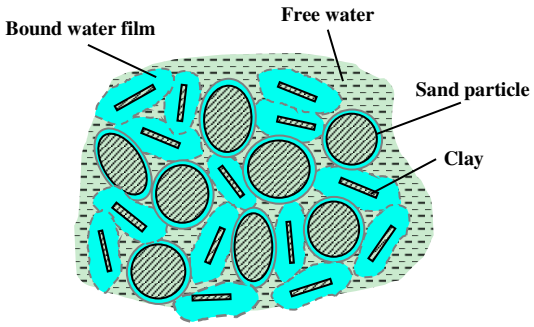

Figure 9. *Schematic diagram of a sand-clay mixture sample*

Based on the above assumptions, the calculation method (*Equation 1*) of the effective porosity n_{eff} is proposed:

$$n_{eff} = n(1 - P_{bw}) \quad \text{(Eq.1)}$$

where P_{bw} is the bound water content in the pore water of the sand-clay mixture.

The effective porosities of the four kinds of sand-clay mixtures are calculated after permeation by tap water and $CaCl_2$ solution, respectively, as shown in *Fig. 10*.

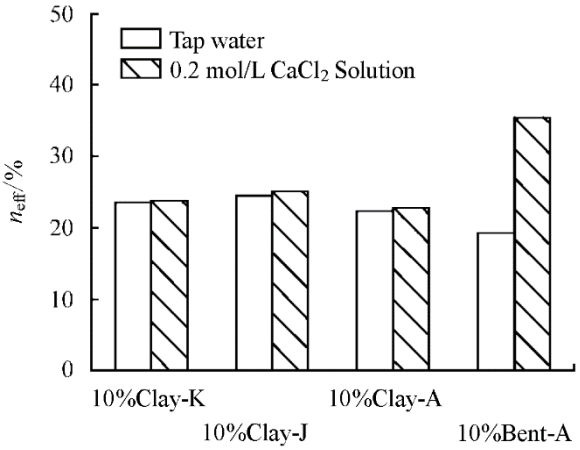

Figure 10. *Effective porosity neff of sand-clay permeated by tap water or $CaCl_2$ solution*

http://www.aloki.hu ● ISSN 1589 1623 (Print) ● ISSN 1785 0037 (Online)
DOI: http://dx.doi.org/10.15666/aeer/1704_98139826

It can be seen directly from *Fig. 10* that for the four kinds of sand-clay mixtures, the final hydraulic conductivity after permeation with $CaCl_2$ solution is increased to varying degrees. This is because although the porosity of the mixture does not change much, or even decreases, the effective porosities of the four kinds of sand-clay mixtures increase, which may be the main reason for the increase of the final hydraulic conductivities of the mixtures. In my opinion, there is a replacement reaction between the calcium ions in the permeant fluid and the univalent metal cations (such as sodium and potassium ions) adsorbed onto the surface of the clay mineral particles. The thickness of the diffused double layer on the surface of the clay mineral particles becomes thinner, and the corresponding bound water content decreases (Gu and Fang, 2009), which results in the increase of the effective porosity and the increase of the hydraulic conductivity of the mixture.

Conclusions

Based on discussions of the test results and further analysis, the following conclusions can be made:

(1) The self-modified flexible wall permeameter is used, and permeability tests of tap water and 0.2 mol/L $CaCl_2$ solution in sand-Clay-K, sand-Clay-J, sand-Clay-A and sand-Bent-A mixtures are conducted. The results show that when the additive amount of clay is 10% and the confining pressure is 100 kPa, compared with the effects of tap water, the hydraulic conductivity of the sand-clay mixture increases in varying degrees when $CaCl_2$ solution is used as the permeant fluid. However, with an increase of the hydraulic conductivity by 10 times, the porosity of $CaCl_2$ solution in the four mixtures decreases slightly after permeation. It is proven that the seepage-control function of the sand-Bent-A mixture used as the material for landfill cut-off walls at the addition rate of 10% can meet the requirement.

(2) The experimental results show that the calcium ion in the permeant fluid is replaced by the univalent cation on the surface of clay mineral particles, which results in the decrease of the thickness of the diffused double layer and the decrease of the bound water content, leading to the increase of the effective porosity. Macroscopically, the hydraulic conductivity of the mixture becomes larger.

(3) In this study, the permeability tests were conducted under calcium chloride solution. However, in fact the contaminants in the landfill leachate may also include inorganic matters and organic matters. Thus, the chemical compatibility of cut-off walls in the presence of composite contaminations, the interaction between clay particle and contaminated fluid is recommended. On-going additional research is aimed at addressing all of the limitations.

Acknowledgements. The authors would like to acknowledge the Open Fund of Joint Technology Transfer Center of Yancheng Polytechnic College (Grant No. YGKF-201810), Key Research and Development Program (Social Development) Project of Zhenjiang (Grant No. SH2018024), National Natural Science Foundation of China (Grant No. 51579119) for supporting this study.

http://www.aloki.hu ● ISSN 1589 1623 (Print) ● ISSN 1785 0037 (Online)
DOI: http://dx.doi.org/10.15666/aeer/1704_98139826

REFERENCES

[1] ASTM Committee D5084. (2010): Standard test methods for measurement of hydraulic conductivity of saturated porous materials using a flexible wall permeameter. – ASTM International.
[2] Devlin, J. F., Parker, B. L. (1996): Optimum hydraulic conductivity to limit contaminant flux through cutoff walls. – Groundwater 34(4): 719-726.
[3] Fan, R. D., Du, Y. J., Liu, S. Y., Chen, Z. B. (2013): Engineering behavior and sedimentation behavior of lead contaminated soil-bentonite vertical cutoff wall backfills. – Journal of Central South University 20(8): 2255-2262.
[4] Fei, P. Y., Ji, R., Zhang, D. L. (2005): Laboratory research on the properties of containment wall material of Shanghai Laogang municipal sanitary waste landfill. – Shanghai Geology (4): 51-53.
[5] Grube, W. E. (1992): Slurry trench cut-off walls for environmental pollution control. – In Slurry Walls: Design, Construction, and Quality Control. ASTM International.
[6] Gu, R. G., Fang, Y. G. (2009): Experimental research on ion effects of ultrafine granular clay seepage. – Rock and Soil Mechanics 30(6): 1595-1598.
[7] Hu, P., Yang, Q. (2012): Experimental study of swelling characteristics of bentonite-sand mixture. – Rock and Soil Mechanics 33(2): 453-458.
[8] Jing, X. D., Ruan, W. J., Dai, G. Z. (2006): Present state of antiseepage techniques used in waste landfill sites. – Journal of Changchun Institute of Technology (Natural Sciences Edition) 7(1): 1-4.
[9] Jo, H. Y., Benson, C. H., Shackelford, C. D., Lee, J. M., Edil, T. B. (2005): Long-term hydraulic conductivity of a geosynthetic clay liner permeated with inorganic salt solutions. – Journal of Geotechnical and Geoenvironmental Engineering 131(4): 405-417.
[10] Jo, H. Y., Katsumi, T., Benson, C. H., Edil, T. B. (2001): Hydraulic conductivity and swelling of nonprehydrated GCLs permeated with single-species salt solutions. – Journal of Geotechnical and Geoenvironmental Engineering 127(7): 557-567.
[11] Katsumi, T., Ishimori, H., Onikata, M., Fukagawa, R. (2008): Long-term barrier performance of modified bentonite materials against sodium and calcium permeant solutions. – Geotextiles and Geomembranes 26(1): 14-30.
[12] Kolstad, D. C., Benson, C. H., Edil, T. B. (2004): Hydraulic conductivity and swell of nonprehydrated geosynthetic clay liners permeated with multispecies inorganic solutions. – Journal of Geotechnical and Geoenvironmental Engineering 130(12): 1236-1249.
[13] Lebedev, A. F. (1936): Soil and groundwaters. – The Academy of Sciences of the USSR, Moscow, Russia.
[14] Lee, J. M., Shackelford, C. D., Benson, C. H., Jo, H. Y., Edil, T. B. (2005): Correlating index properties and hydraulic conductivity of geosynthetic clay liners. – Journal of Geotechnical and Geoenvironmental Engineering 131(11): 1319-1329.
[15] Liang, J. W., Fang, Y. G., Gu, R. G. (2010): Analysis of microelectric field effect of seepage in tiny-particle clay. – Rock and Soil Mechanics 31(10): 3043-3050.
[16] Mesri, G., Olson, R. E. (1971): Mechanisms controlling the permeability of clays. – Clays and Clay Minerals 19(3): 151-158.
[17] Patton, P., Day, S., Byle, M. (2007): Compatibility evaluation of groundwater cutoff wall using salt-resistant bentonite and BFS/cement for deep-mix barrier wall. – In Soil Improvement (pp. 1-11).
[18] Rumer, R. R., Ryan, M. E. (1995): Barrier containment technologies for environmental remediation applications. – Wiley-Interscience, New York.
[19] Shackelford, C. D., Benson, C. H., Katsumi, T., Edil, T. B., Lin, L. (2000): Evaluating the hydraulic conductivity of GCLs permeated with non-standard liquids. – Geotextiles and Geomembranes 18(2-4): 133-161.
[20] Sridharan, A., Rao, S. M., Murthy, N. S. (1986): Compressibility behavior of homogenized bentonite. – Geotechnique 36(4): 551-564.

http://www.aloki.hu ● ISSN 1589 1623 (Print) ● ISSN 1785 0037 (Online)
DOI: http://dx.doi.org/10.15666/aeer/1704_98139826

[21] Yanful, E. K., Shikatani, K. S., Quirt, D. H. (1995): Hydraulic conductivity of natural soils permeated with acid mine drainage. – Canadian Geotechnical Journal 32(4): 624-646.
[22] Yao, Y. C., Bao, Z. W. (2008): Application of vertical cut-off curtain to sanitary landfill site in plain areas. – Environmental Engineering 26(3): 29-32.
[23] Yuan, J. B. (2012): The study of properties of bound water in clayey soils and their quantitative methods. – South China University of Technology, Guangzhou, China.
[24] Min, F., Du, J., Zhang, N., Chen, X., Lv, H., Liu, L., Yu, C. (2019): Experimental study on property change of slurry and filter cake of slurry shield under seawater intrusion. – Tunnelling and Underground Space Technology 88: 290-299.
[25] Zhu, W., Zhang, C. L., Chiu, A. C. (2007): Soil–water transfer mechanism for solidified dredged materials. – Journal of Geotechnical and Geoenvironmental Engineering 133(5): 588-598.

http://www.aloki.hu ● ISSN 1589 1623 (Print) ● ISSN 1785 0037 (Online)
DOI: http://dx.doi.org/10.15666/aeer/1704_98139826

HEAVY METAL CONTENT IN THE BARK OF CAMPHORA TREE IN XIANGTAN AND ITS ENVIRONMENTAL SIGNIFICANCE

ZHANG, Y.[1*] – XIANG, Y. B.[2] – CHEN, W. Y.[1]

[1]*School of Resource, Environment and Safety Engineering, Hunan University of Science and Technology, Taoyuan Road, Xiangtan, Hunan Province, China*

[2]*School of Architecture and Art Design, Hunan University of Science and Technology, Taoyuan Road, Xiangtan, Hunan Province, China*

**Corresponding author*
e-mail: 292278@qq.com; phone: +86-151-7326-5757

(Received 28th Mar 2019; accepted 22nd May 2019)

Abstract. With rapid economic development, Xiangtan, as an old industrial base of China and a famous industrial city in Hunan Province, caused severe pollution, which had a significant impact on people's lives. To understand the heavy metal pollution in Xiangtan, we tested and analyzed the barks of *Cinnamomum camphora* in different functional areas. The article examined the differences and sources of heavy metal contents in the bark of *Cinnamomum camphora* from different functional areas. The results showed that the contents of various heavy metals in the barks of *Cinnamomum camphora* varied considerably and the most common elements of heavy metal pollution were Mn, Pb, and Cr. The activities in different functional areas had a significant influence on the enrichment of heavy metals in the bark of *Cinnamomum camphora*. Heavy metals in the business district mainly came from traffic emissions and various domestic wastes. High population density and household litter affected the heavy metal contents in the Residential District. Heavy metal contents were high in parts of the urban green space due to living garbage or surrounding environment.
Keywords: *pollution, functional areas, spatial distribution, bark, indicator*

Introduction

With the rapid development of the global economy, pollutants containing various heavy metals enter the environment in different ways. Heavy metal pollution can gradually become a serious environmental issue. The hazards of heavy metals including both existing and potential forms have an almost irreversible effect on ecosystems and human health (Sun et al., 2011; Zhang et al., 2012, 1998). Heavy metal pollution has many characteristics, including latency, cumulativeness, long lifespan, and irreversibility. If we do not take immediate and effective measures, it will have a more severe impact. Heavy metals in the environment mainly come from gas emissions, road traffic emissions and industrial emissions (Yao et al., 2012; Zhang et al., 2012). Previous studies showed that heavy metals in plant surface often decreased with increasing distance from pollution sources (Zhu et al., 2007; Chen et al., 2016).

There are various methods to detect atmospheric heavy metal pollution. Broad-leaved and coniferous trees, such as mosses, lichens, vascular plants, and woody-plants, can be utilized to study air pollution (Sun et al., 2011; Huang et al., 1983, 1984; Fang et al., 2000). Because the surface layer of plant contacts more with the atmosphere and is sensitive to environmental changes, it becomes a significant carrier for monitoring air pollution. Though barks do not absorb heavy metals and other pollutants sensitively as mosses do, it is a good indicator of other contaminants, such as electrical conductivity, pH, sulfur, nitrogen, heavy metals, and so on (El-Hasan et al., 2003). Because

http://www.aloki.hu ● ISSN 1589 1623 (Print) ● ISSN 1785 0037 (Online)
DOI: http://dx.doi.org/10.15666/aeer/1704_98279835

Cinnamomum camphora is a street tree and its bark is exposed to the atmosphere for a long time, it has a large contact area with the atmosphere. Barks of *Cinnamomum camphora* not only contained heavy metal elements absorbed from the soil but also accumulated a large amount of dust and particles from the atmosphere (Huang et al., 1983; Zhou et al., 2014). Therefore, this paper chose barks of *Cinnamomum camphora* as an indicator of air pollution to study.

Xiangtan is an old industrial city. In recent years, with the continuous development of industry and economy, the heavy metal contents of Xiangtan have increased sharply. This study tries to analyze the spatial distribution characteristics of heavy metal in the barks of *Cinnamomum camphora* in Xiangtan, reveal the sources and causes of heavy metal pollution, and explore the pollution situation. This study can not only investigate the causes and extent of heavy metal pollution in Xiangtan City but also provide a scientific basis for ecological research in urban areas. It is also helpful to environmental governance, human health, urban eco-environment, and sustainable urban development.

Materials and methods

Research area

Xiangtan City (111°58'E-113°05'E, 27°21'N-28°05'N) is a prefecture-level city in the east-central of Hunan Province, with a total area of 5015 km^2. It is the smallest prefecture-level city in Hunan Province, China. In 2010, the city's resident population was 2.748 million, of which 959,000 were in the urban area, with a population density of 549 people/km^2, ranking second in Hunan Province. The climate of Xiangtan belongs to a subtropical monsoon humid climate with abundant precipitation, sufficient solar and thermal resources. Although the annual rainfall reached 1200-1500 mm, the time distribution was uneven, and the inter-annual variability was considerable (Xiao, 1996).

Xiangtan's geographical position is superior. Many expressways and railways meet and pass here, which is highly beneficial to the economic development of Xiangtan. Simultaneously, Xiangtan, together with Changsha and Zhuzhou, is the "Golden Triangle" urban agglomeration with the most developed politics, economy and culture in Hunan Province (Xiao, 1996). In recent years, Xiangtan's economy has been growing, especially in various industries. Xiangtan has grown up to be a heavy industrial city with mechanical, metallurgical, chemical and textile industries. Main industrial types include coal, metallurgy, chemical fiber, chemical industry, textile, leather, agricultural products' processing, etc. Among them, industrial products with national influence are iron and steel, military products, electromechanical products, and some chemical products.

Sampling and analysis

In January, 2015, the barks of *Cinnamomum camphora* in different functional areas, such as the Residential District (Shuxiangyulin, near the railway station), Commercial District (Bus Station), Industrial District (Xiangtan Iron & Steel Co. Ltd of Hunan Valin, Longpai Food Limited by Share Co. Ltd) and Urban Green District (Baishi Park, Yuhu Park, Yuetang Park, Peace Park), were sampled (*Fig. 1*). The barks of 3-5 selected *Cinnamomum camphora* trees, which have similar age and a 25-45 cm diameter at breast height in one place, were taken from the same side of the trunk at 1.3-1.5 m above the ground surface.

http://www.aloki.hu ● ISSN 1589 1623 (Print) ● ISSN 1785 0037 (Online)
DOI: http://dx.doi.org/10.15666/aeer/1704_98279835

When sampling, the adhesives on the bark's surface were removed with a hard brush, then the barks of 5 × 5 cm^2 were scrape off with a stainless steel knife. To prevent contact pollution and increase the experiment error, polish the bark's surface with sandpaper. The samples were enclosed in a polyethylene self-sealing bag and numbered. Synchronously, the sampling point, sampling time, weather condition, geographical location, altitude and tree height, etc were recorded.

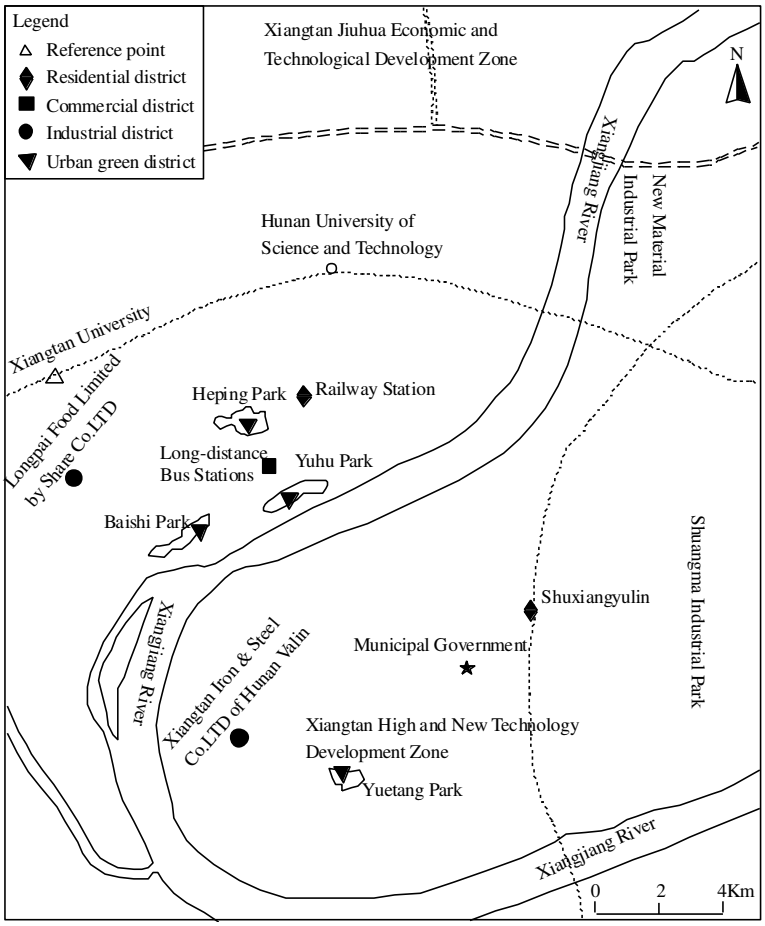

Figure 1. *Schematic diagram of sampling sites*

In the laboratory, the impurities were removed and the samples were baked to a constant weight at 105 °C in a thermostat. Then, the dried sample was ground in an agate mortar through a 100 mesh nylon sieve. Next, 2 ml HCL, 5 ml HNO_3 and 2 ml H_2O_2 were added to 0.5 g ground samples that were digested by microwave digestion (Zhuang et al., 2000). Afterward, the digested samples were heated at 300 °C for 4 h by an electric heating plate to remove the acid. After sample treatment, a FAAS (flame atomic absorption spectrophotometer) was utilized to test the content of heavy metal (Cd, Pb, Cr, Cu, Mn) (Lü, 2008; Sharifi et al., 2017; Kord et al., 2010; Ahmad Afif, 2010; Xie et al., 2009). The correlation between the standard solution was at least 0.99, the error of the heavy metal content of the parallel sample was less than 5%, and every five groups added a blank sample. All experimental data must be subtracted from the blank sample to ensure accuracy.

http://www.aloki.hu ● ISSN 1589 1623 (Print) ● ISSN 1785 0037 (Online)
DOI: http://dx.doi.org/10.15666/aeer/1704_98279835

Results and analysis

Heavy metal contents in the bark of Cinnamomum camphora

Because Xiangtan University is located in the suburb of Xiangtan City, we take the heavy metal contents in the barks of *Cinnamomum camphora* at Xiangtan University as preset reference values to reveal the regional differences due to its good environmental conditions (*Fig. 2*).

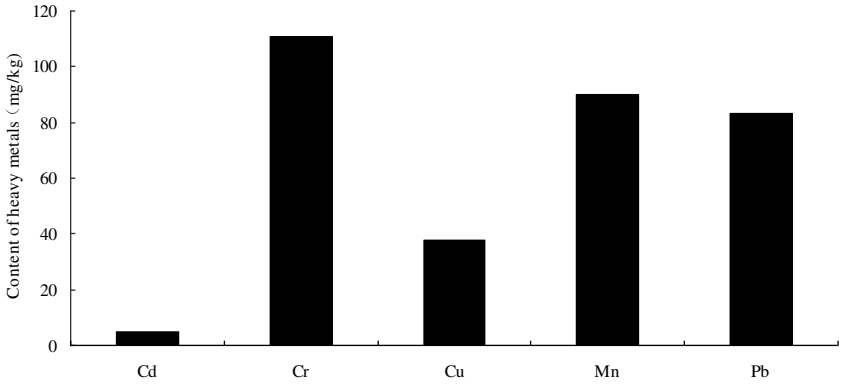

Figure 2. *Contents of heavy metals in the bark of Cinnamomum camphora at Xiangtan University*

The average content of Cd in Xiangtan is 5.35 mg/kg, with a range of 2-10.0 mg/kg; Average content of Cr is 117.35 mg/kg, with a range of 42.0-266.0 mg/kg; Average content of Cu is 44.376 mg/kg, with a range of 23.74-126.42 mg/kg; Average content of Mn is 304.529 mg/kg, with a range of 19.5-1214.56 mg/kg; Average content of Cr is 86.65 mg/kg, with a range of 30.0-220.0 mg/kg (*Tables 1* and *2*). Average heavy metal content in the barks of *Cinnamomum camphora* was Mn > Cr > Pb > Cu > Cd, and the content of Mn reached 304.529 mg/kg. The content of Mn in Xiangtan has a high background value, which is a factor with local characteristics. The above situation may be related to the long-term mining of Mn in Xiangtan Manganese Mine. During over 100 years of mining, tailing, slag and sewage were not treated effectively and timely, resulting in the loss and diffusion of Mn. Manganese can diffuse into the atmosphere and soil through a variety of approaches (Xie et al., 2005; Xi et al., 2008). Plants can absorb manganese through their roots, accepting atmospheric deposition, and absorption function of plants themselves, so that the manganese content in plants reached a higher level.

Heavy metal contents in the barks of Cinnamomum camphora in different functional districts and their sources

Content and spatial distribution of heavy metals in the barks of *Cinnamomum camphora* were different in different functional regions in Xiangtan city (*Table 2*). The content of the heavy metals in each functional district is Industrial Area > residential area > urban green area > commercial area. Among them, the heavy metal content in the Industrial District was the highest, and the maximum value reached 1301.5 mg/kg. The highest content of manganese also appeared in the Industrial District, reaching

http://www.aloki.hu ● ISSN 1589 1623 (Print) ● ISSN 1785 0037 (Online)
DOI: http://dx.doi.org/10.15666/aeer/1704_98279835

736.68 mg/kg. The maximum heavy metal contents in the Residential District reached 947.06 mg/kg, and the contents of Mn, Cr, and Pb were relatively high. Urban Green Districts in this research were mainly urban parks, and their environments are relatively good. Overall, the heavy metal content of the barks of *Cinnamomum camphora* in Urban Green Districts is lower than that in industrial and Residential Districts. However, because Yuetang Park is located close to the old industrial zone of Xiangtan Iron & Steel Co. Ltd of Hunan Valin, environmental pollution around Yuetang Park was severe, and the maximum heavy metal content reached 833.42 mg/kg.

Table 1. *Heavy metal contents in Cinnamomum camphora in Xiangtan (mg/kg)*

Heavy metal	Cd	Cr	Cu	Mn	Pb
Average	5.35	117.35	44.376	304.529	86.65
Range	2.0-10.0	42.0-266.0	23.74-126.42	19.5-1214.56	30.0-220.0
Standard deviation	1.994	51.089	19.242	261.859	42.944

Table 2. *Fundamental characteristics of heavy metal in the barks of Cinnamomum camphora in different functional districts (mg/kg)*

Functional district		Cd	Cr	Cu	Mn	Pb	Total
Residential district	Maximum	8	124	43.82	653.24	118	947.06
	Minimum	4	46	29.16	77.08	60	216.24
	Average	5.3	104	33.66	318.78	79.67	541.41
Commercial district	Maximum	6	162	126.42	222.94	104	621.36
	Minimum	4	78	39.18	84.36	30	235.54
	Average	4.33	113.67	65.81	161.82	59.67	405.3
Industrial district	Maximum	10	266	68.52	736.68	220	1301.2
	Minimum	4	78	39.96	169.14	92	383.1
	Average	6.5	164.25	53.37	405.33	133.75	763.2
Urban green district	Maximum	10	150	65.44	330.86	144	700.3
	Minimum	2	42	23.74	115.36	32	215.1
	Average	5.29	94.57	37.92	221.73	67.57	427.08
Reference point	Maximum	6	150	37.64	149.5	182	525.14
	Minimum	4	106	35.32	69.16	52	266.48
	Average	5	125	36.74	126.68	102.33	395.75

The sources of heavy metal pollution in cities are exceptionally incredible, and the primary pollution sources in diverse functional areas are different. The highest heavy metal content in the barks of *Cinnamomum camphora* in Xiangtan is Mn due to the exploitation of Xiangtan Manganese Mine. However, the content of manganese is different in various functional areas (*Table 3; Fig. 3*). The manganese content in Shuxianglin was 333.96 mg/kg, ranking third in all sampling sites. Besides Mn, the content of Cr and Pb was relatively high, reaching 160 mg/kg and 78 mg/kg respectively. The dense buildings, less greening area, a large population density, large living garbage, living sewage and a large amount of exhaust gas from the combustion of domestic fuel near this district led to the high content of Mn, Cr, and Pb. Besides,

http://www.aloki.hu ● ISSN 1589 1623 (Print) ● ISSN 1785 0037 (Online)
DOI: http://dx.doi.org/10.15666/aeer/1704_98279835

Shuxiangyulin Community is next to Ji'an Road and not far away from the Xiangtan East Automobile Station. Barks of *Cinnamomum camphora* might accumulate a large amount of automobile exhaust and road dust due to the huge traffic flow, which may also be the reason for the high content of Cr and Pb. The minimum values of Cr and Mn appeared near the Railway Station, reaching 68 mg/kg and 78.12 mg/kg. The principal reasons are its location close to the suburbs, the low buildings and the small traffic flow of the adjacent roads.

Table 3. *Heavy metal content in different sampling areas of different functional districts (mg/kg)*

Functional district	Site	Cd	Cr	Cu	Mn	Pb	Total
Residential district	Shuxiangyulin	5	160	31.08	333.96	78	608.04
	Near the railway station	4	68	30.7	78.12	67	247.82
Commercial district	Bus station	5	137	48.83	214.83	92	497.66
Industrial district	Longpai Food Limited by Share Co. Ltd	6	210	39.96	233.28	114	603.24
	Xiangtan Iron & Steel Co. Ltd of Hunan Valin	8	79	62.34	712.89	202	1064.23
Urban green district	Baishi Park	3	101	32.62	127.08	71	334.7
	Yuhu Park	8	54	29.15	119.67	59	269.82
	Yuetang Park	6	82	34.94	304.48	77	504.42
	Peace Park	4	68	33.79	168.82	43	317.61
Reference site	Xiangtan University	5	111	37.64	89.85	83	326.49

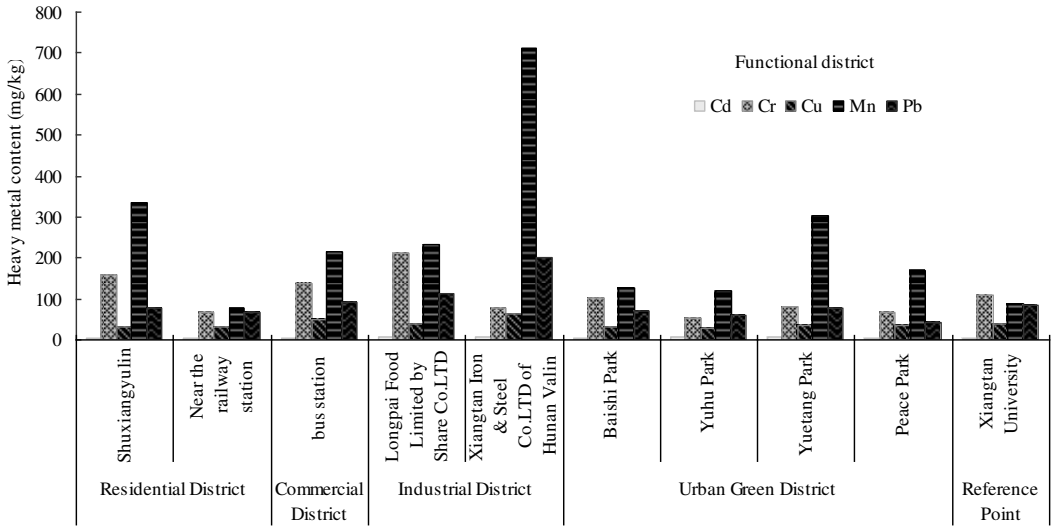

Figure 3. *Contents of heavy metals in the barks of Cinnamomum camphora in different functional areas*

The contents of Cd, Cr, Cu, Mn and Pb in the barks of *Cinnamomum camphora* were high in the Commercial District. The Long-distance Bus Station, as an essential part of the Commercial District, is located in the centre of Xiangtan City and has various food,

http://www.aloki.hu ● ISSN 1589 1623 (Print) ● ISSN 1785 0037 (Online)
DOI: http://dx.doi.org/10.15666/aeer/1704_98279835

accommodation and entertainment industries, resulting in more garbage compared to other areas. Moreover, a large number of heavy metals can be produced by exhaust emissions from vehicle fuel combustion and dust in this district because of the massive traffic volume. These heavy metals will enter the atmosphere, and then accumulate on the surface of the barks of *Cinnamomum camphora* through atmospheric sedimentation and plant adsorption.

In the Industrial District, the heavy metal contents in the barks of *Cinnamomum camphora* are very high (*Tables 2* and *3; Fig. 3*). The maximum value of Mn and Pb both found in Xiangtan Iron & Steel Co. Ltd of Hunan Valin (*Fig. 3*) and reached 712.89 mg/kg, 7.9 times that of the reference point. The content of Pb reached 202 mg/kg, 2.4 times that of the reference point. The main reason why the heavy metal content of Xiangtan Iron & Steel Co. Ltd is so high is that it is a long-standing iron and steel enterprise with a complete set of technological processes, such as coking, sintering, ironmaking, steelmaking, rolled materials and so on. A large number of waste gas, wastewater, and residues containing Mn, Pb, Cd, and other heavy metals can discharge during the production process, and then enter the atmosphere and soil. After atmospheric deposition and rain wash, the heavy metal would accumulate in plants by absorption and adsorption through roots and barks. Therefore, the heavy metal contents in the barks of *Cinnamomum camphora* were high. At Longpai Food Limited by Share Co. Ltd, due to small greening, dense buildings and large traffic volume, the contents of Cr, Mn, Pb, and other heavy metals in the barks of *Cinnamomum camphora* are also relatively high, reaching 210 mg/kg, 233.28 mg/kg and 114 mg/kg, respectively.

Although Yuetang Park is an urban green space, it is located in the old industrial area and has a long history. Besides, it is close to Xiangtan Iron & Steel Co. Ltd, a critical pollutant enterprise. Therefore, the content of Mn in the barks of *Cinnamomum camphora* in this area even reaches a high level of 304.48 mg/kg, which is the place where the maximum content of Mn and Pb appears in urban green space. From *Table 3*, the highest content of Cr appears in Baishi Park, and the content is 101 mg/kg. Baishi Park lies in the old city centre of Xiangtan. There are more residents around it, and the traffic flow near the sampling point is also significant. Similar to other places with the high contents of heavy metal, road dust and living sewage are the main reasons for the high content of Cr in this area.

Conclusion

Heavy metal contents in the barks of *Cinnamomum camphora* had a specific accumulation and could indicate the air pollution condition in Xiangtan. The results showed that:

- The contents of Cr, Mn, and Pb in the barks of *Cinnamomum camphora* were the highest. Among them, the content of Mn exceeded seriously, and the average content was Industrial District > Residential District > Urban Green District > Commercial District. The maximum value of Mn appeared at Xiangtan Iron and Steel Co., with a high value of 712.89 mg/kg, which was 7.9 times the reference point.
- Heavy metals in the barks of *Cinnamomum camphora* mainly were produced by traffic discharge, living waste, manganese mining, and industrial enterprise discharge. The heavy metal contents in the barks of *Cinnamomum camphora* in the industrial area and its adjacent urban green space was high, which was

http://www.aloki.hu ● ISSN 1589 1623 (Print) ● ISSN 1785 0037 (Online)
DOI: http://dx.doi.org/10.15666/aeer/1704_98279835

mainly due to the production and emission of industrial enterprises. For Commercial Districts, the high contents of heavy metal were affected primarily by the traffic flow, automobile exhaust, and domestic waste. Population density and domestic waste were the significant factors affecting the heavy metal in the barks of *Cinnamomum camphora* in Residential Districts. Although some urban green space has a good environment and a vast green area, the heavy metal content in the barks of *Cinnamomum camphora* was high because of the influence of living waste and the surrounding environment.

- Bark has broad application prospects in monitoring environmental heavy metal pollution, but the current research is far from enough. Combining various biological monitoring methods (e.g., moss, leaves, barks, and roots), improving testing techniques and seeking more geochemical means will be the direction of future efforts.

REFERENCES

[1] Ahmad Afif, H. (2010): Biomarker as Indicator of Aerial Dispersal of Heavy Metal within Remediated and Abandoned Tin Mine Site. – Universiti Teknologi Petronas, Perak, Malaysia.

[2] Chen, B., Lu, S., Li, S., Lu, S., Shi, Y., Li, L. (2016): Analysis of heavy metal and sulfur absorption ability of trees under different pollution gradients in Tianjin City. – Research of Soil and Water Conservation 23(1): 175-182.

[3] El-Hasan, T., Al-Omari, H., Jiries, A., Al-Nasir, F. (2002): Cypress tree (Cupressus semervirens L.) bark as an indicator for heavy metal pollution in the atmosphere of Amman City, Jordan. – Environment International 28(6): 513-519.

[4] Fang, Y., Wei, Y., Zhang, X., Yang, K. (2000): Advances in bry-monitoring of atmospheric heavy metal pollution. – Journal of Nanjing Forestry University 24(5): 64-68.

[5] Huang, H., Zhang, C., Zhang, Y., Jiang, D., Wang, Y. (1983): Study on absorption and accumulation of heavy metal pollutants in the woody plants. – Acta Ecologica Sinica 3(4): 11-19.

[6] Huang, H., Zhang, C., Zhang, Y., Jiang, D., Wang, Y. (1984): Study on tolerance of woody-plants to heavy metal pollutants in air. – Acta Phytoecologica et Geobotantica Sinica 8(2): 41-50.

[7] Kord, B., Mataji, A., Babaie, S. (2010): Pine (Pinus Eldarica, Medw.) needles as indicator for heavy metals pollution. – International Journal of Environmental Science & Technology 7(1): 79-84.

[8] Lü, C. (2008): Review on the detection methods of heavy metals. – Resource Development & Market 24(10): 887-890.

[9] Sharifi, R., Baboli, M. J., Roomiani, L. (2017): Essential heavy metal concentrations (Zn, Fe, Cu, Mg and Mn) in muscle tissue of green tiger shrimp, Penaeus semisulcatus, with different size classes. – Journal of Animal & Plant Sciences 27(4): 1402-1407.

[10] Sun, X., Tang, W. (2011): Research on plant monitoring and analysis of Fushun heavy metal pollution in atmosphere. – Environmental Science and Management 36(9): 122-124.

[11] Xi, C., Dai, T., Zhang, H., Liu, W. (2008): Investigation and assessment on pollution of soil heavy metals in Xiangtan City. – Bulletin of Soil and Water Conservation 28(3): 133-137.

[12] Xiao, Z. (1996): Eco-environmental disasters and their developmental tendency in Hunan Province. – Chinese Journal of Ecology 1: 51-56.

http://www.aloki.hu ● ISSN 1589 1623 (Print) ● ISSN 1785 0037 (Online)
DOI: http://dx.doi.org/10.15666/aeer/1704_98279835

[13] Xie, R., Tian, D., Fang, X. (2005): Assessment of pollution of heavy metals on the slag wasteland of Xiangtan manganese mine. – Journal of Central South University of Forestry & Technology 25(2): 38-41.
[14] Xie, Y., Cao, Y. (2009): Determination of heavy metals in corn leaves by atomic absorption spectrophotometry. – Journal of Jilin Institute of Chemical Technology 26(2): 35-39.
[15] Yao, L., Liao, X., Zhang, H., Ling, C., Yu, Z. (1998): Progress and trend of atmospheric heavy metal pollution in China. – Environmental Science and Management 37(9): 41-44.
[16] Yu, G., Yuan, K., Wang, X., Mo, H. (2012): Classification of environmental disaster in Hunan Province. – Disaster Advances 5(4): 195-200.
[17] Zhang, N. (1998): The present situation and prospect of research on heavy metal pollution in soil-plant system. – Chinese Journal of Environmental Engineering 7(4): 30-33.
[18] Zhang, Y., Su, J., Jiang, W., Huang, Z., Xiang, Y., Zeng, F. (2012): Study on the heavy metal pollution evaluation and countermeasures of middle size and small cities in typical drainage area—taking Xiangtan reach of Xiangjiang River as an example. – Research Journal of Chemistry and Environment 16: 172-179.
[19] Zhou, L., Zhang, X., Yang, W., Li, L., Shi, S., Zhang, L., Dong, L., Huang, Y. (2014): Levels and Possible Sources of Organochlorine Pesticides (OCPs) in Camphor (*Cinnamomum camphora*) Tree Bark from Southern Jiangsu, China. – Environmental Science 35(3): 1159-1163.
[20] Zhu, W., Bian, B., Ruan, A. (2007): Analysis of sources of heavy metal contamination in road-deposited sediment from Zhenjiang. – Environmental Science 28(7): 1584-1589.
[21] Zhuang, S., Wang, K. (2000): Study on the relationship between atmospheric heavy metal pollution (Pb, Cd, Cu, Zn) and its accumulations in leaves of urban trees. – Journal of Yantai University (Natural Science and Engineering Edition) 13(1): 33-39.

http://www.aloki.hu ● ISSN 1589 1623 (Print) ● ISSN 1785 0037 (Online)
DOI: http://dx.doi.org/10.15666/aeer/1704_98279835

INCIPIENT CONDITION OF SEDIMENT MOTION IN GREAT DIMENSIONLESS FLOW DEPTH

WANG, R. – YU, G. L.*

SKLOE, CISSE, School of Naval Architecture, Ocean & Civil Engineering, Shanghai Jiao Tong University, Shanghai 200240, China
(phone: +86-186-1621-6478)

**Corresponding author*
e-mail: yugl@sjtu.edu.cn; phone: +86-134-8215-0851

(Received 28th Mar 2019; accepted 22nd May 2019)

Abstract. The incipient condition of granular sediments in great dimensionless flow depth was studied. A series of experimental runs were performed with four kinds of sediments in a 28 m long, 6 m wide flume and the data concerning incipient velocity, water depth and sediment particle size were collected to determine the relationship between incipient velocity and dimensionless water depth. The similarity condition between experimental flow and prototype flow with great dimensionless water depth was analysed according to the logarithmic velocity distribution law in the open channel firstly. The analysis results indicate that water depth cannot be used as a directing-variable for the incipient velocity of granular sediments in great dimensionless flow depth. In order to solve this problem, boundary layer momentum thickness was introduced into flume experiment to replace water depth as the directing-variable. Furthermore, an empirical formula for the incipient velocity of granular sediment in great dimensionless flow depth that includes the proportion of fluid γ, the proportion of granular sediment γ_s, the acceleration of gravity g and the dimensionless water depth (H/d) was proposed and the calculated results are more accurate and reasonable compared to previous studies, especially when the dimensionless water depth is greater than 10^4.
Keywords: *incipient velocity, granular sediment, the ratio of water depth to particle size (H/d), similarity condition, boundary layer momentum thickness*

Introduction

Almost all sediment-related problems in water, including water quality and pollution, scouring, deposition, and issues related to construction and management of reservoirs and canals, and wetland restoration, are associated with the incipient condition of sediment motion (Venditti et al., 2006). In a lake, the bottom currents due to external forces (e.g., winds) can suspend the bottom sediments, thus enhancing the release of contaminants and nutrients from the bed into the water column (Zhang et al., 2018; Zhang and Yu, 2017). The incipient velocity of sediment is an important parameter to estimate sediment motion as well as riverbed evolution, and to solve the engineering problems of riverbed deformation, bank protection engineering, channel stability and other engineering problems (Zou et al., 2017; Mao et al., 2011). The study on the incipient condition of sediment motion has also great significance to the protection of marine ecological environment, hence it has been a hot topic for decades.

There are two major parameters to describe the incipient condition of sediment motion, i.e., threshold bed shear stress (Rijn, 1984; Chien and Wan, 1999; Yu and Lim, 2003; Zhang and Yu, 2017) and incipient velocity (Beheshti et al., 2008; Francisco et al., 2014). Incipient velocity is more widely used in practices, because only when the flow velocity is sufficiently great, the sedimentary particles which belong to a flat-bed can be dislodged and start to move (Righetti and Lucarelli, 2007; Luo, 2011). In

http://www.aloki.hu ● ISSN 1589 1623 (Print) ● ISSN 1785 0037 (Online)
DOI: http://dx.doi.org/10.15666/aeer/1704_98379863

addition, the incipient velocity of sediment is the basic of mechanics of sediment motion and riverbed evolution, and is also an important parameter to solve the sediment problems of riverbed deformation, bank protection engineering, channel stability and other engineering problems (Zou et al., 2017; Mao et al., 2011).

There are a lot of efforts on investigating the incipient condition of sediment motion and many useful formulae have been proposed and successfully applied in practical engineering. As early as 1935, according to the experimental data, Hjulstrom found that when the sediment particle size was 0.2-0.3 mm, the incipient velocity of sediment had a minimum value (Phillips, 1992) and since then, scholars from all over the world carried out many experimental research and theoretical analysis, and derived many formulae for the incipient velocity of sediment from the perspective of mechanics and random process. Xie (1981) recommended several representative former Russia formulae such as Shyamov formula (*Eq. 1*), which can be used to calculate the incipient velocity of the granular sediments with the particle size $d > 0.15$ mm and Goncharov formula (*Eq. 2*).

$$v_c = 1.14\sqrt{\frac{\rho_s - \rho}{\rho} gd}\left(\frac{h}{d}\right)^{\frac{1}{6}} \quad \text{(Eq.1)}$$

$$v_c = 1.07\sqrt{\frac{\rho_s - \rho}{\rho} gd}\lg\left(\frac{h}{d}\right)^{\frac{1}{6}} \quad \text{(Eq.2)}$$

where d = the particle size, v_c = the incipient velocity of sediments, h = the depth of water, ρ and ρ_s were the density of fluid and sediment particle respectively, g = acceleration of gravity, ξ and m were the undetermined coefficients. Considering the viscosity of fine sediment, many Chinese scholars have proposed new formulae for the incipient velocity of sediment. Dou (1960) proposed a formula for the incipient velocity of sediment in shallow water in 1960 and modified it in 1974, such as *Equation 3*.

$$v_c = 0.32(\ln 11\frac{h}{k_s})[(\frac{\rho_s - \rho}{\rho})gd + 0.19(\frac{\varepsilon_k + dh\delta}{d})]^{0.5} \quad \text{(Eq.3)}$$

where $\delta = 0.213 \times 10^4$ cm; $\varepsilon_k = 2.56$ cm^2/s^2, k_s is riverbed roughness, and for the flat bed, $k_s = 0.5$ mm when $d \leq 0.5$ mm and $k_s = d$ when $d > 0.5$ mm. Zhang (1961) proposed *Equation 4*, which is the formula of Wuhan Institute of Hydraulic and Electric Engineering and adopted in Chinese code.

$$v_c = [1.76(\frac{\rho_s - \rho}{\rho})d + 0.000000605(\frac{10 + h}{d^{0.72}})^{0.5}(\frac{h}{d})^{0.14} \quad \text{(Eq.4)}$$

However, the parameters introduced by previous research results which are mostly determined by the flume experiments would affect the accuracy of the formulae, because the water depth in flume is always limited to 0.1-0.5 m, whereas the actual estuary water depth can reach 5-10 m, sometimes even about 20 m (Zeng et al., 2010). Compared with other formulas, the formula (*Eq. 5*) of Sha (1965) payed more attention

http://www.aloki.hu ● ISSN 1589 1623 (Print) ● ISSN 1785 0037 (Online)
DOI: http://dx.doi.org/10.15666/aeer/1704_98379863

to the influence of increased water depth on the incipient velocity of sediment, which was closer to the natural river (Zhang, 2012).

$$v_c = \sqrt{\frac{\rho_s - \rho}{\rho} gdh^{1/5}[266(\frac{\delta}{d})^{1/4} + 0.66\times10^9(0.7-\varepsilon)^4(\frac{\delta}{d})^2]^{1/2}} \quad \text{(Eq.5)}$$

where δ = the film water thickness and $\delta = 0.0001\ mm$; ε was the porosity and $\varepsilon \cong 0.4$). Whereas, Han et al. (1982) considered that the formula of Sha (1965) took the influence of the bonding force caused by contact between sediment particles and the porosity on the incipient velocity of sediment into account, but the mechanical mechanism was not described and expressed clearly. Therefore, the formula for the incipient velocity of sediment needs to be further studied.

The formulae of the incipient velocity of sediment are based on limited water depth which may result in their inapplicability (Zeng et al., 2010). The formula form $v_c = kd^{1/3}h^{1/6}$ is almost adopted to calculate the incipient velocity of non-viscous sediment (Karmer, 1935; He et al., 2002). Nie et al. (2004) summarized dozes of the existing formulas and derived the unified formula (*Eq. 6*), whereas the values of ξ and m were slightly different in different formulae.

$$v_c = \xi\sqrt{\frac{\rho_s - \rho}{\rho} gd}(\frac{h}{d})^m \quad \text{(Eq.6)}$$

In most cases, the value of *m* is 1/6 and the of value ξ is usually between 3. 37 and 7 (Nie, 2004). He et al. (2002) believed that ξ was not a constant, but within a certain range and changed with the relative exposure of particles on the bed surface. However, it is found that the value of ξ at different flow levels is variable according to the analysis of the 246 groups of data on sediment initial motion at Yichang station which is one of the reservoirs of Three Gorges in China (Li et al., 2006). Li et al. (2006) used the normative formula of Wuhan Institute of Hydraulic and Electric Engineering and Shyamov formulae to calculate the incipient velocities of sediment based on the different flow levels at the Yichang station, and there was a huge error between the calculated results and the field measured data, especially in the case of huge flow. In addition, the coefficient ξ of *Equation 6* varies greatly when it is used to calculate the incipient velocities of the granular sediments with different particle sizes in the flow with the same water depth, i.e., Lu (1991) proposed the formulae for the incipient velocity of the pebble in the Yangtze river (its *H/d* range is 80 ~ 1000) and sandy and muddy (the range *H/d* of was 10000 ~ 100000), which based on the field measured data of sediment initial motion in the Yangtze river, but the value of ξ are 0.95 and 1.47, respectively, between which the difference is 1.55 times. Therefore, it is still necessary to study the incipient velocity of sediment under the premise of fully considering the influence of water depth or relative water depth on the incipient velocity of sediment.

To ensure that the formulae for the incipient velocity of sediment obtained by the flume experiments are more accurate and reliable, the similarity conditions between the experimental flow and the prototype flow with great dimensionless water depth should be satisfied (Ferro, 1999; Falcão et al., 2014; Dornbrack and Schumann, 1993; Steward and Tennankore, 1977). According to the force analysis of the sediment particles on the horizontal bed without seepage, only the drag force and the lifting force are favorable to

http://www.aloki.hu ● ISSN 1589 1623 (Print) ● ISSN 1785 0037 (Online)
DOI: http://dx.doi.org/10.15666/aeer/1704_98379863

the initial motion of sediment particles, except the geometric status of sediment particles and the bed roughness (Niven, 2010; Bohorquez and Fernandez-Feria, 2008; Mao et al., 2011). Therefore, the distribution of the flow velocity on vertical line in the experimental flow and the prototype flow with great dimensionless water depth should satisfy the principle of similitude to ensure the accuracy of the experimental results, because the distribution of flow velocity would be affected by different water depth, which would have an impact on the Kinematic similarity between the experiment flow and the prototype flow with great dimensionless water depth. The velocity distribution in experimental flow and natural open channel flow generally adopt the logarithmic formula of velocity distribution (Yu and Tan, 2006; Meftah and Mossa, 2016) and the formula can be written as

$$\frac{u}{u_*} = \frac{1}{k}\ln(\frac{y}{\Delta}) \qquad \text{(Eq.7)}$$

where y = the height from the bed, u = the velocity at the height y, u_* = the friction velocity, κ = the Carmen coefficient, Δ = the rigidity of bed sediment and $\Delta = K_s/30.2$ (Nikuradse, 1933), K_s is the characteristic particle size of the bed surface. Hence, the similarity conditions between the experimental flow and the prototype flow with great dimensionless water depth would be analyzed firstly according to the logarithmic velocity distribution law in open channel.

In this study, a series of experimental runs were conducted and the previous data were collected. Finally, a new formula for the incipient condition of the granular sediment in great dimensionless water depth was proposed. Section 2 described the analysis of Similarity condition between experimental flow and prototype flow with great dimensionless water depth. Section 3 described the derivation and the structure of the empirical formula for the incipient velocity of granular sediment in the flow with great dimensionless water depth. Section 4 described the test materials, experimental setup, and test procedure. In section 5, the experimental results were presented, and the parameters of the empirical formula were determined. In addition, the soundness and the accuracy of this empirical formula were verified by comparing with previous studies. Finally, section 6 presented the main conclusions of the study and the recommendations for future studies.

Theoretical basis

Similarity requirement for sediment motion in different flow depths

In this paper, the similarity condition between the experimental flow and the prototype flow with great dimensionless water depth was analysed based on the logarithmic velocity distribution law in open channel. It is assumed that the experimental flow was to be able to fully simulate the prototype flow with great dimensionless water depth. Some assumptions are made to better illustrate the similarity between the experimental flow and the prototype flow. The flow distributions in an experimental flume and in a prototype flow are shown in *Figure 1,* where the subscript m denotes model (experimental flume) and the subscript p denotes the prototype. H_p and H_m is the flow depth in the experimental flume and in the prototype flow, respectively. Suppose $H_p/Hm = \lambda$. The velocity in the experimental flow at the height y_{m1} and y_{m2}

http://www.aloki.hu ● ISSN 1589 1623 (Print) ● ISSN 1785 0037 (Online)
DOI: http://dx.doi.org/10.15666/aeer/1704_98379863

from the bed surface are assumed as u_{m1} and u_{m2}, and the corresponding velocities in the prototype flow with great dimensionless water depth at the height $y_{p1} = \lambda y_{m1}$ and $y_{p2} = \lambda y_{m2}$ from the bed surface are assumed as u_{p1} and u_{p2}. The particle sizes of the experiment flume bed and corresponding prototype bed are assumed as d_m and d_p, respectively.

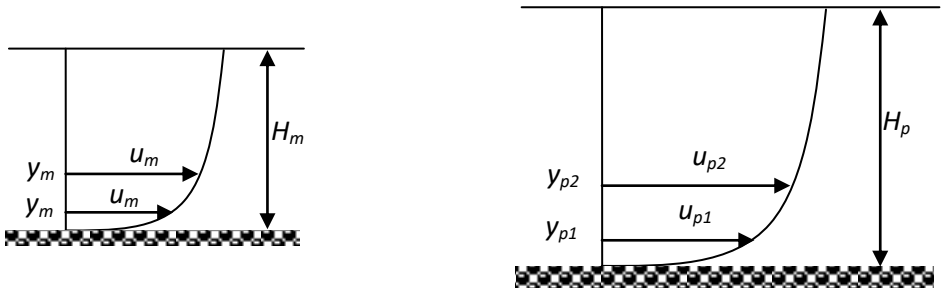

(a) Experimental flow (b) Prototype flow

Figure 1. *Vertical velocity distribution*

Suppose $K_s = d$ (Bennett and Best, 1995; Mianaei et al., 2010) for the uniform sediment. Hence,

$$\frac{u_{m1}}{u_{*m}} = \frac{1}{\kappa}\ln(30.2\frac{y_{m1}}{d_m}) \quad \text{(Eq.8)}$$

$$\frac{u_{m2}}{u_{*m}} = \frac{1}{\kappa}\ln(30.2\frac{y_{m2}}{d_m}) \quad \text{(Eq.9)}$$

$$\frac{u_{p1}}{u_{*m}} = \frac{1}{\kappa}\ln(30.2\frac{y_{p1}}{d_m}) \quad \text{(Eq.10)}$$

$$\frac{u_{p2}}{u_{*m}} = \frac{1}{\kappa}\ln(30.2\frac{y_{p2}}{d_m}) \quad \text{(Eq.11)}$$

Equation 8 is divided by *Equation 9*, and the parameters u_{*m} can be eliminated. In a similar way, *Equation 11* is divided by *Equation 10*, and the parameters u_{*p} can be also eliminated. Hence,

$$\frac{u_{m1}}{u_{m2}} - \frac{u_{p1}}{u_{p2}} = \frac{\ln(30.2\frac{y_{m1}}{dm})}{\ln(30.2\frac{y_{m2}}{d_m})} - \frac{\ln(30.2\frac{y_{p1}}{d_p})}{\ln(30.2\frac{y_{p2}}{d_p})} \quad \text{(Eq.12)}$$

Equation 12 can be further simplified, and the similarity condition between the experimental flow and the prototype flow with great dimensionless water depth can be written as

http://www.aloki.hu ● ISSN 1589 1623 (Print) ● ISSN 1785 0037 (Online)
DOI: http://dx.doi.org/10.15666/aeer/1704_98379863

$$\frac{u_{m1}}{u_{m2}} - \frac{u_{p1}}{u_{p2}} = \frac{\ln(\frac{y_{m2}}{y_{m1}})[\ln(\frac{d_p}{d_m}) - \ln(\lambda)]}{\ln(30.2\frac{y_{m2}}{d_m})\ln(30.2\frac{y_{p2}}{d_p})} \quad \text{(Eq.13)}$$

According to kinematic similarity criteria, it can be seen from *Equation 13*, when $\lambda = d_p/d_m$, u_{m1}/u_{m2} is equal to u_{p1}/u_{p2}. In other words, only when the dimensionless water depth (the ratio of water depth to particle size, H_m/d_m) in experimental flow is the same as that in corresponding prototype flow H_p/d_p, the flow velocity near the particles in experimental flow is similar with that in corresponding prototype flow and the motion of the sediment is similar in both scenarios. Otherwise, if $\lambda < d_p/d_m$, u_{m1}/u_{m2} is larger than u_{p1}/u_{p2} which indicates that the flow velocity near the sediment particles in experimental flow is higher than that in corresponding prototype flow, and the sediment particles in experimental flow would be easier to be dislodged than that in corresponding prototype flow. On the other hand, when $\lambda > d_p/d_m$, u_{m1}/u_{m2} is smaller than u_{p1}/u_{p2}, which indicates that the flow velocity near the sediment particles in experimental flow would be lower than that in corresponding prototype flow, and the sediment particles in experimental flow are then more difficult to be dislodged than that in corresponding prototype flow. It is seen that similarity condition between experimental flow and corresponding prototype flow is that the sediment particle size scale (d_p/d_m) equal to water depth scale (H_p/H_m), that is, $H_p/d_p = H_m/d_m$. Hence, the similarity between experimental flow and corresponding prototype flow is necessary to ensure the similar flow velocity near the sediment particles near bed in experimental flow and corresponding prototype flow.

In line with the similarity analysis between the experimental flow and the prototype flow in great dimensionless water depth, the current formulae deduced from flume experiments may be not suitable for calculating the incipient velocity of the granular sediment motion in great dimensionless depth of water, which requires a wide range of *H/d* in the flume experiment, for example, the water depth varies from 10 to 40 m, and the sediment particle sizes are between 0.2 and 2 mm in the middle reaches of the Yangtze river (Lu, 1991), thus the range of *H/d* is more than 200,000, and, the *H/d* range from 2 to 2030 according to the 272 groups of experimental data collected by author. On the other hand, non-natural sediments such as the homogeneous model sediments are always used in flume experiments (Geiger and Durnford, 2000; Thomas and Calantoni, 2001; Jain and Juans, 2009), and the particle size of the homogeneous model sediment is relatively larger than that of the natural sediments, which cannot be used to simulate the motion of cohesive sediments. Because the particle size of the cohesive sediments is always less than 0.06 mm (Grabowski et al., 2011; Jean Berlamont et al., 1993), and the viscosity between cohesive sediment particles will affect the incipient condition of sediments (Mehta, 1984 and1989; Lumborg and Windelin, 2003). Therefore, the limitation of experimental flume size would affect the accuracy of the existing formulas for the incipient velocity for the granular sediments in the flow with great dimensionless water depth, and and the water depth in flume experiment should not be used as the direct variable of the formulas for the incipient condition of the sediment in the flow with great dimensionless water depth.

http://www.aloki.hu ● ISSN 1589 1623 (Print) ● ISSN 1785 0037 (Online)
DOI: http://dx.doi.org/10.15666/aeer/1704_98379863

Boundary layer momentum thickness calculation

In this paper, boundary layer momentum thickness was introduced into the flume experiment as the independent variable to calculate the incipient velocity of the granular sediment in the flow with great dimensionless water depth. Boundary layer thickness reflects the block effect of bed wall and Roux (2010) regarded that the incipient motion of sediment is mainly affected by the flow near bed, that is, the flow near the boundary layer and the influence of the flow velocity outside the boundary layer on the sediment motion could be ignored in deep water area. Due to the viscous effect of fluid, the change of flow velocity in boundary layer will cause the loss of momentum in the boundary layer. The loss of momentum in the boundary layer can be explained by the momentum thickness of the boundary layer. Therefore, the boundary layer momentum thickness can be taken as a direct factor affecting sediment motion, which should be used to calculate the incipient velocity of sediment, rather than the water depth.

In general, boundary layer momentum thickness δ^1 is used to describe the boundary layer thickness intuitively (Hokenson, 1977), which can be written as follows:

$$\rho\delta^1 U^2 = \int_0^{\delta^*} \rho u(U-u)dy \qquad \text{(Eq.14)}$$

where ρ is the density of water, *kg/m*^{3}; δ^1 is boundary layer momentum thickness; δ^* is the boundary layer thickness, *m*. *U* and *u* are supposed to comply with the logarithmic velocity distribution law (Jonsson, 1966). Therefore, *Equation 14* can be written as

$$\rho\delta^1 = \frac{\delta^*}{\ln(30.2\frac{\delta^*}{d})} - \delta^* - \frac{1}{[\ln(30.2\frac{\delta^*}{d})]^2}\int_0^{\delta^*} \ln^2(30.2\frac{y}{d})dy \qquad \text{(Eq.15)}$$

where *y* is the water depth where the velocity is *u, m/s*. It is assumed that

$$x = 30.2\frac{y}{d} \qquad \text{(Eq.16)}$$

So *Equation 15* can be derived as *Equation 17*.

$$\delta^1 = \frac{\delta^*}{\ln(30.2\frac{\delta^*}{d})} + 2\frac{\delta^*}{\ln^2(30.2\frac{\delta^*}{d})} \qquad \text{(Eq.17)}$$

In the flume scale, the boundary layer thickness is determined by the water depth of the flume, that is $\delta^* = H$, and the boundary layer momentum thickness in shallow water area such as in the flume can be calculated by *Equation 18*.

$$\delta^1 = \frac{H}{\ln(30.2\frac{H}{d})} + 2\frac{H}{\ln^2(30.2\frac{H}{d})} \qquad \text{(Eq.18)}$$

http://www.aloki.hu ● ISSN 1589 1623 (Print) ● ISSN 1785 0037 (Online)
DOI: http://dx.doi.org/10.15666/aeer/1704_98379863

Formula form derivation

In this section the formula form for the incipient velocity of the granular sediment in the flow with great dimensionless water depth was analysed. The incipient motion of sediment is mainly affected by incipient condition which should conclude the characteristics of sediment particles, flow conditions and the relationship between flow conditions and sediment particles (Wang et al., 2008). Hence, the incipient velocity of granular sediment is influenced by the proportion of sediment particle, the proportion of fluid, kinematic viscosity coefficient, salinity, acceleration of gravity besides boundary layer momentum thickness. While the kinematic viscosity coefficient and saltiness can be ignored, because the temperature has little impact on the kinematic viscosity coefficient of fresh water and sea water (Balucani et al., 1996). Therefore, the formula form of the incipient velocity for the granular sediment particle can be written as

$$v_c = f(g, \gamma, \gamma_s, d, \delta^1) \tag{Eq.19}$$

where γ is the proportion of water, kg/m^3; γ_s is the proportion of sediment, kg/m^3. As mentioned above, *Equation 6* is almost adopted as the formula form to calculate the incipient velocity of sediment, therefore the formula form of the granular sediment in the flow with great dimensionless water depth can be expressed as:

$$v_c = \xi(\frac{\gamma_s - \gamma}{\gamma} gd)^a d^b \delta^{1c} \tag{Eq.20}$$

where ξ, a, b, c are constants. In this paper, $d = D_{50}$. It can be deduced that $a = 0.5$, $b = c$ by the dimensional analysis of *Equation 20*. Therefore, the formulary structure of incipient velocity for the granular sediment particle can be written as

$$v_c = \xi(\frac{\gamma_s - \gamma}{\gamma} gd)^a d^{0.5} (\frac{\delta^1}{d})^c \tag{Eq.21}$$

Compared with *Equation 6*, water depth H is replaced by the boundary layer momentum thickness δ^1 in *Equation 21*, which is confirmed to the similarity requirement between the experimental flow and the prototype flow with great dimensionless water depth for sediment initial motion.

Materials and method

Test materials

Four kinds of sediment particles with different particle sizes were used for the tests, which concluded one kinds of model sediments (MS) and three kinds of natural sediments. The homogeneous granular plastic sands were used as the test sediments which can be applied to the model experiment with different scale. The particle size of the homogeneous granular plastic sands in this experiment was 3.2 mm and the proportion of the homogeneous granular plastic sands was 1050 kg/m^3. The natural sediments were from different places: coastal line of Fengxian (FX), Shanghai, China; Huangpu River (HPJ) of Shanghai; coastal line of Zhuhai (ZH), Guangzhou province.

http://www.aloki.hu ● ISSN 1589 1623 (Print) ● ISSN 1785 0037 (Online)
DOI: http://dx.doi.org/10.15666/aeer/1704_98379863

The natural sediments were dried for 24 h in an oven at a temperature of 105°. After that, the dried sediments were sieved through a series of standard sieves with different diameters of holes to screen suitable sediment particle sizes and eliminate impurities such as small stones and shellfish. The determination range of standard sieves in laboratory is 0.038~6 mm. All the grain size and grain density are summarized in *Table 1*.

Table 1. *Grain size and grain density*

Location of sediment	FX	HPJ	ZH
Grain density (g/cm^3)	2.02	2.23	1.98
Median particle size (mm)	0.33	0.84	1.22
Standard deviation of grain size (μm)	1.6	2.6	0.9
Sorting coefficient	1.85	2.11	1.80

In addition, 272 groups of previous data concerning the incipient velocity of granular sediment, water depth and sediment particle size were collected to verify and fit the formula for the incipient velocity for granular sediments in the flow with great dimensionless water depth. The rang of the sediment proportion of the collected data is from 2010 to 2650 kg/m^3, and the rang of the sediment particle sizes of the collected data are from 0.04 to 22.2 mm. The maximum depth selected from the collected data is 0.47 m.

Experiment setup

The flume experiment was performed in the laboratory to examine the incipient velocities of the sediments with different particle size. The layout of the experimental apparatus is shown in *Figure 2*. The experimental flime was a water-circulating rectangle flume with a length of 10 m, width of 1 m, height of 1 m. A rectangular groove with dimensions of 50 cm length, 1 m width, and 5 cm depth was arranged at the bottom of the rectangular flume. The sample box with different sediment particles was placed in a groove during the experiment. The upper surface of the sample box was aligned with the inner wall of the flume to ensure that the inner surface of the flume was flat. Windows are provided on both sides of the flume to facilitate the observation of sediment motion. Two flow straighteners were installed at the upstream and downstream ends of the flume, respectively, to ensure that the water flowed evenly in the test range of the flume. The water inlet and water outlet are on the left side of the flume which can be controlled by the valve. The valves of water inlet and water outlet were closed during the experiment. A pump was arranged under the water-circulating rectangle flume and connected with the flume, flow meter and flow control valve by the pipe. The pump is ISG type vertical pipe centrifugal pump. The lift of this pump is 60 m and the flow is 45 m^3/h. The flow control valve was used to control the flow in the flume. The flow meter is an electromagnetic flowmeter whose nominal diameter is DN6-DN2000 with wide coverage. The flow velocity in the flume was measured by UDV 3000.

http://www.aloki.hu ● ISSN 1589 1623 (Print) ● ISSN 1785 0037 (Online)
DOI: http://dx.doi.org/10.15666/aeer/1704_98379863

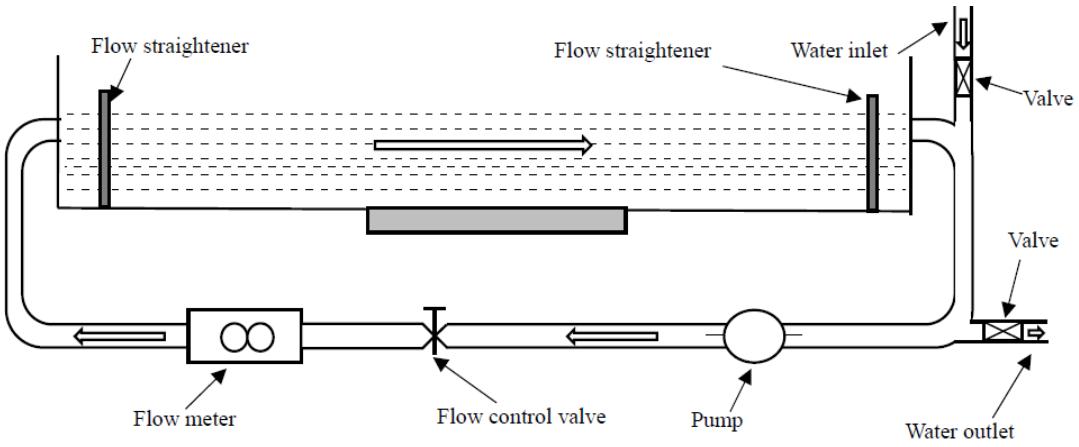

Figure 2. *Experiment setup*

Test procedure

First, tap water was added into the flume through the water inlet on the left side of the flume, and the valve of water outlet was closed at this time. When the water depth reaches a certain level, the valve of water inlet was closed. The depth of the water by artificial control was between 10 and 50 cm. The sample box with the sediment samples inside was then lowered into the square box. Subsequently, the pump was turned on and the flow control valve was then opened slowly. The incipient motion of sediment was observed through the windows on both sides of the flumes. The flow velocity was accelerated very slowly by 1–2 cm/s every minute until a few sediment particles were dislodged from the bed surface, and the flow velocity was recorded at this time. The incipient criterion of sediment is that about 1‰ of the particles dislodged from the bed surface (Kramer, 1935; Chien and Wan, 1983), which also applies to model sediment (Huang et al., 2012). This phenomenon that the sediment particles dislodge from the bed surface continuously took place in both time and space, that is, the sediment motion could always be observed throughout the experiment (Zhang et al., 2017). Because the incipient criterion of sediment processed a certain amount of subjectivity and judgment (He et al., 2003; Huang et al., 2012), there must be some divergent data in the experimental results. In order to minimize the errors of inevitable subjectivity associated with incipient criterion of sediment, the procedure for measuring the flow velocity when the phenomenon that a few sediment particles were dislodged from the bed surface was observed was repeated three times for every sediment samples. Once the incipient criterion of sediment samples was reached, the flow velocity, and the difference of water head were recorded.

Results and discussion

Empirical formula for the incipient velocity for granular sediment in the flow with great dimensionless water depth

In this section, the coefficients ξ and c of *Equation 21* are discussed by means of data fitting and collection. A series of previous data were collected, which include the experimental date of incipient condition of sediment collect by Yang et al. (2006) and a part of the sediment experimental data collected by Brownlie (1981). The basis of the

http://www.aloki.hu ● ISSN 1589 1623 (Print) ● ISSN 1785 0037 (Online)
DOI: http://dx.doi.org/10.15666/aeer/1704_98379863

data screened from the data collected by Brownlie (1981) is that the suspended sediment concentration range of the collected data should be between 0 PPM and 3 PPM, according to the analysis of sediment transport and the distribution of suspended sediment concentration in the fluid when the sediment particles begin to suspend (Ted et al., 1974) and these screened data included the experiment data of Simons, Bishop and Richardson (1965), Yalin and Karahan (1979), Govt. of West Bengal (1965), Casey (1935), Costello (1974), Davies (1971), Guy at al. (1966), Ho (1939), Mavis et al. (1937), Mutter (1971), Nordin (1976), Oerien (1935), Paintal (1971), Pratt (1970), Taylor (1971). The experimental results are shown in *Table 2*. The collected data are shown in the *Appendix*.

Table 2. *Experimental results*

H (m)	Location of sediment							
	FX		HPJ		ZH		MS	
	H/d	V_c (m/s)	H/d	V_c (m/s)	H/d	V_c (m/s)	H/d	V_c (m/s)
0.131	393.94	0.1876	154.76	0.281	106.56	0.2713	40.63	0.0888
0.149	451.52	0.1919	177.38	0.288	122.13	0.2775	46.56	0.0909
0.169	512.12	0.1959	201.19	0.294	138.52	0.2833	52.81	0.0928
0.206	624.24	0.2025	245.24	0.304	168.85	0.2927	64.38	0.0958
0.237	718.18	0.2072	282.14	0.311	194.26	0.2996	74.06	0.0981
0.296	895.45	0.2150	351.79	0.322	242.21	0.3108	92.34	0.1017
0.333	1010.61	0.2194	397.02	0.329	273.36	0.3171	104.22	0.1038
0.366	1109.09	0.2228	435.71	0.334	300	0.3219	114.38	0.1054
0.385	1166.67	0.2247	458.33	0.337	315.57	0.3247	120.31	0.1063
0.426	1290.91	0.2285	507.14	0.343	349.18	0.3302	133.13	0.1081

The coefficients of *Equation 21* were determined respectively using the test results and the collected data with the help of Origin 9.0 and Excel 2017. Firstly, the formal deformation of *Equation 21* was carried out in order to simplify the calculation as follows: the opposite sides of *Equation 21* was taken logarithm respectively, and then the multivariate regression method was used to determine these coefficients. These coefficients were evaluated as follows: $\zeta = 1.74$, $c = 0.18$. The value of $R^2 = 86\%$ indicates that the fit of the obtained model is fairly-good. Hence, the incipient velocity for the granular sediments in the flow with great dimensionless water depth can be expressed as follows:

$$v_c = 1.74\left(\frac{\gamma_s - \gamma}{\gamma} gd\right)^{0.5}\left(\frac{H}{d}\right)^{0.18}\left[\frac{1}{\ln(30.2\frac{H}{d})} + \frac{2}{\ln^2(30.2\frac{H}{d})}\right]^{0.18} \qquad \text{(Eq.22)}$$

As show in *Figure 3,* the curves plotted using the calculated values based on *Equation 22* are in accordance with the experimental data and the collected data, and this formula possesses an acceptable accuracy for calculating V_c, as 86% of the datasets are within a confidence interval with a relative error of 20%.

http://www.aloki.hu ● ISSN 1589 1623 (Print) ● ISSN 1785 0037 (Online)
DOI: http://dx.doi.org/10.15666/aeer/1704_98379863

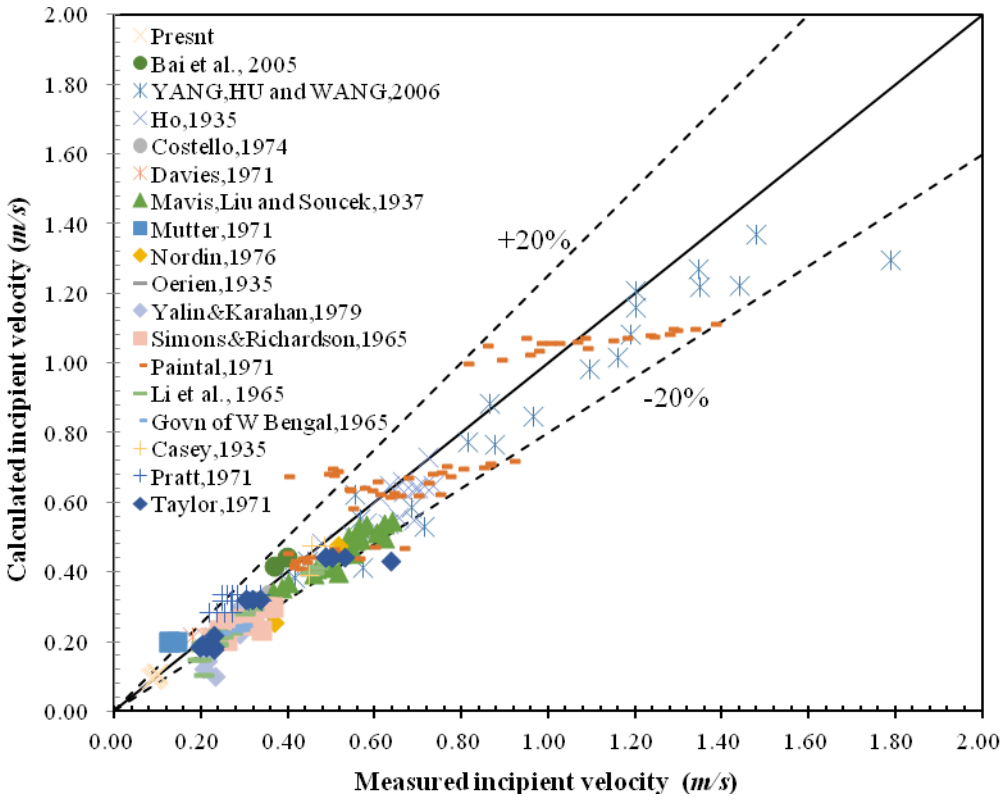

Figure 3. *Comparison between the measured and the calculated incipient velocity*

The incipient velocity of granular sediments in the flow with great dimensionless water depth are plotted according to *Equation 22*, and an incipient velocity diagram is drawn, as shown in *Figure 4*. The incipient velocity of granular sediments in the flow with great dimensionless water depth are plotted as a function of the dimensionless water depth (*H/d*) with the particle size as an independent parameter. It can be seen from *Figure 4* that the incipient velocity of the granular sediments in the flow with great dimensionless water depth increases with the increase of the dimensionless water depth (*H/d*) and the particle size, i.e., the incipient velocity of the granular sediments in the flow with great dimensionless water depth increases from 0.2 m/s to 0.45 m/s when the particle size increases from 0.1 mm to 5 m/s and the great dimensionless water depth is 5000; the incipient velocity of the granular sediments in the flow with great dimensionless water depth increases from 0.2 m/s to 0.625 m/s when the great dimensionless water depth (*H/d*) increases from 5000 to 4000000 and the particle size is 0.5 mm.

Soundness verification this empirical formula

The incipient velocity of granular sediments in the flow with great dimensionless water depth calculated by *Equation 22* proposed in this paper was compared with that calculated by *Equation 4* of Wuhan Institute of Hydraulic and Electric Engineering which has been used as a normative formula for the calculation of incipient velocity of sediment to verify the soundness of *Equation 22*, *Figure 5* depicts the incipient velocities of sediment in the flow with great dimensionless water depth (*H/d*) with various particle size, which are calculated by *Equation 22* and the formula of Wuhan

http://www.aloki.hu ● ISSN 1589 1623 (Print) ● ISSN 1785 0037 (Online)
DOI: http://dx.doi.org/10.15666/aeer/1704_98379863

Institute of Hydraulic and Electric Engineering. The comparison between calculated results of the empirical *Equation 22* and the normative formula of Wuhan Institute of Hydraulic and Electric Engineering clearly indicates the following:

The incipient velocities of the granular sediments calculated by the two formulas both increases with the increase of the dimensionless water depth (*H/d*) and the particle size of granular sediment.

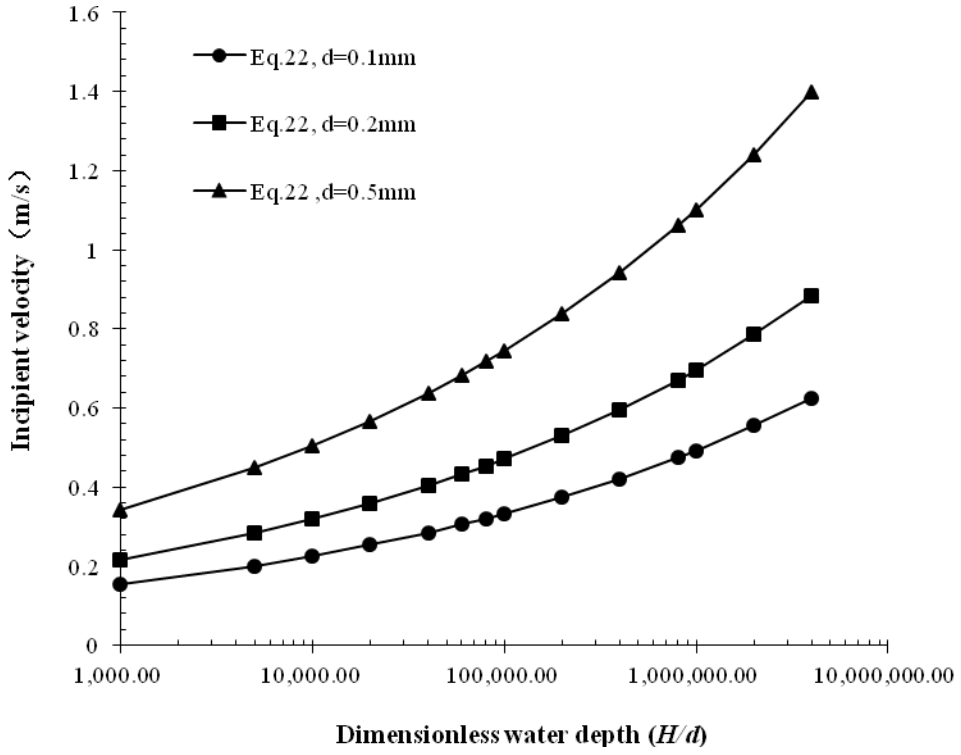

Figure 4. *Incipient velocity diagram*

For $H/d \leq 1 \times 10^4$, the increasing trend of the incipient velocities of the granular sediments calculated by *Equation 16* with the dimensionless water depth (*H/d*) is similar with that calculated by the normative formula of Wuhan Institute of Hydraulic and Electric Engineering, and all increase slowly. Whereas, the incipient velocities of the granular sediments calculated by *Equation 16* is lower than that calculated by the normative formula of Wuhan Institute of Hydraulic and Electric Engineering when the particle size is less than or equal to 0.2 mm. When the particle size is more than 0.2 mm, the incipient velocities of the granular sediments calculated by *Equation 22* is approximately equal that calculated by the normative formula of Wuhan Institute of Hydraulic and Electric Engineering.

For $H/d > 1 \times 10^4$, the increasing trend of the incipient velocities of the granular sediments calculated by *Equation 22* is much slower than that by the normative formula of Wuhan Institute of Hydraulic and Electric Engineering, which demonstrates that there will be a large difference between incipient velocities of granular sediment calculated by *Equation 22* and the normative formula of Wuhan Institute of Hydraulic and Electric Engineering when the dimensionless water depth (*H/d*) is more than 10^4, and the difference increases with the increase of *H/d*. In order to illuminate the

http://www.aloki.hu ● ISSN 1589 1623 (Print) ● ISSN 1785 0037 (Online)
DOI: http://dx.doi.org/10.15666/aeer/1704_98379863

appearance, Wanxian site is taken as an example, which is one of the reservoirs of Three Gorges in China. The particle size of the sediment at Wanxian site is less than 0.16 mm and the depth of water will reach 100 m when the reservoir is full of water (Wang et al., 2010). But the incipient velocities of the sediment at Wanxian site calculated by *Equation 22* and the normative formula of Wuhan Institute of Hydraulic and Electric Engineering are 1.306 m/s and 0.601 m/s respectively, which differ widely.

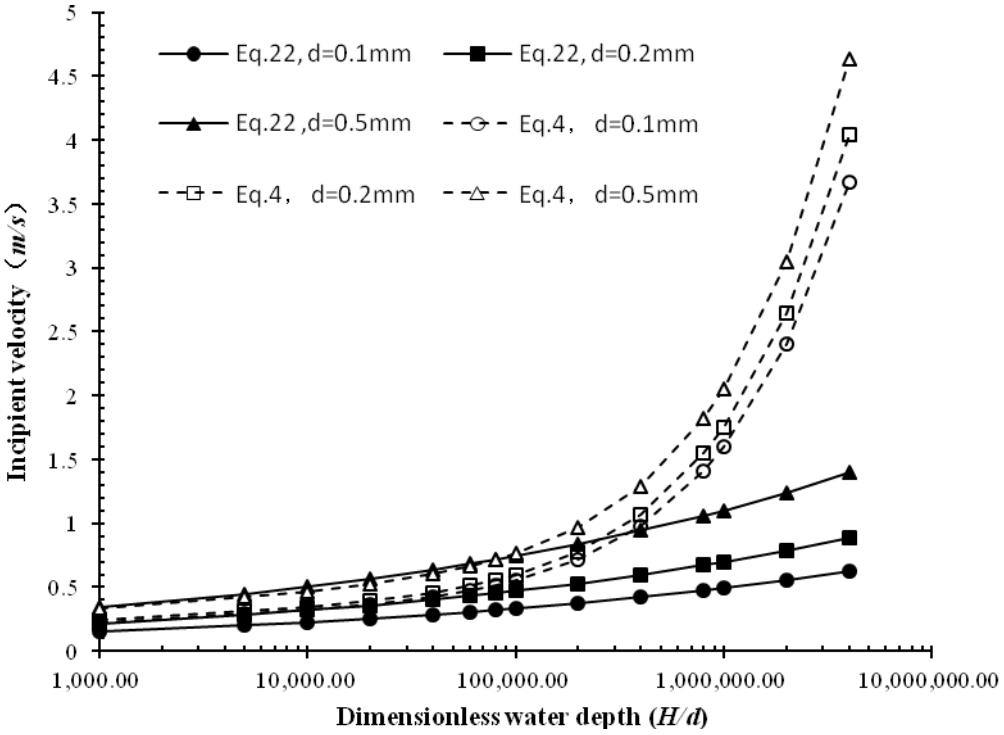

Figure 5. *Comparison between calculated results of the empirical Equation 22 and the normative formula of Wuhan Institute of Hydraulic and Electric Engineering*

Although there is no direct data to determine the rationality of the calculation results *Equation 22* and the formula of Wuhan Institute of Hydraulic and Electric Engineering, it can be concluded that the incipient velocity of granular sediment in the flow with great dimensionless water depth calculated by the formula of Wuhan Institute of Hydraulic and Electric Engineering is certainly higher than the actual situation according to the data of the physical characteristics and environment parameters of the shelf dunes (Zhuang et al., 2004). The area where the depth of water is from 132 to 162 m at continental shelf of the east china sea collected by Zhuang et al. (2004) is taken as the example to verify this claim and there are sand waves with a wavelength of 5 ~ 25 m and a wave height of 0.5 ~ 2 m. In addition, the sediment particle sizes are between 0.125 and 0.188 mm and the local maximum flow velocity is between 0.4 and 0.9 m/s in this area. According to the formula of Wuhan Institute of Hydraulic and Electric Engineering, the incipient velocity of sediment is between 1.43 and 1.91 m/s in this area, while the incipient velocity of sediment calculated by *Equation 22* is between 0.58 and 0.687 m/s. Obviously, the incipient velocity of sediment calculated by the formula of Wuhan Institute of Hydraulic and Electric Engineering is higher than the local maximum flow velocity, which indicates that the sediment particles cannot suspended

http://www.aloki.hu ● ISSN 1589 1623 (Print) ● ISSN 1785 0037 (Online)
DOI: http://dx.doi.org/10.15666/aeer/1704_98379863

and there are no sand waves. It follows that the calculation results of *Equation 22* are more reasonable in this situation, because the local maximum flow velocity can reach the incipient condition of sediment in this area according to *Equation 22*. According to the above analysis, *Equation 22* proposed in this paper is more credible than the normative formula of Wuhan Institute of Hydraulic and Electric Engineering when they are used to calculate the incipient velocity of granular sediment in the flow with great dimensionless water depth.

Accuracy verification of this empirical formula

In the study, the calculation results of the empirical formula were compared with the field measurement data collected by Brownlie (1981) to verify the accuracy of this empirical formula proposed in this paper. Firstly, the field measurement data collected from the extant studies which included Atchafalaya River Data of Toffaleti (1968), South American River & Canal Data of NEDECO (1973), Red River Data of Toffaleti (1968), and Rio Grande River Data of Nordin and Beverage (1965), in which the dimensionless water depth (*H/d*) was less than 10^4. The calculated results and the collected field measurement data were listed in *Table 3*.

Table 3. *Comparisons with extant experimental data (1)*

Rate of flow (m^3/s)	**River width (m)**	**Water depth (m)**	***d* (mm)**	**Sediment concentration (ppm)**	**Extant data (m/s)**	**Calculated velocity (m/s)**	**Data sources**
1073176	313.94	6.889	0.089	4.31	0.396	0.416	Atchafalaya River Data of Toffaleti (1968)
843816	310.89	6.431	0.106	2.80	0.322	0.331	
719226	307.85	6.248	0.096	8.95	0.374	0.319	
637110	307.85	6.218	0.137	5.60	0.333	0.359	
51000	93	1.8	0.12	2.92	0.305	0.282	South American River & Canal Data of NEDECO (1973)
206707	159.41	3.505	0.103	7.88	0.370	0.297	Red River Data of Toffaleti (1968)
2859.9	25.603	0.369	0.396	6	0.303	0.324	Rio Grande River Data of Nordin and Beverage (1965)
2944.8	43.282	0.262	0.343	5	0.262	0.272	
		0.1192	0.102		0.262	0.233	Vanoni (1965)

Then the field experimental data in which the dimensionless water depth (*H/d*) was approximately 10^4 were collected as the correlation data with the calculated results by the empirical formula. The calculated results and the collected field measurement data were listed in *Table 4*.

It can be seen from *Table 3* that when the sediment concentrations are less than or equal to 5 PPM the calculation results by this empirical formula are in good agreement with the data collected from extant studies generally, i.e., Rio Grande River Data of Nordin and Beverage (1965) and South American River & Canal Data of NEDECO (1973). While the incipient velocity of sediment calculated by this empirical formula is lower than the collected field measurement data when the sediment concentrations are more than 5 PPM and approach 10 PPM, for instance, Red River Data of Toffaleti

http://www.aloki.hu ● ISSN 1589 1623 (Print) ● ISSN 1785 0037 (Online)
DOI: http://dx.doi.org/10.15666/aeer/1704_98379863

(1968), because the hydrodynamic condition is considered to have exceeded the incipient condition of sediment according to the analysis of sediment transport and the distribution of suspended sediment concentration in the fluid when the sediment particles begin to suspend (Ted et al., 1974), when the sediment concentrations approach 10 PPM. It can be seen from *Table 4* that the empirical formula can work well when it is used to calculate the incipient of granular sediment in the flow with high dimensionless water depth. *Figure 6* depicts that the calculated values calculated by *Equation 22* and the 20% error lines against measured data.

Table 4. *Comparisons with extant experimental data (2)*

H/D	Water depth (m)	d (mm)	ρ_s (kg/m^3)	Extant data (m/s)	Calculated velocity (m/s)	Data sources
1700.526	0.3231	0.19	1.3	0.24	0.231	Simons, Bishop and Richardson (1965)
1604.211	0.3048	0.19	1.3	0.232	0.229	
1027.407	0.2774	0.18	1.56	0.255	0.253	
1099.286	0.3078	0.24	1.67	0.293	0.261	
1700.526	0.3241	0.19	2.65	0.24	0.231	Guy et al. (1966)
1492.105	0.2835	0.19	2.65	0.264	0.226	
1460	0.2774	0.19	2.65	0.255	0.225	

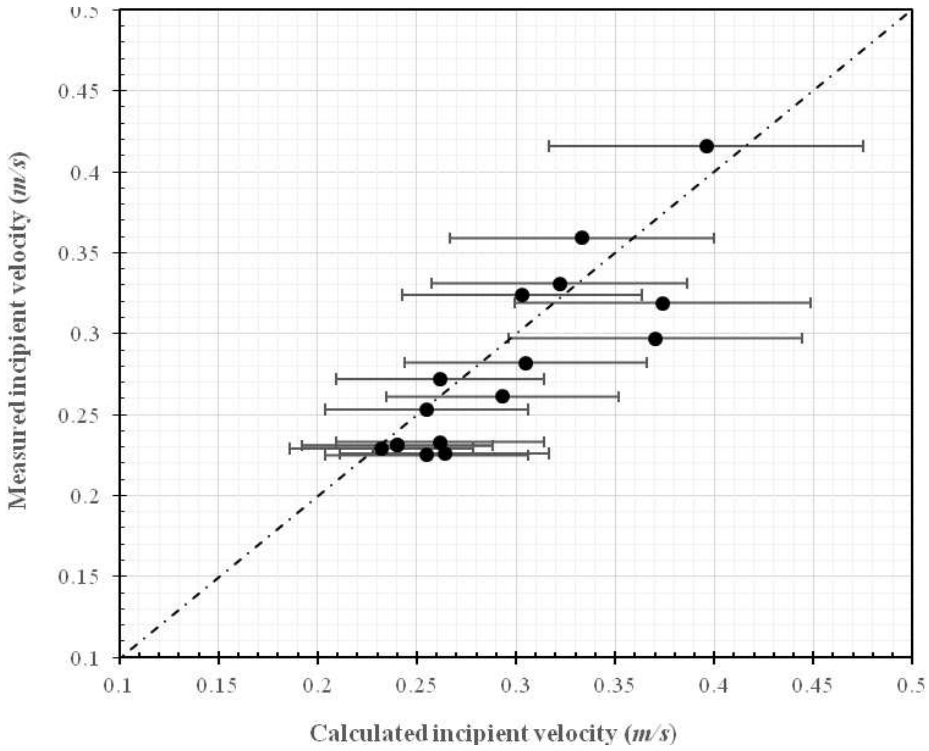

Figure 6. *Comparison between calculated results and measured results*

http://www.aloki.hu ● ISSN 1589 1623 (Print) ● ISSN 1785 0037 (Online)
DOI: http://dx.doi.org/10.15666/aeer/1704_98379863

Conclusion

In this paper, the incipient condition of the granular sediment in the flow with great dimensionless water depth was studied by the method of flume experiment and data fitting. Firstly, the similarity condition between experimental flow and prototype flow with great dimensionless water depth was analysed firstly. Then based on the above analysis, the boundary layer momentum thickness was introduced instead of water depth due to the limitation of the flume experiments. Subsequently, the flume experiment results and a series of extant data were collected and calculated to derive the formula for the incipient velocity of granular sediment in the flow with great dimensionless water depth. The conclusions of this study can be summarized as follows:

The similarity condition between the experimental flow and the prototype flow with great dimensionless water depth is that the ratio of water depth and the particle size of sediment (*H/d*, which is considered as the dimensionless water depth in this paper) in experimental flow is the same with that in prototype flow with great dimensionless water depth, based on the logarithmic velocity distribution law.

Water depth cannot be used as a direct variable in the formula for the incipient condition of the granular sediment in the flow with great dimensionless water depth due to the limitation of flume experiment, which should be replaced by the boundary layer momentum thickness.

An empirical formula for the incipient velocity for the granular sediment in great dimensionless water depth was proposed by introducing boundary layer momentum thickness as an immediate variable. The formula takes boundary layer momentum thickness, particle size and the proportion of sediment and fluid as the main variables. Compared with the normative formula of Wuhan Institute of Hydraulic and Electric Engineering, the increasing trend of the incipient velocities of the granular sediments in the flow with great dimensionless water depth calculated by the two formulas are similar with each other when $H/d \leq 1 \times 10^4$, and all increase slowly, but when $H/d > 1 \times 10^4$, the increasing trend of the incipient velocities of the granular sediments calculated by the formula proposed in this paper is much slower than that by the normative formula of Wuhan Institute of Hydraulic and Electric Engineering. Finally, the accuracy of the proposed formula is verified.

Recommendations for future researches

Firstly, the viscous force between sediment particles should be considered in future researches. Because the sediment particles behave in a cohesive manner when the particle size is less than 500 μm, moreover, the viscous force becomes the main resistance to the initial motion of sediment, and the effect of gravity on the initial motion of sediment can be neglected, when the particle size is less than 60 μm. But there is no convincing result about the incipient condition of cohesive sediment. In future researches, the concept of sediment fluidization can be introduced to study on the incipient conditions of cohesive sediment, and different sediment fluidization level will cause the variation of starting velocity.

Secondly, the application condition and the form of the formula need further study. Because that the research results in this paper are based on logarithmic velocity distribution, which is reliable for the unidirectional flow. However, the applicability of the condition in complex flow field, such as wave or tide, has yet to be verified.

http://www.aloki.hu ● ISSN 1589 1623 (Print) ● ISSN 1785 0037 (Online)
DOI: http://dx.doi.org/10.15666/aeer/1704_98379863

Acknowledgements. This work was financially supported by the National Key Research and Development Program of China (Grant number: 2016YFC0402607). We are also grateful to the anonymous reviewers for their constructive comments and suggestions, which have helped improve the manuscript significantly.

REFERENCES

[1] Bai, Y. C., Xu, D., Zhang, X. Y. (2005): Experimental study on flow turbulence characteristics of open channel on alluvial bed and its relation to incipient motion of bed sediment. – Progress in Natural Science 15(4): 439-445 (in Chinese).

[2] Balucani, U., Brodholt, J. P., Vallauri, R. (1996): Dynamical properties of liquid water. – Journal of Physics: Condensed Matter 8(47): 9269-9274 (https://doi.org/10.1088/0953-8984/8/47/014).

[3] Beheshti, A. A., Ataie-Ashtiani, B. (2008): Analysis of threshold and incipient conditions for sediment movement. – Coastal Engineering 55(5): 423-430 (https://doi.org/10.1016/j.coastaleng.2008.01.003).

[4] Bennett, S. J., Best, J. L. (1995): Mean flow and turbulence structure over fixed, two-dimensional dunes: implications for sediment transport and bedform stability. – Sedimentology 42(3): 491-5123 (https://doi.org/10.1111/j.1365-3091.1995.tb00386.x).

[5] Berlamont, J., Ockenden, M., Toorman, E., Winterwerp, J. (1993): The characterisation of cohesive sediment properties. – Coastal Engineering 21(1): 105-128 (https://doi.org/10.1016/0378-3839(93)90047-c).

[6] Bohorquez, P., Fernandez-Feria, R. (2008): Transport of suspended sediment under the dam-break flow on an inclined plane bed of arbitrary slope. – Hydrol. Process. 22: 2615-2633 (https://doi.org/10.1002/hyp.6858).

[7] Brownlie, W. R. (1981): Compilation of alluvial channel data: laboratory and field. – Rep. No. KH-R-43B, W. M. Keck Lab. of Hydr. and Water Resources., California Institute of Technology, Pasadena, California.

[8] Casey, H. J. (1935): Ueber Geschiebebewegung (On Bed Load, in German). – Mitt. Preuss. Versuchsanstalt f. Wasserbau u. Schiffbau, Berlin.

[9] Chien, N., Wan, Z. (1999): Mechanics of Sediment Transport. – ASCE Press, Reston, VA (https://doi.org/10.1061/9780784404003).

[10] Dornbrack, A., Schumann, U. (1993): Numerical simulation of turbulent convective flow over wavy terrain. – Boundary-Layer Meteorology 65(4): 323-355 (https://doi.org/10.1007/bf00707032).

[11] Costello, W. R. (1974): Development of Bed Configuration in Coarse Sands. – Report 74-1. Department of Earth and Planetary Science. Massachusetts Institute of Technology, Cambridge, Massachusetts.

[12] Davies, T. R. (1971): Summary of experimental data for flume tests over fine sand. – Department of Civil Engineering, University of Southampton.

[13] Dou, G. (1960): Discussion on the incipient velocity of sediment. – Shuili Xuebao 4: 44-60 (in Chinese).

[14] Drake, T. G., Calantoni, J. (2001): Discrete particle model for sheet flow sediment transport in the nearshore. – Journal of Geophysical Research Atmospheres 106(C9): 19858-19868 (https://doi.org/10.1029/2000jc000611).

[15] Falcão, A. F. O., Henriques, J. C. C. (2014): Model-prototype similarity of oscillating-water-column wave energy converters. – International Journal of Marine Energy 6: 18-34 (https://doi.org/10.1016/j.ijome.2014.05.002).

[16] Ferro, V. (1999): Friction factor for gravel-bed channel with high boulder concentration. – J. Hydraul. Eng. 125(7): 771-778 (https://doi.org/10.1061/(asce)0733-9429(1999)125:7(771)).

http://www.aloki.hu ● ISSN 1589 1623 (Print) ● ISSN 1785 0037 (Online)
DOI: http://dx.doi.org/10.15666/aeer/1704_98379863

[17] Francisco, J. M. S. (2014): Shear velocity criterion for incipient motion of sediment. – Water Science and Engineering 7(2): 183-193.
[18] Geiger, S. L., Durnford, D. S. (2000): Infiltration in homogeneous sands and a mechanistic model of unstable flow. – Soil Science Society of America Journal 64(2): 460-469 (https://doi.org/10.2136/sssaj2000.642460x).
[19] Guy, H. P., Simons, D. B., & Richardson, E. V. (1966): Summary of alluvial channel data from flume experiments, 1956-61: US Geol. Survey Prof. Paper 462(1): 11-196 (https://doi.org/10.3133/pp462i).
[20] Han, Q. (1982): Characteristics of incipient sediment motion and incipient velocity. – Journal of Sediment Research 2: 11-26 (in Chinese).
[21] He, W. D., Fang, Z., Yang, J. R., Cao, S. Y. (2002): Study on incipient velocity of sediment. – Shuili Xuebao 33(10): 51-56 (in Chinese).
[22] Hokenson, G. J. (1977): Consistent integral thickness utilization for boundary layers with transverse curvature. – AIAA Journal 15(4): 597-600 (https://doi.org/10.2514/3.7350).
[23] Ho, P. Y. (1939): Abhängigkeit der Geschiebebewegung von der Kornform und der Temperatur. – Preussische Versuchsanstalt für Wasser-, Erdund Schiffbau 37: 43.
[24] Huang, Z. W., Lu, B. W., Wu, N. H. (2012): Study on incipient velocity of sediment in model test. – Jiangxi Hydraulic Science & Technology 38(1): 16-19 (in Chinese).
[25] Jain, A. K., Juans, R. (2009): Preferential mode of gas invasion in sediments: grain-scale model of coupled multiphase fluid flow and sediment mechanics. – JGR Solid Earth 114: B08101 (https://doi.org/10.1029/2008jb006002).
[26] Jonsson, I. G. (1966): Wave boundary layer and friction factors. – Proc.10th Coastal Eng. Conf. ASCE, pp. 127-148 (https://doi.org/10.1061/9780872620087.010).
[27] Kramer, H. (1935): Sand mixtures and sand movement in fluvial models. – Trans. Am. Soc. Civ. Eng. 100(1909): 798-838.
[28] Li, W., Cao, S., Liu, S. (2006): The law of sand transport of Yichang Changjiang station. – Journal of Sichuan University (Engineering Science Edition) 38(1): 26-29 (in Chinese).
[29] Lu, J. (1991): Study on incipient velocity of sediment transport in Yangtze River. – Journal of Yangtze River Scientific Research Institute 8(4): 57-64 (in Chinese).
[30] Lumborg, U., Windelin, A. (2003): Hydrography and cohesive sediment modelling: application to the Rømø Dyb tidal area. – Journal of Marine Systems 38(3): 287-303 (https://doi.org/10.1016/s0924-7963(02)00247-6).
[31] Luo, X., Yang, F. (2011): Derivation of incipient velocity for uniform sediment based on the concept of the angle of repose. – 2011 International Symposium on Water Resource and Environmental Protection. IEEE Xplore 2011 (https://doi.org/10.1109/icicta.2011.31).
[32] Mao, J., Dai, H., He, W. (2011): Calculating incipient velocity of non-uniform sediment through stress analysis. – International Symposium on Water Resource and Environmental Protection, IEEE (https://doi.org/10.1109/iswrep.2011.5893080).
[33] Mavis, F. T., Ho, C., Tu, Y. C., Liu, T. Y., & Soucek, E. (1935): The transportation of detritus by flowing water (I). – Iowa University Studies in Engineering, Bulletin 11.
[34] Meftah, M. B., Mossa, M. (2016): A modified log-law of flow velocity distribution in partly obstructed open channels. – Environmental Fluid Mechanics 16(2): 453-479 (https://doi.org/10.1007/s10652-015-9439-7).
[35] Mehta, A. J. (1984): Characterization of Cohesive Sediment Properties and Transport Processes in Estuaries. – In: Mehta, A. J. (ed.) Estuarine Cohesive Sediment Dynamics, Lecture Notes on Coastal and Estuarine Studies, Volume 14. Springer, New York, pp. 290-325 (https://doi.org/10.1029/ln014p0290).
[36] Mehta, A. J. (1989): On estuarine cohesive sediment suspension behaviour. – JGR Oceans 94(C10): 14303-14314 (https://doi.org/10.1029/jc094ic10p14303).
[37] Meyer-Peter, E., & Muller, R. (1948): Formulas for bed-load transport, – Proceedings of the 2nd Meeting of the International Association for Hydraulic Structures Research. International Association of Hydraulic Research Delft.

http://www.aloki.hu ● ISSN 1589 1623 (Print) ● ISSN 1785 0037 (Online)
DOI: http://dx.doi.org/10.15666/aeer/1704_98379863

[38] Mianael, S. J., Keshavarzi, A. R. (2010): Study of near bed stochastic turbulence and sediment entrainment over the ripples at the bed of open channel using image processing technique. – Stochastic Environmental Research and Risk Assessment 24(5): 591-598.
[39] Mutter, D. G. (1971): A Flume Study of Alluvial Bed Configurations. – Masters thesis submitted to the Faculty of Graduate Studies, University of Alberta.
[40] NEDECO (1973): Rio Magdalena and Canal del Dique Project. Mission Tecnica Colombo-Holandesa. – NEDECO Report, NEDECO, The Hague, The Netherlands.
[41] Nie, R., Liu, X. (2004): Comparison study on incipient motion conditions for cohesive sediment. – Advances in Water Science 15(5): 584-587 (in Chinese).
[42] Nikuradse, J. (1933): Laws of flow in rough pipes (1950 translation). – National Advisory Committee on Aeronautics. Technical Memorandum No 1292, Washington, DC.
[43] Niven, R. K. (2010): Minimization of a free-energy-like potential for non-equilibrium flow systems at steady state. – Philosophical Transactions of The Royal Society B Biological Sciences 365(1545): 1323-31 (https://doi.org/10.1098/rstb.2009.0296).
[44] Nordin, C. F., & Beverage, J. P. (1965): Sediment transport in the Rio Grande. – New Mexico. US Government Printing Office (https://doi.org/10.3133/pp462f).
[45] Nordin, C. F. (1976): Flume studies with fine and coarse sands (No. 76-762). – US Geological Survey, (https://doi.org/10.3133/ofr76762).
[46] O'Brien, M. P. (1936): Notes on the transportation of silt by streams. – Eos, Transactions American Geophysical Union, 17(2), 431-436 (https://doi.org/10.1029/tr017i002p00431).
[47] Paintal, A. S. (1971): Concept of critical shear stress in loose boundary open channels. – Journal of Hydraulic Research 9(1): 91-113 (https://doi.org/10.1080/00221687109500339).
[48] Phillips, J. D. (1992): Nonlinear dynamical systems in geomorphology: revolution or evolution. – Geomorphology 5(3-5): 219-229 9 (https://doi.org/10.1016/0169-555x(92)90005-9).
[49] Pratt, C. J. (1970): Summary of Experimental Data for Flume Tests over 0.49 mm Sand. – Department of Civil Engineering, University of Southhampton, Southhampton, England.
[50] Righetti, M., Lucarelli, C. (2007): May the Shields theory be extended to cohesive and adhesive benthic sediments? – J. Geophys. Res. 112: C05039 (https://doi.org/10.1029/2006jc003669).
[51] Robert, C. G., Droppo, I. G., Wharton, G. (2011): Erodibility of cohesive sediment: The importance of sediment properties. – Earth-Science Reviews 105(4): 101-120 (https://doi.org/10.1016/j.earscirev.2011.01.008.
[52] Rijn, L. C. V. (1984): Sediment transport, Part I: bed load transport. – J. Hydraul. Eng. 110(10): 1431-1456.
[53] Roux, J. P. L. (2010): Sediment entrainment under fully developed waves as a function of water depth, boundary layer thickness, bottom slope and roughness. – Sedimentary Geology 223(1): 143-149 (https://doi.org/10.1016/j.sedgeo.2009.11.006).
[54] Sha, Y. (1965): Introduce Sediment Kinematics. – China Industry Press, Beijing).
[55] Simons, D. B. Bishop, A. A., Richardson, E. V. (1965): Total Bed Material Transport. Proc. – Journal of the Hydraulics Division 91(2): 175-191.
[56] Steward, F. R., Tennankore, K. N. (1977): Similarity criterion for a confined swirling jet system. – Symposium (International) on Combustion 16(1): 1593-1609.
[57] Tang, C. (1963): Initial motion law of sediment. – Shuili Xuebao 3: 1-12 (in Chinese).
[58] Taylor, B. D. (1971): Temperature Effects in Alluvial Streams. – W. M. Keck Laboratory Report KH-R-27, California Institute of Technology, Pasadena, Calif..
[59] Toffaleti, F. B. (1968): A Procedure for Computation of the Total River Sand Discharge and Detailed Distribution, Bed to Surface. – Technical Report No. 5, Committee of Channel Stabilization, United States Army Corps of Engineers.

http://www.aloki.hu ● ISSN 1589 1623 (Print) ● ISSN 1785 0037 (Online)
DOI: http://dx.doi.org/10.15666/aeer/1704_98379863

[60] Vanoni, V. A. (1965): Data used to develop Shields diagram. – In Technical Memorandum 65–2. WM Keck Laboratory of Hydraulics and Water Resources, California Institute of Technology Pasadena (California), USA.
[61] Venditti, J. G., Church, M., Bennett, S. J. (2006): On interfacial instability as a cause of transverse subcritical bed forms. – Water Resour. Res. 42(7): W07423 (https://doi.org/10.1029/2005wr004346).
[62] Wang, T., Liu, X., Huang, E., Nie, R., Cai, B. (2008): Study and comparison on incipient velocity for non-uniform sediment. – Journal of Sichuan University (Engineering Science Edition) 40(1): 16-20 (in Chinese).
[63] Wang, T., Liu, X., Nie, R., Huang, E. (2010): Comparative study on the incipient motion conditions of non-uniform non-cohesive sediment. – Journal of Hydroelectric Engineering 29(6): 126-131 (in Chinese).
[64] West Bengal, Government of. (1965): Study on the Critical Tractive Force Various Grades of Sand. – Annual Report of the River Research Institute, West Bengal, Publication No. 26 Part I, 5-12.
[65] Xie, J. (1981): River Sediment Engineering (Part I). – Water Resources and Electric Power Press, Beijing (in Chinese).
[66] Yalin, M. S., Karahan, E. (1983): On the development of turbulent boundary layer in open channel flows. – Combustion Explosion & Shock Waves 17(5): 545-549(https://doi.org/10.1007/bf00798143).
[67] Yang, S., Hu, J., Wang. X. (2006): Incipient motion of coarse particles in great gradient rivers. – International Journal of Sediment Research 21(3): 220-229.
[68] Yu, G., Lim, S. (2003): Modified manning formula for flow in alluvial channels with sand-beds. – J. Hydraul. Res. 41(6): 597-608 (https://doi.org/10.1080/00221680309506892).
[69] Yu, G., Tan, S. K. (2006): Errors in the bed shear stress as estimated from vertical velocity profile. – Journal of Irrigation and Drainage Engineering 132(5): 490-497 (https://doi.org/10.1061/(asce)0733-9437(2006)132: 5(490)).
[70] Zeng, J., Chen, G., Xiong, S. (2010): Study on incipient velocity of fine sediment in the Qiantang Estuary. – Journal of Waterway and Harbor 31(5): 347-351 (in Chinese).
[71] Zhang, H. (2012): A unified formula for incipient of sediment. – Shuili Xuebao 12(43): 1387-1396 (in Chinese).
[72] Zhang, M., Yu, G. (2017): Critical conditions of incipient motion of cohesive sediments. – Water Resources. Res. 53(9): 7798-7815 (https://doi.org/10.1002/2017wr021066).
[73] Zhang, M., Dolatshah, A., Zhu, W., Yu, G. (2018): Case study on water quality improvement in Xihu Lake through diversion and water distribution. – Water 10(3): 333 (https://doi.org/10.3390/w10030333).
[74] Zhang, R., Xie, J., Chen, W. (1961): River Mechanics. – China Industry Press, Beijing (in Chinese).
[75] Zhuang, Z., Lin, Z., Zhou, J., Liu, Z., Liu, Y. (2004): Environmental conditions for the formation and development of sand dunes (waves) in the continental shelf. – Marine Geology Letters 20(4): 5-10 (in Chinese).
[76] Zou, X., Wang, C., Song, H., Han, Z., Ma, Z. (2017): Experimental measurements of sediment incipient velocity by using B-scan ultrasound imaging device in the water channel. – Measurement 98: 228-236 (https://doi.org/10.1016/j.measurement.2016.12.006).

http://www.aloki.hu ● ISSN 1589 1623 (Print) ● ISSN 1785 0037 (Online)
DOI: http://dx.doi.org/10.15666/aeer/1704_98379863

APPENDIX

Detailed collected data

H/d	Depth (*m*)	*d* (*mm*)	Concentration (*ppm*)	V_c (*m/s*)	Data sources
930.526	0.1768	0.19	1	0.22	Simons, Bishop and Richardson (1965)
705.789	0.1341	0.19	2	0.26	
642.142	0.1798	0.28	1	0.269	
492.766	0.2316	0.47	1.6	0.347	
486.383	0.2286	0.47	2.3	0.353	
480	0.2256	0.47	2.5	0.365	
461.818	0.1524	0.33	3.5	0.319	
350	0.189	0.54	0.5	0.297	Yalin and Karahan (1979) ASCE
1.151	0.0012	1		0.215	
6.276	0.0063	1		0.289	
8.369	0.0047	0.56		0.215	
64.776	0.0065	0.1		0.231	
11.788	0.0047	0.4		0.212	
30.254	0.0057	0.19		0.206	
39.186	0.0055	0.14		0.205	Li and Sun (1965)
821.428	0.115	0.14		0.21	
771.428	0.108	0.14		0.22	
857.142	0.12	0.14		0.2	
28.5	0.057	2		0.45	
30.5	0.061	2		0.46	
38.5	0.077	2		0.47	
49.5	0.099	2		0.49	
48.5	0.097	2		0.49	
61.363	0.054	0.88		0.32	
45.454	0.04	0.88		0.3	
105.263	0.04	0.38		0.24	
115.789	0.044	0.38		0.25	
155.263	0.059	0.38		0.27	
168.421	0.064	0.38		0.24	
215.384	0.056	0.26		0.2	
192.307	0.05	0.26		0.24	
234.615	0.061	0.26		0.21	
188.461	0.049	0.26		0.23	
196.153	0.051	0.26		0.24	
271.428	0.038	0.14		0.19	
264.285	0.037	0.14		0.2	
278.730	0.0878	0.32	0.2	0.243	Govt. of West Bengal (1965)
344.444	0.1085	0.32	0.7	0.271	
391.746	0.1234	0.32	1	0.283	
402.539	0.1268	0.32	1.1	0.288	
427.619	0.1347	0.32	1.1	0.285	
464.444	0.1463	0.32	1.3	0.279	

http://www.aloki.hu ● ISSN 1589 1623 (Print) ● ISSN 1785 0037 (Online)
DOI: http://dx.doi.org/10.15666/aeer/1704_98379863

480	0.1512	0.32	1.8	0.282	
506.984	0.1597	0.32	2.6	0.294	
13.618	0.0335	2.46	1.6	0.447	Casey (1935)
47.561	0.117	2.46	1.6	0.482	
47.439	0.1167	2.46	0.019	0.454	
290.196	0.148	0.51	0.094	0.288	Costello (1974)
288.054	0.1495	0.52	1.679	0.311	
264.167	0.1585	0.6	0.473	0.32	
239.394	0.158	0.66	0.819	0.324	
194.937	0.154	0.79	0.764	0.357	
2032	0.3048	0.15	0.8	0.181	Davies (1971)
2032	0.3048	0.15	0.9	0.21	
706.316	0.1342	0.19	2	0.258	Guy, Simons and Richardson (1966)
642.143	0.1798	0.28	1	0.269	
663.778	0.2987	0.45	0.7	0.242	
548.667	0.2469	0.45	1.2	0.24	
541.778	0.2438	0.45	0.7	0.242	
392.889	0.1768	0.45	0.7	0.238	
392.667	0.1767	0.45	1.4	0.252	
223.556	0.1006	0.45	1	0.225	
337.527	0.3139	0.93	0.4	0.404	
330.968	0.3078	0.93	0.4	0.455	
492.766	0.2316	0.47	0.4	0.347	
486.383	0.2286	0.47	0.4	0.353	
480	0.2256	0.47	0.4	0.365	
69.521	0.2176	3.13	0.1	0.581	Ho (1939)
83.833	0.2624	3.13	0.45	0.656	
45.271	0.1417	3.13	0.73	0.547	
58.339	0.1826	3.13	1.11	0.602	
67.188	0.2103	3.13	1.55	0.631	
78.690	0.2463	3.13	2.89	0.689	
33.195	0.1039	3.13	0.97	0.478	
45.367	0.142	3.13	0.54	0.59	
50.825	0.2216	4.36	0.089	0.633	
56.491	0.2463	4.36	0.19	0.664	
35.573	0.1551	4.36	0.26	0.61	
42.293	0.1844	4.36	0.66	0.667	
46.559	0.203	4.36	0.97	0.698	
50.183	0.2188	4.36	1.79	0.734	
35.525	0.2231	6.28	0.16	0.724	
16.891	0.1061	6.28	1.12	0.714	
18.203	0.1094	6.01	1.3	0.692	
29.019	0.1213	4.18	1.2	0.65	Mavis et al. (1937)
30.837	0.1289	4.18	1.3	0.695	
31.794	0.1329	4.18	1.3	0.715	
22.608	0.0945	4.18	1.3	0.623	

http://www.aloki.hu ● ISSN 1589 1623 (Print) ● ISSN 1785 0037 (Online)
DOI: http://dx.doi.org/10.15666/aeer/1704_98379863

24.067	0.1006	4.18	0.8	0.656	
25.383	0.1061	4.18	0.7	0.660	
25.813	0.1079	4.18	1.3	0.658	
26.244	0.1097	4.18	1.2	0.69	
26.459	0.1106	4.18	2.3	0.713	
25.608	0.0799	3.12	0.9	0.531	
26.955	0.0841	3.12	1.1	0.554	
28.045	0.0875	3.12	2.2	0.567	
30.16	0.0941	3.12	1.9	0.568	
30.481	0.0951	3.12	2.8	0.622	
21.186	0.0661	3.12	2.9	0.532	
22.179	0.0692	3.12	2	0.539	
16.410	0.0512	3.12	2.8	0.523	
15.833	0.0494	3.12	2.8	0.552	
33.054	0.0671	2.03	1.3	0.465	
35.419	0.0719	2.03	1.2	0.481	
37.537	0.0762	2.03	3	0.501	
26.552	0.0539	2.03	2	0.46	
28.818	0.0585	2.03	1.8	0.515	
34.61	0.0488	1.41	2.8	0.366	
24.584	0.0917	3.73	1	0.563	
26.971	0.1006	3.73	1.8	0.581	
28.204	0.1052	3.73	2.3	0.624	
30.08	0.1122	3.73	2.9	0.641	
17.48	0.0652	3.73	1.4	0.539	
19.035	0.071	3.73	1.3	0.56	
20.429	0.0762	3.73	2.3	0.603	
32.679	0.0549	1.68	1.9	0.402	
23.75	0.0399	1.68	2.7	0.386	
41.933	0.1128	2.69	1.133	0.497	Meyer-Peter and Muller (1948)
232.308	0.0604	0.26	3	0.127	Mutter (1971)
233.462	0.0607	0.26	2	0.126	
249.615	0.0649	0.26	2	0.143	
1280	0.32	0.25	0.8	0.369	Nordin (1976)
532.456	0.607	1.14	2.9	0.515	
855	0.3078	0.36	1.9	0.36	O'Brien (1936)
868.611	0.3127	0.36	1.9	0.348	
4.324	0.096	22.2	0.071	0.807	Paintal (1971)
4.739	0.1052	22.2	0.074	0.883	
5.149	0.1143	22.2	0.039	0.949	
5.631	0.125	22.2	0.029	0.967	
5.946	0.132	22.2	0.012	1.079	
6.604	0.1466	22.2	0.058	1.057	
6.73	0.1494	22.2	0.155	1.141	
7.14	0.1585	22.2	0.171	1.173	
7.347	0.1631	22.2	0.396	1.235	

http://www.aloki.hu ● ISSN 1589 1623 (Print) ● ISSN 1785 0037 (Online)
DOI: http://dx.doi.org/10.15666/aeer/1704_98379863

7.69	0.1707	22.2	0.374	1.27
8.239	0.1829	22.2	0.632	1.287
8.401	0.1865	22.2	0.706	1.329
9.131	0.2027	22.2	1.572	1.376
6.455	0.1433	22.2	0.88	1.016
6.455	0.1433	22.2	1.009	0.973
7.14	0.1585	22.2	1.214	1.075
7.414	0.1646	22.2	1.144	1.223
8.306	0.1844	22.2	2.16	1.277
6.455	0.1433	22.2	1.683	0.994
6.28	0.1387	22.2	1.1791	0.849
7.072	0.157	22.2	1.683	0.939
10.201	0.0811	7.95	0.189	0.764
6.742	0.0536	7.95	0.004	0.532
10.767	0.0856	7.95	0.061	0.724
8.516	0.0677	7.95	0.039	0.595
12.264	0.0975	7.95	0.574	0.794
5.522	0.0439	7.95	0.005	0.649
8.201	0.0652	7.95	0.012	0.713
13.421	0.1067	7.95	0.185	0.755
13.648	0.1085	7.95	0.222	0.857
9.623	0.0765	7.95	0.006	0.668
11.27	0.0896	7.95	0.025	0.743
12.956	0.103	7.95	1.1669	0.842
15.409	0.1225	7.95	1.55	0.91
14.566	0.1158	7.95	0.202	0.856
5.786	0.046	7.95	0.007	0.741
7.208	0.0573	7.95	0.006	0.568
6.704	0.0533	7.95	0.001	0.535
5.371	0.0427	7.95	0.026	0.624
5.824	0.0463	7.95	0.01	0.602
6.138	0.0488	7.95	0.008	0.635
6.667	0.053	7.95	0.011	0.585
3.61	0.0287	7.95	0.001	0.54
5.522	0.0439	7.95	0.066	0.692
11.597	0.0922	7.95	0.003	0.504
10.239	0.0814	7.95	0.004	0.495
9.925	0.0789	7.95	0	0.393
10.893	0.0866	7.95	0.001	0.483
12.654	0.1006	7.95	0.005	0.493
43.64	0.1091	2.5	2.5	0.591
38.16	0.0954	2.5	0.192	0.497
33.04	0.0826	2.5	0.032	0.388
40.24	0.1006	2.5	0.686	0.659
32.92	0.0823	2.5	0.092	0.508
16.84	0.0421	2.5	0.002	0.419

http://www.aloki.hu ● ISSN 1589 1623 (Print) ● ISSN 1785 0037 (Online)
DOI: http://dx.doi.org/10.15666/aeer/1704_98379863

19.88	0.0497	2.5	0.01	0.405	
22.8	0.057	2.5	0.014	0.435	
28.04	0.0701	2.5	0.387	0.442	
16.84	0.0421	2.5	0.002	0.443	
24.28	0.0607	2.5	0.01	0.408	
26.84	0.0671	2.5	0.02	0.554	
33.28	0.0832	2.5	0.463	0.506	
26.84	0.0671	2.5	0.266	0.425	
18.4	0.046	2.5	0.012	0.404	
23.04	0.0576	2.5	0.145	0.484	
15.72	0.0393	2.5	0.002	0.441	
637.656	0.3048	0.478	0.77	0.283	
637.659	0.3048	0.478	0.506	0.267	
637.656	0.3048	0.478	0.28	0.248	
637.656	0.3048	0.478	1.37	0.311	
637.656	0.3048	0.478	2.9	0.338	
318.828	0.1524	0.478	2.89	0.272	
318.828	0.1524	0.478	1.54	0.253	
318.828	0.1524	0.478	0.582	0.236	Pratt (1970)
318.828	0.1524	0.478	0.278	0.217	
956.485	0.4572	0.478	0.12	0.247	
956.485	0.4572	0.478	0.262	0.259	
956.485	0.4572	0.478	0.146	0.271	
956.485	0.4572	0.478	0.307	0.283	
956.485	0.4572	0.478	0.632	0.304	
956.485	0.4572	0.478	1.73	0.336	
283.72	0.061	0.215	0.184	0.229	
283.72	0.061	0.215	0.737	0.229	
283.72	0.061	0.215	0.049	0.213	
283.72	0.061	0.215	0.143	0.213	
283.72	0.061	0.215	0.003	0.198	
283.72	0.061	0.215	0.01	0.198	
21.423	0.0602	2.81	0.215	0.502	
21.423	0.0602	2.81	0.051	0.502	
17.864	0.0502	2.81	1.056	0.638	
21.423	0.0602	2.81	0.549	0.532	Taylor (1971)
21.423	0.0602	2.81	0.05	0.487	
21.423	0.0602	2.81	0.023	0.487	
169.747	0.0606	0.357	0.047	0.229	
317.277	0.0606	0.191	1.65	0.229	
244.354	0.0606	0.248	0.025	0.204	
57.009	0.061	1.07	0.053	0.305	
57.009	0.061	1.07	0.036	0.305	
57.009	0.061	1.07	2.06	0.335	
57.009	0.061	1.07	1.125	0.335	
57.009	0.061	1.07	0.423	0.32	

http://www.aloki.hu ● ISSN 1589 1623 (Print) ● ISSN 1785 0037 (Online)
DOI: http://dx.doi.org/10.15666/aeer/1704_98379863

57.009	0.061	1.07	0.255	0.321	
750	0.3	0.4		0.326	Bai et al. (2005)
272.727	0.3	1.1		0.368	
230.769	0.3	1.3		0.398	
2.075	0.083	40	0.108	1.2	Yang et al. (2006)
2.257	0.0903	40	0.648	1.44	
3.49	0.1396	40	4.296	1.79	
5.533	0.083	15		0.964	
4.667	0.035	7.5		0.686	
5.04	0.126	25		1.19	
5.075	0.203	40		1.478	
6	0.021	3.5		0.571	
6	0.009	1.5		0.333	
2.225	0.089	40		1.348	
2.56	0.064	25		1.094	
3	0.021	7		0.714	
2.667	0.04	15		0.875	
2.857	0.01	3.5		0.4	
7.2	0.054	7.5		0.556	
7.714	0.027	3.5		0.444	
10	0.015	1.5		0.333	
7.333	0.11	15		0.864	
8.16	0.204	25		1.201	
3.067	0.023	7.5		0.565	
3.428	0.012	3.5		0.417	
2.867	0.043	15		0.814	
3.28	0.082	25		1.159	
2.975	0.119	40		1.345	

http://www.aloki.hu ● ISSN 1589 1623 (Print) ● ISSN 1785 0037 (Online)
DOI: http://dx.doi.org/10.15666/aeer/1704_98379863

THE ANALYSIS OF CARBON DIOXIDE EMISSIONS FROM TAIWAN'S EXPORT INDUSTRY

LIN, H. C.[1] – ZHANG, W. H.[2] – TSAI, K. H.[3] – CHOU, L. C.[4*]

[1]*Department of Applied Economics, National Chiayi University, 600 Chiayi, RO China*

[2]*School of Politics and Economics, King's College London, WC2R 2LS London, UK*

[3]*Center of Economic Forecasting, Chung-Hua Institution for Economic Research, 114 Taipei, RO China*

[4]*Department of Economics, Wenzhou Business College, 325000 Wenzhou, PR China*

**Corresponding author*
e-mail: zlc@wzbc.edu.cn

(Received 28th Mar 2019; accepted 22nd May 2019)

Abstract. By reviewing Taiwan's economic development after the Second World War, economic activities at various stages are driven by international trade exports, which has led to Taiwan's economic growth and rising per capita income. Therefore, the situation of Taiwan's export industry is of great significance to its development. In this study, the Environmental Input-Output (EIO) model, the World Input-Output Database (WIOD), and Socio-Economic Accounts are used to investigate the CO_2 emissions of Taiwan's export industry sectors and its relationship with other countries. It is analysed how particular export sectors cause carbon dioxide emissions in domestic production supply chains (by tracking downstream to upstream), and how carbon emissions in specific sectors affect export output. The empirical results show that the growth rate of CO_2 emissions in Taiwan's export industry is roughly the same as its GDP growth rate and far lower than Japan and the United States. From the perspective of industry categories, water transport, chemical products and electronic optical products are Taiwan's export sectors with high CO_2 emissions and rapid growth.
Keywords: *environmental input-output (EIO) model, Taiwan export sector, GDP, emission growth rate, supply chain*

Introduction

With island-type economy and poor natural resources, Taiwan takes the export-oriented trade as the most important industry under the government's pursuit of industrial development. At the end of the 20th century, with the development of the Internet and the commercial application of new technologies, the cost of transnational operations of enterprises declined, and information systems made transnational supply chains and management more convenient. As China and Taiwan joined the WTO successively in 2001 and 2002, global trade has become increasingly more achievable under the globalization trend and the elimination of WTO trade barriers. In the past, most of the global trade was concentrated in the North American and EU markets, while in recent years, with the rise of Chinese economy and the expansion of the ASEAN (Association of Southeast Asian Nations) from the first four countries to ten countries, as well as the signing of the Free Trade Agreement (FTA), the focus of trade around the world has been shifted to the Asian region.

In recent years, as China's economy has shown a fast-growing trend for a long term, the open-door policy will inevitably deepen its dependence on international

http://www.aloki.hu ● ISSN 1589 1623 (Print) ● ISSN 1785 0037 (Online)
DOI: http://dx.doi.org/10.15666/aeer/1704_98659880

market (Lu, 2018). Thus, many Taiwanese businessmen have gone to the mainland to invest in the local development (Lin and Yang, 2017; Rigger, 2015), and the industrial division of labor between Taiwan and mainland has shown a weakening vertical division and a more common horizontal division. The proportion of Taiwan's export products in *Table 1* shows that the first major export products in Taiwan are electronic components, and the proportion has increased year by year, reaching 33% in 2016. The second is audio-visual products, accounting for about 10% in the past ten years. The third is metal products, the proportion of which continues to decline, and the proportions of mineral products, petroleum refining products and textiles have also declined due to the change in industrial structure.

Table 1. *Structure of Taiwan's export products (unit: %)*

	2007	**2008**	**2009**	**2010**	**2011**	**2012**	**2013**	**2014**	**2015**	**2016**
Electronic components	22.2	21.4	24.3	24.9	24.1	24.5	25.9	28.2	30.1	33.1
Audio-visual products	11.6	10.0	10.5	11.2	11.7	10.3	10.0	9.7	10.7	10.8
Metal products	11.2	11.0	9.4	9.4	9.7	9.2	8.9	9.1	8.9	8.8
Mechanical products	7.1	7.0	6.1	6.7	7.2	7.3	6.9	7.2	7.5	7.5
Plastic rubber products	7.6	7.7	8.1	8.0	8.1	7.9	8.0	7.6	7.4	7.1
Chemical products	6.0	6.8	6.9	7.0	7.3	6.9	7.0	6.9	6.4	6.1
Optical equipment	7.1	7.6	6.9	7.6	6.7	6.7	6.3	5.6	4.5	4.1
Mineral products	5.7	7.4	5.7	5.3	5.8	7.3	7.8	6.7	4.2	3.9
Petroleum refining products	5.4	7.0	5.3	5.0	5.5	6.9	7.3	6.2	3.6	3.4
Motor products	6.9	6.2	5.7	5.2	4.0	4.2	4.4	4.1	4.1	3.4
Conveyance	3.2	3.5	3.8	3.4	3.3	3.6	3.5	4.1	4.1	3.9
Textiles	4.7	4.2	4.5	4.1	4.1	3.9	3.8	3.8	3.8	3.5

Data source: National Statistics, R.O.C. (Taiwan)

Intermediate goods of various semi-finished products and components account for a high proportion of Taiwan's exports, which are combined with the production factors of exporting countries and sold around the world. In other words, the various interdependent items in international trade form an industrial chain. Nowadays, countries all over the world are developing industrial structures, adjusting economic physique, and claiming to comprehensively improve the self-made rate (Meng et al., 2017; Ritchie et al., 2018), then if Taiwan cannot upgrade its industrial structure and develop an "independent economy" model, it will inevitably be affected by a strong economic impact. The development trend of global trade is particularly significant in the vertical division of labor. The international vertical division of labor is the multi-nationalization of production process, so that the final production of goods is completed through different manufacturing processes in many countries. In Taiwan, the production of components relies on the import of raw materials, which will generate carbon dioxide (CO_2) in the production process. Therefore, this paper intends to understand how much carbon dioxide emissions are generated due to exports, and to explore the correlation analysis of how the downstream export industry can drive carbon dioxide emissions from domestic upstream industry.

This paper explores the comparison of CO_2 emissions between industries in Taiwan and its major exporting countries, and uses the Environmental Input-Output

http://www.aloki.hu ● ISSN 1589 1623 (Print) ● ISSN 1785 0037 (Online)
DOI: http://dx.doi.org/10.15666/aeer/1704_98659880

(EIO) model to provide an in-depth understanding of the sources and structures of CO_2 emissions from the countries. Based on the above research motivation, the main purpose of this paper is to understand the industrial input-output structure and industrial linkage profile of each country according to the input-output tables from the World Input-Output Database (WIOD). The Socio-Economic Accounts from 1995 to 2011, and the old and new versions of WIOD from 1995 to 2011 and from 2000 to 2014 are used to analyze and compare the change in the trends of CO_2 emissions from industrial exports in countries under the global value chain.

Literature review

There are four types of assessment methods for the impact of international trade on the environment in the literature. The first type is Structural Path Analysis (SPA), which refers to the use of input-output analysis to track complex production processes under given final demands. The traditional SPA method only explores one single region, and if the upstream and downstream industrial chains of a product belong to different countries, it will be impossible to discuss the single affiliation problem, such as Lenzen (2003), Peter and Hertwich (2006); the second type is Hybrid Input-Output Analysis, which refers to the use of input-output tables composed of price units and material units to distinguish energy from non-energy, such as Kagawa and Inamura (2001), Dietzenbacher and Stage (2006).

The third type is Multi-regional Input-Output Analysis (MRIO), which refers to that the single-region input-output table is estimated and broken down into a multi-region input-output table under the traditional SPA model framework, so as to calculate the industrial correlation effects on output and pollution emissions in various regions through the final demand and correlation matrix of each region. Since the unit output value, output and even proportion are required for the use of mixed unit model, the difficulty of data collection is a major shortcoming, such as Lenzen et al. (2004), Peter and Hertwich (2006). The fourth type is the EIO model, that is, the use of multi-regional input-output method to extend the regional model derived from the environmental coefficient, so as to gain a deeper understanding of the sources and structures of carbon dioxide emissions from countries' exports and explore climate policies regarding carbon leakage formulated by various countries.

In the past literature, Peter and Hertwich (2006) used the SPA method and the MRIO method to explore the environmental impact brought by the Norwegian international trade. The results show that in terms of household consumption, 80% of the direct emissions of personal fuels environmental impact are the transportation consumption of the households. In the government consumption sector, government expenditures are mainly in the medical treatment, education, and public administration departments, whose public sector has a greater impact on the purchase of transportation vehicles. If compared with households and export sectors, the government's pollution discharge density is relatively low.

Jin et al. (2017) analyzes a few scenarios of Korean CCS projects with a CO_2 pipeline transportation network optimization model for minimizing the total facility cost and pipeline cost. The results for each scenario demonstrate that the effective design and implementation of CO_2 pipeline network enables the lowering of CO_2 units cost. Liu et al. (2016) analyzed the impact of corporate heterogeneity by using

http://www.aloki.hu ● ISSN 1589 1623 (Print) ● ISSN 1785 0037 (Online)
DOI: http://dx.doi.org/10.15666/aeer/1704_98659880

the EIO model, and found that ignoring corporate heterogeneity may lead to overestimation of carbon dioxide emissions from China's export.

Materials and methods

Data description

The database used in this paper comes from the World Input-Output Database (WIOD). Dietzenbacher et al. (2013) and Timmer et al. (2015) give detailed description of its compiling methodology: the World Input-Output Table (WIOT). In the country classification of World Input-Output Table, this paper retained China, India, Japan, South Korea, Taiwan, the United States, and the rest of the countries were merged into other countries, and finally the six major countries were analyzed. The carbon dioxide coefficient (C) is calculated by dividing the CO_2 emissions of each industry in each country of the 35 sectors in 2013 by the corresponding output value. First, calculate the product input coefficient matrix (D) of each country, and then use the D coefficient to calculate the (I-D)^(-1) matrix of domestic correlation table, and calculate the value-added rate (V), then finally perform empirical analysis. Since the Socio Economic Accounts in the WIOD database has not published the 2016 carbon dioxide coefficient data conforming to the new 56-sector classification, so the 56-sector coefficients were not corresponded to the 35-sector classification.

Methods

There are two main methods used to analyze the driving factors of carbon emission growth in the existing literature: Index Decomposition Analysis (IDA) and Structural Decomposition Analysis (SDA) (Hoekstra and van den Bergh, 2003). Some scholars have summarized IDA (Ang, 1995, 2004; Xu and Ang, 2013); and SDA (Rose and Casler, 1996; Su and Ang, 2012). In this paper, based on the results of Liu et al. (2016) that carbon dioxide emissions are closely related to export production, the first is to understand the Input-output analysis (IOA), which is a method of accounting account presentation, and the model building method depends on the input-output table of the country or region. A country's input-output (IO) table shows the flow of inventory and services, while since IO tables have a clear showing of the life cycle of an industry, the relationship between producers and consumers is related to the production chain of entire economy. By taking into account the impact of the entire supply chain IOA, the EIO model is used to estimate specific emissions from trade, thus the estimation formula of CO_2 emissions from national-level export is as follows:

$$CO_{2exp} = \mathrm{C} \cdot (I - A)^{-1} \cdot \mathrm{e} \qquad \text{(Eq.1)}$$

where:
CO_{2exp} = Total carbon dioxide emissions representing the specific exports;
c = 1 × n rows of carbon dioxide emissions, which is the carbon dioxide emissions per unit of economic output;
A = Intermediate input of total output in the n × n input coefficient matrix with the division by sectors;
$(I - A)^{-1}$ = Leontief inverse matrix representing the complete induced output matrix produced by a unit;

http://www.aloki.hu ● ISSN 1589 1623 (Print) ● ISSN 1785 0037 (Online)
DOI: http://dx.doi.org/10.15666/aeer/1704_98659880

e = n × 1 rows of vectors representing exports.

According to the different views on supply chain, exports at the emissions sector level can be tracked from upstream to downstream $(D \rightarrow U)$ or from upstream to downstream $(U \rightarrow D)$:

$$CO_{2exp}^{D \rightarrow U} = \mathrm{C} \cdot (I - A)^{-1} \cdot diag(e) \quad \text{(Eq.2)}$$

$$CO_{2exp}^{U \rightarrow D} = diag(c) \cdot (I - A)^{-1} \cdot e \quad \text{(Eq.3)}$$

In the traditional IO theory, the above two different measures have their own economic explanations, and play different roles in economic analysis. $CO_{2exp}^{D \rightarrow U}$ indicates the carbon dioxide emissions emitted by all industries for exporting certain specific products. In other words, this measure can check the emissions from all the sectors directly or indirectly affected by domestic upstream supply chains. In contrast, $CO_{2exp}^{U \rightarrow D}$ represents the CO_2 emissions of a specific sector's specific export. That is to say, this measure depends on how to show the emissions from specific upstream sectors will affect the final exports of all downstream industries.

Finally, according to the definition, there is no difference between the two measures in CO_2 emissions at national level in terms of export. If we replace imported wealth goods with a ratio v of added value relative to output, to estimate the direct and indirect impact of exports on domestic added value. The following formula can be used to calculate the value-added ratio v of an export product (a 1 × n vector representing each value-added unit by sector). The so-called entity value-added (GDP) can also be estimated by:

$$GDP_{exp} = v \cdot (I - A)^{-1} \cdot \mathrm{e} \quad \text{(Eq.4)}$$

Further use of *Equations2* and *3* to represent the carbon indicator P as emission intensity of export entity can be defined as follows:

$$\mathrm{P} = CO_{2exp} / GDP_{exp} \quad \text{(Eq.5)}$$

This indicator that indicates the value-added export emissions per unit of a country can therefore be considered as a potential environmental cost for national trade. Display export value-added quotas at the industrial level in the same way:

$$GDP_{exp}^{D \rightarrow U} = v \cdot (I - A)^{-1} \cdot \mathrm{diag}(e) \quad \text{(Eq.6)}$$

$$GDP_{exp}^{U \rightarrow D} = diag(v) \cdot (I - A)^{-1} \cdot \mathrm{e} \quad \text{(Eq.7)}$$

In addition, according to *Equation 6,* the specific emissions of carbon intensity export at the industrial level are defined as follows:

$$P^{D \rightarrow U} = CO_{2exp}^{D \rightarrow U} // GDP_{exp}^{D \rightarrow U} = [c \cdot (I - A)^{-1} \cdot diag(e)] // [v \cdot (I - A)^{-1} \cdot diag(e)] \quad \text{(Eq.8)}$$

$$P^{U \rightarrow D} = CO_{2exp}^{U \rightarrow D} // GDP_{exp}^{U \rightarrow D} = c // v \quad \text{(Eq.9)}$$

http://www.aloki.hu ● ISSN 1589 1623 (Print) ● ISSN 1785 0037 (Online)
DOI: http://dx.doi.org/10.15666/aeer/1704_98659880

We define "//" as operational symbol of a vector division. It can be seen that the carbon intensity of carbon emissions depends on the input coefficient c and the value-added rate v of emissions from all upstream sectors when exporting a specific product, while the carbon emissions of specific sectors are based on the carbon intensity of the production sector (sector emissions/added values), showing that all exports are equal to the conventional definition.

Supposing based on production, the estimation of carbon dioxide emissions depends on the amount of energy used, regardless of the type of industry that uses it. In other words, if different types of industries burn the same amount of specific types of energy, the difference in energy efficiency of the enterprise will be reflected in the energy use per unit of output. This also means that if the traditional IO table does not introduce enterprise heterogeneity and does not change the estimate of production base, thus carbon dioxide emission estimates at the industrial or national level may be different. The use of traditional IO tables can lead to overestimation of CO_2 emissions from exports and underestimation of CO_2 emissions from domestic final demand, which is mainly because different types of companies have different market shares in traditional IO tables, and neglecting the heterogeneity of enterprises can lead to overestimation of carbon dioxide emissions from exports.

Therefore, this paper replaces the $(I - A)^{-1}$ matrix with the $(I - A)^{-1}$ matrix, where $(I - A)^{-1}$ indicates the direct plus indirect domestic demand coefficient matrix, also known as the domestic industrial correlation matrix. The domestic industrial correlation matrix $(I - A)^{-1}$ is conducted with the sum of vertical and horizontal analysis to obtain the forward and backward correlation degrees of each industry. If the forward and backward correlation degrees are normalized, sensitivity and influence can be obtained. Industries with high forward correlation (sensitivity greater than one) are easy to support downstream industrial production by providing products for downstream industries. Industries with high backward correlation (influence degree greater than one) are easy to drive the development of other upstream industries, and the demand for upstream industrial products is higher. Industries with both high forward and backward correlation degrees as the important industries can drive the development of other industries. Industries with high forward correlation degree and low backward correlation degree can provide the cooperation for the development of other industries. Industries with low forward correlation degree and high backward correlation degree can drive the development of other industries and are not easily affected by other industries. Industries with both low forward and backward correlation degrees are the industries that are not susceptible to other industries and will not drive the development of other industries.

Results

Main empirical results

This paper collects data from the new version of WIOD (2000-2014) and the old version (1995-2011) to calculate CO_2 emissions, GDP and its intensity (the ratio of CO_2 emissions to GDP, that is, CO_2 emissions per unit of GDP driven by exports) driven by the total exports of major countries (see *Figs. 1* and *4*), the intermediate goods (see *Figs. 2* and *5*) and final goods (see *Figs. 3* and *6*).

http://www.aloki.hu ● ISSN 1589 1623 (Print) ● ISSN 1785 0037 (Online)
DOI: http://dx.doi.org/10.15666/aeer/1704_98659880

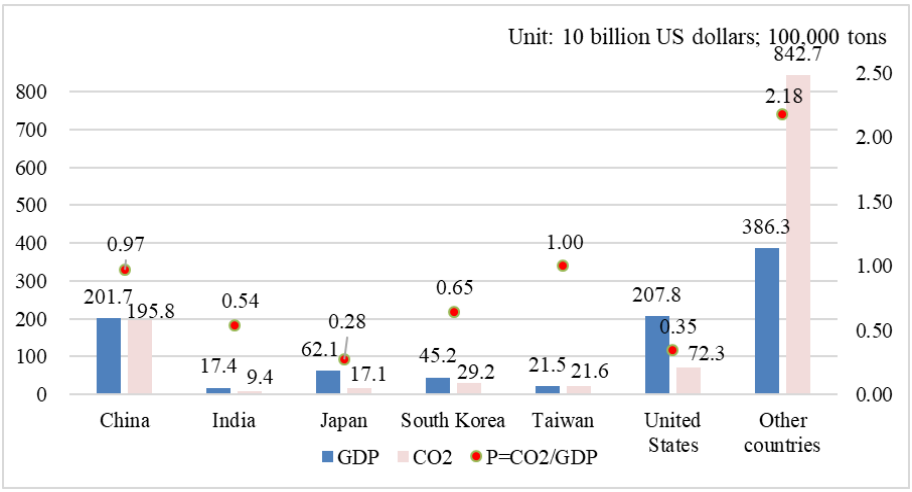

Figure 1. *CO_2 emissions, GDP and its intensity driven by total exports of countries in 2014 (new version)*

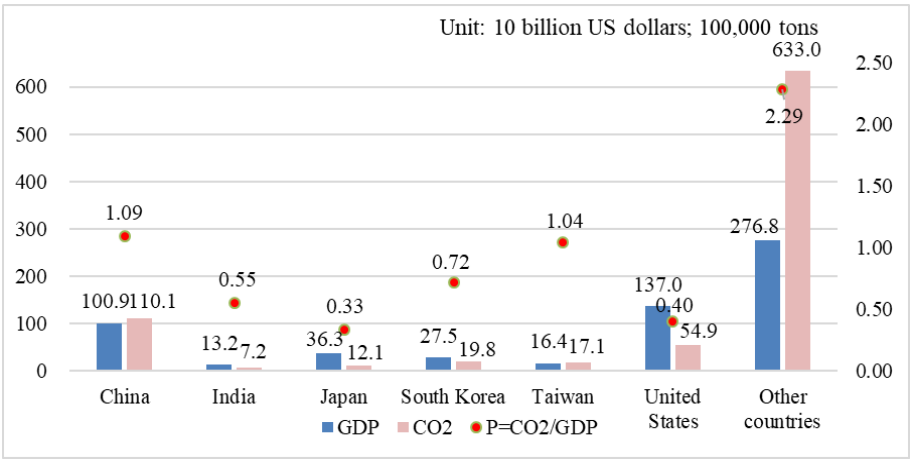

Figure 2. *CO_2 emissions, GDP and its intensity driven by intermediate goods exports of countries in 2014 (new version)*

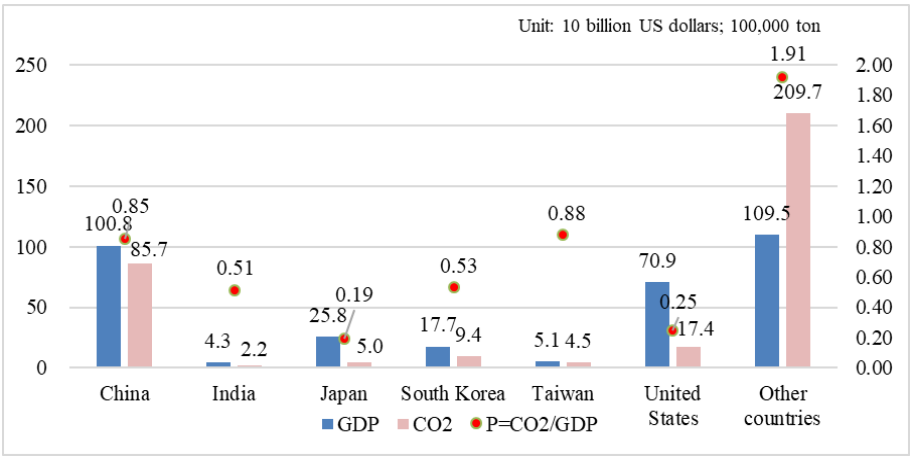

Figure 3. *CO_2 emissions, GDP and its intensity driven by final goods exports of countries in 2014 (new version)*

http://www.aloki.hu ● ISSN 1589 1623 (Print) ● ISSN 1785 0037 (Online)
DOI: http://dx.doi.org/10.15666/aeer/1704_98659880

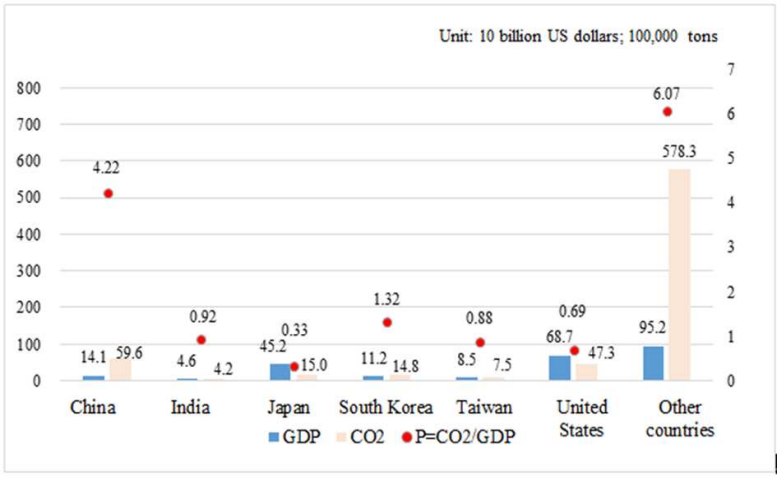

Figure 4. *The export level and intensity of total CO_2 emissions and GDP in 1995 (old version)*

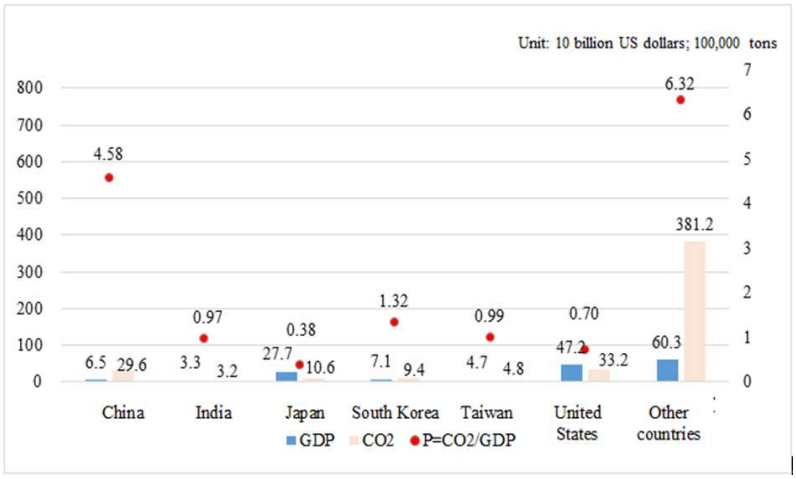

Figure 5. *The export level and intensity of total CO_2 emissions and intermediate goods-driven GDP in 1995 (old version)*

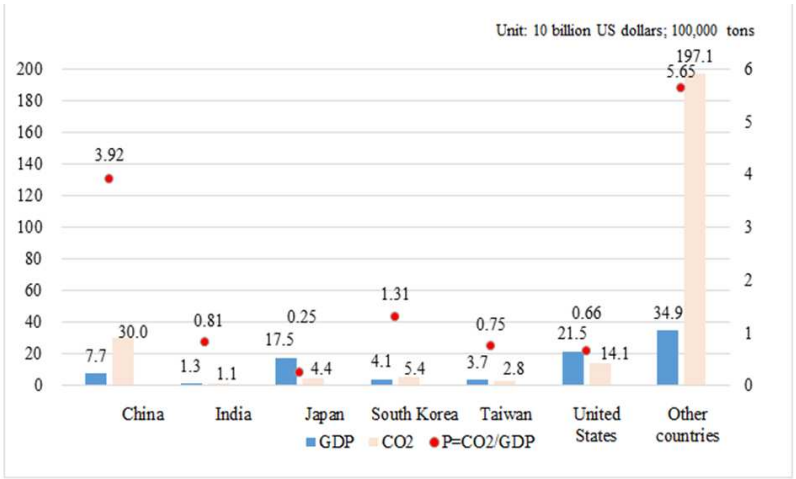

Figure 6. *The export level and intensity of total CO_2 emissions and final goods-driven GDP in 1995 (old version)*

http://www.aloki.hu ● ISSN 1589 1623 (Print) ● ISSN 1785 0037 (Online)
DOI: http://dx.doi.org/10.15666/aeer/1704_98659880

Figure 1 shows the CO_2 emissions, GDP and its intensity driven by total exports of countries in 2014 (new version). China ranks second with CO_2 emission intensity of 0.97 in various countries, including CO_2 emissions of 19.58 billion tons. *Figures 2* and *3* show that the CO_2 emission intensity of 1.09 driven by China's intermediate goods is greater than the CO_2 emission intensity of 0.85 driven by China's final goods, indicating that China's CO_2 emissions mainly come from the intermediate goods. Taiwan's CO_2 emission intensity driven by total exports is the highest, reaching 1.0, but in fact, Taiwan's CO_2 emissions are only 2.1 billion tons, because Taiwan's GDP is only 200 billion US$, only higher than the last ranking of India's 170 billion US$. *Figures 2* and *3* show that the CO_2 emission intensity of 1.04 driven by Taiwan's intermediate goods is greater than the CO_2 emission intensity of 0.88 driven by Taiwan's final goods, indicating that Taiwan's main CO_2 emissions come from the intermediate goods, and intermediate goods and final goods show a ratio of 3:1, showing that Taiwan is an economy that exports intermediate goods. South Korea, which is similar to Taiwan's industrial pattern, ranks third in terms of its CO_2 emission intensity of 0.65 driven by total exports, and its CO_2 emissions of 2.9 billion tons is only 800 million tons more than Taiwan, but its GDP is 450 billion US$. *Figures 2* and *3* show that the CO_2 emission intensity of 0.72 driven by South Korea's intermediate goods is greater than the CO_2 emission intensity of 0.53 driven by South Korea's final goods, indicating that South Korea's main CO_2 emissions mainly come from the intermediate goods. Japan's CO_2 emission intensity driven by total exports is the lowest, with CO_2 emissions of only 1.7 billion tons, but GDP is as high as 620 billion US$, which is three times that of Taiwan. The CO_2 emission intensity of 0.33 driven by Japan's intermediate goods is greater than the CO_2 emission intensity of 0.19 driven by Japan's final goods, indicating that Japan's CO_2 emissions mainly come from the intermediate goods.

Figure 4 shows the level and intensity of CO_2 emissions and GDP total exports in 1995 (old version). China's CO_2 emission intensity is 4.22, which is three times that of South Korea ranking the second, and China's CO_2 emissions are 5.9 billion tons, which ranks the first in the six countries, but China's GDP is only 140 billion US$, only 30 billion US$ higher than South Korea. *Figures 4–6* show that the CO_2 emission intensity of 4.58 driven by China's intermediate goods is greater than the CO_2 emission intensity of 3.92 driven by China's final goods, indicating that in 1995, China was still an intermediate goods-oriented country. Taiwan's CO_2 emission intensity is 0.88, ranking the fourth among the six countries, with CO_2 emissions of 700 million tons and GDP of 80 billion US$. The CO_2 emission intensity of 0.99 driven by Taiwan's intermediate goods is greater than the CO_2 emission intensity of 0.75 driven by Taiwan's final goods, indicating that in 1995, Taiwan was still an intermediate goods export-oriented country. South Korea's CO_2 emission intensity is 1.32, ranking the second among the six countries, with CO_2 emissions of 1.4 billion tons and GDP of 110 billion US$. *Figures 5* and *6* show that the CO_2 emission intensity of 1.32 driven by South Korea's intermediate goods is much the same as the CO_2 emission intensity of 1.31 driven by South Korea's final goods, indicating that in 1995, South Korea's export is complemented by intermediate goods and final goods. Japan's CO_2 emission intensity of 0.33 is almost the same as that of 2014, with CO_2 emissions of 1.5 billion tons and GDP of 450 billion US$. *Figures 5* and *6* show that the CO_2 emission intensity of 0.38 driven by Japan's intermediate goods is much the same as the CO_2 emission intensity of 0.25 driven by Japan's final goods, indicating that in 1995, Japan was an intermediate goods export-oriented country.

http://www.aloki.hu ● ISSN 1589 1623 (Print) ● ISSN 1785 0037 (Online)
DOI: http://dx.doi.org/10.15666/aeer/1704_98659880

Discussion

Analysis and comparison of export-driven CO_2 emission intensity in countries in 1995 and 2014

By comparing the level and intensity of CO_2 emissions and GDP driven by total exports of countries in 1995 and 2014 (see *Figs. 4* and *1*), we can see the rankings of CO_2 emission intensity in 1995 were: China, South Korea, India, Taiwan, the United States and Japan; rankings in 2014 were: Taiwan, China, South Korea, India, the United States and Japan. Taiwan rose from the fourth place to the first place, China, South Korea, and India all ranked down, and the United States and Japan ranked the same. In most countries, the level of CO_2 emissions has declined, except for Taiwan, and Japan which has low intensity. It has shown that Taiwan has grown with the same proportions of CO_2 and GDP in the past 20 years, but other developed countries have doubled.

Analysis of export-driven CO_2 emission paths

In order to concrete our results, *Figures 7–10* compare the CO_2 emissions in each industry and *Table 2* list the industry category and the definition. If we track from downstream industry to the upstream industry (D→U), and from upstream to downstream (U→D), the CO_2 emissions driven by the export of each country are observed, and the carbon dioxide emission paths of the industries in Taiwan are organized, as shown in *Figures 7* and *8*, where, $CO_{2exp}^{D\rightarrow U}$ indicates the carbon dioxide emissions emitted by all industries exporting specific products, which can be used to check the emissions of all sectors directly or indirectly affected by the domestic upstream supply chain, while $CO_{2exp}^{U\rightarrow D}$ indicates the carbon dioxide emissions emitted by specific exports from particular sectors, and it can show how the emissions from specific upstream sectors affect the final exports of all downstream industries.

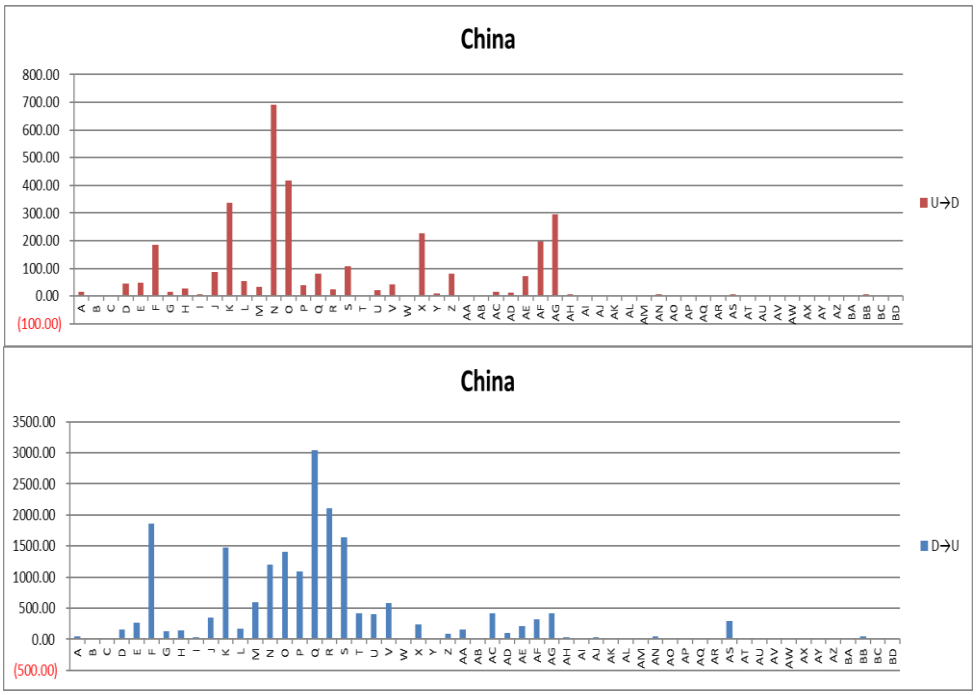

Figure 7. *CO_2 emissions driven by China's exports in 2014: tracking from the downstream industry to the upstream industry (D→U) and from upstream to downstream industry (U→D)*

http://www.aloki.hu ● ISSN 1589 1623 (Print) ● ISSN 1785 0037 (Online)
DOI: http://dx.doi.org/10.15666/aeer/1704_98659880

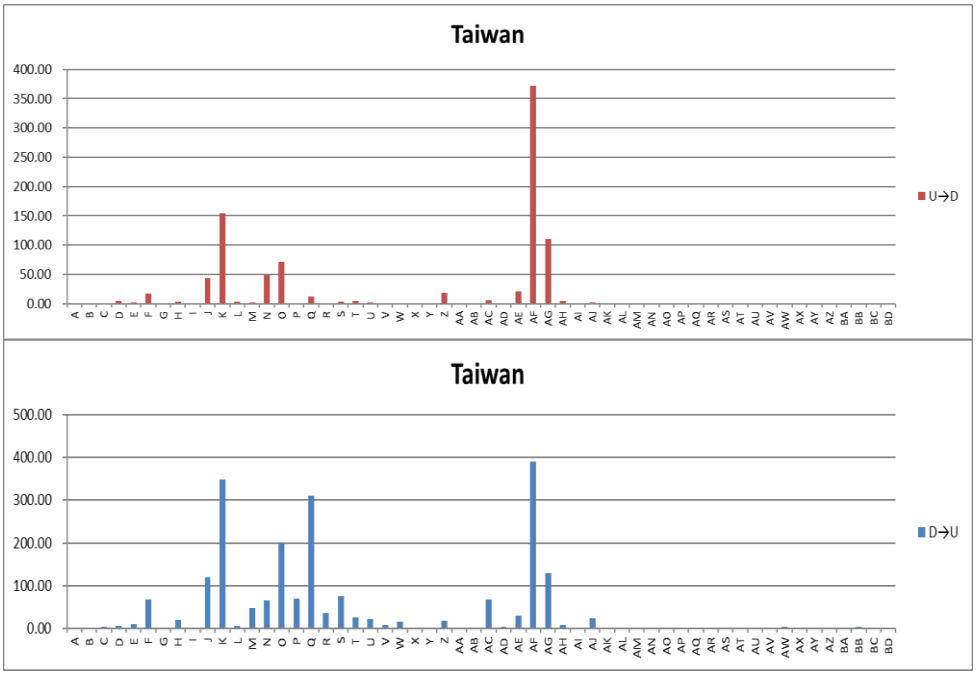

Figure 8. *CO_2 emissions driven by Taiwan's exports in 2014: tracking from the downstream industry to the upstream industry (D→U) and from upstream to downstream industry (U→D)*

Table 2. *Industry category and the definition in Figures 7–10*

Category	Definition
A	Crop and livestock products
B	Forestry logging
C	Fishing aquaculture
D	Mining
E	Food and beverage
F	Textile and apparel
G	Wooden products
H	Paper products
I	Print and copy
J	Coal petroleum products
K	Chemical products
L	Drug products
M	Rubber plastic products
N	Non-metallic mineral products
O	Metal products
P	Metal products (except equipment)
Q	Electronic optical products
R	Electrical equipment manufacturing
S	Transportation equipment manufacturing
T	Car trailer manufacturing
U	Mechanical equipment manufacturing
V	Furniture manufacturing
W	Mechanical equipment repair and installation

http://www.aloki.hu ● ISSN 1589 1623 (Print) ● ISSN 1785 0037 (Online)
DOI: http://dx.doi.org/10.15666/aeer/1704_98659880

X	Electricity-fired fluorine air conditioner supply
Y	Water collection and treatment supply
Z	Waste recycling management
AA	Construction
AB	Trade and repair of automobiles and locomotives
AC	Wholesale trade (except automobiles and locomotives)
AD	Retail (except automobiles and locomotives)
AE	Land pipeline transportation
AF	Water transport
AG	Air transport
AH	Warehousing and transportation
AI	Post Express
AJ	Accommodation activities
AK	Publishing
AL	Audio and video production and publishing
AM	Telecommunications
AN	Computer program consulting related
AO	Financial services (excluding insurance)
AP	Insurance (except compulsory insurance)
AQ	Financial and insurance assistance
AR	Real estate
AS	Legal and accounting advice related
AT	Construction engineering analysis
AU	Scientific research development
AV	Advertising and market research
AW	Other science and technology related to veterinary counseling
AX	Administrative service related
AY	Public administration and compulsory insurance
AZ	Education
BA	Health and social activities
BB	Other social activities
BC	Family (for domestic use)
BD	Related activities of overseas institutions
BE	Leather product

As shown in *Figures 4–7,* the CO_2 emissions driven by China's exports are tracked from the downstream industry to the upstream industry (D→U), that is, CO_2 emissions produced from the input of upstream industry because of the other industries driven by export products, see left bar of *Figures 4–7*. China's major downstream export industry sectors are electronic optical products (300 million tons), electrical equipment manufacturing (210 million tons), textile and apparel (180 million tons), transportation equipment manufacturing (160 million tons). The CO_2 emissions driven by China's exports are tracked from the upstream industry to the downstream industry (U→D) to track the upstream industry, which is to support the CO_2 emissions generated by the downstream industries, see the right bar of *Figures 4–7*. The upstream-supported export

http://www.aloki.hu ● ISSN 1589 1623 (Print) ● ISSN 1785 0037 (Online)
DOI: http://dx.doi.org/10.15666/aeer/1704_98659880

industry sectors are mainly non-metallic mineral products (70 million tons), metal products (40 million tons), and chemical products (30 million tons).

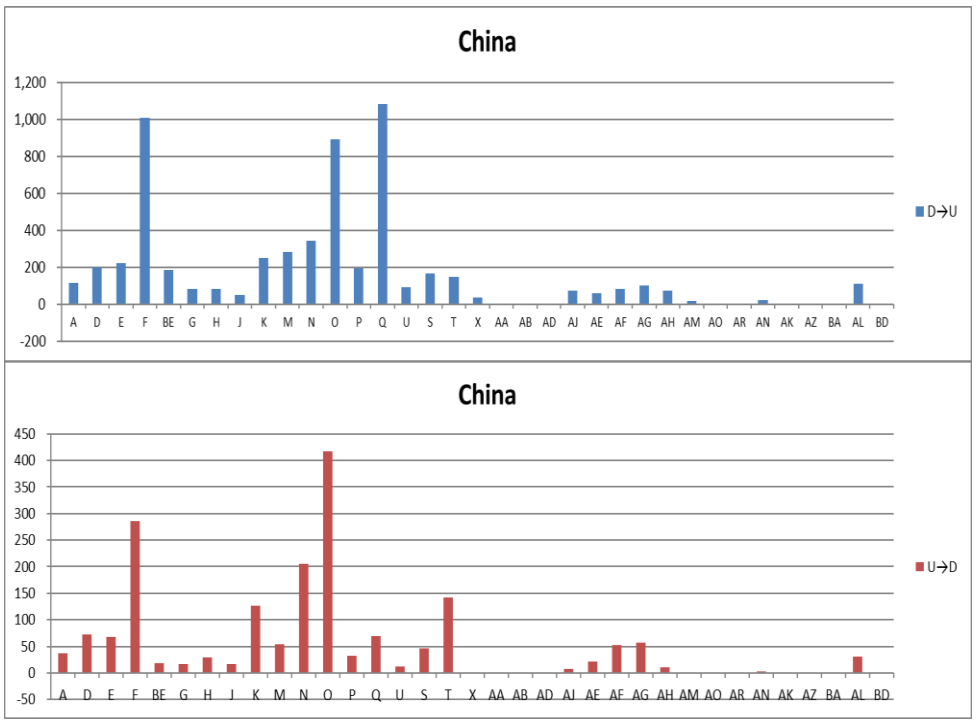

Figure 9. *CO_2 emissions driven by China's exports in 1995: tracking from the downstream industry to the upstream industry (D→U) and from upstream to downstream industry (U→D)*

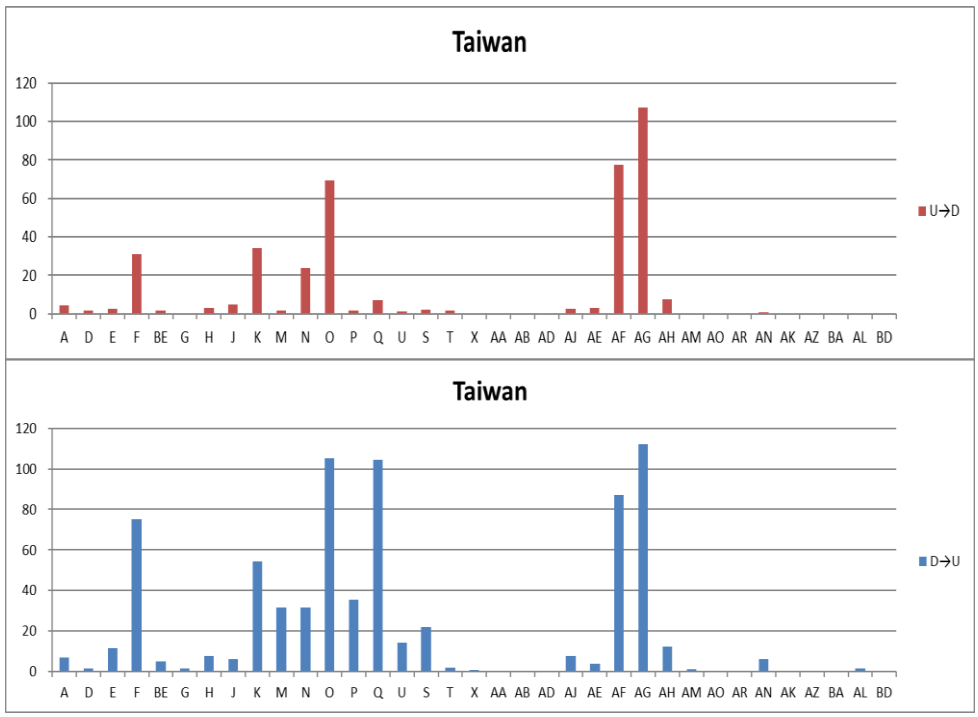

Figure 10. *CO_2 emissions driven by Taiwan's exports in 1995: tracking from the downstream industry to the upstream industry (D→U) and from upstream to downstream industry (U→D)*

http://www.aloki.hu ● ISSN 1589 1623 (Print) ● ISSN 1785 0037 (Online)
DOI: http://dx.doi.org/10.15666/aeer/1704_98659880

The CO_2 emissions driven by Taiwan's exports are tracked from the downstream industry to the upstream industry (D→U), see the left bar of *Figures 4–8*. The major downstream export industry sectors are water transport (about 39 million tons), chemical products (about 35 million tons), and electronic optical products (about 31 million tons). The CO_2 emissions driven by Taiwan's exports tracked from upstream industry to downstream industry (U→D) is shown in the right bar of *Figures 4–9*. The major industrial sectors invested in the upstream are water transport (about 37 million tons), chemical products (about 15 million tons), and air transport (about 11 million tons).

Finally, *Figures 9* and *10* summarize the estimated estimation on CO_2 emissions in China and Taiwan in 1995. The CO_2 emissions driven by exports from 1995 to 2014 are compared and tracked from the downstream industry to the upstream industry (D→U) and from upstream to downstream industry (U→D) see from *Fig 4- Fig 10.* In the CO_2 emissions driven by China's exports tracked from the downstream industry to the upstream industry (D→U), electronic optical products, textile and metal products have the most emissions, while when tracking from upstream to downstream industry (U→D), the metal products, textile and non-metal products have the most emissions. In 2014, China's major downstream industrial sectors added more high CO_2 emissions sectors such as electrical equipment manufacturing, transportation equipment manufacturing and chemical products. In 1995, when CO_2 emissions driven by Taiwan's exports are tracked from the downstream industry to the upstream industry (D→U), the air transport, metal products and electronic optical products have the most emissions, while when tracking from upstream to downstream industry (U→D), the air transport, water transport and metal products have the most emissions. In 2014, Taiwan's high CO_2 emissions sectors are water transport, chemical products and electronic optical products.

Conclusion

The composition of industrial chains is interdependent in international trade. Today, global trade belongs to different countries in the upper, middle and lower reaches of production process of vertical labor division. This paper analyzes trade items and supply chain portfolios from global value chains, and further integrates and compares the carbon emissions from supply chain portfolios across countries. Based on the results of Liu et al. (2016), this paper uses the EIO model to analyze the relationship between trade exports and carbon dioxide emissions in Taiwan and other six countries. The empirical analysis of this paper first analyzes the CO_2 emission intensity driven by countries' exports, where Taiwan's total CO_2 emission intensity is 1.0, topping the highest, with CO_2 emissions of only 2.1 billion tons, which is caused by Taiwan's low GDP of 200 billion US$. The CO_2 emission intensity driven by China's total exports is 0.97, with CO_2 emissions of as high as 19.58 billion tons, but the GDP is 2 trillion US$, resulting in an intensity of only 0.97. The CO_2 emission intensity driven by the US total exports is only 0.35, with CO_2 emissions of 7.2 billion tons, which is caused by the high US GDP as much as 2.07 trillion US$. South Korea, which is similar to Taiwan's industrial pattern, has a CO_2 emission intensity of 0.65 driven by its total exports, with CO_2 emissions of 2.9 billion tons, only 800 million tons more than Taiwan, but the GDP is 450 billion US$. The total CO_2 emission intensity driven by Japan's total exports is 0.28, with CO_2 emissions of only 1.7 billion tons, but the GDP is as high as 620 billion

http://www.aloki.hu ● ISSN 1589 1623 (Print) ● ISSN 1785 0037 (Online)
DOI: http://dx.doi.org/10.15666/aeer/1704_98659880

US$, which is three times that of Taiwan. The results of the analysis show that most developed countries take intermediate goods as the main export type under the global industrial chain, while the exports in less developed countries such as India have a ratio of 1:1 between intermediate goods and final goods, and final goods may even count greater than intermediate goods.

By comparing the level and intensity of CO_2 emissions and GDP total exports in various regions in 1995 and 2004, we can see that Taiwan rose from the fourth to the first place. China, South Korea and India ranked from the first, second and third to second, third and fourth, respectively, the United States and Japan remain unchanged at the fifth and sixth place. In most countries, the level of CO_2 emissions has declined, except for Taiwan, and Japan which has low intensity. It has shown that Taiwan has grown with the same proportions of CO_2 and GDP in the past 20 years, but other developed countries have doubled.

Then, if we track from downstream industry to the upstream industry (D→U), and from upstream to downstream (U→D), the CO_2 emissions driven by the export of Taiwan and mainland are observed, with CO_2 emissions produced from the input of upstream industry because of the other industries driven by China's downstream export products, which means that by tracking from downstream to upstream, China's major downstream export industry sectors are electronic optical products, electrical equipment manufacturing, textile and apparel and transportation equipment manufacturing. The upstream industry in China supports the CO_2 emissions generated by the downstream industries, that is, by tracing from upstream to downstream, the major upstream sectors supporting export industry are non-metallic mineral products, metal products and chemical products. Taiwan's major downstream export industry sectors are water transport, chemical products and electronic optical products, and the major upstream sectors are water transport, chemical products and air transport.

As China launches the carbon trading market, Singapore is expected to introduce a carbon tax in 2019, and many countries around the world have formulated a policy on carbon pricing. Yet it is uncertain whether the carbon tax will bring a huge burden to the economy, only some countries in northern Europe succeeded in maintaining economic growth rate. On the other hand, Australia has abolished the carbon tax, which became a major cause of dragging down the Australian economy. In Taiwan and other countries in the world, environmental mark and carbon footprint mark are more commonly used, that is, how much carbon is emitted from the product or how much energy is used in the product are clearly marked, so that consumers can choose whether to buy lower-carbon products after reading the message. Energy costs such as the use of fuel may rise from the imposition of emission taxes, while people can transform the society into a sustainable development pattern through the change of lifestyle. This paper is mainly to explore the generation and attribution of CO_2 generated by inter-regional economic production and exchange, and to compare the growth rate of CO_2 emissions between different economies. In the follow-up, we will further explore the relationship between environmental shocks, foreign trade changes, and commodity substitutions generated by such economic activities.

Acknowledgements. This paper was supported by Major Project of Humanities and Social Sciences in Colleges and Universities in Zhejiang province during the year 2017-2018 (Grant No. 2018QN089), the MOE Foundation of Humanities and Social Sciences (Grant No. 19YJCGJW011), Talent Project by Qianjiang in Zhejiang province (Grant No. QJC1803005).

http://www.aloki.hu ● ISSN 1589 1623 (Print) ● ISSN 1785 0037 (Online)
DOI: http://dx.doi.org/10.15666/aeer/1704_98659880

REFERENCES

[1] Ang, B. W. (1995): Decomposition methodology in industrial energy demand analysis. – Energy 1: 168-182.
[2] Ang, B. W. (2014): Decomposition analysis for policy making in energy: which is the preferred method? – Energy Policy 32: 1131-1139.
[3] Dietzenbacher, E., Stage, J. (2006): Mixing oil and water? Using hybrid input-output tables in a structural decomposition analysis. – Economic Systems Research 18: 85-95.
[4] Dietzenbacher, E., Los, B., Stehrer, R., Timmer, M. P., de Vries, G. J. (2013): The construction of world input-output tables in the WIOD Project. – Economic Systems Research 25: 71-98.
[5] Hoekstra, R., van den Bergh, J. M. (2003): Comparing structural decomposition analysis and index. – Energy Economics 25: 39-64.
[6] Jin, A. H., Bai, L., Kim, J. Y., Jeong, S. J., Kim, K. S. (2017): Analysis of GHG emission reduction in South Korea using a CO_2 transportation network optimization model. – Energies 10: 1-18.
[7] Kagawa, S., Inamura, H. (2001): A structural decomposition of energy consumption based on a hybrid rectangular input-output framework: Japan's case. – Economic Systems Research 13: 339-363.
[8] Lenzen, M. (2003): Environmentally important paths, linkages and key sectors in the Australian economy. – Structural Change and Economic Dynamics 14: 1-34.
[9] Lenzen, M., Pade, L. L., Munksgaard, J. (2004): CO_2 multipliers in multi-region input-output models. – Economic Systems Research 16: 391-412.
[10] Lin, C., Yang, J. (2017): Research on the Technology Spillover Effect of Taiwanese Investment on Agricultural Products Processing Industry in Mainland China. – In: 2017 International Conference on Education Science and Economic Management (ICESEM 2017). Atlantis Press, Paris.
[11] Liu, Y., Mong, B., Hubacek, K., Xue, J., Feng, K., Gao, Y. (2016): Made in China: a reevaluation of embodied CO_2 emissions in Chinese exports using firm heterogeneity information. – Applied Energy 184: 11106-1113.
[12] Lu, M. (2018): Introduction: The Changing Geographies of China. – In: Li, S. et al. (eds.) Changing China. Routledge, Abingdon, pp. 1-13.
[13] Meng, B., Fang, Y., Guo, J., Zhang, Y. (2017): Measuring China's domestic production networks through trade in value-added perspectives. – Economic Systems Research 29(1): 48-65.
[14] Peter, G. P., Hertwich, E. G. (2006): Structural analysis of international trade: environmental impacts of Norway. – Economic Systems Research 18: 155-181.
[15] Rigger, S. (2015): Taiwanese Business in Mainland China: From Domination to Marginalization? – In: Irwin Crookes, P., Knoerich, J. (eds.) Cross-Taiwan Strait Relations in an Era of Technological Change (pp. 61-76). Palgrave Macmillan, London.
[16] Ritchie, H., Reay, D., Higgins, P. (2018): Sustainable food security in India—Domestic production and macronutrient availability. – PloS One 13(3): e0193766.
[17] Rose, A., Casler, S. (1996): Input-output structural decomposition analysis: a critical appraisal. – Economic Systems Research 8: 33-62.
[18] Su, B., Ang, B. W. (2012): Structural decomposition analysis applied to energy and emissions: some methodological developments. – Energy Economics 34: 177-188.
[19] Timmer, M. P., Dietzenbacher, E., Los, B., Stehrer, R. de Vries, G. J. (2015): An illustrated user guide to the world input output database: the case of global automotive production. – Review of International Economics 23: 575-605.
[20] Xu, X. Y., Ang, B. W. (2013): Index decomposition analysis applied to CO_2 emission studies. – Ecological Economics 93: 313-329.

http://www.aloki.hu ● ISSN 1589 1623 (Print) ● ISSN 1785 0037 (Online)
DOI: http://dx.doi.org/10.15666/aeer/1704_98659880

YIELD AND FEED VALUE OF MAIZE (*ZEA MAYS* L.) GREEN FORAGE OBTAINED FROM EUROPEAN CULTIVARS GROWN IN POLAND

GĄSIOROWSKA, B. – PŁAZA, A. – RZĄŻEWSKA, E.* – WARANICA, M.

Agrotechnology Department, Faculty of Natural Sciences, Siedlce University of Natural Sciences and Humanities, Poland
(e-mail: anna.plaza@uph.edu.pl; barbara.gasiorowska@uph.edu.pl; emilia.rzazewska@uph.edu.pl; szur@uph.edu.pl)

**Corresponding author*
e-mail: emilia.rzazewska@uph.edu.pl

(Received 29th Mar 2019; accepted 13th Jun 2019)

Abstract. This article presents the results of a research conducted to evaluate the production-related value and feeding value of selected maize (*Zea mays* L.) cultivars included in the Common Catalogue of Varieties of Agricultural Plant Species (CCA). The following two factors were examined: A − the harvest date of maize green matter (I − tasseling stage (75% of plants at this stage), II − milk maturity stage (after three weeks), III − wax maturity stage (after another three weeks)); B − cultivars with different times of maturity (Pyroxenia – very early, FAO 130, Codimi – early FAO 200, Moschus – early, FAO 220, Alombo – medium early, FAO 230, Celive – medium early, FAO 245). The results demonstrated that the highest dry matter yield was produced by plants at the wax maturity stage. Cv. Alombo had the highest fresh matter yield. The highest organic matter (OM) digestibility and dry matter (DM) digestibility were determined for maize plants harvested at the wax maturity stage. The earliest maturing cultivars, namely Pyroxenia and Codimi, had the highest organic matter (OM) digestibility and dry matter (DM) digestibility. The highest total protein content and crude ash were recorded for maize plants harvested at the tasseling stage. Cv. Codimi, Moschus, Alombo and Clive produced the highest concentrations of these components.
Keywords: *dry matter yield, green forage chemical composition, organic matter (OM) digestibility, dry matter (DM) digestibility*

Introduction

Soil and climatic conditions of Poland are optimal for the cultivation of maize for silage (Ptaszyńska and Sulewska, 2008). The species represents the most productive fodder crops (Strzetelski et al., 2001; Brzóska, 2001). Harvest date and cultivar selection determine the crop plant make-up and structure, which may lead to substantial differences in yielding, chemical composition and feed value of maize plants (Kowalik, 2001).

As the area under maize production and economic role of maize are on the increase, there is growing demand for better and better cultivars and thus hybrids (Korniewicz et al., 2000; Sulewska et al., 2011). Jha et al. (1998) and Adamczyk (2001) emphasized the fact that the role of new cultivars in modern agriculture is of great importance.

The following factors affect the quality and quantity of harvested yields: agrotechnology (40%), climatic conditions (30%), selected cultivars (30%). Thus, a third of the effect is cultivar-related (Sulewska et al., 2011). As a result, it seems reasonable to examine selected cultivars from other Europeans countries, such as Germany, the Czech Republic, Slovakia and France, in terms of their suitability for cultivation in Poland. The objective of the study was to evaluate the production-related

http://www.aloki.hu ● ISSN 1589 1623 (Print) ● ISSN 1785 0037 (Online)
DOI: http://dx.doi.org/10.15666/aeer/1704_98819887

value and feed value of selected cultivars included in the Common Catalogue of Varieties of Agricultural Plant Species (CCA) harvested at various development stages, which were used as raw materials for the production of whole plant silage from maize cultivated under the soil and climatic conditions of Poland.

Materials and methods

Field research was conducted in 2009-2011 on a private holding located in Kowiesy near Siedlce (52º03' 39'' N, 22º 33' 80'' E). The experiment was carried out on the soil classified as Albic Luvisol (Arenic) characterised by a slightly acid reaction and average available phosphorus, potassium and magnesium contents. Its humus content was 1.28%. The trial was a split-plot arrangement with three replicates. The following two factors were investigated: A − maize green matter harvest date (I − tasseling stage (75% of plants at this stage), II − milk maturity stage (after three weeks), III − wax maturity stage (after another three weeks)); B − cultivars with different earliness of maturity (Pyroxenia – very early FAO 130, Codimi – early FAO 200, Moschus – early FAO 220, Alombo – medium early FAO 230, Celive – medium early FAO 245).

The number of plants per 1 metre was 10, and the sowing rate was established based on previous research by Sulewska (2001). Maize was grown as a continuous crop. Cattle manure was applied at the rate of 30 tha^{-1} in the autumn. In spring, phosphorus and potassium fertilisers were applied at rates matching soil contents of available elements, that is 60 kg Pha^{-1} and 90 kg Kha^{-1}. Nitrogen fertiliser was applied pre-plant at the rate of 92 kg Nha^{-1} in the spring and followed by maize, the nitrogen rate being increased due to an application of Polifoska 6. Maize cultivars were planted in late April. The green matter of maize crop was harvested at three dates as set in the methodology. During harvest, the fresh matter yield of whole plants was determined in each plot, and their average samples were taken for chemical analyses. Dry matter content, total protein content, crude ash content, organic matter digestibility and dry matter digestibility were determined in the sampled material by means of near infrared spectroscopy (NIRS) using the spectrometer NIR Flex N-500.

The results of the study were statistically analysed; ANOVA following the linear model for a two factor split-plot design was performed for each trait examined, and separation of means was obtained by means of Tukey test at the significance level of 0.05.

Results and discussion

The dry matter yield of maize plants

The dry matter yield of maize plants was significantly affected by the experimental factors and their interaction (*Table 1*).

The highest dry matter yield was produced by maize plants harvested at the wax maturity stage. In corresponds to findings reported by Toler et al. (1998), Kowalik (2001), Michalski (2002), Filya (2004), Szempliński et al. (2009), Lynch et al. (2012), Magalhães et al. (2015) and Komainda et al. (2018). In the study discussed here, the dry matter yield of maize plants harvested at the milk stage was lower, it being the lowest when harvest was performed at the tasseling stage. It may be explained by the fact that the dry matter yield of maize plants increases from the tasseling stage to the wax

http://www.aloki.hu ● ISSN 1589 1623 (Print) ● ISSN 1785 0037 (Online)
DOI: http://dx.doi.org/10.15666/aeer/1704_98819887

maturity stage. In the experiment reported here, the highest dry matter of maize plants was produced by the medium early cultivar Alombo, the yields of the maize plants of cv. Pyroxenia, Codimi, Moschus and Celive being significantly lower. Also Sulewska and Koziary (2005), Podkówka et al. (2015), Swanckaert et al. (2016) and Nawab et al. (2017) reported a higher yielding potential of later maturing cultivars. In the current study, an interaction between the experimental factors was confirmed indicating that the highest dry matter yields were supplied by the following cultivars: Pyroxenia, Codimi, Moschus, Alombo and Celive harvested at the wax maturity stage, it being the lowest for all the experimental cultivars harvested at the tasseling stage.

Table 1. *Dry matter yield of maize plants (means across 2009-2011), tha^{-1}*

Cultivars (B)	**Harvest date (A)**			**Means**
	I	**II**	**III**	
Pyroxenia	6.59	13.89	18.04	12.84
Codami	7.11	12.74	19.68	13.18
Moschus	6.57	15.06	20.26	13.97
Alombo	7.98	15.95	23.11	15.68
Celive	7.10	13.82	21.08	14.00
Means	7.07	14.29	20.43	-
ANOVA	P-value		$LSD_{0.05}$	
Harvest date (A)	<0.001		3.63	
Cultivars (B)	<0.001		1.32	
Interaction (AxB)	<0.001		5.40	

The total protein content in plants

Statistical analysis demonstrated a significant influence of the experimental factors and their interaction of total protein content in maize plants (*Table 2*).

The highest total protein content was recorded for maize plants harvested at the tasseling stage. When delayed the harvest date to the milk maturity stage, a significant decrease of total protein content was recorded for maize plants harvested. When harvest is further delayed to the wax maturity stage, no total protein content significant decrease in maize plants is observed.

Table 2. *Total protein content in plants, gkg-1 d.m.*

Cultivars (B)	**Harvest date (A)**			**Means**
	I	**II**	**III**	
Pyroxenia	100.6	82.3	78.5	87.1
Codami	108.7	83.7	80.7	91.0
Moschus	104.9	82.1	80.4	89.1
Alombo	110.1	84.6	76.7	90.5
Celive	111.7	86.5	83.5	93.9
Means	107.2	83.9	79.9	-
ANOVA	P-value		$LSD_{0.05}$	
Harvest date (A)	<0.001		5.9	
Cultivars (B)	<0.001		5.2	
Interaction (AxB)	<0.001		7.8	

It may be explained by fact that the plants harvested in earlier stage are characterized by a higher content of total protein. In corresponds to findings reported by Tolera et al. (1998, 1999), who reported that by delaying the harvest of maize plants, the total

http://www.aloki.hu ● ISSN 1589 1623 (Print) ● ISSN 1785 0037 (Online)
DOI: http://dx.doi.org/10.15666/aeer/1704_98819887

protein content decreases. However, the regress of total protein in the dry matter of plants at the end of vegetation is low. In the study discussed here, the total protein content of maize plants studied cultivars was on the same level, with the exception of the Pyroxenia cultivar.

The concentration of total protein in plants of this cultivar was significantly lower, which has been confirmed in research by other authors (Tolera et al., 1999; Sulewska, 2001; Schttenhelm, 2008; Podkówka et al., 2015). Špelekovă and Galovă (2018) results of research demonstrated higher protein content in maize cultivars from Europe than from the United States. In the present study reported here, the interaction of the studied factors demonstrated that only in the tasseling stage, the total protein content in maize plants of Pyroxenia cultivar was significantly lower than in the other cultivars. At the milk maturity stage and wax maturity stage, no significant differences were found in the total protein content between the studied cultivars. The highest total protein content was recorded from the Codimi, Moschus, Alombo and Celive maize plants harvested in the tasseling stage, significantly lower from all studied maize cultivars harvested in the wax maturity stage.

The crude ash content in plants

The content of crude ash in maize plants was significantly differentiated by the experimental factors studied and their interaction (*Table 3*).

The highest content of crude ash was recorded in maize plants harvested during the tasseling stage. Significantly lower crude ash content was recorded in maize plants harvested at milk maturity stage, the lowest in plants harvested in the wax maturity stage. Also Filya (2004), Yuxiang et al. (2007) and Komainda et al. (2018) demonstrated that by delaying the harvest of maize plants from the stage of early milk to wax maturity stage, the content of crude ash decreases. This should be explained by the fact that plants harvested in earlier stages contain more minerals and more organic components.

Table 3. *Crude ash content in plants, gkg-1 d.m.*

Cultivars (B)	**Harvest date (A)**			**Means**
	I	**II**	**III**	
Pyroxenia	81.3	51.2	38.8	57.1
Codami	77.6	58.8	39.9	58.8
Moschus	80.3	61.5	46.1	62.6
Alombo	83.4	61.3	42.4	62.4
Celive	81.3	60.5	45.7	62.5
Means	80.8	58.7	42.6	-
ANOVA	P-value		$LSD_{0.05}$	
Harvest date (A)	<0.001		3.0	
Cultivars (B)	<0.001		3.9	
Interaction (AxB)	<0.001		5.8	

In own studies, also the cultivars significantly differentiated the content of crude ash in plants. Of these, only the plants of maize of the Pyroxenia cultivar had a significantly lower concentration of crude ash than in the plants of the other cultivars. Also, Tolera et al. (1999), Sulewska (2002), Schttenhelm (2008) and Podkówka et al. (2015) demonstrated that cultivars with a longer growing season contained more crude ash both in whole plants and in grain. In the current study, an interaction between the

http://www.aloki.hu ● ISSN 1589 1623 (Print) ● ISSN 1785 0037 (Online)
DOI: http://dx.doi.org/10.15666/aeer/1704_98819887

experimental factors was confirmed indicating that the highest content of crude ash was recorded in all cultivars of maize plants harvested in the tasseling stage, and the lowest in maize plants of the Pyroxenia and Codmi cultivars harvested at the wax maturity stage.

The organic matter digestibility (OM) of maize plants

Statistical analysis demonstrated a significant influence of the experimental factors and their interaction of organic matter digestibility and dry matter digestibility (*Tables 4 and 5*).

Table 4. *Organic matter digestibility (OM) of maize plants (means across 2009-2011), %*

Cultivars (B)	**Harvest date (A)**			**Means**
	I	**II**	**III**	
Pyroxenia	53.63	66.49	71.65	63.92
Codami	53.76	63.29	71.01	62.69
Moschus	52.91	62.22	69.65	61.59
Alombo	52.28	61.29	69.88	61.15
Celive	53.88	61.87	70.34	62.03
Means	53.29	63.03	70.51	-
ANOVA	P-value		$LSD_{0.05}$	
Termin zbioru (A)	<0.001		1.41	
Odmiany (B)	<0.001		1.84	
Interaction (AxB)	<0.001		2.73	

Table 5. *Dry matter digestibility (DM) of maize plants (means across 2009-2011), %*

Cultivars (B)	**Harvest date (A)**			**Means**
	I	**II**	**III**	
Pyroxenia	52.82	65.09	70.06	62.65
Codami	53.47	61.83	69.52	61.61
Moschus	52.54	60.62	67.95	60.37
Alombo	51.70	59.82	68.11	59.88
Celive	53.33	60.65	68.96	60.98
Means	52.77	61.60	68.92	-
ANOVA	P-value		$LSD_{0.05}$	
Harvest date (A)	<0.001		1.38	
Cultivars (B)	<0.001		1.77	
Interaction (AxB)	<0.001		2.63	

The dry matter digestibility (DM) of maize plants

The highest organic matter (OM) digestibility and dry matter (DM) digestibility were recorded for maize plants harvested at the wax maturity stage. Organic matter digestibility and dry matter digestibility of maize plants harvested at earlier development stages were significantly lower, the finding corresponding to reports by Michalski et al. (2002), Filya (2004), Yuxiang et al. (2007), Rodriges et al. (2008) and Swanckaert et al. (2017). In the present study, there was observed a significantly different response of the experimental cultivars in terms of both organic matter (OM) digestibility and dry matter (DM) digestibility, both kinds of digestibility being the highest for the earliest maturing cultivars, that is Pyroxenia and Codimi. Moreover, the dry matter (DM) digestibility of cv. Celive, which is the latest maturing variety, differed insignificantly from DM digestibility of cv. Pyroxenia and Codimi. The organic matter

http://www.aloki.hu ● ISSN 1589 1623 (Print) ● ISSN 1785 0037 (Online)
DOI: http://dx.doi.org/10.15666/aeer/1704_98819887

(OM) digestibility and dry matter (DM) digestibility of cv. Moschus and Alombo were significantly lower. Also results of research by Tolera et al. (1999), Stejskalova et al. (2011) and Schttenhelm (2008) demonstrated cultivar-related differences between the organic matter digestibility and dry matter digestibility of both grain and green forage of maize plants representing other cultivars. Podkówka et al. (2015) reported that early maturing cultivars had a significantly higher organic substance (OS) digestibility of maize grain compared with medium early and late maturing cultivars. In the study reported here, an interaction between the experimental factors was found which is indicative of the fact that the highest organic matter (OM) digestibility and dry matter (DM) digestibility of all the experimental cultivars were recorded for plants harvested at the wax maturity stage, them being the lowest for cv. Pyroxenia, Codimi, Moschus, Alombo and Celive harvested at the tasseling stage.

Summary

Research on the suitability of cultivating new European cultivars from the Common Catalogue of varieties of Agricultural Plant Species (CCA) in soil and climatic conditions of Poland is fully justified. Therefore, it will be advisable to continuously study new cultivars in terms of dry matter yield and chemical composition of corn forage harvested in various development phases. This will allow the selection of such cultivars from the Common Catalogue of varieties of Agricultural Plant Species (CCA) useful for cultivation in Poland, which will be characterized by the highest yield and favorable chemical composition of forage, which will ensure good quality of silage.

REFERENCES

[1] Adamczyk, J. (2001): The importance of selecting varieties in the cultivation of maize for grain and silage. – Biul. Inf. IŻ - R. XXXIX 1: 29-35. (in Polish).
[2] Brzóska, F. (2001): Nutritional value of fodder from corn. – Biul. Inf. IŻ, R. XXXIX 1: 37-48. (in Polish).
[3] Filya, I. (2004): Nutritive value and aerobic stability of whole crop maize silage harvested at four stages of maturity. – Anim. Feed Sci. Tech. 116: 141-150.
[4] Jha, P. B., Ghosh, J., Nirala, R. B. P. (1998): Genetic variability and character association in fodder maize. – J. Res. Birsa Agric. Univ. 10(2): 139-143.
[5] Komainda, M., Taube, F., Klub, Ch., Antje, H. (2018): The effects of maize (Zea Mays L.) hybrid and harvest date on above-and belowground biomass dynamics, forage yield and quality – A trade-off for carbon inputs? – Eur. Jour. Agron. 92: 51-62.
[6] Korniewicz, A., Kosmala, I., Czarnik-Matusewicz, H., Paleczek, B. (2000): The contents of basic nutrients in the grain of different maize hybrids. – Rocz. Nauk Zoot. 27(1): 289-303. (in Polish).
[7] Kowalik, I. (2001): Variability and correlation of elements of the maize yield structure (Zea mays L.) depending on weather conditions and nitrogen fertilization. – Rocz. AR Poznań, Rol. 61: 77-87. (in Polish).
[8] Lynch, J. P., O'Kiely, P., Doyle, E. M. (2012): Yield, quality and ensilage characteristics of whole-crop maize and of the cob and stover components: harvest date and hybrid effect. – Grass Forage Sci. 67(4): 472-487.
[9] Magalhäes, A., Rolim, M., Duarte, A., Pedrosa, E., Silva, E. (2015): Chemical attributes of soil and dry mass accumulation of maize fertilized with cassava wastewater. – Engen. Agric. 35(3): 458-469.

http://www.aloki.hu ● ISSN 1589 1623 (Print) ● ISSN 1785 0037 (Online)
DOI: http://dx.doi.org/10.15666/aeer/1704_98819887

[10] Michalski, T., Kruczyńska, H., Kowalik, I. (2002): Yields and quality of ensilaging maize depending on the cultivar and mowing height at harvested. – Acta Sci. Pol. Agric. 1(2): 83-92.
[11] Nawab, A., Anjum, M. M. (2017): Effect of Different Nitrogen Rates on Growth, Yield and Quality of Maize. – Mid. East Jour. Agric. Res. 06(1): 107-112.
[12] Podkówka, L., Podkówka, Z., Piwczyński, D., Buko, M. (2015): Effect of cultivar earliness on chemical composition and digestibility of maize grain. – Rocz. Nauk Zoot. 42(2): 155-169. (in Polish).
[13] Ptaszyńska, G., Sulewska, H. (2008): Yield variation of maize hybrids with different growing period in climatic conditions of central wielkopolska region. – Acta Sci. Pol. Agric. 7(3): 93-103. (in Polish).
[14] Rodrigues, A. M., Andueza, D., Picard, F., Cecato, U., Farruggi, A., Baumont, R. (2008): Classification of mountain permanent grasslands based on their feed value. – Biodiversity and animal. Grassland Sci. Europe. 13: 501-503.
[15] Schttenhelm, S. (2008): Chemical composition and methane field of maize hybrids with contrasting maturity. – Eur. Jour. Agron. 29(2-3): 72-78.
[16] Špaleková, A., Gálová, Z. (2018): Comparison of American and European maize (Zea mays L.) protein profiles. – J Cent Eur Agr. 19(2): 453-465.
[17] Stejskalova, M., Hejcmanova, P. Hejcman, M. (2013): Forage value of leaf fodder main European broad-leaved woody species. The role of grassland in a green future. – Grassl. Sci. Europe 18: 85-87.
[18] Strzetelski, A., Jurkiewicz, A., Strzetelski, J. (2001): Maize silage in cattle feed. – Biul. Inf. Inst. Zoot. 39(1): 49-62. (in Polish).
[19] Sulewska, H. (2001): Yielding and nutritive value of maize harvested on green mass depending on some agrotechnical factors. – Rocz. AR Poznań. Rozp. nauk. 315 (in Polish).
[20] Sulewska, H., Koziara, W. (2005): Influence of weather conditions on yielding and plant development of different maturity maize hybrids. – Sci. Pap. Agric. Univ. Poznań, Agric. 5: 35-41.
[21] Sulewska, H., Adamczyk, J., Rejek, D. (2011): Evaluation of the yield of new hybrids of fodder maize (Zea Mays L.) of Smolice Breeding. – Nauka Przy. Tech. 5(1): 1-11.
[22] Swanckaert, J., Pannecoucque, J., Van Waes, J., Cauwer, B., Latre, J., Haesaert, G., Reheul, D. (2016): Harvest date does not influence variety ranking in Belgian forage maize variety trials. – Jour. Agric. Sci. 154(6): 1040-1050.
[23] Szempliński, W., Bogucka, B., Wróbel, E. (2009): Suitability of early and mid-early maize hybrids grown in the province of Warmia and Mazury for silage production. – Acta Sci. Pol. Agric. 8(1): 57-68. (in Polish).
[24] Tolera, A., Sundstol, F., Said, A. N. (1998): The effect of stage of maturity on yield and quality of maize grain and stover. – Anim. Feed Sci. Tech. 75(2): 157-168.
[25] Tolera, A., Berg, T. Sundstol, F. (1999): The effect of variety on maize grain and crop residue yield and nutritive value of the stover. – Anim. Feed Sci. Technol. 79(3): 165-177.
[26] Yuxiang, Ch., Jing, Ch., Daowei, Z. (2007): Effect of harvest date on shearing force of maize stems. – In Liv. Sci. 111(1): 33-44.

http://www.aloki.hu ● ISSN 1589 1623 (Print) ● ISSN 1785 0037 (Online)
DOI: http://dx.doi.org/10.15666/aeer/1704_98819887

THE EFFECTS OF INDUSTRY INCREASE AND URBANIZATION ON AIR POLLUTANTS IN TURKEY: A NONLINEAR AIR QUALITY MODEL

KILINC, B. K.

Department of Statistics, Faculty of Science, Eskisehir Technical University, Eskisehir 26470, Turkey
(e-mail: bkan@eskisehir.edu.tr; phone: +90-222-335-0580; fax: +90-222-320-4910)

(Received 29th Mar 2019; accepted 24th May 2019)

Abstract. Daily concentrations of air pollutants greatly affect air quality as an increase in industry and urbanization deteriorate the environment. For forty cities in Turkey, eleven variables are recorded to investigate the determinants of air pollution presumably by regressing the air pollutants PM10, NO_X, and NO_2. The temperature, wind, human factors such as population, vehicles, manufacturer, and suchlike are used to create a nonlinear air quality model in Turkey due to the multivariate nature of the data. A comparison of the nonparametric models of the concentration of these pollutants, using multivariate adaptive regression splines (MARS), was obtained to estimate the dependence between air pollutants and various factors. Finally, a model for PM10 concentration shows that climate effects are the most significant variables, whereas the predicted models for NO_X and NO_2 indicate that human factors, such as the number of manufacturers and the number of vehicles, are significant variables. In conclusion, the predicted models are easy to interpret and have advantages of capacity to produce the contributions of the factors for each pollutant model. It is advisable for researchers to examine and determine the suitability of their data sets using nonlinear models when atypical observations and high correlations exist in the data.
Keywords: *multivariate adaptive regression splines, nonparametric, multicollinearity, outlier, pollutant*

Introduction

The exposure of ambient air pollutants in industrial or metropolitan cities adversely affect humans, animals, plants, food crops or other living creatures (Lutgens and Tarbuck, 2001; Kelly and Fussell, 2015, 2017). The measurements of meteorological pollution, such as NO_2 (nitrogen dioxide), and PM10 (particulate matter) have become more important due to their harmful effects on human health (Akkoyunlu, 2003; Elbir et al., 2000; Garcia, 2001; Godish, 2004; Garcia, 2006; Lutgens and Tarbuck, 2001). For example, the adverse effects on human health may include coughing, asthma, chronic bronchitis, and cardio vascular morbidity (Lutgens and Tarbuck, 2001; U.S. Department of Interior; Wark et al., 1997; Wang et al., 2004). Ifran and Shaw (2017) investigated the relationship between environmental pollution, energy consumption and the level of urbanization in South Asian countries using by a nonparametric additive model. The European Commission, World Health Organization (WHO) and various national/international environmental agencies have published their standards and air quality guidelines for allowable levels of air pollutants (Cooper and Alley, 2002; Lim, 2005; Surez et al., 2011; Wang et al., 2004).

According to WHO statements, 1.4 out of 2.4 million deaths each year are caused by indoor air pollution while the remaining deaths are due directly to attributable air pollution (Lutgens and Tarbuck, 2001; Wark et al., 1997; Wang et al., 2004). The WHO Air Quality Guidelines provide a Global Update of 205 for threshold values of air pollution. In addition, it reports that 91% of the world population live in places where WHO air quality levels were not met. The WHO guidelines are currently under revision

http://www.aloki.hu ● ISSN 1589 1623 (Print) ● ISSN 1785 0037 (Online)
DOI: http://dx.doi.org/10.15666/aeer/1704_98899903

with an expected new publication in 2020. The latest Global conference on air pollution was organized in Geneva on 20 November 2018. Almost 900 participants registered for the conference, including 70 commitments from countries, cities and organizers discussing how to tackle climate change and related health considerations.

Furthermore, publications from the European Union (EU) regarding emissions of the main air pollutants monitored at more 2500 stations throughout Europe present updated data and its impact. Polices and air quality regimes are aimed at providing the lowest target concentrations of possible pollutants (Holnicki et al., 2017; Isikli et al., 2015). The guidelines apply worldwide and are based on expert evaluations for PM10 and NO_2 (see *Table 1*).

Table 1. *Comparison of limit values*

Average period	EU	Turkey (2017)	Turkey (2018)	Turkey (2019)	Permitted exceedances each year	
					EU (2019)	Turkey (2019)
PM10 (24 h)	50 μg/m^3	70 μg/m^3	60 μg/m^3	50 μg/m^3	35 times/year	35 times/year
NOX (1 year)	30 μg/m^3	-	-	30 μg/m^3	-	-
NO2 (1 h)	200 μg/m^3	270 μg/m^3	260 μg/m^3	250 μg/m^3	18 times/year	18 times/year

(Source: http://ec.europa.eu/environment/air/quality/standards.htm)

PM10, which is often a proxy indicator, for air quality refers to fine particles with a diameter of 10 microns or less, and are tiny solid particles and liquid suspended in a gas. It affects living organisms on a daily basis or over time. As the sources of PM10 can be humans, fossil fuel combustion (primarily from road transport), factories or natural, the increase of PM10 levels can be a cause of mortality or morbidity (Kelly and Fussell, 2015).

The potential risk of PM10 air pollution is critical in certain cities in Turkey, considering that the measured daily PM10 concentrations should be in the range of 50 μg/m^3 from January 1, 2019, due to EU Commission regulations (Istanbul Metropolitan Municipality).

Serious risks are posed to the habitat of humans, animals and plants, not only from exposure of PM10, but also from NO_X (Shi et al., 2014). This is a general term that is used to describe certain gases, namely NO_2 and NO. NO_2 is especially emitted from high temperature combustion processes (power generation, engines in vehicles, heating, and suchlike) and are also produced naturally during thunderstorms by electric discharge. NO_2, a reddish- brown toxic gas, has a sharp and biting odour. The initial product formed is NO (nitric oxide). When NO oxidizes further in the atmosphere, nitrogen dioxide (NO_2) forms. Similarly, studies on NO_2 show that it is mainly due to the eutrophication of lakes and marine environments and acidification of terrestrial ecosystems (Greenfelt et al., 1994).

The concentration levels of NO_2 can also play a significant role in asthma and lung functions. Shao et al. (2006) show that urbanization and industrial developments cause deterioting air quality. The results of their study are that emissions of NO_2 are from industrial and domestic energy production and transportation. When NO_2 is combined

http://www.aloki.hu ● ISSN 1589 1623 (Print) ● ISSN 1785 0037 (Online)
DOI: http://dx.doi.org/10.15666/aeer/1704_98899903

with water, the main component of acid rain, which is one cause for deforestation, is observed (WHO).

With the negative effects of growing population trends and urbanization, the role of such atmospheric pollutants has received increasing attention. Many scientists study on global and regional estimations for such emissions. Seo et al. (2018) examined meteorological conditions together with emissions of air pollutants using long-term measurements in Seoul using by a multiple linear regression model. Sekulic and Kowalski (1992), Friedman and Roosen (1995) used three MARS models for NO_2, SO_2, and PM10 as a function of other measured relevant pollutants in air quality; nitric oxide (NO), carbon monoxide (CO), and ozone (O_3). Donnelly et al. (2017) used a hybrid model including nonparametric regression to describe nonlinear variations in concentration levels with speed, direction and meteorological variables which are employed as inputs to a multiple linear regression. Tao et al. (2017) studied the impact of external pollution and human factors in the forest ecosystems.

It is often assumed that multivariate data should follow a known specific statistical distribution. However, the complex structure of the data and the relationship among various factors may be too complicated to explain general patterns or to model dependency between variables. When examining ecological data, the interaction of several environmental factors have to be recognized carefully and properly analysed.

The aim of this study is to investigate the significant variables by using daily patterns of PM10, NO_X and NO_2 and to provide meaningful future informative models for air quality control and regimes in Turkey. This study is organized as follows. Firstly, the current state of knowledge based on air pollutants in the literature is explained. Secondly, the motivations and data collection concerning our study are described. Next, a novel exploratory modelling technique, multivariate adaptive regression splines (MARS), is introduced by Friedman (1991). The results and comparisons from MARS models for each pollutant follow in the next section. Finally, the highlights of the paper are summarized in the conclusion.

The motivation

One major environmental risk is the concentration of air pollutants due to their harmful influence on health of humans, animals and plants or other living organisms. Low or middle income countries are exposed to pollutants in and around homes from the heating, lighting, traditional stoves used for cooking, polluting fuels on open fires and so on (WHO, 2018). The European Environmental Agency (EEA) indicate that there is an increasing trend of pollutants in urban regions. The WHO Air Quality 2005 document provides a guideline for an assessment of the health effects of air pollutants and guideline values for health risk pollution levels. The EU establishes the standards and objectives for a number of air pollutants in the air to be applied over different periods of time. Although Turkey and Switzerland are not the members of the EU, Turkey at least aims to adapt to EU standards by reaching the air quality limits. *Table 1* shows the limits aimed for in order to achieve the lowest possible concentrations of PM10, NO_X, and NO_2.

There are a number of examples that can be used as sources of air pollution including industrial activity, energy (heating, cooking, lighting, electricity), transportation (vehicles and fuels), waste reduction of forest pollution, increasing numbers of inhabitants, and climate. Addressing the risk factors for air pollution, countries could reduce levels of air pollution to safeguard the public health.

http://www.aloki.hu ● ISSN 1589 1623 (Print) ● ISSN 1785 0037 (Online)
DOI: http://dx.doi.org/10.15666/aeer/1704_98899903

The Ministry of the Environment and Urbanisation is the main institution of the Turkish government that is responsible for transboundary atmospheric pollution control (Yurtseven et al., 2018). The measurements of PM10, NO_x and NO_2 in forty cities organized from the Air Quality Monitoring System are shown in *Figure 1*. These are used to evaluate the priority of the variables that may be sources of the corresponding pollutants. Next, predictions from MARS models are depicted correctly as well as those cities with high levels of pollutants.

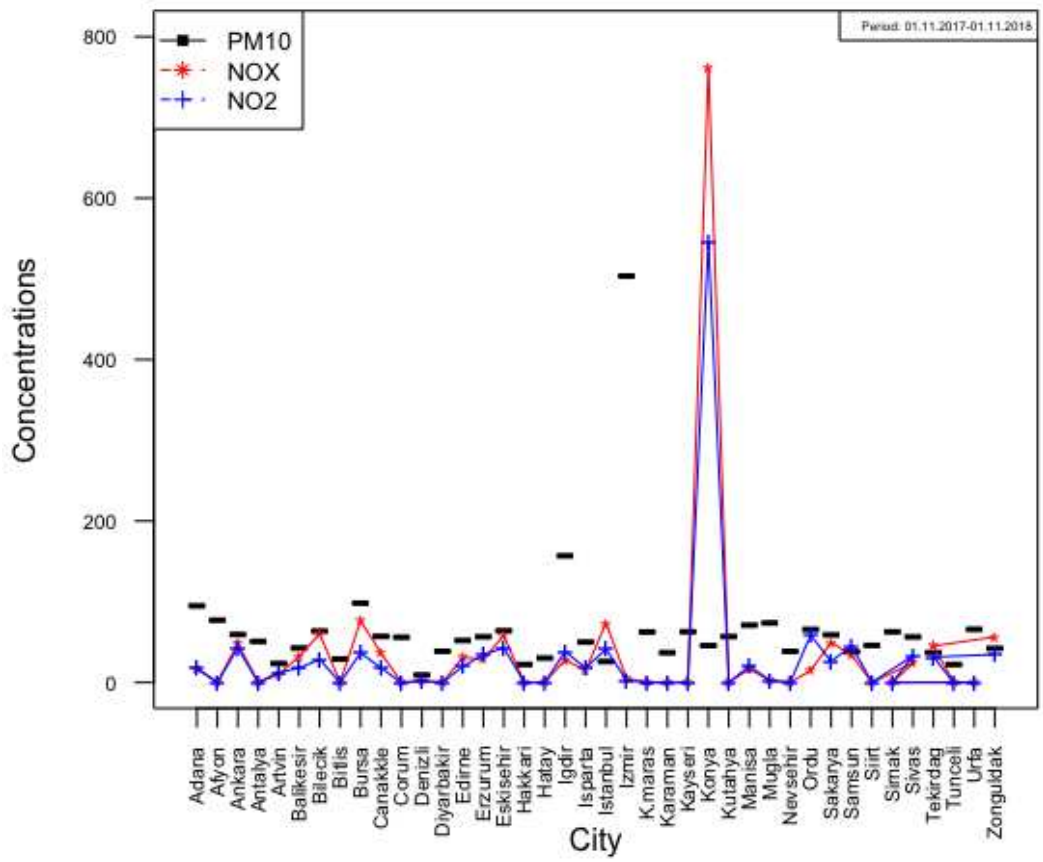

Figure 1. *Scatterplot of the data*

Figure 1 shows concentrations of PM10, NO_X, and NO_2 observed for the forty cities between 1 November, 2017, and 1 November, 2018. It is clear that the emissions peaks of PM10, NO_X and NO_2 occur in some of the cities. Although the trend of the PM10, NO_X, NO_2 is a quasi-sinoidal curve with peaks and valleys, these gases reach the greatest concentrations in Izmir and Konya, respectively. Additionally, certain relationships among variables are given in *Figure 2*.

Materials and methods

Model construction

The measurement of climatic variables is organized by the Ministry of the Environment and Urbanization Measurements and Monitoring Office, Turkey. For forty cities, eleven variables are recorded to investigate the determinants of air pollution

http://www.aloki.hu ● ISSN 1589 1623 (Print) ● ISSN 1785 0037 (Online)
DOI: http://dx.doi.org/10.15666/aeer/1704_98899903

presumably by regressing PM10, NO_X, NO_2 on those related to human ecology and climate. The measurements are collected at monitoring stations located within an industrial area close to the city or within the city limits. The results relating to climate (temperature, wind speed, precipitation, and number of days with precipitation) are average daily measurements (Air Quality Monitoring System).

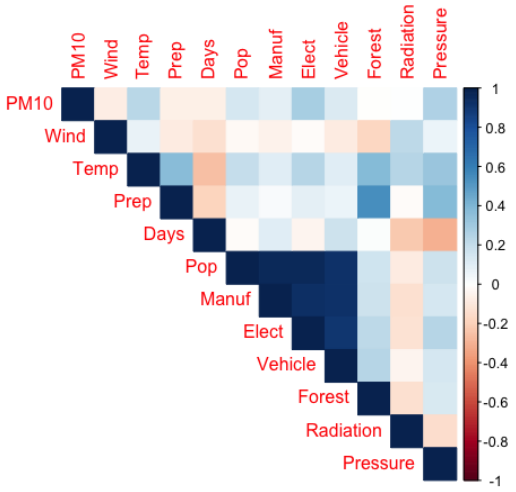

Figure 2. *Correlations among variables*

Addition, the effects of car pollution are widespread and is one of major cause of global warming. The increasing number of people which negatively effects the atmosphere and motorized vehicles can be geo-demographic predictors of the air pollutions and may be useful include in the model. The measurements for Radiation and Pressure are arranged from Turkish State Meteorological Service. The complete list of the data set was created using publicly online related web sources and the names of the variables are given in *Table 2*.

Table 2. *Complete list of variables used in this study*

Factors	Name of the variable	Mean	Min	Max
Average daily temperature period (°C)	Temp	13.6	5.7	19.1
Average daily wind period (km/h)	Wind	2.533	0	20.2
Average daily precipitation (kg/m^2)	Prep	643.9	106.5	1222.1
Average number of days with precipitation	Days	110.1	73.9	438.4
Number of manufacturing enterprises consuming fuel oil	Manuf	218.9	2	2832
Population size (2017)	Pop	1487978	82498	15029231
Electricity consumption (%)	Elect	0.837	0.06	16.719
Number of motorized vehicles (2017)	Vehicle	270708	2048	2755250
Forest area - % of city area (2017)	Forest	32.8	0	68
Radiation in 2016 (kWh/m^2)	Radiation	4.525	3.74	5.21
Average daily pressure	Press	755.4	0	1351.5
Pollutants:				
Particulate matter (µg/m^3 PM10)	PM10	65.14	9.26	503.47
NO_X (µg/m^3)	NO_X	38.15	0	760.56
Nitrite concentration (µg/m^3 NO_2)	NO_2	29.3	0	544.81

http://www.aloki.hu ● ISSN 1589 1623 (Print) ● ISSN 1785 0037 (Online)
DOI: http://dx.doi.org/10.15666/aeer/1704_98899903

Multivariate adaptive regression splines

MARS is a nonparametric approximation of the relationship between a response and a set of independent variables in reflected pairs of simple linear splines (Friedman, 1991). The reflected pairs take the form given in *Equation 1:*

$$(x-t)_+ = \begin{cases} x-t & , x > t \\ 0 & \text{else} \end{cases} \quad \text{(Eq.1)}$$

where the subscript '+' means the argument is a truncated power function.

MARS models do not assume any underlying relationship between the dependent variable and the predictors. This relationship is constructed by an adaptive fitting procedure where piecewise polynomials of degree q (splines) are driven from regressing the dependent variable onto predictors. The MARS model has the following form given in *Equation 2:*

$$y = \beta_0 + \sum_{m=1}^{M} \beta_m h_m(\mathbf{x}) \quad \text{(Eq.2)}$$

where $h_m(\mathbf{x})$ are basis functions and $\beta_0, \cdots, \beta_M$, the unknown parameters for m = 1,…, M. Once the basis functions are investigated then $\beta_0, \cdots, \beta_M$ are estimated by the ordinary least squares method. The basis functions can be represented in *Equation 3* by:

$$h_m^q(\mathbf{x}) = \prod_{k=1}^{K_m} H\left[s_{k,m}\left(x_{v(k,m)} - t_{k,m}\right)\right]_+^q \quad \text{(Eq.3)}$$

with involving the truncated power functions with polynomials of lower order than q, where K_m is the number of variables (interaction order) in the m^{th} basis expansion and the number of splits that give raise to $h_m(\mathbf{x})$. $x_{v(k,m)}$ is the v^{th} variable, $v(k, m)$ label the predictor variables, $1 \leq v(k, m) \leq n$, $t_{k,m}$ is a knot on each of the corresponding variables and represent values on these variables. The quantites $s_{k,m}$ in *Equation 2* take on values + /-1 and indicate the left/right sense of the associated step functions.

The MARS algorithm adaptively selects the basis function set by two iterative approaches; forward and backward selection. It uses the residual squared error in iterations to compare the partition points. The criterion used to set the final model is a modified generalized cross validation (GCV) of the one first proposed by Craven and Wahba in 1979. The difference between the two criteria comes from a penalty term that reflects the complexity of the model in MARS.

The MARS approach allows a nonlinear relationship over different intervals of the vector of the explanatory variables for modeling Y (Sephton, 2001). The relationship between the explanatory variables and the response is fitted by basis functions that are basically splines. The main idea behind MARS is to explore the relationship by splitting the explanatory variables over its region into several intervals and to transform the original input variables over the intervals. MARS fits a spline based model in each interval. Basis Functions (B_i) include knot locations relating to the explanatory variables. B_i can be a single or multivariable interaction term. The final model is a combination of B_i. Model selection is accomplished using the GCV criterion given in *Equation 4:*

$$GCV = \frac{1}{N}\sum_{i=1}^{N}\left(y_i - \hat{f}_M(\mathbf{x})\right)^2 / \left(1 - {}^{C(M)}/_{N}\right)^2 \quad \text{(Eq.4)}$$

http://www.aloki.hu ● ISSN 1589 1623 (Print) ● ISSN 1785 0037 (Online)
DOI: http://dx.doi.org/10.15666/aeer/1704_98899903

where $C(M)$ is the complexity parameter to the corresponding model, and N represents the total number of observations. The final MARS model is the one with the smallest GCV and the largest R^2_{adj}.

Analysis and results

The conventional methods, multiple linear regression (MLR) and principal component analysis are used to address the main determinants of pollutants of PM10, NO_x, NO_2, respectively. Multiple linear regression is used by regressing several predictors listed in *Table 2* on the concentrations of PM10, NOx, and NO_2. The fitted values did not produce statistically significant models except the PM10-model ($F_{PM10;11;28} = 3.002$, $p_{PM10} = 0.0092$, R^2-adj = 0.36; $F_{NOx} = 1.565$, $p_{NOx} = 0.164$, R^2-adj = 0.13; $F_{NO2} = 1.388$, $p_{NO2} = 0.232$, R^2-adj = 0.23). It is also clear from the multiple plots given in the *Appendix* that MLR can not be considered for further analysis.

Next, principal component regression (PCR) is performed to investigate the determinants of the pollutants. The models from PCR did not provide informative contribution in this analysis and are effected by the presence of the outliers. Although the first four components (four eigenvalues greater than 1) explained 84.3% of the total variation among the transformed predictors, the regression models were not statistically found significant ($F_{PM10;4;35} = 0.721$, $p_{PM10} = 0.583$; $F_{NOx;4;35} = 0.951$, $p_{NOx} = 0.446$; $F_{NO2;4;35} = 1.002$, $p_{NO2} = 0.419$). Ultimately, PCR was not appropriate for predicting the responses on several variables.

In this work, a new approach for modelling PM10, NOx, and NO_2 concentrations are developed. MARS models have been used (Milborrow, 2011; Hastie et al., 2003), the basis functions of the models, consisting of linear and second-order splines, are shown in *Tables 3, 4,* and *5*. There are three dependent variables used to build the MARS models; particulate matter less than 10 $\mu g/m3$ (PM10), nitrogen dioxide (NO_2), and nitric oxide (NO_X). The results of MARS computed using all the available observations show a list of 4, 9, and 6 basis functions (B_i) for each of the three MARS models and their coefficients (C_i), respectively.

It should be noted that, MARS constructs nonparametric regression models as an extension of the linear models, and automatically determines the linearities and interactions and models a weighted sum of basis functions (hinge functions). The hinge function $h()$ is x if the first quadrant is greater than 0, and is 0 if x is less than or equal to 0.

The regression equation of PM10, which includes linear form of its term, such as Precipitation and two second order basis functions, can be easily generated using *Table 3* and *Equation 5* as follows:

$$PM10 = 46.002 + 0.466\,B_2 - 0.016B_3 + 0.158\,B_4 \quad \text{(Eq.5)}$$

In *Equation 5,* there are two interaction terms, *B*3 and *B*4, where certain relationships between the variables Pressure and Forest, and the variables Electricity and Pressure found to be important, respectively. Using *Equation 5,* PM10 predictions can be calculated easily. The variation between the predictions and the actual data is presented in *Figure 4*. Similarly, the regression equations for NO_X and NO_2 can be constructed easily from *Tables 4* and *5.*

http://www.aloki.hu ● ISSN 1589 1623 (Print) ● ISSN 1785 0037 (Online)
DOI: http://dx.doi.org/10.15666/aeer/1704_98899903

Table 3. *List of basis function and their coefficients obtained by the MARS model for PM10 pollutant*

C_i	Definition	B_i
46.002	1	B_1
0.466	h(452.3-Prep)	B_2
-0.016	h(452.3-Prep)*Forest	B_3
0.158	Elect* h(Pressure-988.77)	B_4

It is worth to notice that the MARS model for NOX allows us to assess many interactions between different hinge functions. This can be easily seen in *Table 4*. The NO_X model includes three interaction terms between hinge functions and linear terms. For example, $h(13.8-Temp)*Vehicle$ is an interaction effect for those Temp values less than 13.8 and the number of vehicles. Also, the MARS model for NO_X includes linear form of its term such as Vehicle and hinge functions of the variables, Vehicle, Manuf, and Pressure.

Table 4. *List of basis function and their coefficients obtained by the MARS model for NO_x pollutant*

C_i	Definition	B_i
4.07654	1	B_1
0.00077	Vehicle	B_2
-11.01813	h(Manuf-151)	B_3
-0.00064	h(Vehicle-86926)	B_4
-0.59119	h(Pressure-988.77)	B_5
-0.00016	h(13.8-Temp)*Vehicle	B_6
-0.00013	h(Temp-13.8)*Vehicle	B_7
2.63176	h(Manuf-151)*Radiation	B_8
-0.00026	h(988.77-Pressure)	B_9

According to the results of NO_2, the model is constructed by linear and second-order basis functions. There are two linear basis functions and three second-order basis functions where certain relationships between Prep and the variables Manuf, Vehicle, and Pressure are found to be statistically important.

Table 5. *List of basis function and their coefficients obtained by the MARS model for NO_2 pollutant*

C_i	Definition	B_i
2.75336	1	B_1
-0.32477	h(581.8-Prep)	B_2
47.19741	h(4.66-Radiation)	B_3
0.00441	h(581.8-Prep)*Manuf	B_4
-0.000002	h(581.8-Prep)*Vehicle	B_5
0.000304	h(581.8-Prep)* Pressure	B_6

http://www.aloki.hu ● ISSN 1589 1623 (Print) ● ISSN 1785 0037 (Online)
DOI: http://dx.doi.org/10.15666/aeer/1704_98899903

The most significant variables in the prediction of PM10, NO_X and NO_2 can be obtained from each MARS model as well. The list of each model is shown in *Tables 6, 7,* and *8*. These tables list the values of three criteria for estimating variable importance. The *nSubset* criterion indicates the counts of those models that include the variable. More subsets are considered of greater importance. The residual sum of the squares (RSS) criterion calculates the decrease in the RSS for each subset. The variables which cause a large decrease in RSS are considered more important. The last criterion GCV is similar.

Table 6. *Evaluation of the variable importance for the PM10 pollutant model according to Nsubsets, GCV and RSS*

Variable	nSubsets	GCV	RSS
Elect	3	100	100
Pressure	3	100	100
Prep	2	15.5	21.9
Forest	1	14.1	16.66

RSS: residual sum of squares; GCV: generalized cross validation; Nsubsets: number of subset models in which variable occurs

The most important variables in the PM10 prediction given in *Table 6* are obtained from electricity, pressure, precipitation, and forest in order of priority.

Table 7. *Evaluation of the variable importance for the NO_X pollutant model according to Nsubsets, GCV and RSS*

Variable	nSubsets	GCV	RSS
Manuf	8	100	100
Radiation	8	100	100
Temp	6	74.8	67.6
Vehicle	6	74.8	67.6
Pressure	3	28.5	26.3

The results in *Table 7* indicate that the most significant variables are Manufacturer, Radiation, Temperature, Vehicle and Pressure in the prediction of NO_X.

In *Table 8*, the most significant variables in the NO_2 prediction are Precipitation, Manufacturer, Vehicle, Pressure and Radiation.

Table 8. *Evaluation of the variable importance for the NO_2 pollutant model according to Nsubsets, GCV and RSS*

Variable	nSubsets	GCV	RSS
Prep	5	100	100
Manuf	5	100	100
Vehicle	5	87.9	82.6
Pressure	1	23.2	22.0
Radiation	1	15.8	15.8

http://www.aloki.hu ● ISSN 1589 1623 (Print) ● ISSN 1785 0037 (Online)
DOI: http://dx.doi.org/10.15666/aeer/1704_98899903

Furthermore, comparisons between concentrations of PM10, NO_X and NO_2, predicted by the MARS model and observed, are represented by *Figures 3, 4* and *5,* respectively.

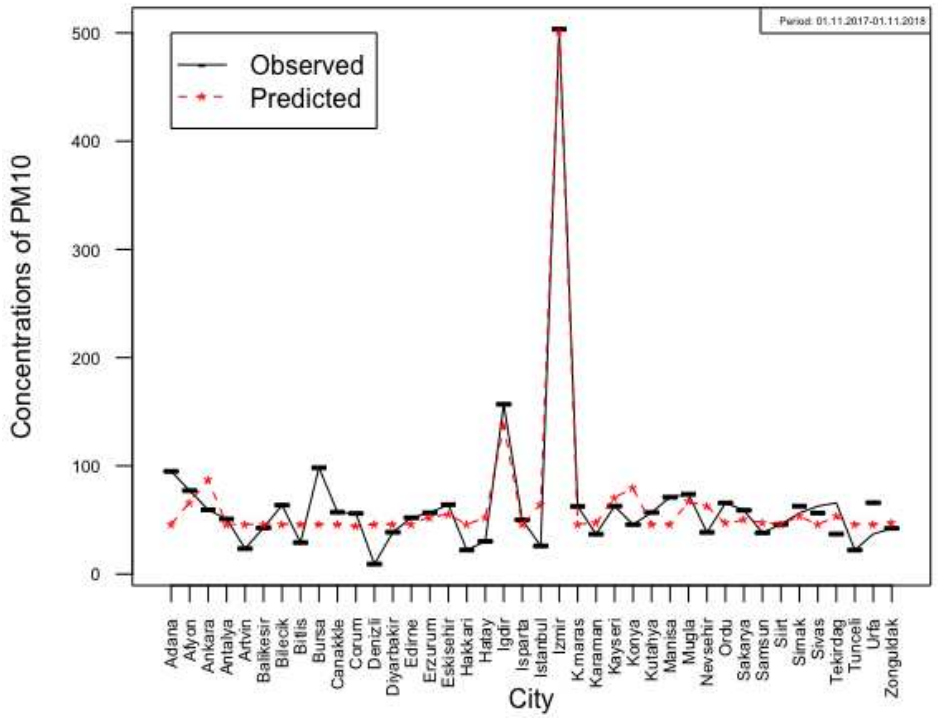

Figure 3. *Comparisons between concentrations of PM10 predicted by the MARS model and those observed*

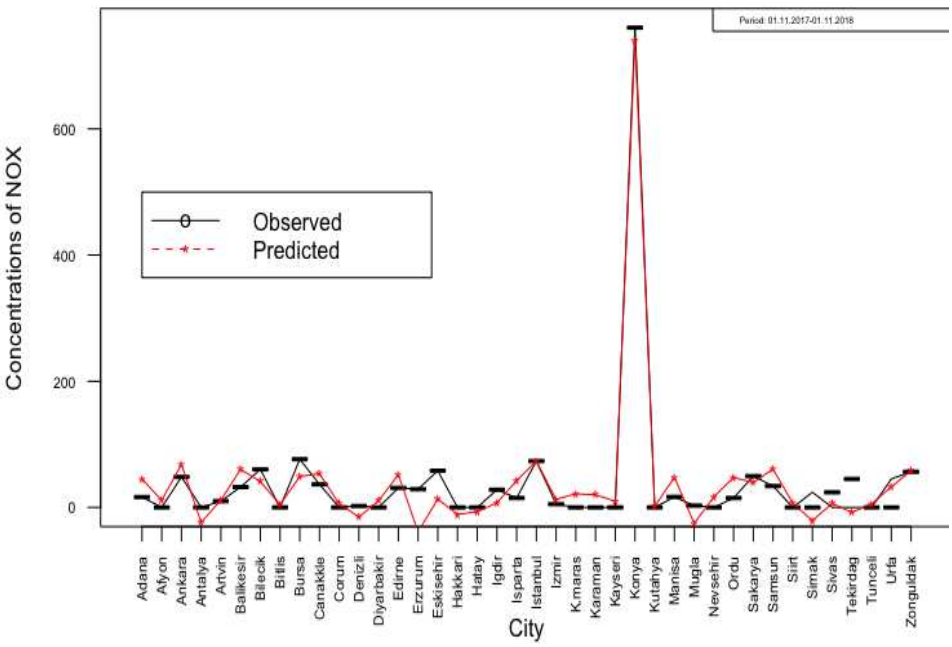

Figure 4. *Comparisons between concentrations of NO_x predicted by the MARS model and those observed*

http://www.aloki.hu ● ISSN 1589 1623 (Print) ● ISSN 1785 0037 (Online)
DOI: http://dx.doi.org/10.15666/aeer/1704_98899903

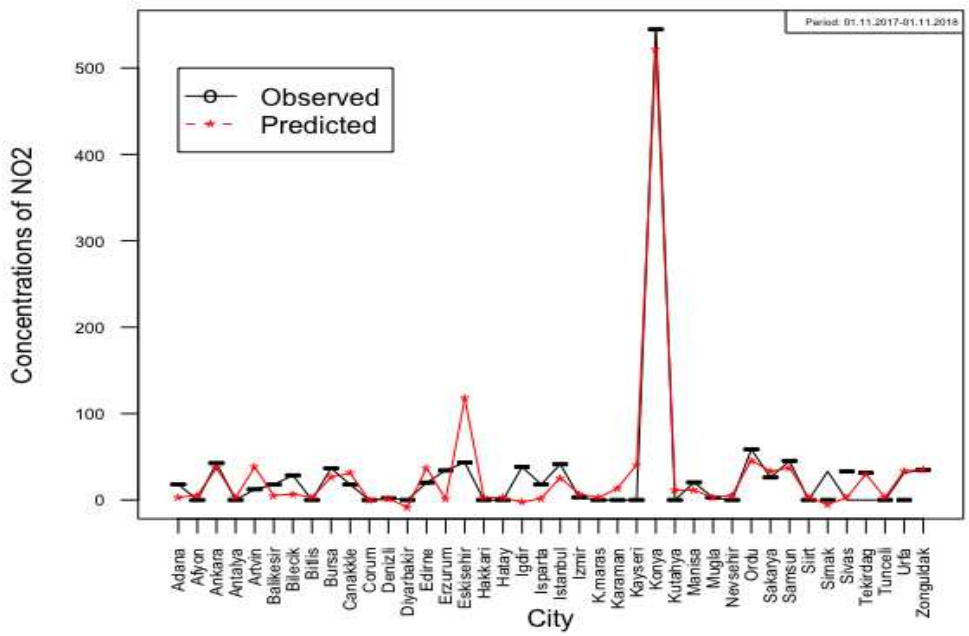

***Figure 5**. Comparisons between concentrations of NO_2 predicted by the MARS model and those observed*

In *Table 9*, an evaluation of the GCV and *R*2 (coefficient of determination) of the models is summarized. A coefficient of determination value indicates how well a model explains and predicts the future. A value of 1.0 is assessed as a perfect fit. For the PM10, NO_X and NO_2 models, the coefficients of determination are 92.5%, 96.2%, and 94.2%, respectively.

***Table 9.** Evaluation of the GCV and R2 that form the models*

Variable	GCV	R^2
PM10-second order	665.114	0.925
NO_X-second order	2294.915	0.962
NO_2-second order	932.613	0.942

Discussion and conclusion

In this research work, three models based on the multivariate adaptive regression splines for the study of considered pollutants PM10, NO_X, and NO_2 are proposed. The main purpose of this study is to increase accuracy in the prediction of three air pollutants when human factors and climate effects are present and physical-chemical parameters are combined. The innovative methodology MARS is applied to a real data set and is able to predict successfully.

One conclusion of this study is to set the order of the most significant variables in the prediction of PM10, NO_X, and NO_2. The priority of the predictor variables involved in the estimation of PM10 are actually related to climate parameters. On the other hand, human factors such as Manufacturer and Vehicles, included in the prediction of NO_X and NO_2, are the most influential parameters followed by Precipitation and Forest, respectively. Furthermore, this paper presents simple statistical models for the

http://www.aloki.hu ● ISSN 1589 1623 (Print) ● ISSN 1785 0037 (Online)
DOI: http://dx.doi.org/10.15666/aeer/1704_98899903

prediction of air pollutants. The results of numerical experiments, based on the application of the MARS technique, confirm high accuracy of daily modelling for pollutants PM10, NO_X, and NO_2.

Finally, the results of this study regarding the development of nonlinear models of three pollutant concentrations are valuable for future projects based on human health. Additionally, the nonlinear modelling of the ecological data with atypical observations can be used to reduce the effects of pollutants and to improve the development of models regarding air quality.

REFERENCES

[1] Air Quality Monitoring System: http://www.havaizleme.gov.tr. – Last Access: 01 November 2018.
[2] Akkoyunlu, A., Ertürk, F. A. (2003): Evaluation of air pollution trends in Istanbul. – International Journal of Environment and Pollution 18: 388-398.
[3] Craven, P., Wahba, G. (1979): Smoothing noisy data with spline functions. – Numerische Mathematik 31: 377-403.
[4] Cooper, C. D., Alley, F. C. (2002): Air Pollution Control. – Waveland Press, New York.
[5] Donnelly, A., Naughton, O., Broderick, B., Misstear, B. (2019): Short-term forecasting of Nitrogen dioxide (NO2) levels using a hybrid statistical and air mass history modelling approach. – Environmental Modelling & Assessment 22(3): 231-241.
[6] Elbir, T., Muezzinoglu, A., Bayram, A. (2000): Evaluation of some air pollution indicators in Turkey. – Environment International 26(1-2): 5-10.
[7] European Commission, Environment: http://ec.europa.eu/environment/air/quality/standards.htm. – Last Access: 11 December 2018.
[8] European Environmental Agency: https://www.eea.europa.eu/publications/corporate _document _2007_2. – Last access: 05 January 2019.
[9] Friedman, J. H. (1991): Multivariate adaptive regression splines. – Annals of Statistics 19: 1-141.
[10] Friedman, J. H., Roosen, C. B. (1995): An introduction to multivariate adaptive regression splines. – Statistical Methods in Medical Research 4: 197-217.
[11] García Nieto, P. J. (2001): Parametric study of selective removal of atmospheric aerosol by coagulation, condensation and gravitational settling. – International Journal of Environmental Health Research 11: 151-162.
[12] García Nieto, P. J. (2006): Study of the evolution of aerosol emissions from coal-fired power plants due to coagulation, condensation, and gravitational settling and health impact. – Journal of Environmental Management 79(4): 372-382.
[13] Grennfelt, P., Hov, O., Derwent, D. (1994): Second generation abatement strategies for NOx, NH3, SO2 and VOC. – Ambio 23: 425-433.
[14] Godish, T. (2004): Air Quality. – Lewis Publishers, Boca Raton, FL.
[15] Hastie, T., Tibshirani, R., Friedman, J. H. (2003): The Elements of Statistical Learning. – Springer-Verlag, New York.
[16] Holnick, P., Kaluszko, A., Nahorski, Z., Stankiewicz, K., Trapp, W. (2017): Air quality modelling for Warsaw agglomeration. – Archives of Environmental Protection 43(1): 48-64.
[17] Irfan, M., Shaw, K. (2017): Modeling the effects of energy consumption and urbanization on environmental pollution in South Asian countries: a nonparametric panel approach. – Quality & Quantity 51: 65-78.
[18] Isikli, E., Ustundag, A., Cevikcan, E. (2015): The effects of environmental risk factors on city life cycle: a link analysis. – Human and Ecological Risk Assessment: An International Journal 21(5): 1379-1394.

http://www.aloki.hu ● ISSN 1589 1623 (Print) ● ISSN 1785 0037 (Online)
DOI: http://dx.doi.org/10.15666/aeer/1704_98899903

[19] Istanbul Metropolitan Municipality: www.ibb.gov.tr. – Last Access: 30 January 2019.
[20] Lim, L. L., Hughes, S. J., Hellawell, E. E. (2005): Integrated decision support system for urban air quality assessment. – Environmental Modelling & Software 20: 947-954.
[21] Lutgens, F. K., Tarbuck, E. J. (2001): The Atmosphere: An Introduction to Meteorology. – Prentice Hall, New York.
[22] Kelly, F. J., Fussell, J. C. (2015): Air pollution and public health: emerging hazards and improved understanding of risk. – Environmental Geochemistry and Health 37(4): 631-649.
[23] Kelly, F. J., Fussell, J. C. (2017): Role of oxidative stress in cardiovascular disease outcomes following exposure to ambient air pollution. – Free Radical Biology and Medicine 110: 345-367.
[24] Milborrow, S. (2011): Earth: Multivariate Adaptive Regression Splines, R package. – Derived from mda:mars by T. Hastie and R. Tibshirani.
[25] Ministry of Environment and Urbanization, Measurements and Monitoring Office: https://www.mgm.gov.tr/kurumsal/istasyonlarimiz.aspx. – Last Access: 01 November 2018.
[26] Related Web Sources: https://www.tobb.org.tr, www.enerjiatlasi.com, www.cmo.org.tr, http://otomobil.haber7.com, https://www.ogm.gov.tr, https://www.nufusu.com.
[27] Sekulic, S. S., Kowalski, B. R. (1992): MARS: a tutorial. – Journal of Chemometrics 6: 199-216.
[28] Seo, J., Park, D. S. R., Kim, J. Y., Youn, D., Lim, Y. B., Kim, Y. (2018): Effects of meteorology and emissions on urban air quality: a quantitative statistical approach to long-term records (1999-2016) in Seoul, South Korea. – Atmospheric Chemistry Physics 18(21): 16121-16137.
[29] Sephton, P. (2001): Forecasting recessions: can we do better on MARS? – Review Federal Reserve Bank of St. Louis 2001(March): 39-49.
[30] Shao, M., Tang, X. Y., Zhang, Y. H., Li, W. J. (2006): City clusters in China: air and surface water pollution. – Frontiers in Ecology and the Environment 4: 353-361.
[31] Shi, P., Xie, P. H., Qin, M., Si, F. Q., Dou, K., Du, K. (2014): Cluster analysis for daily patterns of SO and NO measured by the DOAS system in Xiamen. – Aerosol and Air Quality Research 14: 1455-1465.
[32] Suárez Sánchez, A., García Nieto, P. J, Riesgo Fernández, P., del Coz Díaz, J. J., Iglesias-Rodríguez, F. J. (2011): Application of a SVM-based regression model to the air quality study at local scale in the Avilés urban area (Spain). – Mathematical and Computer Modelling 54(5-6): 1453-1466.
[33] U.S. Department of the Interior, National Park Service, Last Access: 11 December 2018.
[34] Tao, N., Liu, D., Wu, J. (2017): Evaluation study on ecosystem based on system dynamics: A case study of Gongga Mountain. – Journal of Interdisciplinary Mathematics 20(6-7): 1415-1418.
[35] Yurtseven, E., Vehid, S., Bosat, M., Köksal, S., Yurtseven, C. M. (2018): Assessment of ambient air pollution in Istanbul during 2003-2013. – Iranian Journal of Public Health. 47(8): 1137-1144.
[36] Wang, L. K., Pereira, N. C., Hung, Y. T. (2004): Air Pollution Control Engineering. – Humana Press, New York.
[37] Wark, K., Warner, C. F., Davis, W.T. (1997): Air Pollution: Its Origin and Control. 3rd Ed. – Prentice Hall, New Jersey.
[38] World Health Organization (WHO) (2018): https://www.who.int/en. – Last Access: 11 December 2018.

http://www.aloki.hu ● ISSN 1589 1623 (Print) ● ISSN 1785 0037 (Online)
DOI: http://dx.doi.org/10.15666/aeer/1704_98899903

APPENDIX

Because of the nature of this multivariate data set, atypical observations are not easy to identify using univariate approaches. Therefore, we provide four plots; a Scale-Location plot of against fitted values, a Normal Q-Q plot, and a plot of Cook's distances versus row labels for each air pollutants model in *Figures A1, A2* and *A3*.

Figure A1. *Multiple plots for PM10*

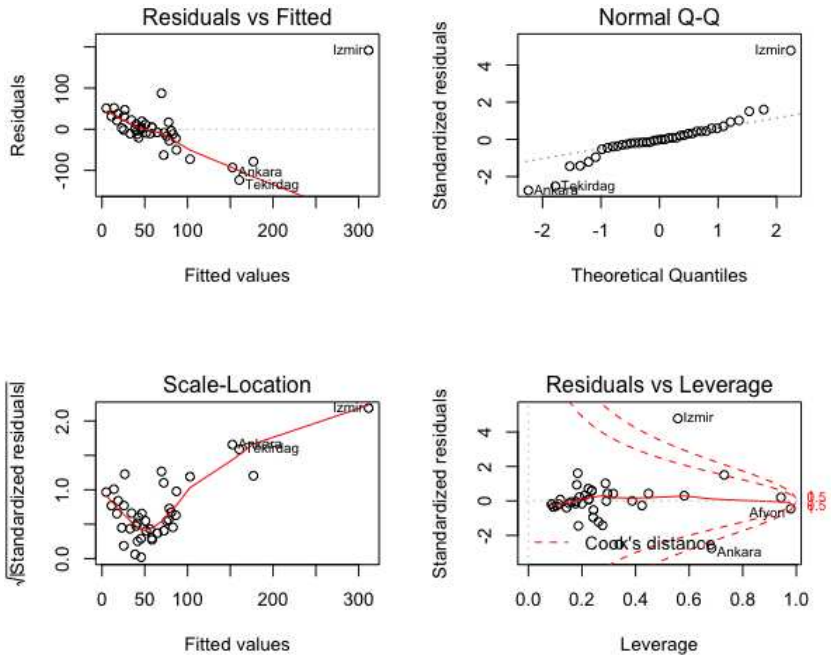

Figure A2. *Multiple plots for NOX*

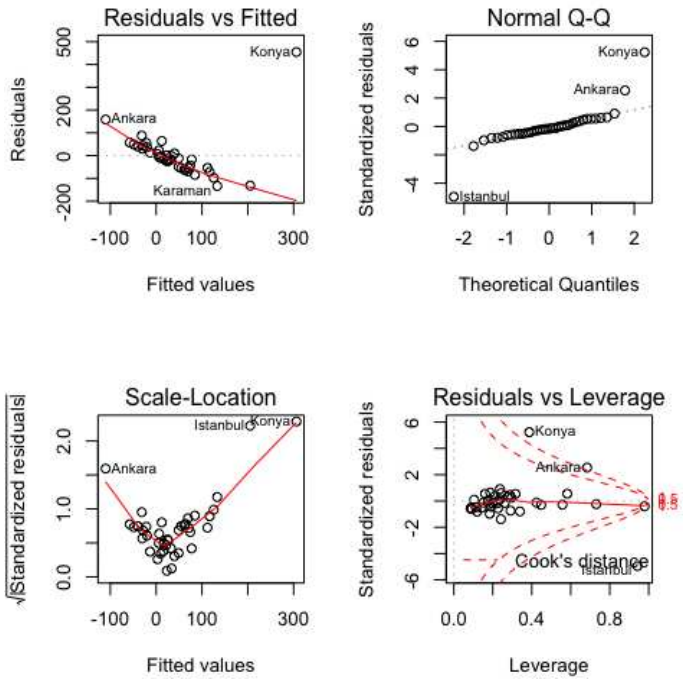

http://www.aloki.hu ● ISSN 1589 1623 (Print) ● ISSN 1785 0037 (Online)
DOI: http://dx.doi.org/10.15666/aeer/1704_98899903

Figure A3. *Multiple plots for NO2*

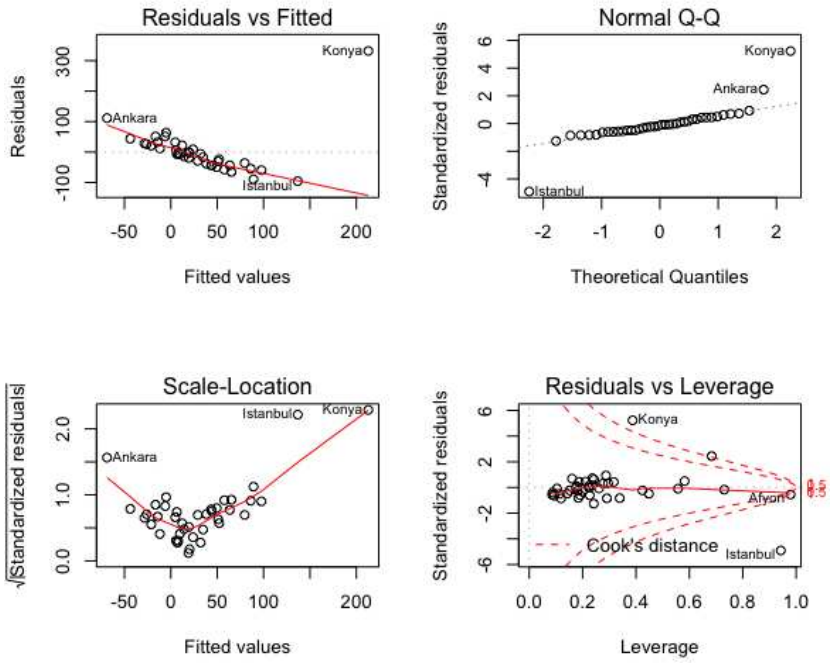

In addition, VIF (Variance Inflation Factor) values for a possible linear model for each pollutant indicates higher degree of multicollinearity 53.4, 21.6, 15.3 and 27.8 for the variables Population, Electricity, Vehicle and Manufacturer, respectively.

http://www.aloki.hu ● ISSN 1589 1623 (Print) ● ISSN 1785 0037 (Online)
DOI: http://dx.doi.org/10.15666/aeer/1704_98899903

QUANTITATIVE ASPECTS OF THE KOH-E-SAFAID RANGE VEGATATION ACROSS THE ALTITUDINAL GRADIENT IN UPPER KURRAM VALLEY, PAKISTAN

HUSSAIN, W.[1*] – BADSHAH, L.[2] – ALI, A.[3]

[1]*Department of Botany, Government Post Graduate College, Parachinar, Pakistan*

[2]*Phytoecology Lab., Department of Botany, University of Peshawar, 25000 Peshawar, Pakistan (e-mail: badshahmasood1@gmail.com, phone: + 92-333-894-4128)*

[3]*Department of Botany, Government AKL Post Graduate College, Matta, Swat, Pakistan (e-mail: asghartk@gmail.com, phone: + 92-333-948-5390)*

**Corresponding author*
e-mail: wahidhussainwahid@gmail.com; phone: + 92-300-371-2148

(Received 30th Mar 2019; accepted 19th Jun 2019)

Abstract. This phytosociological study was conducted during 2015-2018; summed up plant 7 communities of herbs, shrubs and trees at 7 monitoring sites based on elevation, habitats and physiognomic contrast. Quadrate method was employed for the data collection 5 quadrats (10 × 10 m^2) for trees, 10 quadrats (5 × 5 m^2) for shrubs and 15 quadrats (1 × 1 m^2) for herbs at each site. Edaphic attributes were calculated by using standard methods. Based on family importance values Pinaceae was the leading family with an FIV of (374.39) followed by Lamiaceae (350.33), Asteraceae (204.43) and Poaceae (193.67). Seven communities' viz. *Berberis-Themeda-Periploca* community, *Seriphidium-Salvia-Thymus* community and *Indigofera-Quercus-Dichanthium* were established at Sub-Tropical zone. While Temperate Zone comprised of *Juniperus-Picea-Abies* community and *Quercus-Juniperus* community. *Abies-Picea-Rhododendron* community was established at Sub-Alpine zone while *Juniperus-Rheum-Kobresia* community was established at Alpine zone. However, cluster analysis using PAST software and PC-Ord software version 5, classified the vegetation into three groups and four groups based on quantitative value respectively. Vegetation structure and its productivity were governed by soil texture and its chemical composition. The physico-chemical analysis of habitat features revealed that the soil texture was mostly sandy loam and loamy sand with pH ranged from 7.3 to 7.7. Afforestation programs need to be started on wasteland of the area to overcome the impacts of deforestation.
Keywords: *vegetation, phytosociology, edaphic variables, maturity index, similarity index*

Introduction

Study of plant communities and their classification is termed as phytosociology. Primarily phytosociology helps in understanding the multilateral relationships between plants and their environment. It deals with quantitative, qualitative and synthetic attributes of plant communities. Vegetation is an ecological quantification of plant resources (Ali et al., 2018; Timilehin et al., 2017; Badshah et al., 2016). The vegetation of an area is the reflection of its climate, soil, biodiversity, anthropogenic activities and natural resources (Ilyas et al., 2015). The vegetation structure and plant population sizes also indicate species tolerance of existing ecological attributes (Kuma and Shibru, 2015; Sher et al., 2014). The presence and the establishment of the communities reveal the plant type and surroundings condition under which they developed (Hussain et al., 2015; Zhu et al., 2015; Ahmad et al., 2006). The health of any ecosystems is dependent on plant biodiversity and thus the vegetation classification is a prerequisite for ecosystem management and biodiversity conservation. Some of the most important

http://www.aloki.hu ● ISSN 1589 1623 (Print) ● ISSN 1785 0037 (Online)
DOI: http://dx.doi.org/10.15666/aeer/1704_99059924

environmental factors affecting the vegetation are deforestation, erosion, trampling, overgrazing and other ecological factors. In Pakistan two-third of the area is highland type and quick changes in climate and elevation aggravates differences in plant diversity. Pakistan includes variety of land-dwelling ecosystem, with in 18 main geographic regions (Khan et al., 2016; Zoq-ul-Arfeen et al., 2015). Due to non-availability of natural gas and electricity large population of the area depends upon forest wealth for domestic needs. Because of the intense browsing nearly all the pastures have been ruined and need restoration to be sustainable again. Phytosociologically the vegetation and forests of Koh-e-Safaid slopes are Sino-Japanese type (Hussain et al., 2019). The natural forests of Kurram cover about 8% of its area while the Parachinar Forest Department has planted about 6% area. The land under cultivation is 35% while the rest of 47% is barren. The major forest types of the Kurram are dry tropical forest and sub alpine scrub (Hussain et al., 2013). The area is very rich in plant resources however little ecological work has been done in the region. The dry tropical vegetation covers the Southern parts while dry temperate and alpine vegetation types are found in the Northern parts of the area. In the investigated area climate is highland type and it varies at different altitude. The observed changes in the plant communities are due to season, temperature, soil type and time of sampling of the vegetation. During spring and summer many annual show dominance and cause change in the seasonal aspects. They approach each other by sharing the species and that is why 73.5% similarity occurred. However, slight changes were observed in their cover from season to season, but the predominance of annuals changed the community composition. The recorded species exhibit different dominance value due to change in habitat and altitude condition throughout the area. The study area was unexplored in terms of its phytosociology hence present study presents first report of vegetation dynamics of this part of Pakistan.

Materials and methods

Study area

The research work was carried out in Koh-e-Safaid Range Upper Kurram. Kurram is located from 33° 20’ to 34° 10’ north latitudes and 69° 50’ to 70° 50’ east longitudes. The study area covers an area of 3380 km^2, including seven monitoring sites viz. Sub-Tropical South Hills, Sub-Tropical Plain, Sub-Tropical North Hills, Temperate South Facing slopes, Temperate North Facing slopes, Sub alpine and Alpine zone (*Fig. 1*).

Phytosociology

Phytosociological work was carried out in 7 sites based on elevation, species structure, habitats and physiognomic contrast. Vegetation was analyzed by using 5 quadrats (10 × 10 m^2) for trees, 10 quadrats (5 × 5 m^2) for shrubs and 15 quadrats (1 × 1 m^2) for herbs in each site. Density, frequency and cover of each species were recorded and all the values were converted in to IV (Importance value) and FIV (Family importance value). Geographical co-ordinates of each site were noted using GPS. Different plant communities were established based on highest importance value following (Ali et al., 2018; Badshah et al., 2016; Rajendran et al., 2016; Forzieri et al., 2011).

http://www.aloki.hu ● ISSN 1589 1623 (Print) ● ISSN 1785 0037 (Online)
DOI: http://dx.doi.org/10.15666/aeer/1704_99059924

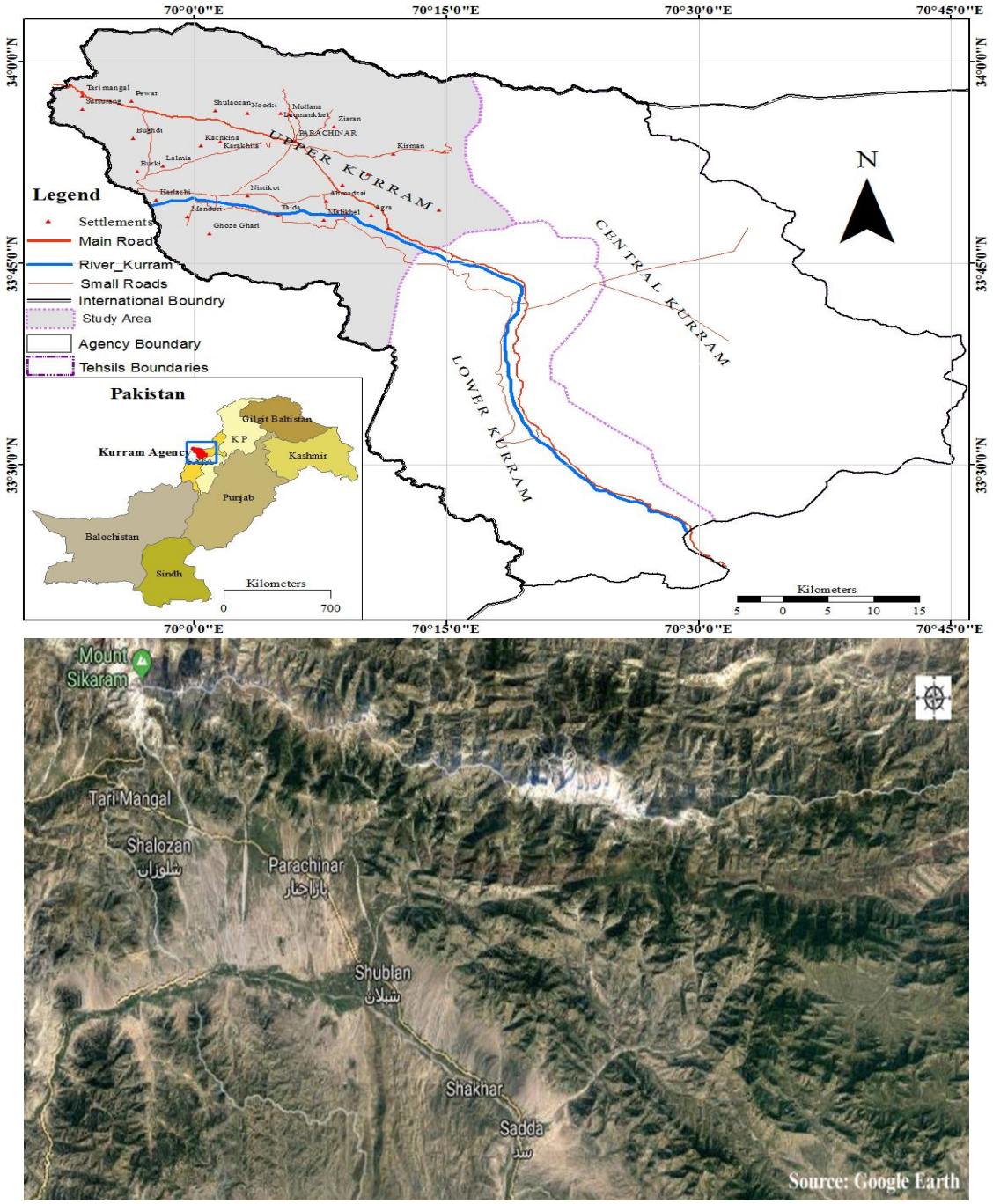

Figure 1. a *Map of the study area.* ***b*** *Google Map of the study area of Upper Kurram Valley*

Data analysis

Cluster analysis was conducted by using PAST software, Wards cluster analysis and Principal Component Analysis tools. It is a classification technique for putting similar objects into clusters. The arrangement is a hierarchical tree like structure is called a dendrogram. These clusters of sampling units may represent different biotic communities. The community classification was made by using Multivariate Statistical Package. The classification was based on structural variations among stands and

http://www.aloki.hu ● ISSN 1589 1623 (Print) ● ISSN 1785 0037 (Online)
DOI: http://dx.doi.org/10.15666/aeer/1704_99059924

dendrogram were made for vegetation stands of the area. A Principal Components Analysis technique was also applied to analyze spatial variations in vegetation by PC-Ord software version 5.

Importance value (IV)

Importance value of each species was calculated by adding all the relative values of RD, RF, RC (Ali et al., 2018; Badshah et al., 2016). The communities were named after the three leading species having the highest importance values.

$$IV = RD + RC + RF$$

Family importance value (FIV)

Importance value of every species in specific families was added together to obtain FIV for all the quantitatively recorded families.

Maturity index

The community maturity index of community was obtained by (Pichi-Sermolli, 1948).

$$\text{Degree of maturity index} = \frac{\text{Frequency values of all species in a stand}}{\text{Total number of species in a stand}}$$

Similarity index

It was applied to compare similarities between different communities. It is the number of species common to both communities. It was calculated by using Sorensen's index (Sorensen, 1948) as modified by (Motyka et al., 1950). It was applied to compare similarities between different communities.

$$IS_{MO} = \frac{2W}{A+B} \times 100$$

where W = Sum of lowest quantitative value of the species pair common to both communities, A = Sum of quantitative value of all species in community A, B = Sum of quantitative value of all species in community B.

Soil analysis

Soil samples of 1 kg from 7 sites were collected from 0-15 cm depth from the selected sites of the study areas. Each of the collected samples was taken in clear polythene bags which were duly labeled and sealed on the spot. Later the soil samples were dried in an oven at 25 to 30 °C. Soil samples were screened for contaminants such as stones, plant roots and other impurities. Soil samples were grounded and passed through a 2.5 mm sieve (Ryan et al., 2001). Standard methods were applied to estimate soil texture (Brady, 1990; Bouyoucos, 1936), pH (Jackson, 1962), organic matter, $CaCO_3$ (Rayan et al., 1997), electrical conductivity (Rhoades, 1996), sodium absorption ratio and sulphates (Richard, 1954). Nitrogen was determined by Kieldahl method of

http://www.aloki.hu ● ISSN 1589 1623 (Print) ● ISSN 1785 0037 (Online)
DOI: http://dx.doi.org/10.15666/aeer/1704_99059924

Bremner and Mulvaney (1982). Phosphorous, Potassium, Calcium and Magnesium were enumerated by Inductively Coupled Plasma Optical Emission Spectroscopy (ICP-OES).

Results

Present study was conducted in Koh-e-Safaid Range Upper Kurram during 2015-2018. Seven monitoring sites were established viz. Sub-Tropical South Hills, Sub-Tropical Plain, Sub-Tropical North Hills, Temperate South Facing slopes, Temperate North Facing slopes, Sub-Alpine and Alpine zone. The study area displays a unique floristic and vegetation structure. The approach of classifying vegetation into 7 different communities agrees with the work of Ali et al. (2018), Ilyas et al. (2018), Badshah et al. (2016), Siddiqui et al. (2015), Sher et al. (2014) and Ahmad et al. (2006). A total of 60 species were recorded in sampling units, of which trees were represented by 09 species, shrubs by 14 species and herbs by 37 species. Based on importance value (IV), a total of seven communities were established at seven monitoring sites. Based on family importance value Pinaceae was the leading family with an FIV of 374.39 followed by Lamiaceae (350.33), Asteraceae (204.43), Poaceae (193.67), Cupressaceae (173.97), Papilonaceae (103.93), Fagaceae (100.3), Berberidaceae (75.64), Polygonaceae (68.23) and Rosaceae with (62.55). Ranunculaceae, Saxifragaceae, Asclepiadaceae, Ericaceae, Boraginaceae, Salicaceae, Elaeagnaceae, Euphorbiaceae, Thymelaeaceae, Valerianaceae, Balsaminaceae, Oleaceae, Primulaceae, Areceaea and Scrophulariaceae had importance values ranging from 48.40 to 10.31. The study area is divided in to four zone i.e. Sub-Tropical zone, Temperate zone, Sub-Alpine and Alpine zone based on altitude, physiognomy, soil type and variance in ecological factors. Based on IV values 7 different communities were established in four ecological zones.

Sub-tropical zone

Sub-tropical south hills (site I)

1. Berberis-Themeda-Periploca community (BTP)

This plant community was reported from north facing slope at southern aspects at elevation of 1525 m. *Berberis lycium* was the dominant species with IV of 36.83. Second dominant species was *Themeda anathera* with an IV of 34.88 forming a close association with *Berberis lycium* at southern lower parts of the sub-tropical zone. *Periploca calophylla* with an IV of 30.98 mostly dispersed among the *Berberis lycium* and *Themeda anathera.* Other prominent member of this community included *Thymus linearis* (29.4 IV), *Aristida purpuea* (27.22 IV) and *Stachys parviflora* (25.54 IV) and *Androsace rotundifolia* (11.22 IV). Common shrubs growing around this community were *Daphne mucronata, Cotoneastor macrophylla, Cotoneastor microphylla, Teucrium stocksianum and Nannorrhops ritchiana.* The only one tree i.e *Olea ferruginea* was sparsely distributed in this community (*Table 2*). Similar communities were also reported by Ali et al. (2018), Badshah et al. (2016), Ilyas et al. (2015) and Forzieri et al. (2011). This plant community was established at Southern aspects at an elevation of 1328 m up to 1525 m. Nitrogen content of the soil was 0.401%, phosphorous 810 µg/g, potassium 8700 µg/g, calcium 32100 µg/g, magnesium 5100 µg/g, sulphur 187 µg/g, sodium 1900 µg/g, iron 81300 µg/g, zinc 73 µg/g,

http://www.aloki.hu ● ISSN 1589 1623 (Print) ● ISSN 1785 0037 (Online)
DOI: http://dx.doi.org/10.15666/aeer/1704_99059924

manganese 731 µg/g and cupper 92 µg/g. Soil pH at this monitoring site was 7.5 and organic matter was found to be 1.8% as shown in *Tables 1* and *2*.

Table 1. *Soil texture and physiochemical characteristics of different sites soil of Koh-e-Safaid Range Kurram*

S. No	Locality		Organic matter %	pH	EC Dsm-1	% Lime $CaCo_3$	HCO_3	Sulphates
1	Sub-Tropical South Hills	Loamy sand	1.8	7.50	1.31	3.9	4.0	0.4
2	Sub-Tropical plain area	Sandy loam	1.7	7.70	1.21	2.6	8.0	0.6
3	Sub-Tropical North Hills	Loamy sand	2	7.66	0.78	7.3	4.8	0.5
4	Temperate North facing slope	Loamy sand	1.9	7.48	1.06	2.8	5.0	4.1
5	Temperate South facing slope	Loamy sand	1.4	7.33	0.85	4.5	3.0	3.5
6	Sub Alpine zone	Sandy loam	2.4	6.50	0.68	7.8	3.5	1.3
7	Alpine zone	Loamy sand	2.42	7.85	1.30	3.0	5.0	7.8

Table 2. *Soil macro and micronutrients in different sites of study area*

S. No	Locality	N_2 %	P µg/g	K µg/g	Ca µg/g	Mg µg/g	S µg/g	Na µg/g	Cl µg/g	Fe µg/g	Mn µg/g	Cu µg/g	Zn µg/g
1	Sub-Tropical South Hills	0.401	810	8700	32100	5100	187	1900	2700	81300	731	92	73
2	Sub-Tropical plain area	0.280	645	7800	39700	6300	263	2600	3500	79000	976	55	84
3	Sub-Tropical North Hills	0.394	571	8300	36200	6800	221	1300	2500	81800	343	95	78
4	Temperate North Facing slope	0.455	435	6580	39800	6200	199	1600	1500	15000	776	105	68
5	Temperate South Facing slope	0.411	650	9900	39300	6500	205	1500	2000	83100	531	109	64
6	Sub-Alpine	0.333	450	5910	36500	5900	175	1800	2000	89200	418	93	53
7	Alpine	0.211	750	1090	39900	5500	163	3300	3500	73200	869	89	82

Sub-tropical plain area (site II)

2. Seriphidium-Salvia-Thymus community (SST)

This herbaceous community was recorded from plains area of Sub-Tropical Zone at an elevation of 1680 m. In this area therophytes dominated the landscape along with sparse distribution of the *Elaeagnus angustifolia.* Dominant species was *Seriphidium kurramense* with IV value of 50.50 followed by *Salvia reflexa* with IV of 42.10. *Salvia reflexa* an invasive species made thick randomly distributed patches in flooded ravines, gullies, along road side, sandy loams and on open fertile clay soils. *Thymus linearis* with an IV value 26.38 was found to be codominant. The other predominant species growing around this community were *Parthenium hysterophorus*, *Artemisia scoparia*, *Cynodon dactylon*, *Conyza canadensis*, *Tagetis minuta* and *Astragalus oplites*. The recorded shrubs in this community were *Daphne mucronata*, *Indigofera heterantha*, *Hertia intermedia* and *Berberis lyceum* (*Table 2*). Ali et al. (2018), Hussain et al. (2016), Badshah et al. (2016), Forzieri et al. (2011) and Wahab et al. (2010) have also reported similar results in their studies. Soil at this locality was sandy loam. Nitrogen content of the soil was 0.280%, phosphorous 645 µg/g, potassium 7800 µg/g, calcium 39700 µg/g, magnesium 6300 µg/g, sulphur 263 µg/g, sodium 2600 µg/g, iron 79000 µg/g, zinc 84 µg/g, manganese 976 µg/g and cupper 55 µg/g. Soil pH at this site was 7.7 and organic matter was found to be 1.7% as shown in *Tables 1* and *2*.

http://www.aloki.hu ● ISSN 1589 1623 (Print) ● ISSN 1785 0037 (Online)
DOI: http://dx.doi.org/10.15666/aeer/1704_99059924

Sub-tropical north hills (site III)

3. Indigofera-Quercus-Dichanthium community (IQD)

This community was recorded from the Sub-Tropical North Hills at an elevation of 2492 m. Thick shrub cover and comparatively thick trees of *Quercus baloot* near the foot hills indicated the disturbed nature of habitats which were under biotic stresses like deforestation and grazing. Dominant species was *Indigofera heterantha var. gerardiana* with an IV value of 42.20 followed by *Quercus baloot* with an IV value of 33.80. These shrubs made thick dispersed patches on mostly treeless open spaces. Codominant species was found to be *Dichanthium annulatum* with an IV value 29.39. Similar communities were recorded by Ali et al. (2018), Ilyas et al. (2015), Badshah et al. (2015 and Ali and Malik (2010). The rest of the species included *Thymus linearis*, *Leptorhabdos parviflora*, *Medicago lupulina, Cotoneastor macrophylla*, *Berberis lycium*, *Impatiens edgeworthii* and *Fragaria nubicola* (*Table 1*). Soil of the area was loamy sand. Nitrogen content of the soil was 0.394%, phosphorous 571 µg/g, potassium 8300 µg/g, calcium 36200 µg/g, magnesium 6800 µg/g, sulphur 221 µg/g and sodium 1300 µg/g. The microelements like iron was recorded 81800 µg/g, zinc 78 µg/g, manganese 343 µg/g and copper 95 µg/g. Soil pH at this site was 7.6 and organic matter was found to be 2% as shown in *Tables 1* and *2*.

Temperate Zone

Temperate north facing slope (site IV)

4. Juniperus-Picea-Abies community (JPA)

This community was recorded on North Facing Slope of Temprate Zone dominated by *Juniperus excelsa* with an IV value of 65.36, almost uniformly distributed in the locality making strong association with the second dominant *Picea smithiana* with an IV value of 51.07. The third dominant species was *Abies pendrow* with an IV 25.89. The tree species were uniformly distributed while the *Juniperus excelsa* was found in open patches among the dominant tree species. The other associated species were *Pedicularis verticilata*, *Aquilegia pubiflora*, *Phlomis bracteosa*, *Salex denticulate*, *Euphorbia wallichii*, *Pinus wallchiana*, *Valeriana jatamansi*, *Quercus semecarpifolia* and *Nepeta kurramensis* (*Table 1*). Badshah et al. (2016), Hussain et al. (2016) and Rashid et al. (2011) also have reported similar results in their studies. This community was recorded from Temperate Zone North facing slope at an elevation of 2200 up to 2450 m. Soil at this locality was loamy sand. Nitrogen content of the soil was 0.455%, phosphorous 435 µg/g, potassium 6580 µg/g, calcium 39800 µg/g, magnesium 6200 µg/g, sulphur 199 µg/g, sodium 1600 µg/g, iron 15000 µg/g, zinc 68 µg/g, manganese 776 µg/g and copper 105 µg/g. Soil pH at this site was 7.4 and organic matter was found to be 1.9% as shown in *Tables 1* and *2*.

Temperate south facing slope (site V)

5. Quercus-Juniperus community (CQJ)

Cedrus-Quercus-Juniperus community was recorded at an elevation of 2450 up to 2700 m on the South Facing Slopes of Temperate Zone. The area had uniformly spread *Cedrus deodara* forest mixed with *Quercus semicarpifolia* and *Juniperus excelsa*. The area was under tremendous biotic stress especially cutting of *Pinus gerardiana, Pinus*

http://www.aloki.hu ● ISSN 1589 1623 (Print) ● ISSN 1785 0037 (Online)
DOI: http://dx.doi.org/10.15666/aeer/1704_99059924

wallichiana, Cedrus deodara for timber wood in past and completely missing of herbage cover due to steep slopes, lacking topsoil and allelopathic effect of shading leaves of *Cedrus, Pinus* and *Juniperus* trees. In this community the dominant species was *Cedrus deodara* with an IV value of (66.39). *Quercus semicarpifolia* with an IV value of (47.71) was codominant making strong association with *Juniperus excelsa* with IV value of (35.29). Only few plants were recorded of *Pinus gerardiana* and it was abundant on Pak-Afghan border. The other important associated members of this community were *Sophora mollis*, *Quercus baloot*, *Pinus wallichiana*, *Piptatherum aequiglume*, *Daphne mucronata, Phlomis cashmeriana* and *Cotoneaster macrophylla* (*Table 1*). Our results are in line with the works of Ali et al. (2018, 2015), Bokhari et al. (2013), Badshah et al. (2015), Ilyas et al. (2015) and Forzieri et al. (2011). Soil at this locality was loamy sand. Nitrogen content of the soil was 0.411%, phosphorous 810 µg/g, potassium 8700 µg/g, calcium 39900 µg/g, magnesium 6500 µg/g, sulphur 205 µg/g, sodium 1500 µg/g, iron 83100 µg/g, zinc 64 µg/g, manganese 531 µg/g and copper 109 µg/g. Soil pH at this site was 7.3 and organic matter was found to be 1.4% as shown in *Tables 1* and *2*.

Sub alpine zone (site VI)

6. Abies-Picea-Rhododendron community (APR)

On the North Facing Slopes *Abies-Picea-Nepeta* community was recorded and comparatively there was thick forest of *Abies pendrow and Pice smithiana.* The *Rhododendron afghanicum* was uniformly distributed on the open space of forest as well as inside the forest. The dominant species was *Abies pendrow* with an IV value 44.25. *Picea smithiana* with an IV value 41.56 was codominant forming a close association with *Rhododendron afghanicum* with an IV value of 33.36. The other associated species were *Nepeta bracteosa*, *Pedicularis verticillata*, *Aquilegia pubiflora, Bistorta amplexicaulis*, *Cynoglossum furcatum*, *Cotoneaster macrophylla*, *Medicago lupina*, *Berberis vulgaris* and *Leptorhabdos parviflora* (*Table 2*). Badshah et al. (2016), Hussain et al. (2016), Forzieri et al. (2011) and Mahmood et al. (2015) also have reported similar results in their studies. Soil at this locality was loamy. Nitrogen content of the soil was 0.333%, phosphorous 450 µg/g, potassium 5910 µg/g, calcium 36500 µg/g, magnesium 5900 µg/g, sulphur 175 µg/g, sodium 1800 µg/g, iron 89200 µg/g, zinc 64 µg/g, manganese 418 µg/g and copper 93 µg/g. Soil pH at this site was 7.4 and organic matter was found to be 2.4% which is typical to the podzolic soil as shown in *Tables 1* and *2*.

Alpine zone (site VII)

7. Juniperus-Rheum-Kobresia community (JRK)

This community was recorded at an elevation of above 2850 m. This is treeless zone and only two shrubs were recorded first one was *Juniper excelsa* and the second was *Rhododendron afghanicum* and dominated by the herbs. The dominant species was *Juniper excelsa* with an IV value of 70.32. *Rheum spiciforme* with an IV value of 45.74 was codominant forming a close association with *Kobresia schoenoides* with an IV value 34.42. The other associative members of the community were *Bergenia stracheyi*, *Thymus serphyllum*, *Morina longifolia*, *Phlomis bracteosa* and *Trifolium repens* (*Table 3*). Badshah et al. (2016), Hussain et al. (2016) and Forzieri et al. (2011) also have reported similar results in their studies. Soil at this locality was sandy loam.

http://www.aloki.hu ● ISSN 1589 1623 (Print) ● ISSN 1785 0037 (Online)
DOI: http://dx.doi.org/10.15666/aeer/1704_99059924

Nitrogen content of the soil was 0.211%, phosphorous 750 µg/g, potassium 1090 µg/g, calcium 39900 µg/g, magnesium 5500 µg/g, sulphur 163 µg/g, sodium 3300 µg/g. The micronutrients like iron was present 73200 µg/g, zinc 82 µg/g, manganese 869 µg/g and copper 89 µg/g. Soil pH at this site was 7.85 and organic matter was found to be 2.42%

Table 3. *Importance value data for plant species*

S. No	Species	Site-I	Site-II	Site-III	Site-IV	Site-V	Site-VI	Site VII
1	*Abies pindrow* (Royle ex. D. Done) Royle	0	0	0	25.89	0	44.25	0
2	*Androsace rotundifolia* Hardw.	11.22	0	0	0	0	0	0
3	*Aquilegia pubiflora* Wall. ex Royle	0	0	0	21.3	12.51	0	0
4	*Aristida cyanantha* Steud.	27.22	0	0	0	0	0	0
5	*Artemisia scoparia* Waldst. & Kitam.	0	23.6	26.8	0	0	0	0
6	*Astragalus oplites* Benth. ex R. Parker	0	16.06	0	0	0	0	0
7	*Bergenia stracheyi* (Hook.f. & Thom.) Engl.	0	0	0	0	0	0	33.44
8	*Berberis lyceum* Royle	36.83	8.42	15.3	0	0	20.14	0
9	*Bistorta amplexicaulis* (D.Don) Greene	0	0	0	0	0	22.49	0
10	*Cedrus deodara* (Roxb. ex Lamb.) G. Don	0	0	0	0	66.39	0	0
11	*Cotoneaster macrophylla* Wall. ex Lindl.	14.37	0	16.3	0	10.87	22.33	0
12	*Cotoneaster microphyllus*Wall. Ex Lindl.	3.6	0	0	0	0	0	0
13	*Conyza Canadensis* (L.) Cronquist	0	24.22	0	0	0	0	0
14	*Cynodon dactylon* (L.) Pers.	22.81	0	0	0	0	0	0
15	*Cynoglossum lanceolatum* Forssk.	0	0	0	0	0	19.31	0
16	*Daphne oleoides* Schreb.	15.37	9.63	0	0	14.45	0	0
17	*Dicanthum annulatum* (Forssk.) Stapf.	0	0	29.39	0	0	0	0
18	*Elaeagnus angustifolia* L.	0	17.8	0	0	0	0	0
19	*Euphorbia wallichii* Hook.f.	0	0	0	16.71	0	0	0
20	*Fragaria nubicola* (Hook.f.) Lindl.ex Lacaita	0	0	7.9	0	0	0	0
21	*Hertia intermedia* (Bioss.) Kuntze	0	21.04	0	0	0	0	0
22	*Impatiens edgeworthii* Hook.f.	0	0	14.2	0	0	0	0
23	*Indigofera heterantha* Brandis	0	8.73	42.2	0	0	0	0
24	*Juniper excelsa* M. Bieb.	0	0	0	65.36	35.29	0	70.32
25	*Kobresia schoenoides* (C. A. Mey.) Steud.	0	0	0	0	0	0	34.42
26	*Leptorhabdos parviflora* (Benth)Benth.	0	0	0	0	0	20.31	0
27	*Medicago lupulina* L.	0	0	17.4	0	0	10.0	0
28	*Morina longifolia* Wall.	0	0	0	0	0	0	26.34
29	*Nannorrhops ritchiana* (Griff) Aitch.	13.98	0	0	0	0	0	0
30	*Nepeta bracteata* Benth	0	0	0	0	0	33.6	0
31	*Nepeta kurramensis* Reech.f.	0	0	0	7.0	0	0	0
32	*Olea ferruginea* (Sol.) Steud.	15.06	0	0	0	0	0	0
33	*Parthenium hysterophorus* L.	0	23.86	0	0	0	0	0
34	*Periploca aphylla* Decne.	30.98	0	0	0	0	0	0
35	*Perovskia atriplicifolia* Benth.	0	8.36	0	0	0	0	0
36	*Pedicularis verticilata* L.	0	0	0	23.18	0	28.57	0
37	*Phlomis bracteosa* Royle ex. Benth.	0	0	0	20.37	0	0	14.24
38	*Phlomis cshmeriana* Royle ex Benth.	0	0	0	0	6.62	0	0
39	*Picea smithiana* (Wall.) Boiss.	0	0	0	51.07	0	41.56	0
40	*Pinus gerardiana* Wall.ex. D.don.	0	0	0	0	9.81	0	0
41	*Pinus wallichiana* A. B. Jacks.	0	0	0	21.08	20.18	0	0
42	*Piptaatherium aequiglume* Roshev.	0	0	29.6	0	18.56	0	0
43	*Quercus baloot* Griff.	0	0	33.8	0	21.93	0	0
44	*Quercus semicrpypholia* Sm.	0	0	13.79	0	47.71	0	0
45	*Rhododendron afghanicum* Aitch. & Hemsl.	0	0	0	0	0	29.56	33.87
46	*Rheum speciforme* Royle	0	0	0	0	0	0	45.74
47	*Salvia reflexa* Hornem.	0	42.1	0	0	0	0	0
48	*Salex denticulate* Anderson	0	0	0	22.77	0	0	0
49	*Stachys parviflora* Benth.	20.54	0	0	0	0	0	0

http://www.aloki.hu ● ISSN 1589 1623 (Print) ● ISSN 1785 0037 (Online)
DOI: http://dx.doi.org/10.15666/aeer/1704_99059924

50	*Syringga afghanica* S. K. Schneid.	0	0	25.9	0	0	0	0
51	*Sericea lespedeza* (Thunb.) Miq.	14.7	0	0	0	0	0	0
52	*Seriphidium kurramense* (Qazilb.) Y.R. Ling	0	50.5	0	0	0	0	0
53	*Sophora mollis* (Royle) Baker	0	0	0	0	28.8	0	0
54	*Tagetis minuta* L.	0	16.47	0	0	0	0	0
55	*Teucrium stocksianum* Boiss.	9.85	0	0	0	0	0	0
56	*Themeda anathera* (Nees ex Steud.) Hack.	34.88	0	0	0	0	0	0
57	*Trifolium repens* L.	0	0	0	0	0	0	13.52
58	*Thymus linearis* var. *linearis* Benth.	29.4	26.38	27.7	6.54	5.57	7.0	2.63
59	*Thymus seriphylum* L.	0	0	0	0	0	0	25.45
60	*Valeriana jatamansi* Jones.	0	0	0	15.46	0	0	0

Site I (Sub-Tropical South Hills), Site II (Sub-Tropical Plain area), Site III (Sub-Tropical North hills), Site IV (Temperate South Facing slope), Site V (Temperate North Facing slope), Site VI (Sub-Alpine zone), Site VII (Alpine Zone)

Ward's cluster analysis

Cluster analysis was conducted by using PAST software applying Wards cluster analysis tool. These clusters are based on IV of the leading species at all monitoring sites and the combined IV of each specie.

Cluster I. Juniper excela – Rhododendron afghanicum community

This group had *Juniper excela* as a leading dominant with a combined IV of 171.21. This member was recorded from Site-IV (65.36 IV), Site-V (35.29 IV) and Site-VII (70.32 IV) while second dominant species was *Rhododendron afghanicum* with a combine IV of 63.43. This species was found at only two sites i.e. Site-VI (29.56 IV) and Site-VII (33.87 IV). *Rheum speciforme*, *Kobresia schoenoides* and *Bergenia stracheyi* were other important members of this group (*Table 3, Fig. 2*).

Cluster II. Picea smithiana – Thymus linearis community

This group had the highest species richness, dominated by *Picea smithiana* with a combined IV of 92.63. It was found at Site-IV (51.07 IV) and Site-VI (41.56 IV). Second dominant species was *Thymus linearis* with a combined IV of 105.22. It was found at Site-I (29.4 IV), Site-II (26.38 IV), Site-III (27.7 IV), Site-IV (6.54 IV), Site-V (5.57 IV), Site-VI (7.0 IV) and Site-VII (2.63 IV). *Berberis lyceum* (combined IV 80.69), *Abies pindrow* (combined IV70.14), *Cotoneaster macrophyla* (combined IV 53.87), *Pedicularis verticilata* (combined IV 51.75) and *Seriphidium kurramense* (combined IV 50.5) were the other prominent plant species of this cluster. This cluster also included *Olea ferruginea* and *Pinus geraardiana* but with lower IV values. *Pinus gerardiana* is an indicator species of Dry Temperate Zone which yields edible seeds (*Table 1, Fig. 2*).

Cluster III. Quercus semicarpifolia – Cedrus deodara community

Quercus semicarpifolia with 66.5 combined IV was dominant member of this group. It was found at Site-III (13.79 IV) and Site-V (52.71 IV). Second dominant species was *Cedrus deodara* having a combined IV of 66.39. *Indigofera heterantha* (50.93 IV), *Quercus baloot* (55.73), *Artimesia scuparia* (50.4 IV) and *Piptatherium aequiglume* (48.16 IV) were other important members of this group (*Table 3, Fig. 2*).

http://www.aloki.hu ● ISSN 1589 1623 (Print) ● ISSN 1785 0037 (Online)
DOI: http://dx.doi.org/10.15666/aeer/1704_99059924

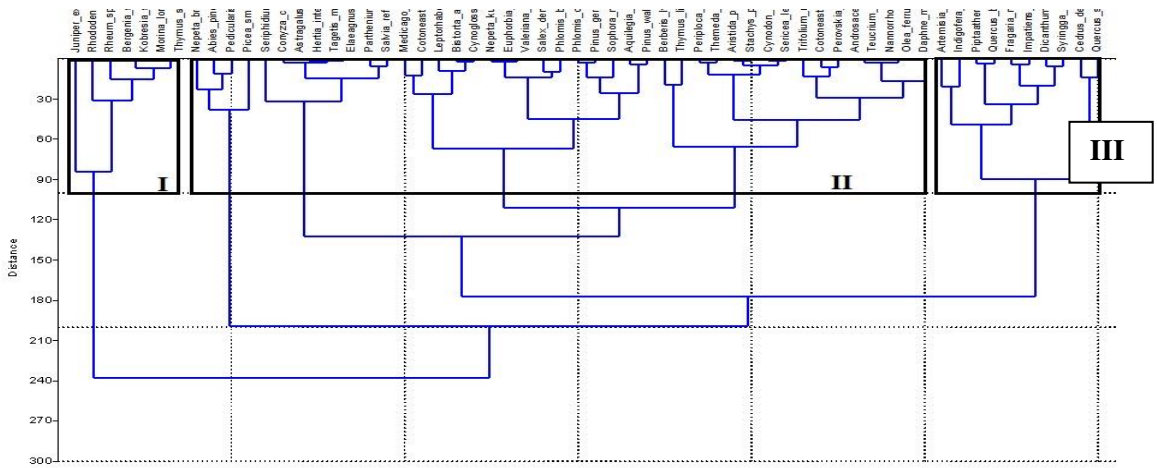

Figure 2. *Cluster dendrogram analysis showing 3 associations based on IV values*

Principal components analysis

Principal Components Analysis is one of the vegetation analysis techniques, which was applied by Pearson in ecology for the first time (Mesdaghi, 2001). Numerous studies have been carried out using PCA in various parts of the world to probe the connection between soil properties and vegetation (Rajendran et al., 2016, Forzieri et al., 2011, Salehi et al., 2005; Taleshi, 2004). Vegetation cover is an important variable in many earth system processes. The aim of this clustering is to analyze spatial variations in vegetation characteristics of Koh-e-Safaid Range Upper Kurram using principal component analysis. PCA was done by PC-Ord software version 5 which classified the vegetation data into 4 major components based on IVs of plant species as shown in the *Figure 3*.

Group 1

The dominant species in this group was *Seriphidium kurramense* with an IV of 50.50, *Berberis lycium* with an IV of 36.83, *Themeda anathera* with an IV of 34.88, *Quercus baloot* with an IV of 33.80, *Dichanthium annulatum* with an IV of 33.60, *Salvia reflex* with an IV of 32.10, *Periploca calophylla* with an IV of 30.98, *Thymus linearis* with an IV of 29.4, *Aristida purpuea* with an IV of 27.22 and *Leptorhabdos parviflora* with an IV of 26.50. The other associative species were *Stachys parviflora*, *Parthenium hysterophorus*, *Artemisia scoparia*, *Cynodon dactylon*, *Conyza canadensis*, *Tagetis minuta* and *Astragalus oplites*. Soil at this site was Sandy loam. Similarly, this group had low amount of N_2, Ca, Mg, Cu, Sulphates and high values of EC, HCO_3, P, K, Ca, Cl, Na, Fe and Zn as compare to other three groups (*Fig. 3*).

Group 2

In this group *Indigofera gerardiana* with an IV value of 52.20 followed by *Quercus baloot* with an IV of 33.80 and *Dichanthium annulatum* with an IV of 33.60 were dominant species. The rest of the associative species were *Thymus linearis*, *Leptorhabdos parviflora*, *Medicago lupulina*, *Cotoneastor macrophylla*, *Berberis lycium*, *Impatiens edgeworthii* and *Fragaria nubicola*. The soil characteristic in group 2

http://www.aloki.hu ● ISSN 1589 1623 (Print) ● ISSN 1785 0037 (Online)
DOI: http://dx.doi.org/10.15666/aeer/1704_99059924

Sub-Tropical North Hills was loamy sand, with low EC, N_2, P, Ca, Na, Mn, Cu, Zn, and Sulphates while $Caco_3$, HCO_3, K, Mg, S, Cl and Fe contents (*Fig. 3*).

Group 3

In this group *Cedrus deodara* with an IV of 66.39 was dominant species followed by *Quercus semicarpifolia* with an IV of 52.71 making strong association with *Juniperus excelsa* with IV of 38.29. The other important associated members of this group were *Sophora mollis*, *Quercus baloot*, *Pinus wallichiana*, *Piptatherum aequiglume*, *Daphne mucronata*, *Phlomis cashmeriana*, *Cotoneaster macrophylla* and *Pinus gerardiana*. Studies on edaphic variables of this group showed that the soil EC was lower than the soil of other groups. Similarly, the amount of HCO_3, P, Mg, Cl, Cu, Na, Mn and Zn contents were low while N, K, S, Ca, Cu, Fe and Sulphates were comparatively (*Fig. 3*).

Group 4

This group was most diverse in terms of species richness having *Juniperus excelsa* as dominant species with an IV of 70.32, *Picea smithiana* with an IV of 51.07, *Rheum speciforme* with an IV of 45.74, *Abies pindrow* with an IV of 44.25, *Kobresia schoenoides* with an IV of 34.42, *Rhododendron afghanicum* with an IV of 33.36, *Nepeta bracteosa* with an IV of 29.56 and *Pedicularis verticillata* with an IV of 28.57. The other associated members were *Thymus seriphylum*, *Morina longifolia*, *Aquilegia pubiflora*, *Bistorta amplexicaulis*, *Aquilegia pubiflora*, *Phlomis bracteosa*, *Cynoglossum furcatum*, *Salex denticulate*, *Cotoneaster macrophylla*, *Euphorbia wallichii*, *Pinus wallchiana*, *Medicago lupina*, *Valeriana jatamansi*, *Berberis vulgaris*, *Phlomis bracteosa* and *Leptorhabdos parviflora*. The characteristics of the soil associative with this group show that the soil EC was lower than the soil of other groups. Similarly, this group had low amount of N, P, Mg, S, Cl, Cu and Zn and high values of HCO_3 K, Ca, Na, Fe and Sulphates as compare to groups (*Fig. 3*).

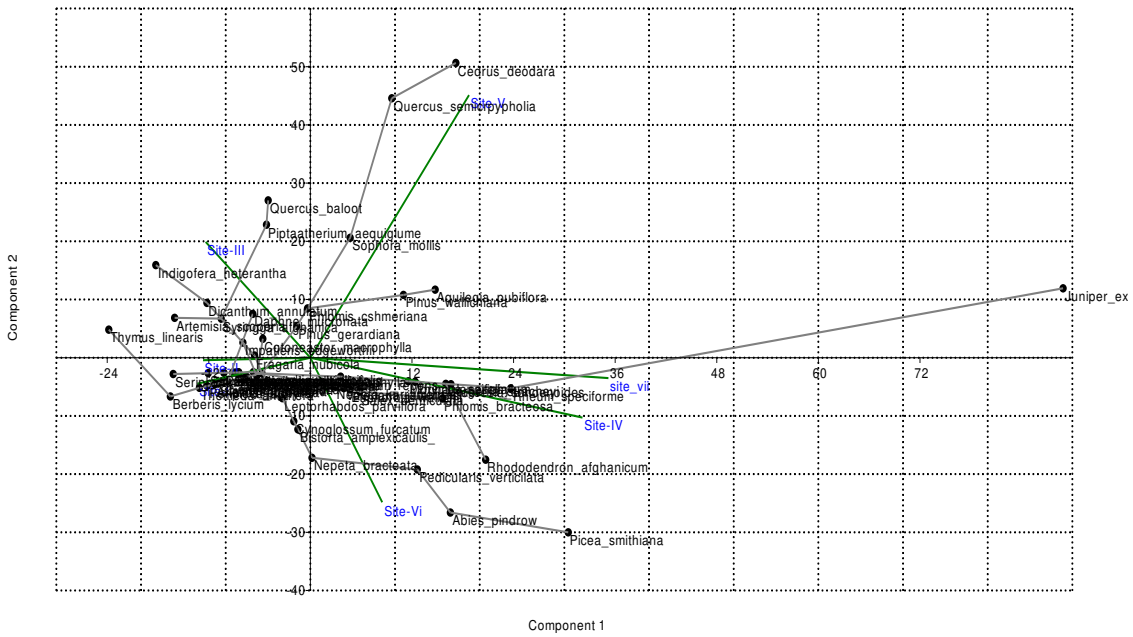

Figure 3. *Principal components analysis showing 4 associations based on IV values*

http://www.aloki.hu ● ISSN 1589 1623 (Print) ● ISSN 1785 0037 (Online)
DOI: http://dx.doi.org/10.15666/aeer/1704_99059924

Maturity index

During the current study the species maturity index ranged from 74.16 to 48.88. The high maturity index was recorded (74.16) both at sub-tropical north zone and temperate south facing zone followed by (72.13) at sub-tropical south zone, (67.49) at sub alpine zone, (64.89) at alpine zone, (64.84) at temperate north facing zone and (48.88) at subtropical plain zone (*Table 4*).

Table 4. *Maturity index*

Sites	Communities	Maturity index
Sub-tropical south hills	*Berberis-Themeda-Periploca*	72.13
Sub-tropical plain area	*Seriphidium-Salvia-Thymus*	48.88
Sub-tropical north hills	*Indigofera-Quercus-Dichanthium*	74.16
Temperate north facing slope	*Juniperus-Picea-Abies*	74.16
Temperate south facing slope	*Cedrus-Quercus-Juniperus*	64.84
Sub-alpine zone	*Abies-Picea- Rhododendron*	67.49
Alpine zone	*Juniperus-Rheum-Kobresia*	64.89

Index of similarity

A similarity index does not consider the relative abundance of species. It is helpful when key concern lies in the absence or presence of species. Degree of similarity between two plant communities allows combining them into an association (Badshah et al., 2010). According to the Motyka's index of similarity (Motyka et al., 1950), *Berberis-Themeda-Periploca* community of Sub-Tropical South Hills was found to be 14.90% like *Seriphedium-Salvia-Thymus* community of Sub-Tropical plain area. The similarity between *Berberis-Themeda-Periploca* community of Sub-Tropical South Hills and *Indigofera-Quercus-Dichanthium* community of Sub-Tropical North Hills was observed 15.81%. The current analysis shows that similarity between *Berberis-Themeda-Periploca* community of Sub-Tropical South Hills and that of *Juniperus-Picea-Abies* community of Temperate Zone North facing slope was 2.18%. The *Berberis-Themeda-Periploca* community of Sub-Tropical South Hills and *Cedrus-Quercus-Juniperus* community of Temperate Zone South facing slope showed 8.16% similarity. The similarity between *Berberis-Themeda-Periploca* community Sub-Tropical South Hills and *Abies-Picea-Rhododendron* of Sub-Alpine Zone was recorded 10.53%. The similarity between *Berberis-Themeda-Periploca* community of Sub-Tropical South Hills and *Juniperus-Rheum-Kobresia* of Alpine zone was 0.87%. The community of Sub-Tropical plain i.e. *Seriphedium-Salvia-Thymus* was 22.48% similar to *Indigofera-Quercus-Dichanthium* community of Sub-Tropical North hills. The *Seriphedium-Salvia-Thymus* community of Sub-Tropical plain was found 2.19% similar to *Juniperus-Picea-Abies* community of Temperate North Facing slope. The *Seriphedium-Salvia-Thymus* community of Sub-Tropical plain was similar to *Cedrus-Quercus-Juniperus* community of Temperate South Facing slope i.e. 5.10%. The *Seriphedium-Salvia-Thymus* community of Sub-Tropical plain was found 5.17% similar to *Abies-Picea-Rhododendron* community of Sub-Alpine Zone. The *Seriphedium-Salvia-Thymus* community of Sub-Tropical plain was observed 0.88% similar to the *Juniperus-Rheum-Kobresia* community of Alpine Zone. The *Indigofera-Quercus-Dichanthium* community of Sub-Tropical North Hills was 2.18% like *Juniperus-Picea-*

http://www.aloki.hu ● ISSN 1589 1623 (Print) ● ISSN 1785 0037 (Online)
DOI: http://dx.doi.org/10.15666/aeer/1704_99059924

Abies community of Temperate Zone North Facing slope and 19.0% similar to *Cedrus-Quercus-Juniperus* Temperate South Facing slope. The *Indigofera-Quercus-Dichanthium* community of Sub-Tropical North Hills showed 16.22% similarity with *Abies-Picea-Rhododendron* community of Sub-Alpine Zone. Similarity between *Indigofera-Quercus-Dichanthium* community Sub-Tropical North Hills and *Juniperus-Rheum-Kobresia* community of Alpine Zone was 0.87%. The *Juniperus-Picea-Abies* community of Temperate North Facing slope showed 24.61% similar to *Cedrus-Quercus-Juniperus* community at Temperate South Facing slope. The *Juniperus-Picea-Abies* community of Temperate North Facing slope was found 32.49% similar to *Abies-Picea-Rhododendron* community at Sub-Alpine Zone. The *Juniperus-Picea-Abies* community of Temperate North Facing slope and *Juniperus-Rheum-Kobresia* community at Alpine Zone showed 27.45% similarity. A 5.50% similarity was recorded between *Cedrus-Quercus-Juniperus* community of Temperate South Facing slope and *Abies-Picea-Rhododendron* community of Sub-Alpine Zone. Comparison of *Cedrus-Quercus-Juniperus* community of Temperate South Facing slope and *Juniperus-Rheum-Kobresia* community at Alpine Zone showed 12.68% similarity while *Abies-Picea-Rhododendron* community of Sub-Alpine Zone and *Juniperus-Rheum-Kobresia* community of Alpine Zone community showed 10.74% similarity (*Table 5*). The current results agree with those of Ilyas et al. (2018), Khan et al. (2016), Urooj et al. (2016), Mehmood et al. (2015), Rashid et al. (2011), Wahab et al. (2010), Ali and Malik (2010) and Mesdaghi (2001), who reported similarities among the plant communities is due to soil properties, ecological and biotic factors.

Table 5. *Similarity index for seven different communities*

	BTP	**SST**	**IQD**	**JPA**	**CQJ**	**APR**	**JRK**
BTP	X	X	X	X	X	X	X
SST	14.90	X	X	X	X	X	X
IQD	15.81	22.48	X	X	X	X	X
JPA	2.18	2.19	2.18	X	X	X	X
CQJ	8.16	5.10	19.0	24.61	X	X	X
APR	10.53	5.17	16.22	32.49	5.50	X	X
JRK	0.87	0.88	0.87	27.45	12.68	10.74	X

BTP-Berberis-Themeda-Periploca community, SST-Seriphidium-Salvia-Thymus community, IQD-Indigofera-Quercus-Dichanthium community, JPA-Juniperus-Picea-Abies community, CQJ- Cedrus-Quercus-Juniperus community, APR-Abies-Picea-Rhododendron community, JRK-Juniperus-Rheum-Kobresia community

Discussion

During the current study the vegetation of the area was classified into seven communities which is in line with the works of Ali et al. (2018, 2015), Badshah et al. (2016) Ilyas et al. (2015), Saurav and Das (2014), Sharma et al. (2014) Saglam (2013), Ahmad et al. (2010), Digiovinazzo et al. (2010), Hussain et al. (2010), Mohler et al. (2006) Munhoz et al. (2006) and Padalia et al. (2004). The research area is under tremendous anthropogenic stress, due to which the vegetation showed clumping rather than a uniform pattern of distribution due to excessive deforestation in the area. Scanty trees and comparatively thick shrub cover at Sub-Tropical North foothills and Temperate zone indicated the disturbed nature of habitat. Due to rapid population and

http://www.aloki.hu ● ISSN 1589 1623 (Print) ● ISSN 1785 0037 (Online)
DOI: http://dx.doi.org/10.15666/aeer/1704_99059924

construction of buildings is the chief reason behind the species loss in this locality. Impacts of soil erosion were more visible at Site I, Site II, III, IV and Site-VII where eroded soils had herbaceous members such as *Plantago major*, *Rumex hastatus, Thymus linearis and Verbascum thapsus* which are indicator species of eroded soils. *Indigofera gerardiana, cotoneaster microphyllus* were observed to form randomly dispersed thick patches at site III, IV, *Juniperus communis*, *Rhododendron afghanicum* and *Salex denticulate* monitoring site V and VI (*Fig. 4*).

Figure 4. *Pictorial view of the study area, (A) A beautiful view of Koh-e-Safaid Range, (B) Sub-alpine vegetation, (C) North facing slopes of temperate site (D) North facing slopes (E) Delphinium brunonianum alpine plant in flowering stage (F) Rhododendron afghanicum of sub-alpine plant in flowering stage (G) Cedrus deodara forest (H) Principal author in field at sub-tropical site at south facing slope (I) measuring canopy cover of Berberis lyceum (J) Principal author showing steep slopes of Alpine zone*

http://www.aloki.hu ● ISSN 1589 1623 (Print) ● ISSN 1785 0037 (Online)
DOI: http://dx.doi.org/10.15666/aeer/1704_99059924

These findings are backed by works of Ali et al. (2018), Dad (2016), Ilyas et al. (2015), Siddiqui et al. (2015) and Ahmad et al. (2010). *Cedrus-Quercus-Juniperus* community was recorded at on the South Facing Slopes of Temperate Zone. The area had uniformly spread thin *Cedrus deodara* forest mixed with *Quercus semicarpifolia* and *Juniperus excelsa*. The area was under tremendous biotic stress especially cutting of *Pinus gerardiana, Pinus wallichiana, Cedrus deodara* for timber wood in past and completely missing of herbage cover due to steep slopes, lacking topsoil and allopathic effect of shading leaves of *Cedrus, Pinus* and *Juniperus* trees. This is line with findings of Ali et al. (2018), Ahmad et al. (2016), Khan et al. (2016), Akhtar and Bergmeier (2015), Shaheen et al. (2015), Sharma et al. (2014), Hussain et al. (2010) and Jabeen and Ahmad (2009). On the North Facing Slopes of Sub-Alpine *Abies-Picea-Rhododendron* community was recorded. The *Rhododendron afghanicum* was uniformly distributed on the open space of forest as well as inside the forest. Forest at this site was found in good health. Deforestation was also not that alarming as compared to that of other monitoring sites. *Juniperus-Rheum-Kobresia* community was recorded at alpine zone. This is treeless zone and only two shrubs were recorded first one was *Juniper excelsa* and the second was *Rhododendron afghanicum* and dominated by the herbs i.e. *Kobresia schoenoides.* This site shrub growth was stunted, and trees were scanty due to unfavorable conditions. These results are in line with the works of Ali et al. (2018), Khan et al. (2016, 2012), Haq et al. (2015), Sharma et al. (2014) and Ahmad et al. (2010, 2006). The soil texture of the research area was typically sandy loam and loamy sand, with pH ranged from 7.3 to 7.7. Organic matter varied from 1.4 to 2.4% and electric conductivity from 0.6 dSm^{-1} to 1.6 dSm^{-1}. The $CaCo_3$ ranged from 2.6 to 7.8%, HCO_3 from 3.0 to 8.0% and sulphates from 0.4 to 7.8% respectively. Nitrogen concentration ranged from 0.280 to 0.569%, phosphorus from 435 to 810 µg/g, potassium from 1090 to 9900 µg/g, calcium from 32100 to 39900 µg/g, magnesium from 5100 to 6800 µg/g and sulphur from 163 to 263 µg/g. The micro nutrients such as iron ranged from 15000 to 89200 µg/g, manganese was enumerated as 343 to 976 µg/g, copper was found to be 55 to 109 µg/g and zinc varied from 53 to 84 µg/g, however, sodium was recorded from 1300 to 3300 µg/g and chlorine as 1500 to 3500 µg/g.

Conclusions

This study reveals results of vegetation mapping based on 140 sampling units at 7 monitoring sites while results of soil analysis cover 18 parameters. Spatial variation among plant communities at different monitoring sites is attributed to variations in edaphic variables, climate and different ecological parameters. Anthropogenic activities, over grazing, natural disasters and erosion are reducing the vegetation cover. Extraction of fuel wood from forest, especially during harsh winters by the local people is alarming. Impacts of anthropogenic pressure are evident from low scores for maturity index (48.88) at Sub-Tropical Plain area. Low values for maturity index indicate inability of the plant communities to cope with anthropogenic, edaphic and climatic stresses. Similarly, low values for similarity index show the heterogeneity among the reported different 7 plant communities. However, cluster analysis using PAST software and PC-Ord software version 5, classified the vegetation into three groups and four groups based on quantitative value. Afforestation programs need to be started on wasteland of the area to overcome the impacts of deforestation. There is severe deforestation pressure on woody and shrubby species especially on *Quercus baloot,*

http://www.aloki.hu ● ISSN 1589 1623 (Print) ● ISSN 1785 0037 (Online)
DOI: http://dx.doi.org/10.15666/aeer/1704_99059924

Quercus semicarpifolia, Cedrus deodara, Abies pindrow, Pinus wallichiana, Indigofera gerardiana, Sophora mollis and Syringa afghanica. Therefore, alternate sources of fuel/timber should be provided, and the area must be protected to promote vegetation cover. Effective measures like afforestation and control of overgrazing are needed to avoid soil erosion.

Acknowledgements. This study is part of the Doctoral work of the principal author. This research did not receive any specific grant from funding agencies in the public, commercial, or not-for-profit sectors.

REFERENCES

[1] Ahmad, M., Husain, T., Sheikh, A. H., Hussain, S. S., Siddiqui, M. F. (2006): Phytosociology and structure of Himalayan forests from different climatic zones of Pakistan. – Pak. J. Bot. 38(2): 361-383.
[2] Ahmad, M., Shoukat, S. S., Khan, D. (2010): Status of vegetation analysis in Pakistan. – Int. J. Biol. Biotech. 7(3): 147-158.
[3] Ahmad, K. S., Ahmad, M., Ahmad, F., Sadia, B. (2016): Edaphic factors as major determinants of plant distribution of temperate Himalayan grasses. – Pak. J. Bot. 48(2): 567-573.
[4] Akhtar, N., Bergmeier, E. (2015): Species richness, alpha and beta diversity of trees, shrubs and herbaceous plants in the woodlands of Swat, Pakistan. – Pak. J. Bot. 47(6): 2107-2113.
[5] Ali, S. M., Malik, R. N. (2010): Vegetation communities of urban open spaces: green belts and parks in Islamabad city. – Pak. J. Bot. 42(2): 1031-1039.
[6] Ali, S., Perveen, A., Qaiser, M. (2015): Vegetation structure and edaphology of Mahaban and Malka (District Buner) KPK, Pakistan. – Pak. J. Bot. 4(7): 15-22.
[7] Ali, A., Badshah, L., Hussain, F. (2018): Vegetation structure and threats to Montane Temperate ecosystems in Hindukush Range, Swat, Pakistan. – *Applied ecology and environmental research*. 16(4): 4789-4811.
[8] Badshah, L., Hussain, F., Akhtar, N. (2010): Vegetation structure of subtropical forest of Tabai, South Waziristan, Pakistan. – Front. Agric. China. 4(2): 232-236.
[9] Badshah, L., Farrukh, H., Zaman, S. (2016): Floristic inventory, ecological characteristics and biological spectrum of plants of Parachinar, Kurram Agency, Pakistan. – Pak. J. Bot. 48(4): 1547-1558.
[10] Bokhari, T. Z., Ahmed, M., Siddique, M. F., Khan, Z. (2013): Forest communities of Azad Kashmir, Pakistan. – FUUAST J. Biol. 3(1): 137.
[11] Bouyoucos, G. J. (1936): Directions for making mechanical analysis of soils by the hydrometer method. – Soil Sci. 42: 225-228.
[12] Brady, N. C. (1990): The Nature and Properties of Soils. 10th Ed. – Macmillan Publishing Co. New York.
[13] Bremner, J., Mulvaney, C. S. (1982): Nitrogen - Total. – In: Page, A. L. et al. (eds.) Methods of Soil Analysis Agronomy Monograph. 9, Part 2, 2nd Ed. American Society of Agronomy, Madison, WI. pp. 595-624.
[14] Dad, J. M. (2016): Distribution, species diversity and composition of plant communities in relation to various affecting factors in an Alpine grassland at Bandipora, Kashmir. – Pak. J. Bot. 48(2): 551-560.
[15] Digiovinazzo, P., Ficetola, G. F., Bottoni, L., Andreis, C., Schioppa, E. P. (2010): Ecological thresholds in herb communities for the management of suburban fragmented forests. – Forest Ecology & Management 259(3): 343-349.
[16] Forzieri, G., Castelli, F., Vivoni, E. R. (2011): Vegetation dynamics within the North American monsoon region. – J. Clim. 24(6): 1763-1783.

http://www.aloki.hu ● ISSN 1589 1623 (Print) ● ISSN 1785 0037 (Online)
DOI: http://dx.doi.org/10.15666/aeer/1704_99059924

[17] Haq, F., Ahmad, H., Iqbal, Z. (2015): Vegetation description and phytoclimatic gradients of subtropical forests of Nandiar Khuwar catchment District Battagram. – Pak. J. Bot. 47(4): 1399-1405.
[18] Hussain, A., Farooq, M. A., Ahmad, M., Akbar, M., Zafar, M. U. (2010): Phytosociology and structure of central Karakoram national park (CKNP) of Northern areas Pakistan. – World App. Sci. J., 9(12): 1443-1449.
[19] Hussain, A., Adhikari, A., Iqbal, C. M., Ayatollahi, S. A., Rahman, A. (2016): New adduct of abietane-type diterpene from Salvia leriifolia Benth. – Nat. Prod. Res. 30(13): 1511-1516.
[20] Hussain, F., Shah, S. M., Badshah, L., Durrani, M. J. (2015): Diversity and ecological characteristics of flora of Mastuj Valley, District Chitral, Hindukush Range, Pakistan. – Pak. J. Bot. 39(2): 339-354.
[21] Hussain, W., Hussain, J., Hussain, S., Shinwari, Z. K., Ali, R., Basir, A. (2013): Ethno-medicinal study of Parachinar, Kurram Valley (FATA) KPK, Pakistan. – JAPS. 3(11): 085-088.
[22] Hussain, W., Badshah, L., Shah, S. A., Hussain, F., Ali, A., Sultan, A. (2019): Salvia reflexa (Lamiaceae): a new record for Pakistan. – Plant Science Today. 6(1): 17-21.
[23] Ilyas, M., Qureshi, R., Akhtar, N., Haq, Z. (2015): Vegetation analysis of Kabal Valley, District Swat, Pakistan using multivariate approach. – Pak. J. Bot. 4(7): 77-86.
[24] Ilyas, M., Qureshi, R., Akhtar, N., Haq, Z. (2018): Vegetation structure of the remnant sub-tropical broad leaves forests from Kabal Valley, Swat, Pakistan. – Pak. J. Bot. 50(1): 217-230.
[25] Jabeen, T., Ahmad, S. S. (2009): Multivariate analysis of environmental and vegetation data of Ayub National Park, Rawalpindi. – Soil & Env. 28(2): 106-112.
[26] Jackson, M. L. (1962): Soil Chemical Analysis. – Constable & Co., Ltd., London, pp. 406-407.
[27] Khan, A., Ahmad, M., Siddiqui, M. F., Iqbal, J., Wahab, M. (2016): Phytosociological analysis of Pine forest at Indus Kohistan, KPK, Pakistan. – Pak. J. Bot. 48(2): 575-580.
[28] Khan, N., Ahmed, M., Siddiqui, M. F., Bibi, S., Ahmed, I. (2012): A phytosociological study of forest and non-forest vegetation of District Chitral, Hindukush Range, Pakistan. – FUUAST J. Bio. 2(1): 91-101.
[29] Kuma, M., Shibru, S. (2015): Floristic composition, vegetation structure, and regeneration status of woody plant species of Oda Forest of Humbo Carbon Project, Wolaita, Ethiopia. – J. Bot. Ethio. 15(01): 01-09.
[30] Mahmood, T., Andleeb, S., Anwar, M., Rais, M., Nadeem, M. S., Akrim, F., Hussain, R. (2015): Distribution, abundance and vegetation analysis of the scaly ant-eater (Manis crassicaudata) in Margalla Hills National Park Islamabad, Pakistan. – JAPS 25(5): 1311-1321.
[31] Mesdaghi, M. (2001): Vegetation Description and Analysis: A Practical Approach. 1st Ed. – Jehad Daneshgahi of Mashhad, Mashhad, p. 161-179.
[32] Mohler, C. L., Marks, P. L., Gardescu, S. (2006): Guide to the Plant Communities of Central Finger Lakes Region. – New York State Agricultural Experiment Station, New York, pp. 7-9.
[33] Motyka, J., Dobrzanski, B., Zawadski, S. (1950): Wstepne badania nad lakami polundnlowowschodneij Lubeiszczyzny. – Ann. Univ. M. Curie-Sklodowska 13: 367-447.
[34] Munhoz, C. B. R., Felfili, J. M. (2006): Phytosociology of the herb-subshrub layer in an area of Campo Sujo, Distrito Federal, Brazil. – Acta Bot. Bras. 20(3). http://dx.doi.org/10.1590/S0102-33062006000300017.
[35] Padalia, H., Chauhan, N., Porwal, M. C., Roy, P. S. (2004): Phytosociological observations on tree species diversity of Andaman Islands, India. – Current Sci. 87: 799-806.

http://www.aloki.hu ● ISSN 1589 1623 (Print) ● ISSN 1785 0037 (Online)
DOI: http://dx.doi.org/10.15666/aeer/1704_99059924

[36] Pichi-Sermolli, R. E. (1948): An index for establishing the degree of maturity in plant communities. – J. Ecol. 36: 85-90.
[37] Rajendran, S., Al-Sayigh, A. R., Al-Awadhi, T. (2016): Vegetation analysis study in and around Sultan Qaboos University, Oman, using Geoeye-1 satellite data. – EJRS. 19(2): 297-311.
[38] Rashid, A., Swati, M. F., Sher, H., Al- Yemeni, M. N. (2011): Phytoecological evaluation with detail floristic appraisal of the vegetation around Malam Jabba, Swat, Pakistan. – Asian Pac. J. Trop. Biomed, 2(11): 461-467.
[39] Rhoades, J. D. (1996): Salinity: Electrical Conductivity and Total Dissolved Solids. – In: Sparks D. L. (ed.) Methods of Soil Analysis: Chemical Methods, Part 3. ASA and SSSA, Madison, WI, pp. 417-435.
[40] Richard, L. A. (1954): Diagnoses and Improvement of Saline and Alkali Soils. – Agriculture Hand Book, 60: USDA, USA.
[41] Ryan, J., George, E., Rashid, A. (1997): Soil and Plant Analysis Laboratory Manual. 2nd Ed. – ICARDA, Aleppo, pp: 7-8.
[42] Saglam, C. (2013): A phytosociological study of the forest, shrub, and steppe vegetation of Kizildag and environs (Isparta, Turkey). – Turk. J. Bot. 37: 316-335.
[43] Salehi, A., Zarinkafsh M., Zahedi G. H., Marvi M. R. (2005): A study of soil physical and chemical properties in relation tree ecological groups in Nam-Khaneh district of Kheirod-Kenar forest. – Iran. J. Nat. Res., 5(8): 567-577.
[44] Saurav, M., Das, A. P. (2014): Plant species richness and phytosociological attributes of the vegetation in the cold temperate zone of Darjilling Himalaya, India. – Int. Res. J. Env. Sci. 3(10): 47-57.
[45] Shaheen, H., Sarwar, R., Firdous, S. S., Dar, M. E. I., Zahidullah., Khan, S. M. (2015): Distribution and structure of conifers with special emphasis on *Taxus baccata* in moist temperate forests of Kashmir Himalayas. – Pak. J. Bot. 47(SI): 71-76.
[46] Sharma, P., Rana, J. C., Devi, U., Randhawa, S. S., Kumar, R. (2014): Floristic diversity and distribution pattern of plant communities along altitudinal gradient in Sangla valley, Northwest Himalaya. – The Sci. World. J. http://dx.doi.org/10.1155/2014/264878.
[47] Sher, Z., Farrukh, H., Badshah, L. (2014): Biodiversity and ecological characterization of the flora of Gadoon Rangeland, District Swabi, Khyber Pukhtunkhwa, Pakistan. – Iran J. Bot. 20(01): 96-108.
[48] Siddiqui, M. F., Ahmed, M., Shaukat, S. S., Khan, N. (2010): Advance multivariate techniques to investigate vegetation-environmental complex of pine forests of moist area of Pakistan. – Pak. J. Bot. 42: 267-293.
[49] Siddiqui, M. F., Salam, A., Ahmad, M., Hussain, M. I., Iqbal, J., Wahab, M. (2015): Present state and future trends of pine forests of Malam Jabba, Swat District, Pakistan. – Pak. J. Bot. 47(6): 2161-2169.
[50] Sorensen, T. (1948): A method of establishing groups of equal amplitudes in plant sociology based on similarity of species content and its application to analyze the vegetation of Darnish commons. – Biol. Skr. 5: 1-34.
[51] Taleshi, H. (2004): Phytosociology of lowland forests in eastern Nowshahr (North of Iran). – M.Sc. Thesis, Tarbiat Modares University (in Persian).
[52] Timilehin, K. E., Olajide, O. S., Ademayowa, O., Olusanya, O. (2017): Floristic composition and structural diversity of Ibodi Monkey Forest, Ibodi, Southwestern Nigeria. – Pak. J. Bot. 49(4): 1359-1371.
[53] Urooj, R., Ahmad, S. S., Ahmad, M. N., Ahmad, H., Nawaz, M. (2016): Ordination study of vegetation analysis around wetland area: a case study of Mangla Dam, Azad Kashmir, Pakistan. – Pak. J. Bot. 48(1): 115-119.
[54] Wahab, M., Ahmad, M., Khan, N., Sarangzai, A. M. (2010): A phytosociological study of pine forest from District Dir, Pakistan. – J. Biol. Biotech. 7(3): 219-226.
[55] Zoq-ul-Arfeen, R., Saleem, A., Mirza, S. N., Akmal, M., Tayyab, H. M., Afzal, O. (2015): Biodiversity and phytosociological studies of upstream and downstream

http://www.aloki.hu ● ISSN 1589 1623 (Print) ● ISSN 1785 0037 (Online)
DOI: http://dx.doi.org/10.15666/aeer/1704_99059924

riparianareas of Pakistan: Special reference to Taunsa Wildlife Sanctuary and Keti Shah Forests. – Pak. J. Agri. Sci. 28(4): 112-121.

[56] Zhu, H., Yong, S., Zhou, H., Wang, C., Yan, L. (2015): Vegetation, floristic composition and species diversity in a tropical mountain nature reserve in southern Yunnan, SW China, with implications for conservation. – Trop. Conserv. Sci. 8(2): 528-546.

http://www.aloki.hu ● ISSN 1589 1623 (Print) ● ISSN 1785 0037 (Online)
DOI: http://dx.doi.org/10.15666/aeer/1704_99059924

ANALYSIS OF THREE-DIMENSIONAL FLUORESCENCE SPECTRUM CHARACTERISTICS OF WATER EXTRACTABLE ORGANIC MATTER IN MOLLISOLS AFTER DIFFERENT YEARS OF CULTIVATION

WANG, T. Y. [1,2#] – ZHAO, X. Y. [1,2#] – WANG, C. Y.[1,2] – HUANG, Z. Y.[1,2] – LIU, S. X. [1,2*]

[1]*College of Resources and Environmental Science, Jilin Agricultural University, Changchun 130118, Jilin Province, China*

[2]*Key Laboratory of Soil Resource Sustainable Utilization for Jilin Province Commodity Grain Bases, Changchun 130118, Jilin Province, China*

**Corresponding author*
e-mail: liushuxia69@163.com

(Received 1st Apr 2019; accepted 13th Jun 2019)

Abstract. Three-dimensional fluorescence technology was applied to analyze the components and structures of the water extractable organic matter (WEOM) in the topsoil (0-20 cm) and a 20-40 cm depth of Mollisol of an uncultivated land or the land after of 5, 20, 50 and 100 years of reclamation, respectively. With the continuous reclamation, the content of the WEOM in the black soil has a tendency of decreasing at first but increasing subsequently. The WEOM reaches its maximum and minimum contents at 86.65 mg/kg and 47.81 mg/kg. The fluorescence intensity of the area III was enhanced. After the reclamation of 100 years, the fluorescence intensity of the areas III and Vreached to the top values, suggesting the maximum contents of fulvic acid-like and humic acid-like organic matters. The emitting lights at the fluorescence peak of the fluorescence area of humic acid-like organic matters also show red shift, indicating the increase of molecular weight, aromaticity and degree of polycondensation. However, the area Ⅳ remained unchanged. The research results showed that: with the reclamation, the components and structure, and the variation of WEOM in soil varies are related to the years of reclamation; the molecular weights, aromaticity and degrees of polycondensation in the WEOM increase evidently with the reclamation.
Keywords: *dissolved organic carbon, fluorescence technology, substance composition, planting years, upland field soil*

Introduction

The water extractable organic matter (WEOM) refers to organic matters dissolved in the soil solution or in the soil solution and a certain proportion of pure water after shaking extraction of organic compounds (Jones and Willett, 2006), and which can pass through the filter membrane of 0.45 μm (Hassouna et al., 2010). It has a tiniest ratio in the total organic carbon of the soil, but gets involved in all kinds of biologic or abiologic processes, such as pedogenesis, carbon distribution and fixation, and environment behaviors of nutrient substances and pollutants in soil, therefore being of important significance (Landgraf et al., 2006). Generally, it is considered that the WEOM mainly comes from the root exudate of the land plants, the hydrolysate of fallen leaves and soil organic matters (McGill et al., 1981), and the metabolites of microorganism (Christ et al., 1996), and is composed of carbon hydrates, long-chain aliphatic compounds and proteins (Hassouna et al., 2010), in which the humic acid and fulvic acid account for about 25%-50%, and the others primarily are proteins, polysaccharides and hydrophilic organic acid (Weishaar et al., 2003). The content,

http://www.aloki.hu ● ISSN 1589 1623 (Print) ● ISSN 1785 0037 (Online)
DOI: http://dx.doi.org/10.15666/aeer/1704_99259935

components and structure of WEOM have been tested influenced by plant types, soil utilization methods, fertilization management, etc. The chemical composition of litter, varying with the plant types, obviously affects the existence of WEOM (Chantigny, 2003). For example, the WEOM has different and orderly reduced contents in the forest, grassland and plough (Wang et al., 2016). The fertilization, such as applying organic fertilizer and chemical fertilizer, shall change the content and structure of WEOM in soil (Liang et al., 2012). As for the soil utilization, after the natural land is reclaimed and turned into farmland, the content of WEOM is obviously reduced. The reclamation of land is regarded as the main reason for the reduction of WEOM (Graham et al., 2012). In terms of the distinctive fluorescence groups in the matters of WEOM, it is possible to analyze the WEOM by the fluorescence characteristics. Li et al. (2013) has researched the components and structure of WEOM in the soil of a farmland with a high maize outcrop by the fluorescence spectrum method, and indicated that the long-term application of nitrogen fertilizer shall affect the composition and structure of WEOM in the black soil, and further there is a parallelism between effect characteristics and application methods.

With fertile soil, the black soil area in the northeast of China ranks among the three largest black soil areas in the world, an extensive part of which has been reclaimed since one hundred years ago and been developed into the main commodity grain base of China with a high production level. Because of the reclamation of black soil, the soil fertility condition changed drastically, showing natural fertility reducing gradually (Provenzano et al., 2004). To a large extent, the natural fertility of soil depends on the quantity and quality of organic carbon in soil. As WEOM is the main part of the active organic carbon pool of soil, it can indicate the variation of quantity and quality of organic matters in soil (Liang et al., 2011). Therefore, this work, in virtue of the 3D fluorescence spectrum technology, has studied the content, composition, and structure of WEOM in the black soil after different years of reclamation, thereby providing a theory basis for deepening the recognition of reclamation's effects on the organic matters and quality of soil to increase the carbon fixation of black soil and improve the soil quality.

Materials and methods

Soil samples were collected in a Mollisol located in Haiqing village, Guojia county, Dehui city, Jilin province situated in the upper part of the corn belt region in China (N44°30'35.41" E125°33'20.90"). Sampling was performed at two depths, topsoil (0-20 cm) and 20-40 cm depth. Samples were taken in five adjacent soil plots of the uncultivated land and the cultivated land after the years of reclamation of 5, 20, 50 and 100, respectively. The soil was planted with maize and was ploughed each spring. With the snake-pattern five-point sampling method, the sampling is conducted in the sites with similar topography conditions and having shortest distance in between to minimize the topography disturbance. The basic physical and chemical properties of the tested soil are listed in *Table 1.*

http://www.aloki.hu ● ISSN 1589 1623 (Print) ● ISSN 1785 0037 (Online)
DOI: http://dx.doi.org/10.15666/aeer/1704_99259935

Table 1. *Basic physicochemical properties of tested samples*

Depth (cm)	Years	W-C (%)	pH	V-W (g/cm3)	A-P (mgkg/)	A-K (mg/kg)	A-N (mg/kg)	T-N (g/kg)
0-20	0	4.68±0.10	7.63±0.14	1.06±0.02	30.54±1.21	283.12±3.83	174.12±2.22	2.25±0.03
	5	3.71±0.17	7.85±0.05	1.01±0.03	22.06±1.34	185.22±4.13	86.34±2.34	1.74±0.02
	20	4.29±0.21	8.04±0.07	1.09±0.05	14.38±1.98	156.34±3.12	76.45±3.02	1.59±0.09
	50	5.02±0.29	7.35±0.12	1.07±0.08	19.72±1.89	200.67±4.23	90.98±3.19	1.85±0.10
	100	5.07±0.32	8.13±0.09	1.32±0.02	3.64±2.11	135.98±2.99	82.65±2.18	1.72±0.11
20-40	0	4.68±0.14	7.63±0.03	1.06±0.09	6.16±2.45	180.76±4.21	77.55±2.98	1.82±0.12
	5	3.93±0.09	8.37±0.11	1.31±0.05	2.42±1.77	59.33±3.08	61.20±1.34	1.47±0.06
	20	6.31±0.15	8.04±0.08	1.12±0.10	3.95±1.20	60.21±4.70	74.43±1.98	1.71±0.01
	50	4.59±0.26	7.64±0.16	1.32±0.11	7.91±1.34	138.55±3.17	84.78±2.31	1.78±0.12
	100	5.07±0.13	8.13±0.15	1.32±0.07	2.55±1.21	55.79±1.99	36.67±2.17	0.75±0.03

W-C: Water content; V-W: Volume weight; A-P: Available phosphorus; A-K: Available potassium; A-N: Available nitrogen; T-N: Total nitrogen

Extraction and determination of the water extractable organic matter

WEOM extract by the steam water. The soil of 25 g in dry weight, having passed through the 2 mm-grade sieve, were put into the triangular flask, and added with the distilled water of 100 ml. The mixture in the flask then was vibrated under the normal temperature for 30 min, and centrifuged by a high-speed centrifugal machine of 8000 rpm for 5 min. After stabilizing for another 5 min, the supernatant was separated from the mixture, and filtrated by the 0.45 μm-grade filter membrane. The collected filtrate was just WEOM, which was used to test the content and analyze the three-dimensional fluorescence spectrum of WEOM. And the concentration of organic carbon in filtrate was measured by the Shimadzu TOC-VCPH analyzer (Li et al., 2013).

Test method

The HATACH F-7000-type fluorescence spectrophotometer produced by Hitachi was used for the fluorescence spectrum analysis of WEOM, with the xenon lamp as the light source of 150 W, the voltage of photomultiplier of 700 V, the silt widths for excitation and emitting lights of 5 nm, the wave length of 220-420 nm and the wavelength interval of 5 nm for excitation lights, and those separately of 280-560 nm and 1 nm for emitting lights (Li et al., 2013), as shown in *Figure 1*.

Determination of basic physicochemical properties of soil were completed with the water content in soil tested by the oven drying method, the pH value by the pH meter, the volume weight by the cutting-ring method, the available phosphorus by the sodium bicarbonate extraction and molybdenum-blue colorimetry, the available potassium by the NH_4OAc extraction and flame photometer, the available nitrogen by the alkaline hydrolysis diffusion method, the total nitrogen by the semimicro-kjeldahl determination, and the soil organic matter (SOM) by the potassium dichromate method with outside heating (Shi and Bao,1908).

Data processing

The data processing and analysis was conducted by virtue of Origin 7.5, SPSS19.0, Excel 2010, etc.

http://www.aloki.hu ● ISSN 1589 1623 (Print) ● ISSN 1785 0037 (Online)
DOI: http://dx.doi.org/10.15666/aeer/1704_99259935

Figure 1. *HATACH F-7000-type fluorescence spectrophotometer*

Results and discussion

Content of the water extractable organic matter in black soil after different years of reclamation

The content of WEOM in black soil after years of reclamation was measured by the organic carbon analyzer (TOC), and the results are listed in *Table 2*. As indicated by the results, the cultivation had certain effects on the WEOM in black soil. In terms of the top soil (0-20 cm underground), the content of WEOM in black soil had a negative growth in the first few years and subsequently recovered to certain levels in the following years. The WEOM has the maximum and minimum contents, i.e. 86.65 mg/kg and 47.81 mg/kg, separately in the uncultivated land and the black soil after 5 years of reclamation and is less abundant in the soil after reclamation of 100 years in comparison with the uncultivated land. However, in the plough (20-40 cm underground), the black soil after 5 years of reclamation had the maximum ratio of WEOM, 124.99 mg/kg, and this content decreased to the lowest of 61.55 mg/kg with the years up to 50. As for SOM, with reclamation, it is subject to a same variation of content both in the top soil and plough, and has been proven more prolific in the top soil comparatively. However, a certain relation of the content of SOM versus soil types has not been figured out.

Basically identical with the results obtained by Graham et al. (2012), one conclusion of this research is that the soil with zero or less human disturbances bears a high content of WEOM, but the content should plummet in the events of some strong disturbances. The obvious changes of WEOM with the exploitation of land indicate it is primarily the land reclamation that should be the reason of the reduction of WEOM in soil. With the natural soil reclaimed, a large drop of WEOM occurred in the soil, and the reduction continued, to the largest extent at the 50th year of reclamation. Subsequently, the reducing was reversed, and the content starts to grow in the succeeding years. We concluded that in order to solve the problems caused by the increasing reclamation and singular plant, more fertilizers should be applied, which prompt in different levels the organic carbons in bodies of animals and plants transforming to those in the soil.

The ratio of WEOM in the total organic matters has a same variation along with its content, which has a reduction of 17.1-44.8% in the cultivated land compared to the uncultivated land. The experiment analysis reveals the content of WEOM varies greatly

http://www.aloki.hu ● ISSN 1589 1623 (Print) ● ISSN 1785 0037 (Online)
DOI: http://dx.doi.org/10.15666/aeer/1704_99259935

in the black soil after different years of reclamation and indicates that the reclamation is the main factor influencing the WEOM content in the black soil.

Table 2. *Variation of the water extractable organic matter contents with reclamation (a, b, c, and d are the grades of variation)*

Depth (cm)	Years	SOM (g/kg)	WEOM (mg/kg)	WEOM/SOM (%)
0-20	0	29.19a	86.65a	0.297
	5	29.27a	75.84b	0.259
	20	25.46b	72.36c	0.284
	50	25.43b	47.81d	0.188
	100	24.15b	71.79c	0.294
20-40	0	28.64a	80.98b	0.283
	5	28.36a	124.99a	0.441
	20	21.41b	71.83c	0.335
	50	23.63b	61.55e	0.26
	100	17.05c	65.28d	0.383

SOM: the soil organic matter; WEOM: the water extractable organic matter

Characteristics of three-dimensional fluorescence spectrum of the water extractable organic matter in black soils after different years of reclamation

Figure 2 is a collection of three-dimensional fluorescence spectrograms of WEOM in soil after different years of reclamation, which reflects great differences between these fluorescence spectrograms. As reported by Chen et al. (2015), a spectrogram shall be divided into 5 sections based on the wavelengths of excitation and emitting lights, the I section representing the tyrosine acid-like protein (for which the wavelength is 220-250 nm/280-330 nm), the II section the tryptophan acid-like protein (the wavelength is 220-250 nm/330-380 nm), the III section the fulvic acid-like substances (the wavelength is 220-250 nm/380-480 nm), the IV section the soluble microbial metabolites acid-like substances (the wavelength is 250-360 nm/280-380 nm), and the V section the humic acid-like substances (the wavelength is 250-420 nm/380-520 nm), respectively.

Suggested by *Figure 2,* the shapes of spectrograms and intensities of fluorescence vary with the reclamation years. The WEOM in all soil types is composed of the tyrosine acid-like protein, tryptophan acid-like protein, fulvic acid-like substances, soluble microbial metabolites acid-like substances, and humic acid-like substances, especially the latter three types. Compared with the uncultivated land being taken as the control group, the cultivated land was shown with evidently intensified fluorescence of the III section, which means the more enrichment of fulvic acid-like substances. After the reclamation of 100 years, the III and V sections reach to the maximum fluorescence intensities, especially for the III section with an evident peak value. Furthermore, in contrast, it is the top soil rather than the plough with the higher fluorescence density, mainly for the fulvic and humic acid-like substances. The difference shall be explained by the continued addition of organic matters into the top soil from the straw stubble per year, which resulted in the growing percentage of organic matters as well as humic organic matters in soil; but the much less organic matters applied to the plough stimulate the relatively lower activity of microorganisms.

http://www.aloki.hu ● ISSN 1589 1623 (Print) ● ISSN 1785 0037 (Online)
DOI: http://dx.doi.org/10.15666/aeer/1704_99259935

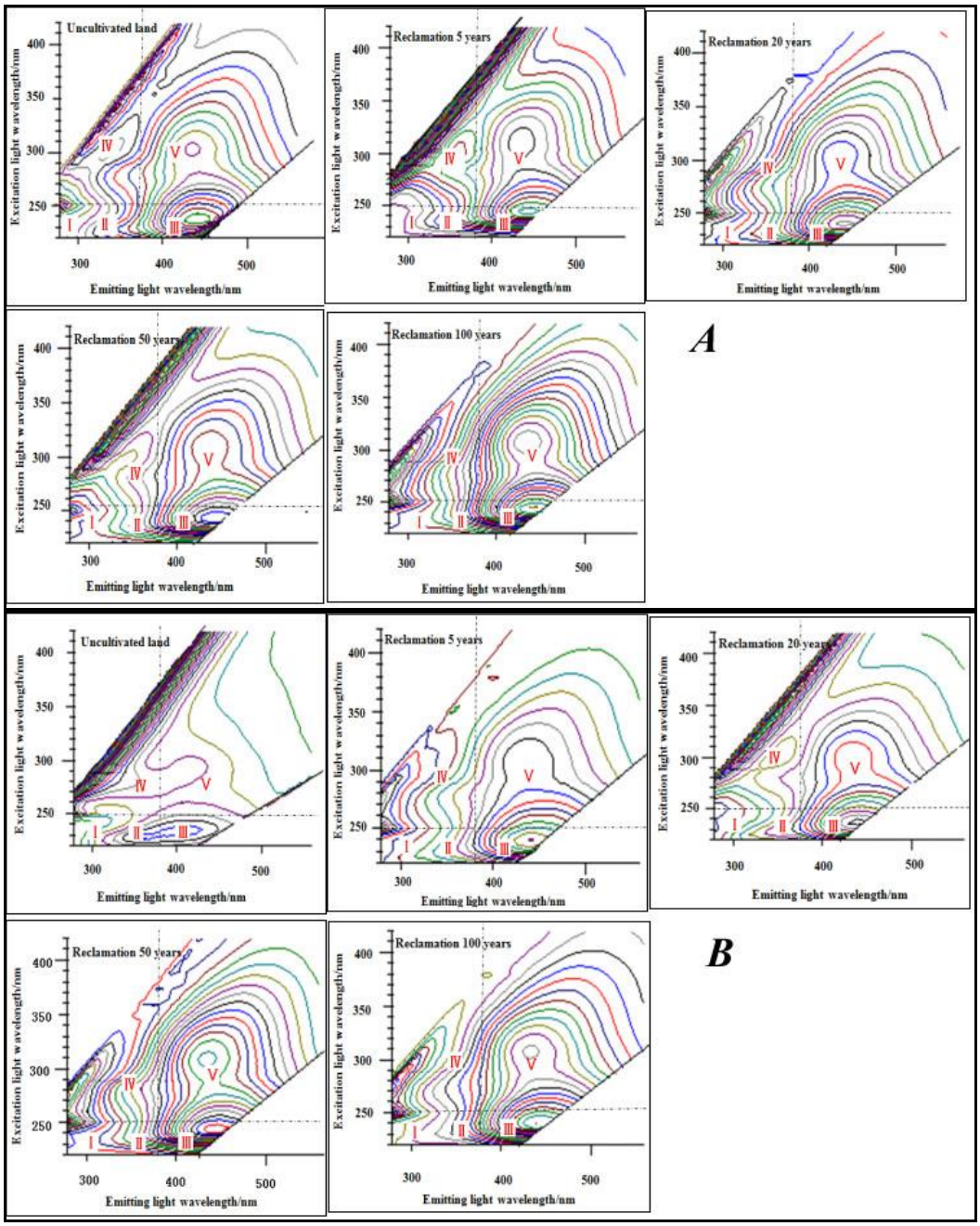

Figure 2. *The black soil of Fluorescence characteristics of the water extractable organic matter after different years of reclamation. (A: topsoil B: plough; the density of isoline represents the intensity of fluorescence I - tyrosine acid-like protein, II - tryptophan acid-like protein, III - fulvic acid-like substances, IV - soluble microbial metabolites acid-like substances, V - humic acid-like substances. The HATACH F-7000-type fluorescence spectrophotometer produced by Hitachi was used for the fluorescence spectrum analysis, with the xenon lamp as the light source of 150 W, the voltage of photomultiplier of 700 V, the silt widths for excitation and emitting lights of 5 nm)*

Basically identical with the results by Li et al. (2013), this research indicates the III and V sections have the most intensified fluorescence, which suggests the fulvic-acid and humic acid organic matters are most abundant in soil. With the fertilizer application

http://www.aloki.hu ● ISSN 1589 1623 (Print) ● ISSN 1785 0037 (Online)
DOI: http://dx.doi.org/10.15666/aeer/1704_99259935

for relieving the problems of reclamation, the fulvic-acid and humic acid organic matters accumulated in soil. The longer the reclamation continued, the more effects were on humic organic matters. It could be explained that with the reclamation, the accumulation of residues of plants gathered more microorganisms and produced a growing number of metabolites. Accordingly, the soil was substantially enriched by many types of fulvic acid and humic acid of complex structures and high aromaticity.

Semi-quantitative analysis of fluorescent substances in black soil after different years of reclamation

To compare the substance composition of black soil after different years of reclamation, the integral computation of fluorescence areas in *Figure 2* has been finished, and the results are shown in *Figure 3*.

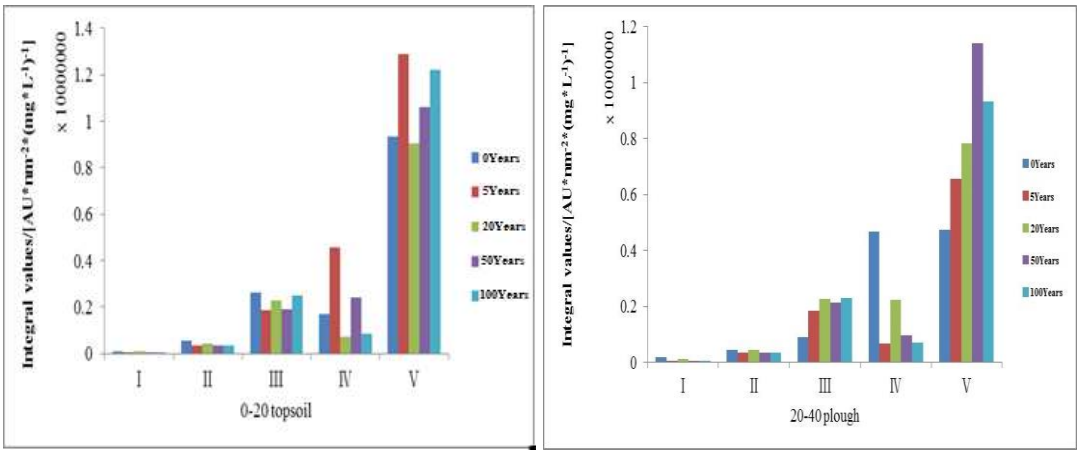

Figure 3. *Integral characteristics of I - V fluorescence areas of the water extractable organic matter after different years of reclamation. (0-20 underground for topsoil, 20-40 underground for plough by the origin)*

Figure 3 indicates the integral values are ordered decreasingly as V, III, IV, II and I. As for the top soil, the integral for the fluorescence area of II descended from 5.4×10^5 AU × nm^{-2} × $(mg \times L^{-1})^{-1}$ to 3.4×10^5 AU × nm^{-2} × $(mg \times L^{-1})^{-1}$, suggesting the less tryptophan acid-like protein in the WEOM; on the contrary, the more enrichment of humic acid-like substances is reflected by the increase of the integral for the fluorescence area of V from 9.3×10^6 AU × nm^{-2} × $(mg \times L^{-1})^{-1}$ to 12.2×10^6 AU × nm^{-2} × $(mg \times L^{-1})^{-1}$. This variation can be explained by the enhanced metabolic activities with reclamation, which utilized the water soluble tyrosine acid-like protein and tryptophan acid-like protein, and converted organic matters in soil to humic acid-like substances. However, the integral for the fluorescence area of III kept nearly stable, which is the sign of the stability of humic acid-like substances in content. As for the plough, it was also subject to the disturbance of reclamation, and the test results with the exception of the increasing content of humic acid are basically same with those in the top soil.

Figure 4 indicates the integral percentages of all sections. Conclusions can be drawn that the tyrosine acid-like protein and tryptophan acid-like protein represented by the I and II sections kept relatively lower integral percentages regardless of the years of reclamation; the percentage of fulvic-acid substances represented by the III section

http://www.aloki.hu ● ISSN 1589 1623 (Print) ● ISSN 1785 0037 (Online)
DOI: http://dx.doi.org/10.15666/aeer/1704_99259935

increases firstly until to the maximum value in the 20th years, and reduced in the following years; the percentage of the V section tended to increase, indicating the rising content of fulvic-acid organic matters in soil; besides, the nearly stable percentage of the IV section reflected the stabilized content of soluble microbial metabolites.

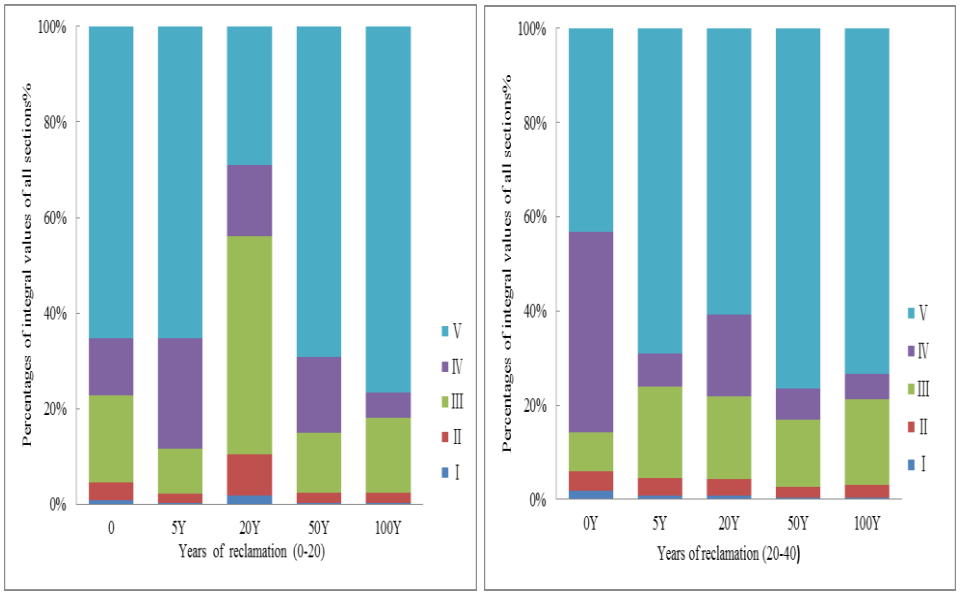

Figure 4. *Percentages of integrals of all sections. (0-20 for topsoil, 20-40 for plough) by the origin*

Analysis of locations of fluorescence peaks and fluorescence intensity

The fluorescence peaks and corresponding wavelengths of excitation and emitting lights for WEOM can characterize their structures and compositions. It is proved that the variation of molecule and aromaticity of a kind of fluorescence substance is reflected by the evolution of wavelengths of excitation and emitting lights at fluorescence peaks. If the wavelength lengthens (i.e. the lights have red shift), the aromaticity and molecule of fluorescence substance is considered increased; if the wavelength shortens (i.e. the lights have blue shift), the aromaticity and molecule of fluorescence substance is considered reduced (Fu et al., 2004). As can be seen in *Table 3,* for the top soil, the I and II areas have red shifts of excitation lights from 225 nm to 240 nm and from 230 nm to 245 nm, respectively. Such red shift suggests the obvious increase of molecules and aromaticity of tyrosine acid-like protein and tryptophan acid-like protein. Accordingly, more abundant proteins were generated in soil with reclamation. The emitting light of fulvic-acid substances at the peak has a red shift from 440 nm to 448 nm, indicating the increases in molecule, aromaticity and the degree of polymerization.

The excitation and emitting lights of the IV area at the peaks have no variation, which reflects the stability of molecule and aromaticity of soluble microbial metabolites acid-like substances. While for the area III, the excitation and emitting lights have red shifts from 235 nm to 245 nm and from 440 nm to 447 nm respectively, which is the sign of increasing content, aromaticity and molecule of fulvic-acid substances in the WEOM. But in comparison with the top soil, the smaller changes of aromaticity and

http://www.aloki.hu ● ISSN 1589 1623 (Print) ● ISSN 1785 0037 (Online)
DOI: http://dx.doi.org/10.15666/aeer/1704_99259935

molecules in the plough shall be explained by the weak disturbance of reclamation to the plough.

Table 3. *Wavelength and fluorescence intensity of excitation/emitting lights at fluorescence peaks for the water extractable organic matter in black soil after different years of reclamation*

Depth (cm)	Years	I		II		III		IV		V	
		Ex/Em (nm)	F	Ex/Em (nm)	F	Ex/Em (nm)	F	Ex/Em (nm)	F	Ex/Em (nm)	F
0-20	0	225/330	251.4	230/380	530.4	235/440	1043	250/380	430.8	250/440	923.7
	5	235/330	166.3	240/380	480.4	245/447	1011	250/380	474.1	250/448	978.1
	20	230/330	186.6	235/380	498.6	240/440	1048	250/380	437.5	250/442	950.3
	50	235/330	122.3	240/380	486.2	245/445	1025	250/380	438	250/443	962.3
	100	235/330	97.8	245/380	579.3	245/442	1302	250/380	533.2	250/444	1172
20-40	0	225/330	277.7	230/360	376.5	235/414	389.2	310/315	1962	310/315	1962
	5	230/330	141.3	235/380	395.3	240/444	823.1	250/380	327.9	250/440	716
	20	225/330	229	235/380	460	235/440	927.2	250/380	357	250/444	774.4
	50	235/330	137.8	240/380	527.5	245/441	1150	250/380	490.6	250/449	1031
	100	230/330	109.8	240/380	490.3	240/440	1089	250/380	435.1	250/445	933.2

Ex/Em: Excitation/emitting lights wavelength; F: Florescence intensity I- tyrosine acid-like protein, II- tryptophan acid-like protein, III- fulvic acid-like substances, IV- soluble microbial metabolites acid-like substances, V- humic acid-like substances

As indicated in *Table 3,* for the topsoil of 0-20 cm underground, the fluorescence intensity decreases with the reclamation, which suggests less tyrosine acid-like protein in the soil. But the increase of the area IV and the obvious increase in the areas III and V of the fluorescence intensity illustrate the rising contents of fulvic-acid, humic-acid and soluble microbial metabolites acid-like substances, respectively. Their increase can be attributed to the growth of content and activity of microorganisms in the soil promoting the transformation into humic humus. And the unclear changes in the area II indicate the nearly stable content of tryptophan acid-like protein regardless of the reclamation.

In this work, excitation and emitting lights of all fluorescence areas have shown red shift regardless of the reclamation years, which is different with the results from Fu et al. (2004). But a same conclusion of the two researches is that the increase of humic acid concentration results in the red shift of fluorescence peaks. The above distinction can be explained by the microorganism decomposition of plant residues, which is suggested the reason for the proliferation of protein-like substances. Therefore, the analysis of the structure and composition of WEOM in soil with the three-dimensional fluorescence spectrum technology in our research shall be an important theoretical basis for the future researches on micro-ecology of soil.

Conclusions

Mainly distributed in the provinces of Jilin and Heilongjiang, the northeast black soil region is an important grain production basis. However, the irrational cultivation

http://www.aloki.hu ● ISSN 1589 1623 (Print) ● ISSN 1785 0037 (Online)
DOI: http://dx.doi.org/10.15666/aeer/1704_99259935

method made the black soil eroded heavily and the water and soil loss increased. Up to now, the area of water and soil loss has accounted for 37.9% of the whole area. That is why the sustainable utilization of black soil and the interaction between the black soil and environment have been raised to the hot topics of researches, especially the researches about the organic matters in black soil.

In this test, 3D fluorescence spectroscopy was used to study the content, composition and structure of soil water-soluble organic matter in black soils with different reclamation years. The following conclusions: (1) the WEOM in soil has an obvious reduction with the transformation of natural soil into farmland soil, and the reduction is shown increasingly clear with reclamation; (2) the fulvic-acid organic matters have large increases in the molecule, aromaticity, and degree of polycondensation with reclamation; (3) the microorganisms in soil can conduct stronger metabolic activities after the reclamation starts, which utilize the tyrosine acid-like and tryptophan acid-like proteins, and convert more organic matters in soil to fulvic-acid organic matters; (4) the wavelength of emitting lights at the fluorescence peak for the humic-acid organic matters lengthens with reclamation, suggesting the increased molecule, aromaticity and degree of polycondensation. But the tyrosine acid-like, tryptophan acid-like proteins and soluble microbial metabolites acid-like substances keep basically stable contents, which indicates few effects of reclamation on their molecules and aromaticity. In the future, fluorescence spectroscopy, mathematical models, metrology chemistry and other methods should be combined to analyze the characteristics of different source components of DOM, as well as the effects of plant species and crop roots on DOM. The relationship between DOM characteristic substances and fluorescence intensity should be established, so that fluorescence quantization of characteristic substances will be carried out.

Acknowledgements. This work was supported by the National key R&D project sub-project (2017YFD0300405--4), Natural Science Foundation of Jilin Province, China (20170101077JC), Outstanding Young Talents Fund Project of Jilin Provincial Department of Science and Technology in 2019 (20190103109JH).

REFERENCES

[1] Chantigny, M. H. (2003): Dissolved and water-extractable organic matter in soils: A review on the influence land use and management practices. – Geoderma 113: 357-380.

[2] Chen, M., Lee, J. H, Hur, J. (2015): Effects of sampling methods on the quantity and quality of dissolved organic matter in sediment pore waters as revealed by absorption and fluorescence spectroscopy. – Environment Science Pollut. Res 22: 14841-14851.

[3] Christ, M. J, David, M. B. (1996): Dynamics of extractable organic carbon in Spodosol forest floors. – Soil Biology and Biochemistry 28: 1171-1179.

[4] Fu, P. Q, Liu, C. Q, Yin, Z. Y. (2004): Characterization of humic acid by three-dimensional excitation emission matrix fluorescence spectroscopy. – Geochimica 33(3): 301-308.

[5] Graham, A. M, Aiken, G. R, Gilmour, C. C. (2012): Dissolved organic matter enhances microbial mercury methylation under sulfidic conditions. – Environmental Science and Technology 46(5): 2715-2723.

[6] Hassouna, D. L, Massiani, C. Dudal, Y. (2010): Changes in water extractable organic matter (WEOM) in a calcareous soil under field conditions with time and soil depth. – Geoderma 155: 75-85.

http://www.aloki.hu ● ISSN 1589 1623 (Print) ● ISSN 1785 0037 (Online)
DOI: http://dx.doi.org/10.15666/aeer/1704_99259935

[7] Jones, D. L, Willett, V. B. (2006): Experimental evaluation of methods to quantify dissolved organic nitrogen (DON) and dissolved organic carbon (DOC) in soil. – Soil Biology & Biochemistry 38: 991-999.
[8] Landgraf, D., Leinweber, P., Makeschin, F. (2006): Cold and hot-water-extractable organic matter as indicators of litter decomposition in forest soils. – Journal of Plant Nutrition and Soil Science 169: 76-82.
[9] Li, M. T, Zhao, L. P, Zhang, J. J. (2013): Effect of temperature, pH and salt on fluorescent quality of water extractable organic matter in black soil. – Journal of Integrative Agriculture 12(7): 1251-1257.
[10] Liang, L., Luo, L., Zhang, S. Z. (2011): Adsorption and desorption of humic and fulvic acids on SiO2 particles at nano- and microscales. – Colloid Surf, A-Physicochem 384: 126-130.
[11] Liang, Q., Chen, H. Q, Gong, Y. S. (2012): 15 years of manure and inorganic fertilizers on soil organic carbon fractions in a wheat-maize system in the north China plain. – Nutrient Cycling in Agroecosystems 92: 21-33.
[12] McGill, W. B, Hunt, H. W, Woodmansee, R. G. (1981): Phoenix a model of the dynamics of carbon and nitrogen in grassland. – Ecol Bull 33: 49-53.
[13] Provenzano, M. R, Dorazio, V., Jerzykiewicz, M., Senesi, N. (2004): Fluorescence behaviour of Zn and Ni complexes of humic acids from different sources. – Chemosphere 55: 885-892.
[14] Shi, R. H., Bao, S. D. (1908): Soil and Agricultural Chemistry Analysis. – Agricultural Publishing House, Beijing.
[15] Wang, Y. T, Shi, H., Liu, X. F. (2016): Spectrofluorometric characterization of soil dissolved organic matter under different vegetation in Loess Hilly Region. – Journal of Plant Nutrition and Fertilizer 22(1): 171-179.
[16] Weishaar, J., Aiken, G., Bergamaschi, B. (2003): Evaluation of specific ultraviolet absorbance as an indicator of the chemical composition and reactivity of dissolved organic carbon. – Environmental Science &Technology 37: 4702-4708.

http://www.aloki.hu ● ISSN 1589 1623 (Print) ● ISSN 1785 0037 (Online)
DOI: http://dx.doi.org/10.15666/aeer/1704_99259935

STUDY ON THE ECOLOGICAL COMPENSATION SHARING IN THE CENTRAL LINE OF THE SOUTH-TO-NORTH WATER DIVERSION PROJECT

LIU, S. J.[1] – ZHANG, W. H.[1*] – YUN, J. W.[1] – KOU, Q. Q.[1] – BAO, L. L.[2] – LIU, J. J.[2]

[1]*Laboratory of Water Resource and Hydrology, College of Resources and Environment Southwest University, Chongqing 400715, China*

[2]*Chongqing Water Conservancy and Electricity Architectural Survey and Design Institute Chongqing 400700, China*

[*]*Corresponding author*
e-mail: swuwater@126.com; phone: +86-136-3782-2374

(Received 2nd Apr 2019; accepted 13th Jun 2019)

Abstract. The way to calculate and share the total amount of ecological compensation for inter-basin water transfer project is directly related to the enthusiasm of the water-receiving area in participating in the ecological protection of the water source area. This paper takes the water source area of the South-to-North Water Diversion Project and the water-receiving areas of Beijing, Tianjin, Hebei and Henan as the research objects, and using the single-index method, the comprehensive index method and the deviation method to make appropriate calculation for the ecological compensation amount of 6.248 billion yuan paid to the water source area each year by the water receiving area. The results show that the method of deviation is more objective, comprehensive and reasonable, which can provide a new idea for the ecological compensation apportion calculation of the Central Line of South-to-North Water Diversion Project.

Keywords: *inter-basin water transfer, water conservation, Shaanxi water source area, resource allocation, water trading, deviation method*

Introduction

Water is the source of all life and an important factor affecting human survival and development. The uneven distribution of water resources makes it necessary to build inter-basin water Diversion facilities between multi-water areas and water-deficient areas. Inter-basin water transfer can alleviate the problem of insufficient water savings in water-scarce areas and the imbalance of water resources in time and space effectively (Chen and Huang, 2006). But it changes the water conditions in the areas it passes through, and it will break the original ecological balance in the process of its application and management at the same time. In order to ensure the sufficiency and cleanliness of the water resources obtained by the water receiving area, it is necessary to do a good job in ecological protection of the water source areas and carry out necessary ecological compensation. Ecological compensation which means paying for ecological or environmental services is based on the purpose of ecological protection and the protection of ecosystems and species diversity through the operation of ecological compensation mechanisms (Hansen et al., 2018). Watershed ecological compensation is a powerful economic tool for addressing water management problems (Thieme et al., 2012). Ecological compensation involves measures to create positive conservation outcomes intended to offset the residual impacts of development (Brown et al., 2014). The inter-basin ecological compensation scheme is the result of the interaction between

http://www.aloki.hu ● ISSN 1589 1623 (Print) ● ISSN 1785 0037 (Online)
DOI: http://dx.doi.org/10.15666/aeer/1704_99379946

upstream and downstream cities, and is of great significance for the guidance of regional economic development (Zhang et al., 2018).

The ecological compensation of the river basin originated from the management and planning of the ecological service market. In the 1960s, soil erosion seriously affected the quality of living environment of the basin residents. To compensate the watershed residents, the US Tennessee Valley Authority (TVA) (Zhang and Liu, 2006) increased the protection of natural resources in the basin, and the prototype of the ecological compensation mechanism has been formed. Wunder et al. (2008) believed that the most ideal ecological compensation should fully integrate ecological services into the market. Ansink and Houba (2011) systematically studied and evaluated the impact and role of market forces in water extraction, delivery, and water pricing. At present, Germany, the United States, Japan and some other countries have accumulated relatively successful experiences and established a relatively complete ecological compensation framework system.

China began to study the issue of ecological compensation in the early 1990s. Zhang et al. (2013) proposed to calculate the amount of ecological compensation based on the loss of the rights to use resource. Cheng and Kai (2018) reviewed the mature theory and scientific mechanism of watershed ecological compensation, analysed the defects and shortcomings of ecological compensation theory, and provided a theoretical reference for the proposed compensation scheme. In addition, starting from the "Eleventh Five-Year Plan" in 2005, China has listed the construction of ecological compensation mechanism as the main point of work, and proposed the requirements for building it. It has been explored to establish an ecological compensation system in many places (Ji, 2018). Jiang et al. (2015) analysed the definition, necessity and principle of ecological compensation in the water source area of the inter-basin water transfer project, and studied the theoretical framework of ecological compensation in the water source area.

China is now doing more qualitative compensation studies, and there are few studies on the methods of quantitative compensation.

This paper calculated the ecological compensation amount that should be paid to the water source area by the water receiving area of the central route of the South-to-North Water Deversion Project, and the compensation amount of the four major water receiving areas in Beijing, Tianjin, Hebei and Henan was obtained.

Materials and methods

Profile of the study area

The Central Line of the South-to-North Water Diversion Project takes water from the Danjiangkou Reservoir. The total length of the main canal is 1432 km, and the annual average water transfer is 95 billion m^3 in recent years. Water is transferred from Hanzhong, Ankang and Shangluo to the main water receiving areas including Beijing, Tianjin, Hebei and Henan. And it provides protection for development of city , industry and agriculture. The diversion route diagram of the South-to-North Water Diversion Project is shown in *Figure 1*.

The cities as Hanzhong, Ankang and Shangluo have humid climates and abundant rainfall. The average annual rainfall of the three cities is 884.2 mm, which is higher than that in Shaanxi Province. The water resources are very rich. In 2017, the total water resources of Hanzhong, Ankang and Shangluo in southern Shaanxi were

http://www.aloki.hu ● ISSN 1589 1623 (Print) ● ISSN 1785 0037 (Online)
DOI: http://dx.doi.org/10.15666/aeer/1704_99379946

33.69 billion m^3, and the water production modulus was more than twice that of the province (Water Resources Department of Shaanxi Province, 2017).

The water source areas are all poor areas. In 2017, the total GDP of the three cities was 306.5 billion yuan, accounting for only 14% of the province's GDP. The per capita GDP rankings of Hanzhong City, Ankang City and Shangluo City are ranked lower in the province (Shaanxi Provincial Bureau of Statistics, 2017). Therefore, the state and the water receiving areas are required to provide certain compensation for water source areas.

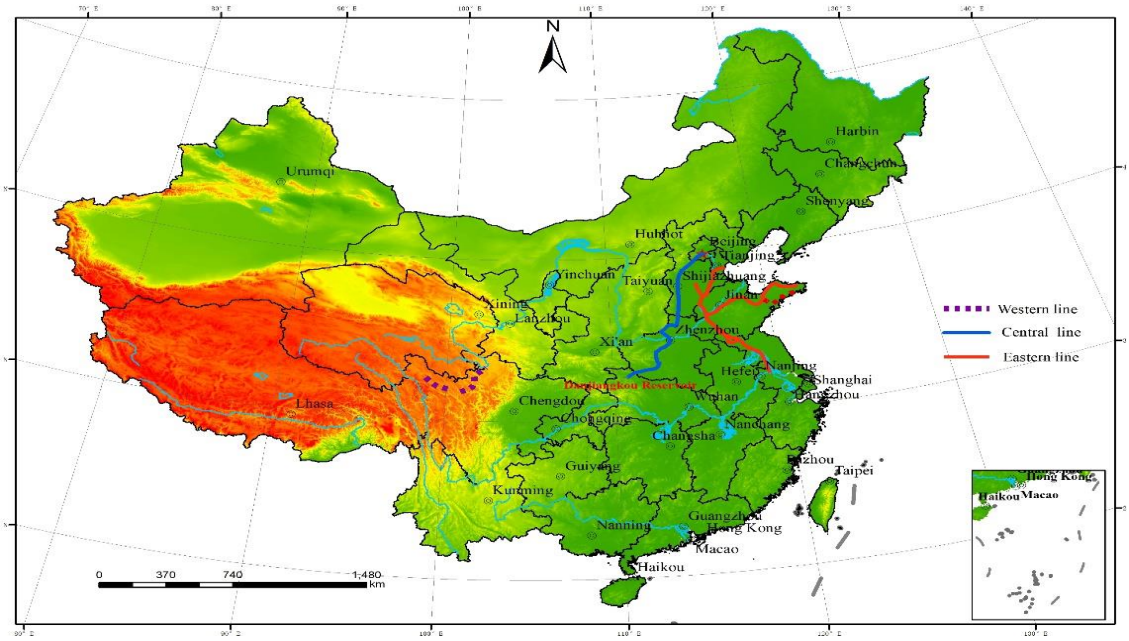

Figure 1. *The circuit diagram of the South-to-North Water Diversion Project*

Data processing

Considering the water and soil conservation construction in the water source area, the water market situation in the water management field, the value of water resources and the opportunity cost of future water resources dispatching, the total amount of ecological compensation is calculated. The compensation amount should be paid by the water receiving areas is 6.248 billion yuan/year. Drawing on the distribution ideas of water conservancy project cost allocation (Wang, 2016) and environmental capacity allocation (Chen et al., 2007), the ecological compensation amount payable for each water receiving area is calculated by using the single index method, the comprehensive index method and the deviation method, respectively.

The research basis of this paper is that the first phase of the South-to-North Water Diversion Project has an annual water transfer of 9.5 billion m^3, and the water transfer from the Shaanxi Water Source Area is 6.65 billion m^3, of which the distribution of water is equal to 0.13 in Beijing, 0.11 in Tianjin, 0.37 in Hebei and 0.4 in Henan.

According to the calculation results, the advantages and disadvantages of various apportion methods are compared and analysed, and a more reasonable apportionment method is determined.

http://www.aloki.hu ● ISSN 1589 1623 (Print) ● ISSN 1785 0037 (Online)
DOI: http://dx.doi.org/10.15666/aeer/1704_99379946

Methods

Single indicator method according to water consumption

According to the water consumption of each water receiving area, the average cost pricing method is used for distribution. (Liu, 2007; Zheng and Zhang, 2006). The calculation method is as shown in *Equation 1*.

$$C_i = \frac{q_i \times C}{\sum_{i=1}^{n} q_i} \quad \text{(Eq.1)}$$

where, C_i is the shared value of the i-th water receiving area; C is the total compensation amount; q_i is the water consumption of the i-th region (i=1, 2 ..., n). The same meaning in the symbolic sense.

Single indicator method according to the maximum payment capacity of the receiving area

According to the per capita GDP of each water receiving area, the corresponding compensation coefficient is determined. The specific method is as follows:

Assume that n water-receiving areas have GDP of GDP_i and population of p_i. The per capita GDP of each region accounts for the ratio of per capita GDP of the water-receiving area, and the calculation method (Zhang, 2003) is shown in *Equation 2*.

$$\alpha_i = \frac{\frac{GDP_i}{p_i}}{\frac{\sum GDP_i}{\sum p_i}} \quad \text{(Eq.2)}$$

Among them, $\alpha_i > 1$ indicates that the level of economic development of the i region is higher than the average level of the water receiving area; $\alpha_i < 1$ indicates that the level of economic development of the i region is lower than the average level of the water receiving area; $\alpha_i = 1$ indicates that the level of economic development of the i region is within the average level of the water receiving area. The proportion of compensation fees for each area β_i is determined according to the ratio of the per capita GDP of each area to the per capita GDP of the area (Zhang, 2003) and the way to caculate it is shown as *Equation 3*.

$$\beta_i = \frac{\alpha_i}{\sum \alpha_i} \quad \text{(Eq.3)}$$

Single indicator method according to the value of ecological environment services

The water diversion project can simultaneously improve the ecological environment service value of the water receiving areas and the water source areas. However, because the value of the ecological environment service of each water receiving area is difficult to define clearly, this paper uses the dry channel coverage and population of water use

http://www.aloki.hu ● ISSN 1589 1623 (Print) ● ISSN 1785 0037 (Online)
DOI: http://dx.doi.org/10.15666/aeer/1704_99379946

to estimate roughly. The specific algorithm is that the ratio of the length of the main canal in each water receiving area to the total length of the main canal and the proportion of water users to the total population of the water receiving area are determined as 4:6, and the compensation is calculated according to the benefit of each receiving area (Cao and Wang, 2009). Calculations can be done according to *Equation 4* and *Equation 5*.

$$C_i = C \times \delta_i \quad \text{(Eq.4)}$$

$$\delta_i = 0.4 \times \frac{l_i}{L} + 0.6 \times \frac{p_i}{P} \quad \text{(Eq.5)}$$

where δ_i is the coefficient of eco-environment service value; l_i is the length of the main canal in the i-th water receiving area; L is the total length of the main canal, which is 1432km; p_i is the water-receiving population of the i-th water receiving area; P is the total population of water users.

Comprehensive indicator method

The comprehensive indicator method is based on the calculation of the selected single-index method which is the comprehensive performance of the single-indicator method. The reasonableness weight of each single-indicator method is evaluated by expert scoring. Drawing on the ideas of the former (Chen et al., 2007) water environment capacity allocation, the proportion of the water consumption, the ability to pay, and the value of the ecological environment service are equal, all of which are 1/3. The methods for calculating them are shown in *Equation 6*, *Equation 7*, and *Equation 8*, respectively.

$$C_i = C \times \frac{\alpha_i + \beta_i + \delta_i}{3} \quad \text{(Eq.6)}$$

$$Q_i = \frac{q_i}{\sum_{i=1}^{n} q_i} \quad \text{(Eq.7)}$$

$$\beta_i = \frac{\alpha_i}{\sum_{i=1}^{n} \alpha_i} \quad \text{(Eq.8)}$$

In above equations, Q_i is the water consumption coefficient; β_i is the coefficient of payment capacity; δ_i is the coefficient of eco-environment service value.

Deviation method

The diviation method is not artificially determining the weighting coefficients of various sharing methods, but determining the weight by the degree of single sharing method approaching the average of multiple sharing methods (Chen et al., 2007). It is a

http://www.aloki.hu ● ISSN 1589 1623 (Print) ● ISSN 1785 0037 (Online)
DOI: http://dx.doi.org/10.15666/aeer/1704_99379946

commonly used and mature sharing method. Suppose there are n kinds of sharing methods, the average value of the sharing is x, and it is assumed that there is a weighting function w_j. When the sharing coefficient x_j of the j-th sharing method deviates from the mean x, it indicates that the accuracy of the sharing of the method is poor, and the obtained weight coefficient should be small; otherwise, the weight coefficient should be large.

The estimate X of the comprehensive sharing coefficient converges to the expected comprehensive sharing coefficient $\bar{x}$ according to the probability.

Results

Calculate according to the function constructed by the above methods and results of the three calculation methods are shown in *Table 1*, *Table 2*, and *Table 3*, respectively.

It can be seen from *Table 1* that according to the water consumption coefficient, the more water is used, the more compensation will be borne. According to the maximum payment capacity of the receiving area, the economic strength is strong, and the per capita GDP is high, so much more is paid. According to the value of the ecological environment service, the area with high canal coverage and more water users will pay more.

Table 1. *Sharing of compensation by single indicator methods (100 million yuan/year)*

Items	Beijing	Tianjin	Hebei	Henan
Water consumption coefficient	0.13	0.11	0.37	0.40
Compensation amount 1	8.11	6.87	23.10	24.97
Ability to pay coefficient	0.35	0.37	0.14	0.13
Compensation amount 2	21.85	23.10	8.74	8.11
Eco-environmental service value coefficient	0.20	0.17	0.21	0.43
Compensation amount 3	12.48	10.61	13.11	26.84

What can be inferred from *Table 2* is that the comprehensive indicator method considers the three impact factors of the single-indicator method, and the calculated result is the average of the three single-indicator methods.

Table 2. *Sharing of compensation by the comprehensive index method (100 million yuan / year)*

Items	Beijing	Tianjin	Hebei	Henan
Comprehensive sharing coefficient	0.23	0.22	0.24	0.32
Compensation amount	14.15	13.52	14.98	19.97

Using the deviation method to calculate the contribution of each water receiving area $C_{Beijing}$, $C_{Tianjin}$, C_{Hebei}, C_{Henan}, the sum is not necessarily equal to the total compensation amount C (Zhou, 2009). Therefore, it is necessary to standardize the amount of the contribution calculated by the deviation method. The calculation of the normalization coefficient is shown in *Equation 9*.

http://www.aloki.hu ● ISSN 1589 1623 (Print) ● ISSN 1785 0037 (Online)
DOI: http://dx.doi.org/10.15666/aeer/1704_99379946

$$\varepsilon = \frac{C}{C_{Beijing} + C_{Tianjin} + C_{Hebei} + C_{Henan}} \quad \text{(Eq.9)}$$

After standardization and adjustment, it can get 1.323 billion yuan/year in Beijing, 1.194 billion yuan/year in Tianjin, 1.40 billion yuan/year in Hebei Province, and 2.331 billion yuan/year in Henan Province.

Table 3. *Sharing of compensation by the deviation method (100 million yuan / year)*

Items	Beijing	Tianjin	Hebei	Henan	Sum
Water weight	0.32	0.35	0.20	0.44	
Payment weight	0.19	0.18	0.32	0.17	
Ecological service weight	0.48	0.47	0.48	0.39	
sharing factor X	0.21	0.19	0.22	0.36	0.97
Compensation amount	12.86	11.61	13.61	22.66	60.67

Comparison of different allocation methods

Make a comparison of calculation results of different methods (*Figure 2*), and compare the advantages and disadvantages of these methods.

Single indicator method: The calculation results are unstable and one-sided. The calculation process is simple, but using different indicators to calculate, the results shared by each water-receiving area are very different, which is easy to lead to doubts about the reliability of the methods and data used.

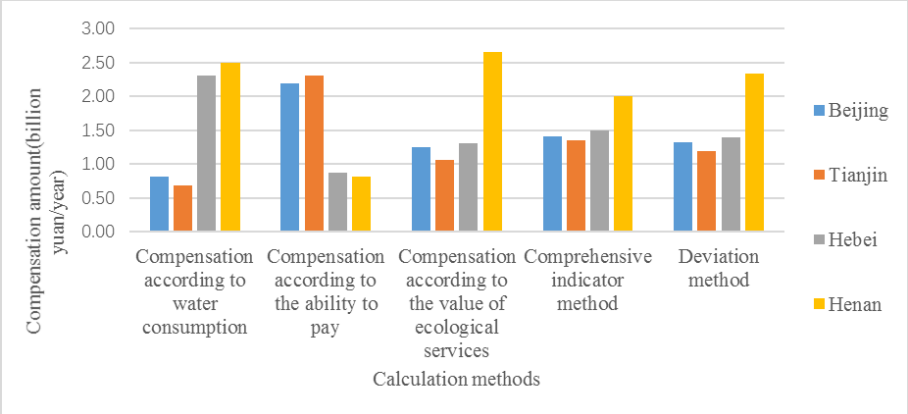

Figure 2. *Comparison of calculation results of different methods*

Comprehensive indicator method: Compared with the comprehensive indicator method, the results are more stable, but the proportion of each individual indicator is artificially determined. It is very subjective, and its objectivity and fairness are easily questioned.

Deviation method: Considering a variety of factors, and the sharing coefficient is determined according to the mathematical model rather than artificial distribution, and the sharing process is transparent and open. Therefore, the method of deviation is a more comprehensive and objective method of compensation.

http://www.aloki.hu ● ISSN 1589 1623 (Print) ● ISSN 1785 0037 (Online)
DOI: http://dx.doi.org/10.15666/aeer/1704_99379946

Discussion

Analysis of the rationality of using the deviation method:

1. It is assumed that the net benefit of national economic use in a certain year after 2018 is B_d, and the annual compensation for ecological construction is C_d. The benefit-to-input ratio is Kd and the way to calculate it is shown in *Equation 10*.

$$K_d = \frac{B_d}{C_d} \quad \text{(Eq.10)}$$

When $K_d \leq 1$, the ecological compensation amount of the water receiving area exceeds the amount of benefits it receives, which will make the project lose its economic significance, so it is necessary to make $K_d > 1$ (Shi et al., 2009). According to the experts of the Yangtze River Water Resources Commission, the direct benefits of the Central Line of the South-to-North Water Diversion Project in terms of water supply and flood control are estimated to have an average annual benefit of 45.6 billion yuan per year. From the difference flat method, the amount of water-receiving burden is 6.248 billion yuan/year, which is far less than the comprehensive benefit of citing water resources, and there is $K_d > 1$.

2. According to the principle of individual rationality, the amount of compensation undertaken by the participating regions should not be greater than the cost of water resources from other sources. Otherwise, the payment will be too high to pay the ecological compensation.

In 2018, the value of surface water resources in Tianjin is 4 yuan/ m^3, and the value of surface water resources in Beijing is about 3.64 yuan/m^3. The value of water resources will continue to increase. The second phase of the Central Line of the South-to-North Water Diversion Project has a water transfer capacity of 6.65 billion m^3/year from Shaanxi, which means that the value of the water resources from Shaanxi water source area of the Central Line of the South-North Water Diversion Project in 2019 is 0.94 yuan/ m^3. It can be seen that the cost of citing water from Shaanxi water source area is much less than the cost of obtaining water resources from other sources.

Conclusions

1. The method of deviation is the most comprehensive and objective method for calculating the ecological compensation sharing method.

2. Using the deviation method to share the ecological compensation amount of Shaanxi water source area, the scores are 1.323 billion yuan/year in Beijing, 1.194 billion yuan/year in Tianjin, and 1.40 billion yuan/year in Hebei Province, Henan. The province has 2.31 billion yuan / year.

This paper only puts forward a basic idea of inter-basin water transfer ecological compensation sharing, and does not give a clear commentary on the specific implementation of ecological compensation. And there is no specific details of the implementation process of an ecological compensation mechanism, such as the way to make collection of compensation funds, methods for solving water pollution problems along the central line of the South-to-North Water Deversion Project and some other measures. It is recommended that future research can be carried out in these directions to ensure a smoother and healthier compensation mechanism.

http://www.aloki.hu ● ISSN 1589 1623 (Print) ● ISSN 1785 0037 (Online)
DOI: http://dx.doi.org/10.15666/aeer/1704_99379946

Acknowledgements. This research is financially supported by "Fundamental Research Funds for the Cen tral Universities No. XDJK2019F002" and Chongqing social livelihood key research and development pr ojects, No.cstc2018jscx-mszdX0052, and the support was gratefully acknowledged.

REFERENCES

[1] Ansink, E., Houba, H. (2011): Market Power in Water Markets. – Journal of Environment al Economics and Management 64(2): 237-252.
[2] Brown, M. A., Clarkson, B. D., Stephens, R. T., Barton, B. J. (2014): Compensating for ecological harm – the 2008 state of play in New Zealand. – New Zealand Journal of Ecology 1: 139-146.
[3] Cao, M. D., Wang, F. Y. (2009): Study on the legal issues of Inter-basin Water Diversion ecological compensation: Taking the water source area (Henan part) of the central route of the South-to-North Water Diversion Project as an example. – Journal of Graduate School of the Chinese Academy of Social Sciences 12: 6-13.
[4] Chen, J., Huang, W. (2006): Risks and countermeasures of Inter-basin Long-distance Water Diversion Project. – China Water Resources 114: 11-14.
[5] Chen, D. J., Lu, J., Jin, S. Q. (2007): Estimation and allocation of water environment capacity of non-point source polluted rivers. – Entironmental science 128: 1416-1423.
[6] Cheng, X., Kai, F. (2018): Research Review of Ecological Compensation Mechanism in Drainage Basin. – Journal North China University Water Resources Electric Power 34: 9-13.
[7] Hansen, K., Duke, E., Bond, C., Purcell, M., Paige, G. (2018): Rancher preferences for a payment for ecosystem services program in Southwestern Wyoming. – Ecological Economics 146: 240-249.
[8] Ji, P. C. (2018): Accelerate the improvement of ecological compensation mechanism in China's river basins. – Environmental Protection: 41-46.
[9] Jiang, R. G., Xie, J. C., Zhu, J. W. (2015): Theoretical framework of ecological compensation in water source area of inter-basin water transfer project. – Bulletin of Soil and Water Conservation 35: 273-277.
[10] Liu, Y. L. (2007): Ecological compensation and watershed ecological co-construction and sharing. – China Water Resources and Hydropower Press, Beijing.
[11] Shaanxi Provincial Bureau of Statistics (2017): Shaanxi Statistical Yearbook. – China Statistics Press.
[12] Shi, S. J., Li, H. E., Lin, Q. C. (2009): Study on the method of sharing ecological compensation amount of inter-basin water transfer. – Journal of Hydraulic Engineering 40: 268-273.
[13] Thieme, M. L., Rudulph, J., Higgins, J., Takats, J. A. (2012): Protected areas and freshwater conservation: a survey of protected area managers in the Tennessee and Cumberland River Basins, USA. – Journal of Environmental Management 109: 189-199.
[14] Wang, H. N. (2016): Hydropower project investment cost sharing method and application. – Communication of Finance and Accounting: 73-77.
[15] Water Resources Department of Shaanxi Province (2017): 2016 Shaanxi Water Resources Bulletin.
[16] Wunder, S., Engel, S., Pagiola, S. (2008): A Comparative Analysis of Payments for Environmental Services Programs in Developed and Developing Countries. – Ecological Economics 65: 834-852.
[17] Zhang, C. L. (2003): Research on compensation mechanism of water resources recover. – China Institute of Water Resources and Hydropower Research, Beijing.
[18] Zhang, H. Y., Liu, G. G. (2006): Design of ecological compensation mechanism for river basins in China. – Environmental Protection 10(A): 49-54.

http://www.aloki.hu ● ISSN 1589 1623 (Print) ● ISSN 1785 0037 (Online)
DOI: http://dx.doi.org/10.15666/aeer/1704_99379946

[19] Zhang, J., Yang, J. X., Chen, X. (2013): Study on the calculation method of water resources ecological compensation quota in river basin. – Chinese Society of Environmental Sciences Academic Annual Meeting: 10W-1097.
[20] Zhang, M., Zhou, J. H., Zhou, R. J. (2018): Interval Multi-Attribute Decision of Watershed Ecological Compensation Schemes Based on Projection Pursuit Cluster. – Water 10: 1280-1282.
[21] Zheng, H. X., Zhang, L. B. (2006): Study on quantitative standards for compensation of watershed ecological services. – Environmental Protection 1(A): 42-46.
[22] Zhou, Z. P. (2009): Application of deviation method in compensation distribution in water-receiving areas. – Information Technology Market Weekly Theoretical Research: 141-142.

http://www.aloki.hu ● ISSN 1589 1623 (Print) ● ISSN 1785 0037 (Online)
DOI: http://dx.doi.org/10.15666/aeer/1704_99379946

ANALYSIS OF CARBON EMISSION REDUCTION AND PRICING FOR SUSTAINABLE CLOSED-LOOP SUPPLY CHAIN CONSIDERING THE QUALITY OF RECYCLED PRODUCTS

WAN, P.* – MA, L. X. – LIU, J. N.

School of Management Engineering, Qingdao University of Technology, Qingdao 266520, Shandong Province, China
(e-mail: 2044772948@qq.com, wpie99@126.com)

**Corresponding author*
e-mail: pengwan@qut.edu.cn; phone: +86-532-8687-5070

(Received 5th Apr 2019; accepted 13th Jun 2019)

Abstract. Sustainable closed-loop supply chains have attracted attention due to environmental protection problems and resource shortages. The quality of recycled products is an important factor in reverse logistics. Based on Stackelberg game theory, we propose two sustainable closed-loop supply chain models: a centralized decision model and a decentralized decision model, and assume that the manufacturer considers the recycling quality level of used products. We compare the differences in the optimal decisions from different decision-makers and analyze the influence of relevant parameters on these decisions in a sustainable closed loop supply chain. From the comparative analysis and numerical analysis, it was observed that the model yields the best decision result and carbon emission reduction level under the centralized decision condition. The recycling quality level is found to be higher in the centralized decision model than in the decentralized decision model, and the sales price is found to be lower in the centralized decision model than in the decentralized decision model. Moreover, the impacts on the carbon emission reduction level, the recycling quality level, and corporate profit are found to be related to the carbon emission preference coefficient of consumers, the recycling effort cost coefficient, and the carbon emission investment cost coefficient.
Keywords: *environmental constraints, game theory, carbon emission, recycling effort, remanufacturing, sustainable supply chain*

Introduction

With the progress in production technology and the diversification of consumer demand, product life cycles are becoming shorter, product upgrades are becoming faster, and the number of eliminated and used products has increased dramatically. At the same time, the Earth's resources are dwindling, and the call for sustainable development is growing. This has made the world's major countries give more consideration to problems of energy conservation and environmental protection. Resource and environmental pressure, as well as laws, regulations, and consumer awareness of environmental protection, are increasing. The recycling and remanufacturing of used products have become a hot issue. Since closed-loop supply chains (CLSCs) have achieved significant results in sustainable development management practices, CLSCs have also become an important topic in the academic area (Savaskan et al., 2004; Savaskan and Van Wassenhove, 2006).

For enterprises, on the one hand, recycling of used products is the responsibility of manufacturers. Recycling of used products can reduce carbon emissions, save resources, reduce negative impacts on the environment, create a good corporate image, and improve the competitiveness of enterprises. On the other hand, enterprises can realize value-added materials, save on costs, and improve their profits through recycling and reuse of used

http://www.aloki.hu ● ISSN 1589 1623 (Print) ● ISSN 1785 0037 (Online)
DOI: http://dx.doi.org/10.15666/aeer/1704_99479963

products (Govindan et al., 2016). From the perspective of recycling, because the time, frequency, and method of a consumer's use of a product may differ, the degree of loss of the product can also be various. According to the different degrees of product loss, we divide recycled products into different quality levels. The quality of recycled products is one of the main factors affecting the operation of a closed-loop supply chain. Low-quality recycled products have a negative effect on enterprises that remanufacture used products (Rahman and Subramanian, 2012). Therefore, the quality level of recycled products is an issue for remanufacturers to consider and is also one of the focuses of our research.

After the Copenhagen climate conference, a low-carbon economy, which pursues a reduction in energy consumption, pollution, and greenhouse gas (GHG) emissions, was listed as one of the most important strategies for global climate change mitigation. Olugu and Wong state that one of the objectives of closed-loop supply chain management is to reduce carbon emissions (Olugu and Wong, 2012). The recycling of used products through a closed-loop supply chain to reduce carbon emissions is a part of reverse logistics. For forward logistics, the manufacturing of new products also needs to consider the problem of reducing carbon emissions. The study of carbon emissions from a sustainable closed-loop supply chain perspective focuses not only on emissions at specific stages of production (such as used product recycling), but also on the social and environmental impacts of a product over its entire life cycle (Metta and Badurdeen, 2013). A carbon emission reduction not only affects the profit of a closed-loop supply chain, but also affects the pricing and recycling decisions of supply chain members. Enterprises need to operate under certain environmental incentives and seek the optimal pricing and emission reduction strategies under the sustainable development goals (Ding et al., 2015).

Carbon emission reduction involves the joint efforts of a sustainable closed-loop supply chain's members. In a closed-loop supply chain where the manufacturer is responsible for recycling, the manufacturer may increase the cost of the product through a low-carbon investment. However, due to consumers' awareness of the environmental features of the product, the cost increase will increase consumers' intention to purchase the product, increase the sales price, and promote increases in the scale of sales. It benefits retailers from a carbon emissions reduction perspective as well. Recycling of used products and investment in new products that reduce carbon emissions have environmental benefits. We consider the following questions: How do manufacturers weigh the impact of recycling quality on carbon reduction levels? How does the retailer decide the selling price? How do the recycling quality level, carbon emission reduction level, recovery rate, consumer preferences, emission reduction and recycling investment coefficient, and other relevant factors affect each other?

This study considers these carbon emissions reduction and pricing decision problems considering recycling quality in the context of a sustainable closed-loop supply chain. Consumer preferences, such as recycling quality, carbon emissions reduction level, and sales price, are used as decision variables to establish a sustainable closed-loop supply chain decision-making model and find out how manufacturers can adjust their own recycling policies and emission reduction investment strategies to maximize revenue. Then, through a numerical simulation, we analyze the impact of recovery rate on recovery quality, emissions reduction level, pricing, and closed-loop supply chain profit. Our goal is not only to enhance the sustainable closed-loop supply chain decision-making optimization theory, but also provide a theoretical basis for enterprises to make emissions

http://www.aloki.hu ● ISSN 1589 1623 (Print) ● ISSN 1785 0037 (Online)
DOI: http://dx.doi.org/10.15666/aeer/1704_99479963

reduction decisions, recycling decisions, and pricing decisions as well as promote the realization of emissions reduction targets.

Our study contributes to the literature in three main regards. First, our study investigates the quality of recycled products in a sustainable closed-loop supply chain for carbon emissions reduction, which complements the existing literature in which sustainable closed-loop supply chains for carbon emissions reduction are not considered (Shu et al., 2018; Xu and Wang, 2018). Second, our work compares a centralized decision CLSC model with a decentralized decision CLSC model for manufacturers who directly recycle used products. We obtain a few appealing management insights. Third, our model analyzes the impact of various factors on decision-making in, and the profits of, CLSCs.

Review of literature

We review the following three streams of literature related to this work: closed-loop supply chains that consider the quality level of recycled products; closed-loop supply chain pricing, and closed-loop supply chains for carbon emissions reduction.

Closed-loop supply chains that consider the quality level of recycled products

Many researchers have discussed the quality level of recycled products in closed-loop supply chains. Guide et al. (2003) studied used product recovery pricing and remanufactured product sales pricing issues for a variety of quality grades. They assumed that the quality grades of used products are sensitive to the recovery cost. Savaskan et al. (2004) assumed that recovery quality is a random variable subject to a uniform distribution, and discussed the selection of recycling strategies in different environments. Dobos and Richter (2006) introduced recycled product quality into a production–recycling system, and assumed that if a recycled product's quality level is too low, it cannot be used in the remanufacturing process. Galbreth and Blackburn (2006) studied the optimal recovery and remanufacturing classification strategy under the condition of uncertain quality of recovered products. In their classification strategy, recycled products are generally treated in one of two ways after testing: if their unit remanufacturing cost is lower than the optimal cost level, they are used in remanufacturing production; otherwise, they are directly abandoned. Mukhopadhyay and Ma (2009) studied optimal procurement and production decisions in remanufacturing systems with uncertain quality of and demand for recycled products. Özkır and Başlıgıl (2012) described the specific features of green supply chain design with consideration of end-of life products and pointed out that considering the quantity and quality of recycled products can improve the system's profitability. Chen et al. (2015) designed a two-stage dynamic closed-loop supply chain that considers uncertainty in the quantity and quality of recycled products as well as differences in the willingness-to-pay of consumers. Jerbia et al. (2018) studied a closed-loop supply chain network design problem. A scenario-based approach was used to model the uncertainties in return rates, revenues, costs, and the quality of returns. Tan and Guo (2019) studied the impact of regulatory environments on the operation of a logistics system that considers the uncertainty in the quality of recycled products and the controllability of the remanufacturing technology level. The models discussed above consider the quality of recycled products in network or channel selection; they do not consider the impact of the quality of recycled products on pricing decisions and carbon emissions reductions. Next, we review the literature on closed-loop supply chain pricing.

http://www.aloki.hu ● ISSN 1589 1623 (Print) ● ISSN 1785 0037 (Online)
DOI: http://dx.doi.org/10.15666/aeer/1704_99479963

Closed-loop supply chain pricing

As an important function of a closed-loop supply chain, pricing has a direct impact on product demand and competitive advantage. Ferrer and Swanminathan (2006) studied closed-loop supply chain pricing decisions in a monopoly environment and explored the effect of various parameters on the Nash equilibrium. Swanminathan and Ferrer (2010) analyzed two-period, multiperiod, and infinite planning horizons in a monopoly environment, and characterized the optimal remanufacturing and pricing strategy. Bulmus et al. (2014) considered differences in recycling quality level, divided used products into several different types, and determined the recycling price of different types of used products and the selling price of new products. Gan et al. (2017) developed a pricing decision model for short life-cycle products in a closed-loop supply chain and found that scaling factors influence both the pricing decisions and the profits of the supply chain's members. Gao et al. (2016) provided centralized and decentralized game-theoretic models of a CLSC and investigated optimal decisions on collection effort and pricing under different channel power structures. Ke et al. (2018) studied a pricing and remanufacturing decision problem in a fuzzy closed-loop supply chain with one manufacturer, two competitive retailers, and one third-party collector. Taleizadeh et al. (2019) studied pricing decisions and discounts on returned products in a multiperiod, multi-echelon, and sustainable closed-loop supply chain. Some researchers have also considered the quality of recycled products when studying pricing in closed-loop supply chains. Zou and Ye (2015) studied pricing strategies for and the coordination mechanism of a supply chain when the remanufacturing cost is random and caused by a recycled product's quality. Taleizadeh et al. (2017) proposed a joint optimization model of pricing strategies, quality levels, effort decisions, and return policies by considering the reference price effect in a three-level supply chain under different channel power structures. The abovementioned studies have taken into account the impact of recycled products' quality level in pricing decisions; however, they did not consider environmental constraints.

Closed-loop supply chains for carbon emissions reduction

The research related to our work concerns carbon emission issues in a closed-loop supply chain. Feng et al. (2017) estimated the economic benefits associated with policy regulations for manufacturers in a low-carbon technology market. They indicated that when the punishment levied on a manufacturer is sizable, the manufacturer will be prone to developing innovative technology. The objective when reducing carbon emissions is not only to respect environmental regulations; it is also to increase profit. Unlike forward supply chains, Brandenburg et al. (2014) believed that environmental and social issues have received very little attention in CLSC models. Carbon emissions have only recently been incorporated into reverse supply chain and CLSC modeling. Govindan et al. (2015) emphasized the need for the investigation of environmental issues and new directions in reverse logistics and closed-loop supply chain research. Fareeduddin et al. (2015) proposed models for three common regulatory policies to optimize not only costs but also emissions in supply chain operations. Tao et al. (2015) studied the CLSC network equilibrium problem in a multiperiod planning horizon, where manufacturers make homogeneous products and have two types of mandatory carbon emission. He et al. (2016) evaluated the impact of consumer free riding on carbon emissions across a product's life cycle in a dual-channel closed-loop supply chain. Bazan et al. (2017) considered the carbon emissions from and the energy cost of a vendor-managed inventory with a consignment stock policy. Xu et

http://www.aloki.hu ● ISSN 1589 1623 (Print) ● ISSN 1785 0037 (Online)
DOI: http://dx.doi.org/10.15666/aeer/1704_99479963

al. (2017) analyzed the effect of considering carbon emissions on the design of both hybrid and dedicated CLSCs. Fang et al. (2017) studied carbon emission reductions under a carbon cap-and-trade scheme and reverse logistics in a production routing problem. Shu et al. (2018) studied optimal decisions for closed-loop supply chains in the framework of social responsibility and explored the impacts of carbon emissions constraints and corporate social responsibility on recycling and remanufacturing decisions. Turki and Rezg (2018) provided an optimal design for a manufacturing/remanufacturing system that differentiates between new and remanufactured products and sorts the used products into three quality levels. Yang et al. (2017) considered two competitive supply chains under the cap-and-trade scheme and studied pricing and carbon emissions reduction decisions. Li et al. (2017) studied the influence of vertical and horizontal cooperation models on the optimal decisions for and performance of a low-carbon closed-loop supply chain with respect to pricing, carbon emissions reduction, used product collection, and profit.

It can be seen from the above literature that the quality level of recycled products has a great impact on the performance of a closed-loop supply chain. Although the quality of recycled products can be graded and the recycling price can vary, this increases the difficulties that recyclers face. It is easier to recycle used products at a set quality level and a fixed price. Therefore, unlike previous research, we consider that the market demand depends on the sale price and the carbon emissions reduction level set by the manufacturer. We carry out the study in accordance with a fixed quality level of recycled products, research pricing and carbon emissions reduction decisions in a closed-loop supply chain, and analyze the sensitivity of the main parameters using a numerical example. We hope to provide a theoretical basis on which related enterprises can make recycling and carbon emissions reduction decisions.

Materials and methods

Assumptions and model description

This section may be divided by subheadings. It should provide a concise and precise description of the experimental results, their interpretation as well as the experimental conclusions that can be drawn.

From an environmental protection perspective, reductions in carbon emissions are conventionally considered to be a burden for manufacturers. This paper considers a closed-loop supply chain composed of a manufacturer and a retailer. The manufacturer uses new materials to make new products and also remanufactures used products. The manufacturer is responsible for recycling used products that are recovered directly from consumers. The retailer is responsible for the sale of the products. In a forward supply chain, the unit cost of manufacturing a new product is c_m, w is the wholesale price of the product as determined by the manufacturer, the selling price of the retailer is p, and the market demand is a linear function of price and the carbon emissions reduction. In a reverse supply chain, the manufacturer divides the used products into different quality levels according to the degree of damage, which is represented by $q\ (0<q<1)$. The unit recovery cost of an old product that the manufacturer recovers from a consumer is represented by $A(q)$, which is a function of the quality of the recovered product. The higher the quality of the recovered product, the higher the recovery cost. $A(q)=aq$, a is the maximum unit recovery price of a used product that the manufacturer pays to the customer. The used product recycling rate is

http://www.aloki.hu ● ISSN 1589 1623 (Print) ● ISSN 1785 0037 (Online)
DOI: http://dx.doi.org/10.15666/aeer/1704_99479963

ε, which is considered to be an exogenous variable, such as government regulations. We only consider carbon emissions in the production process. The manufacturer can improve their carbon emissions reduction technology to reduce the carbon emissions per unit product.

To simplify the research problem and facilitate the analysis, we make the following assumptions:

(1) The manufacturer is the core enterprise of the supply chain and is the leader in the game process. We do not consider an out-of-stock scenario; namely, the production quantity is the market demand. Remanufactured products and new products are sold at the same price, with no difference in quality and performance. Considering the cost advantage, manufacturers give priority to using remanufactured products to meet the market demand. Following Atasu et al. (2013), it is assumed that all recycled products are used in the remanufacturing process. The unit cost of remanufacturing is denoted by $c_r(q)$, and is a function of the quality of the recycled product $\left(c_r(q) < c_m\right)$. Let $c_r(q) = c_m - c_s q$. Then, is the unit cost savings through remanufacturing. To ensure that the remanufacturing process is feasible, let $c_s q < A(q)$, i.e., $a < c_s$.

(2) The manufacturer needs to invest in low-carbon production technologies to reduce its carbon emissions. Only investment in carbon emissions reduction for new products is considered here, and the required capital is a one-time investment, which is independently undertaken by the manufacturer. The reduction rate per unit product is $\lambda(0 < \lambda < 1)$. Following Ghosh and Shah (2012), the emissions reduction cost that the manufacturer pays is $\beta\lambda^2/2$, where β denotes the carbon emissions reduction investment cost coefficient, which is a large number.

(3) To recycle higher-quality used products, manufacturers must pay higher effort costs. Similarly to the cost of the carbon emissions reduction investment, let $I(q) = Kq^2$. $K(K > 0)$ denotes the recycling effort cost coefficient, which is a large number.

(4) The demand is a linear function of the manufacturer's carbon emissions reduction level and the retailer's sales price. Following Liu et al. (2012) and Zhang et al. (2014), the demand function is $D = V - bp + \gamma\lambda$, where V denotes the potential demand scale of the market, b is the sensitivity coefficient of the retail price, and γ is the coefficient of consumers' carbon emissions reduction preferences.

In addition, we assume that both manufacturers and retailers are risk-neutral, and we ignore the carbon emissions of retailers in this study. The subscript c denotes a centralized decision.

Modeling and decision analysis

Based on the above assumptions, let $c(q) = c_m(1-\varepsilon) + c_r(q)\varepsilon$. The simplification $c(q) = c_m - c_s q\varepsilon$, the manufacturer's revenue π_m, and the retailer's revenue π_r are exhibited as follows:

$$\begin{aligned}\max \pi_m &= (p - c_m + \varepsilon c_s q)(V - bp + \gamma\lambda) - a\varepsilon q(V - bp + \gamma\lambda) - (\beta\lambda^2/2) - Kq^2 \\ &= (w - c_m + (c_s q - a)\varepsilon q)(V - bp + \gamma\lambda) - (\beta\lambda^2/2) - Kq^2\end{aligned} \quad \text{(Eq.1)}$$

http://www.aloki.hu ● ISSN 1589 1623 (Print) ● ISSN 1785 0037 (Online)
DOI: http://dx.doi.org/10.15666/aeer/1704_99479963

$$\max \pi_r = (p - w)(V - bp + \gamma\lambda) \quad \text{(Eq.2)}$$

The total supply chain profit is expressed as follows:

$$\pi = \pi_m + \pi_r \quad \text{(Eq.3)}$$

The decentralized decision system for the manufacturer as leader

We assume that, in this situation, the manufacturer is a leader and the retailer is a follower in a Stackelberg game. The partners' action order is given as follows: (1) the manufacturer determines the carbon emissions reduction rate λ, the wholesale price w, and the quality level of recycled products q; then (2) based on the manufacturer's declared decisions, the retailer determines the sales price p.

We first derive the optimal reaction of the retailer.

Proposition 1. In a decentralized decision situation, after determining the wholesale price w, the carbon emissions reduction rate λ, and the recycled product quality level q, the optimal sales price for the retailer is (*Eq. 4*):

$$p^* = \frac{V + \gamma\lambda + bw}{2b} \quad \text{(Eq.4)}$$

Proof of Proposition 1. For *Equation 2,* the first-order partial derivation of π_r to p can be expressed as

$$\frac{\partial \pi_r}{\partial p} = V - 2bp + \gamma\lambda + bw \quad \text{(Eq.5)}$$

We use the second-order partial derivatives to confirm the optimality:

$$\frac{\partial^2 \pi_r}{\partial p^2} = -2b \quad \text{(Eq.6)}$$

Equation 6 indicates that π_r is concave. Therefore, the succeeding first-order conditions can be obtained by setting *Equation 5* to zero

$$V - 2bp + \gamma\lambda + bw = 0 \quad \text{(Eq.7)}$$

We can obtain *Equation 4* by solving *Equation 7;* thus, Proposition 1 is proven.

From *Equation 4* it can be seen that the optimal retail price is a linear function of the carbon emissions reduction level and the wholesale price and increases monotonously. Therefore, manufacturers can influence retailers' optimal pricing decisions through carbon emissions reduction and wholesale price decisions.

Now that we know the retailer's decisions, we can derive the manufacturer's optimal decision. We substitute *Equation 4* into *Equation 1* to obtain the manufacturer's optimal profit function:

http://www.aloki.hu ● ISSN 1589 1623 (Print) ● ISSN 1785 0037 (Online)
DOI: http://dx.doi.org/10.15666/aeer/1704_99479963

$$\max \pi_m = \left(w - c_m + \varepsilon c_s q - a\varepsilon q\right)\left(\frac{V + \gamma\lambda - bw}{2}\right) - \left(\frac{\beta\lambda^2}{2}\right) - Kq^2 \quad \text{(Eq.8)}$$

Proposition 2. In a decentralized decision situation, the manufacturer's optimal decision is obtained as follows:

$$w^* = \frac{\left(c_s - a\right)^2 \beta V b\varepsilon^2 + 2Kc_m\gamma^2 - 4K\beta bc_m - 4K\beta V}{\left(c_s - a\right)^2 \beta b^2\varepsilon^2 + 2K\gamma^2 - 8K\beta b} \quad \text{(Eq.9)}$$

$$\lambda^* = \frac{\left(bc_m - V\right)2K\gamma}{\left(c_s - a\right)^2 \beta b^2\varepsilon^2 + 2K\gamma^2 - 8K\beta b} \quad \text{(Eq.10)}$$

$$q^* = \frac{\left(c_s - a\right)\left(bc_m - V\right)\beta b\varepsilon}{\left(c_s - a\right)^2 \beta b^2\varepsilon^2 + 2K\gamma^2 - 8K\beta b} \quad \text{(Eq.11)}$$

Proof of Proposition 2. To find the optimal wholesale price w, the carbon emission reduction level λ, and the recovery quality level q, the first-order derivative of *Equation 8* to w, λ, and q can be expressed as:

$$\frac{\partial \pi_m}{\partial w} = \frac{V + \gamma\lambda - 2bw + bc_m - b\varepsilon c_s q + ba\varepsilon q}{2} \quad \text{(Eq.12)}$$

$$\frac{\partial \pi_m}{\partial \lambda} = \left(w - c_m + \varepsilon c_s q - a\varepsilon q\right)\left(\frac{\gamma}{2}\right) - \beta\lambda \quad \text{(Eq.13)}$$

$$\frac{\partial \pi_m}{\partial q} = \left(\varepsilon c_s - a\varepsilon\right)\left(\frac{V + \gamma\lambda - bw}{2}\right) - 2Kq \quad \text{(Eq.14)}$$

The Hessian matrix of the objection functions of the manufacturer's profit is expressed as follows:

$$H\left(\pi_m\right) = \begin{bmatrix} -b & \frac{\gamma}{2} & \left(\frac{-b}{2}\right)\left(\varepsilon c_s - a\varepsilon\right) \\ \frac{\gamma}{2} & -\beta & \left(\frac{\gamma}{2}\right)\left(\varepsilon c_s - a\varepsilon\right) \\ \left(\frac{-b}{2}\right)\left(\varepsilon c_s - a\varepsilon\right) & \left(\frac{\gamma}{2}\right)\left(\varepsilon c_s - a\varepsilon\right) & -2K \end{bmatrix} \quad \text{(Eq.15)}$$

According to this paper's assumptions, we derive $\left|H\left(\pi_m\right)_1\right| = -b < 0$ and $\left|H\left(\pi_m\right)_2\right| = \frac{1}{2}\left(2b\beta - \gamma^2\right) > 0$, when $\left|H\left(\pi_m\right)_3\right| = -2b\beta K + \left(\frac{\gamma}{2}\right)^2 2K + \left(\varepsilon c_s - a\varepsilon\right)^2\left(\frac{b}{2}\right)^2\beta < 0$,

http://www.aloki.hu ● ISSN 1589 1623 (Print) ● ISSN 1785 0037 (Online)
DOI: http://dx.doi.org/10.15666/aeer/1704_99479963

which indicates that the Hessian matrix is negative-definite. Hence, π_m is jointly concave in (w, λ, q). Consequently, we can obtain the unique optimal solutions (w^*, λ^*, q^*) with the conditions assumed by the following first-order differential equations:

$$\begin{cases} \dfrac{\partial \pi_m}{\partial w} = \dfrac{V + \gamma\lambda - 2bw + bc_m - b\varepsilon c_s q + ba\varepsilon q}{2} = 0 \\ \dfrac{\partial \pi_m}{\partial \lambda} = \left(w - c_m + \varepsilon c_s q - a\varepsilon q\right)\left(\dfrac{\gamma}{2}\right) - \beta\lambda = 0 \\ \dfrac{\partial \pi_m}{\partial q} = \left(\varepsilon c_s - a\varepsilon\right)\left(\dfrac{V + \gamma\lambda - bw}{2}\right) - 2Kq = 0 \end{cases} \quad \text{(Eq.16)}$$

Solving *Equation 16*, *Equations 9*, *10*, *11* can be obtained; thus, Proposition 2 is proven.

Proposition 3. In the decentralized decision case, the retailer's optimal sales price is

$$p^* = \frac{\left(c_s - a\right)^2 V\beta b\varepsilon^2 - 6KV\beta + 2Kc_m\left(\gamma^2 - \beta b\right)}{\left(c_s - a\right)^2 \beta b^2\varepsilon^2 + 2K\gamma^2 - 8K\beta b} \quad \text{(Eq.17)}$$

Proof of Proposition 3. By Propositions 1 and 2, we can obtain that Proposition 3 holds.

Using *Equations 9, 10, 11, 17, 1, and 2,* π_r^*, π_m^*, and π can be expressed as follows:

$$\pi_r^* = \frac{4b\left(K\beta bc_m - KV\beta\right)^2}{\left(\left(c_s - a\right)^2 \beta b^2\varepsilon^2 + 2K\gamma^2 - 8K\beta b\right)^2} \quad \text{(Eq.18)}$$

$$\pi_m^* = \frac{-\left(bc_m - V\right)^2 \beta K}{\left(\left(c_s - a\right)^2 \beta b^2\varepsilon^2 + 2K\gamma^2 - 8K\beta b\right)} \quad \text{(Eq.19)}$$

$$\pi = 2K\beta\left(6Kb\beta - K\gamma^2 - \left(c_s - a\right)^2 \beta b^2\varepsilon^2\right)\left(\frac{\left(bc_m - V\right)}{\left(c_s - a\right)^2 \beta b^2\varepsilon^2 + 2K\gamma^2 - 8K\beta b}\right)^2 \quad \text{(Eq.20)}$$

The centralized decision system

In the case of centralized decision, manufacturers and retailers jointly determine the sales price, carbon emissions reduction level, and recycled product quality level to maximize the profit of the whole supply chain. Thus, the profit of the whole supply chain is

$$\pi_c = \left(p - c_m + \left(c_s - a\right)\varepsilon q\right)\left(V - bp + \gamma\lambda\right) - \left(\beta\lambda^2 / 2\right) - Kq^2 \quad \text{(Eq.21)}$$

http://www.aloki.hu ● ISSN 1589 1623 (Print) ● ISSN 1785 0037 (Online)
DOI: http://dx.doi.org/10.15666/aeer/1704_99479963

Proposition 4. In the centralized decision case, the optimal decision for the whole supply chain is given as follows:

$$p_c^* = \frac{\left(c_s - a\right)^2 Vb\beta\varepsilon^2 + 2Kc_m\gamma^2 - 2Kbc_m\beta - 2KV\beta}{\left(c_s - a\right)^2 b^2\beta\varepsilon^2 + 2K\gamma^2 - 4Kb\beta} \quad \text{(Eq.22)}$$

$$\lambda_c^* = \frac{\left(2Kbc_m - 2KV\right)\gamma}{\left(c_s - a\right)^2 b^2\beta\varepsilon^2 + 2K\gamma^2 - 4Kb\beta} \quad \text{(Eq.23)}$$

$$q_c^* = \frac{\left(bc_m - V\right)b\beta\left(c_s - a\right)\varepsilon}{\left(c_s - a\right)^2 b^2\beta\varepsilon^2 + 2K\gamma^2 - 4Kb\beta} \quad \text{(Eq.24)}$$

Proof of Proposition 4. To find the optimal sale price p_c, carbon emissions reduction level λ_c, and recovery quality level q_c, the first-order derivative of *Equation 21* to p, λ, and q can be expressed as

$$\frac{\partial\pi_c}{\partial p} = V - bp + \gamma\lambda - b\left(p - c_m + \left(c_s - a\right)\varepsilon q\right) \quad \text{(Eq.25)}$$

$$\frac{\partial\pi_c}{\partial\lambda} = \left(p - c_m + \left(c_s - a\right)\varepsilon q\right)\gamma - \beta\lambda \quad \text{(Eq.26)}$$

$$\frac{\partial\pi_c}{\partial q} = \left(V - bp + \gamma\lambda\right)\left(c_s - a\right)\varepsilon - 2Kq \quad \text{(Eq.27)}$$

The Hessian matrix of the objection functions of the whole supply chain's profit is expressed as follows:

$$H\left(\pi_c\right) = \begin{bmatrix} -2b & \gamma & -b\varepsilon\left(c_s - a\right) \\ \gamma & -\beta & \left(c_s - a\right)\varepsilon\gamma \\ -b\varepsilon\left(c_s - a\right) & \left(c_s - a\right)\varepsilon\gamma & -2K \end{bmatrix} \quad \text{(Eq.28)}$$

According to this paper's assumptions, we derive $\left|H\left(\pi_c\right)_1\right| = -2b < 0$ and $\left|H\left(\pi_c\right)_2\right| = 2b\beta - \gamma^2 > 0$, if $\left|H\left(\pi_c\right)_3\right| = \left(\gamma^2 - 2b\beta\right)2K + \beta b^2\varepsilon^2\left(c_s - a\right)^2 < 0$, which indicates that the Hessian matrix will be negative-definite. Therefore, when $\left(\gamma^2 - 2b\beta\right)2K + \beta b^2\varepsilon^2\left(c_s - a\right)^2 < 0$, i.e. $0 < \varepsilon < \sqrt{\frac{\left(2b\beta - \gamma^2\right)2K}{\beta b^2\left(c_s - a\right)^2}}$, the objection functions of the whole supply chain's revenue are jointly concave in (p , λ , q). For that reason, we can obtain the unique optimal solutions ($p_c^*, \lambda_c^*, q_c^*$) with the conditions assumed by the following first-order differential equations:

http://www.aloki.hu ● ISSN 1589 1623 (Print) ● ISSN 1785 0037 (Online)
DOI: http://dx.doi.org/10.15666/aeer/1704_99479963

$$\begin{cases} \dfrac{\partial \pi_c}{\partial p} = V - bp + \gamma\lambda - b\left(p - c_m + \left(c_s - a\right)\varepsilon q\right) = 0 \\ \dfrac{\partial \pi_c}{\partial \lambda} = \left(p - c_m + \left(c_s - a\right)\varepsilon q\right)\gamma - \beta\lambda = 0 \\ \dfrac{\partial \pi_c}{\partial q} = \left(V - bp + \gamma\lambda\right)\left(c_s - a\right)\varepsilon - 2Kq = 0 \end{cases} \quad \text{(Eq.29)}$$

Solving *Equation 29, Equations 22, 23,* and *24* can be obtained; thus, Proposition 4 is proven.

Using *Equations 22, 23 and 21,* π_c^* can be expressed as follows:

$$\pi_c = \frac{-\left(bc_m - V\right)^2 K\beta}{\left(\left(c_s - a\right)^2 b^2\beta\varepsilon^2 + 2K\gamma^2 - 4Kb\beta\right)} \quad \text{(Eq.30)}$$

Proposition 5. In both centralized decision cases and decentralized decision cases, the supply chain profit, sales price, carbon emissions reduction level, and recycled product quality level satisfy the following relationships:

$$\text{i) } \pi_c^* > \pi \text{, ii) } p_c^* < p^* \text{, iii) } \lambda_c^* > \lambda^* \text{, iv) } q_c^* > q^* .$$

Proof of Proposition 5. Using *Equations 20* and *30*, *Equations 17* and *22*, *Equations 10* and *23*, and *Equations 11* and *24*, respectively, we can obtain

$$\Delta\pi = \pi_c^* - \pi = \frac{\left(-16\right)b^2\left(bc_m - V\right)^2 K^3\beta^3}{\left(\left(c_s - a\right)^2 b^2\beta\varepsilon^2 + 2K\gamma^2 - 4Kb\beta\right)\left(\left(c_s - a\right)^2\beta b^2\varepsilon^2 + 2K\gamma^2 - 8K\beta b\right)^2} > 0 \quad \text{(Eq.31)}$$

$$\Delta p = p_c^* - p^* = \frac{8K^2\beta\left(V - bc_m\right)\left(\gamma^2 - \beta b\right)}{\left(\left(c_s - a\right)^2 b^2\beta\varepsilon^2 + 2K\gamma^2 - 4Kb\beta\right)\left(\left(c_s - a\right)^2\beta b^2\varepsilon^2 + 2K\gamma^2 - 8K\beta b\right)} < 0 \quad \text{(Eq.32)}$$

$$\Delta\lambda = \lambda_c^* - \lambda^* = \frac{-8\beta b\left(bc_m - V\right)K^2\gamma}{\left(\left(c_s - a\right)^2 b^2\beta\varepsilon^2 + 2K\gamma^2 - 4Kb\beta\right)\left(\left(c_s - a\right)^2\beta b^2\varepsilon^2 + 2K\gamma^2 - 8K\beta b\right)} > 0 \quad \text{(Eq.33)}$$

$$\Delta q = q_c^* - q^* = \frac{-4K\left(bc_m - V\right)\left(c_s - a\right)\beta^2 b^2\varepsilon}{\left(\left(c_s - a\right)^2 b^2\beta\varepsilon^2 + 2K\gamma^2 - 4Kb\beta\right)\left(\left(c_s - a\right)^2\beta b^2\varepsilon^2 + 2K\gamma^2 - 8K\beta b\right)} > 0 \quad \text{(Eq.34)}$$

i.e., $\pi_c^* > \pi$, $p_c^* < p^*$, $\lambda_c^* > \lambda^*$, and $q_c^* > q^*$. Thus, Proposition 5 is proven.

Proposition 5 shows that, compared with a decentralized decision, a centralized decision for the supply chain yields greater profits, produces a greater reduction in

http://www.aloki.hu ● ISSN 1589 1623 (Print) ● ISSN 1785 0037 (Online)
DOI: http://dx.doi.org/10.15666/aeer/1704_99479963

carbon emissions, and provides consumers with lower prices, but also has higher requirements for the quality of recycled products.

Results and numerical analysis

We further verify and analyze the above conclusions through numerical examples. The definite values for the relevant parameters are as follows: $V=30$, $b=2$, $\gamma=1$; $a=2$, $K=10$, $\beta=20$, $c_m=6$, $\varepsilon=0.4$, and $c_s=4$. Plugging the above values of the relevant parameters into the models, we obtain the values of the sales price, the carbon emissions reduction rate, the recycled product quality level, the manufacturer's profit, the retailer's profit, and the supply chain's profit in the two models. The two tables below show the effect of the recovery rate intensity on the optimal values in the different model, calculated using the above parameter values.

Table 1 shows that, as the recovery rate increases, the sales price decreases and the total CLSC profit and recycled product quality level increase in the centralized CLSC model. *Table 2* shows that, as the recovery rate increases, the manufacturer's wholesale price decreases, the profit of retailers and manufacturers increases, and the carbon emissions reduction level and recycled product quality level increase. Comparing *Tables 1* and *2,* we can see that both the carbon emissions reduction level and the recovery quality level in the centralized decision case are higher than those in the decentralized decision case. That means that a focus on a centralized decision in a closed-loop supply chain will make it easier to meet emission reduction targets and recycle used products.

Table 1. *The influence of recovery rate on the centralized closed-loop supply chain (CLSC) model*

	Recovery rate intensity								
ε	**0.1**	**0.2**	**0.3**	**0.4**	**0.5**	**0.6**	**0.7**	**0.8**	**0.9**
Total CLSC profit	41.0959	41.3476	41.7741	42.3862	43.2000	44.2381	45.5312	47.1204	49.0612
Sales price	10.5479	10.5207	10.4745	10.4082	10.3200	10.2075	10.0675	9.8953	9.6850
Carbon emissions reduction level	0.2283	0.2297	0.2321	0.2355	0.2400	0.2458	0.2530	0.2678	0.2726
Recycled product quality level	0.0913	0.1838	0.2785	0.3768	0.4800	0.5898	0.7083	0.8377	0.9812

Table 2. *The influence of recovery rate on the decentralized CLSC model*

	Recovery rate intensity								
ε	**0.1**	**0.2**	**0.3**	**0.4**	**0.5**	**0.6**	**0.7**	**0.8**	**0.9**
CLSC profit	30.6713	30.7955	31.0046	31.3019	31.6920	32.1813	32.7781	33.4929	34.3389
Manufacturer's profit	20.3979	20.4597	20.5636	20.7108	20.9032	21.1433	21.4342	21.7800	22.1857
Retailer's profit	10.2734	10.3358	10.4410	10.5911	10.7888	11.0380	11.3439	11.7129	12.1532
Sales price	12.7902	12.7835	12.7723	12.7563	12.7355	12.7095	12.6780	12.6405	12.5965
Carbon emissions reduction level	0.1133	0.1137	0.1142	0.1151	0.1161	0.1175	0.1191	0.1210	0.1233
Recycled product quality level	0.0453	0.0909	0.1371	0.1842	0.2323	0.2819	0.3334	0.3872	0.4437
Wholesale price	10.5238	10.5102	10.4874	10.4551	10.4129	10.3602	10.2964	10.2205	10.1315

The unit cost savings through remanufacturing reflect the manufacturer's remanufacturing capacity, but also affect the supply chain profit and other variables.

http://www.aloki.hu ● ISSN 1589 1623 (Print) ● ISSN 1785 0037 (Online)
DOI: http://dx.doi.org/10.15666/aeer/1704_99479963

The influence of the unit cost savings through remanufacturing on both CLSC models is shown in *Figures 1* and *2*.

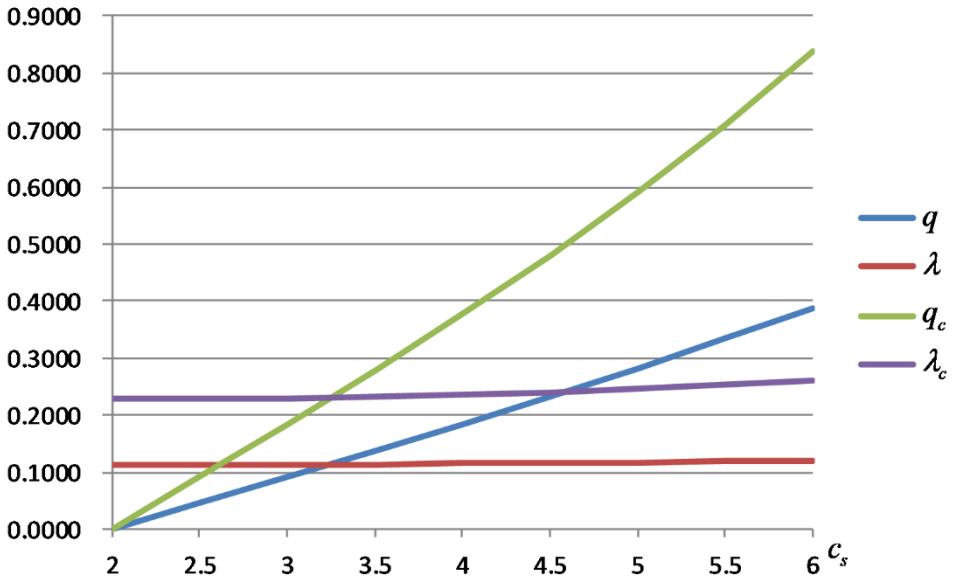

Figure 1. *The effects of C_s on the carbon emissions reduction level and the recycled product quality level*

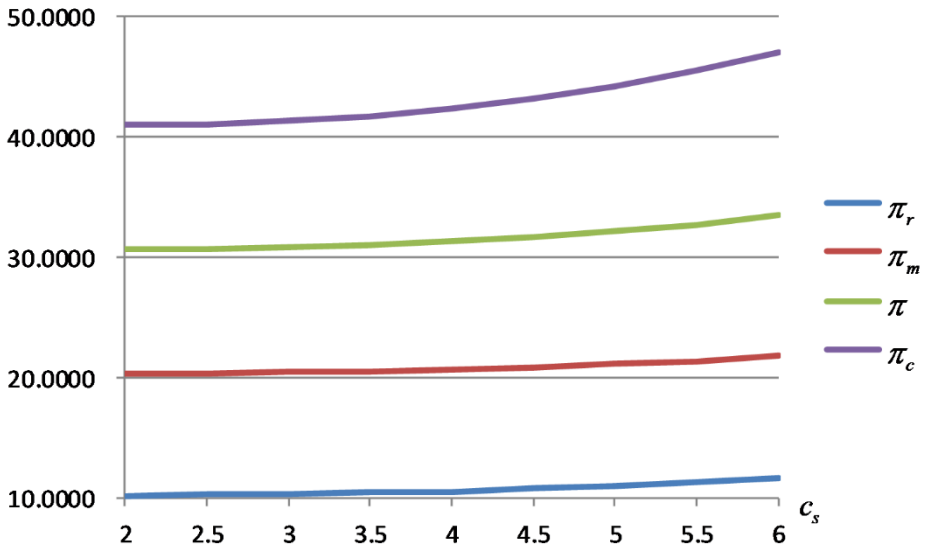

Figure 2. *The effects of C_s on profits*

Figure 1 shows that, as the unit cost saving increases, the recovery quality increases, and the range of variation in the centralized decision case is greater than that in the decentralized decision case. The change in unit cost savings has less of an impact on the carbon emissions reduction level. However, the carbon emissions reduction level in the centralized decision case is still greater than that in the decentralized decision case.

http://www.aloki.hu ● ISSN 1589 1623 (Print) ● ISSN 1785 0037 (Online)
DOI: http://dx.doi.org/10.15666/aeer/1704_99479963

Figure 2 shows that, as the cost savings increase, the profit of the supply chain increases in the decentralized decision case and the centralized decision case, and the profit in the centralized decision case increases faster. This means that, with an increase in cost savings, manufacturers are more willing to recycle used products and earn more from recycling old products. Manufacturers recycle used products more; the lower the unit production costs, and the lower the wholesale prices, the more profit that retailers obtain.

Figure 3 shows that the recovery rate is proportional to the recycled product quality level and the carbon emissions reduction level. In the centralized decision case, the requirements for the quality level of recycled products are higher than those in the decentralized decision case. The impact of recovery rate on the carbon emissions reduction level is not significant. In comparison, the effect of recovery rate on the carbon emissions reduction level in the centralized decision case is better.

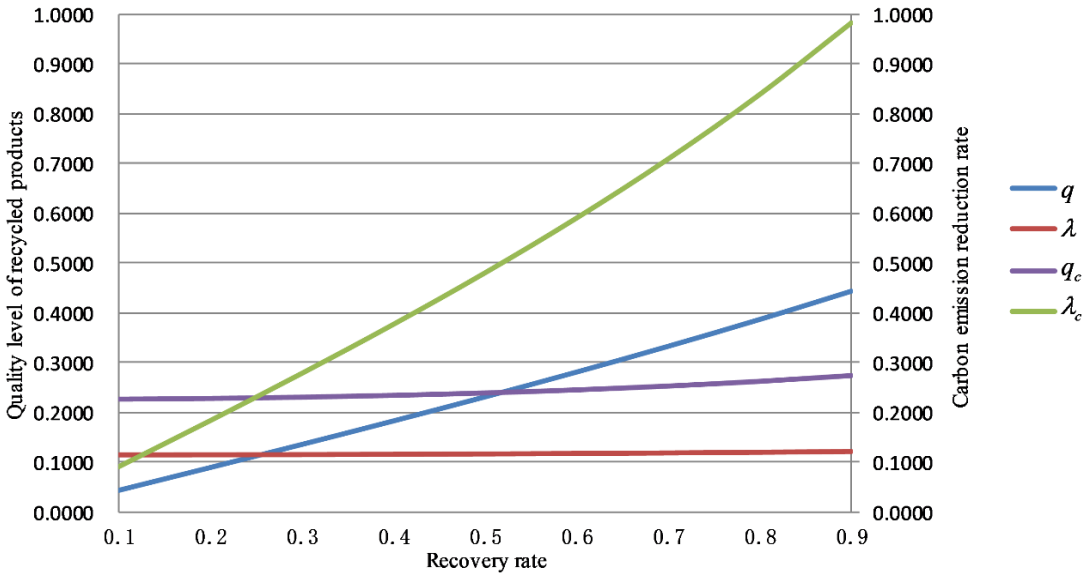

Figure 3. *The effects of ε on the recycled product quality level and the carbon emissions reduction level*

Conclusions and discussion

In this study, we proposed CLSC decision models consisting of a manufacturer and a retailer in which manufacturers recycle used products directly and improve the quality level of the used products through their recycling efforts. We investigated how carbon emissions reduction and pricing decisions in a CLSC are affected by the quality level of recycled products, and how the market demand depends on the sales price and the carbon emissions reduction level.

This paper compared a centralized decision model with a decentralized decision model, and investigated the changes in the optimal recycled product quality level and the profit of the supply chain members, as well as the pricing and carbon emissions reduction decisions, under the two models. The effects of the recovery rate, remanufacturing cost savings, the recovery price, the carbon emissions reduction investment cost coefficient, and the recovery effort cost coefficient on the quality level of recycled products were analyzed. Our conclusions can be summarized as follows:

http://www.aloki.hu ● ISSN 1589 1623 (Print) ● ISSN 1785 0037 (Online)
DOI: http://dx.doi.org/10.15666/aeer/1704_99479963

An increase in the recycling rate and the unit cost savings through remanufacturing will increase the quality level of recycled products as well as the carbon emissions reduction level. However, the increase in the carbon emissions reduction level is not significant.

Compared with the decentralized decision case, the centralized decision case has higher requirements on the quality level of recycled products and is more conducive to the reduction of carbon emissions per unit product.

The sales price in the centralized decision case is lower than that in the decentralized decision case, and the recovery price also has a positive effect on sales pricing. Improving consumers' environmental awareness not only helps the sustainable closed-loop supply chain members set higher prices, but also improves the quality level of recycled products.

Although we have contributed to the literature on closed-loop supply chains, our work has its limitations. First, we assumed that the manufacturer recycles used products that are recovered directly from consumers. However, in reality, used products can also be recycled by retailers or third-party recyclers. Therefore, this study could be extended in the future by considering different recycling channels. Second, we only considered investments in carbon emissions reduction for new products in this paper. Thus, future research could further consider carbon abatement investments in new and remanufactured products together. Third, we considered as identical new products and remanufactured ones. Therefore, future research could consider consumers' different preferences for new products and remanufactured products and study the impact of the quality level of recycled products on sustainable closed-loop supply chain decisions based on consumers' behavioral preferences.

Acknowledgements. The authors thank the editor and the three anonymous referees fo**r** their constructive comments and suggestions. This work was supported by the Humanities and Social Sciences Research Program of Shandong Education Department, No. J18RA088.

REFERENCES

[1] Atasu, A., Toktay, L. B., Van Wassenhove, L. N. (2013): how collection cost structure drives a manufacturer's reverse channel choice. – Production and Operations Management 22: 1089-1102.

[2] Bazan, E., Jaber, M. Y., Zanoni, S. (2017): Carbon emissions and energy effects on a two-level manufacturer-retailer closed-loop supply chain model with remanufacturing subject to different coordination mechanisms. – International Journal of Production Economics 183: 394-408.

[3] Brandenburg, M., Govindan, K., Sarkis, J., Seuring, S. (2014): Quantitative models for sustainable supply chain management: developments and directions. – European Journal of Operational Research 233: 299-312.

[4] Bulmus, S. C., Zhu, S. X., Teunter, R. H. (2014): Optimal core acquisition and pricing strategies for hybrid manufacturing and remanufacturing systems. – International Journal of Production Research 52: 6627-6641.

[5] Chen, W., Kucukyazici, B., Verter, V., Jesús Sáenz, M. (2015): Supply chain design for unlocking the value of remanufacturing under uncertainty. – European Journal of Operational Research 247: 804-819.

http://www.aloki.hu ● ISSN 1589 1623 (Print) ● ISSN 1785 0037 (Online)
DOI: http://dx.doi.org/10.15666/aeer/1704_99479963

[6] Ding, H., Zhao, Q., An, Z., Xu, J., Liu, Q. (2015): Pricing strategy of environmental sustainable supply chain with internalizing externalities. – International Journal of Production Economics 170: 563-575.
[7] Dobos, I., Richter, K. (2006): A production/recycling model with quality consideration. – International Journal of Production Economics 104: 571-579.
[8] Fang, X., Du, Y., Qiu, Y. (2017): Reducing carbon emissions in a closed-loop production routing problem with simultaneous pickups and deliveries under carbon cap-and-trade. – Sustainability-Basel 9: 2198.
[9] Fareeduddin, M., Hassan, A., Syed, M. N., Selim, S. Z. (2015): The impact of carbon policies on closed-loop supply chain network design. – Procedia CIRP 26: 335-340.
[10] Feng, W., Ji, G., Pardalos, P. M. (2017): Effects of government regulations on Manufacturer's behaviors under carbon emission reduction. – Environmental Science and Pollution Research. https://doi.org/10.1007/s11356-017-0891-4.
[11] Ferrer, G., Swaminathan, J. M. (2006): Managing new and remanufactured products. – Management Science 52: 15-26.
[12] Galbreth, M. R., Blackburn, J. D. (2006): Optimal acquisition and sorting policies for remanufacturing. – Production and Operations Management 15: 384-392.
[13] Gan, S., Pujawan, I. N., Suparno, W, B. (2017): Pricing decision for new and remanufactured product in a closed-loop supply chain with separate sales-channel. – International Journal of Production Economics 190: 120-132.
[14] Gao, J., Han, H., Hou, L., Wang, H. (2016): Pricing and effort decisions in a closed-loop supply chain under different channel power structures. – Journal of Cleaner Production 112: 2043-2057.
[15] Ghosh, D., Shah, J. (2012): A comparative analysis of greening policies across supply chain structures. – International Journal of Production Economics 135: 568-583.
[16] Govindan, K., Soleimani, H., Kannan, D. (2015): Reverse logistics and closed-loop supply chain: a comprehensive review to explore the future. – European Journal of Operational Research 240: 603-626.
[17] Govindan, K., Madan, S. K., Kannan, D. (2016): Application of fuzzy analytic network process for barrier evaluation in automotive parts remanufacturing towards cleaner production - a study in an Indian scenario. – Journal of Cleaner Production 114: 199-213.
[18] Guide, V. D. R. J., Teunter, R. H., Van Wassenhove, L. N. (2003): Matching demand and supply to maximize profits from remanufacturing. – Manufacturing & Service Operations Management 5: 303-316.
[19] He, R., Xiong, Y., Lin, Z. (2016): Carbon emissions in a dual channel closed loop supply chain: the impact of consumer free riding behavior. – Journal of Cleaner Production 134: 384-394.
[20] Jerbia, R., Kchaou Boujelben, M., Sehli, M. A., Jemai, Z. (2018): A stochastic closed-loop supply chain network design problem with multiple recovery options. – Computers & Industrial Engineering 118: 23-32.
[21] Ke, H., Wu, Y., Huang, H., Chen, Z. (2018): Optimal pricing decisions for a closed-loop supply chain with retail competition under fuzziness. – Journal of the Operational Research Society 69: 1468-1482.
[22] Li, H., Wang, C., Shang, M., Ou, W. (2017): Pricing, carbon emission reduction, low-carbon promotion and returning decision in a closed-loop supply chain under vertical and horizontal cooperation. – International Journal of Environmental Research and Public Health 14: 1332.
[23] Liu, Z. L., Anderson, T. D., Cruz, J. M. (2012): Consumer environmental awareness and competition in two-stage supply chains. – European Journal of Operational Research 218: 602-613.
[24] Metta, H., Badurdeen, F. (2013): Integrating sustainable product and supply chain design: modeling issues and challenges. – IEEE Transactions on Engineering Management 60: 438-446.

http://www.aloki.hu ● ISSN 1589 1623 (Print) ● ISSN 1785 0037 (Online)
DOI: http://dx.doi.org/10.15666/aeer/1704_99479963

[25] Mukhopadhyay, S. K., Ma, H. (2009): Joint procurement and production decisions in remanufacturing under quality and demand uncertainty. – International Journal of Production Economics 120: 5-17.
[26] Olugu, E. U., Wong, K. Y. (2012): An expert fuzzy rule-based system for closed-loop supply chain performance assessment in the automotive industry. – Expert Systems with Applications 39: 375-384.
[27] Özkır, V., Başlıgıl, H. (2012): Modelling product-recovery processes in closed-loop supply-chain network design. – International Journal of Production Research 50: 2218-2233.
[28] Rahman, S., Subramanian, N. (2012): Factors for implementing end-of-life computer recycling operations in reverse supply chains. – International Journal of Production Economics 140: 239-248.
[29] Savaskan, R. C., Van Wassenhove, L. N. (2006): Reverse channel design: the case of competing retailers. – Management Science 52: 1-14.
[30] Savaskan, R. C., Bhattacharya, S., Van Wassenhove, L. N. (2004): Closed-loop supply chain models with product remanufacturing. – Management Science 50: 239-252.
[31] Shu, T., Liu, Q., Chen, S., Wang, S., Lai, K. (2018): Pricing decisions of CSR closed-loop supply chains with carbon emission constraints. – Sustainability-Basel 10: 4430.
[32] Swaminathan, J. M., Ferrer, G. (2010): Managing new and differentiated remanufactured products. – European Journal of Operational Research 203: 370-379.
[33] Taleizadeh, A. A., Moshtagh, M. S., Moon, I. (2017): Optimal decisions of price, quality, effort level and return policy in a three-level closed-loop supply chain based on different game theory approaches. – European Journal of Industrial Engineering 11: 486-525.
[34] Taleizadeh, A. A., Moshtagh, M. S., Moon, I. (2018): Pricing, product quality, and collection optimization in a decentralized closed-loop supply chain with different channel structures: Game theoretical approach. – Journal of Cleaner Production 189: 406-431.
[35] Tan, Y., Guo, C. (2019): Research on two-way logistics operation with uncertain recycling quality in government multi-policy environment. – Sustainability-Basel 11: 882.
[36] Tao, Z. G., Guang, Z. Y., Hao, S., Song, H. J., Xin, D. G. (2015): Multi-period closed-loop supply chain network equilibrium with carbon emission constraints. – Resources, Conservation and Recycling 104: 354-365.
[37] Turki, S., Rezg, N. (2018): Impact of the quality of returned-used products on the optimal design of a manufacturing/remanufacturing system under carbon emissions constraints. – Sustainability-Basel 10: 3197.
[38] Xu, L., Wang, C. (2018): Sustainable manufacturing in a closed-loop supply chain considering emission reduction and remanufacturing. – Resources, Conservation and Recycling 131: 297-304.
[39] Xu, Z., Pokharel, S., Elomri, A., Mutlu, F. (2017): Emission policies and their analysis for the design of hybrid and dedicated closed-loop supply chains. – Journal of Cleaner Production 142: 4152-4168.
[40] Yang, L., Zhang, Q., Ji, J. (2017): Pricing and carbon emission reduction decisions in supply chains with vertical and horizontal cooperation. – International Journal of Production Economics 191: 286-297.
[41] Zhang, J. Kevin Chiang, W. Y., Liang, L. (2014): Strategic pricing with reference effects in a competitive supply chain. – Omega 44: 126-135.
[42] Zou, Q., Ye, G. (2015): Pricing-decision and coordination contract considering product design and quality of recovery product in a closed-loop supply chain. – Mathematical Problems in Engineering 593123: 1-14.

http://www.aloki.hu ● ISSN 1589 1623 (Print) ● ISSN 1785 0037 (Online)
DOI: http://dx.doi.org/10.15666/aeer/1704_99479963

MITIGATION OF SALINITY STRESS OF PEPPER (*CAPSICUM ANNUUM* L.) BY ARBUSCULAR MYCORRHIZAL FUNGUS, *GLOMUS CONSTRICTUM*

AL-AMRI, S. M

Department of Biology, College of Science and Art, Shaqra University, Shaqra, Saudi Arabia (e-mail: phd1618@hotmail.com, abdelfattaham@yahoo.com)

(Received 8th Apr 2019; accepted 13th Jun 2019)

Abstract. A pot experiment was investigated to study the effect of arbuscular mycorrhizal (AM), *Glomus constrictum* (Trappe) on growth response, photosynthetic pigments, gas exchange parameters, antioxidant enzymes and nutrition of pepper plants irrigated with different concentrations of sea water. Four concentrations (tap water, 10%, 20% and 40% of sea water) were used. Salinity stress markedly reduced all studied parameters, except antioxidant enzymes, of pepper plants. Under saline conditions, AM fungi significantly increased growth parameters, photosynthetic pigments, nutrient contents (except Na^+), gas exchange rate and antioxidant enzymes of pepper plants when compared to non-mycorrhizal ones. Those improvements were linked to mycorrhizal infection degree in pepper. Generally, growth, nutrition, photosynthetic pigments and antioxidant enzymes of pepper appeared to be highly dependent on the AM in salinized soil compared to non-salinized soil. This study suggested that mycorrhizal colonization could be used to mitigate the detrimental effects of salinity, particularly in soils irrigated with high concentration of sea water.
Keywords: *salinity, mycorrhiza, growth, pepper, antioxidant enzymes*

Abbreviations: P_N: net photosynthetic rate; AM: arbuscula rmycorrhizal; AMF: arbuscular mycorrhizal fungi; AMR: arbuscula rmycorrhizal response; Dwt: dry weight; Fwt: fresh weight; *E*: transpiration rate; g_s: stomatal conductance; LA: leaf area; Non-AMF: non-arbuscular mycorrhizal fungi; N: nitrogen; P: phosphorus; K: potassium; Na: sodium; Mg: magnesium; Ca– calcium; CAT: catalase; POX: peroxidase; APX: ascorbate peroxidase.

Introduction

Water salinity is a very important environmental problem, particularly in Saudi Arabia, decreasing plant growth and yields worldwide, and affecting about 10% of the world's global land (Abdel-Ghani, 2009; Al-Amri et al., 2013; Abdel-Fattah et al., 2016). The saline area is still extending due to irrigation and land clearing (Abdel-Fattah et al., 2013; Sheng et al., 2013). Increasing salt concentration in soil suppresses the plant ability to absorb and uptake water, negatively decreases metabolic processes, nutrient absorbance, root hydraulic conductivity and all photosynthetic rates, all of these results in negatively affecting the plant ability to grow (Al-Karaki et al., 2001; Abdel-Fattah and Asrar, 2012).

Pepper (*Capsicum annuum* L.) is an important vegetable plant in Saudi Arabia. Raising growth of pepper plant through improving the productivity area as increasing the cultivated area in salinized newly reclaimed lands is the major important national target. Increasing salt tolerance of vegetables, horticultures and economic plants is required to tolerate the increase in food production in many regions of the world in general and Saudi Arabia in particular (Al-Amri et al., 2013). Expansion of salt-tolerant vegetables or desalinization of soil by washing excessive salts in not enough to remove this problem (Kumar et al., 2010; Abdel-Fattah et al., 2016). Recently, application of biological agents like mycorrhizal symbiosis as a practical applied technology to

http://www.aloki.hu ● ISSN 1589 1623 (Print) ● ISSN 1785 0037 (Online)
DOI: http://dx.doi.org/10.15666/aeer/1704_99659978

mitigate salt stress effects on plant growth and development has customary a great attention (Poss et al., 1985; Abdel-Fattah and Asrar et al., 2012; Al-Amri et al., 2013).

Several investigators have concluded that the existence of the arbuscular mycorrhizal plants grown in saline stress conditions (Pond et al., 1984; Kumar et al., 2010; Wu et al., 2010; Asrar et al., 2014). Furthermore, the biotechnological application of arbuscular mycorrhizal fungi in salinized soil may increase plant tolerance and growth via mitigating the adverse effect of salt stress in various plants (Juniper and Abbott, 1993; Daei et al., 2009; Abdel-Fattah and Asrar, 2012). Under salinity stress conditions, plant tolerance and production are complicated different mechanisms. In this connection, arbuscular mycorrhizal fungi has several mechanisms to increase salt tolerance of associated plants through stimulating nutrient uptake (Evelin et al., 2009; Abdel-Fattah et al., 2013); decreasing the uptake of Na^+ and preventing their movement to aerial parts of plant (Daei et al., 2009); increasing water uptake (Al-Karaki, 2006; Asrar et al., 2012); maintaining ionic balance by increasing and/or selective uptake of nutrients (Kumar et al., 2010); increasing of some antioxidant defense enzyme activities (catalase, peroxidase, superoxide dismutase and ascorbate peroxidase) and molecules like carotenoids, glutathione and tocopherols (Ibrahum et al., 2011); accumulating of polyamines like spermine and spermidine in associated host plants and regulating the osmotic status of plants through maintaining the turgor pressure of the leaves, and stimulating the photosynthetic and transpiration rate, and water use efficiency in the host plants (Juniper and Abbott, 2006; Auge et al., 2008).

Due to the detrimental effects of salt stress on different plants species and the function of arbuscular mycorrhizal fungi in improving the salinity tolerance, the present study was evaluated to study the efficiency of arbuscular mycorrhizal fungus (*Glomus constrictum*, Trappe) for enhancing plant growth, photosynthetic pigments, nutrition, gas exchange and some antioxidant enzymes of Pepper plants grown in soil irrigated with different concentrations of sea water.

Materials and methods

Experimental design

The experiment with a (2 × 4) factorial design was done. The treatments consisted of two arbuscular mycorrhizal onces [*Glomus constrictum* (AMF) and non-inoculated (--AMF)] and four levels {0.0% (control), 15%, 30% and 60% of sea water} g Kg^{-1} and 0.5 g kg^{-1} soil]. The sea water was obtained from the Red sea, Gadda, Saudi Arabia. Each of the eight treatments was replicated ten times (one plant per each pot) to give 90 pots as total.

Inoculum preparation of arbuscular mycorrhizal fungus

The inoculums mycorrhizal fungus, *Glomus constrictum* (Trappe), was isolated from saline site of Shaqra region using the wet sieving method of Gerdmann and Nicolson (1963). The spores of AM were left to multiply for 4 monthes in greenhouse under controlled environmental conditions. The mycorrhizal inoculums consisting of 10 g of rhizoplane soil (approx. 600 spores) and 0.5 g of colonized onion root pieces with a colonized level of 80% were inoculated to each pot. The mycorrhizal inoculums were added at 5 cm depth the pepper seedlings upon planting.

http://www.aloki.hu ● ISSN 1589 1623 (Print) ● ISSN 1785 0037 (Online)
DOI: http://dx.doi.org/10.15666/aeer/1704_99659978

Plant and growth conditions

Seeds of Pepper (*Capsicum annuum* L.*)* were surface disinfected by soaking in 7% sodium hypochlorite for 10 min then rewashed with deionized sterilized water and left to germinate for 48 h on wetted sterilized filter paper in dark at 25 °C. Similar sterilized germinated seedlings were transplanted (one plant/pot) into 20 cm diameter plastic pots containing 3 kg of autoclaved (120 °C for 3 separate consequent time) sandy loam soil. Soil characteristics were: pH (water) = 7.31; available nitrogen (15.0 mg kg^{-1}); available phosphorus (5.12 mg kg^{-1}); potassium (40 mg kg^{-1}); magnesium (53 mg kg^{-1}) and organic matter (0.33%). All pots were irrigated by tap water (control) until the second week, and then the pots were divided into four groups for salinity treatments. The 1st group irrigated with tap water (control), the 2nd, 3rd and 4th groups were irrigated with 15, 30 and 50% sea water respectively. Chemical analysis of sea water are: Cl^-, 21.5 g/l; Na^+, 12.5 g/l; K^+, 0.49 g/l; salinity, 38.2 g/kg; pH 8.2 and its electrical conductivity was 48 mmhos/cm. Half of all pots treated or non-treated with different concentrations of sea water were inoculated with the mycorrhizal fungus, *Glomus constrictum* (as described before). Arbuscular mycorrhizal inoculums were added 3 cm below the seedlings at planting time. The non-mycorrhizal treatments (-AMF) were provided with filtered washings of an equal amount of the mycorrhizal soil inoculum to provide the same associated microorganisms without AM spores. All pots were arranged in a complete randomized blocks design in a glasshouse of Experimental Station of Plant Production Department, College of Food and Agriculture Sciences, King Saud University under controlled conditions of 550 μmol m^{-2} s^{-1} light intensity, 23/18 °C day/night temperatures, 70–80% relative humidity and 16-h photoperiod. Plants for all treatments received 32 mg sulfur (K_2SO_4) pot^{-1} as a nutrient solution after four weeks of planting. All plants were watered regularly with the corresponding irrigation sea water level. Ten plants for each treatment were harvested 10 weeks after planting.

Growth parameters

At harvest, the plants for each harvest were carefully uprooted with minimum disturbance of roots. The roots were washed with tap water to remove adherent soil particles and the shoot height per plant was measured. Roots and shoots fresh and dry weights (after drying the samples at 80 °C for 48 h in oven) were recorded. Leaf area was determined using a leaf area meter (Li-Cor, Lincoin, NE). Arbuscular mycorrhizal growth responses (AMR) for each estimated parameter was calculated following Menge et al. (1978) using the following formula: (parameter value of mycorrhizal treatment (AMF) - parameter value of non-mycorrhizal treatment (-AMF)/{parameter value of non-mycorrhizal treatment (-AMF)} × 100.

Estimation of photosynthetic pigments

Photosynthetic pigments content (chlorophyll ‘a’, and “b”, carotenoids and total pigments) of the fully mature third leaves for each treatment was determined by extraction in 85% aqueous acetone for 5 min. The homogenate samples were centrifuged at 8000 rpm for 10 min. The supernatant was made up to 10 ml with acetone and it measured spectrophotometrically against a blank of aqueous acetone The concentrations of the pigments were determined using the equations of Abdel-Fattah et al. (2013).

http://www.aloki.hu ● ISSN 1589 1623 (Print) ● ISSN 1785 0037 (Online)
DOI: http://dx.doi.org/10.15666/aeer/1704_99659978

Measurement of photosynthesis, transpiration and stomatal conductance

Net photosynthetic rate (*A*), transpiration rate (*E)* and stomatal conductance (g_s) of the mature third leaves were measured by using Li-Cor, 8400XT, Lincoln. NE, USA. Leaf was fitted into leaf chamber. Gas exchange measurements were made in the growth chamber under saturated light conditions and adjusted to an intensity of 480 μmol m^{-1} s^{-1}. Four replicates for each treatment were used.

Nutrient analysis

Root and shoot samples for each tratment were oven-dried, grounded. A known weight of the dried material was extracted in a digestion flask containing 10 ml of three acid mixture (HNO_3:H_2SO_4: 60% HCL, at the ratio of 3:2:1 (v/v/v), respectively) in kjeldahed digestion flask. Phosphorus (P) was determined by the vanadate-molybdate colorimetric method (Jackson, 1973). Calcium (Ca^{++}), potassium (K^+), magnesium ($Mg^{++)}$ and sodium (Na^+) in digested samples by using atomic absorption (model unicam 969). Total nitrogen (N) was analyzed using Kjeldahl method (Nelson and Sommers1973).

Estimation the activities of antioxidant enzymes (Catalase, peroxidase andascorbate peroxidase)

Antioxidant enzymes were analyzed by homogenization of a known leaf fresh weight in 50 mM cold phosphate buffer (pH 7.0) containing 1 mM EDTA (Ethylene Diamine tetra acetic acid) and 5 mM ascorbic acid in case of ascorbate peroxidase assay (Gajewska and Sklodowska, 2008). Peroxidase (POX) and Catalase activitties (CAT) were estimated according to the method of Aebi (1983). The specific enzyme activity of CAT and POX was expressed as μmol of H_2O_2 consumed/min. Ascorbate peroxidase (XPX) activity was assayed using the method of Nakano and Asada (1981) and the specific activity of this enzyme was expressed as μmol oxidized ascorbate/min.

Mycorrhizal colonization

After harvest, the root systems for each treatment were washed carefully with tap water to remove all the adhering soil particles. Randomly sampled roots from five plants per treatment were cut into 0.5 to 1 cm pieces, then cleared with 10% KOH solution and stained with 0.05% trypan blue in lactophenol (Phillips and Hayman, 1970) for estimated of mycorrhizal colonization.40 root segments of each treatment were putted on slides and were examined with a light microscope (Carl Zeiss, Japan) at 40x magnification, where visually were allocated six classes of mycorrhizal colonization (from 0 to 5, depending on the occurrence of mycorrhizal structure in the root segment) and four levels of arbuscular abundance (from A0 to A3). With this values, mycorrhizal colonization levels [Frequency of mycorrhizal colonization (F %), the intensity of mycorrhizal colonization (M %) and arbuscular frequency (A %)] of the stained roots were estimated according to Trouvelot et al. (1986) using the “Mycocalc” software (http://www.dijon.inra.fr /mychintec/mycocalcprg/download.html).

Statistical analysis

All results were statistical analyzed using two-factor analysis of variance (ANOVA). Means of all treatments were divided by Duncan’s multiple range tests by the least

http://www.aloki.hu ● ISSN 1589 1623 (Print) ● ISSN 1785 0037 (Online)
DOI: http://dx.doi.org/10.15666/aeer/1704_99659978

significant difference (LSD, $P \leq 0.05$) method using the Costat software. All of the measurements were performed five times for each treatment. The means and calculated standard error (SE) are recorded.

Results

Growth responses

Sea water stress significantly reduced biomass of shoots and roots, leaf area and shoot length of both mycorrhizal (AMF) and nonmycorrhizal (-AMF) pepper plants compared with control treatment (irrigated with tap water) and the rate of reduction increased with increasing sea water concentration in the soil. However, the reduction in most growth criteria was more pronounced in non-mycorrhizalkal pepper plants (*Table 1*). In this connection; Leaves of mycorrhizal pepper plants grown at higher concentrations of sea water were highly greener and less senescent than those in the non-AM plants (*Fig. 1*). Values of mycorrhizal dependency of pepper plants (AMR) in responding to AMF colonization were significantly increased with increasing sea water concentration in soil.

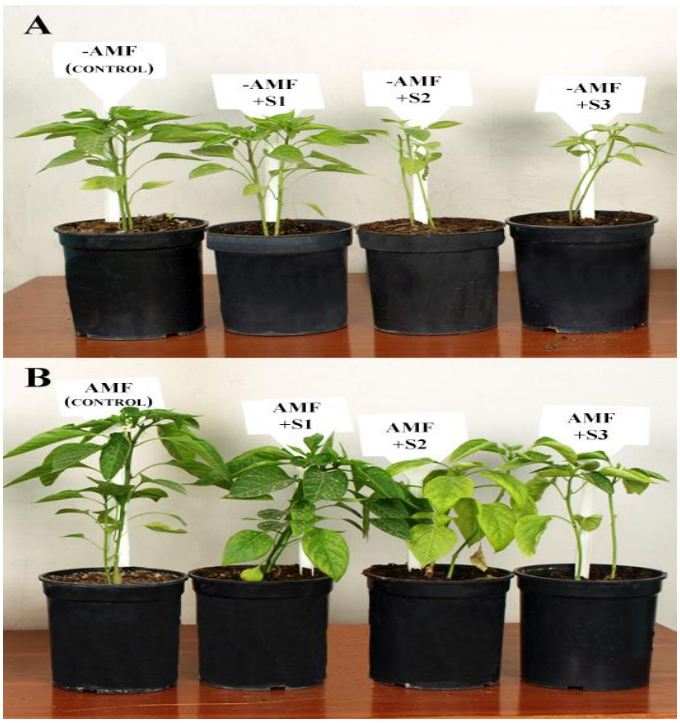

Figure 1. *Growth of non-mycorrhizal (-AMF) [A] and Mycorrhizal (AMF) [B] Pepper plants grown in soil irrigated with different concentrations of sea water [Control (0.0), S1 (10%), S2 (20%) and S3 (40%)]. The leaves of non-mycorrhizal pepper plants were more senescent (less green) than those of mycorrhizal plants*

Photosynthetic pigments

The photosynthetic pigments content (chlorophyll a, chlorophyll b and carotenoids) in mycorrhizal leaves of pepper plants were significantly greater than those of non-mycorrhizal plants grown either with or without sea water irrigated in soil (*Table 2*).

http://www.aloki.hu ● ISSN 1589 1623 (Print) ● ISSN 1785 0037 (Online)
DOI: http://dx.doi.org/10.15666/aeer/1704_99659978

Such increases in these contents were linked to the degree of mycorrhizal colonization. In most cases, this increase in carotenoides content in leaves of pepper plants in response to mycorrhizal effects was increased with increasing sea water concentration in the soil, particularly 40%. On contrary, no significant differences chlorophyll "b" was observed between mycorrhizal plants irrigated with 10% sea water and control treatment (*Table 2*).

Table 1. *Growth parameters of mycorrhizal (AMF) and non-mycorrhizal (-AMF) pepper plants grown in soil irrigated with different concentrations of sea water*

Treatments		Fresh weight (g plant^{-1})		Dry weight (g plant^{-1})		Shoot height (cm plant^{-1})	Leaf area (mm^2 plant^{-1})
Sea water conc. (%)	AMF status	Shoot	Root	Shoot	Root		
Control (0.0)	-AMF	14.15 ± 0.96^{D}	1.58 ± 0.09^{B}	3.51 ± 0.44^{BC}	0.84 ± 0.05^{B}	28.5 ± 1.25^{C}	250 ± 8.11^{C}
	AMF	18.00 ± 0.98^{A}	2.01 ± 0.17^{A}	4.11 ± 0.57^{AB}	0.93 ± 0.09^{A}	40.1 ± 2.41^{A}	350 ± 9.21^{A}
	AMR (%)	27.2 ± 1.37	27.1 ± 2.09	17.1 ± 1.05^{B}	10.7 ± 0.96	40.7 ± 1.95	40.0 ± 1.38
10%	-AMF	14.00 ± 0.85^{D}	1.90 ± 0.13^{AB}	3.21 ± 0.45^{C}	0.77 ± 0.10^{B}	25.3 ± 1.05^{CD}	245 ± 7.99^{C}
	AMF	17.90 ± 0.54^{A}	2.11 ± 0.22^{A}	4.00 ± 0.53^{A}	0.88 ± 0.16^{AB}	39.1 ± 2.11^{A}	352 ± 9.01^{A}
	AMR (%)	27.90 ± 1.97	11.2 ± 1.98	24.6 ± 1.58	14.3 ± 0.93	59.5 ± 2.99	43.7 ± 1.37
20%	-AMF	13.38 ± 0.59^{D}	1.54 ± 0.19^{B}	2.99 ± 0.33^{CD}	0.70 ± 0.09^{C}	23.2 ± 1.08^{D}	238 ± 8.04^{CD}
	AMF	17.62 ± 0.98^{B}	1.93 ± 0.21^{AB}	3.87 ± 0.54^{B}	0.82 ± 0.08^{AB}	35.1 ± 2.11^{B}	340 ± 8.62^{AB}
	AMR (%)	30.90 ± 1.87	25.3 ± 1.99	29.4 ± 1.97	17.1 ± 0.83	51.3 ± 2.95	42.8 ± 1.88
40%	-AMF	12.10 ± 0.89^{E}	0.89 ± 0.08^{D}	2.11 ± 0.55^{D}	0.55 ± 0.03^{D}	18.8 ± 1.01^{E}	200 ± 6.25^{D}
	AMF	15.99 ± 0.54^{C}	1.11 ± 0.29^{C}	3.28 ± 0.58^{BC}	0.69 ± 0.04^{C}	29.6 ± 1.22^{C}	310 ± 8.11^{B}
	AMR (%)	32.20 ± 2.01	24.7 ± 1.89	55.4 ± 2.15	25.5 ± 1.34	57.4 ± 2.95	55.0 ± 2.08

Values in each column (except AMR) followed by the same letter(s) are not significantly different at $P \leq 0.05$ (Duncan's multiple range test). AMF: arbuscular mycorrhizal fungi, -AMF: non-mycorrhizal fungi, AMR: arbuscular mycorrhizal response. Each value represents the mean of five replicates ± standard error

Table 2. *Photosynthetic pigments in leaves of mycorrhizal (AMF) and non-mycorrhizal (-AMF) pepper plants grown in soil irrigated with different concentrations of sea water*

Treatments		Chlorophyll content (μg g^{-1}fwt.)		
Sea water conc. (%)	AMF status	Chlorophyll "a"	Chlorophyll "b"	Carotenoides
Control (0.0)	-AMF	830 ± 10.22^{C}	400 ± 4.22^{B}	680 ± 7.22^{B}
	AMF	1340 ± 18.22^{A}	570 ± 4.24^{A}	850 ± 9.54^{A}
	AMR (%)	61.4 ± 2.44	42.5 ± 0.87	25.0 ± 0.31
10%	-AMF	670 ± 9.25^{D}	290 ± 2.48^{C}	450 ± 3.99^{CD}
	AMF	1050 ± 11.47^{B}	480 ± 3.99^{A}	530 ± 2.41^{C}
	AMR (%)	56.7 ± 1.99	65.5 ± 1.49	17.8 ± 0.27
20%	-AMF	490 ± 7.22^{E}	225 ± 1.33^{D}	405 ± 4.14^{D}
	AMF	620 ± 8.71^{D}	290 ± 1.30^{C}	$.455 \pm 4.00^{CD}$
	AMR (%)	26.5 ± 1.05	28.9 ± 0.85	12.3 ± 0.19
40%	-AMF	360 ± 4.17^{F}	165 ± 0.73^{E}	215 ± 2.45^{F}
	AMF	400 ± 3.58^{EF}	195 ± 0.89^{CD}	338 ± 2.98^{E}
	AMR (%)	11.1 ± 0.84	18.8 ± 0.22	57.2 ± 1.97

Values in each column (except AMR) followed by the same letter(s) are not significantly different at $P \leq 0.05$ (Duncan's multiple range test). AMF: arbuscular mycorrhizal fungi, -AMF: non-mycorrhizal fungi, AMR: arbuscular mycorrhizal response. Each value represents the mean of five replicates ± standard error

http://www.aloki.hu ● ISSN 1589 1623 (Print) ● ISSN 1785 0037 (Online)
DOI: http://dx.doi.org/10.15666/aeer/1704_99659978

Gas exchange parameters

Generally, g_s, *A* and *E* in mycorrhizal leaves of pepper plants were highly significant than those in non-mycorrhizal plants grown either in soil irrigated with or without sea water (*Table 3*), and the effect was more noticed in soil irrigated with higher concentrations of sea water. Such increases in gas exchange parameters were highly related to the degree of the mycorrhizal colonization for each treatment. Furthermore, the dependency of pepper plants on mycorrhizal fungi for improving gas exchange parameters was increased with increasing sea water concentration in soil. The differences in g_s, *A* and *E* in pepper leaves were not significant between mycorrhizal plants grown in soil irrigated with 10% sea water and control treatment.

Table 3. *Net photosynthetic rate (A), transpiration rate (E) and stomatal conductance (g_s) in leaves of mycorrhizal (AMF) and non-mycorrhizal (-AMF) pepper plants grown in soil irrigated with different concentrations of sea water*

Treatments		Gas exchange parameters		
Sea water conc. (%)	**AMF status**	***A*** **(µmol m^{-2} s^{-1})**	***E*** **(mmol m^{-2} s^{-1})**	**g_s (mol m^{-2} s^{-1})**
Control (0.0)	-AMF	12.99 ± 0.80^{C}	$10.11 \pm 0.75B^{C}$	0.125 ± 0.021^{C}
	AMF	15.61 ± 0.88^{A}	12.24 ± 0.74^{A}	0.198 ± 0.023^{A}
	AMR (%)	20.17 ± 1.01	21.07 ± 1.41	58.40 ± 3.23
10%	-AMF	12.98 ± 0.69^{C}	09.88 ± 0.54^{C}	0.111 ± 0.020^{C}
	AMF	15.71 ± 0.71^{A}	12.20 ± 0.70^{A}	0.188 ± 0.035^{A}
	AMR (%)	21.03 ± 1.24	23.48 ± 1.92	69.40 ± 3.98
20%	AMF	10.11 ± 0.68^{D}	08.54 ± 0.57^{CD}	0.090 ± 0.019^{D}
	AMF	13.99 ± 0.66^{B}	11.88 ± 0.70^{B}	0.160 ± 0.027^{B}
	AMR (%)	38.38 ± 2.99	39.11 ± 1.98	77.80 ± 3.98
40%	AMF	08.65 ± 0.58^{E}	05.90 ± 0.44^{D}	0.055 ± 0.012^{E}
	AMF	12.11 ± 0.75^{CD}	09.24 ± 0.80^{C}	0.098 ± 0.017^{D}
	AMR (%)	40.00 ± 2.87	56.61 ± 2.60	78.20 ± 3.97

Values in each column (except AMR) followed by the same letter(s) are not significantly different at $P \leq 0.05$ (Duncan's multiple range test). AMF: arbuscular mycorrhizal fungi, -AMF: non-mycorrhizal fungi, AMR: arbuscular mycorrhizal response. Each value represents the mean of five replicates ± standard error

Antioxidant enzymes

Sea water stress significantly increased the antioxidant enzyme activities (CAT, POX and APX) in leaves of mycorrhizal and non-mycorrhizal pepper plants as compared to the control treatments (*Table 4*). However, mycorrhizal colonization significantly improved the contents of antioxidant enzyme activities than those in leaves of non-mycorrhizal plants, regardless of sea water treatments. This increase in antioxidant activities in leaves of pepper plants in response to mycorrhizal effects was increased with increasing sea water concentration in the soil, particularly in case of POX and APX.. On the other hand, no significant differences in APX activity was observed between mycorrhizal and non-mycorrhizal plants grown in soil irrigated with normal water.

http://www.aloki.hu ● ISSN 1589 1623 (Print) ● ISSN 1785 0037 (Online)
DOI: http://dx.doi.org/10.15666/aeer/1704_99659978

Table 4. *Antioxidant enzymes {catalase (CAT), Peroxidase (POX) and Ascorbate peroxidase (APX) in leaves of mycorrhizal (AMF) and non-mycorrhizal (-AMF) pepper plants grown in soil irrigated with different concentrations of sea water*

Treatments		Antioxidant enzymes		
Sea water conc. (%)	**AMF status**	**CAT (µmol H_2O_2/min)**	**POX (µmol H_2O_2/min)**	**APX (µmol oxidized ascorbate/min)**
Control (0.0)	-AMF	$140 \pm 3.80^{E*}$	0.93 ± 0.032^{D}	4.50 ± 0.78^{D}
	AMF	180 ± 4.41^{D}	1.11 ± 0.092^{CD}	4.68 ± 0.77^{D}
	AMR (%)	28.6 ± 1.07	19.3 ± 1.05	04.0 ± 0.42
10%	-AMF	145 ± 3.69^{E}	1.01 ± 0.040^{CD}	4.90 ± 0.76^{C}
	AMF	180 ± 4.05^{F}	1.26 ± 0.082^{C}	5.30 ± 0.79^{BC}
	AMR (%)	26.2 ± 1.13	24.7 ± 1.99	08.0 ± 0.55
20%	-AMF	189 ± 4.11^{F}	1.30 ± 0.18^{C}	5.25 ± 0.57^{BC}
	AMF	230 ± 4.65^{C}	1.88 ± 0.17^{B}	5.80 ± 0.57^{B}
	AMR (%)	21.7 ± 1.48	44.6 ± 2.55	10.4 ± 0.89
40%	-AMF	280 ± 5.88^{B}	1.55 ± 0.041^{B}	5.92 ± 0.88^{B}
	AMF	345 ± 5.96^{A}	2.30 ± 0.060^{A}	6.95 ± 0.89^{A}
	AMR (%)	23.2 ± 0. 95	48.4 ± 2.22	17.4 ± 1.11

Values in each column (except AMR) followed by the same letter(s) are not significantly different at $P \leq 0.05$ (Duncan's multiple range test). AMF: arbuscular mycorrhizal fungi, -AMF: non-mycorrhizal fungi, AMR: arbuscular mycorrhizal response. Each value represents the mean of five replicates ± standard error

Mycorrhizal colonization levels

Mycorrhizal colonization levels (frequency (F%), intensity (M%) of mycorrhizal colonization and arbuscular development (A%)) in root tissues of pepper plants were significantly affected by sea water stress in soil. Both intensity of mycorrhizal colonization (M%) and arbuscular frequency (A%) were significantly decreased in pepper root tissues with increasing concentration of sea water in soil (*Table 5*). On the other hand, no significant differences were observed in the frequency of mycorrhizal colonization (F%) in root tissues between mycorrhizal plants irrigated with or without sea water concentration. On the contrary; no significant differences were observed in the intensity of mycorrhizal colonization (M%) between AMF plants grown either in soil irrigated with 10% sea water and control treatment. No mycorrhizal colonization was observed in the non-inoculated pepper plants.

Nutrient content

Increasing sea water concentration in soil significantly reduced N, P, Mg, Ca and K concentrations, but increased sodium in the shoots of mycorrhizal and non-mycorrhizal pepper plants. However, P, N, K, Ca and Mg contents in shoot tissues of the AM plants, in most cases, were significantly greater than those in non-mycorrhizal pepper plants grown in soil irrigated with or without sea water concentrations (*Table 6*). Such stimulations in nutrients content in response to the mycorrhizal effects were highly increased with increasing sea water concentration in the soil. AM-inoculated plants exhibited reduction in Na concentration in shoot tissues compared to non-mycorrhizal

http://www.aloki.hu ● ISSN 1589 1623 (Print) ● ISSN 1785 0037 (Online)
DOI: http://dx.doi.org/10.15666/aeer/1704_99659978

control plants in either soil irrigated with different concentration of sea water and control treatment (*Table 6*). The rate of reduction in Na content in response to mycorrhizal effects (AMR) was increased highly with increasing sea water concentration in the soil. On the other hand, no significant differences in Mg content in shoot tissues were observed between mycorrhizal and non-mycorrhizal pepper plants at control and 20% sea water treatments

Table 5. *Frequency of mycorrhizal infection (F %) Intensity of mycorrhizal colonization (M %) and arbuscular frequency (A %) in the root tissues of mycorrhizal (AMF) and non-mycorrhizal (-AMF) pepper plants grown in soil irrigated with different concentrations of sea water*

Treatments		Level of mycorrhizal colonization (%)		
Sea water conc. (%)	**AMF status**	**F**	**M**	**A**
Control (0.0)	-AMF	0.0^{C}	0.0^{C*}	0.0^{C*}
	AMF	95.2 ± 4.11^{A}	80.3 ± 3.99^{A}	61.8 ± 2.63^{A}
10%	-AMF	0.0^{C*}	0.0^{C*}	0.0^{C*}
	AMF	93.7 ± 4.01^{A}	75.6 ± 3.540^{A}	57.0 ± 2.47^{A}
20%	-AMF	0.0^{C*}	0.0^{C*}	0.0^{C*}
	AMF	82.8 ± 3.58^{A}	71.3 ± 3.54^{AB}	48.7 ± 1.99^{B}
40%	-AMF	0.0^{C*}	0.0^{C*}	0.0^{C*}
	AMF	79.9 ± 3.65^{A}	66.5 ± 2.60^{B}	41.9 ± 1.037^{B}

Values in each column (except AMR) followed by the same letter(s) are not significantly different at $P \leq 0.05$ (Duncan's multiple range test). AMF: arbuscular mycorrhizal fungi, -AMF: non-mycorrhizal fungi. Each value represents the mean of five replicates ± standard error

Table 6. *Nutrients (N, P, K) and minerals (Ca, Mg, Na) content in leaves of mycorrhizal (AMF) and non-mycorrhizal (-AMF) pepper plants grown in soil irrigated with different concentrations of sea water*

Treatments		Nutrients and minerals content [mg g^{-1} (Dwt)]					
Water status	**AMF status**	**N**	**P**	**K**	**Ca**	**Mg**	**Na**
Control (0.0)	-AMF	2.80 ± 0.17^{C}	0.17 ± 0.052^{B}	38.9 ± 1.55^{B}	16.2 ± 0.88^{AB}	11.1 ± 0.55^{A}	12.0 ± 0.111^{E}
	AMF	3.18 ± 0.18^{A}	0.30 ± 0.081^{A}	42.2 ± 1.68^{A}	17.4 ± 0.89^{A}	11.5 ± 0.55^{A}	11.3 ± 0.17^{E}
	AMR (%)	13.6 ± 1.11	82.4 ± 3.22	9.65 ± 0.44	7.40 ± 0.54	3.60 ± 0.042	$- 05.83 \pm 0.44$
10%	-AMF	2.81 ± 0.15^{C}	0.16 ± 0.045^{B}	34.2 ± 1.32^{C}	13.7 ± 0.77^{C}	10.8 ± 0.59^{B}	19.6 ± 0.98^{C}
	AMF	3.20 ± 0.15^{A}	0.30 ± 0.084^{A}	39.5 ± 1.44^{AB}	15.1 ± 0.71^{B}	11.5 ± 0.61^{A}	16.6 ± 0.88^{D}
	AMR (%)	13.9 ± 1.051	87.5 ± 3.85	15.5 ± 0.88	9.56 ± 0.52	6.48 ± 0.098	$- 15.31 \pm 1.04$
20%	-AMF	2.45 ± 0.14^{D}	0.12 ± 0.034^{C}	26.6 ± 0.99^{E}	12.05 ± 0.68^{C}	08.7 ± 0.33^{C}	22.2 ± 1.05^{B}
	AMF	3.01 ± 0.15^{B}	0.27 ± 0.077^{AB}	32.2 ± 1.01^{C}	13.75 ± 0.66^{C}	09.6 ± 0.37^{C}	18.5 ± 1.55^{CD}
	AMR (%)	22.9 ± 1.55	125 ± 5.14	21.1 ± 0.98	14.1 ± 1.01	10.3 ± 0.99	$- 16.67 \pm 1.85$
40%	-AMF	2.05 ± 0.091^{E}	0.09 ± 0.004^{D}	22.7 ± 0.57^{E}	7.02 ± 0.33^{F}	06.5 ± 0.12^{D}	28.9 ± 1.74^{A}
	AMF	2.92 ± 0.10^{BC}	0.25 ± 0.014^{B}	29.9 ± 0.59^{D}	9.00 ± 0.571^{D}	08.1 ± 0.15^{C}	21.3 ± 1.88^{B}
	AMR (%)	42.4 ± 2.05	178 ± 7.40	31.7 ± 1.41	28.2 ± 1.33	24.6 ± 1.99	-26.30 ± 2.11

Values in each column (except AMR) followed by the same letter(s) are not significantly different at $P \leq 0.05$ (Duncan's multiple range test). AMF: arbuscular mycorrhizal fungi, -AMF: non-mycorrhizal fungi, AMR: arbuscular mycorrhizal response. Each value represents the mean of five replicates ± standard error

http://www.aloki.hu ● ISSN 1589 1623 (Print) ● ISSN 1785 0037 (Online)
DOI: http://dx.doi.org/10.15666/aeer/1704_99659978

Discussion

Salinity of soil is one of the severe abiotic stress problems particularly in arid and semi-arid area like Saudi Arabia. It directly negatively affecting the majority of arable lands worldwide, limiting the growth and production of most of the economically important crop, vegetable and horticulture plants (Giri et al., 2003; Al-Karaki, 2006; Kaya et al., 2009; Ibrahim et al., 2011; Abdel-Fattah and Asrar, 2012; Asrar et al., 2014; Elhindi et al., 2017). Augmenting salt concentration in soil decreases the plant ability to absorb water, negatively affect all metabolic processes and osmotic balance, nutrient absorption, water relations and net photosynthetic rate. All of these results adversely affecting plant growth and productivity (Ojala et al., 1983; Zuccarini, 2007; Scharnagl et al., 2018).

It is evident from the present investigation that sea water stress significantly decreased of estimated growth parameters of mycorrhizal and non-mycorrhizal pepper plants compared to the control plants. However, mycorrhizal fungi improved growth and biomass of pepper plants grown in either sea water stressed or control soils when comparing with non-mycorrhizal plants. The dependency of pepper plants on mycorrhizal fungi was highly increased with increasing sea water concentration soil. These results are entirely consistent with earlier studies on other crop and vegetable plant species (Giri et al., 2007; Al-Amri et al., 2013; Sheng et al., 2013). Enhancement of growth in mycorrhizal pepper plants irrigated with different concentrations of sea water has been related partially to mycorrhizal enhancement of host plant P, N and K nutrition (Poss et al., 1985; Garg and Chandel, 2011; Evelin et al., 2012).

Interestingly, AM pepper plants had higher K, Ca, P and N contents than non-mycorrhizal plants grown at sea water stress treatment. In this connection, pepper plant tolerance to sea water stress was improved highly by mycorrhizal fungi. The obtained results suggested that improving growth of pepper plants duo to mycorrhizal colonization is a manifest of increased nutrients content and maintaining favorable ionic ratios than non-mycorrhizal pepper plants. These results are confirmed by the most previous studies (Kaya et al., 2009; Kumar et al., 2010; Scharnagl et al., 2018). Furthermore, improved P, N, K and Ca contents by mycorrhizal fungi in pepper plants grown under sea water stress conditions may contribute to the maintenance of vacuolar membrane integrity and facilitate the compartmentalization of Na ions with vacuoles (Cantrell and Linderman, 2001). Preventation of Na ion from interfering in metabolic pathways of growth and yield, thereby mitigated the toxicity of sea water stress (Poss et al., 1985; Abdel-Fattah and Asrar, 2012). Lower Na in the mycorrhizal plants than non-mycorrhizal plants may be explained by the dilution effect due to growth enhancement (Giri and Mukherjee, 2004; Al-Karaki, 2006). In addition, Mycorrhizal inoculation can increase K^+ absorption under sea water stress conditions. The higher K^+: Na^+ ratio helps not only to prevent the disruption of various K-mediated enzymatic processes and inhibition of protein synthesis but also are beneficial in influencing the ionic balance of the cytoplasm or Na^+ efflux from plants (Colla et al., 2008; Zuccarini and Okurowska, 2008).

Photosynthetic pigments like chlorophyll have been proposed as one of the most parameters of salt tolerance in plants (Sirivastava et al., 1998) and also carotenoids are responsible for reducing of single oxygen (Bourgou et al., 2012). In this connection, it is evident from the present investigation that the photosynthetic pigments in leaves of mycorrhizal pepper plants were significantly higher than those in non-mycorrhizal plants grown in soil irrigated with sea water. The dependency of pepper plants on AM

http://www.aloki.hu ● ISSN 1589 1623 (Print) ● ISSN 1785 0037 (Online)
DOI: http://dx.doi.org/10.15666/aeer/1704_99659978

fungi was increased highly with increasing sea water concentration in soil. These results are in line with results of Elhindi et al. (2017) and Scharnagl et al. (2018). Furthermore, mycorrhiza improving Mg^{++} support a higher chlorophyll concentration. Effective Mg^{++} uptake helps by increasing the chlorophyll content and hence stimulating photosynthetic efficiency and plant growth (Camprubi et al., 2012; Metwally and Abdelhameed, 2018). Of particular interest in this study that g_s, P_N and E were highly significant in the AM pepper plants than in the non-mycorrhizal plants grown in soil irrigated with or without different concentrations of sea water. Such increased in the contents of gas water exchange were linked to the degree of mycorrhizal colonization. These results are in the same line of those obtained by Auge et al. (2008), Abdel-Fattah et al. (2013), Metwally and Abdelhameed (2018).

Sea water stress in soil not only affect the growth and production of pepper plant but also the levels of mycorrhizal colonization in associated pepper plants. These results were in agreement with the previous findings (Aroca et al., 2013; Abdel-Fattah et al., 2016; Elhindi et al., 2017). Based on the previous results of Jiang and Zhang (2002), who reported that antioxidant enzymes play an important role in scavenging of reactive oxygen species (ROS) and hence averting the oxidative stress induced damaging effects on several sensitive molecules like nucleic acids, proteins and lipids The present study demonstrated that the activities of CAT, POX and APX in mycorrhizal plants were significantly higher than in non-mycorrhizal pepper plants grown either in soil irrigated with or without sea water. Such stimulation in antioxidant activities in response to the mycorrhizal effect were significantly increased with increasing sea water concentration in soil. In this connection, several investigators reported that mycorrhizal symbiosis helps plants to alleviate or reduced salt stress by enhancing the activities of antioxidant enzymes (Tang et al., 2009; Metwally and Abdelhameed, 2018).

Conclusion

Arbuscular mycorrhizal colonization has a great contribution from pepper plant to alleviate salinity stress imposed by irrigation with different concentrations of sea water through improving growth, increasing nutrient contents, stimulating gas exchange parameters, presentation of Na^+ content and transfer by the roots to the shoots and some metabolic contents of pepper plants. These benefits in response to mycorrhizal inoculation were greatly increased with increasing sea water concentration in soil, suggesting that pepper plants was highly depended on mycorrhizal fungi particularly at higher concentration of sea water. However, more investigations are required to explain in details the relationship between the molecular of AM efficiency for plant growth and other metabolic activates in different varieties of plants under salinity stress conditions.

Acknowledgements. The author would like to thank the Deanship of Scientific Research, Shaqra University, Saudi Arabia for supporting this work.

Author contribution. The author designed and formed the experiments and analyzed the results. In addition, the author wrote, edited and revised the paper and approved the final version of the manuscript to be published.

http://www.aloki.hu ● ISSN 1589 1623 (Print) ● ISSN 1785 0037 (Online)
DOI: http://dx.doi.org/10.15666/aeer/1704_99659978

REFERENCES

[1] Abdel-Fattah, G. M., Asrar, A. A. (2012): Arbuscular mycorrhizal fungal application to improve growth and tolerance of wheat (*Triticum aestivum* L.) plants grown in saline soil. – Acta Physiol Plantarum 34: 267-277.

[2] Abdel-Fattah, G. M., Ibrahim, A. H., Al-Amri, S. M., Shoker, A. E. (2013): Synergistic effect of arbuscular mycorrhizal fungi and spermine on amelioration of salinity stress of wheat (*Triticum aestivum* L. cv. gimiza). – Aust. J. Crop Sci. 7: 1525-1532.

[3] Abdel-Fattah, G. M., Rabie, G. H., Lamis, D., Rabab, A. M. (2016): The impact of arbuscular mycorrhizal fungi on growth and physiological parameters of cowpea plants grown under salt stress conditions. – Int. J. Appl. Sci. Biotechnology 4: 372-379.

[4] Abdel-Ghani, A. H. (2009): Response of wheat varieties from semi-arid regions of Jordan to salt stress. – J. Agron. Crop Science 195: 55-65.

[5] Aebi, H. (1983): Catalase. – In: Bergmeyer, H. (Ed.), Methods of Enzymatic Analysis. Weinheim-Verlagchemie, Weinheim, pp. 273-286.

[6] Al-Amri, S. M., Al-Whaibi, M. H., Abdel-Fattah, G. M., Siddiqui, M. H. (2013): Role of mycorrhizal fungi in tolerance of wheat genotypes to salt stress. – African J. Microbiol. Res. 7: 1286-1295.

[7] Al-Karaki, G. N. (2006): Nursery inoculation of tomato with arbuscular mycorrhizal fungi and subsequent performance under irrigation with saline water. – Scientia Horticulturae 109: 1-7.

[8] Al-Karaki, G. N., Hammad, R., Rusan, M. (2001): Response of two tomato cultivars differing in salt tolerance to inoculation with mycorrhizal fungi under salt stress. – Mycorrhiza 11: 43-47.

[9] Aroca, R., Ruiz-Lozano, J. M., Lopez-Raez, J. A. (2013): Arbuscular mycorrhizal symbiosis influences strigolactone production under salinity and alleviates salt stress in lettuce plants. – J. Plant Physiol. 170: 47-55.

[10] Asrar, A., Abdel-Fattah, G., Elhindi, K., Abdel-Salam, E. (2014): The impact of arbuscular mychorrhizal fungi in improving growth, flower yield and tolerance of *kalanchoe (Kalanchoe blossfeldiana* Poelin) plants grown in NaCl-stress conditions. – Journal of Food, Agriculture & Environment 12: 105-112.

[11] Auge, R. M., Toler, H. D., Sams, C. E., Nasim, G. (2008): Hydraulic conductance and water potential gradients in squash leaves showing mycorrhiza-induced increases in stomatal conductance. – Mycorrhiza 18: 115-121.

[12] Bourgou, S., Bettaie, I., Hamrouni, I., Marzouk, B. (2012): Effect of NaCl on fatty acids, phenolics and antioxidant activity of *Nigella sativa* organs. – Acta Physiol. Plantarum 34: 379-386.

[13] Camprubi, A., Abril, M., Estaun, V., Calvet, C. (2012): Contribution of arbuscular mycorrhizal symbiosis to the survival of psammophilic plants after sea water flooding. – Plant Soil 35: 97-107.

[14] Cantrell, I. C., Linderman, R. G. (2001): Preinoculation of lettuce and onion with VA mycorrhizal fungi reduces deleterious effects of soil salinity. – Plant and Soil 233: 269-281.

[15] Colla, G., Rouphael, Y., Cardarelli, M., Tullio, M., Rivera, C. M., Rea, E. (2008): Alleviation of salt stress by arbuscular mycorrhizal in *Zucchini* plants grown at low and high phosphorus concentration. – Biology and Fertility of Soils 44: 501-509.

[16] Daei, G., Ardekani, M. R., Rejali, F., Teimuri, S., Miransari, M. (2009): Alleviation of salinity stress on wheat yield, yield components and nutrient uptake using arbuscular mycorrhizal fungi under field conditions. – J. Plant Physiol. 166: 617-625.

[17] Elhindi, K. M., Sharaf El-Din, A., Elgorban, A. M. (2017): The impact of arbuscular mycorrhizal fungi in mitigating salt-induced adverse effect in sweet basil (*Ocimum basilicum* L.). – Saudi Journal of Biological Science 24: 170-179.

http://www.aloki.hu ● ISSN 1589 1623 (Print) ● ISSN 1785 0037 (Online)
DOI: http://dx.doi.org/10.15666/aeer/1704_99659978

[18] Evelin, H., Kapoor, R., Giri, B. (2009): Arbuscular mycorrhizal fungi in alleviation of salt stress: a review. – Ann Botany 104: 1263-1280.
[19] Evelin, H., Giri, B., Kapoor, R. (2012): Contribution of *Glomus intraradices* inoculation to nutrient acquisition and mitigation of ionic imbalance in NaCL-stressed *Trigonella graecum*. – Mycorrhiza 22: 203-217.
[20] Gajewska, E., Sklodowska, M. (2007): Effect of nickel on ROS content and antioxidative enzyme activities in wheat leaves. – Bio Metals 20: 27-36.
[21] Garg, N., Chandel, S. (2011): Effect of mycorrhizal inoculation on growth, nitrogen fixation and nutrient uptake in *Cicer arietinum* L. under salt stress. – Turk. J. Agric. 35: 205-214.
[22] Gerdemann, J. W., Nicolson, T. H. (1936): Spores of mycorrhizal endogone species extracted from soil by wet sieving and decanting. – Trans. Brit. Mycol. Soc. 46: 235-244.
[23] Giri, B., Mukherjee, K. G. (2004): Mycorrhizal inoculant alleviates salt stress in *Sesbania aegyptiaca* and *Sesbania grandiflora* under field conditions: evidence for reduced sodium and improved magnesium uptake. – Mycorrhiza 14: 307-312.
[24] Giri, B., Kapoor, R., Mukerji, K. G. (2003): Influence of arbuscular mycorrhizal fungi and salinity on growth, biomass and mineral nutrition of *Acacia auriculiformis*. – Biology and Fertility of Soils 38: 170-175.
[25] Giri, B., Kapoor, R., Mukerji, K. G. (2007): Improved tolerance of *Acacia nilotica* to salt stress by arbuscular mycorrhiza, *Glomus fasciculatum*, may be partly related to elevated K^+/Na^+ ratios in root and shoot tissues. – Microbial Ecology 54: 753-760.
[26] Ibrahim, H. A., Abdel-Fattah, G. M., Eman, F. M., AbdEl_Aziz. M. H., Shohr, A. E. (2011): Arbuscular mycorrhizal fungi and spermine alleviate the adverse effects of salinity stress on electrolyte leakage and productivity of wheat plants. – Phyton-Ann Rel Bot. 51: 261-276.
[27] Jackson, M. L.: Soil Chemical Analysis. – Prentice Hall of India Ltd., New Delhi.
[28] Jiang, M., Zhang, J. (2002): Water stress-induced abscissic acid accumulation triggers the increased generation of reactive oxygen species and up-regulates the activities of antioxidant enzymes in maize-leaves. – Journal of Experimental Botany 53: 2401-2410.
[29] Juniper, S., Abbott, L. K. (1993): Vesicular-arbuscular mycorrhizas and soil salinity. – Mycorrhiza 4: 45-57.
[30] Juniper, S., Abbott, L. K. (2006): Soil salinity delays germination and limits growth of hyphae from propagules of arbuscular mycorrhizal fungi. – Mycorrhiza 16: 371-379.
[31] Kaya, C., Ashraf, M., Sonmez, O., Aydemir, S., Tuna, A. L., Cullu, M. A. (2009): The influence of arbuscular mycorrhizal colonization on key growth parameters and fruit yield of pepper plants grown at high salinity – Scientia Horticulturae 121: 1-6.
[32] Kumar, A., Sharma, S., Mishra, S. (2010): Influence of arbuscular mycorrhizal (AM) fungi and salinity on seedling growth, solute accumulation and mycorrhizal dependency of *Jatropha curcas* L. – J Plant Growth Regul. 29: 297-306.
[33] Metwally, R., Abdelhameed, R. (2018): Synergistic effect of arbuscular mycorrhizal fungi on growth and physiology of salt-stressed *Trigonella foenum*-graecum plants. – Biocatalysis and Agricultural Biotechnology 16: 538-544.
[34] Menge, J. A., Johnson, E. L. V., Platt, R. G. (1978): Mycorrhizal dependency of several citrus cultivars under three nutrient regimes. – New Phytol. 81: 553-559.
[35] Nakano, Y., Asada, K. (1981): Hydrogen peroxide is scavenged by ascorbate-specific peroxidase in spinach chloroplasts. – Plant Cell Physiol. 22: 867-880.
[36] Nelson, D. W., Sommers, L. E. (1973): Determination of total nitrogen in plant material. – Agro. J. 65: 109-112.
[37] Ojala, J. C., Jarrel, W. M., Menge, J. A., Johnson, E. L. V. (1983): Influence of mycorrhizal fungi on the mineral nutrition and yield of onion in saline soil. – Agron J. 75: 255-259.

http://www.aloki.hu ● ISSN 1589 1623 (Print) ● ISSN 1785 0037 (Online)
DOI: http://dx.doi.org/10.15666/aeer/1704_99659978

[38] Phillips, J. M., Hayman, D. S. (1970): Improved procedures for clearing roots and staining parasitic and vesicular-arbuscular mycorrhizal fungi for rapid assessment of infection. – Trans. Brit. Mycol. Soc. 55: 158-161.
[39] Pond, E. C., Menge, J. A., Jarrell, W. M. (1984): Improved growth of tomato in salinized soil by vesicular arbuscular mycorrhizal fungi collected from saline sites – Mycologia 76: 74-84.
[40] Poss, J. A., Pond, E. C., Menge, J. A., Jarrell, W. M. (1985): Effect of salinity on mycorrhizal onion and tomato in soil with and without additional phosphate – Plant and Soil 88**:** 307-319.
[41] Scharnag, K., Sanchez, V., Wettberg, E. (2018): The impact of salinity on mycorrhizal colonization of a rare legume, *Galactia smallii* in south Florida pine rocklands. – BNC Res. Notes 11: 2-5.
[42] Sheng, M., Lalande, R., Hamel, C., Zladi, N. (2013): Effect of long-term tillage and mineral phosphorus fertilization on arbuscular mycorrhizal fungi in a humid continental zone of Eastern Canada. – Plant Soil 369: 599-613.
[43] Sirivastava, T. P., Gupta, S. C., Lal, P, Muralia N, Kumar, N. (1998): Effect of salt stress on physiological and biochemical parameters of wheat. – Ann Arid Zone 27: 197-204.
[44] Tang, M., Chen, H., Huang, J. C., Tian, Z. Q. (2009): AM fungi effects on the growth and physiology of *Zea mays* seedlings under diesel stress. – Soil Biol. Biochem. 41: 936-940.
[45] Trouvelot, A., Kough, J., Gianinazzi-Pearson, V. (1986): Evaluation of VA Infection Levels in Root Systems. Research for Estimation Methods Having a Functional Significance. – In: Gianinazzi-Pearson, V., Gianinazzi, S. (eds.) Physiological and Genetical Aspects of Mycorrhizae. INRA Press, Paris, pp. 217-221.
[46] Wu, Q. S., Zon, Y. N., Liu, W., Ye, X. E., Zai, H. E., Zhao, L. J. (2010): Alleviation of salt stress in citrus seedlings inoculated with mycorrhiza: changes in leaf antioxidant defense systems. – Plant Soil Environ. 56: 470-475.
[47] Zuccarini, P. (2007): Mycorrhizal infection ameliorates chlorophyll content and nutrient uptake of lettuce exposed to saline irrigation. – Plant, Soil and Environment 53: 283-289.
[48] Zuccarini, P., Okurowska, P. (2008): Effects of mycorrhizal colonization and fertilization on growth and photosynthesis of sweet basil under salt stress. – Journal of Plant Nutrition 31: 497-513.

http://www.aloki.hu ● ISSN 1589 1623 (Print) ● ISSN 1785 0037 (Online)
DOI: http://dx.doi.org/10.15666/aeer/1704_99659978

EFFECTS OF TECHNICAL FACTORS TOWARDS ACHIEVING THE THERMOPHILIC TEMPERATURE STAGE IN COMPOSTING PROCESS AND THE BENEFITS OF CLOSED RECTOR SYSTEM COMPARED TO CONVENTIONAL METHOD – A MINI REVIEW

ALKARIMIAH, R.[1*] – SUJA', F.[2]

[1]*School of Civil Engineering, Universiti Sains Malaysia, 14300 Pulau Pinang, Malaysia*

[2]*Faculty of Engineering and Built Environment, Universiti Kebangsaan Malaysia, 43600 Bangi, Selangor, Malaysia*
(phone: +60-38-911-8364/8911/8354, fax: +60-38-911-8355)

**Corresponding author*
e-mail: cerosnani@usm.my; phone: +60-45-996-264; fax: +60-45-996-906

(Received 9th Apr 2019; accepted 19th Jun 2019)

Abstract. Composting is the process of organic biological decomposition in aerobic and controlled conditions. Many factors can affect the composting process, and almost all are related. Some factors that majorly affect the composting process also influence the stage or direction of the process. This paper focuses on the technical factors that affect the composting process' achievement of the thermophilic phase, particularly in a closed reactor system. At the same time, this paper will be discussed about the benefits and comparison between close reactor system and the conventional pile method. The technical factors that are discussed in-depth in this mini review paper are the rotation or turning frequency, aeration rates, and the initial moisture of the compost mixture for closed reactor composting system. All three factors significantly cause increased thermophilic temperature in the closed reactor. Basically, there are 3 important phases in the composting process, which are the mesophilic phase, thermophilic phase, and maturation phase. In the composting process, it is crucial that the thermophilic temperature is reached. By increasing the thermophilic temperature, the number of thermophilic microorganisms also increases, causing the rapid degradation of bio-waste
Keywords: *aeration rates, initial moisture, rotation/turning frequency, thermophilic temperature*

Introduction

The problem of residual waste streams from the industry has worsened. Before industrialization, the production and decomposition of organic matter were essentially balanced. Composting, in general, is not only important in preventing the accumulation of organic waste from harming the environment, but also to recycle nutrients and organic matter. A proper composting process effectively destroys pathogens and weed seeds because in the process a high temperature (55–65 °C) is achieved through the metabolic heat generated by microorganisms in the thermophilic phase (Petric and Selambasic, 2008).

Among the benefits of composting is that plant nutrients are conserved, and harmful substances are transformed into non-hazardous substances; thus, producing reusable products (Liu, 2000). Composting materials from organic waste can also improve the structure of the water-holding capacity of the soil (Mohammad et al., 2012). Furthermore, the benefit of composting nowadays is not limited to landfills, but also for controlling and preventing environmental pollution. Composting materials are now used

http://www.aloki.hu ● ISSN 1589 1623 (Print) ● ISSN 1785 0037 (Online)
DOI: http://dx.doi.org/10.15666/aeer/1704_99799996

to control soil erosion on highways. It also works for cleaning runoff in running water and for recovering soil contaminated with heavy metals or toxic organic compounds (Bhattarai et al., 2011).

Compost stability and maturity have an important impact on the application of the compost's final product in land use. The use of immature and unstable compost products because of an incomplete biodegradation process can negatively affect germination and reduce plant fertility, which causes competing absorption of oxygen and toxicity (Zhang et al., 2017). The application of unstable and immature compost would fix nitrogen in the soil and limit plant growth because it competes for oxygen in the rhizosphere and discharges toxic substances (Bernal et al., 2009). According to many researchers, matured compost products from composting at thermophilic temperature are eco-friendlier (Bernal et al., 1998; Yang et al., 2013; He et al., 2014).

Most of the composting system used is conventional technology which is by adapting the pile method. The pile method, if not properly maintained, will cause many problems, for example the presence of wild animals and require more sophisticated operation controls and require large space and a need long time to produce the product. Hence, composting using mechanical methods such as closed reactors is easier and able to overcome problems resulting from composting rather than using pile methods. The goal of the reactor's mechanical design is to accelerate the composting process through optimum maintenance for active microbes during composting and to minimize adverse effects on the environment (Bertoldi et al., 1983). Mechanical systems can process large amounts of waste without taking up much space, and they offer good control of the environmental conditions such as temperature, moisture content, and airflow rate (Alkoaik et al., 2018). The mechanical system is usually closed, however there are researchers using an open reactor system. However, mechanical closed reactor systems have good control which makes it more suitable for composting in large quantities (Bhamidimarri and Pandey, 1996; Haug, 1993). In general, pile methods and mechanical methods can be distinguished on several criteria such as capital costs, operational costs, land requirements, operating controls and so on (Habsah, 2008). *Table 1* describes the comparison of both pile and closed mechanical methods. From the table below, pile composting method are more exposed to the influenced of weather, which will at the same time influence the temperature rise of the pile. Adapting pile/windrow system also lead to leachate contamination posing a risk of groundwater contamination GHG emissions, space limitation and emission of greenhouse gases (Rich and Bharti, 2015). Zhu-Barker et al. (2017) mentioned that windrow composting system is a source of greenhouse gases (GHG) that contribute to climate change. In their study, found that pile compost during the rainy season with cooler temperature resulted in oxygen depleted environment that generated the highest CH_4 and lowest N_2O emissions. Chen et al. (2015) also studied the N_2O emission during the composting of dairy manure by windrow system. They found out pile turning altered the distributions of NO_3^- and NO_2^- in the compost materials and dramatically influenced surface windrow N_2O emissions.

The process of composting is a biological one and thus involves various microorganisms. These organisms will break down organic matter and organic compounds. The identification of microorganisms capable of decomposing certain compounds is very useful in the composting process. Organic waste is decomposed during the process of fertilization by replacing microbial communities with complex and critical substrata such as cellulose, lignin, and hemicellulose (Hiroaki et al., 2006).

http://www.aloki.hu ● ISSN 1589 1623 (Print) ● ISSN 1785 0037 (Online)
DOI: http://dx.doi.org/10.15666/aeer/1704_99799996

Composting-related organisms can be classified into two classes, namely mesophyll and thermophile. Classification of microorganisms according to the temperature in which they live and grow. Temperature plays an important role in the composting process, as it affects microbial activity. Hoseini and Abdul Aziz (2013) also indicate temperature as a key factor for determining the progress of the composting process; a higher temperature (thermophilic conditions) results in a higher decomposition of organic matter (OM).

Several researchers concluded that using a single-maturity index was insufficient to indicate compost maturity and stability (Rashad et al., 2010). However, many other researchers used the thermophilic stage of the composting process as a key factor for specifying the success of the entire process (Sarkar et al., 2016; Han et al., 2018; Koyama et al., 2018; Gou et al., 2017; Awasthi et al., 2017; Hoseini and Abdul Aziz 2013; Li et al., 2014). Therefore, this paper discusses and reviews the factors that significantly impact thermophilic temperature achievement, especially in a closed reactor, either lab-scale or pilot-scale. The factors that are discussed include rotation/turning frequency, aeration rate, and initial moisture of the compost mixture.

Table 1. *Comparison between pile composting and mechanical methods. (Source: Habsah, 2008)*

Criteria	Pile method	Closed mechanical reactor
Capital Cost	Low	High
Operational cost	Low	Low
Land requirement	High	Low. Can increase if the resulting compost needs to be matured in a pile method
Ventilation control	Limited. Unless forced aeration is done	No limit
Operation control	Turning frequency, parameter correction (moisture, pH, C/N)	Airflow rate, dynamic of turning process, parameter correction (moisture, pH, C/N), recycling
Sensitivity to weather changes	Sensitive. Need to be covered with plastic canvas	Can operate at any weather. But it depends on the material
Odor control	Depending on the organic material used	Good
Problem in operation	Easily influenced by uncertain weather	Potential for short circuit, complex mechanical process

Thermophilic temperature

Temperature is a substantial measurement that could affect the composting process and the microbial activity during composting (Sun et al., 2017; Morales et al., 2016; Zhao et al., 2016). At the same time, it is also a function of the process. During the aerobic composting process, there are three phases affecting the microbial population. The first is the mesophilic phase (ambient temperature up to 45 °C), followed by the thermophilic phase (45 °C- > 60 °C) and finally returning to the mesophilic phase (45 °C to the surrounding temperature) as shown in *Figure 1*. Temperature does not only affect the metabolic process of microorganisms, but these parameters are also seen to affect the density and composition of microbes in the compost mass (Liang et al., 2003). Because temperature impacts microbiological processes, important responses and other elements of the composting process are also affected by temperature changes (Epstein, 1997). It was reported that a composting temperature set to 55 °C, enabled the

http://www.aloki.hu ● ISSN 1589 1623 (Print) ● ISSN 1785 0037 (Online)
DOI: http://dx.doi.org/10.15666/aeer/1704_99799996

killing off of pathogens and sanitization of compost material (Gea et al., 2005). Stentiford (1996) also found that maximum temperatures of 55-65 °C were necessary to destroy pathogens, but temperatures within the range of 45-55 °C must be maintained for maximum biodegradation in the composting process. Additionally, temperatures below 20 °C and more than 60 °C have been shown to reduce microbial activity (Liang et al., 2006). However, Wong et al. (2001) agreed that a 60 °C temperature was the most ideal condition to produce optimum reproducibility in the composting process.

In the early mesophilic phase, mesophilic and fungal bacterial populations number 10^8 and 10^6 for each 1 g of wet compost. Meanwhile, the thermophilic and actinomycet bacterial population is 10^4 and the thermophilic fungi population is 10^3 for every 1 g of wet compost. A summary of the bacterial, fungal and actinomycet populations at every composting phase is shown in *Table 2*.

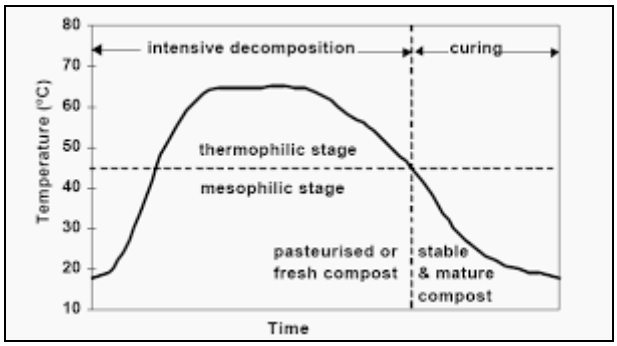

Figure 1. *Temperature profile and growth of microorganisms in compost heap*

Table 2. *Comparison between pile composting and mechanical methods. (Source: Abu Zahrim, 2004)*

Microbe	Mesophilic Early stage < 40 °C	Thermophilic 40- > 60 °C	Thermophilic to maturation phase
Bacteria			
Mesophilic	10^8	10^6	10^{11}
Thermophilic	10^4	10^9	10^7
Actinomycete			
Thermophilic	10^4	10^8	10^5
Fungi			
Mesophilic	10^6	10^3	10^5
Thermophilic	10^3	10^7	10^6

The increase in temperature is significant for the activity and growth of mesophilic organisms during the initial phase of composting such as lactic acid bacteria, Gram-negative bacteria, yeast, and fungi (Steger et al., 2005). At the thermophilic stage of the composting process, thermophilic organisms dominate the degradation process. The bacterial species that dominate the thermophilic phase of the composting process belong to the genus *Bacillus spp*. and *Thermus thermophiles* (Steger et al., 2005). Siu-Rodas et al. (2018), in their study, found that three out of twenty isolated strains showed higher enzymatic activity and were identified as *Bacillus subtilis*; the study composted coffee residue at a pile temperature of 57 °C. They also discovered that the isolation of

http://www.aloki.hu ● ISSN 1589 1623 (Print) ● ISSN 1785 0037 (Online)
DOI: http://dx.doi.org/10.15666/aeer/1704_99799996

microorganisms from composting piles in the thermophilic stage allowed for the identification of three *B. subtilis strains*, where the enzymatic extracts showed activity on CMC and crystal cellulose, confirming the existence of endo- and exocellulases. These cellulases could be used in several industries, such as in the preparation of animal foods, fruit juice extraction, and clarification and bleaching of recycled paper. The differences in microbial community were observed clearly at different composting temperatures. The genus *Bacillus* was dominant at 50 °C to 70 °C, while the genus *Geobacillus* increased with the escalation of temperature and dominated at 70 °C (Bhatia et al., 2013; Ivanov et al., 2001). All these bacteria genera play an important role in the degradation of complex substrates.

The mode of composting and the control levels have a great impact on composting temperature. The highest degree of temperature control is usually obtained in mechanical systems. Large-scale reactors (10–300 l) often comprise a self-heating phase (Lashermes et al., 2012). Previously, Petiot and de Guardia (2004) reported small-volume reactors resulting in a rapid decrease of temperature due to the reactors' limited amounts of organic substrates and heat losses. Meanwhile, the temperature inside the full-scale reactor declined slowly and gradually. However, temperature, regardless of the method used, is rarely uniform for the entire mass of composting material. The center point of the mass of compost material tends to be warmer than the mass of the composting material on the cooler outer edge. Ali et al. (2014) revealed that the temperature at the inlet zone, middle zone, and outlet zone of the drum varied between 50 °C to 60 °C, 50 °C to 54 °C, and 30–28 °C (ambient temperature or slightly higher, signifying the end of the active thermophilic phase), respectively. The variation in temperature range in the three zones inside the reactor is attributed to the microbial activity and accessibility of degradable substances.

Some methods for heating up the pile have been extensively studied to confirm the standard operations for composting. Normally there are 2 methods to heating up the pile. Artificial heating is one of the methods to increase the composting temperature; however, it incurs high cost and energy consumption (Xie et al., 2017). Besides, recent studies have revealed that inoculating microorganisms (bacteria and fungi) in the composting would be beneficial for the composting to pass the start-up period and achieve thermophilic stage even under cold-climate temperature (Gou et al., 2017; Sarkar et al., 2010; Awasthi et al., 2014; Awasthi, 2017).

Elango et al. (2009) investigated the optimal value for reducing the municipal solid waste (MSW) composting time in a thermophilic bioreactor in aerobic conditions. In their study, the thermophilic temperature reached 65–70 °C within 14 to 21 days of the composting process. After 21 days, the temperature declined gradually, reaching 40 °C at day 40. They conclude that the use of a thermophilic bioreactor enabled the stabilization of the final compost and led to the production of good humus. At the same time, they also mentioned that the higher the temperature, the longer the retention time in the bioreactor and, in turn, the higher reduction in C/N and volatile solids.

Bai and Wang (2011) studied the biodegradation of organic matter (OM) during the aerobic thermophilic phase of human faecal matter. They used a closed reactor system and a thermo-controlled water heater to control the temperature. Under the controlled thermophilic temperature of 60 °C and with moisture maintained at 60%, more than 70% of faecal organic matter was obtained in the two-week composting process. They also observed that under thermophilic conditions, ammonification and nitrifications were reduced because of a lack of ammonifying and nitrification bacterial activity. On

http://www.aloki.hu ● ISSN 1589 1623 (Print) ● ISSN 1785 0037 (Online)
DOI: http://dx.doi.org/10.15666/aeer/1704_99799996

the other hand, thermophilic composting led to more organic nitrogen content being retained without loss of phosphorus (P) in the compost products. Thermophilic composting treatment could also affect the abundance of tetracycline resistance genes (TRGs) especially in the composting of animal manure (including human manures). Kang et al. (2017) reported that short thermophilic composting treatment is insufficient to remove TRGs in the pig manure composting process. The devoting of inactivation of TRGs contain in the animal manure is crucial, because it will be a major source of antibiotic pollution in the soil if the animal manure did not undergo proper thermophilic composting process prior to used directly to the soil.

Besides that, increase in thermophilic temperature in the composting process will help exploit NH^{3+} gas recovery and would allow the production of a nitrogen source that is free from pathogens and heavy metals (Koyama et al., 2018). During the thermophilic stage, aerobic microorganisms degrade the organic nitrogen of the fresh material into dissolved nitrogen, which, in turn, degrades to NH_4^+ -N; some element of NH_4^+-N then vaporizes as NH^{3+} gas. Pagans et al. (2006) also confirmed that NH^{3+} emission increased at a higher temperature. Various environmental conditions, including temperature, strongly impact the microbial community and cause additional differences in nitrogen dynamics (Wang et al., 2017). Koyama et al. (2018) mentioned in their study that ammonia recaptured from aquacultural sludge could potentially be used for the cultivation of high-value microalgae and the commercial production of medicines, cosmetics, or health supplements. Therefore, in any composting system, the main principle that researchers apply is to develop a composting system that is able to achieve the thermophilic phase. This is because the thermophiles isolated from the high temperature during composting can be further used to develop an inoculum that accelerates the degradation process (Sarkar et al., 2016).

Technical factors affecting thermophilic temperature increase in composting process

A controlled composting process is crucial to achieving a short processing time at lower costs, and to obtain products that are free of pathogens and odors (Bertoldi et al., 1983). Decomposition is a slow process and offers very slight control of the process conditions such as moisture, temperature, and air supply (Schulze, 1961). Temperature is an important factor in the composting process and depends on the activity of the microbes. Besides that, other parameters that affect the composting process is moisture and oxygen level. Hence, it is essential to identify factors that can significantly increase thermophilic temperature. The subtopics below discuss how rotation/turning frequency, feeding ratio, initial moisture content and aeration rate affect the temperature of the composting process.

Rotation/turning frequency

Rotation/turning frequency of compost mass is one of the factors affecting the composting rate and quality of compost produced (Tiquia et al., 1997). Rotation or turning for composting can also be performed in a closed reactor system. The main function of rotation in this type of system is to expose compost materials to fresh air, increase oxygen levels, and release heat and gas once the compost products are decomposed (Rynk Richard, 2001). Rotation in a closed system can also reduce air pollution and facilitate the mixing process of the compost pile (Tiquia and Tam, 1998).

http://www.aloki.hu ● ISSN 1589 1623 (Print) ● ISSN 1785 0037 (Online)
DOI: http://dx.doi.org/10.15666/aeer/1704_99799996

There are many advantages for adapting optimum rotation frequency for the closed reactor system. The main advantages of rotation operation for closed reactor system are to provide ventilation, reduce particle size, ensure that composting materials have the highest temperature, renew microbial activity, and provide fresh material for microbial colonization, so that the ammonia accumulated in the internal void space of the compost is released; thus yielding more uniform compost quality (Diaz et al., 2002; Hackett et al., 1999; Thambirajah and Kuthubutheen, 1989; Biddlestone and Gray, 1991; Parkinson et al., 2004). The rotation process also may increase the functional free air space in the compost (El Kader et al., 2007). Increased free air space can directly increase air renewal or the area of the gas/liquid interface. In addition, increasing free air space increases both oxygen diffusion and the insulation coefficient. This leads to heat production and temperature increase in the compost pile inside the reactor.

Rotation is a preliminary mechanism for controlling ventilation and temperature in composting systems (Tiquia et al., 1997). It is an essential variable in composting and provides both homogenization and aeration to the waste mixture. Furthermore, it controls the composting mixture temperature, the kinetics of the process, and the end-product sanitation (Smith et al., 2006). Normally, the compost piled through a turning process may experience a reduction in volume by 55% to 72% (Larney et al., 2000). This reduction is found in the form of mass elements such as C, K, and Na in the compost (Tiquia et al., 2002). Agamuthu (2001) suggests that the turning process should be carried out regularly to ensure that the mass of the compost material contains a moisture content of more than 70%.

However, the disadvantage of high frequency of the rotation process is it may affect the temperature of the compost pile. Therefore, the rotation process must be controlled to ensure that high temperatures are maintained in the compost pile inside the system. Ahmad (2001) states that an excessive rotation process could cause the compost mass to turn cold and dry up, which will indirectly destroy fungi and actinomycetes. Parkinson et al. (2004) also suggest that too much rotation in the composting process would result in the loss of nitrogen in the form of ammonia gas to the atmosphere. This may affect the quality of the compost products, as it may lack important nutrients such as nitrates that are useful for plants. Wan Razali et al. (2012) also mentioned, the fluctuation of temperature in the composting process especially in vessel composting cannot be avoided because of the sludge addition and mechanical turning effect.

Kalamdhad and Kazmi (2009) studied the impact of the rotation process in rotary drum reactors on the quality and stability of the resulting compost product. In their study, the organic waste used was a mixture of cattle stools, wooden ashes, and rotten green vegetables. They found that there was a close correlation between the quality of the compost produced with the frequency of rotation in terms of the value of nitrogen and phosphorus.

Fewer turning frequency would not yield rapid composting, but might be satisfactory for avoiding anaerobic conditions, odors, and maintaining high temperature. A higher turning frequency causes lower temperature and higher moisture loss. In study conducted by Smars et al. (2001), the rotation was limited to only 10-20 min per day. Rodriguez et al. (2012) suggested 12 rotations per hour as necessary for reaching optimal conditions to ensure that the composting would reach high thermophilic temperatures of up to 70 °C. They also argued that a combination of several optimal variables and appropriate reactor designs was essential to ensure that the composting process rapidly achieved thermophilic temperatures and obtained quality final products.

http://www.aloki.hu ● ISSN 1589 1623 (Print) ● ISSN 1785 0037 (Online)
DOI: http://dx.doi.org/10.15666/aeer/1704_99799996

Table 3 shows the variation of turning frequency for rotary reactor by different references.

Table 3. *Variation of rotation frequency for closed reactor*

Variation of rotation frequency	Reactor	Reference
4 rotations/h every 15 min	Hermetic rotary drum	Scoton et al. (2016)
12 rotations/h and 48 rotations/h	Rotary drum	Rodriguez et al. (2012)
1 rotation/day for 2 weeks	Rotary drum	Villasenor et al. (2011)
1 rotation/day	Full scale rotary drum composter	Bhatia et al. (2013)
3 rotations every 6 h/12 h/18 h/24 h	Rotary drum composter	Kalamdhad and Kazmi (2009)
1 rotation/day for 2 weeks and 1 or 2 rotations/week	Pilot scale closed rotary drum	Fernandez et al. (2010)
2 rotations/day	Full scale continuous rotary drum	Ali et al. (2014)
4 rotations/day	Rotary drum composter	Sharma et al. (2018)

Aeration rate

Oxygen is important for promoting microbial activity in the compost because composting is an aerobic process (involves the presence of oxygen). Therefore, aeration is required for the production of metabolic heat from aerobic microbes. There are three main principles of aeration that can supply oxygen (O_2) during the process of composting: natural aeration, passive aeration, and active aeration (Epstein, 1997). Aeration, moisture content, and temperature are major factors that affect the composting process because these parameters are interdependent (Talib et al., 2014). A lack of oxygen will result in anaerobic conditions to occur in the compost pile (Polsprasert, 1986). Failure in adjusting for a good aeration system will cause a slow decomposition of organic matter, unpleasant odors, delayed maximum temperature, a low maximum temperature, and slow water removal rate (Diaz et al., 2002; Ferrer et al., 2001; Haug, 1993). Besides, excessive aeration may increase costs and slow down the composting process through heat, water, and ammonia losses. Based on a study conducted by Guo et al. (2012), the aeration rate is a major factor influencing the stability of the compost.

Natural aeration occurs when there is diffusion and natural movement of air in the compost pile. This type of aeration is cheap, easy, and does not require special equipment. Active aeration involves the construction of porous pipes under the compost pile to promote the spread of oxygen gas into the compost waste materials. Meanwhile, passive aeration is highly reliant on the porosity of the matrix pipe because this method uses natural absorption and movement of air inside the pipeline to facilitate the spreading of air into the compost pile. However, using an air ventilation system in the composting process could interfere with temperature stabilization in the compost pile (Barrington et al., 2003). Compared to active aeration, passive aeration modes produce better composting rates. This is because the passive aeration process does not produce a cooling effect on the stack of compost material and can reduce the effect of nitrogen loss to the environment (Habsah, 2008). The lower the aeration rate, the longer the thermophilic temperature stage can be maintained in the composting process (Zang et al., 2016). Otherwise, Alkoaik et al. (2018) in their study mentioned that for the continually rotating drum natural aeriation is suggested by making holes of appropriate size on the drum surface. This is because, the pressure difference between inside and outside the rotating drum will induced aeriation.

http://www.aloki.hu ● ISSN 1589 1623 (Print) ● ISSN 1785 0037 (Online)
DOI: http://dx.doi.org/10.15666/aeer/1704_99799996

Kasinski et al. (2016) also stated that the application of passive aeration at a larger scale simultaneously permits the thermophilic temperature to be maintained during municipal solid waste composting process and constrains microbial activity in the reactor. Passive aeration permits thermophilic temperature levels in larger-scale composting processes to be retained, which, in turn, allows that biodegradation has occurred and microbial activity has not been repressed. Guo et al. (2012) conducted a statistical analysis on the effect of aeration rate, moisture content, and C/N ratio on the stability and maturity of compost pig feces and corn stalk. Their results showed that the aeration rate had a significant influence on the change in temperature ($p = 0.023$). Meanwhile, Talib et al. (2014) found that excessive aeration rate would increase energy conversion, thereby reducing temperature and moisture content. Charles et al. (2009) studied the effect of pre-aeration to start up batch thermophilic anaerobic digestion. They found that a pre-aeration of 48 h generated sufficient biological heat to increase the temperature of bulk municipal solid waste to 60 °C. Ambient temperature and aeration rate also affected the composting process. Han et al. (2018) investigated the effect of ambient temperature and aeration on thermophilic aerobic composting and found that although the ambient temperature increased in the summer, the upgraded aeration frequency during that season might have accelerated heat loss. They conclude that ambient temperature and aeration frequency influenced the average and highest temperatures of the composting materials. On the other hand, different composting materials and the type of composting system used in different works of literature provide a wide range of aeration rates (Mason, 2007). *Table 4* shows the optimum aeration rate for different organic waste composting and raw materials.

Table 4. *Optimal aeration rates and thermophilic temperature*

Optimum aeration rate	Type of waste	Range of thermophilic temperature	Reference
0.4 L min^{-1} kg^{-1} OM	Extraction of tomatoes, peppers, grass, and eggplant	62–65 °C	Kulcu and Yaldiz (2004)
0.25 L min^{-1} kg^{-1} VS	Dairy manure and rice straw		Luo et al. (2008)
0.6 L min^{-1} kg^{-1} for the active phase and 0.4 L min^{-1} kg^{-1} in the maturation phase	Municipal solid waste	70–73 °C	Rasapoor et al. (2009)
0.24, 0.48, 0.72 L kg^{-1} dry matter (DM) min^{-1}	Pig feces and corn stalk	> 50 °C	Guo et al. (2012)
0.1 Lmin^{-1} m^{-3}	Chicken manure, paddy stalk, grass	73–74 °C	Shen et al. (2011)
0.26 Lmin^{-1} kg^{-1} OM	EFB rabbit manure	70 °C	Talib et al. (2014)
33.5 L/h/kg of initial waste mass	Municipal waste	70–73 °C	Kasinski et al. (2016)
42–48 m^3 min^{-1}	Municipal sewage sludge	53–80 °C	Han et al. (2018)

Initial moisture content

Moisture content in the composting process can affect microbial activity and, in turn, affect the temperature and decomposition rate of composting materials. Moisture content can also affect the composition of the microbial population (Coppola et al.,

http://www.aloki.hu ● ISSN 1589 1623 (Print) ● ISSN 1785 0037 (Online)
DOI: http://dx.doi.org/10.15666/aeer/1704_99799996

1983). The optimum moisture content in the composting process is between 50% and 60% (Liang et al., 2003; Eipstein, 1997; Tiquia et al., 1997; Schulze, 1961; Poincelot, 1975). For moisture content that is below 40%, microbial activity can be reduced, but if moisture content exceeds 60%, anaerobic conditions may occur due to a wedged pore space. Excessive moisture will result in the problem of nutrient loss and pathogens leaking out in leachate form. This condition may also interfere with airflow and temperature in the compost pile. According to Metcalf and Eddy (2003), the optimum moisture content of a non-reactor system (pile method) is 60% and 65% for a reactor system (mechanical method).

The change in moisture content in composting varies depending on the composting method, the bulking agent, and the raw materials used (Day and Shaw, 2001). The initial moisture level of past experiments varied and was dependent on the concentration of the compost mixture and material (Villasenor et al., 2011). According to Liang et al. (2003), the moisture content process, as well as the temperature to increase microbial activity, should be given more priority in the composting process. Another study agreed, mentioning that optimum moisture content would accelerate the flow of oxygen, which, in turn, increases the activity of microbes, accelerates decomposition, and increases the thermophilic temperature and reduce odor (Goldstein, 2002; Liang et al., 2003; Schaub and Leonard, 1996).

Luo et al. (2008) found that increasing the volumetric mixing ratios of the bulking agent for sewage sludge in the upper half zone of the compost pile could increase the temperature increment rate, achieve uniform temperature distribution, prolong the thermophilic temperature stage, and kill most pathogenic organisms in different layers of the pile, given that the initial moisture content of the mixture was adjusted to about 60%. They also suggested that high initial moisture content in the compost mixture for co-composting gave very low composting effectiveness because of an absence of the thermophilic stage in both the top and middle layers of the pile. Otherwise, excessive moisture will inhibit airflow in the system and will not allow the temperature to increase (Sarkar et al., 2016).

Tiquia et al. (1996) found that different moisture levels in the compost pile gave a different effect on temperature. At 50% and 60% initial moisture levels, the highest temperature achieved was around 64–69 °C. Meanwhile, at 70% moisture content, the pile would cool early and the production of microbial activity and biomass decrease, whereas the highest temperature achieved was 58 °C. Zang et al. (2016), in their study, observed a relationship between initial moisture content and thermophilic temperature for which moisture content significantly influenced composting temperature ($p < 0.001$). High initial moisture content may cause limited oxygen transfer and diffusion and increased heat capacity of the compost. On the other hand, composting temperature can also be affected by feedstock mix ratio, as feedstock ratio may relate to the initial moisture content. However, Petric et al. (2009) demonstrated that for composting of poultry manure and wheat straw, relatively high initial moisture content was better for achieving higher temperatures and retaining them for longer times. A wide range of optimum moisture content indicates: i) the complex dynamic nature of the composting process, with changes in particle size and structure occurring over time, and ii) the necessity for more fundamental and inclusive parameters to understand the physical and biological interactions controlling the composting process (Zavala and Funamizu, 2005). *Table 5* shows the different initial moisture content (%) for different type of waste.

http://www.aloki.hu ● ISSN 1589 1623 (Print) ● ISSN 1785 0037 (Online)
DOI: http://dx.doi.org/10.15666/aeer/1704_99799996

High moisture content can also lead to increased losses of ammonia, which must be controlled with the addition of suitable additives. The findings of Petric et al. (2009) suggest that initial moisture content of around 69% can be considered as suitable for the efficient composting of poultry manure mixed with wheat straw. Otherwise, Sarkar et al. (2016) mentioned that composting would be at its most efficient if the important thermophilic phase was reached and only if the moisture content was kept around 60%. Ali et al. (2014) determined that the reduction of moisture content in the inlet, middle, and outlet zones during composting in a rotary drum reactor caused a higher degree of temperature and evaporation losses to the surrounding air. The moisture content tended to decrease due to the combination of high-temperature levels and aeration during the thermophilic temperature phase (Lashermes et al., 2012; Villasenor et al., 2011). Hence, in order to control the optimum moisture content in the composting process, the continuous monitoring of the moisture in the compost mixture must be carried out regularly. Some studies conclude that the moisture content of the compost mixture in a closed reactor and its stabilization at about 50% (± 2%) could lead to increased stabilization of temperature at the thermophilic level (Kasinski et al., 2016; Liang et al., 2003).

Table 5. *Initial moisture content for different type of waste*

Initial moisture content (%)	Type of waste	Reference
< 64	Bio toilet	Zavala and Funamizu (2005)
60	Pig manure and corn stalks	Zang et al. (2016)
> 60	Municipal solid waste	Elango et al. (2009)
75	Vegetable waste	Ali et al. (2014)
66	Sewage sludge, branches, grass dipping and leaves	Lashermes et al. (2012)
70-75	Cattle manure and rice straw	Hoseini and Aziz (2013)
± 67	Chicken manure and carnation waste	Kulcu et al. (2008)
60	Sawdust and human feces	Bai and Wang (2011)
60	Green waste, sugar beet pulp and paper waste	Zhang and Sun (2018)
75-82	Flower waste, cow dung	Sharma et al. (2018)

Conclusion

Optimizing the process of composting is an important step in obtaining an effective process and good compost quality. The commonly used method of composting in plantations is the pile method. Normally, the pile method, along with the periodic turning process, is adopted. As mentioned in many studies, composting using this method invites many problems, especially the composting period process, which is too long (usually taking more than 80 days for the entire process), the presence of wild animals such as snakes, and also its requirement for more sophisticated operational controls along with its large space and also the concern of GHG gas emission that can lead to the increasing of greenhouse gas emission to the atmosphere. Therefore, composting using mechanical methods in a closed reactor is easier and is able to overcome the problems resulting from composting using the pile method. However, in a closed-reactor composting process, inadequate stabilization of the compost normally occurs due to its short residence time in a biologically active system (Singh et al., 2009;

http://www.aloki.hu ● ISSN 1589 1623 (Print) ● ISSN 1785 0037 (Online)
DOI: http://dx.doi.org/10.15666/aeer/1704_99799996

Kalamdhad et al., 2008). Due to the absence of extensive reviews of thermophilic temperature rise in closed reactors, this paper presents the basic knowledge to a new researcher in composting studies to obtain optimum composting process quality. For closed reactors, aeration rate, rotation frequency and initial moisture content of compost materials play an important role in the effort to achieve optimum temperature of composting. On the other hand, Rich and Bharti (2015) also mentioned that, the material used of the closed reactor manufacturing which is metal, and a good conductor is also as essential to retain the temperature of compost material in the reactor.

Although the composting method via closed reactors has proven to be technically effective, there are many other aspects of the operation that need to be improved, so that existing system facilities can implement the method more efficiently. One of the most important aspects of using rotary drum reactors is its air diversion system, which stimulates the decomposition of microbes in organic waste. The exothermic process plays an important role in increasing the composting temperature from ambient to thermophilic temperature. For a closed reactor, rotation is one of the methods to supply air to organic waste. An optimum rotation process is important to expose fresh organic waste to the microbial population and thus freeing the accumulated ammonia in the air composite material, while at the same time maintaining the temperature of the compost heap in the reactor.

Vigilant control of the composting process at the microbial level comprises four interrelated factors: metabolic heat generation, temperature, aeration, and moisture content. A critical element of control is the maintenance of temperature within a required range since temperature both imitates prior microbial activity and strongly regulates the current rate of activity. This key relationship has previously been proven via the assessment of the response of this ecosystem to temperature using physical and chemical measurements. From the reviewed literature, it can be concluded that a fewer rotation/turning frequency allows the high temperature in the compost material inside the reactor to be maintained. Passive aeration is a more favorable condition for supplying air in the closed reactor and to retain the thermophilic temperature in the compost pile. Finally, the moisture content must be kept around ± 60% to increase microbial activity without inhibiting the thermophilic-stage temperature.

REFERENCES

[1] Abu Zahrim, Y. (2004): Pengkomposan enapcemar perawatan ais sisa industri. – M. Eng Thesis. Universiti Kebangsaan Malaysia.
[2] Agamuthu, P. (2001): Solid Waste: Principle and Management with Malaysian Case Studies. – University of Malaya Press, Kuala Lumpur.
[3] Ahmad, J. (2001): Proses pengkomposan bahan-bahan organik dari aliran sisa pejal domestic dengan menggunakan reaktor aerobic. – Tesis Msc. Universiti Sains Malaysia.
[4] Ali, M., Kazmi, A. A., Ahmed, N. (2014): Study on effects of temperature, moisture and pH in degradation and degradation kinetics of aldrin, endosulfan, lindane pesticides during full-scale continuous rotary drum composting. – Chemosphere 102: 68-75.
[5] Alkoaik, F. N., Abdel-Ghany, A. M., Rashwan, M. A., Fulleros, R. B., Ibrahim, M. N. (2018): Energy analysis of a rotary drum bioreactor for composting tomato plant residues. – Energies 11(449): 2-14.
[6] Awasthi, M. K., Pandey, A. K., Khan, J., Bundela, P. S., Wong, J. W. C., Selvam, A. (2014): Evaluation of thermophilic fungal consortium for organic municipal solid waste composting. – Bioresource Technology 168: 214-221.

http://www.aloki.hu ● ISSN 1589 1623 (Print) ● ISSN 1785 0037 (Online)
DOI: http://dx.doi.org/10.15666/aeer/1704_99799996

[7] Awasthi, M. K., Selvam, A., Lai, K. M., Wong, J. W. C. (2017): Critical evaluation of post-consumption food waste composting employing thermophilic bacterial consortium. – Bioresour. Technol. 245: 665-672.
[8] Bai, F., Wang, X. (2011): Biodegradation of Organic matter and holding of N, P during aerobic thermophilic composting of human feces. – Procedia Environmental Sciences 10: 2631-2637.
[9] Barrington, S., Choiniere, D., Trigui, M., Knight, W. (2003): Compost convective airflow under passive aeration. – Bioresource Technology 86: 259-266.
[10] Bernal, M. P., Paredes, C., Sanchez-Monedero, M. A., Roig, A. (1998): Carbon mineralization from organik waste at different composting stages during their incubation with soil. – Agr. Ecosyst. Environ. 69: 175-189.
[11] Bernal, M. P., Alburquerque, J. A., Moral, R. (2009): Composting of animal manures and chemical criteria for compost maturity assessment. A review. – Bioresour. Technol. 100: 5444-5453.
[12] Bertoldi, M., Vallini, G., Pera, A. (1983): The biology of composting: a review. – Waste Management Res. 1(2): 157-176.
[13] Bhamidimarri, S. M. R. Pandey, S. P. (1996): Aerobic thermophilic composting of piggery solid wastes. – Water Science & Technology 33(8): 89-94.
[14] Bhatia, A., Madan, S., Sahoo, J., Ali, M., Pathania, R., Kazmi, A. A. (2013): Diversity of bacterial isolates during full scale rotary drum composting. – Waste Management 33: 1595-1601.
[15] Bhattarai, R., Kalita, P. K., Yatsu, S., Howard, H. R., Svendsen, N. G. (2011): Evaluation of compost blankets for erosion control from disturbed lands. – Journal of Environmental Management 92: 803-812.
[16] Biddlestone, A. J. Gray, K. R. (1988): A Review of Aerobic Biodegradation of Solid Waste. – In: Houghton, D. R., Smith, R. N. Eggins, H. O. W. (eds.) Biodeteriotion 7. Elsevier Science Publisher Ltd, Amsterdam, pp 825-839.
[17] Charles, W., L. Walker, L., Cord-Ruwisch, R. (2009): Effect of pre-aeration and inoculum on the start-up of batch thermophilic anaerobic digestion of municipal solid waste. – Bioresource Technology 100: 2329-2335.
[18] Chen, R., Wang, Y., Wang, W., Wei, S., Jing, Z., Lin, X. (2015): N_2O emissions and nitrogen transformation during windrow composting of dairy manure. – Journal of Environmental Management 160: 121-127.
[19] Coppola, S., Dumontet, S. Marino, P. (1983): Composting Raw Sewage Sludge in Mixture with Organic or Inert Bulking Agents. – In: Stentiford, E. I. (ed.) Proceeding of the International Conference on Composting of Solid Waste and Slurries. The University of Leeds, England, pp 125-147.
[20] Day, M. Shaw, K. (2001): Biological, Chemical and Physical Processes of Composting. – In: Stofella, P. J., Kahn, B. A. (eds.) Compost Utilization in Horticulture Cropping Systems. : Lewis Publisher, USA.
[21] Diaz, M. J., Madejon, E., Lopez, R. Cabrera, F. (2002): Composting of vinasse and cotton gin wastes by using two different systems. – Resource, Conservations and Recycling 34: 235-248.
[22] Epstein, E. (1997): The Science of Composting. – Technomic Publishing Company, Inc, USA.
[23] Elango, D., Thinakaran, N., Panneerselvam, P., Sivanesan, S. (2009): Thermophilic composting of municipal solid waste. – Applied Energy 86: 663-668.
[24] El Kader, N. A., Robin, P., Paillat, J. M., Leterme, P. (2007): Turning, compacting and the addition of water as factors affecting gaseous emissions in farm manure composting. – Bioresource Technology 98: 2619-2628.
[25] Fernandez, F. J., Sanchez-Arias, V., Rodriguez, L., Villasenor, J. (2010): Feasibility of composting combinations of sewage sludge, olive mill waste and winery waste in a rotary drum reactor. – Waste Management 30: 1948-1956.

http://www.aloki.hu ● ISSN 1589 1623 (Print) ● ISSN 1785 0037 (Online)
DOI: http://dx.doi.org/10.15666/aeer/1704_99799996

[26] Ferrer, J., Paez, G., Marmol, Z., Ramones, E., Chandler, C., Marin, M., Ferrer, A. (2001): Agronomic use of biotechnologically processed grape wastes. – Bioresource Technology 76(1): 39-44.
[27] Gea, T., Artolla, A., Sanchez, A. (2005): Composting of de-inking sludge from the recycled paper manufacturing industry. – Bioresource Technology 96(10): 1161-1167.
[28] Goldstein, N. (2002): Quick to implement odour reduction techniques. – Bio Cycle 1: 29.
[29] Gou, C., Wang, Y., Zhang, X., Lou, Y., Gao, Y. (2017): Inoculation with a psychrotrophic-thermophilic complex microbial agent accelerates onset and promotes maturity of dairy manure-rice straw composting under cold climate conditions. – Bioresource Technology 243: 339-346.
[30] Guo, M., Liang, F., Yu, A. Yang, L. (2012): Evaluation of stability and maturity during forced-aeration composting of chicken manure and sawdust at different C/N ratios. – Chemosphere 78: 614-619.
[31] Habsah, N. M. S. (2008): Pengkomposan sisa taman menggunakan kaedah timbunan statik berudara dan drum berputar. – Tesis M.Eng, Universiti Sains Malaysia, Pulau Pinang, pp. 1-227.
[32] Hackett, G. A. R., Easton, C. A. Duff, S. J. B. (1999): Composting of pulp and paper mill fly ash with wastewater treatment sludge. – Bioresource Technology 70: 217-224.
[33] Han, Z., Sun, D., Wang, H., Li, R., Bao, Z., Qi, F. (2018): Effects of ambient temperature and aeration frequency on emissions of ammonia and greenhouse gases from a sewage sludge aerobic composting plant. – Bioresource Technology 270: 457-466.
[34] Haug, R. T. (1993): The Practical Handbook of Compost Engineering. – McGraw-Hill International Editions, New York.
[35] He, X. S., Xi, B. D., Cui, D. Y., Liu, Y., Tan, W. B., Pan, H. W., Li, D. (2014): Influence of chemical and structural evolution of dissolved organic matter on electron transfer capacity during composting. – Journal of Hazardous Material 268(15): 256-263.
[36] Hiroaki, T., Kodaira, S., Kimoto, A., Nashimoto, M. Takagi, M. (2006): Microbial communities in the garbage composting with rice hull as an amendment revealed by culture dependent and independent approaches. – Journal Bioscience Bioengineering 101(1): 42-50.
[37] Hosseini, S. M., Abdul Aziz, H. (2013): Evaluation of thermochemical pretreatment and continuous thermophilic condition in rice straw composting process enhancement. – Bioresource Technology 133: 240-247.
[38] Ivanov, M. V., Lysenko, A. M., Petrunyaka, V. V., Ivanova, A. E., Nazina, T. N., Poltaraus, A. B., Tourova, T. P., Belyaev, S. S., Grigoryan, A. A., Novikova, E. V., Osipov, G. A. (2001): Taxonomic study of aerobic thermophilic bacilli: descriptions of *Geobacillus subterraneus* gen. nov., sp. nov. and *Geobacillus uzenensis* sp. nov. from petroleum reservoirs and transfer of *Bacillus stearothermophilus*, *Bacillus thermocatenulatus*, *Bacillus thermoleovorans*, *Bacillus kaustophilus*, *Bacillus thermodenitrificans* to *Geobacillus* as the new combinations *G. stearothermophilus*, *G. th.* – Int. J. Syst. Evol. Microbiol. 51: 433-446.
[39] Kang, Y., Li, Q., Xia, D., Shen, M., Mei, L., Hua, J. (2017): Short-term thermophilic treatment cannot remove tetracyclineresistance genes in pig manures but exhibits controlling effects ontheir accumulation and spread in soil. – Journal of Hazardous Materials 340: 213-220.
[40] Kalamdhad, A. S. Kazmi, A. A. (2009): Effects of turning frequency and compost stability and some chemical characteristics in a rotary drum composter. – Chemosphere 74: 1327-1334.
[41] Kalamdhad, A. S., Pasha, M., Kazmi, A. A. (2008): Stability evaluation of compost by respiration methods in a rotary drum composter. – Res Cons Recy. 52: 829-34.
[42] Kasinski, S., Slota, M., Markowski, M., Kaminska, A. (2016): Municipal waste stabilization in a reactor with an integrated active and passive aeration system. – Waste Management 50: 31-38.

http://www.aloki.hu ● ISSN 1589 1623 (Print) ● ISSN 1785 0037 (Online)
DOI: http://dx.doi.org/10.15666/aeer/1704_99799996

[43] Koyama, M., Nagao, N., Syukrib, F., Abd Rahim, A., Kamarudin, M. S., Todac, T., Mitsuhashia, T., Nakasakia, K. (2018): Effect of temperature on thermophilic composting of aquaculture sludge: NH_3 recovery, nitrogen mass balance, and microbial community dynamics. – Bioresource Technology 265: 207-213.
[44] Kulcu, R., Yaldiz, O. (2004): Effects of air flow directions on composting process temperature profile. – Waste Management 28: 1766-1772.
[45] Kulcu, R., Sonmez, I., Yaldiz, O., Kaplan, M. (2008): Composting of spent mushroom compost, carnation wastes, chicken and cattle manures. – Bioresource Technology 99(17): 8259-8264.
[46] Larney, F. J., Olson, A. F., Carcamo, A. A. Chang, C. (2000): Physical changes during active and passive composting of beef feedlof manure in winter and summer. – Bioresource Technology 75: 139-148.
[47] Lashermes, G., Barriuso, E., Le Villio-Poitrenaud, M., Houot, S. (2012): Composting in small laboratory pilots: Performance and reproducibility. – Waste Management 32: 271-277.
[48] Liu, J. (2000): Composting and use of compost as a soil amendment. – Ph.D thesis. Department of Astronomy and Soil Science, University of Hawaii.
[49] Li, R., Li, L., Huang, R., Sun, Y., Mei, X., Shen, B., Shen, Q. (2014): Variations of culturable thermophilic microbe numbers. and bacterial communities during the thermophilic phase of composting. – World J Microbiol Biotechnol 30: 1737-1746.
[50] Liang, C., Das, K. C. McClendon, R. W. (2003): The influence of temperature and moisture contents regimes on the aerobic microbial activity of a biosolids composting blend. – Bioresource Technology 86(2): 131-137.
[51] Liang, Y., Leonard, J. J., Feddes, J. J. R., McGill, W. B. (2006): Influence of carbon and buffer amendment on ammonia volatilization in composting. – Bioresource Technology 97(5): 748-761.
[52] Luo, W., Chen, T. B., Zheng, G. D., Gao, D., Zhang, Y. A. Gao, W. (2008): Effect of moisture adjustments on vertical temperature distribution during forced-aeration static-pile composting of sewage sludge. – Resources, Conservation Recycling 52: 635-642.
[53] Mason, I. G. (2007): A study of power, kinetics and modellling in the composting process. – Tesis Ph.D, University of Canterbury, Christchurch, New Zealand: 1-230.
[54] Metcalf Eddy. (2003): Wastewater Engineering Treatment and Reuse. – McGraw-Hill, Inc., New York.
[55] Mohammad, N., Alam, M. Z., Kabbashi, N. A. Ahsan, A. (2012): Effective composting of oil palm industrial waste by filamentous fungi: A review. – Resource, Conservation & Recycling 58: 69-78.
[56] Morales, A. B., Bustamante, M. A., Marhuenda-Egea, F. C., Moral, R., Ros, M., Pascual, J. A. (2016): Agri-food sludge management using different co-composting strategies: study of the added value of the composts obtained. – J. Clean. Prod. 121: 186-197.
[57] Pagans, E., Barrena, R., Font, X., Sánchez, A. (2006): Ammonia emissions from the composting of different organic wastes. Dependency on process temperature. – Chemosphere 62: 1534-1542.
[58] Parkinson, R., Gibbs, P., Burchett, S. Misselbrook, T. (2004): Effect of turning regime and seasonal weather conditions on nitrogen and phosphorus losses during aerobic composting. – Bioresource Technology 916: 171-178.
[59] Petiot, C., de Guardia, A. (2004): Composting in a laboratory reactor: a review. – Compost Science & Utilization 12: 69-79.
[60] Petric, I., Selimbasic, V. (2008): Composting of poultry manure and wheat straw in a closed reactor: optimum mixture ratio and evolution of parameters. – Biodegradation 19: 53-63.
[61] Petric, I., Šestan, A., Šestan, I. (2009): Influence of initial moisture content on the composting of poultry manure with wheat straw. – Biosystem Engineering 104(1): 125-134.

http://www.aloki.hu ● ISSN 1589 1623 (Print) ● ISSN 1785 0037 (Online)
DOI: http://dx.doi.org/10.15666/aeer/1704_99799996

[62] Poincelot, R. P. (1975): The Biochemistry and Methodology of Composting. – Bull. 754. The Connecticut Agr. Expt. Station, New Haven, CT.
[63] Polprasert, C., Edwards, P., Rajput, V. S. C., Pacharaprakiti, C. (1986): Integrated biogas technology in the tropics 1. Performance of small-scale digesters. – Waste Management & Research 4(2): 197-213.
[64] Rasapoor, M., Nasrabadi, T., Kamali, M. Hoveidi, H. (2009): The effects of aeration rates on generated compost quality, using aerated static pile method. – Waste Management 29: 570-573.
[65] Rashad, F. M., Saleh, W. D., Moselhy, M. A. (2010): Bioconversion of rice straw and certain agro industrial wastes to amendments for organic farming systems: 1. Composting, quality, stability and maturity indices. – Bioresource Technology 101: 5952-5960.
[66] Rich, N., Bharti, A. (2015): Assessment of different types of in-vessel composters and its effect on stabilization of MSW compost. – International Research Journal of Engineering and Technology 2(3): 37-42.
[67] Rodriguez, L., Maria, I. C., Valentin, G. A., Villasenor, J. (2012): Domestic sewage sludge composting in a rotary drum reactor: optimizing the thermophilic stage. – Journal of Environmental Management 112: 284-291.
[68] Rynk, R. Richard, T. L. (2001): Commercial Compost Production System. – In: Stofella, P. J., Khan, B. A. (eds.) Compost Utilization in Horticulture Cropping Systems, pp: 36-55. Lewis Publisher, USA.
[69] Sarkar, S., Banerjee, R., Chanda, S., Das, P., Ganguly, S., Pal, S. (2010): Effectiveness of inoculation with isolated *Geobacillus* strains in the thermophilic stage of vegetable waste composting. – Bioresource Technology 101: 2892-2895.
[70] Sarkar, S., Pal, S., Sunanda Chanda, S. (2016): Optimization of a vegetable waste composting process with a significant thermophilic phase. – Procedia Environmental Sciences 35: 435-440.
[71] Schaub, S. M. Leonard, J. J. (1996): Composting: an alternative waste management option for food processing industries. – Trends in Food Science and Technology 7: 263-268.
[72] Schulze, K. L. (1961): Continuous thermophilic composting. – Applied Microbiology 10: 108-122.
[73] Scoton, E. J., Battistelle, R. A. G., Bezerra. B. S., Akutsu, J. (2016): A sewage sludge co composting process using respirometric monitoring method in hermetic rotary reactor. – Journal of Cleaner Production 121: 169-175.
[74] Sharma, D., Yadav, K. D., Kumar, S. (2018): Role of sawdust and cow dung on compost maturity during rotary drum composting of flower waste. – Bioresource Technology 264: 285-289.
[75] Shen, Y., Ren, L., Li, G., Chen, T., Guo, R. (2011): Influence of aeration on CH_4, N_2O and NH_3 emissions during aerobic composting of a chicken manure and high C/N waste mixture. – Waste Management 31: 33-38.
[76] Singh, Y. T., Kalamdhad, A. S., Ali, M., Kazmi, A. A. (2009): Maturation of primary stabilized compost from rotary drum composter. – Resources, Conservation and Recycling 53: 386-392.
[77] Siu-Rodas, Y., Calixto-Romoa, M. D. L. A., Guillén-Navarro, K., Sánchez, J. E., Zamora-Brise˜noa, J. A., Lorena Amaya-Delgado, L. (2018): Bacillus subtilis with endocellulase and exocellulase activities isolated in the thermophilic phase from composting with coffee residues. – Rev Argent Microbiol. 50(3): 234-243.
[78] Smars, S., Beck-Friis, B., Jonsson, H. Kirchmann, H. (2001): An advanced experimental composting reactor for systematic simulation studies. – Journal of Agriculture Engineering Research 78(4): 415-422.

http://www.aloki.hu ● ISSN 1589 1623 (Print) ● ISSN 1785 0037 (Online)
DOI: http://dx.doi.org/10.15666/aeer/1704_99799996

[79] Smith, D. R., Cawton, D. L., Sloan, J. J., Freeman, T. M. (2006): In-vessel mechanical rotating drum composting of institutional food residuals. – Compost. Sci. Util. 14: 155-161.
[80] Steger, K., Eklind, Y., Olsson, J., Sundh, I. (2005): Microbial community growth and utilization of carbon constituents during thermophilic composting at different oxygen levels. – Microbial Ecology 50: 163-171.
[81] Stentiford, E. I. (1996): Composting Control: Principle and Practice. – In: de Bertoldi, M., Sequi, P., Lemans, B. P., Papi, T. (eds.). The Science of Composting: Part 1. Blackie Academic and Professional, Blackie, Glasgow.
[82] Sun, Q., Wu, D., Zhang, Z., Zhao, Y., Xie, X., Wu, J., Lu, Q., Wei, Z. (2017): Effect of cold-adapted microbial agent inoculation on enzyme activities during composting start-up at low temperature. – Bioresource Technology 244: 635-640.
[83] Talib, A. T., Mokhtar, M. N., Baharuddin, A. S., Sulaiman, A. (2014): Effect of aeration rate on degradation process of oil palm empty fruit bunch with kinetic-dynamic modelling. – Bioresource Technology 169: 428-438.
[84] Thambirajah, J. J. Kuthubutheen, A. J. (1989): Composting of palm press fibre. – Biological Wastes 27: 257-269.
[85] Tiquia, S. M. Tam, N. F. Y. (1998): Composting of spent pig litter in turned and forced-aerated piles. – Environmental Pollution 99: 329-337.
[86] Tiquia, S. M., Tam, N. F. Y. Hodgkis, I. J. (1996): Microbial activities during composting of spent manure sawdust litter at different moisture content. – Bioresource Technology 55: 201-205.
[87] Tiquia, S. M., Tam, N. F. Y. Hodgkis, I. J. (1997): Effects of turning frequency on composting of spent pig-manure sawdust litter. – Bioresource Technology 62(1-2): 37-42.
[88] Tiquia, S. M., Wan, J. H. C., Tam, N. F. Y. (2002): Dynamics of yard trimmings composting as determined by dehydrogenase activity, ATP content, arginine ammonification, and nitrification potential. – Process Biochemistry 37(10): 1057-1065.
[89] Villasenor, J., Rodriguez, I. Fernandez, F. J. (2011): Composting domestic sewage sludge with natural zeolites in a rotary drum reactor. – Bioresource Technology 102: 1447-1454.
[90] Wan Razali, W. A., Baharuddin, A. S., Talib, A. T., Sulaiman, A., Naim, M. N., Hassan, M. A., Shirai, Y. (2012): Degradation of oil palm empty fruit bunches (OPEFB) fibre during composting process using in-vessel composter. – BioResource 7(4): 4786-4805.
[91] Wang, X., Pan, S., Zhang, Z., Lin, X., Zhang, Y., Chen, S. (2017): Effects of the feeding ratio of food waste on fed-batch aerobic composting and its microbial community. – Bioresource Technology 224: 397-404.
[92] Wong, J. W. C., Mak, K. F., Chan, N. W., Lam, A., Fang, M., Zhou, L. X., Wu, Q. T., Liao, X. D. (2001): Co-composting of soybean residues and leaves in Hong Kong. – Bioresource Technology 76(2): 99-106.
[93] Xie, X. Y., Zhao, Y., Sun, Q. H., Wang, X. Q., Cui, H. Y., Zhang, X., Li, Y. J., Wei, Z. M. (2017): A novel method for contributing to composting start-up at low temperature by inoculating cold-adapted microbial consortium. – Bioresource Technology 238: 39-47.
[94] Yang, F., Li, G. X., Yang, Q. Y., Luo, W. H. (2013). Effect of bulking agents on maturity and gaseous emissions during kitchen waste composting. – Chemosphere 93(7): 1393-1399.
[95] Zang, B., Li, S., Michel Jr. F., Li, G., Luo, Y., Zhang, D., Li, Y. (2016): Effects of mix ratio, moisture content and aeration rate on sulfur odor emissions during pig manure composting. – Waste Management 56: 498-505.
[96] Zavala, M. A. L., Funamizu, N. (2005): Effect of moisture content on the composting process in a biotoilet system. – Compost Science & Utilization 13(3): 208-216.
[97] Zhang, L. Sun, X. (2018): Influence of sugar beet pulp and paper waste as bulking agents on physical, chemical, and microbial properties during green waste composting. – Bioresource Technology 267: 182-191.

http://www.aloki.hu ● ISSN 1589 1623 (Print) ● ISSN 1785 0037 (Online)
DOI: http://dx.doi.org/10.15666/aeer/1704_99799996

[98] Zhang, X., Zhao, Y., Zhu, L., Cui, H., Jia, L., Xie, X., Li, J., Wei, Z. (2017): Assessing the use of composts from multiple sources based on the characteristics of carbon mineralization in soil. – Waste Management 70: 30-36.
[99] Zhao, X. Y., He, X. S., Xi, B. D., Gao, R., Tan, W. B., Zhang, H., Li, D. (2016): The evolution of water extractable organic matter and its association with microbial community dynamics during municipal solid waste composting. – Waste Management 56: 79-87.
[100] Zhu-Barker, X., Bailey, S. K., U, K. T. P., Burger, M., Horwath, W. R. (2017): Greenhouse gas emissions from green waste composting windrow. – Waste Management 59: 70-79.

http://www.aloki.hu ● ISSN 1589 1623 (Print) ● ISSN 1785 0037 (Online)
DOI: http://dx.doi.org/10.15666/aeer/1704_99799996

EFFECT OF DIFFERENT IRRIGATION LEVELS ON PHYSIOLOGICAL PERFORMANCE OF SOME DROUGHT TOLERANT MELON (*CUCUMIS MELO* L.) GENOTYPES

AKHOUNDNEJAD, Y.[1*] – DASGAN, H. Y.[2]

[1]*Faculty of Agriculture, Depatment of Horticultur, Sirnak university, 73300 Idil, Sirnak, Turkey*

[2]*Faculty of Agriculture, Depatment of Horticultur, Cukurova university, Adana, Turkey*

[*]*Corresponding author*
e-mail: yakhoundnejad@sirnak.edu.tr; phone: +90-544-864-5435

(Received 9th Apr 2019; accepted 19th Jun 2019)

Abstract. This study was conducted for determining drought tolerance in melon genotypes. In order to reduce the negative effects of the climatic changes on vegetable production, new melon cultivars that are tolerant to water stress are being developing. For this purpose, 9 melon genotypes that were previously found as drought tolerant have been tested in field conditions. In order to determine field performance of the melon genotypes three irrigation treatments with different water levels have been realized; 100% (control), 50% and 0% irrigations. In 50% and 0% irrigated plants, the above mentioned parameters have been compared versus their control plants. Some Physiological parameters were investigated. The investigated parameters were: Total fruit yield (kg/ha), brix in fruit (%), leaf stoma conductance (mmol/m^2/s), membrane damage on leaf cells (%), leaf water potential (MPa), leaf osmotic potential (MPa), leaf temperature (^{o}C), K and Ca concentrations in leaf (%), water use efficiency (g/Liter) of the genotypes According to the results melon genotypes were sorted from highest to lowest levels for their stress tolerance.
Keywords: *irrigation, Cucumis melo, drought, physiological*

Introduction

Abiotic stresses, such as drought, salinity, extreme temperatures, chemical toxicity and oxidative stress are serious threats to agriculture and result in the deterioration of the environment. Abiotic stress is the primary cause of crop loss worldwide, reducing average yields for most major crop plants by more than 50% (Boyer, 1982; Bray et al., 2000). Drought, salinity, extreme temperatures and oxidative stress are often interconnected, and may induce similar cellular damage. For example, drought and/or salinization are manifested primarily as osmotic stress, resulting in the disruption of homeostasis and ion distribution in the cell (Serrano et al., 1999; Zhu, 2001). Drought and salinity are becoming particularly widespread in many regions, and may cause serious salinization of more than 50% of all arable lands by the year 2050 (Wang et al., 2003). Abiotic stress leads to a series of morphological, physiological, biochemical and molecular changes that adversely affect plant growth and productivity (Wang et al., 2001). The effect of increased drought stress results in a decrease in germination rate, seedling viability, collective length, root length and shoot length (Kızlgeci, 2017). In this study we studied 9 melon genotypes to appraise the drought stress performance of these genotypes, according to physiological parameters in Adana of Turkey.

http://www.aloki.hu ● ISSN 1589 1623 (Print) ● ISSN 1785 0037 (Online)
DOI: http://dx.doi.org/10.15666/aeer/1704_999710012

Materials and methods

As plant material, 9 melon genotypes, gathered from different parts of Turkey country, were used (*Table 1 and Fig. 1*). These genotypes were previously used in UNDP-MDG-F 1680 project. Study 3. was performed, with the practice, in open field in the conditions of Adana- Cukurova (37°01'49.1"N 35°22'03.0"E, and elevation 23 m) in 2011 spring-summer. One of the applications (1) is thought as control and completely 100% irrigation being watered parcels, other one (2) is being watered as much half as of controlled one in other words being 50% irrigation limited watered parcels, and the last one(3) is being watered as 0%irrigation of the controlled limited watered parcels.

Table 1. *Melon genotypes*

Genotypes No	Genotypes No
Mln-4	CU-159
Mln-20	CU-213
Mln-23	CU-280
Mln27	CU-311
Mln-28	

Figure 1. *Melon genotypes used in the experiment*

The amount of the water, which will be given to the melon plants, was determined according to; the amount of water evapoquantityd from the evaporation pan, the kcp coefficient for melon, test area, and the quantity of vegetation depending on the field of plant growth. Randomized block experiment was established, as 3 recurrence in experimental design and each recurrence being 5 plants. While melons were being planted,

http://www.aloki.hu ● ISSN 1589 1623 (Print) ● ISSN 1785 0037 (Online)
DOI: http://dx.doi.org/10.15666/aeer/1704_999710012

row space was organized as 180 cm and the row was organized as 50 cm. The melon seedlings planted on the field were watered in optimum level the same as controlled plants in all 3 applications until they growed for 69 days. The application of water stress of 50% and 0% of the control was started on 55 days after they were planted. Different watering stress applied in experiment were done after first blossom. In addition, analyzes were performed after the first fruit formation was seen. The nutrition of the melon plants were done equally in all 3 applications. For this, for a 10000 m^2 purely 140 kg ha^{-1} N, 95 kg ha^{-1} P2O5, 220 kg ha^{-1} K2O, 20 kg ha^{-1} MgO and 40 kg ha^{-1} CaO; were used (Gunay, 2005). Physical and chemical properties of the orchard soil from depth of 0–30 cm (*Table 2*). In the experiment, the monthly minimum, average, rainfall and maximum temperature and humidity values for years 2011 are shown in *Figs. 2, 3* and *4*, respectively.

Table 2. *Physical and chemical properties of the orchard soil from depth of 0–30 cm*

Soil parameters		Value
pH	--	8.1
EC	(dSm^{-1})	0.3
N	(%)	0.19
P	(kg P_2O_5/ha)	63
K	(kg K_2O/ha)	150.36
Ca	(kg CaO/ha)	1990.1
Mg	(kg MgO/ha)	240.3
Fe	(ppm)	185
Mn	(ppm)	2.82
Zn	(ppm)	0.28
Cu	(ppm)	0.34

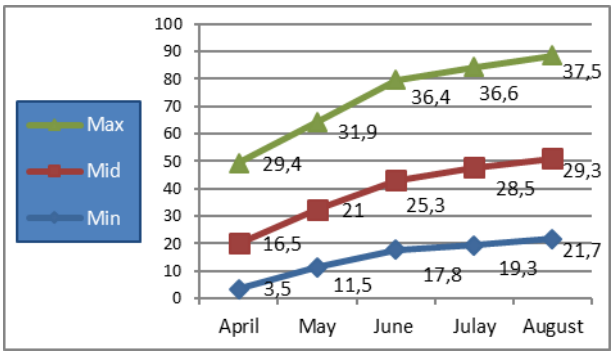

Figure 2. *2011 spring summer period during Max, Mid, Min temperature values (°C)*

Physiological parameters shown below were examined.

Ca and K concentration in green parts of melon genotype (%)

Before the fruit formation of melon plant, the 5th leaf as of the tip was taken and washed in pure water in order to remove dust and similar substances on it. It will be kept in the etuve at 70ºC for 48 hours. After drying, the leaves will be ground until becoming powdery. 0.200 grams will be weighed and burned in the combustion unit for 6 hours at 550ºC. It was dissolved in 1/3 HCL acid ratio and passed through filter paper. Values were determined with FS 220 Atomic Absorption Spectrophotometer brand device.

http://www.aloki.hu ● ISSN 1589 1623 (Print) ● ISSN 1785 0037 (Online)
DOI: http://dx.doi.org/10.15666/aeer/1704_999710012

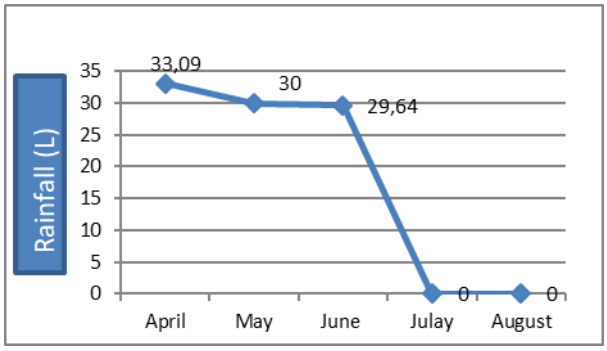

Figure 3. *2011 spring summer period during rainfall (L)*

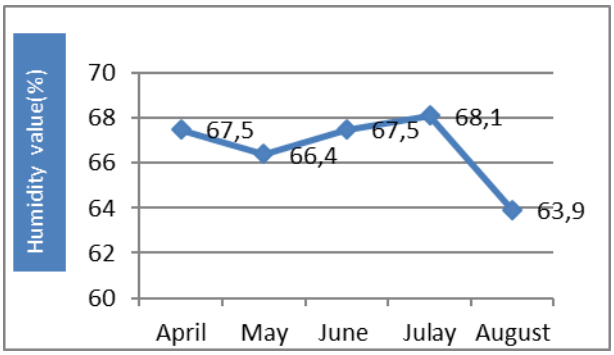

Figure 4. *2011 spring summer period recorded during trial Max, Mid, Min Monthly air relative humidity values (%)*

Membrane damage stages in green parts of melon genotypes (%)

In order to determine the damage rate of membrane cells of different melon genotypes, 5 discs (1 cm diameter metal pipe) were taken from the 4th and 5th leaf of the melon plant down from the tip between the hours of 9: 00-11: 00 and after putting into 20 ml of pure water, they were waited for 4 hours and measured with Ec meter. After measuring, when equilibrated to room temperature after it was kept at 100ºC for 10 minutes, measured with the EC meter again and calculated with the following formula (Dlugokecka and Kacperska-Palacz, 1978; Fan and Blake, 1994).

The formula of the Membrane Loss Index on the green component is

$$(Lt - Lc / 1\text{-}Lc) \times 100 \qquad \text{(Eq.1)}$$

where
Lt: EC measurement of stress plants before autoclaving /EC measurement after autoclave.
Lc: EC measurement of control plants before autoclaving /EC measurement after autoclave.

http://www.aloki.hu ● ISSN 1589 1623 (Print) ● ISSN 1785 0037 (Online)
DOI: http://dx.doi.org/10.15666/aeer/1704_999710012

Determination of Leaf Stoma Permeability (mmol m^{-2} s^{-1})

In the melon plant, in order to determine stomata of the leaves as of the 4th part of tip, measurement was done between the hours of 9:00-10:00 in sunny weather by using AP4 model porometer of Delta T Brand Devices.

Determination of Leaf Osmotic Potential (MPa)

Between the hours of 9:00 and 10:00, after taking samples from the 4 leaves from the tip of experimental melon plant, they were kept at the -20ºC and taken to the lab. 1 gram of the green component was mixed with 19 ml of distilled water. After filtering with 0.45 µm scale, the liquid samples were taken from 50 µl scale samples and measured by Gonatec brand and 030 model osmometer device. Besides, values were calculated as (MPa).

Determination of Leaf Water Potential (MPa)

In the Soilmoisture brand portable pressure circle, it was measured by taking samples from the 4th leaf from the tip of melon plant between the hours of 9:00-10:00.

Water Use Efficiency (g / L)

In the experiment, the amount of water given at different levels of stress was recorded at each stage. In addition, the amount of harvest in each stage of the experiment was recorded in each harvest. At the end of the experiment, the water use efficiency of each genotype was calculated by dividing the sum of each genotype by the amount of water spent. Water Usage Efficiency (g / L) formula is calculated by

Total yield (g / plant) / Amount of water supplied (L / plant) (Eq.2)

The data obtained from the experiment by using JMP packaged software was analyzed statistically and mean was compared according to Tukey test. In the study, changes in physiological parameters recorded and measured in melon genotypes cultivated with 50% and 0% irrigation applications, which is water stress applications in two different levels, were calculated as percentages compare to non-stress control plants (% 100 application). In total 10 parameters, the mean of the changes according to the control of both water stress applications was taken. A special method "weighed classification method", was developed for this study. Accordingly, scores were assigned to each of the selected parameters according to their significance level (*Table 3*), and the averages of the changes were multiplied by the score gained the parameters in the weighed classification system.

After parameters were multiplied by it'sown multiplier, all parameters were added. According to the total score obtained, 9 melon genotypes were arranged as from the best performing to the least performing. Watering time was carried out as once a week. The amount of irrigation water to be applied to plants according to the evaporation values read daily from the evaporation tank (Class Apan) was calculated by means of the following equality. In the study, "Full Plastic" drip irrigation laterals, placed with 50 cm spaces with a diameter of 16 mm and a flow rate of 2 L/h were used in the drip irrigation system. The amount of irrigation water given to the plants in the experiment was determined by the following formula. Water usage efficiency of melon genotypes is shown below (*Table 4*).

http://www.aloki.hu ● ISSN 1589 1623 (Print) ● ISSN 1785 0037 (Online)
DOI: http://dx.doi.org/10.15666/aeer/1704_999710012

$$IR = A * E\ pan * kcp * P \quad \text{(Eq.3)}$$

where

IR: Amount of water applied (m^3).
A: Size of the parcel (ha).
E pan: Evaporation amount (mm).
kcp: Coefficient of plant (melon) (0.80).
P-cover: Flora %.
P-cover: Plant Crown Width (cm) / Row spacing (cm).

Table 3. *Score according to significant level of melon experiment*

Parameters	Point
Total fruit yield	30
leaf osmotic potential	6
leaf stoma conductance	12
leaf water potential	9
leaf temperature	7
Membrane damage on leaf cells	8
Ca concentrations in leaf	6
K concentrations in leaf	6
Brix in fruit	7
Water use efficiency	9
Total	100

Table 4. *Water use efficiency of the melon genotypes (g/ Liter)*

Application	Stress before (04.04.2011 —26.05.2011)	Stress after (08.06.2011—20.07.2011)	Rain*	Total water
100%	31.2L	50.57L	55.61L	137.38L
50%	31.2L	25.28L	55.61L	112.09L
0%	31.2L	-	55.61L	86.81L

*Rainfall date: (01.04.2011-30.04.2011) 33.06L, (01.05.2011-31.05.2011) 30L, (01.06.2011-31.06.2011) 29.64L

Results and discussion

The results of ANOVA for physiological properties are in *Table 5*. Statistical data analysis for the leaf stoma conductance, leaf water potential, Ca, K concentrations in leaf, Membrane damage on leaf cells, Water use efficiency and Total fruit yield the analysis of variance, stress and genotypes x stress interactions were found significant but the genotypes were insignificant for leaf stoma conductance, Brix in fruit and leaf temperature. The average value of leaf stoma conductance under drought stress 50% and 0% irrigation of melon genotypes tested has been 140.39, 83.6, respectively and the mean of control plants has been 107.74.

Decrease 50% and 0% irrigation indices has occurred as 46.22%, -27,86%, respectively according to control of melon genotypes under drought stress (*Table 6*). The average value of leaf temperature under drought stress 50% and 0% irrigation of melon genotypes tested has been 27.34°C, 31.28°C, respectively and the mean of control plants has been 29.80°C. Increase 50% and 0% irrigation indices has occurred as 3.83%, 5.86%, respectively according to control of melon genotypes under drought stress (*Table 7*). Turner et al. (1998) reported that as the osmotic potential decreases, stoma conductivity decreases in sorghum

http://www.aloki.hu ● ISSN 1589 1623 (Print) ● ISSN 1785 0037 (Online)
DOI: http://dx.doi.org/10.15666/aeer/1704_999710012

and sunflowers. Similar results were obtained in chickpea (Mafakheri, 2010), sugar beet (Dadkhah, 2010), tomato (Zhou et al., 2017) and hazelnut (Silva et al., 2011). During drought, leaves are exposed to both heat and water deficiency stress (Clarke et al., 1993).

Table 5. *Analysis of variance and physiological properties of melon genotypes*

Analysis of variance	Total fruit yield	Leaf osmotic potential	Leaf stoma conductance	Leaf water potential	Leaf temperature	Membrane damage on leaf cells	Ca	K	Brix in fruit	Water use efficiency
Stress(s)	**	**	**	*	ns	**	**	*	ns	**
Genotypes(G)	**	ns	**	ns	ns	*	**	*	ns	**
S*G	**	ns	*	*	ns	*	**	*	ns	**
CV(%)	4.25	-6.02	4.34	-8.93	1.52	4.32	8.38	8.36	3.01	3.37

ns = not significantly, (*) and (**) are significant at 0.05 and 0.01, respectively

Table 6. *In the applications of melon genotypes quantities in different 50% and 0% irrigation under the normal condition and drought stress condition; leaf stoma conductance quantity of (%) change by to control*

Genotypes No	**100% irrigation (mmol/m2/s)**	**50% irrigation (mmol/m2/s)**	**0% irrigation (mmol/m2/s)**	**50% irrigation change by to control (%)**	**0% irrigation change by to control (%)**
Mln-4	257a	105de	68.68c	-59.14	-89.04
Mln-20	66f	149.3b	94.3b	126.21	-36.84
Mln-23	69.67f	96e	88.3bc	37.79	-8.02
Mln-27	151b	349ba	38.3e	131.32	-19.43
Mln-28	59.33g	78.67f	84.6d	32.60	-12.80
Cu-159	97.67d	118c	107a	20.81	-9.32
CU-213	123c	144.3b	92b	17.32	-36.24
Cu-280	65fg	111cd	73.3d	70.77	-33.96
CU-311	81e	112cd	106.3a	38.27	-5.09
Mean	107.74	140.39	83.6	46.22	-27.86
LSD $_{0.05}$	6.02	12.21	6.95	-	-

Table 7. *In the applications of melon genotypes quantities in different 50% and 0% irrigation under the normal condition and drought stress condition; leaf temperature quantity of (%) change by to control*

Genotypes No	**100% irrigation (ºC)**	**50% irrigation (ºC)**	**0% irrigation (ºC)**	**50% irrigation change by to control (%)**	**0% irrigation change by to control (%)**
Mln-4	26.25g	32.31ab	33.22a	23.09	26.55
Mln-20	33.03a	28.90gh	30.12d	-12.50	-8.81
Mln-23	28.20ef	31.13cd	32.65a	10.39	15.78
Mln-27	31.74b	29.70fe	29.29d	-6.43	-7.72
Mln-28	30.48c	28.43h	27.74e	-6.73	-8.99
Cu-159	28.94de	31.80bc	32.45ab	9.88	12.13
CU-213	27.27f	33.01a	33.14a	21.05	21.53
Cu-280	29.47d	30.66de	31.13c	4.04	5.63
CU-311	32.89a	30.16ef	31.79bc	-8.30	-3.34
Mean	29.80	27.34	31.28	3.83	5.86
LSD $_{0.05}$	0.82	0.81	0.77	-	-

http://www.aloki.hu ● ISSN 1589 1623 (Print) ● ISSN 1785 0037 (Online)
DOI: http://dx.doi.org/10.15666/aeer/1704_999710012

As the leaf temperature increased, a decrease in the transpiration rates of the leaves was observed. All of the melon genotypes were increased leaf temperature under salt and drought stress. The best performers in terms of leaf stoma conductance have been selected by taking into account the % change quantities 50% and 0% irrigation of the melon genotypes in the experiment in comparison to their control in drought stress application. These genotypes are respectively; Mln-27 (131.32%) and Cu311 (-5.09%), and the most affected 50% and 0% irrigation of melon genotypes from the percentage change in the drought stress compared to control have been Mln-4(-70%) and Mln-4 (-89.04%), respectively (*Table 6*). The best performers in terms of leaf temperature have been selected by taking into account the % change quantities 50% and 0% irrigation of the melon genotypes in the experiment in comparison to their control in drought stress application. These genotypes are respectively; Mln-20 (-12.50%) and Mln-20 (-8.81%), and the most affected 50% and 0% irrigation of melon genotypes from the percentage change in the drought stress compared to control have been Mln4 (23.09%) and Mln4 (26.55%), respectively (*Table 7*). Leaf temperature of all melon genotypes increased under drought stress. Lack of water and salinity cause stoma closure, a reduced transpiration rate, and high canopy leaf temperature (Halim et al., 1990). During drought, leaves are exposed to both heat and water deficiency stress (Clarke et al., 1993). As a result of the decrease in the transpiration rates of the leaves, the leaf temperature increases. All melon genotypes increased leaf temperature under salt and drought stress. Mohammadian et al. (2001) asserted that sugar beet becomes fading in the conditions of drought in response to the lack of water and tend to spread to the soil and thus increased the effective area exposed to the sun, so the decreased transpiration rates of these leaves increase the temperature of the leaf. Azevedo et al. (2004) reported that leaf temperature increased with salinity.

The average value of leaf water potential, osmotic potentialunder drought stress 50% and 0% irrigation of melon genotypes tested has been -0.32, -0.32 in 50% irrigation and -0.27, -0.26 in 0% irrigation the mean of control plants has been -0.54, -0.16, respectively (*Tables 8, 9*). It may cause to holding relatively large volumes of protoplasts in the inhibition of photosynthesis under low osmotic potential (Matthews and Boyer, 1984; Chaves et al., 2002; Grzesıak et al., 2006). Leaf water potential and osmotic potential of all melon genotypes decreased under salt and drought stress.

Table 8. *In the applications of melon genotypes quantities in different 50% and 0% irrigation under the normal condition and drought stress condition; leaf water potential quantity of (%) change by to control*

Genotypes No	100% irrigation (MPa)	50% irrigation (MPa)	0% irrigation (MPa)	50% irrigation change by to control (%)	0% irrigation change by to control (%)
Mln-4	-0.61de	-0.26c	-0.14b	-57.38	-77.05
Mln-20	-0.68e	-0.45e	-0.45f	-33.82	-23.17
Mln-23	-0.47ab	-0.33d	-0.24c	-29.79	-48.94
Mln-27	-0.59cd	-0.53f	-0.58e	-10.17	-14.71
Mln-28	-0.53bc	-0.43e	-0.35d	-18.87	-33.96
Cu-159	-0.44a	-0.18b	-0.11ab	-59.09	-75.00
CU-213	-0.42a	-0.12a	-0.09a	-79.31	-84.48
Cu-280	-0.58cd	-0.16ab	-0.10ab	-61.90	-76.19
CU-311	-0.54bd	-0.43e	-0.33d	-20.37	-38.89
Mean	-0.54	-0.32	-0.27	-41.19	-52.49
$LSD_{0.05}$	0.082	0.055	0.037	-	-

http://www.aloki.hu ● ISSN 1589 1623 (Print) ● ISSN 1785 0037 (Online)
DOI: http://dx.doi.org/10.15666/aeer/1704_999710012

However, resistant genotypes showed high water potential in both stress conditions. Levitt (1972), Ashraf and Oleary (1996), Anyia and Herzog (2004), Xu and Zhou (2008), Fahad et al. (2017) and Echevarri-Zomeno et al. (2009) suggested that leaf water potential may differ between durable and sensitive cultures of different crops. In addition, drought tolerant plants are expected to have a much lower osmotic potential than those that are susceptible to drought when exposed (Ashraf and Oleary, 1996). Considering the 50% and 0% irrigation in the experiment, the best genotypes showing the best response in terms of leaf water potentialwere selected. These genotypes are respectively; Mln 27 (-10.17%) and Mln27 (-14.71%), and the most affected 50% and 0% irrigation of melon genotypes from the percentage change in the drought stress compared to control have been Cu213 (-79.31%) and Cu213 (-84.48%), respectively (*Table 8*). Considering the 50% and 0% irrigation in the experiment, the best genotypes showing the best response in terms of osmotic potential were selected. These genotypes are respectively; Mln27 (11.65%) and Mln27 (12.5%), and the most affected 50% and 0% irrigation of melon genotypes from the percentage change in the drought stress compared to control have been Mln4 (-17.24%) and CU213 (35.85%), respectively (*Table 9*).

Table 9. *In the applications of melon genotypes quantities in different 50% and 0% irrigation under the normal condition and drought stress condition; leaf osmotic potential quantity of (%) change by to control*

Genotypes No	100% irrigation (MPa)	50% irrigation (MPa)	0% irrigation (MPa)	50% irrigation change by to control (%)	0% irrigation change by to control (%)
Mln-4	-0.1490a	-0.12	-0.14a	-17.24	-6.42
Mln-20	-0.1520a	-0.45	-0.20c	196.05	31.58
Mln-23	-0.1776b	-0.32	-0.23d	80.18	29.50
Mln-27	-0.1433a	-0.16	-0.18b	11.65	12.5
Mln-28	-0.1496a	-0.43	-0.34ef	187.43	128.19
Cu-159	-0.1640ab	-0.18	-0.24d	9.76	46.34
CU-213	-0.1526a	-0.53	-0.34ef	247.31	-35.85
Cu-280	-0.1450a	-0.26	-0.34f	74.50	134.48
CU-311	-0.1776b	-0.43	-0.33e	142.12	85.81
Mean	-0.16	-0.32	-0.26	103.53	47.35
LSD $_{0.05}$	0.02	ns	0.01	-	-

ns = not significantly

The average value of Ca concentrations in leaf under drought stress 50% and 0% irrigation of melon genotypes tested has been 4.03 and 3.22, respectively and the mean of control plants has been 5.13. Decrease 50% and 0% irrigation indices have occurred as 17.77%, 35.37% respectively according to control of melon genotypes under drought stress (*Table 10*). The average value of K concentrations in leaf under drought stress 50% and 0% irrigation of melon genotypes tested has been 4.03 and 3.22, respectively and the mean of control plants has been 5.13. Decrease 50% and 0% irrigation indices have occurred as 19.63%, 30.05%, respectively according to control of melon genotypes under drought stress (*Table 11*). In the present experiment, calcium (Ca) levels in the leaves were significantly lower in the water-stressed plants and supplemented potassium (K) enhanced leaf Ca. In this study, It is clearly seen that under 0% drought stress, calcium concentration is significantly lower than potassium concentration (*Tables 10, 11*). Similar results were reported in Pearlmillet (Ashraf et al., 2002). Calcium plays a

http://www.aloki.hu ● ISSN 1589 1623 (Print) ● ISSN 1785 0037 (Online)
DOI: http://dx.doi.org/10.15666/aeer/1704_999710012

vital role in maintaining membrane stability and permeability (Mengel and Kirkby, 1987). Higher Ca concentrations in plant tissues can also help with better crop health with improved yields in stress conditions (Cachorro et al., 1994).

Considering the 50% and 0% irrigation in the experiment, the best genotypes showing the best response in terms Ca and K concentrations in leaf were selected. This genotypeis respectively; Mln 28 and the most affected 50% and 0% irrigation of melon genotypes from the percentage change in the drought stress compared to control have been mln 4 and Cu213, respectively (*Tables 10, 11*).

Table 10. *In the applications of melon genotypes quantities in different 50% and 0% irrigation under the normal condition and drought stress condition; Ca concentrations in leaf quantity of (%) change by to control*

Genotypes No	100% irrigation (%)	50% irrigation (%)	0% irrigation (%)	50% irrigation change by to control (%)	0% irrigation change by to control (%)
Mln-4	7.56a	2.81e	1.49d	-62.83	-80.29
Mln-20	7.50a	7.19a	7.53a	-4.13	0.40
Mln-23	4.55d	2.22f	1.54c	-51.21	-66.15
Mln-27	3.44e	3.76d	3.45c	9.30	0.29
Mln-28	3.49c	4.47c	3.79c	28.08	8.60
Cu-159	3.01f	2.22f	1.13d	-26.25	-62.46
CU-213	5.42c	2.79e	0.49e	-48.52	-90.96
Cu-280	5.79b	4.29cd	3.86c	-25.91	-33.33
CU-311	5.39c	6.55b	5.69b	21.52	5.57
Mean	5.13	4.03	3.22	-17.77	-35.37
LSD $_{0.05}$	0.22	0.24	0.49	-	-

Table 11. *In the applications of melon genotypes quantities in different 50% and 0% irrigation under the normal condition and drought stress condition; K concentrations in leaf quantity of (%) change by to control*

Genotypes No	100% irrigation (%)	50% irrigation (%)	0% irrigation (%)	50% irrigation change by to control (%)	0% irrigation change by to control (%)
Mln-4	3.56a	1.21cd	0.65b	-66.01	-81.74
Mln-20	2.84c	2.66b	2.45b	-6.34	-13.73
Mln-23	2.49de	1.45c	1.05c	-41.77	-57.83
Mln-27	3.50a	3.67a	3.45a	4.86	-1.43
Mln-28	2.57d	3.87a	3.17a	50.58	23.35
Cu-159	2.42de	0.77de	0.58d	-68.18	-76.03
CU-213	3.35ab	0.77e	0.39d	-77.01	-88.36
Cu-280	2.29e	2.68b	2.75b	17.03	20.09
CU-311	3.24b	3.57a	3.41a	10.19	5.25
Mean	2.918	2.29	1.989	-19.63	-30.05
LSD $_{0.05}$	0.24	0.45	0.33	-	-

Knight et al. (1997) showed that osmotic stress increases the cytosolic free calcium in Arabidopsis seedlings and these changes in Ca^{2+} levels can mediate the expression of drought-induced genes with protective functions. Potassium nutrient can management has the potential to minimum the influences of drought stress in cotton (Zahoor et al., 2016) and Similar study (Kusvuran and Dasgan, 2011). Askari et al. (2017) rapored that drought stress highest effect on reducing content of chlorophyll index and concentration

http://www.aloki.hu ● ISSN 1589 1623 (Print) ● ISSN 1785 0037 (Online)
DOI: http://dx.doi.org/10.15666/aeer/1704_999710012

of N and P nutrition element in leafage, while concentrations of K, Zn, Fe, Cu and Na raised with drought stress. The lower tolerability of plants with K-deficiency can be attributed to the role of K in stoma regulation, which is the main mechanism that controls the water balance in plants. This may also be due to the role of K as the major osmoticum in the vacuole, even maintain a high tissue water potential in severe drought conditions.

The average value of membrane damage on leaf cells under drought stress 50% and 0% irrigation of melon genotypes tested has been 7.23 and 8.00, respectively (*Table 12*). The cell membrane is one of the main cellular targets common to different stresses (Levitt, 1972). The extent of its damage is commonly used as a measure of tolerance to various stresses in plants such as freezing heat (Dexter, 1956), drought (Blum and Ebercon, 1981; Tiwari et al., 2016) and salt (Leopold and Willing, 1983). Bewley (1979) reviewed drying tolerance in high plants and concluded that the critical properties of desiccant tolerance depend on their ability to limit membrane damage during water stress and to regain membrane integrity and membrane-related activities on rehydration.

Table 12. *In the applications of melon genotypes quantities in different 50% and 0% irrigation under the normal condition and drought stress condition; membrane damage on leaf cells quantity of (%) change by to control*

Genotypes No	50% Irrigation	0% Irrigation
Mln-4	8.20b	5.58f
Mln-20	4.72f	5.48f
Mln-23	6.74d	5.34f
Mln-27	7.53c	11.56b
Mln-28	9.06a	13.07a
Cu-159	8.14bc	8.40d
CU-213	8.52ab	5.80f
Cu-280	6.63d	7.47e
CU-311	5.54e	9.32c
Mean	7.23	8.00
$LSD_{0.05}$	0.63	0.49

The average Brix value in the fruit under drought stress was 50% and 0% irrigation of the tested melon genotypes was 6.74, 8.62 respectively, and the control plants average was 6.28. According to control, 50% and 0% irrigation indexes of melon genotypes under drought stress, were 10.75% and 47.91%, respectively (*Table 13*). The Brix value was found higher forthe melon by less irrigation (Shmueli and Golsberg, 1971; Bhella, 1985; Lester et al., 1994). In contrast to the other observed parameters, the linear regression test has a value of 0.60 and 0.32 r2 for the sub-surface drip irrigation system. Brix and r2 values are better explained as 0.27 and 0.4 for the surface drip irrigation system. However, Fabeiro et al. (2002) detected in their conducted study that the value of Birx decreases as irrigation increases.

Considering the 50% and 0% irrigation in the experiment, the best genotypes showing the best response in terms of Brix of fruit were selected. These genotypes are respectively; Mln (32.39%) and Mln (125.51%), and the most affected 50% and 0% irrigation of melon genotypes from the percentage change in the drought stress compared to control have been Cu213 (-15.71%) and Cu213 (-12.42%), respectively (*Table 13*).

http://www.aloki.hu ● ISSN 1589 1623 (Print) ● ISSN 1785 0037 (Online)
DOI: http://dx.doi.org/10.15666/aeer/1704_999710012

Table 13. *In the applications of melon genotypes quantities in different 50% and 0% irrigation under the normal condition and drought stress condition; brix in fruit quantity of (%) change by to control*

Genotypes No	100% irrigation (%)	50% irrigation (%)	0% irrigation (%)	50% irrigation change by to control (%)	0% irrigation change by to control (%)
Mln-4	7.12	6.85	6.33	-3.79	-11.10
Mln-20	5.77	6.71	8.48	16.29	46.97
Mln-23	5.42	6.11	7.55	12.73	39.30
Mln-27	5.41	6.13	12.20	13.31	125.51
Mln-28	4.94	6.54	10.25	32.39	107.49
Cu-159	8.56	8.55	9.58	-0.12	11.92
CU-213	6.24	5.26	5.46	-15.71	-12.50
Cu-280	7.55	8.39	9.62	11.13	27.42
CU-311	5.49	6.08	8.12	10.75	47.91
Mean	6.28	6.74	8.62	8.55	39.50
LSD $_{0.05}$	ns	ns	ns	-	-

ns = not significantly

The average value of water use efficiency under drought stress 50% and 0% irrigation of melon genotypes tested has been 13.71, 19.77 respectively and the mean of control plants has been 12.05. Increase 50% and 0% irrigation indices has occurred as 37.90%, 93.85% respectively according to control of melon genotypes under drought stress (*Table 14*). Causes and effects of drought and salt stresses, which was basically justifiable by their salt- and water retention ability (Khodadadi Dehkordi, 2017). The average value of total fruit yield under drought stress 50% and 0% irrigation of melon genotypes tested has been 13470, 16190 (kg/ha) respectively and the mean of control plants has been 14690 (kg/ha) (*Table 15*). Water stress significantly reduced the fruit yield of the melon plant. Similar results (Srinivas et al., 1989) were obtained from melon and watermelon by Bhella (1985). In our previous study, a decrease in melon fruit yield was seen due to water stress (Kirnak et al., 2005).

Table 14. *In the applications of melon genotypes quantities in different 50% and 0% irrigation under the normal condition and drought stress condition; water use efficiency quantity of (%) change by to control*

Genotypes No	100% irrigation (%)	50% irrigation (%)	0% irrigation (%)	50% irrigation change by to control (%)	0% irrigation change by to control (%)
Mln-4	10.85d	9.61f	8.16g	-10.32	-25.70
Mln-20	9.89d	17.78b	26.38a	79.76	156.58
Mln-23	14.96b	17.70b	21.55d	18.34	41.79
Mln-27	9.77d	18.30a	24.95b	87.89	156.95
Mln-28	7.88e	11.35e	23.19c	43.18	192.79
Cu-159	13.65c	14.16c	19.23e	9.67	31.60
CU-213	29.12a	11.62e	21.46d	-61.54	-31.09
Cu-280	7.35e	13.34d	18.28e	81.28	137.25
CU-311	4.94f	9.56f	14.77f	92.83	184.50
Mean	12.05	13.71	19.77	37.90	93.85
LSD $_{0.05}$	ns	0.30	1.17	-	-

ns = not significantly

http://www.aloki.hu ● ISSN 1589 1623 (Print) ● ISSN 1785 0037 (Online)
DOI: http://dx.doi.org/10.15666/aeer/1704_999710012

Table 15. *In the applications of melon genotypes quantities in different 50% and 0% irrigation under the normalcondition and drought stress condition; Total fruit yield quantity of (%) change by to control*

Genotypes No	100% irrigation (kg/ha)	50% irrigation (kg/ha)	0% irrigation (kg/ha)	50% irrigation change by to control (%)	0% irrigation change by to control (%)
Mln-4	13080c	9680e	6550	-25.99	-49.92
Mln-20	11780d	18070ab	20890	53.40	77.33
Mln-23	16900b	17220b	18030	1.89	6.69
Mln-27	11550d	18350a	20930	58.87	81.21
Mln-28	9000e	12340d	18720	37.11	108.00
Cu-159	15770b	13380c	15660	-15.16	-0.70
CU-213	34570a	11700d	17720	-66.16	-48.74
Cu-280	8440e	13320c	14710	57.82	74.29
CU-311	5790f	9590e	12460	65.63	115.20
Mean	14100	1374	16190	-	-
LSD $_{0.05}$	115.29	92.85	ns	-	-

ns = not significantly

The best performers in terms of water use efficiency and total fruit yield have been selected by taking into account the % change quantities 50% and 0% irrigation of the melon genotypes in the experiment in comparison to their control in drought stress application. These genotypes are respectively; Mln27 and Mln 28 (*Tables 14, 15*).The ranking of genotypes is shown in the *Table 16*. Classification of the 9 melon genotypes for their drought responses to tolerant, mild tolerant, susceptible in this *Table 17*.

Table 16. *The experiment melon genotypes grown under irrigation 50% and 0% compared to the control parameters are recorded and measured changes in Physiological quantities weighted rating process is done, the highest score genotipten until the lowest point genotipe*

Genotype No	Weighted Rating
Mln-28	5343
CU-311	4526
Mln-27	4519
Mln-20	4321
Cu-280	3029
Mln-23	-19
Cu-159	-956
Mln-4	-2452
CU-213	-3397

Table 17. *Classification of the 9 melon genotypes for their drought responses*

Tolerant	Mild Tolerant	Susceptible
CU-311	Mln-23	Mln-4
Mln-28	Cu-159	CU-213
Mln-27		
Mln-20		
Cu-280		

http://www.aloki.hu ● ISSN 1589 1623 (Print) ● ISSN 1785 0037 (Online)
DOI: http://dx.doi.org/10.15666/aeer/1704_999710012

Conclusion

After that, our ongoing studies will be included that Mln 28 and CU 311 genotypes which are the most tolerant selected for the second times repeating of "drought stress performance in the field" and the most suitable for commercial improving by doing the selection of melon genotypes, and an evidence variety. The need for reinforcing the tolerance levels of genotypes in drought stress conditions will be more apparent after the second re-experiment by the prominence of hopeful lines.

Acknowledgements. This study was made possible through a part of TUBITAK- KAMAG 109 G099 No 'F1 TURKEY Vegetable Varieties and Qualified Line Development Project.

REFERENCES

[1] Anyia, A. O., Herzog, H. (2004): Genotypic variability in drought performance and recovery in cowpea under controlled environment. – J. Agron. Crop Sci. 190: 151-159.
[2] Ashraf, M., Oleary, J. W. (1996): Effect of drought stress on growth, water relatıons, and gas exchange of two lınes of sunflower dıfferıngın degree of salt tolerance. – Int. J. Plant Sci. 157(6): 729-732.
[3] Ashraf, M., Ashfaq, M., Ashraf, M. Y. (2002): Effects of increasedsupply of potassium on growth andnutrient content in pearl millet under water stress. – Biologia Plantarum 45: 141-144.
[4] Askari, A., Ardakani, M. R., Vazan, S., Paknejad, F., Hosseini, Y. (2017): The effect of mycorrhizal symbiosis and seed priming on the amount of chlorophyll index and absorption of nutrients under drought stress in sesame plant under field conditions. – Applied ecology and environmental research 16(1): 335-357.
[5] Azevedo, N. A., Prisco, J. T., Filho, J. E., Lacerda, C. F., Silva, J. V., Costa, P. H., Filho, E. G. (2004): Effects of salt stress on plant growth, stomatal response and solute accumulation of different maize genotypes. – Braz. J. Plant Physiol. 16(1): 31-38.
[6] Bewley, J. D. (1979): Physiological aspects of desiccation tolerance. – Annu Rev Plant Physiol 30: 195-238.
[7] Bhella, H. S. (1985): Muskmelon growth. Yield and nutrient as influenced by planting method and trickle irrigation. – J Am Soc Hortic Sci 110: 793-796.
[8] Blum, A., Ebercon, A. (1981): Cell membrane stability as a measure of drought and heat tolerance in wheat. – Crop Sci 21: 43-47.
[9] Boyer, J. S. (1982): Plant productivity and environment. – Science 218: 443-448.
[10] Bray, E. A., Bailey-Serres, J., Weretilnyk, E. (2000): Responses to abiotic stresses. – In: Gruissem, W., Buchannan, B., Jones, R. (eds.) Biochemistry and molecular biology of plants. American Society of Plant Physiologists, Rockville, MD, pp 1158-1249.
[11] Cachorro, P., Ortiz, A., Cerda, A. (1994): Implications of calcium on theresponse of Phaseolus vulgaris L. to salinity. – Plant and Soil 159: 205-212.
[12] Chaves, M. M., Pereira, J. S., Maroco, J., Rodrigues, M. L., Ricardo, C. P. P., Osorio, M. L., Carvalho, I., Faria, T., Pinheiro, C. (2002): How plants cope with water stress in the field, Photosynthesis and Growth. – Annals of Botany 89: 907-916.
[13] Clarke, N., Hetschkun, H., Jones, C., Boswell, E., Marfaing, H. (1993): Identification of stress tolerance traits in sugar beet. – In: Jackson, M. B., Black, C. R. (eds.) Interacting Stress on Plants in a Changing Climate. Springer-Verlag, Berlin, pp. 511-524.
[14] Dadkhah, A. R. (2010): Effect of long term salt stress on gas exchange and leaf carbohydquantity contents in two sugar beet (Beta vulgaris L.) cultivars. – Res. J. Biol. Sci. 5(8): 512-516.

http://www.aloki.hu ● ISSN 1589 1623 (Print) ● ISSN 1785 0037 (Online)
DOI: http://dx.doi.org/10.15666/aeer/1704_999710012

[15] Dexter, S. T. (1956): Evaluation of crop plants for winter hardiness. – Adv Agron 8: 203-209.
[16] Dlugokecka, E., Kacperska-Palacz, A. (1978): Re-examination of electrical conductivity method for estimation of drought in-jury. – Biologia Plantarum (Prague) 20: 262-267.
[17] Echevarrıa-Zomeno, S., Arıza, D., Jorge, I., Lenz, C., Jesusvjorrı, N. A., Navarro, R. (2009): Changes ın the protein profile of Quercus ılex leaves in response to drought stress and recovery. – J. Plant Physiol. 166: 233-245.
[18] Fabeiro, C., de Santa Olalla, F. M., de Juan, J. A. (2002): Production of muskmelon (Cucumis melo L.) under controlled deficit irrigation in a semi-arid climate. – Agric Water Manag 54: 93-105.
[19] Fahad, S., Bajwa, A. A., Nazir, U., Anjum, S. A., Farooq, A., Zohaib, A., Sadia, S., Nasim, W., Adkins, S., Saud, S., Ihsan, M. Z., Alharby, H., Wu, C., Wang, D., Huang, J. L. (2017): Crop production under drought and heat stress: plant responses and management options. – Front. Plant Sci. 8: 1147. 10.3389/fpls.01147.
[20] Fan, S., Blake, T. G. (1994): Absisic acid ınduced electrolyte leakage in woody spe-cies with contrasting ecological require-ments. – Plant Physiol. 89: 817-823.
[21] Grzesiak, M. T., Grzesiak, S., Skoczowski, A. (2006): Changes of leaf water potential and gas exchange during and after drought in triticale and maize genotypes differing in drought tolerance. – Photosynthetica 44(4): 561-568.
[22] Gunay, A. (2005): Special Vegetable Growing. – Chapter, Tomato Breeding: 318-343.
[23] Halim, R. A., Buxton, D. R., Hattendorf, M. J., Carlson, R. E. (1990): Crop water stress ındex and forage quality relationships in alfalfa. – Agric. J. 82: 906-909.
[24] Khodadadi Dehkordi, D. (2017): Effect of superabsorbent polymer on salt and drought resistance of eucalyptus globules. – Applied ecology and environmental research 15(4): 1791-1802.
[25] Kirnak, H., Higgs, D., Kaya, C., Tas, I. (2005): Effects of irrigation and nitrogen quantitys on growth, yield,and quality of muskmelon in semiarid regions. – Journal of Plant Nutrition 28: 621-638.
[26] Knight, S. L., Rogers, R. B., Smith, M. A. L., Spomer, L. A. (1997): Effects of NaCl salinity on miniature dwarf tomato 'Micro-Tom': I. Growth analyses and nutrient composition. – Journal of Plant Nutrition15: 2315-2327.
[27] Kusvuran, S., Dasgan Y. H., Abak, K. (2011): Responses of different melon genotypes to drought stress. – Yuzuncu Yil University Journal of Agricultural Sciences 21: 209-219.
[28] Leopold, A. C., Willing, R. P. (1983): Evidence of toxicity effects of salt on membranes. – In: Staples, R. C., Toenniessen, G. H. (eds.) Plant improvement for irrigated crop production under increasing saline conditions. John Wiley and Sons, New York, pp 678-685.
[29] Lester, G. E., Oebker, N. F., Coons, J. (1994): Preharvest furrow and drip irrigation schedule effects on postharvest muskmelon quality. Postharvest Biol Thechnol 4: 57-63.
[30] Levitt, J. (1972): Responses of Plants to Environmental Stresses. – Academic Press, New York.
[31] Mafakheri, A. (2010): Effect of drought stress on yield, proline and chlorophyll contents in three chickpea cultivars. – Aust. J. Crop Sci. 4(8): 580-585.
[32] Matthews, M. A., Boyer, J. S. (1984): Acclimation of photosynthesis to low water potentials. – Plant Physiol. 74: 161-166.
[33] Mengel, K., Kirkby, E. A. (1987): Principles of Plant Nutrition. – Dordrecht, the Netherlands: KluwerAcademic.
[34] Mohammadian, R., Khoyi, F. R., Rahimian Moghaddam, H. M, Ghassemi Golezani, K., Sadeghian, S. Y. (2001): The effects of early season drought on stomatal conductance, leaf-air temperature difference and proline accumulation in sugar beet genotypes. – J. Agric. Sci. Technol. 3: 181-192.

http://www.aloki.hu ● ISSN 1589 1623 (Print) ● ISSN 1785 0037 (Online)
DOI: http://dx.doi.org/10.15666/aeer/1704_999710012

[35] Serrano, R., Mulet, J. M., Rios, G., Marquez, J. A., de Larrinoa, I. F., Leube, M. P., Mendizabal, I., Pascual-Ahuir, A., Proft, M., Ros, R., Montesinos, C. (1999): A glimpse of the mechanisms of ion homeostasis during salt stress. – J Exp Bot 50: 1023-1036.
[36] Shmueli, M., Golsberg, D. (1971): Sprinkler, furrow and trickle irrigation of muskmelon in an arid zone. – HortScience 6: 557-559.
[37] Silva, E. N., Ribeiro, R. V., Silva, S. L.,Viegas, R. A., Silveire, J. A. (2011): Salt stress induced damages on the photosynthesis of physic nut young plants. – Sci. Agric. 68(1): 62-68.
[38] Srinivas, K., Hedge, D. M., Havanagi, G. V. (1989): Plant water relations, canopy temperature, yield and water-use efficiency of watermelon Citrullus lanatus (Thunb.) Matsum et Nakai under drip and furrow irrigation. – Journal of Horticultural Science 64: 115-124.
[39] Tiwari, S., Puneet, C. L., Chandra, S. C., Nautiyal, S. (2016): Pseudomonas putida attunes morphophysiological: biochemicaland molecular responses in Cicer arietinum L. during drought stress and recovery. – Plant Physiol. Biochem. 99: 108-117.
[40] Turner, N. C., Begg, J. E., Tonnet, M. L. (1998): Osmotic adjustment of sorghum and sunflower crops in response to water deficits and its influence on the water potential at which stomta close. – Aust. J. Plant Physiol. 5(5): 597-608.
[41] Wang, W. X., Vinocur, B., Shoseyov, O., Altman, A. (2001): Biotechnology of plant osmotic stress tolerance. physiological and molecular considerations. – Acta Hort 560: 285-292.
[42] Wang, W. X., Vinocur, B., Altman, A. (2003): Plant responses to drought, salinity and extreme temperatures: towards genetic engineering for stress tolerance. – Planta 218: 1-14.
[43] Xu, Z., Zhou, G. (2008): Responses of leaf stomatal density to water status and its relationship with photosynthesis in a grass. – J. Exp. Bot. 59(12): 3317-3325.
[44] Zahoor, R., Dong, H., Abid, M., Zhao, W., Wang, Y., Zhou, Z. (2017): Potassium fertilizer improves drought stress alleviation potential in cotton by enhancing photosynthesis and carbohydrate metabolism. – Environmental and Experimental Botany 137: 73-83.
[45] Zhou, R., Yu, X., Ottosen, C., Rosenqvist, E., Zhao, L., Wang, Y., Yu, W., Zhao, T., Wu, Z. (2017): Drought stress had a predominant effect over heat stress on three tomato cultivars subjected to combined stress. – BMC Plant Biology 17: 24.
[46] Zhu, J. K. (2001): Plant salt tolerance. – Trends Plant Sci 6: 66-71.

http://www.aloki.hu ● ISSN 1589 1623 (Print) ● ISSN 1785 0037 (Online)
DOI: http://dx.doi.org/10.15666/aeer/1704_999710012